PDF Output of CLIC (clustering by inferred co-expression)

Dataset:

Num of genes in input gene set: 20

Total number of genes: 16493

CLIC PDF output has three sections:

1) Overview of Co-Expression Modules (CEMs)

- Heatmap shows pairwise correlations between all genes in the input query gene set.
- Red lines shows the partition of input genes into CEMs, ordered by CEM strength.
- Each row shows one gene, and the brightness of squares indicates its correlations with other genes.
- Gene symbols are shown at left side and on the top of the heatmap.

2) Details of each CEM and its expansion CEM+

- Top panel shows the posterior selection probability (dataset weights) for top GEO series datasets.
- Bottom panel shows the CEM genes (blue rows) as well as expanded CEM+ genes (green rows).
- Each column is one GEO series dataset, sorted by their posterior probability of being selected.
- The brightness of squares indicates the gene's correlations with CEM genes in the corresponding dataset.
- CEM+ includes genes that co-express with CEM genes in high-weight datasets, measured by LLR score.

3) Details of each GEO series dataset and its expression profile:

- Top panel shows the detailed information (e.g. title, summary) for the GEO series dataset.
- Bottom panel shows the background distribution and the expression profile for CEM genes in this dataset.

Overview of Co-Expression Modules (CEMs) with Dataset Weighting

Num of Genes in Query Geneset: 20. Num of CEMs: 0.

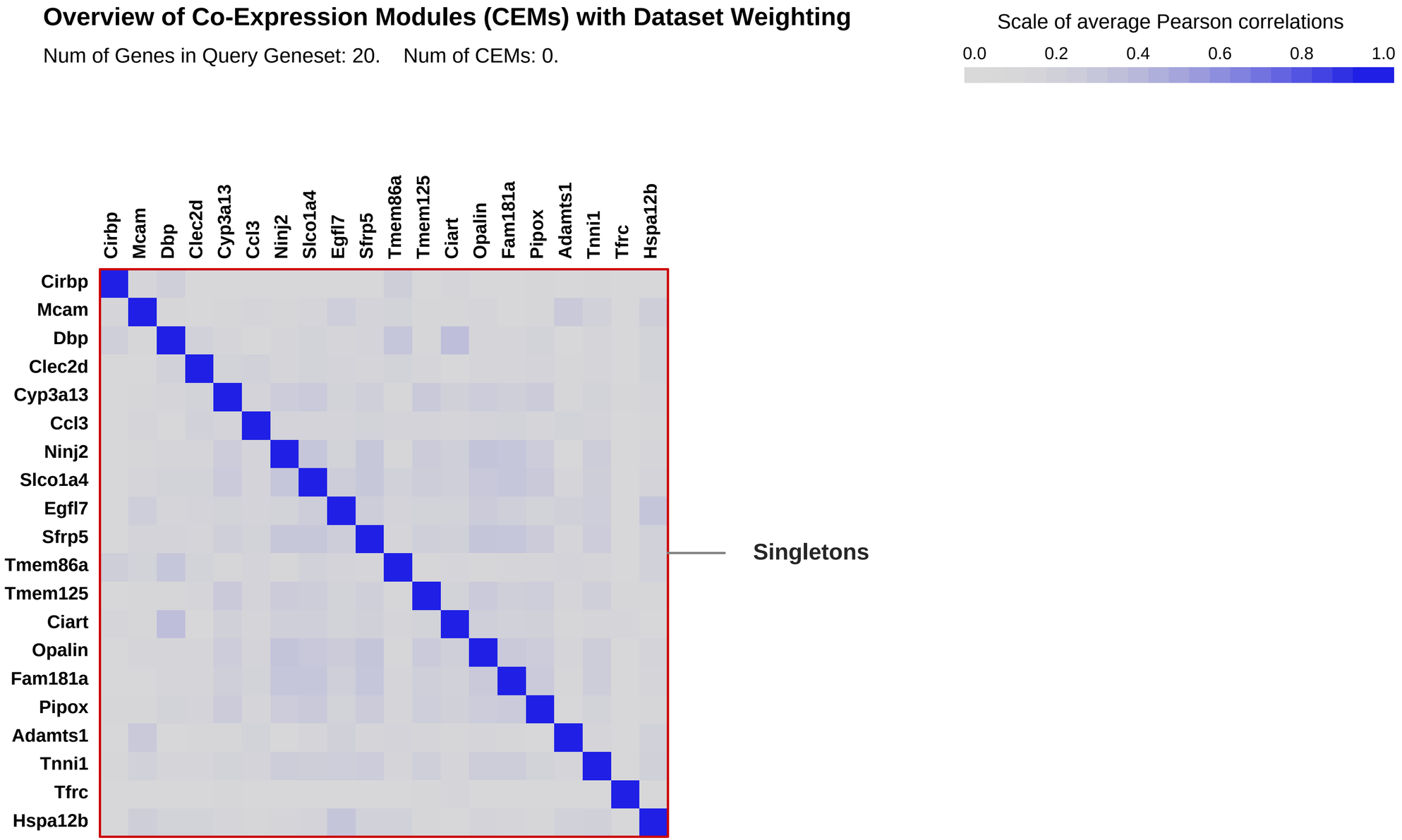

GEO Series "GSE56482" Expression Profiles

Num of samples in this series: 8

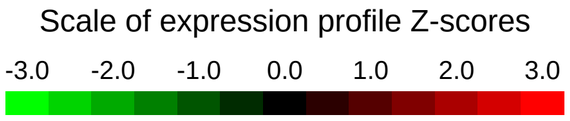

GEO Link:	**http://www.ncbi.nlm.nih.gov/geo/query/acc.cgi?acc=GSE56482**
Status:	**Public on Jul 04 2014**
Title:	**Expression Data comparing Gene Expression in 27-day old testes of wild-type and Brwd1-/- mice**
Organism:	**Mus musculus**
Experiment type:	**Expression profiling by array**
Platform:	**GPL1261**
Pubmed ID:	
Summary & Design:	**Summary:** **Brwd1-/- mice are infertile with post-meiotic defects in the male. BRWD1 contains bromodomains and may function as a transcriptional regulator important for post-meiotic development in the male germline.** **This microarray compares post-meiotic gene expression between WT and mutant mice.** **Overall design:** **We collected total RNA from testes of 27-day old WT and Brwd1-/- (MT) mice. At this age, germ cells have completed meiosis and are mid-way in post-meiotic development. Any gene expression changes in spermatids would be apparent at this time-point. We decided to do this with 4 WT and 4 Brwd1-/- mice.**

Background corr dist: **KL-Divergence = 0.0388, L1-Distance = 0.0285, L2-Distance = 0.0010, Normal std = 0.6239**

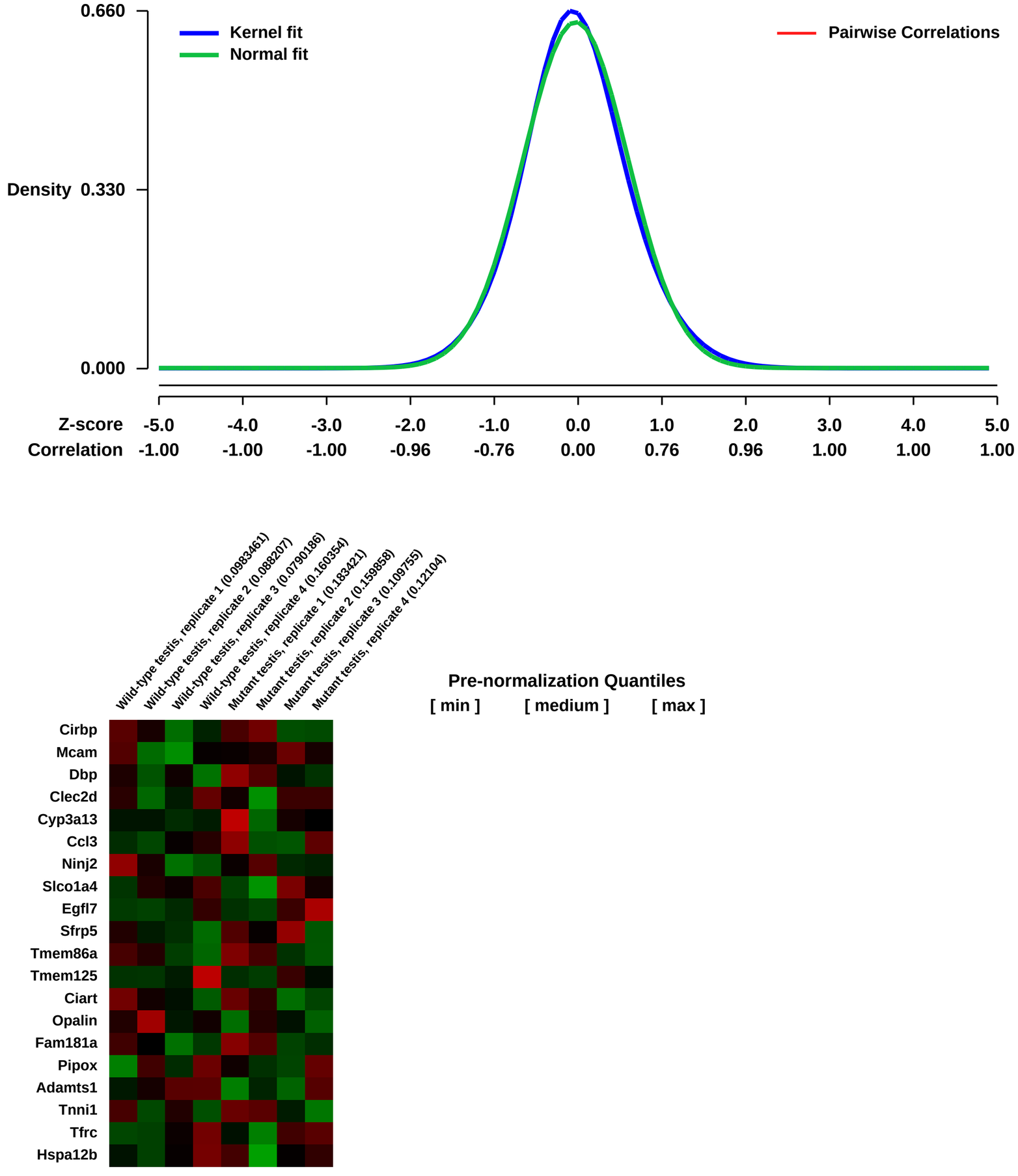

GEO Series "GSE37000" Expression Profiles

Num of samples in this series: 47

Scale of expression profile Z-scores

-3.0 -2.0 -1.0 0.0 1.0 2.0 3.0

GEO Link:	http://www.ncbi.nlm.nih.gov/geo/query/acc.cgi?acc=GSE37000
Status:	Public on Nov 01 2012
Title:	The transcriptional landscape of hematopoietic stem cell ontogeny
Organism:	Mus musculus
Experiment type:	Expression profiling by array
Platform:	GPL1261
Pubmed ID:	23122293
Summary & Design:	**Summary:** Transcriptome analysis of adult hematopoietic stem cells (HSC) and their progeny has informed our understanding of blood differentiation and leukemogenesis, but a similarly transformative analysis of the embryonic origins of hematopoiesis is lacking. To address this issue, we acquired gene expression profiles of developing HSC purified from over 2500 dissected murine embryos and adult mice, and applied a network biology-based analysis to reconstruct the gene regulatory networks of sequential stages of HSC development. We found that embryonic hematopoietic elements clustered into three distinct transcriptional states characteristic of the definitive yolk sac, HSCs emerging from hemogenic endothelium, and definitive HSCs. We functionally validated several candidate transcriptional regulators of HSC ontogeny by morpholino-mediated knock-down in zebrafish embryos, confirming changes in the expression of HSC markers runx1 and c-myb in the aorta-gonads-mesonephros (AGM), the site of definitive HSC specification. Moreover, we found that HSCs derived from differentiating embryonic stem cells in vitro (ESC-HSC) most closely resemble definitive HSC, yet lack a signature indicative of specification by Notch signaling, which likely accounts for their deficient lymphoid development. Our analysis and accompanying web resource will accelerate the characterization of regulators of HSC ontogeny, facilitate efforts to direct hematopoietic differentiation and cell fate conversion, and serve as a model to study the origins of other adult stem cells. **Overall design:** Hematopoietic stem cells and their precursors were isolated from mouse embryos and distinct stages and sites during development, purified by fluorescence activated cell sorting, and gene expression profiled on Affymetrix arrays. We also profiled HSCs and their precurors derived by in vitro differentitation of embryonic stem cells [expression data from GSE16925 and GSE14012 was used for mESCs, available at http://hsc.hms.harvard.edu/].

Background corr dist: KL-Divergence = 0.3392, L1-Distance = 0.0693, L2-Distance = 0.0137, Normal std = 0.2669

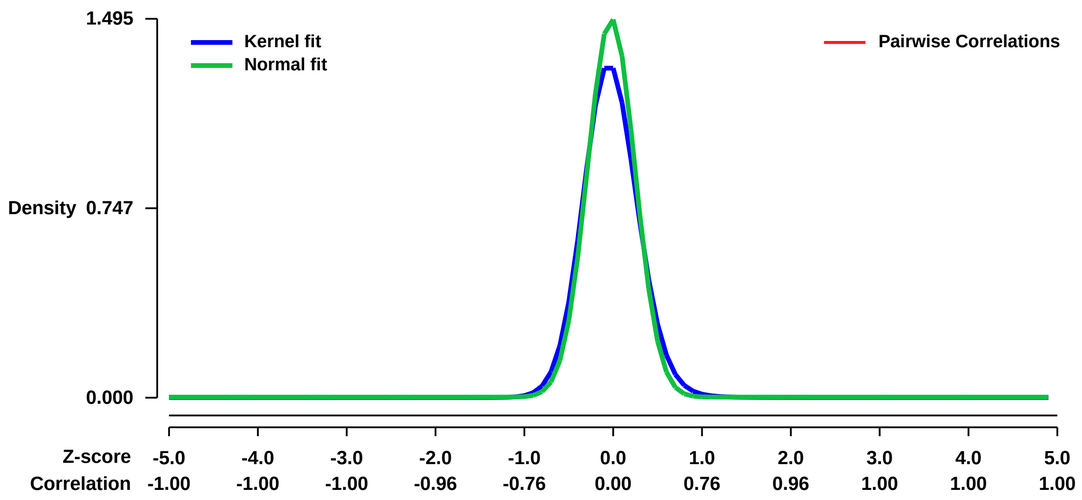

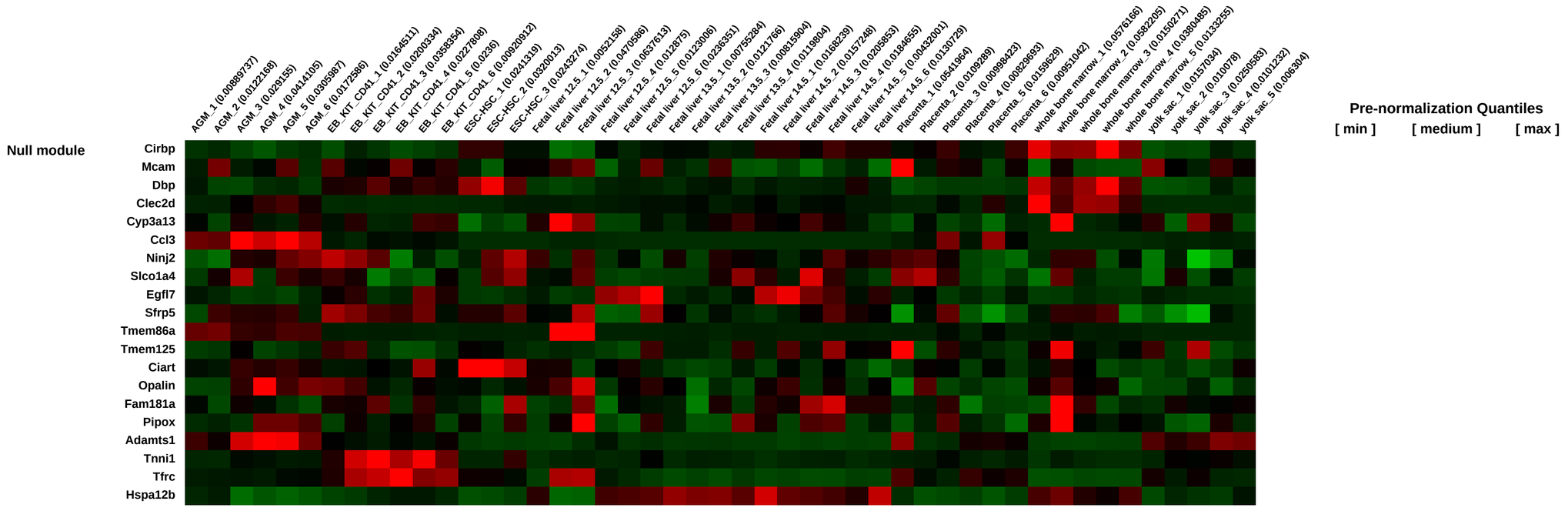

GEO Series "GSE25778" Expression Profiles

Num of samples in this series: 6

Scale of expression profile Z-scores

-3.0 -2.0 -1.0 0.0 1.0 2.0 3.0

GEO Link:	http://www.ncbi.nlm.nih.gov/geo/query/acc.cgi?acc=GSE25778
Status:	Public on Dec 03 2010
Title:	Genome profiling of mouse pulmonary epithelial type II cells
Organism:	Mus musculus
Experiment type:	Expression profiling by array
Platform:	GPL1261
Pubmed ID:	
Summary & Design:	**Summary:** Pulmonary alveoli contain two distinct populations of epithelial cells. Type II cells produce pulmonary surfactant lipids and surfactant-associated proteins (SP) required for maintaining alveolar surface tension at the air-liquid interface and host defense against respiratory pathogens. Type II cells are also progenitors for epithelial type I cells, a terminally differentiated elongated cell that covers microvascular endothelial cells and participates in gas exchange. Despite some indirect evidence, it is unknown whether subpopulations of type II cells exist. We created a line of transgenic mice expressing enhanced green fluorescent protein (EGFP) under control of the human SP-C promoter. Expression of EGFP may define a subpopulation of type II cells because it is 1) expressed in approximately 10% of type II cells, 2) appears much later in embryonic development than SP-C, and 3) selectively proliferates in mice infected with influenza A virus. To determine whether EGFP defines a unique subpopulation of type II cells, RNA was isolated from EGFP-positive and negative type II cells and hybridized to affymetrix arrays. Of the genes detected in EGFP-positive cells, most were equally detected in EGFP-negative cells. However, approximately 350 genes were selectively elevated â¥5-fold in EGFP-positive cells and 1500 genes selectively expressed by EGFP-negative cells. These findings suggest EGFP defines a subpopulation of type II epithelial cells in this line of transgenic mice. **Overall design:** Type II cells were harvested from approximately 10 young adult (8-week) mice and sorted into EGFP-positive (sample EGFP-1) and EGFP-negative (sample nonEGFP-1) populations using a B-D FACSVantage SE cell sorter. RNA was prepared from approximately two million cells and hybridized to Affymetrix M430 2.0 array as a one by one comparison. The isolation and gene expression analysis of EGFP-positive and EGFP-negative type II cells was repeated a second (using EGFP-2 and nonEGFP-2 samples) and third (using EGFP-3 and nonEGFP-3 samples) time.

Background corr dist: KL-Divergence = 0.0244, L1-Distance = 0.0296, L2-Distance = 0.0011, Normal std = 0.7429

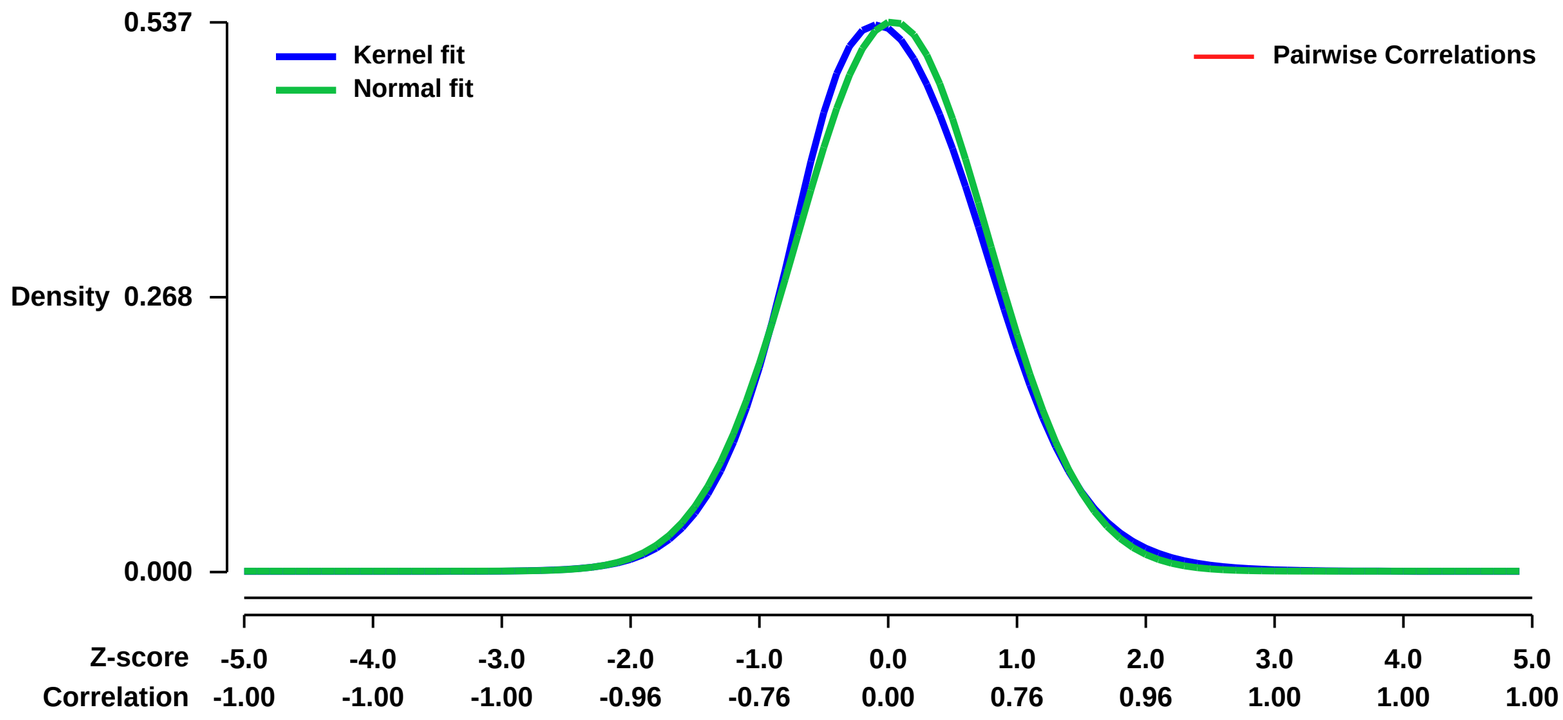

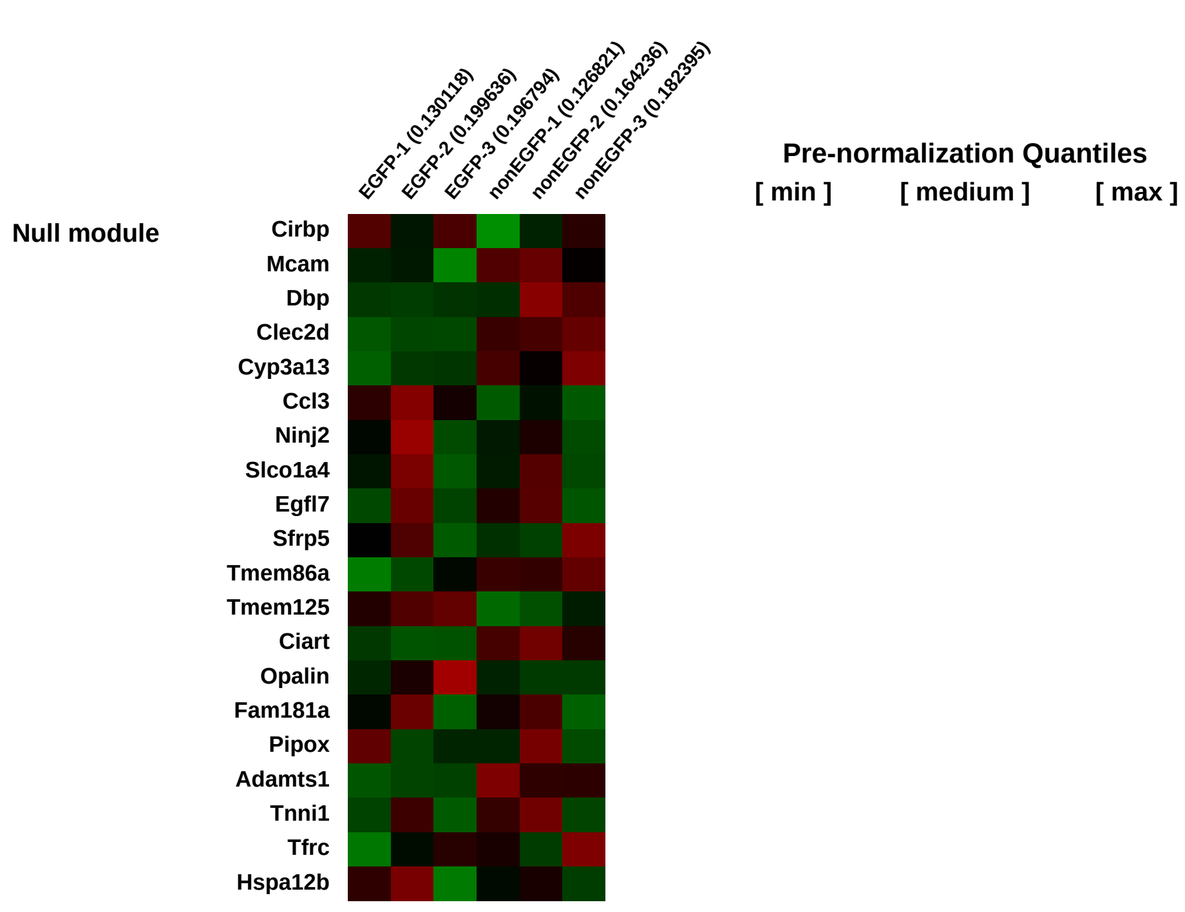

GEO Series "GSE28687" Expression Profiles

Num of samples in this series: 10

Scale of expression profile Z-scores

-3.0 -2.0 -1.0 0.0 1.0 2.0 3.0

GEO Link:	http://www.ncbi.nlm.nih.gov/geo/query/acc.cgi?acc=GSE28687
Status:	Public on Oct 01 2011
Title:	Defective K-Ras Oncoproteins Initiate Cancer In Vivo and Evolve to Overcome Impaired Effector Binding
Organism:	Mus musculus
Experiment type:	Expression profiling by array
Platform:	GPL1261
Pubmed ID:	23637129
Summary & Design:	**Summary:** The oncogenic proteins expressed in human cancer cells are exceedingly difficult targets for drug discovery due to intrinsic properties of the Ras GTPase switch. As a result, recent efforts have largely focused on inhibiting Ras-regulated kinase effector cascades, particularly the Raf/MEK/ERK and PI3 kinase/Akt/mTOR pathways. We constructed murine stem cell leukemia virus (MSCV) vectors encoding oncogenic K-RasD12 with additional â second siteâ amino acid substitutions that that impair PI3 kinase/Akt or Raf/MEK/ERK activation and performed bone marrow transduction/transplantation experiments in mice. In spite of attenuated signaling properties, defective K-Ras oncoproteins induced aggressive clonal T lineage acute lymphoblastic leukemia (T-ALL). These leukemias exhibited a high frequency of somatic Notch1 mutations, which is also true of human T-ALL. Multiple independent T-ALLs restored full oncogenic Ras activity by acquiring â third siteâ mutations within the viral KrasD12 transgenes. Other leukemias with undetectable PTEN and elevated phosphoryated Akt levels showed a similar gene expression profile to human early T progenitor (ETP) T-ALL. Expressing oncoproteins that are defective for specific functions is a general strategy for assessing requirements for tumor maintenance and uncovering potential mechanisms of drug resistance in vivo. In addition, our observation that defective Kras oncogenes regain potent cancer initiating activity strongly supports simultaneously targeting distinct components of Ras signaling networks in the substantial fraction of cancers with RAS mutations. **Overall design:** WT Balb/c mice were lethally irradiated and transplanted with WT Balb/c bone marrow cells transduced with MSCV-IRES-Kras mutant-GFP vectors. Mice developed T-cell lymphoproliferative disease.

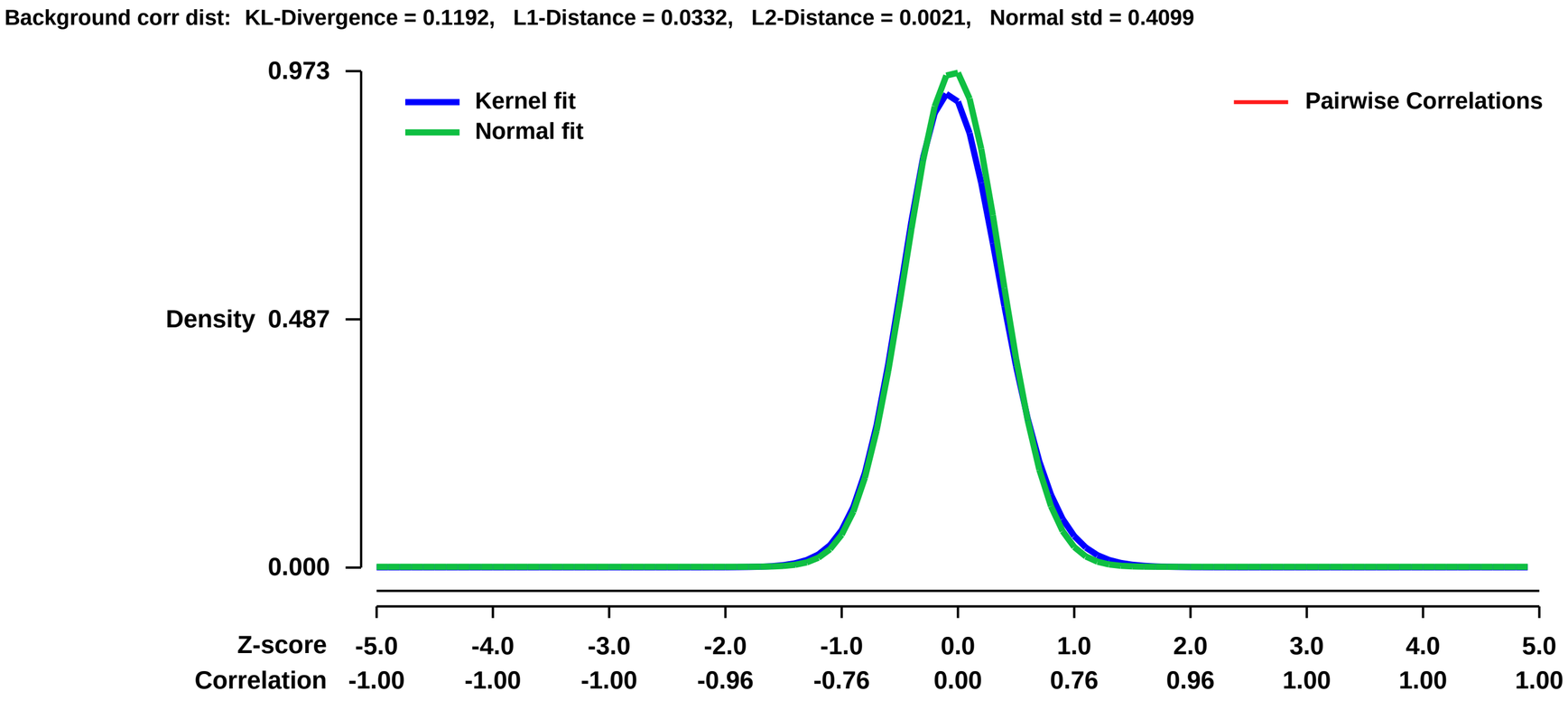

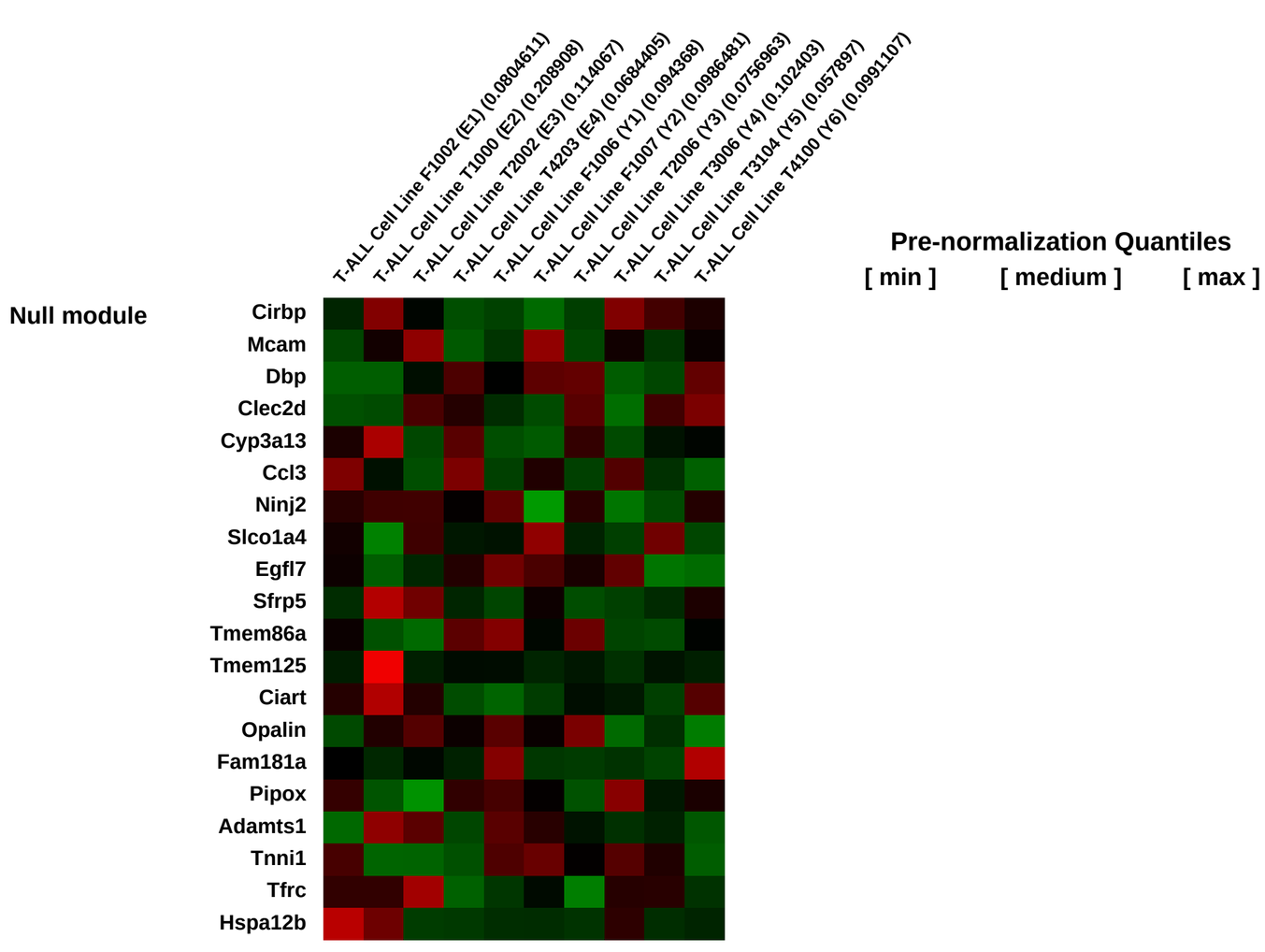

GEO Series "GSE9018" Expression Profiles

Num of samples in this series: 9

Scale of expression profile Z-scores

-3.0 -2.0 -1.0 0.0 1.0 2.0 3.0

GEO Link:	**http://www.ncbi.nlm.nih.gov/geo/query/acc.cgi?acc=GSE9018**
Status:	**Public on Dec 27 2007**
Title:	**IgA impact on distal small intestine after colonization with B. thetaiotaomicron**
Organism:	**Mus musculus**
Experiment type:	**Expression profiling by array**
Platform:	**GPL1261**
Pubmed ID:	**18005754**
Summary & Design:	**Summary:** **Wildtype B6, Rag1-/- B6 and Rag1-/- B6 mice harboring the 225.4 IgA producing hybridoma were colonized for 10 days with Bacteroides thetaiotaomicron** **Keywords: RNA Expression Array** **Overall design:** **Distal small intestine segments were snap frozen immediately after the mice were sacrificed, and small intestine divided into 16 equal segments, segments 10, 11, 12 and 14 were pooled and RNA extracted.**

Background corr dist: **KL-Divergence = 0.0788, L1-Distance = 0.0223, L2-Distance = 0.0008, Normal std = 0.4803**

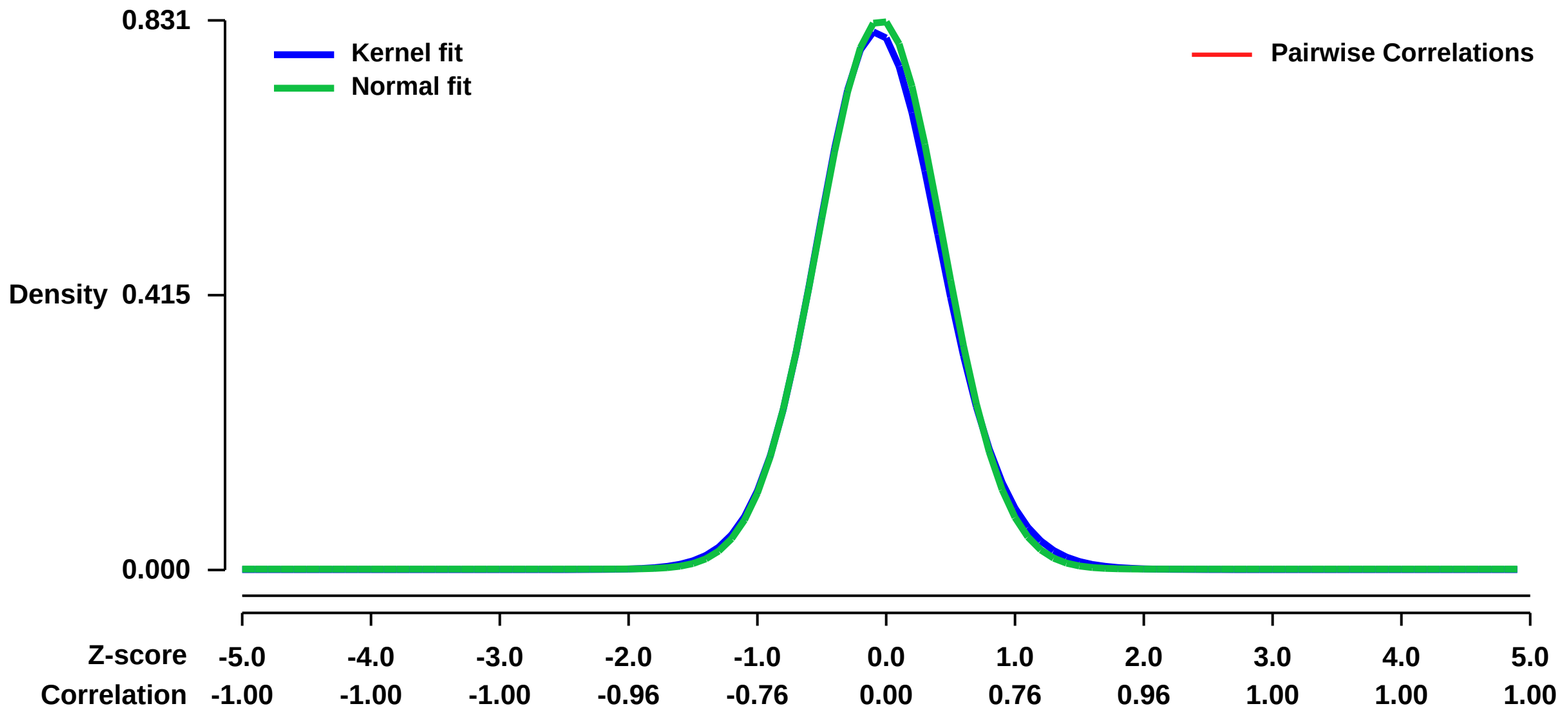

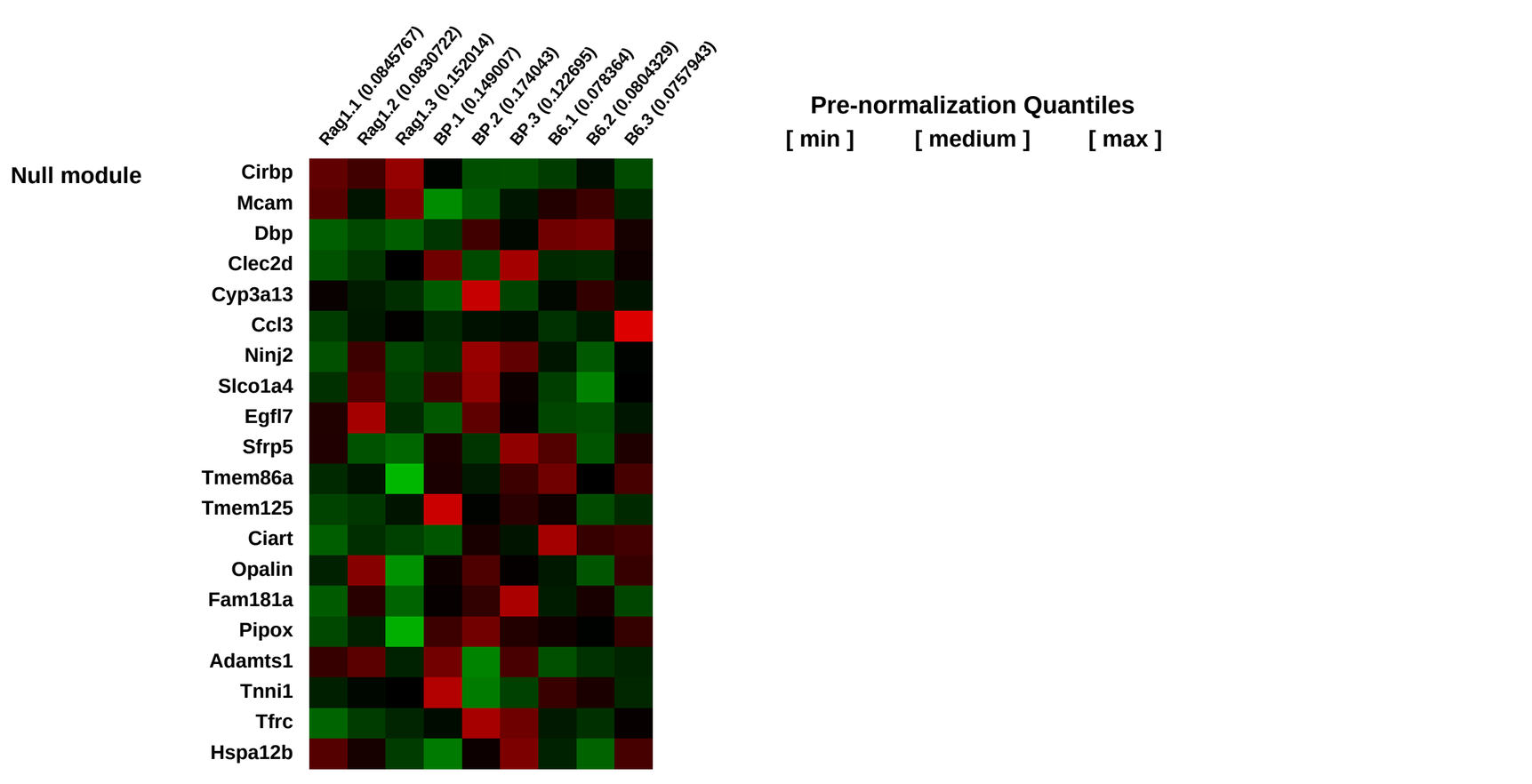

GEO Series "GSE31150" Expression Profiles

Num of samples in this series: 6

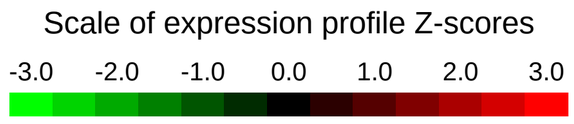

GEO Link:	http://www.ncbi.nlm.nih.gov/geo/query/acc.cgi?acc=GSE31150
Status:	Public on Nov 19 2012
Title:	The role of Raf-1 kinase inhibitor protein in the regulation of pancreatic beta cell proliferation in mice
Organism:	Mus musculus
Experiment type:	Expression profiling by array
Platform:	GPL1261
Pubmed ID:	22926403
Summary & Design:	**Summary:** **AIMS/HYPOTHESIS: Manoeuvres aimed at increasing beta cell mass have been proposed as regenerative medicine strategies for diabetes treatment. Raf-1 kinase inhibitor protein 1 (RKIP1) is a common regulatory node of the mitogen-activated protein kinase (MAPK) and nuclear factor ¸”B (NF-¸”B) pathways and therefore may be involved in regulation of beta cell homeostasis. The aim of this study was to investigate the involvement of RKIP1 in the control of beta cell mass and function.** **METHODS: Rkip1 (also known as Pebp1) knockout (Rkip1 (-/-)) mice were characterised in terms of pancreatic and glucose homeostasis, including morphological and functional analysis. Glucose tolerance and insulin sensitivity were examined, followed by assessment of glucose-induced insulin secretion in isolated islets and beta cell mass quantification through morphometry. Further characterisation included determination of endocrine and exocrine proliferation, apoptosis, MAPK activation and whole genome gene expression assays. Capacity to reverse a diabetic phenotype was assessed in adult Rkip1 (-/-) mice after streptozotocin treatment.** **RESULTS: Rkip1 (-/-) mice exhibit a moderately larger pancreas and increased beta cell mass and pancreatic insulin content, which correlate with an overall improvement in whole body glucose tolerance. This phenotype is established in young postnatal stages and involves enhanced cellular proliferation without significant alterations in cell death. Importantly, adult Rkip1 (-/-) mice exhibit rapid reversal of streptozotocin-induced diabetes compared with control mice.** **CONCLUSIONS/INTERPRETATION: These data implicate RKIP1 in the regulation of pancreatic growth and beta cell expansion, thus revealing RKIP1 as a potential pharmacological target to promote beta cell regeneration.** **Overall design:** **Pancreatic gene expression of Rkip-1 (Raf kinase inhibitor 1) knockout (KO) and wild type (WT) mice, including three biological replicates in each group.**

Background corr dist: KL-Divergence = 0.0457, L1-Distance = 0.0163, L2-Distance = 0.0003, Normal std = 0.5868

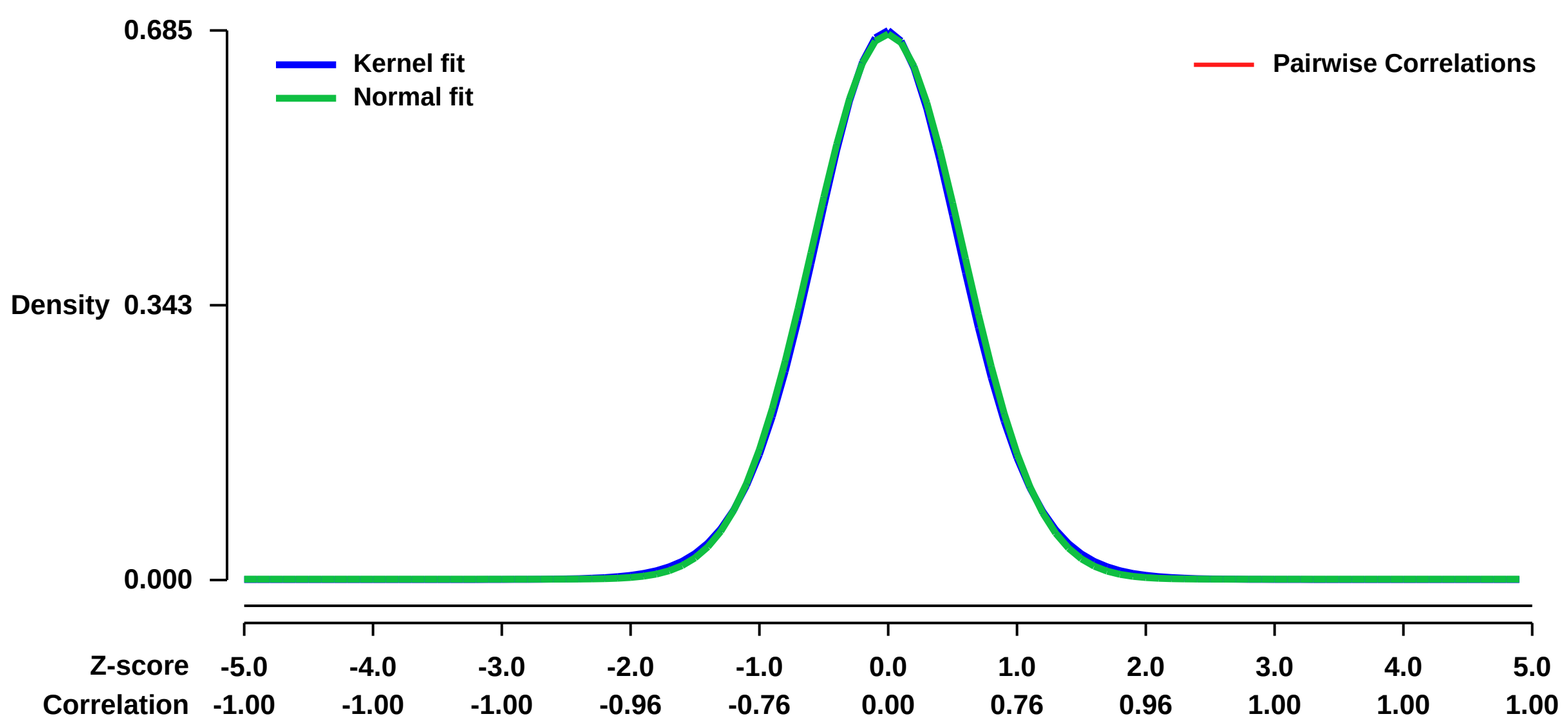

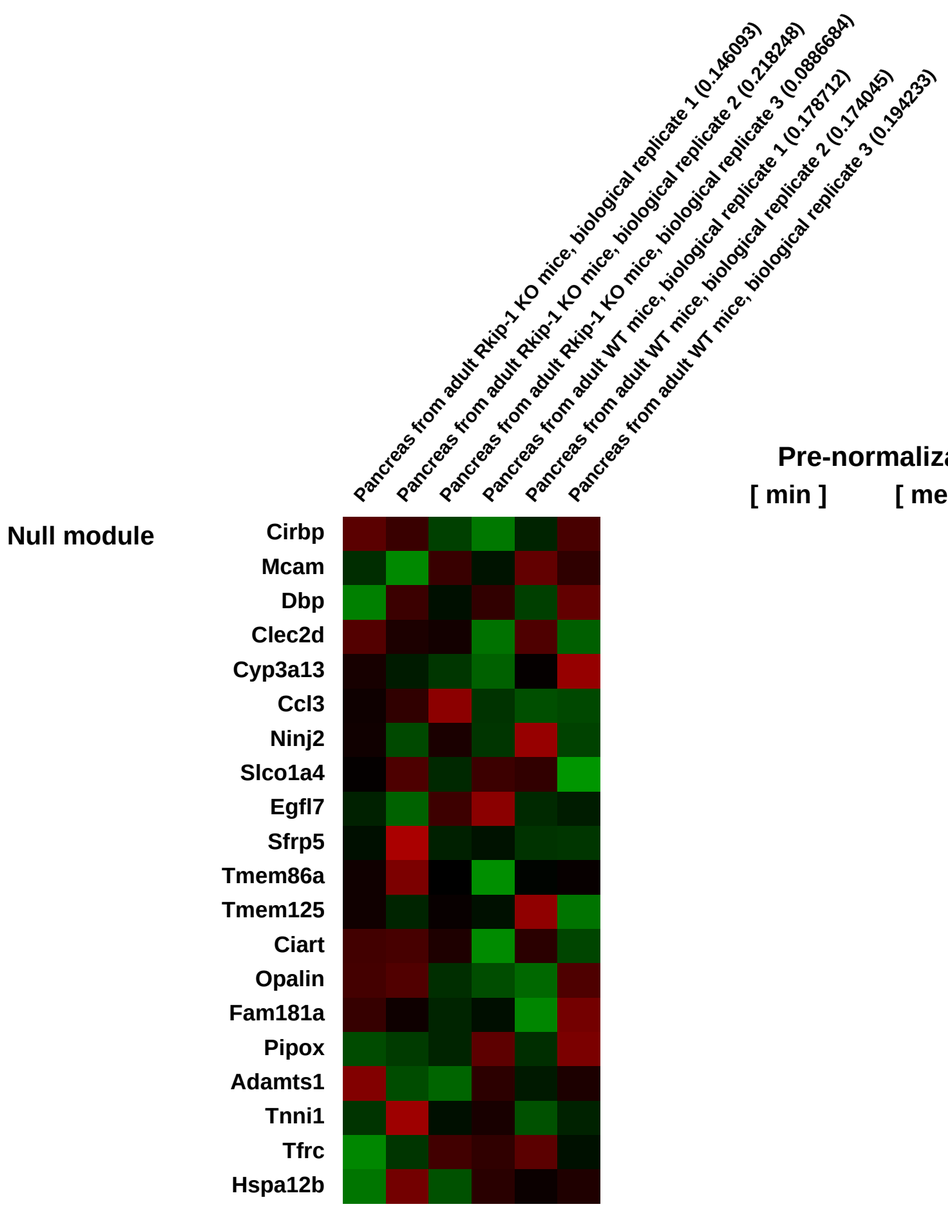

GEO Series "GSE7333" Expression Profiles

Num of samples in this series: 6

Scale of expression profile Z-scores

-3.0 -2.0 -1.0 0.0 1.0 2.0 3.0

GEO Link:	http://www.ncbi.nlm.nih.gov/geo/query/acc.cgi?acc=GSE7333
Status:	Public on Mar 29 2007
Title:	miR-1-2 knockout versus wild-type hearts
Organism:	Mus musculus
Experiment type:	Expression profiling by array
Platform:	GPL1261
Pubmed ID:	17397913
Summary & Design:	**Summary:** **microarray was done on Heart tissue from ko and wt** **MicroRNAs (miRNAs) are genomically encoded small RNAs used by organisms to regulate the dosage of proteins generated from messenger RNA transcripts. The in vivo requirement of specific miRNAs in mammals is unknown, and reliable prediction of mRNA targets remains problematic. Here, we show that miRNA biogenesis in the mouse heart is essential for cardiogenesis. Furthermore, targeted deletion of the muscle-specific miRNA, miR-1-2, revealed numerous functions in the heart, including regulation of cardiac morphogenesis, electrical conduction, and cell cycle control. Analyses of miR-1 complementary sequences in mRNAs upregulated upon miR-1-2 deletion revealed an enrichment of miR-1 ""seed matches"" and a strong tendency for potential miR-1 binding sites to be located in physically accessible regions. These findings indicate that subtle alteration of miRNA dosage can have profound consequences in mammals and demonstrate the utility of mammalian loss-of-function models in revealing physiologic miRNA targets.** **Keywords: miRNA** **Overall design:** **Heart tissues from 3 wild type and 3 miR-1-2 knockout mice at postnatal days 10 were used and total RNA was extracted by Trizol. Expression level was compared between wild type and miR-1-2 knockout mice. The affy package from R/Bioconductor was used to generate RMA values.**

Background corr dist: KL-Divergence = 0.0216, L1-Distance = 0.0241, L2-Distance = 0.0009, Normal std = 0.7218

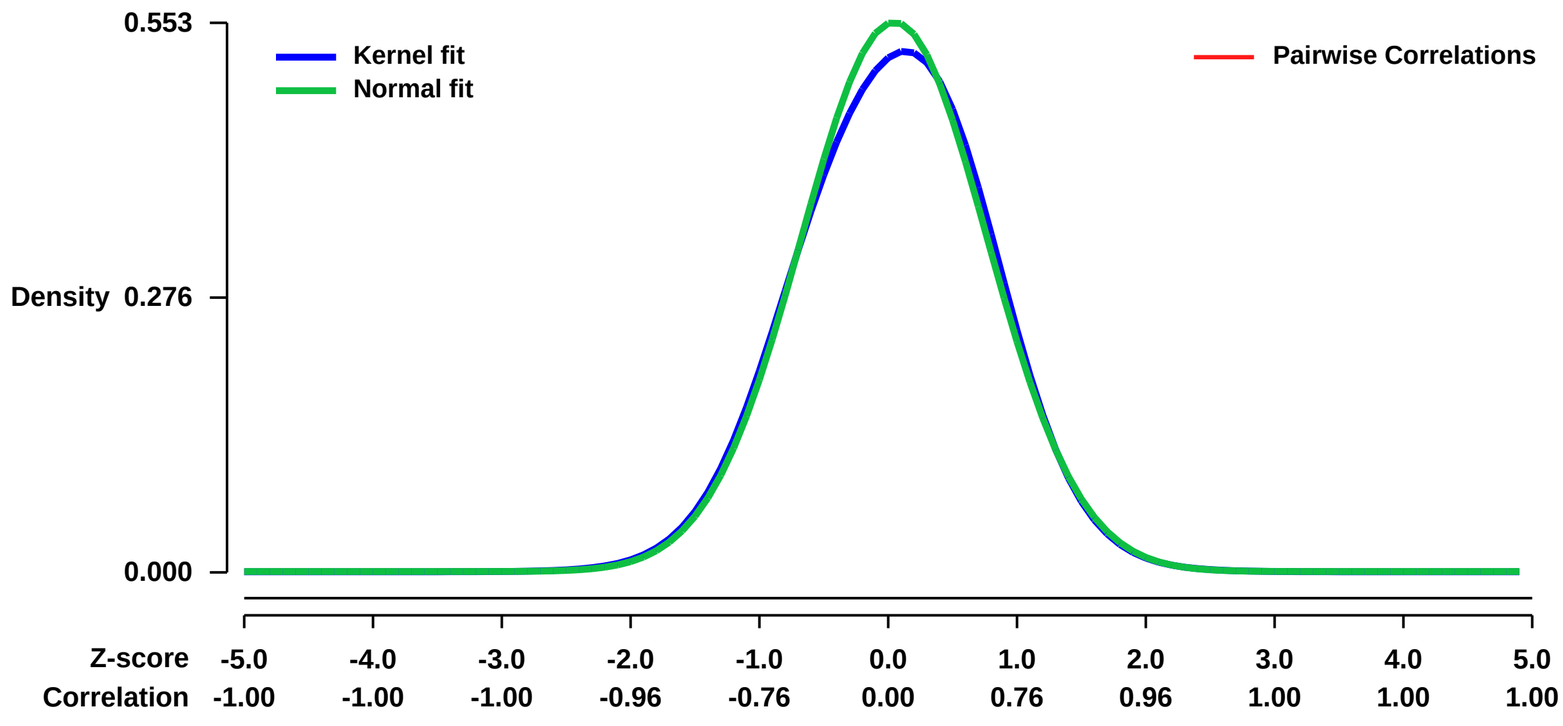

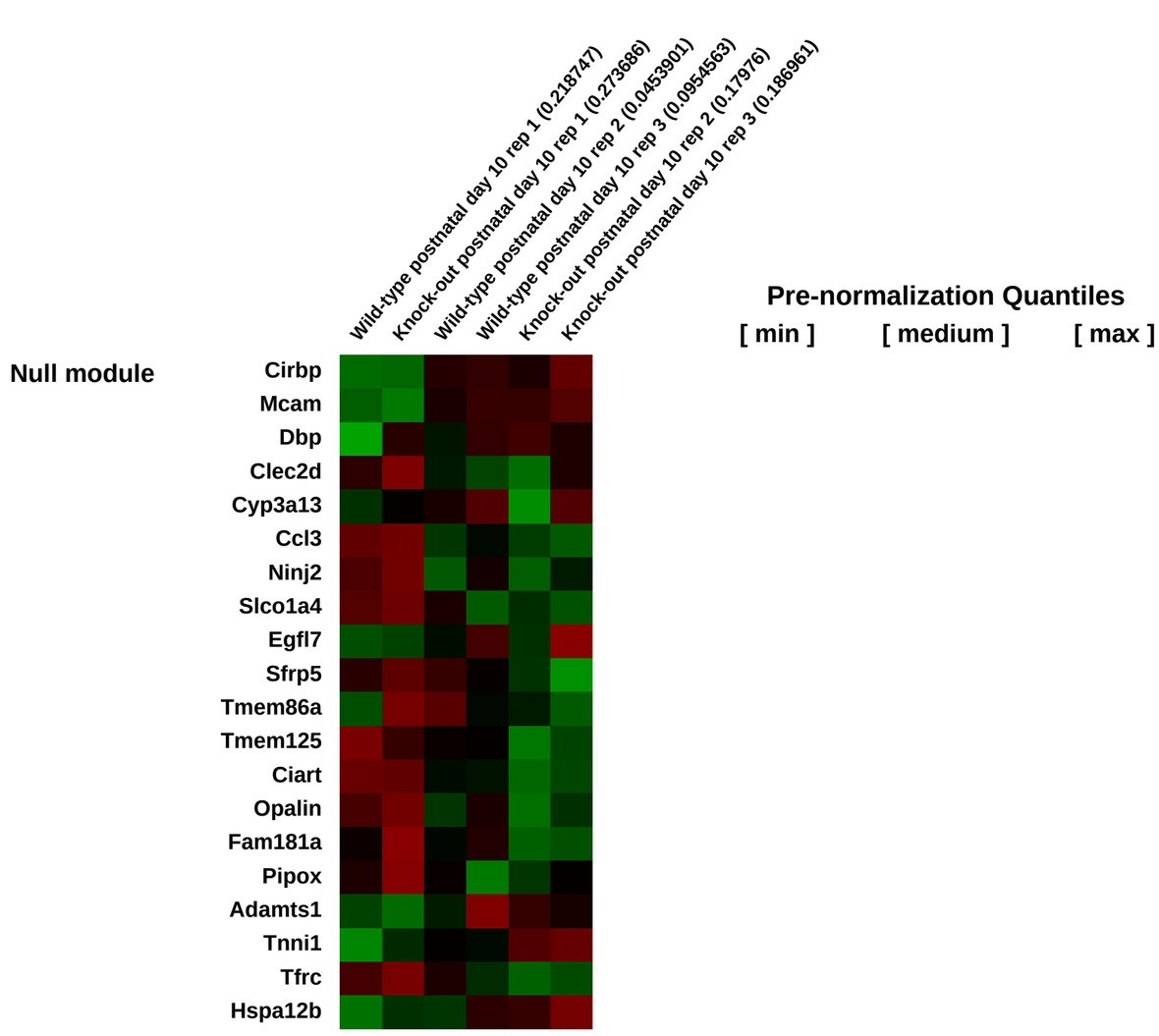

GEO Series "GSE51355" Expression Profiles

Num of samples in this series: 16

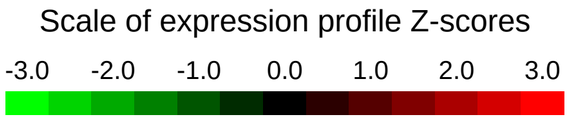

GEO Link:	**http://www.ncbi.nlm.nih.gov/geo/query/acc.cgi?acc=GSE51355**
Status:	**Public on Feb 10 2014**
Title:	**Metabolic programs orchestrated by the activated Ha-ras and ˛†-catenin oncoproteins in mouse liver tumors [mRNA]**
Organism:	**Mus musculus**
Experiment type:	**Expression profiling by array**
Platform:	**GPL1261**
Pubmed ID:	
Summary & Design:	**Summary:** **The process of hepatocarcinogenesis in the diethylnitrosamine (DEN) initiation/phenobarbital (PB) promotion mouse model involves the selective clonal outgrowth of cells harboring oncogene mutations in Ha-ras, B-raf, or Ctnnb1. Here, we have characterized mouse liver tumors harboring either Ctnnb1 or Ha-ras mutations via integrated molecular profiling at the transcriptional and translational and post-translational levels. In addition, metabolites of the intermediary metabolism were quantified by high resultion 1H magic angle nuclear magnetic resonance (HR-MAS NMR). We have identified tumor characteristic genotype-specific differences in mRNA and miRNA expression, protein levels, and post-translational modifications and in metabolite levels that facilitate the molecular and biochemical stratification of tumor phenotypes. Bioinformatic integration of these data at the pathway level led to novel insights into tumor genotype-specific aberrant cell signaling and in particular to a better understanding of alterations in pathways of the cell intermediary metabolism, which are driven by the constitutive activation of the ˛†-Catenin and Ha-ras oncoproteins in tumors of the two genotypes.** **Overall design:** **Male C3H/HeJ mice received a single i.p. injection of DEN (10 or 90´µg/g body weight) at 2, or 6 weeks of age. After a treatment-free interval of 2 weeks, the C3H/HeJ mice were either kept on a diet containing 0.05% PB or on a PB-free control diet for 28 to 36 weeks before they were sacrificed. Ha-ras- or Ctnnb1-mutated tumors and control tissues were isolated and either flash frozen in liquid nitrogen and stored at -80´℃, or prepared for immunohistochemistry.**

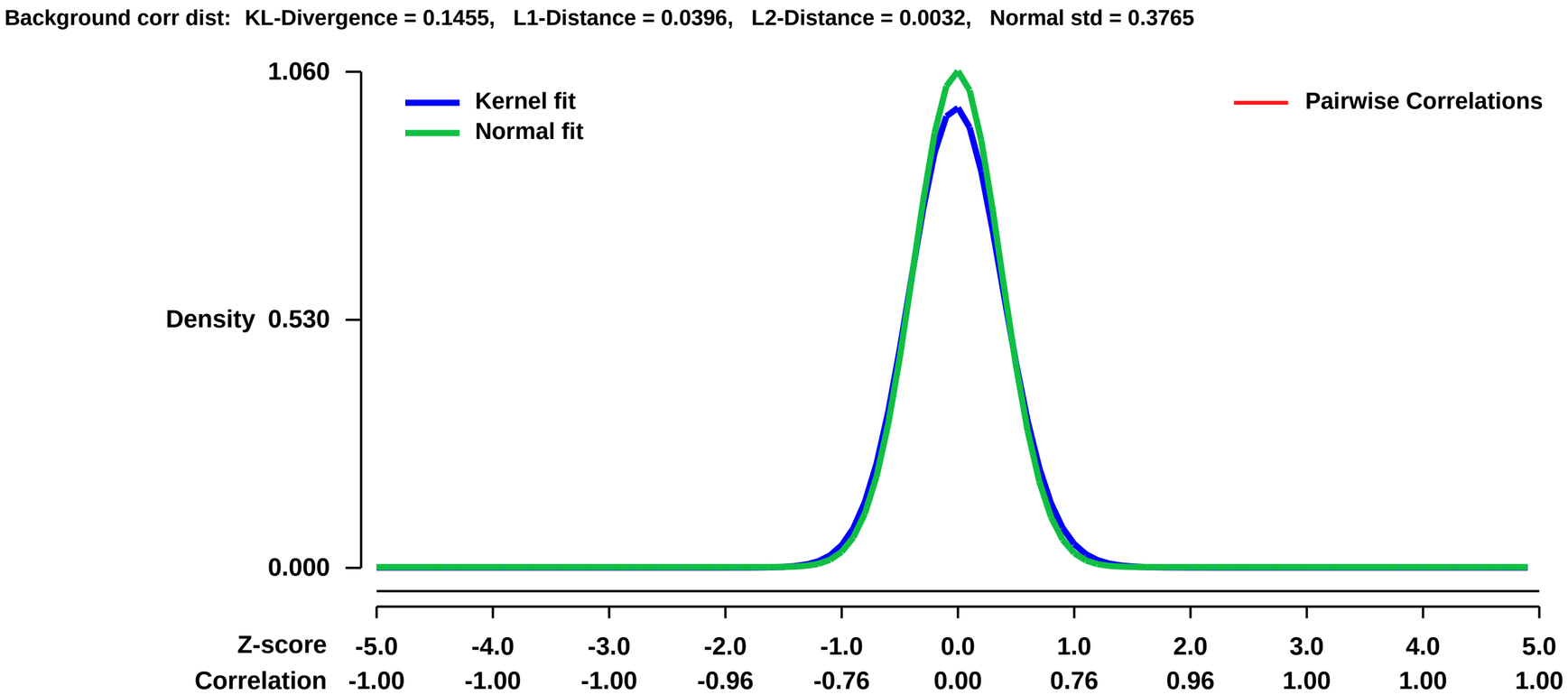

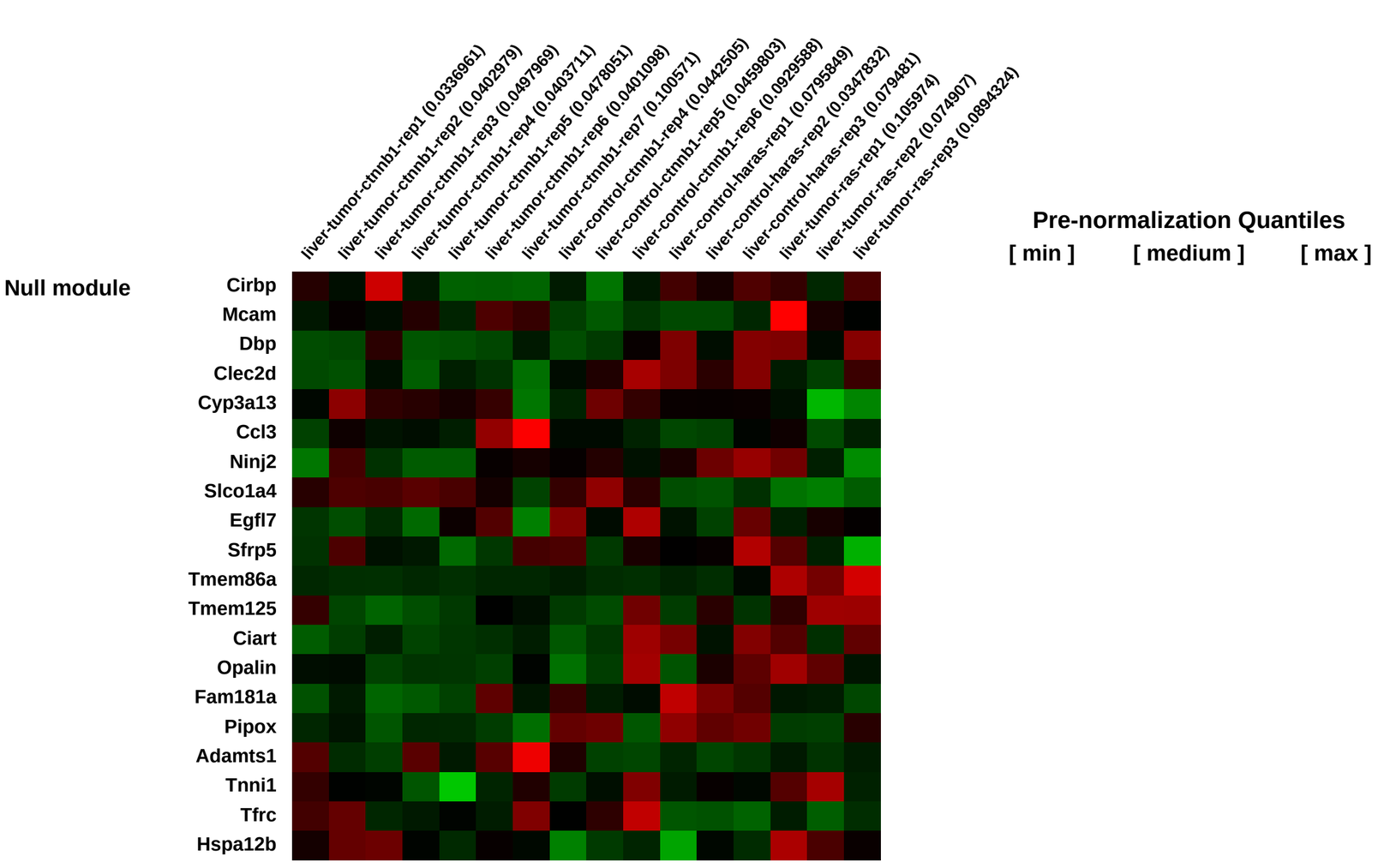

GEO Series "GSE17925" Expression Profiles

Num of samples in this series: 12

Scale of expression profile Z-scores

-3.0 -2.0 -1.0 0.0 1.0 2.0 3.0

GEO Link:	http://www.ncbi.nlm.nih.gov/geo/query/acc.cgi?acc=GSE17925
Status:	Public on Sep 03 2009
Title:	Gene expression from TCDD treated C57BL6/J and human Aryl hydrocarbon Receptor expressing primary mouse hepatocytes
Organism:	Mus musculus
Experiment type:	Expression profiling by array
Platform:	GPL1261
Pubmed ID:	20044593
Summary & Design:	**Summary:** The human and mouse aryl hydrocarbon receptor (hAHR and mAHRb) share limited (58%) transactivation domain sequence identity. Compared to the mAHRb allele, the hAHR displays 10-fold lower relative affinity for prototypical ligands such as 2,3,7,8 tetrachlorodibenzo-p-dioxin (TCDD). However, in previous studies we have demonstrated that the hAHR can display a higher relative ligand binding affinity than the mAHRb for specific AHR ligands such as indirubin. Each receptor has also been shown to differentially recruit LXXLL co-activator-motif proteins and to utilize different TAD subdomains in gene transactivation. Using hepatocytes isolated from C57BL6/J mice (Ahrb/b) and AHRTtr transgenic mice which express hAHR protein specifically in hepatocytes, we investigated whether the hAHR and mAHRb differentially regulate genes. Microarray and quantitative-PCR analysis of Ahrb/b and AHRTtr primary-mouse hepatocytes treated with 10 nM TCDD revealed that a number of established AHR target genes such as Cyp1a1 and Cyp1b1 are significantly induced by both receptors. Remarkably, of the 1752 genes induced by mAHRb and 1186 genes induced by hAHR, only 265 genes (<10%) were significantly activated by both receptors in response to TCDD. Conversely of the 1100 and 779 genes significantly repressed in mAHRb and hAHR hepatocytes respectively, only 462 (<25%) genes were significantly repressed by both receptors in response to TCDD treatment. Genes identified as differentially expressed are known to be involved in a number of biological pathways, including cell proliferation and inflammatory response which suggests that compared to the mAHRb, the hAHR may play contrasting roles in TCDD-induced toxicity and endogenous AHR-mediated gene regulation. **Overall design:** Isolated mouse hepatocytes from wild type and treated with 10nM TCDD for 6h were analyzed. 1 array per mouse (3 mice per treatment group) was used.GeneChip´fi Operating Software (Affymetrix) was utilized to preprocess CAB/CEL files generated from the 12 scanned microarrays which represented hepatocytes isolated from one mouse each. Data quality was initially assessed by checking the array image, B2 oligo performance, average background to noise ratios, poly-A controls, hybridization controls and the 3' to 5' probe-set ratios for control genes (e.g. ˆ-actin or GAPDH). Microarray data was normalized using Probe Logarithmic Intensity Error Approximation PLIER-MM algorithm (Affymetrix Expression Consoleâ¢ Software 1.1). Normalized microarray data outputs from TCDD and control treated Ahrb/band AHRTtr hepatocytes were compared for differential expression using Significance Analysis of Microarrays (SAM, version 2.23A (Pan 2002; Tusher et al. 2001)) with 100 permutations, KNN-10.

Background corr dist: KL-Divergence = 0.1387, L1-Distance = 0.0308, L2-Distance = 0.0018, Normal std = 0.3861

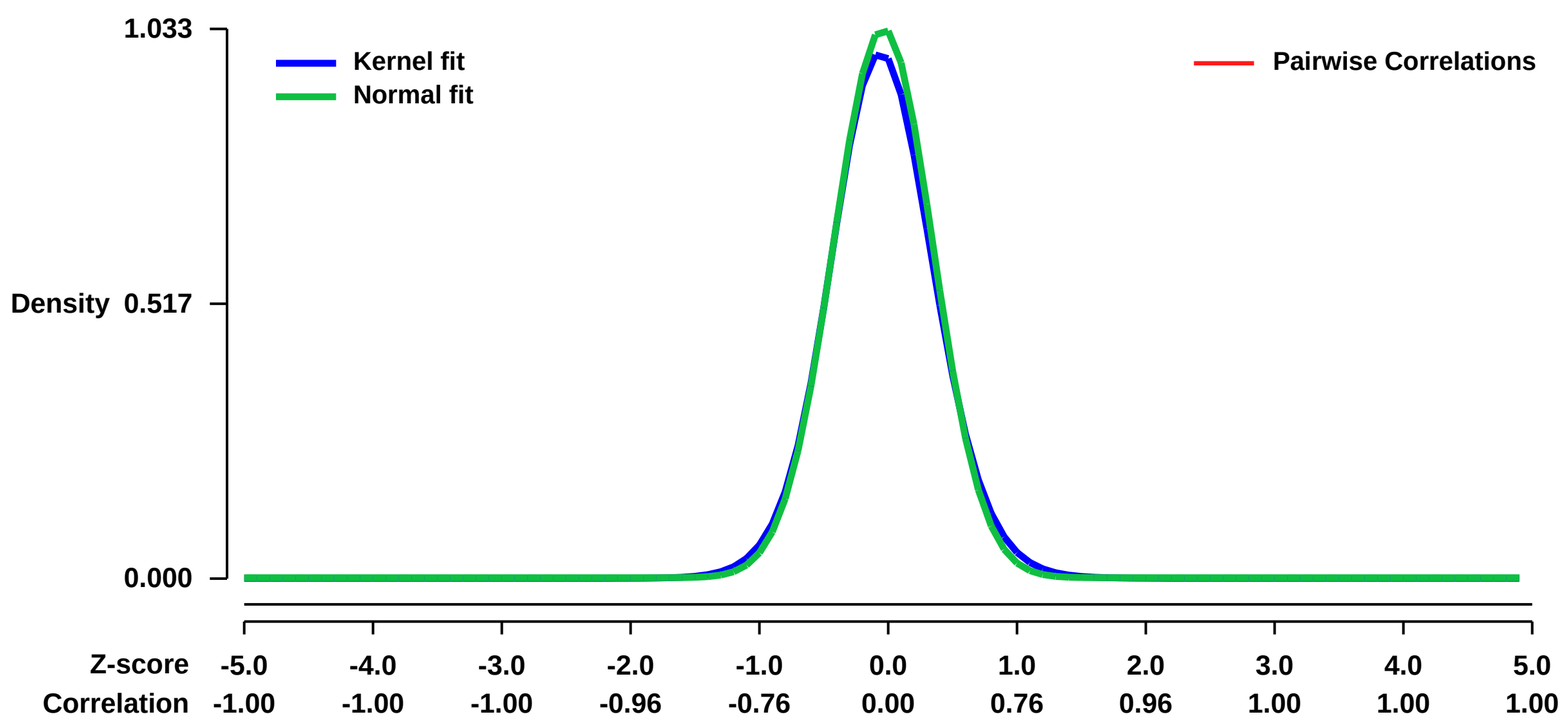

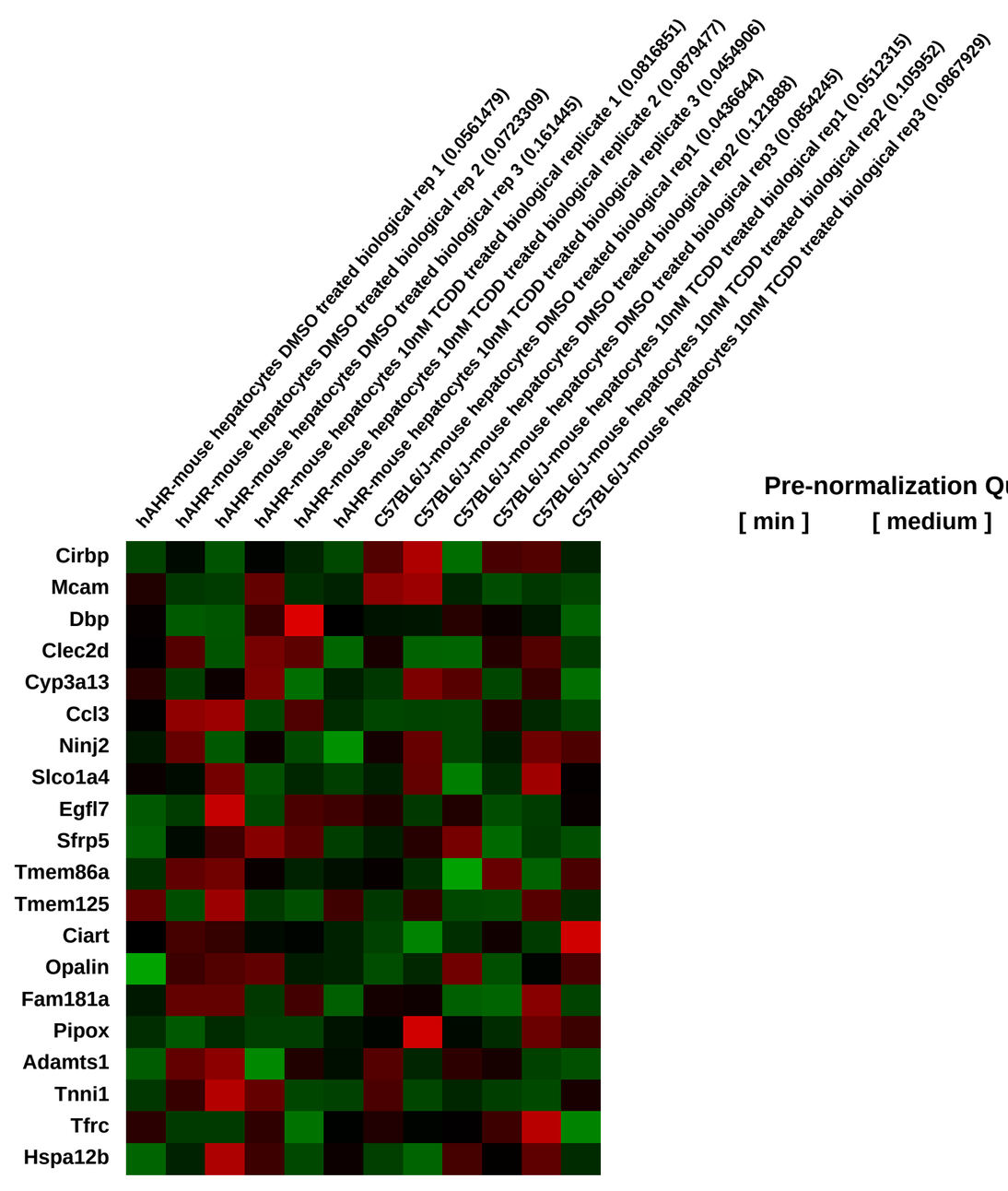

Null module

GEO Series "GSE45895" Expression Profiles

Num of samples in this series: 27

Scale of expression profile Z-scores

-3.0 -2.0 -1.0 0.0 1.0 2.0 3.0

GEO Link:	http://www.ncbi.nlm.nih.gov/geo/query/acc.cgi?acc=GSE45895
Status:	Public on Apr 10 2013
Title:	EphrinB2 Regulation by PTH and PTHrP Revealed by Molecular Profiling in Differentiating Osteoblasts
Organism:	Mus musculus
Experiment type:	Expression profiling by array
Platform:	GPL1261
Pubmed ID:	18627264
Summary & Design:	**Summary:** With the aim of identifying new pathways and genes regulated by PTH(1-34) and PTH-related protein 1-141 [PTHrP(1-141)] in osteoblasts, this study was carried out using a mouse marrow stromal cell line, Kusa 4b10, that acquires features of the osteoblastic phenotype in long-term culture conditions. After the appearance of functional PTH receptor 1 (PTHR1) in Kusa 4b10 cells, they were treated with either PTH(1-34) or PTHrP(1-141), and RNA was subjected to Affymetrix whole mouse genome array. **Overall design:** NOTE: This work has been published in 2008 (PMID 18627264); Since the original normalised data for this project is unavailable, the data has been re-normalised using a standard method for GEO submission in 2013. Therefore, the re-normalized data represented in this records may differ slightly from the original normalized data in the publication.

Background corr dist: KL-Divergence = 0.1060, L1-Distance = 0.0288, L2-Distance = 0.0017, Normal std = 0.4275

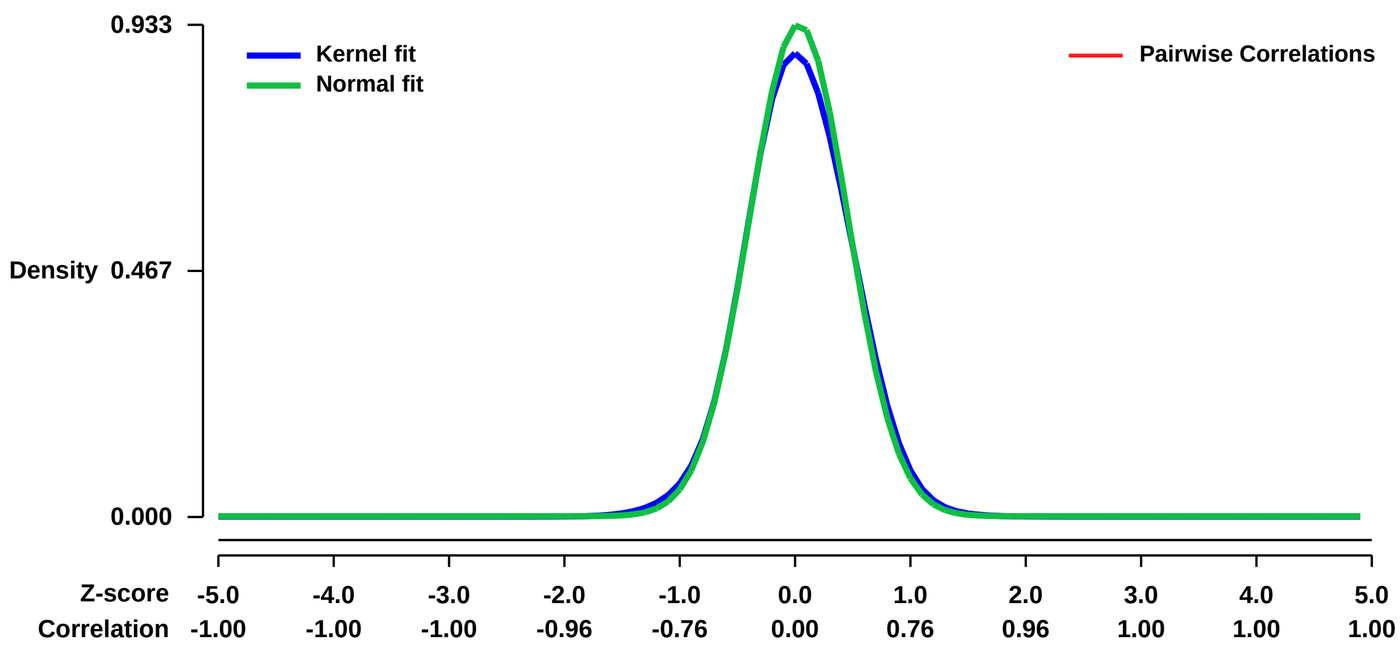

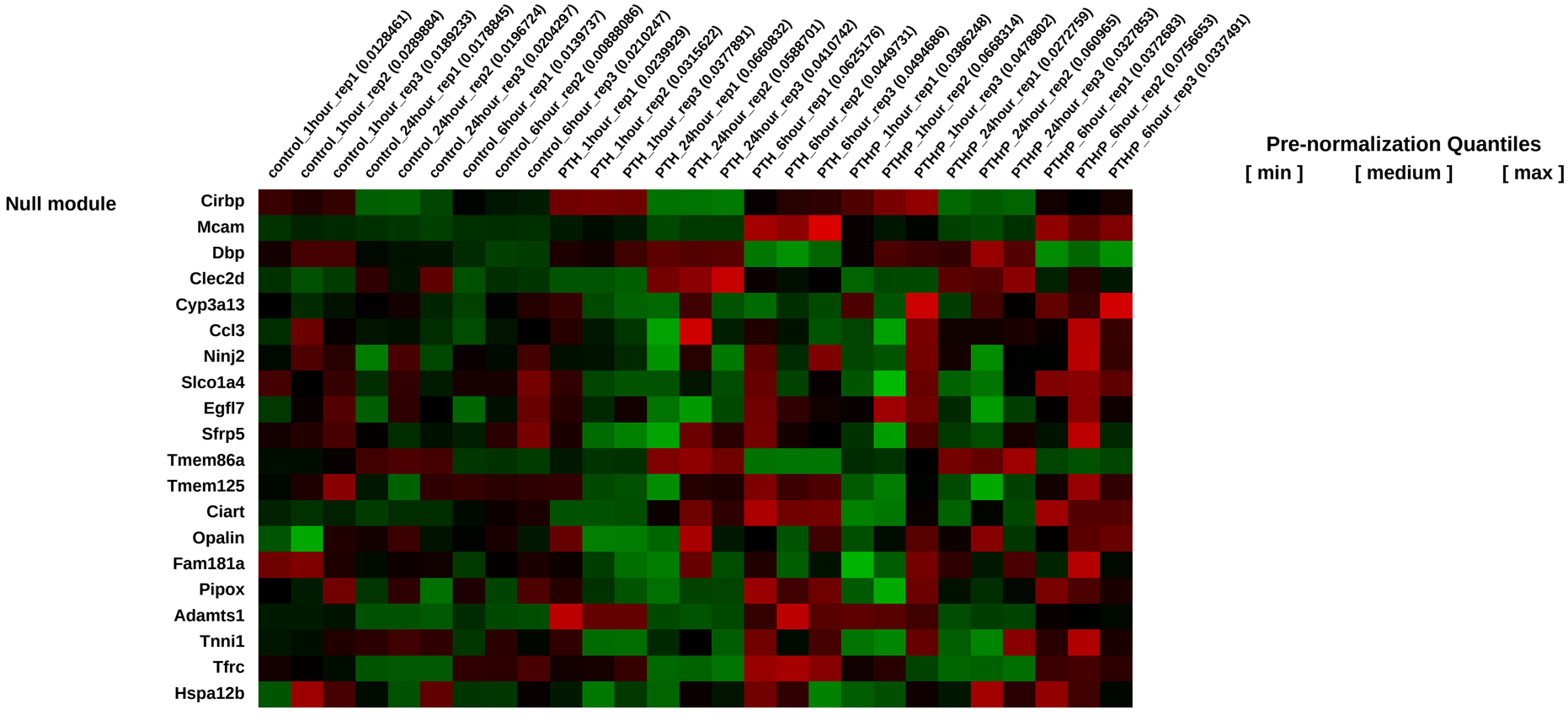

GEO Series "GSE10478" Expression Profiles

Num of samples in this series: 6

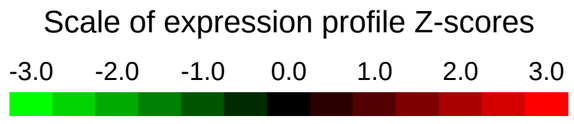

GEO Link:	http://www.ncbi.nlm.nih.gov/geo/query/acc.cgi?acc=GSE10478
Status:	Public on Dec 31 2008
Title:	Curative and beta cell regenerative effects of alpha1 antitrypsin treatment in autoimmune diabetic NOD mice
Organism:	Mus musculus
Experiment type:	Expression profiling by array
Platform:	GPL1261
Pubmed ID:	18852471
Summary & Design:	**Summary:** In this study, we performed the gene expression analysis of the Normal, Diabetic and AAT treated NOD mice to elucidate the transcriptional changes induced by AAT. This will assist in identifying the biological processes / pathways involved in curative mechanism of AAT. **Keywords: alpha1 antitrypsin treatment** **Overall design:** Duplicate samples of Normal, Diabetic and AAT treated NOD mice were analyzed.

Background corr dist: KL-Divergence = 0.0339, L1-Distance = 0.0268, L2-Distance = 0.0010, Normal std = 0.6490

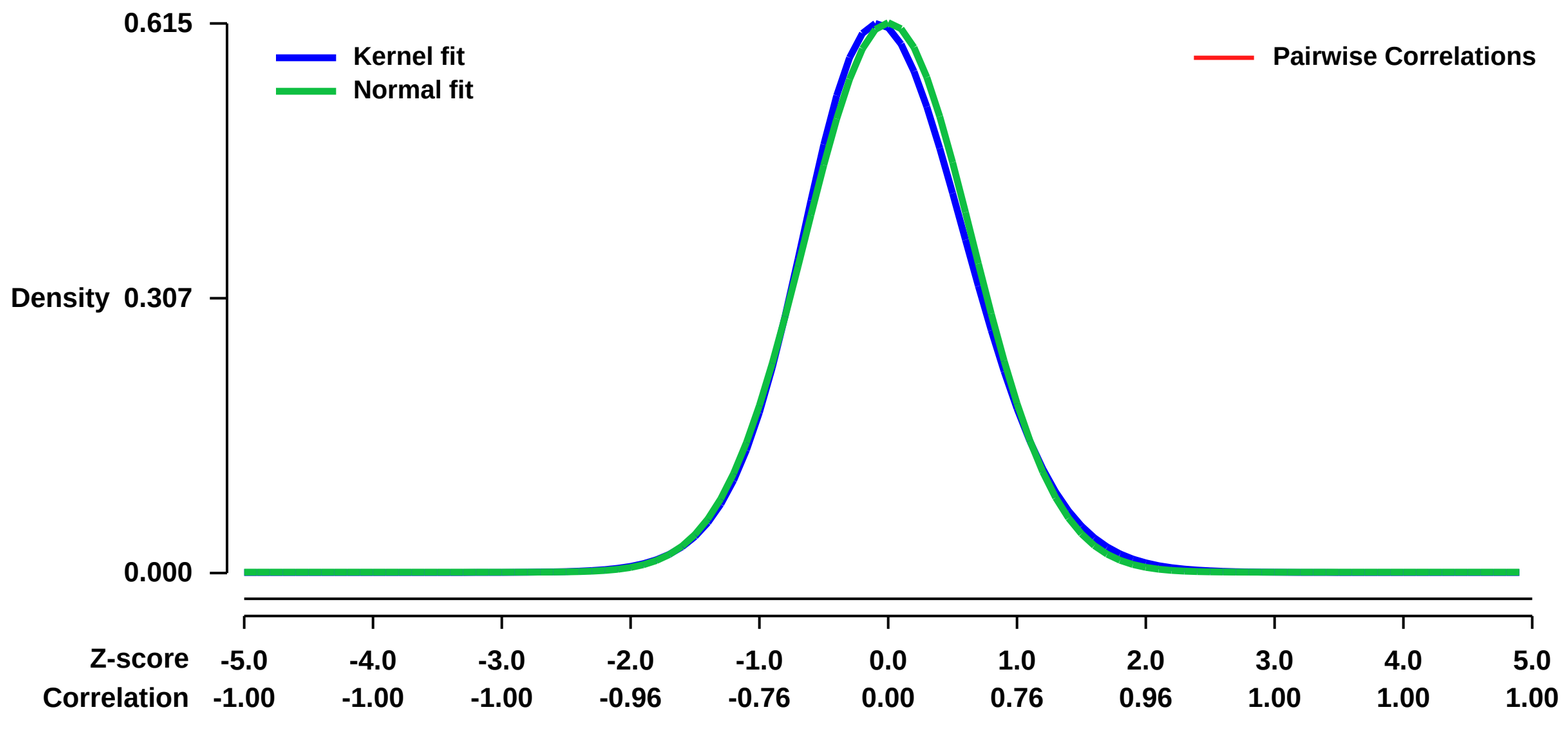

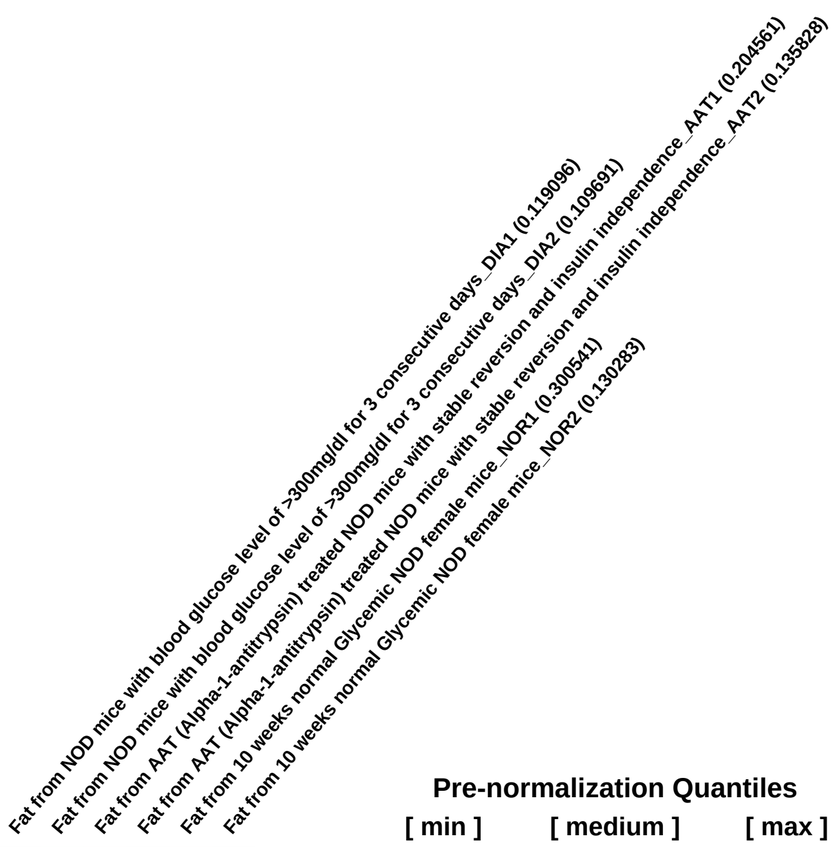

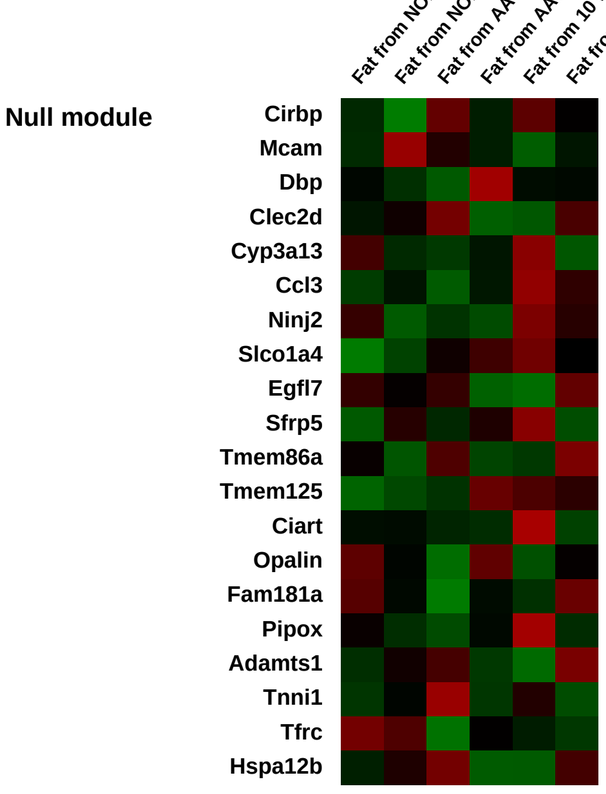

GEO Series "GSE44175" Expression Profiles

Num of samples in this series: 18

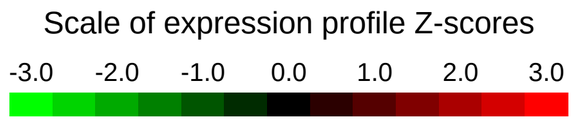

GEO Link:	http://www.ncbi.nlm.nih.gov/geo/query/acc.cgi?acc=GSE44175
Status:	Public on Feb 09 2013
Title:	Expression data from mouse embyonic stem cell, neural progenitor and neuron
Organism:	Mus musculus
Experiment type:	Expression profiling by array
Platform:	GPL1261
Pubmed ID:	23775126
Summary & Design:	**Summary:** The effect of HMGN1 protein on gene expression of mouse ESC, NP and Neurons were investigated by comparing the transcriptome between Hmgn1+/+ and Hmgn1 -/- cells. **Overall design:** three cell types, two genotypes, three reps per sample type

Background corr dist: KL-Divergence = 0.0123, L1-Distance = 0.0320, L2-Distance = 0.0019, Normal std = 0.8462

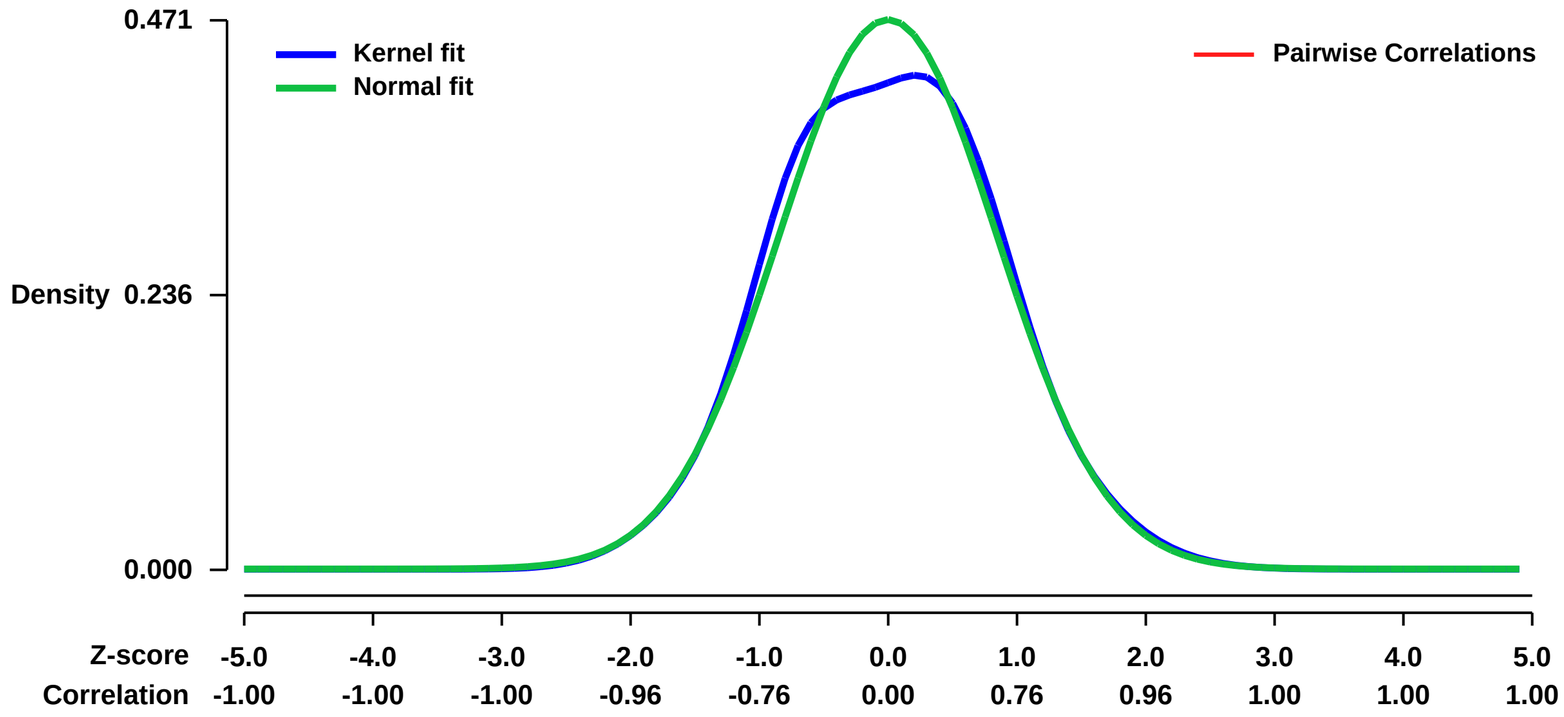

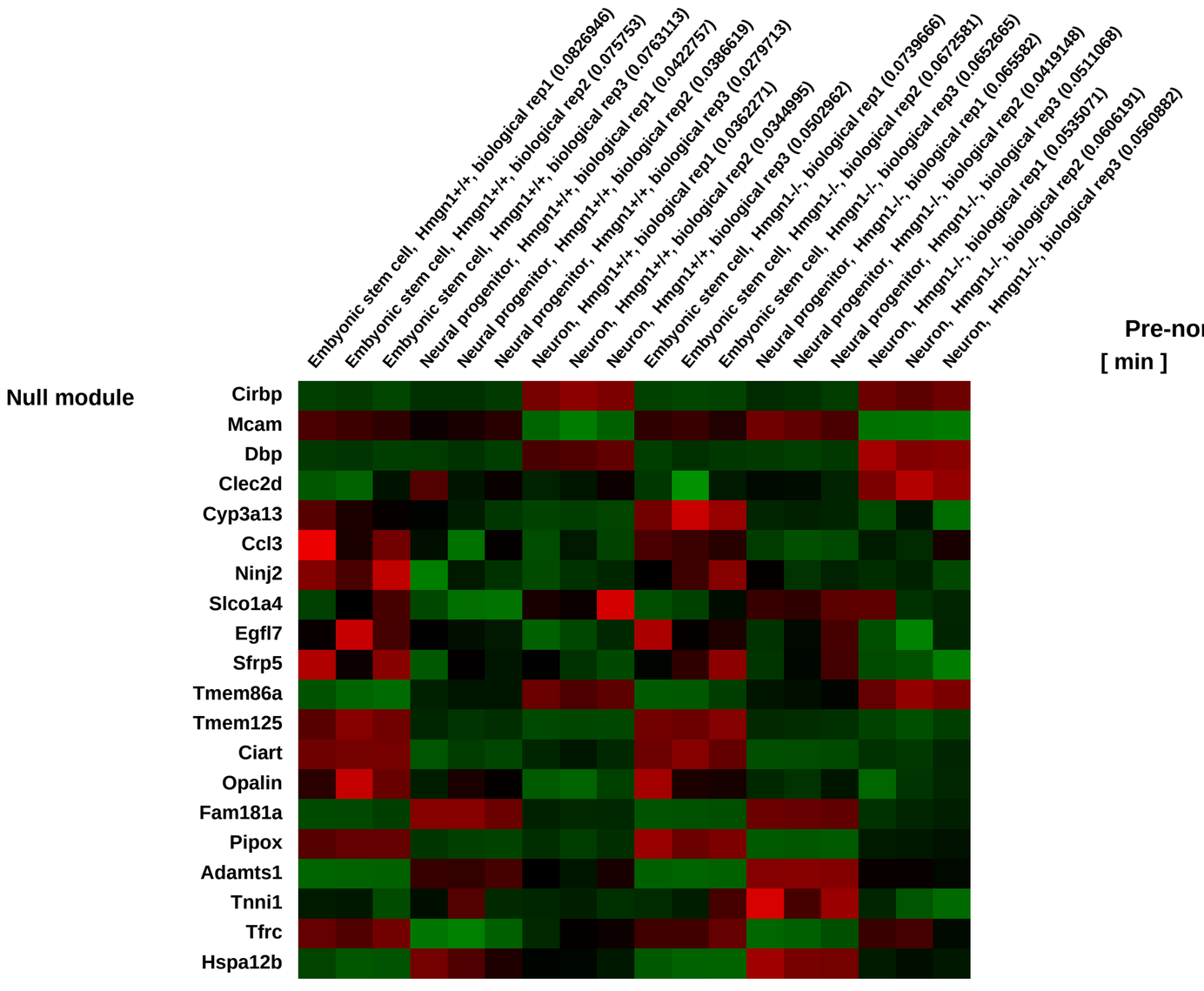

GEO Series "GSE31406" Expression Profiles

Num of samples in this series: 12

Scale of expression profile Z-scores

-3.0 -2.0 -1.0 0.0 1.0 2.0 3.0

GEO Link:	http://www.ncbi.nlm.nih.gov/geo/query/acc.cgi?acc=GSE31406
Status:	Public on Apr 01 2014
Title:	Gene expression analyses of PR action in the uteri of SRC-2 mutant mice
Organism:	Mus musculus
Experiment type:	Expression profiling by array
Platform:	GPL1261
Pubmed ID:	24571987
Summary & Design:	**Summary:** Ovarian estrogen (E2) and progesterone (P4) are indispensable for embryo-implantation and endometrial stromal decidualization; however, the molecular mechanisms that underpin these reproductive processes are unclear. Steroid receptor coregulator-2 (SRC-2) belongs to the multifunctional SRC/p160 family which also includes SRC-1 and SRC-3. Sharing strong sequence homology, all three SRCs exert diverse regulatory effects by modulating the transcriptional potency of nuclear receptor family members, including the estrogen and progesterone receptor (ER and PR respectively). Importantly, absence of SRC-2 in PR positive cells in the epithelial, stromal, and myometrial compartments of the murine uterus results in a striking infertility defect. This reproductive phenotype highlights a key role for SRC-2 in uterine function which is not shared with other coregulators. Intriguingly, abrogation of uterine SRC-2 does not block embryo apposition or attachment to the apical surface of luminal epithelial cells of the endometrium but rather prevents P4-dependent local decidualization of the sub-epithelial stroma. Remarkably, epithelial-specific ablation of SRC-2 in the murine uterus does not compromise endometrial functionality, again underscoring the unique importance of stromal derived SRC-2 in uterine function. The stromal decidualization defect resulting from SRC-2 ablation is reflected at the molecular level by a marked attenuation in P4 responsive target genes known to be critical for P4 dependent decidualization (i.e. ERBB receptor feedback inhibitor 1, Follistatin and Fkbp5). Conversely, the induction of E2 or P4 target genes involved in embryo implantation (i.e. leukemia inhibitory factor (LIF) and Indian hedgehog (Ihh) respectively) is not affected by SRC-2â s absence. As with mouse studies, decidualization of primary human stromal cells (HESCs) in culture is blocked by SRC-2 knockdown; however, HESC decidualization is unaffected by knockdown of SRC-1 or SRC-3. As a consequence of SRC-2 knockdown, molecular studies disclose a striking decrease in the induction of a subset of P4 target genes (i.e. WNT4 and FKBP5) which are essential for the stromal-epithelioid transformation step, the cellular hallmark of endometrial decidualization. Collectively, these studies not only showcase the evolutionary importance of SRC-2 in endometrial biology but also suggest that deregulation of this coregulator may underpin a spectrum of hormone-dependent uterine pathologies such as endometriosis and endometrial cancer. **Overall design:** multiple group comparison

Background corr dist: KL-Divergence = 0.0933, L1-Distance = 0.0314, L2-Distance = 0.0013, Normal std = 0.4618

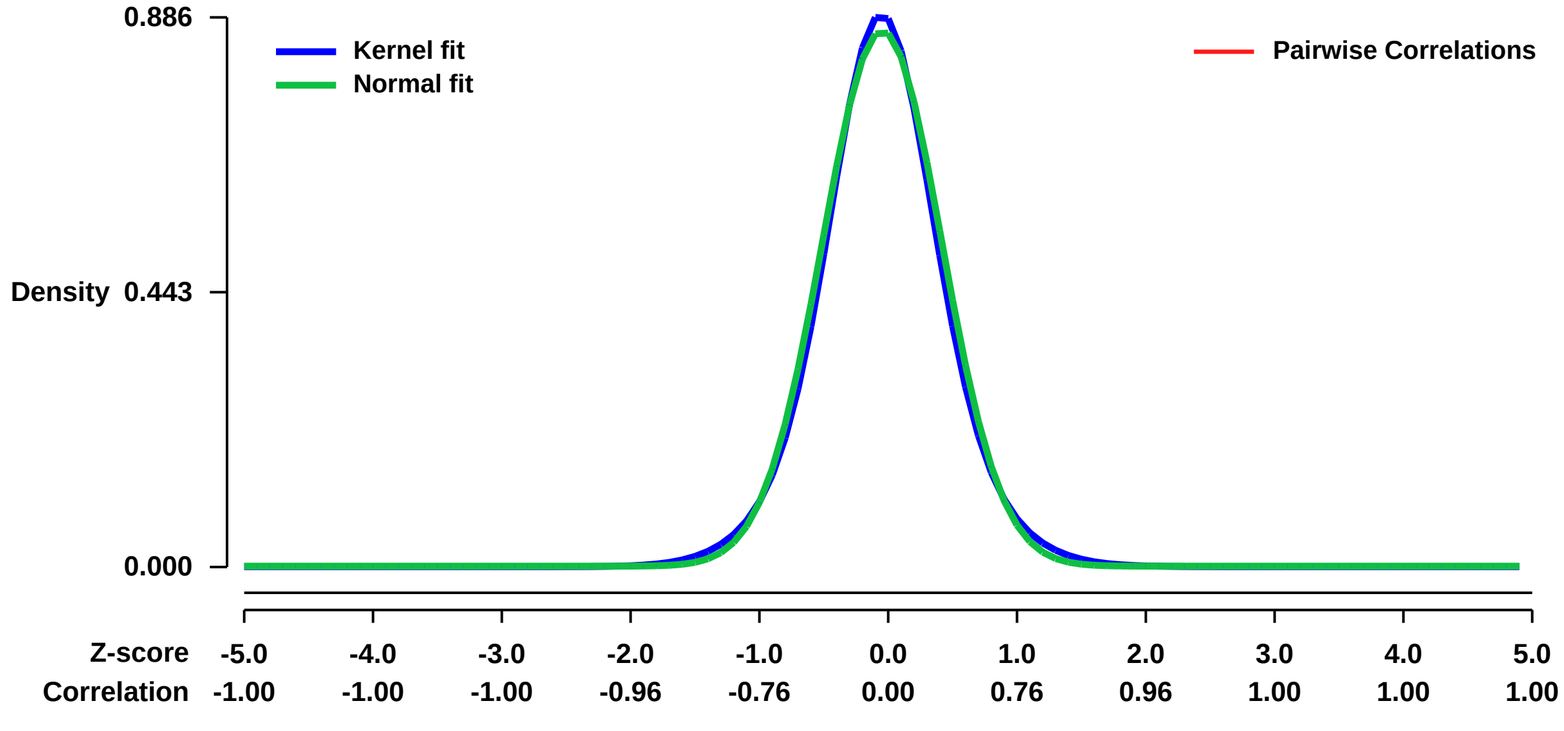

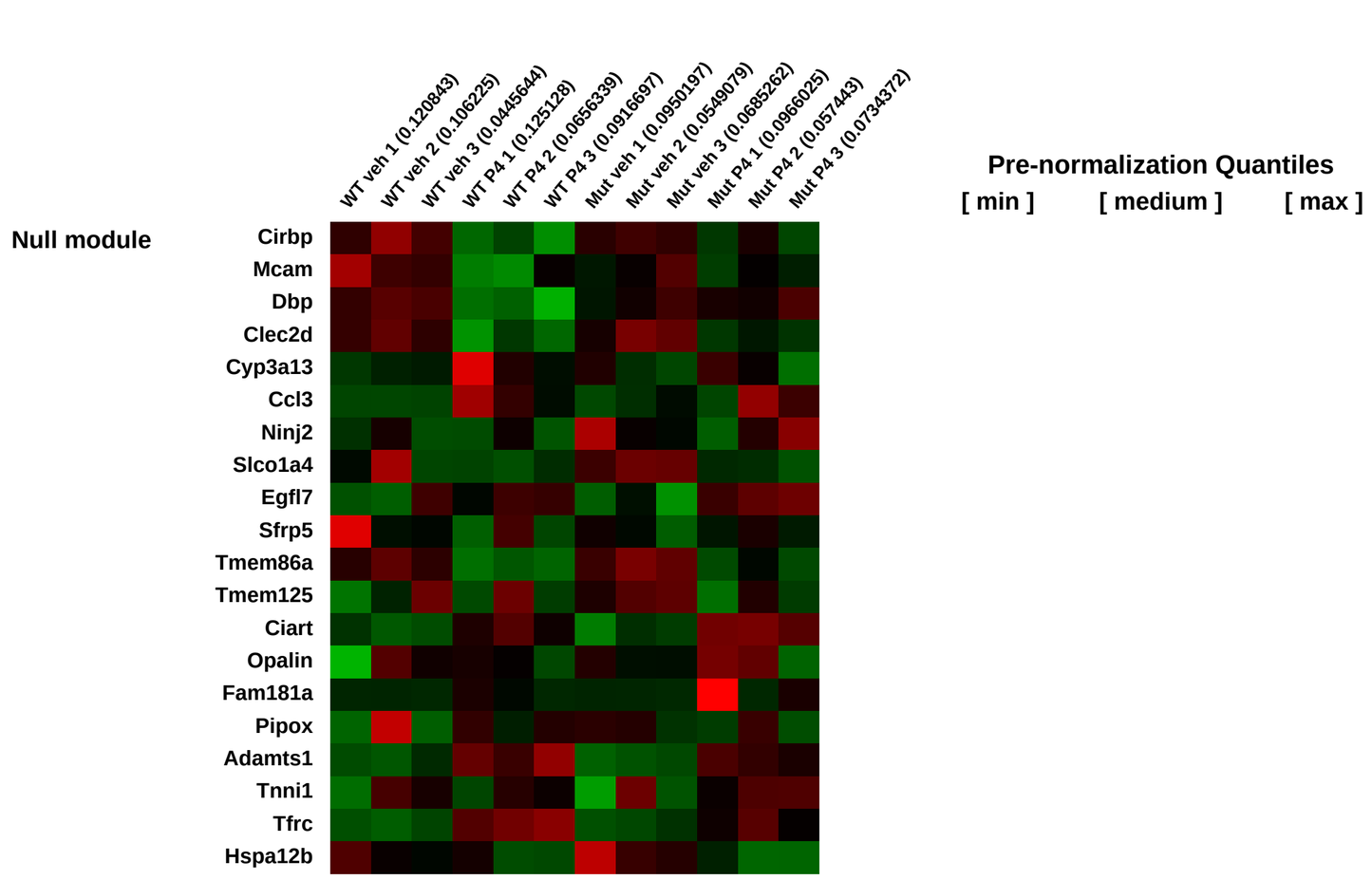

GEO Series "GSE7155" Expression Profiles

Num of samples in this series: 9

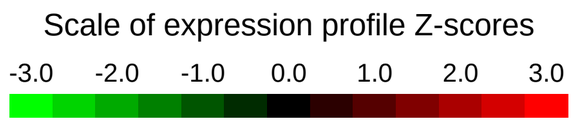

GEO Link:	http://www.ncbi.nlm.nih.gov/geo/query/acc.cgi?acc=GSE7155
Status:	Public on Jul 30 2007
Title:	Expression data from adult laboratory mouse brain hemispheres
Organism:	Mus musculus
Experiment type:	Expression profiling by array
Platform:	GPL1261
Pubmed ID:	17936574
Summary & Design:	**Summary:** Inbred congenic strain B6.C6.132.54/Vad was created using C57BL/6ByJ background and BALB/cJ donor strains. Flanking background markers at chr. 6: 75.9 Mb (rs4226008, NCBI Mouse Build 36 / dbSNP Build 126) and 122.3 Mb (rs3023093), and limiting donor markers at 81.9 Mb (rs4226024) and at 91.8 Mb (rs3712161) defined the introgressed region. We concluded the segment size must be between 9.9 Mb and 46.4 Mb. In a Quantitative Trait Gene identification study we compared brain (without cerebellum) gene expression between progenitors and congenics. Such comparisons can facilitate identification of cis-regulated genes and to establish genetic control of a complex phenotype whose expression is associated with the introgressed chromosome segment. We used microarrays to detail the global programme of gene expression underlying cellularisation and identified distinct classes of up-regulated genes during this process. **Keywords:** strain comparison **Overall design:** Experiments were carried out in three batches. In each batch 10 animals per strain were used. After processing each hemisphere separately, 10 hemispheres were pooled for one high-density oligonucleotide microarray (Mouse Genome 430 2.0, Affymetrix, Santa Clara, CA). For each strain 3 oligonucleotide microarrays were used (n=3). We used adult, untreated, male mice (n=30, 90 mice in toto).

Background corr dist: KL-Divergence = 0.0759, L1-Distance = 0.0218, L2-Distance = 0.0007, Normal std = 0.4870

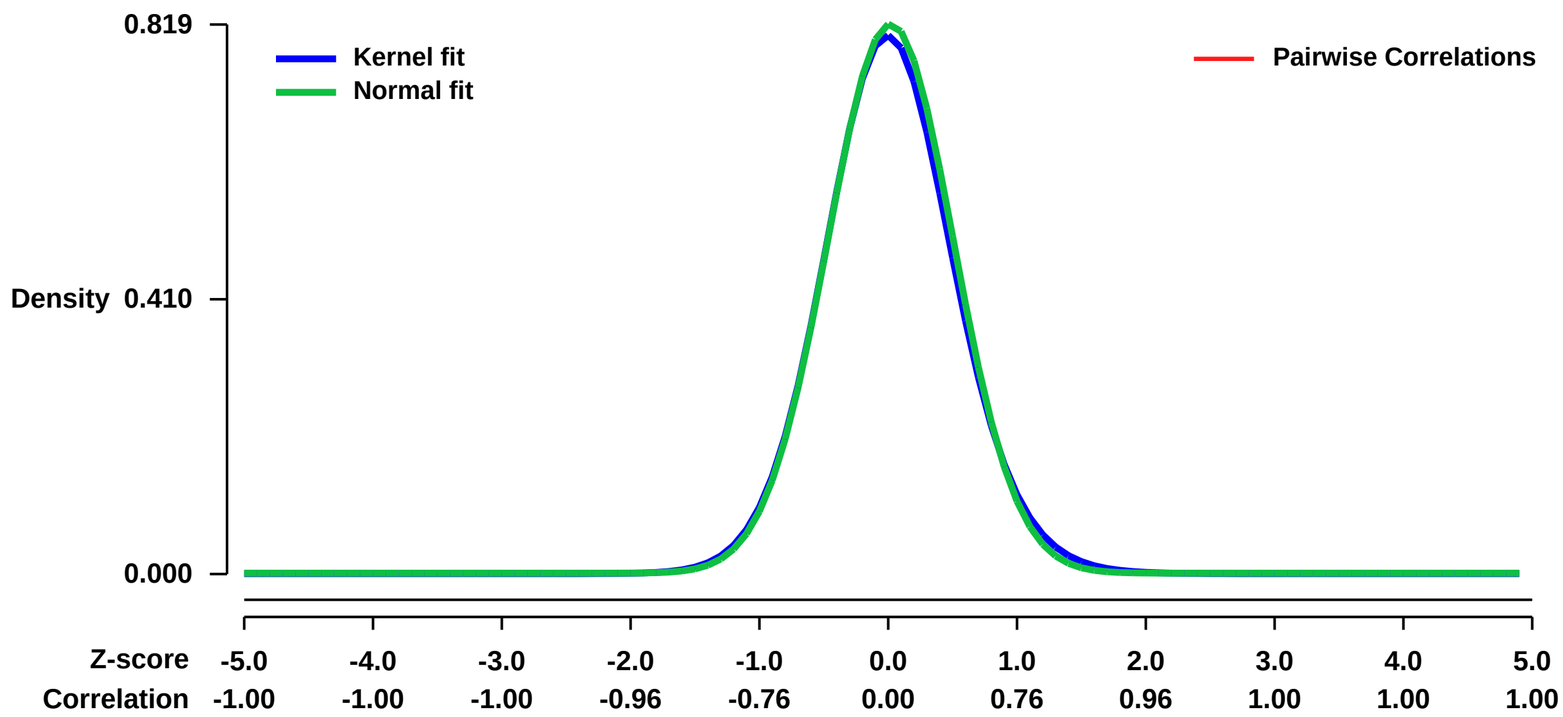

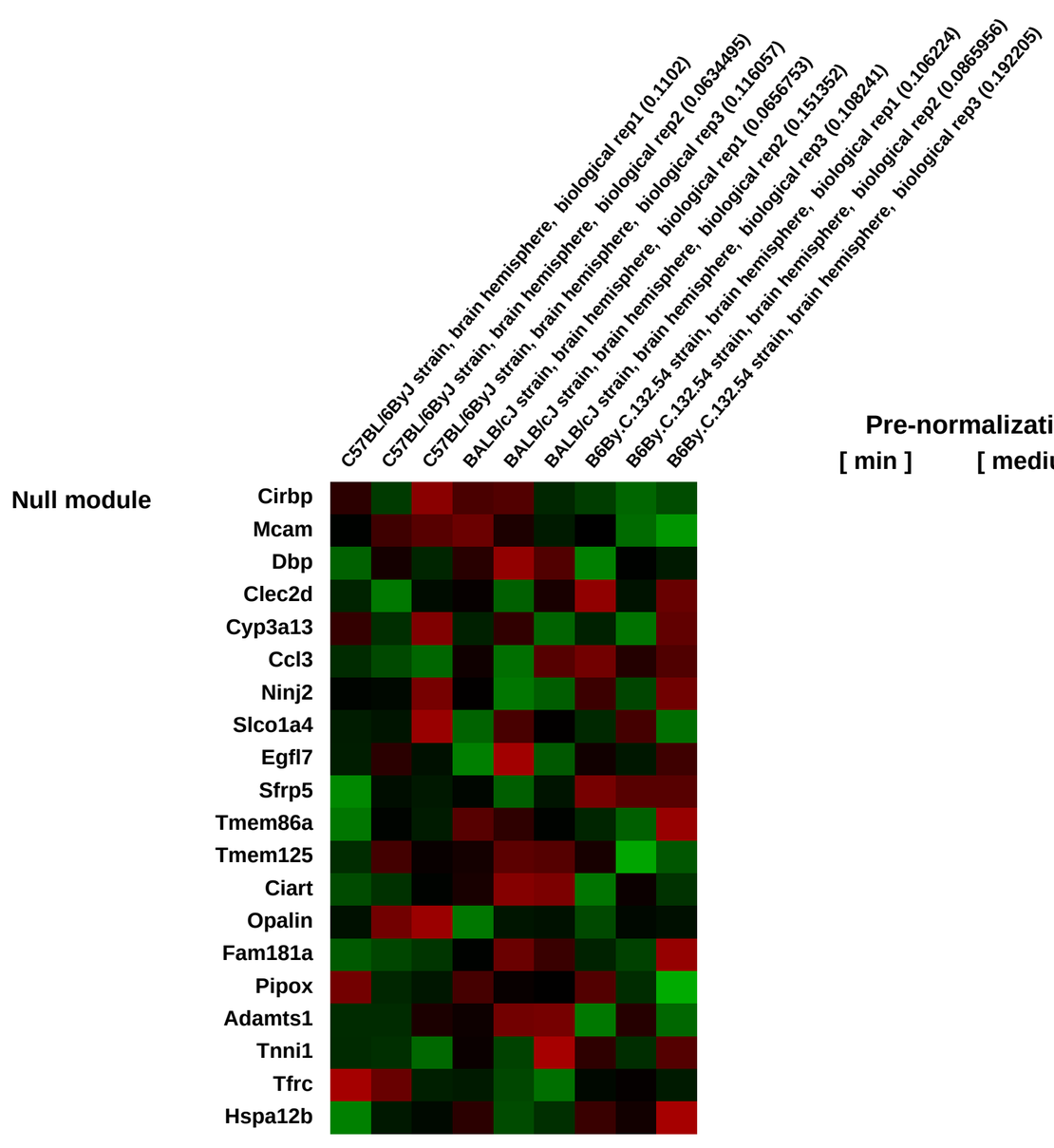

GEO Series "GSE5817" Expression Profiles

Num of samples in this series: 21

Scale of expression profile Z-scores

-3.0 -2.0 -1.0 0.0 1.0 2.0 3.0

GEO Link:	http://www.ncbi.nlm.nih.gov/geo/query/acc.cgi?acc=GSE5817
Status:	Public on Sep 12 2006
Title:	marsh-affy-mouse-232749
Organism:	Mus musculus
Experiment type:	Expression profiling by array
Platform:	GPL1261
Pubmed ID:	18799476
Summary & Design:	**Summary:** Malformations of cortical development are the underlying eitiology of many cases of Mental Retardation and Epilepsy. Subtle, below the resolution of current MRI, cortical dysplasias are probably involved in many cases of MR, Epilepsy and Autism for which no diagnosis can currently be made. Therefore, understanding the process of cortical development will be vital in diagnosing and eventual treatment of many patients with these conditions. More specifically, the cortex forms from two major populations of neuroblasts which reach their final destination in the cortex by differerent mechanisms. One is radial migration from ventricular neuroblasts to the cortical plate. These cells are excititory projection neurons and glia. The second pathway is from the ventral ganglionic eminences and tangential migration of the interneuronal population of primarily inhibitory neurons. Much less is known about the control of the latter process, and many of these currently undiagnosed subtle malformations may stem from abnormalities of this tangential migration. This project focuses on the understanding the control of the tangentially migrating inhibitory interneurons. We aim to uncover the transcriptional differences between two distinct neuronal populations, GFP positive cells in the ganglionic emience and GFP positive cells within the cortical plate, in order to understand the genetic control of tangential migration. We will acomplish this aim by targeting two different labeled transcripts againts the affymetrix mouse genome arrays. We hypothesis that there will be distinct differences in mRNA transcription profiles between the ganglionic eminence and cortical plate within developing interneurons. The differences in transcript profiles will be genes that regulate the migration and differentiation of these developing neurons. Transgenic mice have been generated which express green flourscent protien (GFP) based on the activity of the Dlx 5-6 promotor. Dlx 5-6 are highly regulated genes, and are expressed only in developing interneurons with in the embryonic brain. The expression of this gene begins at around E8 within the medial and lateral ganglionic eminence (GE) and then remain present as cells born within these regions migrate out into the developing cortex. Therefore, we can take advantage of these mice by harvesting embryos at a midpoint in their development (E13.5-14.5) and dissect out GFP positive cells from the ganglionic eminence and from the cortical plate. In order to obtain enough cells to extract sufficent mRNA, we have choosen to perform microdisction of the entire GE and entire cortical plate then break up the tissue into single cell suspension and Florescent activated cell sort (FACs) the populations of GFP + and GFP - cells. We then will extract the total RNA from the GFP postive cell populations using a Trizol based method and purify the RNA with a Quiagen column purification method. The purified RNA will then be amplified using the Affymetrix 1 or 2 round T7 based amplification procedure in order to generate the microgram quantities of labelled cRNA. The labelled biotin cRNA will be sent to the microarray consortium for hybridization againt the Affy mouse genome chip. Three embryos will be pooled in order to obtain sufficent RNA and 6 GFP positive GE and cortical plate samples will be used. The six replicates will be obtained from at least 3 different pregnant mice. **Keywords: other** **Overall design:**

Background corr dist: KL-Divergence = 0.1016, L1-Distance = 0.0943, L2-Distance = 0.0158, Normal std = 0.5231

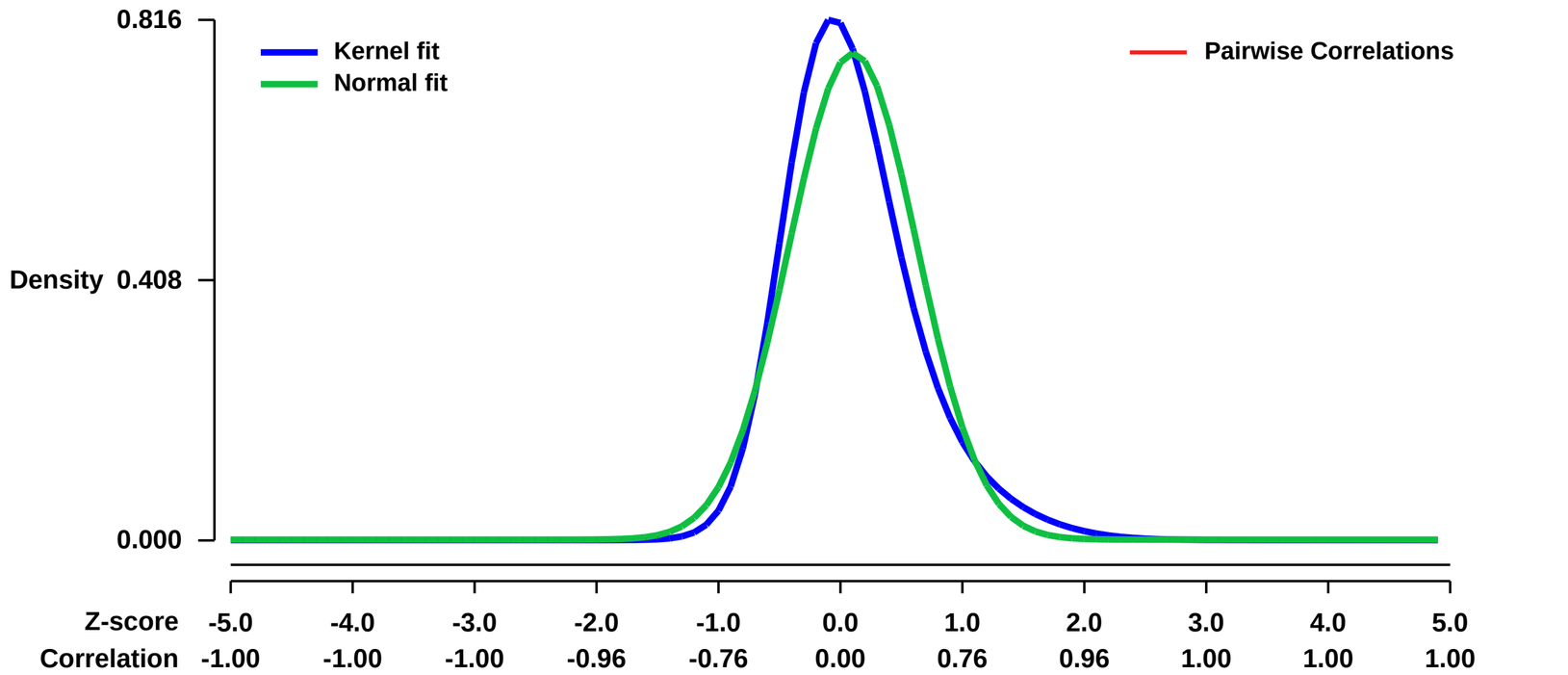

GEO Series "GSE43581" Expression Profiles

Num of samples in this series: 12

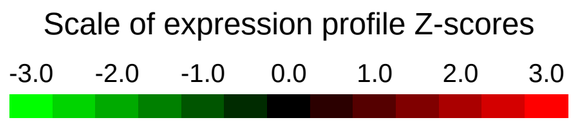

GEO Link:	**http://www.ncbi.nlm.nih.gov/geo/query/acc.cgi?acc=GSE43581**
Status:	**Public on Jan 18 2013**
Title:	**Hepatic glucose sensing is required to preserve beta-cell glucose competence**
Organism:	**Mus musculus**
Experiment type:	**Expression profiling by array**
Platform:	**GPL1261**
Pubmed ID:	**23549084**
Summary & Design:	**Summary:** **We assessed the impact of glucose transporter Glut2 gene inactivation in adult mouse liver (LG2KO mice). This suppressed hepatic glucose uptake but not glucose output. In the fasted state, expression of carbohydrate responsive element-binding protein (ChREBP) and its glycolytic and lipogenic target genes was abnormally elevated. Feeding, energy expenditure, and insulin sensitivity were identical in LG2KO and control mice. Glucose tolerance was normal early after Glut2 inactivation but intolerance developed at later time. This was caused by progressive impairment of glucose-stimulated insulin secretion even though beta-cell mass and insulin content remained normal. Liver transcript profiling revealed a coordinate down-regulation of cholesterol biosynthesis genes in LG2KO mice. This was associated with reduced hepatic cholesterol in fasted mice and a 30 percent reduction in bile acid production. We showed that chronic bile acids or FXR agonist treatment of primary islets increases glucose-stimulated insulin secretion, an effect not seen in islets from fxr-/- mice. Collectively, our data show that glucose sensing by the liver controls beta-cell glucose competence, through a mechanism that likely depends on bile acid production and action on beta-cells.** **Overall design:** **three replicates each of ps_ctrl_refed, ps_tamox_refed, ps_ctrl_fasted, ps_tamox_fasted**

Background corr dist: KL-Divergence = 0.0709, L1-Distance = 0.0372, L2-Distance = 0.0028, Normal std = 0.4933

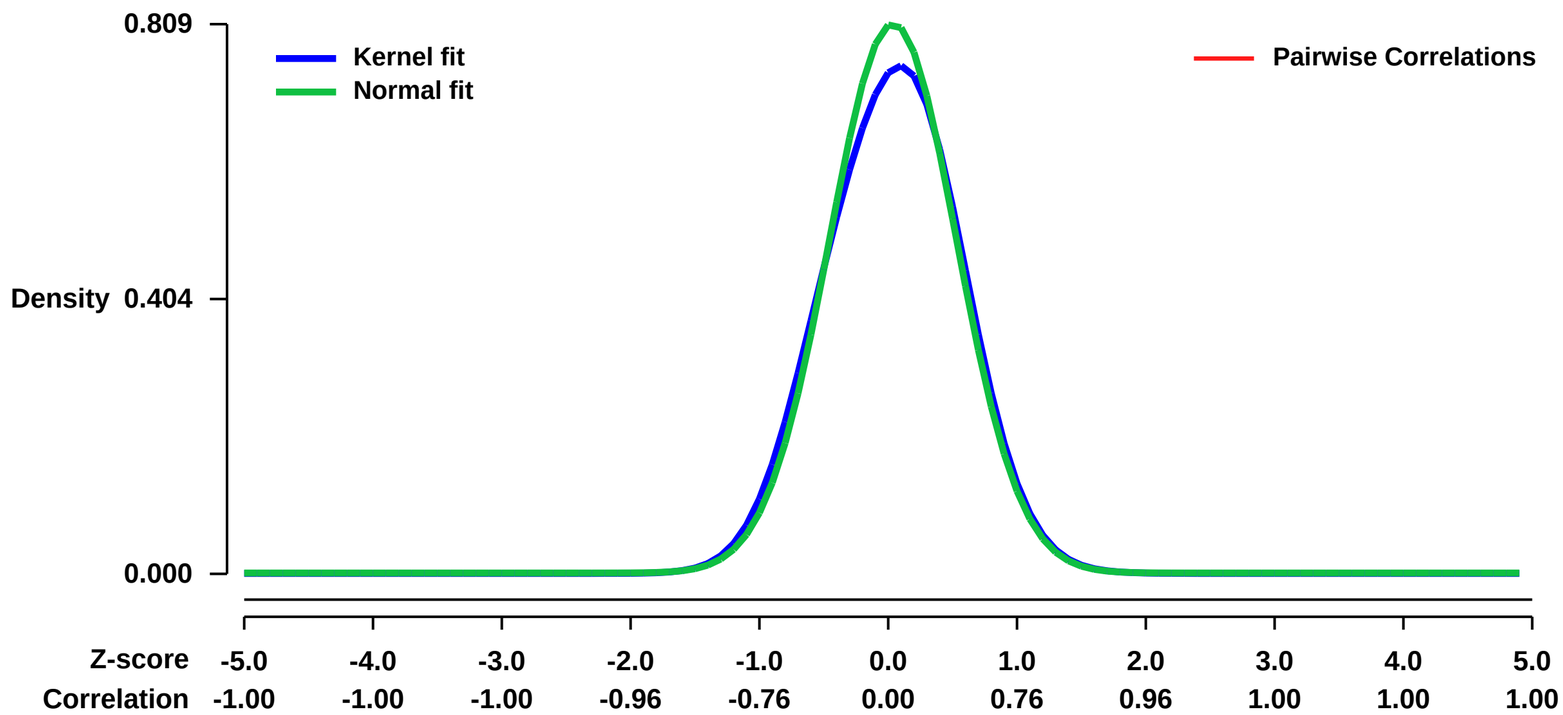

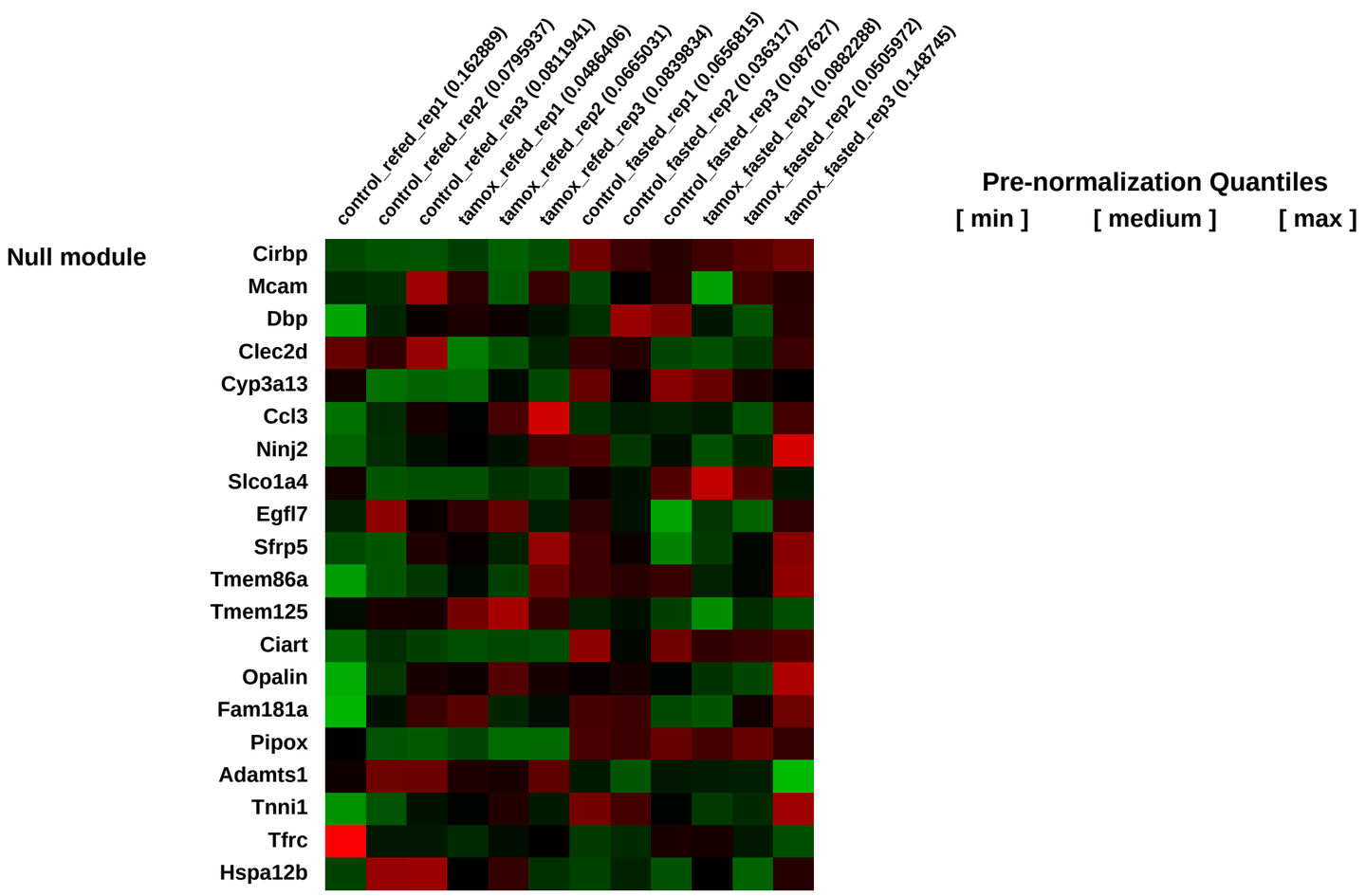

GEO Series "GSE9735" Expression Profiles

Num of samples in this series: 9

Scale of expression profile Z-scores

-3.0 -2.0 -1.0 0.0 1.0 2.0 3.0

GEO Link:	**http://www.ncbi.nlm.nih.gov/geo/query/acc.cgi?acc=GSE9735**
Status:	**Public on Nov 29 2008**
Title:	**B6_IL1218_WAP**
Organism:	**Mus musculus**
Experiment type:	**Expression profiling by array**
Platform:	**GPL1261**
Pubmed ID:	
Summary & Design:	**Summary:** **Dataset of IL-12+IL-18 trated and Yersinia enterocolitica infected C57BL/6 NK cells** **Keywords: infection response** **Overall design:** **3 conditions, 3 biological replicates each**

Background corr dist: **KL-Divergence = 0.0617, L1-Distance = 0.0954, L2-Distance = 0.0121, Normal std = 0.7100**

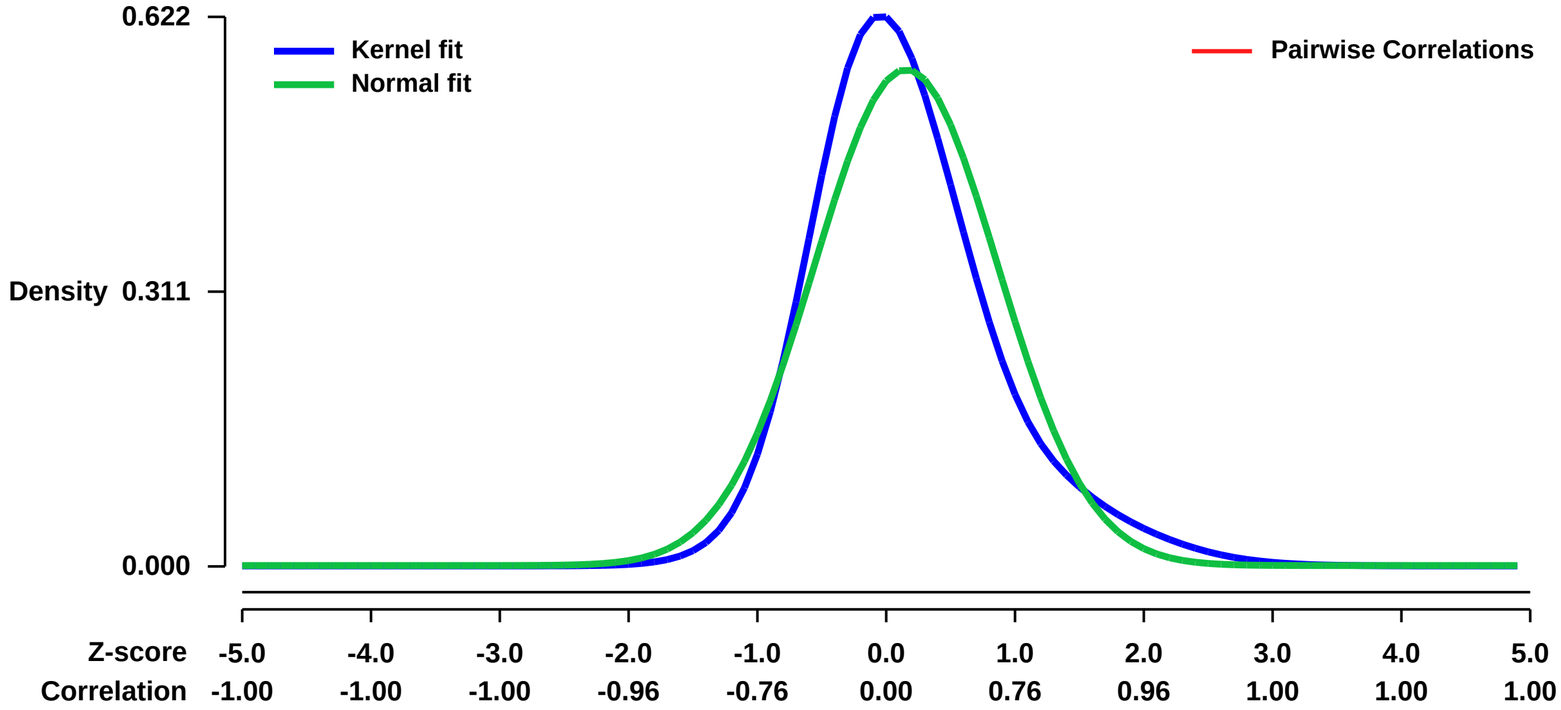

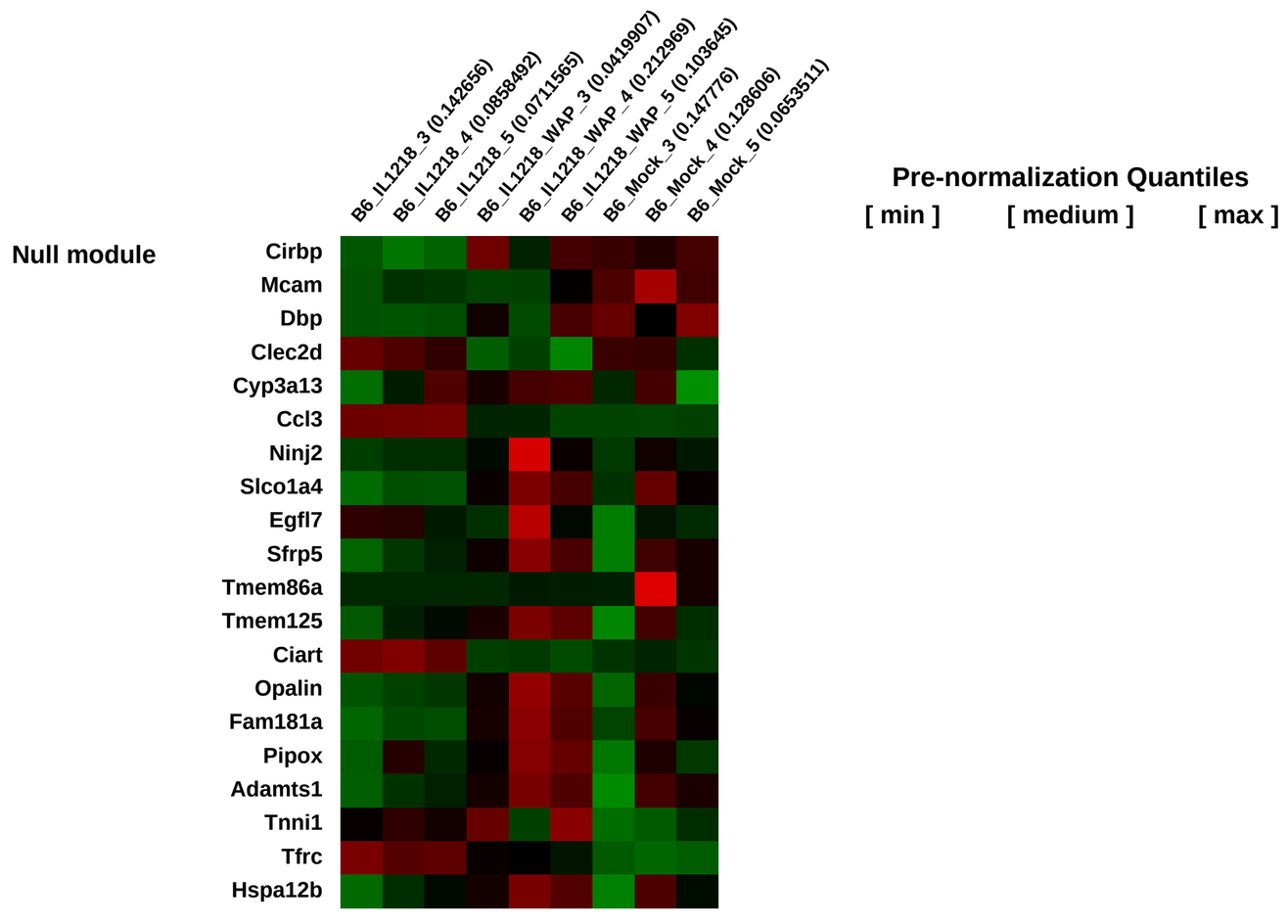

GEO Series "GSE50822" Expression Profiles

Num of samples in this series: 12

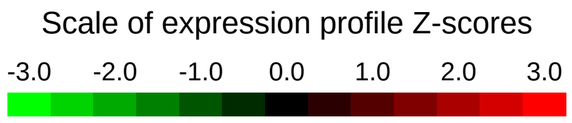

GEO Link:	http://www.ncbi.nlm.nih.gov/geo/query/acc.cgi?acc=GSE50822
Status:	Public on Dec 31 2013
Title:	Differential neuronal targeting of a new and 2 known calcium channel ¸†4 subunit splice variants correlates with their regulation of gene expression
Organism:	Mus musculus
Experiment type:	Expression profiling by array
Platform:	GPL1261
Pubmed ID:	24453333
Summary & Design:	**Summary:** The ¸† subunits of voltage-gated calcium channels regulate surface expression and gating of CaV1 and CaV2 ¸–1 subunits, and thus contribute to neuronal excitability, neurotransmitter release and calcium-induced gene regulation. In addition certain ¸† subunits are targeted into the nucleus, where they directly interact with the epigenetic machinery. Whereas their involvement in this multitude of functions is reflected by a great molecular heterogeneity of ¸† isoforms derived from four genes and abundant alternative splicing, little is known about the roles of individual ¸† variants in specific neuronal functions. In the present study, an alternatively spliced ¸†4 subunit lacking the variable N-terminus (¸†4e) is identified. It is highly expressed in mouse cerebellum and cultured cerebellar granule cells (CGC) and modulates P/Q-type calcium currents in tsA cells and CaV2.1 surface expression in neurons. Compared to the other two known full-length ¸†4 variants (¸†4a, ¸†4b) ¸†4e is most abundantly expressed in the distal axon, but lacks nuclear targeting properties. To examine the importance of nuclear targeting of ¸†4 subunits for transcriptional regulation, we performed whole genome expression profiling of CGCs from lethargic mice individually reconstituted with ¸†4a, ¸†4b, and ¸†4e. Notably, the number of genes regulated by each ¸†4 splice variant correlated with the rank order of their nuclear targeting properties (¸†4b> ¸†4a> ¸†4e). Together these findings support isoform-specific functions of ¸†4 splice variant in neurons, with ¸†4b playing a dual role in channel modulation and gene regulation, while the newly detected ¸†4e variant serves exclusively in calcium channel-dependent functions. We used microarrays to identify gene expression changes caused by ¸†4 splice variants (¸†4a, ¸†4b and ¸†4e) of the voltage gated calcium channel in cultured cerebellar granule cells of lethargic mice **Overall design:** Cultured cerebellar granule cells from lethargic (129/SvJ background) mice reconstituted with the ¸†4 splice variants (¸†4a, ¸†4b and ¸†4e) were compared to eGFP transfected controls

Background corr dist: KL-Divergence = 0.0838, L1-Distance = 0.0264, L2-Distance = 0.0011, Normal std = 0.4649

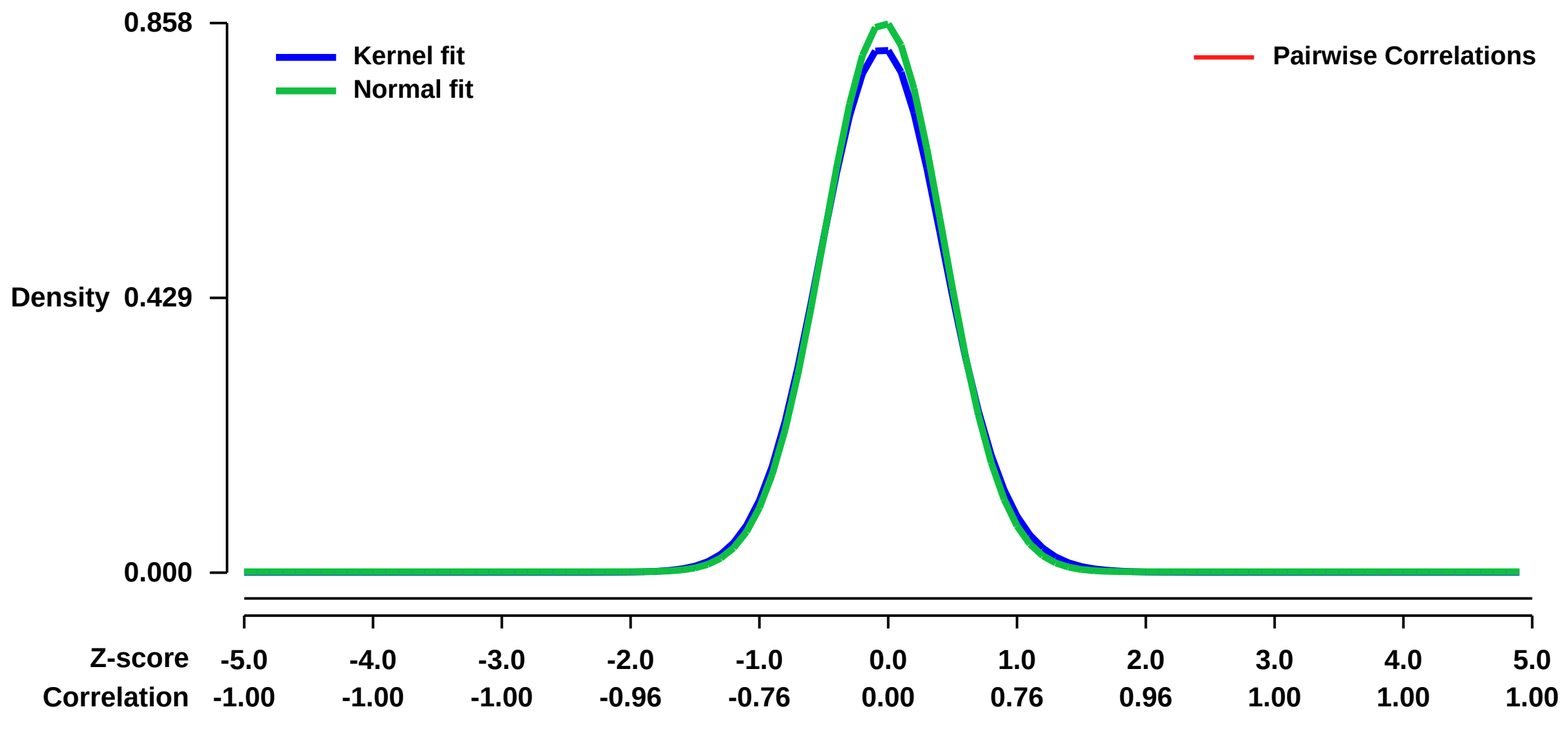

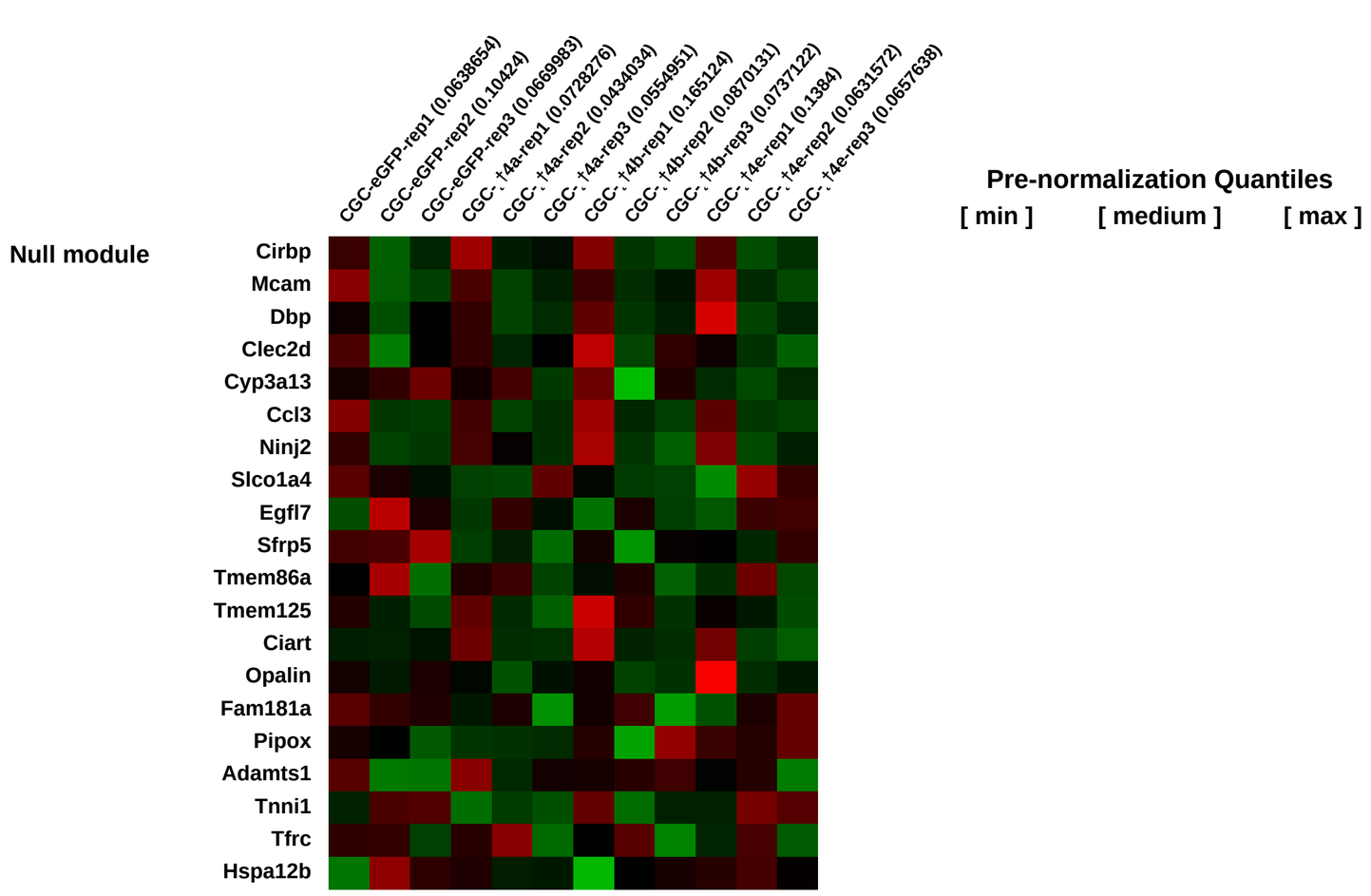

GEO Series "GSE13611" Expression Profiles

Num of samples in this series: 8

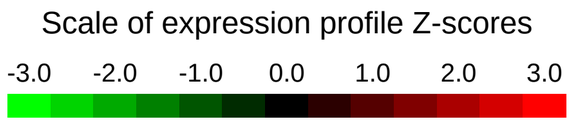

GEO Link:	http://www.ncbi.nlm.nih.gov/geo/query/acc.cgi?acc=GSE13611
Status:	Public on Aug 15 2009
Title:	Affymetrix gene expression AID-GFP-positive vs AID-GFP-negative
Organism:	Mus musculus
Experiment type:	Expression profiling by array
Platform:	GPL1261
Pubmed ID:	19732723
Summary & Design:	**Summary:** Affymetrix gene expression AID-GFP-positive vs AID-GFP-negative **Overall design:** Affymetrix gene expression AID-GFP-positive vs AID-GFP-negative

Background corr dist: KL-Divergence = 0.0067, L1-Distance = 0.0275, L2-Distance = 0.0010, Normal std = 0.9603

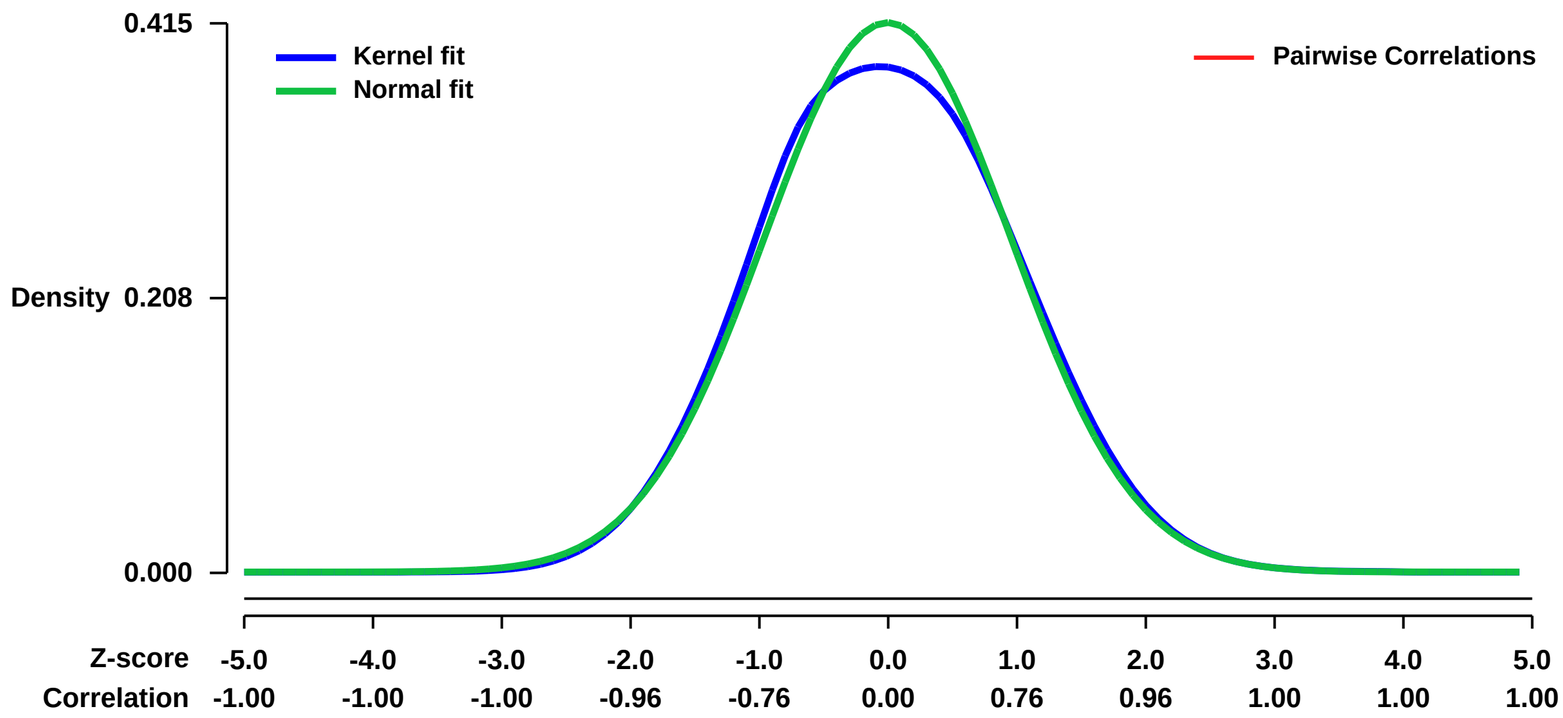

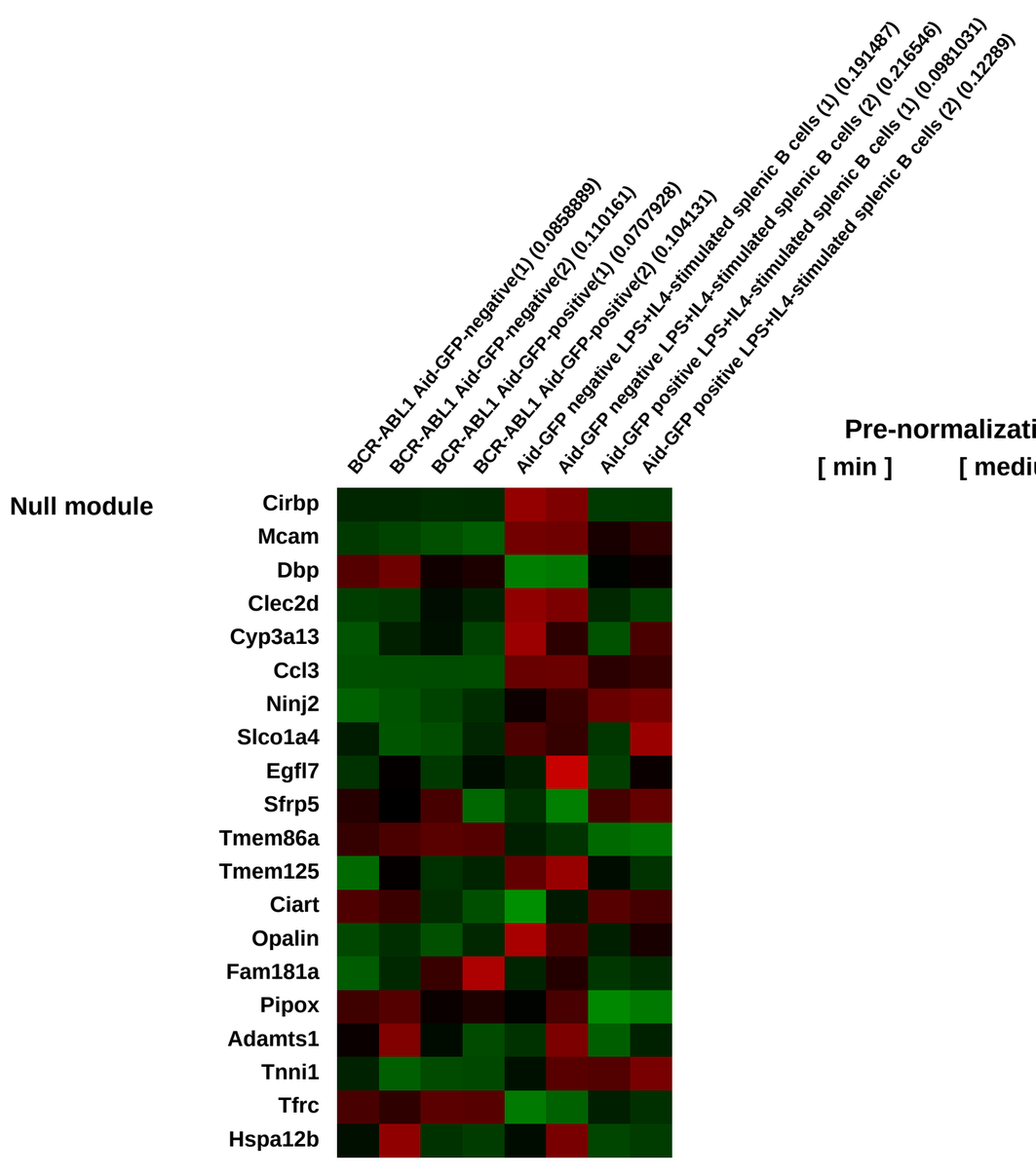

GEO Series "GSE35825" Expression Profiles

Num of samples in this series: 9

Scale of expression profile Z-scores

-3.0 -2.0 -1.0 0.0 1.0 2.0 3.0

GEO Link:	http://www.ncbi.nlm.nih.gov/geo/query/acc.cgi?acc=GSE35825
Status:	Public on Feb 15 2012
Title:	Type I and II Interferon-Stimulated Genes in Murine Primary Bone Marrow Macrophages
Organism:	Mus musculus
Experiment type:	Expression profiling by array
Platform:	GPL1261
Pubmed ID:	22371602
Summary & Design:	**Summary:** We used microarrays to compare interferon-alpha (IFNa)- and interferon-gamma (IFNg)-stimulated genes under an equivalent biological input. The goal was to compare IFNa- and IFNg-stimulated genes, as well as to identify common and distinct sets of type I and II ISGs. **Overall design:** Bone marrow macrophages derived from mouse bone marrow in M-CSF for 7 days. The cells were stimulated with 62U/mL IFNa and 1U/mL of IFNg for 2.5 hrs in culture. These concentrations induced equivalent STAT1 phosphorylation in BMMs.

Background corr dist: KL-Divergence = 0.0865, L1-Distance = 0.0224, L2-Distance = 0.0007, Normal std = 0.4706

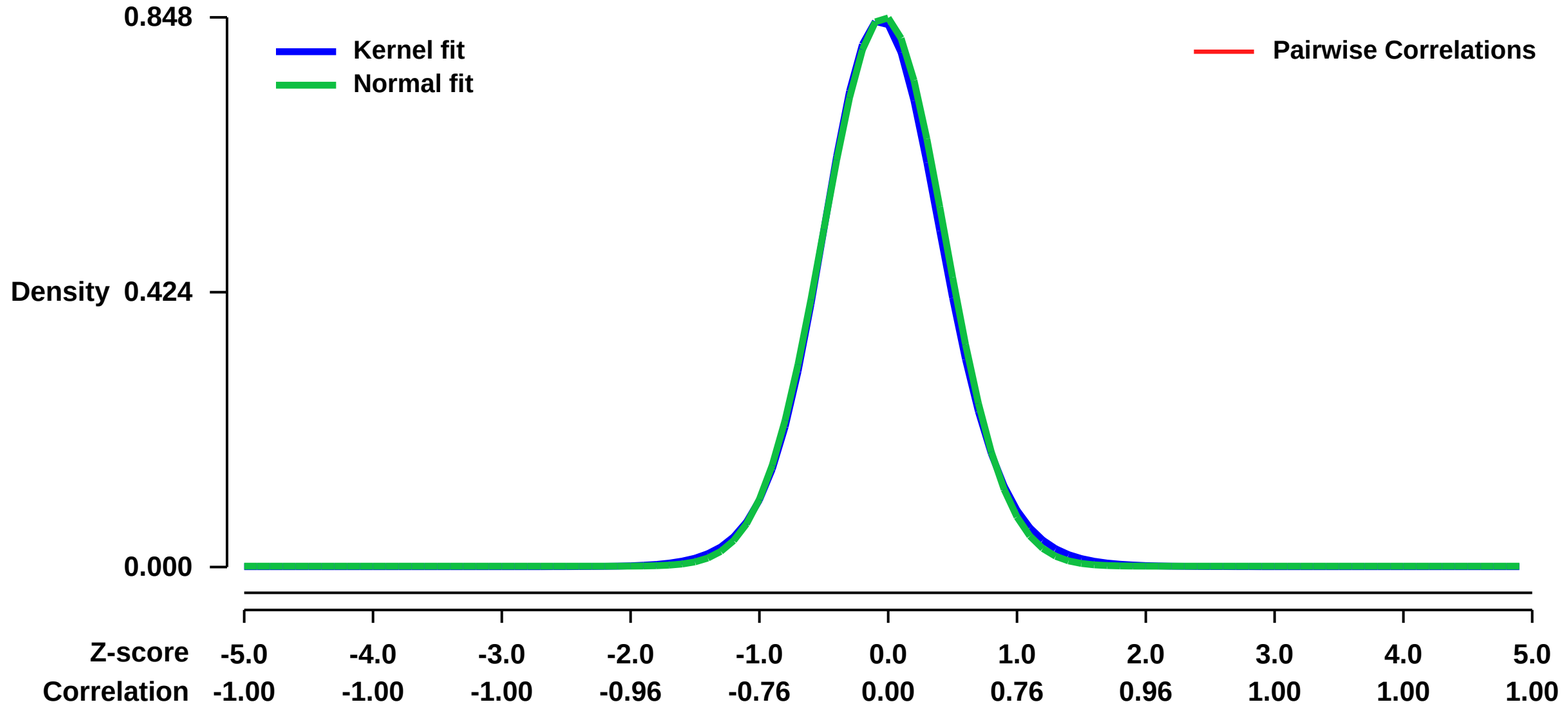

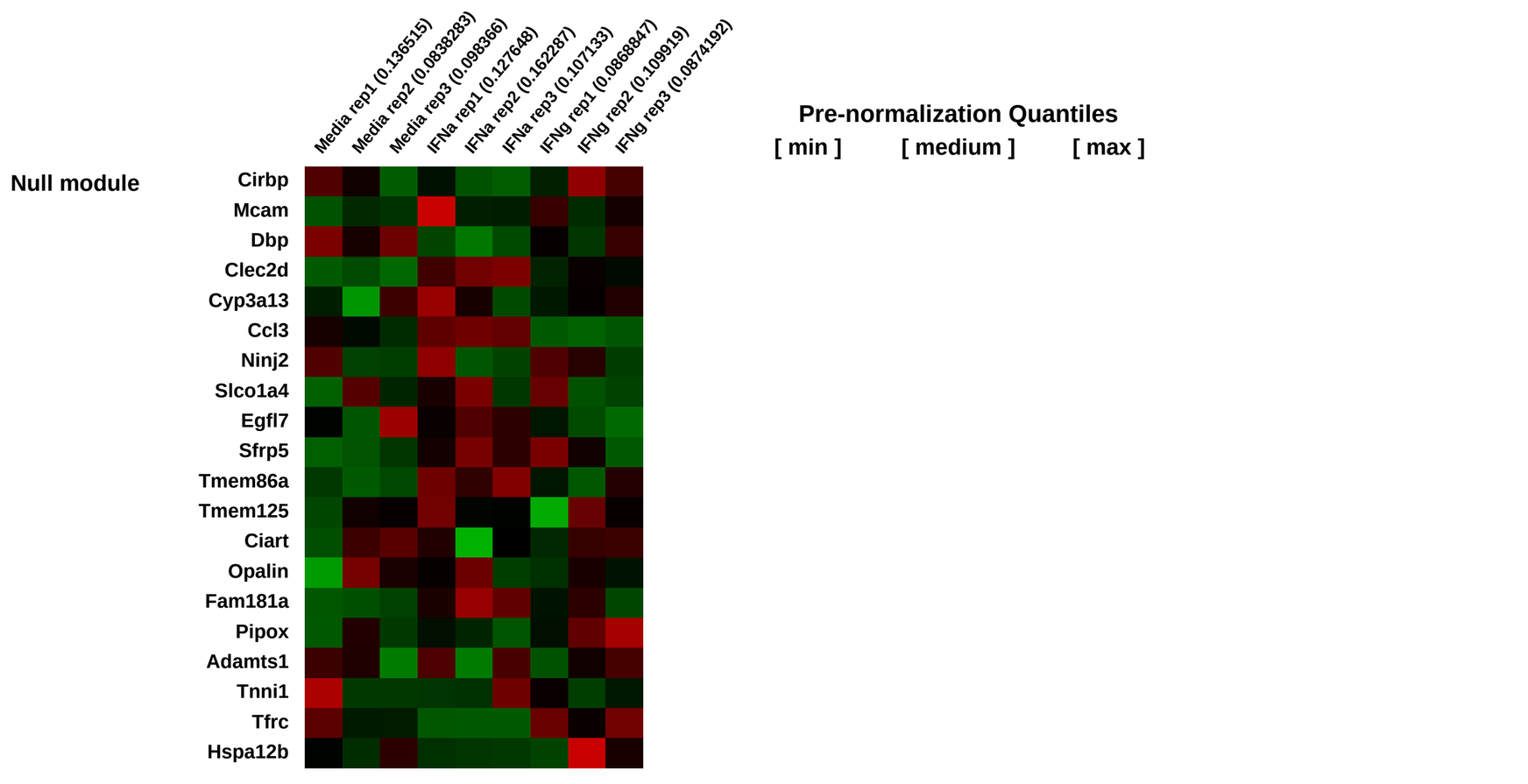

GEO Series "GSE28389" Expression Profiles

Num of samples in this series: 20

Scale of expression profile Z-scores

-3.0 -2.0 -1.0 0.0 1.0 2.0 3.0

GEO Link:	http://www.ncbi.nlm.nih.gov/geo/query/acc.cgi?acc=GSE28389
Status:	Public on Apr 05 2011
Title:	[E-MTAB-368] Transcription profiling by array of mouse embryos at 8 different stages
Organism:	Mus musculus
Experiment type:	Expression profiling by array
Platform:	GPL1261
Pubmed ID:	21427719
Summary & Design:	**Summary:** **Transcription profiling of mouse development** **The experiment were perfomed as a part of our Vertebrate Evo-Devo project. The aim of the project is to compare transcription profiles of normal (unmanipulated, wild-type, whole embryo) vertebrate embryos.** **Overall design:** **Total RNA was collected from wild type C57BL/6 mice, whole embryos at 8 different stages (Stages:E7.5, E8.5, E9.5, E10.5, E12.5, E14.5, E16.5, E18.5), and hybridized to Affymetrix Mouse Genome 430 2.0 Array. All the stages contains data from 2 to 3 biological replications. Each staged-samples consists of pooled total RNA from several whole embryos.**

Background corr dist: **KL-Divergence = 0.0441, L1-Distance = 0.0355, L2-Distance = 0.0018, Normal std = 0.5966**

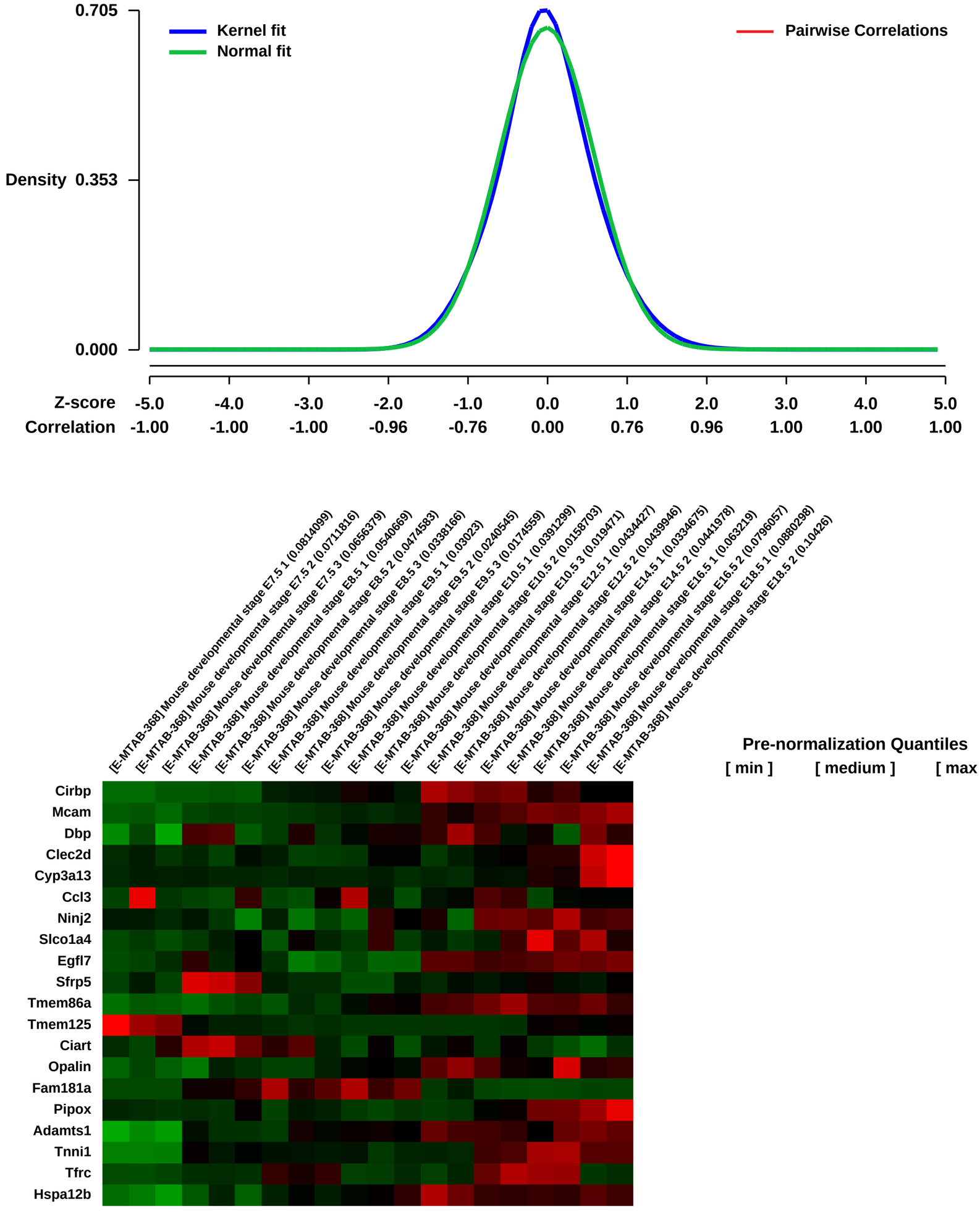

GEO Series "GSE31378" Expression Profiles

Num of samples in this series: 9

Scale of expression profile Z-scores

-3.0 -2.0 -1.0 0.0 1.0 2.0 3.0

GEO Link:	http://www.ncbi.nlm.nih.gov/geo/query/acc.cgi?acc=GSE31378
Status:	Public on Aug 16 2013
Title:	Host cell gene expression in Human respiratory syncytial virus (HRSV) infected mouse macrophage cells at 4, 24 hours post infection
Organism:	Mus musculus
Experiment type:	Expression profiling by array
Platform:	GPL1261
Pubmed ID:	23506210
Summary & Design:	**Summary:** We used the microarray data to analyze host cells response on mouse macrophage cells infected with HRSV **Overall design:** The HRSV infected mouse macrophage cells were harvested at 4 and 24 hpi and RNA extraction was performed using standard protocol as described by Affymetrix. The aim of this experiment is to analyze host cell response to HRSV infection.

Background corr dist: KL-Divergence = 0.0597, L1-Distance = 0.0481, L2-Distance = 0.0032, Normal std = 0.5745

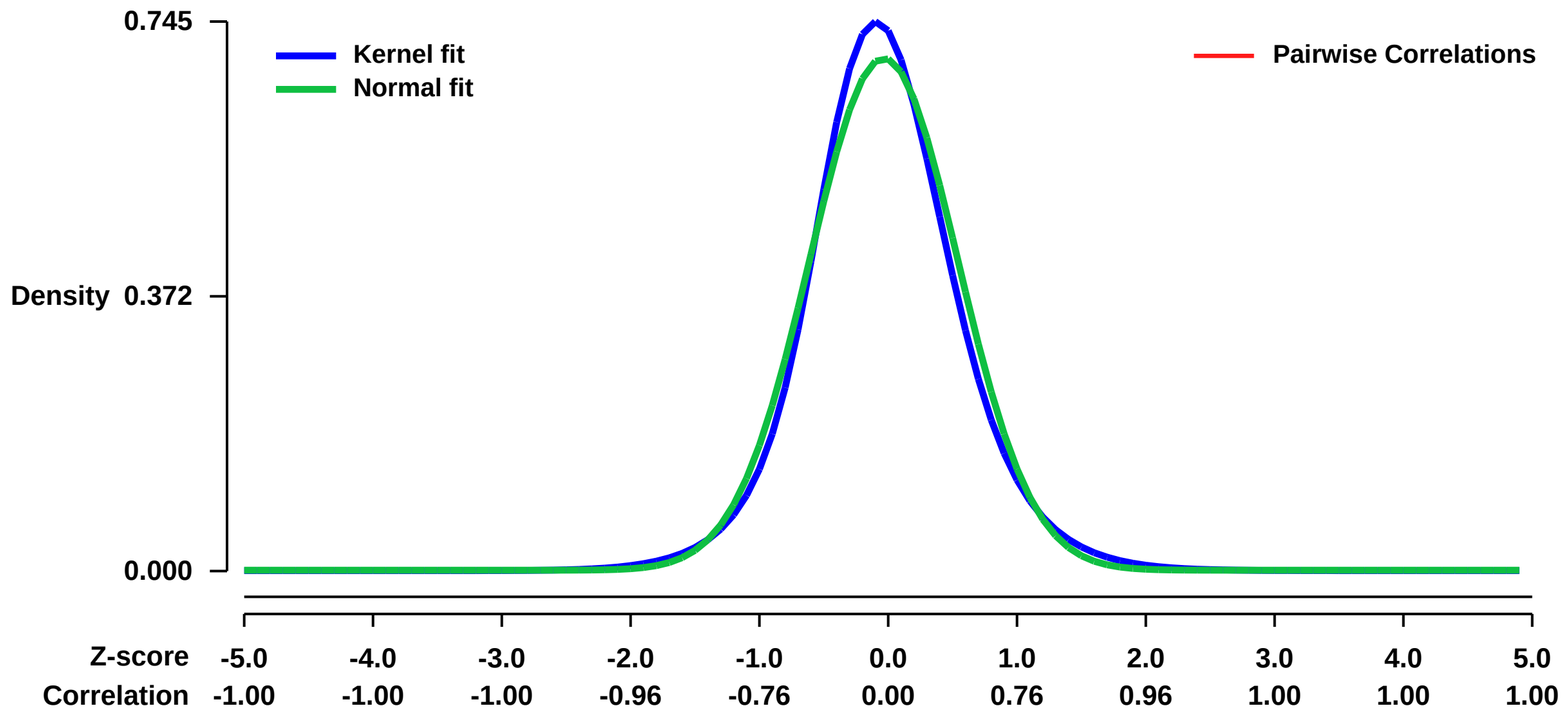

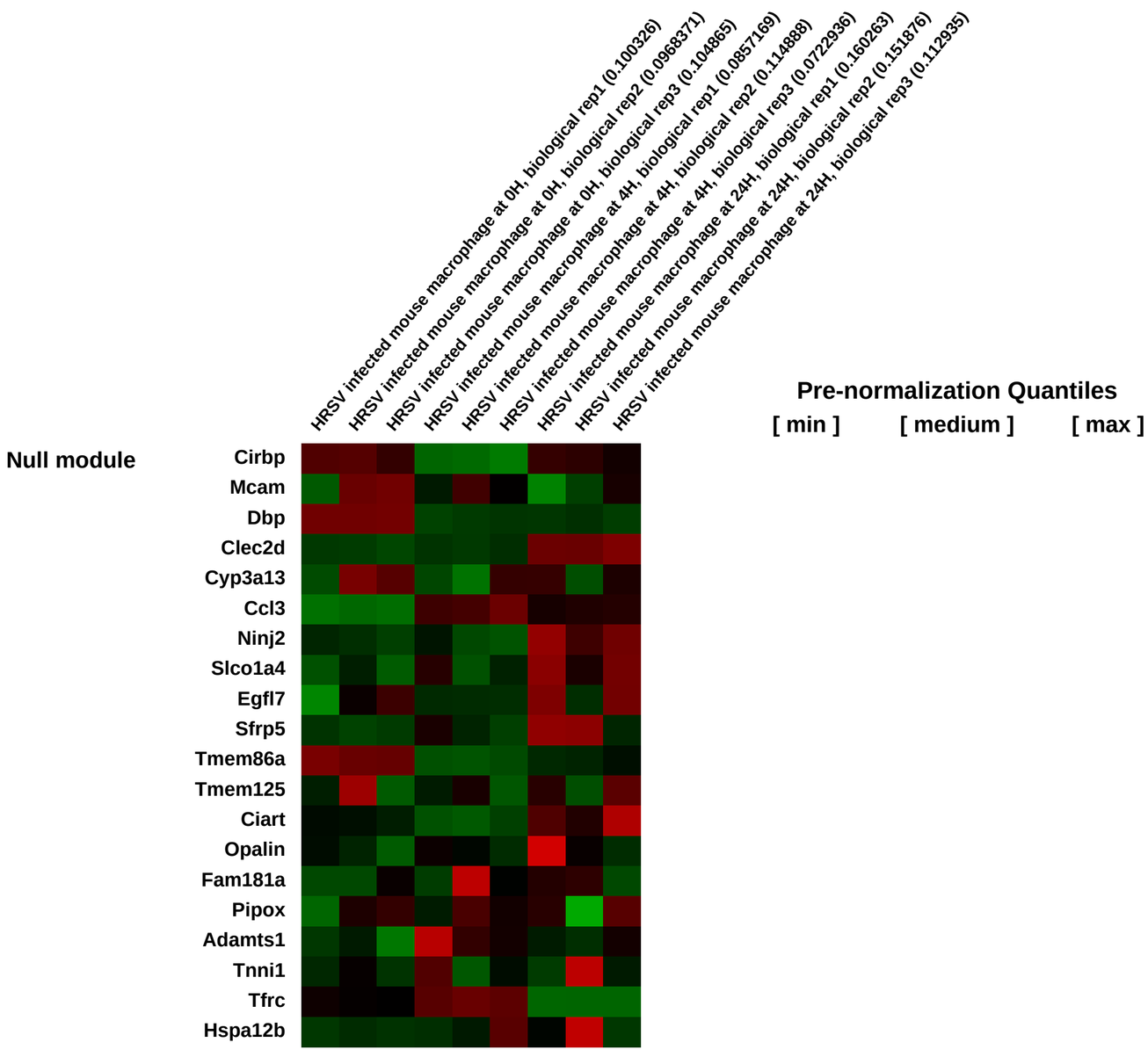

GEO Series "GSE40156" Expression Profiles

Num of samples in this series: 42

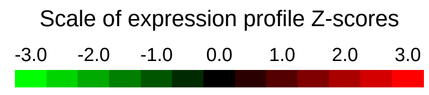

GEO Link: http://www.ncbi.nlm.nih.gov/geo/query/acc.cgi?acc=GSE40156

Status: Public on Oct 30 2013

Title: Transcript atlases reveal that artery tertiary lymphoid organs but not secondary lymphoid organs control key steps of atherosclerosis T cell immunity in aged apoe-/- mice.

Organism: Mus musculus

Experiment type: Expression profiling by array

Platform: GPL1261

Pubmed ID:

Summary & Design:

Summary:
Tertiary lymphoid organs (TLOs) emerge in response to nonresolving inflammation but their roles in adaptive immunity remain unknown. Here, we explored artery TLOs (ATLOs) to delineate atherosclerosis T cell responses in apoe-/- mice during aging. Though the T cell repertoire showed systemic age-associated contractions in size and modifications in subtype composition and activation, wt and apoe-/- mice were equally affected. In contrast, ATLOs - but not wt aortae, apoe-/- aorta segments without ATLOs or atherosclerotic plaques - promoted T cell recruitment, altered characteristics of T cell motility, primed and imprinted T cells in situ, generated CD4+/FoxP3-, CD4+/FoxP3+, CD8+/FoxP3- effector and central memory cells, and converted naˆflve CD4+/FoxP3- T cells into induced Treg cells. ATLOs also showed substantially increased antigen presentation capability by conventional dendritic cells (DCs) and monocyte-derived DCs but not by plasmacytoid DCs. Thus, the senescent immune system specifically employs ATLOs to control dichotomic atherosclerosis T cell immune responses. We assembled transcriptome maps of wt and apoe-/- aortae and aorta-draining RLNs and identified ATLOs as major sites of atherosclerosis-specific T cell responses during aging: Transcriptome atlases of wt and apoe-/- abdominal aortae and associated draining RLNs were constructed from laser capture microdissection (LCM)-based whole genome mRNA expression microarrays yielding 6 maps: wt adventitia (tissue-1); wt RLN (tissue-2); apoe-/- ATLOs (tissue-3); apoe-/- RLN (tissue-4); apoe-/- adventitia without adjacent plaques (tissue-5), and plaques (tissue-6). Several two-tissue comparisons within the transcriptome atlases are noteworthy: Unexpectedly, transcriptomes of wt and apoe-/- RLNs were virtually identical; additonal data revealed that transcriptomes of RLNs were strikingly similar to those of inguinal LNs which do not drain the aorta adventitia (as shown of India ink injection experiments of surgically exposed aortae); in sharp contrast, wt adventitia versus ATLOs revealed 1405 differentially expressed transcripts many of which encoded members of GO terms immune response and inflammatory response; the ATLO-plaque comparison also showed > 1000 differentially expressed transcripts; however, wt adventitia versus apoe-/- adventitia without plaque showed few genes (< 5 % of differentially expressed transcripts of the wt adventitia-ATLO comparison). Thus, the aorta transcriptome atlases support the conclusion that neither aorta-draining apoe-/- RLNs nor ILNs participate in atherosclerosis-specific T cell responses. In addition, they demonstrate that T cell responses in the diseased aorta are highly territorialized. Finally, these data show that the immune responses carried out in ATLOs differ significantly from those carried out in plaques. We next identified three major clusters within the transcriptome atlases through ANOVA analyses and application of strict filters: An adventitia cluster, a plaque/ATLO cluster, and a LN/plaque cluster. The total number of differentially expressed genes in each cluster were examined for GO terms immune response, inflammatory response, T cell activation, positive regulation of T cell response, and T cell proliferation. Within the adventitia cluster, similarities of transcriptomes of wt adventitia and apoe-/- adventitia without associated plaque versus ATLOs indicate that a robust number of immune response-regulating genes are selectively expressed in ATLOs which are located within a distance of few ´µm of the adventitia without associated plaques indicating a very high degree of territoriality of the atherosclerosis T cell response. Furthermore, unlike the total number of differentially regulated transcripts, the majority of transcripts among GO terms immune response and inflammatory response, was up-regulated. Inspection of the plaque/ATLO cluster provided further information: The majority of immune response regulating genes where expressed at a higher level in ATLOs when compared to plaques though plaques also contained a significant number of immune response regulating genes; the reverse is true for genes regulating inflammation. Finally, the lymph node cluster revealed that though the majority of immune response regulating genes resides in both wt and apoe-/- RLNs (with little differences between them) ATLOs express a selected set of immune response regulating genes at a higher level when compared to LNs. In addition, the inflammatory component of ATLOs when compared to LNs is documented by the finding that many more genes regulating inflammation reside in ATLOs even when compared to those of plaques.

Key words:

T cell response in atherosclerosis; Laser capture microdissection; transcriptome atlas of atherosclerosis.

Citations:

Grˆbner R. et al. Lymphotoxin beta receptor signaling promotes tertiary lymphoid organogenesis in the aorta adventitia of aged ApoE-/- mice. J Exp Med 2009 Jan 16;206(1):233-48. PMID: 19139167;

Moos M. et al. The lamina adventitia is the major site of immune cell accumulation in standard chow-fed apolipoprotein E-deficient mice. Arterioscler Thromb Vasc Biol. 2005 Nov;25(11):2386-91. Epub 2005 Sep 22. PMID: 16179593;

Beer M. et al. Laser-capture microdissection of hyperlipidemic/ApoE-/- mouse aorta atherosclerosis. Methods Mol Biol. 2011;755:417-28. PMID: 21761324;

Weih F. et al. Control of Dichotomic Innate and Adaptive Immune Responses by Artery Tertiary Lymphoid Organs in Atherosclerosis. Front Physiol. 2012;3:226. Epub 2012 Jul 6. PMID: 22783198.

Overall design:
Wild-type and apoE-deficient mice on the C57BL/6J genetic background were maintained on a standard mouse chow. Total aortae were removed at the age of 6 (n=3), 32 (n=3), or 78 (n=3) w and microarrays were prepared from total RNA extracts or extracts of atherosclerotic lesions and adventitiae obtained by the use of a laser dissection microscope. In addition, aorta associated LNs or distant LNs were prepared from both mouse genotypes.

Background corr dist: KL-Divergence = 0.1004, L1-Distance = 0.0740, L2-Distance = 0.0098, Normal std = 0.4788

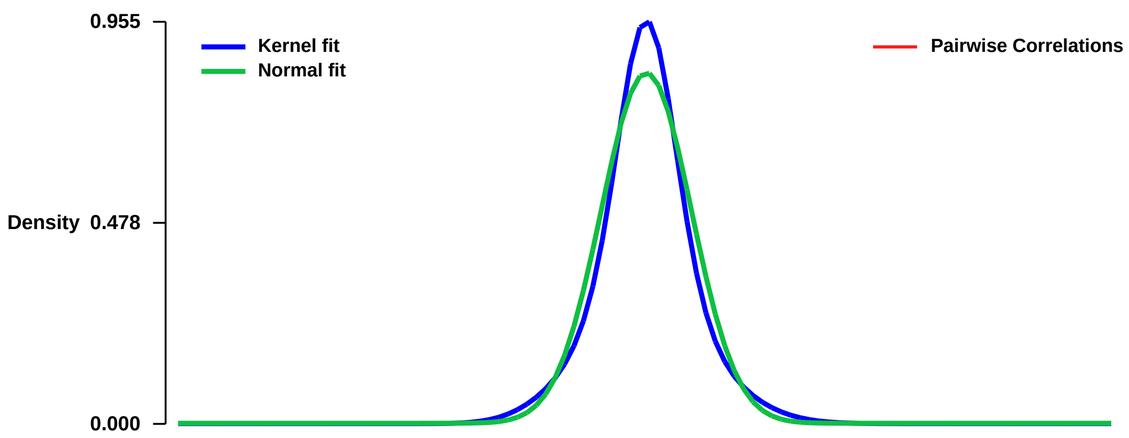

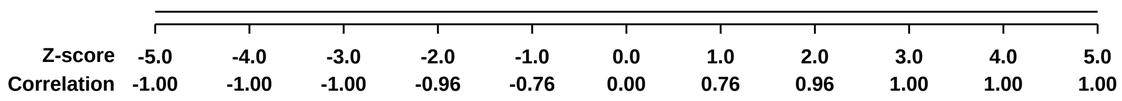

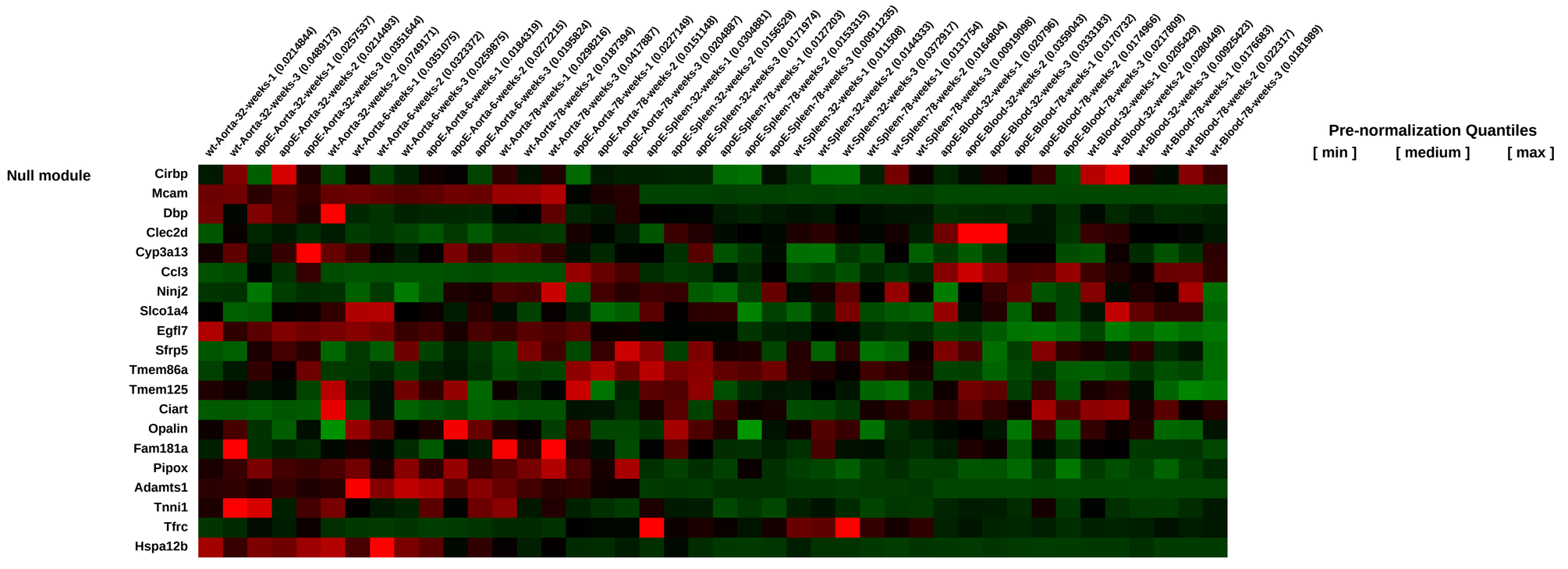

GEO Series "GSE9725" Expression Profiles

Num of samples in this series: 16

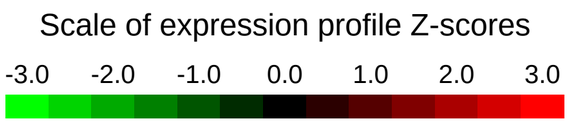

GEO Link:	http://www.ncbi.nlm.nih.gov/geo/query/acc.cgi?acc=GSE9725
Status:	Public on Dec 13 2007
Title:	Gene expression data after acute withdrawal of TERT in mouse skin
Organism:	Mus musculus
Experiment type:	Expression profiling by array
Platform:	GPL1261
Pubmed ID:	18208333
Summary & Design:	**Summary:** TERT is an essential protein component of telomerase, a ribonuclearprotein complex that protects chromosomal ends. Ectopic expression of TERT in mouse skin activates hair follicle stem cells and induces active growth phase of hair cycles, called anagen. This activity of TERT is independent of its reverse transcriptase function, indicating that this is a non-telomeric function of TERT. We performed time-course microarray analysis using conditional bi-transgenic mice (iK5-TERT) to understand the mechanism of this novel non-telomeric function of TERT. Keywords: Time course, 2 cohorts (control, experimental) **Overall design:** Hair follicles of iK5-TERT mice at postnatal day 60 is in TERT-induced anagen. To those mice, we injected either PBS, to maintain TERT transgene expression, or doxycycline, to rapidly extinguish transgene expression. We then took time-course dorsal skin biopsies (0,6,12,24 hr) of these mice and analyzed differential gene expressions using Affymetrix Genechips and various bioinformatic tools, including SAM, to discover TERT-regulated genes.

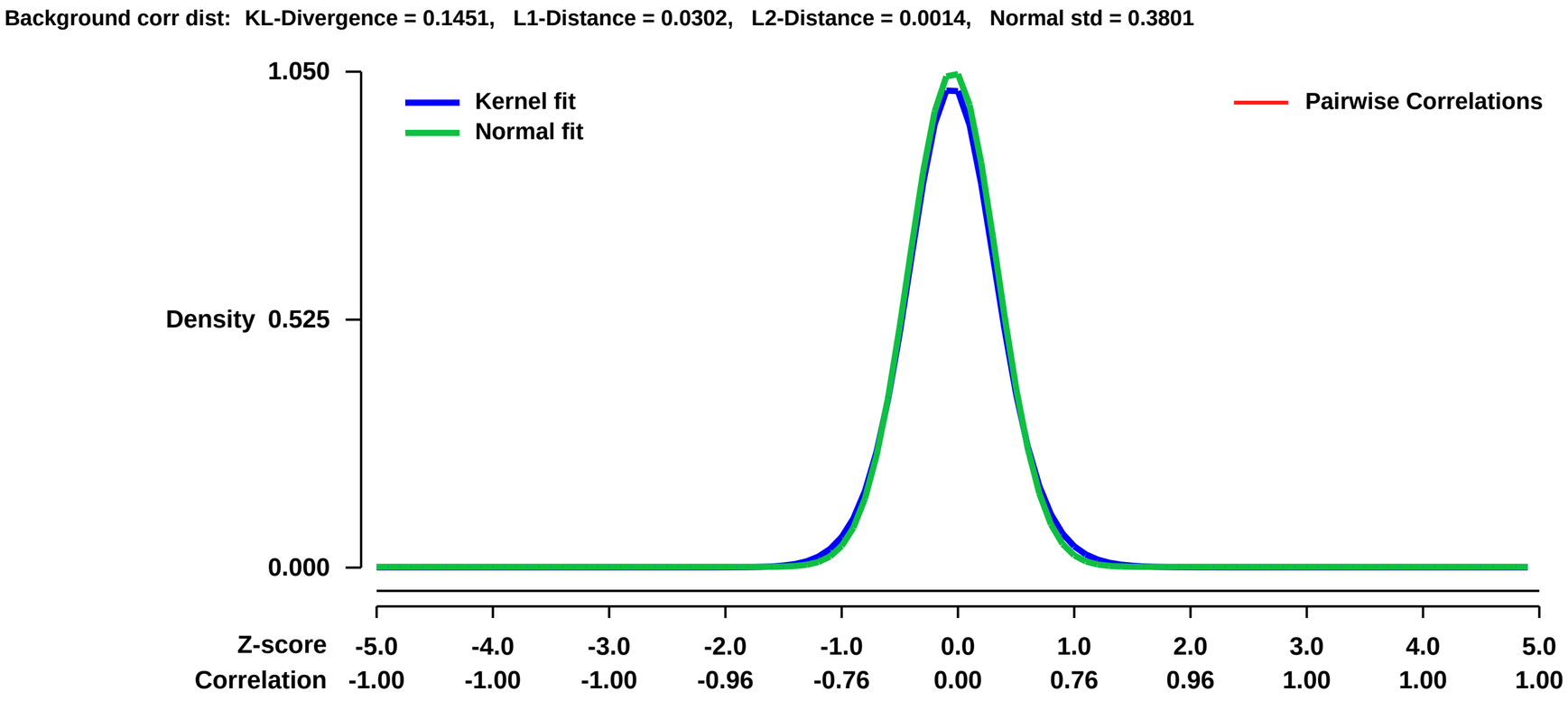

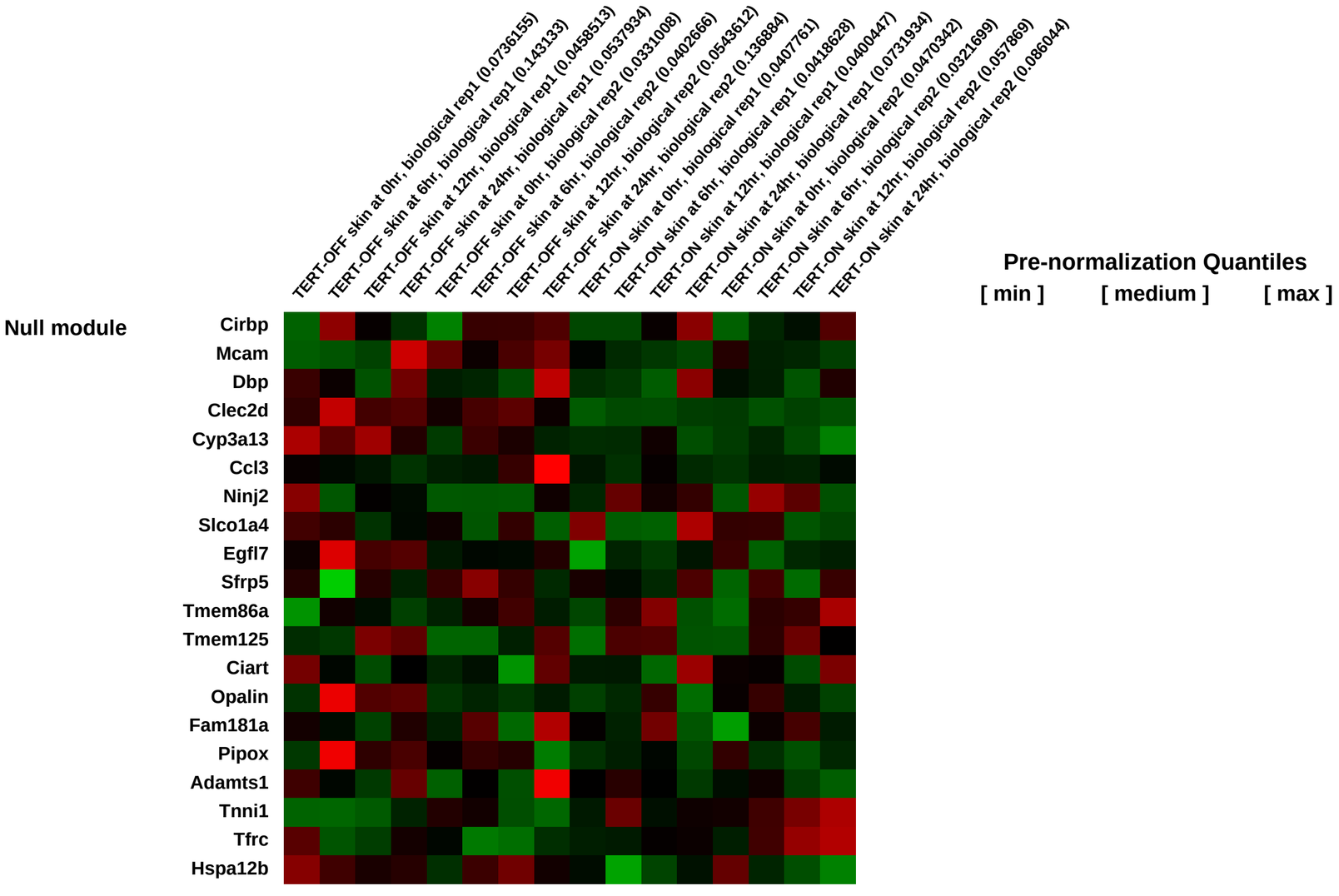

GEO Series "GSE12986" Expression Profiles

Num of samples in this series: 10

Scale of expression profile Z-scores

-3.0 -2.0 -1.0 0.0 1.0 2.0 3.0

GEO Link:	http://www.ncbi.nlm.nih.gov/geo/query/acc.cgi?acc=GSE12986
Status:	Public on Feb 01 2010
Title:	Expression of Cdx2 or Gata3 in R1 mouse embryonic stem cells
Organism:	Mus musculus
Experiment type:	Expression profiling by array
Platform:	GPL1261
Pubmed ID:	20081188
Summary & Design:	**Summary:** To identify whether Cdx2 or Gata3 can activate trophoblast specific gene expression when expressed in R1 ES cells. To assess the dependency of Gata3 activity on Cdx2, Gata3 was also expressed in Cdx2-null ES cells. **Keywords: gene expression** **Overall design:** a fusion construct of either Cdx2 or Gata3 and the tamoxifen responsive estrogen receptor ligand binding domain was expressed in R1 ES cells. Cell were induced with tamoxifen for 6 days to activate the transcription factor and cultured under trophoblast stem cell conditions

Background corr dist: **KL-Divergence = 0.0488, L1-Distance = 0.0298, L2-Distance = 0.0015, Normal std = 0.5634**

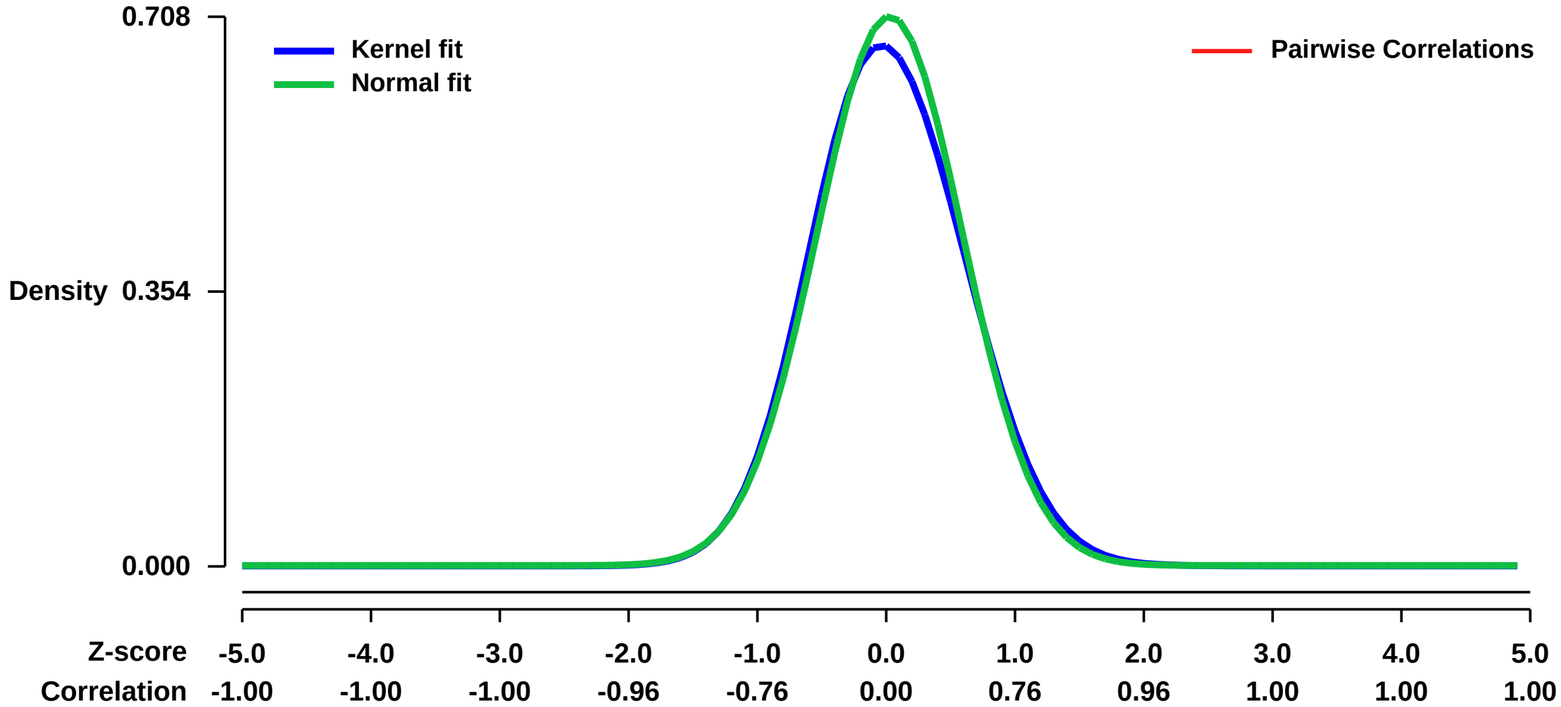

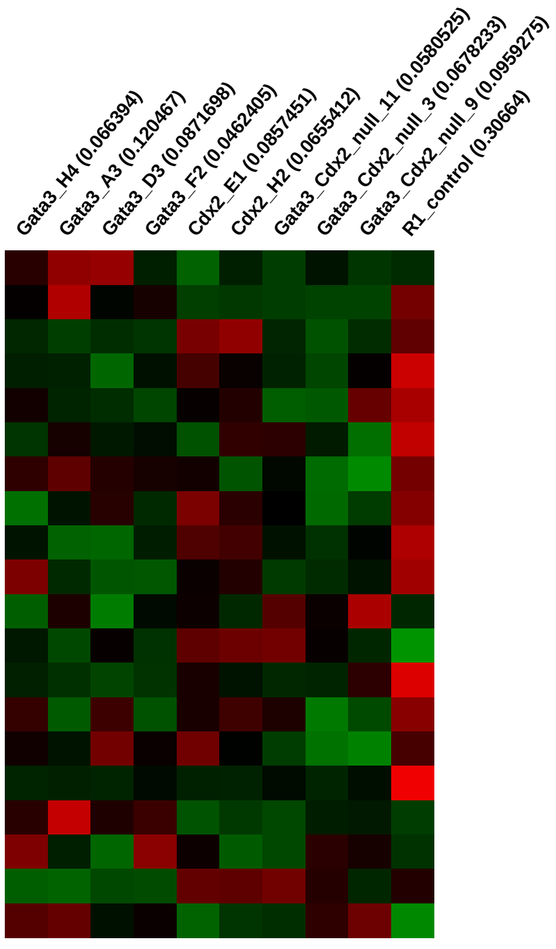

GEO Series "GSE26668" Expression Profiles

Num of samples in this series: 6

Scale of expression profile Z-scores

-3.0 -2.0 -1.0 0.0 1.0 2.0 3.0

GEO Link:	http://www.ncbi.nlm.nih.gov/geo/query/acc.cgi?acc=GSE26668
Status:	Public on Mar 23 2011
Title:	Expression data from E13.5 Fz4-/-Fz8-/- and Fz4+/+Fz8-/- kidneys
Organism:	Mus musculus
Experiment type:	Expression profiling by array
Platform:	GPL1261
Pubmed ID:	21343368
Summary & Design:	**Summary:** Fz4 and Fz8 cooperate in regulating the branching morhpogenesis of the developing kidney during mouse embryonic development, hence determines the eventual kidney size. We used microarrays to study the global gene expression profiles regulated by Fz4 and Fz8 signaling during early kidney development, and to understand the collaboration between the signaling events mediated by Fz4 and Fz8 **Overall design:** Kidney rudiments were dissected from E13.5 mouse embryos for RNA extraction and hybridization on Affymetrix MOE430.2 arrays. Three biological replicates of each genotype were analyzed.

Background corr dist: KL-Divergence = 0.0193, L1-Distance = 0.0128, L2-Distance = 0.0002, Normal std = 0.7424

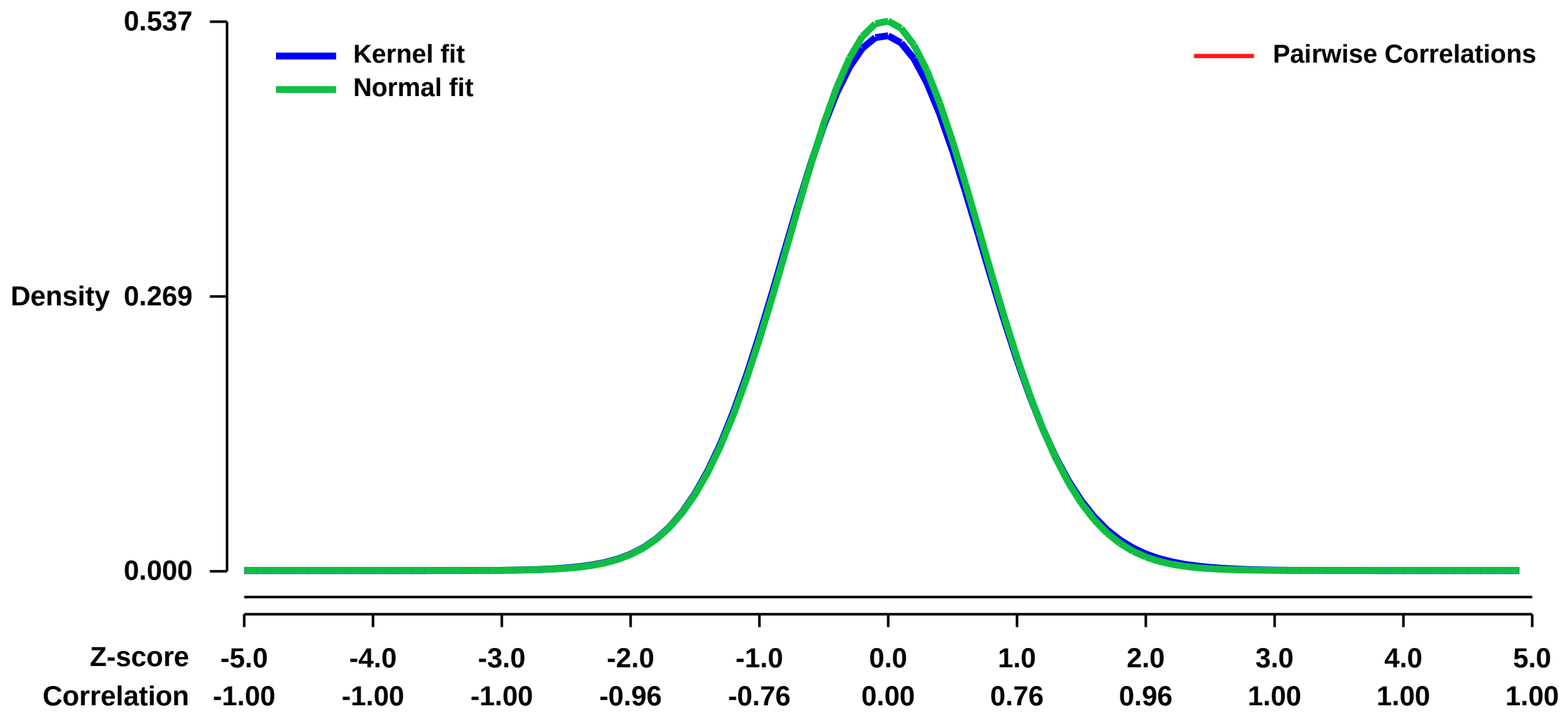

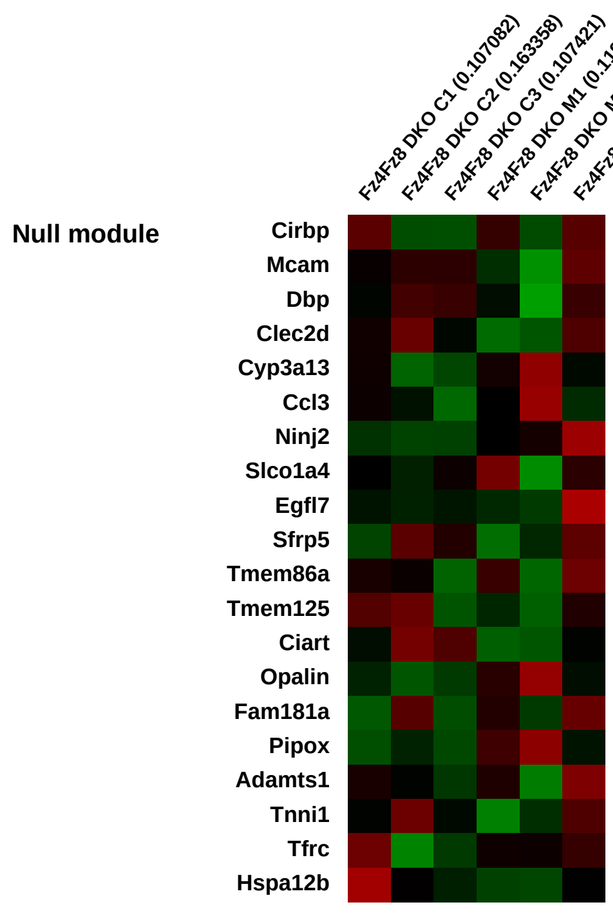

GEO Series "GSE30318" Expression Profiles

Num of samples in this series: 12

Scale of expression profile Z-scores

-3.0 -2.0 -1.0 0.0 1.0 2.0 3.0

GEO Link:	http://www.ncbi.nlm.nih.gov/geo/query/acc.cgi?acc=GSE30318
Status:	Public on May 23 2012
Title:	Expression data from murine Fancc-deficient hematopoietic stem and progenitor cells
Organism:	Mus musculus
Experiment type:	Expression profiling by array
Platform:	GPL1261
Pubmed ID:	22653977
Summary & Design:	**Summary:** We used gene expression microarrays to identify genes whose expression was influenced differently by TNFa in Fancc-deficient mice compared to wild type (WT) mice. To identify genes whose expression was directly or indirectly influenced by Fancc, we looked in particular for genes either suppressed or induced by TNF in WT cells that were not affected by TNF in Fancc-deficient cells. **Overall design:** Enriched populations of KSL cells (marrow mononuclear cells sorted for the c-Kit+/Sca-1+/Lineage (Lin)- fraction from WT and Fancc-deficient mice were exposed for 24 hours in vitro to either hematopoietic growth factors alone (IL-6, IL-11, Flt3L, and SCF) or to those factors plus TNFa (10 ng/ml) after which RNA was prepared and hybridized to Affymetrix microarrays (MOE430 2.0).

Background corr dist: KL-Divergence = 0.1174, L1-Distance = 0.0288, L2-Distance = 0.0013, Normal std = 0.4109

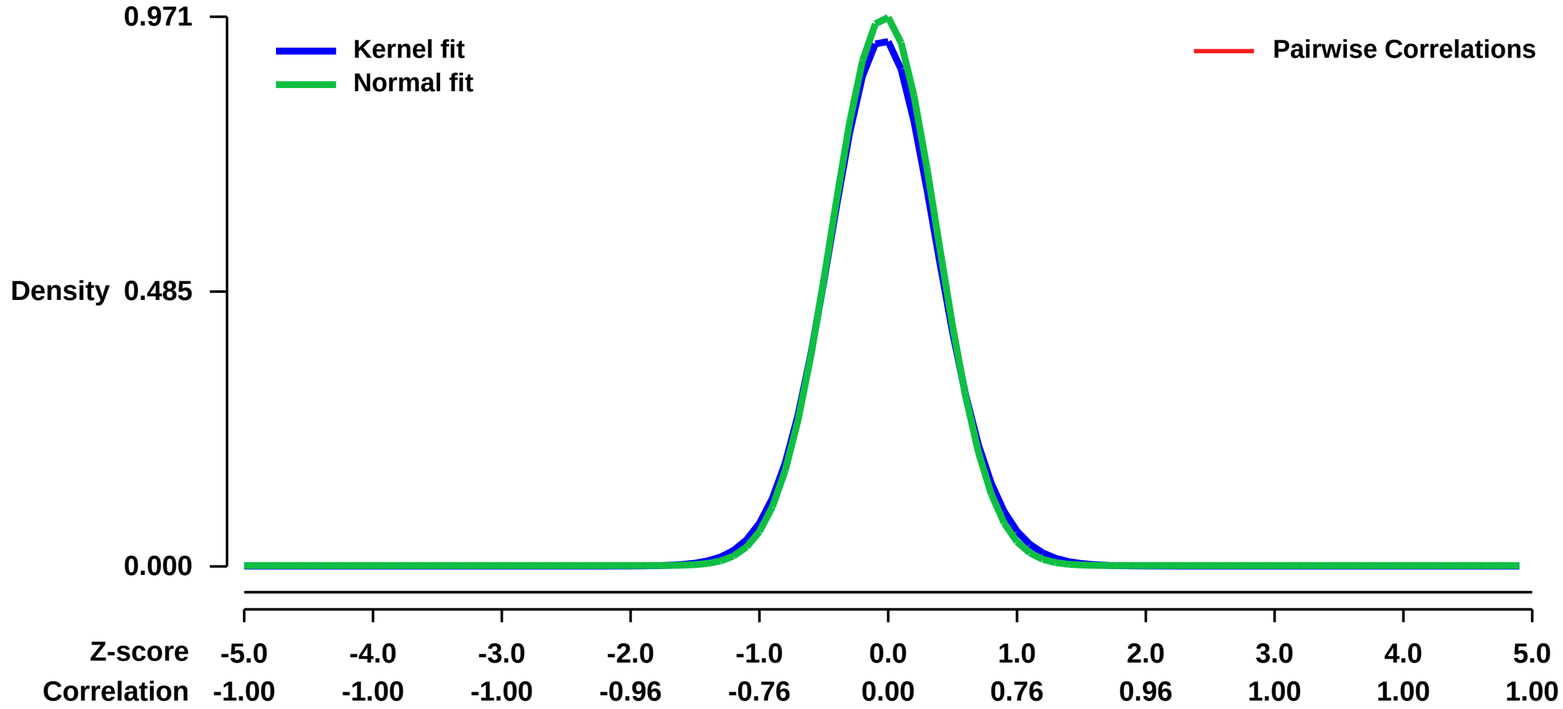

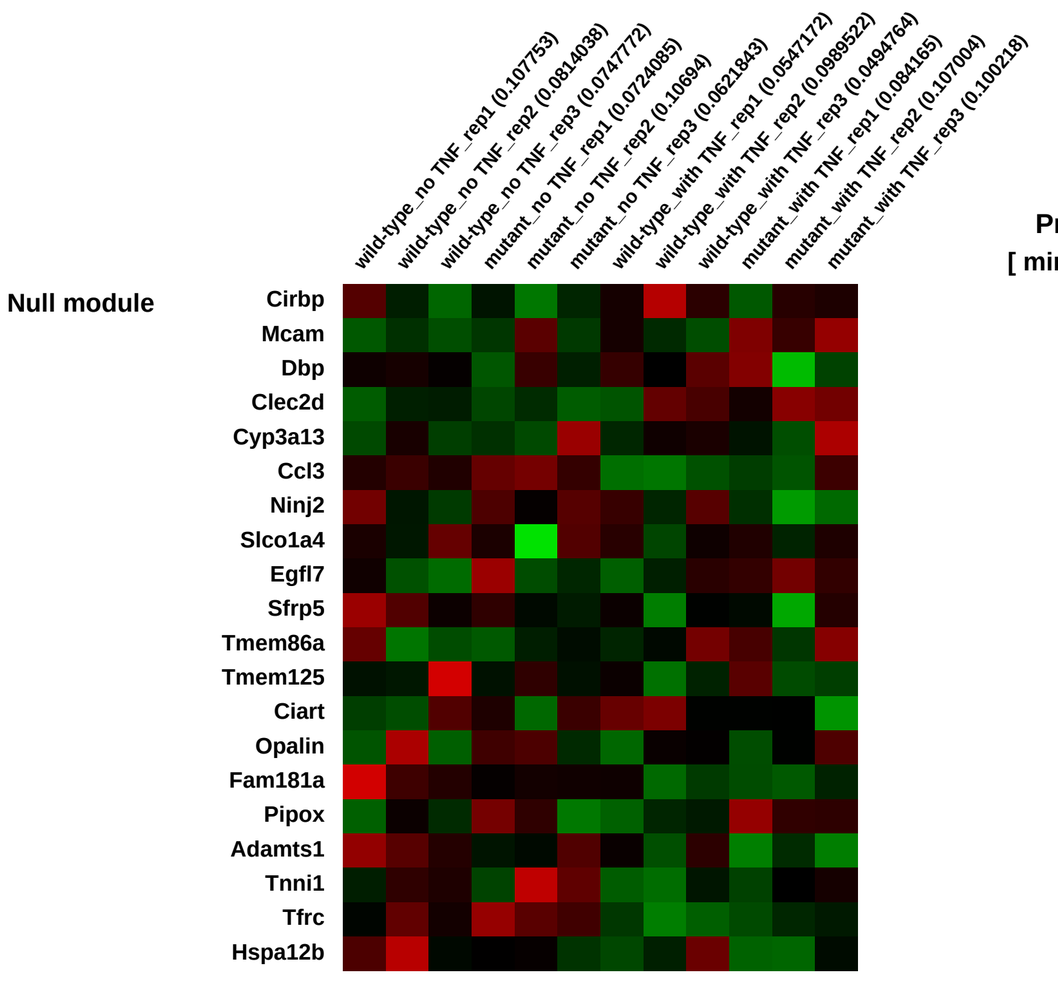

GEO Series "GSE36814" Expression Profiles

Num of samples in this series: 20

Scale of expression profile Z-scores

-3.0 -2.0 -1.0 0.0 1.0 2.0 3.0

GEO Link:	http://www.ncbi.nlm.nih.gov/geo/query/acc.cgi?acc=GSE36814
Status:	Public on Jun 24 2013
Title:	Role for DNA methylation in response to Gata4 activation in embryonic stem cell-derived mesoderm
Organism:	Mus musculus
Experiment type:	Expression profiling by array
Platform:	GPL1261
Pubmed ID:	23825962
Summary & Design:	**Summary:** During embryogenesis, many key transcription factors are used repeatedly, achieving different outcomes depending on cell type and developmental stage. The epigenetic modification of the genome functions as a memory of a cellâ s developmental history, and it has been proposed that such modification shapes the cellular response to transcription factors. To investigate the role of DNA methylation in the response to transcription factor Gata4, we examined expression profiles of Dnmt3a-/-Dnmt3b-/- ES cell-derived mesoderm cells cultured for 4 days with or without Gata4 activation, as well as the wild-type counterparts, using Affymetrix microarrays. **Overall design:** Wild-type and Dnmt3a-/-Dnmt3b-/- (DKO) ES cell clones stably expressing dexamethasone (Dex)-inducible Gata4 were generated by introducing an expression plasmid for Gata4 fused with the ligand-binding domain of the human glucocorticoid receptor (Gata4GR) driven by the CAG promoter, by electroporation. For mesoderm differentiation, 1 x 10^5 ES cells were plated on a type IV collagen-coated 10-cm dish and cultured for 4 days. Cultured cells were harvested and collected as single-cell suspensions using 0.25% trypsin-EDTA, followed by incubation in differentiation medium at 37¸ C to allow cell-surface markers to recover. Flk1(+)/PDGFRalpha(+) double-positive (DP) cells, which are considered equivalent to the lateral plate mesoderm, were sorted by FACS-Aria (BD Biosciences). Sorted DP cells were further cultured on type IV collagen-coated culture dishes in the absence or presence of 100 nM Dex for 4 days. For reference data, primitive endoderm (PE) cells were directly differentiated from undifferentiated ES cells by addition 100 nM Dex in ES cell-maintenance medium.

Background corr dist: KL-Divergence = 0.1205, L1-Distance = 0.0293, L2-Distance = 0.0014, Normal std = 0.4098

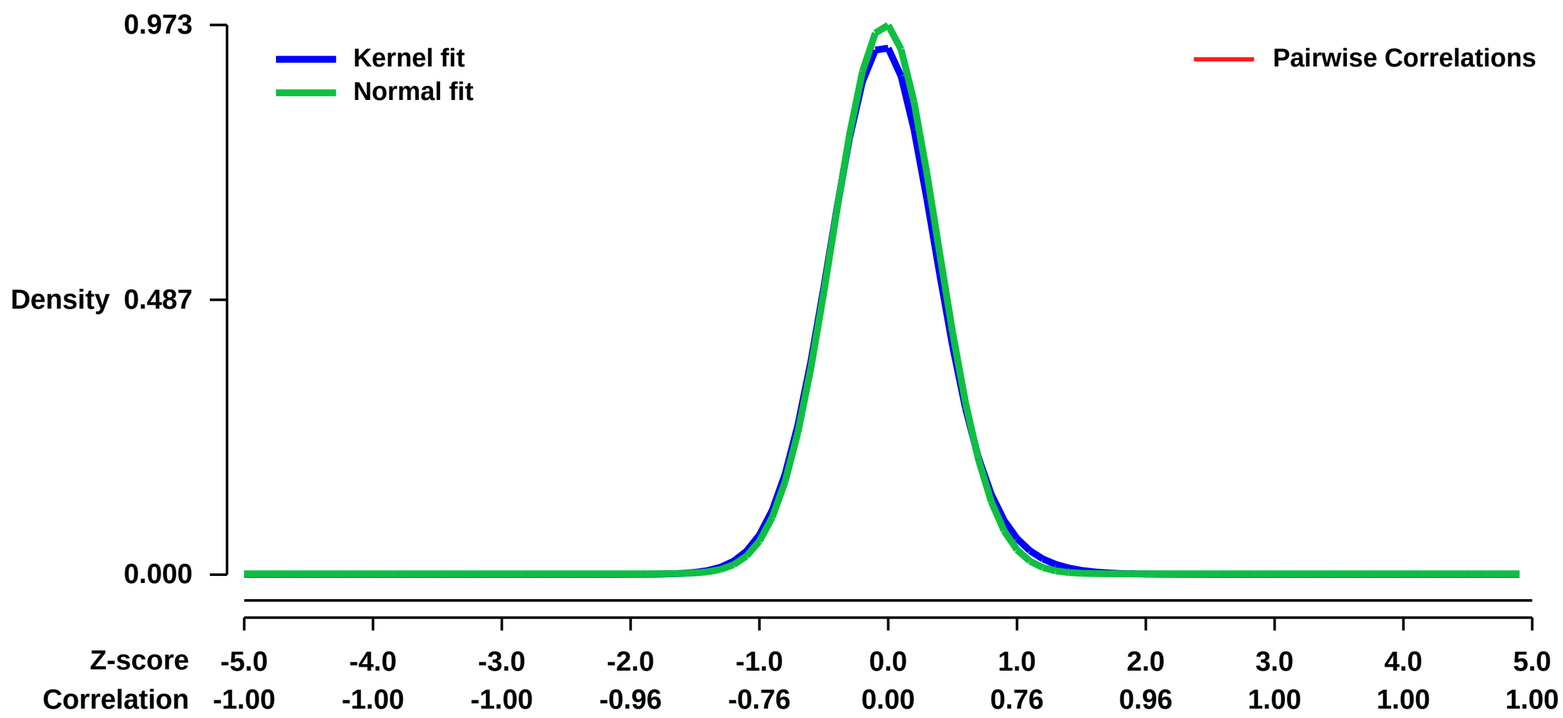

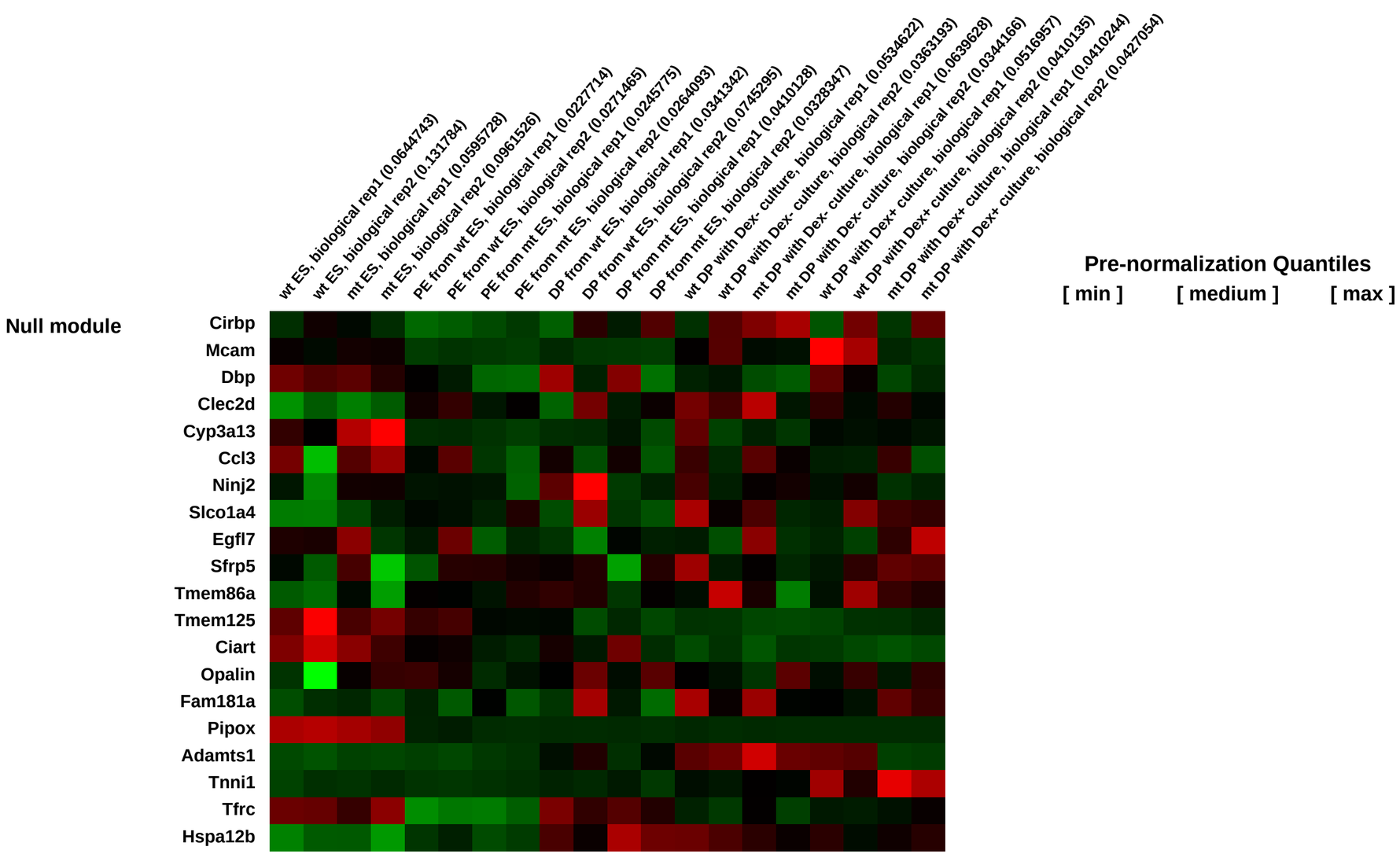

GEO Series "GSE24625" Expression Profiles

Num of samples in this series: 12

Scale of expression profile Z-scores

-3.0 -2.0 -1.0 0.0 1.0 2.0 3.0

GEO Link:	http://www.ncbi.nlm.nih.gov/geo/query/acc.cgi?acc=GSE24625
Status:	Public on Jan 01 2012
Title:	Transcriptome in 129sv and Crx-/- pineal gland at ZT (Zeitgeber time) 6 and ZT20
Organism:	Mus musculus
Experiment type:	Expression profiling by array
Platform:	GPL1261
Pubmed ID:	21797868
Summary & Design:	**Summary:** The cone-rod homeobox gene (Crx) encodes Crx, a transcription factor selectively expressed in two cell types, retinal photoreceptors and the melatonin secreting pinealocytes of the pineal gland. In this report the role of Crx in regulating gene expression in the mammalian pineal gland was extended using Affymetrix GeneChip technology. Deletion of Crx results in broad modulation of the mouse pineal transcriptome, including a >2-fold downregulation of 543 genes and a >2-fold upregulation of 745 genes. In addition to Crx, there was a >10-fold downregulation of 13 other genes. Of special interest was the discovery of a link between Crx and the homeobox gene Hoxc4, which was upregulated ~20-fold in the Crx-/- pineal gland. Analysis of night and day expression of genes indicated that a set of 51 genes exhibited differential expression in control animals. Of these genes, only eight were also differentially expressed in Crx-/- animals. This group included Aanat, which encodes the enzyme that controls the daily rhythm in melatonin synthesis in the vertebrate pineal gland. Accordingly, Crx appears to be essential for the 24-hour rhythmic component of expression of some genes in the pineal gland. In the Crx-/- mouse pineal gland, 41 genes exhibited differential night/day expression that was not seen in control animals, suggesting that Crx may function to modulate rhythmic expression of these genes as well. Together, the results of this investigation indicate that Crx broadly modulates the pineal transcriptome, perhaps in part through suppressive effects on expression of the homeobox gene Hoxc4. **Overall design:** Log(2) fold change independently of time of day. Up regulated genes: genes which are up regulated in Crx-/- compared to the control; down regulated genes: genes which are down regulated in Crx-/- compared to the control.

Background corr dist: KL-Divergence = 0.0827, L1-Distance = 0.0236, L2-Distance = 0.0009, Normal std = 0.4734

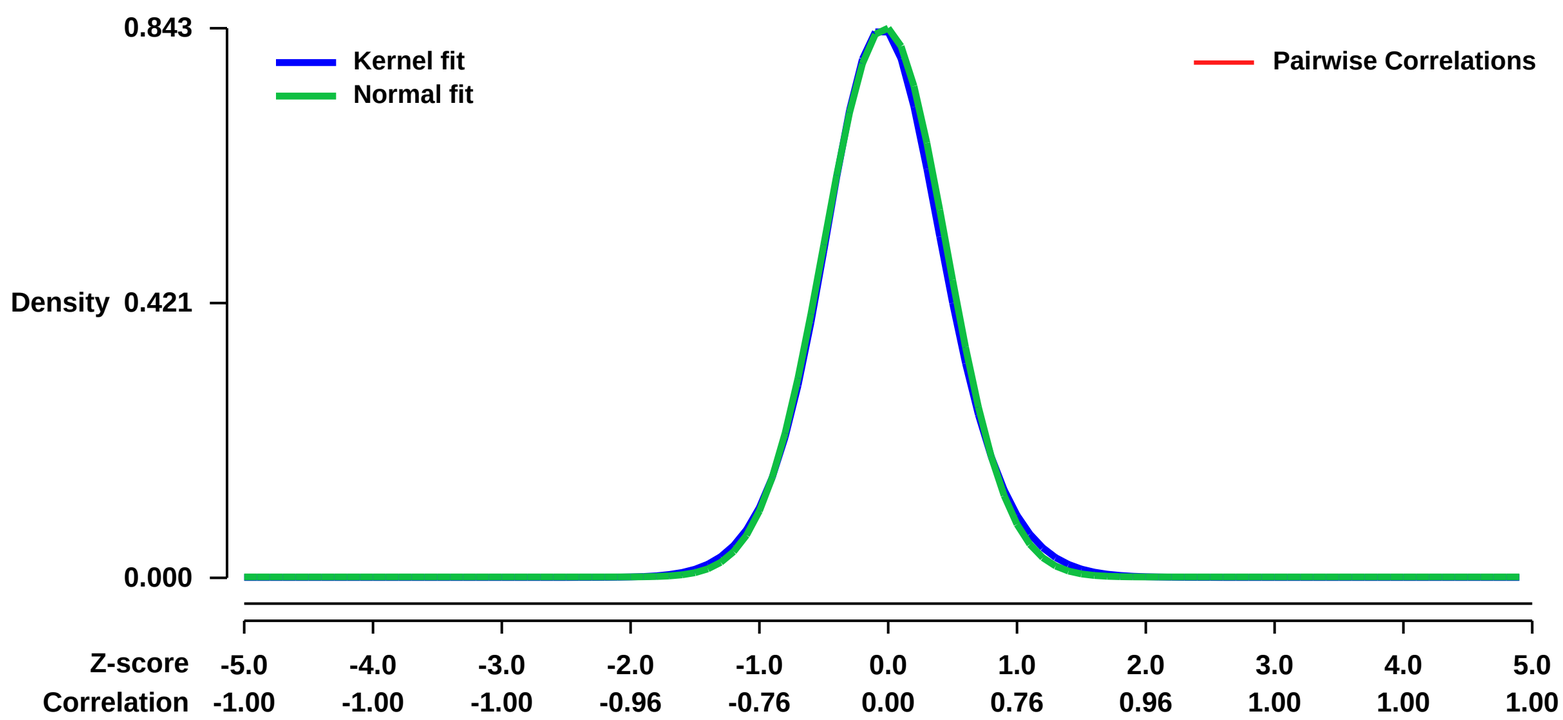

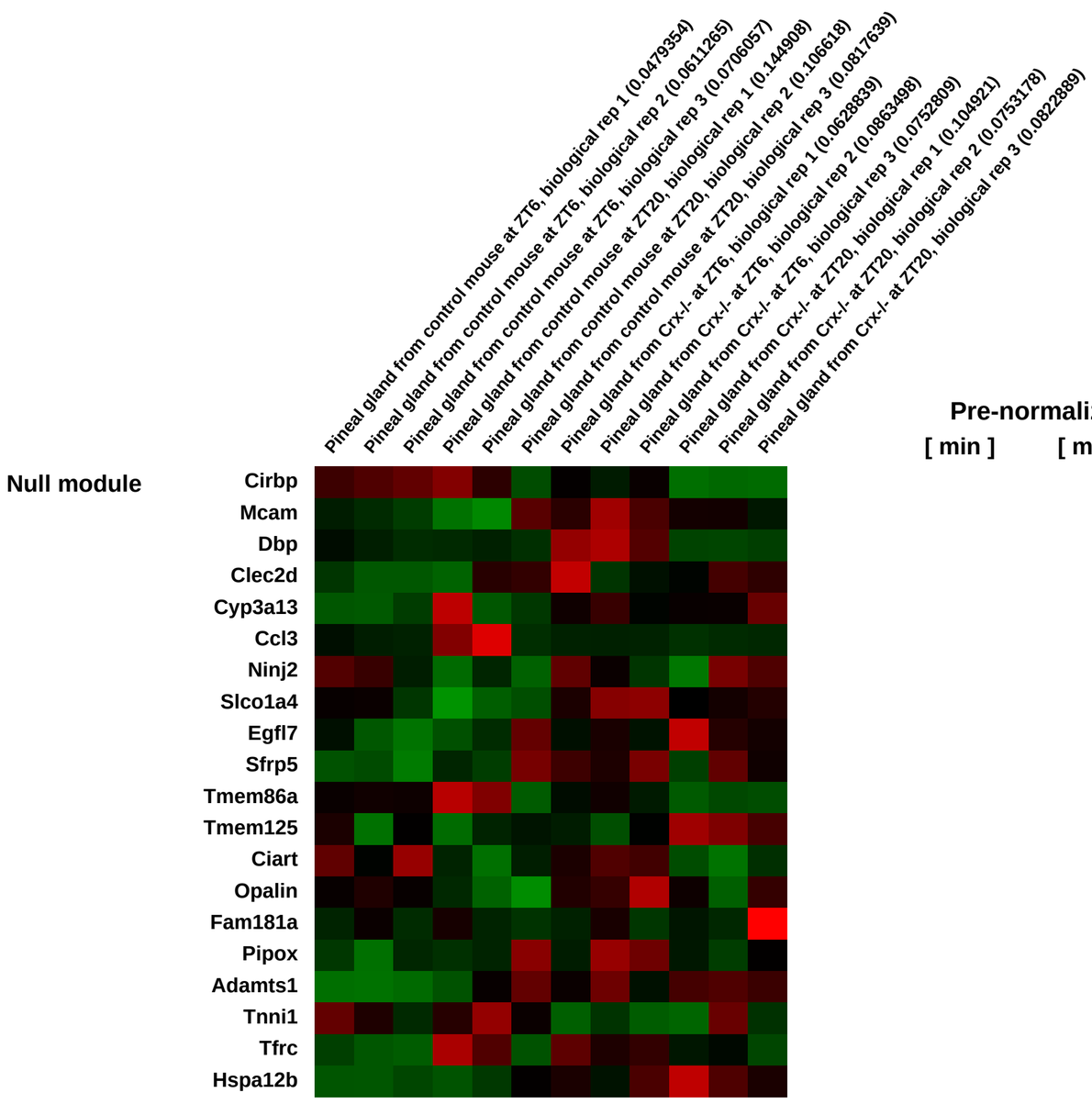

GEO Series "GSE9330" Expression Profiles

Num of samples in this series: 8

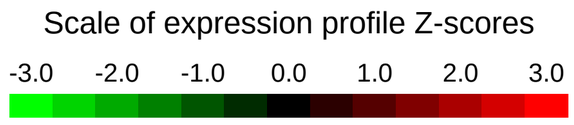

GEO Link:	http://www.ncbi.nlm.nih.gov/geo/query/acc.cgi?acc=GSE9330
Status:	Public on Dec 15 2007
Title:	Expression data from wild type and Ctip2-/- (Bcl11b) mutant mouse striatum at P0
Organism:	Mus musculus
Experiment type:	Expression profiling by array
Platform:	GPL1261
Pubmed ID:	18199763
Summary & Design:	**Summary:** Striatal medium spiny neurons (MSN) are critically involved in motor control, and their degeneration is a principal component of Huntingtonâ s disease. We find that the transcription factor Ctip2 (also known as Bcl11b) is central to MSN differentiation and striatal development. Within the striatum, it is expressed by all MSN, while it is excluded from essentially all striatal interneurons. In the absence of Ctip2, MSN do not fully differentiate, as demonstrated by dramatically reduced expression of a large number of MSN markers, including DARPP-32, FOXP1, Chrm4, Reelin, MOR1, GluR1, and Plexin-D1. Furthermore, MSN fail to aggregate into patches, resulting in severely disrupted patch-matrix organization within the striatum. Finally, heterotopic cellular aggregates invade the Ctip2-/- striatum suggesting a failure by MSN to repel these cells in the absence of Ctip2. In order to investigate the molecular mechanisms that underlie Ctip2-dependent differentiation of MSN and that underlie the patch-matrix disorganization in the mutant striatum, we directly compared gene expression between wild type and mutant striatum at P0. Because CTIP2-expressing MSN constitute 90-95% of the neurons within the striatum, we reasoned that we should be able to detect changes in medium spiny neuron gene expression in Ctip2 null mutants. We microdissected out small regions of striatum at matched locations in wild type and Ctip2-/- mutant littermates at P0 and investigated gene expression with Affymetrix microarrays. We selected the 153 most significant genes and further analyzed them to identify a smaller set of genes of potentially high biological relevance. In order to verify the microarray data and define the distribution of the identified genes in the striatum, we performed in situ hybridization or immunohistochemistry for 12 selected genes: Plexin-D1, Ngef, Nectin-3, Kcnip2, Pcp4L1, Neto1, Basonuclin 2, Fidgetin, Semaphorin 3e, Secretagogin, Unc5d, and Neurotensin. We find that all these genes are either specifically downregulated (Plexin-D1, Ngef, Nectin-3 Kcnip2, Pcp4L1, Neto1), or upregulated (Basonuclin 2, Fidgetin, Semaphorin 3e, Secretagogin, Unc5d, Neurotensin), in the Ctip2-/- striatum, confirming and extending the microarray results. Together, these data indicate that Ctip2 is a critical regulator of MSN differentiation, striatal patch development, and the establishment of the cellular architecture of the striatum. **Keywords:** mutant analysis **Overall design:** Matched regions of striatum from wild type and Ctip2-/- mice were obtained via 500 ´µm diameter punch biopsies performed in the center of the developing striatum in acutely sectioned 300 ´µm coronal slices of the brain at postnatal day 0 (P0). Sections were matched rostro-caudally between wild type and null mutant tissue, and fiduciary landmarks were used to assure reproducible microdissection of comparable regions. RNA was extracted using the StrataPrep Total RNA Mini Kit (Stratagene, La Jolla, CA), and RNA quality was assayed using a bioanalyzer (Agilent Technologies, Paola Alto, CA). To ensure reproducibility and biological significance, microarrays were performed with RNA samples from three independent wild type, one heterozygote, and four Ctip2-/- mice (biological replicates). Microarray data were normalized using the RMA function within Bioconductor (Irizarry et al., 2003). Statistical significance of gene expression differences between wild type and knockout was determined using Statistical Analysis of Micrarrays (SAM) (Tusher et al., 2001). Using a SAM d-score cutoff of > 2 or < -2, we selected the 153 most significant genes and further analyzed them to identify a smaller set of genes of potentially high biological relevance.

Background corr dist: KL-Divergence = 0.0229, L1-Distance = 0.0600, L2-Distance = 0.0051, Normal std = 0.7875

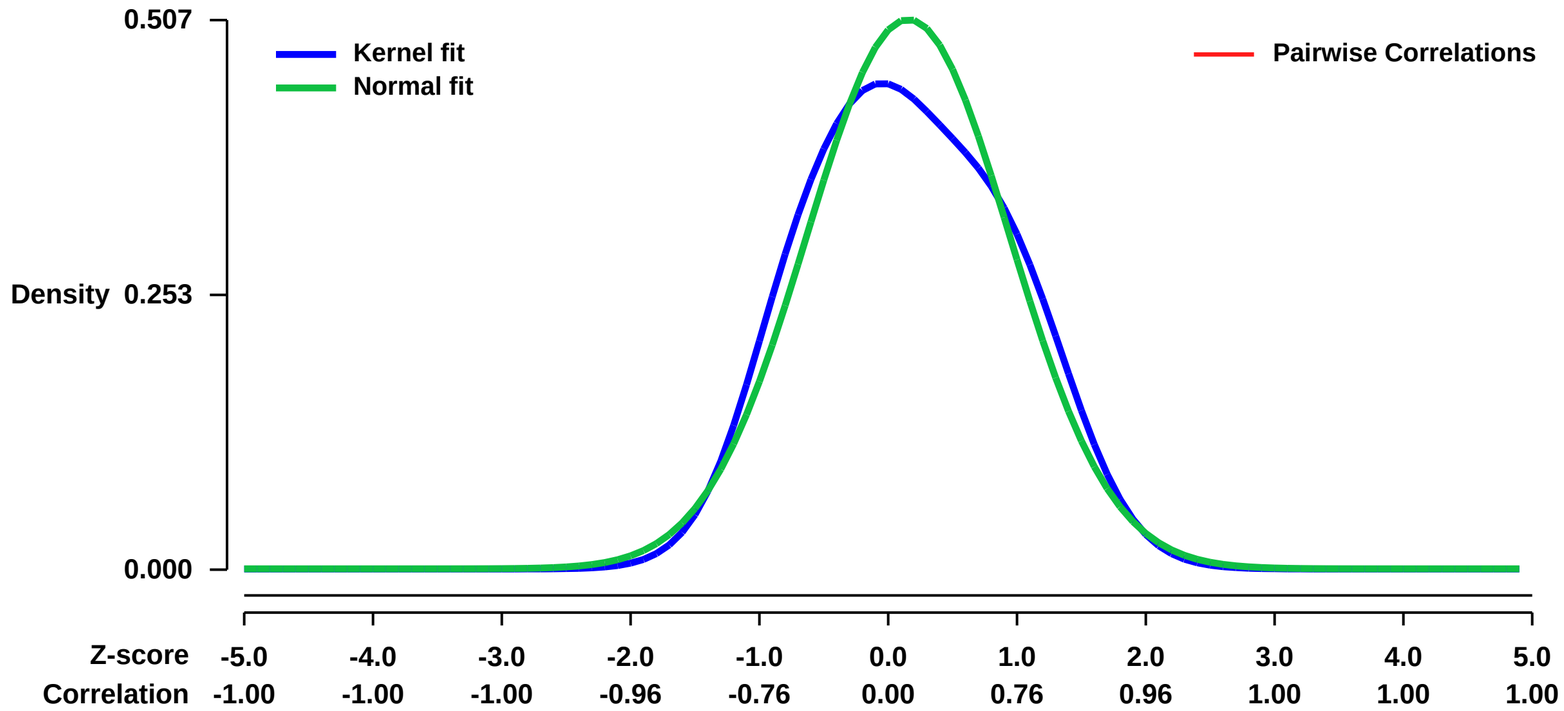

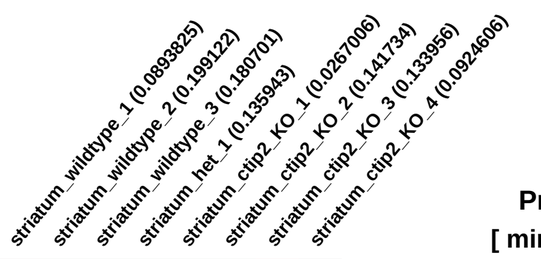

Pre-normalization Quantiles

[min] [medium] [max]

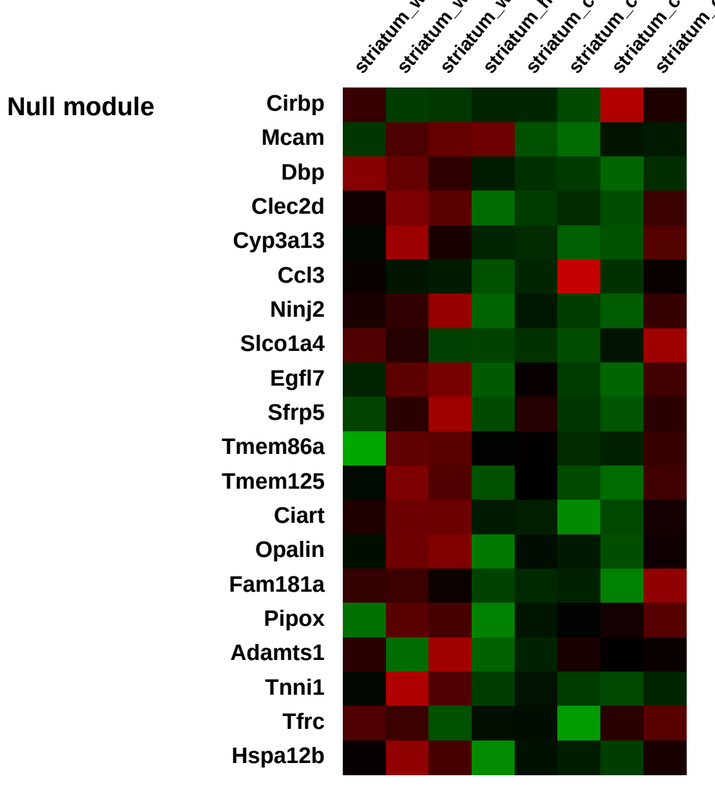

GEO Series "GSE13799" Expression Profiles

Num of samples in this series: 18

Scale of expression profile Z-scores

-3.0 -2.0 -1.0 0.0 1.0 2.0 3.0

GEO Link:	**http://www.ncbi.nlm.nih.gov/geo/query/acc.cgi?acc=GSE13799**
Status:	**Public on Jan 15 2009**
Title:	**Hippocampal gene expression changes during age-related cognitive decline**
Organism:	**Mus musculus**
Experiment type:	**Expression profiling by array**
Platform:	**GPL1261**
Pubmed ID:	
Summary & Design:	**Summary:** **Comparison of hippocampal gene expression between normal young animals and older animals with good spatial memory and older animals with poor spatial memory** **Overall design:** **The hippocampus from animals with good spatial memory (unimpaired) were compared to animals with poor spartial memory (impaired)**

Background corr dist: **KL-Divergence = 0.3011, L1-Distance = 0.0677, L2-Distance = 0.0128, Normal std = 0.2791**

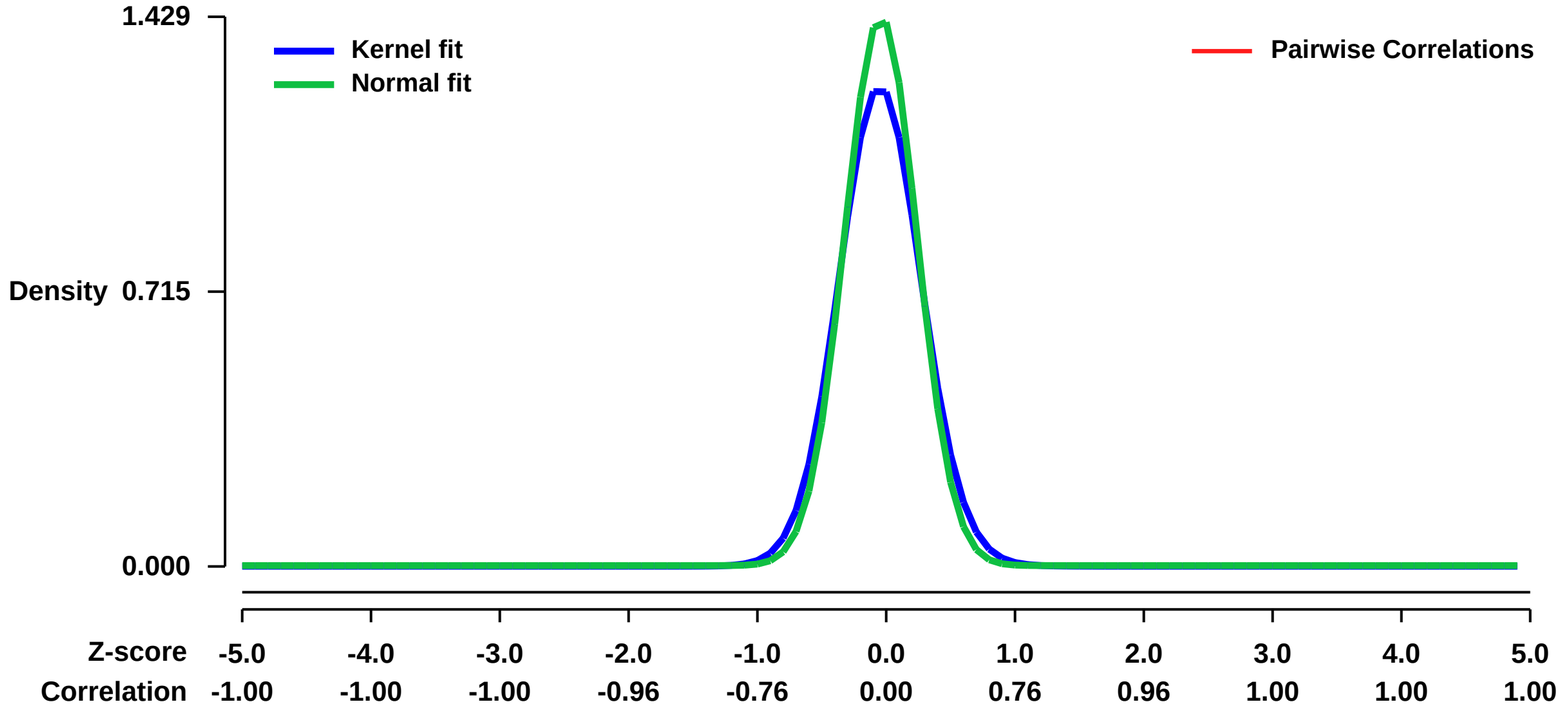

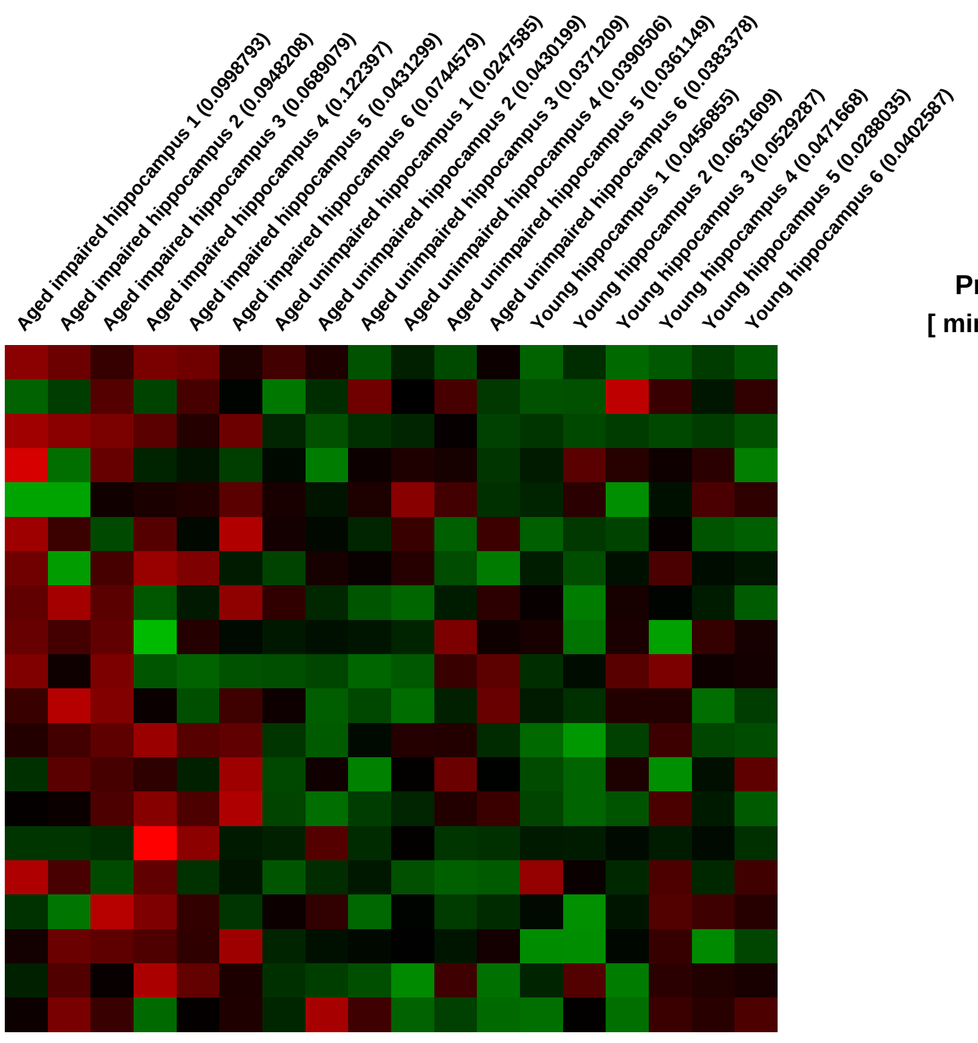

GEO Series "GSE8836" Expression Profiles

Num of samples in this series: 56

Scale of expression profile Z-scores

-3.0 -2.0 -1.0 0.0 1.0 2.0 3.0

GEO Link:	http://www.ncbi.nlm.nih.gov/geo/query/acc.cgi?acc=GSE8836
Status:	Public on Dec 01 2007
Title:	CLL in Em-TCL1 mice provides a biologically relevant model to unravel and reverse immune deficiency in human cancer.
Organism:	Mus musculus
Experiment type:	Expression profiling by array
Platform:	GPL1261
Pubmed ID:	19332800
Summary & Design:	**Summary:** Immune deficiency is common in cancer, but the biological basis for this and ways to reverse it remains elusive. Here we present a mouse model of B cell chronic lymphocytic leukemia (CLL) that recapitulates changes in the non-malignant circulating T cells seen in patients with this illness.1 To validate this model, we examined changes in T cell gene expression, protein expression and function in Em-TCL1 transgenic mice as they developed CLL 2,3 and demonstrate that development of CLL in these transgenic mice is associated with changes in impaired T cell function and in gene expression in CD4 and CD8 T cells similar to those observed in patients with this disease. Infusion of CLL cells into non-leukemia bearing Em-TCL1 mice rapidly induces these changes, demonstrating a causal relationship between leukemia and the induction of T cell changes. This model allows dissection of the molecular changes induced in CD4 and CD8 T cells by interaction with leukemia cells and further supports the concept that cancer results in complex abnormalities in the immune microenvironment. Gene expression profiling was performed to determine whether Em-TCL1 murine model of chronic lymphocytic leukemia (CLL) mimics T cell defects induced by CLL cells in patients with CLL. Keywords: comparative gene expression profiling analysis. **Overall design:** CD4 T cells and CD8 T cells were obtained from spleens of B6C3 and Em-TCL1 transgenic murine model of CLL or from peripheral blood mononuclear cells of previously untreated patients with CLL and healthy individuals (Pubmed ID: 15965501). Gene expression profiling was performed using total RNA and the data were analysed to compare gene expression profile of CLL to healthy within or between the species.

Background corr dist: KL-Divergence = 0.4566, L1-Distance = 0.0842, L2-Distance = 0.0228, Normal std = 0.2347

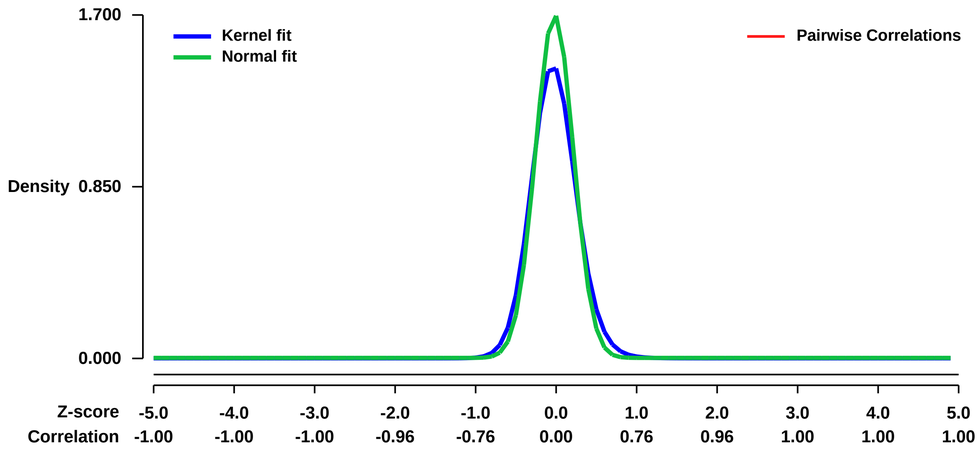

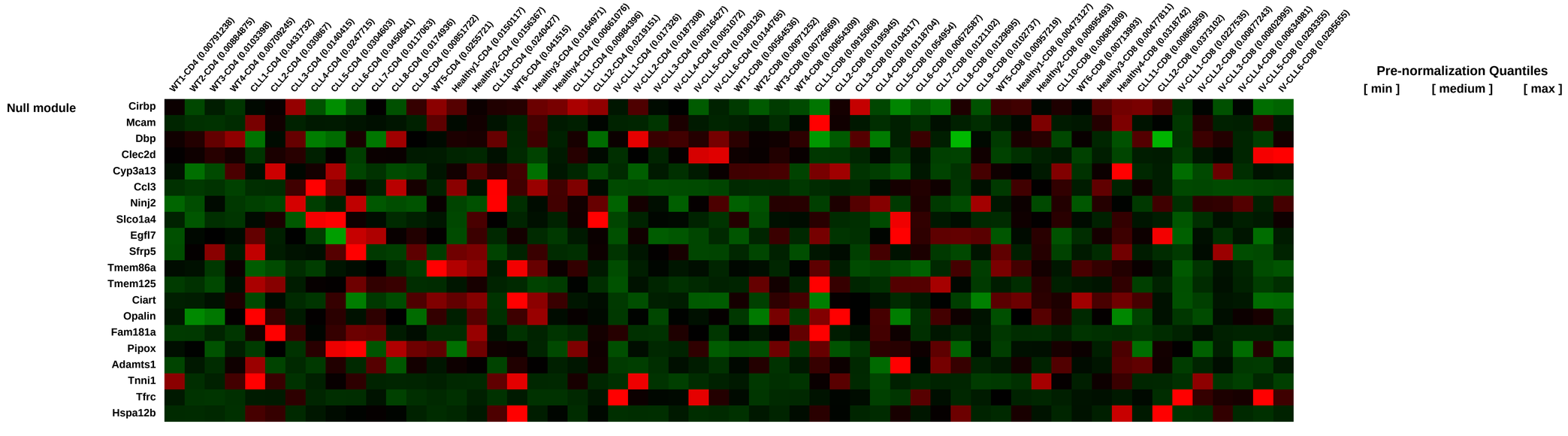

GEO Series "GSE38335" Expression Profiles

Num of samples in this series: 9

Scale of expression profile Z-scores

-3.0 -2.0 -1.0 0.0 1.0 2.0 3.0

GEO Link:	http://www.ncbi.nlm.nih.gov/geo/query/acc.cgi?acc=GSE38335
Status:	Public on May 31 2012
Title:	JAK2 Naive and Persitent Murine BaF3 cells infected with MPLW515L
Organism:	Mus musculus
Experiment type:	Expression profiling by array
Platform:	GPL1261
Pubmed ID:	22820254
Summary & Design:	**Summary:** Transcriptional profiling of Murine BaF3 cells infected with MPLW515L grown under either normal conditions (Naive) or in 0.8 uM INCB18424 for 4-6 weeks (Persistent). Naive and Persistent cells were then treated with either DMSO (Control) or 0.8 uM INCB18424 for 4 hours. Goal was to determine transcriptional changes conditioned upon sensitivity/resistance of BaF3 MPLW515L mutants to JAK1/2 specific inhibitor. **Overall design:** 3 condition experiment consiting of: 1) Naive cells treated with DMSO (Control) , 2) Naˆflve cells treated with 0.8 uM INCB18424 for 4 hours (Acute) and 3) Persistent cells treated with 0.8 uM INCB18424 for 4 hours (Persistent). Biological replicates: 3 DMSO control replicates, 3 Acute replicates, 3 Persistent replicates.

Background corr dist: KL-Divergence = 0.0258, L1-Distance = 0.0561, L2-Distance = 0.0057, Normal std = 0.7359

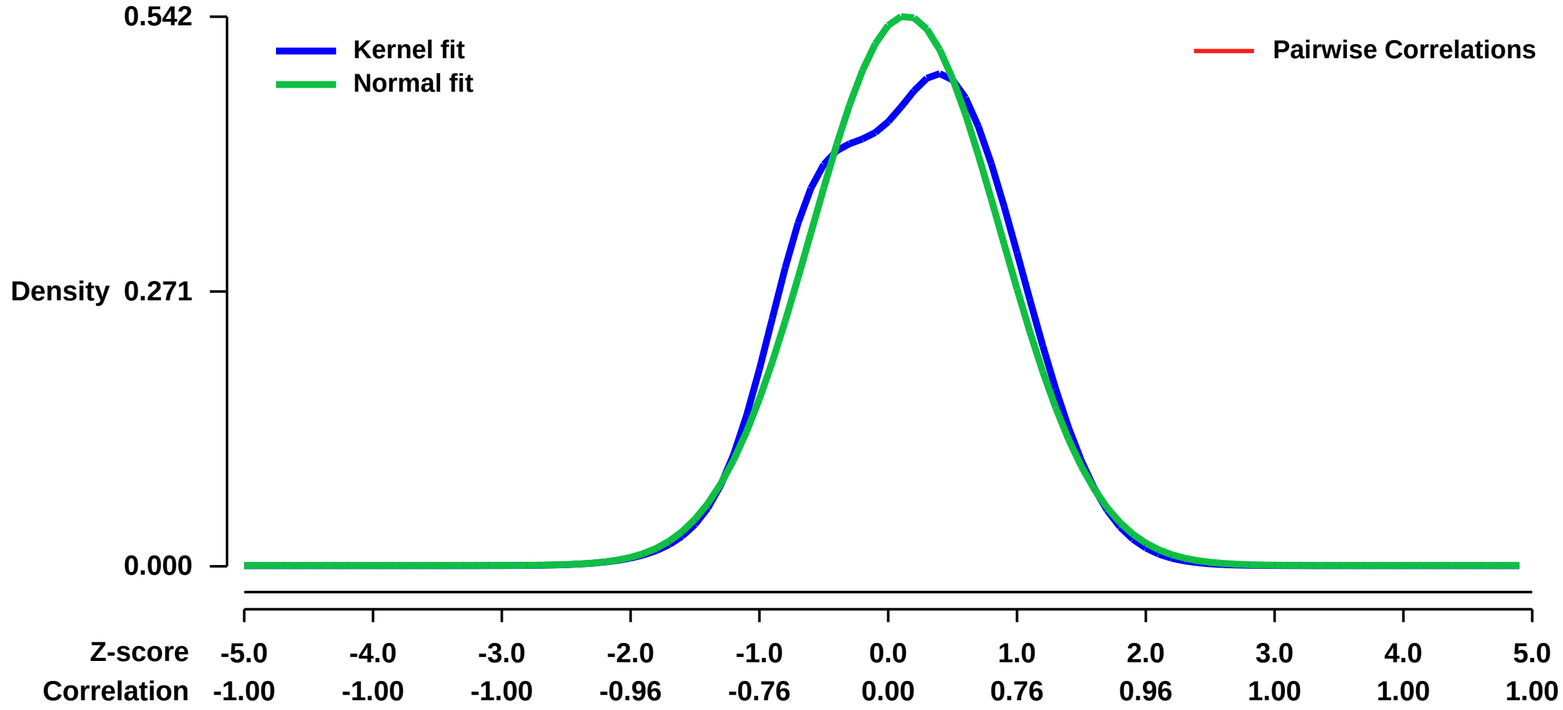

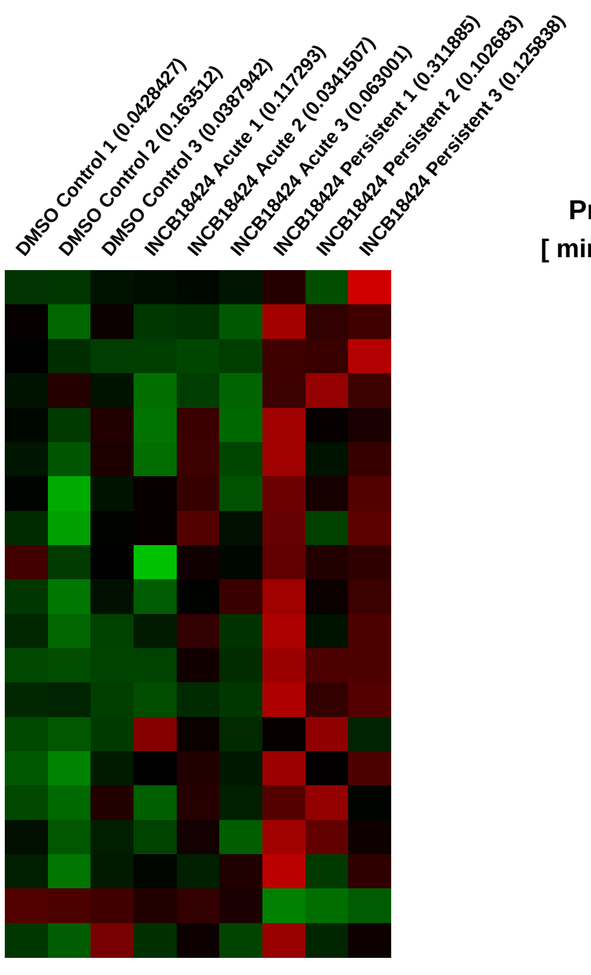

GEO Series "GSE45043" Expression Profiles

Num of samples in this series: 12

Scale of expression profile Z-scores

-3.0 -2.0 -1.0 0.0 1.0 2.0 3.0

GEO Link:	http://www.ncbi.nlm.nih.gov/geo/query/acc.cgi?acc=GSE45043
Status:	Public on May 29 2013
Title:	Age-mediated transcriptomic changes in adult mouse substantia nigra
Organism:	Mus musculus
Experiment type:	Expression profiling by array
Platform:	GPL1261
Pubmed ID:	23638090
Summary & Design:	**Summary:** Substantia nigra pars compacta (SNpc) is highly sensitive to normal aging and selectively degenerates in Parkinson's disease. Until now, molecular mechanisms behind SNpc aging have not been fully investigated using high throughput techniques. Here, aging-associated early changes in transcriptome of SNpc were investigated comparing late middle-aged (18 months old) to young (2 months old) mice. **Overall design:** Three age groups of C57 wild type mice were used in microarray analysis: young (2 months old), middle aged (10 months old), and late-middle aged (18 months old) mice. Four replicates were included in each age group and each replicate was pooled from 4 mice (4 mice/replicate x 4 replicates x 3 age groups). Total RNA was isolated from SNpc for hybridization on Affymetrix microarrays.

Background corr dist: KL-Divergence = 0.0738, L1-Distance = 0.0392, L2-Distance = 0.0021, Normal std = 0.5110

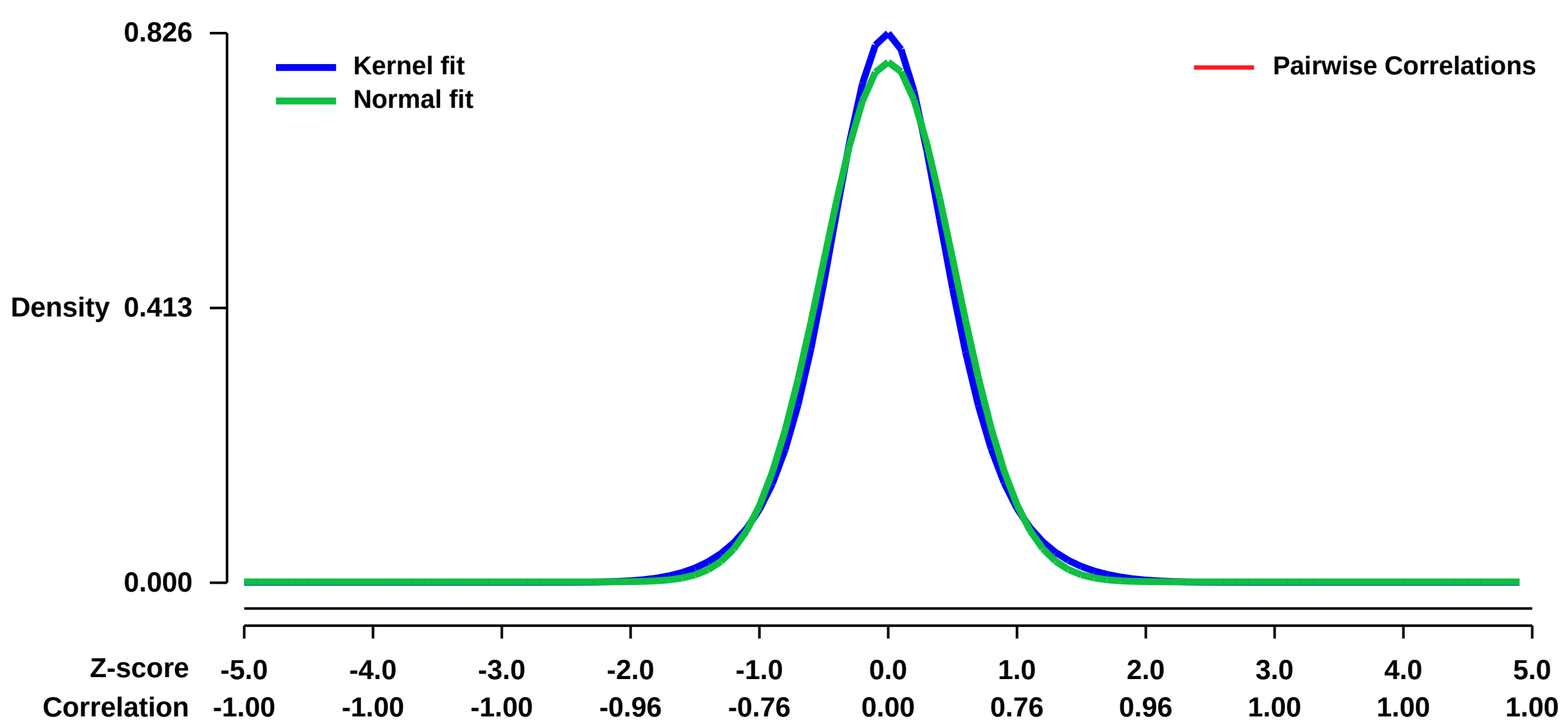

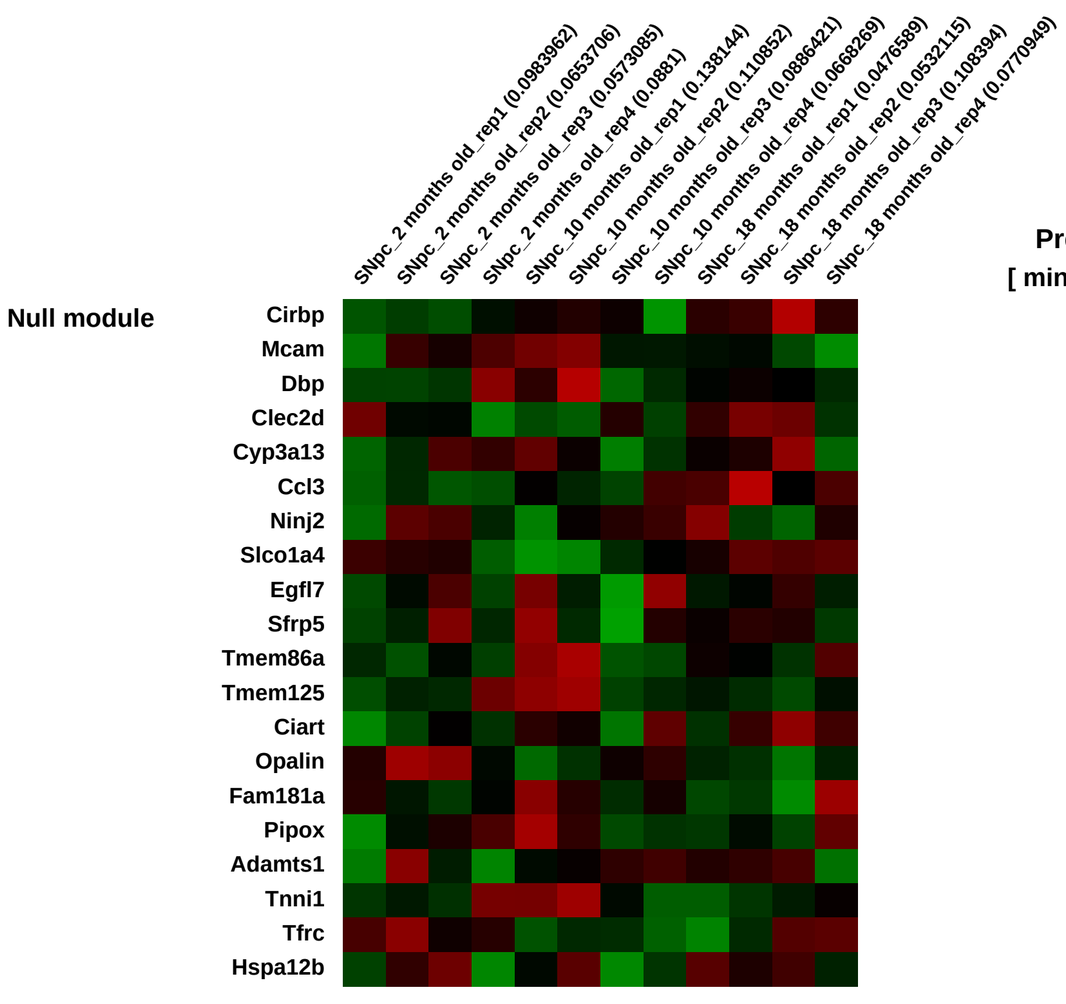

GEO Series "GSE3463" Expression Profiles

Num of samples in this series: 12

Scale of expression profile Z-scores

-3.0 -2.0 -1.0 0.0 1.0 2.0 3.0

GEO Link: http://www.ncbi.nlm.nih.gov/geo/query/acc.cgi?acc=GSE3463
Status: Public on Dec 17 2005
Title: Expression profiling of mouse gonadal somatic cells
Organism: Mus musculus
Experiment type: Expression profiling by array
Platform: GPL1261
Pubmed ID: 16399799

Summary & Design:

Summary:
Gene expression profiling of FACS sorted GFP+ve cells from sexed gonads of transgenic pSF1-eGFP mice

Keywords: Time course and comparison of sexes

Overall design:
Experiment is both a time course and an assesment of sex specific expression in SF1+ve somatic gonadal cells. Each time point and sex has been profiled in triplicate

Background corr dist: KL-Divergence = 0.0488, L1-Distance = 0.0488, L2-Distance = 0.0033, Normal std = 0.6164

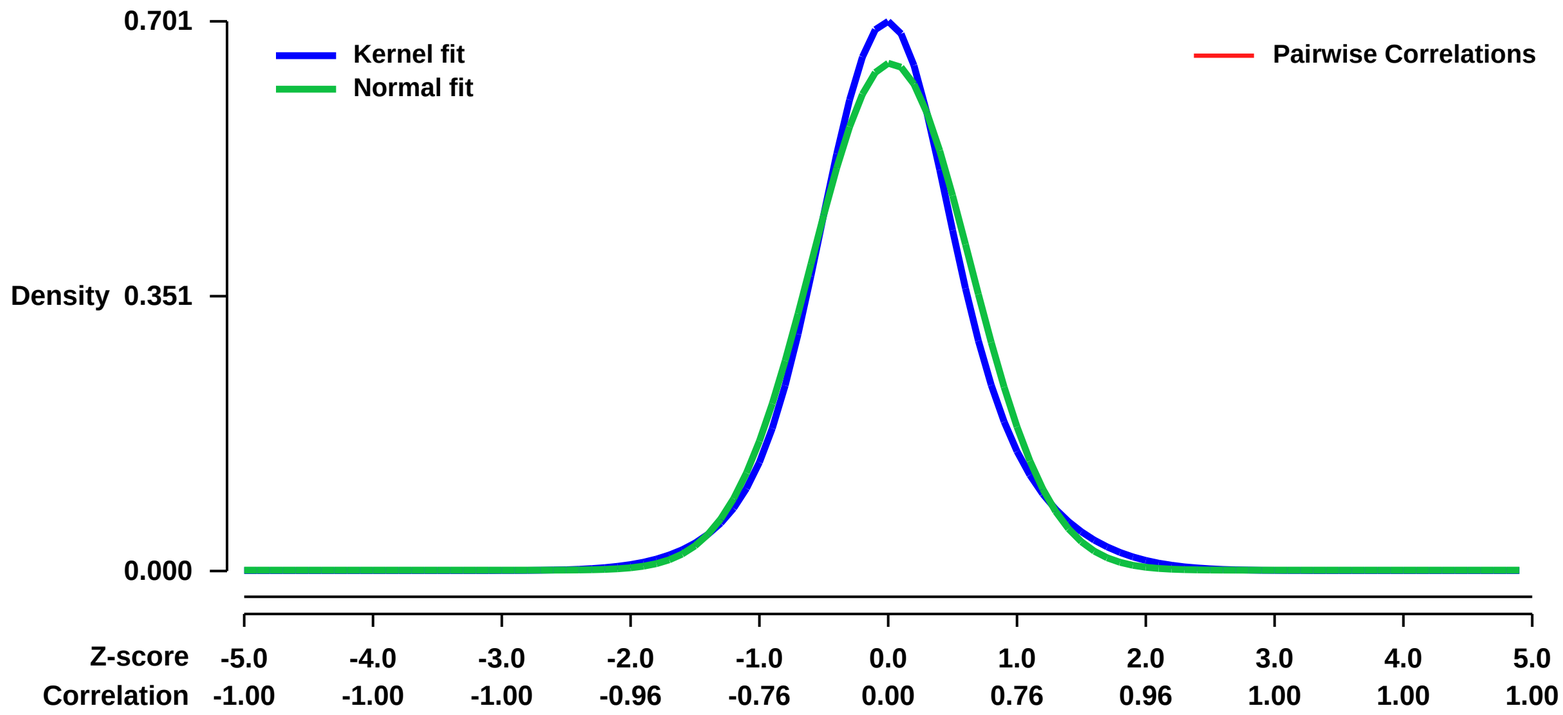

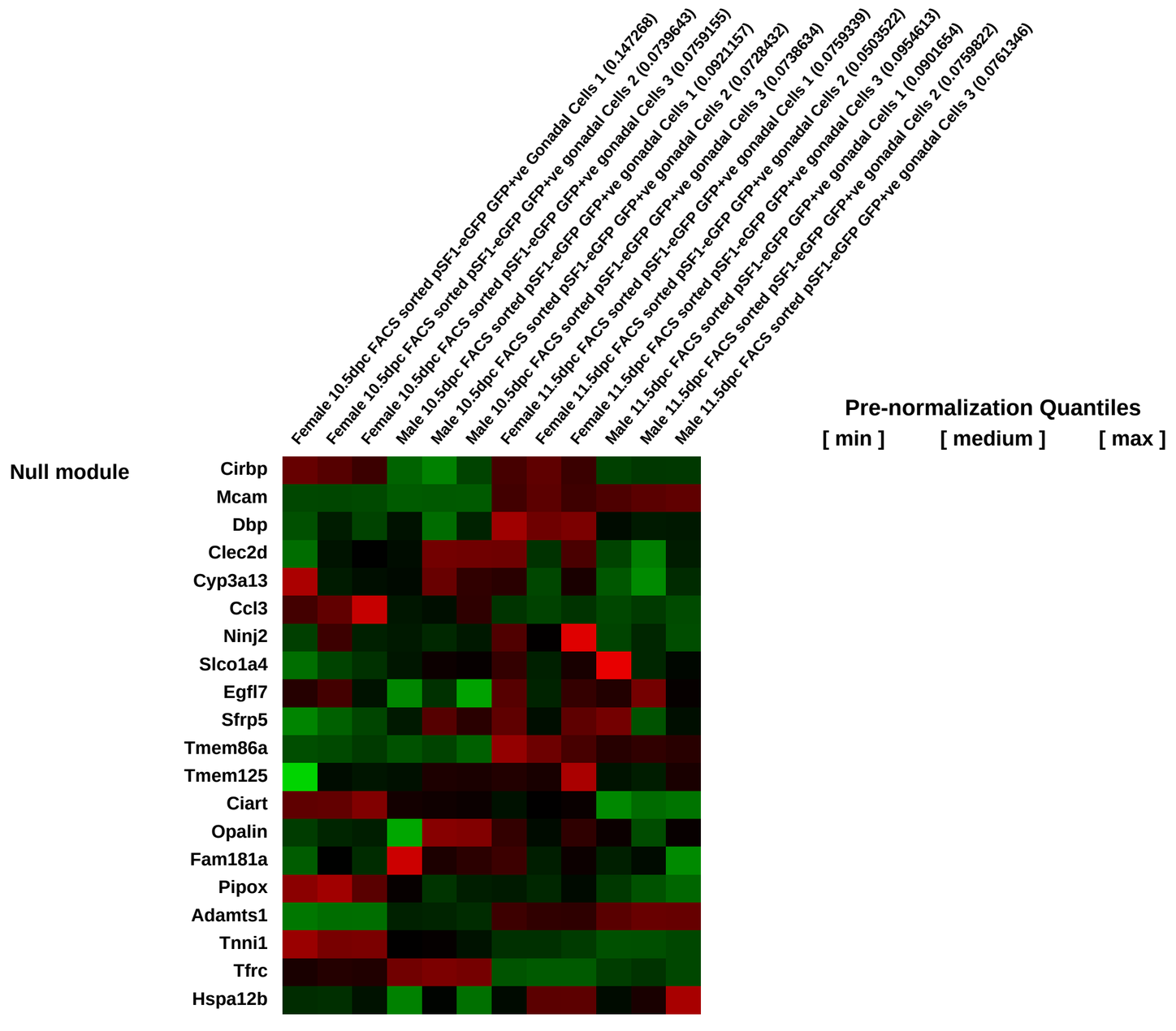

GEO Series "GSE39557" Expression Profiles

Num of samples in this series: 15

Scale of expression profile Z-scores

-3.0 -2.0 -1.0 0.0 1.0 2.0 3.0

GEO Link:	http://www.ncbi.nlm.nih.gov/geo/query/acc.cgi?acc=GSE39557
Status:	Public on Jul 02 2013
Title:	Expression data from genetically engineered mouse models (GEMMs)
Organism:	Mus musculus
Experiment type:	Expression profiling by array
Platform:	GPL1261
Pubmed ID:	23403635
Summary & Design:	**Summary:** 3 Cell lines from Apc, p53 (AP) GEMMs were compared to 12 cell lines from Apc, Kras, p53 (AKP) GEMMs. Mouse 430 2.0 arrays were used to determine genomic expression differences between the two genotypes (AP and AKP). **Overall design:** RNA was extracted from 3 AP and 10 AKP cell lines using the Qiagen RNEasy kit, and hybridized to individual Affymetrix mouse 430 2.0 chips as per manufacturer's instructions

Background corr dist: KL-Divergence = 0.1709, L1-Distance = 0.0613, L2-Distance = 0.0093, Normal std = 0.3784

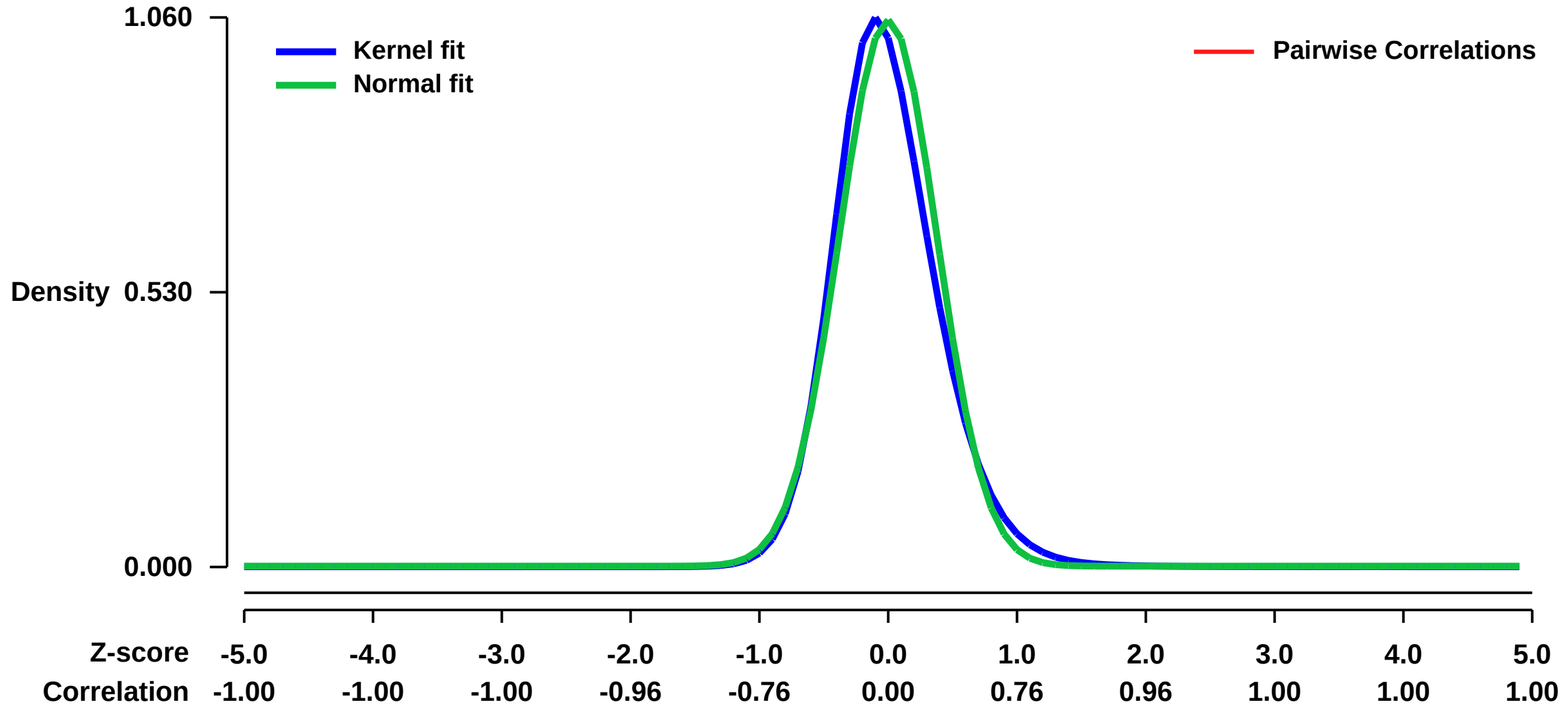

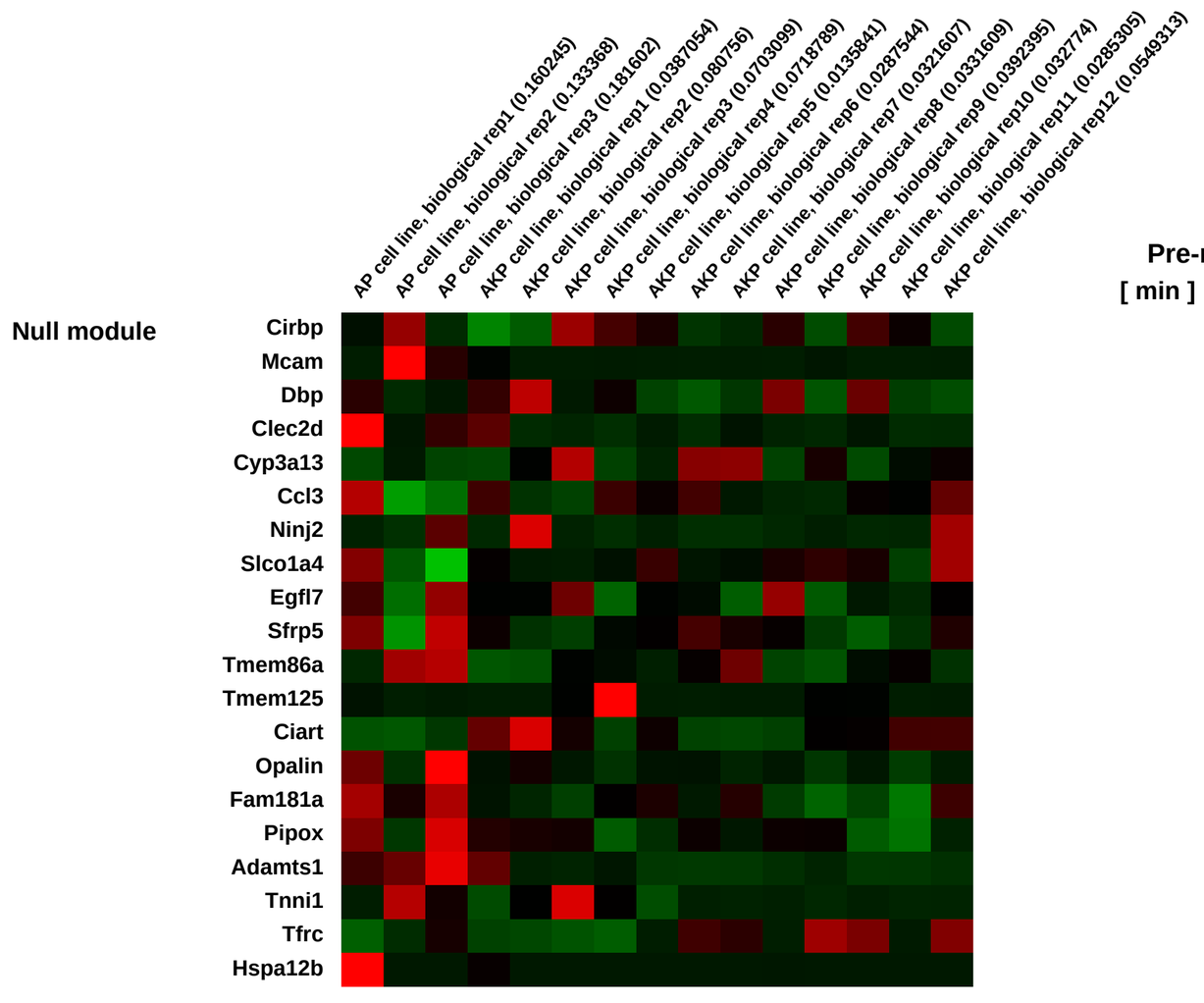

GEO Series "GSE11496" Expression Profiles

Num of samples in this series: 16

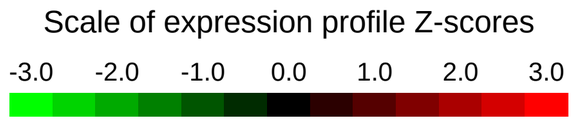

GEO Link:	http://www.ncbi.nlm.nih.gov/geo/query/acc.cgi?acc=GSE11496
Status:	Public on Nov 10 2009
Title:	Expression data from Gcn2 wild-type and knockout mouse liver perfused with or without methionine
Organism:	Mus musculus
Experiment type:	Expression profiling by array
Platform:	GPL1261
Pubmed ID:	19509078
Summary & Design:	**Summary:** In eukaryotes, regulation of mRNA translation enables a fast, localized and finely tuned expression of gene products. Within the translation process, the first stage of translation initiation is most rigorously modulated by the actions of eukaryotic initiation factors (eIFs) and their associated proteins. These 11 eIFs catalyze the joining of the tRNA, mRNA and rRNA into a functional translation complex. Their activity is influenced by a wide variety of extra- and intracellular signals, ranging from global, such as hormone signaling and unfolded proteins, to specific, such as single amino acid imbalance and iron deficiency. Their action is correspondingly comprehensive, in increasing or decreasing recruitment and translation of most cellular mRNAs, and specialized, in targeting translation of mRNAs with regulatory features such as a 5â terminal oligopyrimidine tract (TOP), upstream open reading frames (uORFs), or an internal ribosomal entry site (IRES). In mammals, two major pathways are linked to targeted mRNA translation. The target of rapamycin (TOR) kinase induces translation of TOP and perhaps other subsets of mRNAs, whereas a family of eIF2 kinases does so with mRNAs containing uORFs or an IRES. TOR targets translation of mRNAs that code for proteins involved in translation, an action compatible with its widely accepted role in regulating cellular growth. The four members of the eIF2 kinase family increase translation of mRNAs coding for stress response proteins such as transcription factors and chaperones. Though all four kinases act on one main substrate, eIF2, published literature demonstrates both common and unique effects by each kinase in response to its specific activating stress. This suggests that the activated eIF2 kinases regulate the translation of both a global and a specific set of mRNAs. Up to now, few studies have attempted to test such a hypothesis; none has been done in mammals. We use array analysis to determine the global mRNA shift into polysomes following a stress response, and to compare the translational response following activation of GCN2 versus PERK, two of the four eIF2alpha kinases. **Overall design:** Gcn2 wild-type or knockout mouse liver were perfused with complete amino acids media or media lacking methionine for RNA extraction and hybridization of Affymetrix microarrays. RNA was extracted from unfractionated liver samples and polysome fraction of samples separated on sucrose density gradient. To minimize biological variations, we pooled RNA from two perfused liver samples to use in each array analysis. The conditions were total and polysome fraction of Gcn2+/+, +Met or -Met; total and polysome fraction of Gcn2-/-, +Met or -Met. Each array analysis was done in duplicate.

Background corr dist: KL-Divergence = 0.2327, L1-Distance = 0.0508, L2-Distance = 0.0061, Normal std = 0.3119

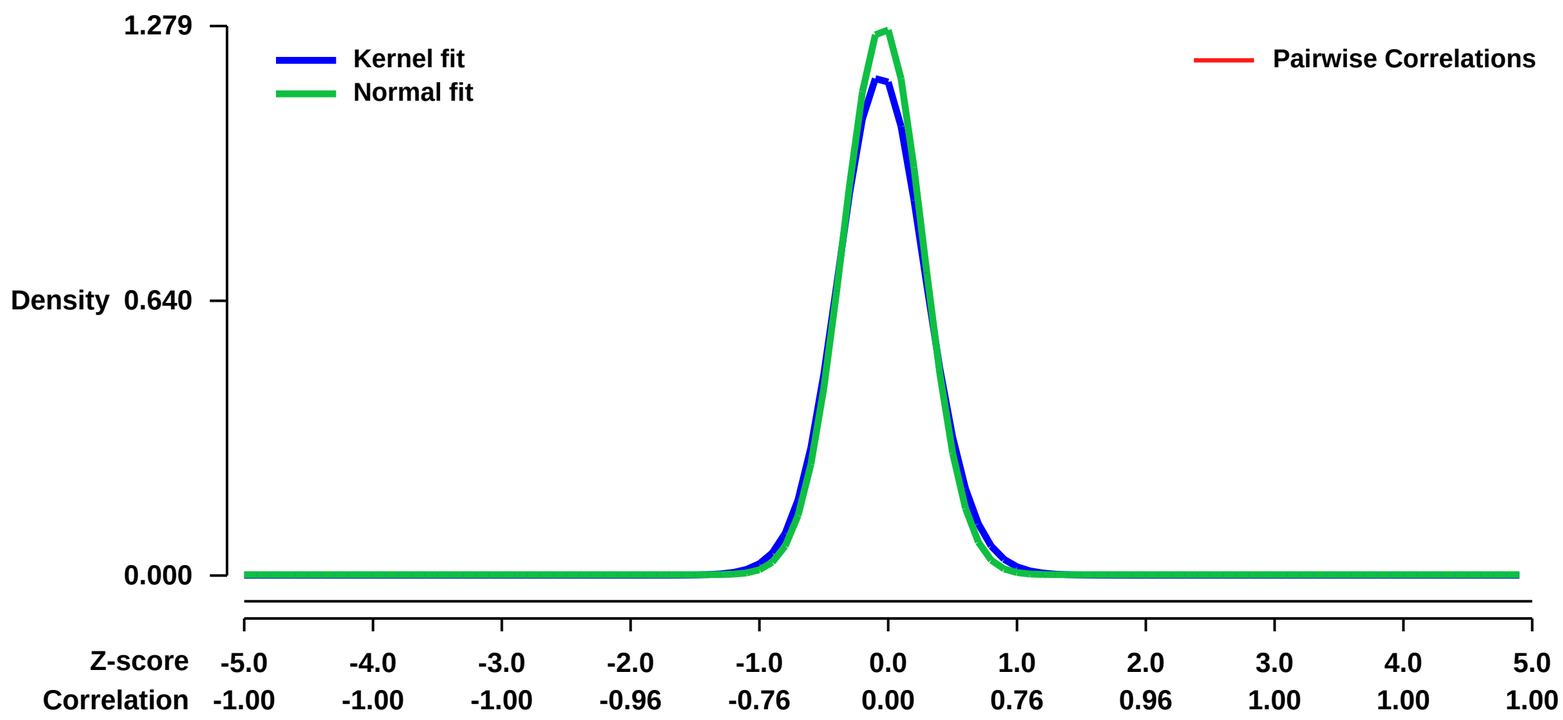

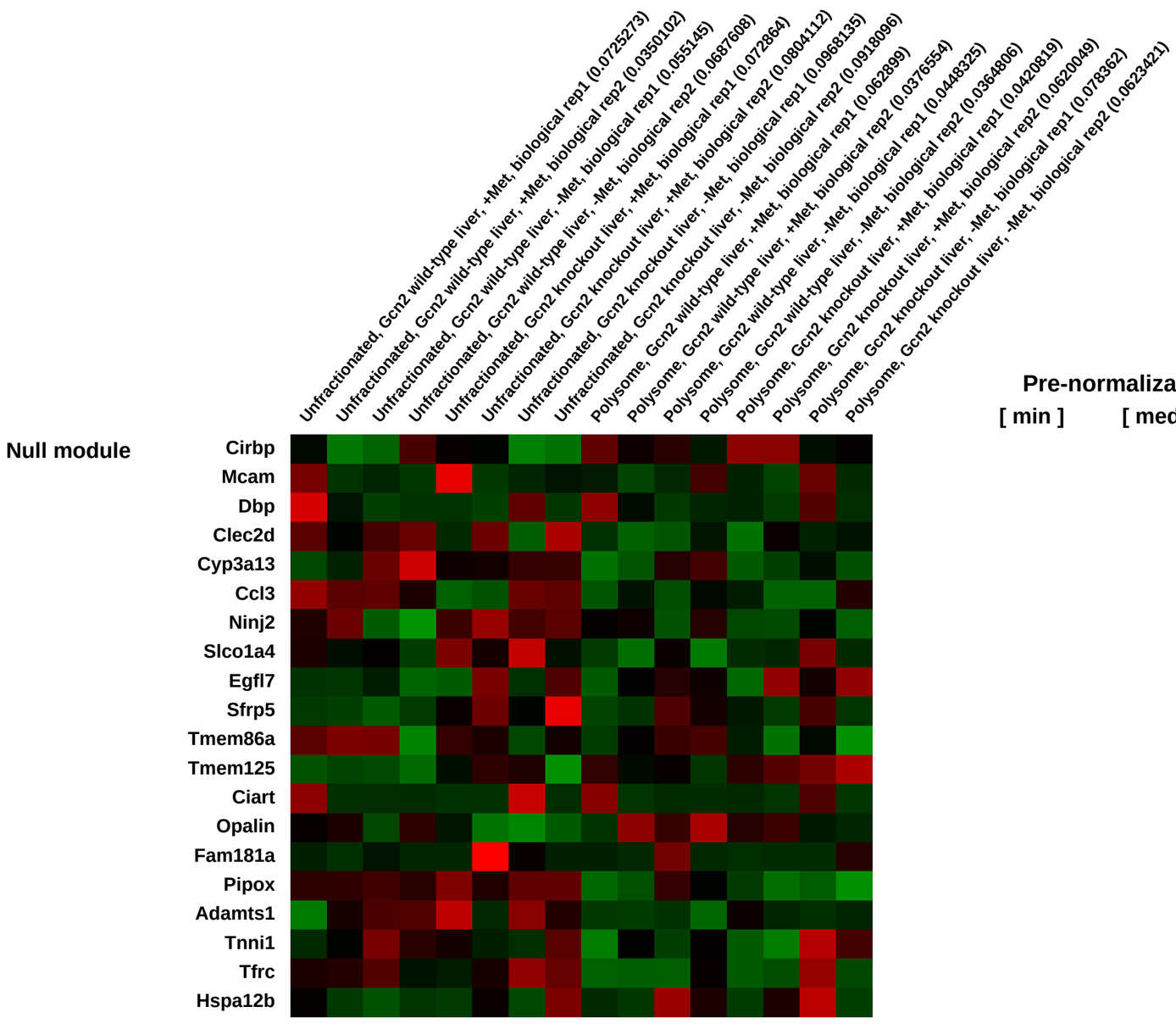

GEO Series "GSE22180" Expression Profiles

Num of samples in this series: 60

Scale of expression profile Z-scores

-3.0 -2.0 -1.0 0.0 1.0 2.0 3.0

GEO Link:	http://www.ncbi.nlm.nih.gov/geo/query/acc.cgi?acc=GSE22180
Status:	Public on Oct 02 2010
Title:	In vitro carcinogenicity testing with Balb/c 3T3 Cells treated with various chemical carcinogens
Organism:	Mus musculus
Experiment type:	Expression profiling by array
Platform:	GPL1261
Pubmed ID:	20713471
Summary & Design:	**Summary:** Background: Information on the carcinogenic potential of chemicals is only availably for High Production Volume products. There is however, a pressing need for alternative methods allowing for the chronic toxicity of substances, including carcinogenicity, to be detected earlier and more reliably. Here we applied advanced genomics to a cellular transformation assay to identify gene signatures useful for the prediction of risk for carcinogenicity. Methods: Genome wide gene expression analysis and qRT-PCR were applied to untransformed and transformed Balb/c 3T3 cells that exposed to 2, 4-diaminotoluene (DAT), benzo(a)pyrene (BaP), 2-Acetylaminoflourene (AAF) and 3-methycholanthrene (MCA) for 24h and 120h, at different concentrations, respectively. Furthermore, various bioinformatics tools were used to identify gene signatures predicting for the carcinogenic risk. Results: Bioinformatics analysis revealed distinct datasets for the individual chemicals tested while the number of significantly regulated genes increased with ascending treatment concentration of the cell cultures. Filtering of the data revealed a common gene signature that comprised of 13 genes whose regulation in cancer tissue has already been established. Strikingly, this gene signature was already identified prior to cell transformation therefore confirming the predictive power of this gene signature in identifying carcinogenic risks of chemicals. Comparison of fold changes determined by microarray analysis and qRT-PCR were in good agreement. Conclusion: Our data describes selective and commonly regulated carcinogenic pathways observed in an easy to use in vitro carcinogenicity assay. Here we defined a set of genes which can serve as a simply assay to predict the risk for carcinogenicity by use of an alternative in vitro testing strategy. **Overall design:** Balb/c 3T3 cells were seeded at 200 cells in each 60 x 15 mm culture dish with 4 ml M10F, using six culture dishes for every treatment. When cells reached a confluence of 60-65%, the culture medium was removed and replaced with fresh medium containing all tested chemicals at a specific concentration and two time points (24 and 120h). First we treated the cells both 24h and 120h with concentrations reported in the literature (0.5´µM BaP, 50´µM DAT, 25´µM AAF and 2´µM MCA). In a second approach IC20 concentrations were investigated for each chemical at both time points. The concentrations determined for IC20 ranged from 1.5 ´µM BaP to 700 ´µM DAT for 24h of treatment, and from 0.1 ´µM BaP or MCA to 10´µM AAF for 120h of treatment. Balb/c 3T3 cells treated with 0.75% DMSO alone were kept as controls. Each experiment was run in triplicate.

Background corr dist: KL-Divergence = 0.0902, L1-Distance = 0.0536, L2-Distance = 0.0063, Normal std = 0.4799

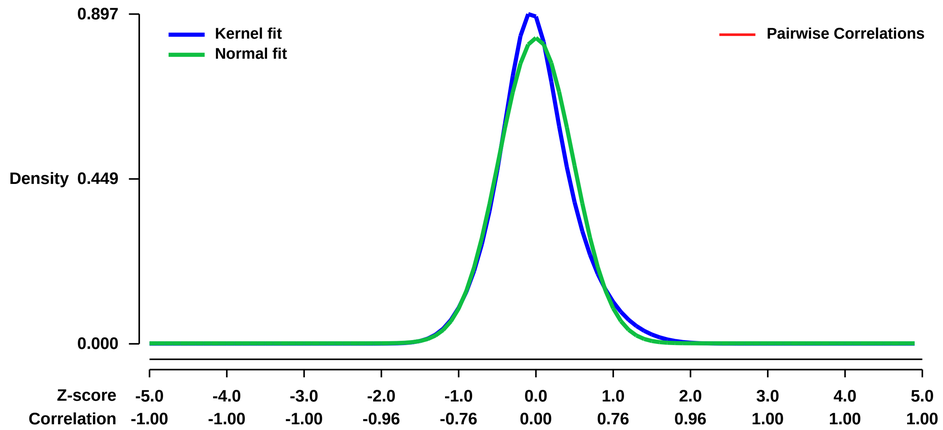

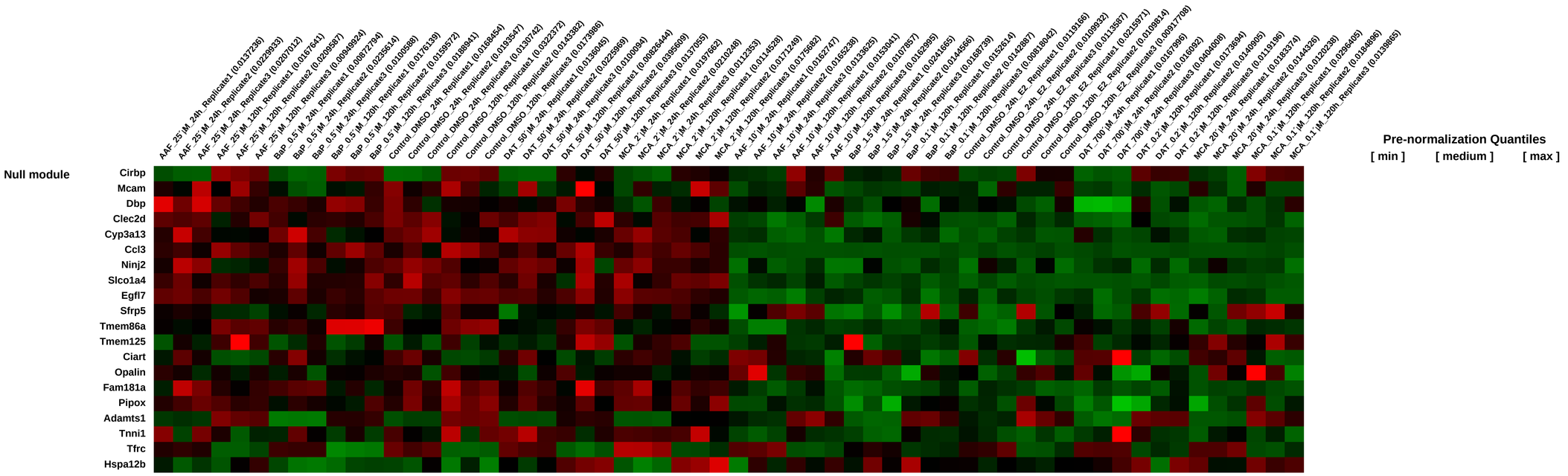

GEO Series "GSE32681" Expression Profiles

Num of samples in this series: 61

Scale of expression profile Z-scores

-3.0 -2.0 -1.0 0.0 1.0 2.0 3.0

GEO Link: http://www.ncbi.nlm.nih.gov/geo/query/acc.cgi?acc=GSE32681
Status: Public on Oct 07 2011
Title: Alterations in gene expression in lacrimal and salivary glands of male NOD mice due to LTBR-Ig treatment relative to control antibody
Organism: Mus musculus
Experiment type: Expression profiling by array
Platform: GPL1261
Pubmed ID: 22044682

Summary & Design:

Summary:
NOD mice were injected once a week with LTBR-Ig to block the LTBR-pathway, or with control monoclonal antibody MOPC from age 8 to 16 weeks old. Extraorbital lacrimal glands or submaxillary glands were dissected and total mRNA prepared. Each sample was either the combined lacrimals (2) from each mouse or individual salivary glands. There were 4 mice in each treatment group. Total mRNA was isolated and the quality was assessed using the Agilent 2100 Bioanalyzer (Agilent Technologies, Palo Alto, CA). Reverse transcription to prepare cDNA was performed using Invitrogen M-MLV system. The purpose was to determine changes in gene expression in glands due to blockade of the LTBR-pathway.

Overall design:
Differential Gene Expression in NOD mouse lacrimal and salivary glands after LTBR-Ig treatment

Background corr dist: KL-Divergence = 0.1256, L1-Distance = 0.0724, L2-Distance = 0.0108, Normal std = 0.4503

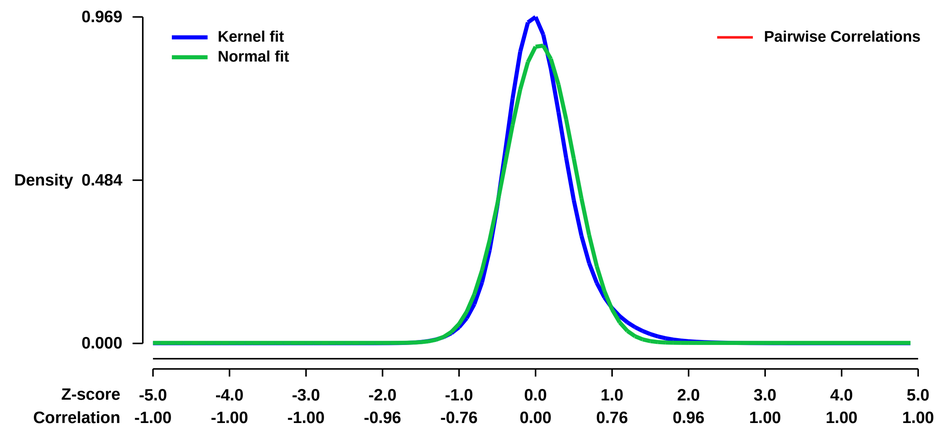

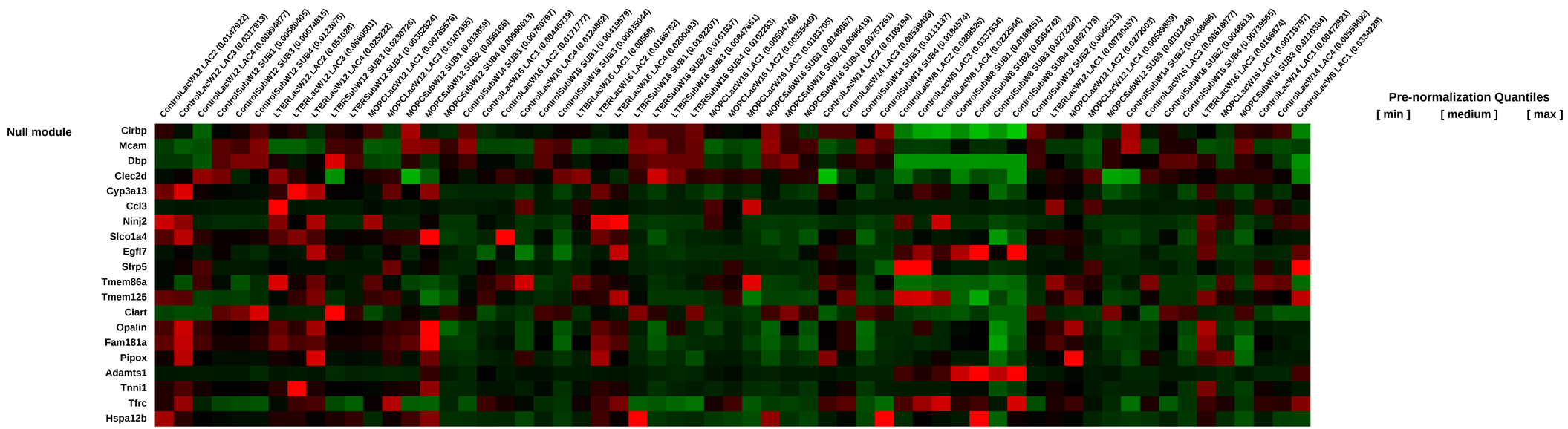

GEO Series "GSE26355" Expression Profiles

Num of samples in this series: 6

Scale of expression profile Z-scores

-3.0 -2.0 -1.0 0.0 1.0 2.0 3.0

GEO Link:	http://www.ncbi.nlm.nih.gov/geo/query/acc.cgi?acc=GSE26355
Status:	Public on Jan 01 2011
Title:	Expression data from early and late born Atoh1 lineages within the E14.5 rhombomere 1 and isthmus
Organism:	Mus musculus
Experiment type:	Expression profiling by array
Platform:	GPL1261
Pubmed ID:	21440680
Summary & Design:	**Summary:** Following neural tube closure at around E9.5, the rhombic lip within the rhombomere 1/isthmus region (""upper rhombic lip"") produces a sequence of neuronal lineages that populate the brainstem and cerebellum. The transcription factor Atoh1 (Math1) is required for this specialized neurogenesis, although the genetic programs that delineate the temporal cell fate changes downstream of Atoh1 are not well characterized. We examined the gene expresion changes that take place within Atoh1 lineages **Overall design:** We purified early (E10.5) and late (E13.5) born Atoh1 expressing cells from E14.5 embryos using a transgenic labeling strategy, and analyzed differences in gene expression across the two populations using the microarray data shown below.

Background corr dist: KL-Divergence = 0.0310, L1-Distance = 0.0295, L2-Distance = 0.0010, Normal std = 0.6844

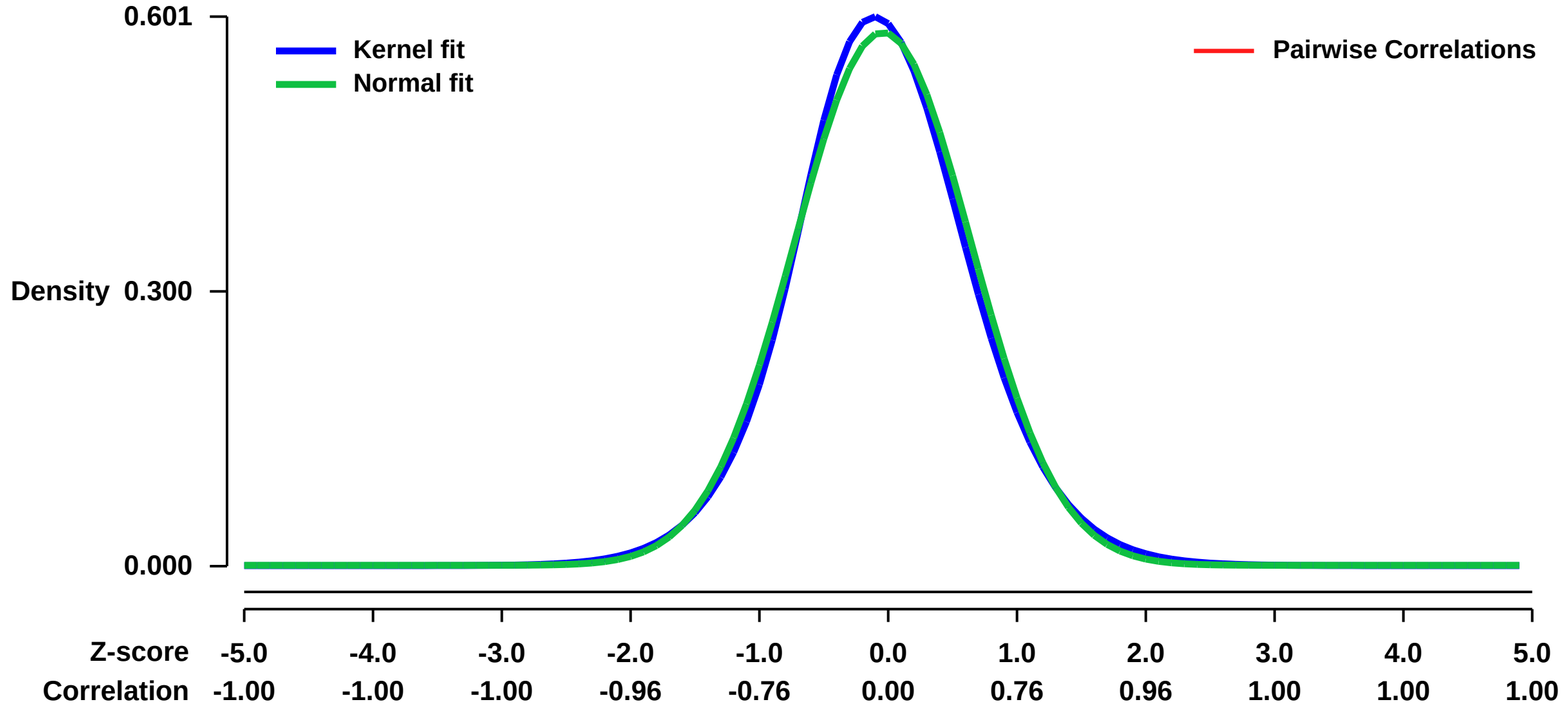

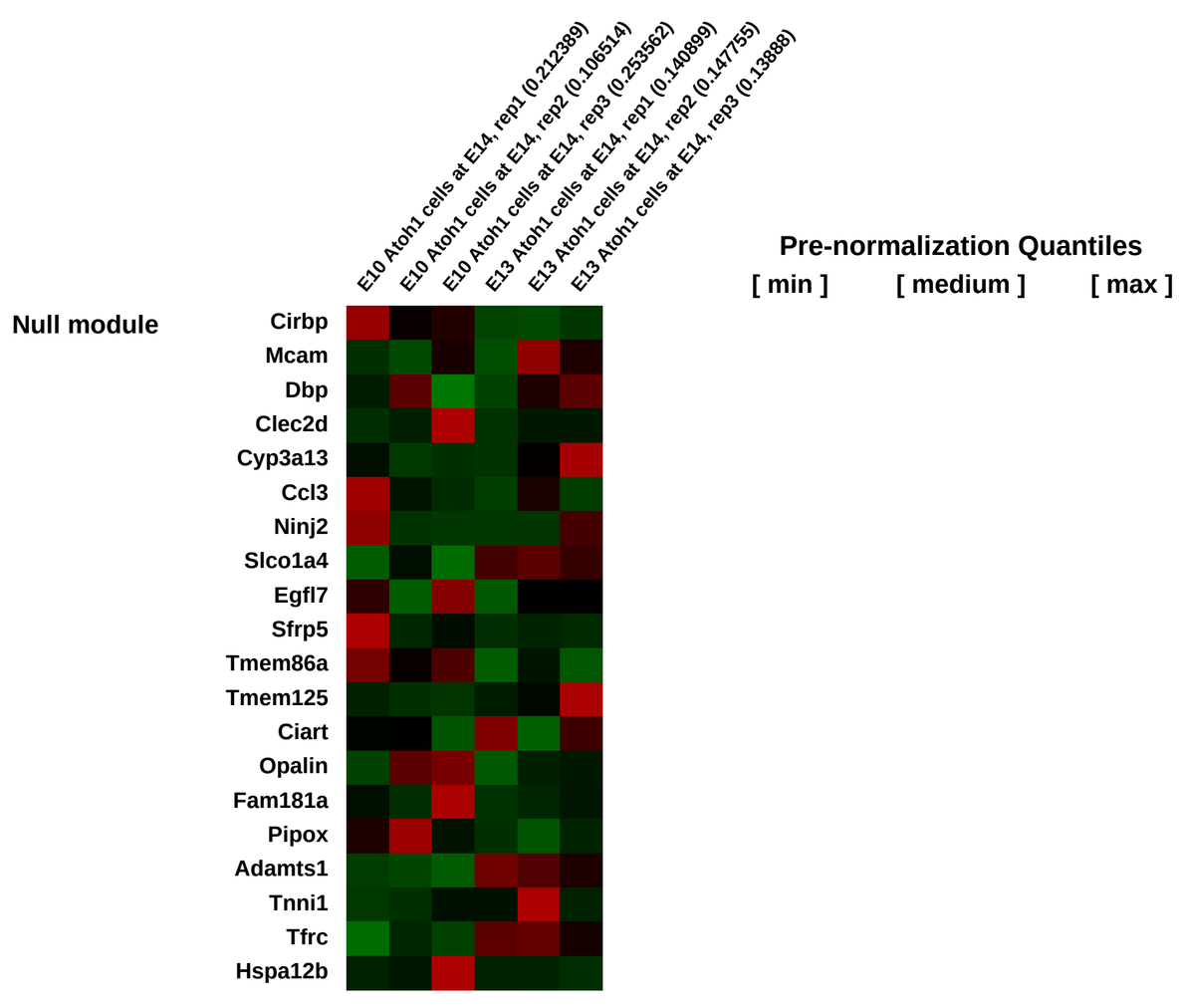

GEO Series "GSE13333" Expression Profiles

Num of samples in this series: 6

Scale of expression profile Z-scores

-3.0 -2.0 -1.0 0.0 1.0 2.0 3.0

GEO Link:	http://www.ncbi.nlm.nih.gov/geo/query/acc.cgi?acc=GSE13333
Status:	Public on Mar 01 2009
Title:	Srf conditional knockout in the mouse liver
Organism:	Mus musculus
Experiment type:	Expression profiling by array
Platform:	GPL1261
Pubmed ID:	19205030
Summary & Design:	**Summary:** Serum response factor (SRF) is a transcription factor that binds to the serum response element (SRE) of genes that are expressed in response to mitogens. SRF plays essential roles in muscle and nervous system development; however, little is known about the role of SRF during liver growth and function. To examine the function of SRF in the liver, we generated mice in which the Srf gene was specifically disrupted in hepatocytes. The survival of mice lacking hepatic SRF activity was lower than that of control mice; moreover, surviving mutant mice were smaller and had lower blood glucose and triglyceride levels compared with control mice. Srf-deficient livers were also smaller than control livers, hepatocyte morphology was abnormal, and liver-cell proliferation and viability was compromised. Gene array and quantitative RT-PCR analysis of SRF depleted livers revealed a reduction in mRNAs encoding components of the growth hormone/IGF1 pathway, cyclins, several metabolic regulators, and cytochrome p450 enzymes. Conclusion: SRF is essential for hepatocyte proliferation and survival, liver function, and control of postnatal body growth by regulating hepatocyte gene expression. **Overall design:**

Background corr dist: KL-Divergence = 0.0330, L1-Distance = 0.0376, L2-Distance = 0.0020, Normal std = 0.6811

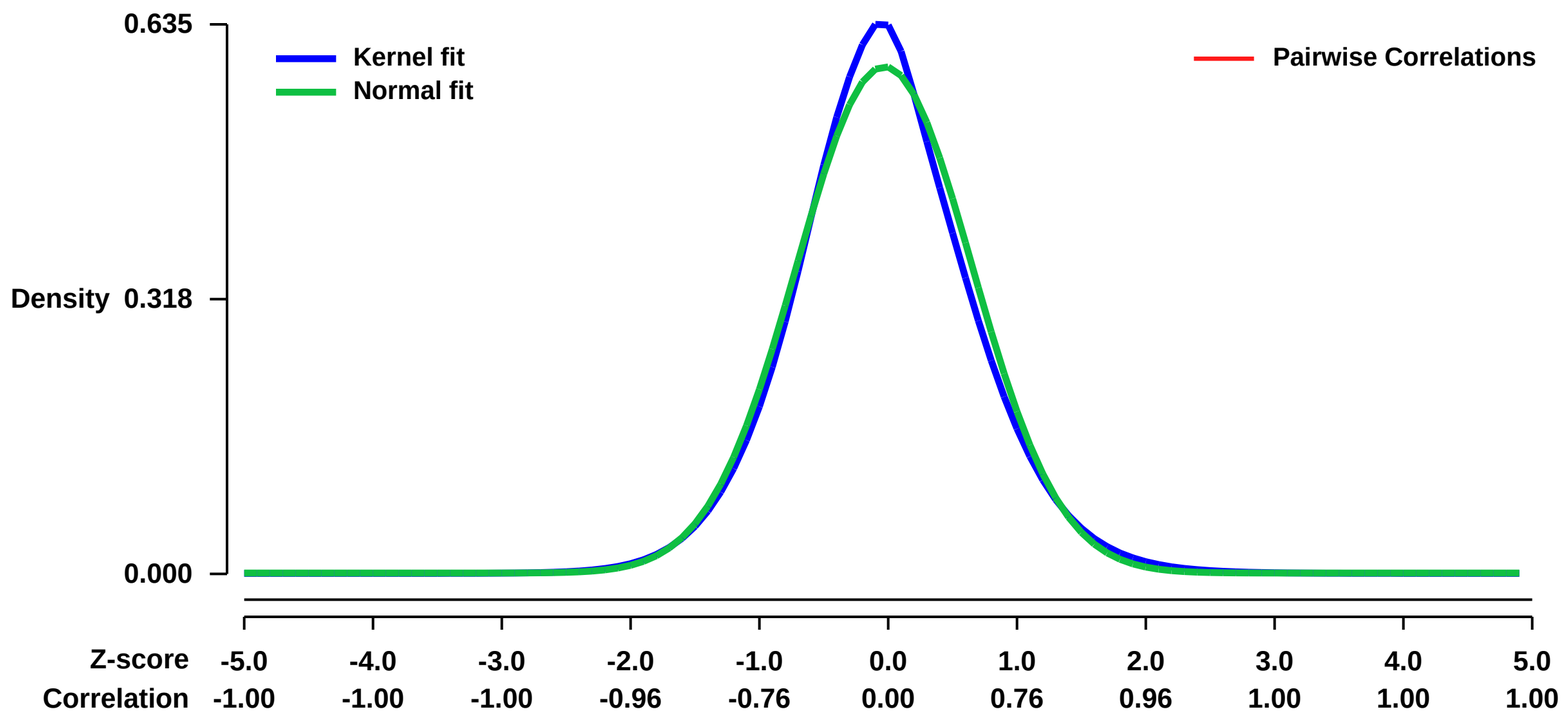

Pre-normalization Quantiles

[min] [medium] [max]

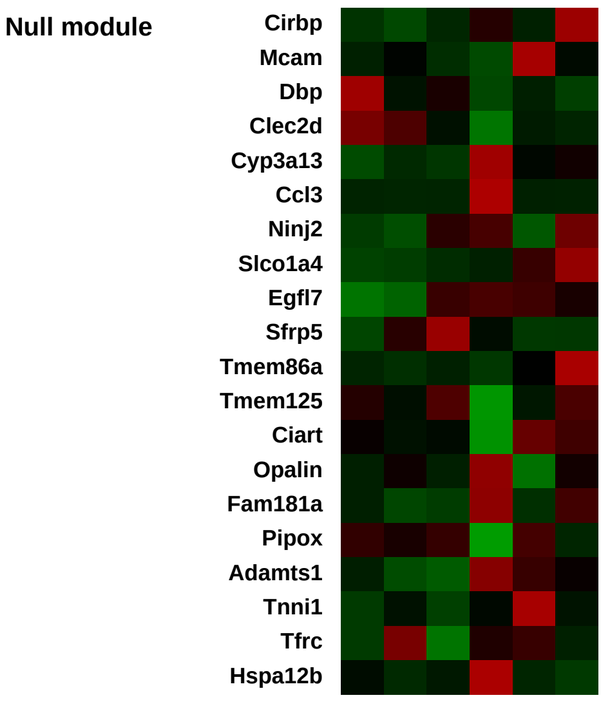

GEO Series "GSE3126" Expression Profiles

Num of samples in this series: 6

Scale of expression profile Z-scores

-3.0 -2.0 -1.0 0.0 1.0 2.0 3.0

GEO Link:	http://www.ncbi.nlm.nih.gov/geo/query/acc.cgi?acc=GSE3126
Status:	Public on Dec 31 2005
Title:	Comparison of HNF4 null mouse embryonic livers with control mouse embryonic livers
Organism:	Mus musculus
Experiment type:	Expression profiling by array
Platform:	GPL1261
Pubmed ID:	16714383
Summary & Design:	**Summary:** To study the role of hepatic nuclear factor alpha (HNF4a in hepatogenesis, we used loxP-Cre technology to eliminate it from developing mouse livers. A comparison of control and experimental livers revealed that hepatocytes lacking HNF4a_failed to fully differentiate. Specifically, HNF4a null liver cells failed to express genes that are markers of mature hepatocytes including Gys2, Pck1, and G6pc. These cells also failed to form normal cellular junctions, which are critical for establishment of the hepatic epithelium [Parviz et al. (2003) Nat.Genet. 34, 292-96]. Because HNF4a functions as a transcription factor, we hypothesized that it regulates liver development by controlling the expression of genes whose products are essential in executing cellular differentiation and morphogenesis. To identify these genes, we compared expression profiles between HNF4a null and wild type E18.5 fetal livers using Affymetrix gene arrays. We identified 564 genes whose expression was decreased by at least 2.5-fold and 34 genes whose expression was increased by at least 2.5-fold when HNF4a was eliminated from hepatocytes. These represent genes involved in diverse molecular pathways, reflecting the pleiotropic phenotype of HNF4a null livers. Our goal was to use the information from the gene arrays to define the mechanisms through which HNF4a controls the generation of the hepatic epithelium. We identified 27 genes from our list of downregulated genes with either defined or predicted roles in cellular junctions and/or adhesion. Most striking was that loss of HNF4a altered the expression of genes encoding proteins involved in virtually all types of cellular junctions including tight junctions (Cldn1, Cldn-2, Cldn-12, Ocln, F11r/Jam1, Cxadr, Crb3), adherens junctions (Cdh1), desmosomes (Dsc2, Pkp2, Krt2-8), and gap junctions (Gjb1, Gjb2). Using immunoblotting and immunohistochemistry, we found that the expression of proteins representing each of these junction types was reduced or absent. Analysis of these genes for the presence of putative HNF4a binding sites revealed that 25 of 27 contain such sites. We have used chromatin immunoprecipitation to confirm that HNF4a occupies several of these sites in vivo, including Cdh1, Cldn1, and F11r/Jam1. From these data, we conclude that HNF4a is a central mediator of the fully differentiated hepatocyte gene expression program and that it orchestrates the expression of cell junction and adhesion proteins required for establishing the hepatic epithelium. Keywords: E18.5 fetal hnf4 null and control mouse livers **Overall design:** comparison of three hnf4 null livers to three control

Background corr dist: KL-Divergence = 0.0251, L1-Distance = 0.0111, L2-Distance = 0.0001, Normal std = 0.6969

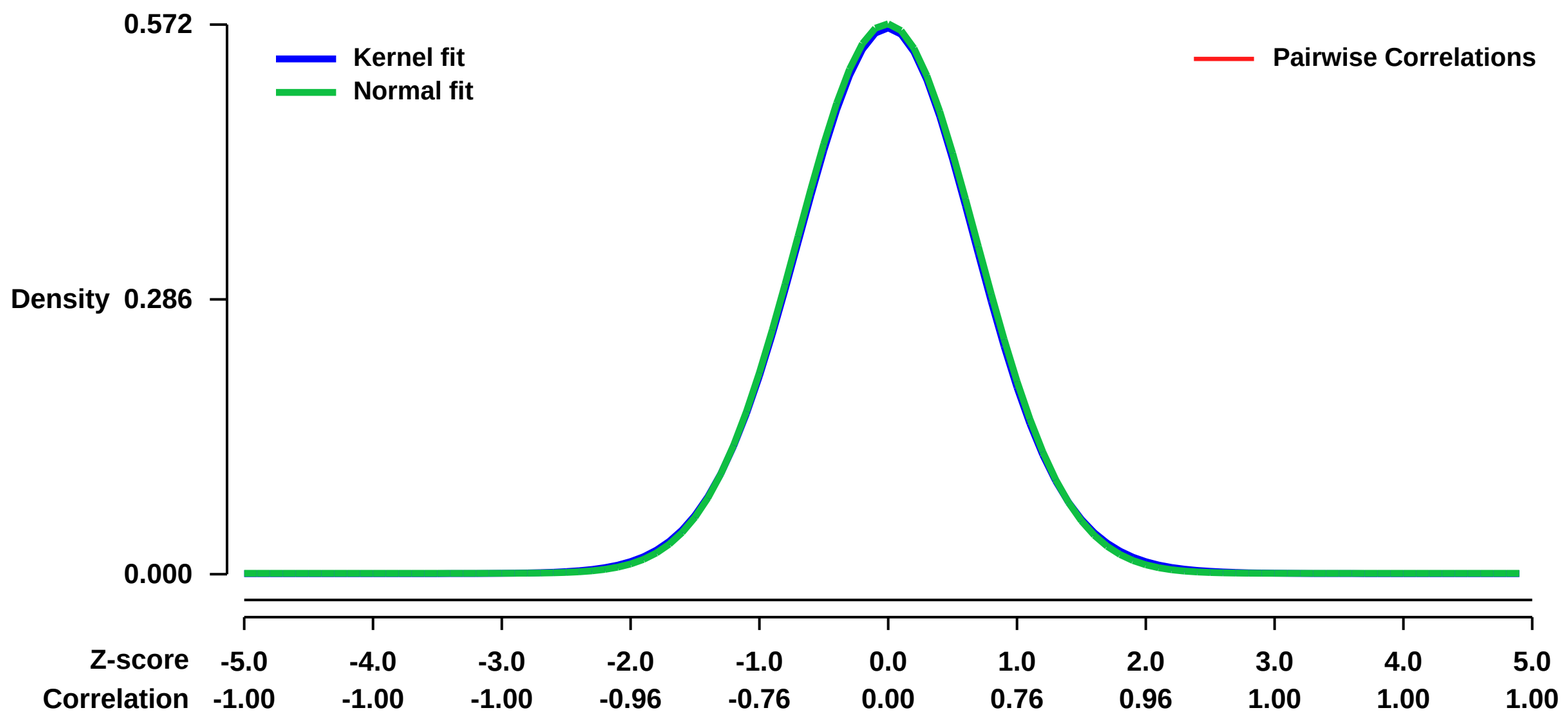

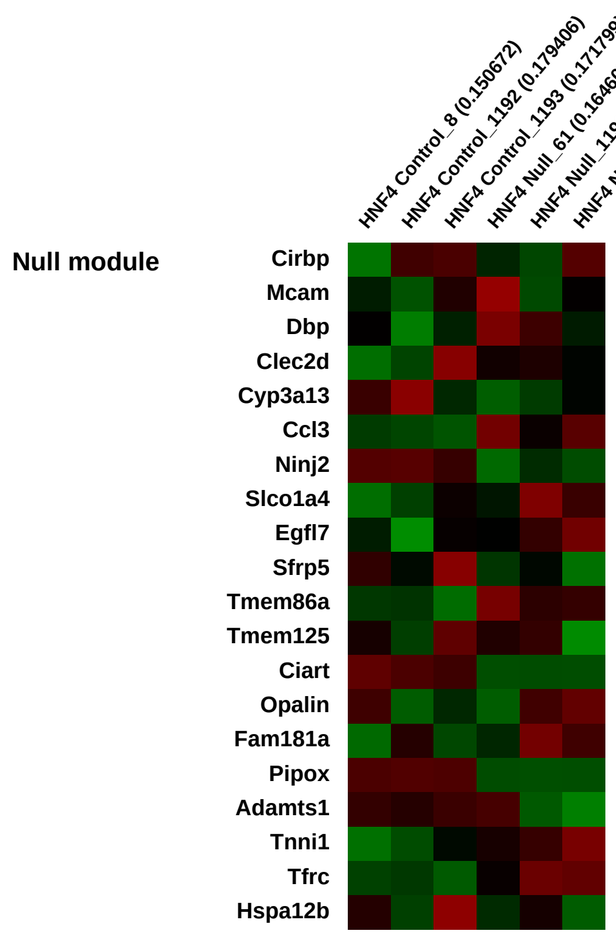

GEO Series "GSE35366" Expression Profiles

Num of samples in this series: 78

Scale of expression profile Z-scores

-3.0 -2.0 -1.0 0.0 1.0 2.0 3.0

GEO Link: http://www.ncbi.nlm.nih.gov/geo/query/acc.cgi?acc=GSE35366

Status: Public on Jan 26 2012

Title: Global developmental gene expression and pathway analysis of normal brain development and mouse models of human neuronal migration defects

Organism: Mus musculus

Experiment type: Expression profiling by array

Platform: GPL1261

Pubmed ID: 21423666

Summary & Design:

Summary:
Proper cortical development relies on the balance of neuronal migration and proliferation. We investigated the gene expression differences of mouse knock-outs for Lissencephaly in humans.

Our analysis suggests that gene expression and pathway analysis in mouse models of a similar disorder or within a common pathway can be used to define novel candidates for related human diseases.

Overall design:
We investigated the developing brain of four mutants and wild-type mice using expression microarrays, bioinformatic analyses, and in vivo/in vitro experiments to address whether mutations in different members of the LIS1 neuronal migration complex lead to similar and/or distinct global gene expression alterations.

Background corr dist: KL-Divergence = 0.0409, L1-Distance = 0.0353, L2-Distance = 0.0024, Normal std = 0.5985

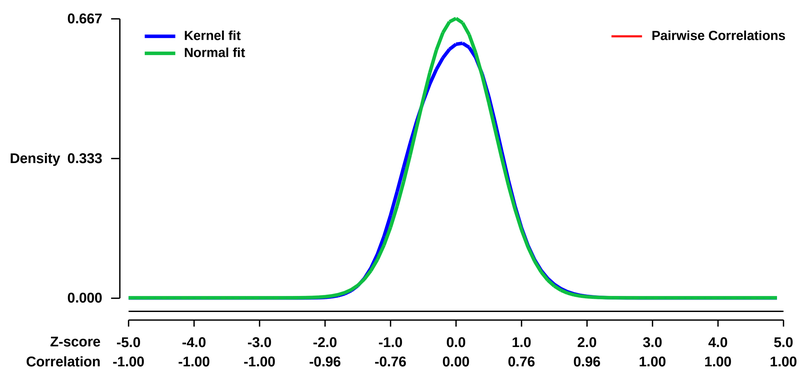

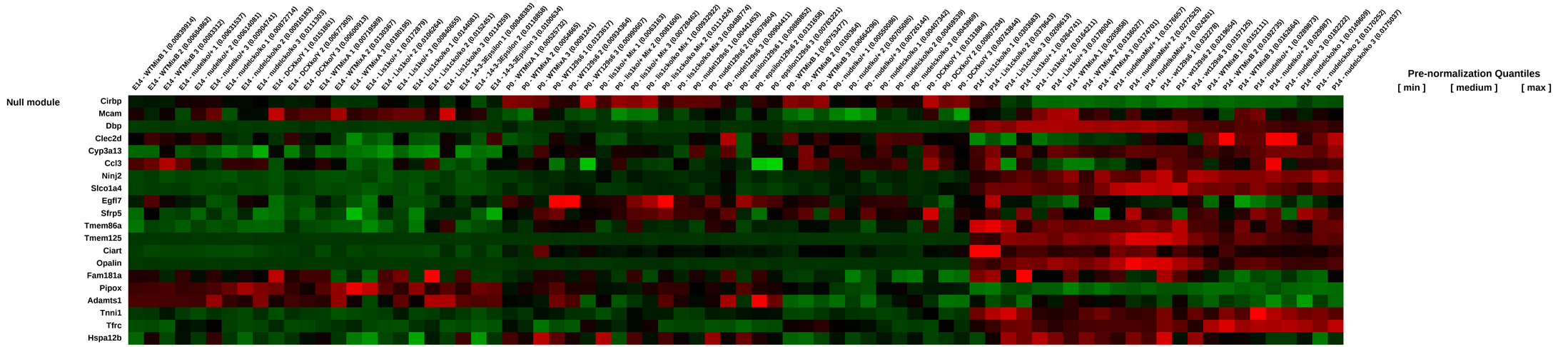

GEO Series "GSE35077" Expression Profiles

Num of samples in this series: 26

Scale of expression profile Z-scores

-3.0 -2.0 -1.0 0.0 1.0 2.0 3.0

GEO Link:	http://www.ncbi.nlm.nih.gov/geo/query/acc.cgi?acc=GSE35077
Status:	Public on Mar 13 2012
Title:	A gene expression database for retinal neuron subtypes
Organism:	Mus musculus
Experiment type:	Expression profiling by array
Platform:	GPL1261
Pubmed ID:	22407321
Summary & Design:	**Summary:** The goal of this experiment was to define gene expression patterns of thirteen mouse retinal neuron subsets, labeled by expression of fluorescent proteins in transgenic mice. **Overall design:** Neurons expressing xFPs were purified by flow cytometry. Thirteen different neuron subtypes were compared. Two biological replicates, originating from different litters, were collected for each cell type. RNA was extracted from sorted cells and prepared for hybridization to Affymetrix microarrays.

Background corr dist: KL-Divergence = 0.1251, L1-Distance = 0.0402, L2-Distance = 0.0027, Normal std = 0.4194

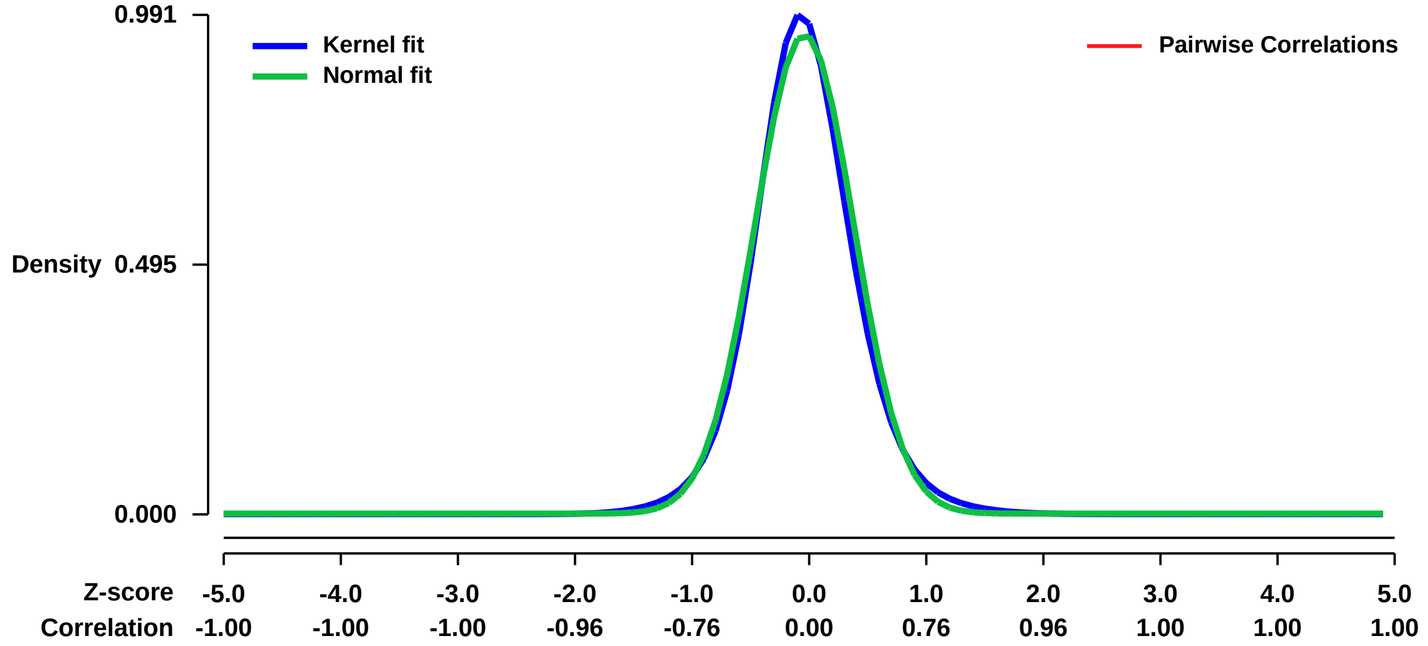

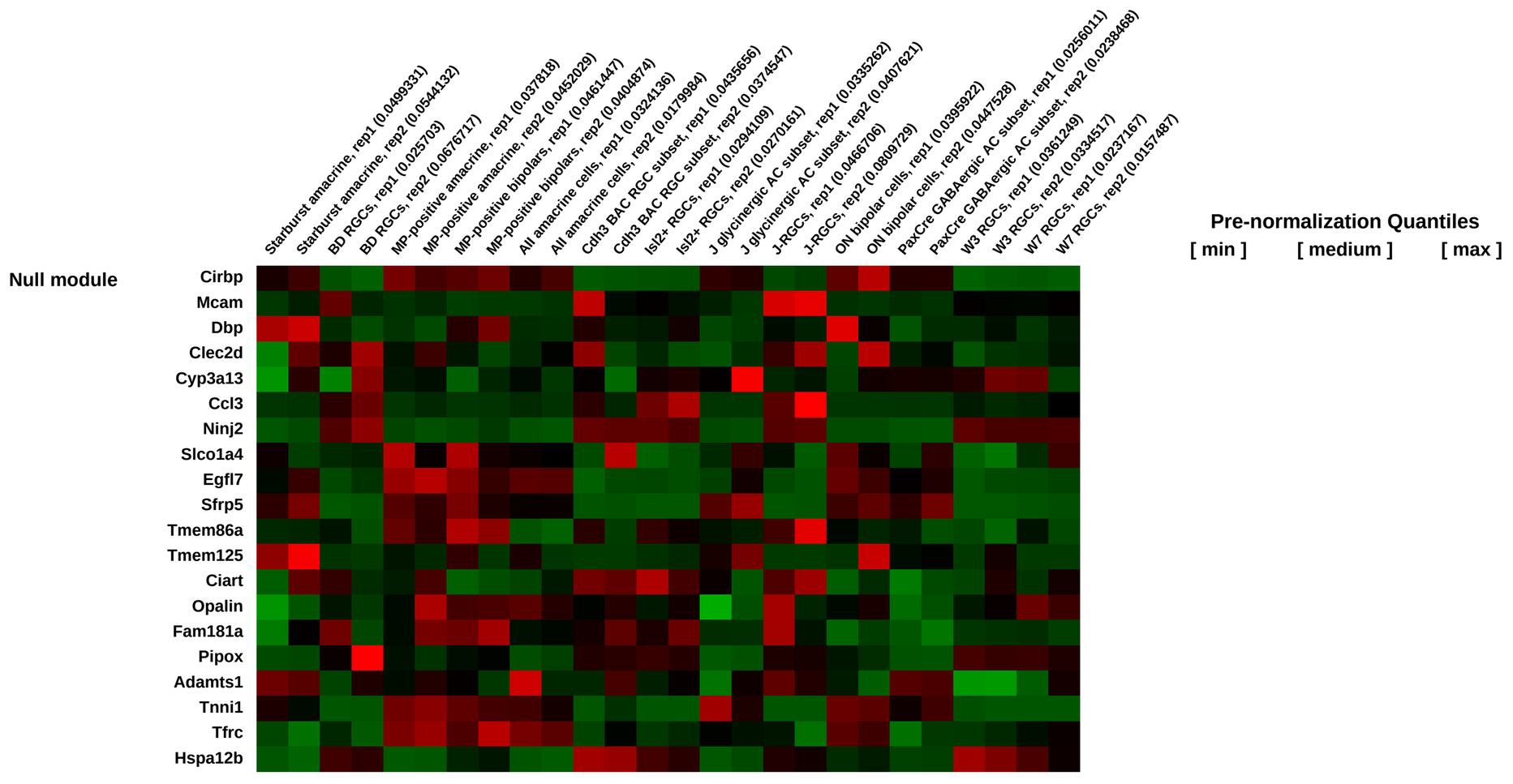

GEO Series "GSE48261" Expression Profiles

Num of samples in this series: 14

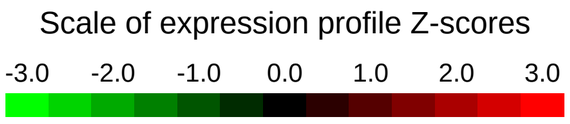

GEO Link:	http://www.ncbi.nlm.nih.gov/geo/query/acc.cgi?acc=GSE48261
Status:	Public on Mar 20 2014
Title:	Gene expression in mouse hematopoietic stem and multi-potent progenitor cells with temporally defined divisional histories
Organism:	Mus musculus
Experiment type:	Expression profiling by array
Platform:	GPL1261
Pubmed ID:	24749072
Summary & Design:	**Summary:** **Homeostatic hematopoietice stem cells (HSCs) with greater divisional history lose repopulating potential after very few cell divisions. Divisional history overrides both phenotype and immediate quiescence in determining functional activity. In GFP label retaining system GFP is progressively diluted when cells proceed through a cascade of divisions.** **We used a GFP label retaining system and performed microarray expression analyses to track the changes in the gene expression profile of bone marrow (BM) LSK cells that relates to divisional history during homeostasis.** **Overall design:** **Chromatins are dynamically labeled in a double transgenic mouse (huCD34-tTA X Tet-O-H2B-GFP) by the expression of GFP tagged Histone2B. The expression is driven by a human CD34 promoter active specifically in all bone marrow (BM) hematopoietic stem and multi-potent progenitor cells. This is a pulse/chase Tet-off system where cells constantly label with GFP. Upon administration of Doxycyclin (Dox) to GFP labeled animals, further labeling is stopped during the chase period. With each round of cell division, the newly synthesized endogenous H2B will dilute H2B-GFP by one-half, whereas cells that donâ t divide will retain GFP labeling. Therefore, the level of GFP reflects how many times cells have divided over the period of Dox treatment (chase). Animals were treated with Dox for 12 weeks starting at the age of 6-8 weeks. After chase, BM Lineage negative, Sca1+, Kit+ (LSK) cells with varying GFP levels were sorted for mRNA extraction. GFP levels were ranked from 0 to 4 based on the kinetic analysis of GFP fully labeled LSK cells and obvious peaks in the GFP histogram of LSK cells after Dox treatment. There is approximately 1-2 cell divisions between each level of GFP.**

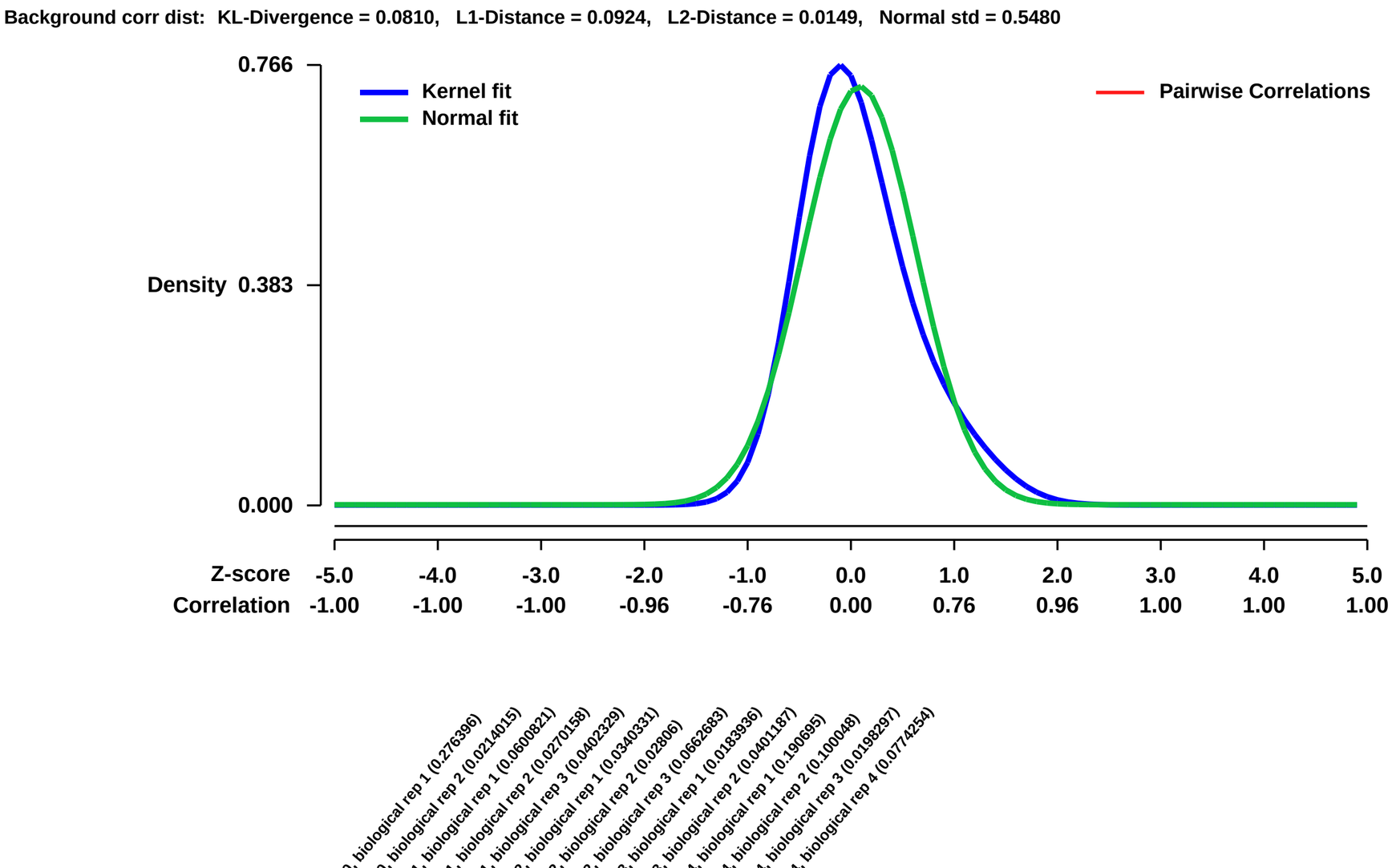

GEO Series "GSE36838" Expression Profiles

Num of samples in this series: 18

Scale of expression profile Z-scores

-3.0 -2.0 -1.0 0.0 1.0 2.0 3.0

GEO Link:	http://www.ncbi.nlm.nih.gov/geo/query/acc.cgi?acc=GSE36838
Status:	Public on Mar 28 2012
Title:	Expression profiling of the effect of high-fat diet, low-fat diet, CR and exercise on mice liver
Organism:	Mus musculus
Experiment type:	Expression profiling by array
Platform:	GPL1261
Pubmed ID:	22509016
Summary & Design:	**Summary:** Dietary interventions are effective ways to extend or shorten lifespan. By examining midlife hepatic gene expressions in mice under different dietary conditions, which resulted in different lifespans and aging-related phenotypes, we were able to identify genes and pathways that modulate the aging process. We found that pathways transcriptionally correlated with diet-modulated lifespan and physiological changes were enriched for lifespan-modifying genes. **Overall design:** At the age of 5 weeks, animals were randomly assigned to one of the 6 intervention groups (n = 30 for each group): feeding of a low-fat diet (10% fat, D12450B, Research Diets) ad libitum (LF) or with 30% calorie restriction (LF+CR) or with voluntary running exercise (LF+Ex), feeding of a high-fat diet (60% fat, D12492, Research Diets) ad libitum (HF) or with 30% calorie restriction (HF+CR) or with voluntary running exercise (HF+Ex). All mice were housed individually during the study. The daily consumption of food in LF and HF groups was recorded over a week and averaged to determine the amount of food for the following week for the LF+CR and HF+CR groups, respectively. After 1 week acclimation in cage with the locked running wheels, mice in the LF+Ex and HF+Ex groups were allowed free access to a running wheel, and the running distance and time were recorded automatically by the equipment. The hepatic transcriptional level for 3 mice from each intervention group at 62 weeks of age was analyzed using Affymetrix Mouse Genome 430 2.0 Arrays.

Background corr dist: KL-Divergence = 0.1729, L1-Distance = 0.0467, L2-Distance = 0.0048, Normal std = 0.3511

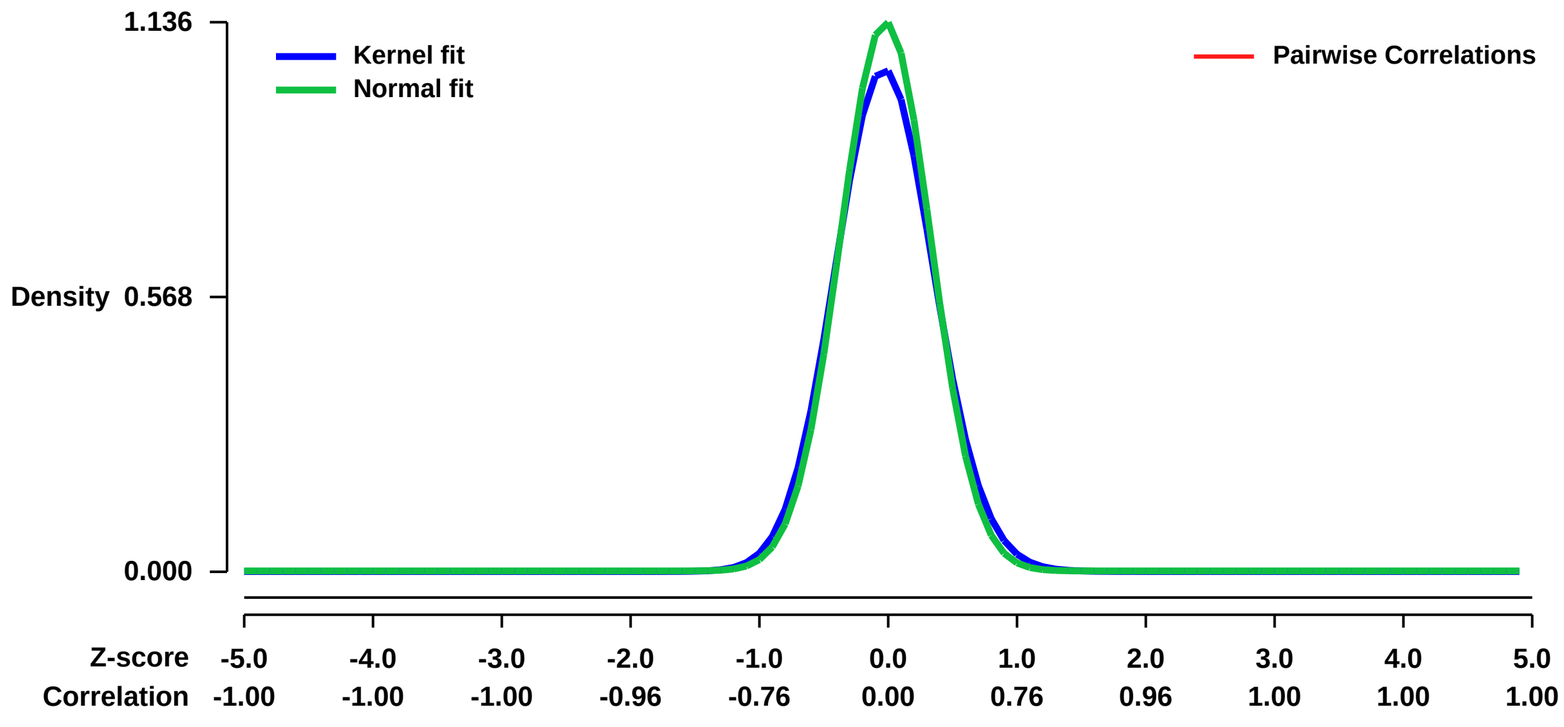

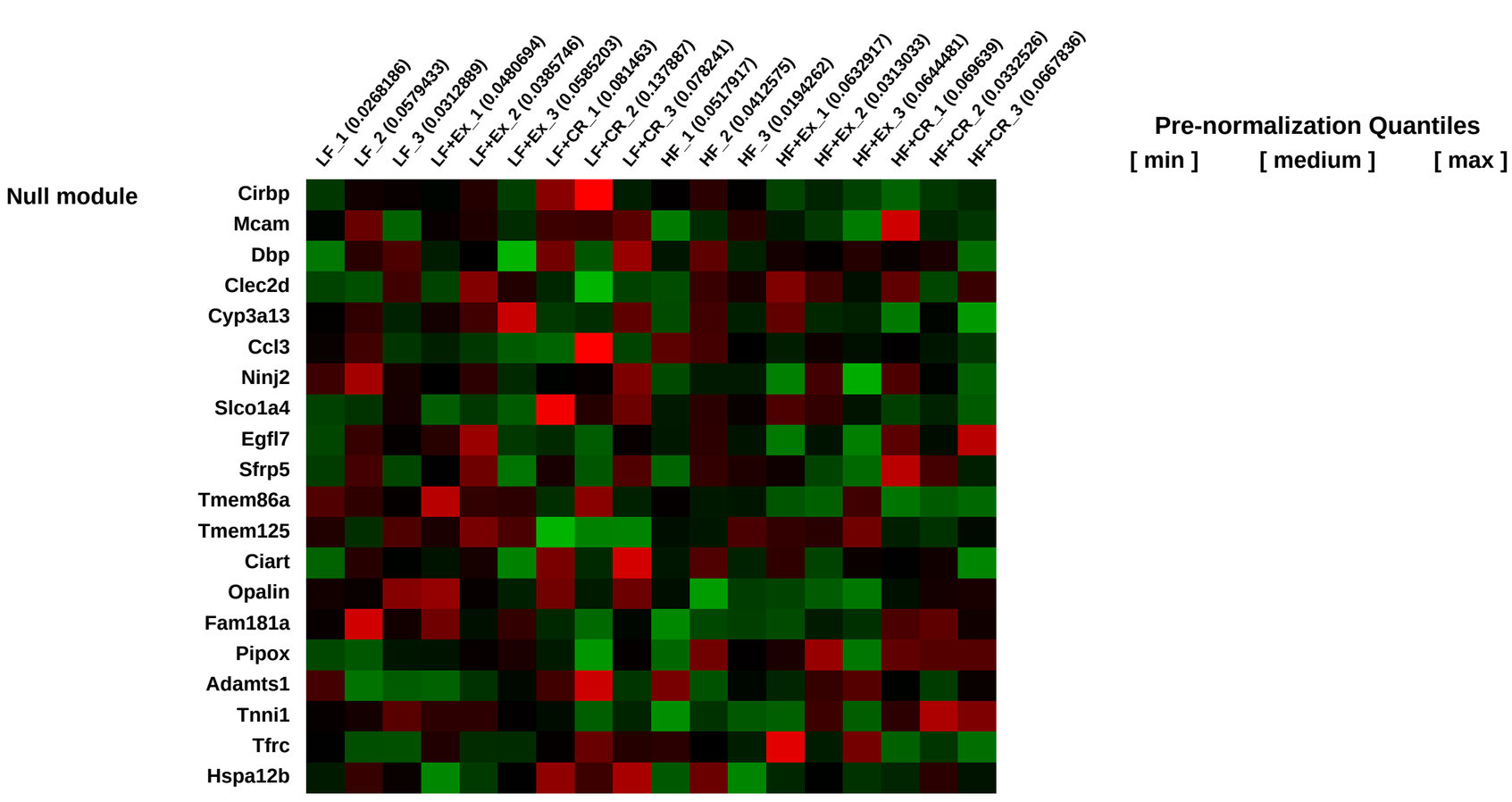

GEO Series "GSE6383" Expression Profiles

Num of samples in this series: 6

Scale of expression profile Z-scores

-3.0 -2.0 -1.0 0.0 1.0 2.0 3.0

GEO Link:	http://www.ncbi.nlm.nih.gov/geo/query/acc.cgi?acc=GSE6383
Status:	Public on Mar 12 2007
Title:	Mouse small intestine epithelium vs. mesenchyme
Organism:	Mus musculus
Experiment type:	Expression profiling by array
Platform:	GPL1261
Pubmed ID:	17299133
Summary & Design:	**Summary:** During organogenesis of the intestine, reciprocal crosstalk between the endodermally-derived epithelium and the underlying mesenchyme is required for regional patterning and proper differentiation. Though both of these tissue layers participate in patterning, the mesenchyme is thought to play a prominant role in the determination of epithelial phenotype during development and in adult life. However, the molecular basis of this instructional dominance is unclear. In fact, surprisingly little is known about the cellular origins of many of the critical signaling molecules and the gene transcriptional events that they impact. Here, we profile genes that are expressed in separated mesenchymal and epithelial compartments of the perinatal mouse intestine. The data indicate that the vast majority of soluble modulators of signaling pathways such as Hedgehog, Bmp, Wnt, Fgf and Igf are expressed predominantly or exclusively by the mesenchyme, accounting for its ability to dominate instructional crosstalk. We also catalog the most highly enriched transcription factors in both compartments and find evidence for a major role for Hnf4alpha and Hnf4 gamma in the regulation of epithelial genes. Finally, we find that while epithelially enriched genes tend to be highly tissue-restricted in their expression, mesenchymally-enriched genes tend to be broadly expressed in multiple tissues. Thus, the unique tissue-specific signature that characterizes the intestinal epithelium is instructed and supported by a mesenchyme that itself expresses genes that are largely non-tissue specific. **Keywords: comparative genomic hybridization: epithelium vs. mesenchyme** **Overall design:** Mouse small intestine (E18.5) is separated to epithelium and mesenchyme. Total RNA is extracted from epithelium and mesenchyme. There are 6 samples in this microarray experiment: 3 for epithelium and 3 for mesenchyme. Samples are hybridized the affymetrix Mouse Genome 430 2.0 Array. We compare the gene expression between epithelium and mesenchyme to study the gene expression profiles in these two compartments.

Background corr dist: KL-Divergence = 0.0057, L1-Distance = 0.0149, L2-Distance = 0.0002, Normal std = 0.9832

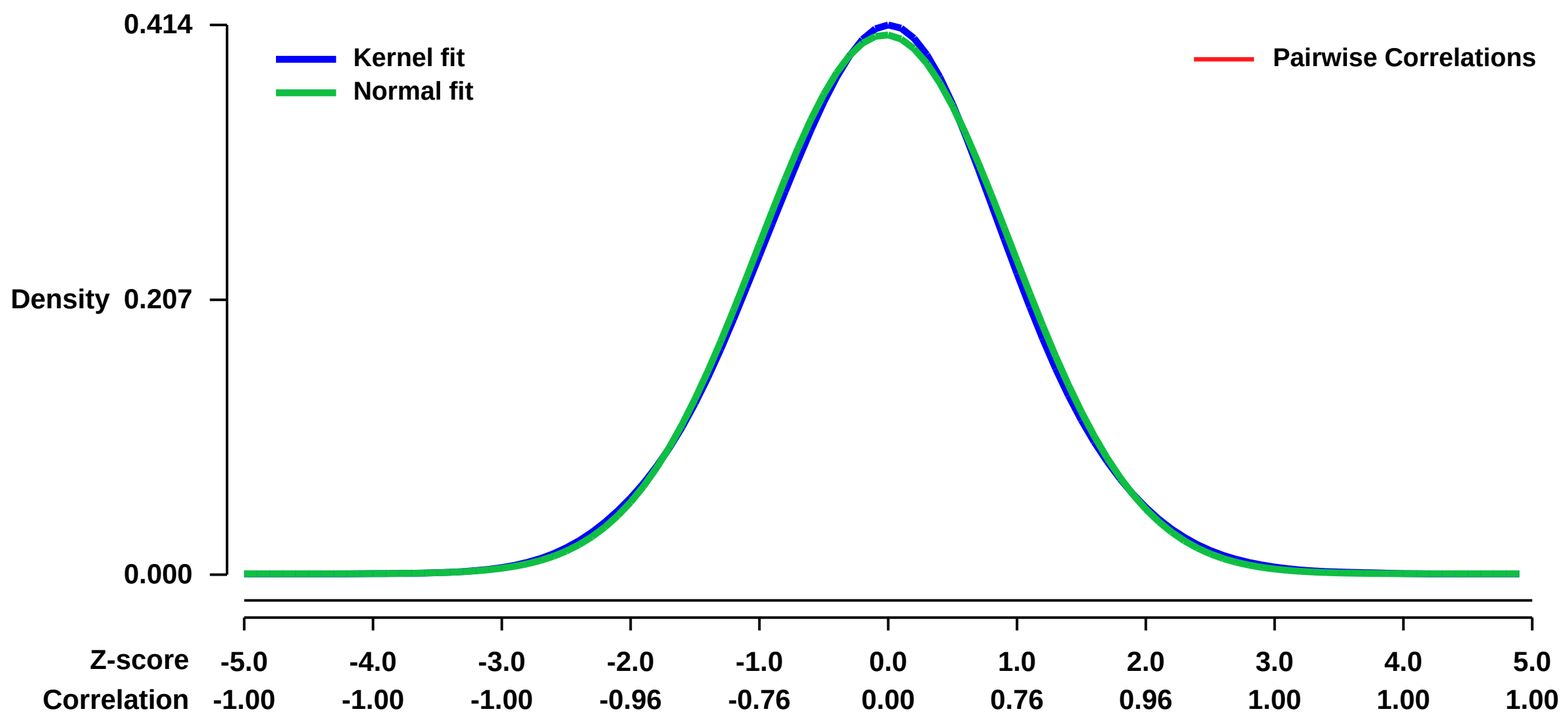

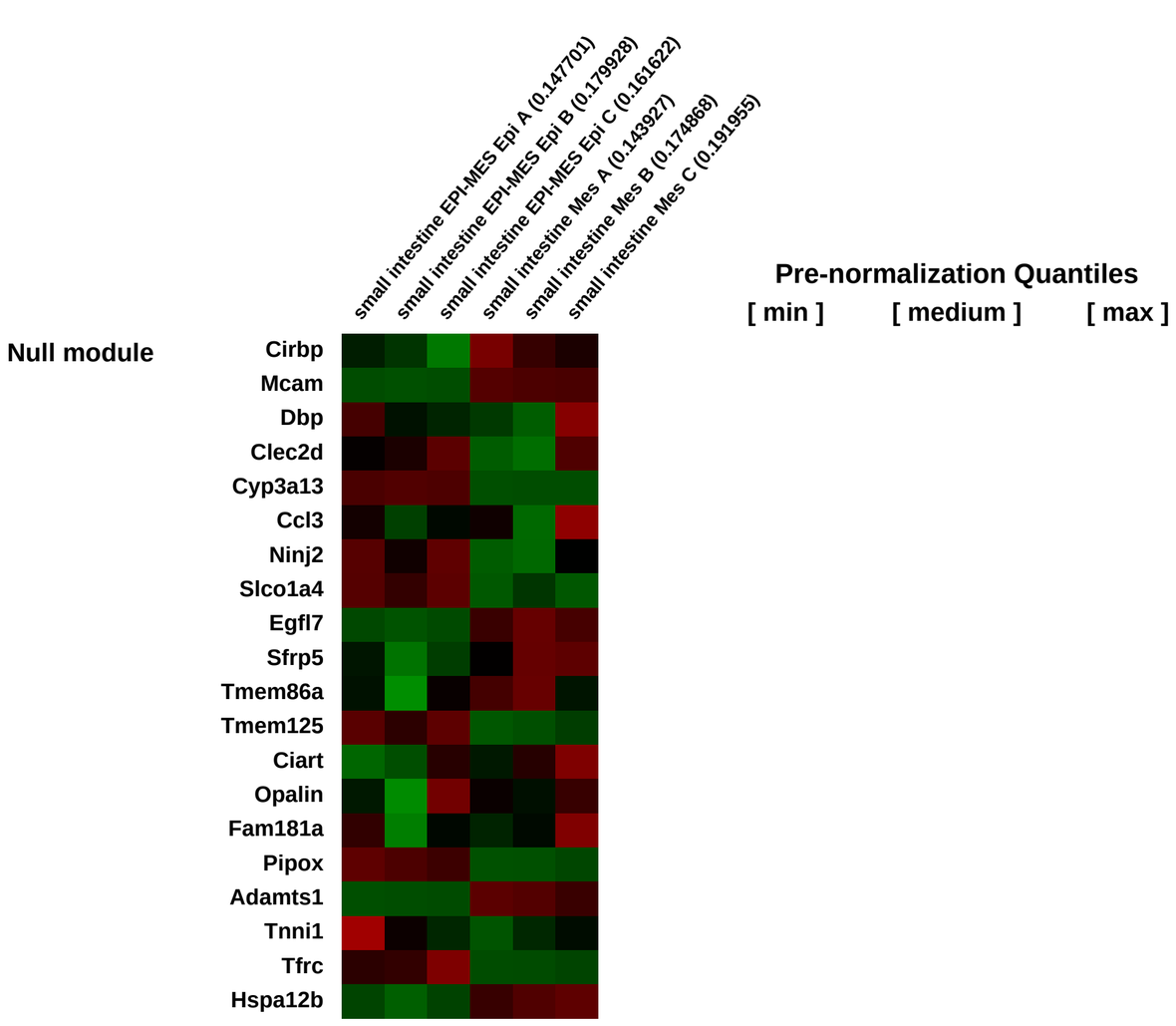

GEO Series "GSE2924" Expression Profiles

Num of samples in this series: 13

Scale of expression profile Z-scores

-3.0 -2.0 -1.0 0.0 1.0 2.0 3.0

GEO Link: http://www.ncbi.nlm.nih.gov/geo/query/acc.cgi?acc=GSE2924
Status: Public on Jul 12 2006
Title: Immunodomination leads to selective expansion of the fittest CD8 T cells
Organism: Mus musculus
Experiment type: Expression profiling by array
Platform: GPL1261
Pubmed ID:

Summary & Design:

Summary:
During the course of infection, T cells are confronted with a multitude of non self epitopes but only respond to a few epitopes and neglect other potentially immunogenic peptides. Restriction of T cell responses to a small number of selected epitopes (immunodominance) is a central feature of immune responses. Immunodominance is considered to be disadvantageous to the host because it allows pathogens to escape by selectively mutating the relevant epitope(s). Using Affymetrix microarrays, we compared the gene expression profile of unprimed CD8 T cells to that of effector CD8 T cells specific for a dominant (H7a) and a nondominant (HY) Ag. Our key finding is that T cells specific for the dominant and nondominant Ags displayed similar gene expression profiles except for a few gene transcripts, such as Gzma, Sell, Il7r and Klrg1, that contribute to the fitness of effector CD8 T cells. The differences between HY- and H7a-specific CD8 T cells were validated by real-time PCR and flow cytometry analyses. We propose that, by leading to selective expansion of the fittest CD8 effector T cells, immunodominance may be beneficial to the host. Inhibition of T cell response to nondominant Ags would ensure that host resources (APCs, cytokines) for which T cells compete are devoted to T cells that have the best effector potential. One implication is that, in general, favouring expansion of the fittest effector T cells may be more important that increasing the diversity of the T cell repertoire.

Keywords: comparative gene profile, cell type comparaison, H7a, HY

Overall design:
B10.H7b female mice were primed by i.p. injection of a cell mixture containing 2 x 107 B10 male splenocytes and 2 x 107 B10.H7b male splenocytes. On day 14 after priming, splenocytes were labeled with anti-CD8 Ab as well as H7a- and HY-Tet labeled with different fluorochromes. Then, three populations of splenocytes were purified using a FACS cell sorting: HYTet+ (n=4), H7aTet+ (n=4), and Tet- (n=5) CD8 T cells. RNA of sorted T cells was extracted and linearly amplified, cRNA was prepared, and Affymetrix Mouse Genome 430 2.0 oligonucleotide arrays were used to analyze gene expression.

Background corr dist: KL-Divergence = 0.1532, L1-Distance = 0.0497, L2-Distance = 0.0059, Normal std = 0.3740

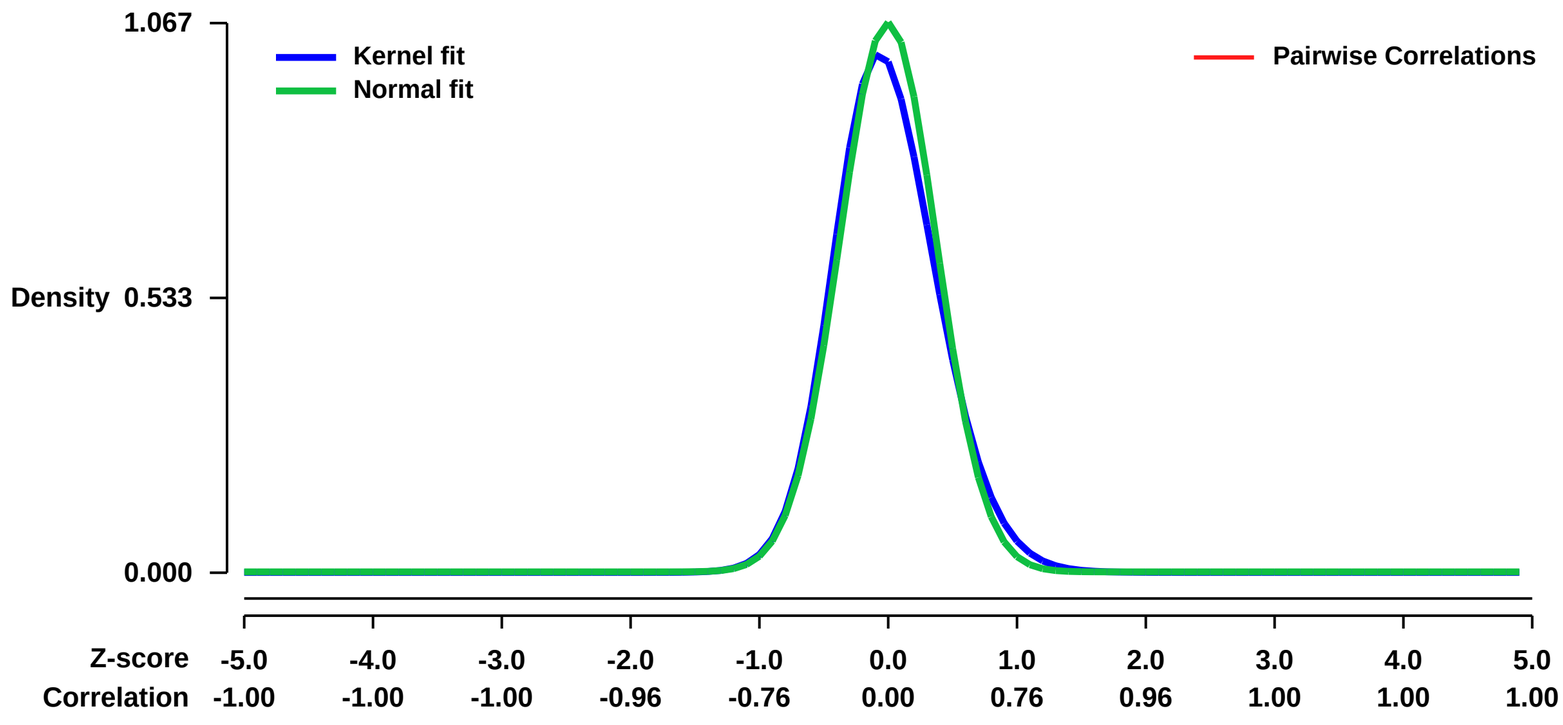

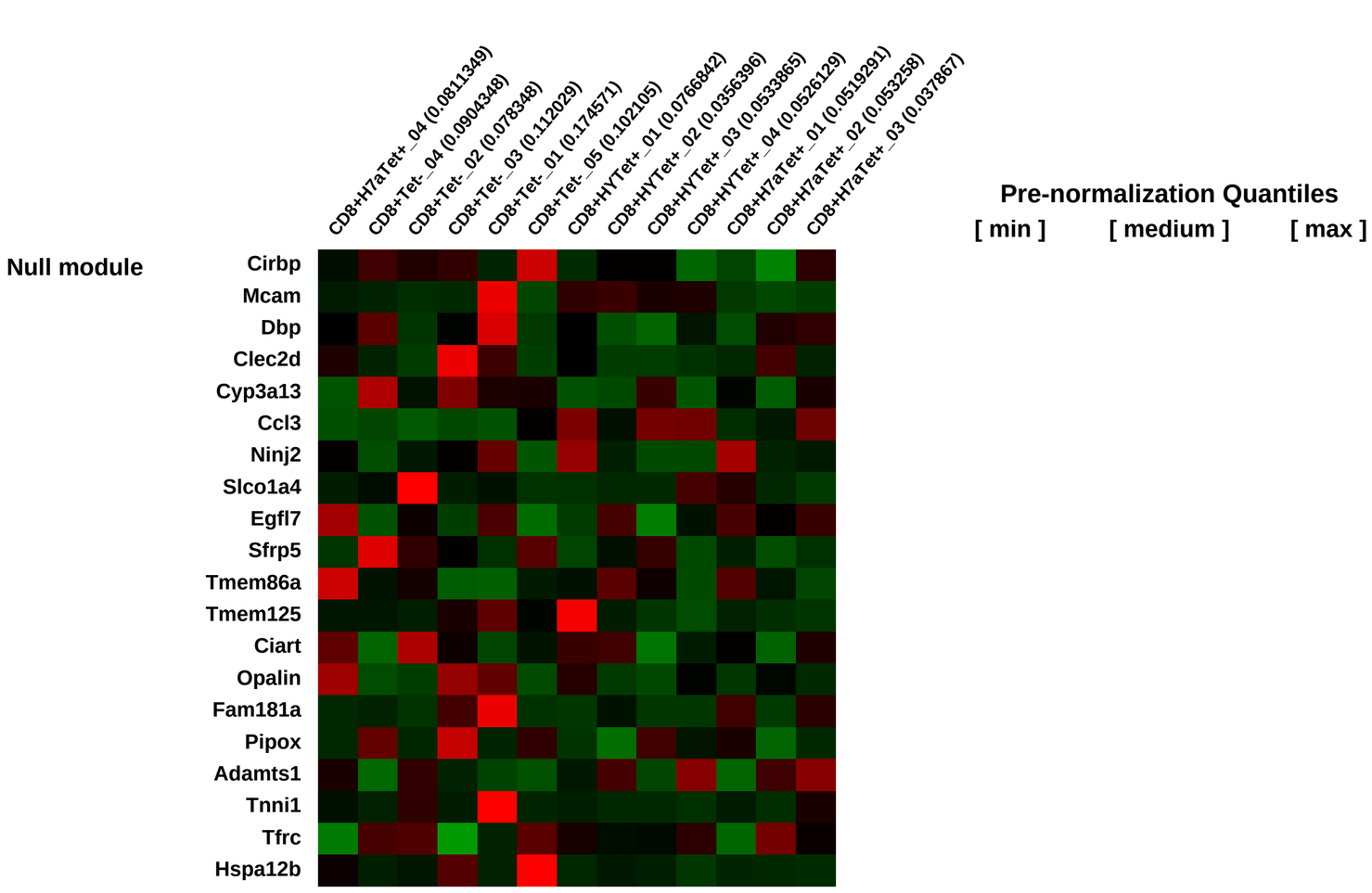

GEO Series "GSE13129" Expression Profiles

Num of samples in this series: 12

Scale of expression profile Z-scores

-3.0 -2.0 -1.0 0.0 1.0 2.0 3.0

GEO Link:	**http://www.ncbi.nlm.nih.gov/geo/query/acc.cgi?acc=GSE13129**
Status:	**Public on Oct 15 2008**
Title:	**Analysis of genes regulated by FoxD3 in B16-F10 mouse melanoma cells**
Organism:	**Mus musculus**
Experiment type:	**Expression profiling by array**
Platform:	**GPL1261**
Pubmed ID:	
Summary & Design:	**Summary:** **We wished to examine the genes regulated by FoxD3 in pigment cells to gain understanding in how FoxD3 represses melanoblast specification in the neural crest. For technical reasons, we could not use neural crest cells, so we used melanoma cells, since they are derived from neural crest cells. To this end, we transfected B16-F10 mouse melanoma cells with constructs expressing FoxD3, or FoxD3-VP16, in which the C-terminal portion of FoxD3 (which contains the transcriptional repression domain) has been replaced by the VP16 transcriptional activation domain.** **Overall design:** **24 hours after transfection, EGFP-positive cells were collected by FACS and those cells were subjected to microarray analysis.**

Background corr dist: **KL-Divergence = 0.0752, L1-Distance = 0.0365, L2-Distance = 0.0027, Normal std = 0.4935**

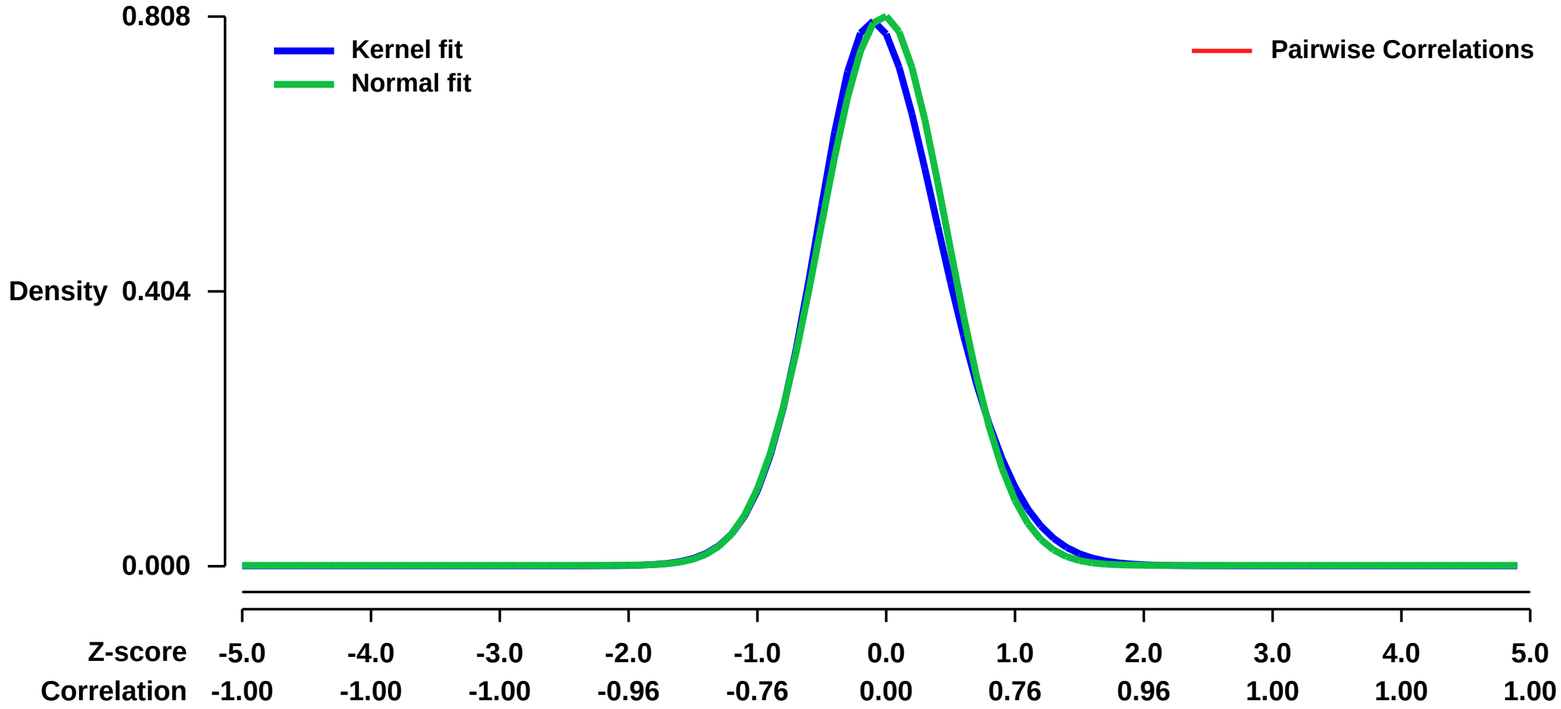

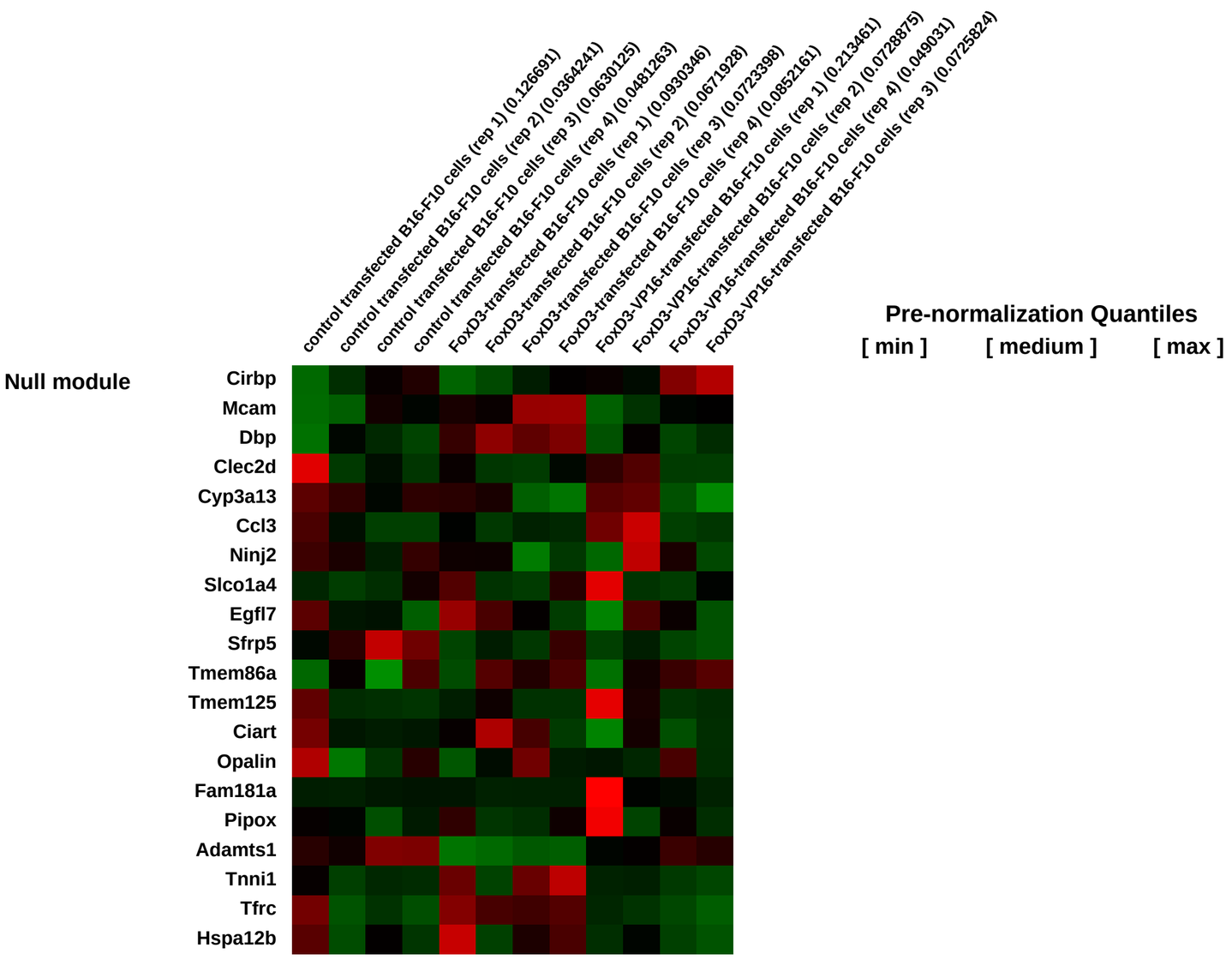

GEO Series "GSE41558" Expression Profiles

Num of samples in this series: 8

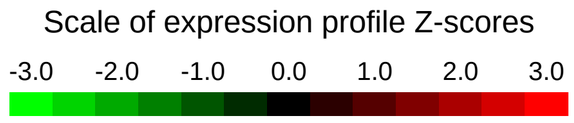

GEO Link:	http://www.ncbi.nlm.nih.gov/geo/query/acc.cgi?acc=GSE41558
Status:	Public on Oct 13 2012
Title:	SRC-2 Coactivator Deficiency Decreases Functional Reserve in Response to Pressure Overload of Mouse Heart
Organism:	Mus musculus
Experiment type:	Expression profiling by array
Platform:	GPL1261
Pubmed ID:	23300926
Summary & Design:	**Summary:** A major component of the cardiac stress response is the simultaneous activation of several gene regulatory networks. Interestingly, the transcriptional regulator steroid receptor coactivator-2, SRC-2 is often decreased during cardiac failure in humans. We postulated that SRC-2 suppression plays a mechanistic role in the stress response and that SRC-2 activity is an important regulator of the adult heart gene expression profile. Genome-wide microarray analysis, confirmed with targeted gene expression analyses revealed that genetic ablation of SRC-2 activates the â fetal gene programâ in adult mice as manifested by shifts in expression of a) metabolic and b) sarcomeric genes, as well as associated modulating transcription factors. While these gene expression changes were not accompanied by changes in left ventricular weight or cardiac function, imposition of transverse aortic constriction (TAC) predisposed SRC-2 knockout (KO) mice to stress-induced cardiac dysfunction. In addition, SRC-2 KO mice lacked the normal ventricular hypertrophic response as indicated through heart weight, left ventricular wall thickness, and blunted molecular signaling known to activate hypertrophy. Our results indicate that SRC-2 is involved in maintenance of the steady-state adult heart transcriptional profile, with its ablation inducing transcriptional changes that mimic a stressed heart. These results further suggest that SRC-2 deletion interferes with the timing and integration needed to respond efficiently to stress through disruption of metabolic and sarcomeric gene expression and hypertrophic signaling, the three key stress responsive pathways. **Overall design:** For microarray analysis, 250ng of RNA isolated from total heart (RNeasy kit, Qiagen) for each sample was labeled using the new standard Affymetrix linear amplification protocol using the 3' IVT Express Kit. This was reverse-transcribed and cRNA was produced and biotinylated via in vitro transcription. A hybridization cocktail containing Affymetrix spike-in controls and 15 ¸…g fragmented, labeled cRNA was loaded onto a GeneChip´fi Mouse 430 2.0 array. The array was hybridized for 16 hours at 45´ºC with rotation at 60 rpm then washed and stained with a strepavidin, R-phycoerythrin conjugate stain using the FS 450_0001 Fluidics protocol setting. Signal amplification was done using biotinylated antistreptavidin. The stained array was scanned on the Affymetrix GeneChip´fi Scanner 3000. The images were analyzed and quality control metrics recorded using Affymetrix Command Console v3. Experiments were run using Affymetrix MG 430 2.0 chip with 45,101 probesets representing 20,757 unique genes. There were 8 experiments in 2 groups: WT-unstressed â 4 experiments, and KO-unstressed â 4 experiments. QC parameters for all experiments were within the acceptable limits. We used the following software packages for data QC, statistical analysis and presentation of the results: Affymetrix Expression Console (www.affymetrix.com), Partek (www.partek.com), BRB Array Tools (linus.nci.nih.gov/BRB-ArrayTools.html), and dChip (biosun1.harvard.edu/complab/dchip). Expressions were estimated using the RMA (Multi-Array Analysis) method [38] with Partek software. Differentially expressed genes were found using the RVM (Random Variance Model) t-test, which is designed for small sample size experiments [39]. We used BRB Array Tools software, developed by Dr. Richard Simon and the BRB-ArrayTools Development Team. All genes were included in the comparison. For the genes represented by more than one probeset, we used the most highly expressed probeset. The cutoffs for differentially expressed genes were False Discovery Rate (FDR) = 0.05 [40].

Background corr dist: KL-Divergence = 0.0856, L1-Distance = 0.0220, L2-Distance = 0.0008, Normal std = 0.4644

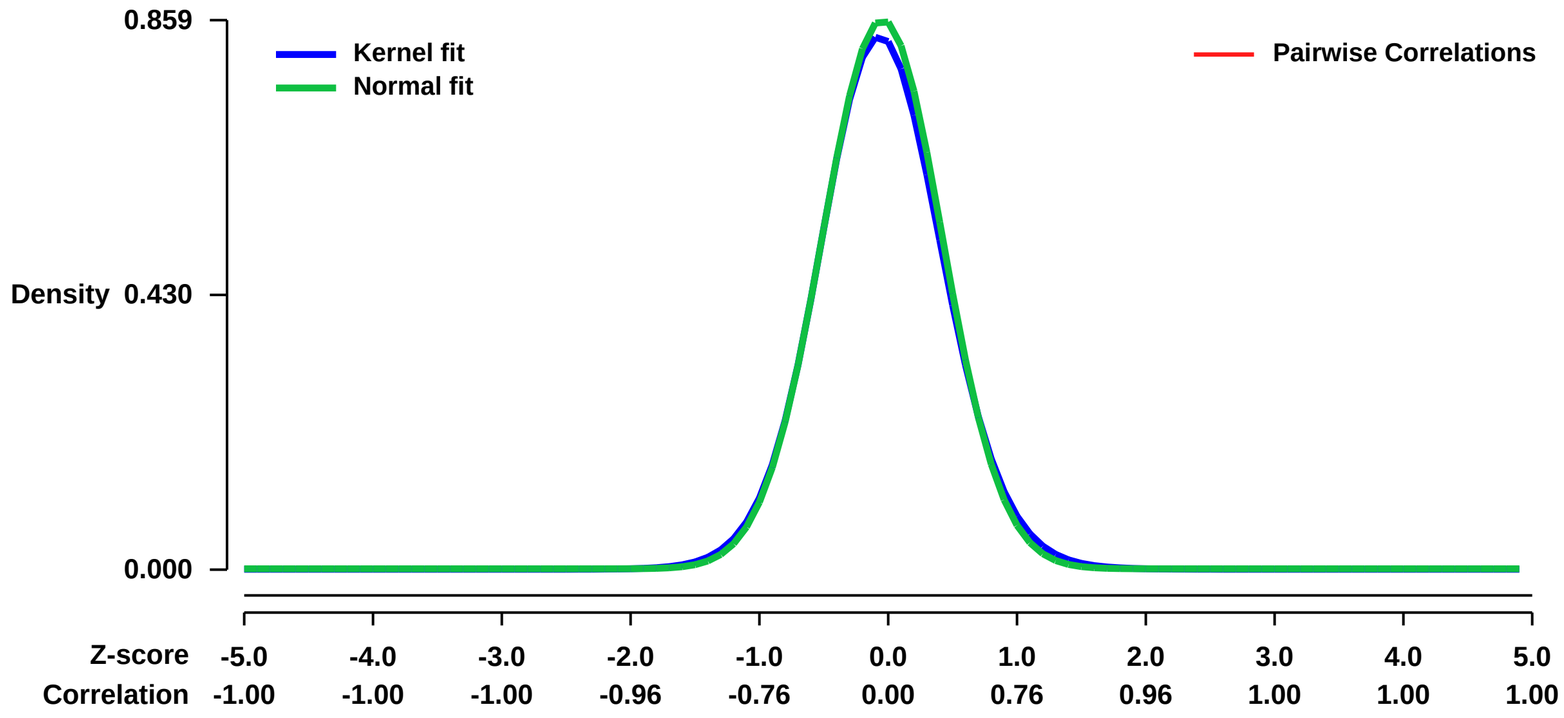

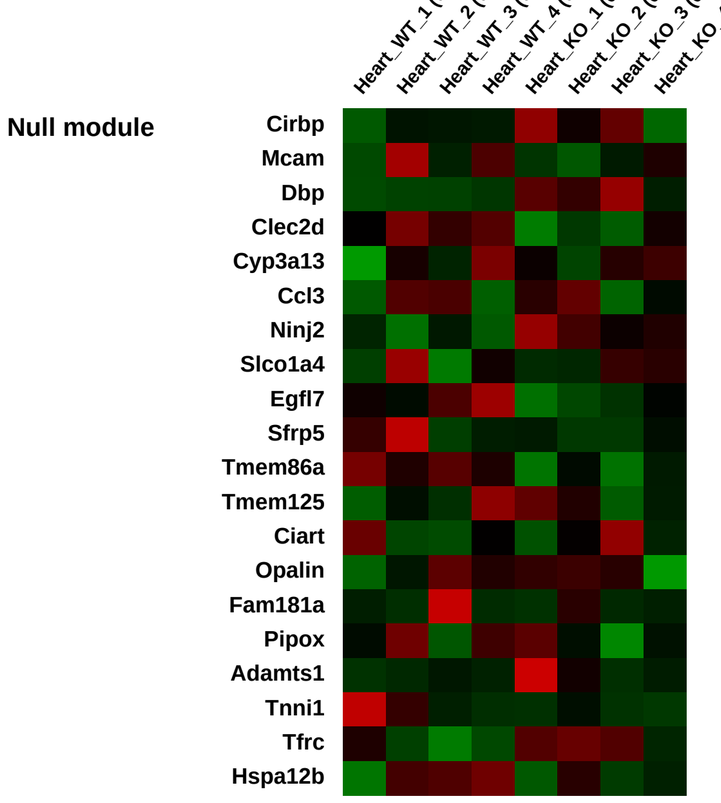

GEO Series "GSE29648" Expression Profiles

Num of samples in this series: 10

Scale of expression profile Z-scores

-3.0 -2.0 -1.0 0.0 1.0 2.0 3.0

GEO Link:	http://www.ncbi.nlm.nih.gov/geo/query/acc.cgi?acc=GSE29648
Status:	Public on Jun 02 2011
Title:	The impact of a phytoestrogen-rich diet on cardiac gene expression in the context of HCM
Organism:	Mus musculus
Experiment type:	Expression profiling by array
Platform:	GPL1261
Pubmed ID:	22778230
Summary & Design:	**Summary:** A soy diet worsens the progression of an inherited form of hypertrophic cardiomyopathy (HCM) in male mice when compared to casein-fed mice. Females are largely resistant to this diet effect and better preserve cardiac function. We hypothesized that the abundant phytoestrogens found in soy are mainly responsible for this diet-dependent phenotype. Indeed, feeding male mice a phytoestrogen-supplemented casein-based diet can recapitulate the negative outcome seen when male mice are fed a standard soy-based diet. To gain mechanistic insights into disease pathogenesis, we used Affymetrix microarrays to profile gene expression in left ventricular tissue from 2 month old HCM male and female mice as well as wild-type littermate controls. These mice were fed a phytoestrogen (genistein + daidzein)-supplemented casein-based diet. We identified a number of molecular pathways that could explain both the male and female phenotypes. **Overall design:** Hearts from male and female wild-type or HCM C57BL/6 mice fed a phytoestrogen-supplemented (genistein and daidzein mix) casein-based diet were excised at 2 months of age. Total RNA was extracted from left ventricles. Biotin-labeled amplified RNA was hybridized to Affymetrix Mouse Genome 430 2.0 microarrays.

Background corr dist: KL-Divergence = 0.0353, L1-Distance = 0.0826, L2-Distance = 0.0103, Normal std = 0.7445

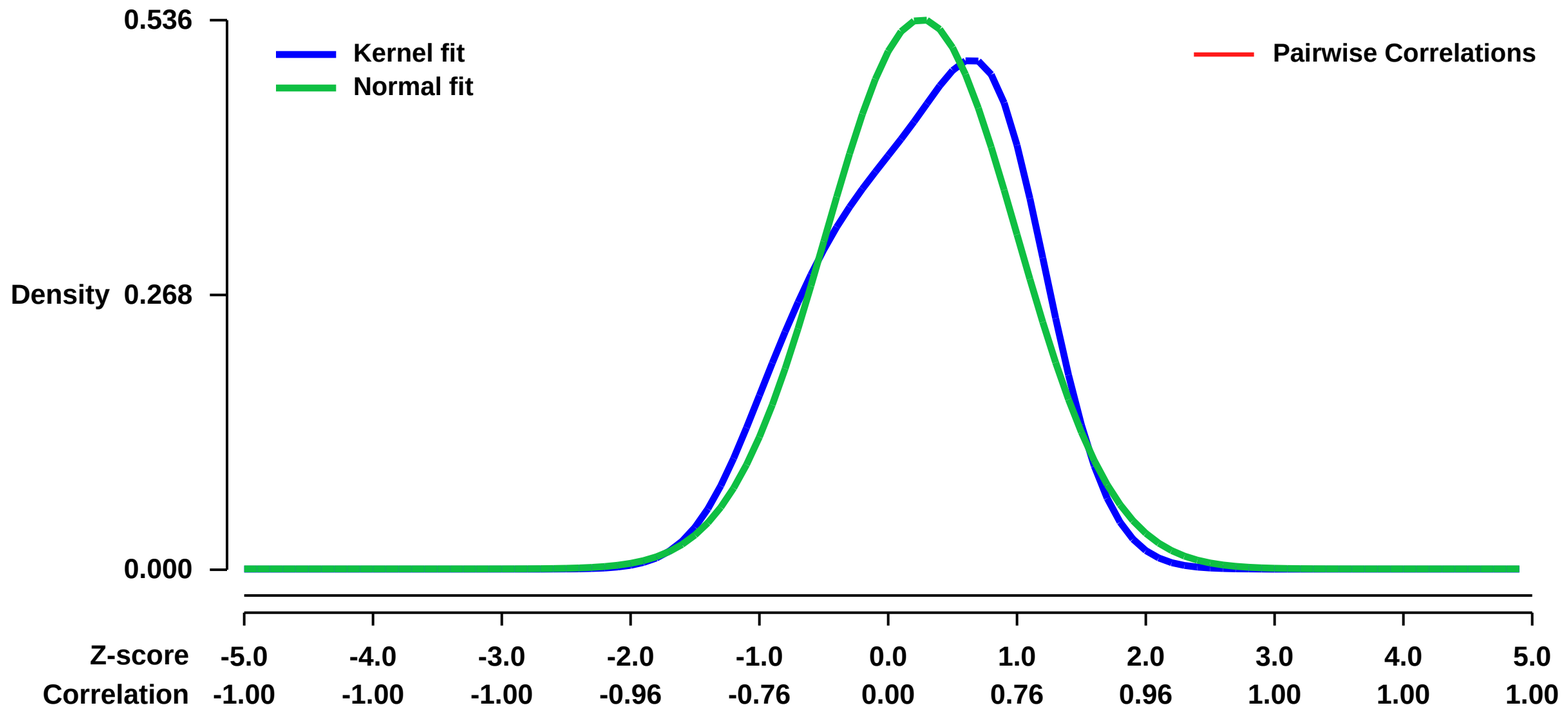

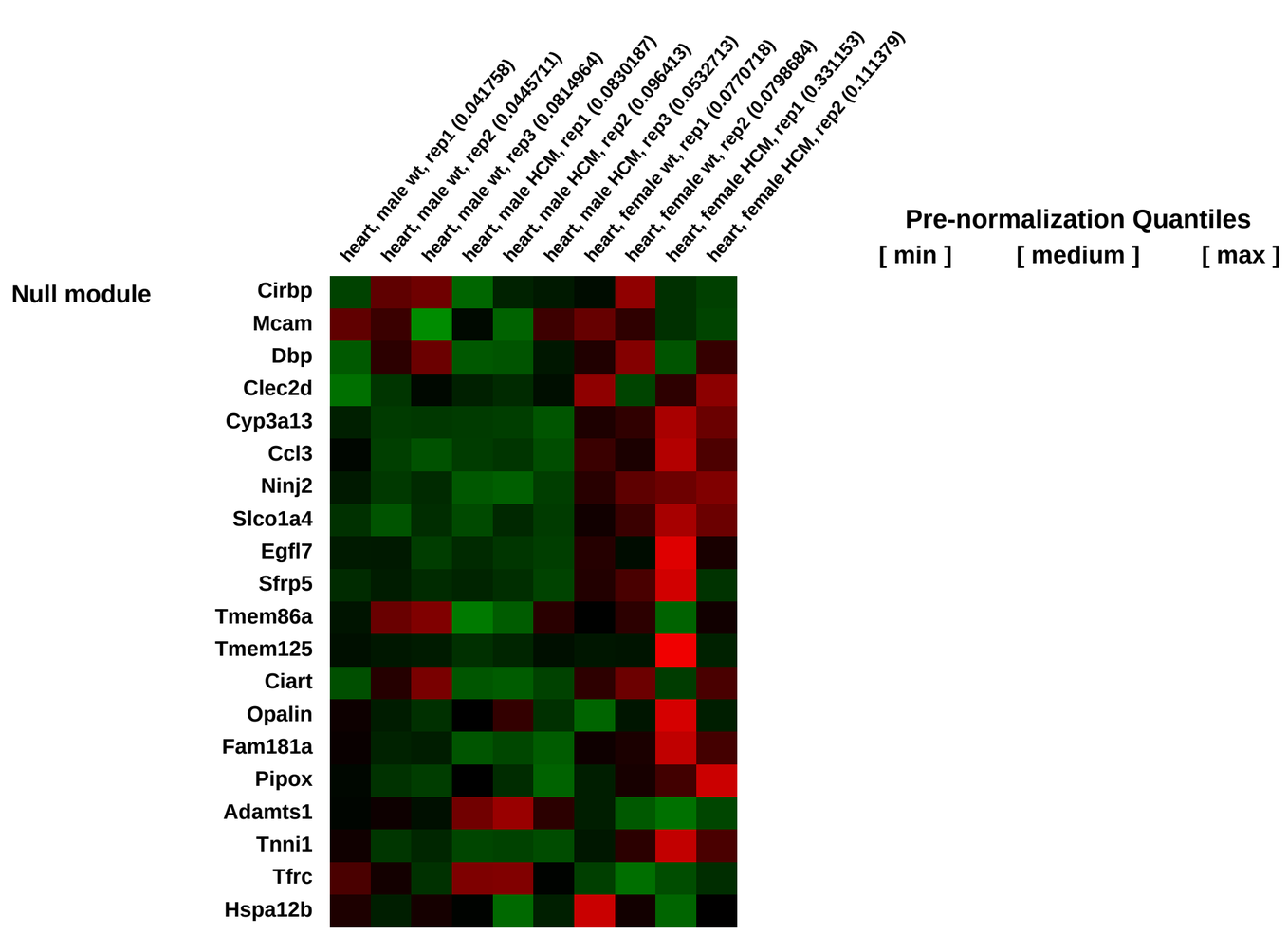

GEO Series "GSE11680" Expression Profiles

Num of samples in this series: 10

Scale of expression profile Z-scores

-3.0 -2.0 -1.0 0.0 1.0 2.0 3.0

GEO Link:	http://www.ncbi.nlm.nih.gov/geo/query/acc.cgi?acc=GSE11680
Status:	Public on Oct 08 2008
Title:	Gene expression differences between high and low exploratory genetically identical mice
Organism:	Mus musculus
Experiment type:	Expression profiling by array
Platform:	GPL1261
Pubmed ID:	18836535
Summary & Design:	**Summary:** Genetically identical inbred mice exhibit substantial stable individual variability in exploratory behavior. We used microarrays to look at gene expression differences in the hippocampus in female mice separated by stable differences in exploratory behavior **Overall design:** Balb c/J offspring were briefly separated from mothers for 15 minutes each morning on postnatal days 1-14 (handled group) or left undisturbed. At 8 weeks of age mice were tested in the open-field and light-dark behavioral paradigms to verify a handling-induced behavioral phenotype. 2 weeks after behavioral testing, animals were sacrificed and the CA1 region was microdissected. CA1 regions were stored at -20C in RNA later. RNA was extracted from 8 samples (4 handled and 4 non-handled) using Trizol. RNA was extracted from second group of animals (7 handled and 10 non-handled) using Qiagen RNA/DNA columns. All total RNA samples were double round amplied and labeled using standard Affymetrix protocols and hybridized to Mouse 430_2.0 arrays in parallel.

Background corr dist: KL-Divergence = 0.1115, L1-Distance = 0.0448, L2-Distance = 0.0044, Normal std = 0.4277

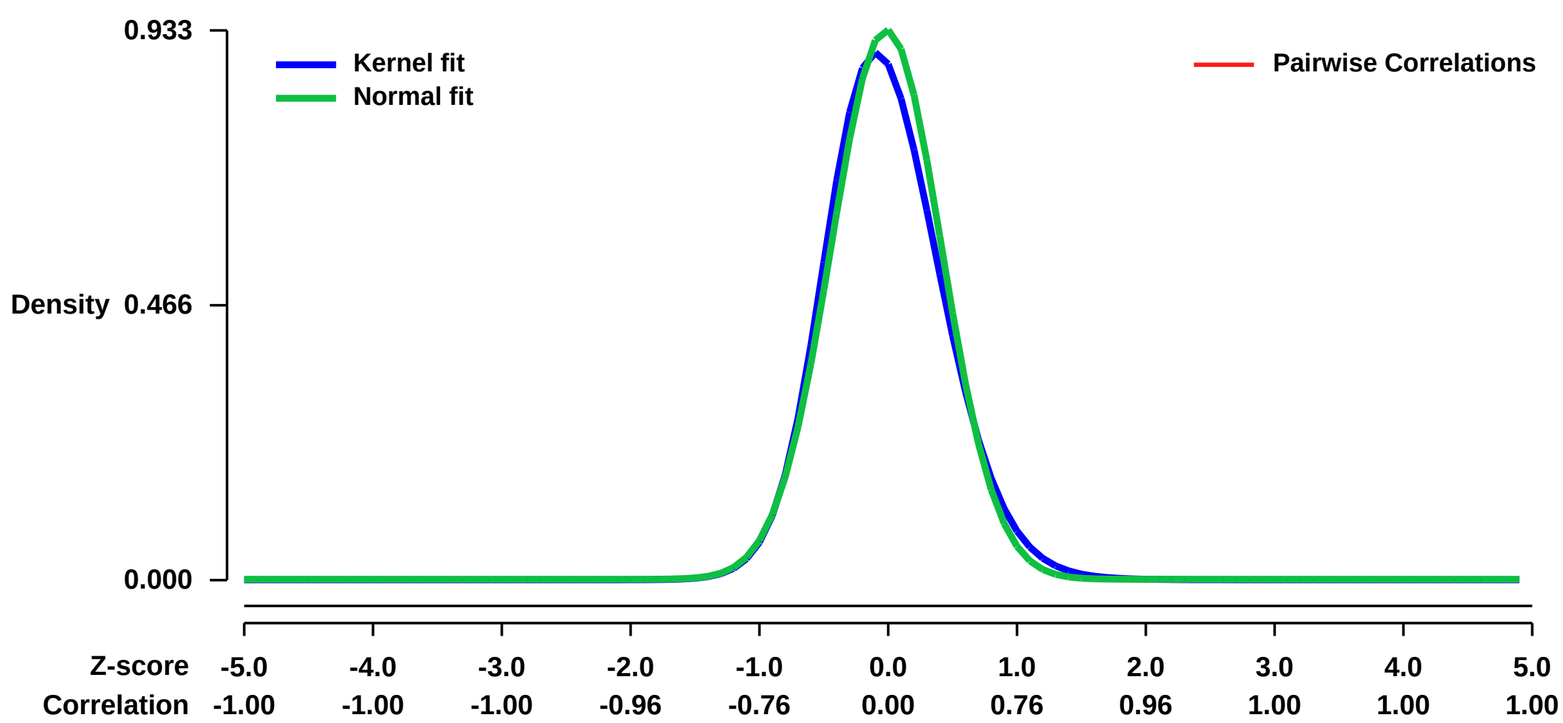

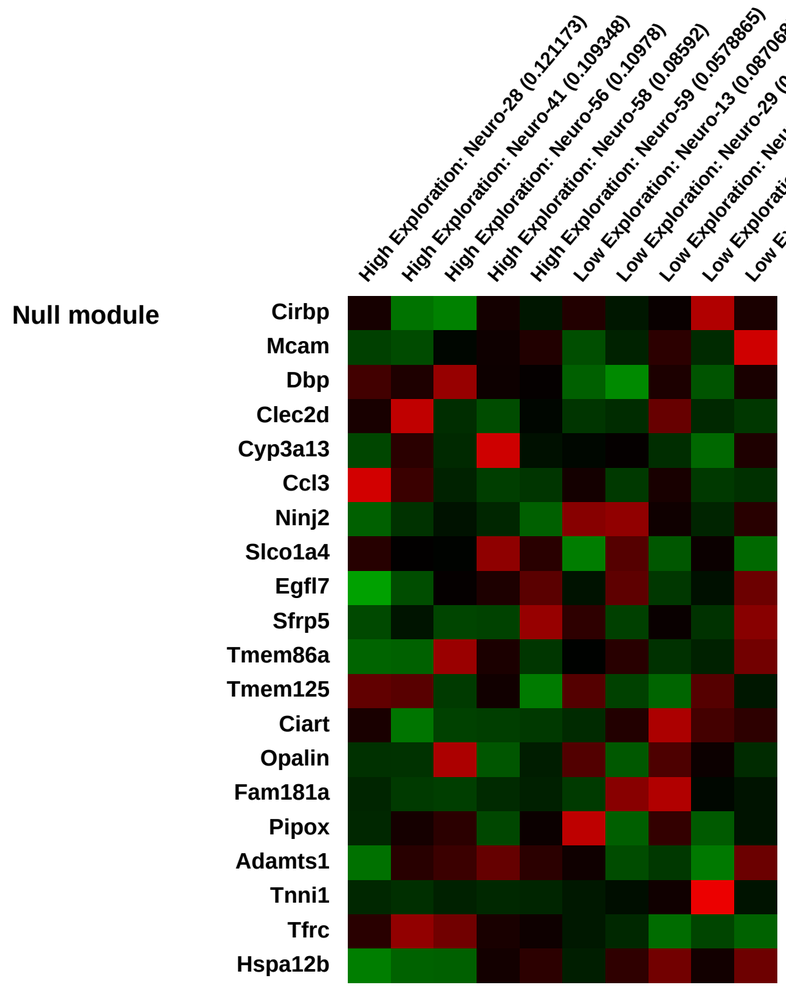

GEO Series "GSE22448" Expression Profiles

Num of samples in this series: 6

Scale of expression profile Z-scores

-3.0 -2.0 -1.0 0.0 1.0 2.0 3.0

GEO Link:	http://www.ncbi.nlm.nih.gov/geo/query/acc.cgi?acc=GSE22448
Status:	Public on Dec 22 2010
Title:	Gene expression data from wild-type and Nlrc5 knockout GM-CSF induced bone marrow dendritic cells infected with Newcastle Disease virus.
Organism:	Mus musculus
Experiment type:	Expression profiling by array
Platform:	GPL1261
Pubmed ID:	21148033
Summary & Design:	**Summary:** Nlrc5 is encoding a Nod-like receptor protein NLRC5/NOD27. To check the involvement of Nlrc5 in antiviral response, we examined gene expression profile in wild-type and Nlrc5 knockout GM-CSF bone marrow macrophage with using microarrays. **Overall design:** Bone marrow cells were cultured with GM-CSF and harvested on day 6. The induced dendritic cells were then stimulated with NDV at moi 1, collected at 0, 2, and 4 hours after infection. Total RNA was extracted and subjected to microarray experiment according to manufactures' instructions.

Background corr dist: KL-Divergence = 0.0228, L1-Distance = 0.0249, L2-Distance = 0.0011, Normal std = 0.7158

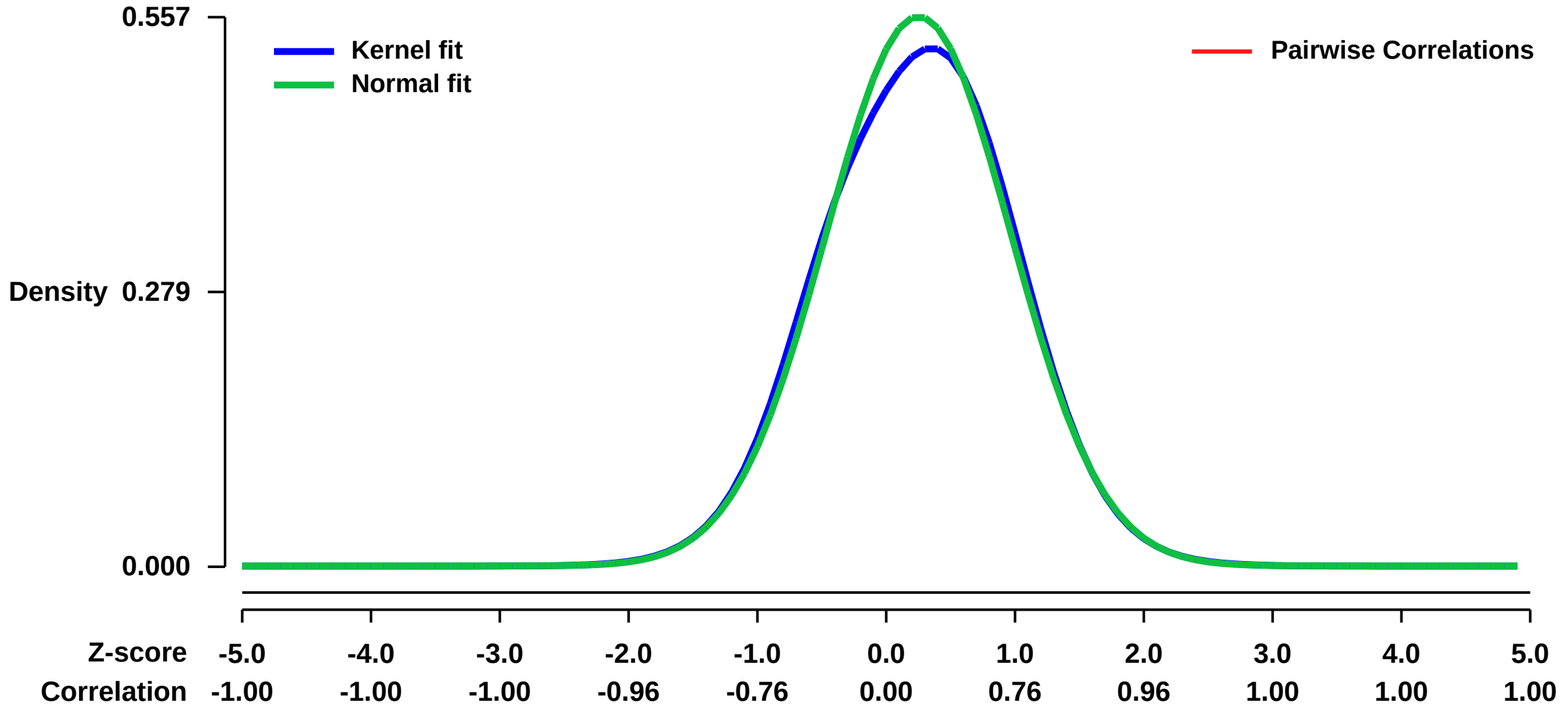

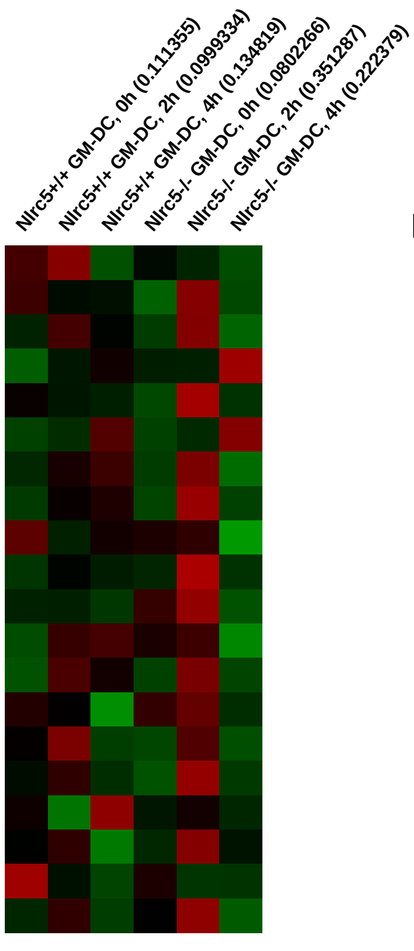

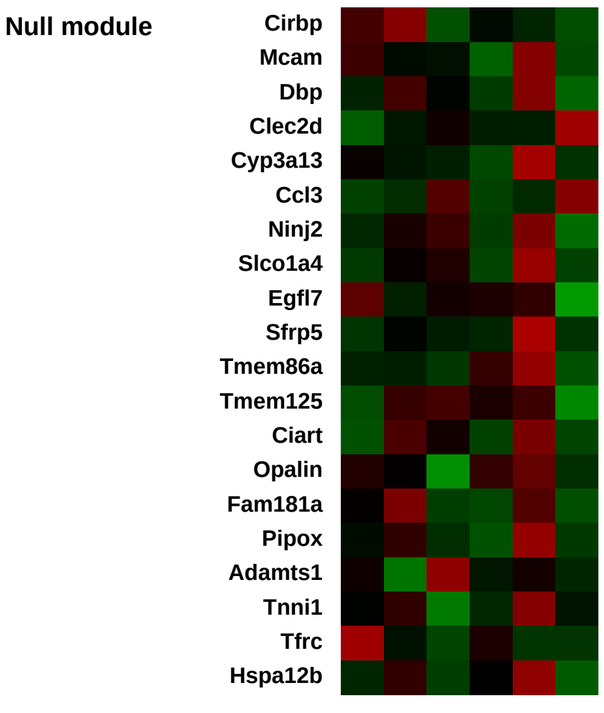

GEO Series "GSE3962" Expression Profiles

Num of samples in this series: 8

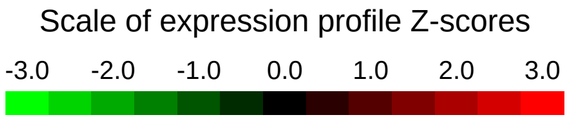

GEO Link:	**http://www.ncbi.nlm.nih.gov/geo/query/acc.cgi?acc=GSE3962**
Status:	**Public on Jun 30 2006**
Title:	**Mouse oocyte and one-cell embryo polysomal mRNA**
Organism:	**Mus musculus**
Experiment type:	**Expression profiling by array**
Platform:	**GPL1261**
Pubmed ID:	**16860309**
Summary & Design:	**Summary:** **Transcriptional activation in mammalian embryos occurs in a stepwise manner. In mice, it begins at the late one-cell stage, followed by a minor wave of activation at the early two-cell stage, and then the major genome activation (MGA) at the late two-cell stage. Cellular homeostasis, metabolism, cell cycle, and developmental events are orchestrated before MGA by time-dependent changes in the array of maternal transcripts being translated (i.e., the translatome). Despite the importance of maternal mRNA and its correct recruitment for development, neither the array of recruited mRNA nor the regulatory mechanisms operating have been well characterized. We present the first comprehensive analysis of changes in the maternal component of the zygotic translatome during the transition from oocyte to late one-cell stage embryo, revealing global transitions in the functional classes of translated maternal mRNAs, and apparent changes in the underlying cis-regulatory mechanisms.** **Keywords: Time course** **Overall design:** **Batches of 160-500 MII oocytes or one-cell embryos. 4 independent replicates per sample kind. Lysed and processed for polysomal mRNA extraction. Two rounds of IVT.**

Background corr dist: KL-Divergence = 0.0406, L1-Distance = 0.0621, L2-Distance = 0.0062, Normal std = 0.6589

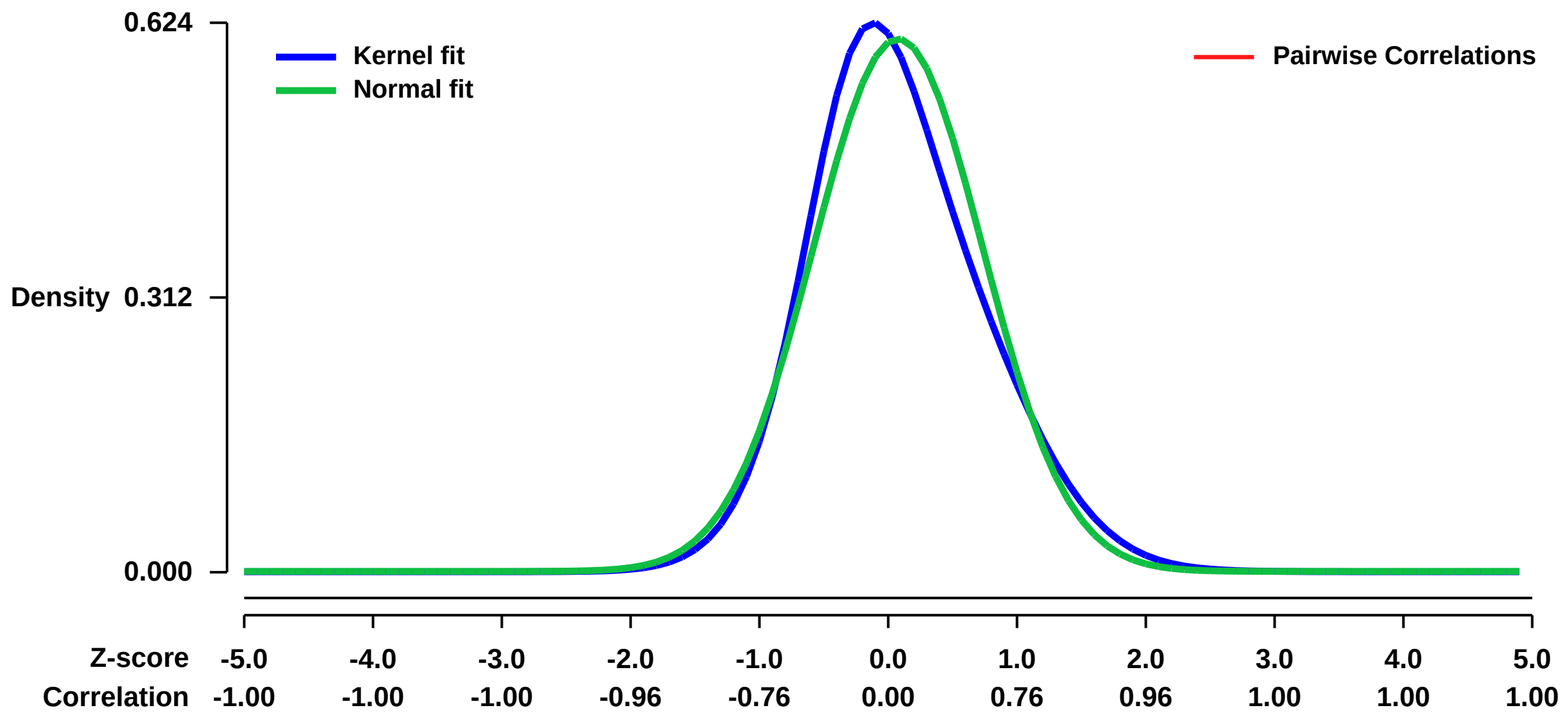

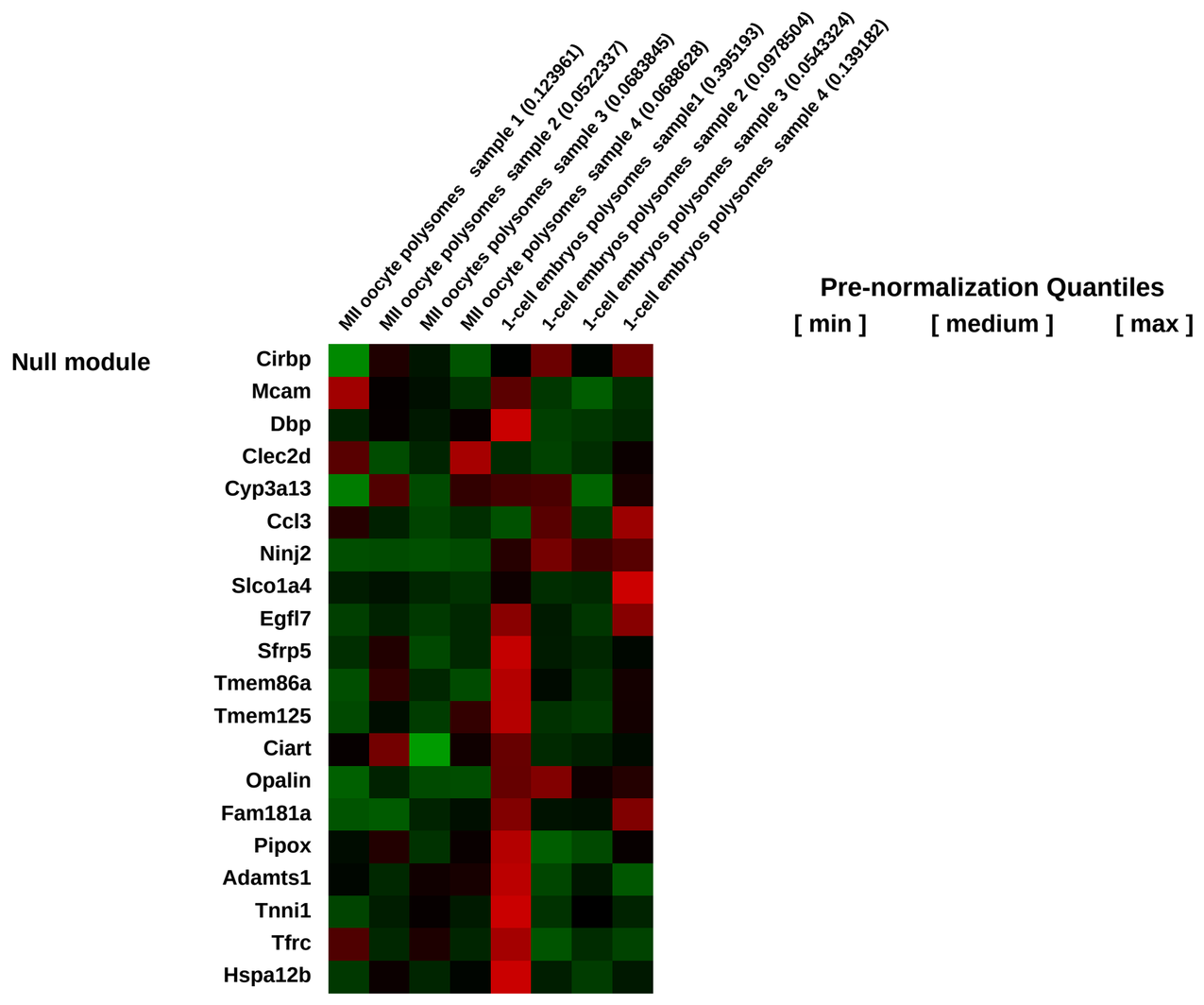

GEO Series "GSE28261" Expression Profiles

Num of samples in this series: 72

Scale of expression profile Z-scores

-3.0 -2.0 -1.0 0.0 1.0 2.0 3.0

GEO Link: http://www.ncbi.nlm.nih.gov/geo/query/acc.cgi?acc=GSE28261
Status: Public on Mar 30 2011
Title: Whole blood gene expression in female Balb/c mice following 2-week Pb exposure and subsequent 2-week recovery period
Organism: Mus musculus
Experiment type: Expression profiling by array
Platform: GPL1261
Pubmed ID:

Summary & Design:

Summary:
Background: Current evidence indicates that even low-level lead (Pb) exposure can have detrimental effects, especially in children. We tested the hypothesis that Pb exposure alters gene expression patterns in peripheral blood cells and that these changes reflect dose-specific alterations in the activity of particular pathways.

Methodology/Principal Finding: Using Affymetrix Mouse Genome 430 2.0 arrays, we examined gene expression changes in the peripheral blood of female Balb/c mice following exposure to per os lead acetate trihydrate or plain drinking water for two weeks and after a two-week recovery period. Data sets were RMA-normalized and dose-specific signatures were generated using established methods of supervised classification and binary regression. Pathway activity was analyzed using the ScoreSignatures module from GenePattern.

Conclusions/Significance: The low-level Pb signature was 93% sensitive and 100% specific in classifying samples a leave-one-out crossvalidation. The high-level Pb signature demonstrated 100% sensitivity and specificity in the leave-one-out crossvalidation. These two signatures exhibited dose-specificity in their ability to predict Pb exposure and had little overlap in terms of constituent genes. The signatures also seemed to reflect current levels of Pb exposure rather than past exposure. Finally, the two doses showed differential activation of cellular pathways. Low-level Pb exposure increased activity of the interferon-gamma pathway, whereas high-level Pb exposure increased activity of the E2F1 pathway.

Overall design:
We isolate total RNA from 72 mouse whole blood samples. These included samples following a 2-week exposure to lead acetate trihydrate (untreated controls = 7; Low Pb 5ug/mL drinking water = 15; High Pb 50ug/mL drinking water = 15) and additional samples following a 2-week recovery period with plain drinking water (untreated controls = 7; Low Pb group = 15; High Pb group = 13).

Background corr dist: KL-Divergence = 0.1437, L1-Distance = 0.0741, L2-Distance = 0.0158, Normal std = 0.3837

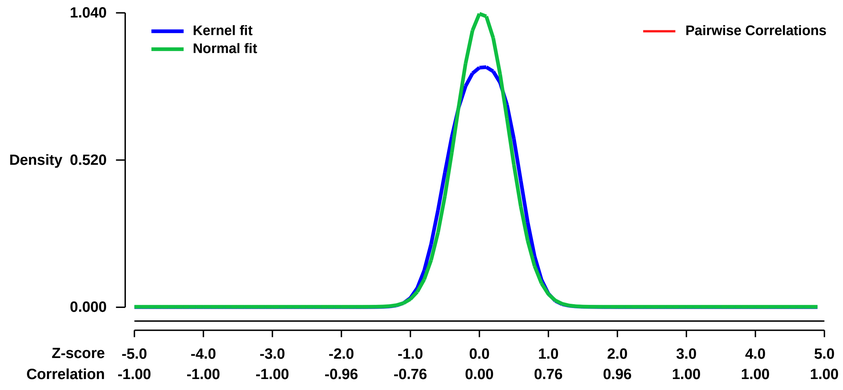

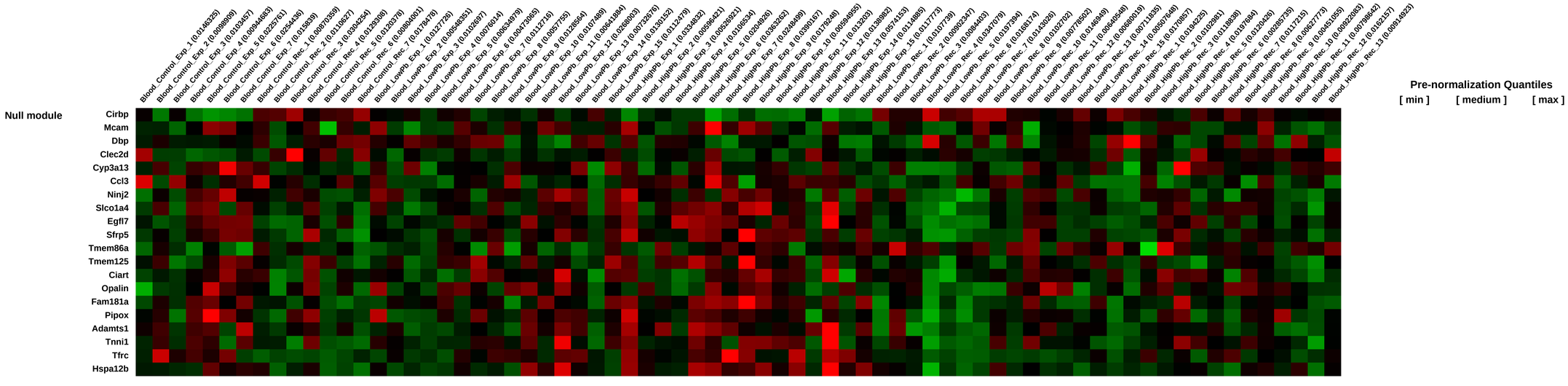

GEO Series "GSE4749" Expression Profiles

Num of samples in this series: 6

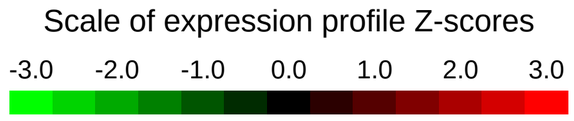

GEO Link:	**http://www.ncbi.nlm.nih.gov/geo/query/acc.cgi?acc=GSE4749**
Status:	**Public on Feb 20 2008**
Title:	**Microarray based comparison of gene expression in stria vascularis of 129S6 mice lacking slc26a4 and wildtype controls**
Organism:	**Mus musculus**
Experiment type:	**Expression profiling by array**
Platform:	**GPL1261**
Pubmed ID:	**17187680**
Summary & Design:	**Summary:** **To see for differential expression of genes in the stria vascularis of wild type and pendrin knockout mice** **Keywords: Knockout vs Control** **Overall design:** **Six samples in total of stria vascularis RNA were analyzed. Triplicates from wild type and pendrin knockout mice were run and analyzed.**

Background corr dist: **KL-Divergence = 0.0292, L1-Distance = 0.0187, L2-Distance = 0.0004, Normal std = 0.6723**

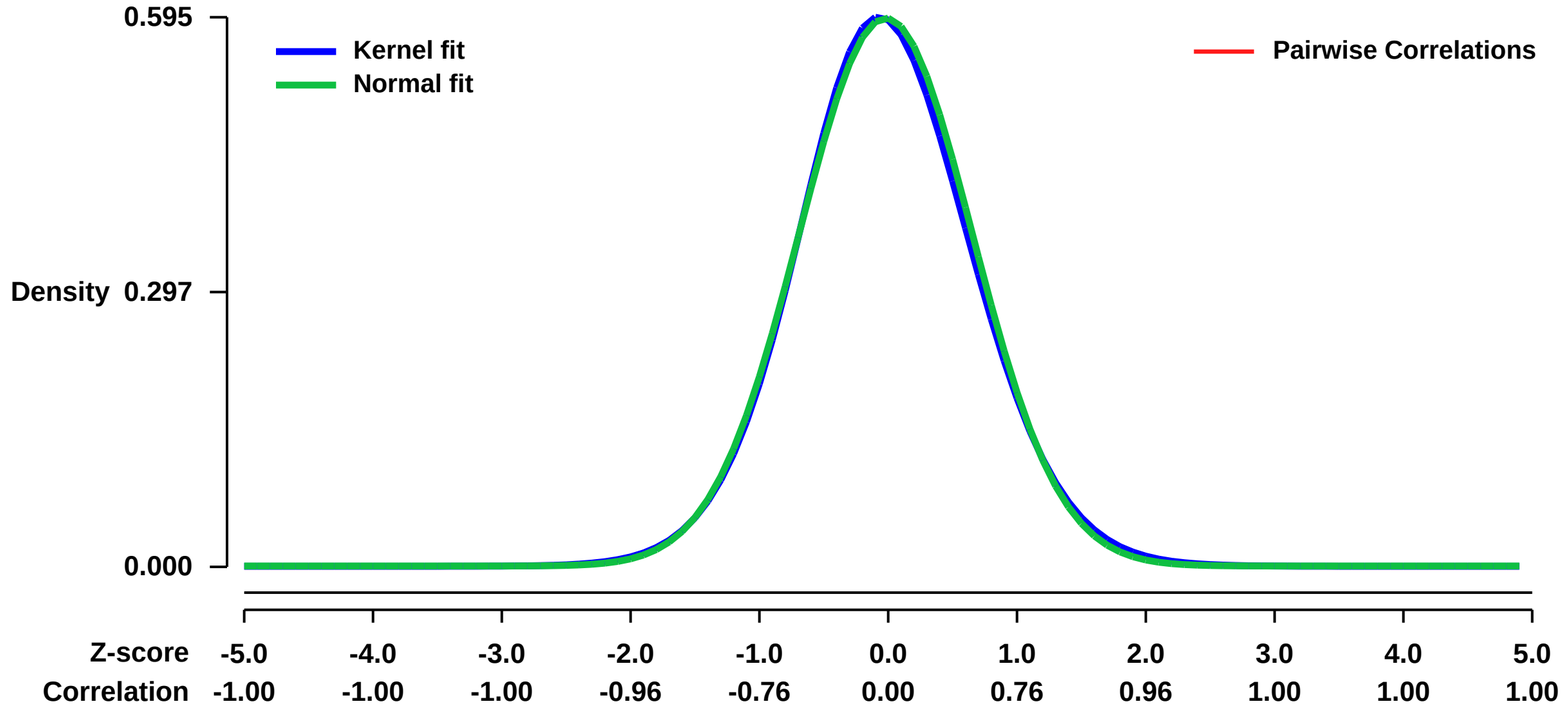

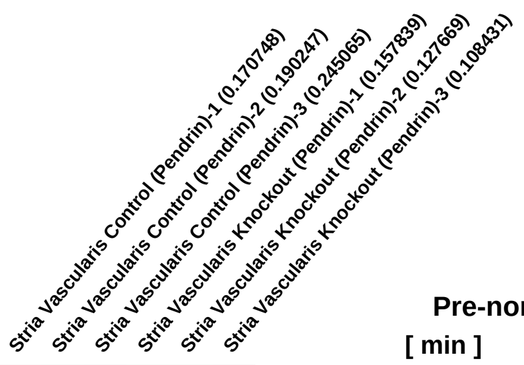

Pre-normalization Quantiles

[min] [medium] [max]

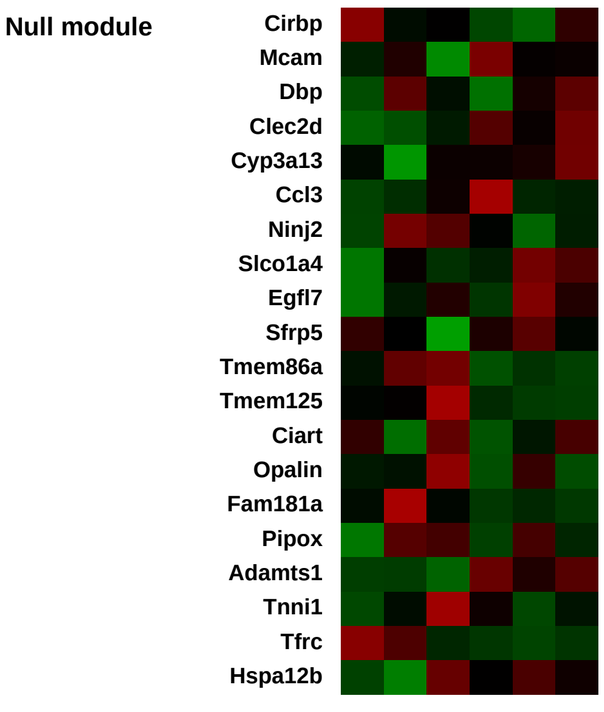

GEO Series "GSE5959" Expression Profiles

Num of samples in this series: 6

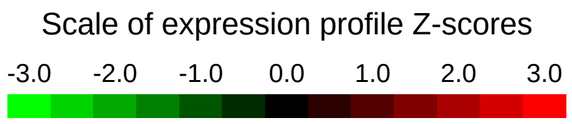

GEO Link:	http://www.ncbi.nlm.nih.gov/geo/query/acc.cgi?acc=GSE5959
Status:	Public on Oct 29 2006
Title:	Expression differences in the liver of a congenic mouse with low serum IGF-1
Organism:	Mus musculus
Experiment type:	Expression profiling by array
Platform:	GPL1261
Pubmed ID:	17584978
Summary & Design:	**Summary:** Several studies have shown that bone mineral density (BMD), a clinically measurable predictor of osteoporotic fracture, is the sum of genetic and environmental influences. In addition, serum IGF-1 levels have been correlated to both BMD and fracture risk. We previously identified a Quantitative Trait Locus (QTL) for Bone Mineral Density (BMD) on mouse Chromosome (Chr) 6 that overlaps a QTL for serum IGF-1. The B6.C3H-6T (6T) congenic mouse is homozygous for C57BL/6J (B6) alleles across the genome except for a 30 cM region on Chr 6 that is homozygous for C3H/HeJ (C3H) alleles. This mouse was created to study biology behind both the BMD and the serum IGF-1 QTLs and to identify the gene(s) underlying these QTLs. Female 6T mice have lower BMD and lower serum IGF-1 levels at all ages measured. As the liver is the major source of serum IGF-1, we examined differential expression in the livers of fasted female B6 and 6T mice by microarray. **Keywords:** Genetic variation **Overall design:** The experimental design of this experiment was a simple two-factor experiment, with three biological replicates of each factor (in this case mouse strain, B6.C3H-6T vs. C57BL/6J). Each sample represented one mouse; no samples were pooled. No technical replicated were done.

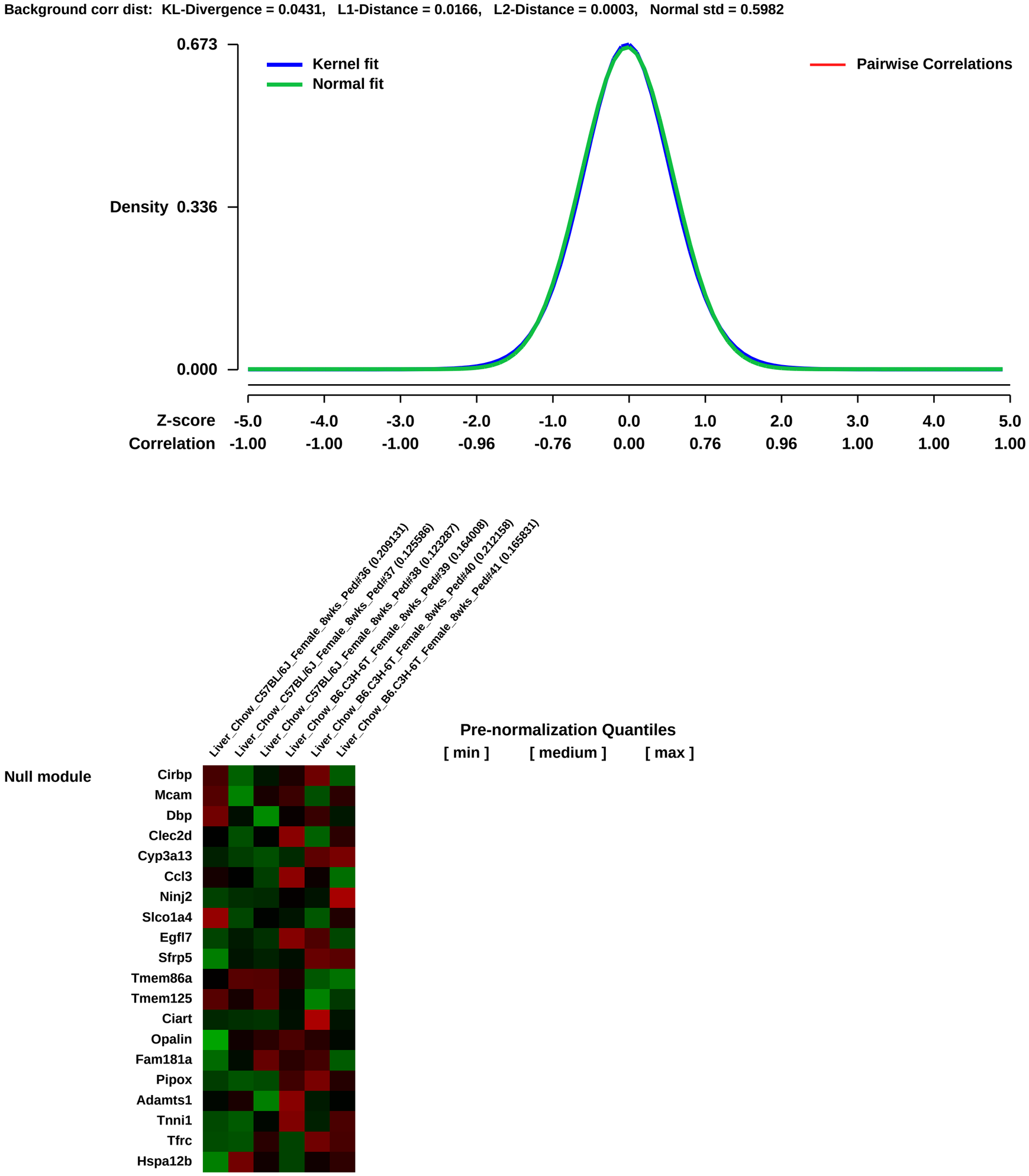

GEO Series "GSE40284" Expression Profiles

Num of samples in this series: 6

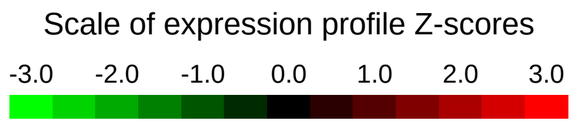

GEO Link:	http://www.ncbi.nlm.nih.gov/geo/query/acc.cgi?acc=GSE40284
Status:	Public on Jun 25 2013
Title:	Gene expression data of Lsd1fl/fl and Lsd1fl/fl Mx1Cre CD150+ CD48- lin- c-Kit+ Sca-1+ LT-HSCs
Organism:	Mus musculus
Experiment type:	Expression profiling by array
Platform:	GPL1261
Pubmed ID:	23795291
Summary & Design:	**Summary:** We discovered that mice that lack Lsd1 in hematopoietic cells were exhibited increased frequencies of CD150+ CD48- lin- c-Kit+ Sca-1+ LT-HSCs, but completely lacked the lin- c-Kit+ Sca-1- myeloid progenitor compartment. To determine the genes altered by Lsd1-loss, CD150+ CD48- lin- c-Kit+ Sca-1+ LT-HSCs from Lsd1fl/fl and Lsd1fl/fl Mx1Cre mice were FACS-purified to be analyzed by gene expression profiling. **Overall design:** Primary CD150+ CD48- lin- c-Kit+ Sca-1+ LT-HSCs were isolated by FACS-sorting, from the bone marrow of Lsd1fl/fl and Lsd1fl/fl Mx1Cre animals, one week after the final p(I:C) dose. Total RNA from three biological replicates per genotype was extracted with the RNeasy Micro Kit (QIAGEN), treated with DNaseI, reverse transcribed. RNA extracted from CD150+ CD48- lin- c-Kit+ Sca-1+ cells was amplified with the Ovation Pico WTA RNA Amplification System 2 (NuGEN Technologies). Single-stranded cDNA amplification products were purified using QIAquick PCR Purification Kit (QIAGEN) and labeled with the FL-Ovation cDNA Biotin Module V2 (NuGEN). The Biotin-labeled cDNA was used to hybridize to Affymetrix expression arrays using the Mouse Genome 430 2.0 array platform. Primary CD150+ CD48- lin- c-Kit+ Sca-1+ LT-HSCs were isolated by FACS-sorting, from the bone marrow of Lsd1fl/fl and Lsd1fl/fl Mx1Cre animals, one week after the final p(I:C) dose. Total RNA from three biological replicates per genotype was extracted with the RNeasy Micro Kit (QIAGEN), treated with DNaseI, reverse transcribed. RNA extracted from CD150+ CD48- lin- c-Kit+ Sca-1+ cells was amplified with the Ovation Pico WTA RNA Amplification System 2 (NuGEN Technologies). Single-stranded cDNA amplification products were purified using QIAquick PCR Purification Kit (QIAGEN) and labeled with the FL-Ovation cDNA Biotin Module V2 (NuGEN). The Biotin-labeled cDNA was used to hybridize to Affymetrix expression arrays using the Mouse Genome 430 2.0 array platform.

Background corr dist: KL-Divergence = 0.0508, L1-Distance = 0.0643, L2-Distance = 0.0068, Normal std = 0.6243

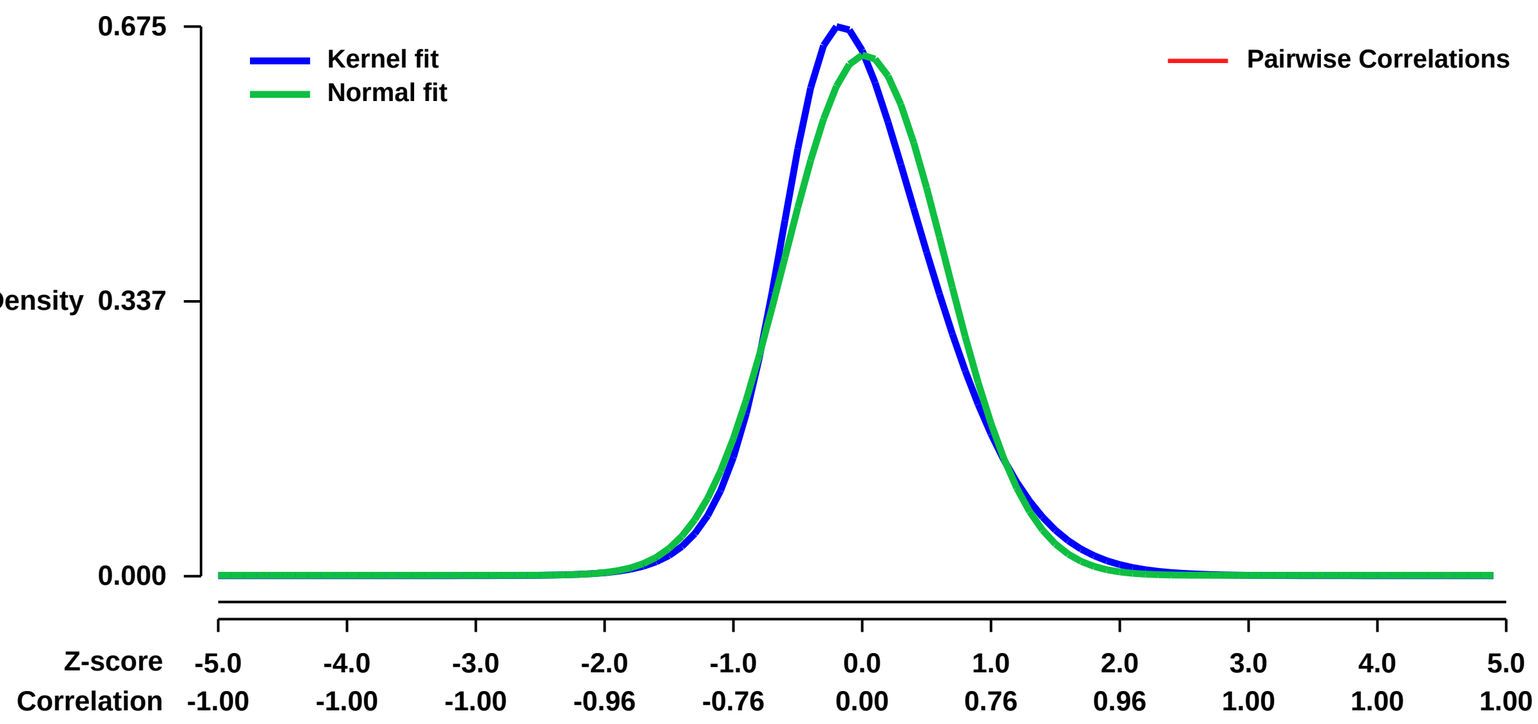

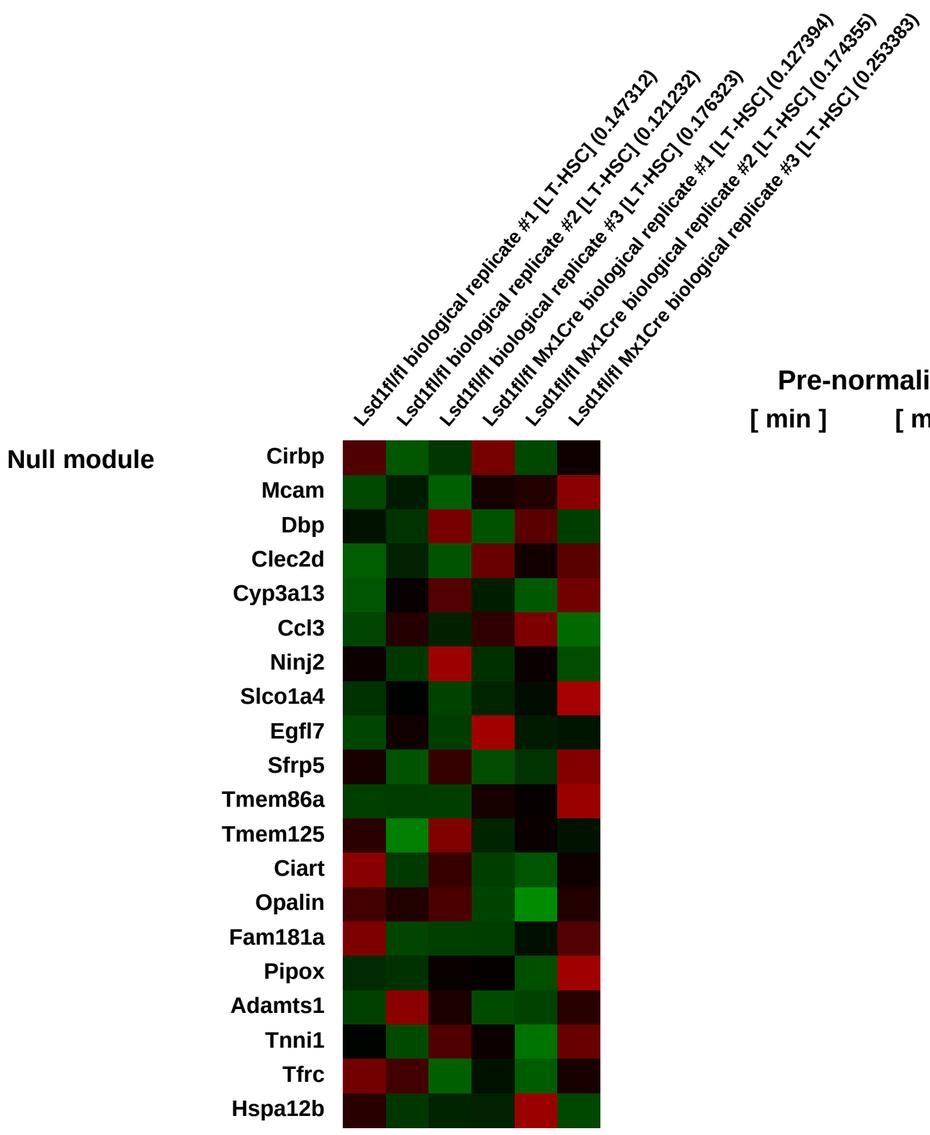

GEO Series "GSE33726" Expression Profiles

Num of samples in this series: 48

Scale of expression profile Z-scores

-3.0 -2.0 -1.0 0.0 1.0 2.0 3.0

GEO Link:	http://www.ncbi.nlm.nih.gov/geo/query/acc.cgi?acc=GSE33726
Status:	Public on Dec 01 2012
Title:	The circadian clock coordinates ribosome biogenesis.
Organism:	Mus musculus
Experiment type:	Expression profiling by array
Platform:	GPL1261
Pubmed ID:	23300384
Summary & Design:	**Summary:** Evolutionary conserved biological rhythms play a fundamental role in the physiology and behavior of all light-sensitive organisms. Generation of rhythmic expression of clock-controlled genes is orchestrated by a molecular circadian clock constitutes by interconnected negative feedback loops of transcription factors. In this study, we want to characterize gene which also present a rhythmic translation through the characterization of genes with a rhythmic polysomal/total RNA ratio. **Overall design:** Analyze of gene expression in liver total RNA and polysomal RNA harvested every 2 hrs during 2 series of 48 hrs, 2 mice per samples

Background corr dist: KL-Divergence = 0.2369, L1-Distance = 0.0556, L2-Distance = 0.0060, Normal std = 0.3249

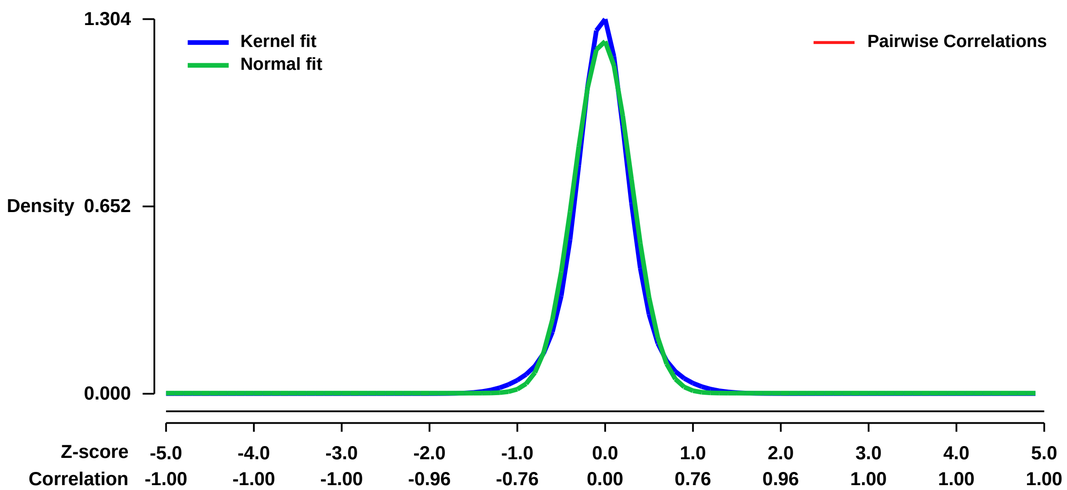

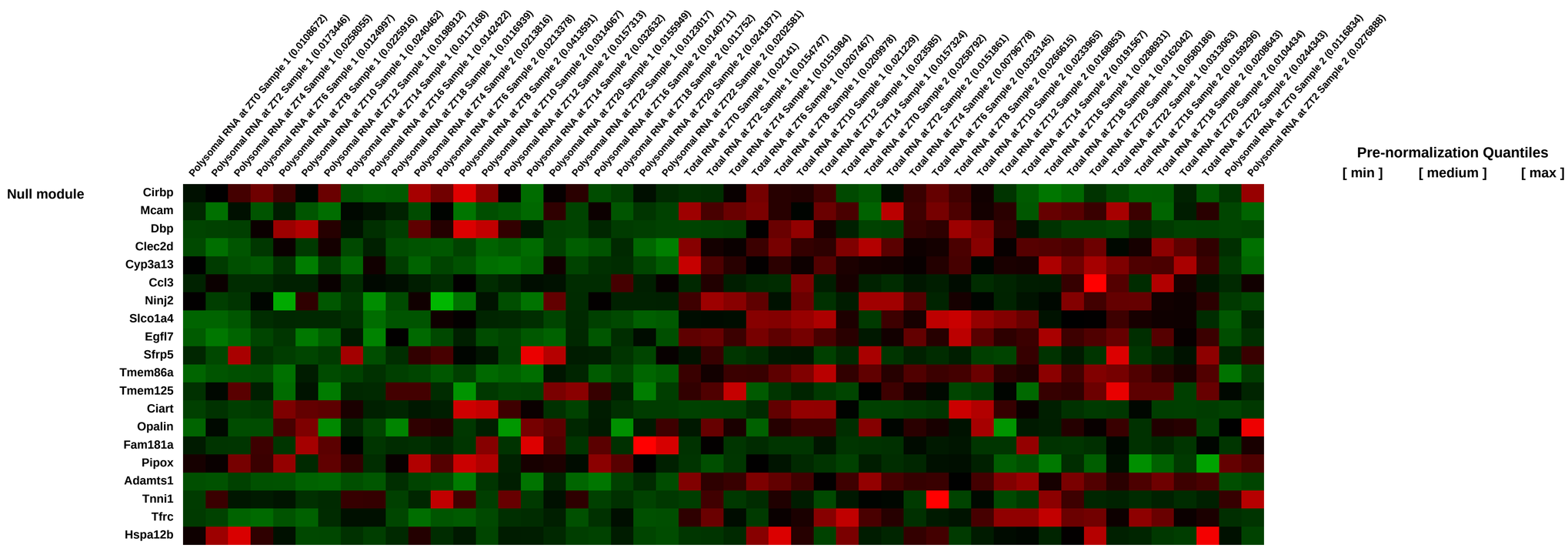

GEO Series "GSE28025" Expression Profiles

Num of samples in this series: 18

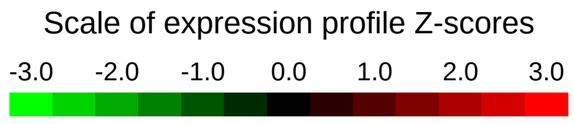

GEO Link:	**http://www.ncbi.nlm.nih.gov/geo/query/acc.cgi?acc=GSE28025**
Status:	**Public on Oct 19 2011**
Title:	**Comparative gene expression analysis of repro9/repro9 and wild type testes from 14 and 17 day mice**
Organism:	**Mus musculus**
Experiment type:	**Expression profiling by array**
Platform:	**GPL1261**
Pubmed ID:	**21750041**

Summary & Design:

Summary:
Repro9 in an allele of Mybl1 (A-Myb) transcription factor obtained in ENU screen to identify alleles causing mouse infertility. Repro9/repro9 mutant males are infertile due to meiotic arrest at pachytene stage. Mutants show wide range of abnormalities including inefficient chromosome synapsis, sex body formation and progression through meiotic cycle. Females are unaffected. To determine genes transcriptionally regulated by MYBL1 we analyzed gene expression profiles of wild type and repro9/repro9 mutant testis at 14 and 17 days postpartum. Analysis revealed many misregulated genes, in majority downregulated, at day 14 pp and even more at day 17 pp, probably due to secondary effects of meiotic arrest. Significantly misregulated genes were characterized by Gene Ontology. Comparative gene expression analysis uncovered potential targets of MYBL1 regulation that play roles in regulation of transcription, cell cycle, apoptosis, protein phosphorylation and ubiquitination, chromosome organization and others.

Abstract:The transcriptional regulation of mammalian meiosis is poorly characterized, due to few genetic and ex vivo models. From a genetic screen, we identify the transcription factor MYBL1 as a male-specific master regulator of several critical meiotic processes. Spermatocytes bearing a novel separation-of-function allele (Mybl1repro9) had subtle defects in autosome synapsis in pachynema, a high incidence of unsynapsed sex chromosomes, incomplete double strand break (DSB) repair on synapsed pachytene chromosomes, and a lack of crossing-over. MYBL1 protein appears in pachynema, and its mutation caused specific alterations in expression of diverse genes, including some translated postmeiotically. These data, coupled with chromatin immunoprecipitation (ChIP-chip) experiments and bioinformatic analysis of promoters, identified direct targets of MYBL1 regulation. Meiosis in mutant females appears unaffected. These results reveal that MYBL1 is a master regulator of meiotic genes that are involved in multiple processes in spermatocytes, including chromosome synapsis, recombination, and cell cycle progression through pachynema.

Overall design:
RNA was extracted from wt and repro9/repro9 mutant testis from 14 and 17 days old mice. This two time points were selected for sample enrichment in early/midpachytene and latepachytene/diplotene spermatocytes, respectively. Total testis RNA from wild-type (â¥3) and mutant (â¥3) mice was reverse-transcribed into double stranded cDNA, and biotin-labeled cRNA (GeneChip IVT labeling kit, Affymetrix, Santa Clara, CA) was hybridized to Affymetrix mouse genome 430 2.0 GeneChips containing. The raw data was processed using Affymetrix GCOS software. Two-way ANOVA analysis resolved differentially expressed (DE) genes either between genotypes and/or days using MeV(version 4.6.1) on log2-transformed expression values. Results were multiple test corrected with the Benjamini-Hochberg method to control the false discovery rate (FDR) in R. ~800 genes significant at FDR<=0.025 were selected as differentially expressed for downstream analysis.

Background corr dist: KL-Divergence = 0.0601, L1-Distance = 0.0440, L2-Distance = 0.0033, Normal std = 0.5461

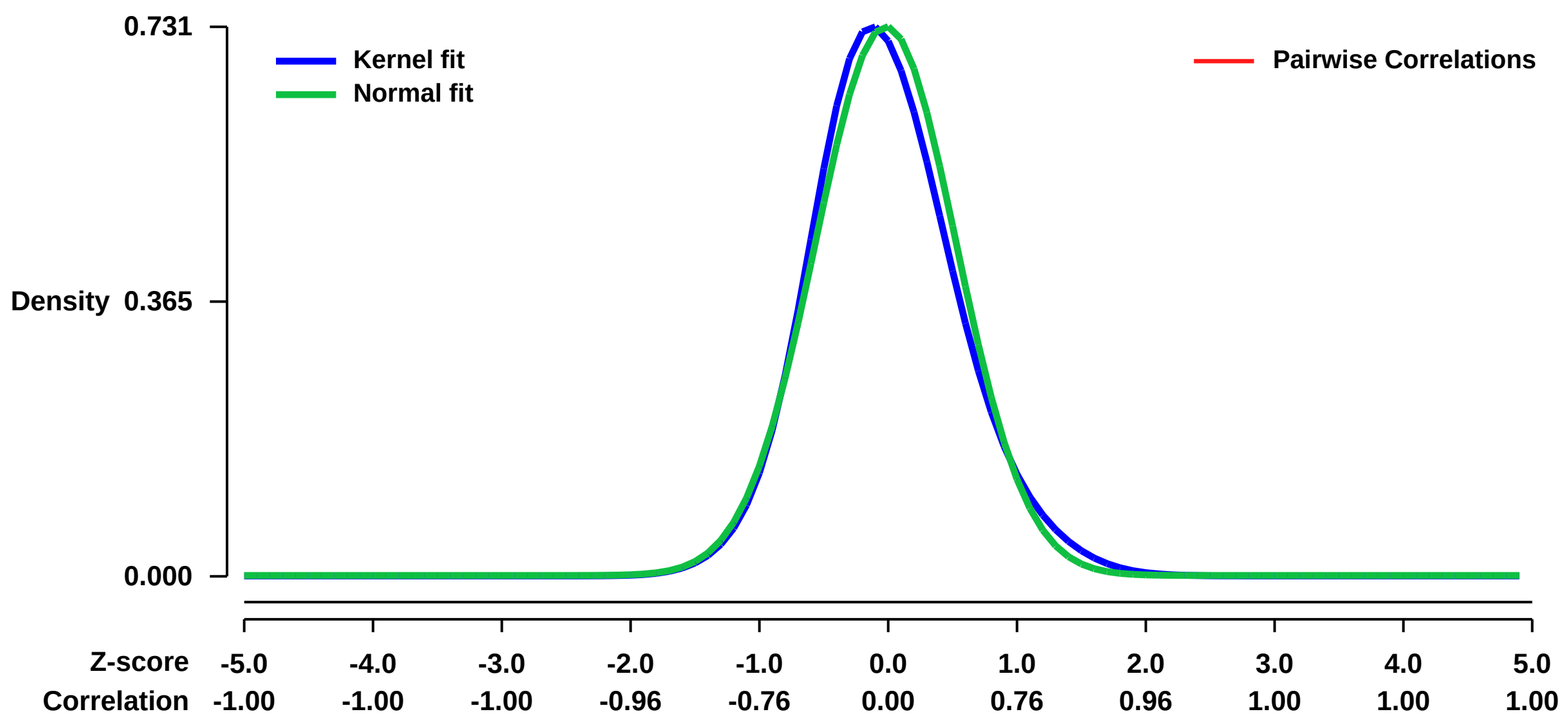

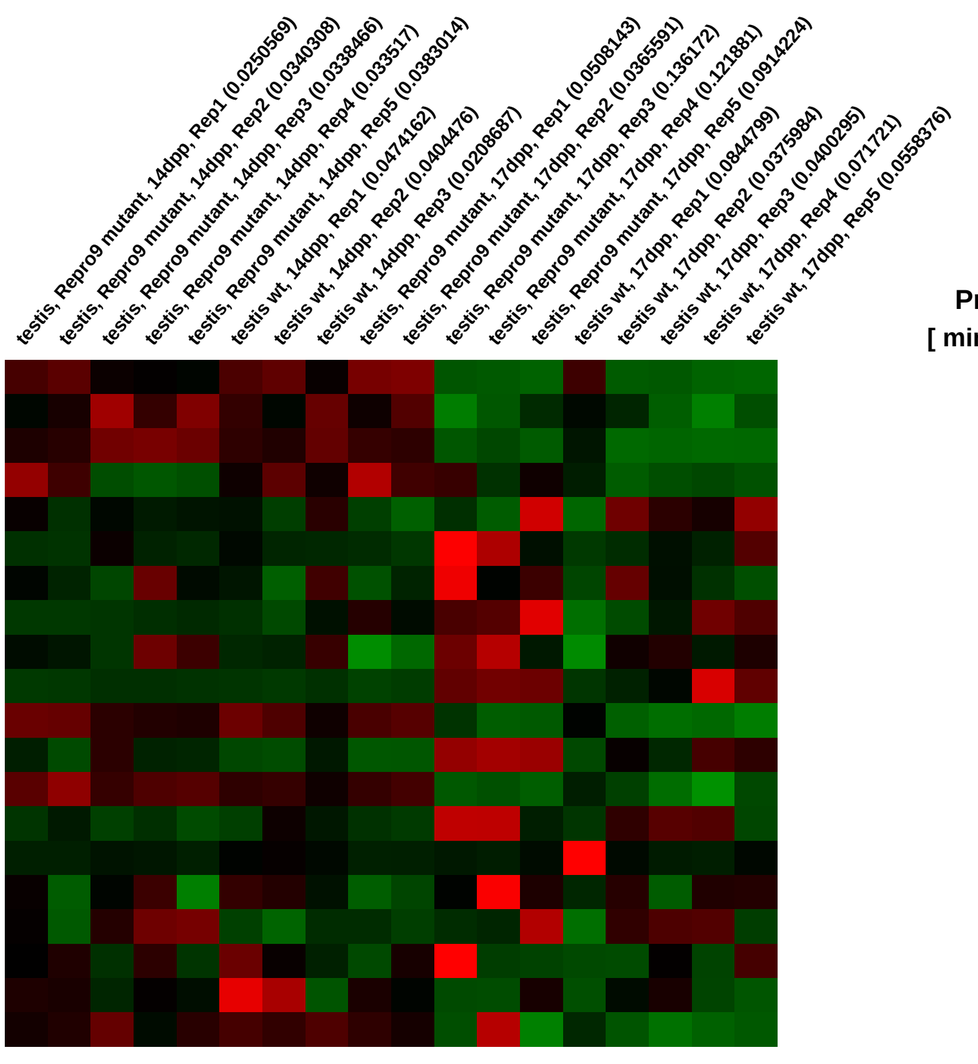

GEO Series "GSE43145" Expression Profiles

Num of samples in this series: 12

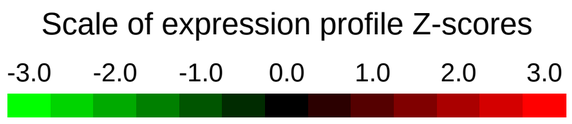

GEO Link:	**http://www.ncbi.nlm.nih.gov/geo/query/acc.cgi?acc=GSE43145**
Status:	**Public on Dec 27 2012**
Title:	**Expression data of mouse gastric tumors (TNF KO-Gan and BALB/c-Gan mice)**
Organism:	**Mus musculus**
Experiment type:	**Expression profiling by array**
Platform:	**GPL1261**
Pubmed ID:	
Summary & Design:	**Summary:** **Gan mice express Wnt1, Ptgs2, and Ptges, which develop inflammation-associated gastric tumors (Oshima et al, Gastroenterology 131: 1086, 2006). We examined the role of TNF-alpha in tumorigenesis by construction of TNF-/- Gan mice. We also examined genetic background difference in tumor phenotype by changing Gan mouse background from C57BL/6(B6) to BALB/c.** **Microarray analyses were performed to examine changes of expression profiles in tumors by TNF gene disruption or by changing genetic background.** **Overall design:** **Total RNA was prepared from B6 Gan mice (n=3: Gan1-Gan3), B6-Gan TNF-/- mice (n=3: Gan(TNF KO)1-Gan(TNF KO)3), BALB-Gan mice (n=3: Gan(BALB/c)1-Gan(BALB/c)3), and wid-type normal glandular stomach (n=3: WT1-WT3). We used Affymetrix microarrays for hybridization, and examined expression profiles.**

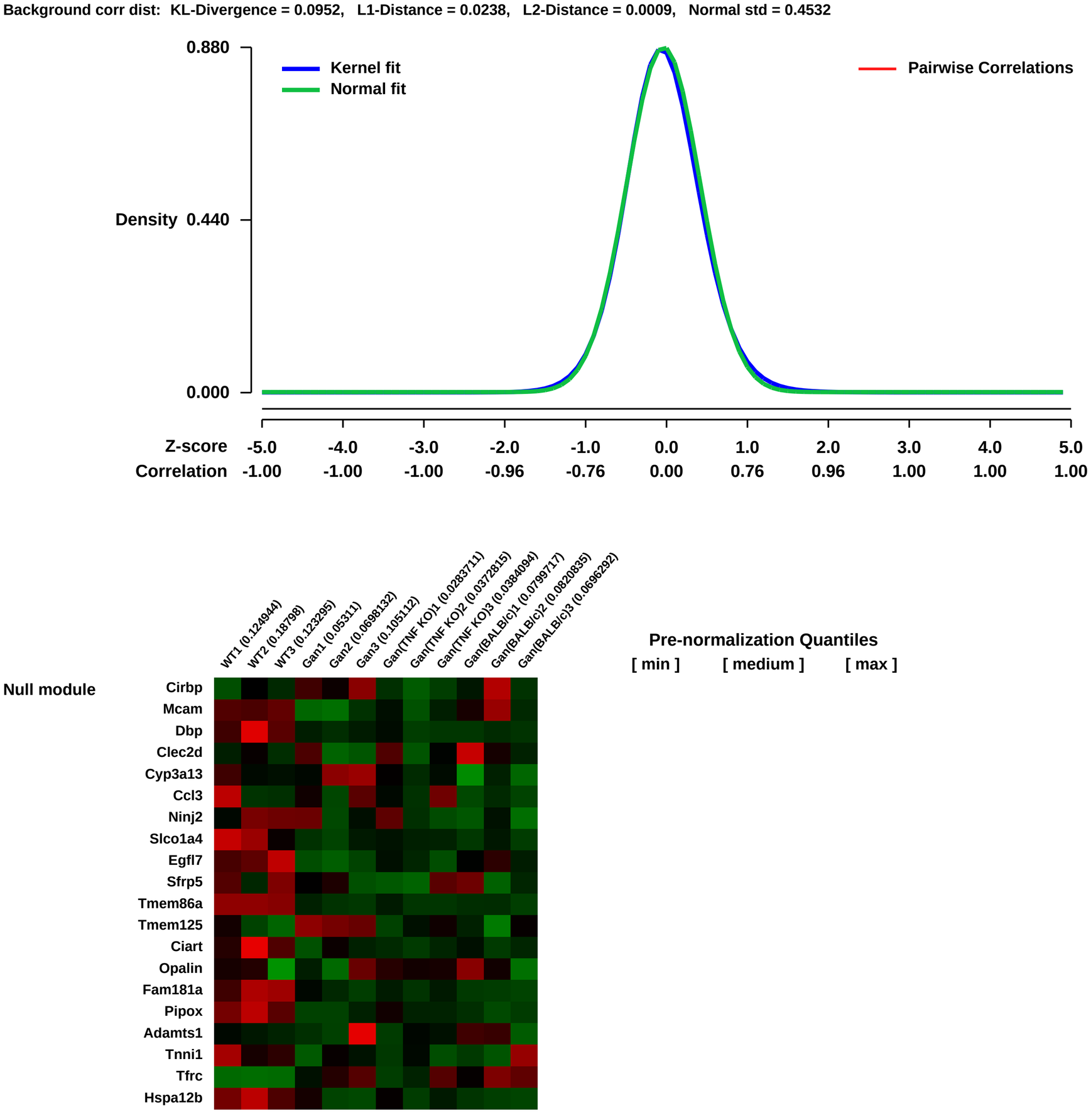

GEO Series "GSE13563" Expression Profiles

Num of samples in this series: 6

Scale of expression profile Z-scores

-3.0 -2.0 -1.0 0.0 1.0 2.0 3.0

GEO Link:	**http://www.ncbi.nlm.nih.gov/geo/query/acc.cgi?acc=GSE13563**
Status:	**Public on Nov 15 2008**
Title:	**Pilot study: Basal gene expression in bone**
Organism:	**Mus musculus**
Experiment type:	**Expression profiling by array**
Platform:	**GPL1261**
Pubmed ID:	**23182809**
Summary & Design:	**Summary:** **Pilot study** **Analysis of basal gene expression of the protective bones of the skull (parietals), weight-bearing bones of the limb (ulnae) and mandibular bone and teeth #!#** **Overall design:** **RNA extraction from normal bone**

Background corr dist: **KL-Divergence = 0.0312, L1-Distance = 0.0280, L2-Distance = 0.0008, Normal std = 0.6863**

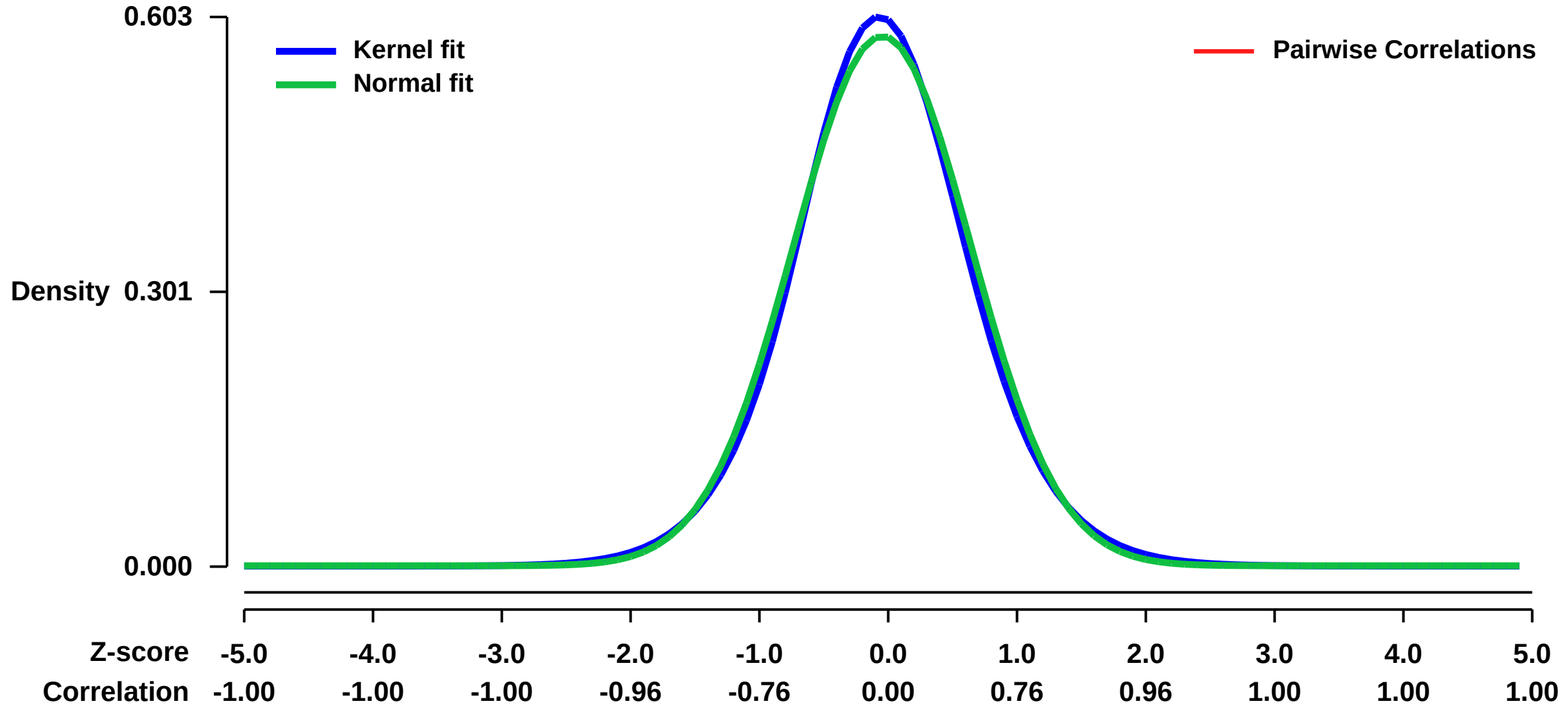

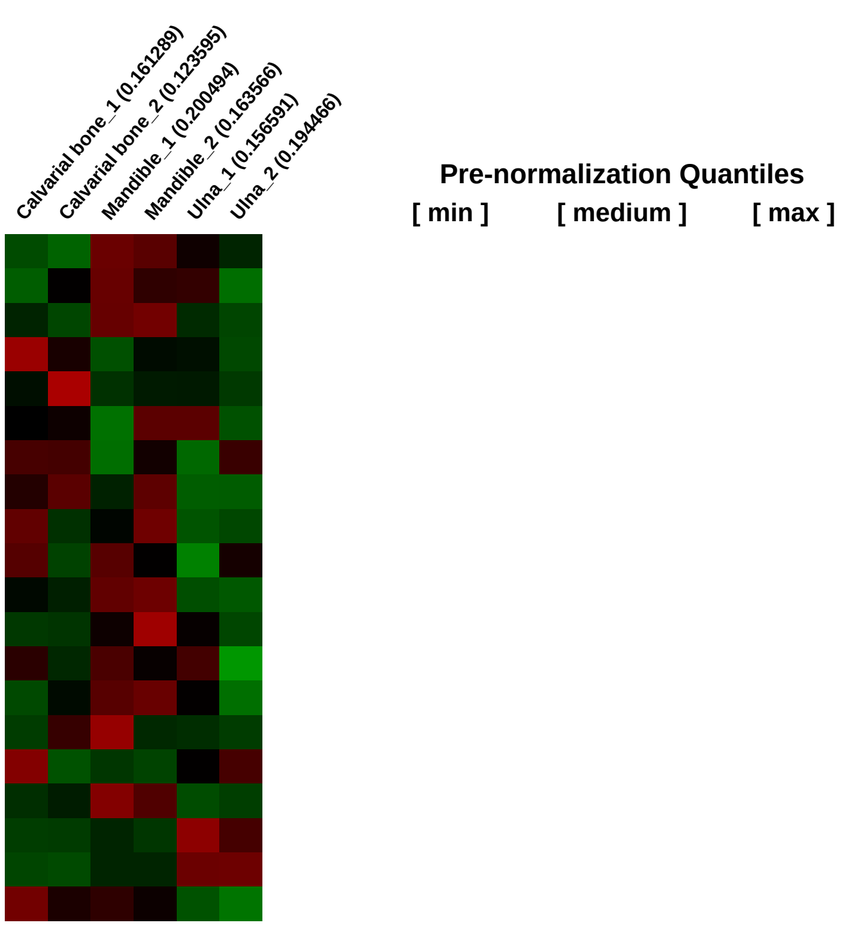

GEO Series "GSE13493" Expression Profiles

Num of samples in this series: 6

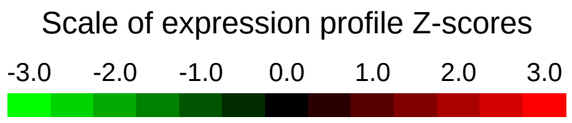

GEO Link:	http://www.ncbi.nlm.nih.gov/geo/query/acc.cgi?acc=GSE13493
Status:	Public on Mar 31 2009
Title:	Expression data from developing thymocytes of N15TCR transgenic Rag2 deficient mice
Organism:	Mus musculus
Experiment type:	Expression profiling by array
Platform:	GPL1261
Pubmed ID:	19027330
Summary & Design:	**Summary:** T cell development relies on the precise developmental control of various cellular functions for appropriate positive and negative selection. Previously, gene expression profiling of peptide-driven negative selection events in the N15 TCR class I MHC-restricted mouse and D011.10 TCR class II MHC-restricted mouse has offered insights into the coordinate engagement of biological processes affecting thymocyte development. However, there has been little comparable detailed in vivo global genome expression analysis reported for positive selection. We used microarrays to identify the genes differentially expressed during CD8 single positive T cell development in N15 TCR transgenic Rag2 deficient mice. **Overall design:** We have analyzed gene expression in the individual populations as development proceeds from DP, intermediate (Int), to SP subsets. To this end, we sorted the individual populations from six age and sex matched 5-6 week old N15 TCR tg+/+ RAG-2-/- H-2b mice for two independent experiments. For sorting subpopulations, cells were stained with anti-CD4 (L3T4) and anti-CD8 (Ly-2) antibodies (Pharmingen, San Diego, CA USA) and DP, Int and SP thymocytes were sorted on a MoFlo (Cytomation, Fort Collins, CO USA).

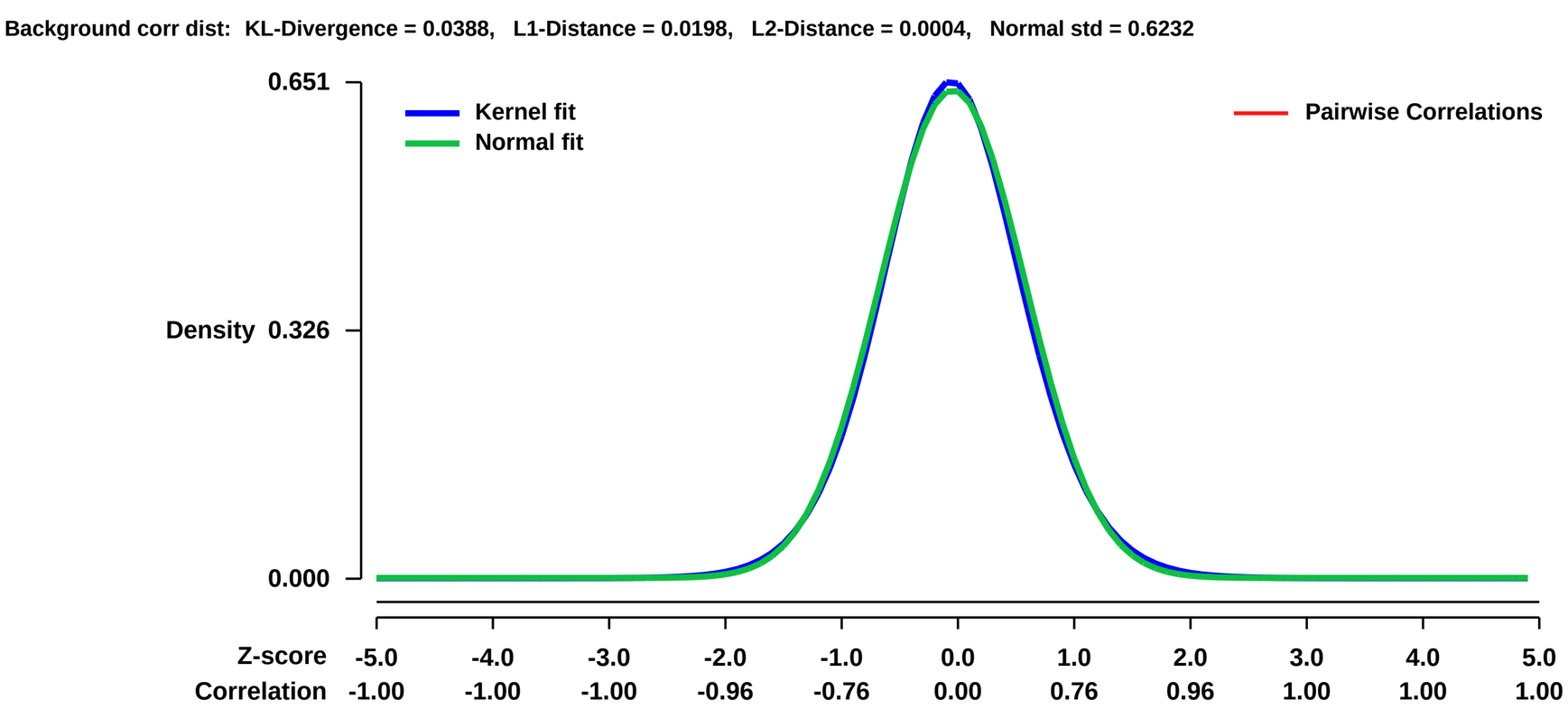

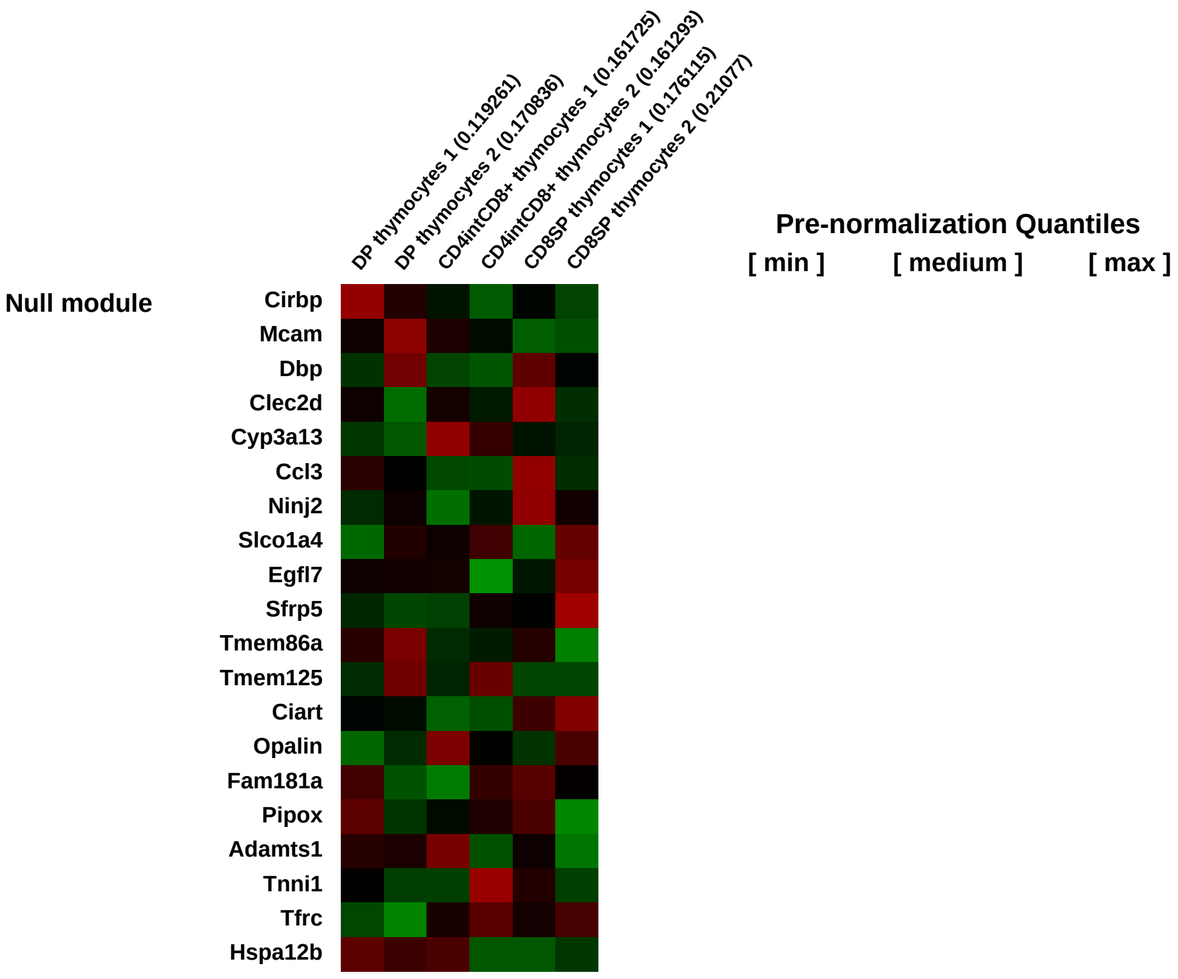

GEO Series "GSE26024" Expression Profiles

Num of samples in this series: 20

Scale of expression profile Z-scores

-3.0 -2.0 -1.0 0.0 1.0 2.0 3.0

GEO Link:	http://www.ncbi.nlm.nih.gov/geo/query/acc.cgi?acc=GSE26024
Status:	Public on Apr 12 2011
Title:	Evaluating Gene Expression in C57BL/6J and DBA/2J Mouse Striatum Using RNA-Seq and Microarray
Organism:	Mus musculus
Experiment type:	Expression profiling by array
Platform:	GPL1261
Pubmed ID:	21455293
Summary & Design:	**Summary:** **C57BL/6J (B6) and DBA/2J (D2) are two of the most commonly used inbred mouse strains in neuroscience research. However, the only currently available mouse genome is based entirely on the B6 strain sequence. Subsequently, oligonucleotide microarray probes are based solely on this B6 reference sequence, making their application for gene expression profiling comparisons across mouse strains dubious due to their allelic sequence differences, including single nucleotide polymorphisms (SNPs). The emergence of next-generation sequencing (NGS) and the RNA-Seq application provides a clear alternative to oligonucleotide arrays for detecting differential gene expression without the problems inherent to hybridization-based technologies. Using RNA-Seq, an average of 22 million short sequencing reads were generated per sample for 21 samples (10 B6 and 11 D2), and these reads were aligned to the mouse reference genome, allowing 16,183 Ensembl genes to be queried in striatum for both strains. To determine differential expression, 'digital mRNA counting' is applied based on reads that map to exons. The current study compares RNA-Seq (Illumina GA IIx) with two microarray platforms (Illumina MouseRef-8 v2.0 and Affymetrix MOE 430 2.0) to detect differential striatal gene expression between the B6 and D2 inbred mouse strains. We show that by using stringent data processing requirements differential expression as determined by RNA-Seq is concordant with both the Affymetrix and Illumina platforms in more instances than it is concordant with only a single platform, and that instances of discordance with respect to direction of fold change were rare. Finally, we show that additional information is gained from RNA-Seq compared to hybridization-based techniques as RNA-Seq detects more genes than either microarray platform. The majority of genes differentially expressed in RNA-Seq were only detected as present in RNA-Seq, which is important for studies with smaller effect sizes where the sensitivity of hybridization-based techniques could bias interpretation.** **Overall design:** *****This submission represents the microarray component of the study**

Background corr dist: KL-Divergence = 0.2201, L1-Distance = 0.0390, L2-Distance = 0.0034, Normal std = 0.3159

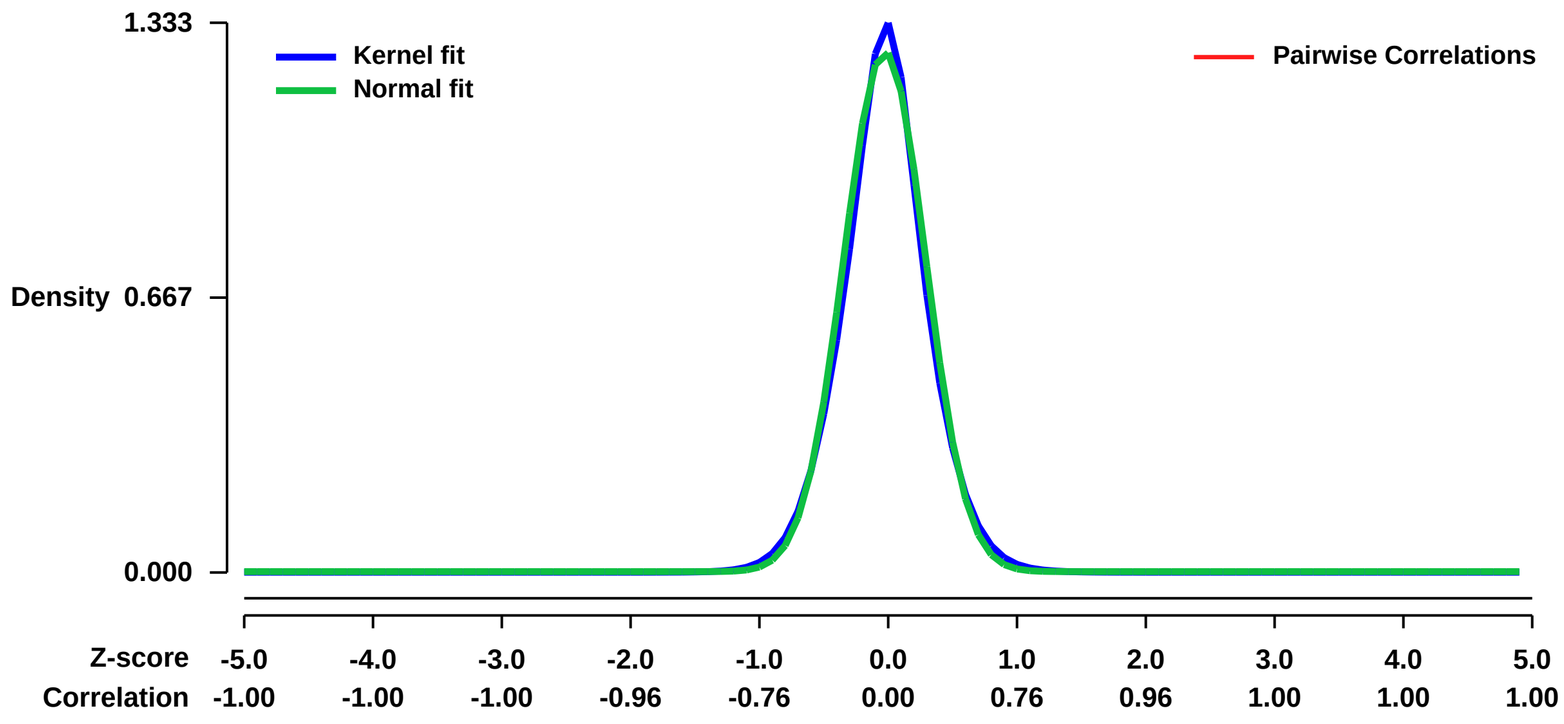

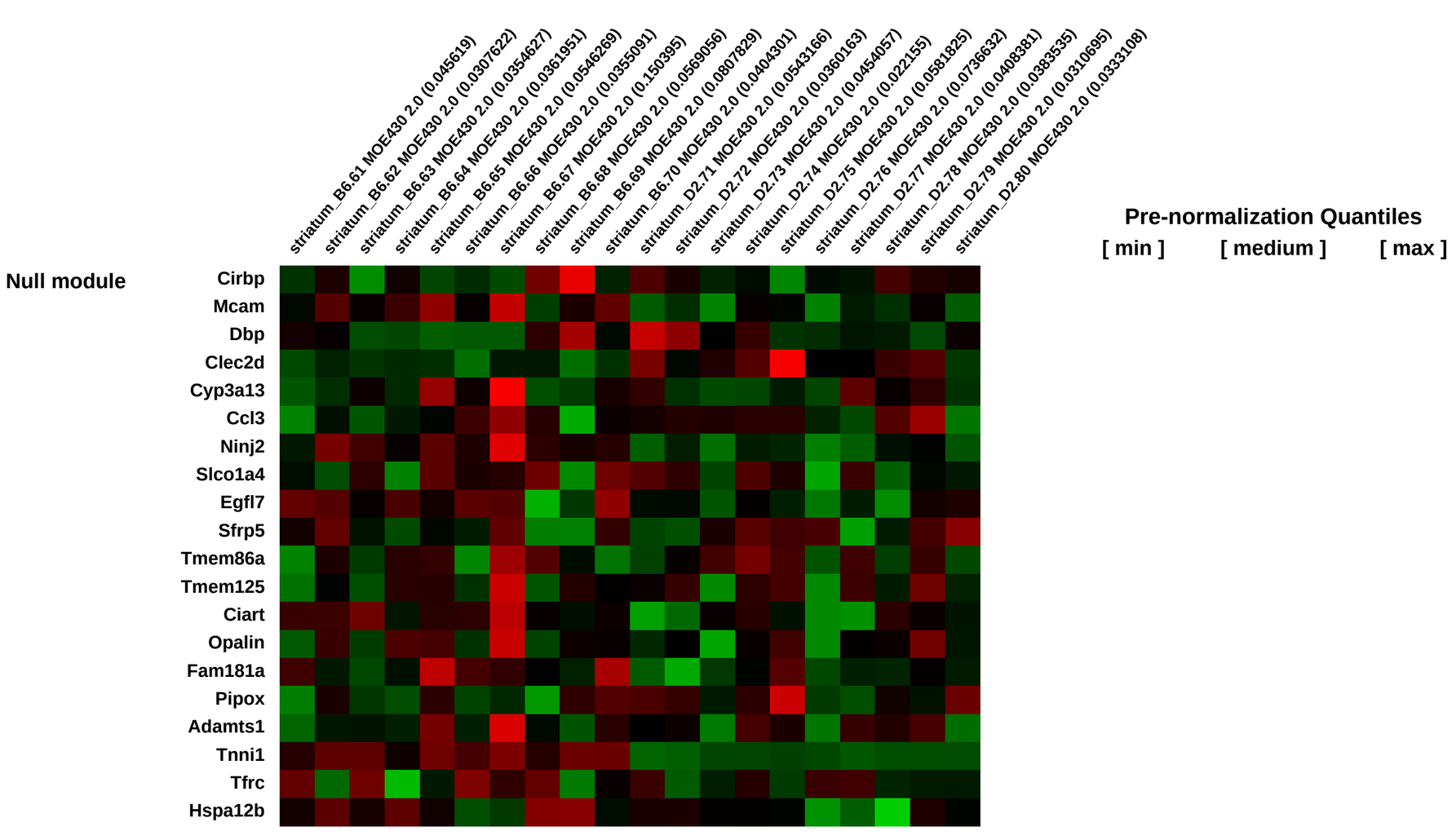

GEO Series "GSE6875" Expression Profiles

Num of samples in this series: 8

Scale of expression profile Z-scores

-3.0 -2.0 -1.0 0.0 1.0 2.0 3.0

GEO Link:	http://www.ncbi.nlm.nih.gov/geo/query/acc.cgi?acc=GSE6875
Status:	Public on Jan 26 2007
Title:	Development of Regulatory T cell Precursors in the Absence of a Functional Foxp3 Protein
Organism:	Mus musculus
Experiment type:	Expression profiling by array
Platform:	GPL1261
Pubmed ID:	17273171
Summary & Design:	**Summary:** To analyze gene expression in in regulatory T cell precursors that develop in the absence of a functional Foxp3 protein as compared to that of normal regulatory T cells **Keywords: Cell type comparison** **Overall design:** Murine wild-type and mutant (delta) Foxp3 alleles were tagged with EGFP reporters. CD4 positive T cells expressing the respective tagged Foxp3 allele (Foxp3/EGFP and delta Foxp3/EGFP) were isolated from hemizygous male mice by cell sorting using FACS. CD4 positive cells that did not express the EGFP tag were a isolated. Total RNA was prepared and used in the array studies.

Background corr dist: KL-Divergence = 0.0619, L1-Distance = 0.0225, L2-Distance = 0.0006, Normal std = 0.5327

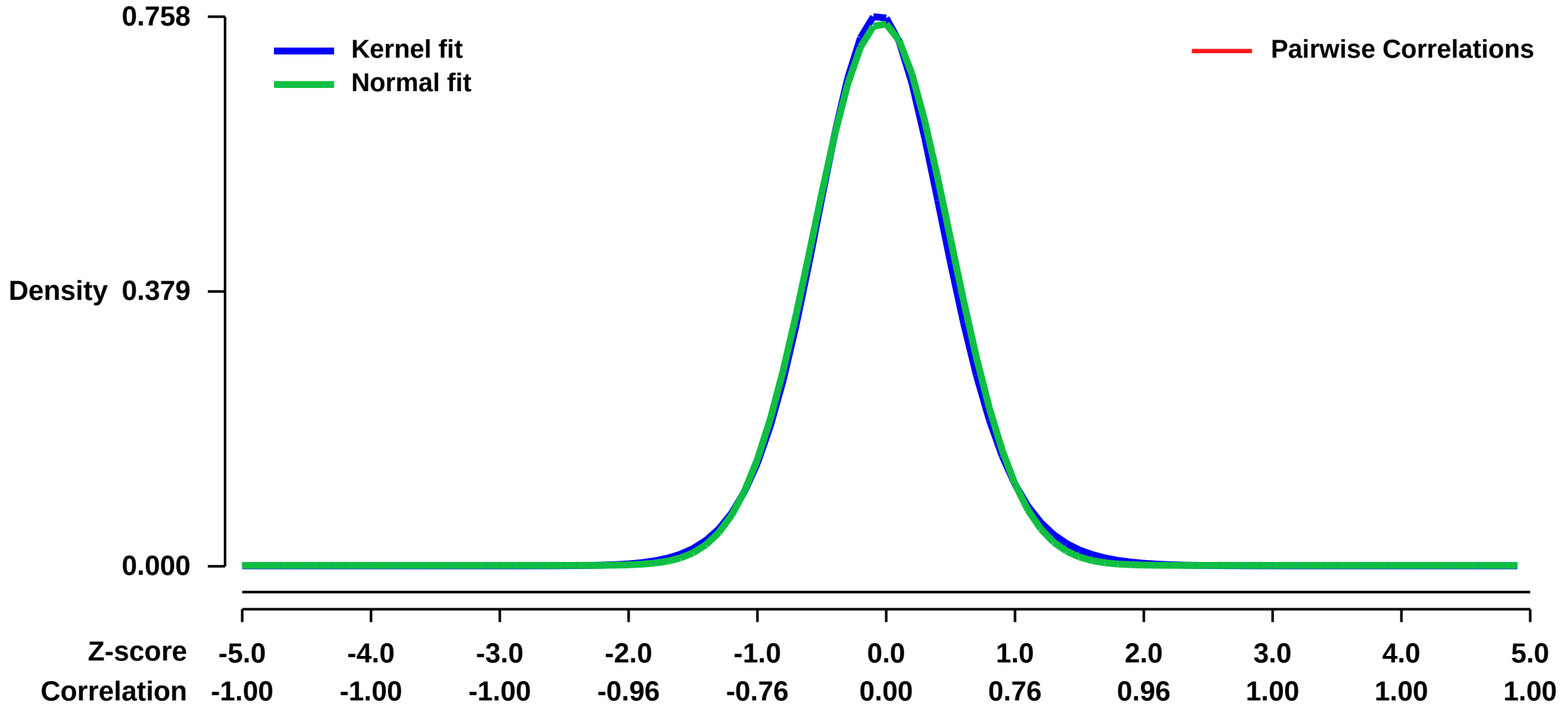

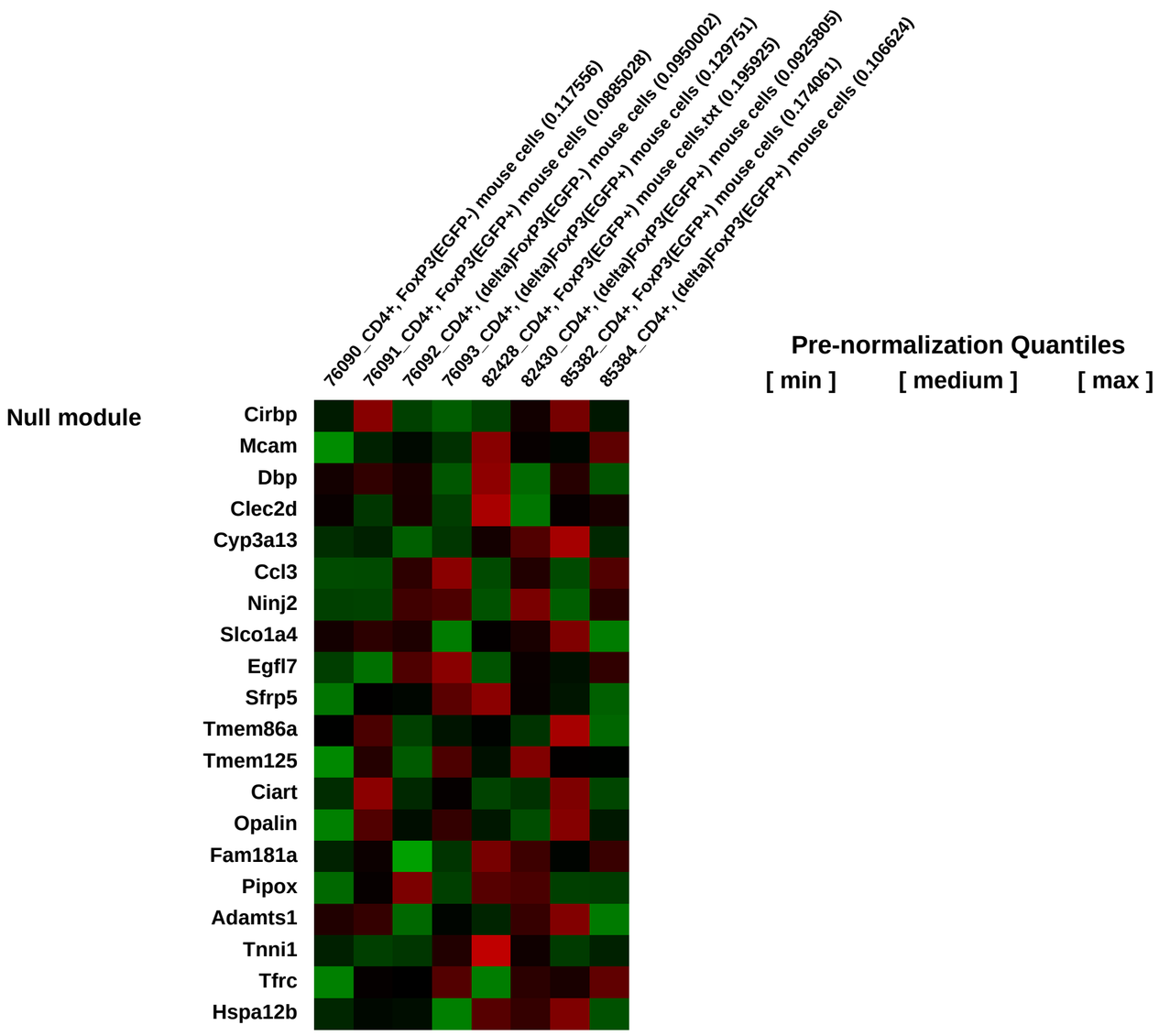

GEO Series "GSE18800" Expression Profiles

Num of samples in this series: 25

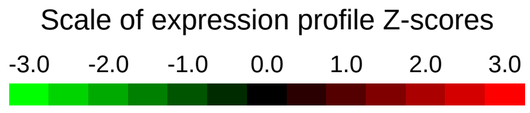

GEO Link:	**http://www.ncbi.nlm.nih.gov/geo/query/acc.cgi?acc=GSE18800**
Status:	**Public on Oct 30 2009**
Title:	**Effect of PGF receptor FP on bleomycin-induced pulmonary fibrosis in mice**
Organism:	**Mus musculus**
Experiment type:	**Expression profiling by array**
Platform:	**GPL1261**
Pubmed ID:	**19966781**
Summary & Design:	**Summary:** **We purposed to examine the effect of PGF receptor FP in development of bleomycin-induced pulmonary fibrosis in mice. We performed gene expression analysis in the lung of WT and FP-KO mice on Days 0, 7 and 14. We found out that fibrosis-related genes such as various isoforms of collagen, which were induced on Day 7 and continued to increase or remained unchanged on Day 14, were induced to less extent in FP-KO mice. In contrast, expression of inflammation-related genes peaked on Day 7 similarly in WT and FP-KO mice. These results suggest that FP functions in fibrosis-phase, not in peak inflammation phase, and facilitates fibrogenesis by enhancing expression of fibrosis-related genes.** **Overall design:** **compared with those in WT mice.**

Background corr dist: KL-Divergence = 0.2049, L1-Distance = 0.0359, L2-Distance = 0.0021, Normal std = 0.3323

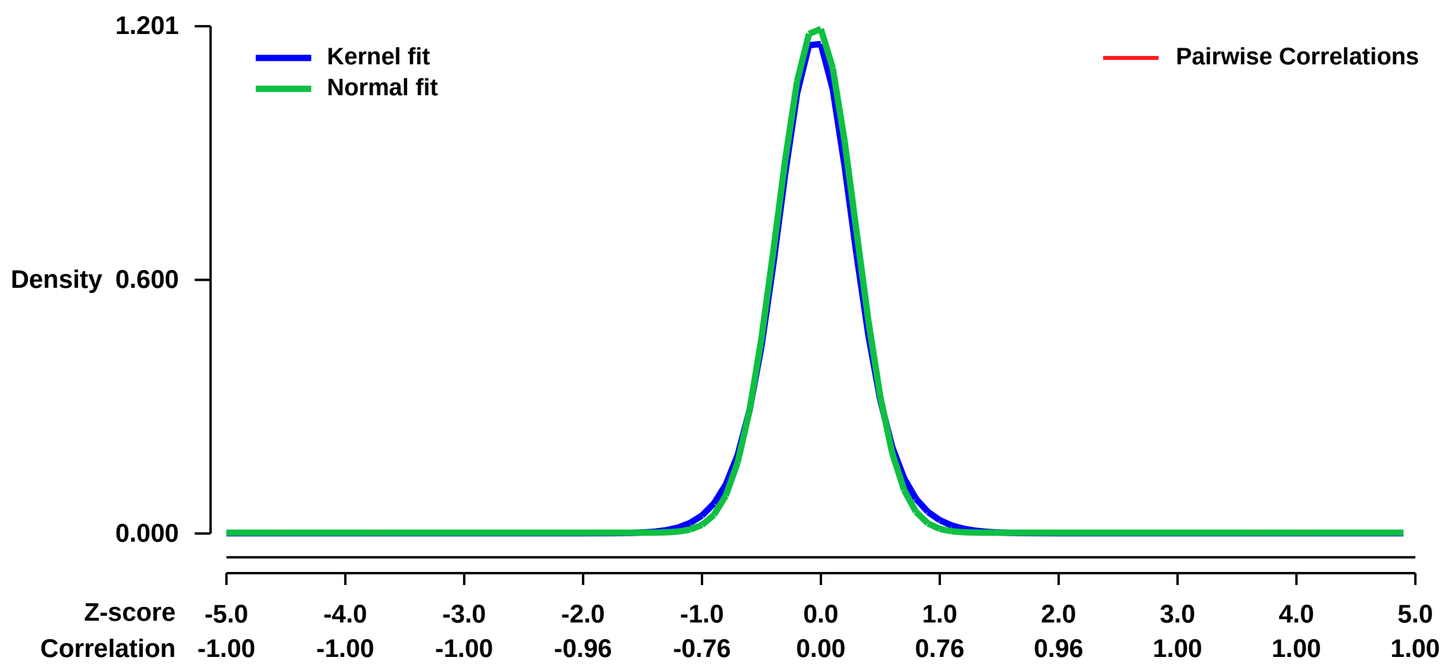

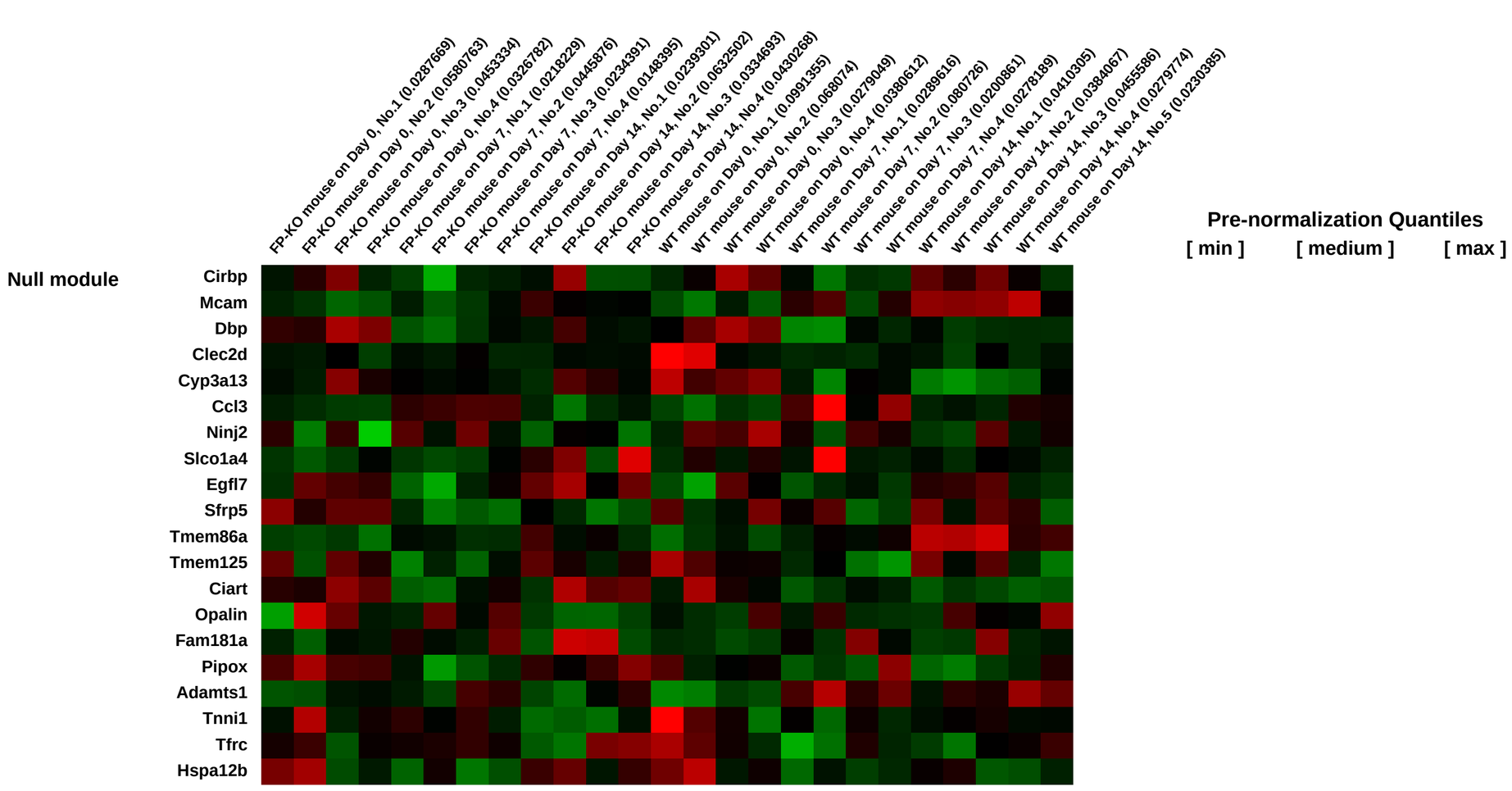

GEO Series "GSE54678" Expression Profiles

Num of samples in this series: 6

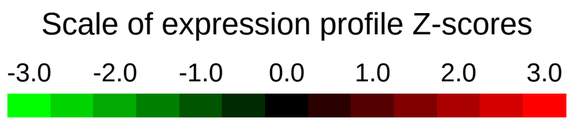

GEO Link:	**http://www.ncbi.nlm.nih.gov/geo/query/acc.cgi?acc=GSE54678**
Status:	**Public on Jun 30 2014**
Title:	**A pivotal role of SRC-2 in Metastatic and Castration Resistant Prostate Cancer**
Organism:	**Mus musculus**
Experiment type:	**Expression profiling by array**
Platform:	**GPL1261**
Pubmed ID:	
Summary & Design:	**Summary:** **SRC-2 is frequently amplified or overexpressed in metastatic prostate cancer patients. In this study, we used genetically engineered mice, overexpressing SRC-2 specifically in the prostate epithelium as a mouse model to examine the role of SRC-2 in prostate tumorigenesis. Over-expression of SRC-2 in PTEN heterozygous mice accelerates PTEN mutation induced tumor progression and develops a metastasis-prone cancer.** **We used microarrays to examine the molecular profile of prostate-specific SRC-2 overexpression adult dorsal-lateral prostate in comparison with that of control PTENF/+ heterozygous deletion mice.** **Overall design:** **total RNA was extracted from dorsal-lateral prostate of 7 months old-PTEN flox/+ control and PTEN flox/+; Rosa26-SRC-2 OE/+ adult mice, followed by gene expression profiling using Affymetrix microarrays. Each sample contains pooled prostate RNA from 3 mice.**

Background corr dist: **KL-Divergence = 0.0300, L1-Distance = 0.0202, L2-Distance = 0.0004, Normal std = 0.6761**

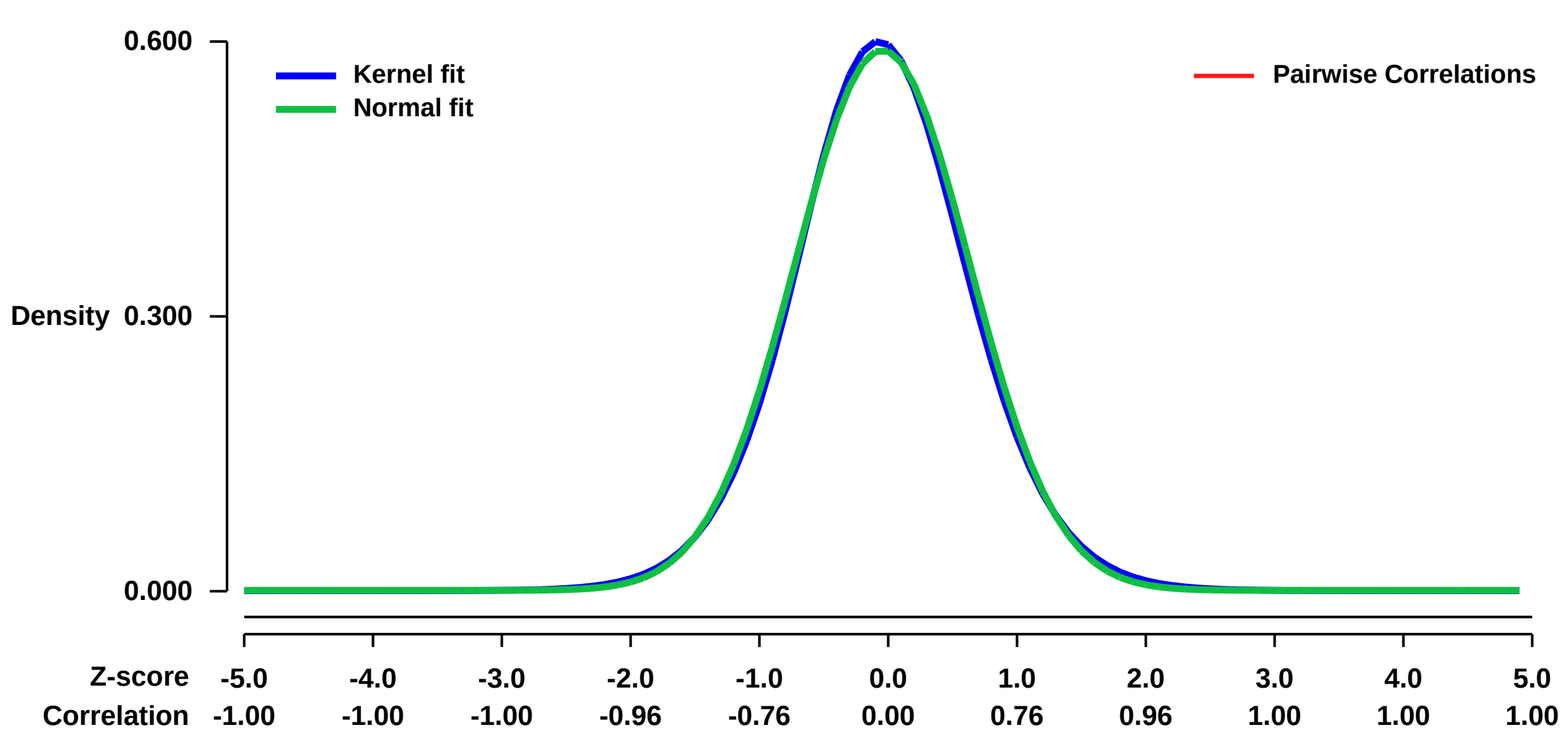

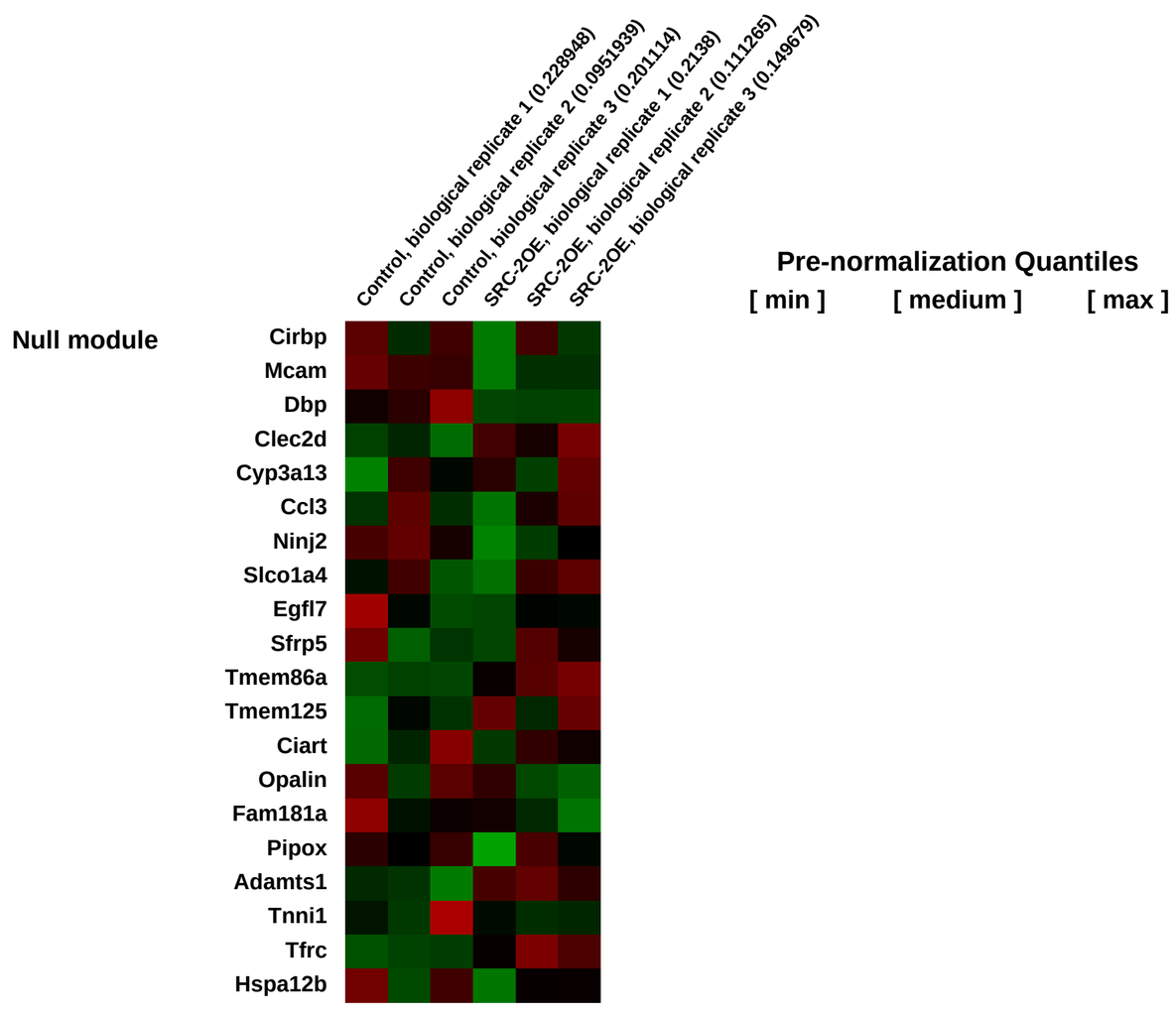

GEO Series "GSE22434" Expression Profiles

Num of samples in this series: 8

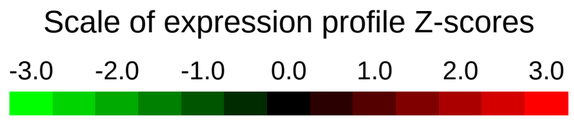

GEO Link:	http://www.ncbi.nlm.nih.gov/geo/query/acc.cgi?acc=GSE22434
Status:	Public on Jun 18 2010
Title:	Expression data from Evi1-transduced primary bone marrow cells
Organism:	Mus musculus
Experiment type:	Expression profiling by array
Platform:	GPL1261
Pubmed ID:	21289308
Summary & Design:	**Summary:** Evi1 is essential for proliferation of hematopoietic stem cells and implicated in the development of myeloid disorders. Particularly, high Evi1 expression defines one of the largest clusters in acute myeloid leukemia and is significantly associated with extremely poor prognosis. Improvement of the therapeutic outcome of leukemia with activated Evi1 is one of the most challenging issues. However, mechanistic basis of Evi1-mediated leukemogenesis has not been fully elucidated. Here we show that Evi1 directly represses PTEN transcription in the murine bone marrow, which leads to activation of AKT/mTOR signaling. In a murine bone marrow transplantation model, Evi1 leukemia showed remarkable sensitivity to an mTOR inihibitor rapamycin. Furthermore, we found that Evi1 binds to several polycomb group proteins and recruits polycomb repressive complexes for PTEN downregulation, which reveals a novel epigenetic mechanism of AKT/mTOR activation in leukemia. Expression analyses and chromatin immunoprecipitation assays using human samples indicate that our findings in mice models are recapitulated in human leukemic cells. Dependence of Evi1-expressing leukemic cells on AKT/mTOR signaling provides the first example of targeted therapeutic modalities that suppress the leukemogenic activity of Evi1. The PTEN/AKT/mTOR signaling pathway and the Evi1-polycomb interaction can be promising therapeutic targets for leukemia with activated Evi1. **Overall design:** 5-FU-primed mononuclear bone marrow cells harvested from C57/B6 mice were retrovirally transduced with Evi1-GFP or GFP. GFP positive cells were sorted and analyzed by Affymetrix´fi Mouse Genome 430 2.0 Array´fi for gene expression. Four independent experiments were performed.

Background corr dist: KL-Divergence = 0.0778, L1-Distance = 0.0209, L2-Distance = 0.0006, Normal std = 0.4805

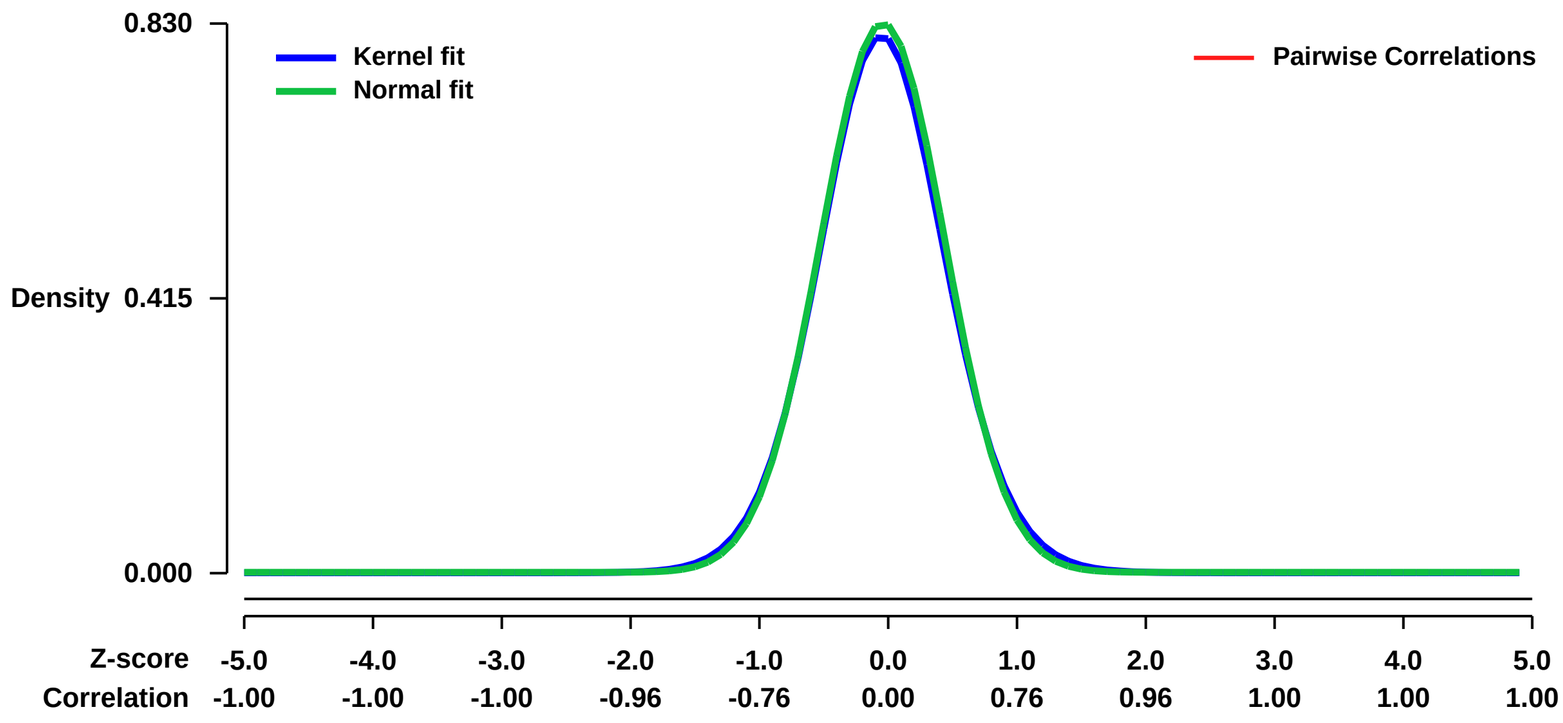

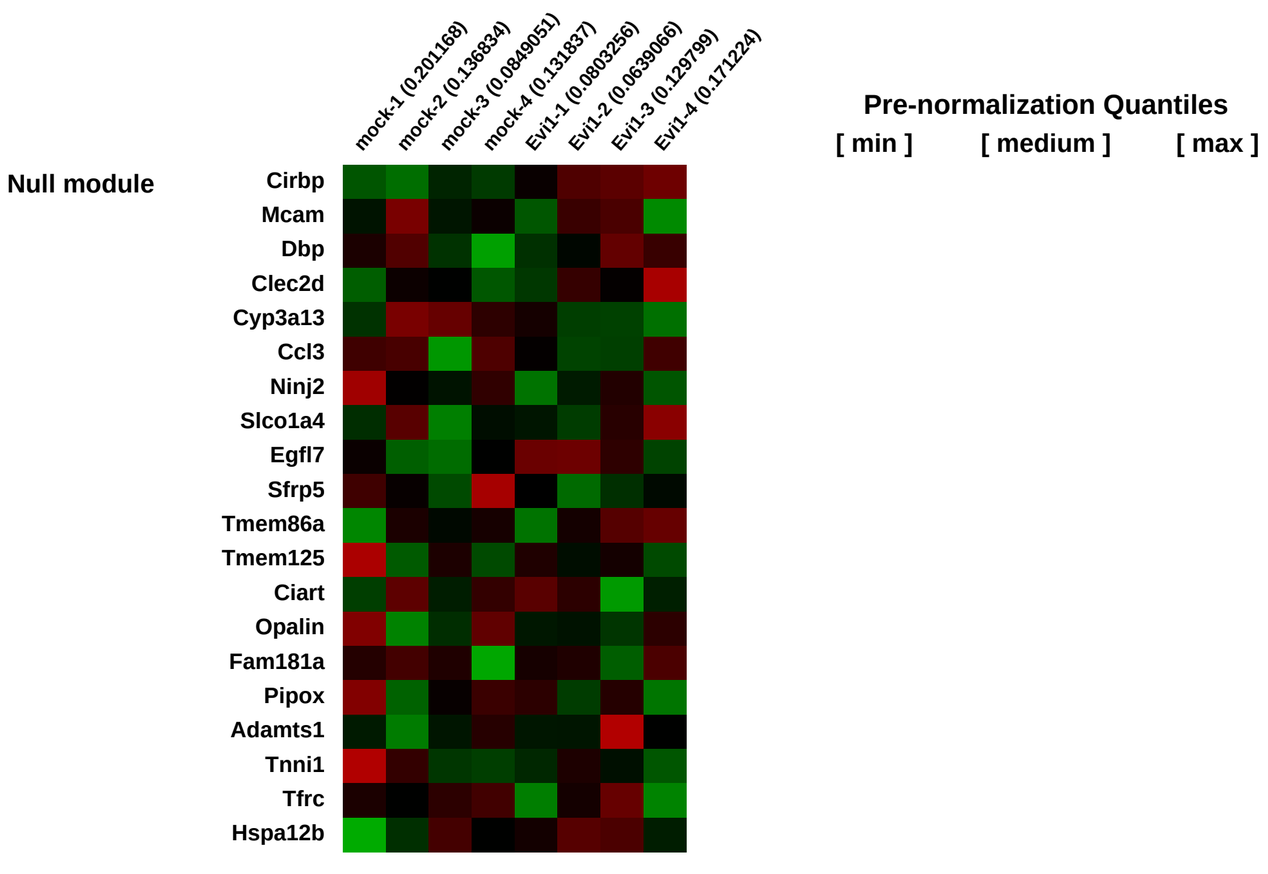

GEO Series "GSE12454" Expression Profiles

Num of samples in this series: 13

Scale of expression profile Z-scores

-3.0 -2.0 -1.0 0.0 1.0 2.0 3.0

GEO Link:	http://www.ncbi.nlm.nih.gov/geo/query/acc.cgi?acc=GSE12454
Status:	Public on Aug 01 2009
Title:	The SWI/SNF protein ATRX co-regulates pseudoautosomal genes that have translocated to autosomes in the mouse genome
Organism:	Mus musculus
Experiment type:	Expression profiling by array
Platform:	GPL1261
Pubmed ID:	18842153
Summary & Design:	**Summary:** Pseudoautosomal regions (PAR1 and PAR2) in eutherians retain homologous regions between the X and Y chromosomes that play a critical role in the obligatory X-Y crossover during male meiosis. Genes that reside in the PAR1 are exceptional in that they are rich in repetitive sequences and undergo a very high rate of recombination. Remarkably, murine PAR1 homologs have translocated to various autosomes, reflecting the complex recombination history during the evolution of the mammalian X chromosome. We now report that the SNF2-type chromatin remodeling protein ATRX controls the expression of eutherians ancestral PAR1 genes that have translocated to autosomes in the mouse. In addition, we have identified two potentially novel mouse PAR1 orthologs. We propose that the ancestral PAR1 genes share a common epigenetic environment that allows ATRX to control their expression. **Overall design:** At P0.5, n = 4 biological replicates of littermate-matched wt/ko pairs (for pair #2 there is one wt and 2 Atrx-null samples (2A & 2B) and we count this as 2 pairs).

Background corr dist: KL-Divergence = 0.0342, L1-Distance = 0.0308, L2-Distance = 0.0011, Normal std = 0.6463

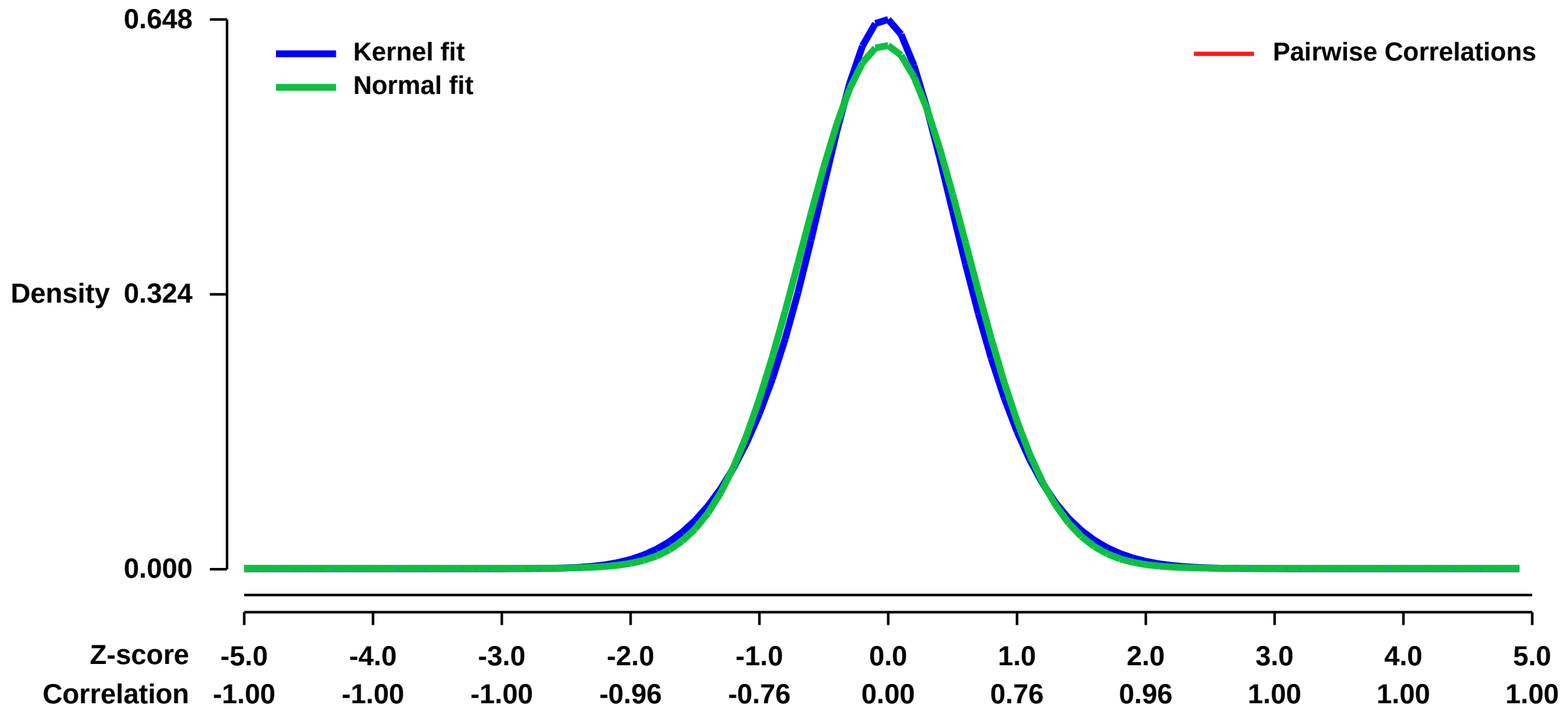

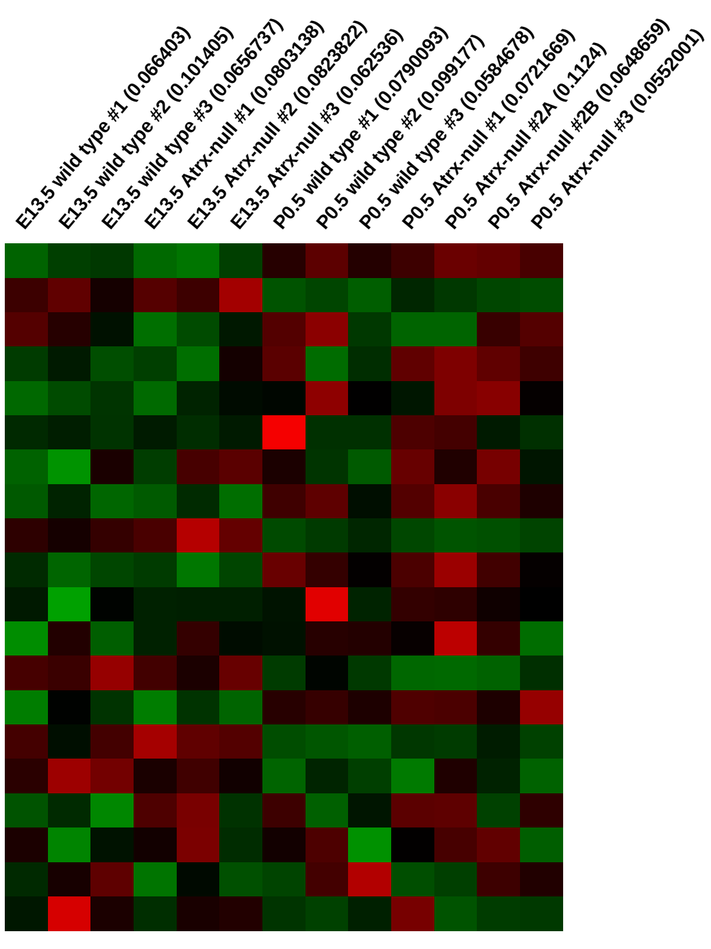

GEO Series "GSE22006" Expression Profiles

Num of samples in this series: 19

Scale of expression profile Z-scores

-3.0 -2.0 -1.0 0.0 1.0 2.0 3.0

GEO Link:	**http://www.ncbi.nlm.nih.gov/geo/query/acc.cgi?acc=GSE22006**
Status:	**Public on Sep 29 2010**
Title:	**Medulloblastoma tumors derived from Ptch+/-p53-/- transgenic mouse allografted in nude mice**
Organism:	**Mus musculus**
Experiment type:	**Expression profiling by array**
Platform:	**GPL1261**
Pubmed ID:	
Summary & Design:	**Summary:** **Nude mice were allografted with medulloblastoma tumors derived from Ptch+/-p53-/- transgenic mouse and treated with vehicle or NVP-LDE225.** **Overall design:** **RNA was prepared from tumours from vehicle or NVP-LDE225 treated nude mice allografted with medulloblastoma tumors derived from Ptch+/-p53-/- transgenic mouse and hybridized on the Affymetrix Mouse Genome 430A 2.0 RNA expression microarray.**

Background corr dist: **KL-Divergence = 0.2745, L1-Distance = 0.0620, L2-Distance = 0.0103, Normal std = 0.2907**

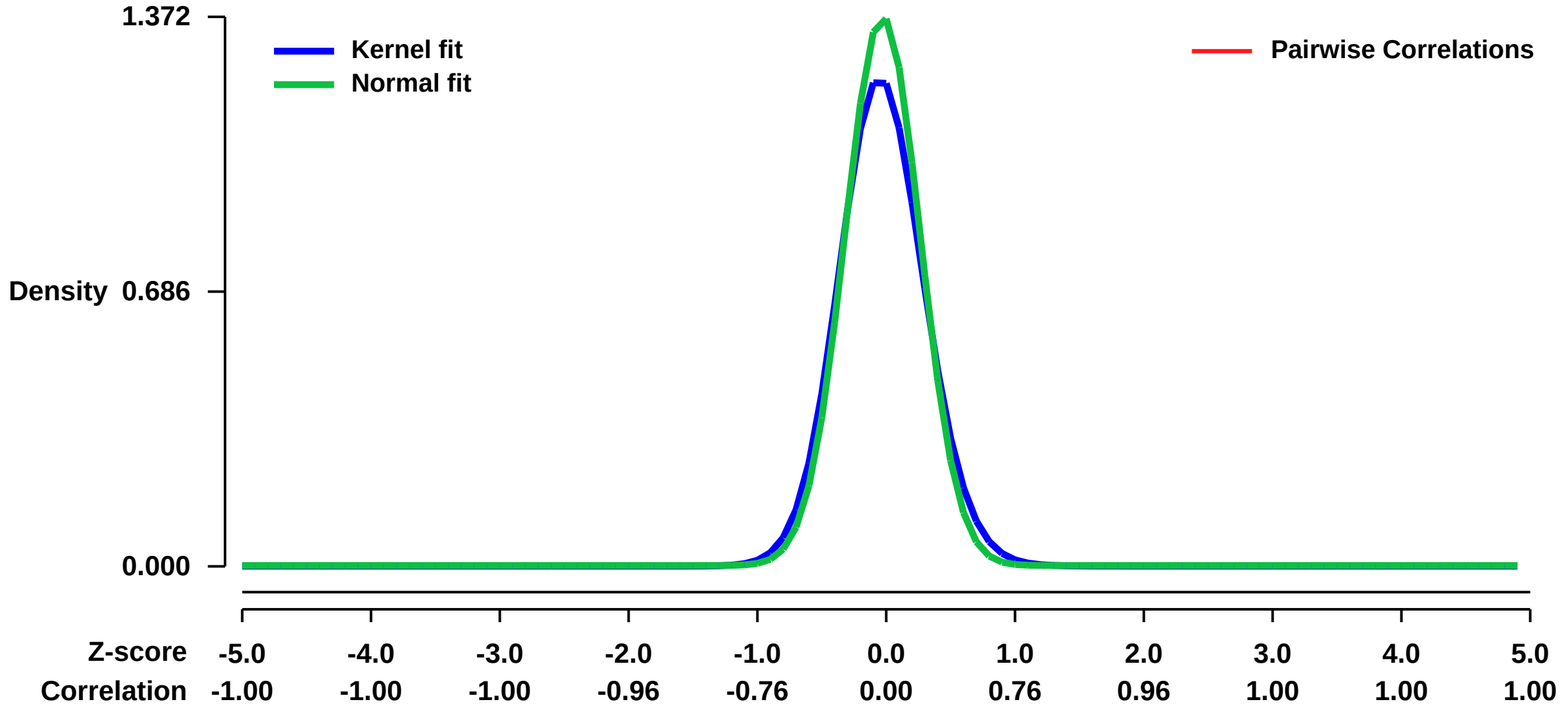

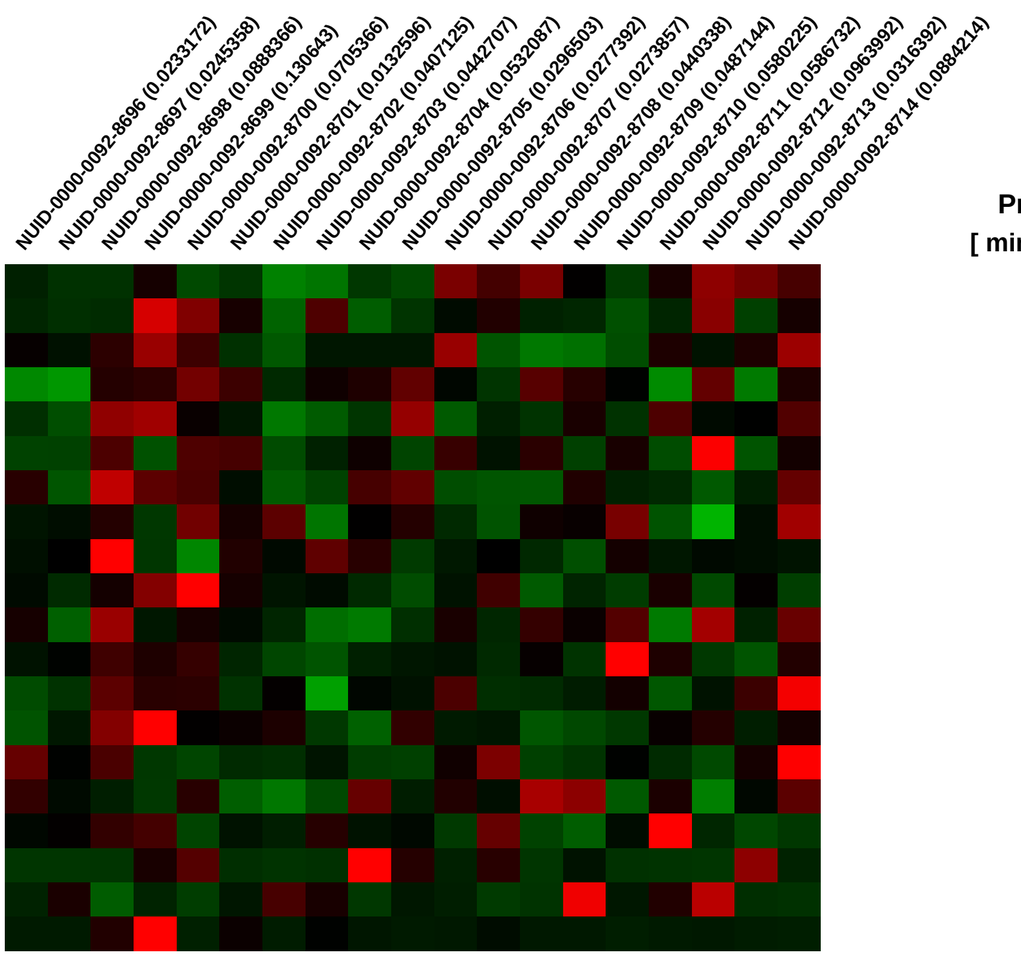

GEO Series "GSE20727" Expression Profiles

Num of samples in this series: 15

Scale of expression profile Z-scores

-3.0 -2.0 -1.0 0.0 1.0 2.0 3.0

GEO Link:	http://www.ncbi.nlm.nih.gov/geo/query/acc.cgi?acc=GSE20727
Status:	Public on Mar 10 2011
Title:	Reactive oxygen species induced gene expression changes on dendritic cells
Organism:	Mus musculus
Experiment type:	Expression profiling by array
Platform:	GPL1261
Pubmed ID:	22974541
Summary & Design:	**Summary:** **Identification of ROS induced genes on dendritic cells** **Dendritic cells were incubated for 15 min with or without a ROS inhibitor (DPI), washed extensively and incubated for 30 min with a chemical allergen (DNFB), hydrogen peroxide, and vehicle alone in HBSS containing DPI or vehicle. After washed extensively, the samples were post-incubated for 5.5 h with DNFB, hydrogen peroxide, or vehicle in complete culture medium containing DPI or vehicle.** **Overall design:** **Total RNA was extracted from cells treated with a chemical allergen, hydrogen peroxide, and vehicle alone in the presence or absence of a ROS inhibitor.**

Background corr dist: **KL-Divergence = 0.1500, L1-Distance = 0.0334, L2-Distance = 0.0023, Normal std = 0.3745**

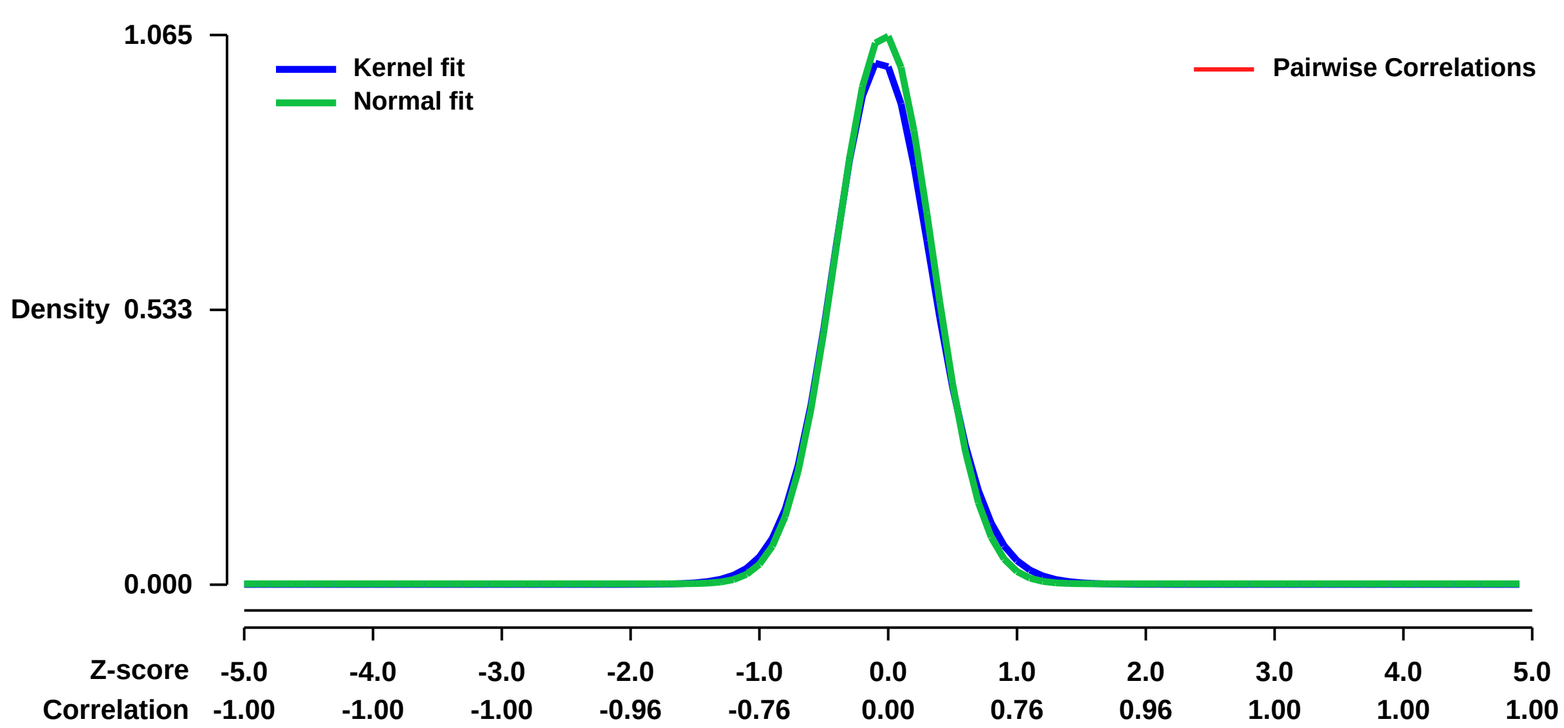

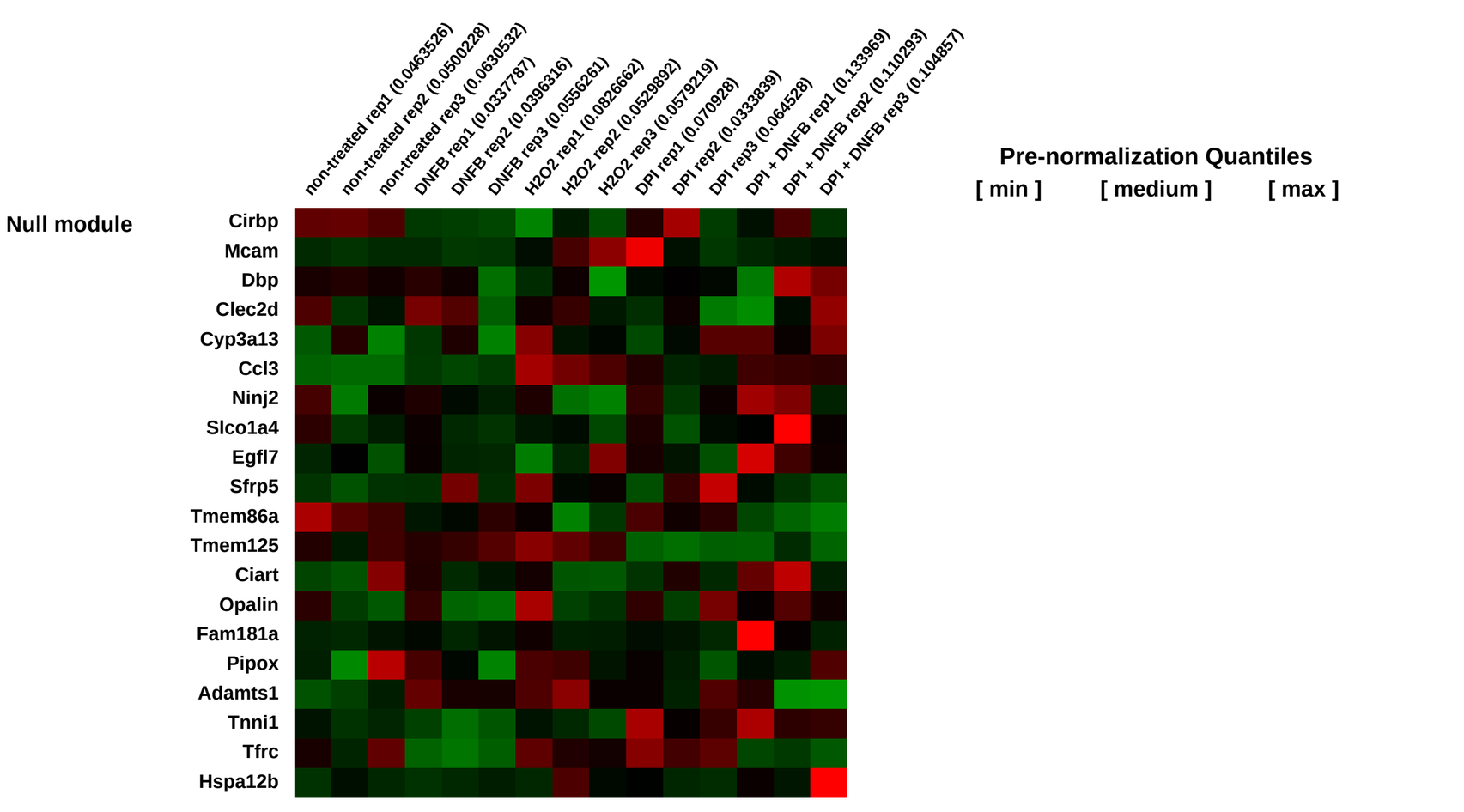

GEO Series "GSE38283" Expression Profiles

Num of samples in this series: 7

Scale of expression profile Z-scores

-3.0 -2.0 -1.0 0.0 1.0 2.0 3.0

GEO Link:	http://www.ncbi.nlm.nih.gov/geo/query/acc.cgi?acc=GSE38283
Status:	Public on May 28 2012
Title:	Expression data from normal brain/glioma associated macrophages
Organism:	Mus musculus
Experiment type:	Expression profiling by array
Platform:	GPL1261
Pubmed ID:	24371228
Summary & Design:	**Summary:** Tumor associated macrophages are contributing to local invasion, angiogensis, and metastasis during the progression of many kinds of tumor including glioma We used microrray to study the difference of expression of glioma associated macrophages and normal brain tissue associated macrophages **Overall design:** The macrophgages were isolated based on the markers of GFP and F4/80+ from Gl261 glioma and normal brain, RNA were extracted for microarray analysis

Background corr dist: KL-Divergence = 0.0613, L1-Distance = 0.0320, L2-Distance = 0.0017, Normal std = 0.5371

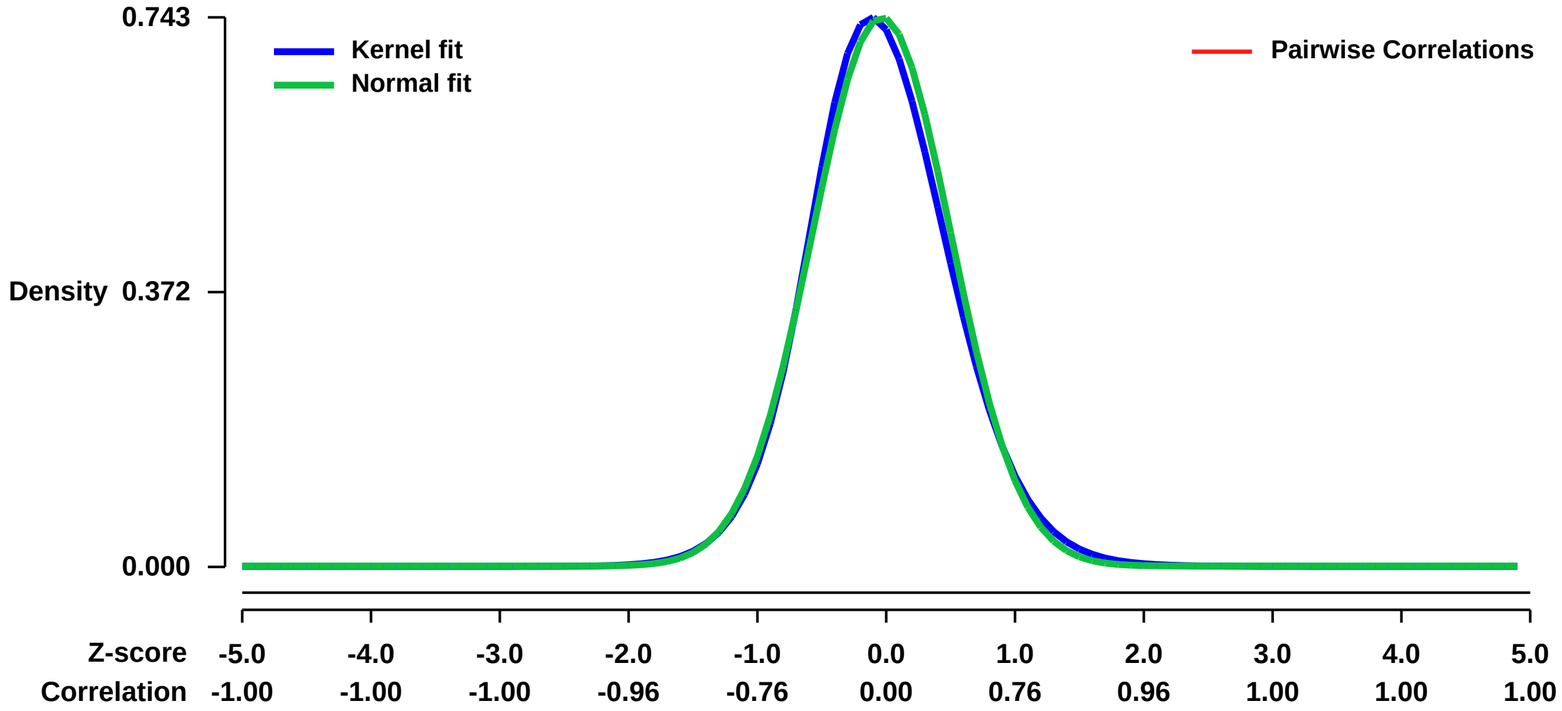

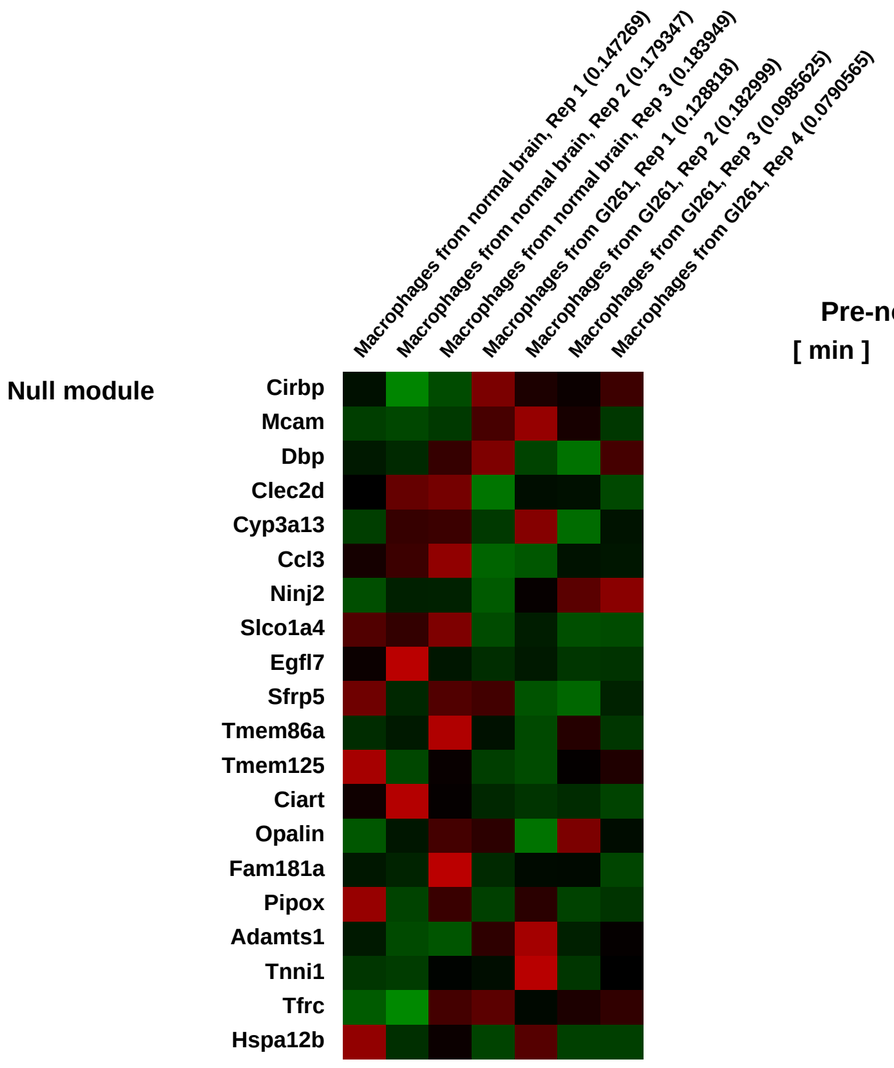

GEO Series "GSE13805" Expression Profiles

Num of samples in this series: 7

Scale of expression profile Z-scores

-3.0 -2.0 -1.0 0.0 1.0 2.0 3.0

GEO Link:	http://www.ncbi.nlm.nih.gov/geo/query/acc.cgi?acc=GSE13805
Status:	Public on Dec 02 2009
Title:	Expression data from wild type and calreticulin deficient murine embryonic stem cells
Organism:	Mus musculus
Experiment type:	Expression profiling by array
Platform:	GPL1261
Pubmed ID:	20506533
Summary & Design:	**Summary:** Primordial genomic challenge compromises embryonic development and survival, and surveillance of deployed transcriptional programs may provide an early opportunity to forecast phenotype abnormalities. Here, comparisons between wild-type and calreticulin-ablated embryonic stem cells revealed transcriptome shifts precipitated by calreticulin loss. Bioinformatic analysis identified down and up-regulation in 1187 and 418 genes, respectively. Cardiovascular development precedes other organogenic programs, and examination of cardiogenic genes revealed a map of calreticulin-calibrated expression profiles that encompass the developmental regulators, Ccnd1, Ccnd2 and Notch1. Interrogation of primary function in the resolved network forecasted abnormalities during myocardial development. Whole embryo magnetic resonance imaging, verified by pathoanatomical analysis, diagnosed prominent ventricular septal defect. Correlation clustering and network resolution of probesets associated with protein folding/chaperoning and calcium handling demonstrated 14 and 19 genes, respectively, modulated by calreticulin deficiency. Calreticulin deletion provoked ontological re-prioritization of gene expression, molecular transport and protein trafficking that translated into multiple subcellular functional outcomes. Individual stem cell-derived cardiomyocytes lacking calreticulin demonstrated a disorganized contractile apparatus with mitochondrial paucity and architectural aberrations. Thus, bioinformatic deconvolution of primordial embryonic stem cell transcriptomes enables predictive phenotyping of defective developmental networks that coalesce from complex systems biology hierarchies. **Keywords:** Comparison of embryonic stem cell genomes between wild type and calreticulin knockouts **Overall design:** Stem cells cultured in triplicate (or more) were pooled to provide raw material per sample. Each sample represents material collected from three technical replicates or more. In this manner, two wild type samples, and five derived from calreticulin knockout samples, were obtained. Although sample content contains material from three or more technical replicates harvested contemporaneously, each sample is a distinct biological replicate. Total RNA was extracted from each of the samples and RNA pools were profiled on Affymetrix Mouse 430 2.0 Arrays to identify global gene expression changes invoked by genomic ablation of calreticulin.

Background corr dist: KL-Divergence = 0.0370, L1-Distance = 0.0281, L2-Distance = 0.0009, Normal std = 0.6423

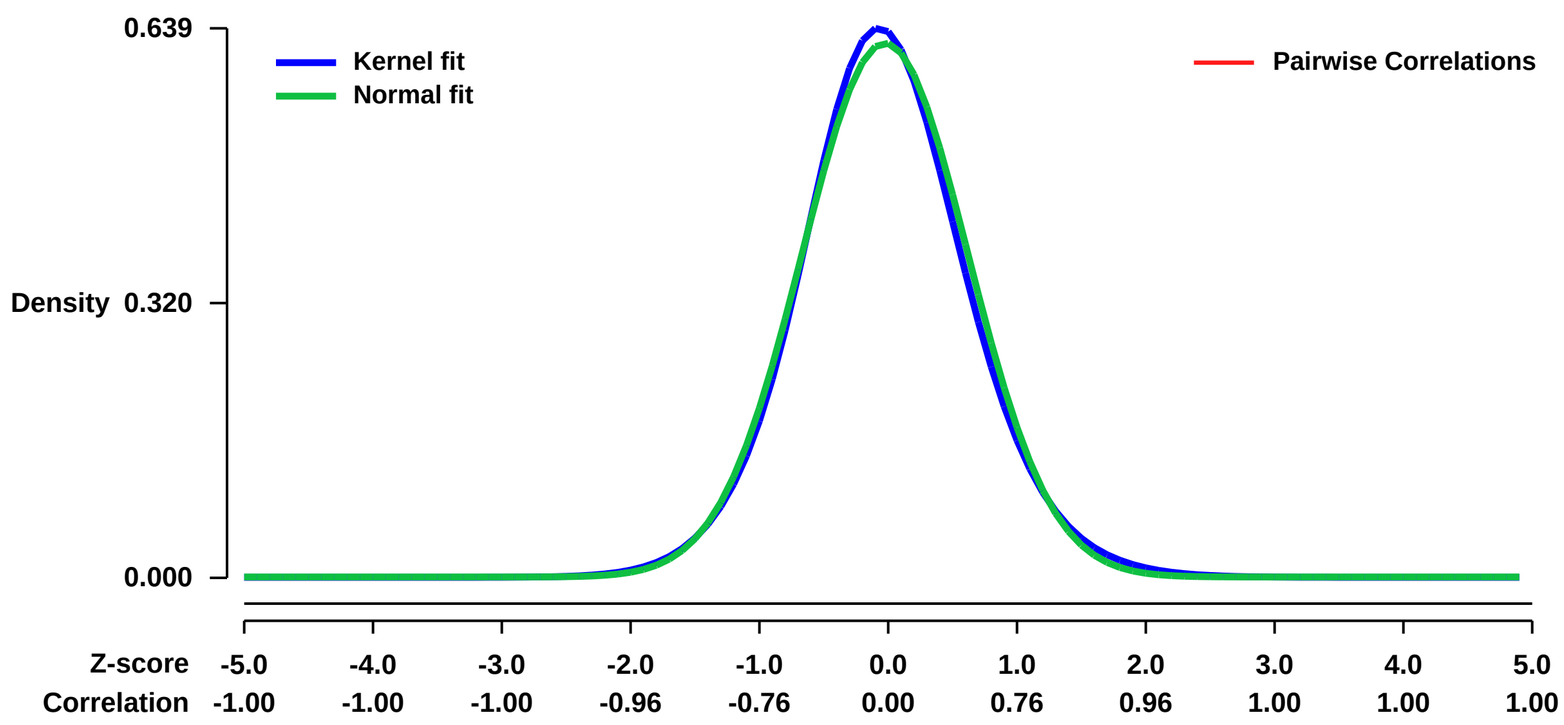

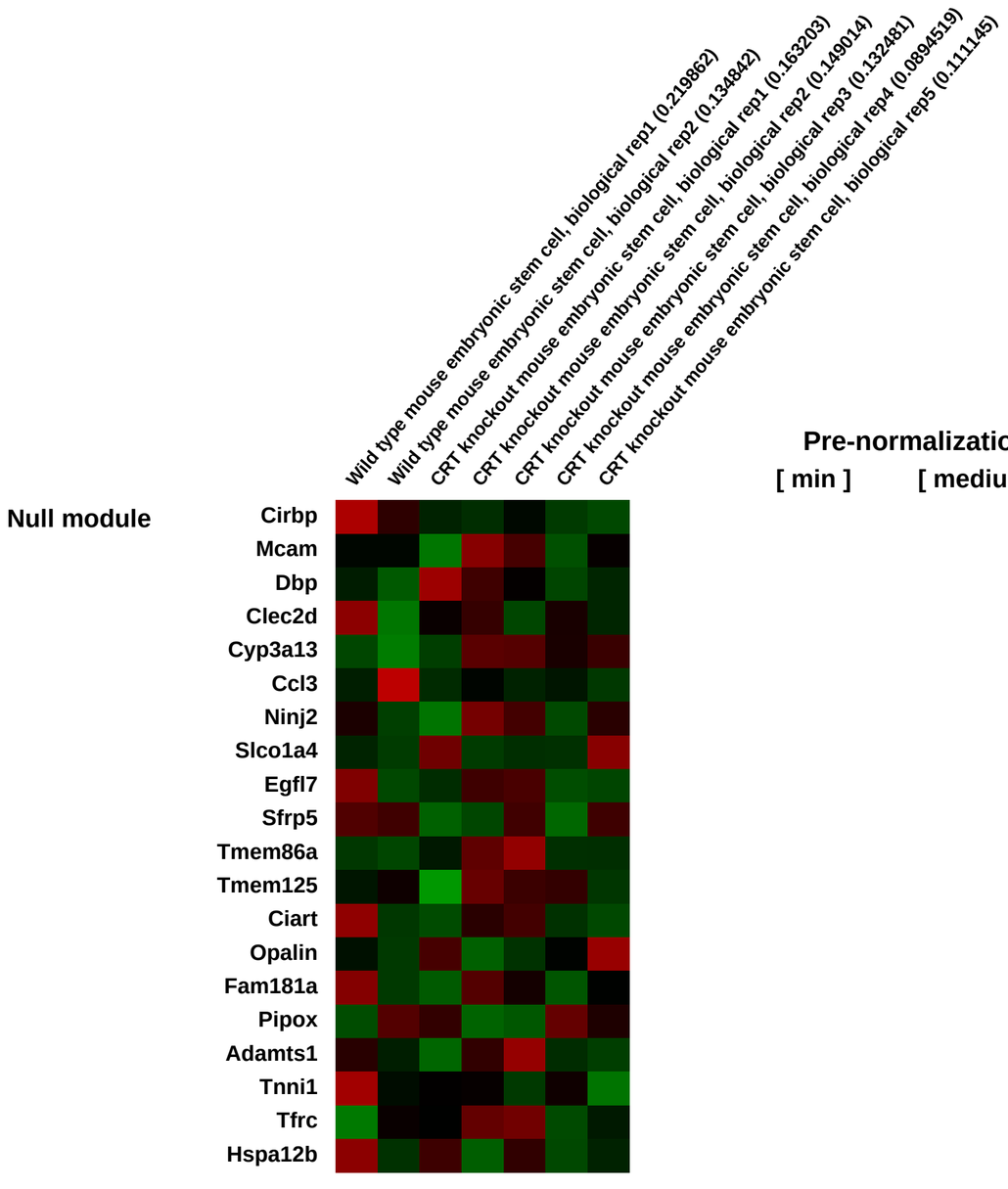

GEO Series "GSE45143" Expression Profiles

Num of samples in this series: 6

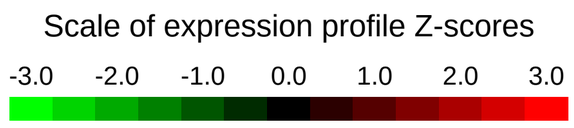

GEO Link:	http://www.ncbi.nlm.nih.gov/geo/query/acc.cgi?acc=GSE45143
Status:	Public on Aug 01 2013
Title:	Pax6 is required for normal cell cycle exit and the differentiation kinetics of retinal progenitor cells.
Organism:	Mus musculus
Experiment type:	Expression profiling by array
Platform:	GPL1261
Pubmed ID:	24073291
Summary & Design:	**Summary:** The coupling between cell-cycle exit and onset of differentiation is a common feature throughout the developing nervous system, but the mechanisms that link these processes are mostly unknown. Although the transcription factor Pax6 was implicated in both proliferation and differentiation of multiple regions within the CNS, its contribution to the transition between these successive states remains elusive. To gain insight into the role of Pax6 during the transition from proliferating progenitors to differentiating precursors, we investigated cell-cycle and transcriptomic changes occurring in Pax6- retinal progenitor cells (RPCs). Our analyses revealed a unique cell-cycle phenotype of the Pax6-deficient RPCs, which included a reduced number of cells in the S phase, an increased number of cells exiting the cell cycle, and delayed differentiation kinetics of Pax6- precursors. These alterations were accompanied by co-expression of factors that promote (Ccnd1, Ccnd2, Ccnd3) and inhibit (P27kip1 and P27kip2) the cell cycle. Further characterization of the changes in transcription profile of the Pax6-deficient RPCs revealed abrogated expression of multiple factors which are known to be involved in regulating proliferation of RPCs, including the transcription factors Vsx2, Nr2e1, Plagl1 and Hedgehog signaling. These findings provide novel insight into the molecular mechanism mediating the pleiotropic activity of Pax6 in RPCs. The results further suggest that rather than conveying a linear effect on RPCs, such as promoting their proliferation and inhibiting their differentiation, Pax6 regulates multiple transcriptional networks which function simultaneously, thereby conferring the capacity to proliferate, assume multiple cell fates and execute the differentiation program into retinal lineages. **Overall design:** The data contains 3 control and 3 Pax6 negative samples representing biological repeats. Each sample was prepared from ~1.8 million cells taken from the distal retina of either E12 alpha-Cre or Pax6 floxed alpha-Cre animals. Distally located retinal progenitors expressing Cre and eGFP were separated using FACS.

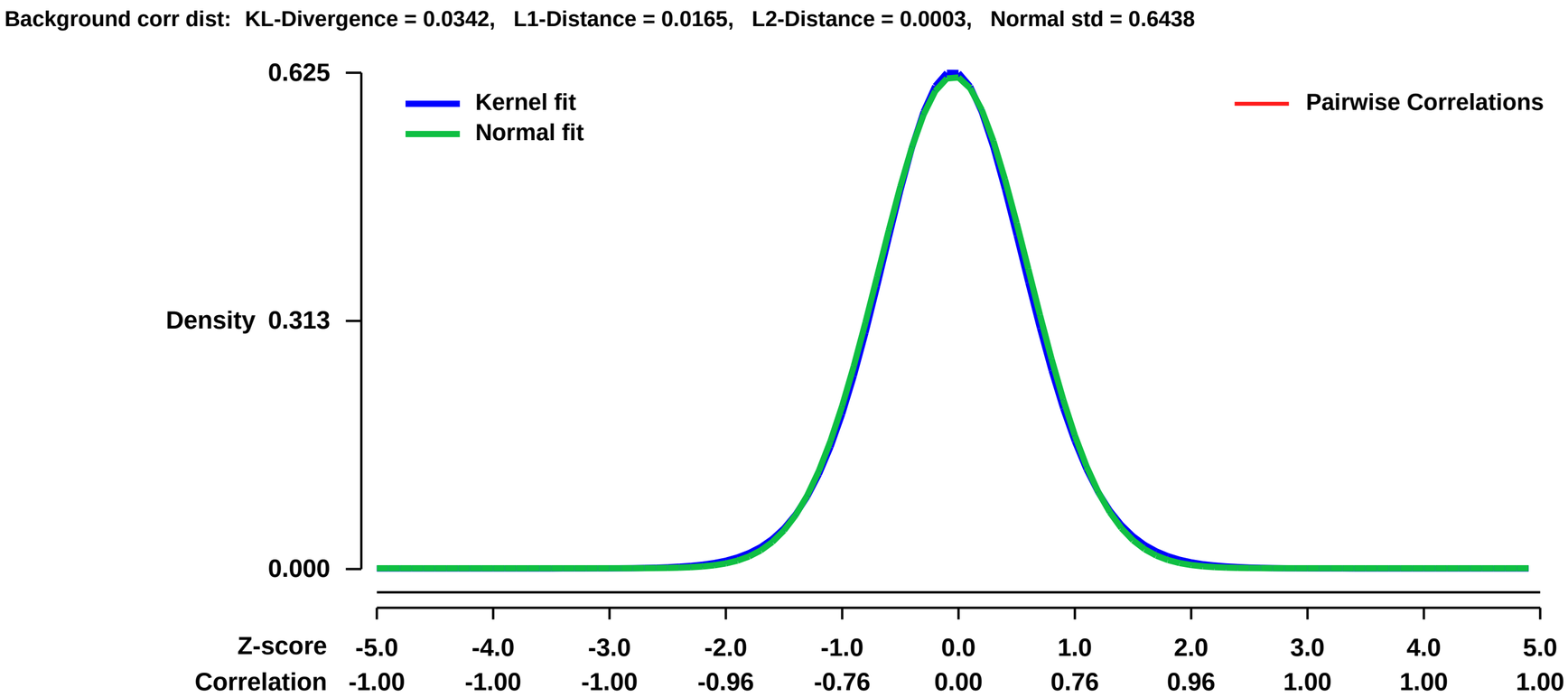

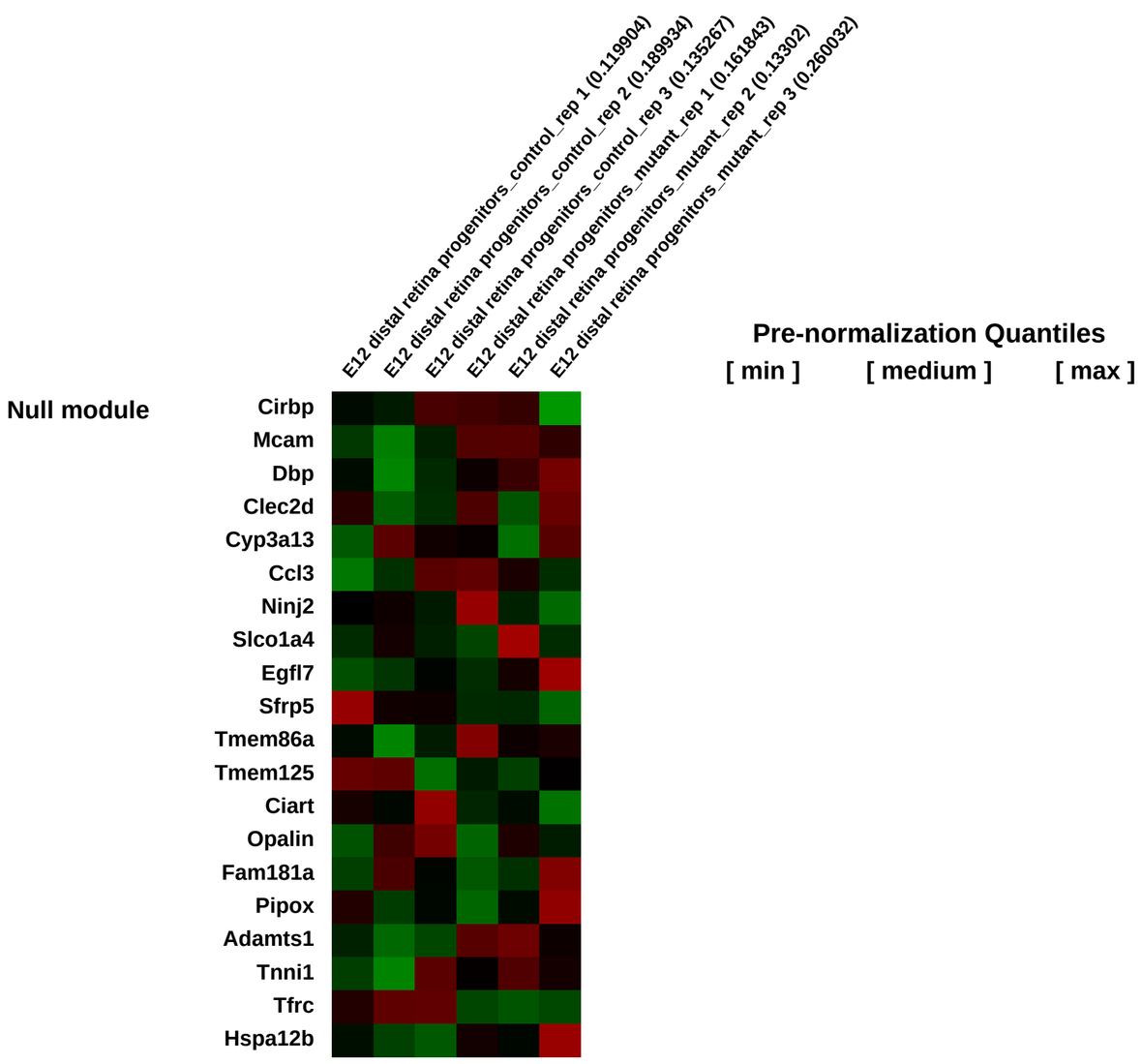

GEO Series "GSE7948" Expression Profiles

Num of samples in this series: 13

Scale of expression profile Z-scores

-3.0 -2.0 -1.0 0.0 1.0 2.0 3.0

GEO Link:	http://www.ncbi.nlm.nih.gov/geo/query/acc.cgi?acc=GSE7948
Status:	Public on Jun 22 2009
Title:	In vitro modeling of primordial germ cell development
Organism:	Mus musculus
Experiment type:	Expression profiling by array
Platform:	GPL1261
Pubmed ID:	19578360
Summary & Design:	**Summary:** Transgenic StellaGFP ESCs were used to derive primordial germ cells during embryoid body (EB) differentiation, and microarry analysis used to compared FACS sorted Stella-positive cells of day 7 Ebs with the parental ESCs and Stella-negative cells of day 7 Ebs. **Keywords: in vitro, primordial germ cells, embryonic stem cells, stella** **Overall design:** Four replicates of Stella-positive day 7 cells were compared to two replicates of stella-negative day 7 cells. Also, there were three replicated of FACS sorted Stella-negative ESCs, two replicated of FACS-sorted Stella-postive ESCs, and two replicates of unsorted StellaGFP ESCs.

Background corr dist: KL-Divergence = 0.0827, L1-Distance = 0.0355, L2-Distance = 0.0024, Normal std = 0.4733

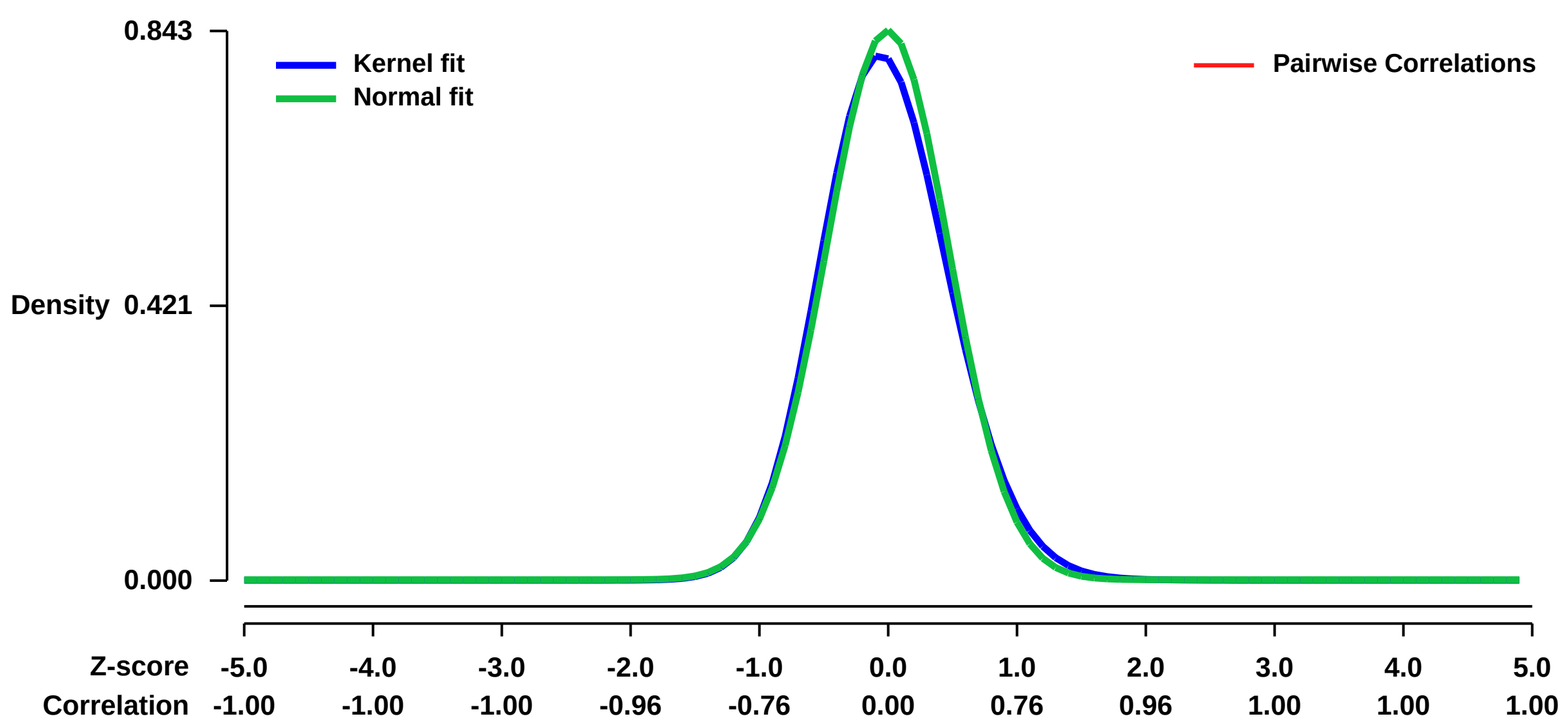

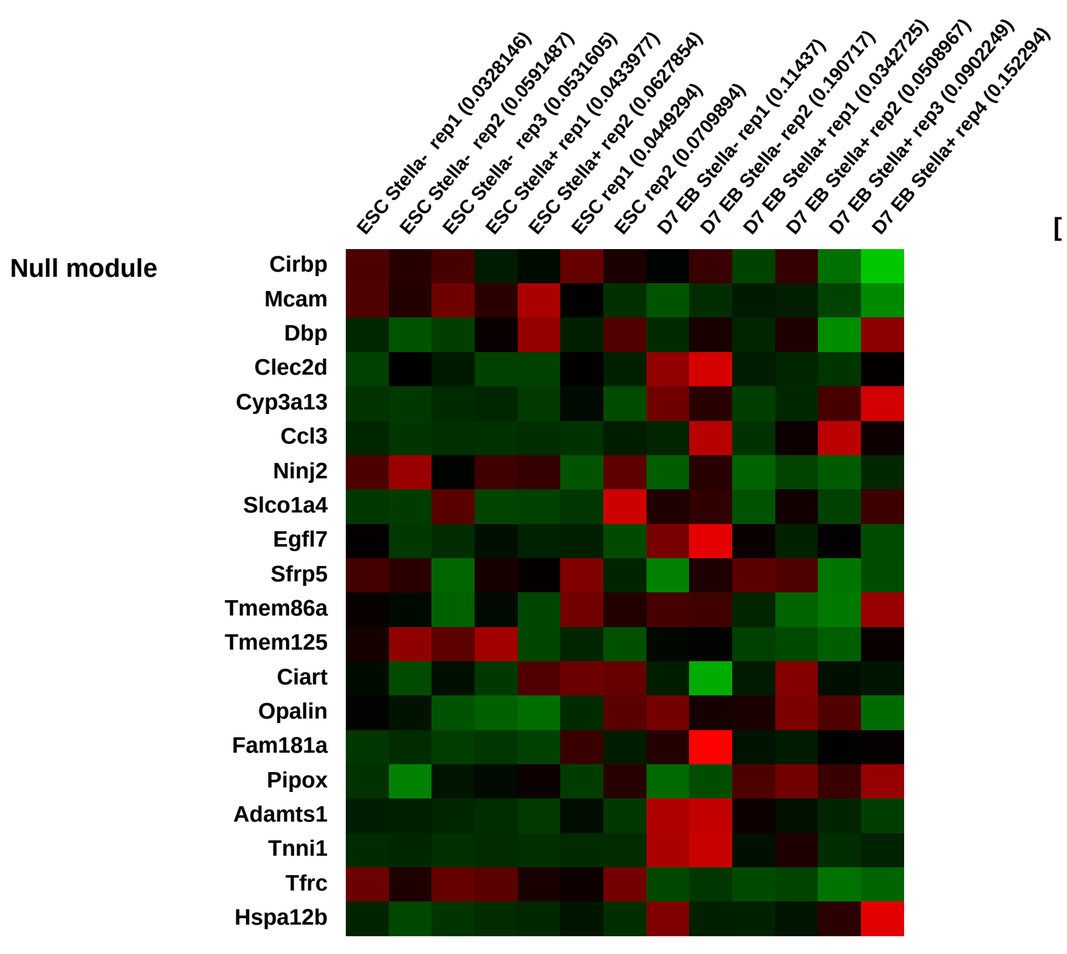

GEO Series "GSE42061" Expression Profiles

Num of samples in this series: 12

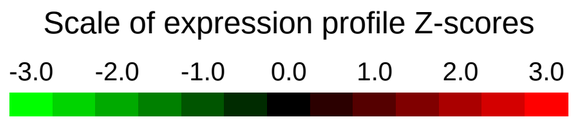

GEO Link:	**http://www.ncbi.nlm.nih.gov/geo/query/acc.cgi?acc=GSE42061**
Status:	**Public on Nov 07 2012**
Title:	**hyperlipidemia impaired innate response**
Organism:	**Mus musculus**
Experiment type:	**Expression profiling by array**
Platform:	**GPL1261**
Pubmed ID:	
Summary & Design:	**Summary:** **To explore the effect of hyperlipidemia on macrophages' innate immune response to Porphyromonas gingivalis invasion** **Overall design:** **12 samples, 3 replicates in 4 groups, with cells from hyperlipidemic ApoE deficient mice and nonhyperlipidemic C57BL/6 mice stimulate with or without P.gingivalis(Pg)**

Background corr dist: **KL-Divergence = 0.0969, L1-Distance = 0.0429, L2-Distance = 0.0028, Normal std = 0.4676**

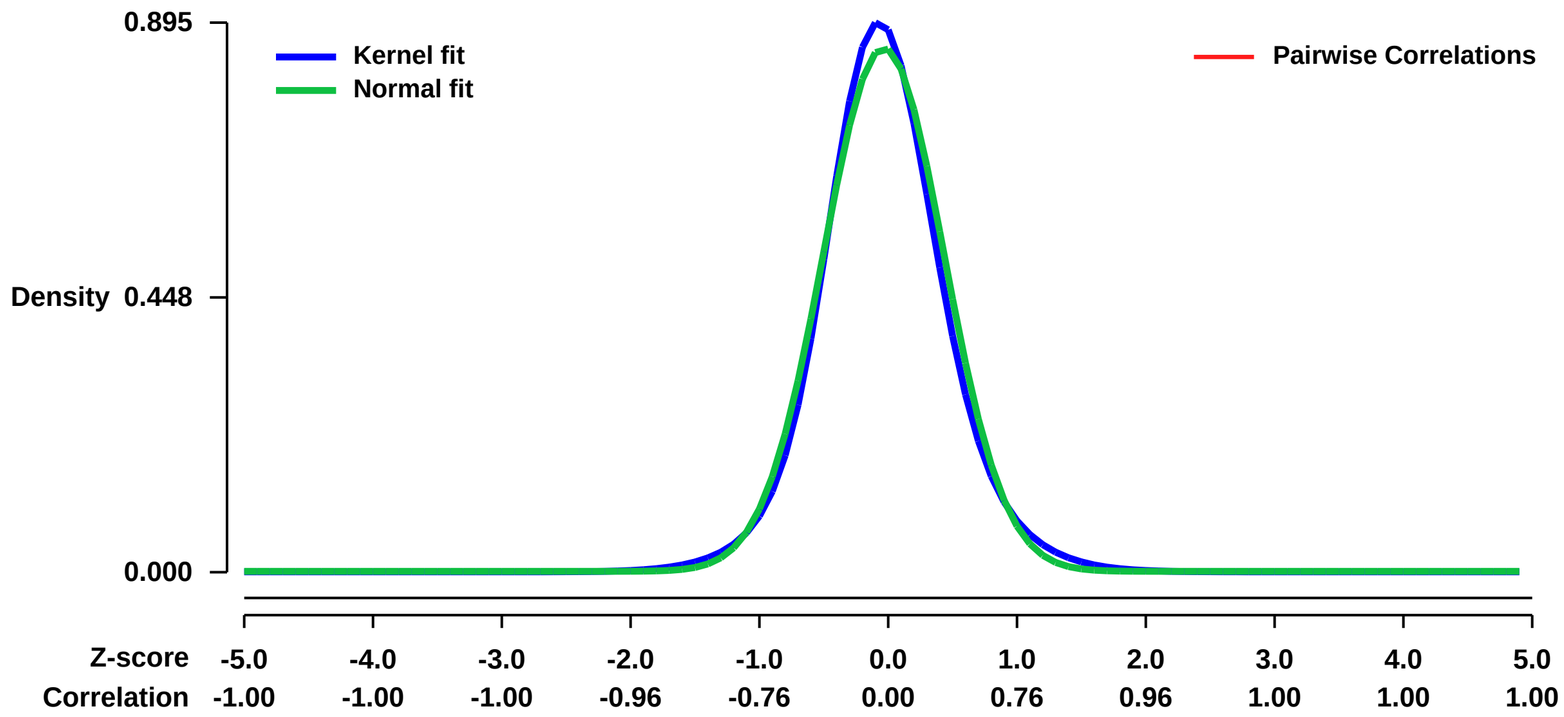

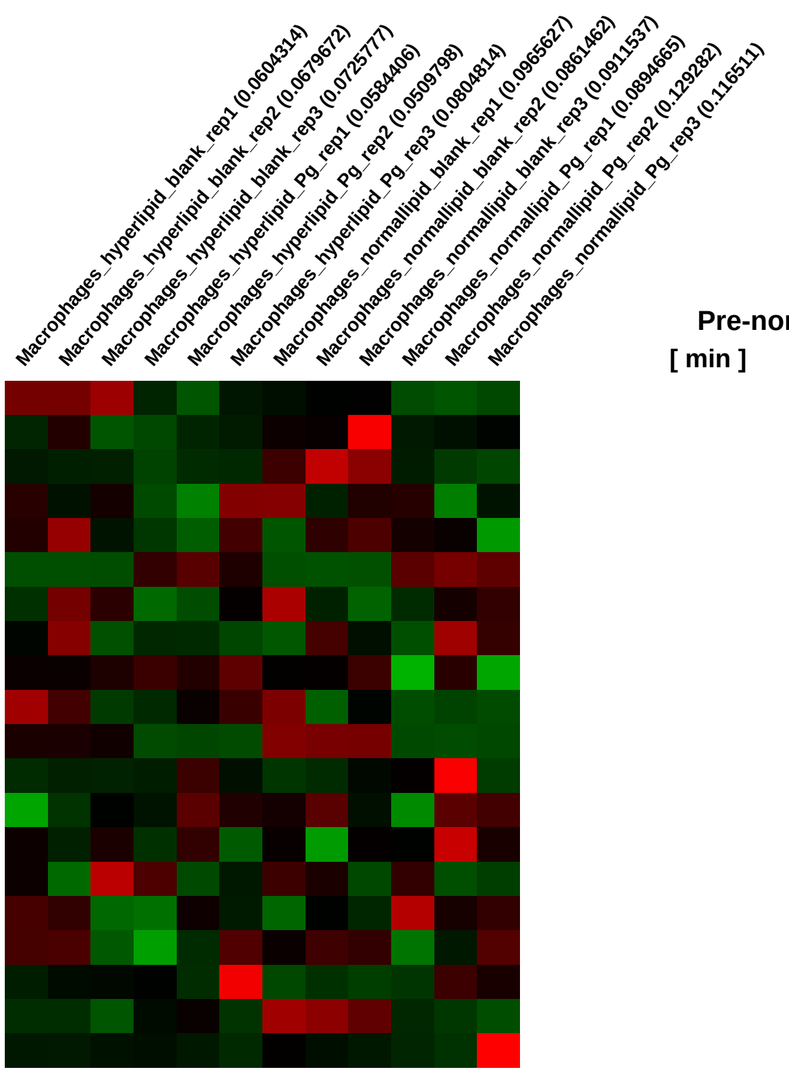

GEO Series "GSE21576" Expression Profiles

Num of samples in this series: 10

Scale of expression profile Z-scores

-3.0 -2.0 -1.0 0.0 1.0 2.0 3.0

GEO Link:	http://www.ncbi.nlm.nih.gov/geo/query/acc.cgi?acc=GSE21576
Status:	Public on Sep 01 2010
Title:	Expression profiles of laser dissected colon tumor samples of wild-type mice and vil-Cre-Bcl9-/-/Bcl9l-/- mice
Organism:	Mus musculus
Experiment type:	Expression profiling by array
Platform:	GPL1261
Pubmed ID:	20682801
Summary & Design:	**Summary:** To investigate the impact of ablating Bcl9/Bcl9l on tumorigenesis, 6-8- week-old mice were exposed first to a single dose dimethylhydrazine (DMH, 44 mg/kg body weight), which is metabolized in the liver to carcinogenic azoxymethane (AOM), followed by 7 days oral administration of 2 % dextrane sulfate sodium (DSS) in the drinking water. This regimen results in the emergence of dysplastic adenomas, which progress to differentiated adenocarcinomas that are morphologically similar to human colorectal adenocarcinomas and typically harbor ˛†-catenin stabilizing mutations of GSK3ˆ phosphorylation sites. Accordingly, these tumors present hallmarks of active Wnt signaling such as accumulation of nuclear ˛†-catenin and expression of Wnt target genes. **Overall design:** Total RNA of laser dissected samples from five different tumors each of two wild-type mice and three vil-Cre-Bcl9-/-/Bcl9l-/- mice was collected and resulting amplified cDNA hybridized to Affymetrix Mouse Genome 430 2.0 arrays. Samples are labeled as follows: Genotype_TumorID_MouseID_UniqueID.

Background corr dist: KL-Divergence = 0.1042, L1-Distance = 0.0294, L2-Distance = 0.0015, Normal std = 0.4299

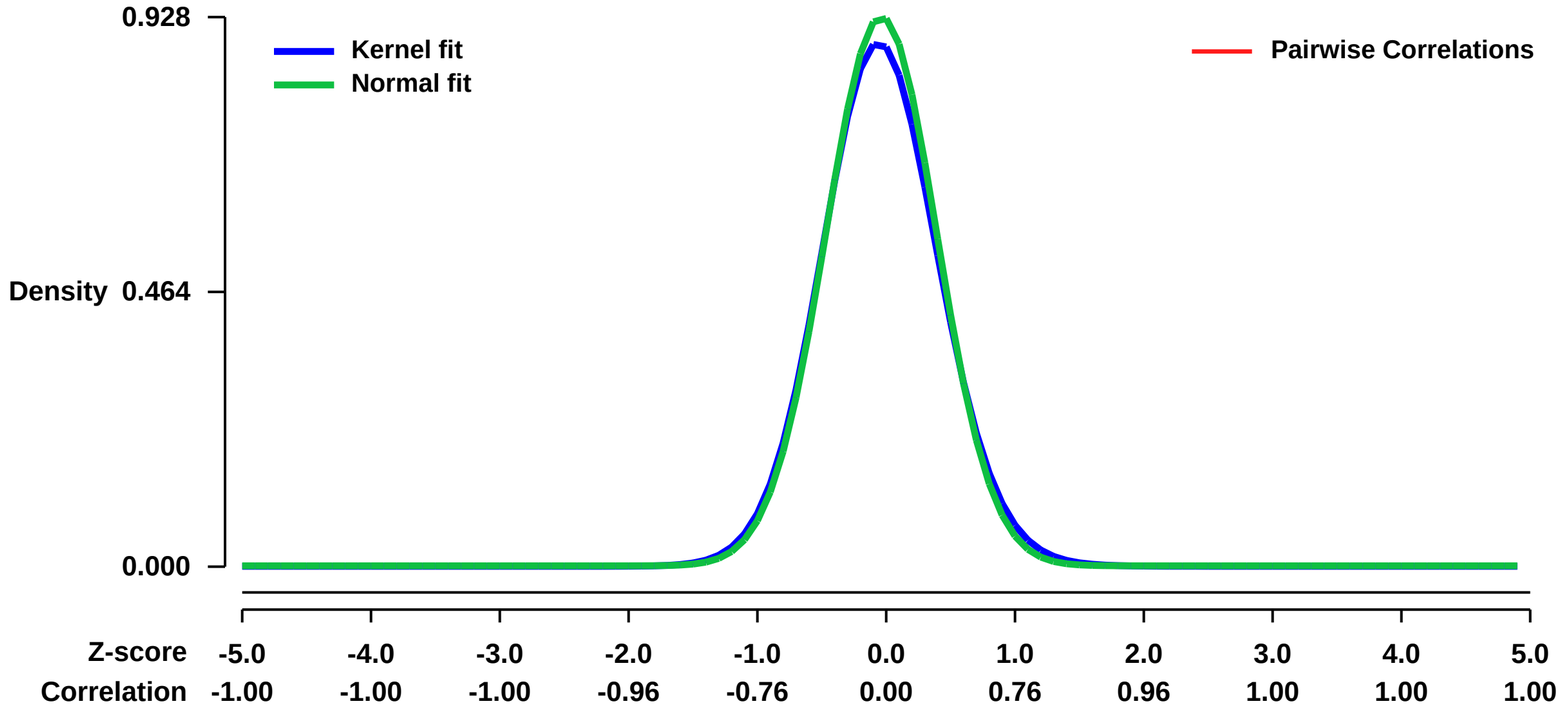

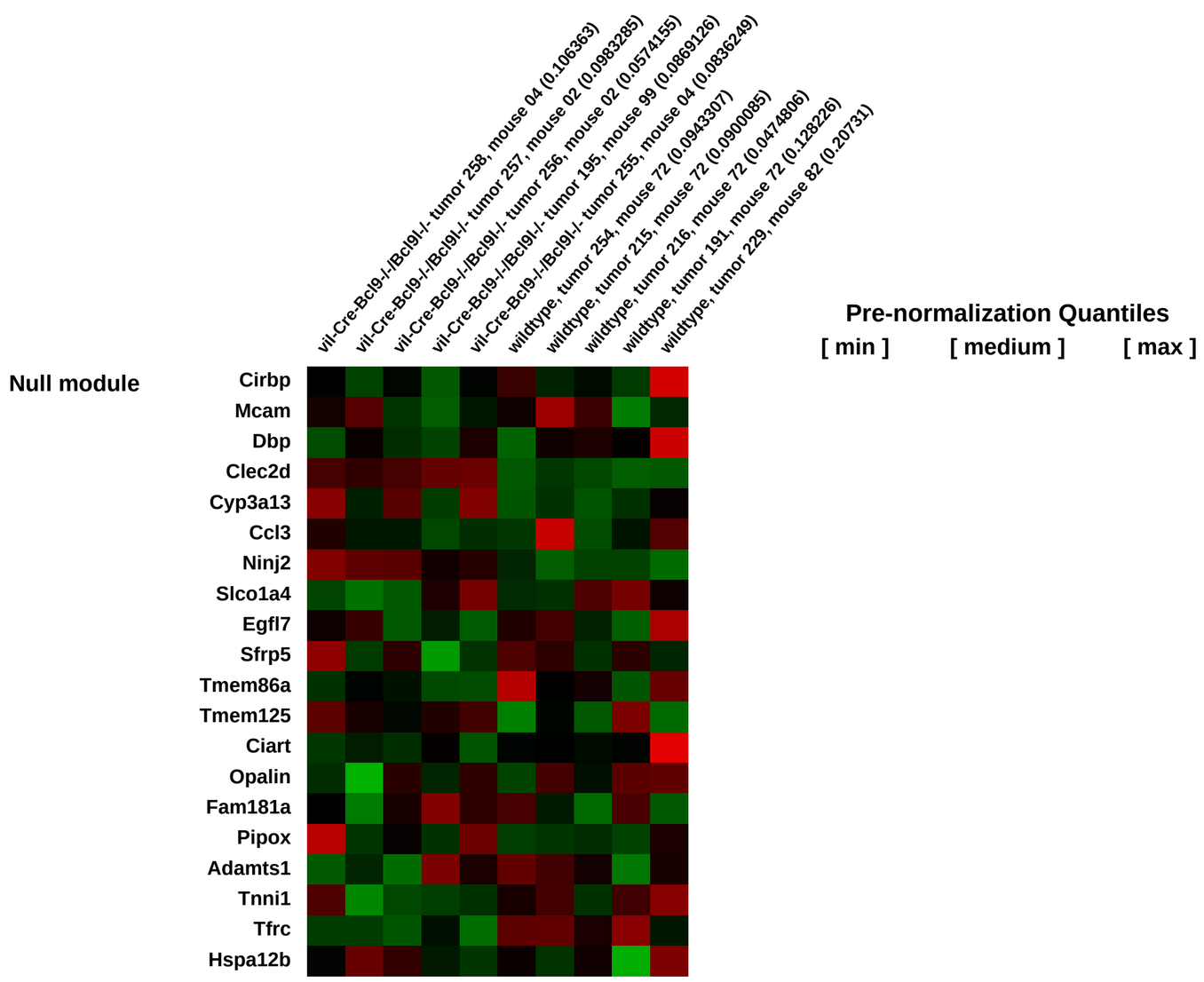

GEO Series "GSE15155" Expression Profiles

Num of samples in this series: 12

Scale of expression profile Z-scores

-3.0 -2.0 -1.0 0.0 1.0 2.0 3.0

GEO Link:	http://www.ncbi.nlm.nih.gov/geo/query/acc.cgi?acc=GSE15155
Status:	Public on Jan 04 2010
Title:	Gene profiling of quiescent and activated skeletal muscle satellite cells by an in vivo approach
Organism:	Mus musculus
Experiment type:	Expression profiling by array
Platform:	GPL1261
Pubmed ID:	19962952
Summary & Design:	**Summary:** The satellite cell of skeletal muscle provides a paradigm for quiescent and activated tissue stem cell states. We have carried out transcriptome analyses by comparing satellite cells from adult skeletal muscles, where they are mainly quiescent, with cells from growing muscles, regenerating (mdx) muscles, or with cells in culture, where they are activated. Our study gives new insights into the satellite cell biology during activation and in respect with its niche. We used microarrays to study the global programme of gene expression underlying adult satellite cell quiescence compared to activation states and to identify distinct classes of up-regulated genes in these two different states **Overall design:** Skeletal muscle satellite cells were isolated by flow cytrometry using the GFP fluorescence marker from Pax3GFP/+ mice skeletal muscle. The transcriptome of quiescent satellite cells from adult Pax3GFP/+ muscle was compared to the transcriptome of activated satellite cells obtained from three different samples: 1) regenerating Pax3GFP/+:mdx/mdx muscle (Ad.mdx) , 2) growing 1 week old Pax3GFP/+ muscle (1wk), and 3) adult Pax3GFP/+ cells after 3 days in culture (Ad.cult).

Background corr dist: KL-Divergence = 0.0419, L1-Distance = 0.0196, L2-Distance = 0.0005, Normal std = 0.5936

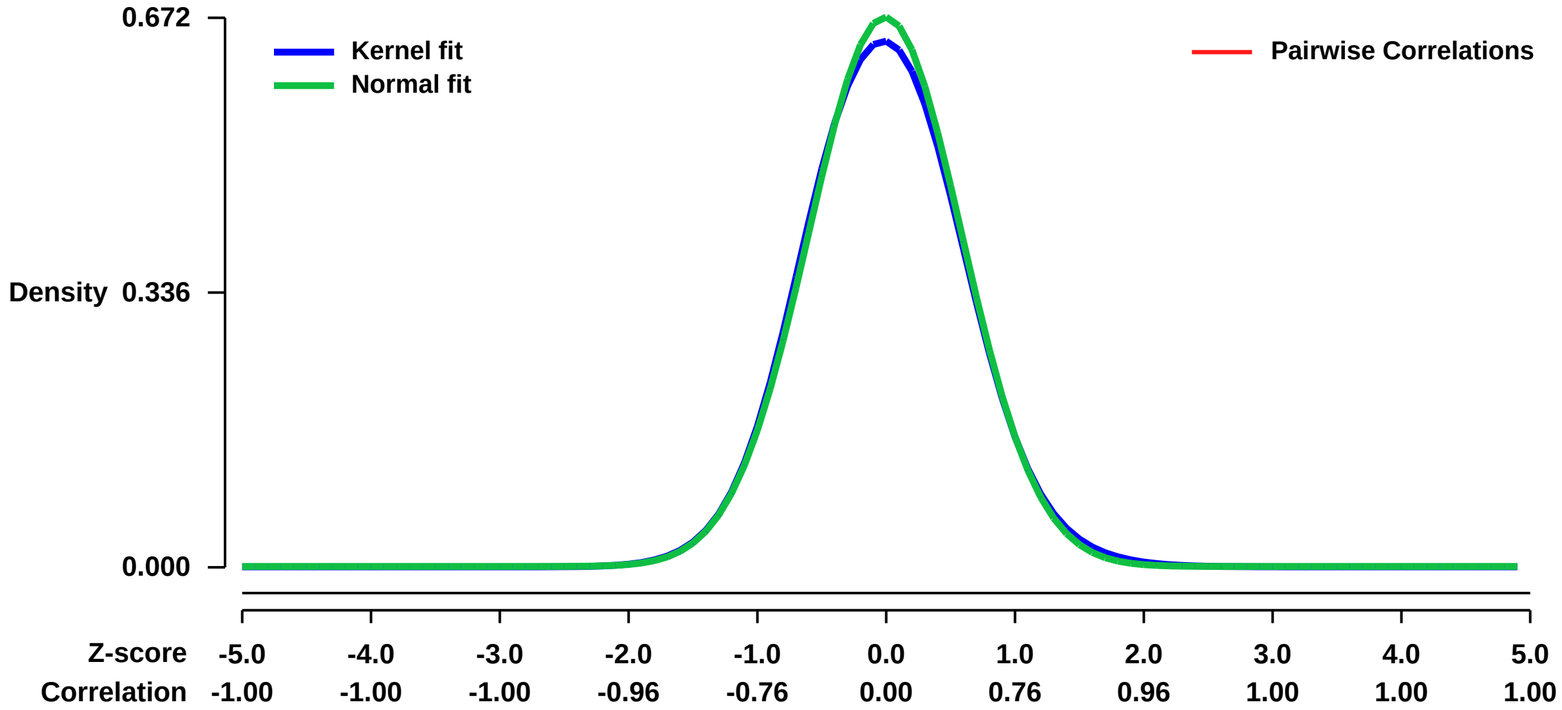

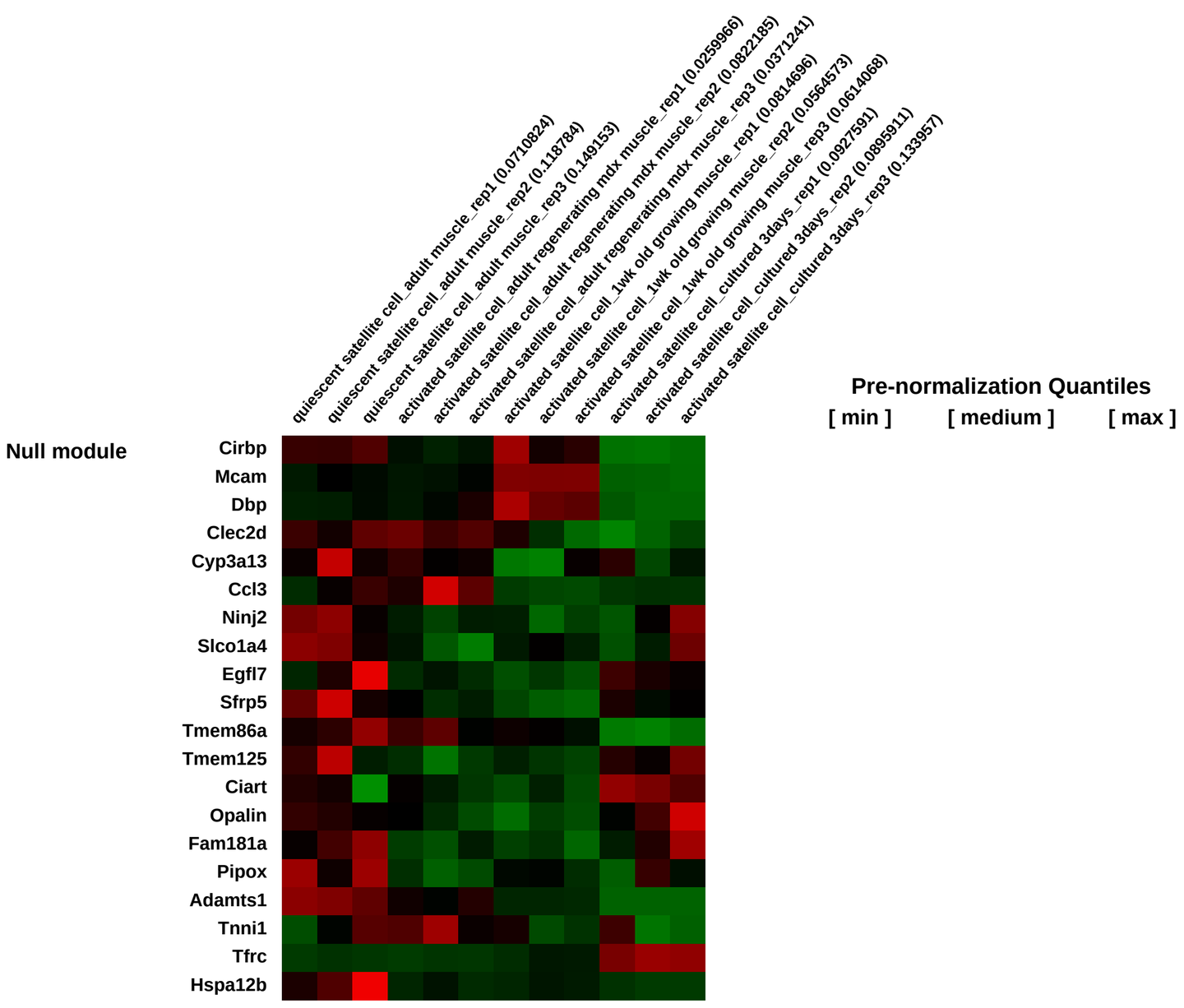

GEO Series "GSE12337" Expression Profiles

Num of samples in this series: 16

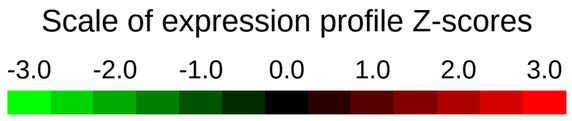

GEO Link:	http://www.ncbi.nlm.nih.gov/geo/query/acc.cgi?acc=GSE12337
Status:	Public on Aug 06 2008
Title:	Transcriptomic analysis of PPARalpha-dependent alterations during cardiac hypertrophy
Organism:	Mus musculus
Experiment type:	Expression profiling by array
Platform:	GPL1261
Pubmed ID:	18812456
Summary & Design:	**Summary:** Findings suggest that PPARalpha plays a decisive role in the development of hypertrophy, affecting the functional outcome of the heart. Unfortunately, information on the nature of PPARalpha-dependent processes in cardiac hypertrophy is fragmentary and incomplete. The primary aim of this study was to identify the processes and signaling pathways regulated by PPARalpha in hearts challenged by a chronic pressure overload by means of whole genome transcriptomic analysis. Second, we wanted to gain insight how PPARalpha modulates the identified processes, e.g. by trans-activation or by trans-repression. **Keywords: 28 days of TAC** **Overall design:** Wild-type and PPARalpha-/- mice were sham-operated or subjected to TAC for 28 days. Left ventricular gene expression profile was determined using Affymetrix 430 2.0 arrays containing over 45,000 probe sets (covering over 34,000 mouse genes) to detect PPARalpha-related differences in cardiac gene expression under basal conditions and after imposition of a sustained hemodynamic stress.

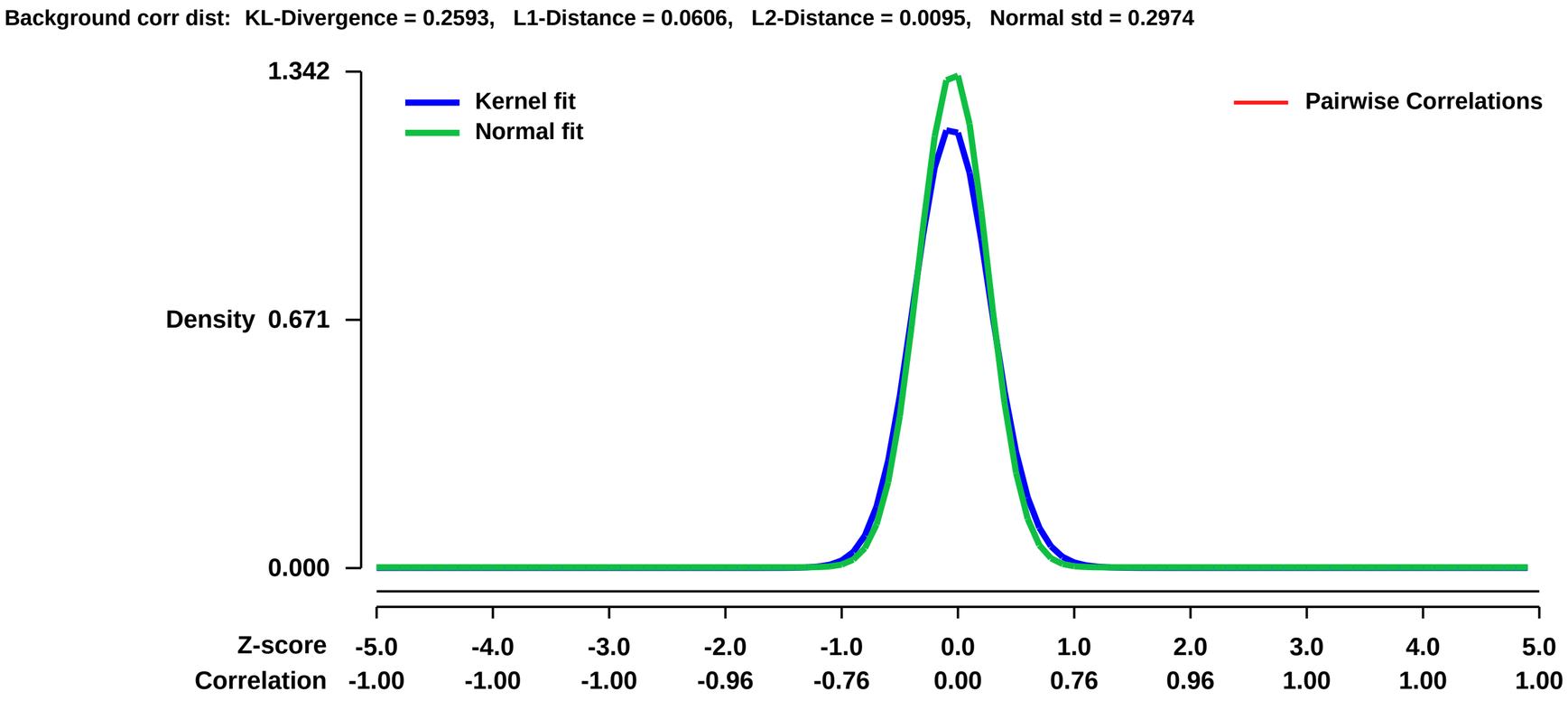

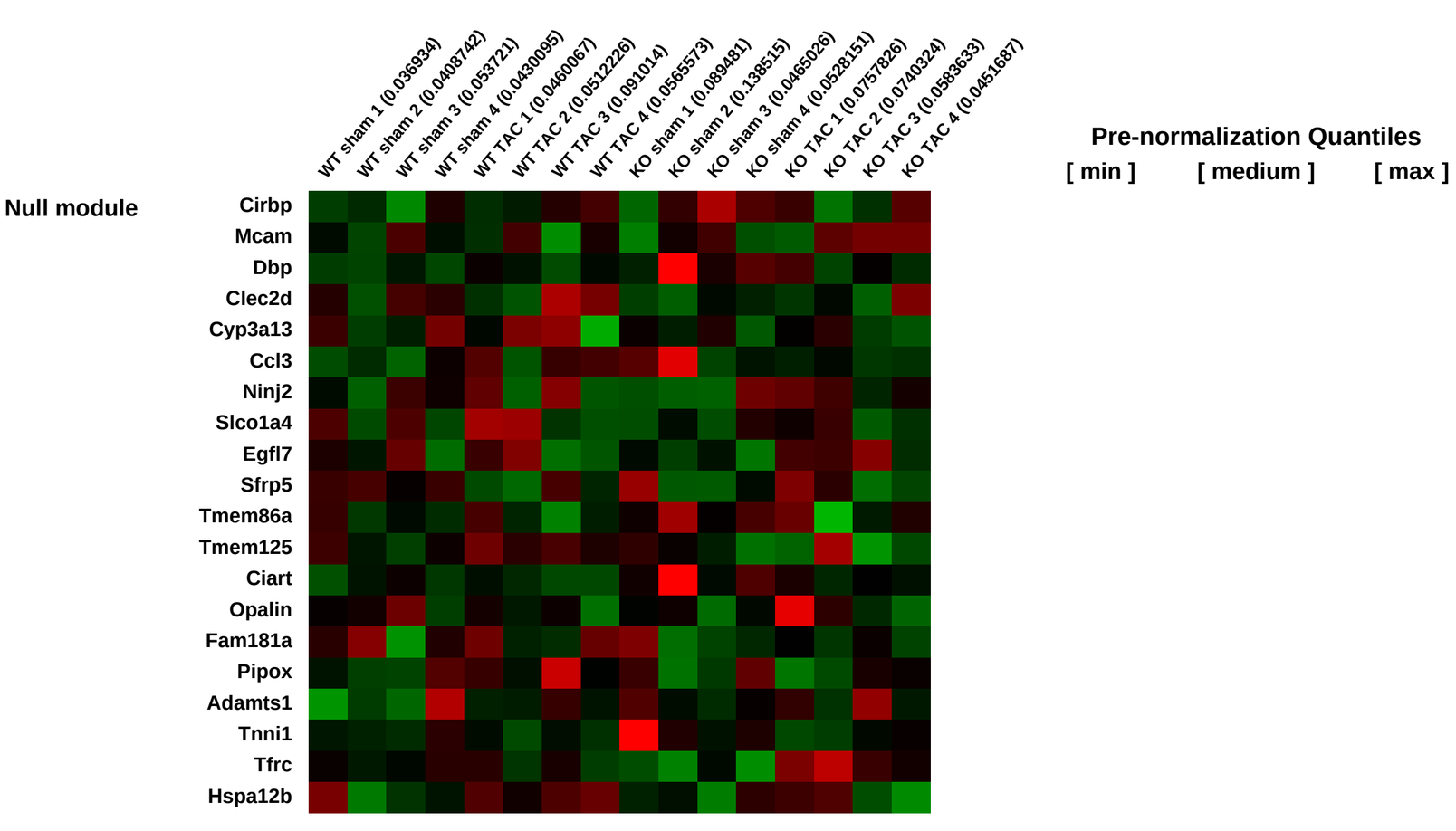

GEO Series "GSE19534" Expression Profiles

Num of samples in this series: 26

Scale of expression profile Z-scores

-3.0 -2.0 -1.0 0.0 1.0 2.0 3.0

GEO Link:	http://www.ncbi.nlm.nih.gov/geo/query/acc.cgi?acc=GSE19534
Status:	Public on Jul 22 2010
Title:	Alpha-synuclein deficiency affects brain Foxp1 expression and ultrasonic vocalization
Organism:	Mus musculus
Experiment type:	Expression profiling by array
Platform:	GPL1261
Pubmed ID:	20056137
Summary & Design:	**Summary:** Alpha-synuclein is an abundant protein implicated in synaptic function and plasticity, but the molecular mechanism of its action is not understood. Missense mutations and gene duplication/triplication events result in Parkinson's disease, a neurodegenerative disorder of old age with impaired movement and emotion control. Here, we systematically investigated the striatal as well as the cerebellar transcriptome profile of alpha-synuclein-deficient mice via a genome-wide microarray survey in order to gain hypothesis-free molecular insights into the physiological function of alpha-synuclein. A genotype-dependent, specific and strong downregulation of forkhead box P1 (Foxp1) transcript levels was observed in all brain regions from postnatal age until old age and could be validated by qPCR. In view of the co-localization and heterodimer formation of FOXP1 with FOXP2, a transcription factor with a well established role for vocalization, and the reported regulation of both alpha-synuclein and FOXP2 expression during avian song learning, we performed a detailed assessment of mouse movements and vocalizations in the postnatal period. While there was no difference in isolation-induced behavioral activity in these animals, the alpha-synuclein-deficient mice exhibited an increased production of isolation-induced ultrasonic vocalizations (USVs). This phenotype might also reflect the reduced expression of the anxiety-related GABA-A receptor subunit gamma 2 (Gabrg2) we observed. Taken together, we identified an early behavioral consequence of alpha-synuclein deficiency and accompanying molecular changes, which supports the notion that the neural connectivity of sound or emotion control systems is affected. **Overall design:** Factorial design comparing SNCA knock-out mice with wild type littermates in two different tissues (striatum, cerebellum) at two different timepoints (6 and 21 month)

Background corr dist: KL-Divergence = 0.0459, L1-Distance = 0.0209, L2-Distance = 0.0004, Normal std = 0.5868

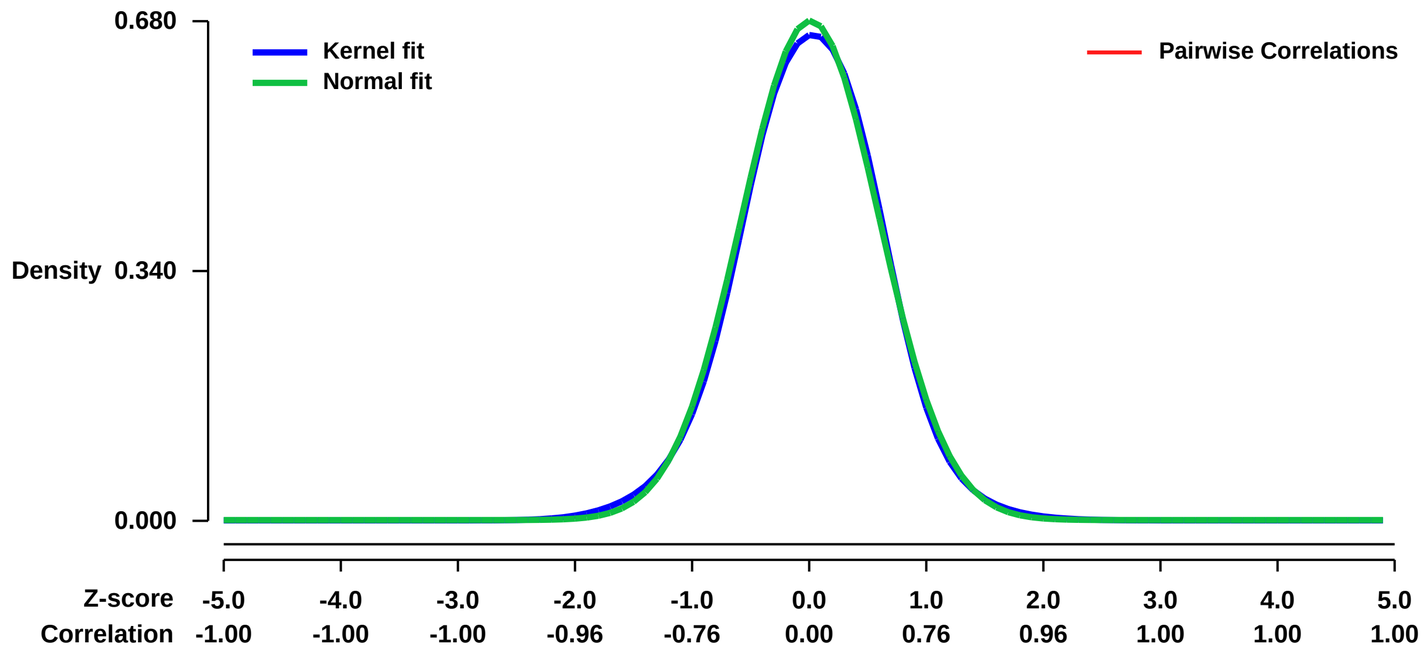

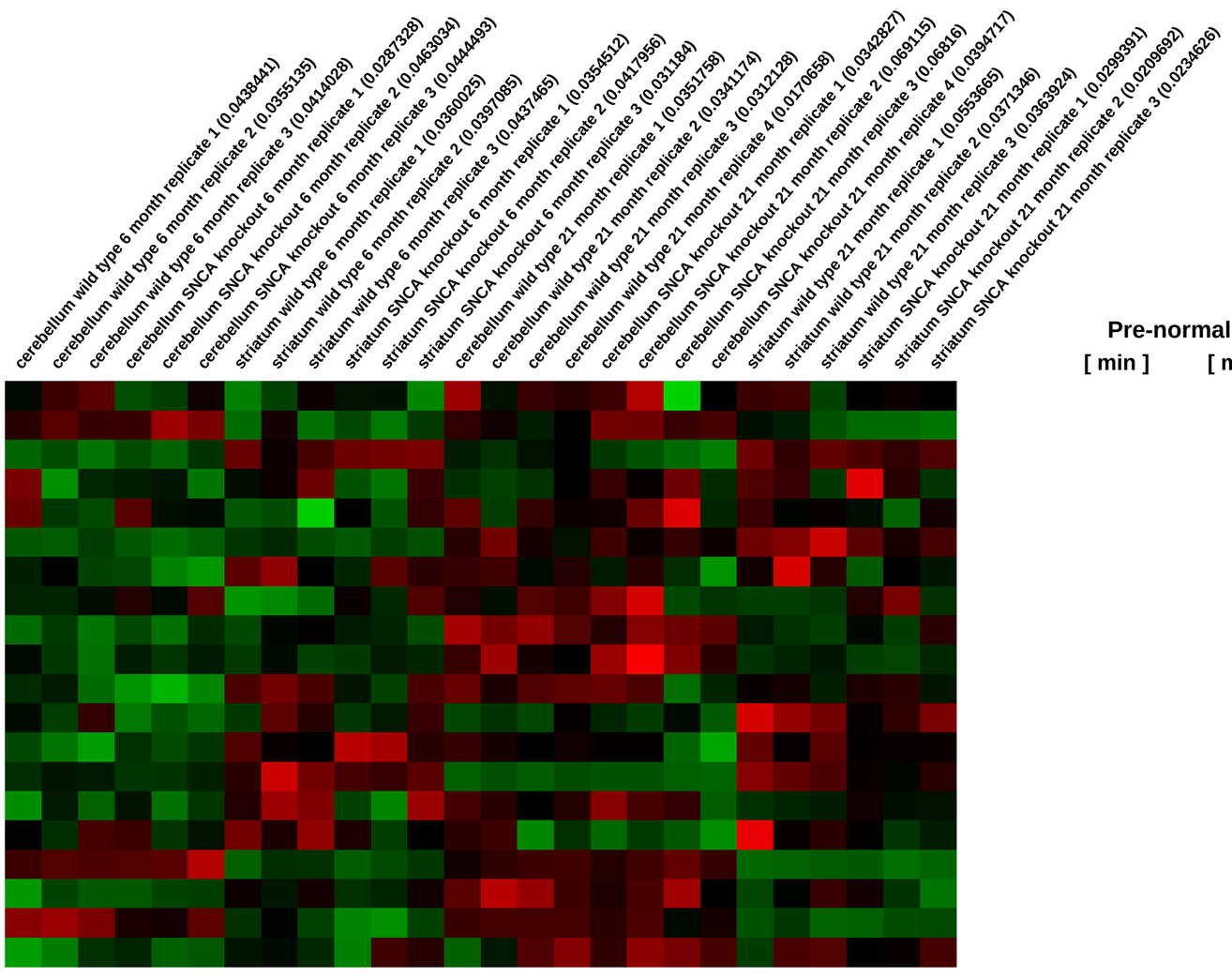

GEO Series "GSE25645" Expression Profiles

Num of samples in this series: 17

Scale of expression profile Z-scores

-3.0 -2.0 -1.0 0.0 1.0 2.0 3.0

GEO Link:	http://www.ncbi.nlm.nih.gov/geo/query/acc.cgi?acc=GSE25645
Status:	Public on May 09 2011
Title:	Ebf1 or Pax5 Haploinsufficiency Synergizes with STAT5 Activation to Initiate Acute Lymphoblastic Leukemia
Organism:	Mus musculus
Experiment type:	Expression profiling by array
Platform:	GPL1261
Pubmed ID:	21606506
Summary & Design:	**Summary:** STAT5 is critical for differentiation, proliferation and survival of progenitor B cells suggesting a possible role in Acute Lymphoblastic Leukemia (ALL). Herein, we show increased expression of activated STAT5 in ALL patients, which correlates with treatment outcome. Mutations in Ebf1 and Pax5, genes critical for B cell development have also been identified in human ALL. To determine whether mutations in Ebf1 or Pax5 synergize with STAT5 activation to induce ALL we crossed mice expressing a constitutively active form of STAT5 (Stat5b-CA) with mice heterozygous for Ebf1 or Pax5. Haploinsufficiency of either Pax5 or Ebf1 synergized with Stat5b-CA to rapidly induce ALL in 100% of the mice. The leukemic cells displayed reduced expression of both Pax5 and Ebf1 but this had little affect on most EBF1 or PAX5 target genes. However, a subset of these genes was deregulated and included a large percentage of potential tumor suppressor genes and oncogenes. Further, most of these genes appear to be jointly regulated by both EBF1 and PAX5. Our findings suggest a model whereby small perturbations in a self-reinforcing network of transcription factors critical for B cell development, specifically PAX5 and EBF1, cooperate with STAT5 activation to initiate ALL. **Overall design:** Gene expression profiling was performed on cells isolated from lymph nodes of Stat5b-CA x Ebf1+/- and Stat5b-CA x Rag2-/- leukemic mice and pre B cells sorted from bone marrow of C57BL/6 mice and Stat5b-CA transgenic mice. 17 Samples.

Background corr dist: KL-Divergence = 0.0897, L1-Distance = 0.0378, L2-Distance = 0.0030, Normal std = 0.4540

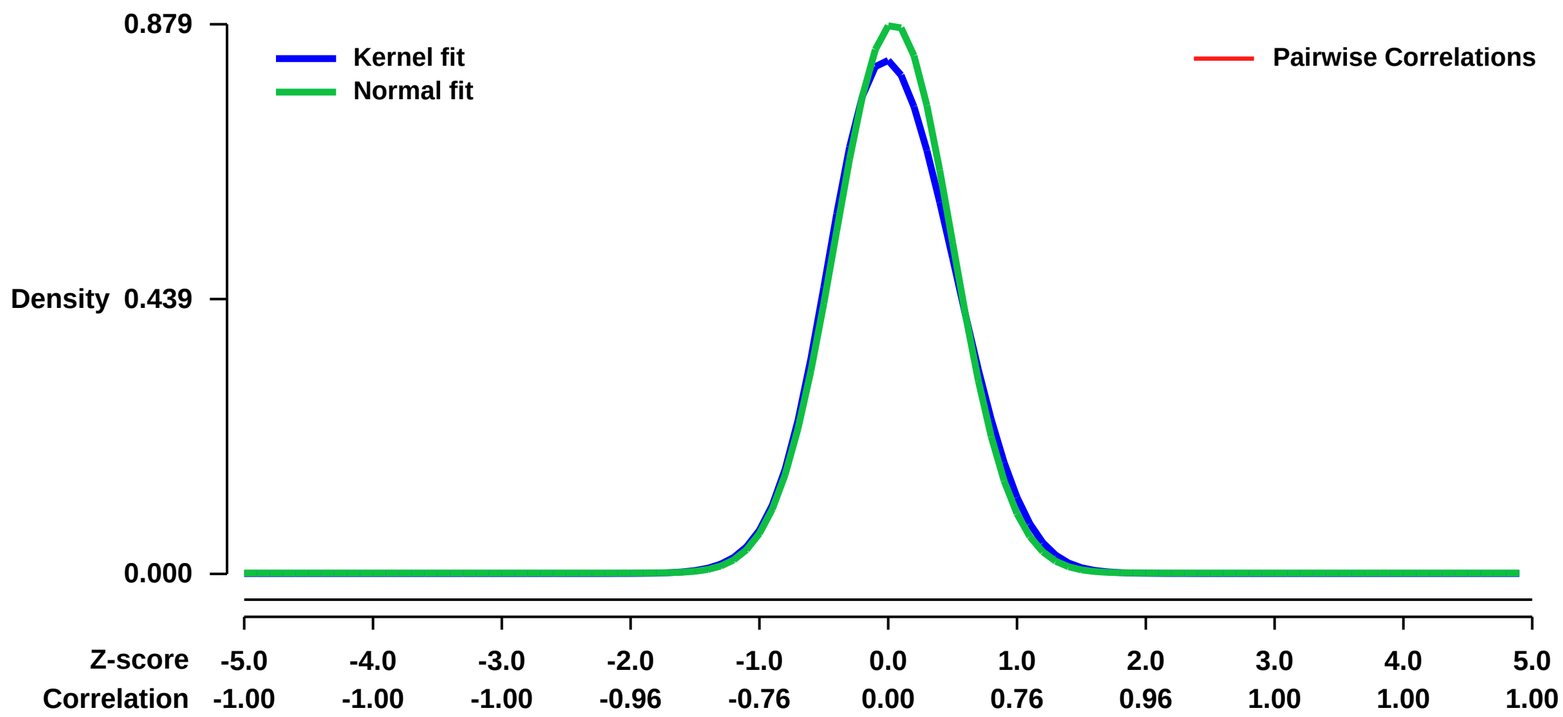

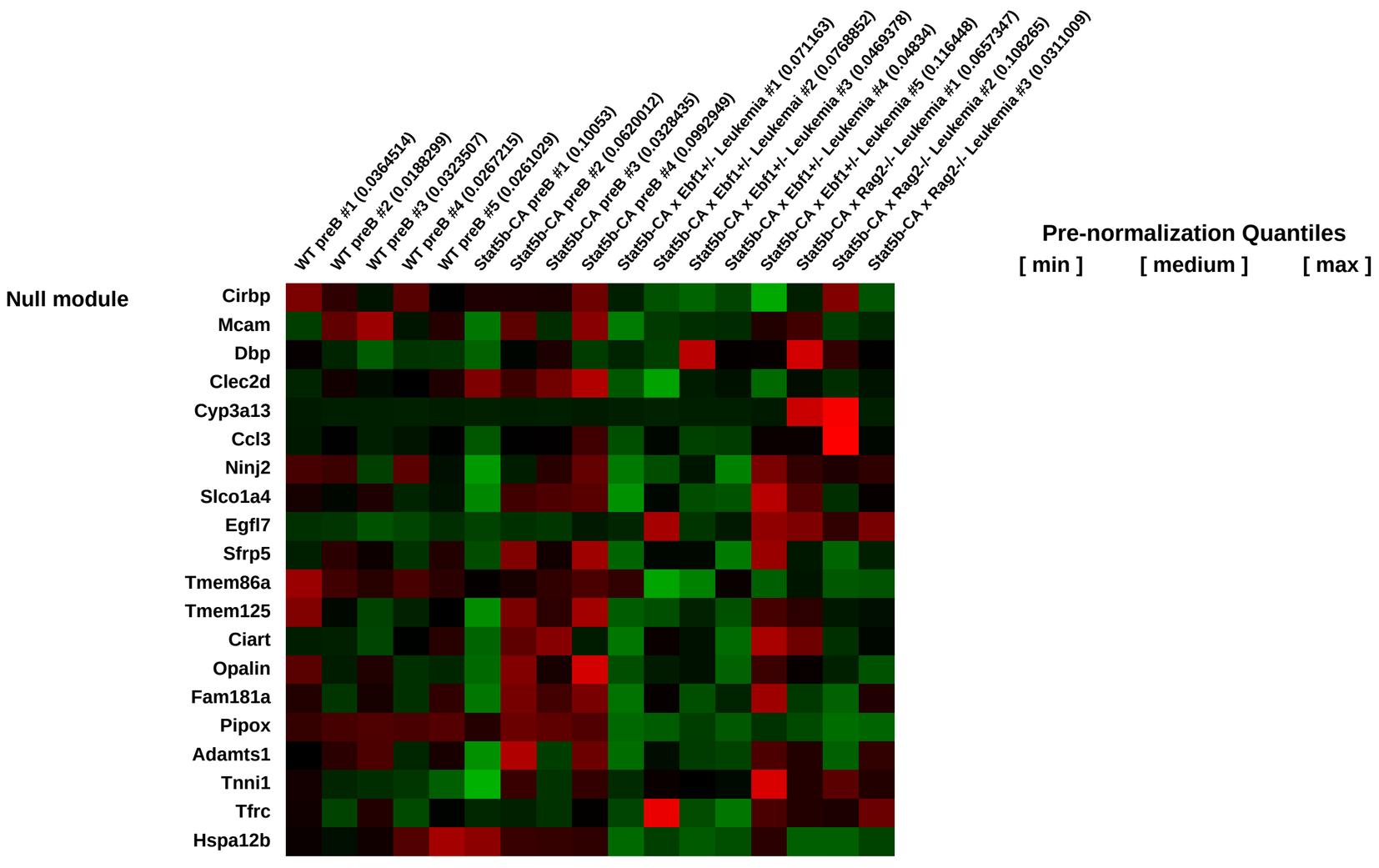

GEO Series "GSE16751" Expression Profiles

Num of samples in this series: 6

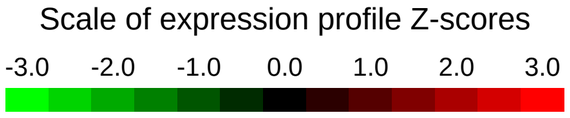

GEO Link:	http://www.ncbi.nlm.nih.gov/geo/query/acc.cgi?acc=GSE16751
Status:	Public on Jun 24 2009
Title:	Activation-induced cytidine deaminase accelerates clonal evolution in BCR-ABL1-driven acute lymphoblastic leukemia
Organism:	Mus musculus
Experiment type:	Expression profiling by array
Platform:	GPL1261
Pubmed ID:	
Summary & Design:	**Summary:** Activation-Induced Cytidine Deaminase (AID) is required for somatic hypermutation and immunoglobulin (Ig) class switch recombination in germinal center B lymphocytes. Occasionally, AID targets non-Ig genes, thereby contributing to B cell lymphomagenesis. We recently reported aberrant expression of AID in BCR-ABL1-driven acute lymphoblastic leukemia (ALL). To elucidate the biological significance of aberrant AID expression, we studied loss of AID function in a murine model of BCR-ABL1 ALL. Mice transplanted with BCR-ABL1-transduced AID-/- bone marrow had prolonged survival as compared to mice transplanted with leukemia cells generated from AID+/+ bone marrow. Consistent with a causative role of AID in genetic instability, AID-/- leukemia had a decreased frequency of amplifications, deletions and a lower frequency of mutations in non-Ig genes including Pax5 and Rhoh as compared to AID+/+ leukemias. AID-/- and AID+/+ ALL cells showed a markedly distinct gene expression pattern as determined by principle component analysis, with 2,365 genes differentially expressed. In contrast to AID+/+ leukemia, AID-/- ALL cells failed to downregulate a number of tumor suppressor genes such as Rhoh, Cdkn1a (p21), and Blnk (SLP65). We conclude that AID accelerates clonal evolution in BCR-ABL1 ALL by enhancing genetic instability, aberrant somatic hypermutation, and by transcriptional inactivation of tumor suppressor genes. **Overall design:** We used microarrays to detect differences in gene expression profiles between AID expressing leukemia and AID deficient leukemia

Background corr dist: KL-Divergence = 0.0295, L1-Distance = 0.0170, L2-Distance = 0.0003, Normal std = 0.6752

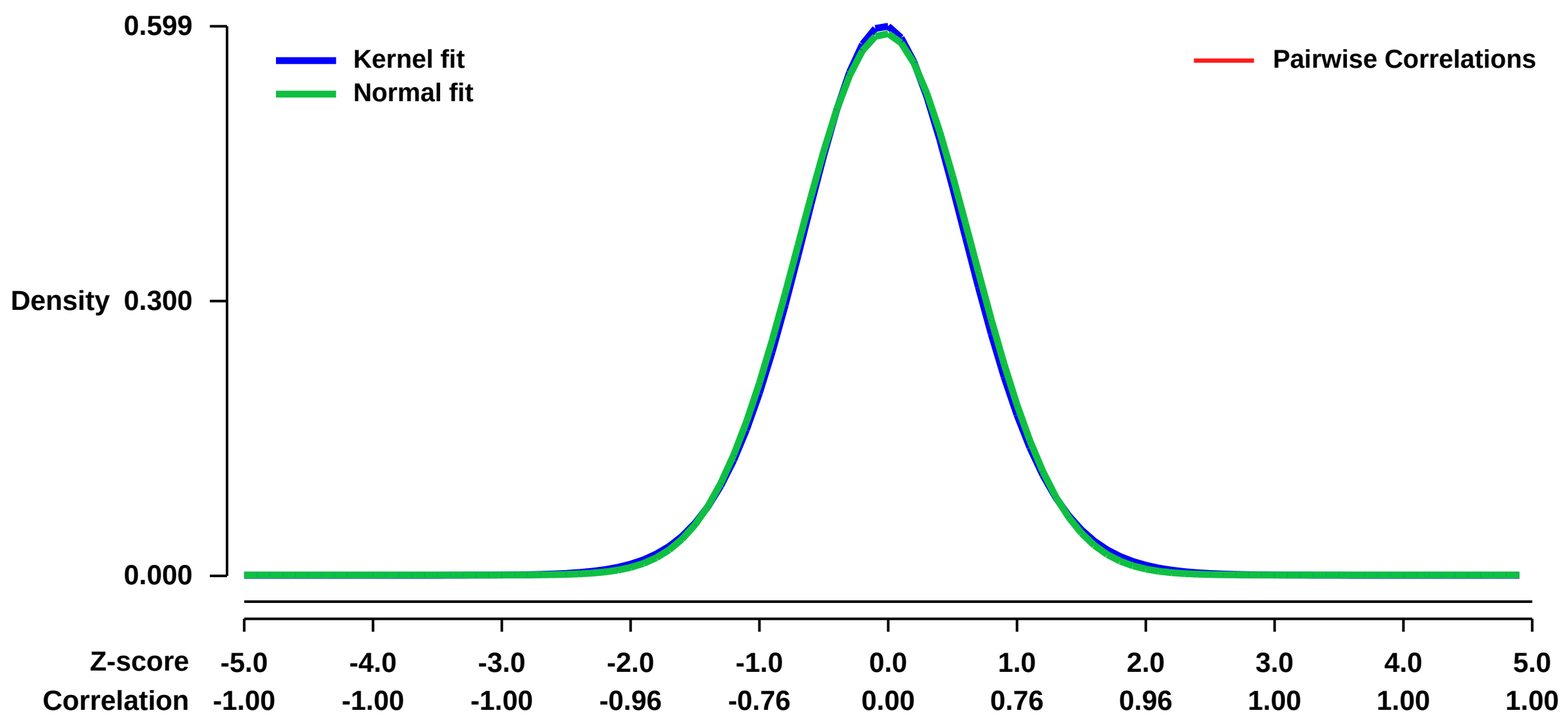

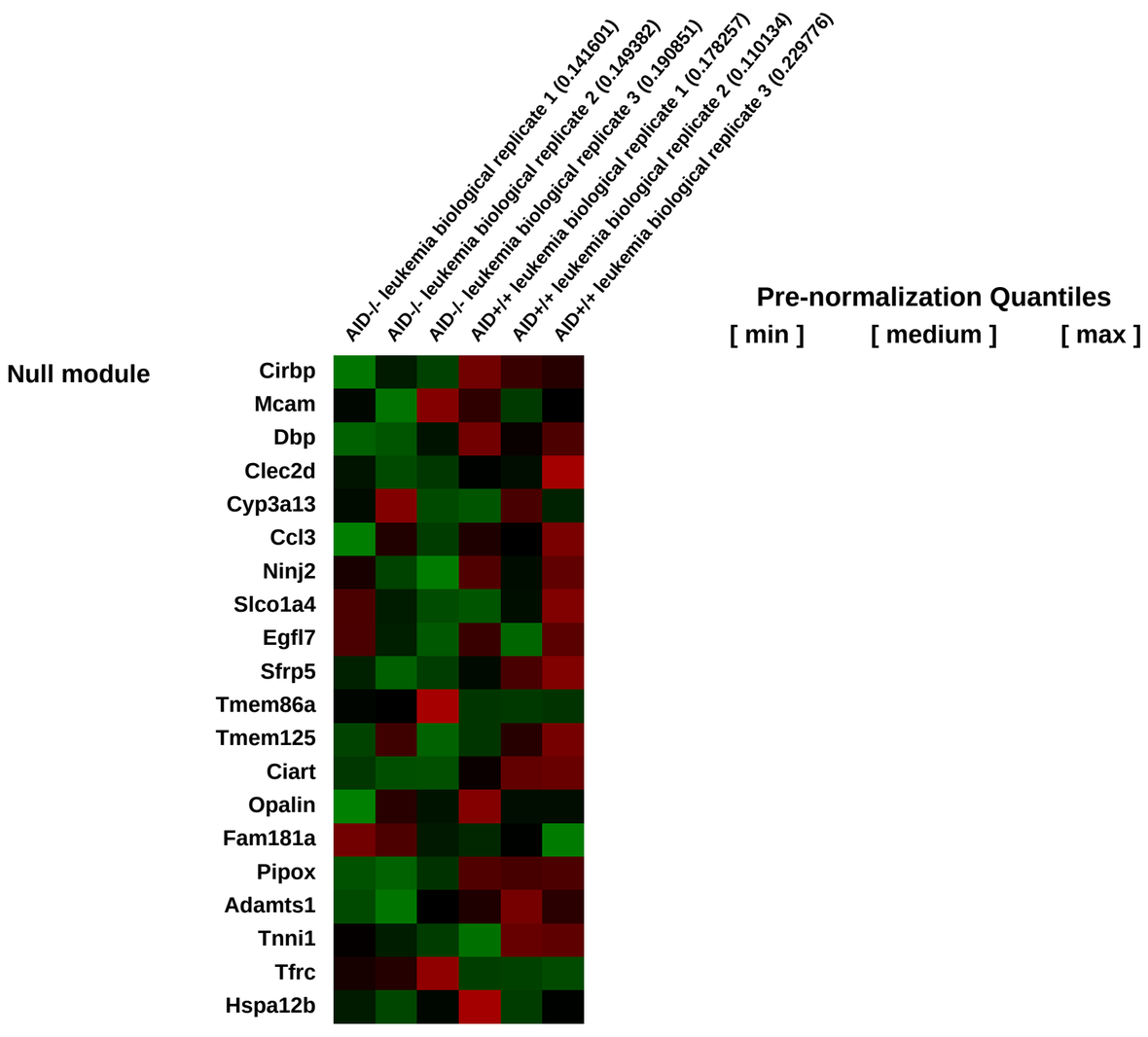

GEO Series "GSE23584" Expression Profiles

Num of samples in this series: 36

Scale of expression profile Z-scores

-3.0 -2.0 -1.0 0.0 1.0 2.0 3.0

GEO Link:	http://www.ncbi.nlm.nih.gov/geo/query/acc.cgi?acc=GSE23584
Status:	Public on Dec 31 2011
Title:	The Identification of Genetic Factors Influencing Susceptibility to Staphylococcus aureus Infection in mice susceptible and resistant to S. aureus infection
Organism:	Mus musculus
Experiment type:	Expression profiling by array
Platform:	GPL1261
Pubmed ID:	22690378
Summary & Design:	**Summary:** It has been shown that inbred strains of mice exhibit variable susceptibility to S. aureus infection, but the specific genes responsible for this differential phenotype are unknown. Using ISHM to identify genomic regions associated with the phenotypes, we considered genes within those interval to be candidate genes and used the gene expression patterns of the genes contained in the region to determine whether the genes are differentially expressed between the 2 phenotypically different groups of mice. **Overall design:** To identify genes differentially expressed between mice susceptible and resistant to S. aureus infection that could contribute to host susceptibility to S. aureus infection, we compared the gene expression profiles between 2 groups of mice where 3 were susceptible (A/J, BALBcBy/J, AKR/J) and resistant (C57BL/J, C3H/HeJ, NOD/ShiLtJ) to S. aureus. The susceptible group had high bacterial count values in the kidney while the resistant group had low values.

Background corr dist: KL-Divergence = 0.0904, L1-Distance = 0.0952, L2-Distance = 0.0201, Normal std = 0.4948

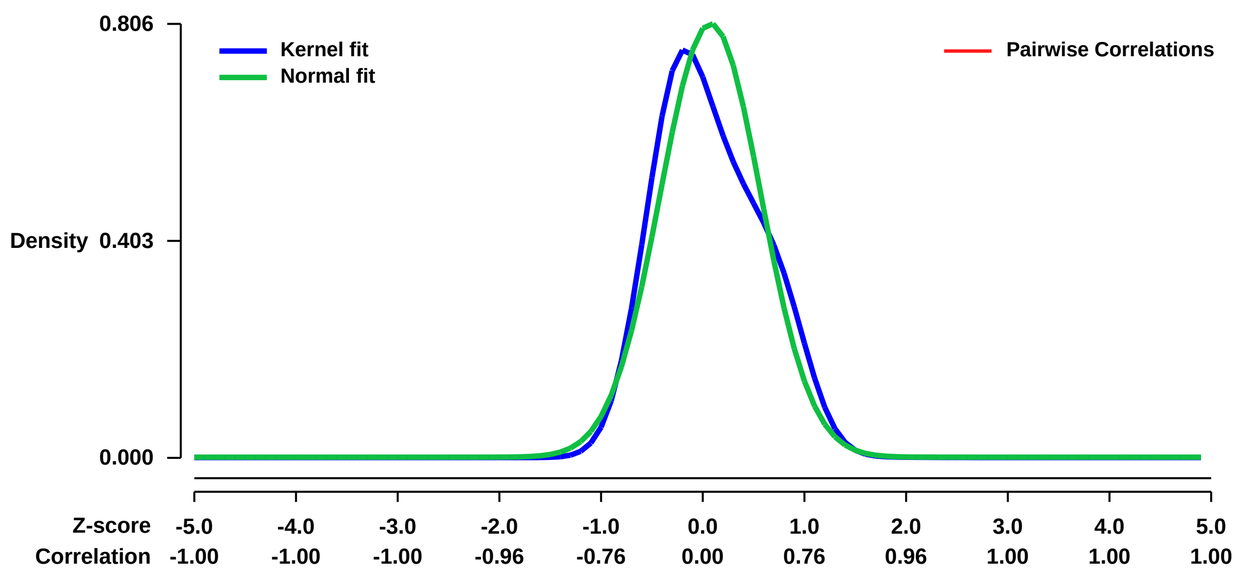

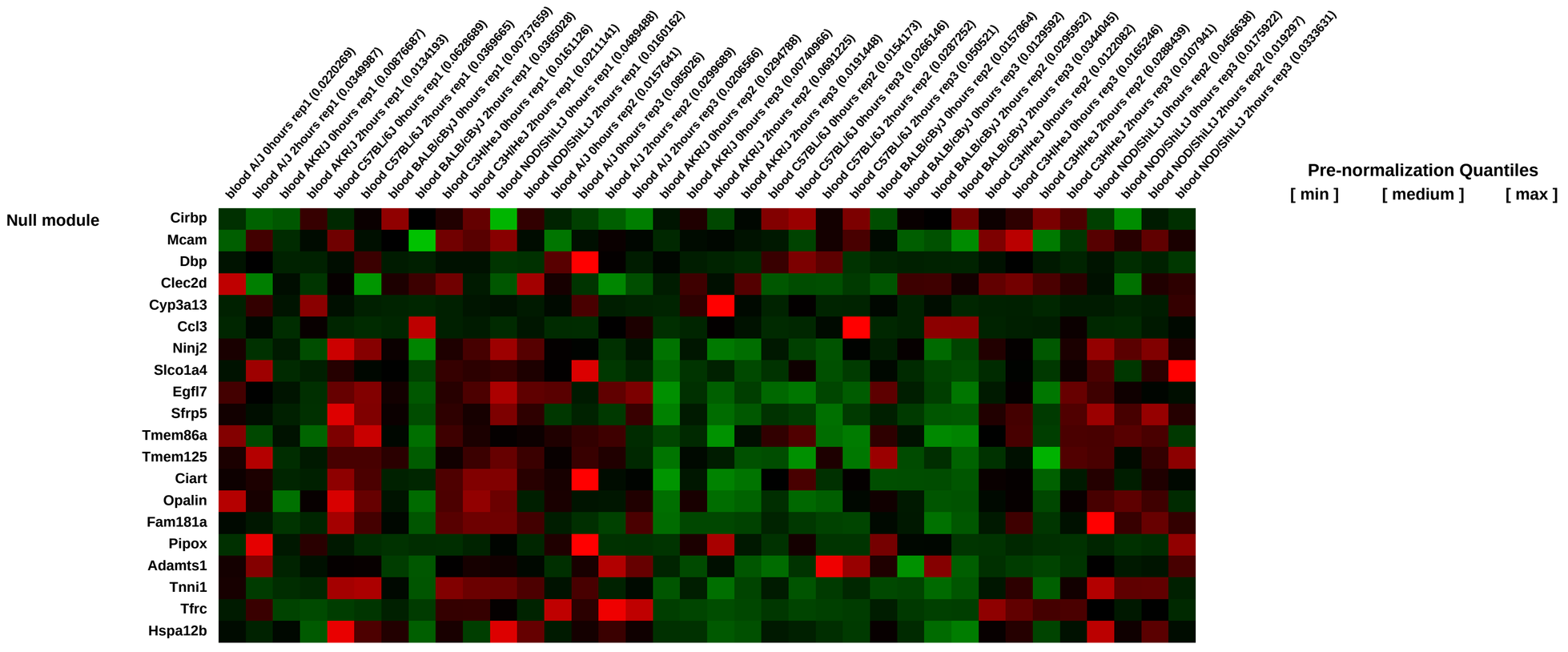

GEO Series "GSE5038" Expression Profiles

Num of samples in this series: 9

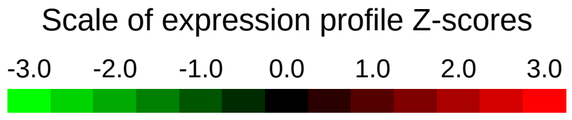

GEO Link:	**http://www.ncbi.nlm.nih.gov/geo/query/acc.cgi?acc=GSE5038**
Status:	**Public on Jun 09 2006**
Title:	**zhang-affy-mouse-308606**
Organism:	**Mus musculus**
Experiment type:	**Expression profiling by array**
Platform:	**GPL1261**
Pubmed ID:	

Summary & Design:

Summary:
In our original grant we proposed to use the NR3B-null mouse model to study the role of NR3B subunit in motor neuron function. We have now successfully generated NR3B null mice. Interestingly, NR3B-null mice invariably die at age P4-P8. Our preliminary examination indicates that the motor strength of these mice is severely impaired prior to death. As we continue to explore the cause of death in NR3B null mice, we propose to conduct gene profiling experiments to search for transcription changes in the brain related to ablation of the NR3B gene. We have used the facility provided by the NINDS/NIMH Microarray Consortium to identify genes that show abnormal expression patterns in these mice. We would like to compare these changes with that opccured in SOD1 mice, a mouse model of motor neuron diseases. Analysis of these genes will help to identify changes in networks and pathways that may cause the death of NR3B-null mice. These studies will further help to elucidate the functional role of NR3B in motor neurons.

We will compare samples from motor neurons of wild type and SOD1 mice to identify genes that show abnormal expression patterns, which may be implicated in the death of SOD1 mice and shared with the same changes in NR3B-null mice.

We hypothesize that genes with their transcription level changing significantly in SOD1 mutant mice will be associated with the molecular mechanism underlying the death of motor neurons.

We like to compare motor neuron and spinal cord smaples from SOD1 mice at the age prior to the disease onset. Total RNA from total 9 samples will be purified, each from ~200 motor neurons obtained by Laser Capture Microdissection and the total spinal cord. Extracted RNAs will be subjected to one or two rounds of amplification and the obtained cRNA will be biotinylated. The purified cRNA will be sent to the NINDS/NIMH Microarray Consortium be used to hybridize the GeneChip Mouse Genome 430 2.0 Array. The hybridization, scanning, and initial data analysis of these GeneChips will be conducted by the Consortium staff. We will analyze the collected data further after data collection. We will first identify genes that show significant changes between wild-type and SOD1 mice and then compare that with the result from NR3B null mice.

Keywords: other

Overall design:

Background corr dist: **KL-Divergence = 0.0309, L1-Distance = 0.0667, L2-Distance = 0.0062, Normal std = 0.7668**

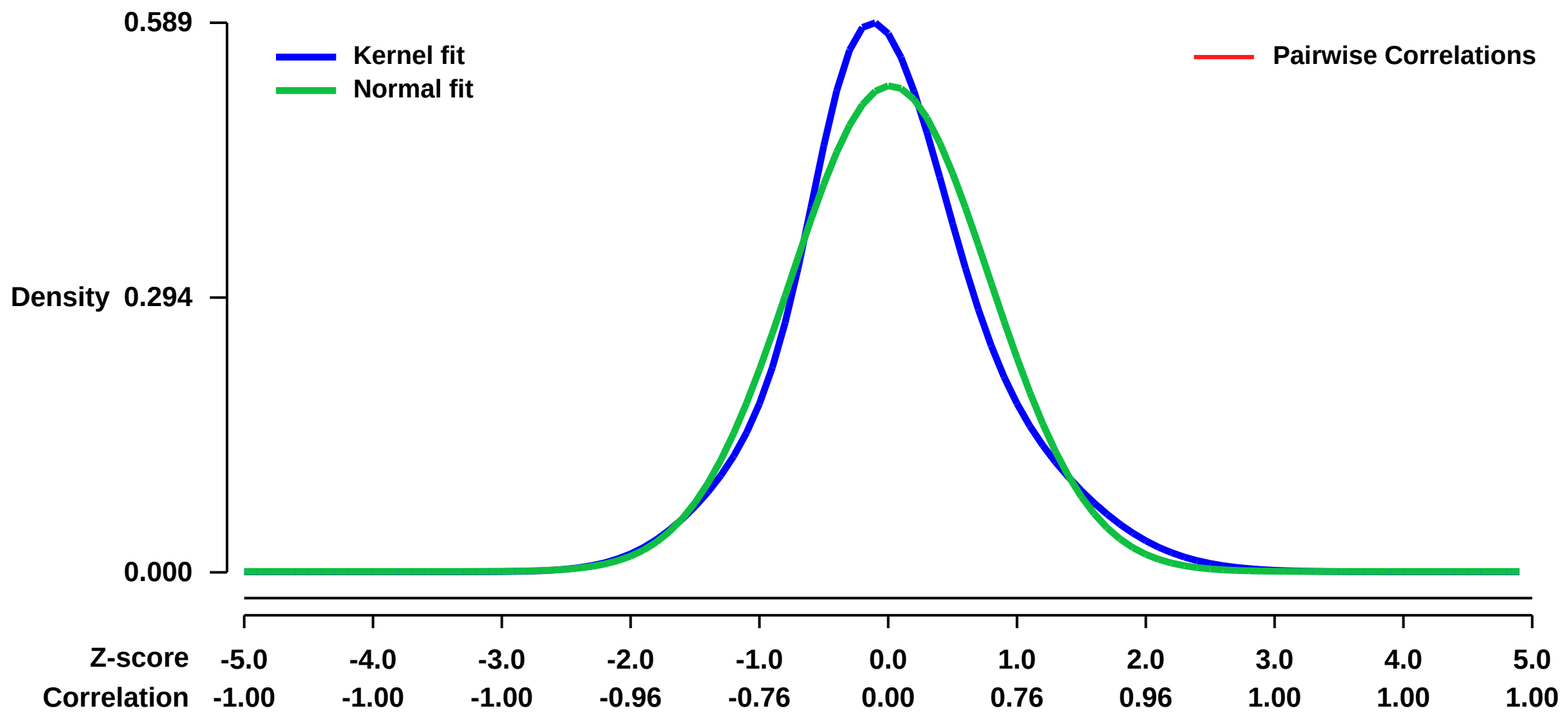

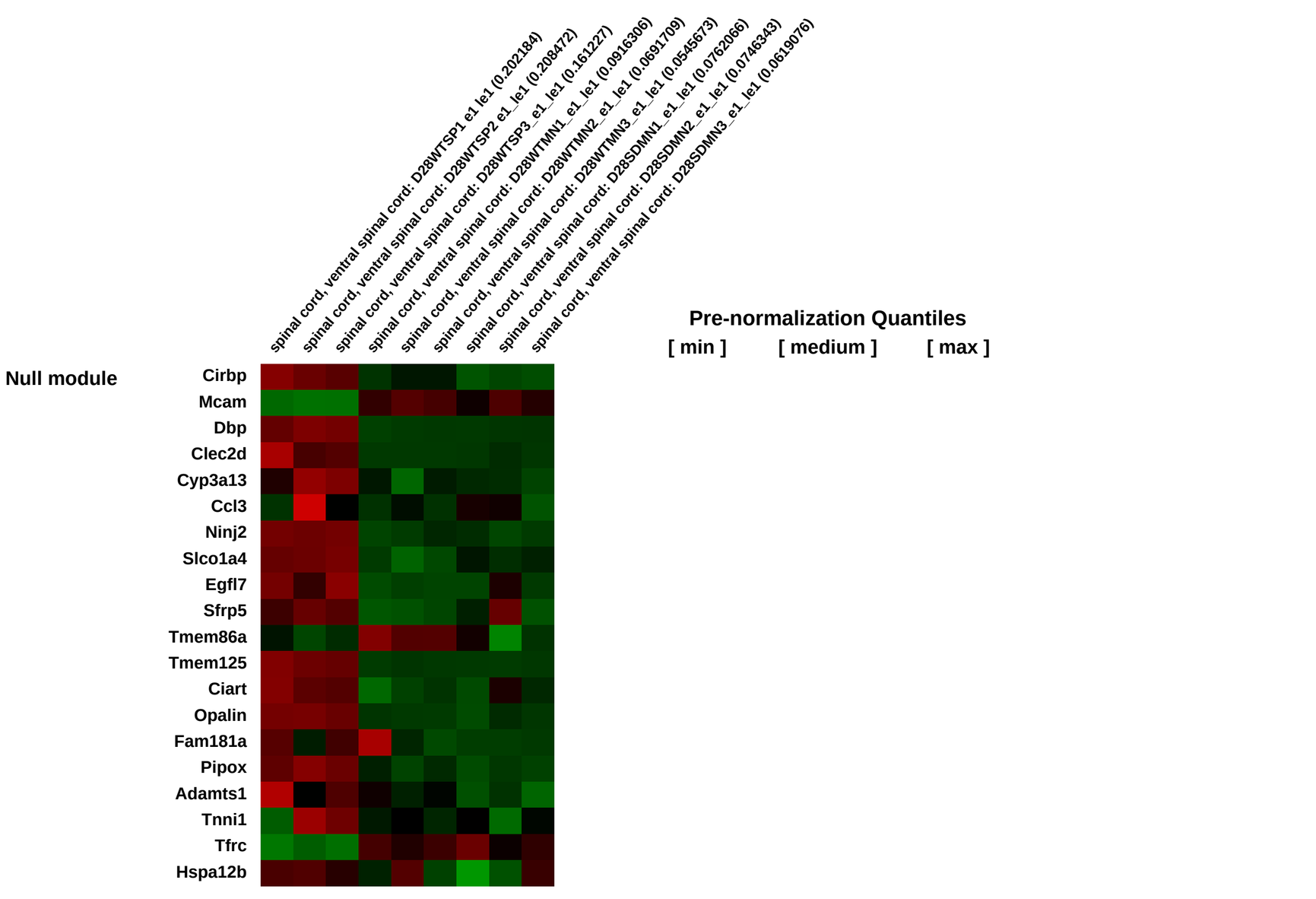

GEO Series "GSE47967" Expression Profiles

Num of samples in this series: 18

Scale of expression profile Z-scores

-3.0 -2.0 -1.0 0.0 1.0 2.0 3.0

GEO Link:	http://www.ncbi.nlm.nih.gov/geo/query/acc.cgi?acc=GSE47967
Status:	Public on Dec 31 2013
Title:	Cooperation of estrogen and oocytes on gene expression in mouse cumulus cells
Organism:	Mus musculus
Experiment type:	Expression profiling by array
Platform:	GPL1261
Pubmed ID:	24035995
Summary & Design:	**Summary:** Oocyte-derived paracrine factors and estrogens cooperate to regulate the function and development of mouse cumulus cells. **Overall design:** Cumulus oocyte complexes (COCs) were isolated from ovaries of mice. Oocytes were removed from some complexes (OOX). Groups were cultured with/without oocytes with/without estrogen and then cumulus cell transcriptome analyzed by microarrays.

Background corr dist: KL-Divergence = 0.0790, L1-Distance = 0.0474, L2-Distance = 0.0046, Normal std = 0.4812

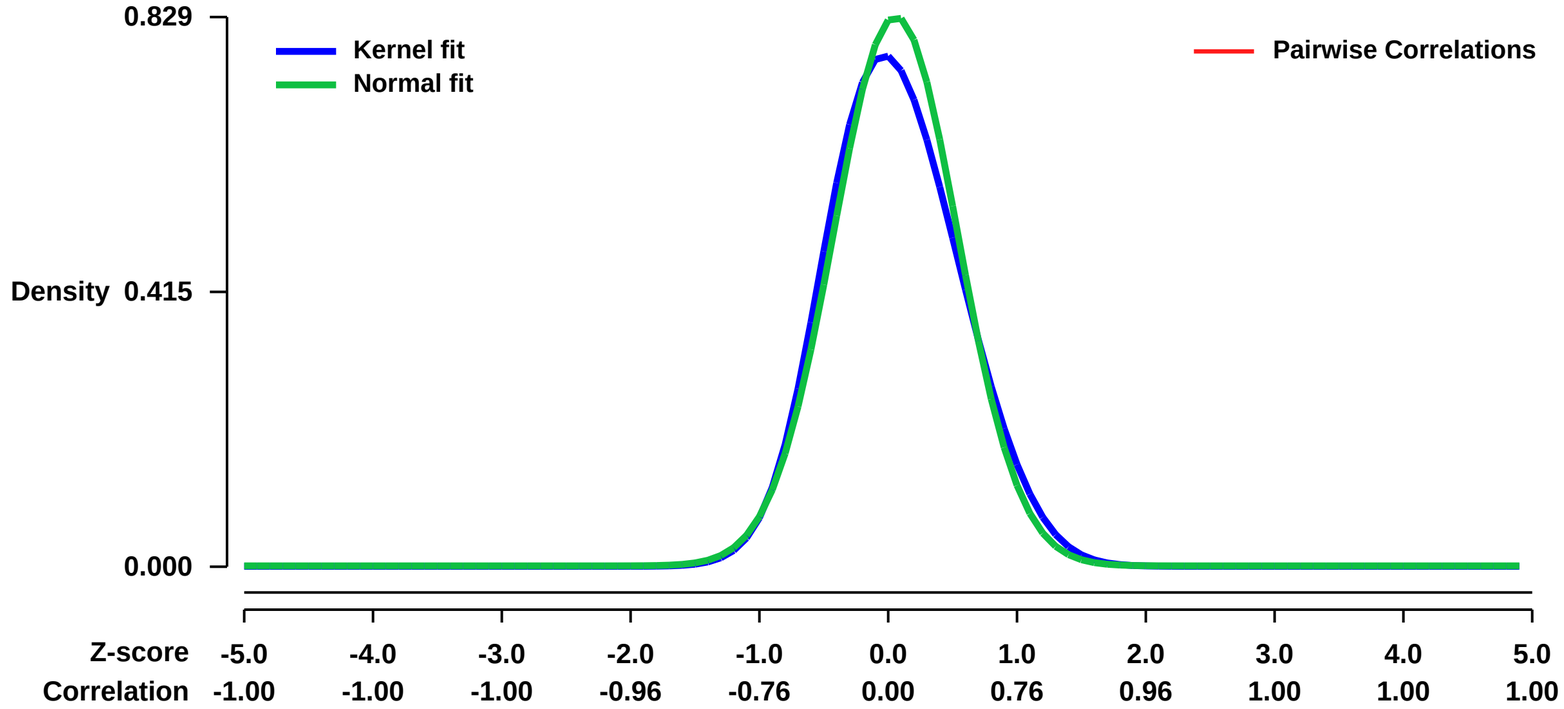

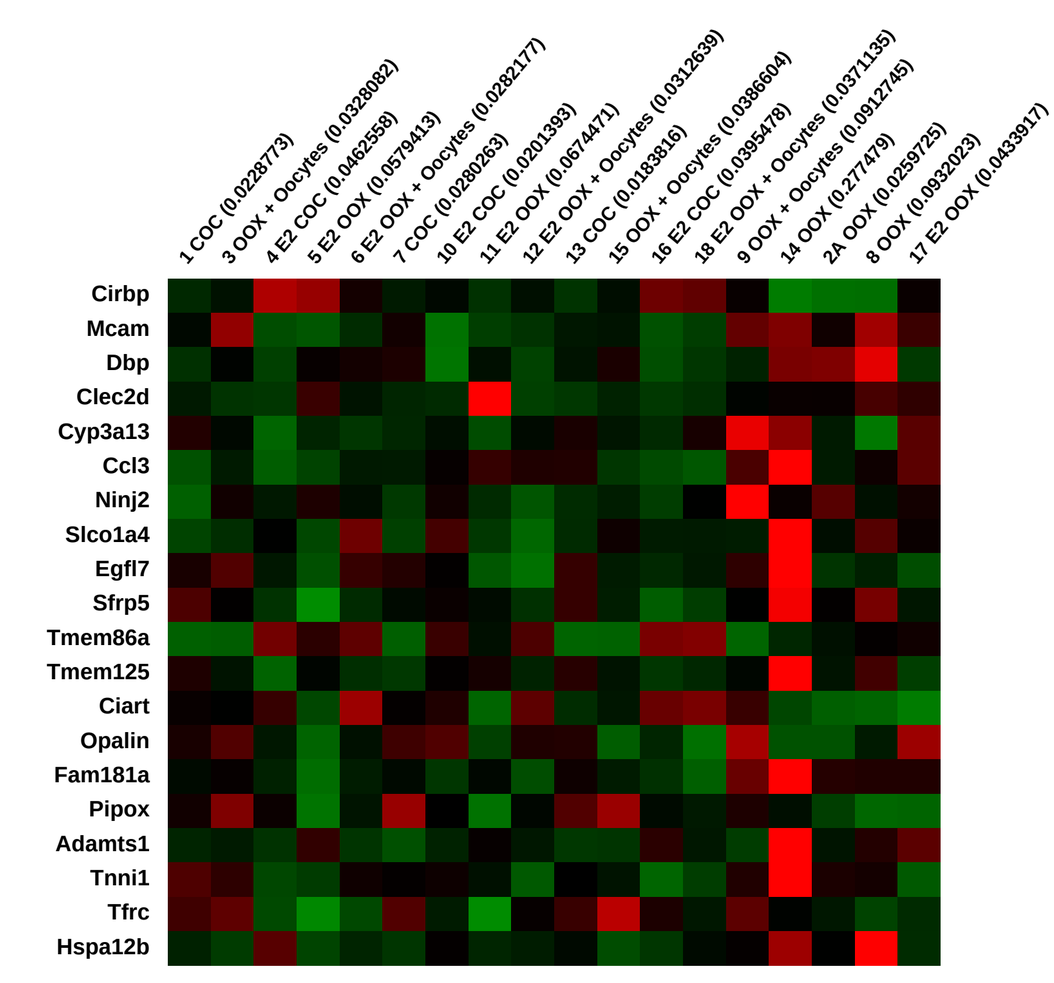

GEO Series "GSE9316" Expression Profiles

Num of samples in this series: 12

Scale of expression profile Z-scores

-3.0 -2.0 -1.0 0.0 1.0 2.0 3.0

GEO Link:	http://www.ncbi.nlm.nih.gov/geo/query/acc.cgi?acc=GSE9316
Status:	Public on Oct 17 2007
Title:	Gene Microarray analysis of Th17 cells
Organism:	Mus musculus
Experiment type:	Expression profiling by array
Platform:	GPL1261
Pubmed ID:	18025126
Summary & Design:	**Summary:** **Th17 cells are enriched by sorting FR4-CD4+ T cells from SKG mice. A large number of Th17 cells also develop spontaneously when CD4+ T cells from IFN-g-deficient (IFN-g-/-) BALB/c mice are transferred to T cell-deficient RAG2-deficient (RAG2-/-) mice and subjected to homeostatic proliferation, whereas they fail to develop in similar transfer of IL-6-deficient (IL-6-/-) CD4+ T cells to IL-6-/- RAG2-/- mice.** **To explore the functional molecules specifically expressed by Th17 cells, we conducted Gene Microarray analysis between 10-month-old SKG FR4-CD4+ cells and age-matched BALB/c FR4-CD4+ cells, and between IFN-g-/- CD4+ cells transferred to RAG2-/- mice and IL-6-/- CD4+ T cells transferred to IL-6-/- RAG2-/- mice. The analysis revealed that 1,556 and 115 genes were up-regulated in 10-month-old SKG FR4-CD4+ and IFN-g-/- CD4+ T cells after homeostatic proliferation, respectively, with 29 genes shared by the two groups of genes. The 29 genes included those encoding cytokines, chemokines, and their receptors, such as IL-1 receptor type1 (IL-1R1), IL-17, IL-22, IL-21, CCR6, and CCL20.** **Keywords: cell type comparison** **Overall design:** **We conducted Gene Microarray analysis between 10-month-old SKG FR4-CD4+ cells and age-matched BALB/c FR4-CD4+ cells, and between IFN-g-/- CD4+ cells transferred to RAG2-/- mice and IL-6-/- CD4+ T cells transferred to IL-6-/- RAG2-/- mice using GeneChip Mouse Genome 430 2.0 Array (Affymetrix). Each gruop has three replicates.**

Background corr dist: KL-Divergence = 0.1064, L1-Distance = 0.0366, L2-Distance = 0.0023, Normal std = 0.4418

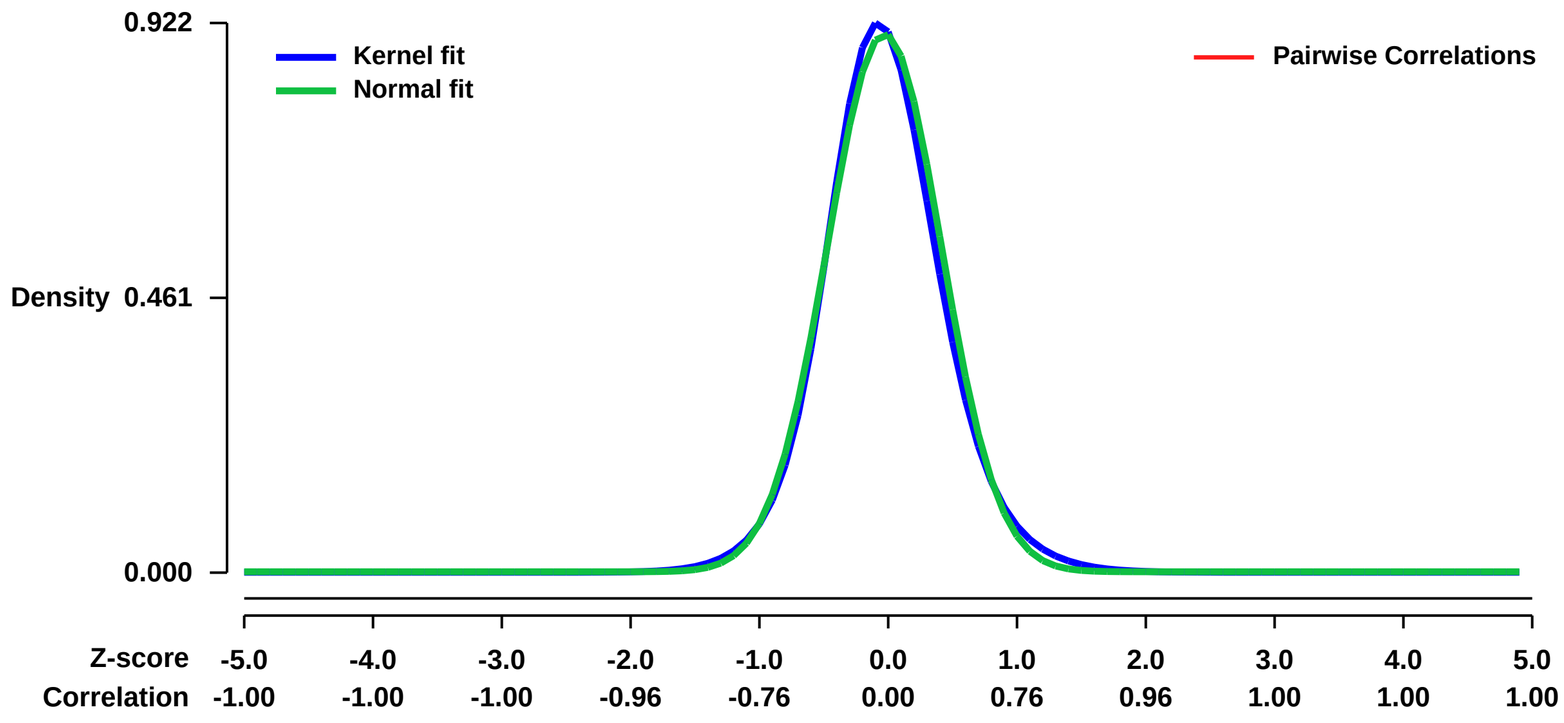

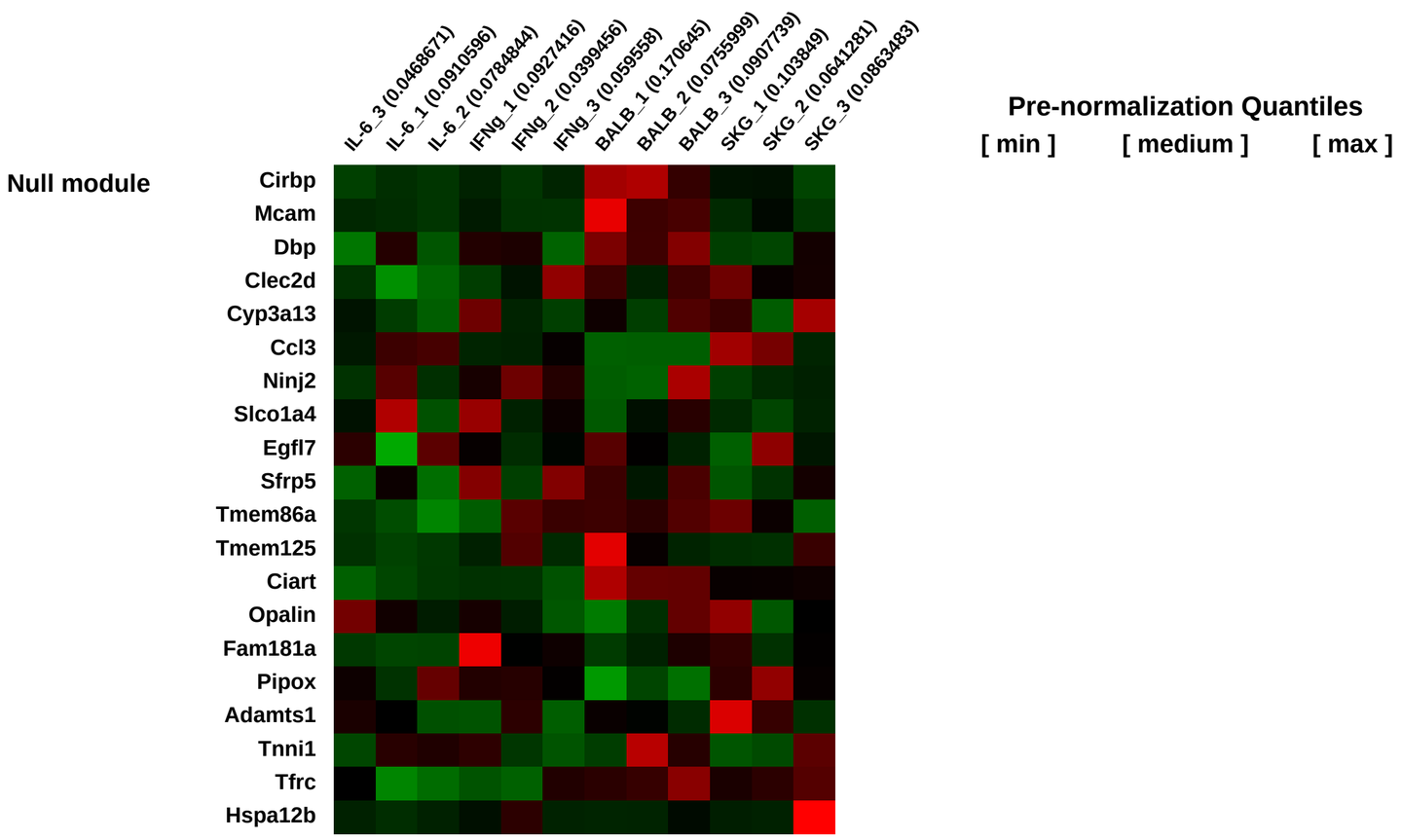

GEO Series "GSE13590" Expression Profiles

Num of samples in this series: 12

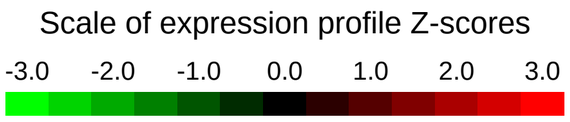

GEO Link:	http://www.ncbi.nlm.nih.gov/geo/query/acc.cgi?acc=GSE13590
Status:	Public on Nov 14 2008
Title:	Experimental identification of microRNA-140 targets by silencing and overexpressing miR-140
Organism:	Mus musculus
Experiment type:	Expression profiling by array
Platform:	GPL1261
Pubmed ID:	20071455
Summary & Design:	**Summary:** MicroRNAs (miRNAs) are short noncoding RNA molecules regulating the expression of mRNAs. Target identification of miRNAs is computationally difficult due to the relatively low homology between miRNAs and their targets. We present here an experimental approach to target identification where the cartilage-specific miR-140 was overexpressed and silenced in cells it is normally expressed in separate experiments. Expression of mRNAs was profiled in both experiments and the intersection of mRNAs repressed by miR-140 overexpression and derepressed by silencing of miR-140 was identified. The intersection contained only 49 genes, although both treatments affected the accumulation of hundreds of mRNAs. These 49 genes showed a very strong enrichment for the miR-140 seed sequence implying that the approach is efficient and specific. 21 of these 49 genes were predicted to be direct targets based on the presence of the seed sequence. Interestingly, none of these were predicted by the published target prediction methods we used. One of the potential target mRNAs, Cxcl12, was experimentally validated by Northern blot analysis and a luciferase reporter assay. **Overall design:** Each condition was profiled in triplicate. For over-expression experiment cells were transfected with siRNA-140 (miR-140 mimick) or siRNA-96 (as a control). For suppresion experiment cells were transfected with LNA-antimicroRNA-140 (suppressing endogenous miR-140) or LNA-antimicroRNA-449 (as a control).

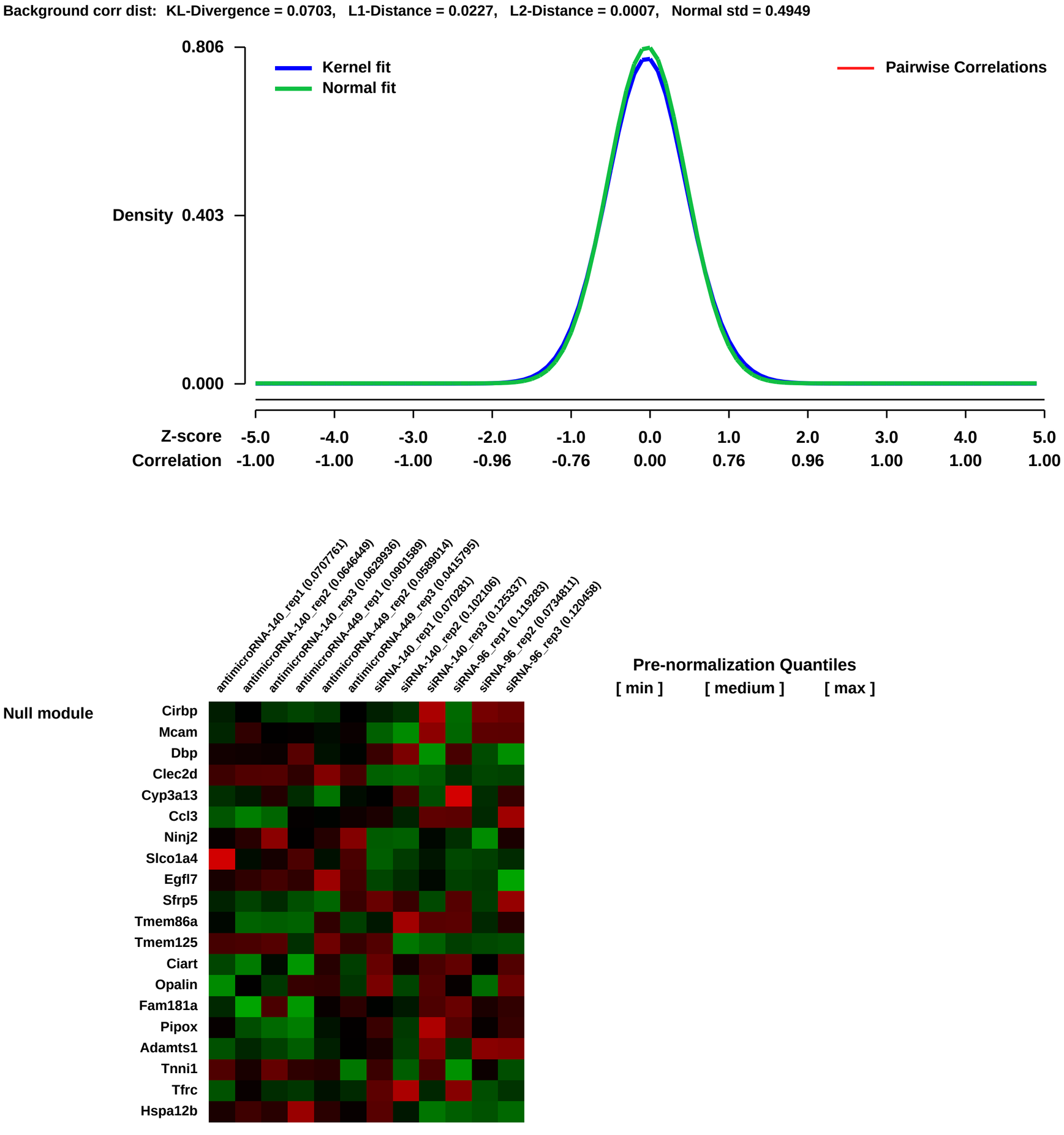

GEO Series "GSE15587" Expression Profiles

Num of samples in this series: 6

Scale of expression profile Z-scores

-3.0 -2.0 -1.0 0.0 1.0 2.0 3.0

GEO Link:	http://www.ncbi.nlm.nih.gov/geo/query/acc.cgi?acc=GSE15587
Status:	Public on Feb 24 2011
Title:	Identification of Metastasis-prone Lung Adenocarcinoma Cell Population That Is Sensitive to Notch Inhibition
Organism:	Mus musculus
Experiment type:	Expression profiling by array
Platform:	GPL1261
Pubmed ID:	21403400
Summary & Design:	**Summary:** Tumor cells that give rise to metastatic disease are a primary cause of cancer-related death and have not been fully elucidated in patients with lung cancer. Here, we addressed this question by using tissues from a mouse that develops metastatic lung adenocarcinoma owing to expression of mutant K-ras and p53. We identified a metastasis-prone population of tumor cells that differed from those with low metastatic capacity on the basis of having sphere-forming capacity in Matrigel cultures, increased expression of CD133 and Notch ligands, and relatively low tumorigenicity in syngeneic mice. Knockdown of jagged1 or pharmacologic inhibition of its downstream mediator phosphatidylinositol 3-kinase abrogated the metastatic but not the tumorigenic activity of these cells. We conclude from these studies on a mouse model of lung adenocarcinoma that CD133 and Notch ligands mark a population of metastasis-prone tumor cells and that the efficacy of Notch inhibitors in metastasis prevention should be explored. Keywords: two group comparison Overall design: 344SQ subcutaneous tumors (from a lung adenocarcinoma cell line derived from a KrasLA1/+; p53R172HdelG/+ mouse that metastasizes widely following subcutaneous injection into syngeneic mice) were sorted by flow cytometry into CD133high and CD133low fractions. RNA samples from these fractions were processed and analyzed on Affymetrix Mouse Expression Array 430A 2.0 chips.

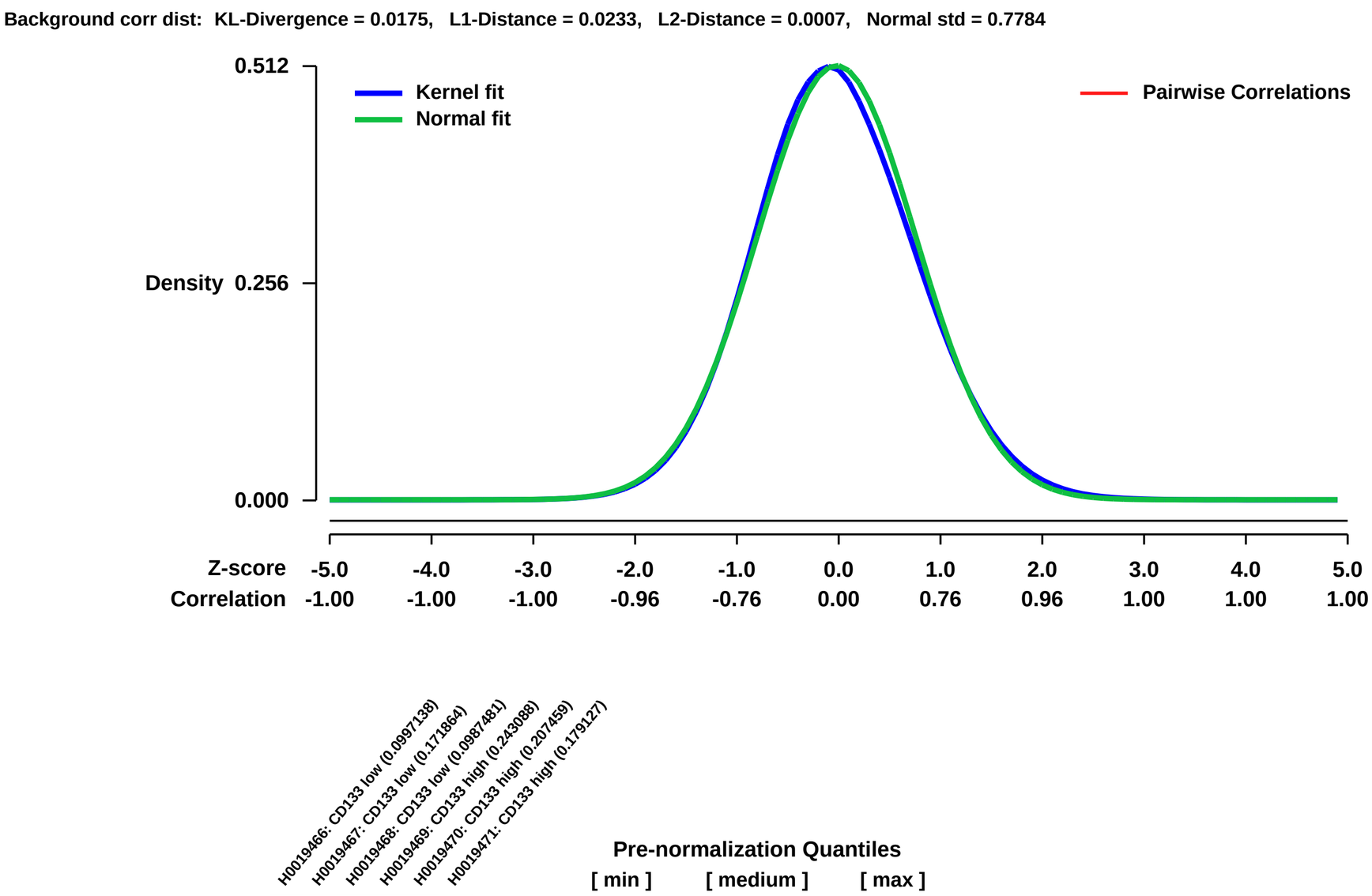

GEO Series "GSE10535" Expression Profiles

Num of samples in this series: 6

Scale of expression profile Z-scores

-3.0 -2.0 -1.0 0.0 1.0 2.0 3.0

GEO Link:	http://www.ncbi.nlm.nih.gov/geo/query/acc.cgi?acc=GSE10535
Status:	Public on Feb 21 2008
Title:	Retinal transcripts level alteration in the prCAD -/- mouse, a model for retinal degeneration
Organism:	Mus musculus
Experiment type:	Expression profiling by array
Platform:	GPL1261
Pubmed ID:	15872101
Summary & Design:	**Summary:** This experiment was designed to identify transcripts that exhibit changes in abundance in the context of retinal degeneration by comparing transcript levels in adult wild type and prCAD -/- mouse retinas. **Keywords: genetic mutant analysis** **Overall design:** Retinas were dissected from ~4 weeks old mice. Retinas from 3 prCAD knockout mice or wild type 129 mice were pooled for each sample and 3 replicate of wild type and mutant samples were analysed.

Background corr dist: KL-Divergence = 0.0328, L1-Distance = 0.0125, L2-Distance = 0.0001, Normal std = 0.6456

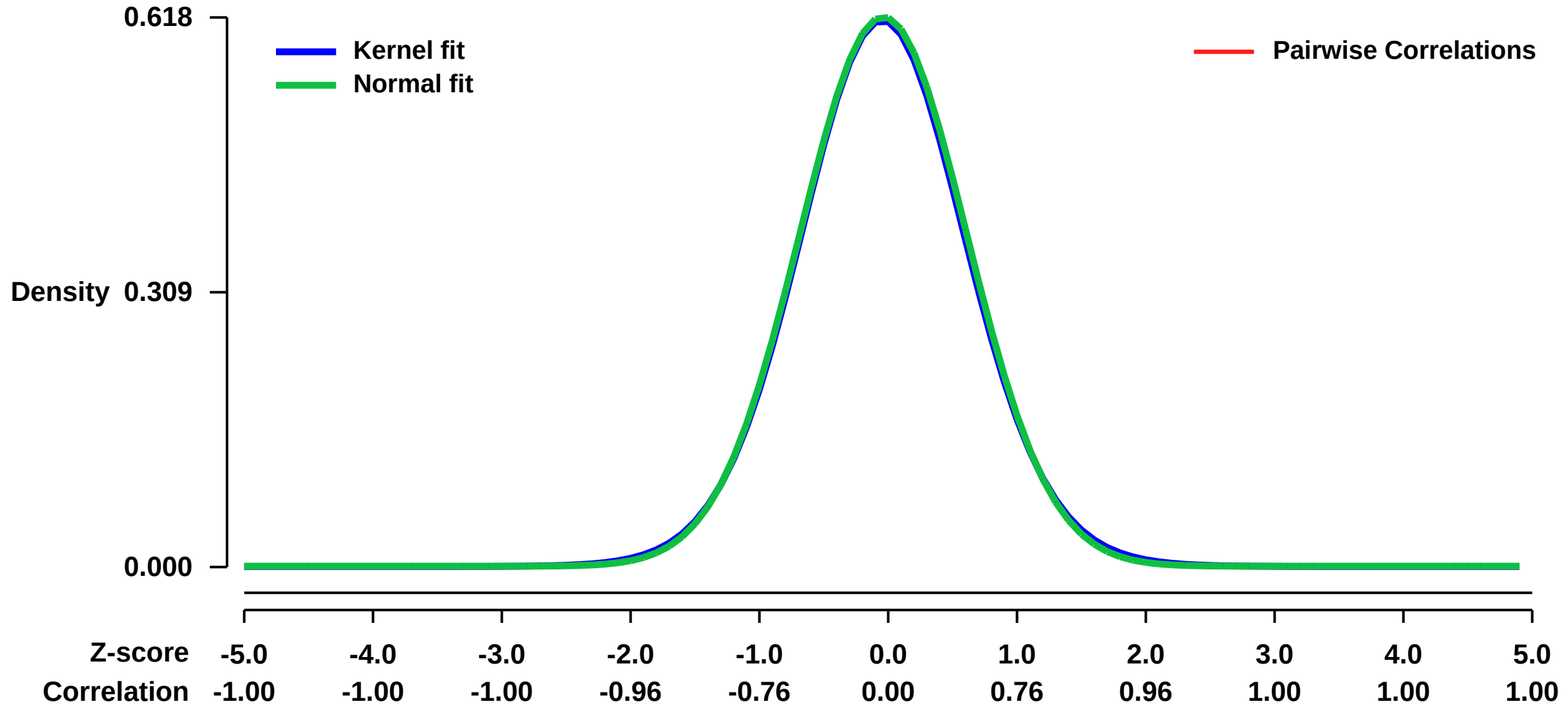

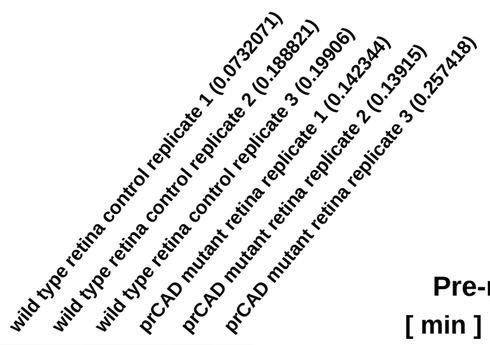

Pre-normalization Quantiles

[min] [medium] [max]

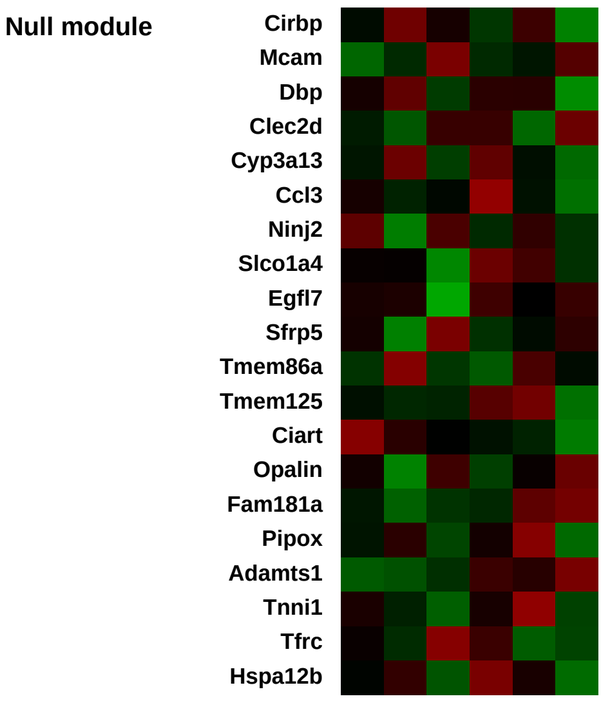

GEO Series "GSE13364" Expression Profiles

Num of samples in this series: 6

Scale of expression profile Z-scores

-3.0 -2.0 -1.0 0.0 1.0 2.0 3.0

GEO Link:	http://www.ncbi.nlm.nih.gov/geo/query/acc.cgi?acc=GSE13364
Status:	Public on Oct 28 2008
Title:	Expression data from BWF1 mice
Organism:	Mus musculus
Experiment type:	Expression profiling by array
Platform:	GPL1261
Pubmed ID:	20200542
Summary & Design:	**Summary:** Microarray analysis was performed on BWF1 mice spleenocyte cells in control and pCONS treated mice. Microarray analysis identified many genes differentially expressed in control vs pCONS treated mice spleenocytes. Some of the genes were uperegulated and some of the genes were down regulated. Microarray analysis was performed in CD4, CD8, and whole spleenocyte WBC cells. Keywords: One week after pCONS injection **Overall design:** RNA was isolated from the mice spleenocytes from control and pCONs treated mice one week after treatment.

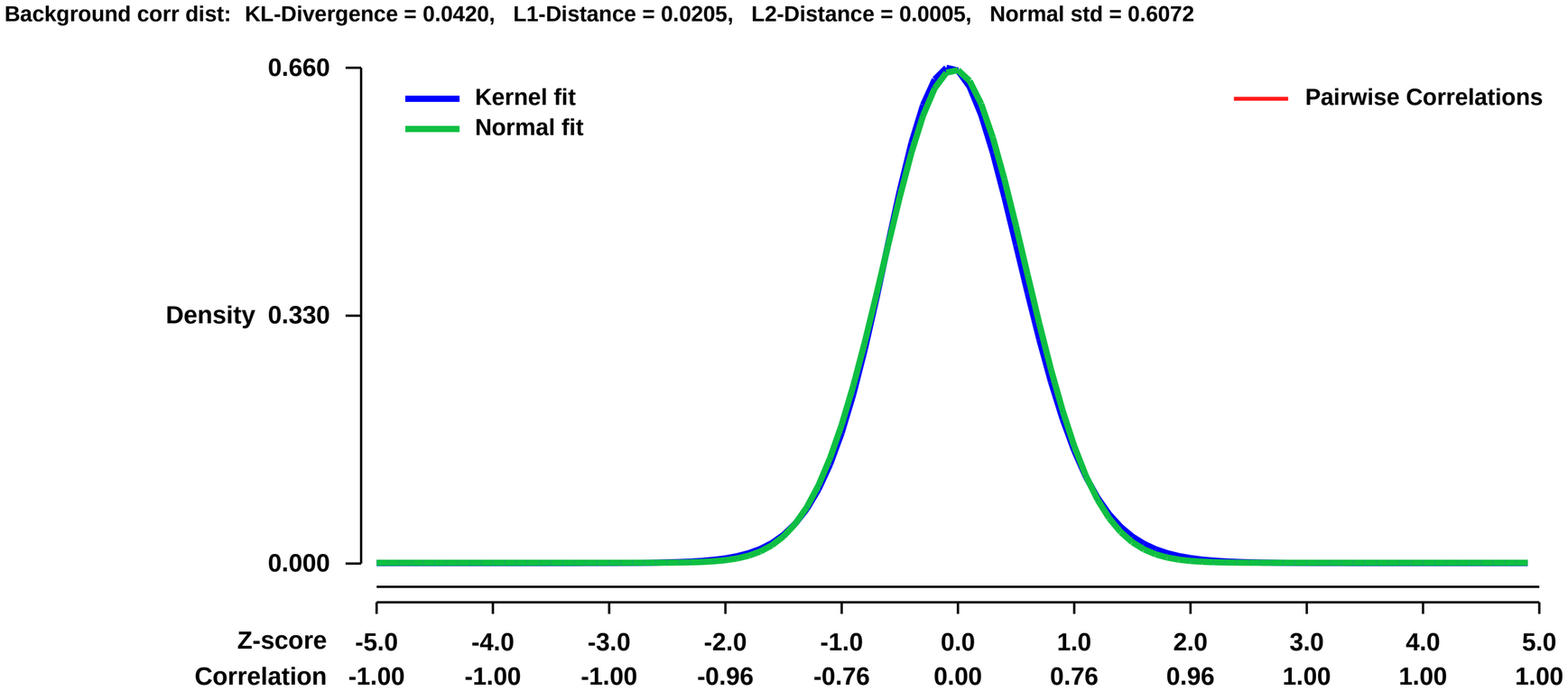

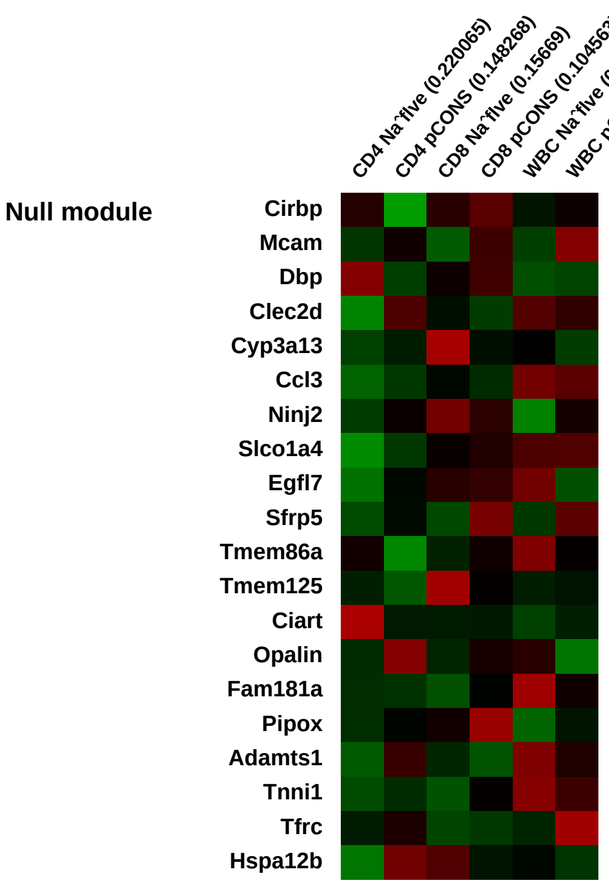

GEO Series "GSE14906" Expression Profiles

Num of samples in this series: 6

Scale of expression profile Z-scores

-3.0 -2.0 -1.0 0.0 1.0 2.0 3.0

GEO Link:	http://www.ncbi.nlm.nih.gov/geo/query/acc.cgi?acc=GSE14906
Status:	Public on Feb 18 2010
Title:	The Gene Expression Analysis in E12.5 Mouse Hearts with GATA4-FOG2 Interaction Loss
Organism:	Mus musculus
Experiment type:	Expression profiling by array
Platform:	GPL1261
Pubmed ID:	19578715
Summary & Design:	**Summary:** In order to identify the targets of GATA4-FOG2 action in mammalian heart development we performed Affymetrix microarray comparisons of gene expression in normal and mutant at embryonic (E) day E12.5 hearts. We compared RNA samples from both Fog2-null and Gata4ki/ki mutant E12.5 hearts to the wild-type control E12.5 hearts. We reasoned that as the phenotypes of the Fog2 knockout and Gata4ki/ki mutation (a V217G mutation that specifically cripples the interaction between GATA4 and FOG proteins) are similar, we should expect to identify a similar set of differentially expressed genes in both experiments. As an additional control, we expected to find the Fog2 gene expression absent in the mutant (null) Fog2 cardiac sample, but not Gata4ki/ki sample. **Overall design:** We have analyzed 6 RNA samples total (3 from control hearts, 2 from FOG2 null hearts and 1 from GATA4ki hearts)

Background corr dist: KL-Divergence = 0.0388, L1-Distance = 0.0213, L2-Distance = 0.0005, Normal std = 0.6215

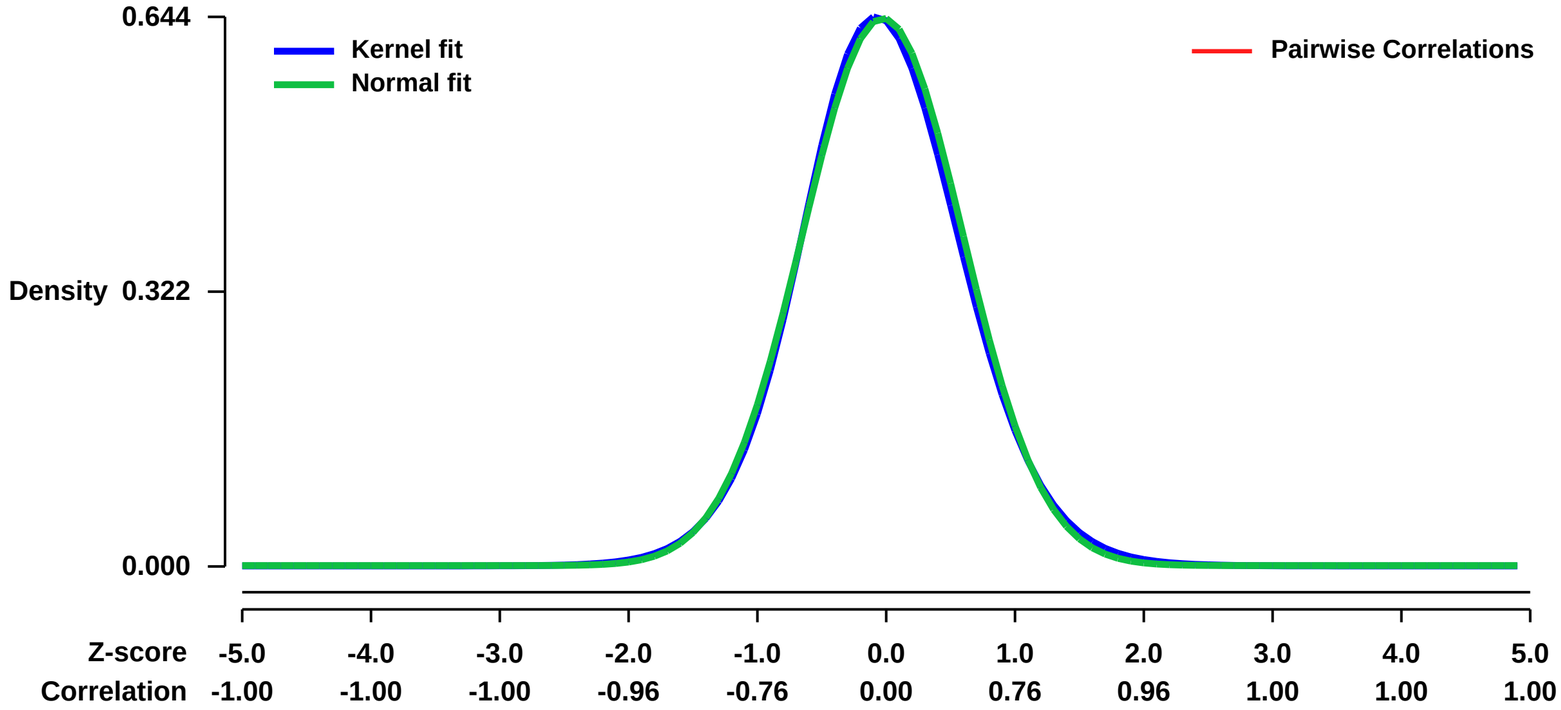

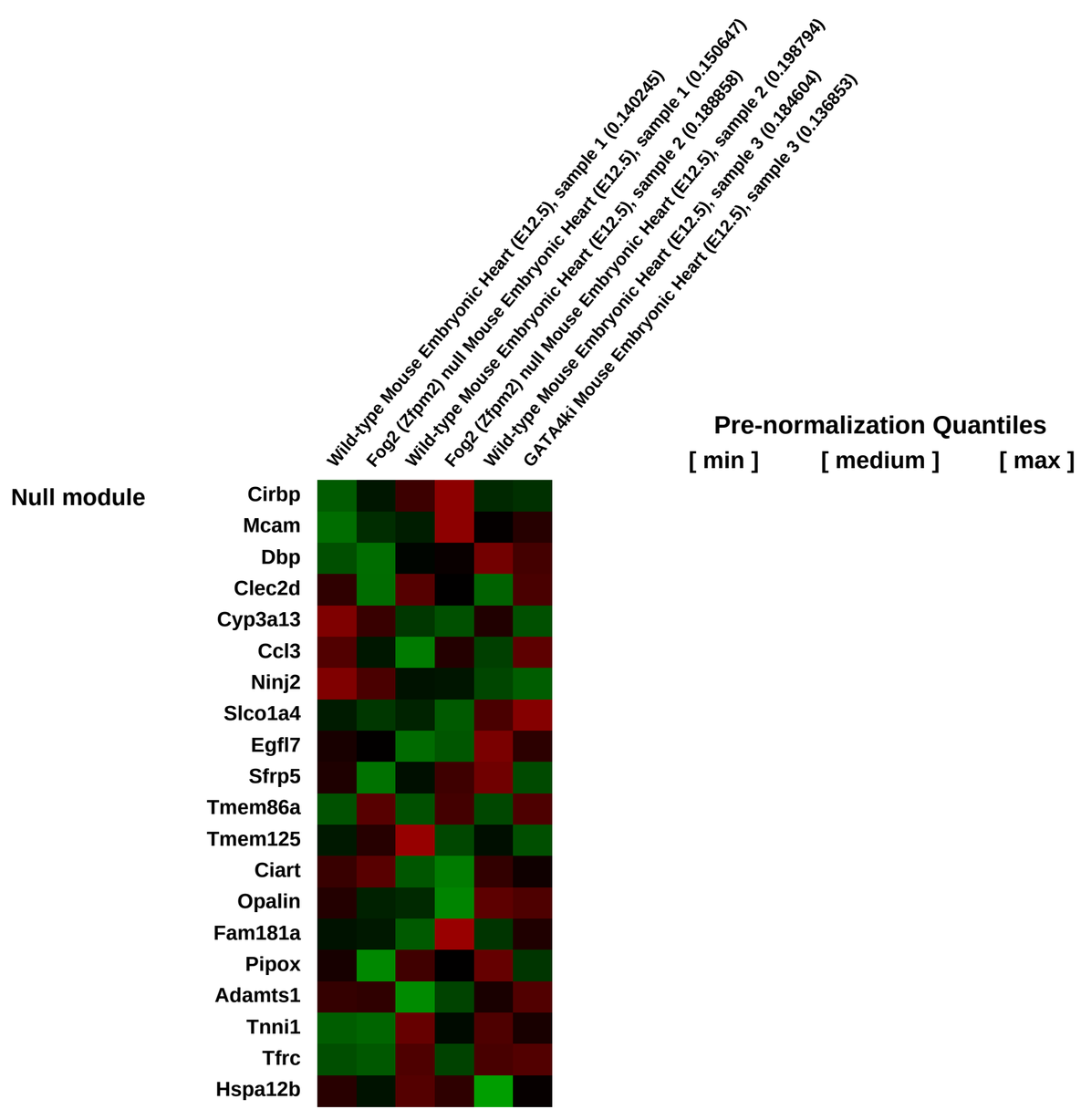

GEO Series "GSE9312" Expression Profiles

Num of samples in this series: 6

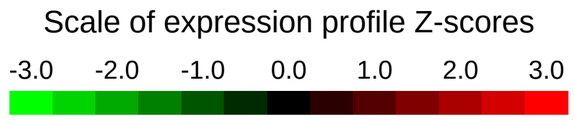

GEO Link:	**http://www.ncbi.nlm.nih.gov/geo/query/acc.cgi?acc=GSE9312**
Status:	**Public on Apr 12 2008**
Title:	**MIA overexpression**
Organism:	**Mus musculus**
Experiment type:	**Expression profiling by array**
Platform:	**GPL1261**
Pubmed ID:	
Summary & Design:	**Summary:** **In experiments using tissue recombinants and mesenchyme-free culture, we have demonstrated that the entire embryonic respiratory tract epithelium, from the trachea to the distal lung tips, exhibits substantial plasticity in its eventual phenotype that is dependent on the inductive cues it receives from its associated mesenchyme. This observation led us to speculate that the differences between embryonic trachea and lung are defined by limited subset of genes, and that the molecular comparison of these two tissues might provide new information on genes that are important for both lung and trachea development. Microarray experiments designed to identify genes differentially expressed in the E11.5 lung and trachea showed that melanoma inhibitory activity (Mia1) was expressed only in the lung. Mia1 was abundantly expressed during early lung development, but was virtually absent by the end of gestation. Bitransgenic mice expressing MIA under the control of the SFTPC promoter after E16.5, the age when Mia1 is normally silenced, died from respiratory failure at birth with morphologically immature lungs associated with reduced levels of saturated phosphatidylcholine and mature SP-B. Microarray analysis showed significant reductions expression of Sftpa, Sftpb, Abca3, Aqp5, Lzp-s, Scd2, and Aytl2 in lungs misexpressing MIA.** **Keywords: genotype comparison** **Overall design:** **To assess the effect of misexpressing MIA on overall lung gene expression, we analyzed RNA from day E18.5 lungs of bitransgenic and control littermates by microarray (Affymetrix MOE430 chip).**

Background corr dist: KL-Divergence = 0.0335, L1-Distance = 0.0178, L2-Distance = 0.0003, Normal std = 0.6480

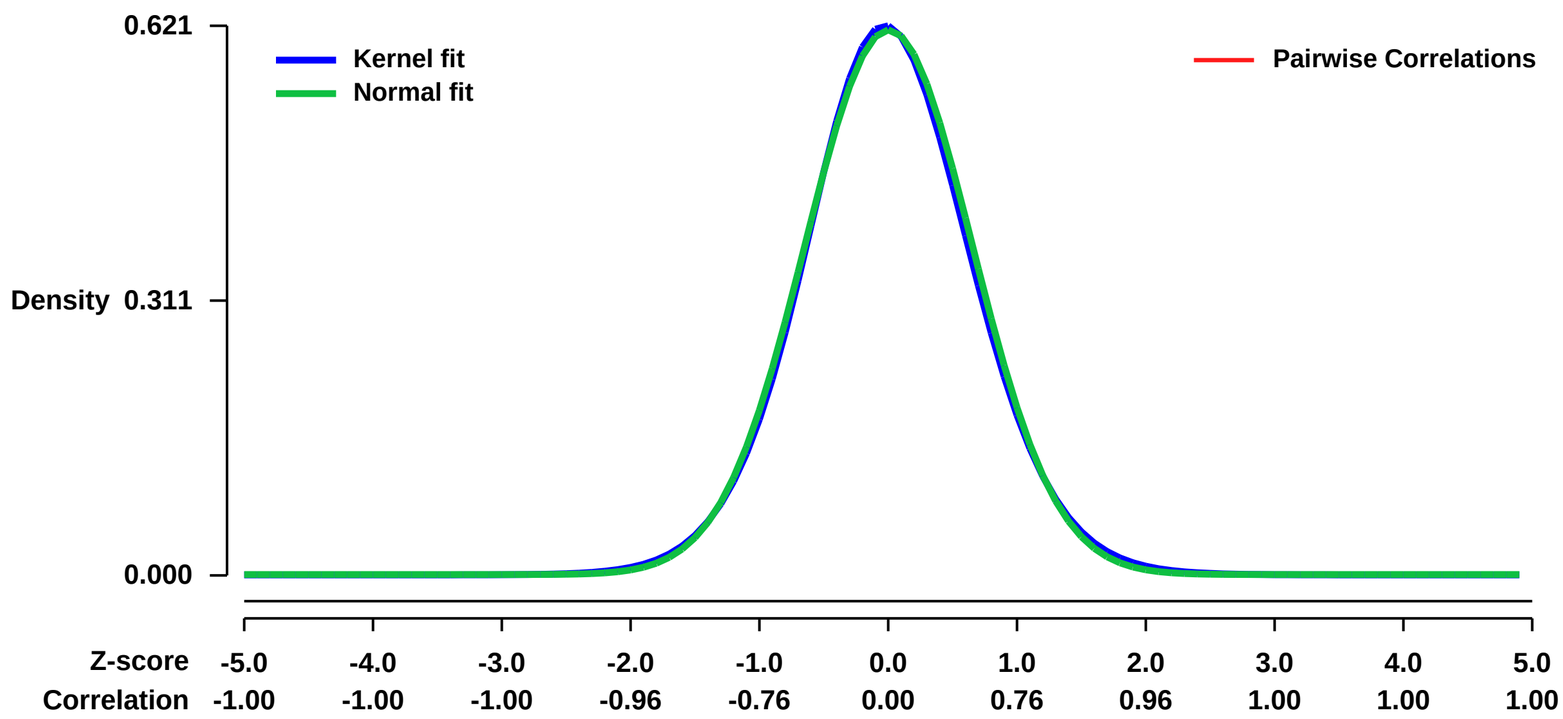

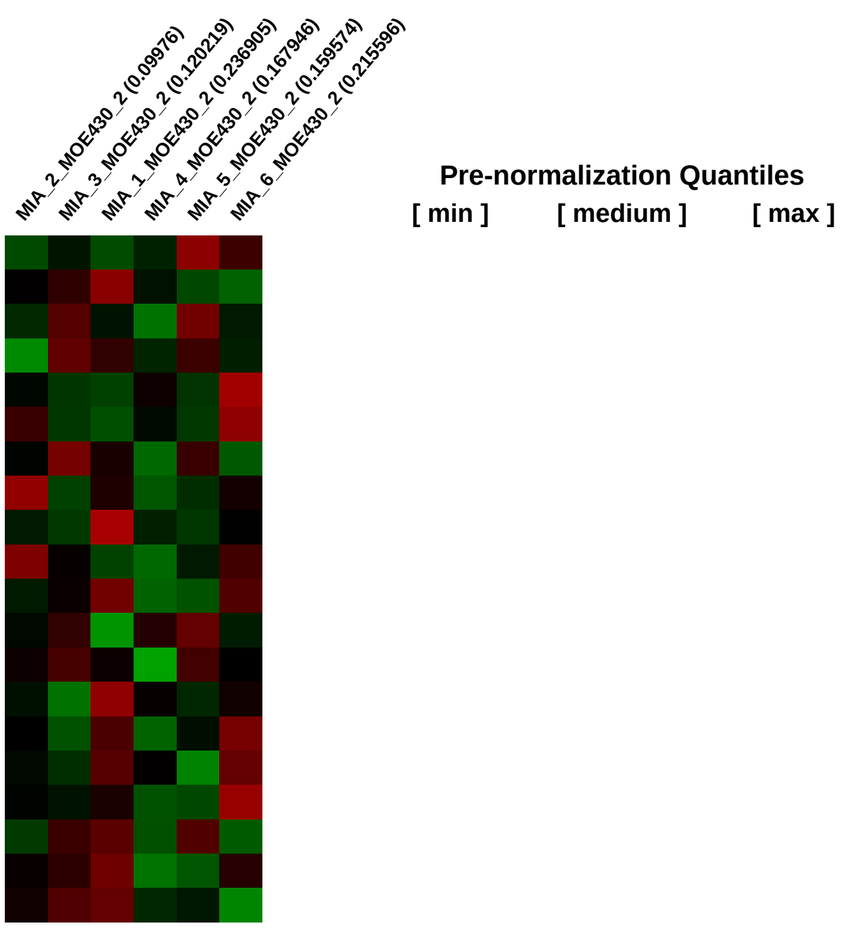

GEO Series "GSE29081" Expression Profiles

Num of samples in this series: 6

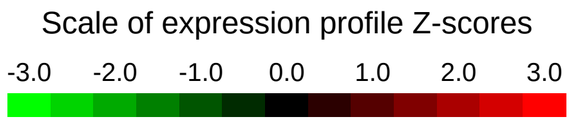

GEO Link:	http://www.ncbi.nlm.nih.gov/geo/query/acc.cgi?acc=GSE29081
Status:	Public on Sep 13 2011
Title:	Cerebellar gene expression analysis of Gb5-deficient mice
Organism:	Mus musculus
Experiment type:	Expression profiling by array
Platform:	GPL1261
Pubmed ID:	21883221
Summary & Design:	**Summary:** Gb5 is a divergent, evolutionarily-conserved, member of the heterotrimeric G protein b subunit family that is expressed principally in brain and neuronal tissue. Among Gb isoforms, Gb5 is unique in its ability to heterodimerize with members of the R7 subfamily of the regulator of G protein signaling (RGS) proteins that contain G protein-g like (GGL) domains. Previous studies employing Gb5 knockout mice have shown that Gb5 is an essential stabilizer of GGL domain-containing RGS proteins and regulates the deactivation of retinal phototransduction and the proper functioning of retinal bipolar cells. The purpose of this study is to better understand the functions of Gb5 in the brain outside the visual system by employing molecular biology, immunohistochemistry and confocal imaging technologies. We show here that mice lacking Gb5 have a markedly abnormal neurologic phenotype that includes neurobehavioral developmental delay, wide-based gait, motor learning and coordination deficiencies, and hyperactivity. Using immunohistochemical analysis and a green fluorescent reporter of Purkinje cell maturation we show that the phenotype of Gb5-deficient mice includes, in part, delayed development of the cerebellar cortex, an abnormality that likely contributes to the neurobehavioral phenotype. Multiple neuronally-expressed genes are dysregulated in cerebellum of Gb5 KO mice. **Overall design:** Brain tissues from WT and KO with three biological replications of mice were collected, frozen in liquid nitrogen, and stored at -70 ´℃

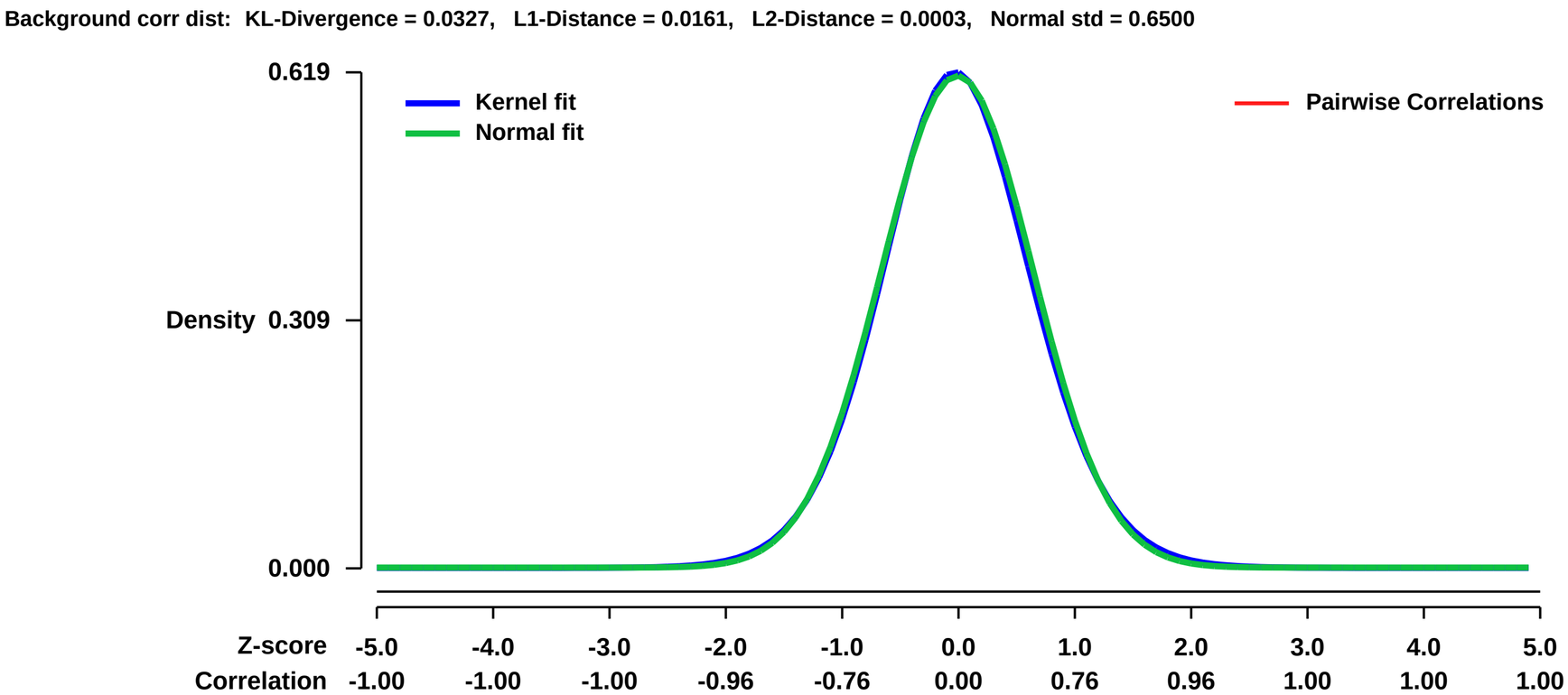

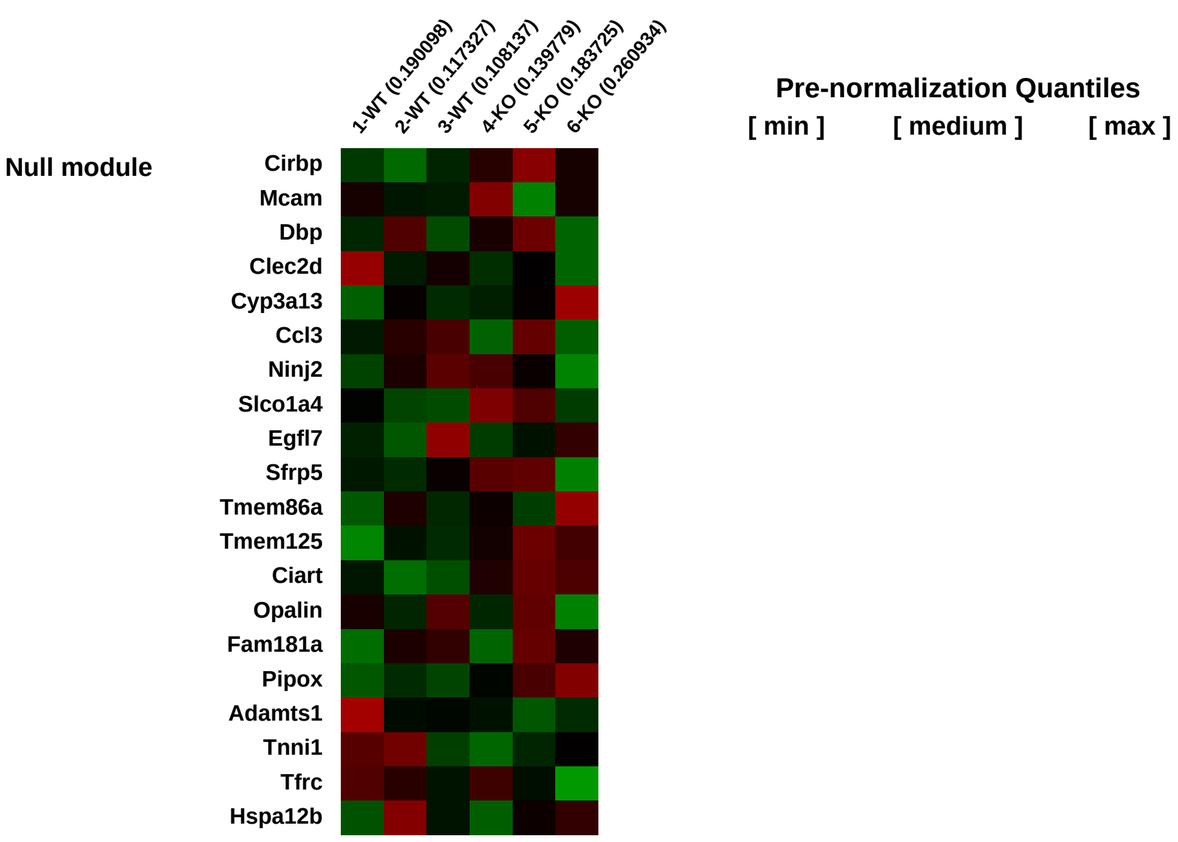

GEO Series "GSE38257" Expression Profiles

Num of samples in this series: 14

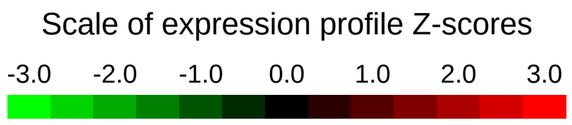

GEO Link:	http://www.ncbi.nlm.nih.gov/geo/query/acc.cgi?acc=GSE38257
Status:	Public on Dec 21 2012
Title:	A Novel Tumor suppressor network in squamous malignancies
Organism:	Mus musculus
Experiment type:	Expression profiling by array
Platform:	GPL1261
Pubmed ID:	23145321
Summary & Design:	**Summary:** The specific ablation of Rb1 gene in stratified epithelia (RbF/F;K14cre) promotes proliferation and altered differentiation but is insufficient to produce spontaneous tumors. The pRb relative, p107, compensates some of the functions of pRb in these tissues, however RbF/F;K14cre;p107-/- mice die postnatally. Acute pRb loss in stratified epithelia, using an inducible mouse model (RbF/F;K14creERTM), shows that p107 exerts specific tumor suppressor functions in its absence. After simultaneous absence of pRb and p107, p53 transcriptional function is impaired and Pten expression is reduced. All mutant mice develop spontaneous squamous tumors carcinomas rapidly. Gene expression analysis of mouse tumors, besides supporting the impaired p53 function and the susceptibility to Akt/mTOR inhibitors, also revealed significant overlap with human squamous carcinomas. Thus, RbF/F;K14creERTM;p107-/- may constitute a new mouse model for these malignancies. Collectively, these data demonstrate the existence of a previously unreported functional connection between pRb, Pten and p53 tumor suppressors, through p107, of a particular relevance in squamous tumor development. **Overall design:** Gene expression was compared between normal mouse skin and carcinomas arising in the skin of RbF/F;K14creERTM;p107-/- mouse. All mice were treated with tamoxifen.

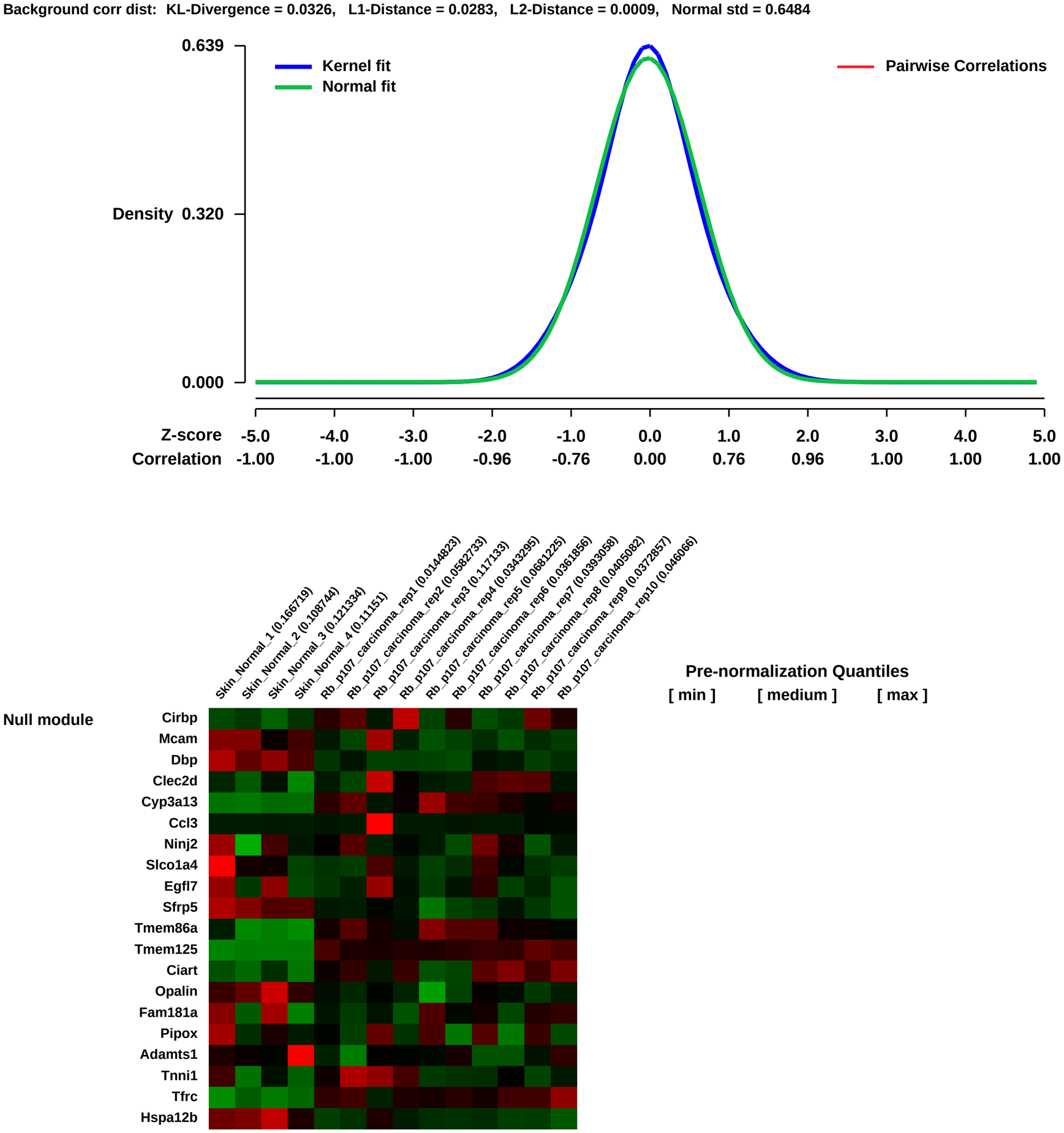

GEO Series "GSE48622" Expression Profiles

Num of samples in this series: 16

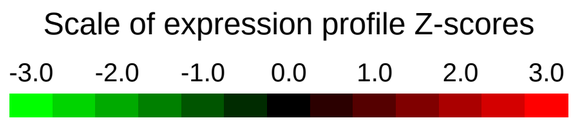

GEO Link:	**http://www.ncbi.nlm.nih.gov/geo/query/acc.cgi?acc=GSE48622**
Status:	**Public on Jul 10 2013**
Title:	**Transcriptional Profiling of Neuronal APP/APLP2 Double-Conditional Knockout Mice.**
Organism:	**Mus musculus**
Experiment type:	**Expression profiling by array**
Platform:	**GPL1261**
Pubmed ID:	**20855613**
Summary & Design:	**Summary:** **Gene expression analysis of 2-month-old APP/APLP2 double-conditional Knockout (N-dCKO) mice and littermate APLP2 knockout controls, APP knockout and wildtype controls.** **Overall design:** **Mouse hippocampus were dissected for RNA extraction and hybridization on Affymetrix microarrays.**

Background corr dist: **KL-Divergence = 0.2702, L1-Distance = 0.0634, L2-Distance = 0.0108, Normal std = 0.2920**

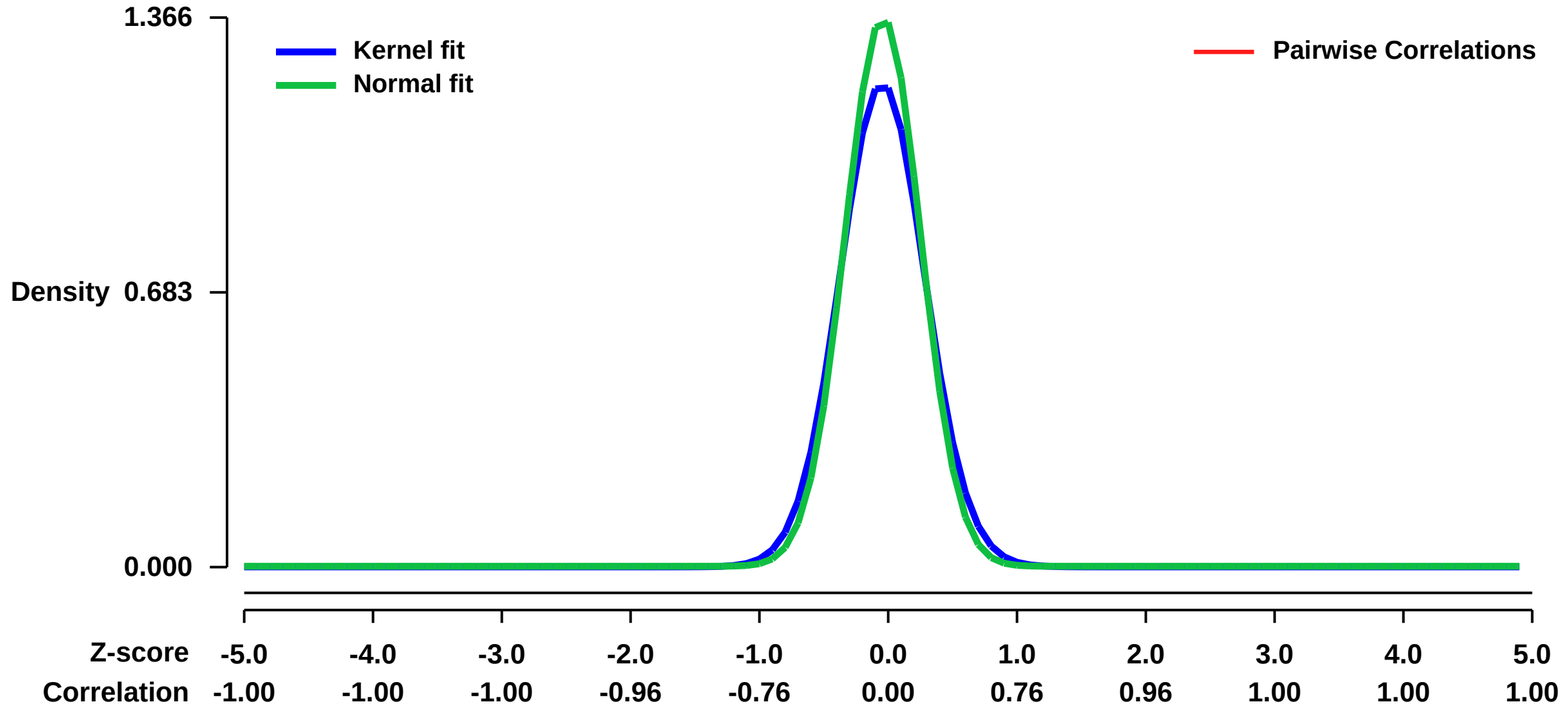

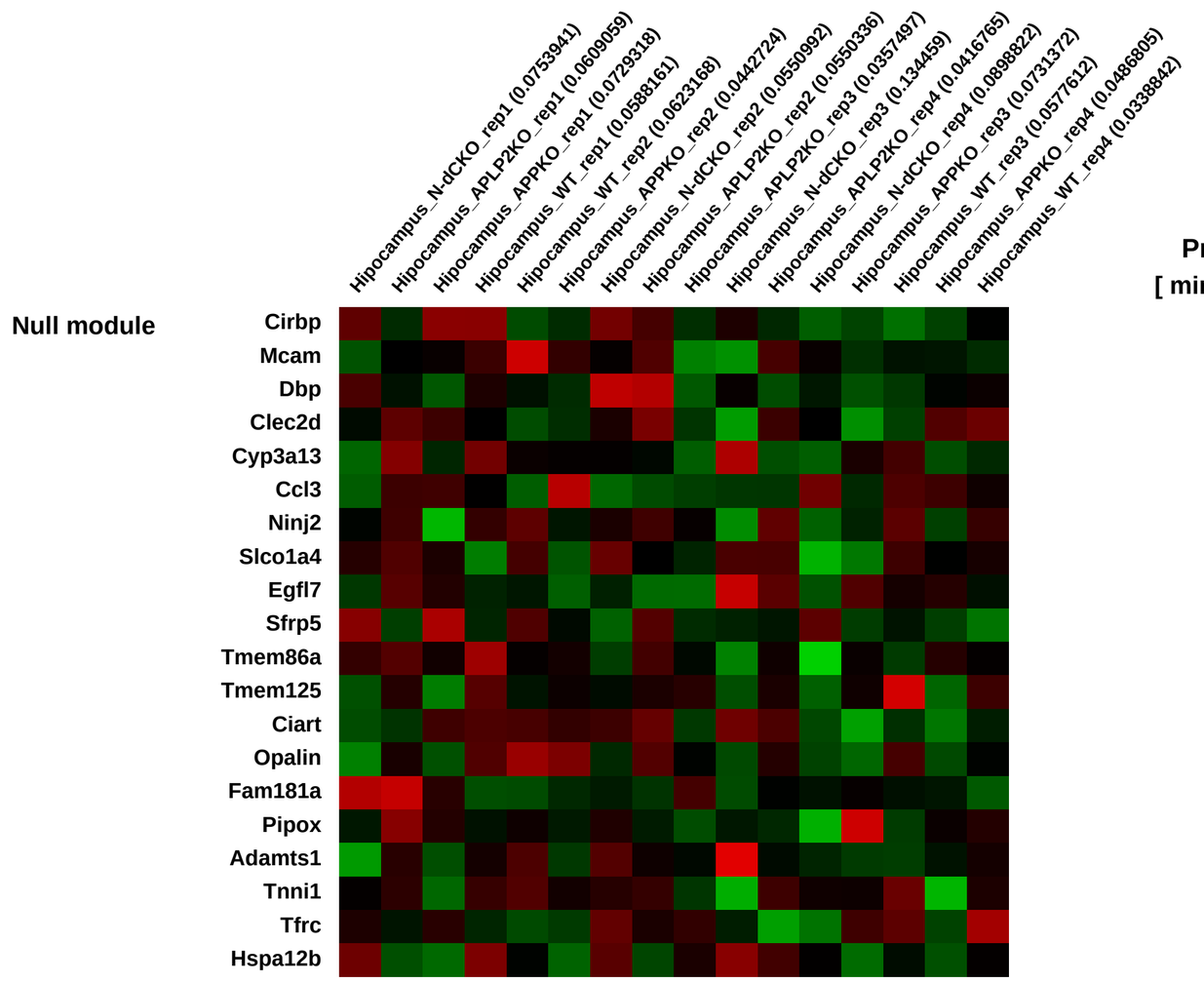

GEO Series "GSE25825" Expression Profiles

Num of samples in this series: 8

Scale of expression profile Z-scores

-3.0 -2.0 -1.0 0.0 1.0 2.0 3.0

GEO Link:	**http://www.ncbi.nlm.nih.gov/geo/query/acc.cgi?acc=GSE25825**
Status:	**Public on Dec 03 2010**
Title:	**Expression data from MxCre;E2F1-/-2-/-3f/f Cd11B myeloid cells**
Organism:	**Mus musculus**
Experiment type:	**Expression profiling by array**
Platform:	**GPL1261**
Pubmed ID:	**21115501**
Summary & Design:	**Summary:** **To understand the underlying cause for the observed apoptosis in E2f1-3 deficient myeloid cells. We compared gene expression profiles of Cd11b+ sorted myeloid cells isolated from bone marrow of control (E2F1-/-) and experimental (Mxcre;E2F1-/-2-/-3f/f) mice.** **Overall design:** **RNA was extracted from Cd11b cells from bone marrow of eight-week-old mice after FACS sorting with FITC- cojugated Cd11b antibody.**

Background corr dist: **KL-Divergence = 0.0635, L1-Distance = 0.0189, L2-Distance = 0.0006, Normal std = 0.5182**

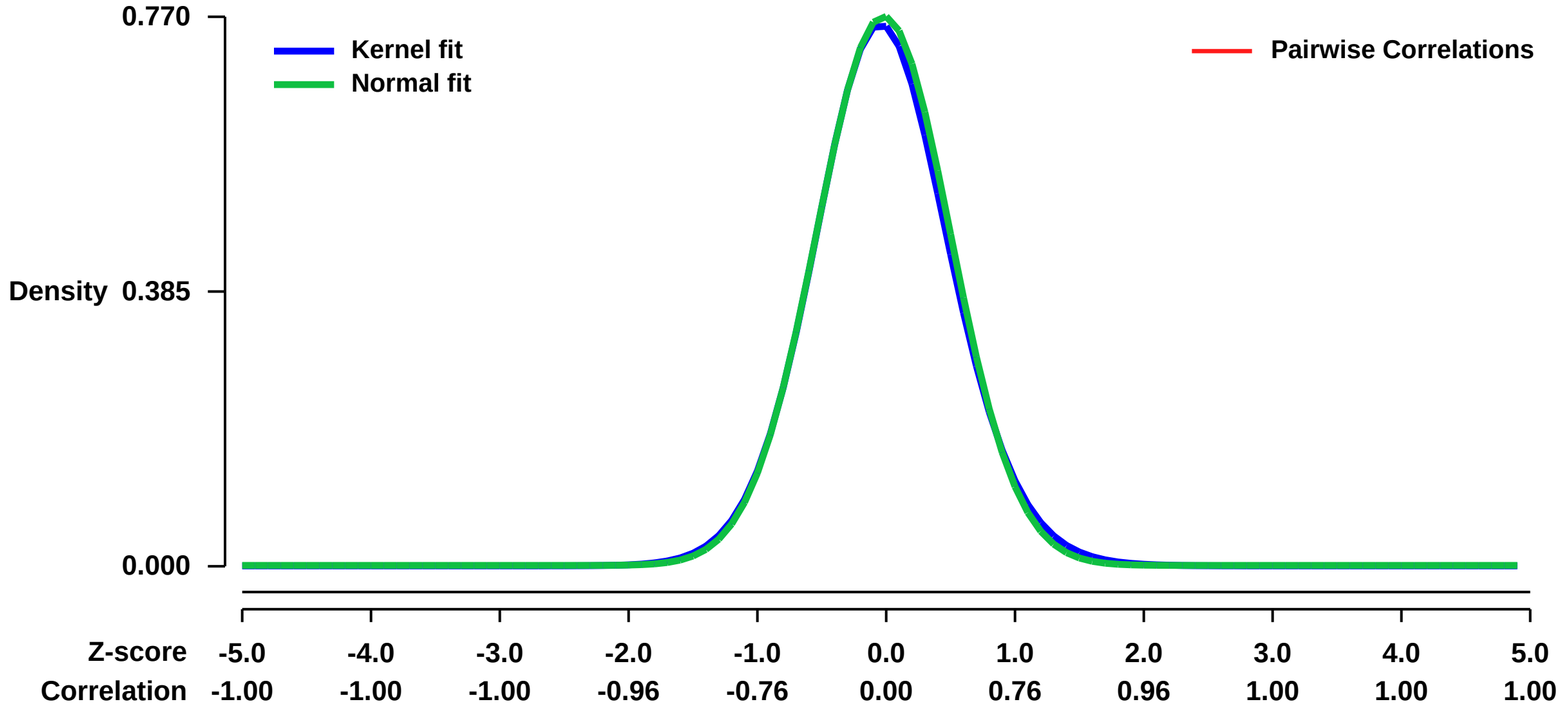

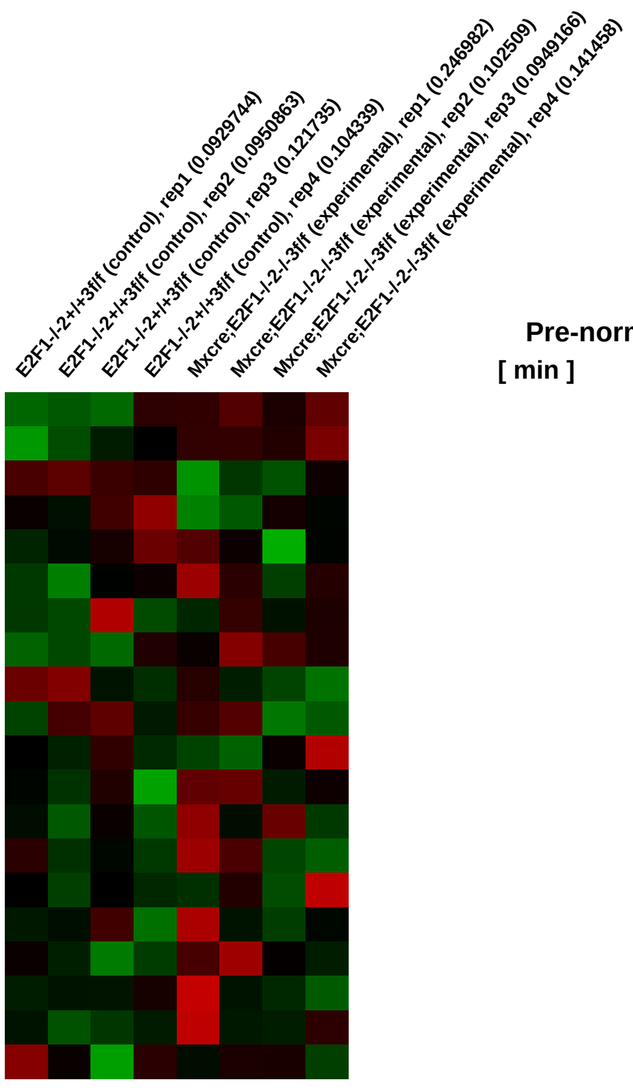

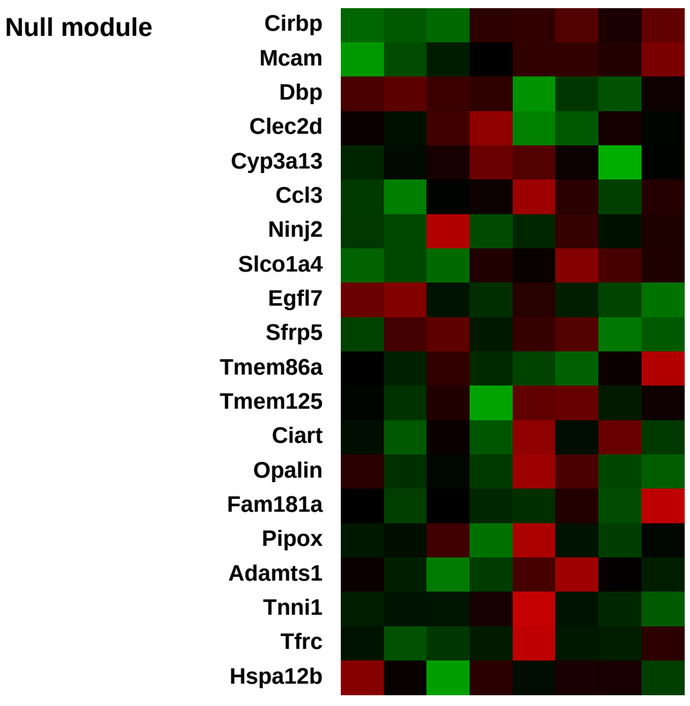

GEO Series "GSE7685" Expression Profiles

Num of samples in this series: 12

Scale of expression profile Z-scores

-3.0 -2.0 -1.0 0.0 1.0 2.0 3.0

GEO Link: http://www.ncbi.nlm.nih.gov/geo/query/acc.cgi?acc=GSE7685
Status: Public on Sep 01 2007
Title: Transcriptional profiling of growth plate chondrocyte differentiation yields insight into endochondral ossification
Organism: Mus musculus
Experiment type: Expression profiling by array
Platform: GPL1261
Pubmed ID: 20084171

Summary & Design:

Summary:
A variety of cell cultures models and in vivo approaches have been used to study gene expression during chondrocyte differentiation. The extent to which the in vitro models reflect bona fide gene regulation in the growth plate has not been quantified. In addition, studies that evaluate global gene expression changes among different growth plate zones are limited. To address these issues, we completed a microarray screen of three growth plate zones derived from manually segmented embryonic mouse tibiae. Classification of genes differentially expressed between each respective growth plate zone, functional categorization as well as characterization of gene expression patterns, cytogenetic loci, signaling pathways and functional motifs confirmed documented data and pointed to novel aspects of chondrocyte differentiation. Parallel comparisons of the microdissected tibiae data set to our previously completed micromass culture screen further corroborated the suitability of micromass cultures for modeling gene expression in chondrocyte development. The micromass culture system demonstrated striking similarities to the in vivo microdissected tibiae screen; however, the micromass system was unable to accurately distinguish gene expression differences in the hypertrophic and mineralized zones of the growth plate. These studies will allow us to better understand zone-specific gene expression patterns in the growth plate. Ultimately, this work will help define both the genomic context in which genes are expressed in the long bones and the extent to which the micromass culture system is able to recapitulate chondrocyte development in endochondral ossification.

Keywords: Growth plate microdissection

Overall design:
Samples: Total RNA

Background corr dist: KL-Divergence = 0.0886, L1-Distance = 0.0335, L2-Distance = 0.0017, Normal std = 0.4750

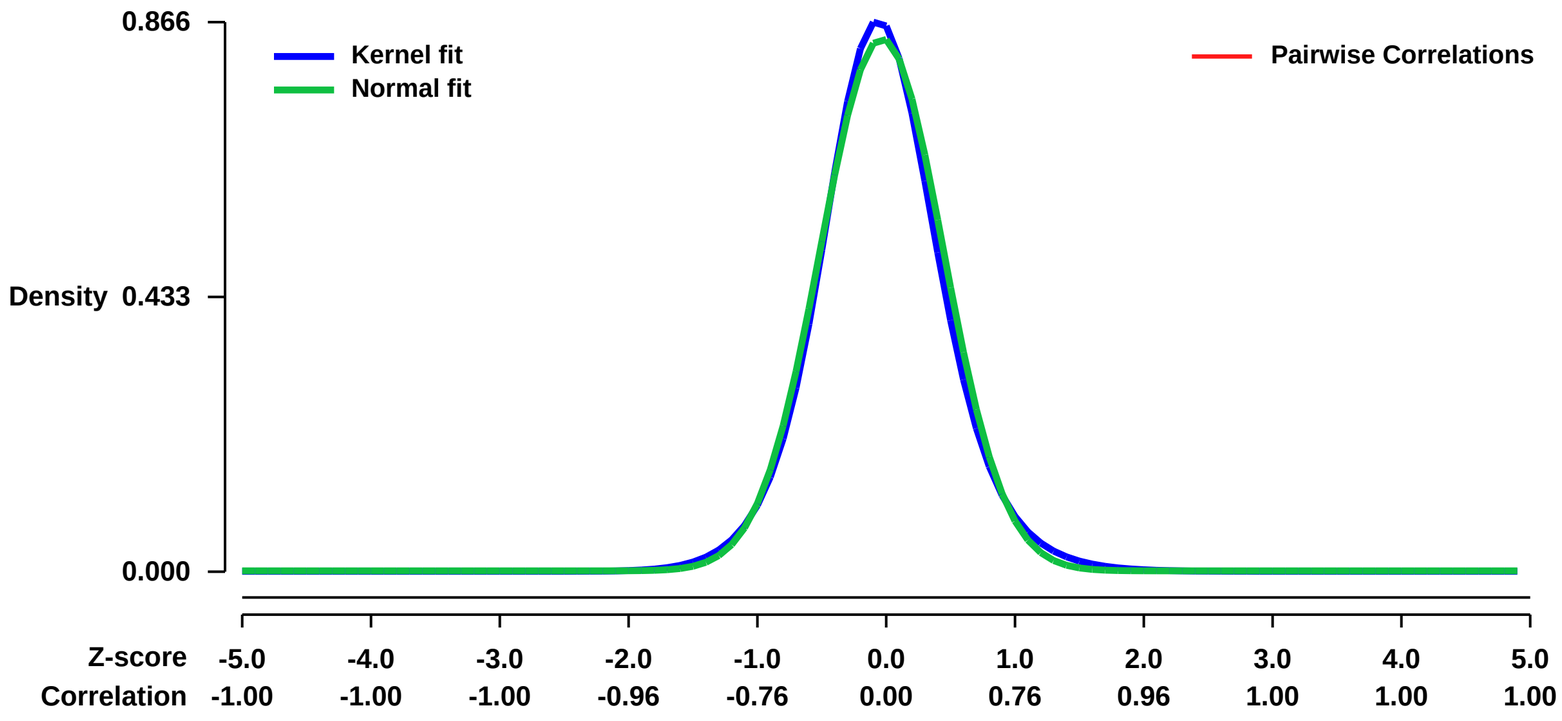

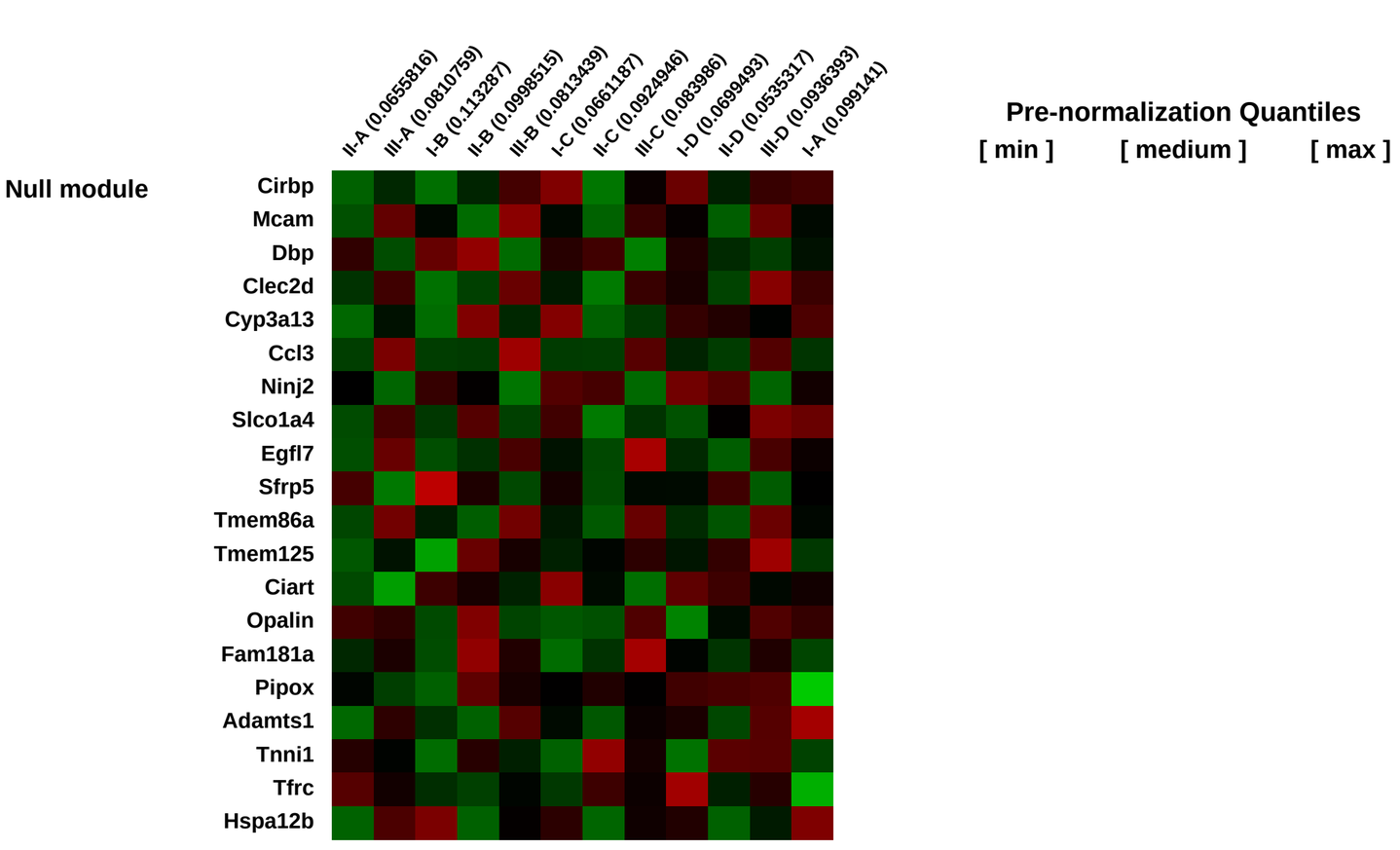

GEO Series "GSE38304" Expression Profiles

Num of samples in this series: 8

Scale of expression profile Z-scores

-3.0 -2.0 -1.0 0.0 1.0 2.0 3.0

GEO Link:	http://www.ncbi.nlm.nih.gov/geo/query/acc.cgi?acc=GSE38304
Status:	Public on Sep 24 2012
Title:	Gene Expression Profiles of MYC+ and MYC- mouse Germinal Center B cells
Organism:	Mus musculus
Experiment type:	Expression profiling by array
Platform:	GPL1261
Pubmed ID:	23001145
Summary & Design:	**Summary:** Germinal centers (GC) arise within B cell follicles upon antigenic challenge. In the dark zones (DZ) of GCs, B cells proliferate and hypermutate their immunoglobulin genes, and mutants with increased affinity are positively selected in the light zone (LZ) to either differentiate into plasma and memory cells, or re-enter the DZ for further refinement. However, the molecular circuits governing GC positive selection are not known. Here, we show that the GC reaction requires the biphasic regulation of c-MYC expression, involving its transient induction during early GC commitment, its repression by BCL6 in DZ B cells, and its re-induction in a subpopulation of positively selected LZ B cells destined to DZ re-entry. Accordingly, acute disruption of MYC function in vivo leads to GC collapse, indicating an essential role in GC physiology. These results have implications for our understanding of GC selection and the role of MYC deregulation in B cell lymphomas. We used microarrays to determine the global gene expression programs that distinguish MYC+ GC B cells from their MYC- negative counterparts. **Overall design:** GFPMYC+ and GFPMYC- GC B cell subpopulations were collected by Fluorescence Activated Cell Sorting (FACS) from B cell enriched fractions of splenic mononuclear cell pools of GFPMYC knock-in mice (12 days after SRBC immunization). 5-20ng of total RNA (RIN>9) for each sample was used as a template for linear cDNA amplification (Ovation RNA amplification Kit, NuGen). cDNA was labeled using the Encore Biotin Labeling Kit (NuGen) and hybridized to Affymetrix Mouse 430.2 gene expression arrays.

Background corr dist: KL-Divergence = 0.0656, L1-Distance = 0.0311, L2-Distance = 0.0016, Normal std = 0.5216

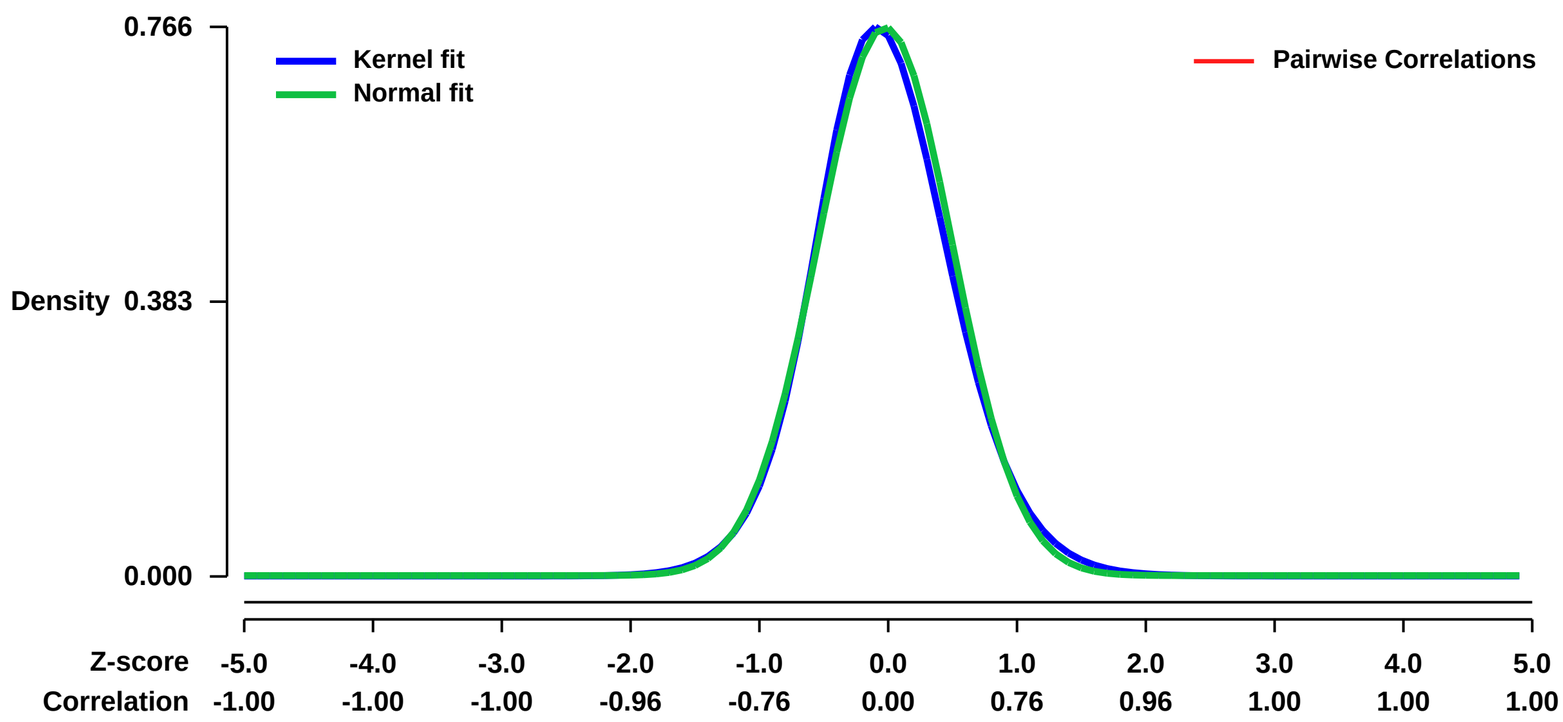

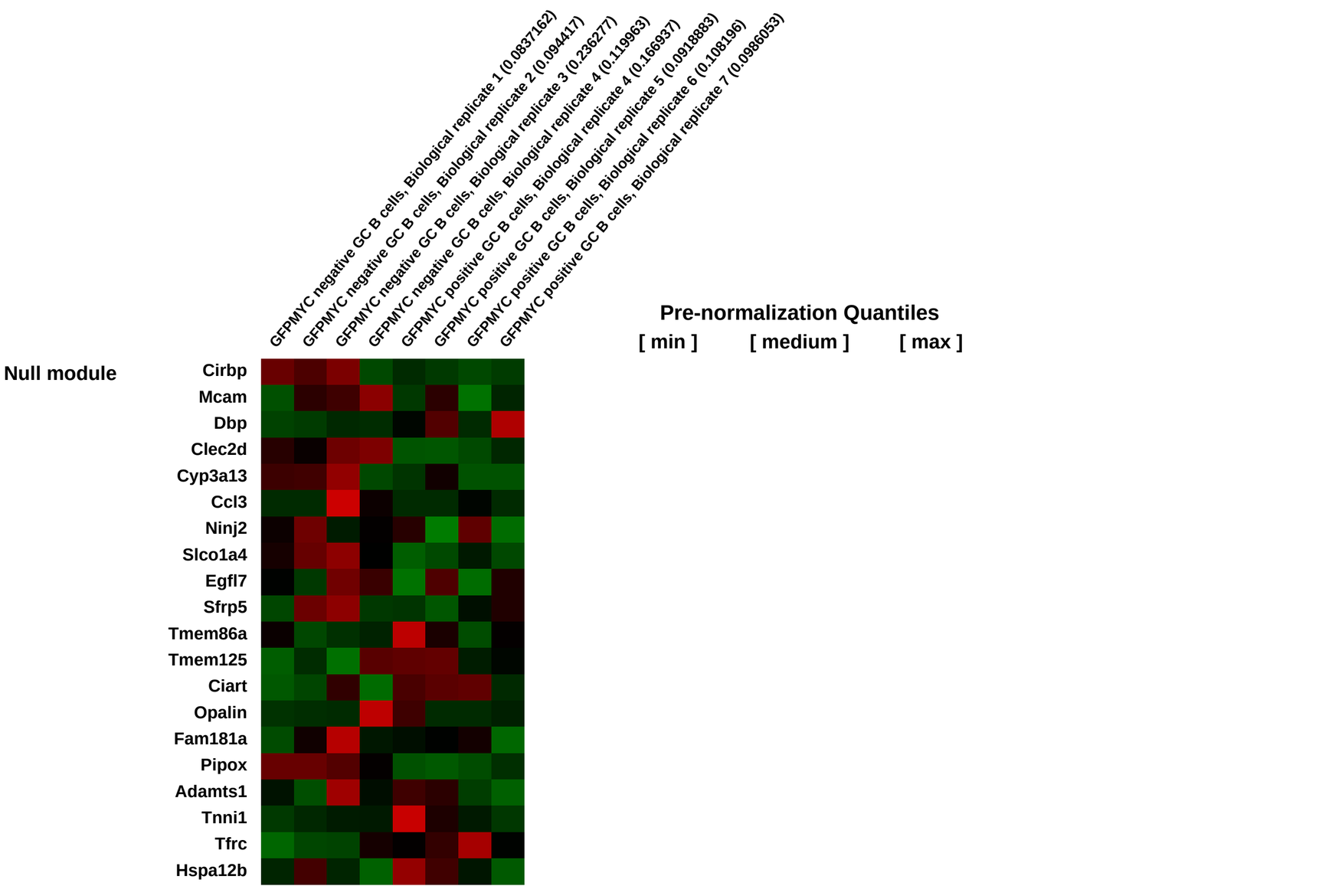

GEO Series "GSE17745" Expression Profiles

Num of samples in this series: 6

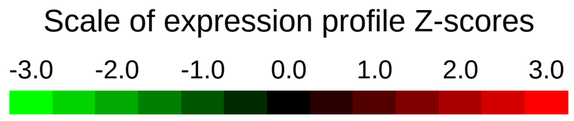

GEO Link:	**http://www.ncbi.nlm.nih.gov/geo/query/acc.cgi?acc=GSE17745**
Status:	**Public on Aug 20 2011**
Title:	**Identification of genes regulated by the RANK IVVY motif in macrophages**
Organism:	**Mus musculus**
Experiment type:	**Expression profiling by array**
Platform:	**GPL1261**
Pubmed ID:	
Summary & Design:	**Summary:** **Identification of genes regulated by RANK RVVY motif in macrophages by gene expression analysis of TNFR1-/-R2-/- BMMs expressing a chimeric receptor consisting of the external domain of mouse TNFR1 linked to the transmembrane and intracellular domain of mouse RANK (WT) and NFR1-/-R2-/- BMMs expressing a chimeric receptor consisting of the external domain of mouse TNFR1 linked to the transmembrane and intracellular domain of mouse RANK bearing inactivating mutations in the IVVY motif (Mu).** **Overall design:** **three replicates: rep1, rep2, and rep3**

Background corr dist: **KL-Divergence = 0.0309, L1-Distance = 0.0597, L2-Distance = 0.0044, Normal std = 0.7758**

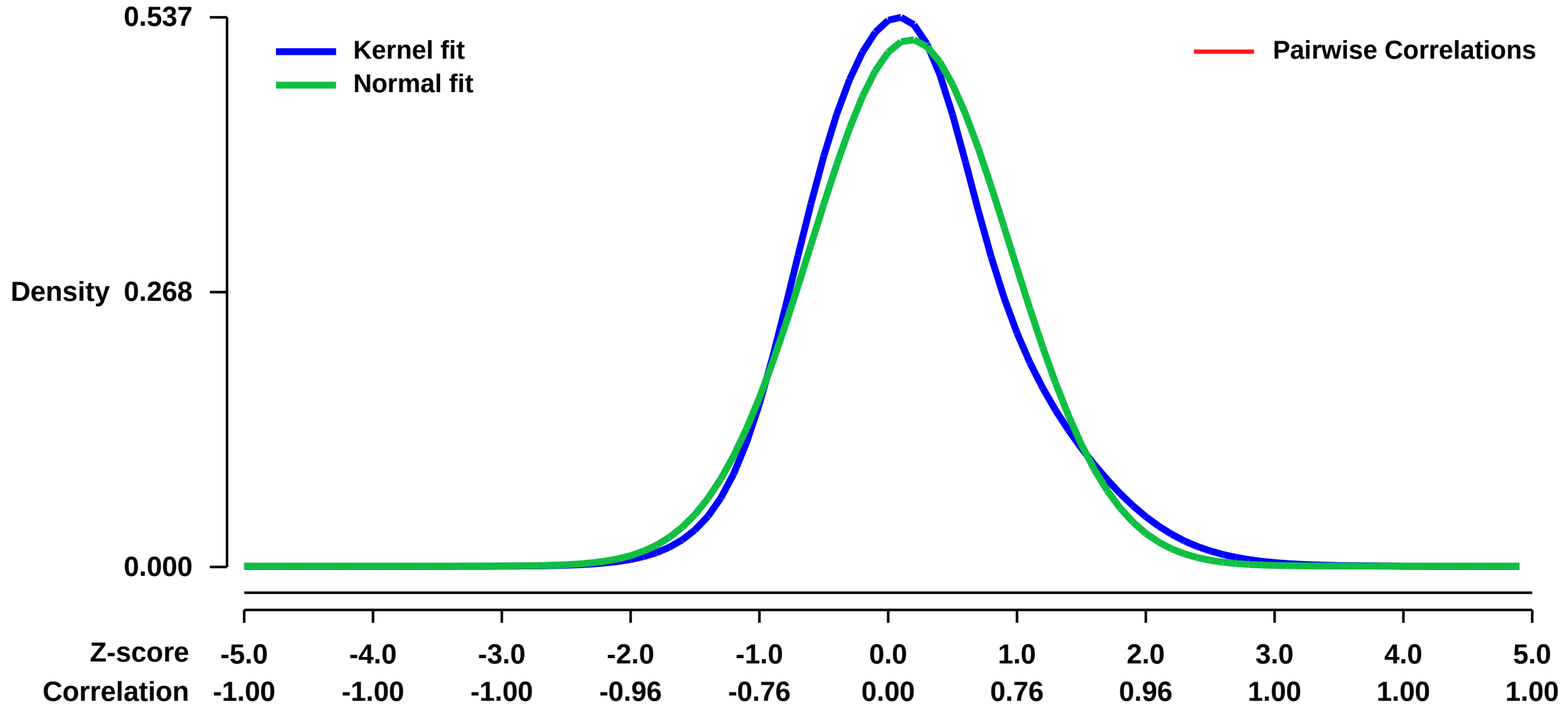

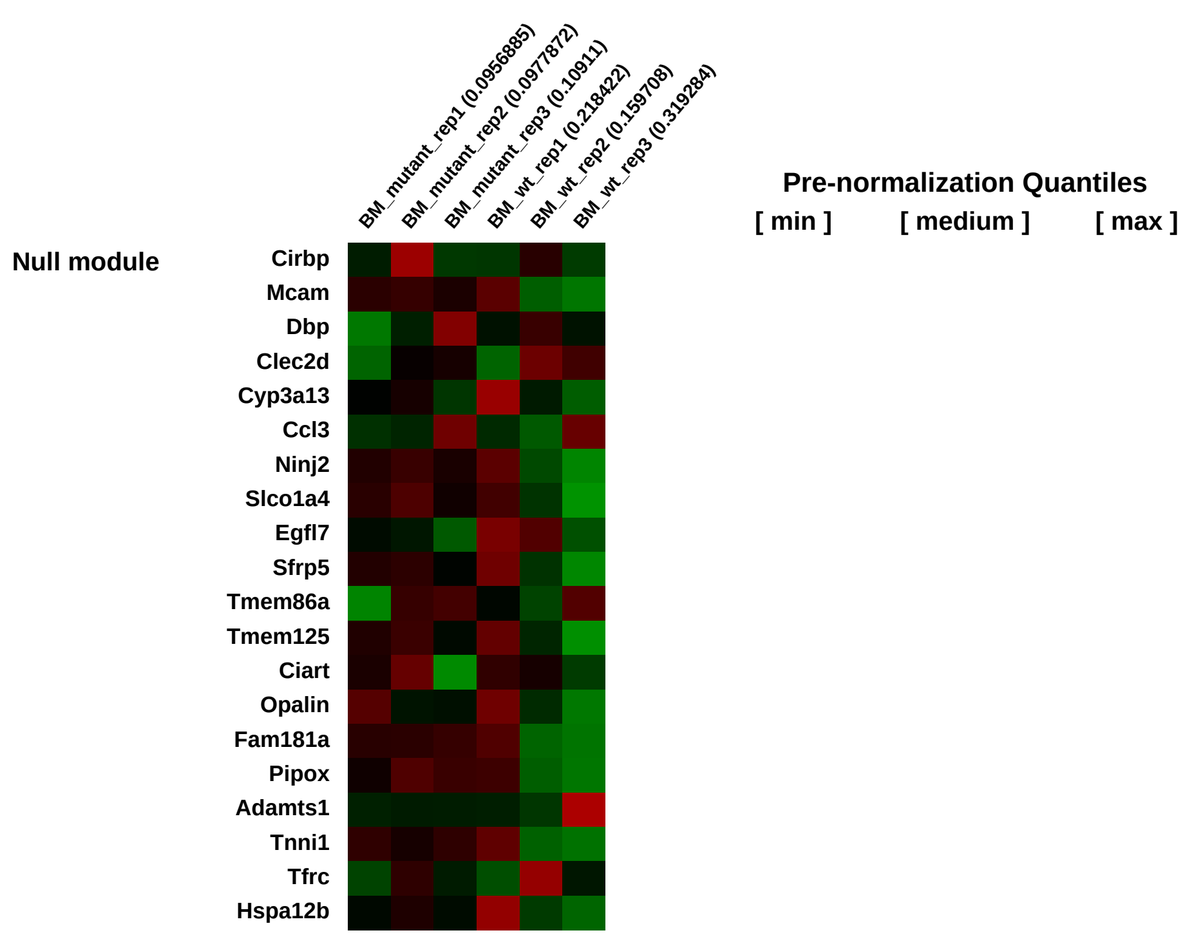

GEO Series "GSE9509" Expression Profiles

Num of samples in this series: 18

Scale of expression profile Z-scores

-3.0 -2.0 -1.0 0.0 1.0 2.0 3.0

GEO Link:	http://www.ncbi.nlm.nih.gov/geo/query/acc.cgi?acc=GSE9509
Status:	Public on Dec 01 2007
Title:	A transcriptional repressor and co-repressor induced by the STAT3-regulated anti-inflammatory signaling pathway.
Organism:	Mus musculus
Experiment type:	Expression profiling by array
Platform:	GPL1261
Pubmed ID:	18025162
Summary & Design:	**Summary:** IL-10 regulates anti-inflammatory signaling via the activation of STAT3, which in turn controls the induction of a gene expression program whose products execute inhibitory effects on pro-inflammatory mediator production. Here we show that IL-10 induces the expression of an ETS family transcriptional repressor, ETV3 and a helicase family co-repressor, SBNO2 (Strawberry notch homolog 2) in mouse and human macrophages. IL-10-mediated induction of ETV3 and SBNO2 expression was dependent upon both STAT3, and co-stimulus through the TLR pathway. We also observed that ETV3 expression was strongly induced by the STAT3 pathway induced by IL-10 but not STAT3 signaling activated by IL-6, which cannot activate the anti-inflammatory signaling pathway. ETV3 and SBNO2 specifically repressed NF-kB-mediated transcription and can physically interact. Collectively our data suggest that ETV3 and SBNO2 are components of the pathways that contribute to the downstream anti-inflammatory effects of IL-10. We compared expression profiles of macrophages isolated from IL-10 -/- mice. Macrophages were treated with either LPS or LPS plus IL-10. Treatment times were 10, 20 and 30 minutes. Keywords: time-course, treatment response, gene expression analysis **Overall design:** Mouse IL-10 -/- macrophages were isolated and purified and set up in culture medium containing LPS or LPS plus IL-10. A total of 18 samples were analyzed. This set contains three replicates of each treatment condition where treatment (LPS versus LPS plus IL-10) and time (10min, 20min and 30min) were varied.

Background corr dist: KL-Divergence = 0.1615, L1-Distance = 0.0290, L2-Distance = 0.0013, Normal std = 0.3670

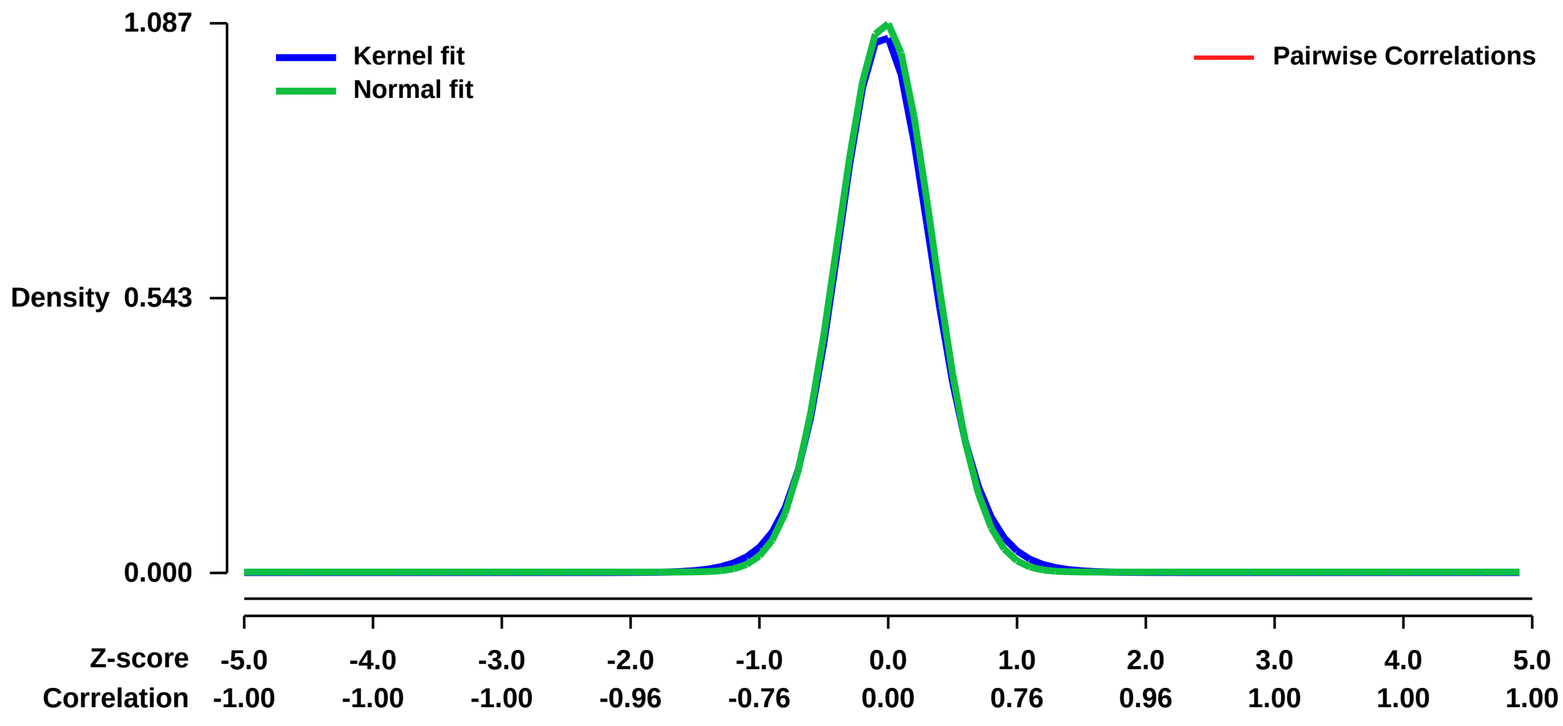

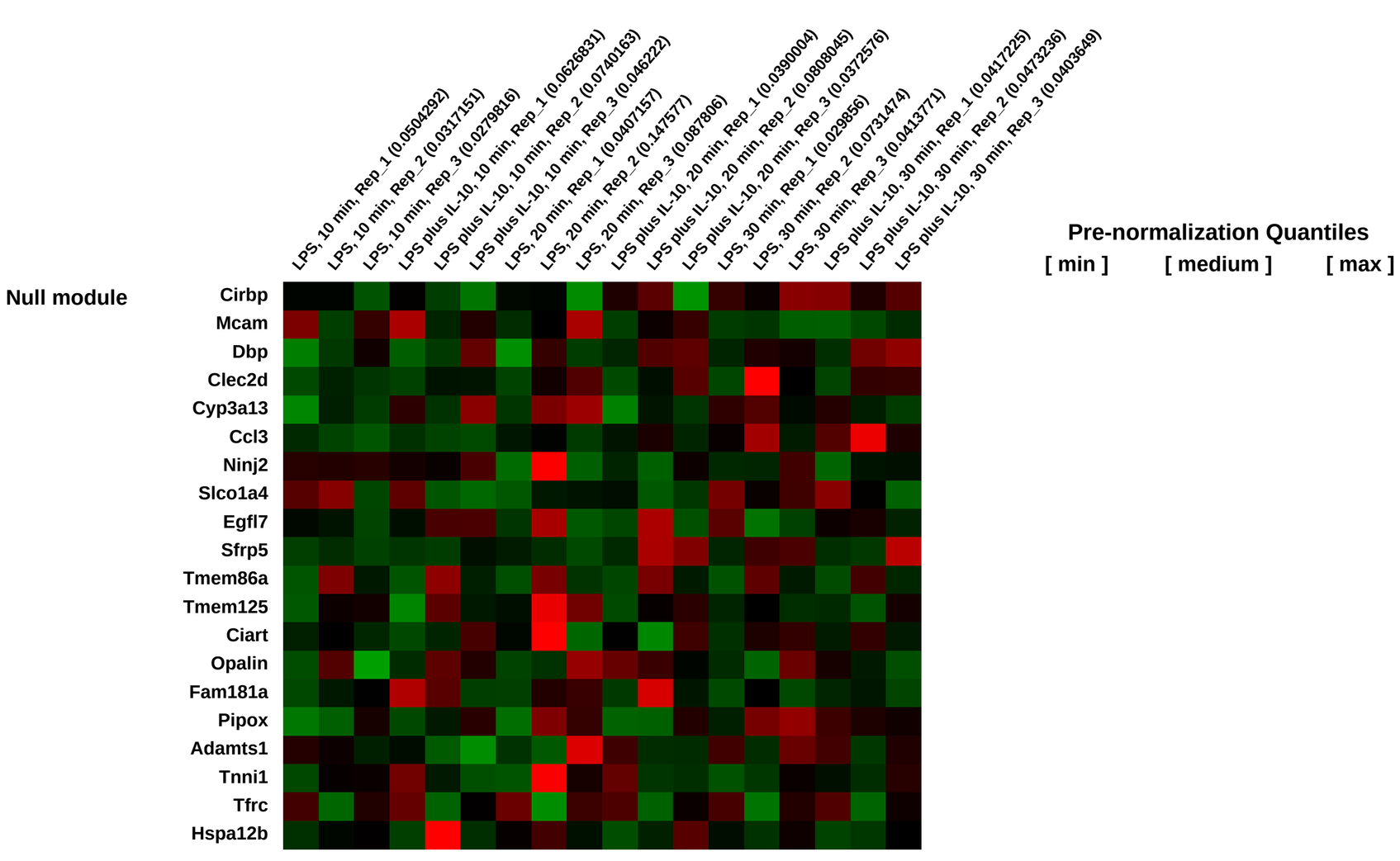

GEO Series "GSE36229" Expression Profiles

Num of samples in this series: 14

Scale of expression profile Z-scores

-3.0 -2.0 -1.0 0.0 1.0 2.0 3.0

GEO Link:	http://www.ncbi.nlm.nih.gov/geo/query/acc.cgi?acc=GSE36229
Status:	Public on Dec 25 2012
Title:	Dynamic changes in the functions of Klf5 in maturing mouse corneas revealed by the changes in its target genes at postnatal days 11 and 56
Organism:	Mus musculus
Experiment type:	Expression profiling by array
Platform:	GPL1261
Pubmed ID:	23024760
Summary & Design:	**Summary:** **Purpose: Klf5 plays a critical role in the mouse ocular surface (Kenchegowda et al., 2011. Dev Biol. 356:5-18). Here, we compare wild-type (WT) and Klf5-conditional null (Klf5CN) corneal gene expression at postnatal day-11 (PN11) and PN56 to identify the Klf5-target genes. Methods: Gene expression was compared using Affymetrix microarrays with QPCR validation. Transient transfection assays examined the effect of Klf5 on selected target gene promoter activities. Whole-mount corneal immunofluorescent staining examined neovascularization and CD45+ macrophage influx. Results: Expression of 714 and 753 genes was increased, and 299 and 210 genes decreased in PN11 and PN56 Klf5CN corneas, respectively, with 366 concordant increases, 72 concordant decreases and 3 discordant changes. Canonical pathway analysis identified 35 and 34 significantly (p<0.001) enriched pathways at PN11 and PN56, respectively, with 24 common pathways. PN56 Klf5CN corneas shared 327 increases and 91 decreases with the previously described Klf4CN corneas (Swamynathan et al., 2008. IOVS 49:3360-70). Angiogenesis and immune response-related genes were affected consistent with lymphangiogenesis and macrophage influx in Klf5CN corneas, respectively. Expression of 1574 genes was increased and 1915 decreased, in the WT PN56 compared with PN11 corneas. Expression of many collagens, matrix metalloproteinases and other extracellular matrix associated genes decreased in WT corneas between PN11 and PN56, while that of solute carrier family members increased. Conclusions: Differences in PN11 and PN56 corneal Klf5-target genes reveal dynamic changes in Klf5 functions during corneal maturation. Klf4- and Klf5-target genes do not overlap, consistent with their non-redundant roles in the mouse cornea.** **Overall design:** **Wild type and Klf5-conditional null mouse corneal gene expression at postnatal day-11 and -56 was compared by Affymetrix mouse whole genome 430 2 arrays. Four age-matched PN56 WT and Klf5CN mice, and 3 age-matched PN11 WT and Klf5CN mice each were used for comparison of corneal gene expression by microarrays. Two dissected corneas from each mouse were pooled for isolation of total RNA using the RNeasy Mini kit (Qiagen, Germantown, MD). The quality and integrity of the isolated total RNA was confirmed using an Agilent Bioanalyzer. Total RNAs were amplified and labeled using a 3' IVT Express Kit (Affymetrix Inc., Santa Clara, CA), and hybridized to Affymetrix MG 430 2 chips following the protocol suggested by the manufacturer.**

Background corr dist: KL-Divergence = 0.0791, L1-Distance = 0.0304, L2-Distance = 0.0014, Normal std = 0.4870

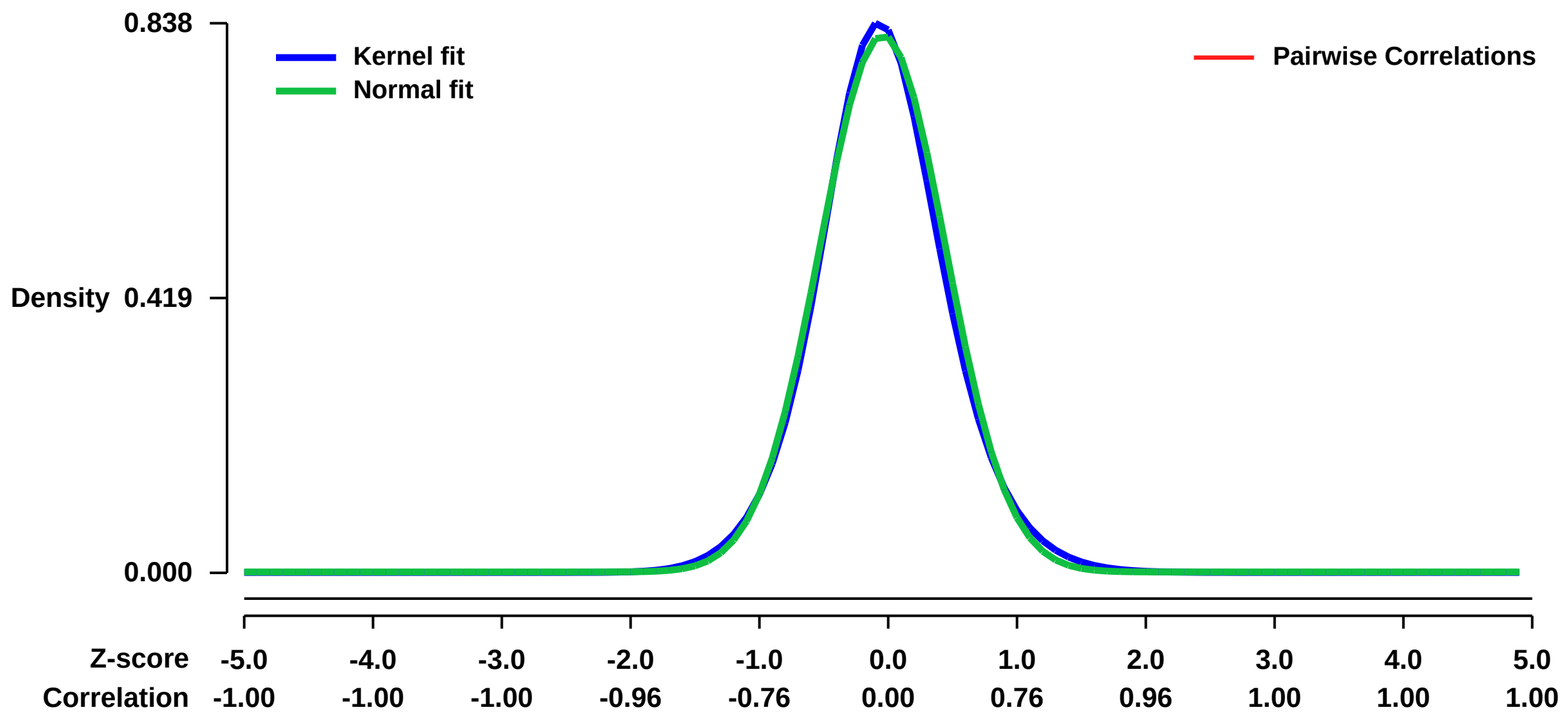

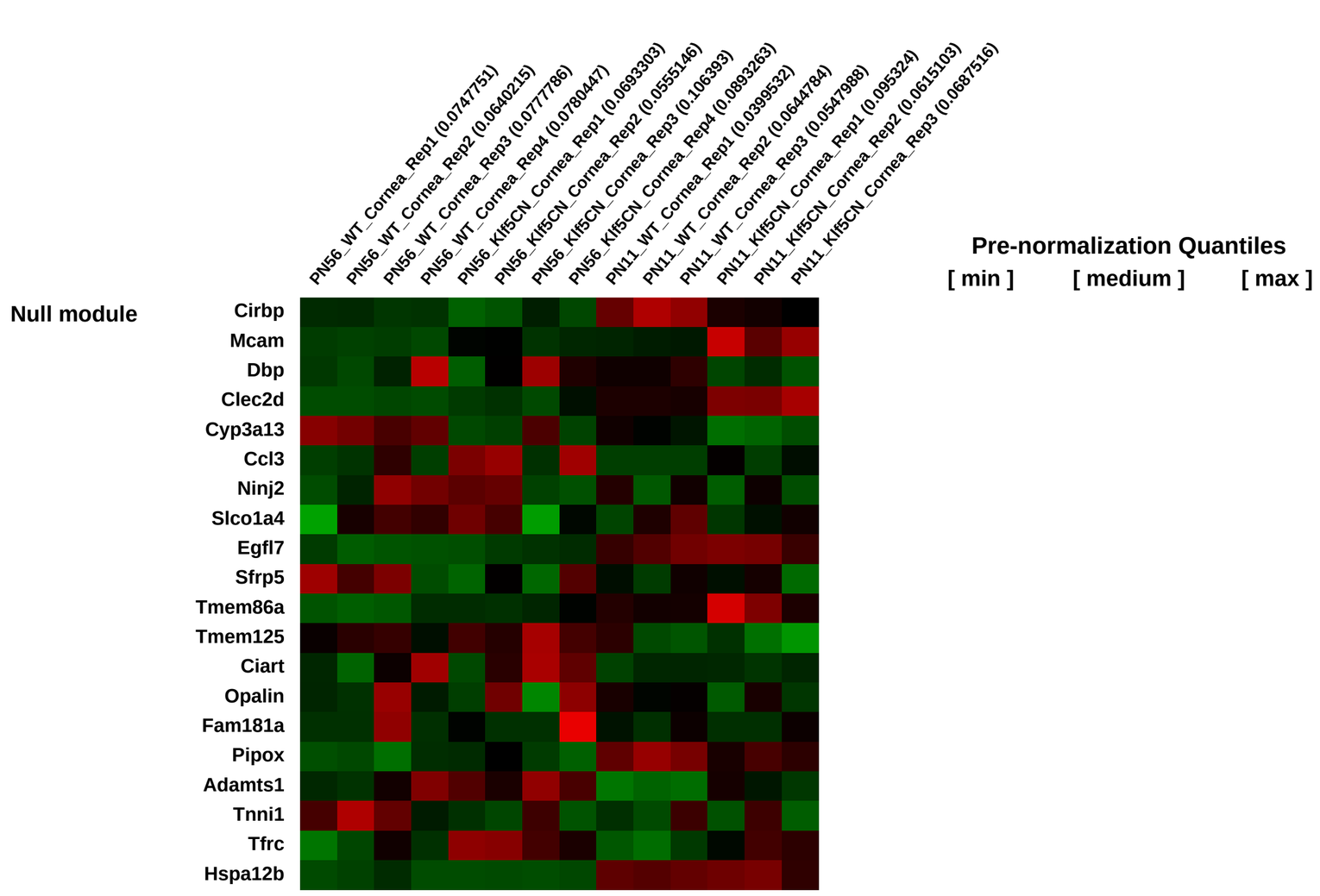

GEO Series "GSE16874" Expression Profiles

Num of samples in this series: 12

Scale of expression profile Z-scores

-3.0 -2.0 -1.0 0.0 1.0 2.0 3.0

GEO Link:	http://www.ncbi.nlm.nih.gov/geo/query/acc.cgi?acc=GSE16874
Status:	Public on Dec 07 2010
Title:	Expression in wild type and TgDREAM mouse B cells unstimulated or 2 days after LPS+IL4 stimulation
Organism:	Mus musculus
Experiment type:	Expression profiling by array
Platform:	GPL1261
Pubmed ID:	21059893
Summary & Design:	**Summary:** DREAM/KChIP-3 is a calcium-dependent transcriptional repressor highly expressed in immune cells. Transgenic mice expressing a dominant active DREAM mutant show reduced serum immunoglobulin levels. In vitro assays show that reduced immunoglobulin secretion is an intrinsic defect of transgenic B cells that occurs without impairment in plasma cell differentiation but with an accelerated entry in cell division and an increase in class switch recombination. B cells from DREAM knockout mice did not show any phenotype, due to compensation by endogenous KChIP-2. Expression arrays revealed modified expression of Edem1 and Derlin3, two proteins related to the ER-associated degradation pathway and of Klf9, a cell-cycle regulator. Our results disclose a function of DREAM and KChIP-2 in Ig subclass production in B lymphocytes. **Overall design:** We used Affymetrix microarrays (GeneChip Mouse Genome 430 2.0) to compare global gene expression in wild type (WT) versus transgenic B cells (Tg), unstimulated and 2 days after LPS + IL4 stimulation. For ech type of sample three hybridizations were carried-out (independent biological replicates).

Background corr dist: KL-Divergence = 0.0300, L1-Distance = 0.0974, L2-Distance = 0.0115, Normal std = 0.9421

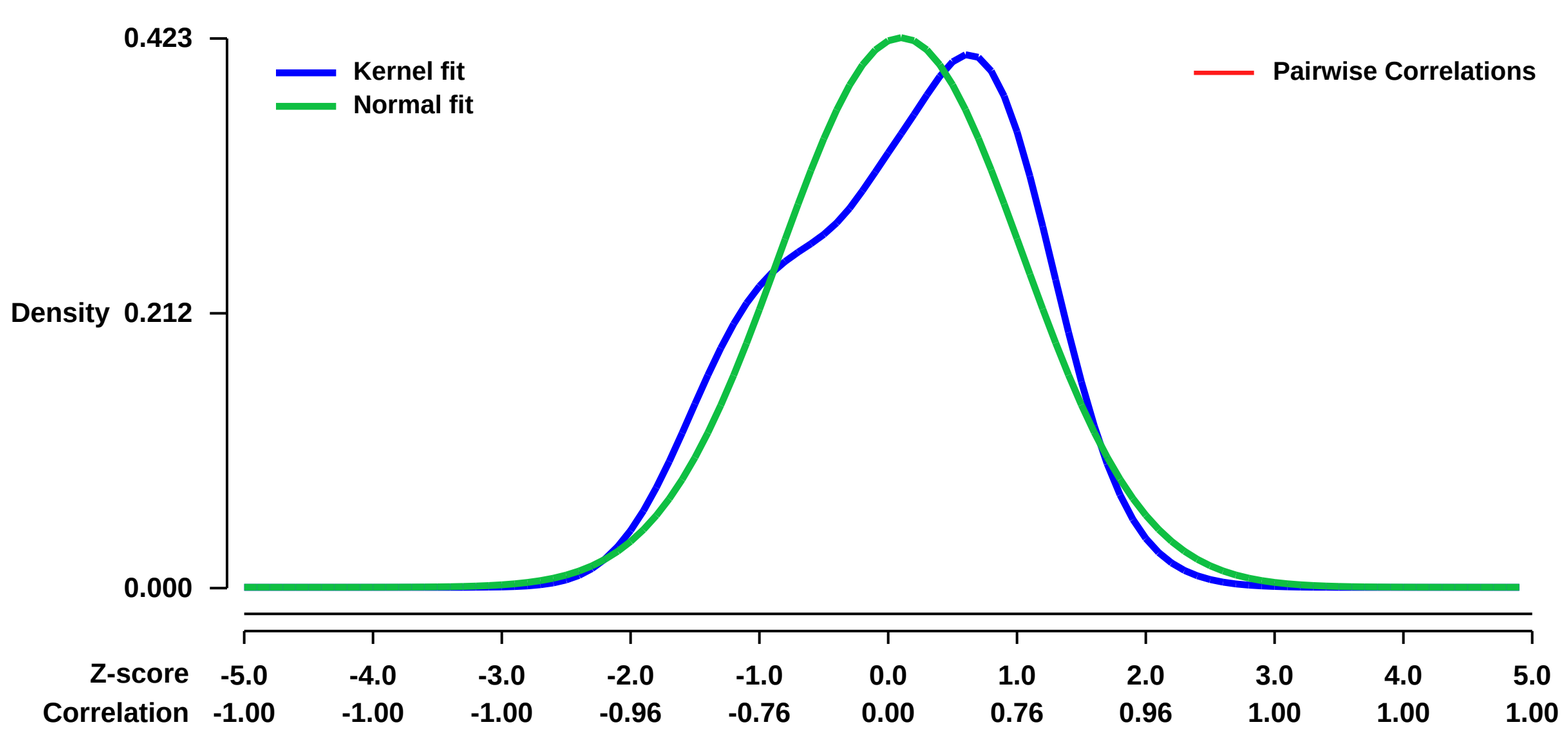

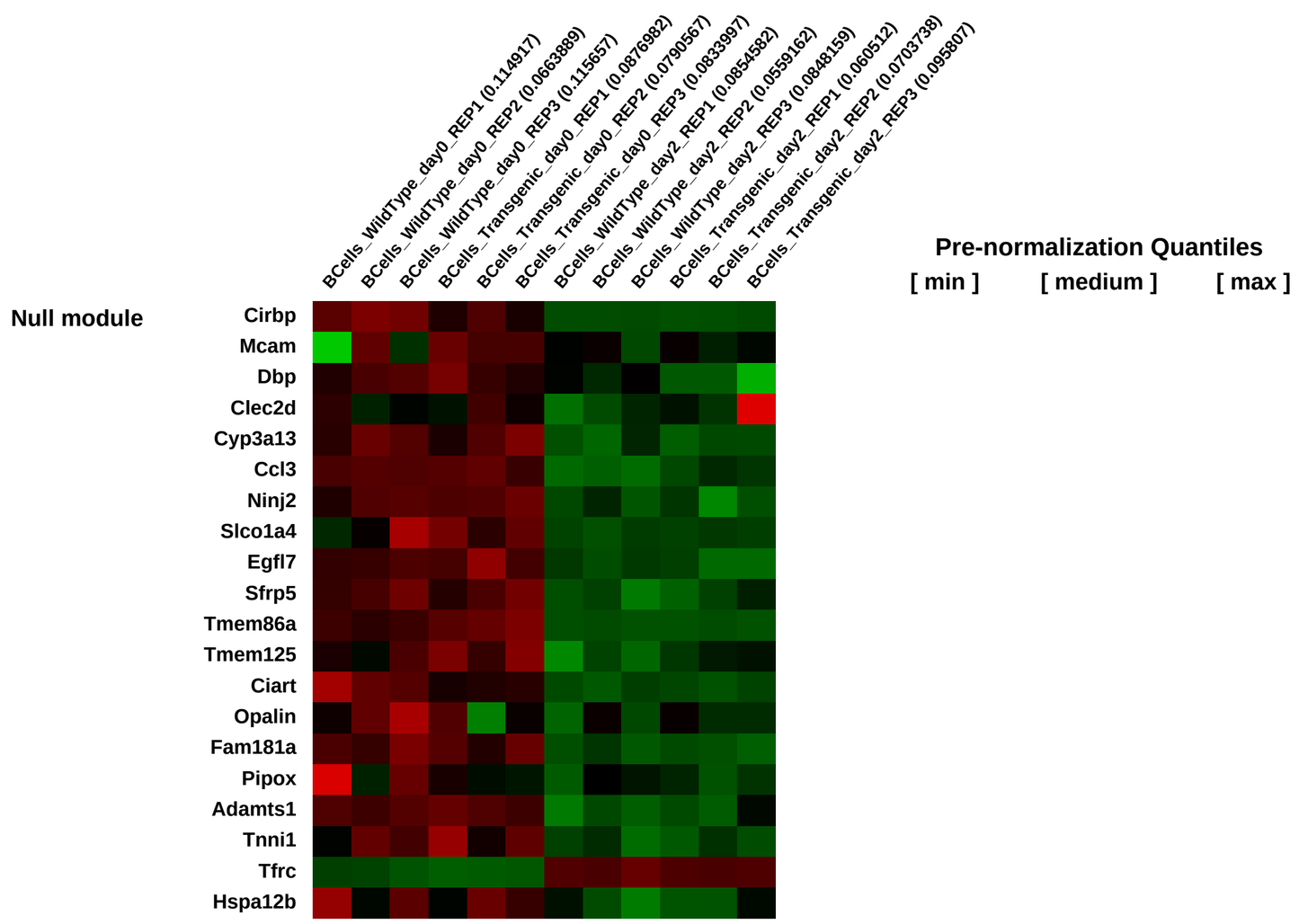

GEO Series "GSE55525" Expression Profiles

Num of samples in this series: 71

Scale of expression profile Z-scores

-3.0 -2.0 -1.0 0.0 1.0 2.0 3.0

GEO Link:	http://www.ncbi.nlm.nih.gov/geo/query/acc.cgi?acc=GSE55525
Status:	Public on May 08 2014
Title:	Hematopoietic stem cell quiescence attenuates DNA damage repair and response contributing to age-dependent DNA damage accumulation
Organism:	Mus musculus
Experiment type:	Third-party reanalysis
Platform:	GPL1261
Pubmed ID:	
Summary & Design:	**Summary:** Comprehensive analysis of gene expression in hematopoietic stem and progenitor cells from young and old mice. **Overall design:** Gene expression profiling of young and old mouse hematopoietic stem and progenitor cells by Gene Expression Commons system.

Background corr dist: KL-Divergence = 0.2290, L1-Distance = 0.0620, L2-Distance = 0.0107, Normal std = 0.3181

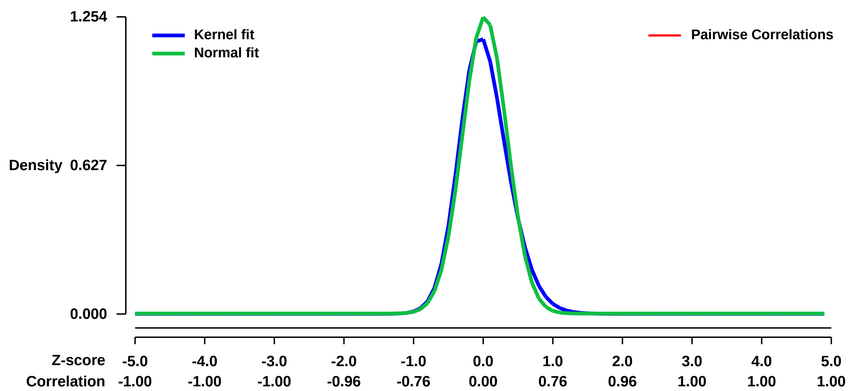

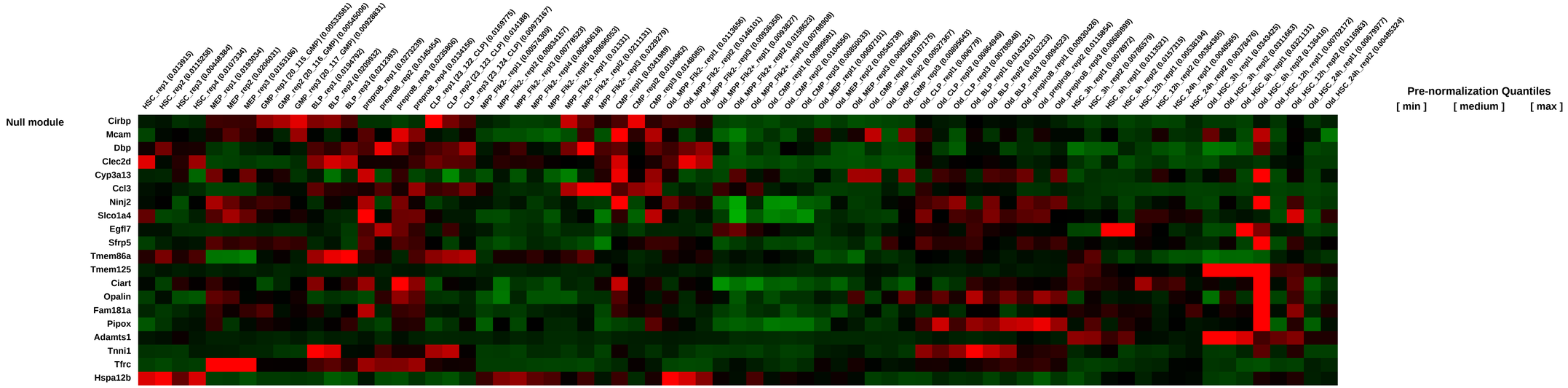

GEO Series "GSE30873" Expression Profiles

Num of samples in this series: 6

Scale of expression profile Z-scores

-3.0 -2.0 -1.0 0.0 1.0 2.0 3.0

GEO Link:	http://www.ncbi.nlm.nih.gov/geo/query/acc.cgi?acc=GSE30873
Status:	Public on Jul 23 2011
Title:	Effects of caspase-8 deletion in the intestinal epithelium
Organism:	Mus musculus
Experiment type:	Expression profiling by array
Platform:	GPL1261
Pubmed ID:	21921917
Summary & Design:	**Summary:** Caspase-8 is a cystein protease involved in regulating apoptosis. The function of caspase-8 was studied in the intestinal epithelium, using mice with an intestinal epithelial cell specific deletion of caspase-8. We used microarrays to investigate the difference of the global programme of gene expression in intestinal epithelial cells of control and caspase-8 deficient mice. **Overall design:** Intestinal epithelial cells were isolated from 3 control mice and 3 mice with a conditional deletion of caspase-8 in the intestinal epithelium. RNA was isolated and subjected to Affymetrix gene chip analysis.

Background corr dist: KL-Divergence = 0.0388, L1-Distance = 0.0228, L2-Distance = 0.0006, Normal std = 0.6268

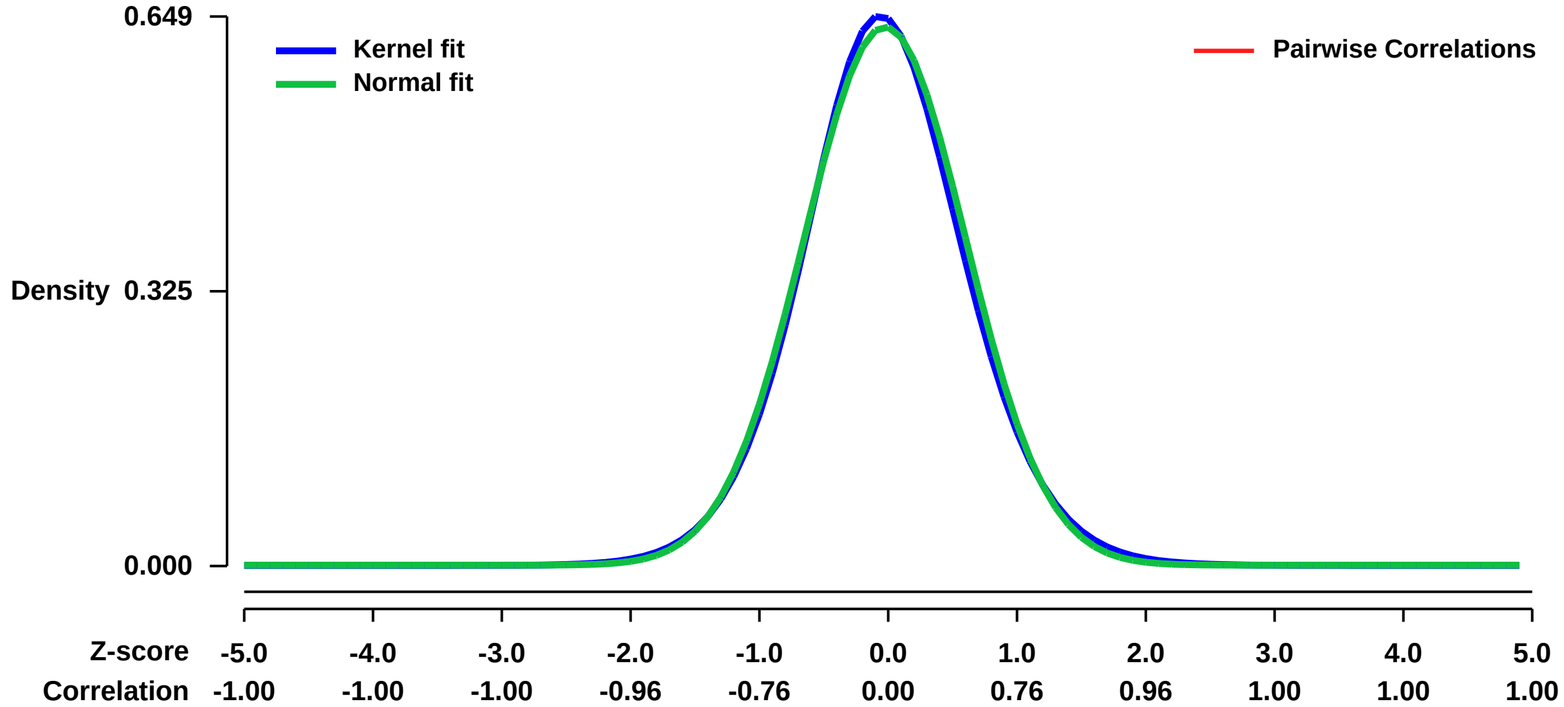

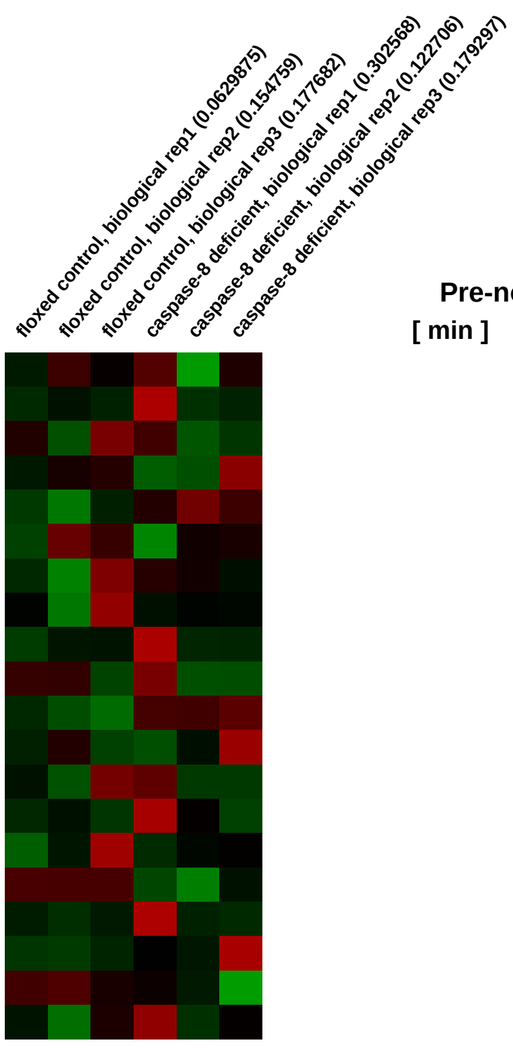

GEO Series "GSE44162" Expression Profiles

Num of samples in this series: 6

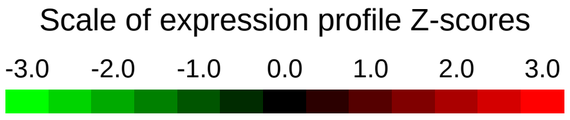

GEO Link:	http://www.ncbi.nlm.nih.gov/geo/query/acc.cgi?acc=GSE44162
Status:	Public on Apr 10 2013
Title:	Let-7 represses Nr6a1 and a mid-gestation developmental program in adult fibroblasts [3p arrays]
Organism:	Mus musculus
Experiment type:	Expression profiling by array
Platform:	GPL1261
Pubmed ID:	23630078
Summary & Design:	**Summary:** MicroRNAs (miRNAs) are critical to proliferation, differentiation, and development. Here, we characterize gene expression in murine Dicer-null adult mesenchymal stem cell lines, a fibroblast cell type. Loss of Dicer leads to de-repression of let-7 targets at levels that exceed 10-100 fold with increases in transcription. Direct and indirect targets of this miRNA belong to a mid-gestation embryonic program that encompasses known oncofetal genes as well as oncogenes not previously associated with an embryonic state. Surprisingly, this mid-gestation program represents a distinct period that occurs between the pluripotent state of the inner cell mass at embryonic day 3.5 and the induction of let-7, upon differentiation, at embryonic day 10.5. Within this mid-gestation program, we characterize the let-7 target Nr6a1, an embryonic transcriptional repressor that regulates gene expression in adult fibroblasts following miRNA loss. In total, let-7 is required for the continual suppression of embryonic gene expression in adult cells, a mechanism that may underlie its tumor suppressive function. **Overall design:** Three dicer heterozygotes and 3 dicer null sarcoma cell lines.

Background corr dist: KL-Divergence = 0.0360, L1-Distance = 0.0203, L2-Distance = 0.0005, Normal std = 0.6381

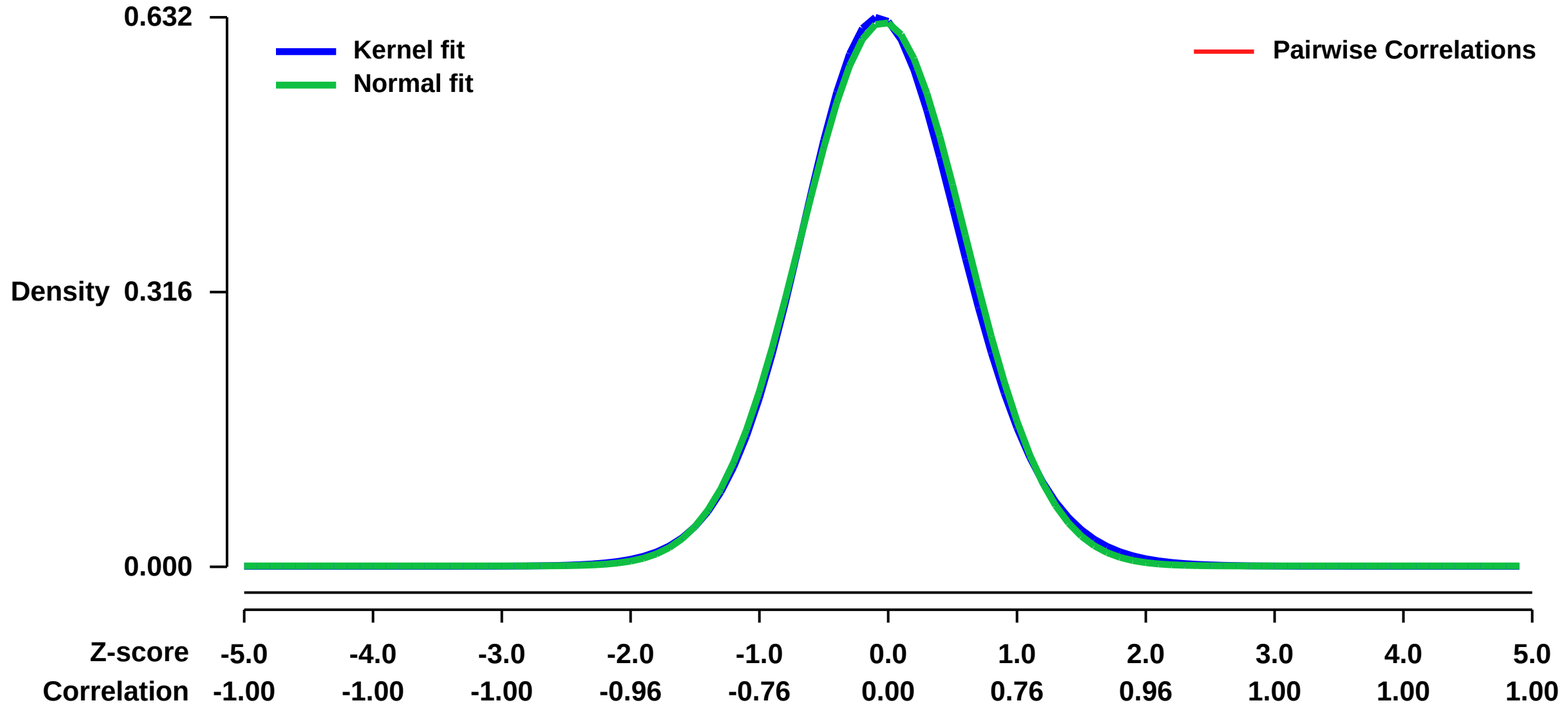

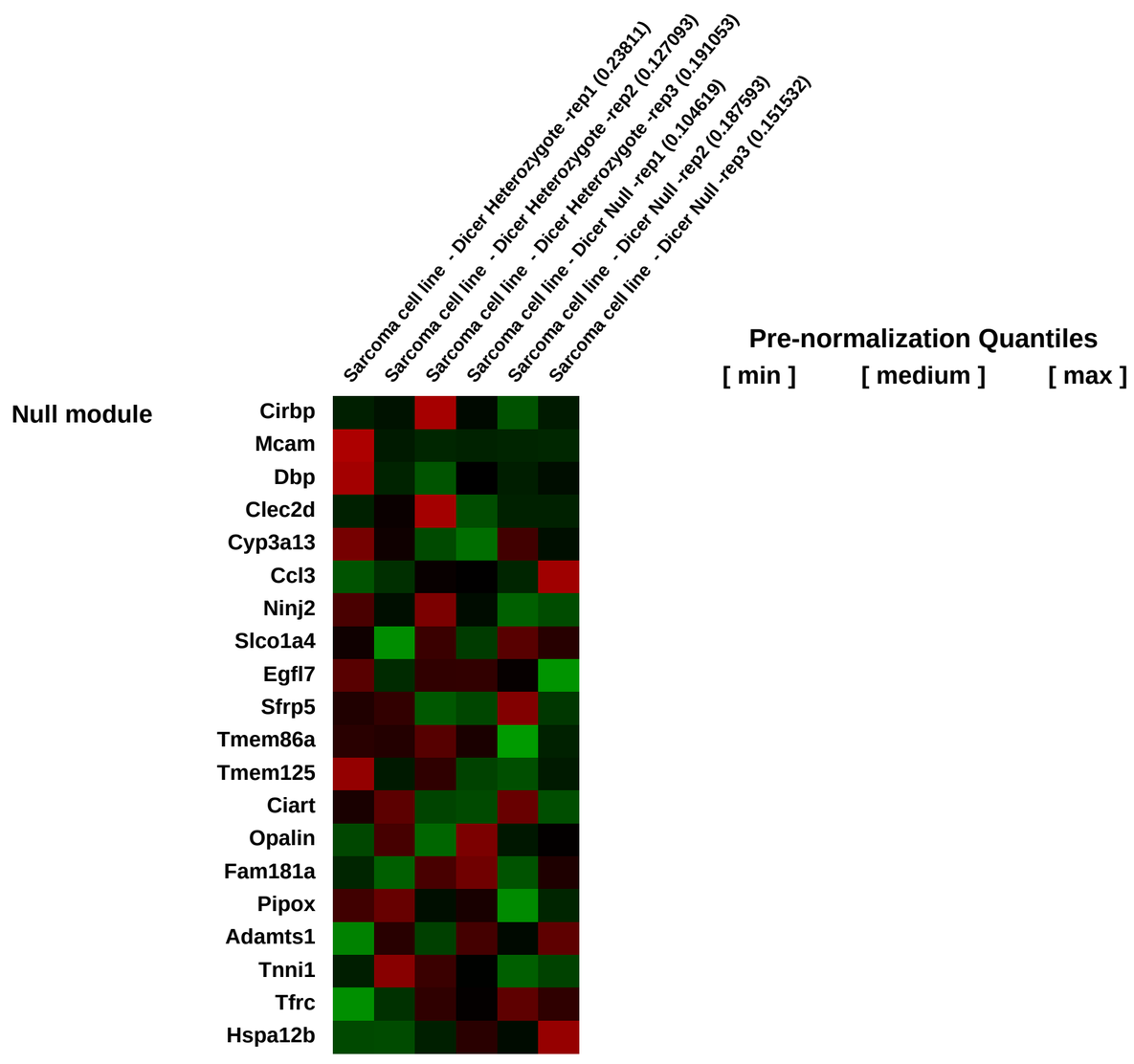

GEO Series "GSE49030" Expression Profiles

Num of samples in this series: 24

Scale of expression profile Z-scores

-3.0 -2.0 -1.0 0.0 1.0 2.0 3.0

GEO Link:	**http://www.ncbi.nlm.nih.gov/geo/query/acc.cgi?acc=GSE49030**
Status:	**Public on Oct 23 2013**
Title:	**Genome-wide profiling of the activity-dependent hippocampal transcriptome**
Organism:	**Mus musculus**
Experiment type:	**Expression profiling by array**
Platform:	**GPL1261**
Pubmed ID:	**24146943**
Summary & Design:	**Summary:** **Activity-dependent gene expression is central for sculpting neuronal connectivity in the brain. Despite the importance for synaptic plasticity, a comprehensive analysis of the temporal changes in the transcriptomic response to neuronal activity is lacking. In a genome wide survey we identified genes that were induced at 1, 4, 8, or 24 hours following neuronal activity in the hippocampus.** **Overall design:** **3 month old male mice were injected with kainic acid or isotonic saline solution. Animals were sacrificed by cervical luxation 1, 2, 4, 8, or 24 h after onset of the first seizure, and RNA was extracted from the hippocampal region.**

Background corr dist: **KL-Divergence = 0.1663, L1-Distance = 0.0450, L2-Distance = 0.0044, Normal std = 0.3569**

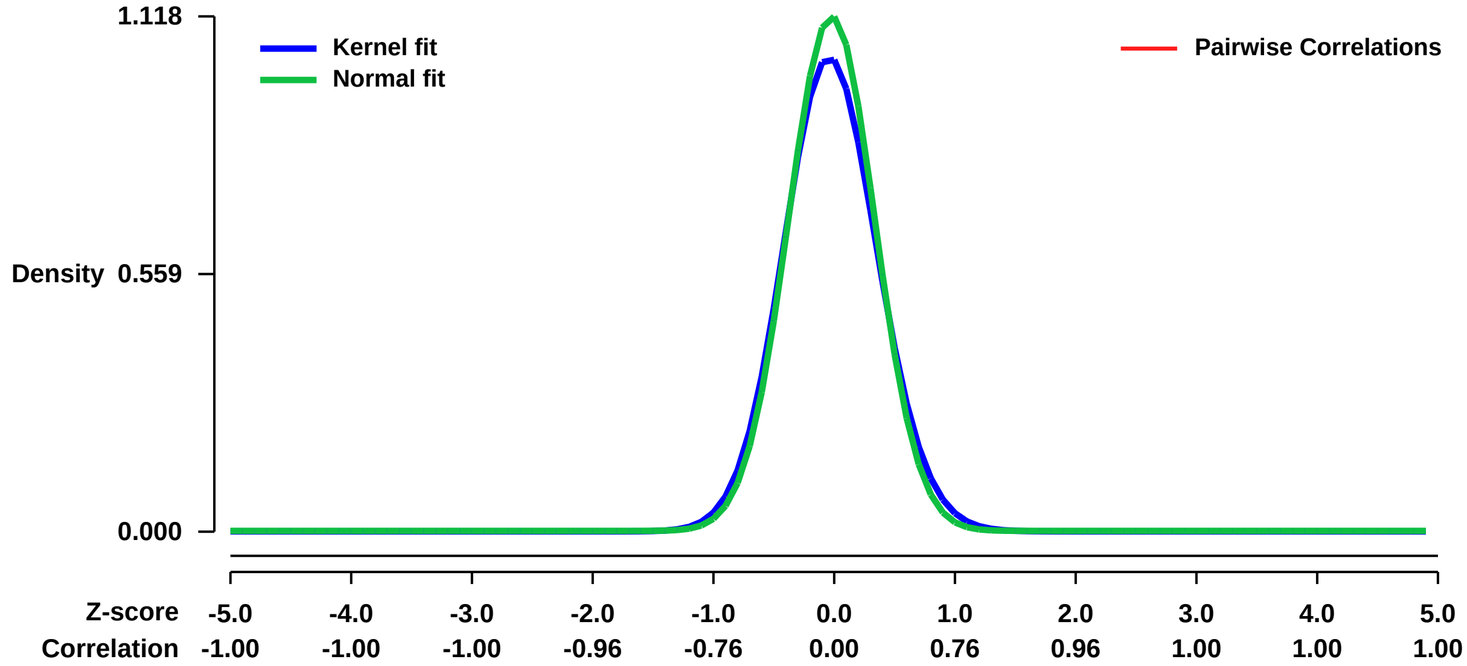

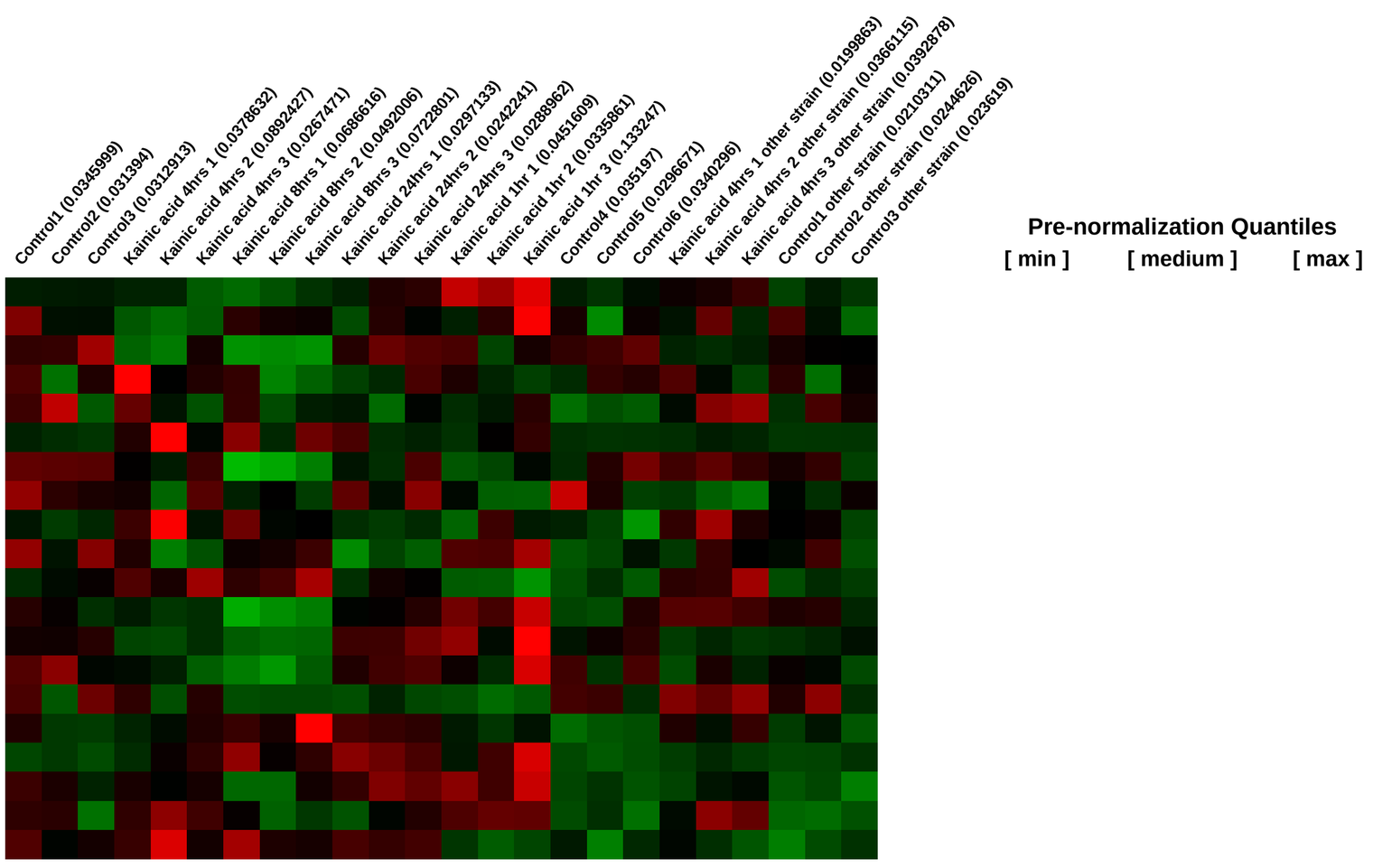

Null module

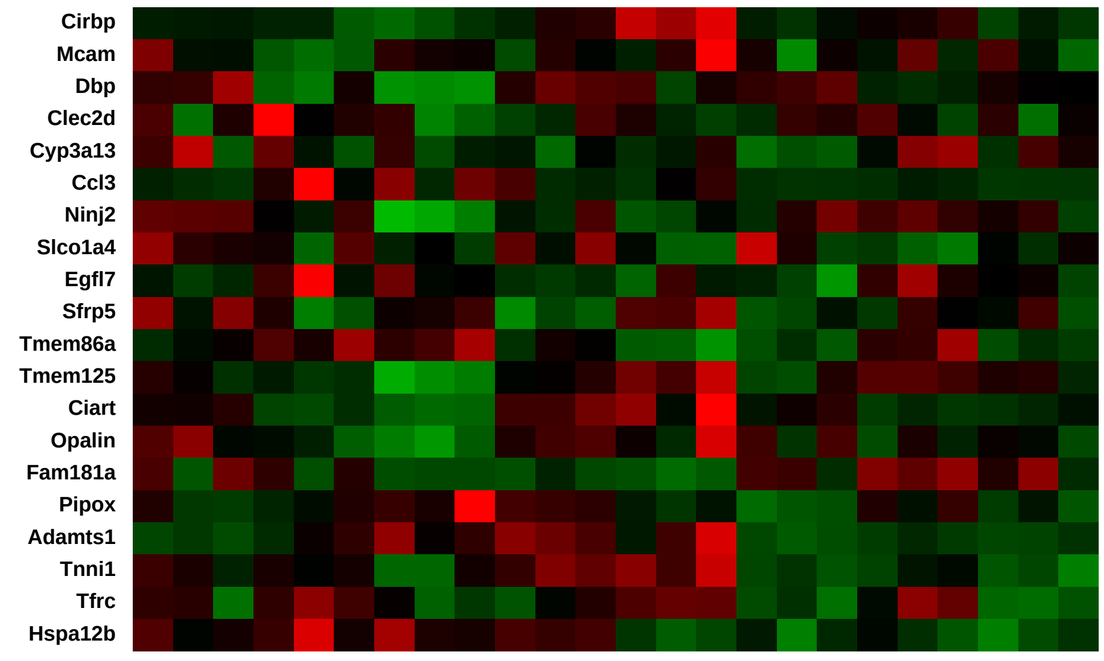

GEO Series "GSE51932" Expression Profiles

Num of samples in this series: 8

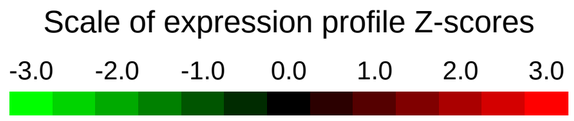

GEO Link:	http://www.ncbi.nlm.nih.gov/geo/query/acc.cgi?acc=GSE51932
Status:	Public on Nov 22 2013
Title:	Expression data from murine irf4-/- and irf4+/+ mature B cells purified by magnetic cell separation
Organism:	Mus musculus
Experiment type:	Expression profiling by array
Platform:	GPL1261
Pubmed ID:	24323359
Summary & Design:	**Summary:** Gene expression profiling of murine irf4-/- and irf4+/+ splenic B cells identifies genes regulated by the transcription factor IRF4 in quiescent mature B cells. **Overall design:** B cells from 12-week old irf4-/- and irf4+/+ littermate mice were isolated by magnetic depletion of non-B cells from splenic mononuclear cells. RNA was isolated. Labeled cRNA was hybridized to microarrays and genes specifically expressed in irf4-/- vs. irf4+/+ samples.

Background corr dist: KL-Divergence = 0.0828, L1-Distance = 0.0205, L2-Distance = 0.0007, Normal std = 0.4714

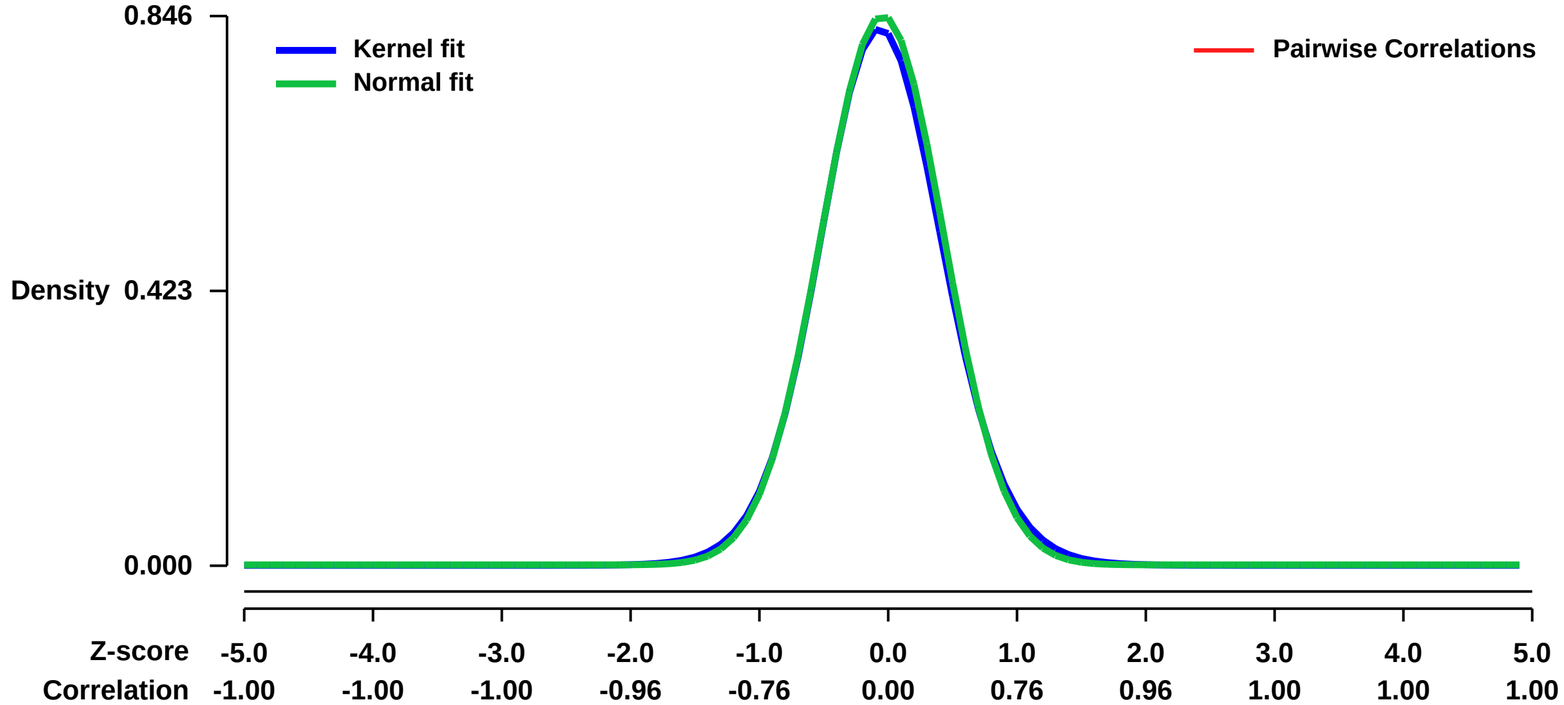

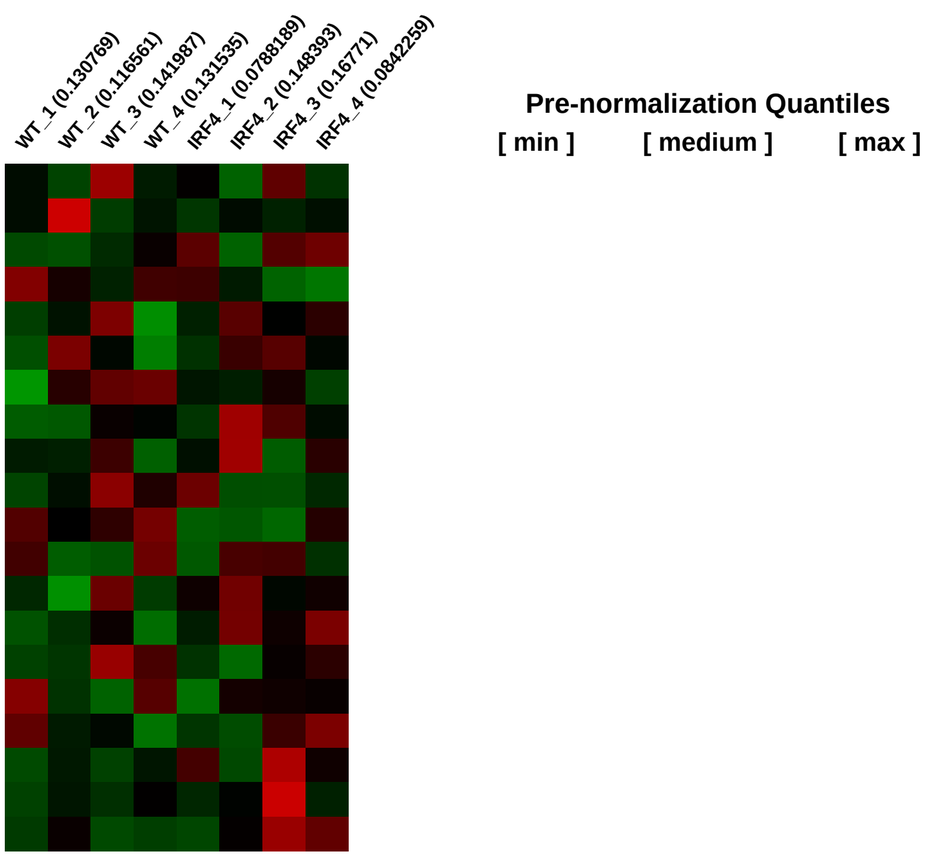

GEO Series "GSE29241" Expression Profiles

Num of samples in this series: 6

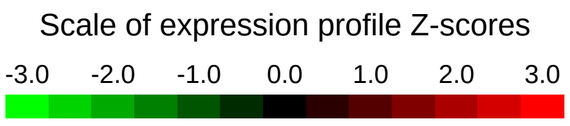

GEO Link:	http://www.ncbi.nlm.nih.gov/geo/query/acc.cgi?acc=GSE29241
Status:	Public on Nov 13 2011
Title:	Dendritic cell lineage commitment is instructed by distinct cytokine signals
Organism:	Mus musculus
Experiment type:	Expression profiling by array
Platform:	GPL1261
Pubmed ID:	22078373
Summary & Design:	**Summary:** Dendritic cells (DC) develop from hematopoietic stem cells, which is guided by instructive signals through cytokines. DC development progresses from multipotent progenitors (MPP) via common DC progenitors (CDP) into DC. Flt3 ligand (Flt3L) signaling via the Flt3/Stat3 pathway is of pivotal importance for DC development under steady state conditions. Additional factors produced during steady state or inflammation, such as TGF-beta1 or GM-CSF, also influence the differentiation potential of MPP and CDP. Here, we studied how gp130, GM-CSF and TGF-beta1 signaling influence DC lineage commitment from MPP to CDP and further into DC. We observed that activation of gp130 signaling promotes expansion of MPP. Additionally, gp130 signaling inhibited Flt3L-driven DC differentiation, but had little effect on GM-CSF-driven DC development. The inflammatory cytokine GM-CSF induces differentiation of MPP into inflammatory DC and blocks steady state DC development. Global transcriptome analysis revealed a GM-CSF-driven gene expression repertoire that primes MPP for differentiation into inflammatory DC. Finally, TGF-beta1 induces expression of DC-lineage affiliated genes in MPP, including Flt3, Irf-4 and Irf-8. Under inflammatory conditions, however, the effect of TGF- beta1 is altered: Flt3 is not upregulated, indicating that an inflammatory environment inhibits steady state DC development. Altogether, our data indicate that distinct cytokine signals produced during steady state or inflammation have a different outcome on DC lineage commitment and differentiation. **Overall design:** - GM-TNFa-DC_2

Background corr dist: KL-Divergence = 0.0220, L1-Distance = 0.0160, L2-Distance = 0.0003, Normal std = 0.7247

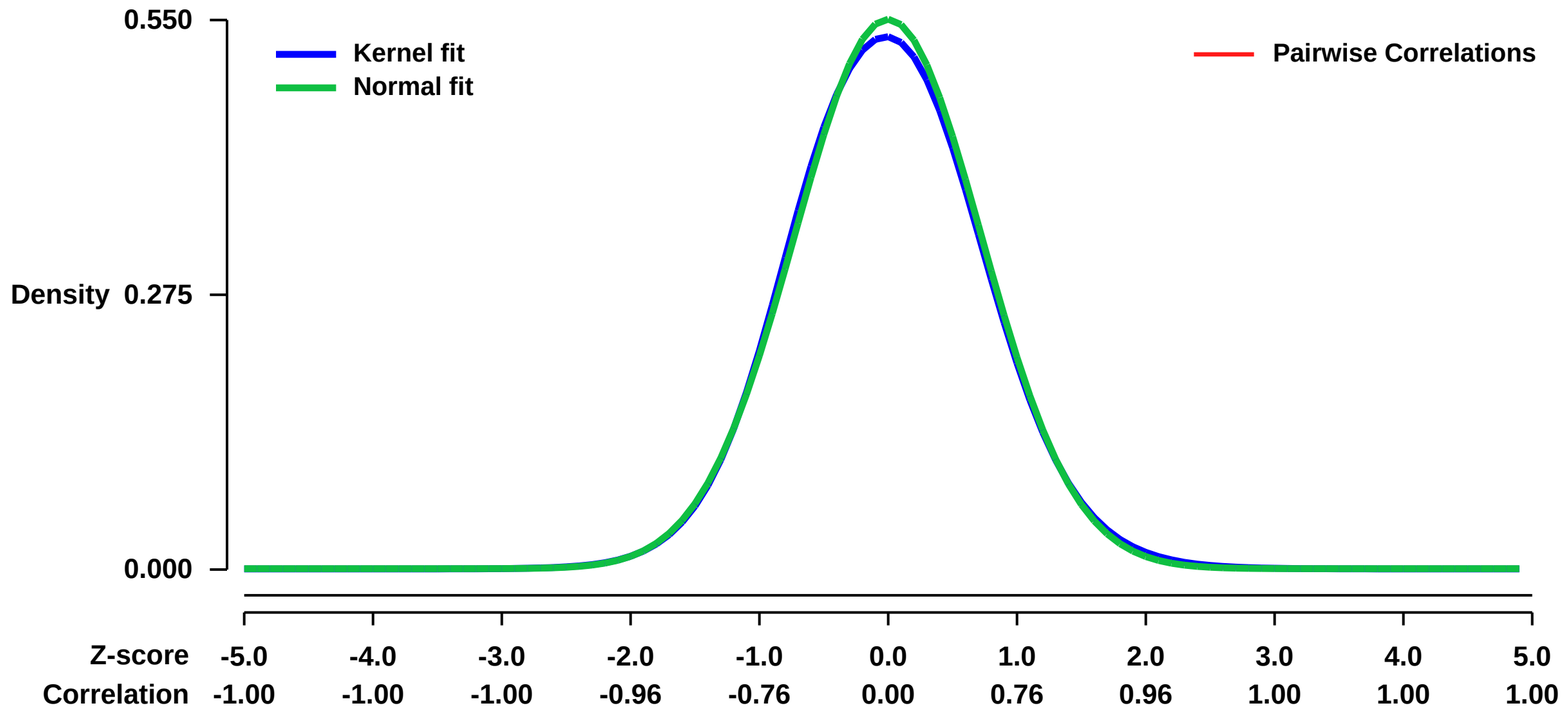

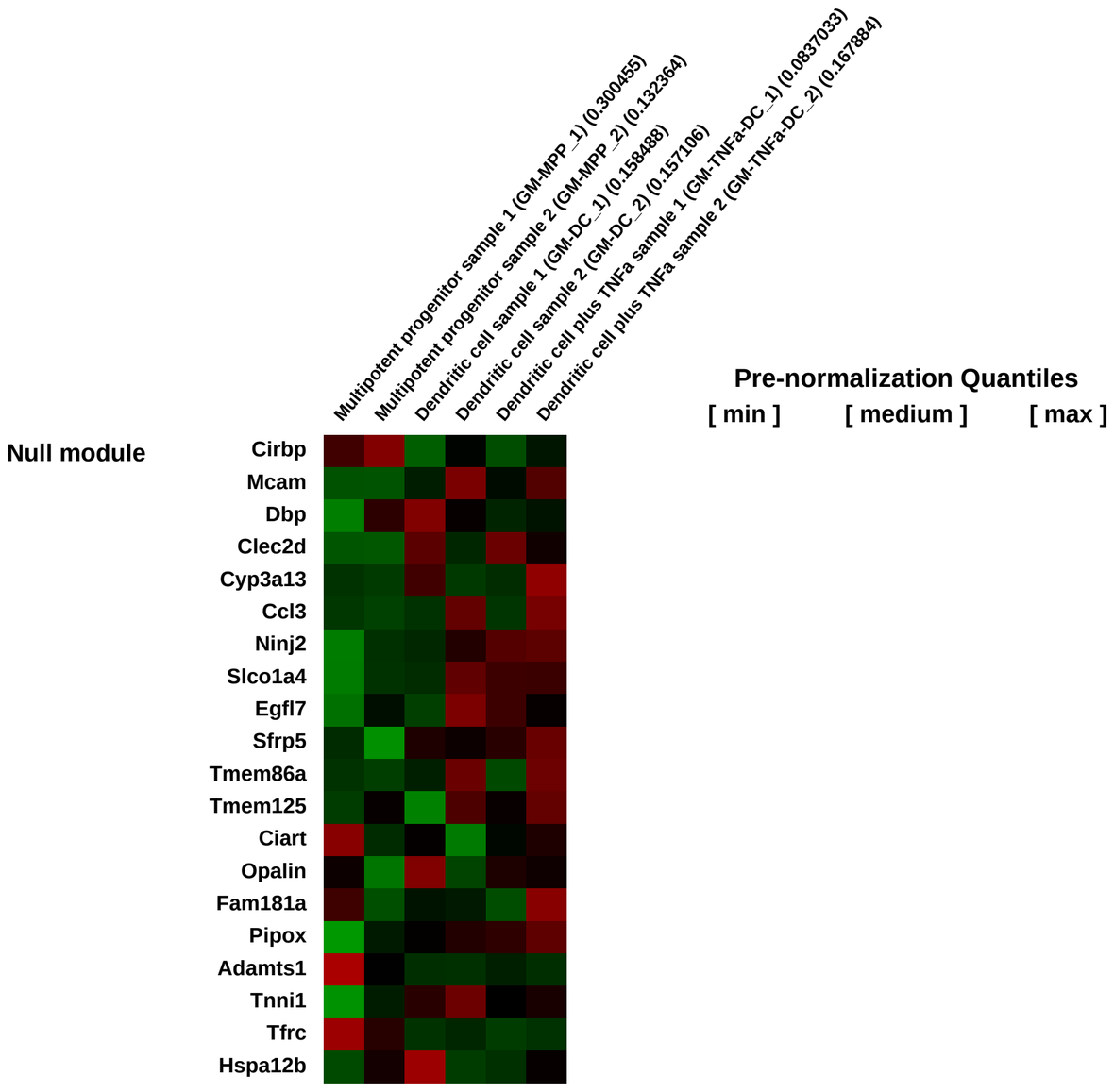

GEO Series "GSE57797" Expression Profiles

Num of samples in this series: 23

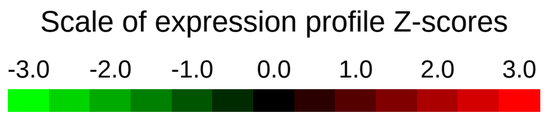

GEO Link:	**http://www.ncbi.nlm.nih.gov/geo/query/acc.cgi?acc=GSE57797**
Status:	**Public on Jul 13 2014**
Title:	**Expression data from the subclones of Lewis Lung Carcinoma (LLC) cells**
Organism:	**Mus musculus**
Experiment type:	**Expression profiling by array**
Platform:	**GPL1261**
Pubmed ID:	
Summary & Design:	**Summary:** **Medium conditioned by LLC cells stimulates thermogenic gene expression when added onto primary adipocytes. We generated single cell colonies from parental LLC cells. Media conditioned by the subclones stimulated thermogenic gene expression in primary adipocytes at varying degrees.** **Subclones 2, 3, 6 and 28 produce significantly larger amount of thermogenic activity than the subclones 18, 19, 23 and 24. We compared gene expression profiles of these subclones to identify secreted factors enriched in the more thermogenic clones.** **Overall design:** **LLC subclones were cultured under conditioned medium preparation conditiones and total RNA was extracted from biological replicates.**

Background corr dist: KL-Divergence = 0.2154, L1-Distance = 0.0344, L2-Distance = 0.0019, Normal std = 0.3269

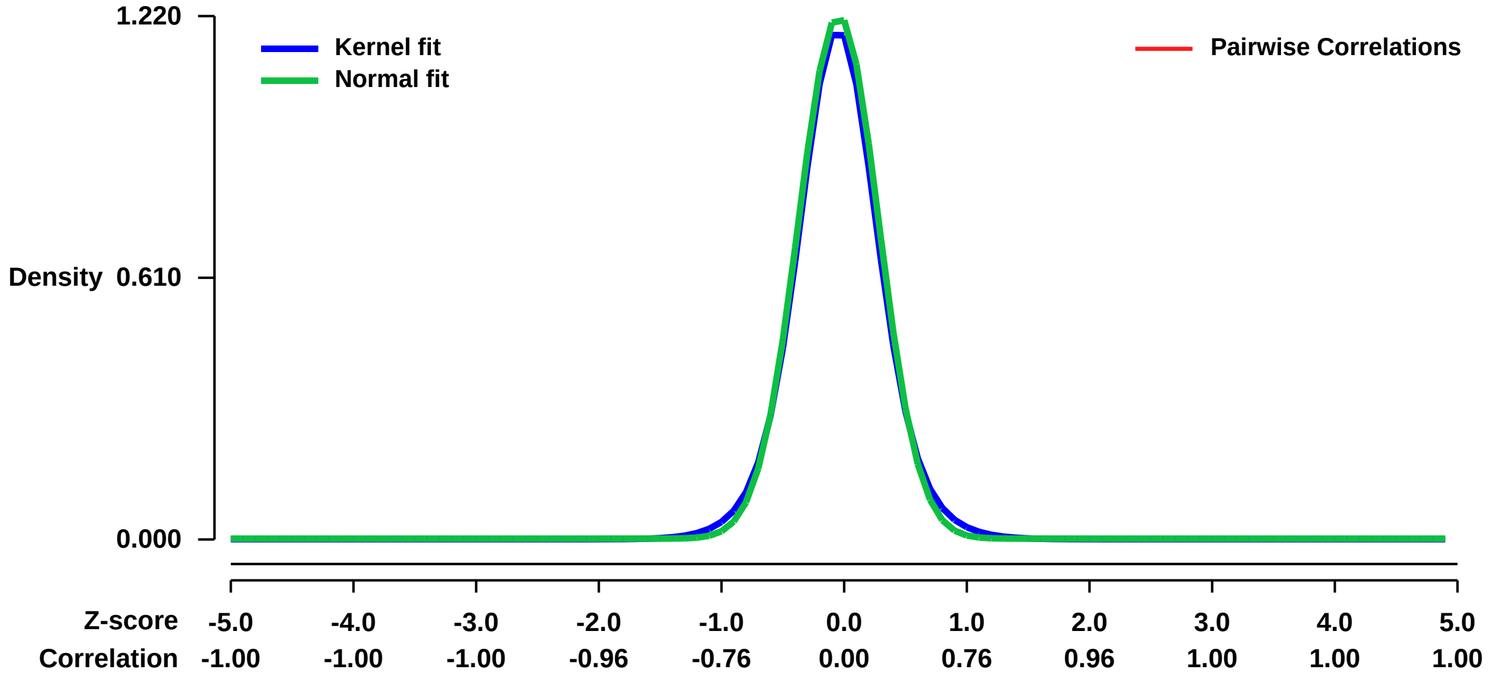

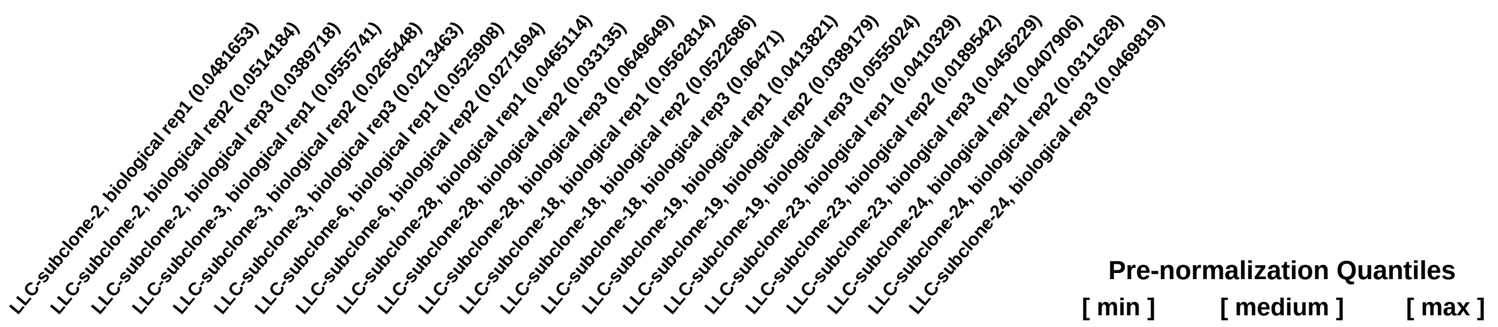

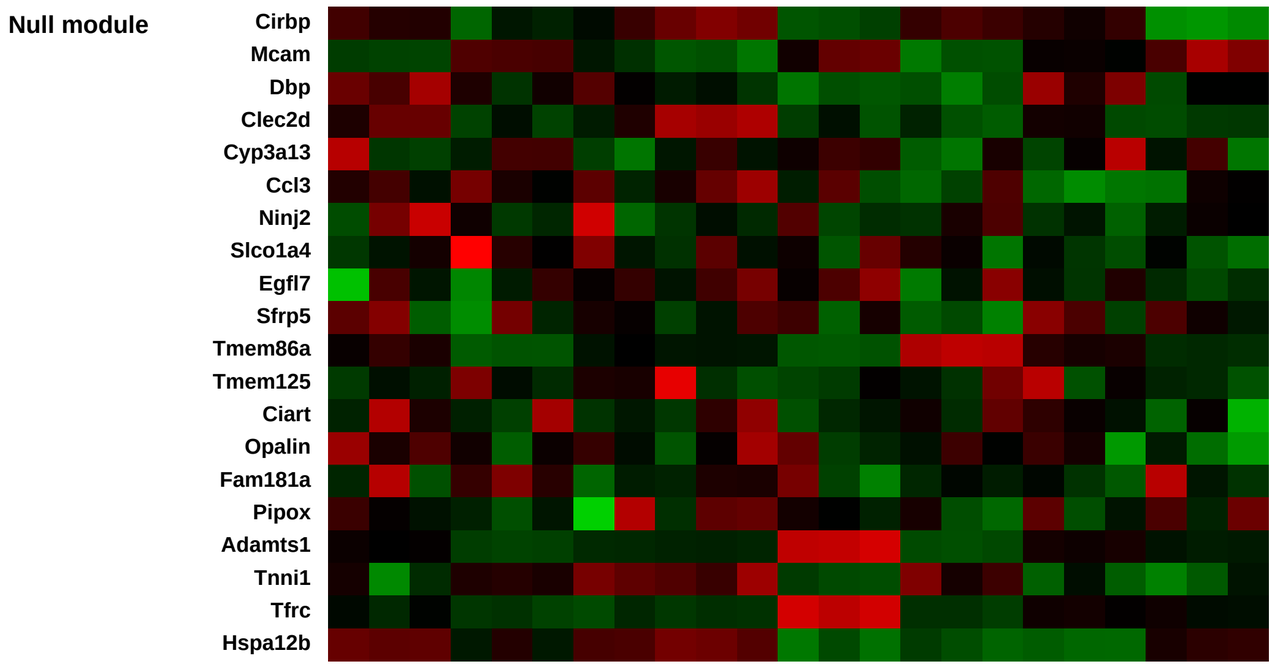

GEO Series "GSE2161" Expression Profiles

Num of samples in this series: 8

Scale of expression profile Z-scores

-3.0 -2.0 -1.0 0.0 1.0 2.0 3.0

GEO Link:	http://www.ncbi.nlm.nih.gov/geo/query/acc.cgi?acc=GSE2161
Status:	Public on Feb 02 2005
Title:	Identification of genes that are dysregulated in the telencephalon of Dlx1/2 mutants. Rubenstein-2R01MH049428-11
Organism:	Mus musculus
Experiment type:	Expression profiling by array
Platform:	GPL1261
Pubmed ID:	
Summary & Design:	**Summary:** **The Dlx homeodomain transcription factors are implicated in regulating the function of inhibitory neurons; therefore understanding their functions will provide insights into disorders such as epilepsy, mental retardation, autism and cerebral palsy.** **Identify genes that are dysregulated in the telencephalon of Dlx1/2 mutants. I am sending separate samples of the Basal Ganglia (BG) and cortex (Ctx).** **Comparing gene expression in the embryonic basal ganglia and cortex in wild type and dlx1/2 mutant mice will provide information regarding the types of genes that are downstream of Dlx1/2 function.** **Perform gene array analyses in duplicate or triplicate; compare expression profile of total RNA from wild type and dlx1/2 telencephalons. I am sending separate samples of the Basal Ganglia (BG) and cortex. I want to perform gene expression comparison between: 1) wild type and dlx1/2 basal ganglia (BG) 2) wild typee and dlx1/2 cortex (ctx) Age of all mice has been indicated as 14 days to satisfy system requirements, however all mice are embryonic day 14.5.** **Keywords: other** **Overall design:**

Background corr dist: **KL-Divergence = 0.0460, L1-Distance = 0.0154, L2-Distance = 0.0002, Normal std = 0.5784**

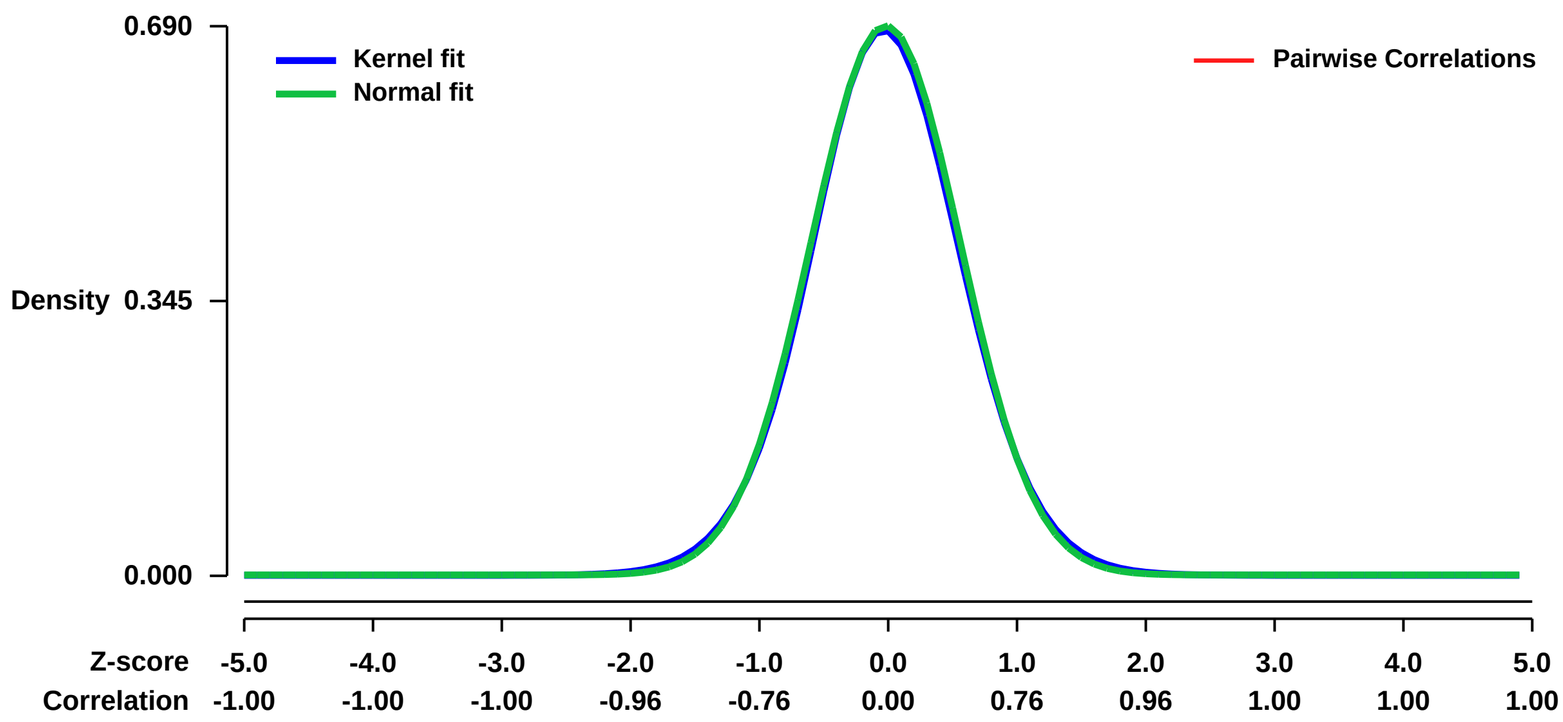

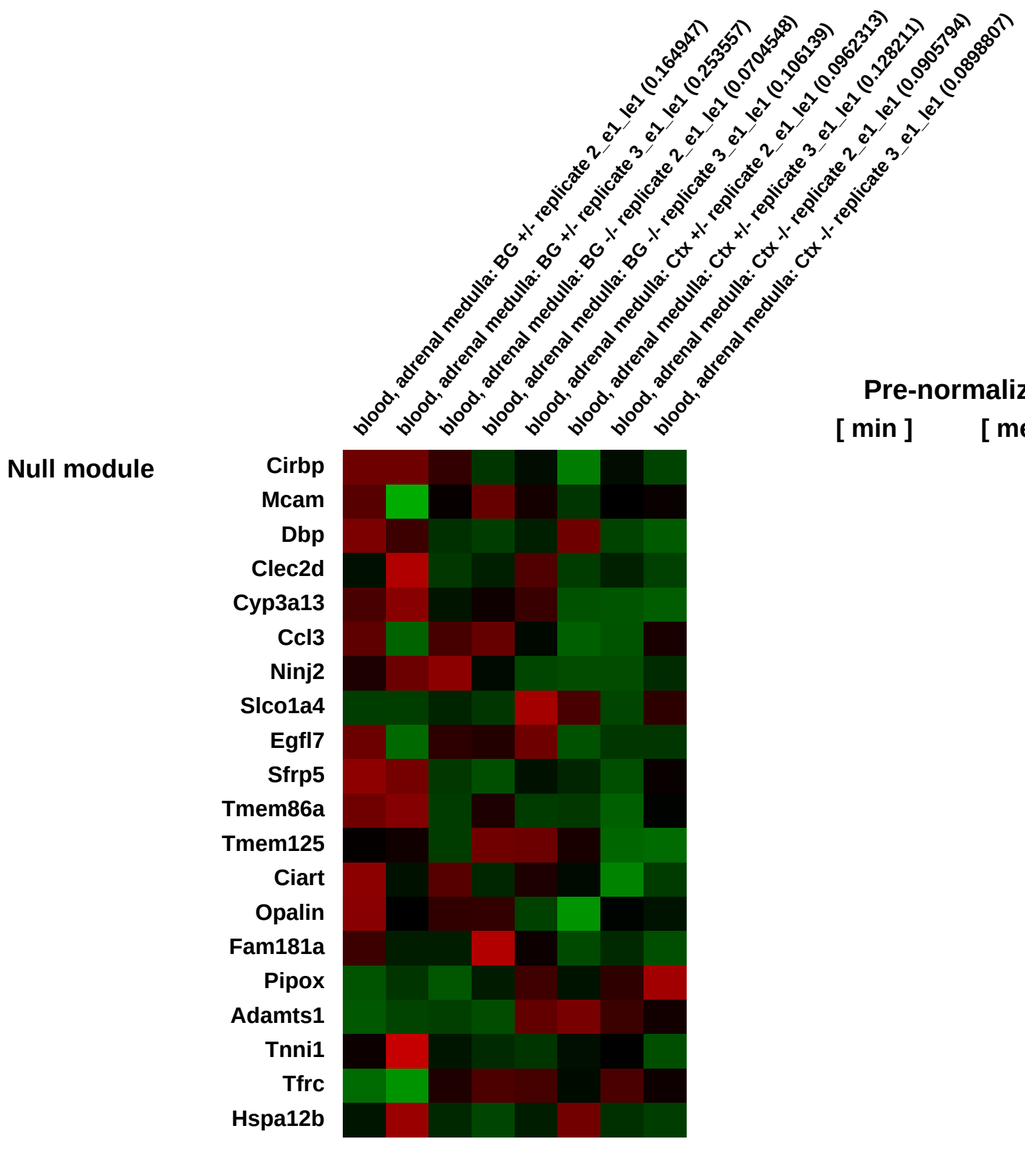

GEO Series "GSE45968" Expression Profiles

Num of samples in this series: 6

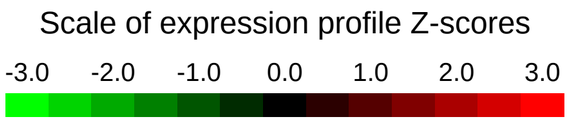

GEO Link:	http://www.ncbi.nlm.nih.gov/geo/query/acc.cgi?acc=GSE45968
Status:	Public on Apr 11 2013
Title:	Gene expression profiling of the tongue in Tgfbr2 mutant mouse models
Organism:	Mus musculus
Experiment type:	Expression profiling by array
Platform:	GPL1261
Pubmed ID:	23950180
Summary & Design:	**Summary:** The overall goal of this project is to investigate the role of TGF-beta signaling in tongue development in order to study the contribution of cranial neural crest (CNC) cells towards the patterning of cranial mesoderm for proper tongue formation. Here, we conducted gene expression profiling of embryonic tongue tissue from wild type mice as well as those with a neural crest specific conditional inactivation of the Tgfbr2 gene. The latter mice provide a model of microglossia, a common congenital birth defect which is frequently observed with several syndromic conditions. **Overall design:** To investigate the mechanism of microglossia resulting from dysfunctional TGF-Beta signaling during muscle development, we analyzed neural crest specific conditional inactivation of Tgfbr2 in mice (Tgfbr2fl/fl;Wnt1-Cre). We performed microarray analyses of tongue tissue of Tgfbr2fl/fl;Wnt1-Cre mutant mice and Tgfbr2fl/fl control mice at embryonic day E14.5 (n=3 per genotype) to examine the genes regulated by Tgf-beta during tongue muscle development.

Background corr dist: KL-Divergence = 0.0267, L1-Distance = 0.0183, L2-Distance = 0.0003, Normal std = 0.6951

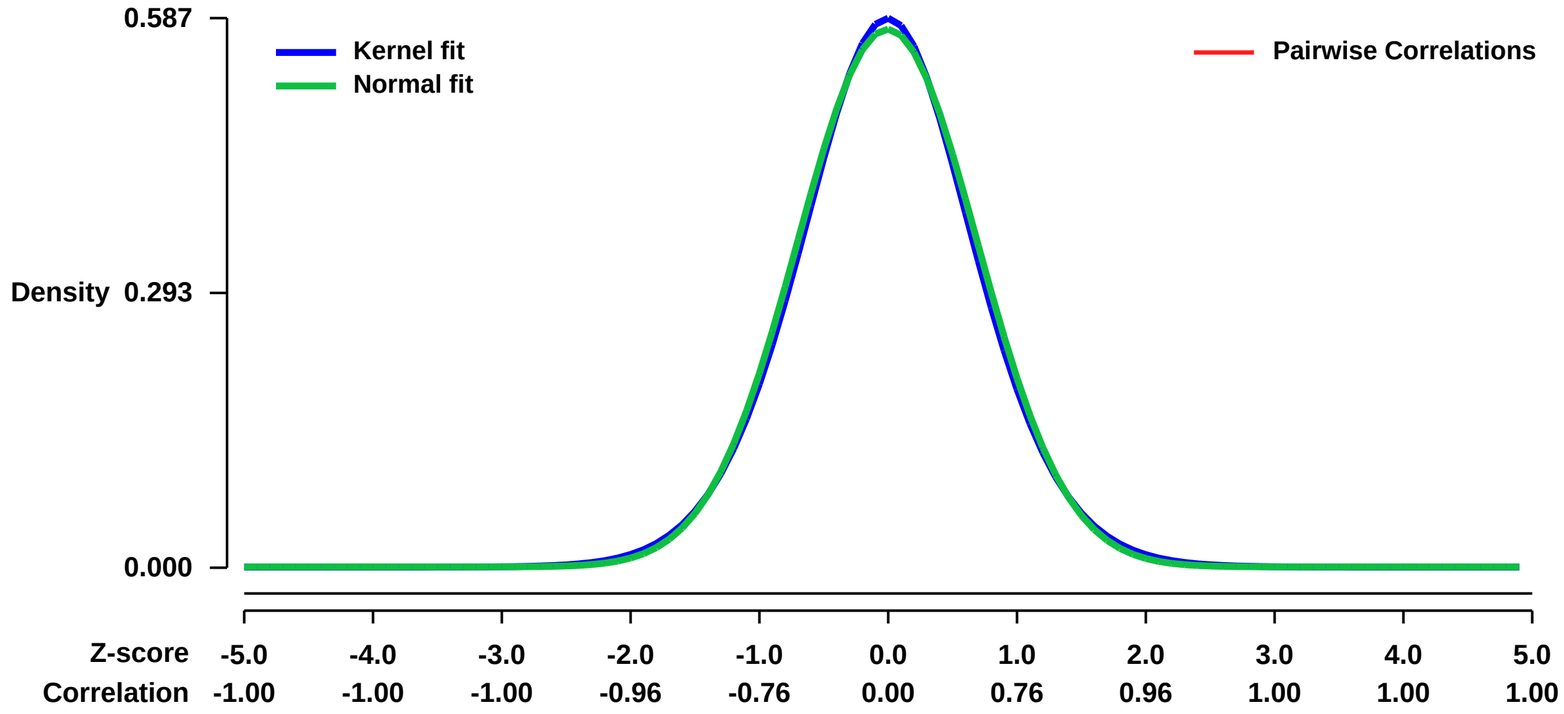

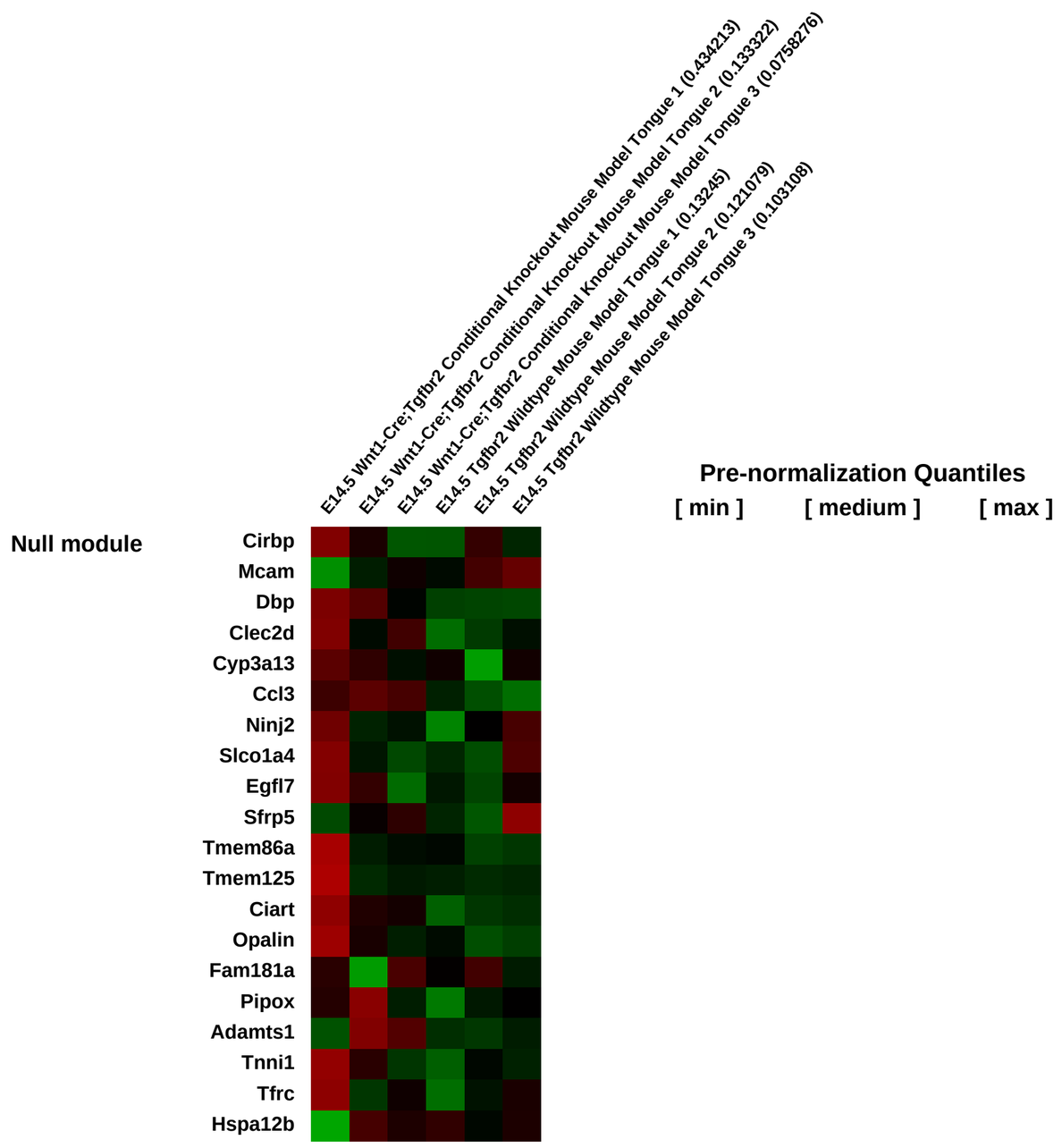

GEO Series "GSE39034" Expression Profiles

Num of samples in this series: 9

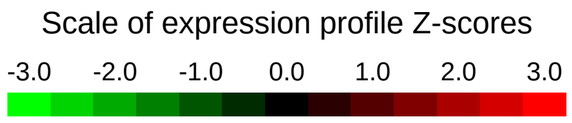

GEO Link:	http://www.ncbi.nlm.nih.gov/geo/query/acc.cgi?acc=GSE39034
Status:	Public on Nov 29 2012
Title:	Mammalian cells acquire epigenetic hallmarks of human cancer during immortalization
Organism:	Mus musculus
Experiment type:	Expression profiling by array
Platform:	GPL1261
Pubmed ID:	23143272
Summary & Design:	**Summary:** Progression to malignancy requires cells to overcome senescence and switch to an immortal phenotype. Thus, exploring the genetic and epigenetic changes that occur during senescence/immortalization may help elucidate crucial events that lead to cell transformation. In the present study, we have globally profiled DNA methylation in relation to gene expression in primary, senescent and immortalized mouse embryonic fibroblasts. **Overall design:** Primary, senescent and immortalized mouse fibroblasts obtained from three independent embryos. Compare immortalized versus primary and senescent versus primary cells.

Background corr dist: KL-Divergence = 0.0790, L1-Distance = 0.0213, L2-Distance = 0.0007, Normal std = 0.4801

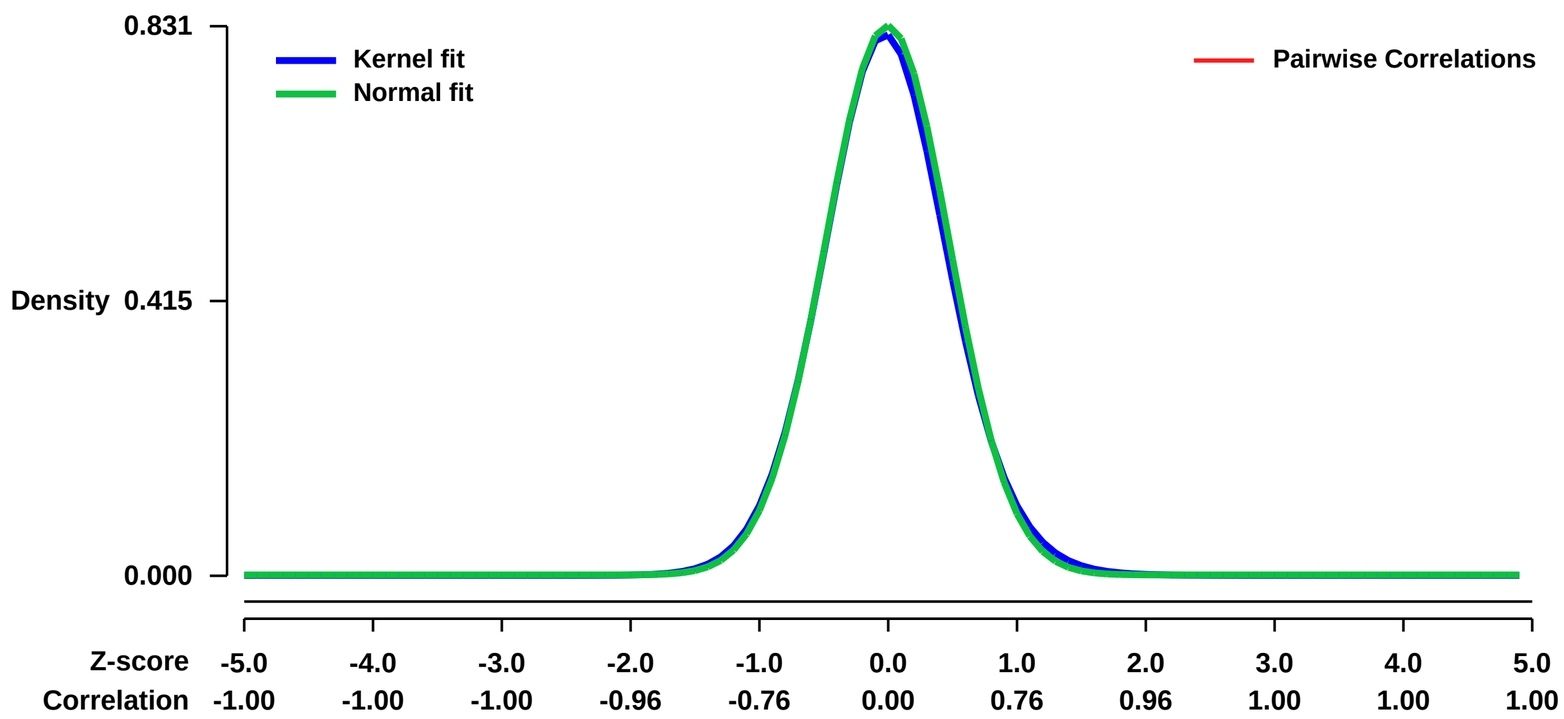

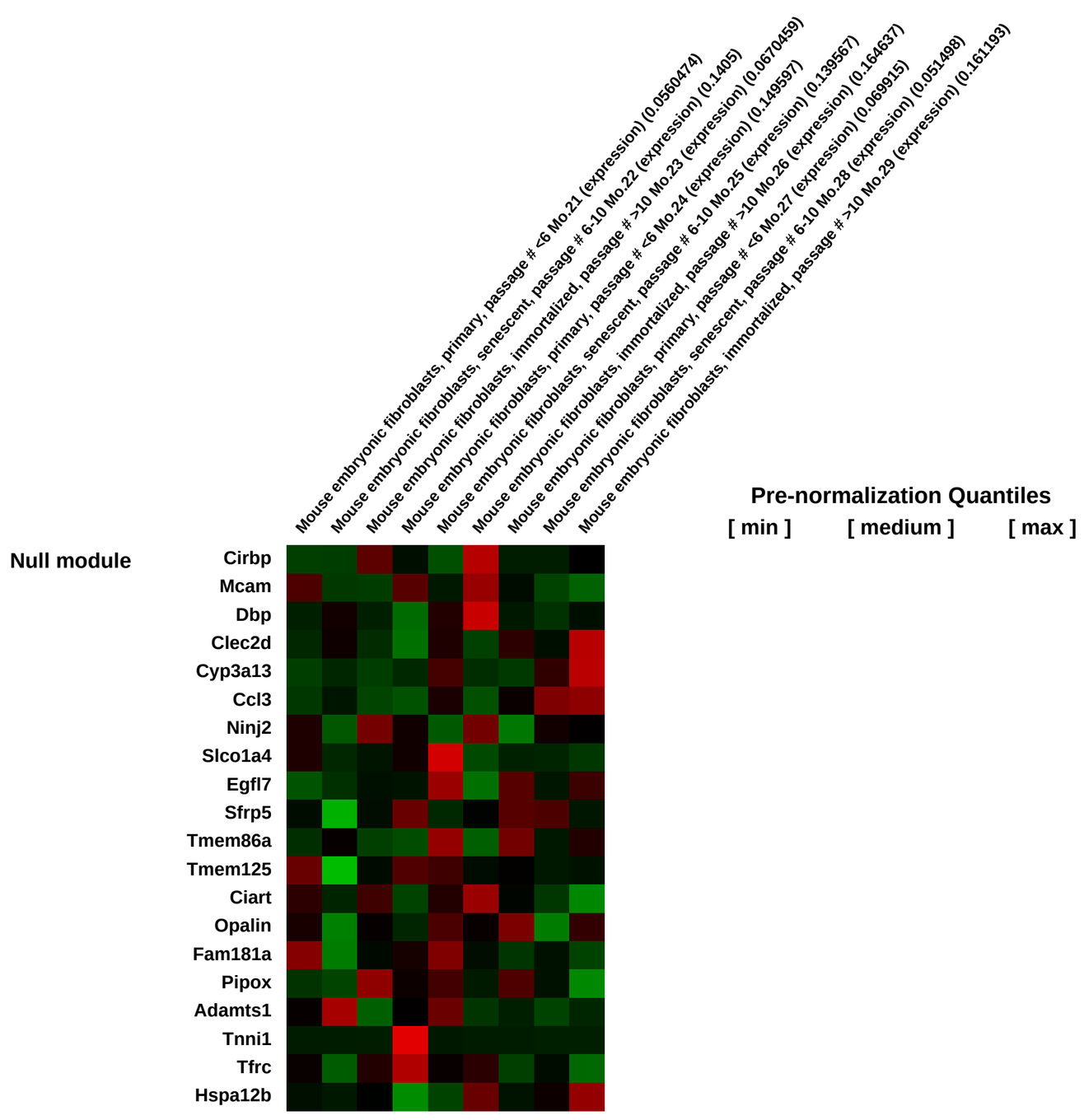

GEO Series "GSE17739" Expression Profiles

Num of samples in this series: 24

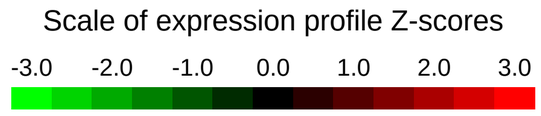

GEO Link:	**http://www.ncbi.nlm.nih.gov/geo/query/acc.cgi?acc=GSE17739**
Status:	**Public on Oct 22 2009**
Title:	**Circadian gene profiling in the distal nephron and collecting ducts**
Organism:	**Mus musculus**
Experiment type:	**Expression profiling by array**
Platform:	**GPL1261**
Pubmed ID:	**19805330**
Summary & Design:	**Summary:** **Renal excretion of water and major electrolytes exhibits a significant circadian rhythm. This functional periodicity is believed to result, at least in part, from circadian changes in secretion/reabsorption capacities of the distal nephron and collecting ducts. Here, we studied the molecular mechanisms underlying circadian rhythms in the distal nephron segments, i.e. distal convoluted tubule (DCT) and connecting tubule (CNT) and, the cortical collecting duct (CCD). Temporal expression analysis performed on microdissected mouse DCT/CNT or CCD revealed a marked circadian rhythmicity in the expression of a large number of genes crucially involved in various homeostatic functions of the kidney. This analysis also revealed that both DCT/CNT and CCD possess an intrinsic circadian timing system characterized by robust oscillations in the expression of circadian core clock genes (clock, bma11, npas2, per, cry, nr1d1) and clock-controlled Par bZip transcriptional factors dbp, hlf and tef. The clock knockout mice or mice devoid of dbp/hlf/tef (triple knockout) exhibit significant changes in renal expression of several key regulators of water or sodium balance (vasopressin V2 receptor, aquaporin-2, aquaporin-4, alphaENaC). Functionally, the loss of clock leads to a complex phenotype characterized by partial diabetes insipidus, dysregulation of sodium excretion rhythms and a significant decrease in blood pressure. Collectively, this study uncovers a major role of molecular clock in renal function.** **Keywords: time course** **Overall design:** **We examined the temporal profiles of gene expression in mouse distal nephron segments and collecting ducts. The RNA was extracted from microdissected distal convoluted tubules and connecting tubules (DCT/CNT samples) or, cortical collecting ducts (CCD samples). Animals were sacrificed for microdissection every 4 hours, i.e. at ZT0, ZT4, ZT8, ZT12, ZT16 and ZT20 (ZT â Zeitgeber (circadian) time, indicates time of light-on as ZT0 and time of light-off as ZT12). The microarray hybridization was performed in duplicates on two pools of RNA composed of equivalent amounts of RNA prepared from five animals at each ZT time-point.**

Background corr dist: KL-Divergence = 0.0374, L1-Distance = 0.0298, L2-Distance = 0.0014, Normal std = 0.6138

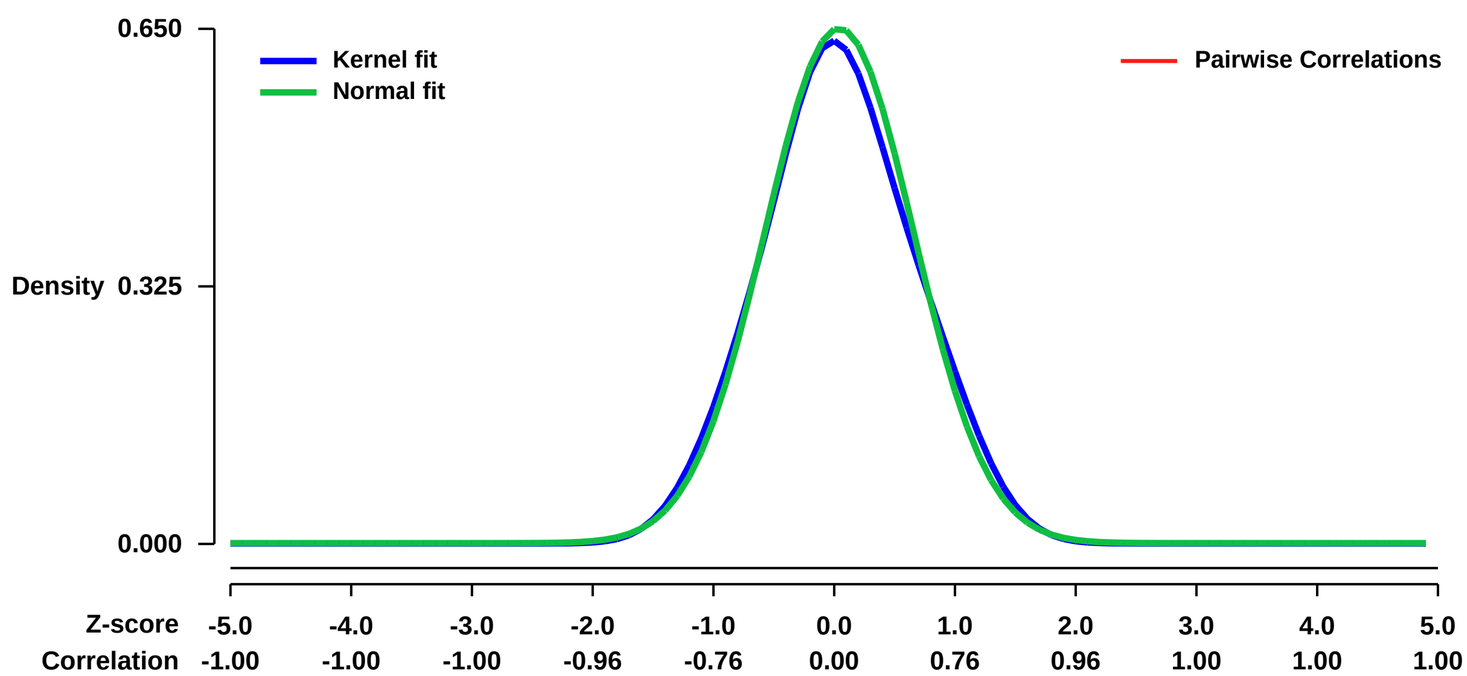

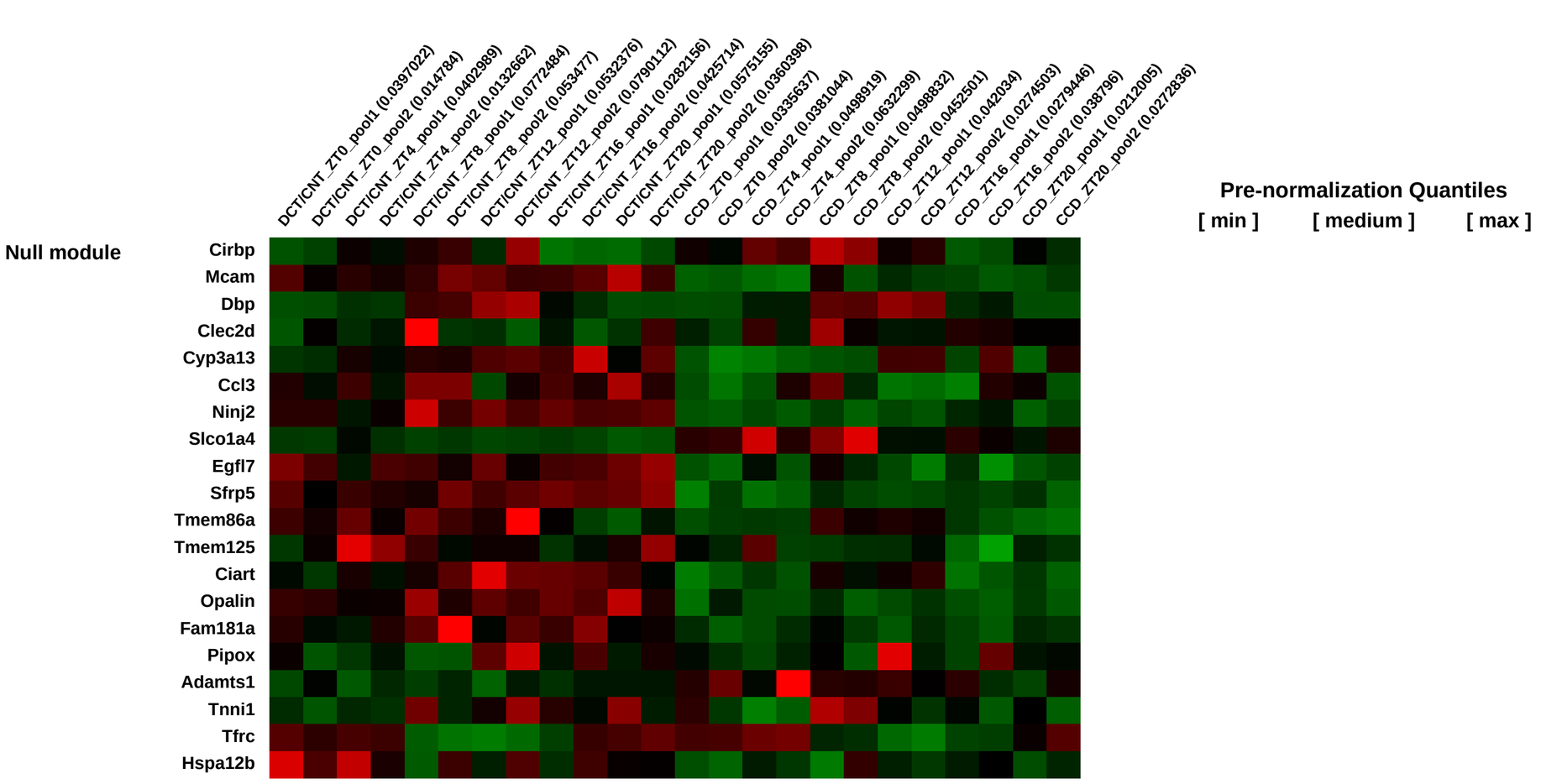

GEO Series "GSE24276" Expression Profiles

Num of samples in this series: 6

Scale of expression profile Z-scores

-3.0 -2.0 -1.0 0.0 1.0 2.0 3.0

GEO Link:	http://www.ncbi.nlm.nih.gov/geo/query/acc.cgi?acc=GSE24276
Status:	Public on Sep 22 2010
Title:	Fz1Fz2 double knock out mouse palate microarray (E13.5)
Organism:	Mus musculus
Experiment type:	Expression profiling by array
Platform:	GPL1261
Pubmed ID:	20940229
Summary & Design:	**Summary:** The closure of an open anatomical structure by the directed growth and fusion of two tissue masses is a recurrent theme in mammalian embryology, and this process plays an integral role in the development of the palate, ventricular septum, neural tube, urethra, diaphragm, and eye. In mice, targeted mutations of the genes encoding frizzled1 (Fz1) and frizzled2 (Fz2) show that these highly homologous integral membrane receptors play an essential and partially redundant role in closure of the palate and ventricular septum, and in the correct positioning of the cardiac outflow tract. When combined with a mutant allele of the planar cell polarity (PCP) gene Vangl2 (Vangl2Lp), Fz1 and/or Fz2 mutations also cause defects in neural tube closure and mis-orientation of inner ear sensory hair cells. These observations indicate that frizzled signaling is involved in diverse tissue closure processes, defects in which account for some of the most common congenital anomalies in humans. **Overall design:** Supplementary file below reports fold change data.

Background corr dist: KL-Divergence = 0.0240, L1-Distance = 0.0129, L2-Distance = 0.0002, Normal std = 0.7002

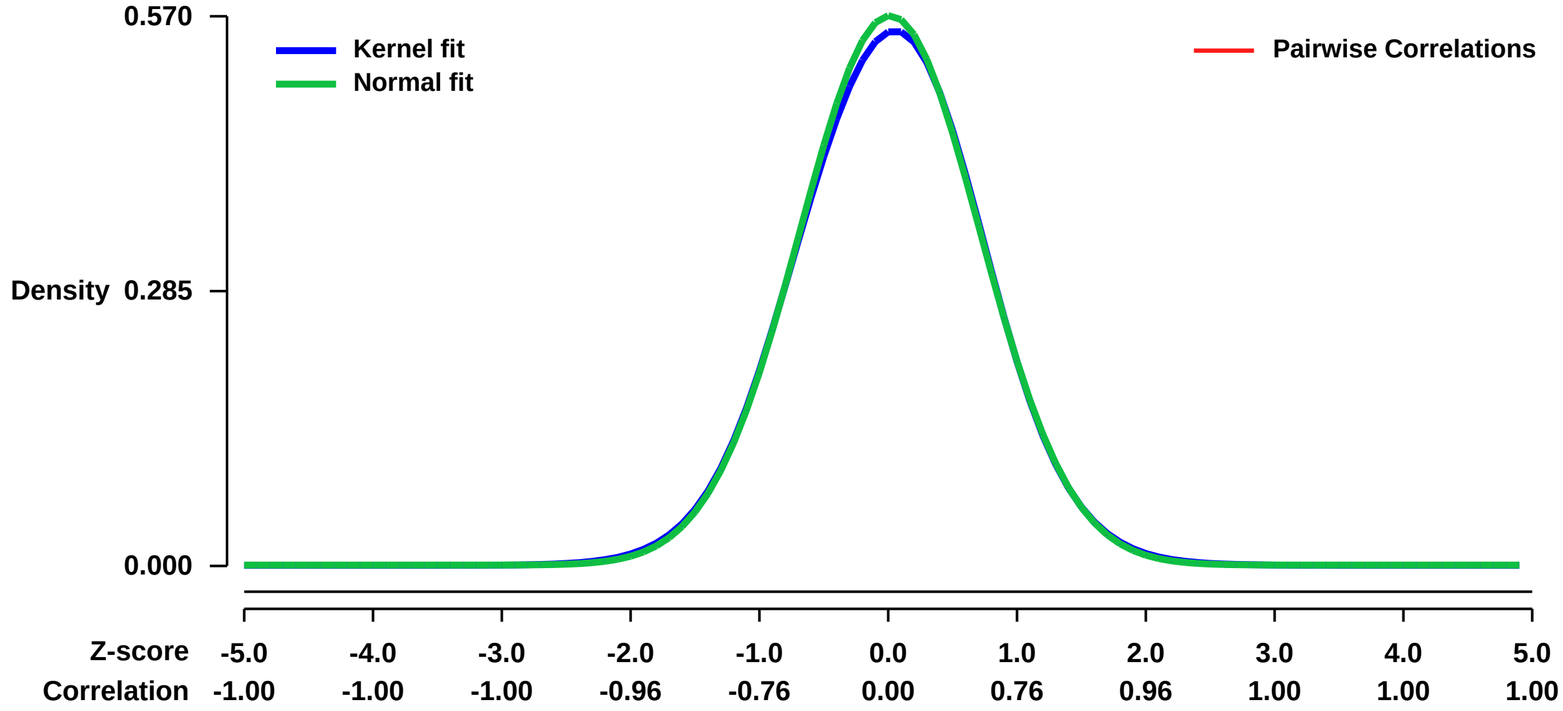

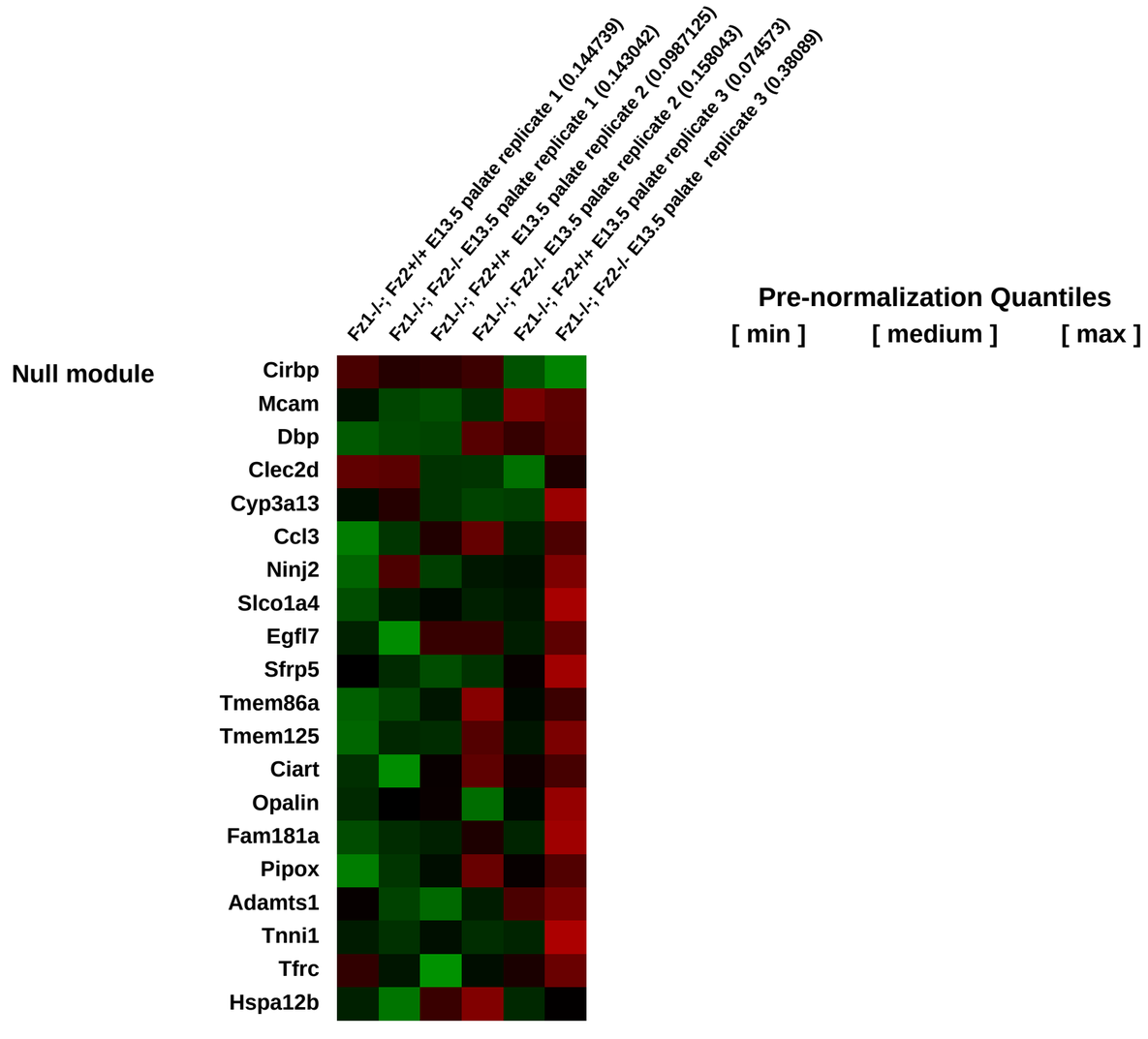

GEO Series "GSE6678" Expression Profiles

Num of samples in this series: 18

Scale of expression profile Z-scores

-3.0 -2.0 -1.0 0.0 1.0 2.0 3.0

GEO Link:	http://www.ncbi.nlm.nih.gov/geo/query/acc.cgi?acc=GSE6678
Status:	Public on Jan 09 2007
Title:	Palmitoyl protein thioesterase-1 knockout mice hofma-affy-mouse-370000
Organism:	Mus musculus
Experiment type:	Expression profiling by array
Platform:	GPL1261
Pubmed ID:	
Summary & Design:	**Summary:** **Infantile neuronal ceroid lipofuscinosis (aka infantile Batten disease) is a severe neurodegenerative disorder of early childhood characterized by cortical atrophy, blindness and seizures, leading to premature death in the first decade. The disorder is caused by deficiency in a soluble lysosomal enzyme, palmitoyl protein thioesterase-1 (PPT1). PPT1 knockout mice faithfully reproduce the features of the human disease, with motor deterioration, blindness, seizures, and death before 10 months of age. The progression of events leading from enzyme deficiency to organ failure is poorly defined. The neuronal ceroid lipofuscinoses are of particular interest because of the similarities between the accumulated material and lipofuscin that is associated with normal aging.** **We will determine changes in gene expression that occur during the course of neurodegeneration in PPT1 knockout as compared to control mice.** **Gene expression profiling of brain tissue from PPT1 knockout mice as compared to normal controls will provide insights into the mechanism of neurodegeneration. Comparison of this profile with gene expression profiles associated with normal aging may provide insights into the contribution of lipofuscin to aging and neurodegeneration.** **PPT1 knockout mice on a C57BL/6 background will be sacrificed under CO2 and whole brains removed and frozen under liquid nitrogen. Three mice will be used for each time point. Data points will be collected at 3 months, 5 months and 8 months of age. Normal age- and sex-matched C57BL/6 mice will be used as controls.** **Keywords: gene knockout** **Overall design:**

Background corr dist: KL-Divergence = 0.2682, L1-Distance = 0.0557, L2-Distance = 0.0079, Normal std = 0.2938

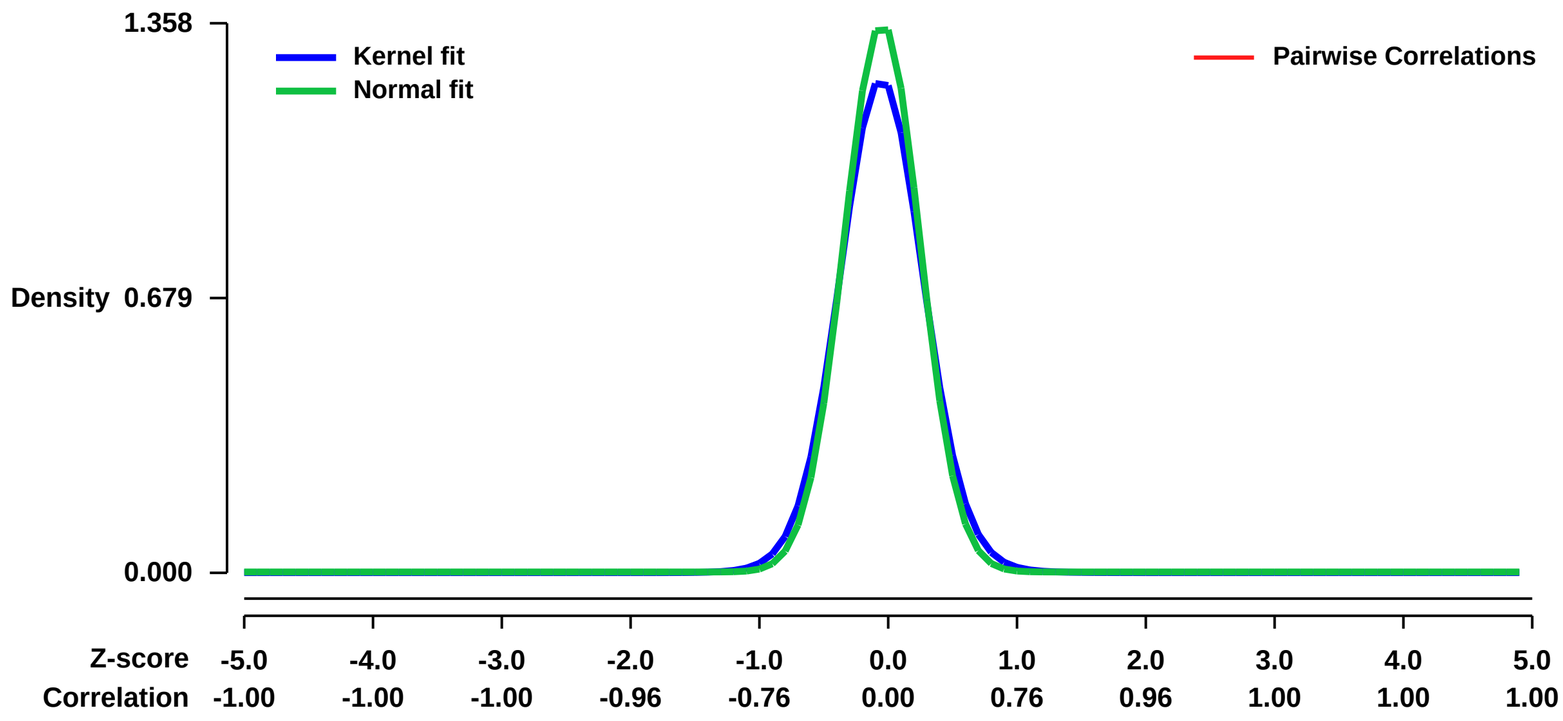

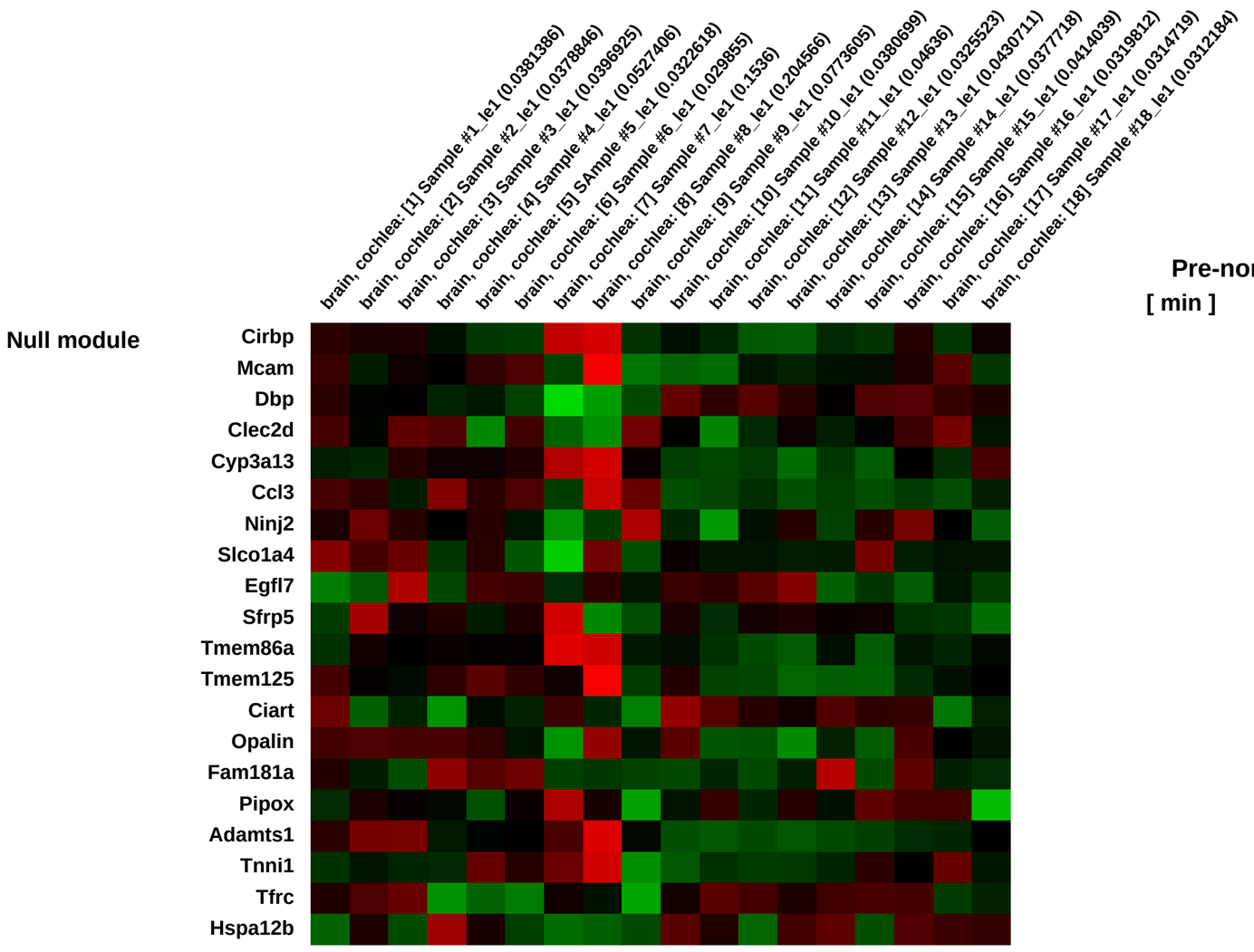

GEO Series "GSE44923" Expression Profiles

Num of samples in this series: 16

Scale of expression profile Z-scores

-3.0 -2.0 -1.0 0.0 1.0 2.0 3.0

GEO Link:	http://www.ncbi.nlm.nih.gov/geo/query/acc.cgi?acc=GSE44923
Status:	Public on Mar 06 2013
Title:	An Epigenetic Component of Hematopoietic Stem Cell Aging Amenable to Reprogramming Into a Young State
Organism:	Mus musculus
Experiment type:	Expression profiling by array
Platform:	GPL1261
Pubmed ID:	23476050
Summary & Design:	**Summary:** Aging of hematopoietic stem cells (HSCs) leads to several functional changes, including alterations affecting self-renewal and differentiation. While it is well established that many of the age-induced changes are intrinsic to HSCs, less is known about the stability of this state. Here, we entertained the hypothesis that HSC aging is driven by the acquisition of permanent genetic mutations. To examine this issue at a functional level in vivo, we applied induced pluripotent stem (iPS) cell reprogramming of aged hematopoietic progenitors and allowed the resulting aged-derived iPS cells to reform hematopoiesis via blastocyst complementation. Next, we functionally characterized iPS-derived HSCs in primary chimeras and following the transplantation of 're-differentiated' HSCs into new hosts; the gold standard to assess HSC function. Our data demonstrate remarkably similar functional properties of iPS-derived and endogenous blastocyst-derived HSCs, despite the extensive chronological and proliferative age of the former. Our results therefore favor a model in which an underlying, but reversible, epigenetic component is a hallmark of HSC aging rather than being driven by an increased DNA mutation burden. **Overall design:** Hematopoietic stem cells (HSC) have been sorted out from young and aged steady-state mice, and from recipients transplanted with young and aged bone marrow. Generated iPS and commercially available ES cells were also sorted and analyzed.

Background corr dist: KL-Divergence = 0.0286, L1-Distance = 0.0494, L2-Distance = 0.0038, Normal std = 0.7036

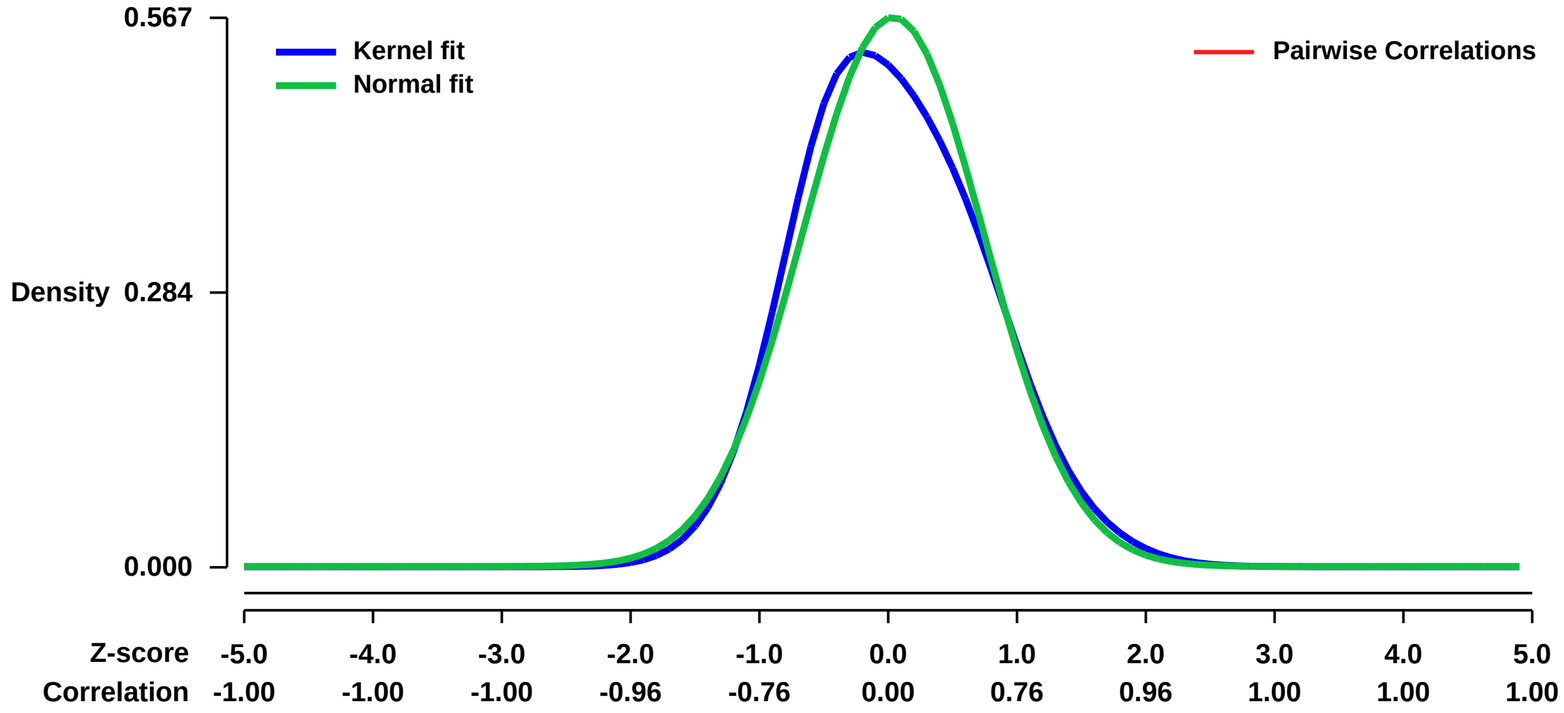

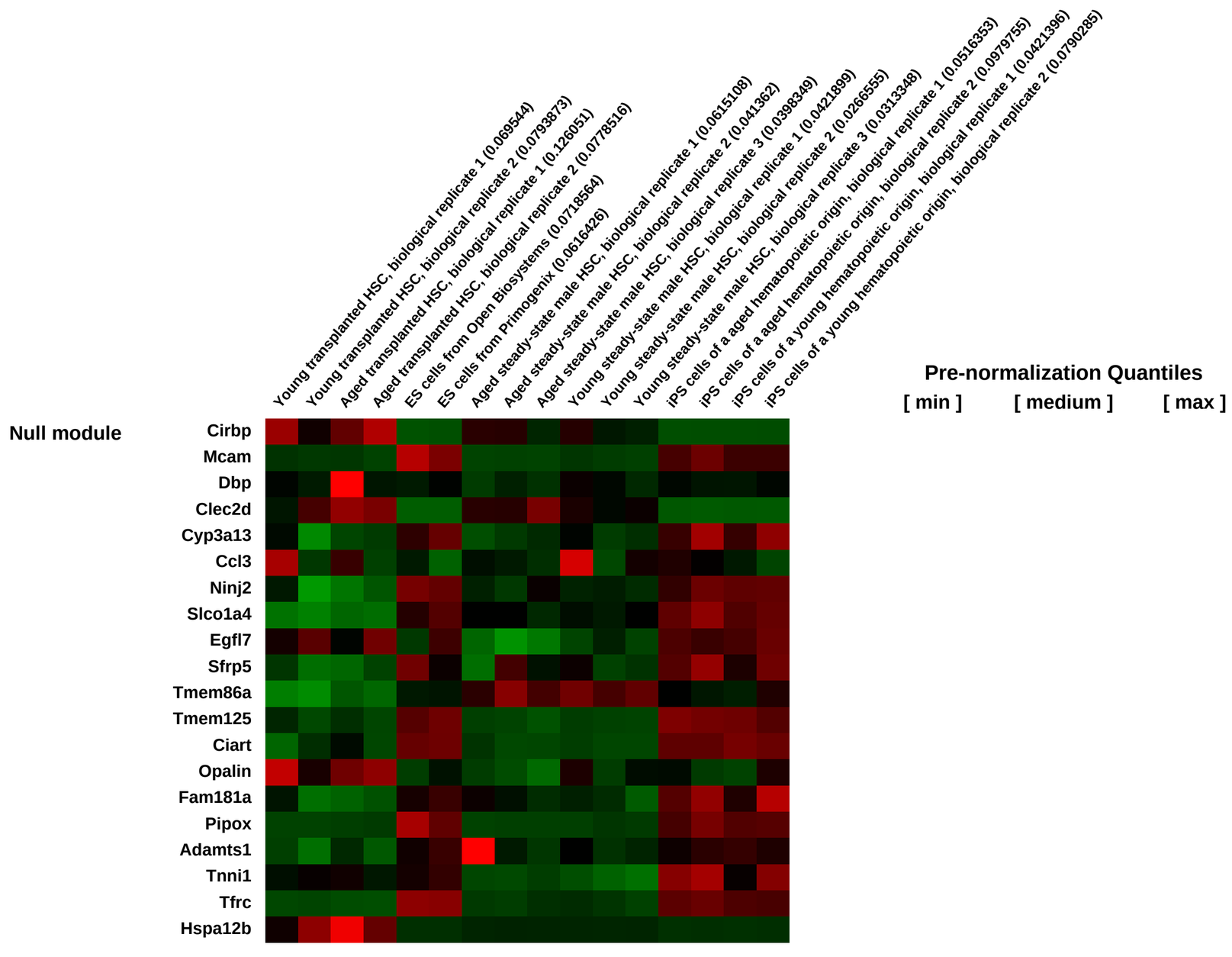

GEO Series "GSE35044" Expression Profiles

Num of samples in this series: 9

Scale of expression profile Z-scores

-3.0 -2.0 -1.0 0.0 1.0 2.0 3.0

GEO Link:	http://www.ncbi.nlm.nih.gov/geo/query/acc.cgi?acc=GSE35044
Status:	Public on Jan 17 2012
Title:	Expression profiles of Telomerase+ vs. ALT+ G3 Atm-/-TERT-ER T-cell lymphomas
Organism:	Mus musculus
Experiment type:	Expression profiling by array
Platform:	GPL1261
Pubmed ID:	22341440
Summary & Design:	**Summary:** We used microarray profiling to document the difference between telomerase+ vs. ALT+ T-cell lymphomas developed on G3 Atm-/-TERT-ER genetic background. **Overall design:** T-cell lymphomas were developed in G3 Atm-/-TERT-ER mice with 4-OHT treatment. These cells were either maintained on SCID mice treated with 4-OHT or vehicle. Cells maintained on vehicle eventually developed ALT-dependent resistance. We used microarray to profile telomerase+ tumors vs. ALT+ tumors from the same parental lines.

Background corr dist: KL-Divergence = 0.0830, L1-Distance = 0.0208, L2-Distance = 0.0006, Normal std = 0.4711

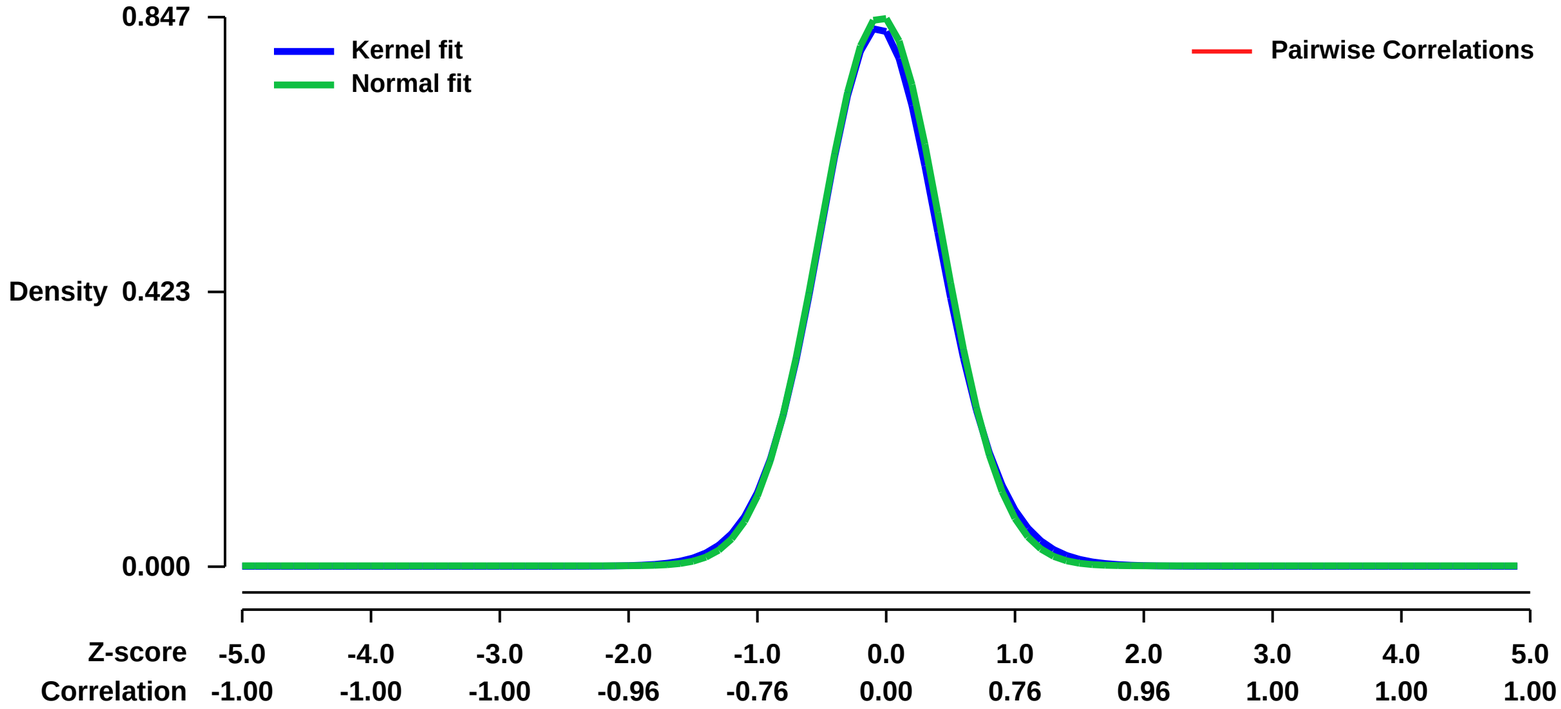

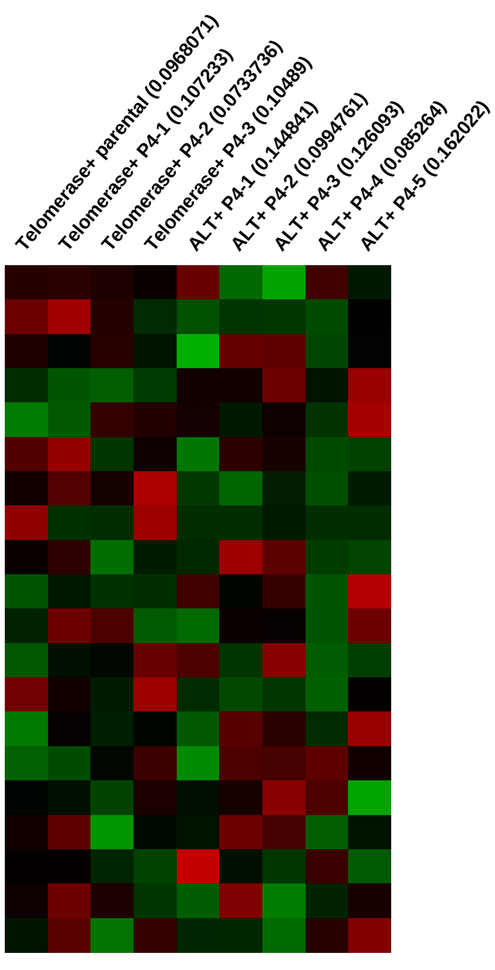

GEO Series "GSE45583" Expression Profiles

Num of samples in this series: 8

Scale of expression profile Z-scores

-3.0 -2.0 -1.0 0.0 1.0 2.0 3.0

GEO Link:	**http://www.ncbi.nlm.nih.gov/geo/query/acc.cgi?acc=GSE45583**
Status:	**Public on Mar 29 2013**
Title:	**A hypomorphic Lsd1 allele results in heart development defects in mice.**
Organism:	**Mus musculus**
Experiment type:	**Expression profiling by array**
Platform:	**GPL1261**
Pubmed ID:	
Summary & Design:	**Summary:** **Microarray characterization of Lsd1 knock-outs compared to littermate controls** **Microarrays were employed to identify transcripts that were differentially modulated in the hearts of wild-type and Lsd1-hypomorphic late-stage embryos.** **Overall design:** **Late-stage embryonic hearts were isolated from wild-type and Lsd1-hypomorphic hearts, in order to isolate RNA for hybridization on Affymetrix microarrays. We sought to identify gene products that are differentially regulated between the two genotypes, in order to explain the observed ventricular septal defects in the hypomorphic animals.**

Background corr dist: **KL-Divergence = 0.0787, L1-Distance = 0.0212, L2-Distance = 0.0005, Normal std = 0.4781**

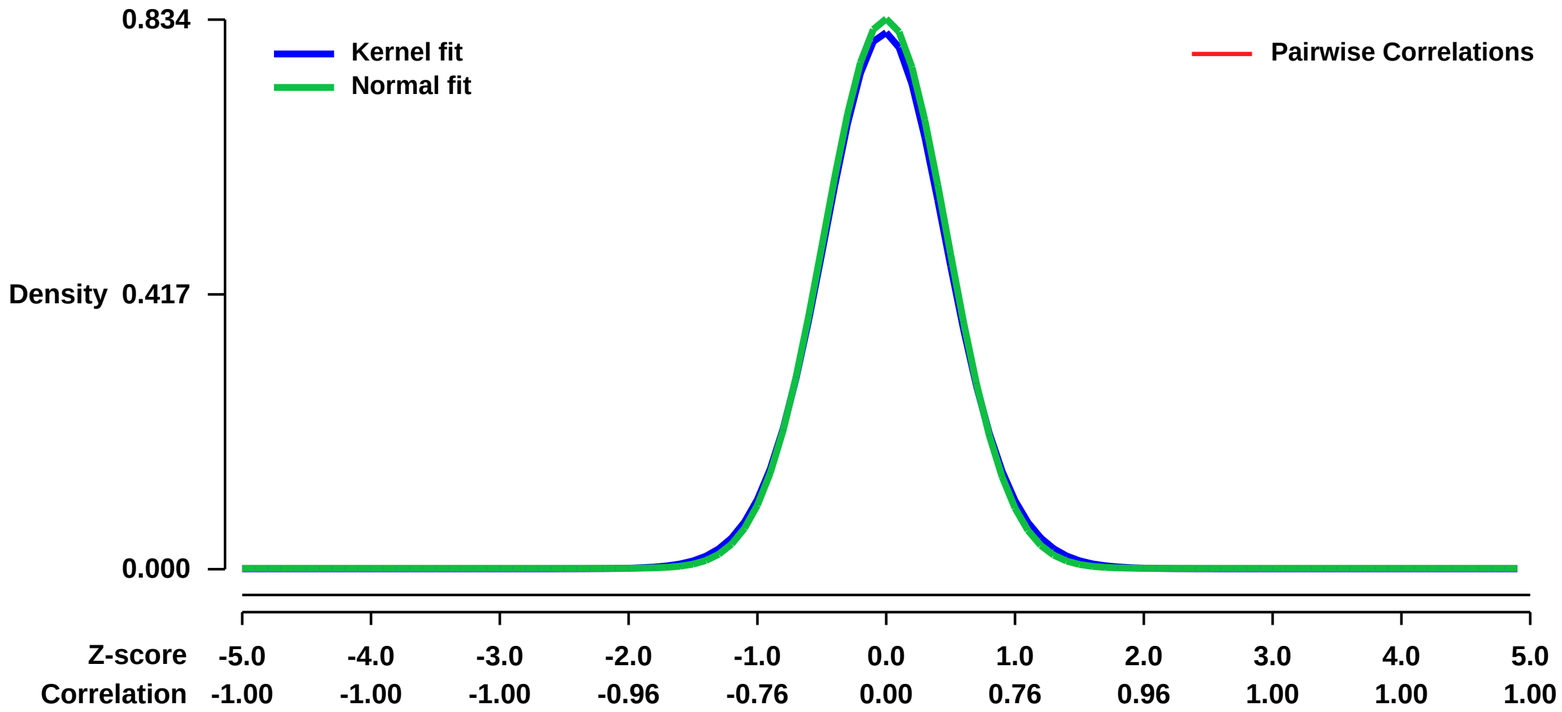

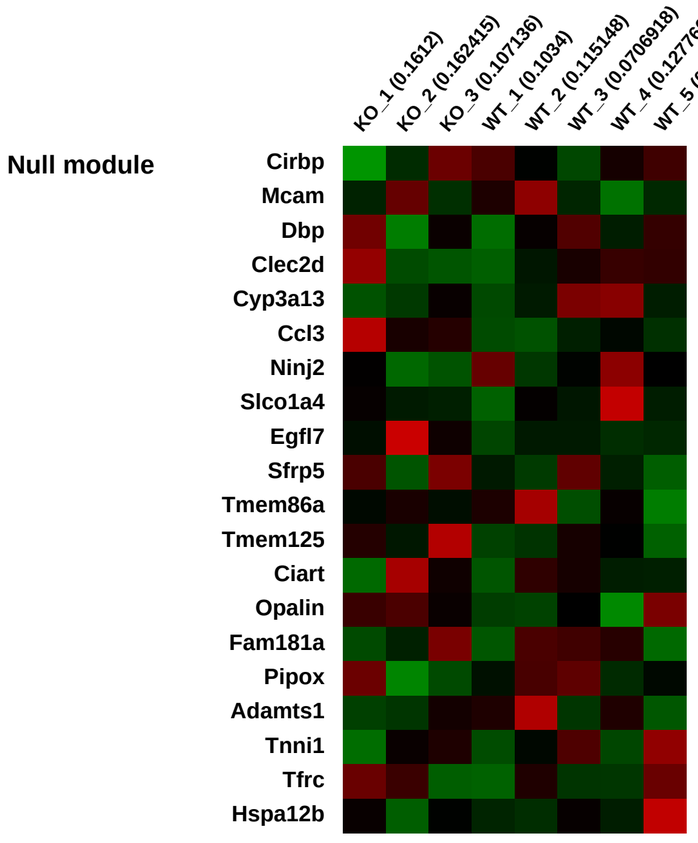

GEO Series "GSE25768" Expression Profiles

Num of samples in this series: 6

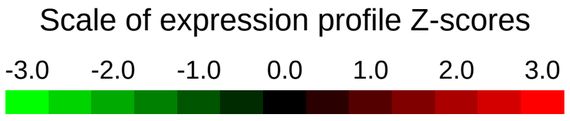

GEO Link:	http://www.ncbi.nlm.nih.gov/geo/query/acc.cgi?acc=GSE25768
Status:	Public on Dec 03 2010
Title:	Model of heart failure induced by mild thiol-blocking with cystamine
Organism:	Mus musculus
Experiment type:	Expression profiling by array
Platform:	GPL1261
Pubmed ID:	21711241
Summary & Design:	**Summary:** Depletion of cardiac ATP content is a characteristic feature of heart failure in patients and experimental animal models. To analyze the impact of insufficient ATP supply on heart function we inhibited cellular respiration by disulfide poisoning with the mild thiol-blocking agent, cystamine. We chose 4 month-old apolipoprotein E (apoE)-deficient mice, which are highly vulnerable to increased oxygen and ATP demands. After 4 weeks of cystamine treatment (300 mg/kg in drinking water), echocardiography and histology analyses demonstrated that apoE-deficient mice had developed heart failure with cardiac dilation. The microarray gene expression study of heart tissue from cystamine-treated apoE-deficient mice relative to untreated mice confirmed the development of heart failure showing up-regulation heart failure-specific genes by mild thiol-blocking with cystamine. **Overall design:** Microarray gene expression profiling was performed with heart tissue isolated from three study groups: (i) cystamine-treated 5 month-old apolipoprotein- (apoE)- deficient mice with symptoms of heart failure, (ii) untreated 5 month-old apoE- deficient mice, and (iii) age-matched, untreated, non-transgenic B6 control mice.

Background corr dist: KL-Divergence = 0.0389, L1-Distance = 0.0232, L2-Distance = 0.0006, Normal std = 0.6303

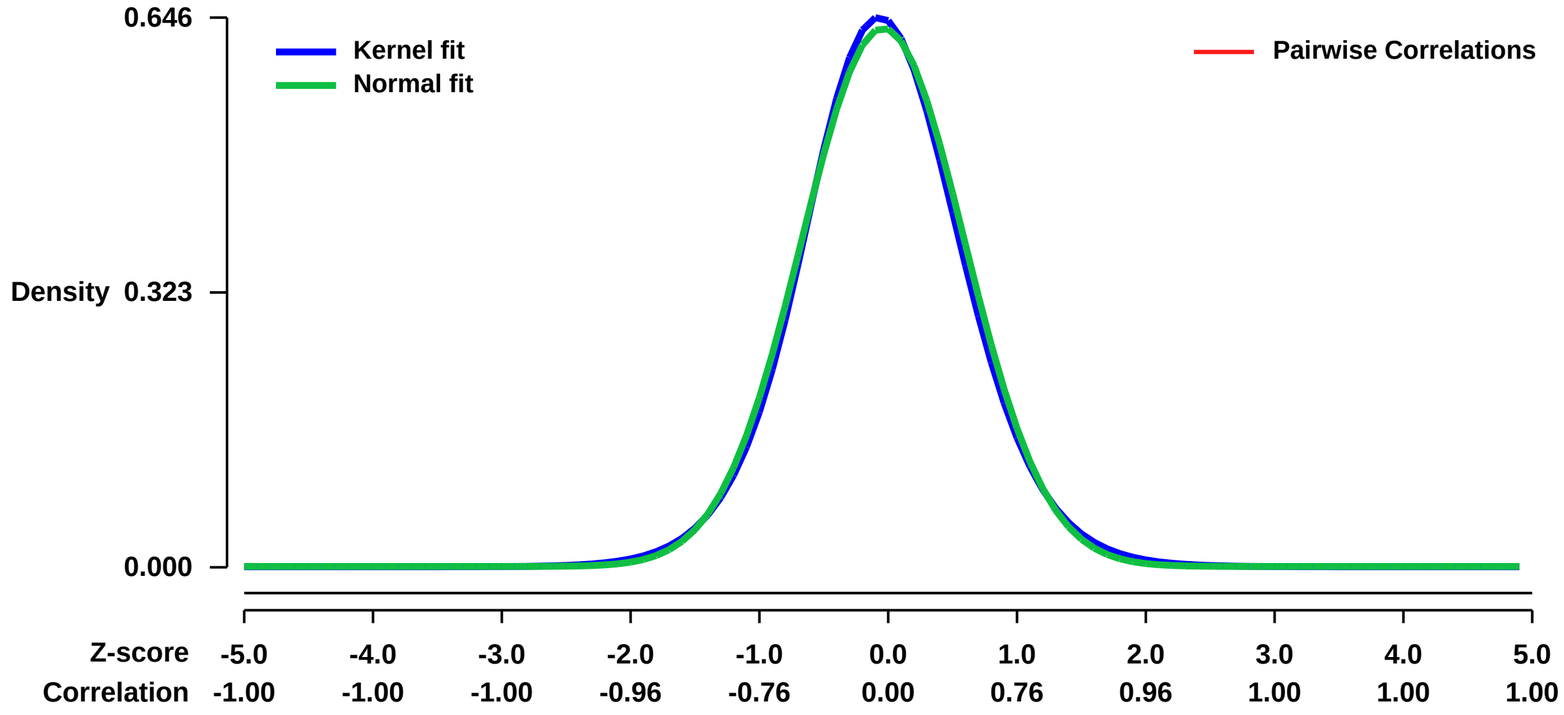

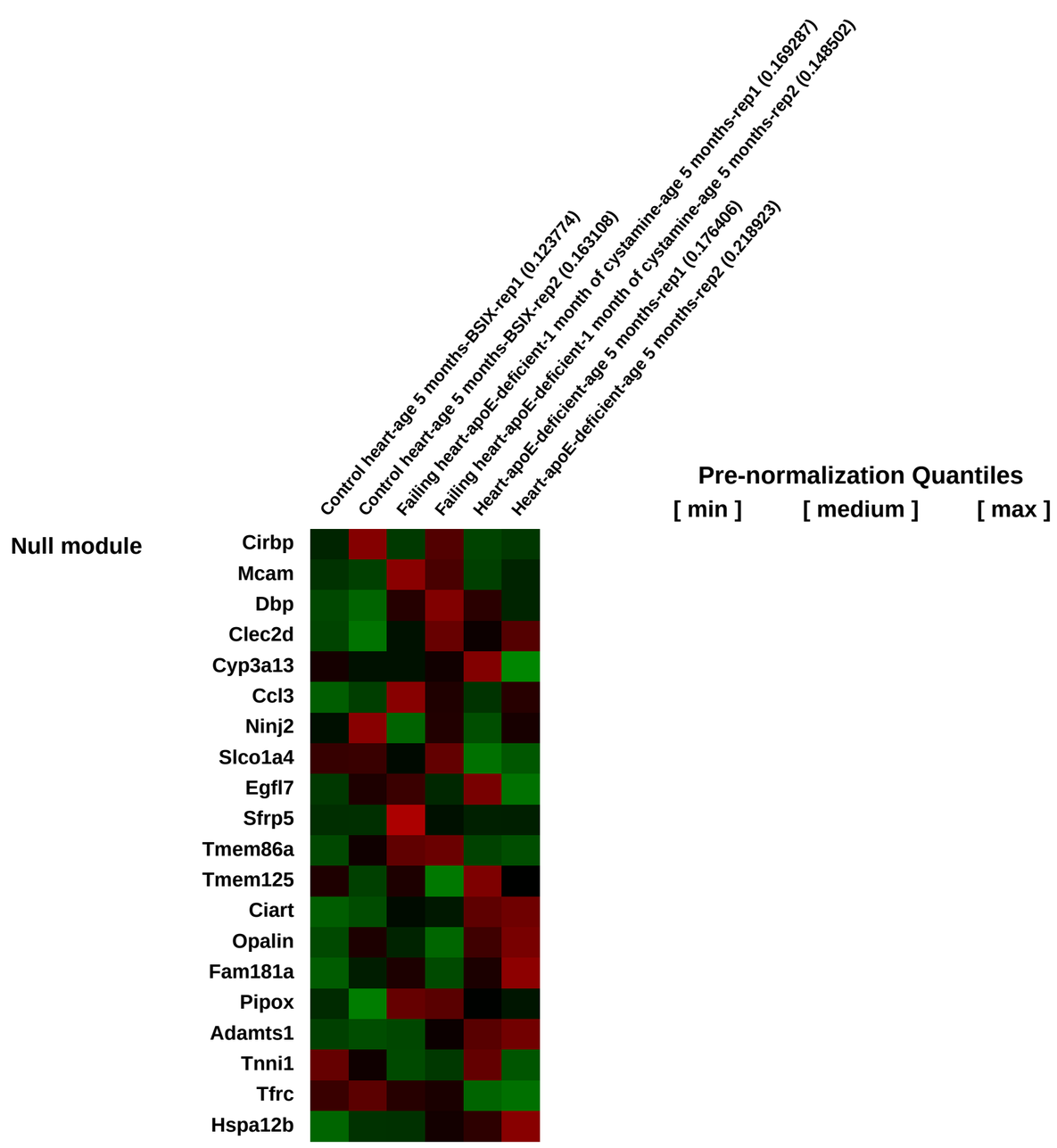

GEO Series "GSE5976" Expression Profiles

Num of samples in this series: 12

Scale of expression profile Z-scores

-3.0 -2.0 -1.0 0.0 1.0 2.0 3.0

GEO Link:	http://www.ncbi.nlm.nih.gov/geo/query/acc.cgi?acc=GSE5976
Status:	Public on Jul 01 2008
Title:	Mesp1-induced gene expression changes
Organism:	Mus musculus
Experiment type:	Expression profiling by array
Platform:	GPL1261
Pubmed ID:	18593559
Summary & Design:	**Summary:** During gastrulation, cells of the prospective mesoderm ingress through the primitive streak and acquire fates based on complex spatial and temporal cues. Progenitors of the cardiogenic mesoderm are first found at E6.5 in the posterior lateral epiblast and subsequently migrate laterally and anteriorly to form the cardiac crescent at E7.5, when regionalized cell fates are first delineated . Lineage tracing and heterotopic transplantation studies suggest that precursors in the earliest heart field possess potential to generate myocardium, endocardium, and pericardium. The mechanisms by which inductive signals in the primitive streak effect the development of this pancardiac progenitor field, however, remain poorly understood In mice, the earliest restricted progenitors of the cardiovascular system are marked by expression of the basic helix-loop-helix transcription factor, Mesp1. We therefore use microarray analysis to determine the early and intermediate effects of transiently forced Mesp1 expression during ES cell differentiation. **Keywords: time course** **Overall design:** ES cells bearing a targeted, doxycycline inducible Mesp1 transgene were differentiated in the absence or presence of DKK1 from day 0-4, either with or without transient doxycycline treatment from day 2-4.

Background corr dist: KL-Divergence = 0.0893, L1-Distance = 0.0268, L2-Distance = 0.0010, Normal std = 0.4657

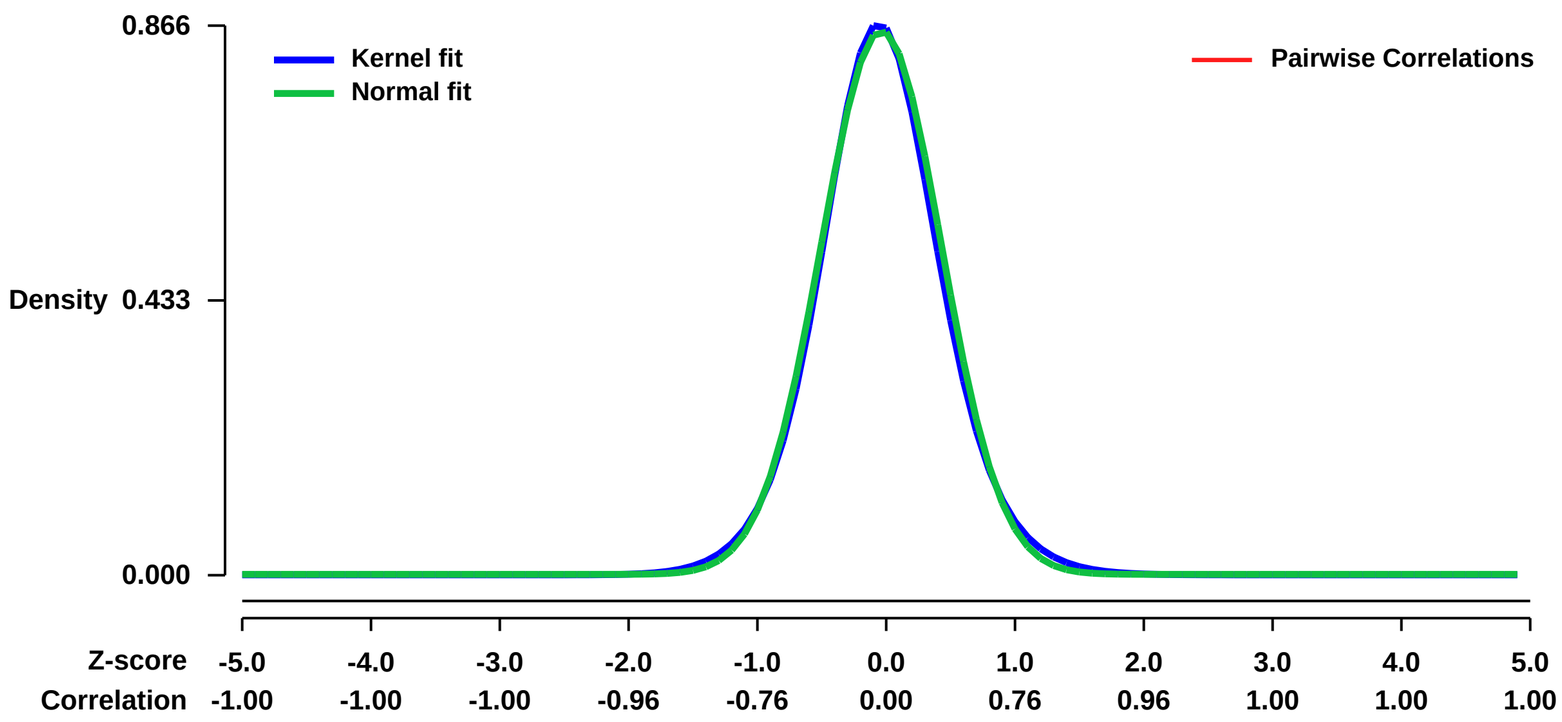

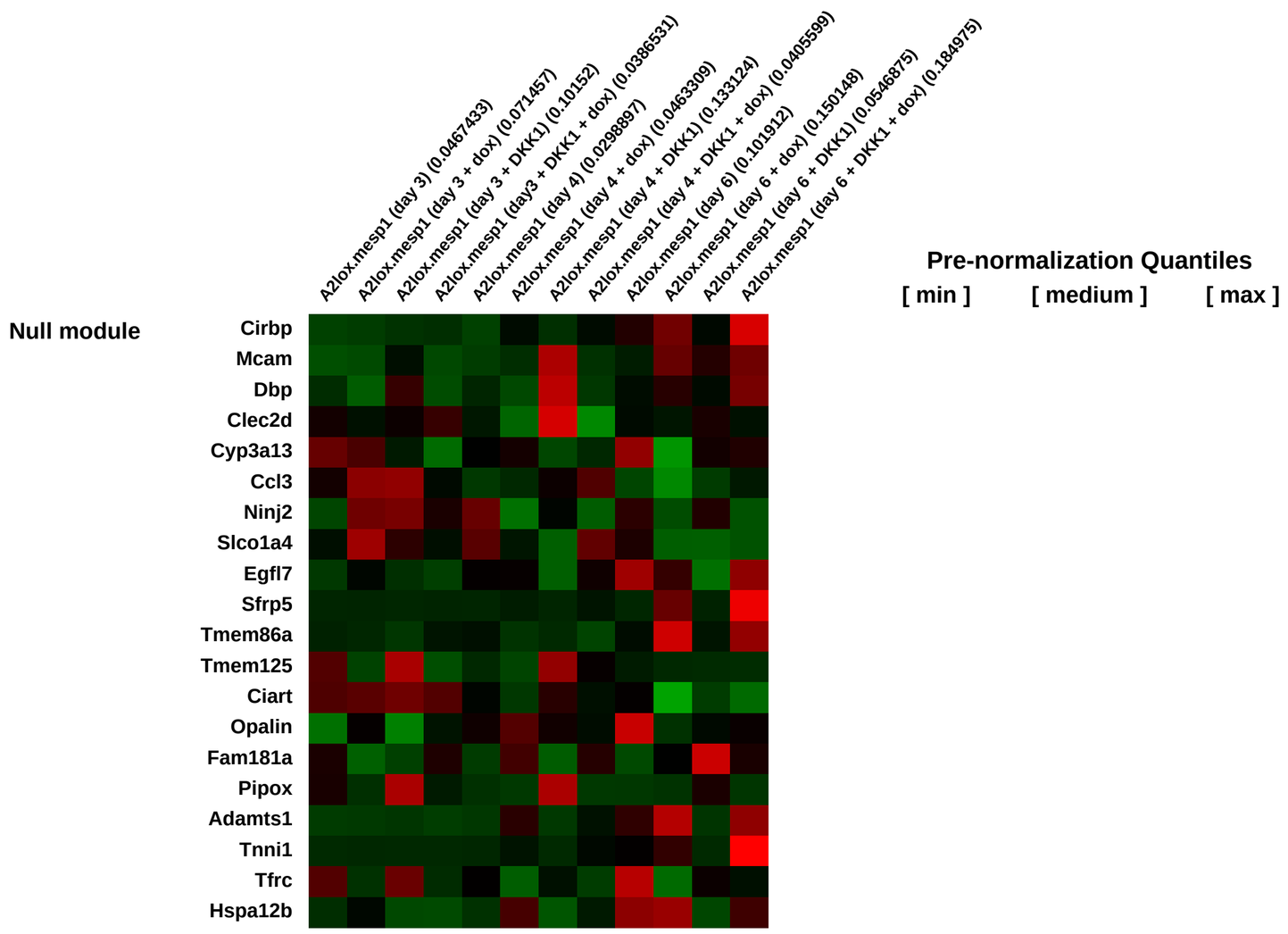

GEO Series "GSE10343" Expression Profiles

Num of samples in this series: 18

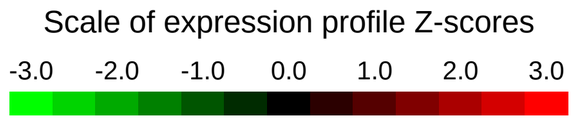

GEO Link:	http://www.ncbi.nlm.nih.gov/geo/query/acc.cgi?acc=GSE10343
Status:	Public on Feb 02 2008
Title:	Murine Acute Lung Injury
Organism:	Mus musculus
Experiment type:	Expression profiling by array
Platform:	GPL1261
Pubmed ID:	19136373

Summary & Design:

Summary:
With advances in supportive therapy in the last two decades, mortality rates from ALI/ARDS have improved somewhat, but remain around 30 to 40% with significant morbidity in survivors. Several promising treatments are in various stages of evaluation, but many have failed to prove beneficial in large randomized clinical trials (RCT). The first definitive step forward in ALI therapeutics occurred recently as a result of a large RCT demonstrating a mortality decrease from 40 to 31% with the use of low-volume ventilation strategies. From this, it is clear that the opportunity for successful intervention in ALI exists. However, therapeutic advances remain frustrated by the lack of complete understanding of ALI pathophysiology. This stresses the importance of integrating basic and clinical research of the molecular pathogenesis of this disease. The conclusions of a recent National Heart, Lung, and Blood Institute (NHLBI) Working Group on ALI support this type of research as a priority for future investigations of ALI. One of the areas of research given priority by this ALI Working Group is the issue of ALI severity progression and the role of cells of innate immunity in this process. Currently, the processes that determine which ALI patients progress to ARDS and which do not are unclear. As with many phenotype differences, there is most likely a genetic component involved. The basis for this has been demonstrated. For example, a surfactant protein B (SP-B) polymorphism appears to increase a patientâ s risk of developing ALI from pneumonia. Additionally, a polymorphism in the promoter region of the gene for interleukin-6 (IL-6) has been associated with a poor prognosis in patients with ARDS. Understanding the intracellular processes of these genes and the cells expressing them in ALI progression could lead to the identification of molecular markers of ALI severity and eventually to the development of targeted therapies. An examination of genetically uniform animals will provide a clearer insight into the interaction between immune cells in ALI progression as well as guide future human experiments.

Keywords: Time Series Design, ALI - acute lung injury, ARDS - acute respiratory distress syndrome, CLP - cecal ligation and puncture

Overall design:
Specific Aim 1. We will prospectively collect and bank RNA from peripheral blood CD4+ T lymphocytes (Th1 and Th2 subsets) and platelets from cecal ligation and puncture-treated BALB/c mice using a negative selection technique. Specific Aim 2. Four mice will undergo whole blood sampling at each of 3 time points (t = 0, 24, and 48 hours). Time 0 represents the point of CLP. Specific Aim 3. The temporal series of 3 cell types pooled within each time point will be expression profiled (3 time points x 3 cell types x MOE430A array = 9 profiles) in order to generate a map of potential cell-cell interactions and a prioritization model for examining these further.

Background corr dist: KL-Divergence = 0.1806, L1-Distance = 0.0717, L2-Distance = 0.0134, Normal std = 0.3626

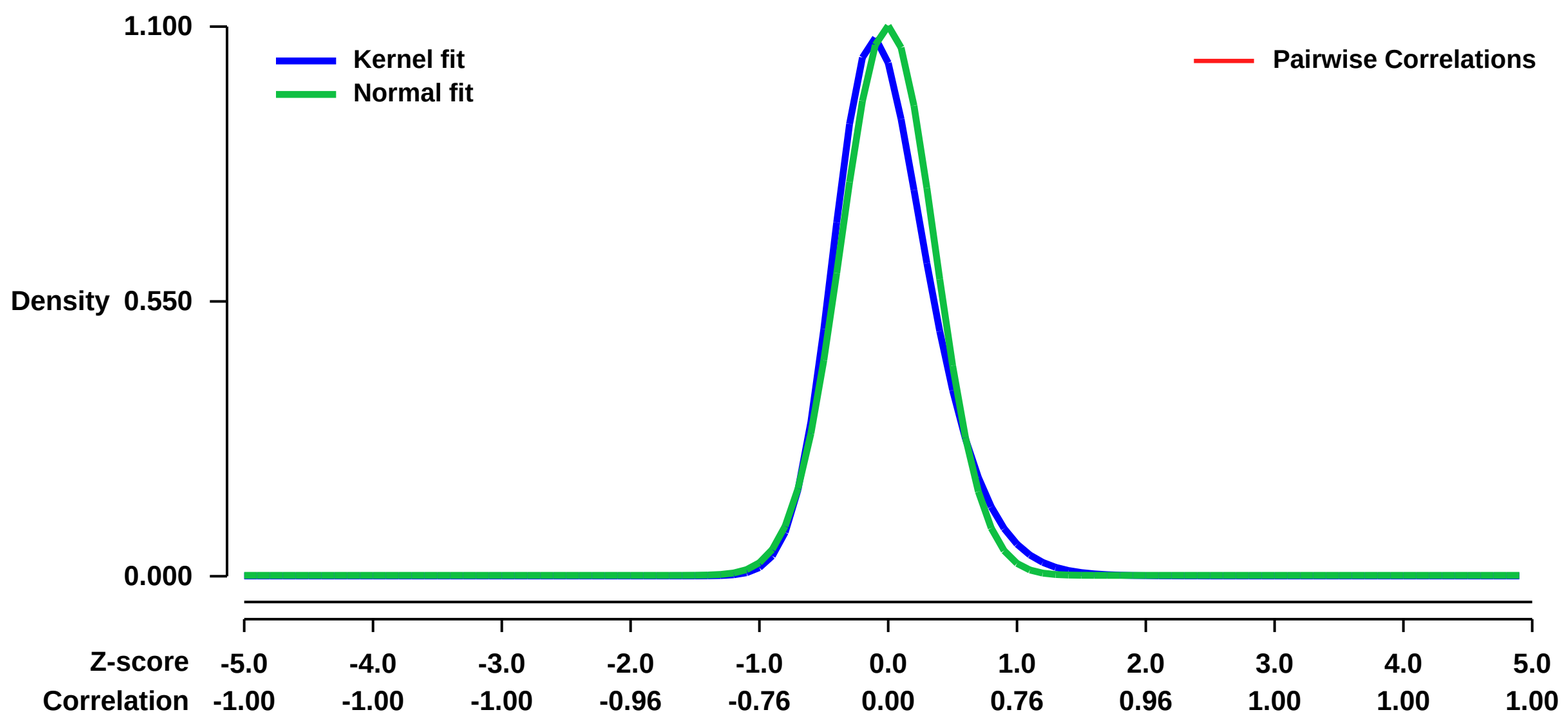

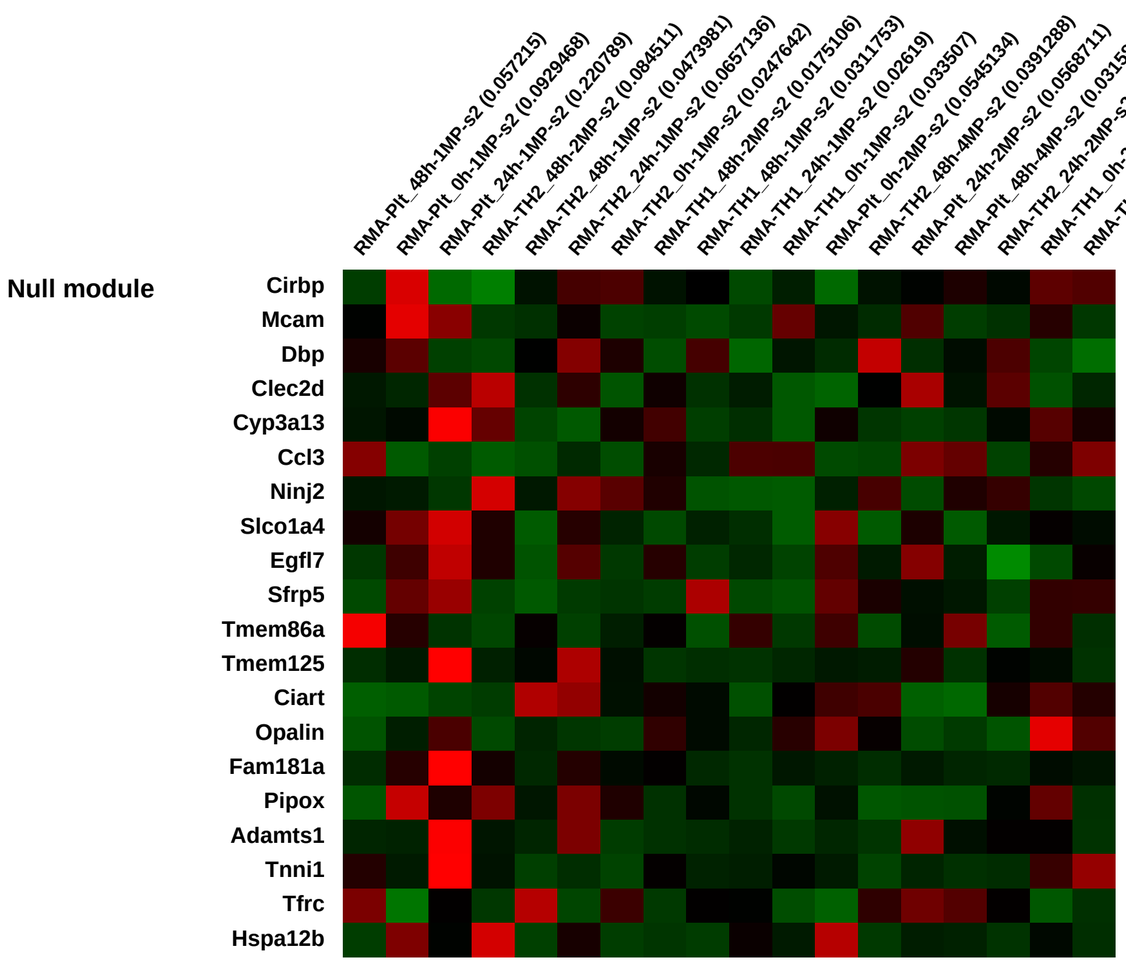

GEO Series "GSE21379" Expression Profiles

Num of samples in this series: 10

Scale of expression profile Z-scores

-3.0 -2.0 -1.0 0.0 1.0 2.0 3.0

GEO Link:	http://www.ncbi.nlm.nih.gov/geo/query/acc.cgi?acc=GSE21379
Status:	Public on Apr 20 2010
Title:	Expression Data from WT and Sh2d1a-/- in vivo follicular helper CD4 T cells (TFH) versus non follicular helper CD4 T cells (non-TFH)
Organism:	Mus musculus
Experiment type:	Expression profiling by array
Platform:	GPL1261
Pubmed ID:	20525889
Summary & Design:	**Summary:** CD4 T cell help is critical for both the generation and maintenance of germinal centers, and T follicular helper (TFH) cells are the CD4 T cell subset required for this process. SAP (SH2D1A) expression in CD4 T cells is essential for germinal center development. However, SAP-deficient mice have only a moderate defect in TFH differentiation as defined by common TFH surface markers. CXCR5+ TFH cells are found within the germinal center as well as along the boundary regions of T/B cell zones. Here we show that germinal center associated T cells (GC TFH) can be identified by their co-expression of CXCR5 and the GL7 epitope, allowing for phenotypic and functional analysis of TFH and GC TFH populations. Here we show GC TFH are a functionally discrete subset of further polarized TFH cells, with enhanced B cell help capacity and a specialized ability to produce IL-4 in a TH2-independent manner. Strikingly, SAP-deficient mice have an absence of the GC TFH subset and SAP- TFH are defective in IL-4 and IL-21 production. We further demonstrate that SLAM (Slamf1, CD150), a surface receptor that utilizes SAP signaling, is specifically required for IL-4 production by GC TFH. GC TFH cells require IL-4 and IL-21 production for optimal help to B cells. These data illustrate complexities of SAP-dependent SLAM family receptor signaling, revealing a prominent role for SLAM receptor ligation in IL-4 production by germinal center CD4 T cells but not in TFH and GC TFH differentiation. **Overall design:** Analysis of in vivo antigen-specific (LCMV-specific, SMARTA TCR transgenic) WT and Sh2d1a-/- follicular helper CD4 T cells (CXCR5high),versus non-follicular helper CD4 T cells (CXCR5low), eight days after viral infection.

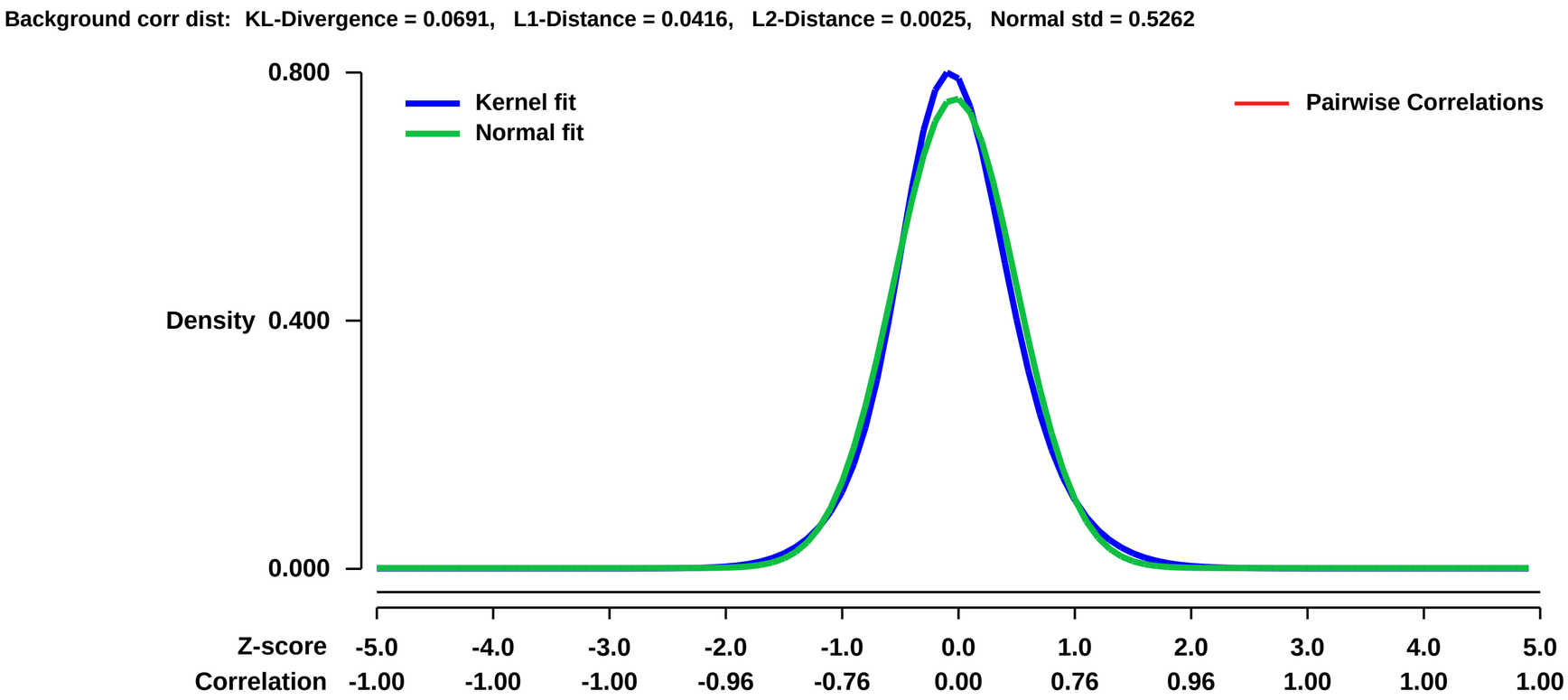

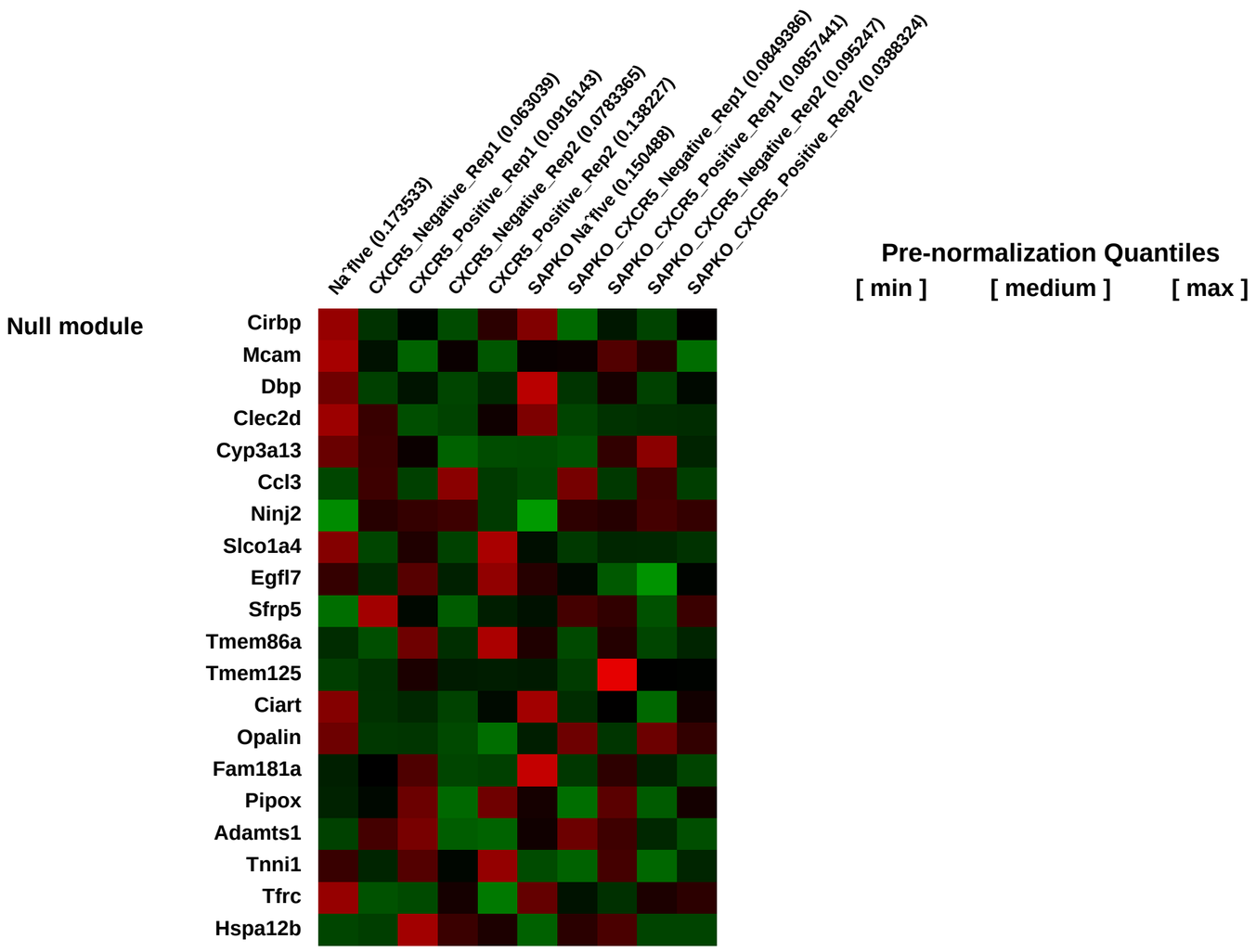

GEO Series "GSE42777" Expression Profiles

Num of samples in this series: 12

Scale of expression profile Z-scores

-3.0 -2.0 -1.0 0.0 1.0 2.0 3.0

GEO Link:	http://www.ncbi.nlm.nih.gov/geo/query/acc.cgi?acc=GSE42777
Status:	Public on Aug 13 2013
Title:	Gene expression microarray analysis on the dentate gyrus of Schnurri-2 knockout and wild-type control mice
Organism:	Mus musculus
Experiment type:	Expression profiling by array
Platform:	GPL1261
Pubmed ID:	23389689
Summary & Design:	**Summary:** Schnurri-2 (Shn-2), an NF-kappa B site-binding protein, tightly binds to the enhancers of major histocompatibility complex (MHC) class I genes and inflammatory cytokines, which have been shown to harbor common variant single nucleotide polymorphisms associated with schizophrenia. Shn-2 knockout mice show behavioral abnormalities that strongly resemble those of schizophrenics. We performed gene expression microarray analysis of dentate gyri from Shn-2 knockout and wild-type control mice. **Overall design:** Dentate gyrus RNA isolated from six Shn-2 knockout and six control wild-type mice were compared.

Background corr dist: KL-Divergence = 0.1212, L1-Distance = 0.0259, L2-Distance = 0.0009, Normal std = 0.4091

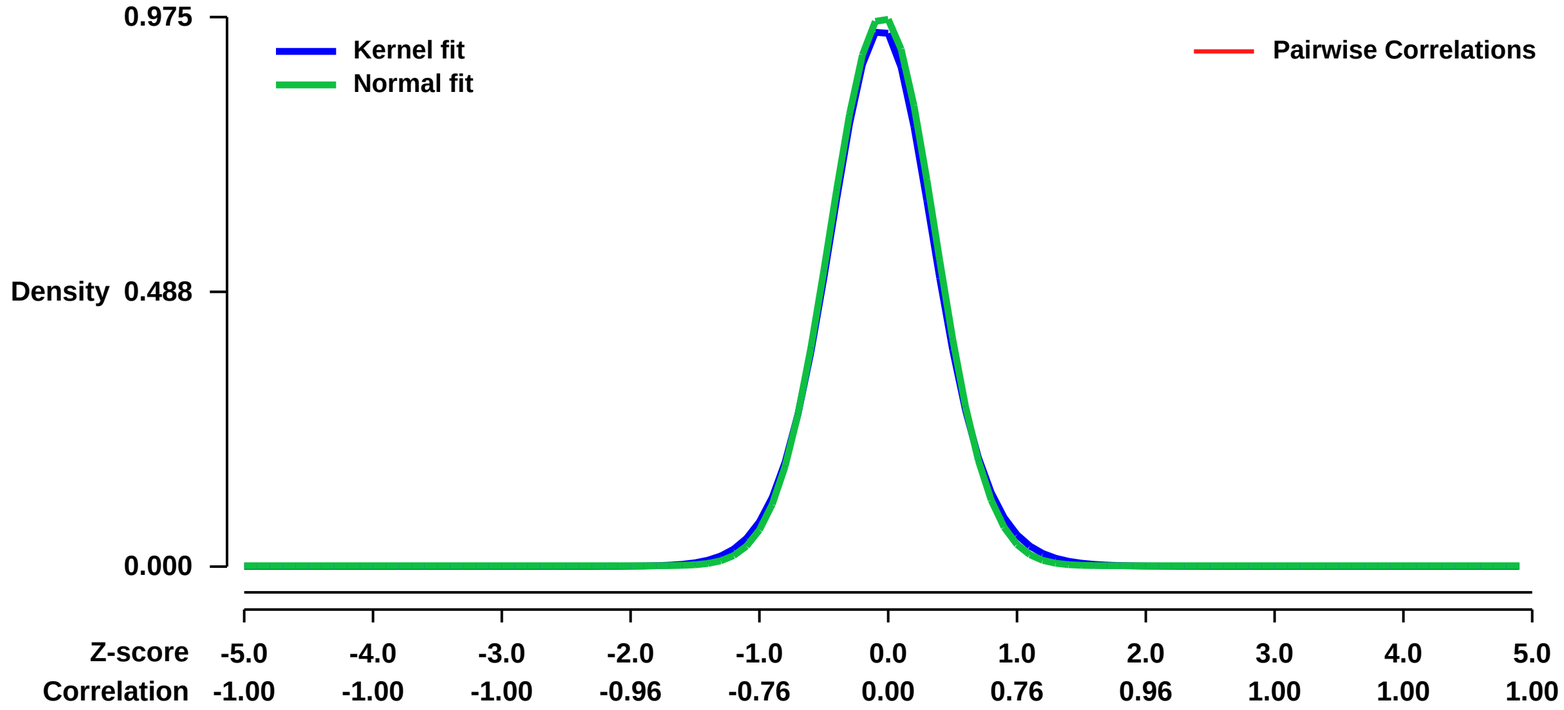

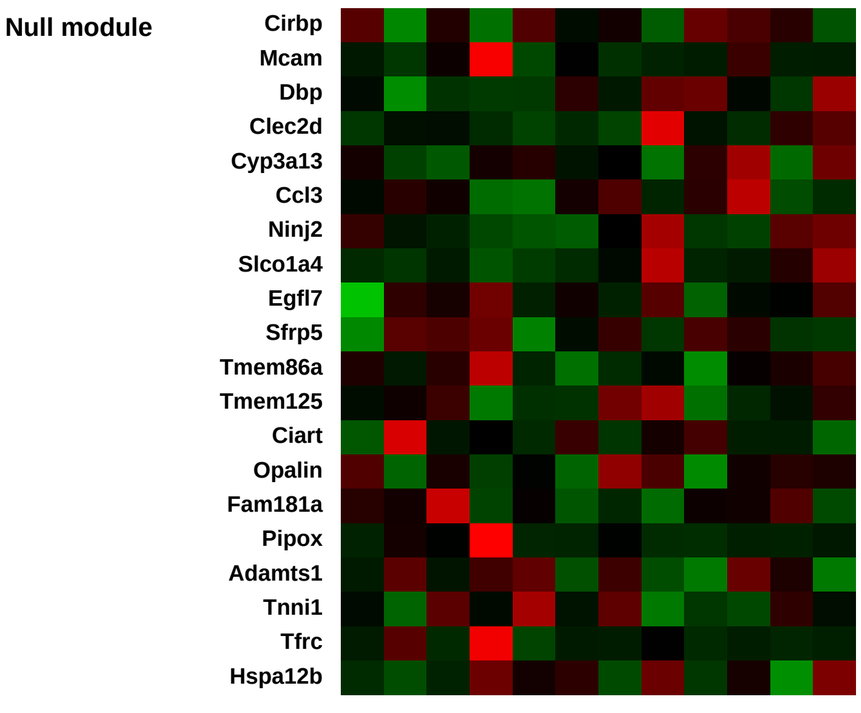

GEO Series "GSE51075" Expression Profiles

Num of samples in this series: 12

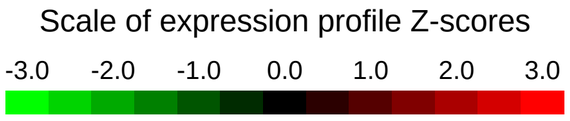

GEO Link:	http://www.ncbi.nlm.nih.gov/geo/query/acc.cgi?acc=GSE51075
Status:	Public on Sep 22 2013
Title:	Transcriptional responses of murine macrophages to the adenylate cyclase toxin of Bordetella pertussis
Organism:	Mus musculus
Experiment type:	Expression profiling by array
Platform:	GPL1261
Pubmed ID:	17890046
Summary & Design:	**Summary:** Three different recombinant forms of CyaA were used to investigate transcriptional responses of murine bone marrow-derived macrophages (BMDMs) using Affymetrix Mouse Genome Genechips. These forms were enzymically active, invasive CyaA, nonenzymically active, invasive CyaA (CyaA*) and non-enzymically active, non-invasive CyaA (proCyaA*). BMMs, treated with 20 ng/ml of CyaA for 24 h, showed over 1000 significant changes in gene transcription compared with control cells. CyaA caused an increase in transcription of many inflammatory genes and genes associated with various signalling cascades such as those involved in cyclic AMP-dependent protein kinase A signalling. Most strikingly, CyaA caused down-regulation of numerous genes involved in cell proliferation. CyaA* at 20 ng/ml significantly up-regulated the transcription of only twelve genes after 24 h whereas proCyaA* at this concentration significantly increased the transcription of only two genes. **Overall design:** The effect of administration of three different recombinant forms of pertussis toxin to mouse bone marrow derived macrophages are compared with a vehicle only contol 24 hours after treatment in technical triplicate measurements

Background corr dist: KL-Divergence = 0.0967, L1-Distance = 0.0706, L2-Distance = 0.0078, Normal std = 0.5189

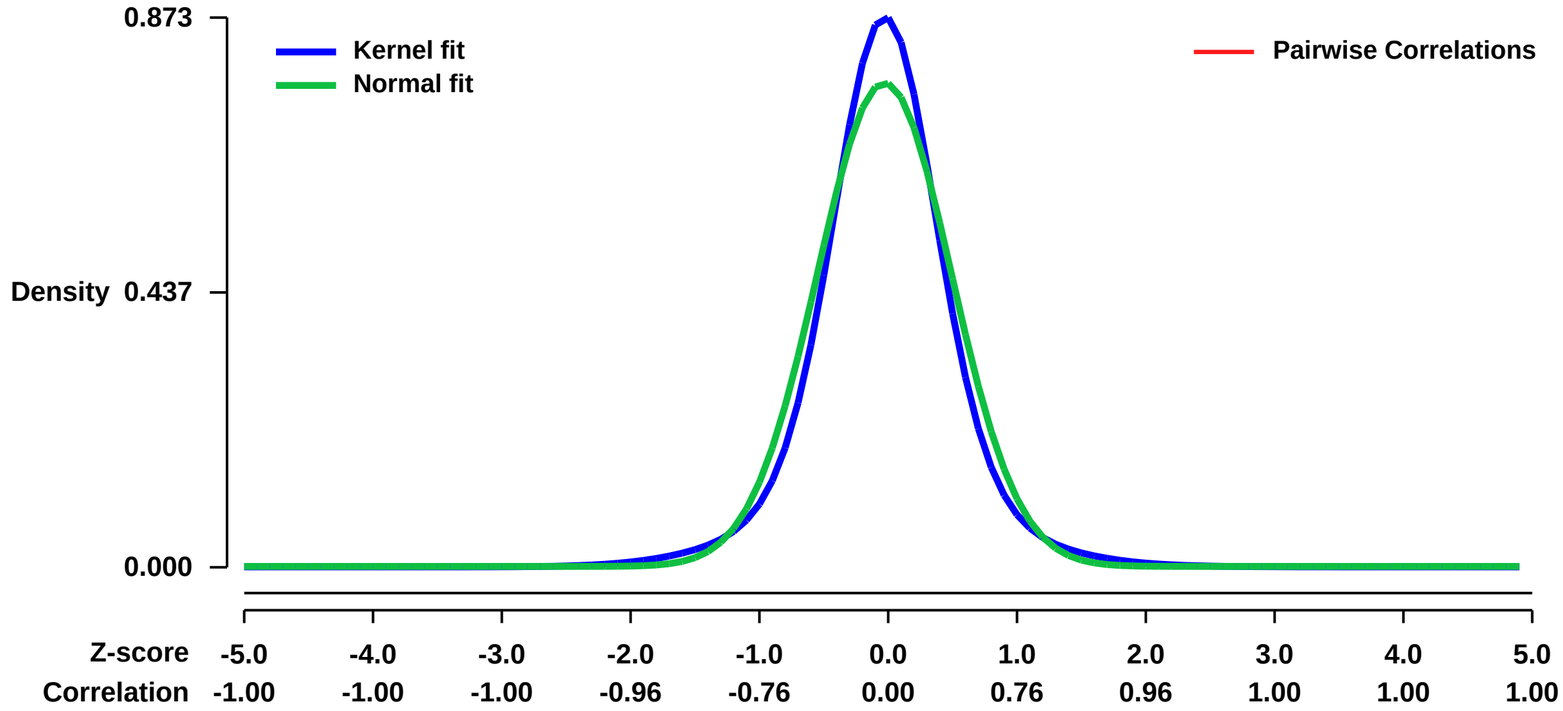

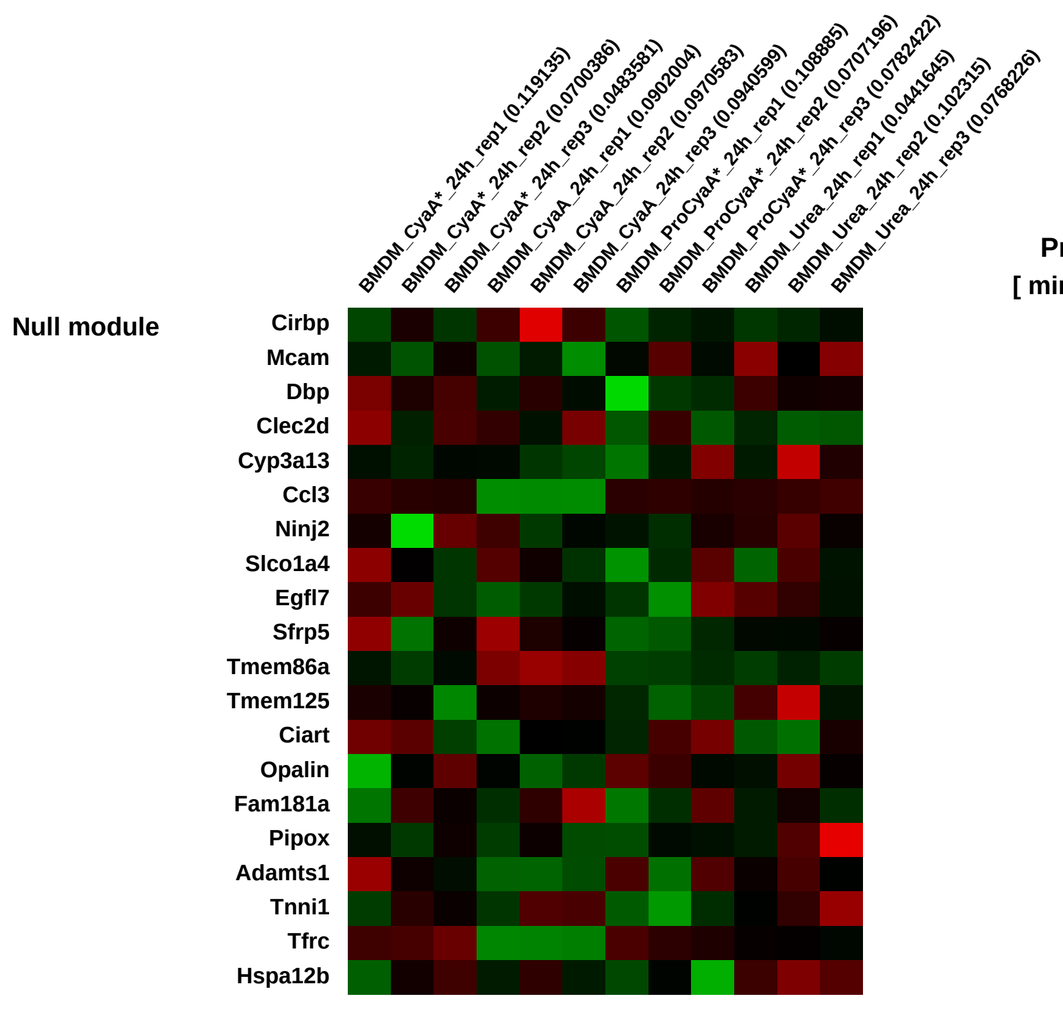

GEO Series "GSE5124" Expression Profiles

Num of samples in this series: 6

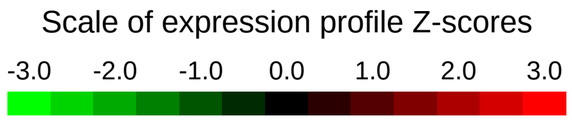

GEO Link:	http://www.ncbi.nlm.nih.gov/geo/query/acc.cgi?acc=GSE5124
Status:	Public on Aug 28 2006
Title:	Hoxb1 gene expressing Hox-A1 protein: Altered transcriptional profile in rhombomere 4 at E10.5
Organism:	Mus musculus
Experiment type:	Expression profiling by array
Platform:	GPL1261
Pubmed ID:	16890163
Summary & Design:	**Summary:** This study analyzed mRNA profiles in rhombomere 4 of E10.5 mouse knock-in embryos expressing either normal endogenous Hox-B1 protein or the paralogous Hox-A1 protein from the Hoxb1 locus. The Hox-A1 protein was found to be detectably less efficacious than Hox-B1 in promoting neurogenesis in the basal plate of rhombomere 4 and its transcriptional profile shared several similarities with the Hoxb1 mutant. **Keywords:** gene swap, knock-in, hindbrain development, rhombomere 4 **Overall design:** GFP-positive cells were FACS-sorted from dissected hindbrains of entire litters of E10.5 mouse embryos expressing either normal endogenous Hox-B1 protein or the paralogous Hox-A1 protein from the Hoxb1 locus, either one tagged with IRES-tauGFP. Three independent biological replicates of each genotype were analyzed. Total RNA was isolated, amplified and hybridized to Affymetrix Mouse Genome 430 2.0 Arrays.

Background corr dist: KL-Divergence = 0.0481, L1-Distance = 0.0204, L2-Distance = 0.0005, Normal std = 0.5814

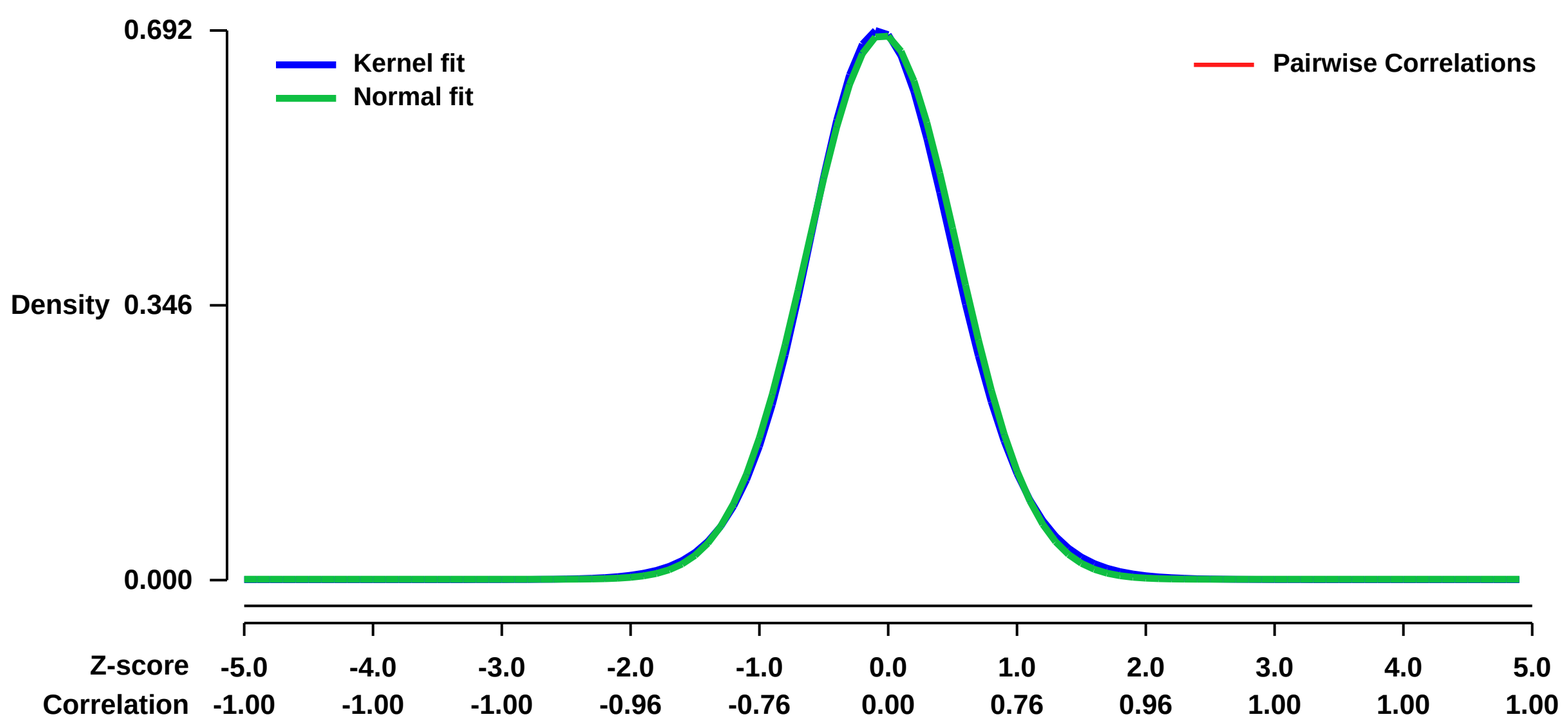

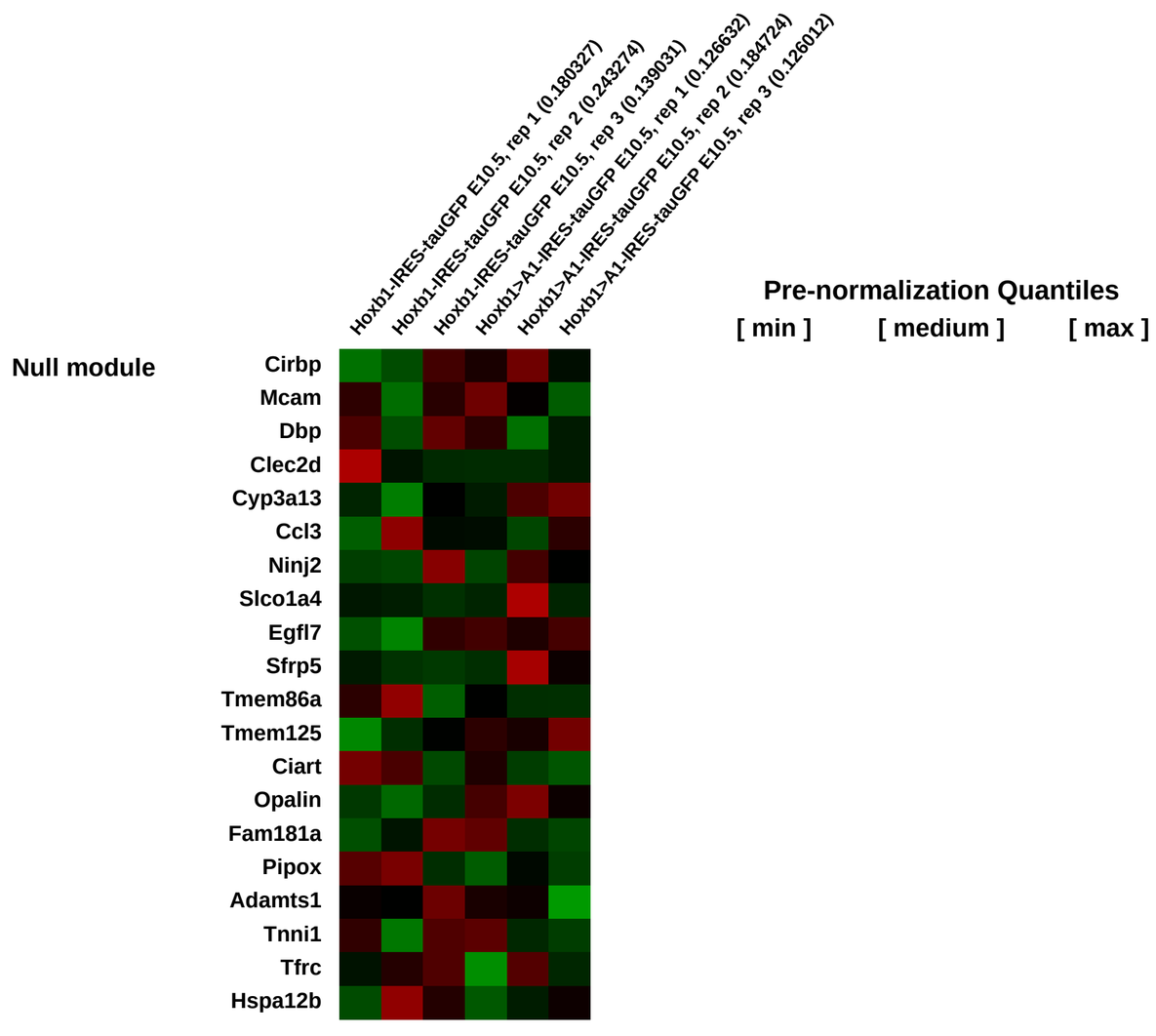

GEO Series "GSE52022" Expression Profiles

Num of samples in this series: 8

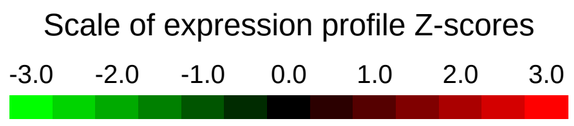

GEO Link:	**http://www.ncbi.nlm.nih.gov/geo/query/acc.cgi?acc=GSE52022**
Status:	**Public on Dec 01 2013**
Title:	**Genome wide analysis of transcriptome and microRNAs in early stage of Alzheimerâ s disease (mRNA)**
Organism:	**Mus musculus**
Experiment type:	**Expression profiling by array**
Platform:	**GPL1261**
Pubmed ID:	
Summary & Design:	**Summary:** **We addressed the integrated analysis of mRNA and miRNA expression levels of Tg6799 AD model mice at 4 month and 8 months of age. Total 8 gene cluster modules for co-expression network were predicted from transcriptome data and 6 modules were show relation with AD or aging. We constructed early stage AD network using data integration between mRNA and miRNA profiles and predicted miRNAs strongly involved in module regulation. We found that ARRDC3 showed AD mutation dependent changes of expression and was related metabolic dysfunction in early stage AD.** **These results demonstrate that candidate genes on the simultaneous profiling of mRNA and miRNA expressions in genome wide can be used for the understanding of non-coding RNA related gene expression in early stage AD. We suggested that our results could be future candidate to be developed as early biomarkers in progressive AD pathology. This result can be used for the further application in neurodegenerative diseases.** **Overall design:** **Tg6799 transgenic mice were purchased from The Jackson Laboratory (USA) and were housed under a 12h light-dark cycle with free access to food and water. Female Tg6799 mice are maintained until 4 months and 8 months of age (for littermate control: LM and mutant subjects: MT). RNA samples were isolated from hippocampus of mice using TRI-Reagent (Sigma-Aldrich, St. Louis, MO) according to the manufacturerâ s instructions. Gene expression was analyzed with GeneChip´fi Mouse Genome 430 2.0 Arrays (Affymetrix, Santa Clara, CA), which is comprised of over 45,000 probe sets representing approximately 28,700 well-characterized mouse genes. The Ion Total RNA-Seq Kit v2 (Lifetechnologies, USA) was used for the preparation of micro RNA libraries according to the manufacturer's instructions. Total numbers of subject used are as followed: 1) LM 4 months : MT 4 months : LM 8 months : MT 8 months (2:4:2:4) for screening mRMA and miRNA, 2) LM 4 months : MT 4 months : LM 8 months : MT 8 months (4:4:4:4) for expression verification. Tg6799 transgenic mice were purchased from The Jackson Laboratory (USA) and were housed under a 12h light-dark cycle with free access to food and water. Female Tg6799 mice are maintained until 4 months and 8 months of age (for littermate control: LM and mutant subjects: MT). RNA samples were isolated from hippocampus of mice using TRI-Reagent (Sigma-Aldrich, St. Louis, MO) according to the manufacturerâ s instructions. Gene expression was analyzed with GeneChip´fi Mouse Genome 430 2.0 Arrays (Affymetrix, Santa Clara, CA), which is comprised of over 45,000 probe sets representing approximately 28,700 well-characterized mouse genes. The Ion Total RNA-Seq Kit v2 (Lifetechnologies, USA) was used for the preparation of micro RNA libraries according to the manufacturer's instructions. Total numbers of subject used are as followed: 1) LM 4 months : MT 4 months : LM 8 months : MT 8 months (2:4:2:4) for screening mRMA and miRNA, 2) LM 4 months : MT 4 months : LM 8 months : MT 8 months (4:4:4:4) for expression verification.**

Background corr dist: KL-Divergence = 0.0823, L1-Distance = 0.0215, L2-Distance = 0.0006, Normal std = 0.4710

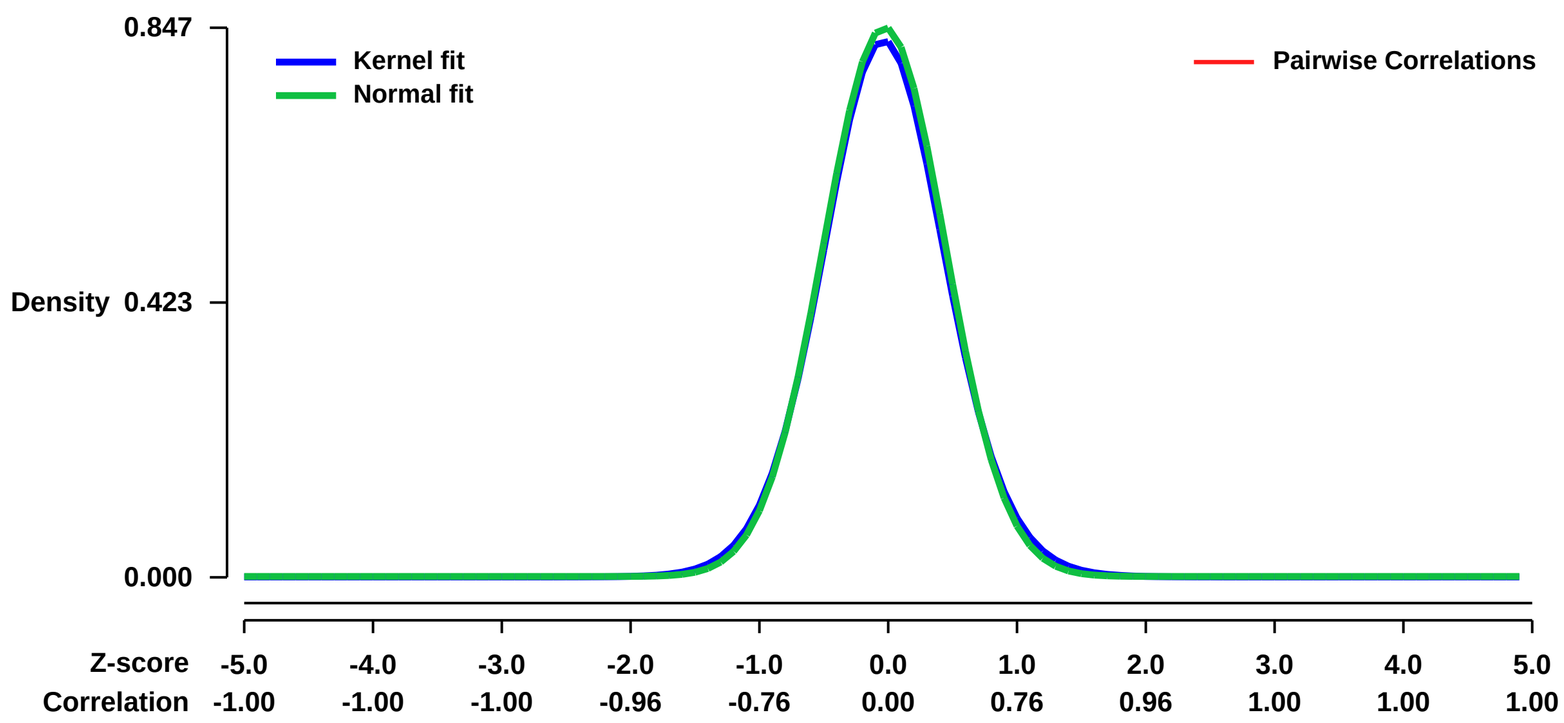

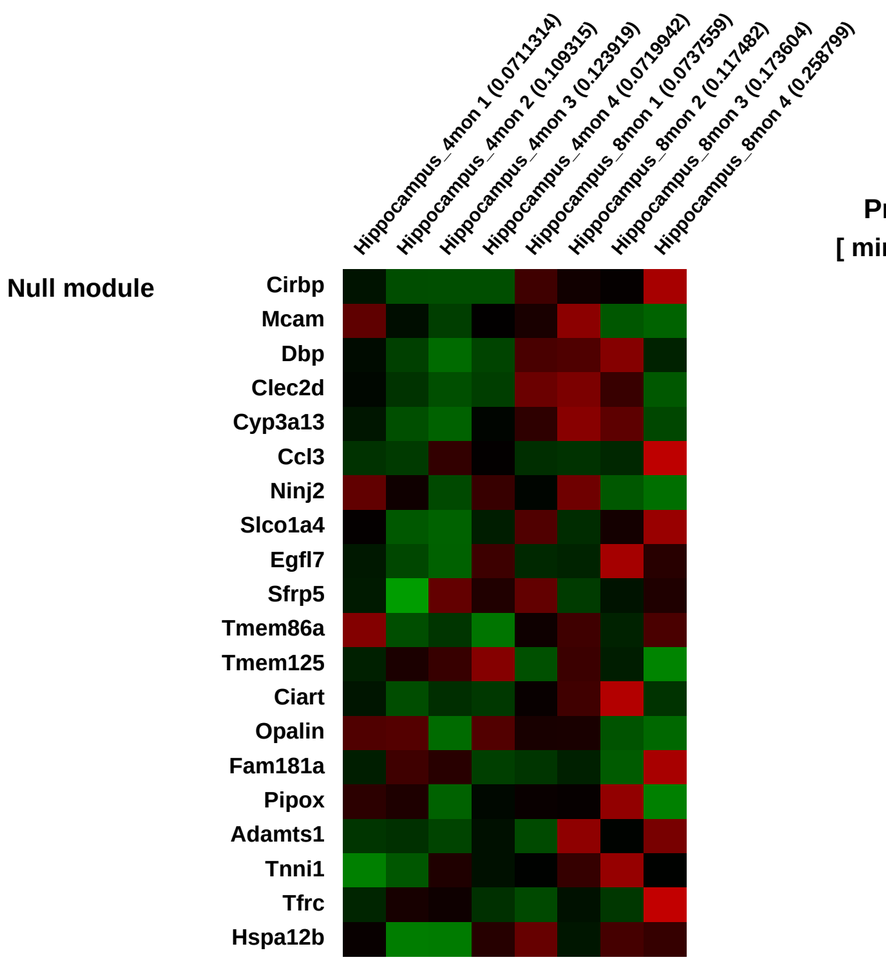

GEO Series "GSE25286" Expression Profiles

Num of samples in this series: 10

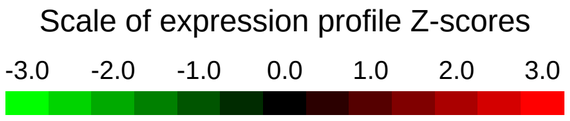

GEO Link:	**http://www.ncbi.nlm.nih.gov/geo/query/acc.cgi?acc=GSE25286**
Status:	**Public on May 01 2012**
Title:	**mRNA expression profile in a murine model of hyperoxia-induced bronchopulmonary dysplasia**
Organism:	**Mus musculus**
Experiment type:	**Expression profiling by array**
Platform:	**GPL1261**
Pubmed ID:	
Summary & Design:	**Summary:** **We performed miRNA and mRNA profiling at postnatal day 14 and day 29 to compare hyperoxia-induced bronchopulmonary dysplasia and wild type. We built potential miRNA-mRNA interaction networks specific to brochopulmonary dysplasia.** **Overall design:** **Replicated time course of mouse lung development at 2 time points (P14, P29). Three replicates per time point for bronchopulmonary dysplasia induced by hyperoxia mouse lung, and two replicates per time point for wild type mouse lung. This dataset represents the mRNA expression profiling component of the study.**

Background corr dist: **KL-Divergence = 0.0273, L1-Distance = 0.0359, L2-Distance = 0.0021, Normal std = 0.6782**

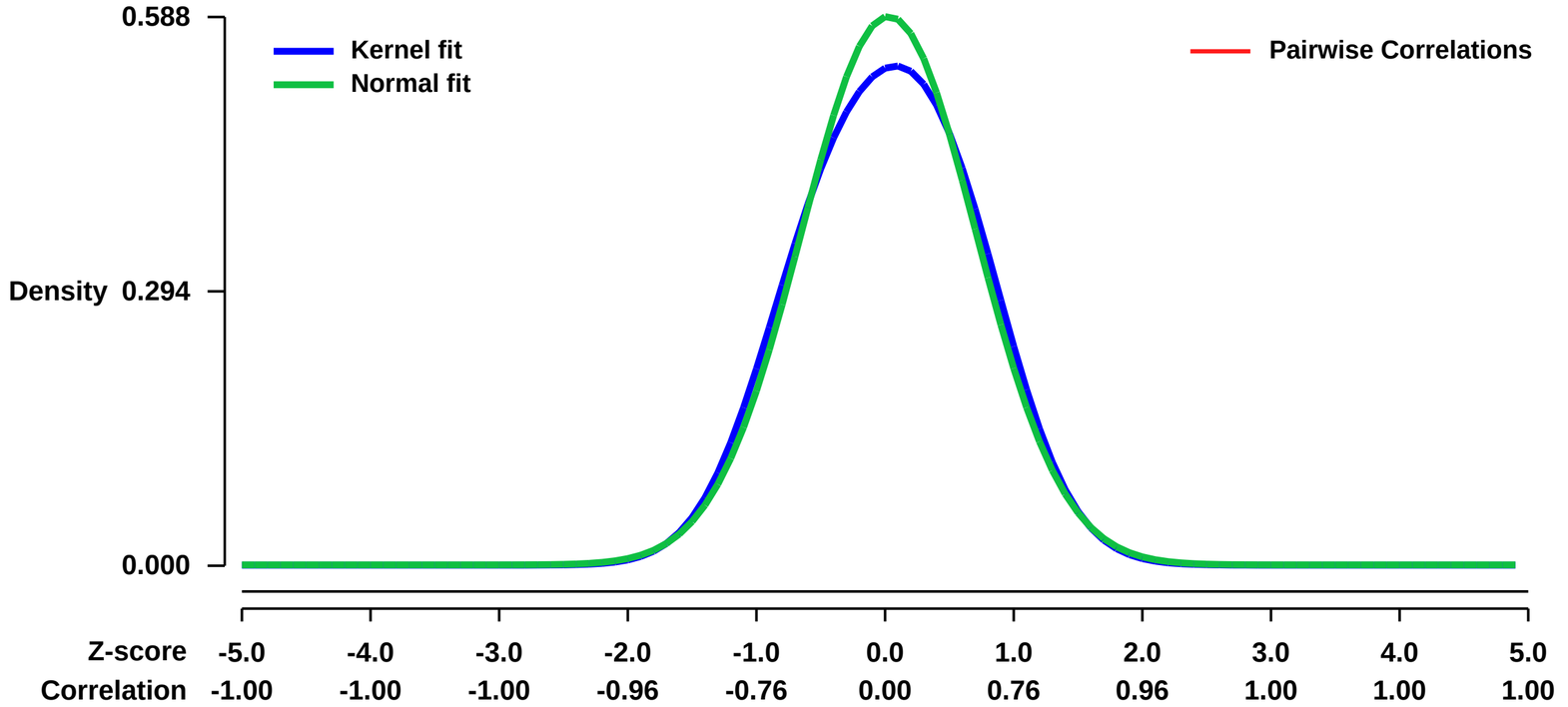

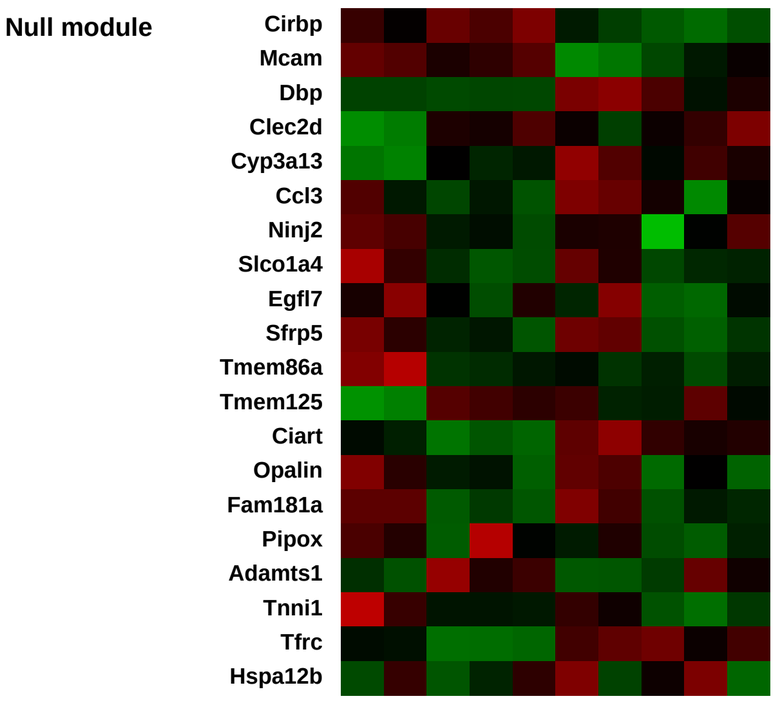

GEO Series "GSE3595" Expression Profiles

Num of samples in this series: 6

Scale of expression profile Z-scores

-3.0 -2.0 -1.0 0.0 1.0 2.0 3.0

GEO Link:	http://www.ncbi.nlm.nih.gov/geo/query/acc.cgi?acc=GSE3595
Status:	Public on Jun 10 2006
Title:	Identification of potential KLF7 target genes in olfactory sensory neurons
Organism:	Mus musculus
Experiment type:	Expression profiling by array
Platform:	GPL1261
Pubmed ID:	17123745
Summary & Design:	**Summary:** KLF7 null mice show profound axonal growth defects in the olfactory epithelium. The goal of this study was the identification of potential KLF7 target genes in olfactory sensory neurons. Keywords: Molecular analysis of knockout mice. **Overall design:** Olfactory epithelia were isolated from 3 wildtype and 3 mutant 1 day old pups and the RNA isolated, labeled and hybridized to one chip each.

Background corr dist: KL-Divergence = 0.0329, L1-Distance = 0.0446, L2-Distance = 0.0027, Normal std = 0.6976

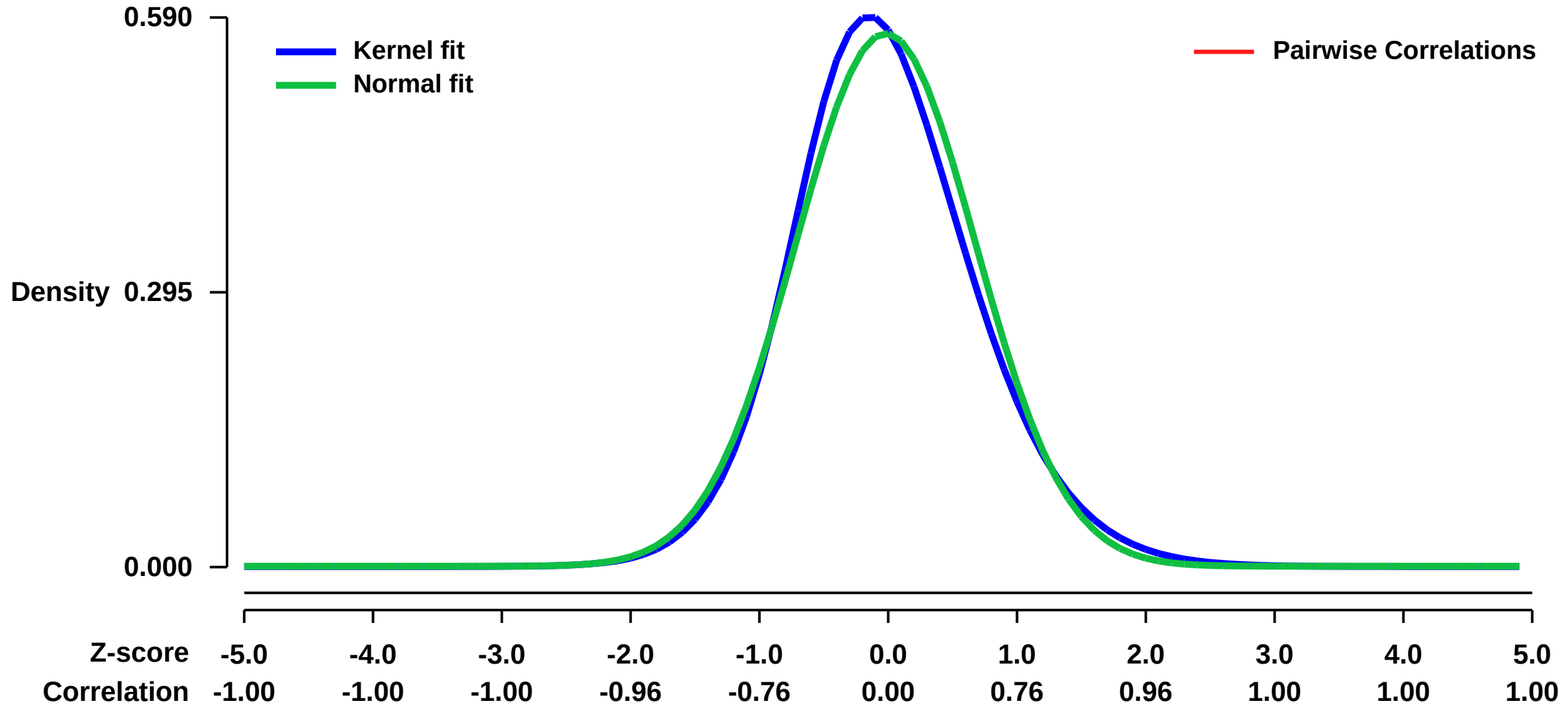

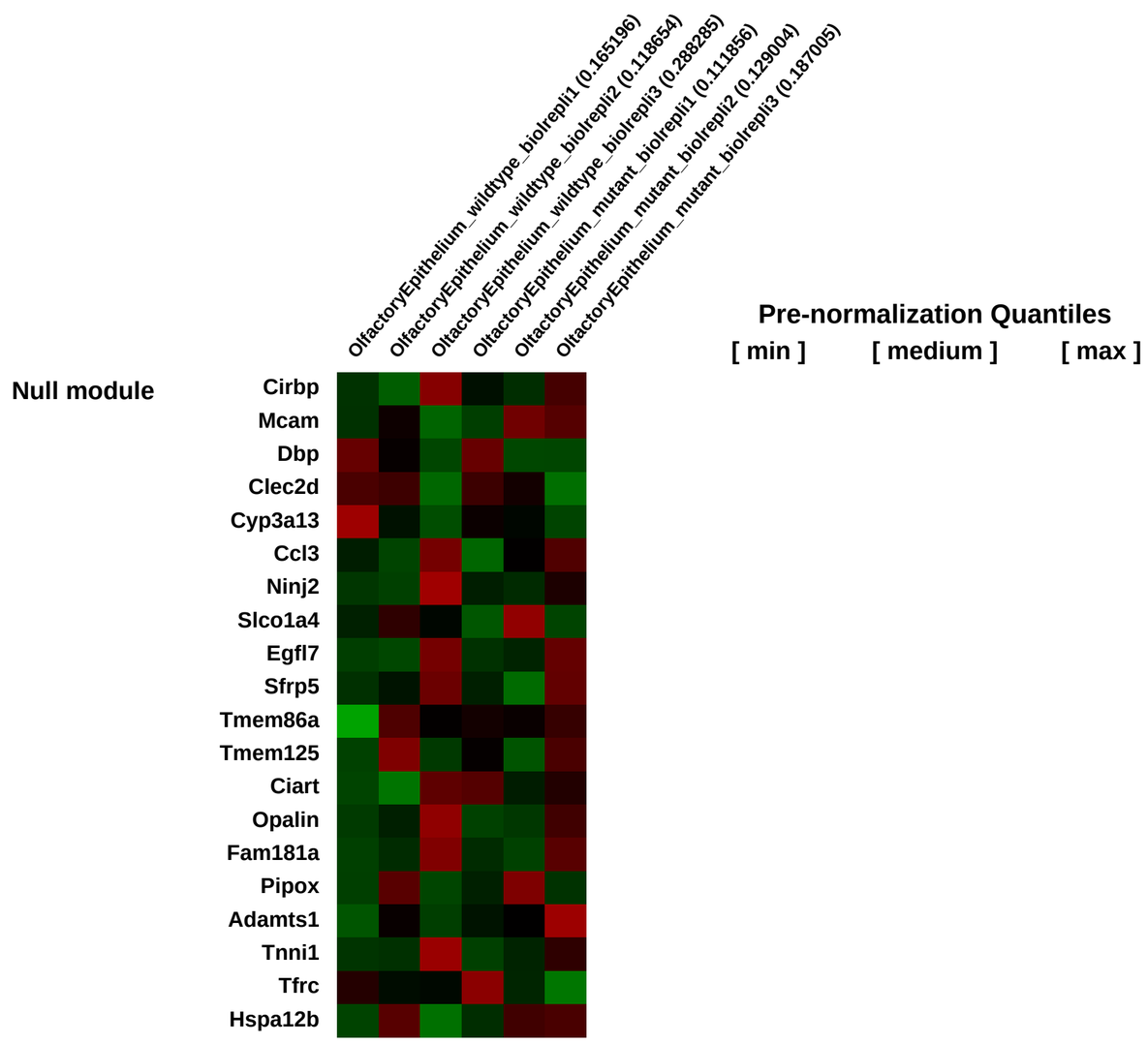

GEO Series "GSE51628" Expression Profiles

Num of samples in this series: 15

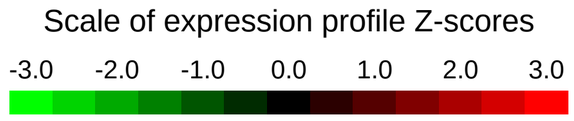

GEO Link:	**http://www.ncbi.nlm.nih.gov/geo/query/acc.cgi?acc=GSE51628**
Status:	**Public on Oct 24 2013**
Title:	**Effects of acute Notch activation on the mammary epithelial compartment in vivo**
Organism:	**Mus musculus**
Experiment type:	**Expression profiling by array**
Platform:	**GPL1261**
Pubmed ID:	
Summary & Design:	**Summary:** **Notch signaling is widely implicated in mouse mammary gland development and tumorigenesis. To investigate the effects of acute activation of Notch signaling in the mammary epithelial compartment, we generated bi-transgenic MMTV-rtTA; TetO-NICD1 (MTB/TICNX) mice that conditionally express a constitutively active NOTCH1 intracellular domain (NICD1) construct in the mammary epithelium upon doxycycline administration.** **Overall design:** **Two timepoints (48h and 96h) of doxycycline induction in TetO-NICD1 (TICNX; control) and MMTV-rtTA; TetO-NICD1 (MTB/TICNX) mice with 3-4 replicates per timepoint**

Background corr dist: **KL-Divergence = 0.0788, L1-Distance = 0.0320, L2-Distance = 0.0014, Normal std = 0.4893**

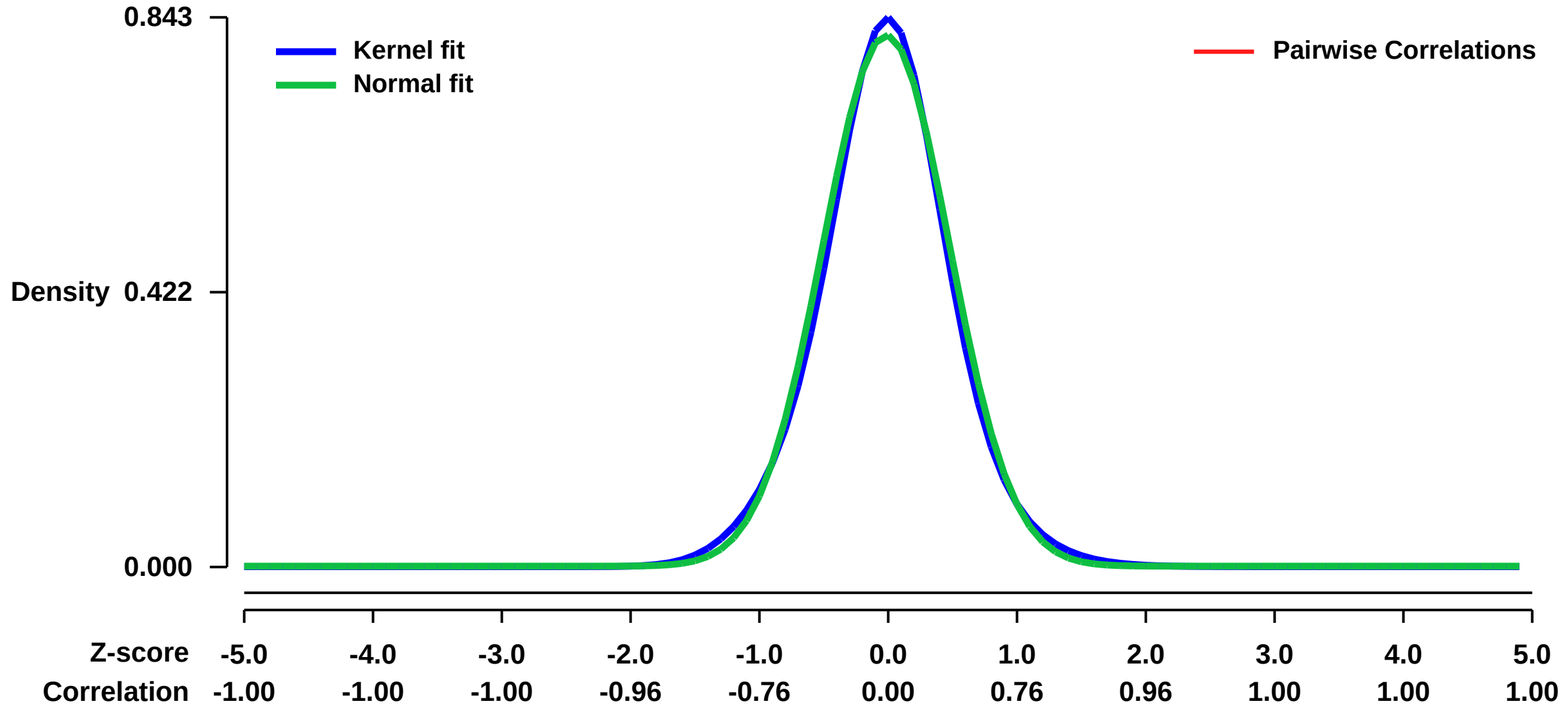

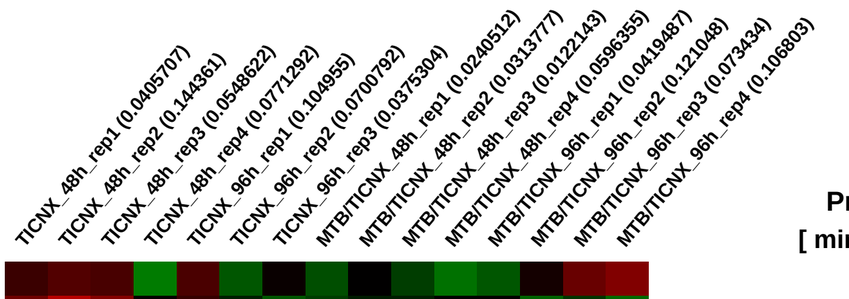

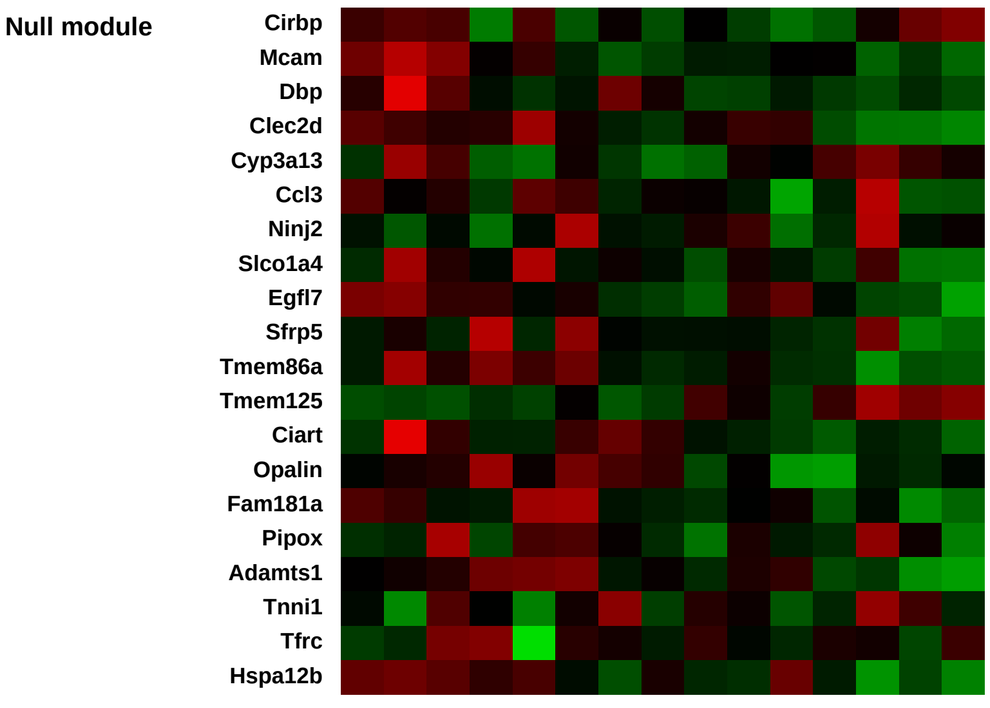

GEO Series "GSE18308" Expression Profiles

Num of samples in this series: 6

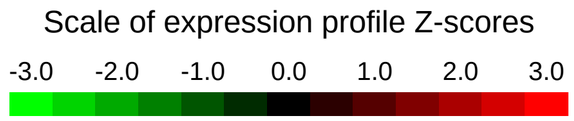

GEO Link:	**http://www.ncbi.nlm.nih.gov/geo/query/acc.cgi?acc=GSE18308**
Status:	**Public on Jan 01 2010**
Title:	**FoxOs cooperatively regulate diverse pathways governing neural stem cell homeostasis**
Organism:	**Mus musculus**
Experiment type:	**Expression profiling by array**
Platform:	**GPL1261**
Pubmed ID:	**19896444**
Summary & Design:	**Summary:** **FoxOs cooperatively regulate diverse pathways governing neural stem cell homeostasis** **Overall design:** **expression profile between six independant neural stem cell lines (three FoxO null and three wild type) were compared**

Background corr dist: **KL-Divergence = 0.0468, L1-Distance = 0.0219, L2-Distance = 0.0006, Normal std = 0.5893**

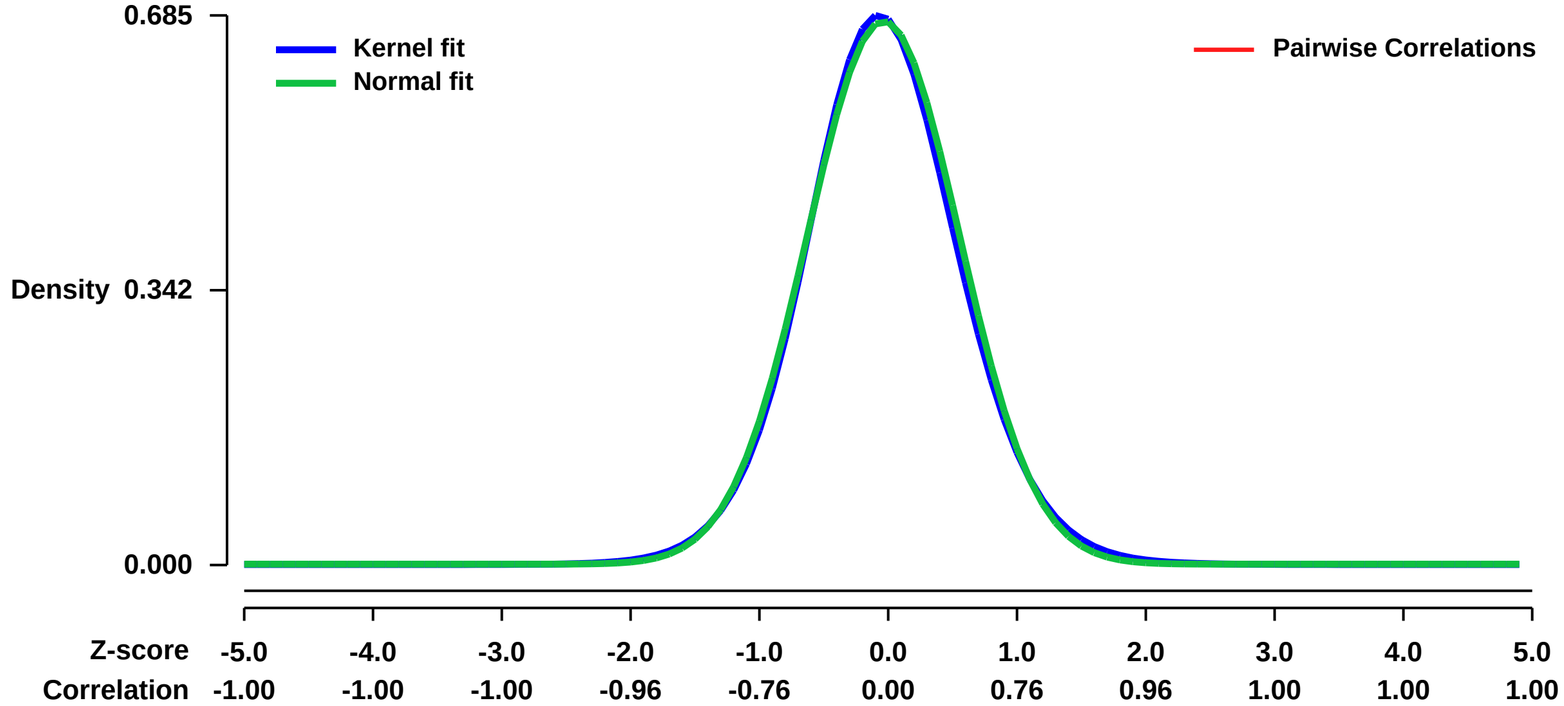

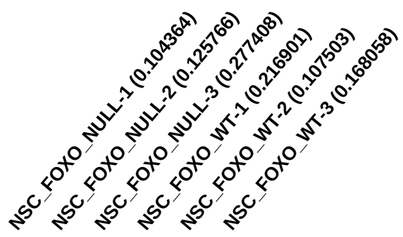

Pre-normalization Quantiles

[min] [medium] [max]

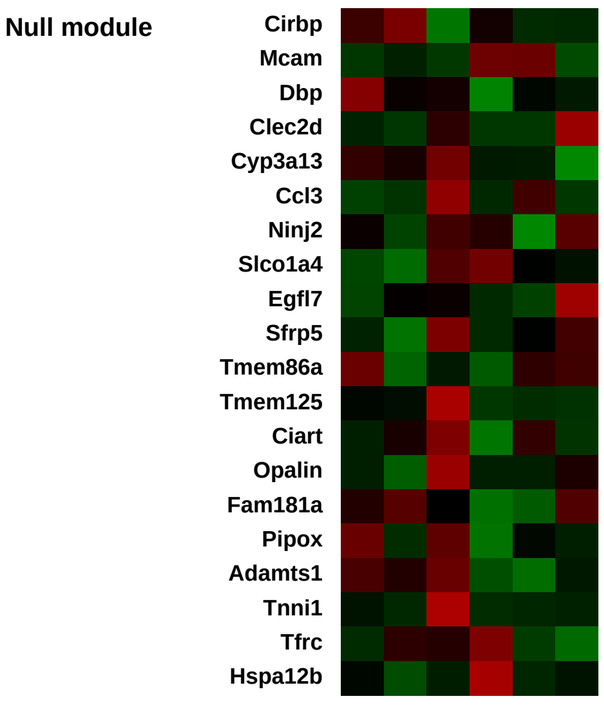

GEO Series "GSE39355" Expression Profiles

Num of samples in this series: 7

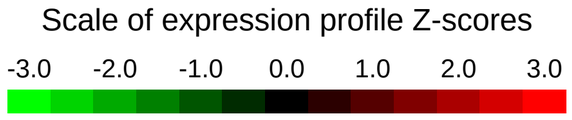

GEO Link:	http://www.ncbi.nlm.nih.gov/geo/query/acc.cgi?acc=GSE39355
Status:	Public on Mar 01 2013
Title:	Expression profiling of mouse primary prostate luminal cells from WT and T-ETV1 mice, which contains human ETV1 cDNA under the endogenous Tmprss2 promoter.
Organism:	Mus musculus
Experiment type:	Expression profiling by array
Platform:	GPL1261
Pubmed ID:	23512661
Summary & Design:	**Summary:** Chromosomal rearrangements involving ETS factors, ERG and ETV1, occur frequently in prostate cancer. We here examine mouse prostate cells from WT mice with s with T-ETV1 mice, which contains express the truncated human ETV1 under the endogenous Tmprss2 promoter. ETV1 expression can be tracked by GFP expression. **Overall design:** Primary prostate cells were isolated and luminal prostate cells were FACS-sorted by CD49F+ Sca1- from the lineage (CD31, CD45, Ter119) negative fraction. Total RNA was extracted from three biological replicates, and amplified using NuGEN V2cDNA amplification kit. This was used to hybridize to Affymetrix expression arrays using the Mouse Genome 430 2.0 platform.

Background corr dist: KL-Divergence = 0.0642, L1-Distance = 0.0279, L2-Distance = 0.0012, Normal std = 0.5311

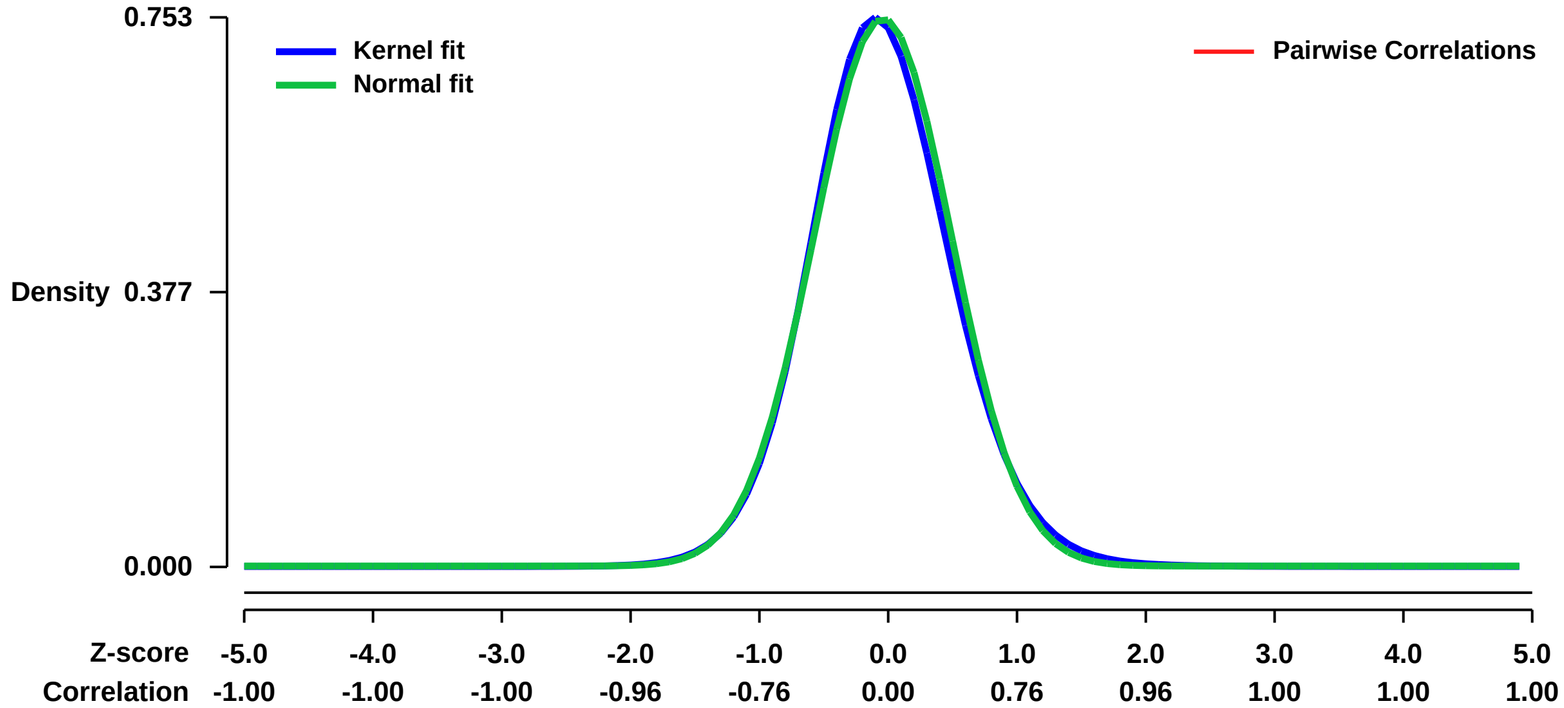

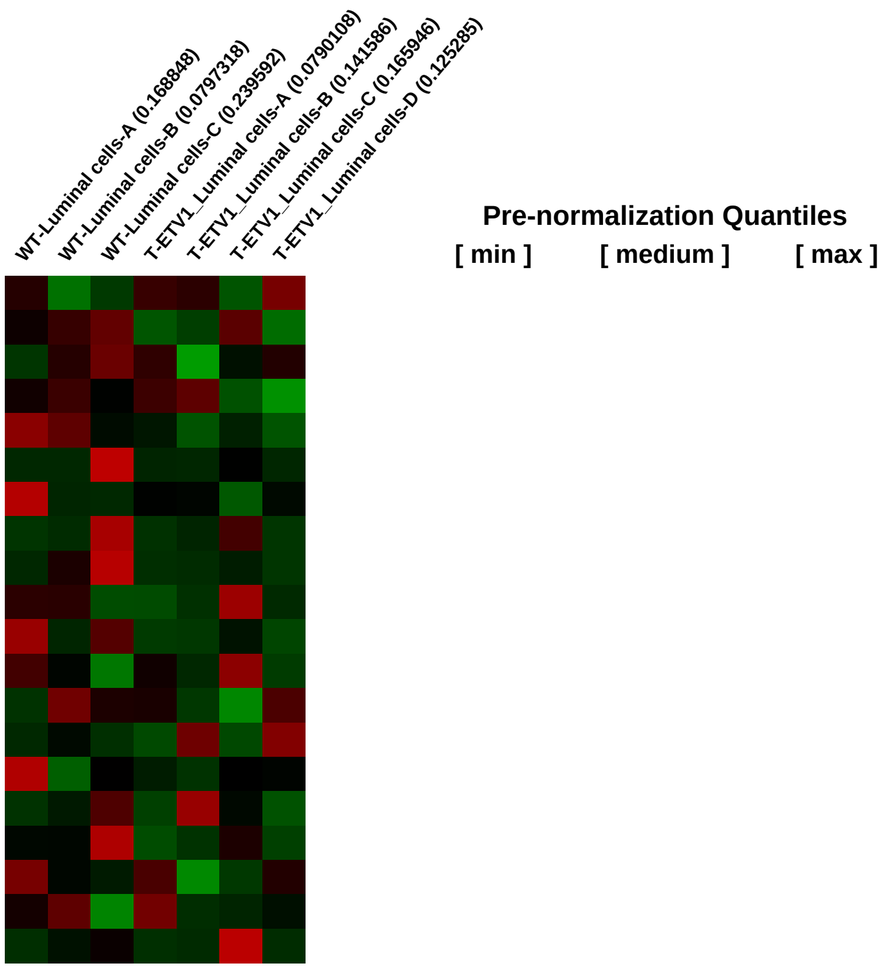

GEO Series "GSE7225" Expression Profiles

Num of samples in this series: 9

Scale of expression profile Z-scores

-3.0 -2.0 -1.0 0.0 1.0 2.0 3.0

GEO Link:	http://www.ncbi.nlm.nih.gov/geo/query/acc.cgi?acc=GSE7225
Status:	Public on Oct 22 2007
Title:	Identification and characterization of the changed transcripts in cumulus cells of Bmp15-/- and Bmp15-/-Gdf9+/--DM mice.
Organism:	Mus musculus
Experiment type:	Expression profiling by array
Platform:	GPL1261
Pubmed ID:	21047911
Summary & Design:	**Summary:** Mouse oocytes control cumulus cell metabolic processes that are deficient in the oocytes themselves and this delegation is necessary for oocyte development. Oocyte-derived bone morphogenetic factor 15 (BMP15) and growth differentiation factor 9 (GDF9) appear to be key regulators of follicular development. The effect of these factors on cumulus cell function before the preovulatory surge of luteinizing hormone (LH) was assessed by analysis of the transcriptomes of cumulus cells from wildtype (WT), Bmp15-/-, and Bmp15-/- Gdf9+/- double mutant (DM) mice using microarray analysis. The biological themes associated with the most highly-affected transcripts were identified using bioinformatic approaches, IPA and GenMAPP/MAPPFinder. There were 5,332, 7,640, and 2,651 transcripts identified to be significantly changed in the comparisons of Bmp15-/- vs. WT, DM vs. WT, and DM vs. Bmp15-/- respectively by the criteria of FC (fold change) p <0.01. Among theses changed transcripts, 744 were commonly changed in all three pair-wise comparisons, and hence were considered to be the most highly affected transcripts by mutation of Bmp15 and Gdf9. IPA Analyses revealed that metabolism was the major theme associated with the most highly-changed transcripts: glycolysis and sterol biosynthesis were the two most significantly affected pathways. Most of the transcripts encoding enzymes for sterol biosynthesis were down-regulated in both mutant cumulus cells and in WT cumulus cell after oocytectomy. Similarly, there was a reduction of de novo-synthesized cholesterol in these cumulus cells. This suggests that oocytes regulate cumulus cell metabolism, particularly sterol biosynthesis, by promoting the expression of corresponding transcripts. Furthermore, in WT-mice, Mvk, Pmvk, Fdps, Sqle, Cyp51, Sc4mol, and Ebp, which encode enzymes in the sterol biosynthetic pathway, were found to be expressed robustly in cumulus cells, but expression was barely detectable in oocytes. Levels of de novo-synthesized cholesterol were significantly higher in cumulusâ enclosed oocytes than denuded oocytes. These results indicate that mouse oocytes are deficient in their ability to synthesize cholesterol and require cumulus cells to provide them with products of the sterol biosynthetic pathway. Oocyte-derived BMP15 and GDF9 may promote this metabolic pathway in cumulus cells as compensation for their own deficiencies. **Keywords:** Gdf9, Bmp15, cumulus cells, transcriptome, metabolism, sterol biosynthesis, genotype comparison, microarray, ingenuity pathways analyses. **Overall design:** GC_430_2_GES05_0169_033105_1.CEL

Background corr dist: KL-Divergence = 0.0629, L1-Distance = 0.0203, L2-Distance = 0.0005, Normal std = 0.5154

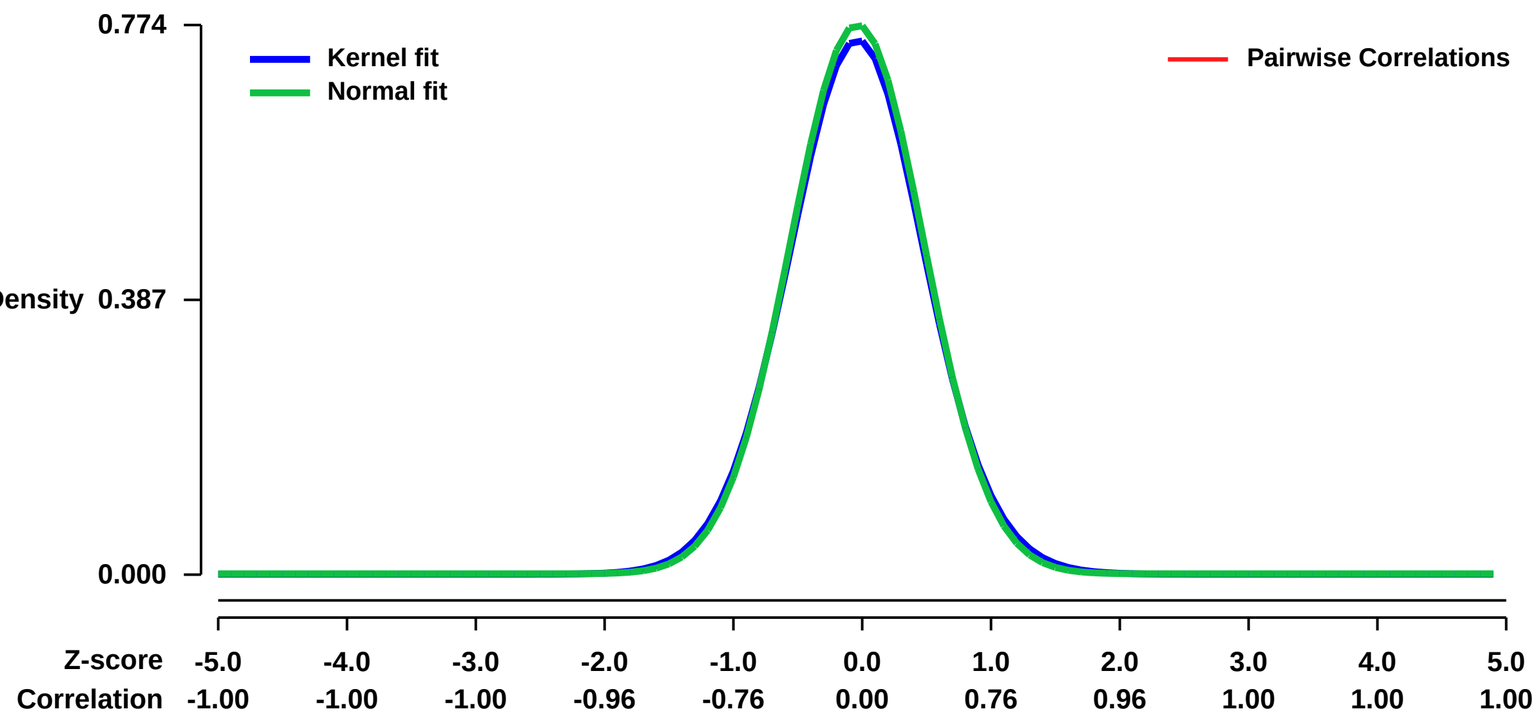

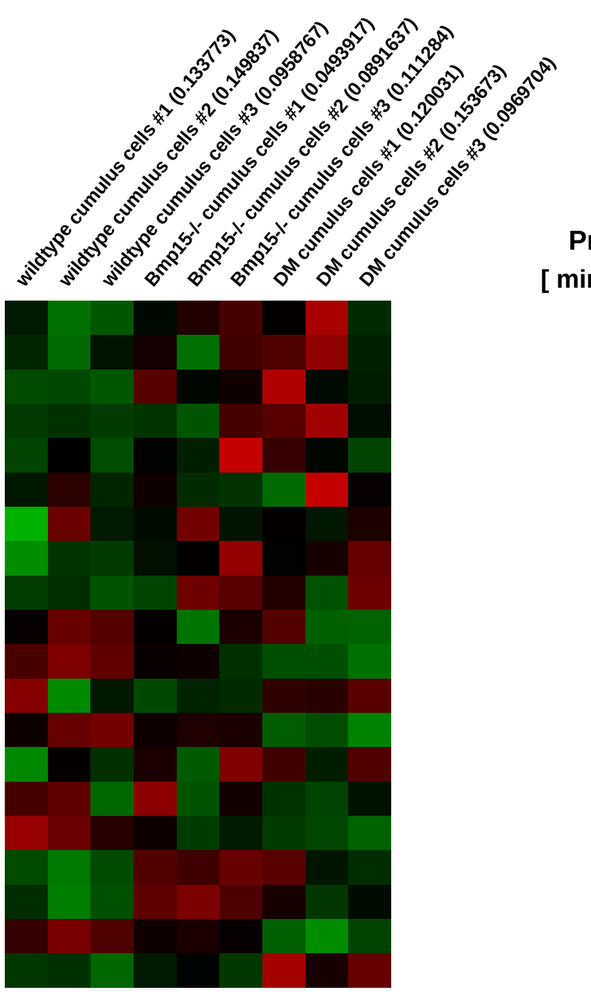

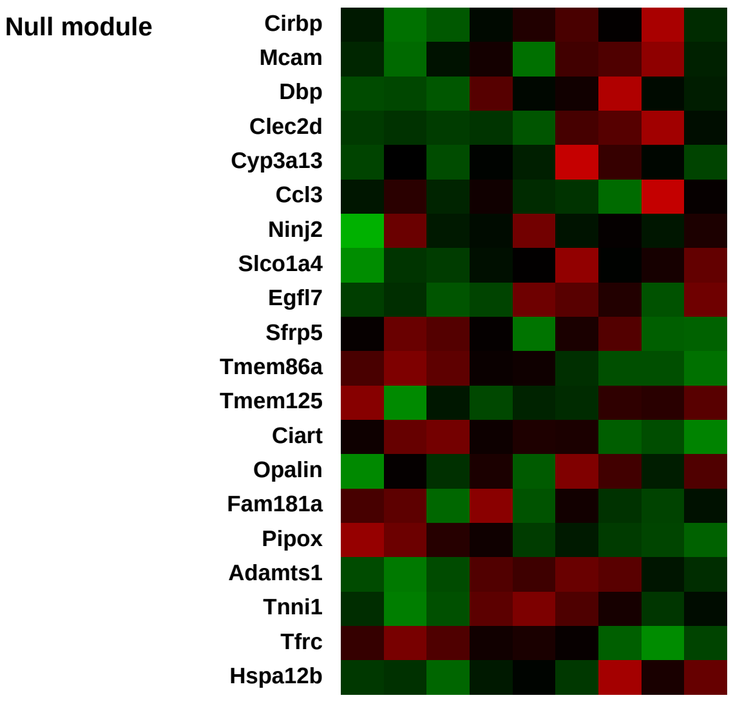

GEO Series "GSE27713" Expression Profiles

Num of samples in this series: 7

Scale of expression profile Z-scores

-3.0 -2.0 -1.0 0.0 1.0 2.0 3.0

GEO Link:	http://www.ncbi.nlm.nih.gov/geo/query/acc.cgi?acc=GSE27713
Status:	Public on Aug 07 2012
Title:	Genome-wide analysis of gene expression patterns in mir-122 knockout mice livers
Organism:	Mus musculus
Experiment type:	Expression profiling by array
Platform:	GPL1261
Pubmed ID:	22820290
Summary & Design:	**Summary:** To invesigate the physiology roles of mir-122 in liver, we performed expression profiling of mir-122 knockout mice and the control B6/129 mice. **Overall design:** Total RNA was extracted from four mir-122 knockout mice and three control mice of 2 months of age. Gene expression was quantified by robust multi-array analysis (RMA) using the Genomic Suite software from Partek.

Background corr dist: KL-Divergence = 0.0468, L1-Distance = 0.0155, L2-Distance = 0.0003, Normal std = 0.5728

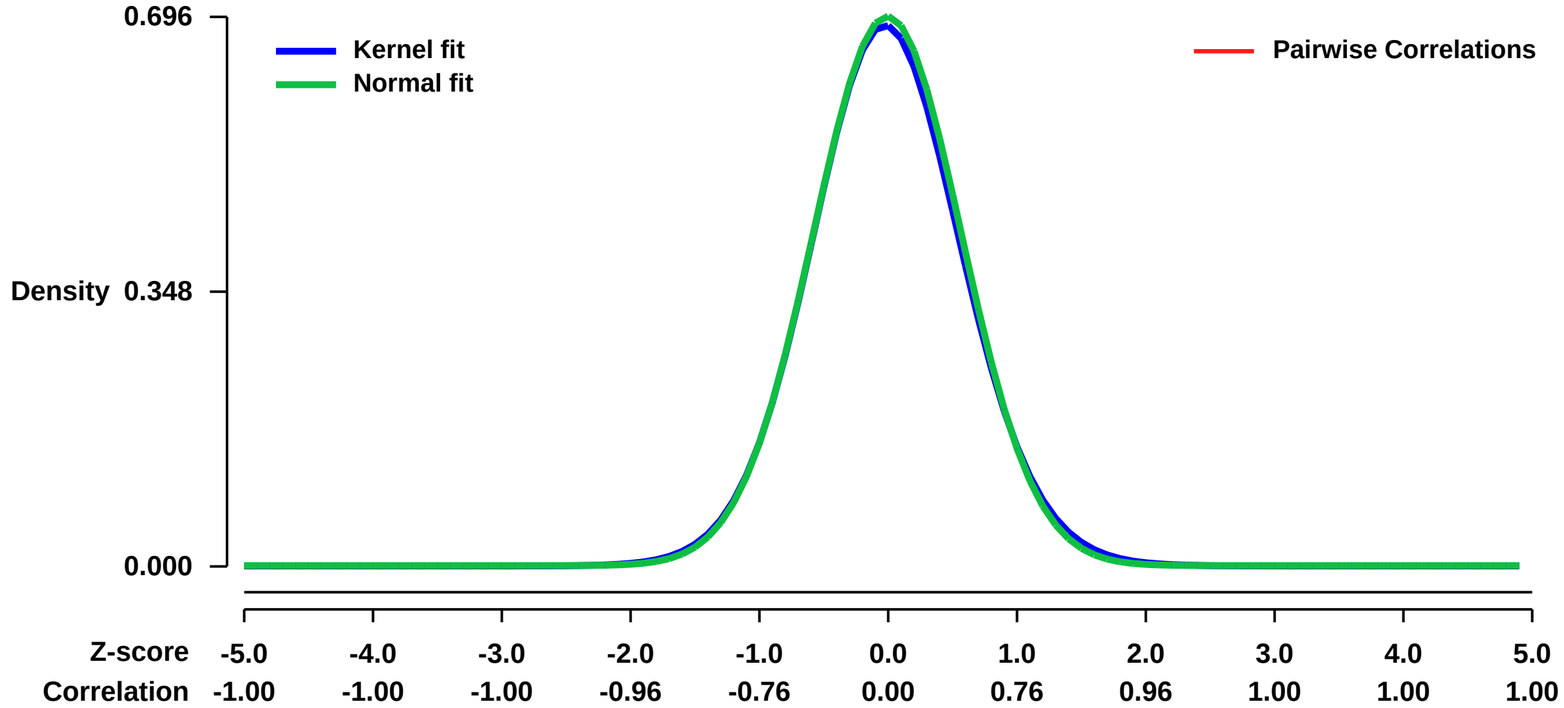

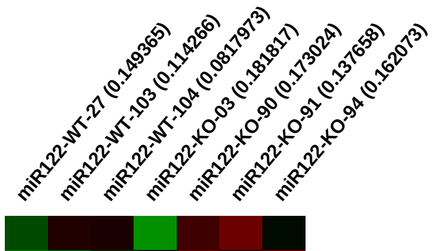

Pre-normalization Quantiles

[min] [medium] [max]

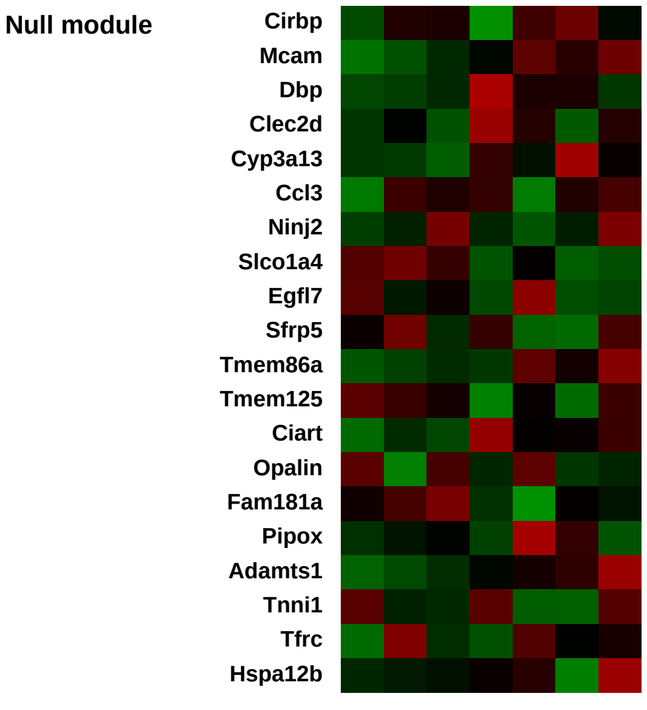

GEO Series "GSE9630" Expression Profiles

Num of samples in this series: 59

Scale of expression profile Z-scores

-3.0 -2.0 -1.0 0.0 1.0 2.0 3.0

GEO Link:	http://www.ncbi.nlm.nih.gov/geo/query/acc.cgi?acc=GSE9630
Status:	Public on Nov 17 2007
Title:	Expression data from mouse liver
Organism:	Mus musculus
Experiment type:	Expression profiling by array
Platform:	GPL1261
Pubmed ID:	18396267
Summary & Design:	**Summary:** Exposure to high levels of arsenic in drinking water is associated with several types of cancers including lung, bladder and skin, as well as vascular disease and diabetes. Drinking water standards are based primarily on epidemiology and extrapolation from higher dose experiments, rather than measurements of phenotypic changes associated with chronic exposure to levels of arsenic similar to the current standard of 10ppb, and little is known about the difference between arsenic in food as opposed to arsenic in water. Measurement of phenotypic changes at low doses may be confounded by the effect of laboratory diet, in part because of trace amounts of arsenic in standard laboratory chows, but also because of broad metabolic changes in response to the chow itself. Finally, this series contrasts 8hr, 1mg/kg injected arsenic with the various chronic exposures, and also contrasts the acute effects of arsenic, dexamethasone or their combination. Male C57BL/6 mice were fed on two commercially available laboratory diets (LRD-5001 and AIN-76A) were chronically exposed, through drinking water or food, to environmentally relevant concentrations of sodium arsenite, or acutely exposed to dexamethasone. **Keywords:** dose response **Overall design:** Another group animals, fed on the AIN 76A diet, was IP injected with dexamethasone (1 mg/kg), sodium arsenite (1mg/kg), both dexamethosone and arsenite, or saline alone.

Background corr dist: KL-Divergence = 0.2465, L1-Distance = 0.0752, L2-Distance = 0.0169, Normal std = 0.3041

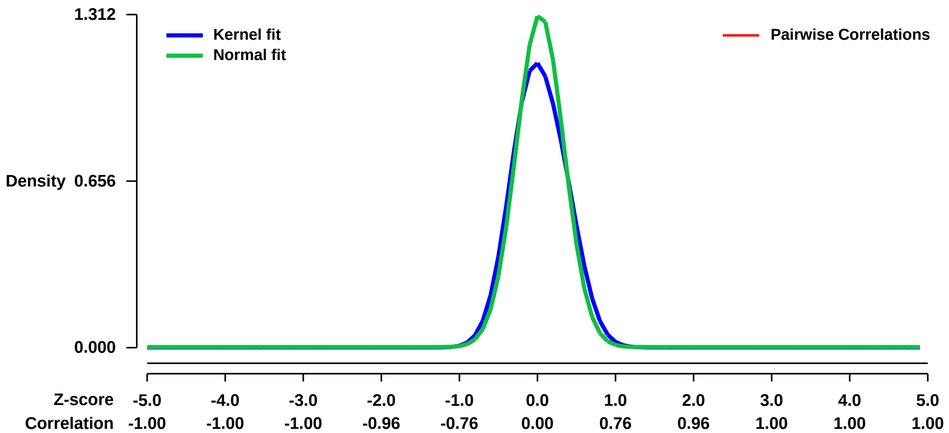

Z-score	-5.0	-4.0	-3.0	-2.0	-1.0	0.0	1.0	2.0	3.0	4.0	5.0
Correlation	-1.00	-1.00	-1.00	-0.96	-0.76	0.00	0.76	0.96	1.00	1.00	1.00

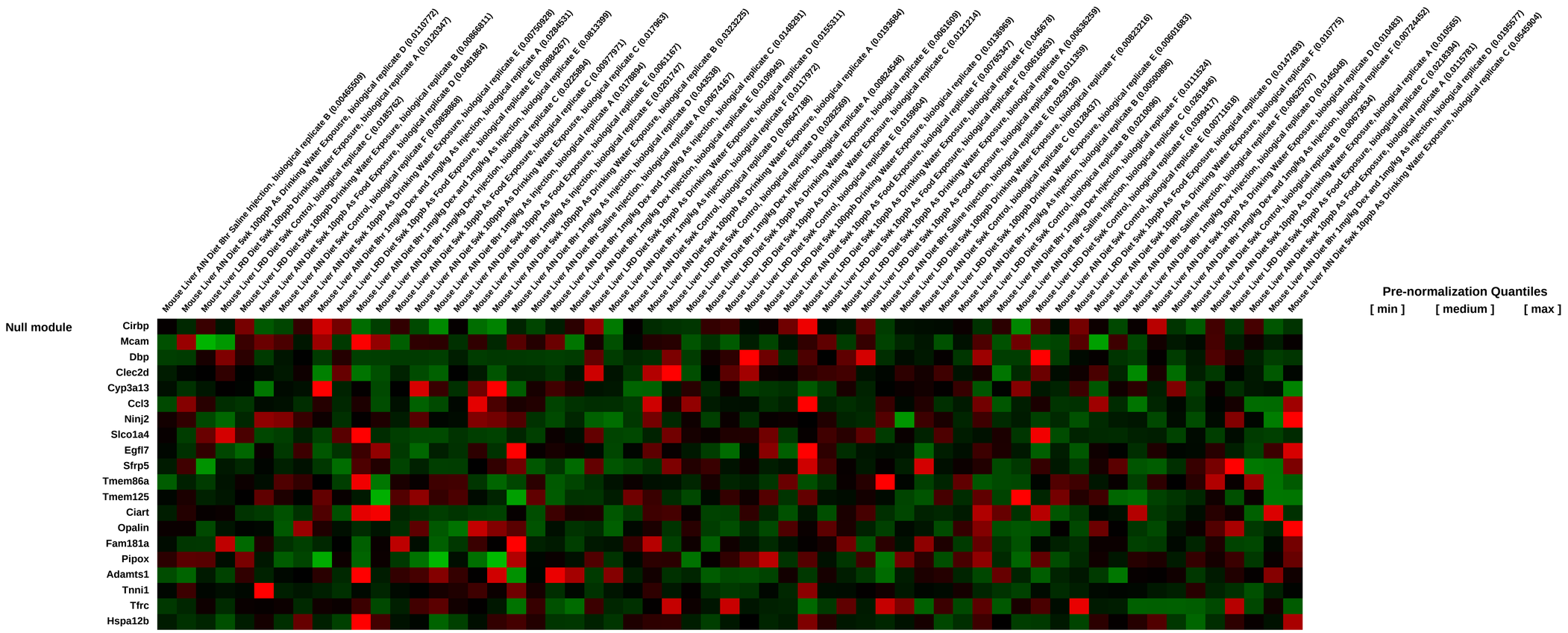

GEO Series "GSE18396" Expression Profiles

Num of samples in this series: 6

Scale of expression profile Z-scores

-3.0 -2.0 -1.0 0.0 1.0 2.0 3.0

GEO Link:	http://www.ncbi.nlm.nih.gov/geo/query/acc.cgi?acc=GSE18396
Status:	Public on Jun 30 2010
Title:	Dmrt1 (doublesex and mab-3 related transcription factor 1) knockout expression analyses in E13.5 testes in S6 background
Organism:	Mus musculus
Experiment type:	Expression profiling by array
Platform:	GPL1261
Pubmed ID:	20007774
Summary & Design:	**Summary:** Dmrt1 (doublesex and mab-3 related transcription factor 1) is a conserved transcriptional regulator of male differentiation required for testicular development in vertebrates. In mice of the 129Sv strain, loss of Dmrt1 causes a high incidence of teratomas. Mutant 129Sv germ cells undergo apparently normal differentiation up to embryonic day 13.5 (E13.5), but some cells fail to arrest mitosis and ectopically express pluripotency markers. Expression analysis and chromatin immunoprecipitation identified DMRT1 target genes whose misexpression may underly teratoma formation. **Overall design:** Comparison of E13.5 testes gene expression between Dmrt1(+/-) and Dmrt1(-,-) animals that show high incidence of teratoma formation.

Background corr dist: KL-Divergence = 0.0394, L1-Distance = 0.0172, L2-Distance = 0.0003, Normal std = 0.6150

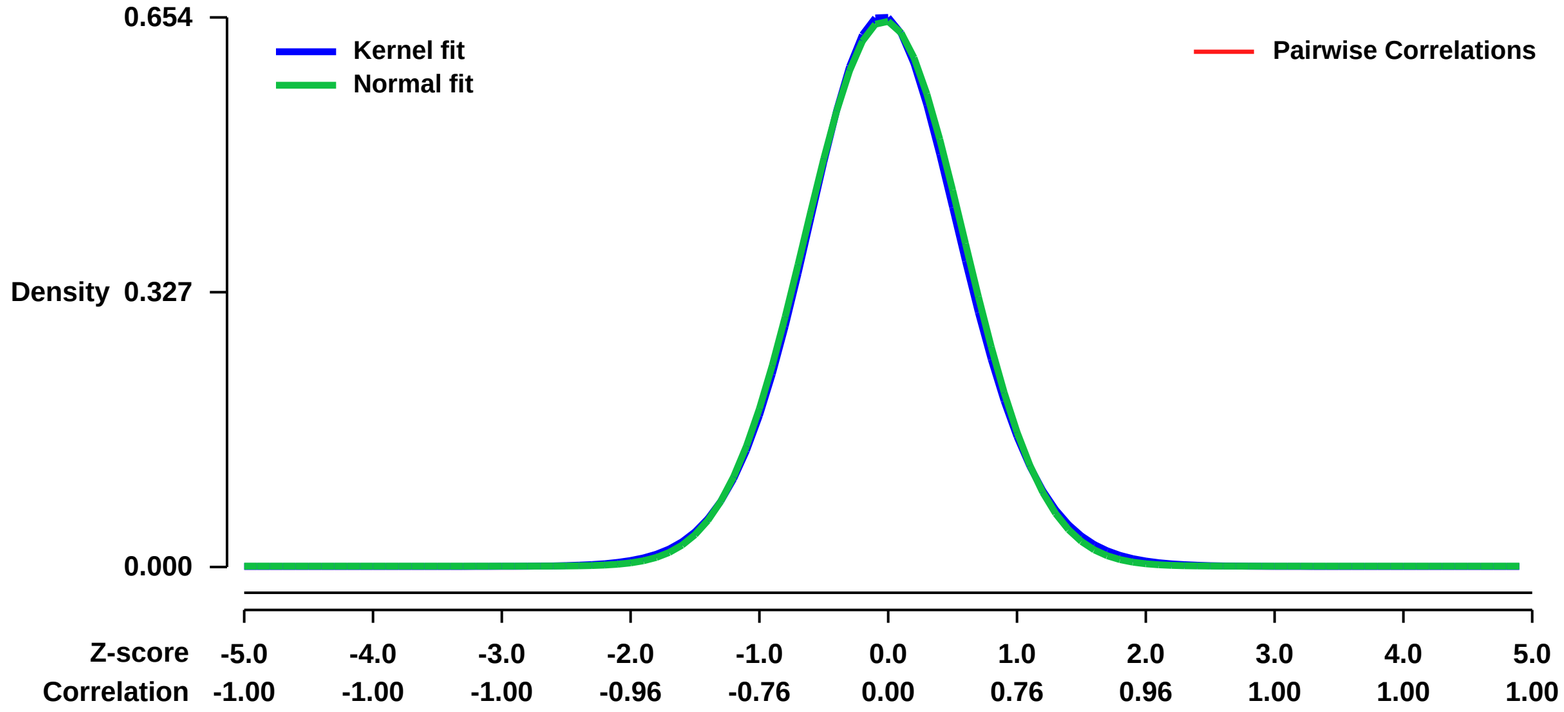

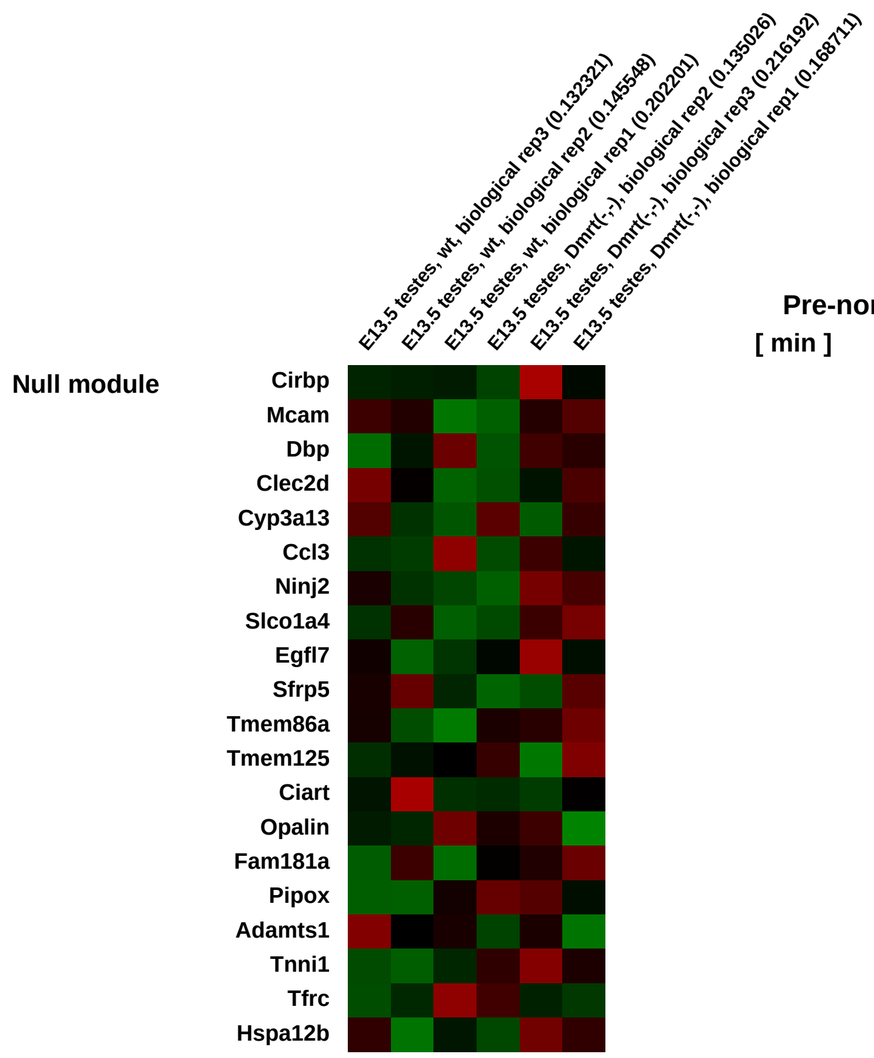

GEO Series "GSE32937" Expression Profiles

Num of samples in this series: 8

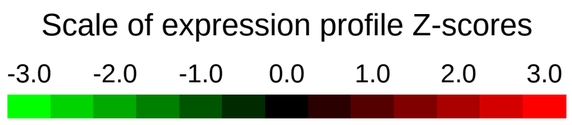

GEO Link:	**http://www.ncbi.nlm.nih.gov/geo/query/acc.cgi?acc=GSE32937**
Status:	**Public on Oct 13 2011**
Title:	**MicroRNA-29 in Aortic Dilation: Implications for Aneurysm Formation**
Organism:	**Mus musculus**
Experiment type:	**Non-coding RNA profiling by array**
Platform:	**GPL1261**
Pubmed ID:	**21903938**
Summary & Design:	**Summary:** **We compared the aorta of 6-weeks-old mice (young) with 18-months-old mice (old). Using the publicly available tools Sylamer and DIANA-mirExTra, we identified an enrichment for miR-29 binding sites in the 3'UTR of genes downregulated in the aged aortas. We subsequently showed that inhibition of miR-29 in aged mice prevented dilation of the aorta.** **Overall design:** **aortas of 6 week old and 18 month old mice**

Background corr dist: **KL-Divergence = 0.0766, L1-Distance = 0.0196, L2-Distance = 0.0005, Normal std = 0.4847**

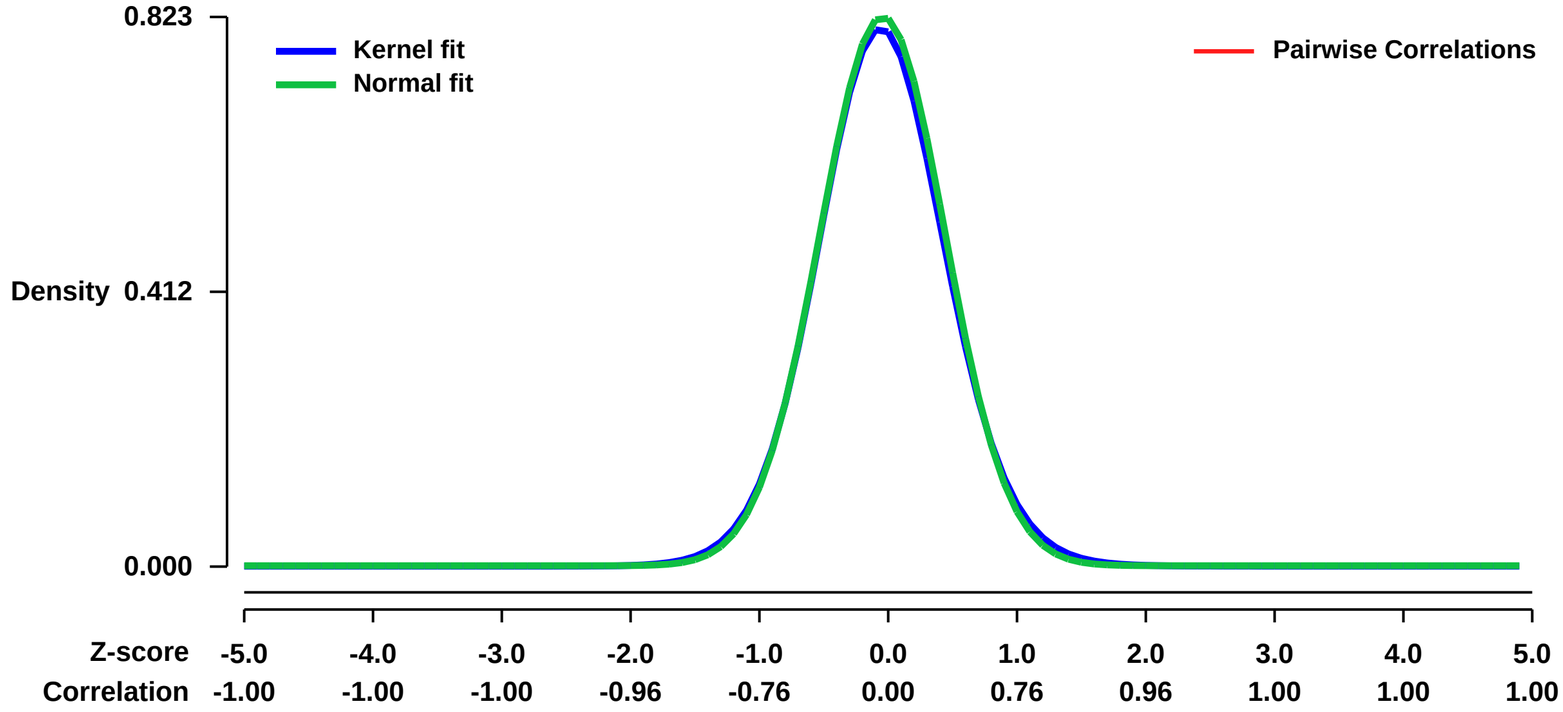

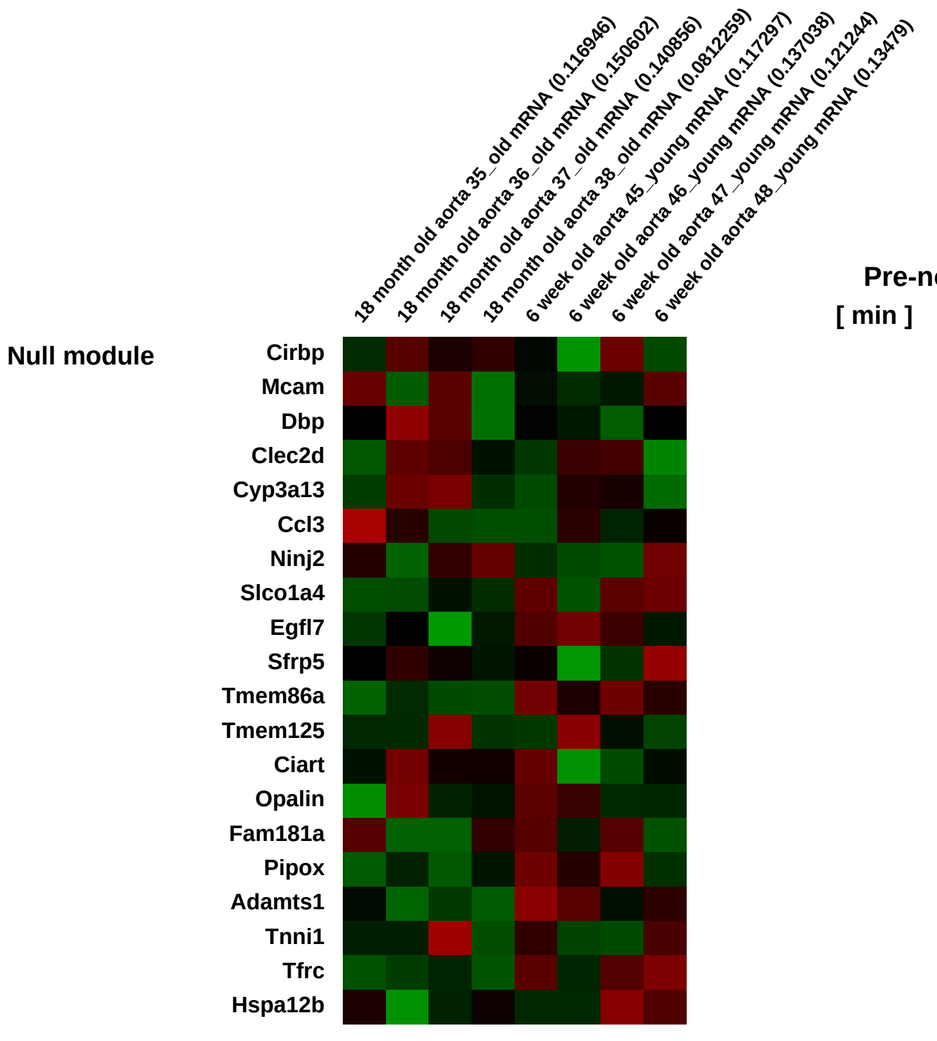

GEO Series "GSE23496" Expression Profiles

Num of samples in this series: 9

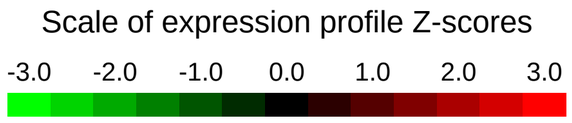

GEO Link:	http://www.ncbi.nlm.nih.gov/geo/query/acc.cgi?acc=GSE23496
Status:	Public on Dec 31 2011
Title:	Expression data from osteocytes in virgin,lactating and post lactation mice
Organism:	Mus musculus
Experiment type:	Expression profiling by array
Platform:	GPL1261
Pubmed ID:	22308018
Summary & Design:	**Summary:** We have previously shown that during lactation, osteocytes directly remodel their perilacunar and pericanalicular matrix, thereby mobilizing calcium and contributing to maternal bone loss. To identify genes potentially responsible for perilacunar remodeling, microarray analysis was performed on osteocytes from CD-1 virgin and lactating mice and mice sacrificed on day 7 post weaning. By comparing how gene expression changes in osteocytes among virgin, lactation and post lactation, the goal is to identify the genes osteocytes use to remodel their perilacunar matrix **Overall design:** To identify genes responsible for perilacunar remodeling, microarray analysis was performed on tibiae from CD-1 virgin and lactating mice and mice sacrificed on day 7 post weaning. Periosteum and bone marrow were removed from the tibiae and the bone fragments underwent sequential collagenase/trypsin digestion and were examined histologically to ensure removal of all surface cells and confirm osteocyte enrichment prior to RNA extraction. Microarray Affy M430 arrays, n=3 per group were performed and Genepattern and Bioconductor were used to analyse the microdata.

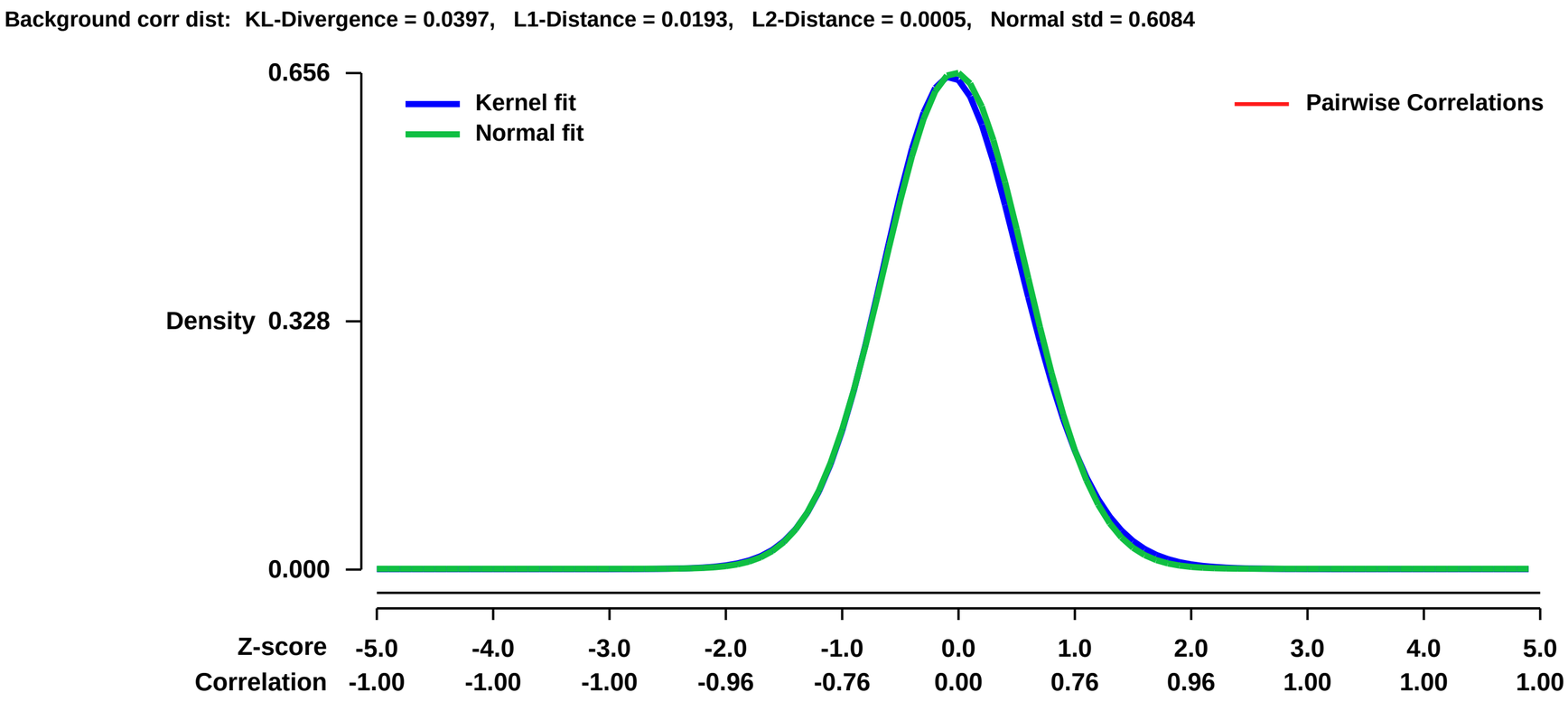

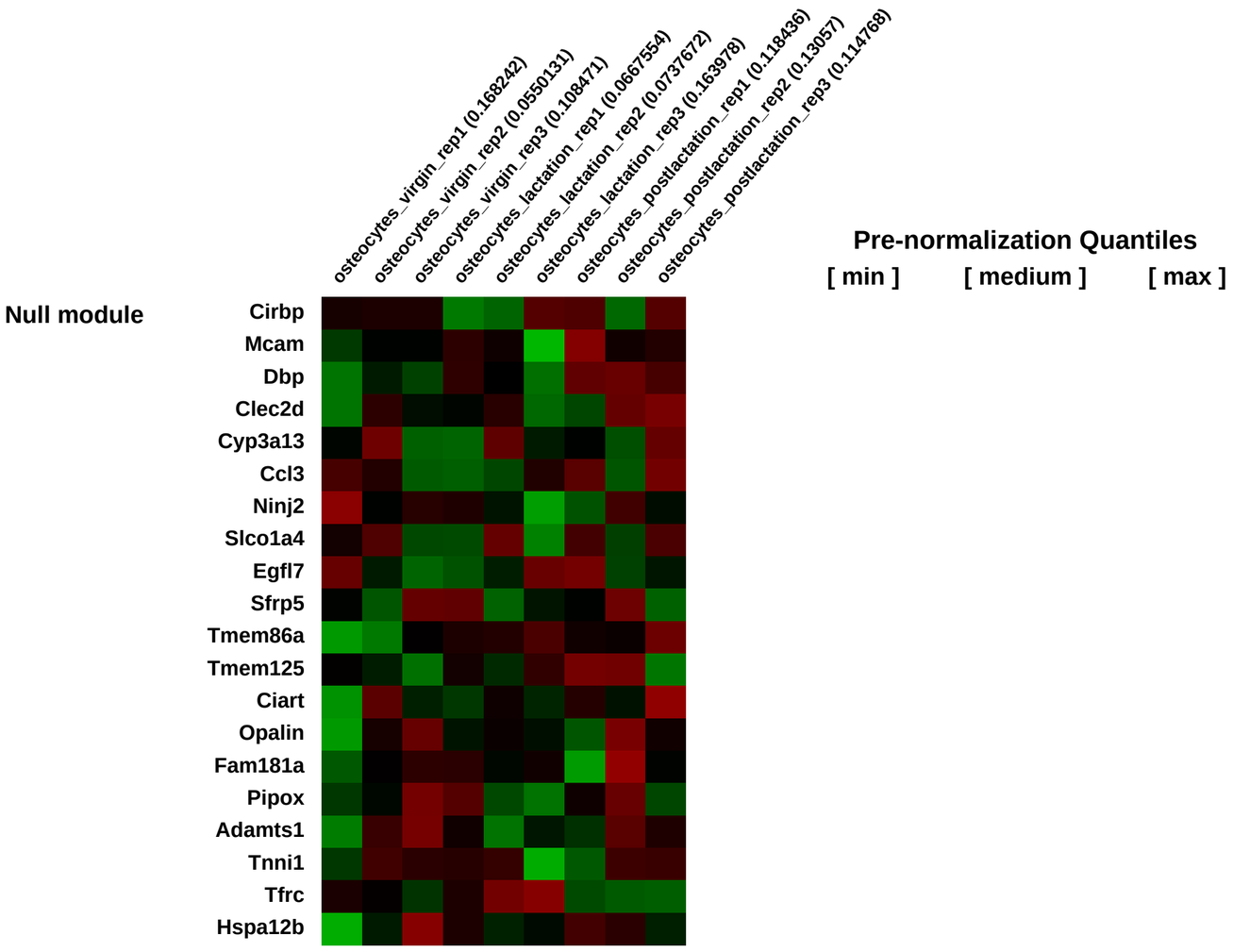

GEO Series "GSE29097" Expression Profiles

Num of samples in this series: 18

Scale of expression profile Z-scores

-3.0 -2.0 -1.0 0.0 1.0 2.0 3.0

GEO Link:	**http://www.ncbi.nlm.nih.gov/geo/query/acc.cgi?acc=GSE29097**
Status:	**Public on May 06 2011**
Title:	**Gene expression between high and low altitude Mus musculus domesticus**
Organism:	**Mus musculus domesticus**
Experiment type:	**Expression profiling by array**
Platform:	**GPL1261**
Pubmed ID:	
Summary & Design:	**Summary:** **Analysis of gene expression profiles is an attractive method for discovering how animals respond to environmental challenges in nature. Compared to low altitudes, high altitudes are characterized by reduced partial pressures of oxygen (hypoxia) and cooler ambient temperatures** **To better understand how mammals cope with high altitudes, we trapped wild house mice (Mus musculus domesticus) from 3 populations in La Paz, Bolivia (3000 - 3600 m) and 3 populations in Lima, Peru (0 â 200 m). Affymetrix GeneChip´fi Mouse Genome 430 2.0 Arrays were use to measure mRNA abundance in the livers of these mice.** **Overall design:** **Eighteen male house mice were trapped from three different locations (3 mice per location)at high alttiude (La Paz, Bolivia, 3600 m) and from three locations at low altiditude (Lima, Peru, 100 m). Total mRNA was extracted from the livers and used for hybridization of Affymetrix GeneChip Mouse expression set 420.**

Background corr dist: **KL-Divergence = 0.1874, L1-Distance = 0.0537, L2-Distance = 0.0069, Normal std = 0.3400**

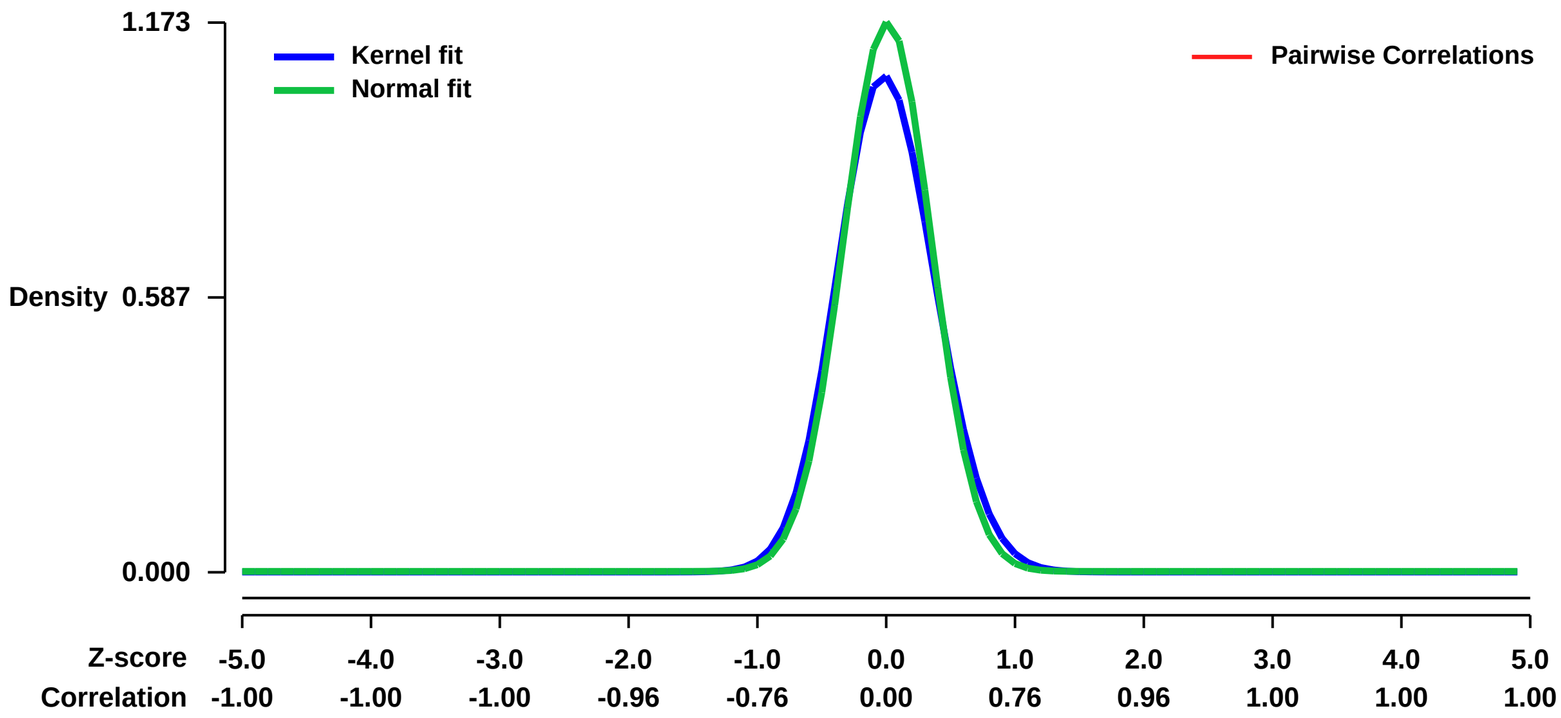

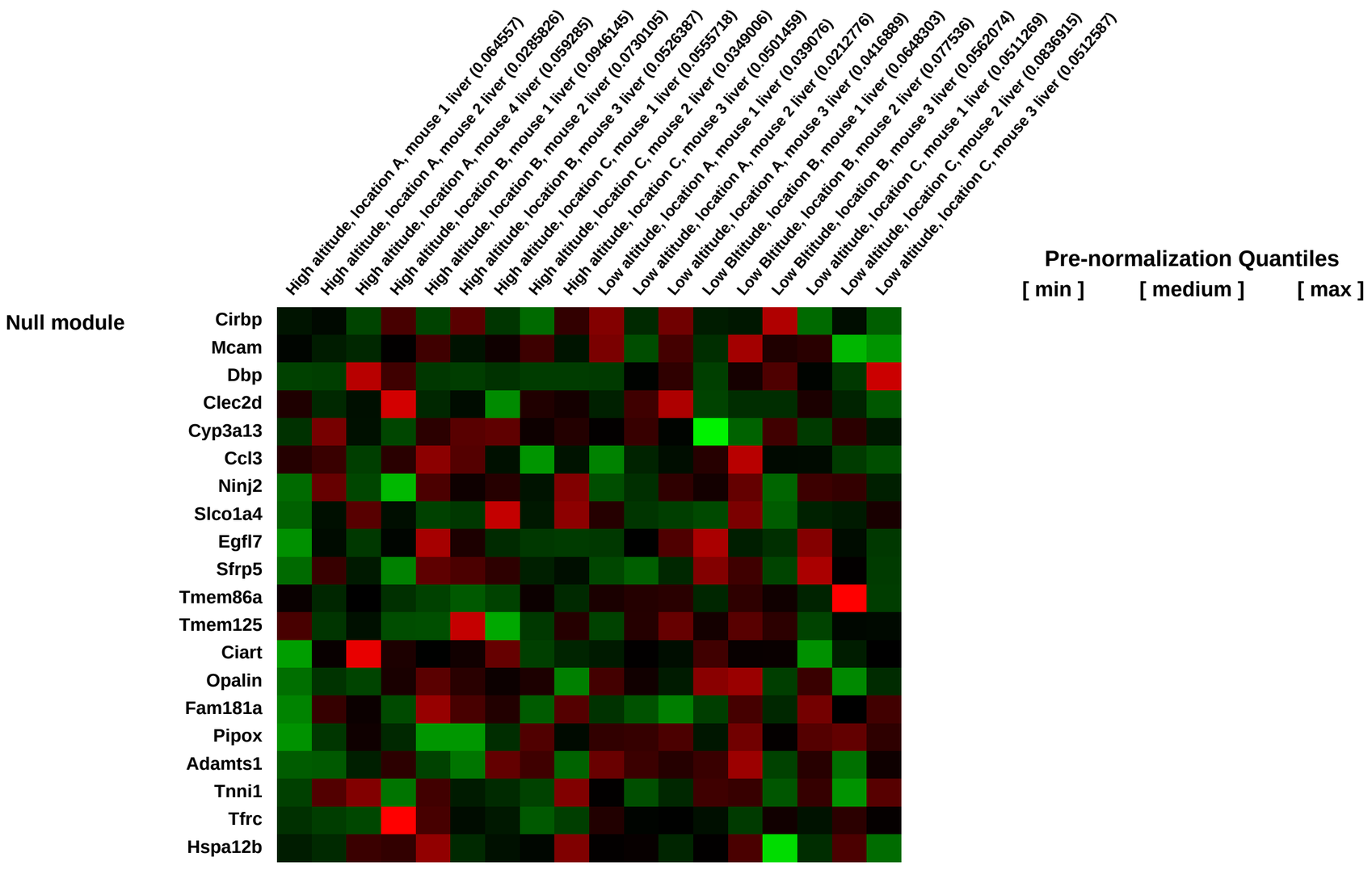

GEO Series "GSE15914" Expression Profiles

Num of samples in this series: 9

Scale of expression profile Z-scores

-3.0 -2.0 -1.0 0.0 1.0 2.0 3.0

GEO Link:	http://www.ncbi.nlm.nih.gov/geo/query/acc.cgi?acc=GSE15914
Status:	Public on Oct 01 2009
Title:	Interleukin-7 promotes monocyte/macrophage arrest on endothelial cells
Organism:	Mus musculus
Experiment type:	Expression profiling by array
Platform:	GPL1261
Pubmed ID:	21804111
Summary & Design:	**Summary:** **Background: It is recognized that atherosclerosis can regresses at least in animal models. However, little is known about the mechanisms. We induced regression of advanced atherosclerosis in apolipoprotein E deficient (APOE´›/´›) mice and studied underlying mechanisms. Unexpectedly, our study led to the role of interleukin-7 (IL-7) in atherogenesis.** **Methods and Results: We treated APOE´›/´› mice fed a high cholesterol diet for 30 weeks to induce advanced lesions with a helper-dependent adenoviral vector expressing human apoE3 (HDAd-gE3), and analyzed the regression of atherosclerosis after 41 weeks. Using microarray analysis, we identified IL-7 as one of most significantly affected genes by lowering cholesterol. To answer why IL-7 is downregulated by reduced cholesterol, we studied effects of IL-7 on endothelial cells (ECs). Our major findings were (1) long-term lowering cholesterol induced regression of advanced atherosclerosis. (2) Microarray analysis identified multiple signaling pathways affected by lowering cholesterol. (3) Correction for multiple testing revealed that IL-7 expression was downregulated, whereas gamma-sarcoglycan and ˆ´–-actin were upregulated. (4) Oxidized LDL upregulated IL-7 expression in macrophages but not in aorta ECs or smooth muscle cells. (5) IL-7 increased the expression of cell adhesion molecules and chemokine in ECs and promoted monocyte adhesion to ECs. (6) Systemic elevation of IL-7 induced inflammatory response and recruited monocyte/macrophage to the lesions without increasing plasma cholesterol.** **Conclusion: Our finding suggest that IL-7 inflames endothelium and triggers the adhesion/recruitment of monocyte/macrophages to the atherosclerotic lesions and thus plays a direct role in development of atherosclerosis.** **Key Words: arteriosclerosis, gene therapy, hypercholesterolemia, interleukins, cell adhesion molecules** **Overall design:** **12039: E3: vector control**

Background corr dist: KL-Divergence = 0.0908, L1-Distance = 0.0240, L2-Distance = 0.0008, Normal std = 0.4532

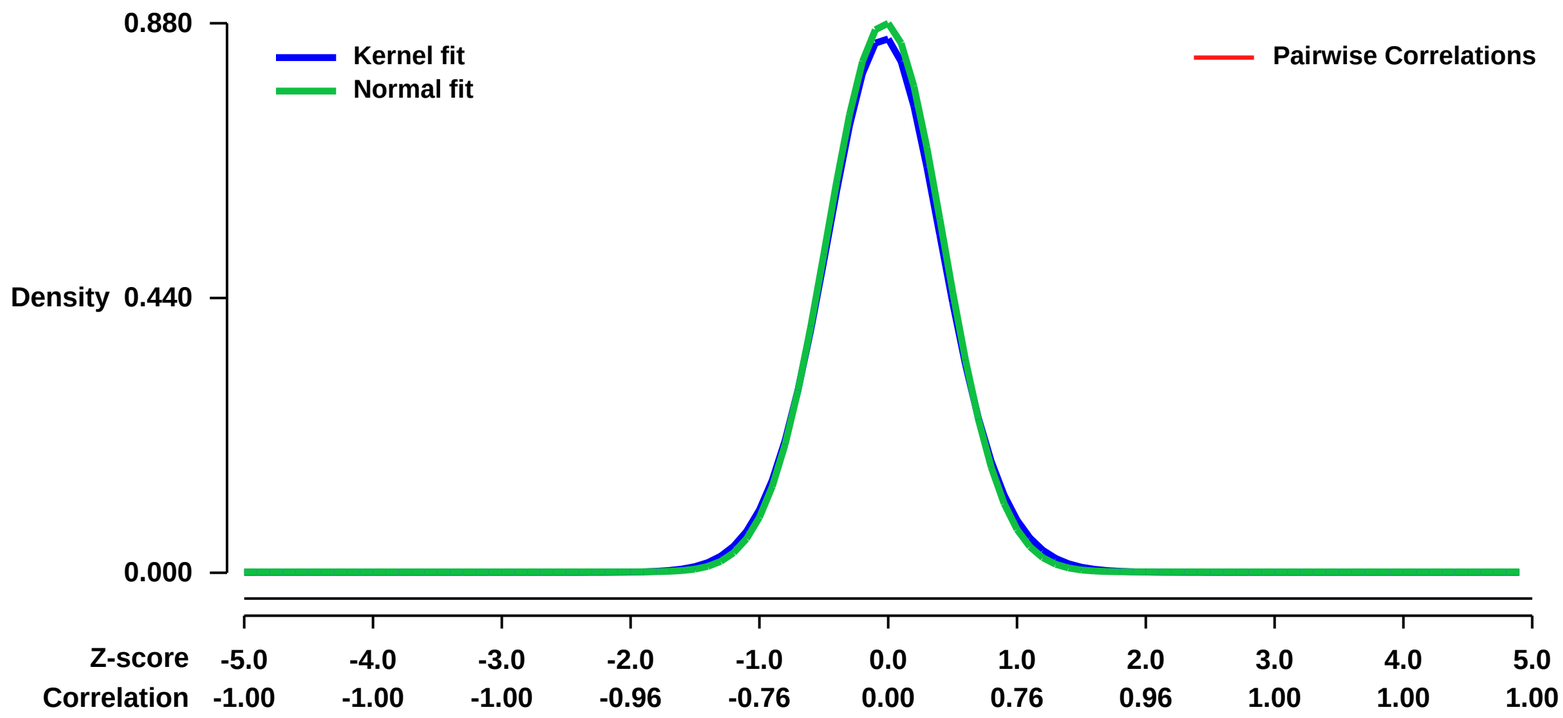

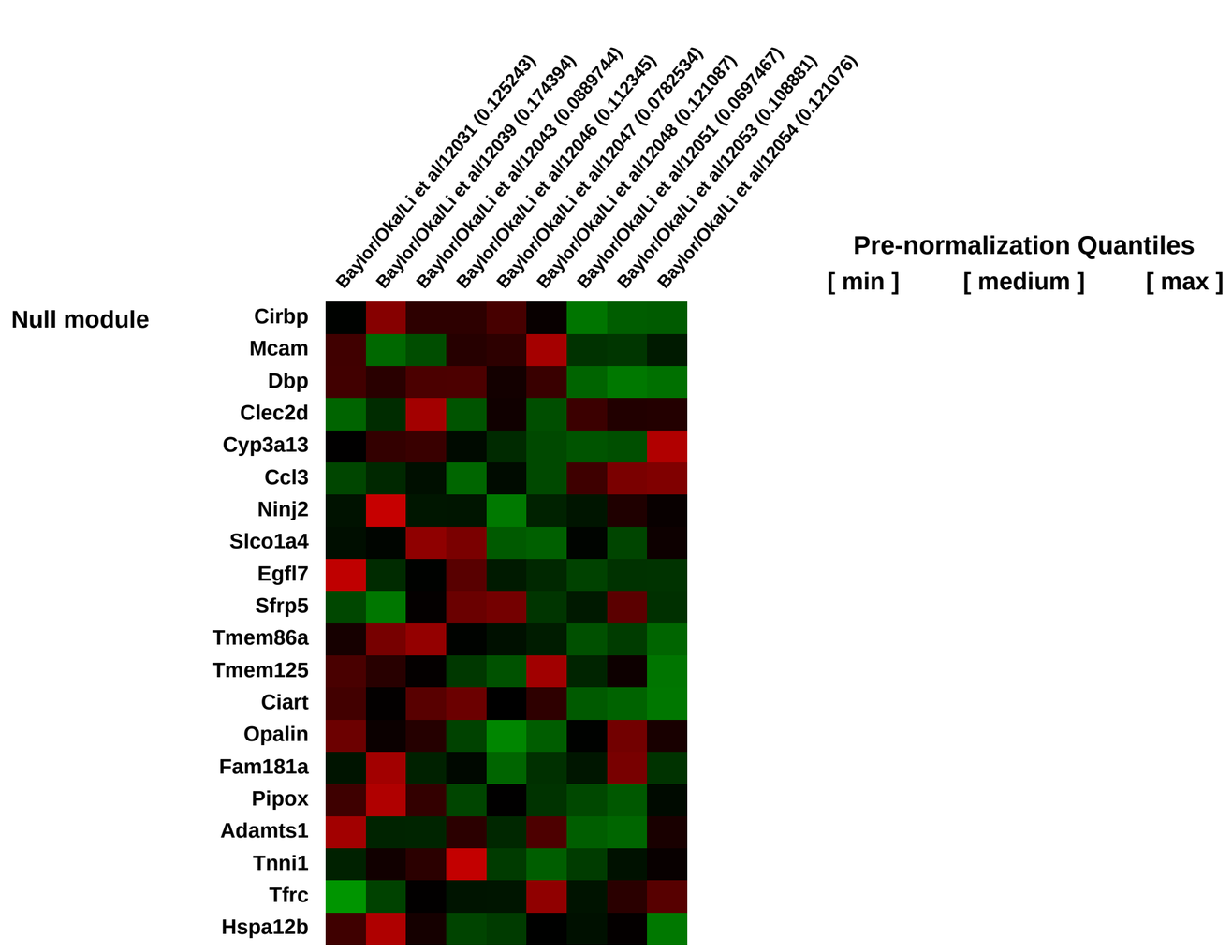

GEO Series "GSE40087" Expression Profiles

Num of samples in this series: 15

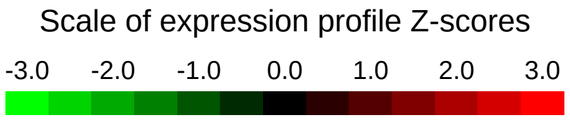

GEO Link:	**http://www.ncbi.nlm.nih.gov/geo/query/acc.cgi?acc=GSE40087**
Status:	**Public on Nov 13 2012**
Title:	**Expression data from Middle Ear Mucosal Metaplasia in Mice**
Organism:	**Mus musculus**
Experiment type:	**Expression profiling by array**
Platform:	**GPL1261**
Pubmed ID:	
Summary & Design:	**Summary:** **Chronic Otitis Media (OM) develops after sustained inflammation and is characterized by secretory middle ear epithelial metaplasia and effusion, most frequently mucoid. Non-typeable Haemophilus influenzae (NTHi), the most common acute OM pathogen, is known to activate inflammation and mucin expression in vitro and in animal models of OM. The goals of this study were to: examine expression profiling epithelial effects of NTHi challenge in murine middle ears.** **We used microarrays to detail examine the global programme of gene expression underlying epithelial effects of NTHi challenge in murine middle ears during this study.** **Overall design:** **Weekly transtympanic inoculation of Balb/c mice with 300 ´µg/ml of NTHi lysates vs saline was performed. Bacteria were grown on chocolate agar at 37´”C in 5% CO2 overnight and inoculated in brain heart infusion (BHI) broth supplemented with 3.5 mg of nicotinamide adenine dinucleotide per ml. After overnight incubation, bacteria were subcultured into 5 ml of fresh brain heart infusion (BHI) and upon reaching log phase growth, NTHi were washed and suspended in phosphate-buffered saline (PBS) followed by sonication for lysis. Three transtympanic inoculation of 6 Balb/c mice middle ears (3 animals, 6 ears) with 50 uL of 300 ug/ml of NTHi bacterial lysate and 6 Balb/c mice middle ears (3 animals, 6 ears) with 50 uL of 1X phosphate buffered saline (PBS) were carried out weekly over 4 weeks (injection on days 7, 14, and 21). On day 28, the mice were euthanized and their bullae harvested. Expression microarray analysis was performed at 1 and 7 days. Microarray findings were validated in independent animal samples and in a cultured murine middle ear epithelial cell (mMEEC) line.**

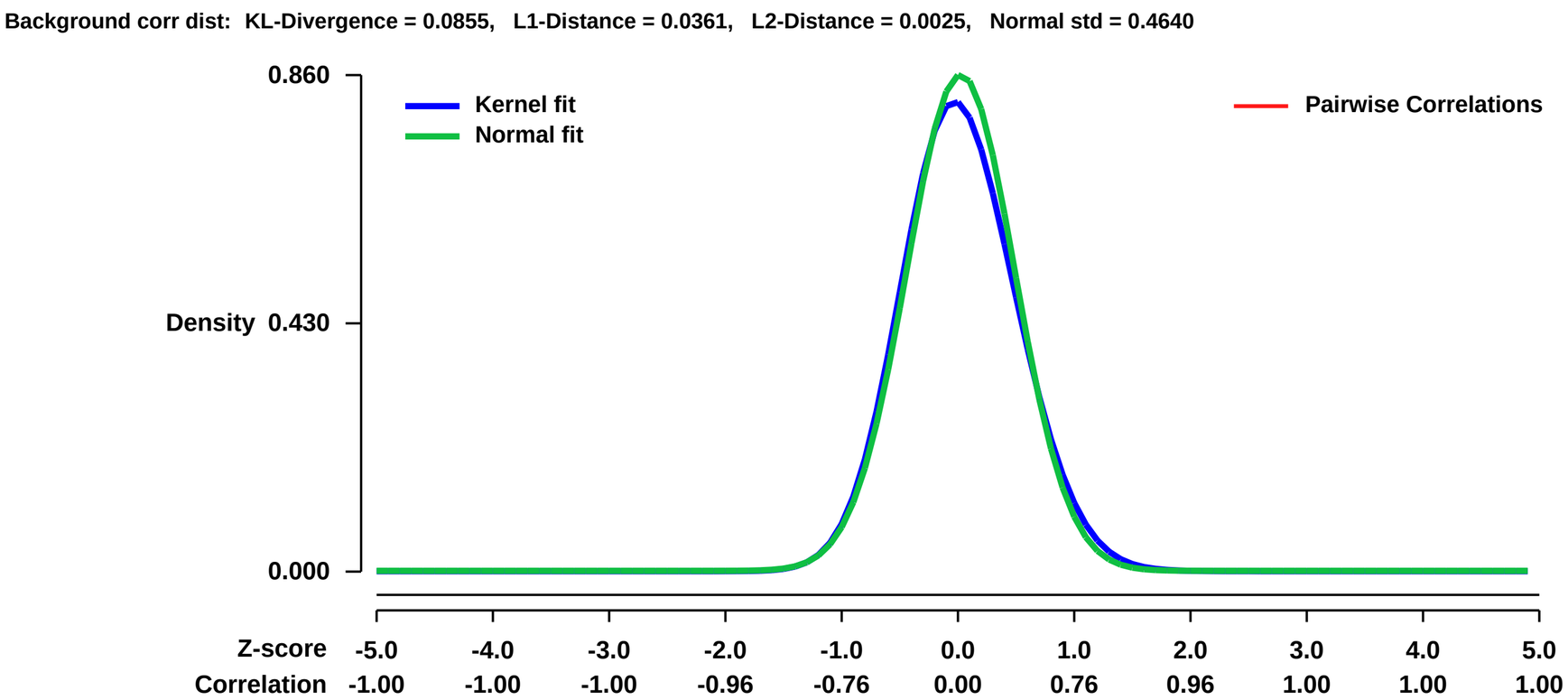

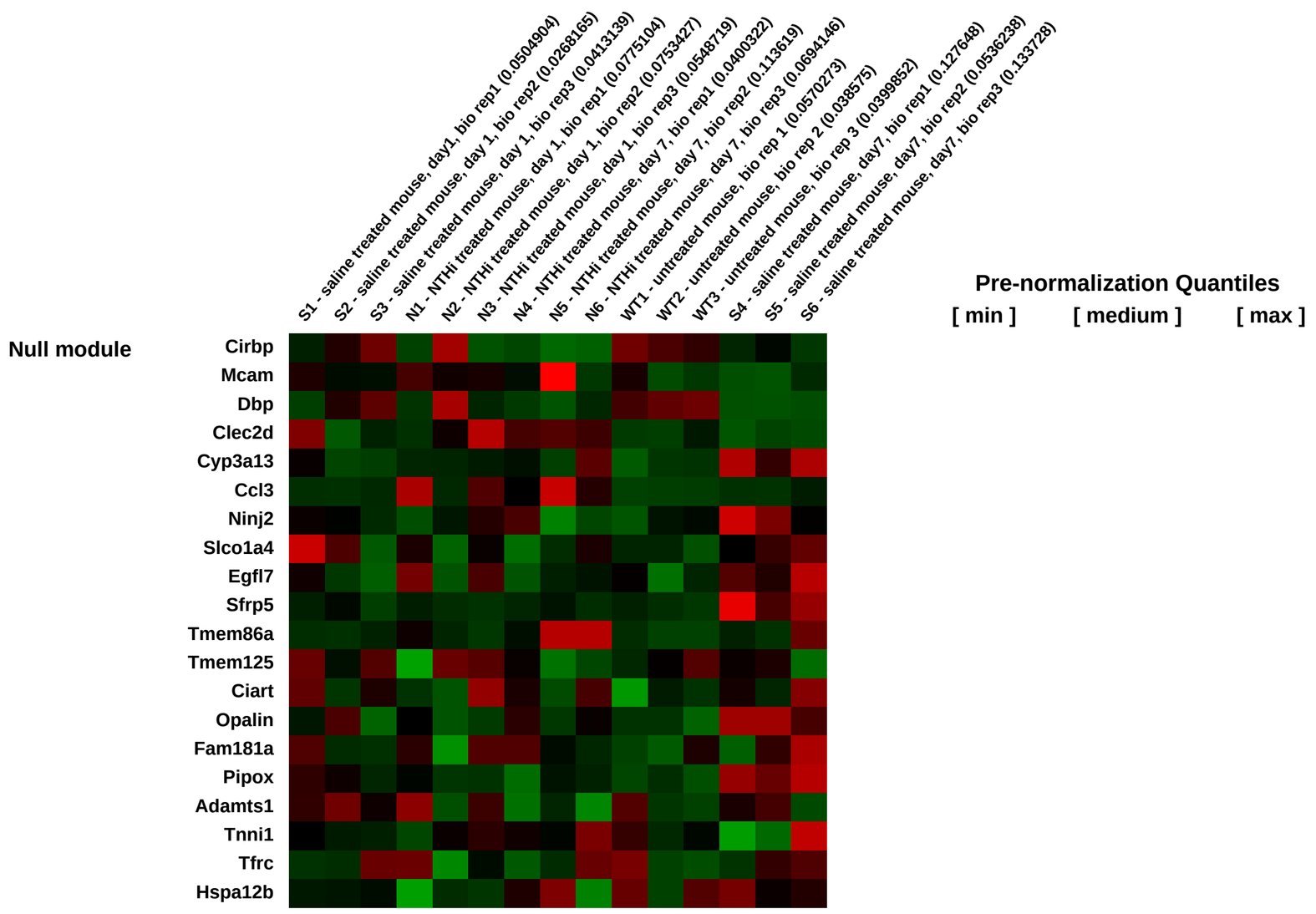

GEO Series "GSE35247" Expression Profiles

Num of samples in this series: 15

Scale of expression profile Z-scores

-3.0 -2.0 -1.0 0.0 1.0 2.0 3.0

GEO Link:	http://www.ncbi.nlm.nih.gov/geo/query/acc.cgi?acc=GSE35247
Status:	Public on Jan 21 2012
Title:	Genome unstable murine prostate cancers acquire genomic aberrations and bone metastatic features of the human disease
Organism:	Mus musculus
Experiment type:	Genome variation profiling by genome tiling array
Platform:	GPL1261
Pubmed ID:	22341455
Summary & Design:	**Summary:** Gene copy numbers of prostate tumors of G3 and G4 generations of LSL-mTert PB-Pten/p53 mouse model **Overall design:** Prostate tumors were developed in G3 and G4 generations of LSL-mTert PB-Pten/p53 mice. These tumors were profiled with affy and aCGH. We used affy gene expression to correlate with the copy number alterations in the mouse prostate tumors.

Background corr dist: KL-Divergence = 0.2052, L1-Distance = 0.0483, L2-Distance = 0.0055, Normal std = 0.3318

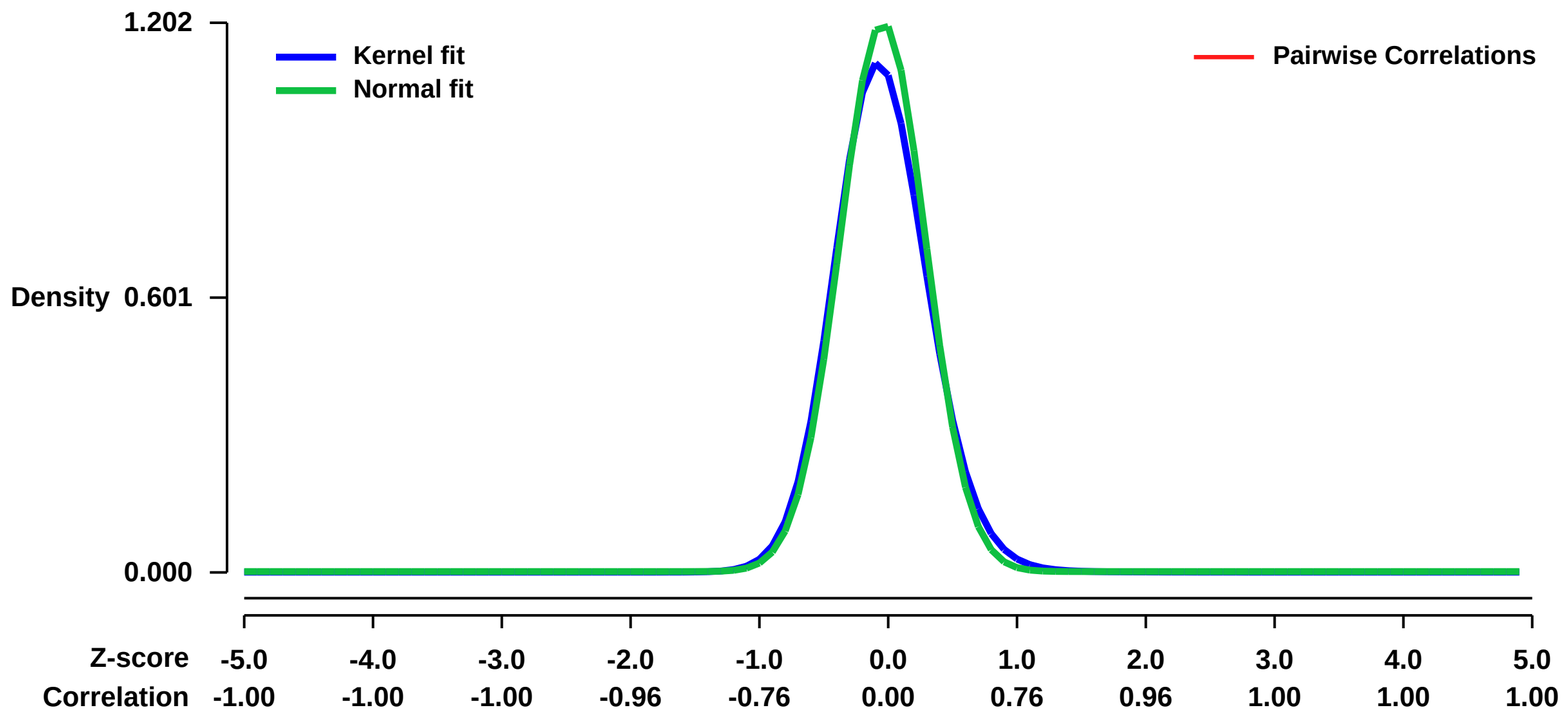

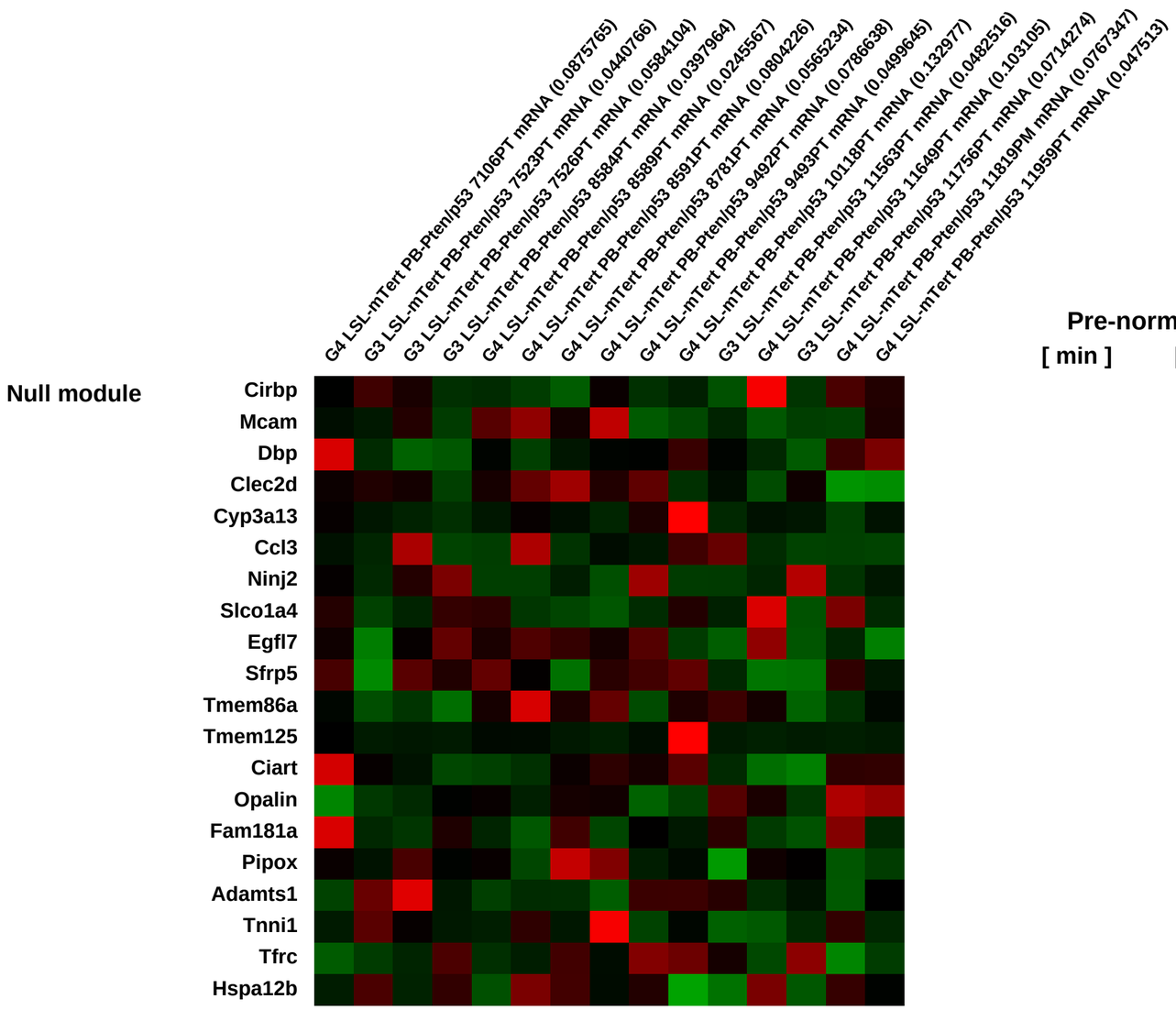

GEO Series "GSE15401" Expression Profiles

Num of samples in this series: 18

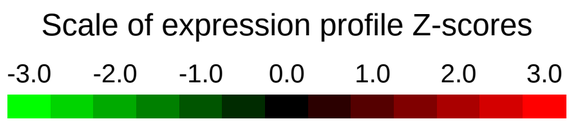

GEO Link:	http://www.ncbi.nlm.nih.gov/geo/query/acc.cgi?acc=GSE15401
Status:	Public on Aug 09 2010
Title:	Expression data from mouse aorta during and following transient hyperglycaemia
Organism:	Mus musculus
Experiment type:	Expression profiling by array
Platform:	GPL1261
Pubmed ID:	20844862
Summary & Design:	**Summary:** Immediate and early effects of transient hyperglycaemia were examined using fully- reversible transgenic diabetic mice. Transient hyperglycaemia altered expression of 769 arterial genes, of which 200 did not reverse following recovery from hyperglycaemia. Many such genes are known to promote atherogenesis, including several implicated in arterial calcification and inflammation. This supports the view that hyperglycaemia causes not only very early deleterious changes in arterial gene expression but that to a large extent these persist for some time after restoration of normal blood glucose levels in vivo. Together, results support the contention that avoiding excess CVD risk in diabetes requires very early correction of hyperglycaemia. **Overall design:** As shown previously (Pelengaris et al., 2002 Cell), c-MycERTAM protein is activated in pancreatic beta cells of adult transgenic mice, by daily intraperitoneal (IP) administration of tamoxifen (TAM; Sigma-Aldrich, Dorset, UK) (1 mg/0.2 ml in peanut oil). Inactivation of c-MycERTAM protein was achieved through withdrawal of TAM. Adult female mice, 3-6 months of age, inbred into CBA-C57Bl/6 background and maintained under barrier conditions, were treated with TAM for up to 7 days (Myc â ONâ) and then monitored during recovery for more than 4 months (140 days) (Myc â OFFâ). Experimental timepoints were: Days 2, 4 and 7: c-Myc â ONâ ; days 0, 11, 26: c-Myc â OFFâ . Biological replicates: each timepoint included 3 biological replicates (n=3 mice).

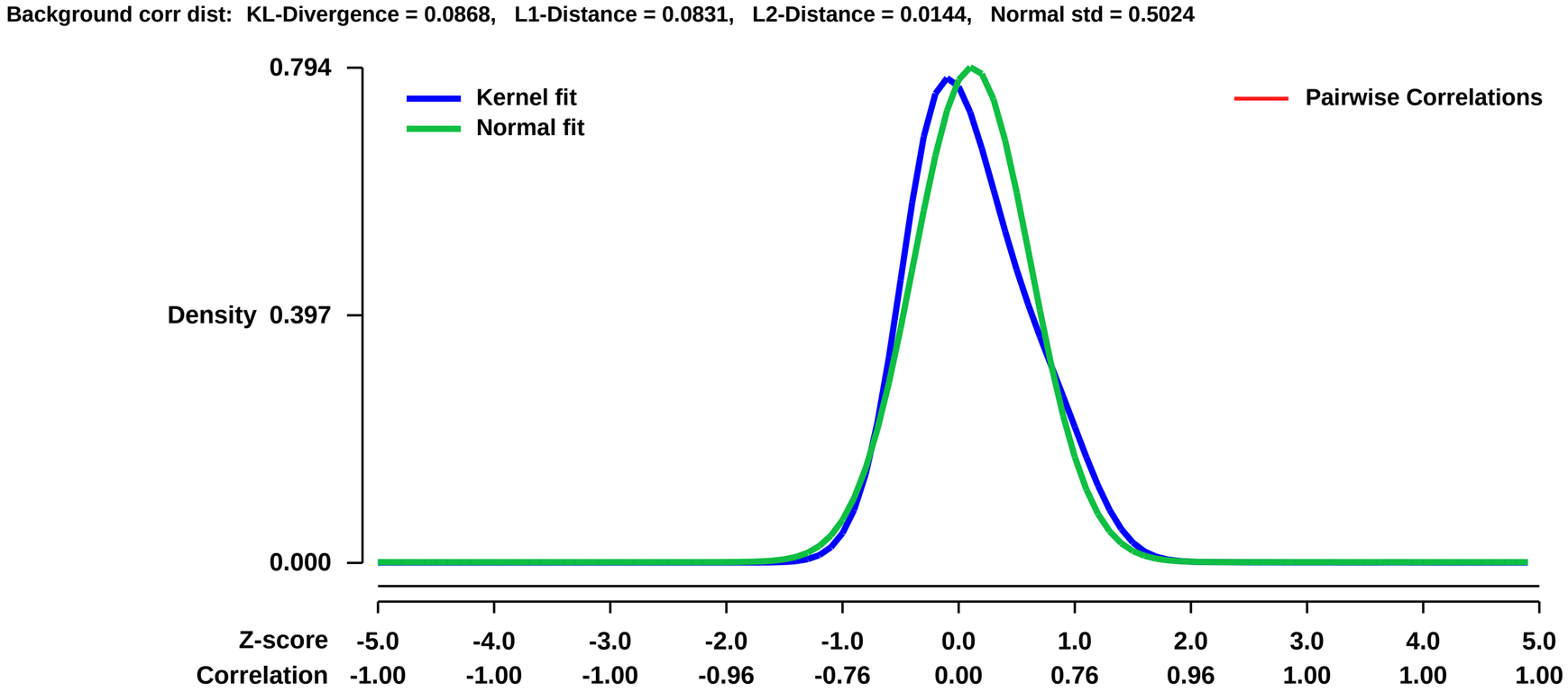

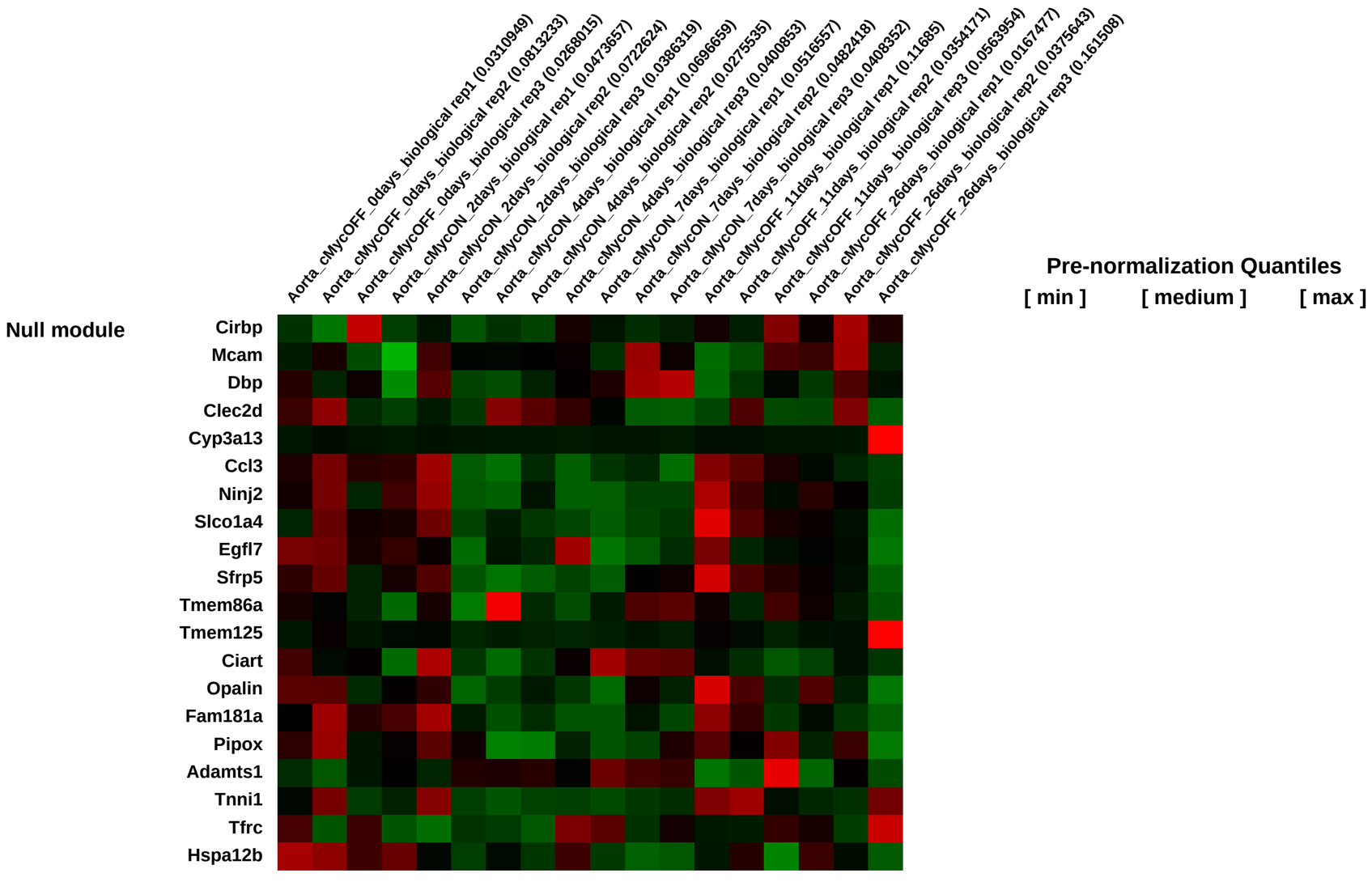

GEO Series "GSE51243" Expression Profiles

Num of samples in this series: 7

Scale of expression profile Z-scores

-3.0 -2.0 -1.0 0.0 1.0 2.0 3.0

GEO Link:	http://www.ncbi.nlm.nih.gov/geo/query/acc.cgi?acc=GSE51243
Status:	Public on Sep 28 2013
Title:	Comparison of the transcriptome of TEL-JAK2- versus activated NOTCH1 (ICN1)-induced T cell acute lymphoblastic leukemias (mouse)
Organism:	Mus musculus
Experiment type:	Expression profiling by array
Platform:	GPL1261
Pubmed ID:	24268771
Summary & Design:	**Summary:** The TEL-JAK2 fusion oncogene and the ICN1 activated allele of NOTCH1 are the result of specific chromosomal translocations in T cell acute lymphoblastic leukemia (T-ALL). Mouse models of these diseases (TEL-JAK2 transgenic mice; Carron C. et al. Blood (2000); a bone marrow transplantation model for ICN1-induced T-ALL) were used to compare the transcriptional program specific to each oncoprotein in mouse models of these leukemias. Tumor load was >50% leukemic cells in all selected organs. **Overall design:** Leukemic cells were collected from the thymus of terminally-ill TEL-JAK2 leukemic mice and bone marrow of terminally-ill ICN1 leukemic mice. RNA was extracted from each sample and processed for hybridization to Affymetrix arrays.

Background corr dist: KL-Divergence = 0.0331, L1-Distance = 0.0151, L2-Distance = 0.0003, Normal std = 0.6426

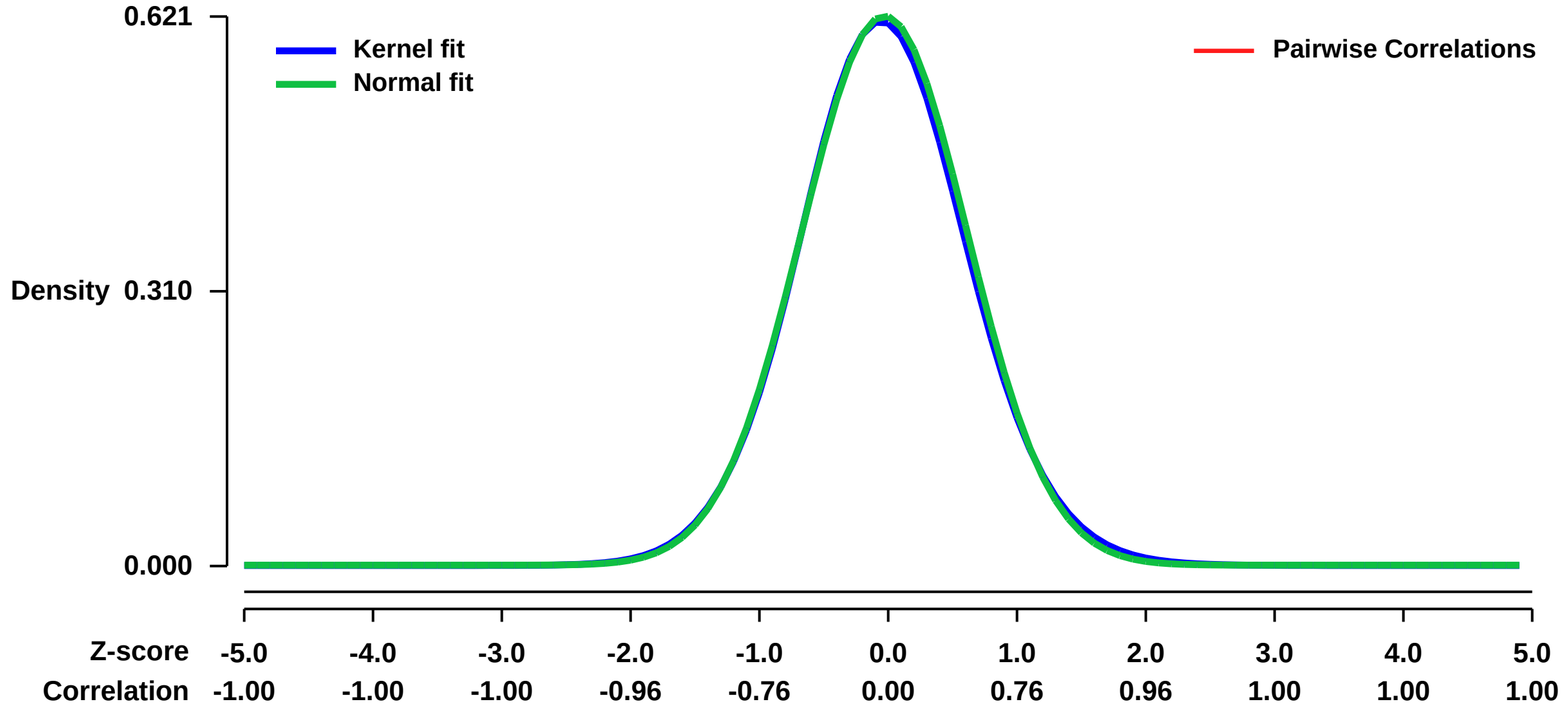

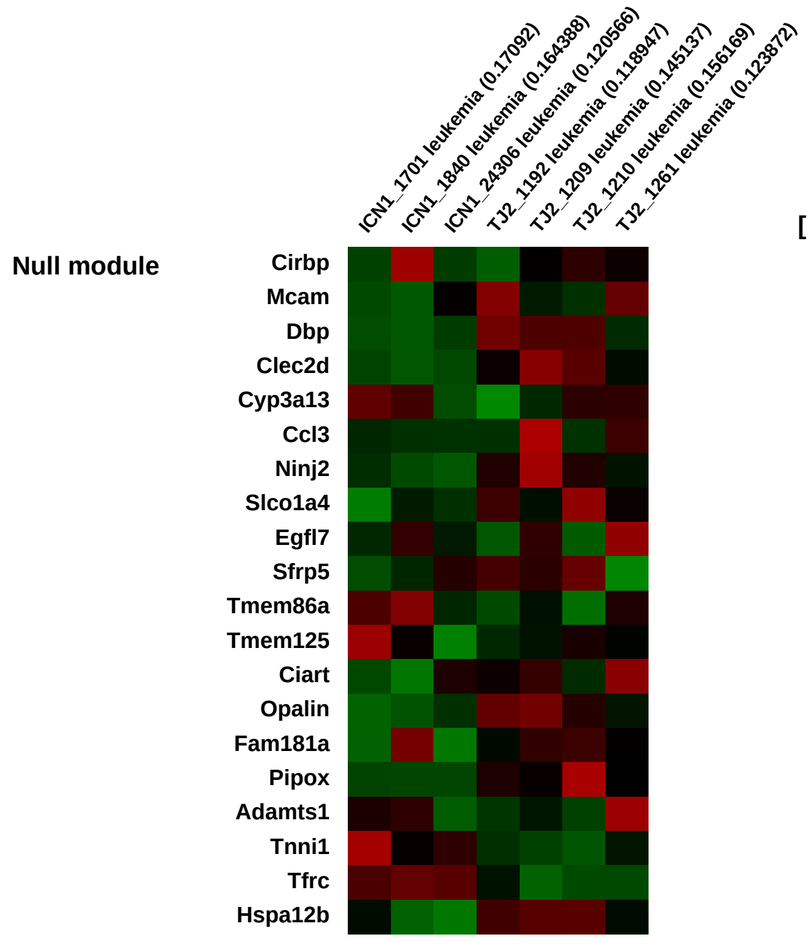

GEO Series "GSE38754" Expression Profiles

Num of samples in this series: 40

Scale of expression profile Z-scores

-3.0 -2.0 -1.0 0.0 1.0 2.0 3.0

GEO Link:	http://www.ncbi.nlm.nih.gov/geo/query/acc.cgi?acc=GSE38754
Status:	Public on Jun 16 2012
Title:	Temporal changes of gene expression in mouse heart, kidney and lung during juvenile growth
Organism:	Mus musculus
Experiment type:	Expression profiling by array
Platform:	GPL1261
Pubmed ID:	19036884
Summary & Design:	**Summary:** Temporal changes of gene expression from 1-wk- to 4-wk and 8-wk-old mouse in heart, kidney and lung. Mammalian somatic growth is rapid in early postnatal life but then slows and eventually ceases in multiple tissues. We hypothesized that there exists a postnatal gene expression program that is common to multiple tissues and is responsible for this coordinate growth deceleration. Consistent with this hypothesis, microarray analysis identified >1600 genes that were regulated with age coordinately in kidney, lung, and heart of juvenile mice, including many genes that regulate proliferation. As examples, we focused on three growth-promoting genes, Igf2, Mest, and Peg3, that were markedly downregulated with age. We conclude that there exists an extensive genetic program occurring during postnatal life. Many of the involved genes are regulated coordinately in multiple organs, including many genes that regulate cell proliferation. At least some of these are themselves apparently regulated by growth, suggesting that, in the embryo, a gene expression pattern is established that allows for rapid somatic growth of multiple tissues but then, during postnatal life, this growth leads to negative-feedback changes in gene expression that in turn slow and eventually halt somatic growth, thus imposing a fundamental limit on adult body size. **Overall design:** To compare gene expression between fast-growing animals and more slowly growing animals, we extracted total mRNA from kidney and lung in 1-wk, 4-wk, and 8-wk-old mice (5 animals each).

Background corr dist: KL-Divergence = 0.1315, L1-Distance = 0.0443, L2-Distance = 0.0038, Normal std = 0.4135

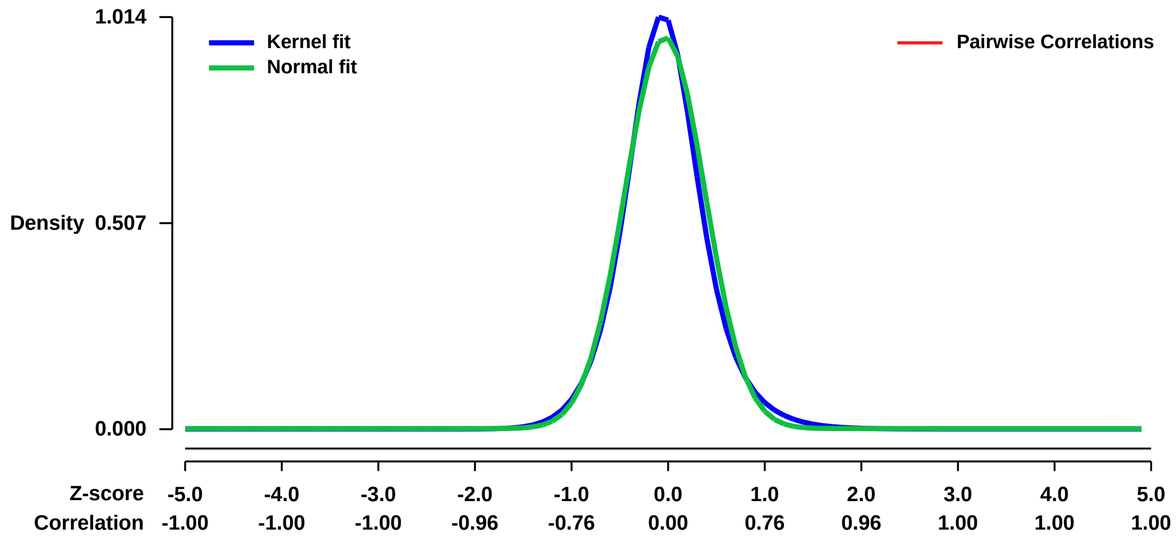

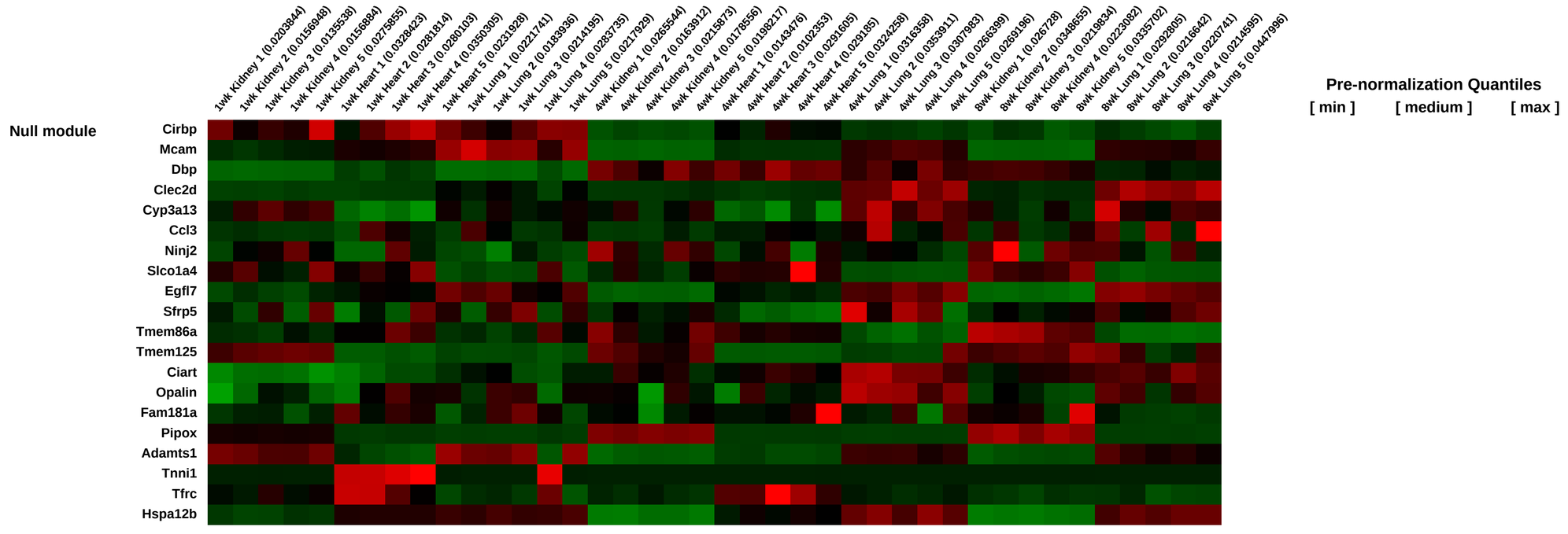

GEO Series "GSE28887" Expression Profiles

Num of samples in this series: 12

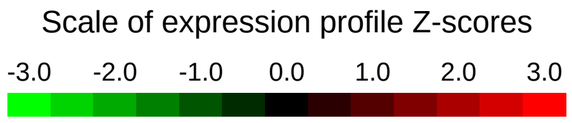

GEO Link:	**http://www.ncbi.nlm.nih.gov/geo/query/acc.cgi?acc=GSE28887**
Status:	**Public on Apr 28 2011**
Title:	**Gene expression profile of Age associated B cells, Follicular B cells, and B1 cells**
Organism:	**Mus musculus**
Experiment type:	**Expression profiling by array**
Platform:	**GPL1261**
Pubmed ID:	**21543762**
Summary & Design:	**Summary:** **We performed gene expression profile of different B cell populations found in old (18 months old) C57BL/6 female mouse (B1 cells were recovered from both young and old C57BL/6 mice). Mice were naˆflve and healthy (no autoimmunity was detected at the time of the experiment).** **Overall design:** **Different B cell populations were sorted using flow cytometry and RNA was isolated.**

Background corr dist: **KL-Divergence = 0.0909, L1-Distance = 0.0280, L2-Distance = 0.0014, Normal std = 0.4689**

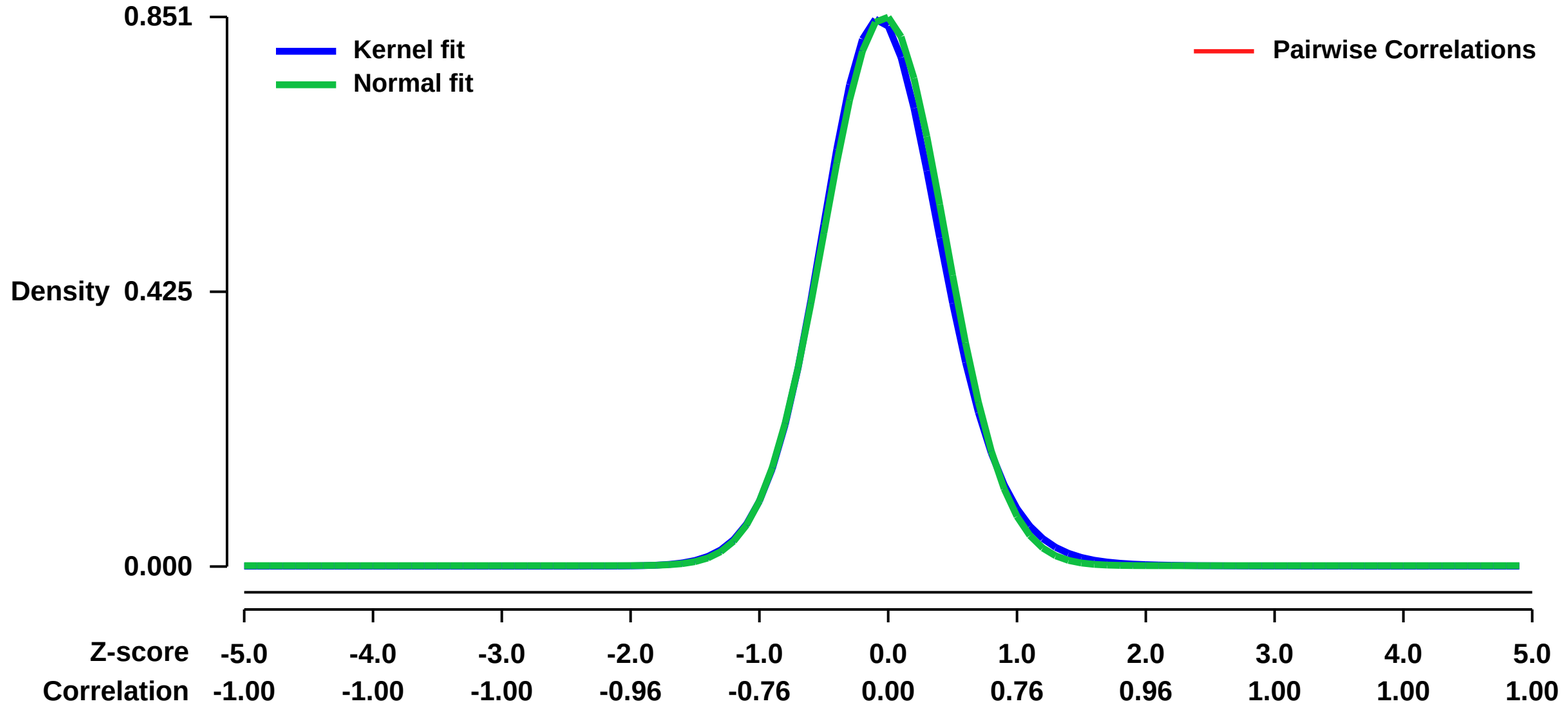

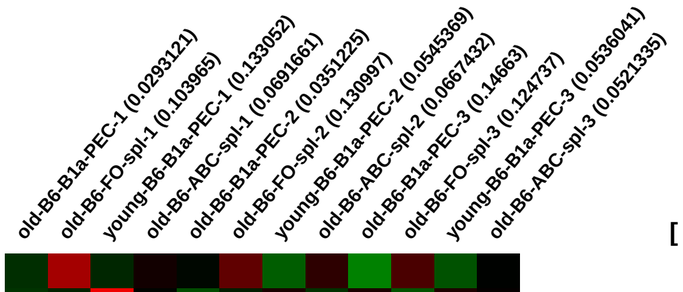

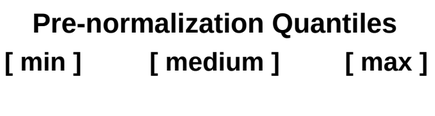

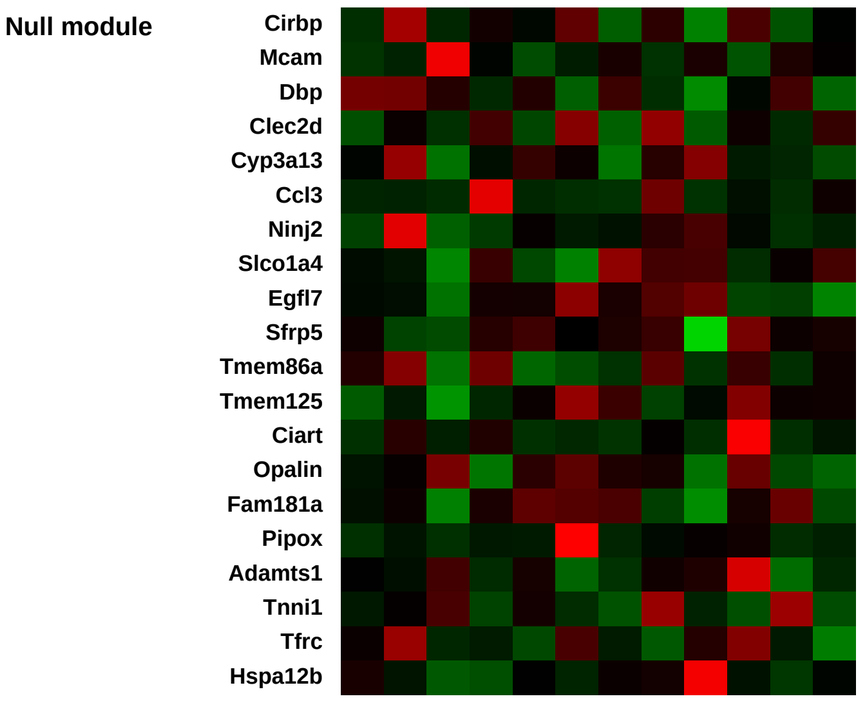

GEO Series "GSE16564" Expression Profiles

Num of samples in this series: 15

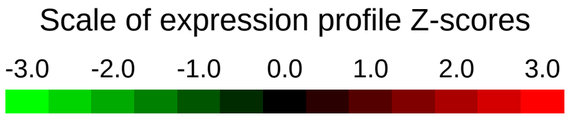

GEO Link:	http://www.ncbi.nlm.nih.gov/geo/query/acc.cgi?acc=GSE16564
Status:	Public on Jun 13 2009
Title:	Expression data from AtT20 mouse pituitary gland cells following overexpression or down regulation of NSBP1
Organism:	Mus musculus
Experiment type:	Expression profiling by array
Platform:	GPL1261
Pubmed ID:	19748358
Summary & Design:	**Summary:** Chromatin architectural protein NSBP1/HMGN5 belongs to the family of HMGN proteins which specifically interact with nucleosomes via Nucleosome Binding Domain, unfold chromatin and affect transcription. Mouse NSBP1 is a new and uncharacterized member of HMGN protein family. NSBP1 is a nuclear protein which is localized to euchromatin, binds to linker histone H1 and unfolds chromatin. We analyzed the effect of altered expression levels of mouse NSBP1 protein on global gene expression profile in AtT20 pituitary cells. We found that NSBP1 modulates the fidelity of cellular transcription in the nucleosome binding-dependent manner. **Overall design:** Stable clones overexpressing wild type mouse NSBP1 protein or mutated NSBP1SE protein which does not bind to nucleosomes were generated by retroviral infection of AtT20 cells. siRNA treatment was applied to down regulate NSBP1 in the cells. Total RNA was collected from biological triplicates and analyzed by Affymetrix expression arrays.

Background corr dist: KL-Divergence = 0.0509, L1-Distance = 0.0344, L2-Distance = 0.0022, Normal std = 0.5561

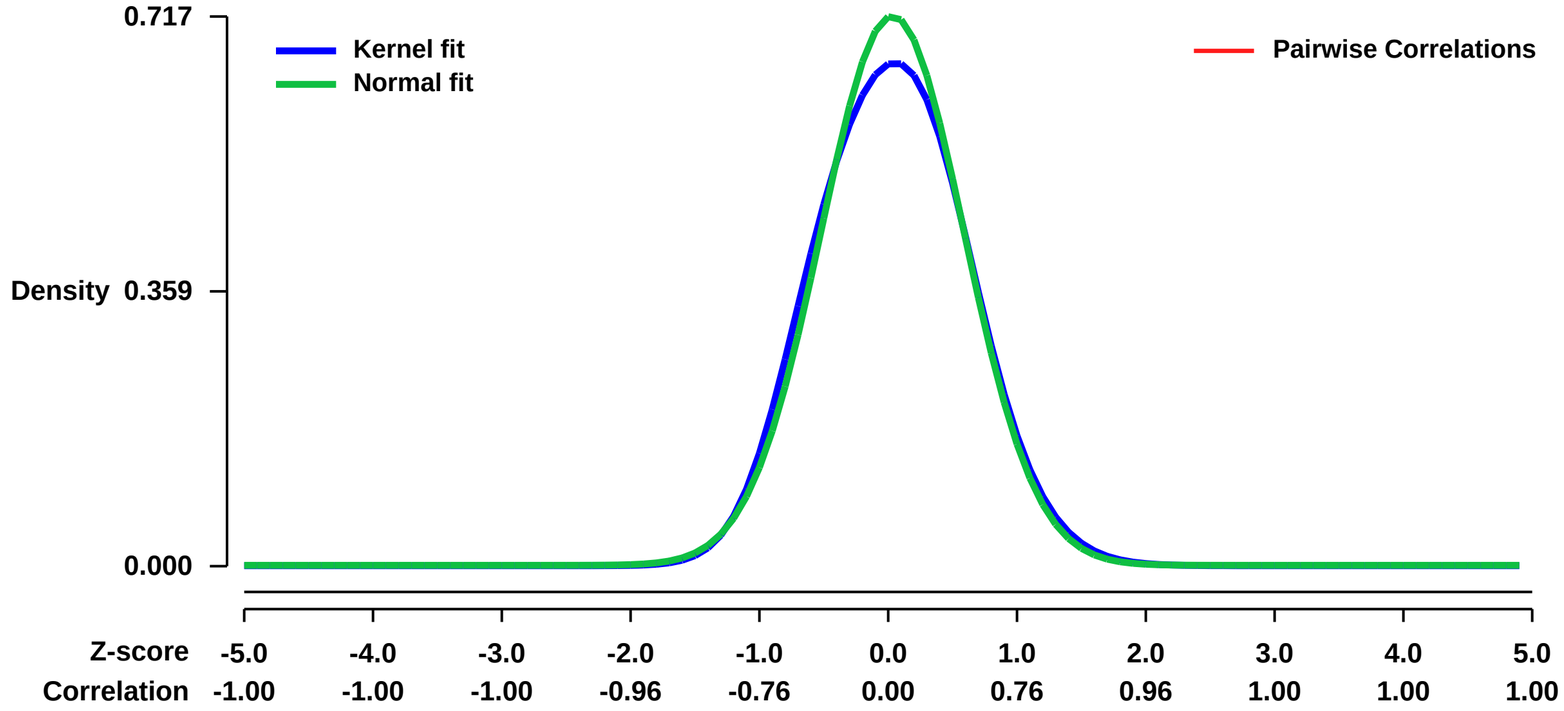

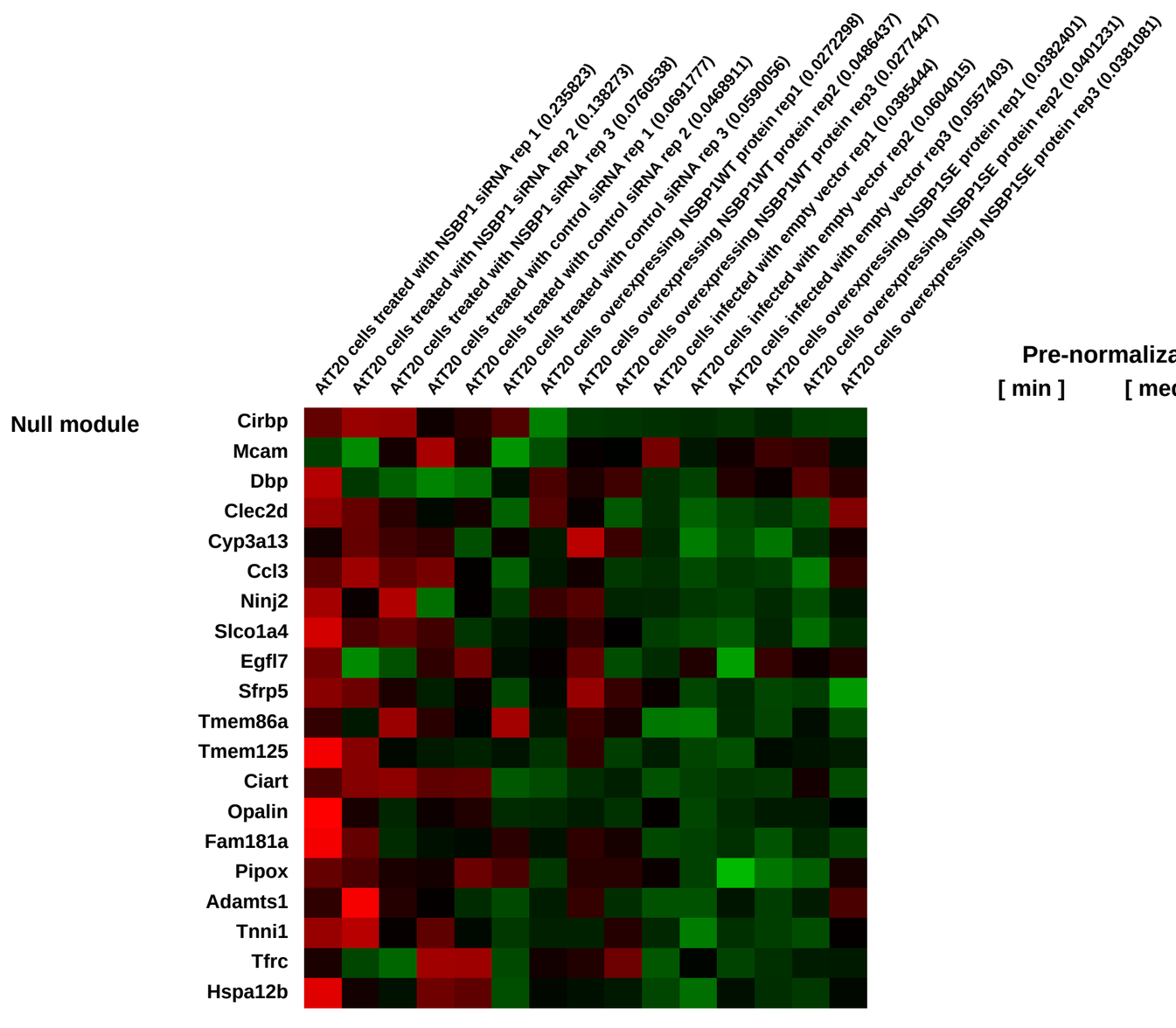

GEO Series "GSE10589" Expression Profiles

Num of samples in this series: 6

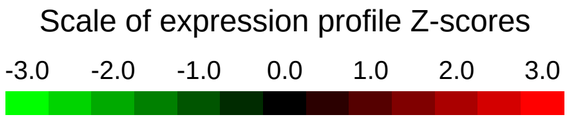

GEO Link:	http://www.ncbi.nlm.nih.gov/geo/query/acc.cgi?acc=GSE10589
Status:	Public on Feb 19 2009
Title:	Comparison of gene expression between the thyroid of mice lacking Slc26a4 and heterzygous controls.
Organism:	Mus musculus
Experiment type:	Expression profiling by array
Platform:	GPL1261
Pubmed ID:	19692489
Summary & Design:	**Summary:** Determination of differential expression of genes in the thyroid of pendrin (Slc26a4) heterozygous and knockout mice at a time point corresponding to maximal thyroid gland activity, postnatal day 15 (P15). **Keywords:** Differential expression under disease state **Overall design:** A total of Six samples of thyroid RNA obtained from P15 mice were analyzed. Triplicates from pendrin (Slc26a4) heterozygous and knockout mice were run and analyzed.

Background corr dist: KL-Divergence = 0.0392, L1-Distance = 0.0183, L2-Distance = 0.0004, Normal std = 0.6178

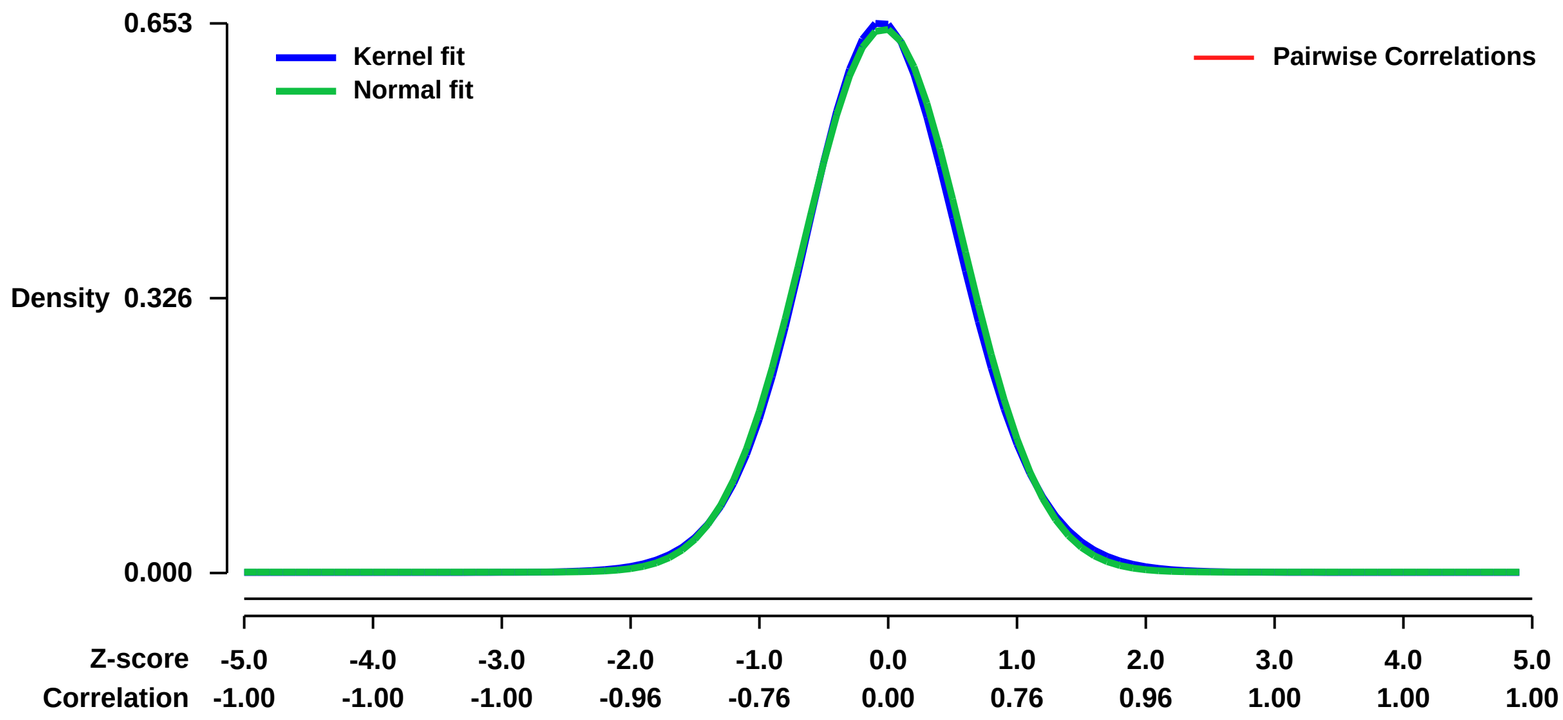

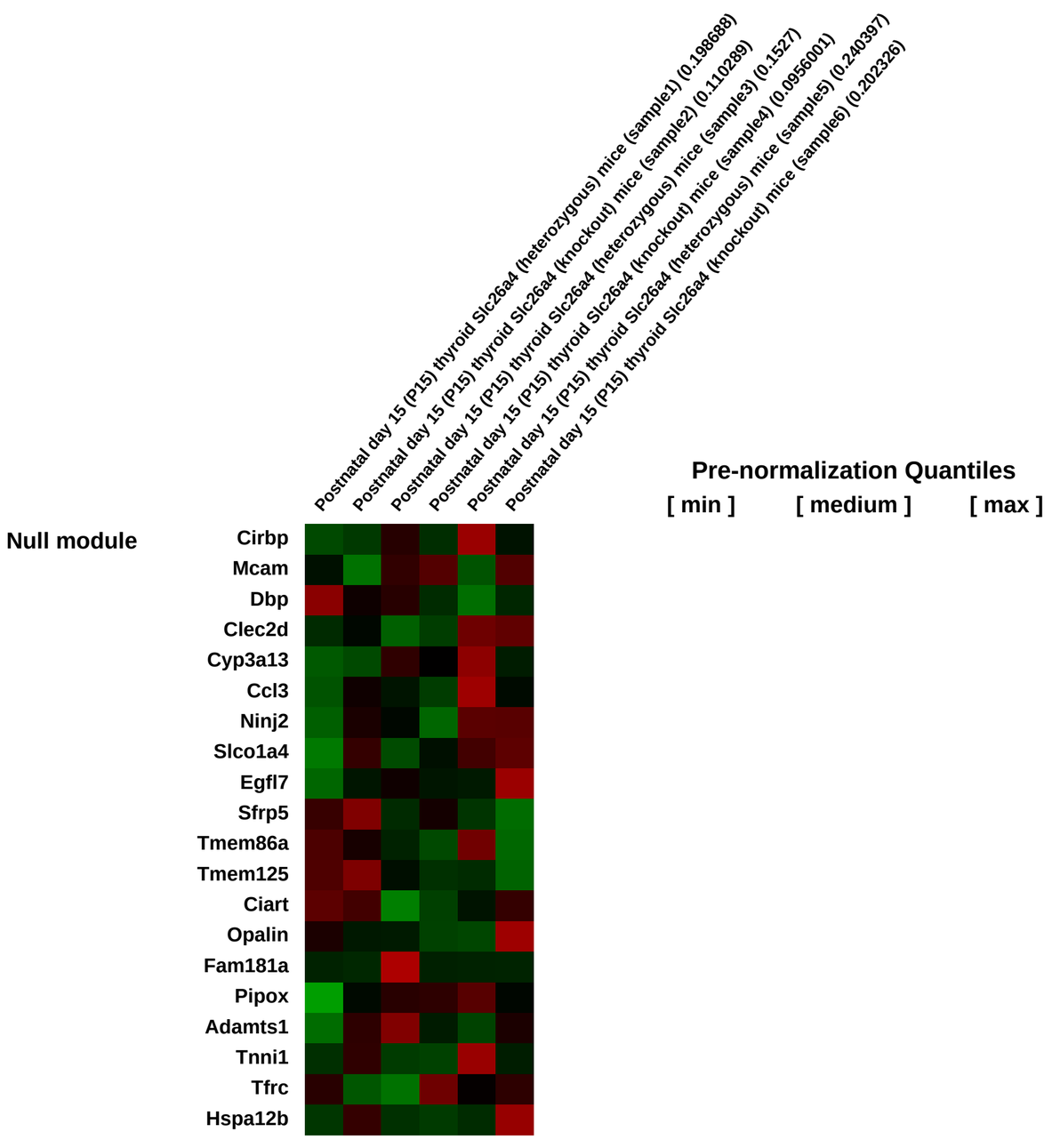

GEO Series "GSE4034" Expression Profiles

Num of samples in this series: 24

Scale of expression profile Z-scores

-3.0 -2.0 -1.0 0.0 1.0 2.0 3.0

GEO Link:	http://www.ncbi.nlm.nih.gov/geo/query/acc.cgi?acc=GSE4034
Status:	Public on Jan 13 2006
Title:	Rapid selection response for contextual fear conditioning in a cross between C57BL/6J and A/J (palme-affy-mouse-198967)
Organism:	Mus musculus
Experiment type:	Expression profiling by array
Platform:	GPL1261
Pubmed ID:	18363093
Summary & Design:	**Summary:** These data are from the brains (amygdala and hippocampus) of mice originally derived from a cross between C57BL/6J and A/J inbred strains. We used short-term selection to produce outbred mouse lines with differences in contextual fear conditioning, which is a measure of fear learning. We selected for a total of 4 generations. Fear learning differed in the selected lines and this difference was stronger with each successive generation of selection. We identified several QTLs for the selection response, including a highly significant QTL at the tyr locus (p < 9.6(-10)). We used Affymetrix microarrays to identify many differentially expressed genes in the amygdala and hippocampus of mice from the final generation of selection. Amygdala and hippocampus samples were rapidly dissected out of experimentally naˆflve mice from each selected line. Three samples were pooled and hybridized to each array. Experimentally naˆflve mice were used because the behavior of the mice can be reliably a nticipated due to their lineage. Thus these gene expression differences are not due to the response to human handling, foot shock or fear-inducing conditioned stimuli. We have a second similar study that focuses on a different selected population that was based on C57BL/6J and DBA/2J mice (see GES4035). **Overall design:**

Background corr dist: KL-Divergence = 0.2053, L1-Distance = 0.0437, L2-Distance = 0.0032, Normal std = 0.3474

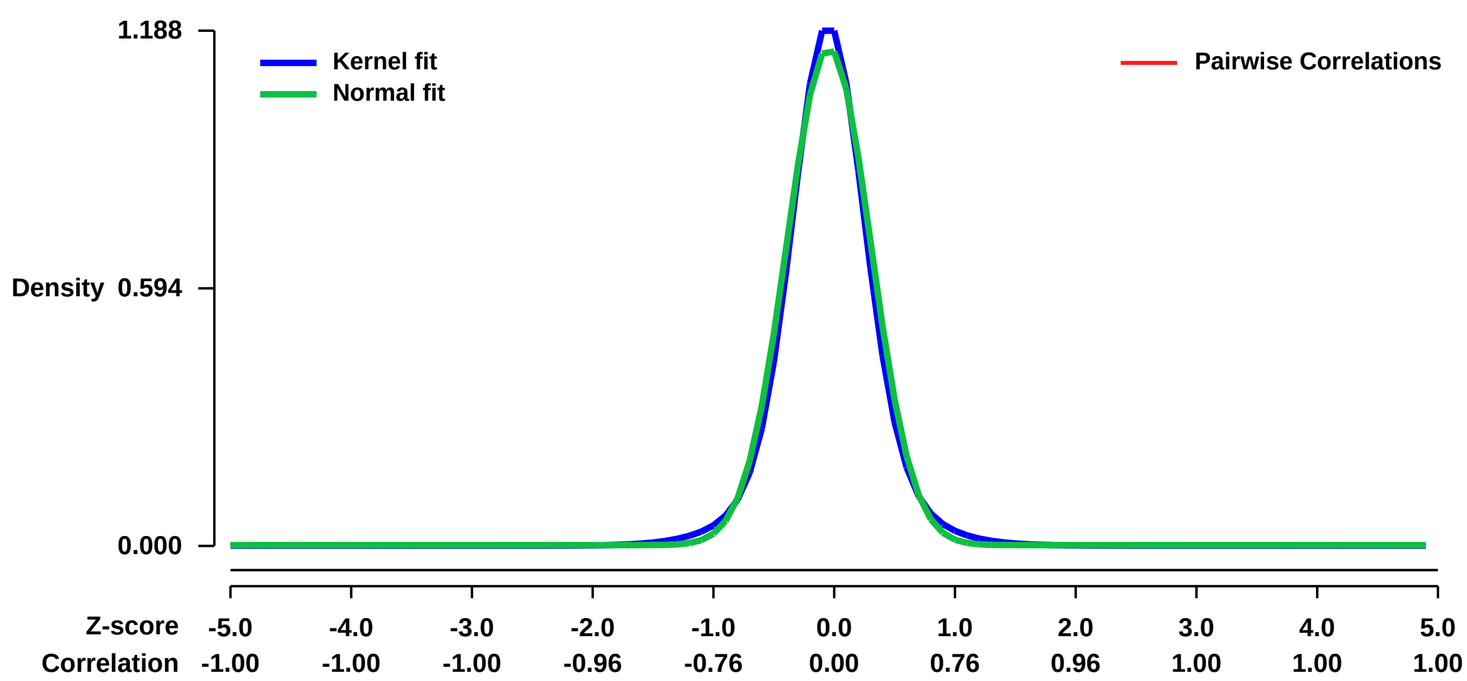

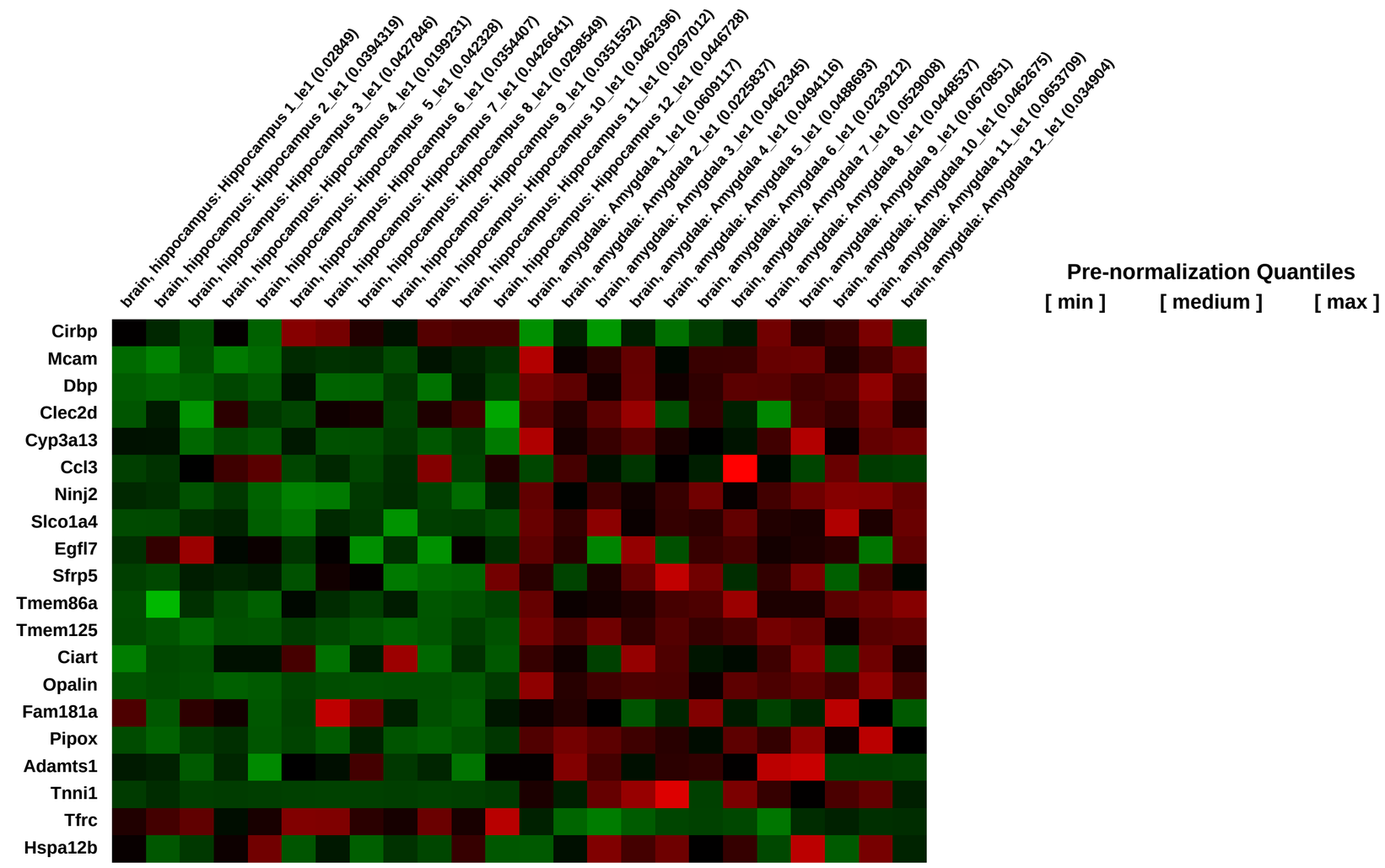

GEO Series "GSE14929" Expression Profiles

Num of samples in this series: 38

Scale of expression profile Z-scores

-3.0 -2.0 -1.0 0.0 1.0 2.0 3.0

GEO Link: http://www.ncbi.nlm.nih.gov/geo/query/acc.cgi?acc=GSE14929
Status: Public on Jun 23 2009
Title: Myocardial expression data from gnotobiotic wild-type and Ppara-/- mice
Organism: Mus musculus
Experiment type: Expression profiling by array
Platform: GPL1261
Pubmed ID: 20529848

Summary & Design:

Summary:
Germ free (GF) and conventionalized (CONV-D) wild-type C57Bl/6 male mice in the CARB-fed, 24h fasted, and 30d trained states; plus GF and CONV-D CARB-fed Ppara-/- mice. CARB-fed indicates a standard polysaccharide-rich mouse chow diet.

CONV-D mice are those that received a microbiota transplant from conventionally raised mice 2-3 weeks before experiment was initiated

Keywords: RNA Expression Array

Overall design:
Hearts from six to ten week-old GF and CONV-D mice, from the following eight treatment groups (GF, CONV-D) X (CARB-fed [wild-type], 24h fast [wild-type], 30d trained [wild-type], Ppara-/- [CARB-fed])

Background corr dist: KL-Divergence = 0.2177, L1-Distance = 0.0406, L2-Distance = 0.0032, Normal std = 0.3220

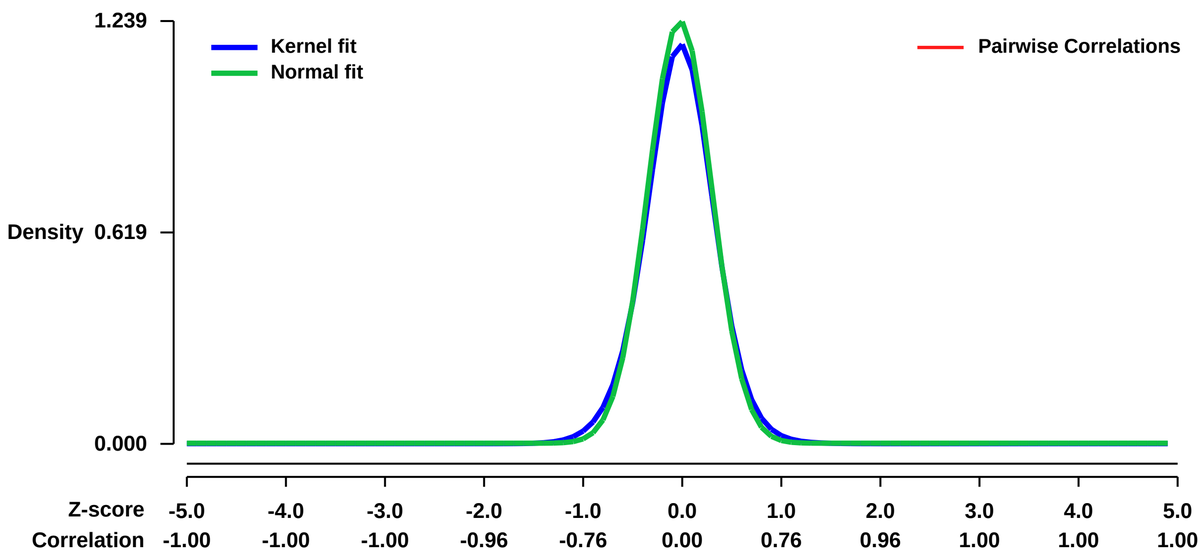

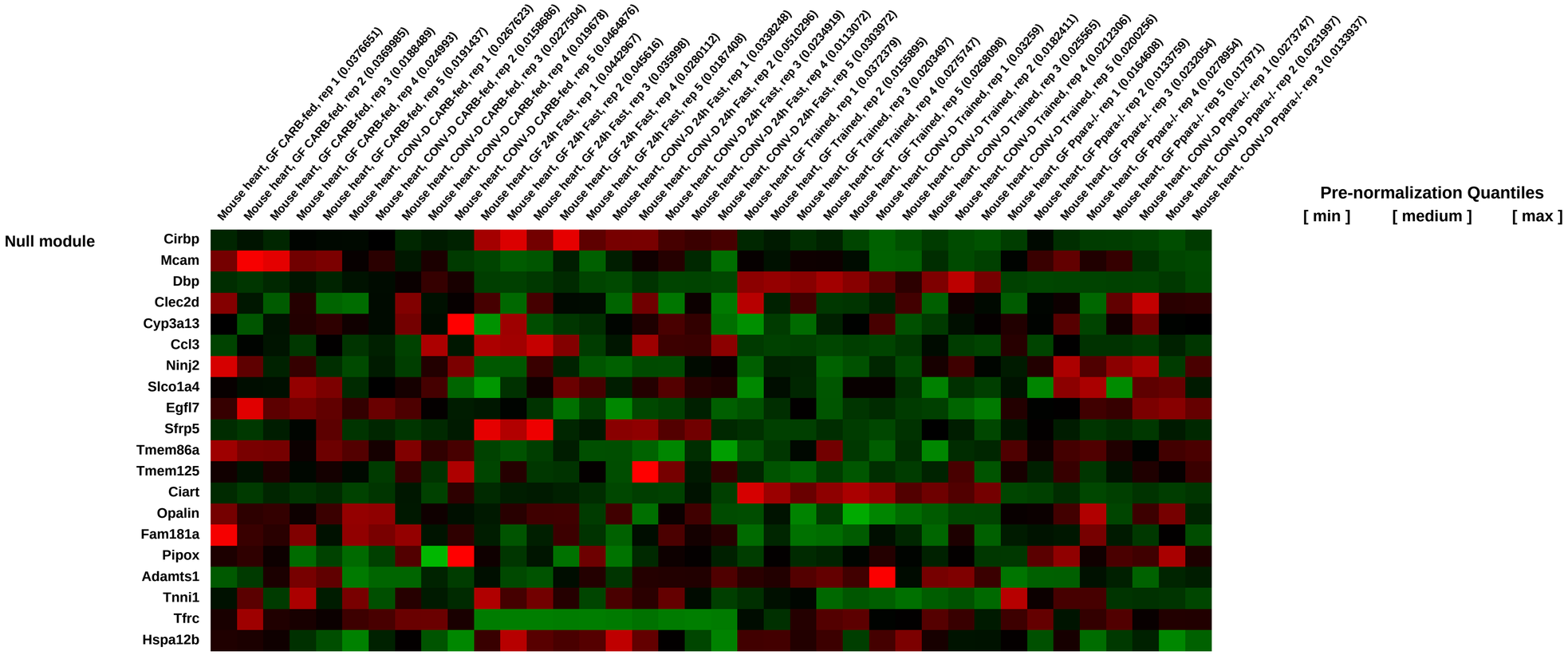

GEO Series "GSE32214" Expression Profiles

Num of samples in this series: 6

Scale of expression profile Z-scores

-3.0 -2.0 -1.0 0.0 1.0 2.0 3.0

GEO Link:	http://www.ncbi.nlm.nih.gov/geo/query/acc.cgi?acc=GSE32214
Status:	Public on Oct 31 2011
Title:	Expression profiling of erythroid developmental subsets isolated from mouse fetal liver.
Organism:	Mus musculus
Experiment type:	Expression profiling by array
Platform:	GPL1261
Pubmed ID:	22076376
Summary & Design:	**Summary:** The S1 and S3 erythroid developmental subsets were isolated using flow cytometry and the cell surface markers CD71 and Ter119 as described by Pop et. al. 2010 (PMID: 20877475) Expression profiles for S1 and S3 subsets were generated using Affymetrix GeneChips. Results were used to identify genes that are differentially expressed during erythropoiesis. **Overall design:** Single cell suspensions were prepared by mechanically dissociating whole fetal livers obtained from E12.5 to E13.5 Balb/C mouse embryos. Cells were stained for CD71, Ter119, and a cocktail containing lineage-specific antibodies. S1 and S3 erythroid developmental subsets were identified and isolated using flow cytometric sorting as described by Pop et. al. 2010 (PMID: 20877475). S1 and S3 subsets were isolated on 3 seperate days to generate total RNA (biological replicates). 20 ng of total RNA from each biological replicate was converted to cDNA, linearly amplified and biotinylated using Ovation reagents (Nugen, San Carlos, CA). Samples were hybridized to Mouse Genome 430 2.0 Arrays (Affymetrix, Santa Clara, CA). Microarray suite 5 (MAS5) processed sample data were normalized to the average of 18SRNA (AFFX-18SRNAMur/X00686_M_at), GAPDH (AFFX-GapdhMur/M32599_3_at) and ¸†-actin (1419734_at) expression values. These gene expression profiles were performed as part of the manuscript by Shearstone et. al. Global DNA Demethylation During Erythropoiesis In Vivo

Background corr dist: KL-Divergence = 0.0491, L1-Distance = 0.0863, L2-Distance = 0.0176, Normal std = 0.6771

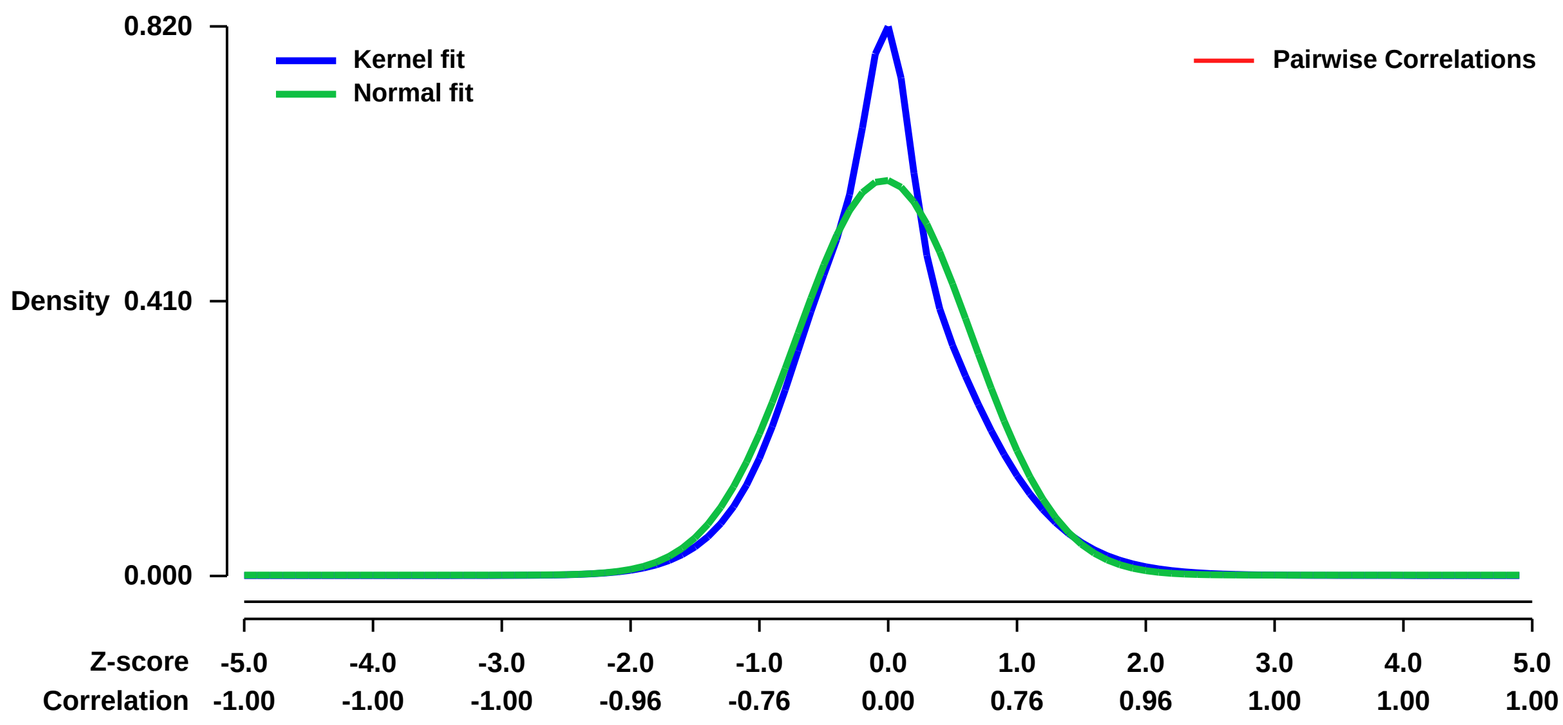

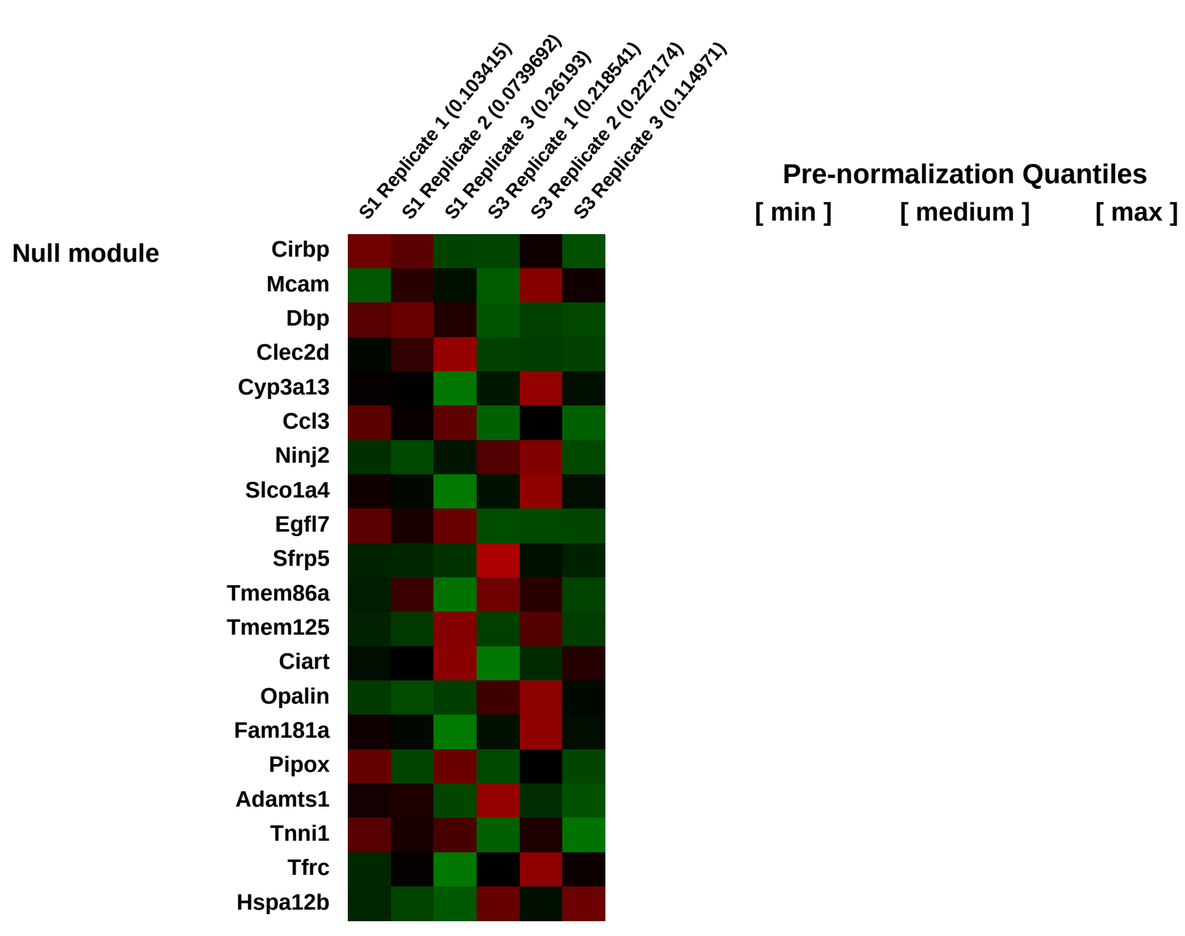

GEO Series "GSE49237" Expression Profiles

Num of samples in this series: 8

Scale of expression profile Z-scores

-3.0 -2.0 -1.0 0.0 1.0 2.0 3.0

GEO Link:	http://www.ncbi.nlm.nih.gov/geo/query/acc.cgi?acc=GSE49237
Status:	Public on Dec 31 2013
Title:	Analysis of TBR1 downnstream target genes in embryonic forebrains
Organism:	Mus musculus
Experiment type:	Expression profiling by array
Platform:	GPL1261
Pubmed ID:	24441682
Summary & Design:	**Summary:** **TBR1 is a forebrain specific T-box transcription factor. Tbr1-/- mice have been characterized by defective axonal projections from cerebral cortex and abnormal neuronal migration of cerebral cortex and amygdala.** **To investigate how TBR1 regulates neural development, the gene expression profile of Tbr1-/- brains was compared with WT littermates.** **Overall design:** **Total RNAs purified from forebrains at embryonic day 16.5 were hybridized on Affymetrix microarrays**

Background corr dist: KL-Divergence = 0.0472, L1-Distance = 0.0231, L2-Distance = 0.0006, Normal std = 0.5812

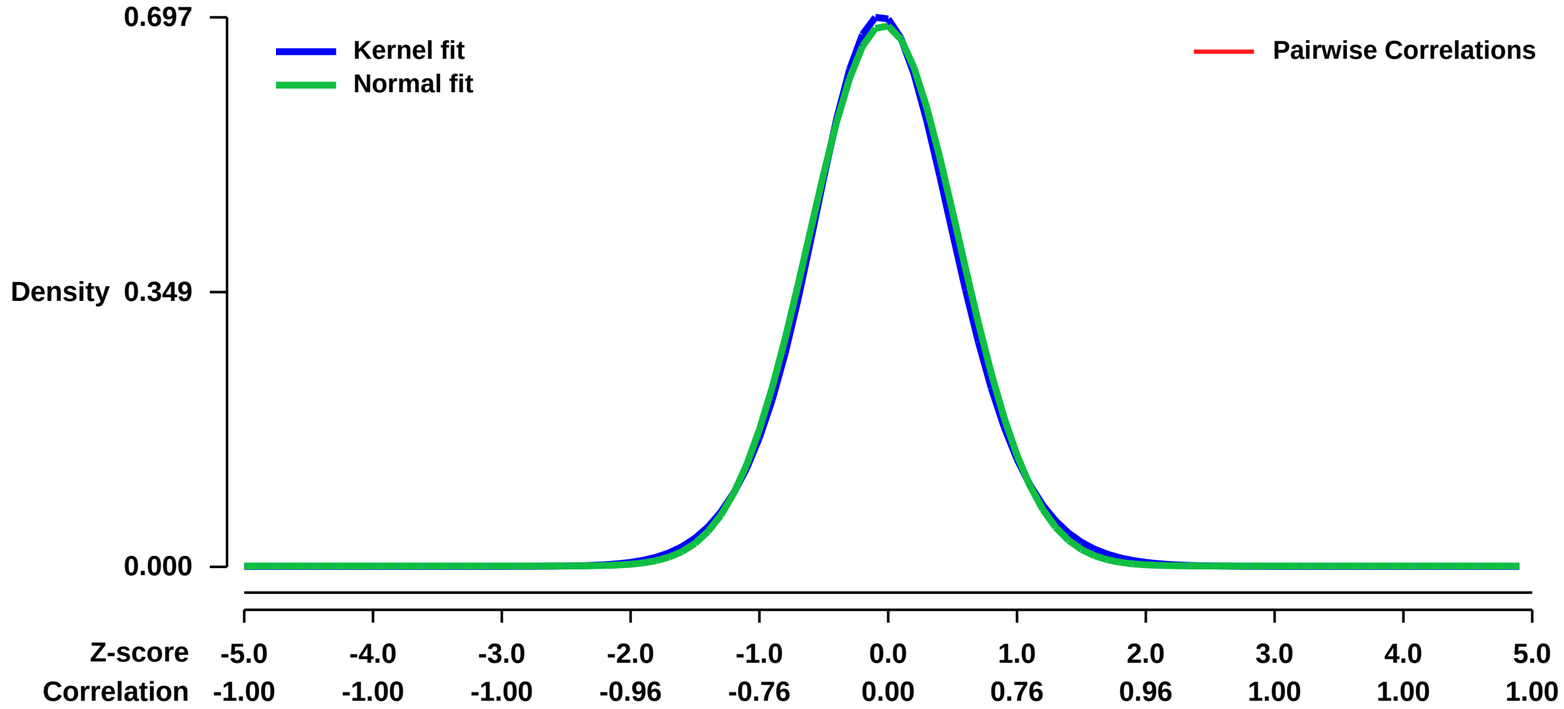

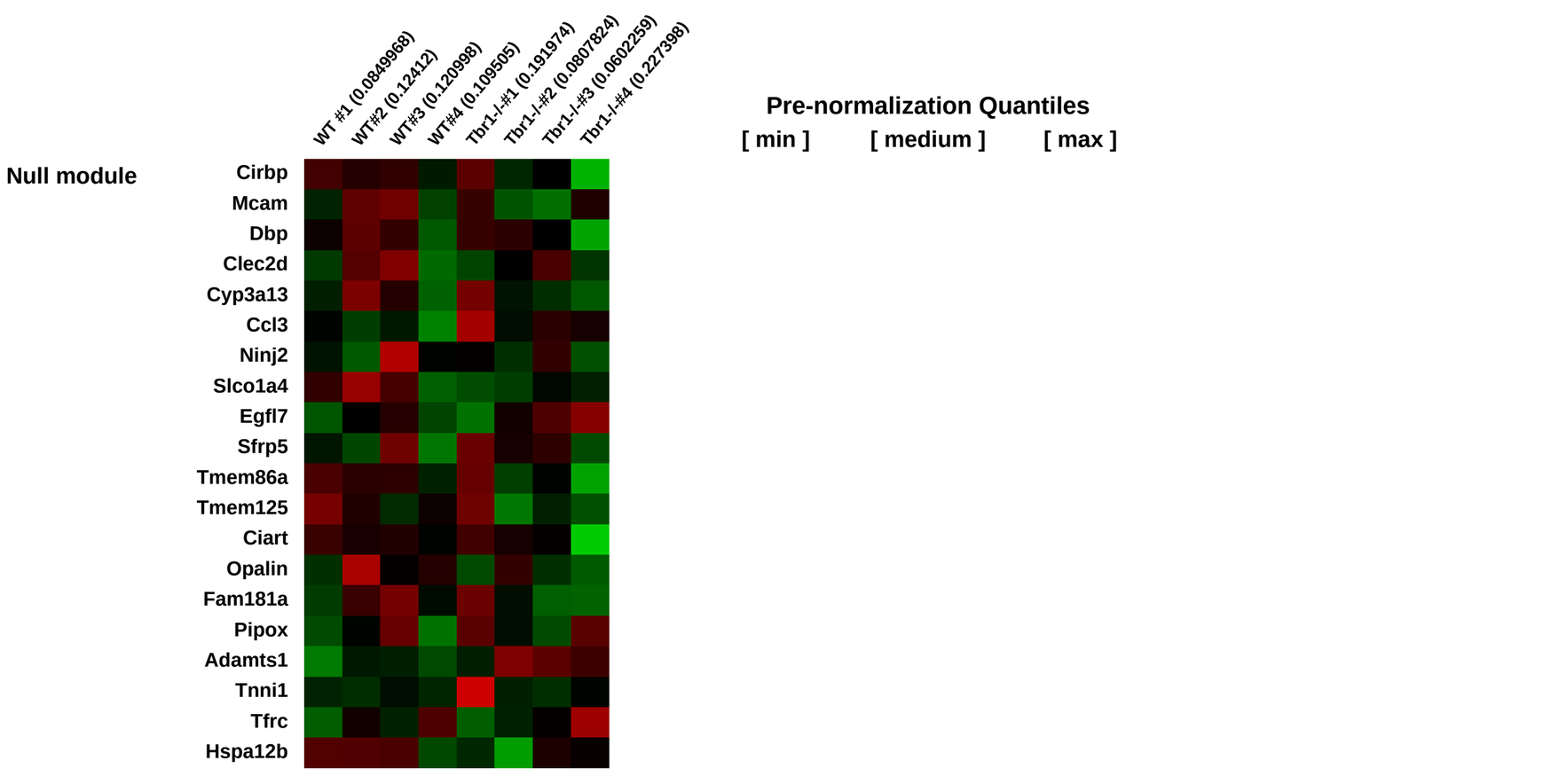

GEO Series "GSE21224" Expression Profiles

Num of samples in this series: 16

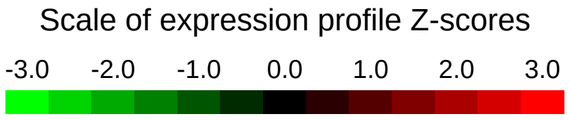

GEO Link:	http://www.ncbi.nlm.nih.gov/geo/query/acc.cgi?acc=GSE21224
Status:	Public on Oct 01 2010
Title:	Transcriptional ontogeny of the developing liver
Organism:	Mus musculus
Experiment type:	Expression profiling by array
Platform:	GPL1261
Pubmed ID:	22260730
Summary & Design:	**Summary:** We characterized gene expression changes in the developing mouse liver at gestational days (GD) 11.5, 12.5, 13.5, 14.5, 16.5, and 19.5 and in the neonate (postnatal day (PND) 7 and 30) using full-genome microarrays and compared these changes to that in the adult liver. The fetal liver, and to a lesser extent the neonatal liver, exhibited dramatic differences in gene expression compared to adults. Canonical pathway analysis of the fetal liver signature demonstrated increases in functions important in cell replication and DNA fidelity whereas most metabolic pathways of intermediary metabolism were suppressed. Comparison of the dataset to a number of previously published datasets revealed 1) a striking similarity between the fetal liver and that of the pancreas in both mice and humans, 2) a nucleated erythrocyte signature in the fetus and 3) suppression of most xenobiotic metabolism genes throughout development, except a number of transporters associated with expression in hematopoietic cells. **Keywords:** gene expression/microarray **Overall design:** We characterized gene expression changes in the developing mouse liver at gestational days (GD) 19 and in the neonate (postnatal day (PND) 7 and 30) using full-genome microarrays and compared these changes to that in the adult liver. Total RNA was isolated from liver samples and gene expression analyzed using Affymetrix Mouse 430 2.0 GeneChips. Data from 16 samples, with four mice in each of the four age groups, were analyzed.

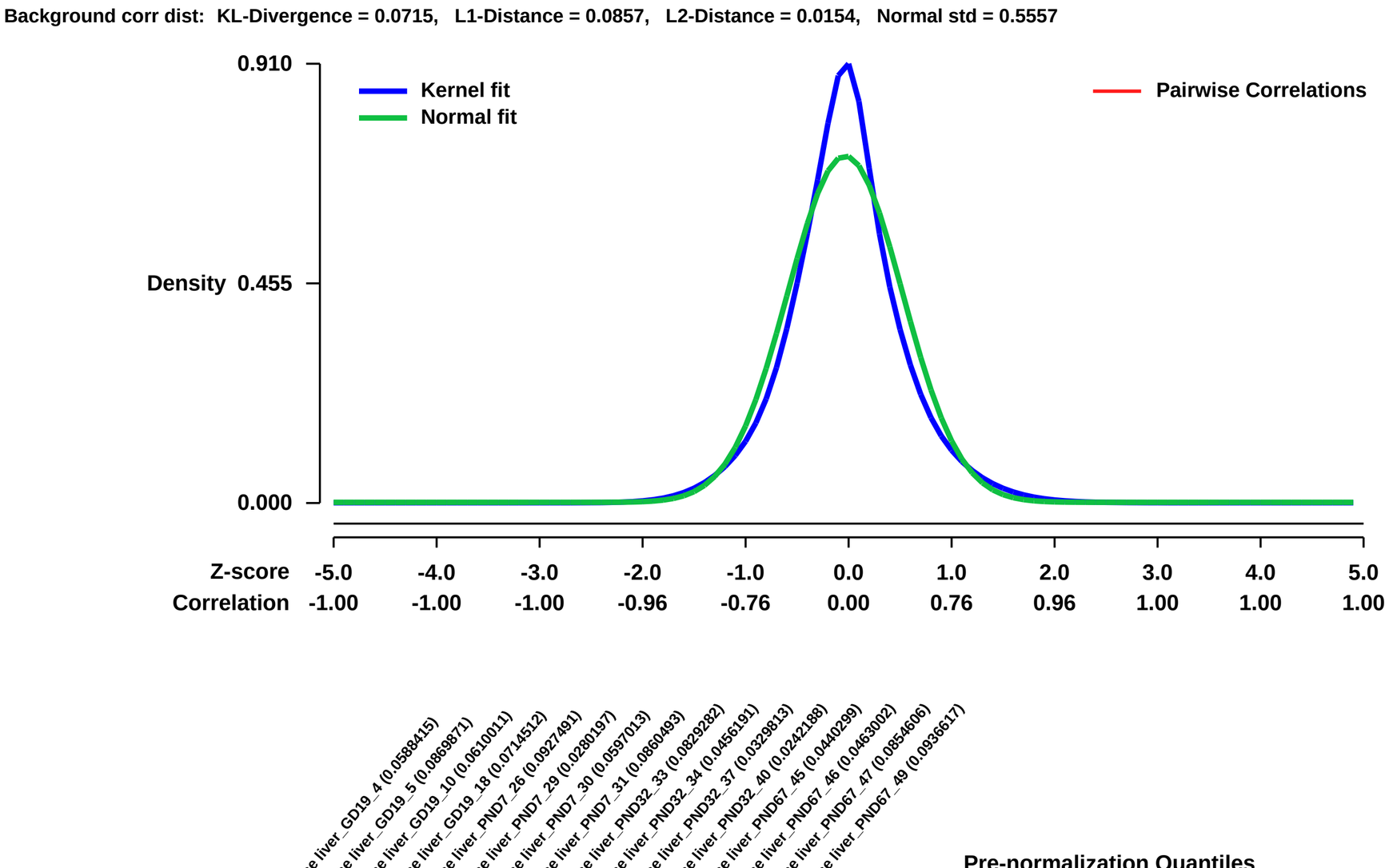

GEO Series "GSE24873" Expression Profiles

Num of samples in this series: 48

Scale of expression profile Z-scores

-3.0 -2.0 -1.0 0.0 1.0 2.0 3.0

GEO Link:	http://www.ncbi.nlm.nih.gov/geo/query/acc.cgi?acc=GSE24873
Status:	Public on Oct 19 2011
Title:	IL-17-induced NF-kB activation via CIKS/Act1: Physiologic significance and signaling mechanisms
Organism:	Mus musculus
Experiment type:	Expression profiling by array
Platform:	GPL1261
Pubmed ID:	21335551
Summary & Design:	**Summary:** Interleukin-17 (IL-17) is essential in host defense against extracellular bacteria and fungi, especially at mucosal sites, but it also contributes significantly to inflammatory and autoimmune disease pathologies. Binding of IL-17 to its receptor leads to recruitment of the adaptor protein CIKS/Act1 via heterotypic association of their respective SEFIR domains and to activation of the transcription factor NF-kB; it is not known whether CIKS and/or NF-kB are required for all gene induction events. Here we report that CIKS is essential for all IL-17 induced immediate-early genes in primary mouse embryo fibroblasts, while NF-kB is profoundly involved.´ We also identify a novel sub-domain in the N-terminus of CIKS that is essential for IL-17-mediated NF-kB activation. This domain is both necessary and sufficient for the interaction between CIKS and TRAF6, an adaptor required for NF-kB activation.´ The ability of decoy peptides to block this interaction may provide a new therapeutic strategy for intervention in IL-17-driven autoimmune and inflammatory diseases. **Keywords:** strain comparisons **Overall design:** strain comparisons

Background corr dist: KL-Divergence = 0.5409, L1-Distance = 0.0905, L2-Distance = 0.0273, Normal std = 0.2178

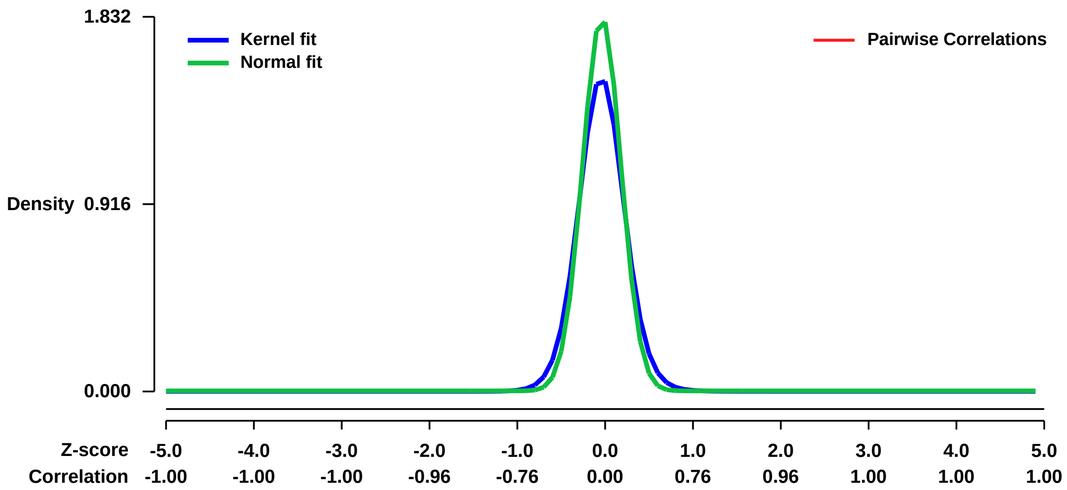

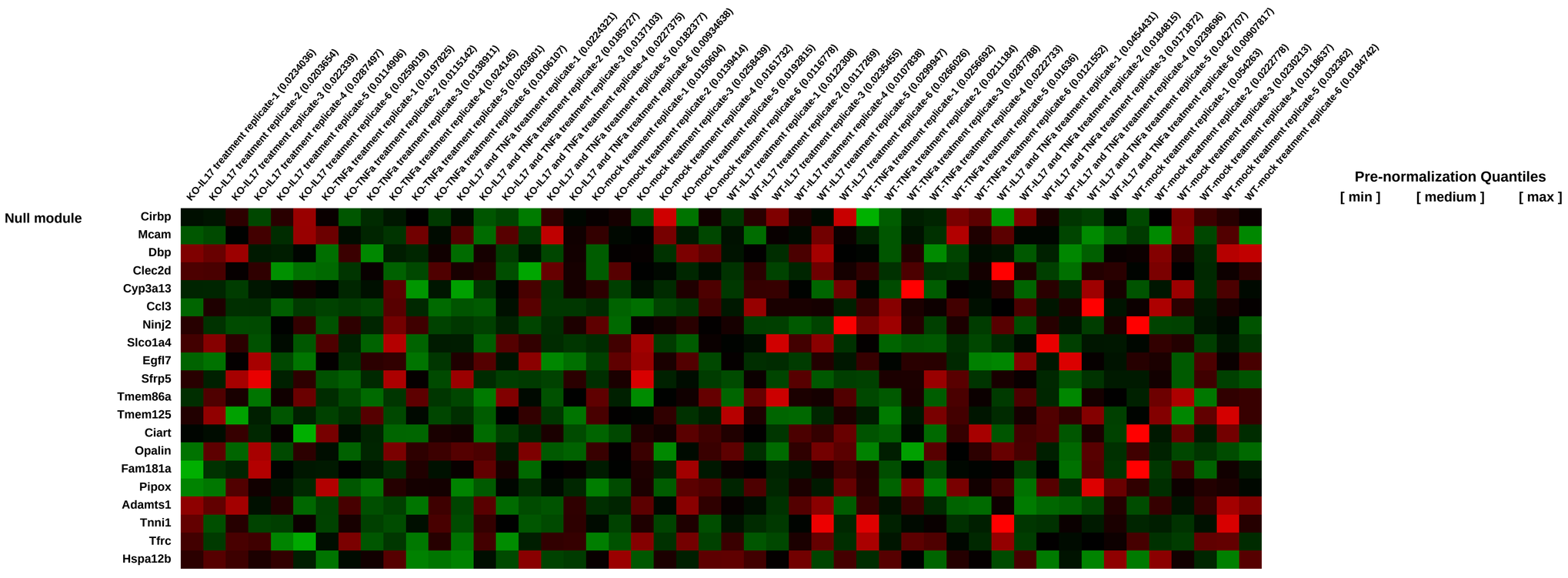

GEO Series "GSE18891" Expression Profiles

Num of samples in this series: 9

Scale of expression profile Z-scores

-3.0 -2.0 -1.0 0.0 1.0 2.0 3.0

GEO Link:	http://www.ncbi.nlm.nih.gov/geo/query/acc.cgi?acc=GSE18891
Status:	Public on Nov 05 2009
Title:	Foxl2 mediated expression data from KK1 granulosa cells
Organism:	Mus musculus
Experiment type:	Expression profiling by array
Platform:	GPL1261
Pubmed ID:	20167115
Summary & Design:	**Summary:** The Foxl2 transcription factor is required for ovarian function during follicular development. Our approach to begin to understand Foxl2 function is through the identification of Foxl2 regulated genes in the ovary. Transiently transfected KK1 mouse granulosa cells were used to identify genes that are potentially regulated by Foxl2. KK1 cells were transfected in three groups (mock, activated, and repressed) and twenty-four hours later RNA was isolated and submitted for Affymetrix microarray analysis. **Overall design:** To increase the potential of Foxl2 to alter gene expression levels of putative target genes, two fusions were constructed consisting of Foxl2 fused to the activation domain of the Herpes simplex virus VP16 transcription factor (Foxl2-VP16) and Foxl2 fused to the repression domain of the murine MAD transcription factor (Foxl2-MAD). Levels of gene expression were compared between mock transfected cells and those that were transfected with Foxl2-VP16 and Foxl2-MAD, respectively.

Background corr dist: KL-Divergence = 0.0983, L1-Distance = 0.0276, L2-Distance = 0.0014, Normal std = 0.4429

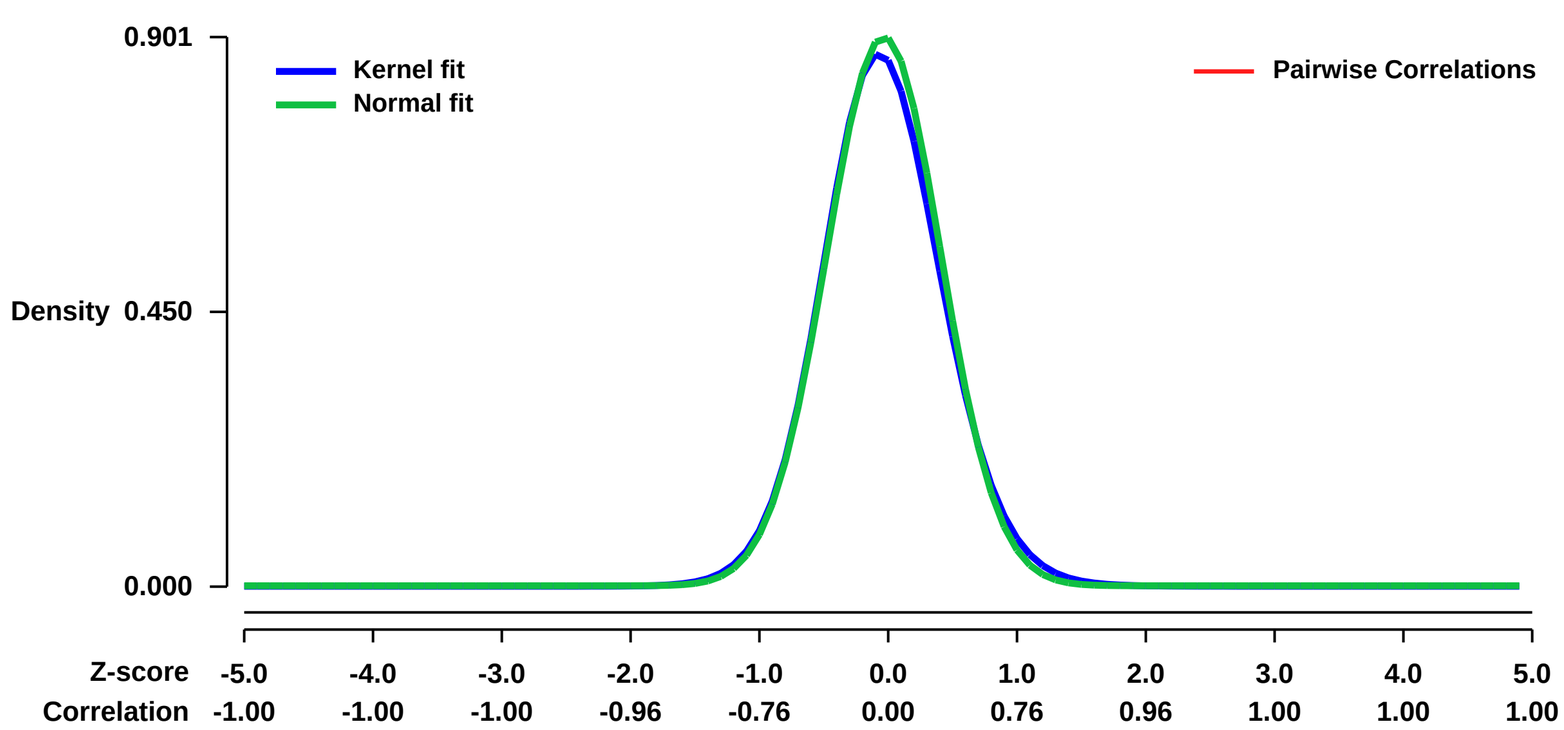

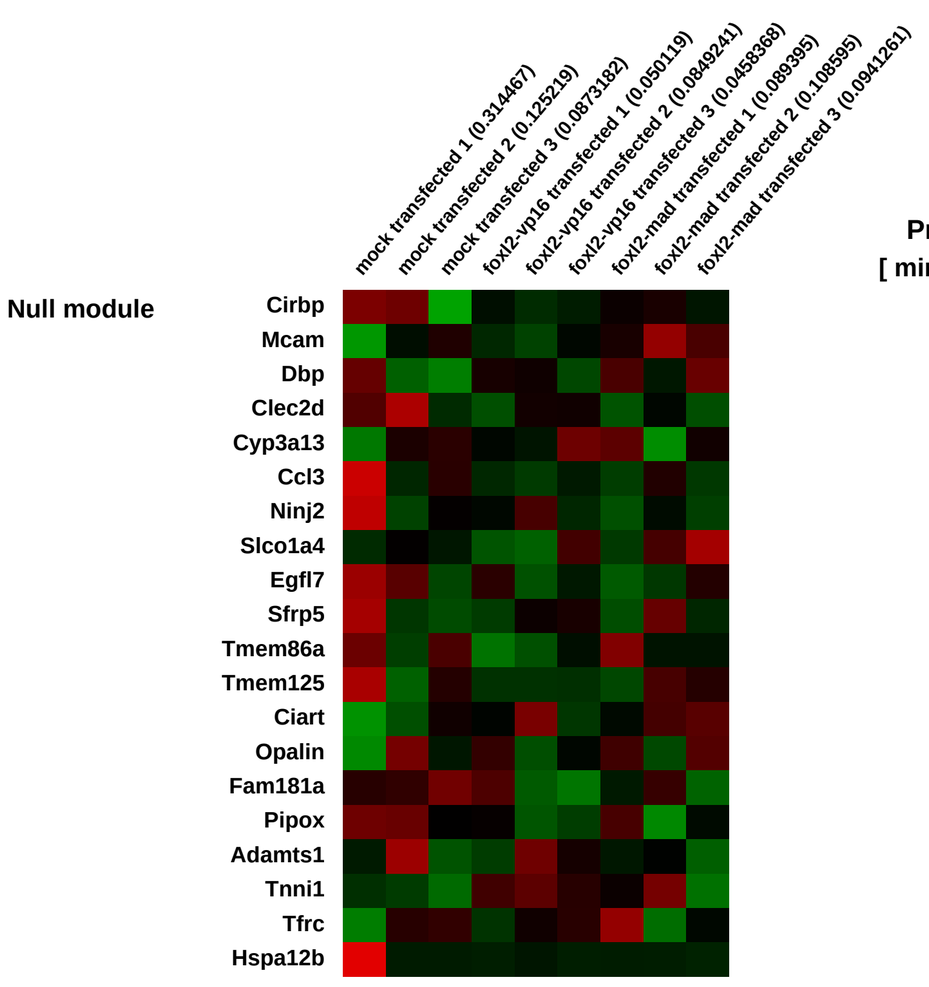

GEO Series "GSE32386" Expression Profiles

Num of samples in this series: 13

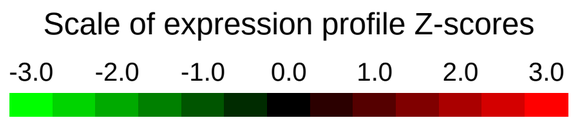

GEO Link:	**http://www.ncbi.nlm.nih.gov/geo/query/acc.cgi?acc=GSE32386**
Status:	**Public on Apr 01 2012**
Title:	**Expression profiling of murine neuroblastoma in transgenic mice**
Organism:	**Mus musculus**
Experiment type:	**Expression profiling by array**
Platform:	**GPL1261**
Pubmed ID:	**22764207**
Summary & Design:	**Summary:** **Neuroblastoma is an embryonal tumor arising from the neural crest. It can be mimicked in mice by neural crest-specific overepxression of oncogenes such as MYCN or mutated ALK.** **Overall design:** **Expression profiling of murine neuroblastoma driven by MYCN were compared to those driven by mutated ALK or both oncogenes. Mouse normal adrenal tissue served as a control.**

Background corr dist: **KL-Divergence = 0.0643, L1-Distance = 0.0382, L2-Distance = 0.0025, Normal std = 0.5410**

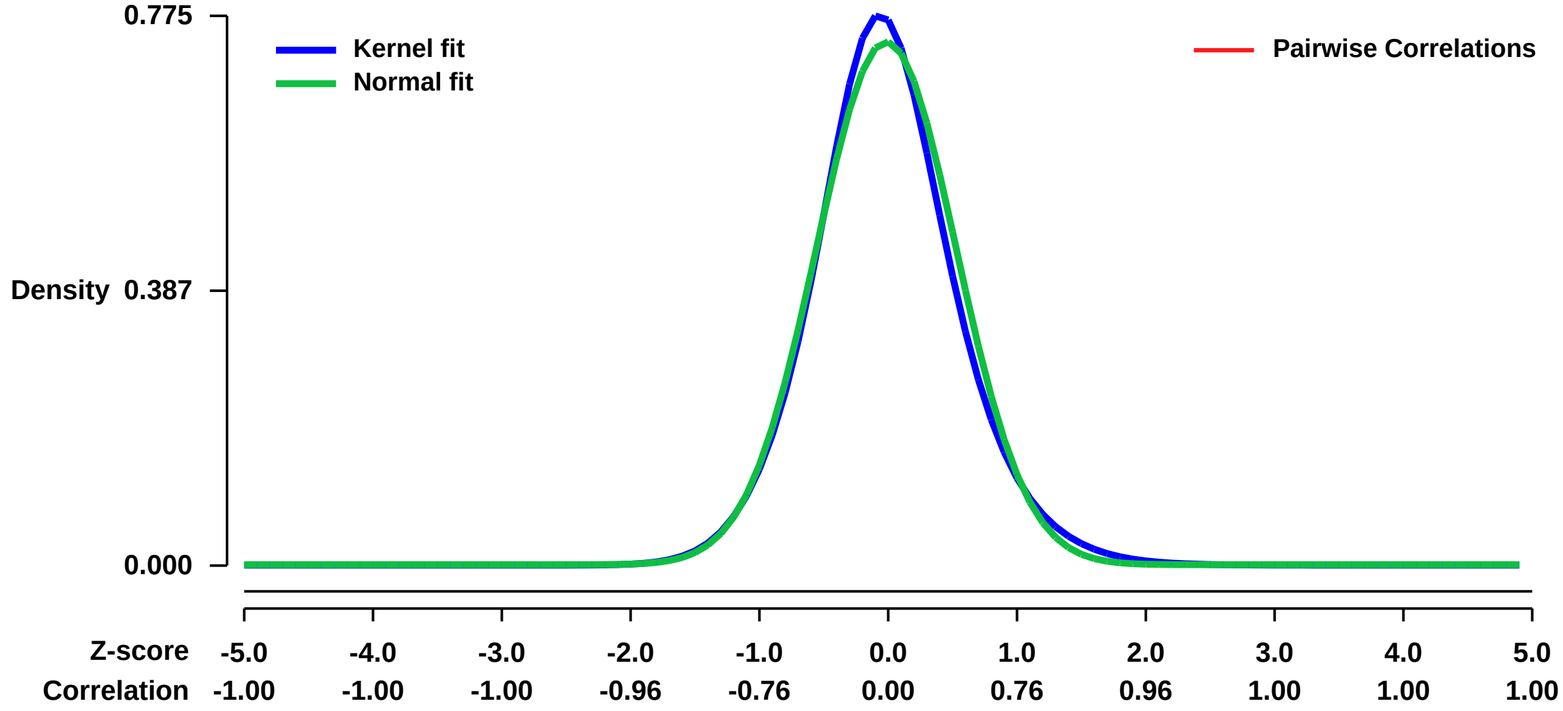

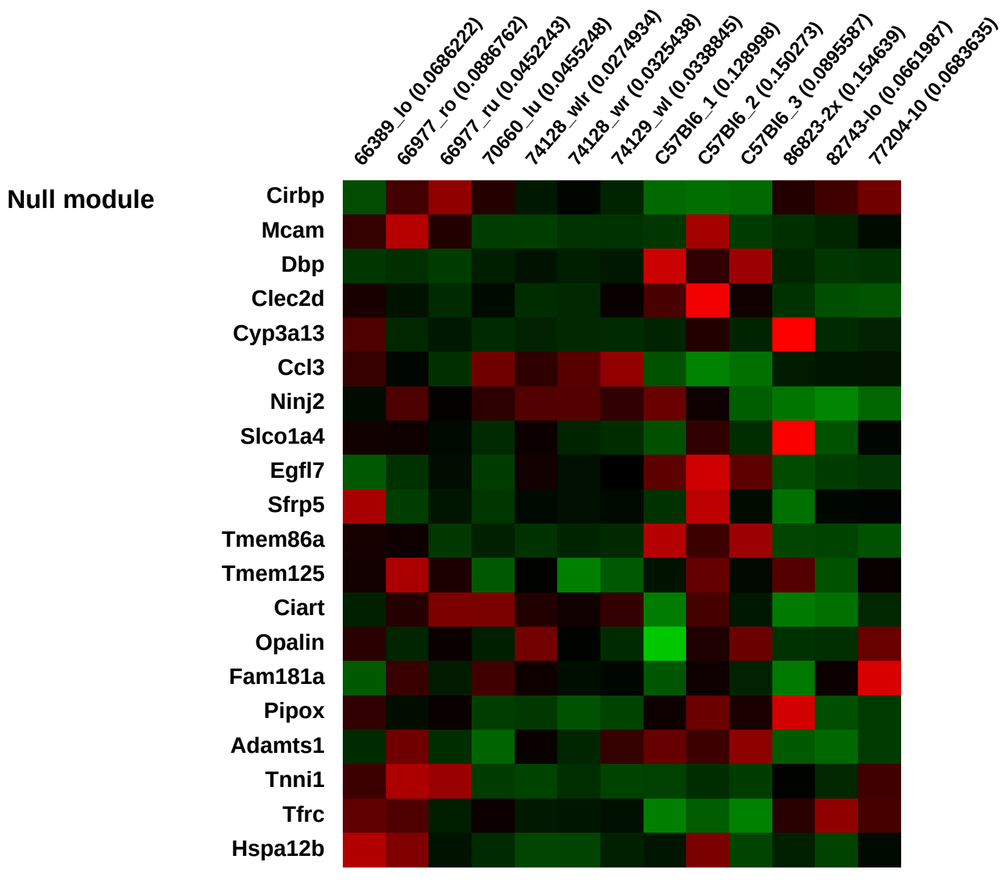

GEO Series "GSE11572" Expression Profiles

Num of samples in this series: 12

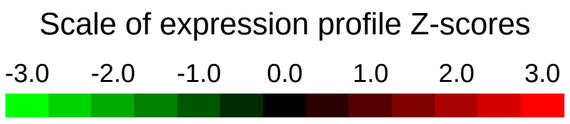

GEO Link:	**http://www.ncbi.nlm.nih.gov/geo/query/acc.cgi?acc=GSE11572**
Status:	**Public on Jul 31 2012**
Title:	**Klf4**
Organism:	**Mus musculus**
Experiment type:	**Expression profiling by array**
Platform:	**GPL1261**
Pubmed ID:	
Summary & Design:	**Summary:** **Klf4 is the zinc finger transcription factor indispensable for terminal maturation of epithelial tissues and part of group of proteins for the generation of pluripotent embryonic stem cells from differentiated tissues. No definitive in-vivo-function of Klf4 in the hematopoietic system has been established yet. We show here that Klf4 directly guides the transcriptional program for terminal differentiation of Ly-6Chigh monocytes. Klf4 suppresses transcripts of the interferon immune response and induces a proinflammatory cytokine transcriptional program.** **Concordantly, Klf4 hematopoietic deficiency in mice results in an enhanced Th1 but impaired Th17 immune response, and, consequently, those mice are resistant towards the induction of experimental autoimmune encephalitis (EAE). We here identify Klf4 is a transcription factor required for ontogenesis and function of Ly-6Chigh monocytes at the interface of innate and acquired immunity.** **Overall design:** **Williams,D.A., Tao,W., Yang,F., Kim,C., Gu,Y., Mansfield,P., Levine,J.E., Petryniak,B., Derrow,C.W., Harris,C., Jia,B., Zheng,Y., Ambruso,D.R., Lowe,J.B., Atkinson,S.J., Dinauer,M.C., and Boxer,L. (2000). Dominant negative mutation of the hematopoietic-specific Rho GTPase, Rac2, is associated with a human phagocyte immunodeficiency. Blood 96, 1646-1654.**

Background corr dist: KL-Divergence = 0.0401, L1-Distance = 0.0249, L2-Distance = 0.0010, Normal std = 0.5949

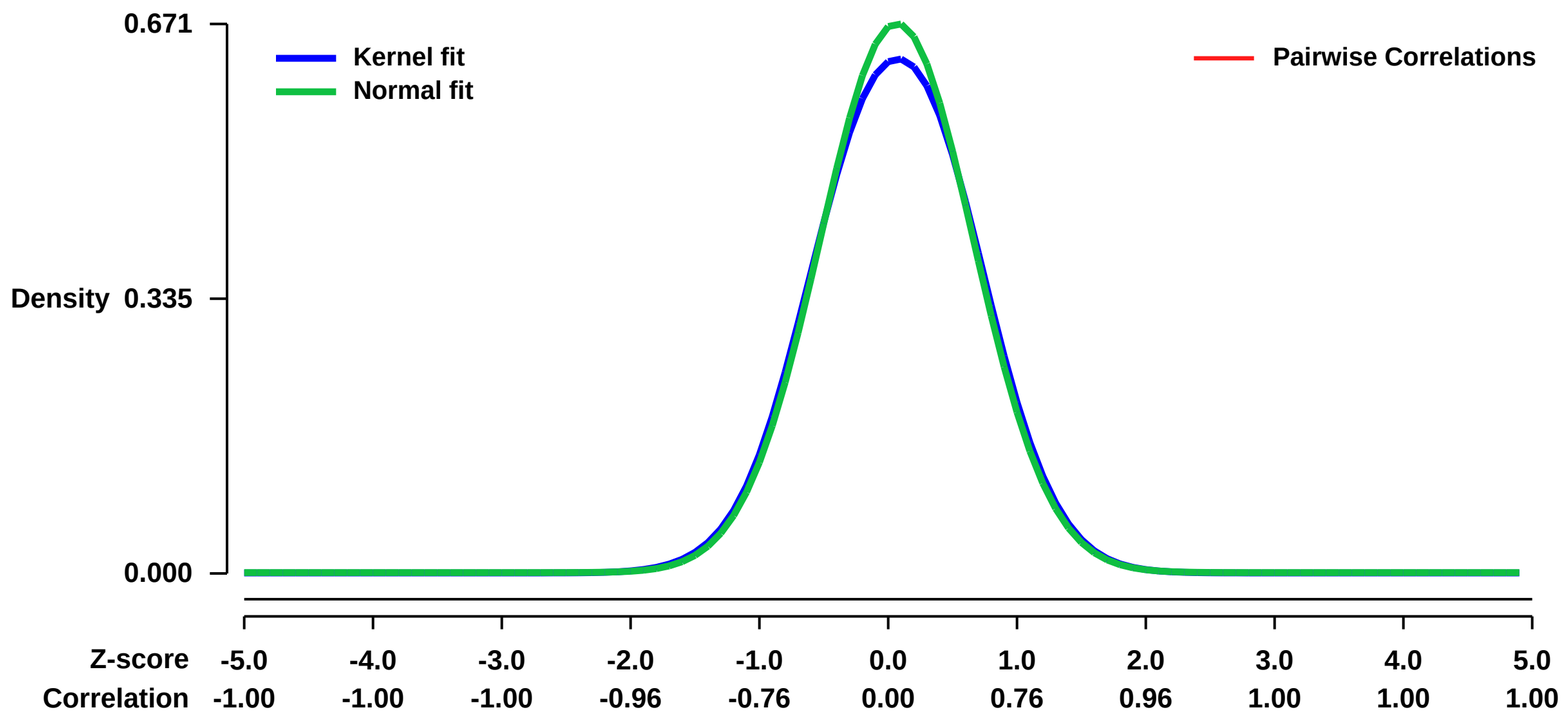

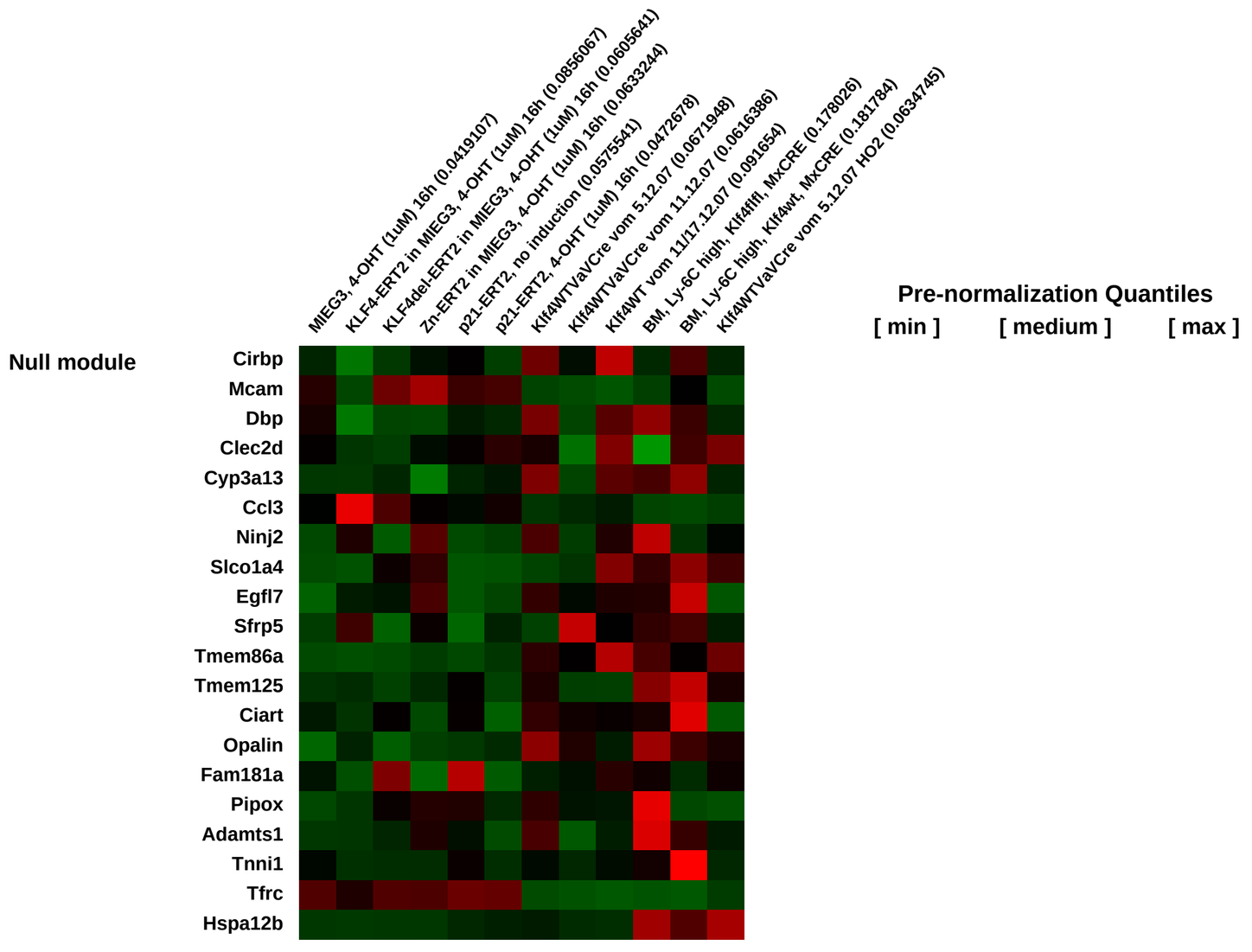

GEO Series "GSE8034" Expression Profiles

Num of samples in this series: 17

Scale of expression profile Z-scores

-3.0 -2.0 -1.0 0.0 1.0 2.0 3.0

GEO Link:	http://www.ncbi.nlm.nih.gov/geo/query/acc.cgi?acc=GSE8034
Status:	Public on May 29 2008
Title:	Prospective isolation of functionally distinct radial glial subtypes - lineage and transcriptome analysis
Organism:	Mus musculus
Experiment type:	Expression profiling by array
Platform:	GPL1261
Pubmed ID:	18372191
Summary & Design:	**Summary:** Since the discovery of radial glia as the source of neurons, their heterogeneity in regard to neurogenesis has been described by clonal and time-lapse analysis in vitro. However, the molecular determinants specifying neurogenic radial glia differently from radial glia that mostly self-renew remain ill-defined. Here, we isolated two radial glial subsets that co-exist at mid-neurogenesis in the developing cerebral cortex and their immediate progeny. While one subset generates neurons directly, the other is largely non-neurogenic but also gives rise to Tbr2-positive basal precursors, thereby contributing indirectly to neurogenesis. Isolation of these distinct radial glia subtypes allowed determining interesting differences in their transcriptome. These transcriptomes were also strikingly different from the transcriptome of radial glia isolated at the end of neurogenesis. This analysis therefore identifies, for the first time, the lineage origin of basal progenitors and the molecular differences of this lineage in comparison to directly neurogenic and gliogenic radial glia. **Overall design:** Comparison of radial glial subtypes

Background corr dist: KL-Divergence = 0.1566, L1-Distance = 0.0331, L2-Distance = 0.0024, Normal std = 0.3712

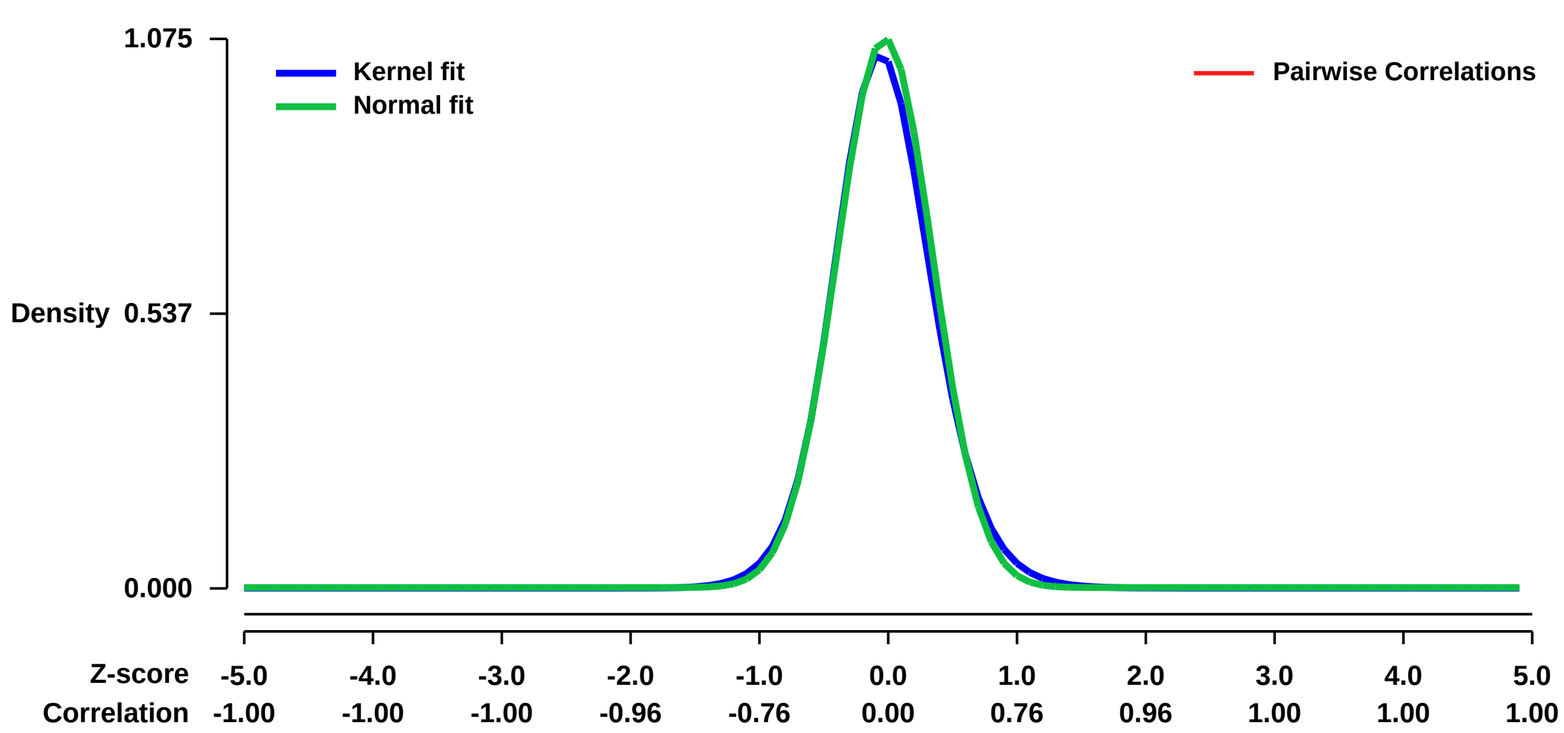

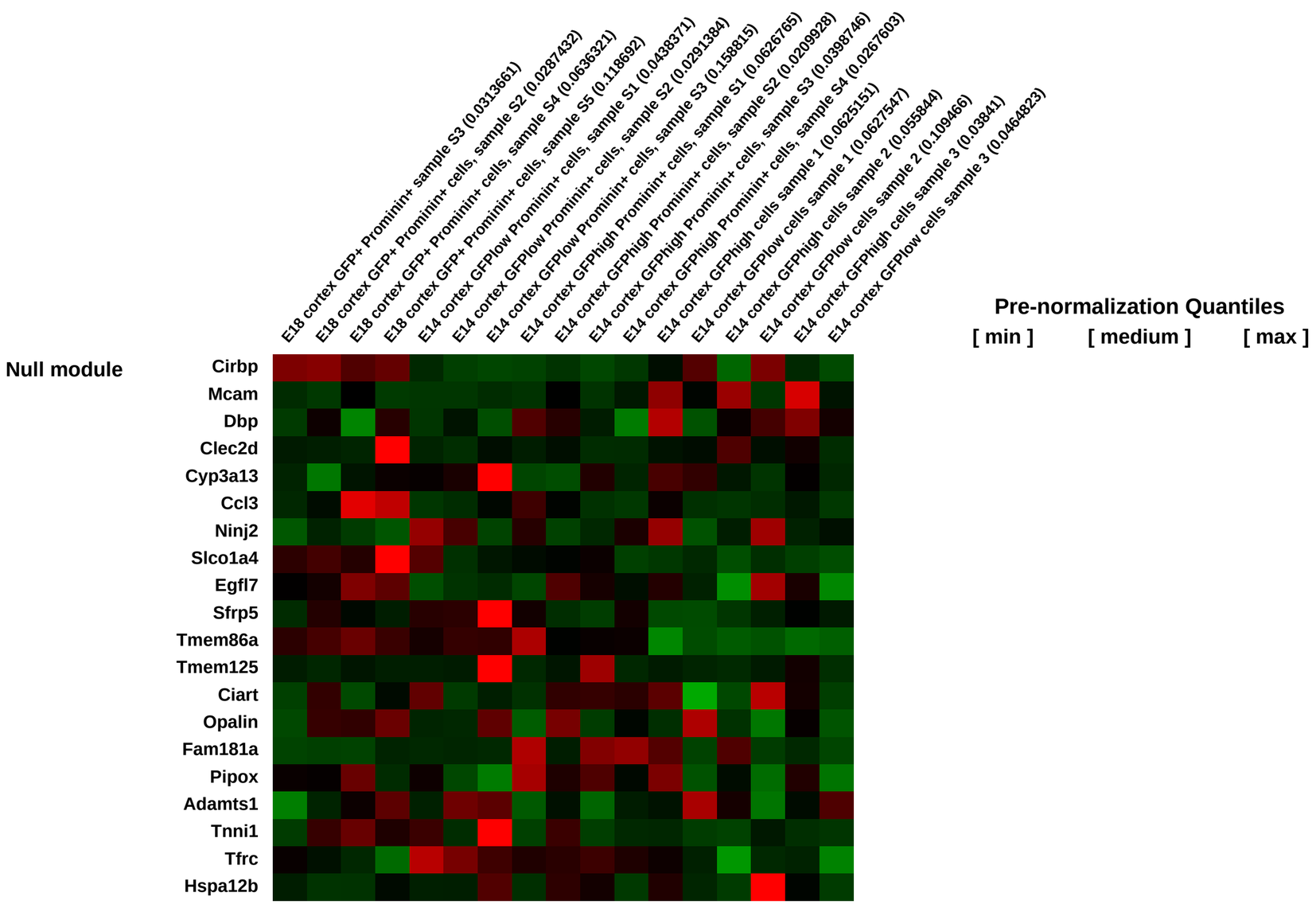

GEO Series "GSE13033" Expression Profiles

Num of samples in this series: 6

Scale of expression profile Z-scores

-3.0 -2.0 -1.0 0.0 1.0 2.0 3.0

GEO Link:	http://www.ncbi.nlm.nih.gov/geo/query/acc.cgi?acc=GSE13033
Status:	Public on Dec 01 2008
Title:	Differentially expressed genes in brain tissue from HtrA2 knockout mice
Organism:	Mus musculus
Experiment type:	Expression profiling by array
Platform:	GPL1261
Pubmed ID:	19023330
Summary & Design:	**Summary:** Cellular stress responses can be activated following functional defects in organelles such as mitochondria and the endoplasmic reticulum. Mitochondrial dysfunction caused by loss of the serine protease HtrA2 leads to a progressive movement disorder in mice and has been linked to parkinsonian neurodegeneration in humans. Here we demonstrate that loss of HtrA2 results in transcriptional up-regulation of nuclear genes characteristic of the integrated stress response, including the transcription factor CHOP, selectively in the brain. We also show that loss of HtrA2 results in the accumulation of unfolded proteins in the mitochondria, defective mitochondrial respiration and enhanced production of reactive oxygen species that contribute to the induction of CHOP expression and to neuronal cell death. CHOP expression is also significantly increased in Parkinsonâ s disease patientsâ brain tissue. We therefore propose that this brain-specific transcriptional response to stress may be important in the advance of neurodegenerative diseases. **Keywords:** genotype comparison **Overall design:** This experiment was set out to identify genes that are differentially expressed in brain tissue from the cortex of HtrA2 knockout (KO) mice compared to wild type (WT) littermates. We chose a cortical region since there is no evidence of neuronal loss in this region enabling us to compare mRNA transcripts in identical cellular populations. Brains of littermate WT and HtrA2 KO mice were dissected to obtain cortex tissue at post-natal day 29 (P29). RNA was isolated and samples were processed for hybridisation (6 samples in total, 3 replicates for each genotype).

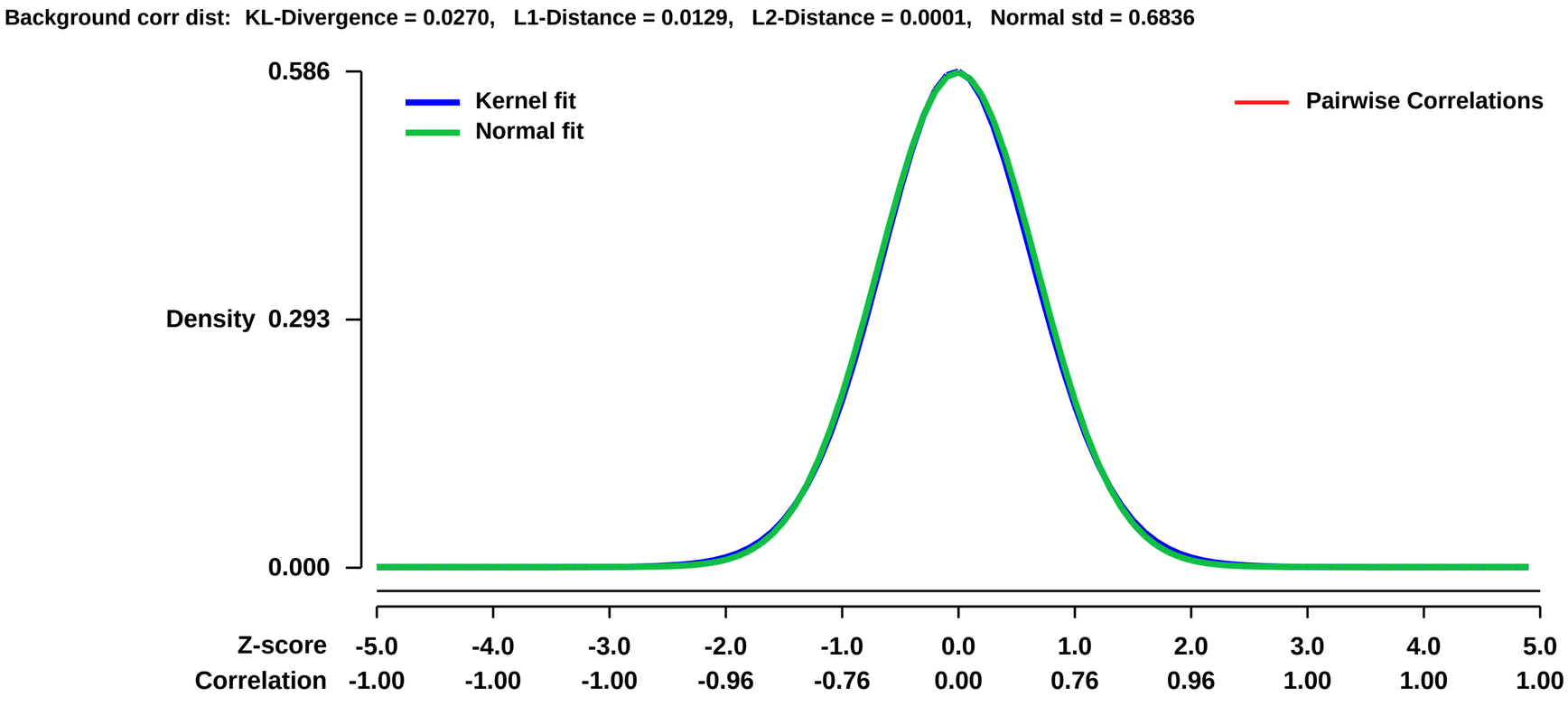

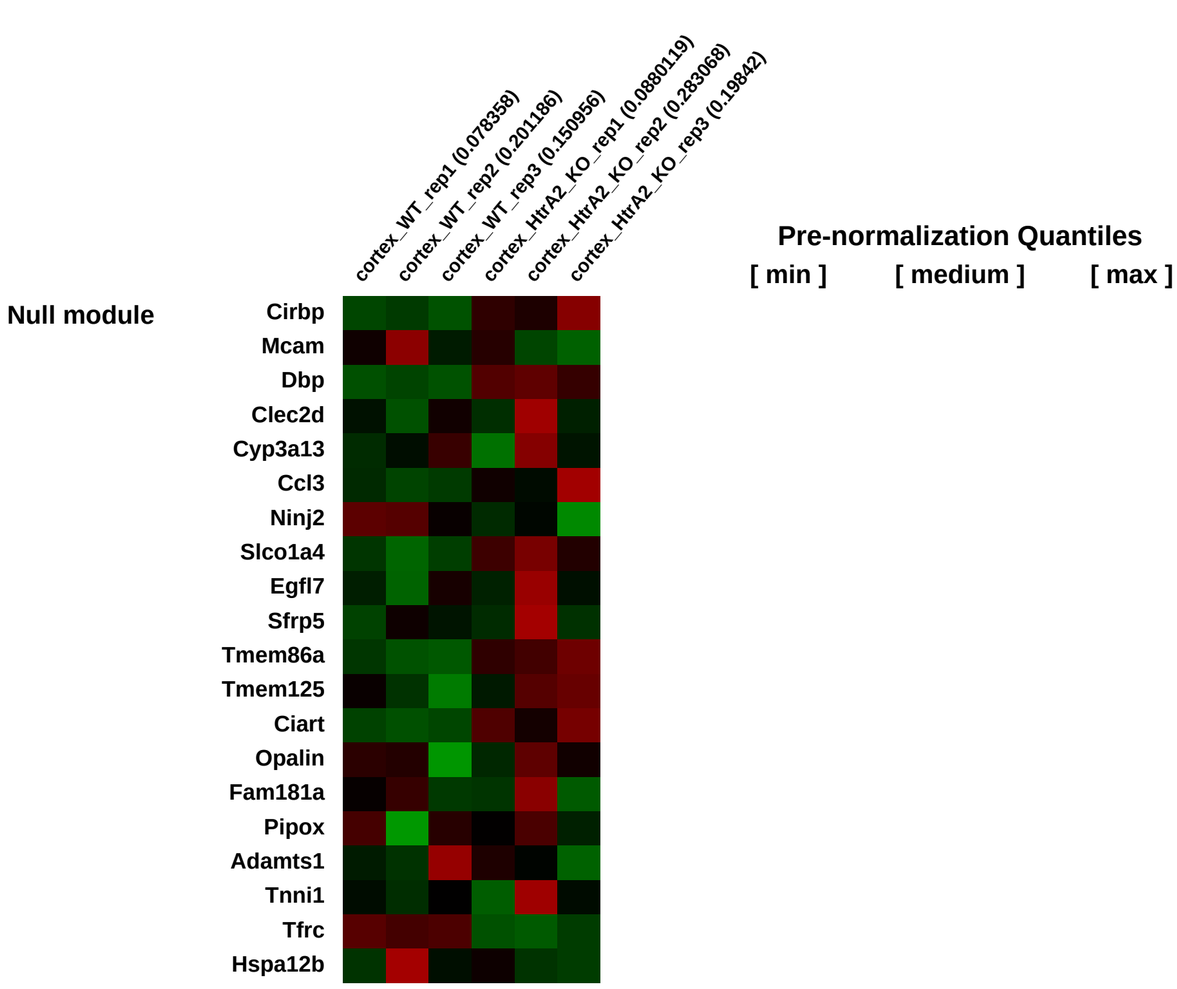

GEO Series "GSE19181" Expression Profiles

Num of samples in this series: 6

Scale of expression profile Z-scores

-3.0 -2.0 -1.0 0.0 1.0 2.0 3.0

GEO Link:	http://www.ncbi.nlm.nih.gov/geo/query/acc.cgi?acc=GSE19181
Status:	Public on Dec 23 2010
Title:	Expression data from macroH2A shRNA lines
Organism:	Mus musculus
Experiment type:	Expression profiling by array
Platform:	GPL1261
Pubmed ID:	21179167
Summary & Design:	**Summary:** Cancer is a disease of both genetic and epigenetic changes. While increasing evidence demonstrates that oncogenic progression entails chromatin-mediated changes such as DNA methylation, the role of histone variants in cancer initiation and progression currently remains unexplored. Here, we report that the histone variant macroH2A (mH2A) suppresses tumour progression of malignant melanoma. We hypothesized that loss of mH2A could contribute to melanoma progression by relieving repression of cell cycle- and metastasis-related genes. To gain insight into the transcriptional state of mH2A1 and mH2A2-deficient cells, we examined their gene expression profiles using Affymetrix microarrays. **Overall design:** Murine B16-F1 cells with lentiviral shRNAs against mH2A1 and mH2A2 were generated along with control shRNA (against GFP) and used for the microarray analysis. Two independent biological replicates were used.

Background corr dist: KL-Divergence = 0.0449, L1-Distance = 0.0241, L2-Distance = 0.0007, Normal std = 0.5998

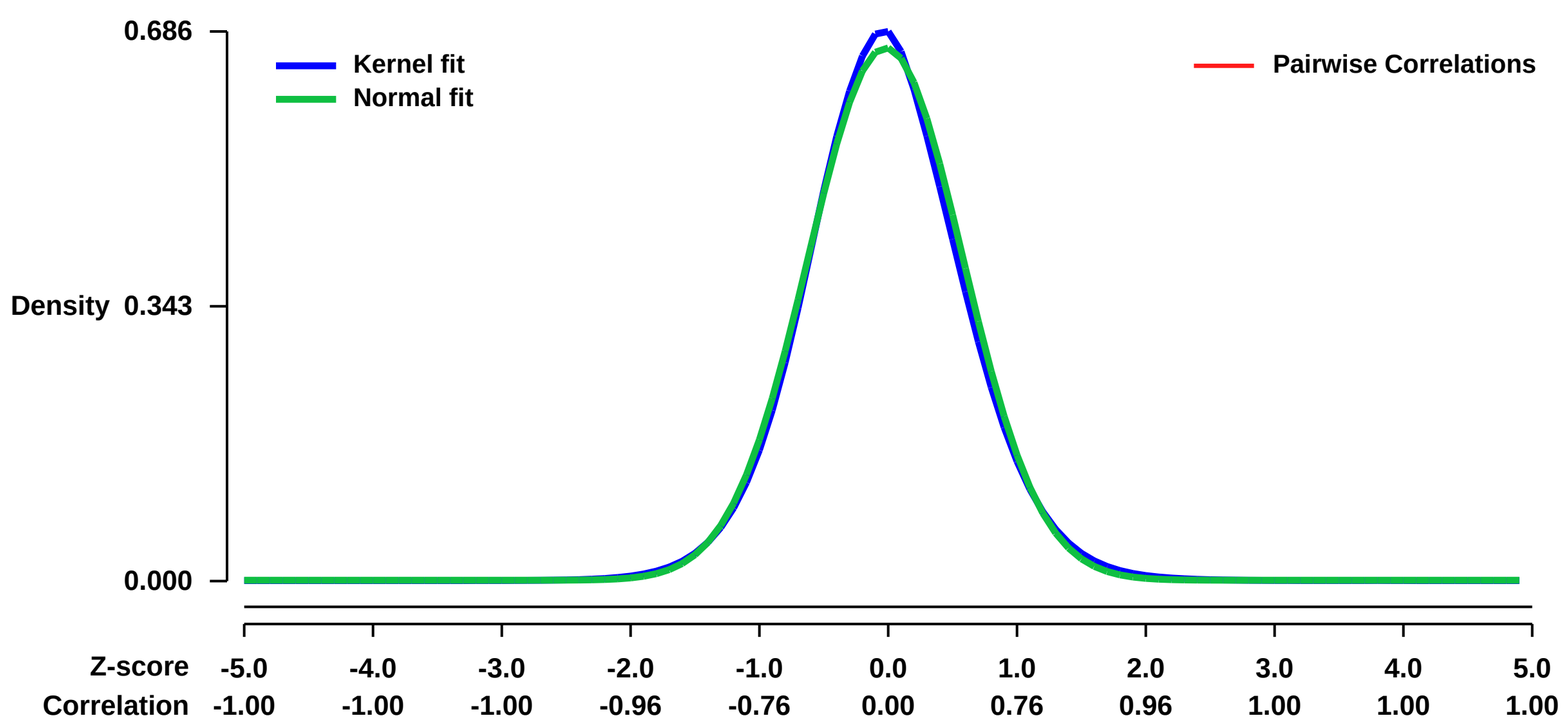

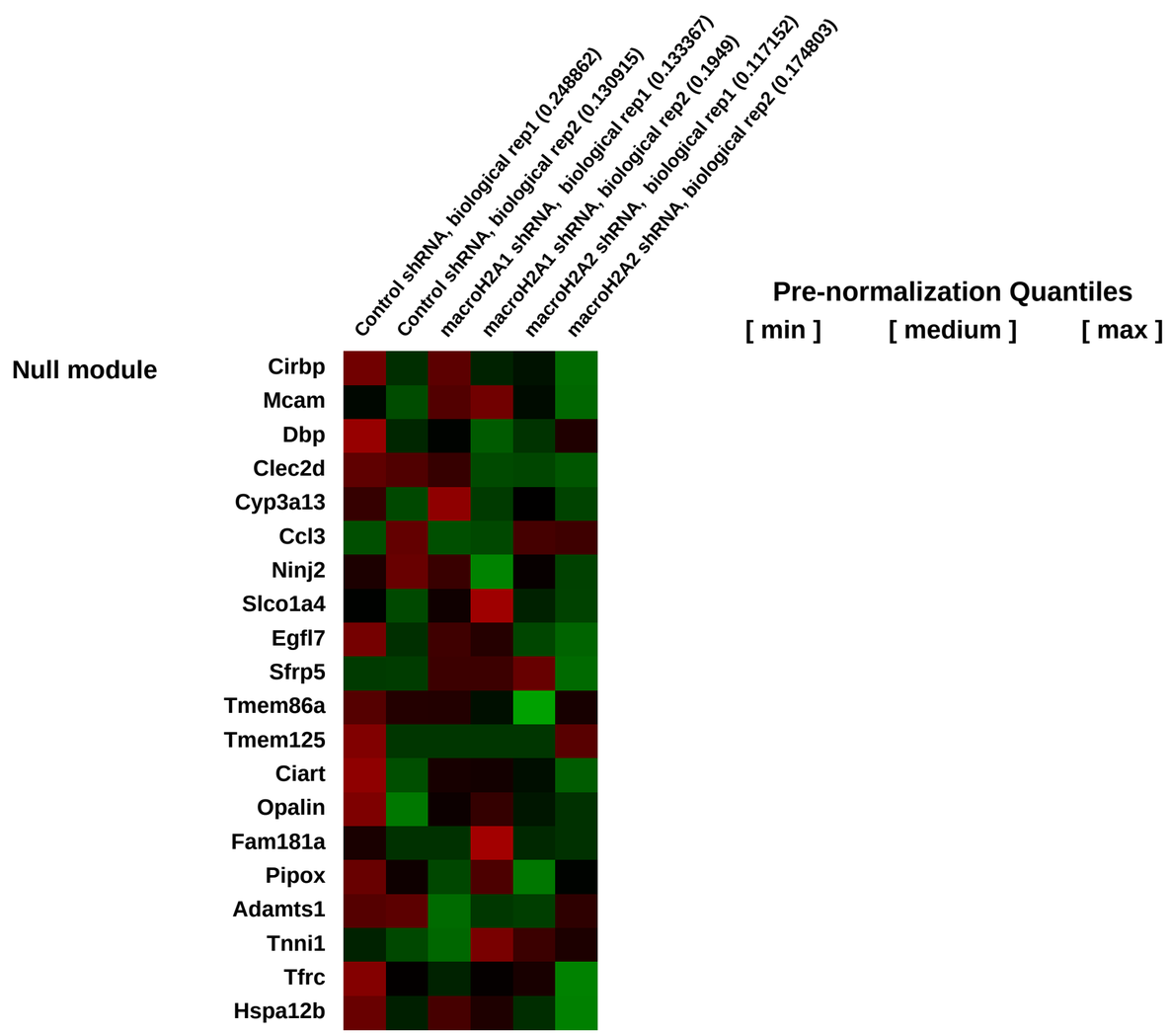

GEO Series "GSE18500" Expression Profiles

Num of samples in this series: 35

Scale of expression profile Z-scores

-3.0 -2.0 -1.0 0.0 1.0 2.0 3.0

GEO Link: http://www.ncbi.nlm.nih.gov/geo/query/acc.cgi?acc=GSE18500
Status: Public on Dec 31 2009
Title: Mast cells in response to some pathogens elicit a transcriptional program devoid of type I IFN response
Organism: Mus musculus
Experiment type: Expression profiling by array
Platform: GPL1261
Pubmed ID: 20421474

Summary & Design:

Summary:
Although mast cells elicit proinflammatory and type I IFN responses upon VSV infection, in response to L.monocytogenes (L.m) or S. Typhimurium (S.t), such cells elicit a transcriptional program devoid of type I IFN response.

Balanced induction of proinflamatory and type I interferon (IFN) responses upon activation of Toll like receptors (TLRs) determines the outcome of microbial infections and the pathogenesis of autoimmune and other inflammatory diseases. Mast cells, key components of the innate immune system, are known for their debilitating role in allergy and autoimmune syndromes. However, their potential role in anti-microbial host defenses is increasingly being acknowledged. How mast cells interact with microbes and the nature of responses triggered thereof is not well characterized. Here we show that in response to TLR activation by Gram-positive and negative bacteria or their components like LPS, unlike macrophages, mast cells elicit pro-inflammatory but not type I IFN responses. We demonstrate that in mast cells, the bound bacteria and TLR ligands remain trapped at the cell surface and do not undergo internalization - a prerequisite for type I IFN induction. Such cells could, however, elicit type I IFNs in response to vesicular stomatitis virus (VSV), which accesses the cytosolic RIG-I receptor. Although important for anti-viral immunity, a strong type I IFN response is known to contribute to pathogenesis during bacterial infection. Thus, while endowed with the capacity to elicit type I IFNs in response to viral infection, the fact that mast cells only elicit pro-inflammatory responses upon bacterial infection illustrates that mast cells, key effector cells of the innate immune system, are well adjusted for optimal anti-bacterial and anti-viral responses.

Overall design:
Gene Expression levels were determined by the Affymetrix MOE 430 2.0 GeneChips. Signal Intensities were calculated using the RMA algorithm and for statistical analysis we applied GeneSpring GX 10 software suite (Agilent Technologies, Waldbronn, Germany). MultiExperiment Viewer (MEV) software version 4.4 of the Institute for Genomic Research was used for clustering algorithm data analysis and visualization.

Background corr dist: KL-Divergence = 0.1240, L1-Distance = 0.0285, L2-Distance = 0.0012, Normal std = 0.4128

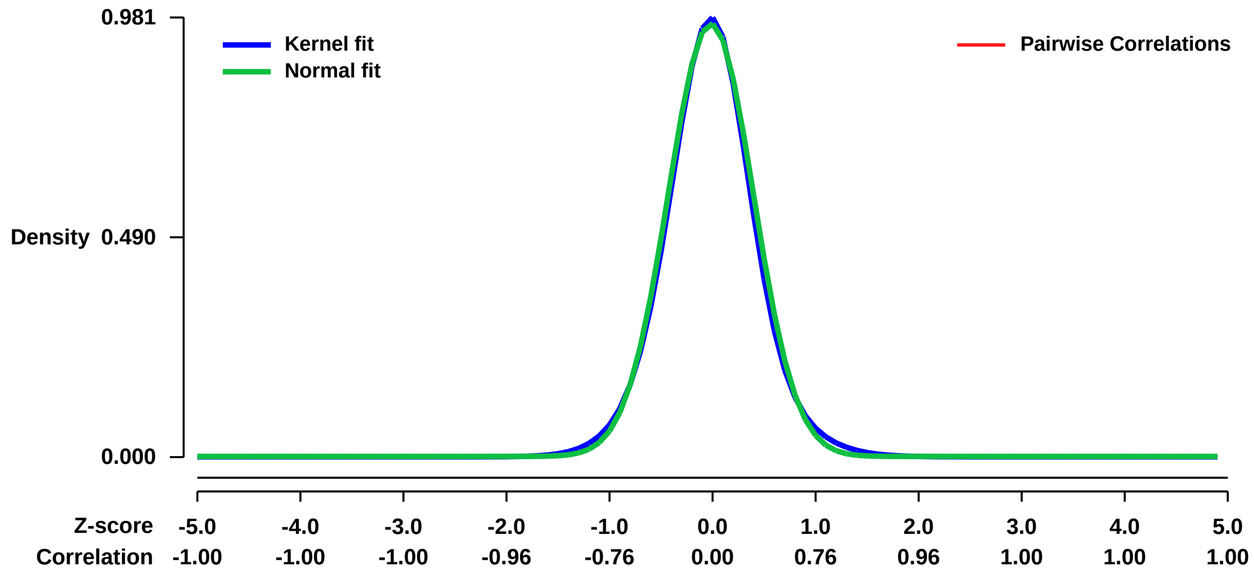

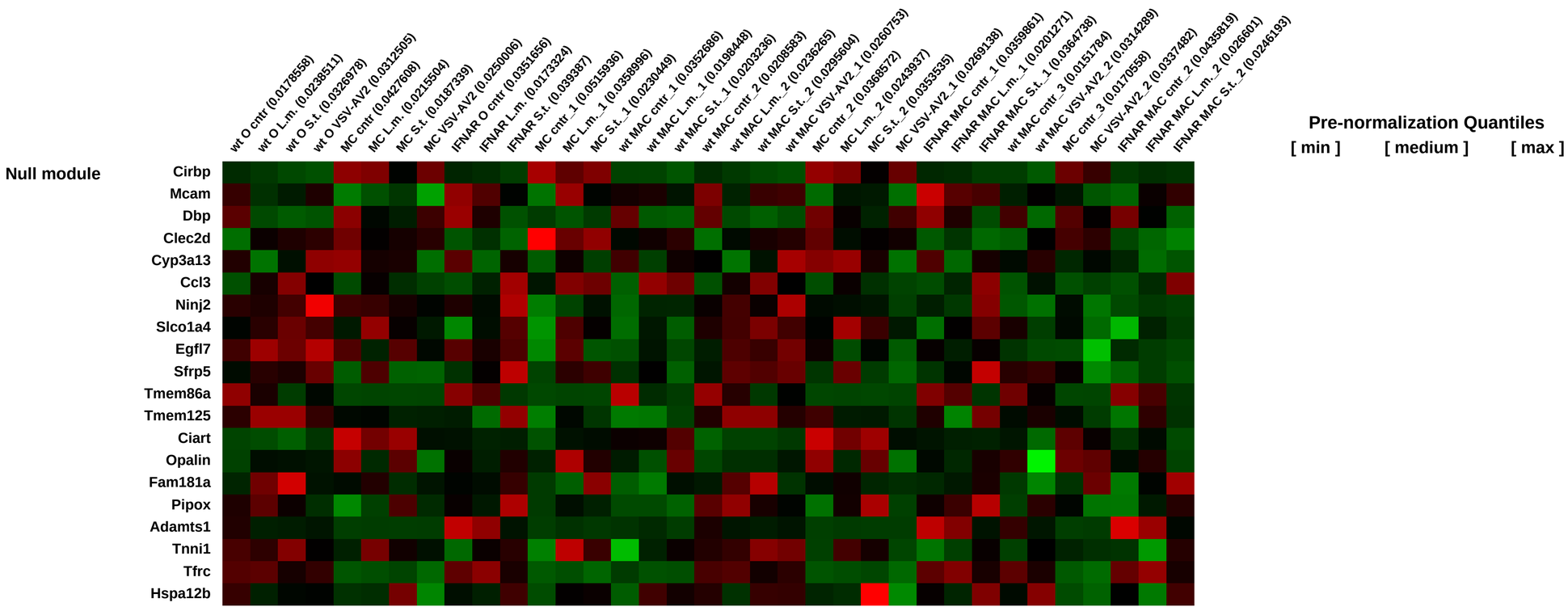

GEO Series "GSE7897" Expression Profiles

Num of samples in this series: 60

Scale of expression profile Z-scores

-3.0 -2.0 -1.0 0.0 1.0 2.0 3.0

GEO Link: http://www.ncbi.nlm.nih.gov/geo/query/acc.cgi?acc=GSE7897

Status: Public on Aug 09 2008

Title: Expression data from Mouse Lymphoma

Organism: Mus musculus

Experiment type: Expression profiling by array

Platform: GPL1261

Pubmed ID: 18922927

Summary & Design:

Summary:
We have made use of the E$_\mu$...-myc transgenic mouse, a model for the study of B-cell lymphoma development that is initiated through a defined genetic alteration, to explore the contributions of additional somatic alterations that contribute to the heterogeneity of the resulting tumors. As one example of such heterogeneity, we have focused on the observation that lymphomas develop in E$_\mu$...-myc mice with a variable time of onset. Twenty-five early-onset, 25 late-onset lymphomas and 10 normal samples were each assayed on an Affymetrix Mouse Genome 430 2.0 array.

Keywords: Myc induced lymphomas with various time-of-onset

Overall design:
To focus on events that might distinguish early and late onset tumors, we performed genome-wide expression analyses of early- and late-onset lymphomas from E$^+\mu$myc transgenic mice using expression microarray techniques. Total RNA was prepared from 25 early-onset (32-76 days, 62.6+/-11.0 days, median 65 days), 25 late-onset tumors (253-649 days, 391.5+/-101.8 days, median 398 days) and 10 normal tissues (lymph nodes or spleen, 38-438 days, 181.0+/-175.2 days, median 62.5 days) and subjected to Affymetrix GeneChip analyses.

Background corr dist: KL-Divergence = 0.3081, L1-Distance = 0.0449, L2-Distance = 0.0038, Normal std = 0.2815

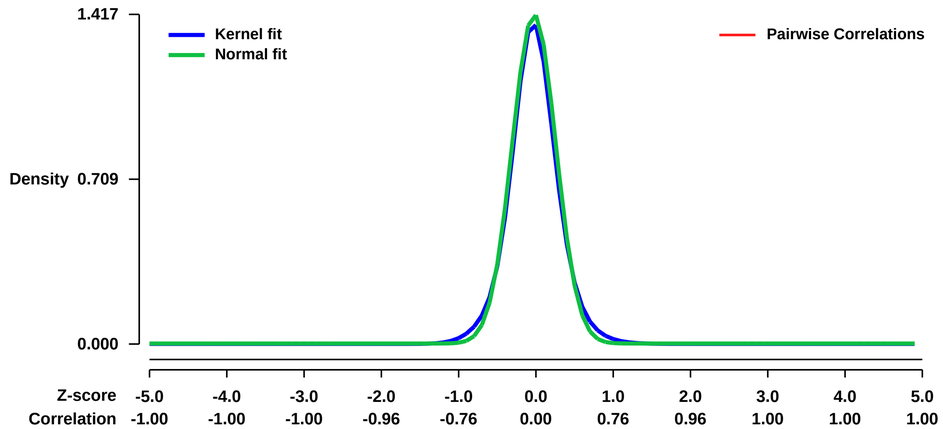

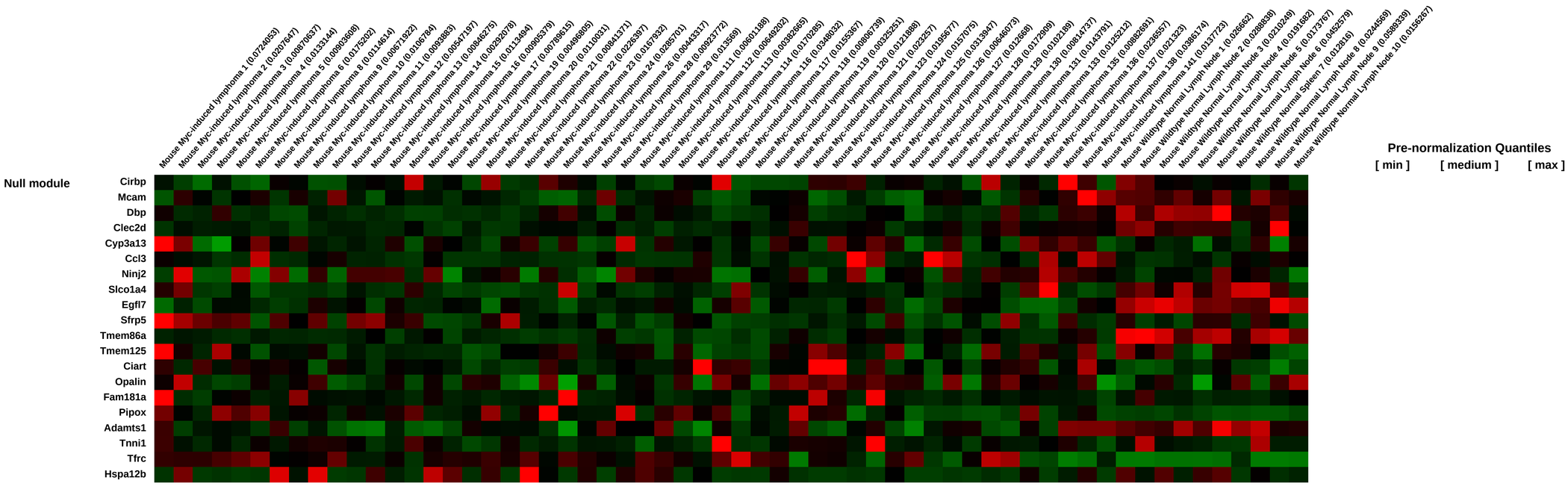

GEO Series "GSE21755" Expression Profiles

Num of samples in this series: 25

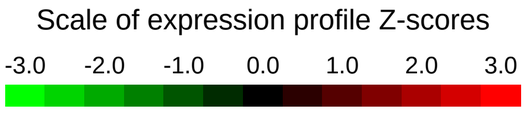

GEO Link:	http://www.ncbi.nlm.nih.gov/geo/query/acc.cgi?acc=GSE21755
Status:	Public on Jul 30 2010
Title:	Rapamycin effect on Wild Type and TSC deficient Mouse Embryonic Fibroblasts : Time Course
Organism:	Mus musculus
Experiment type:	Expression profiling by array
Platform:	GPL1261
Pubmed ID:	20670887
Summary & Design:	**Summary:** Aberrant activation of the mammalian target of rapamycin (mTOR) complex 1 (mTORC1) is a common molecular event in a large variety of pathological settings, including genetic tumor syndromes, cancer, and obesity. However, the cell intrinsic consequences of mTORC1 activation remain poorly defined. Here, we identify global trancriptional changes in TSC1 and TSC2 null MEFs, which exhibit constitutive activation of mTORC1, compared to wild-type littermate control lines. A rapamycin time course is included to determine those changes that are dependent on mTORC1 signaling, revealing mTORC1 induced and repressed transcripts. In order to identify mTORC1-dependent transcriptional changes, we compared wild-type MEFs to both Tsc1-/- and Tsc2-/- MEFs following serum starvation, where mTORC1 signaling is off in wild-type cells and fully active in TSC-deficient cells. All cell lines were serum-starved for 24 h, and the Tsc1-/- and Tsc2-/- cells were treated with a time course of rapamycin prior to the isolation of mRNA for microarray analysis. **Overall design:** Immortalized wild-type (Tsc2+/+ p53-/-), Tsc1-/- (p53+/+, 3T3-immortalized), and Tsc2-/- (p53-/-, derived from a littermate of the wild-type cell line) MEFs are the three cell lines used in this study and were derived in the laboratory of David J. Kwiatkowski (Brigham and Women's Hospital, Harvard Medical School, Boston, MA). Wild-type and null MEFs were grown to 70% confluence in 10 cm plates and were serum starved for 24 h in the presence of vehicle (DMSO) for 24 h or rapamycin (20 nM) for 2, 6, 12, or 24 h. All vehicle-treated samples (0 h time points) were plated in triplicate and all rapamycin time course samples were plated in duplicate. For each replicate, expression analysis was performed by hybridization to an Affymetrix Mouse 430_2 oligonucleotide microarray chip.

Background corr dist: KL-Divergence = 0.1004, L1-Distance = 0.0271, L2-Distance = 0.0010, Normal std = 0.4442

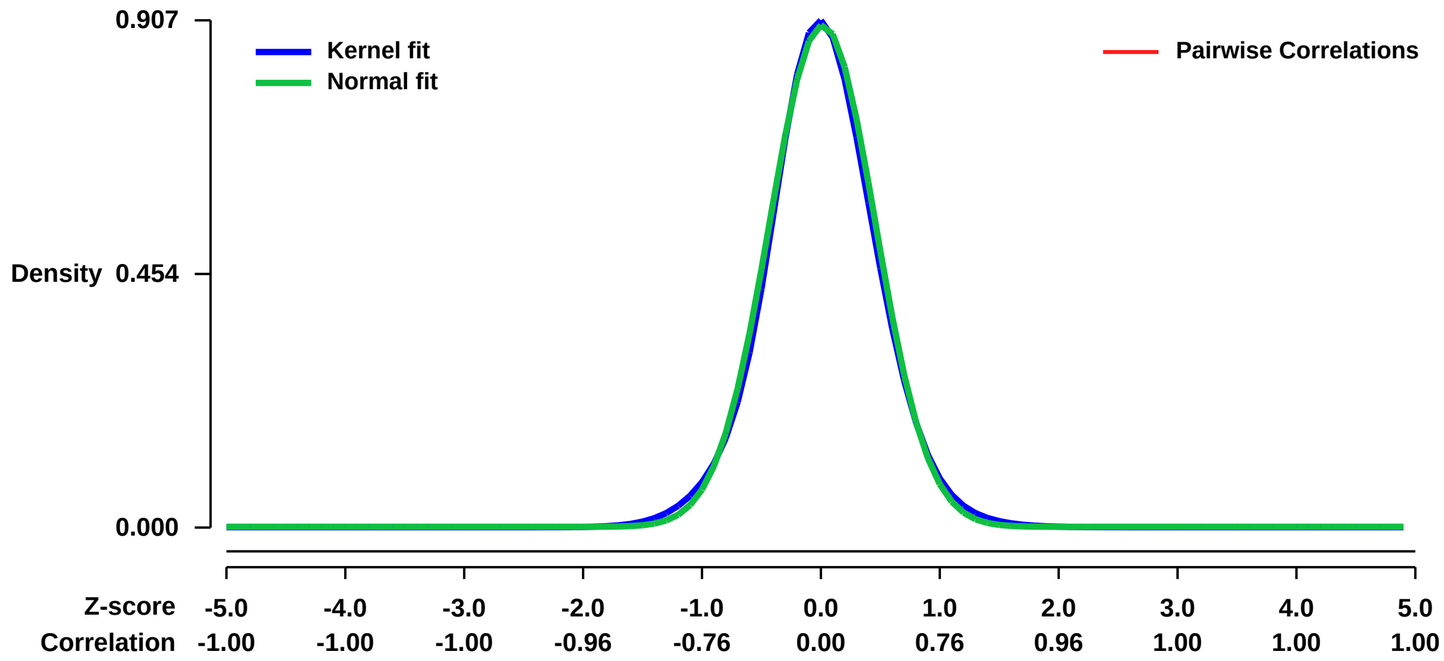

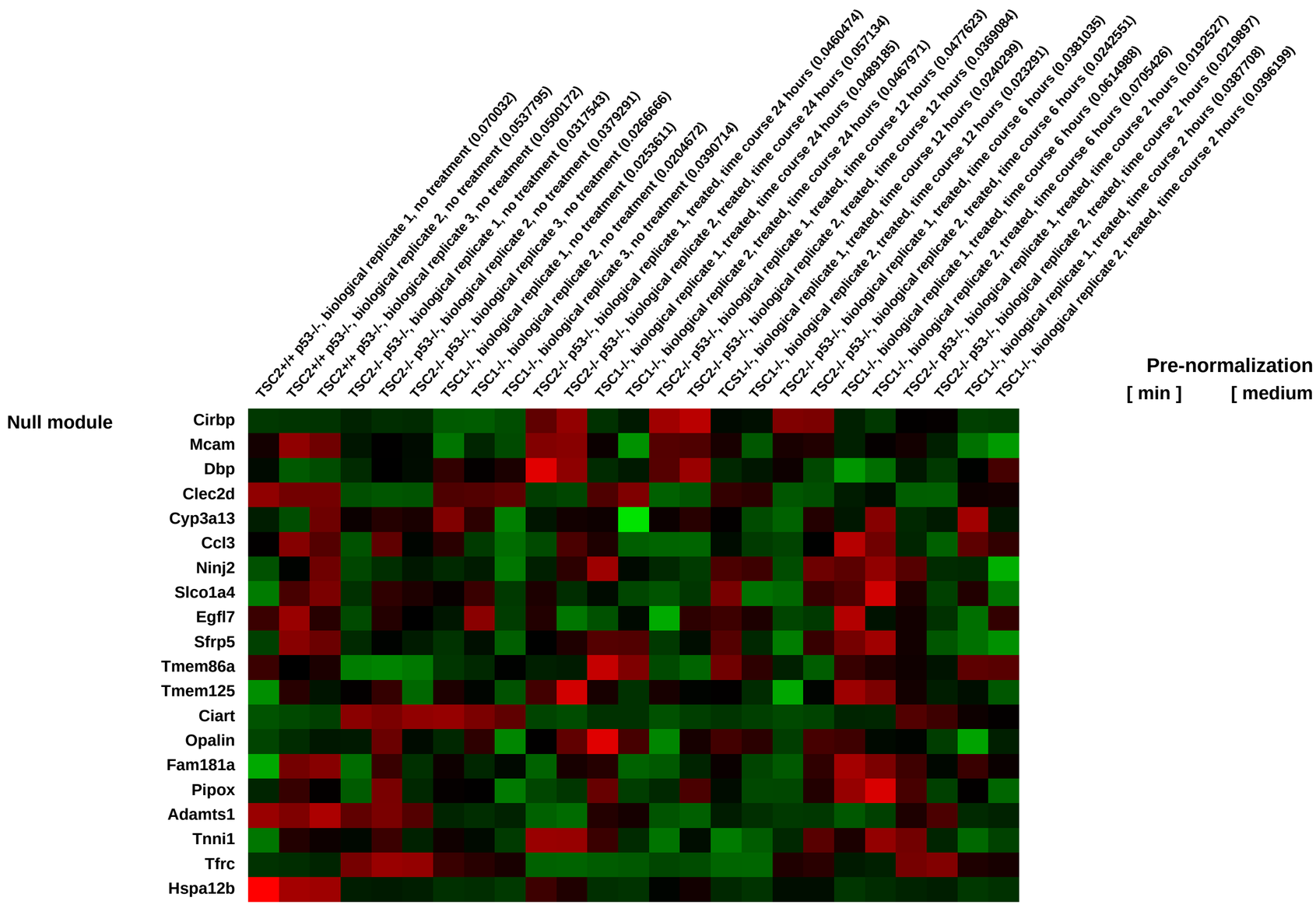

GEO Series "GSE23182" Expression Profiles

Num of samples in this series: 12

Scale of expression profile Z-scores

-3.0 -2.0 -1.0 0.0 1.0 2.0 3.0

GEO Link:	http://www.ncbi.nlm.nih.gov/geo/query/acc.cgi?acc=GSE23182
Status:	Public on Jul 28 2010
Title:	Systemic inflammation modulates Fc receptor expression on microglia in chronic neurodegeneration
Organism:	Mus musculus
Experiment type:	Expression profiling by array
Platform:	GPL1261
Pubmed ID:	21572034
Summary & Design:	**Summary:** To investigate the inflammatory response in neurodegenerative disease during an episode of systemic inflammation using the ME7 prion model. Comparison of ME7-infected mice with mice innoculated with Normal brain homogenate (NBH). 18 weeks post-innoculation mice were administered 500ug/kg LPS or an equivalent volume of saline as a control. **Overall design:** Total RNA was extracted from the hippocampus, amplified and reverse transcribed to cDNA using WT ovation kit and hybridised to mouse 430_2.0 Affymetrix Arrays. There were three biological replicates (individual mice) per group.

Background corr dist: KL-Divergence = 0.1371, L1-Distance = 0.0285, L2-Distance = 0.0013, Normal std = 0.3892

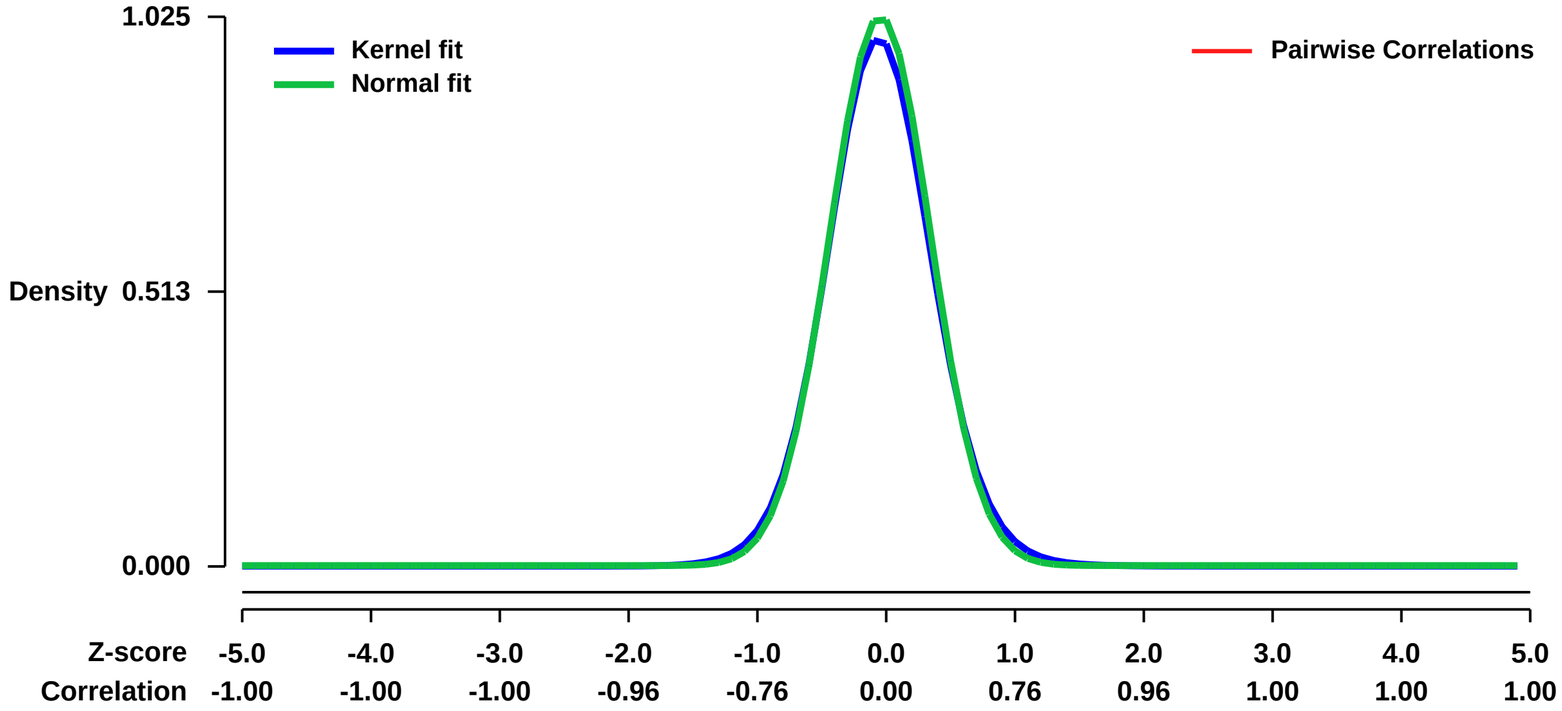

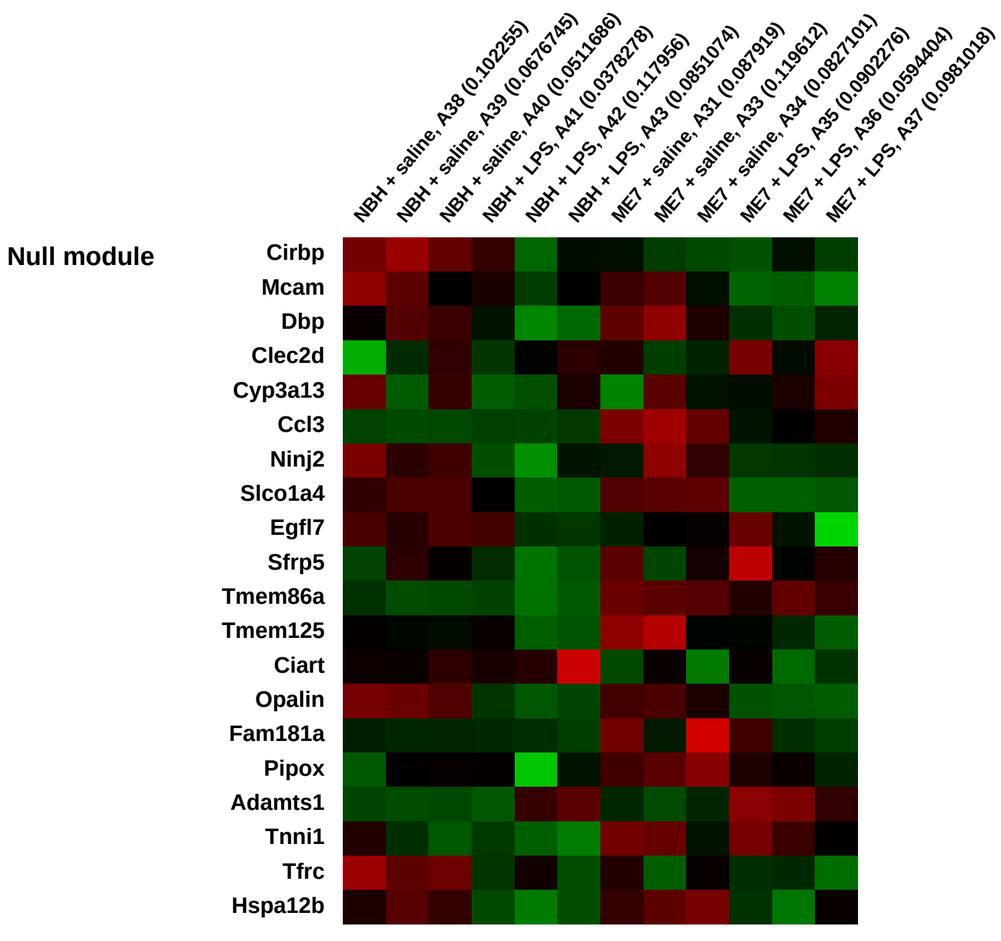

GEO Series "GSE32034" Expression Profiles

Num of samples in this series: 14

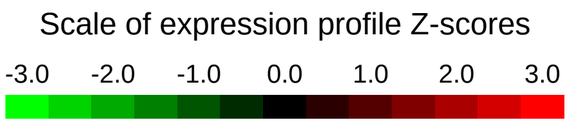

GEO Link:	http://www.ncbi.nlm.nih.gov/geo/query/acc.cgi?acc=GSE32034
Status:	Public on Oct 03 2012
Title:	Tissue-specific differences in PPAR‹‡ control of macrophage function.
Organism:	Mus musculus
Experiment type:	Expression profiling by array
Platform:	GPL1261
Pubmed ID:	22855714
Summary & Design:	**Summary:** PPAR‹‡ is known for its anti-inflammatory actions in macrophages. However, which macrophage populations express PPAR‹‡ in vivo and how it regulates tissue homeostasis in the steady state and during inflammation is not completely understood. We show that lung and spleen macrophages constitutively expressed PPAR‹‡, while other macrophage populations did not. Recruitment of monocytes to sites of inflammation was associated with induction of PPAR‹‡ as they differentiated to macrophages. Its absence in these macrophages led to failed resolution of inflammation, characterized by persistent, low-level recruitment of leukocytes. Conversely, PPAR‹‡ agonists supported an earlier cessation in leukocyte recruitment during resolution of acute inflammation and likewise suppressed monocyte recruitment to chronically inflamed atherosclerotic vessels. In the steady state, PPAR‹‡ deficiency in macrophages had no obvious impact in the spleen but profoundly altered cellular lipid homeostasis in lung macrophages. Reminiscent of pulmonary alveolar proteinosis, LysM-Cre x PPAR‹‡flox/flox mice displayed mild leukocytic inflammation in the steady-state lung and succumbed faster to mortality upon infection with S. pneumoniae. Surprisingly, this mortality was not due to overly exuberant inflammation, but instead to impaired bacterial clearance. Thus, in addition to its anti-inflammatory role in promoting resolution of inflammation, PPAR‹‡ sustains functionality in lung macrophages and thereby has a pivotal role in supporting pulmonary host defense. **Overall design:** The two major subsets of monocytes (Ly-6C+ and Ly-6Clo) from 12-week old C57Bl/6 mice were sorted and the RNA extracted and hybridized to Affymetrix GeneChip´fi 430 2.0 arrays. We pooled leukocytes from 5 mice for each sort and sorted 3 to 4 separate times for 3 to 4 biological replicates.

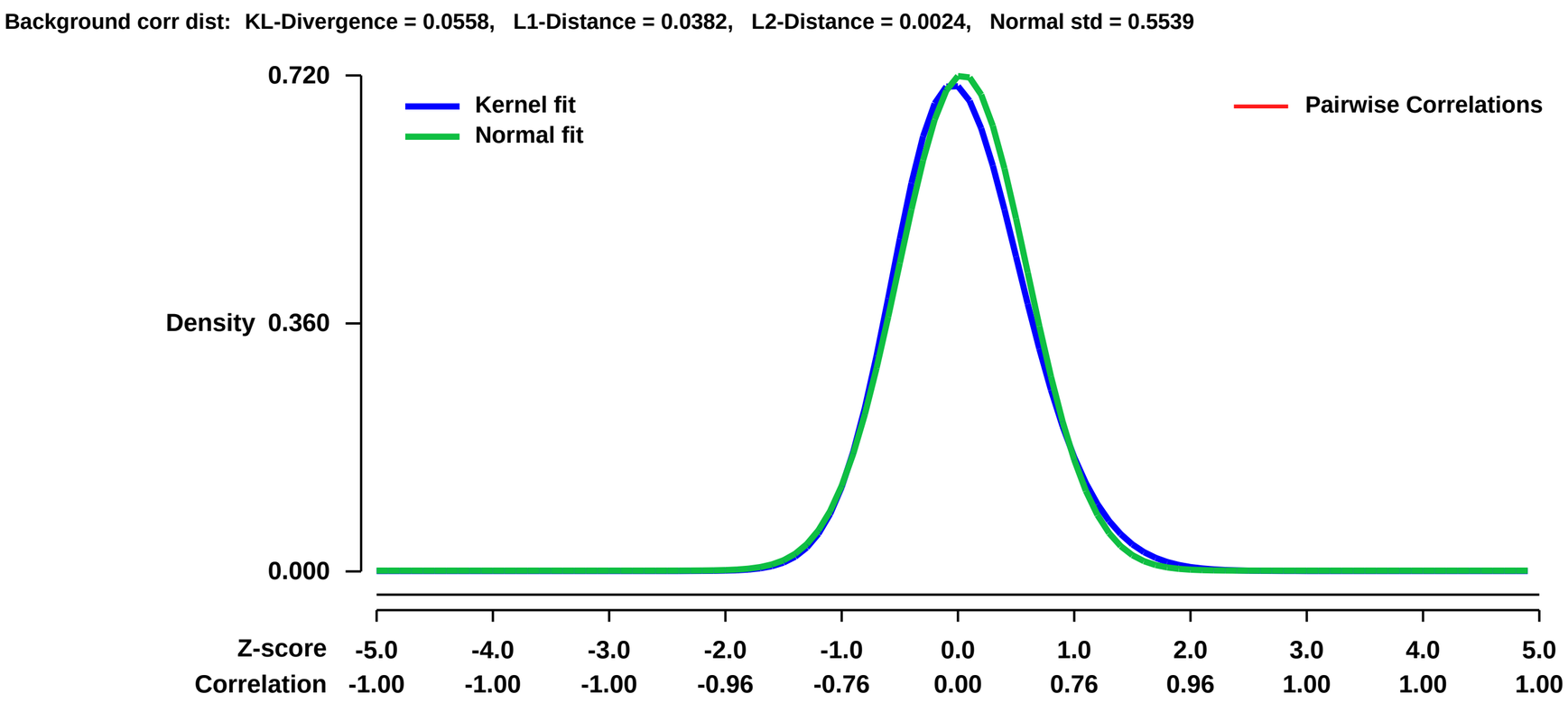

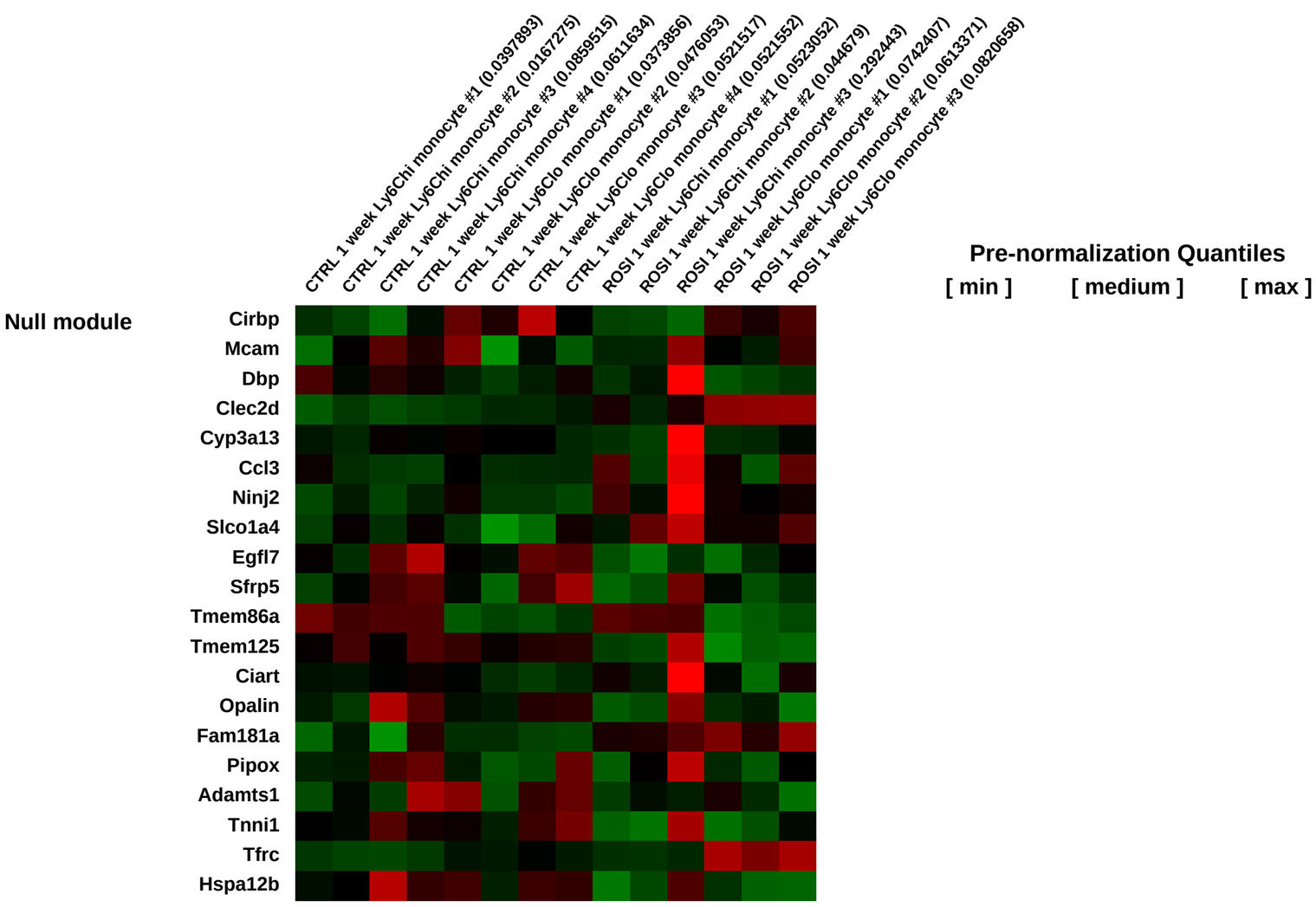

GEO Series "GSE3203" Expression Profiles

Num of samples in this series: 16

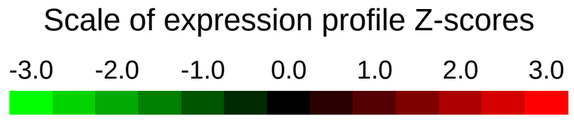

GEO Link:	http://www.ncbi.nlm.nih.gov/geo/query/acc.cgi?acc=GSE3203
Status:	Public on Aug 26 2006
Title:	Influenza virus infection-induced gene expression changes of regional B cells are mediated in part through type I IFN
Organism:	Mus musculus
Experiment type:	Expression profiling by array
Platform:	GPL1261
Pubmed ID:	17237394
Summary & Design:	**Summary:** Influenza virus infection-induced gene expression changes of regional B cells are mediated at least in part through type I Interferon: Our objective is to determine whether the influenza virus-infection induced gene expression changes in regional lymph node B cells are facilitated at least in part through type I interferon. Our specific aim is to compare the gene expression profile of highly FACS-purified B cells in the regional lymph nodes of wildtype and IFNR-/- mice prior to and 48h following infection with influenza virus infection and to contrast this expression profile with that of FACS-purified wildtype B cells activated in vitro with IFN-beta +/- anti-CD86 for 12h. Keywords: Infection-induced responses **Overall design:** We analyzed gene expression from mouse lymph node B cells purified by flow cytometric sorting using single channel oligonucleotide microarrays. There were 4 groups: 1) wild type uninfected mice (control group), 2) wild type mice infected with influenza (flu) for 2 days, 3) IFNR-/- mice infected with flu for 2 days, 4) cells stimulated with IFN-b in vitro for 17 h. Each group contained 4 biological replicates obtained from independent experiments. There were 16 total samples and each was measured on a separate array.

Background corr dist: KL-Divergence = 0.0926, L1-Distance = 0.0269, L2-Distance = 0.0011, Normal std = 0.4486

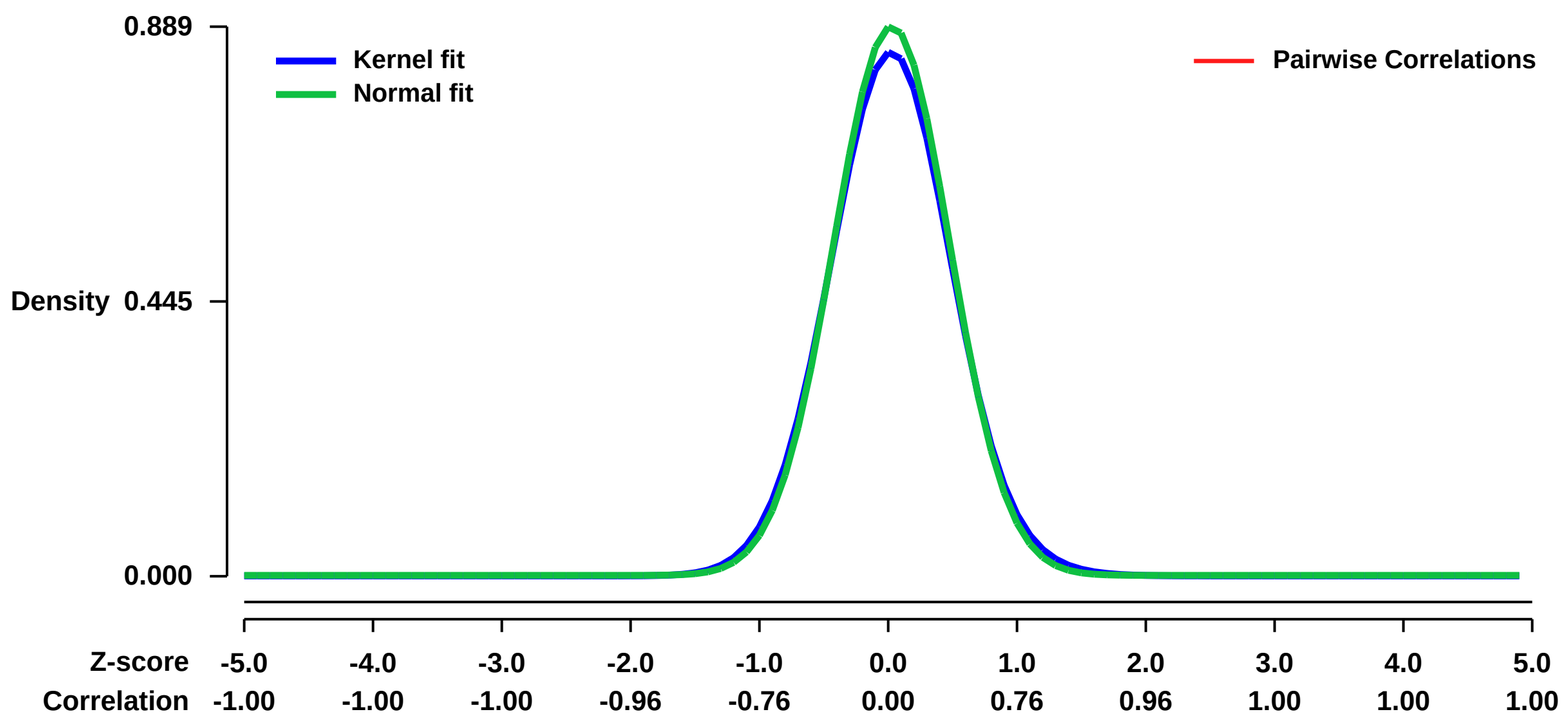

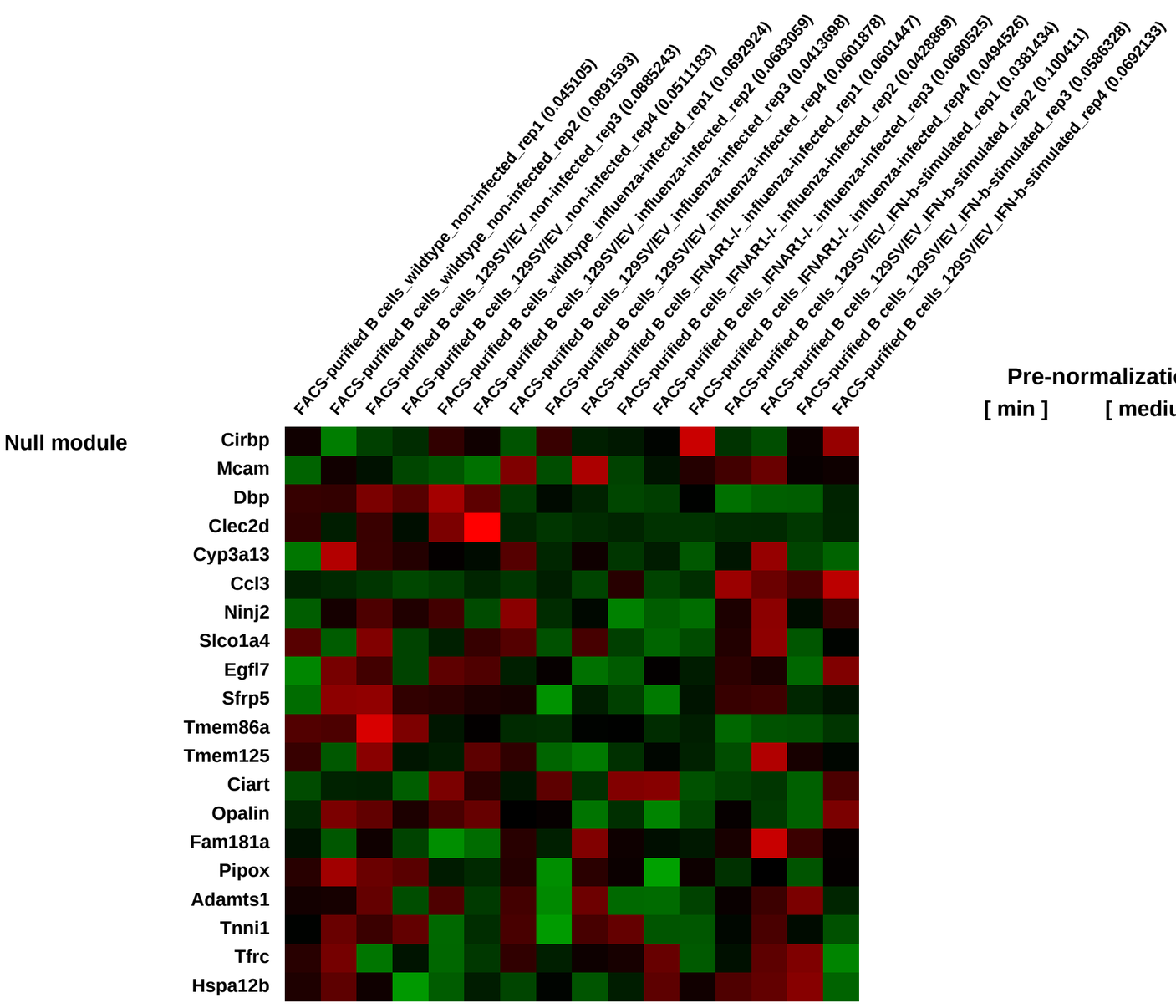

GEO Series "GSE23178" Expression Profiles

Num of samples in this series: 6

Scale of expression profile Z-scores

-3.0 -2.0 -1.0 0.0 1.0 2.0 3.0

GEO Link:	http://www.ncbi.nlm.nih.gov/geo/query/acc.cgi?acc=GSE23178
Status:	Public on Jul 29 2010
Title:	Expression data analysis in lungs from mice induced for pulmonary arterial hypertension (PAH) by inhalation of Stachybotrys chartarum spores
Organism:	Mus musculus
Experiment type:	Expression profiling by array
Platform:	GPL1261
Pubmed ID:	23157700
Summary & Design:	**Summary:** It has been reported that repeated intra-tracheal instillation of S. chartarum spores induced significant pulmonary arterial remodeling in mice, which resulted in pathological changes like human pulmonary arterial hypertension (PAH) and elevation right ventricle systolic pressure. Then, we used microarrays to know the complex molecular mechanisms that underlie pathogenesis of PAH. **Overall design:** Isolates of Stachybotrys chartarum were used. Ddy mice were anesthetized and the spore suspension was intratracheally injected 12 times, i.e. 1^ 104 spores into each mouse at 4-5 day intervals for 8 weeks. Mice were sacrificed one week after the final injection and then examined. Lung tissue specimens from mice model of PAH (n=3) and normal controls (n=3) were obtained. RNA targets preparation were performed according to the manufacturer's protocol using GeneChip(R) 3' IVT Express Kit (Affymetrix). One hundred nanograms of total RNA was converted into double-stranded cDNA template for transcription. In vitro transcription synthesized amplified RNA (aRNA) and incorporated a biotin-conjugated nucleotide. After purification and fragmentation of aRNA, 12.5 ug of them was hybridized to GeneChip(R) Mouse Genome 430 2.0 Array (Affymetrix).The Probe Array was scanned using a GeneChip(R) Scanner 3000 7G.

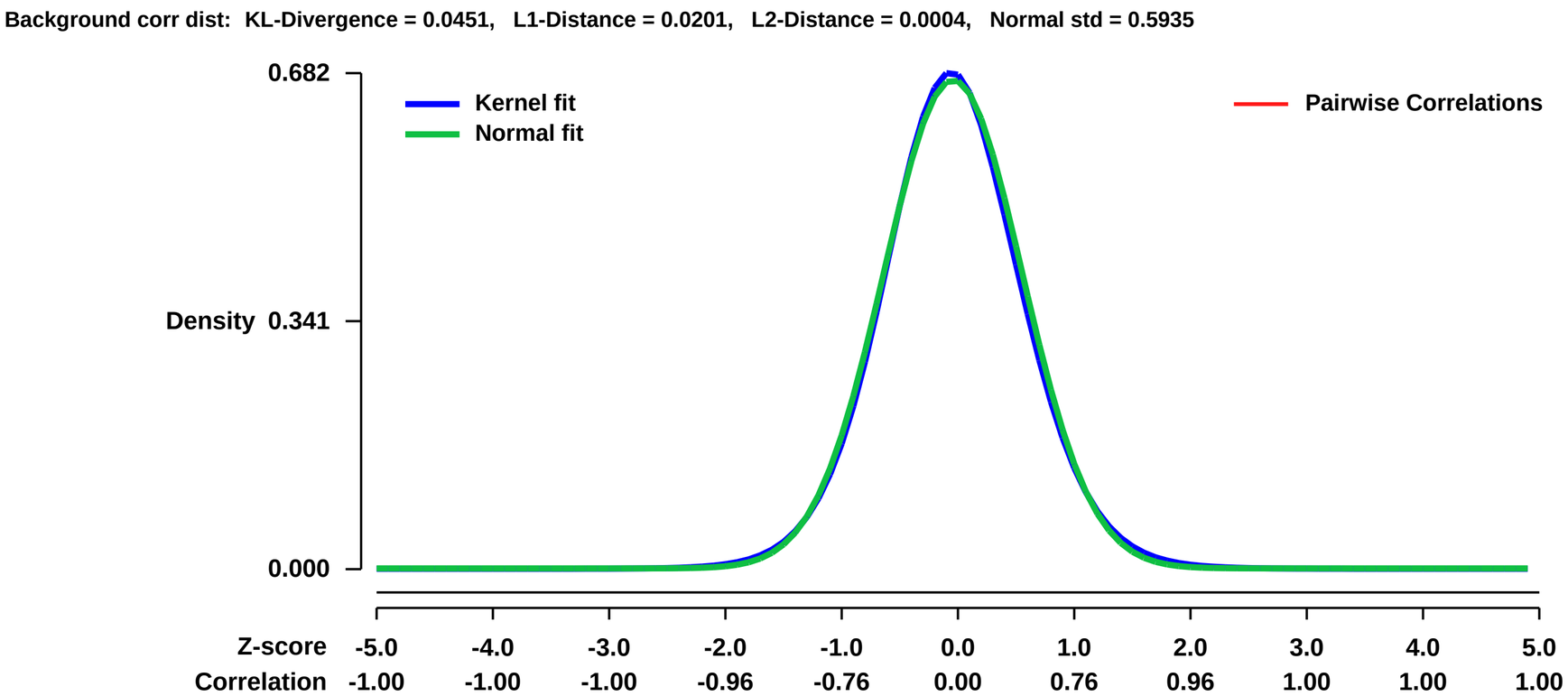

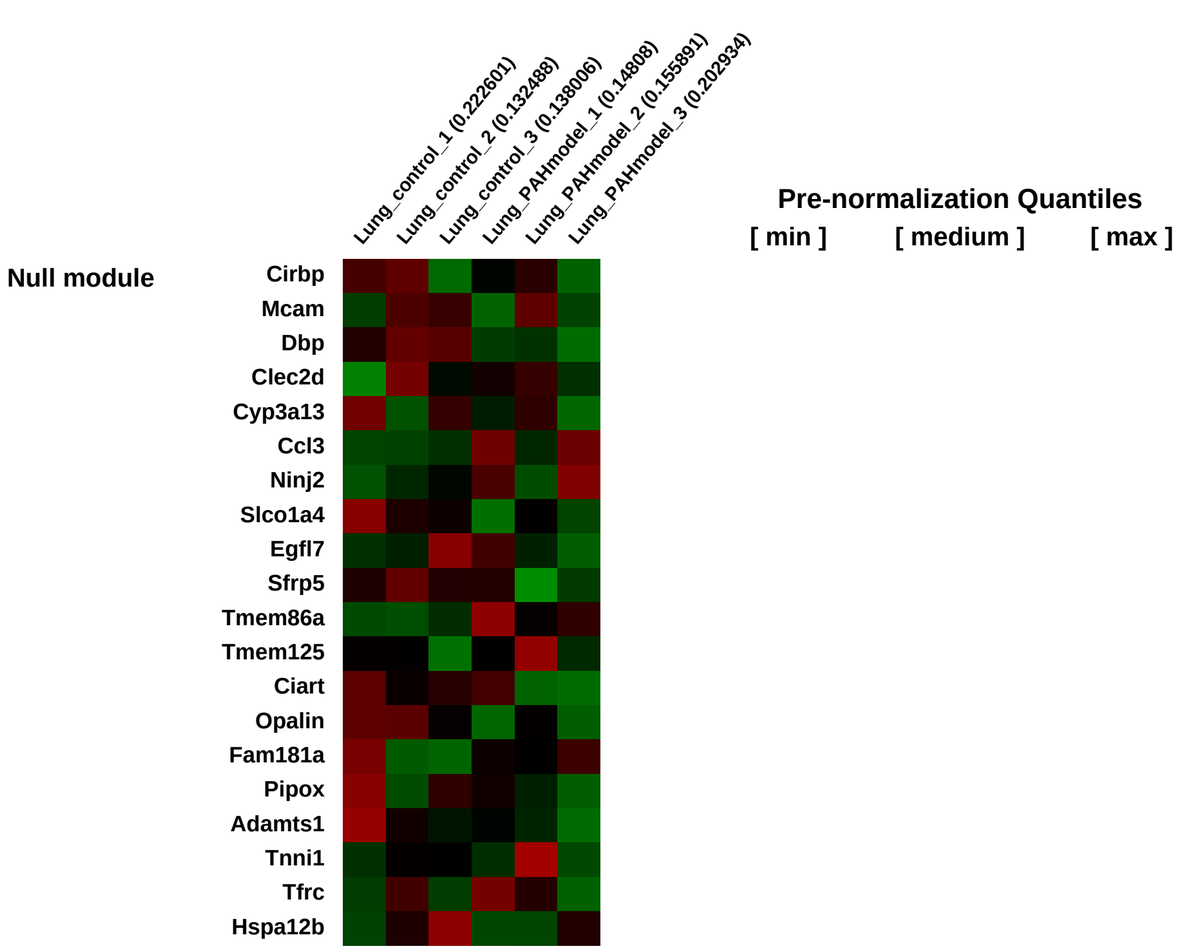

GEO Series "GSE24705" Expression Profiles

Num of samples in this series: 33

Scale of expression profile Z-scores

-3.0 -2.0 -1.0 0.0 1.0 2.0 3.0

GEO Link:	http://www.ncbi.nlm.nih.gov/geo/query/acc.cgi?acc=GSE24705
Status:	Public on May 31 2011
Title:	mRNA expression data from iPSCs, ntESCs and iPSC-nt-ESCs
Organism:	Mus musculus
Experiment type:	Expression profiling by array
Platform:	GPL1261
Pubmed ID:	21624975
Summary & Design:	**Summary:** We generated three kinds of genetically identical mouse reprogrammed cells: induced pluripotent stem cells (iPSCs), nuclear transfer embryonic stem cells (ntESCs) and iPSC-nt-ESCs that are established after successively reprogramming of iPSCs by nuclear transfer (NT). NtESCs show better developmental potential than iPSCs, whereas iPSC-nt-ESCs display worse developmental potential than iPSCs. We used microarrays to distinguish the gene expression differences among three pluriptoent stem cells and identified that imprinted genes had a similar expression pattern in iPSCs and iPSC-nt-ESCs. **Overall design:** We sought to obtain genetic identical pluripotent stem cell lines in order to minimize genetic variations among different reprogrammed cells. To that end, we established a genetically homogenous secondary reprogramming system, in which mouse embryonic fibroblasts (MEFs) carrying doxycycline (dox)-inducible lentiviruses expressing Oct4, Sox2, Klf4 and c-Myc were isolated and used as donors for different reprogramming experiments. We generated iPSCs after plating MEFs in the presence of dox in ES culture conditions, and then derived ntESCs after transplantation of the nucleus from the same MEFs into enucleated oocyte. Furthermore, we successively reprogrammed iPSCs by means of NT and established a set of nt-iPSC lines. Pluripotent stem cells generated from different reprogramming strategies were for RNA extraction and hybridization on Affymetrix microarrays.

Background corr dist: KL-Divergence = 0.1788, L1-Distance = 0.0475, L2-Distance = 0.0039, Normal std = 0.3601

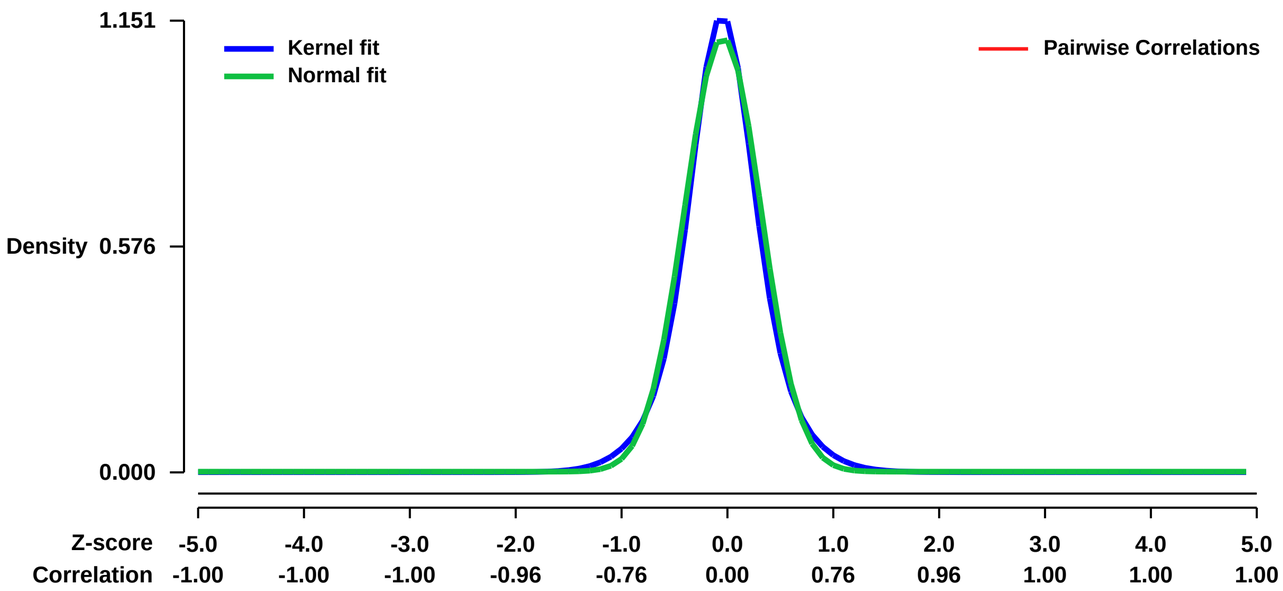

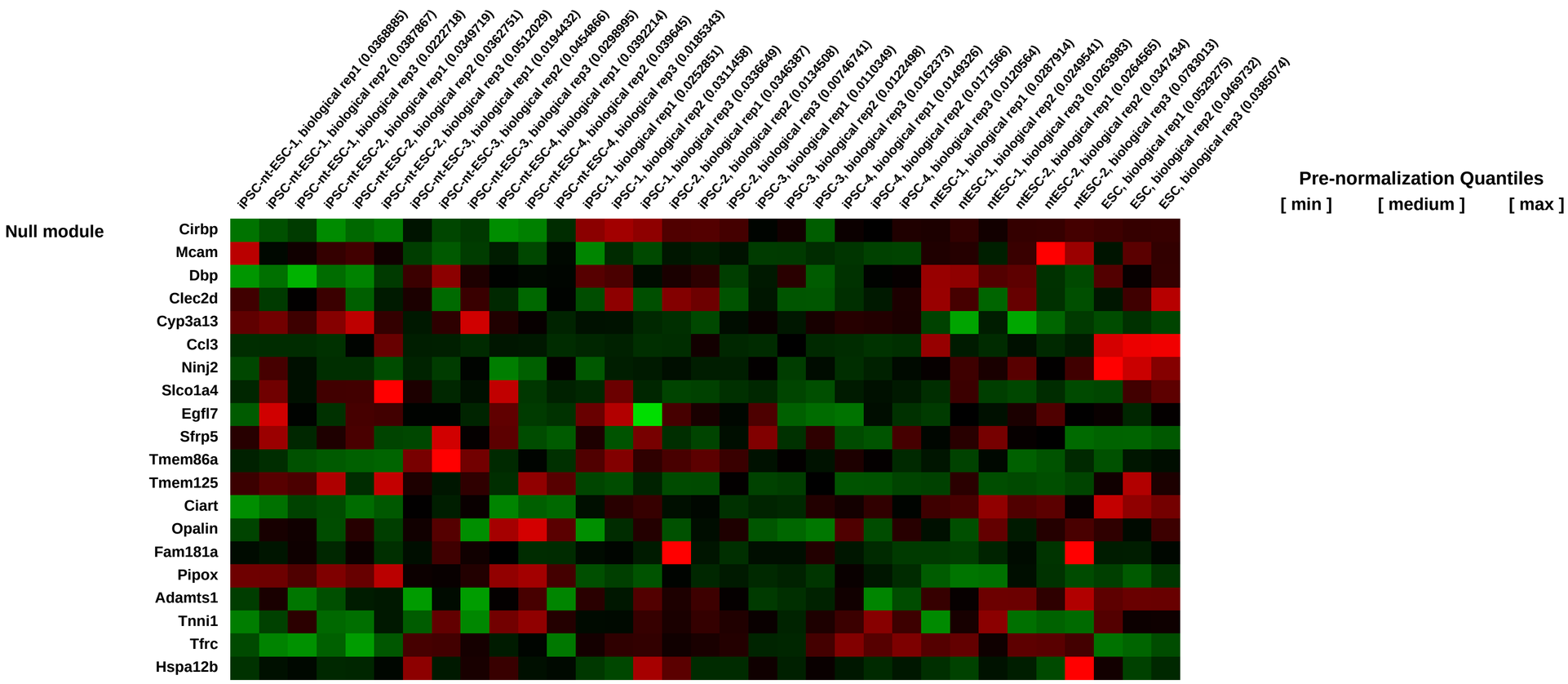

GEO Series "GSE49274" Expression Profiles

Num of samples in this series: 35

Scale of expression profile Z-scores

-3.0 -2.0 -1.0 0.0 1.0 2.0 3.0

GEO Link:	http://www.ncbi.nlm.nih.gov/geo/query/acc.cgi?acc=GSE49274
Status:	Public on Nov 21 2013
Title:	Antigen availability determines CD8+ T cell-dendritic cell interaction kinetics and T cell fate decisions.
Organism:	Mus musculus
Experiment type:	Expression profiling by array
Platform:	GPL1261
Pubmed ID:	24054328
Summary & Design:	**Summary:** This experiment compares the transciptional changes in antigen specific murine CD8 T cells (P14 T cells) after exposure in vivo to dendritic cells (DC) pulsed with low dose cognate peptide (1uM KAVYNFATC), high dose cognate peptide (100uM KAVYNFATC) or no antigen. Splenic dendritic cells were freshly isolated, peptide pulsed, washed and then adoptively transferred s.c. to the right footpad of C57BL/6 hosts. After 18h, freshly isolated P14 CD8 T cells were labelled with CMFDA and adoptively transferred iv. Two hours after T cell transfer, anti-L selectin antibody was given iv. At 12 and 24 hours, recipients were sacrificed and The right popliteal LN was harvested at 12 or 24h post T cell transfer and a single cell suspension was created and stained with PE CD4, B220 and CD19 (dump channel). Cells were then sorted on a FacsARIA for being non-doublets, CMFDA positive and dump channel negative. **Overall design:** This experiment compares the transciptional changes in antigen specific murine CD8 T cells (P14 T cells) after exposure in vivo to dendritic cells (DC) pulsed with low dose cognate peptide (1uM KAVYNFATC), high dose cognate peptide (100uM KAVYNFATC) or no antigen. Splenic dendritic cells were freshly isolated, peptide pulsed, washed and then adoptively transferred s.c. to the right footpad of C57BL/6 hosts. After 18h, freshly isolated P14 CD8 T cells were labelled with CMFDA and adoptively transferred iv. Two hours after T cell transfer, anti-L selectin antibody was given iv. At 12 and 24 hours, recipients were sacrificed and The right popliteal LN was harvested at 12 or 24h post T cell transfer and a single cell suspension was created and stained with PE CD4, B220 and CD19 (dump channel). Cells were then sorted on a FacsARIA for being non-doublets, CMFDA positive and dump channel negative. The experiment was conducted for 39 samples out of which 35 passsed transcriptional quality control tests. The phenotypic distribution for the 35 samples includes: (1) high dose (100uM KAVYNFATC) cognate peptide pulsed samples harvested at 12h post T cell transfer: 6 biological replicates (2) high dose (100uM KAVYNFATC) cognate peptide pulsed samples harvested at 24h post T cell transfer: 7 biological replicates (3) low dose (1uM KAVYNFATC) cognate peptide pulsed samples harvested at 12h post T cell transfer: 6 biological replicates (4) low dose (1uM KAVYNFATC) cognate peptide pulsed samples harvested at 24h post T cell transfer: 9 biological replicates (5) no antigen pulsed samples harvested at 12h post T cell transfer: 3 biological replicates (6) no antigen pulsed samples harvested at 24h post T cell transfer: 4 biological replicates.

Background corr dist: KL-Divergence = 0.1895, L1-Distance = 0.0623, L2-Distance = 0.0105, Normal std = 0.3401

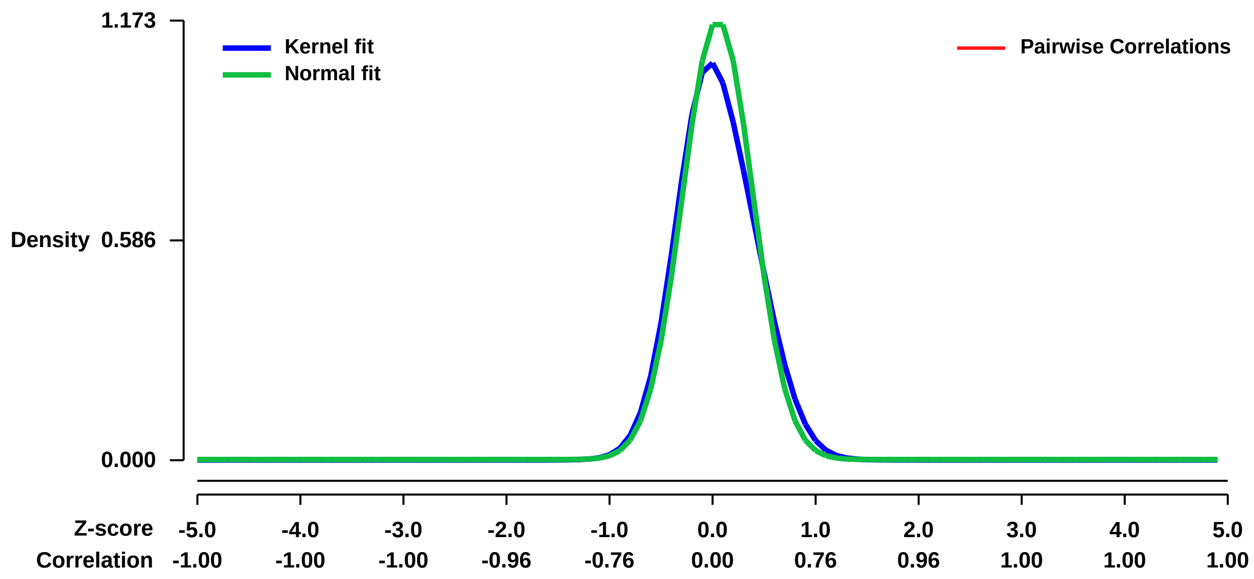

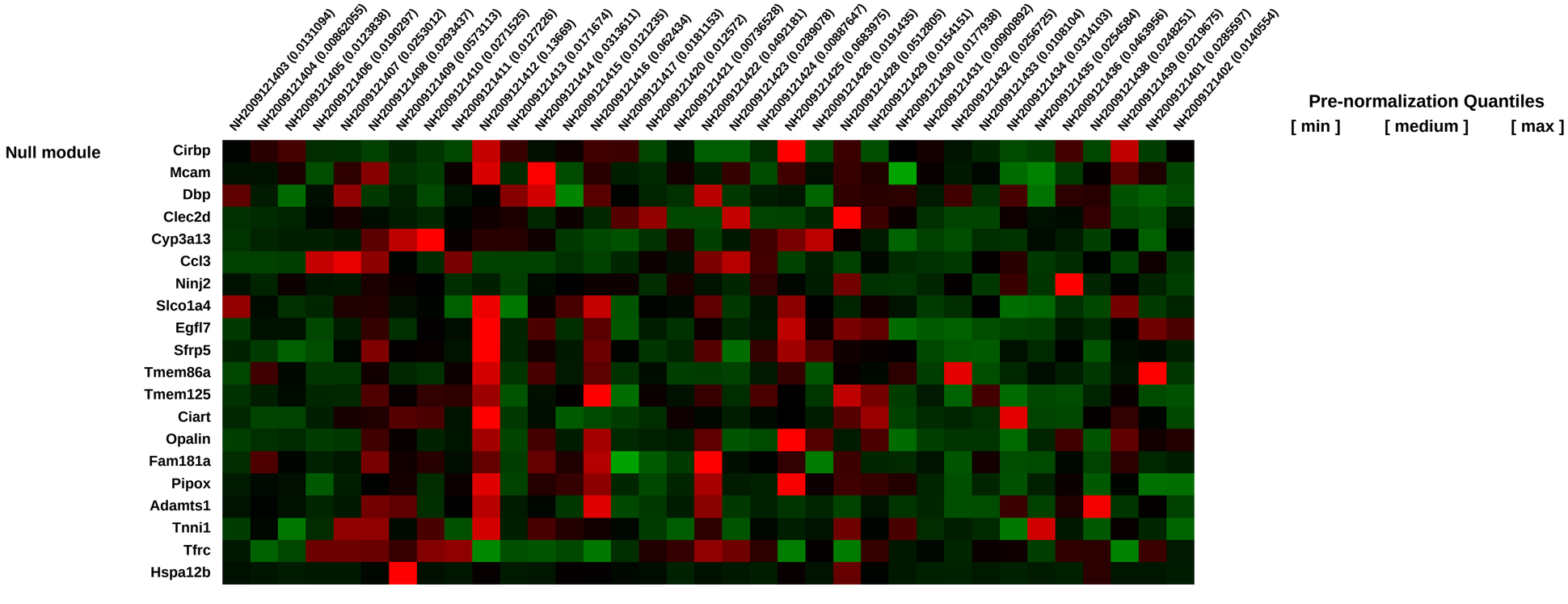

GEO Series "GSE30138" Expression Profiles

Num of samples in this series: 51

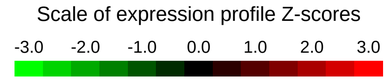

GEO Link:	http://www.ncbi.nlm.nih.gov/geo/query/acc.cgi?acc=GSE30138
Status:	Public on Dec 31 2011
Title:	Global Gene Expression Analysis of Murine Limb Development
Organism:	Mus musculus
Experiment type:	Expression profiling by array
Platform:	GPL1261
Pubmed ID:	22174793
Summary & Design:	**Summary:** Detailed information about stage-specific changes in gene expression is crucial for understanding the gene regulatory networks underlying development and the various signal transduction pathways contributing to morphogenesis. Here, we describe the global gene expression dynamics during early murine limb development, when cartilage, tendons, muscle, joints, vasculature, and nerves are specified and the musculoskeletal system of the limbs is established. We used whole-genome microarrays to identify genes with differential expression at 5 stages of limb development (E9.5 to 13.5), during fore-limb and hind-limb patterning. We found that the onset of limb formation is characterized by an up-regulation of transcription factors, which is followed by a massive activation of genes during E10.5 and E11.5 which tampers off at later time points. Among 3520 genes identified as significantly up-regulated in the limb, we find ~30% to be novel, dramatically expanding the repertoire of candidate genes likely to function in the limb. Hierarchical and stage-specific clustering identified expression profiles that correlate with functional programs during limb development and are likely to provide new insights into specific tissue patterning processes. Here we provide for the first time, a comprehensve analysis of developmentally regulated genes during murine limb development, and provide some novel insights into the expression dynamics governing limb morphogenesis. **Overall design:** Fifty- one arrays were analyzed, consisting of whole fore-limb and hind-limb bud RNA (experimental) and whole embryo RNA (reference) samples from E9.5 to E13.5 DPC mouse (FVB strain). Embryos were not pooled to generate samples. Each time point has 3 to 5 biological replicates for limb bud samples, duplicates for whole embryos. Comparisons were made between limb bud samples and whole embryo at the same stage, fore-limb samples of different stages, hind-limb samples of different stages, and fore-limb samples compared to hind-limb samples at the same or the next stage.

Background corr dist: KL-Divergence = 0.0710, L1-Distance = 0.0466, L2-Distance = 0.0047, Normal std = 0.4968

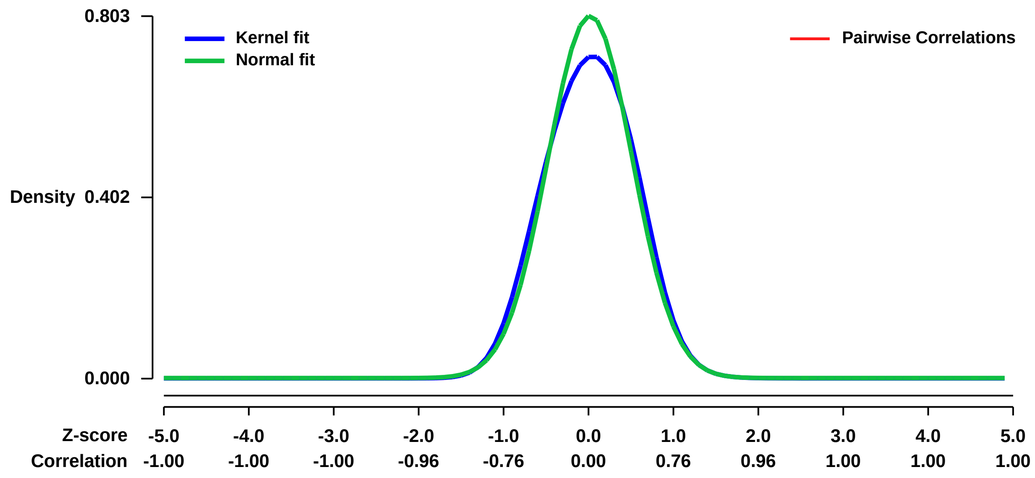

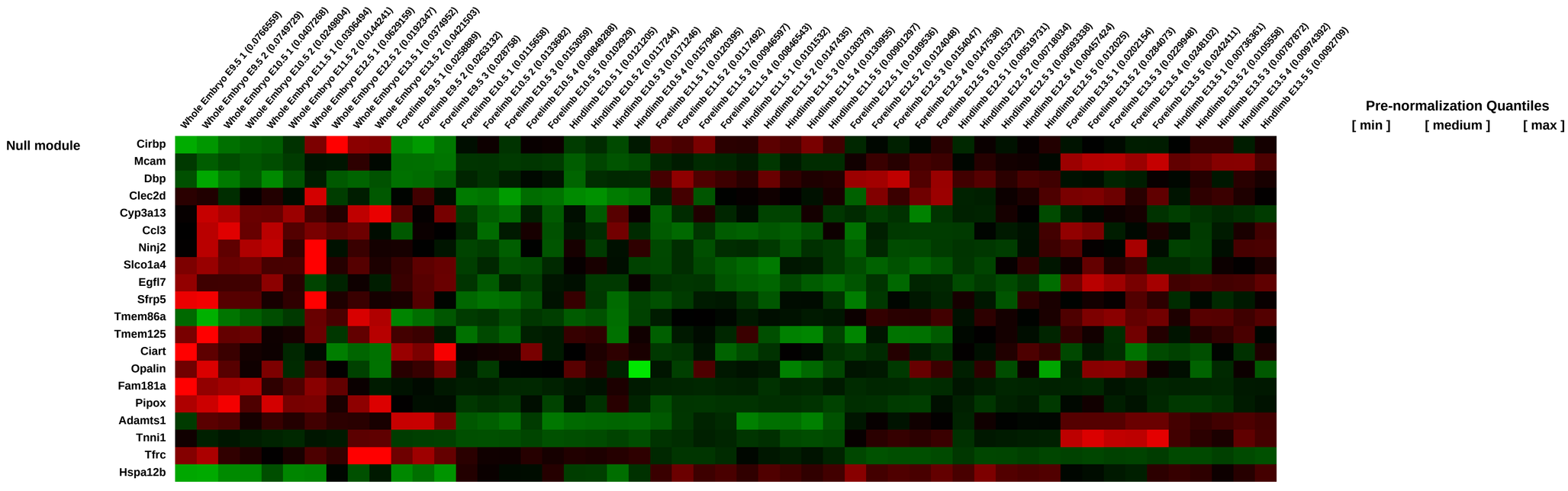

GEO Series "GSE48203" Expression Profiles

Num of samples in this series: 9

Scale of expression profile Z-scores

-3.0 -2.0 -1.0 0.0 1.0 2.0 3.0

GEO Link:	http://www.ncbi.nlm.nih.gov/geo/query/acc.cgi?acc=GSE48203
Status:	Public on Jun 21 2013
Title:	Expression data from tumoral thymocytes and DP thymocytes expressing an activated form of b-catenin in mouse T cells
Organism:	Mus musculus
Experiment type:	Expression profiling by array
Platform:	GPL1261
Pubmed ID:	23801632
Summary & Design:	**Summary:** To assess the importance of the Wnt pathway during T cell develoment, we generated a mouse line (R26-¸†cat) in which high levels of active ¸†-catenin are maintained throughout T cell development. Young R26-¸†cat mice (6-week-old) show a differentiation block at the CD4+CD8+ DP stage. All R26-¸†cat mice develop T cell leukemias with a DP phenotype at 5-6 months of age. To identify the molecular pathways involved in tumor development, we profiled the global gene expression of transformed and pre-transformed DP cells. **Overall design:** Thymocytes from 6-week-old mice (with a normal sized thymus and a polyclonal thymocyte population) were used to define the pre-transformed transcriptome. RNA from control and pre-leukemic R26-¸†cat DP thymocytes as well as R26-¸†cat total tumor cells were extracted and used for transcriptome analysis.

Background corr dist: KL-Divergence = 0.0301, L1-Distance = 0.0269, L2-Distance = 0.0010, Normal std = 0.6711

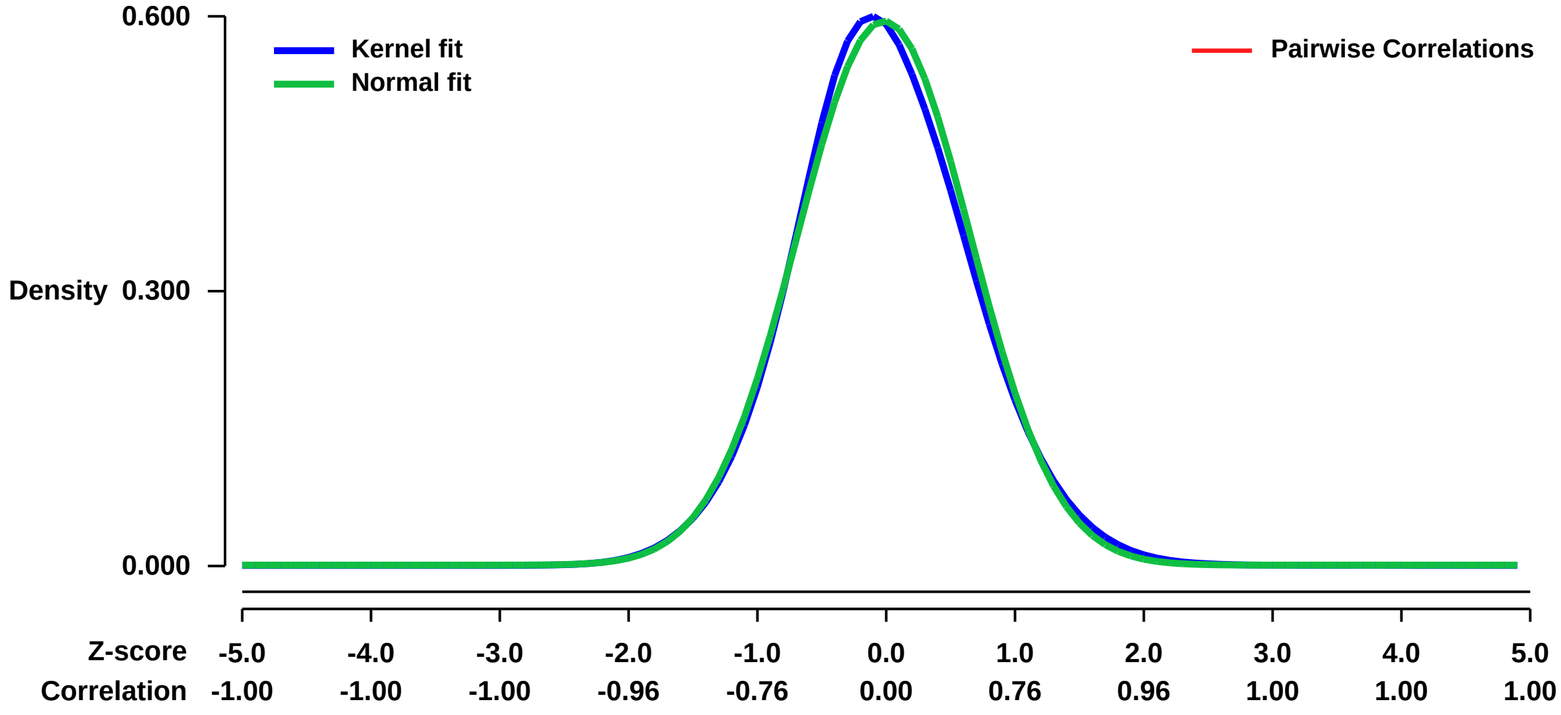

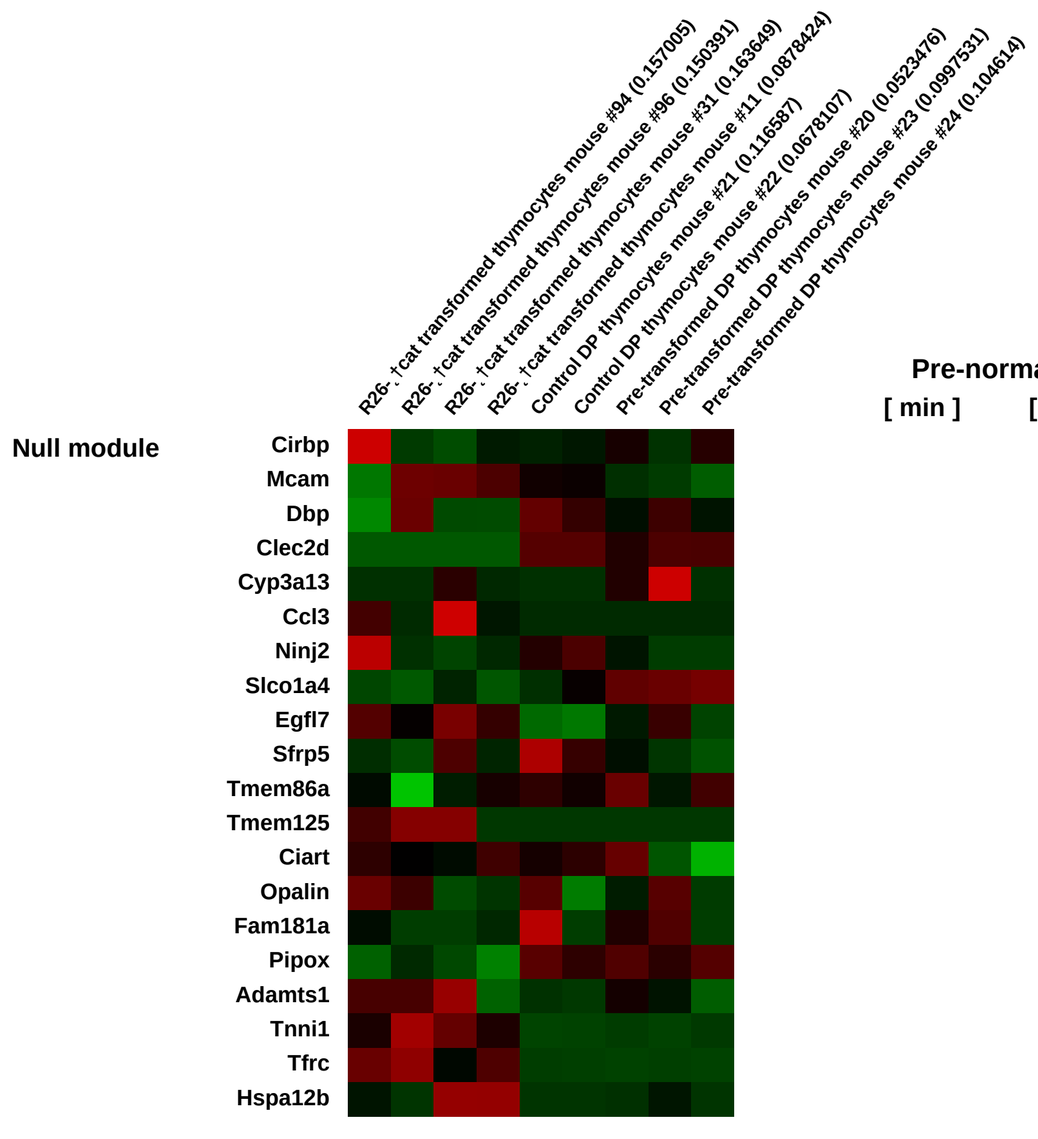

GEO Series "GSE21041" Expression Profiles

Num of samples in this series: 6

Scale of expression profile Z-scores

-3.0 -2.0 -1.0 0.0 1.0 2.0 3.0

GEO Link:	http://www.ncbi.nlm.nih.gov/geo/query/acc.cgi?acc=GSE21041
Status:	Public on Jul 15 2010
Title:	Transcriptome analysis of miR-144/451-null bone marrow erythroid cells
Organism:	Mus musculus
Experiment type:	Expression profiling by array
Platform:	GPL1261
Pubmed ID:	20679398
Summary & Design:	**Summary:** microRNA miR-144/451 is highly expressed during erythropoiesis. We deleted the miR-144/451 gene locus in mice and compared the transcriptomes of miR-144/451-null bone marrow erythroid precursors to stage-matched wild-type control cells. **Overall design:** Ter119+/CD71+/FSC-high bone marrow erythroblasts were sorted directly into Trizol LS reagent. Total RNAs extracted from three miR-144/451 knock-out and three wide type mice were analyzed using Affymetrix Mouse Genome 430 2.0 Arrays.

Background corr dist: KL-Divergence = 0.0360, L1-Distance = 0.0159, L2-Distance = 0.0003, Normal std = 0.6337

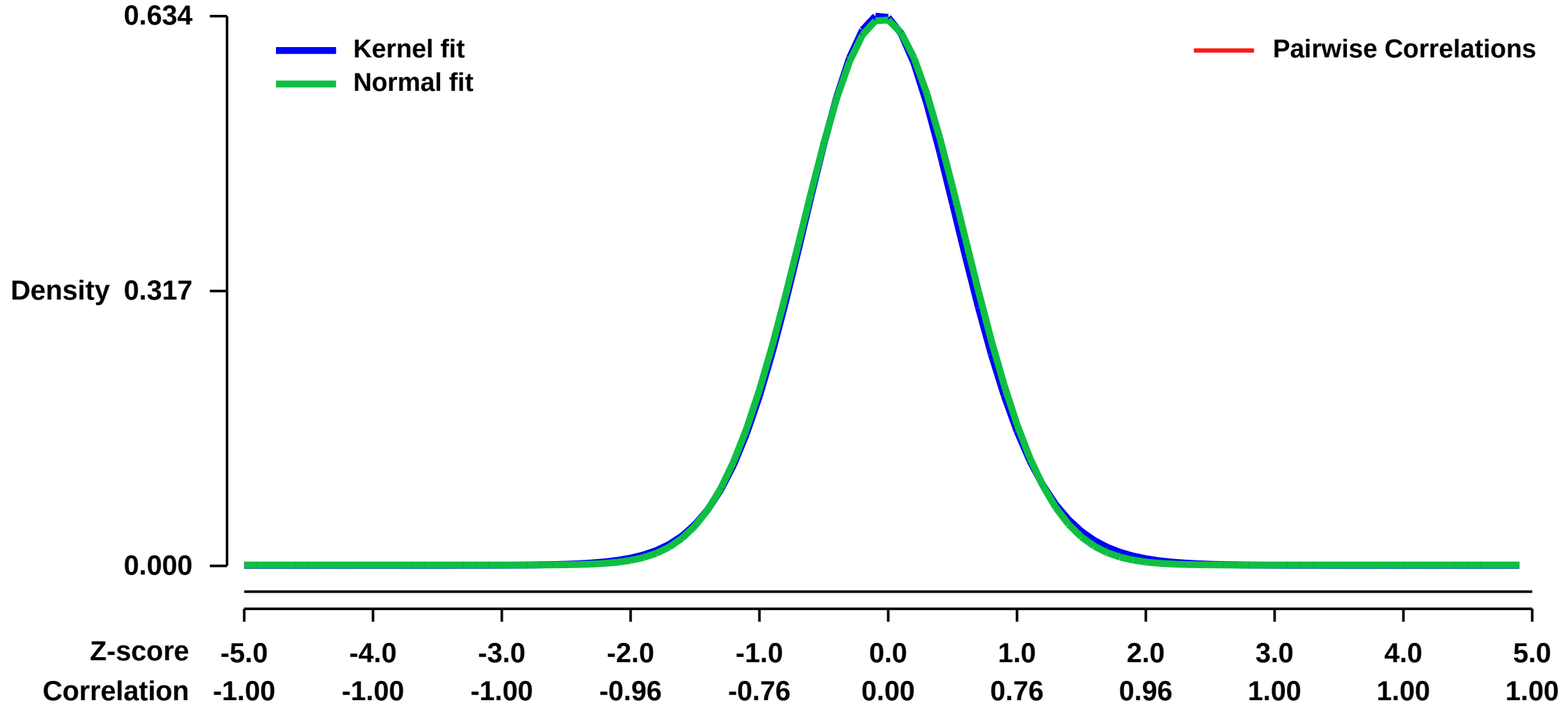

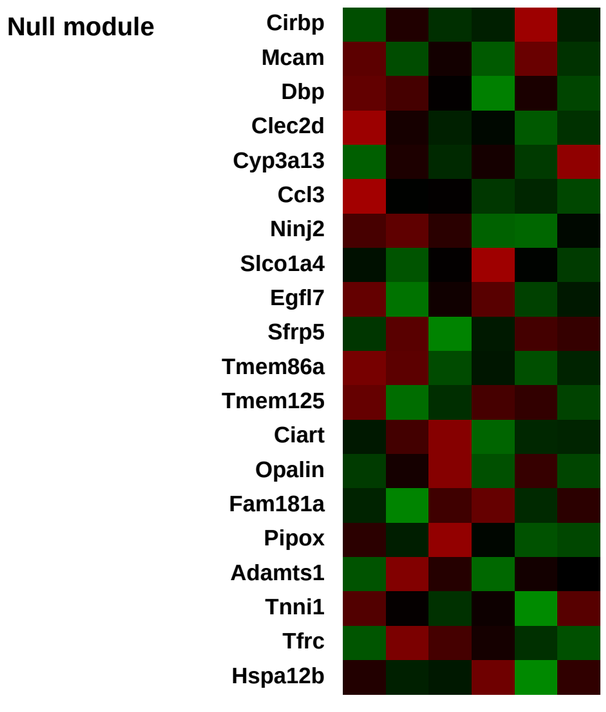

GEO Series "GSE10239" Expression Profiles

Num of samples in this series: 12

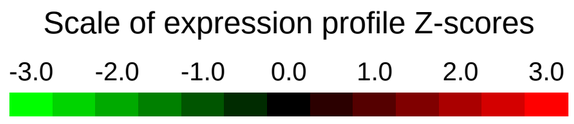

GEO Link:	http://www.ncbi.nlm.nih.gov/geo/query/acc.cgi?acc=GSE10239
Status:	Public on Jan 23 2008
Title:	Functional and Genomic Profiling of Effector CD8 T Cell Subsets
Organism:	Mus musculus
Experiment type:	Expression profiling by array
Platform:	GPL1261
Pubmed ID:	18316415
Summary & Design:	**Summary:** Using killer cell lectin-like receptor G1 as a marker to distinguish terminal effector cells from memory precursors, we found that despite their diverse cell fates both subsets possessed remarkably similar gene expression profiles and functioned as equally potent killer cells. However, only the memory precursors were capable of making IL-2 thus defining a novel effector cell that was cytotoxic, expressed granzyme B, and produced inflammatory cytokines in addition to IL-2. This effector population then differentiated into long-lived protective memory T cells capable of self-renewal and rapid re-call responses. Mechanistic studies showed that cells that continued to receive antigenic stimulation during the later stages of infection were more likely to become terminal effectors. Importantly, curtailing antigenic stimulation towards the tail-end of the acute infection enhanced the generation of memory cells. These studies support the decreasing potential model of memory differentiation and show that the duration of antigenic stimulation is a critical regulator of memory formation **Keywords:** Infection Type **Overall design:** An important question in memory development is understanding the differences between effector CD8 T cells that die versus effector cells that survive and give rise to memory cells. In this study we provide a comprehensive phenotypic, functional and genomic profiling of terminal effectors and memory precursors, towards better understanding the generation of these subsets. The two effector subsets were FACS purified during the early expansion phase (Days 4-5 post-infection) and extensively analyzed for their phenotypic (eg. CD127, CD62L, CD27, Bcl-2, Granzyme B, etc.) and functional properties (cytokine production, cytotoxicity, homeostatic proliferation, recall proliferation), and gene expression profiles (by genome-wide microarray analyses). Mechanistic studies involving the extent of proliferation and duration of antigen stimulation on memory differentiation potential of effectors were also performed using adoptive transfer techniques.

Background corr dist: KL-Divergence = 0.0430, L1-Distance = 0.0323, L2-Distance = 0.0019, Normal std = 0.5846

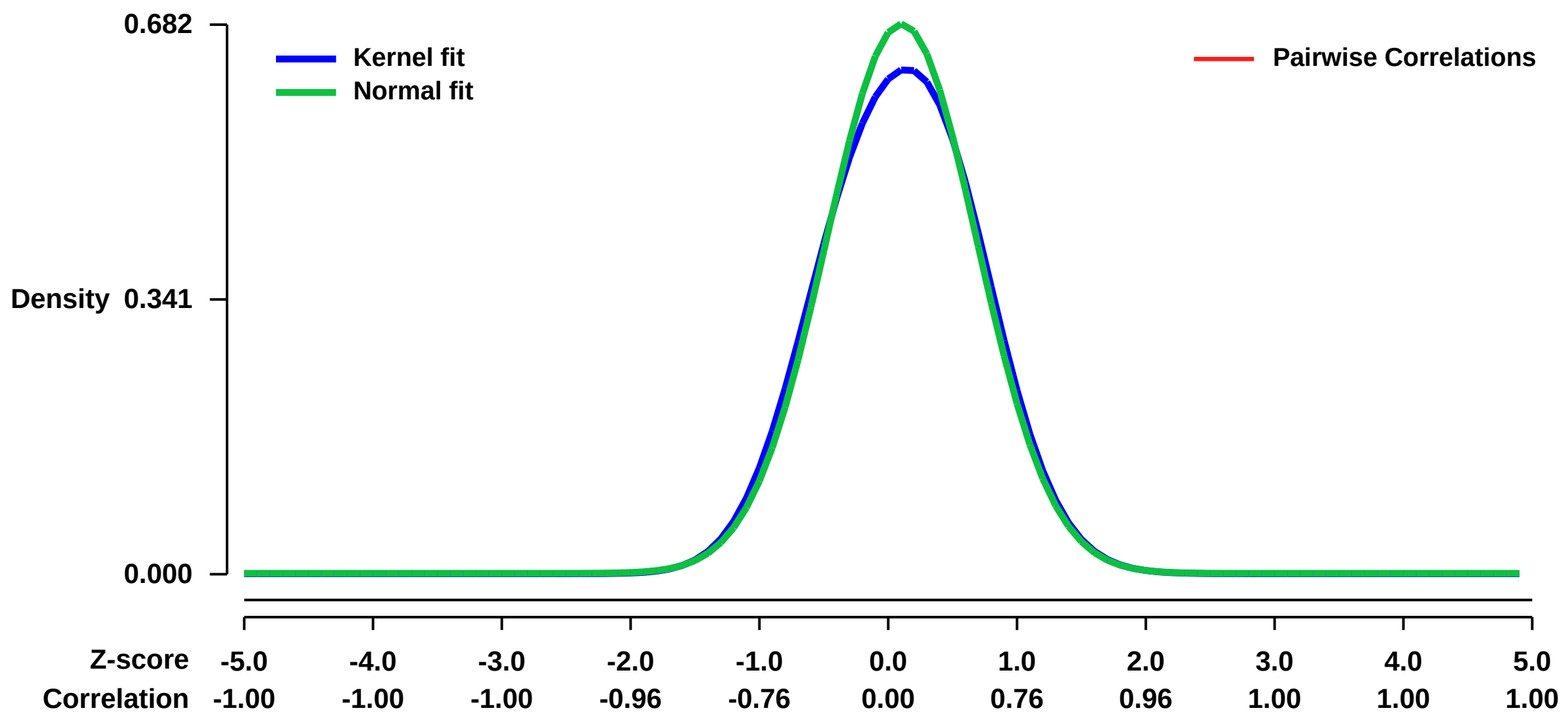

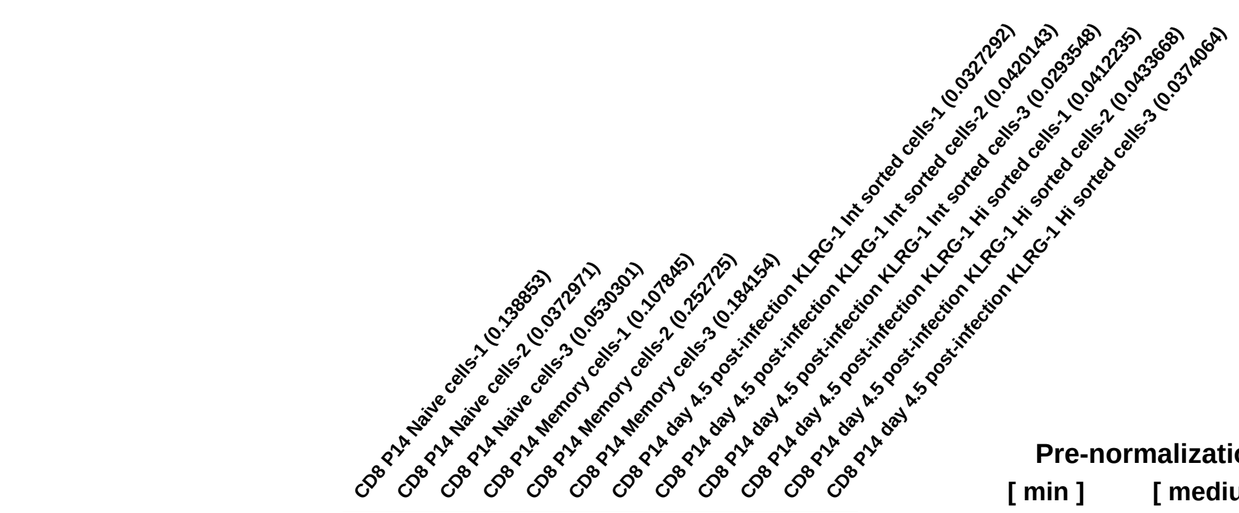

GEO Series "GSE18991" Expression Profiles

Num of samples in this series: 8

Scale of expression profile Z-scores

-3.0 -2.0 -1.0 0.0 1.0 2.0 3.0

GEO Link:	**http://www.ncbi.nlm.nih.gov/geo/query/acc.cgi?acc=GSE18991**
Status:	**Public on Oct 15 2010**
Title:	**Overexpression of Hoxd4 transcription factor alters transcriptional profiles in mouse chondrocytes at E18.5**
Organism:	**Mus musculus**
Experiment type:	**Expression profiling by array**
Platform:	**GPL1261**
Pubmed ID:	
Summary & Design:	**Summary:** **Homeobox genes of the Hox class are required for proper patterning of skeletal elements and play a role in cartilage differentiation. In transgenic mice with overexpression of Hoxd4 during cartilage development, we observed severe defects, namely physical instability of cartilage, accumulation of immature chondrocytes, and decreased maturation to hypertrophy. To define the molecular basis underlying these defects, we performed gene expression profiling using the Affymetrix microarray platform.** **Overall design:** **Embryos were dissected from four different mouse litters at E18.5. Embryos from each litter were grouped according their genotype: TA=control; TR=transgenic.**

Background corr dist: **KL-Divergence = 0.0923, L1-Distance = 0.0235, L2-Distance = 0.0008, Normal std = 0.4509**

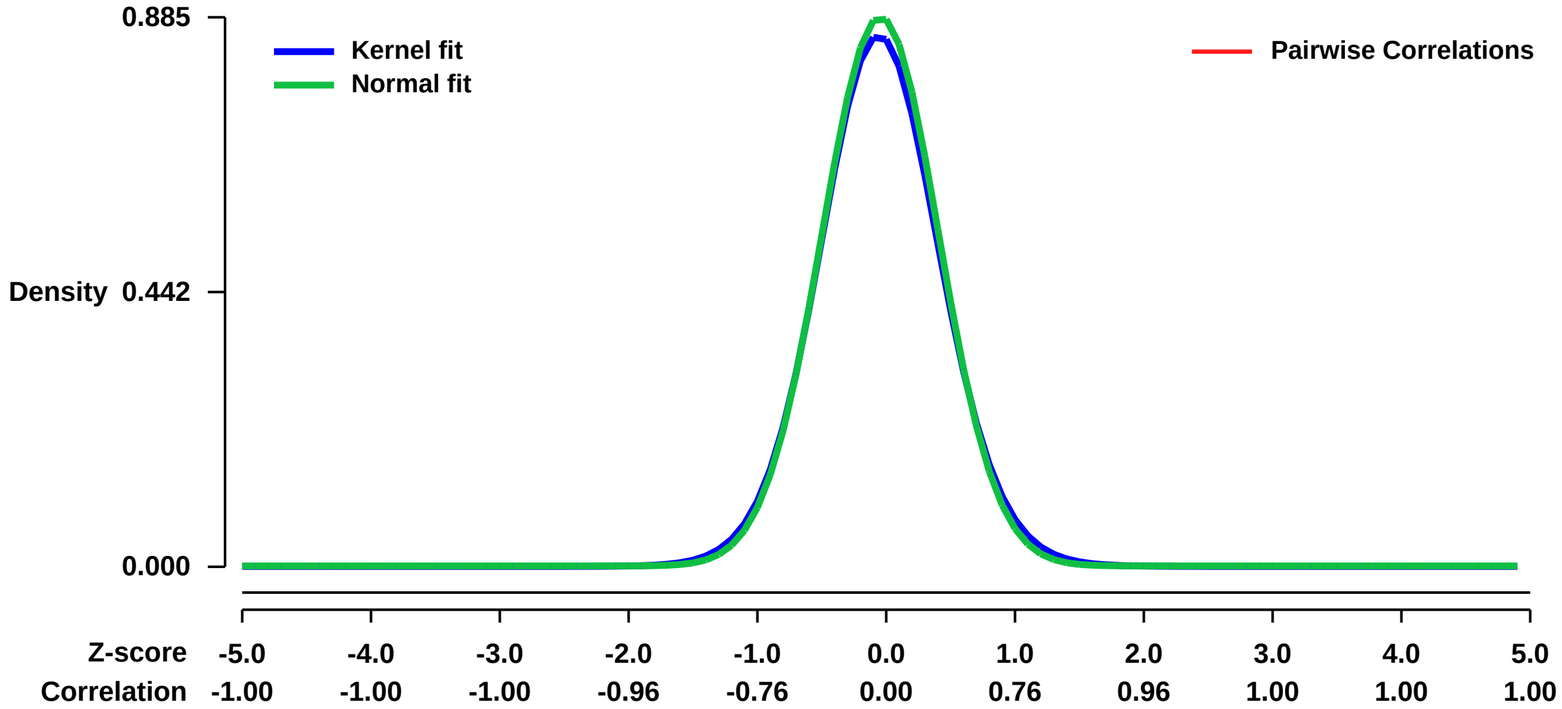

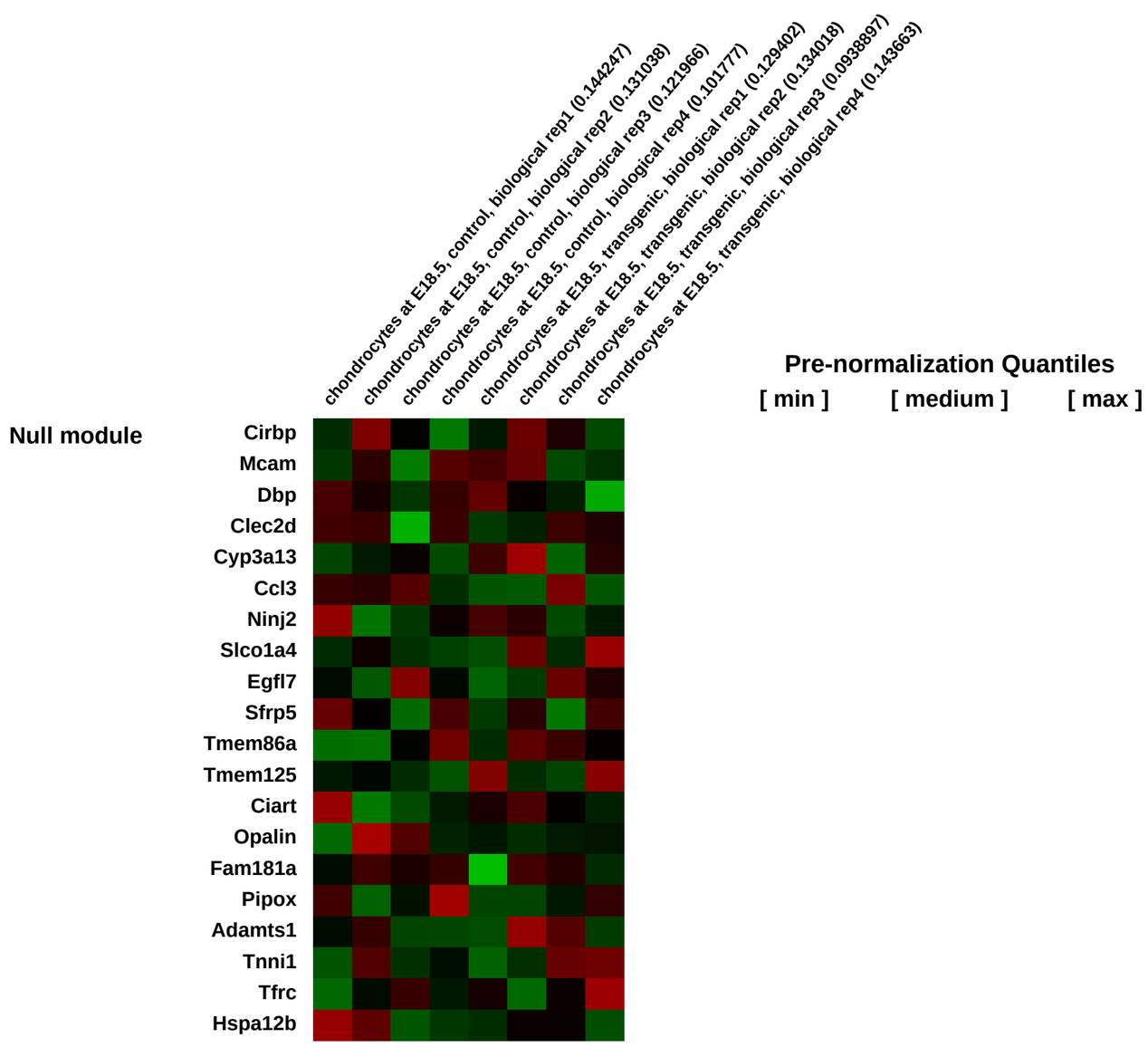

GEO Series "GSE11220" Expression Profiles

Num of samples in this series: 44

Scale of expression profile Z-scores

-3.0 -2.0 -1.0 0.0 1.0 2.0 3.0

GEO Link:	http://www.ncbi.nlm.nih.gov/geo/query/acc.cgi?acc=GSE11220
Status:	Public on Apr 23 2008
Title:	Timecourse of developing mouse placenta, with placental and decidual tissues profiled separately
Organism:	Mus musculus
Experiment type:	Expression profiling by array
Platform:	GPL1261
Pubmed ID:	18340042
Summary & Design:	**Summary:** We used full genome microarrays to profile the full lifetime of the mouse placenta from embryonic day 8.5 (e8.5), at the time of chorioallantoic fusion, until postnatal day 0 (P0). At each stage, the fetal placenta and maternal decidual tissues were dissected and profiled separately Keywords: time course **Overall design:** Mouse placentas were obtained from timed pregnant female mice at each timepoint, and fetal tissues were used to confirm embryo staging. Fetal placenta and maternal decidual tissues were dissected and pooled separately for each litter prior to RNA extraction and hybridization on Affymetrix microarrays.

Background corr dist: KL-Divergence = 0.1391, L1-Distance = 0.0310, L2-Distance = 0.0019, Normal std = 0.3911

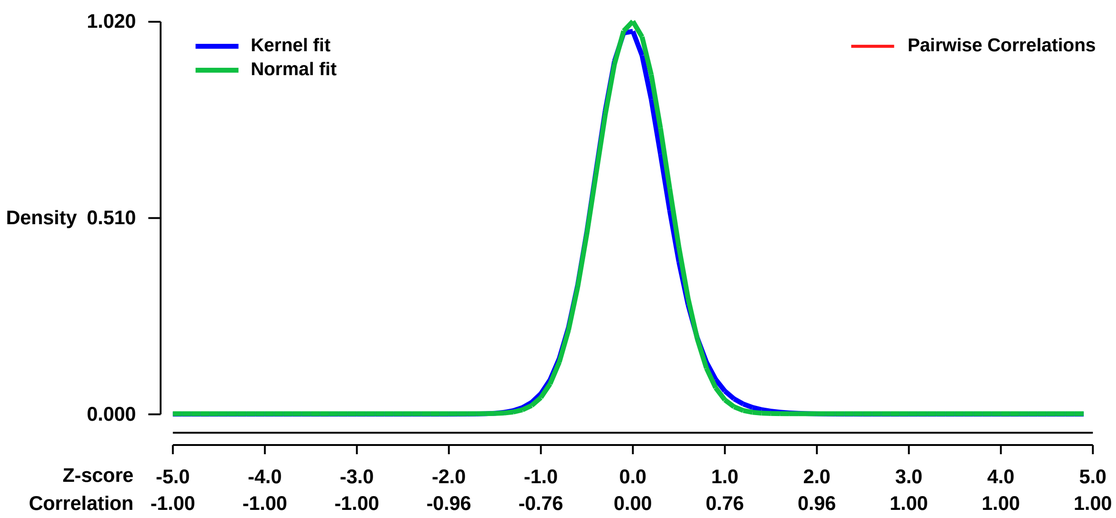

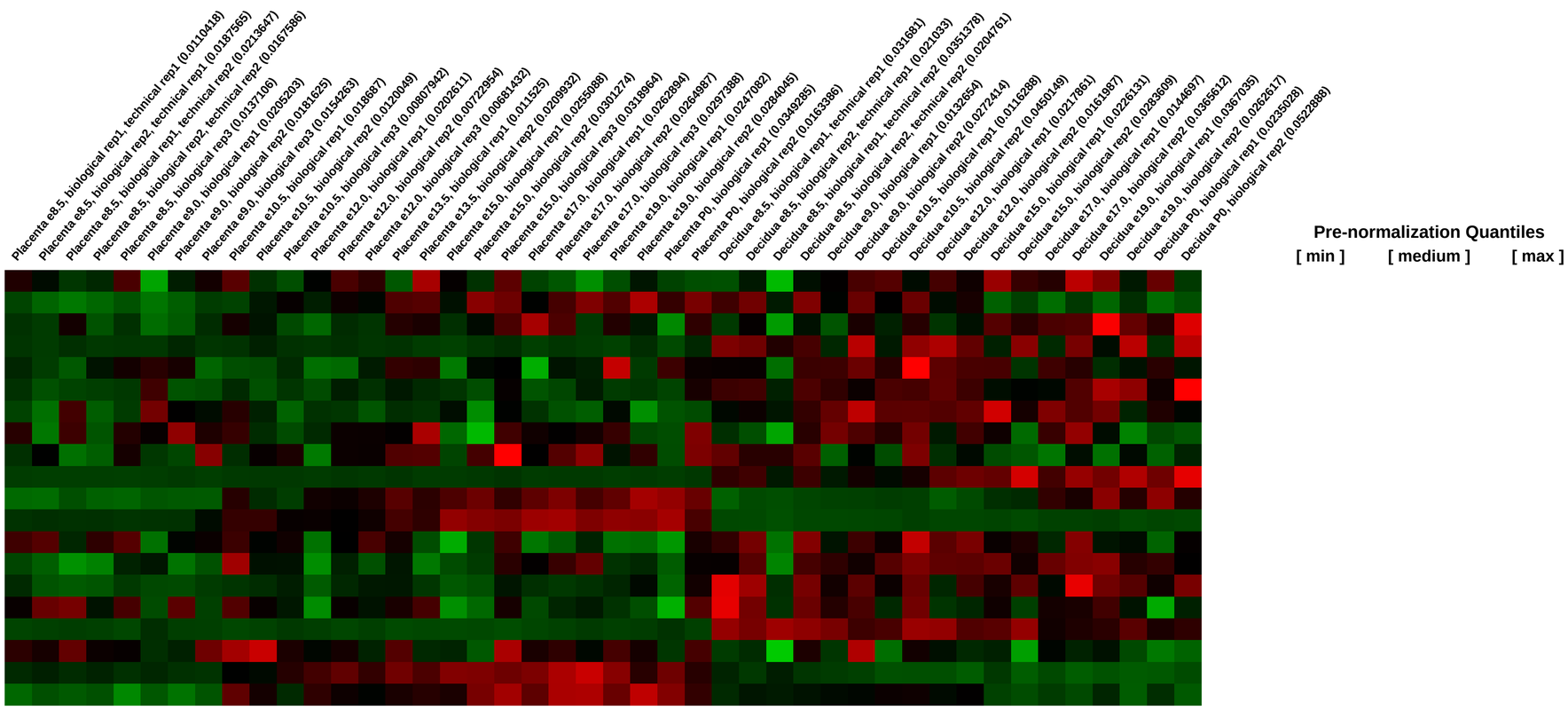

GEO Series "GSE13692" Expression Profiles

Num of samples in this series: 8

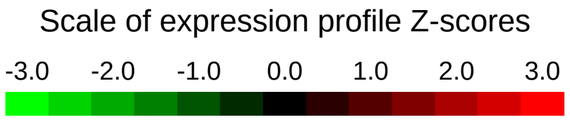

GEO Link:	http://www.ncbi.nlm.nih.gov/geo/query/acc.cgi?acc=GSE13692
Status:	Public on Feb 06 2009
Title:	Expression profiling of MLL-AF10 myeloid leukemia cellular subsets
Organism:	Mus musculus
Experiment type:	Expression profiling by array
Platform:	GPL1261
Pubmed ID:	19200802
Summary & Design:	**Summary:** Leukemia cells from mice with MLL-AF10 AML were fractionated into separate sub-populations on the basis of c-kit expression, which correlates with MLL LSC frequency (Somervaille and Cleary, 2006). The sorted AML sub-populations exhibited substantial differences in their frequencies of AML CFCs/LSCs (mean 14-fold) and morphologic features, consistent with a leukemia cell hierarchy with maturation through to terminally differentiated neutrophils. **Overall design:** Leukemic splenocytes from four mice with MLL-AF10 AML were sub-fractionated in to c-kit high and c-kit negative sub-populations by FACS.

Background corr dist: KL-Divergence = 0.0464, L1-Distance = 0.0346, L2-Distance = 0.0017, Normal std = 0.6099

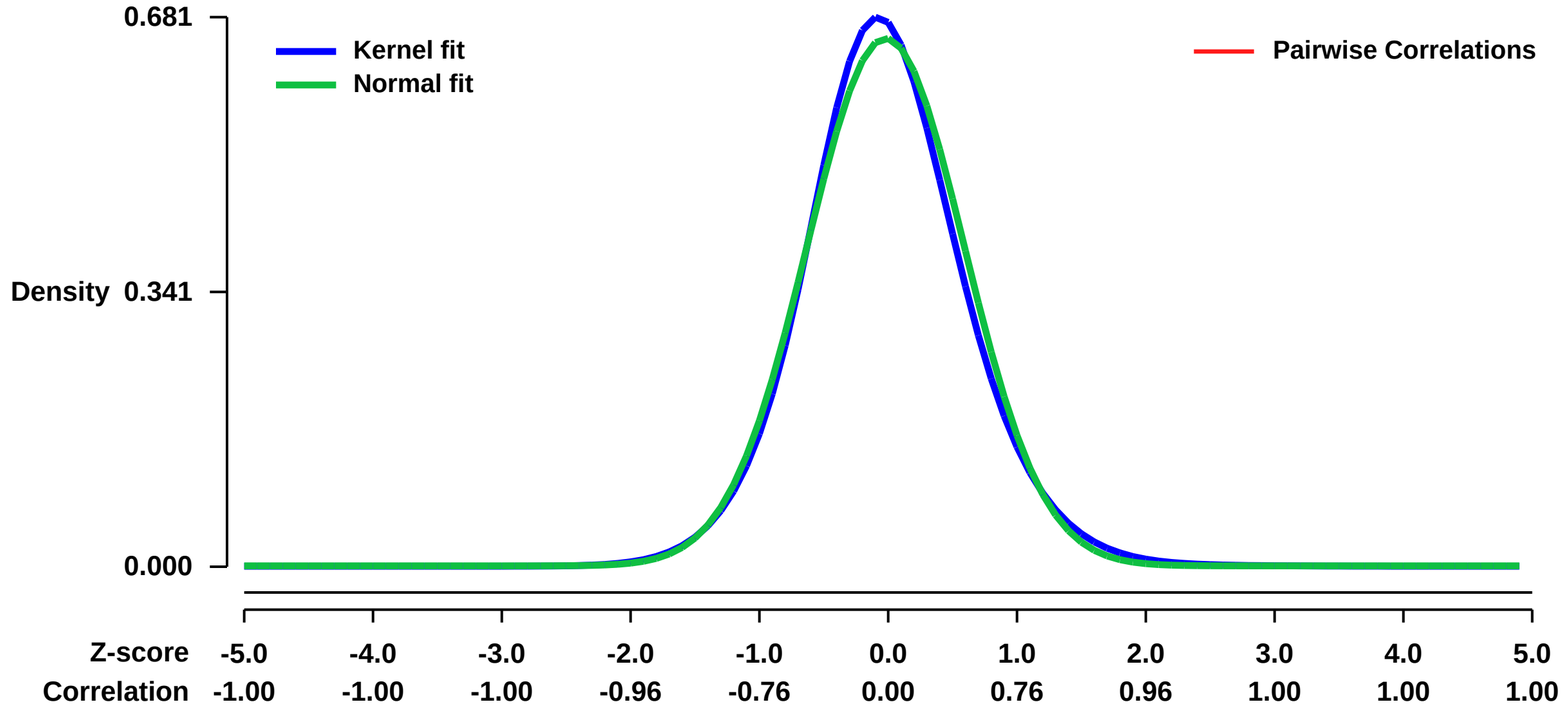

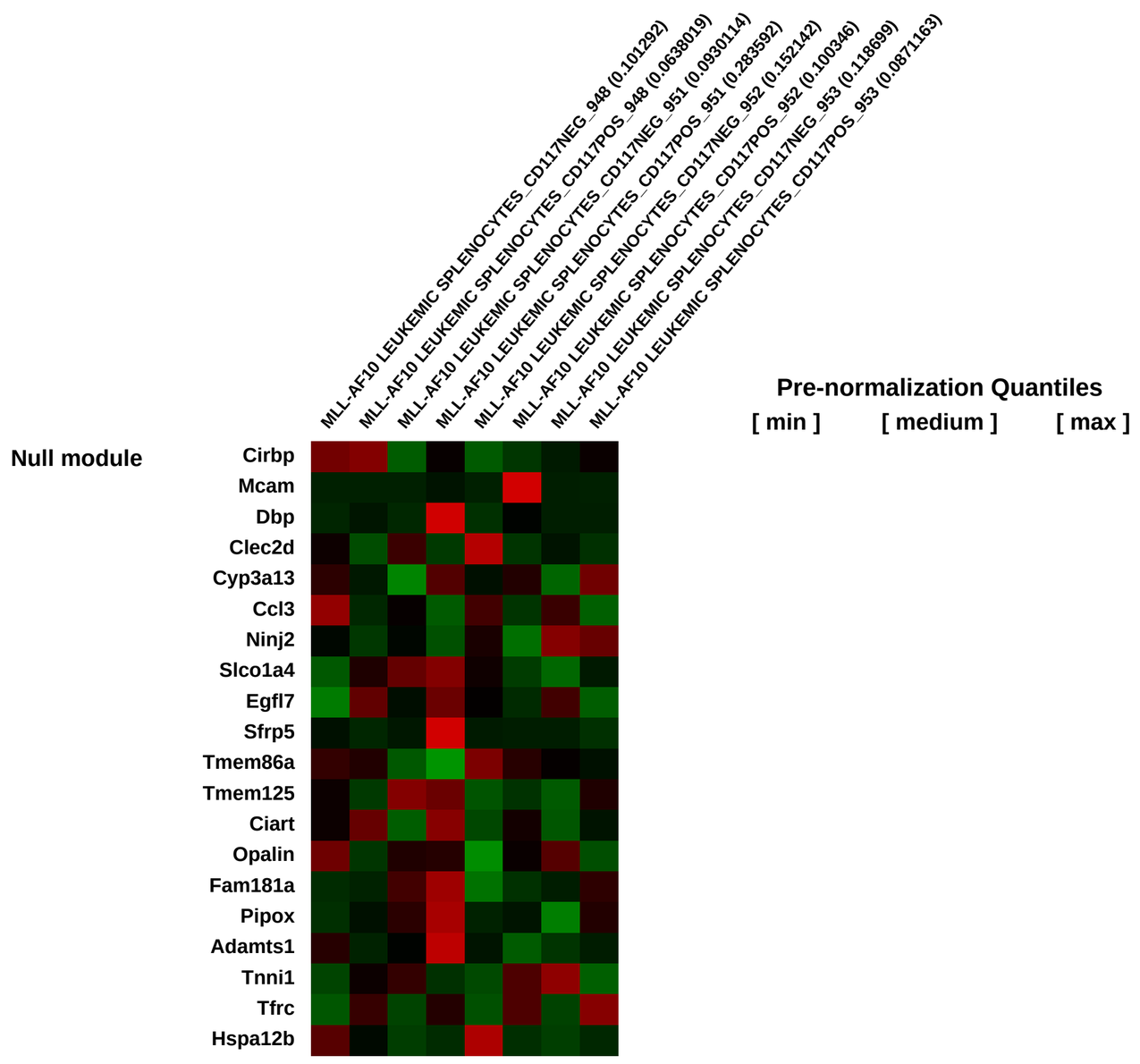

GEO Series "GSE4758" Expression Profiles

Num of samples in this series: 24

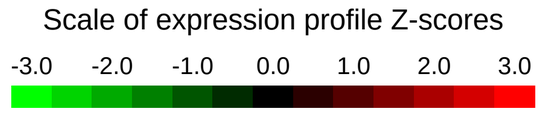

GEO Link:	**http://www.ncbi.nlm.nih.gov/geo/query/acc.cgi?acc=GSE4758**
Status:	**Public on May 02 2006**
Title:	**conra-affy-mouse-89474**
Organism:	**Mus musculus**
Experiment type:	**Expression profiling by array**
Platform:	**GPL1261**
Pubmed ID:	

Summary & Design:

Summary:
Parkinsonâ s disease (PD) and Dementia with Lewy bodies (DLB) are the two most common examples of synucleinopathies, i.e. human disorders that display intracellular deposition of the Alpha-synuclein (aSYN) protein. The two forms of aSYN deposits, intracellular Lewy bodies and Lewy neurites, are in the PD brain primarily found in the substantia nigra whereas in DLB brains they are diffusely spread in cortical and limbic areas. We are currently analyzing the protective effects on aSYN pathology by the molecular chaperone hsp70 in mice overexpressing wildtype human aSYN. Moreover, transgenic mice overexpressing hsp70 have been cross-bred with the aSYN mouse line. Intriguingly, the aSYN / hsp70 double transgenics display a pronounced reduction in biochemically assessed aSYN aggregation. Gene expression of these mice will not only provide insight into the disease mechanisms of aSYN pathology but its prevention by the overexpression of hsp70, leading to new potential avenues of treatment.

Project 1: To investigate and compare alterations in gene expression profiles of brains from wild-type mice and mice overexpressing wildtype human aSYN, human hsp70 and aSYN / hsp70, respectively.

The comparison of the expression profiles of the groups of mice: aSYN, Hsp70, aSYN/ Hsp70 and non-transgenic littermates will help to identify the genes that are involved in the mediation of aggregation toxicity of aSYN expression as well as the genes that may mediate an attenuation of aSYN pathology in hsp70-coexpressors.

Project 1: Selection of animals Mice of 4 month old (n=6) of age of each background (aSYN, Hsp70, aSYN/ Hsp70 and non-transgenic littermates) will be used for RNA-extraction for a total of 24 mice. Preparation of samples For the proposed experiments, we will use the recommended procedures, as outlined by the consortium, for extracting and purifying RNA from whole brain homogenate. Briefly, RNA will be extracted by the trizol method and purified by using the RNeasy MinElute Cleanup (QIAGEN Inc., USA). RNA labeling and hybridization procedures will be carried out by the microarray consortium. SPECIAL NOTE: The samples will be sent upon availability. Gene Expression Microarray Analysis Six mice will be included in each group per timepoint to generate statistically testable data and limit the possible confound of individual mouse gene expression variations. The genome expression will be evaluated through the use of the GeneChip´fi Mouse Genome 430 2.0 Array (Affymetrix) for each individual mouse constituting a total of 24 arrays for the proposed study. Gene expression data interpretation will be assisted by the Microarray Consortium Center bioinformatics core.

Keywords: time-course

Overall design:

Background corr dist: KL-Divergence = 0.2005, L1-Distance = 0.0460, L2-Distance = 0.0046, Normal std = 0.3320

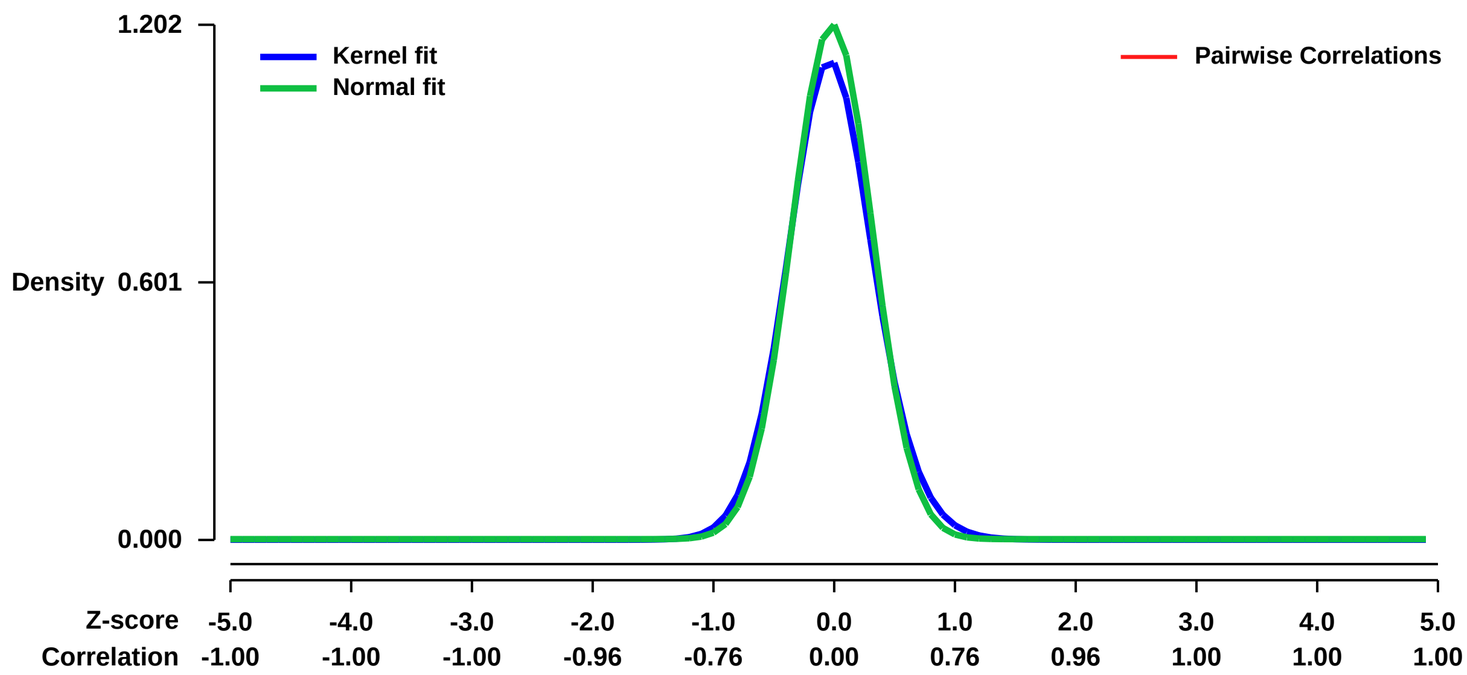

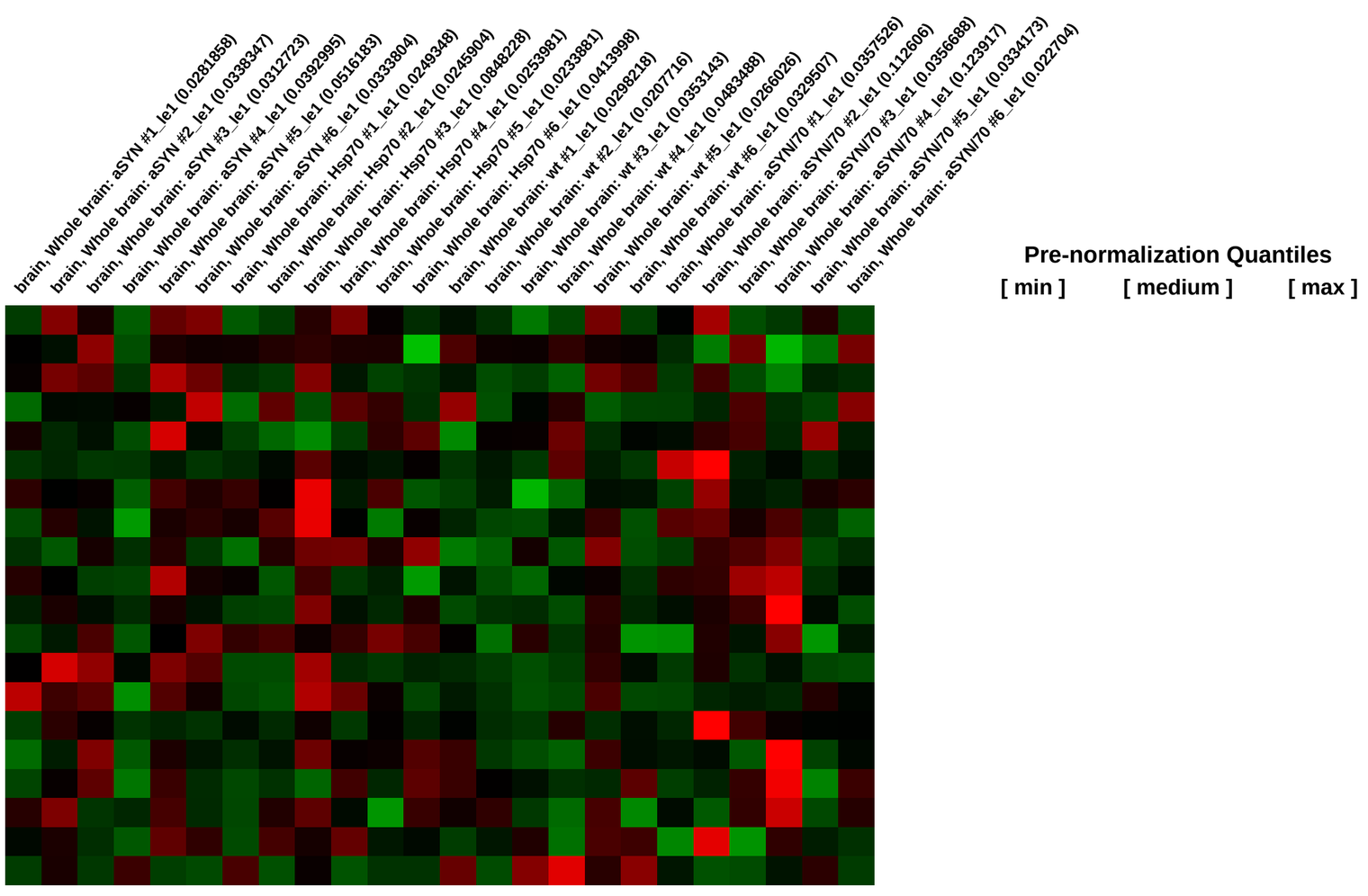

GEO Series "GSE12950" Expression Profiles

Num of samples in this series: 6

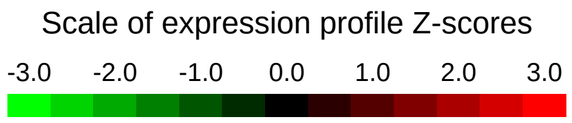

GEO Link:	**http://www.ncbi.nlm.nih.gov/geo/query/acc.cgi?acc=GSE12950**
Status:	**Public on Nov 01 2008**
Title:	**Gene expression profile of testes from three mouse strains, AKR/N, C57BL/6 and MRL/MpJ+/+**
Organism:	**Mus musculus**
Experiment type:	**Expression profiling by array**
Platform:	**GPL1261**
Pubmed ID:	
Summary & Design:	**Summary:** **Cryptorchidism and scrotal heating result in abnormal spermatogenesis but the mechanism(s) proscribing this temperature sensitivity are unknown. It was previously reported that the AKR/N or MRL/MpJ-+/+ mouse testis is more heat resistant than the testis from the C57BL/6 strain. We have attempted to probe into the mechanism(s) involved in heat sensitivity by examining global gene expression profiles of normal and heat-treated testes from C57BL/6, AKR/N and MRL/MpJ-+/+ mice by microarray analysis. In the normal C57BL/6 testis, 415 and 416 transcripts were differentially expressed (at least two-fold higher or lower) when compared to the normal AKR/N and MRL/MpJ-+/+ testis, respectively. The AKR/N and MRL/MpJ-+/+ strains revealed 268 differentially expressed transcripts between them. There were 231 transcripts differentially expressed between C57BL/6 and two purported heat-resistant strains, AKR/N and MRL/MpJ-+/+.** **Overall design:** **Total RNA of testes from 3 different strains of mice, C57BL/6, AKR/N and MRL/MpJ-+/+, were analyzed using microarray 430.20 chip. All mice were 8 weeks old, 2 mice/strain.**

Background corr dist: KL-Divergence = 0.0405, L1-Distance = 0.0184, L2-Distance = 0.0003, Normal std = 0.6139

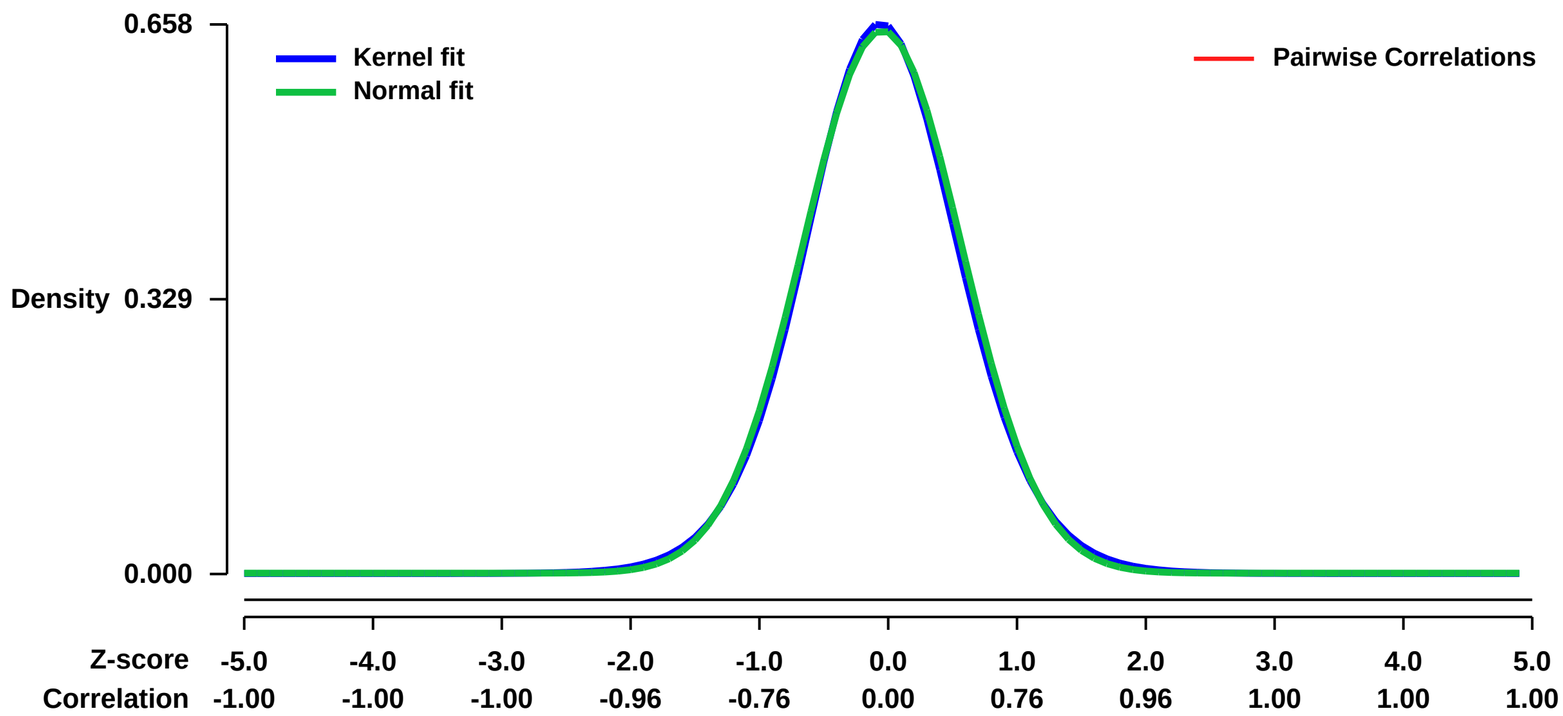

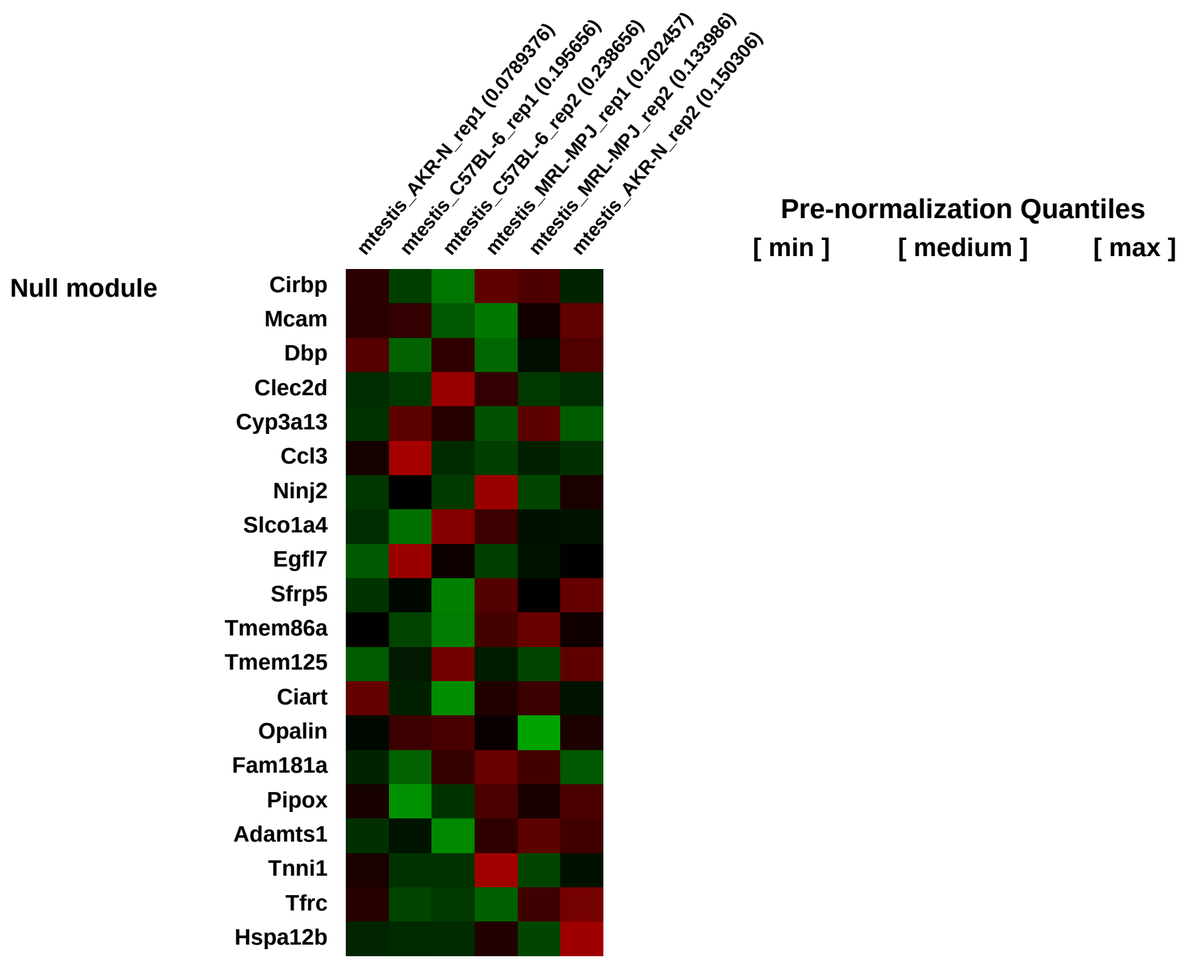

GEO Series "GSE8039" Expression Profiles

Num of samples in this series: 32

Scale of expression profile Z-scores

-3.0 -2.0 -1.0 0.0 1.0 2.0 3.0

GEO Link:	http://www.ncbi.nlm.nih.gov/geo/query/acc.cgi?acc=GSE8039
Status:	Public on Oct 30 2007
Title:	Gene Expression in Transgenic Mice Expressing CD30L on T Cells
Organism:	Mus musculus
Experiment type:	Expression profiling by array
Platform:	GPL1261
Pubmed ID:	
Summary & Design:	**Summary:** CD30L and CD30 are cell-surface glycoproteins in the TNF and TNFR superfamilies, respectively. Their expression is limited to immune cells and is tightly regulated. Cell surface expression of CD30 is restricted to subpopulations of activated T and B cells. CD30L is expressed primarily on activated T cells and subpopulations of B cells. The significance of CD30/CD30L interactions in immune regulation is not fully understood. Reported activities of CD30/CD30L in immune responses imply roles in regulation of secondary memory and antibody responses. Depending on the experimental system, both positive and negative regulation of immunoglobulin class switching and antibody production have been reported. Additionally, the biological activity of CD30/CD30L in animals has been difficult to assess due to the restricted and tightly regulated expression of this receptor-ligand pair. We generated transgenic mice with constitutive T cell specific overexpression of CD30L as a tool to help unravel the consequences of CD30/CD30L interactions in vivo. CD30L transgenic mice displayed a phenotype and responses to antigen challenge supporting a role for CD30/CD30L in promoting immunoglobulin class switching and antibody production. CD30L transgenic mice had increased numbers of germinal centers, elevated class-switched immunoglobulin isotypes, increased germinal center B cells and plasma cells, upregulation of genes indicative of B-cell activity, and exaggerated antibody responses to immune challenge. Interestingly, despite the heightened B-cell activity in CD30L transgenic mice, CD30L overexpression on T cells did not result in overt autoimmunity. Our results demonstrate that overexpression of CD30L on T cells promotes T cell-dependent B cell responses characterized by secondary antibody responses. **Keywords:** Transgenic vs. wild-type **Overall design:** Spleen, thymus, mesenteric lymph nodes and peripheral lymph nodes where samples from both CD30L transgenic and non-transgenic littermates (4 mice per group.)

Background corr dist: KL-Divergence = 0.1279, L1-Distance = 0.0705, L2-Distance = 0.0114, Normal std = 0.4192

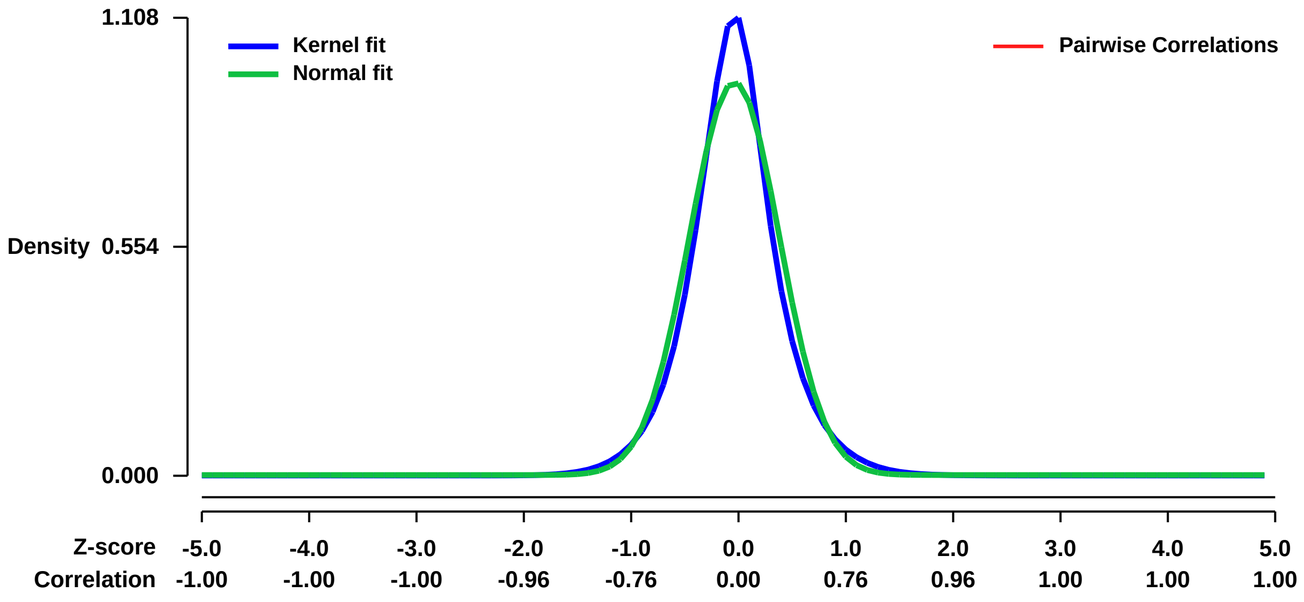

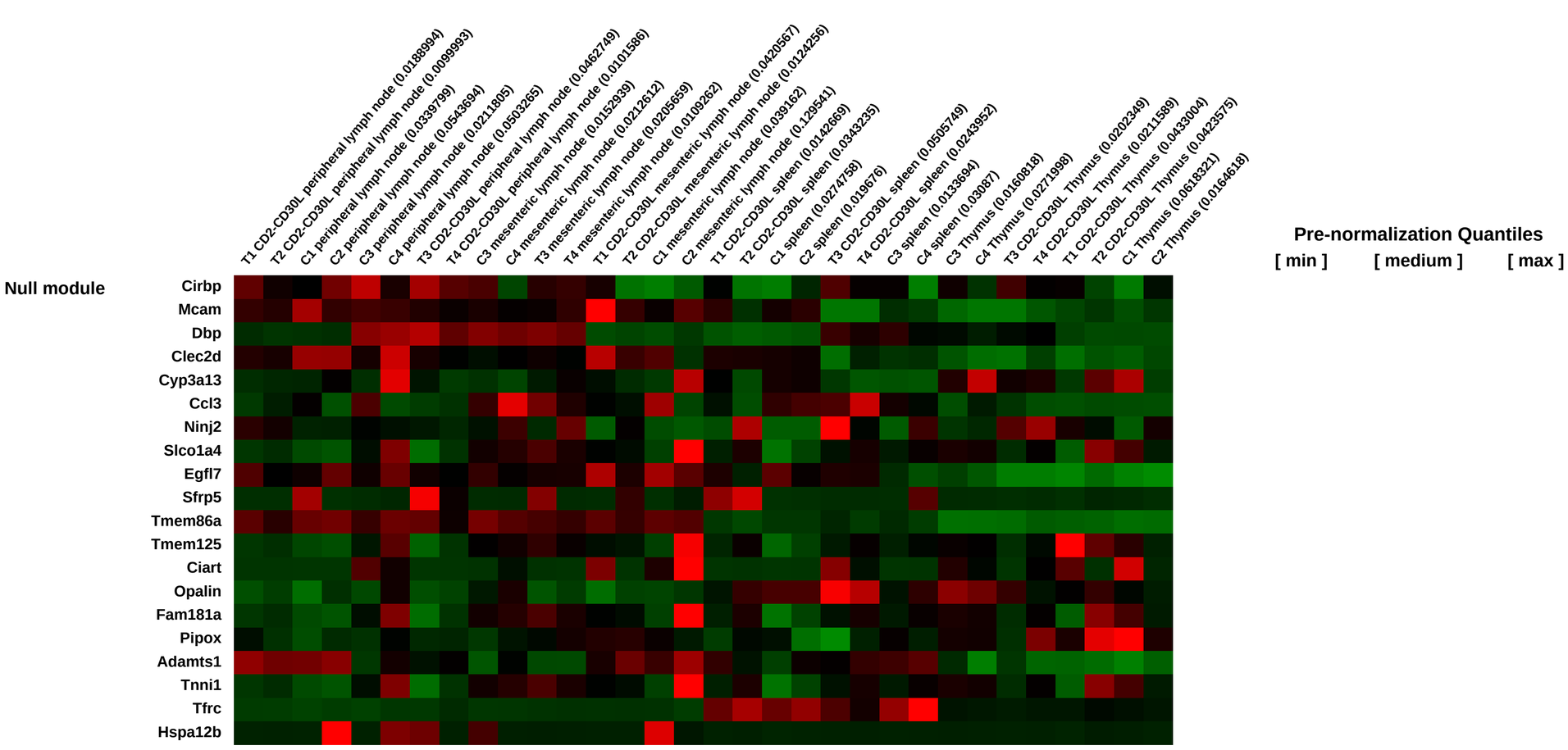

GEO Series "GSE14406" Expression Profiles

Num of samples in this series: 54

Scale of expression profile Z-scores

-3.0 -2.0 -1.0 0.0 1.0 2.0 3.0

GEO Link:	http://www.ncbi.nlm.nih.gov/geo/query/acc.cgi?acc=GSE14406
Status:	Public on Jan 31 2009
Title:	Oligodendroglial precursor cell line [Oli-neu] undergoing differentiation into myelin basic protein-producing cells
Organism:	Mus musculus
Experiment type:	Expression profiling by array
Platform:	GPL1261
Pubmed ID:	19139271
Summary & Design:	**Summary:** Inadequate remyelination of brain white matter lesions has been associated with a failure of oligodendrocyte precursors to differentiate into mature, myelin-producing cells. In order to better understand which genes play a specific role in oligodendrocyte differentiation we performed time dependent, genome-wide gene expression studies of mouse Oli-neu cells as they differentiate into myelin basic protein-producing cells, following treatment with three different agents. Our data indicate that different inducers activate distinct pathways that ultimately converge into the differentiated state where regulated gene sets overlap maximally. In order to also gain insight into the functional role of genes that are regulated in this process, we silenced 88 of these genes using siRNA, and identified multiple repressors of spontaneous differentiation of Oli-neu, most of which were confirmed in rat primary oligodendrocyte precursors cells. Among these repressors were CNPase, a well-known myelin constituent, and three phosphatases, each known to negatively control MAP kinase cascades. We show that a novel inhibitor for one of the identified genes, dual-specificity phosphatase DUSP10/MKP5, was also capable of inducing oligodendrocyte differentiation in primary oligodendrocyte precursors. Oligodendrocytic differentiation feedback loops may therefore yield pharmacological targets to treat disease related to dysfunctional myelin deposition **Keywords:** time course **Overall design:** triplicates for 3 times points 10h, 24h, 72h in 6 conditions, Forskolin, Insulin, Dexamethasone, Retinoic Acid, PD174265, Untreated. Arrays were done in two distinct experiments 1 and 2. Some replicates are missing because of lab operating issues

Background corr dist: KL-Divergence = 0.3521, L1-Distance = 0.0454, L2-Distance = 0.0041, Normal std = 0.2629

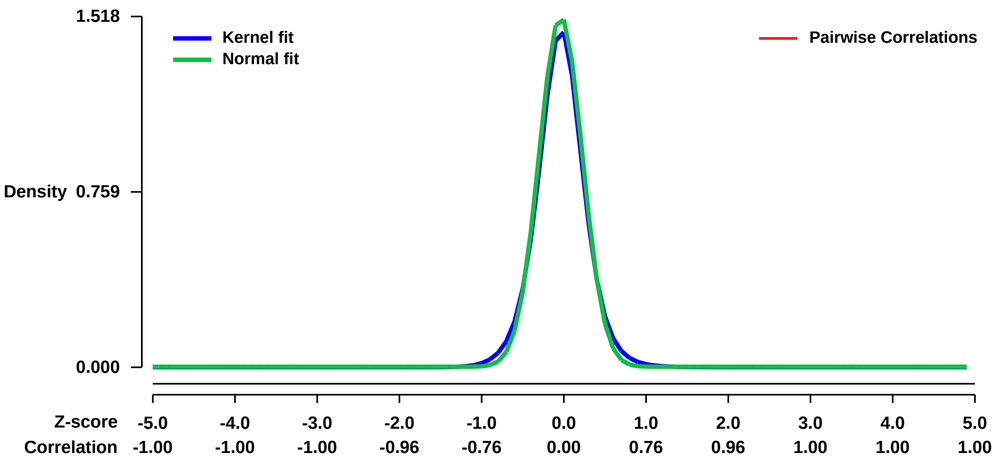

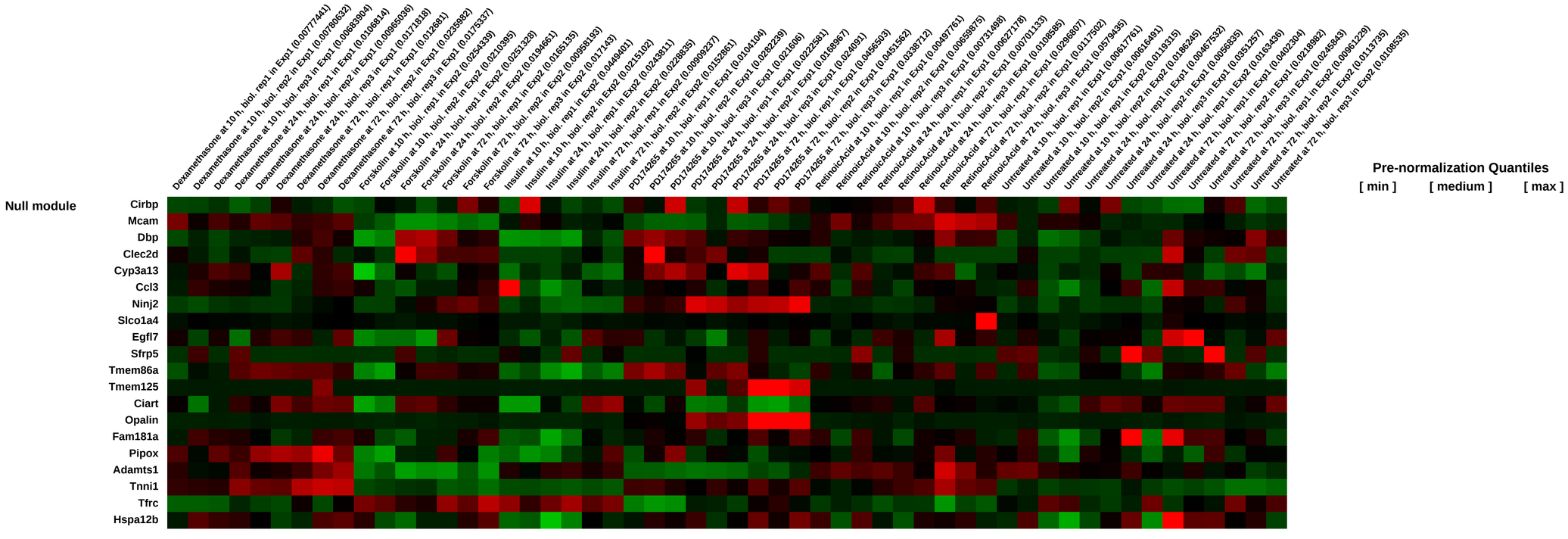

GEO Series "GSE13283" Expression Profiles

Num of samples in this series: 10

Scale of expression profile Z-scores

-3.0 -2.0 -1.0 0.0 1.0 2.0 3.0

GEO Link:	http://www.ncbi.nlm.nih.gov/geo/query/acc.cgi?acc=GSE13283
Status:	Public on Dec 05 2008
Title:	Mouse Erythroleukemia (MEL) Cells Expressing Tagged Versions of BCL11A
Organism:	Mus musculus
Experiment type:	Expression profiling by array
Platform:	GPL1261
Pubmed ID:	19056937
Summary & Design:	**Summary:** Differences in the amount of fetal hemoglobin (HbF) that persists into adulthood affect the severity of sickle cell disease and the beta-thalassemia syndromes. Genetic association studies have identified sequence variants in the gene BCL11A that influence HbF levels. Here we examine BCL11A as a potential regulator of HbF expression. The high HbF BCL11A genotype is associated with reduced BCL11A expression. Moreover, abundant expression of full-length forms of BCL11A is developmentally restricted to adult erythroid cells. Down-regulation of BCL11A expression in primary adult erythroid cells leads to robust HbF expression. Consistent with a direct role of BCL11A in globin gene regulation, we find that BCL11A occupies several discrete sites in the beta-globin gene cluster. BCL11A emerges as a therapeutic target for reactivation of HbF in beta-hemoglobin disorders. Expression clone label: FBB (4 different subclones, with 2 arrays each), Control label: MelBirA Keywords: cell type comparsion **Overall design:** Microarray expression analysis from parental control mouse erythroleukemia (MEL) cells containing the BirA enzyme (MelBirA cells) and cells containing tagged versions (FLAG-Biotag) of BCL11A. Two control datasets and eight datasets from four subclones containing tagged BCL11A are included.

Background corr dist: KL-Divergence = 0.1217, L1-Distance = 0.0300, L2-Distance = 0.0015, Normal std = 0.4045

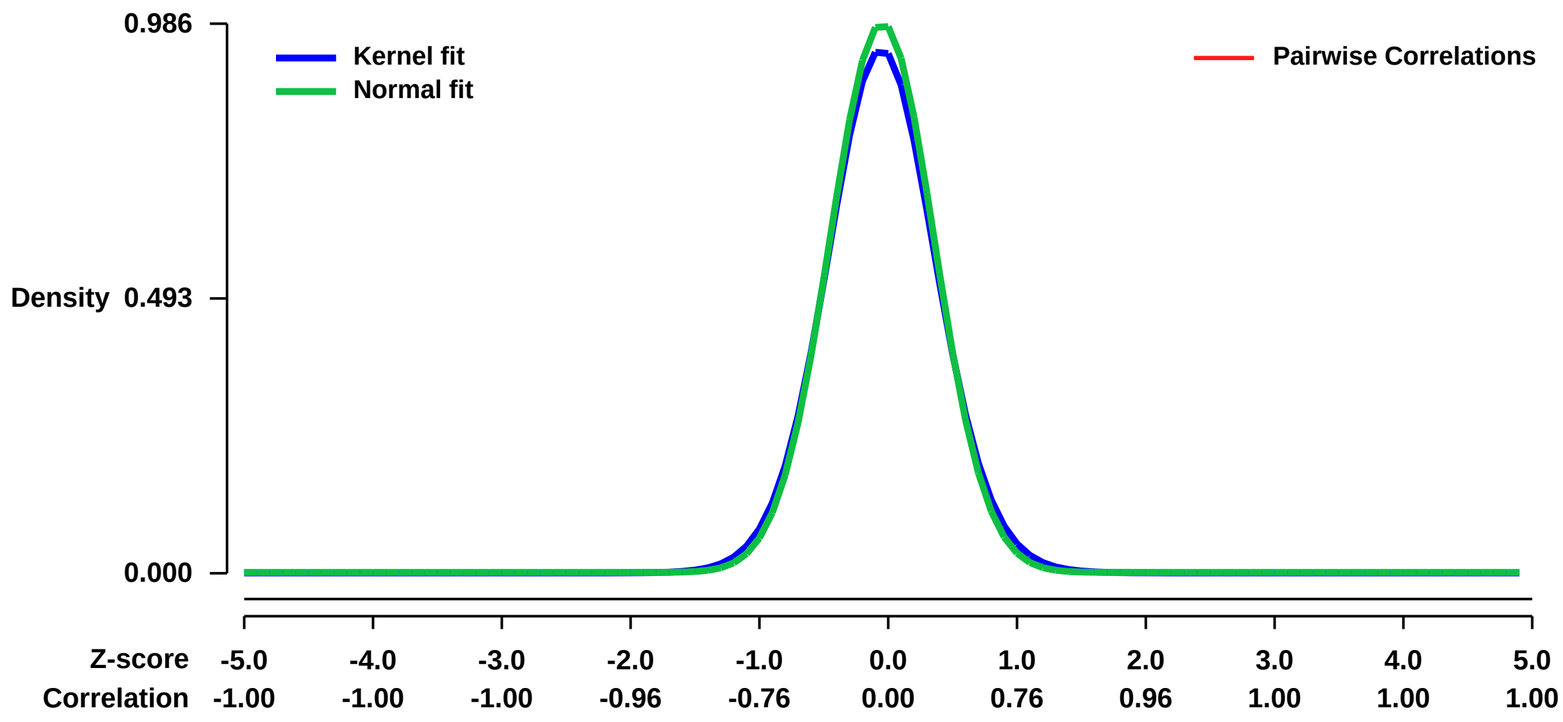

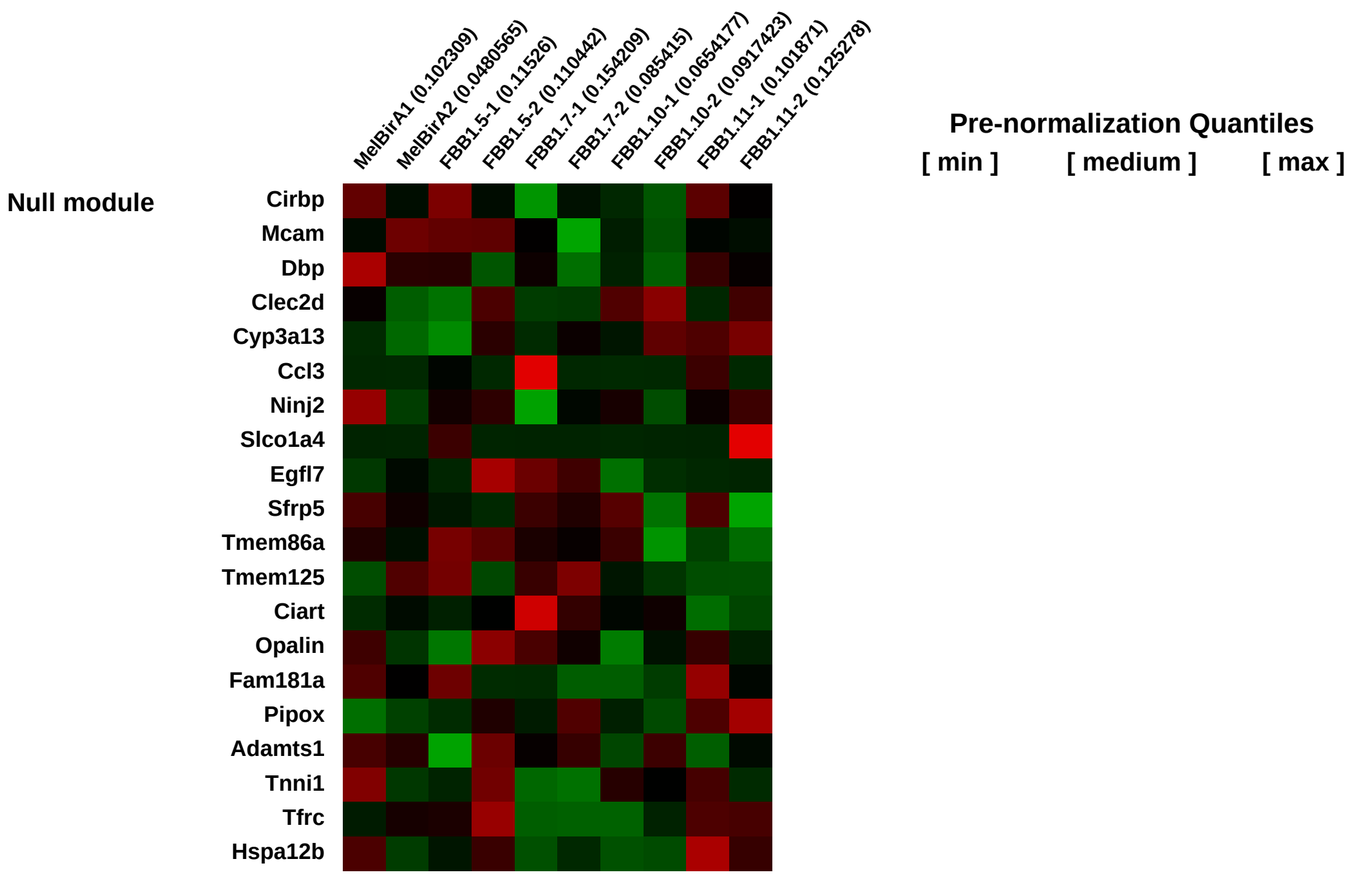

GEO Series "GSE15324" Expression Profiles

Num of samples in this series: 8

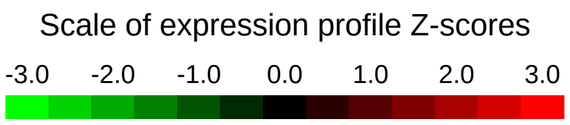

GEO Link:	http://www.ncbi.nlm.nih.gov/geo/query/acc.cgi?acc=GSE15324
Status:	Public on Mar 24 2009
Title:	Control of CD8+ T cell proliferation by the transcription factor ELF4
Organism:	Mus musculus
Experiment type:	Expression profiling by array
Platform:	GPL1261
Pubmed ID:	19412182
Summary & Design:	**Summary:** Transcription factors that regulate quiescence, proliferation, and homing of lymphocytes are critical for effective immune system function. In the present study, we demonstrated that the transcription factor ELF4 directly activates the tumor suppressor KLF4 downstream of T cell receptor (TCR) signaling to induce cell cycle arrest in naˆflve CD8+ T cells. Elf4- and Klf4-deficient mice accumulated CD8+CD44hi T cells during steady-state conditions and generated more memory T cells after immunization. The homeostatic expansion of CD8+CD44hi T cells in Elf4-null mice resulted in a redistribution of cells to non-lymphoid tissue due to reduced expression of the transcription factor KLF2, and the surface proteins CCR7 and CD62L. This work describes the combinatorial role of lymphocyte-intrinsic factors in the control of T cell homeostasis, activation and homing. **Overall design:** RNAs isolated from wild type and Elf4 -/- CD8+ T cells were used in Affimetrix oligonucleotide arrays either untreated or after 3.5 days of activation.

Background corr dist: KL-Divergence = 0.0407, L1-Distance = 0.0476, L2-Distance = 0.0029, Normal std = 0.6550

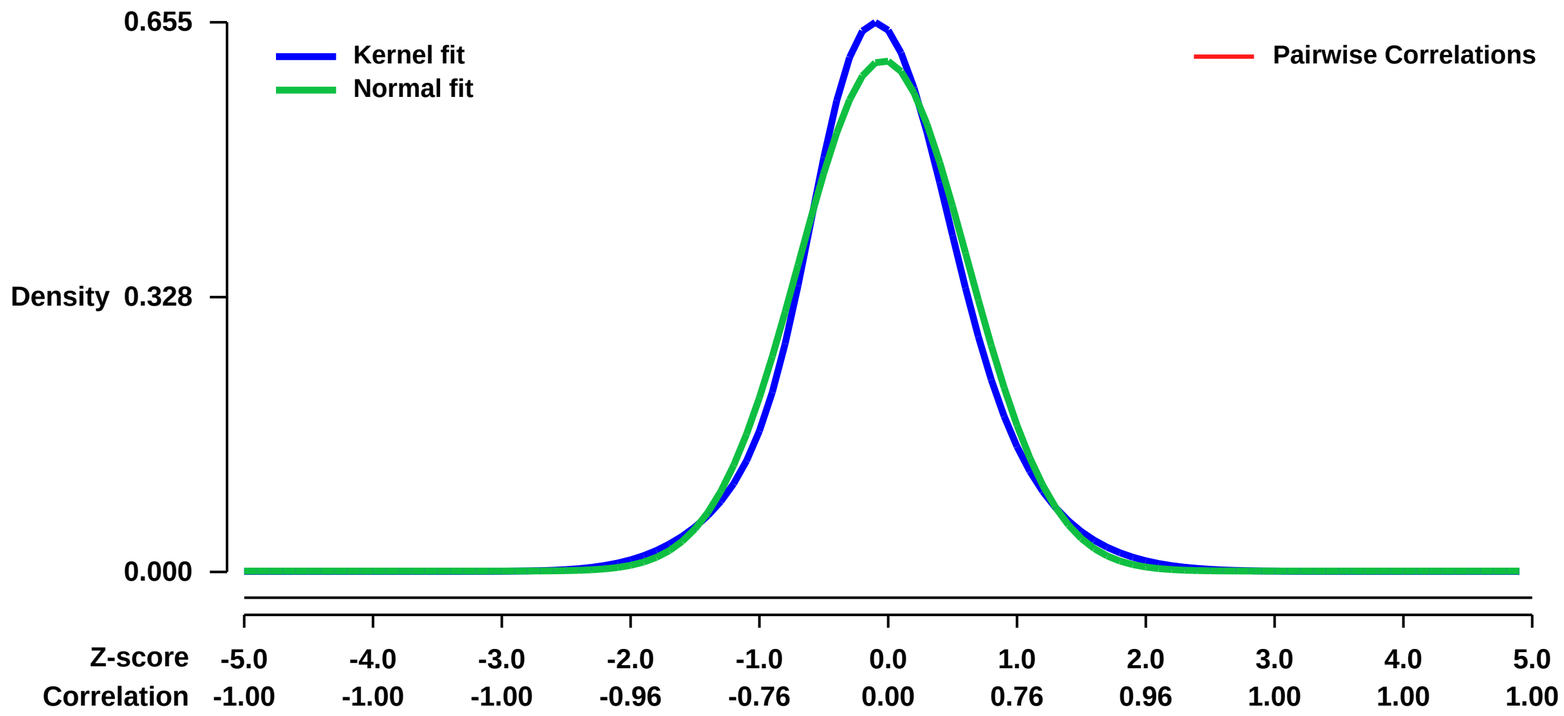

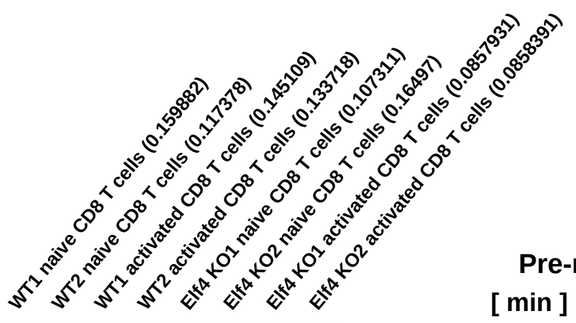

Pre-normalization Quantiles

[min] [medium] [max]

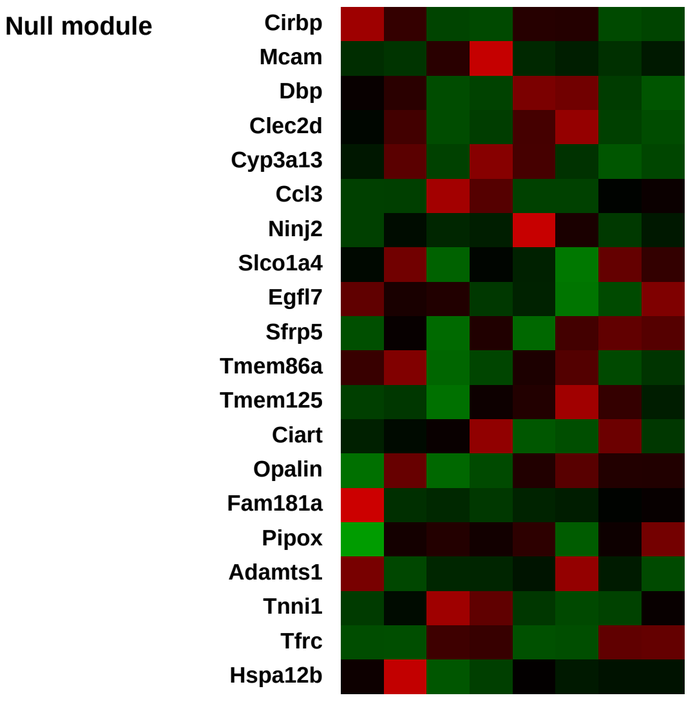

GEO Series "GSE24813" Expression Profiles

Num of samples in this series: 10

Scale of expression profile Z-scores

-3.0 -2.0 -1.0 0.0 1.0 2.0 3.0

GEO Link:	http://www.ncbi.nlm.nih.gov/geo/query/acc.cgi?acc=GSE24813
Status:	Public on Aug 24 2011
Title:	Gene expression data of BCR-ABL1 transformed myeloid cells from BCL6 wild-type and BCL6 knockout mice treated with and without Imatinib and RI-BPI
Organism:	Mus musculus
Experiment type:	Expression profiling by array
Platform:	GPL1261
Pubmed ID:	21911423
Summary & Design:	**Summary:** To identify differences in the gene regulation between BCL6+/+ and BCL6-/- CML cells a gene expression analysis has been performed. We investigated the gene expression pattern in BCL6+/+ cells in the presence or absence of Imatinib and a combination of Imatinib and RI-BPI (a novel retro-inverso BCL6 peptide inhibitor). In BCL6-/- CML cells, we investigated the gene expression pattern in the presence or absence of Imatinib. **Overall design:** BCR-ABL1 transformed myeloid cells from BCL6+/+ mice were cultured in the presence or absence of 10´µM Imatinib or 10´µM Imatinib and 20´µM RI-BPI for 16 hours. BCR-ABL1 transformed myeloid cells from BCL6-/- mice were cultured in the presence or absence of 10´µM Imatinib. Two samples for each condition were processed.

Background corr dist: KL-Divergence = 0.0654, L1-Distance = 0.0414, L2-Distance = 0.0023, Normal std = 0.5423

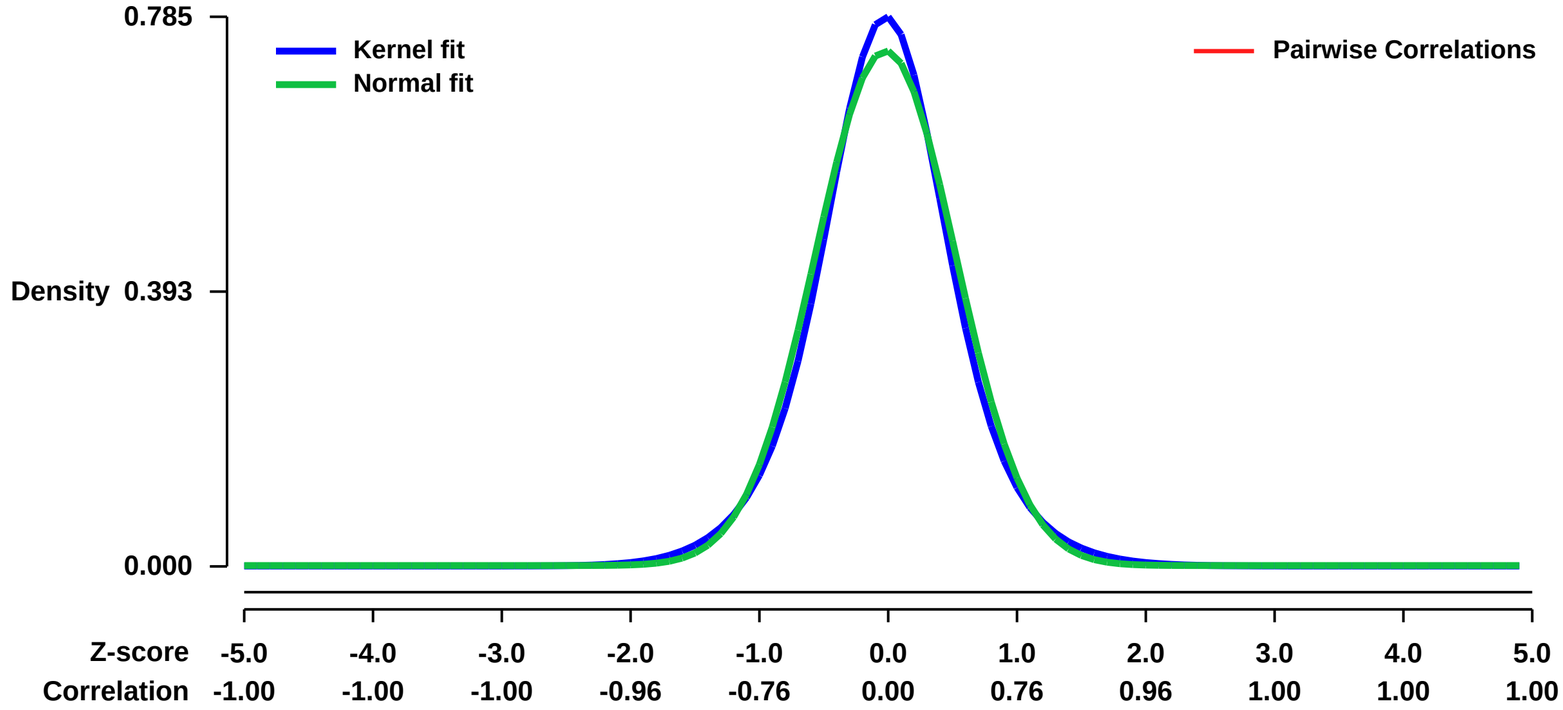

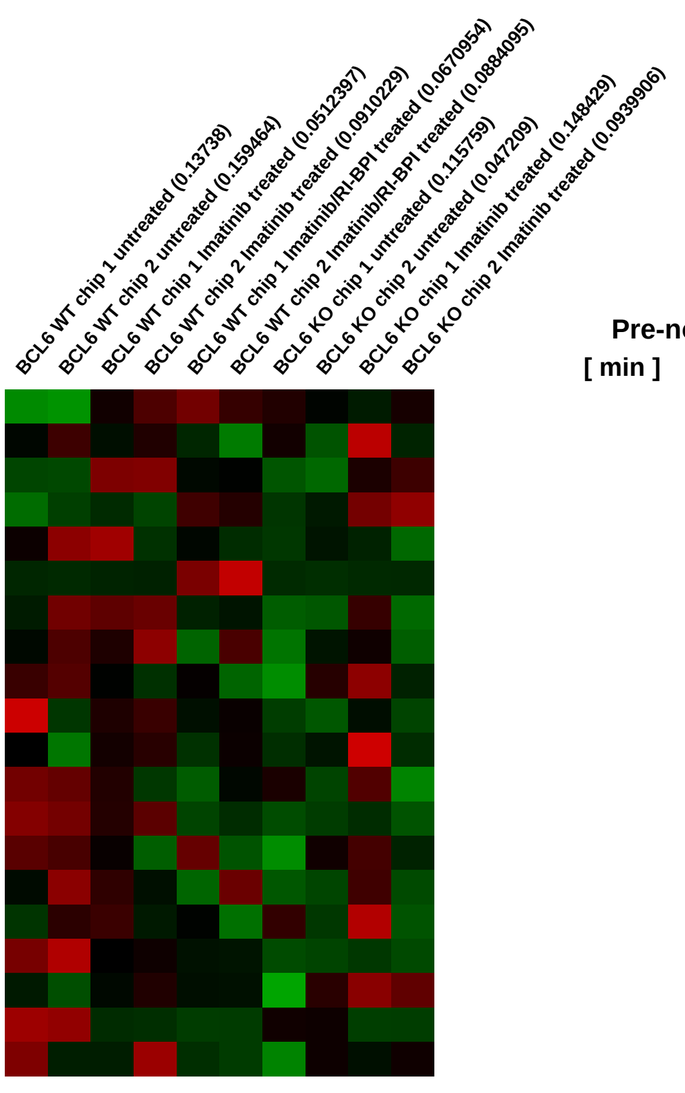

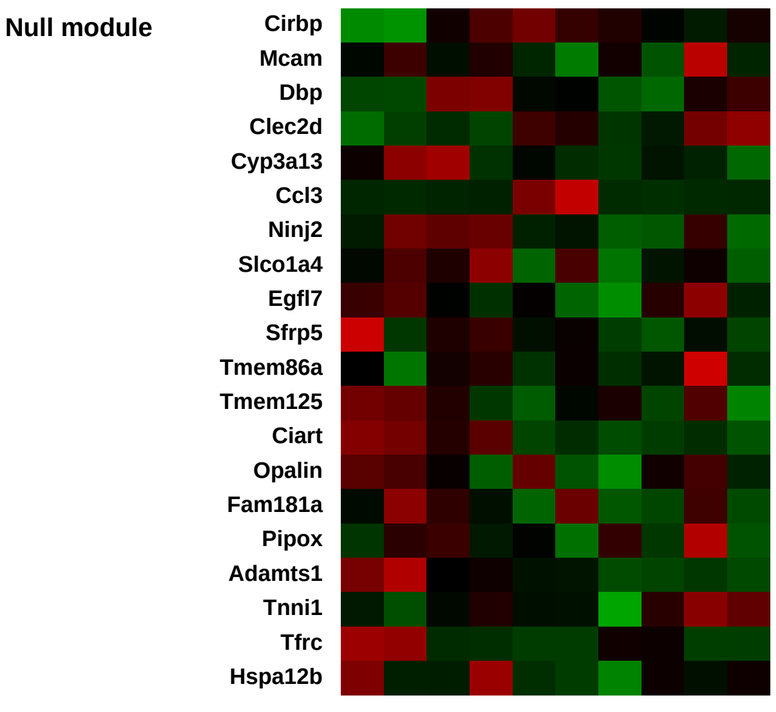

GEO Series "GSE26076" Expression Profiles

Num of samples in this series: 12

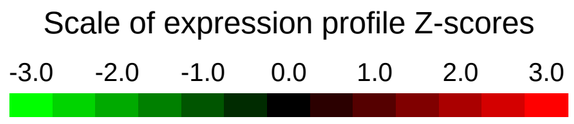

GEO Link:	http://www.ncbi.nlm.nih.gov/geo/query/acc.cgi?acc=GSE26076
Status:	Public on Jun 15 2011
Title:	Mouse conjunctival forniceal gene expression during postnatal development and its regulation by Kruppel-like factor 4
Organism:	Mus musculus
Experiment type:	Expression profiling by array
Platform:	GPL1261
Pubmed ID:	21398290
Summary & Design:	**Summary:** **Purpose: To identify the changes in postnatal mouse conjunctival forniceal gene expression and their regulation by Klf4 around eye opening stage when the goblet cells first appear.** **Methods: Laser-capture-microdissection was used to collect conjunctival forniceal epithelial cells from postnatal-day (PN) 9, PN14 and PN20 wild-type (WT), and PN14 Klf4-conditional null (Klf4CN) mice, where goblet cells are absent, developing, present, and missing, respectively. Microarrays were used to compare gene expression among these four groups. Expression of selected genes was validated by Q-RT-PCR, and spatiotemporal expression assessed by in situ hybridization. Results: We identified 668, 251, 1160 and 139 genes that were upregulated and 492, 377, 1419 and 57 genes that were downregulated between PN9 and PN14, PN14 and PN20, PN9 and PN20, and PN14 WT and Klf4CN conjunctiva, respectively. Transcription factors Spdef, FoxA1 and FoxA3 that regulate goblet cell development in other mucosal epithelia, and epithelial specific Ets (ESE) transcription factor family members were upregulated during conjunctival development. Mesenchymal-epithelial transition (MET) was favored and diverse pathways related to glycoprotein biosynthesis, mucosal immunity, signaling, endocytic and neural regulation were affected during conjunctival development. Conjunctival Klf4-target genes differed significantly from the previously identified corneal Klf4-target genes, implying tissue-dependant regulatory targets for Klf4.** **Conclusions: We have identified the changes in gene expression accompanying mouse conjunctival development and the role of Klf4 in this process. These studies provide new probes to study conjunctival epithelial development and function, and reveal that the gene regulatory network required for goblet cell development is conserved across different mucosal epithelia.** **Overall design:** **Three independent samples in each of four developmental groups**

Background corr dist: KL-Divergence = 0.1081, L1-Distance = 0.0315, L2-Distance = 0.0019, Normal std = 0.4256

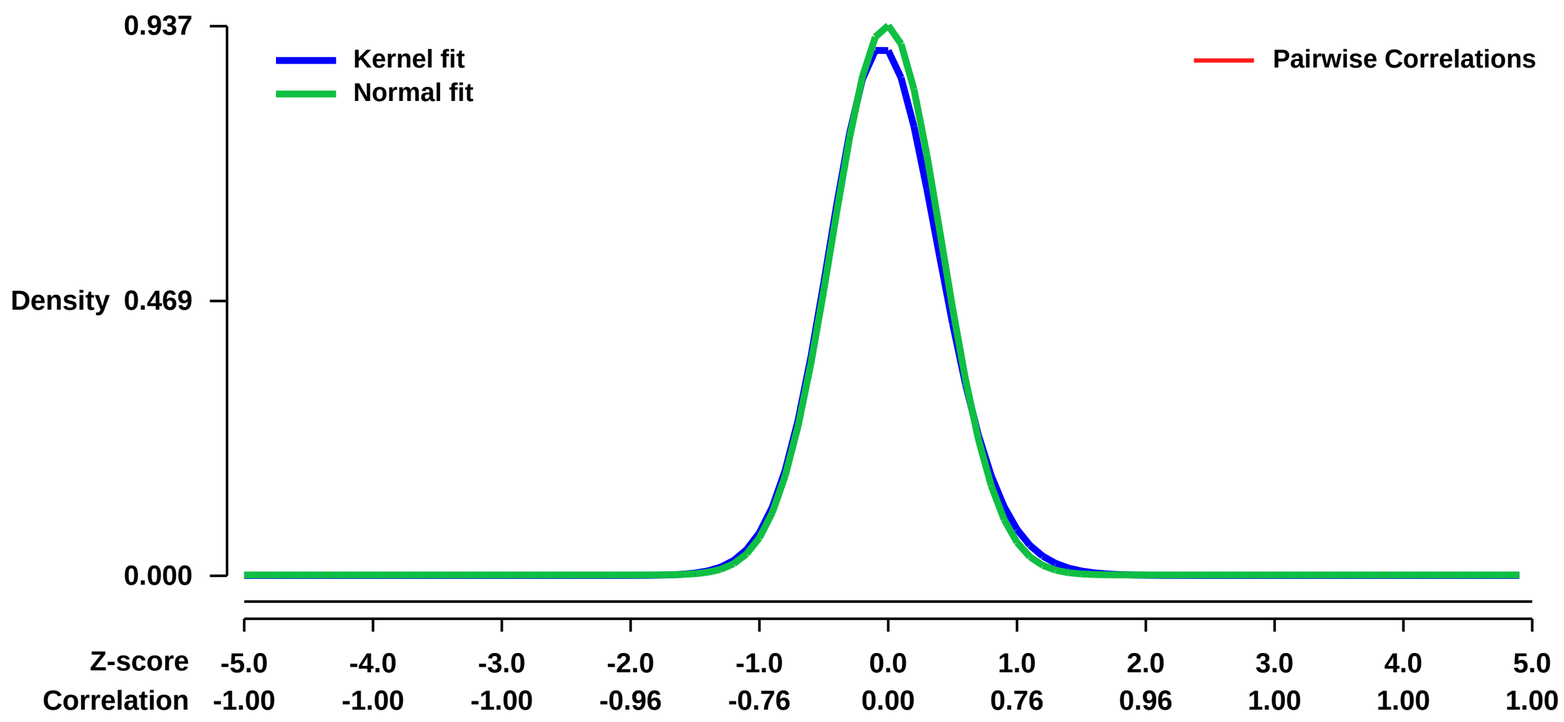

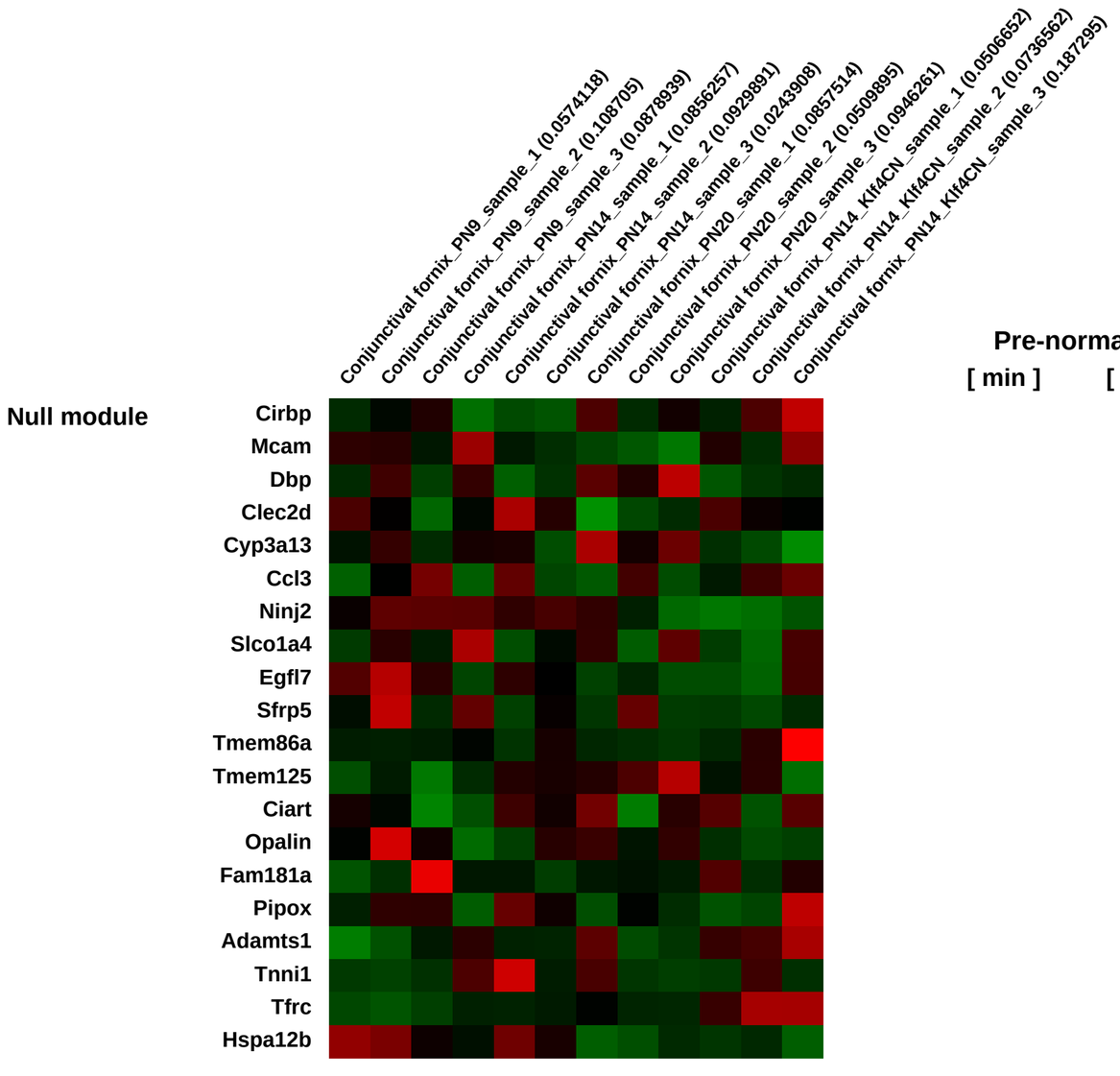

GEO Series "GSE4656" Expression Profiles

Num of samples in this series: 7

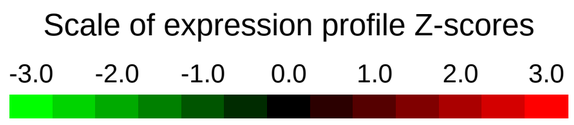

GEO Link:	http://www.ncbi.nlm.nih.gov/geo/query/acc.cgi?acc=GSE4656
Status:	Public on Mar 11 2007
Title:	day3 brown fat from wt compared to day3 from Gyk ko
Organism:	Mus musculus
Experiment type:	Expression profiling by array
Platform:	GPL1261
Pubmed ID:	17406644
Summary & Design:	**Summary:** Glycerol kinase (GK) is at the interface of fat and carbohydrate metabolism and has been implicated in insulin resistance and type 2 diabetes mellitus (T2DM). To define GKâ s role in insulin resistance, we examined gene expression in brown adipose tissue in a glycerol kinase (Gyk) knockout (KO) mouse model using microarray analysis. Global gene expression profiles of KO mice were distinct from wild type (WT) with 668 genes that were differentially expressed. These included genes involved in lipid metabolism, carbohydrate metabolism, insulin signaling, and insulin resistance. Real-Time (RT) PCR analysis confirmed the differential expression of selected genes involved in lipid and carbohydrate metabolism. PathwayAssist analysis confirmed direct and indirect connections between GK and genes in lipid metabolism, carbohydrate metabolism, insulin signaling, and insulin resistance. Network Component Analysis (NCA) showed that the transcription factors, peroxisome proliferator-activated receptor gamma (PPAR-¿‡), sterol regulatory element binding factor 1 (SREBP-1), SREBP-2, signal transducer and activator of transcription 3 (STAT3), STAT5, trans-acting transcription factor 1 (SP1), CCAAT/enhancer binding protein alpha (CEBP-¿–), cAMP responsive element binding protein 1 (CREB), glucocorticoid receptor (GR), and PPAR-¿– have altered activity in the KO mice. NCA also revealed the individual contribution of these transcription factors on the expression of genes altered in the microarray data. This study elucidates the transcription network of Gyk and further confirms a role for Gyk, a simple Mendelian disorder, in insulin resistance and T2DM, a common complex genetic disorder. **Keywords:** genotype state analysis **Overall design:** 7 samples are analyzed; 3 wildtype and 4 KO. the WT samples are used as control and KO samples are used as the experimental group.

Background corr dist: KL-Divergence = 0.0613, L1-Distance = 0.0172, L2-Distance = 0.0003, Normal std = 0.5265

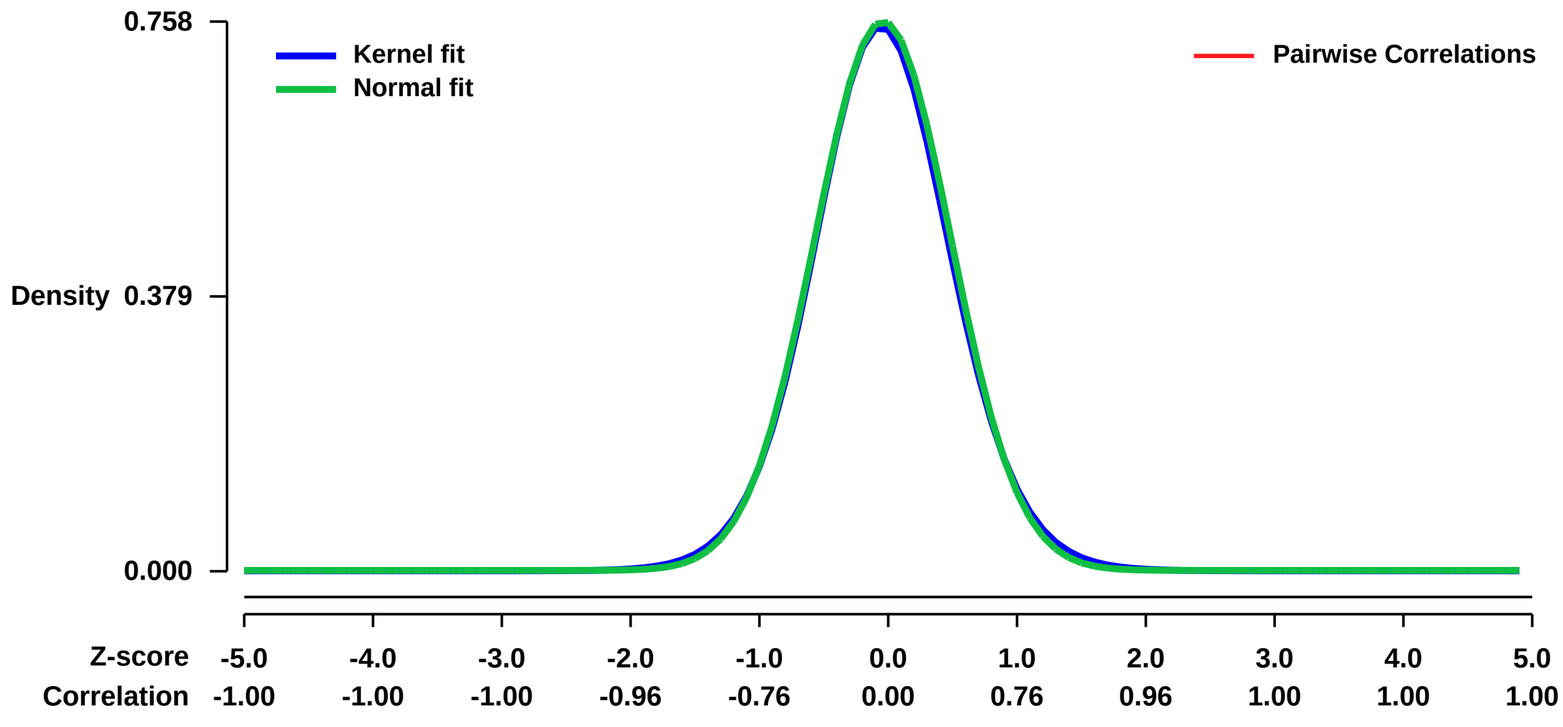

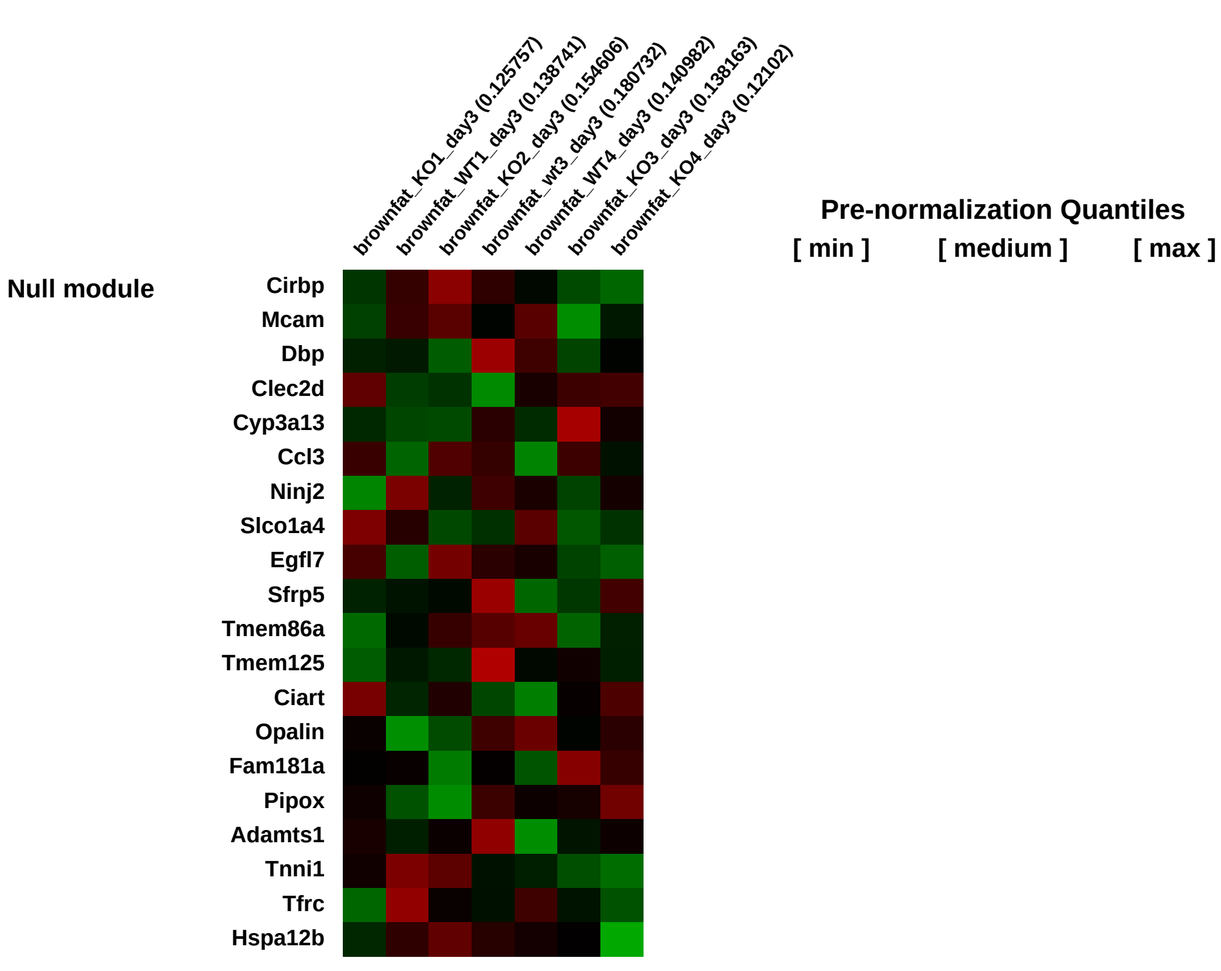

GEO Series "GSE13106" Expression Profiles

Num of samples in this series: 10

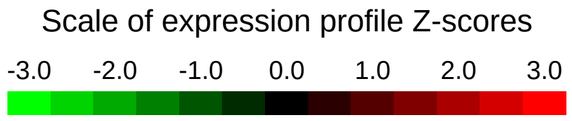

GEO Link:	http://www.ncbi.nlm.nih.gov/geo/query/acc.cgi?acc=GSE13106
Status:	Public on Sep 09 2009
Title:	Regulated SMAD signalling in development
Organism:	Mus musculus
Experiment type:	Expression profiling by array
Platform:	GPL1261
Pubmed ID:	19517569
Summary & Design:	**Summary:** Phosphorylation and subsequent nuclear translocation of SMAD proteins determine the cellular response to activin. Here we identify a novel means by which activin signalling is regulated to enable developmental stage-specific SMAD gene transcription. In response to activin A, immature proliferating mouse Sertoli cells exhibit nuclear accumulation of SMAD3, but not SMAD2, although both proteins are phosphorylated. In post-mitotic differentiating cells, both SMAD2 and SMAD3 accumulate in the nucleus. Furthermore, immature Sertoli cells are sensitive to activin dosage; at higher concentrations maximal SMAD3 nuclear accumulation is observed, accompanied by a small, but significant, increase in nuclear SMAD2. Microarray analysis confirmed that differential SMAD utilization correlated with altered transcriptional outcomes and identified new activin target genes, Gja1 and Serpina5, which are known to be required for Sertoli cell development and male fertility. In immature Sertoli cells, genetic or transient knockdown of SMAD3 enhanced SMAD2 nuclear accumulation in response to activin, with increased Serpina5 mRNA levels associated with nuclear localized SMAD2. In transgenic mice with altered activin bioactivity that display male fertility phenotypes, testicular Gja1 and Serpina5 mRNA levels reflected altered in vivo activin levels. We conclude that regulated nuclear accumulation of phosphorylated SMAD2 is a novel determinant of developmentally regulated activin signalling. **Overall design:** Murine 15dpp Sertoli Cell treated with 0ng, 5ng activin (duplicates). Total 10 samples.

Background corr dist: KL-Divergence = 0.0442, L1-Distance = 0.0746, L2-Distance = 0.0079, Normal std = 0.6871

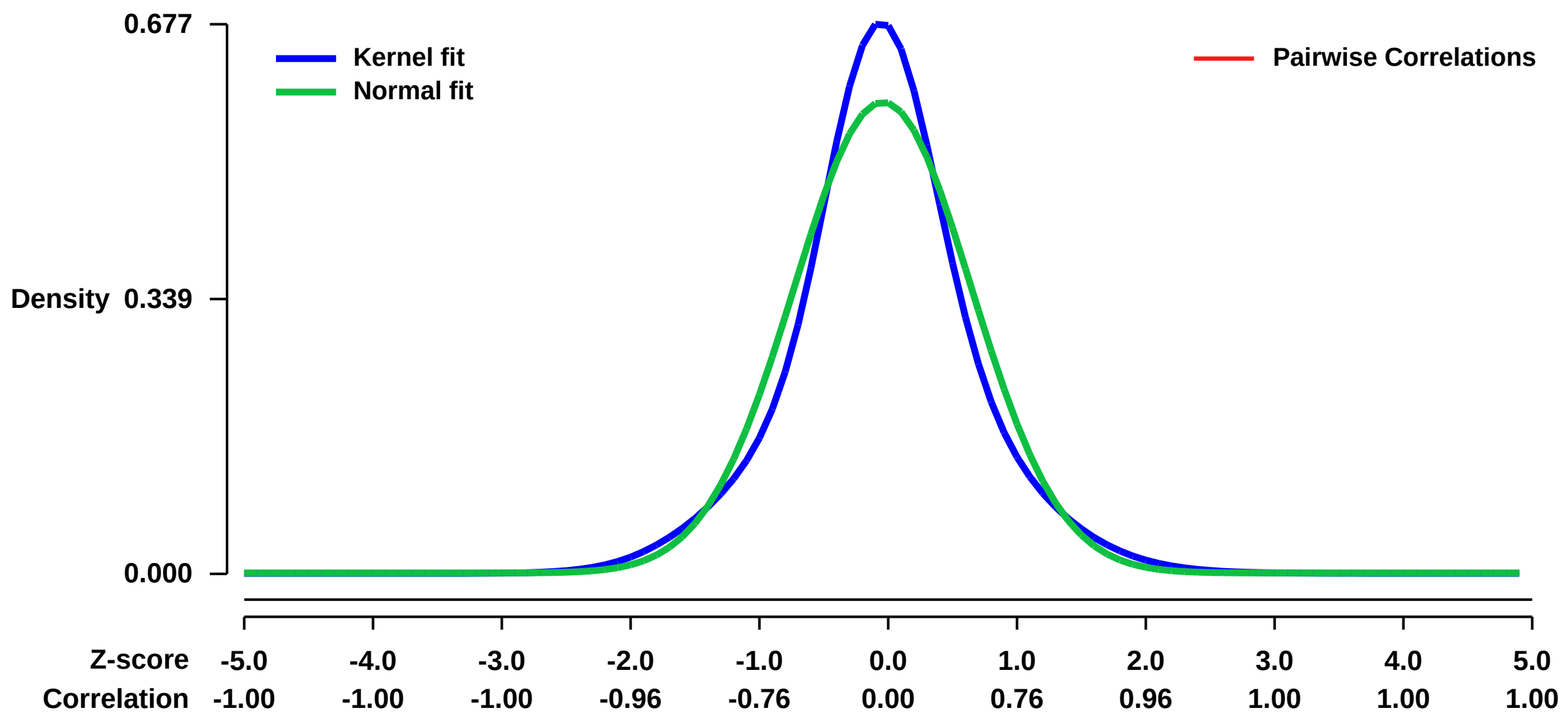

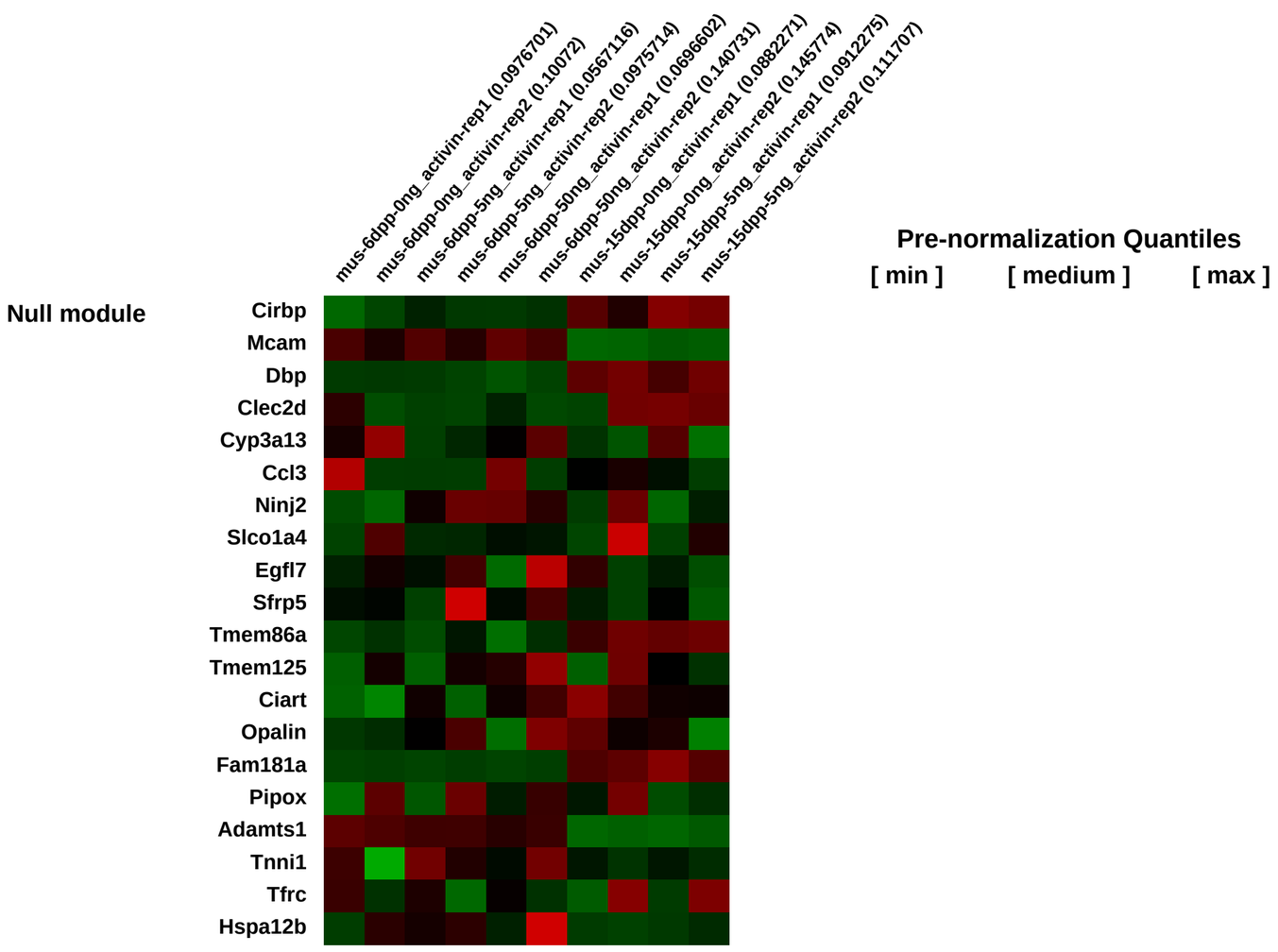

GEO Series "GSE43927" Expression Profiles

Num of samples in this series: 19

Scale of expression profile Z-scores

-3.0 -2.0 -1.0 0.0 1.0 2.0 3.0

GEO Link:	http://www.ncbi.nlm.nih.gov/geo/query/acc.cgi?acc=GSE43927
Status:	Public on Feb 04 2014
Title:	Exposure to Propylthiouracil in Pregnant Mice Potentiates the Transcriptional Response to Thyroid Hormone in the Fetal Cerebral Cortex
Organism:	Mus musculus
Experiment type:	Expression profiling by array
Platform:	GPL1261
Pubmed ID:	24436321
Summary & Design:	**Summary:** Although the effects of thyroid hormones (TH) on the brain development have been extensively studied perinatally, effects of TH of maternal origin on the fetal brain development have been largely unexplored. We applied a high throughput study on the mouse models with aberrant TH levels on gestation day (GD) 16, before the onset of fetal thyroid function. Although 3 day treatment with methimazole (MMI) and perchlorate significantly decreased TH levels in fetal cerebral cortex, few changes in the abundance of mRNA were revealed by the microarray analysis. Injection TH to dams 12 hours before sacrifice on GD 16 induced 161 genes significantly changed in fetal cortex. Nine out of 10 selected genes were confirmed with RT-PCR, including known TH responsive gene Klf9 and other novel TH responsive genes such as Appbp2, Ppap2b and Fgfr1op2. TH regulation of the expression of these genes was also confirmed with cultured N2a˛† cells. Thyroid responsive elements (TREs) in the promoters of these genes were identified using electrophoresis mobility shift assay. TH effect on microRNA (miRNA) expression in developing cortex on GD 16 and postnatal day (PND) 15 was investigated with microarray and RT-PCR. Some of miRNAs and precursors decreased in fetal cortex from the dams injected with TH on GD 16, including miR-16 and miR-106. Using 3â untranslate region reporter vector, we identified Klf9 is one of the target genes of miR-106, while Ppap2b is the target of miR-16. These results indicated that TH regulation on gene expression could through TR-TRE interaction and through regulating target miRNA expression. This study is the first report to identify TH responsive genes and miRNAs genome wide in the early fetal brain; it provides evidence to further understand the mechanism of TH effect on brain development. **Overall design:** 1 of 20 samples removed due to poor quality.

Background corr dist: KL-Divergence = 0.2258, L1-Distance = 0.0571, L2-Distance = 0.0081, Normal std = 0.3144

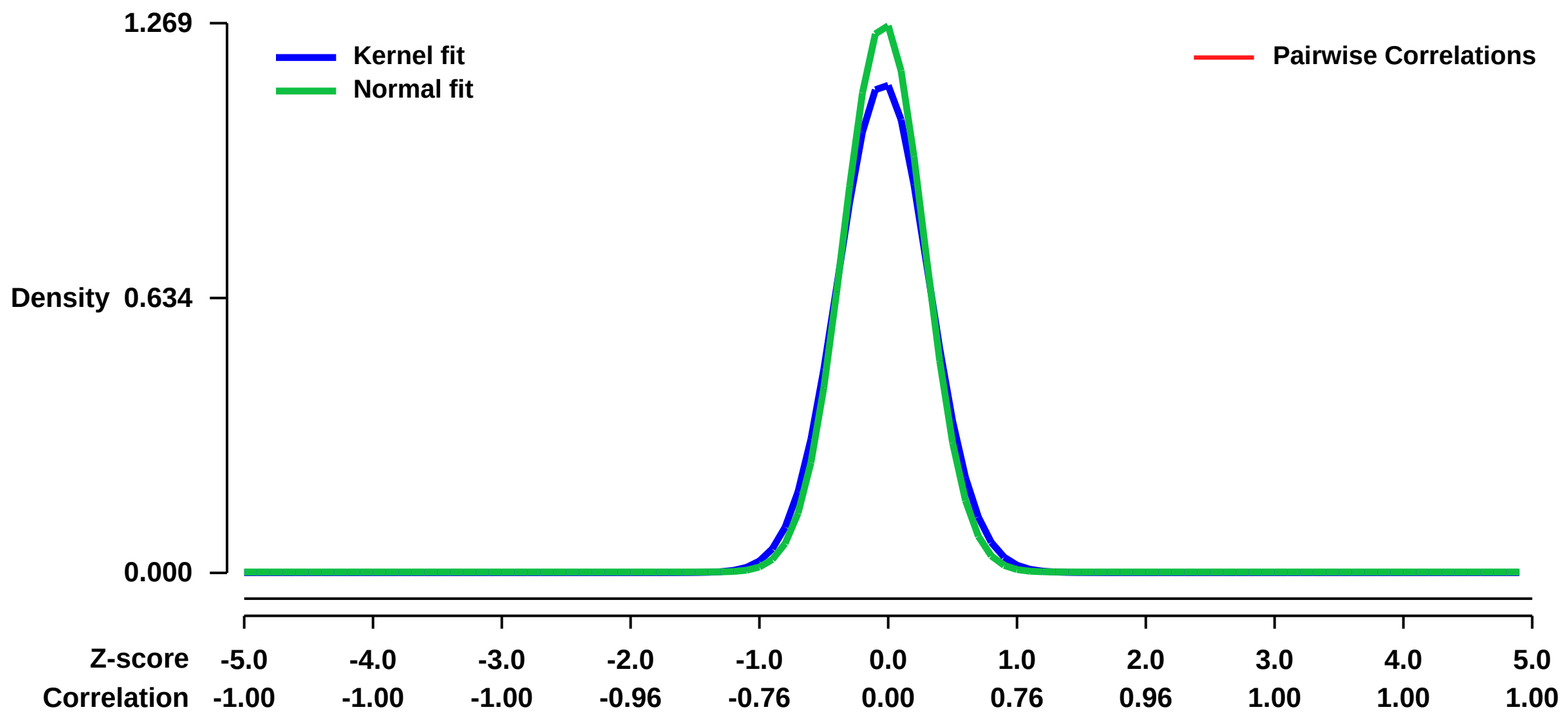

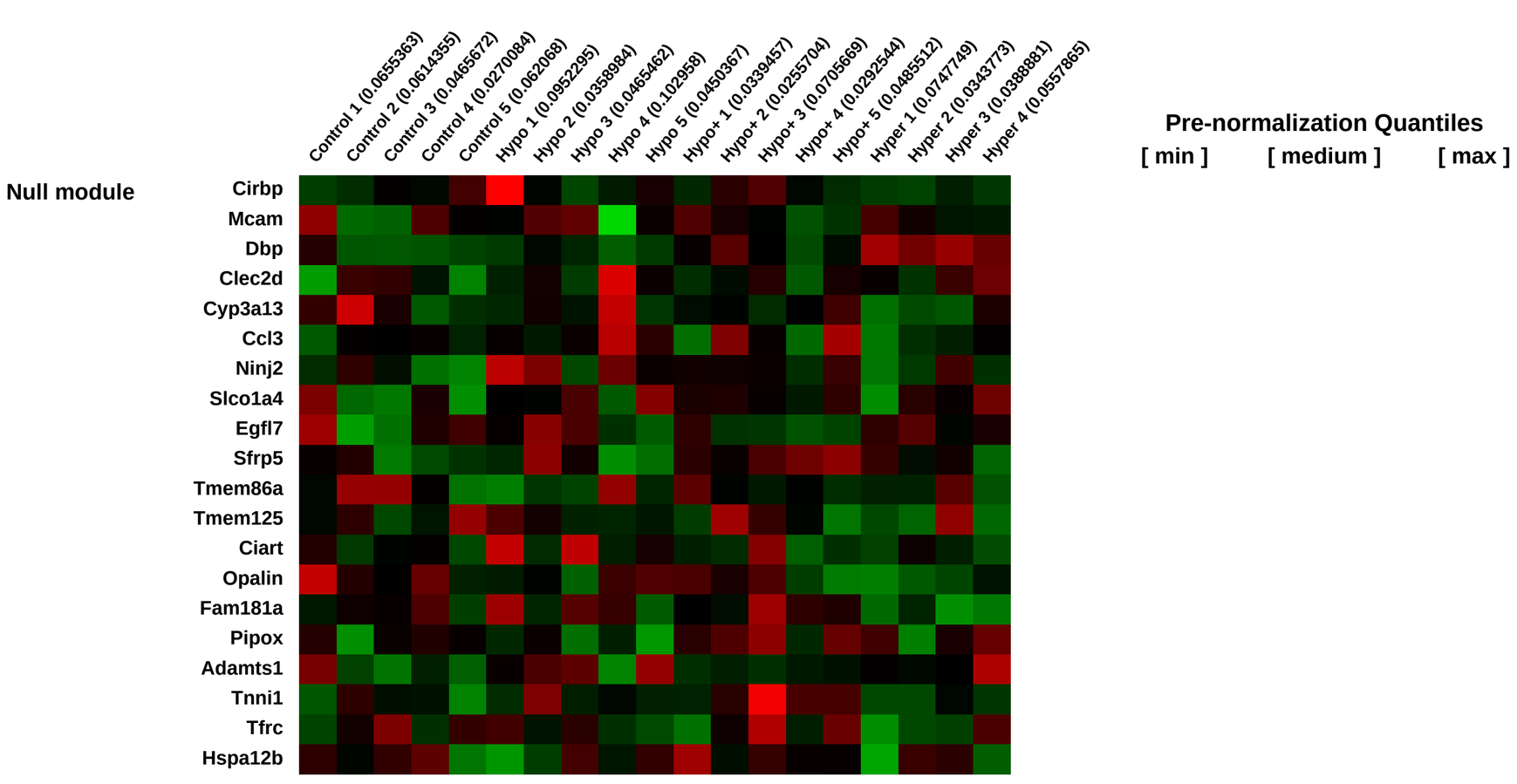

GEO Series "GSE3293" Expression Profiles

Num of samples in this series: 8

Scale of expression profile Z-scores

-3.0 -2.0 -1.0 0.0 1.0 2.0 3.0

GEO Link:	http://www.ncbi.nlm.nih.gov/geo/query/acc.cgi?acc=GSE3293
Status:	Public on Dec 31 2005
Title:	Leptin Regulated Mouse Gallbladder Genes
Organism:	Mus musculus
Experiment type:	Expression profiling by array
Platform:	GPL1261
Pubmed ID:	17463181
Summary & Design:	**Summary:** Gallstone disease is a major contributor to health care costs in the United States. Approximately 12 % of the U.S. population has gallstones. As a result, more than 700,000 cholecystectomies are performed in this country each year. Many of these patients are obese and have a positive family history; but surprisingly, little is known about the link between obesity, genetics and gallstone formation. Obese individuals have been shown to have supersaturated bile, larger gallbladder fasting volumes and impaired gallbladder emptying. We have recently demonstrated that leptin plays a role in gallbladder motility. In an effort to understand the genetic basis for these observations, we tested the hypothesis that leptin would alter gallbladder gene expression. Methods: Affymetrix oligonucleotide microarrays 430 2.0 were used to compare gallbladder gene expression profiles from 12 week old control saline-treated leptin-deficient (Lep ob) and from leptin-treated Lep ob female mice. Analyses were performed on pooled RNA (n=4) from the gallbladders of 12 saline-treated Lep ob mice and from 12 Lep ob mice which were administered daily IP 5 ug/g of recombinant murine leptin for 4 weeks. Resulting data were analyzed utilizing Gene Chip Operating Software or MAS 5.0. Results: Of the genes analyzed 314 were upregulated and 108 were downregulated by leptin administration. Numerous genes related to gallstone pathogenesis, gallbladder absorption/secretion, inflammatory cytokines, and insulin resistance were altered by leptin. **Keywords: comparitive response to leptin** **Overall design:** Female B6.V-lepob obese mice (n=24) aged 7 weeks were obtained from The Jackson Laboratory (Bar Harbor, ME). Upon arrival, mice were placed on a standard chow diet and were allowed to acclimate for 1 week before starting the experiment. For leptin treatments, mice received daily intraperitoneal injections of either recombinant mouse leptin (R&D Systems, Minneapolis, MN) (n=12) at a dose of 5 ´¡g/g body weight or with saline as a control (n=12) for 4 weeks. At 12 weeks of age, mice were fasted overnight with free access to water. The following morning the mice underwent cholecystectomy. Three gallbladders were pooled to create 4 pools in each treatment and total RNA was isolated. Affymetrix murine 430 2.0 arrays were utilized to examine altered gallbladder gene expression as a result of leptin administration. The resulting data was analyzed utlizing Gene Chip Operating Software or MAS 5.0.

Background corr dist: KL-Divergence = 0.0763, L1-Distance = 0.0225, L2-Distance = 0.0008, Normal std = 0.4847

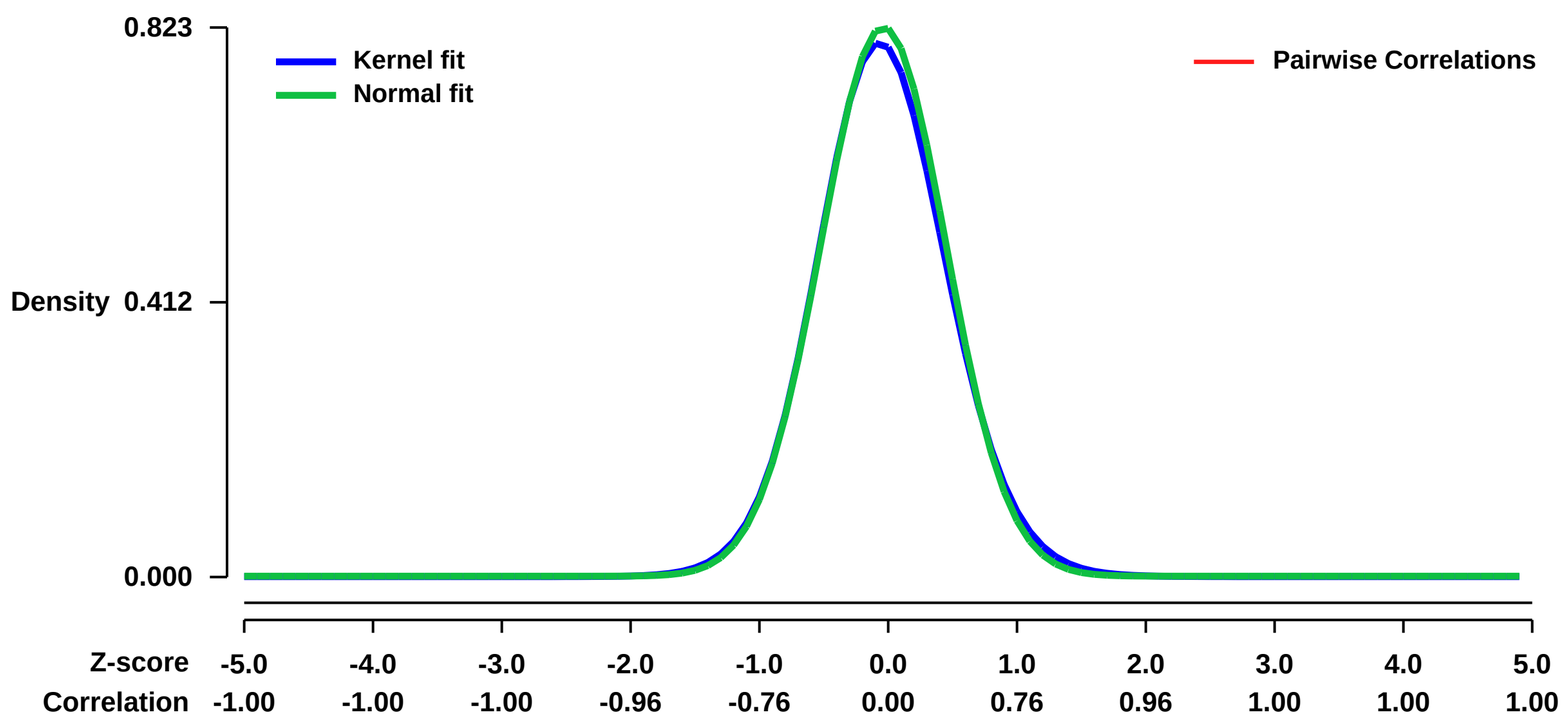

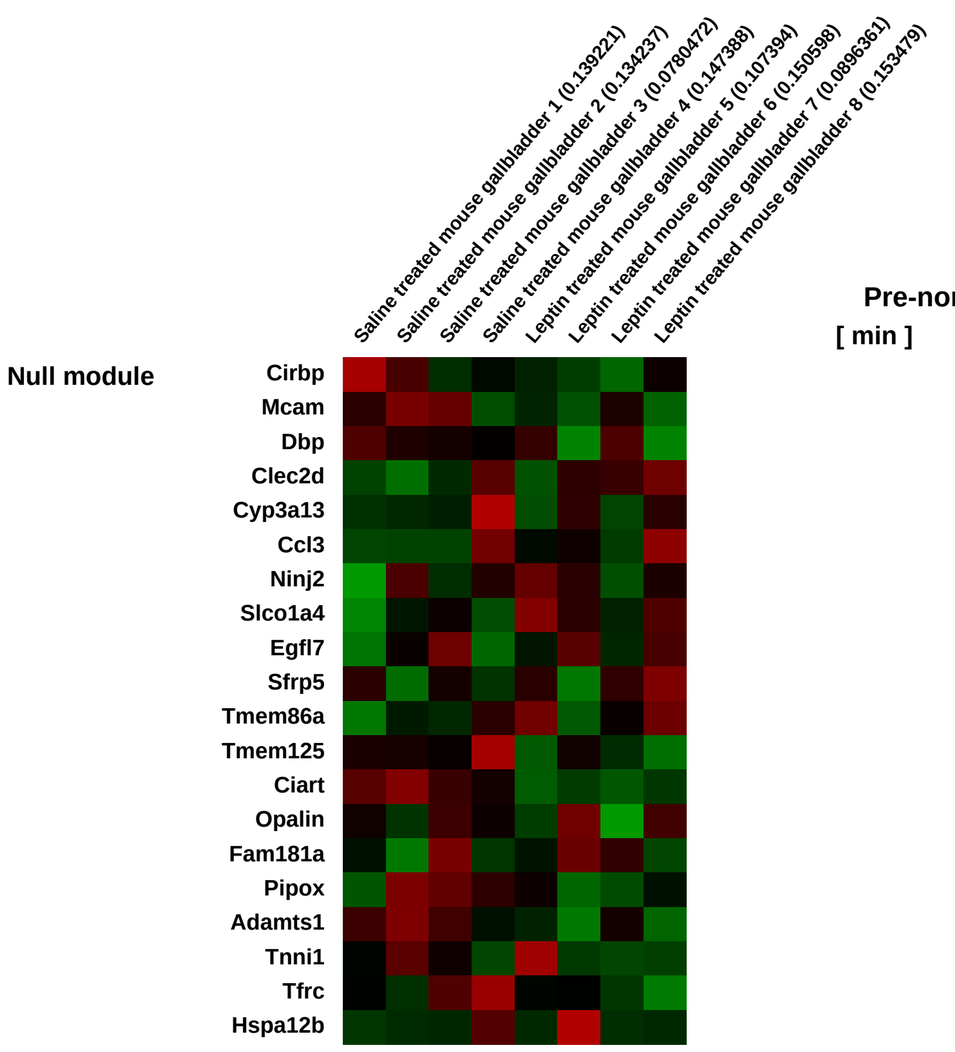

GEO Series "GSE50865" Expression Profiles

Num of samples in this series: 12

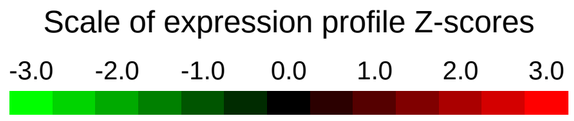

GEO Link:	http://www.ncbi.nlm.nih.gov/geo/query/acc.cgi?acc=GSE50865
Status:	Public on Sep 13 2013
Title:	Expression Data For BRD4 Inhibition
Organism:	Mus musculus
Experiment type:	Expression profiling by array
Platform:	GPL1261
Pubmed ID:	24373973
Summary & Design:	**Summary:** BRD4 Inhibition of spindle cell malignant peripheral nerve sheath tumor (sMPNST) tumor cells **Overall design:** Cells were treated with Brd4 shRNA (3 days) or 500 nM JQ1 (2 days) before RNA isolation

Background corr dist: KL-Divergence = 0.1079, L1-Distance = 0.0335, L2-Distance = 0.0015, Normal std = 0.4420

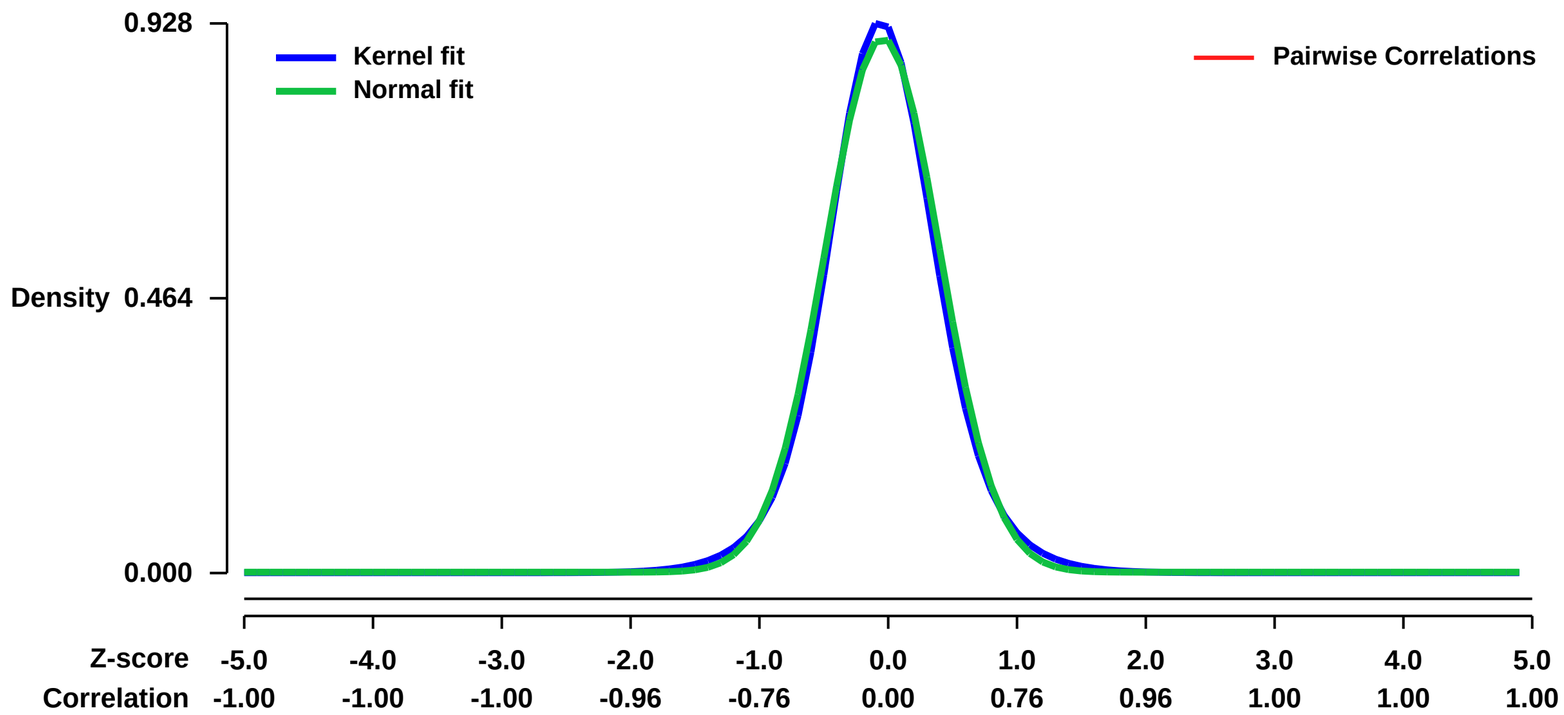

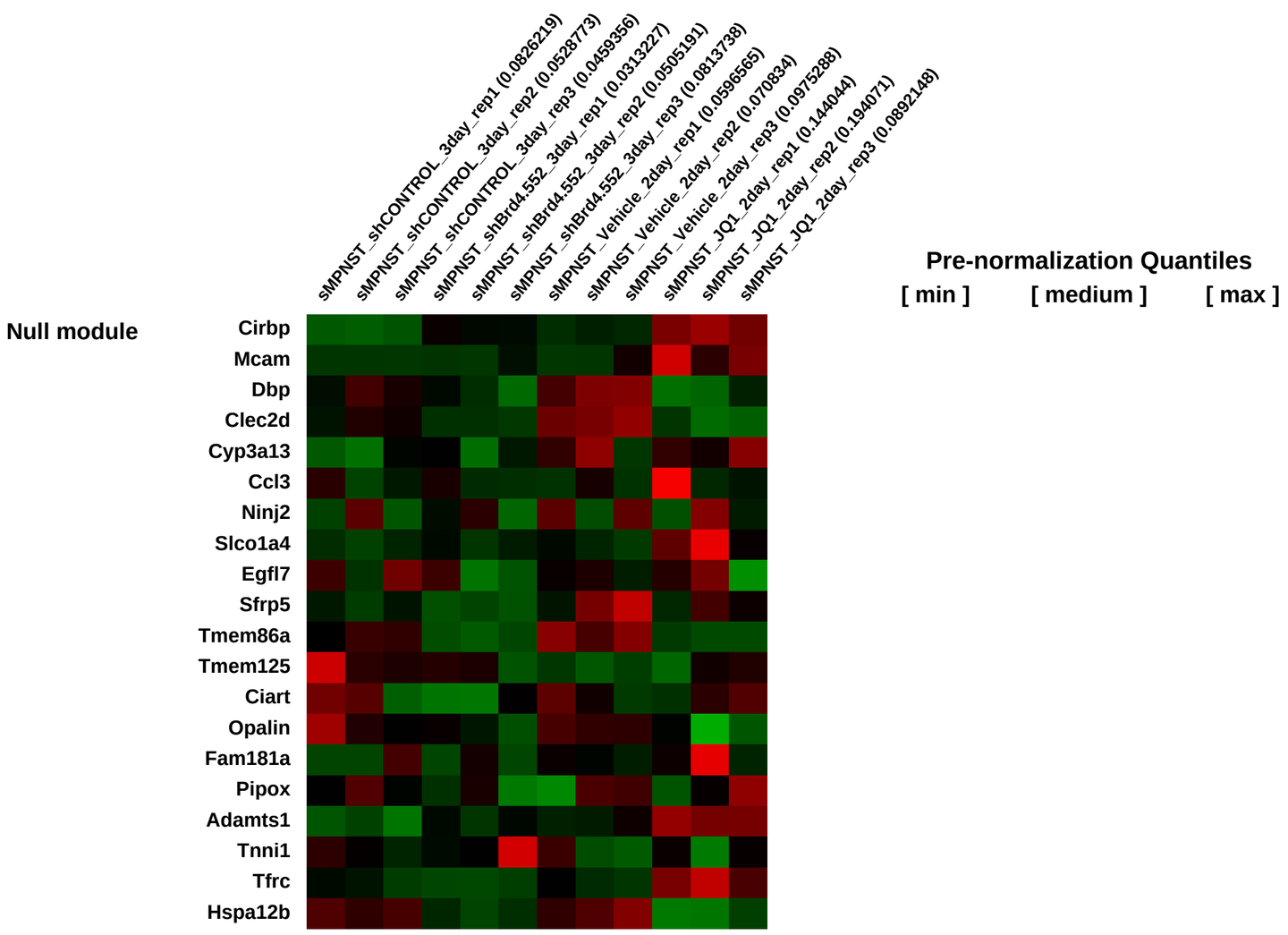

GEO Series "GSE32328" Expression Profiles

Num of samples in this series: 24

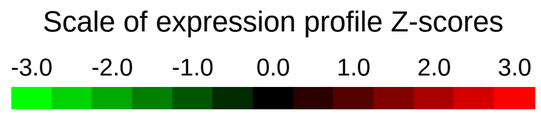

GEO Link:	**http://www.ncbi.nlm.nih.gov/geo/query/acc.cgi?acc=GSE32328**
Status:	**Public on Sep 23 2011**
Title:	**Macrophage response to serum in culture medium**
Organism:	**Mus musculus**
Experiment type:	**Expression profiling by array**
Platform:	**GPL1261**
Pubmed ID:	
Summary & Design:	**Summary:** **Most cell culture experiments utilize media containing fetal calf serum. Results are often interpreted regarding importance to human pathways. We studied gene expression in mouse macrophages grown in the absence of serum, and in fetal calf serum, mouse serum, and human serum using genome wide expression systems in resting conditions and after stimulation with lipopolysaccharide.** **Overall design:** **We cultured mouse bone marrow derived macrophages in media containing no serum, or 5% fetal calf, or mouse or human serum. The experiment was performed in conditions without or with stimulation by LPS. We harvested the cells at 4 hours after stimulation and analyzed whole genome mRNA expression by microarray as a proxy for transcriptional responses. Three replicate experiments were performed.**

Background corr dist: **KL-Divergence = 0.0879, L1-Distance = 0.0267, L2-Distance = 0.0009, Normal std = 0.4698**

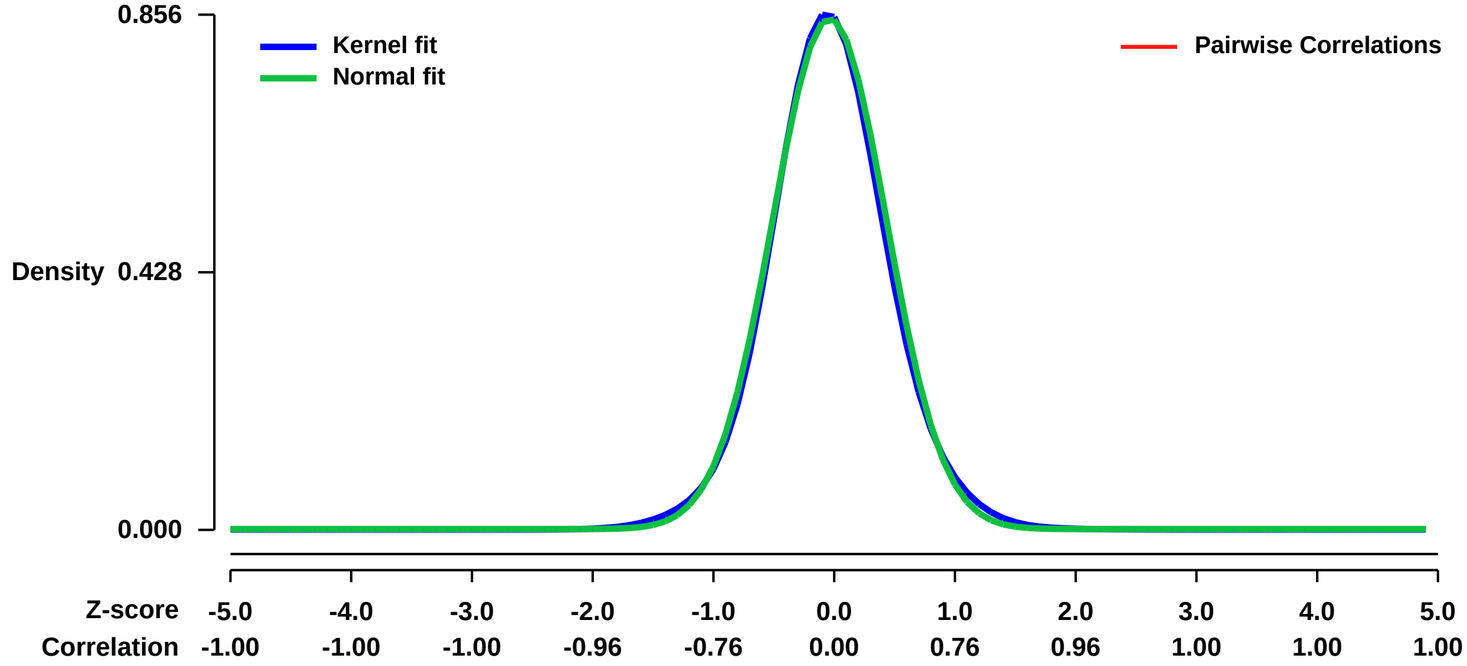

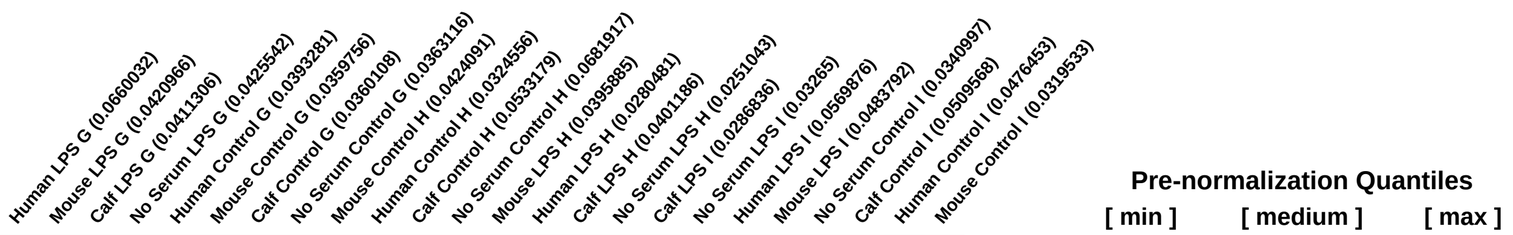

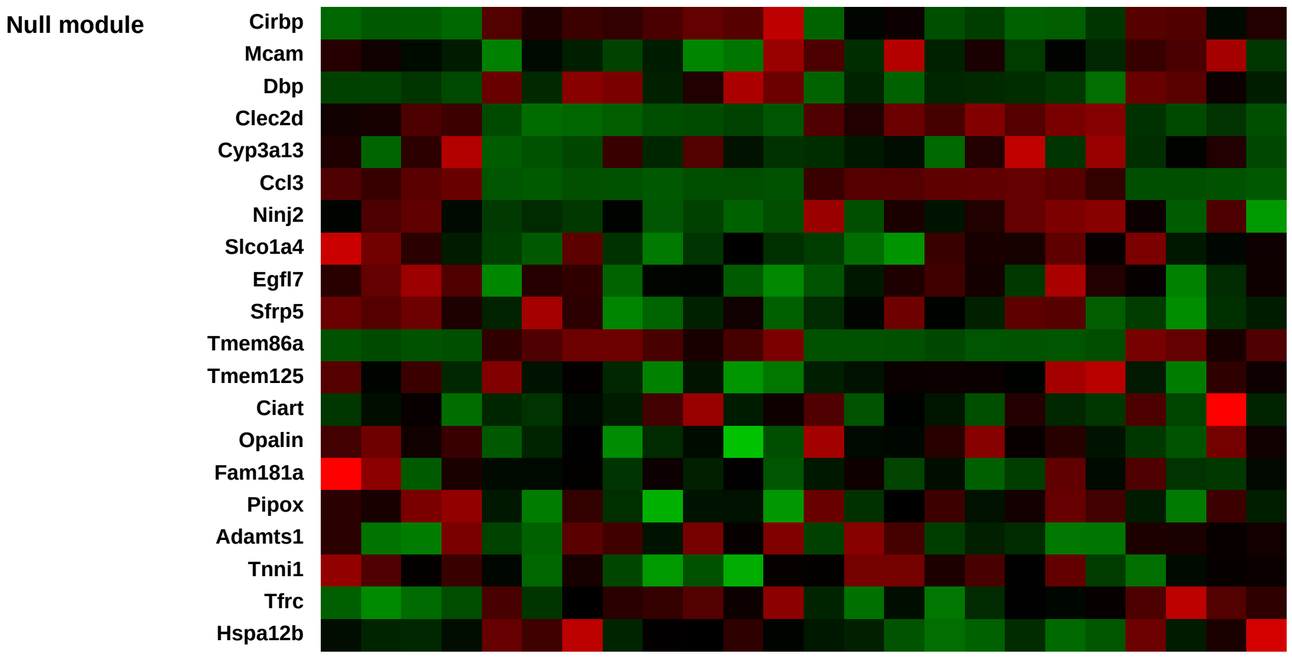

GEO Series "GSE46169" Expression Profiles

Num of samples in this series: 30

Scale of expression profile Z-scores

-3.0 -2.0 -1.0 0.0 1.0 2.0 3.0

GEO Link:	http://www.ncbi.nlm.nih.gov/geo/query/acc.cgi?acc=GSE46169
Status:	Public on Apr 19 2013
Title:	Expression data from mouse SEOC tumors
Organism:	Mus musculus
Experiment type:	Expression profiling by array
Platform:	GPL1261
Pubmed ID:	22617326
Summary & Design:	**Summary:** We have developed mouse models for serous epithelial ovarian cancer (SEOC) based on conditional inactivation of p53 and Rb tumor suppression (RB-TS) in combination with or without Brca1/2 following injection of adenovirus expressing Cre recombinase into the ovarian bursa. These models develop metastatic (Stage IV) disease with key histopathological features resembling human SEOC.To determine whether these mouse tumors resemble human SEOC at the molecular level, we conducted global gene expression analysis on 27 ovarian carcinomas and 3 pooled normal ovarian surface epithelium samples (single epithelial layer isolated from ovarian surface by laser capture). **Overall design:** RNA was isolated from flash frozen ovarian tumors or from ovarian surface epithelial cells microdissected from frozen sections using PixCell IIe laser capture microdissection instrument.

Background corr dist: KL-Divergence = 0.2110, L1-Distance = 0.0470, L2-Distance = 0.0054, Normal std = 0.3277

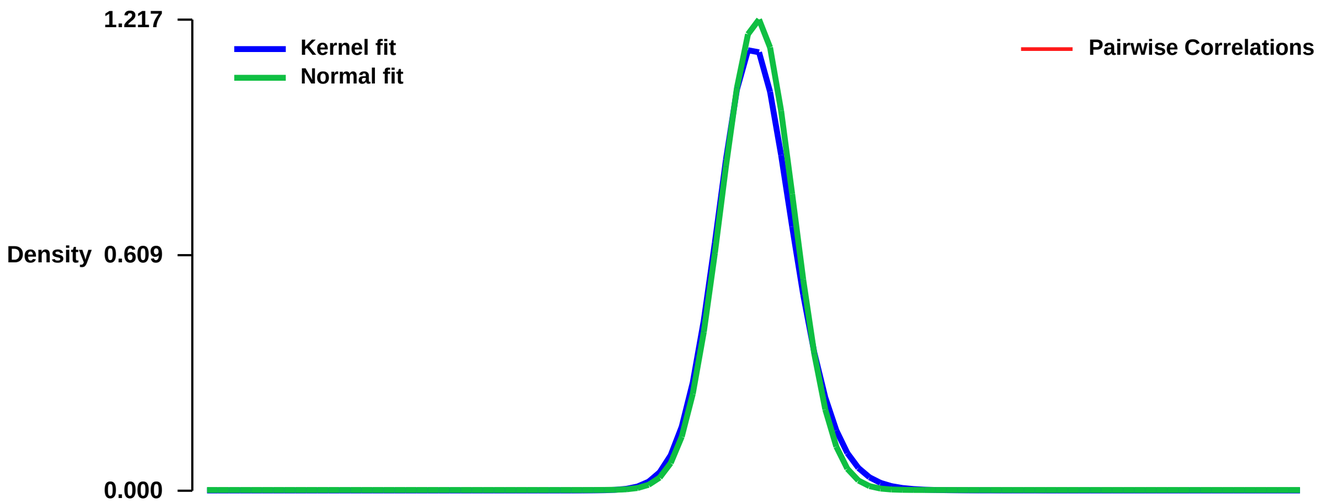

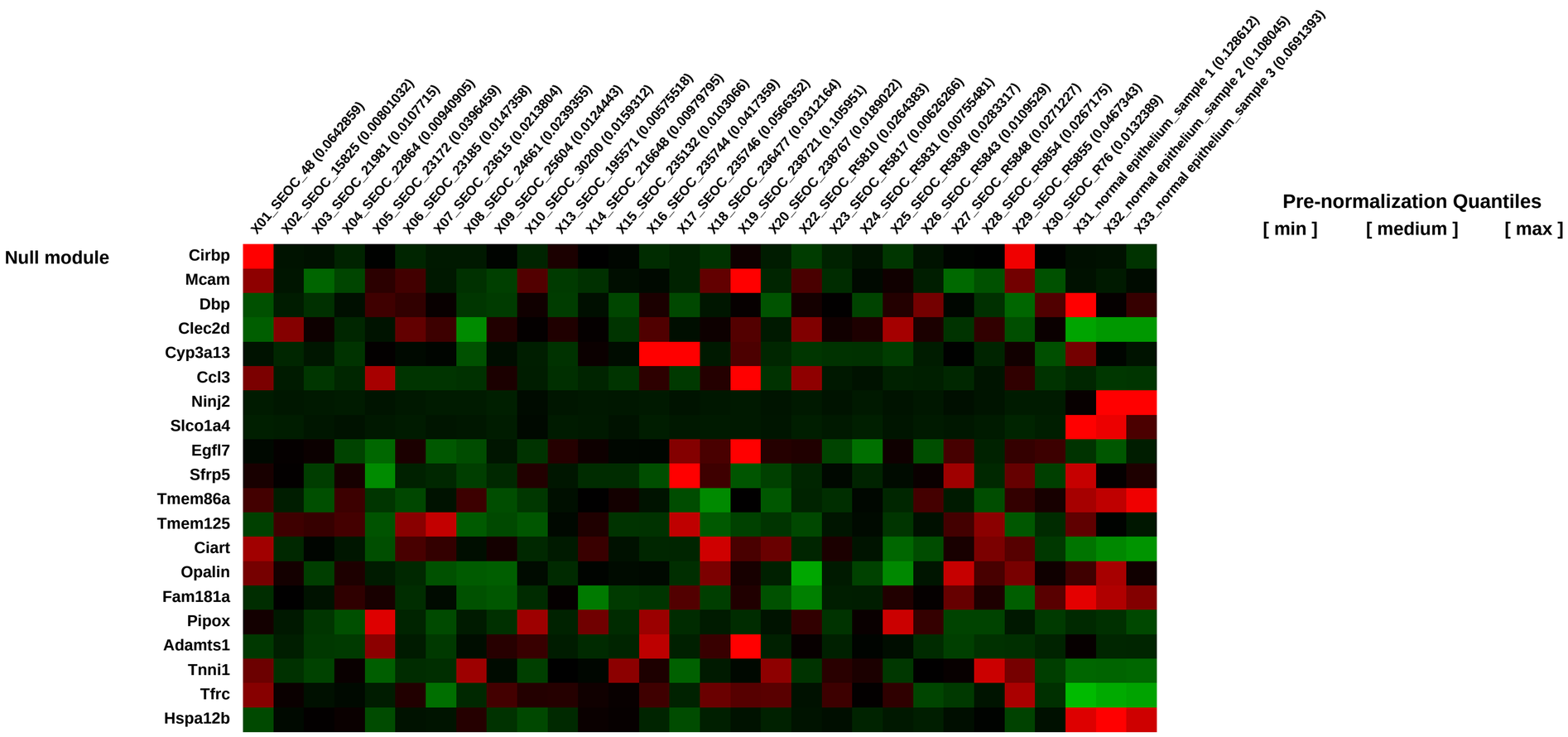

GEO Series "GSE21996" Expression Profiles

Num of samples in this series: 14

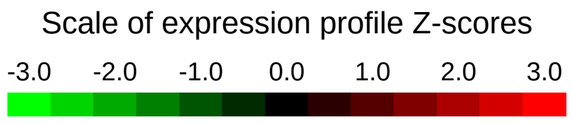

GEO Link:	**http://www.ncbi.nlm.nih.gov/geo/query/acc.cgi?acc=GSE21996**
Status:	**Public on Jan 23 2013**
Title:	**Trpm4-induced gene expression changes in Th1 and Th2 cells**
Organism:	**Mus musculus**
Experiment type:	**Expression profiling by array**
Platform:	**GPL1261**
Pubmed ID:	**20656926**
Summary & Design:	**Summary:** **T helper cell subsets have unique calcium (Ca2+) signals when activated with identical stimuli. The regulation of these Ca2+ signals and their correlation to the biological function of each T cell subset remains unclear. Trpm4 is a Ca2+-activated cation channel that we found is expressed at higher levels in Th2 cells compared to Th1 cells. Inhibition of Trpm4 expression increased Ca2+ influx and oscillatory levels in Th2 cells and decreased influx and oscillations in Th1 cells. This inhibition of Trpm4 expression also significantly altered T cell cytokine production and motility. Our experiments revealed that decreasing Trpm4 levels divergently regulates nuclear localization of NFAT. Consistent with this, gene profiling did not show Trpm4 dependent transcriptional regulation and T-bet and GATA-3 levels remain identical. Thus, Trpm4 is expressed at different levels on T helper cells and plays a distinctive role in T cell function by differentially regulating Ca2+ signaling and NFAT localization.** **T helper cell gene expression levels when Trpm4 is inhibited by siRNA or dominant negative Trpm4 construct.** **Overall design:** **The ion channel Trpm4 was inhibited in Th1 or Th2 cells using either siRNA or a dominant negative Trpm4 retrovirus and changes in gene profiles were analyzed.**

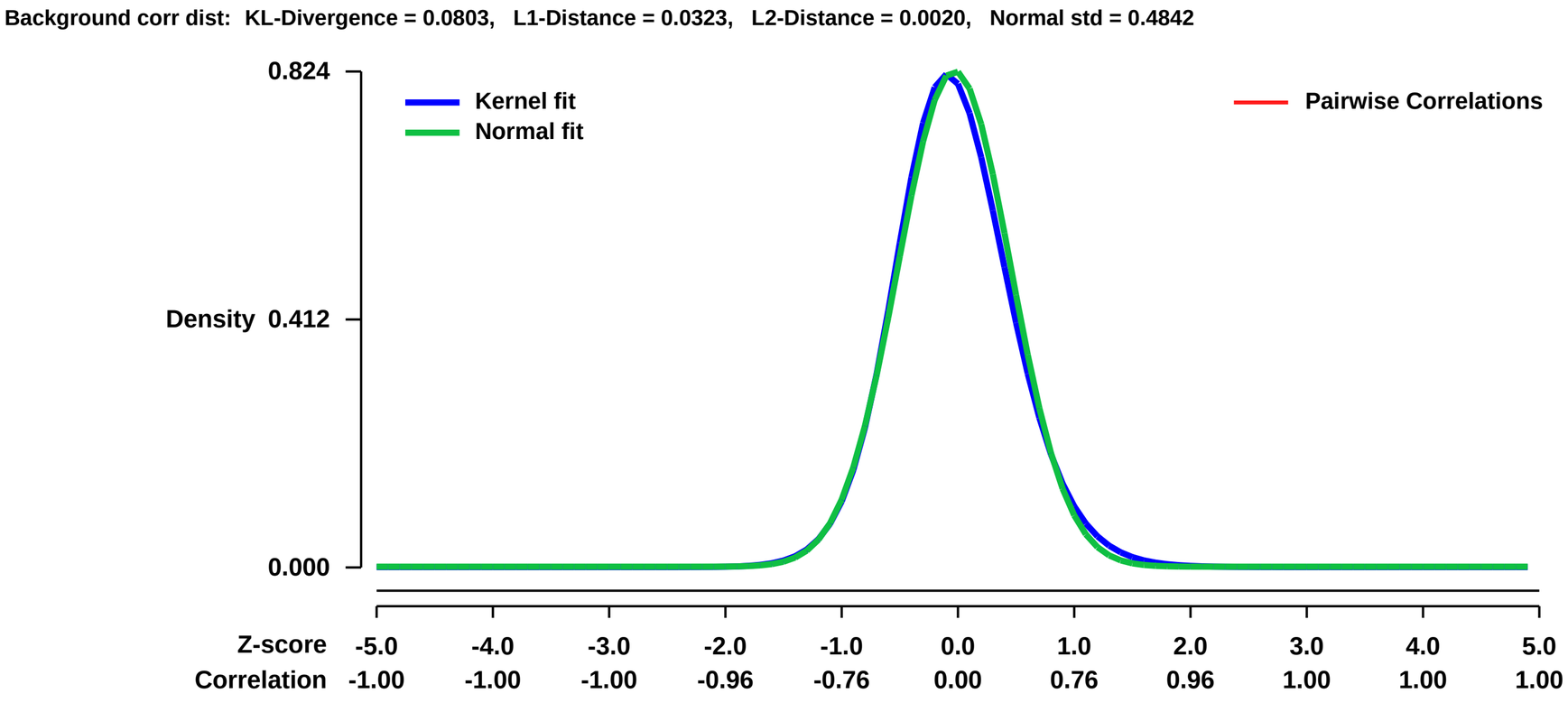

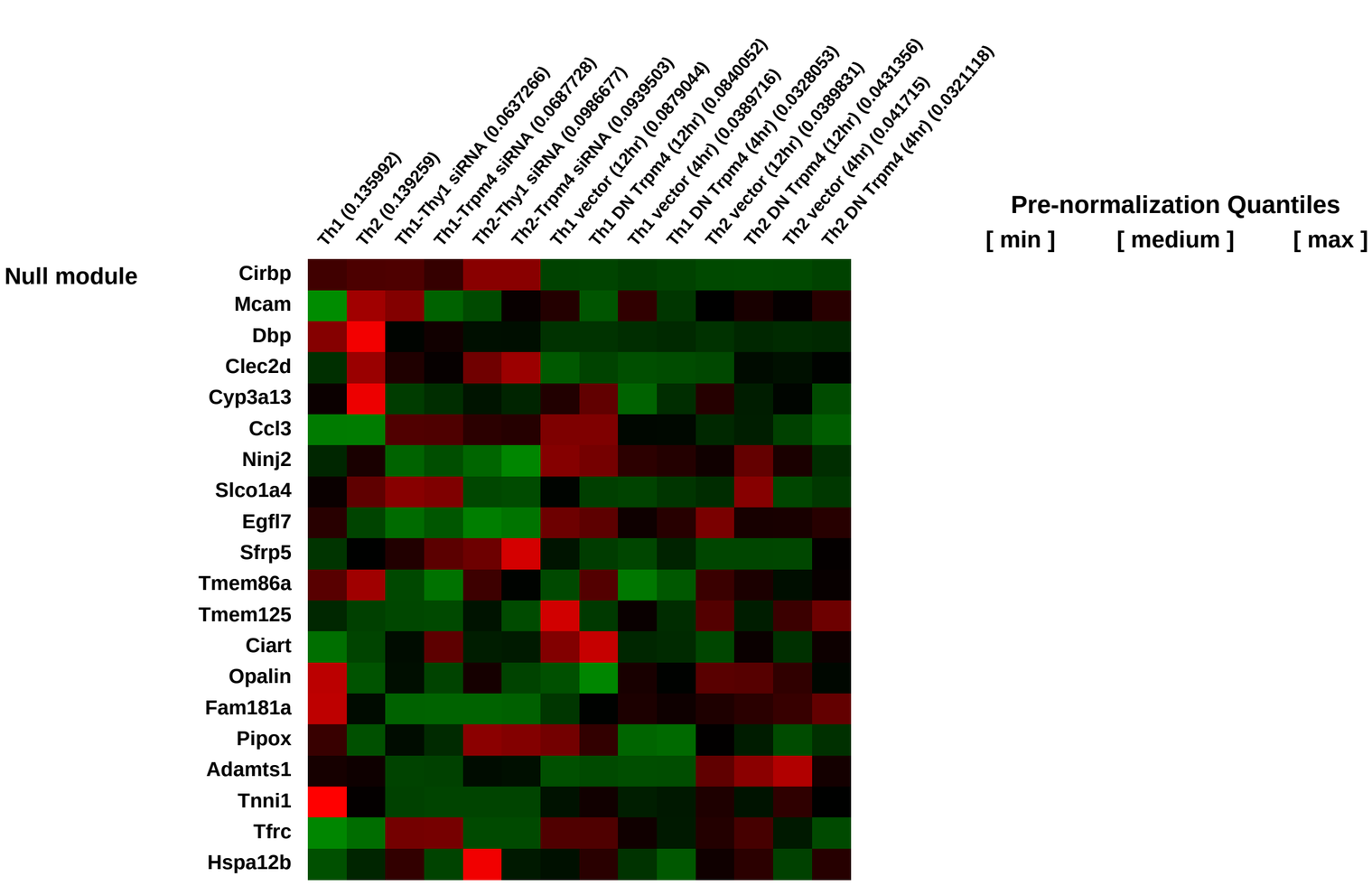

GEO Series "GSE22506" Expression Profiles

Num of samples in this series: 12

Scale of expression profile Z-scores

-3.0 -2.0 -1.0 0.0 1.0 2.0 3.0

GEO Link:	http://www.ncbi.nlm.nih.gov/geo/query/acc.cgi?acc=GSE22506
Status:	Public on Jun 26 2010
Title:	Unacylated Ghrelin Rapidly Modulates Lipogenic and Insulin Signaling Pathway Gene Expression in Metabolically Active Tissues of GHSR Deleted Mice
Organism:	Mus musculus
Experiment type:	Expression profiling by array
Platform:	GPL1261
Pubmed ID:	20668691
Summary & Design:	**Summary:** Background: There is increasing evidence that unacylated ghrelin (UAG) improves insulin sensitivity and glucose homeostasis; however, the mechanism for this activity is not fully understood since a UAG receptor has not been discovered. Methodology/Principal Findings: To assess potential mechanisms of UAG action in vivo, we examined rapid effects of UAG on genome-wide expression patterns in fat, muscle and liver of growth hormone secretagogue receptor (GHSR)-ablated mice using microarrays. Expression data were analyzed using Ingenuity Pathways Analysis and Gene Set Enrichment Analysis. Regulation of subsets of these genes was verified by quantitative PCR in an independent experiment. UAG acutely regulated clusters of genes involved in glucose and lipid metabolism in all three tissues, consistent with enhancement of insulin sensitivity. Conclusions/Significance: Fat, muscle and liver are central to the control of lipid and glucose homeostasis. UAG rapidly modulates the expression of metabolically important genes in these tissues in GHSR-deleted mice indicating a direct, GHSR-independent, action of UAG to improve insulin sensitivity and metabolic profile. **Overall design:** White adipose tissue (gonadal), muscle and liver collected from female GHSR knockout mice 6 hours after ip. injection with saline or unacylated ghrelin (20 nmol/kg). Two replicates.

Background corr dist: KL-Divergence = 0.0581, L1-Distance = 0.0487, L2-Distance = 0.0038, Normal std = 0.5847

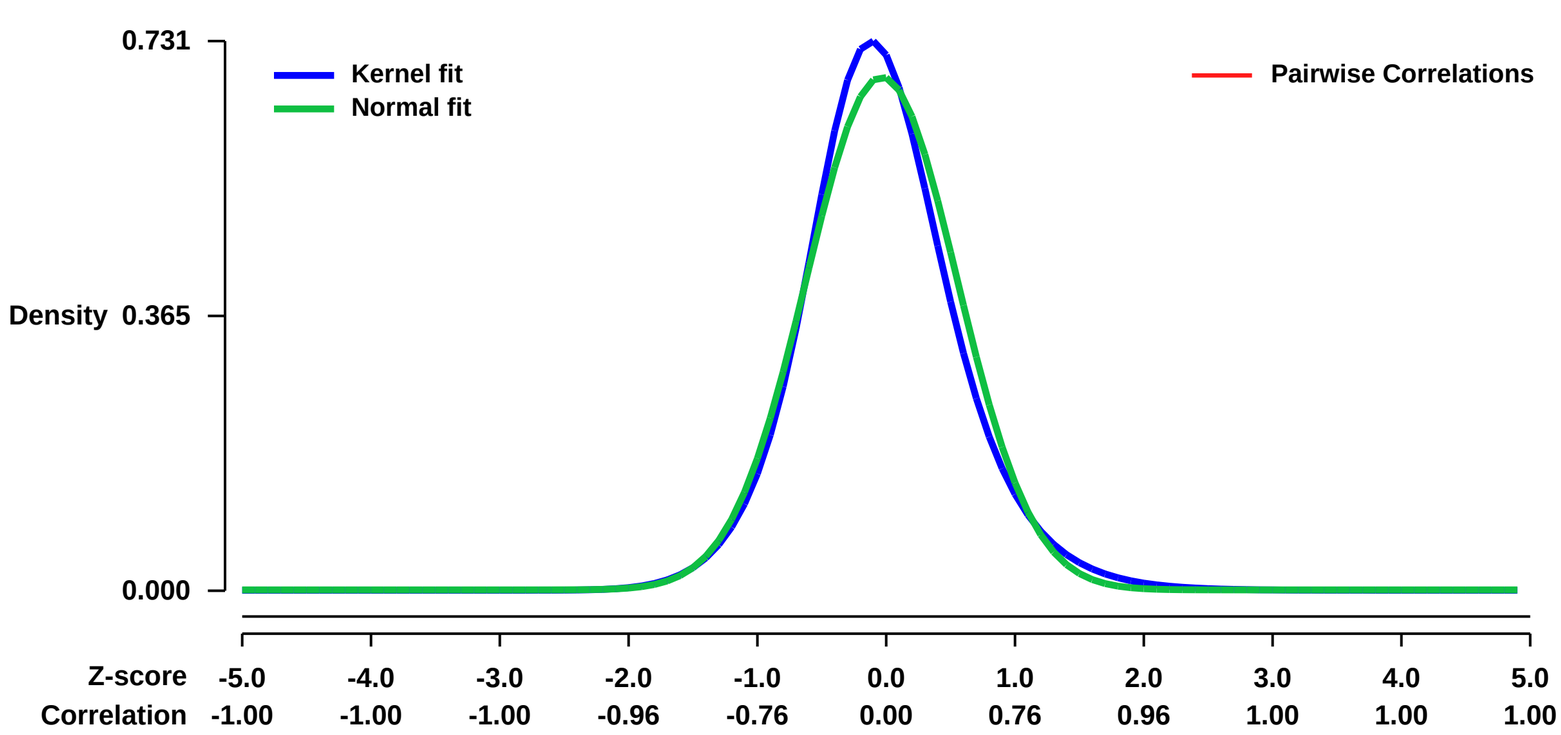

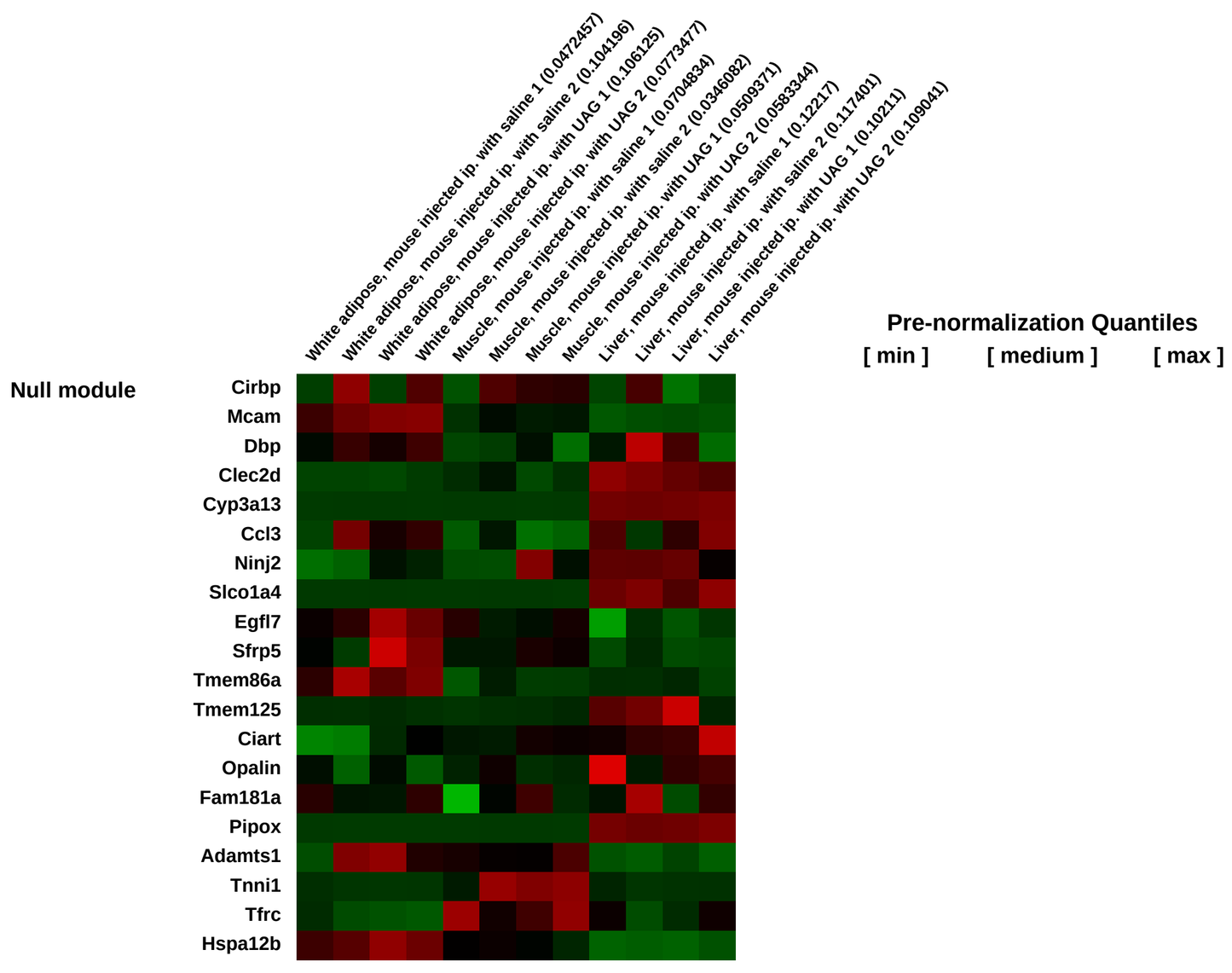

GEO Series "GSE14366" Expression Profiles

Num of samples in this series: 24

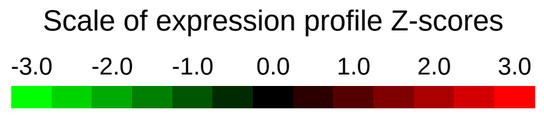

GEO Link:	http://www.ncbi.nlm.nih.gov/geo/query/acc.cgi?acc=GSE14366
Status:	Public on Jan 10 2009
Title:	Analysis of the retinal gene expression after hypoxic preconditioning identifies candidate genes for neuroprotection
Organism:	Mus musculus
Experiment type:	Expression profiling by array
Platform:	GPL1261
Pubmed ID:	18261226
Summary & Design:	**Summary:** Neuroprotective therapies for retinal degeneration may be used to rescue retinal cells and preserve vision. Hypoxic preconditioning stabilizes the transcription factor HIF-1¸ – in the retina and strongly protects photoreceptors in an animal model of light-induced retinal degeneration. Our data suggest that neuroprotection after hypoxic preconditioning of the retina is the result of the differential expression of a multitude of genes which may act in concert to protect visual cells against a toxic insult. Keywords: hypoxic preconditioning, neuroprotection, transcription-profile, retina **Overall design:** In total 24 samples were analyzed on Affymetrix mouse 430.2 arrays, the samples represent different durations of regeneration (none = 0 h, 2 h, 4 h and 16 h) from hypoxic or normoxic treatments, that were tested in triplicates.

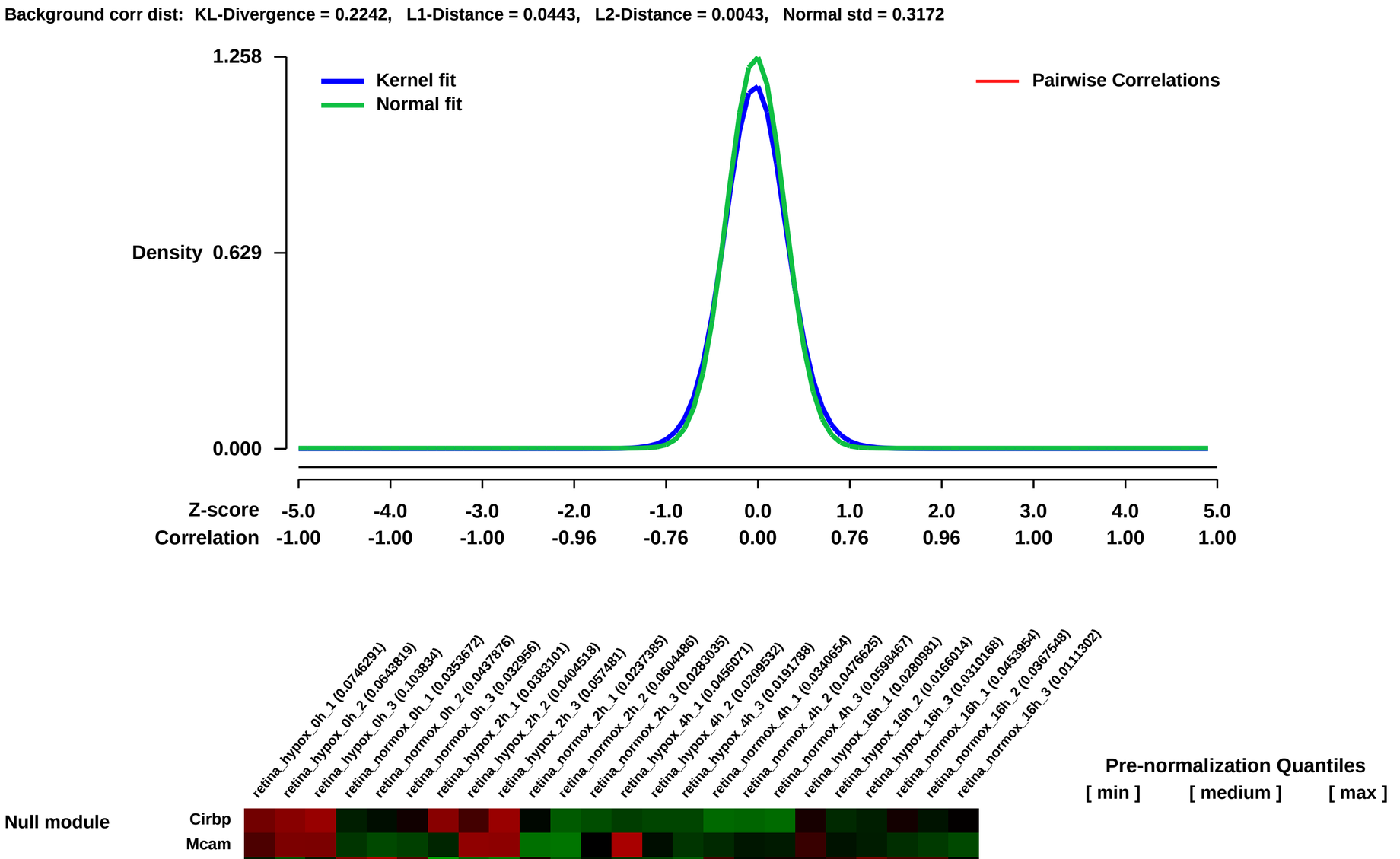

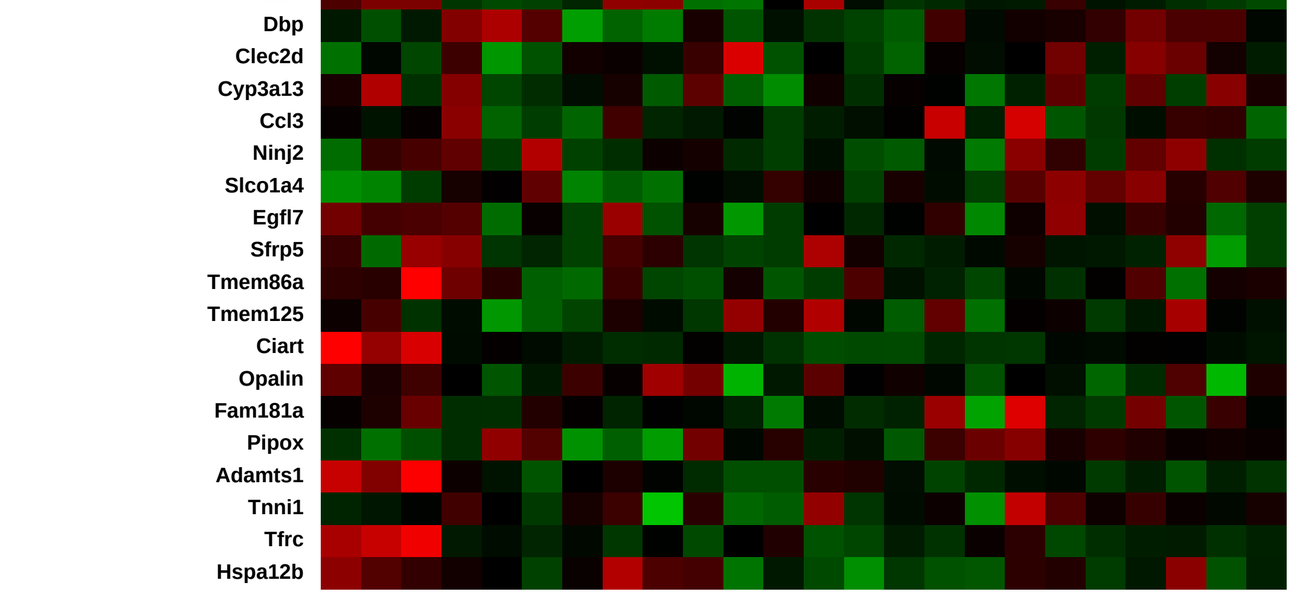

GEO Series "GSE23925" Expression Profiles

Num of samples in this series: 6

Scale of expression profile Z-scores

-3.0 -2.0 -1.0 0.0 1.0 2.0 3.0

GEO Link:	http://www.ncbi.nlm.nih.gov/geo/query/acc.cgi?acc=GSE23925
Status:	Public on Sep 07 2010
Title:	Gene expression in germinal center light zone, dark zone, and naˆflve B cells
Organism:	Mus musculus
Experiment type:	Expression profiling by array
Platform:	GPL1261
Pubmed ID:	21074050
Summary & Design:	**Summary:** Microarrays of gene expression in mouse germinal center B cells photoactivated in the light zone or dark zone, and of naˆflve cells for comparison. We used microarray data to identify genes differentially expressed by B cells in the light and dark zones of the germinal center. **Overall design:** Light and dark zone cells were photoactivated in day 7 germinal centers and sorted by flow cytometry. Naˆflve splenic B cells(IgD+CD19+) were sorted for comparison.

Background corr dist: KL-Divergence = 0.0123, L1-Distance = 0.0424, L2-Distance = 0.0027, Normal std = 0.8861

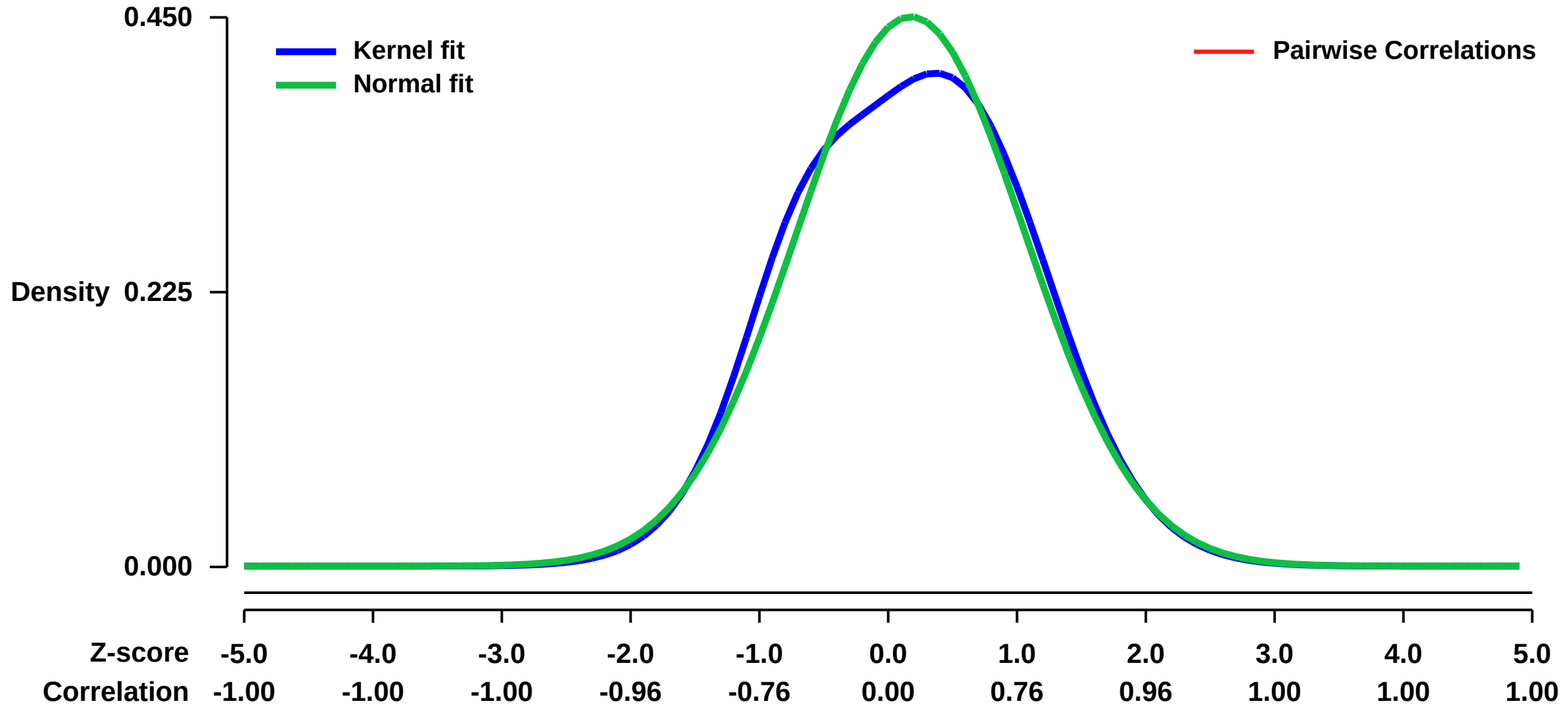

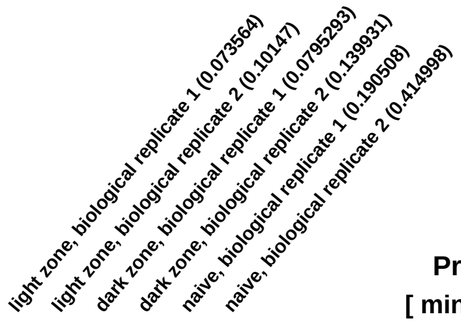

Pre-normalization Quantiles

[min] [medium] [max]

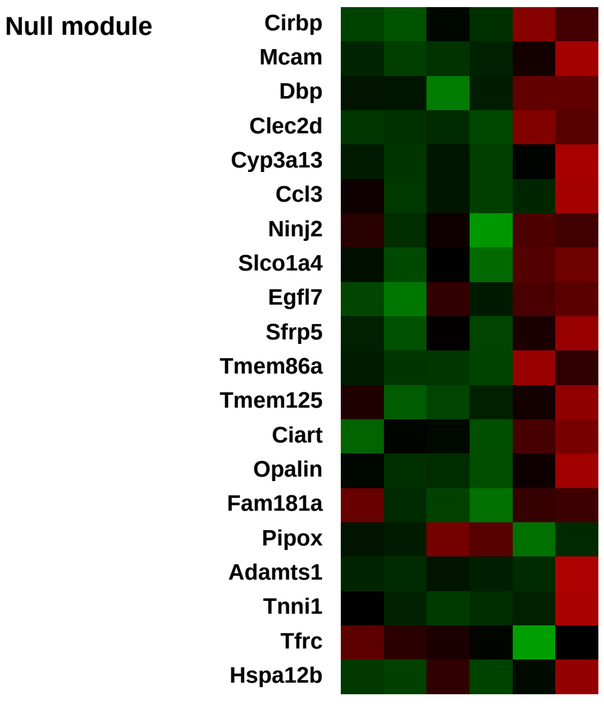

GEO Series "GSE40513" Expression Profiles

Num of samples in this series: 6

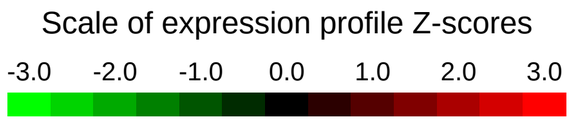

GEO Link:	**http://www.ncbi.nlm.nih.gov/geo/query/acc.cgi?acc=GSE40513**
Status:	**Public on Oct 16 2012**
Title:	**Gene expression profile of mouse breast cancer V720 cells treated with vehicle or PD 0332991**
Organism:	**Mus musculus**
Experiment type:	**Expression profiling by array**
Platform:	**GPL1261**
Pubmed ID:	**23079655**
Summary & Design:	**Summary:** **D-cyclins represent components of cell cycle machinery. To test the efficacy of targeting D-cyclins in cancer treatment, we engineered mouse strains which allow acute and global ablation of individual D-cyclins in a living animal. Ubiquitous shutdown of cyclin D1 or inhibition of cyclin D associated kinase activity in mice bearing ErbB2-driven mammary carcinomas halted cancer progression and triggered tumor-specific senescence, without compromising the animals' health. Ablation of cyclin D3 in mice bearing T-cell acute lymphoblastic leukemias (T-ALL) triggered tumorspecific apoptosis. Such selective killing of leukemic cells can be also achieved by inhibiting cyclin D associated kinase activity in mouse and human T-ALL models. Hence, contrary to what one might expect from ablation of a cell cycle protein, acute shutdown of a D-cyclin leads not only to cell cycle arrest, but it also triggers tumor cell senescence or apoptosis, and it affects different tumor types through distinct cellular mechanisms. Inhibiting cyclin D-activity represents a highly-selective anticancer strategy which specifically targets cancer cells without significantly affecting normal tissues.** **Overall design:** **Mouse breast cancer V720 cells were cultured in the presence of the CDK4/6 inhibitor PD 0332991 (PD; 1 microM) or vehicle (VO) for 24 hrs. Experiment was done in biological triplicate. A total of 6 RNA samples (3 vehicle treated and 3 PD 0332991 treated samples) were used for microarray expression analysis.**

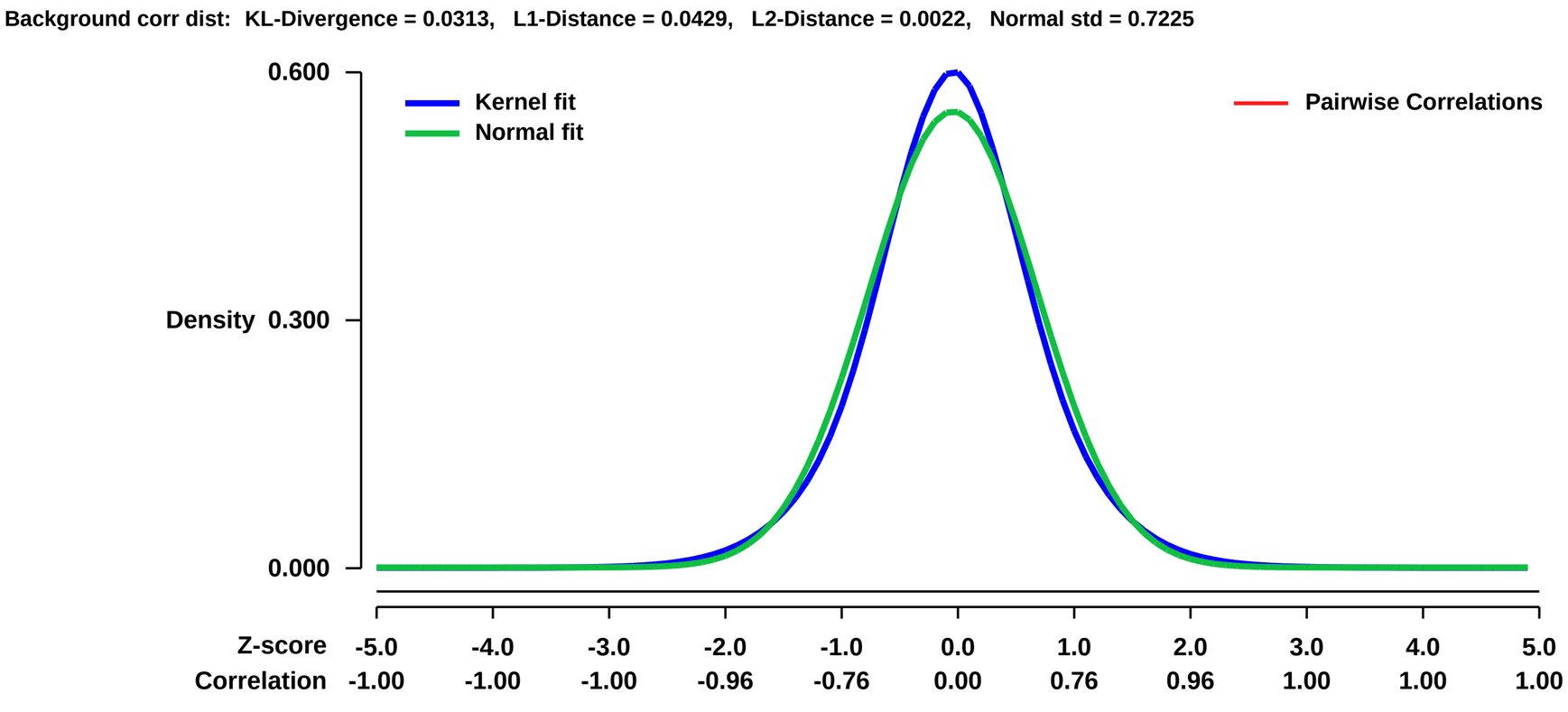

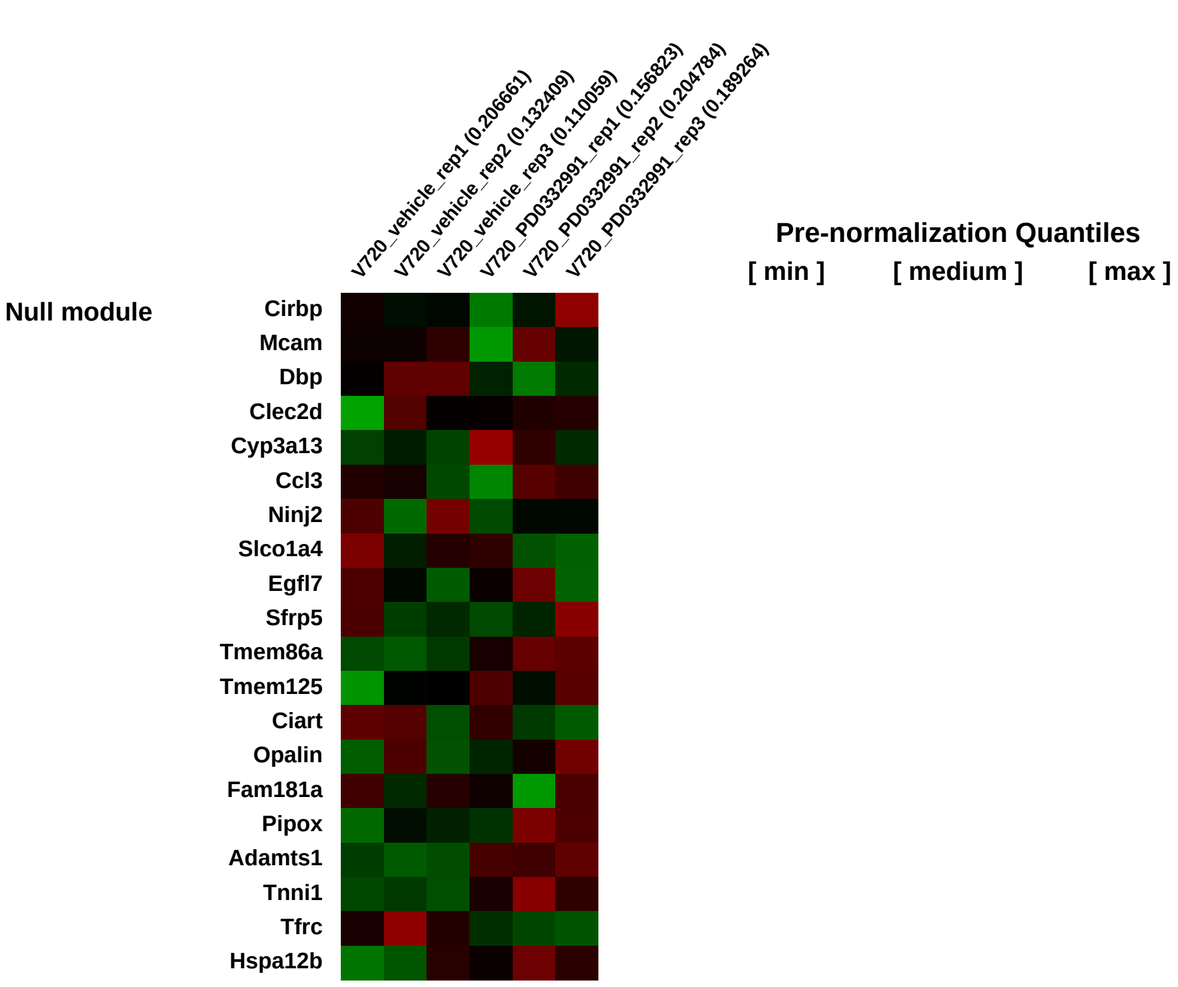

GEO Series "GSE50687" Expression Profiles

Num of samples in this series: 38

Scale of expression profile Z-scores

-3.0 -2.0 -1.0 0.0 1.0 2.0 3.0

GEO Link:	http://www.ncbi.nlm.nih.gov/geo/query/acc.cgi?acc=GSE50687
Status:	Public on Jan 31 2014
Title:	Expression data from testes of the mouse X-chromosome substitution strains
Organism:	Mus musculus
Experiment type:	Expression profiling by array
Platform:	GPL1261
Pubmed ID:	24743563
Summary & Design:	**Summary:** To investigate the evolutionary divergence of transcriptional regulation between the mouse subspecies, we performed transcriptome analysis by microarray on testes from the X-chromosome substitution strain, which carries different subspecies-derived X chromosome on the host subspecies genome. Transcription profiling showed that large-scale aberrations in gene expression were occurred on the introgressed X chromosome. This improper expression was restored by introducing chromosome 1 from the same donor strain as the X chromosome, suggesting that the genetic incompatibility between trans-acting regulatory gene(s) on chromosome 1 and X-linked downstream genes might be a cause of the misregulation. **Overall design:** Testes were collected from 5- and 7-day-old males for RNA extraction and the microarray experiments were performed by using Affymetrix microarrays. Testes from three different males for each strain were tested independently. Tested males are from control C57BL/6J (B6) strain, MSM strain, X-chromosome substitution strain (B6-ChrXMSM), partial X-chromosome substitution strain 1 (B6-ChrXTMSM), partial X-chromosome substitution strain 2 (XS39-tel), and restored (B6-ChrXTMSM X B6-Chr1MSM) F1.

Background corr dist: KL-Divergence = 0.1752, L1-Distance = 0.0398, L2-Distance = 0.0028, Normal std = 0.3593

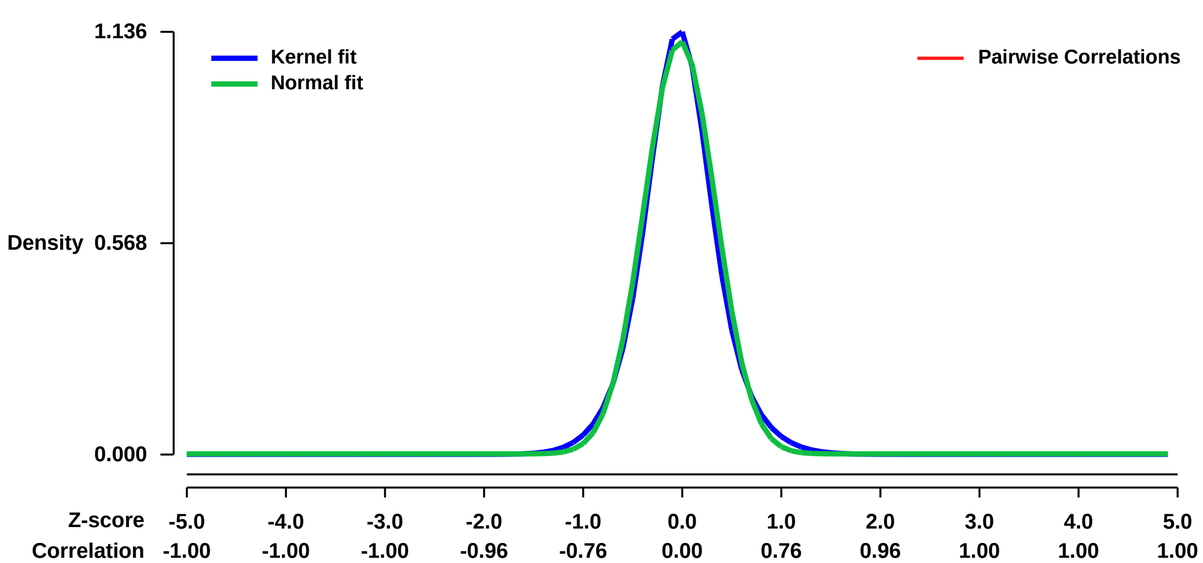

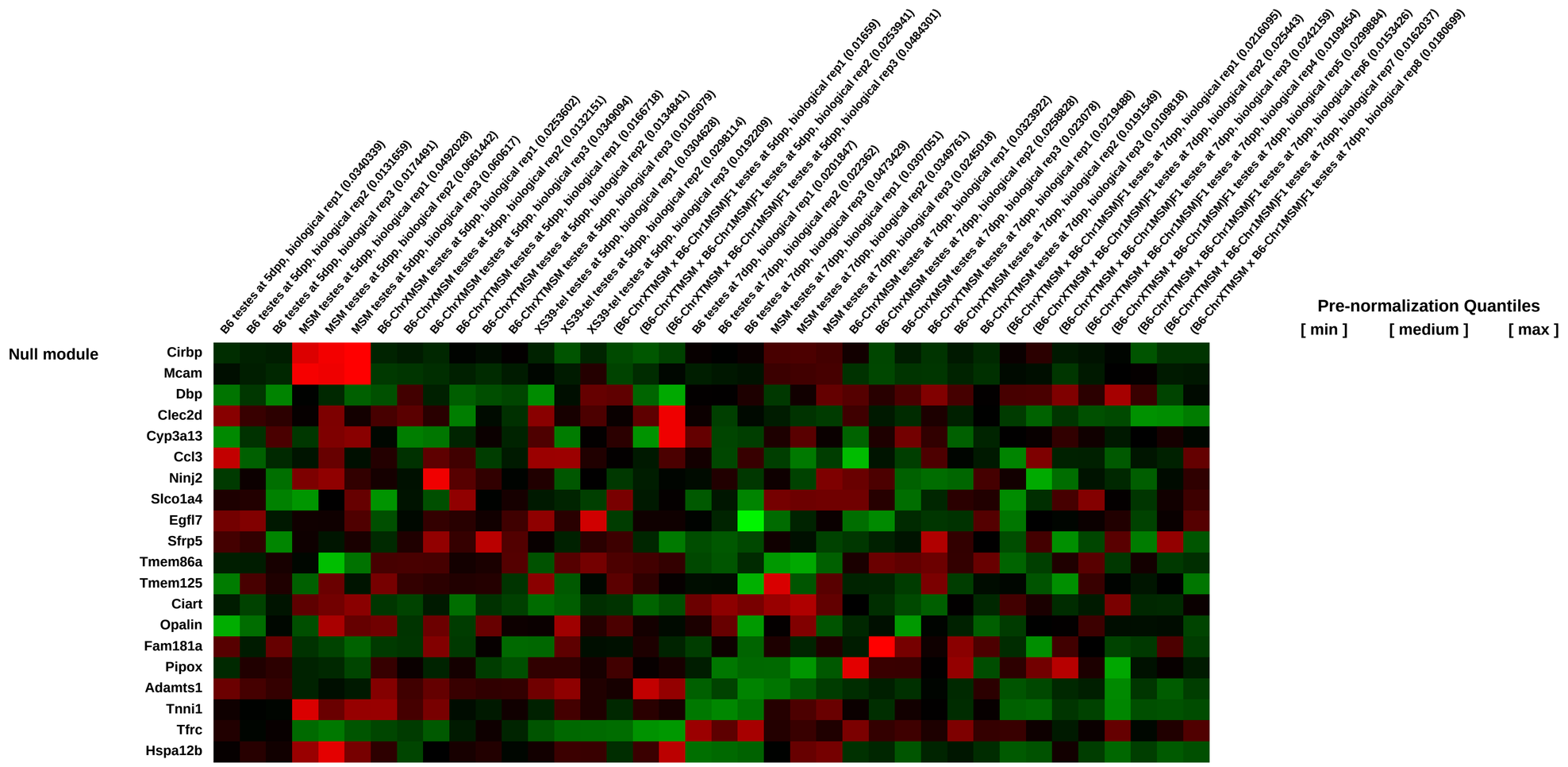

GEO Series "GSE46854" Expression Profiles

Num of samples in this series: 20

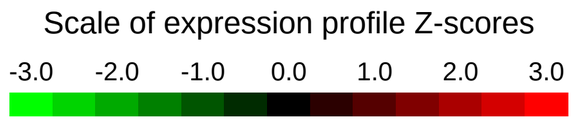

GEO Link:	http://www.ncbi.nlm.nih.gov/geo/query/acc.cgi?acc=GSE46854
Status:	Public on Aug 04 2013
Title:	Induction of the mouse germ cell fate by transcription factors in vitro [exp2]
Organism:	Mus musculus
Experiment type:	Expression profiling by array
Platform:	GPL1261
Pubmed ID:	23913270
Summary & Design:	**Summary:** The germ cell lineage ensures the continuity of life through the generation of male and female gametes, which unite to form a totipotent zygote. We have established a culture system that recapitulates the mouse germ-cell specification pathway: Using cytokines, embryonic stem cells (ESCs)/induced pluripotent stem cells (iPSCs) are induced into epiblast-like cells (EpiLCs) and then into primordial germ cell-like cells (PGCLCs) with capacity both for spermatogenesis and oogenesis, creating an opportunity for understanding and regulating mammalian germ cell development in both sexes in vitro. Here we show that, without cytokines, simultaneous over-expression of three transcription factors (TFs), Blimp1 (also known as Prdm1), Prdm14 and Tfap2c (also known as AP2‚ÄĘ), directs EpiLCs, but not ESCs, swiftly and highly efficiently into a PGC state with endogenous transcription circuitry. The induction of the PGC state on EpiLCs minimally requires Prdm14 but not Blimp1 or Tfap2c. The TF-induced PGC state reconstitutes key transcriptome and epigenetic reprogramming in PGCs, but bypasses a mesodermal program that accompanies PGC specification in vivo and in vitro by cytokines including BMP4. Importantly, the TF-induced PGC-like cells robustly contribute to spermatogenesis and fertile offspring. Our findings provide not only a novel insight into the transcriptional logic that creates a germ cell state, but also a foundation for the TF-based reconstitution and regulation of mammalian gametogenesis. **Overall design:** Aim of this analysis is identification of genes whose expression was altered by each of key transcription factor for transcription factor-induced primordial germ cells (TF-PGCLCs) induction (Blimp1 (B), Prdm14 (P14), and Tfap2c (A)). Both of epiblast-like cells (EpiLCs) (Hayashi et al., 2011, Cell) and aggregates of EpiLCs cultured with doxycycline on day 1 were harvested for 5 cell lines, including BP14A (Clone #3-3), B (#2-4), P14 (#7-109), A (#8-2), and the parental clone (BVSCR26rtTA embryonic stem cells). Total RNA was isolated and analyzed. Two biological duplicates for each cell type were included.

Background corr dist: KL-Divergence = 0.1480, L1-Distance = 0.0511, L2-Distance = 0.0045, Normal std = 0.3974

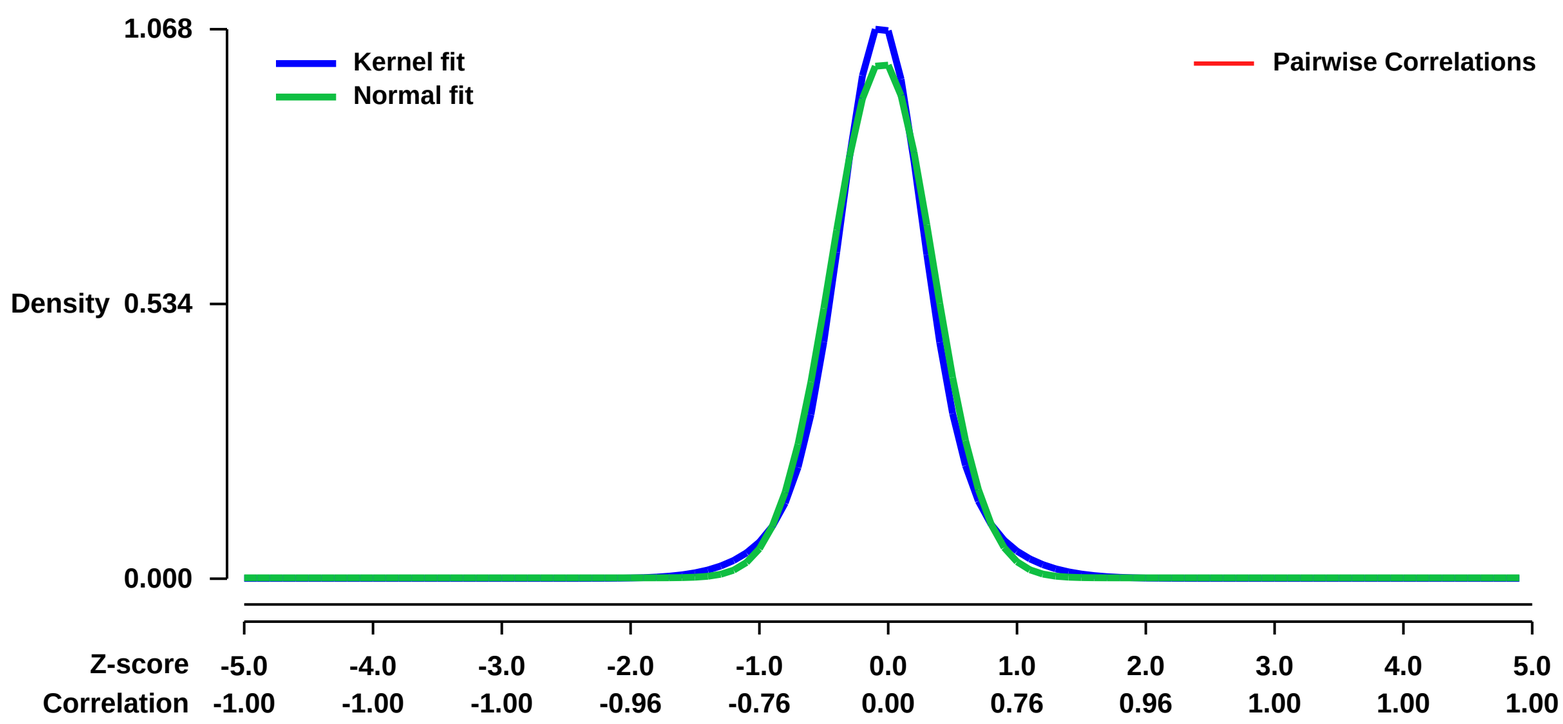

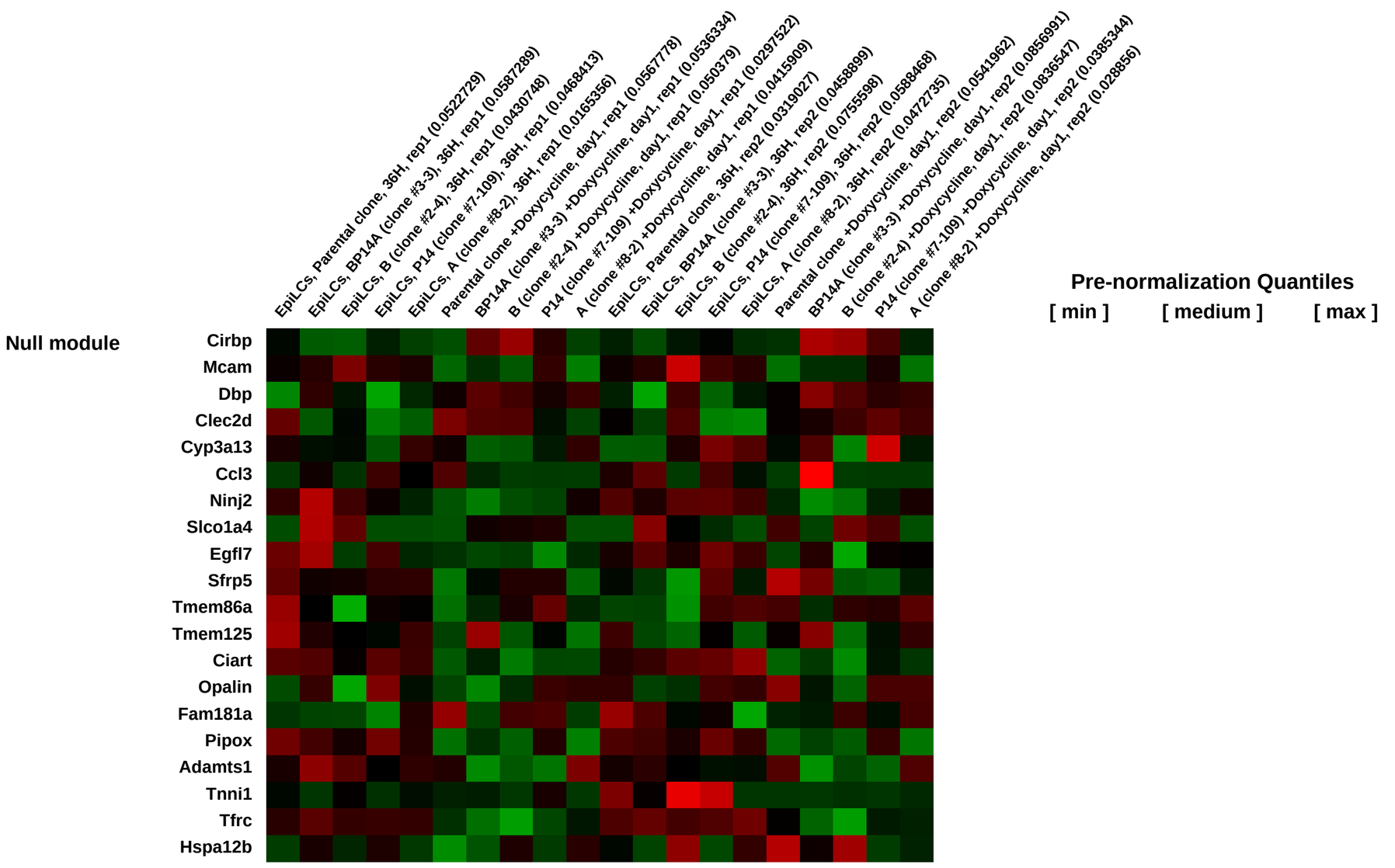

GEO Series "GSE15741" Expression Profiles

Num of samples in this series: 6

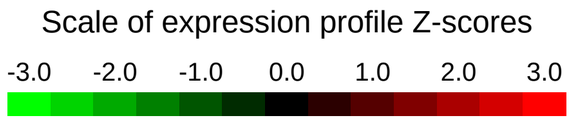

GEO Link:	http://www.ncbi.nlm.nih.gov/geo/query/acc.cgi?acc=GSE15741
Status:	Public on Nov 10 2009
Title:	Gene expression profiles of forced miR-200 expression in 344SQ lung adenocarcinoma cells with high metastatic potential
Organism:	Mus musculus
Experiment type:	Expression profiling by array
Platform:	GPL1261
Pubmed ID:	19759262
Summary & Design:	**Summary:** Metastatic disease is a primary cause of cancer-related death, and factors governing tumor cell metastasis have not been fully elucidated. Here we addressed this question by using tumor cell lines derived from mice that develop metastatic lung adenocarcinoma owing to expression of mutant K-ras and p53. A feature of metastasis-prone tumor cells that distinguished them from metastasis-incompetent tumor cells was plasticity in response to changes in their microenvironment. They transited reversibly between epithelial and mesenchymal states, forming highly polarized epithelial spheres in 3-dimensional culture that underwent epithelial-mesenchymal transition (EMT) following treatment with transforming growth factor-beta or injection into syngeneic mice. This plasticity was entirely dependent upon the microRNA-200 family, which decreased during EMT. Forced expression of miR-200 abrogated the capacity of these tumor cells to undergo EMT, invade, and metastasize and conferred transcriptional features of metastasis-incompetent tumor cells. We conclude that microenvironmental cues direct tumor metastasis by regulating miR-200 expression. **Overall design:** Cell lines from p53R172Hâ g/+ K-rasLA1/+ mice were derived from tumor tissues removed at autopsy from two different mice (#344 and #393). The tissues were minced, placed in culture, and passed serially in RPMI 1640 supplemented with 10% fetal bovine serum (FBS), which yielded mass populations of tumor cells derived from primary lung tumors (344P and 393P), mediastinal lymph nodes (344LN and 393LN), and a subcutaneous site (344SQ). Stable 344SQ cell lines expressing the miR-200b-200a-429 cluster or control vector were generated by transduction with lentivirus vectors. GFP positive transfectant pools were selected by growth in RPMI 1640 with 10% FBS and puromycin. RNA samples of miR-200b-200a-429 knockup versus control (from triplicate cultures of each) were processed and analyzed on Affymetrix Mouse Expression Array 430A 2.0 chips.

Background corr dist: KL-Divergence = 0.0327, L1-Distance = 0.0246, L2-Distance = 0.0007, Normal std = 0.6647

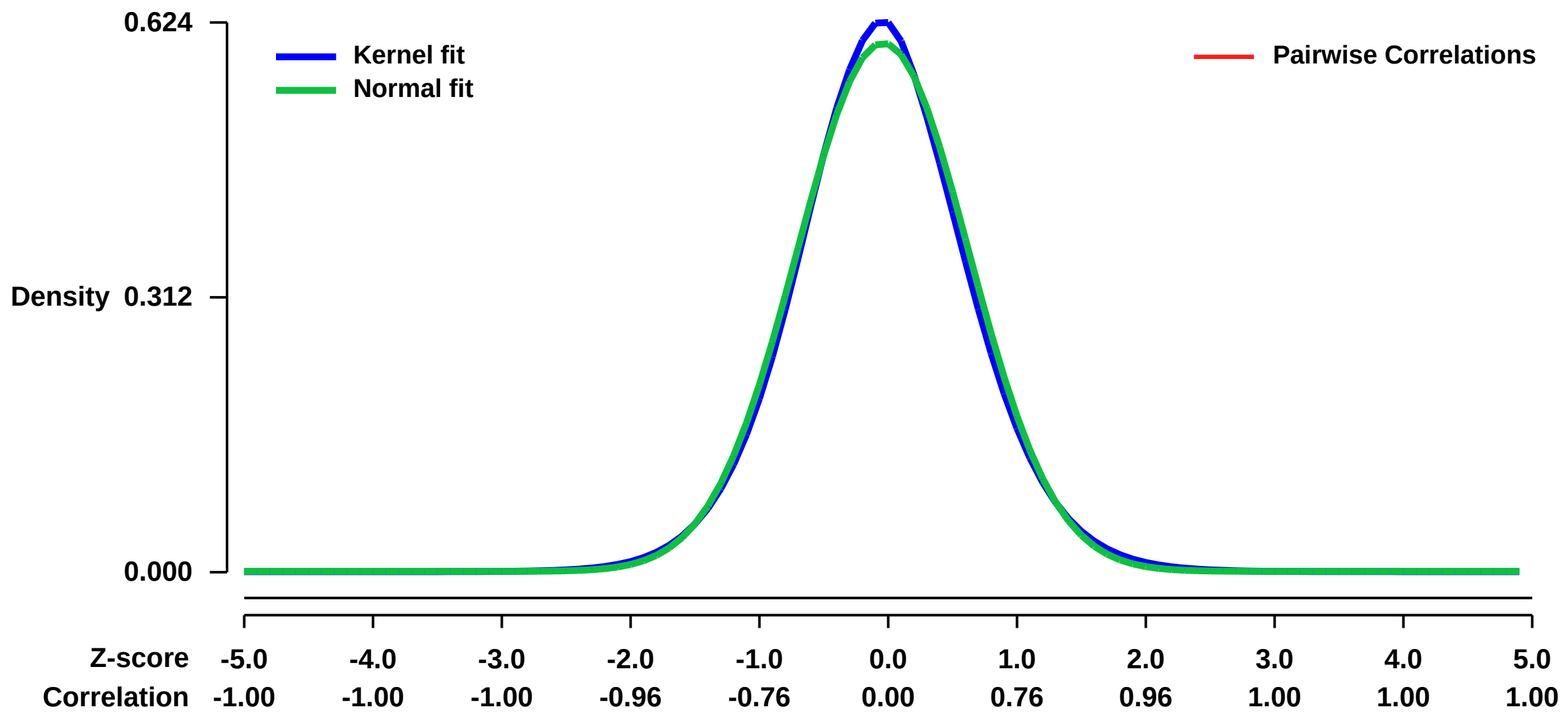

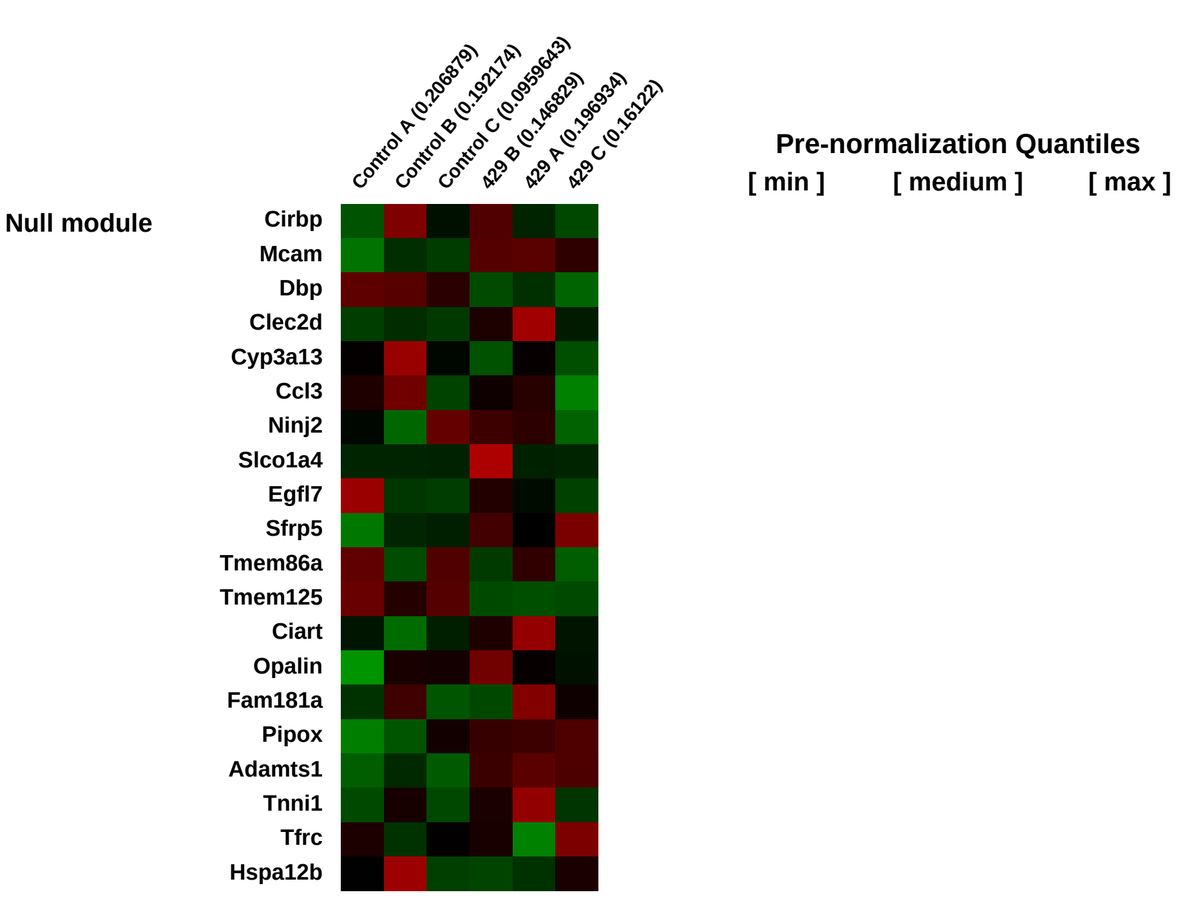

GEO Series "GSE50794" Expression Profiles

Num of samples in this series: 60

Scale of expression profile Z-scores

-3.0 -2.0 -1.0 0.0 1.0 2.0 3.0

GEO Link:	http://www.ncbi.nlm.nih.gov/geo/query/acc.cgi?acc=GSE50794
Status:	Public on Jul 01 2014
Title:	GEMM CRC collection analysis
Organism:	Mus musculus
Experiment type:	Expression profiling by array
Platform:	GPL1261
Pubmed ID:	24742783
Summary & Design:	**Summary:** A collection of genetically engineered mouse models (GEMM) of colorectal cancer (CRC) were created, and primary tumors from these GEMMs were analyzed. Primary CRC tumors from these GEMMs were genotyped to confirm that they contain the core genetic lesions of interest, including APC, P53, KRAS, and BRAF. Primary tumors from GEMMs with combinations of lesions of interest were analyzed by whole genome expression, and their expression profiles were compared to determine how they segregate. Signatures were then generated from GEMM tumors of interest and compared to human clinical datasets with expression and outcome data. **Overall design:** Primary tumors from CRC GEMMs with different combinations of mutant alleles of interested were generated and analyzed. Alleles include mutant forms of APC (A), P53 (P), KRAS (K) and BRAF (B).

Background corr dist: KL-Divergence = 0.0675, L1-Distance = 0.0585, L2-Distance = 0.0063, Normal std = 0.5460

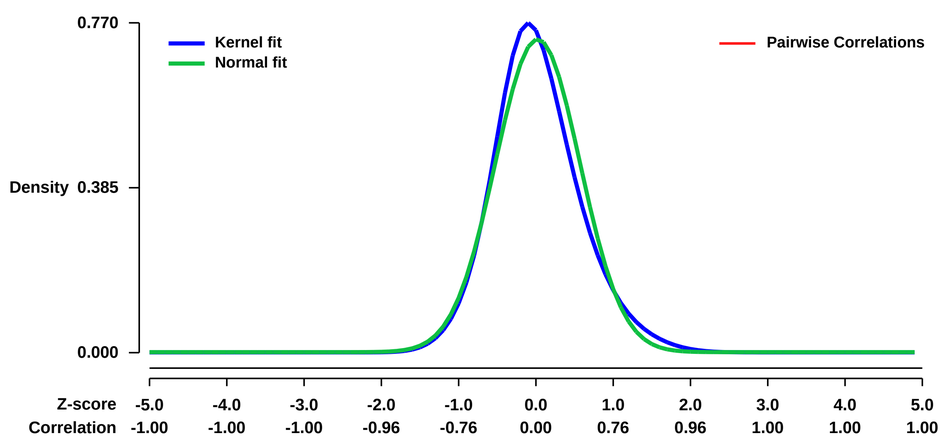

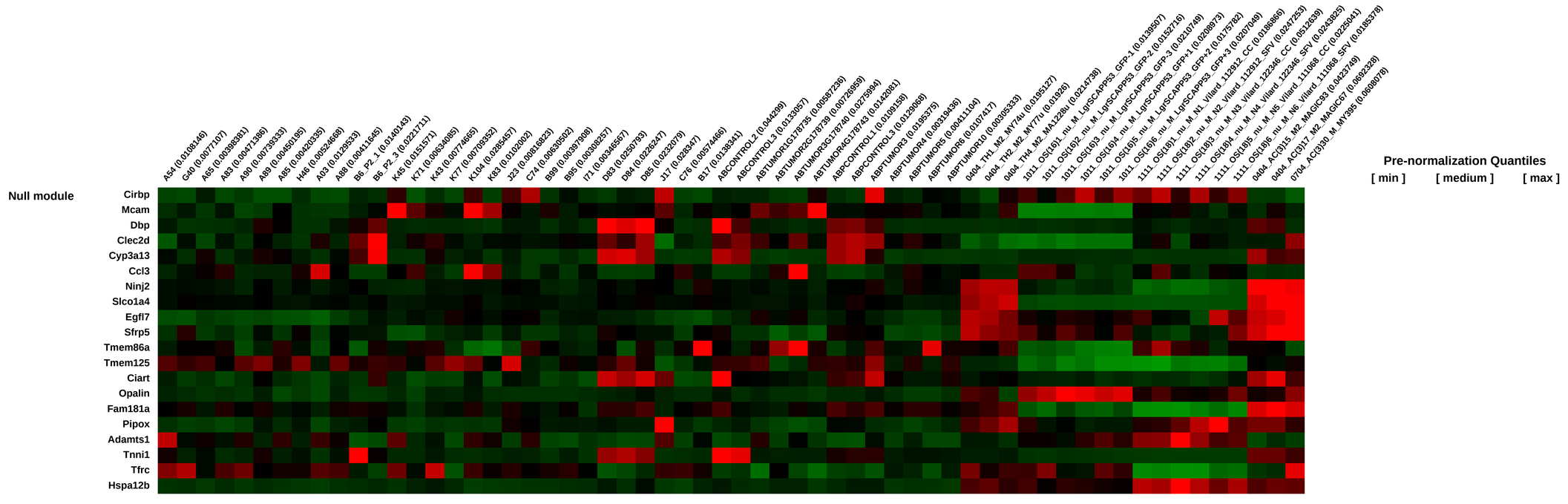

GEO Series "GSE18534" Expression Profiles

Num of samples in this series: 15

Scale of expression profile Z-scores

-3.0 -2.0 -1.0 0.0 1.0 2.0 3.0

GEO Link:	http://www.ncbi.nlm.nih.gov/geo/query/acc.cgi?acc=GSE18534
Status:	Public on Jun 01 2010
Title:	Mouse small cell lung cancer model
Organism:	Mus musculus
Experiment type:	Expression profiling by array
Platform:	GPL1261
Pubmed ID:	20406986
Summary & Design:	**Summary:** A mouse model for human small cell lung carcinoma (SCLC) has been developed based on evidence in human tumors that the tumor suppressor functions of RB and p53 are defective in more than 90% of SCLC cases. We also developed another mouse model also combines loss of p130 (Rbl2), an RB-related gene, with deletion of RB and p53. These two mouse tumors were shown to closely resemble human SCLC. **Overall design:** The goal of this array experiment is to assess genome-wide gene expression of those mouse tumors and determine the similarity of the mouse models to human SCLC. Gene expression from Mouse Rb/p53 (n=10) and Rb/p53/p130 primary tumors (n=3) as well as tumor-free adult mouse lungs (n=2) was measured using the Affymetrix GeneChip Mouse Genome 430-2.0 arrays.

Background corr dist: KL-Divergence = 0.0991, L1-Distance = 0.0337, L2-Distance = 0.0022, Normal std = 0.4651

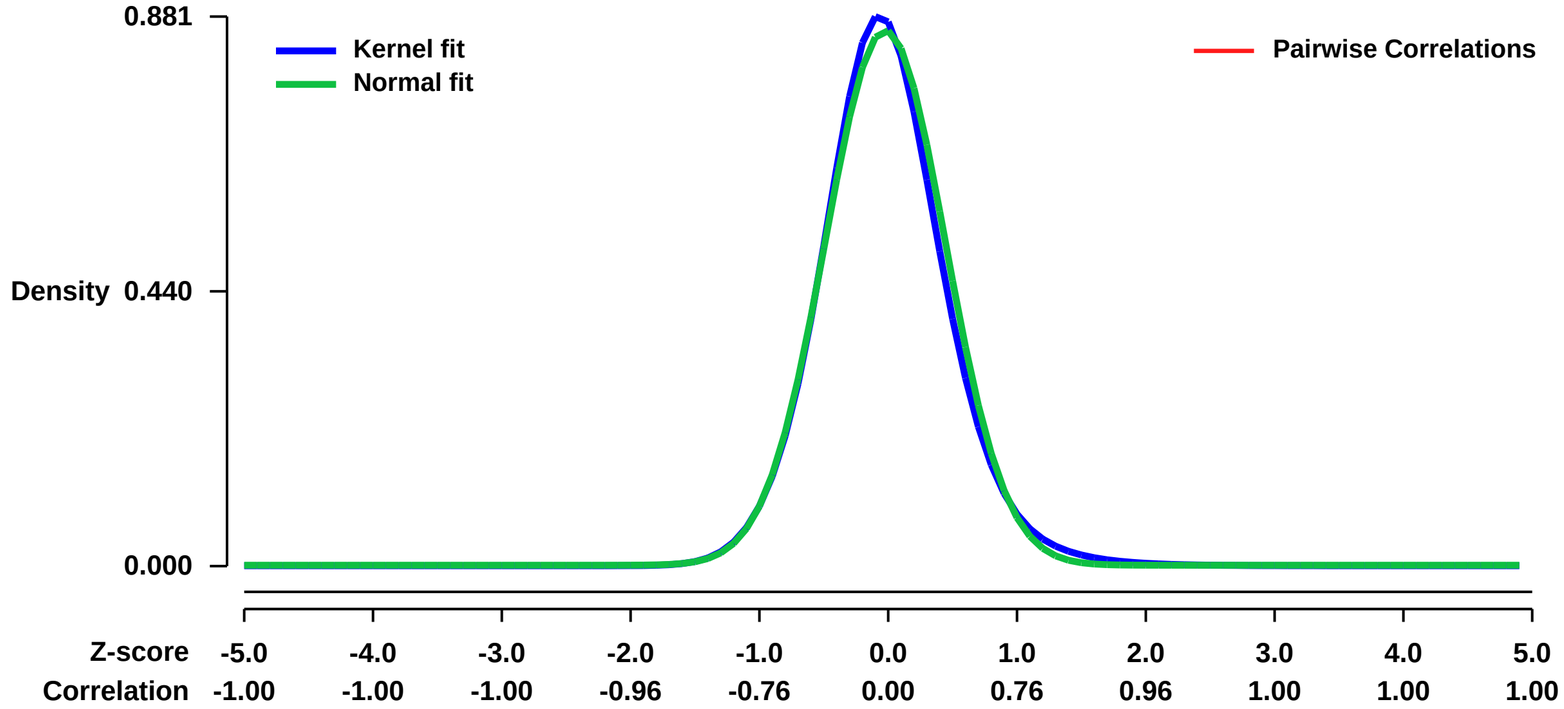

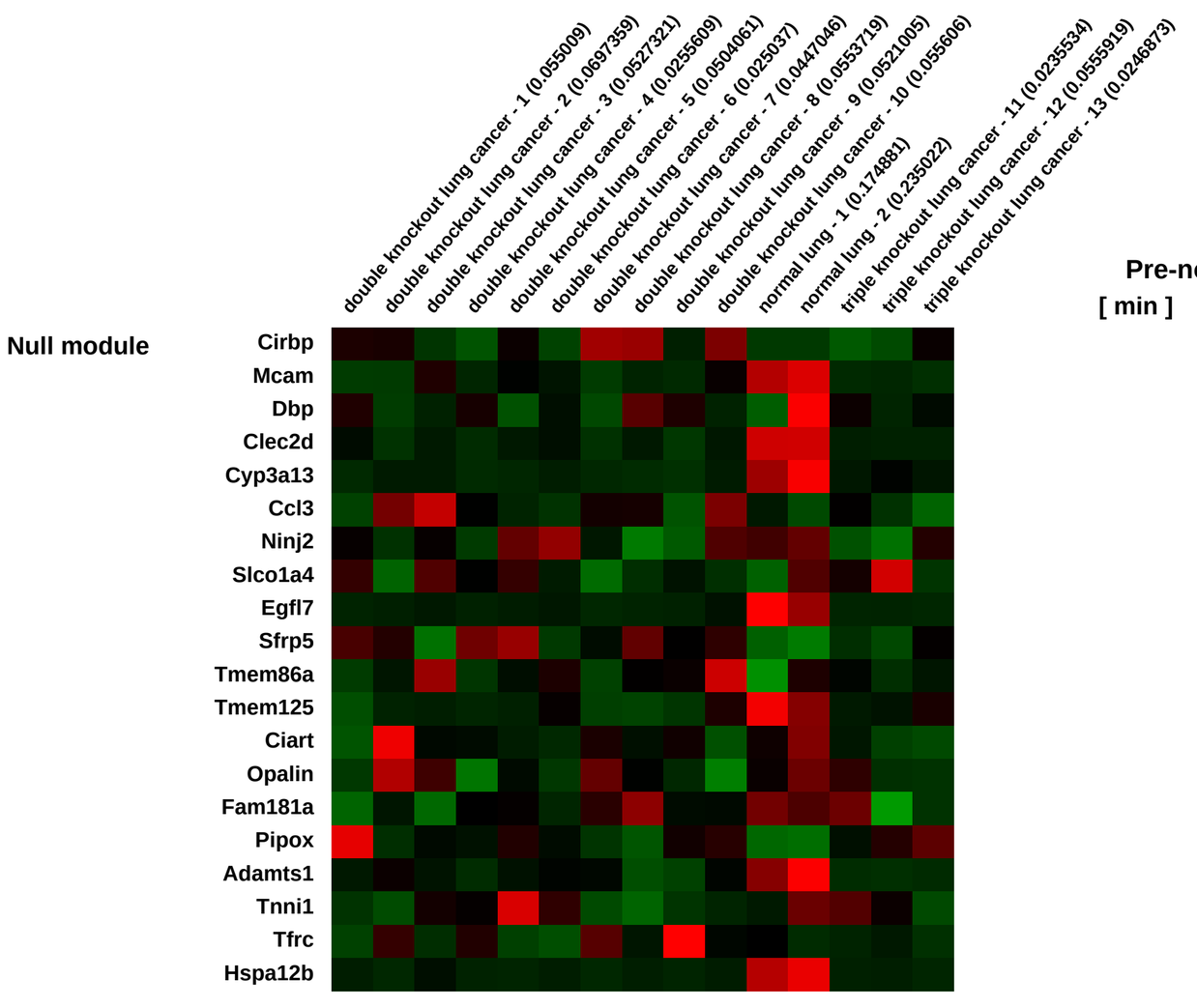

GEO Series "GSE22283" Expression Profiles

Num of samples in this series: 8

Scale of expression profile Z-scores

-3.0 -2.0 -1.0 0.0 1.0 2.0 3.0

GEO Link:	http://www.ncbi.nlm.nih.gov/geo/query/acc.cgi?acc=GSE22283
Status:	Public on Jul 06 2011
Title:	expression data in lung of mice bearing inducible FGF18 transgene
Organism:	Mus musculus
Experiment type:	Expression profiling by array
Platform:	GPL1261
Pubmed ID:	21878612
Summary & Design:	**Summary:** Better understanding alveolarization mechanisms could help improving prevention and treatment of diseases characterized by reduced alveolar number, especially bronchopulmonary dysplasia (BPD). Although signaling through fibroblast growth factor (FGF) receptors is essential for alveolarization, involved ligands are unidentified. FGF18 whose expression peaks during alveolar septation is likely to be involved. Herein, a mouse model of inducible, lung-targeted FGF18-transgene was used to advance the onset of FGF18 expression, and genome-wide expression changes were determined. keywords: transgenic mice, alveolarization, angiogenesis, fibrosis, epithelial-mesenchymal transition. **Overall design:** Four pairs of simple and double transgenic pups issued from 4 different litters were selected on the basis of FGF18 transgene induction. RNA from the mice lung were extracted and hybridized on Affymetrix microarrays.

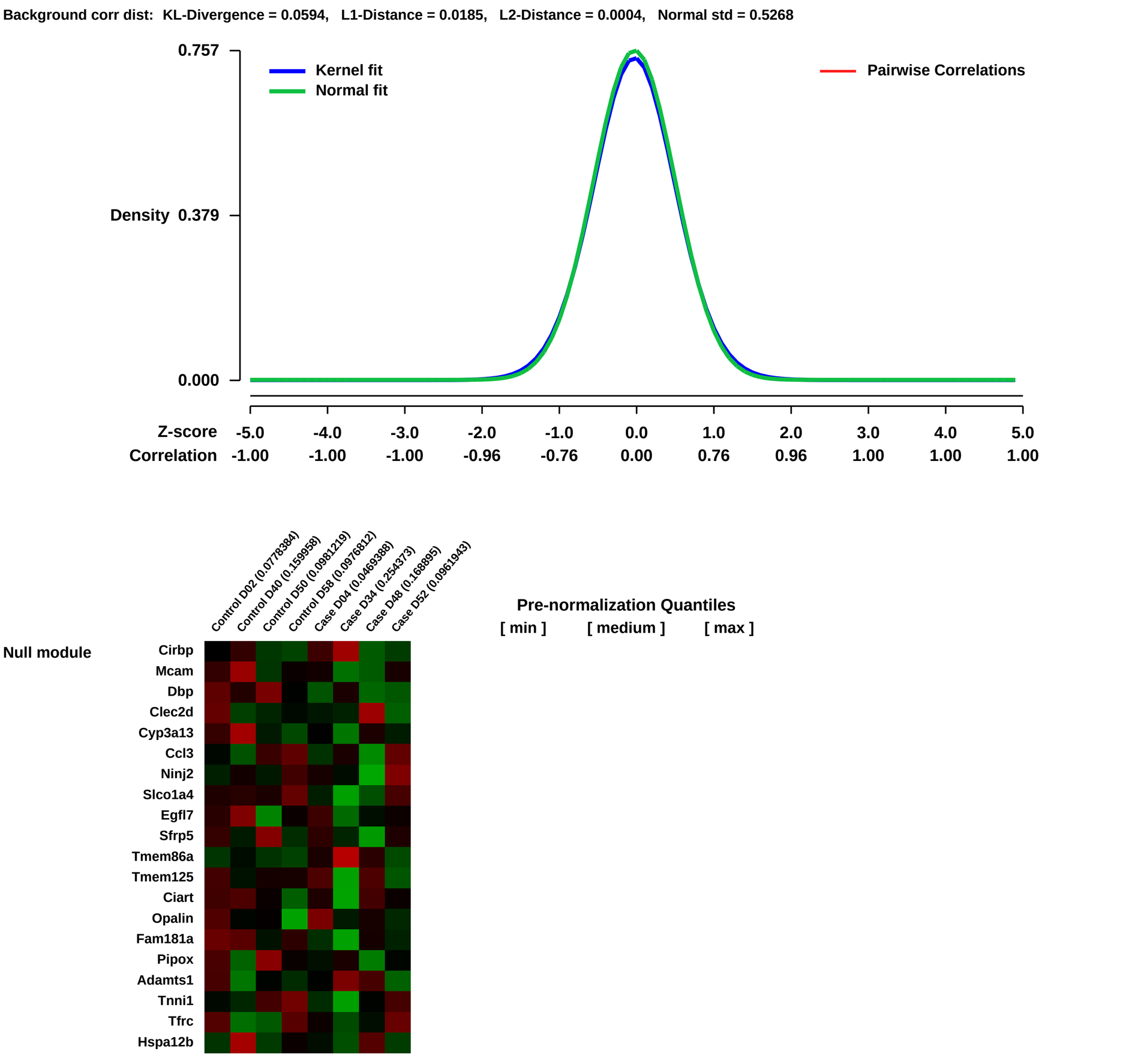

GEO Series "GSE29632" Expression Profiles

Num of samples in this series: 42

Scale of expression profile Z-scores

-3.0 -2.0 -1.0 0.0 1.0 2.0 3.0

GEO Link: http://www.ncbi.nlm.nih.gov/geo/query/acc.cgi?acc=GSE29632
Status: Public on May 25 2012
Title: Effect of Nrf2 deletion in postnatal lung development and BPD phenotype in newborn mice
Organism: Mus musculus
Experiment type: Expression profiling by array
Platform: GPL1261
Pubmed ID:

Summary & Design:

Summary:
Background: Nrf2 is an essential cytoprotective transcription factor. However, association of Nrf2 in organ development and neonatal disease is rarely examined. Hyperoxia exposure to newborn rodents generates pulmonary phenotypes which resemble bronchopulmonary dysplasia (BPD) of prematurity.

Methods: To investigate the role of Nrf2 in lung maturation and BPD pathogenesis, Nrf2-deficient (Nrf2-/-) and wild-type (Nrf2+/+) neonates were exposed to air or hyperoxia (O2). Transcriptome analysis determined Nrf2-directed mechanisms in premature lung. Lung injury was assessed by bronchoalveolar lavage analysis and histopathology.

Results: In Nrf2-/- neonates, basal expression of cell cycle machinery, redox balance, and lipid/carbohydrate metabolism genes were suppressed while immunity genes were overexpressed compared to Nrf2+/+ pups. O2-induced mortality and pulmonary inflammation/injury were significantly higher in Nrf2-/- than in Nrf2+/+. Lung DNA lesion and oxidation were greater in Nrf2-/- than in Nrf2+/+, constitutively and after O2. Nrf2-dependent genes modulated cellular growth/proliferation, defense, immunity, and lipid metabolism against hyperoxia. Bioinformatic elucidation of Nrf2 binding motifs and augmented O2-induced inflammation in genetically deficient neonates validated Gpx2 and Marco as Nrf2 effectors.

Conclusion: Overall, Nrf2 in underdeveloped lungs orchestrated cell cycle, morphogenesis, and immunity as well as cellular defense constitutively and under oxidant stress. Results provide putative molecular mechanisms of Nrf2-directed lung alveolarization and BPD of prematurity.

Overall design:
PARALLEL study design with 42 samples comparing 14 groups of age (P1 to P4 corresponding to day 0 to day 3 animals), gene, and exposure: (4 groups Nrf+/+ wild type P1-P4 air exposure) (4 groups Nrf -/- knockout P1-P4 air exposure), (3 groups Nrf+/+ wild type P2-P4 with 100 percent O2 (hyperoxia exposure) and 3 groupsNrf -/- knockout P2-P4 with 100 percent O2 (hyperoxia exposure)) Biological replicates: 3 per group

Background corr dist: KL-Divergence = 0.2661, L1-Distance = 0.0498, L2-Distance = 0.0062, Normal std = 0.2972

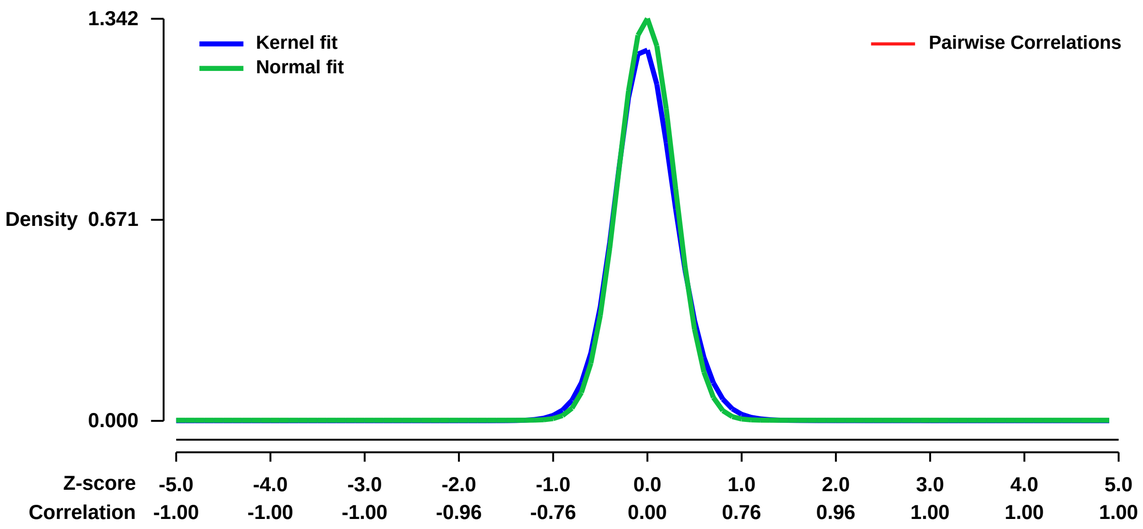

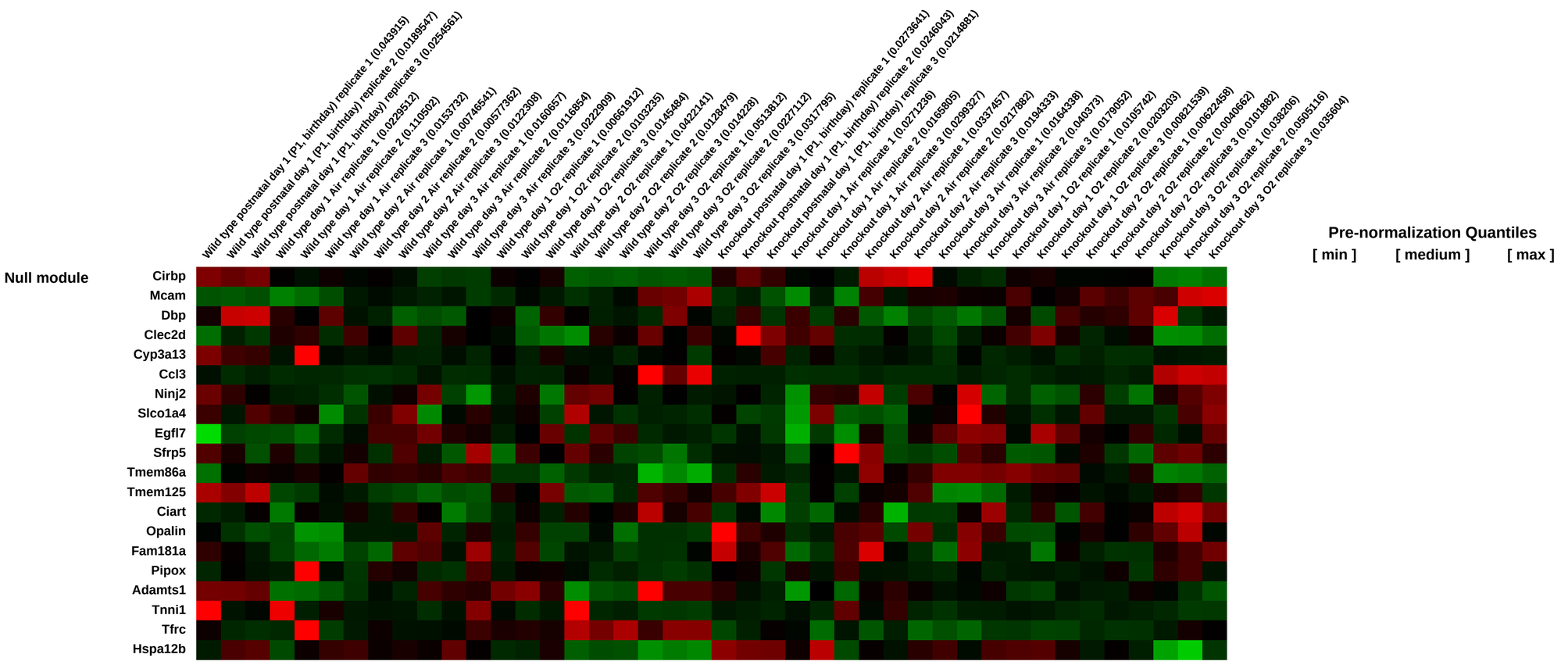

GEO Series "GSE34065" Expression Profiles

Num of samples in this series: 6

Scale of expression profile Z-scores

-3.0 -2.0 -1.0 0.0 1.0 2.0 3.0

GEO Link:	http://www.ncbi.nlm.nih.gov/geo/query/acc.cgi?acc=GSE34065
Status:	Public on Jan 01 2013
Title:	Expression data from mesodermal Tbx1-knockout otic vesicles and periotic mesenchyme at E11.5
Organism:	Mus musculus
Experiment type:	Expression profiling by array
Platform:	GPL1261
Pubmed ID:	
Summary & Design:	**Summary:** **The T-box transcription factor Tbx1 is expressed in the otic vesicle and surrounding periotic mesenchyme during inner ear development. Mesenchymal Tbx1 is essential for inner ear development, with conditional mutants displaying defects in both auditory and vestibular systems. We have previously identified reduced expression of retinoic acid metabolic genes in the periotic mesenchyme of mesoderm conditional Tbx1 mutants, using the T-Cre mouse line, implicating retinoic acid in mesenchymal-epithelial signaling downstream of Tbx1 in the periotic mesenchyme.** **In order to identify downstream effectors of mesenchymal-epithelial signaling downstream of mesenchymal Tbx1, we have utilized a gene profiling approach comparing embryonic day 11.5 otic vesicle and surrounding periotic mesenchyme from T-Cre-mediated conditional Tbx1 mutants (Mest-KO) and conditional heterozygous control litter mates (control). This data was used in conjunction with OV-only data (GSE34064) to identify expression changes within the periotic mesenchyme.** **Overall design:** **E11.5 T-Cre-mediated conditional Tbx1 mutants (Mest-KO) and control (T-Cre conditional Tbx1 heterozygotes) embryos were microdissected to isolate the otic vesicle and surrounding periotic mesenchyme. Left and right ears from 3 embryos of the same genotype were pooled for each chip, and 3 biological replicates of each chip were performed.**

Background corr dist: KL-Divergence = 0.0473, L1-Distance = 0.0220, L2-Distance = 0.0006, Normal std = 0.5858

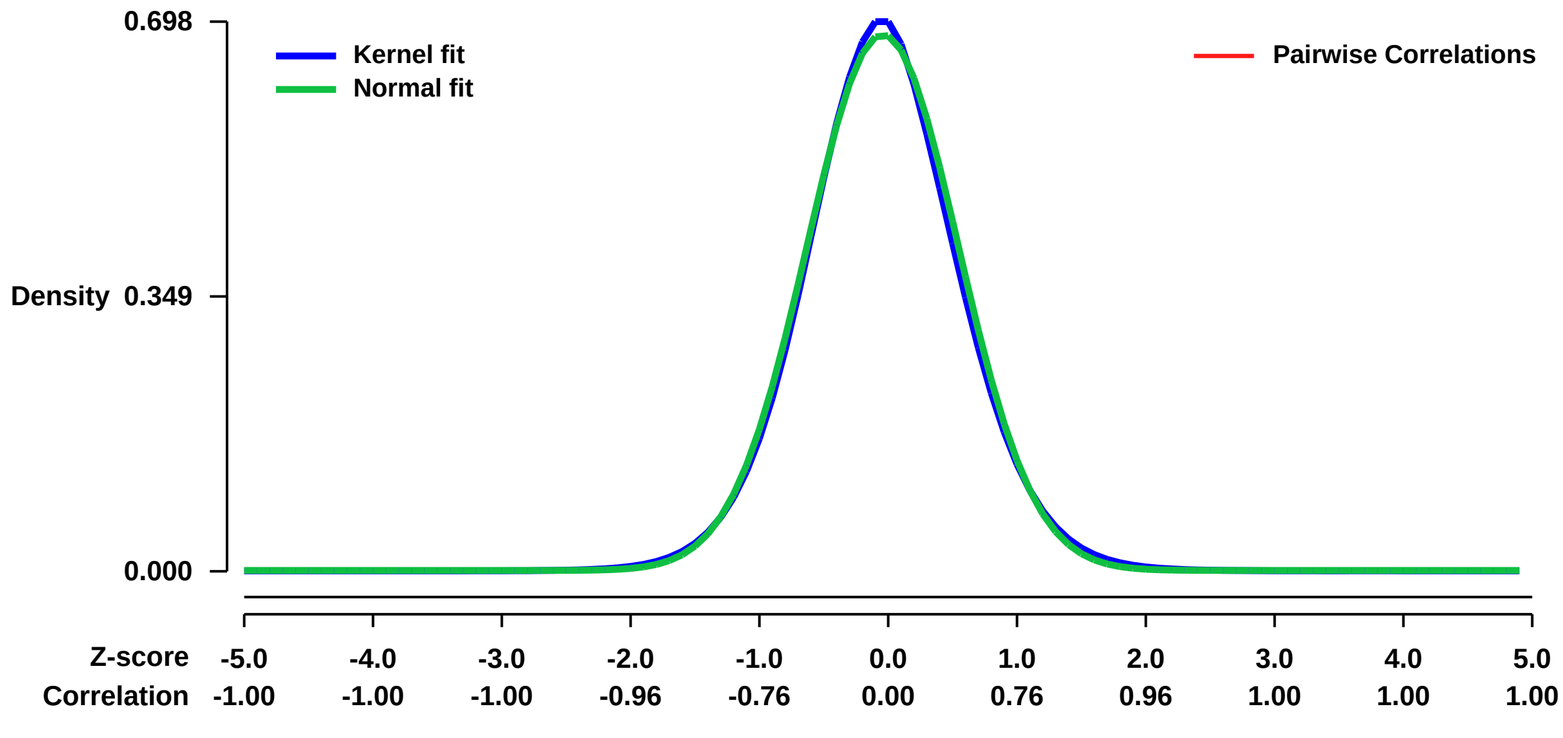

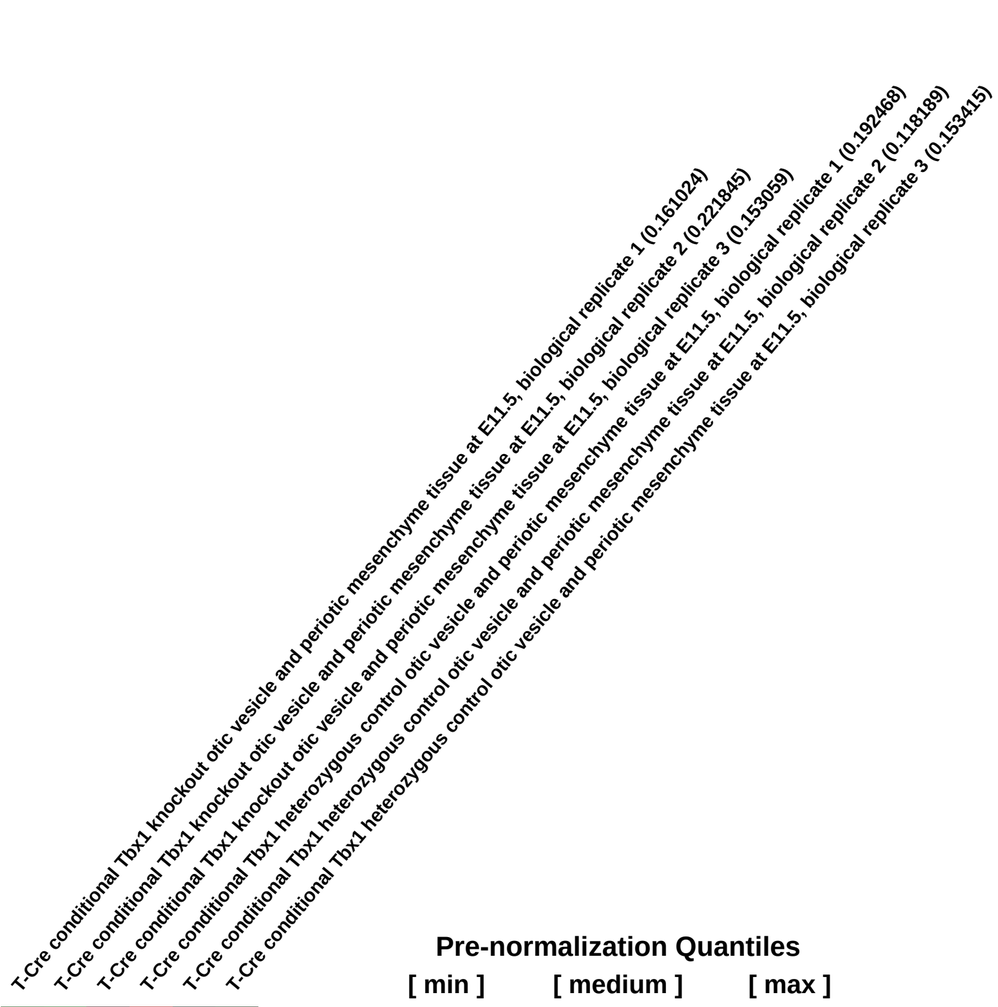

Pre-normalization Quantiles

[min] [medium] [max]

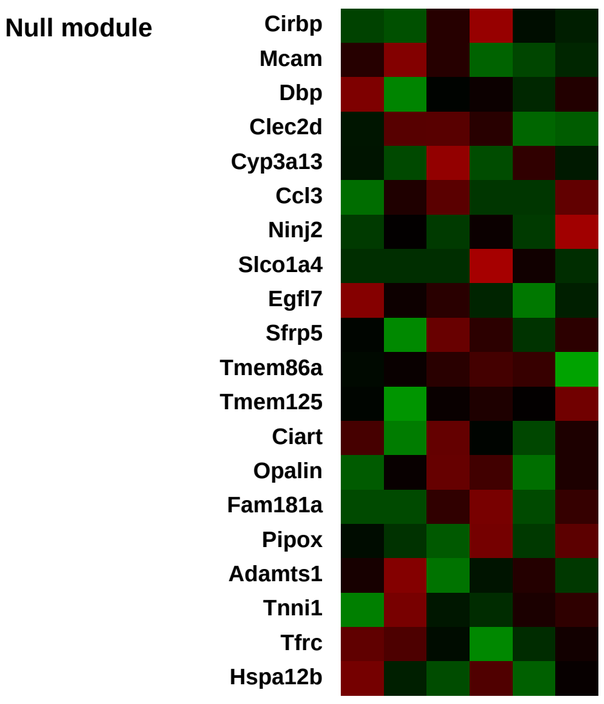

GEO Series "GSE36810" Expression Profiles

Num of samples in this series: 16

Scale of expression profile Z-scores

-3.0 -2.0 -1.0 0.0 1.0 2.0 3.0

GEO Link:	http://www.ncbi.nlm.nih.gov/geo/query/acc.cgi?acc=GSE36810
Status:	Public on Mar 27 2012
Title:	Expression data from mouse lungs exposed in-utero and/or as an adult to second-hand smoke (SHS)
Organism:	Mus musculus
Experiment type:	Expression profiling by array
Platform:	GPL1261
Pubmed ID:	22962063
Summary & Design:	**Summary:** Second-hand smoke (SHS) exposure during pregnancy has adverse effects on offspring. We used microarrays to characterize the gene expression changes caused by in-utero exposure and adult exposure to SHS in adult mouse lungs. **Overall design:** Left lungs from Balb/c male mice were collected at 15 weeks of age for RNA extraction and hybridization on Affymetrix mouse 430 2.0 microarrays. Based on their smoke exposure status, there are 4 groups of mice, each exposed in-utero to filtered-air or SHS and as an adult to filtered-air or SHS. We extracted RNA from 4 animals from each group for microarray analysis (N = 16 samples).

Background corr dist: KL-Divergence = 0.0998, L1-Distance = 0.0238, L2-Distance = 0.0008, Normal std = 0.4416

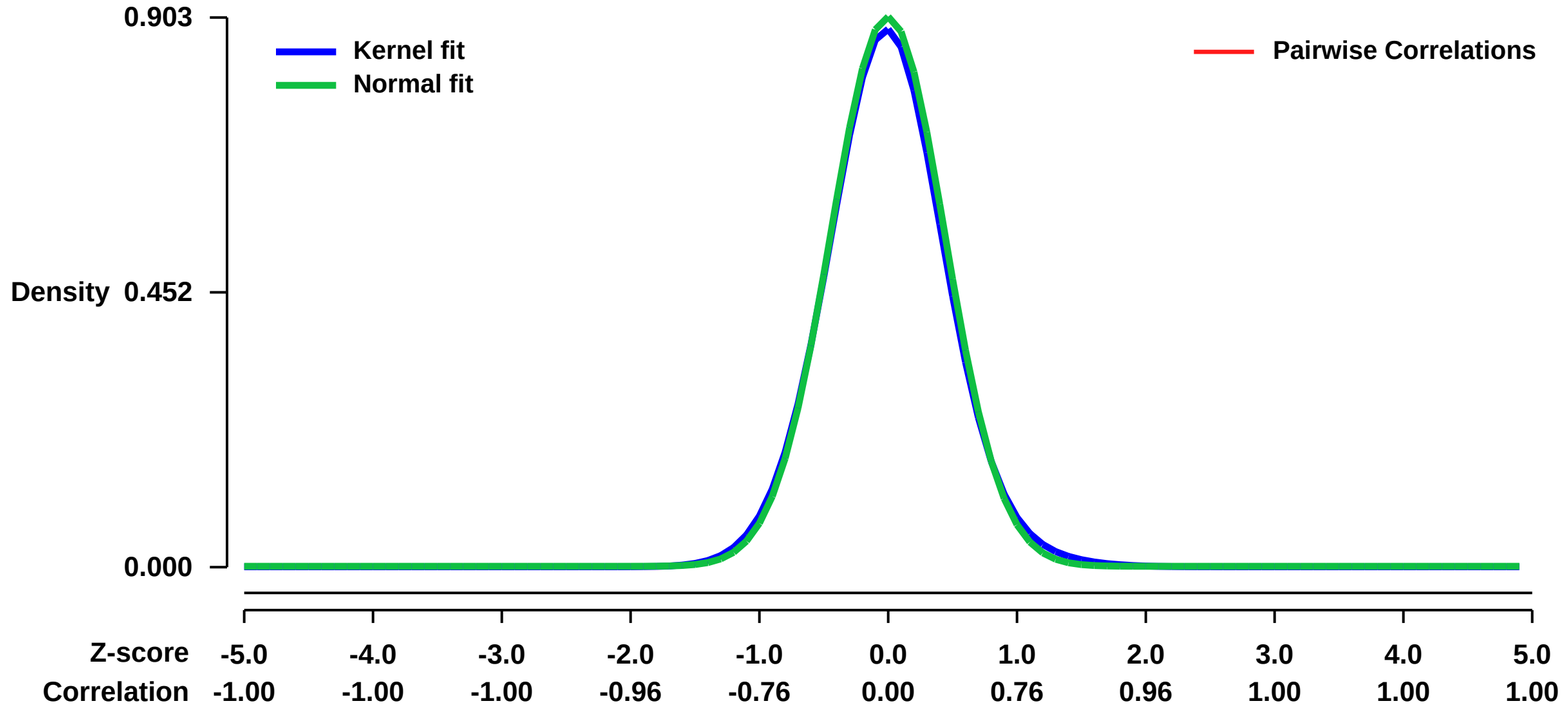

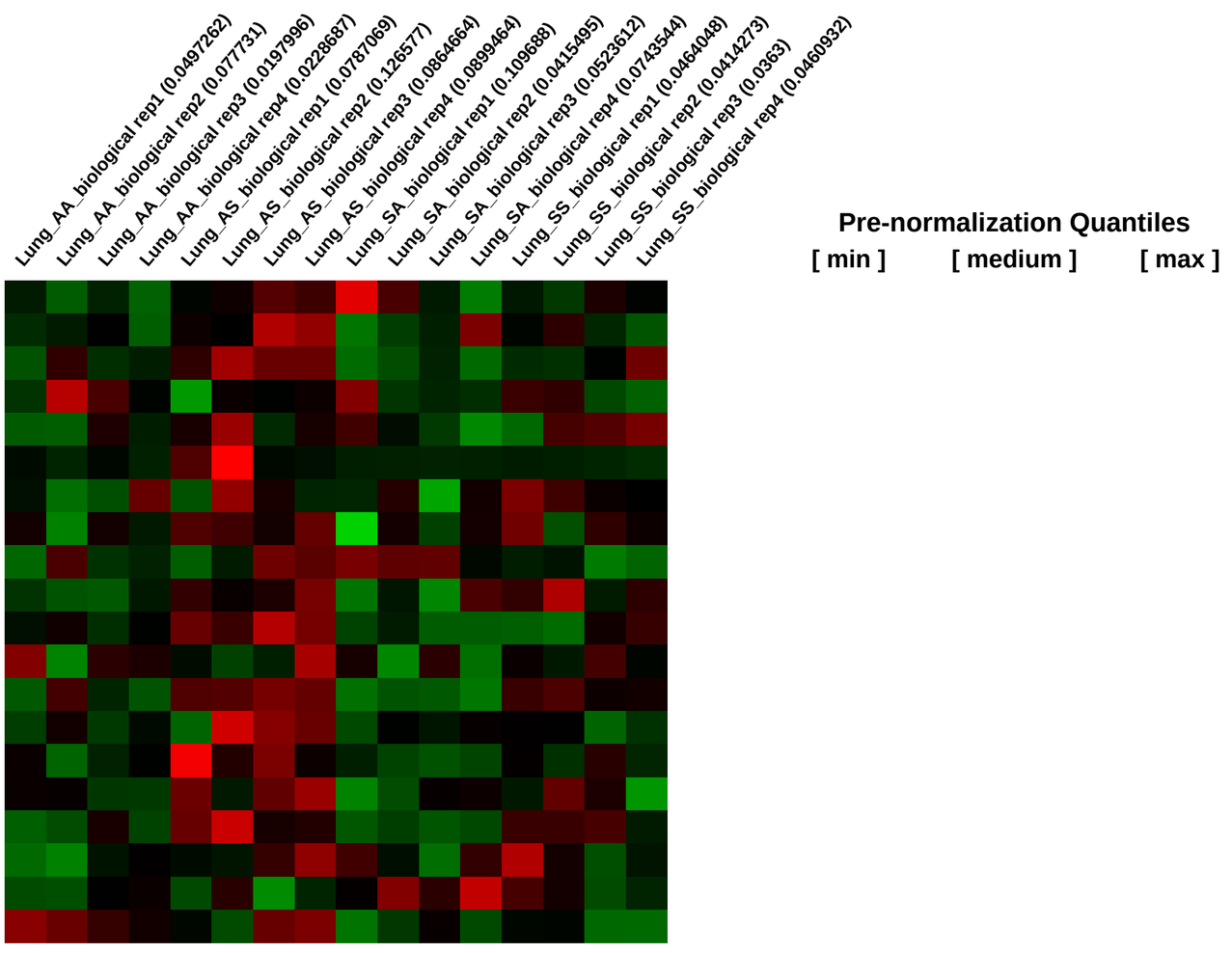

GEO Series "GSE9975" Expression Profiles

Num of samples in this series: 36

Scale of expression profile Z-scores

-3.0 -2.0 -1.0 0.0 1.0 2.0 3.0

GEO Link:	http://www.ncbi.nlm.nih.gov/geo/query/acc.cgi?acc=GSE9975
Status:	Public on Sep 30 2009
Title:	newly transcribed RNA (nt-RNA) for IFN alpha and gamma time course
Organism:	Mus musculus
Experiment type:	Expression profiling by array
Platform:	GPL1261
Pubmed ID:	18658122
Summary & Design:	**Summary:** Expression data from NIH-3T3 cells treated with mock, 100 U/ml IFN alpha or 100 U/ml gamma for 1 or 3h on nt-RNA labeled for 30-60 min at different times of interferon treatment Differential gene expression caused by IFN alpha or gamma was analyzed in newly transcribed RNA (nt-RNA) of NIH-3T3 cells treated for 1 or 3 h. RNA was labeled for 30 to 60 min and separated from total cellular RNA (tc-RNA) following Trizol RNA preparation and thiol-specific biotinylation We used microarrays to analyze the effects of IFNalpha and gamma treatment in newly transcribed RNA (nt-RNA) Keywords: time course **Overall design:** NIH-3T3 cells (5th to 15th passage after thawing) were split 24 h before start of the experiment. When starting the experiment 80% confluency was reached. The experiment was started by applying fresh, prewarmed, CO2-equilibrated medium containing either mock, 100U/ml IFN alpha or 100 U/ml IFN gamma. Labeling was either started simultaneously, 30 or 150 minutes later.

Background corr dist: KL-Divergence = 0.0632, L1-Distance = 0.0569, L2-Distance = 0.0049, Normal std = 0.5658

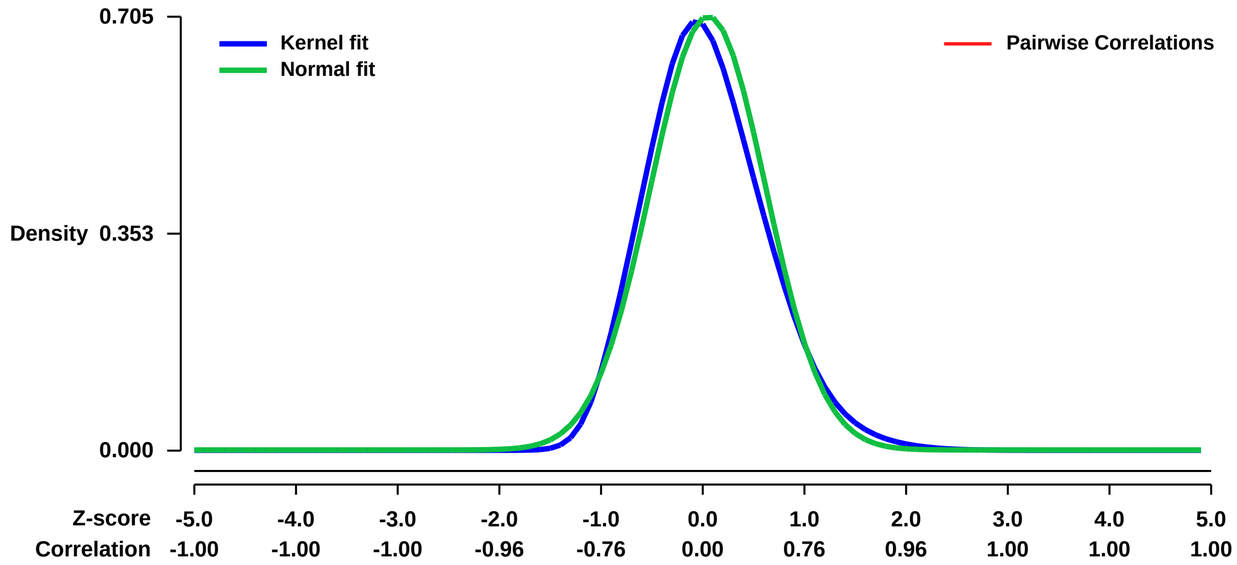

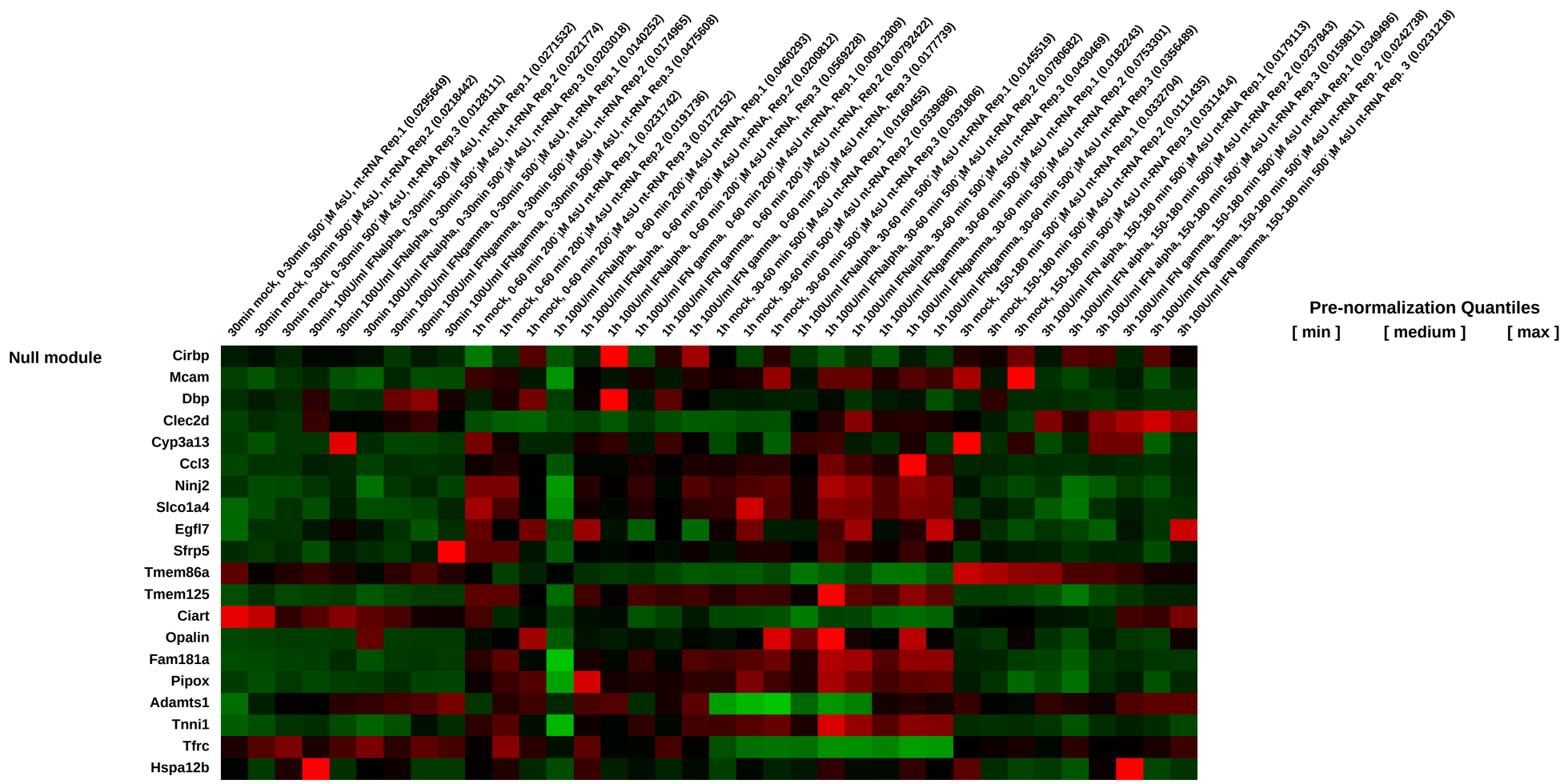

GEO Series "GSE7762" Expression Profiles

Num of samples in this series: 36

Scale of expression profile Z-scores

-3.0 -2.0 -1.0 0.0 1.0 2.0 3.0

GEO Link:	http://www.ncbi.nlm.nih.gov/geo/query/acc.cgi?acc=GSE7762
Status:	Public on Jun 14 2007
Title:	Morphine effects on striatal transcriptome in four inbred mouse strains
Organism:	Mus musculus
Experiment type:	Expression profiling by array
Platform:	GPL1261
Pubmed ID:	17598886
Summary & Design:	**Summary:** Chronic opiate use produces molecular and cellular adaptations in the nervous system, leading to tolerance, physical dependence and addiction. Genome-wide comparison of morphine-induced changes in brain transcription of mouse strains with different opioid-related phenotypes provides an opportunity to discover the relationship between gene expression and behavioral response to the drug. **Keywords:** Drug response **Overall design:** Microarray experiment was designed to determine the impact of genetic background on the transcriptional effects of morphine in the striatum. The effects of single (20 mg/kg, s.c.) and repeated morphine administration (10-40 mg/kg, 3 times daily for 5 days) were analyzed in four inbred mouse strains (129P3/J. DBA/2J, C57BL/6J, SWR/J). Twelve experimental groups were compared. Control animals received injections of saline. Three independent biological replicates of the microarray were prepared for each experimental group. For each array, independent pools of total RNA from three animals were prepared.

Background corr dist: KL-Divergence = 0.3024, L1-Distance = 0.0656, L2-Distance = 0.0117, Normal std = 0.2790

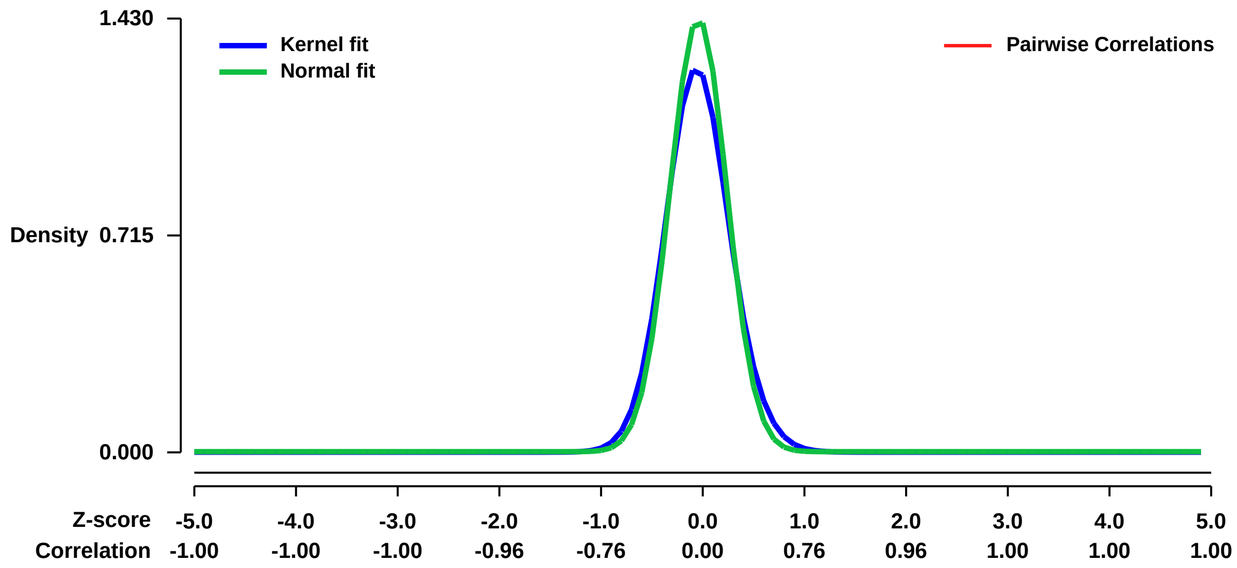

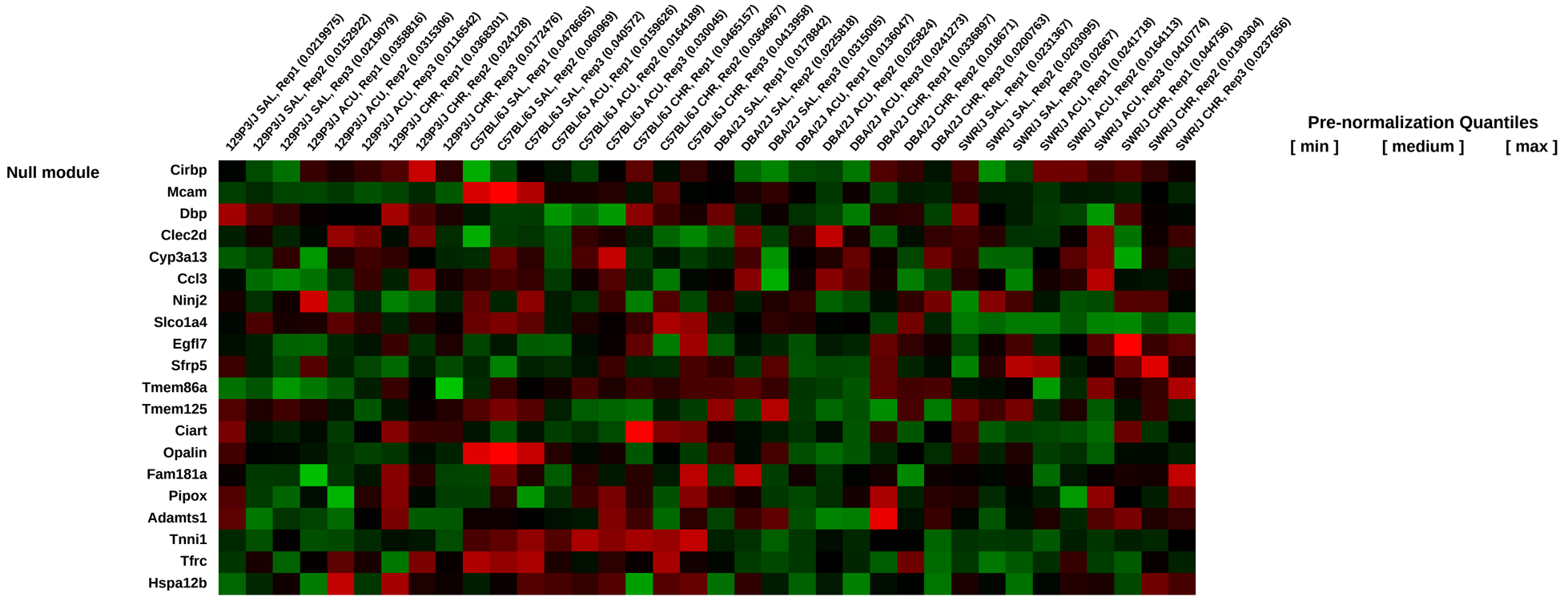

GEO Series "GSE10162" Expression Profiles

Num of samples in this series: 6

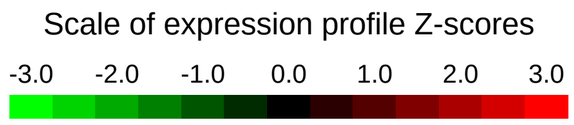

GEO Link:	http://www.ncbi.nlm.nih.gov/geo/query/acc.cgi?acc=GSE10162
Status:	Public on Apr 03 2008
Title:	Transcriptional Adaptation to Clcn5 Knockout in Proximal Tubules of the Mouse Kidney
Organism:	Mus musculus
Experiment type:	Expression profiling by array
Platform:	GPL1261
Pubmed ID:	18349385
Summary & Design:	**Summary:** Dent disease has multiple defects attributed to proximal tubule malfunction including low molecular weight proteinuria, aminoaciduria, phosphaturia and glycosuria. In order to understand the changes in kidney function of the Clc5 transporter gene knockout mouse model of Dent disease, we examined gene expression profiles from proximal tubules of mouse kidneys. Overall 720 genes are expressed differentially in the proximal tubules of the Dent Clcn5 knockout mouse model compared to those of control wild type mice. The fingerprint of these gene changes may help us to understand the phenotype of Dent disease. Keywords: gene knockout, mouse, Clcn5, Dent's disease **Overall design:** 3 microarrays each of wild type and knockout mouse proximal tubule were processed

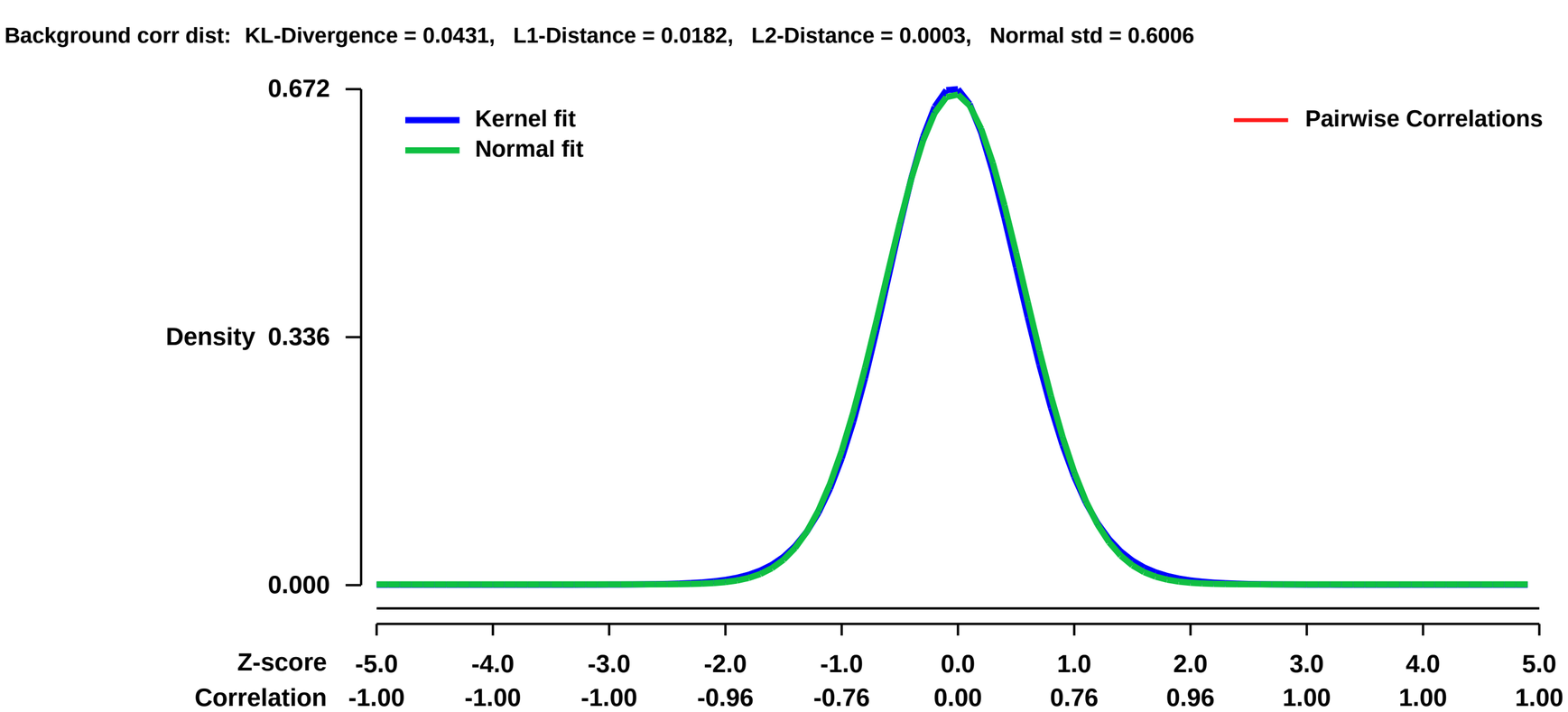

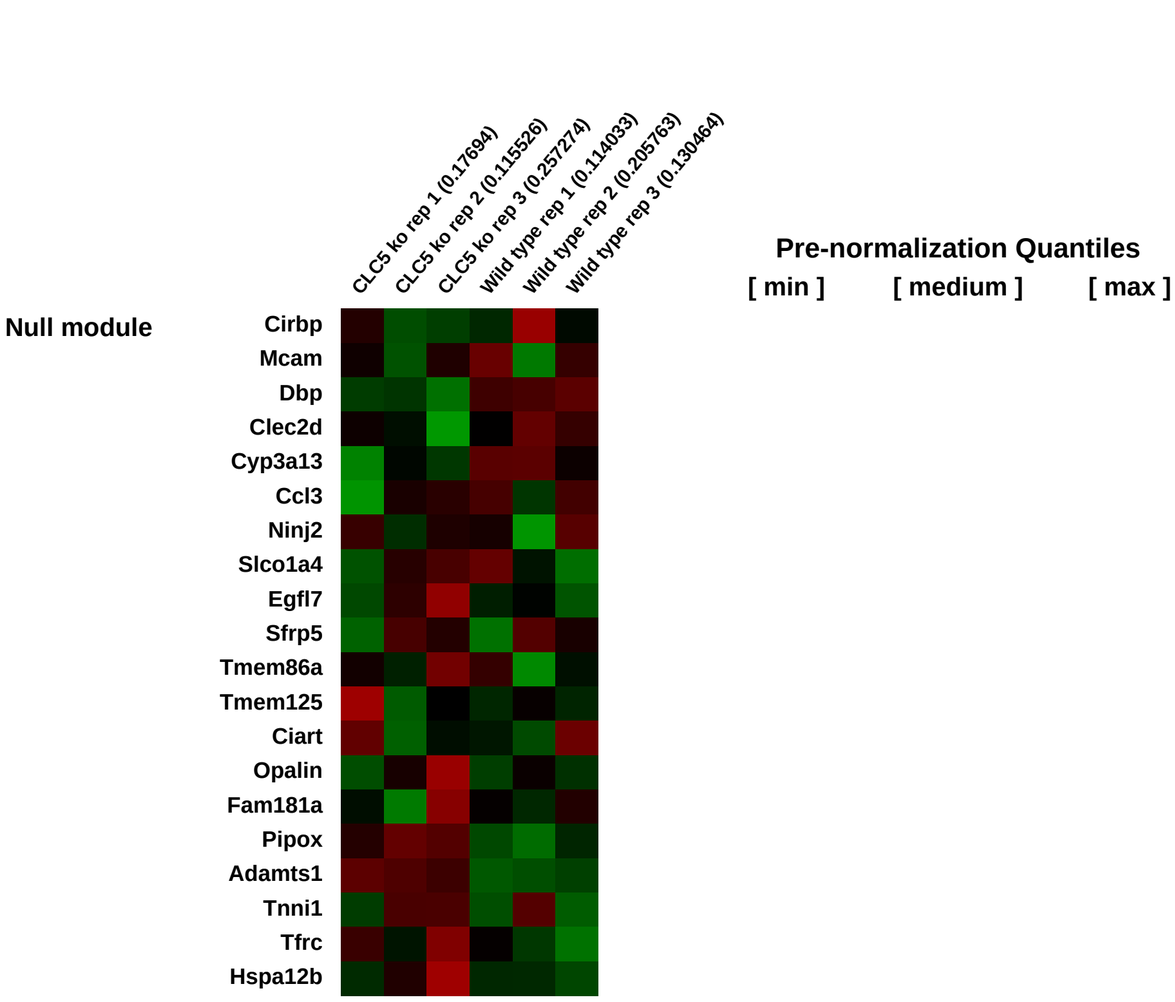

GEO Series "GSE12693" Expression Profiles

Num of samples in this series: 6

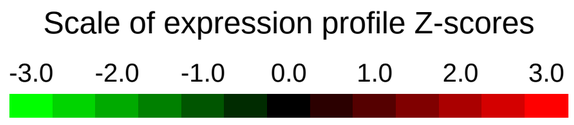

GEO Link:	http://www.ncbi.nlm.nih.gov/geo/query/acc.cgi?acc=GSE12693
Status:	Public on Apr 09 2009
Title:	Hepatic gene expression profile of mice exposed to social stress
Organism:	Mus musculus
Experiment type:	Expression profiling by array
Platform:	GPL1261
Pubmed ID:	19106182
Summary & Design:	**Summary:** Social stress is well known to be involved in the occurrence and exacerbation of mental illness, and also various life-style related diseases such as hyperinsulinemia, hyperglycemia, cardiovascular diseases and cancer. However, there is little information on tissue-specific gene expression in response to social stress, which reflects our daily life. Liver is one of the most important organs, owing to its biological functions such as energy metabolic homeostasis, metabolization and detoxification of endo- and exogenous substances. In order to elucidate the mechanism underlying response to social stress in the liver, we investigated hepatic gene expression in mice exposed to isolation stress using DNA microarray. Male BALB/c mice (4 weeks old) were housed 5 per cage for 10 days acclimatization. Then mice were exposed to isolation stress for 30 days. After stress treatment, the mouse liver RNA was subjected to DNA microarray analysis. Taking the false discovery rate into account, isolation stress altered expression of 420 genes. Moreover, Gene Ontology analysis of these differentially expressed genes indicated that isolation stress remarkably down-regulated lipid metabolism-related pathway through peroxisome proliferator-activated receptor-alpha (PPARalpha), while lipid biosynthesis pathway regulated by sterol regulatory element binding factor-1 (SREBF-1), Golgi vesicle transport and secretory pathway-related genes were significantly up-regulated. These results suggested that isolation for 30 days, mild and consecutive social stress, not only regulate the systems for lipid metabolism but also cause the endoplasmic reticulum stress in mouse liver. **Overall design:** Male BALB/c mice (4 weeks old, Japan SLC, Shizuoka, Japan) weighing 14-18 g were housed 5 per cage. After acclimatization for 10 days, the mice were exposed to isolation (1 mouse per cage). All cages were placed in a foam plastic box in order to avoid social contact. To enhance the feeling of isolation, the bed volume in each cage for the isolated mice was reduced to one-tenth of that in the control group. The weight of bedding chips was about 2 g. All mice were housed in an air-conditioned room (room temperature: 23 ´– 1´℃, humidity: 55 ´– 5 %) under 12 h dark/12 h light cycles, with free access to tap water and MF diet (Oriental Yeast Co., Tokyo, Japan).

Background corr dist: KL-Divergence = 0.0484, L1-Distance = 0.0220, L2-Distance = 0.0006, Normal std = 0.5821

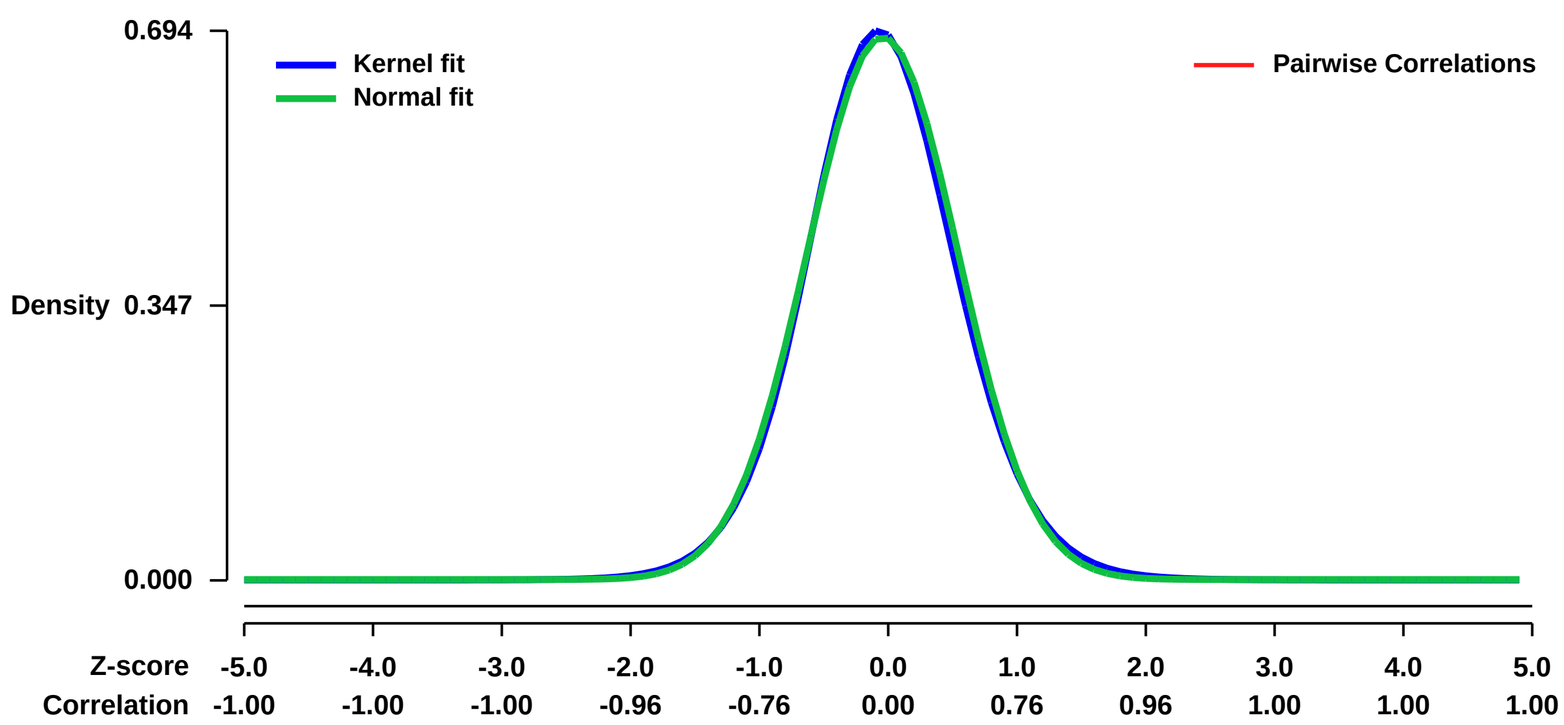

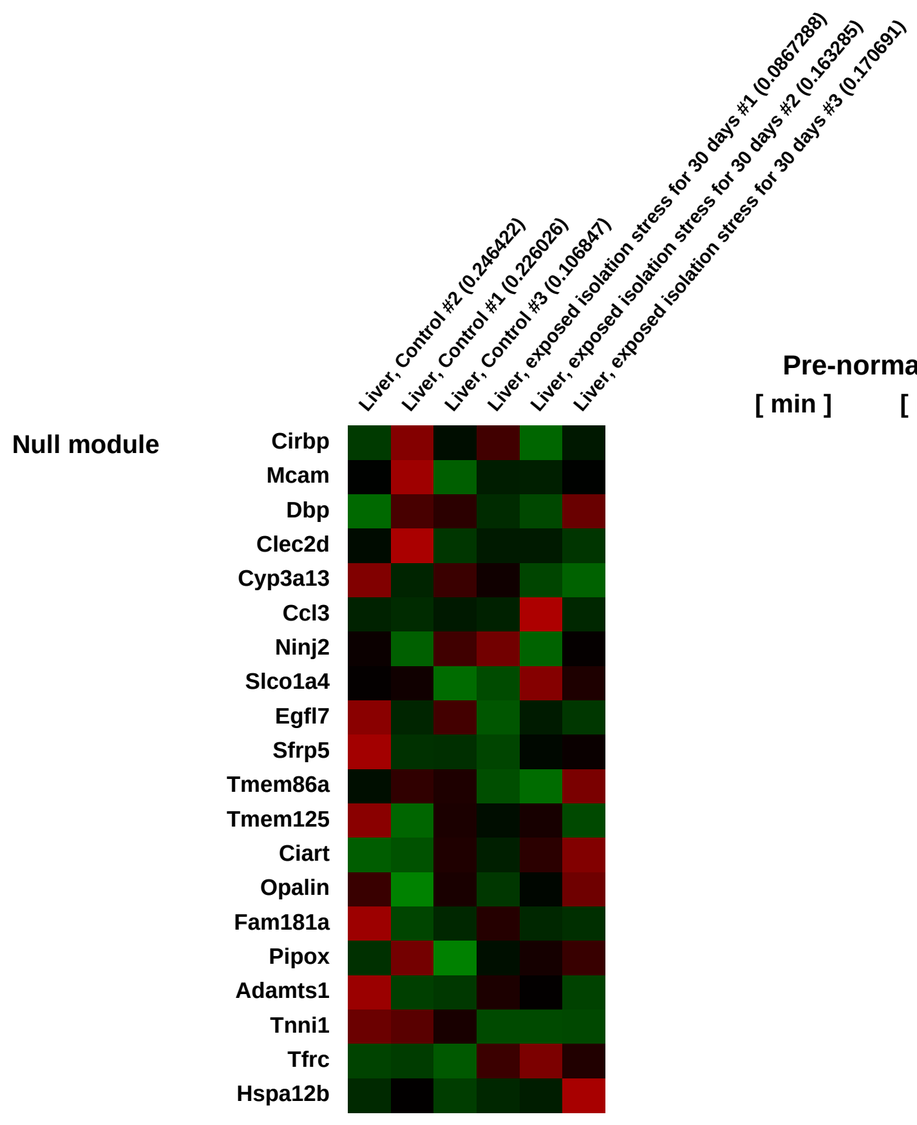

GEO Series "GSE31646" Expression Profiles

Num of samples in this series: 11

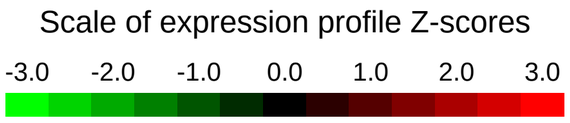

GEO Link:	http://www.ncbi.nlm.nih.gov/geo/query/acc.cgi?acc=GSE31646
Status:	Public on Mar 31 2012
Title:	Adipose tissue in the presence or absence of kinin B1 receptors
Organism:	Mus musculus
Experiment type:	Expression profiling by array
Platform:	GPL1261
Pubmed ID:	
Summary & Design:	**Summary:** We studied adipose tissue from wild type mice, kinin B1 receptor knockout mice (B1KO), and B1KO mice with rescued expression of kinin B1 receptor selectively in fat. We used microarrays to detail the gene expression profile of the epididymal fat of these mice. **Overall design:** Three-month-old mice were killed and tissue was collected for RNA processing and microarray analysis.

Background corr dist: KL-Divergence = 0.1556, L1-Distance = 0.0390, L2-Distance = 0.0031, Normal std = 0.3671

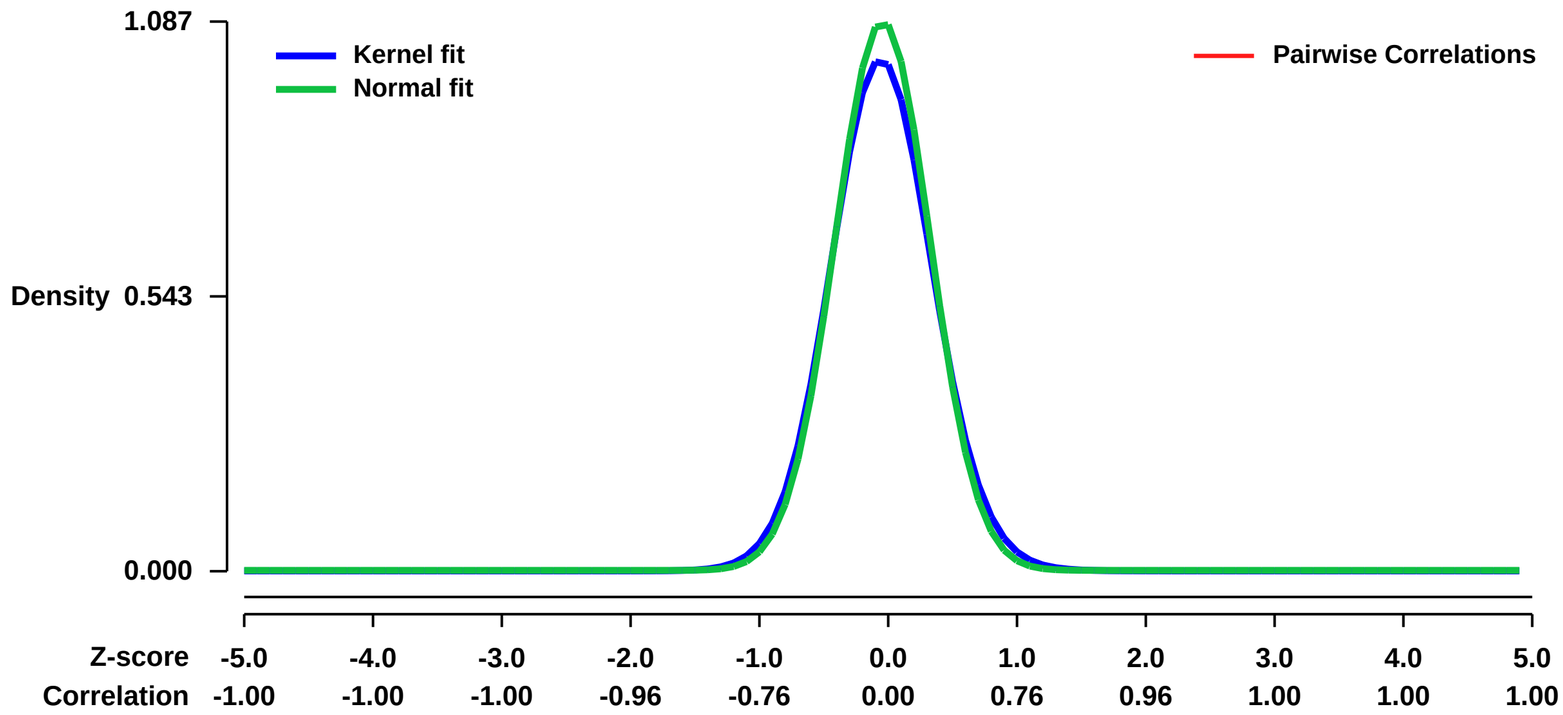

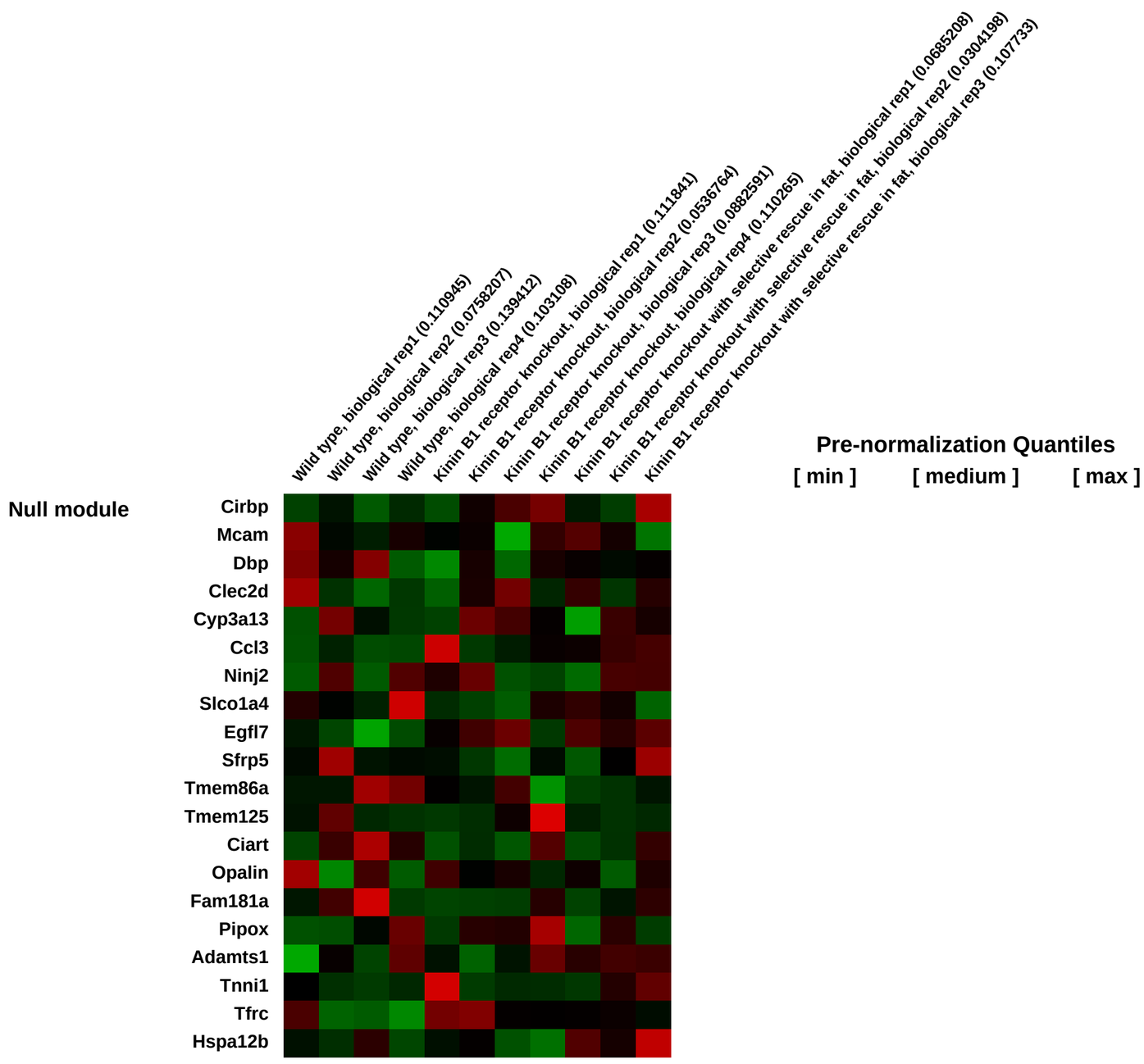

GEO Series "GSE2197" Expression Profiles

Num of samples in this series: 6

Scale of expression profile Z-scores

-3.0 -2.0 -1.0 0.0 1.0 2.0 3.0

GEO Link:	http://www.ncbi.nlm.nih.gov/geo/query/acc.cgi?acc=GSE2197
Status:	Public on Mar 01 2005
Title:	DC response to ISD vs CpG
Organism:	Mus musculus
Experiment type:	Expression profiling by array
Platform:	GPL1261
Pubmed ID:	16413926
Summary & Design:	**Summary:** **Bone marrow-derived dendritic cells were left untreated or stimulated with lipid-transfected double-stranded DNA or CpG oligonucleotides for four hours before harvesting.** **Keywords: other** **Overall design:**

Background corr dist: **KL-Divergence = 0.0357, L1-Distance = 0.0292, L2-Distance = 0.0011, Normal std = 0.6498**

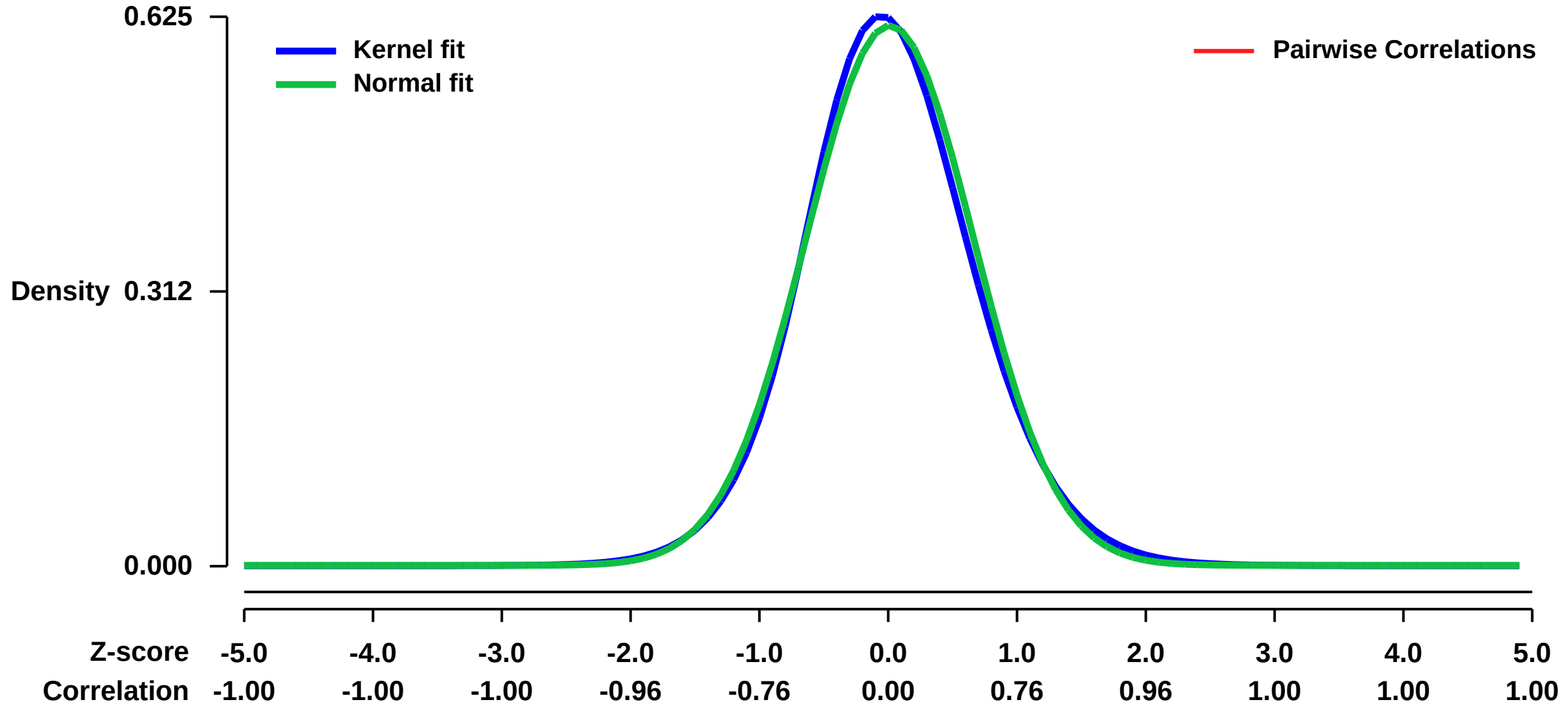

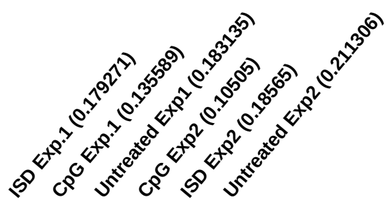

Pre-normalization Quantiles

[min] [medium] [max]

Null module

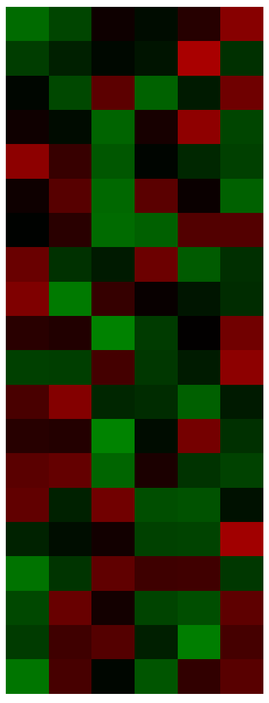

GEO Series "GSE7676" Expression Profiles

Num of samples in this series: 10

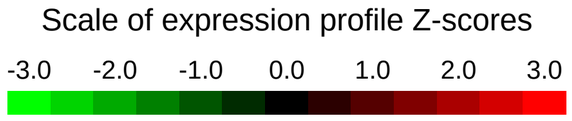

GEO Link:	**http://www.ncbi.nlm.nih.gov/geo/query/acc.cgi?acc=GSE7676**
Status:	**Public on Jun 30 2008**
Title:	**Changes in gene expression following Protocadherin 12 knockout**
Organism:	**Mus musculus**
Experiment type:	**Expression profiling by array**
Platform:	**GPL1261**
Pubmed ID:	**18477666**
Summary & Design:	**Summary:** **Protocadherin 12 (Pcdh12) is a transmembrane adhesive protein with homophilic adhesive properties and expressed in endothelial cells, the glycogen trophoblast cells of the placenta, and the mesangial cells of kidney glomeruli. Pcdh12-deficient mice are alive although they show alterations in placenta development.** **To reveal Pcdh12-associated pathways, 45,000 - Affymetrix probe arrays were used on Pcdh12 knockout and control placentas.** **Keywords: Comparative gene knockout results** **Overall design:** **To identify genes whos expression was modified by Pcdh12 deficiency, we examined global gene expression profiles of whole E12.5 knockout placentas (Pcdh12 -l-) and their wild-type (WT â Pcdh12+l+) littermates, using the Affymetrix Murine Genome 430 2.0 microarrays. Gestation day 12 was chosen as it is the period at which placentas already formed distinct layers, but organogenesis is still very active. Total RNA was extracted from five Pcdh12 knockout embryos and five normal placentas. RNA were tested for integrity on Agilent 2100 BioAnalyzer, prior to cRNA synthesis and chip hybridization (performed by the Institute of Genetics and Molecular and Cellular Biology, Strasbourg, France).**

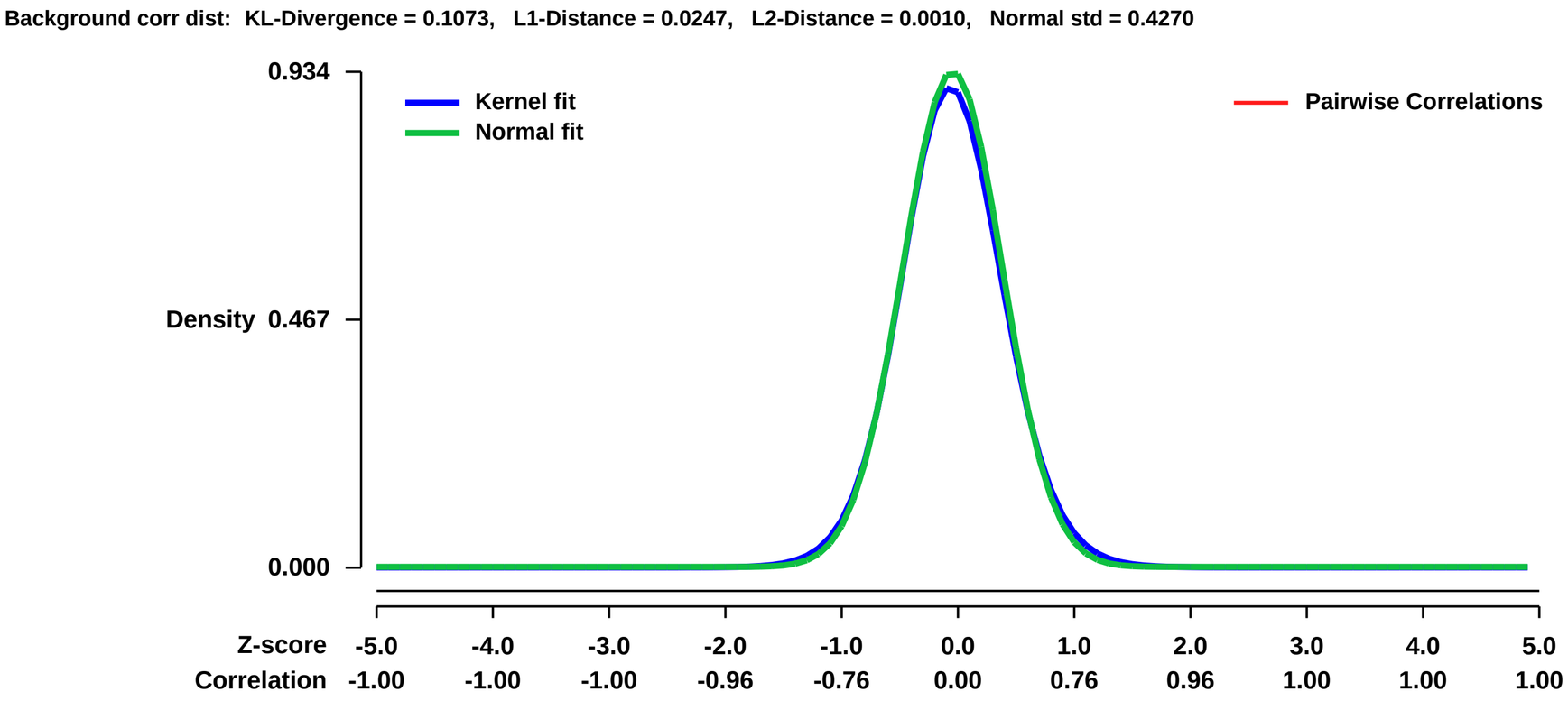

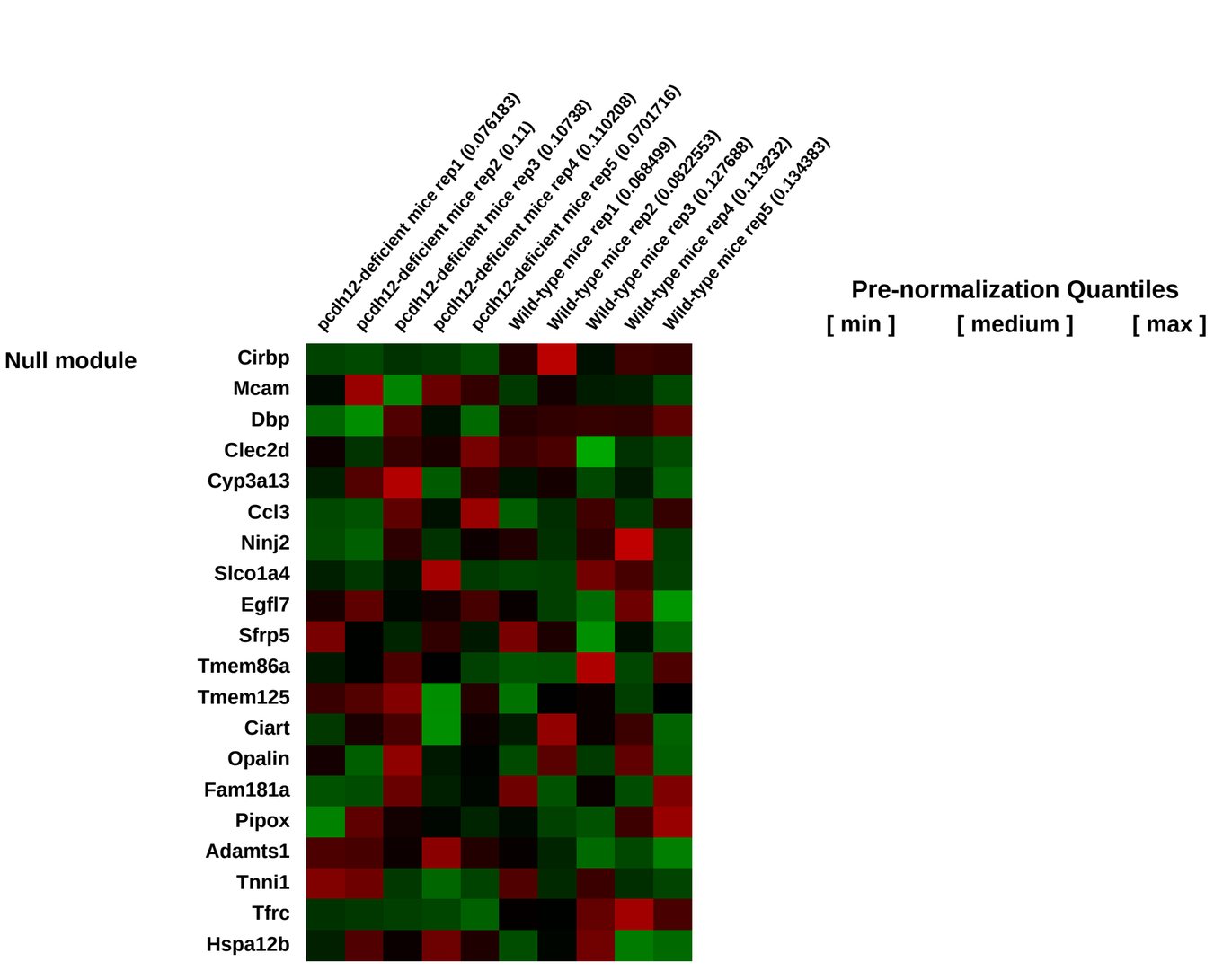

GEO Series "GSE30865" Expression Profiles

Num of samples in this series: 68

Scale of expression profile Z-scores

-3.0 -2.0 -1.0 0.0 1.0 2.0 3.0

GEO Link:	http://www.ncbi.nlm.nih.gov/geo/query/acc.cgi?acc=GSE30865
Status:	Public on Jul 22 2011
Title:	Gene expression of polyoma middle T antigen induced mammary tumors [NZB x PyMT]
Organism:	Mus musculus
Experiment type:	Expression profiling by array
Platform:	GPL1261
Pubmed ID:	22308418
Summary & Design:	**Summary:** Mouse genetic crosses were established between the PyMT model of metastatic breast cancer and NZB strain. Tumors were harvested from the animals for gene expression analysis to identify genes and network modules associated with progression to distant metastatic disease. **Overall design:** Gene expression of 68 samples from the NZB crosses were assayed on Affymetrix chips

Background corr dist: KL-Divergence = 0.0881, L1-Distance = 0.0712, L2-Distance = 0.0127, Normal std = 0.4866

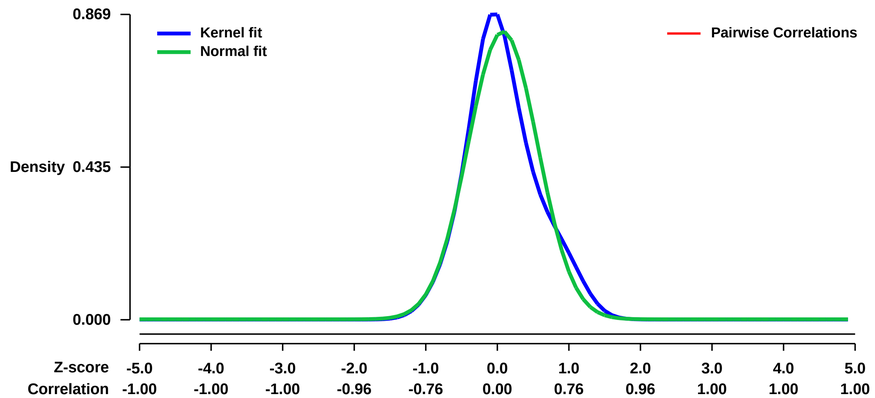

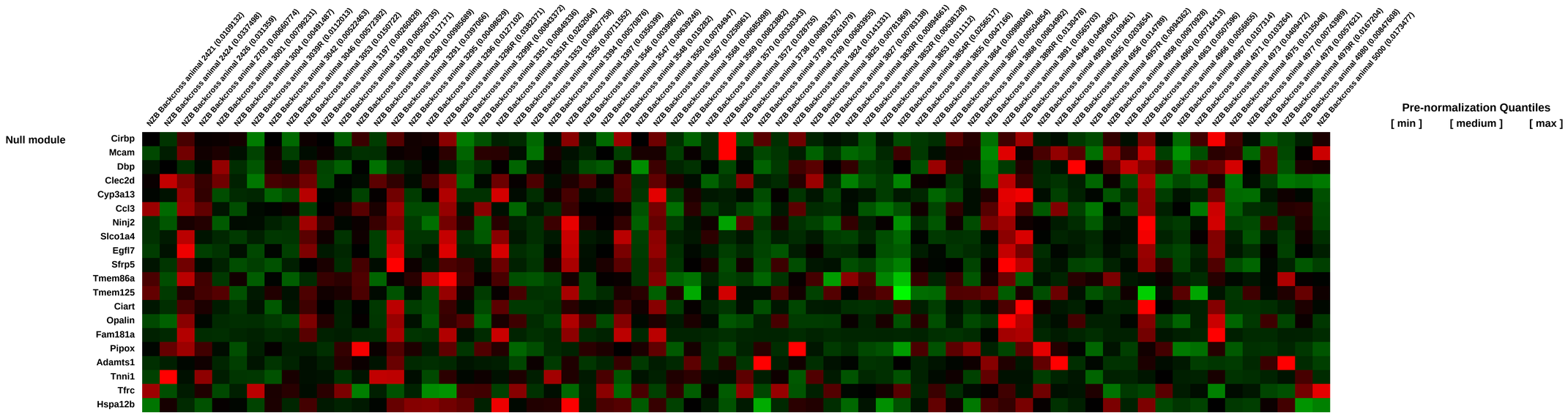

GEO Series "GSE42601" Expression Profiles

Num of samples in this series: 6

Scale of expression profile Z-scores

-3.0 -2.0 -1.0 0.0 1.0 2.0 3.0

GEO Link:	http://www.ncbi.nlm.nih.gov/geo/query/acc.cgi?acc=GSE42601
Status:	Public on Jun 01 2013
Title:	Expression data from wild-type and Dazap1 mutant mouse testes
Organism:	Mus musculus
Experiment type:	Expression profiling by array
Platform:	GPL1261
Pubmed ID:	23965306
Summary & Design:	**Summary:** Deleted in Azoospermia Associated Protein 1 (DAZAP1) is a ubiquitous RNA-binding protein that is highly expressed in the testis. It is a component of the hnRNP particles and shuttles between the nucleus and the cytoplasm. Mice expressing the DAZAP1-Fn mutant protein manifest both growth retardation and spermatogenic arrest before meiosis I. To elucidate the biological function(s) of DAZAP1 and to search for its natural RNA substrates, we compared the expression profiles of wild-type and Dazap1 mutant testes by cDNA microarrays. **Overall design:** We used wild-type and Dazap1 mutant mouse testes. Each genotype has three replicates. 6 total samples were analyzed.

Background corr dist: KL-Divergence = 0.0070, L1-Distance = 0.0271, L2-Distance = 0.0008, Normal std = 0.9770

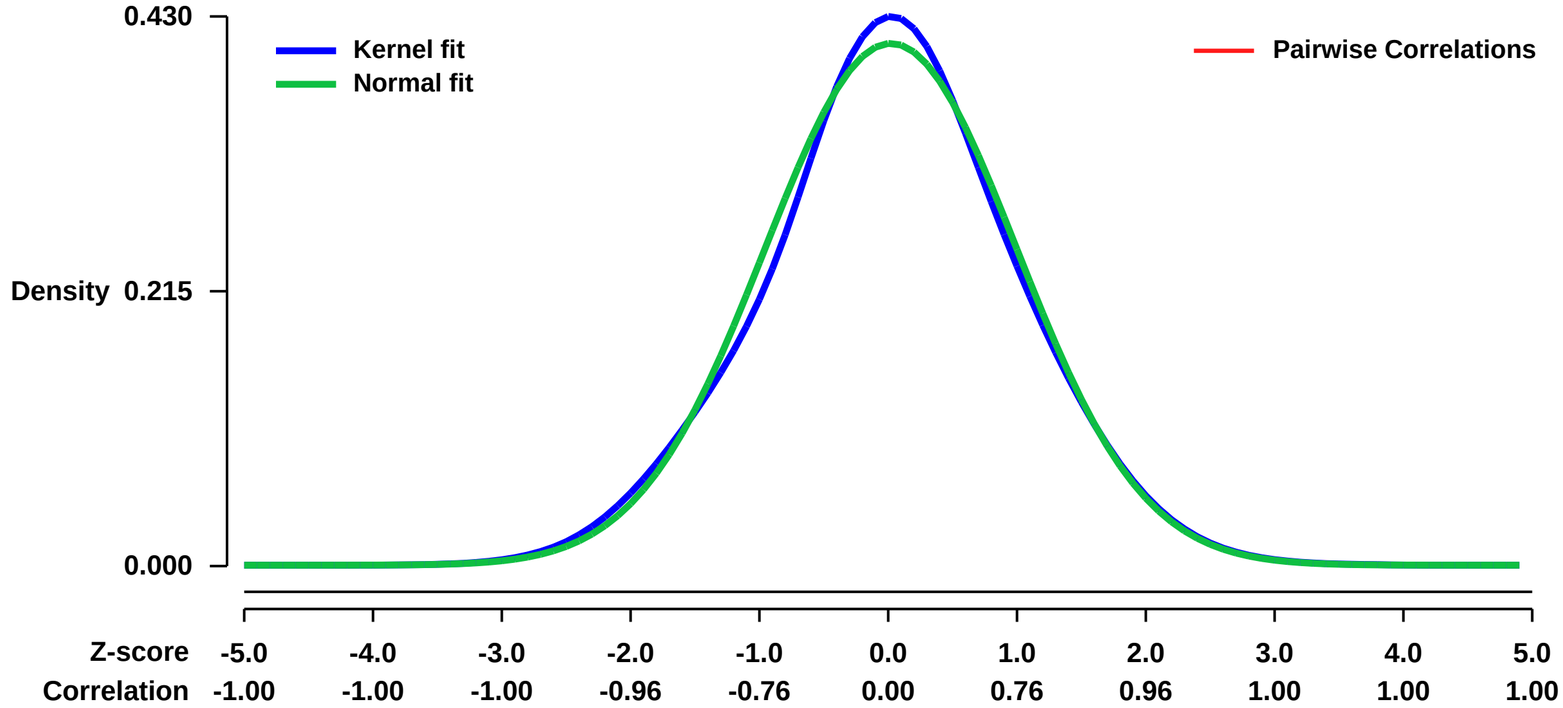

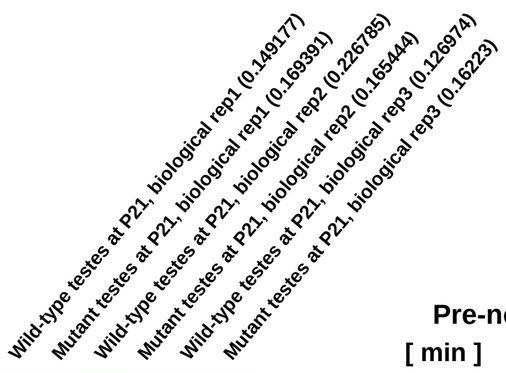

Pre-normalization Quantiles

[min] [medium] [max]

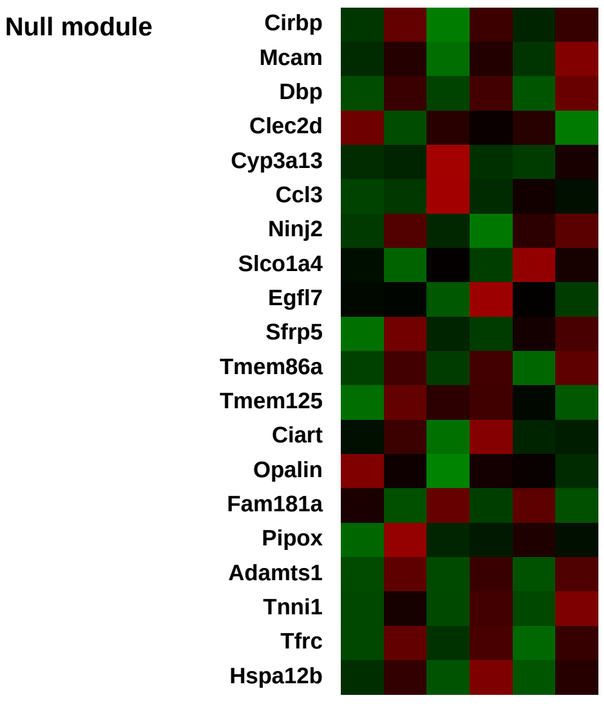

GEO Series "GSE24683" Expression Profiles

Num of samples in this series: 8

Scale of expression profile Z-scores

-3.0 -2.0 -1.0 0.0 1.0 2.0 3.0

GEO Link:	http://www.ncbi.nlm.nih.gov/geo/query/acc.cgi?acc=GSE24683
Status:	Public on Mar 31 2012
Title:	Dicer knockout mouse subcutaneous preadipocytes
Organism:	Mus musculus
Experiment type:	Expression profiling by array
Platform:	GPL1261
Pubmed ID:	22958919
Summary & Design:	**Summary:** Dicer is required for miRNA processing and RNA interference. Here we knocked out Dicer in SV40 T antigen immortalized subcutaneous preadipocytes isolated from Dicer flox mice by transducing these cells with adenoviruses harboring Cre recombinase. Control cells were transduced with adenovirus harboring GFP. We used microarrays to detail the gene expression profile of Dicer knockout preadipocytes. **Overall design:** Four days after adenovirus infection, cells were harvested for RNA isolation and hybridization on Affymetrix microarrays. At this point, Dicer knockout was confirmed by several methods.

Background corr dist: KL-Divergence = 0.0810, L1-Distance = 0.0212, L2-Distance = 0.0006, Normal std = 0.4734

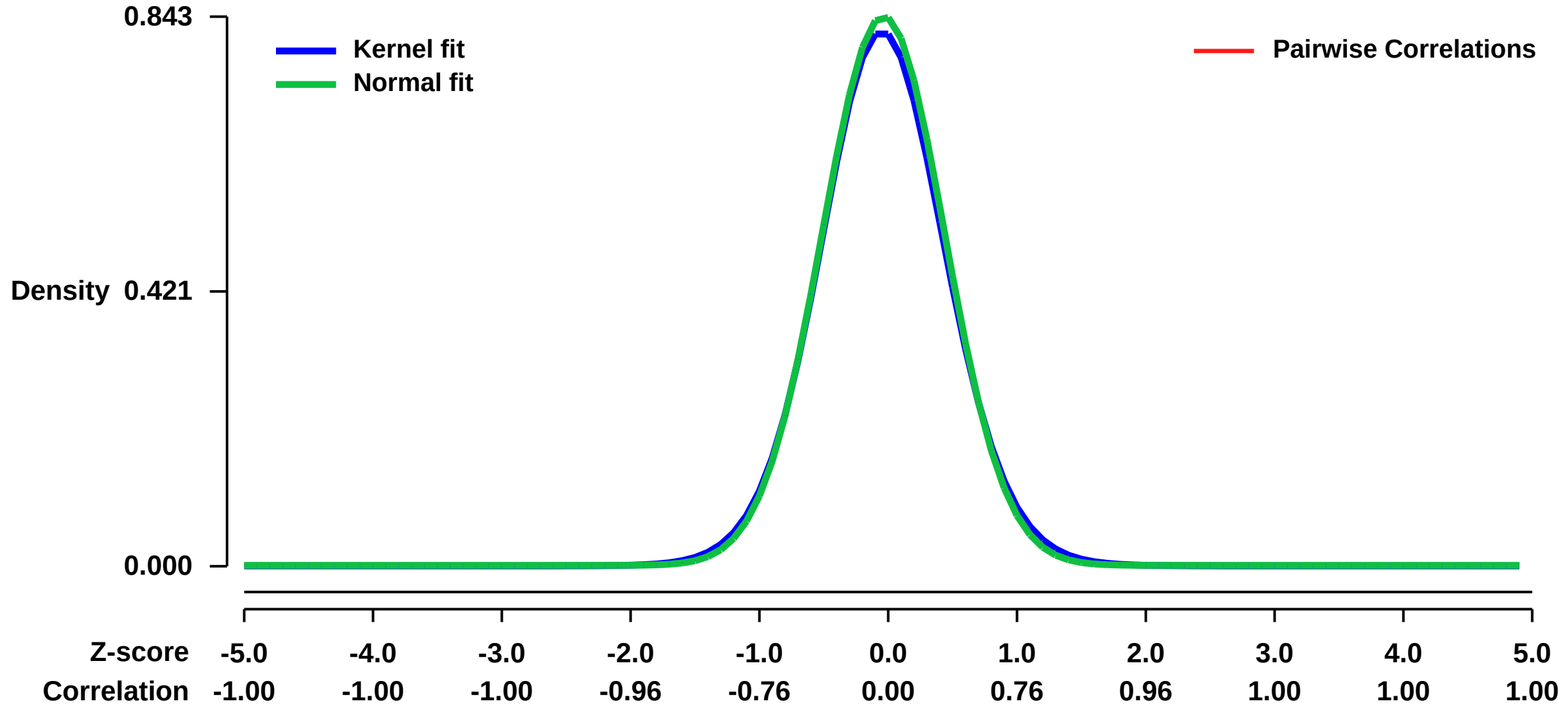

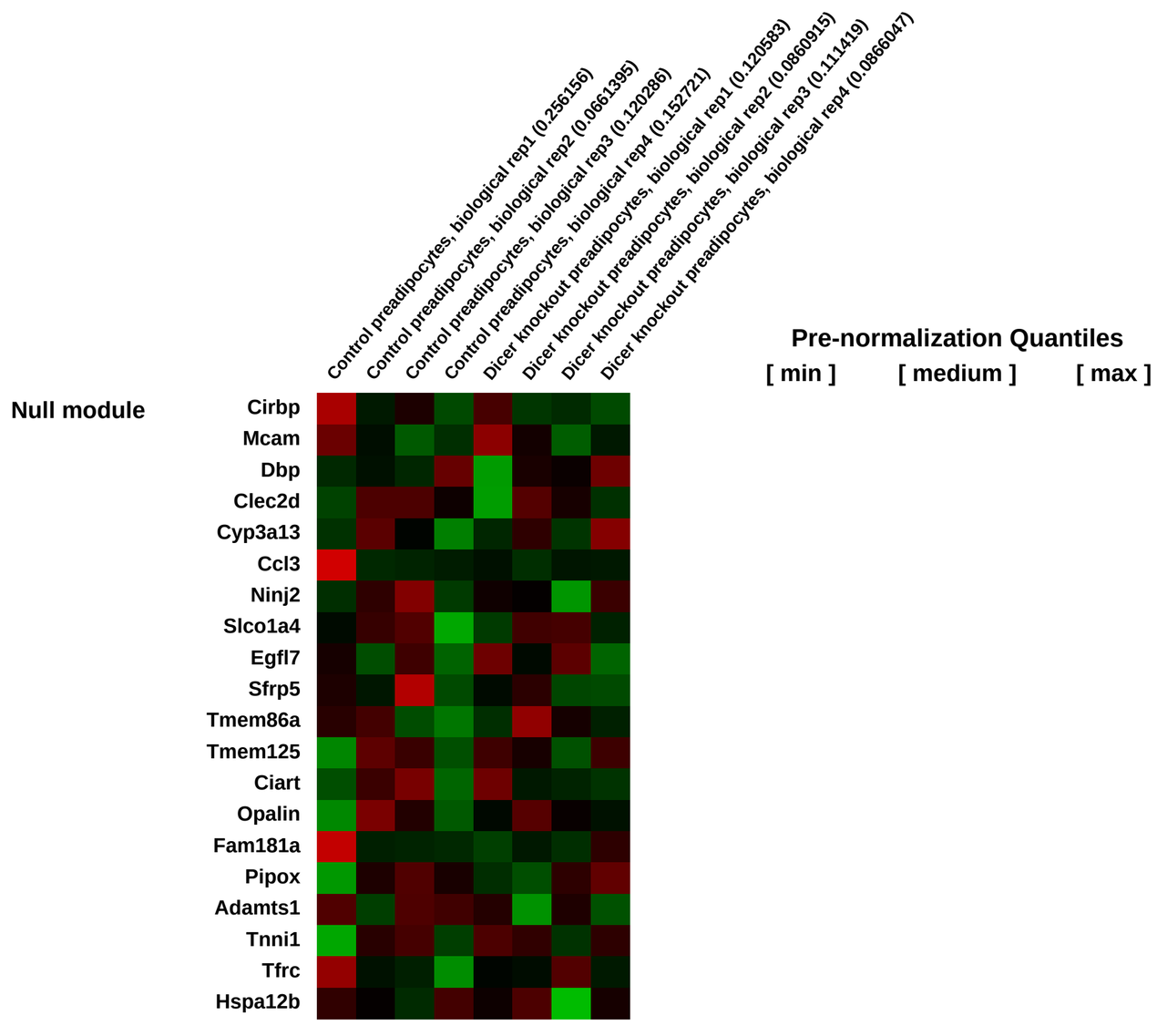

GEO Series "GSE50603" Expression Profiles

Num of samples in this series: 12

Scale of expression profile Z-scores

-3.0 -2.0 -1.0 0.0 1.0 2.0 3.0

GEO Link:	http://www.ncbi.nlm.nih.gov/geo/query/acc.cgi?acc=GSE50603
Status:	Public on Sep 05 2013
Title:	Effect of L-Proline on mouse embryonic stem cells (ESCs)
Organism:	Mus musculus
Experiment type:	Expression profiling by array
Platform:	GPL1261
Pubmed ID:	24319666
Summary & Design:	**Summary:** We found that the non-essential amino acid L-Proline (L-Pro) acts as a signaling molecule that promotes the conversion of embryonic stem cells (ESCs) into mesenchymal-like, spindle-shaped, highly motile, invasive pluripotent stem cells. This embryonic stem cell-to-mesenchymal-like transition (esMT) is accompanied by a genome-wide remodeling of the transcriptome We used microarrays to elucidate whether a diverse transcriptional program is the basis of the morphological and motility differences between ESCs and L- Proline treated ESCs (PiCs) **Overall design:** Total RNA was extracted from Control (ESCs) and L-Proline treated mouse embryonic stem cells (PiCs) and hybridized on Affimetrix microarrays.

Background corr dist: KL-Divergence = 0.0532, L1-Distance = 0.0337, L2-Distance = 0.0015, Normal std = 0.5680

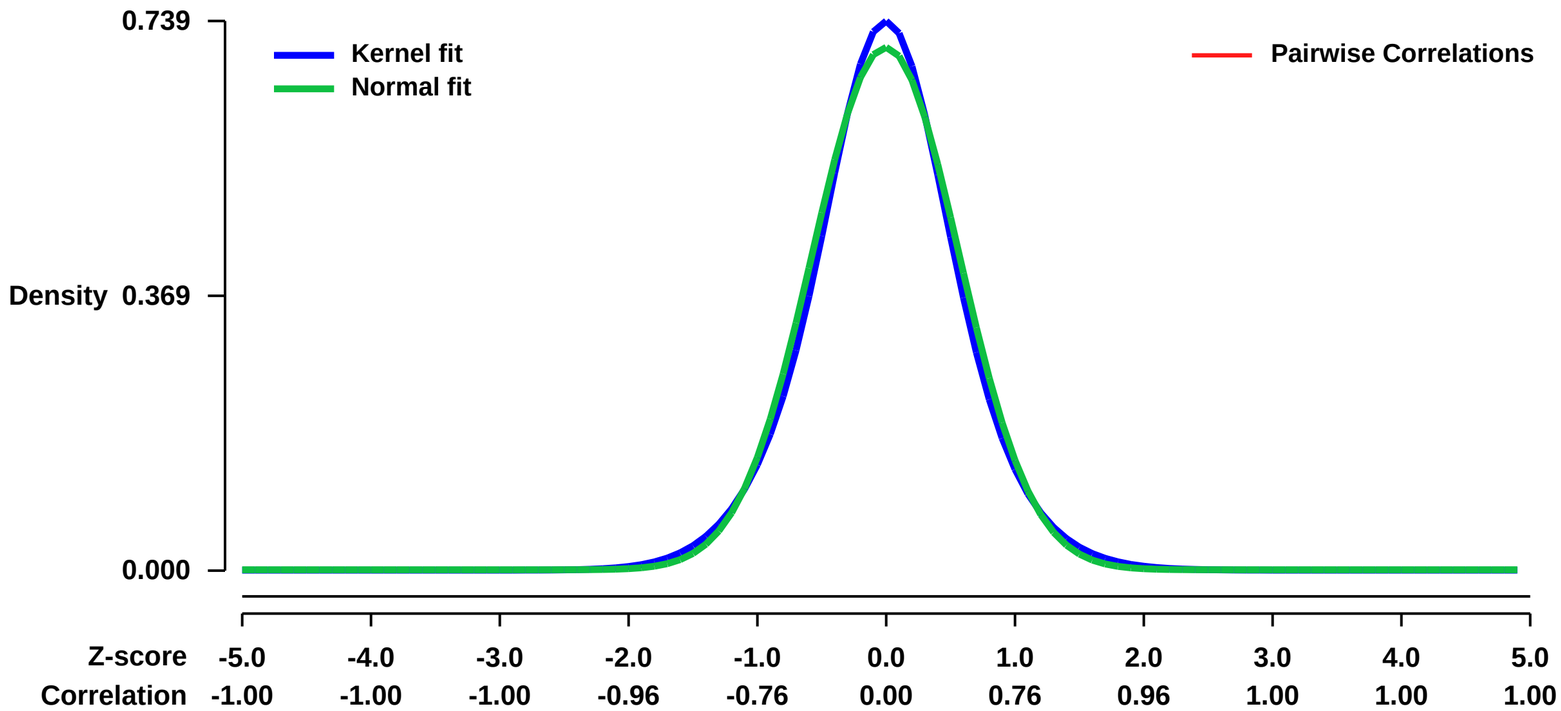

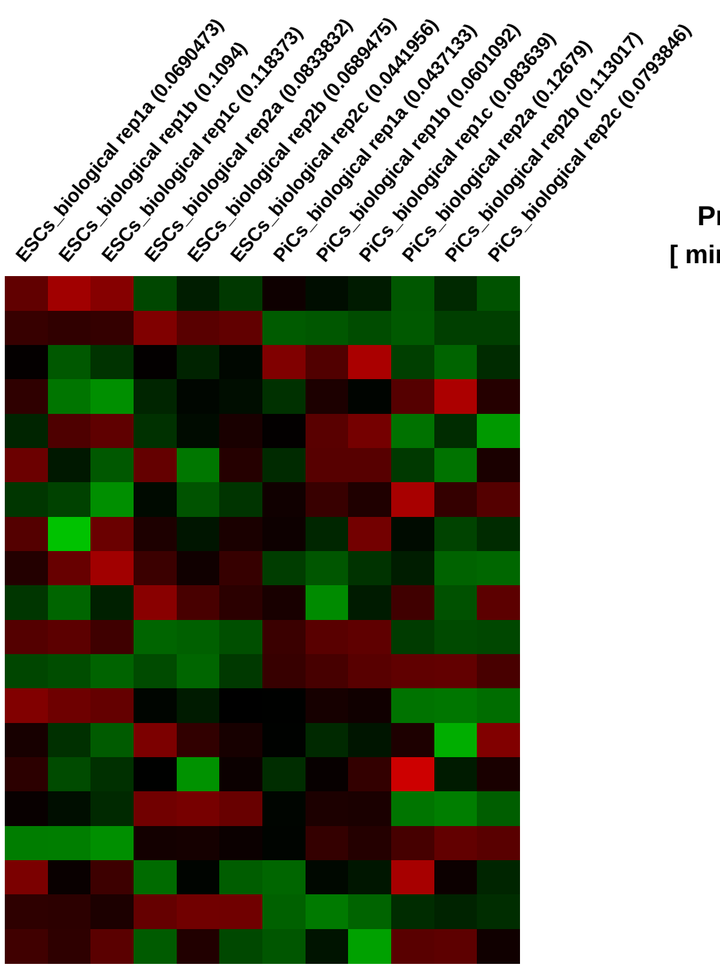

GEO Series "GSE38136" Expression Profiles

Num of samples in this series: 24

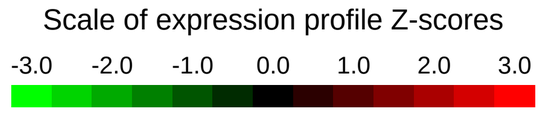

GEO Link:	http://www.ncbi.nlm.nih.gov/geo/query/acc.cgi?acc=GSE38136
Status:	Public on May 30 2012
Title:	Hepatic gene expression in BALB/c mice fed a quercetin diet
Organism:	Mus musculus
Experiment type:	Expression profiling by array
Platform:	GPL1261
Pubmed ID:	19496084
Summary & Design:	**Summary:** We showed that diets containing 0.1% or 0.5% quercetin lowered the STZ-induced increase in blood glucose levels and improved plasma insulin levels. A cluster analysis of the hepatic gene expressions showed that 0.5% quercetin diet suppressed STZ-induced alteration of gene expression. Gene set enrichment analysis (GSEA) and quantitative RT-PCR analysis showed that the quercetin diets had their greatest suppressive effect on the STZ-induced elevation of expression of cyclin dependent kinase inhibitor p21(WAF1/Cip1) (Cdkn1a). In this experiment, we determined the effect of quercetin on healthy control BALB/c mice that were fed the AIN93G diet containing 0, 0.1, 0.5 or 1% quercetin for 2 weeks. GSEA and one-way ANOVA did not detect any significant changes in hepatic gene expression in normal mice as a result of a quercetin diet. Using a linear modeling approach and the empirical Bayes statistics, we found that Ubc were significantly reduced by both the 0.5% and 1% quercetin. **Overall design:** Six-week-old male mice were divided into 4 groups of 6 mice each, housed in groups of 3 per cage, and fed a standard purified AIN-93G diet containing 0% (Control), 0.1% (0.1), 0.5% (0.5), or 1% quercertin (1.0) for 2 weeks.

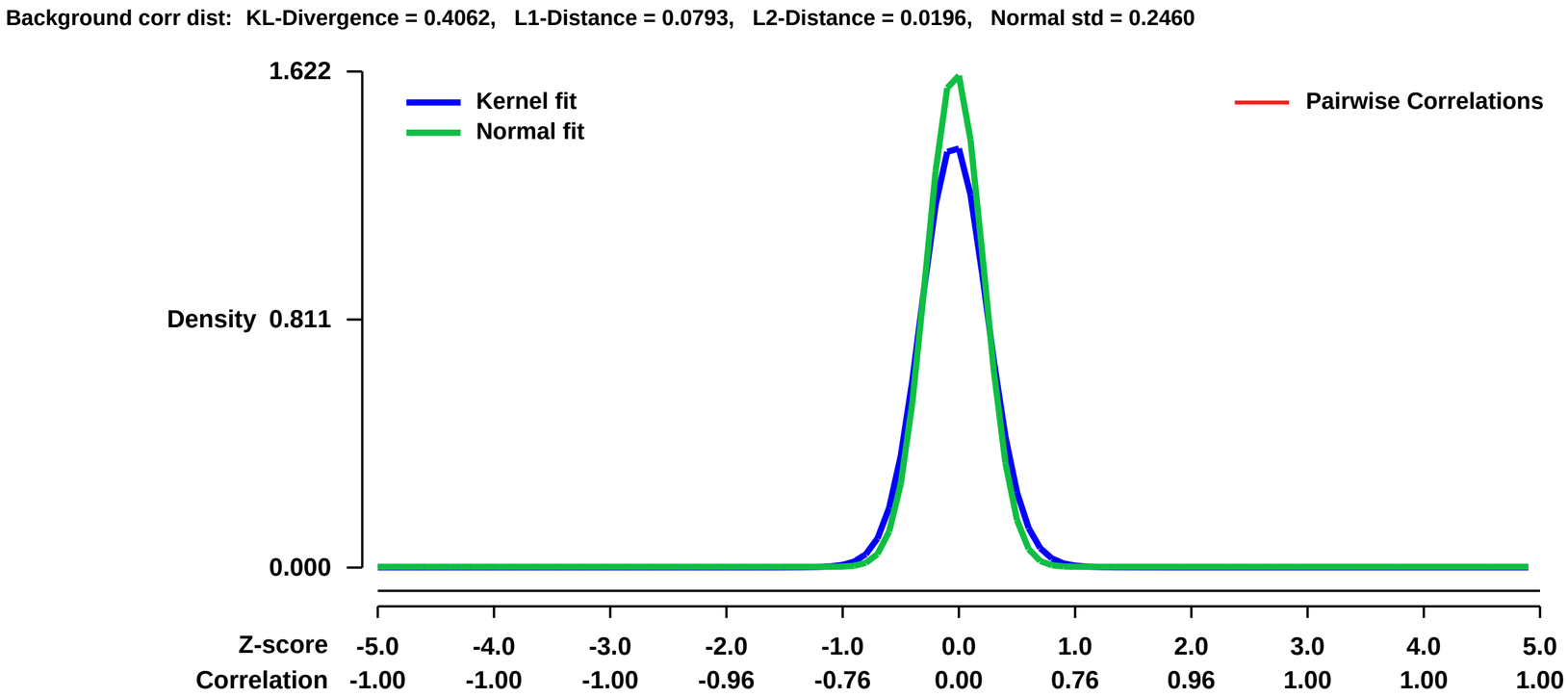

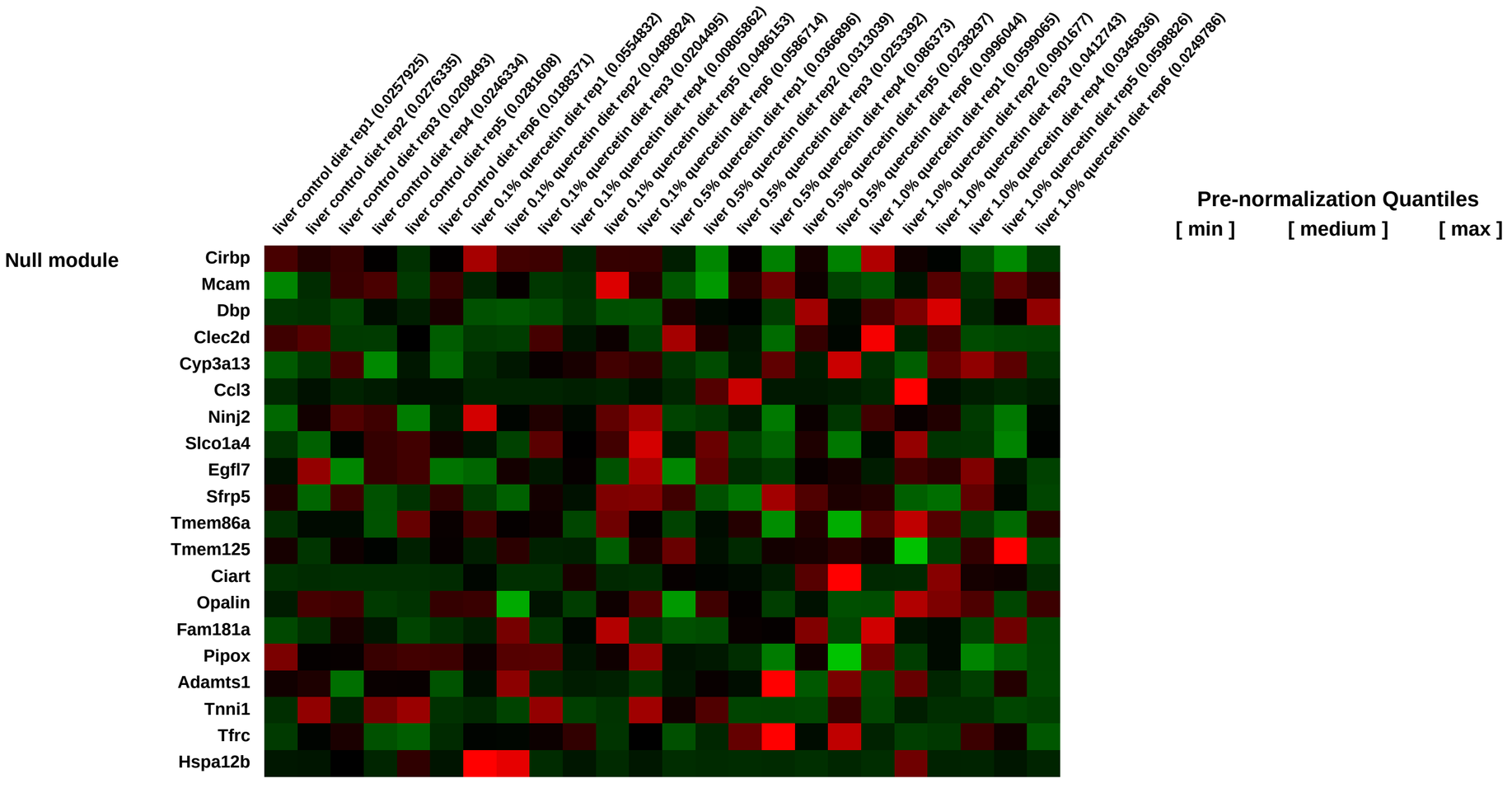

GEO Series "GSE28093" Expression Profiles

Num of samples in this series: 6

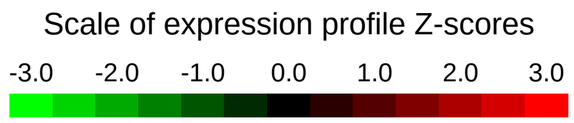

GEO Link:	**http://www.ncbi.nlm.nih.gov/geo/query/acc.cgi?acc=GSE28093**
Status:	**Public on Jun 01 2011**
Title:	**Expression profile of OPC senescence**
Organism:	**Mus musculus**
Experiment type:	**SNP genotyping by SNP array**
Platform:	**GPL1261**
Pubmed ID:	**20404145**
Summary & Design:	**Summary:** **To identify factors involved in OPC senescence, we compared gene expressions between OPC-CG4, OPC-FCS and OPC-Rev.** **Overall design:** **We established OPC senescence model system, in which OPC become senescent in the presence of high concentration of FCS. This phenotypes were kept even when the medium was switched to their optimal serum-free medium.**

Background corr dist: **KL-Divergence = 0.0321, L1-Distance = 0.0147, L2-Distance = 0.0002, Normal std = 0.6545**

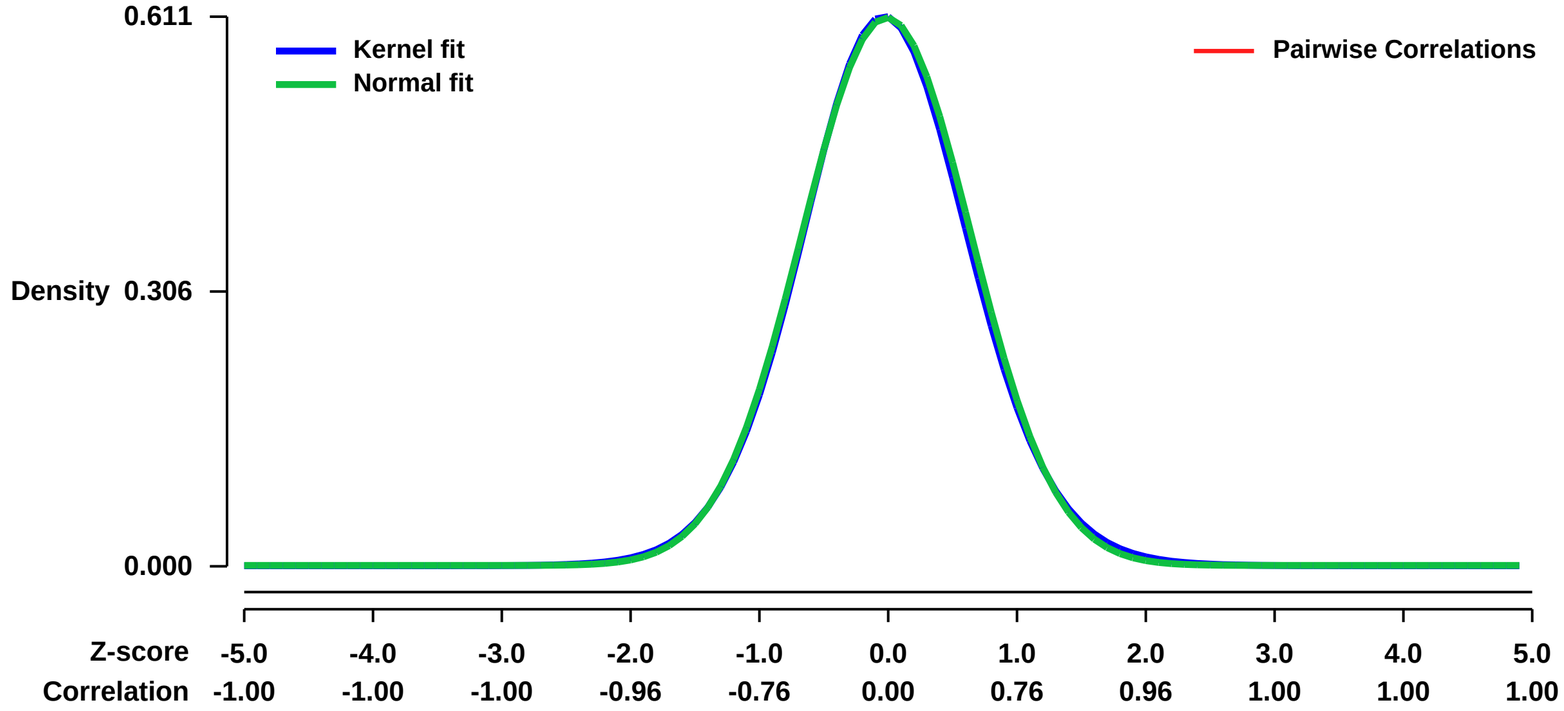

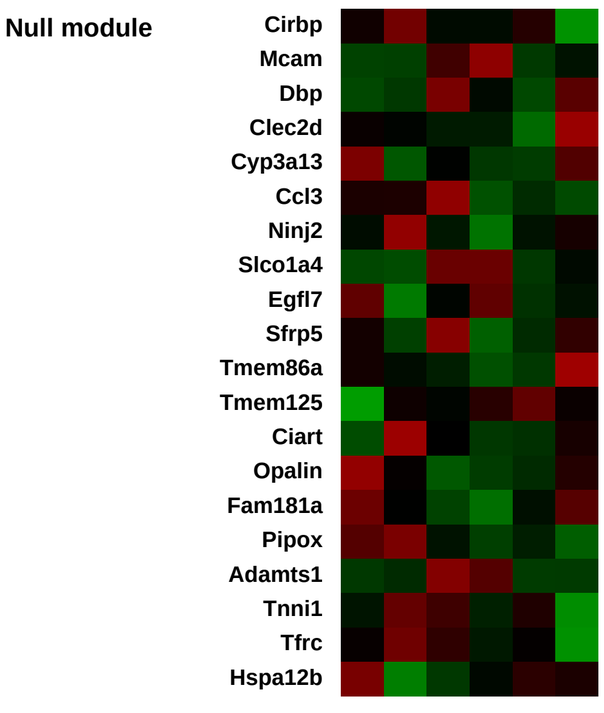

GEO Series "GSE11434" Expression Profiles

Num of samples in this series: 10

Scale of expression profile Z-scores

-3.0 -2.0 -1.0 0.0 1.0 2.0 3.0

GEO Link:	http://www.ncbi.nlm.nih.gov/geo/query/acc.cgi?acc=GSE11434
Status:	Public on May 15 2008
Title:	Ventilator-induced lung injury in C57BL\6 mice
Organism:	Mus musculus
Experiment type:	Expression profiling by array
Platform:	GPL1261
Pubmed ID:	19447895
Summary & Design:	**Summary:** This study was undertaken to examine differential gene expression across the whole genome during short-term ventilator-induced lung injury in mice, a commonly used model of acute lung injury, as compared with spontaneous ventilation. **Keywords: Disease state analysis** **Overall design:** Mice were anesthetized with isoflurane followed by ketamine/xylaxine. Saline (0.25 ml) was given every hour ip. A tracheotomy tube was placed and the mice were ventilated with an initial peak airway pressure of 20 cmH2O approximating a tidal volume of 20 ml/kg and without end-expiratory pressure. Ventilation was continued for 3h. Tidal volume was not adjusted. Body temperature was monitored with a digital rectal thermometer and maintained at 37C with a heating table and external heating lamp. Control mice were treated identically, but were not mechanically ventilated (i.e. breathed spontaneously). There were 5 biological relicates in each group.

Background corr dist: KL-Divergence = 0.1024, L1-Distance = 0.0264, L2-Distance = 0.0012, Normal std = 0.4335

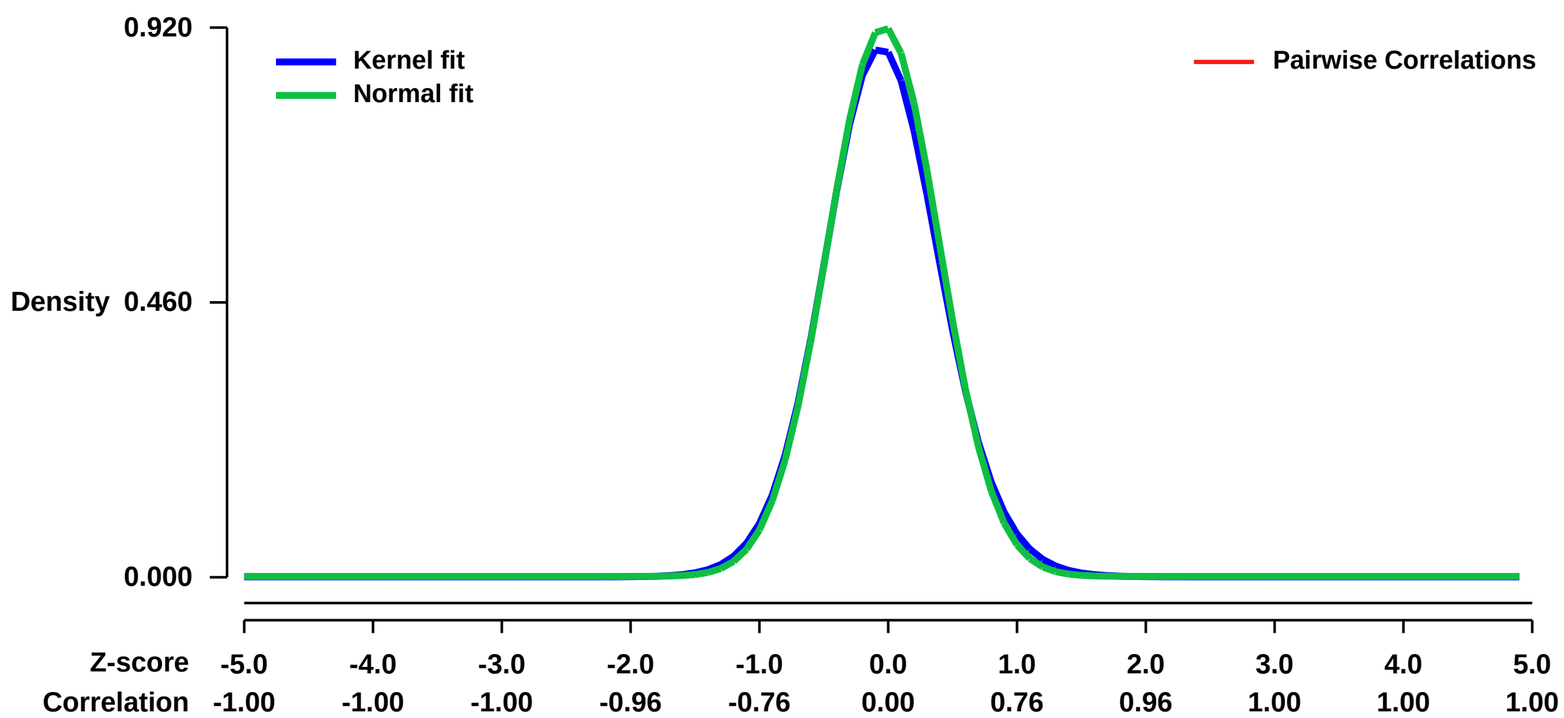

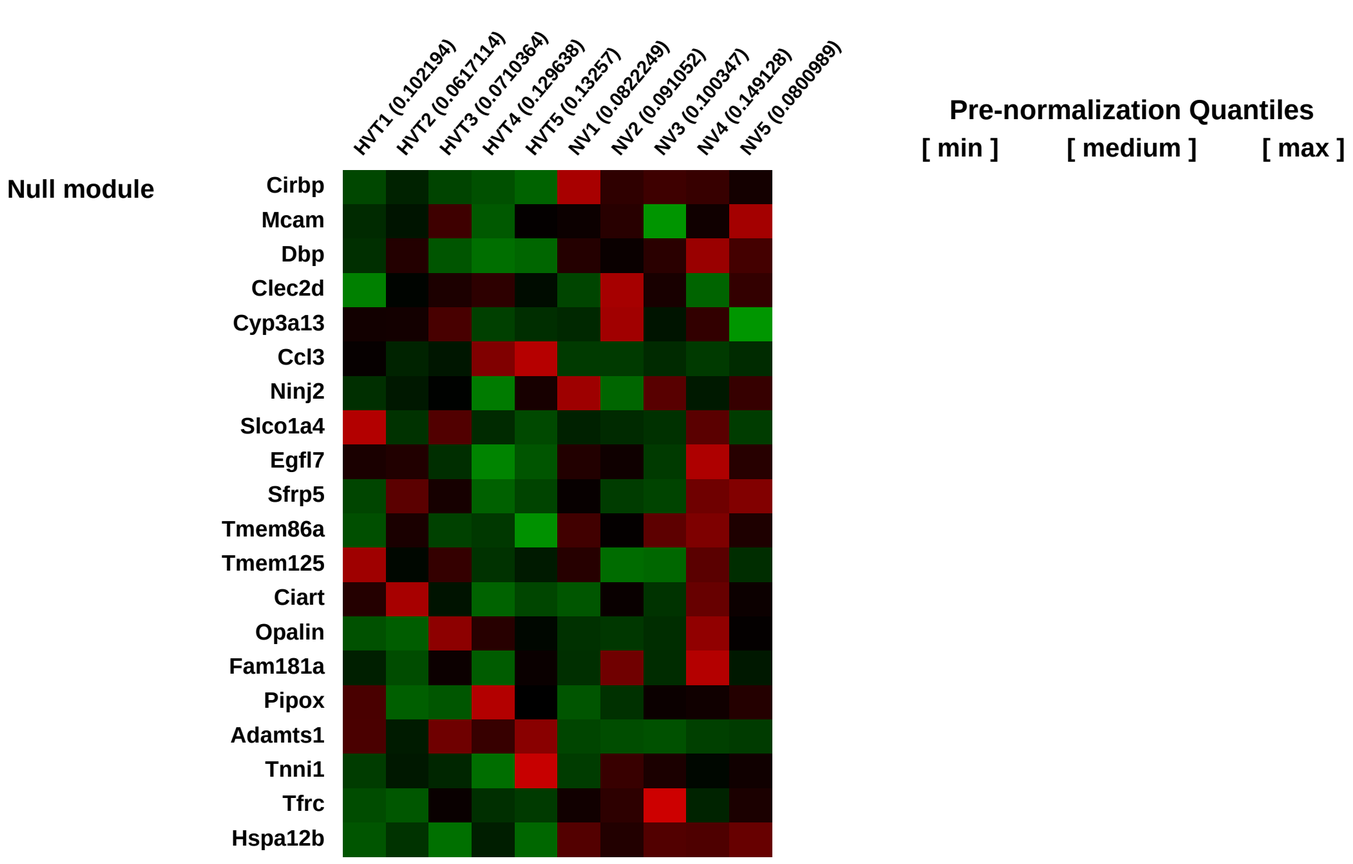

GEO Series "GSE37415" Expression Profiles

Num of samples in this series: 24

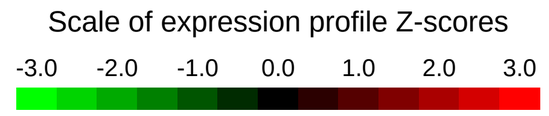

GEO Link:	http://www.ncbi.nlm.nih.gov/geo/query/acc.cgi?acc=GSE37415
Status:	Public on May 18 2012
Title:	Phloridzin reduces blood glucose levels and alters hepatic gene expression in normal BALB/c mice
Organism:	Mus musculus
Experiment type:	Expression profiling by array
Platform:	GPL1261
Pubmed ID:	22538082
Summary & Design:	**Summary:** We previously showed that a diet containing phloridzin suppressed the blood glucose levels in streptozotocin-induced diabetic mice most likely by inhibiting glucose absorption from the small intestine. In this study, we showed that 0.5% and 1% phloridzin diets significantly reduce the blood glucose levels in healthy normal BALB/c mice after 7 days of feeding. To understand the effect of the high continuing intake of dietary phloridzin on normal mouse livers, we analyzed the hepatic gene expressions in mice fed diets containing 0%, 0.1%, 0.5%, or 1% phloridzin for 14 days using DNA microarrays. **Overall design:** Six-week-old male mice were divided into 4 groups of 6 mice each, housed in groups of 3 per cage, and fed a standard purified AIN-93G diet containing 0% (Con), 0.1% (Phlorizin0.1), 0.5% (Phlorizin0.5), or 1% phloridzin (purity > 97%) (Phlorizin1.0) for 2 weeks.

Background corr dist: KL-Divergence = 0.2189, L1-Distance = 0.0354, L2-Distance = 0.0021, Normal std = 0.3236

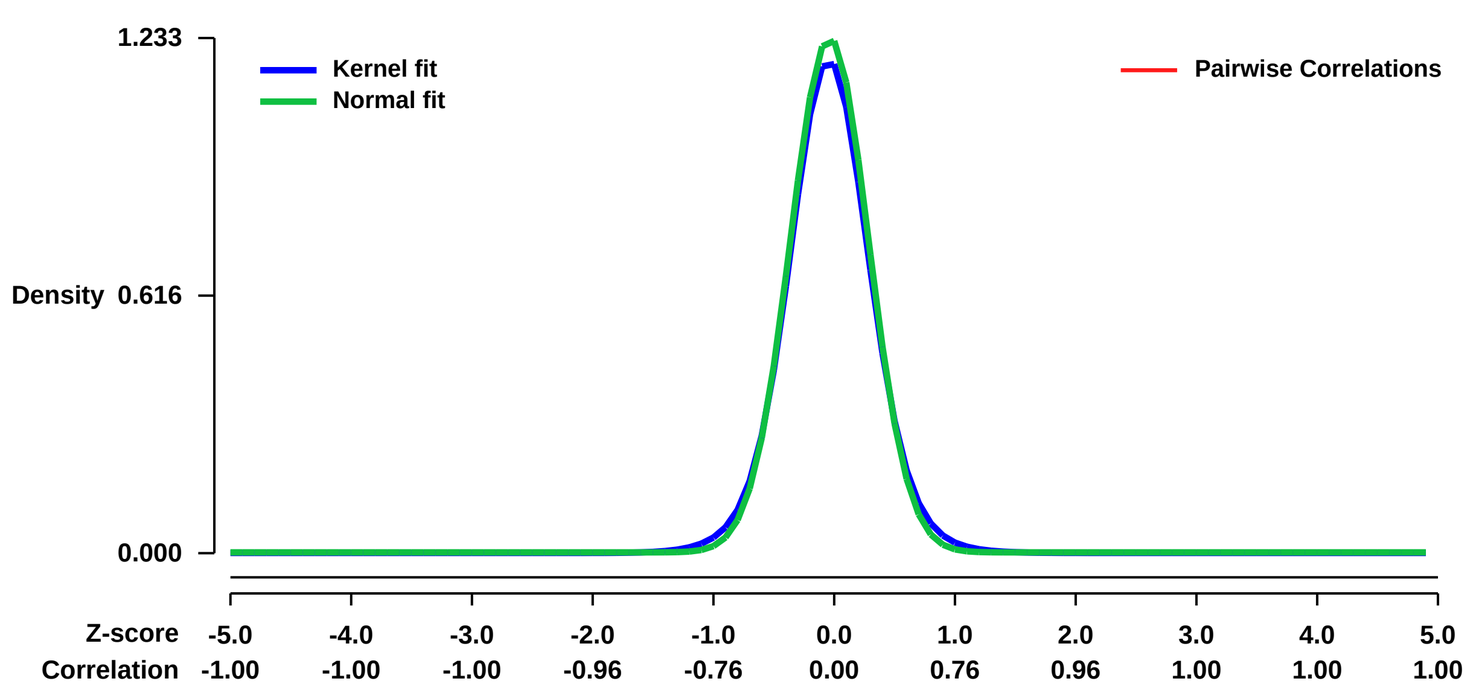

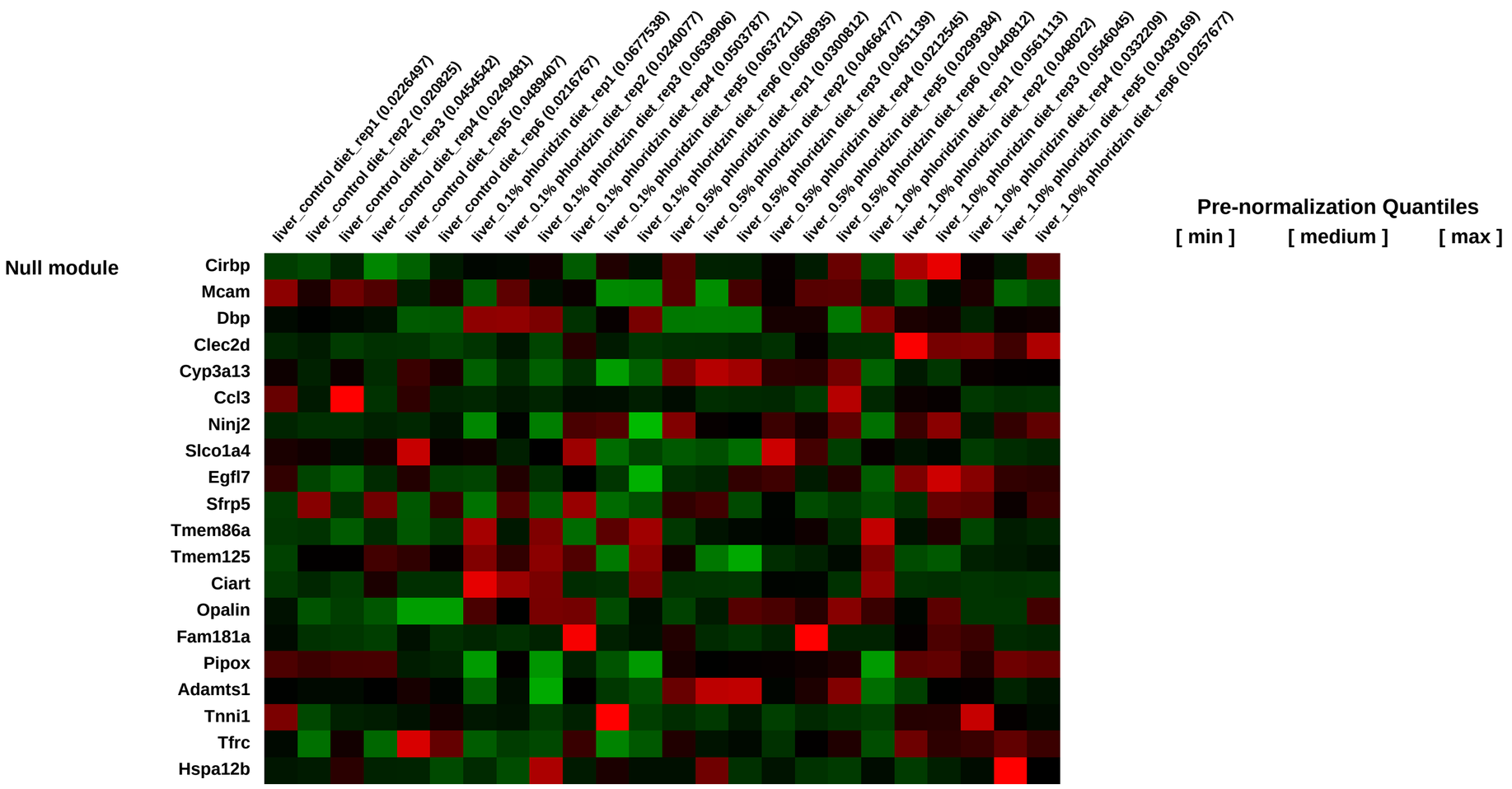

GEO Series "GSE27195" Expression Profiles

Num of samples in this series: 6

Scale of expression profile Z-scores

-3.0 -2.0 -1.0 0.0 1.0 2.0 3.0

GEO Link:	http://www.ncbi.nlm.nih.gov/geo/query/acc.cgi?acc=GSE27195
Status:	Public on Sep 01 2011
Title:	Ciliary neurotrophic factor induces genes associated with inflammatory response and gliosis in the retina: A gene profiling study of flow-sorted, Muller (glial) cells
Organism:	Mus musculus
Experiment type:	Expression profiling by array
Platform:	GPL1261
Pubmed ID:	21637858
Summary & Design:	**Summary:** Our data suggest that CNTF remodels the transcription profile of Mˆ…ller (glial) cells leading to induction of networks associated with transcription, cell cycle regulation and inflammatory response. CNTF also appears to function as an inducer of gliosis in the retina. These studies provide new insights into the biological functions of cytokines in the retina. **Overall design:** Muller glial cells treated with CNTF for 1 and 3 days

Background corr dist: KL-Divergence = 0.0457, L1-Distance = 0.0255, L2-Distance = 0.0008, Normal std = 0.5956

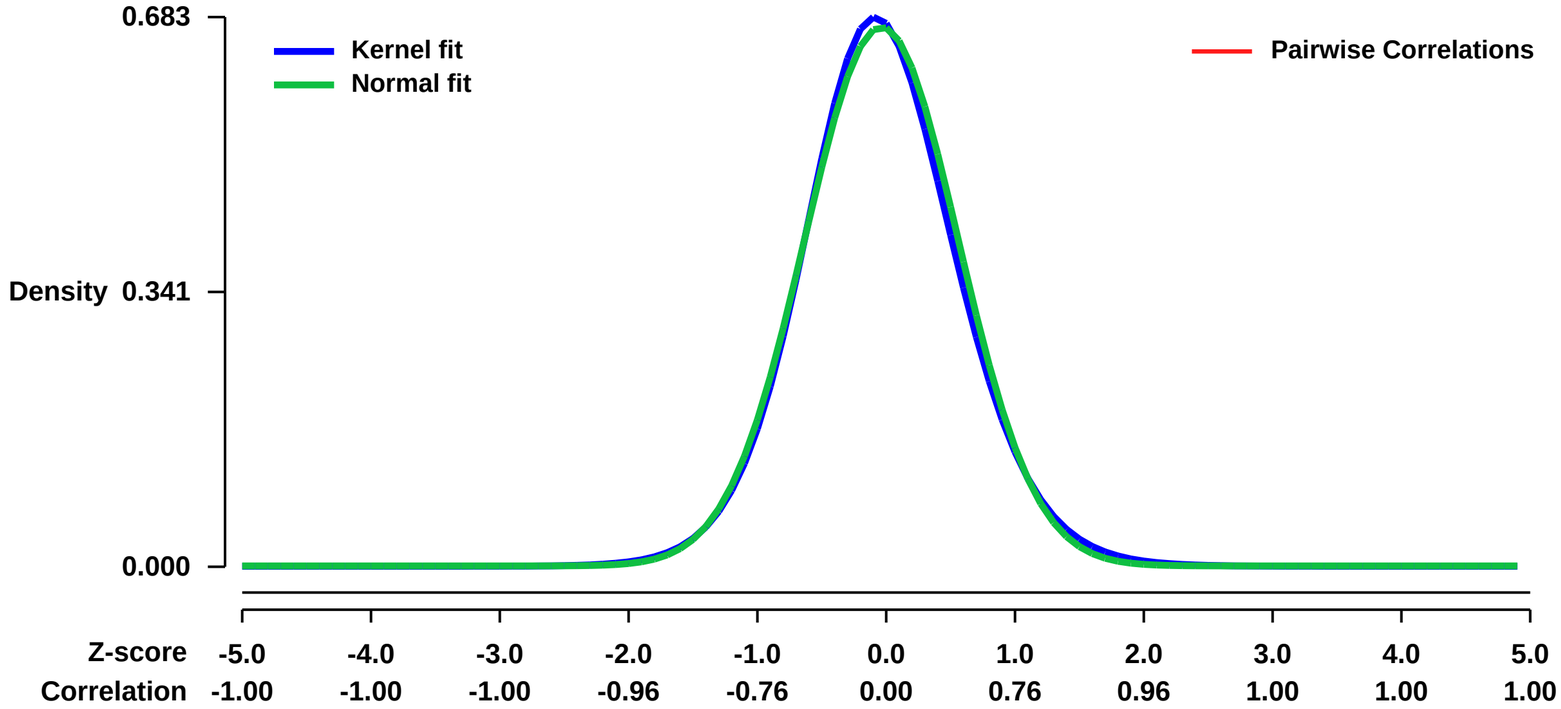

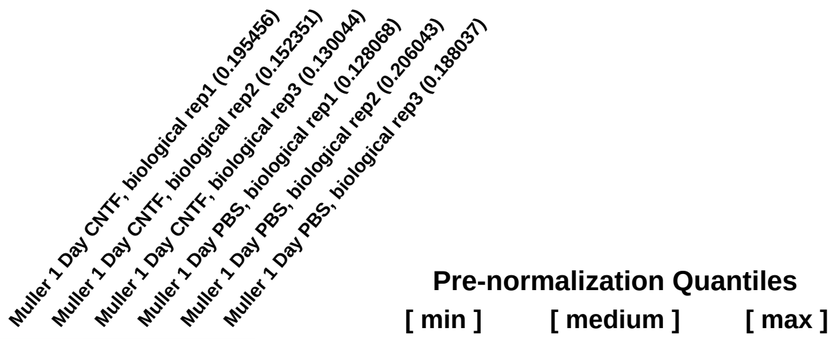

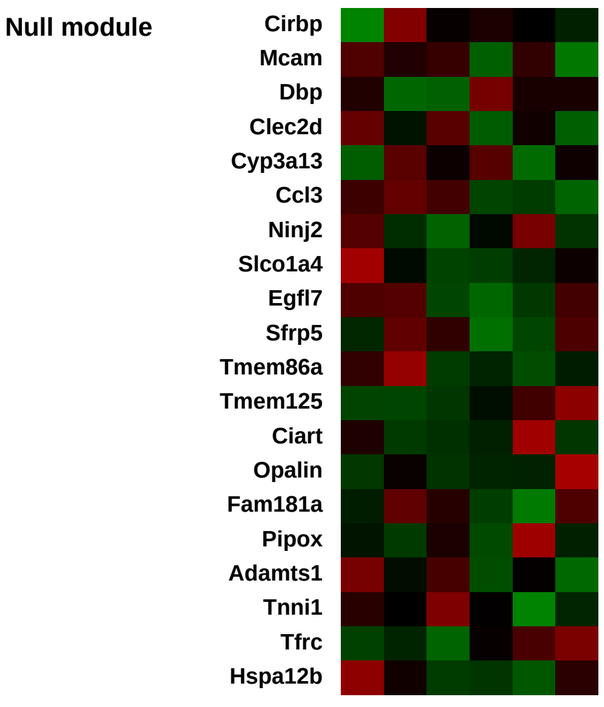

GEO Series "GSE8788" Expression Profiles

Num of samples in this series: 6

Scale of expression profile Z-scores

-3.0 -2.0 -1.0 0.0 1.0 2.0 3.0

GEO Link:	http://www.ncbi.nlm.nih.gov/geo/query/acc.cgi?acc=GSE8788
Status:	Public on Aug 17 2007
Title:	Comparison of gene expression pattern between Wild-type and Trib1-deficient mice (Gene chip data for JEM 20070183)
Organism:	Mus musculus
Experiment type:	Expression profiling by array
Platform:	GPL1261
Pubmed ID:	17724128
Summary & Design:	**Summary:** The purpose of this experiment was to compare the gene expression pattern between wild-type and Trib1-deficient macrophages in response to LPS. **Keywords: Comparison of gene expression pattern between Wild-type and Trib1-deficient mice** **Overall design:** Two samples to define ""LPS-inducible gene"" and 4 samples (2 for wild-type and the rests for Trib1-deficient mice) for comparison.

Background corr dist: KL-Divergence = 0.0435, L1-Distance = 0.0258, L2-Distance = 0.0009, Normal std = 0.6043

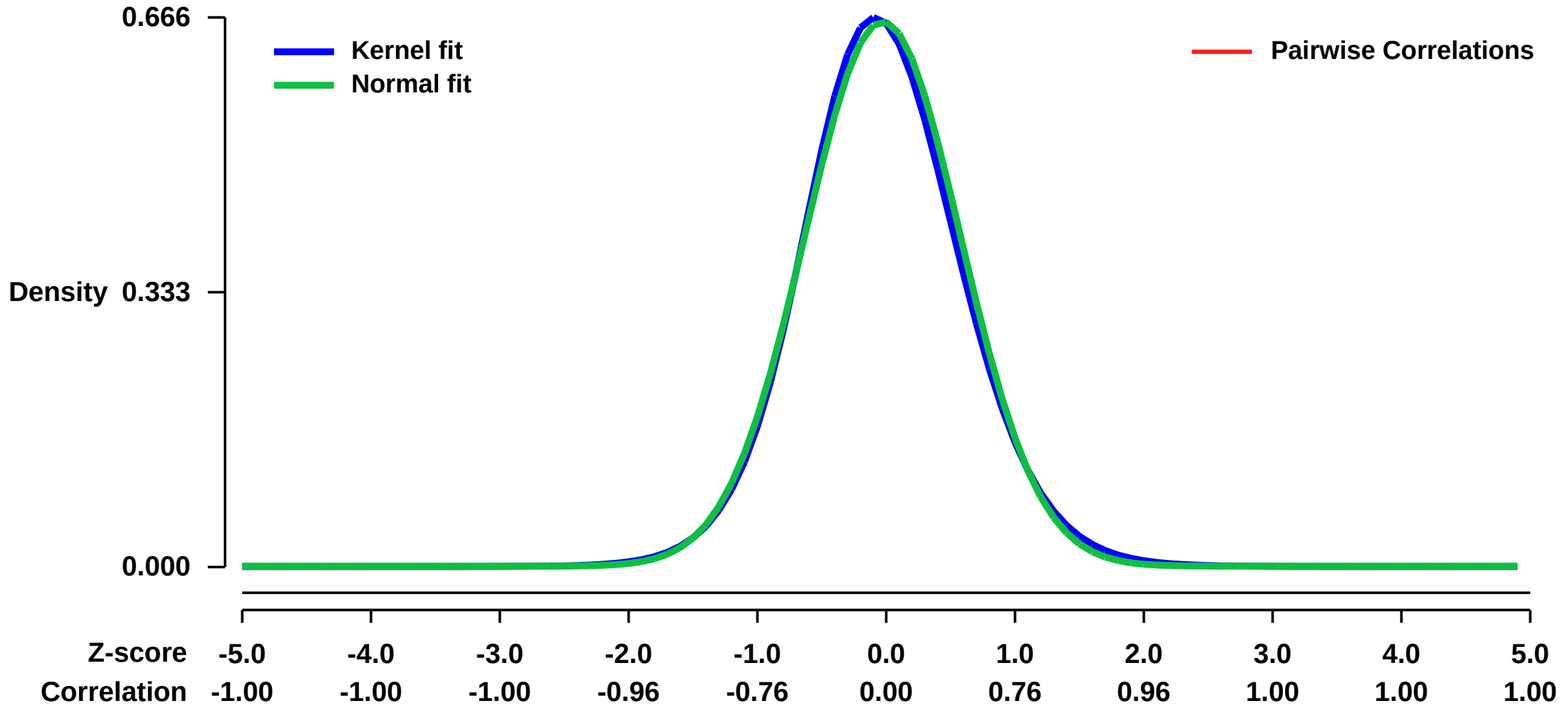

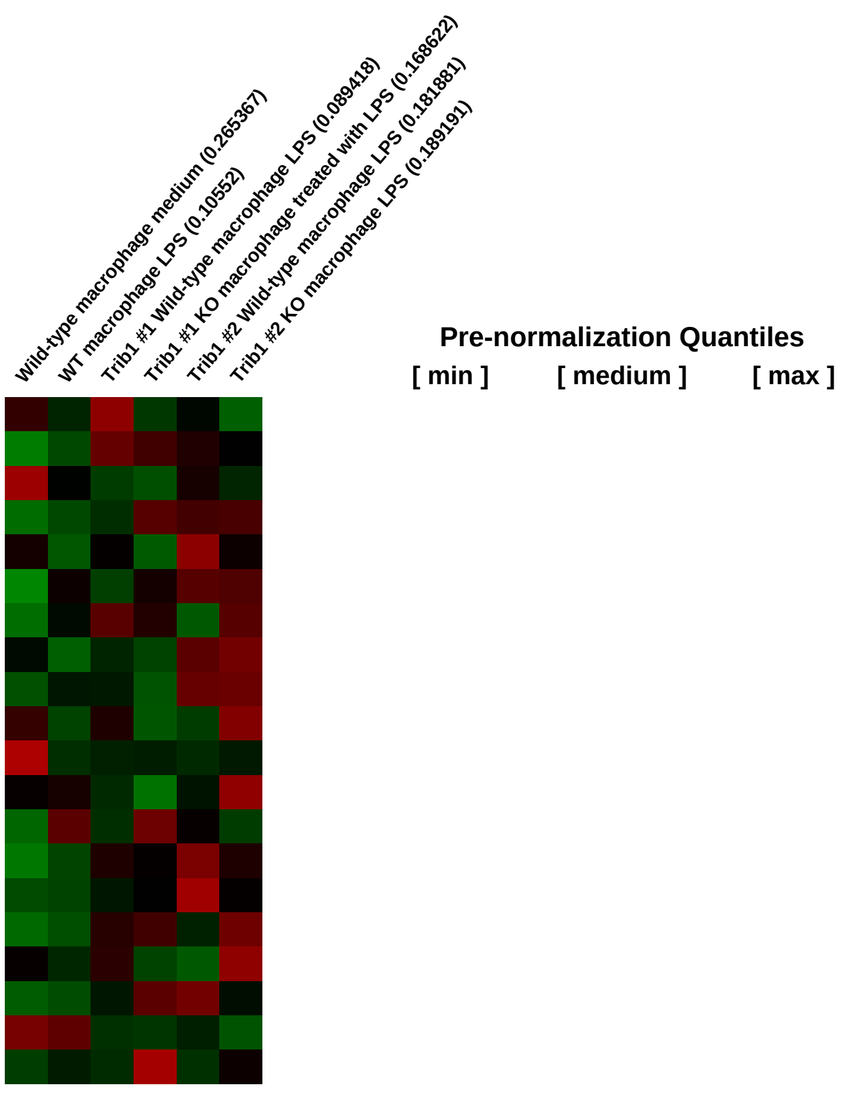

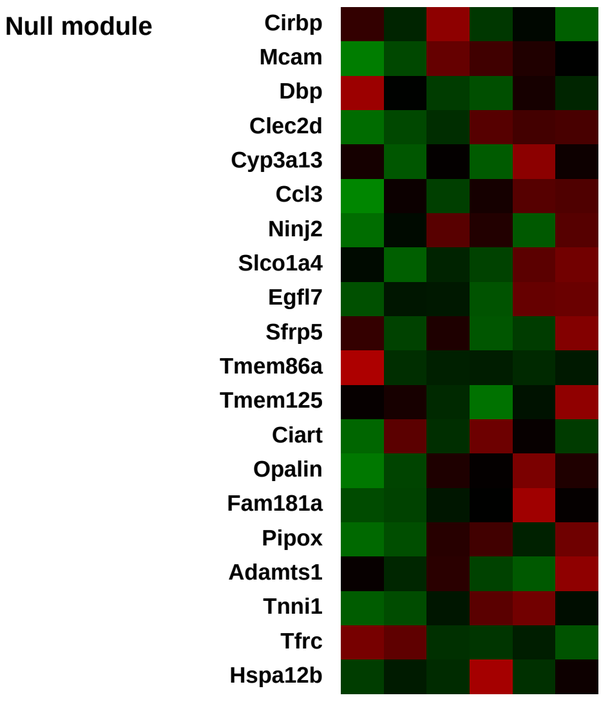

GEO Series "GSE43620" Expression Profiles

Num of samples in this series: 8

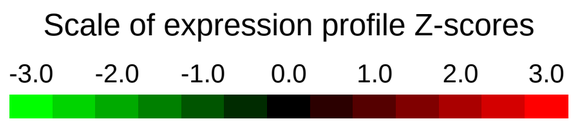

GEO Link:	http://www.ncbi.nlm.nih.gov/geo/query/acc.cgi?acc=GSE43620
Status:	Public on Jan 19 2014
Title:	Effects of sodium tungstate administration in Irs2 -/- mice
Organism:	Mus musculus
Experiment type:	Expression profiling by array
Platform:	GPL1261
Pubmed ID:	24253047
Summary & Design:	**Summary:** Relative beta cell deficit and increased beta cell apoptosis are hallmarks of type 2 diabetes (T2D). The Insulin/Insulin Growth Factor (Igf) signaling pathway is an established regulator of beta cell survival and is found downregulated in human T2D islets. The Insulin Receptor Substrate 2 (Irs2) plays a central role in the coordination of this pathway in beta cells. Thus, Irs2 knockout mice (Irs2 -/-) exhibit increased beta cell apoptosis that leads to a progressive decline of beta cell mass and hyperglycaemia. In this study, we sought to determine whether the anti-diabetic compound sodium tungstate could prevent the onset of diabetes in Irs2 -/- mice. Oral administration of tungstate resulted in an overall improvement in whole-body glucose tolerance in Irs2 -/- mice which correlated with increased beta cell mass. Enhanced beta cell mass was due to a dramatic reduction of beta cell apoptosis without changes in proliferation. Whole genome gene profiling analysis of islets isolated from treated Irs2 -/- mice confirmed a broad impact of tungstate on cell death pathways. Mechanistically, tungstate induced Erk1/2 phosphorylation in islets in vitro and, in agreement, treated Irs2 -/- islets exhibited increased basal Erk1/2 phosphorylation. Tungstate also downregulated expression of apoptosis-related genes in Irs2-/- islets in vitro, uncovering a direct effect of this compound in islets. All together, our data demonstrate that tungstate can restore beta cell mass and glucose homeostasis in a context of deficient Insulin/Igf signaling. This study underscores the importance of developing strategies specifically designed to arrest beta cell apoptosis as a means to prevent progressive beta cell failure in diabetes. **Overall design:** 10-week old WT and Irs2 -/- mice were randomly divided into two treatment group, in a total of 4 experimental groups. For 21 days one group received distilled water as drinking water (untreated group) whilst the other received ad libitum a solution of 2mg/ml of sodium tungstate in distilled water (treated group). For each experimental group 2 independent samples were analysed, in a total of 8 samples.

Background corr dist: KL-Divergence = 0.0481, L1-Distance = 0.0167, L2-Distance = 0.0003, Normal std = 0.5662

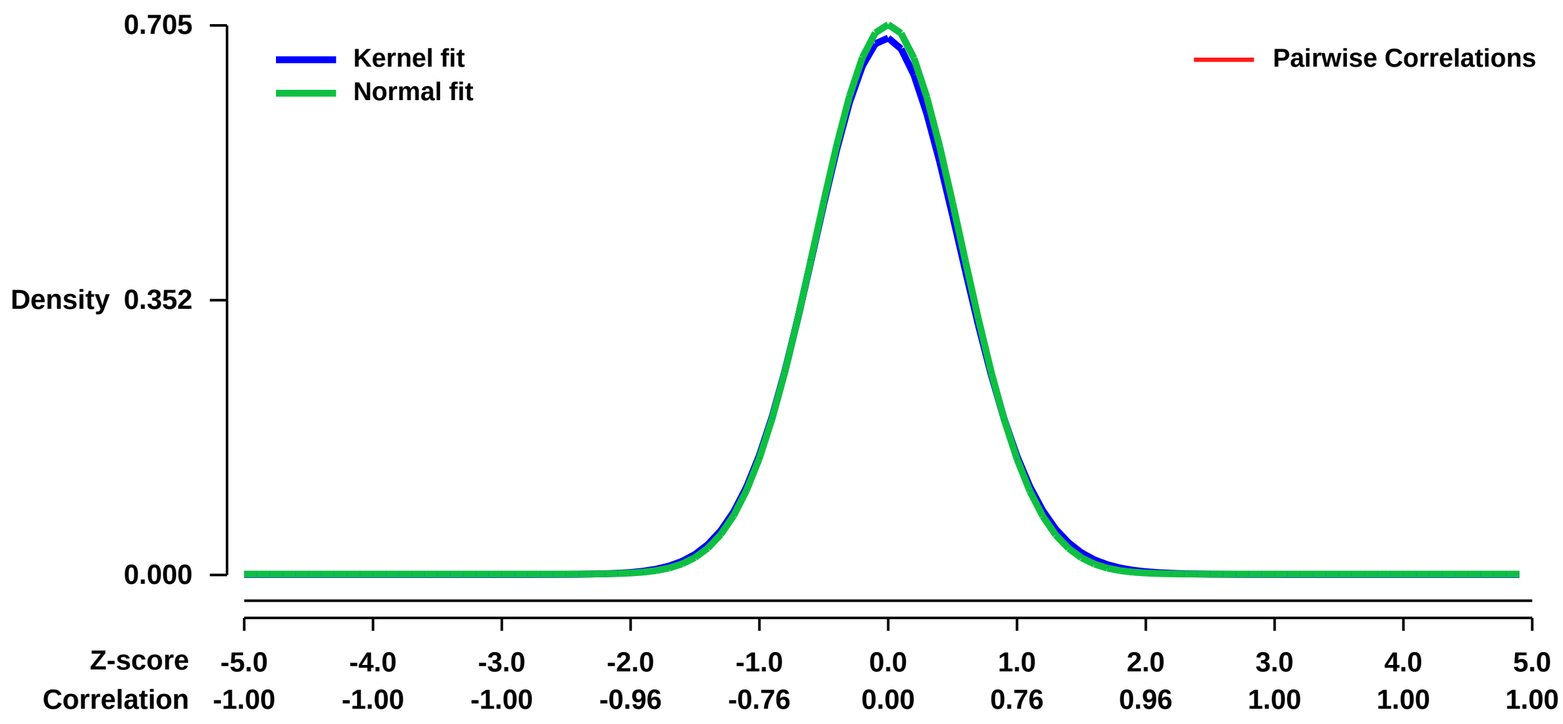

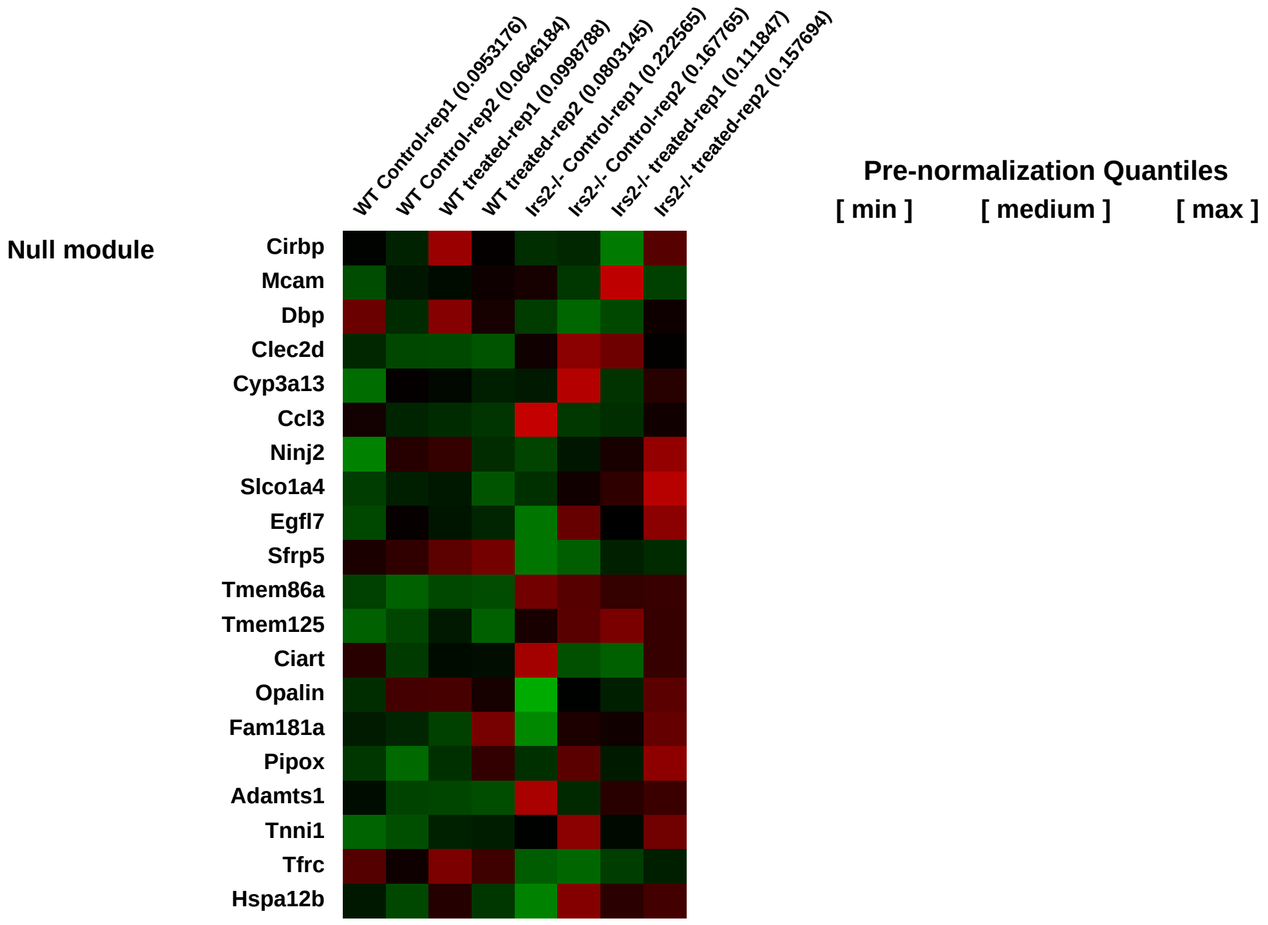

GEO Series "GSE26096" Expression Profiles

Num of samples in this series: 10

Scale of expression profile Z-scores

-3.0 -2.0 -1.0 0.0 1.0 2.0 3.0

GEO Link:	http://www.ncbi.nlm.nih.gov/geo/query/acc.cgi?acc=GSE26096
Status:	Public on Jan 03 2011
Title:	Widespread targeted chromatin remodeling during the initial phase of somatic cell reprogramming [expression]
Organism:	Mus musculus
Experiment type:	Expression profiling by array
Platform:	GPL1261
Pubmed ID:	21211784
Summary & Design:	**Summary:** Despite rapid progress in characterizing transcription factor-driven reprogramming of somatic cells to an induced pluripotent stem (iPS) cell state, many mechanistic questions still remain. To gain insight into the earliest events in the reprogramming process, we systematically analyzed the transcriptional and epigenetic changes that occur during early factor induction after discrete numbers of divisions. We observed rapid, genome-wide changes in the euchromatic histone modification, H3K4me2, at more than a thousand loci including large subsets of pluripotency or developmentally related gene promoters and enhancers. In contrast, patterns of the repressive H3K27me3 modification remained largely unchanged except for focused depletion specifically at positions where H3K4 methylation is gained. These chromatin regulatory events precede transcriptional changes within the corresponding loci. Our data provide evidence for an early, organized, and population-wide epigenetic response to ectopic reprogramming factors that clarify the temporal order through which somatic identity is reset during reprogramming. **Overall design:** Gene expression was measured by Affymetric microarrays during the initial phase of the reprogramming of mouse embryonic fibroblasts.

Background corr dist: KL-Divergence = 0.0618, L1-Distance = 0.0293, L2-Distance = 0.0012, Normal std = 0.5376

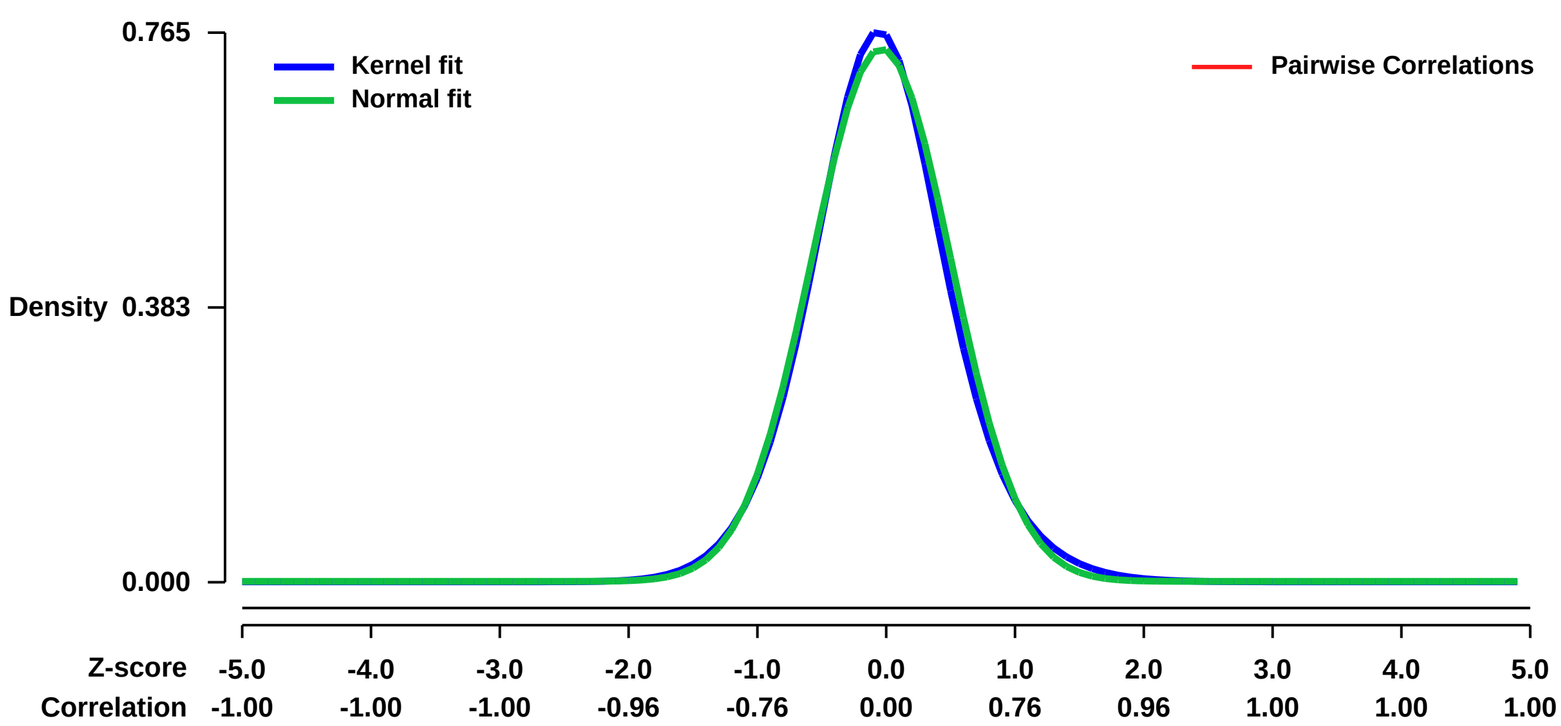

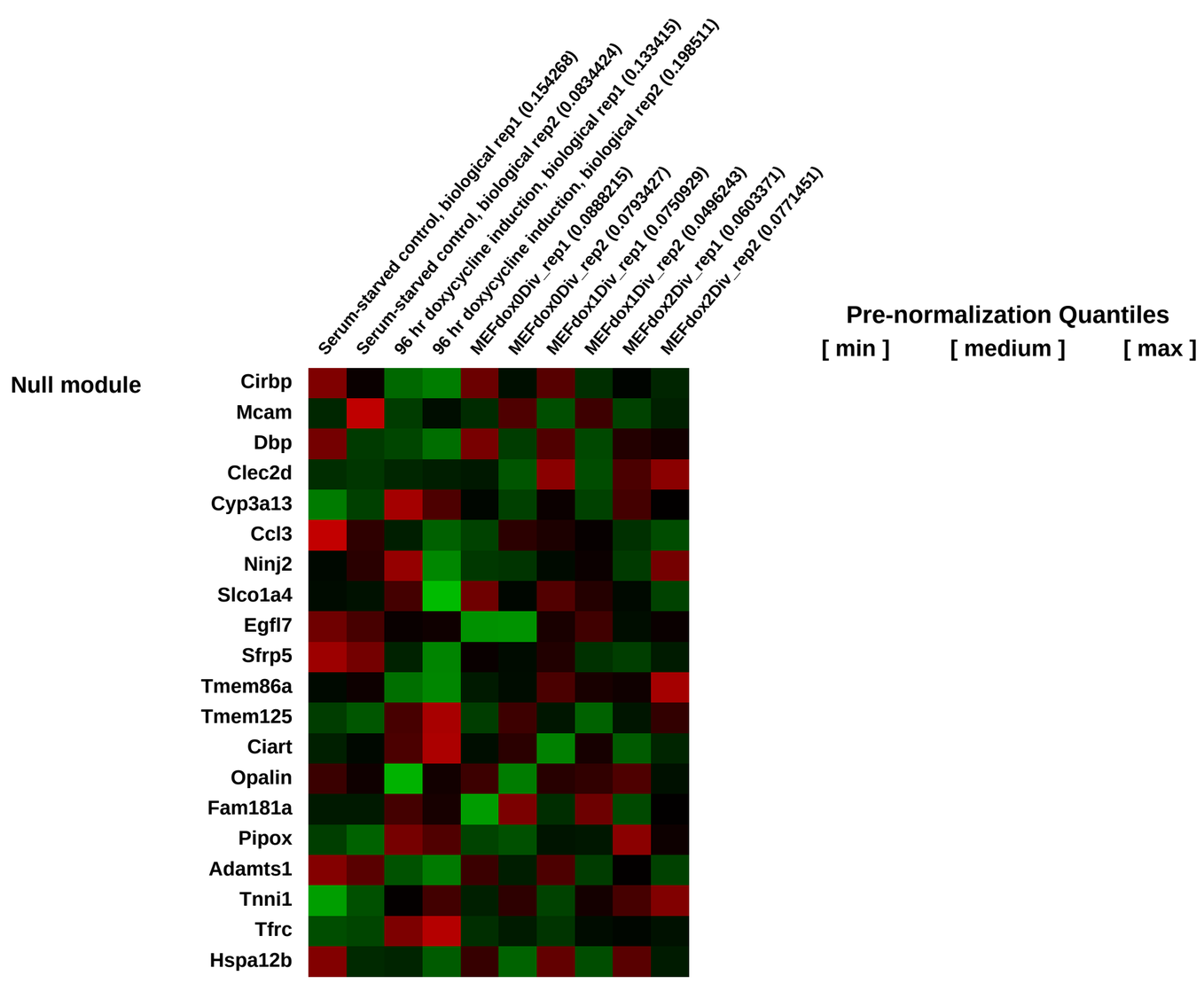

GEO Series "GSE28731" Expression Profiles

Num of samples in this series: 10

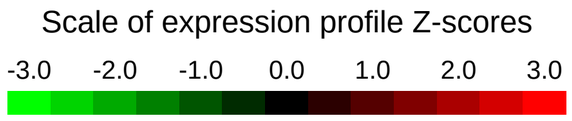

GEO Link:	http://www.ncbi.nlm.nih.gov/geo/query/acc.cgi?acc=GSE28731
Status:	Public on Jan 11 2013
Title:	Effects of Hsp72 on astrocyte activation following stroke in the mouse
Organism:	Mus musculus
Experiment type:	Expression profiling by array
Platform:	GPL1261
Pubmed ID:	22940431
Summary & Design:	**Summary:** **Astrogliosis is a hallmark of the response to brain ischemia, comprised of changes in gene expression and morphology. Hsp72 protects from cerebral ischemia, and although several mechanisms of protection have been investigated, effects on astrocyte activation are unknown. To identify potential mechanisms of protection, gene expression was assessed in mice subjected to middle cerebral artery (MCAO) or sham surgery, of either wildtype (WT) or Hsp72-overexpressing (Hsp72Tg) mice. After stroke, both genotypes exhibited genes related to cell death, stress response, and immune response. Furthermore, genes indicative of astrocyte activation, including cytoskeletal proteins and cytokines, were upregulated. To measure astrocyte activation after stroke, detailed histological and morphological analyses were performed in the cortical penumbra after stroke using unbiased stereology. Consistent with other reports, we observed a marked and persistent increase in glial fibrillary acidic protein (GFAP) as soon as 3 hours after MCAO. In contrast, vimentin immunoreactivity appeared 12-24 hours after stroke, peaked at 72 hours, and returned to baseline after 30 days. Surprisingly, no change in overall astrocyte number was observed based on glutamine synthetase (GS) immunoreactivity. To determine if Hsp72Tg mice exhibited altered astrocyte activation compared to WT controls, morphological evaluation by fractal analysis was used. Overexpression of Hsp72 reduced astrocyte cell area, arbor area, and to a lesser extent fractal dimension, 72 hours following stroke. In conclusion, in vivo overexpression of Hsp72 alters gene expression following stroke, including genes involved in astrocyte activation, and decreases astrocyte activation acutely following MCAO. Thus, modulation of astrogliosis may be a neuroprotective mechanism exerted by Hsp72 after ischemia.** **Overall design:** **A total of 10 samples were analyzed, with 5 of each genotype, wildtype (WT) and Hsp72-overexpressing (Hsp72Tg) mice. Of the 5 in each group, 3 received middle cerebral artery occlusion (MCAO) and 2 received a sham surgery. The sham samples serve as the controls for the MCAO samples in each genotype. All samples were taken from the ischemic or control hemisphere 24 hours after surgery.**

Background corr dist: KL-Divergence = 0.0829, L1-Distance = 0.0224, L2-Distance = 0.0006, Normal std = 0.4685

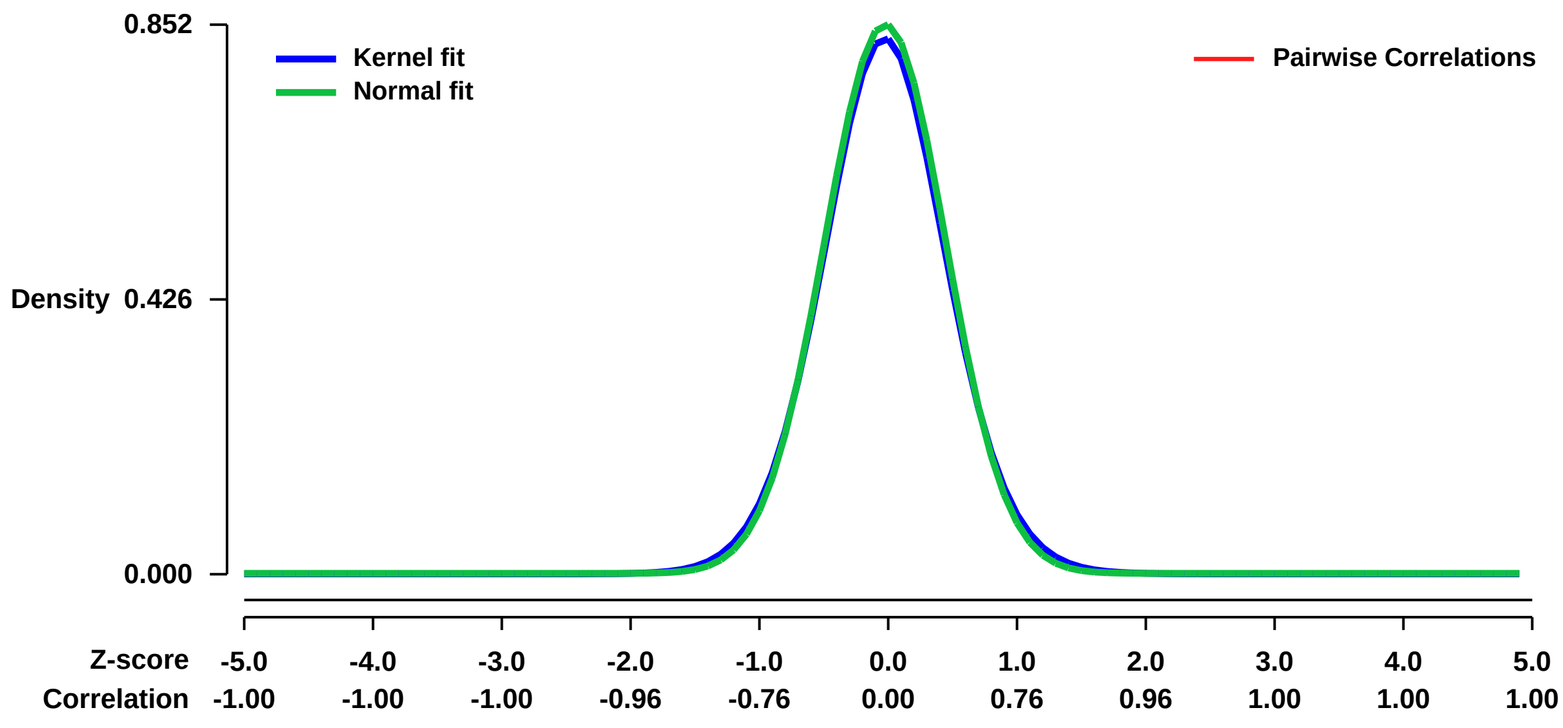

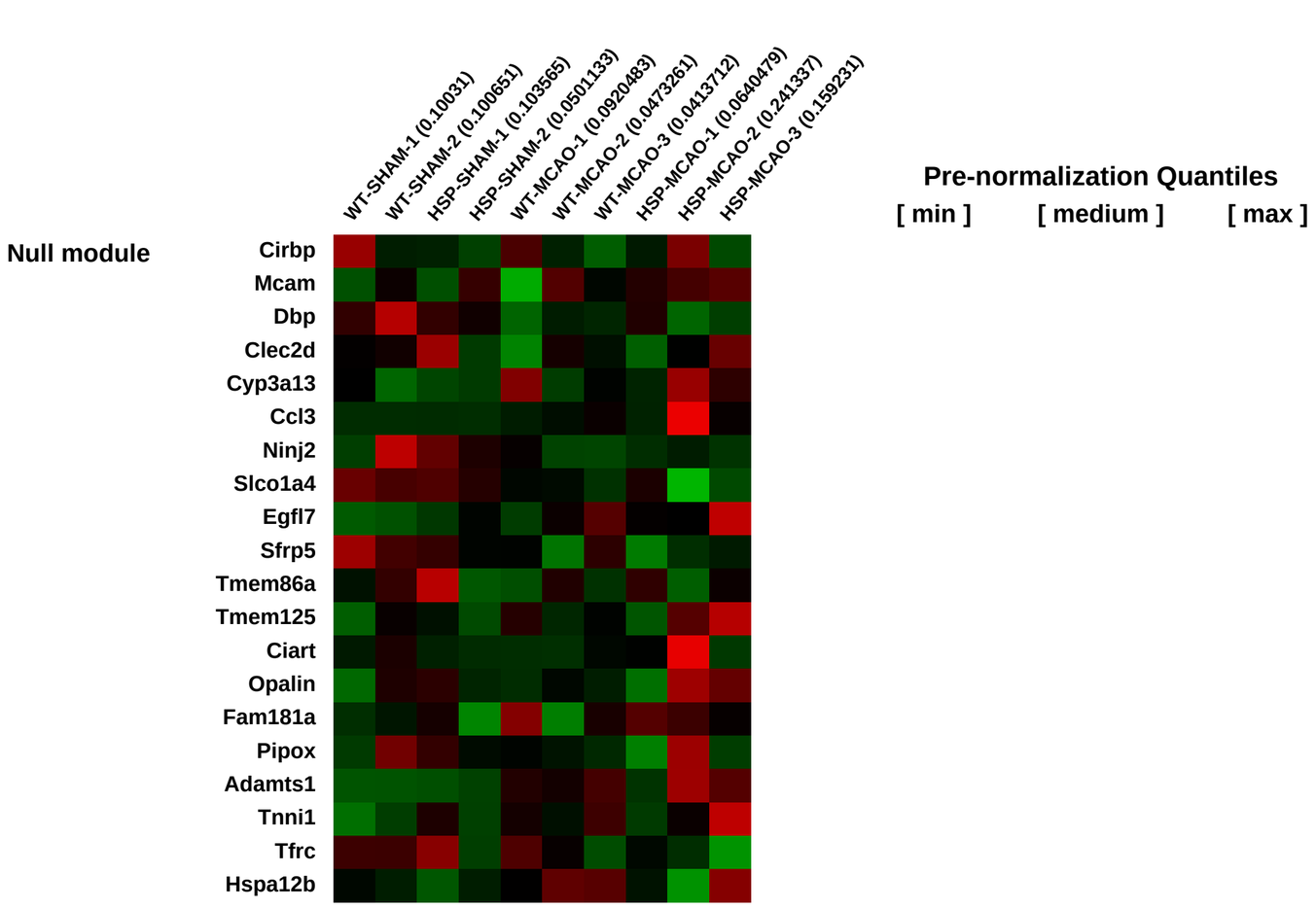

GEO Series "GSE33121" Expression Profiles

Num of samples in this series: 10

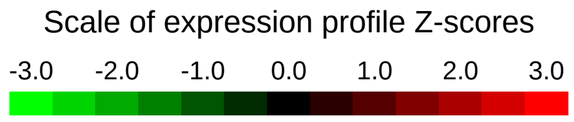

GEO Link:	**http://www.ncbi.nlm.nih.gov/geo/query/acc.cgi?acc=GSE33121**
Status:	**Public on Dec 15 2011**
Title:	**Expression data from ESC and in vitro derived somatic cells and germ cells**
Organism:	**Mus musculus**
Experiment type:	**Expression profiling by array**
Platform:	**GPL1261**
Pubmed ID:	**22194959**
Summary & Design:	**Summary:** **We performed gene expression profiling on in vitro derived PGCs, undifferentiated ESCs, and somatic cells from the EB to examine germ cell expression in ESC-derived cells** **Overall design:** **All cells were collected using fluorescence activated cell sorting to isolate SSEA1+/cKit+ ESCs, SSEA1+/cKitbright PGCs, Oct4-gfp+/cKitbright PGCs, and SSEA1-/cKit- somatic cells and Oct4-gfp-/cKit- somatic cells.**

Background corr dist: **KL-Divergence = 0.0409, L1-Distance = 0.0340, L2-Distance = 0.0016, Normal std = 0.6170**

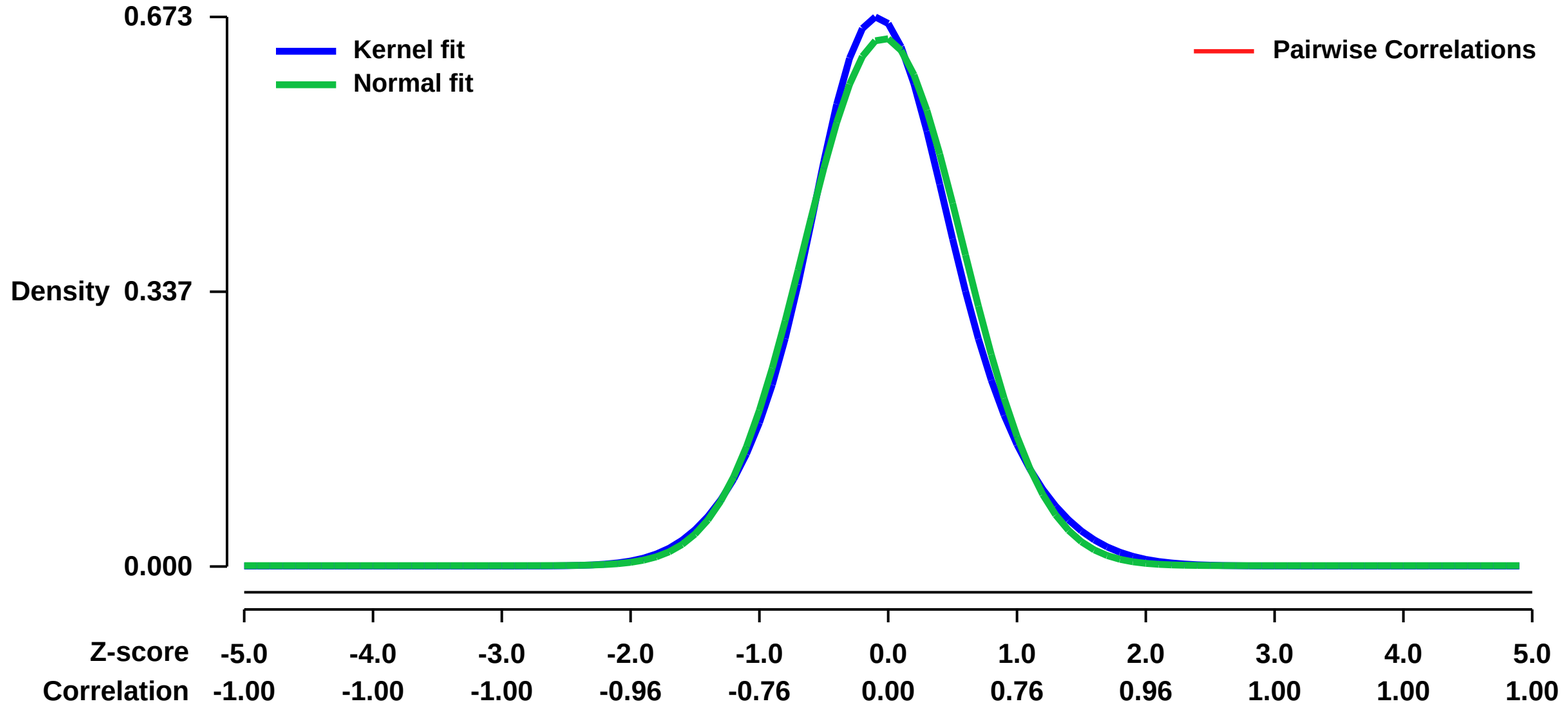

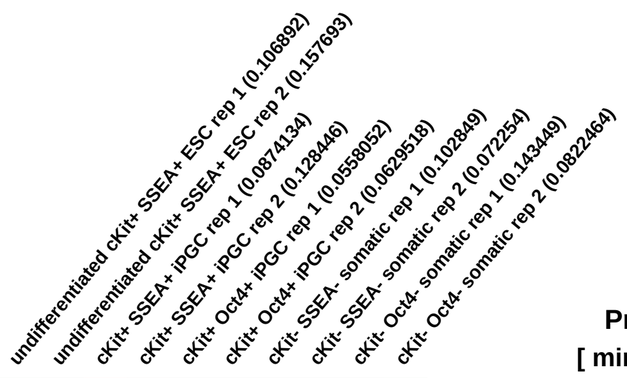

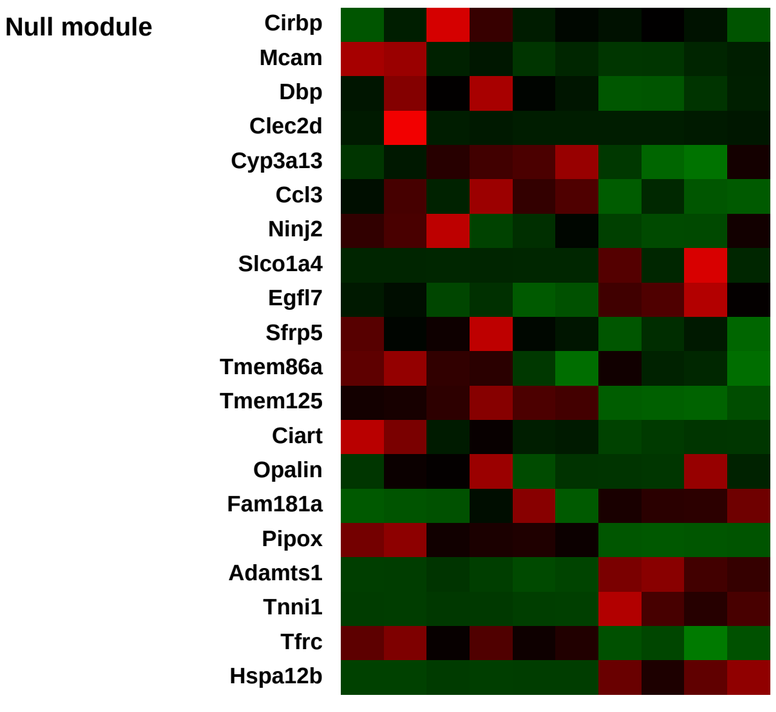

GEO Series "GSE10071" Expression Profiles

Num of samples in this series: 10

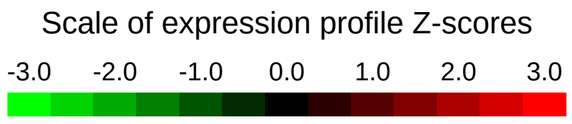

GEO Link:	http://www.ncbi.nlm.nih.gov/geo/query/acc.cgi?acc=GSE10071
Status:	Public on Jan 04 2008
Title:	NUP98-NSD1 links H3K36 methylation to Hox-A gene activation and leukaemogenesis
Organism:	Mus musculus
Experiment type:	Expression profiling by array
Platform:	GPL1261
Pubmed ID:	17589499
Summary & Design:	**Summary:** Nuclear receptor-binding SET domain protein 1 (NSD1) prototype is a family of mammalian histone methyltransferases (NSD1, NSD2/MMSET/WHSC1, NSD3/WHSC1L1) that are essential in development and are mutated in human acute myeloid leukemia (AML), overgrowth syndromes, multiple myeloma and lung cancers. In AML, the recurring t(5;11)(q35;p15.5) translocation fuses NSD1 to nucleoporin-98 (NUP98). Here, we present the first characterization of the transforming properties and molecular mechanisms of NUP98-NSD1. We demonstrate that NUP98-NSD1 induces AML in vivo, sustains self-renewal of myeloid stem cells in vitro, and enforces expression of the HoxA7, HoxA9, HoxA10 and Meis1 proto-oncogenes. Mechanistically, NUP98-NSD1 binds genomic elements adjacent to HoxA7 and HoxA9, maintains histone H3 Lys 36 (H3K36) methylation and histone acetylation, and prevents EZH2-mediated transcriptional repression of the Hox-A locus during differentiation. Deletion of the NUP98 FG-repeat domain, or mutations in NSD1 that inactivate the H3K36 methyltransferase activity or that prevent binding of NUP98-NSD1 to the Hox-A locus precluded both Hox-A gene activation and myeloid progenitor immortalization. We propose that NUP98-NSD1 prevents EZH2-mediated repression of Hox-A locus genes by colocalizing H3K36 methylation and histone acetylation at regulatory DNA elements. This report is the first to link deregulated H3K36 methylation to tumorigenesis and to link NSD1 to transcriptional regulation of the Hox-A locus. **Keywords:** expression analysis **Overall design:**

Background corr dist: KL-Divergence = 0.0759, L1-Distance = 0.0227, L2-Distance = 0.0009, Normal std = 0.4842

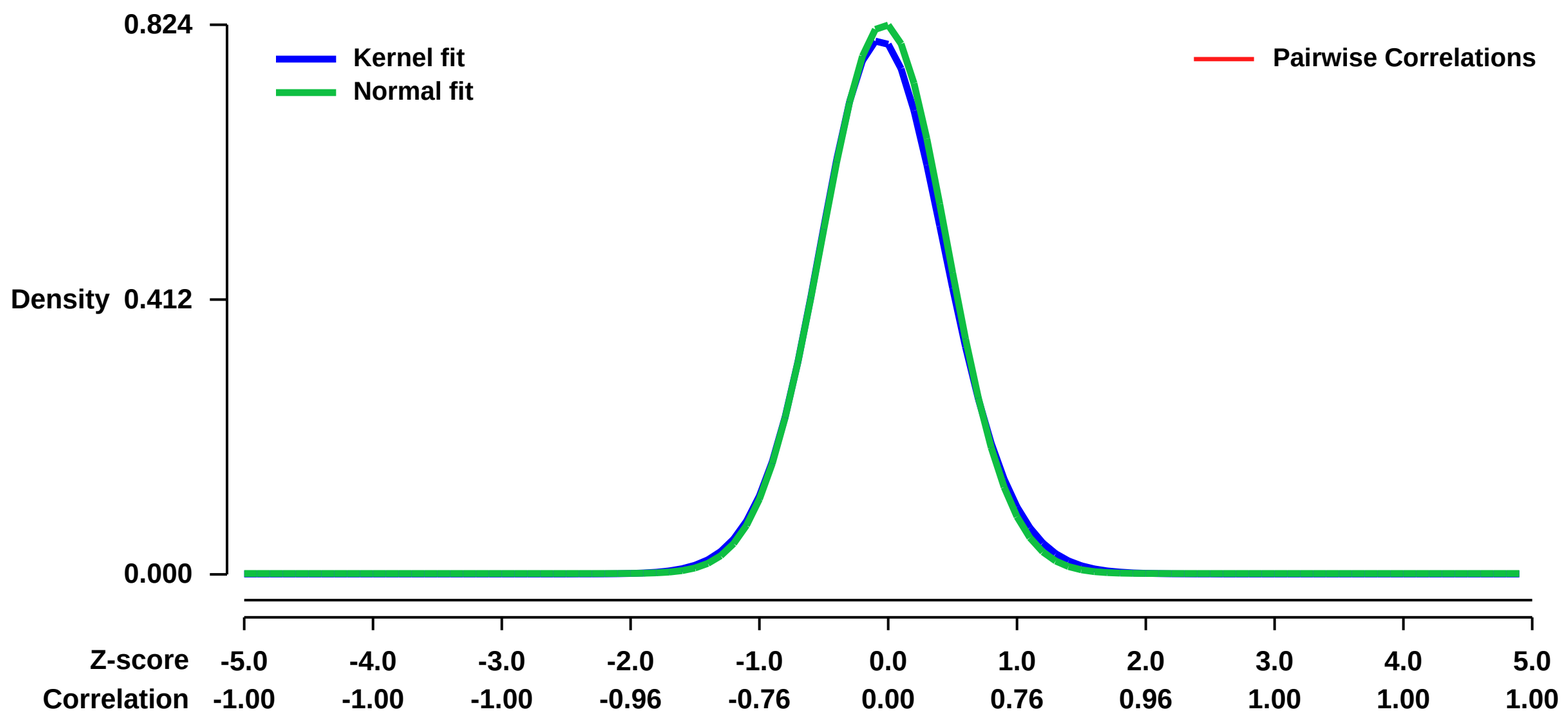

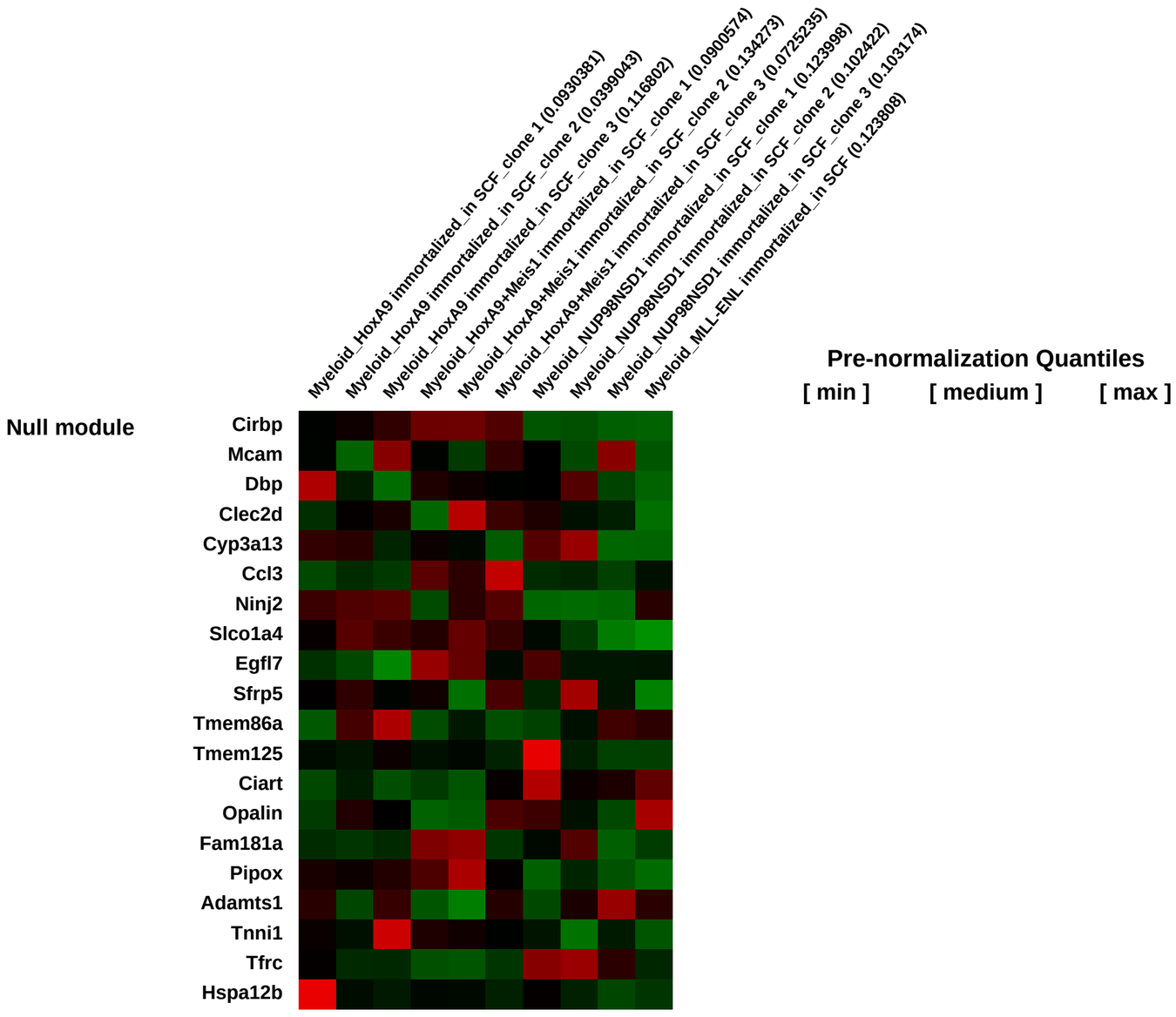

GEO Series "GSE19528" Expression Profiles

Num of samples in this series: 8

Scale of expression profile Z-scores

-3.0 -2.0 -1.0 0.0 1.0 2.0 3.0

GEO Link:	http://www.ncbi.nlm.nih.gov/geo/query/acc.cgi?acc=GSE19528
Status:	Public on Jan 22 2010
Title:	Effect of c-Myb deficiency on pre-selection DP thymocytes
Organism:	Mus musculus
Experiment type:	Expression profiling by array
Platform:	GPL1261
Pubmed ID:	20142358
Summary & Design:	**Summary:** Comparing the mRNA expression profiles of c-Myb deficient and c-Myb sufficient Tcra-/- DP thymocytes. Results provide insight into the role of c-Myb in the regulation of survival and differentiation during the pre-selection DP stage where c-Myb expression is abundant during T cell development. **Overall design:** DP thymocytes were purified from four c-Myb deficient and four c-Myb sufficient mice over magnetic columns. RNA from each biological replicate was individually hybridized onto a total of eight MOE430 2.0 Chips.

Background corr dist: KL-Divergence = 0.0791, L1-Distance = 0.0206, L2-Distance = 0.0007, Normal std = 0.4804

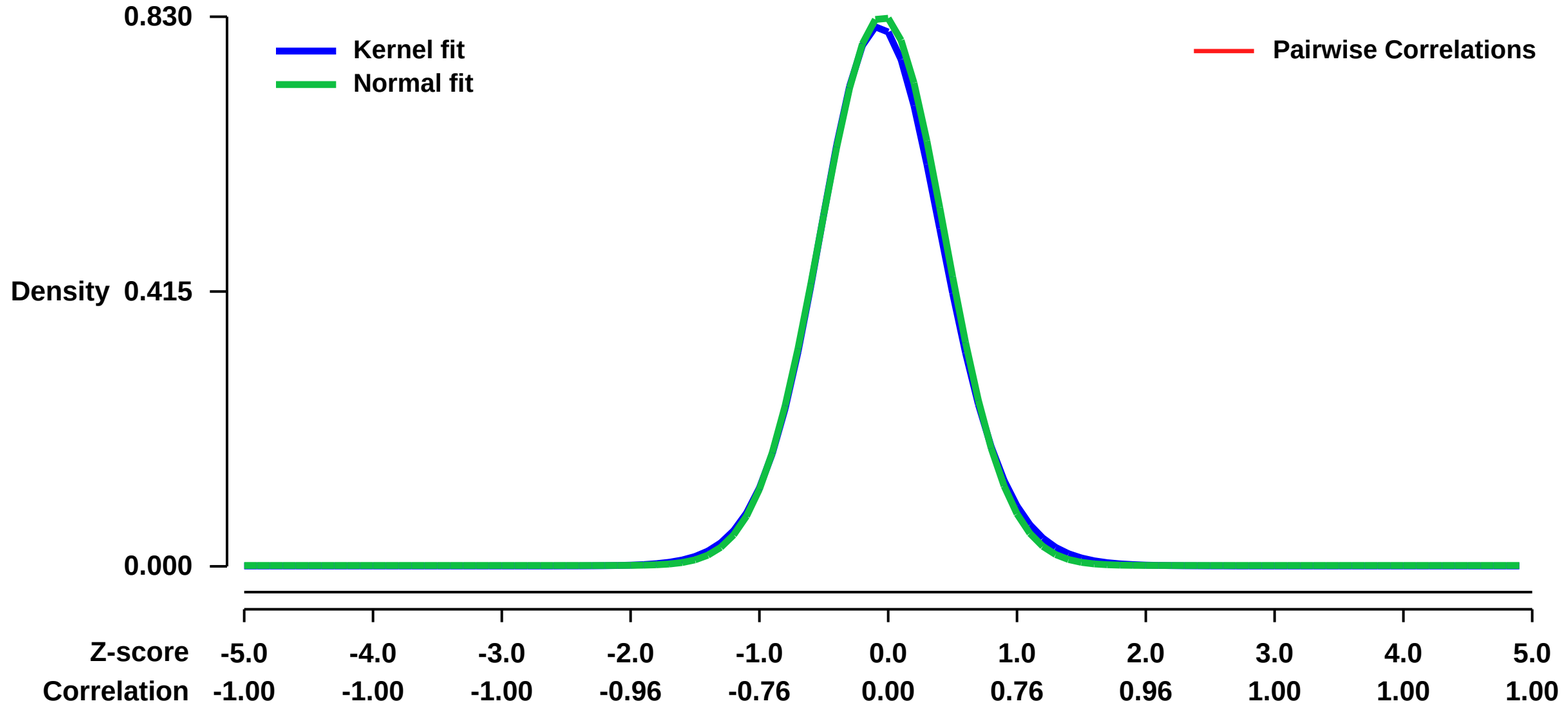

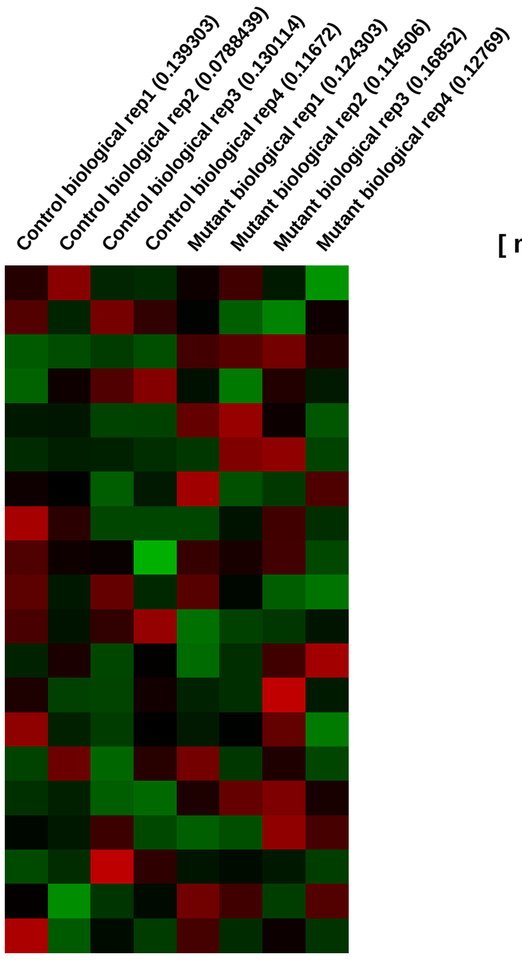

GEO Series "GSE13062" Expression Profiles

Num of samples in this series: 24

Scale of expression profile Z-scores

-3.0 -2.0 -1.0 0.0 1.0 2.0 3.0

GEO Link:	http://www.ncbi.nlm.nih.gov/geo/query/acc.cgi?acc=GSE13062
Status:	Public on Nov 23 2009
Title:	The effects of temporally restricted feeding on hepatic gene expression of Cry1, Cry2 double KO mice
Organism:	Mus musculus
Experiment type:	Expression profiling by array
Platform:	GPL1261
Pubmed ID:	19940241
Summary & Design:	**Summary:** Restricted feeding impacts the hepatic circadian clock of WT mice. Cry1, Cry2 double KO mice lack a circadian clock and are thus expected to show rhythmical gene expression in the liver. Imposing a temporally restricted feeding schedule on these mice shows how the hepatic circadian clock and rhythmic food intake regulate rhythmic transcription in parallel **Overall design:** Cry1, Cry2 double KO mice were entrained either to ad libitum or temporally restricted feeding (tRF) schedules. Food was made available to mice under the tRF regimen only between ZT(CT)1 and ZT(CT)9. Mice were then released into constant darkness while the respective feeding schedules were still maintained. Liver tissue was collected on the second day of constant darkness at the indicated timepoints. Total RNA was extracted and 5ug of RNA was used in the standard Affymetrix protocol for amplification, labeling and hybridization

Background corr dist: KL-Divergence = 0.1620, L1-Distance = 0.0794, L2-Distance = 0.0131, Normal std = 0.4340

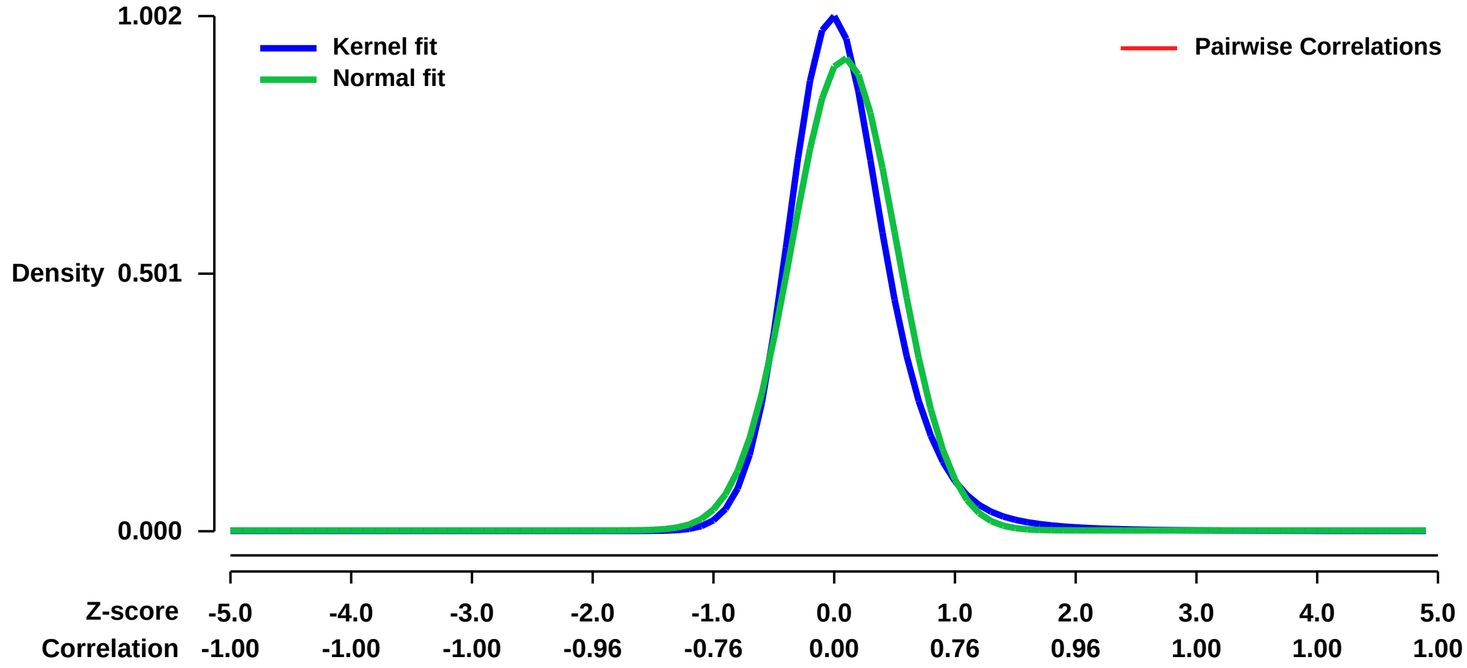

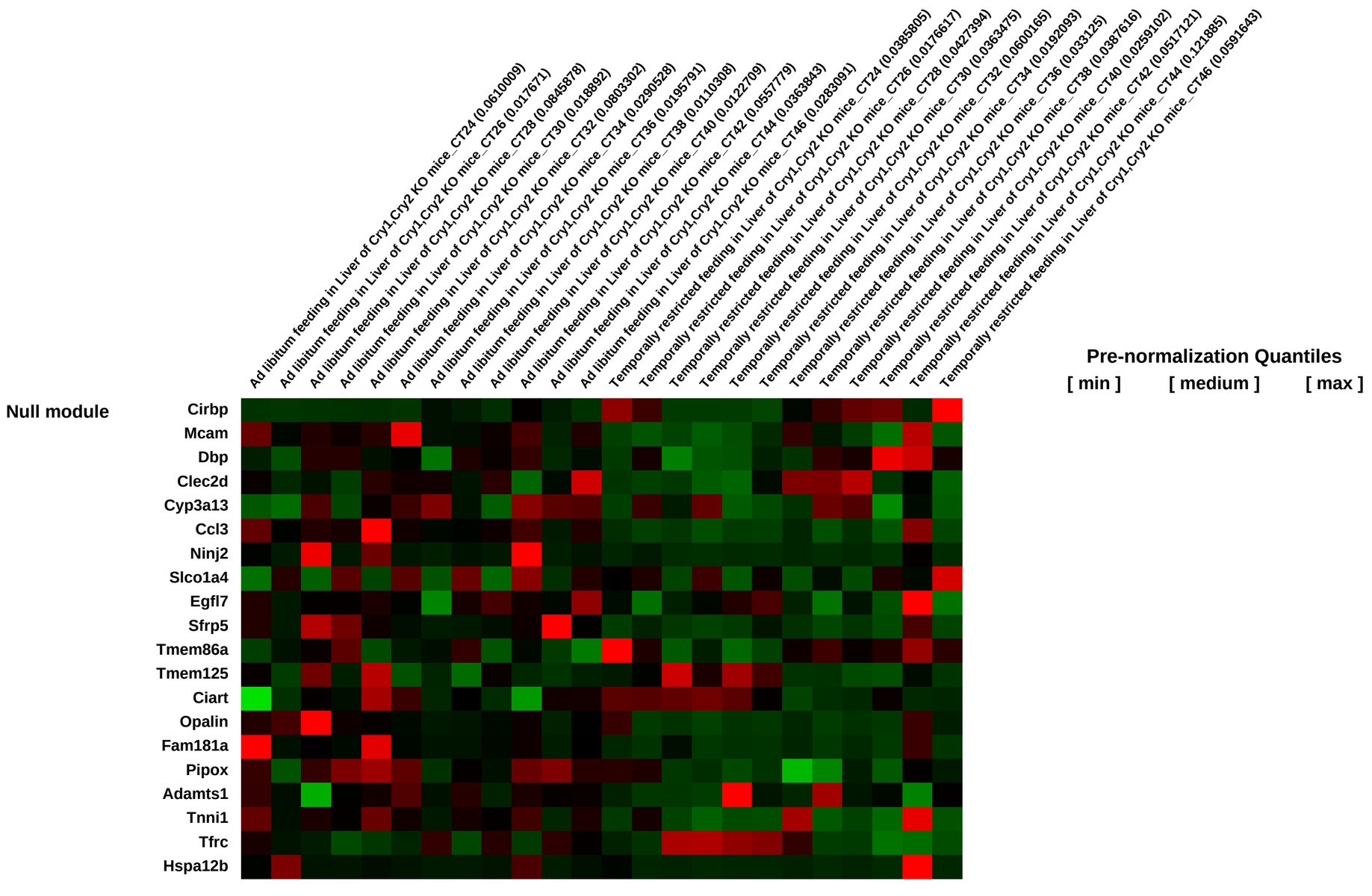

GEO Series "GSE35734" Expression Profiles

Num of samples in this series: 6

Scale of expression profile Z-scores

-3.0 -2.0 -1.0 0.0 1.0 2.0 3.0

GEO Link:	http://www.ncbi.nlm.nih.gov/geo/query/acc.cgi?acc=GSE35734
Status:	Public on Jun 04 2012
Title:	Screening of genes involved in chromosome segregation in meiosis I
Organism:	Mus musculus
Experiment type:	Expression profiling by array
Platform:	GPL1261
Pubmed ID:	22648182
Summary & Design:	**Summary:** Prophase I of meiosis involves dynamic chromosome segregation processes including synapsis, meiotic recombination, and cohesion. Genetic defects in genes participating in these processes consistently cause reproduction failure in mice. To identify candidate genes responsible for infertility or recurrent pregnancy loss in humans, we performed expression profiling of male and female gonads of mice undergoing meiotic prophase I. **Overall design:** Both male and female gonads at 15.5 days postcoitum, neonatal day 1 and 10 weeks postpartum were dissected from mice for RNA extraction and subjected to hybridization on Affymetrix microarrays.

Background corr dist: KL-Divergence = 0.0426, L1-Distance = 0.0540, L2-Distance = 0.0033, Normal std = 0.8424

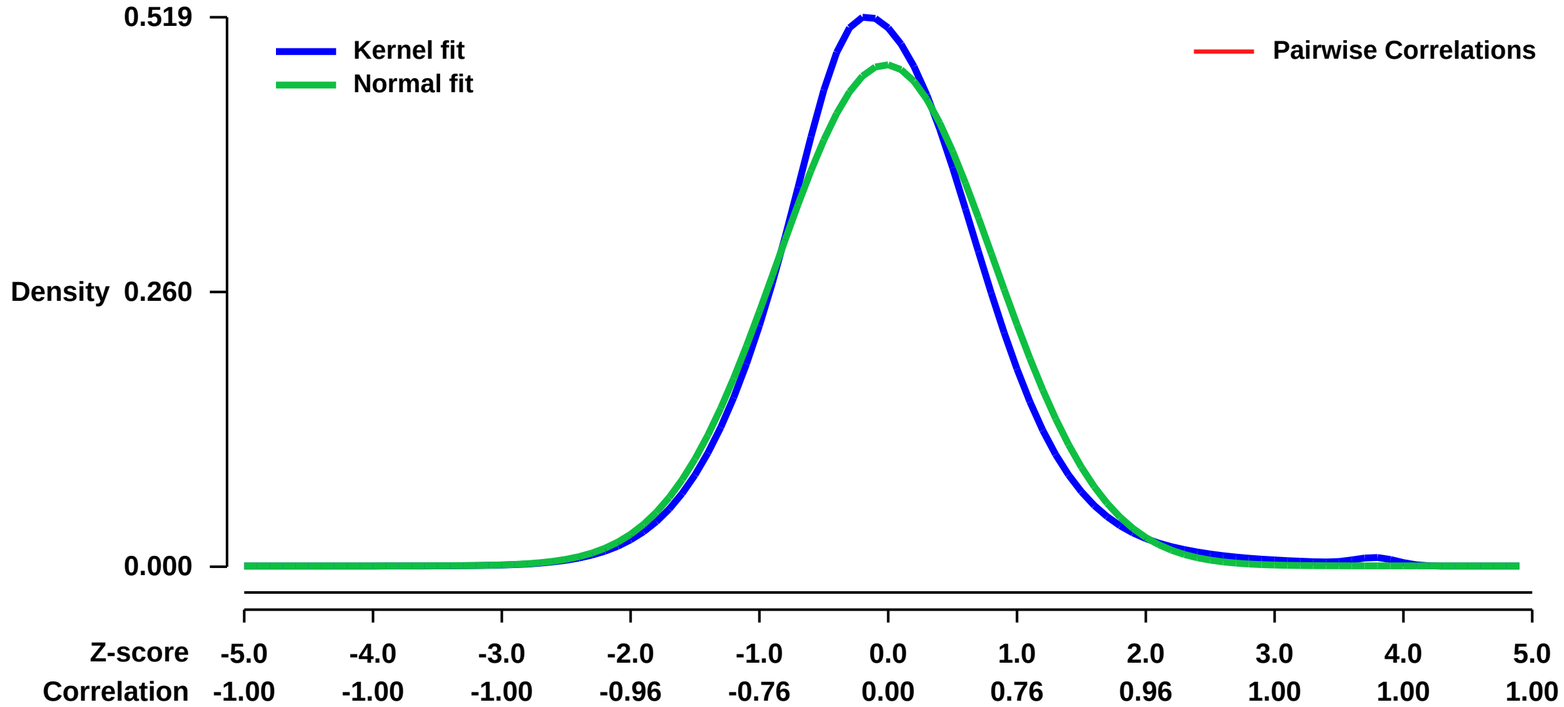

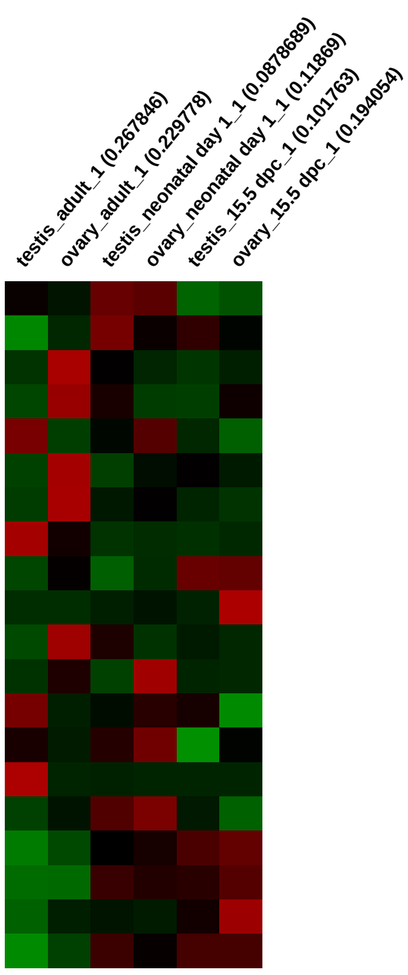

GEO Series "GSE18907" Expression Profiles

Num of samples in this series: 12

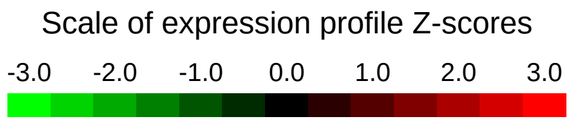

GEO Link:	http://www.ncbi.nlm.nih.gov/geo/query/acc.cgi?acc=GSE18907
Status:	Public on Mar 19 2011
Title:	Gene expression profiling of pregnant and virgin mouse lung and liver
Organism:	Mus musculus
Experiment type:	Expression profiling by array
Platform:	GPL1261
Pubmed ID:	21646719
Summary & Design:	**Summary:** Metastasis depends on the ability of tumor cells to establish a relationship with the newly seeded host tissue that is conducive to their survival and proliferation. Recent evidence suggests that tumor cells regulate their own dissemination by preparing permissive â metastatic nichesâ within host tissues. However, the factors that are implicated in rendering tissues permissive for metastatic tumor growth have yet to be fully elucidated. Breast tumors arising during pregnancy display highly aggressive behaviour and early metastatic proclivity, raising the possibility that pregnancy may constitute a physiological condition of permissiveness for tumor dissemination. We show that during murine gestation, both the rate and degree of metastatic tumor growth are enhanced irrespective of tumor type and that decreased natural killer (NK) cell activity is responsible for the observed increase in experimental metastasis. We identify gene expression changes in pregnant mouse lung and liver that bear striking similarity with reported pre-metastatic niche signatures and several of the up-regulated genes are indicative of myeloid-cell infiltration. We provide evidence, that CD11b+ Gr-1+ myeloid-derived suppressor cells accumulate in pregnant mice and exert an inhibitory effect on NK cell activity, thereby enhancing metastatic tumor growth. MDSC have never been evoked in the context of pregnancy and our observations suggest that they may represent a further shared mechanism of immune suppression occurring during gestation and tumor growth. **Overall design:** Three chips were done per organ (liver/lung) and per condition (virgin/pregnant), with equal amounts of RNA from two mice pooled for one chip.

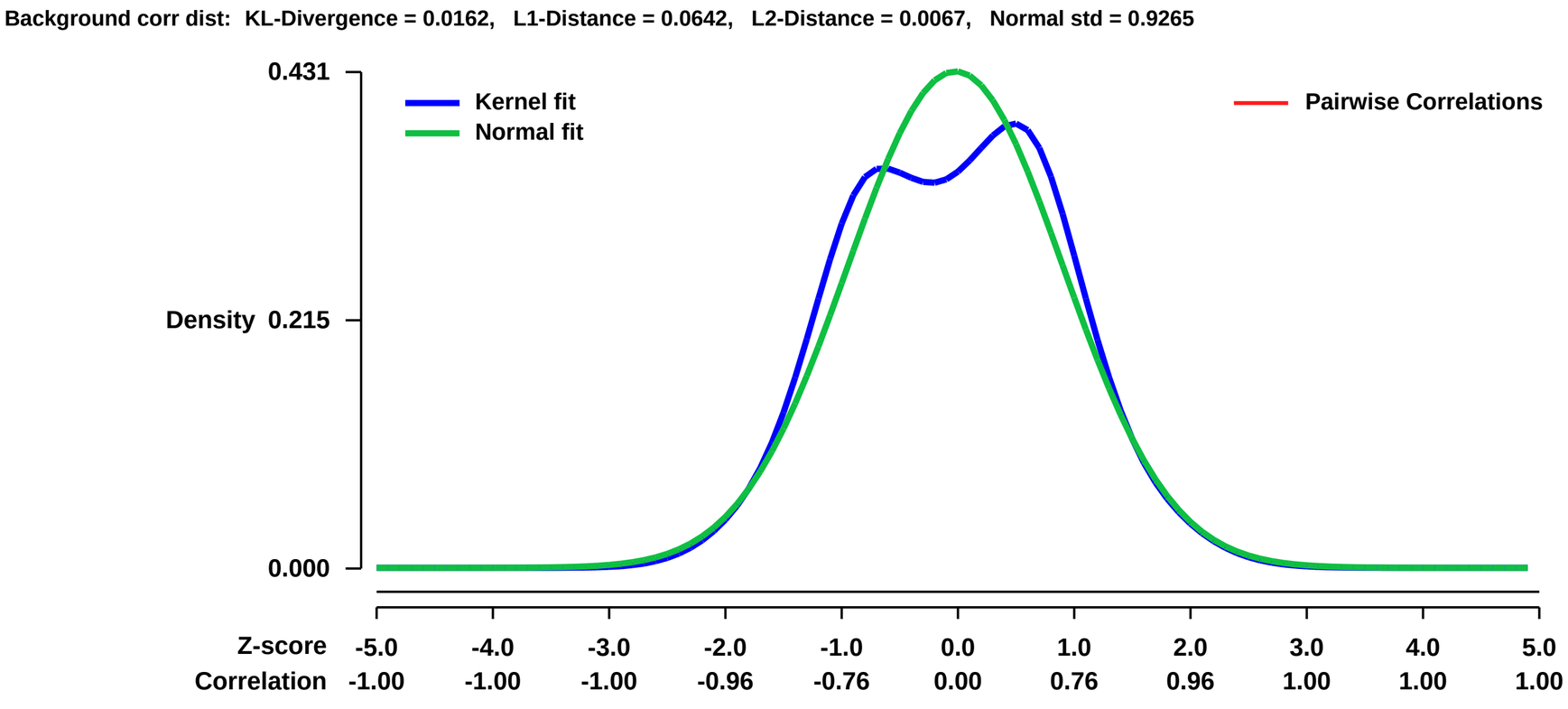

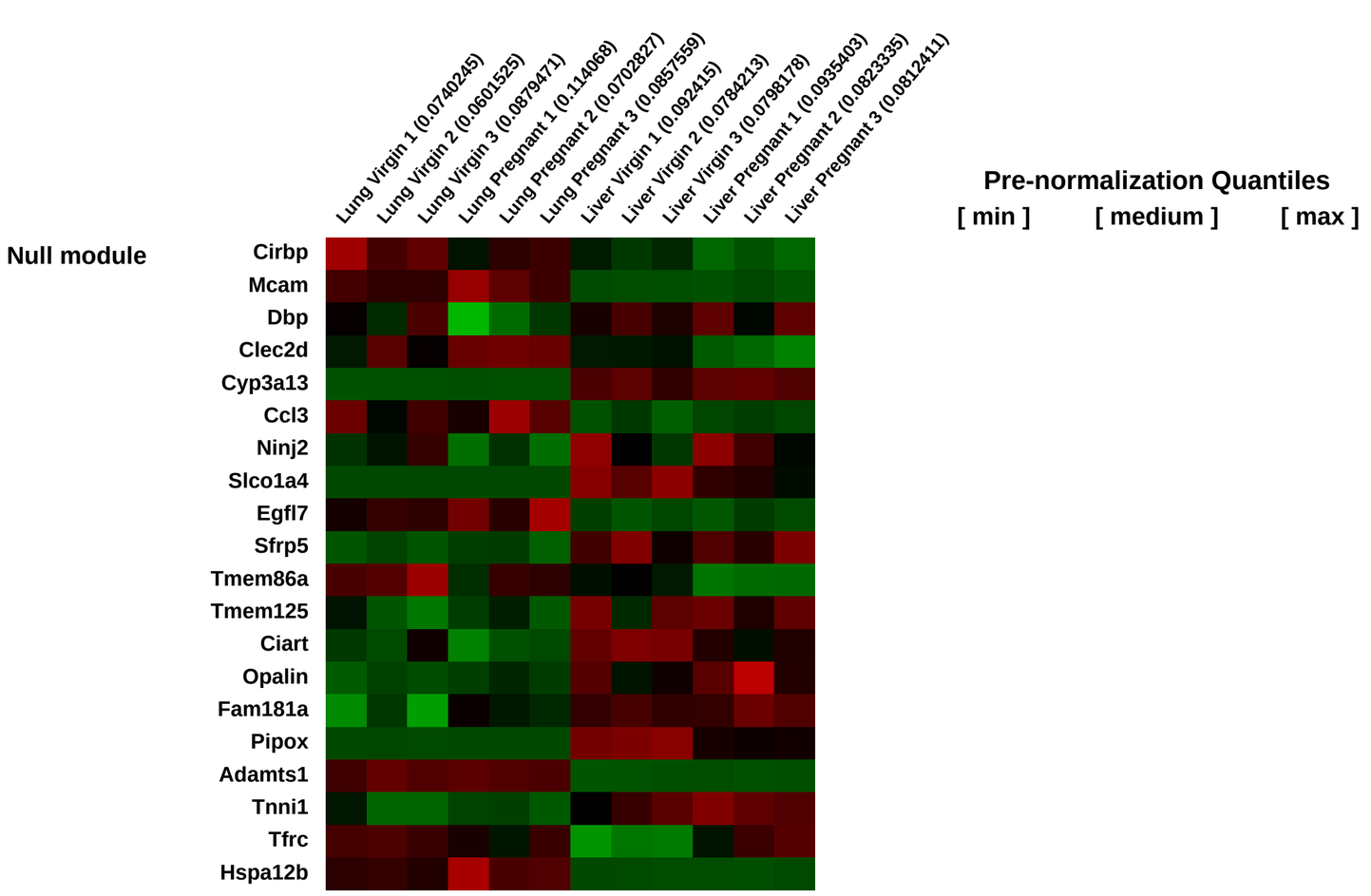

GEO Series "GSE13693" Expression Profiles

Num of samples in this series: 9

Scale of expression profile Z-scores

-3.0 -2.0 -1.0 0.0 1.0 2.0 3.0

GEO Link:	http://www.ncbi.nlm.nih.gov/geo/query/acc.cgi?acc=GSE13693
Status:	Public on Feb 06 2009
Title:	Gene expression profiling of normal mouse myeloid cell populations
Organism:	Mus musculus
Experiment type:	Expression profiling by array
Platform:	GPL1261
Pubmed ID:	19200802
Summary & Design:	**Summary:** Normal myeloid lineage cell populations (C57BL/6 mice, aged 4-10 weeks, male or female) with three distinct immunophenotypes were prospectively isolated and characterized. In preparation for FACS sorting, bone marrow cells were separated into c-kit+ and c-kit- fractions using an AutoMACS device. C-kit+ cells were further fractionated based on Gr1 and Mac1 expression, and absence of lineage antigen expression (B220, TER119, CD3, CD4, CD8 and IL7R$_{\epsilon}$–), by cell sorting. C-kit+ Gr1+ Mac1lo/- and c-kit+ Gr1+ Mac1+ displayed cytologic features of undifferentiated hematopoietic cells or myeloblasts, whereas c-kit- Gr1+ Mac1+ cells were mature neutrophils. **Overall design:** See summary.

Background corr dist: KL-Divergence = 0.0176, L1-Distance = 0.0380, L2-Distance = 0.0018, Normal std = 0.8108

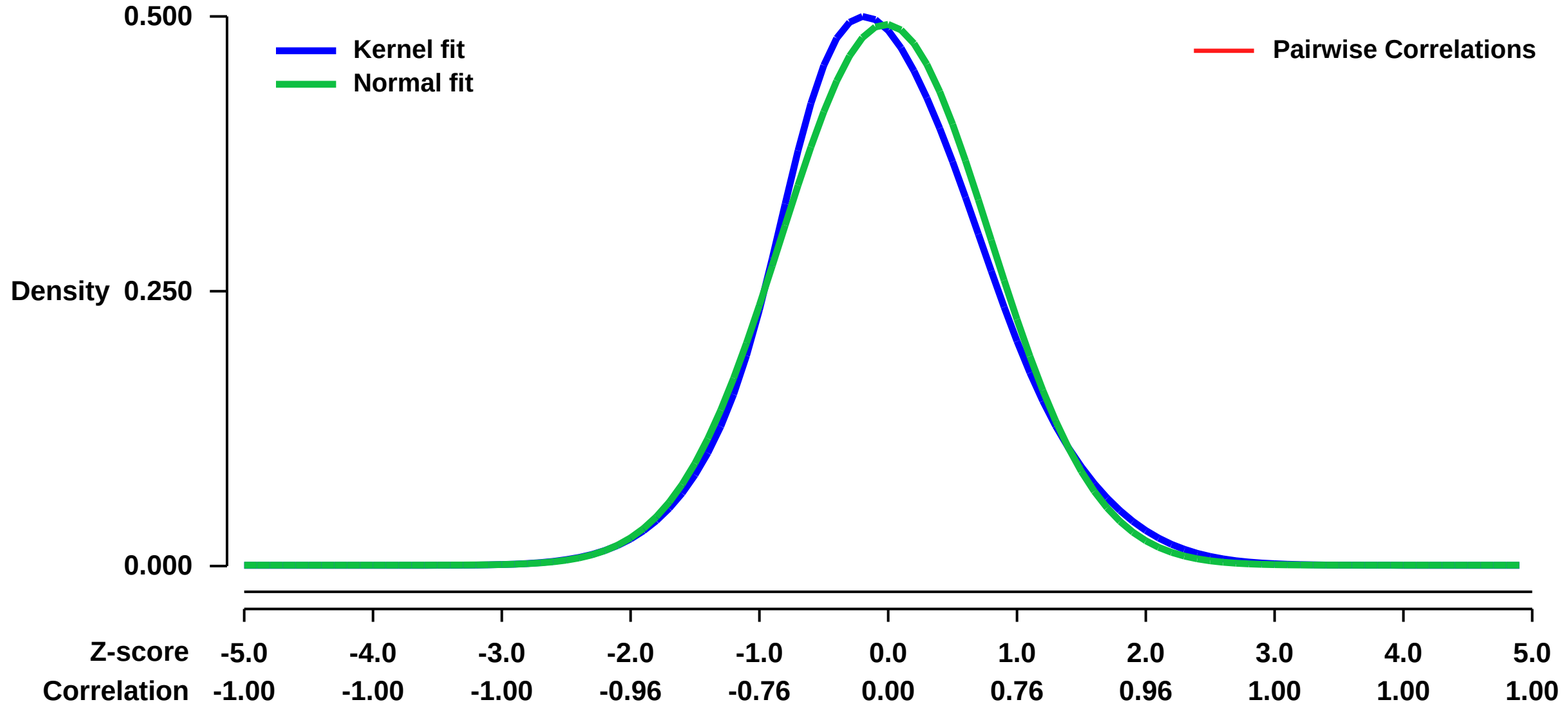

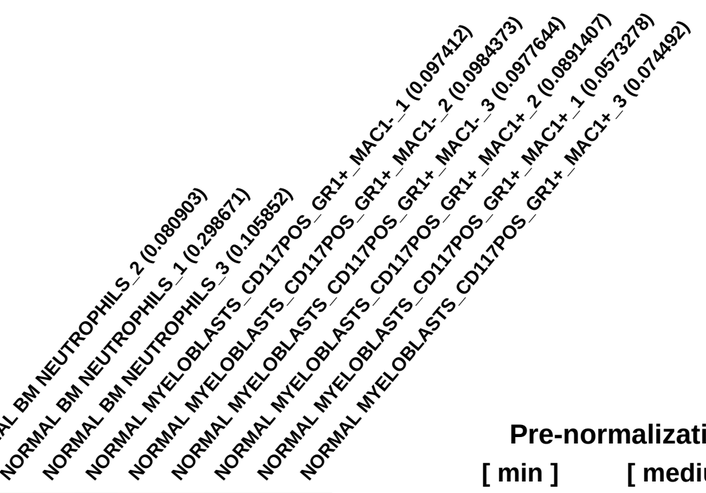

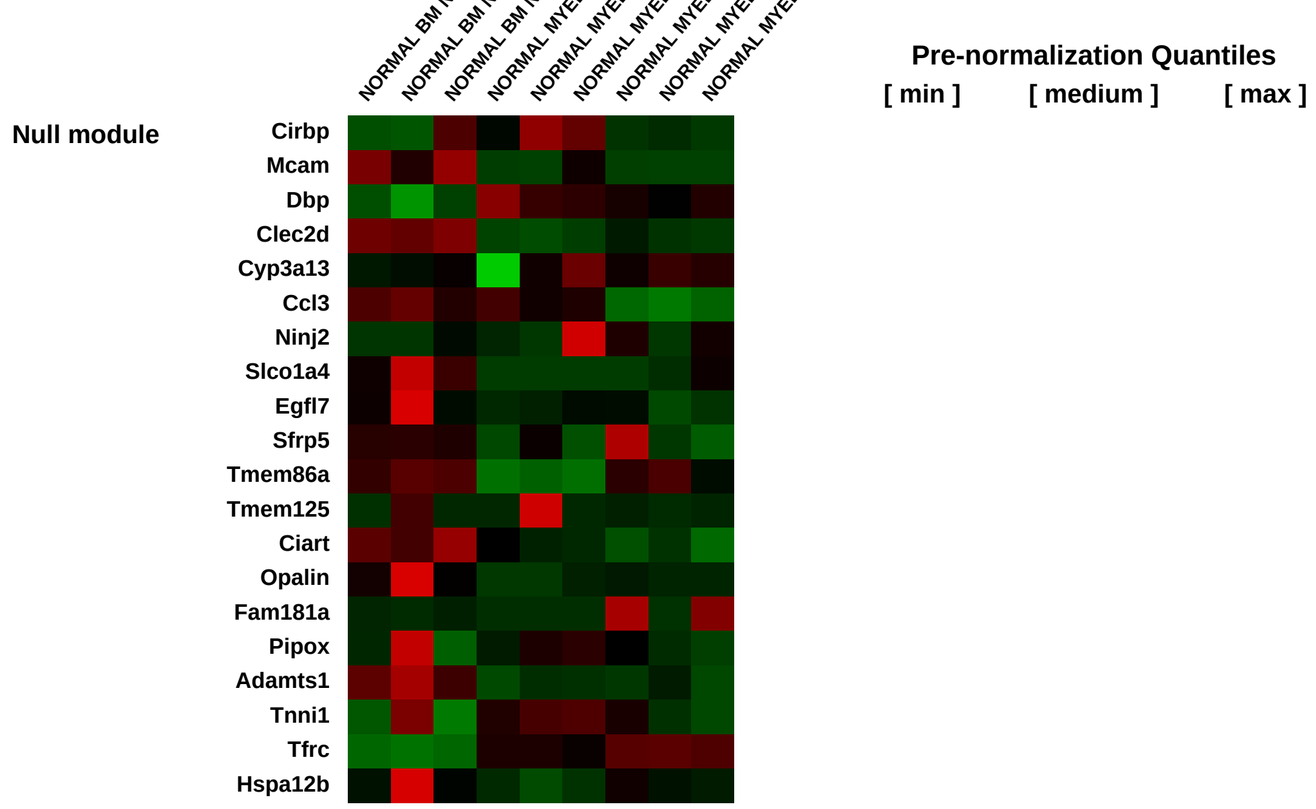

GEO Series "GSE33891" Expression Profiles

Num of samples in this series: 19

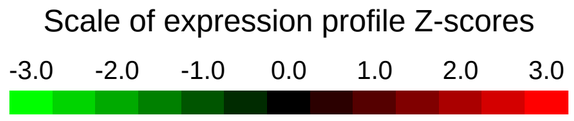

GEO Link:	**http://www.ncbi.nlm.nih.gov/geo/query/acc.cgi?acc=GSE33891**
Status:	**Public on Nov 22 2012**
Title:	**The role for TNF-alpha in murine type 1 and 2 diabetes**
Organism:	**Mus musculus**
Experiment type:	**Expression profiling by array**
Platform:	**GPL1261**
Pubmed ID:	
Summary & Design:	**Summary:** **To search for new therapeutic targets for type 1 & 2 diabetes, we have applied genome wide transcriptional profiling and systems biology oriented bioinformatics analysis to examine the impact of the Power mix(PM) and Alpha-1 Anti-Trypsin(AAT) regimens upon pancreatic lymph node (PLN) and fat, a crucial tissue for insulin dependent glucose disposal, in new onset diabetic NOD mice.** **Overall design:** **Transcriptional profiles of fat and PLNs in normal (non diabetic) NOD mice (NOR), new onset diabetic (DIA), new onset diabetic NOD mice treated with AAT or PM were perfromed in this study**

Background corr dist: **KL-Divergence = 0.0927, L1-Distance = 0.0417, L2-Distance = 0.0036, Normal std = 0.4528**

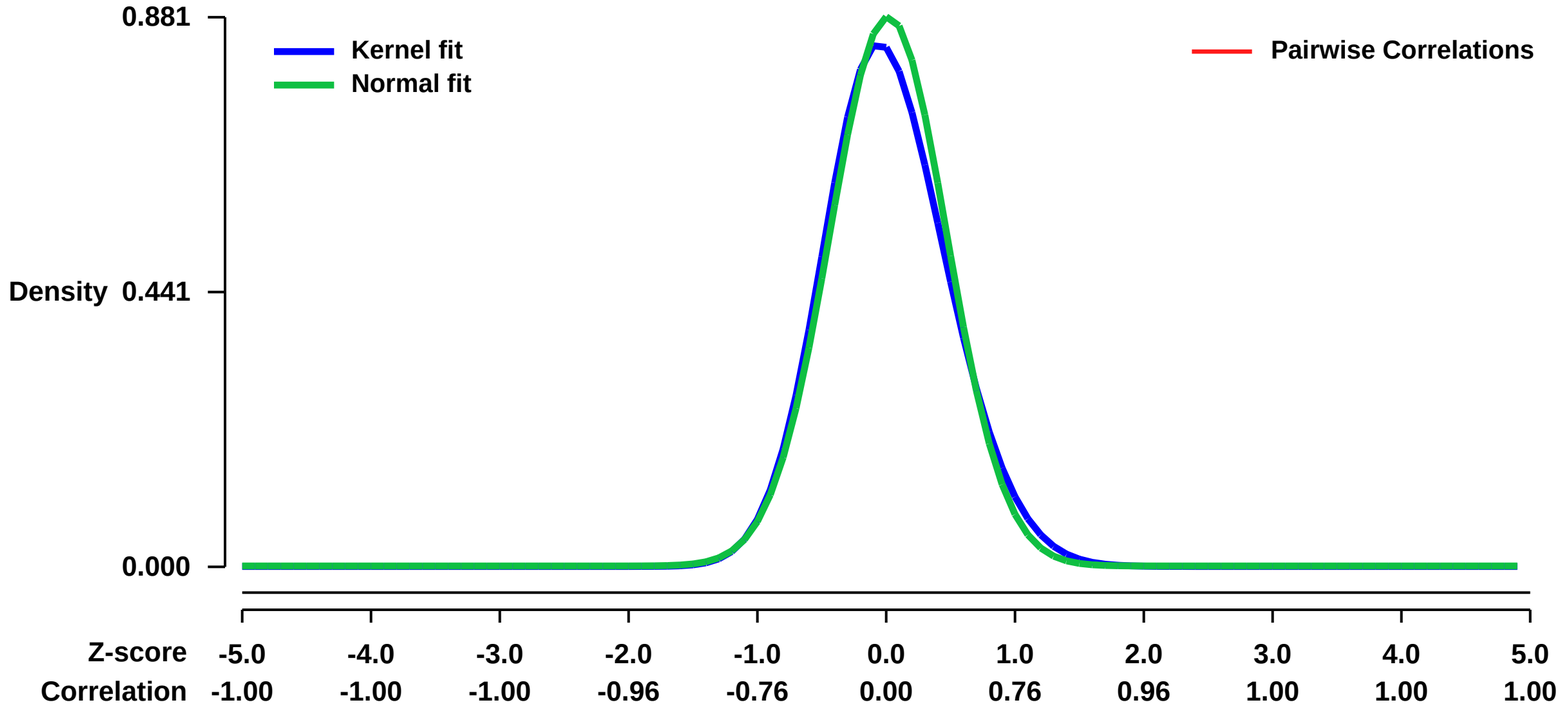

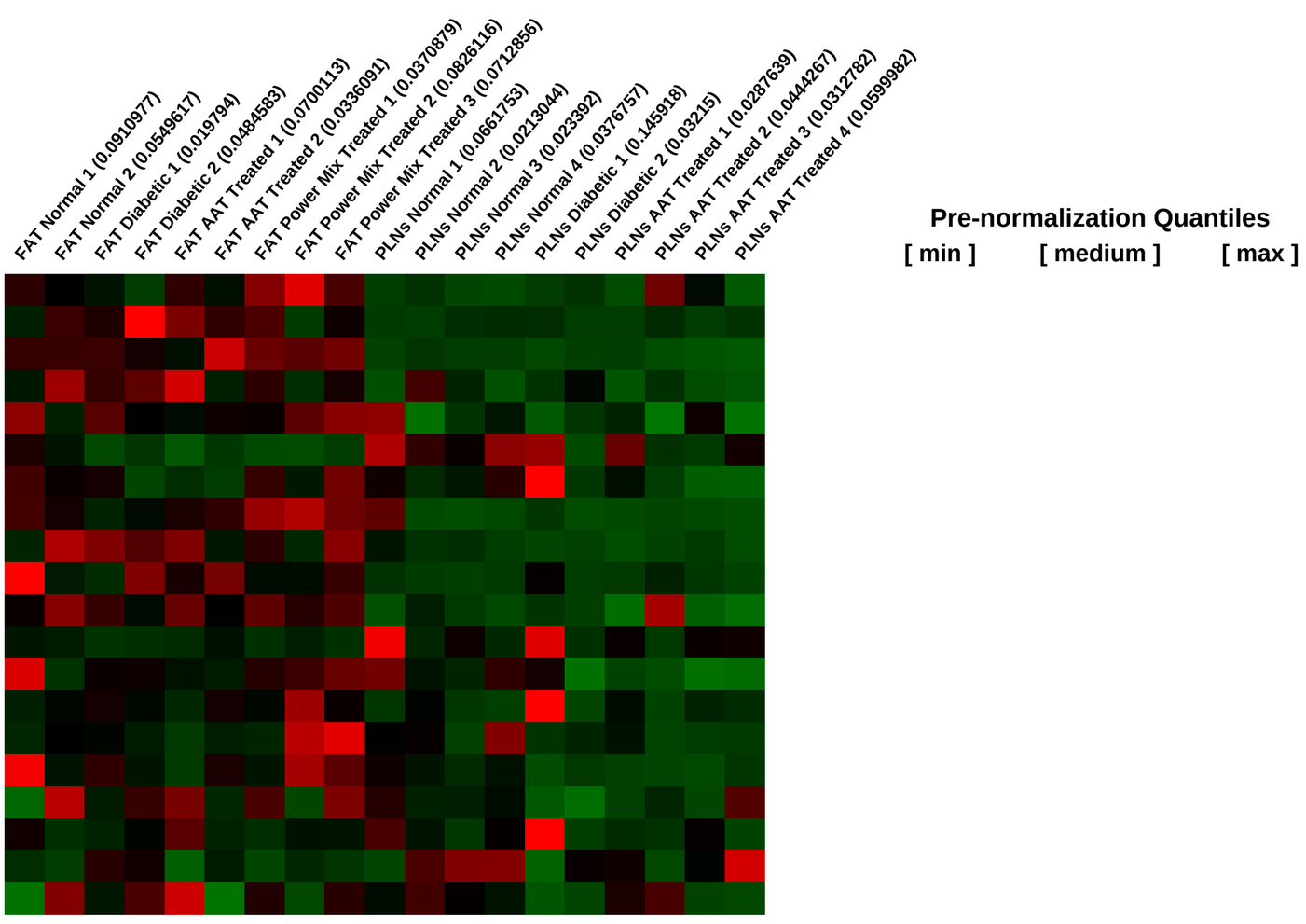

GEO Series "GSE19403" Expression Profiles

Num of samples in this series: 12

Scale of expression profile Z-scores

-3.0 -2.0 -1.0 0.0 1.0 2.0 3.0

GEO Link:	http://www.ncbi.nlm.nih.gov/geo/query/acc.cgi?acc=GSE19403
Status:	Public on Dec 10 2009
Title:	Dysregulation of the Wnt pathway inhibits timely myelination and remyelination in the mammalian CNS
Organism:	Mus musculus
Experiment type:	Expression profiling by array
Platform:	GPL1261
Pubmed ID:	21706018
Summary & Design:	**Summary:** The progressive loss of CNS myelin in patients with multiple sclerosis (MS) has been proposed to result from the combined effects of damage to oligodendrocytes and failure of remyelination. A common feature of demyelinated lesions is the presence of oligodendrocyte precursors (OLPs) blocked at a premyelinating stage. However, the mechanistic basis for inhibition of myelin repair is incompletely understood. To identify novel regulators of OLP differentiation, potentially dysregulated during repair, we performed a genome-wide screen of 1040 transcription factor-encoding genes expressed in remyelinating rodent lesions. We report that â…50 transcription factor-encoding genes show dynamic expression during repair and that expression of the Wnt pathway mediator Tcf4 (aka Tcf7l2) within OLPs is specific to lesionedâ but not normalâ adult white matter. We report that ¸†-catenin signaling is active during oligodendrocyte development and remyelination in vivo. Moreover, we observed similar regulation of Tcf4 in the developing human CNS and lesions of MS. Data mining revealed elevated levels of Wnt pathway mRNA transcripts and proteins within MS lesions, indicating activation of the pathway in this pathological context. We show that dysregulation of Wntâ¸†-catenin signaling in OLPs results in profound delay of both developmental myelination and remyelination, based on (1) conditional activation of ¸†-catenin in the oligodendrocyte lineage in vivo and (2) findings from APCMin mice, which lack one functional copy of the endogenous Wnt pathway inhibitor APC. Together, our findings indicate that dysregulated Wntâ¸†-catenin signaling inhibits myelination/remyelination in the mammalian CNS. Evidence of Wnt pathway activity in human MS lesions suggests that its dysregulation might contribute to inefficient myelin repair in human neurological disorders. **Overall design:** 12 samples total. Two variables in the experiment: genotype (wild type or Olig2cre/DA-Cat) and Developmental stage (Day 4 or Day 15). 4 phenotypes in total with 3 biological replicates for each phenotype.

Background corr dist: KL-Divergence = 0.0423, L1-Distance = 0.0614, L2-Distance = 0.0055, Normal std = 0.6512

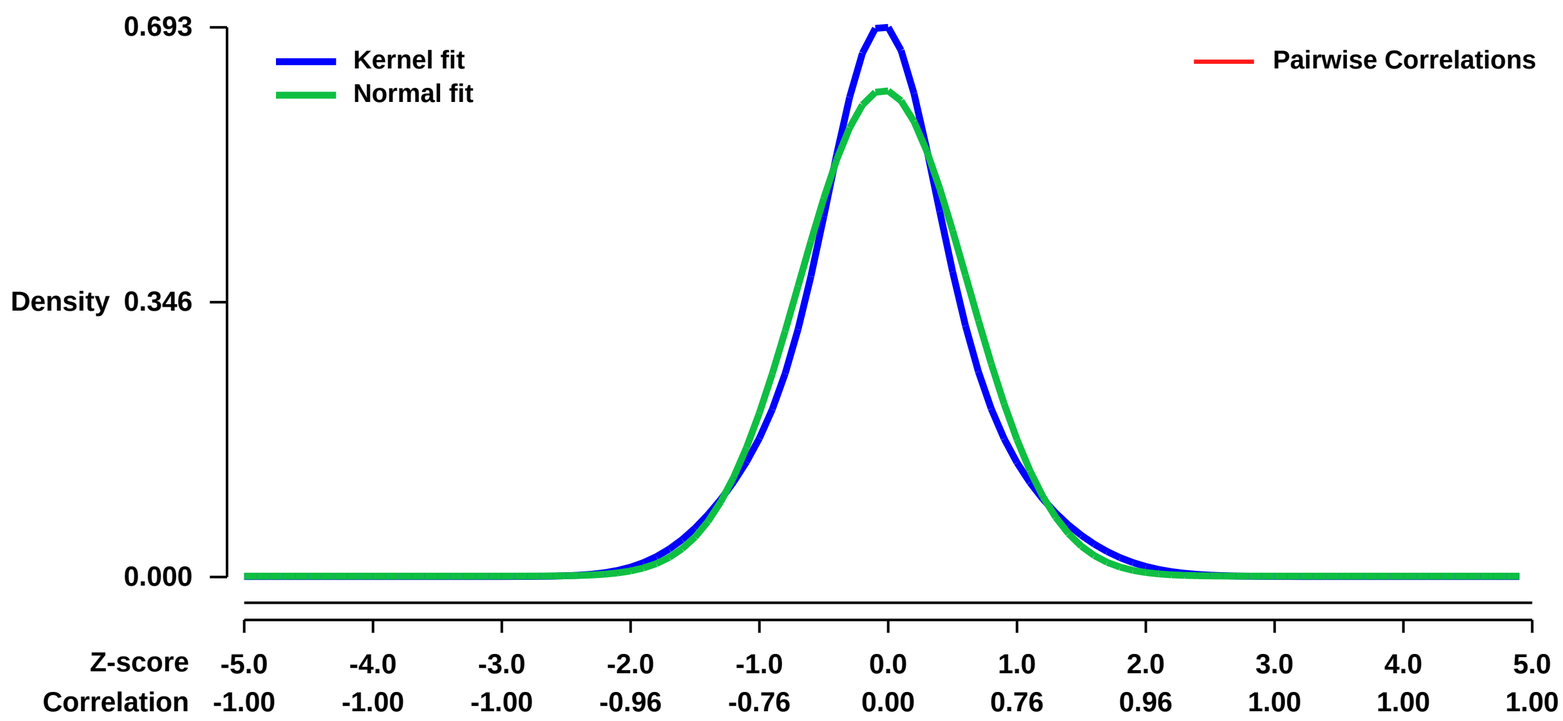

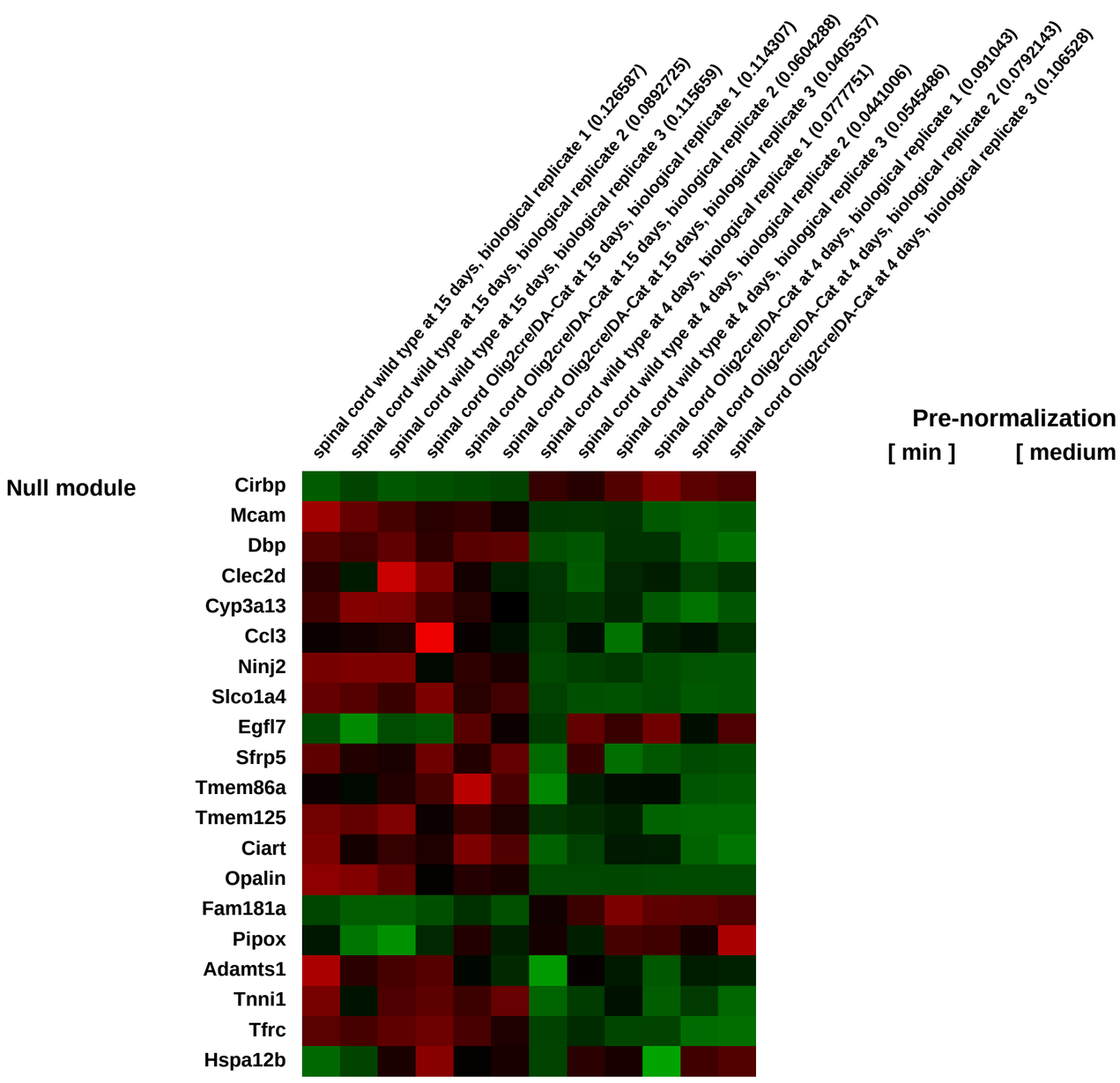

GEO Series "GSE45229" Expression Profiles

Num of samples in this series: 20

Scale of expression profile Z-scores

-3.0 -2.0 -1.0 0.0 1.0 2.0 3.0

GEO Link:	http://www.ncbi.nlm.nih.gov/geo/query/acc.cgi?acc=GSE45229
Status:	Public on Apr 16 2013
Title:	Unique pharmacological actions of atypical neuroleptic quetiapine: possible role in cell cycle/fate control
Organism:	Mus musculus
Experiment type:	Expression profiling by array
Platform:	GPL1261
Pubmed ID:	23549417
Summary & Design:	**Summary:** Quetiapine is an atypical neuroleptic with a pharmacological profile distinct from classic neuroleptics. It is currently approved for treating patients with schizophrenia, major depression and bipolar I disorder. However, its cellular effects remain elusive. We used microarrays to characterize RNA transcript levels in the brains of mice chronically treated with quetiapine, the neuroleptic haloperidol, or vehicle. We further characterized particular RNA transcripts in cortical cell cultures. **Overall design:** Mice were given one of 5 treatments (vehicle, 1 mg/kg haloperidol, 0.3 mg/kg haloperidol, 100 mg/kg quetiapine, 10 mg/kg quetiapine). Pooled tissue samples were used for microarray analysis of gene expression in the frontal cortex (FC) and striatum (STR). Frontal cortex gene targets were subsequently verified with quantitative real-time PCR (qRT-PCR) from the same cohort of mice and an independent cohort.

Background corr dist: KL-Divergence = 0.1111, L1-Distance = 0.0722, L2-Distance = 0.0098, Normal std = 0.4609

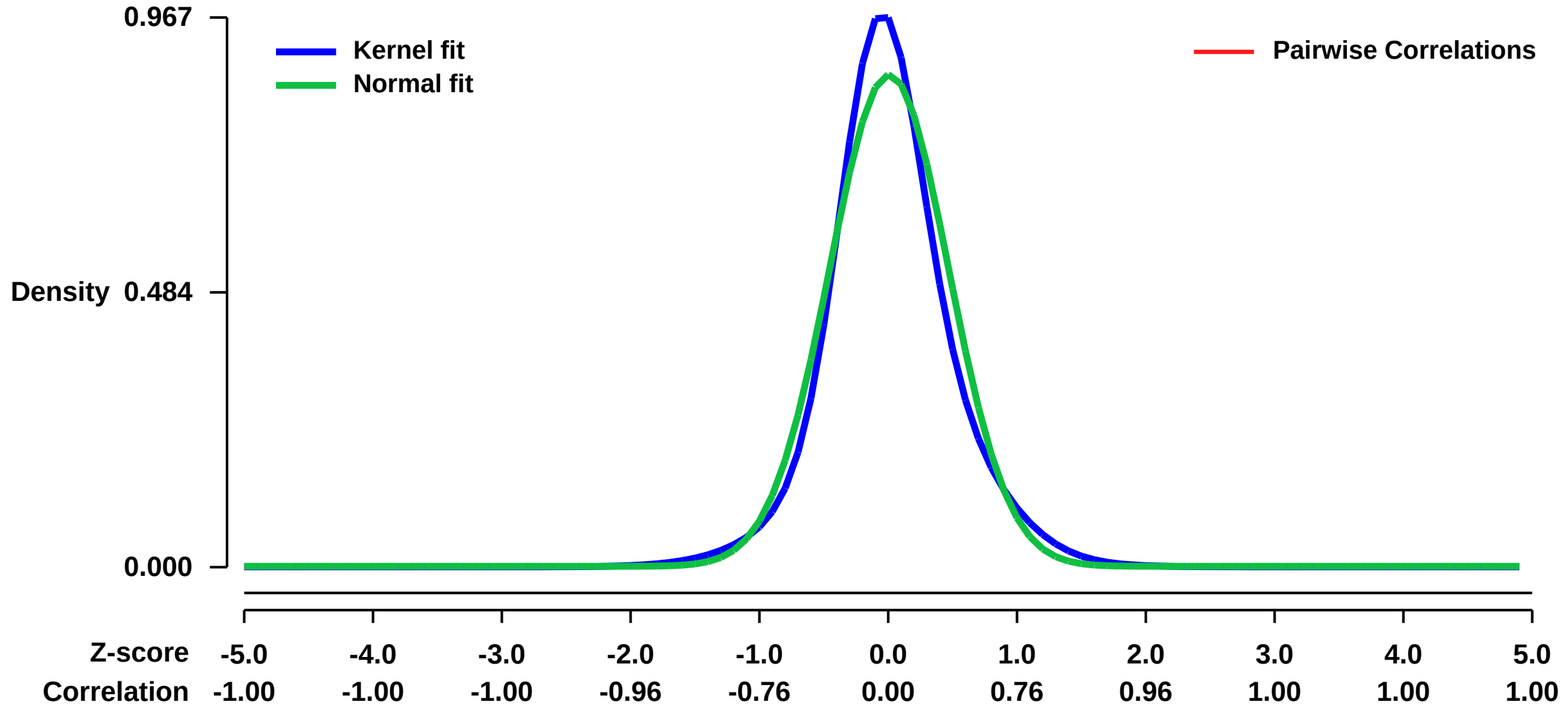

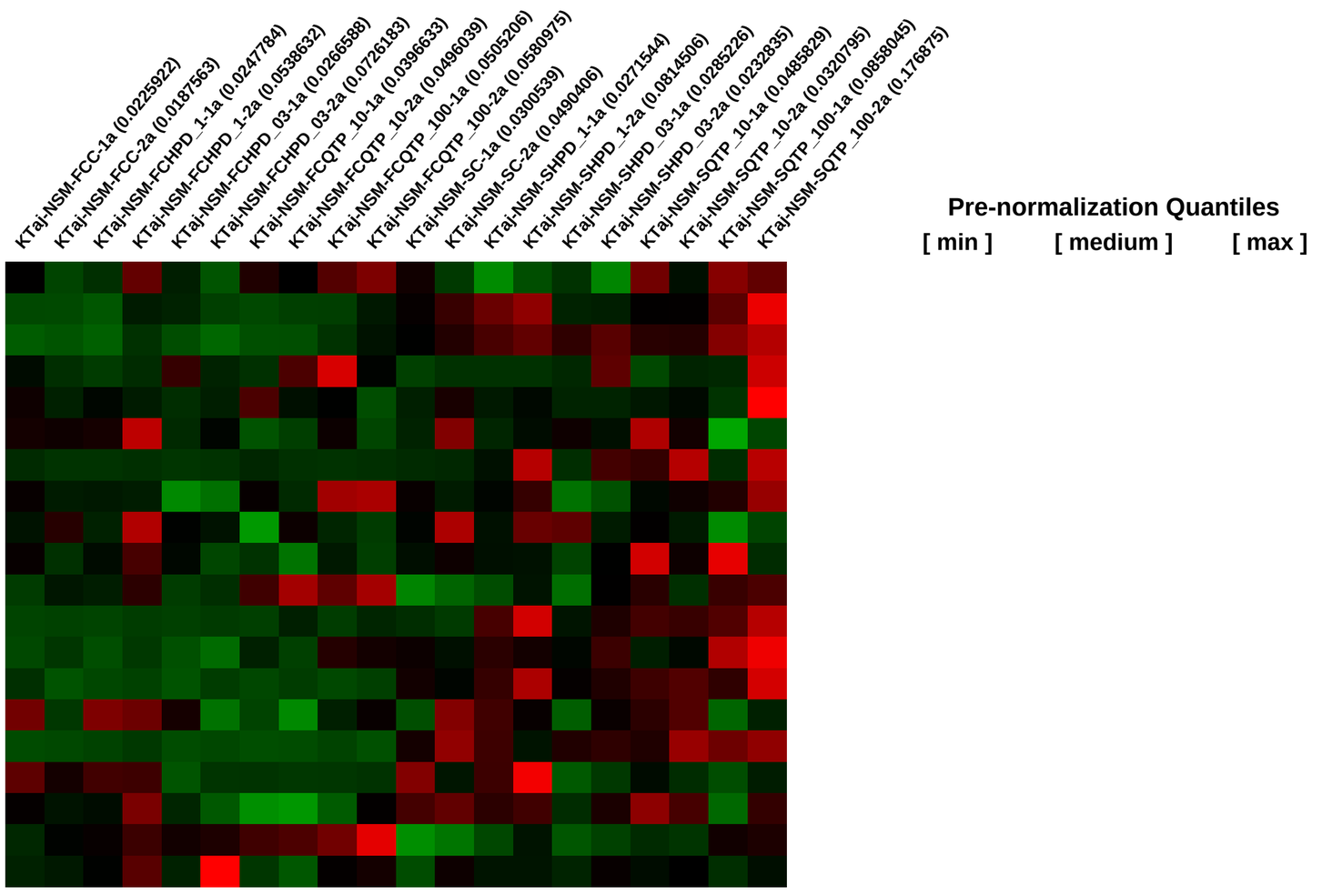

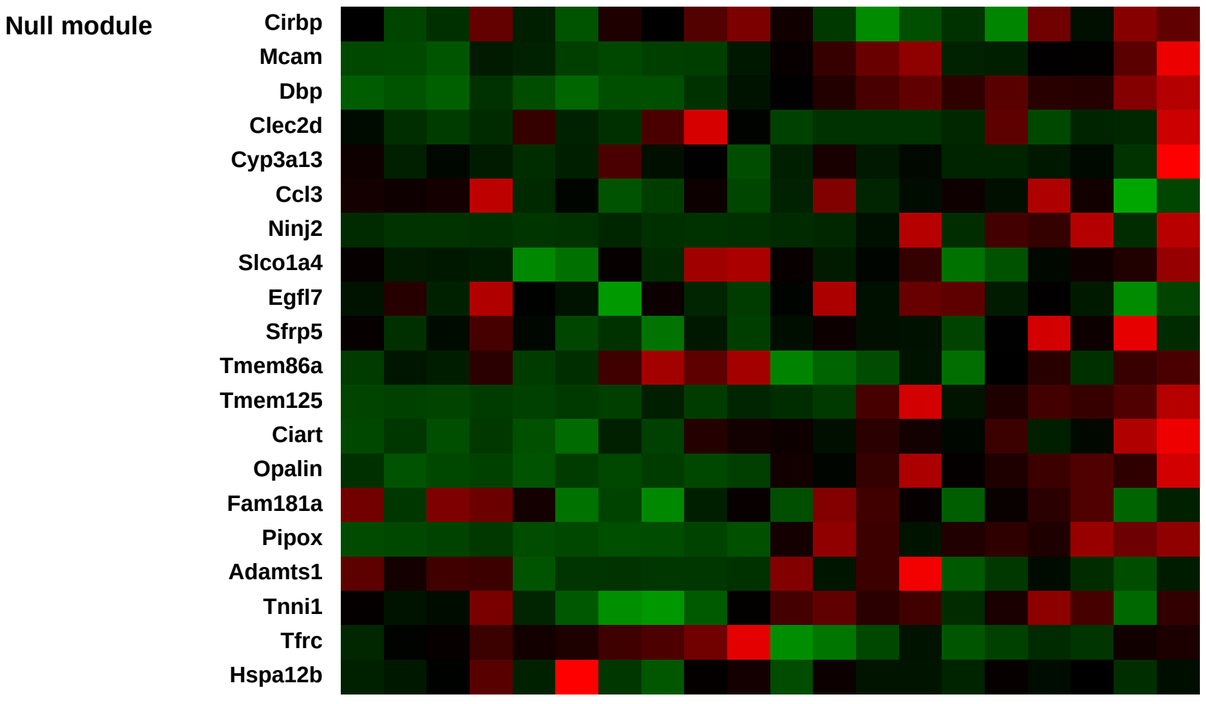

GEO Series "GSE30561" Expression Profiles

Num of samples in this series: 6

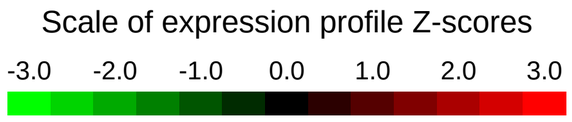

GEO Link:	**http://www.ncbi.nlm.nih.gov/geo/query/acc.cgi?acc=GSE30561**
Status:	**Public on Nov 01 2011**
Title:	**Expression data from mouse embryonic stem cells lacking the Alkbh1 gene**
Organism:	**Mus musculus**
Experiment type:	**Expression profiling by array**
Platform:	**GPL1261**
Pubmed ID:	

Summary & Design:

Summary:
AlkB homolog 1 (ALKBH1) is one of nine members of the AlkB homologs in mammals. Most Alkbh1-deficient mice die during embryonic development, and survivors have severe defects in tissues originating from the ectodermal lineage. We hypothesized the phenotype to rely upon aberrant epigenetic regulation and provided evidence for ALKBH1 to be a histone H2A demethylase. We used a whole genome expression microarray to detail differentially expressed genes in embryonic stem cells lacking the Alkbh1 gene and identified distinct classes of up- and down-regulated genes during this process.

Overall design:
Wild type and Alkbh-/- embryonic stem cells were established to identify differentially expressed genes at day 0, undifferentiated cells. We sought to obtain a subset of genes possibly explaining the observed phenotype. Total RNA was extracted and hybridized on Affymetrix GeneChips. 3 parallels were analyzed from each of the two genotypes.

Background corr dist: **KL-Divergence = 0.0310, L1-Distance = 0.0211, L2-Distance = 0.0004, Normal std = 0.6731**

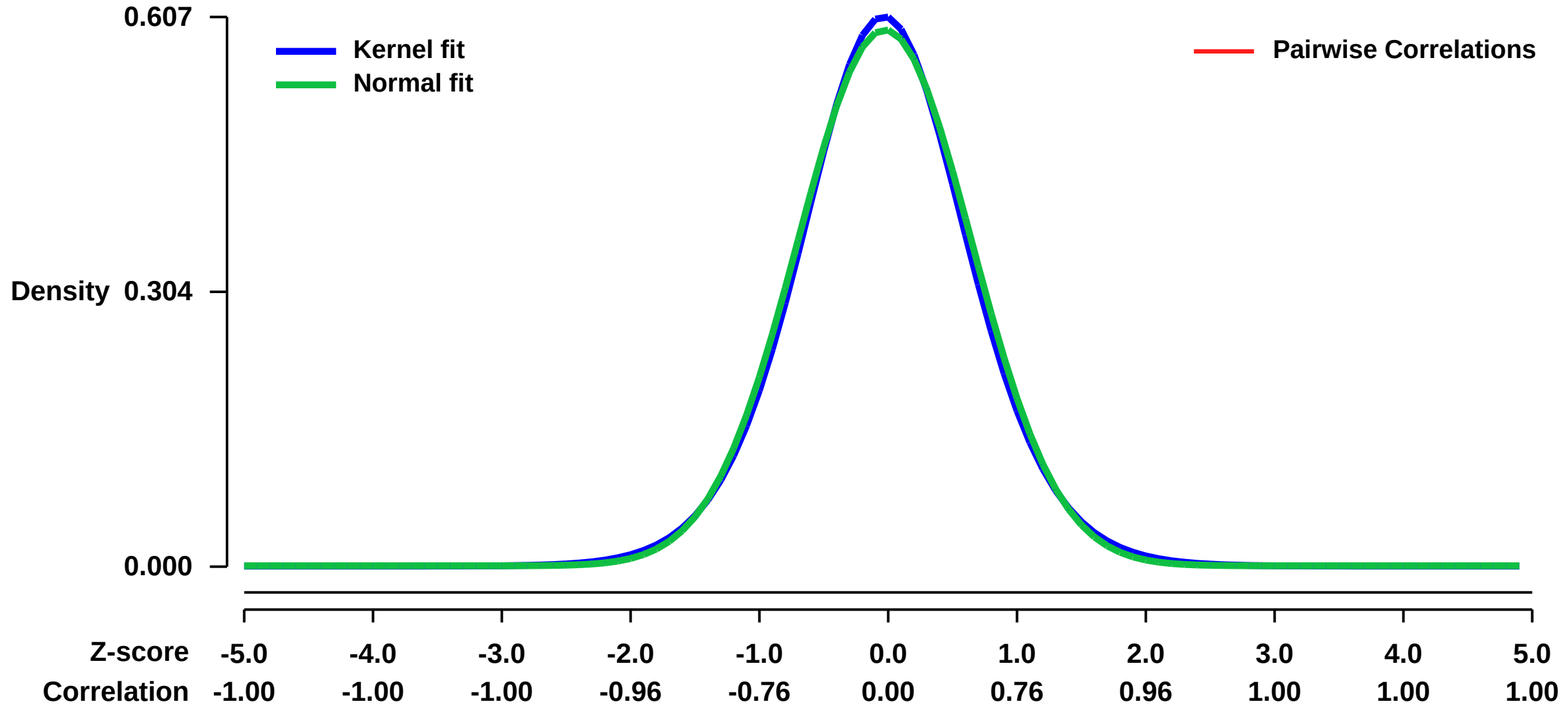

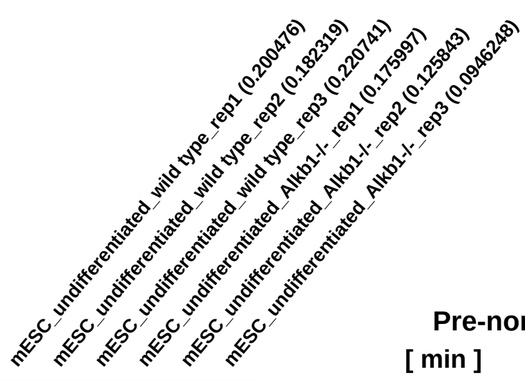

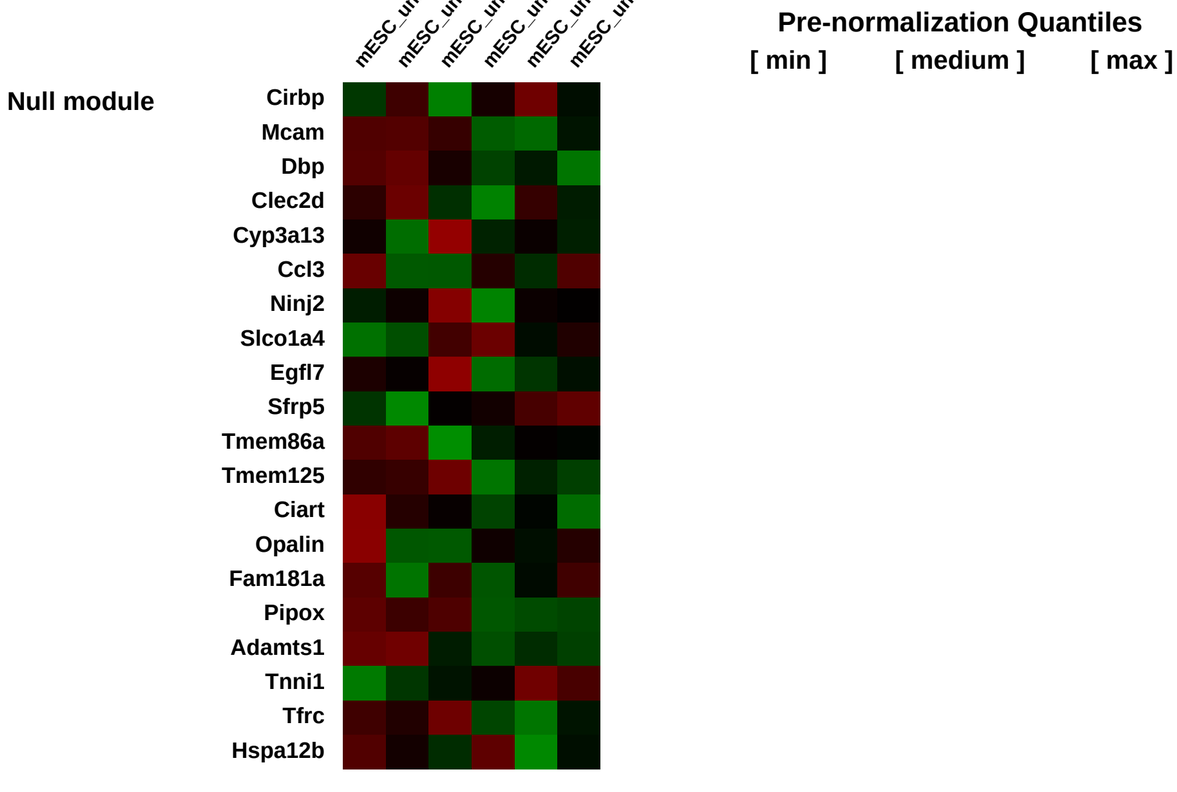

GEO Series "GSE34863" Expression Profiles

Num of samples in this series: 8

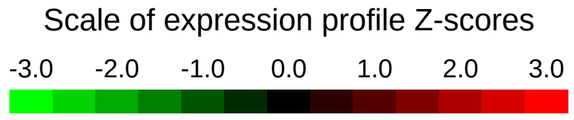

GEO Link:	http://www.ncbi.nlm.nih.gov/geo/query/acc.cgi?acc=GSE34863
Status:	Public on Jan 05 2012
Title:	Expression in IFN-gamma treated control and Atg5-/- macrophages
Organism:	Mus musculus
Experiment type:	Expression profiling by array
Platform:	GPL1261
Pubmed ID:	22520467
Summary & Design:	**Summary:** Type-I (‹–/‹†) and -II (‹‡) interferons (IFN), through an incompletely understood combination of redundant and unique mechanisms, are essential for host resistance to viral infection. We report a requirement for the Atg5-Atg12/Atg16L1 autophagosome elongation complex in IFN‹‡-mediated control of murine norovirus in macrophages. We use microarrays to compare transcriptional changes induced in control and Atg5 deficient macrophages by IFN‹‡ treatment. **Overall design:** Bone marrow derived macrophages were generated from Atg5flox/flox and Atg5flox/flox+LysM cre mice and treated with media alone or 100U/ml of IFN‹‡ for 14 hrs. RNA was extracted using Trizol (Invitrogen) and 10 ´µg of RNA hybridized to Affymetrix microarrays.

Background corr dist: KL-Divergence = 0.0360, L1-Distance = 0.0137, L2-Distance = 0.0002, Normal std = 0.6209

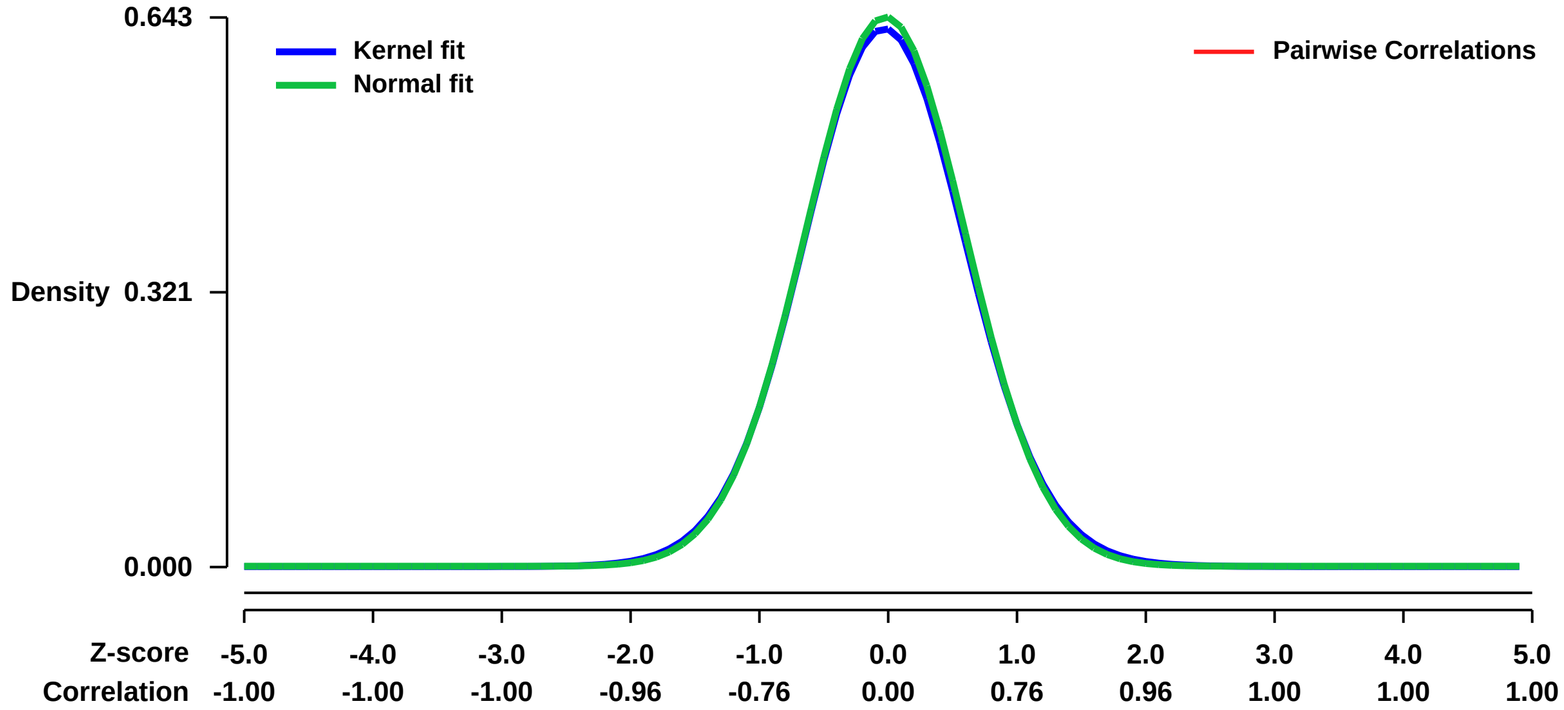

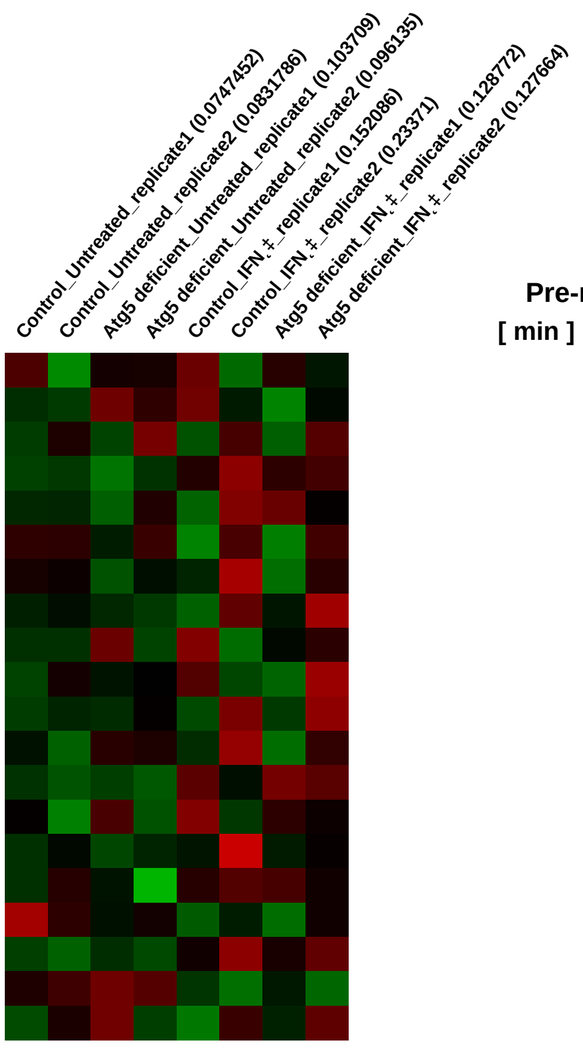

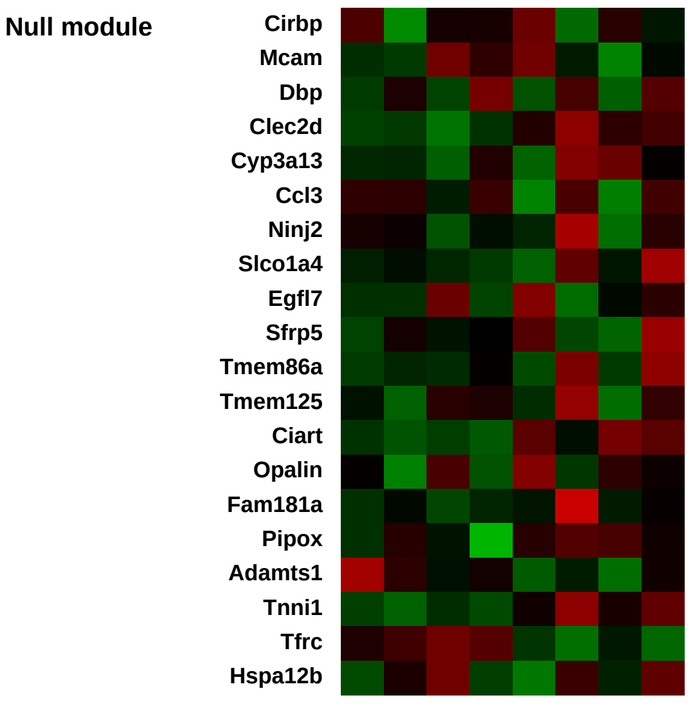

GEO Series "GSE50821" Expression Profiles

Num of samples in this series: 14

Scale of expression profile Z-scores

-3.0 -2.0 -1.0 0.0 1.0 2.0 3.0

GEO Link:	http://www.ncbi.nlm.nih.gov/geo/query/acc.cgi?acc=GSE50821
Status:	Public on May 08 2014
Title:	Restoring Systemic GDF11 Levels Reverses Age-Related Dysfunction in Mouse Skeletal Muscle
Organism:	Mus musculus
Experiment type:	Expression profiling by array
Platform:	GPL1261
Pubmed ID:	24797481
Summary & Design:	**Summary:** In this study, we investigated signaling pathways in Skeletal muscle precursors that are altered with aging and age-related deficits in muscle regenerative potential. We performed fluorescence activated cell sorting (FACS) to obtain highly purified skeletal muscle satellite cells from young, middle-aged and old mice. Parabiosis experiments indicate that impaired regeneration in aged mice is reversible by exposure to a young circulation, suggesting that young blood contains humoral ""rejuvenating"" factors that can restore regenerative function. Here, we demonstrate that the circulating protein growth differentiation factor 11 (GDF11) is a rejuvenating factor for skeletal muscle. Supplementation of systemic GDF11 levels, which normally decline with age, by heterochronic parabiosis or systemic delivery of recombinant protein, reversed functional impairments and restored genomic integrity in aged muscle stem cells (satellite cells). Increased GDF11 levels in aged mice also improved muscle structural and functional features and increased strength and endurance exercise capacity. These data indicate that GDF11 systemically regulates muscle aging and may be therapeutically useful for reversing age-related skeletal muscle and stem cell dysfunction. **Overall design:** We used Affymetrix Mouse Genome array to identify global transcriptional changes associated with age in skeletal muscle precursors.

Background corr dist: KL-Divergence = 0.1316, L1-Distance = 0.0442, L2-Distance = 0.0043, Normal std = 0.3912

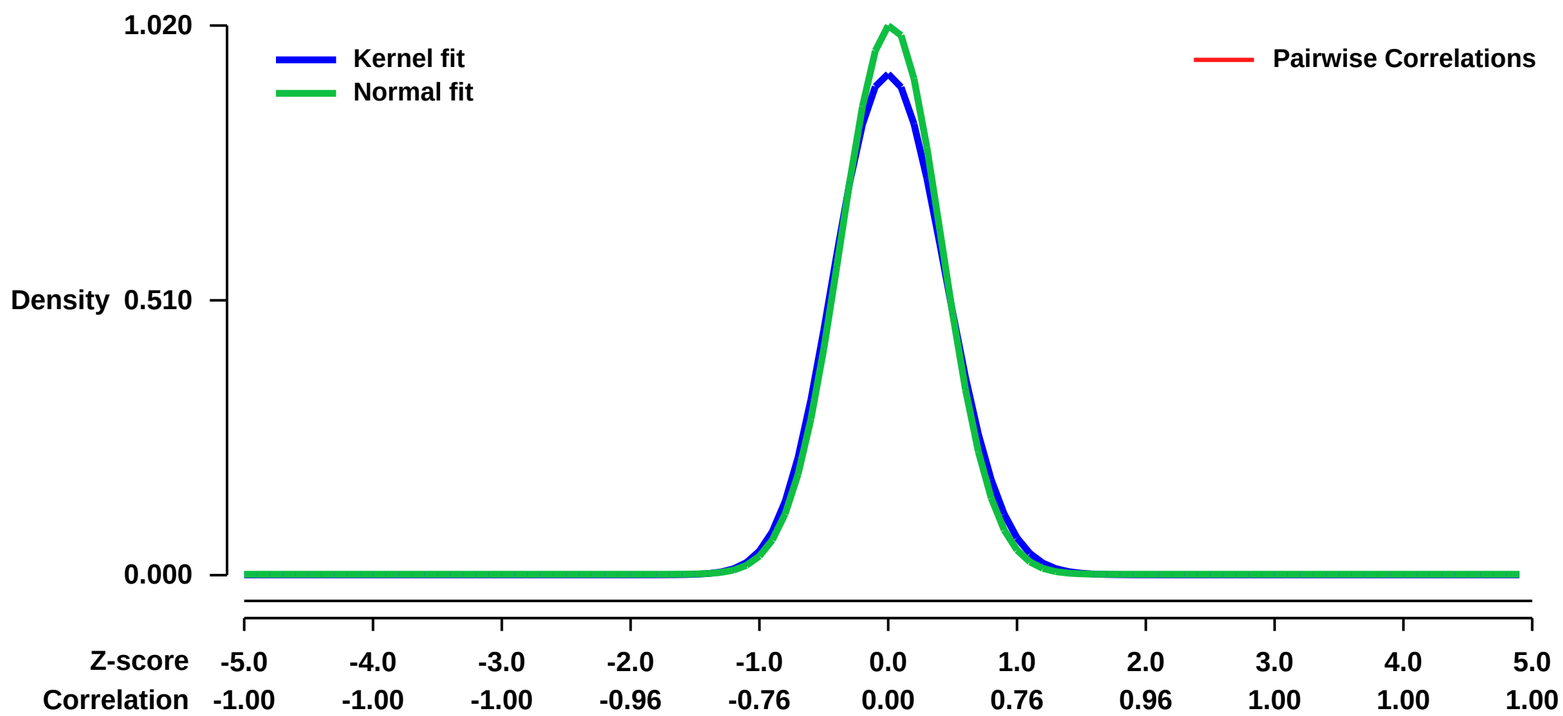

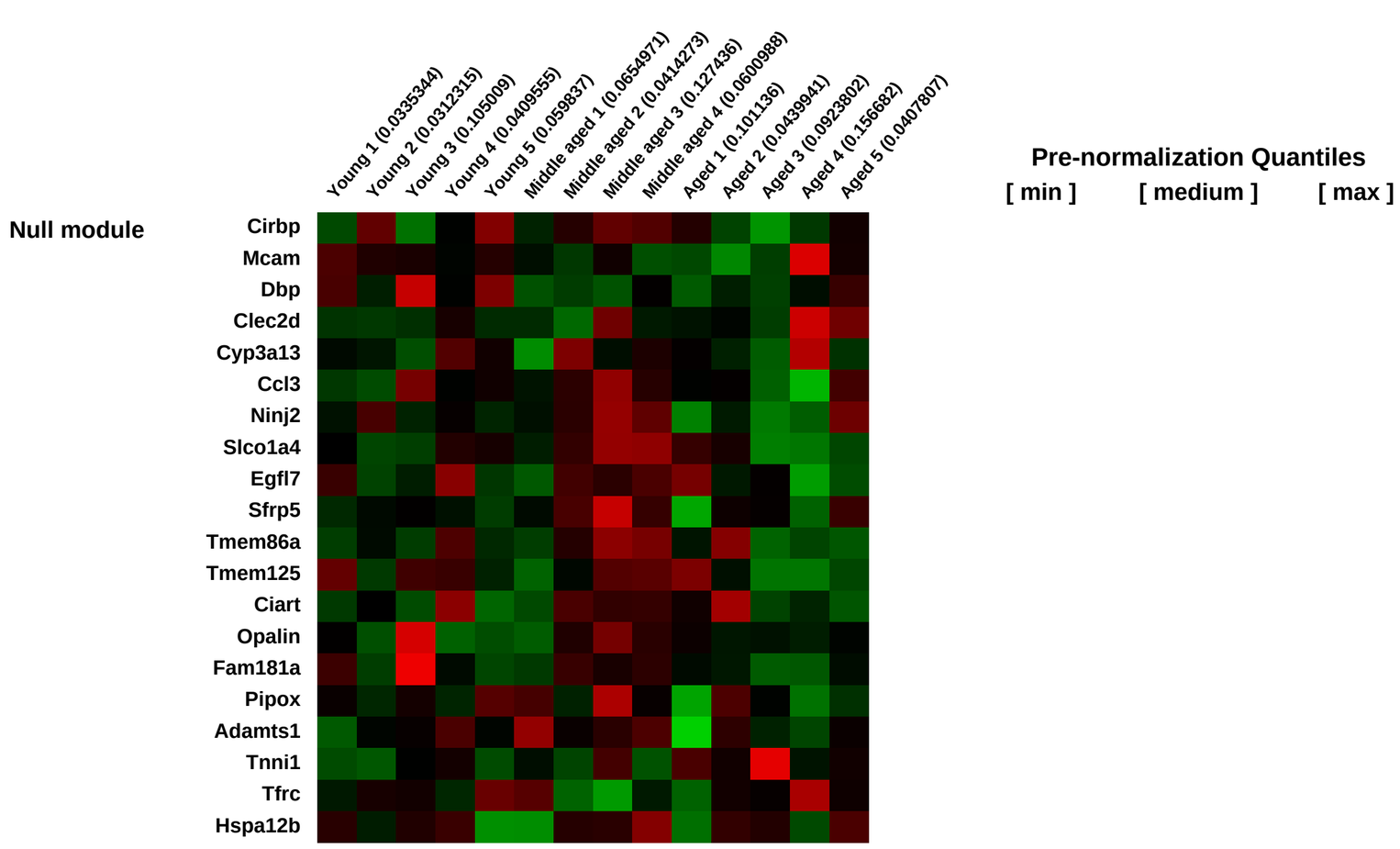

GEO Series "GSE41759" Expression Profiles

Num of samples in this series: 14

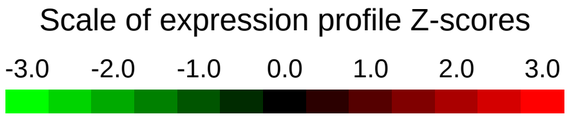

GEO Link:	**http://www.ncbi.nlm.nih.gov/geo/query/acc.cgi?acc=GSE41759**
Status:	**Public on Apr 19 2013**
Title:	**Differential Gene Expression and Mitochondrial Dysfunction in Imprinting center deletion (PWS- IC del) Mouse model of Prader-Willi Syndrome**
Organism:	**Mus musculus**
Experiment type:	**Expression profiling by array**
Platform:	**GPL1261**
Pubmed ID:	
Summary & Design:	**Summary:** **Prader-Willi syndrome (PWS) is a genetic disorder caused by deficiency of imprinted gene expression from the paternal chromosome 15q11-15q13 and clinically characterized by neonatal hypotonia, short stature, cognitive impairment, hypogonadism, hyperphagia, morbid obesity and diabetes. Previous clinical studies suggest that a defect in energy metabolism may be involved in the pathogenesis of PWS. Assessment of enzyme activities of mitochondrial oxidative phosphorylation (OXPHOS) complexes in the brain, heart, liver and muscle were assessed.** **We used microarrays to detail the global programme of gene expression underlyingthe PWS and identified distinct classes of disregulated genes during this process.** **Overall design:** **Skeletal (quadriceps) muscle Vastus Lateralis and whole brain samples from the mutant mice and their wild-type age-matched littermates were analyzed by microarray technology using the Mouse Genome 430 2.0 arrays (Affymetrix).**

Background corr dist: **KL-Divergence = 0.0080, L1-Distance = 0.0325, L2-Distance = 0.0010, Normal std = 0.9775**

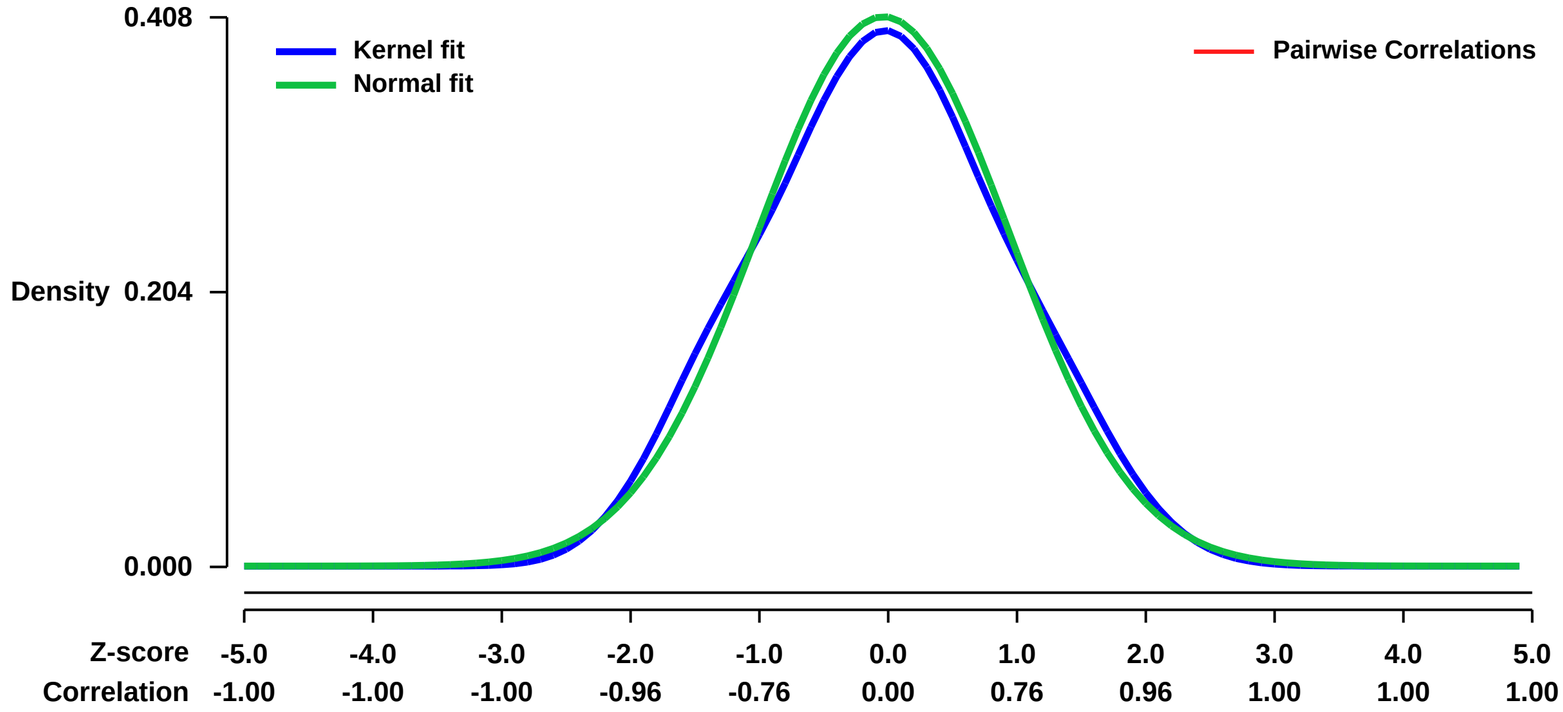

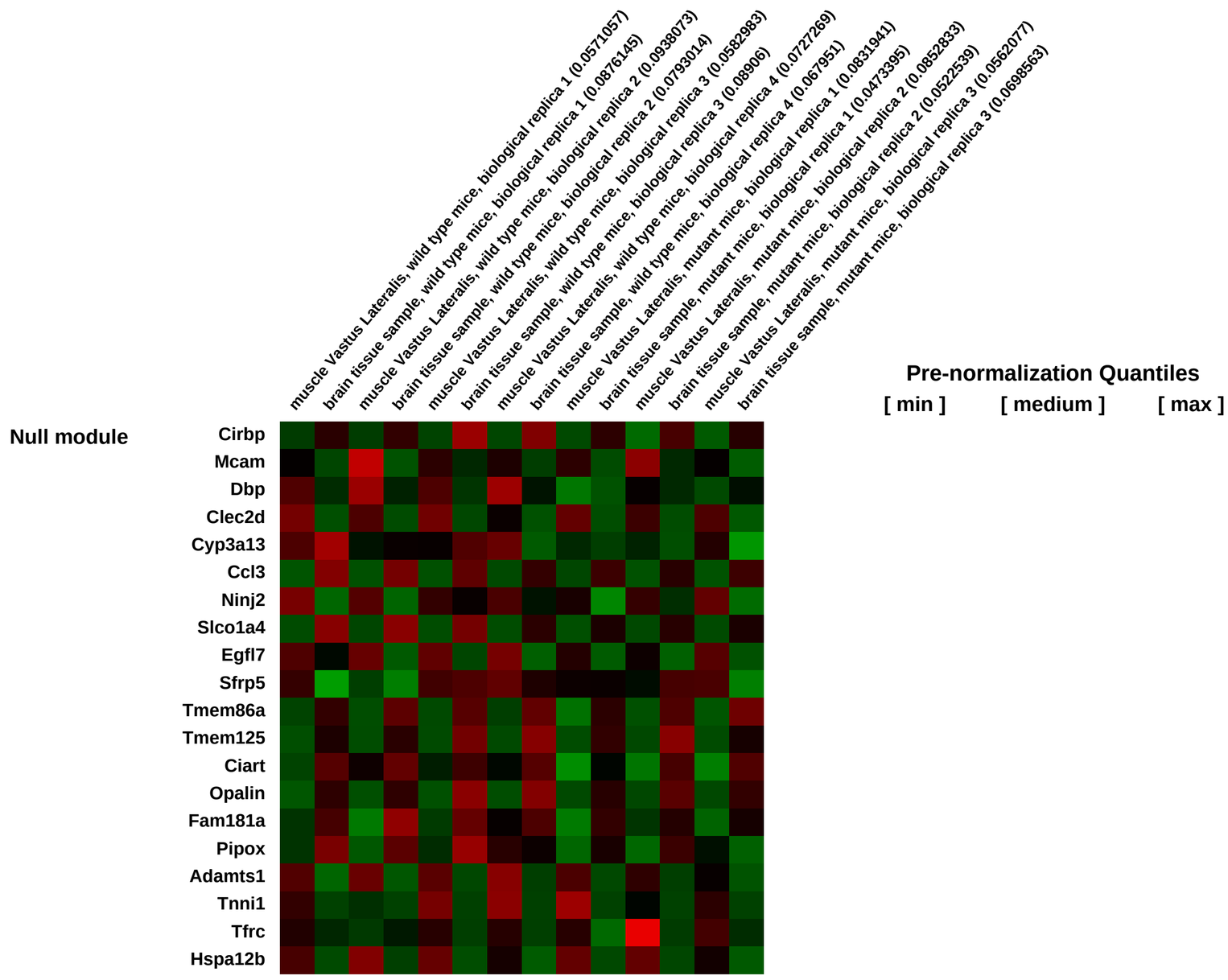

GEO Series "GSE38031" Expression Profiles

Num of samples in this series: 8

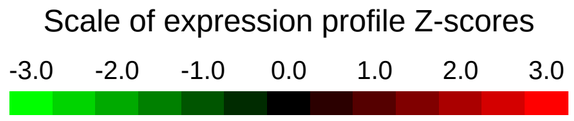

GEO Link:	**http://www.ncbi.nlm.nih.gov/geo/query/acc.cgi?acc=GSE38031**
Status:	**Public on Jul 25 2013**
Title:	**DNA damage-induced differentiation of NSC**
Organism:	**Mus musculus**
Experiment type:	**Expression profiling by array**
Platform:	**GPL1261**
Pubmed ID:	**24052948**
Summary & Design:	**Summary:** **Murine ES-derived neural stem cells (NSC) were not irradiated (ctrl) or irradiated with 10Gy and cultured for 7 days (irr).** **The goal was to study the gene expression changes in NSC at d7 after irradiation.** **Overall design:** **Total RNA was extracted from 4 ctrl and 4 irr samples (biological quadruplicates).**

Background corr dist: **KL-Divergence = 0.0114, L1-Distance = 0.0339, L2-Distance = 0.0011, Normal std = 0.9128**

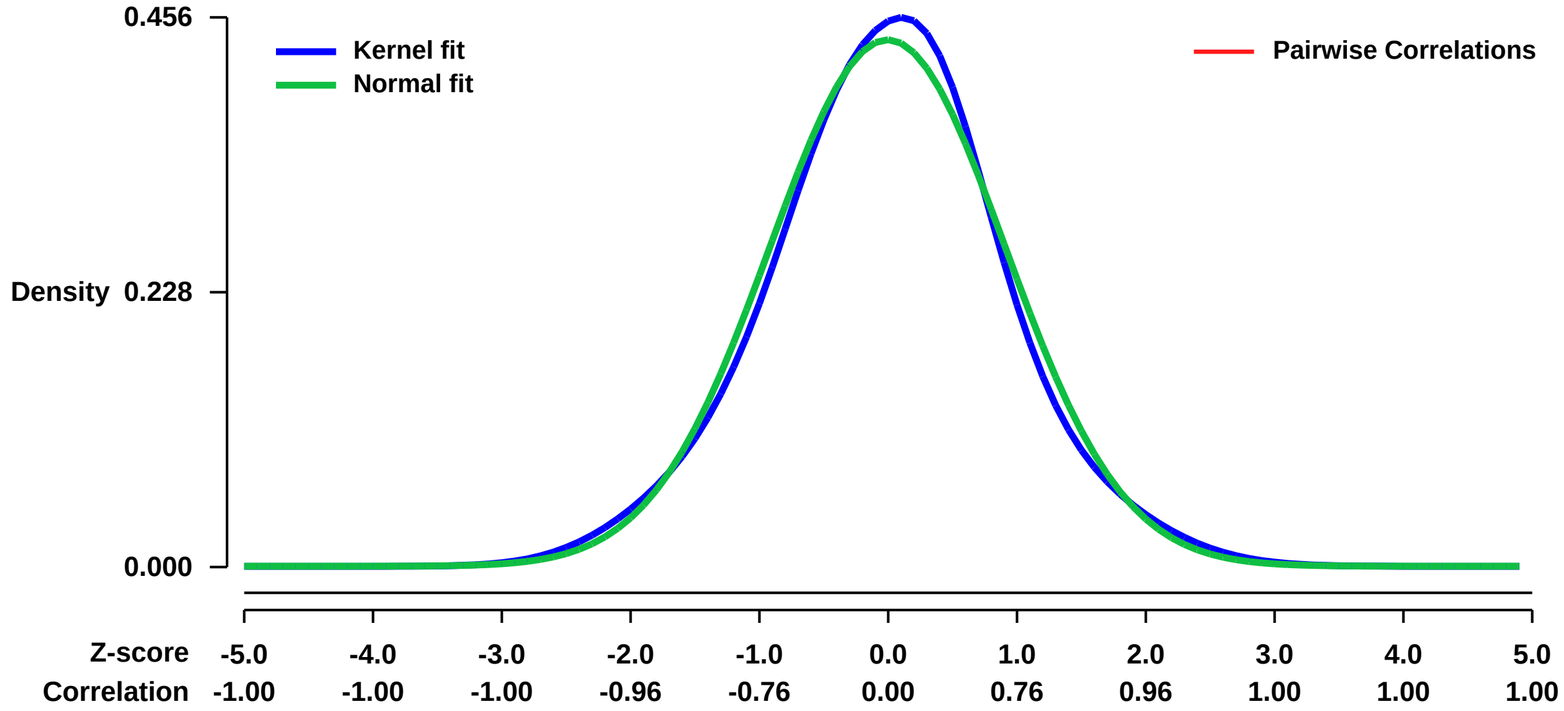

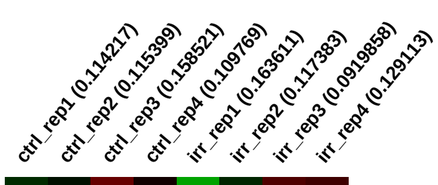

Pre-normalization Quantiles

[min] [medium] [max]

Null module

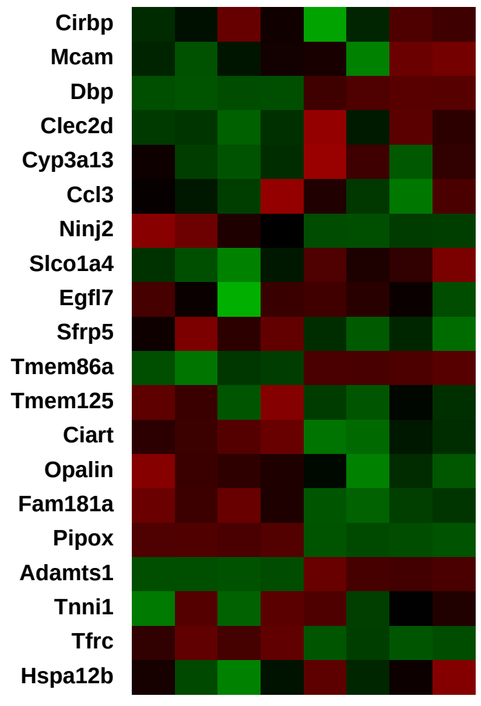

GEO Series "GSE23040" Expression Profiles

Num of samples in this series: 6

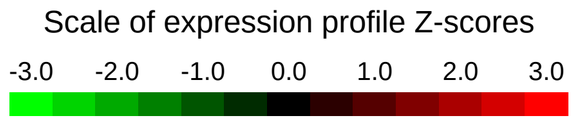

GEO Link:	http://www.ncbi.nlm.nih.gov/geo/query/acc.cgi?acc=GSE23040
Status:	Public on Jan 01 2011
Title:	Loss of Hepatocyte-Nuclear-Factor-1$_{\alpha}$– Impacts on Adult Mouse Intestinal Epithelial Cell Growth and Cell Lineages Differentiation
Organism:	Mus musculus
Experiment type:	Expression profiling by array
Platform:	GPL1261
Pubmed ID:	20808783
Summary & Design:	**Summary:** Although hepatocyte-nuclear-factor-1$_{\alpha}$– (Hnf1$_{\alpha}$–) is crucial for pancreas and liver functions, it is believed to play a limited functional role for intestinal epithelial functions. The aim of this study was to assess the consequences of abrogating Hnf1$_{\alpha}$– on the maintenance of adult small intestinal epithelial functions. Methodology/Principal Findings An Hnf1$_{\alpha}$– knockout mouse model was used. Assessment of histological abnormalities, crypt epithelial cell proliferation, epithelial barrier, glucose transport and signalling pathways were measured in these animals. Changes in global gene expression were also analyzed. Mice lacking Hnf1$_{\alpha}$– displayed increased crypt proliferation and intestinalomegaly as well as a disturbance of intestinal epithelial cell lineages production during adult life. This phenotype was associated with a decrease of the mucosal barrier function and lumen-to-blood glucose delivery. The mammalian target of rapamycin (mTOR) signalling pathway was found to be overly activated in the small intestine of adult Hnf1$_{\alpha}$– mutant mice. The intestinal epithelium of Hnf1$_{\alpha}$– null mice displayed a reduction of the enteroendocrine cell population. An impact was also observed on proper Paneth cell differentiation with abnormalities in the granule exocytosis pathway. Conclusions/Significance Together, these results unravel a functional role for Hnf1$_{\alpha}$– in regulating adult intestinal growth and sustaining the functions of intestinal epithelial cell lineages. **Overall design:** HNF1alpha was knocked out. A total of 3 control and 3 mutant littermate individuals were sacrificed at 4 months of age. The jejunum was harvested and total RNA was isolated from each individual. Each RNA sample was independently used to generate probes to screen Affymetrix chips.

Background corr dist: KL-Divergence = 0.0372, L1-Distance = 0.0151, L2-Distance = 0.0002, Normal std = 0.6258

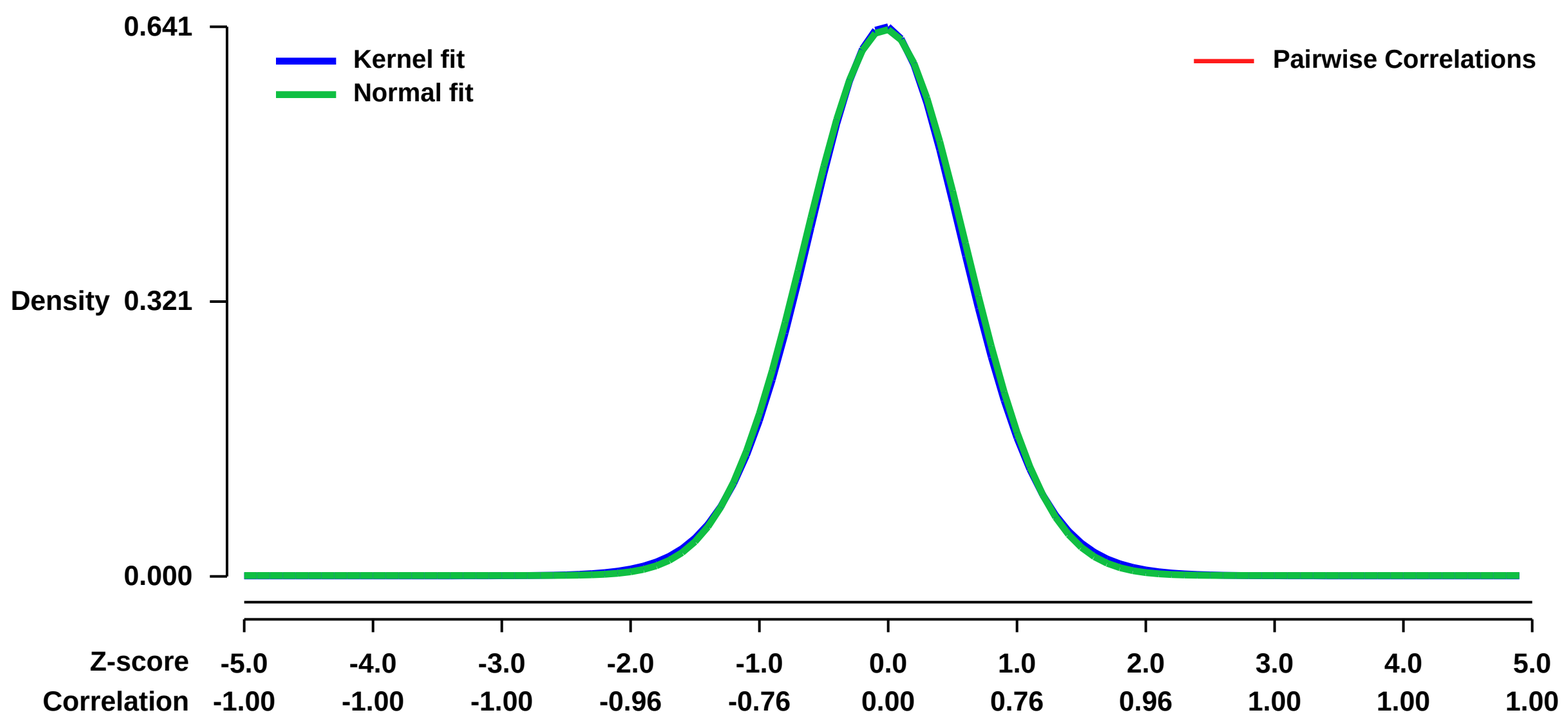

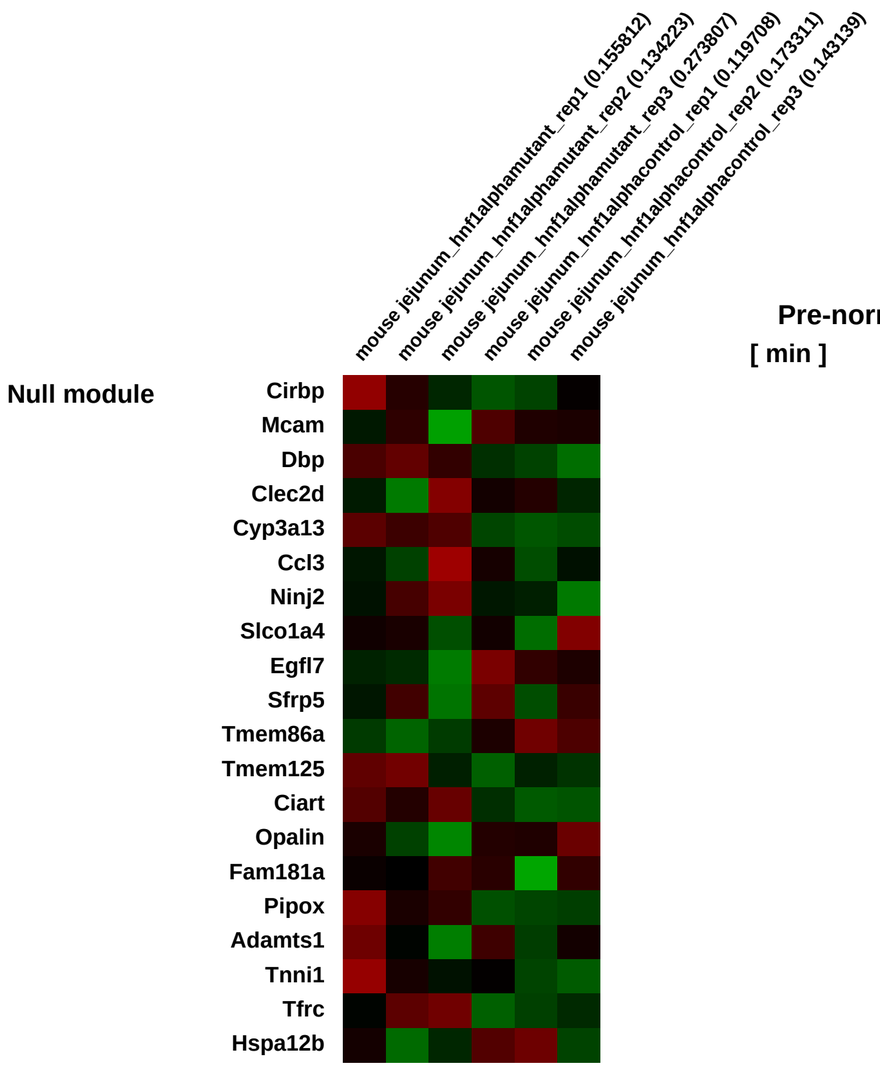

GEO Series "GSE25908" Expression Profiles

Num of samples in this series: 111

Details of this dataset are not shown due to large number of samples and the page size limit.

Find details in http://www.ncbi.nlm.nih.gov/geo/query/acc.cgi?acc=GSE25908

Background corr dist: KL-Divergence = 0.6449, L1-Distance = 0.0921, L2-Distance = 0.0285, Normal std = 0.2023

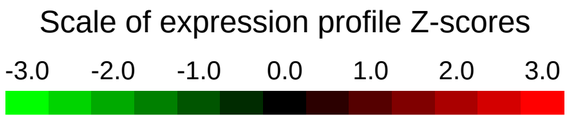

GEO Series "GSE12581" Expression Profiles

Num of samples in this series: 16

Scale of expression profile Z-scores

-3.0 -2.0 -1.0 0.0 1.0 2.0 3.0

GEO Link:	http://www.ncbi.nlm.nih.gov/geo/query/acc.cgi?acc=GSE12581
Status:	Public on Dec 01 2008
Title:	Gene expression profiles of the lymphoid and non-lymphoid leukemias induced by the Graffi murine leukemia retrovirus
Organism:	Mus musculus
Experiment type:	Expression profiling by array
Platform:	GPL1261
Pubmed ID:	21135260
Summary & Design:	**Summary:** We used the microarrays to obtain the cancerous signatures of T-cell, B-cell, erythroid and megakaryoblastic leukemias in mice. **Keywords: cell type comparison** **Overall design:** 16 samples are included, 13 corresponding to leukemic samples and 3 corresponding to control samples. Each control sample corresponds to the pooled RNA of 12 mice.

Background corr dist: KL-Divergence = 0.1679, L1-Distance = 0.0535, L2-Distance = 0.0073, Normal std = 0.3639

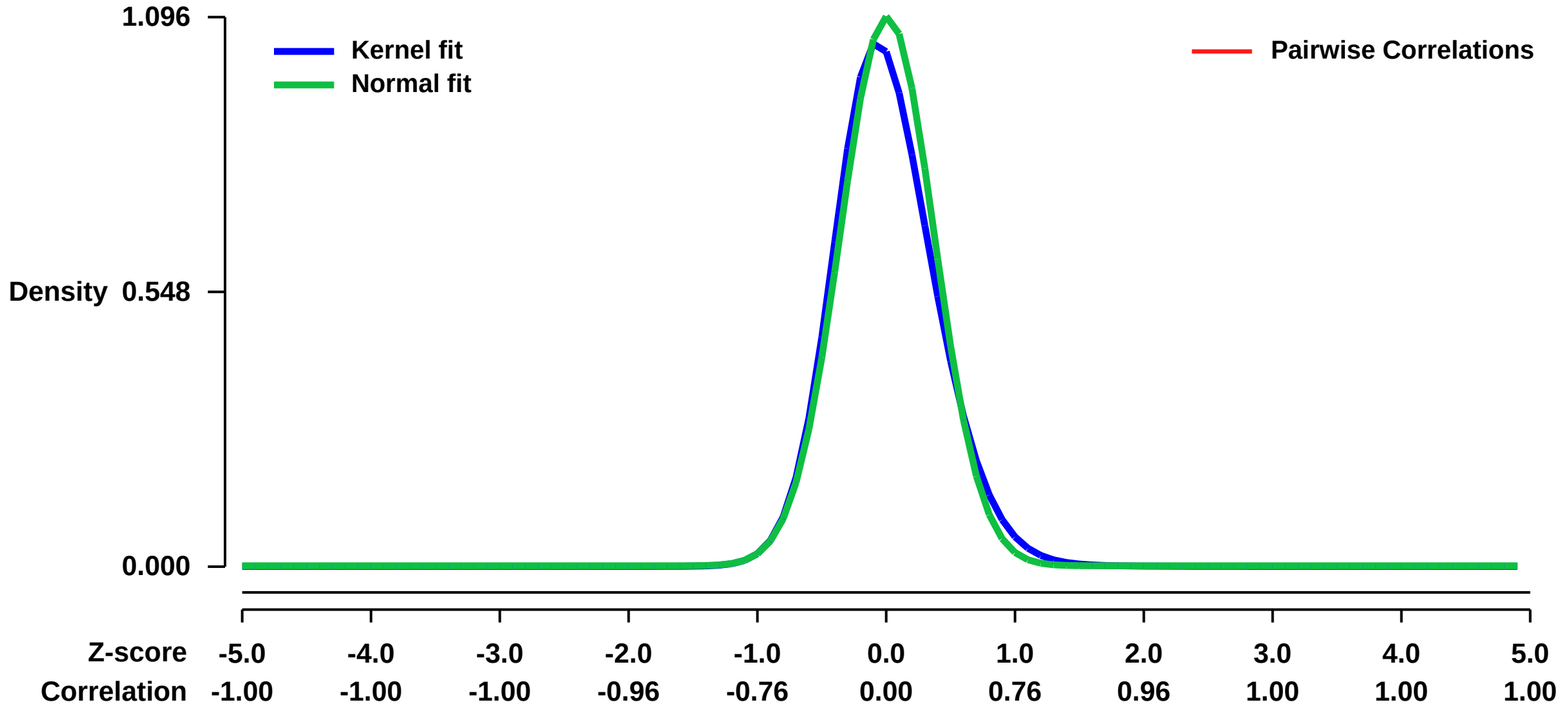

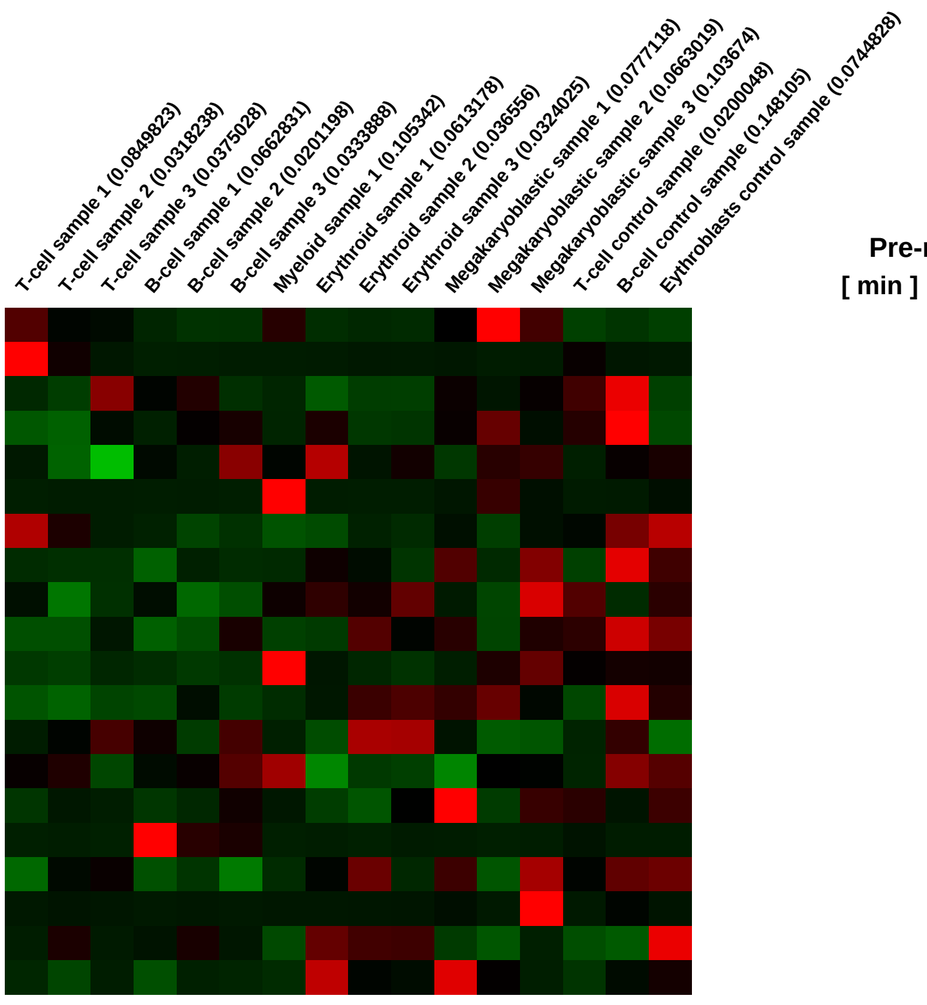

GEO Series "GSE6933" Expression Profiles

Num of samples in this series: 15

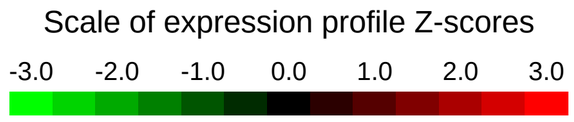

GEO Link:	**http://www.ncbi.nlm.nih.gov/geo/query/acc.cgi?acc=GSE6933**
Status:	**Public on Oct 11 2007**
Title:	**Unique Molecular Signature of Multipotent Adult Progenitor Cells (Affy)**
Organism:	**Mus musculus**
Experiment type:	**Expression profiling by array**
Platform:	**GPL1261**
Pubmed ID:	**17683608**
Summary & Design:	**Summary:** **We compare the transcriptome of embryonic stem cells (ESCs), adult stem cells with apparent greater differentiation potential such as multipotent adult progenitor cells (MAPCs), mesenchymal stem cells (MSCs) and neurospheres (NS). Mouse and rat MAPCs were used in this study and two different array platforms (Affymetrix and NIA) were used for mouse samples.** **Keywords: mRNA expression profiling, oligonucleotide microarrays, stem cells** **Overall design:** **Three mRNA samples (biological replicates) per cell type taken at different passage number were compared. Cell types include mouse ESCs, mouse MSCs and three clones isolated using mouse MAPC culture condition: mMAPC-1, mMAPC-2 and mClone-3. mMAPC-1 and mClone-3 were obtained from same bone marrow isolation, mMAPC-2 was obtained in a different bone marrow isolation. Two clones derived from same rat bone marrow using rat MAPC culture conditions were compared. Three mRNA samples (biological replicates) per clone were taken at different passage numbers**

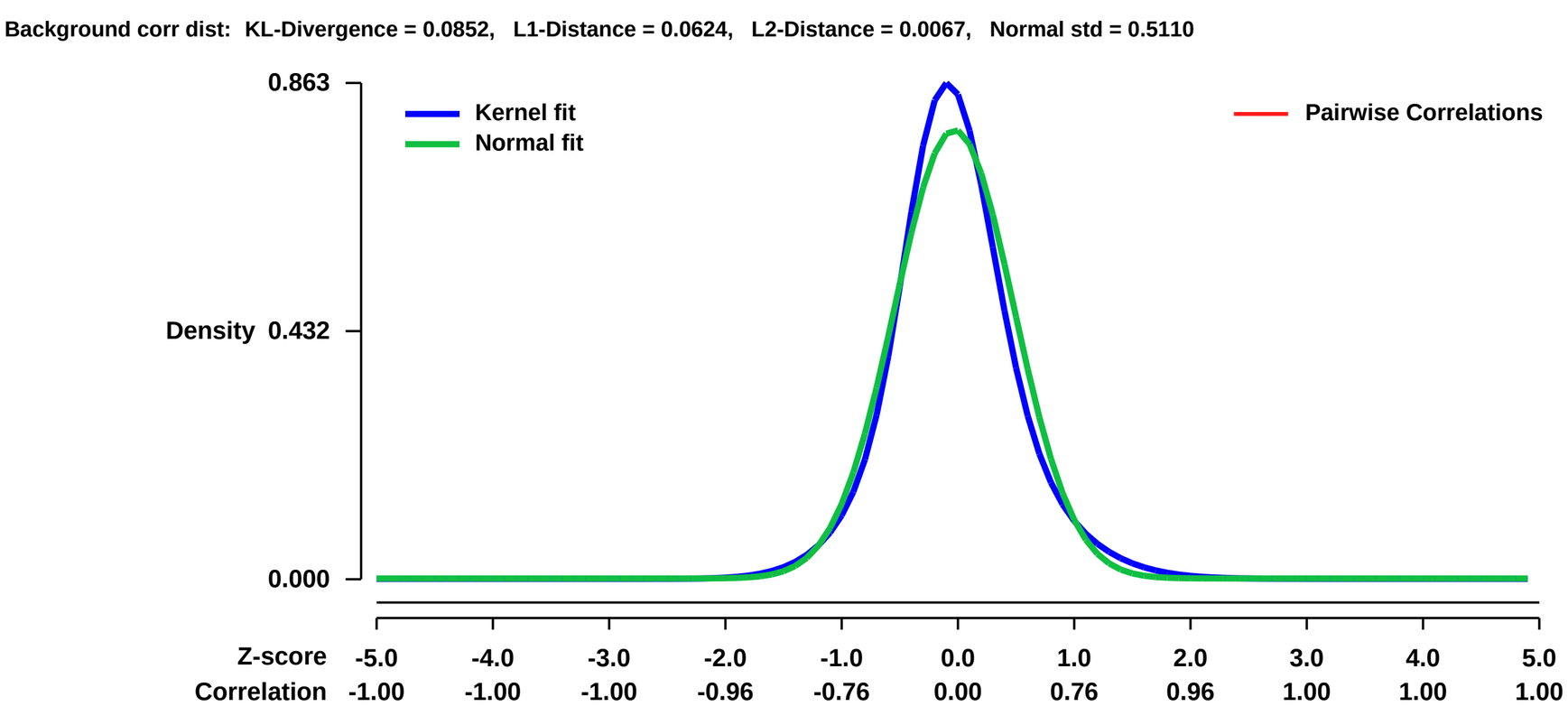

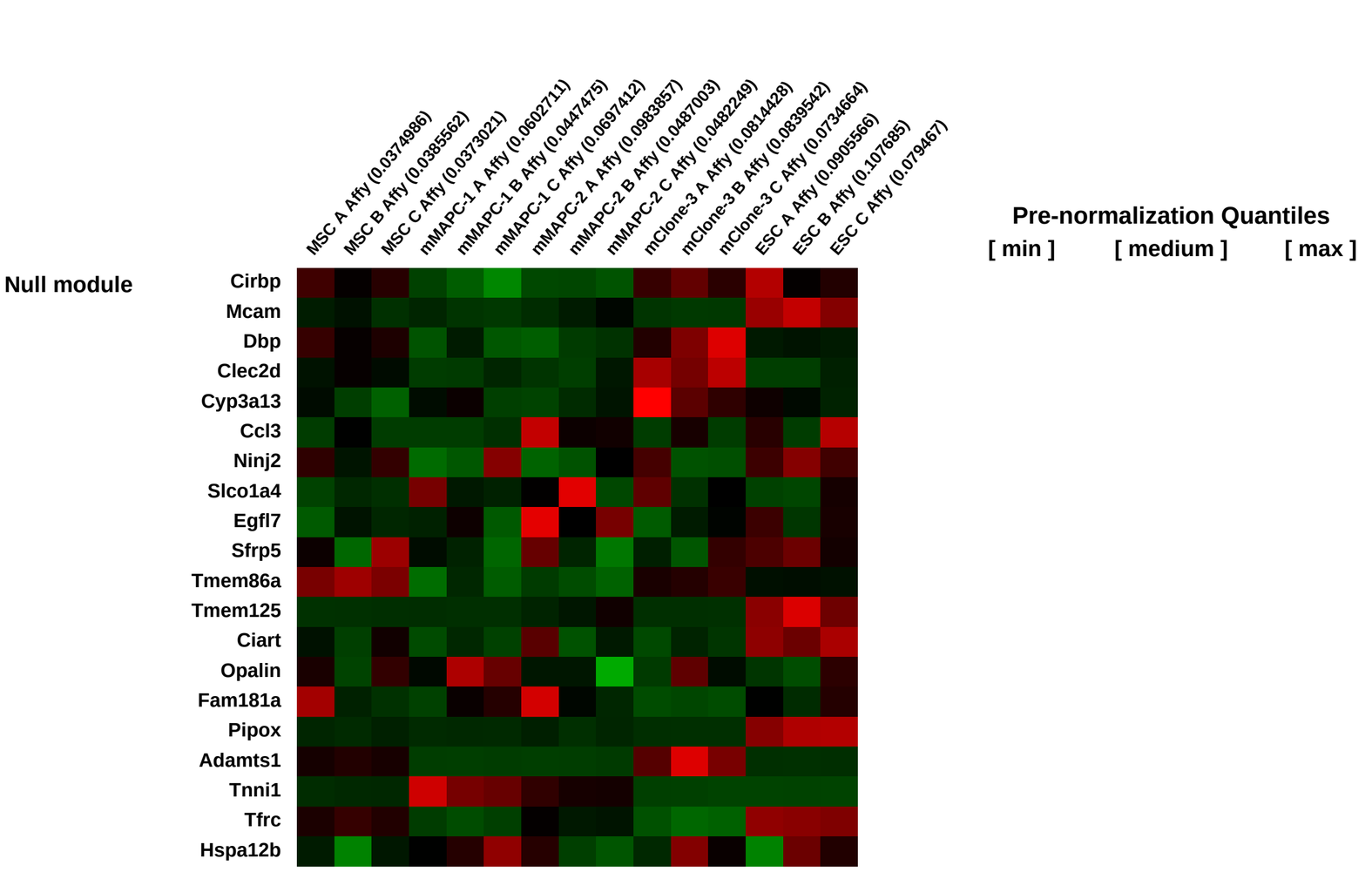

GEO Series "GSE50813" Expression Profiles

Num of samples in this series: 24

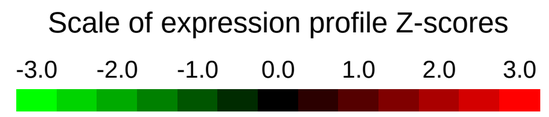

GEO Link:	http://www.ncbi.nlm.nih.gov/geo/query/acc.cgi?acc=GSE50813
Status:	Public on Dec 31 2013
Title:	Prevention of mammary tumor progression by silencing HoxA1 via intraductal injection of nanoparticle-formulated siRNA
Organism:	Mus musculus
Experiment type:	Expression profiling by array
Platform:	GPL1261
Pubmed ID:	24382894
Summary & Design:	**Summary:** Silencing HoxA1 in vivo by intraductal delivery of nanoparticle-formulated siRNA reduced mammary tumor incidence by 75% , reduced cell proliferation, and prevented loss of ER and PR expression. **Overall design:** 8 week wild type FVB mouse whole mammary gland and 8week to 20 week transgenic FVB C3(1)-SV40Tag mouse whole mammary gland

Background corr dist: KL-Divergence = 0.1026, L1-Distance = 0.0245, L2-Distance = 0.0008, Normal std = 0.4380

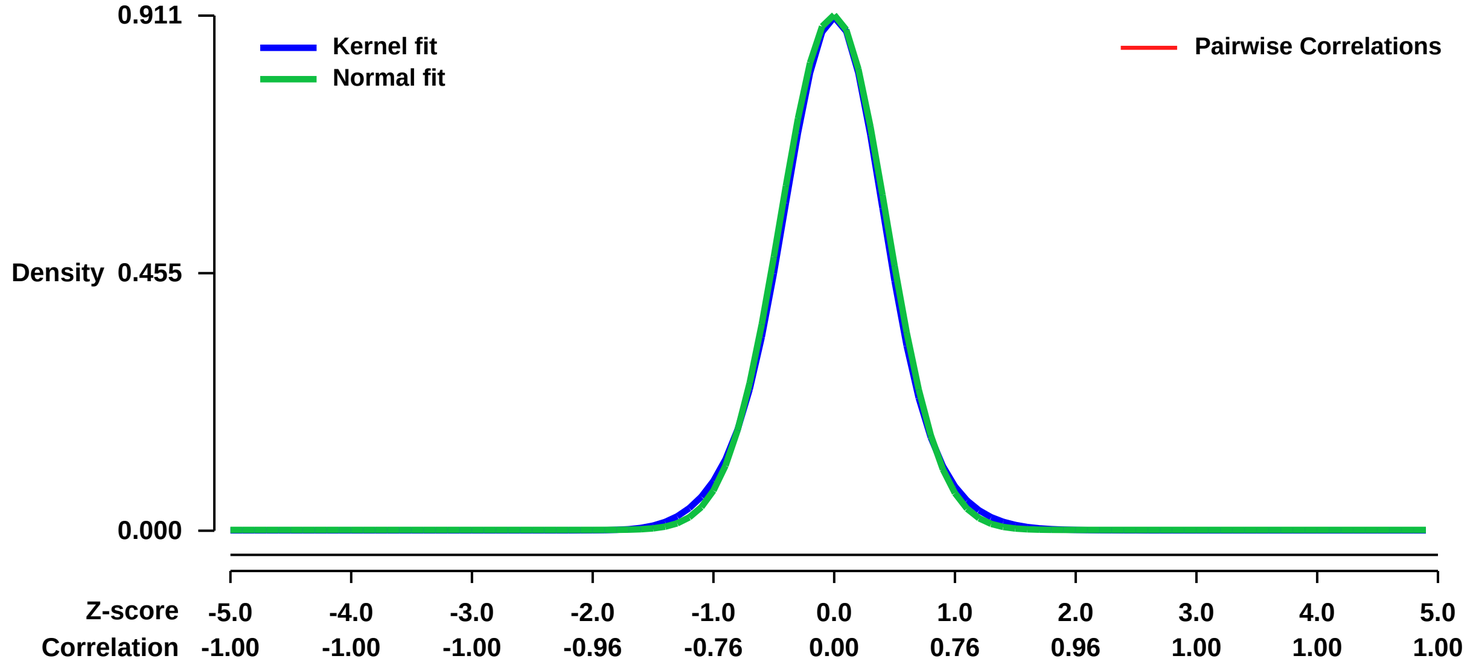

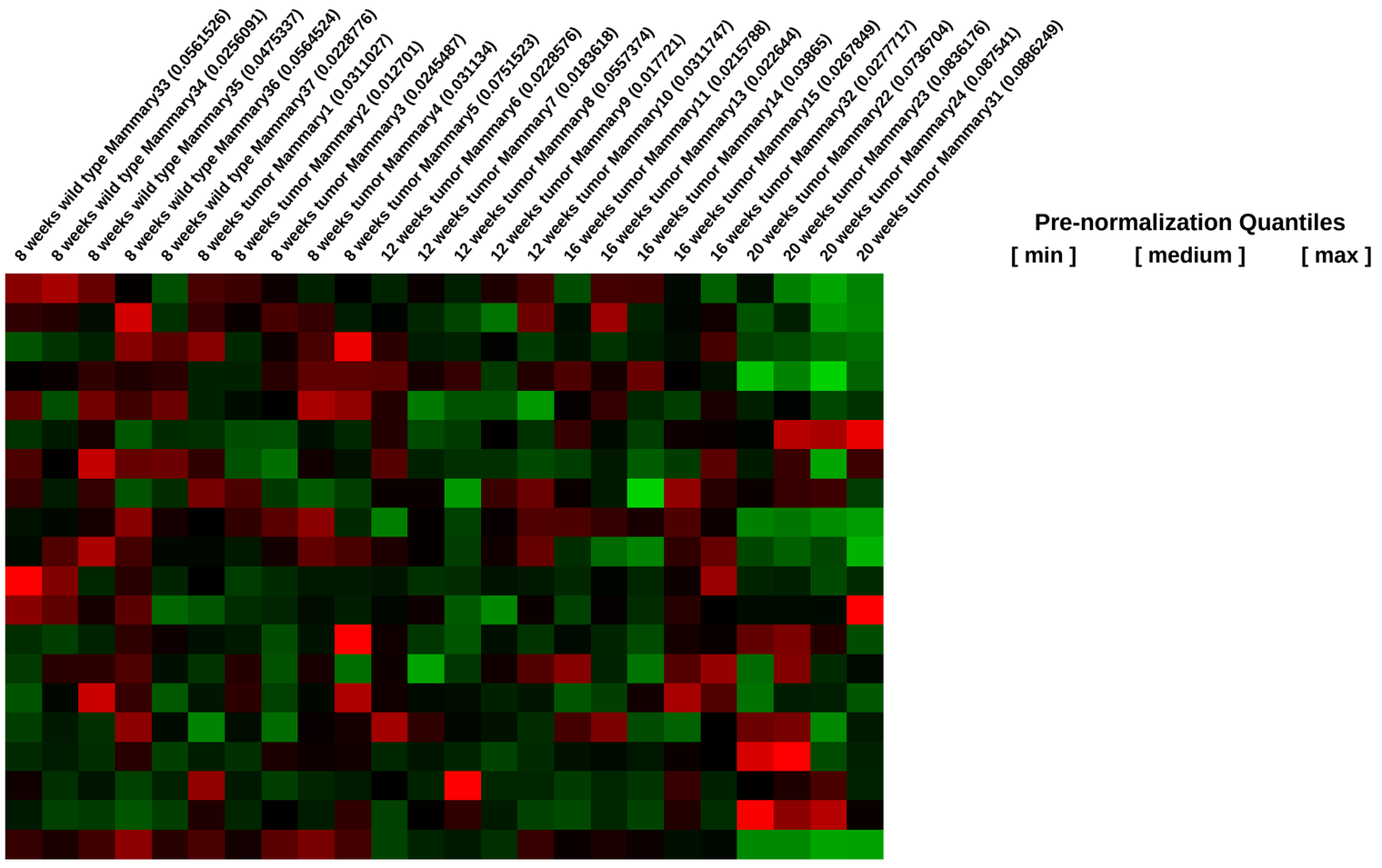

GEO Series "GSE28035" Expression Profiles

Num of samples in this series: 9

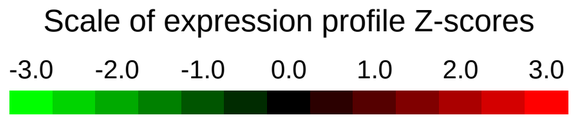

GEO Link:	**http://www.ncbi.nlm.nih.gov/geo/query/acc.cgi?acc=GSE28035**
Status:	**Public on Mar 19 2011**
Title:	**Expression data from mouse oral keratinocyte**
Organism:	**Mus musculus**
Experiment type:	**Expression profiling by array**
Platform:	**GPL1261**
Pubmed ID:	**21676921**
Summary & Design:	**Summary:** **Keratinocytes are the major constituent of epithelial cells at mucosal surfaces and skin, which cover organs, internal cavities and the body. Traditionally, keratinocytes have been considered as an inert component of the multilayered epithelium to protect the subepithelial compartments from the pathogenic microorganisms, toxic stimuli and physical trauma. However, accumulated researches of the airway, gastrointestinal tract and skin have demonstrated that keratinocytes function in the development of the immune system, promotion of pathologic inflammation and even impose diverse decisions on immune cells.** **We used microarrays to detail the global gene expression of oral keratinocyte during oral adaptive immune response.** **Overall design:** **Oral keratinocyte were collected at three time points (control, 48h and 96h) in oral adaptive immune response for RNA extraction and hybridization on Affymetrix microarrays**

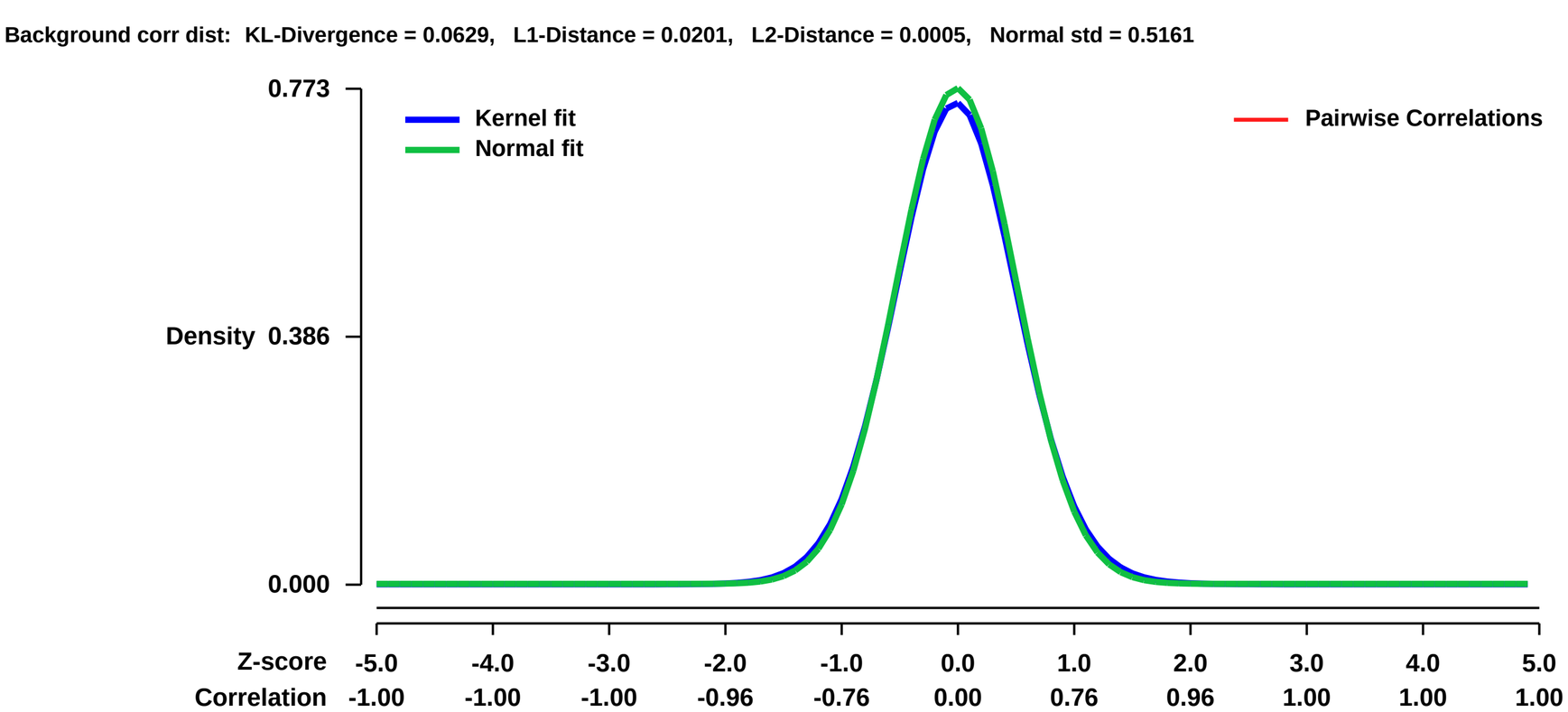

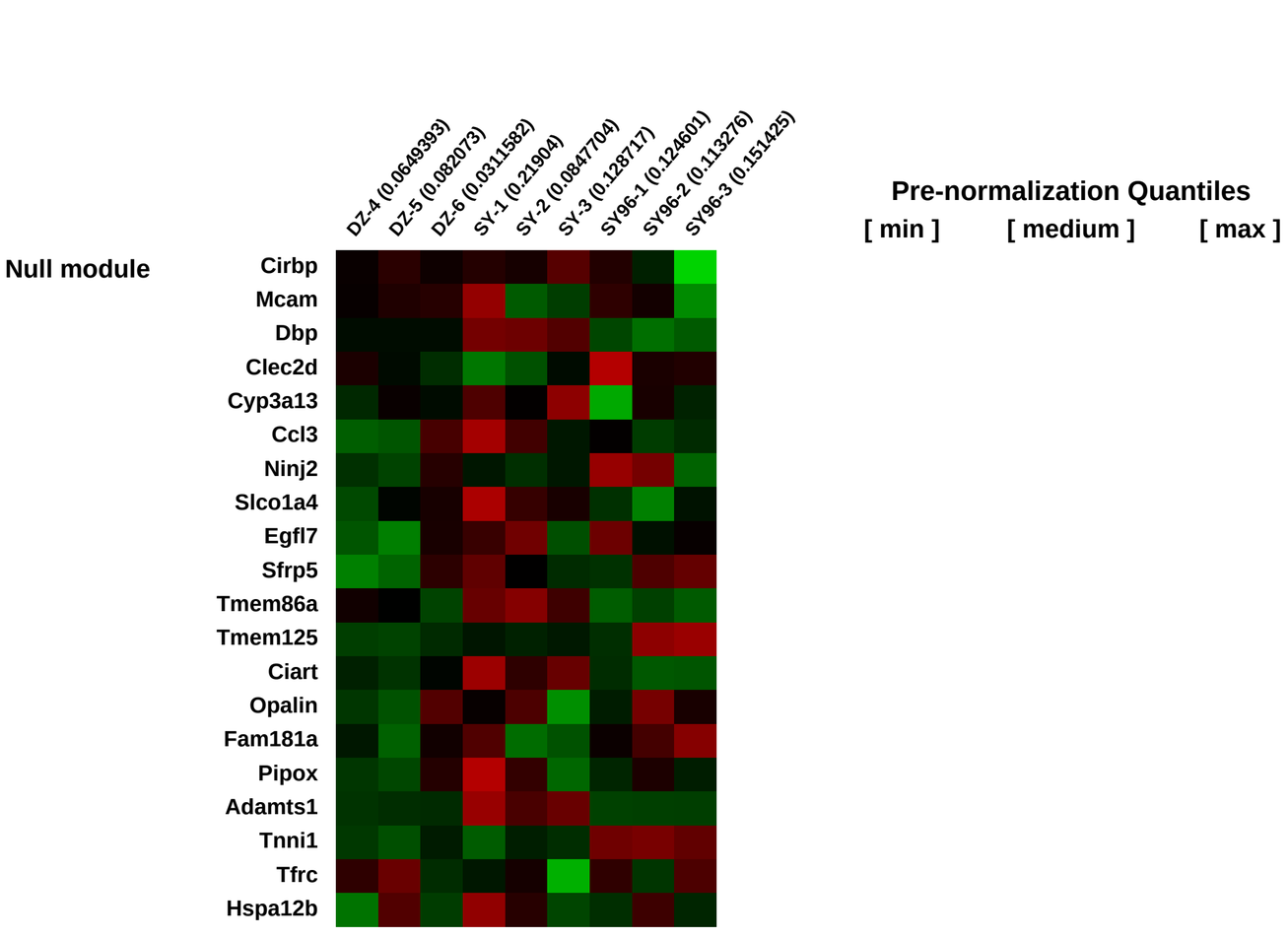

GEO Series "GSE41005" Expression Profiles

Num of samples in this series: 8

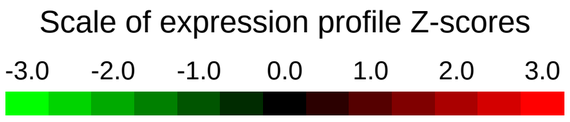

GEO Link:	http://www.ncbi.nlm.nih.gov/geo/query/acc.cgi?acc=GSE41005
Status:	Public on Sep 20 2012
Title:	HSF1 mediated Gene regulation in T cells at normal (37C) and febrile (40C) temperatures
Organism:	Mus musculus
Experiment type:	Expression profiling by array
Platform:	GPL1261
Pubmed ID:	24043900
Summary & Design:	**Summary:** HSF1 is a major transcriptional regulator of heat shock responses. Many cells activate HSF1 in response to heat shock temperatures (>42oC) and other cellular stress causing agents. Unlike other cell types, T cells activate HSF1 in response to T cell activation or when exposed to febrile (40oC) temperatures, suggesting a role for HSF1 beyond the heat-shock response. We used microarray analysis and HSF1 knock-out mice to study the HSF1 mediated gene regulation in activated T cells under normal and fever temperatures. **Overall design:** T cells were purifed from spleen and lymphnodes using miltenyi anti-CD3 magnetic beads and were activated for 5 hr with plate bound anti-CD3 at normal (37oC) and febrile(40oC) temperatures in triplicate cultures. Total RNA from triplicate cultures were extracted, pooled and processed for hybridization on to whole mouse genome 430 2.0 affymetrix microarray chips.

Background corr dist: KL-Divergence = 0.0781, L1-Distance = 0.0198, L2-Distance = 0.0005, Normal std = 0.4824

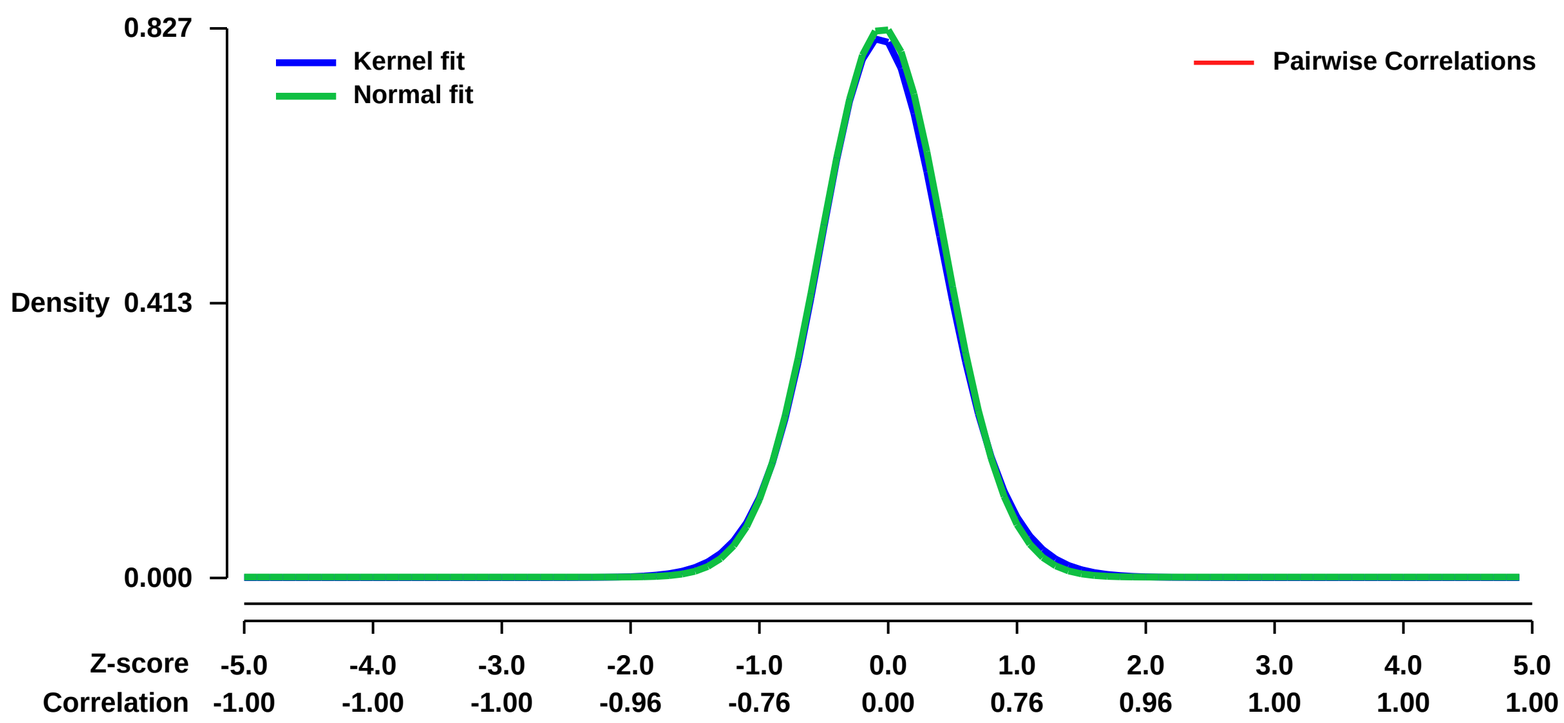

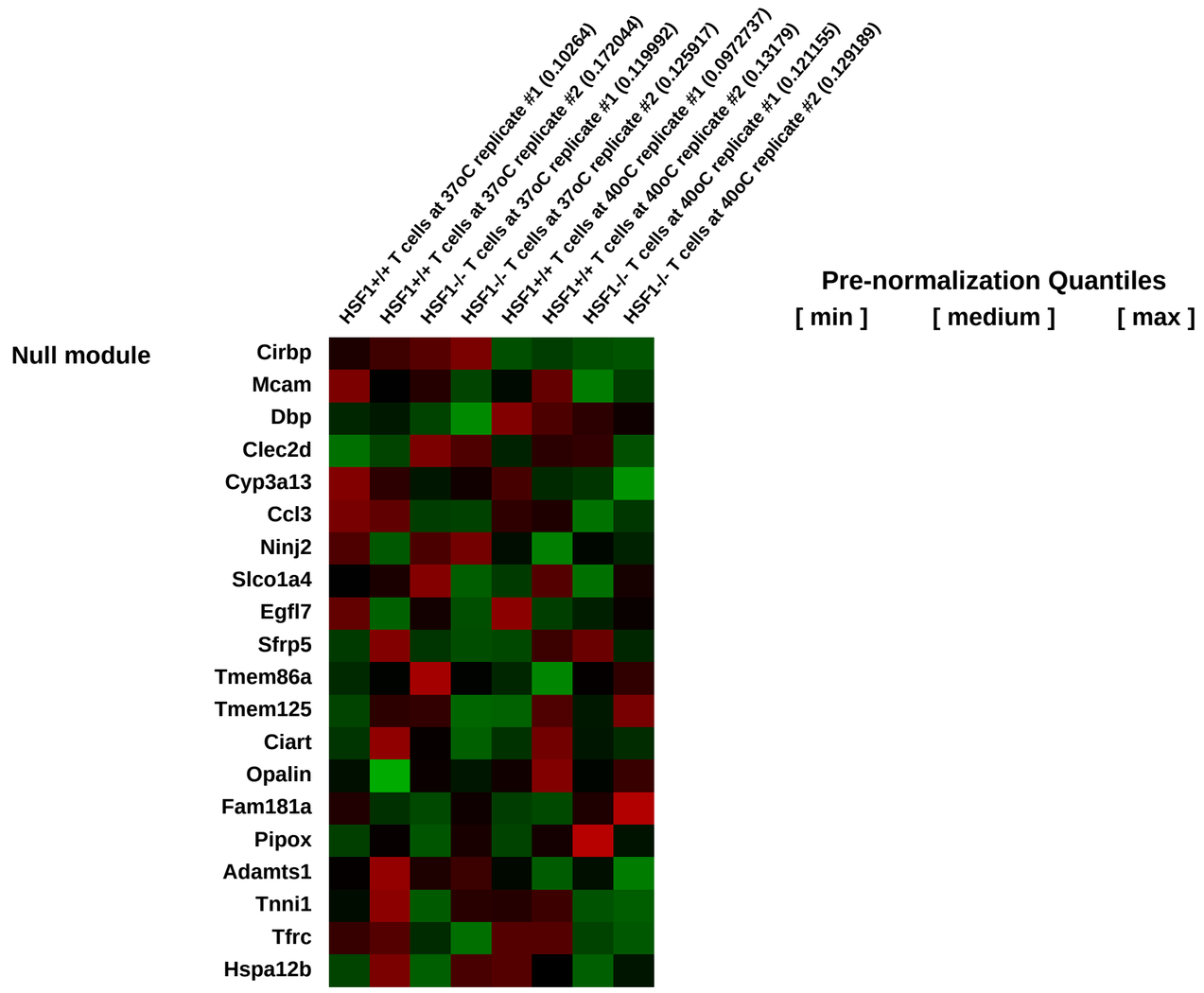

GEO Series "GSE14478" Expression Profiles

Num of samples in this series: 7

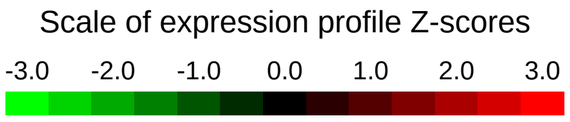

GEO Link:	http://www.ncbi.nlm.nih.gov/geo/query/acc.cgi?acc=GSE14478
Status:	Public on Jan 31 2009
Title:	SCL knockouts in mouse megakaryocytes
Organism:	Mus musculus
Experiment type:	Expression profiling by array
Platform:	GPL1261
Pubmed ID:	19211936
Summary & Design:	**Summary:** The bHLH transcription factor stem cell leukemia gene (Scl) is a master regulator for hematopoiesis essential for hematopoietic specification and proper differentiation of the erythroid and megakaryocyte lineages. However, the critical downstream targets of Scl remain undefined. Here, we identified a novel Scl target gene, transcription factor myocyte enhancer factor 2 C (Mef2C) from Sclfl/fl fetal liver progenitor cell lines. Analysis of Mef2C-/- embryos showed that Mef2C, in contrast to Scl, is not essential for specification into primitive or definitive hematopoietic lineages. However, adult VavCre+Mef2Cfl/fl mice exhibited platelet defects similar to those observed in Scl deficient mice. The platelet counts were reduced, while platelet size was increased and the platelet shape and granularity was altered. Furthermore, megakaryopoiesis was severely impaired in vitro. ChIP-on-chip analysis revealed that Mef2C is directly regulated by Scl in megakaryocytic cells, but not in erythroid cells. In addition, an Scl independent requirement for Mef2C in B-lymphoid homeostasis was observed in Mef2C-deficient mice, characterized as severe age-dependent reduction of specific B cell progenitor populations reminiscent of premature aging. In summary, this work identifies Mef2C as an integral member of hematopoietic transcription factors with distinct upstream regulatory mechanisms and functional requirements in megakaryocyte and B-lymphoid lineages. **Overall design:** ¸ /¸ cell line, and the Scl ¸ /¸ cell line was transduced with Scl retrovirus to re-introduce Scl expression (Scl ¸ /¸ +Scl cell line). Megakaryocyte differentiation was enhanced by adding Tpo for 5 days before harvesting the cells. RNA was extracted with Trizol (Gibco BRL) and RNEasy (Qiagen) kits. Differential gene expression between Sclfl/fl, Scl ¸ /¸ and Scl ¸ /¸ +Scl cell lines was analyzed by Affymetrix MOE430_2 microarray in the microarray core facility at the Dana-Farber Cancer Institute.

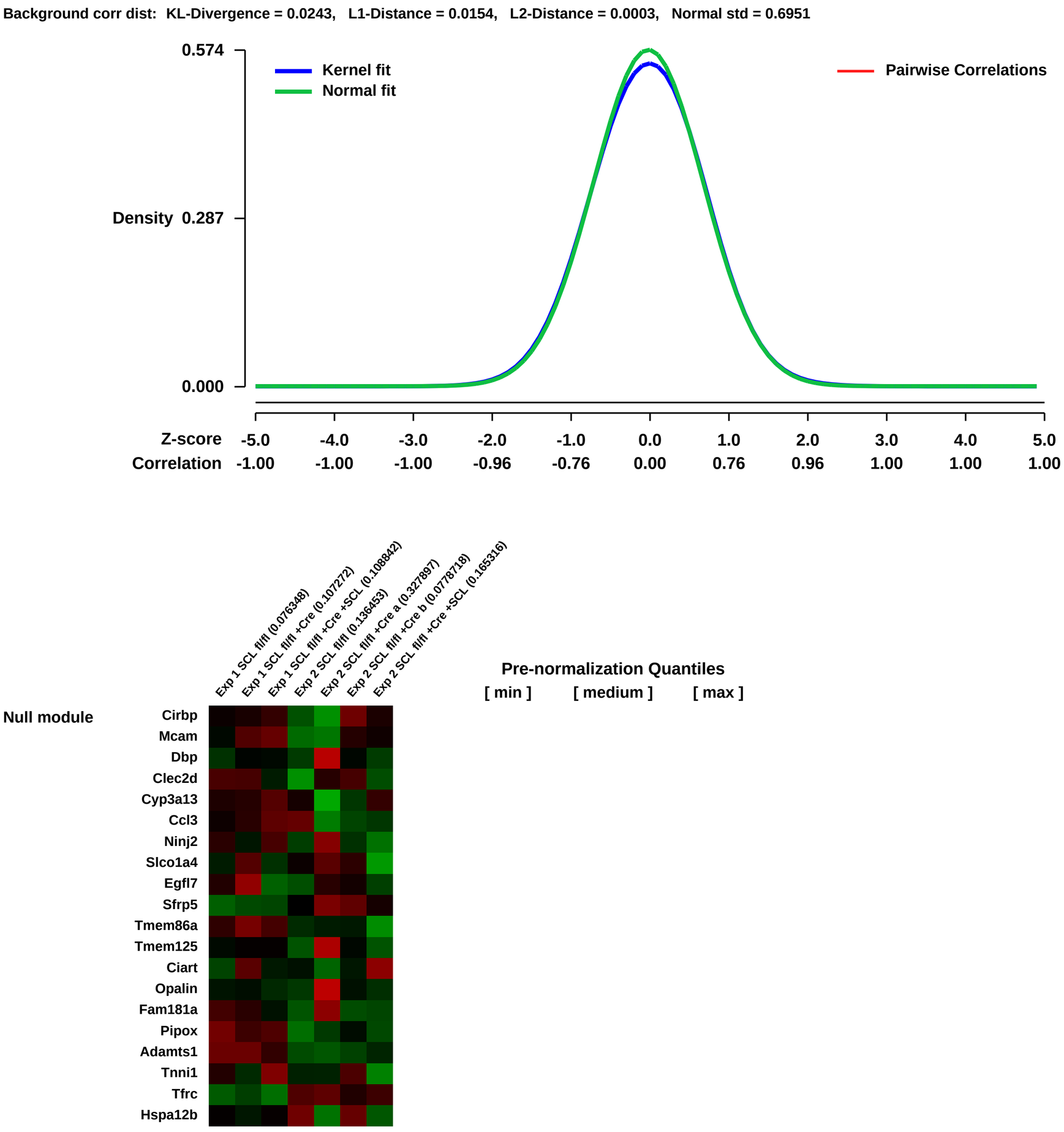

GEO Series "GSE57817" Expression Profiles

Num of samples in this series: 9

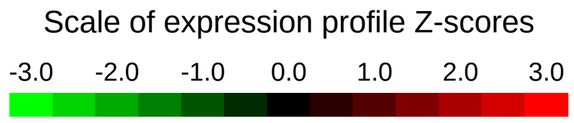

GEO Link:	**http://www.ncbi.nlm.nih.gov/geo/query/acc.cgi?acc=GSE57817**
Status:	**Public on May 21 2014**
Title:	**Towards epigenetic understanding and therapy of insulin resistance by intranuclear insulin [mouse liver gene expression]**
Organism:	**Mus musculus**
Experiment type:	**Expression profiling by array**
Platform:	**GPL1261**
Pubmed ID:	
Summary & Design:	**Summary:** **There is evidence indicating the involvement of DNA methylation memory in maintaining gene expression patterns associated with insulin resistance. Although the exact mechanism remains unknown, it has been proved that insulin resistance is correlated to low heat shock protein (HSP) expression.** **We reveal that intranuclear insulin can reduce HSP DNA methylation level to up-regulate HSP protein expression and result in long term cure of hyperglycemia.** **Overall design:** **Type 2 diabetes KKAy mouse were selected in our experiments.Three conditions were compared with three replicates each. These are:(1) Untreated KKAy mouse (2) Insulin treated KKAy mouse(Insulin); (3) Biomineralized insulin treated KKAy mouse(BI).**

Background corr dist: **KL-Divergence = 0.1152, L1-Distance = 0.0293, L2-Distance = 0.0015, Normal std = 0.4140**

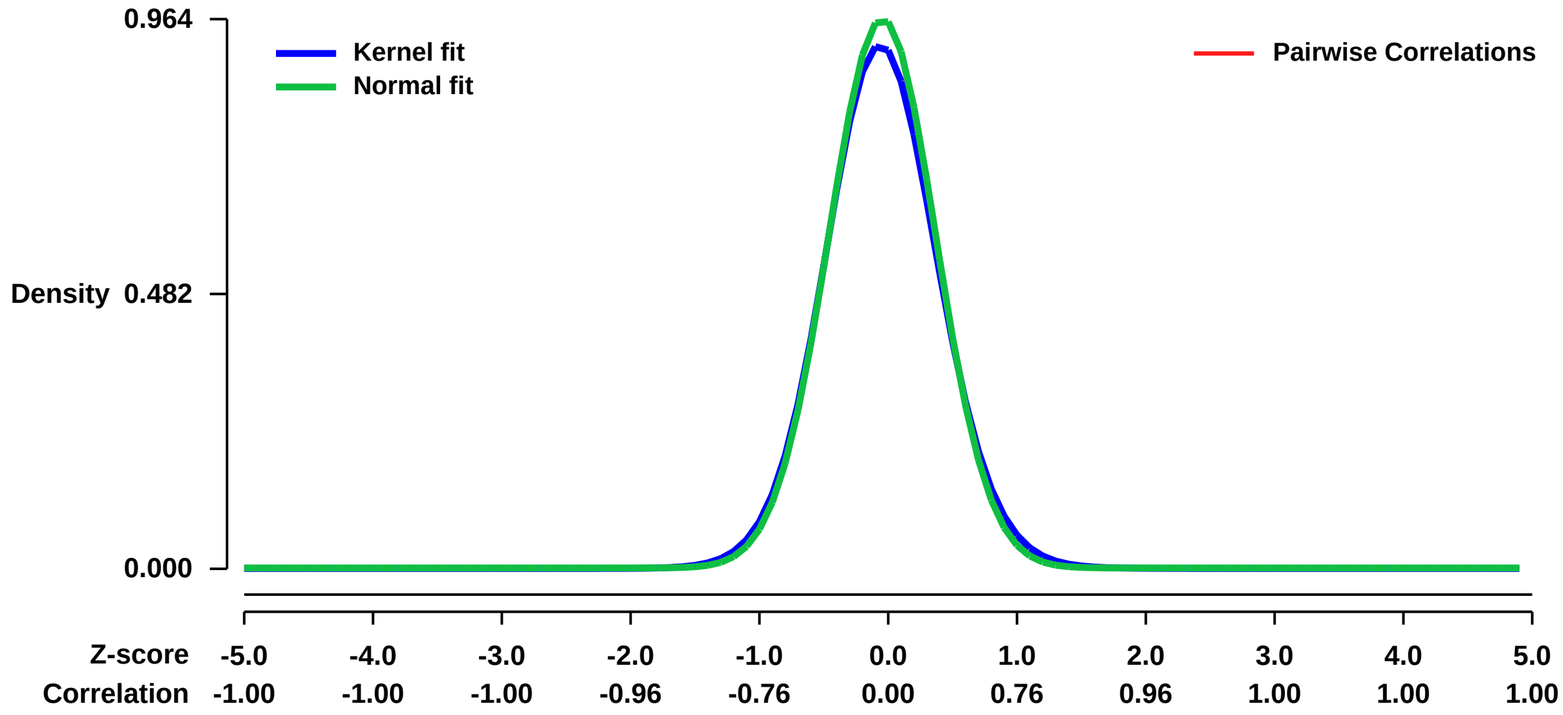

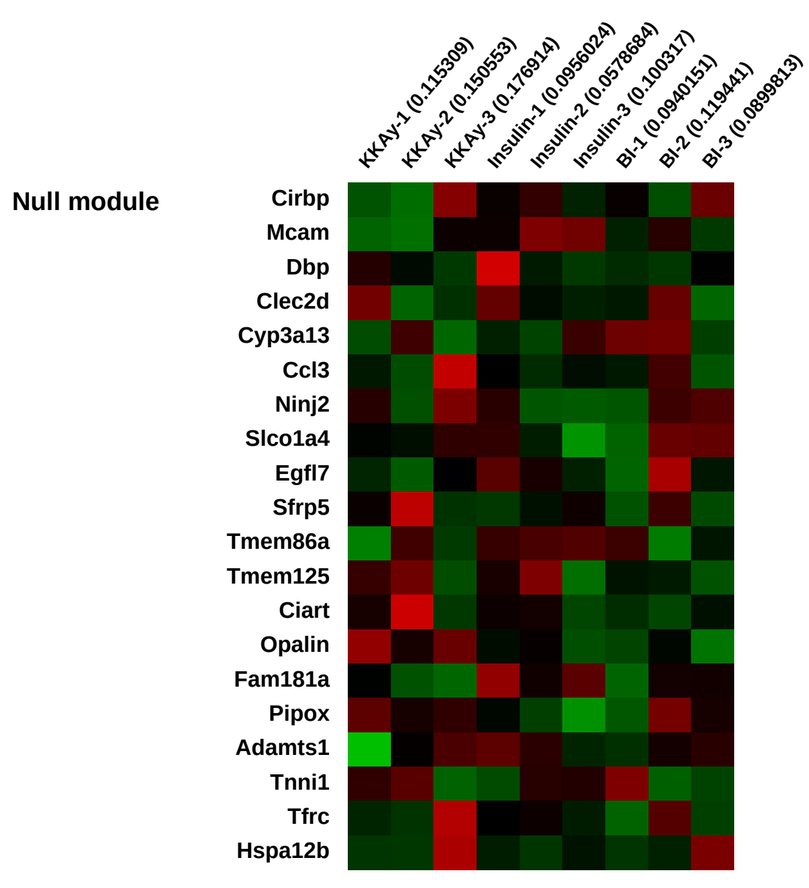

GEO Series "GSE47414" Expression Profiles

Num of samples in this series: 18

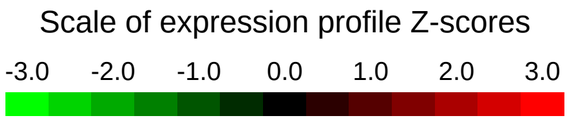

GEO Link:	http://www.ncbi.nlm.nih.gov/geo/query/acc.cgi?acc=GSE47414
Status:	Public on Jun 12 2013
Title:	Expression data from bone marrow macrophage derived from lean and obese mice after 1,4, and 24h exposition to P.gingivalis
Organism:	Mus musculus
Experiment type:	Expression profiling by array
Platform:	GPL1261
Pubmed ID:	
Summary & Design:	**Summary:** Obesity is a chronic inflammatory disease that weakens macrophage innate immune response to infections. Since M1 polarization is crucial during acute infectious diseases, we hypothesized that diet-induced obesity inhibits M1 polarization of macrophages in the response to bacterial infection. Using a computational approach in conjunction with microarray data, we identified switching genes that may differentially control the behavior of response pathways in macrophages from lean and obese mice. **Overall design:** Bone marrow macrophages (BMMϕ) from lean and obese mice were exposed to live Porphyromonas gingivalis (P. gingivalis) for three incubation times (1 h, 4 h and 24 h). cDNA from BMMϕ of lean and obese mice were hybridized on Affymetrix Mouse Genome 430 2.0 Arrays. Hybridization was performed on three replicates at each time point (18 arrays total).

Background corr dist: KL-Divergence = 0.0932, L1-Distance = 0.0325, L2-Distance = 0.0014, Normal std = 0.4688

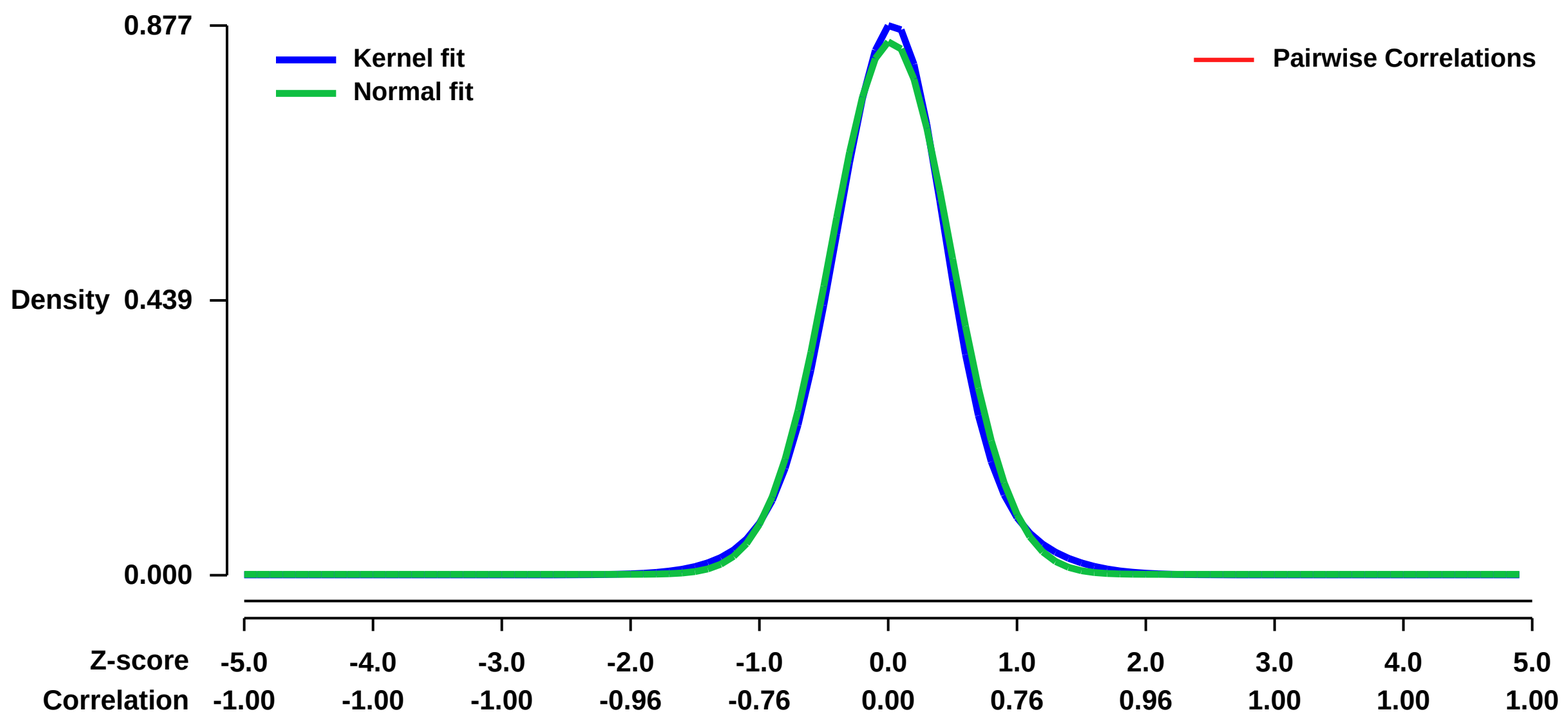

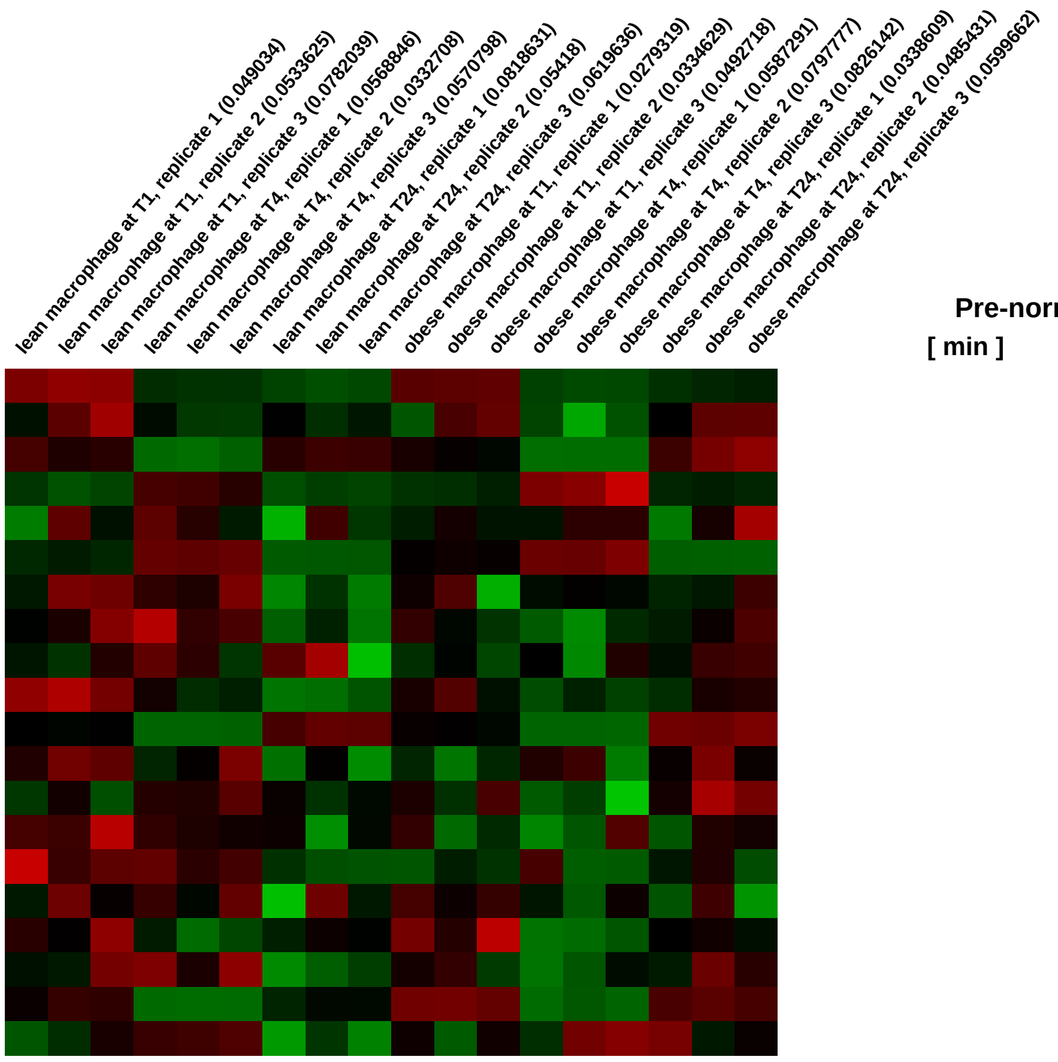

GEO Series "GSE20500" Expression Profiles

Num of samples in this series: 6

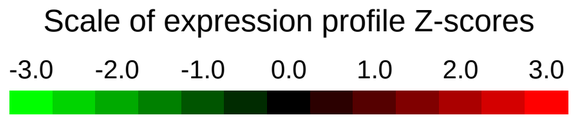

GEO Link:	http://www.ncbi.nlm.nih.gov/geo/query/acc.cgi?acc=GSE20500
Status:	Public on Feb 14 2011
Title:	T cell genes regulated by retinoic acid
Organism:	Mus musculus
Experiment type:	Expression profiling by array
Platform:	GPL1261
Pubmed ID:	20664575
Summary & Design:	**Summary:** This is to determine the T cell genes regulated by retinoic acid. **Overall design:** 2 arrays were used for each group

Background corr dist: KL-Divergence = 0.0330, L1-Distance = 0.0460, L2-Distance = 0.0029, Normal std = 0.7128

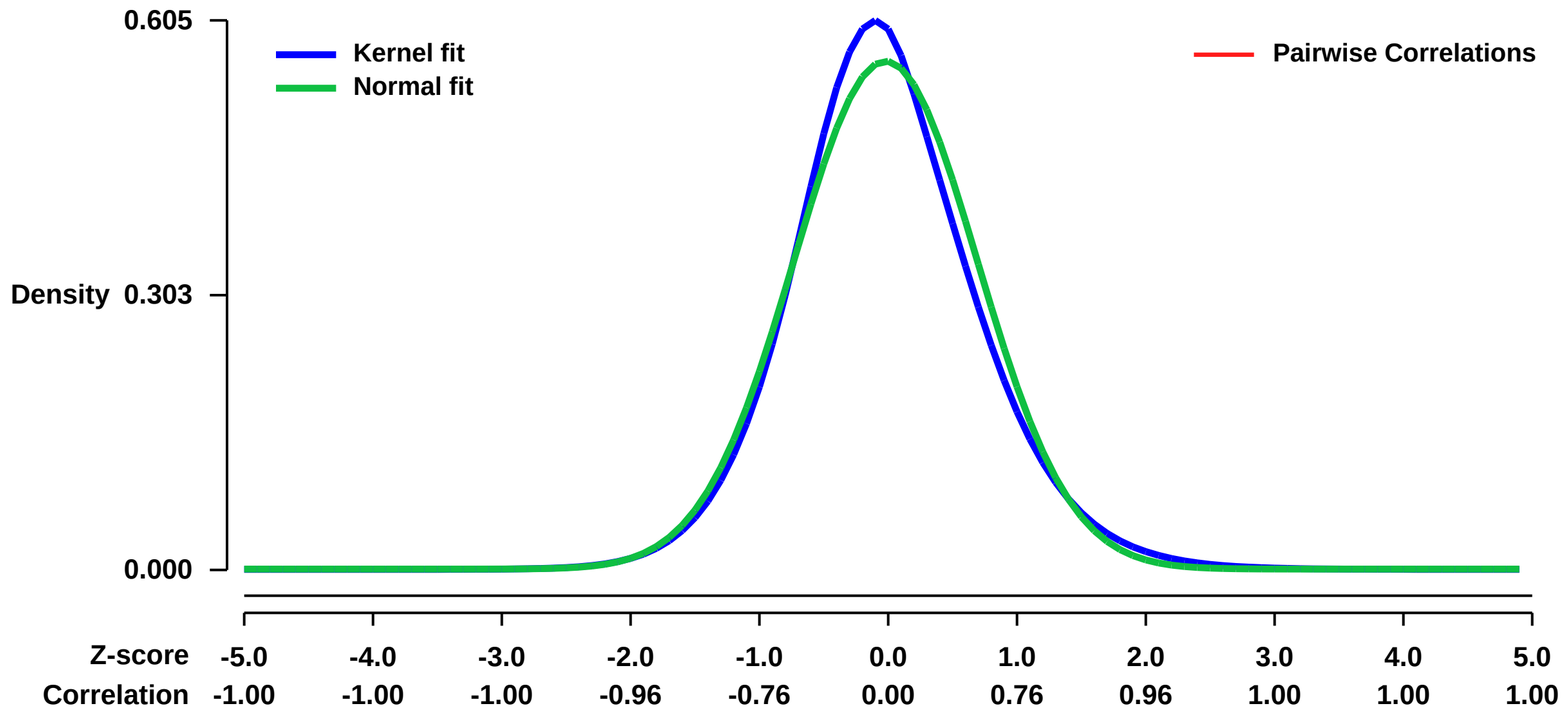

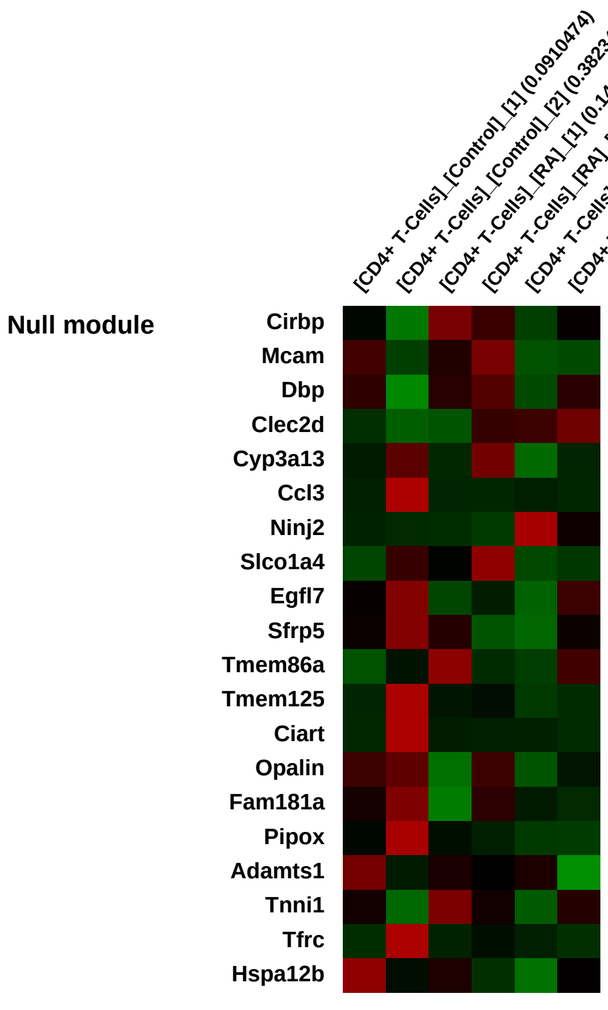

GEO Series "GSE1074" Expression Profiles

Num of samples in this series: 12

Scale of expression profile Z-scores

-3.0 -2.0 -1.0 0.0 1.0 2.0 3.0

GEO Link:	http://www.ncbi.nlm.nih.gov/geo/query/acc.cgi?acc=GSE1074
Status:	Public on Mar 11 2004
Title:	Strain-dependent effects of alcohol on early mouse embryos
Organism:	Mus musculus
Experiment type:	Expression profiling by array
Platform:	GPL1261
Pubmed ID:	17200951
Summary & Design:	**Summary:** **EXPERIMENT: Microarray expression profiles derived from the cranial neural folds (headfold) of neurulation-stage mouse embryos 3.0h after maternal alcohol exposure on 8 d.p.c.** **ANIMAL MODEL: Pregnancies from 2 substrains of C57BL/6 mice that differ in relative risk of Fetal Alcohol Syndrome (FAS): C57BL/6J (B6J) high-risk condition, and C57BL/6NCrl (B6N) low-risk condition.** **EXPOSURE: Dams dosed with ethanol (EtOH) by intraperitoneal injection at 2.9 g EtOH per kg body weight. Controls received vehicle (saline) alone. A third group of dams received EtOH + 4.0 mg/kg PK11195, a specific high-affinity ligand to the 18 KDa mitochondrial peripheral benzodiazepine receptor site.** **INTERVAL: High blood alcohol content must be sustained in dams for several hours to invoke FAS and is traditionally accomplished by a double injection of EtOH 4.0h apart. Since these embryos were harvested for genetic analysis 1h before dams would have gotten the second alcohol injection, the interval represents a snapshot of the critical response, prior to the second maternal injection that invokes greater risk. Counter-exposure to PK11195 significantly lowers the adverse response of B6J embryos to EtOH.** **PLATFORM: Two independent assays run. The first dataset (PE), run April 2002 â January 2003, used samples pooled from 2 litters (PE) and the platform was a two-channel MPS621 array (http://www.lifesciences.perkinelmer.com/). This platform has 4800 sequence-verified gene elements derived from over 50 different human cDNA libraries reflecting a variety of well-annotated cellular processes and disease pathways. The second dataset (AF), run between May 2005 â November 2005, used samples pooled from 1 litter and the platform was Affymetrix GeneChip´fi Mouse Genome 430A 2.0 Array (http://www.affymetrix.com/). The MG430A 2.0 platform has 45,102 oligonucleotide probe cells representing approximately 14,000 well-characterized genes in the draft mouse genome assembly. The corresponding GEO samples are GSM12218 - GSM12227 for the two-channel PE arrays, and GSM136067 - GSM136078 for the one-channel AF arrays.** **Keywords = fetal alcohol syndrome** **Keywords = alcohol-related birth defects** **Keywords = EtOH** **Keywords = PK11195** **Keywords = embryo** **Keywords = strain differences** **Keywords: Ordered** **Overall design:** **Assay of early mouse embryos during pathogenesis of Fetal Alcohol Syndrome (FAS). Replicate RNA samples were arrayed by one-channel oligonucleotide (Affymetrix) or two-channel cDNA (Perkin-Elmer) platforms.**

Background corr dist: **KL-Divergence = 0.0731, L1-Distance = 0.0209, L2-Distance = 0.0005, Normal std = 0.4915**

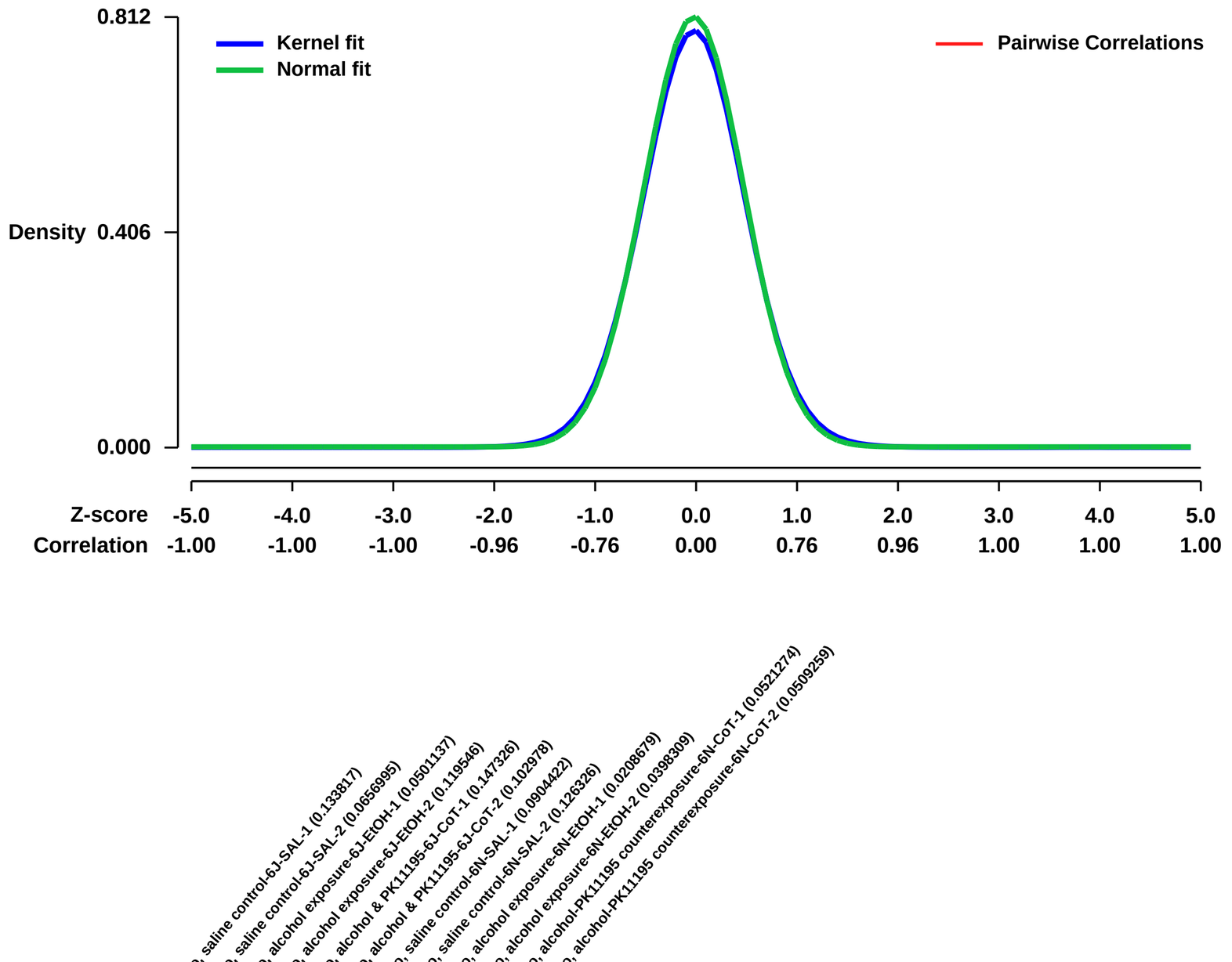

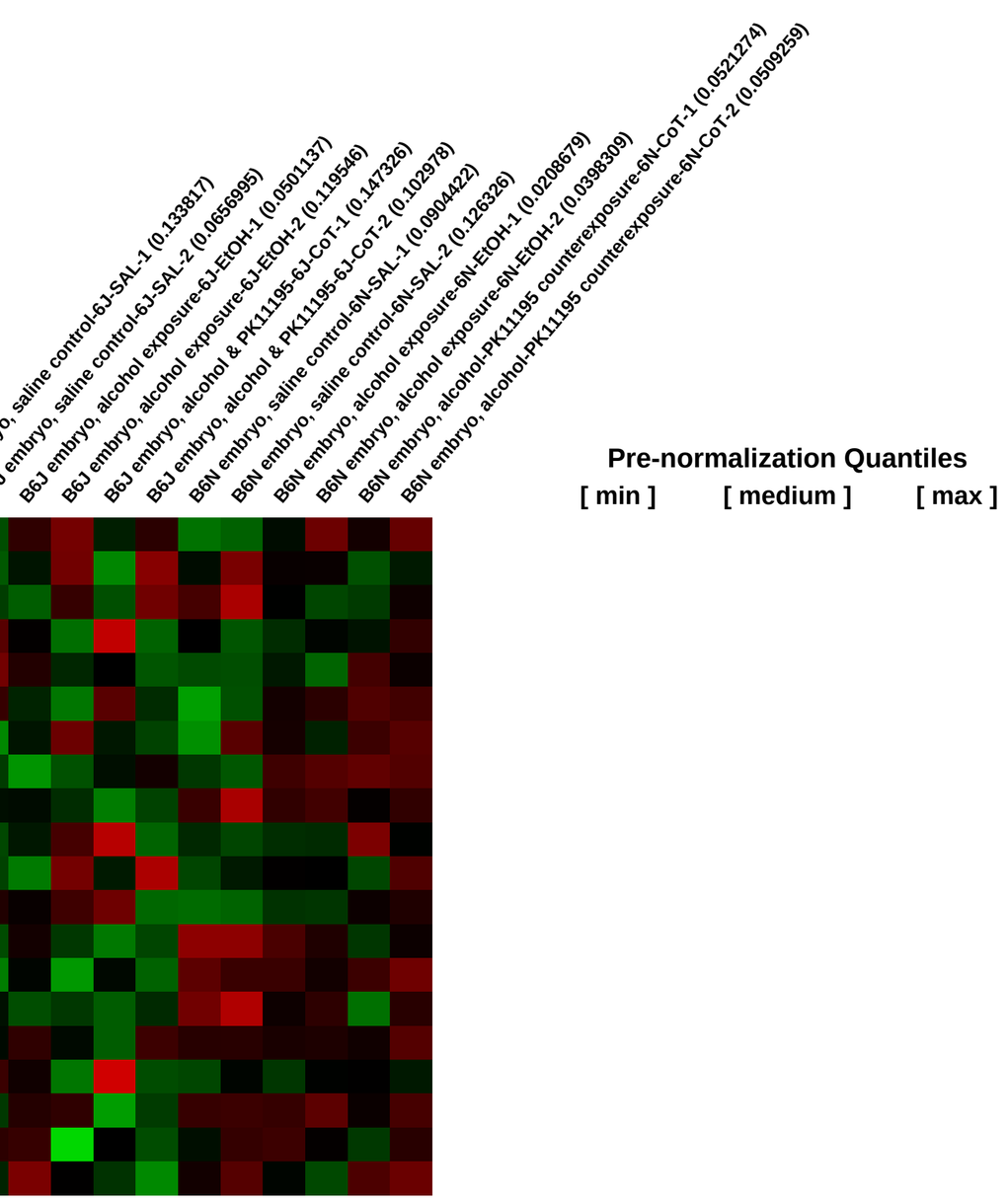

GEO Series "GSE50824" Expression Profiles

Num of samples in this series: 19

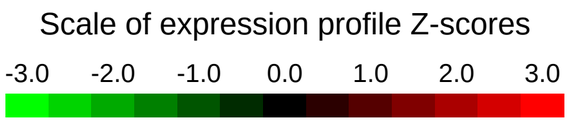

GEO Link:	http://www.ncbi.nlm.nih.gov/geo/query/acc.cgi?acc=GSE50824
Status:	Public on Sep 13 2013
Title:	The identification and tumorigenecity of neuronal progenitors in developing cerebellum
Organism:	Mus musculus
Experiment type:	Expression profiling by array
Platform:	GPL1261
Pubmed ID:	24141309
Summary & Design:	**Summary:** It is generally believed that cerebellar granule neurons originate exclusively from granule neuron precursors (GNPs) in the external germinal layer (EGL). Here we identify a rare population of neuronal progenitors in the developing cerebellum that expresses Nestin. Although Nestin is widely considered a marker for multipotent stem cells, these Nestin-expressing progenitors (NEPs) are committed to the granule neuron lineage. Unlike conventional GNPs, which reside in the outer EGL and proliferate extensively, NEPs reside in the deep part of the EGL and are quiescent. Expression profiling reveals that NEPs are distinct from GNPs, and in particular, express markedly reduced levels of genes associated with DNA repair. Consistent with this, upon aberrant activation of Sonic hedgehog (Shh) signaling, NEPs exhibit more severe genomic instability and give rise to tumors more efficiently than GNPs. These studies identify a novel progenitor for cerebellar granule neurons and a novel cell of origin for medulloblastoma. **Overall design:** 4 samples of Nestin expressing progenitors (NEPs), 4 samples of Math1 positive cells (GNPs) and 3 samples of Neural stem cells (CD133+ NSCs) were used for microarray analysis to determine the distinct genetic profile of NEPs. 4 samples of NEP-derived tumor and 4 samples of GNP-derived tumor were used to determine the similarity of those tumors by microarray analysis.

Background corr dist: KL-Divergence = 0.1108, L1-Distance = 0.0321, L2-Distance = 0.0019, Normal std = 0.4402

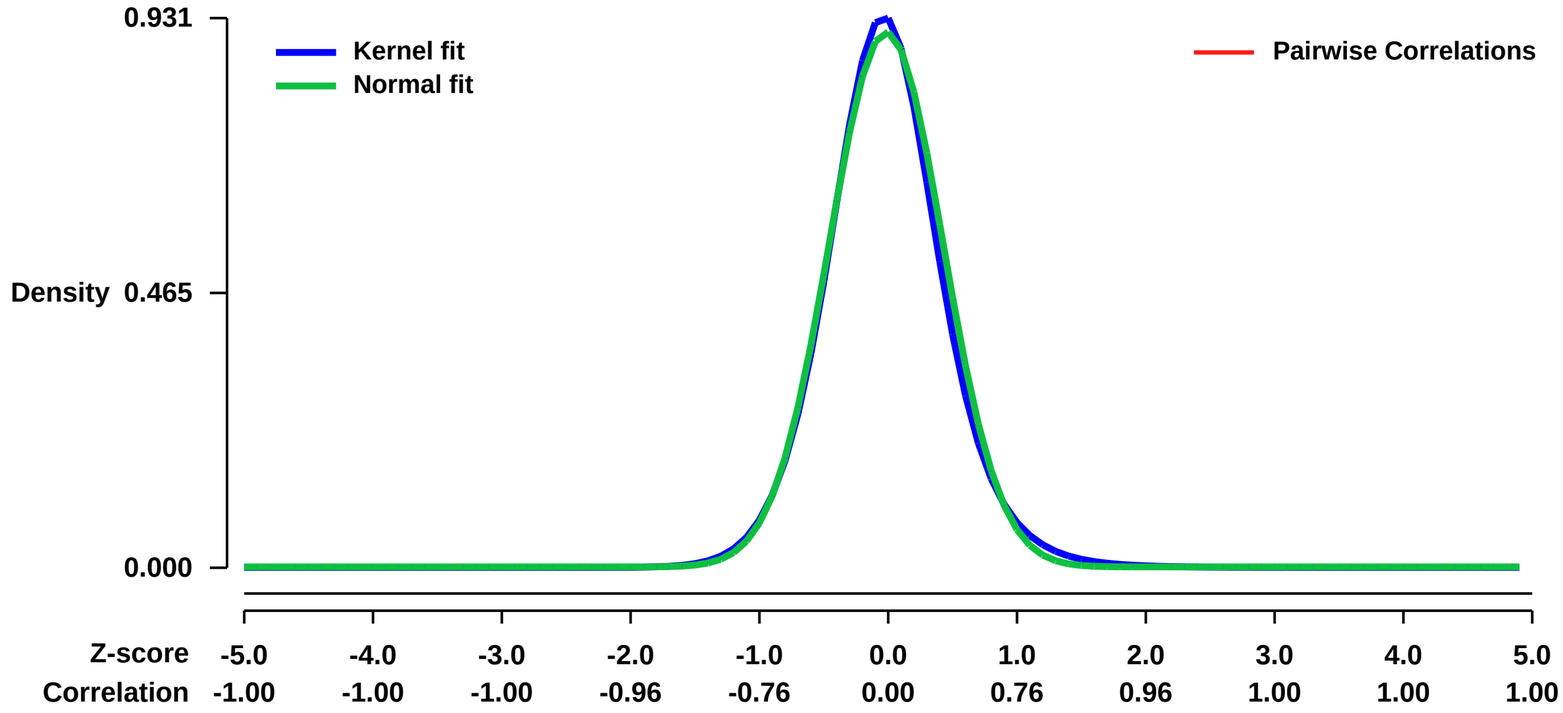

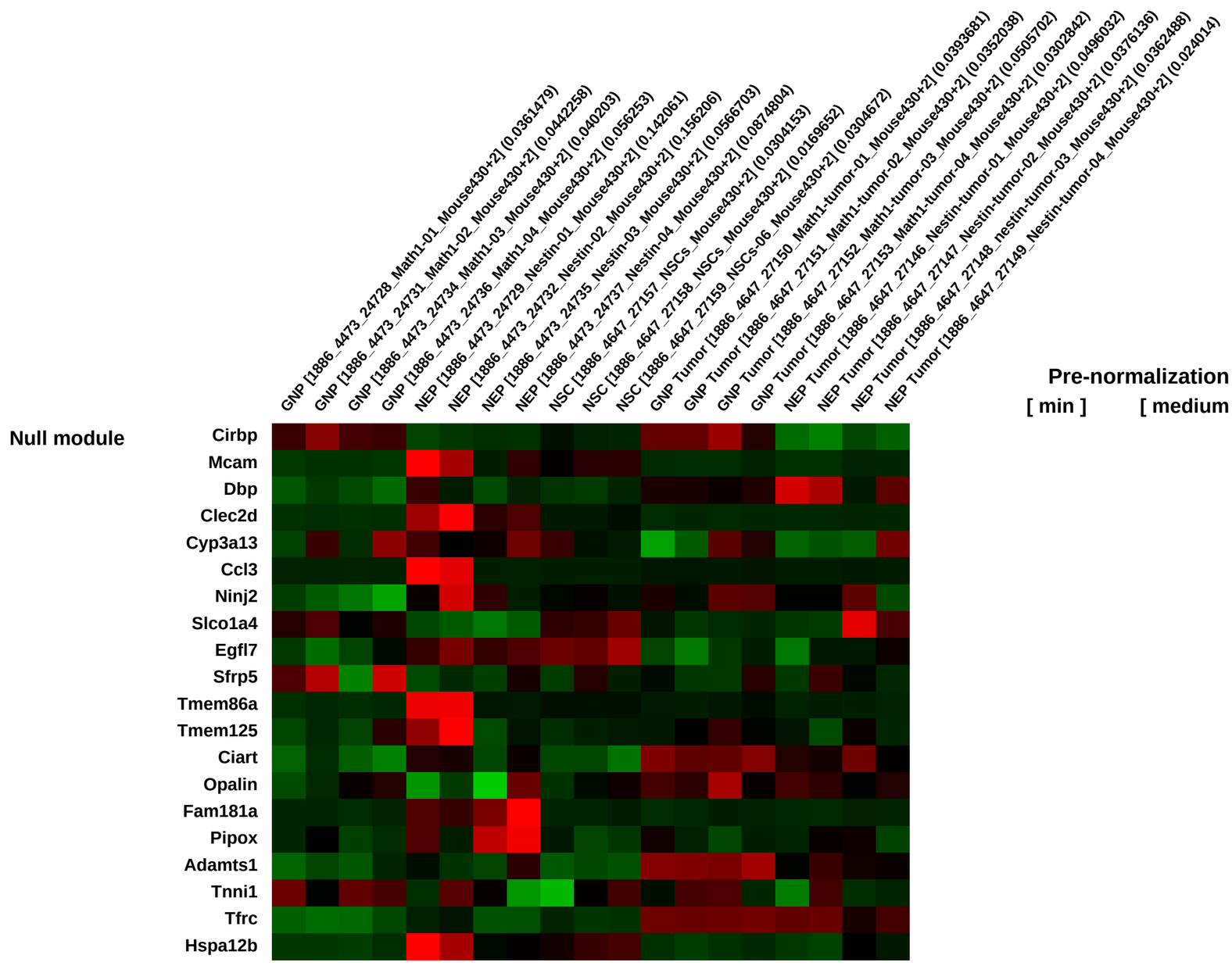

GEO Series "GSE23833" Expression Profiles

Num of samples in this series: 12

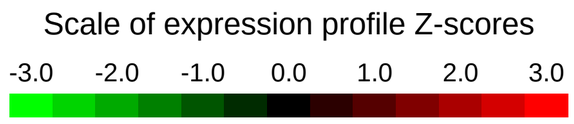

GEO Link:	**http://www.ncbi.nlm.nih.gov/geo/query/acc.cgi?acc=GSE23833**
Status:	**Public on Sep 01 2010**
Title:	**The Forkhead factor FoxQ1 influences epithelial differentiation**
Organism:	**Mus musculus**
Experiment type:	**Expression profiling by array**
Platform:	**GPL1261**
Pubmed ID:	**20717954**
Summary & Design:	**Summary:** **The Forkhead family of transcription factors comprises numerous members and is implicated in various cellular functions, including cell growth, apoptosis, migration and differentiation.In this study we identified the Forkhead factor FoxQ1 as increased in expression during TGF-beta1 induced changes in epithelial differentiation, suggesting functional roles of FoxQ1 for epithelial plasticity.The repression of FoxQ1 in mammary epithelial cells led to a change in cell morphology characterized by an increase in cell size, pronounced cell-cell contacts and an increased expression of several junction proteins (e.g. E-cadherin). In addition, FoxQ1 knock-down cells revealed rearrangements in the actin-cytoskeleton and slowed down cell cycle G1-phase progression.Furthermore, repression of FoxQ1 enhanced the migratory capacity of coherent mammary epithelial cells.Gene expression profiling of NM18 cells indicated that FoxQ1 is a relevant downstream mediator of TGF-beta1 induced gene expression changes. This included the differential expression of transcription factors involved in epithelial plasticity, e.g. Ets-1, Zeb1 and Zeb2.In summary, this study has elucidated the functional impact of FoxQ1 on epithelial differentiation** **Overall design:**

Background corr dist: KL-Divergence = 0.0453, L1-Distance = 0.0772, L2-Distance = 0.0080, Normal std = 0.6930

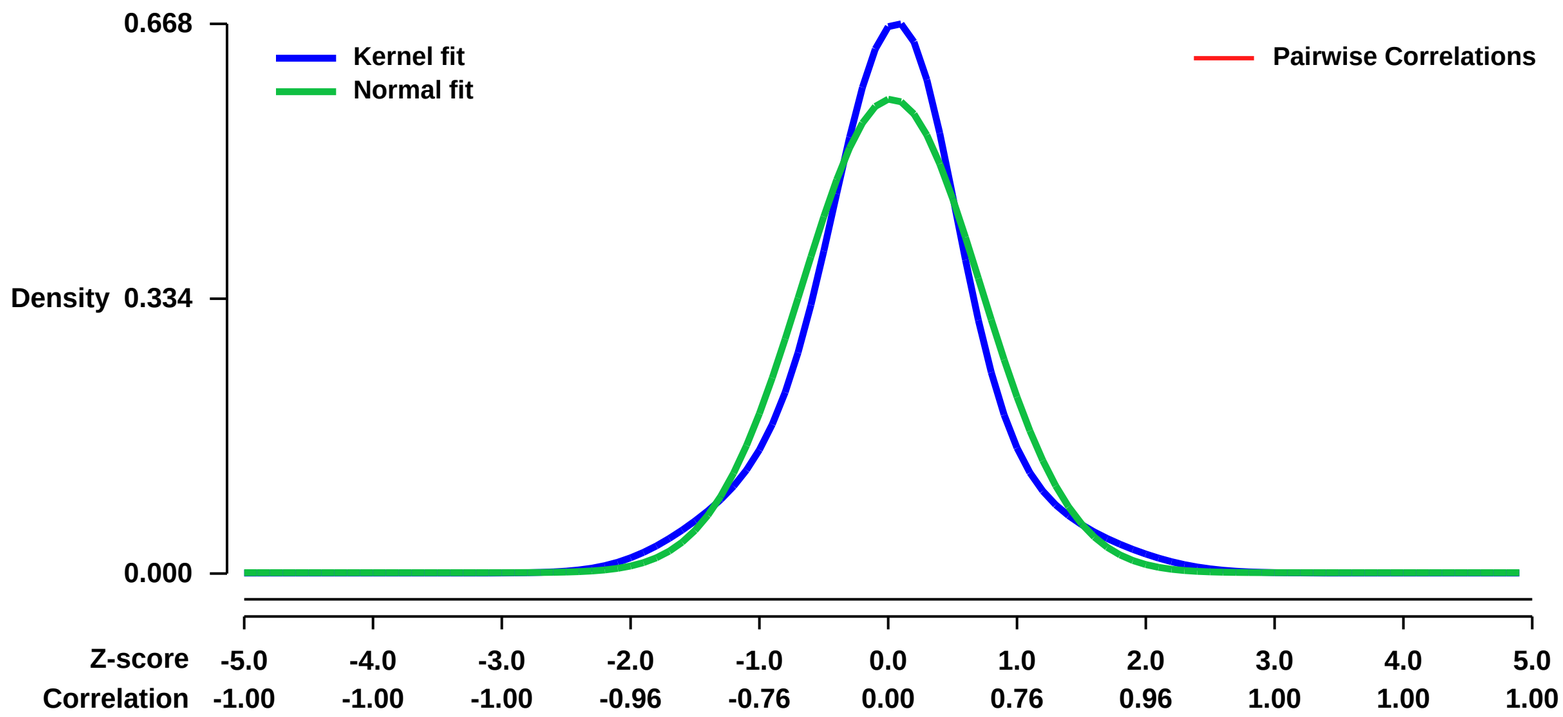

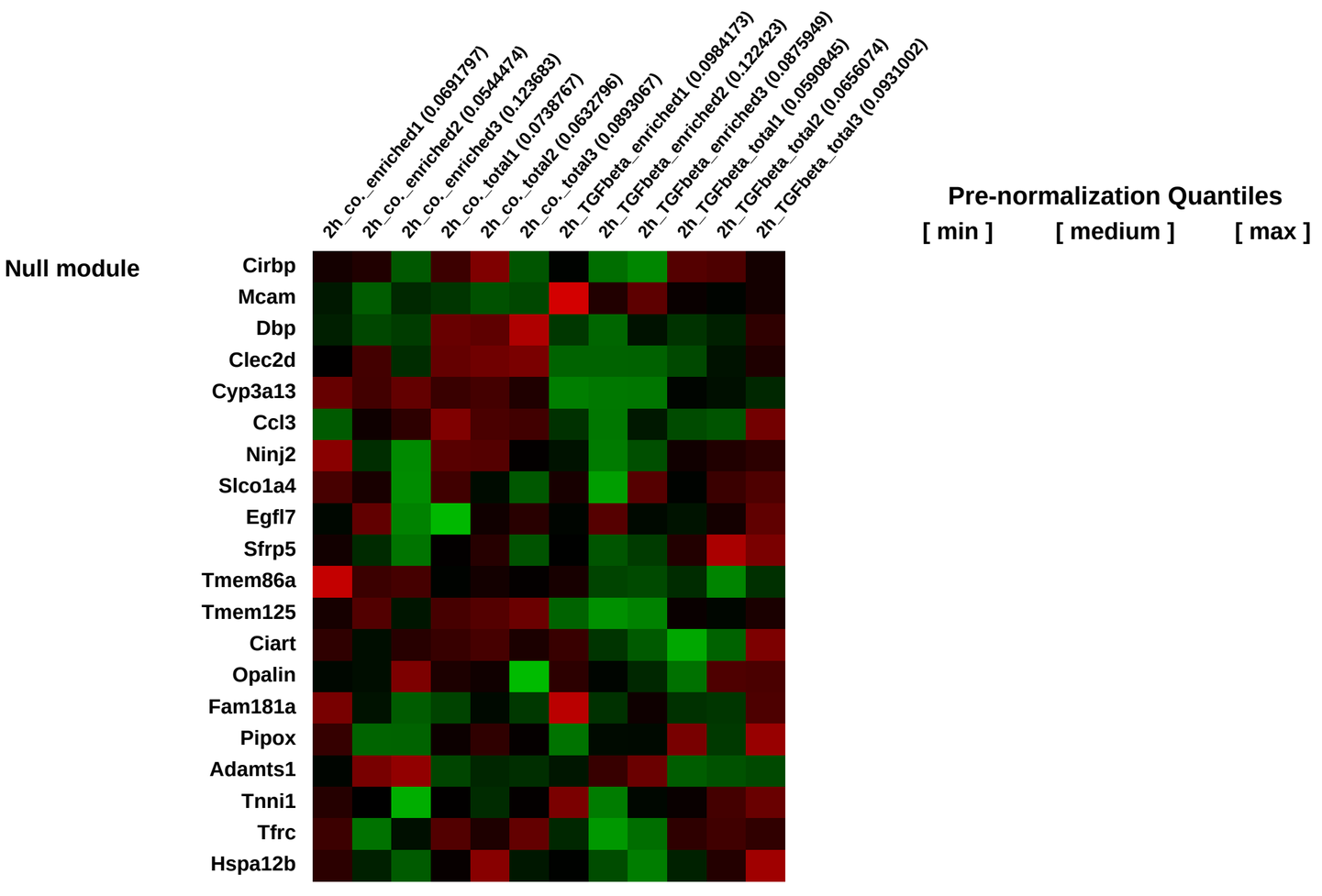

GEO Series "GSE53986" Expression Profiles

Num of samples in this series: 16

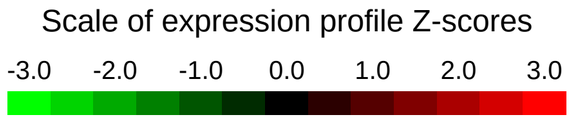

GEO Link:	**http://www.ncbi.nlm.nih.gov/geo/query/acc.cgi?acc=GSE53986**
Status:	**Public on Mar 31 2014**
Title:	**NRROS negatively regulates ROS in phagocytes during host defense and autoimmunity**
Organism:	**Mus musculus**
Experiment type:	**Expression profiling by array**
Platform:	**GPL1261**
Pubmed ID:	**24739962**
Summary & Design:	**Summary:** **Production of reactive oxygen species (ROS) is one of the important antimicrobial mechanisms of phagocytic cells. Enhanced oxidative burst requires these cells to be primed with agents such as IFNg and LPS with a synergistic effect of these agents on the level of the burst. However, excessive ROS generation will lead to tissue damage and has been implicated in a variety of inflammatory and autoimmune disease. Therefore, this process needs to be tightly regulated. In order to understand the genes regulating this process, we will treat bone marrow derived macrophages with above mentioned priming agents and study the gene expression.** **We used microarrays to determine the changes in gene expression that occur in bone marrow derived macrophages after treatment with IFNg, LPS, or a combination of IFNg and LPS** **Overall design:** **Four condition experiment; Biological replicates: four replicates per condition**

Background corr dist: KL-Divergence = 0.1364, L1-Distance = 0.0322, L2-Distance = 0.0018, Normal std = 0.3981

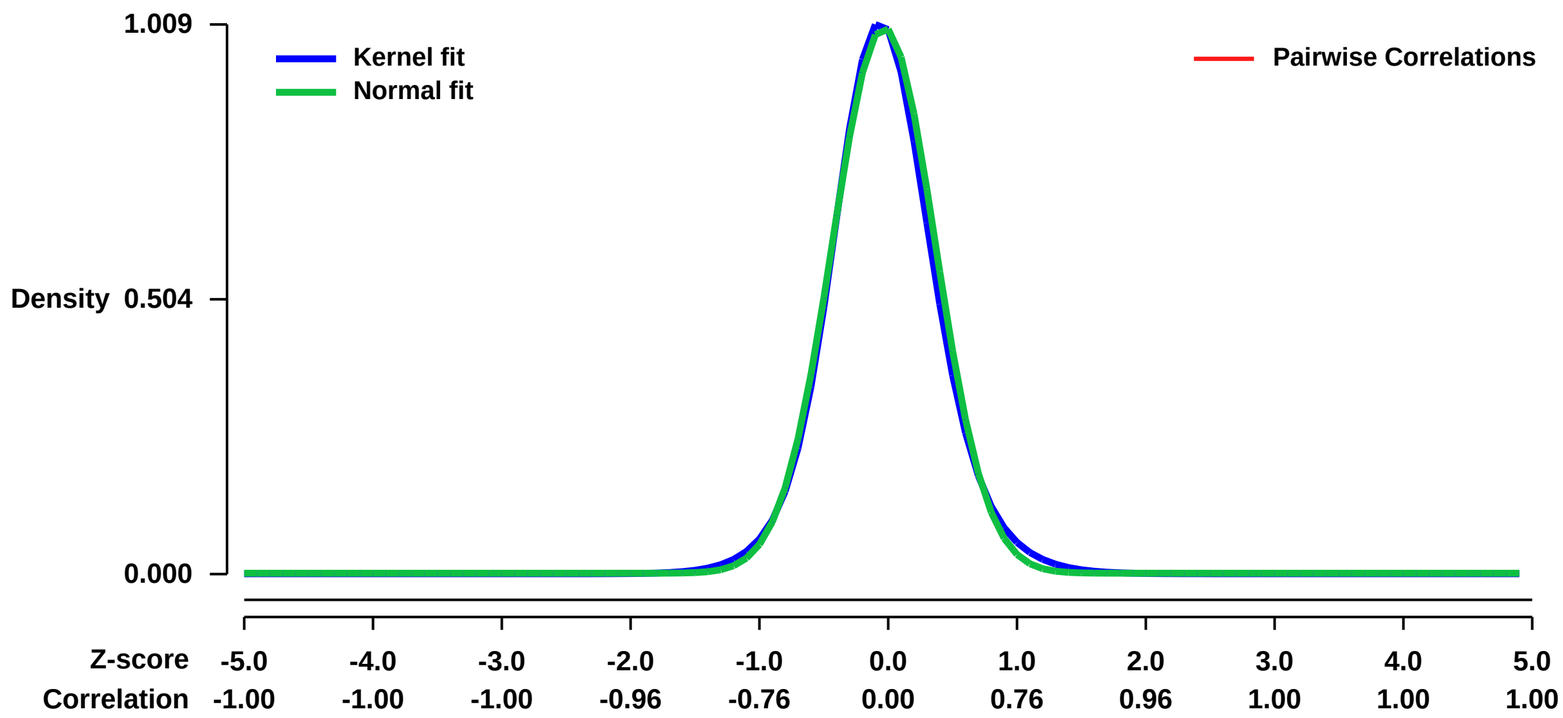

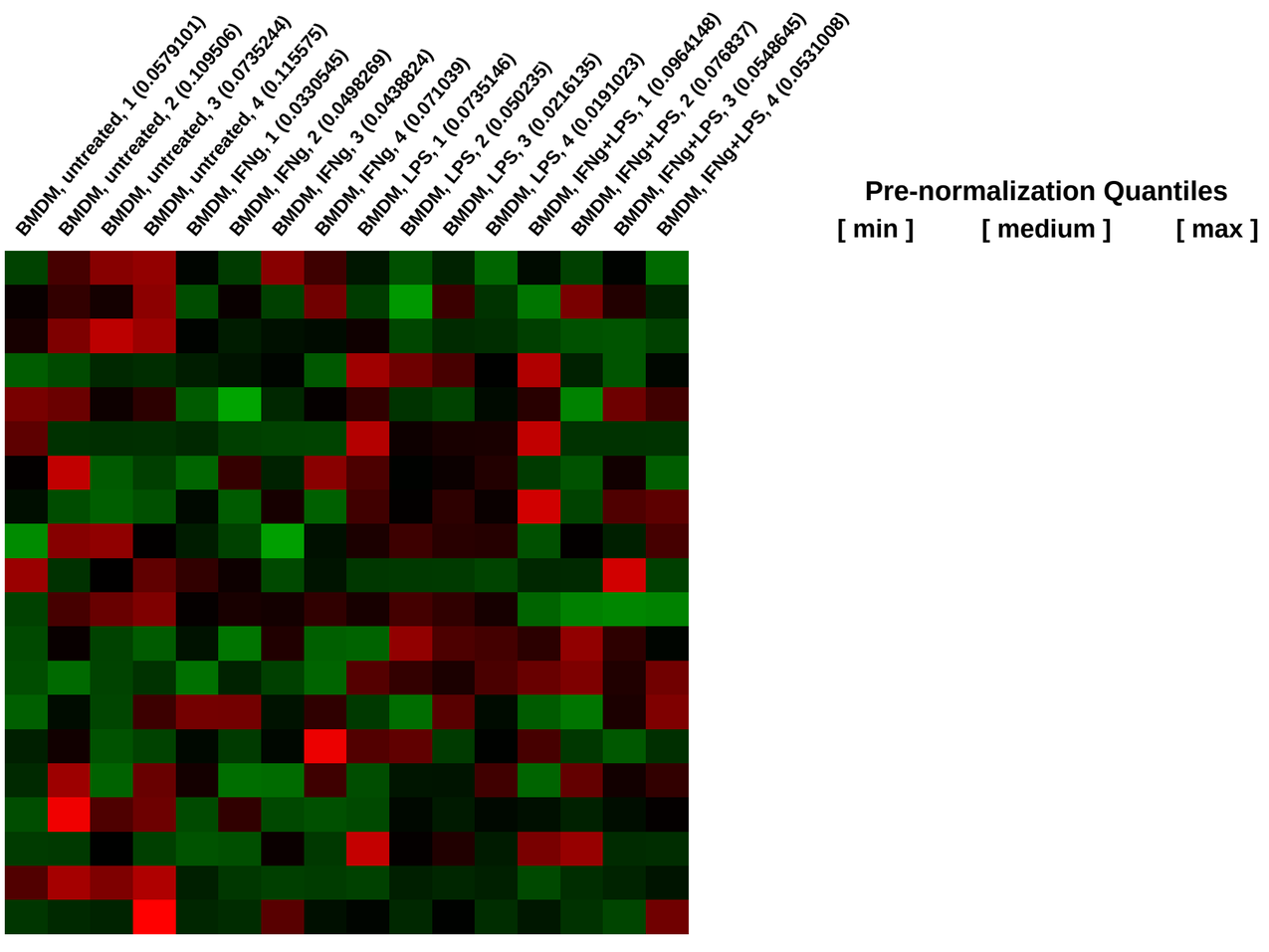

GEO Series "GSE12001" Expression Profiles

Num of samples in this series: 6

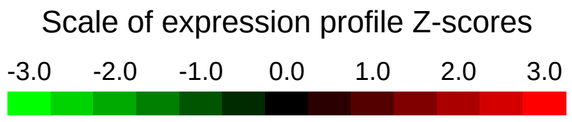

GEO Link:	http://www.ncbi.nlm.nih.gov/geo/query/acc.cgi?acc=GSE12001
Status:	Public on Jul 31 2008
Title:	Wild-type neutrophils and miR-223 null neutrophils
Organism:	Mus musculus
Experiment type:	Expression profiling by array
Platform:	GPL1261
Pubmed ID:	18668037
Summary & Design:	**Summary:** **This array analysis is to study the regulation of target messagesâ expression in murine neutrophils versus miR-223 null neutrophils.** **Overall design:** **Three arrays for wild-type neutrophils and miR-223 null neutrophils**

Background corr dist: **KL-Divergence = 0.0437, L1-Distance = 0.0189, L2-Distance = 0.0004, Normal std = 0.5982**

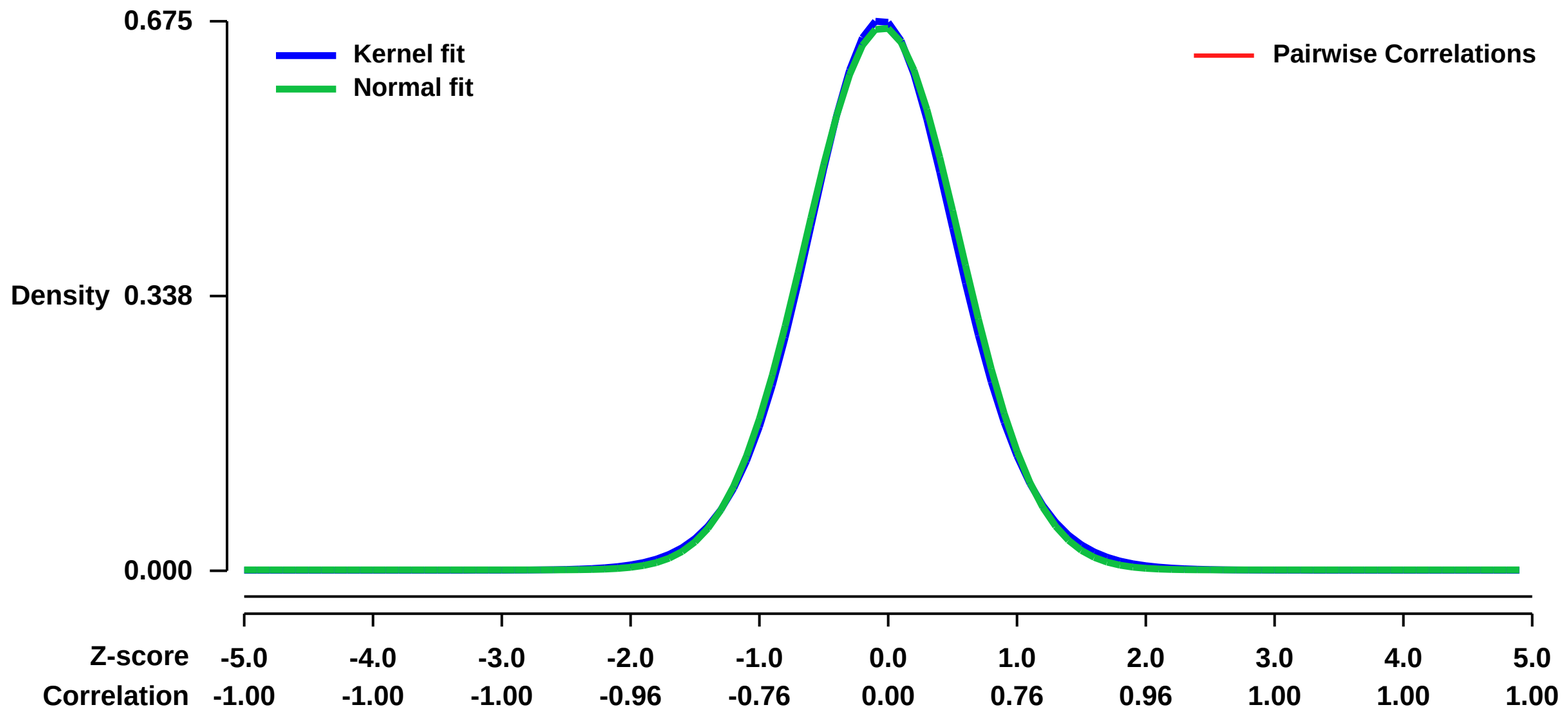

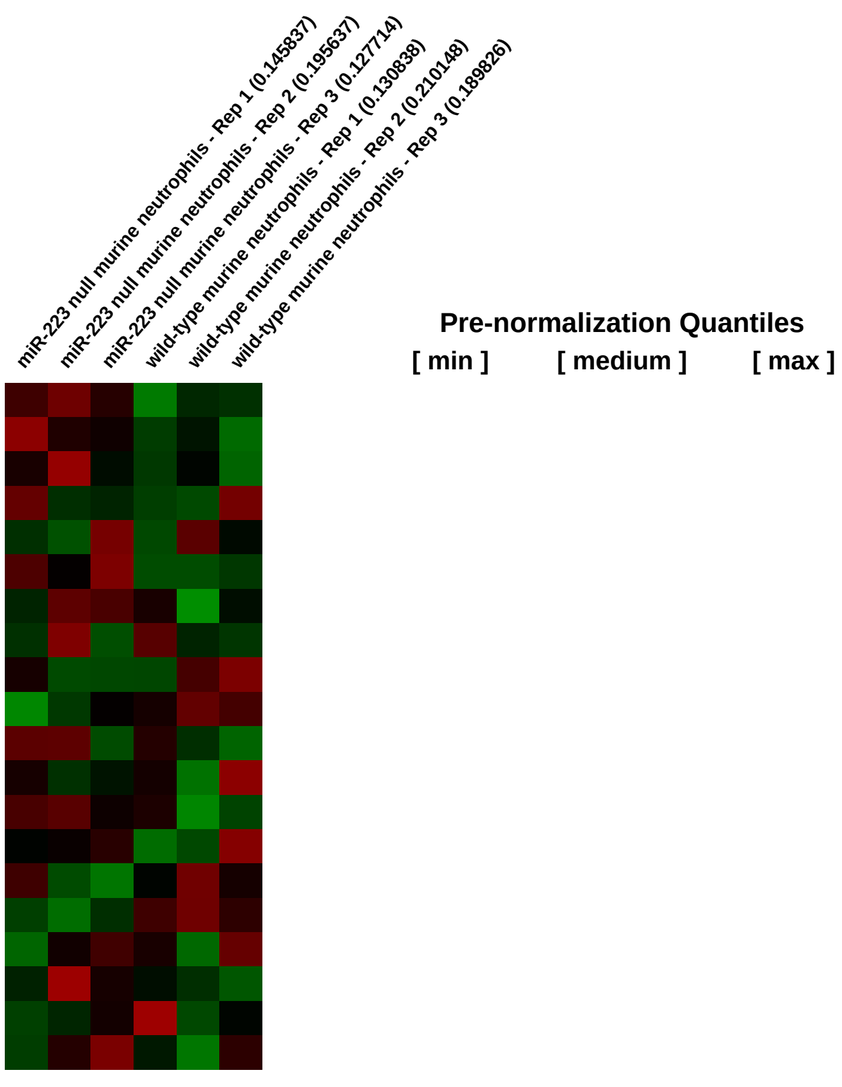

GEO Series "GSE38574" Expression Profiles

Num of samples in this series: 32

Scale of expression profile Z-scores

-3.0 -2.0 -1.0 0.0 1.0 2.0 3.0

GEO Link:	http://www.ncbi.nlm.nih.gov/geo/query/acc.cgi?acc=GSE38574
Status:	Public on Jun 08 2012
Title:	Gene expression data from Ldlr-/-, Apob100/100, Mttp flox/flox Mx1-Cre mice at different stages of atherosclerosis development
Organism:	Mus musculus
Experiment type:	Expression profiling by array
Platform:	GPL1261
Pubmed ID:	18369455
Summary & Design:	**Summary:** Gene expression profiles from the aortic arch of Ldlr-/-Apob100/100 Mttpflox/flox Mx1-Cre mice at different stages of atherosclerosis development **Overall design:** Total RNAs from the aortic arch were collected at different time points during atherosclerosis development (10, 20, 30, 40, 50, and 60 weeks of age), 4-7 mice per time point.

Background corr dist: KL-Divergence = 0.3656, L1-Distance = 0.0660, L2-Distance = 0.0123, Normal std = 0.2582

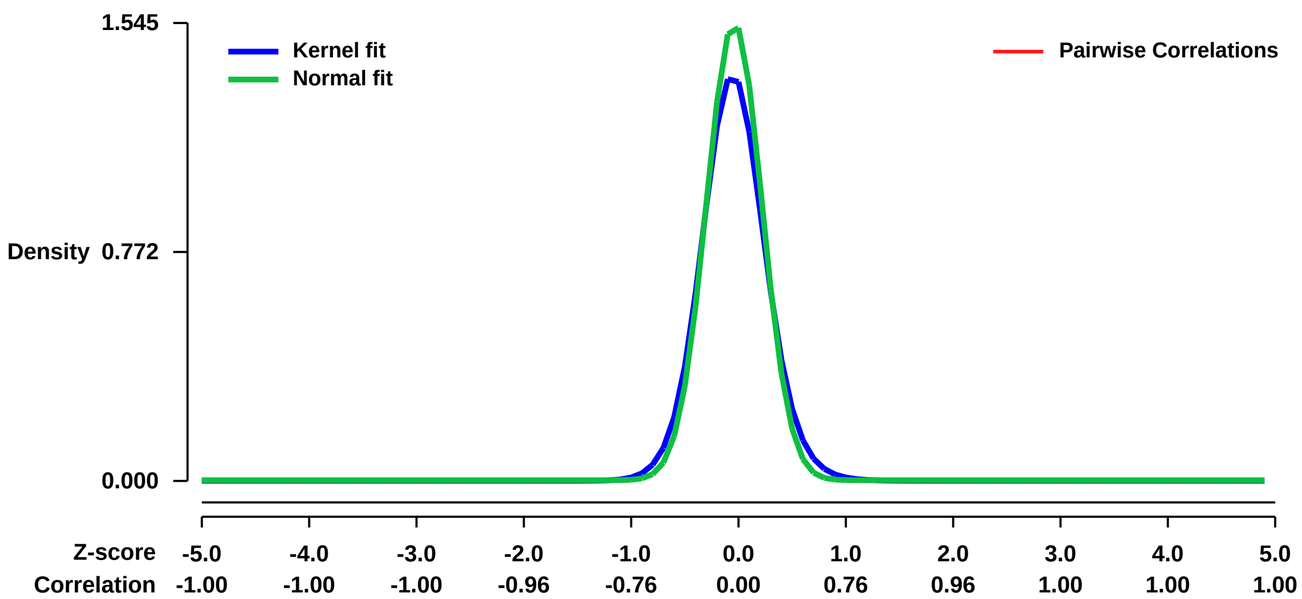

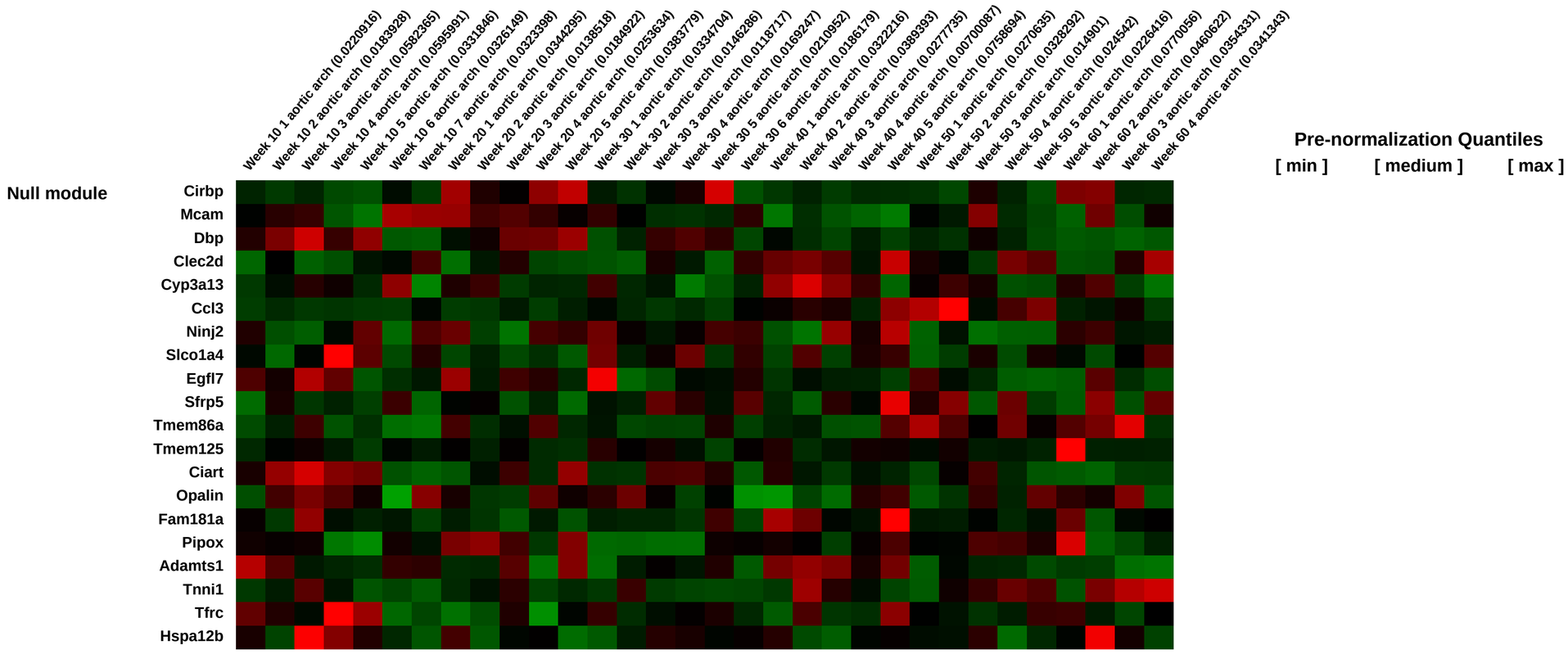

GEO Series "GSE3583" Expression Profiles

Num of samples in this series: 9

Scale of expression profile Z-scores

-3.0 -2.0 -1.0 0.0 1.0 2.0 3.0

GEO Link:	http://www.ncbi.nlm.nih.gov/geo/query/acc.cgi?acc=GSE3583
Status:	Public on Jun 20 2007
Title:	Huntington's disease: Gene expression changes caused by Hdh CAG mutation or 3-nitropropionic acid in striatal cells
Organism:	Mus musculus
Experiment type:	Expression profiling by array
Platform:	GPL1261
Pubmed ID:	17708681
Summary & Design:	**Summary:** Affymetrix MG430 2.0 expression levels of wild-type (STHdhQ7/Q7), 3NP-treated wild-type (STHdhQ7/Q7+3-NP), and mutant (STHdhQ111/Q111) striatal cells **Keywords: Pharmacological and genetic HD cell culture models** **Overall design:** Investigation of HD disease mechanism by gene expression profiling of two HD model systems

Background corr dist: KL-Divergence = 0.0454, L1-Distance = 0.0173, L2-Distance = 0.0003, Normal std = 0.5904

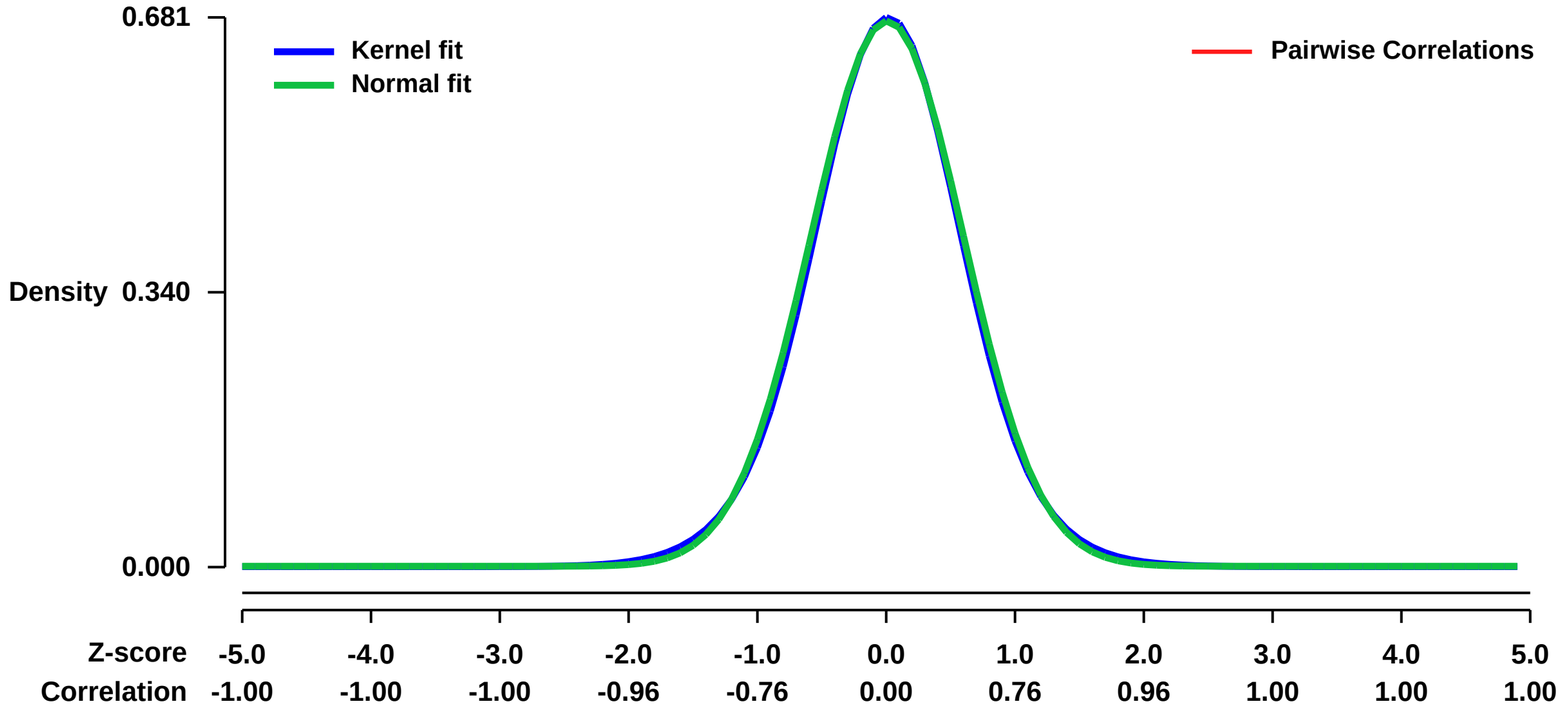

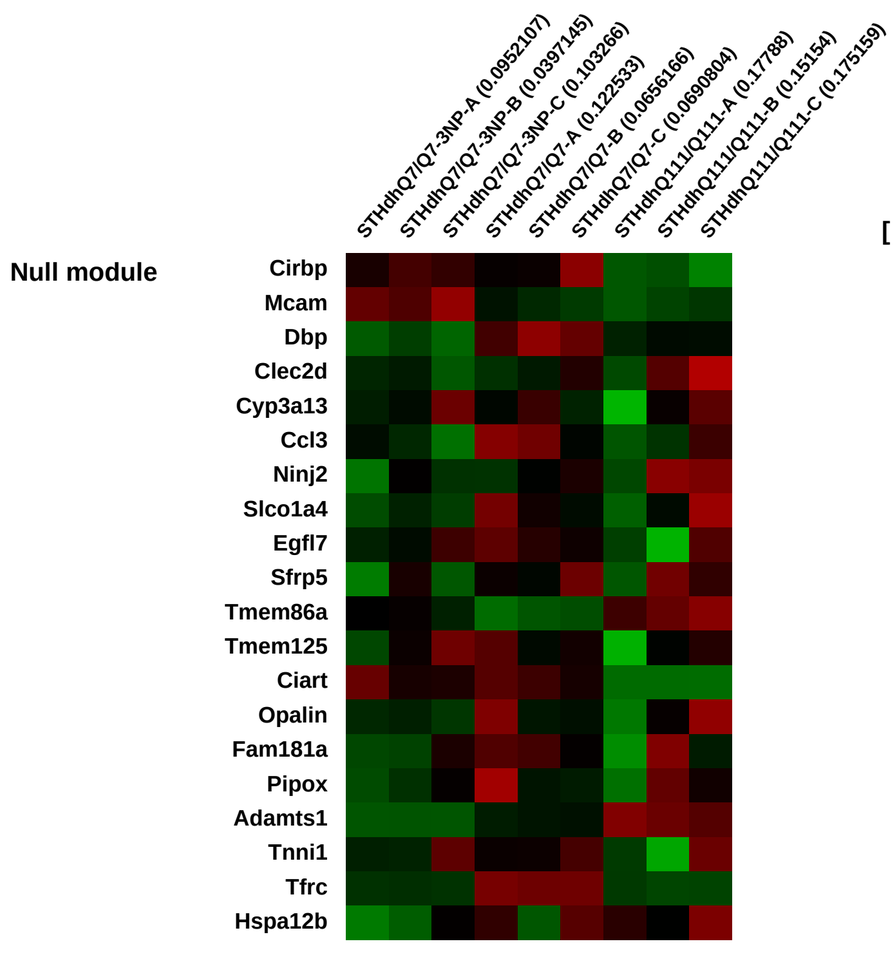

GEO Series "GSE41895" Expression Profiles

Num of samples in this series: 12

Scale of expression profile Z-scores

-3.0 -2.0 -1.0 0.0 1.0 2.0 3.0

GEO Link:	**http://www.ncbi.nlm.nih.gov/geo/query/acc.cgi?acc=GSE41895**
Status:	**Public on Jan 01 2014**
Title:	**Dmrt1 (doublesex and mab-3 related transcription factor 1) conditional knockout expression analysis of E15.5 testes.**
Organism:	**Mus musculus**
Experiment type:	**Expression profiling by array**
Platform:	**GPL1261**
Pubmed ID:	
Summary & Design:	**Summary:** **Dmrt1 (doublesex and mab-3 related transcription factor 1) is a conserved transcriptional regulator of male differentiation required for testicular development in vertebrates. This study examines the result of conditional removal of Dmrt1 in E15.5 testes tissue in B6 and 129Sv strains.** **Overall design:** **This study examines the result of conditional removal of Dmrt1 in E15.5 testes tissue in B6 and 129Sv strains.**

Background corr dist: **KL-Divergence = 0.0803, L1-Distance = 0.0298, L2-Distance = 0.0015, Normal std = 0.4748**

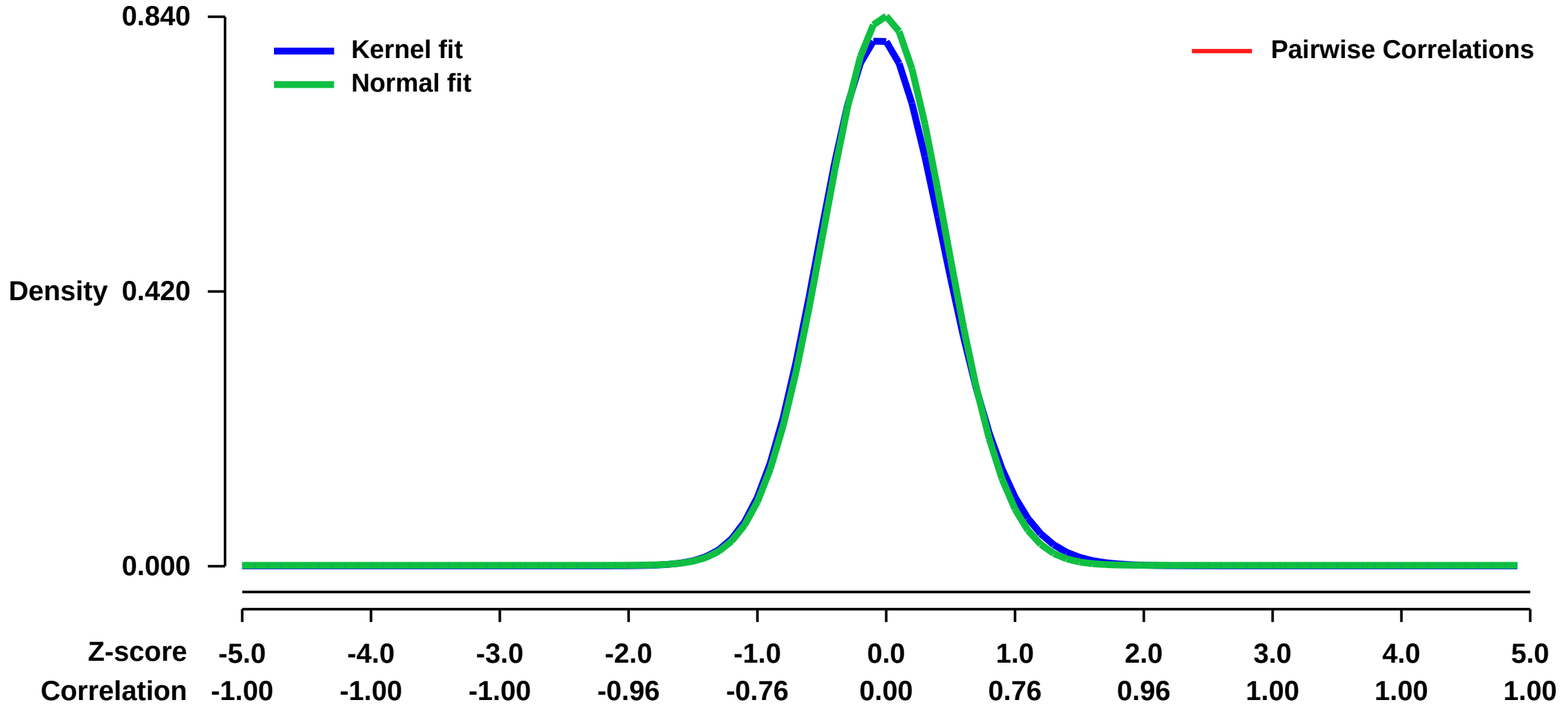

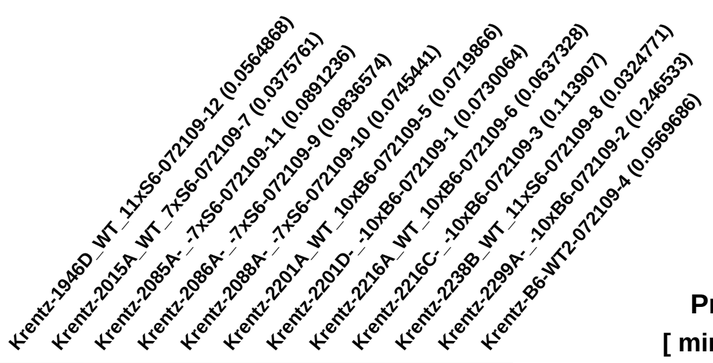

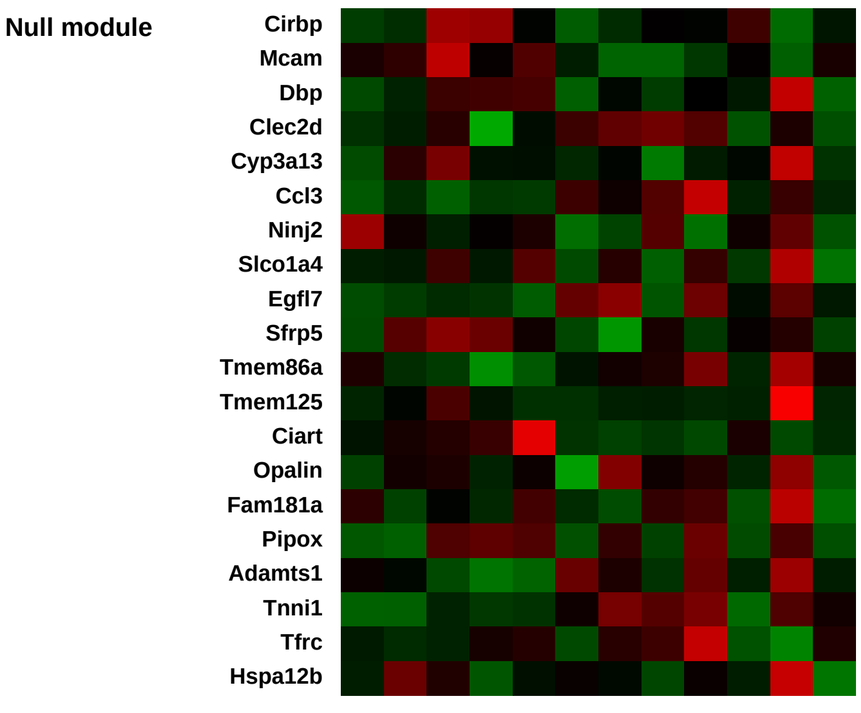

GEO Series "GSE11035" Expression Profiles

Num of samples in this series: 6

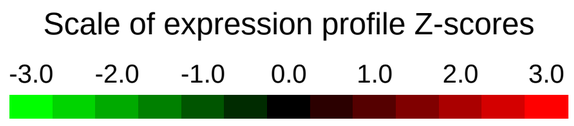

GEO Link:	http://www.ncbi.nlm.nih.gov/geo/query/acc.cgi?acc=GSE11035
Status:	Public on Jun 01 2008
Title:	Effect of 5HTT knockout and heterozygosity in whole mouse lung
Organism:	Mus musculus
Experiment type:	Expression profiling by array
Platform:	GPL1261
Pubmed ID:	19426553

Summary & Design:

Summary:
Rationale: While modulation of the serotonin transporter (5HTT) has shown to be a risk factor for pulmonary arterial hypertension for almost 40 years, there is a lack of in vivo data about the broad molecular effects of pulmonary inhibition of 5HTT. Previous studies have suggested effects on inflammation, proliferation, and vasoconstriction. The goal of this study was to determine which of these were supported by alterations in gene expression in serotonin transporter knockout mice. Methods: Eight week old normoxic mice with a 5-HTT knock-out (5HTT-/-) and their heterozygote(5HTT+/-) or wild-type(5HTT+/+) littermates had right ventricular systolic pressure(RVSP) assessed, lungs collected for RNA, pooled, and used in duplicate in Affymetrix array analysis. Representative genes were confirmed by quantitative RT-PCR and western blot. Results: RVSP was normal in all groups. Only 124 genes were reliably changed between 5HTT-/- and 5HTT+/+ mice. More than half of these were either involved in inflammatory response or muscle function and organization; in addition, some matrix, heme oxygenase, developmental, and energy metabolism genes showed altered expression. Quantitative RT-PCR for examples from each major group confirmed changes seen by array, with an intermediate level in 5HTT+/- mice. Conclusions: These results for the first time show the in vivo effects of 5HTT knockout in lungs, and show that many of the downstream mechanisms suggested by cell culture and ex vivo experiments are also operational in vivo. This suggests that the effect of 5HTT on pulmonary vascular function arises from its impact on several systems, including vasoreactivity, proliferation, and immune function.

Keywords: Genetic modification

Overall design:
Comparison of whole lung total RNA from pools of wild-type, heterozygote, and knockout 5HTT mice to determine the pulmonary effects of loss of 5HTT expression.

Background corr dist: KL-Divergence = 0.0496, L1-Distance = 0.0187, L2-Distance = 0.0004, Normal std = 0.5747

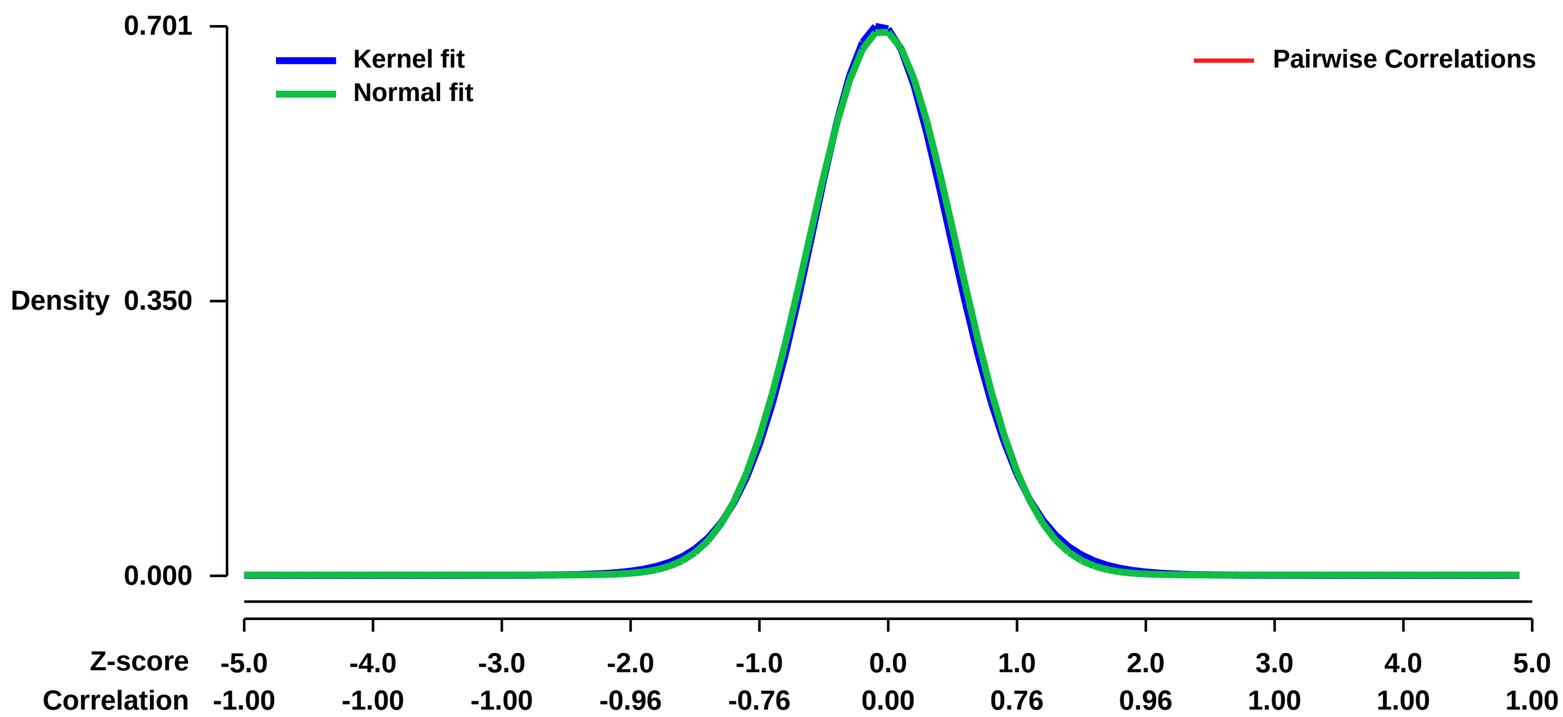

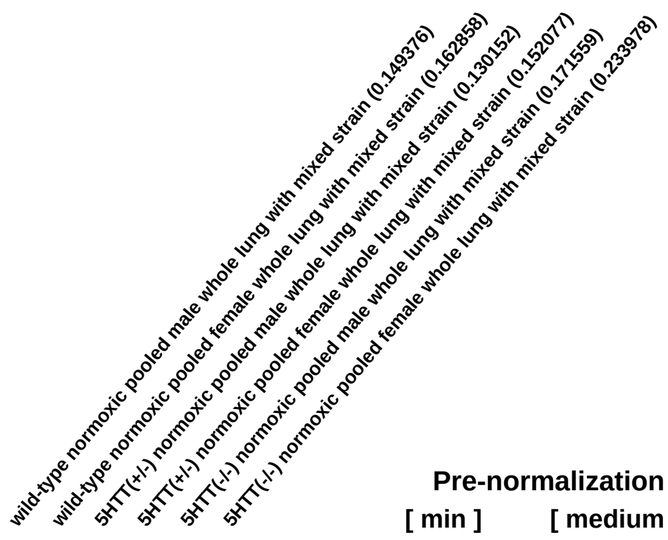

GEO Series "GSE4260" Expression Profiles

Num of samples in this series: 6

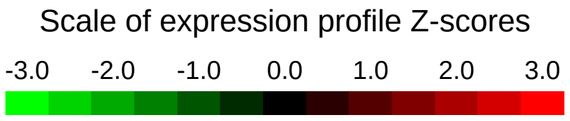

GEO Link:	http://www.ncbi.nlm.nih.gov/geo/query/acc.cgi?acc=GSE4260
Status:	Public on Feb 17 2006
Title:	Cumulus-oocyte complex temporal expression
Organism:	Mus musculus
Experiment type:	Expression profiling by array
Platform:	GPL1261
Pubmed ID:	16455817
Summary & Design:	**Summary:** Cumulus-oocyte complexes were isolated a seperate time-points to generate temporal complexes. Targets from two biological replicates at each time point (0h, 8h, 16h post-hCG treatment) were generated and the expression profiles were determined using Affymetrix GeneChip Mouse Genome 430 2.0 Arrays. Comparisons between the sample groups allow the identification of genes with temporal expression patterns. **Keywords: time course** **Overall design:** 2 eCG-primed (48h) pooled cumulus-oocyte complexes, 2 eCG-primed (48h) hCG-treated (8h) pooled cumulus-oocyte complexes, and 2 eCG-primed (48h) hCG-treated (16h) pooled cumulus-oocyte complexes replicates were analyzed

Background corr dist: KL-Divergence = 0.0244, L1-Distance = 0.0244, L2-Distance = 0.0006, Normal std = 0.7316

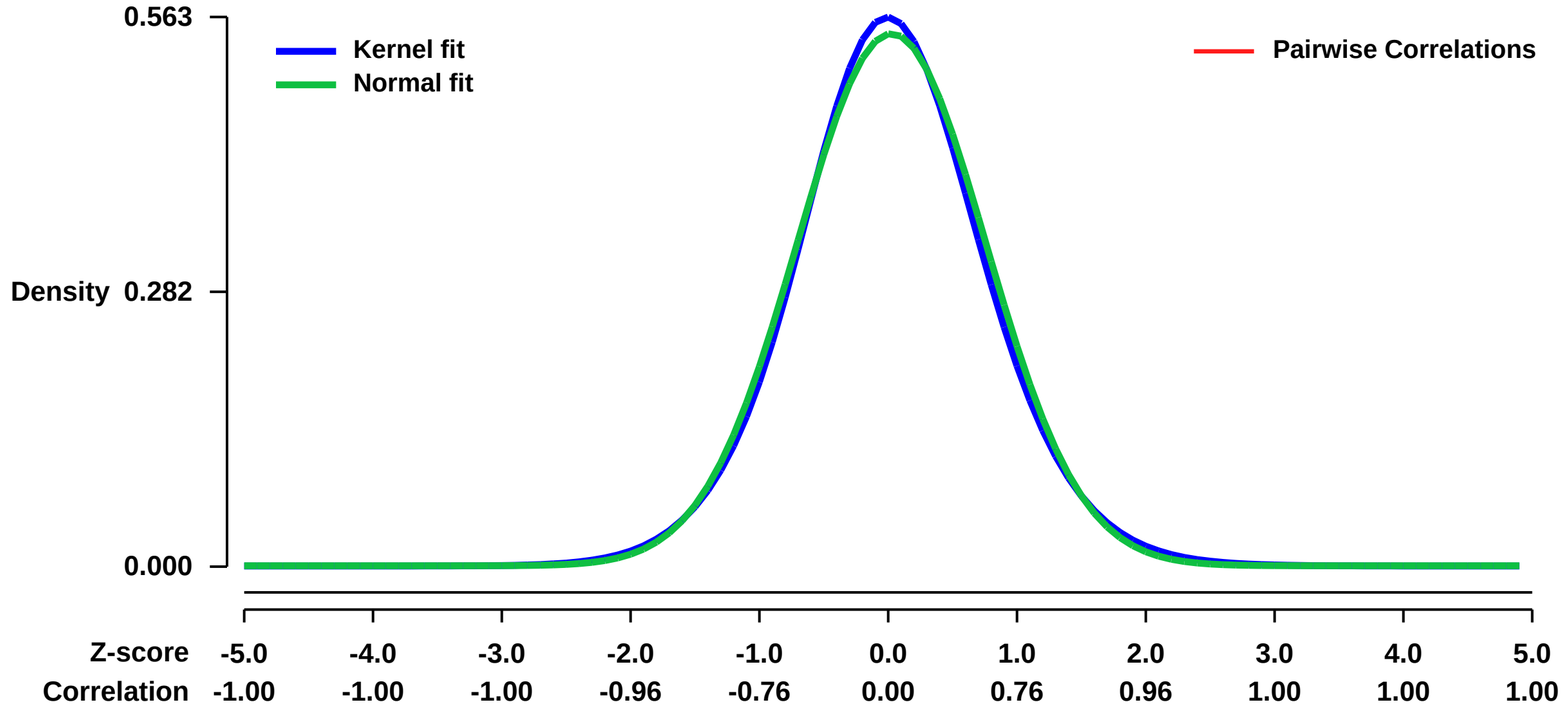

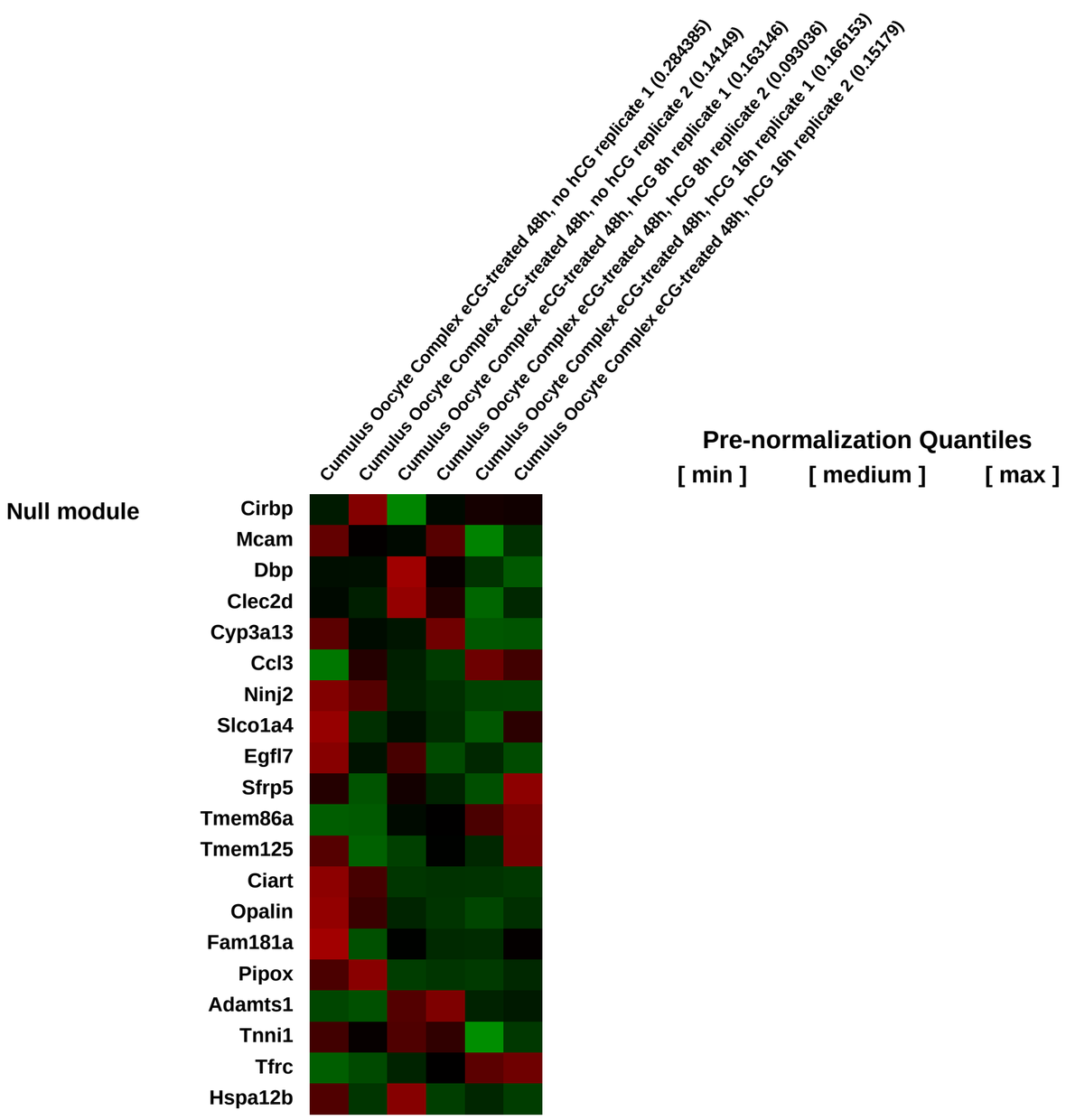

GEO Series "GSE32529" Expression Profiles

Num of samples in this series: 224

Details of this dataset are not shown due to large number of samples and the page size limit.

Find details in http://www.ncbi.nlm.nih.gov/geo/query/acc.cgi?acc=GSE32529

Background corr dist: KL-Divergence = 0.0225, L1-Distance = 0.0447, L2-Distance = 0.0023, Normal std = 0.7763

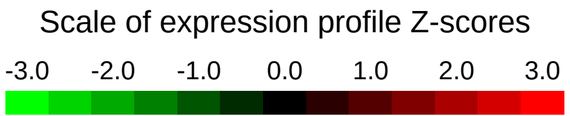

GEO Series "GSE16002" Expression Profiles

Num of samples in this series: 9

Scale of expression profile Z-scores

-3.0 -2.0 -1.0 0.0 1.0 2.0 3.0

GEO Link:	**http://www.ncbi.nlm.nih.gov/geo/query/acc.cgi?acc=GSE16002**
Status:	**Public on Sep 30 2010**
Title:	**Molecular Events Initiating B Cell Fate Specification**
Organism:	**Mus musculus**
Experiment type:	**Expression profiling by array**
Platform:	**GPL1261**
Pubmed ID:	**20971928**
Summary & Design:	**Summary:** **Functional genomics comparison of EBFko, Pax5ko, and RAG2ko cell lines.** **Identify gene signatures associated with specfication and commitment to the B cell fate.** **Overall design:** **Cultured cells harvested and for RNA extraction and hybridization to Affymetrix 430 2.0 Arrays.**

Background corr dist: **KL-Divergence = 0.0727, L1-Distance = 0.0236, L2-Distance = 0.0008, Normal std = 0.5007**

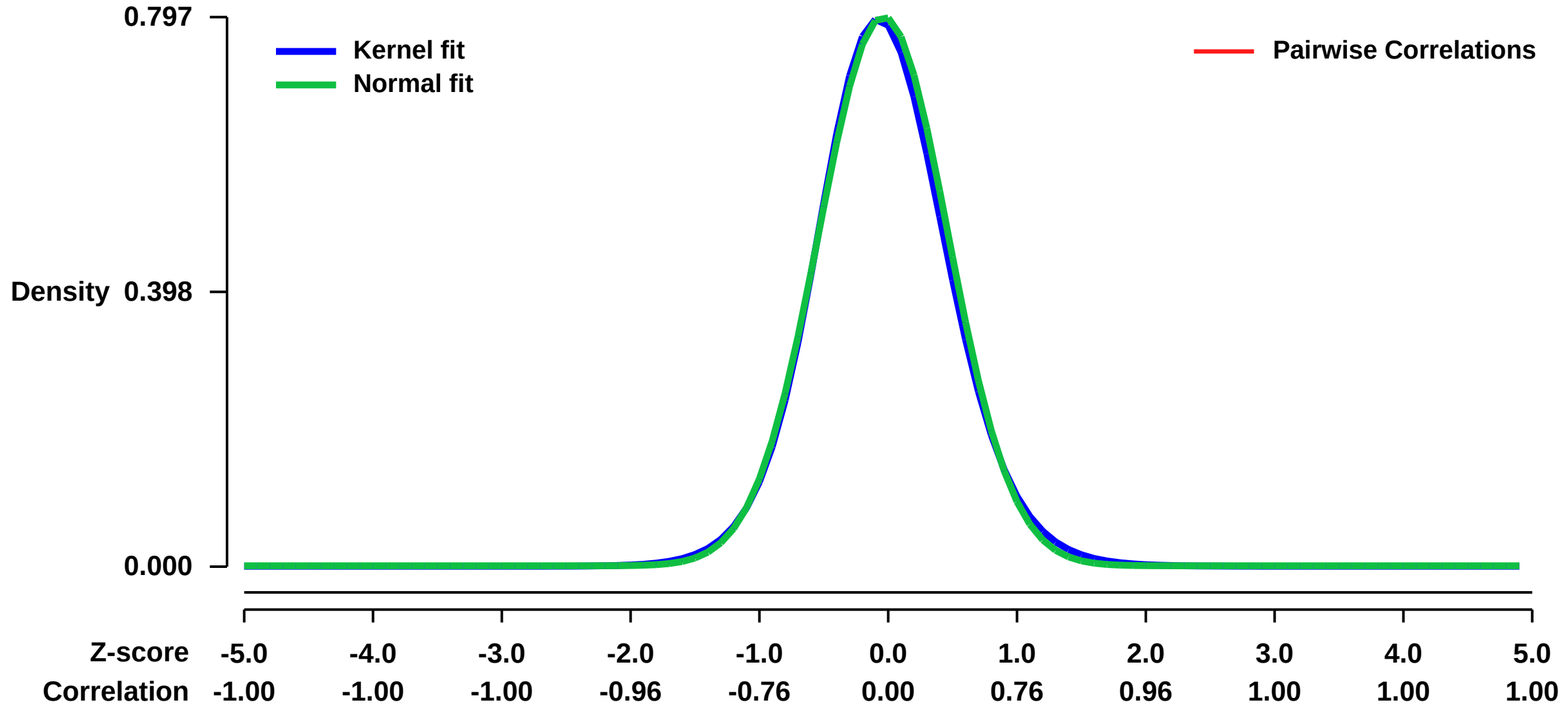

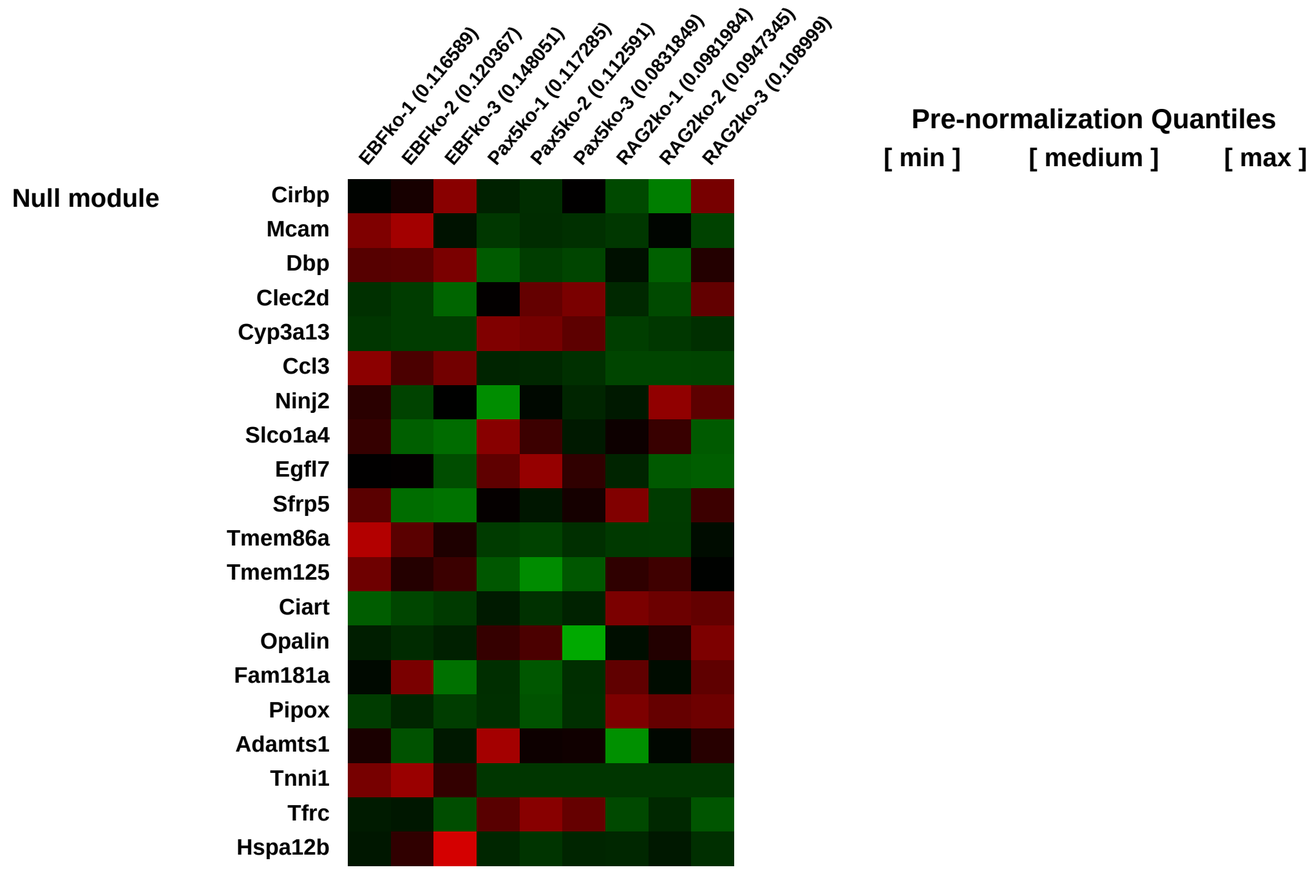

GEO Series "GSE27630" Expression Profiles

Num of samples in this series: 8

Scale of expression profile Z-scores

-3.0 -2.0 -1.0 0.0 1.0 2.0 3.0

GEO Link:	http://www.ncbi.nlm.nih.gov/geo/query/acc.cgi?acc=GSE27630
Status:	Public on Feb 05 2013
Title:	The transcription factor Otx2 regulates choroid plexus development and function
Organism:	Mus musculus
Experiment type:	Expression profiling by array
Platform:	GPL1261
Pubmed ID:	23364326
Summary & Design:	**Summary:** The choroid plexuses (ChPs) are the main regulators of cerebrospinal fluid (CSF) composition and thereby also control the composition of a principal source of signaling molecules that is in direct contact with neural stem cells in the developing brain. The regulators of ChP development mediating the acquisition of a fate that differs from the neighboring neuroepithelial cells are poorly understood. Here, we demonstrate in mice a crucial role for the transcription factor Otx2 in the development and maintenance of ChP cells. Deletion of Otx2 by the Otx2-CreERT2 driver line at E9 resulted in a lack of all ChPs, whereas deletion by the Gdf7-Cre driver line affected predominately the hindbrain ChP, which was reduced in size, primarily owing to an increase in apoptosis upon Otx2 deletion. Strikingly, Otx2 was still required for the maintenance of hindbrain ChP cells at later stages when Otx2 deletion was induced at E15, demonstrating a central role of Otx2 in ChP development and maintenance. Moreover, the predominant defects in the hindbrain ChP mediated by Gdf7-Cre deletion of Otx2 revealed its key role in regulating early CSF composition, which was altered in protein content, including the levels of Wnt4 and the Wnt modulator Tgm2. Accordingly, proliferation and Wnt signaling levels were increased in the distant cerebral cortex, suggesting a role of the hindbrain ChP in regulating CSF composition, including key signaling molecules. Thus, Otx2 acts as a master regulator of ChP development, thereby influencing one of the principal sources of signaling in the developing brain, the CSF. **Overall design:** We performed gene expression microarray analysis of fourth ventricular choroid plexus tissue from Otx2 k.o. mice compared to wildtype mice from the same litters.

Background corr dist: KL-Divergence = 0.0475, L1-Distance = 0.0207, L2-Distance = 0.0005, Normal std = 0.5785

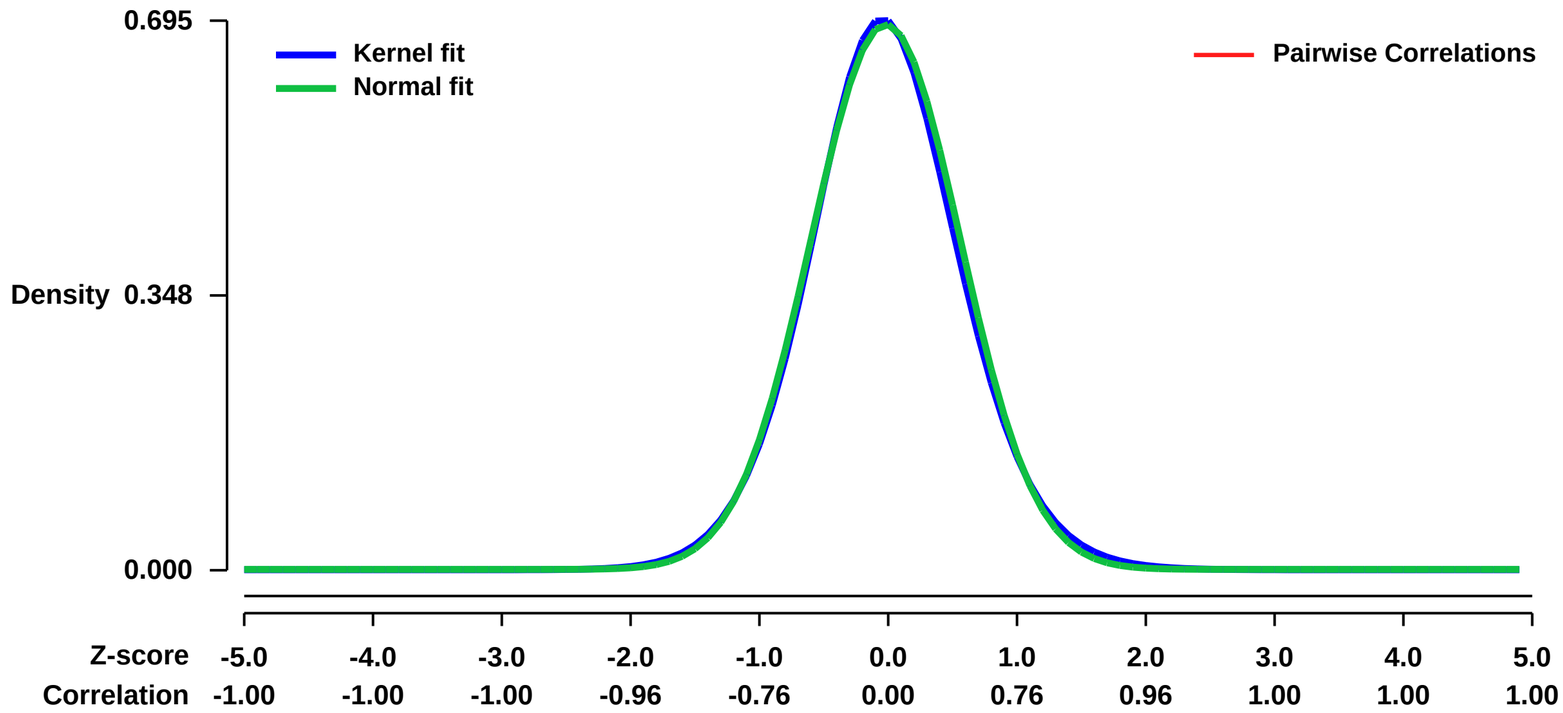

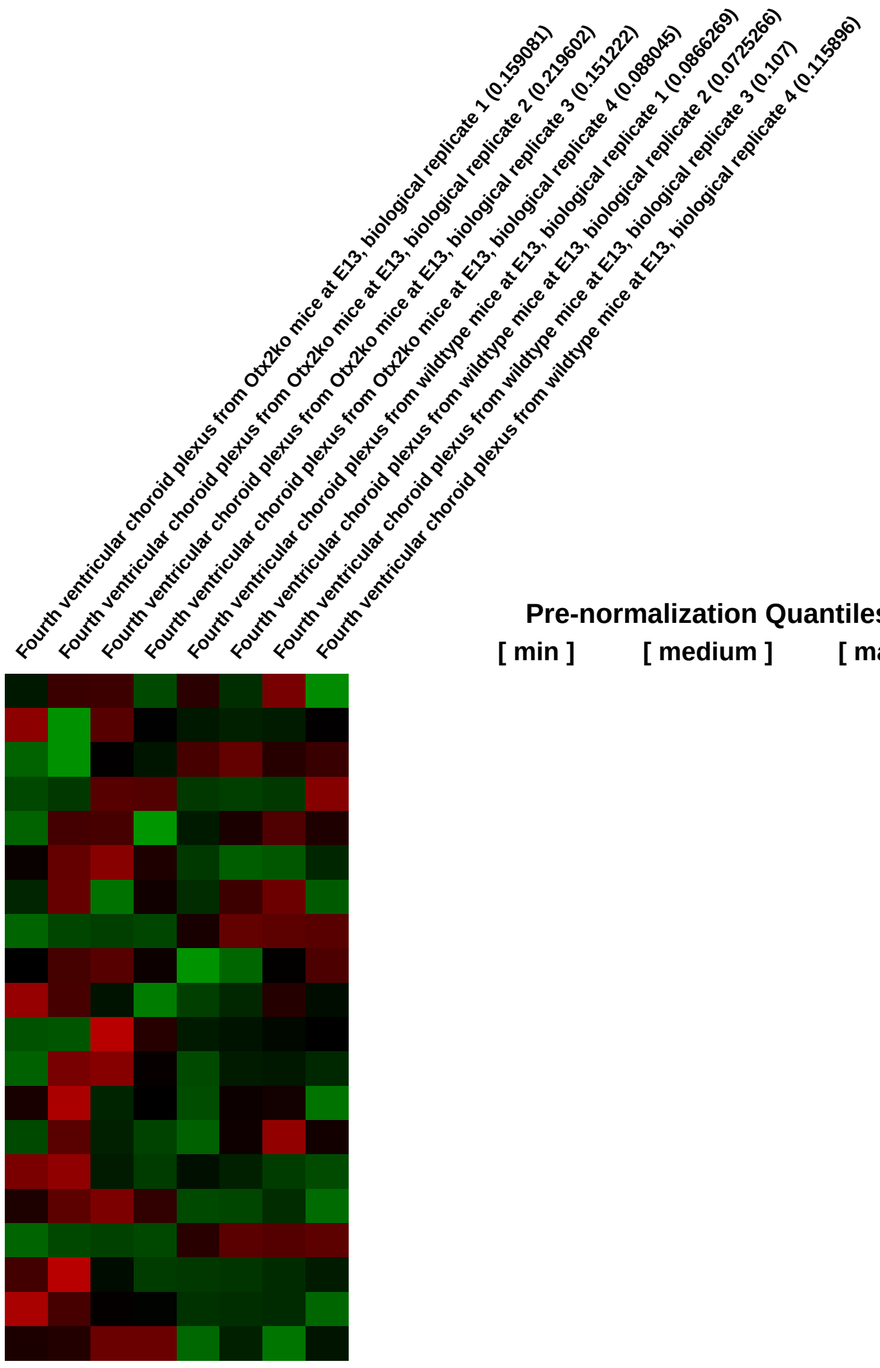

GEO Series "GSE33199" Expression Profiles

Num of samples in this series: 64

Scale of expression profile Z-scores

-3.0 -2.0 -1.0 0.0 1.0 2.0 3.0

GEO Link:	http://www.ncbi.nlm.nih.gov/geo/query/acc.cgi?acc=GSE33199
Status:	Public on Feb 29 2012
Title:	A mouse model of the most aggressive subgroup of human medulloblastoma [Mouse430_2]
Organism:	Mus musculus
Experiment type:	Expression profiling by array
Platform:	GPL1261
Pubmed ID:	22340591
Summary & Design:	**Summary:** Mouse models of medulloblastoma are compared to human subgroups through microarray expression and other measures **Overall design:** This study contrasts mouse medullablastomas from a range of mouse genetic models. For Shh-type medulloblastoma [dka001-005, 009, 033 and 034] and [dka050-057], spontaneous medulloblastomas from [Cdkn2c-/-; Trp53FI/FI; Nestin-Cre] and [Cdkn2c-/-; Ptch1+/-] (Uziel et al.,2005 Genes Dev) were used, respectively. For Myc [dka010-022, 037, 046, 049 and 058-71] and Mycn [dka023-032, 036 and 047] were generated by orthotopic injection of either Myc or Mycn overexpression in Cdkn2c-/-, Trp53-/- cerebellar cells into immunocompromised nude mice. For Wnt-type medulloblastomas [pgr003, 016 and 066], spontaneously developed tumors from CTNNB1+/lox (ex3); BLBP-Cre; Trp53FI/FI (Gibson et al., Nature, 2010) were removed for RNA extraction.

Background corr dist: KL-Divergence = 0.3359, L1-Distance = 0.0564, L2-Distance = 0.0083, Normal std = 0.2699

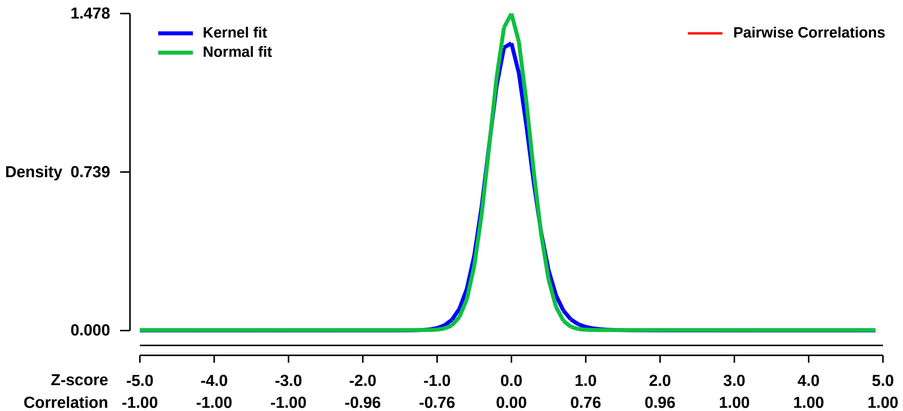

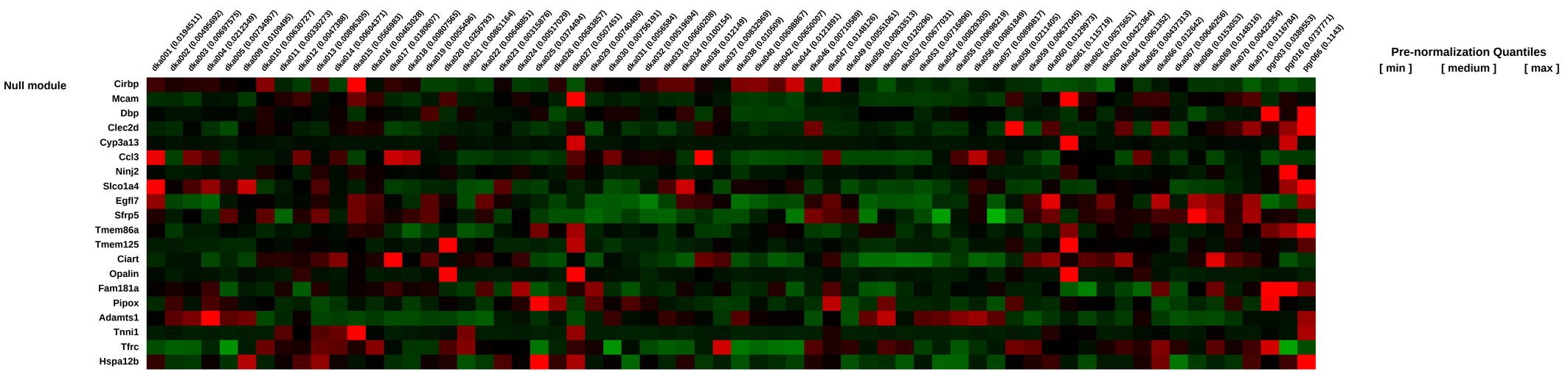

GEO Series "GSE29318" Expression Profiles

Num of samples in this series: 9

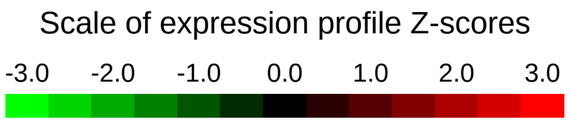

GEO Link:	http://www.ncbi.nlm.nih.gov/geo/query/acc.cgi?acc=GSE29318
Status:	Public on Jul 12 2011
Title:	Expression profile of FAC-sorted murine retinal cells
Organism:	Mus musculus
Experiment type:	Expression profiling by array
Platform:	GPL1261
Pubmed ID:	21743009
Summary & Design:	**Summary:** Microarray experiments were performed using FAC-sorted young photoreceptors to analyze their transcriptome in comparison to remaining retinal cells at same developmental stage and retinal progenitors. **Overall design:** For each replicate, retinae of 6 to 8 postnatal day 0 pNestin-GFP or postnatal day 4 rhoEGFP mice were dissected and FAC-sorted based on GFP expression. RNA of fractions was isolated and subsequently analyzed with microarray experiment.

Background corr dist: KL-Divergence = 0.0360, L1-Distance = 0.0199, L2-Distance = 0.0006, Normal std = 0.6174

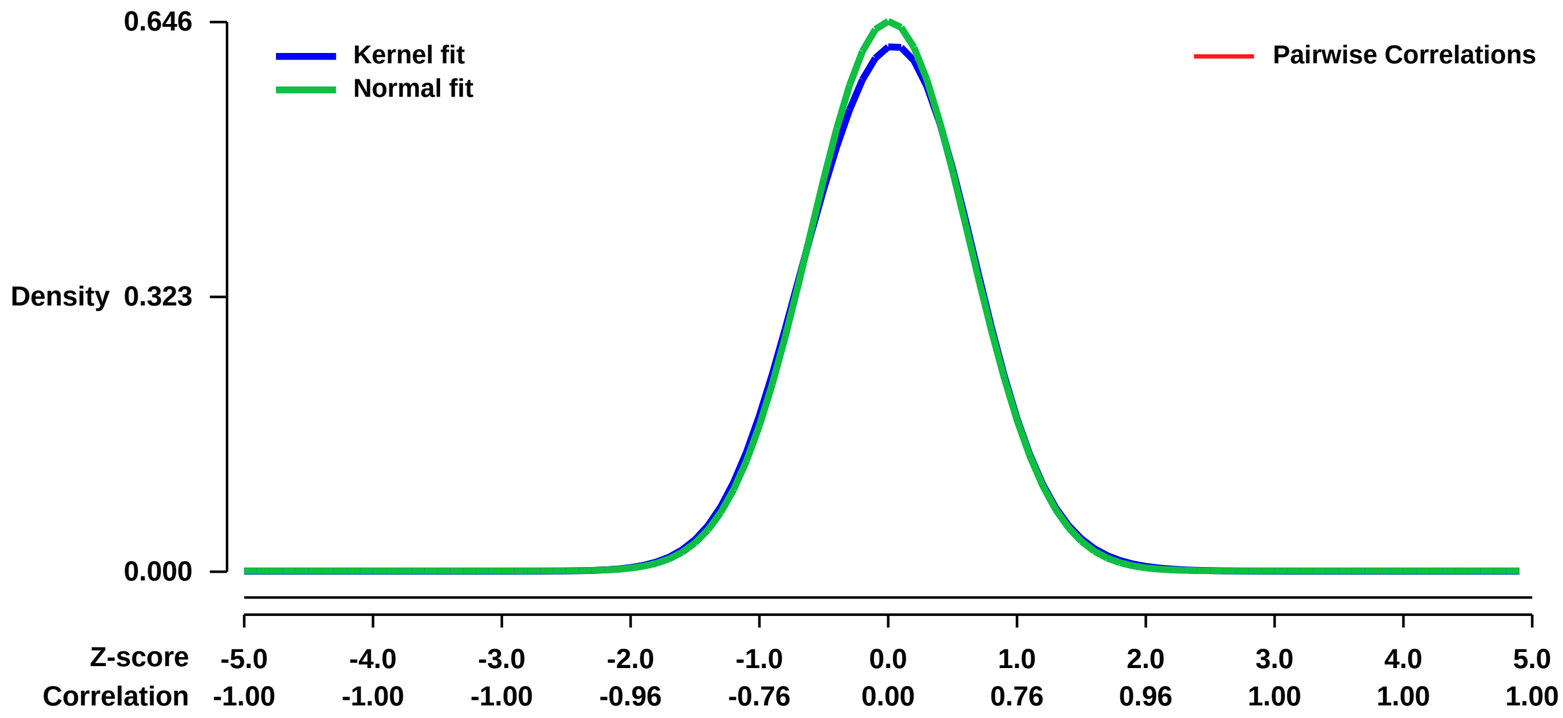

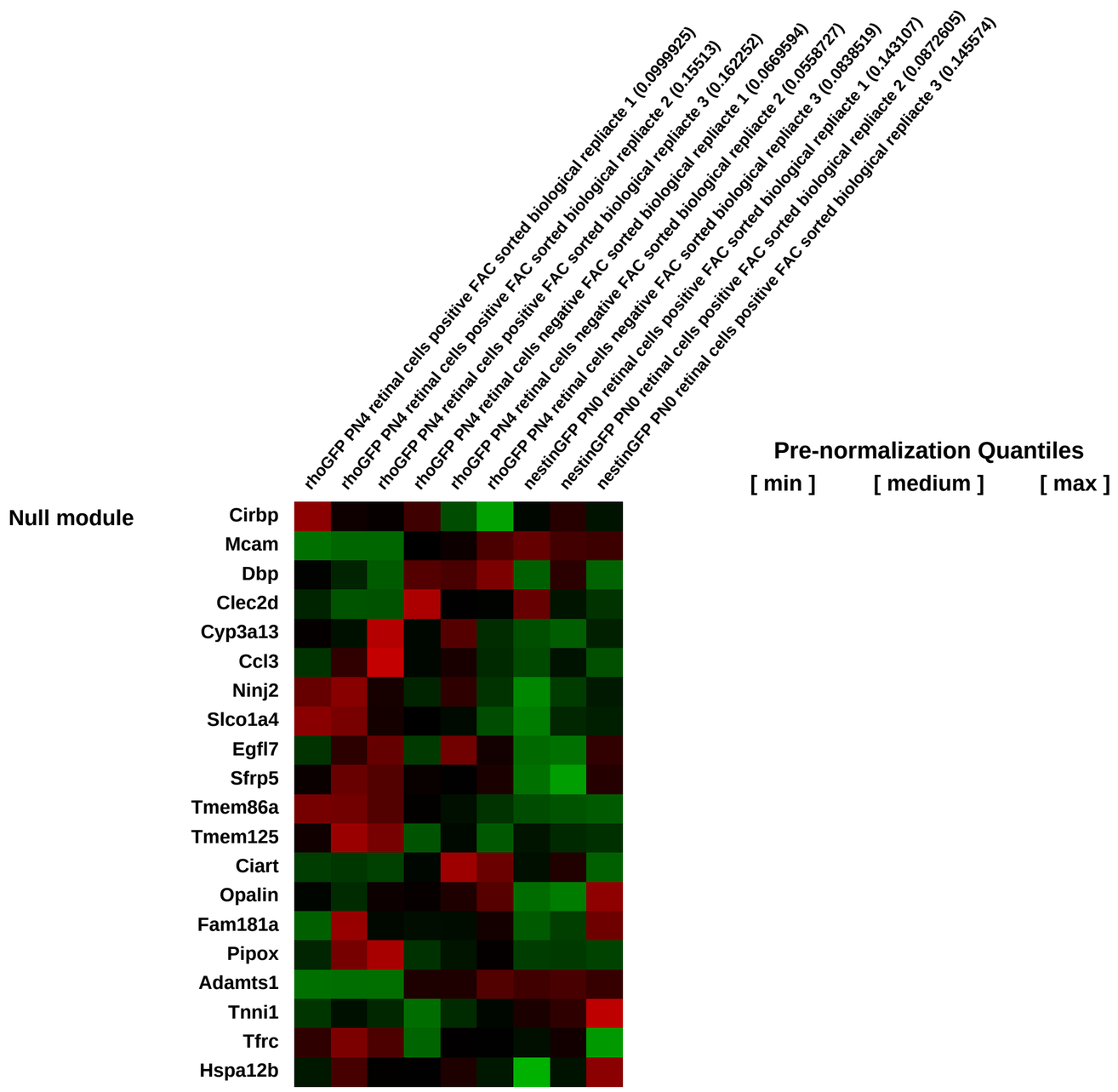

GEO Series "GSE30688" Expression Profiles

Num of samples in this series: 9

Scale of expression profile Z-scores

-3.0 -2.0 -1.0 0.0 1.0 2.0 3.0

GEO Link:	**http://www.ncbi.nlm.nih.gov/geo/query/acc.cgi?acc=GSE30688**
Status:	**Public on Jul 15 2011**
Title:	**Gene expression profiles of mouse sentinel lymph nodes (SLNs) in xenotransplanted and non tumor bearing CB17 SCID.**
Organism:	**Mus musculus**
Experiment type:	**Expression profiling by array**
Platform:	**GPL1261**
Pubmed ID:	
Summary & Design:	**Summary:** **Cutaneous melanoma first metastasizes into sentinel lymph nodes that control the lymphatic drain from the area of the primary tumor. This observation is used clinically for melanoma patients with primary melanomas thicker than 1mm (tumor stage â¥T2a), for these patients sentinel lymph node biopsy has become an important and routinely performed diagnostic procedure. The importance of sentinel node analysis is reflected by a significant better prognosis of melanoma patients with tumor free sentinel nodes compared to patients with metastatic sentinel nodes. Although intensively studied, not much is known about mechanisms responsible for the development of melanoma metastasis.To analyze gene expression in mouse SLNs of M24met tumor bearing animals as compared to tumor free control animals, SLNs were taken at different time points and analyzed for the presence of human M24met to classify SLNs into control, negative, macro metastatic SLN. After categorized SLNs were subjected to microarray analysis.** **Overall design:** **To analyze gene expression in mouse SLNs of human M24met tumor bearing animals as compared to tumor free control animals, SLNs were taken at different time points and analyzed for the presence of human M24met to classify SLNs into control, negative, macro metastatic SLN. Briefly, explanted SLNs were stored in RNA later (Ambion, Austin, TX) and DNA as well as RNA was extracted using AllPrep DNA/RNA Mini Kit and RNeasy Micro Kit (Qiagen, Valencia, CA) according to manufacturerâ s instructions. To detect human cells in mouse SLNs we used a polymerase chain reaction method for the detection of a human-specific 850-bp fragment of the alpha-satellite DNA on human chromosome 17. For analysis of gene expression RNA from control SLN from tumor free animals (control), RNA from tumor negative SLN (negative), and RNA from macro metastatic SLN (positive) from tumor bearing animals was used to analyze gene expression on Mouse Genome 430A 2.0 Arrays (Affymetrix, Santa Clara, CA)**

Background corr dist: KL-Divergence = 0.0518, L1-Distance = 0.0285, L2-Distance = 0.0014, Normal std = 0.5507

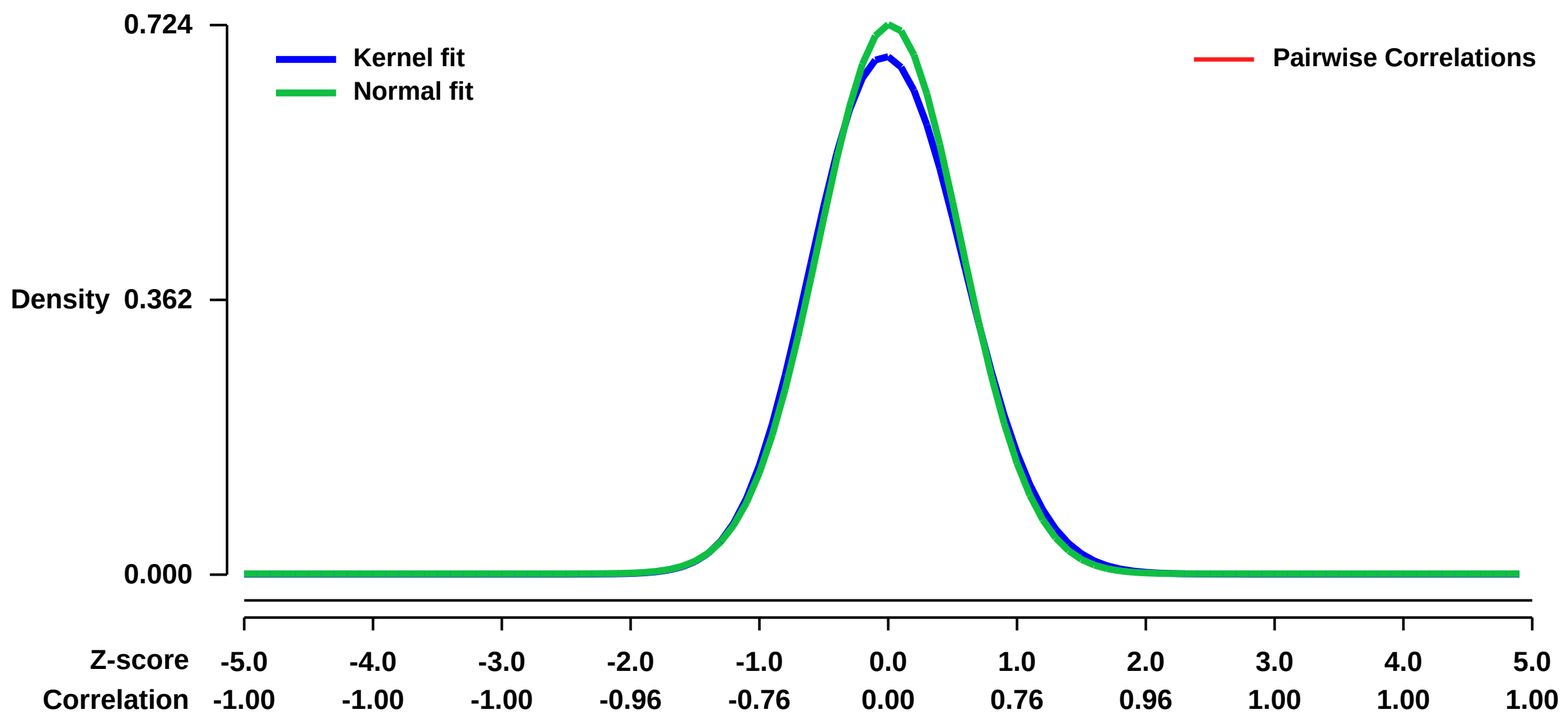

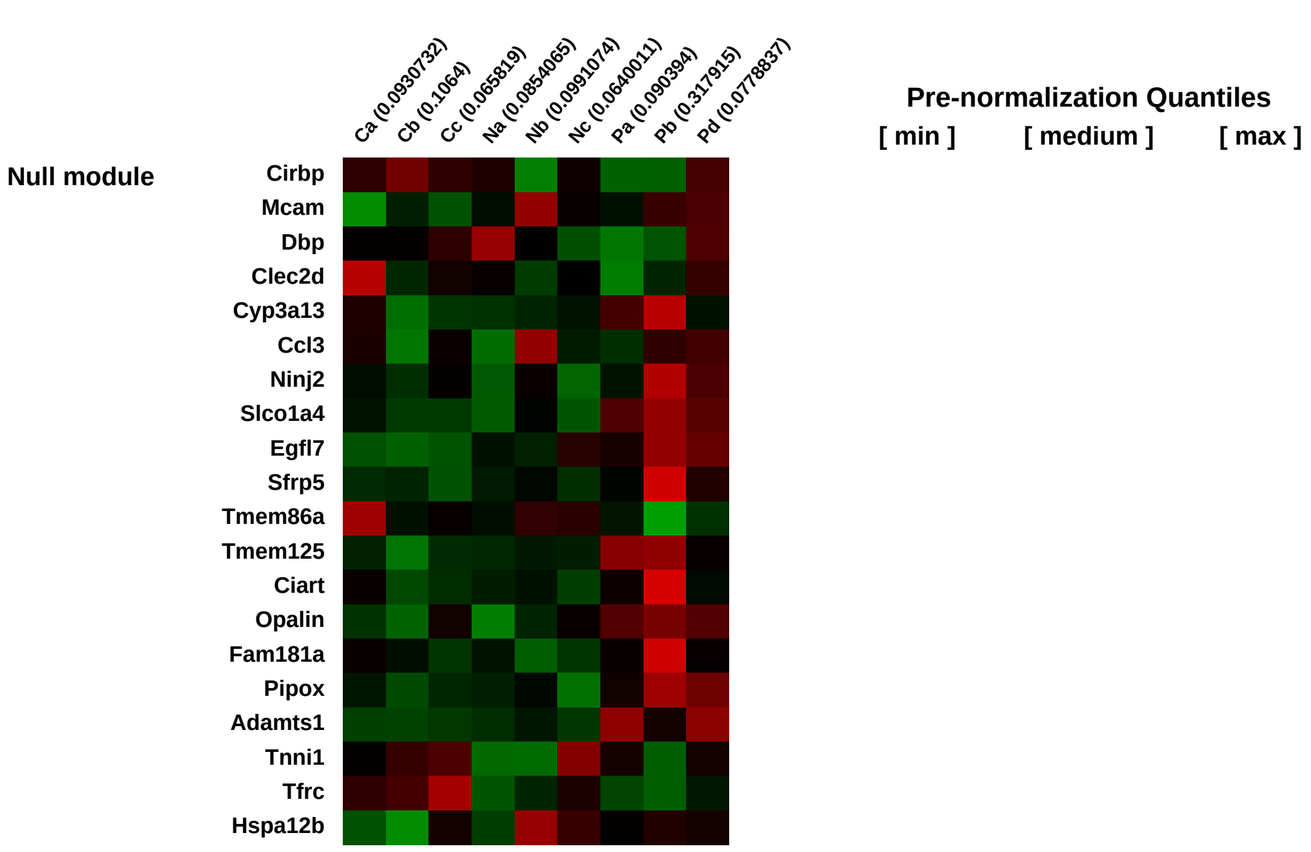

GEO Series "GSE47719" Expression Profiles

Num of samples in this series: 6

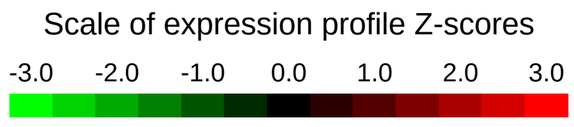

GEO Link:	http://www.ncbi.nlm.nih.gov/geo/query/acc.cgi?acc=GSE47719
Status:	Public on Jan 28 2014
Title:	Derivation and maintenance of murine trophoblast stem cells under defined conditions
Organism:	Mus musculus
Experiment type:	Expression profiling by array
Platform:	GPL1261
Pubmed ID:	
Summary & Design:	**Summary:** **Trophoblast stem (TS) cells are in vitro equivalents to the precursor cells of the placenta. In mice, TS cells can be derived either from polar trophectoderm (TE) of blastocyst outgrowths or from postimplantation extraembryonic ectoderm (ExE), originating from polar TE. Since their first successful derivation in 1998 TS cells have been cultured in serum-rich medium in the presence of fibroblast growth factor 4 (FGF4), the cofactor heparin and embryonic fibroblast conditioned medium. Here, we developed and tested a simple medium consisting of ten chemically defined ingredients for routine culture of TS cells. The defined medium (TX medium) supports growth and self-renewal of TS cells grown on Matrigel-coated dishes over multiple (>20) passages. TS cells cultured under these conditions retain expression of key trophoblast stem cell-associated markers. Global gene expression profiling of cells cultured in standard and TX media conditions revealed that 99.6 % of genes are similarly expressed. DNA methylation profiling confirmed the faithful propagation of epigenomic characteristics of TS cells cultured in TX compared to standard media. Importantly, TX media also supported the derivation of new TS cell lines directly from post implantation embryos. In addition, TS cells cultured in TX retain their ability to differentiate into all derivatives of the trophectodermal lineage in vitro and give rise to haemorrhagic lesions in nude mice, indistinguishable from cells grown in standard conditions. Further, injection into blastocysts proofs chimerization potential after TX culture. The fact that TX media formulation no longer requires fetal bovine serum and conditioned medium facilitates and standardizes the culture of this extraembryonic lineage in vitro. Cell culture. TS cell lines TS-LacZ and TS-L5 have been derived from blastocysts and post implantation embryos us according to standard protocols. Cells were grown on tissue culture plastic (TPP) at 37´℃ in humidified incubators containing 5% CO2 (Heraeus). For conventional stem cell culture cells were cultured in serum containing medium supplemented with 70% CM, 25 ng/ml human recombinant FGF4 (Reliatech) and 1 ´µg/ml Heparin (Sigma-Aldrich), hereafter named TS medium. For differentiation experiments TS medium without CM, FGF4 and heparin (TS -CMF4H) was used. For stem cell culture in defined medium cells were cultured on Matrigel-coated dishes in TX medium. TX medium formulation: DMEM/F12 (Life Technologies), 64 mg/l l-ascorbic acid-2-phosphate magnesium (Sigma), 14 microg/l sodium selenite (Sigma-Aldrich), 25 ng/ml human recombinant FGF4 (Reliatech), 19.4 mg/l insulin (Sigma-Aldrich), 543 mg/l NaHCO3 (Sigma-Aldrich), 10.7 mg/l holo-transferrin (Sigma-Aldrich), 2 ng/ml human recombinant TGF-beta1 (Peprotech), 1 microg/ml Heparin (Sigma-Aldrich), 2 mM L-glutamine (PAN-biotech), 1% penicillin and streptomycin (PAN-biotech). Medium was prepared without growth factors, stored at 4´℃ and used within two weeks. FGF4, heparin and TGFˆ were added to the medium prior to use. Medium was changed every other day. Cells were passaged when sub confluent, by incubation in trypsin-EDTA (PAN-biotech) for 4 min at 37´℃. The enzyme was inactivated by addition of trypsin inhibitor (Life Technologies) in defined culture and by serum containing medium in case of conventional culture. Cells were dissociated and plated in fresh medium. Passage numbers are represented as x + y, where x represents the passage number at which cells were transferred to TX medium, and y being the passage number in TX. For cryopreservation, cells were harvested and pellets were re-suspended either in FBS/10%DMSO (standard conditions) or in KnockOut Serum Replacement/10%DMSO (Life Technologies). Plate coating. Tissue culture dishes for culture of TS cells in TX medium were coated with growth factor reduced Matrigel (BD Biosciences), which was diluted 1:30 in ice cold DMEM/F12 and incubated over night at 4´℃. Coating solution was aspirated immediately before plating cells. For initial coating tests, plates were incubated either with Matrigel, poly-L-lysine, gelatine or fibronectin, respectively. Poly-L-lysine was used at 0.01 % (w/v) in PBS (PAN-biotech) for 30 min at 37´℃ and washed once with PBS prior to use. Gelatine coating was performed with 0.1% (w/v) gelatine solution in PBS for 30 min at 37´℃. Dishes were incubated with fibronectin solution (16.7 ´µg/ml) for 30 min in the incubator, washed once with PBS and used thereafter. Isolation of TS cells from post-implantation (E6.5) embryos Embryos were dissected in PBS on day E6.5 and transferred in PBS/10% (v/v) FBS and kept on ice. Before dissociation, embryos were washed in PBS twice. Whole conceptuses were transferred into an U-bottom 96-well plate and incubated in 40 ´µl trypsin-EDTA (PAN-biotech) for 15 min in the incubator. The content of the well was pipetted up and down several times and transferred to a 24 well plate on pre-plated irradiated MEFS (gammaMEFs) in either TS medium with 1.5x FGF4 and heparin concentration (TS+1.5xF4H) or TX medium with 1.5x FGF4 and heparin (TX+1.5xF4H). TS cell colonies appeared after 2-4 days. Immunofluorescent staining, western blotting. Before staining, cells were washed with PBS once and fixed for 10 min with 4% paraformaldehyde (Sigma-Aldrich). Permeabilization of the cells was performed with 0.5 % (v/v) Triton X-100 (Sigma-Aldrich) in PBS for 10 min and subsequent incubation for 30 min in blocking buffer (2% bovine serum albumin [Sigma-Aldrich], 0.1% (v/v) Triton X-100 in PBS). Samples were incubated overnight at 4´℃ with the following primary antibodies: Cdx2 (1:200, Cdx2-88, BioGenex Inc), Eomes (1:500,ab23345, Abcam), Tfap2c (1:300, sc-8977, Santa Cruz). After three washing steps, detection was performed with appropriate Alexa Fluor-conjugated antibodies (Invitrogen) at a 1:500 dilution in blocking buffer for 1 h at room temperature in the dark. After secondary antibody incubation, nuclei were stained with Hoechst (Sigma-Aldrich). Cells stained without primary antibodies served as controls. Western blotting was performed with 23 ´µg of cell lysates from TS cells cultured in TS and TX media by SDS-polycrylamide gel electrophoresis and blotted onto PVDF membranes. Membranes were blocked with 5% (v/v) BSA or 5% (v/v) non-fat milk powder in TBST (TBS with 0.1% Tween). Membranes were incubated with primary antibodies at room temperature for 2 h, washed three times with TBST and labeled with HRP conjugated antibodies (Dako) for 1 h at room temperature. After three washing steps with TBST, membranes were incubated in ECL substrate (Thermo Scientific). RNA isolation and analysis. RNA was isolated from cells using the RNeasy Minikit (Qiagen) according to the manufacturer's protocol. 500 ng total RNA was used for cDNA synthesis by RevertAidPremium (Thermo Scientific). For gene expression microarray analysis, RNA quality was tested using the Agilent 2100 Bioanalyzer (Agilent Technologies). 100 ng total RNA were used for cDNA synthesis. Biotin labeling and fragmentation were performed according to the Affymetrix user manual. cRNA was hybridized for 16h to Mouse Genome 430 2.0 GeneChip expression arrays (Affymetrix). After hybridization, arrays were washed and stained automatically on a GeneChip Fluidics station 450 (Affymetrix) and scanned with a GeneChip scanner 3000 7G (Affymetrix).** **Overall design:** **TSLacZTX: Mouse trophoblast stem cell LacZ cell line cultered in defined TX medium, 1 biological rep**

Background corr dist: KL-Divergence = 0.0443, L1-Distance = 0.0179, L2-Distance = 0.0003, Normal std = 0.5945

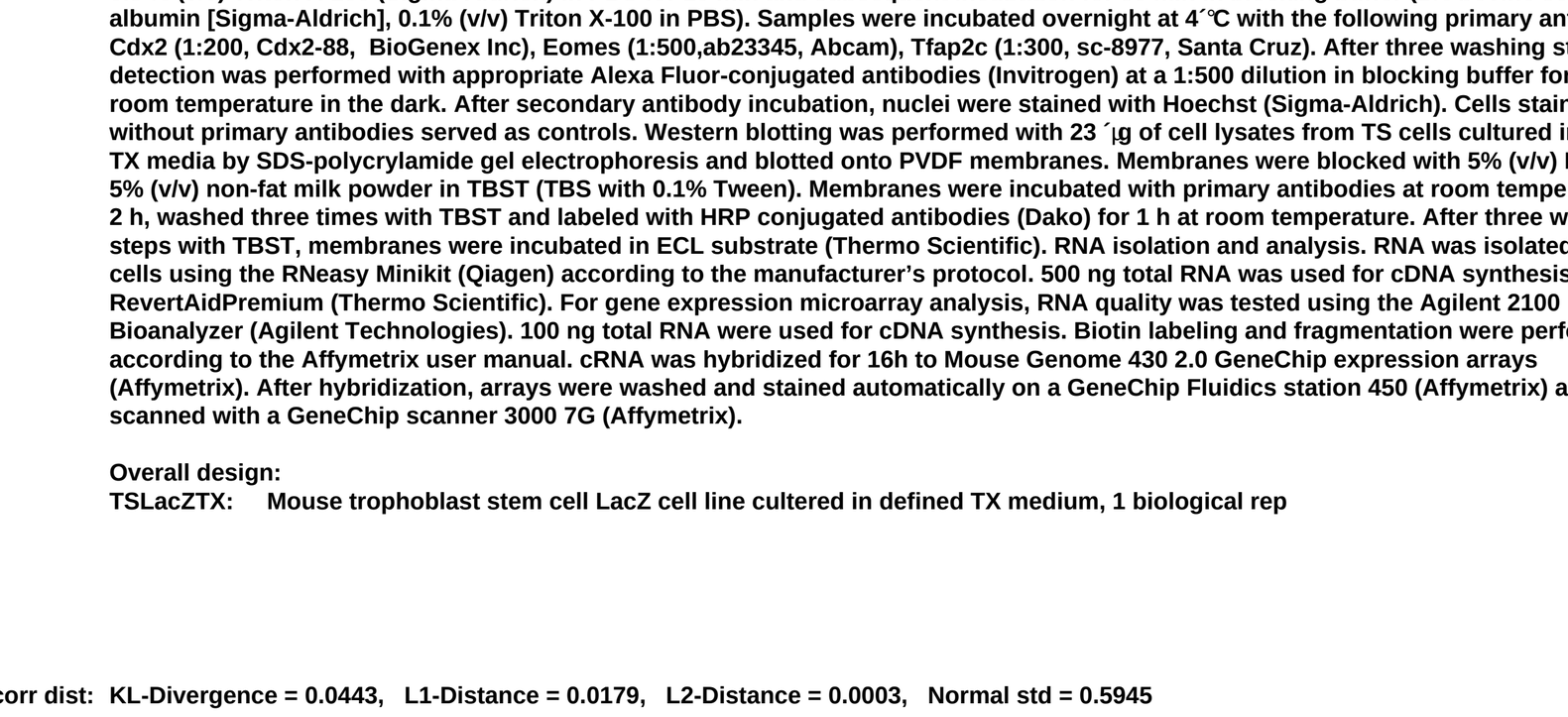

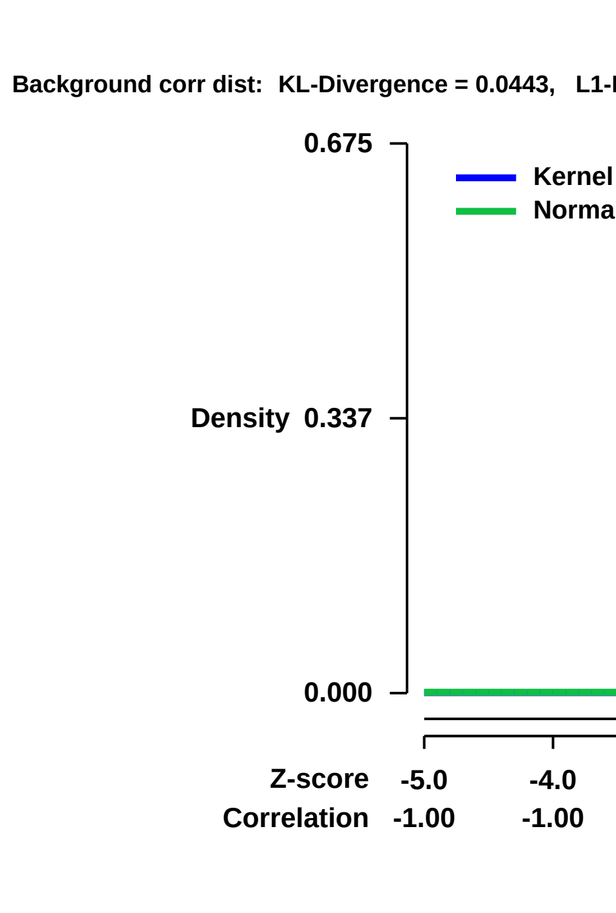

GEO Series "GSE22381" Expression Profiles

Num of samples in this series: 12

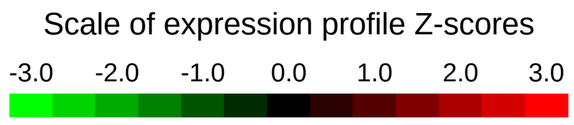

GEO Link:	http://www.ncbi.nlm.nih.gov/geo/query/acc.cgi?acc=GSE22381
Status:	Public on Jul 01 2011
Title:	Identification of downstream transcriptional targets of Dlx5 during early mouse inner ear (otocyst/otic vesicle) development
Organism:	Mus musculus
Experiment type:	Expression profiling by array
Platform:	GPL1261
Pubmed ID:	21227998

Summary & Design:

Summary:
Several transcription factors are known to be expressed in discrete regions of the otic vesicle and Dlx5 is one of those that is expressed highly in the presumptive dorsal vestibular region. Mice lacking Dlx5 have vestibular defects. Specifically, they fail to form the endolymphatic duct (a defect visible as early as E10) as well as the anterior and posterior semi-circular canals. The lateral canal does form but is smaller, whereas the saccule, the utricle and the cochlea appear relatively normal. The goal of this study was to use microarrays to identify differentially expressed genes between wild-type and Dlx5-null otic vesicles microdissected from E10 and 10.5 and identify downstream targets of Dlx5 by searching the immediate 3kb promoter regions of the differentially expressed genes for homeodomain binding sites followed by chromatin immunoprecipitation in an otic vesicle-derived cell line over-expressing Dlx5.

Normal vestibular morphogenesis is compromised in mice lacking Dlx5, a member of the Distal-less family of homeobox transcription factors. We identified its direct downstream targets in the developing mouse inner ear by gene expression profiling wild-type and Dlx5 null otic vesicles from embryonic stages E10 and E10.5. Four hundred genes were differentially expressed in mutants when compared to wild-type in at least one of the two stages. To further constrain the list of likely direct targets of Dlx5, we examined the genomic DNA sequences in the 3kb promoter regions immediately proximal to the transcriptional start sites of these genes. We searched for (i) one or more previously described binding site for Dlx5, (ii) one or more novel 12bp-long motifs with a canonical homeodomain response element (HDRE) shared by promoters of two or more genes, and (iii) 100% conservation of the 12bp-long HDRE-containing motifs in promoter regions of human orthologs. Forty genes passed one or more of these filters, 12 of which are known to be expressed in the developing otic vesicle in domains that at least partially overlap with that of Dlx5 in one or both stages that we examined. Chromatin immunoprecipitation using a Dlx5 antibody confirmed direct binding of Dlx5 to promoter regions of seven of these genes (Atbf1, Bmper, Large, Lrrtm1, and Msx1, all of which were down-regulated in mutants, and Ebf1 and Lhx1, both of which were up-regulated in mutants) in an otic vesicle-derived cell line over-expressing Dlx5. Gene expression profiling of this cell line showed that Bmper and Lrrtm1 transcripts were up-regulated, further supporting their identification as direct targets of Dlx5 activity.

Overall design:
Otic vesicles from wild-type and Dlx5-null embryos were microdissected from mouse developmental stages E10 and E10.5 and expression profiled in duplicate for each stage and genotype. Dlx5-transfected and empty vector-transfected 2B1 cell line samples were also profiled in duplicate (independent cell cultures).

Background corr dist: KL-Divergence = 0.0129, L1-Distance = 0.0464, L2-Distance = 0.0028, Normal std = 0.8888

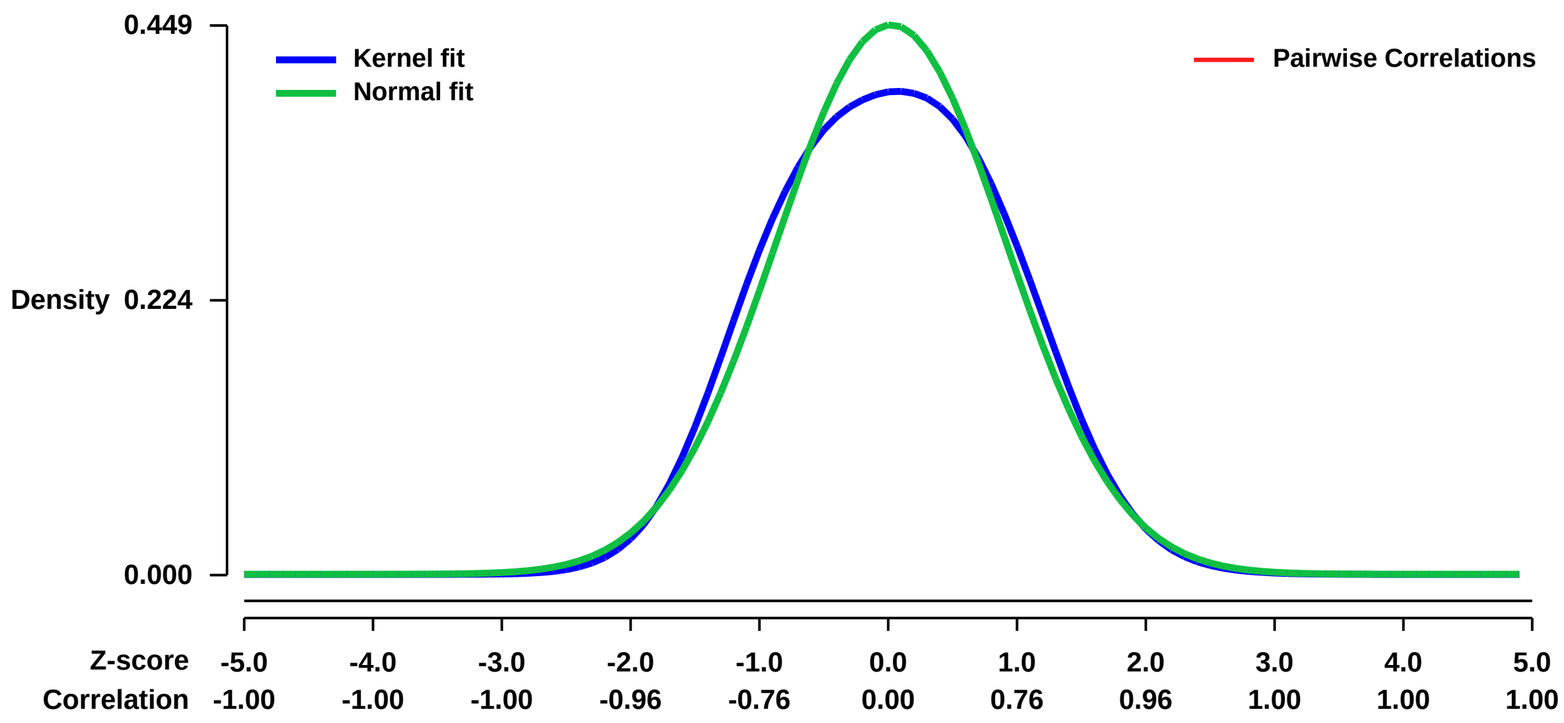

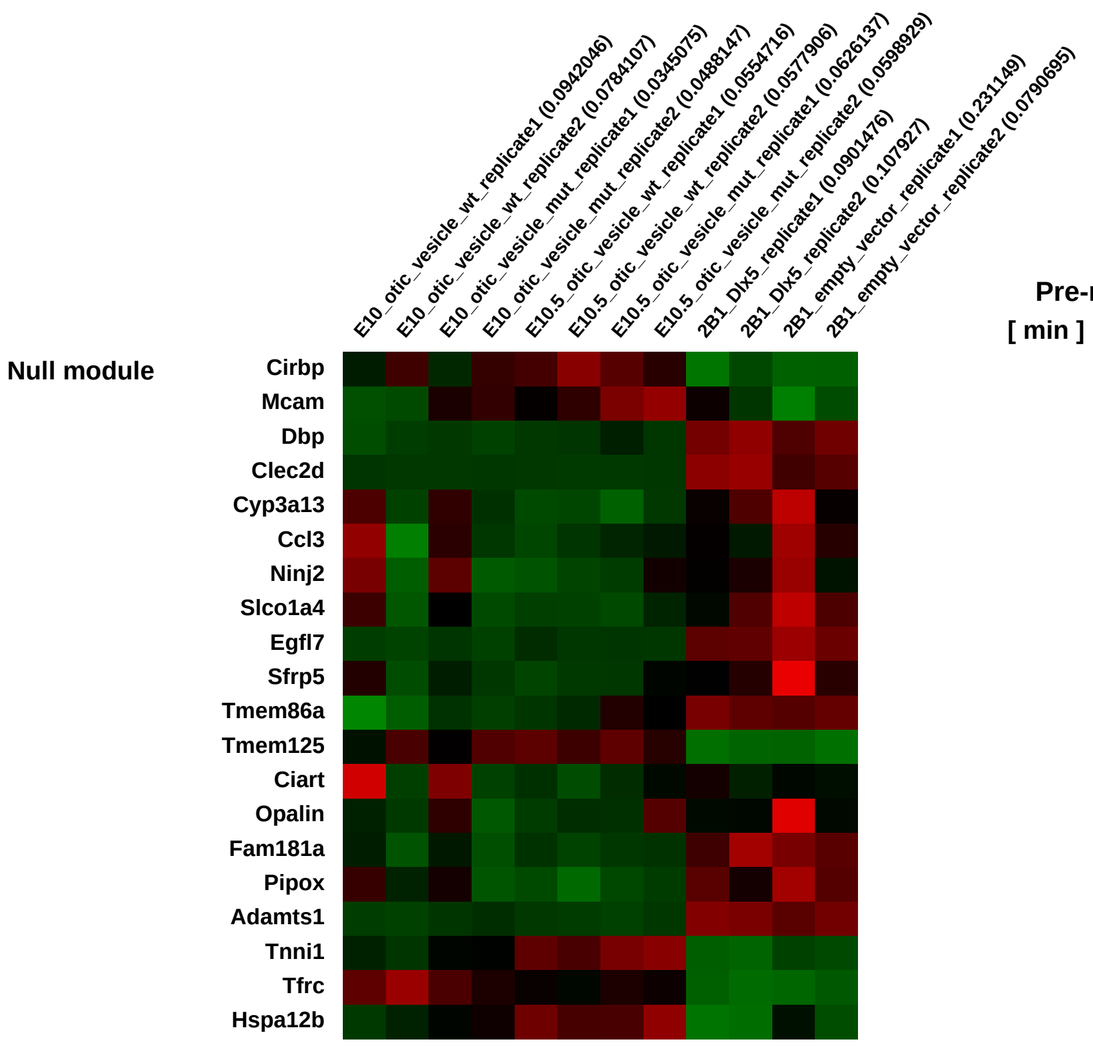

GEO Series "GSE25515" Expression Profiles

Num of samples in this series: 6

Scale of expression profile Z-scores

-3.0 -2.0 -1.0 0.0 1.0 2.0 3.0

GEO Link:	**http://www.ncbi.nlm.nih.gov/geo/query/acc.cgi?acc=GSE25515**
Status:	**Public on Dec 25 2012**
Title:	**Effect of Lira treatment on heart in obese mice**
Organism:	**Mus musculus**
Experiment type:	**Expression profiling by array**
Platform:	**GPL1261**
Pubmed ID:	
Summary & Design:	**Summary:** **C57BL/6 Male mice were treated with high fat diet at the age of 8 weeks and continue the diet for 16 weeks(4 mo) and then injected them with placebo/drug for 1 week before scarifice. Their were sacrifised at the age of 6 months.** **Drug: Lira is used to reduce morbidity and mortality due to obesity and its effect on heart.** **Overall design:** **10 C57BL/6 Male mice under high fat diet for 16 weeks treated with eithe Placebo/drug were chosen for the microarray analysis. Heart from each mouse was disected and the left ventricle was used for TRNA extraction.**

Background corr dist: **KL-Divergence = 0.0493, L1-Distance = 0.0195, L2-Distance = 0.0004, Normal std = 0.5757**

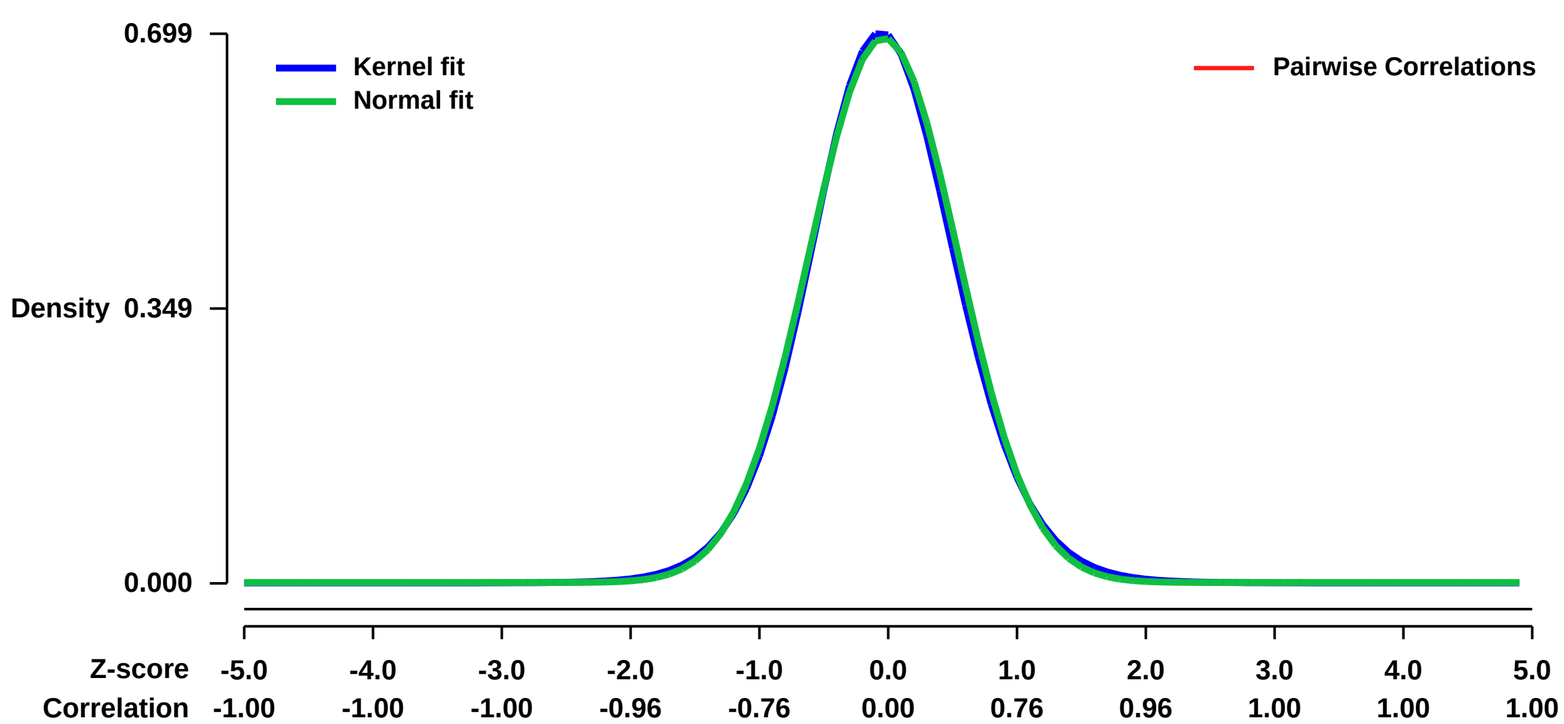

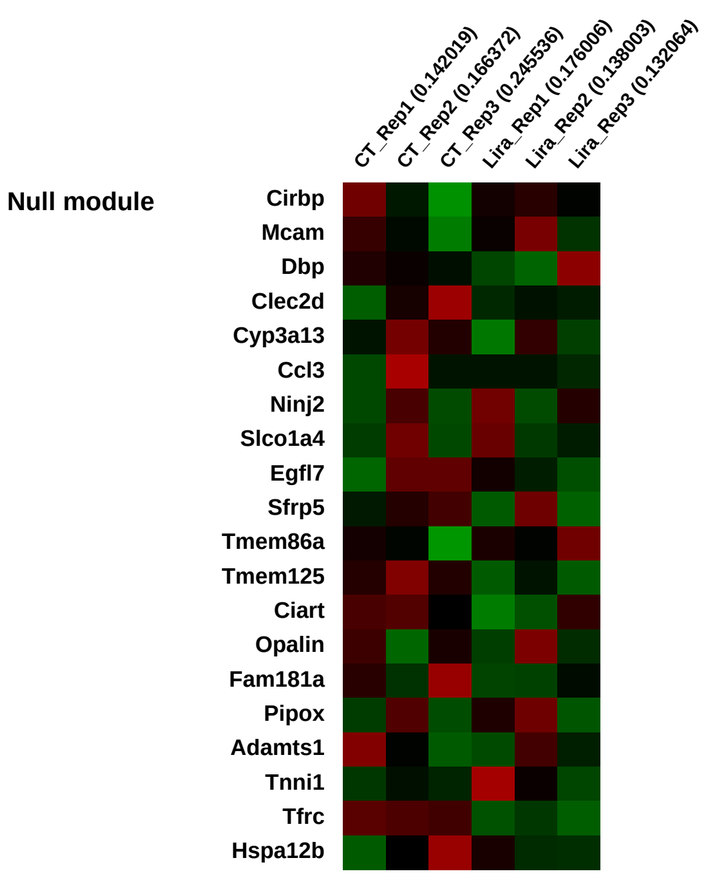

GEO Series "GSE5298" Expression Profiles

Num of samples in this series: 8

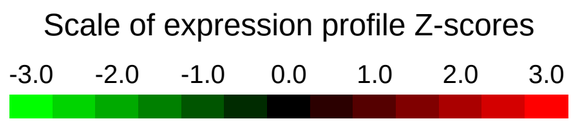

GEO Link:	http://www.ncbi.nlm.nih.gov/geo/query/acc.cgi?acc=GSE5298
Status:	Public on Jul 14 2006
Title:	Development of heart valves requires Gata4 expression in endothelial-derived cells
Organism:	Mus musculus
Experiment type:	Expression profiling by array
Platform:	GPL1261
Pubmed ID:	16914500
Summary & Design:	**Summary:** Cardiac malformations due to aberrant development of the atrioventricular (AV) valves are among the most common forms of congenital heart disease. At localized swellings of extracellular matrix known as the endocardial cushions, the endothelial lining of the heart undergoes an epithelial to mesenchymal transition (EMT) to form mesenchymal progenitors of the AV valves. Further growth and differentiation of these mesenchymal precursors results in formation of portions of the atrial and ventricular septae, and generation of thin, pliable valves. The transcription factor Gata4 is expressed in the endothelium and mesenchyme of the AV valves. Using a Tie2-Cre transgene, we selectively inactivated Gata4 within endothelial-derived cells. Mutant endothelium failed to undergo EMT, resulting in hypocellular cushions. Mutant cushions had decreased levels of Erbb3, an EGF-family receptor essential for EMT in the atrioventricular cushions. In Gata4 mutant embryos, Erbb3 downregulation was associated with impaired activation of Erk, which is also required for EMT. Expression of a Gata4 mutant protein defective in interaction with Friend of Gata (FOG) cofactors rescued the EMT defect, but resulted in decreased proliferation of mesenchyme and hypoplastic cushions that failed to septate the ventricular inlet. We demonstrate two novel functions of Gata4 in development of the AV valves. First, Gata4 functions as an upstream regulator of an Erbb3-Erk pathway necessary for EMT, and second, Gata4 acts to promote cushion mesenchyme growth and remodeling. **Keywords: genetic modification** **Overall design:** For RNA analysis, four mutant and four control RNA samples were prepared (Pico-Pure RNA Isolation Kit, Arcturus), each consisting of 10 microdissected AVCs. Probe was prepared from 50 ng total RNA using an isothermal amplification protocol (NuGen), and hybridized to Affymetrix Mouse 430 2.0 microarrays. Two control samples were excluded because of excessive noise.

Background corr dist: KL-Divergence = 0.0176, L1-Distance = 0.0303, L2-Distance = 0.0014, Normal std = 0.7687

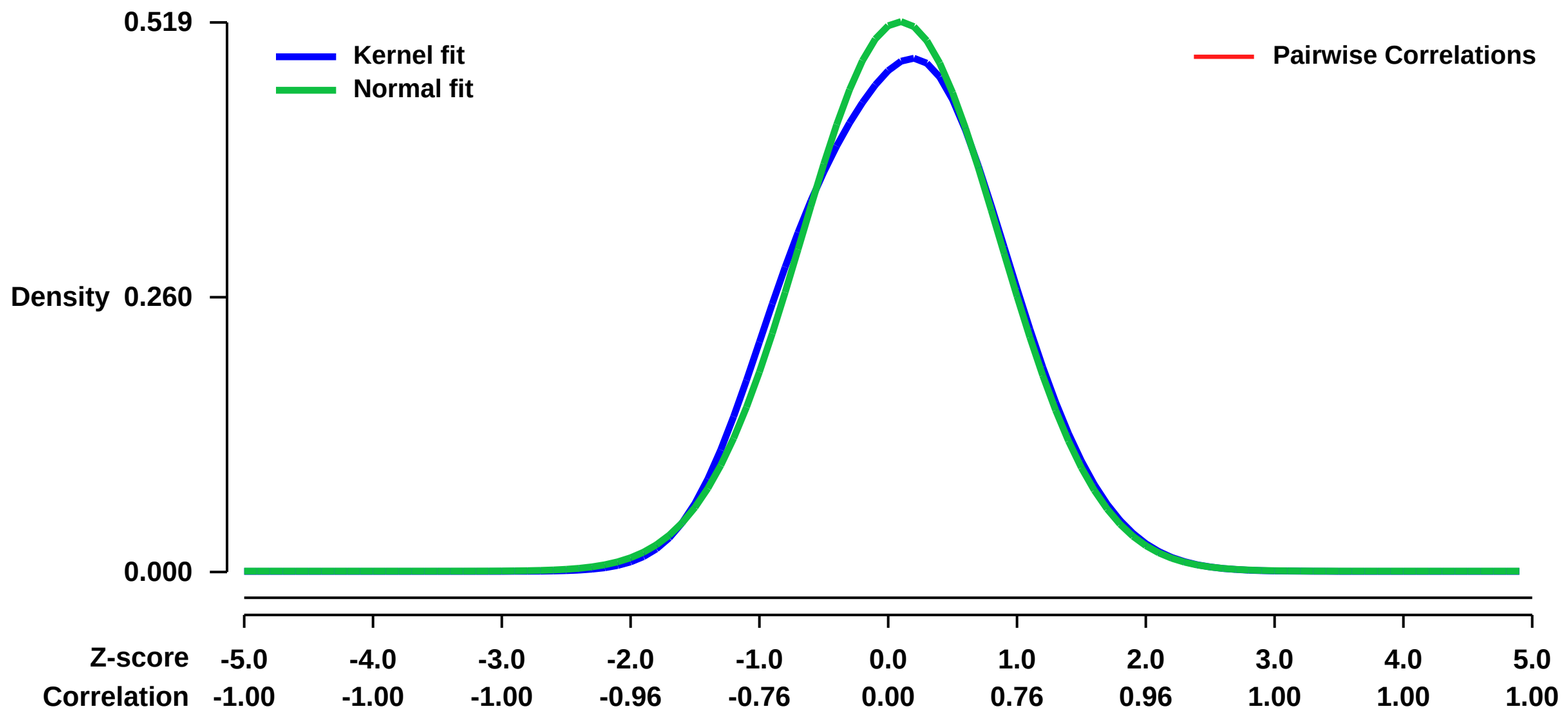

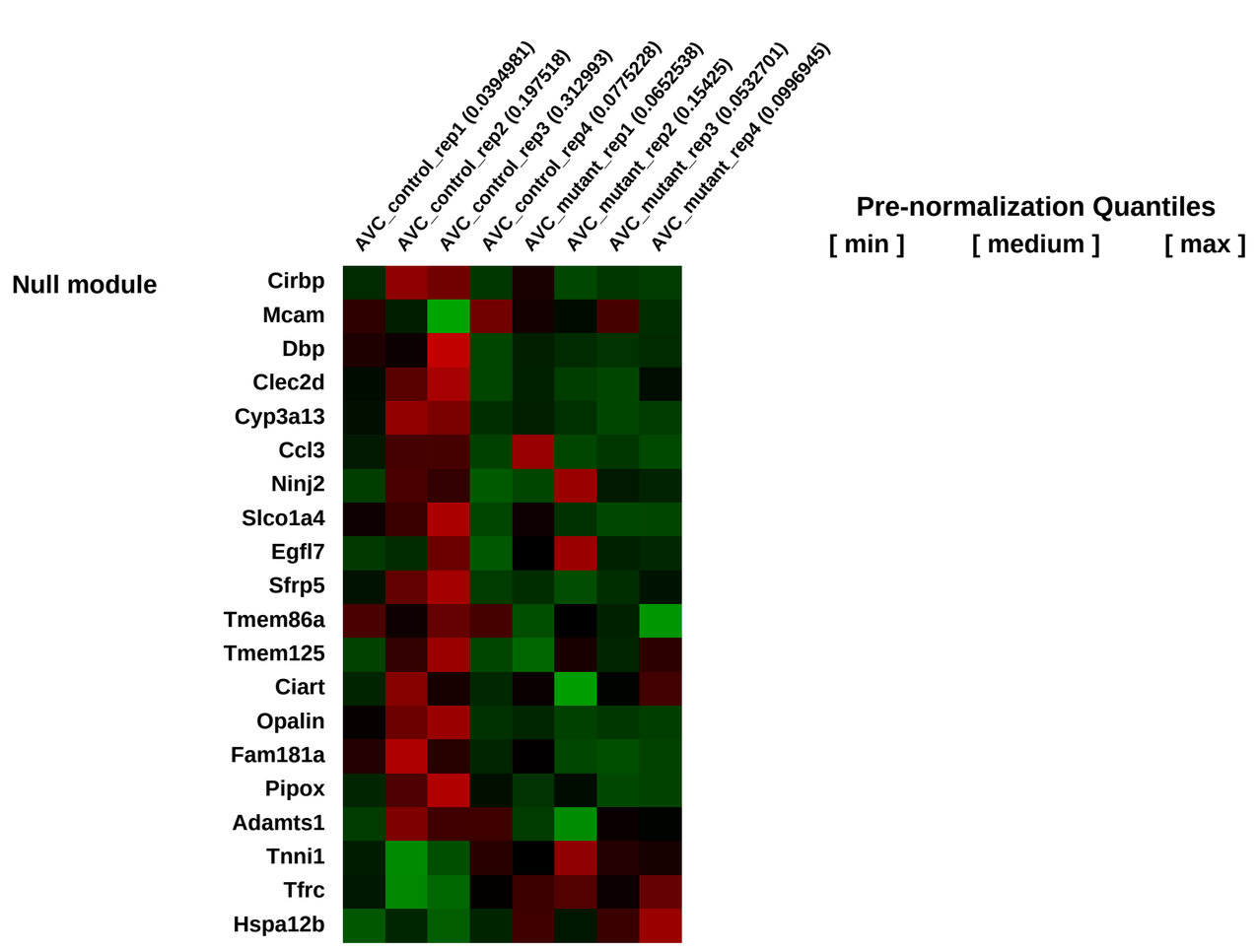

GEO Series "GSE44261" Expression Profiles

Num of samples in this series: 12

Scale of expression profile Z-scores

-3.0 -2.0 -1.0 0.0 1.0 2.0 3.0

GEO Link:	http://www.ncbi.nlm.nih.gov/geo/query/acc.cgi?acc=GSE44261
Status:	Public on Feb 13 2013
Title:	Gene expression data from mouse CD8 T cells
Organism:	Mus musculus
Experiment type:	Expression profiling by array
Platform:	GPL1261
Pubmed ID:	23563690
Summary & Design:	**Summary:** Determing the influence of lipid metabolism on murine T cell blastogenesis. Gene expression studies from purified spleen and lymph node T cells with conditional deletion of the SREBP Cleavage Activating Protein (SCAP) ex vivo or activated with plate-bound anti-CD3 and CD28 antibodies for 6 h. **Overall design:** CD8 T cells were purified from T cell specific Scap deficient mouse spleens (KO, n=3) and control littermate (WT, n=3). The cells from each mouse were used for RNA extraction at either quiescent (T0) or 6 h activation (T6).

Background corr dist: KL-Divergence = 0.1140, L1-Distance = 0.0274, L2-Distance = 0.0011, Normal std = 0.4275

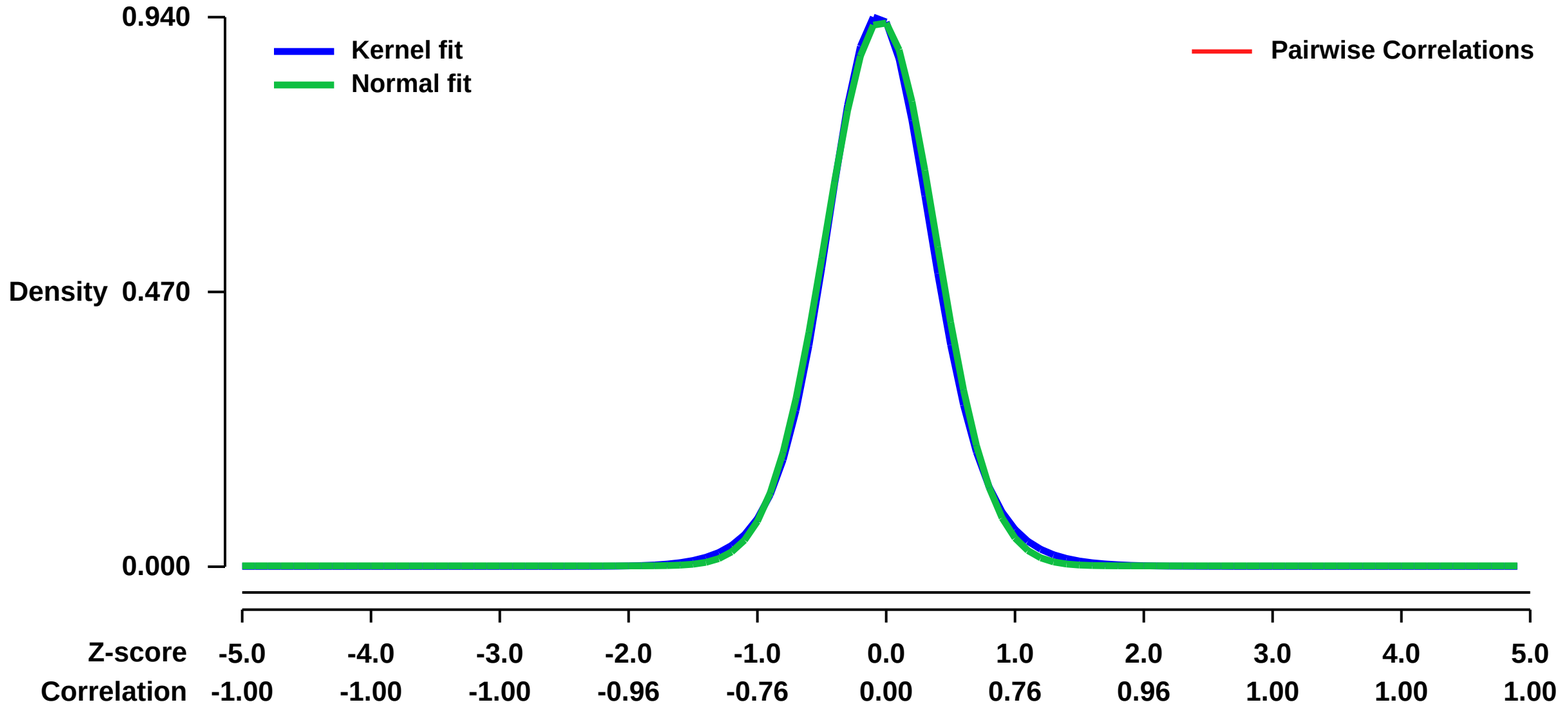

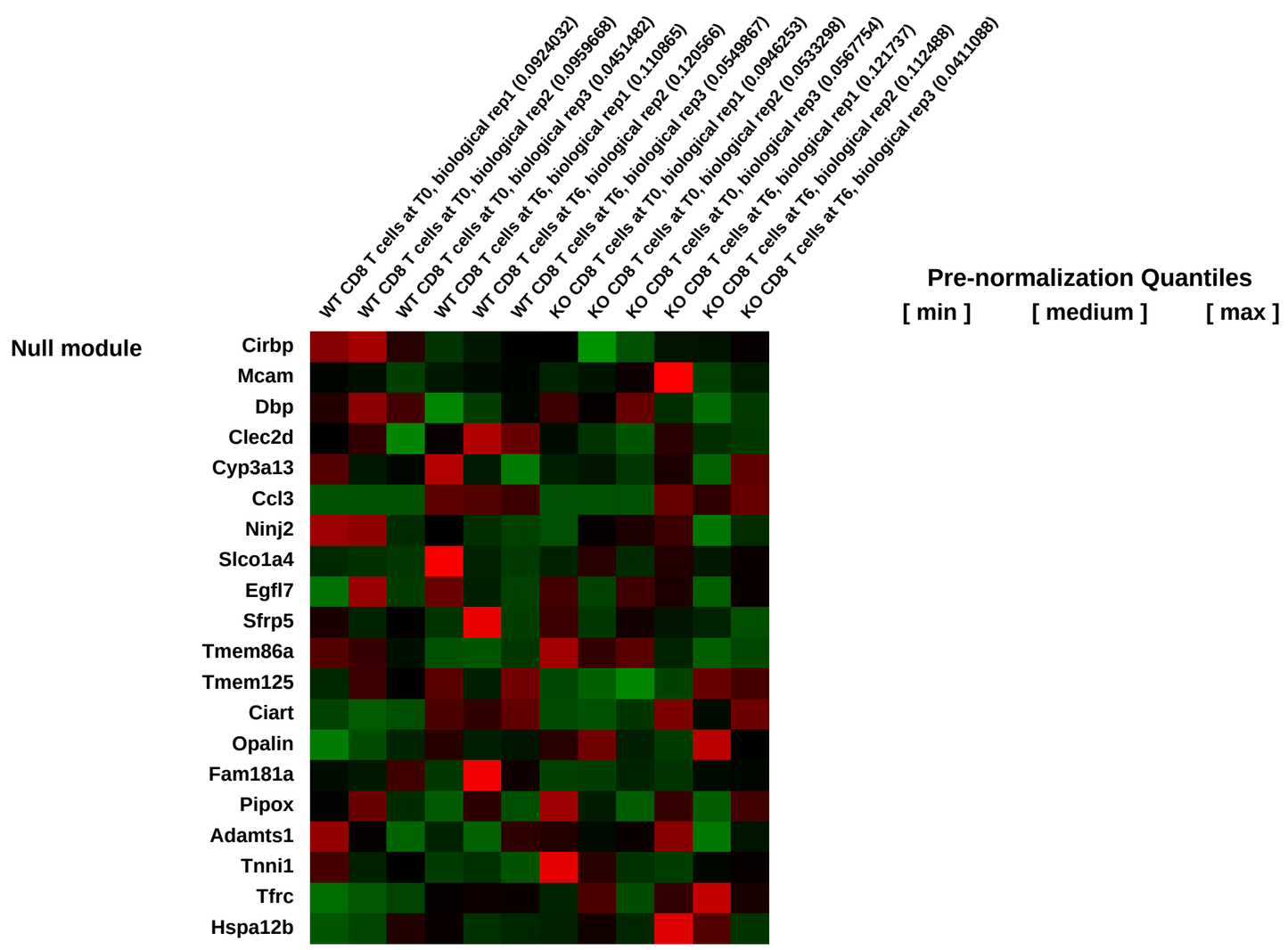

GEO Series "GSE9297" Expression Profiles

Num of samples in this series: 27

Scale of expression profile Z-scores

-3.0 -2.0 -1.0 0.0 1.0 2.0 3.0

GEO Link:	**http://www.ncbi.nlm.nih.gov/geo/query/acc.cgi?acc=GSE9297**
Status:	**Public on Nov 01 2008**
Title:	**Genomic profile of IL10-/- knocked out colitis model**
Organism:	**Mus musculus**
Experiment type:	**Expression profiling by array**
Platform:	**GPL1261**
Pubmed ID:	
Summary & Design:	**Summary:** **Objetives: study and characterization of the IL10-/- knocked out colitis model in mice at genomic level and the study of the influence of bacteria in the development of the disease.** **Keywords: Differentially expressed genes analysis** **Overall design:** **RNA was extracted from homogenized full-thickness colonic tissues in Trizol´fi reagent (Invitrogen) and purified with RNeasy affinity columns (Qiagen), according to manufacturer´·s protocol. The microarray analysis was performed by Progenika Biopharma (Bilbao, Spain) on GeneChip´fi Rat Genome 230 2.0 Array (Affymetrix). All sample labeling (biotin), hybridization, staining and scanning procedures were carried out using Affimetrix, standard protocols (www.affymetrix.com). Normalization was carried out using Bioconductor sofware (affyPLM package).**

Background corr dist: **KL-Divergence = 0.1442, L1-Distance = 0.0387, L2-Distance = 0.0024, Normal std = 0.3895**

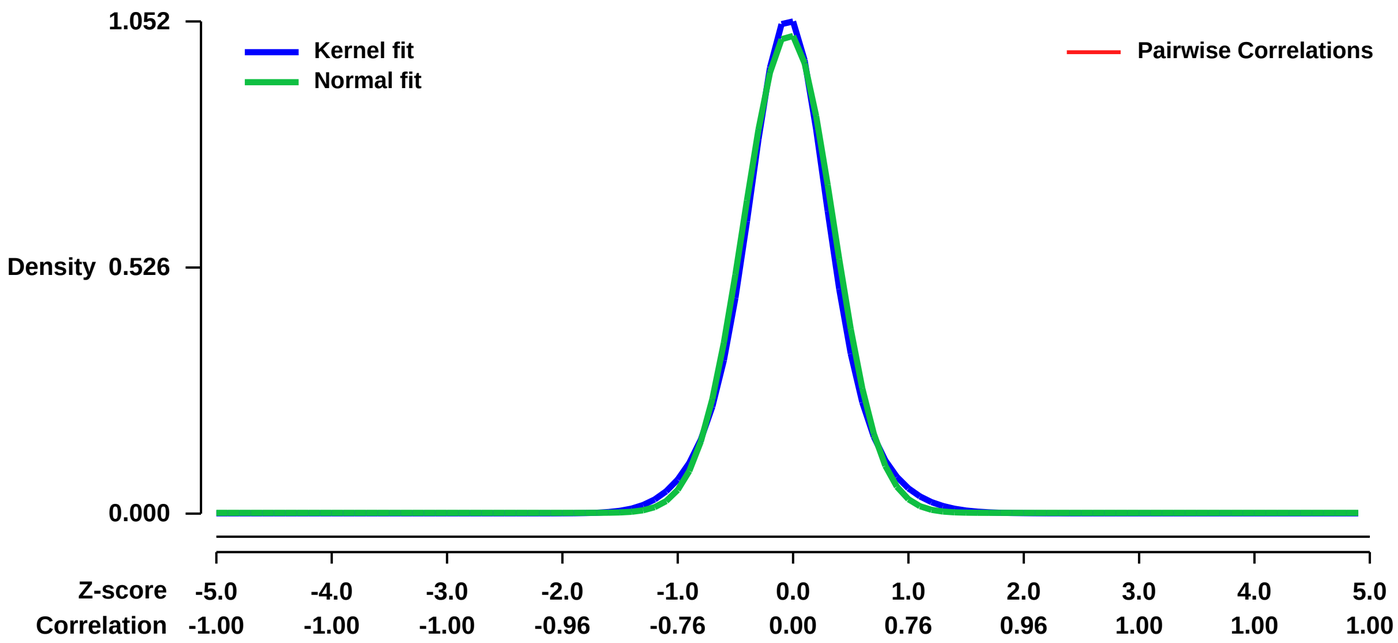

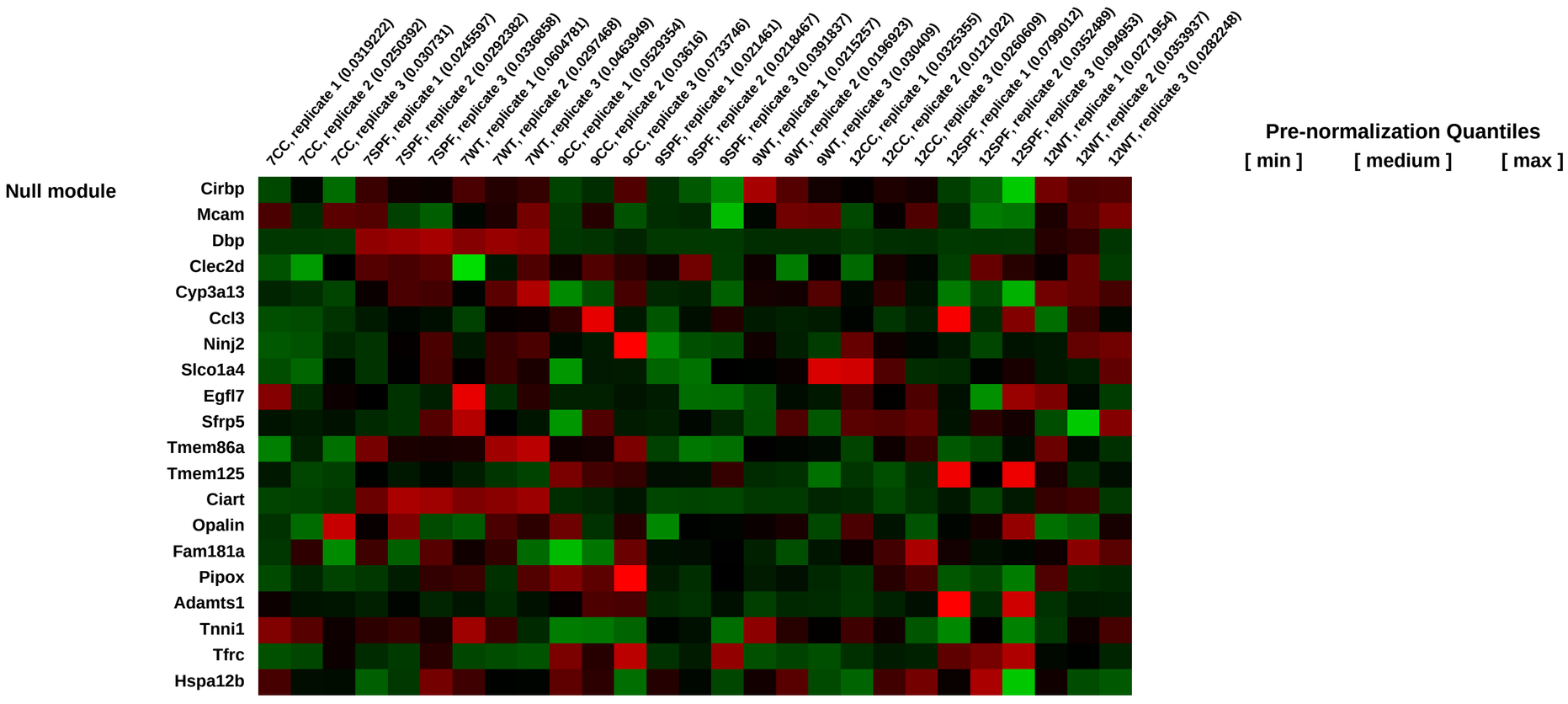

GEO Series "GSE16496" Expression Profiles

Num of samples in this series: 102

Details of this dataset are not shown due to large number of samples and the page size limit.

Find details in http://www.ncbi.nlm.nih.gov/geo/query/acc.cgi?acc=GSE16496

Background corr dist: KL-Divergence = 0.3007, L1-Distance = 0.0716, L2-Distance = 0.0154, Normal std = 0.2865

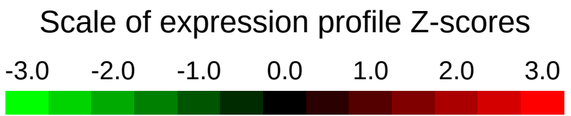

GEO Series "GSE11013" Expression Profiles

Num of samples in this series: 6

Scale of expression profile Z-scores

-3.0 -2.0 -1.0 0.0 1.0 2.0 3.0

GEO Link:	http://www.ncbi.nlm.nih.gov/geo/query/acc.cgi?acc=GSE11013
Status:	Public on Nov 30 2009
Title:	Gene expression rates in a mouse model for Potocki-Lupski Syndrome
Organism:	Mus musculus
Experiment type:	Expression profiling by array
Platform:	GPL1261
Pubmed ID:	18469339
Summary & Design:	**Summary:** To identify gene(s) that are modified in their relative expression levels in the Potocki-Lupski Syndrome mouse model and map to the rearranged region, i.e. possible candidate genes at the source of the PTLS-like phenotypes shown by the PTLS mouse, we comp **Keywords: disease model, expression profiling** **Overall design:** We profiled the hippocampi of three Dp(11)17/+ and three wild type males, all six in a pure C57BL/6-Tyr c-Brd genetic background.

Background corr dist: KL-Divergence = 0.0399, L1-Distance = 0.0164, L2-Distance = 0.0003, Normal std = 0.6127

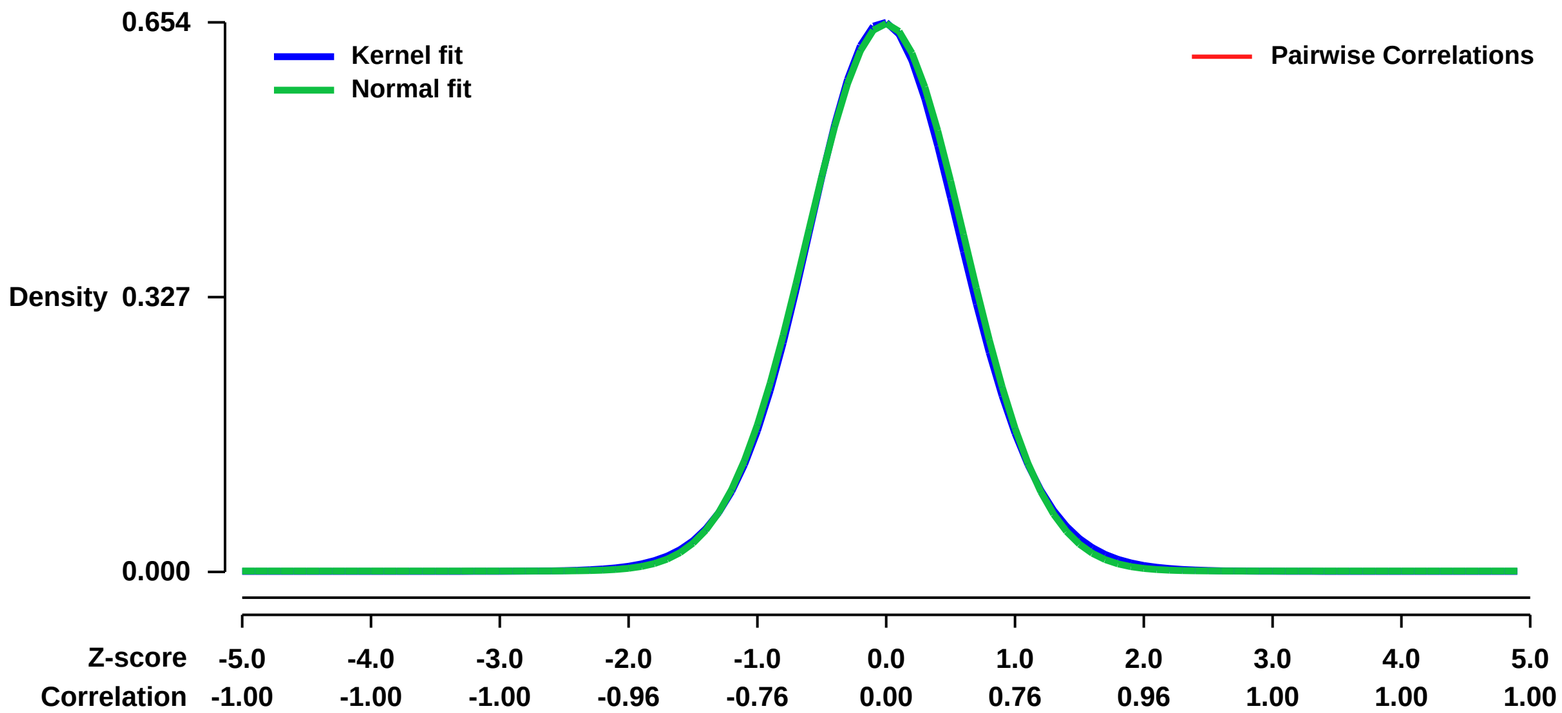

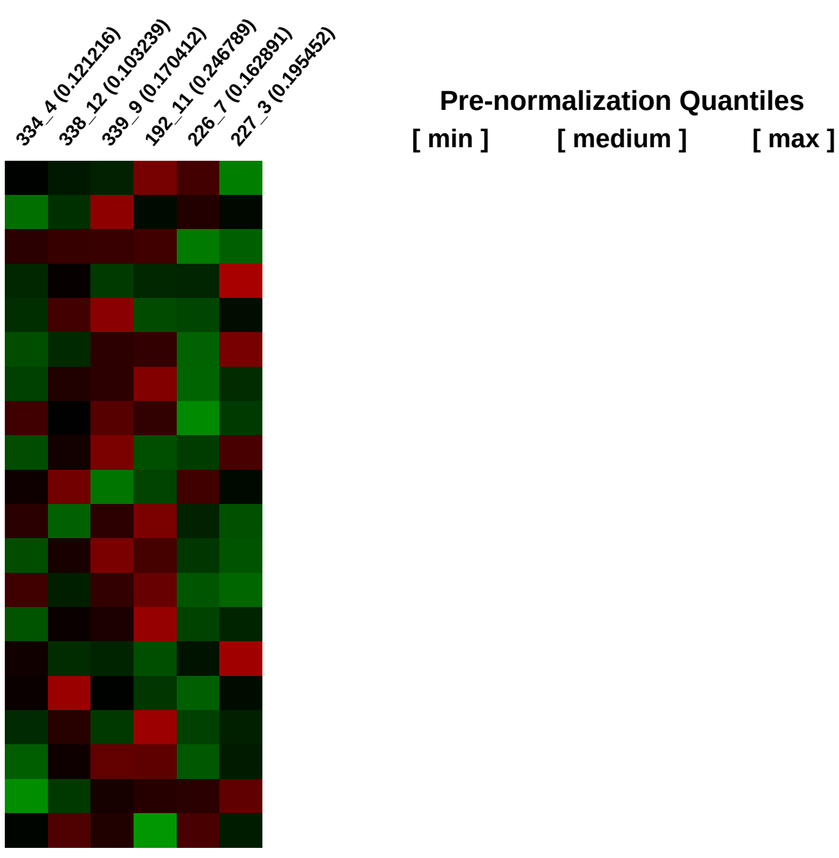

GEO Series "GSE39583" Expression Profiles

Num of samples in this series: 21

Scale of expression profile Z-scores

-3.0 -2.0 -1.0 0.0 1.0 2.0 3.0

GEO Link:	http://www.ncbi.nlm.nih.gov/geo/query/acc.cgi?acc=GSE39583
Status:	Public on Sep 11 2012
Title:	Transcriptional response of cap mesenchyme (undifferentiated nephron progenitors) to Wnt activation
Organism:	Mus musculus
Experiment type:	Expression profiling by array
Platform:	GPL1261
Pubmed ID:	22902740
Summary & Design:	**Summary:** During mammalian kidney development, mesenchymal nephron progenitors (cap mesenchyme) differentiate into the epithelial cells that go on to form the nephron. Although differentiation of nephron progenitors is triggered by activation of Wnt/b-catenin signaling, constitutive activation of Wnt/b-catenin signaling blocks epithelialization of nephron progenitors. Full epithelialization of nephron progenitors requires transient activation of Wnt/b-catenin signaling. We performed transcriptional profiling of nephron progenitors responding to constitutive or transient activation of Wnt/b-catenin signaling. **Overall design:** Nephron progenitors were FACS-isolated from BAC transgenic Six2GFPcre-positive embryonic kidneys at E16.5. Cells were aggregated by centrifugation at 850g for 5min and incubated in 10%FBS/DMEM containing either 4uM BIO or the equal volume of DMSO for 24hrs or 48hrs.

Background corr dist: KL-Divergence = 0.1948, L1-Distance = 0.0359, L2-Distance = 0.0026, Normal std = 0.3386

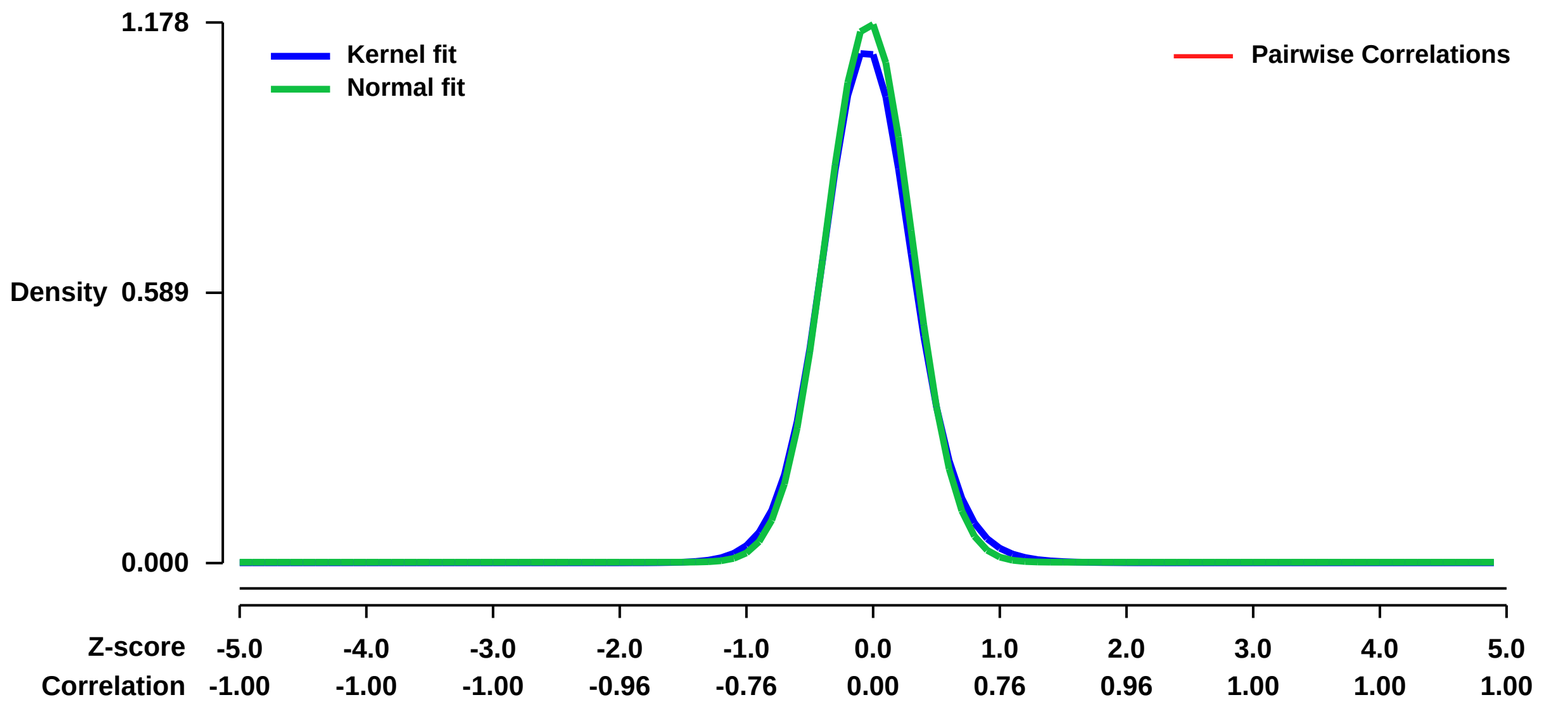

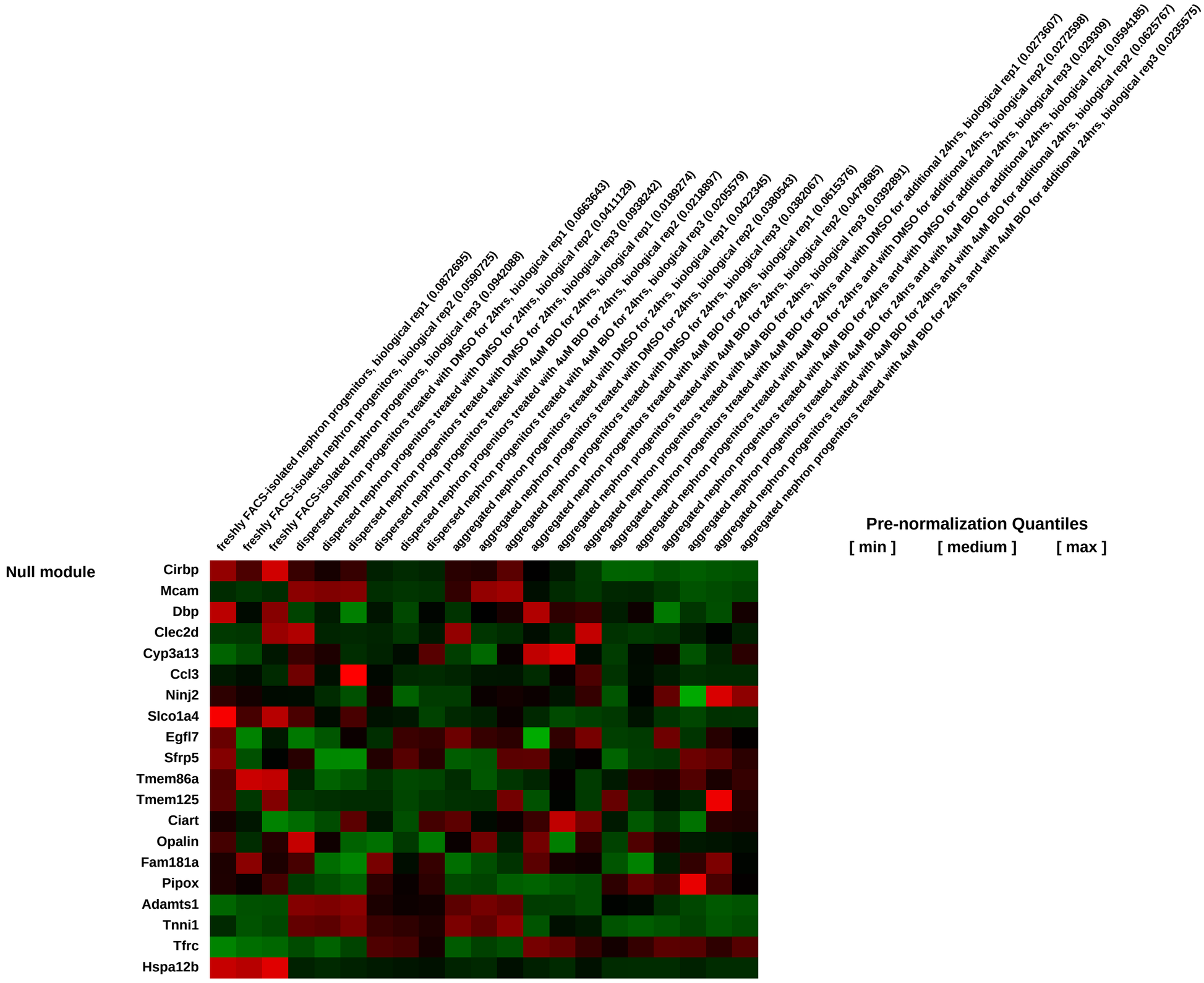

GEO Series "GSE13402" Expression Profiles

Num of samples in this series: 7

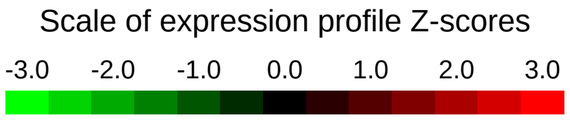

GEO Link:	http://www.ncbi.nlm.nih.gov/geo/query/acc.cgi?acc=GSE13402
Status:	Public on May 01 2009
Title:	SPARC-null vs. wild-type lens epithelium
Organism:	Mus musculus
Experiment type:	Expression profiling by array
Platform:	GPL1261
Pubmed ID:	19401199
Summary & Design:	**Summary:** SPARC is a matricellular glycoprotein involved in regulation of the extracellular matrix, growth factors, adhesion, and migration. SPARC-null mice have altered basement membranes and develop posterior sub-capsular cataracts with cell swelling and equatorial vacuoles. Exchange of fluid, nutrients, and waste products in the avascular lens is driven by a unique circulating ion current. Here we demonstrate that SPARC-null mouse lenses exhibit abnormal circulation of fluid, ion, and small molecules which leads to altered fluorescein distribution in vivo, loss of resting membrane polarization, and altered distribution of small molecules. Microarray analysis of SPARC-null lenses showed changes in gene expression of ion channels and receptors, matrix and adhesion genes, cytoskeleton, immune response genes, and cell signaling molecules. Our results demonstrate that the regulation of SPARC on cell-capsular matrix interactions can influence the circulation of fluid and ions in the lens, and the phenotype in the SPARC-null mouse lens is the result of multiple intersecting pathways. **Overall design:** Lens epithelial cells from 7 lenses of littermate mice were isolated by laser capture microdissection. 3 wild-type lenses from 3 different mice and 4 knock-out lenses from 3 different mice were used as biological replicates.

Background corr dist: KL-Divergence = 0.0641, L1-Distance = 0.0214, L2-Distance = 0.0007, Normal std = 0.5196

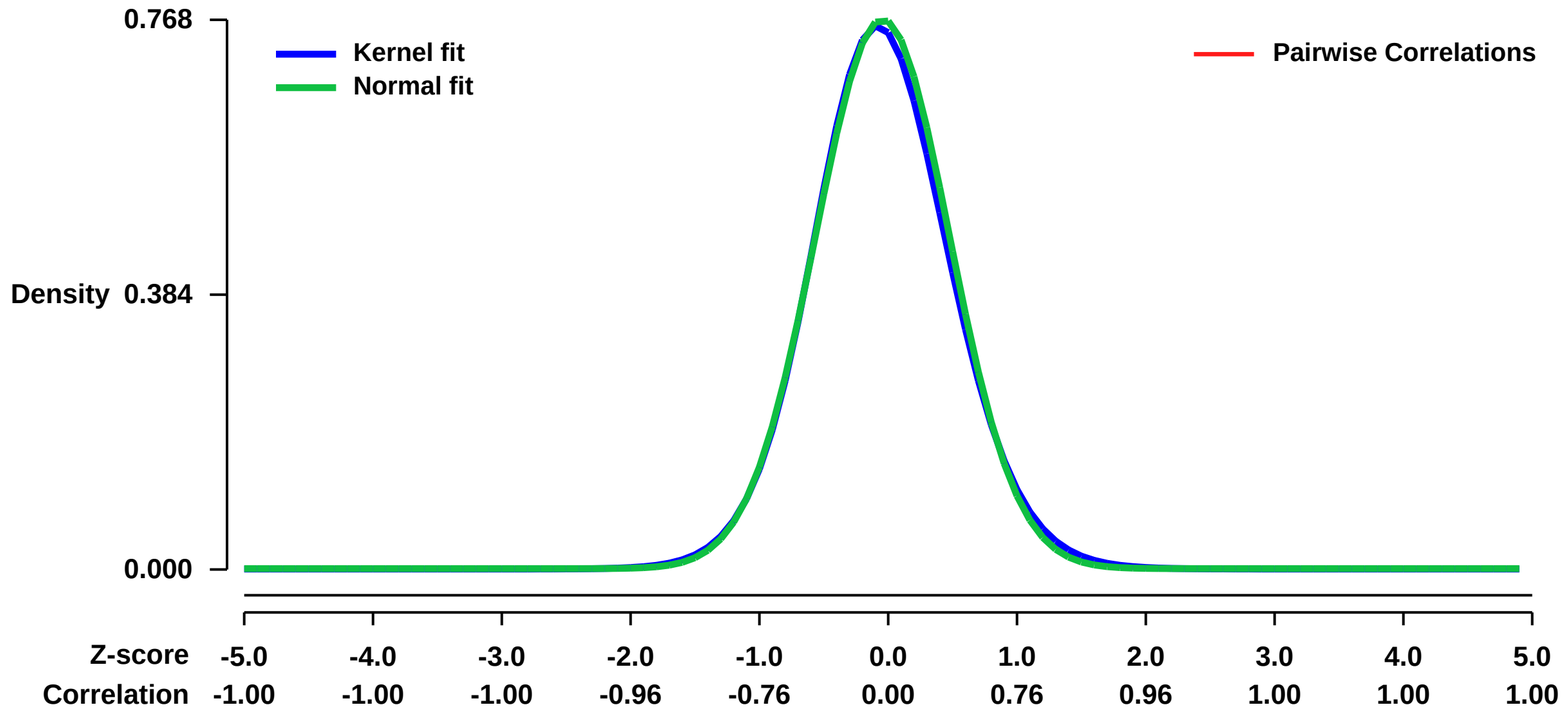

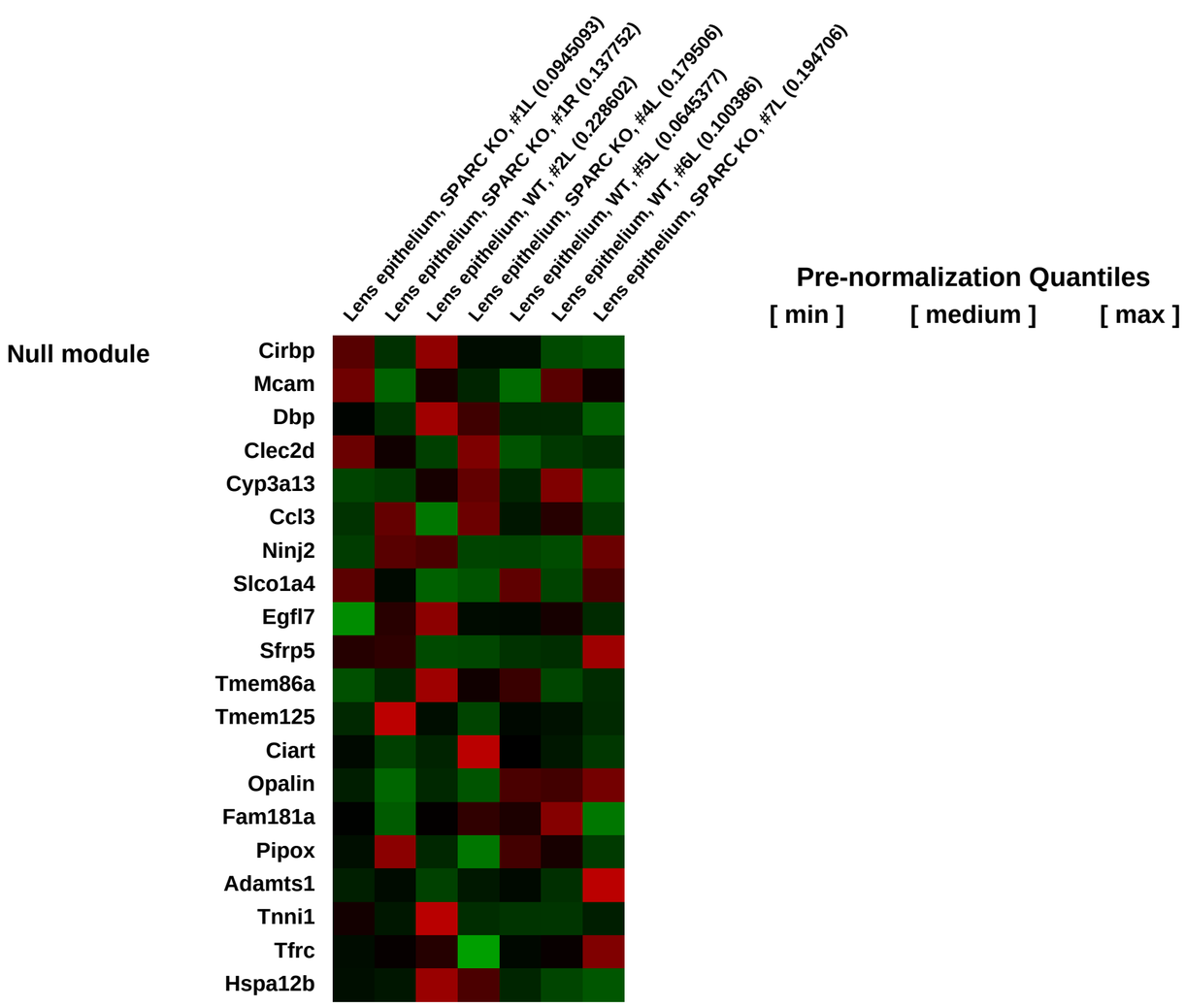

GEO Series "GSE7302" Expression Profiles

Num of samples in this series: 6

Scale of expression profile Z-scores

-3.0 -2.0 -1.0 0.0 1.0 2.0 3.0

GEO Link:	http://www.ncbi.nlm.nih.gov/geo/query/acc.cgi?acc=GSE7302
Status:	Public on May 01 2007
Title:	Expression data from bone marrow hematopoietic stem cell CD34 Flt3 subfractions
Organism:	Mus musculus
Experiment type:	Expression profiling by array
Platform:	GPL1261
Pubmed ID:	17433729
Summary & Design:	**Summary:** Lineage negativ Sca1+ Kit+ bone marrow cells (containing putative hematopoietic stem cells) subfractionation based on CD34 and FLT3 identifies three functionally destinc subpopulations (LSKCD34-FLT3-, LSKCD34+FLT3- & LSKCD34+FLT3+). **Keywords: cell type comparison** **Overall design:** Lineage negativ Kit+ Sca1+ (LSK) hematopoietic stem cell subpopulations were FACS sorted based on their CD34/FLT3 expression. Subsequently RNA was extracted, labelled and hybridized to Affymetrix microarrays. We sought to obtain expression pattern changes that might explain the difference in function between the functionally destinct LSK subpopulations.

Background corr dist: KL-Divergence = 0.0326, L1-Distance = 0.0147, L2-Distance = 0.0002, Normal std = 0.6494

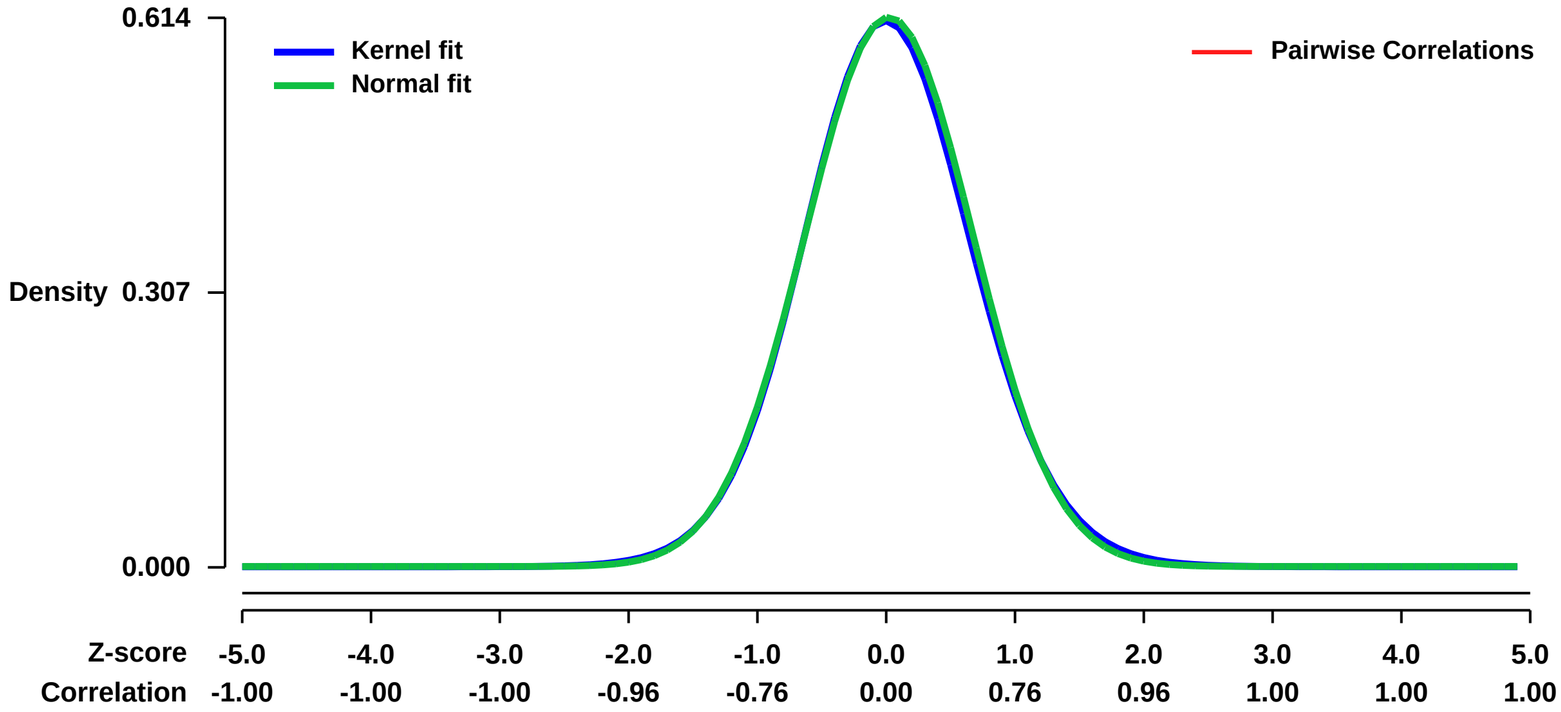

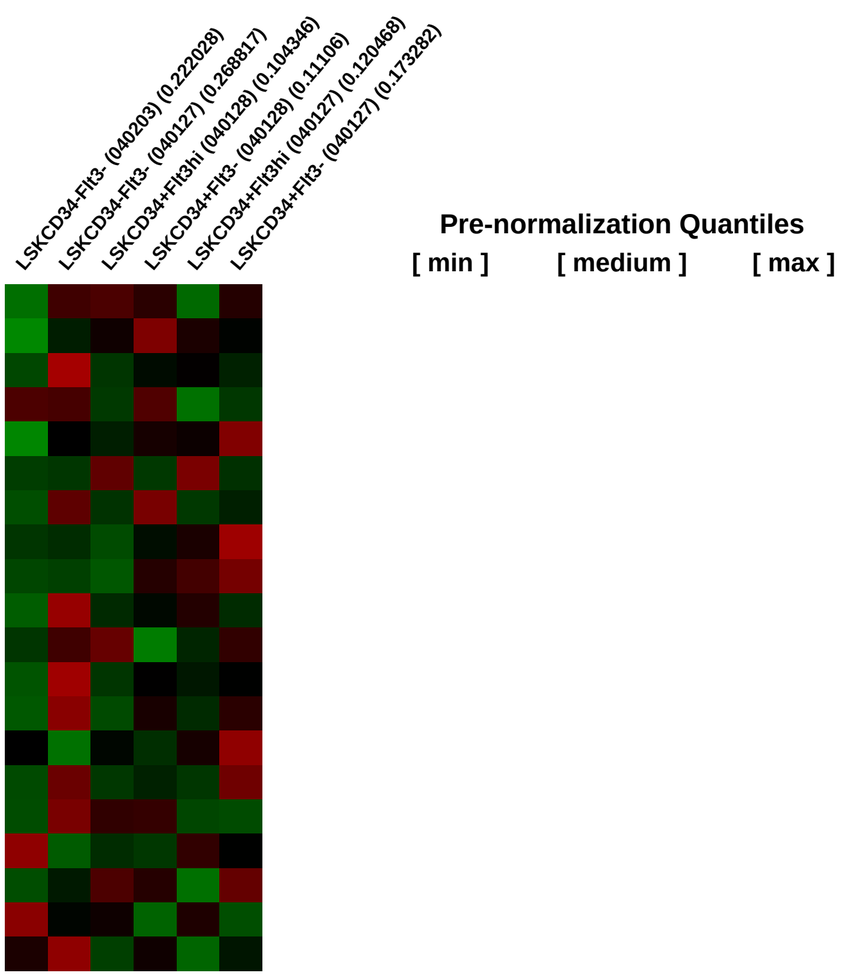

GEO Series "GSE24920" Expression Profiles

Num of samples in this series: 19

Scale of expression profile Z-scores

-3.0 -2.0 -1.0 0.0 1.0 2.0 3.0

GEO Link:	**http://www.ncbi.nlm.nih.gov/geo/query/acc.cgi?acc=GSE24920**
Status:	**Public on Oct 21 2012**
Title:	**Gene Expression in Myotonic Dystrophy**
Organism:	**Mus musculus**
Experiment type:	**Expression profiling by array**
Platform:	**GPL1261**
Pubmed ID:	
Summary & Design:	**Summary:** **In order to examine the changes in gene expression between normal and myotonic dystrophic animals, gene expression array studies were done with extensor digitorum longus (EDL) of transgenic HSALR line 20b mice using Affymetrix MOE430 2.0 microarrays.** **We used EDL muscle from transgenic HSALR line 20b mice, maintained as homozygotes in an FVB inbred background and wild-type FVB mice purchased from Taconic.** **Overall design:** **Affymetrix gene expression arrays were performed on HSALR and wild type EDL muscle**

Background corr dist: **KL-Divergence = 0.2353, L1-Distance = 0.0438, L2-Distance = 0.0042, Normal std = 0.3125**

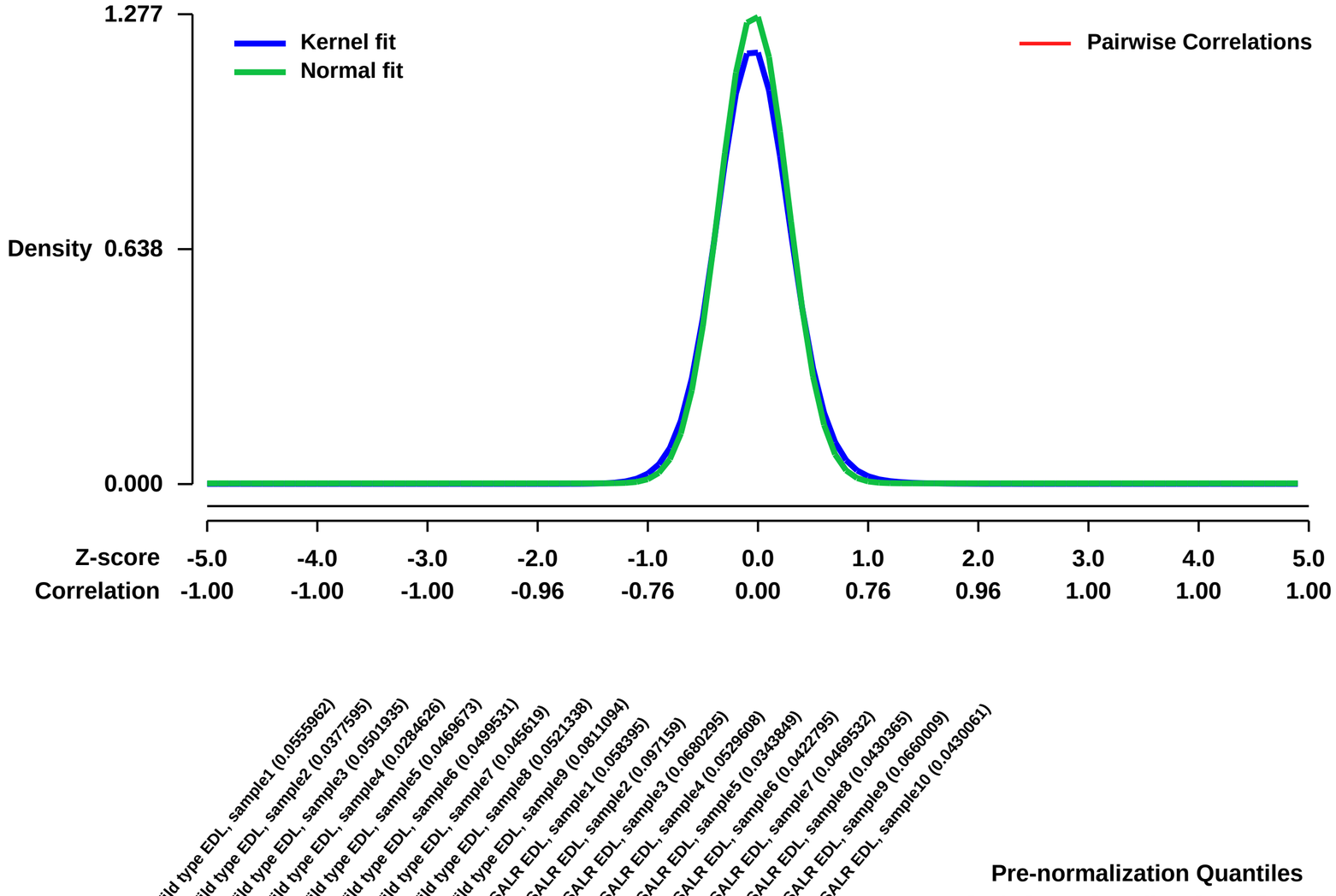

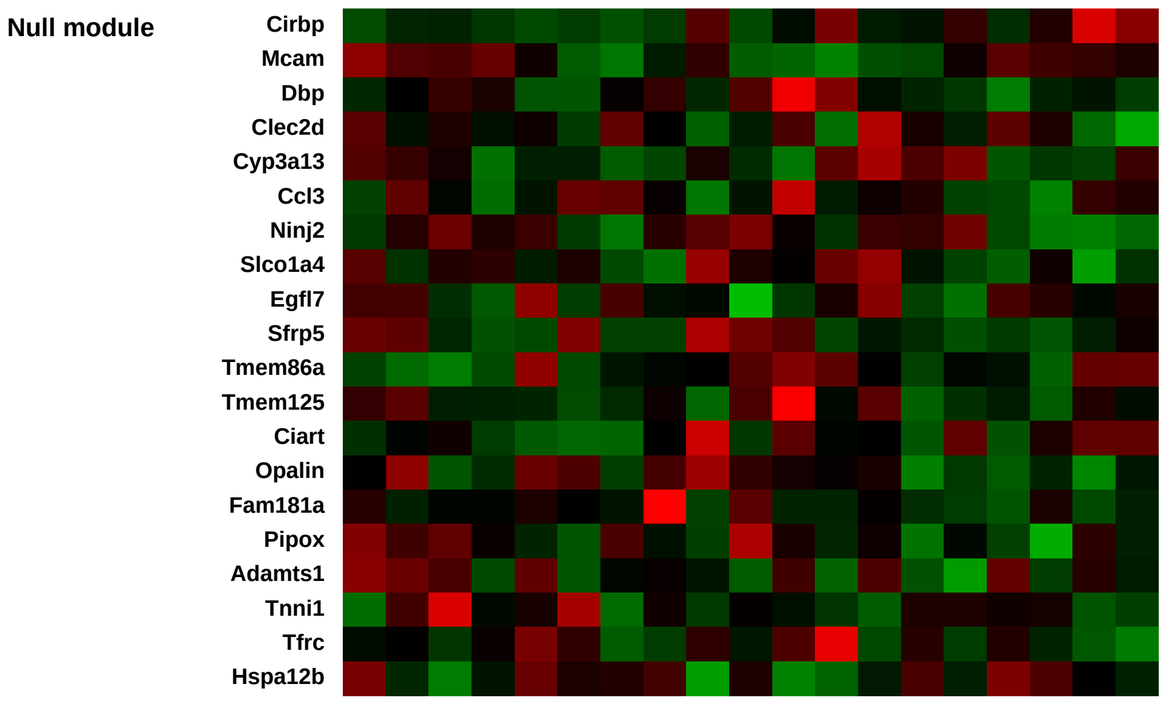

GEO Series "GSE10192" Expression Profiles

Num of samples in this series: 24

Scale of expression profile Z-scores

-3.0 -2.0 -1.0 0.0 1.0 2.0 3.0

GEO Link:	http://www.ncbi.nlm.nih.gov/geo/query/acc.cgi?acc=GSE10192
Status:	Public on Jan 15 2009
Title:	PPAR Controls Gene Expression in MSC Cells
Organism:	Mus musculus
Experiment type:	Expression profiling by array
Platform:	GPL1261
Pubmed ID:	19115254
Summary & Design:	**Summary:** Rosiglitazone (Rosi), a member of the thiazolidinedione class of drugs used to treat type 2 diabetes, activates the adipocyte-specific transcription factor peroxisome proliferator-activated receptor gamma (PPARg). This activation causes bone loss in animals and humans, at least in part due to suppression of osteoblast differentiation from marrow mesenchymal stem cells (MSC). In order to identify mechanisms by which PPARg2 suppresses osteoblastogenesis and promotes adipogenesis in MSC, we have analyzed the PPARg2 transcriptome in response to Rosi. A total of 4,252 transcriptional changes resulted when Rosi (1 uM) was applied to the U-33 marrow stromal cell line, stably transfected with PPARg2 (U-33/g2), as compared to non-induced U-33/g2 cells. Differences between U-33/g2 and U-33 cells stably transfected with empty vector (U-33/c) comprised 7,928 transcriptional changes, independent of Rosi. Cell type-, time- and treatment-specific gene clustering uncovered distinct patterns of PPARg2 transcriptional control of MSC lineage commitment. The earliest changes accompanying Rosi activation of PPARg2 included adjustments in morphogenesis, Wnt signaling, and immune responses, as well as sustained induction of lipid metabolism. Expression signatures influenced by longer exposure to Rosi provided evidence for distinct mechanisms governing the repression of osteogenesis and stimulation of adipogenesis. Our results suggest interactions that could lead to the identification of a â masterâ regulatory scheme controlling osteoblast differentiation. **Keywords:** rosiglitazone, PPARgamma, microarray, time course, gene expression, stem cells **Overall design:** U-33/g2 and U-33/c cells were cultured in the presence or absence of Rosi and gene expression was monitored at three different time points (2, 24, 72h) after exposure to the agonist. Each time point corresponds to a separate stage of Rosi-treated U-33/g2 cell conversion from the osteoblast-like phenotype to the adipocyte-like phenotype and includes induction (2h), intermediate alterations in phenotype progression (24h), and a terminally differentiated adipocytic with completely suppressed osteoblastic phenotype (72h). The experiment is a full factorial design performed in replicate.

Background corr dist: KL-Divergence = 0.0462, L1-Distance = 0.0784, L2-Distance = 0.0103, Normal std = 0.6400

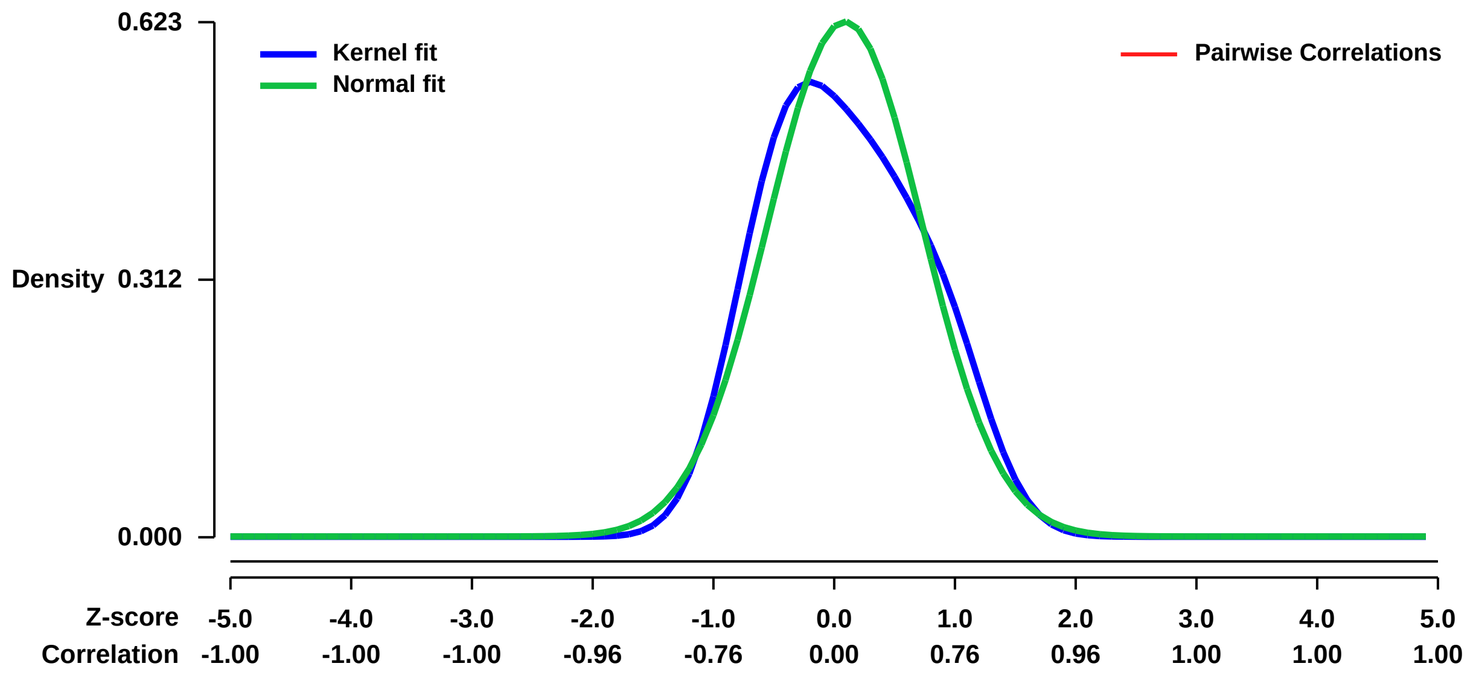

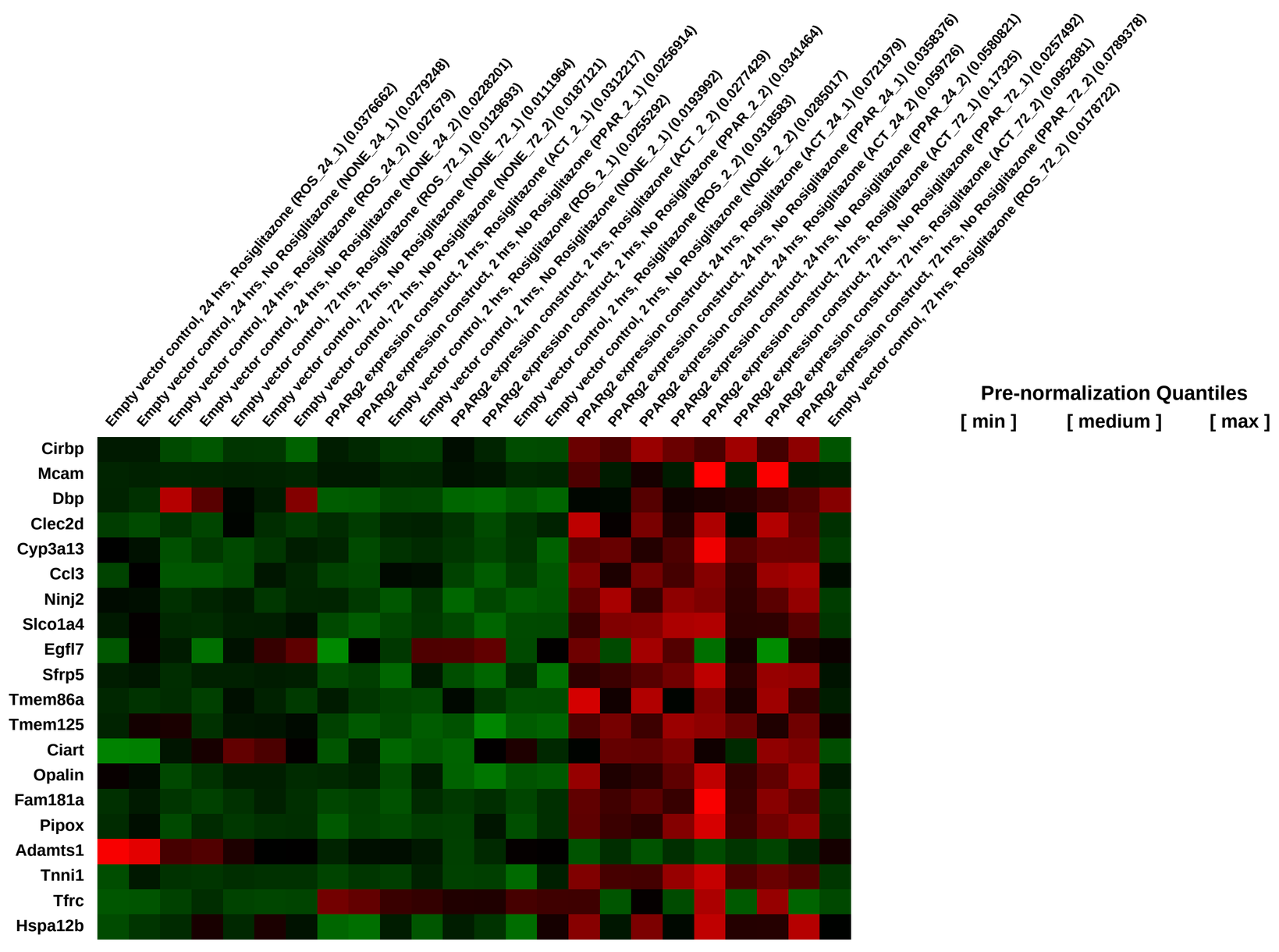

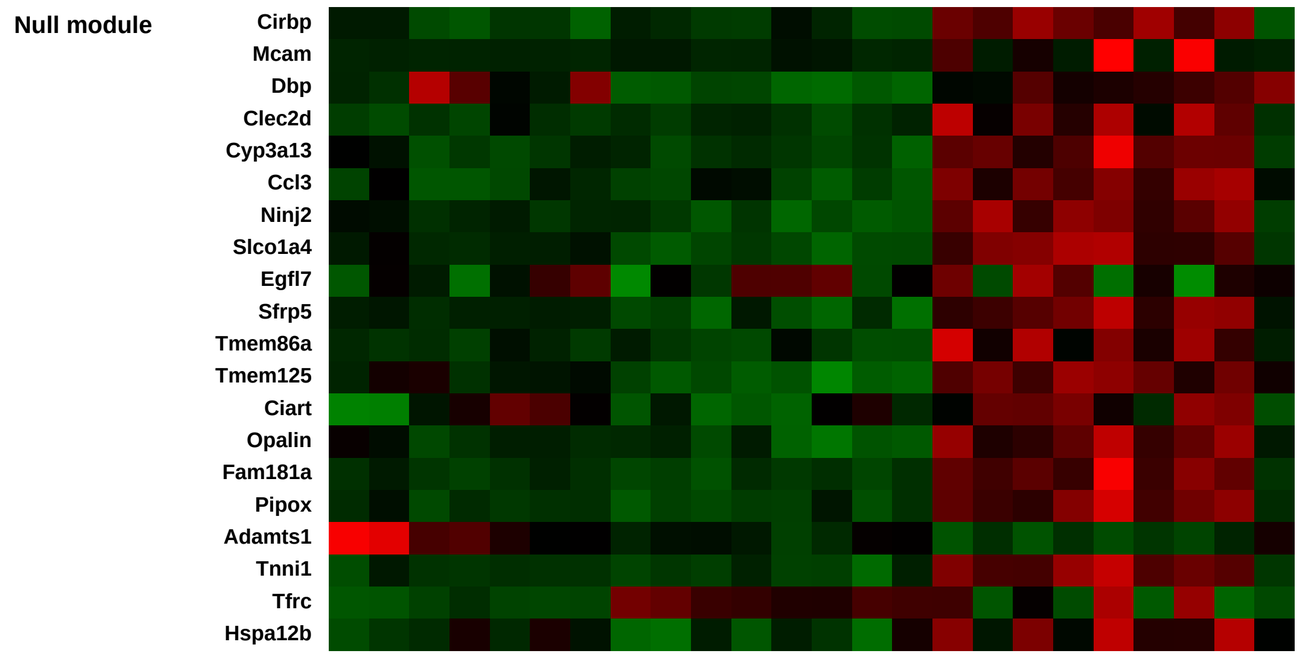

GEO Series "GSE24078" Expression Profiles

Num of samples in this series: 6

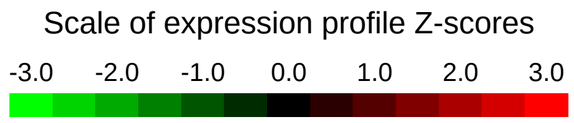

GEO Link:	**http://www.ncbi.nlm.nih.gov/geo/query/acc.cgi?acc=GSE24078**
Status:	**Public on Sep 11 2010**
Title:	**Expression data from SSEA1+ differentiated murine embryonic stem cells**
Organism:	**Mus musculus**
Experiment type:	**Expression profiling by array**
Platform:	**GPL1261**
Pubmed ID:	
Summary & Design:	**Summary:** **SSEA1+ cells sorted from mouse embryonic stem cells differentiated for 4 days in 10uM Retinoic acid do not form teratomas when transplated into SCID mice while Pten-/- cells do.** **We used microarrays to identify genes and pathways besides Pten that could explain this difference in tumorigenicity.** **Keywords: wild type vs Pten-/-** **Overall design:** **Wild type and Pten mutant SSEA1 positive differentiated cells were compared as the wild type cells were non-tumorigenic upon transplant to SCID mice and the Pten-/- cells were tumorigenic.**

Background corr dist: **KL-Divergence = 0.0388, L1-Distance = 0.0202, L2-Distance = 0.0005, Normal std = 0.6194**

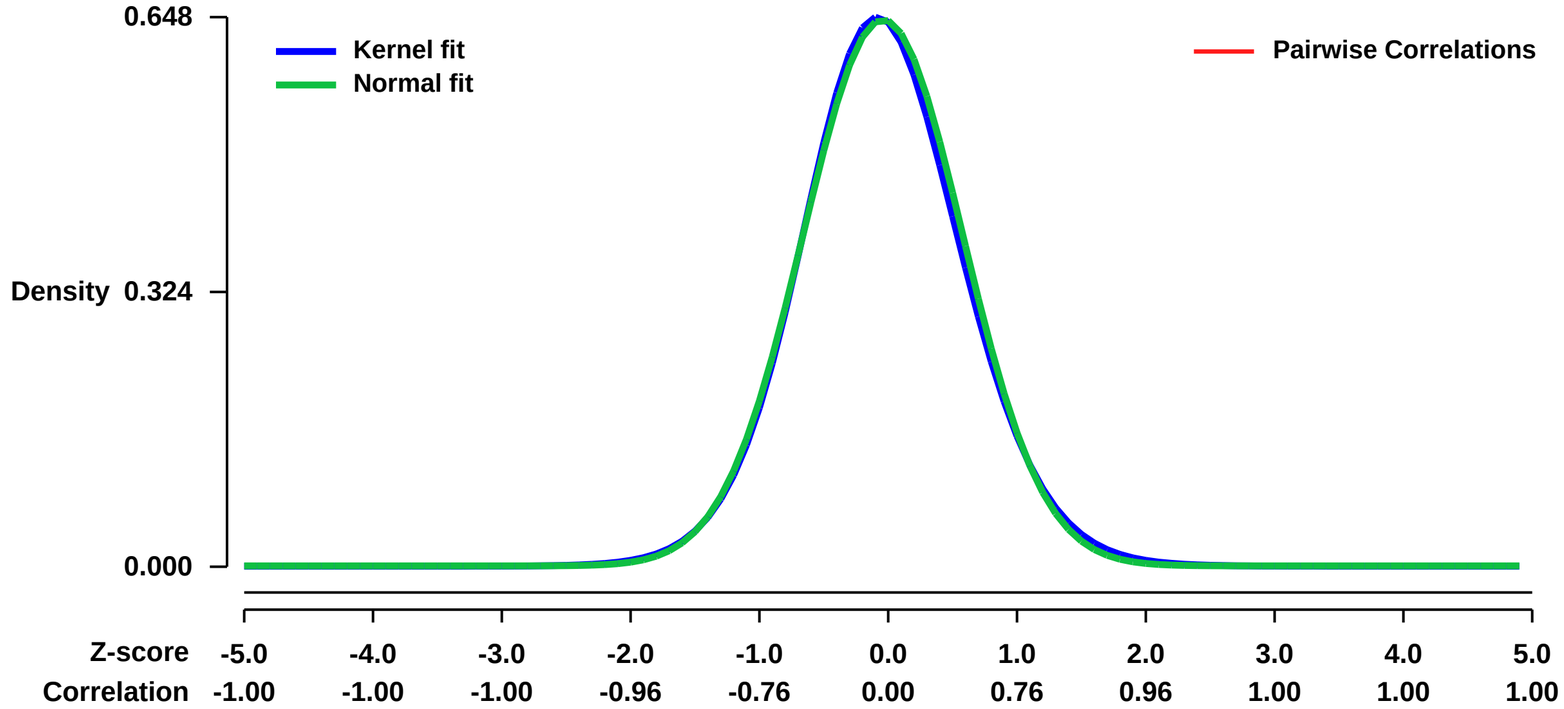

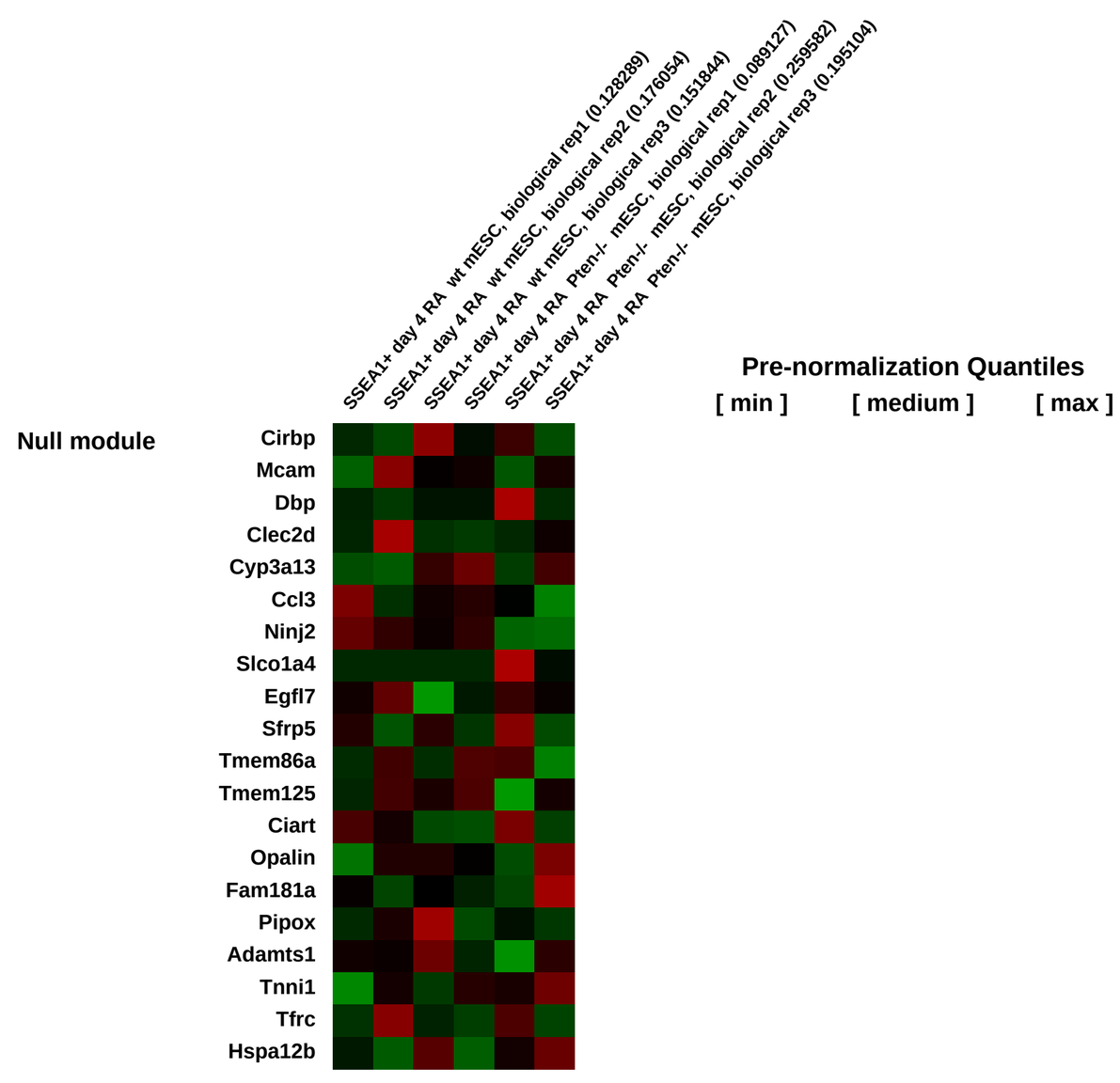

GEO Series "GSE37191" Expression Profiles

Num of samples in this series: 12

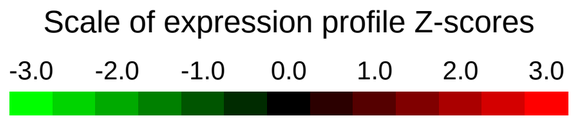

GEO Link:	http://www.ncbi.nlm.nih.gov/geo/query/acc.cgi?acc=GSE37191
Status:	Public on Jan 01 2013
Title:	Gene expression profiling reveals mast cell-dependent inflammation in the meninges in early EAE.
Organism:	Mus musculus
Experiment type:	Expression profiling by array
Platform:	GPL1261
Pubmed ID:	23267561
Summary & Design:	**Summary:** The meninges are generally considered relatively inert tissues that house the CSF and provide protection for the brain and spinal cord. However, our previous studies using Kit mutant (Kit W/Wv) mast cell-deficient mice demonstrated that mast cells residing in the dura mater and pia mater exacerbate the severity of experimental autoimmune encephalomyelitis (EAE), the rodent model of the CNS demyelinating disease, multiple sclerosis. These data suggest that the meninges are sites of active immune responses in disease. Gene expression profiles of meningeal tissue from wild type and mast cell deficient mice prior to and at day 6 post-EAE induction were found highly distinct. Increases in both mast cell- and neutrophil-associated transcripts were among the notable disease-related changes observed in wild type mice. Kinetic analyses show that meningeal mast cells are activated within 24 hours of disease induction to express multiple mediators including IL-1b and TNF as well as the neutrophil chemoattractant, CXCL2, an observation corresponding with an influx of neutrophils to the meninges. Neutrophil recruitment as well as the disease-related loss of BBB integrity is dependent on mast cell-derived TNF. These data provide unequivocal evidence that the meninges are sites of early inflammatory events in EAE. Mast cells residing within these tissues promote disease by orchestrating an early and efficient immune cell co-localization resulting in a robust local inflammatory response and a breach of the proximal BBB. We hypothesize that these events reflect an aberrant manifestation of the normal immune surveillance role of the meninges in infection settings. **Overall design:** Immunized WT and Kit W/Wv mice were sacrificed on Day 6 post-immunization and perfused with PBS as were naˆflve littermate control mice. The dura mater was immediately removed from the calvarium of the skull and pooled (10 mice/group, 4 groups). RNA was isolated using SV Total RNA Isolation System (Promega). Each pool was analyzed in technical triplicates. Briefly, cRNA was synthesized and amplified/labeled using the Affymetrix Express Kit, then fragmented and hybridized to the The GeneChip´fi Mouse Genome 430 2.0 Array in accordance to the Affymetrix GeneChip expression analysis technical manual (Affymetrix, Santa Clara, CA). After hybridization, arrays were washed and stained with Affymetrix fluidics protocol FS450_0001 and scanned with a 7G Affymetrix GeneChip Scanner. Image data were analyzed with Affymetrix Expression Consoleâ¢ software and normalized with Robust Multichip Analysis (RMA; www.bioconductor.org/) to determine signal log ratios (CITE: Gentleman, R.C., Carey, V.J., Bates, D.M., Bolstad, B., Dettling, M., Dudoit, S., Ellis, B., Gautier, L., Ge, Y., Gentry, J., et al. (2004). Bioconductor: open software development for computational biology and bioinformatics. Genome Biol 5, R80.). The mean fold change was calculated from 3 independent technical replicates for each of the four experimental conditions and assessed by a non-parametric rank product test (CITE: Hong, F., Breitling, R., McEntee, C.W., Wittner, B.S., Nemhauser, J.L., and Chory, J. (2006). RankProd: a bioconductor package for detecting differentially expressed genes in meta-analysis. Bioinformatics 22, 2825-2827). Heat maps were generated with Genesis (Cite: Sturn, A., Quackenbush, J. and Trajanoski, Z. (2002) Genesis: cluster analysis of microarray data. Bioinformatics, 18, 207-208).

Background corr dist: KL-Divergence = 0.1081, L1-Distance = 0.0249, L2-Distance = 0.0009, Normal std = 0.4256

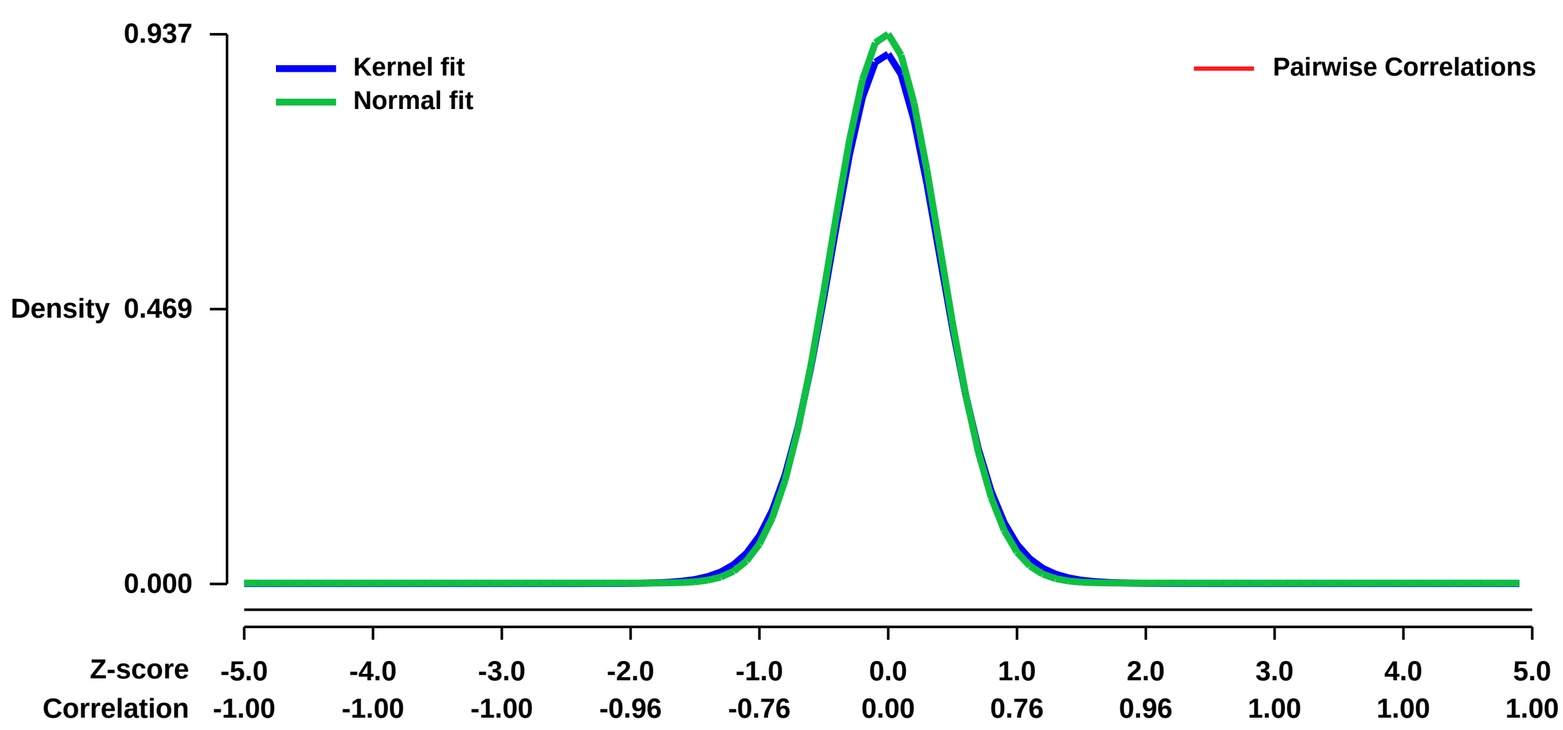

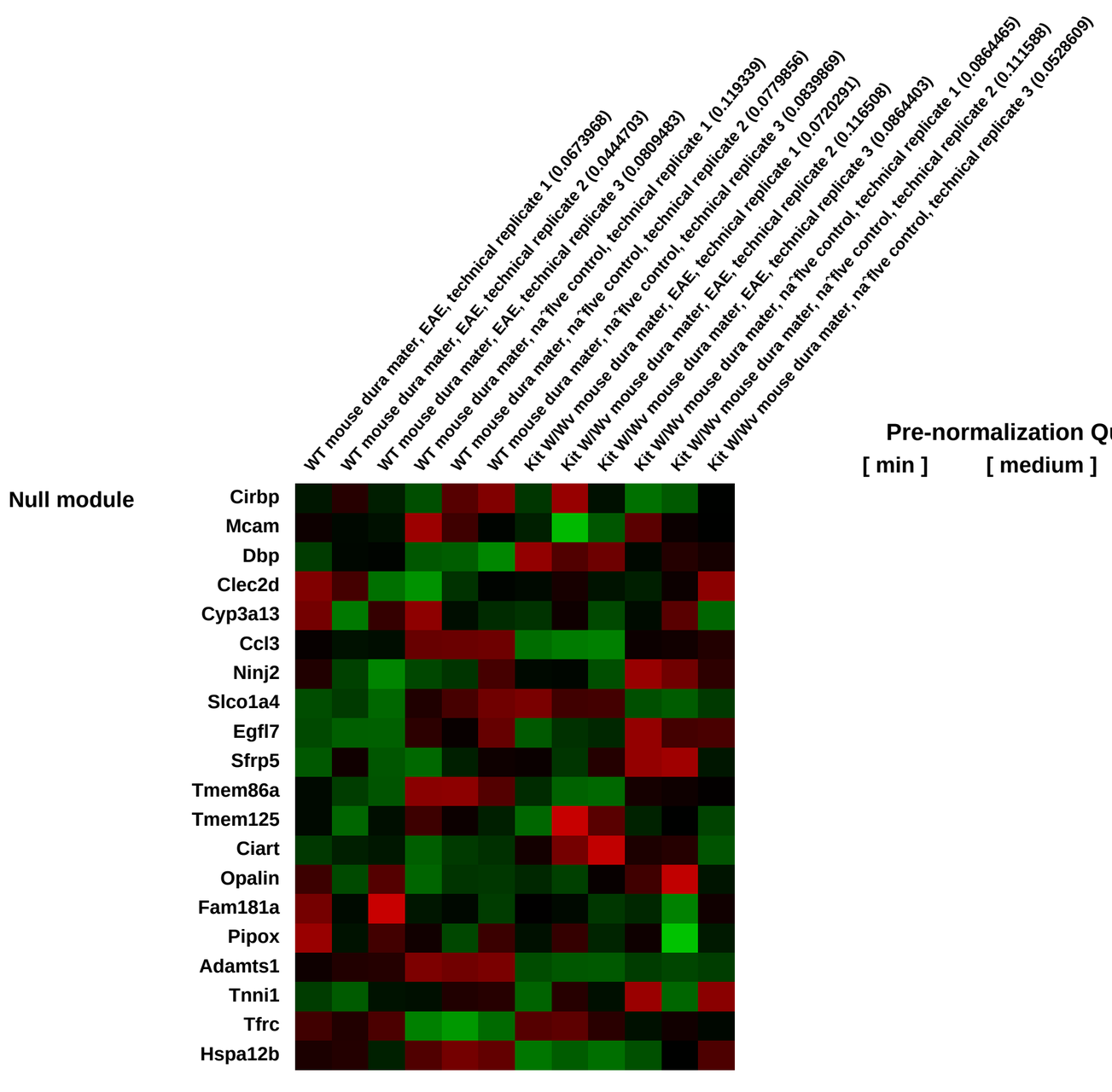

GEO Series "GSE38880" Expression Profiles

Num of samples in this series: 12

Scale of expression profile Z-scores

-3.0 -2.0 -1.0 0.0 1.0 2.0 3.0

GEO Link:	**http://www.ncbi.nlm.nih.gov/geo/query/acc.cgi?acc=GSE38880**
Status:	**Public on Jul 01 2012**
Title:	**Subtherapeutic antibiotics alter the murine colonic microbiome and early life adiposity**
Organism:	**Mus musculus**
Experiment type:	**Expression profiling by array**
Platform:	**GPL1261**
Pubmed ID:	
Summary & Design:	**Summary:** **Early life exposure to antibiotics alters the gut microbiome. These alterations lead to changes in metabolic homeostasis and an increase in host adiposity. We used microarrays to identify metabolic genes that may be up- or down-regulated secondary to antibiotic exposure.** **Low dose antibiotics have been widely used as growth promoters in the agricultural industry since the 1950â s, yet the mechanisms for this effect are unclear. Because antimicrobial agents of different classes and varying activity are effective across several vertebrate species, we hypothesized that such subtherapeutic administration alters the population structure of the gut microbiome as well as its metabolic capabilities. We generated a model of adiposity by giving subtherapeutic antibiotic therapy (STAT) to young mice and evaluated changes in the composition and capabilities of the gut microbiome. STAT administration increased adiposity in young mice and altered hormones related to metabolism. We observed substantial taxonomic changes in the microbiome, changes in copies of key genes involved in the metabolism of carbohydrates to short-chain fatty acids (SCFA), increases in colonic SCFA levels, and alterations in the regulation of hepatic metabolism of lipids and cholesterol. In this model, we demonstrate the alteration of early life murine metabolic homeostasis through antibiotic manipulation.** **Overall design:** **C57BL6 mice were divided into low-dose penicillin or control groups. Given antibiotics via drinking water after weaning. Sacrificed and liver sections collected for RNA extraction.**

Background corr dist: KL-Divergence = 0.1531, L1-Distance = 0.0396, L2-Distance = 0.0031, Normal std = 0.3687

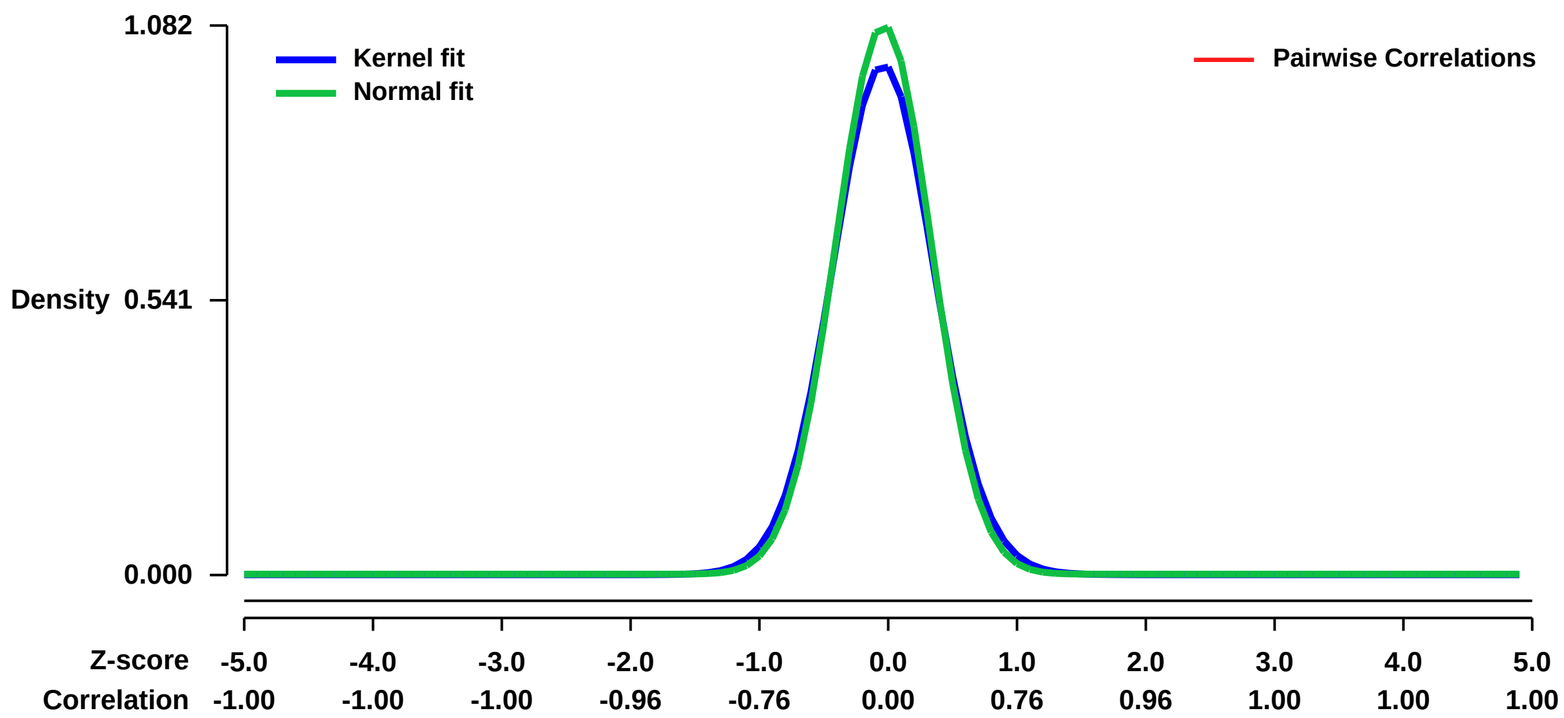

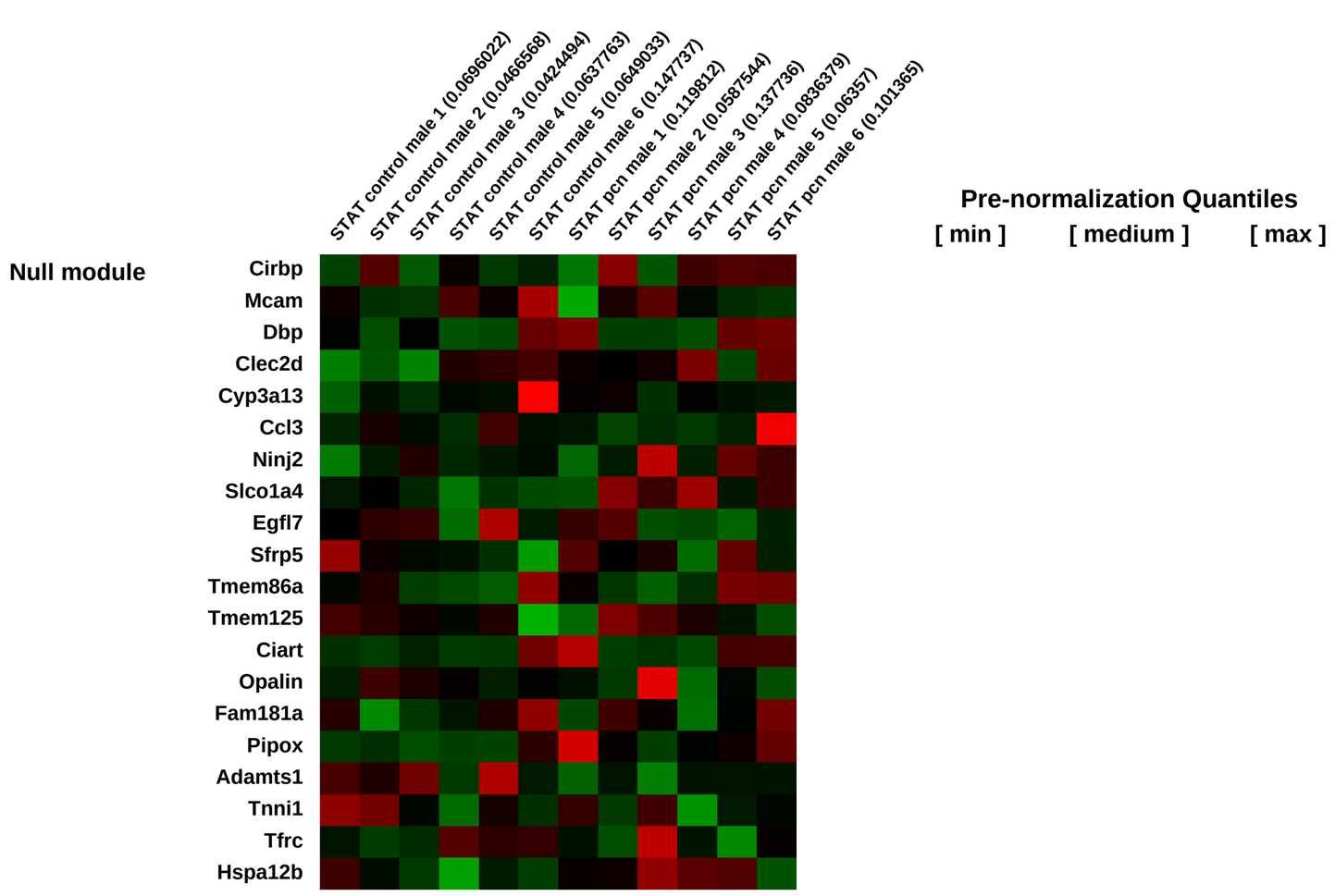

GEO Series "GSE14891" Expression Profiles

Num of samples in this series: 8

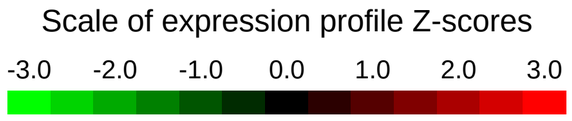

GEO Link:	http://www.ncbi.nlm.nih.gov/geo/query/acc.cgi?acc=GSE14891
Status:	Public on Feb 19 2009
Title:	Expression data of LPS-stimulated macrophages from wild-type and Zc3h12a-/- mice.
Organism:	Mus musculus
Experiment type:	Expression profiling by array
Platform:	GPL1261
Pubmed ID:	19322177
Summary & Design:	**Summary:** Lipopolysaccharide (LPS), a Toll-like receptor (TLR) 4 ligand, induces the expression of various genes including proinflammatory cytokines, and the expression is modified by the presence of Zc3h12a. We used microarrays to examine influence of Zc3h12a deficiency in LPS-inducible gene expression. Keywords: Time course after LPS (100 ng/ml) stimulation **Overall design:** Peritoneal macrophages from wild-type and Zc3h12a-/- mice were stimulated with LPS for 0, 1, 2 and 4 hours, followed by RNA extraction. Then hybridization on affymetrix microarrays was performed.

Background corr dist: KL-Divergence = 0.0555, L1-Distance = 0.0263, L2-Distance = 0.0011, Normal std = 0.5497

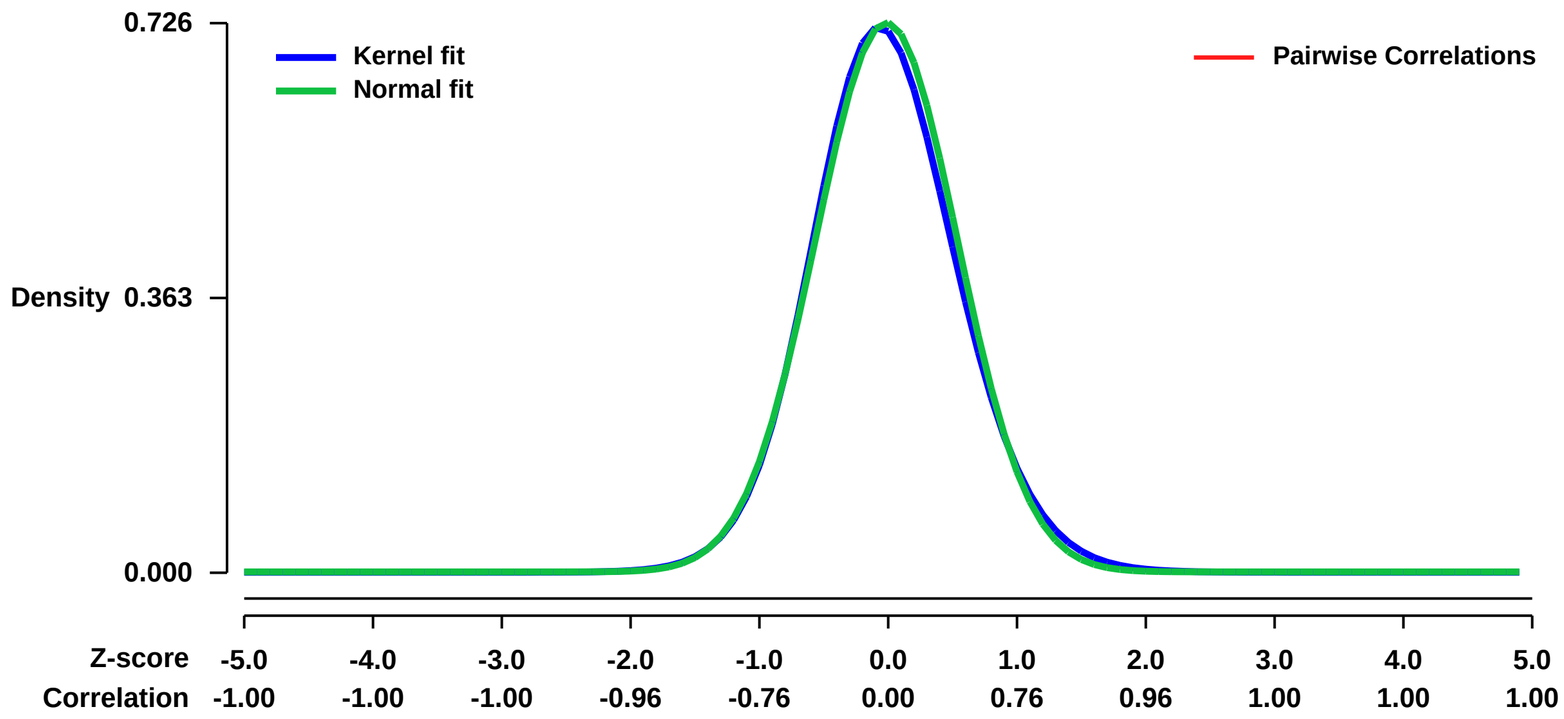

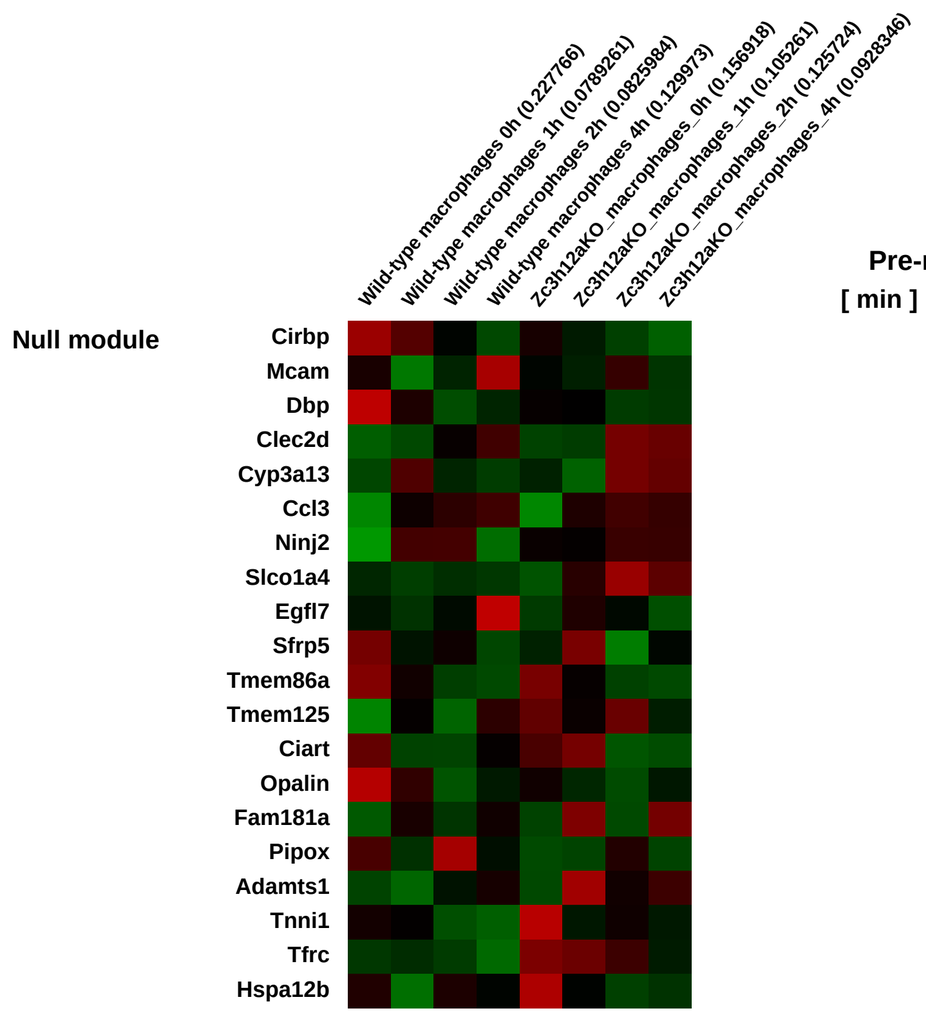

GEO Series "GSE6065" Expression Profiles

Num of samples in this series: 100

Scale of expression profile Z-scores

-3.0 -2.0 -1.0 0.0 1.0 2.0 3.0

GEO Link:	http://www.ncbi.nlm.nih.gov/geo/query/acc.cgi?acc=GSE6065
Status:	Public on Oct 21 2006
Title:	Murine host cell response to Aeromonas infection
Organism:	Mus musculus
Experiment type:	Expression profiling by array
Platform:	GPL1261
Pubmed ID:	17897183
Summary & Design:	**Summary:** **Aims: To assess the virulence of multiple Aeromonas spp. using two models, a neonatal mouse assay and a mouse intestinal cell culture.** **Methods and Results: Transcriptional responses to both infection models were evaluated using microarrays. After artificial infection with a variety of Aeromonas spp., mRNA extracts from the two models were processed and hydridized to murine microarrays to determine host gene response. Definition of virulence was determined based on host mRNA production in murine neonatal intestinal tissue and mortality of infected animals. Infections of mouse intestinal cell cultures were then performed to determine whether this simpler model system's mRNA responses correlated to neonatal results and therefore be predictive of virulence of Aeromonas spp. Virulent aeromonads up-regulated transcripts in both models including multiple host defense gene products (chemokines, regulation of transcription and apoptosis, cell signaling). Avirulent species exhibited little or no host response in neonates. Mortality results correlated well with both bacterial dose and average fold change of up-regulated transcripts in the neonatal mice.** **Conclusions: Cell culture results were less discriminating but showed promise as potentially being able to be predictive of virulence. Jun oncogene up-regulation in murine cell culture is potentially predictive of Aeromonas virulence.** **Significance and Impact of the Study: Having the ability to determine virulence of waterborne pathogens quickly would potentially assist public health officials to rapidly assess exposure risks.** **Keywords: Aeromonas; Virulence; Gene expression; Host response** **Overall design:** **Two infection models were assessed, live, whole animals (neonatal Swiss Webster mice) and a murine small intestinal cell culture. Biological replicates (n=5) were infected with different Aeromonas species/strains and compared to uninfected controls.**

Background corr dist: KL-Divergence = 0.0734, L1-Distance = 0.0755, L2-Distance = 0.0103, Normal std = 0.5327

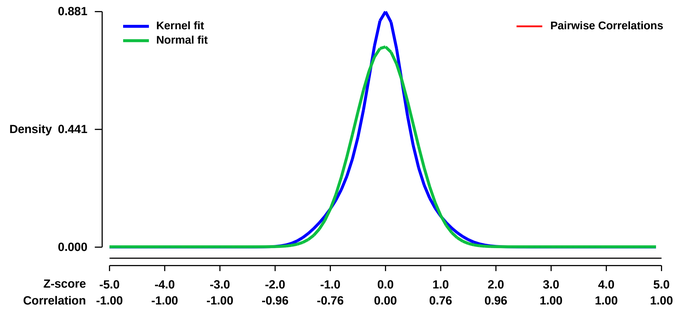

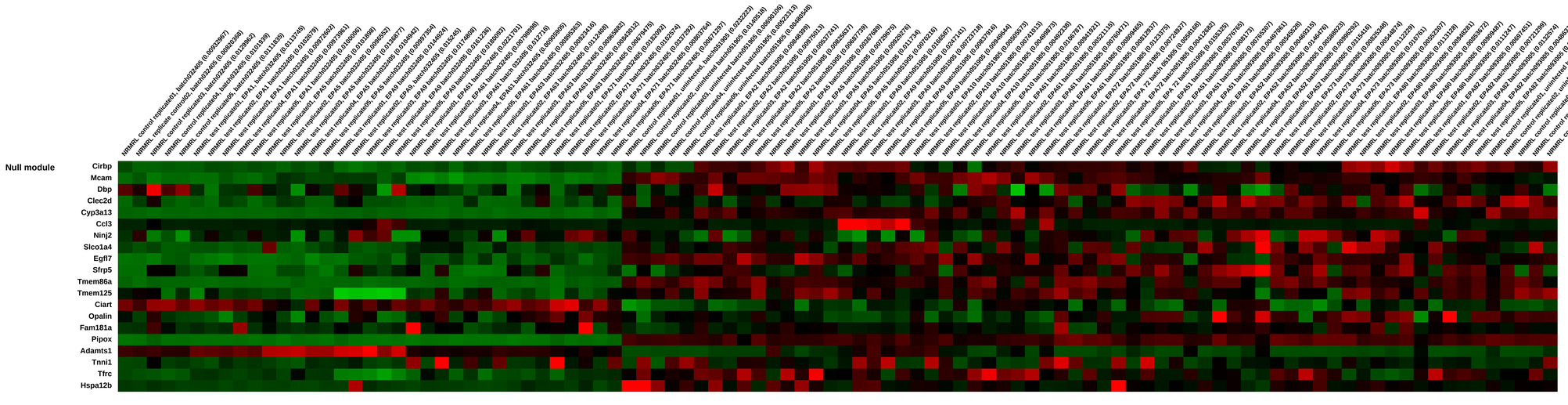

GEO Series "GSE18742" Expression Profiles

Num of samples in this series: 13

Scale of expression profile Z-scores

-3.0 -2.0 -1.0 0.0 1.0 2.0 3.0

GEO Link:	http://www.ncbi.nlm.nih.gov/geo/query/acc.cgi?acc=GSE18742
Status:	Public on Dec 17 2010
Title:	Increased Expression of Angiogenic Genes in the Brains of Mouse Meg3-null Embryos
Organism:	Mus musculus
Experiment type:	Expression profiling by array
Platform:	GPL1261
Pubmed ID:	20392836
Summary & Design:	**Summary:** MEG3 (Maternally Expressed Gene 3) is a non-coding RNA that is highly expressed in the normal human brain and pituitary. Expression of MEG3 is lost in gonadotroph-derived clinically non-functioning pituitary adenomas. Meg3 knock-out mice were generated to identify targets and potential functions of this gene in embryonic development and tumorigenesis. Gene expression profiles were compared in the brains of Meg3-null embryos and wild-type litter-mate controls using microarray analysis. Microarray data were analyzed with GeneSifter which uses Kyoto Encyclopedia of Genes and Genomes (KEGG) pathways and Gene Ontology (GO) classifications to identify signaling cascades and functional categories of interest within the data set. Differences were found in signaling pathways and ontologies related to angiogenesis between wild-type and knock-out embryos. Quantitative RT-PCR and histological staining showed increased expression of some VEGF pathway genes and increased cortical microvessel density in the knock-out embryos. These results are consistent with reported increases in VEGF signaling observed in human clinically non-functioning pituitary adenomas. In conclusion, Meg3 may play an important role in control of vascularization in the brain and may function as a tumor suppressor by preventing angiogenesis. **Overall design:** biological replicate: 148_15 KO, 219_12 KO, 238_1 KO, 238_5 KO, 250_1 KO, 250_3 KO, 262_1 KO

Background corr dist: KL-Divergence = 0.1145, L1-Distance = 0.0270, L2-Distance = 0.0012, Normal std = 0.4164

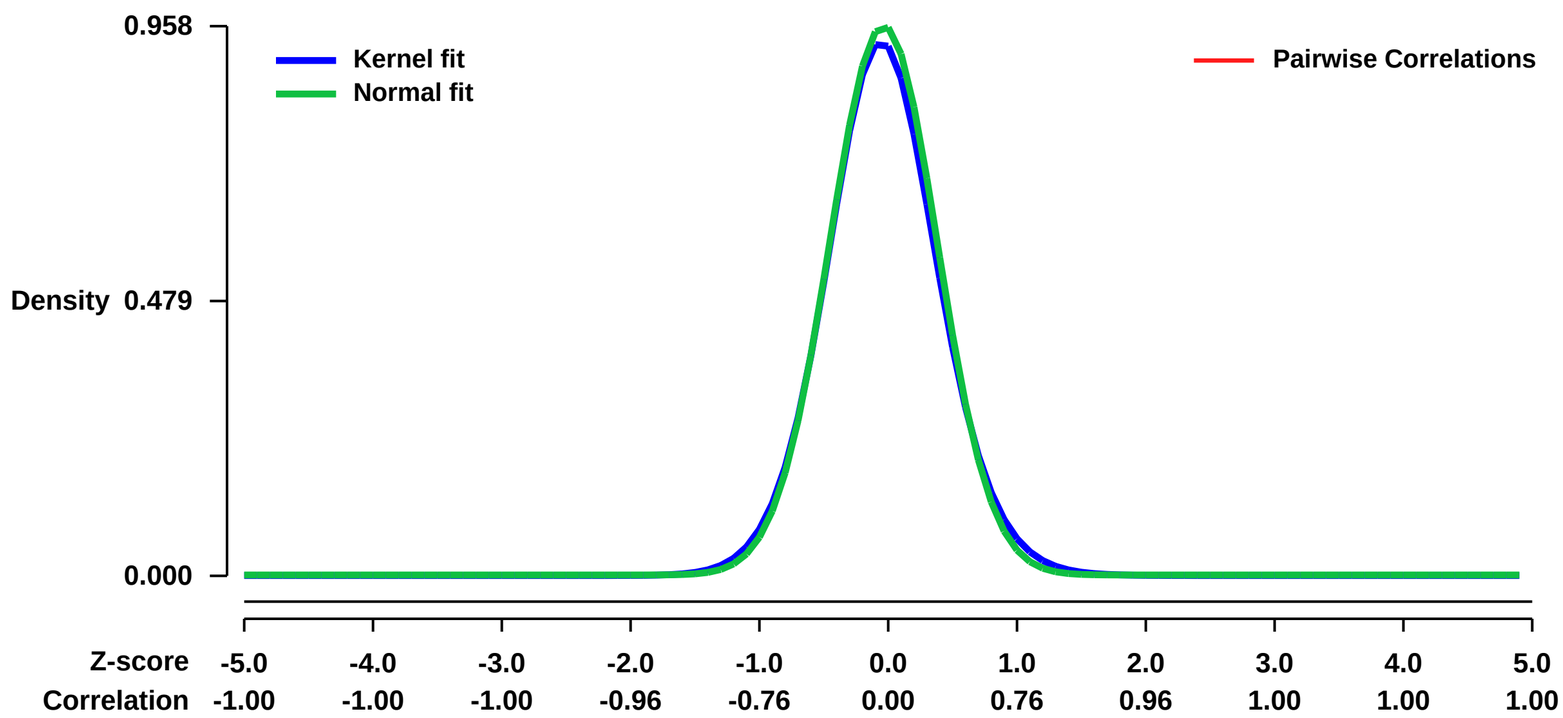

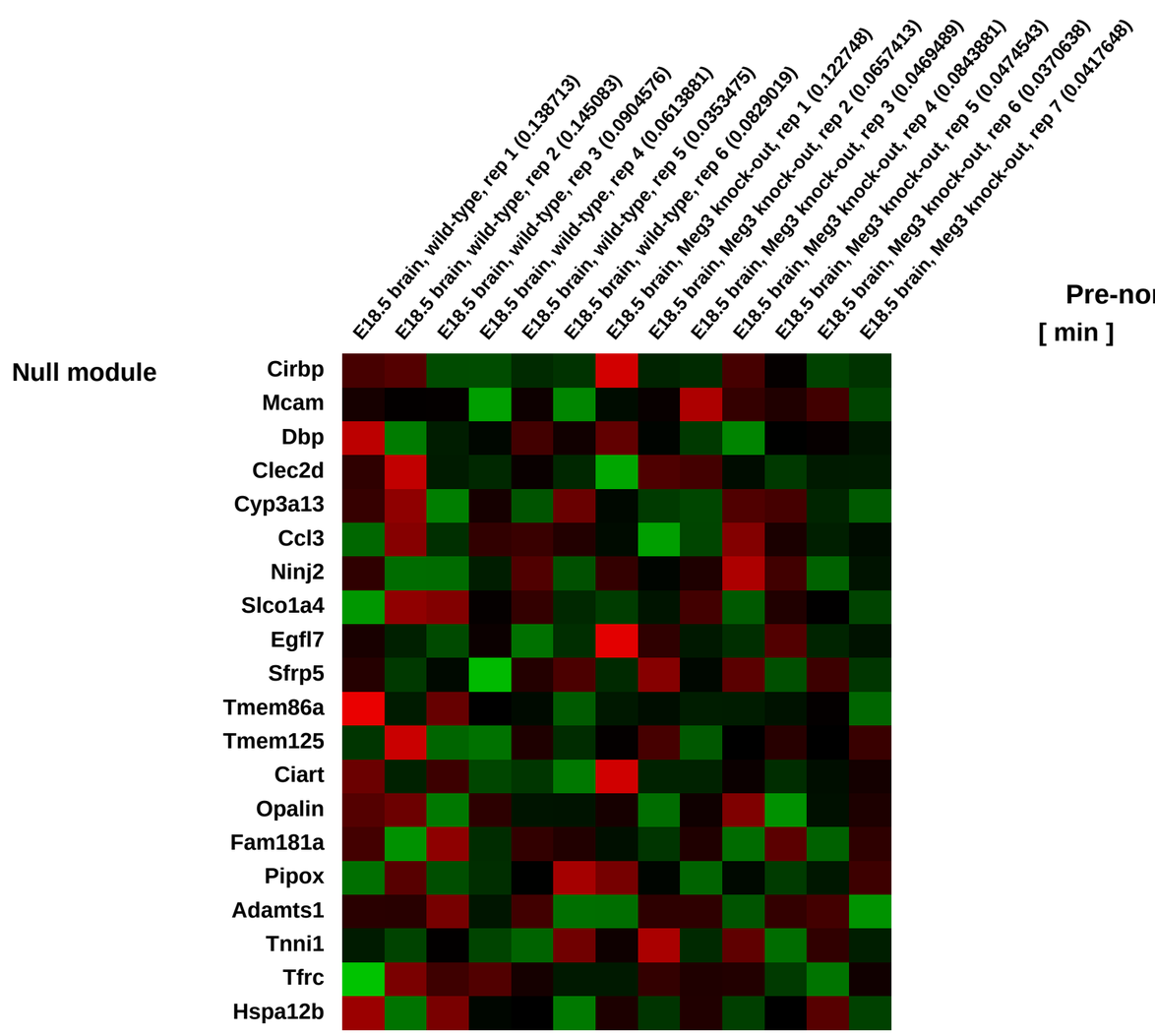

GEO Series "GSE22527" Expression Profiles

Num of samples in this series: 6

Scale of expression profile Z-scores

-3.0 -2.0 -1.0 0.0 1.0 2.0 3.0

GEO Link:	http://www.ncbi.nlm.nih.gov/geo/query/acc.cgi?acc=GSE22527
Status:	Public on Jun 23 2010
Title:	Anti-CD3 therapy permits regulatory T cells to surmount T cell receptor-specified peripheral niche constraints
Organism:	Mus musculus
Experiment type:	Expression profiling by array
Platform:	GPL1261
Pubmed ID:	20679403
Summary & Design:	**Summary:** Treatment with anti-CD3 is a promising therapeutic approach for autoimmune diabetes, but its mechanism of action remains unclear. Foxp3+ regulatory T (Treg) cells may be involved, but the evidence has been conflicting, and there is great uncertainty as to possible mechanistic connections. We investigated this issue in mice derived from the NOD model, which were engineered mice in which Treg populations were perturbed, or could be manipulated by acute ablation or transfer. The data highlighted the involvement of Foxp3+ cells in anti-CD3 action. Rather than a generic influence on all Treg cells, the therapeutic effect seemed to involve an striking expansion of previously constrained Treg cell populations; this expansion occurred not through conversion from Foxp3- Tconv cells but from a dramatic proliferative expansion. We found that Treg cells are normally constrained by TCR-specific niches in secondary lymphoid organs, and that intraclonal competition restrains their possibility for conversion and expansion in the spleen and lymph nodes, much as niche competition limits their selection in the thymus. The strong perturbations induced by anti-CD3 overcame these niche limitations, in a process dependent on receptors for trophic cytokines, interleukin-2 receptor (IL-2R) and IL-7R. **Keywords: Treatment response** **Overall design:** All gene expression profiles were obtained from highly purified T cell populations sorted by flow cytometry. RNA from 5 - 50 x 104 cells was amplified, labeled, and hybridized to Affymetrix M430v2. Raw data were preprocessed with the RMA algorithm in GenePattern, and averaged expression values were used for analysis.

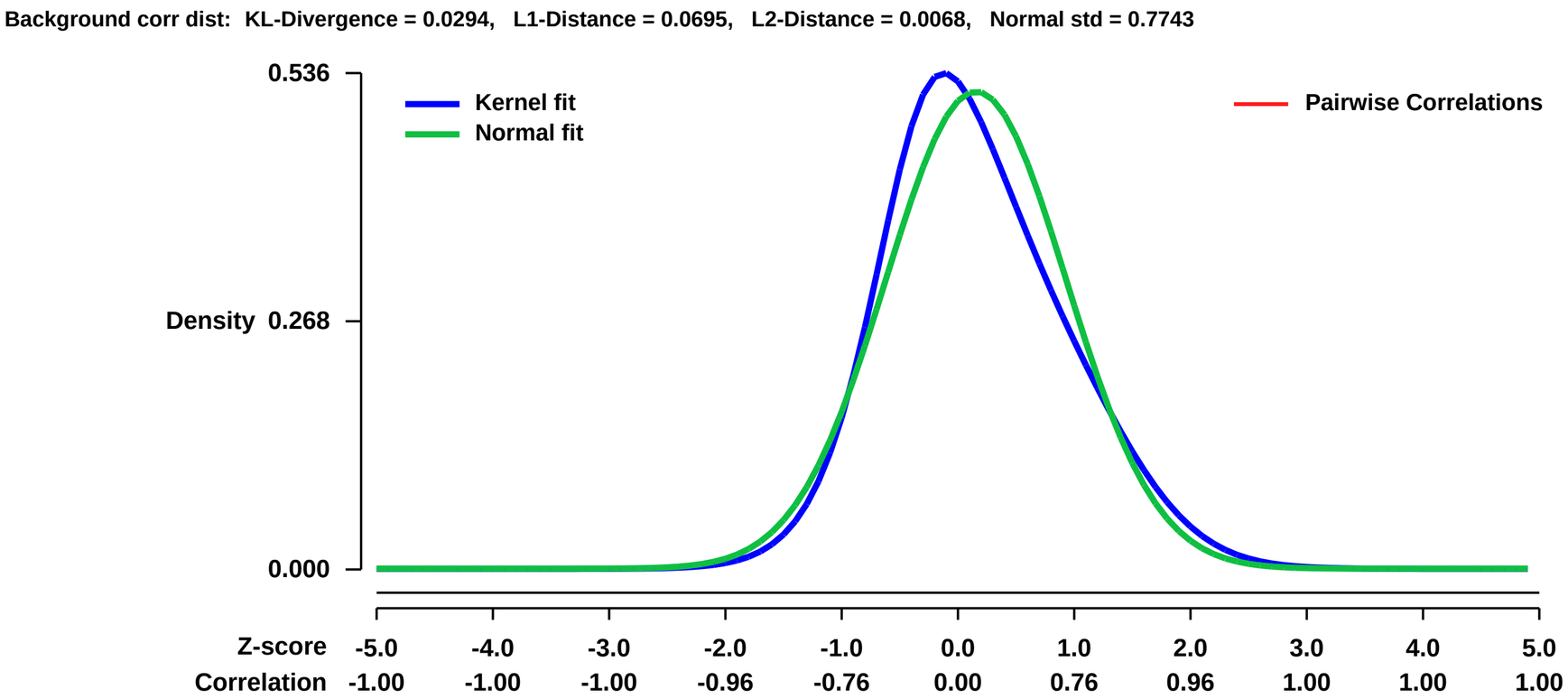

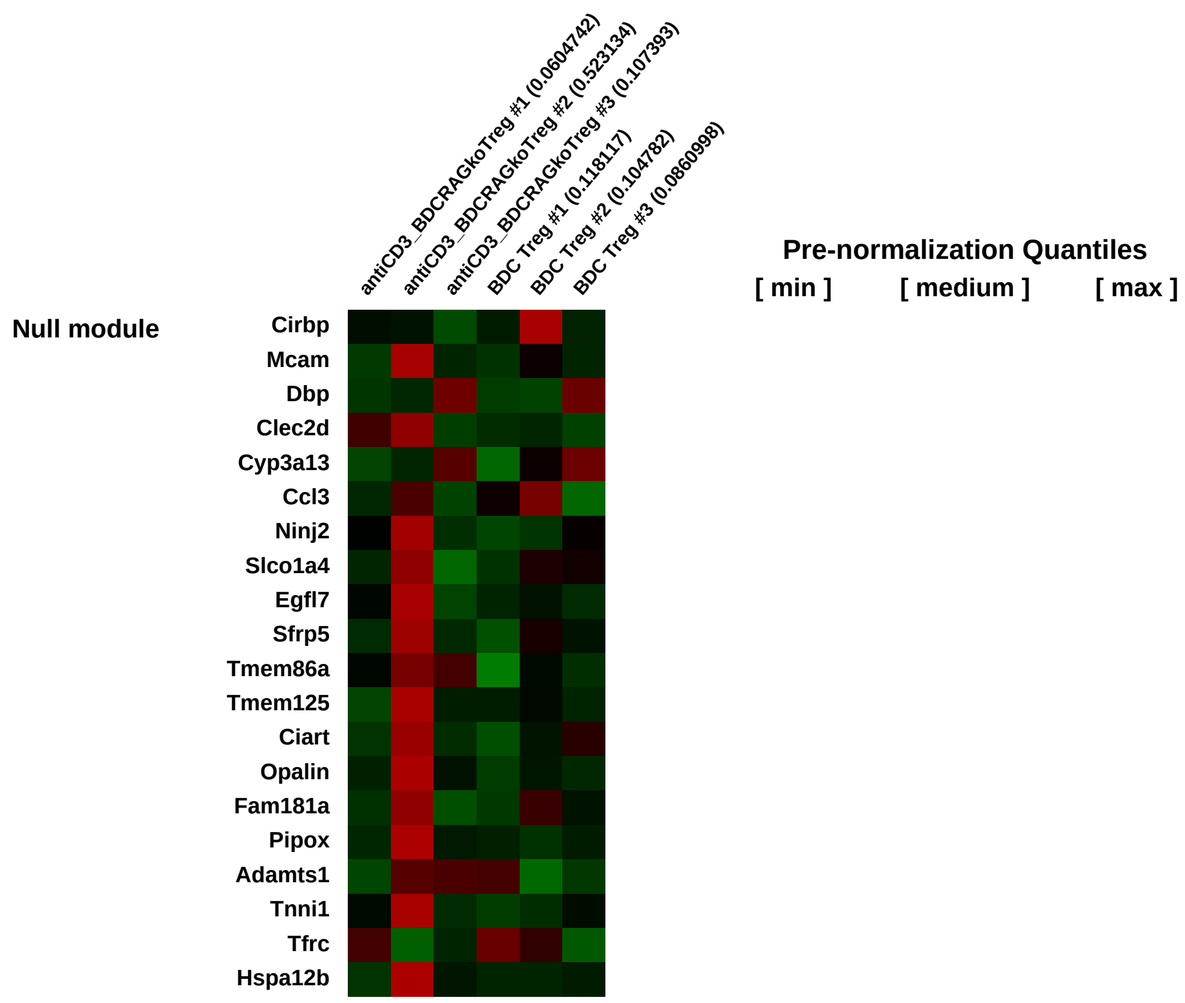

GEO Series "GSE45820" Expression Profiles

Num of samples in this series: 6

Scale of expression profile Z-scores

-3.0 -2.0 -1.0 0.0 1.0 2.0 3.0

GEO Link: http://www.ncbi.nlm.nih.gov/geo/query/acc.cgi?acc=GSE45820
Status: Public on May 19 2014
Title: Expression data from murine cardiac fibroblasts and endothelial cells following Transverse Aortic Constriction
Organism: Mus musculus
Experiment type: Expression profiling by array
Platform: GPL1261
Pubmed ID:

Summary & Design:

Summary:
Accumulation of activated cardiac fibroblasts plays a key role in heart failure progression. These cells deposit excessive extracellular matrix that leads to mechanical stiffness, myocyte uncoupling and ischemia. To investigate whether two developmentally distinct cardiac fibroblast populations exhibit distinct expression profiles in response to cardiac injury, and therefore might necessitate distinct therapeutic targeting, we performed microarray analysis on FACS sorted cells. Tie2cre lineage traced CFs, non Tie2cre lineage traced cardiac fibroblasts and endothelial cells were isolated from left ventricle of SHAM operated and banded hearts at the onset of fibrosis, one week after surgery.

We used microarrays to detail the global programme of gene expression in cardiac fibroblasts and endothelium following pressure overload. Tie2cre lineage traced, non-tie2cre lineage traced fibroblasts and endothelial cells were sorted from left ventricle of 3 SHAM operated and 3 TAC operated adult male Black Swiss mice.

Overall design:
Tie2cre lineage traced, non-tie2cre lineage traced fibroblasts and endothelial cells were sorted from left ventricle of 3 SHAM operated and 3 Transaortic Constriction (TAC) operated adult male Black Swiss mice for RNA extraction and Affymetrix microarray analysis. Hypertrophy in TAC animals, an lack of hypertrophy in SHAM operated animals, was evaluated by hemodynamic measurements before surgery and one week after surgery. Cells were isolated one week after surgery.

Background corr dist: KL-Divergence = 0.0132, L1-Distance = 0.0279, L2-Distance = 0.0011, Normal std = 0.8360

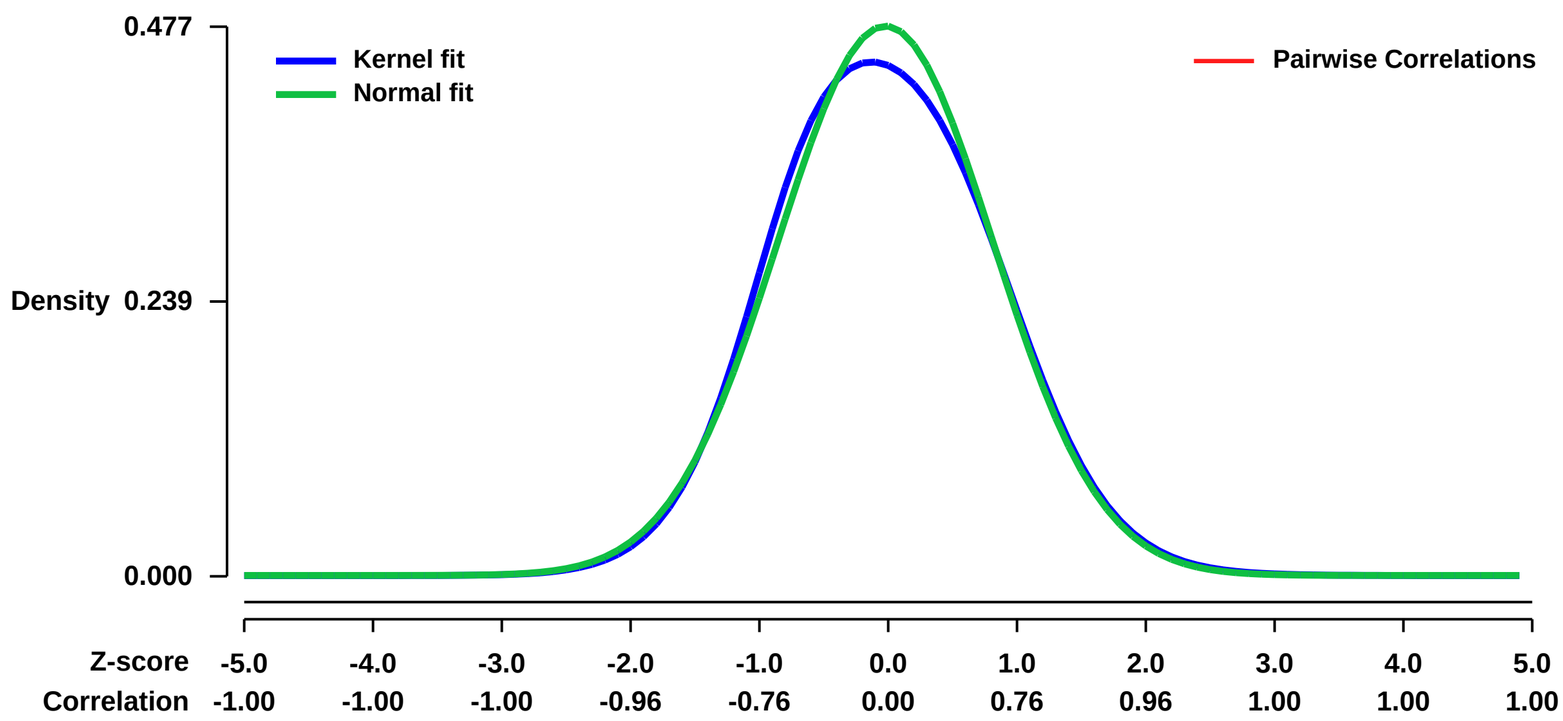

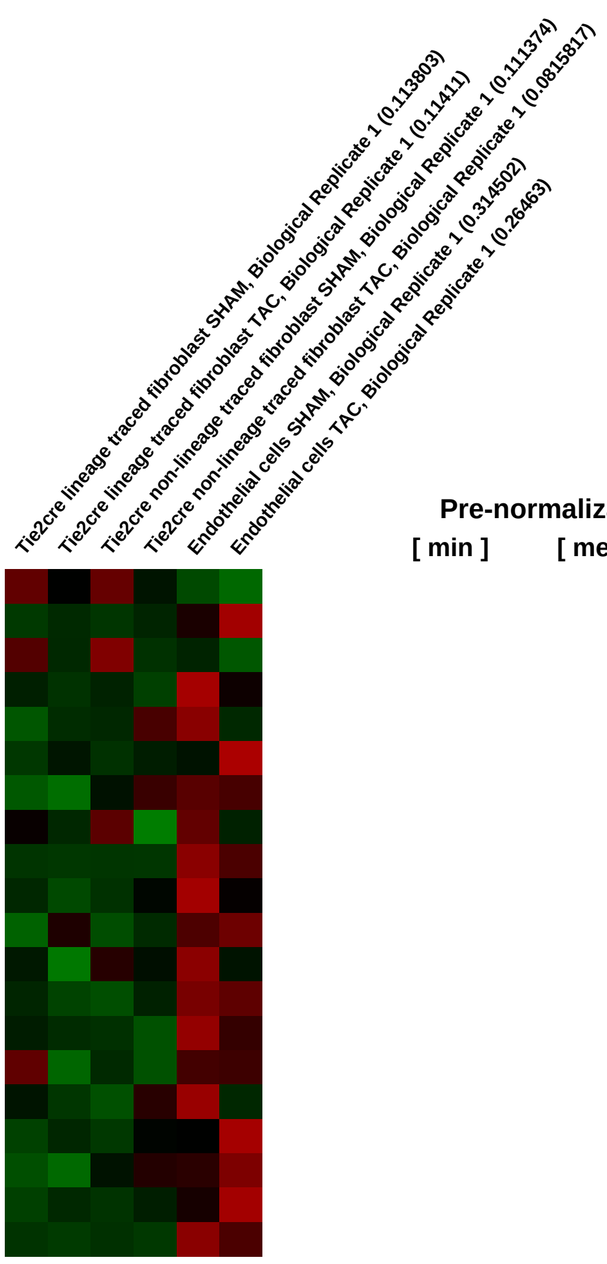

GEO Series "GSE51213" Expression Profiles

Num of samples in this series: 16

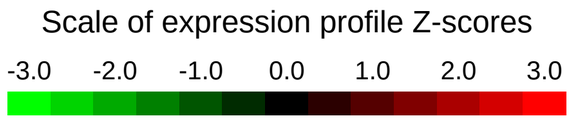

GEO Link:	http://www.ncbi.nlm.nih.gov/geo/query/acc.cgi?acc=GSE51213
Status:	Public on Sep 26 2013
Title:	Effect of chronic glucocorticoid (GC) treatment on neonatal mouse whole cerebellum and whole lung
Organism:	Mus musculus
Experiment type:	Expression profiling by array
Platform:	GPL1261
Pubmed ID:	
Summary & Design:	**Summary:** Dexamethasone (1ug/g, Dex) or vehicle (saline) injected into postnatal days 0-7 (P0 to P7) of C57BL6J mouse pups every day. Whole organ were harvested at P7. **Overall design:** KEYWORDS: cell type comparison, treatment comparison.

Background corr dist: KL-Divergence = 0.0258, L1-Distance = 0.0164, L2-Distance = 0.0003, Normal std = 0.6871

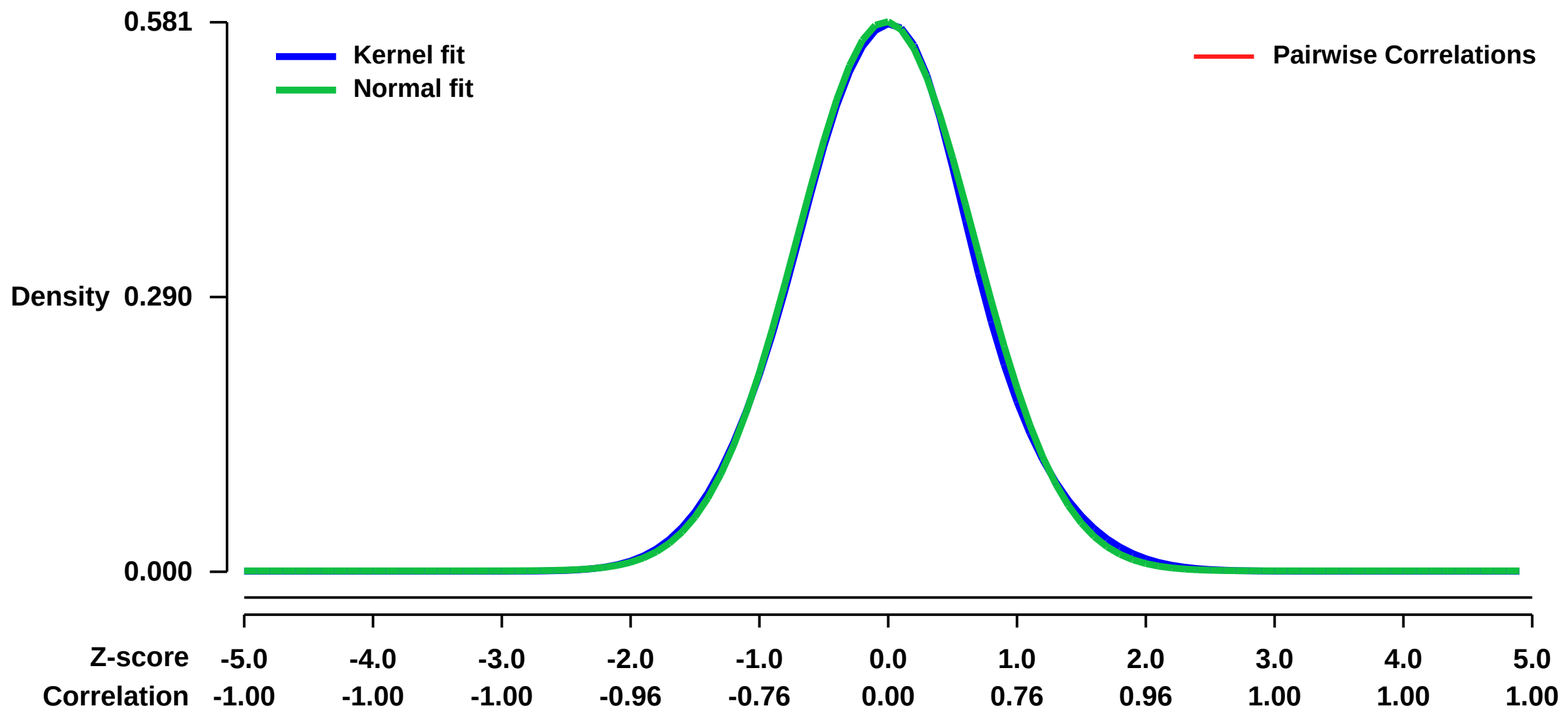

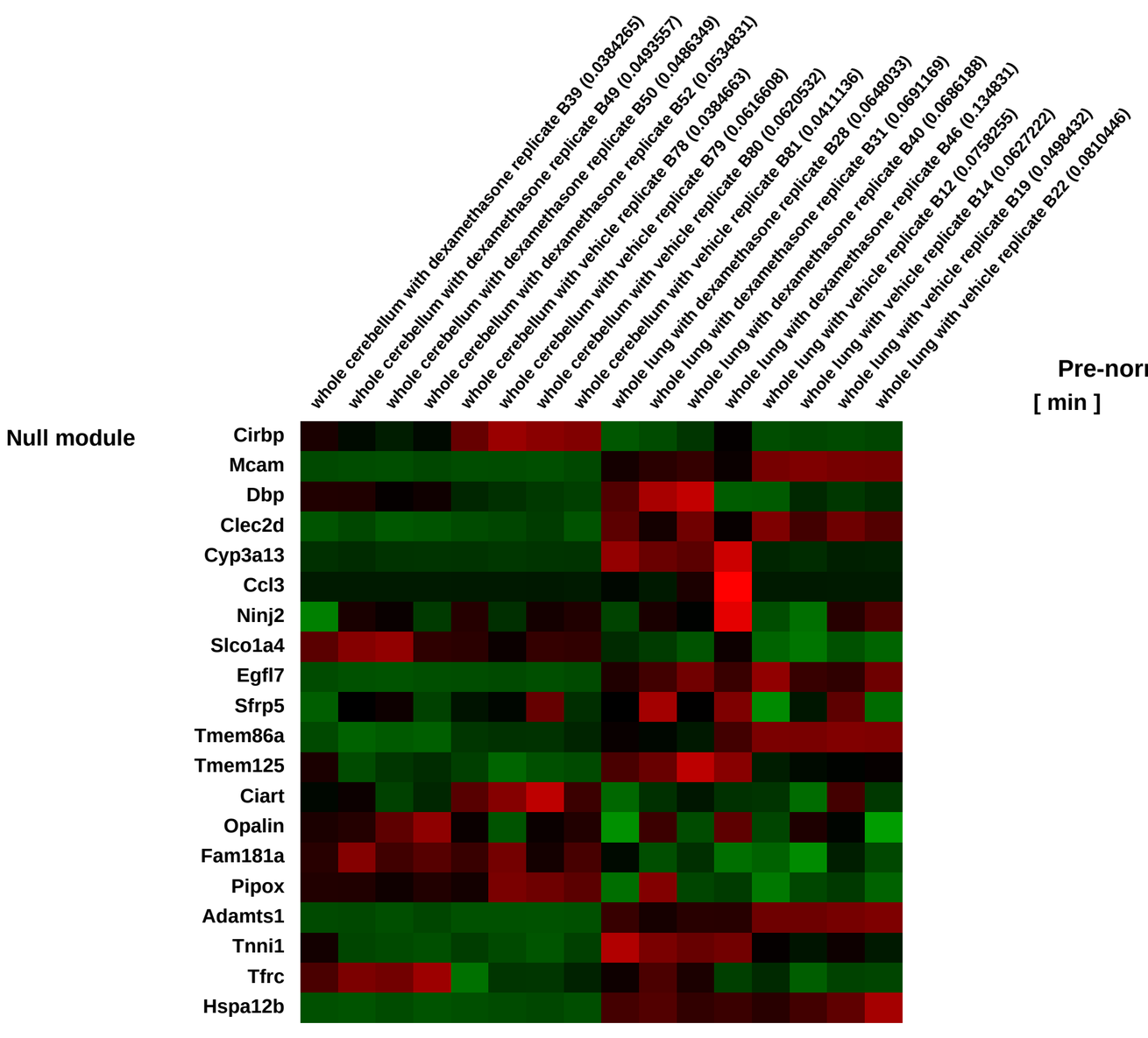

GEO Series "GSE49346" Expression Profiles

Num of samples in this series: 6

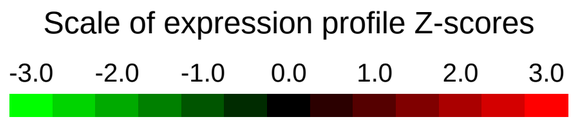

GEO Link:	http://www.ncbi.nlm.nih.gov/geo/query/acc.cgi?acc=GSE49346
Status:	Public on Mar 07 2014
Title:	Expression data from adult ATII and E18 Bipotent progenitor cells in the mouse lung
Organism:	Mus musculus
Experiment type:	Expression profiling by array
Platform:	GPL1261
Pubmed ID:	24499815
Summary & Design:	**Summary:** **Alveoli are thin-walled sacs that serve as the gas exchange units of the lung. They are affected in devastating lung diseases including COPD, Idiopathic Pulmonary Fibrosis, and the major form (adenocarcinoma) of lung cancer, the leading cause of cancer deaths. The alveolar epithelium is composed of two morphologically distinct cell types: alveolar type (AT) 1 cells, exquisitely thin cells across which oxygen diffuses to reach the blood, and AT2 cells, specialized surfactant-secreting cells. Classical studies suggested that AT1 cells arise from AT2 cells during development and following injury, but more recent studies suggest other sources. Here we use histological and marker analysis, lineage tracing, and clonal analysis in mice to identify alveolar progenitor and stem cells and map their locations and potential in vivo. The results show that AT1 and AT2 cells arise independently during development from a bipotential progenitor. After birth, new AT1 cells derive from rare, long-lived, self-renewing AT2 cells, each producing a slowly expanding clonal focus of regenerated alveoli contiguous with the founder AT2 cell. This stem cell function of AT2 cells is broadly activated by diffuse AT1 cell injury, and AT2 self-renewal can be induced in vitro by EGF ligands and permanently activated in vivo by AT2 cell-specific targeting of the oncogenic KrasG12D allele, efficiently transforming AT2 cells into monoclonal adenomatous tumors that rapidly enlarge and prove fatal. Thus, there is a developmental switch in alveolar progenitor cells after birth, when mature AT2 cells function as facultative stem cells that contribute to local alveolar renewal, repair, and cancer. We propose that short-range signals from dying AT1 cells regulate AT2 stem cell activity: a signal transduced by EGFR-KRAS controls AT2 self-renewal and is hijacked during oncogenic transformation, and a separate signal controls reprogramming to AT1 cell fate.** **Overall design:** **To compare expression between ATII and E18 BP populations, RNA was isolated from either population purified by FACS. Two populations are analyzed with 3 biological replicates per population.**

Background corr dist: KL-Divergence = 0.0359, L1-Distance = 0.0425, L2-Distance = 0.0025, Normal std = 0.6765

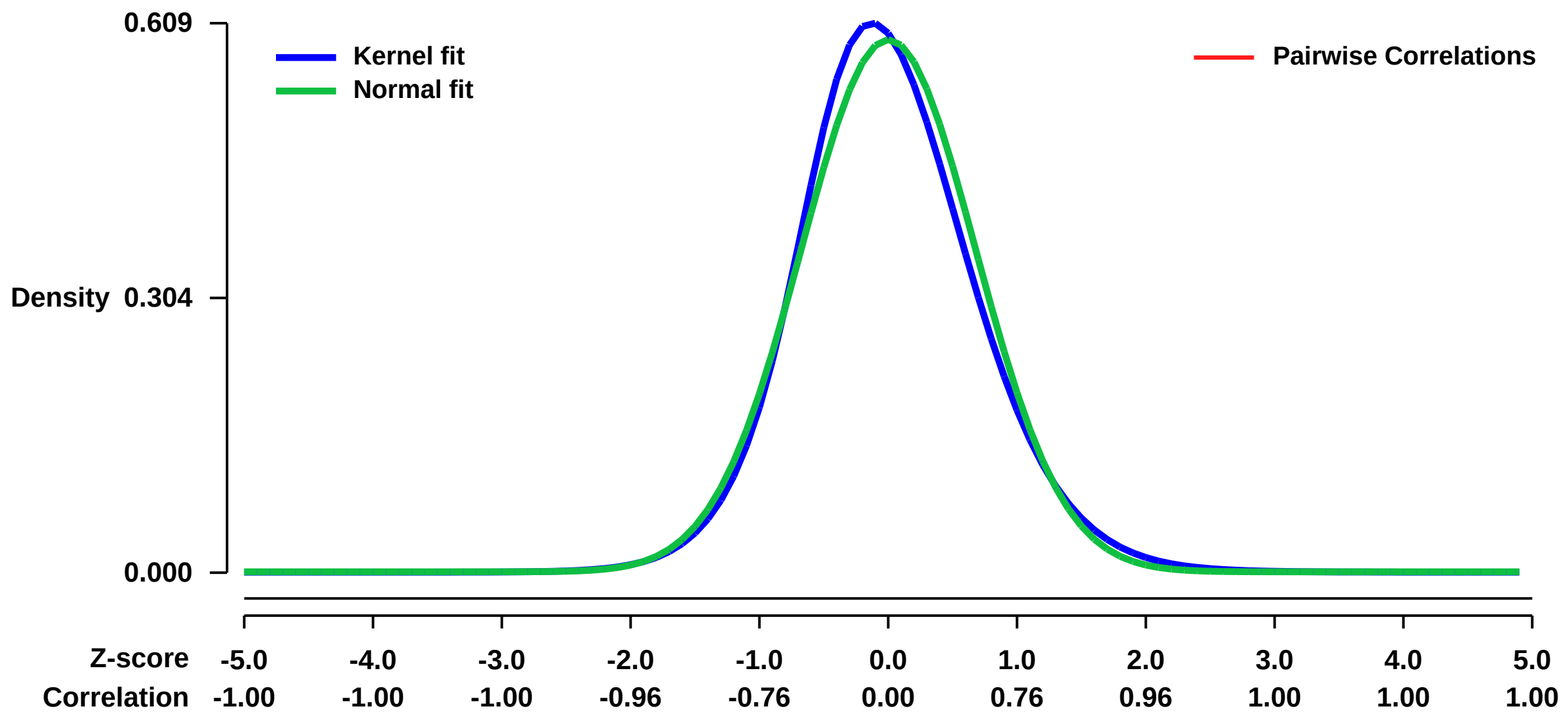

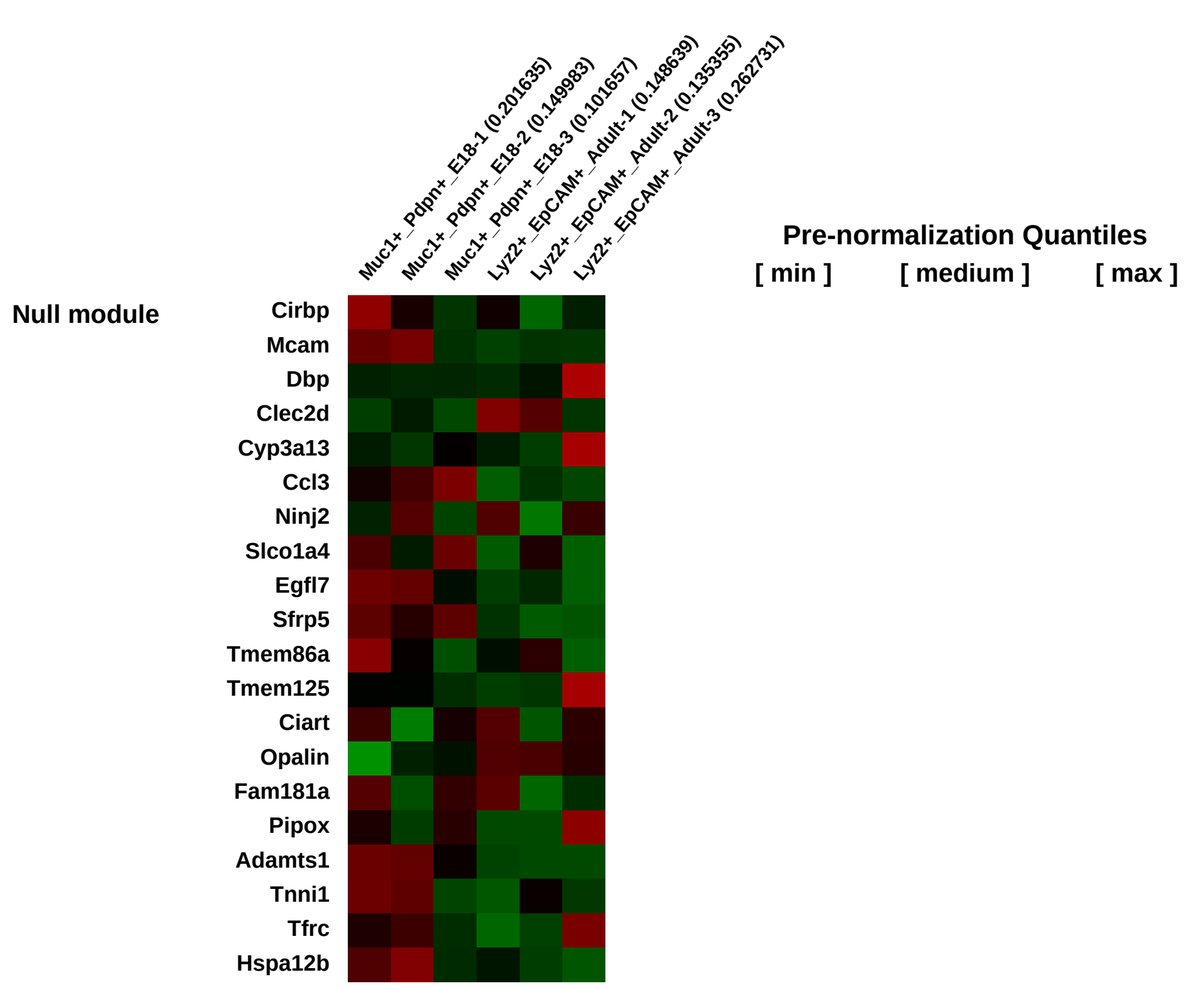

GEO Series "GSE41910" Expression Profiles

Num of samples in this series: 12

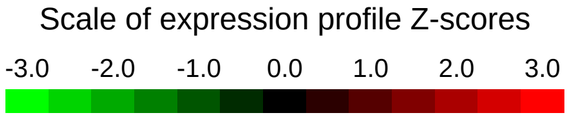

GEO Link:	http://www.ncbi.nlm.nih.gov/geo/query/acc.cgi?acc=GSE41910
Status:	Public on Feb 19 2013
Title:	Gene expression profiling of gastrocnemius of mini muscle mice
Organism:	Mus musculus
Experiment type:	Expression profiling by array
Platform:	GPL1261
Pubmed ID:	23362141
Summary & Design:	**Summary:** Few studies have investigated heterogeneity of selection response in replicate lines subjected to equivalent selection. We developed 4 replicate lines of mice based on high levels of voluntary wheel running (high runner or HR lines) while also maintaining 4 non-selected control lines. This led to the unexpected discovery of the HR mini-muscle (HRmini) phenotype, recognized by a 50% reduction in hindlimb muscle mass, which became fixed in 1 of the 4 HR selected lines. Here, we report genome-wide expression profiling describing transcriptome differences between HRnormal and HRmini medial gastrocnemius. This work provides a resource for understanding differences in muscle phenotypes in populations exhibiting high running capacity. **Overall design:** Male mice were used from an animal model of 4 closed lines selectively bred for high voluntary wheel-running behaviour (HR) and 4 control lines bred without intentional selection, described in Swallow et al. Animals used in the current work were sampled from generation 37 at a mean age of 84 days (range = 79-86). For microarray analysis, we used gastrocnemius muscles (including both lateral and medial portions) from HRmini line #3 and HRnormal line #8 (n = 6, in each group). To obtain sufficient RNA, gastrocnemius samples of HRmini were pooled from left and right limbs from each animal, whereas HRnormal gastrocnemius was sampled from either left or right limb only.

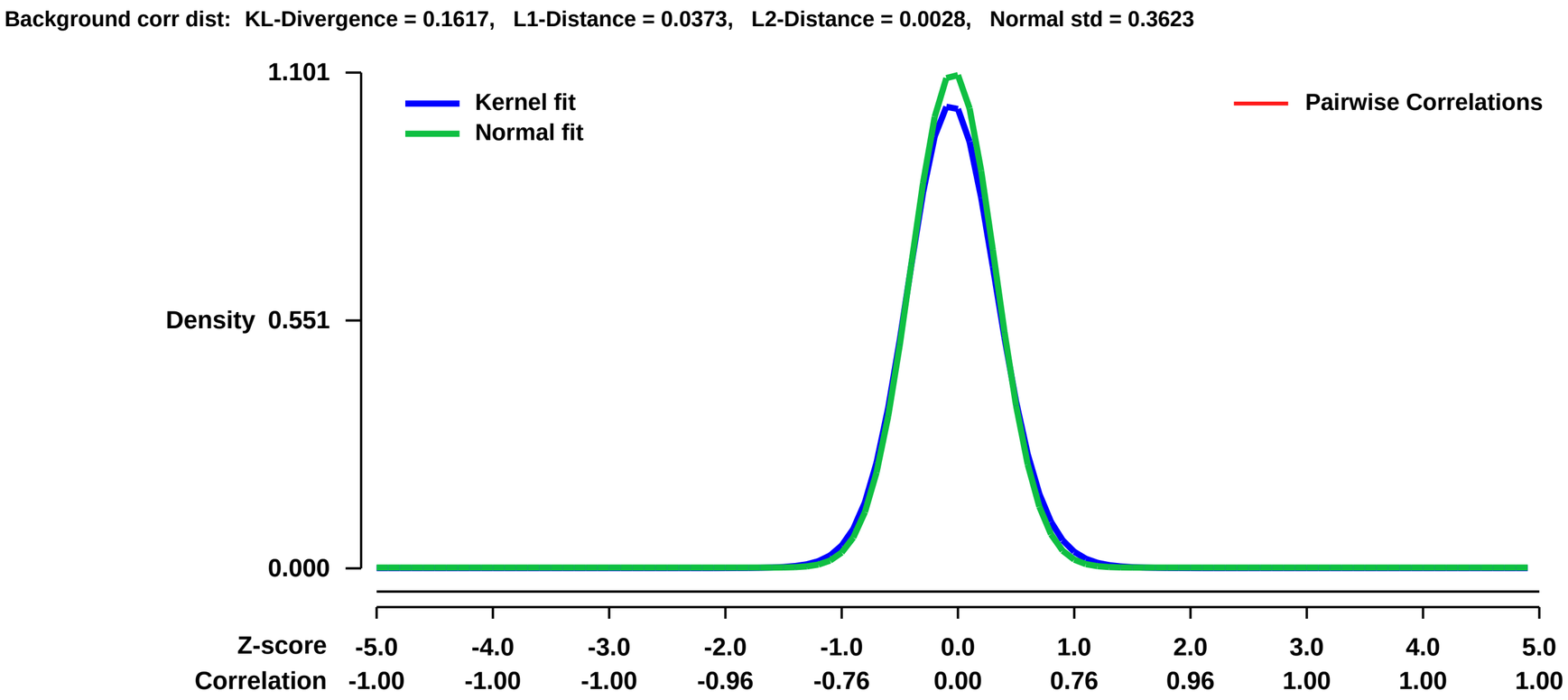

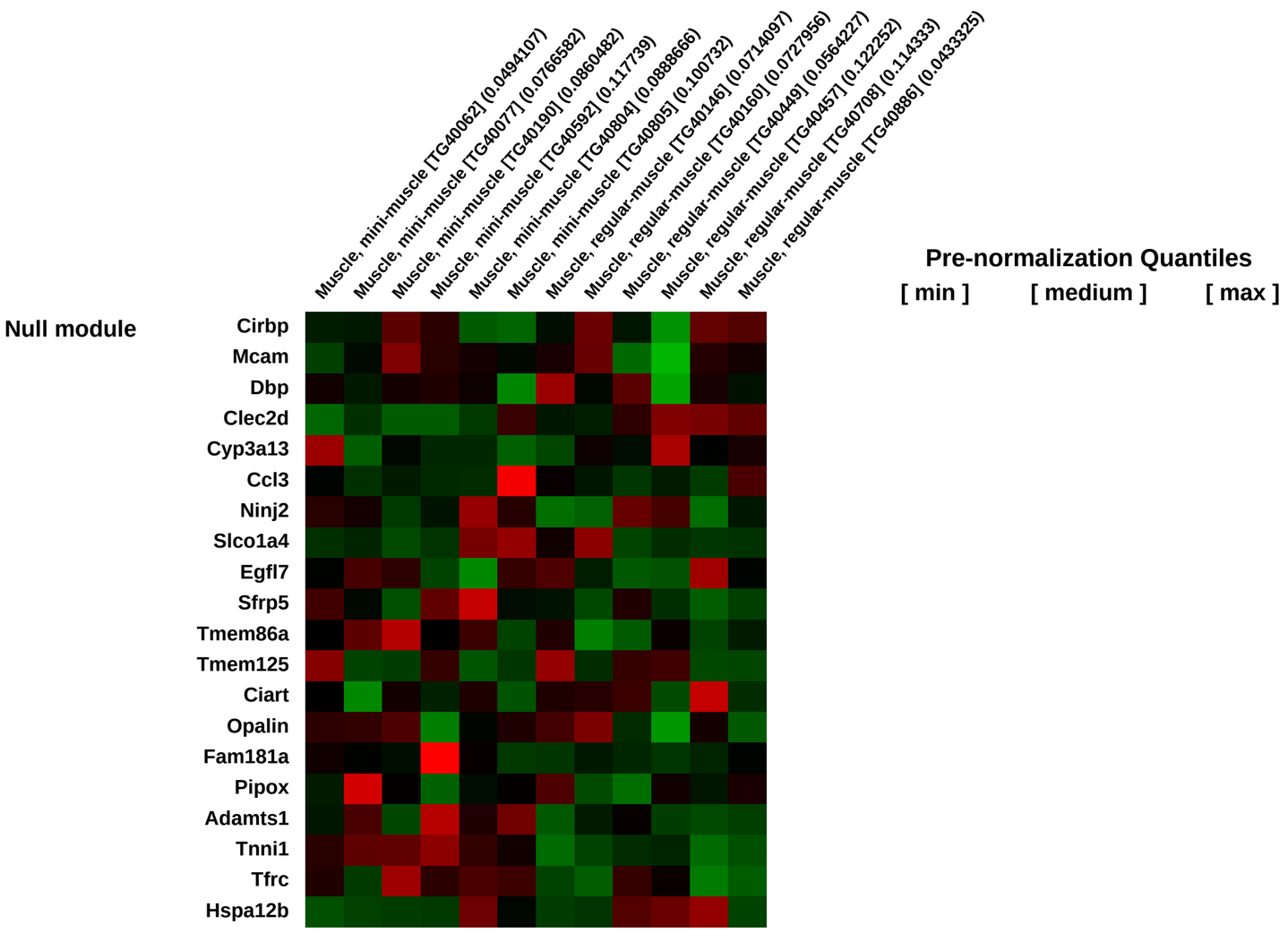

GEO Series "GSE11859" Expression Profiles

Num of samples in this series: 27

Scale of expression profile Z-scores

-3.0 -2.0 -1.0 0.0 1.0 2.0 3.0

GEO Link:	http://www.ncbi.nlm.nih.gov/geo/query/acc.cgi?acc=GSE11859
Status:	Public on Jun 24 2008
Title:	Acquisition of granule neuron precursor identity and Hedgehog-induced medulloblastoma in mice.
Organism:	Mus musculus
Experiment type:	Expression profiling by array
Platform:	GPL1261
Pubmed ID:	18691547
Summary & Design:	**Summary:** Origins of the brain tumor, medulloblastoma, from stem cells or restricted pro-genitor cells are unclear. To investigate this, we activated oncogenic Hedgehog signaling in multipotent and lineage-restricted CNS progenitors. We observed that normal unipo-tent cerebellar granule neuron precursors (CGNP) derive from hGFAP+ and Olig2+ rhombic lip progenitors. Hedgehog activation in a spectrum of early and late stage CNS progenitors generated similar medulloblastomas, but not other brain cancers, indicating that acquisition of CGNP identity is essential for tumorigenesis. We show in human and mouse medulloblastoma that cells expressing the glia-associated markers Gfap and Olig2 are neoplastic and that they retain features of embryonic-type granule lineage progenitors. Thus, oncogenic Hedgehog signaling promotes medulloblastoma from lineage-restricted granule cell progenitors. Gene expression profiling of cerebellar tumors generated from various early and late stage CNS progenitor cells. **Overall design:** Group comparisons with biological replicates

Background corr dist: KL-Divergence = 0.1816, L1-Distance = 0.0304, L2-Distance = 0.0019, Normal std = 0.3517

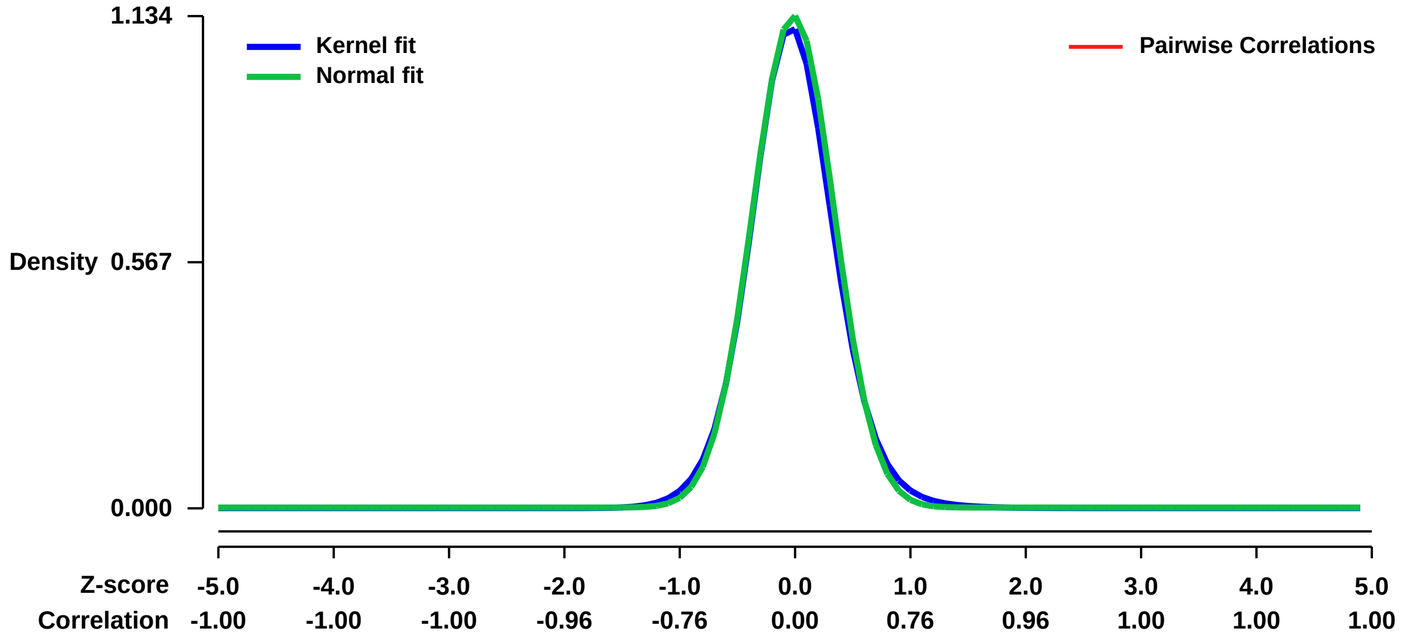

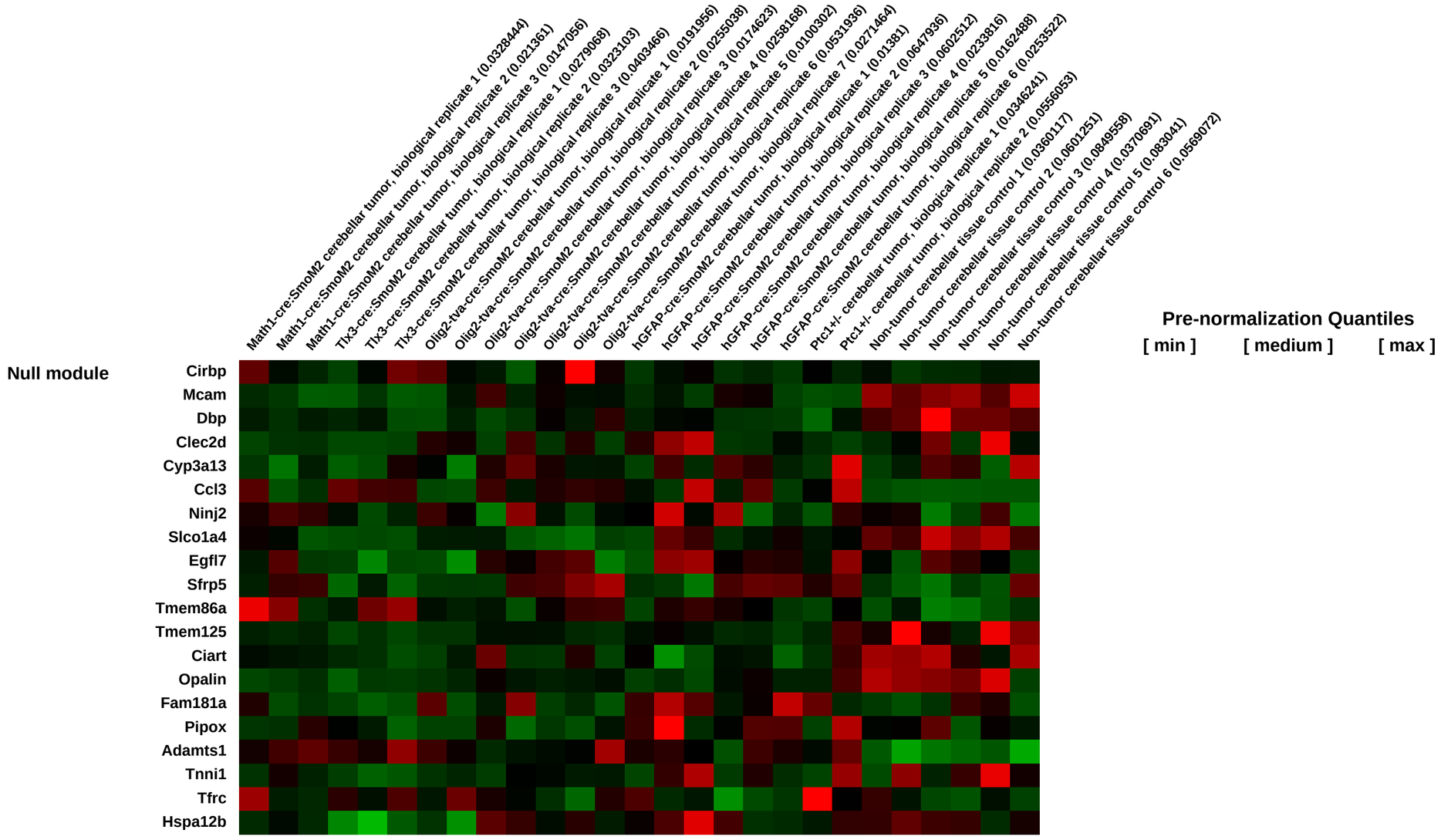

GEO Series "GSE38837" Expression Profiles

Num of samples in this series: 6

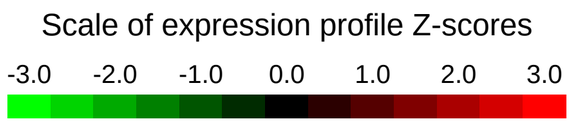

GEO Link:	http://www.ncbi.nlm.nih.gov/geo/query/acc.cgi?acc=GSE38837
Status:	Public on Apr 11 2014
Title:	Zbtb20-mediated repression of genes in developing CA1 pyramidal neurons
Organism:	Mus musculus
Experiment type:	Expression profiling by array
Platform:	GPL1261
Pubmed ID:	23283686
Summary & Design:	**Summary:** The transcriptional repressor Zbtb20 is essential for specification of hippocampal CA1 pyramidal neurons. Moreover, ectopic expression of Zbtb20 is sufficient to transform subicular and retrosplenial areas of D6/Zbtb20S mice to CA1. We used microarrays to identify genes that are repressed by Zbtb20 in developing CA1 pyramidal neurons in the CA1-transformed cortex of D6/Zbtb20S mice. **Overall design:** For RNA extraction and hybridization on Affymetrix microarrays, we isolated the CA1-transformed subiculum and retrosplenial cortex from postnatal day 1 D6/Zbtb20S mice, as well as corresponding areas from their wildtype littermates. Total RNA was extracted using the RNeasy Lipid Tissue Mini Kit (Qiagen). Each RNA sample represents a pool of RNA obtained from dissected tissues of seven animals.

Background corr dist: KL-Divergence = 0.0353, L1-Distance = 0.0136, L2-Distance = 0.0002, Normal std = 0.6349

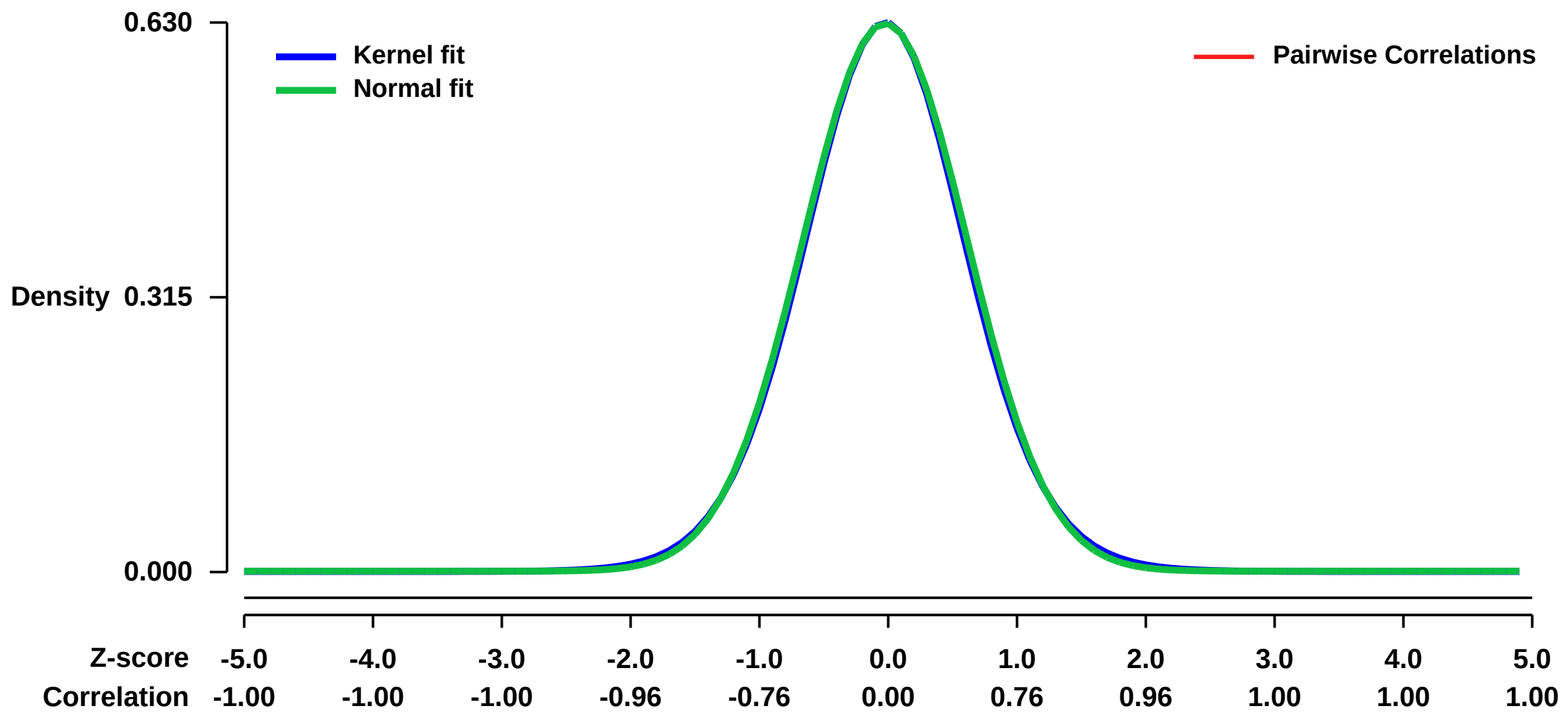

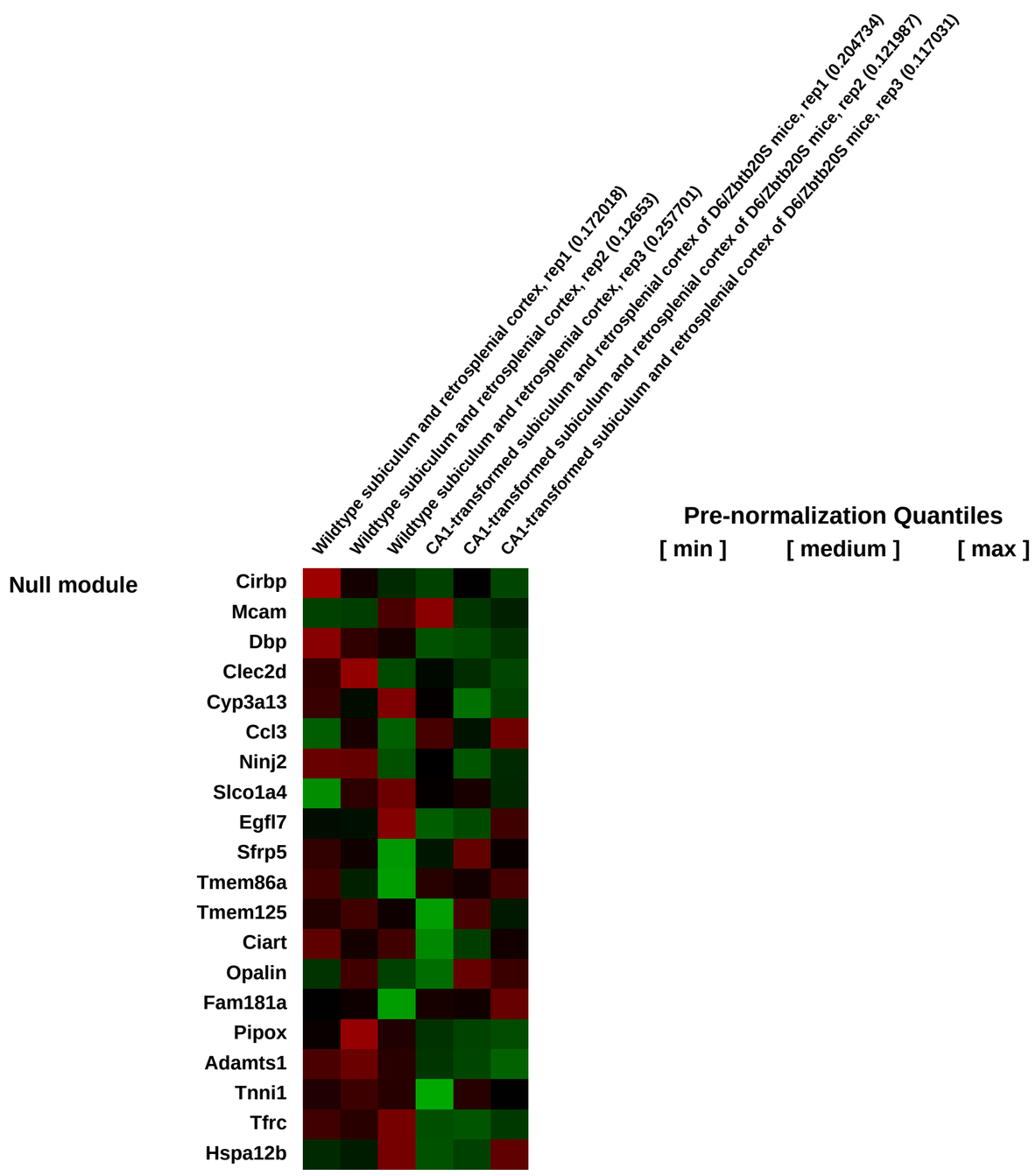

GEO Series "GSE49194" Expression Profiles

Num of samples in this series: 14

Scale of expression profile Z-scores

-3.0 -2.0 -1.0 0.0 1.0 2.0 3.0

GEO Link:	http://www.ncbi.nlm.nih.gov/geo/query/acc.cgi?acc=GSE49194
Status:	Public on Oct 01 2013
Title:	Expression data from neurospheres derived from the neocortex, striatum and subventricular zones of the adult mouse brain
Organism:	Mus musculus
Experiment type:	Expression profiling by array
Platform:	GPL1261
Pubmed ID:	23974433
Summary & Design:	**Summary:** Differential gene expression profiles of neurospheres derived from different regions of the adult brain. In this dataset, we include data on triplicated biological samples from each of the following brain regions: neocortex, striatum, and subventricular zone. We also include duplicated data on neurospheres derived from the dorsal and ventralforebrain neural tubes and one spinal cord of E14.5 mouse embryos for comparison. **Overall design:** Fourteen samples were analyzed in total. To compare the expression profiles across the samples, Affymetrix GeneChip Mouse Genome 430 2.0 Array Platform (total 41,170 probes) was used, and the data were analyzed using Silicon Genetics GeneSpring Software GX7.3.1. The data was normalized to median settings across the entire probe set and samples, and transcripts that are expressed across triplicated samples at levels two-fold or higher than the rest of the samples were considered as significantly enriched in particular biological samples. Comparisons between adult and embryonic samples also identified genes enriched in adult brain-derived samples.

Background corr dist: KL-Divergence = 0.0913, L1-Distance = 0.0376, L2-Distance = 0.0026, Normal std = 0.4673

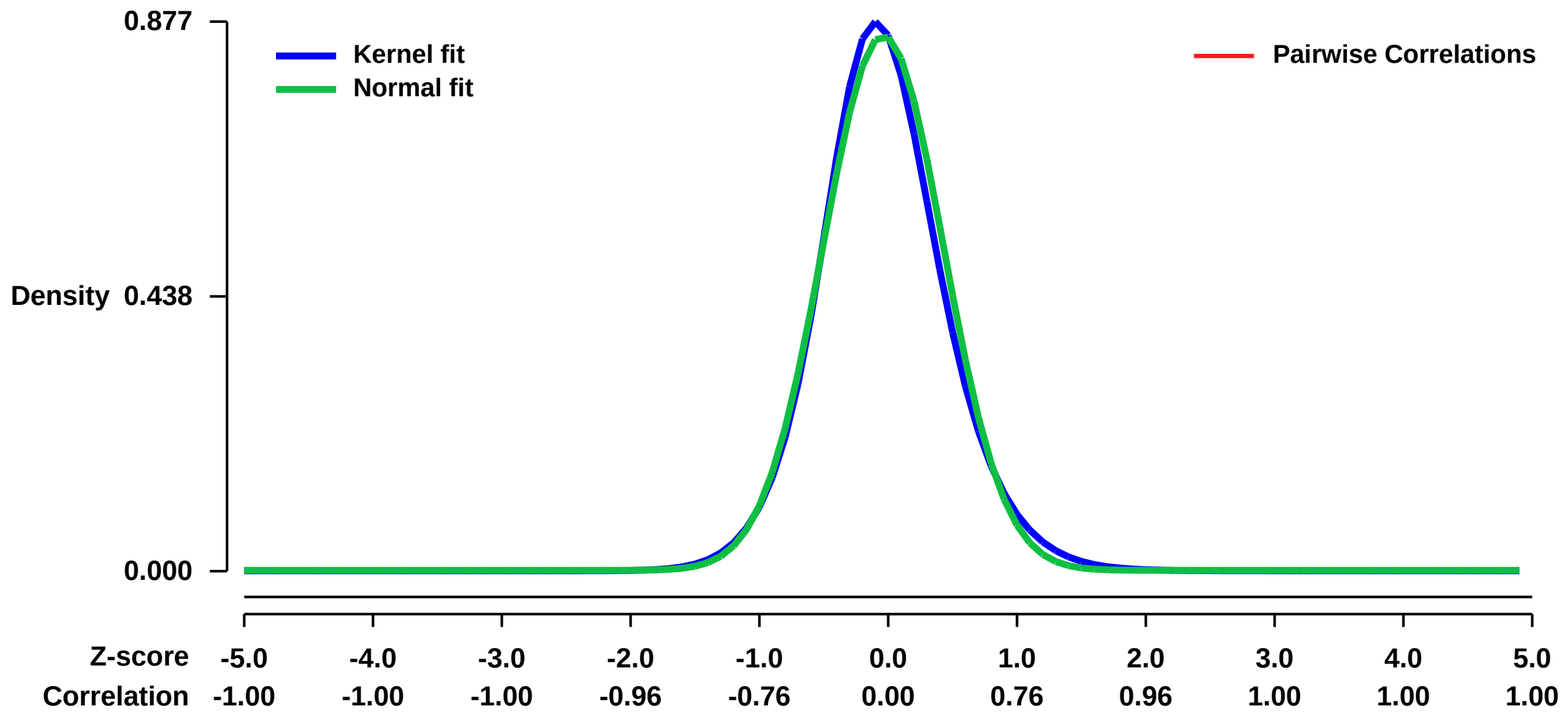

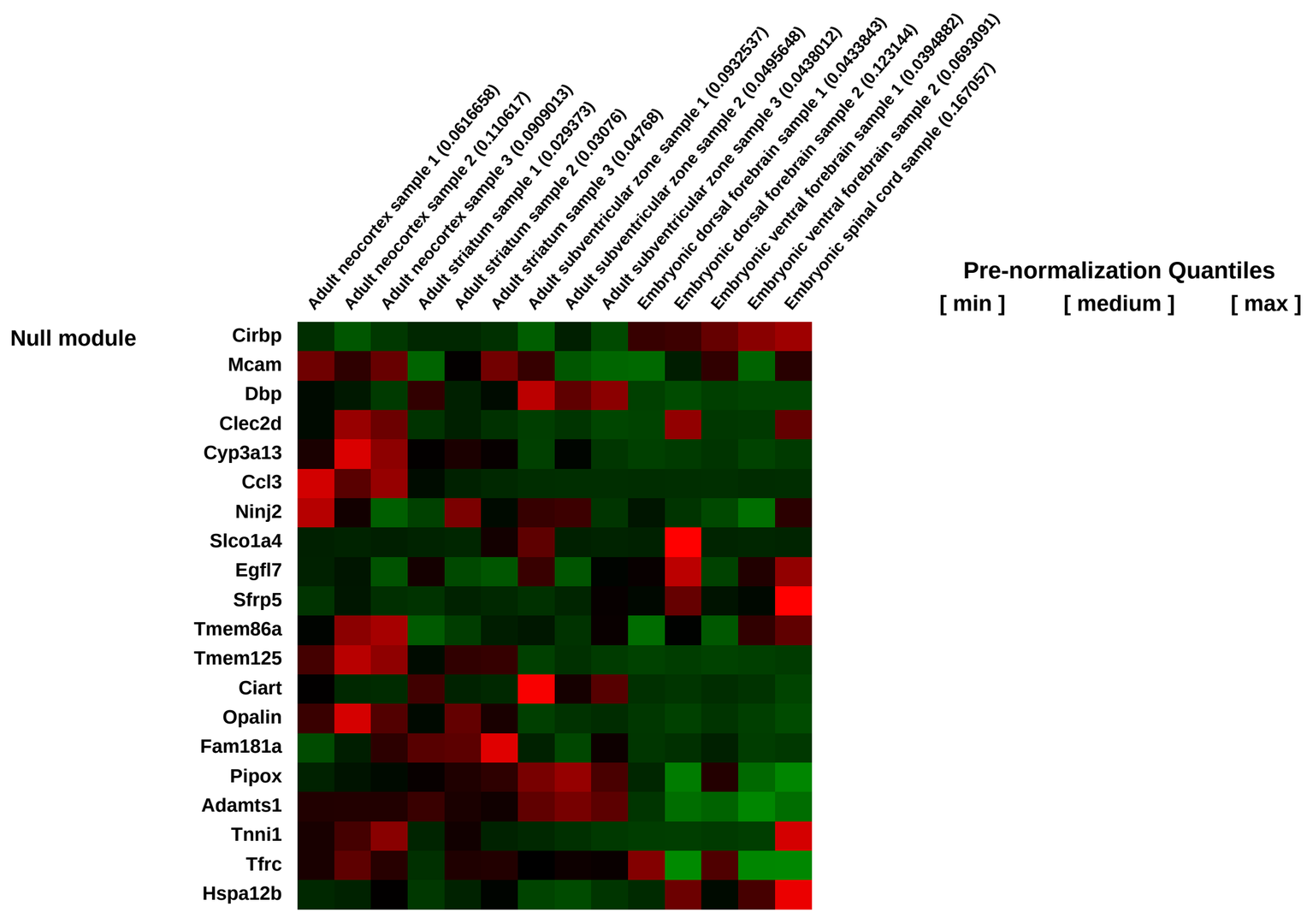

GEO Series "GSE36530" Expression Profiles

Num of samples in this series: 6

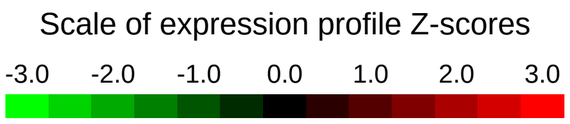

GEO Link:	http://www.ncbi.nlm.nih.gov/geo/query/acc.cgi?acc=GSE36530
Status:	Public on Mar 13 2013
Title:	Expression data for program activation by IR-induced DNA breaks in G1 phase Murine PreB cells
Organism:	Mus musculus
Experiment type:	Expression profiling by array
Platform:	GPL1261
Pubmed ID:	23496831
Summary & Design:	**Summary:** The objective of this set of samples is to identify genes that are differentially expressed following the introduction of DNA double strand breaks (DSBs) by ionizing radiation in wild-type murine pre-B cells. The data generated in this project will be compared to the data generated in GSE9024, in which genes that are differentially expressed following the introduction of DNA double strand breaks (DSBs) by the Rag proteins in murine pre-B cells were examined. In order to understand the differences between the physiologic and genotoxic responses to DSB DNA damage, we need to compare cells that are all in the same compartment of the cell cycle. We are therefore examining the response to IR-induced damage in cells that are arrested in G1, which would correspond to our previous study of G1 arrested cells with Rag-induced breaks. This will illuminate the difference directly, allowing us to better understand the signaling responses to the different types of DNA damage. **Overall design:** Murine v-abl-transformed pre-B cells were treated with 3 uM STI571 for 48 hours. The cell type is Wild type (3 biological replicates). For each wild type cell line, cells were treated with 1 Gy ionizing radiation or no ionizing radiation. Each sample was hybridized once using Affymetrix Mouse Genome 2.0 GeneChip arrays (Mouse 430 v2, Affymetrix, Santa Clara, CA). Data were analyzed using the unirradiated samples as the controls.

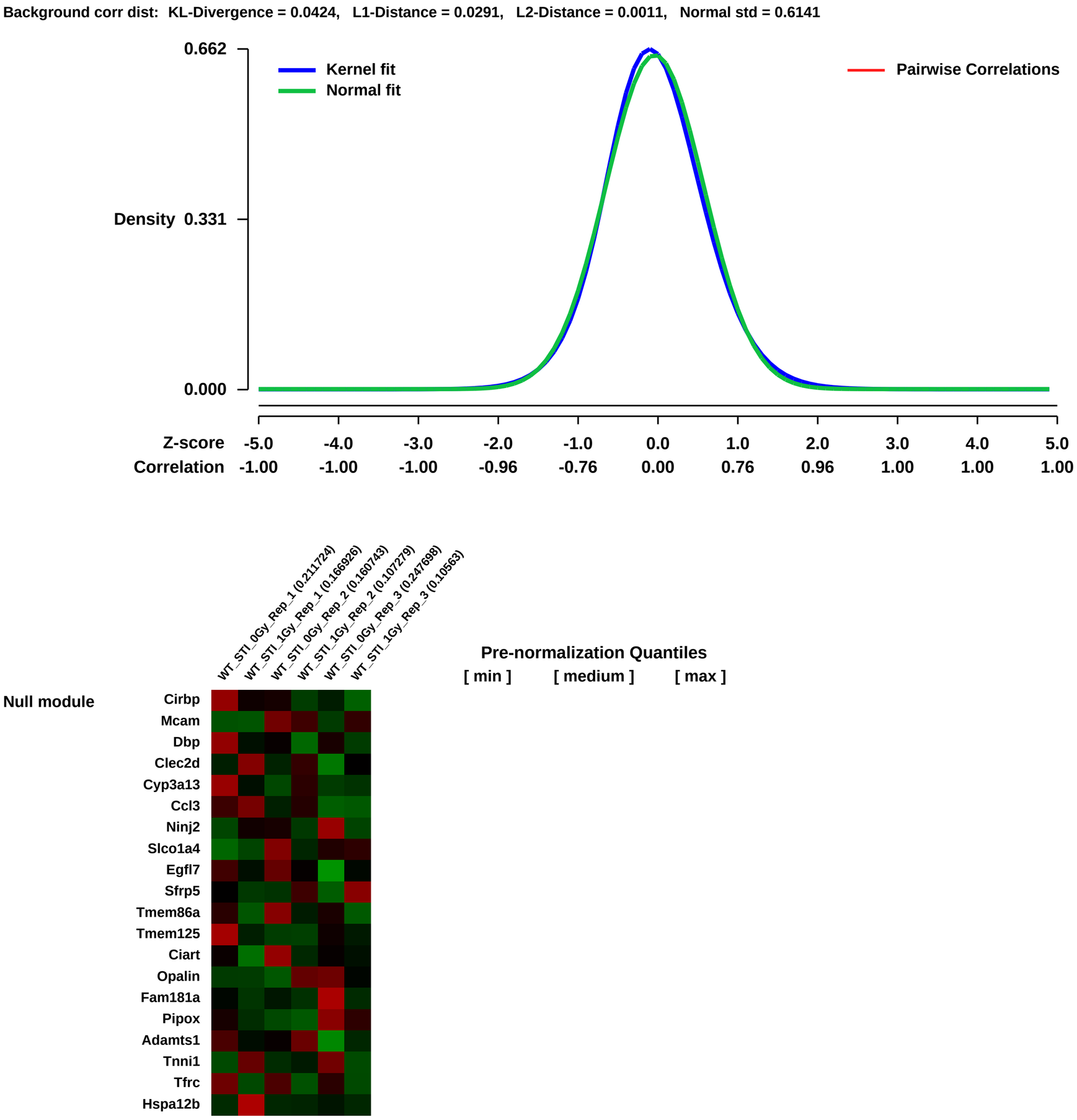

GEO Series "GSE47811" Expression Profiles

Num of samples in this series: 12

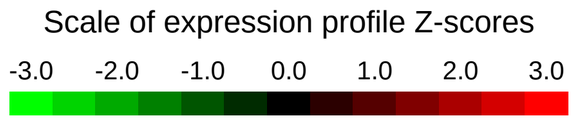

GEO Link:	http://www.ncbi.nlm.nih.gov/geo/query/acc.cgi?acc=GSE47811
Status:	Public on Jun 12 2013
Title:	Pancreatic cancer biomarkers in mouse saliva
Organism:	Mus musculus
Experiment type:	Expression profiling by array
Platform:	GPL1261
Pubmed ID:	23880764
Summary & Design:	**Summary:** This is a pilot study. We are trying to detect potential salivary biomarkers in mice with a pancreatic tumor. Global gene expression profiling has shown great promise in high-throughput biomarker discovery for early disease detection in body fluids such as saliva, which is accessible, cost-effective, and non-invasive. However, this goal has not been fully realized because saliva, like many clinical samples, contains partially fragmented and degraded RNAs that are difficult to amplify and detect with prevailing technologies. Here, using nanogram scale salivary RNA as a proof-of-principle example, we describe our progress with a novel poly-A tail independent mRNA amplification strategy combined with the Affymetrix GeneChip Exon arrays. We defined a Salivary Exon Core Transcriptome (SECT) with highly similar expression profiles in healthy individuals verified by quantitative PCR. Informatics analysis of SECT provided important mechanistic insight to their potential origin and function. Finally we demonstrated the diagnostic potential of true exon level expression profiling approach with salivary exon biomarkers that accurately discriminated gender in healthy individuals. Recent studies have demonstrated that discriminatory salivary biomarkers can be readily detected upon the development of systemic diseases such as pancreatic cancer, breast cancer, lung cancer and ovarian cancer. However, the utility of salivary biomarkers for the detection of systemic diseases has been undermined due to the absence of biological and mechanistic rationale why distal diseases from the oral cavity would lead to the development of discriminatory biomarkers in saliva. Here, we examine the hypothesis that pancreatic tumor-derived exosomes are mechanistically involved in the development of pancreatic cancer-discriminatory salivary transcriptomic biomarkers. We first developed a pancreatic cancer mouse model that yielded discriminatory salivary biomarkers by implanting the mouse pancreatic cancer cell line Pan02 into the pancreas of the syngeneic host C57BL/6. The role of pancreatic cancer-derived exosomes in the development of discriminatory salivary biomarkers was then tested by engineered a Pan02 cell line that is suppressed for exosome biogenesis, implanted into the C56BL/6 mouse and examine if the discriminatory salivary biomarker profile was ablated or disrupted. Suppression of exosome biogenesis results in the ablation of discriminatory salivary biomarker development. This study supports that tumor-derived exosomes provide a mechanism in the development of discriminatory biomarkers in saliva and distal systemic diseases. **Overall design:** We analyzed saliva from 6 healthy mice and 6 mice with a pancreatic tumor using the Affymetrix Mouse Exon Genome 430 2.0 platform. Array data was processed by dChip. No techinical replicates were performed.

Background corr dist: KL-Divergence = 0.1253, L1-Distance = 0.0807, L2-Distance = 0.0154, Normal std = 0.4325

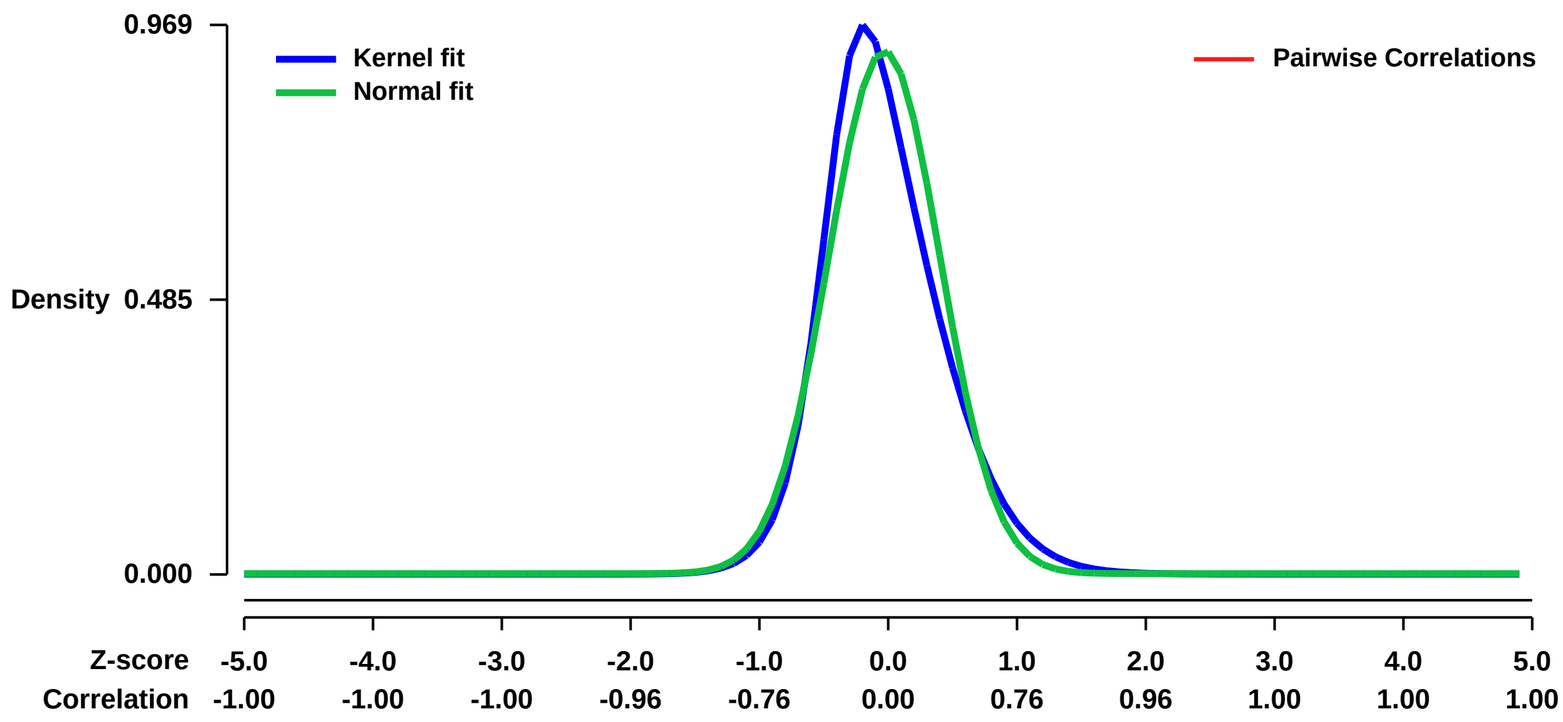

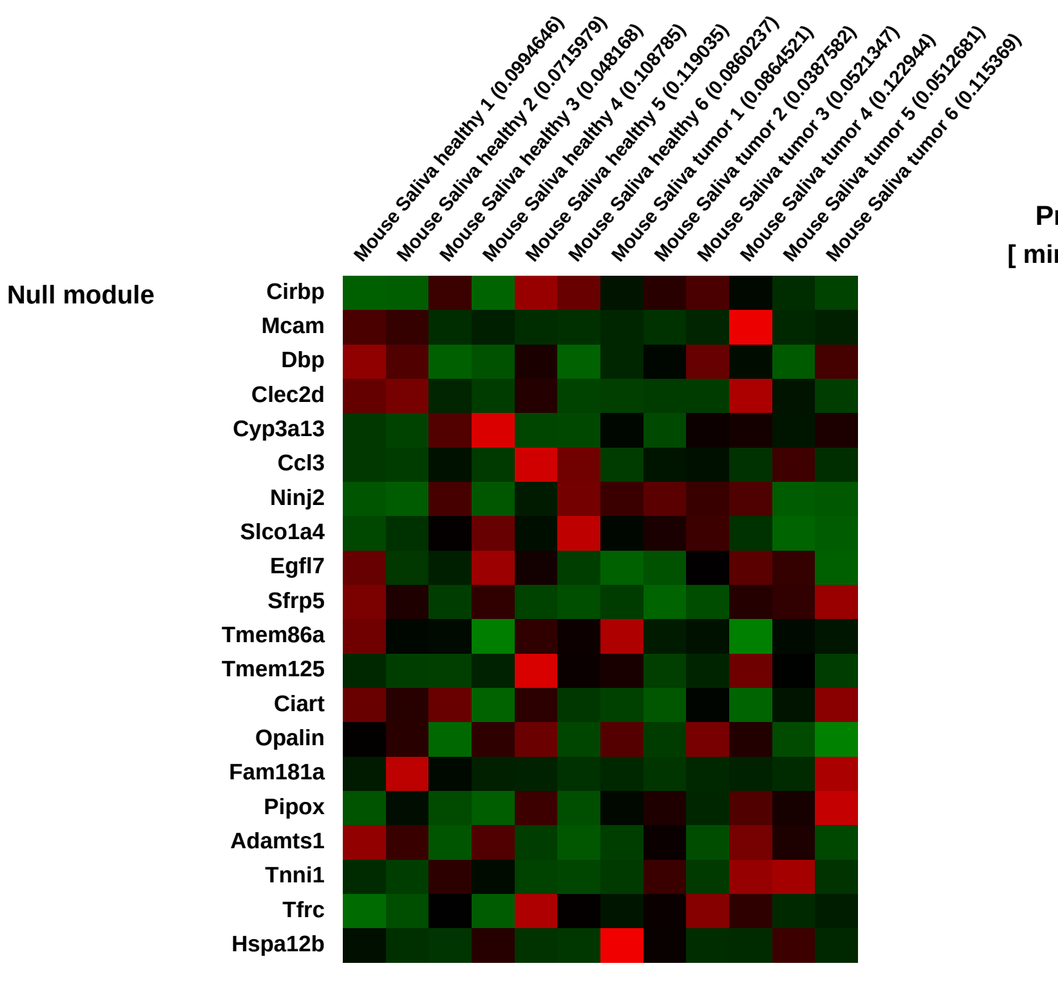

GEO Series "GSE4189" Expression Profiles

Num of samples in this series: 14

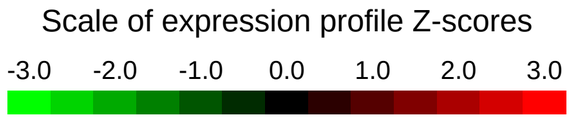

GEO Link:	http://www.ncbi.nlm.nih.gov/geo/query/acc.cgi?acc=GSE4189
Status:	Public on Feb 08 2006
Title:	The Oct4 and Nanog transcription network that regulates pluripotency in mouse embryonic stem cells
Organism:	Mus musculus
Experiment type:	Expression profiling by array
Platform:	GPL1261
Pubmed ID:	16518401
Summary & Design:	**Summary:** **A) We profiled gene expression changes during ES cell differentiation** **B) We profiled gene expression changes when Pou5f1 or Nanog is knockdown upon RNAi** **Keywords: Array Based** **Overall design:** **B) We used siRNA to knockdown Pou5f1 or Nanog in mouse ES cells. The RNAs from control and knockdown cells were hybridized onto Affymetrix Mouse Genome 430 2.0 microarrays**

Background corr dist: **KL-Divergence = 0.0760, L1-Distance = 0.0402, L2-Distance = 0.0021, Normal std = 0.5187**

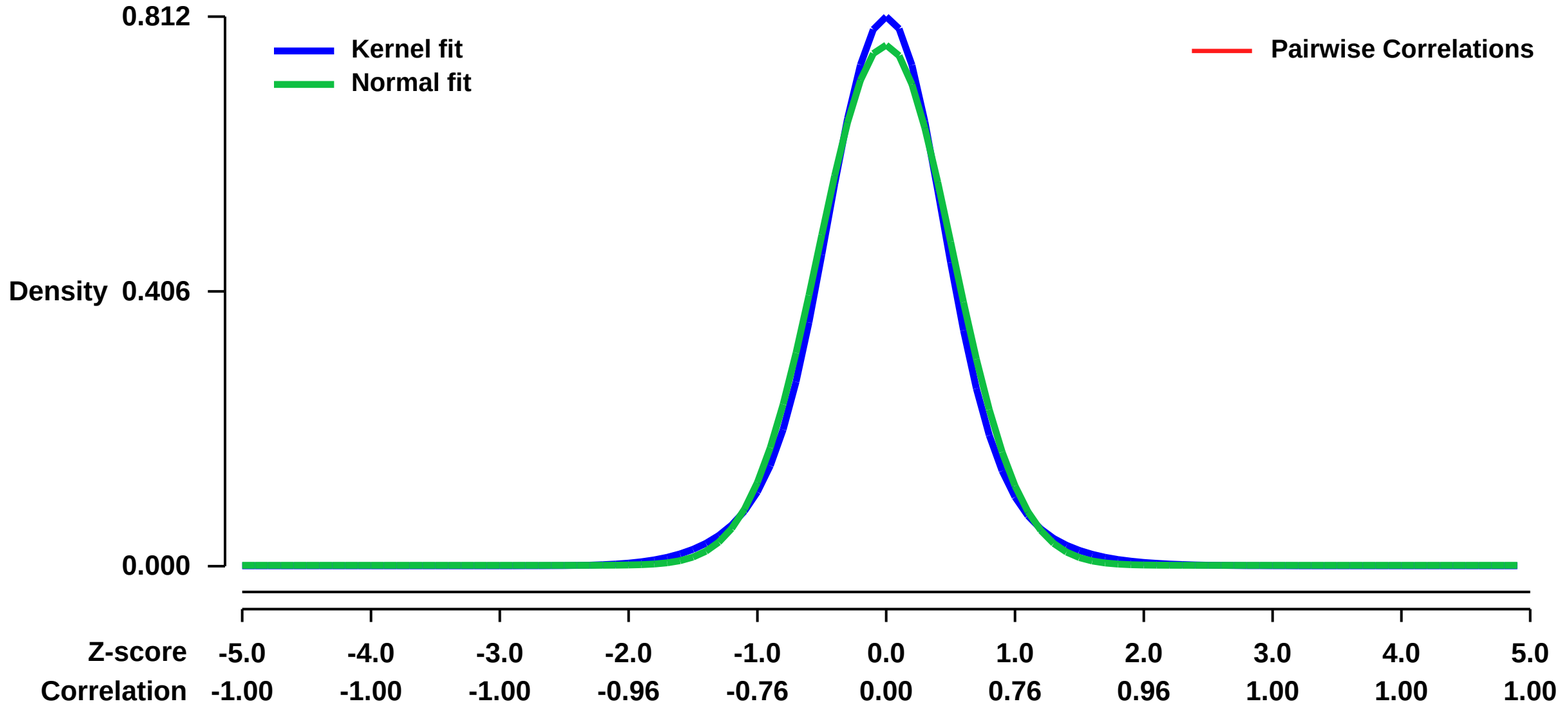

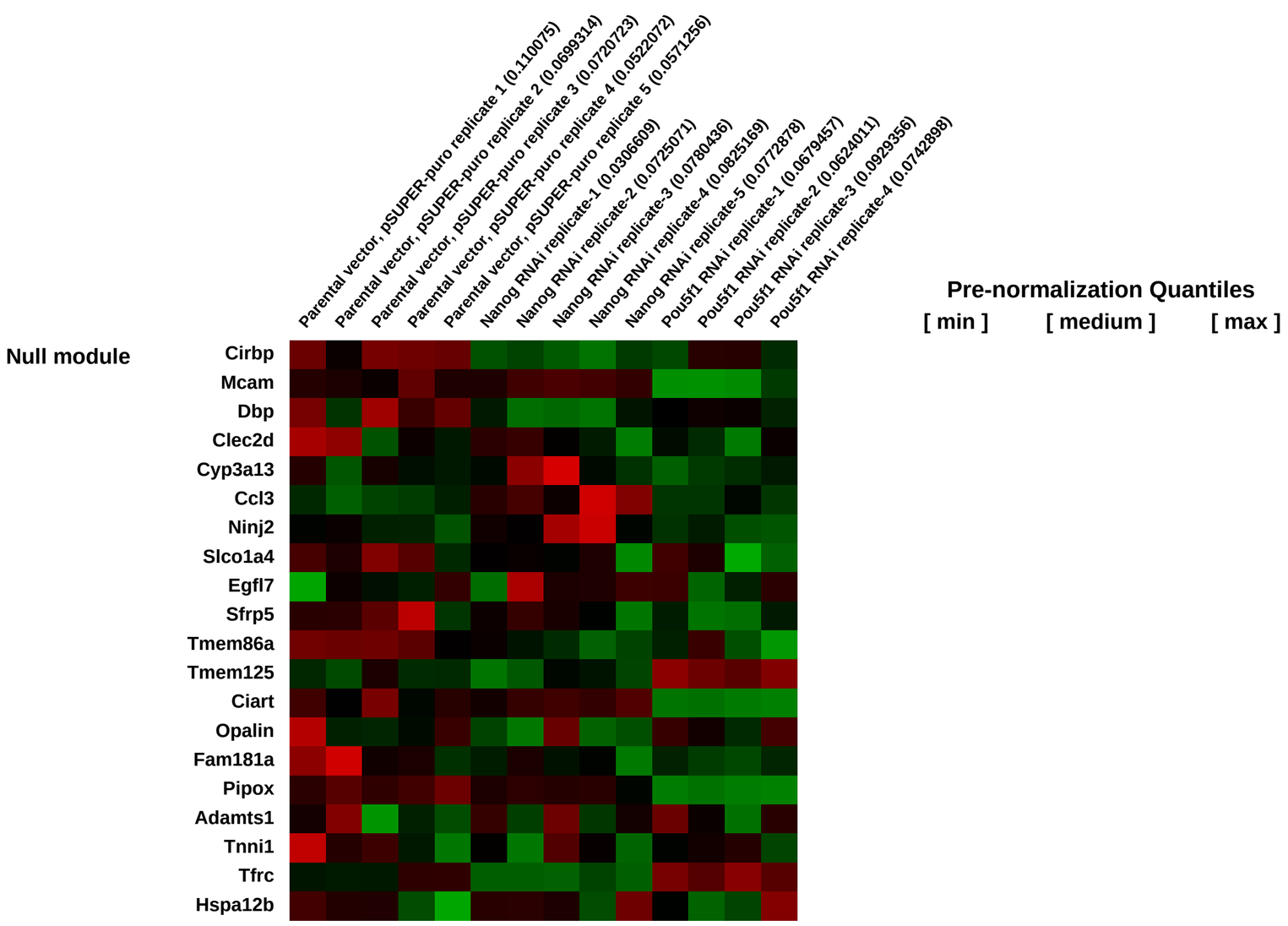

GEO Series "GSE11419" Expression Profiles

Num of samples in this series: 6

Scale of expression profile Z-scores

-3.0 -2.0 -1.0 0.0 1.0 2.0 3.0

GEO Link:	http://www.ncbi.nlm.nih.gov/geo/query/acc.cgi?acc=GSE11419
Status:	Public on Jul 12 2010
Title:	GeneChip expression profiling of Glud1 (glutamate dehydrogenase 1) transgenic mice
Organism:	Mus musculus
Experiment type:	Expression profiling by array
Platform:	GPL1261
Pubmed ID:	20529287
Summary & Design:	**Summary:** **Glud1 (glutamate dehydrogenase 1) transgenic mice release more excitatory neurotransmitter glutamate to synaptic cleft throughout lifespan and show signs of accelerated aging.** **Here we compared transcriptomic profiles of these animals to their wild-type counterparts. The hippocampus was used for the analysis.** **Keywords: transgenic analysis** **Overall design:** **Three Glud1 transgenic mice vs. three age-matched wide-type mice. Age: 9-month-old. Tissue: hippocampus.**

Background corr dist: **KL-Divergence = 0.0484, L1-Distance = 0.0189, L2-Distance = 0.0004, Normal std = 0.5788**

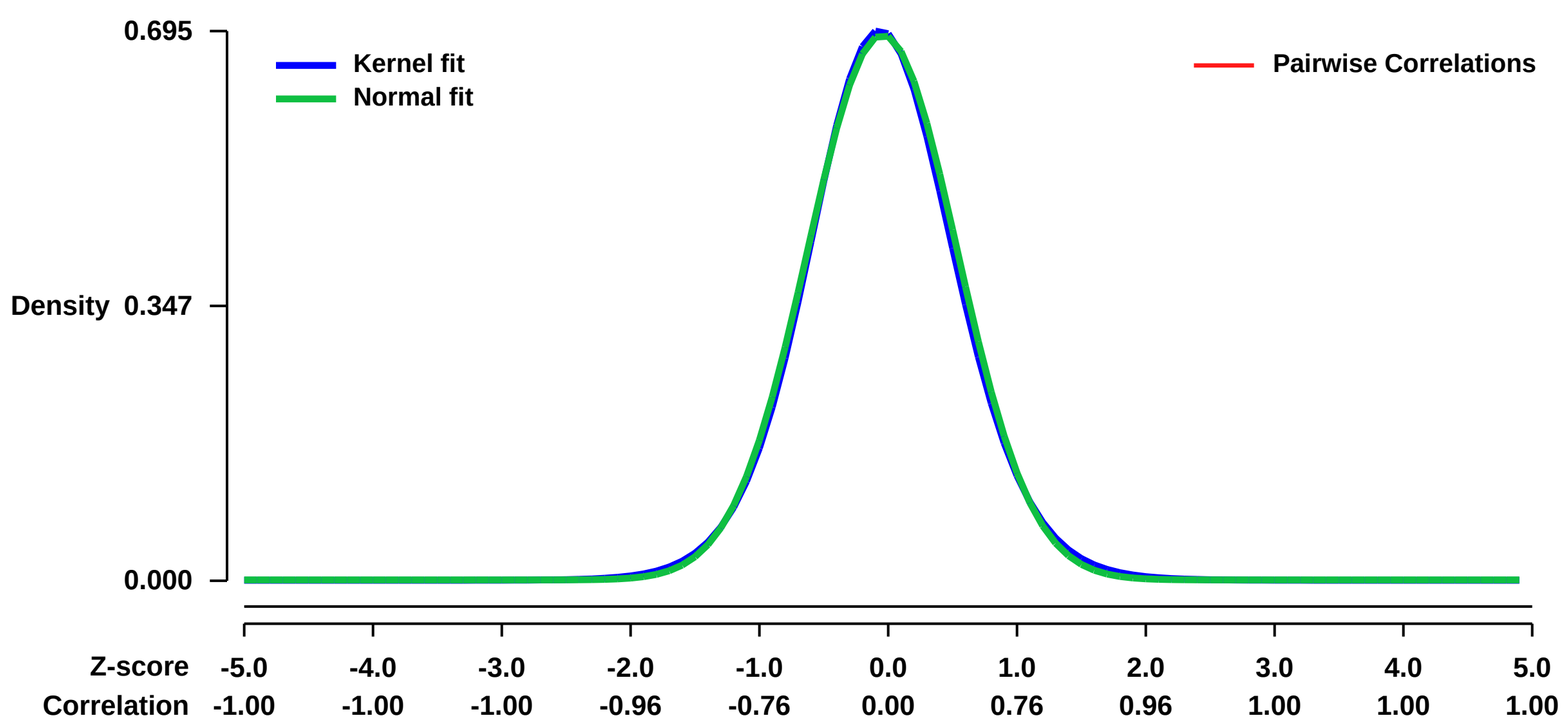

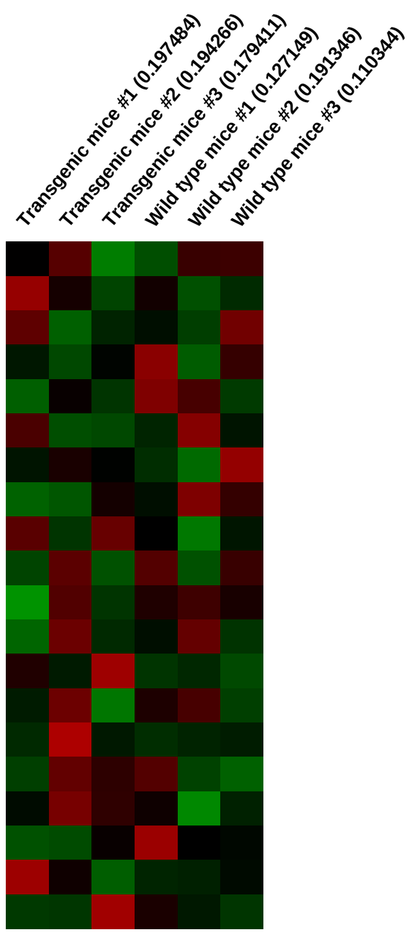

GEO Series "GSE12956" Expression Profiles

Num of samples in this series: 10

Scale of expression profile Z-scores

-3.0 -2.0 -1.0 0.0 1.0 2.0 3.0

GEO Link:	http://www.ncbi.nlm.nih.gov/geo/query/acc.cgi?acc=GSE12956
Status:	Public on Feb 26 2010
Title:	Arx acts as a key selector gene of the ventral telencephalon mainly through its repression transcriptional activity
Organism:	Mus musculus
Experiment type:	Expression profiling by array
Platform:	GPL1261
Pubmed ID:	23968833
Summary & Design:	**Summary:** The homeobox containing gene Arx is expressed during ventral telencephalon development and it is required for correct GABAergic interneuron tangential migration from the ganglionic eminences to the olfactory bulbs, cerebral cortex and striatum. Its human ortholog is associated with a variety of neurological clinical manifestations whose syntoms are compatible with a loss of cortical interneurons and altered basal ganglia related-activities in humans. Herein, we reported the identification by global expression profiling of a group of genes whose expression is consistently altered in Arx mutant ganglionic eminences. Following analysis revealed the striking ectopic expression in the ganglionic eminences of a number of genes normally not, or only marginally, expressed in the ventral telencephalon. Among them, we functionally analyzed Ebf3, whose ectopic expression in ventral telencephalon is preventingneuronal tangential migration. Further, we showed that Arx is sufficient to repress Ebf3 endogenous expression and that its silencing in Arx mutant tissue might marginally rescue tangential cell movements. Together, these data provide an initial analysis of the molecular pathways regulated by Arx and how their networking might regulate those specific cellular processes during telencephalon development strongly altered by loss of Arx. **Overall design:** Three timed-pregnant Arx heterozygous dams crossed with C57Bl/6 males were sacrificed at E14.5, the embryos harvested and placed into cold PBS. After brain isolarion, meninges and olfactory bulbs were removed, and the ventral telencephalon separated from the overlying cerebral cortex. The same procedure was repeated for 5 wt and 5 Arx mutant embryos.

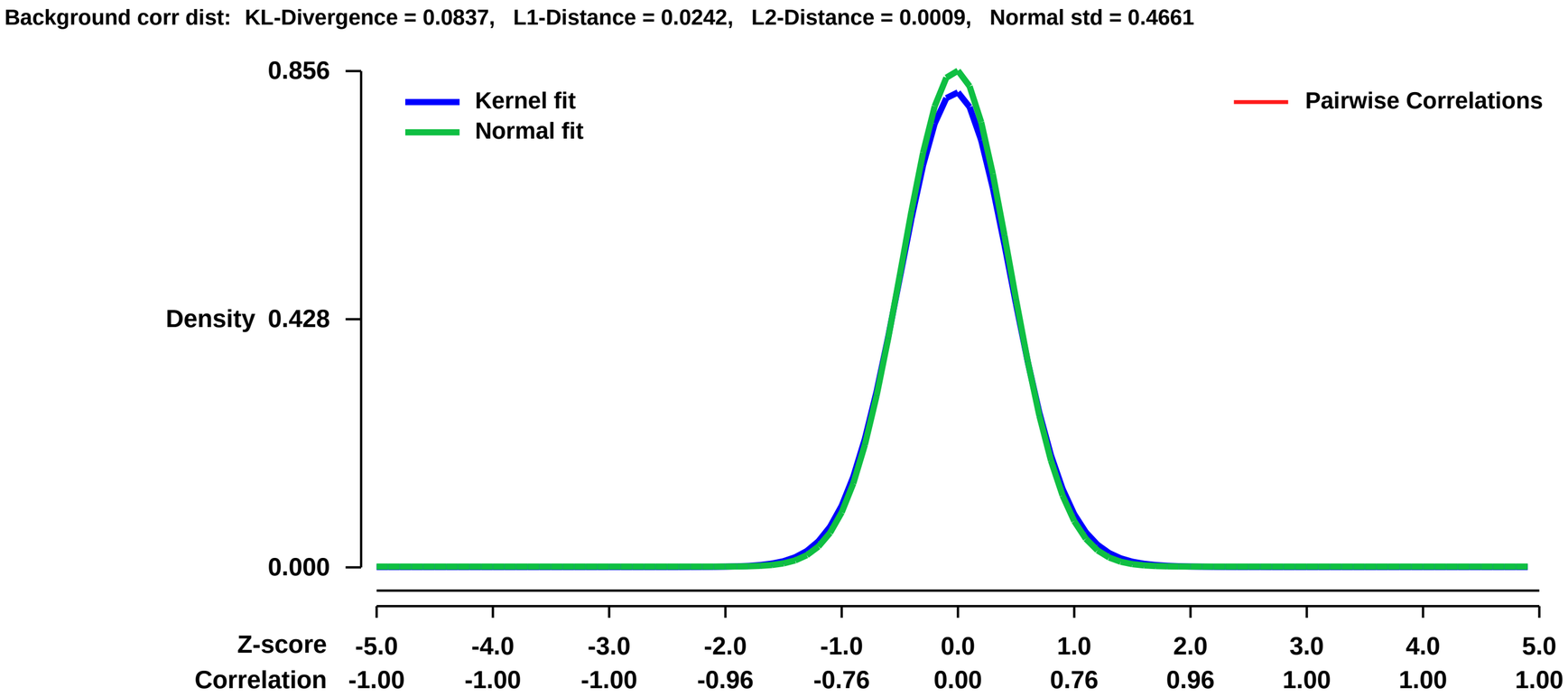

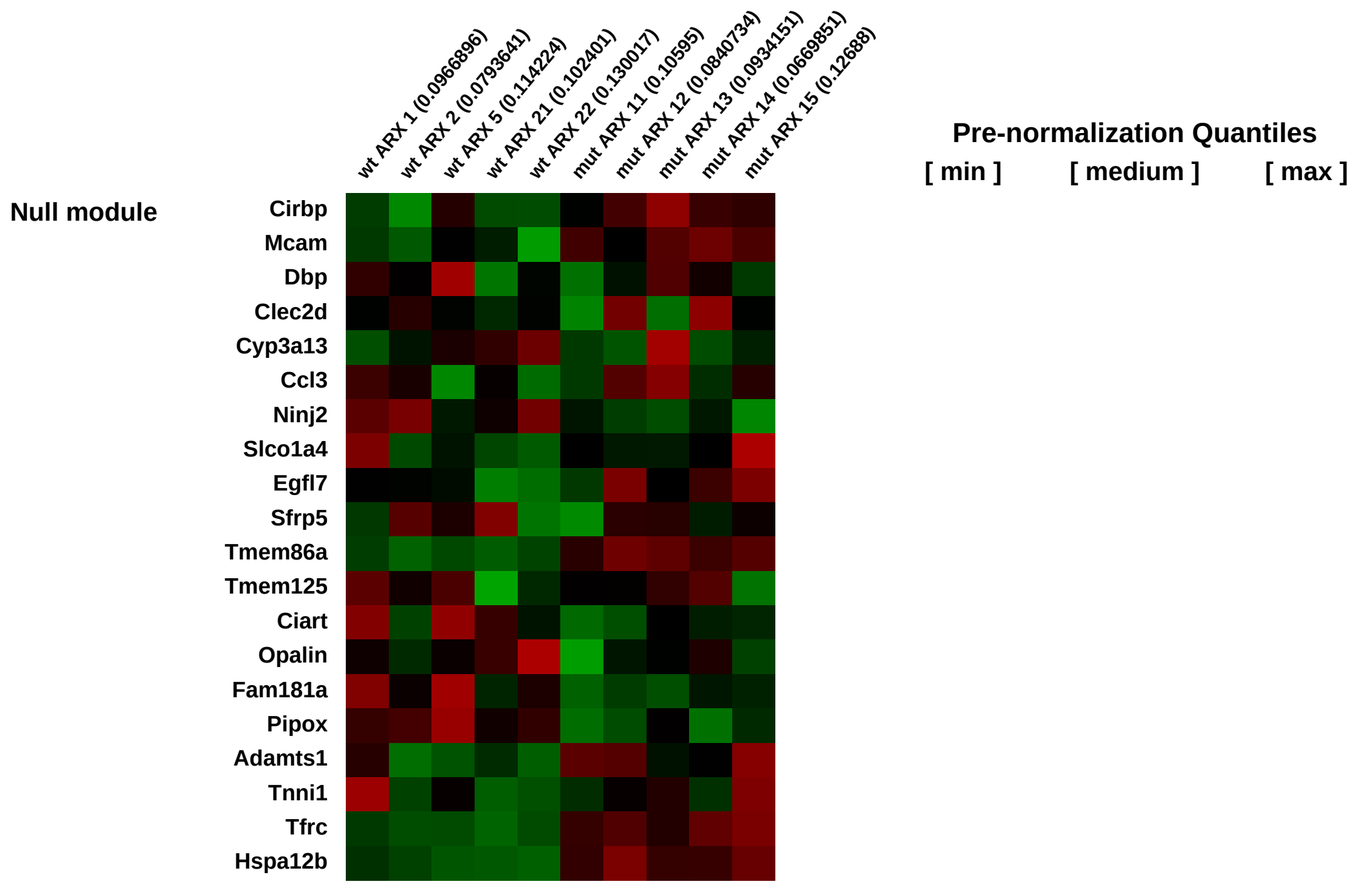

GEO Series "GSE5921" Expression Profiles

Num of samples in this series: 6

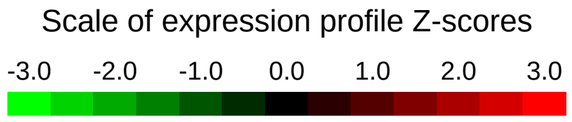

GEO Link:	http://www.ncbi.nlm.nih.gov/geo/query/acc.cgi?acc=GSE5921
Status:	Public on Sep 26 2007
Title:	Differential expression of BMP4-regulated genes associated with commitment of C3H10T1/2 cells into adipocytes
Organism:	Mus musculus
Experiment type:	Expression profiling by array
Platform:	GPL1261
Pubmed ID:	17204246
Summary & Design:	**Summary:** C3H10T1/2 stem cells are committed to the adipocyte lineage by treatment with BMP-4 and grown to postconfluence. When subjected to our standard differentiation protocol, the committed cells differentiate into adipocytes in a manner indistinguishable from that of 3T3-L1 preadipocytes. In contrast, C3H10T1/2 cells not committed with BMP-4 remain undifferentiated despite treatment with differentiation inducers. The molecular basis of the commitment process, however, has not been elucidated. Since postconfluent uncommitted and committed C3H10T1/2 cells respond differently to the differentiation inducers, it was reasoned that the two cell types differed at the gene expression level. Therefore, we undertook microarray gene expression profiling to detect changes between the two cell populations at postconfluence to identify expressed genes that may be responsible for the dramatic change in phenotype. **Keywords: control vs treated** **Overall design:** C3H10T1/2 cells were plated and treated with 50 ng/ml BMP4 and grown to postconfluence. Control samples were treated in the same manner were not given BMP4. Total RNA was collected at postconfluence. There were 3 replicates each for control and treated cells.

Background corr dist: KL-Divergence = 0.0414, L1-Distance = 0.0193, L2-Distance = 0.0004, Normal std = 0.6115

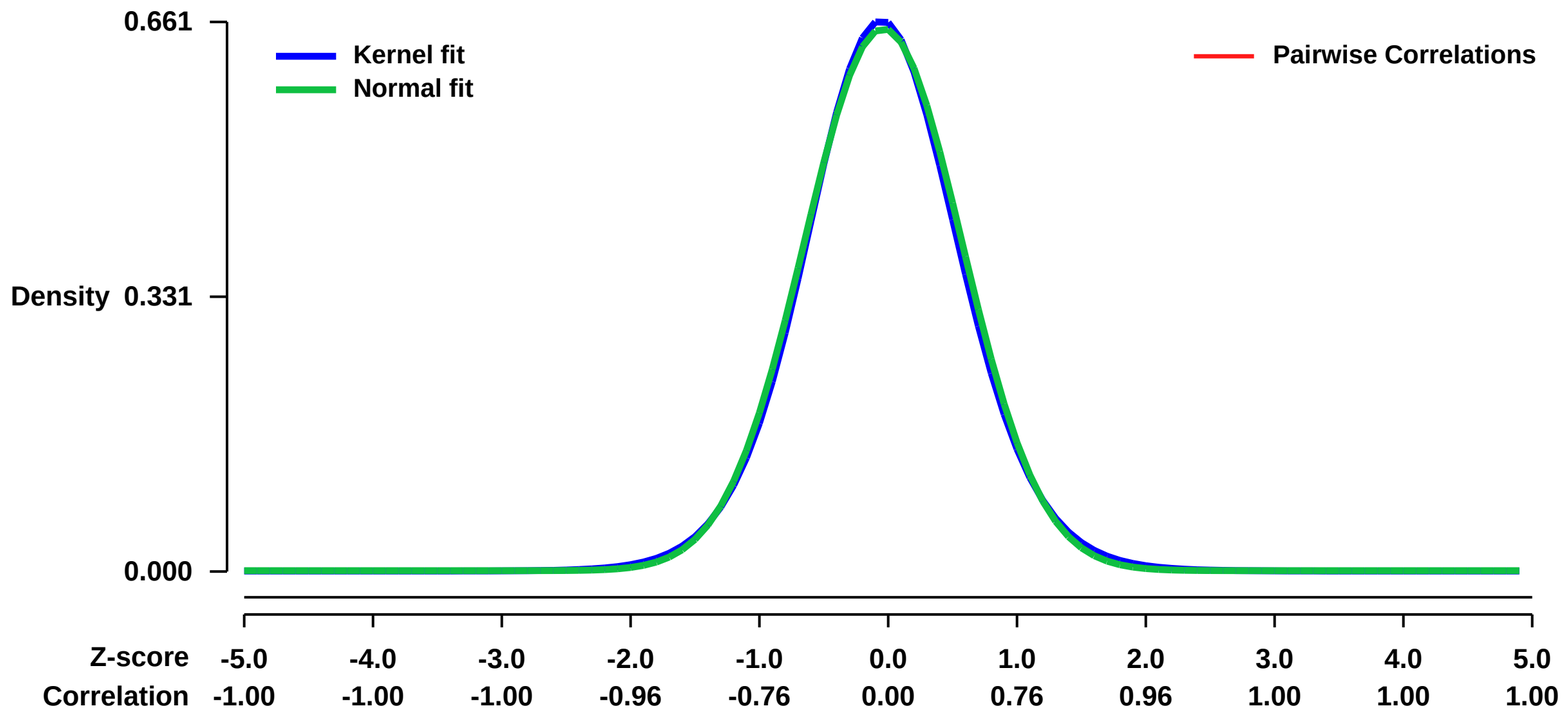

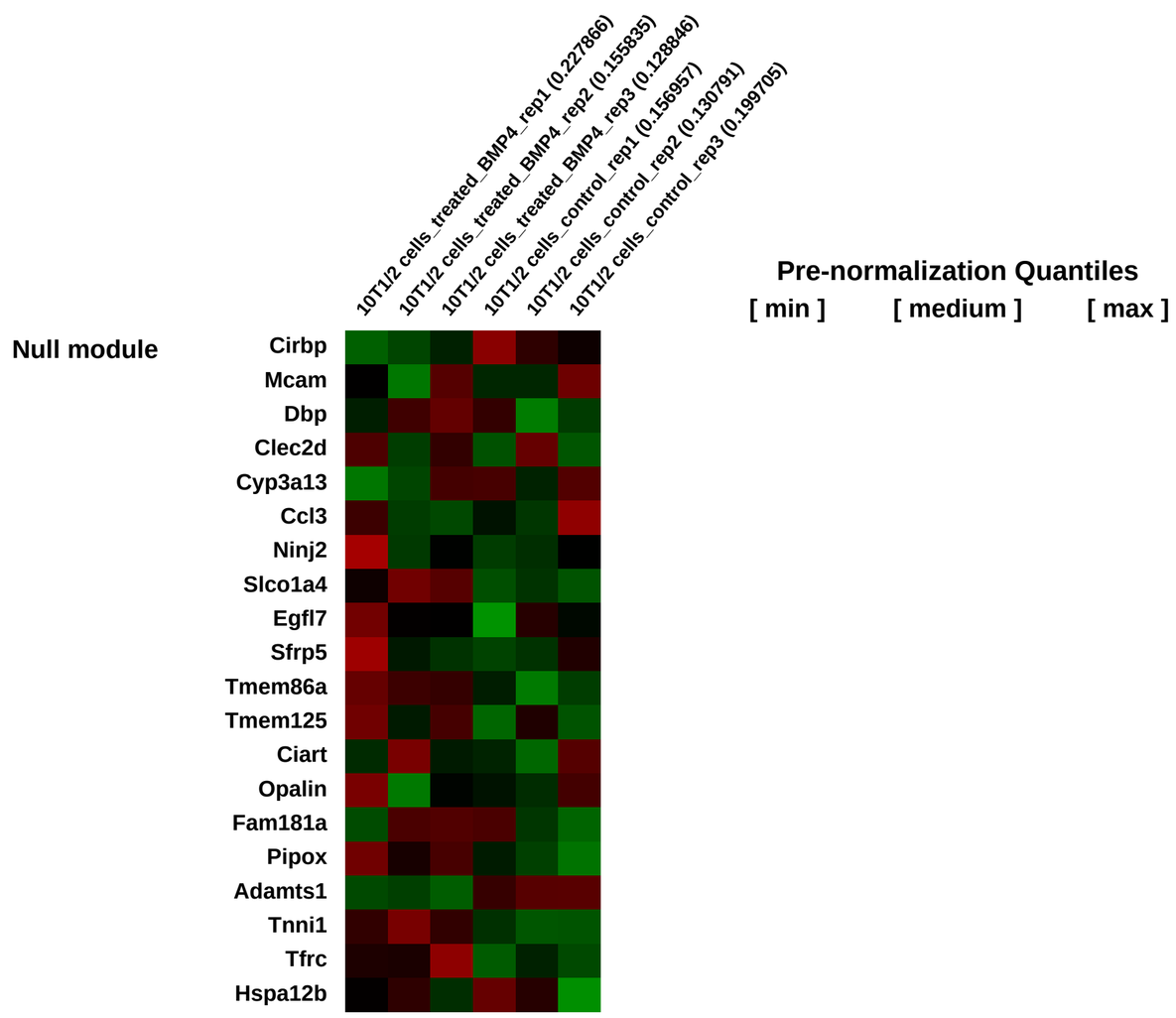

GEO Series "GSE36665" Expression Profiles

Num of samples in this series: 6

Scale of expression profile Z-scores

-3.0 -2.0 -1.0 0.0 1.0 2.0 3.0

GEO Link:	http://www.ncbi.nlm.nih.gov/geo/query/acc.cgi?acc=GSE36665
Status:	Public on Apr 15 2012
Title:	Gene expression profiling of Wwox targeted ablation in mouse mammary epithelial cells
Organism:	Mus musculus
Experiment type:	Expression profiling by array
Platform:	GPL1261
Pubmed ID:	22574198
Summary & Design:	**Summary:** The WWOX gene has been implicated in human cancers, including breast cancer.The development and tumorigenesis between human and mouse mammary glands (MGs) share similar molecular details and signal transduction pathways. We established mouse line that specifically knockout the expression of WWOX gene in the MG epithelial cells (MECs) by crossing BK5-cre mice with our WWOX flox stain. In order to study the gene expression profile in the subpopulation MECs, we isolated the organoids from the 4th MGs of both BK5-cre +; WWOX flox/flox (KO) mice and their WT counterparts (BK5-cre -; WWOX flox/flox), 3 mice each genotype. The total RNA from the mouse MG organoids was extracted and purified by TRIzol/RNeasy Kit and their integrity was checked on Agilent RNA 6000 Nanochip. The goal is to identify the significant perturbation in tumorigenic pathways in these cells induced by WWOX ablation. **Overall design:** Mammary gland epithelial organoids samples and gene expression profiles were deribed from three WWOX-KO mice (BK5-cre +; WWOX flox/flox) and from three WWOX-WT mice (BK5-cre -; WWOX flox/flox)

Background corr dist: KL-Divergence = 0.0345, L1-Distance = 0.0188, L2-Distance = 0.0004, Normal std = 0.6428

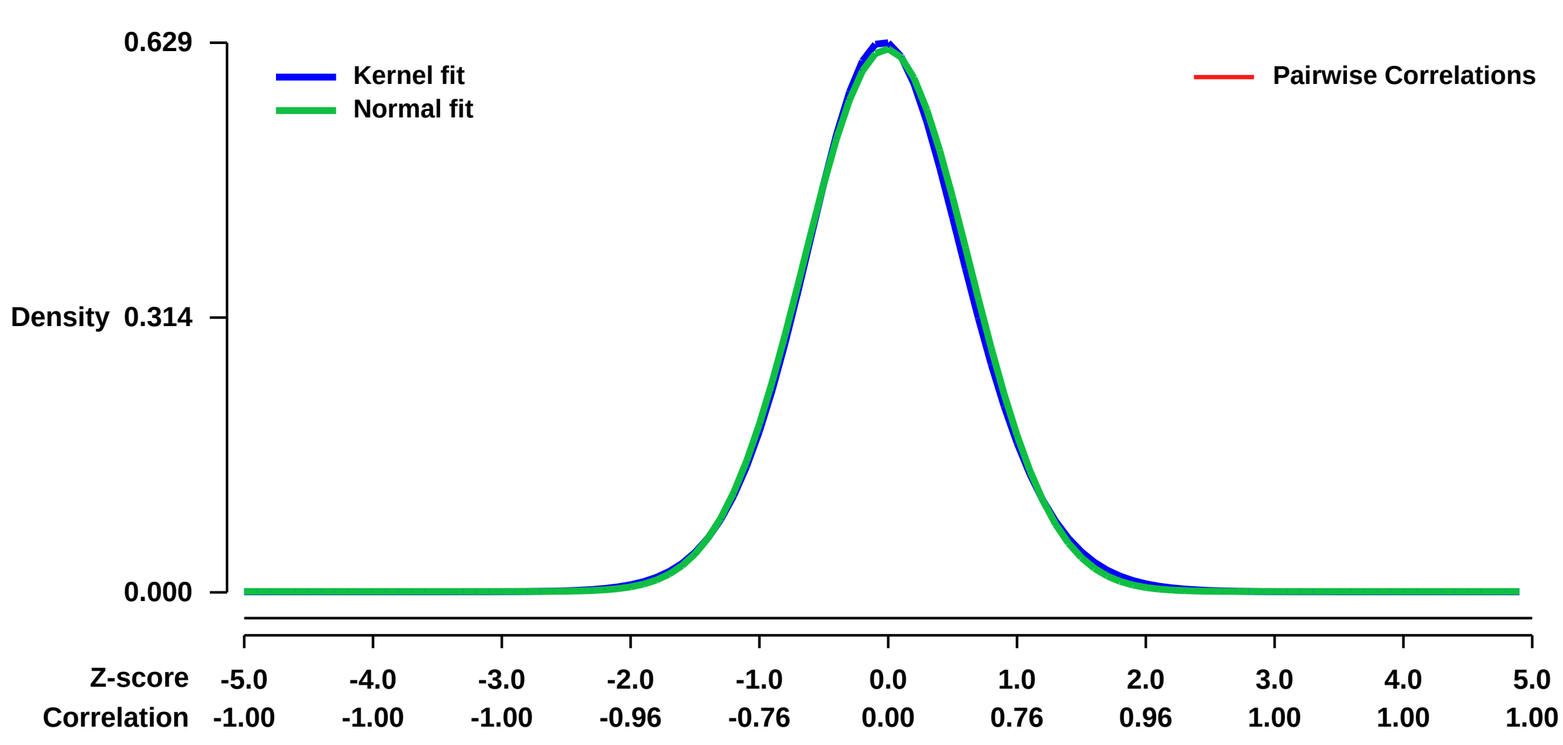

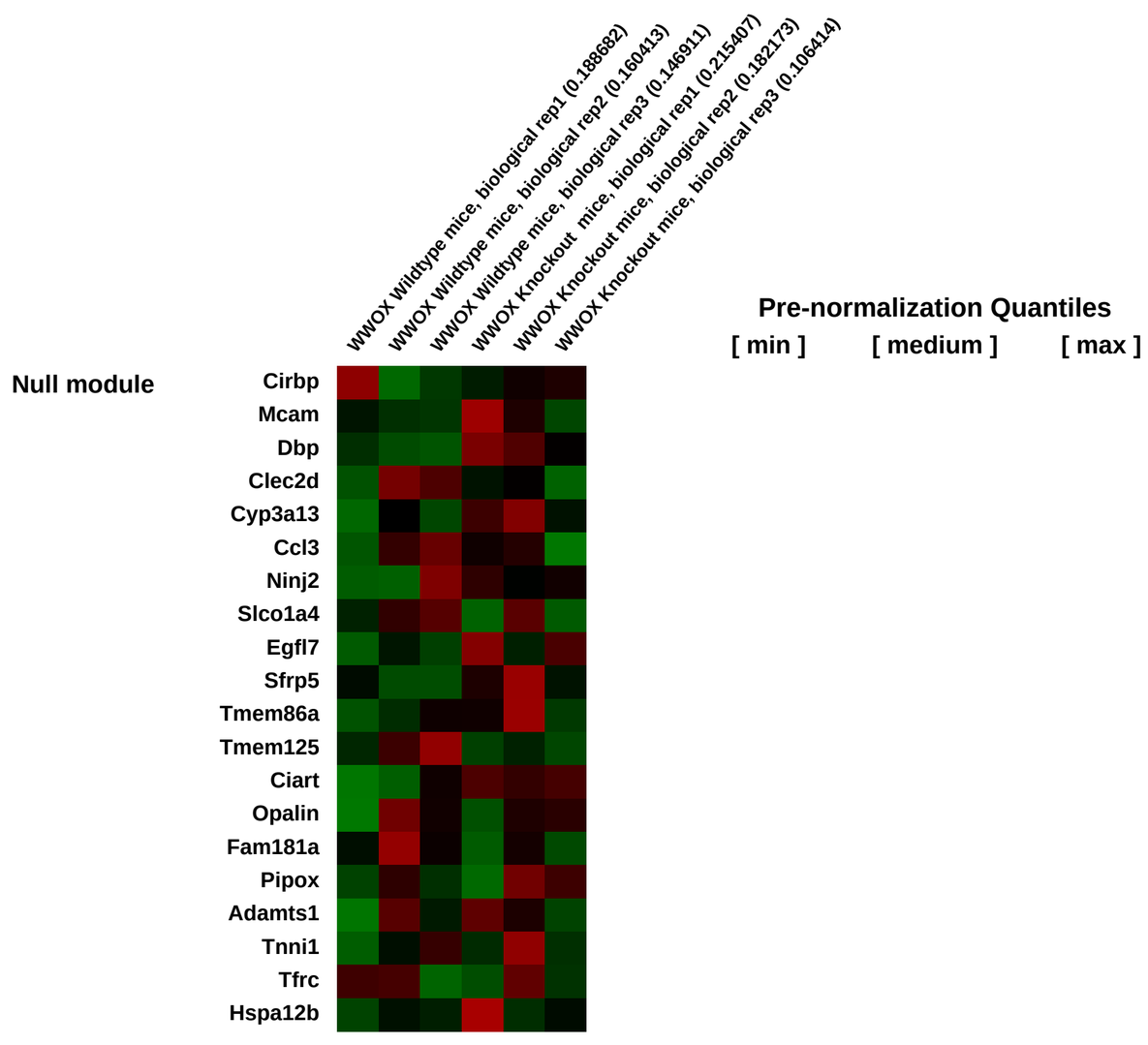

GEO Series "GSE11274" Expression Profiles

Num of samples in this series: 20

Scale of expression profile Z-scores

-3.0 -2.0 -1.0 0.0 1.0 2.0 3.0

GEO Link:	http://www.ncbi.nlm.nih.gov/geo/query/acc.cgi?acc=GSE11274
Status:	Public on Jul 15 2009
Title:	Induction of Pluripotency in Adult Unipotent Germline Stem Cells
Organism:	Mus musculus
Experiment type:	Expression profiling by array
Platform:	GPL1261
Pubmed ID:	19570517
Summary & Design:	**Summary:** Mouse and human stem cells with features similar to those of embryonic stem cells have been derived from testicular cells. Although pluripotent stem cells have been obtained from defined germline stem cells (GSCs) of mouse neonatal testis, only multipotent stem cells have been obtained so far from defined cells of mouse adult testis. In this study we describe a robust and reproducible protocol for obtaining germline-derived pluripotent stem (gPS) cells from adult unipotent GSCs. Pluripotency of gPS cells was confirmed by in vitro and in vivo differentiation, including germ cell contribution and transmission. As determined by clonal analyses, gPS cells indeed originate from unipotent GSCs. We propose that the conversion process requires a GSC culture microenvironment that depends on the initial number of plated GSCs and the length of culture time. **Overall design:** - ESC_like_3

Background corr dist: KL-Divergence = 0.1113, L1-Distance = 0.0446, L2-Distance = 0.0038, Normal std = 0.4495

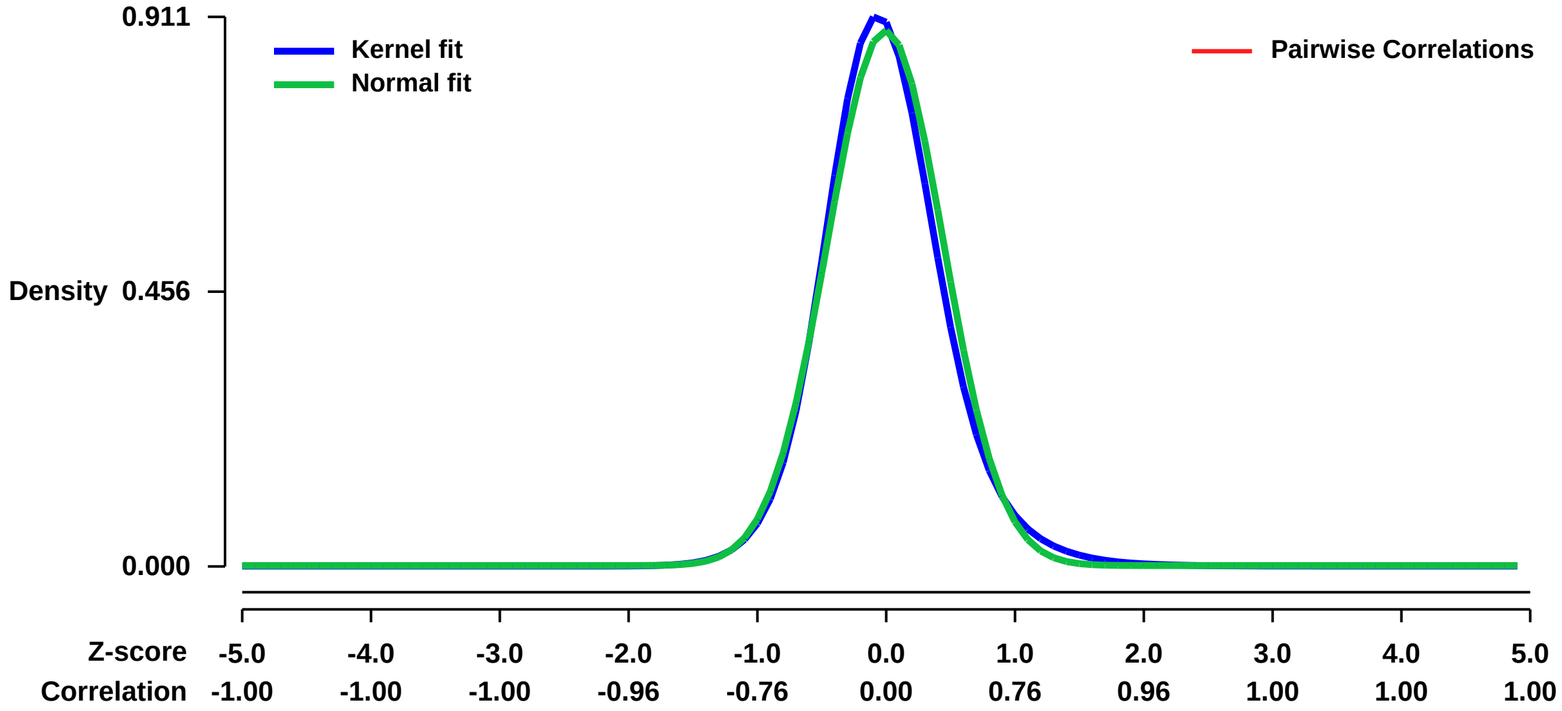

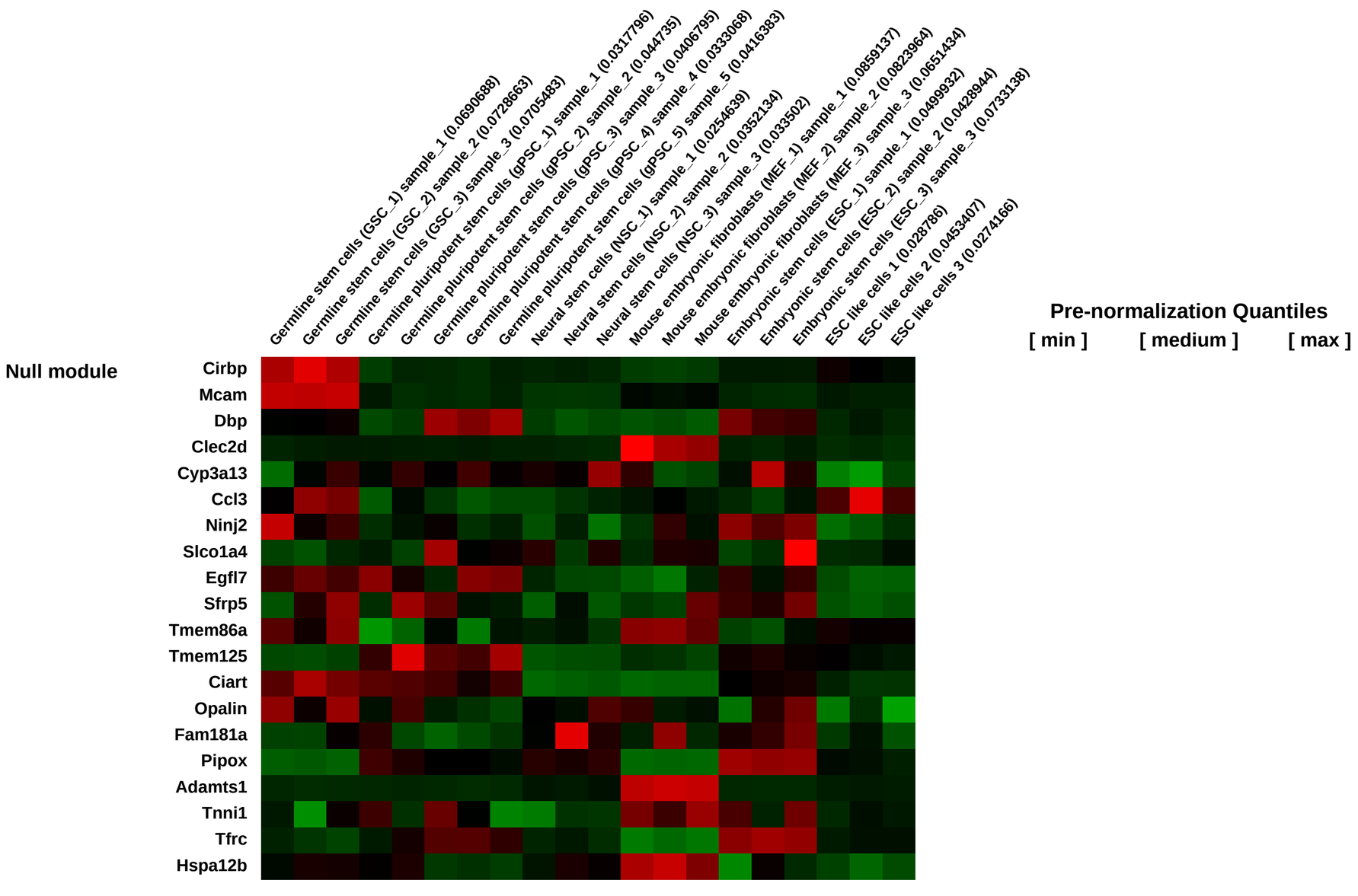

GEO Series "GSE22922" Expression Profiles

Num of samples in this series: 8

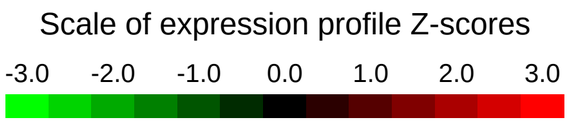

GEO Link: http://www.ncbi.nlm.nih.gov/geo/query/acc.cgi?acc=GSE22922

Status: Public on Jan 30 2013

Title: The Molecular Signature Induced by HMGA1 During Lymphoid Tumorigenesis

Organism: Mus musculus

Experiment type: Expression profiling by array

Platform: GPL1261

Pubmed ID:

Summary & Design:

Summary:
We are exploring the molecular pathways activated during lymphoid transformation with the long term goal of developing better therapies. Our focus is the HMGA1a oncogene because our studies indicate that it plays an important role in aggressive human lymphoid leukemia and lymphoma. We have developed the transgenic mouse over-expressing HMGA1a in lymphoid cells that develop aggressive lymphoid tumors by 8-10 months with histopathologic findings resembling human T-cell acute lymphocytic leukemia. By analyzing the gene expression profiles of our HMGA1a mouse model we plan to identify molecular pathways activated by HMGA1a in lymphoid transformation. Results from these studies will enhance our understanding of the pathogenesis of lymphoid malignancies and should lead to the development of better therapies.

Overall design:
A total of 20,669 genes represented on the Affymetrix Mouse 430 2.0 GeneChipTM array were screened with cRNA prepared from lymphoid cells of HMGA1a transgenic mice at different stages in tumorigenesis. These mice develop lymphoid tumors with complete penetrance at 8-12 months of age. We isolated RNA from splenocytes at 2 months (before tumors develop) and at 12 months (after tumors are well-established). These results were compared to splenocytes from control littermates. We used two statistical approaches to define differentially expressed genes, including a parametric (Partek genomics suite analysis) and nonparametric (CAM) approach.

Background corr dist: KL-Divergence = 0.0637, L1-Distance = 0.0182, L2-Distance = 0.0004, Normal std = 0.5171

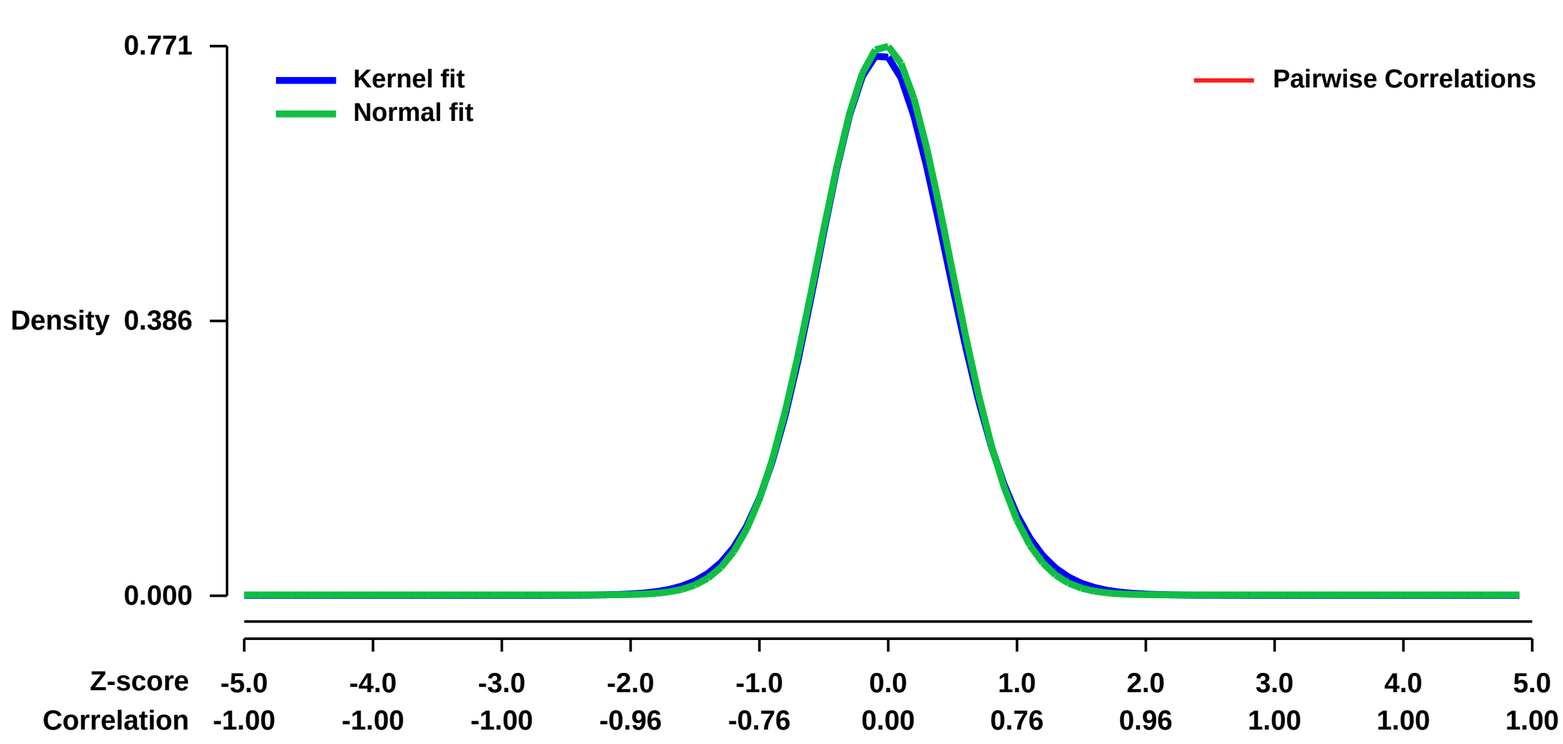

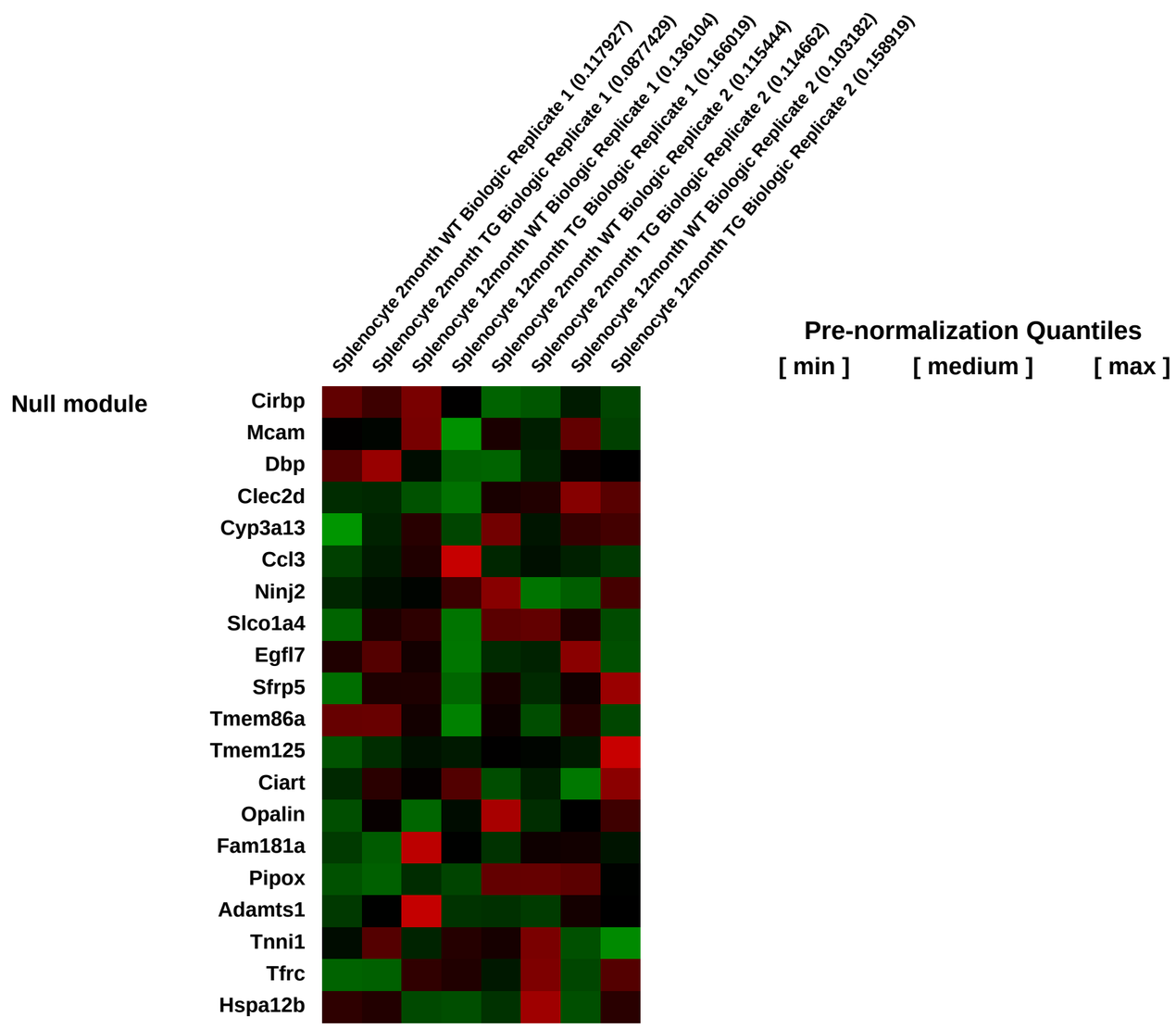

GEO Series "GSE46242" Expression Profiles

Num of samples in this series: 12

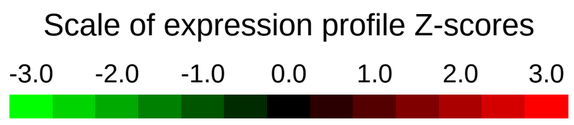

GEO Link:	http://www.ncbi.nlm.nih.gov/geo/query/acc.cgi?acc=GSE46242
Status:	Public on Apr 21 2013
Title:	Egr2-dependent expression in T cell anergy
Organism:	Mus musculus
Experiment type:	Expression profiling by array
Platform:	GPL1261
Pubmed ID:	23548837
Summary & Design:	**Summary:** T cell anergy is one of the mechanisms contributing to peripheral tolerance, particularly in the context of progressively growing tumors and in tolerogenic treatments promoting allograft acceptance. We recently reported that early growth response gene 2 (Egr2) is a critical transcription factor for the induction of anergy in vitro and in vivo, which was identified based on its ability to regulate the expression of inhibitory signaling molecules diacylglycerol kinase (DGK)-a and -z. We reasoned that other transcriptional targets of Egr2 might encode additional factors important for T cell anergy and immune regulation. Thus, we conducted two sets of genome-wide screens: gene expression profiling of wild type versus Egr2-deleted T cells treated under anergizing conditions, and a ChIP-Seq analysis to identify genes that bind Egr2 in anergic cells. Merging of these data sets revealed 49 targets that are directly regulated by Egr2. Among these are inhibitory signaling molecules previously reported to contribute to T cell anergy, but unexpectedly, also cell surface molecules and secreted factors, including lymphocyte-activation gene 3 (Lag3), Class-I-MHC-restricted T cell associated molecule (Crtam), Semaphorin 7A (Sema7A), and chemokine CCL1. These observations suggest that anergic T cells might not simply be functionally inert, and may have additional functional properties oriented towards other cellular components of the immune system. **Overall design:** T cell-specific Egr2 deletion was mediated by use of a Cre-expressing adenovirus and a CAR Tg x Egr2flox/flox mouse in which CAR is expressed exclusively in the T cell compartment from a Lck promoter/CD2 enhancer cassette. OVA-specific Th1 cell clones were generated from CAR Tg x Egr2flox/flox mice. CAR Tg x Egr2flox/flox Th1 T cells were infected with an empty (EV) or a Cre-expressing adenovirus. Upon confirmation of Egr2 deletion by immunoblot, the T cells were left untreated (Control) or anergized (Anergic) by immobilized anti-CD3 for 16 hours, and microarray was conducted after 1 day of rest in culture medium. The microarray analysis was performed three times using three sets of independently manipulated samples

Background corr dist: KL-Divergence = 0.0916, L1-Distance = 0.0260, L2-Distance = 0.0009, Normal std = 0.4594

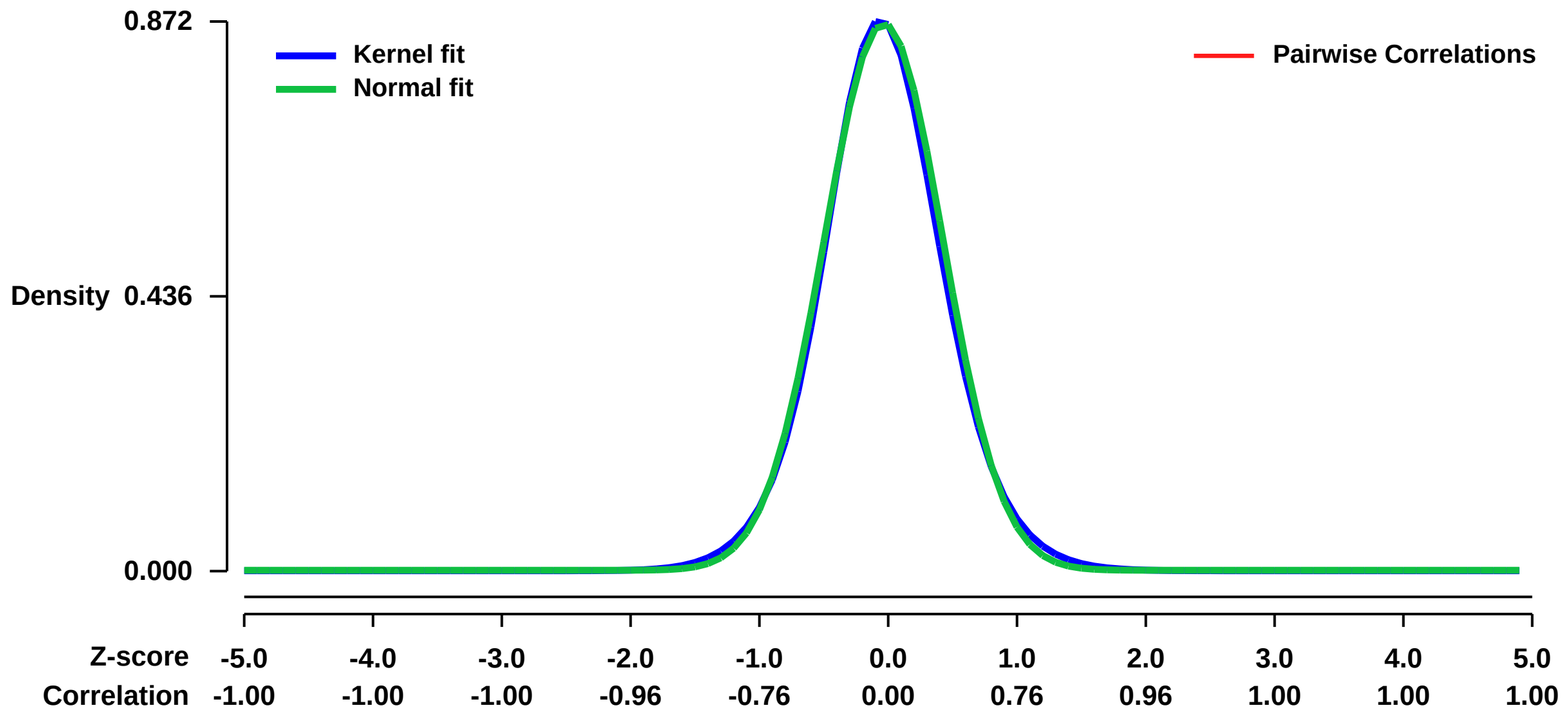

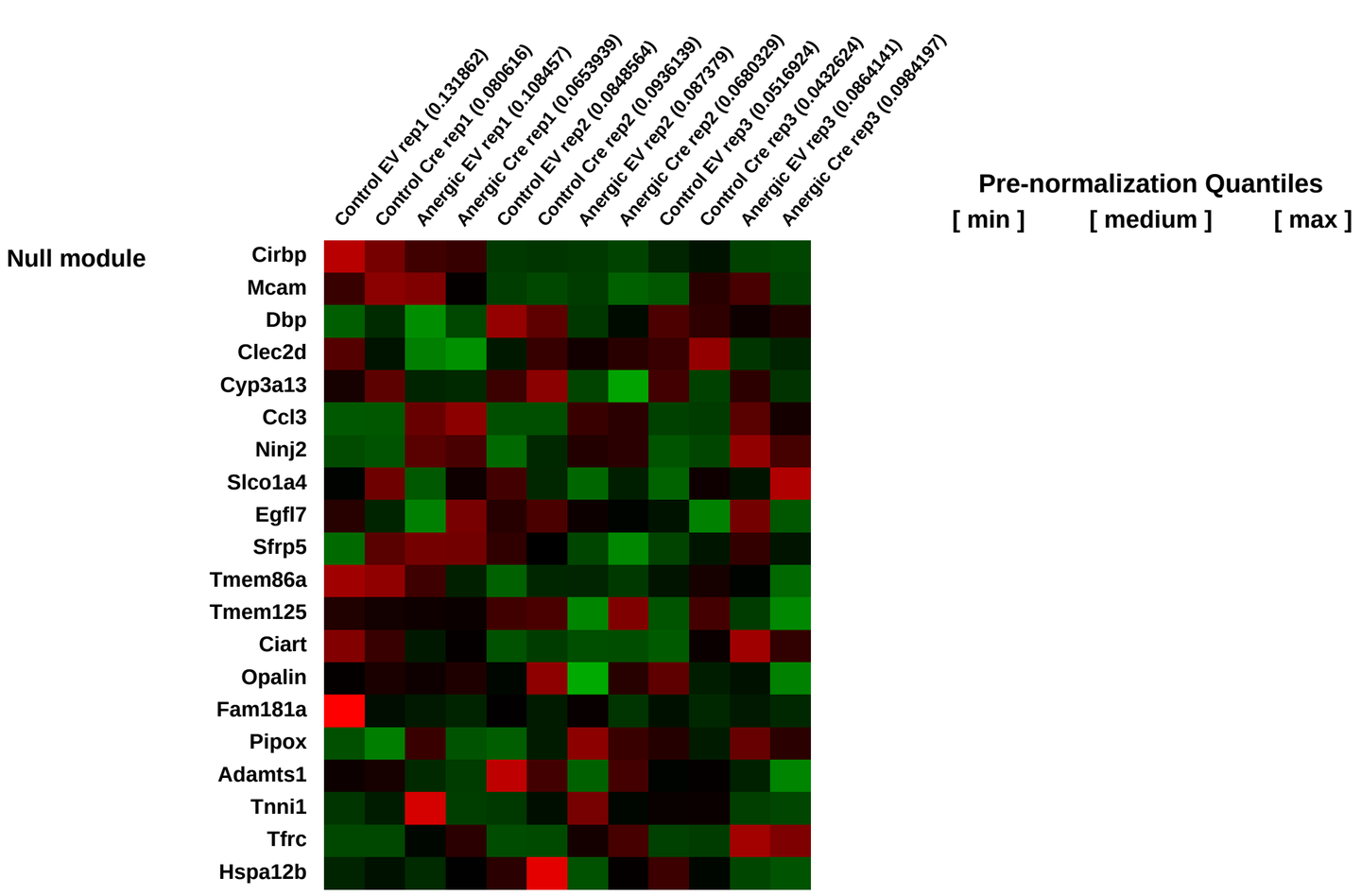

GEO Series "GSE2433" Expression Profiles

Num of samples in this series: 10

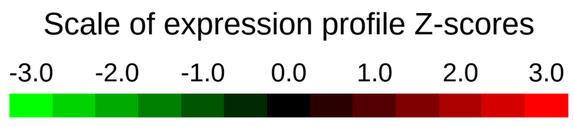

GEO Link:	**http://www.ncbi.nlm.nih.gov/geo/query/acc.cgi?acc=GSE2433**
Status:	**Public on May 14 2005**
Title:	**Expression profiling of GATA-1 wild type and mutant fetal megakaryocytes**
Organism:	**Mus musculus**
Experiment type:	**Expression profiling by array**
Platform:	**GPL1261**
Pubmed ID:	**15895080**
Summary & Design:	**Summary:**

Background:

Children with Down syndrome (DS) are predisposed to acute megakaryoblastic leukemia (AMKL, or AML M7) and a related myeloid disorder, referred to as transient myeloproliferative disorder (TMD), or transient leukemia (TL). Recently, acquired mutations in the erythroid/megakaryocytic lineage-specific transcription factor GATA-1 have been identified in megakaryoblasts from virtually all DS patients with AMKL (DS-AMKL), as well as in nearly all DS neonates with TMD. These mutations prevent synthesis of full-length GATA-1, but lead to synthesis of a truncated GATA-1 protein (GATA-1s) that lacks the N-terminal transactivation domain.

To determine the in vivo requirement of GATA-1 N-terminal domain in hematopoiesis and to model DS megakaryocytic leukemia initiated by GATA-1 mutation, we generated a GATA-1 knockin allele with a truncation at this domain (GATA-1deltaN). ES cells bearing this mutant allele generated a unique type of large Thrombopoietin (Tpo)-dependent megakaryocytes-containing colonies, when differentiated in vitro. Fetal livers from mice carrying this mutant allele contained elevated numbers of CD41+ cells throughout embryonic development, especially during mid-gestation. In in vitro hematopoietic colony assays, mutant cells from yolk sacs and mid-gestation fetal livers gave rise to a large number of macroscopic hyperproliferative megakaryocytic colonies (CFU-MKs). Consistent with that, when mutant fetal liver progenitors were cultured in liquid medium in the presence of Tpo, the derived megakaryocytes displayed marked hyperproliferation and grew for longer period of time than WTs.

Specific aims:

To understand the molecular basis for the megakaryocytic hyperproliferation phenotype of the GATA-1deltaN mutants, we plan to profile gene expression patterns of fetal liver-derived primary megakaryocytes and megakaryocytic progenitors from the GATA-1deltaN mutants and compare them with WTs, as well as GATA-1deltaNeodeltaHS mutants (GATA-1â megakaryocytes).

Experimental design:

E12.5 fetal livers were harvested from either GATA-1 WT and mutant embryos. Single cell suspensions were made from these livers and the cells were cultured in liquid medium in the presence of Tpo for 3 days. On day 3, primary megakaryocytes were enriched by a BSA gradient, and further enriched by anti-CD41 antibody and magnetic microbeads. Megakaryocytic progenitors were collected by FACS sorting for small cells in the same culture that express low level of CD41. Total RNAs were then prepared from these two populations and submitted for microarray profiling.

Conclusions:

When examining genes that are normally upregulated upon megakaryocyte differentiation (many of this class are megakaryocyte-specific genes), we found in GATA-1deltaN megakaryocytes, the majority of these genes are upregulated, although not to the full extent as seen in WTs. In contrast, this class of genes is largely not upregulated in GATA-1deltaNeodeltaHS megakaryocytes, which are blocked at an immature stage of differentiation. Genes that are downregulated during megakaryocyte differentiation include those that are normally repressed by GATA-1. Among genes that are not properly downregulated in GATA-1deltaN megakaryocytes, five transcription factors (Myc, Myb, GATA-2, PU.1, Ikaros) are of particular interest. Inadequate GATA-1s-mediated repression of transcription factors required for proliferation of hematopoietic progenitors (Myc, Myb and GATA-2) and for specifying lineage choices other than megakaryocyte/erythrocyte (PU.1 and Ikaros) may contribute to hyperproliferation of GATA-1deltaN megakaryocytes.

Keywords = GATA-1

Keywords = megakaryocyte

Keywords = mouse model

Keywords: other

Overall design:

Background corr dist: KL-Divergence = 0.0391, L1-Distance = 0.0161, L2-Distance = 0.0003, Normal std = 0.6072

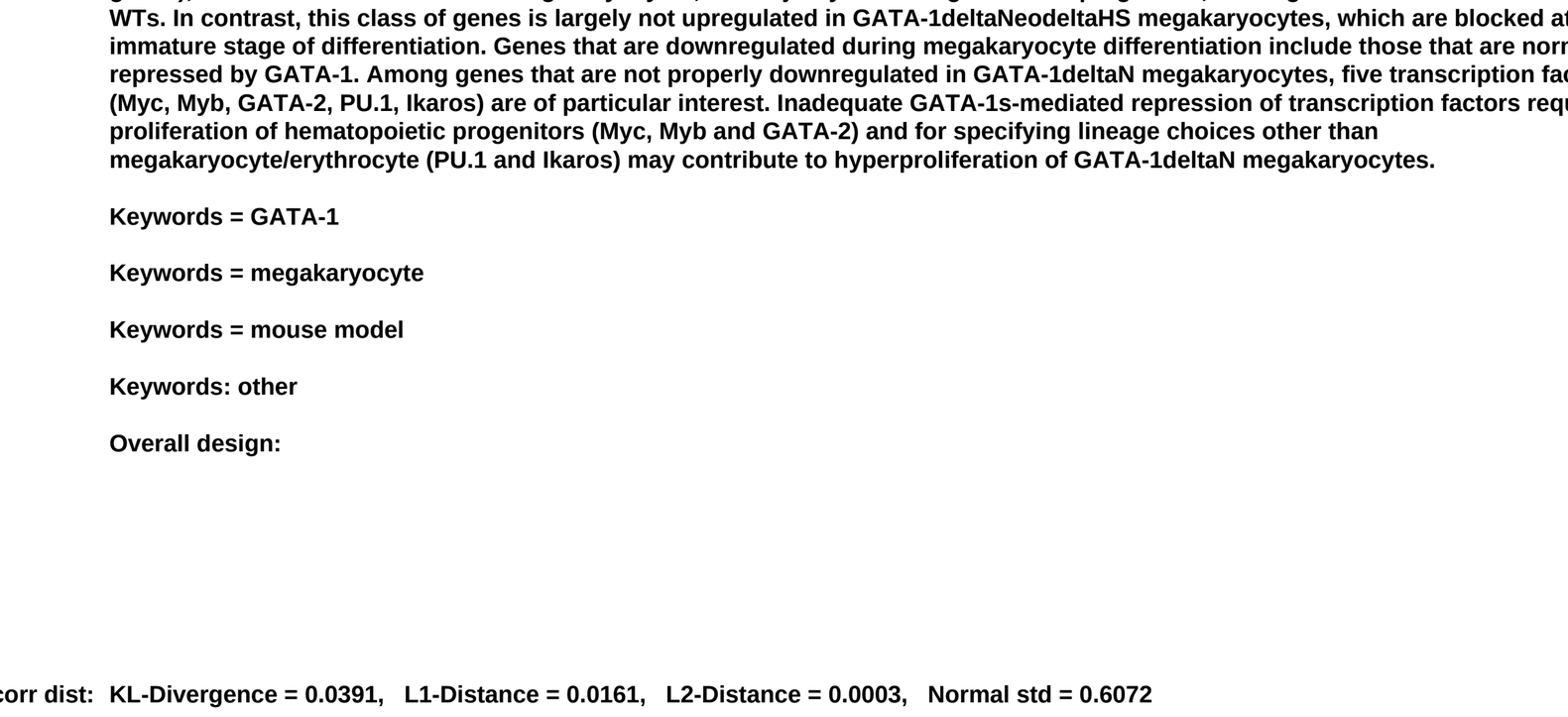

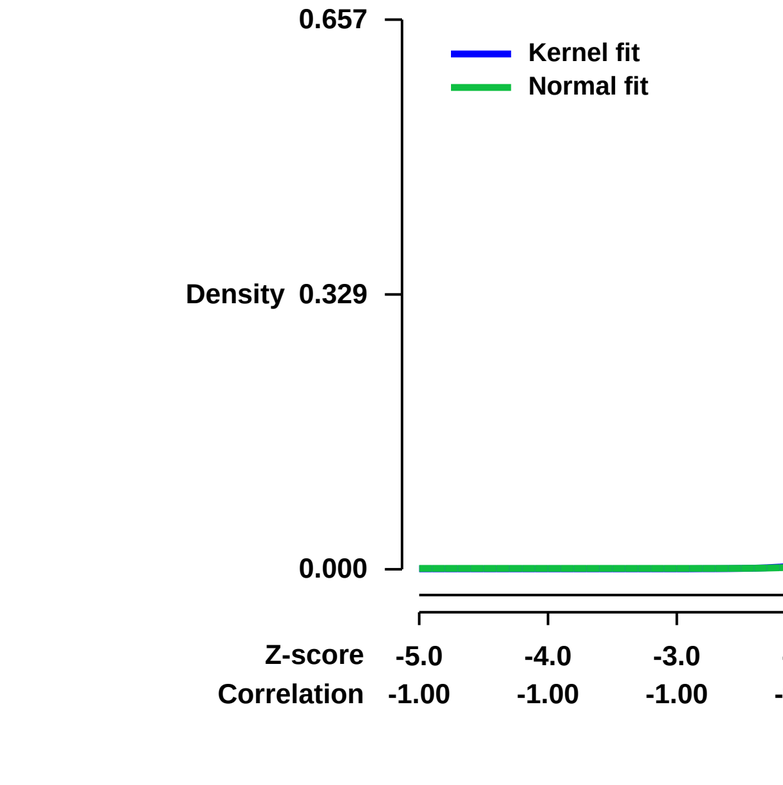

GEO Series "GSE1806" Expression Profiles

Num of samples in this series: 22

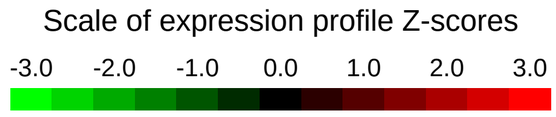

GEO Link:	**http://www.ncbi.nlm.nih.gov/geo/query/acc.cgi?acc=GSE1806**
Status:	**Public on Sep 27 2005**
Title:	**Skeletal muscle allotypes**
Organism:	**Mus musculus**
Experiment type:	**Expression profiling by array**
Platform:	**GPL1261**
Pubmed ID:	
Summary & Design:	**Summary:** **Expression profiling of 8 skeletal muscles from adult C57BL mice. Extraocular, temporalis, anterior digastric, sternocleidomastoid, triceps, diaphragm, quadraceps femoris (vastus lateralis), and tibialis anterior were evaluated using Affymetrix 430 v.2 arrays.** **Keywords: parallel sample** **Overall design:**

Background corr dist: **KL-Divergence = 0.2825, L1-Distance = 0.0525, L2-Distance = 0.0067, Normal std = 0.2886**

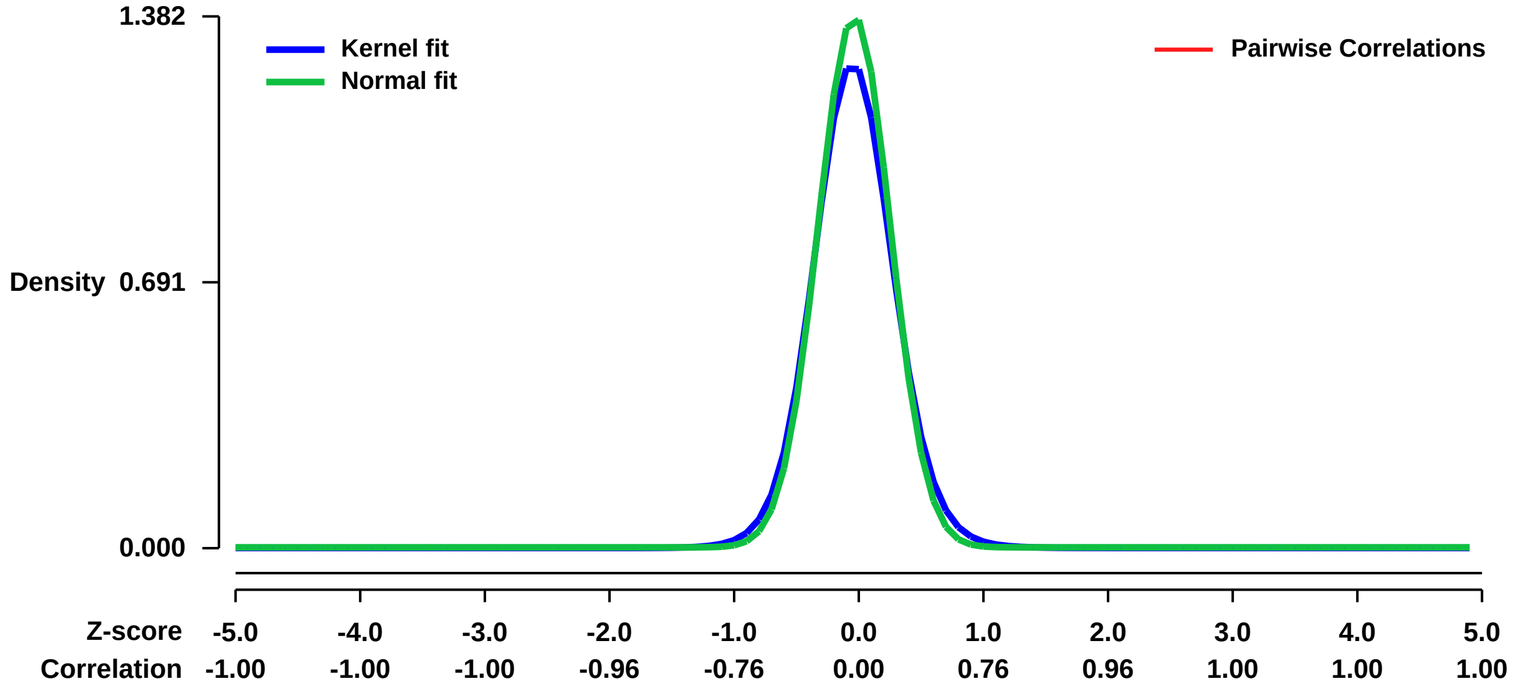

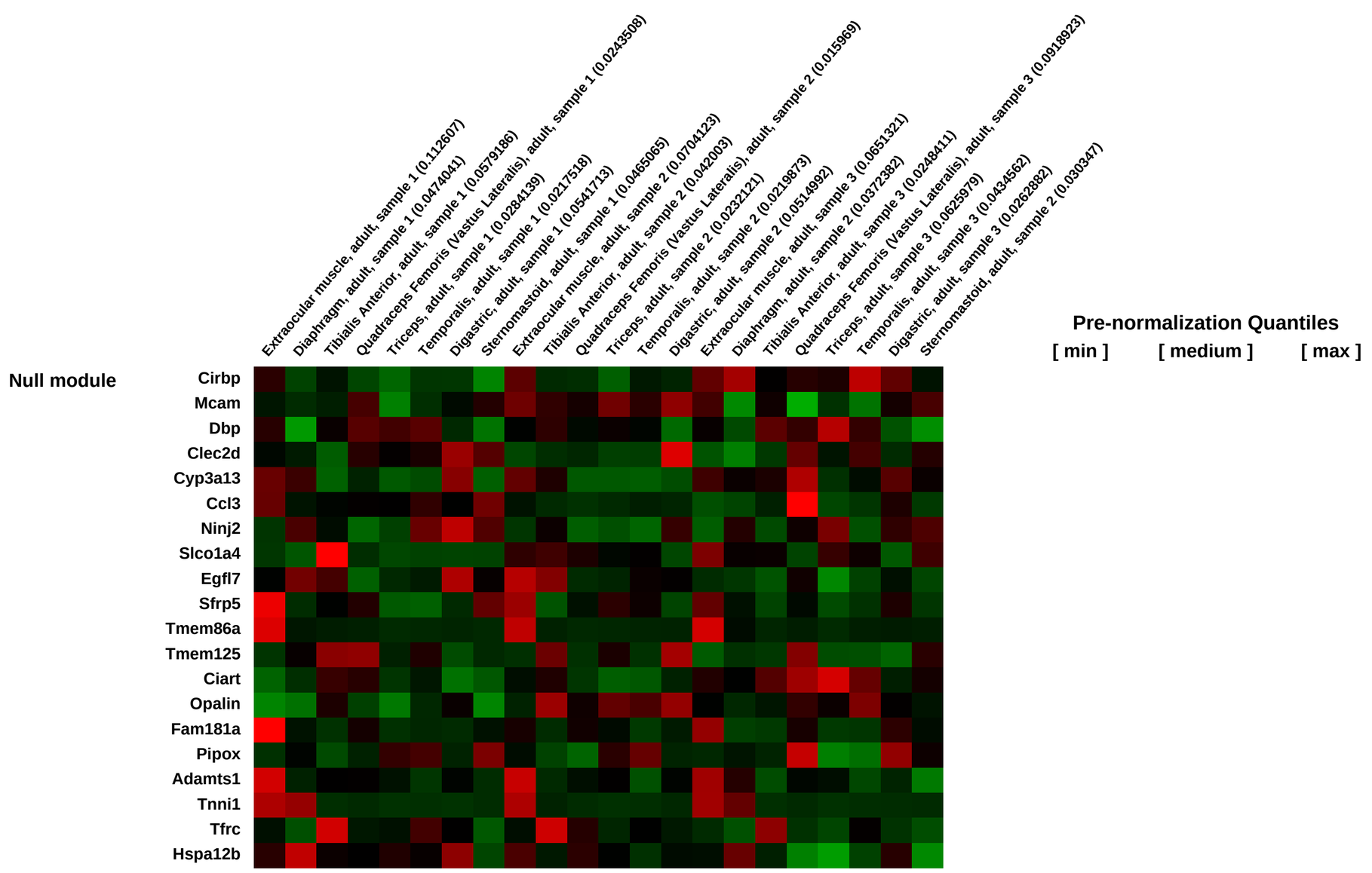

GEO Series "GSE26403" Expression Profiles

Num of samples in this series: 6

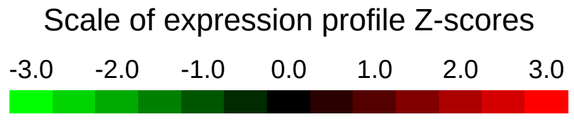

GEO Link:	http://www.ncbi.nlm.nih.gov/geo/query/acc.cgi?acc=GSE26403
Status:	Public on Jan 03 2011
Title:	Gene therapy of Mpl -/- mouse LSK cells
Organism:	Mus musculus
Experiment type:	Expression profiling by array
Platform:	GPL1261
Pubmed ID:	21289307
Summary & Design:	**Summary:** Comparison of Mpl-/- mouse LSK cells, either treated with control (GFP) or Mpl lentivirus. Lineage negative bone marrow cells were isolated and transduced and transplanted into Mpl-/- recipient mice. After transplantation and follow up mice were sacrificed and LSK (lineage negative, Sca-1 positive, cKit positive) cells were isolated by FACS. RNA was isolated using RNeasy Micro Kit (Qiagen GmbH, Hilden, Germany) and RNA was amplified for microarray hybridization using the Nugen Ovation system (Nugen Technologies, AC Bemmel, Netherlands). The resulting material was hybridized to Affymetrix Mouse 430 2.0 arrays. RMA normalization and summarization was performed in R 2.10 using Bioconductor packages. The aim was to show the normalization of Mpl associated gene expression. **Overall design:** 3 control (GFP transduced) samples of Mpl -/- mouse LSK cells and 3 treatment (Mpl transduced) samples of Mpl -/- mouse LSK cells.

Background corr dist: KL-Divergence = 0.0346, L1-Distance = 0.0714, L2-Distance = 0.0073, Normal std = 0.7501

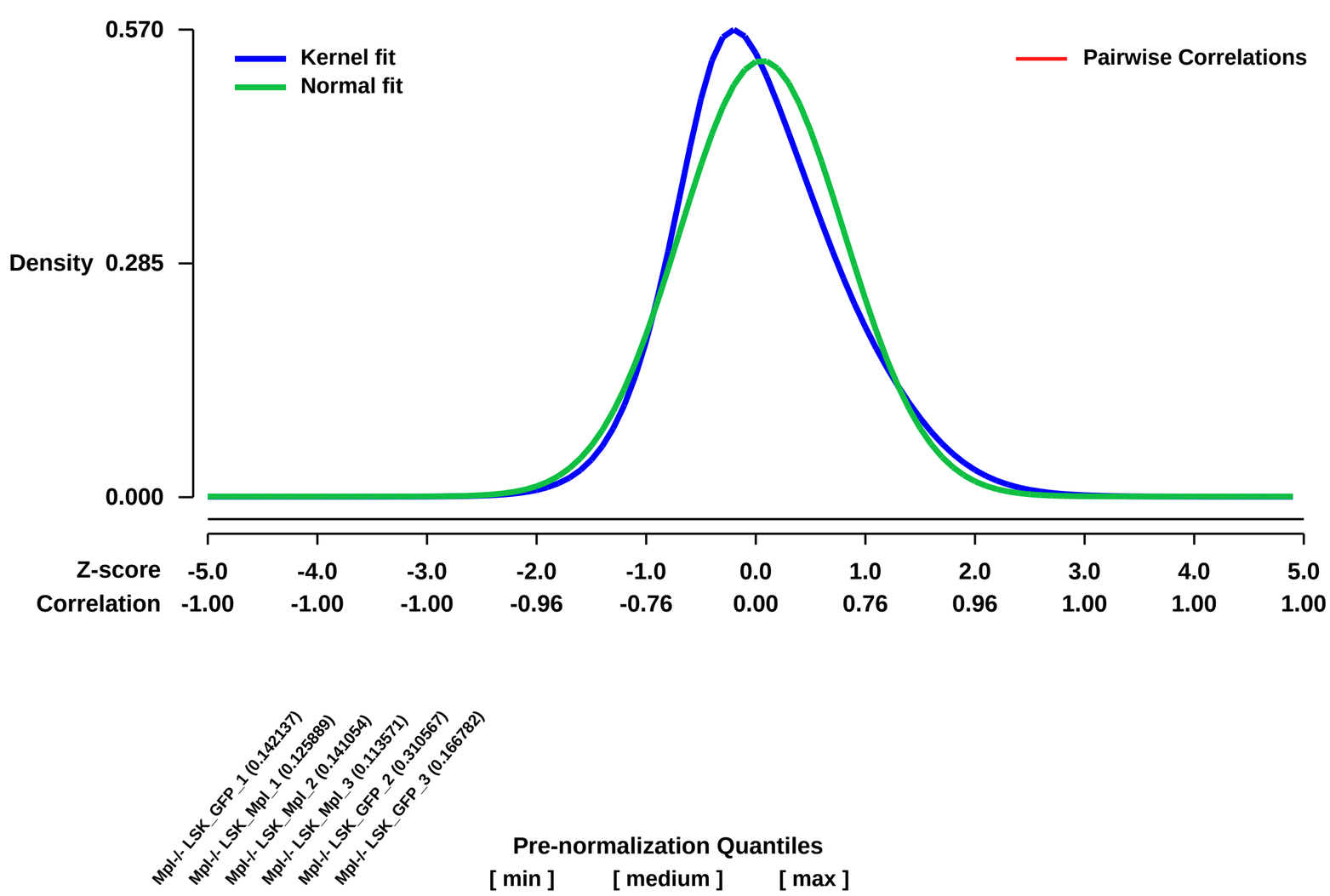

Pre-normalization Quantiles

[min] **[medium]** **[max]**

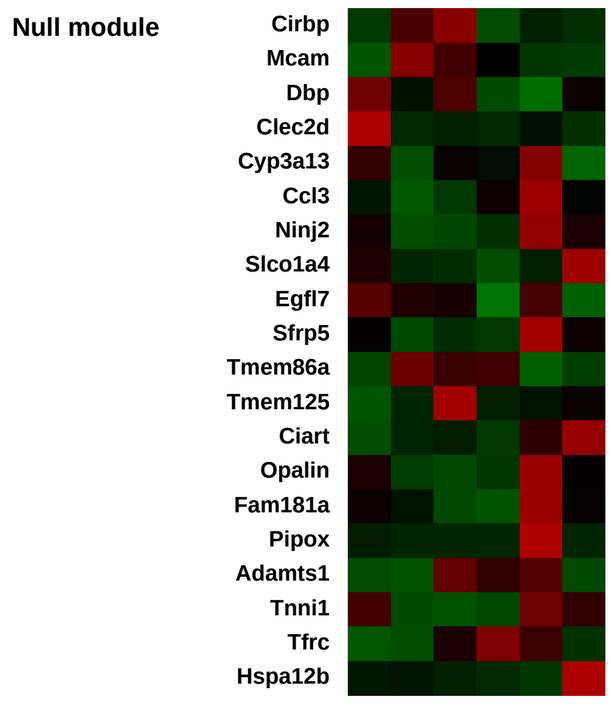

GEO Series "GSE18135" Expression Profiles

Num of samples in this series: 18

Scale of expression profile Z-scores

-3.0 -2.0 -1.0 0.0 1.0 2.0 3.0

GEO Link:	http://www.ncbi.nlm.nih.gov/geo/query/acc.cgi?acc=GSE18135
Status:	Public on Jan 15 2010
Title:	Gene Expression Profile of Androgen Modulated Genes in the Murine Fetal Developing Lung
Organism:	Mus musculus
Experiment type:	Expression profiling by array
Platform:	GPL1261
Pubmed ID:	20064212
Summary & Design:	**Summary:** Accumulating evidences suggest that sex affects lung development. During the fetal period, male lung maturation is delayed compared with female and surfactant production appears earlier in female than in male fetal lungs. We analyzed by microarrays the expression of genes showing a sexual difference and those modulated by endogenous androgens (flutamide). **Overall design:** Following flutamide or vehicle administration to pregnant mothers, fetal mouse lungs were studied at gestational day 17 (GD17) and GD18. RNA was extracted and hybridized on Affymetrix microarrays.

Background corr dist: KL-Divergence = 0.0822, L1-Distance = 0.0567, L2-Distance = 0.0049, Normal std = 0.5081

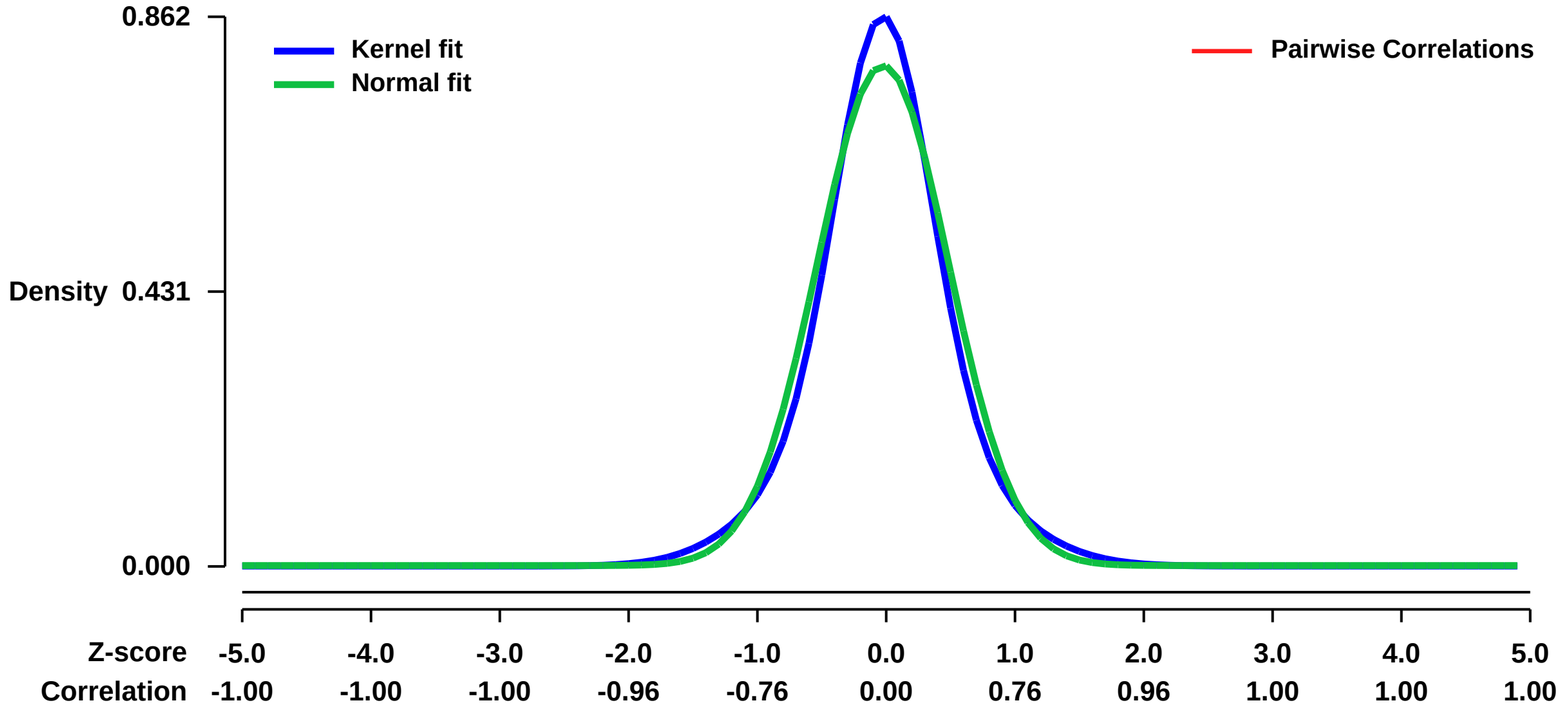

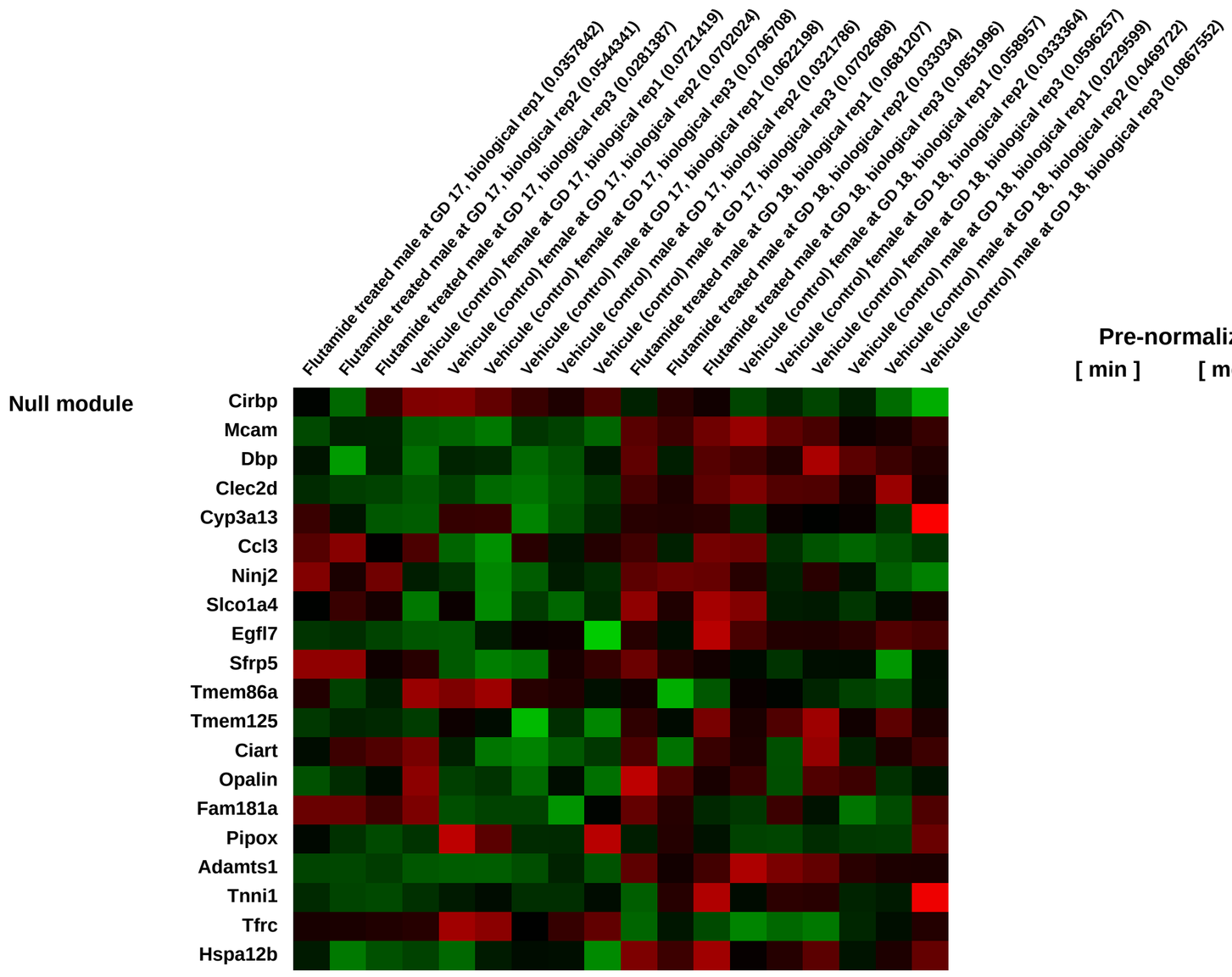

GEO Series "GSE47049" Expression Profiles

Num of samples in this series: 6

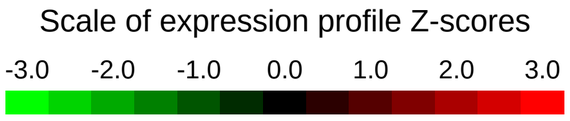

GEO Link:	**http://www.ncbi.nlm.nih.gov/geo/query/acc.cgi?acc=GSE47049**
Status:	**Public on May 09 2014**
Title:	**Expression data from wild type and Gata6-deficient tissue resident peritoneal macrophages**
Organism:	**Mus musculus**
Experiment type:	**Expression profiling by array**
Platform:	**GPL1261**
Pubmed ID:	**24762537**
Summary & Design:	**Summary:** **Tissue resident macrophages are notoriously heterogeneous, exhibiting discrete phenotypes as a consequence of tissue- and micro-anatomical niche-specific functions, but the molecular basis for this is not understood. We resolved a restricted transcriptional profile for the self-renewing population of peritoneal resident macrophages, which is expressed during homeostasis and inflammation and distinct from other Mˆ . Prominent within this profile was the expression of Gata6. This study represents a characterisation of the role of Gata6 in peritoneal resident macrophage phenotype. We used microarrays to determine the patterns of gene expression in peritoneal resident Mˆ in the absence of GATA-6 against wild type.** **Overall design:** **Conditional 'floxed' Gata6 deficient sex-matched mice between 7 weeks old were compared against wild type**

Background corr dist: **KL-Divergence = 0.0407, L1-Distance = 0.0228, L2-Distance = 0.0006, Normal std = 0.6176**

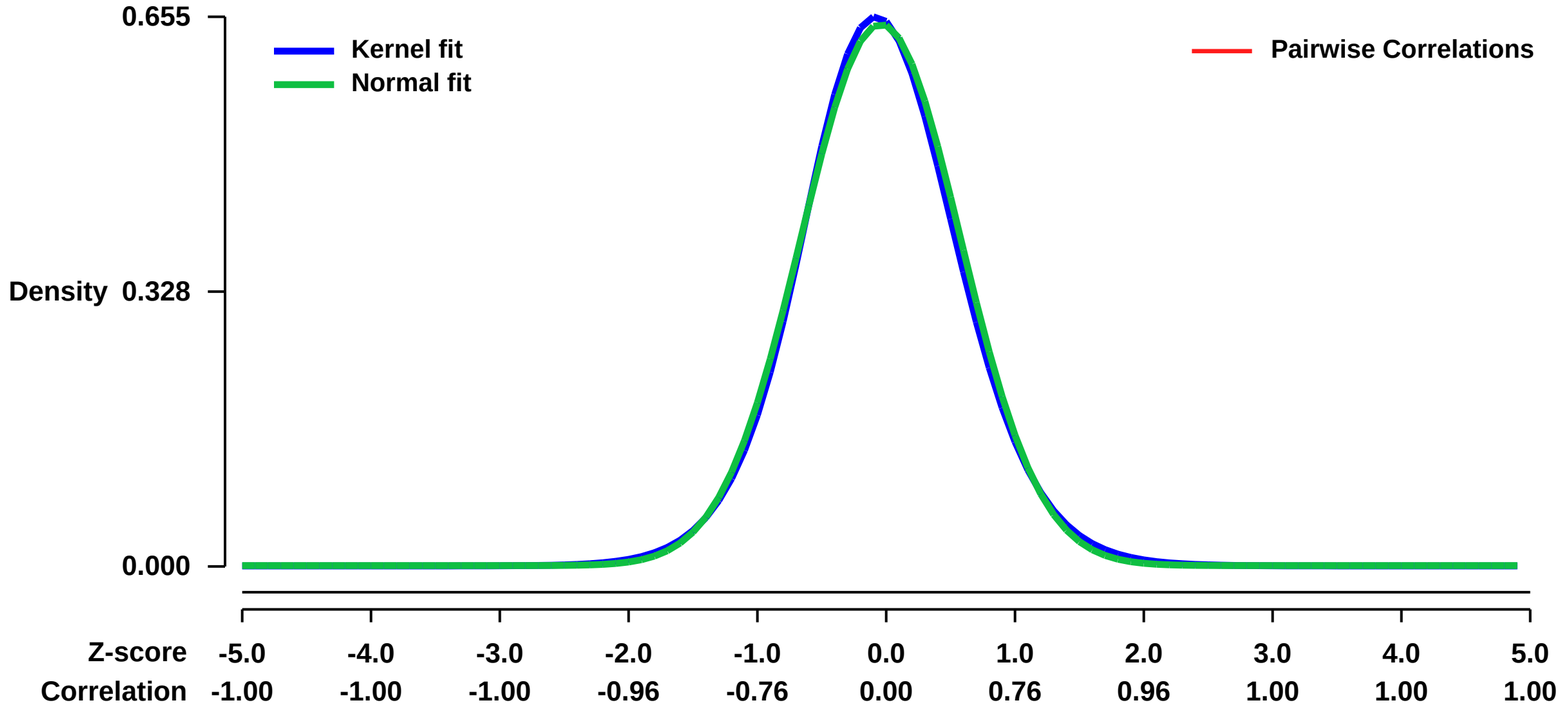

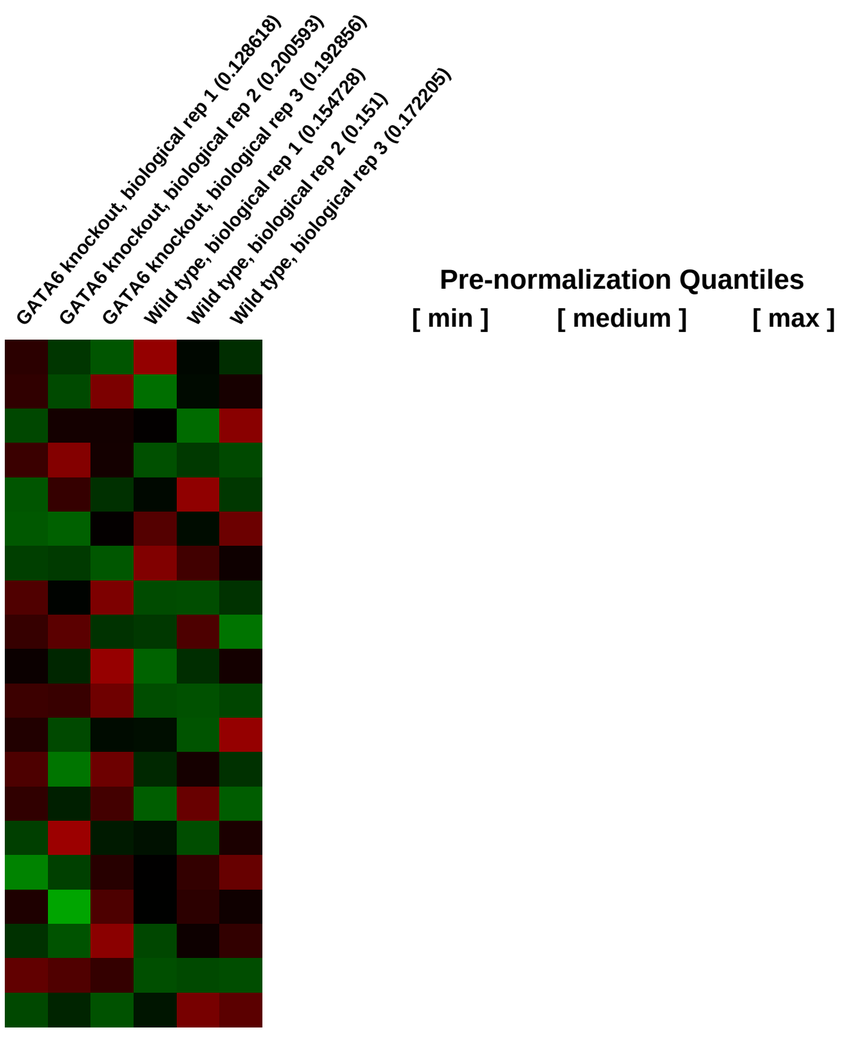

GEO Series "GSE16555" Expression Profiles

Num of samples in this series: 12

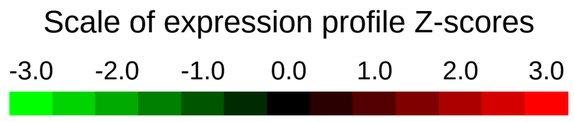

GEO Link:	http://www.ncbi.nlm.nih.gov/geo/query/acc.cgi?acc=GSE16555
Status:	Public on Jun 23 2010
Title:	Over-expression and knockdown of KLF5
Organism:	Mus musculus
Experiment type:	Expression profiling by array
Platform:	GPL1261
Pubmed ID:	20639455

Summary & Design:

Summary:
Activation of the Ras/Erk pathway upregulates expression of the Kruppel-like Factor 5 (KLF5) transcription factor, and KLF5 is a downstream mediator of Ras oncogenic signaling. Specifically, in bladder and colon cancer cell lines KLF5 upregulates the Ras-pathway target gene cyclin D1, and facilitates entry into the S phase of the cell cycle. Ras mutations are common in lung cancer, but a role for KLF5 in lung tumorigenesis has not been defined. To this end, we manipulated KLF5 expression in four Ras-mutant human lung adenocarcinoma cell lines to find that KLF5 significantly modulates anchorage-independent growth, a mutant Ras phenotype. However, in a mouse model of human lung adenocarcinoma, K-RasG12D does not critically require Klf5 to mediate oncogenesis or induce cyclin D1 expression.

Patients with lung tumors expressing high levels of KLF5 have significantly better prognosis than those with low or no KLF5 expression (opposite of mutant Ras prognosis). The latter may be explained by KLF5 transcriptional repression of the ATP-binding cassette, sub-family G (WHITE), member 2 (ABCG2), an anthracycline transporter. In agreement with this, KLF5 knockdown cells display significantly more Hoechst â side populationâ and resistance to doxorubicin. In summary, while KLF5 is not an obligate partner in Ras oncogenic signaling, KLF5 control of ABCG2 expression is significant to patient survival.

Overall design:
Total RNA was extracted from H441 cells transduced with KLF5-specific shRNA (KD), KLF5 over expression (OE) and MSCV empty vertor (NT) respectively. The cRNAs was then hybridized to Human Genome U133 Plus 2.0 Arrays (Affymetrix) according to manufacturerâ s protocol.

Background corr dist: KL-Divergence = 0.0806, L1-Distance = 0.0262, L2-Distance = 0.0010, Normal std = 0.4778

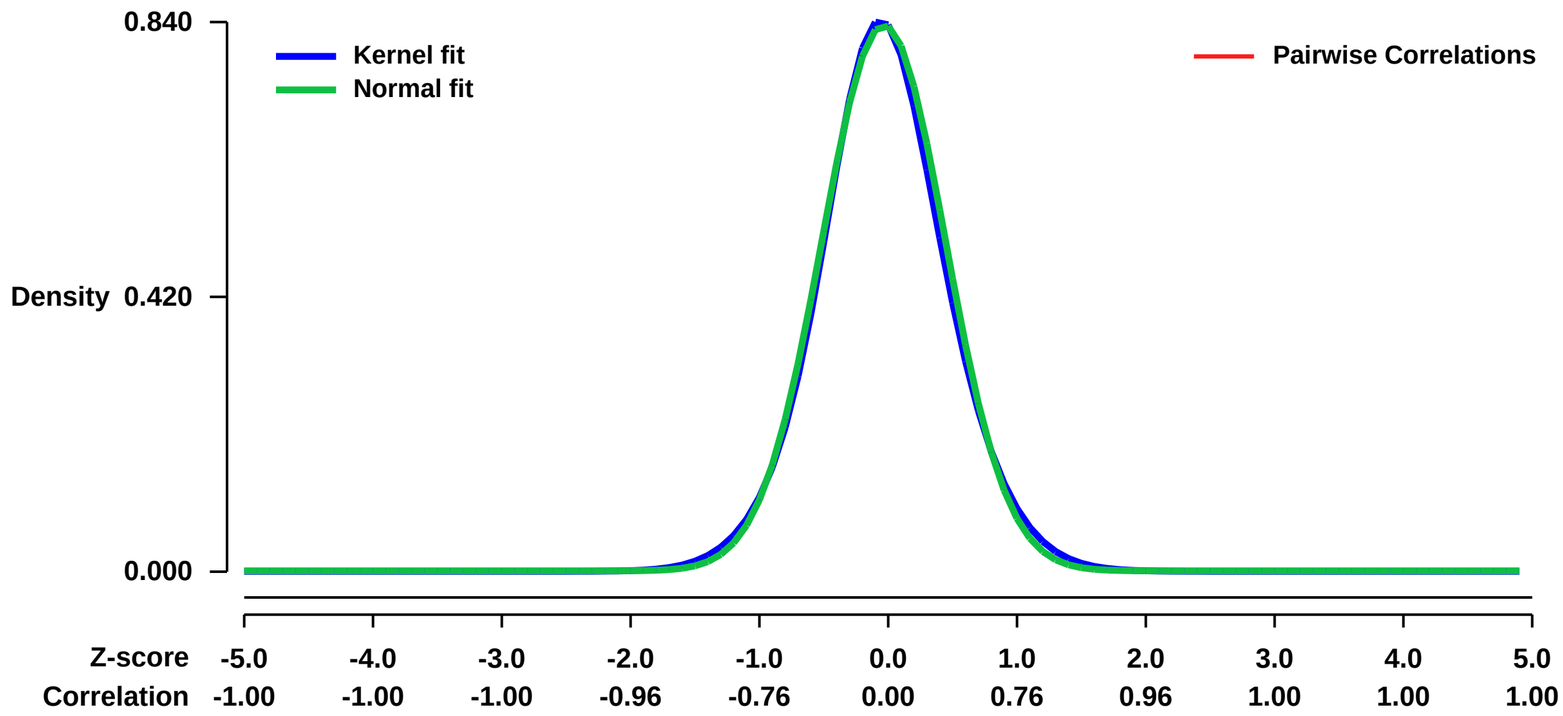

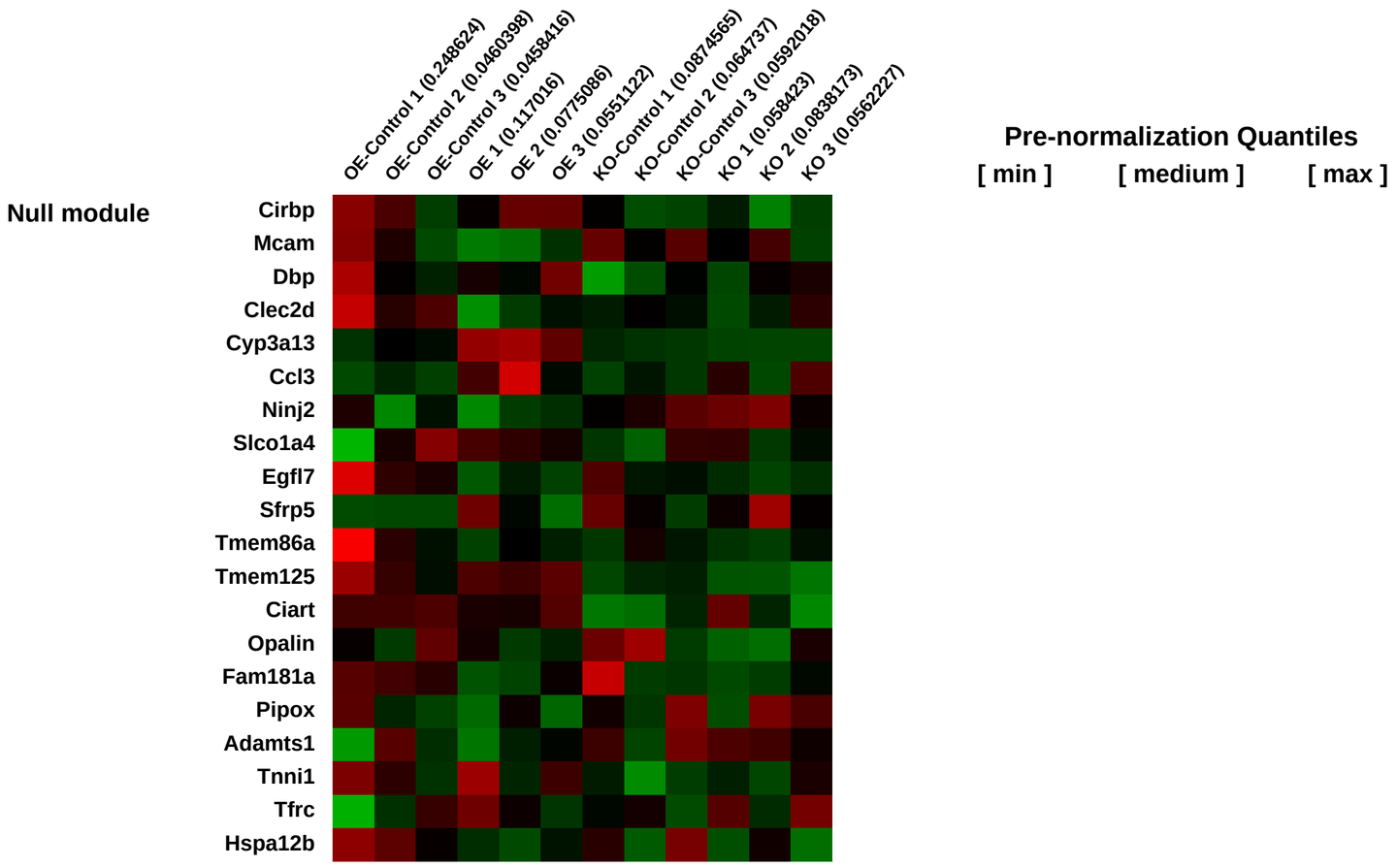

GEO Series "GSE3653" Expression Profiles

Num of samples in this series: 16

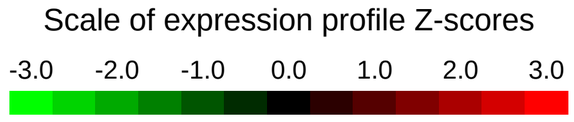

GEO Link:	http://www.ncbi.nlm.nih.gov/geo/query/acc.cgi?acc=GSE3653
Status:	Public on Jul 01 2006
Title:	Inducible Ngn3 Embryonic Stem Cells
Organism:	Mus musculus
Experiment type:	Expression profiling by array
Platform:	GPL1261
Pubmed ID:	16809427
Summary & Design:	**Summary:** Expression of the proendocrine gene neurogenin 3 (Ngn3) is required for the development of pancreatic islets. In order to better characterize the molecular events regulated by Ngn3 during development, we have determined the expression profile of differentiating murine embryonic stem cells (mESCs) uniformly induced to overexpress Ngn3. An ESC line was created that allows for the induction of Ngn3 by adding doxycycline (Dox) to the culture medium. Genome-wide microarray analysis was performed to identify genes regulated by Ngn3 in a variety of both undifferentiated and differentiated conditions. Characterization of pancreatic developmental markers during embryoid body (EB) formation revealed an optimum context for Ngn3 induction. Neuroendocrine genes including neurogenic differentiation 1 (NeuroD1) and single minded 1 (Sim1) were found to be significantly upregulated. Genes regulated by Ngn3 independent of the context were analyzed using systematic gene ontology tools and revealed Notch signaling as the most significantly regulated signaling pathway (p=0.009). This result is consistent with the hypothesis that Ngn3 expression makes the cell competent for Notch signaling to be activated and conversely, more sensitive to Notch signaling inhibition. Indeed, EBs induced to express Ngn3 were significantly more sensitive to gamma-secretase inhibitor-mediated Notch signaling inhibition (p<0.0001). Moreover, we find that Ngn3 induction in differentiating ESCs results in significant increases in insulin, glucagon, and somatostatin transcription. **Keywords:** Ngn3 induction, embryonic stem cell differentiation **Overall design:** 16 embryonic stem cell (ESC) samples (8 groups in duplicate) were processed for microarray analysis using the Affymetrix Mouse Genome 430 2.0 GeneChip. The samples included the parental Ainv15 ESC line (1) undifferentiated (Ainv15 ESC), (2) differentiated for 3 days as embryoid bodies (Ainv15 EB3) or (3) for 10 days as embryoid bodies (Ainv15 EB10). The remaining samples included tetracycline inducible Ngn3 ESC line derived from the parental Ainv15 ESC line (4) after differentiation and addition of doxycycline for 3 days without embryoid body formation (Ngn3 ES3 ON), (5 and 6) after differentiation as embryoid bodies for 3 days with (Ngn3 EB3 ON) or without (Ngn3 EB3 OFF) doxycycline, and (7 and 8) after differentiation as embryoid bodies for 10 days with (Ngn3 EB10 ON) or without (Ngn3 EB10 OFF) doxycycline.

Background corr dist: KL-Divergence = 0.1062, L1-Distance = 0.0773, L2-Distance = 0.0115, Normal std = 0.5090

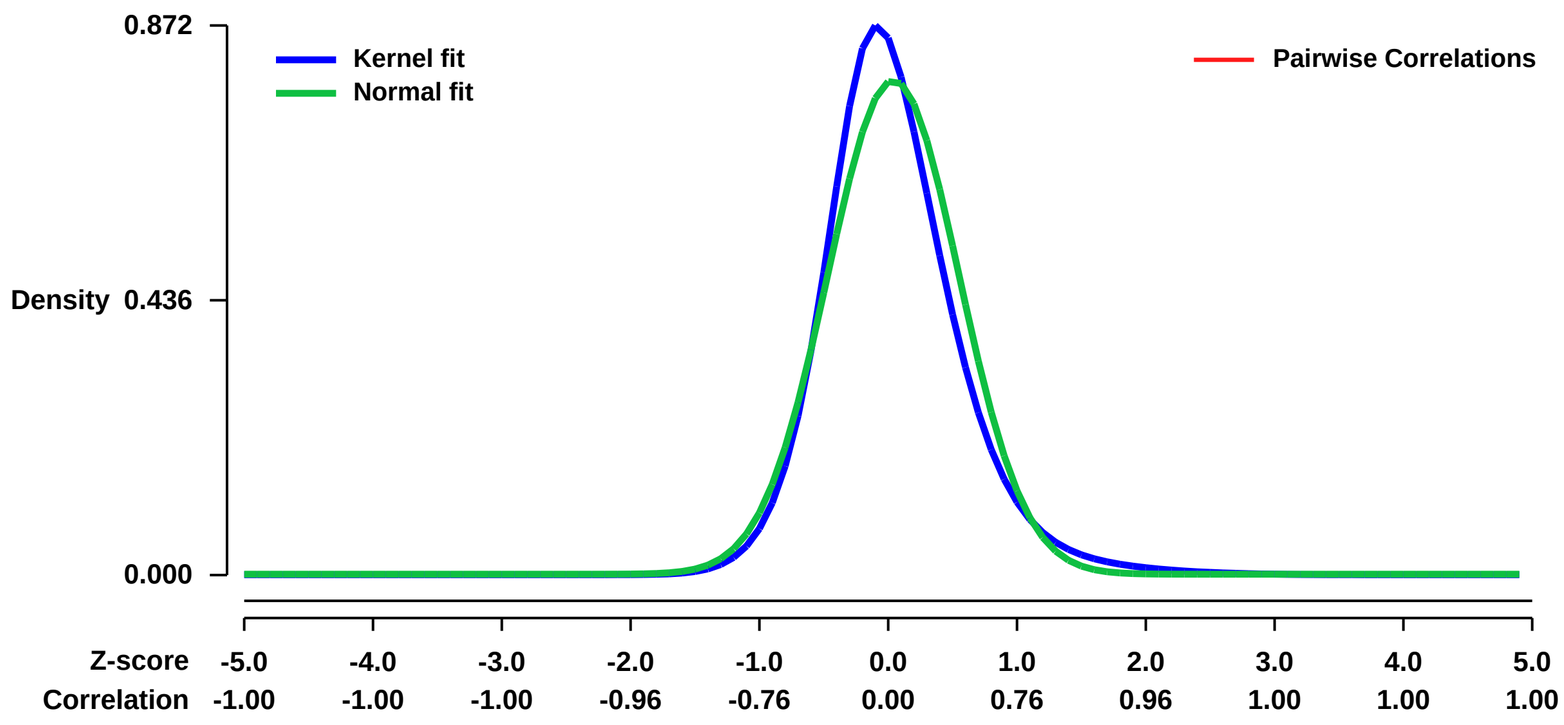

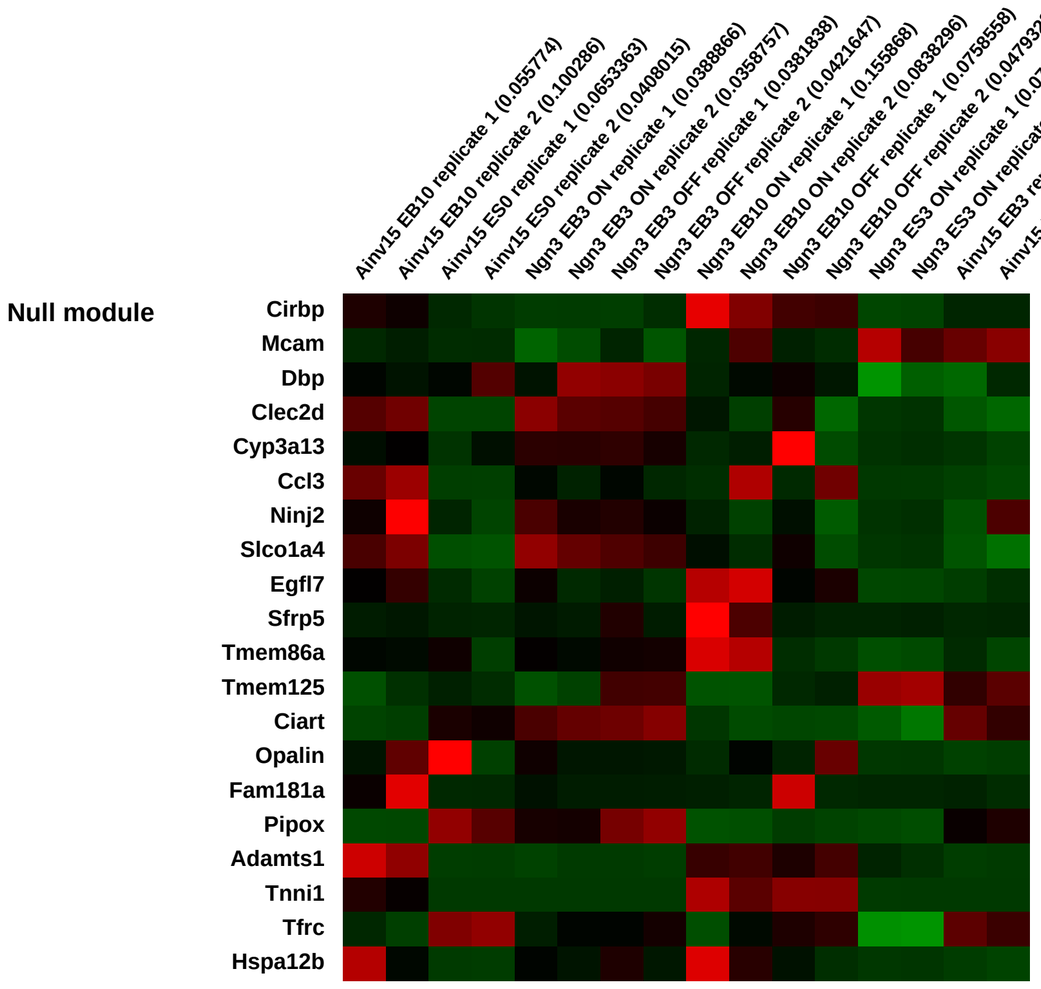

GEO Series "GSE14344" Expression Profiles

Num of samples in this series: 6

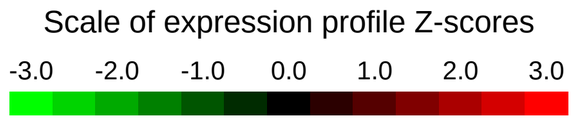

GEO Link:	http://www.ncbi.nlm.nih.gov/geo/query/acc.cgi?acc=GSE14344
Status:	Public on Jan 20 2009
Title:	esBAF is an essential component of the core pluripotency transcriptional network
Organism:	Mus musculus
Experiment type:	Genome binding/occupancy profiling by high throughput sequencing
Platform:	GPL1261
Pubmed ID:	19279218
Summary & Design:	**Summary:** Distinctive SWI/SNF-like ATP-dependent chromatin remodeling esBAF complexes are indispensable for the maintenance and pluripotency of mouse embryonic stem (ES) cells. To understand the mechanism underlying the roles of these complexes in ES cells, we performed high-resolution genome-wide mapping of the core ATPase subunit, Brg, using ChIP-Seq technology. We find that that esBAF, as represented by Brg, binds to genes encoding components of the core ES transcriptional circuitry, including Polycomb group proteins. esBAF colocalizes extensively with Oct4, Sox2 and Nanog genome-wide, and shows distinct functional interactions with Oct4 and Sox2 at its target genes. Surprisingly, no significant colocalization of esBAF with PRC2 complexes, represented by Suz12, is observed. Lastly, esBAF co-binds with Stat3 and Smad1 genome-wide, consistent with a direct and critical role in LIF and BMP signaling essential to maintain pluripotency. Taken together, our studies indicate that esBAF is both an essential component of the core pluripotency transcriptional network, and might also be a critical component of the LIF and BMP signaling pathways essential for maintenance of self-renewal and pluripotency. **Overall design:** Brg knockdown effect on expression, Brg ChIP-Seq

Background corr dist: KL-Divergence = 0.0061, L1-Distance = 0.0122, L2-Distance = 0.0002, Normal std = 0.9472

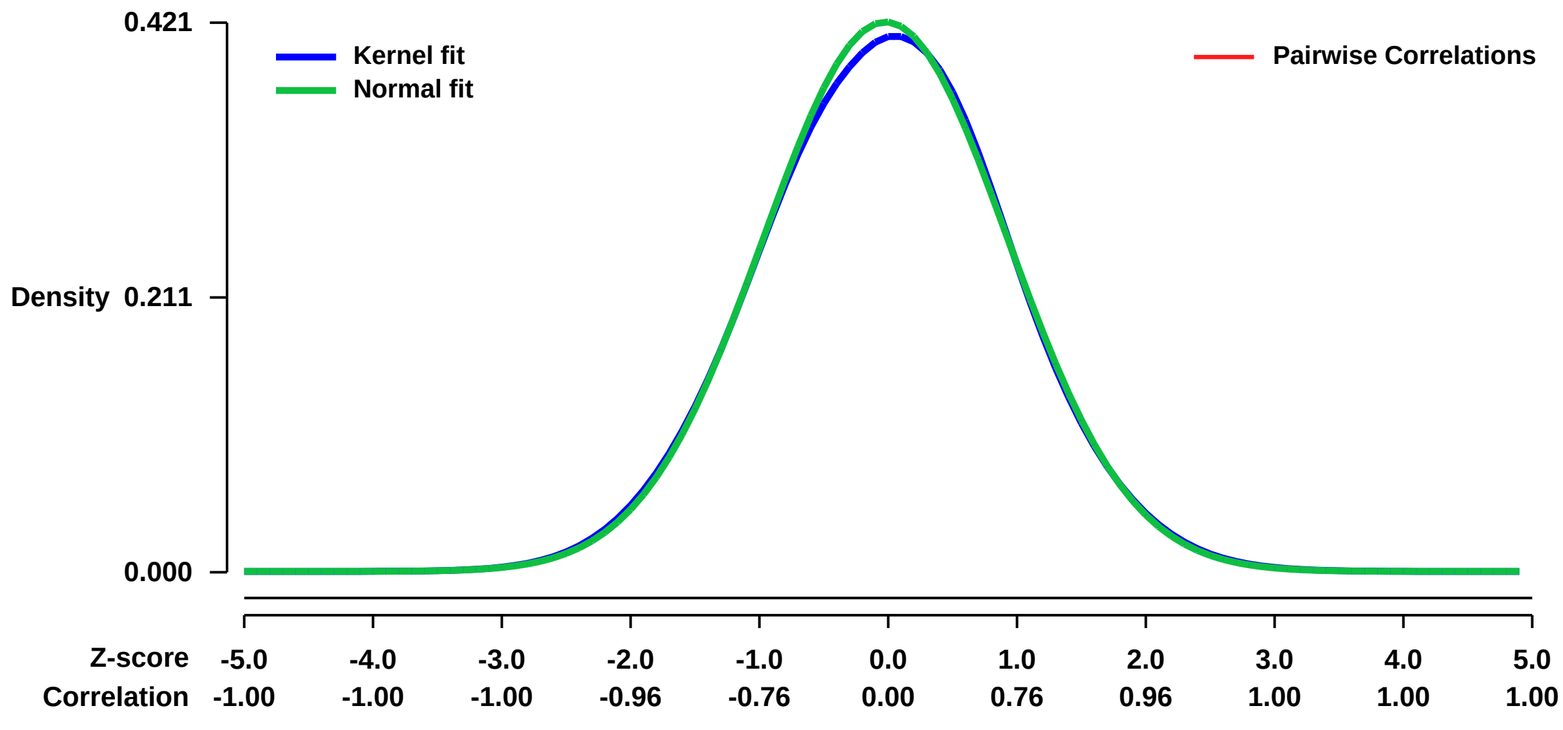

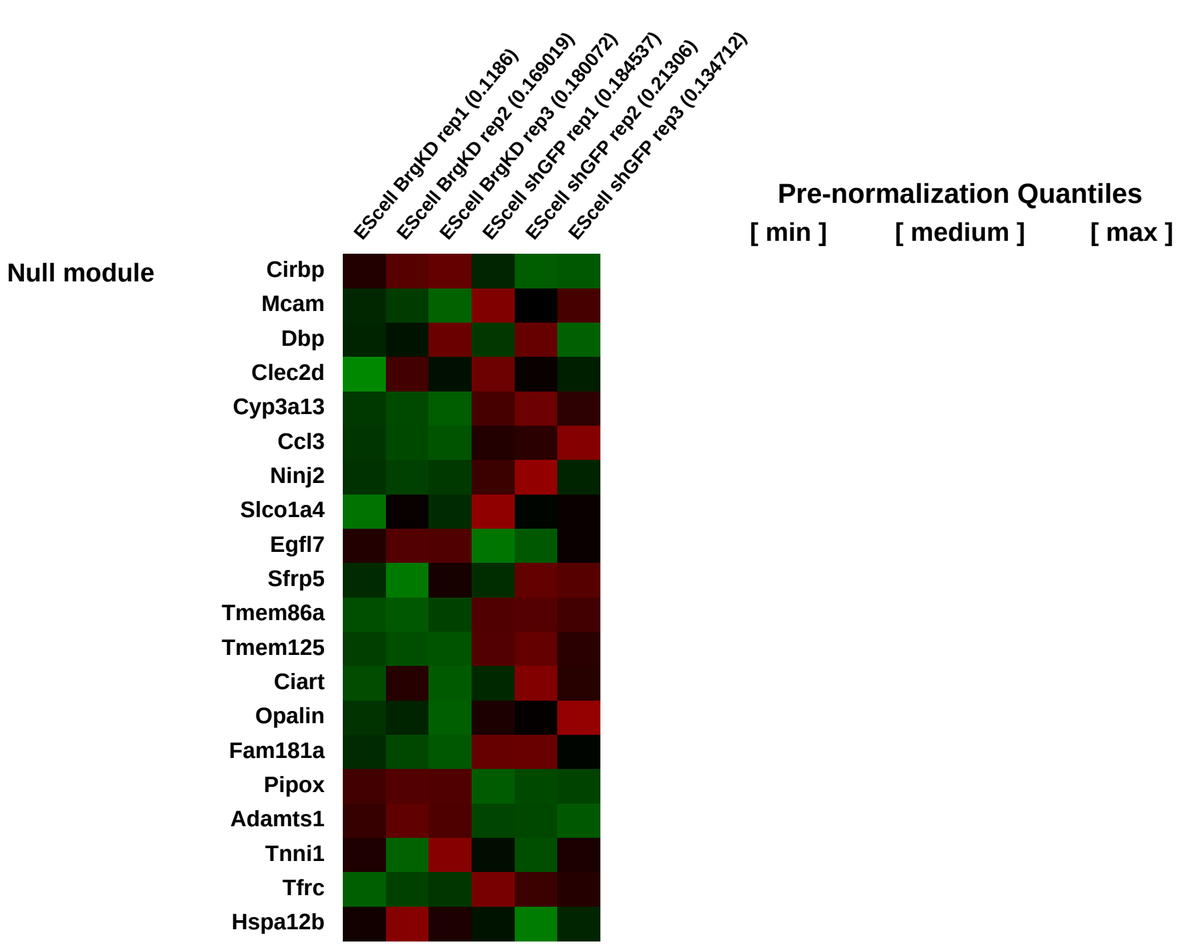

GEO Series "GSE14698" Expression Profiles

Num of samples in this series: 12

Scale of expression profile Z-scores

-3.0 -2.0 -1.0 0.0 1.0 2.0 3.0

GEO Link:	**http://www.ncbi.nlm.nih.gov/geo/query/acc.cgi?acc=GSE14698**
Status:	**Public on Feb 02 2010**
Title:	**Microarray Experiments for mice lacking or with the Stat5a and 5b genes in blood cells that were treated w/o CMP**
Organism:	**Mus musculus**
Experiment type:	**Expression profiling by array**
Platform:	**GPL1261**
Pubmed ID:	
Summary & Design:	**Summary:** **GM-CSF controls the development of granulocytes but little is known about the contribution of the downstream mediating transcription factor STAT5A/B. To elucidate this pathway, we generated mice lacking the Stat5a and 5b genes in blood cells. Peripheral neutrophils were decreased and administration of 5-FU and GM-CSF failed to induce granulopoiesis in Stat5a/b-mutant mice. CMPs were isolated and cultured with GM-CSF. #!#** **Overall design:** **Microarray Experiments for mice lacking or with the Stat5a and 5b genes in blood cells that were treated w/o CMP**

Background corr dist: **KL-Divergence = 0.0827, L1-Distance = 0.0372, L2-Distance = 0.0028, Normal std = 0.4743**

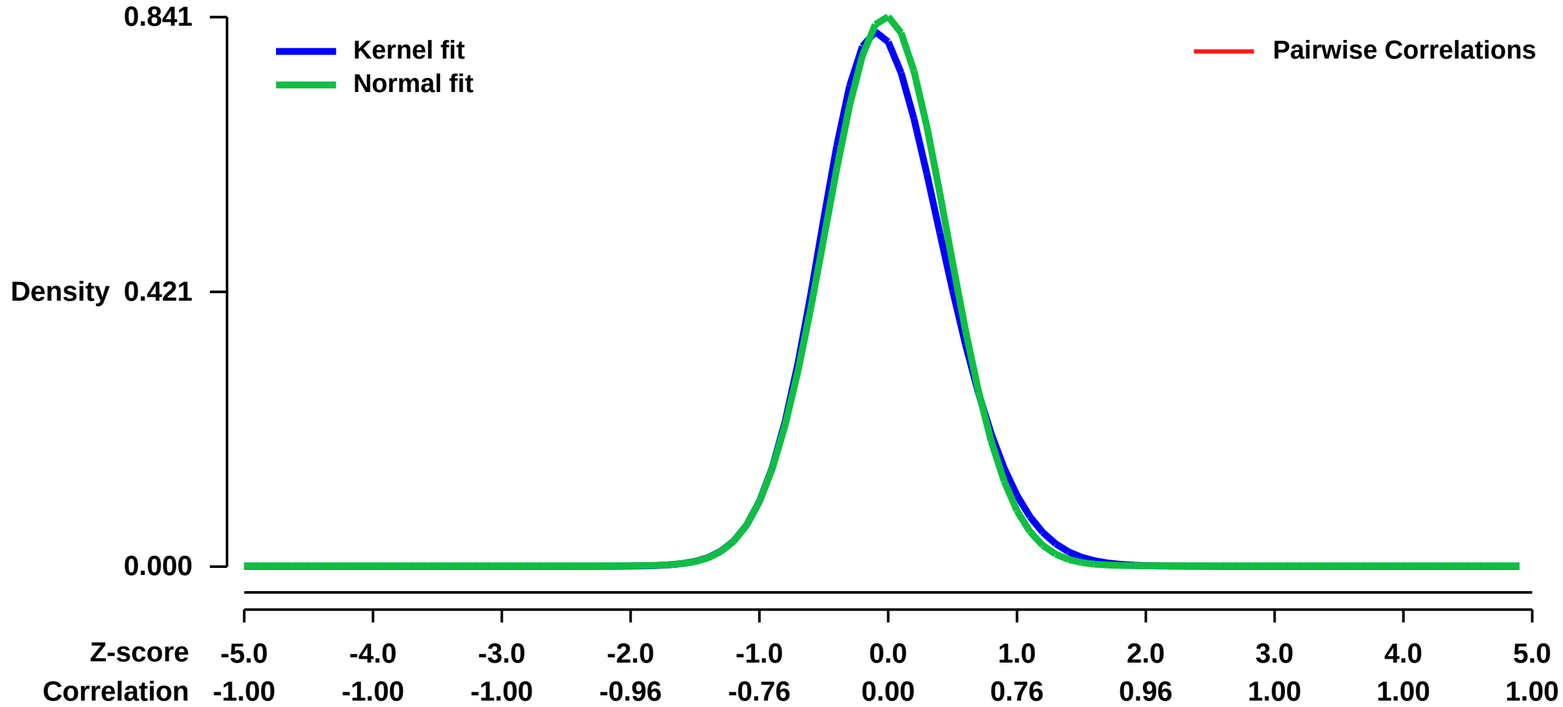

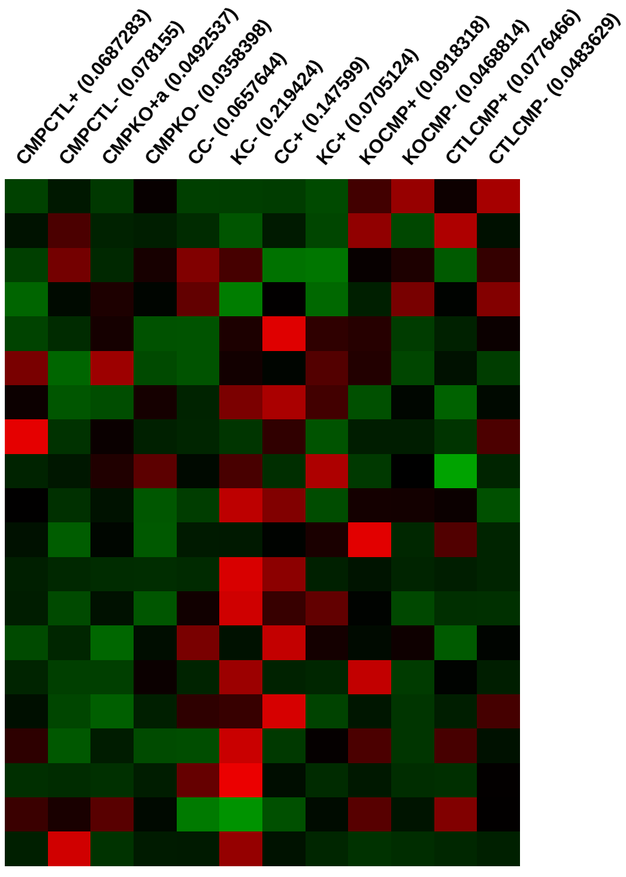

GEO Series "GSE34215" Expression Profiles

Num of samples in this series: 6

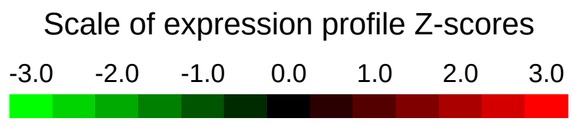

GEO Link:	http://www.ncbi.nlm.nih.gov/geo/query/acc.cgi?acc=GSE34215
Status:	Public on Dec 06 2012
Title:	Knockout of GPx4 gene in mouse keratinocyte
Organism:	Mus musculus
Experiment type:	Expression profiling by array
Platform:	GPL1261
Pubmed ID:	23364477
Summary & Design:	**Summary:** Comparative analysis of gene expression in cultured primary keratinocytes isolated from newborn control (K14-cre; GPx4fl/+) and knockout (K14-cre; GPx4fl/fl) mice. Selenoproteins are essential for skin function, as targeted abolition of selenoproteins in epidermal tissue results in newborn mice manifesting gross abnormalities of skin and hair, accompanied by retarded growth and premature death. To investigate whether lack of a single selenoprotein could induce similar phenotypic effect in mice, we generated keratinocyte-specific knockout mice lacking glutathione peroxidase 4 (GPx4), an essential selenoprotein in skin, to examine phenotypic changes resulting from the lack of GPx4 in skin. Ablation of GPx4 results in focal alopecia and disturbed hair follicle morphogenesis, with GPx4 being essential during early stages of hair follicle morphogenesis as well as for keratinocyte adhesion and proliferation in culture. **Overall design:** We have generated mice with selective removal of the GPx4 gene in keratinocytes under the control of Keratin-14-cre (K14-cre) promoter. Comparative microarray analysis was performed on RNA samples taken from pooled primary keratinocytes from knockout and control mice from the same litter. Array replicates were performed using RNA samples from three different litters.

Background corr dist: KL-Divergence = 0.0401, L1-Distance = 0.0263, L2-Distance = 0.0009, Normal std = 0.6210

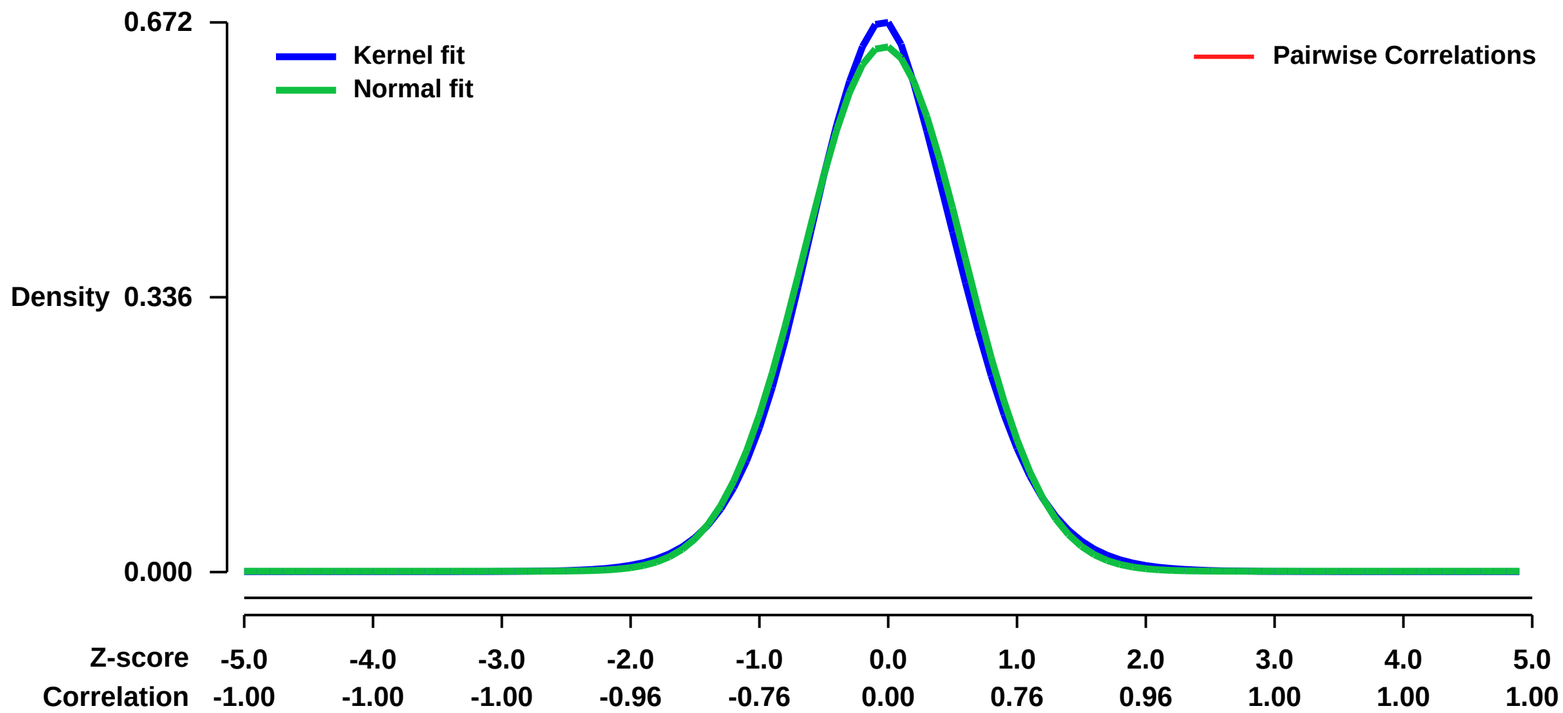

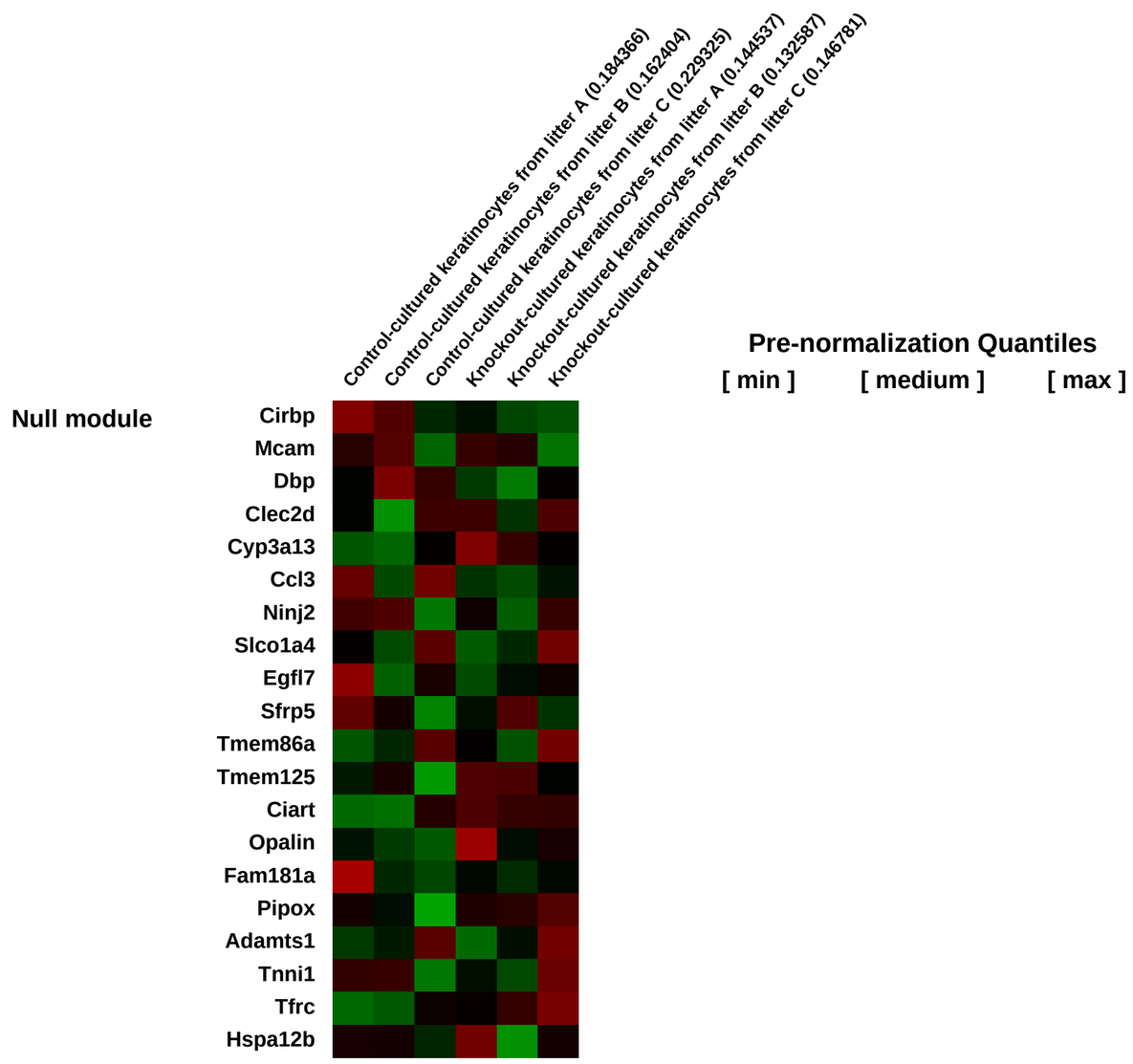

GEO Series "GSE21842" Expression Profiles

Num of samples in this series: 8

Scale of expression profile Z-scores

-3.0 -2.0 -1.0 0.0 1.0 2.0 3.0

GEO Link:	http://www.ncbi.nlm.nih.gov/geo/query/acc.cgi?acc=GSE21842
Status:	Public on May 15 2010
Title:	Physiological Jak2V617F expression causes a lethal myeloproliferative neoplasm with differential effects on hematopoietic stem and progenitor cells
Organism:	Mus musculus
Experiment type:	Expression profiling by array
Platform:	GPL1261
Pubmed ID:	20541703
Summary & Design:	**Summary:** We report a Jak2V617F knock-in mouse myeloproliferative neoplasm (MPN) model resembling human polycythemia vera (PV). The MPN is serially transplantable and we demonstrate that the hematopoietic stem cell (HSC) compartment has the unique capacity for disease initiation but does not have a selective competitive advantage over wild type HSCs. In contrast, myeloid progenitor populations are expanded and skewed towards the erythroid lineage, but cannot transplant the disease. Treatment with a JAK2 kinase inhibitor ameliorated the MPN phenotype, but did not eliminate the disease-initiating population. These findings provide insights into the consequences of JAK2 activation on HSC differentiation and function and have the potential to inform therapeutic approaches to JAK2V617F positive MPN. **Overall design:** LKS cells were isolated from wild type (n=4) and JAK2V617F mutant mice (n=4). RNA was extracted using Qiagen RNeasy Micro Kit according to manufacturers instruction and amplified using NUGEN amplification kit. cDNA was fragmented and biotinylated before hybridization onto Affymetrix Mouse Expression Array 430 2.0.

Background corr dist: KL-Divergence = 0.0704, L1-Distance = 0.0212, L2-Distance = 0.0006, Normal std = 0.4959

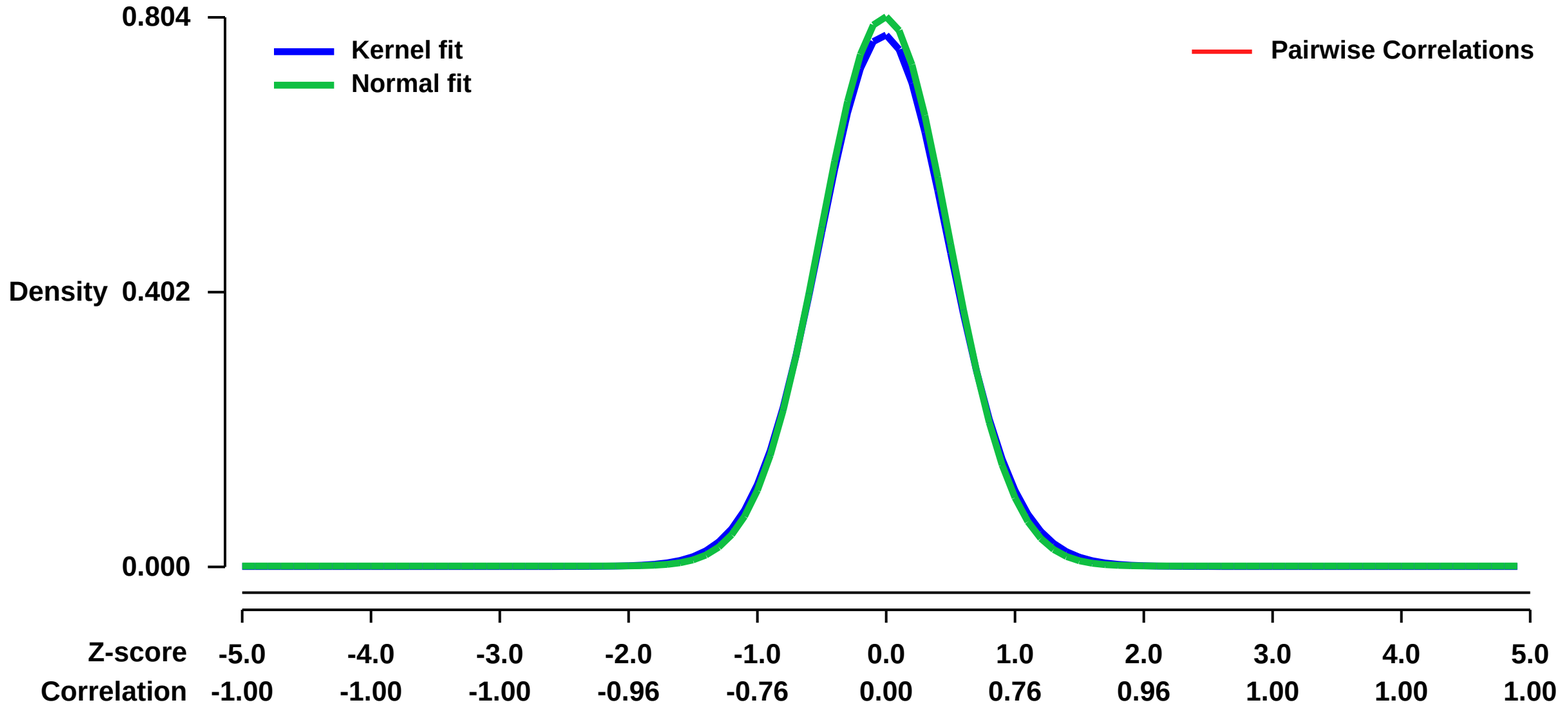

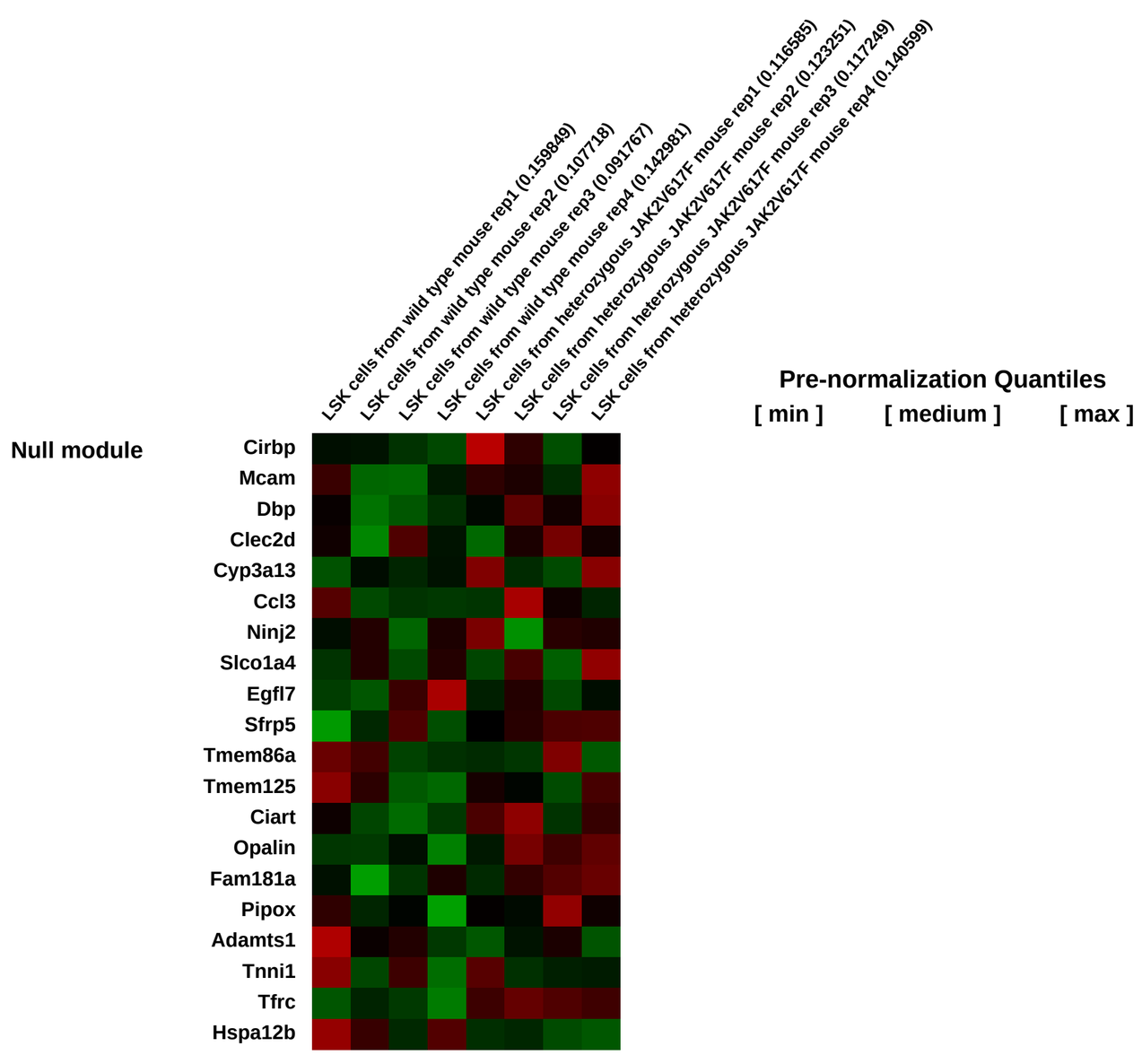

GEO Series "GSE4818" Expression Profiles

Num of samples in this series: 21

Scale of expression profile Z-scores

-3.0 -2.0 -1.0 0.0 1.0 2.0 3.0

GEO Link:	**http://www.ncbi.nlm.nih.gov/geo/query/acc.cgi?acc=GSE4818**
Status:	**Public on May 12 2006**
Title:	**Gene expression profiling of whole testes in embryonic (gestational day 11, 12, 14, 16 & 18) and postnatal day 2 mice. (GUDMAP Series ID: 3)**
Organism:	**Mus musculus**
Experiment type:	**Expression profiling by array**
Platform:	**GPL1261**
Pubmed ID:	
Summary & Design:	**Summary:** **The overall objective of this proposal is to map the temporal and spatial dynamics of gene expression in the fetal mouse testis at key developmental timepoints. Urogenital tract malformations are the most common birth defects in males and their incidence together with other male reproductive health concerns such as reduced fertility and testicular cancer are reportedly on the rise in the human population. To better understand the impact of genetic factors and environmental influences on testicular development, it is important to first understand normal gene expression patterns and signaling cascades within the fetal testis during development. The goal of this study is to identify cell-specific genes that can be used as biomarkers for key differentiation events.** **Keywords: developmental time course** **Overall design:** **Day to day comparison in whole testes throughout development with triplicates at each time point. Each sample is a pair of testes from a single animal and each animal is taken from a different dam.**

Background corr dist: KL-Divergence = 0.1571, L1-Distance = 0.0451, L2-Distance = 0.0046, Normal std = 0.4081

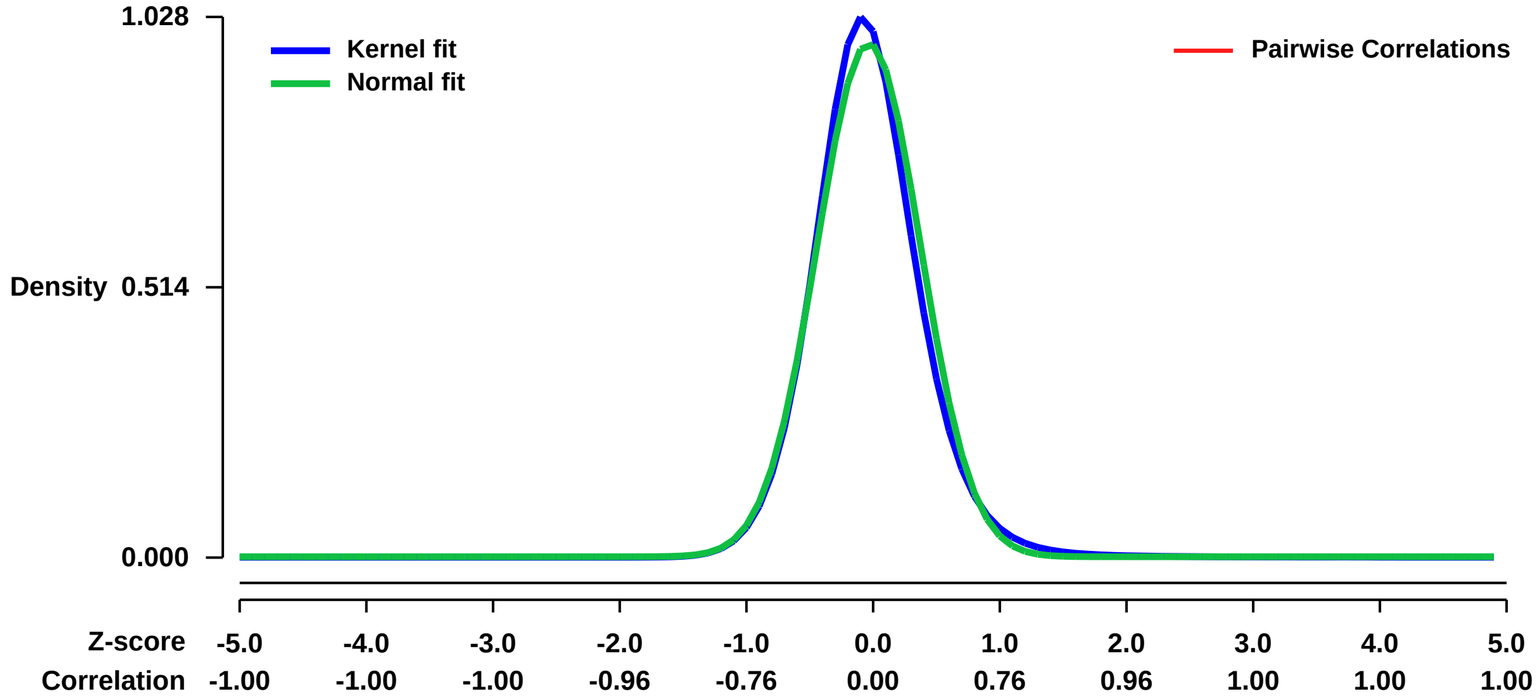

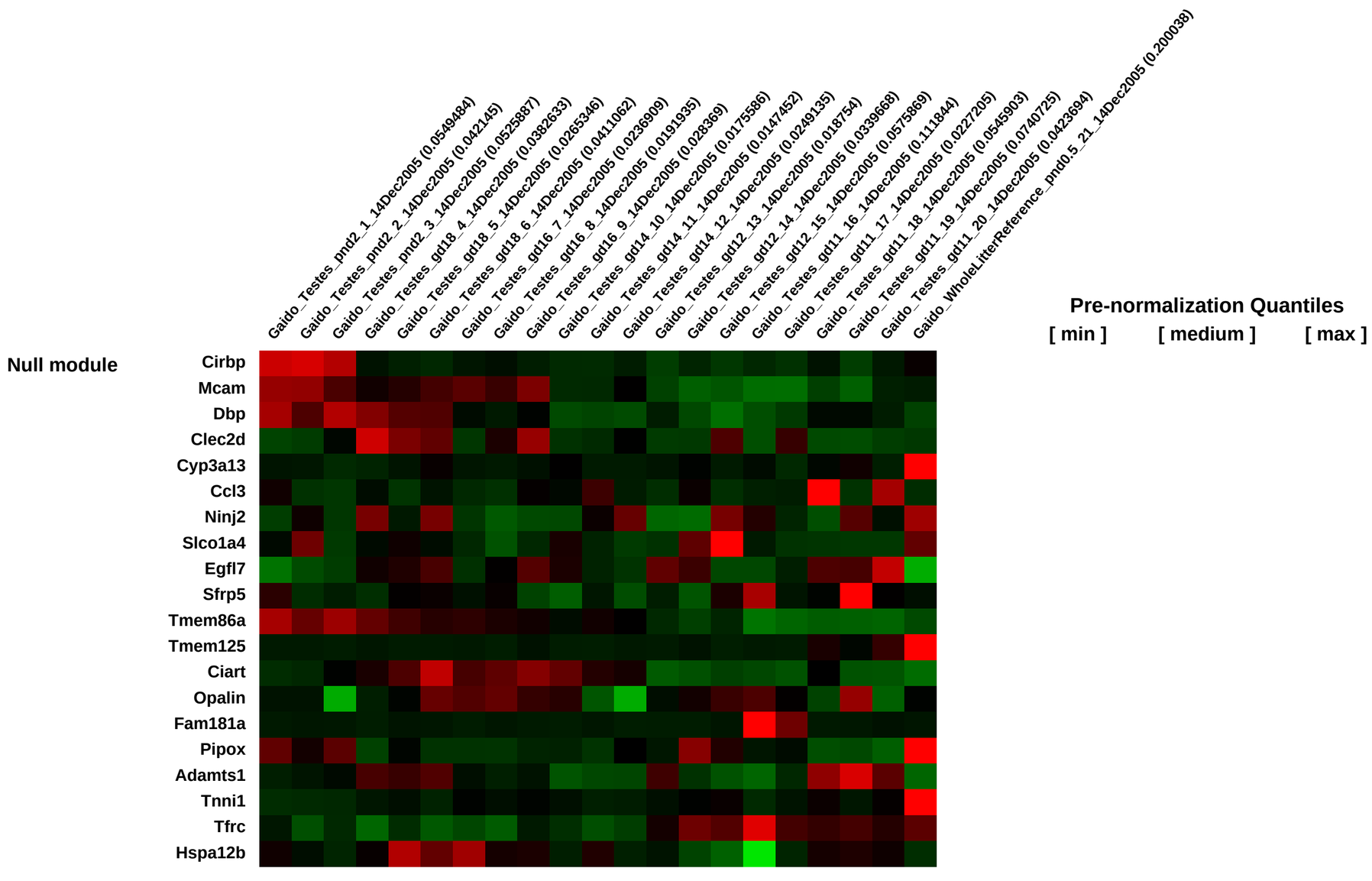

GEO Series "GSE33761" Expression Profiles

Num of samples in this series: 9

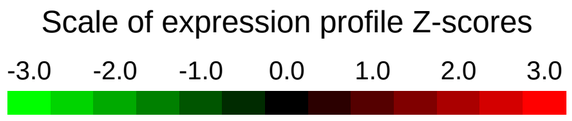

GEO Link:	**http://www.ncbi.nlm.nih.gov/geo/query/acc.cgi?acc=GSE33761**
Status:	**Public on Apr 25 2012**
Title:	**Gene expression in adipose tissue of intrauterine growth restricted (IUGR) and Macrosomic animals that developed in a crowded uterine horn**
Organism:	**Mus musculus**
Experiment type:	**Expression profiling by array**
Platform:	**GPL1261**
Pubmed ID:	
Summary & Design:	**Summary:** **Animals that are growth restricted in utero may show rapid postnatal growth that ultimately results in adult obesity. Macrosomic animals at birth typically remain large and are also obese as adults. Our goal was to examine the differences between animals that reach obesity in different ways. We also aimed to examine gene expression in animals that start out lean and stay lean compared to those that start out lean and become fat.** **We used microarrays to detail gene expression in adipose tissue.** **Overall design:** **3 samples each from IUGR animals with rapid postnatal growth (IH), IUGR animals with slower postnatal growth (IL), and macromsomic animals (M).**

Background corr dist: **KL-Divergence = 0.0966, L1-Distance = 0.0243, L2-Distance = 0.0010, Normal std = 0.4445**

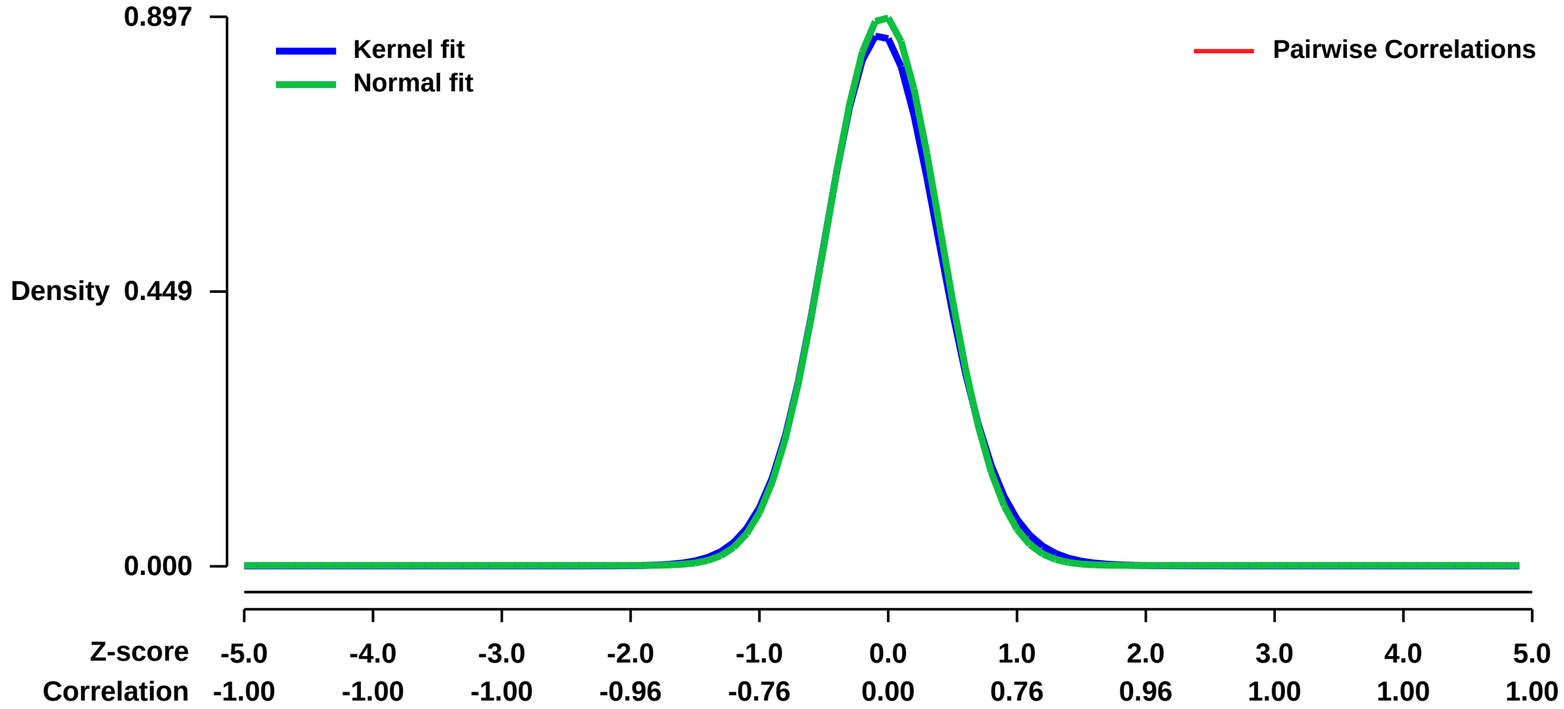

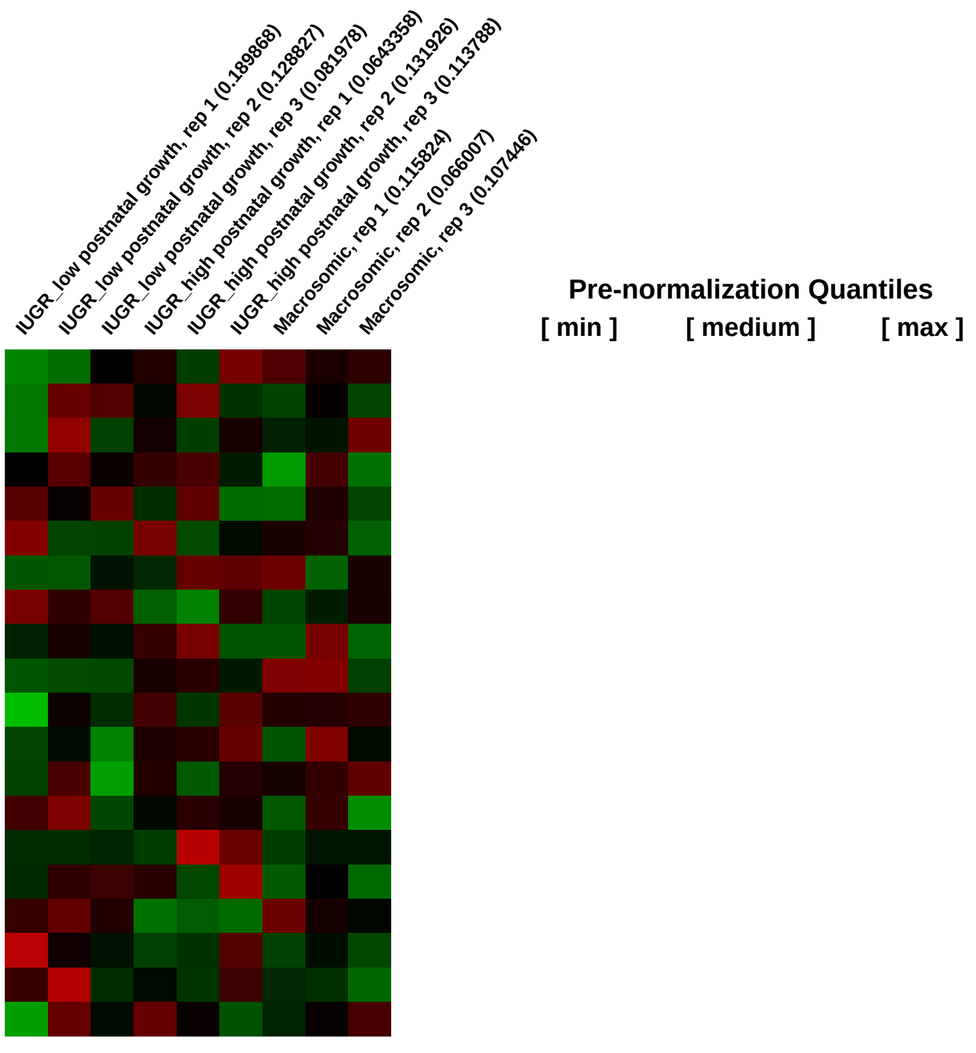

GEO Series "GSE41807" Expression Profiles

Num of samples in this series: 6

Scale of expression profile Z-scores

-3.0 -2.0 -1.0 0.0 1.0 2.0 3.0

GEO Link:	**http://www.ncbi.nlm.nih.gov/geo/query/acc.cgi?acc=GSE41807**
Status:	**Public on Oct 25 2012**
Title:	**Expression data from adult (9 month-old) and young (4 month-old) hearts from C57BL/6J mice**
Organism:	**Mus musculus**
Experiment type:	**Expression profiling by array**
Platform:	**GPL1261**
Pubmed ID:	
Summary & Design:	**Summary:** **G protein-coupled receptor kinase 2 (GRK2) has emerged as a key regulator of cardiac function and myocardial structure. Cardiac GRK2 is increased in heart failure and ischemia in humans, whereas genetic inhibition of GRK2 is cardioprotective in animal models of these pathologies. However, the mechanistic basis underlying these effects are not fully understood. We have used adult GRK2 hemizygous mice (GRK2+/-) as a model to assess the effects of a sustained systemic inhibition of GRK2 in heart tissue with age.** **We used microarrays to determine the global programme of gene expression underlying cardioprotection with age in GRK2 hemizygous mice in comparation with their wild-type littermates.** **Overall design:** **9 month-old and 4 month-old mice hearts were collected for RNA extraction and hybridization on Affymetrix microarrays.**

Background corr dist: **KL-Divergence = 0.0358, L1-Distance = 0.0129, L2-Distance = 0.0001, Normal std = 0.6285**

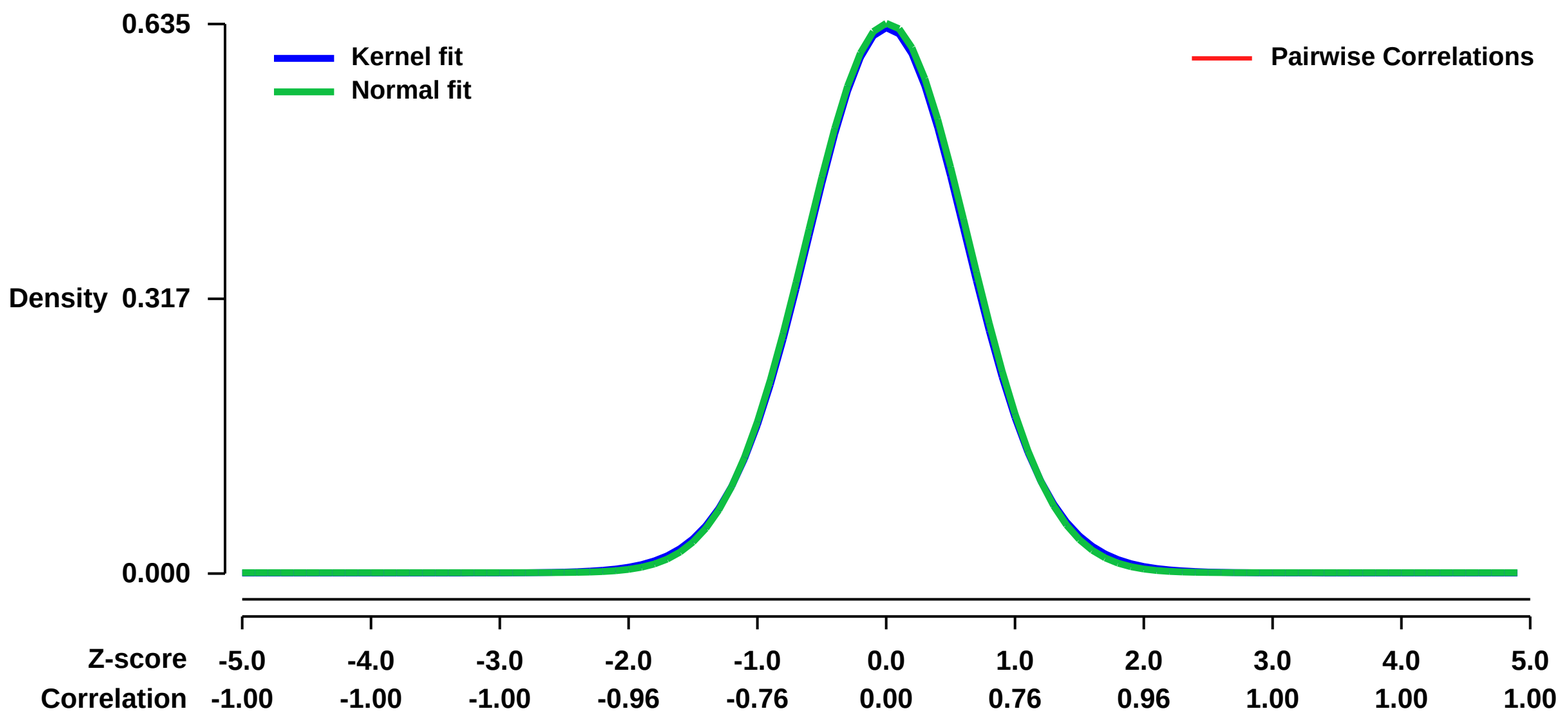

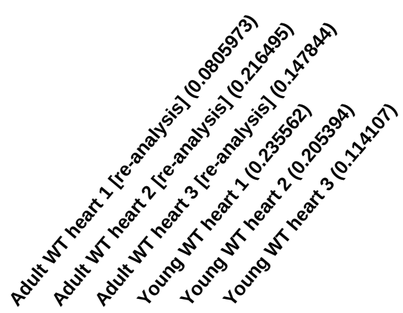

Pre-normalization Quantiles

[min] [medium] [max]

Null module

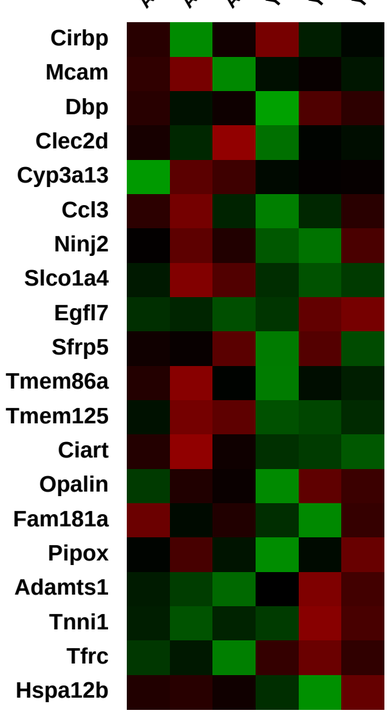

GEO Series "GSE14004" Expression Profiles

Num of samples in this series: 9

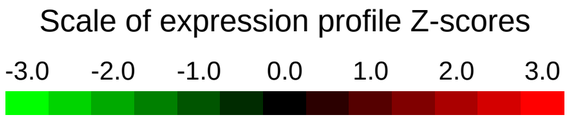

GEO Link:	**http://www.ncbi.nlm.nih.gov/geo/query/acc.cgi?acc=GSE14004**
Status:	**Public on Jan 14 2009**
Title:	**Re-expression of GATA2 Cooperates with PPAR gamma Depletion to Revert the Adipocyte Phenotype**
Organism:	**Mus musculus**
Experiment type:	**Expression profiling by array**
Platform:	**GPL1261**
Pubmed ID:	**19136559**
Summary & Design:	**Summary:** **The nuclear receptor PPAR gamma is required for adipocyte differentiation, but its role in mature adipocytes is less clear. Here we report that knockdown of PPAR gamma expression in 3T3-L1 adipocytes returned the expression of most adipocyte genes towards preadipocyte levels. Consistently, down regulated but not up regulated genes showed strong enrichment of PPAR gamma binding. Surprisingly, not all adipocyte genes were reversed and the adipocyte morphology was maintained for an extended period after PPAR gamma depletion. To explain this, we focused on transcriptional regulators whose adipogenic regulation was not reversed upon PPAR gamma depletion. We identified GATA2, a transcription factor whose down-regulation early in adipogenesis is required for preadipocyte differentiation, remaining low after PPAR gamma knockdown. Forced expression of GATA2 in mature adipocytes complemented PPAR gamma depletion and impaired adipocyte functionality with a more preadipocyte- like gene expression profile. Ectopic expression of GATA2 in adipose tissue in vivo had similar effect on adipogenic gene expression. These results suggest that PPAR gamma-independent down regulation of GATA2 prevents reversion of mature adipocytes after PPAR gamma depletion.** **Keywords: cell type comparison, Gata2, PPAR gamma, adipocyte, preadipocytes, differentiation** **Overall design:** **Technical replicates: PPAR gamma siRNA 1, PPAR gamma siRNA 2, PPAR gamma siRNA 3**

Background corr dist: KL-Divergence = 0.0294, L1-Distance = 0.0232, L2-Distance = 0.0006, Normal std = 0.6966

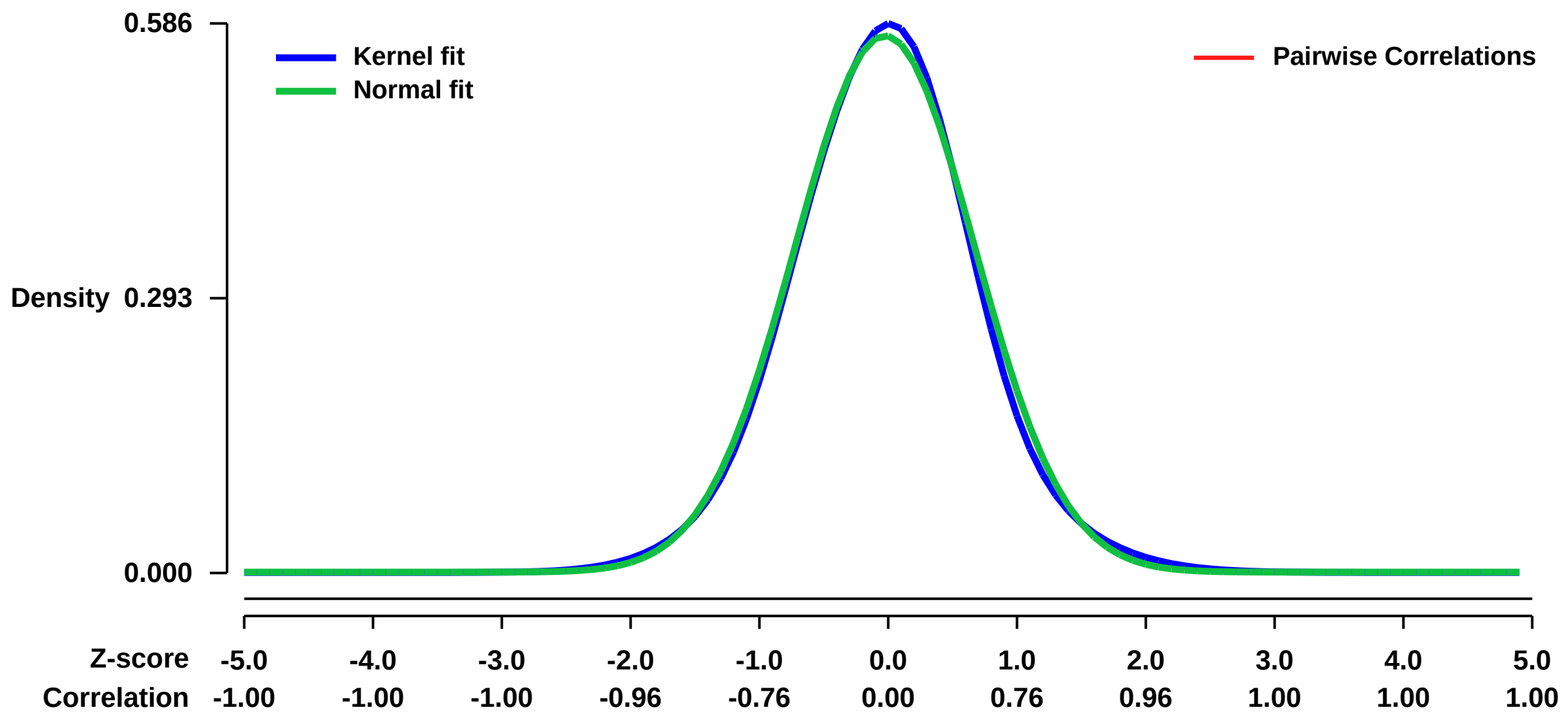

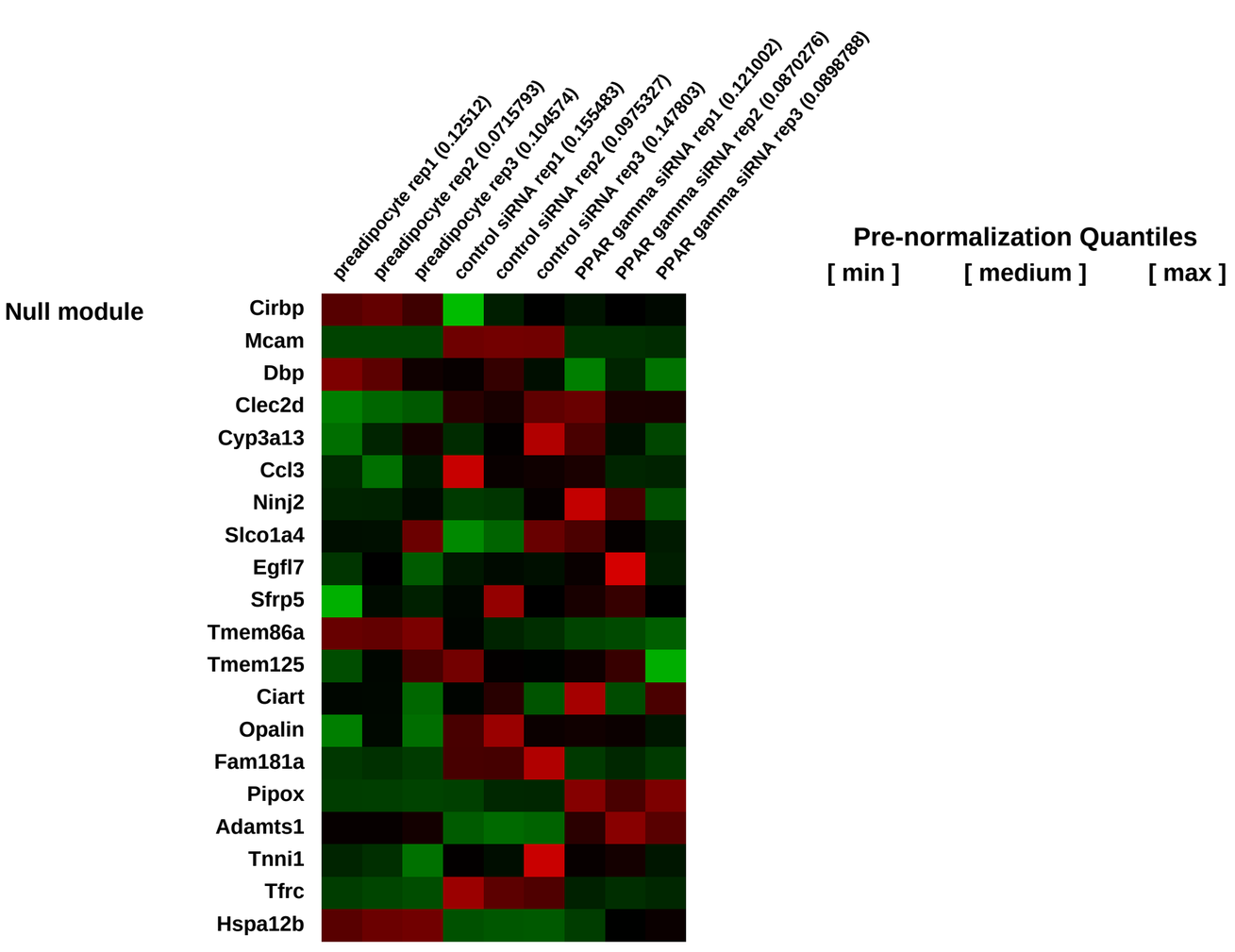

GEO Series "GSE21054" Expression Profiles

Num of samples in this series: 8

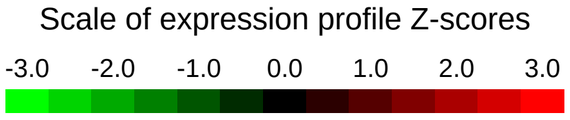

GEO Link:	**http://www.ncbi.nlm.nih.gov/geo/query/acc.cgi?acc=GSE21054**
Status:	**Public on Sep 13 2010**
Title:	**Differential roles of Sall4 isoforms in ES cell pluripotency: expression**
Organism:	**Mus musculus**
Experiment type:	**Expression profiling by array**
Platform:	**GPL1261**
Pubmed ID:	**20837710**
Summary & Design:	**Summary:** **Murine embryonic stem cells (ESCs) are defined by continuous self-renewal and pluripotency. A diverse repertoire of protein isoforms arising from alternative splicing are expressed in ES cells without defined biological roles. Sall4, a transcription factor essential for pluripotency, exists as two isoforms (Sall4a and Sall4b). By genome-wide location analysis, we have determined that Sall4b, and not Sall4a, binds preferentially to highly expressed loci in ES cells. Sall4a and Sall4b binding sites are distinguished by both epigenetic marks at target loci and their clustering with binding sites of other pluripotency factors. When ESCs expressing a single isoform of Sall4 are generated, Sall4b alone could maintain the pluripotent state, although it could not completely suppress all differentiation markers. Sall4a and Sall4b collaborate in maintenance of the pluripotent state, but play distinct roles. Our work is novel in establishing such isoform-specific differences in ES cells.** **Overall design:** **Cells infected with an empty lentivirus (Wt) are compared with cells missing both isoforms of Sall4 (WT+shRNA) or a single isoform (Sall4aIMM+shRNA or Sall4bIMM+shRNA). ES cells expressing a single isoform of Sall4 (either Sall4a or Sall4b) were generated by using a lentivirally based shRNA (Open Biosystems TRC0000097821) that depleted both endogenous isoforms and then adding back a single isoform cDNA that was immune to the shRNA. Transcriptome analysis was performed 48 hrs after infection to identify changes in gene expression at various loci when only a single isoform of Sall4 was present.**

Background corr dist: KL-Divergence = 0.0685, L1-Distance = 0.0207, L2-Distance = 0.0006, Normal std = 0.5015

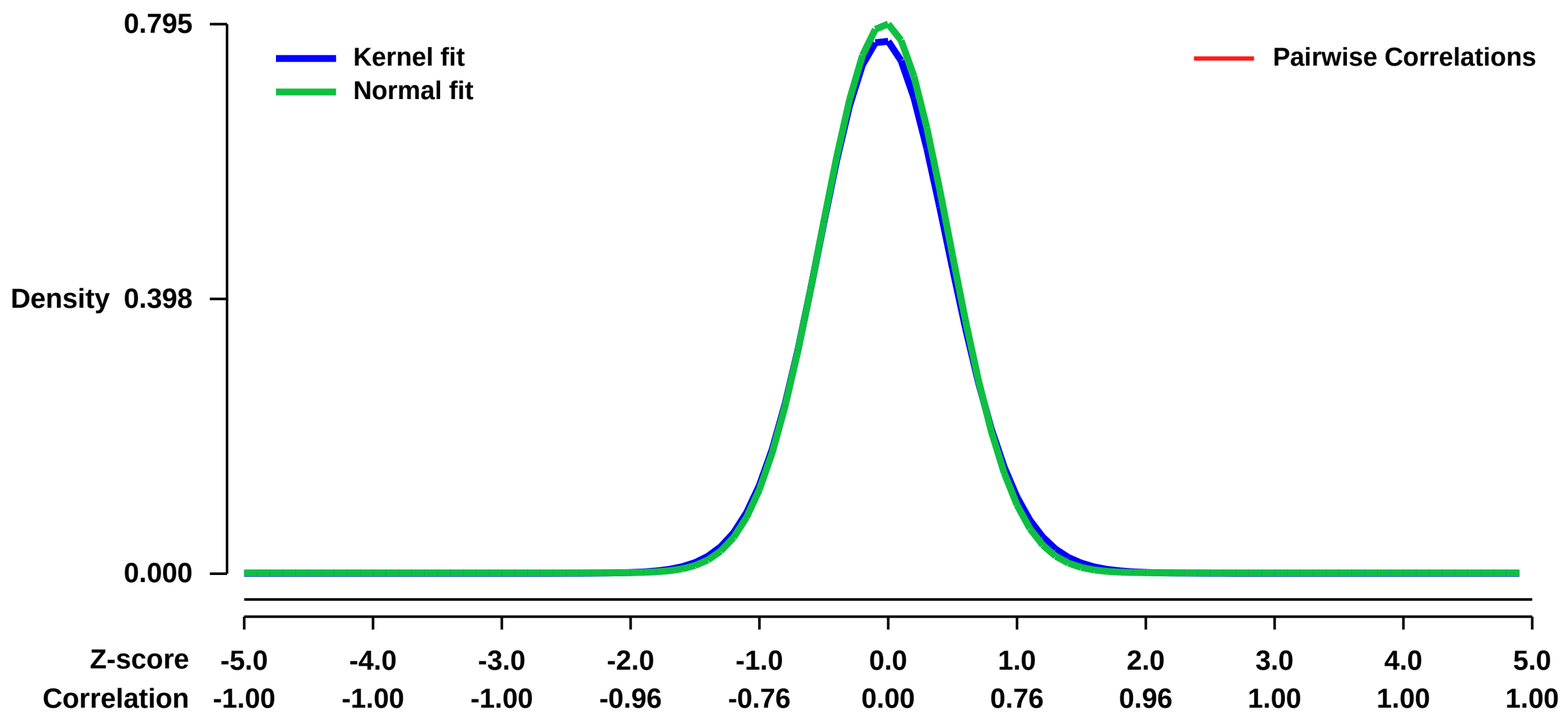

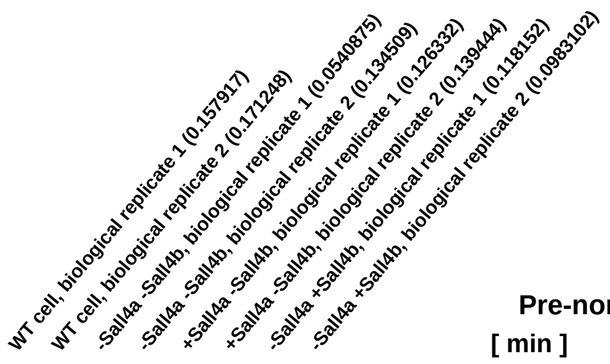

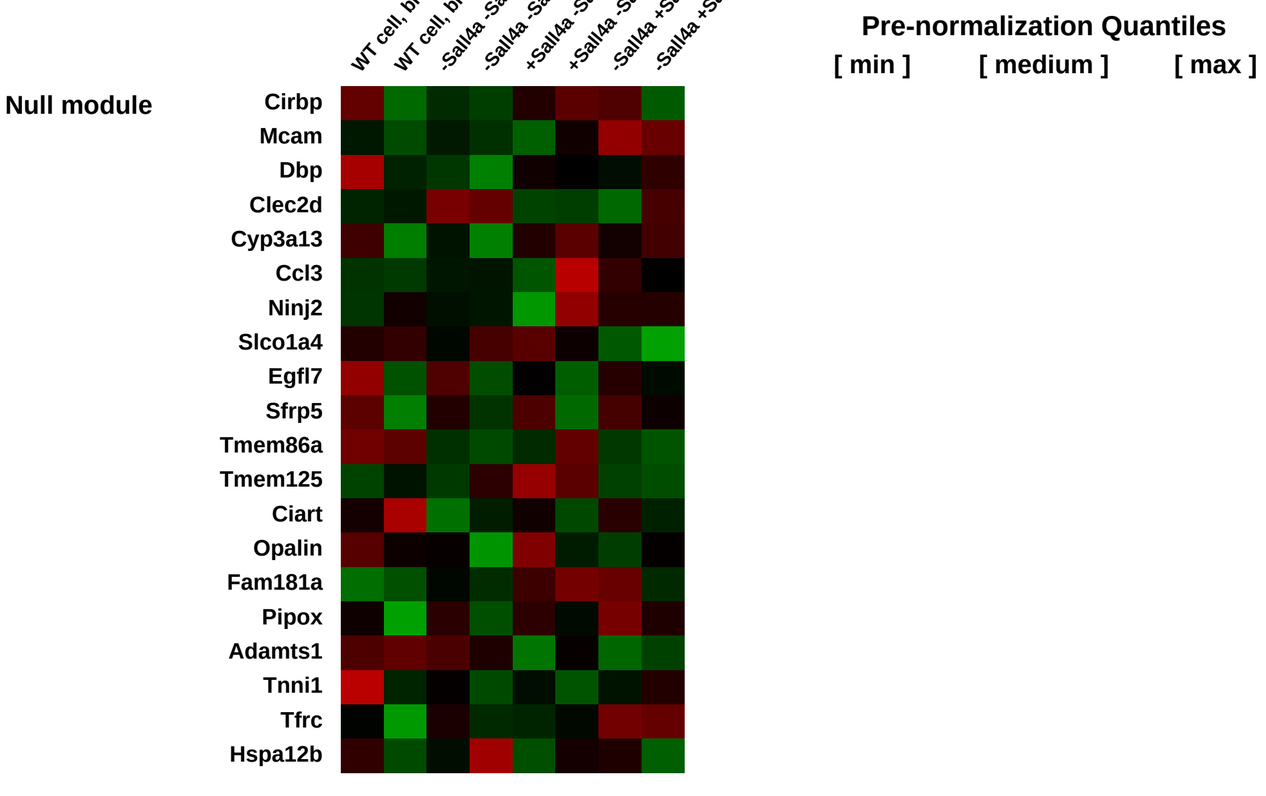

GEO Series "GSE25257" Expression Profiles

Num of samples in this series: 6

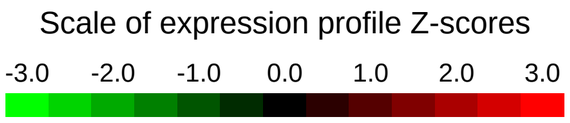

GEO Link:	**http://www.ncbi.nlm.nih.gov/geo/query/acc.cgi?acc=GSE25257**
Status:	**Public on Nov 11 2010**
Title:	**Expression data from wild-type and Zmpste24-/- mouse embryonic fibroblasts (MEFs) at an early passage (passage 3, P3)**
Organism:	**Mus musculus**
Experiment type:	**Expression profiling by array**
Platform:	**GPL1261**
Pubmed ID:	
Summary & Design:	**Summary:** **Zmpste24 is a metalloproteinase processing prelamin A into mature lamin A, a nuclear structure protein. Zmpste24-/- mice which accumulate prelamin A in cells recapitulate accelerated aging phenotypes observed in human premature aging disorder, Hutchinson Gilford progeria sydrome (HGPS). Zmpste24-/- mouse embryonic fibroblasts (MEFs) exhibited genomic instabiliy and accelerated aging at cellular level, which is premature senescence.** **We performed microarray analysis on Zmpste24-/- MEFs, compared to wild-type littermates' MEFs, at an early passage (P3), which is a pre-symptom stage before cellular senescence occurs in the mutant MEFs, in order to examine gene expression profile and figure out the underneath mechanism triggering the premature aging process.** **Overall design:** **Early passage wild-type and Zmpste24-/- MEFs were collected for RNA extraction, the quality of RNAs were determinded by Electrophoresis Assay (2100 Bioanalyzer, Agilent) and RNA extractions were used for hybridization on Affymetrix microarrays.**

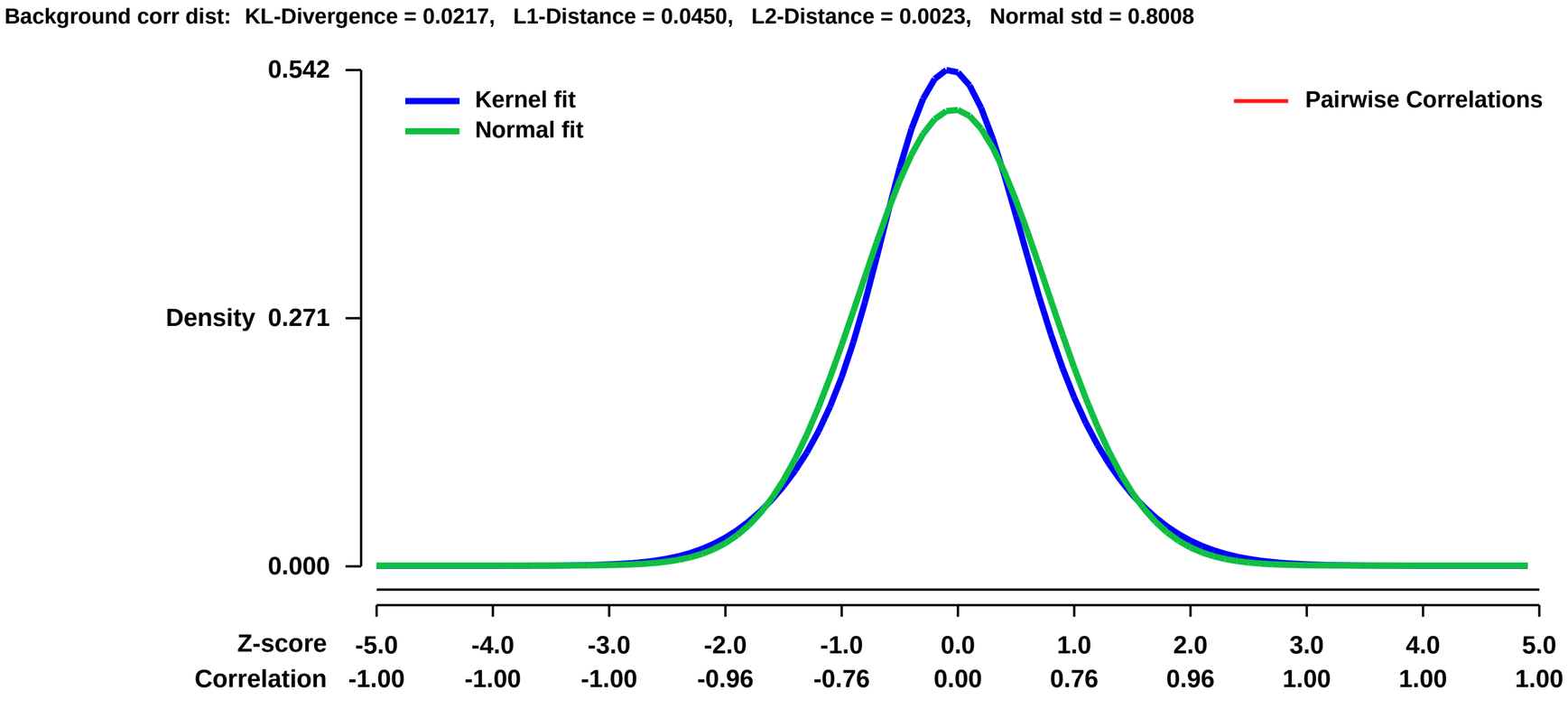

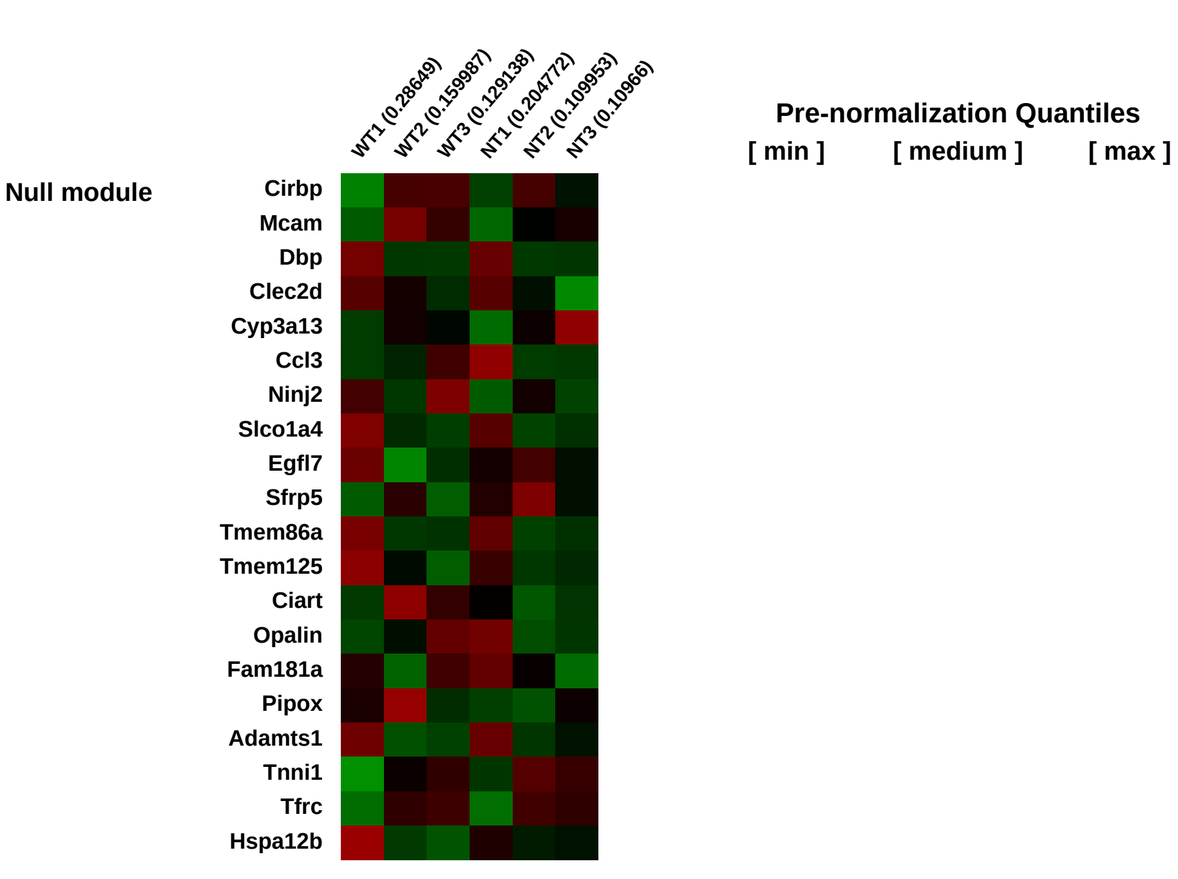

GEO Series "GSE17728" Expression Profiles

Num of samples in this series: 12

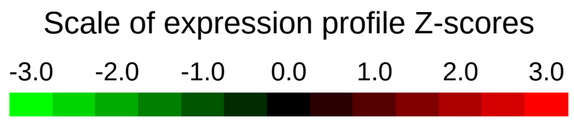

GEO Link:	http://www.ncbi.nlm.nih.gov/geo/query/acc.cgi?acc=GSE17728
Status:	Public on May 26 2012
Title:	Blood gene expression profile from mouse C57Bl/10 exposed to chronic hypoxia
Organism:	Mus musculus
Experiment type:	Expression profiling by array
Platform:	GPL1261
Pubmed ID:	22629407
Summary & Design:	**Summary:** In order to study the gene expression profile in C57Bl/10 mouse blood, we exposed three different groups of animals. First was exposed to PO2 21% or normoxia. The second was exposed to chronic hypoxia (from PO2 21% to PO2 8%) and the third was also exposed to the same chronic hypoxia (CH) protocol but followed by two weeks under normoxia, and called as recovery group. The blood was extracted from inferior vena cava, the RNA was extracted, amplified and hybridized to Affimetrix MOE 430 V2.o chip. The results were analyzed using Partek Genome suite software. Using two fold cuttoff and 0% FDR parameters, we observed genes 512 diferentially expressed, of which one gene was up-regulated in both hypoxic and recovery condition, 202 were up-regulated during CH and then down-regulated after the recovery, 18 genes were down-regulated afteh CH and the up-regulated after recovery, ans finally 9 genes were down-regulated in both CH and recovery conditions. **Overall design:** Each group of C57Bl/10 mouse had 4 individuals and they were divided into three different groups of animals. First was exposed to PO2 21% or normoxia for 14 days. The second was exposed to chronic hypoxia (from PO2 21% to PO2 8%) and the third was also exposed to the same chronic hypoxia (CH) protocol but followed by two weeks under normoxia, and called as recovery group. After the exposure period, the animals were anaesthetized with a mix of Ketamine (100 mg/mL) and xylasine (20 mg/mL) in a proportion of 1:1. A incison was made on abdominal area and from kidneis and liver area of inferior vena cava venus blood was collected The blood was extracted from inferior vena cava. Then, the RNA was extracted, amplified and hybridized to Affimetrix MOE 430 V2.o chip. The results were analyzed using Partek Genome suite software. Using two fold cuttoff and 0% FDR parameters, we observed genes 512 diferentially expressed, of which one gene was up-regulated in both hypoxic and recovery condition, 202 were up-regulated during CH and then down-regulated after the recovery, 18 genes were down-regulated afteh CH and the up-regulated after recovery, ans finally 9 genes were down-regulated in both CH and recovery conditions.

Background corr dist: KL-Divergence = 0.0545, L1-Distance = 0.0470, L2-Distance = 0.0038, Normal std = 0.5640

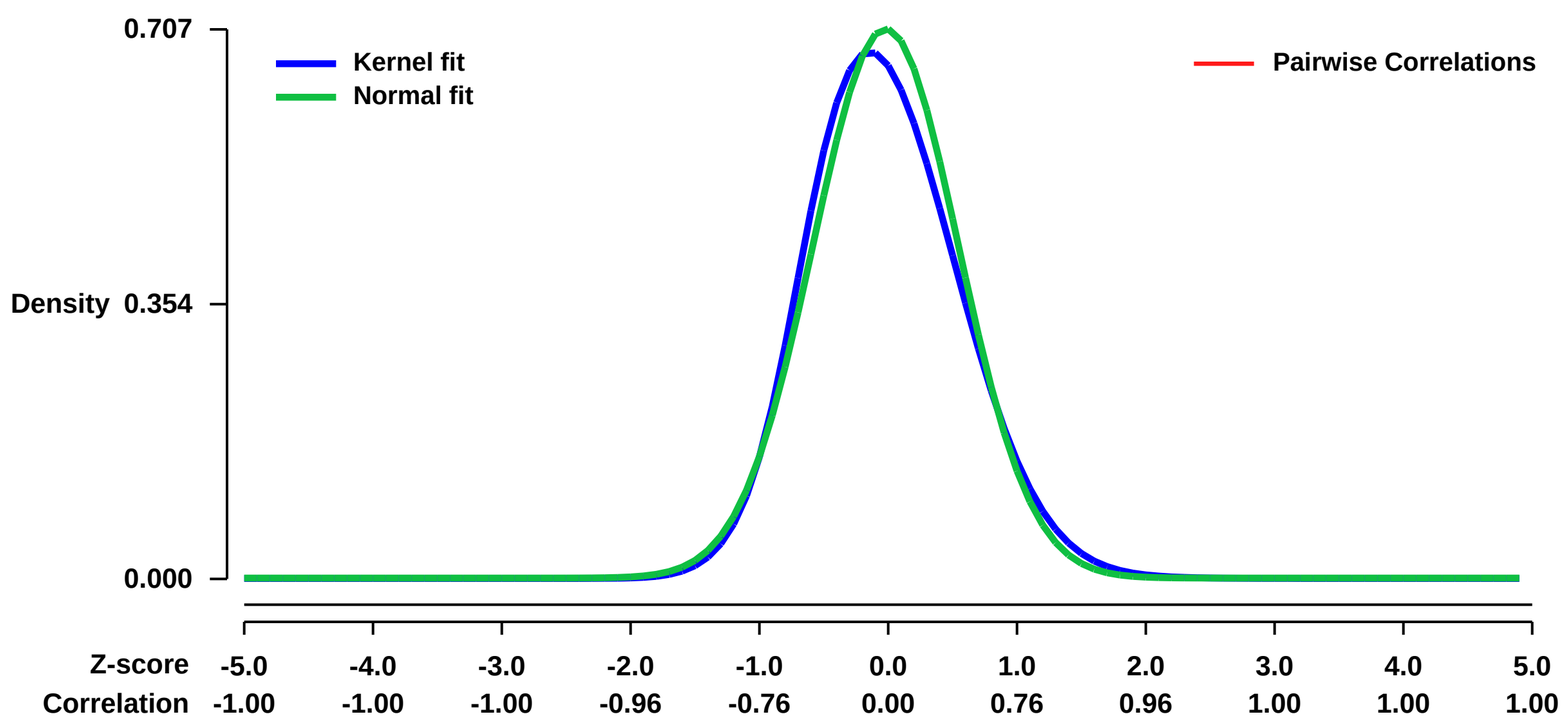

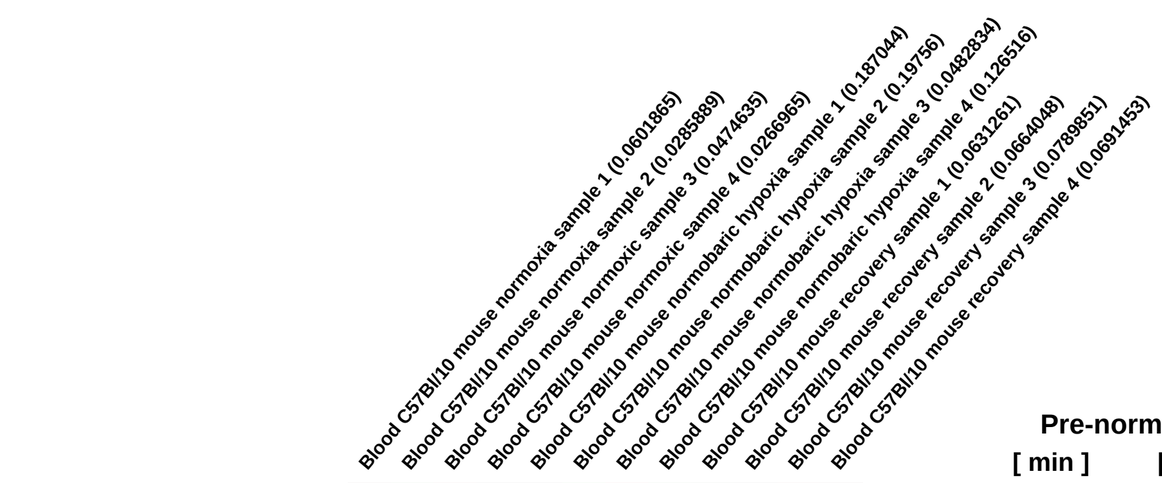

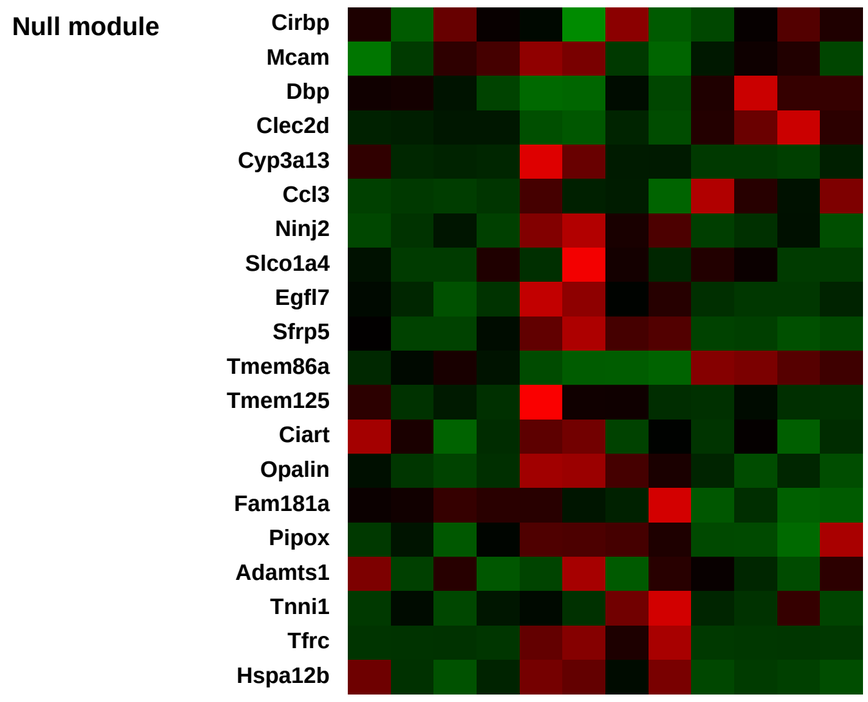

GEO Series "GSE27019" Expression Profiles

Num of samples in this series: 6

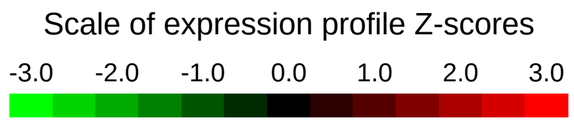

GEO Link:	**http://www.ncbi.nlm.nih.gov/geo/query/acc.cgi?acc=GSE27019**
Status:	**Public on Aug 01 2012**
Title:	**Role of transcriptional regulators IFRD1 and IFRD2 in intestinal lipid absorption and obesity**
Organism:	**Mus musculus**
Experiment type:	**Expression profiling by array**
Platform:	**GPL1261**
Pubmed ID:	
Summary & Design:	**Summary:** **Because of the epidemic rise of obesity worldwide, the identification of novel target genes for pharmacological treatment of obesity and related disorders is becoming of high importance. IFRD1 and IFRD2 are members of a novel transcriptional regulators family. Intestinal over-expression of mouse homologue of IFRD1 promoted intestinal triglyceride uptake and induced whole body adiposity in mice. To further elucidate the role of IFRD1 and IFRD2 in vivo, we generated mice lacking both mouse homologues of IFRD1 (TIS7) and IFRD2 (SKMc15) genes. Here, we report that mice deficient in TIS7 and SKMc15 genes, despite normal calorie intake had severely reduced amount of adipose tissue, were resistant to diet-induced obesity and displayed high glucose tolerance. Lower dietary fat entry into the circulation suggested that this phenotype resulted from impaired intestinal lipid transport. We identified down-regulation of CD36, a fatty acid transporter, both on RNA and protein levels. Reporter assays indicated that TIS7 and SKMc15 transcriptionally regulated CD36 expression and CD36 overexpression partially restored fatty acid uptake in vitro. Hence, our study suggested that TIS7 and SKMc15 play an important role in the regulation of the lipid metabolism and might represent a novel strategy for treatment of disorders caused by excess fat intake.** **To determine whether decreased intestinal lipid absorption might be caused by changes in expression of lipid processing and transport molecules, we performed Affymetrix microarray analyses of total RNA samples isolated from the jejunum of HFD-fed WT type and dKO animals. The moderated t-test was used to calculate p-values for significance of differential gene expression between 3 dKO and 3 wild type mice. These raw p-values were adjusted for multiple hypothesis testing using the method from Benjamini and Hochberg for a strong control of the false discovery rate (FDR) and genes with thus adjusted p-values < 0.05 were considered significant.** **Overall design:** **Age-matched (7-10 week old) male wild type and TIS7 (Ifrd1) SKMc15 (Ifrd2) double knock out mice (C57Bl6 background) were caged individually and maintained from 3 weeks up to 8 weeks on a synthetic high saturated fat (HFD) diet (Ssniff). Small intestines (jejunum) were harvested for total RNA isolation. RNAs from 3 WT and 3 dKO mice were subjected to Affymetrix based whole genome gene expression analysis (Mouse 430.2 GeneChip).**

Background corr dist: KL-Divergence = 0.0401, L1-Distance = 0.0172, L2-Distance = 0.0003, Normal std = 0.6130

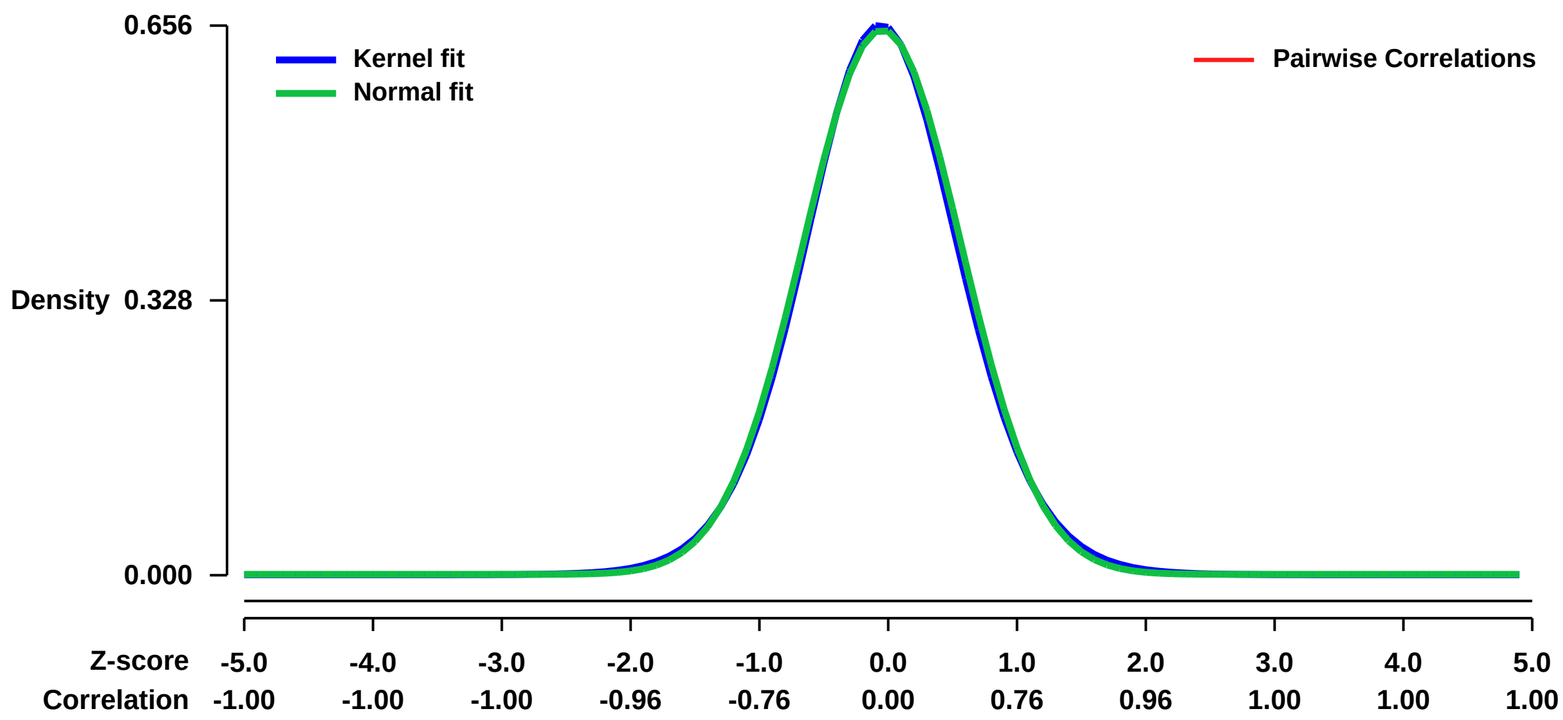

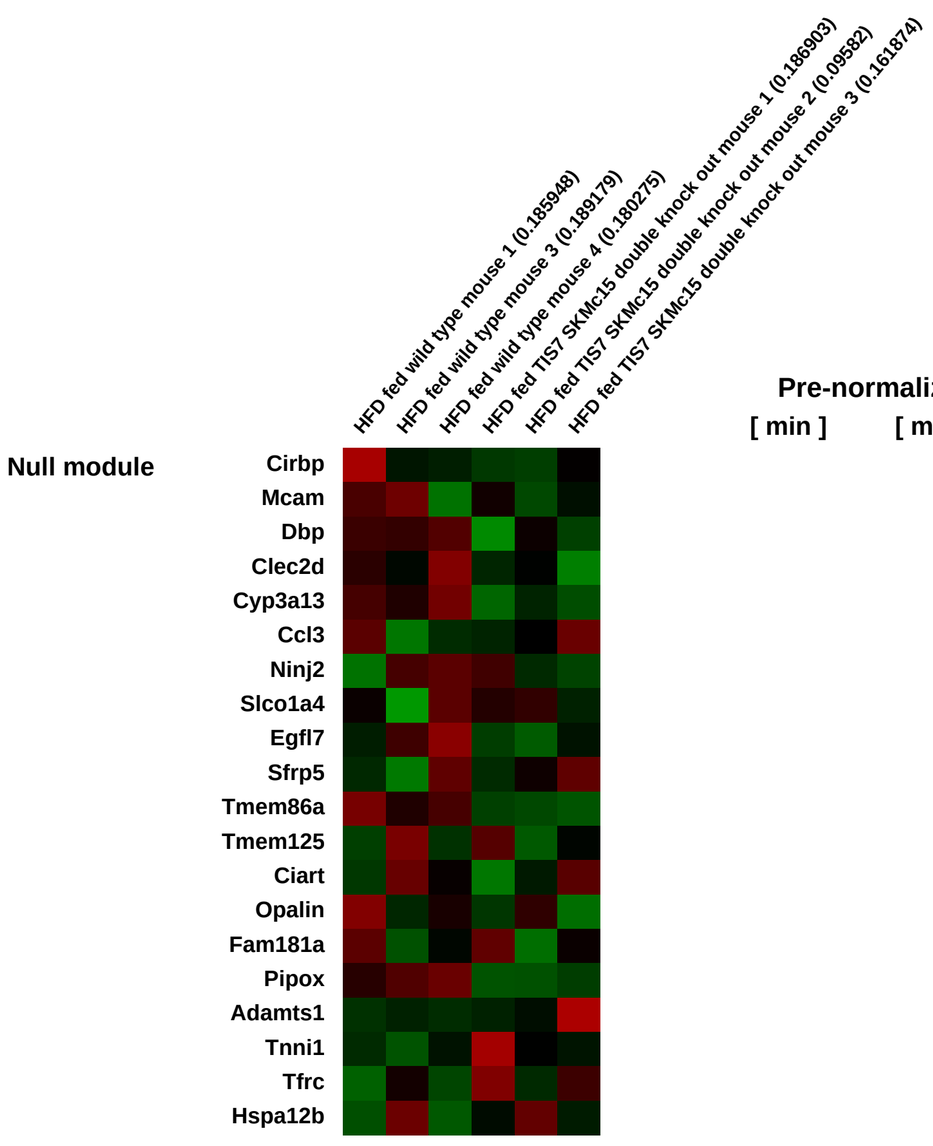

GEO Series "GSE12333" Expression Profiles

Num of samples in this series: 6

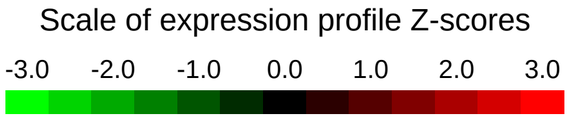

GEO Link:	http://www.ncbi.nlm.nih.gov/geo/query/acc.cgi?acc=GSE12333
Status:	Public on Aug 04 2009
Title:	Retinoic Acid Delivery within Embryoid Bodies Induces an Early Streak Phenotype in vitro
Organism:	Mus musculus
Experiment type:	Expression profiling by array
Platform:	GPL1261
Pubmed ID:	19162317
Summary & Design:	**Summary:** During embryogenesis, cell specification and tissue formation is directed by the concentration and temporal presentation of morphogens, and similarly, pluripotent embryonic stem cells differentiate in vitro into various phenotypes in response to morphogen treatment. Embryonic stem cells are commonly differentiated as three dimensional spheroids called embryoid bodies (EBs); however, differentiation within EBs is typically heterogeneous and disordered. Here we show that spatiotemporal control of microenvironmental cues embedded directly within EBs enhances the homogeneity, synchrony and organization of differentiation. Degradable polymer microspheres releasing retinoic acid within EBs induce the formation of cystic spheroids closely resembling the early streak mouse embryo, with an exterior of visceral endoderm enveloping an epiblast layer. These results demonstrate that controlled morphogen presentation to stem cells more efficiently directs cell differentiation and tissue formation, thereby improving developmental biology models and enabling the development of regenerative medicine therapies and cell diagnostics. **Overall design:** Triplicate control and experiment EBs were processed for microarray.

Background corr dist: KL-Divergence = 0.0339, L1-Distance = 0.0253, L2-Distance = 0.0007, Normal std = 0.6623

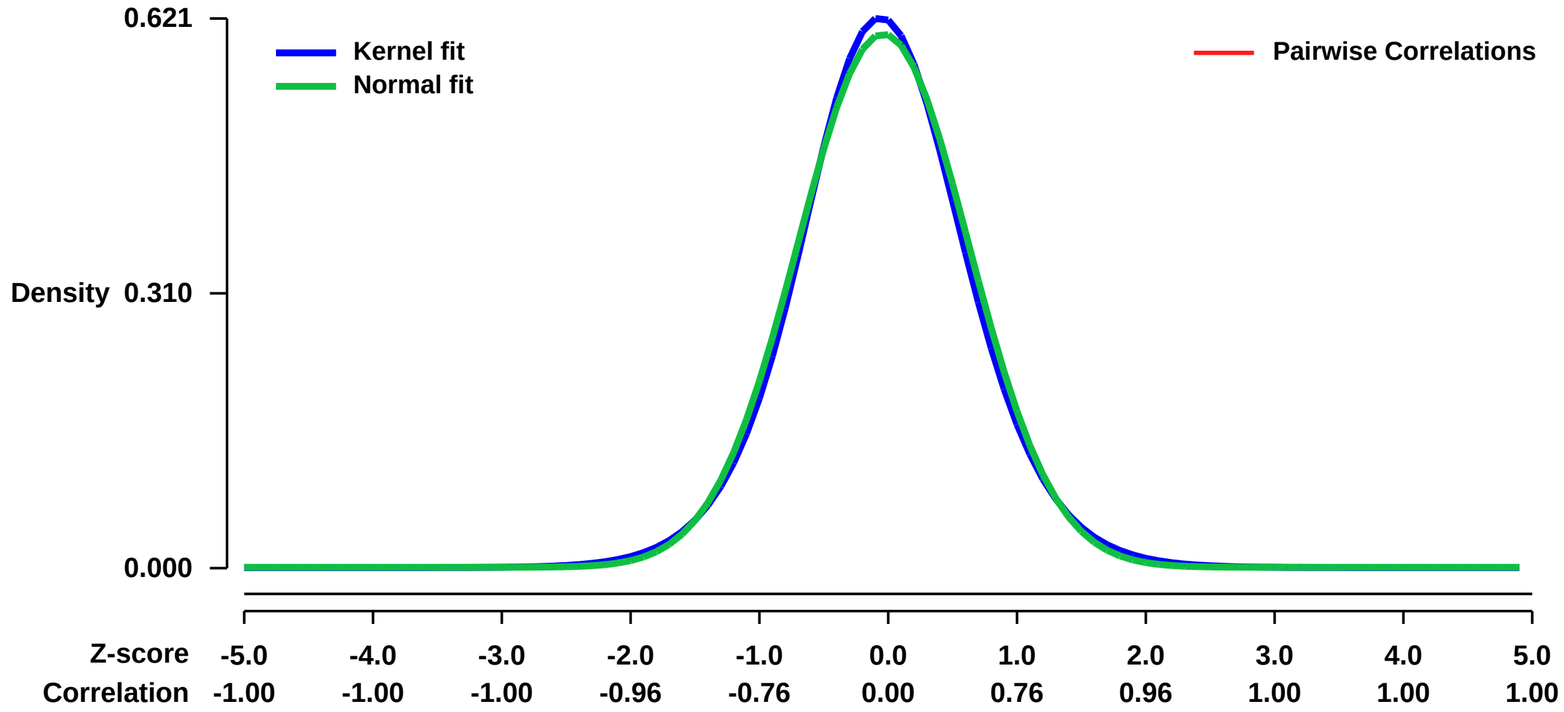

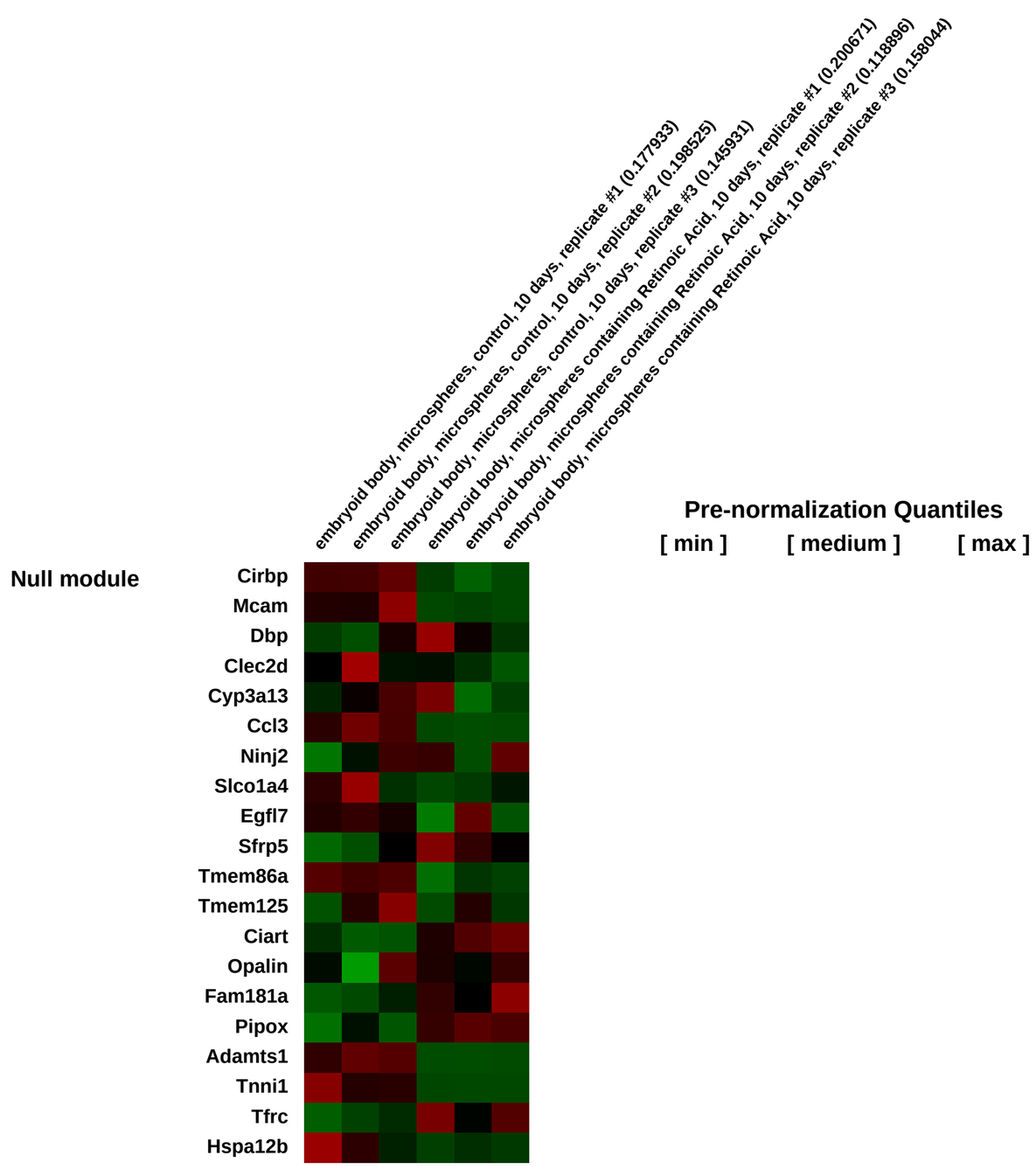

GEO Series "GSE13421" Expression Profiles

Num of samples in this series: 8

Scale of expression profile Z-scores

-3.0 -2.0 -1.0 0.0 1.0 2.0 3.0

GEO Link:	http://www.ncbi.nlm.nih.gov/geo/query/acc.cgi?acc=GSE13421
Status:	Public on Nov 01 2008
Title:	CBA/CaJ mouse cochlea gene expression profile
Organism:	Mus musculus
Experiment type:	Expression profiling by array
Platform:	GPL1261
Pubmed ID:	19277783
Summary & Design:	**Summary:** This data set is intended as a public resource documenting the identity of roughly 10,000 genes that are abundantly expressed in the mouse cochlea. The data have many uses, including for making comparisons with proteomics studies, and for comparisons of expression profiles with other mouse strains and with other species. The CBA/CaJ strain was chosen because of its lack of known vulnerabilities to premature cochlear degeneration or to extreme reactions to cochlear stresses. It may therefore be considered a â normalâ mouse. No experimental manipulations were done on the mice of this study. Contamination of the results by genes expressed in the surrounding petrous bone and from those in blood cells was minimized. **Keywords: normal controls** **Overall design:** 8 replicates, pooled ears from each of 8 mice

Background corr dist: KL-Divergence = 0.0701, L1-Distance = 0.0211, L2-Distance = 0.0007, Normal std = 0.5048

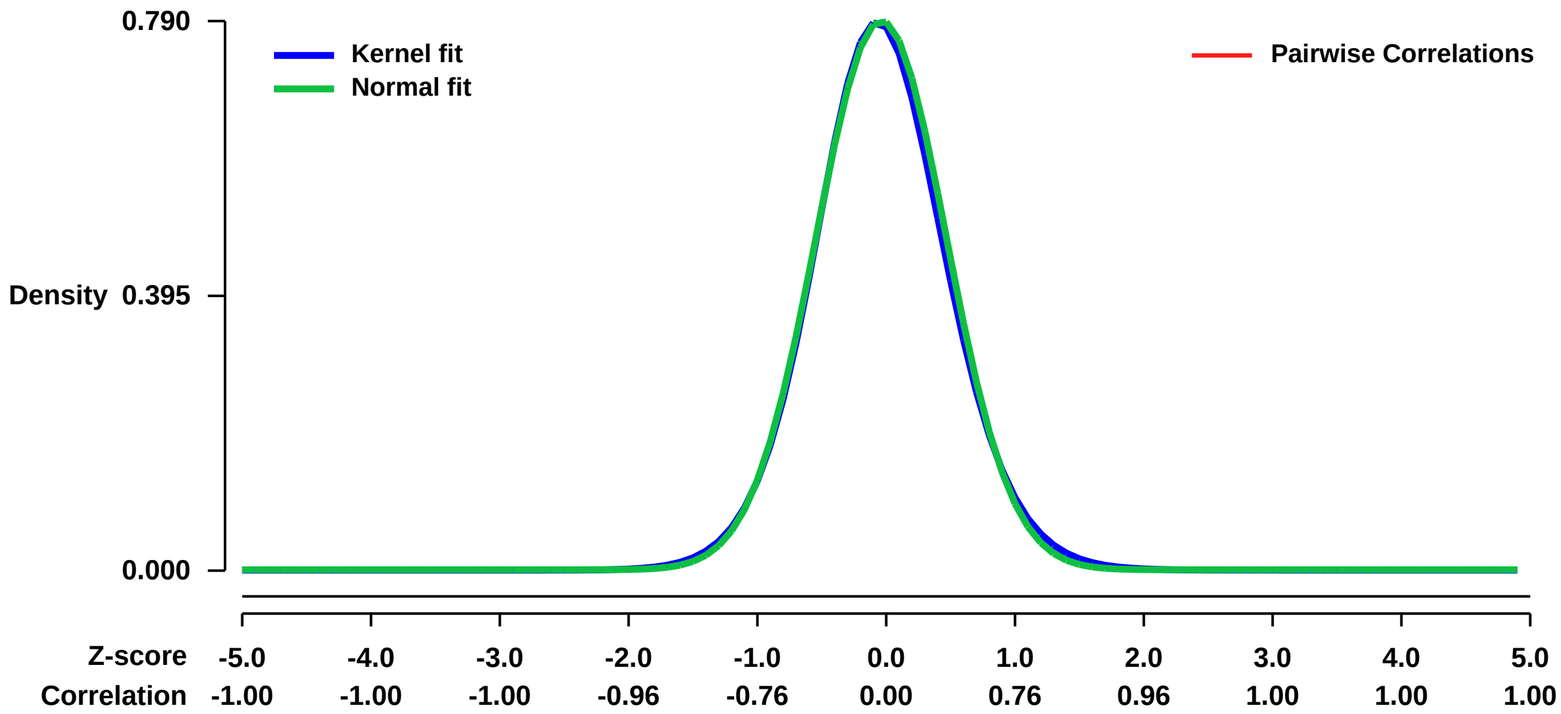

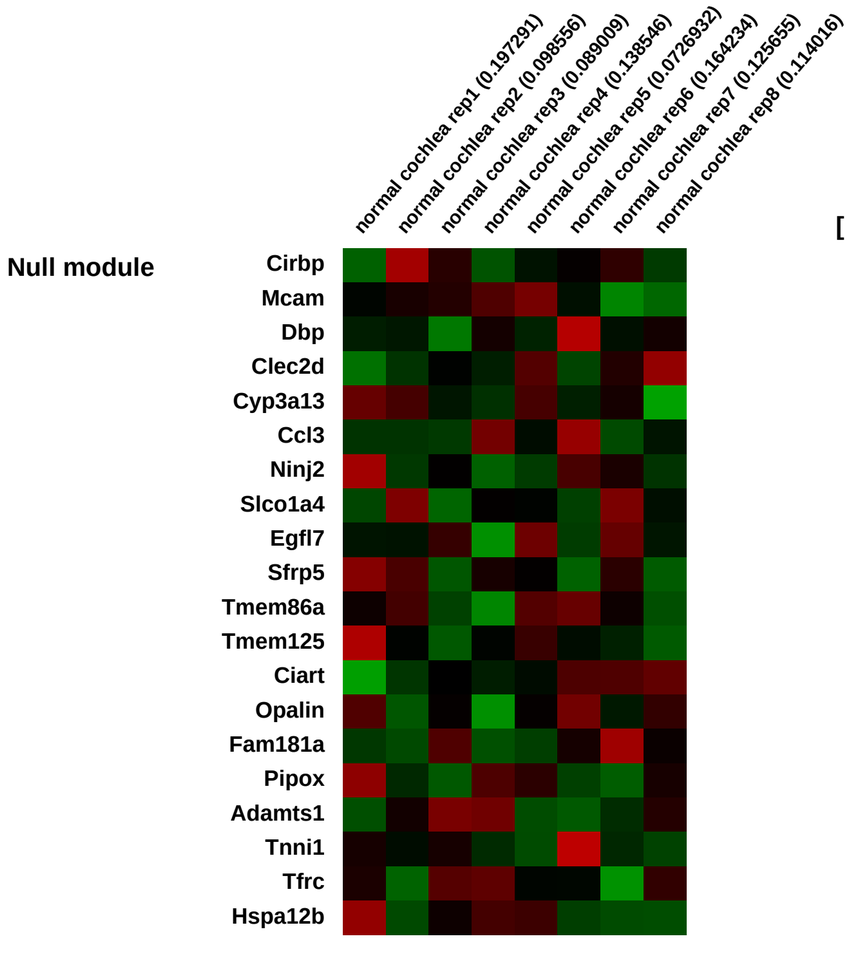

GEO Series "GSE1479" Expression Profiles

Num of samples in this series: 36

Scale of expression profile Z-scores

-3.0 -2.0 -1.0 0.0 1.0 2.0 3.0

GEO Link:	**http://www.ncbi.nlm.nih.gov/geo/query/acc.cgi?acc=GSE1479**
Status:	**Public on Jun 24 2004**
Title:	**C57BL/6 Benchmark Set for Early Cardiac Development**
Organism:	**Mus musculus**
Experiment type:	**Expression profiling by array**
Platform:	**GPL1261**
Pubmed ID:	
Summary & Design:	**Summary:** **Timed matings were performed using C57BL/6 mice and pregnant females sacrificed starting at embryonic day (E) 10.5, and then in daily intervals until E14.5. Gene expression was be further analyzed at E16.5 and E18.5, to monitor changes in gene expression related to maturation of the heart. At stage 10.5, the rostral and caudal parts of the embryo were removed and the middle part, which includes the heart, was subjected to expression analysis. From embryonic day 11.5 on, we isolated embryonic hearts and separated the ventricular from the atrial chambers.** **Keywords = heart** **Keywords = development** **Keywords = cardiac** **Keywords: time-course** **Overall design:**

Background corr dist: **KL-Divergence = 0.2433, L1-Distance = 0.0423, L2-Distance = 0.0035, Normal std = 0.3083**

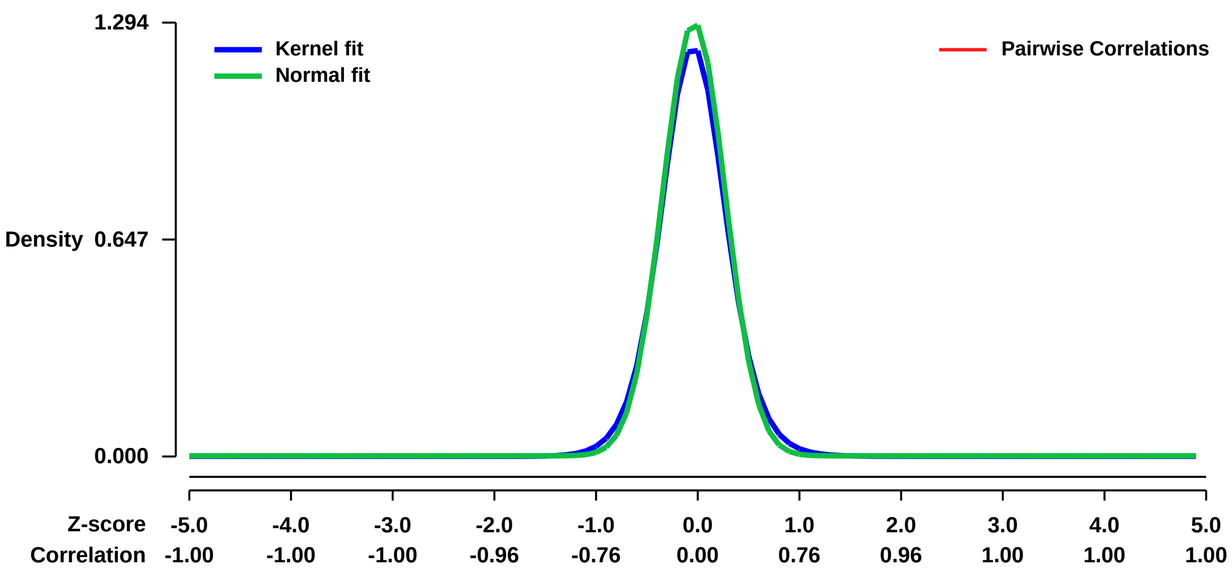

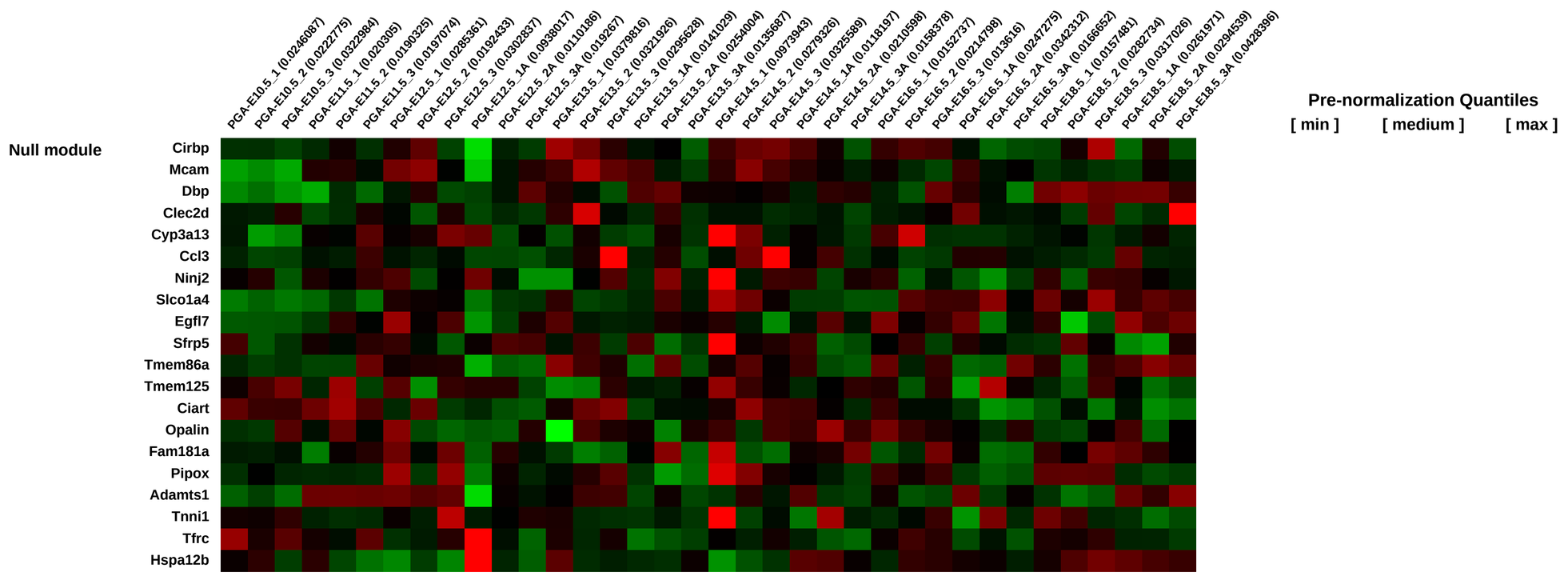

GEO Series "GSE11684" Expression Profiles

Num of samples in this series: 16

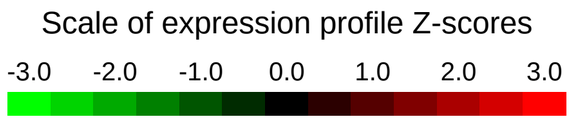

GEO Link:	http://www.ncbi.nlm.nih.gov/geo/query/acc.cgi?acc=GSE11684
Status:	Public on Nov 10 2009
Title:	Expression data from Perk wild-type and knockout mouse liver perfused without or with 2,5-di-tert-butylhydroquinone
Organism:	Mus musculus
Experiment type:	Expression profiling by array
Platform:	GPL1261
Pubmed ID:	19509078

Summary & Design:

Summary:
In eukaryotes, regulation of mRNA translation enables a fast, localized and finely tuned expression of gene products. Within the translation process, the first stage of translation initiation is most rigorously modulated by the actions of eukaryotic initiation factors (eIFs) and their associated proteins. These 11 eIFs catalyze the joining of the tRNA, mRNA and rRNA into a functional translation complex. Their activity is influenced by a wide variety of extra- and intracellular signals, ranging from global, such as hormone signaling and unfolded proteins, to specific, such as single amino acid imbalance and iron deficiency. Their action is correspondingly comprehensive, in increasing or decreasing recruitment and translation of most cellular mRNAs, and specialized, in targeting translation of mRNAs with regulatory features such as a 5â terminal oligopyrimidine tract (TOP), upstream open reading frames (uORFs), or an internal ribosomal entry site (IRES). In mammals, two major pathways are linked to targeted mRNA translation. The target of rapamycin (TOR) kinase induces translation of TOP and perhaps other subsets of mRNAs, whereas a family of eIF2 kinases does so with mRNAs containing uORFs or an IRES. TOR targets translation of mRNAs that code for proteins involved in translation, an action compatible with its widely accepted role in regulating cellular growth. The four members of the eIF2 kinase family increase translation of mRNAs coding for stress response proteins such as transcription factors and chaperones. Though all four kinases act on one main substrate, eIF2, published literature demonstrates both common and unique effects by each kinase in response to its specific activating stress. This suggests that the activated eIF2 kinases regulate the translation of both a global and a specific set of mRNAs. Up to now, few studies have attempted to test such a hypothesis; none has been done in mammals.

We use array analysis to determine the global mRNA shift into polysomes following a stress response, and to compare the translational response following activation of GCN2 versus PERK, two of the four eIF2alpha kinases.

Keywords: stress response, comparative genomic

Overall design:
Perk wild-type or knockout mouse liver were perfused without or with 2,4-di-tert-butylhydroquinone (tBuHQ) for RNA extraction and hybridization of Affymetrix microarrays. RNA was extracted from unfractionated liver samples and polysome fraction of samples separated on sucrose density gradient. To minimize biological variations, we pooled RNA from two perfused liver samples to use in each array analysis. The conditions were total and polysome fraction of Perk+/+, -tBuHQ or +tBuHQ; total and polysome fraction of Perk-/-, -tBuHQ or +tBuHQ. Each array analysis was done in duplicate.

Background corr dist: KL-Divergence = 0.2098, L1-Distance = 0.0435, L2-Distance = 0.0042, Normal std = 0.3267

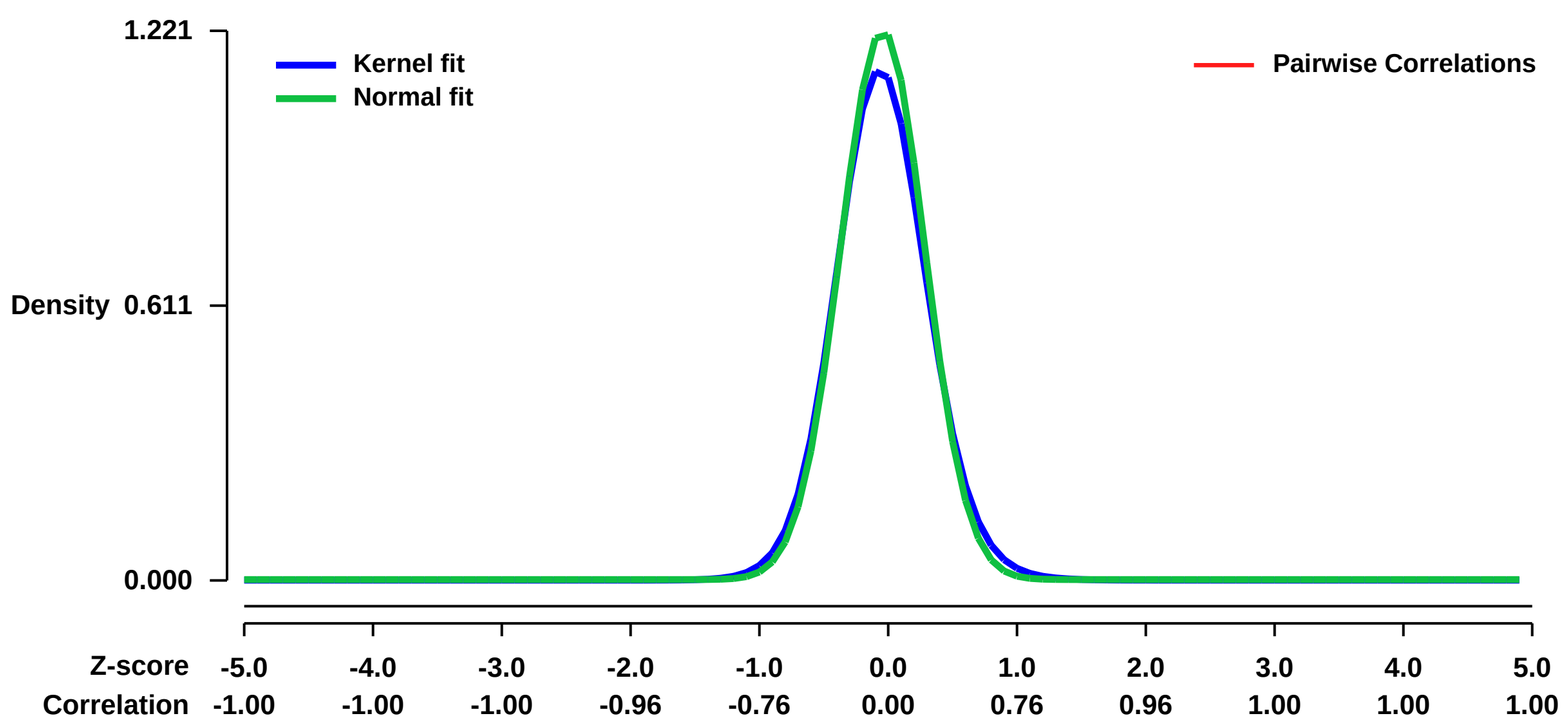

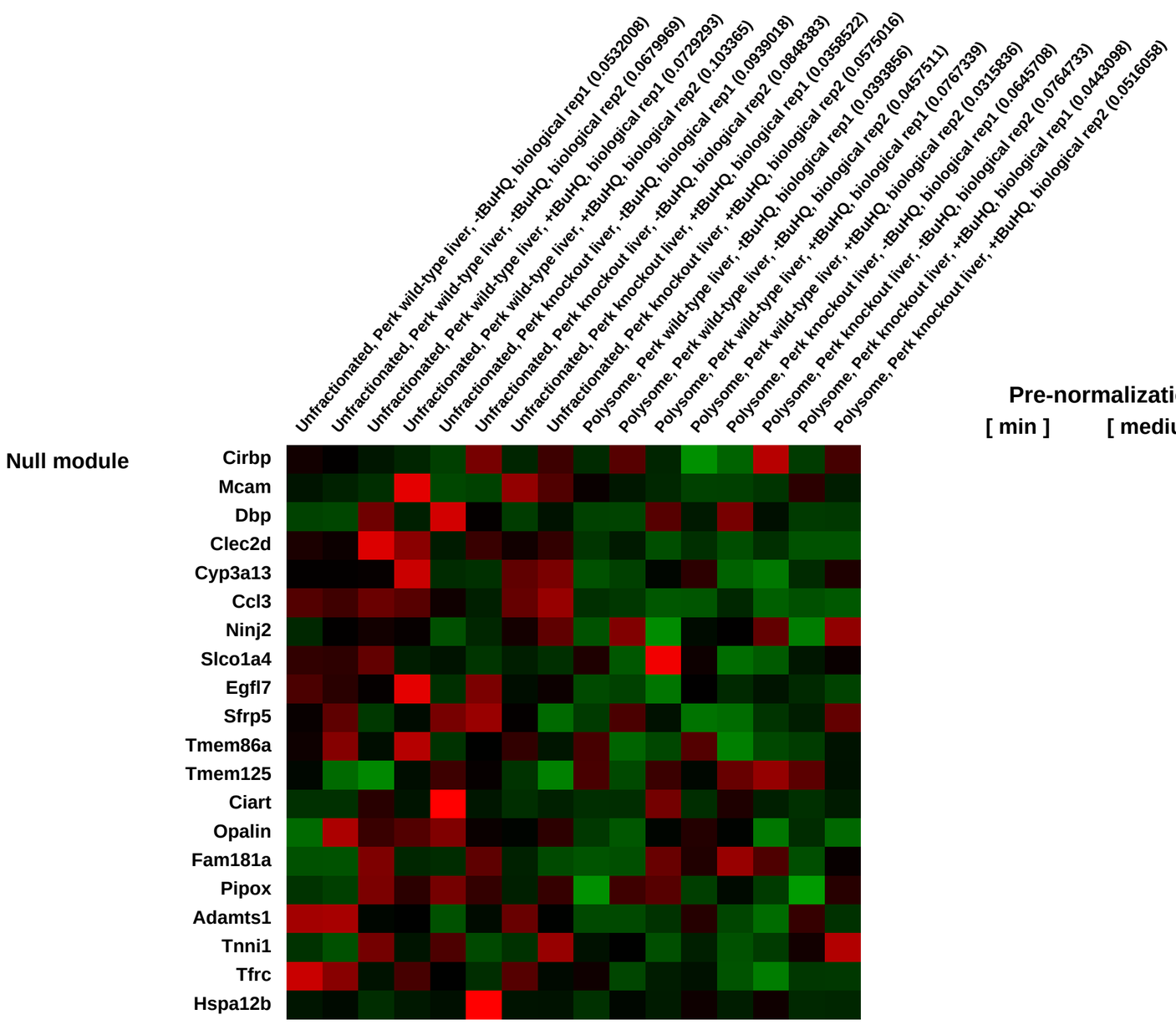

GEO Series "GSE10627" Expression Profiles

Num of samples in this series: 51

Scale of expression profile Z-scores

-3.0 -2.0 -1.0 0.0 1.0 2.0 3.0

GEO Link:	http://www.ncbi.nlm.nih.gov/geo/query/acc.cgi?acc=GSE10627
Status:	Public on Feb 25 2008
Title:	Mll-AF9 induced changes in gene expression in various hematopoietic cells
Organism:	Mus musculus
Experiment type:	Expression profiling by array
Platform:	GPL1261
Pubmed ID:	18455126
Summary & Design:	**Summary:** The pathways by which oncogenes, such as MLL-AF9, initiate transformation and leukemia in humans and mice are incompletely defined. In a study of target cells and oncogene dosage, we found that Mll-AF9, when under endogenous regulatory control, efficiently transformed LSK (Lin- Sca1+ c-kit+) stem cells while committed granulocyte-monocyte progenitors (GMPs) were transformation-resistant and did not cause leukemia. Mll-AF9 was expressed at higher levels in hematopoietic stem (HSC) than GMP cells. Mll- AF9 gene dosage effects were directly shown in experiments where GMPs were efficiently transformed by the high dosage of Mll-AF9 resulting from retroviral transduction. Mll-AF9 up-regulated expression of 196 genes in both LSK and progenitor cells, but to higher levels in LSKs than in committed myeloid progenitors. **Keywords:** mutant hematopoietic cells **Overall design:** Comparison of gene expression profiles among four types of hematopoietic cells (GMP, CMP, CLP and HSC), FACS sorted from wild type and Mll-AF9 knock-in mice. The goal was to identify genes differentially expressed in each Mll-AF9 cell type compared to the corresponding wild type cells.

Background corr dist: KL-Divergence = 0.3051, L1-Distance = 0.0613, L2-Distance = 0.0102, Normal std = 0.2794

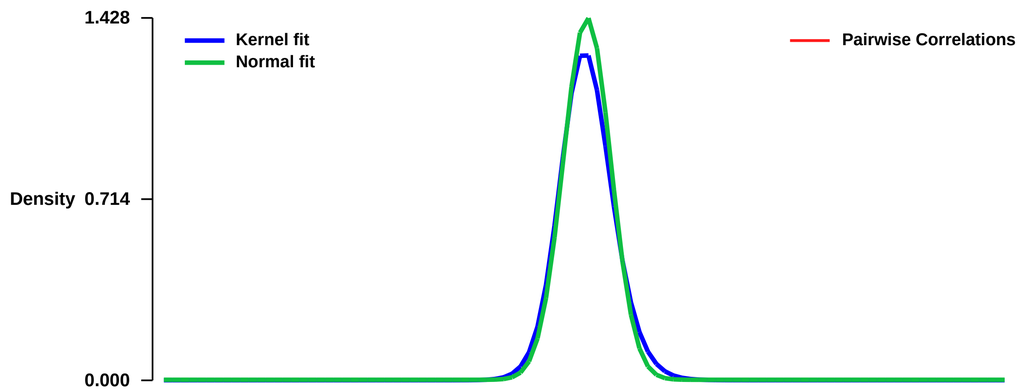

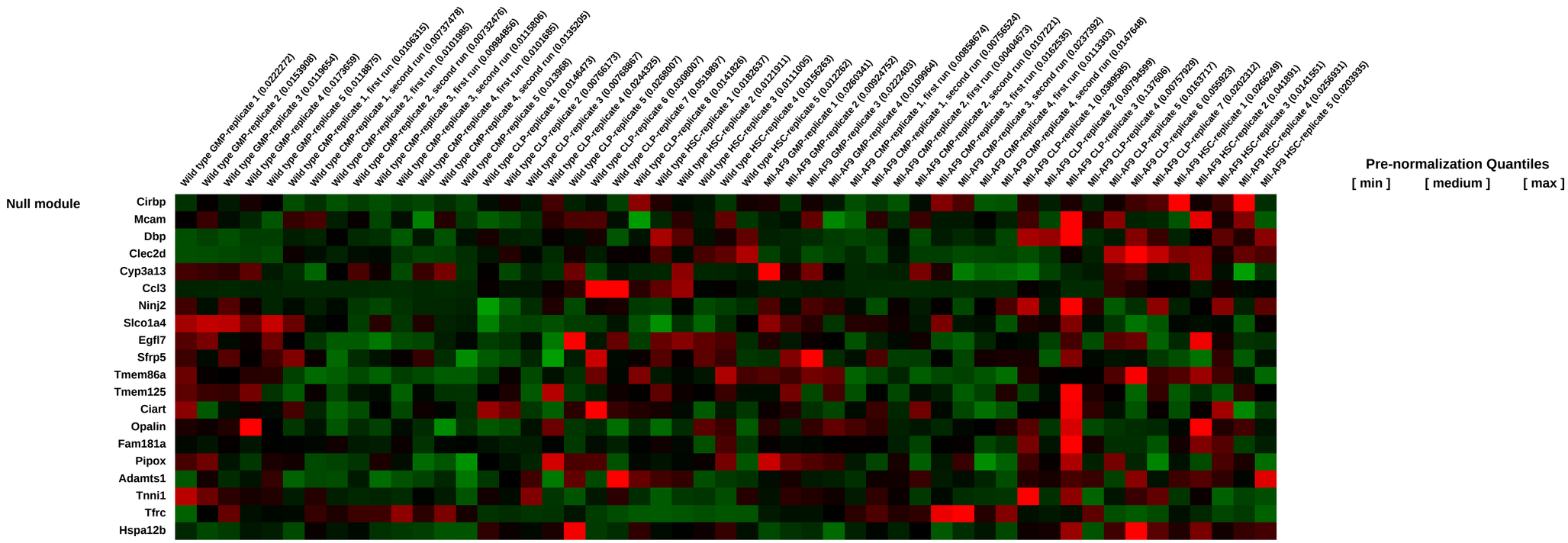

GEO Series "GSE4332" Expression Profiles

Num of samples in this series: 8

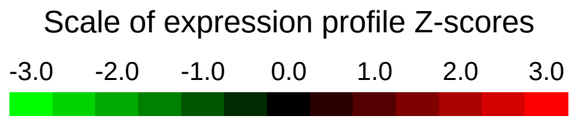

GEO Link:	http://www.ncbi.nlm.nih.gov/geo/query/acc.cgi?acc=GSE4332
Status:	Public on Mar 15 2006
Title:	Cell intrinsic alterations underlie hematopoietic stem cell aging
Organism:	Mus musculus
Experiment type:	Expression profiling by array
Platform:	GPL1261
Pubmed ID:	15967997
Summary & Design:	**Summary:** **Loss of immune function and an increased incidence of myeloid leukemia are two of the most clinically significant consequences of aging of the hematopoietic system. To better understand the mechanisms underlying hematopoietic aging, we evaluated the cell intrinsic functional and molecular properties of highly purified long-term hematopoietic stem cells (LT-HSCs) from young and old mice. We found that LT-HSC aging was accompanied by cell autonomous changes, including increased stem cell self-renewal, differential capacity to generate committed myeloid and lymphoid progenitors, and diminished lymphoid potential. Expression profiling revealed that LT-HSC aging was accompanied by the systemic down-regulation of genes mediating lymphoid specification and function and up-regulation of genes involved in specifying myeloid fate and function. Moreover, LT-HSCs from old mice expressed elevated levels of many genes involved in leukemic transformation. These data support a model in which age-dependent alterations in gene expression at the stem cell level presage downstream developmental potential and thereby contribute to age-dependent immune decline, and perhaps also to the increased incidence of leukemia in the elderly.** **Groups of assays that are related as part of a time series.** **Keywords: time_series_design** **Overall design:** **5 old mice and 3 young mice**

Background corr dist: KL-Divergence = 0.0603, L1-Distance = 0.0196, L2-Distance = 0.0006, Normal std = 0.5299

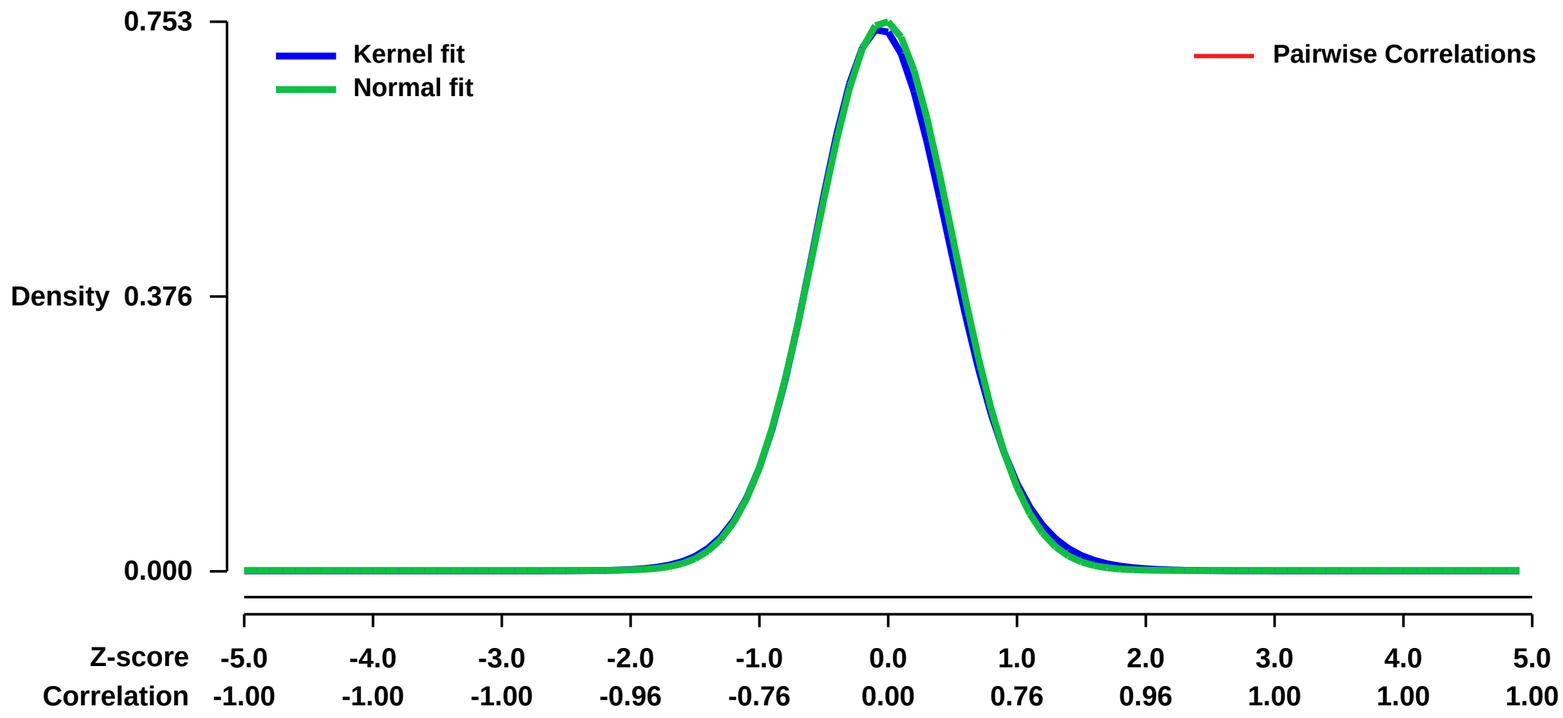

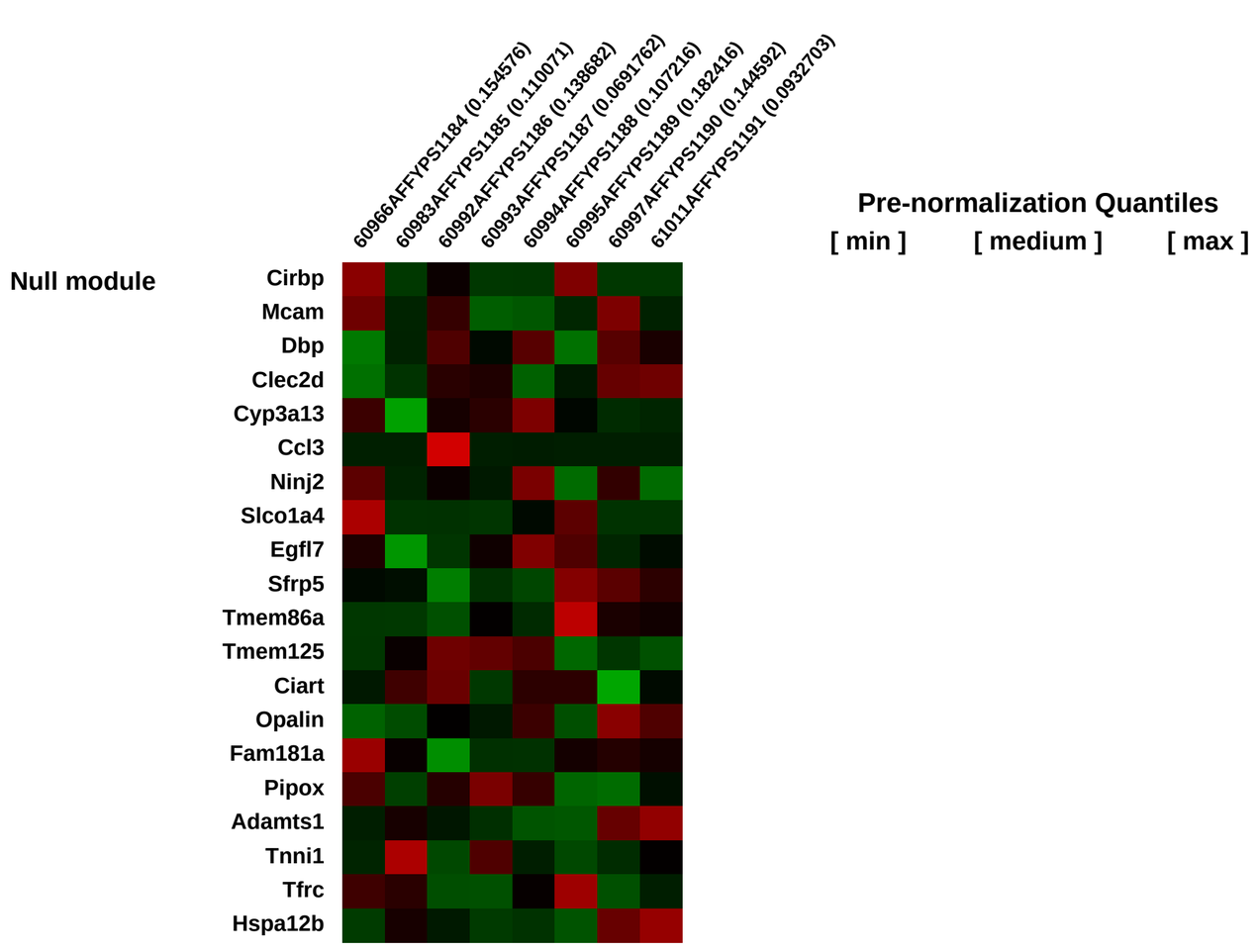

GEO Series "GSE27888" Expression Profiles

Num of samples in this series: 12

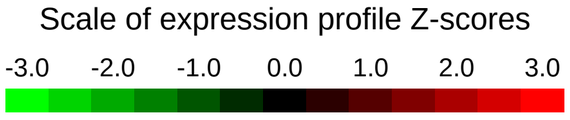

GEO Link:	http://www.ncbi.nlm.nih.gov/geo/query/acc.cgi?acc=GSE27888
Status:	Public on May 10 2011
Title:	Comparative transcriptome analysis of APPs¸–-DM and APLP2-KO brains
Organism:	Mus musculus
Experiment type:	Expression profiling by array
Platform:	GPL1261
Pubmed ID:	21522131
Summary & Design:	**Summary:** Despite its key role in Alzheimer pathogenesis, the physiological function(s) of the amyloid precursor protein (APP) and of its proteolytic fragments are still poorly understood. The secreted APPs¸– ectodomain has been shown to be involved in neuroprotection and synaptic plasticity. The ¸‡-secretase generated APP intracellular domain, AICD, functions as a transcriptional regulator in heterologous reporter assays although its role for endogenous gene regulation has remained controversial. Previously, we have generated APPs¸– knockin (KI) mice expressing solely the secreted ectodomain APPs¸–. Here, we generated double mutants (APPs¸–-DM) by crossing APPs¸–-KI mice onto an APLP2-deficient background and show that APPs¸– rescues the postnatal lethality of the majority of APP/APLP2 double knockout mice. Despite normal CNS morphology and unaltered basal synaptic transmission, young APPs¸–-DM mice already showed pronounced hippocampal dysfunction, impaired spatial learning and a deficit in LTP. To gain further mechanistic insight into which domains/proteolytic fragments are crucial for hippocampal APP/APLP2 mediated functions, we performed a DNA microarray transcriptome profiling of prefrontal cortex and hippocampus of adult APLP2-KO (APLP2-/-) and APPs¸–-DM mice (APP¸–/¸–APLP2-/- mice).Interestingly, this analysis failed to reveal major genotype-related transcriptional differences. Expression differences between cortex and hippocampus were, however, readily detectable. **Overall design:** Prefrontal cortices and hippocampi of adult mice (38 - 40 weeks) of the following genotypes were analyzed: APLP2-KO (APLP2-/-) (n=3) and APPs¸–-DM (APP¸–/¸–APLP2-/-) (n=3).

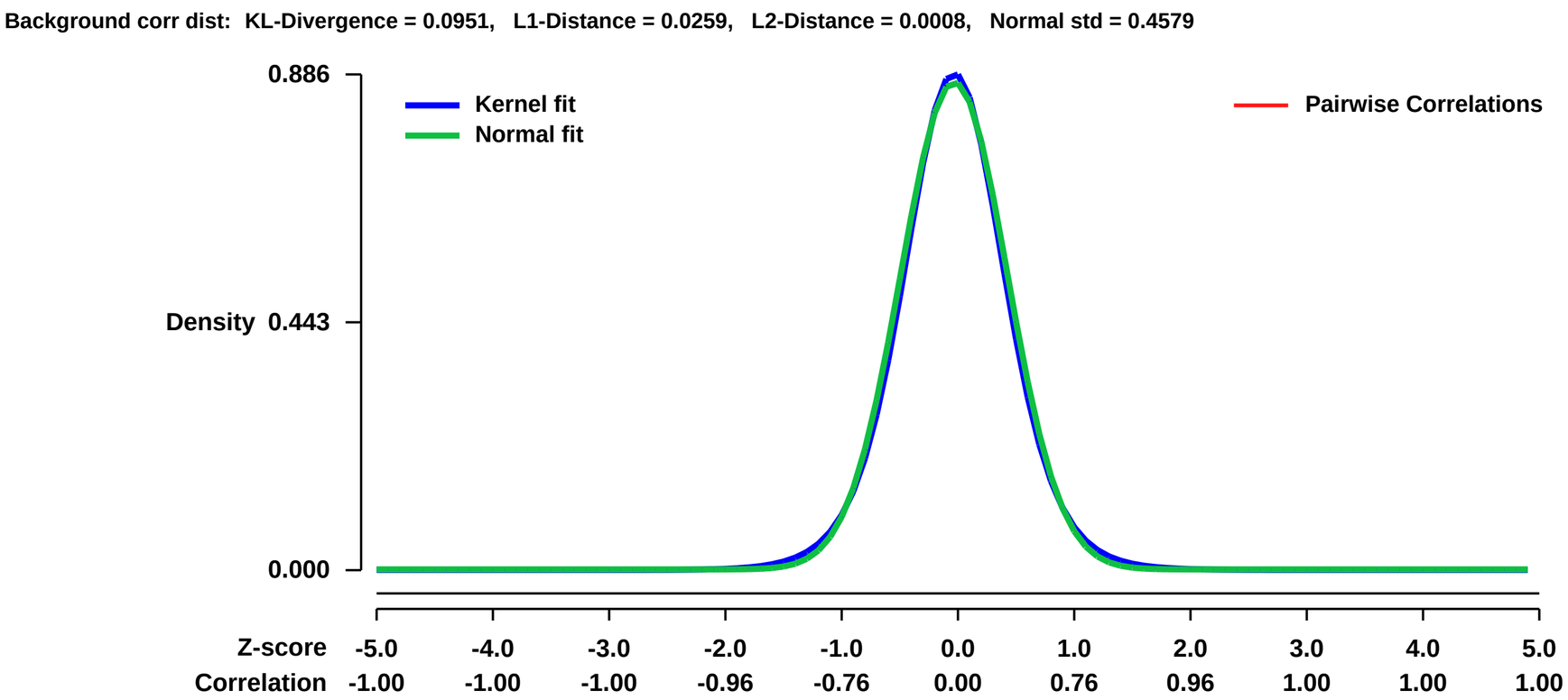

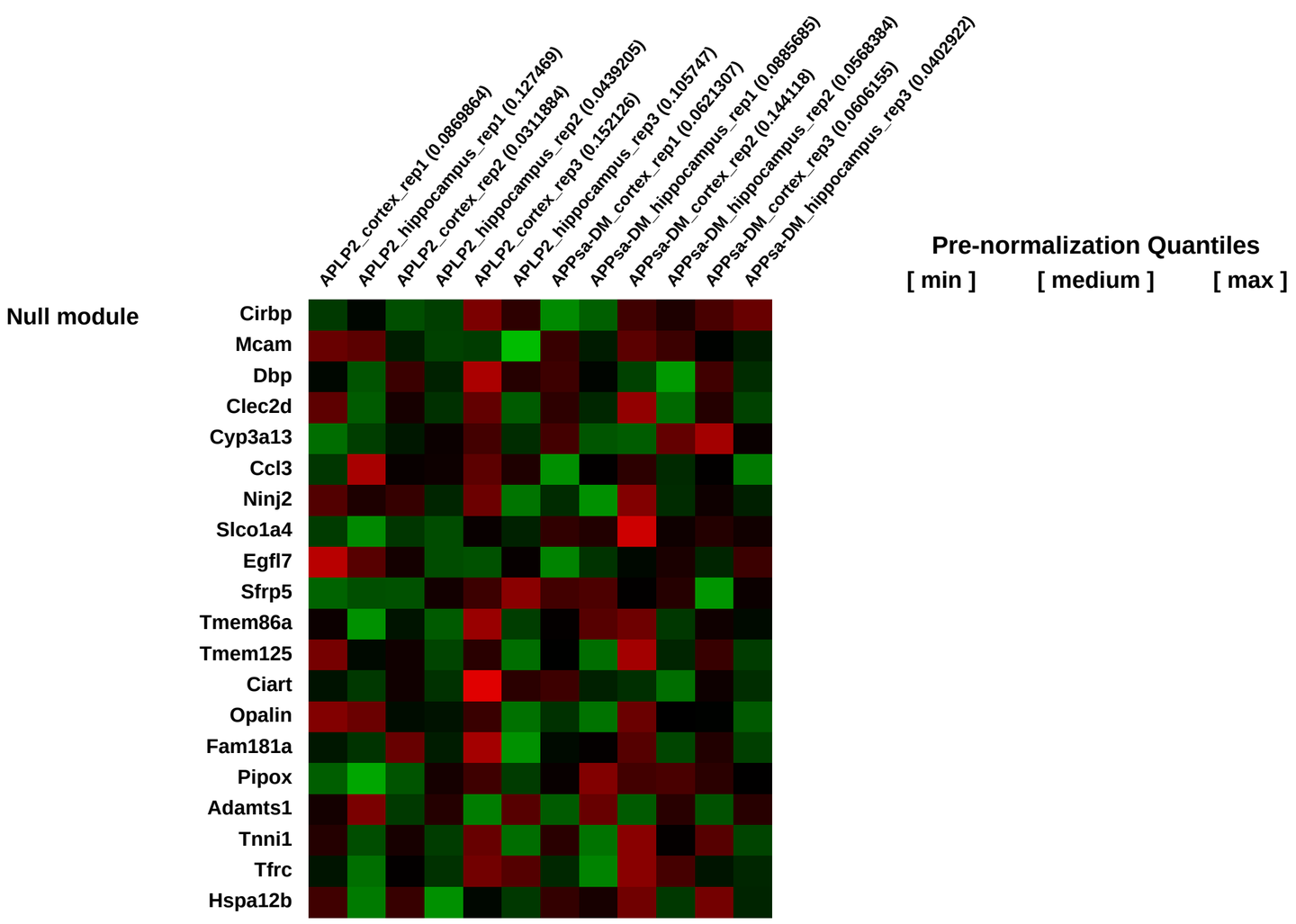

GEO Series "GSE51678" Expression Profiles

Num of samples in this series: 13

Scale of expression profile Z-scores

-3.0 -2.0 -1.0 0.0 1.0 2.0 3.0

GEO Link:	**http://www.ncbi.nlm.nih.gov/geo/query/acc.cgi?acc=GSE51678**
Status:	**Public on Jun 23 2014**
Title:	**Microarray profiling of STEP knockout mouse striatum**
Organism:	**Mus musculus**
Experiment type:	**Expression profiling by array**
Platform:	**GPL1261**
Pubmed ID:	
Summary & Design:	**Summary:** **STEP (striatal-enriched tyrosine phosphatase) is a brain-specific phosphatase named for its robust expression in striatum. Brains from homozygous and heterozygous STEP knockout mice and wild-type littermates were harvested, and striatum microdissected. RNA was extracted and hybridized to Affymetrix 230_2 microarray chips.** **Overall design:** **n=4-5 per group. Wild-type littermates were compared with STEP +/- and -/-**

Background corr dist: **KL-Divergence = 0.1091, L1-Distance = 0.0348, L2-Distance = 0.0022, Normal std = 0.4212**

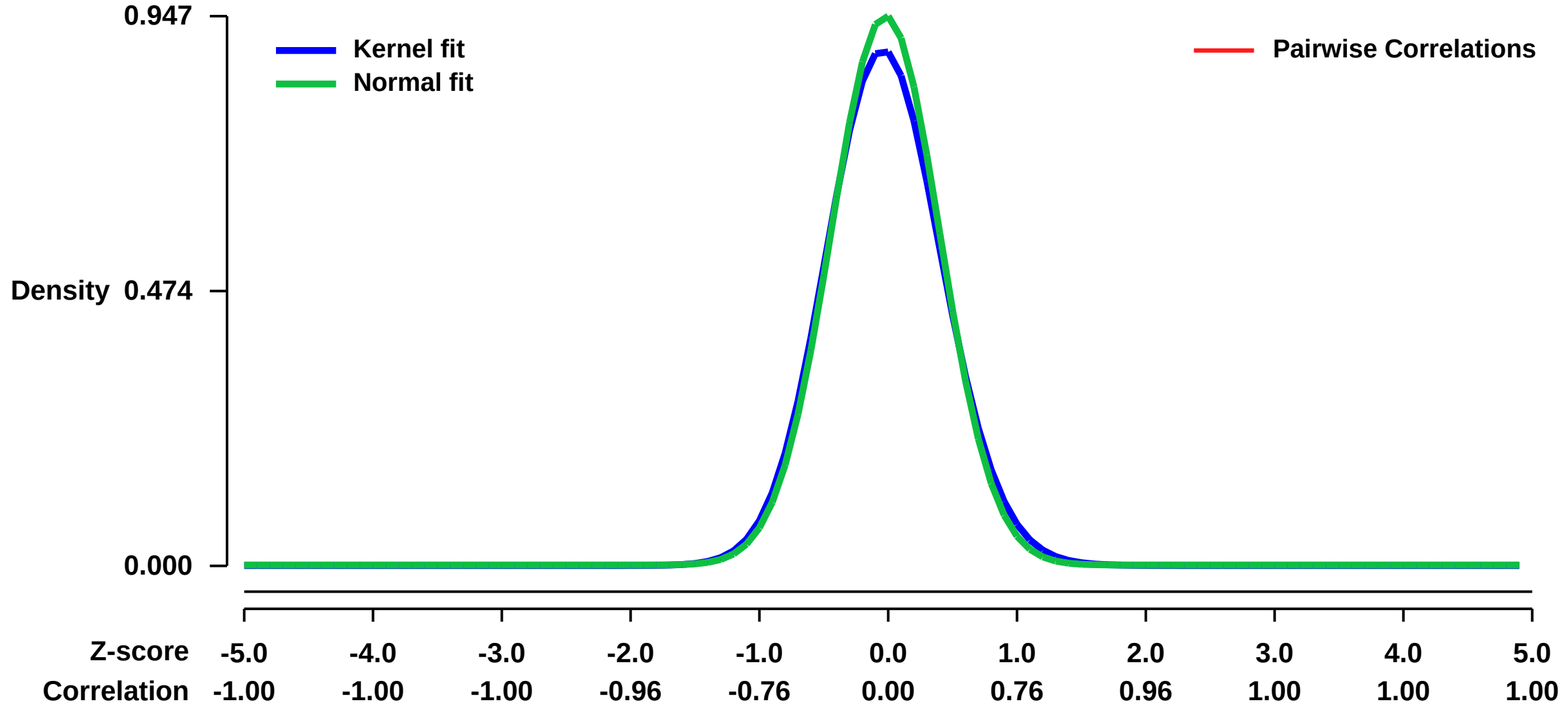

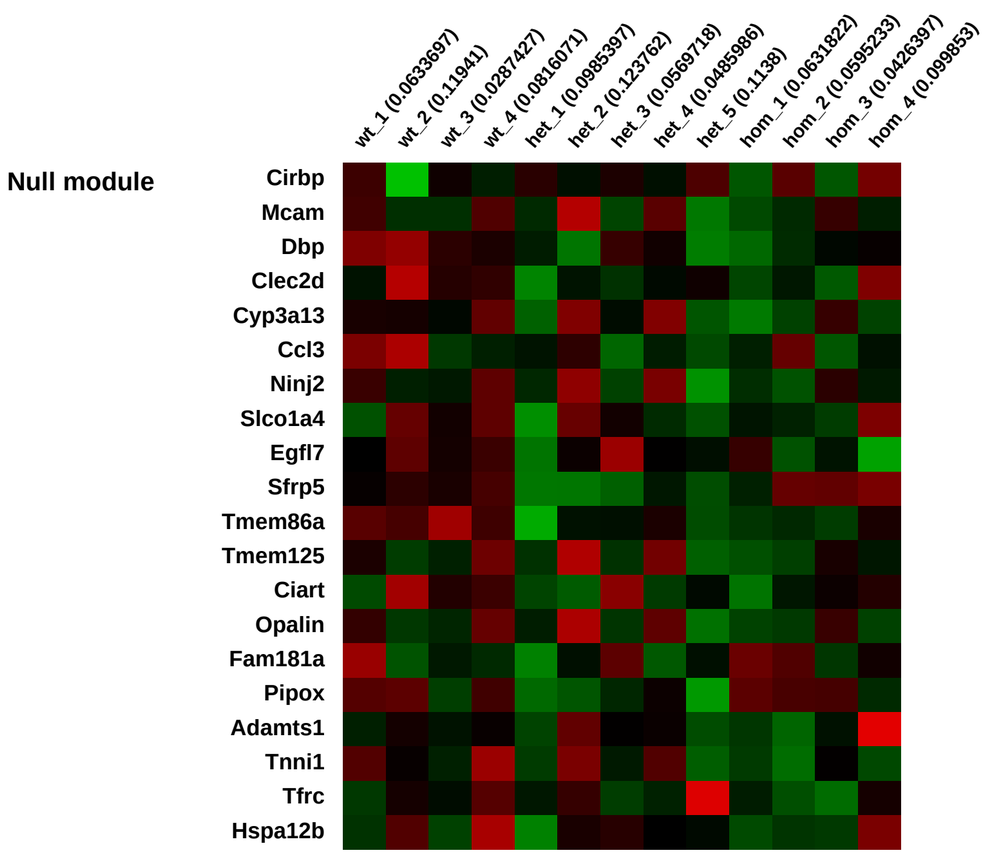

GEO Series "GSE39555" Expression Profiles

Num of samples in this series: 24

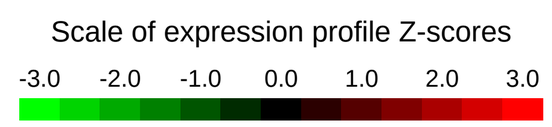

GEO Link:	http://www.ncbi.nlm.nih.gov/geo/query/acc.cgi?acc=GSE39555
Status:	Public on Oct 17 2012
Title:	Genome-wide expression study of the responses of murine NK cells and dendritic cell subsets to MCMV infection
Organism:	Mus musculus
Experiment type:	Expression profiling by array
Platform:	GPL1261
Pubmed ID:	23084923
Summary & Design:	**Summary:** Murine Cytomegalovirus (MCMV) infection leads to the activation of various immune cells, including dendritic cells (DCs) and Natural Killer (NK) cells. This activation is partly driven by innate cytokines including IFN-I, which are induced early after infection. The objective was to address the role of different innate cytokines in shaping DC subsets and NK cell responses, in particular the role of cell intrinsic responses to IFN-I. In order to decipher the specific impact of cell-intrinsic IFN-I on cell subsets, we performed a genome-wide expression analysis on CD45.1 WT and CD45.2 IFNAR-/- splenic conventional DC (cDC) subsets and NK cells isolated from C57BL/6 [CD45.1 WT / CD45.2 IFNAR-KO] mixed bone marow chimera mice. **Overall design:** This study includes data from cDC subsets (CD8a and CD11b) and NK cells purified by flow cytometry sorting from the spleen of bone marrow chimera (BMC) mice, under steady-state or MCMV condition. Two independent replicates were made for each cell type, from two independent pools of spleens from uninfected or d1.5 MCMV-infected BMC 5-8 mice, and were hybridized on 3 separate batches of gene chips.

Background corr dist: KL-Divergence = 0.1860, L1-Distance = 0.0500, L2-Distance = 0.0059, Normal std = 0.3425

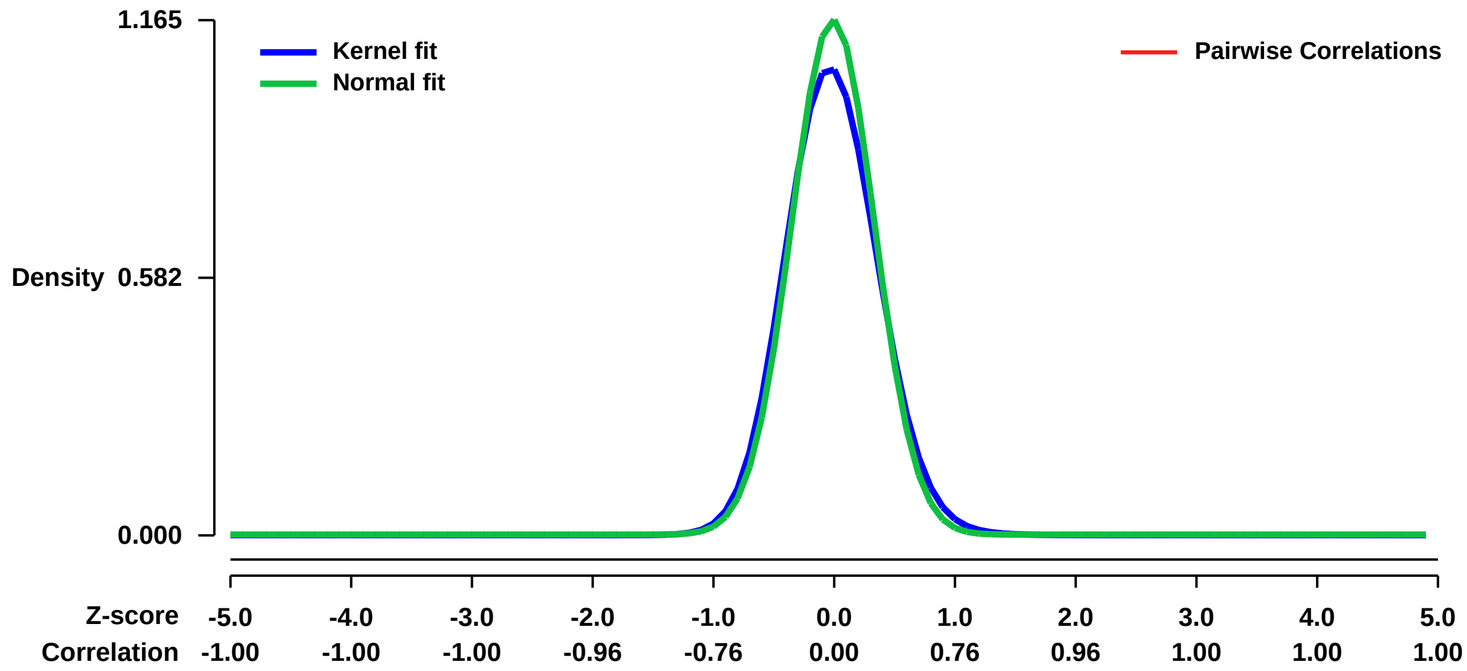

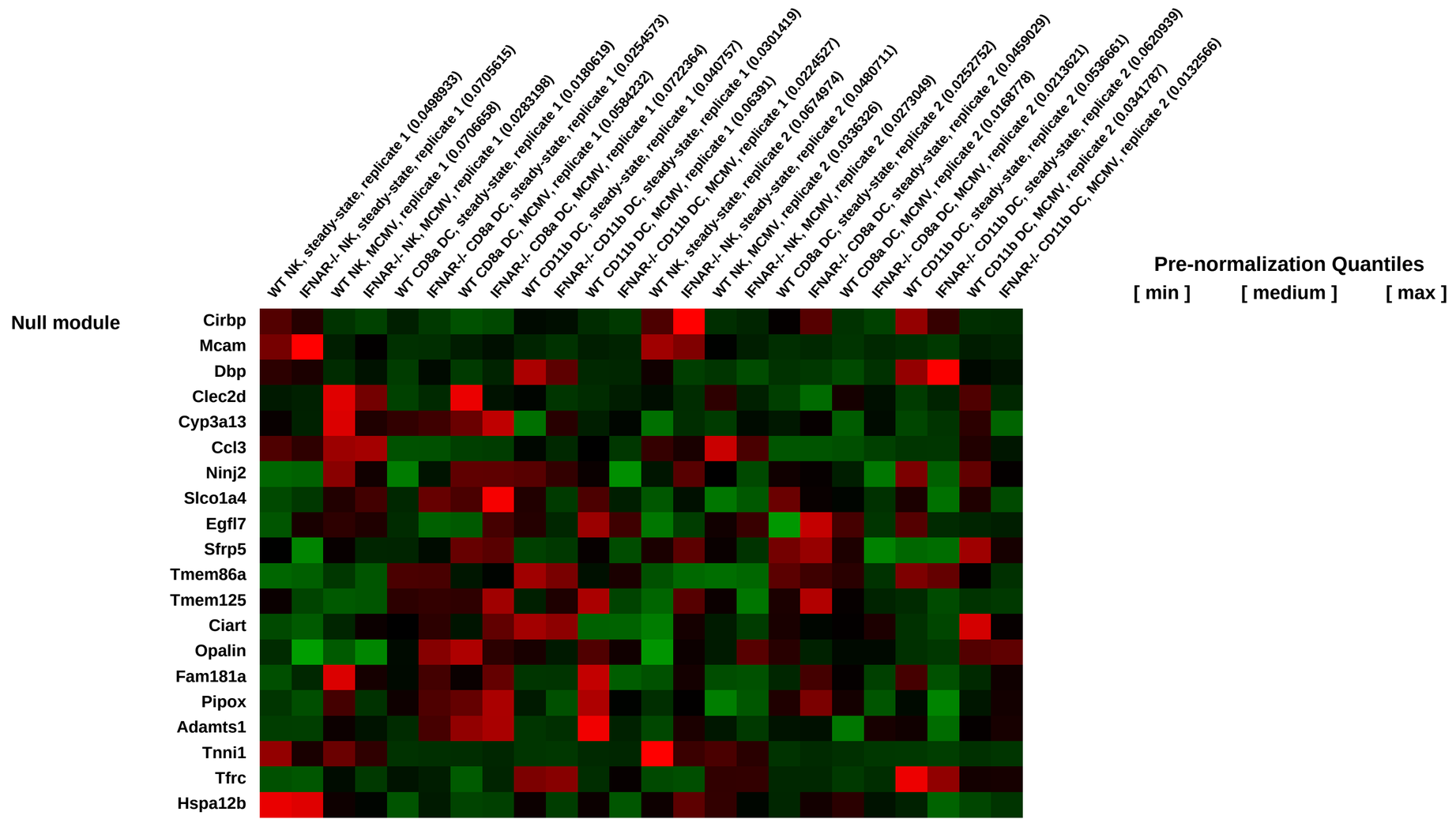

GEO Series "GSE6540" Expression Profiles

Num of samples in this series: 12

Scale of expression profile Z-scores

-3.0 -2.0 -1.0 0.0 1.0 2.0 3.0

GEO Link:	http://www.ncbi.nlm.nih.gov/geo/query/acc.cgi?acc=GSE6540
Status:	Public on Dec 14 2007
Title:	Expression data from olfactory epithelium of Lip-C-treated mice compared to Lip-O-treated control mice
Organism:	Mus musculus
Experiment type:	Expression profiling by array
Platform:	GPL1261
Pubmed ID:	17848607
Summary & Design:	**Summary:** Microarray analysis of gene expression in the olfactory epithelium of macrophage depleted mice to study the role of macrophages in regulating neurodegeneration, neuroprotection, and neurogenesis of olfactory sensory neurons **Keywords: comparison of gene expression level in sham and 48 hr OBX Lip-O mice versus Lip-C mice** **Overall design:** Olfactory epithelium from LIp-C-treated and Lip-O-treated mice was microdissected for RNA extraction and hybridization on Affymetrix microarrays. We compared levels of gene expression in macrophage-depleted and non-depleted sham and 48 hr OBX mice using a 2x2 ANOVA and pairwise comparisons to identify molecular mechanisms of macrophage-mediated neurodegeneration, neuroprotection, and neurogenesis and to validate the gene expression patterns using real-time RT-PCR and immunohistochemistry

Background corr dist: KL-Divergence = 0.1195, L1-Distance = 0.0264, L2-Distance = 0.0010, Normal std = 0.4100

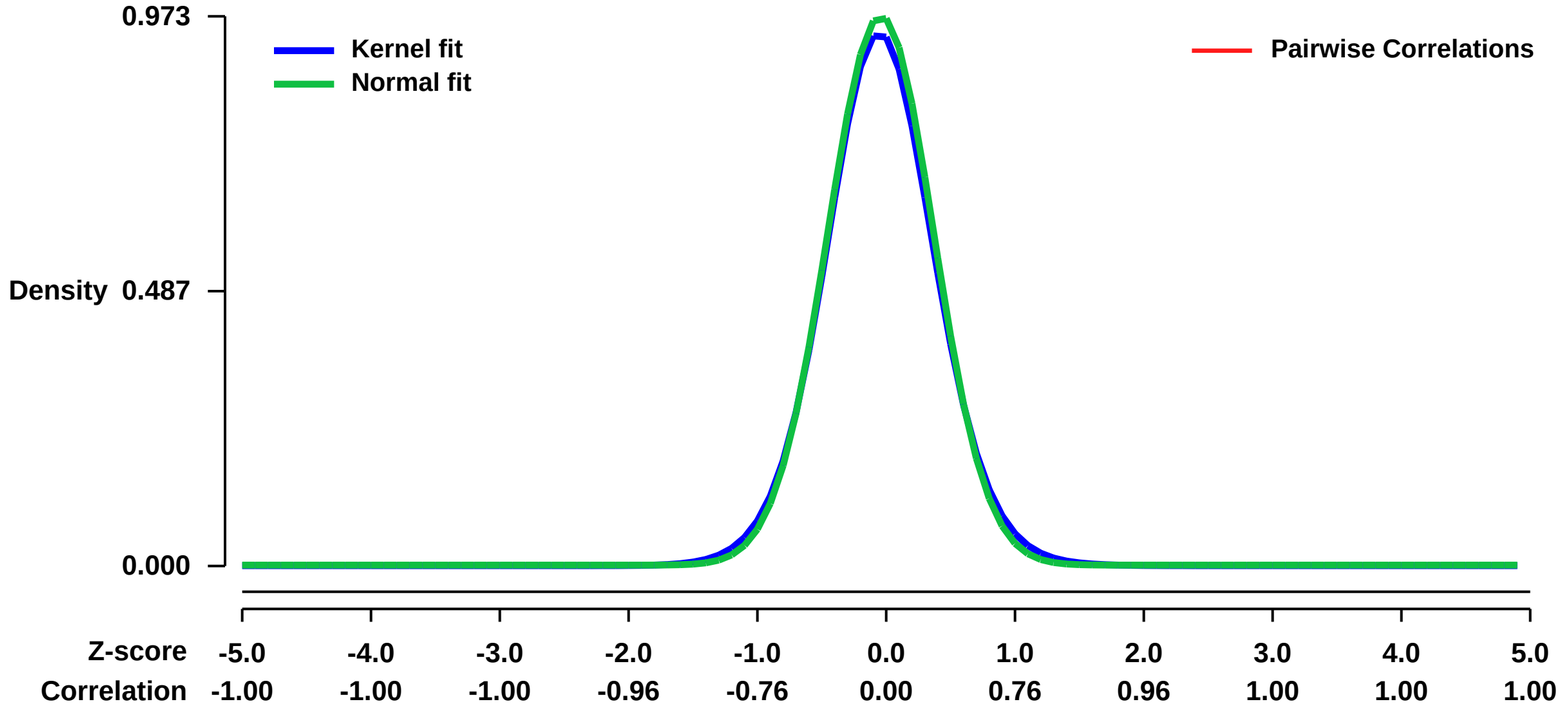

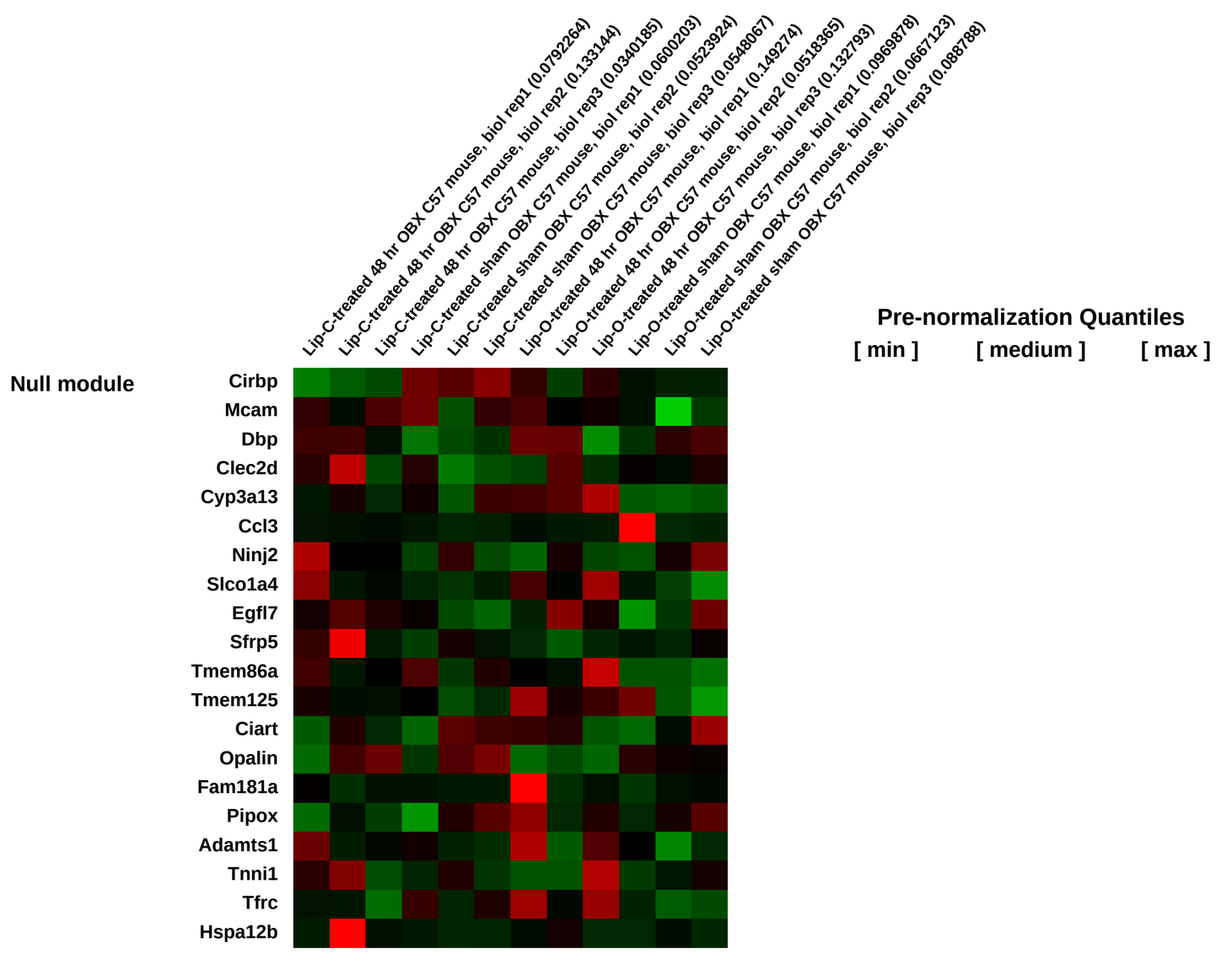

GEO Series "GSE51417" Expression Profiles

Num of samples in this series: 60

Scale of expression profile Z-scores

-3.0 -2.0 -1.0 0.0 1.0 2.0 3.0

GEO Link:	http://www.ncbi.nlm.nih.gov/geo/query/acc.cgi?acc=GSE51417
Status:	Public on Apr 15 2014
Title:	Comparative Iron Oxide Nanoparticle Cellular Dosimetry and Response in Mice by the Inhalation and Liquid Cell Culture Exposure Routes
Organism:	Mus musculus
Experiment type:	Expression profiling by array
Platform:	GPL1261
Pubmed ID:	
Summary & Design:	**Summary:** To identify the molecular impact of SPIO nanoparticle inhalation exposure on lung tissue. Transcriptional responses were measured by global microarray analysis of mouse lung. **Overall design:** Male Balb/c mice were exposed to aerosolized SPIO nanoparticles using a nano-aerosol generation and inhalation system . Exposure was performed using two groups of 30 male Balb/c mices (60 total). One group of 30 was exposed to aerosolized SPIO nanopartic

Background corr dist: KL-Divergence = 0.3759, L1-Distance = 0.0792, L2-Distance = 0.0189, Normal std = 0.2550

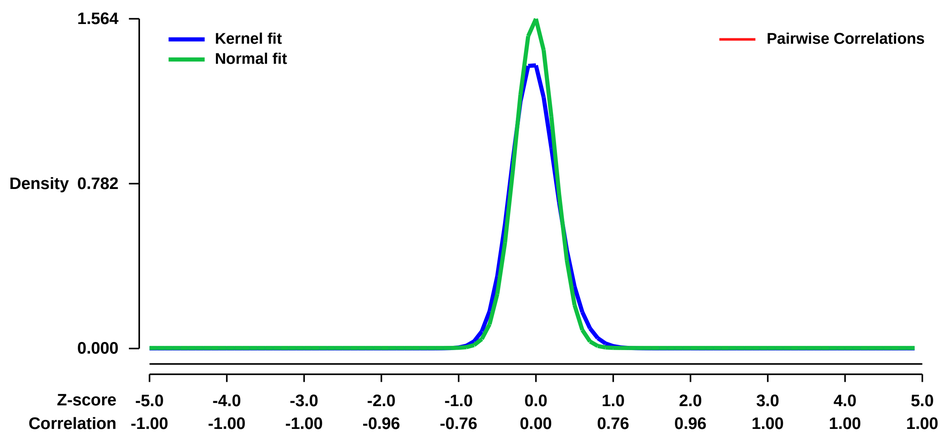

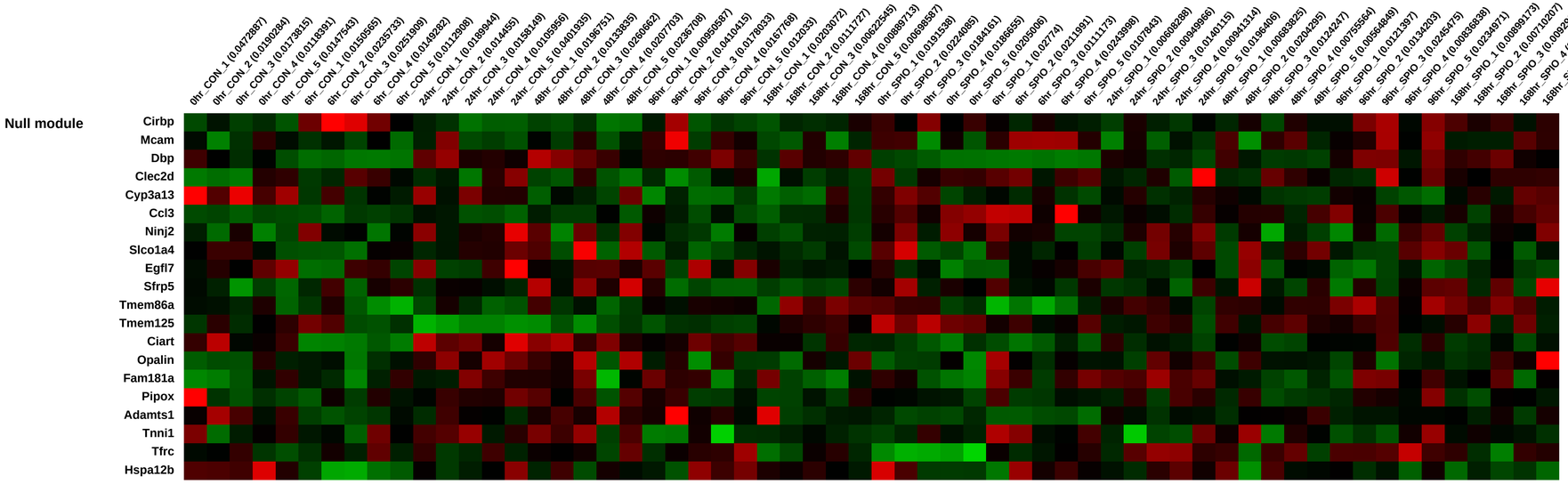

GEO Series "GSE7404" Expression Profiles

Num of samples in this series: 144

Details of this dataset are not shown due to large number of samples and the page size limit.

Find details in http://www.ncbi.nlm.nih.gov/geo/query/acc.cgi?acc=GSE7404

Background corr dist: KL-Divergence = 0.3751, L1-Distance = 0.0810, L2-Distance = 0.0209, Normal std = 0.2582

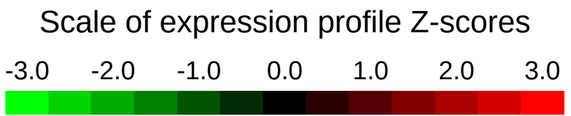

GEO Series "GSE34006" Expression Profiles

Num of samples in this series: 6

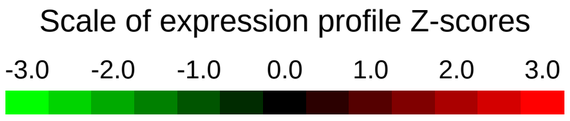

GEO Link:	**http://www.ncbi.nlm.nih.gov/geo/query/acc.cgi?acc=GSE34006**
Status:	**Public on Jun 01 2012**
Title:	**Role of Adenosine 2A Receptors (A2AR) on regulatory T cells (Tregs)**
Organism:	**Mus musculus**
Experiment type:	**Expression profiling by array**
Platform:	**GPL1261**
Pubmed ID:	**22835488**
Summary & Design:	**Summary:** **The adenosine 2A receptor (A2AR) is expressed on regulatory T cells (Tregs), but the functional significance is currently unknown. We compared the gene expression between wild-type (WT) and A2AR knockout (KO) Tregs and between WT Tregs treated with vehicle or a selective A2AR agonist.** **Overall design:** **FACS-sorted GFP positive Tregs from WT or A2AR KO FoxP3GFP mouse spleen and lymph nodes were incubated 18 hr with vehicle (DMSO), a separate set of WT Tregs were incubated with the selective A2AR agonist ATL1222 10 nM (Dogwood Pharmaceuticals, Inc.) for 18 hr prior to RNA isolation.**

Background corr dist: **KL-Divergence = 0.0480, L1-Distance = 0.0198, L2-Distance = 0.0004, Normal std = 0.5813**

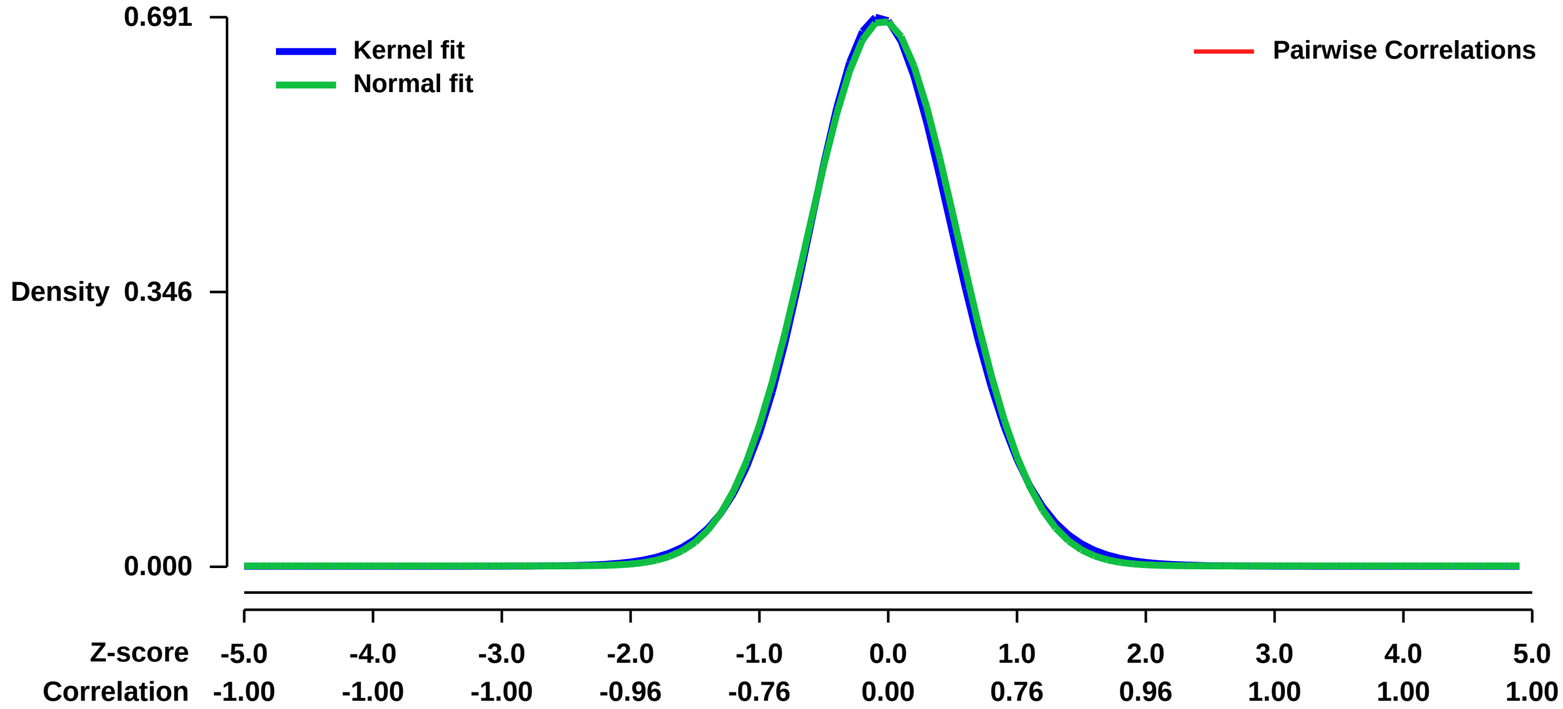

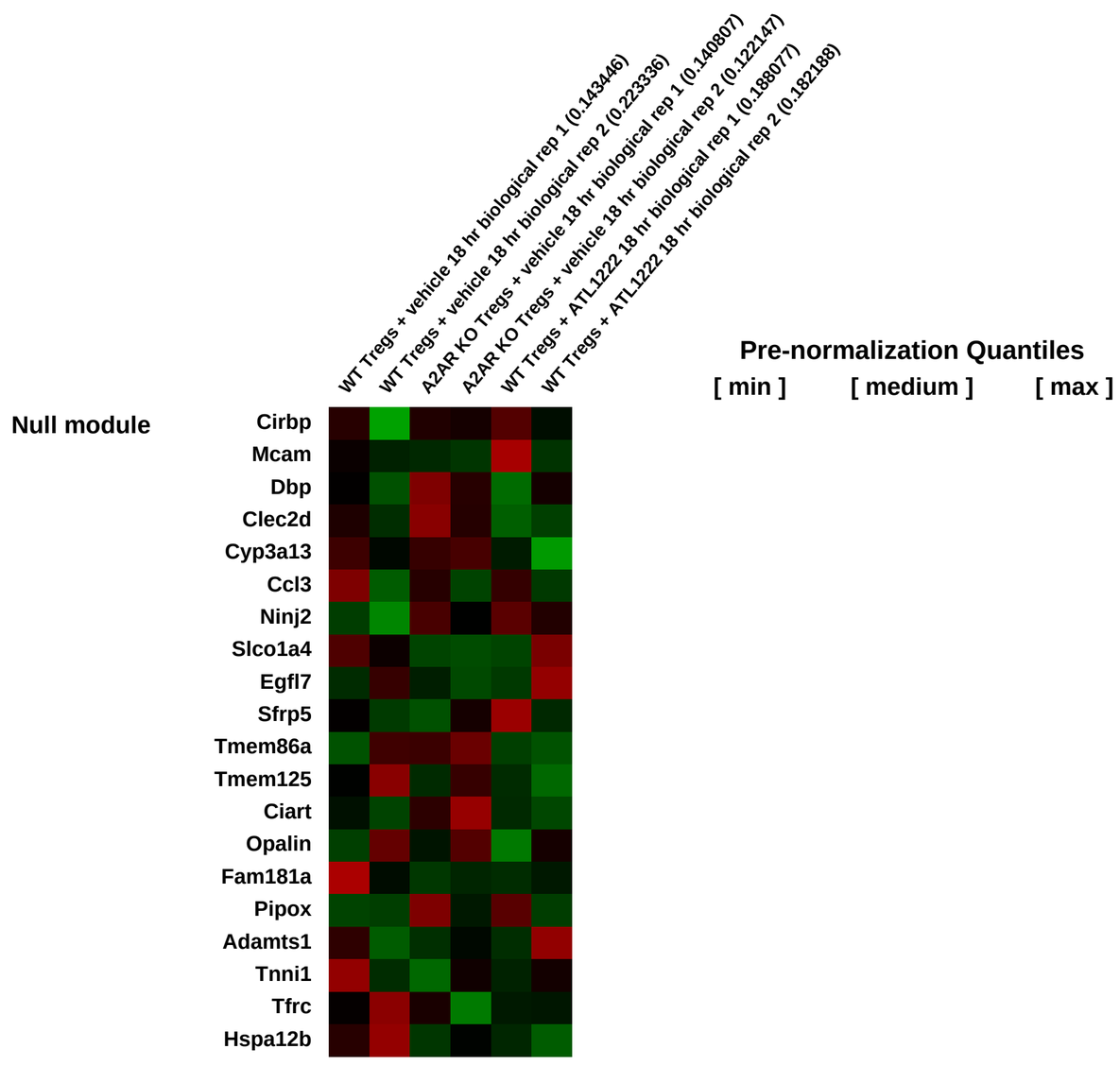

GEO Series "GSE22903" Expression Profiles

Num of samples in this series: 24

Scale of expression profile Z-scores

-3.0 -2.0 -1.0 0.0 1.0 2.0 3.0

GEO Link:	http://www.ncbi.nlm.nih.gov/geo/query/acc.cgi?acc=GSE22903
Status:	Public on Nov 14 2011
Title:	Ribosomal deficiencies in Diamond-Blackfan anemia impair translation of transcripts essential for differentiation of murine and human erythroblasts
Organism:	Mus musculus
Experiment type:	Expression profiling by array
Platform:	GPL1261
Pubmed ID:	22058113
Summary & Design:	Summary: Diamond Blackfan Anemia (DBA) is associated with developmental defects and profound anemia. Mutations in genes encoding a ribosomal protein of the small (e.g. Rps19) or large (e.g. Rpl11) ribosomal subunit are found in over half of these patients. The mutations cause ribosomal haploinsufficiency, which reduces overall translation efficiency of cellular mRNAs. We reduced expression of *Rps19* or *Rpl11* in mouse erythroblasts and investigated mRNA polyribosome association, which revealed deregulated translation initiation of specific transcripts. Among these were *Bag1*, encoding a Hsp70 co-chaperone, and *Csde1*, encoding an RNA binding protein, both expressed at increased levels in erythroblasts. Their translation initiation is cap-independent and starts from an internal ribosomal entry site (IRES), which appeared sensitive to knock down of Rps19 or Rpl11. Mouse embryos lacking Bag1 die at embryonic day E13.5 with reduced erythroid colony forming cells in the fetal liver, and low Bag1 expression impairs erythroid differentiation in vitro. Reduced expression of Csde1 impairs proliferation and differentiation of erythroid blasts. Protein but not mRNA expression of *BAG1* and *CSDE1* was reduced in erythroblasts cultured from DBA patients. Our data suggest that impaired IRES-mediated translation of mRNAs expressed at increased levels in erythroblasts contributes to the erythroid phenotype of DBA. Overall design: 3 biological replicates of erythroblasts treated with different shRNA were used for polyribosomal sucrose gradients; RNA was extracted from gradients in 2 samples - mRNA associated with polyribosomes (poly) and the rest (sub).

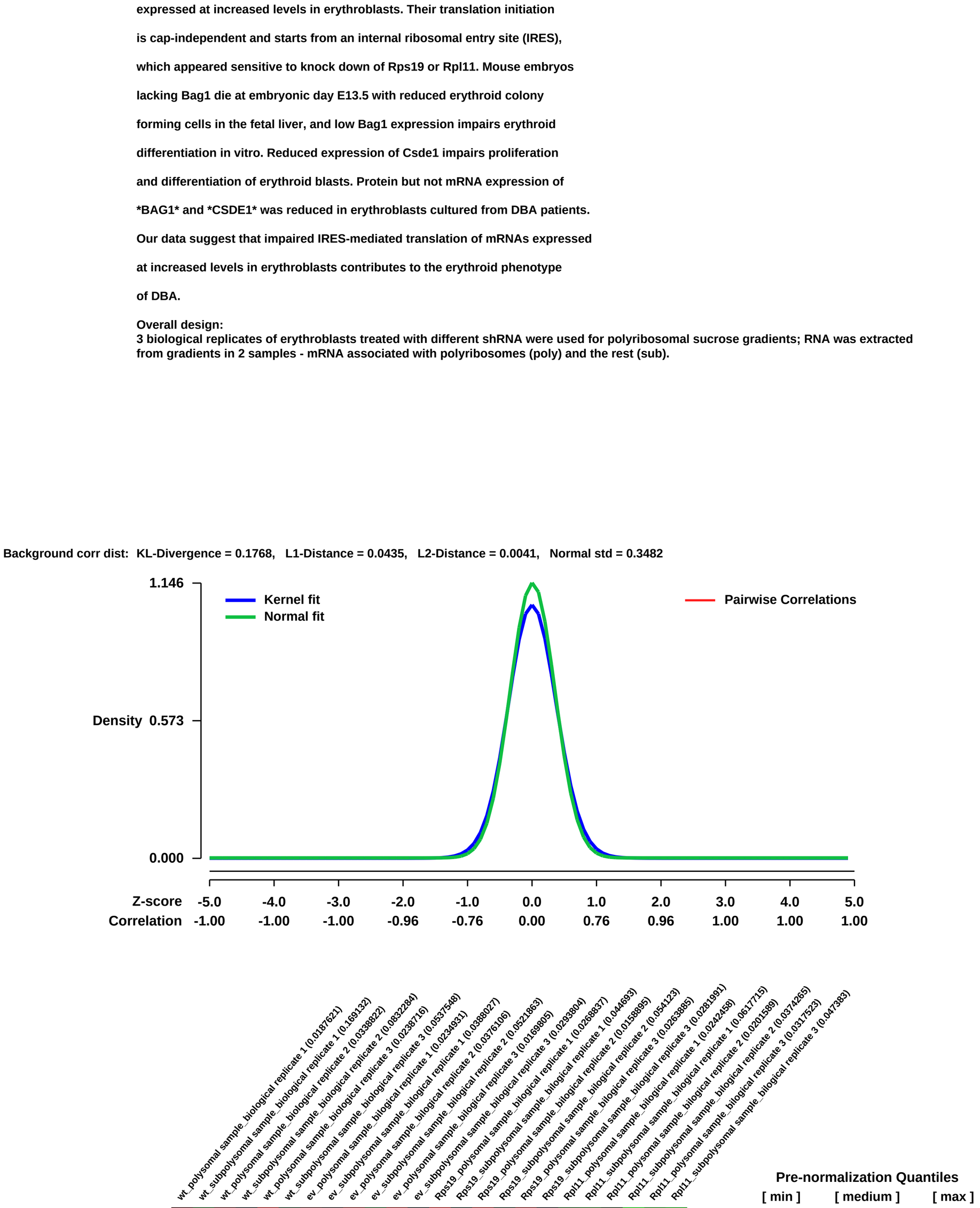

GEO Series "GSE7810" Expression Profiles

Num of samples in this series: 9

Scale of expression profile Z-scores

-3.0 -2.0 -1.0 0.0 1.0 2.0 3.0

GEO Link:	http://www.ncbi.nlm.nih.gov/geo/query/acc.cgi?acc=GSE7810
Status:	Public on May 18 2007
Title:	Comparative analysis of gene expression WT and Nrf2-/- mice Type II cells
Organism:	Mus musculus
Experiment type:	Expression profiling by array
Platform:	GPL1261
Pubmed ID:	17895394
Summary & Design:	**Summary:** We hypothesize that gene expression in the Type II cells of Nrf2+/+ and Nrf2-/- mice are divergent thus contributing the cell growth. More specifically, type II cells from Nrf2-/- mice have increased reactive oxygen species that cause the impaired cell growth. In order to test these hypotheses at the gene expression level, we utilized microarray analysis to examine transcriptional differences between Nrf2+/+ and Nrf2-/- cells. **Keywords: comparative expression profiling** **Overall design:** . This study utilizes microarray analysis to test these hypotheses. Three sets of type II cells were isolated from lungs from both Nrf2+/+ and Nrf2-/- mice and grown for 5 days. RNA was isolated and used for global gene expression profiling (Affymetrix Mouse 430 2.0 array). Statistically significant gene expression was determined as a minimum 6 counts of 9 pairwise comparisons, minimum 1.5-fold change, and p < 0.05. Further, Absolute | FC - FC SEM | >= 1.5.

Background corr dist: KL-Divergence = 0.0624, L1-Distance = 0.0171, L2-Distance = 0.0003, Normal std = 0.5241

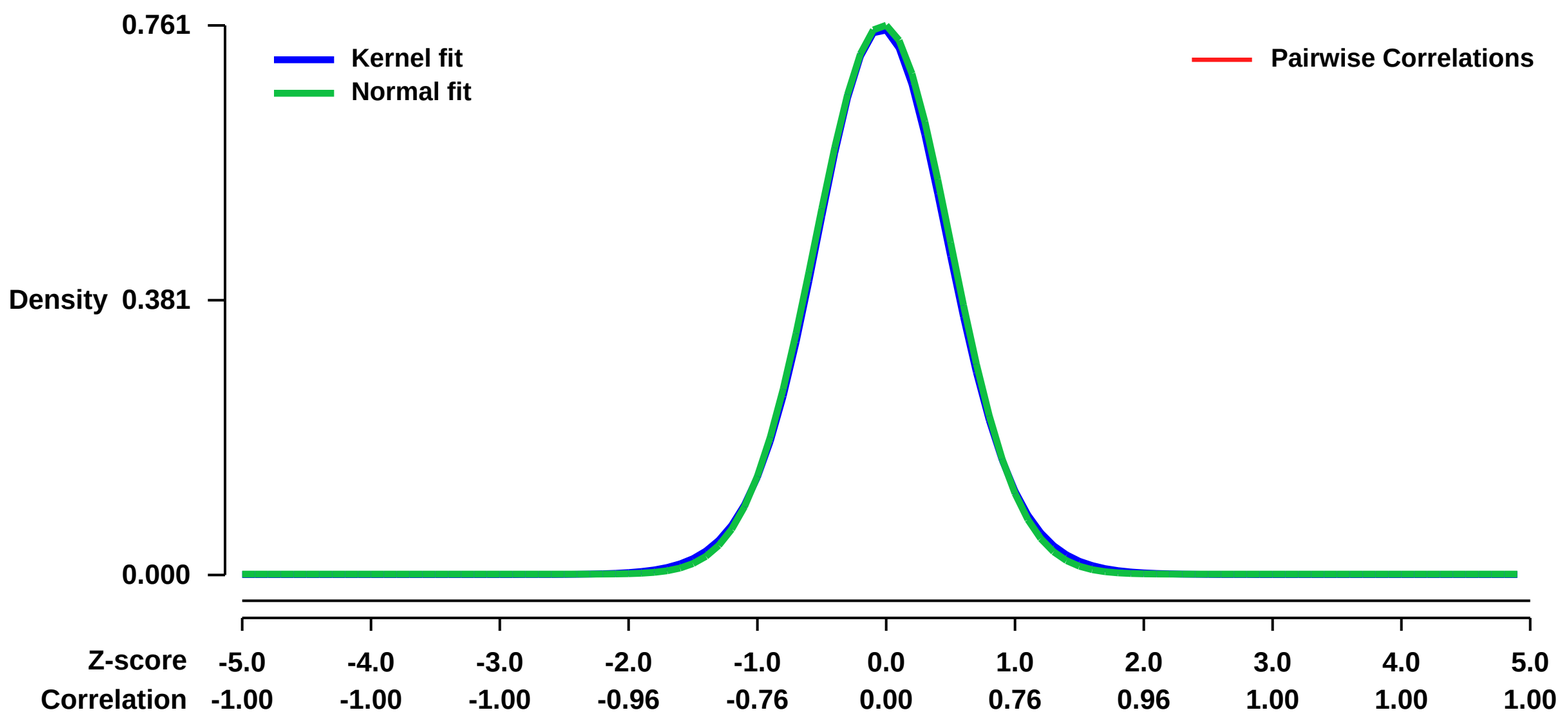

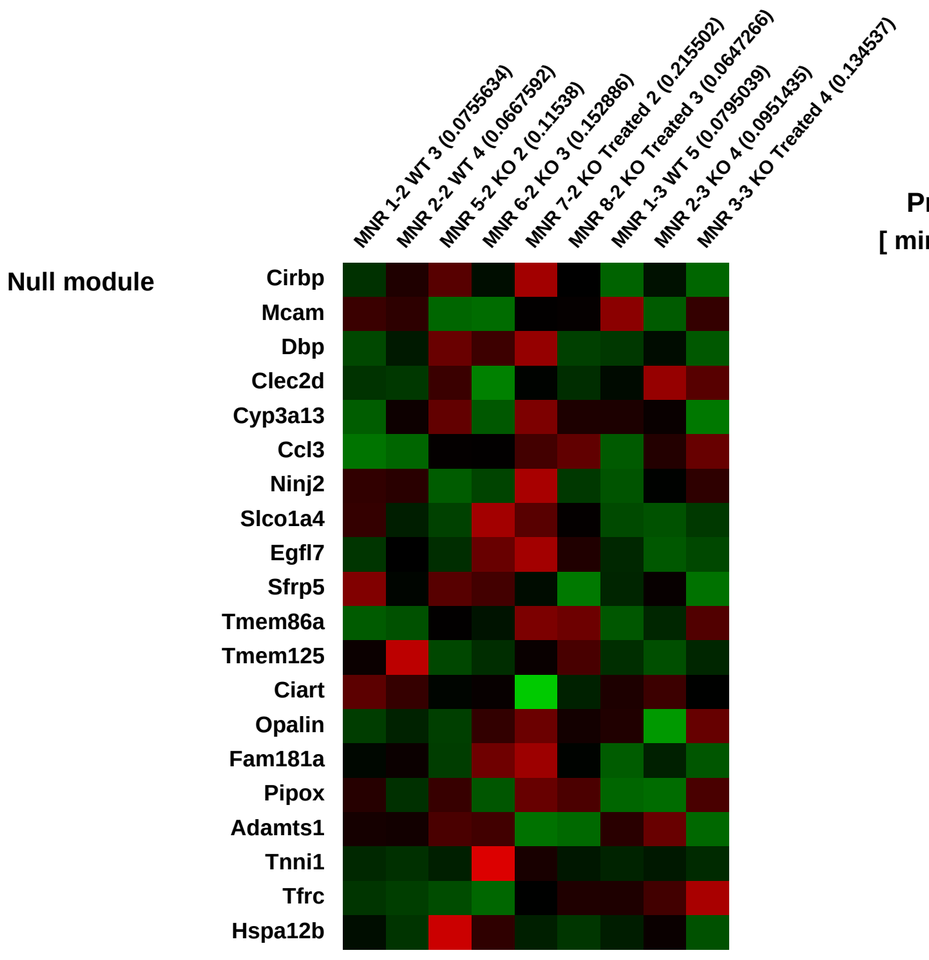

GEO Series "GSE13553" Expression Profiles

Num of samples in this series: 10

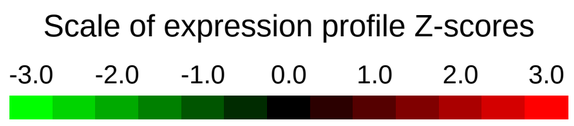

GEO Link:	http://www.ncbi.nlm.nih.gov/geo/query/acc.cgi?acc=GSE13553
Status:	Public on Nov 19 2008
Title:	The effect of dietary CLA on mammary tumorigenesis
Organism:	Mus musculus
Experiment type:	Expression profiling by array
Platform:	GPL1261
Pubmed ID:	20624750
Summary & Design:	**Summary:** Conjugated linoleic acid (CLA), a class of fatty acids found in beef and dairy products, has been shown to inhibit tumorigenesis in a variety of cancer model systems. Based on previously well-documented anti-tumor activity of CLA in rodent models of breast cancer, a pilot study was initiated to examine the effect of dietary CLA in a well-established transgenic model of breast cancer. Western blots were performed for the detection of AKT, c-Src, ERK1/2, and Cdc24. CLA significantly increased tumor burden ($p<0.1$) independent of an increase in oncogenic signaling. Mammary gland whole mounts indicated a loss of mammary adipose and extensive epithelial expansion in CLA-treated animals. Microarray analysis indicated a significant reduction in cytoskeletal related genes with at least a two-fold decrease in five out of six CLA-fed animals compared to untreated controls. Reduction of Cdc42, a key regulator of cell adhesion and cytoskeletal arrangements, was confirmed at the protein level by western blot ($p<0.01$). These findings suggest that dietary CLA may advance the malignant phenotype by promoting a loss of cell polarity and adhesion in the mammary gland epithelium. This action may have serious clinical implications for a subset high-risk population and warrants further investigation. **Overall design:** Virgin, four-week-old PyV-mT mice were administered a diet of a mixed-isomer CLA formulation (1% wt/wt) (N=6) or control AIN96G diet (N=5) for four weeks. Measurements of food disappearance, weights and palpations were recorded weekly. All animals were euthanized at eight weeks of age. Formalin-fixed, paraffin-embedded mammary gland tissue was used for H&E and trichrome staining and immunohistochemistry for Ki67. Tissue levels of CLA were measured by gas chromatography. Thoracic mammary glands were fixed in glacial acetic acid:ethanol and carmine stained. cDNA microarray was performed on RNA from 6 CLA-fed mice and 4 control mice using the Affymetrix 430 2.0 mouse genome chips.

Background corr dist: KL-Divergence = 0.1131, L1-Distance = 0.0294, L2-Distance = 0.0015, Normal std = 0.4170

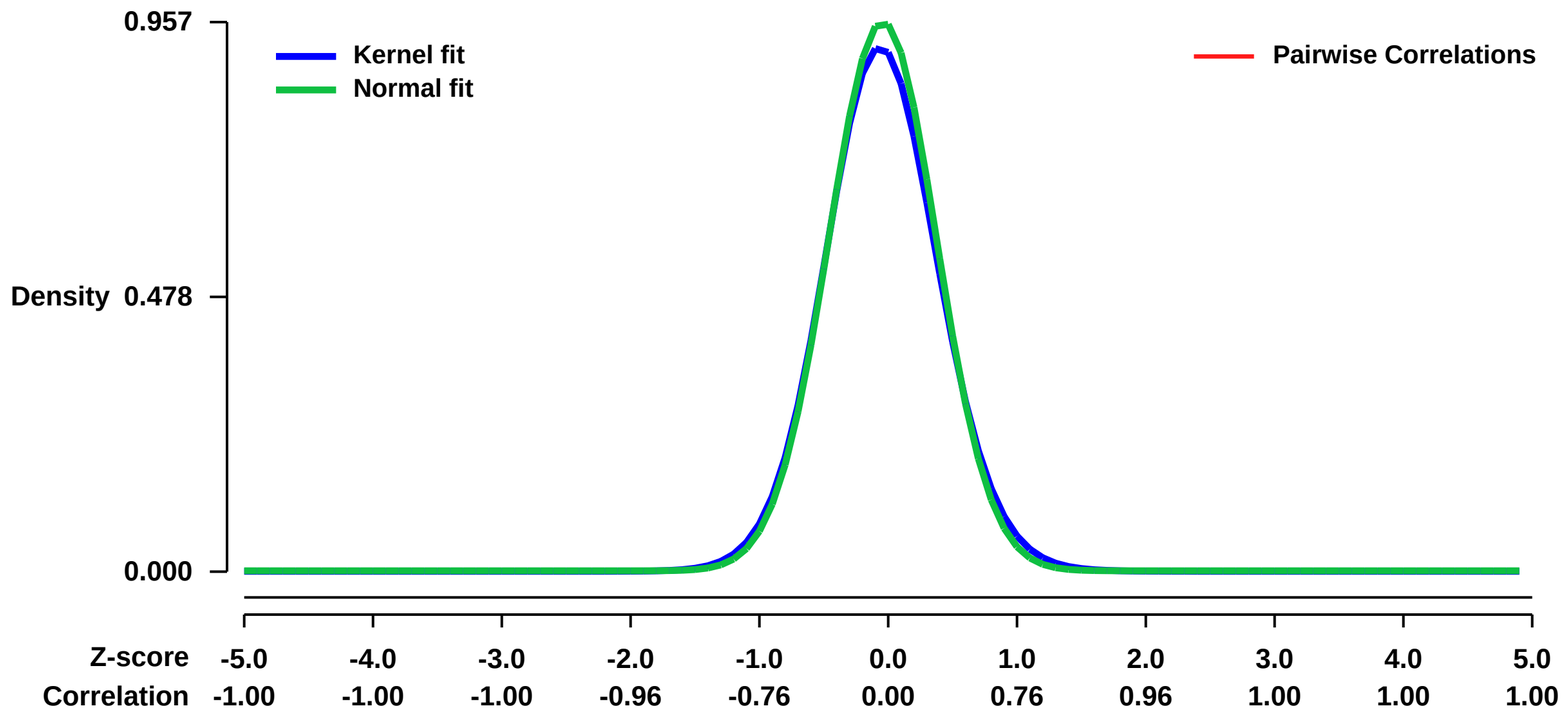

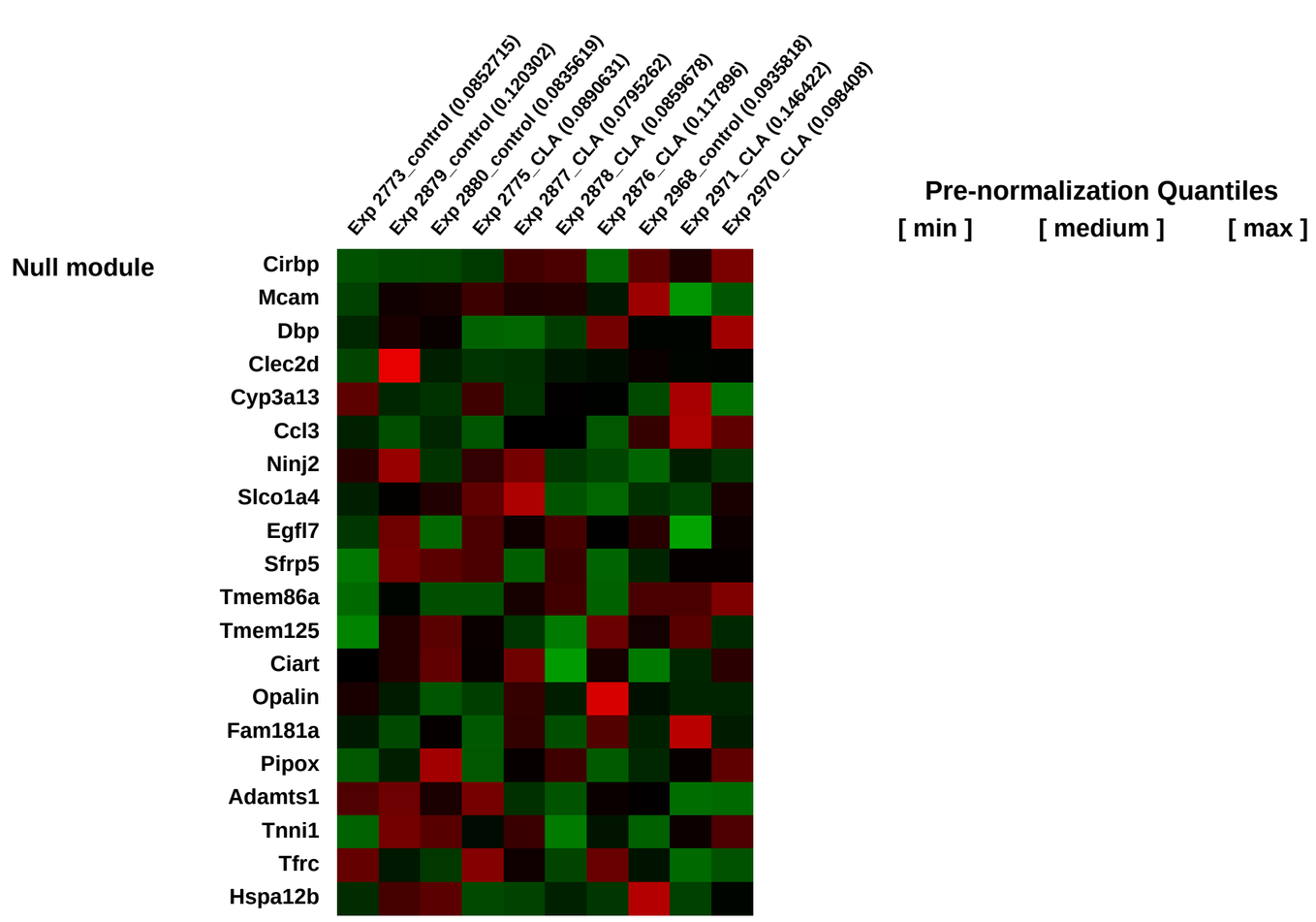

GEO Series "GSE34765" Expression Profiles

Num of samples in this series: 6

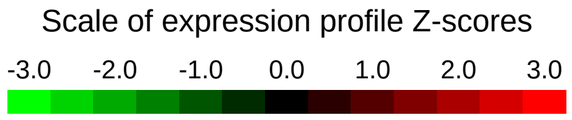

GEO Link:	http://www.ncbi.nlm.nih.gov/geo/query/acc.cgi?acc=GSE34765
Status:	Public on Sep 30 2012
Title:	Transcriptomic analysis of the cerebellum of daDREAM mice
Organism:	Mus musculus
Experiment type:	Expression profiling by array
Platform:	GPL1261
Pubmed ID:	22563308
Summary & Design:	**Summary:** DREAM (downstream regulatory element antagonist modulator) is a Ca2+-binding protein that binds DNA and represses transcription in a Ca2+-dependent manner. Previous studies have shown a role for DREAM in cerebellar function regulating the expression of the sodium/calcium exchanger3 (NCX3) in cerebellar granules to control Ca2+ homeostasis and survival of these neurons. To achieve a more global view of the genes regulated by DREAM in the cerebellum, we performed a genome-wide analysis in transgenic cerebellum expressing a Ca2+-insensitive/CREB-independent dominant active mutant DREAM (daDREAM). Our results indicate that DREAM is a major transcription factor in the cerebellum that regulates genes important for cerebellar development. **Overall design:** We used Affymetrix microarrays (GeneChip Mouse Genome 430 2.0) to compare global gene expression in wild type (WT) versus transgenic cerebellum cells. For ech type of sample three hybridizations were carried-out (independent biological replicates).

Background corr dist: KL-Divergence = 0.0144, L1-Distance = 0.0300, L2-Distance = 0.0013, Normal std = 0.8079

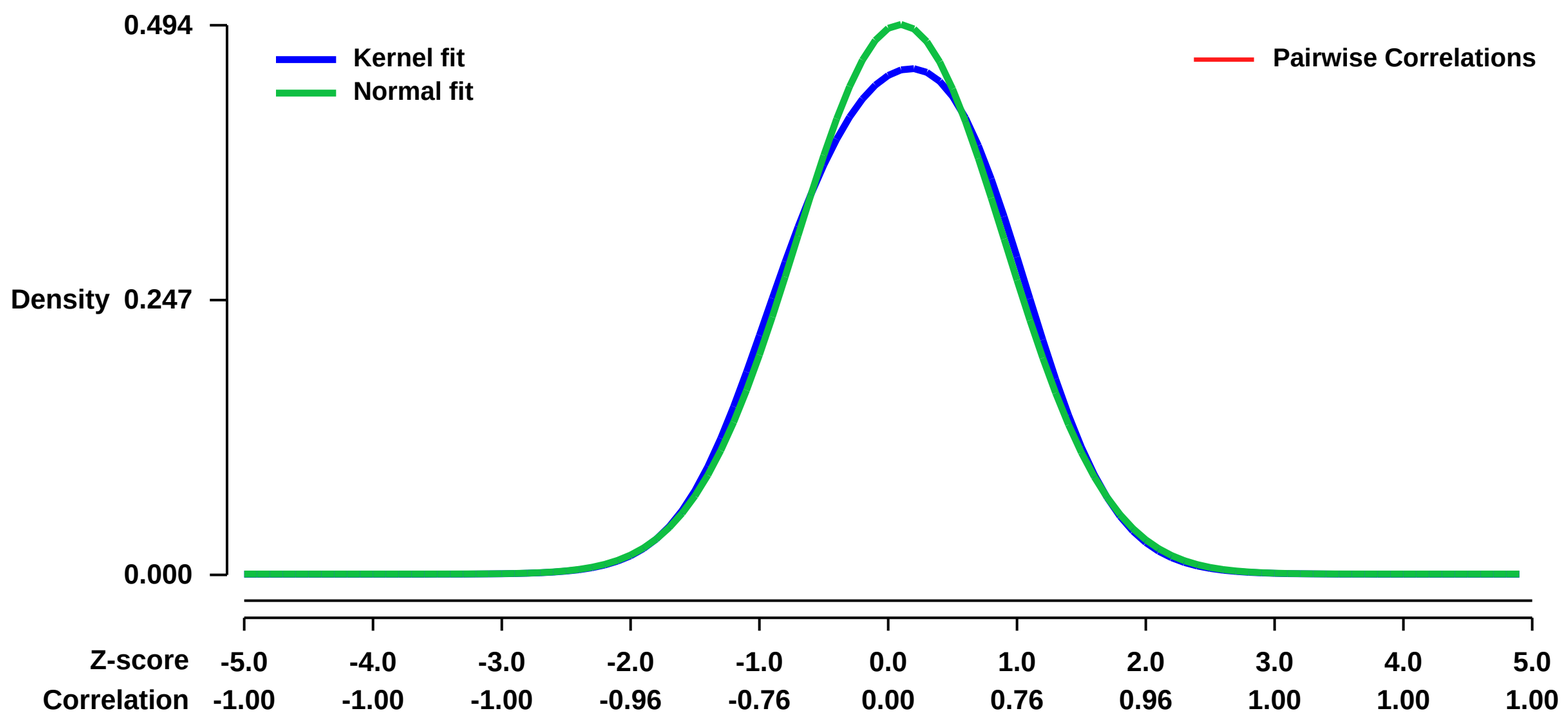

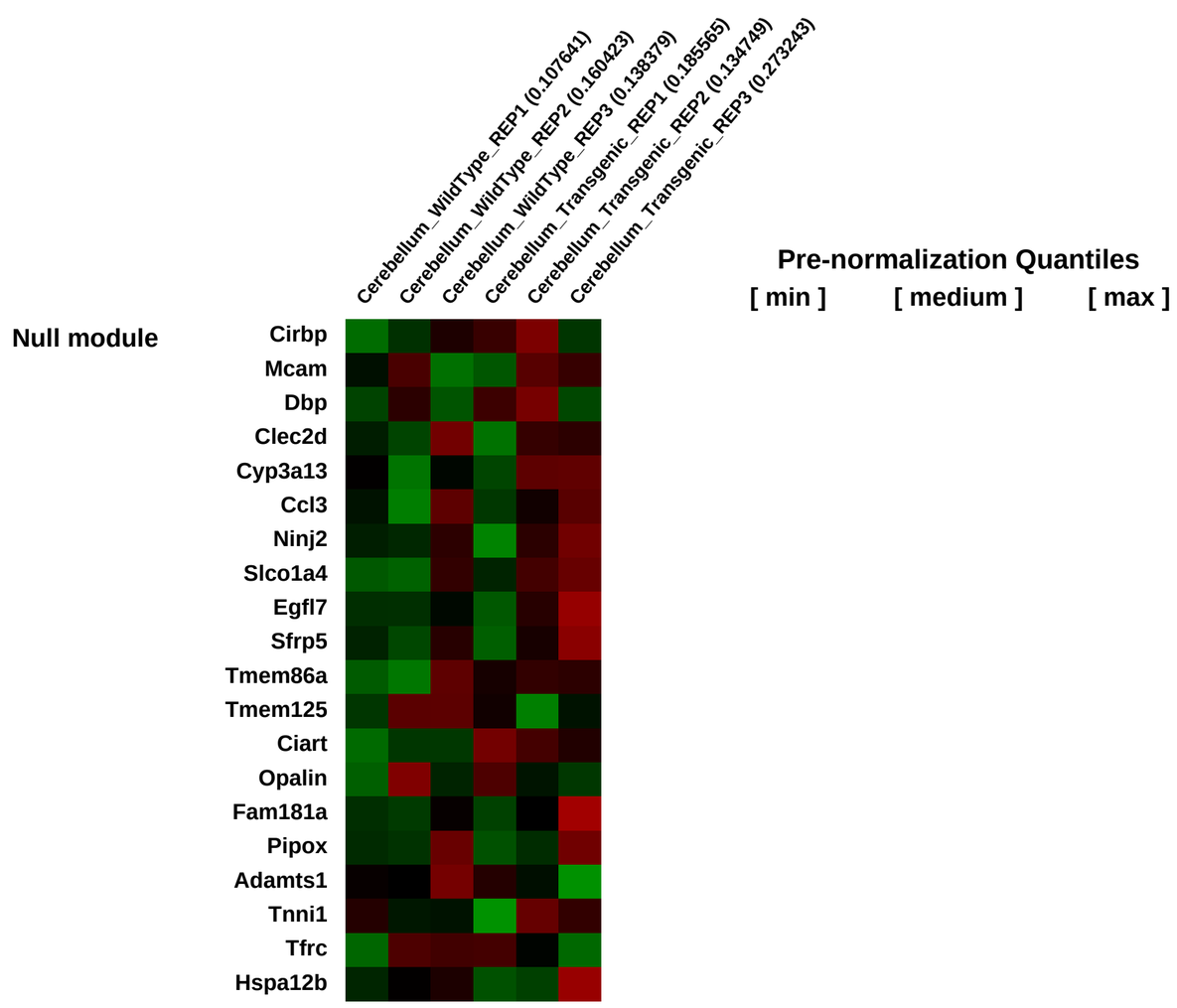

GEO Series "GSE29681" Expression Profiles

Num of samples in this series: 32

Scale of expression profile Z-scores

-3.0 -2.0 -1.0 0.0 1.0 2.0 3.0

GEO Link: http://www.ncbi.nlm.nih.gov/geo/query/acc.cgi?acc=GSE29681
Status: Public on Jun 01 2014
Title: Expression data from WT and R6/2 mice treated with HSP90 inhibitor NVP-HSP990
Organism: Mus musculus
Experiment type: Expression profiling by array
Platform: GPL1261
Pubmed ID:

Summary & Design:

Summary:
Huntingtonâ s disease (HD) is a neurodegenerative disorder that is associated with the deposition of proteinaceous aggregates in the brains of HD patients and mouse models. Previous studies have suggested that wide-scale disruption of protein homeostasis occurs in protein folding diseases. Protein homeostasis can be maintained by activation of the heat shock response (HSR) via the transcription factor heat shock factor 1 (HSF1), the pharmacological activation of which can be achieved by Hsp90 inhibition and has been demonstrated to be beneficial in cell and invertebrate models of HD. Whether the HSR is functional in HD and whether its activation has therapeutic potential in mammalian HD models is currently unknown. To address these issues, we used a novel, brain penetrant Hsp90 inhibitor to activate the HSR in brain after systemic administration. Microarrays, quantitative PCR and western blotting showed that the HSR becomes impaired with disease progression in two mouse models of HD and that this originates at the level of transcription.

Huntingtonâ s disease (HD) is a neurodegenerative disorder that is associated with the deposition of proteinaceous aggregates in the brains of HD patients and mouse models. Previous studies have suggested that wide-scale disruption of protein homeostasis occurs in protein folding diseases. Protein homeostasis can be maintained by activation of the heat shock response (HSR) via the transcription factor heat shock factor 1 (HSF1), the pharmacological activation of which can be achieved by Hsp90 inhibition and has been demonstrated to be beneficial in cell and invertebrate models of HD. Whether the HSR is functional in HD and whether its activation has therapeutic potential in mammalian HD models is currently unknown. To address these issues, we used a novel, brain penetrant Hsp90 inhibitor to activate the HSR in brain after systemic administration. Microarrays, quantitative PCR and western blotting showed that the HSR becomes impaired with disease progression in two mouse models of HD and that this originates at the level of transcription.

Overall design:
mRNA expression analysis was performed by microarray in 12 week old R6/2 and WT mice treated with vehicle or HSP990 for 4h (12mg/kg).The following number of replicates was analysed for each genotype: 7 for WT+vehicle, 10 for WT+HSP990, 7 for R6/2+vehicle and 8 for R6/2+HSP990. Microarray quality control was performed using the software package provided on RACE (http://race.unil.ch).

Background corr dist: KL-Divergence = 0.2496, L1-Distance = 0.0430, L2-Distance = 0.0036, Normal std = 0.3048

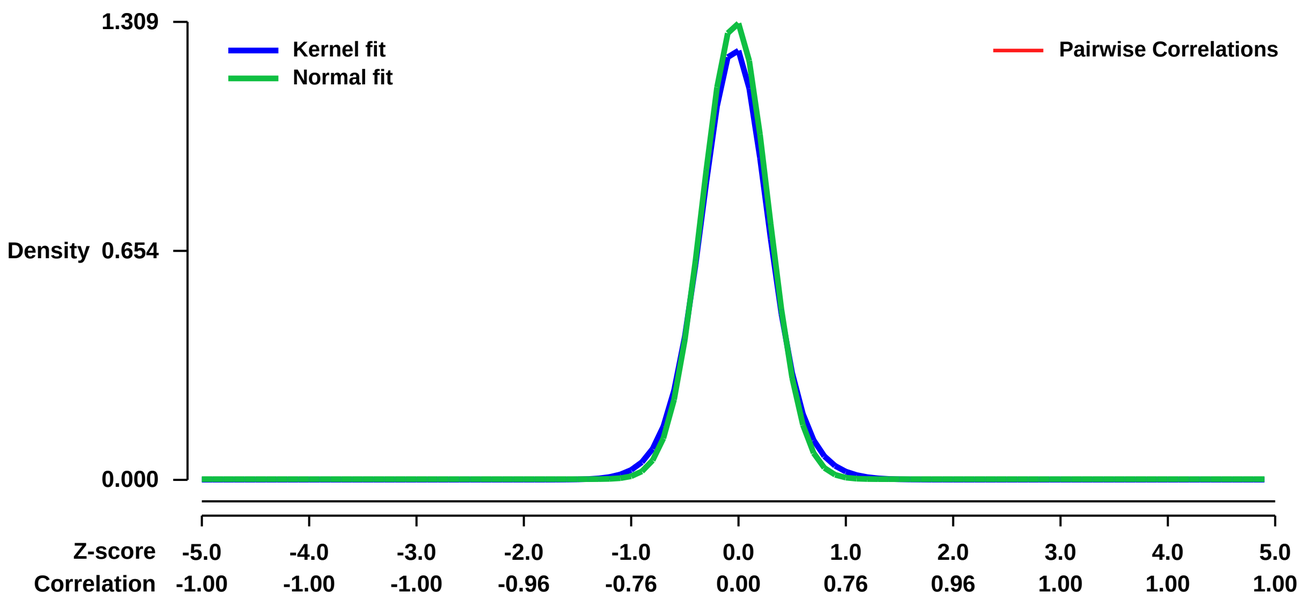

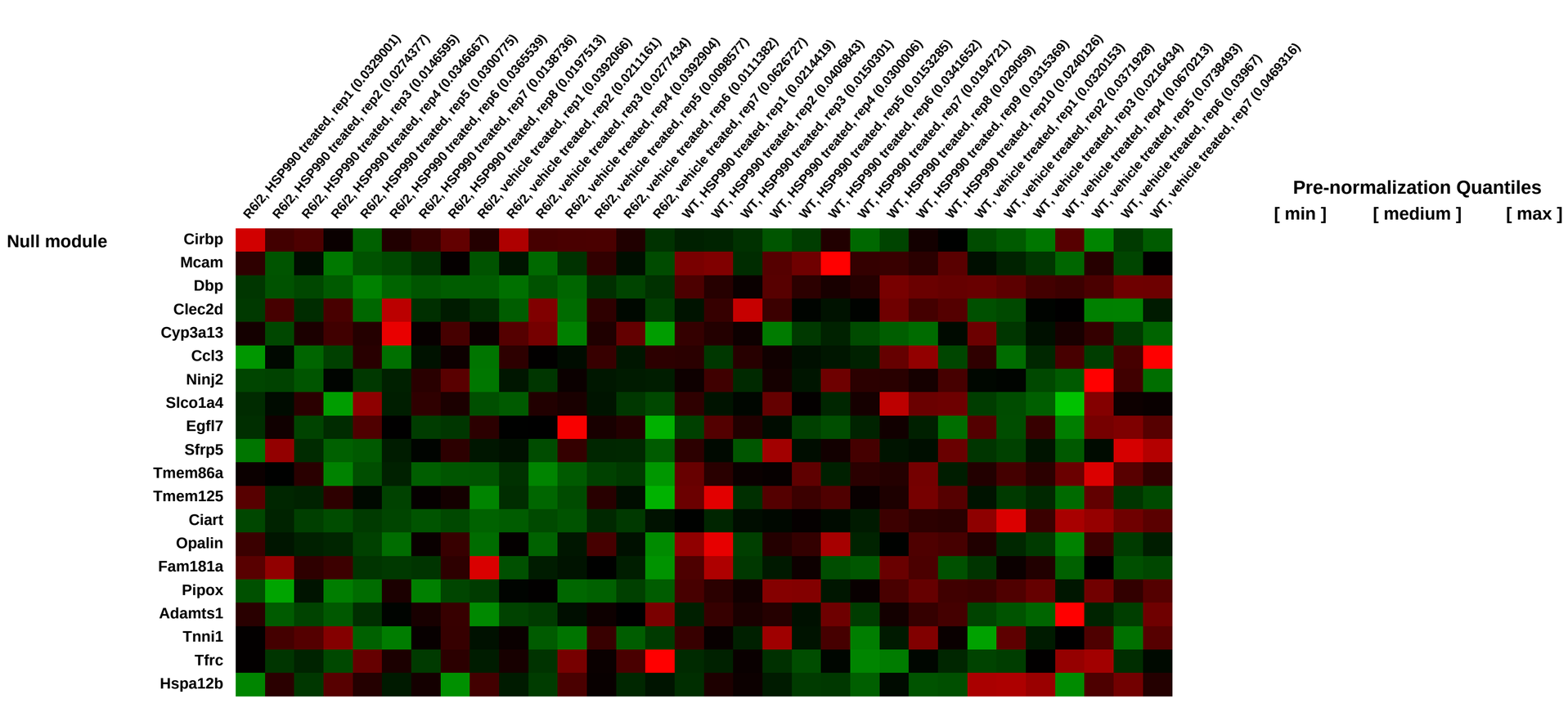

GEO Series "GSE51365" Expression Profiles

Num of samples in this series: 28

Scale of expression profile Z-scores

-3.0 -2.0 -1.0 0.0 1.0 2.0 3.0

GEO Link:	http://www.ncbi.nlm.nih.gov/geo/query/acc.cgi?acc=GSE51365
Status:	Public on Oct 18 2013
Title:	Latent gammaherpesvirus 68 infection induces distinct transcriptional changes in different organs
Organism:	Mus musculus
Experiment type:	Expression profiling by array
Platform:	GPL1261
Pubmed ID:	24155394
Summary & Design:	**Summary:** Previous studies identified a role for latent herpesvirus infection in cross-protection to infection and exacerbation of chronic inflammatory diseases. Here, we compared the gene expression signature from livers, spleens and brains of mice infected with wild-type gammaherpesvirus 68 (MHV68), a mutant virus defective in the establishment of latency (ORF73.stop) or mockulum. We identified over 600 genes differentially expressed in organs of mice latently infected with MHV68 and found distinct sets of genes linked to different pathways were altered in spleen compared to liver. Several of the most differentially expressed latency-specific genes (e.g. IFN‸‡, Cxcl9, Ccl5) are associated with known latency-specific phenotypes. **Overall design:** RNA was extracted from livers, spleens and brains of 7-9 week old male C57Bl/6 mice infected with gammaherpesvirus 68 (MHV68), a virus defective in establishment of latency (ORF73.stop) or mockulum. RNA from 3-4 mice per treatment was pooled and analyzed by M430 2.0 Affymetrix Gene Chip. Three biologic replicates were analyzed for all conditions, except mock livers, for which four biologic replicates were analyzed.

Background corr dist: KL-Divergence = 0.0674, L1-Distance = 0.0734, L2-Distance = 0.0082, Normal std = 0.6075

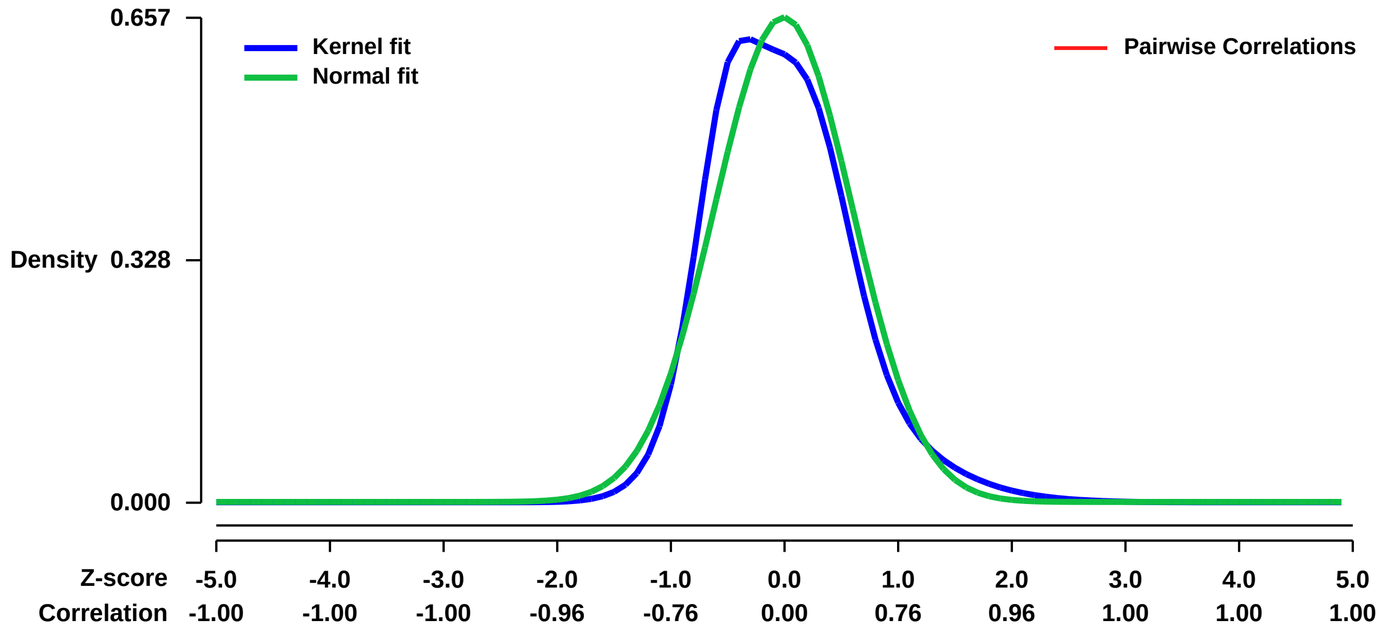

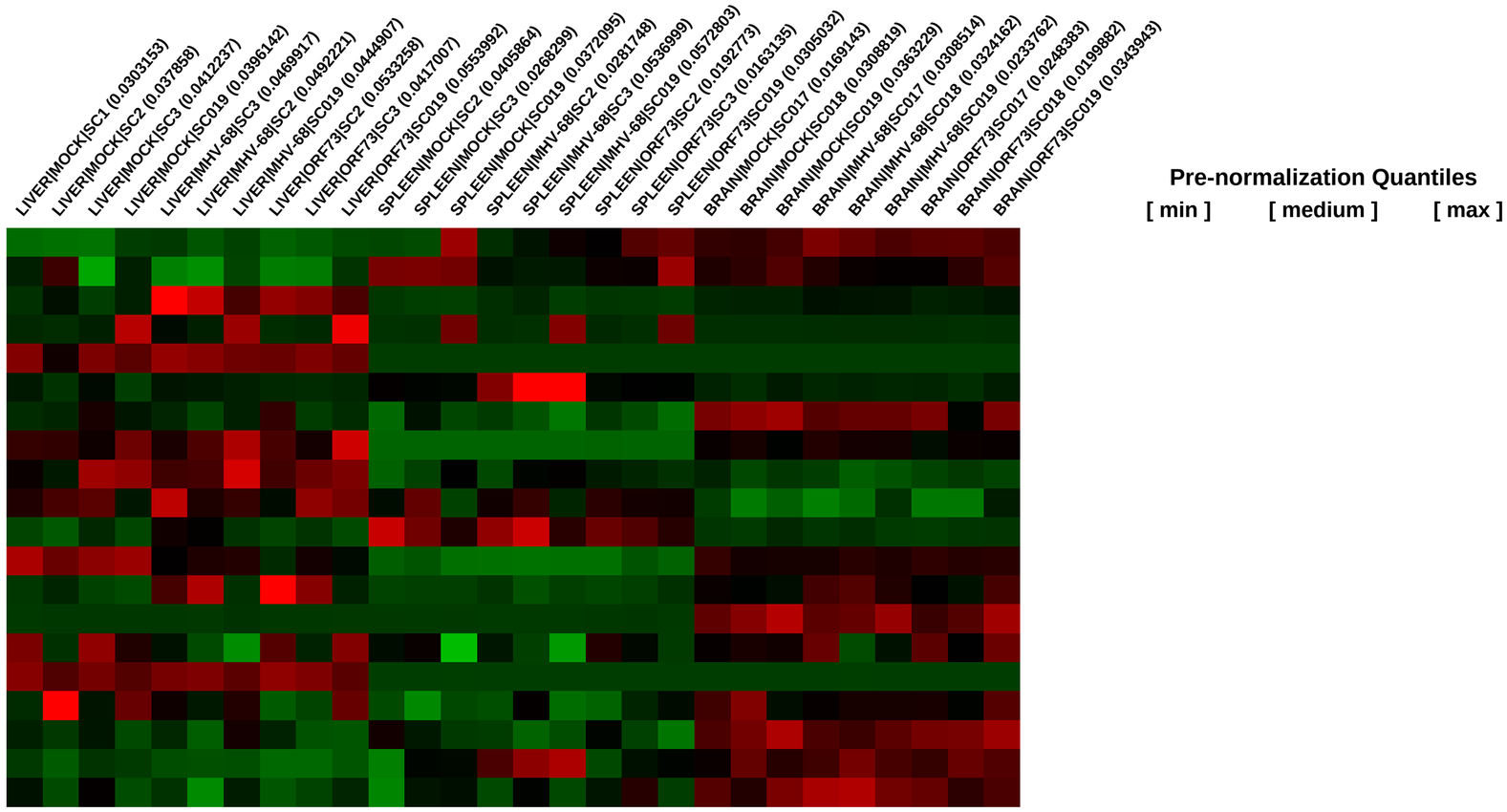

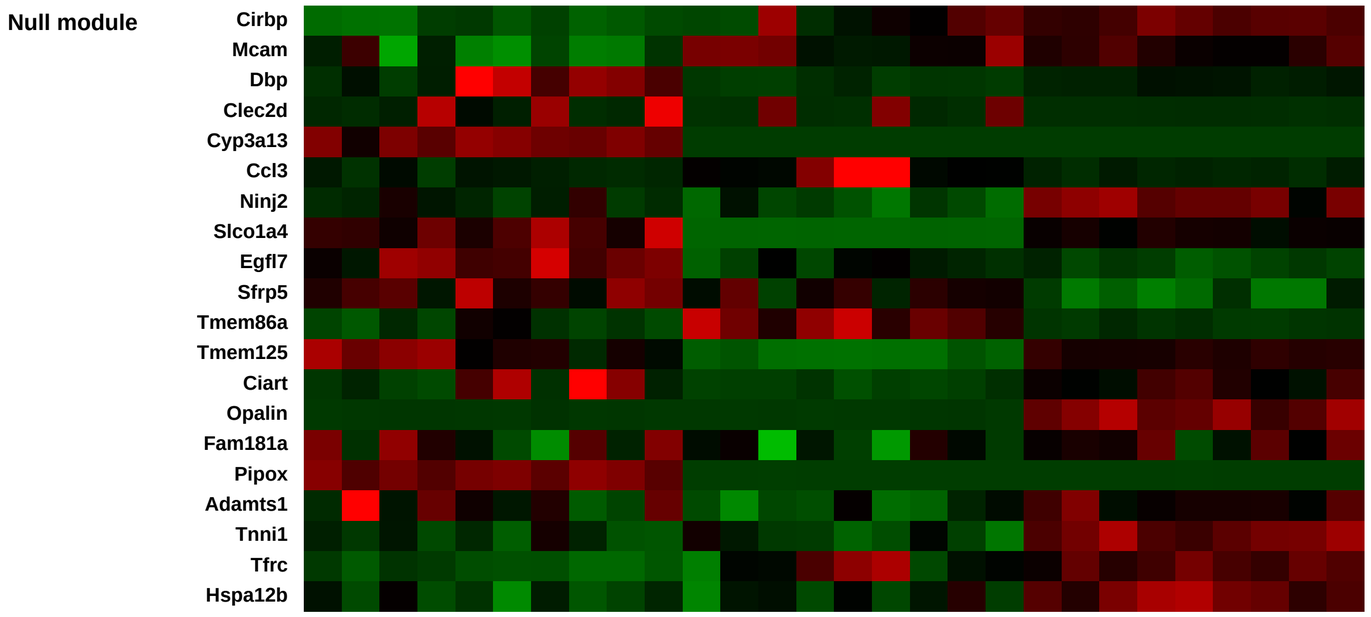

GEO Series "GSE31004" Expression Profiles

Num of samples in this series: 8

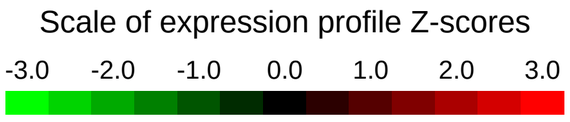

GEO Link:	**http://www.ncbi.nlm.nih.gov/geo/query/acc.cgi?acc=GSE31004**
Status:	**Public on Dec 15 2011**
Title:	**Effects of Nicotine on the Fetal Mouse Palate Development and Transcriptome**
Organism:	**Mus musculus**
Experiment type:	**Expression profiling by array**
Platform:	**GPL1261**
Pubmed ID:	
Summary & Design:	**Summary:** **Nonsyndromic cleft palate is a common birth defect (1:700) with a complex etiology involving both genetic and environmental risk factors. Nicotine, a major teratogen present in tobacco products, was shown to cause alterations and delays in the developing fetus. To demonstrate the effect of nicotine on craniofacial development, particularly palatogenesis, we delivered three different doses of nicotine (1.5, 3.0 and 4.5 mg/kg/day) into pregnant BALB/c mice throughout their entire pregnancy using subcutaneous osmotic mini-pump. We assessed the pups for morphological anomalies, as well as genome-wide mRNA (transcriptome) microarray analysis. Consistent administration of nicotine caused developmental retardation, still birth, low birth weight, and significant palatal size and shape abnormality in the pups. However, it did not cause obvious cleft palate. The microarray data analysis using IPA identified differential expression of genes involved in various biological pathways, particularly cancer, genetic diseases, and tissue development in response to consistent nicotine exposure. 6232 up-regulated and 6310 down-regulated genes were detected in nicotine-treated groups compared to the control. Moreover, 45% of the genes associated with cleft palate were found to be affected by nicotine. Alterations of a subset of differentially expressed genes were illustrated with hierarchal clustering and RT-PCR. We concluded that consistent nicotine exposure during pregnancy interferes with normal growth and development of the fetus including palatogenesis; however, this interference does not result in cleft palate, rather smaller palate size with persistent MES. To our knowledge, this is the first experiment revealing the impact of nicotine on the fetal palate transcriptome in mice.** **Overall design:** **Total 8 samples were analyzed. Using an osmotic minipump, duplicate samples from palates of either sterile physiological saline or nicotine (1.5 mg/kg/day, 3.0 mg/kg/day, or 4.5 mg/kg/day)-treated newborn pups.**

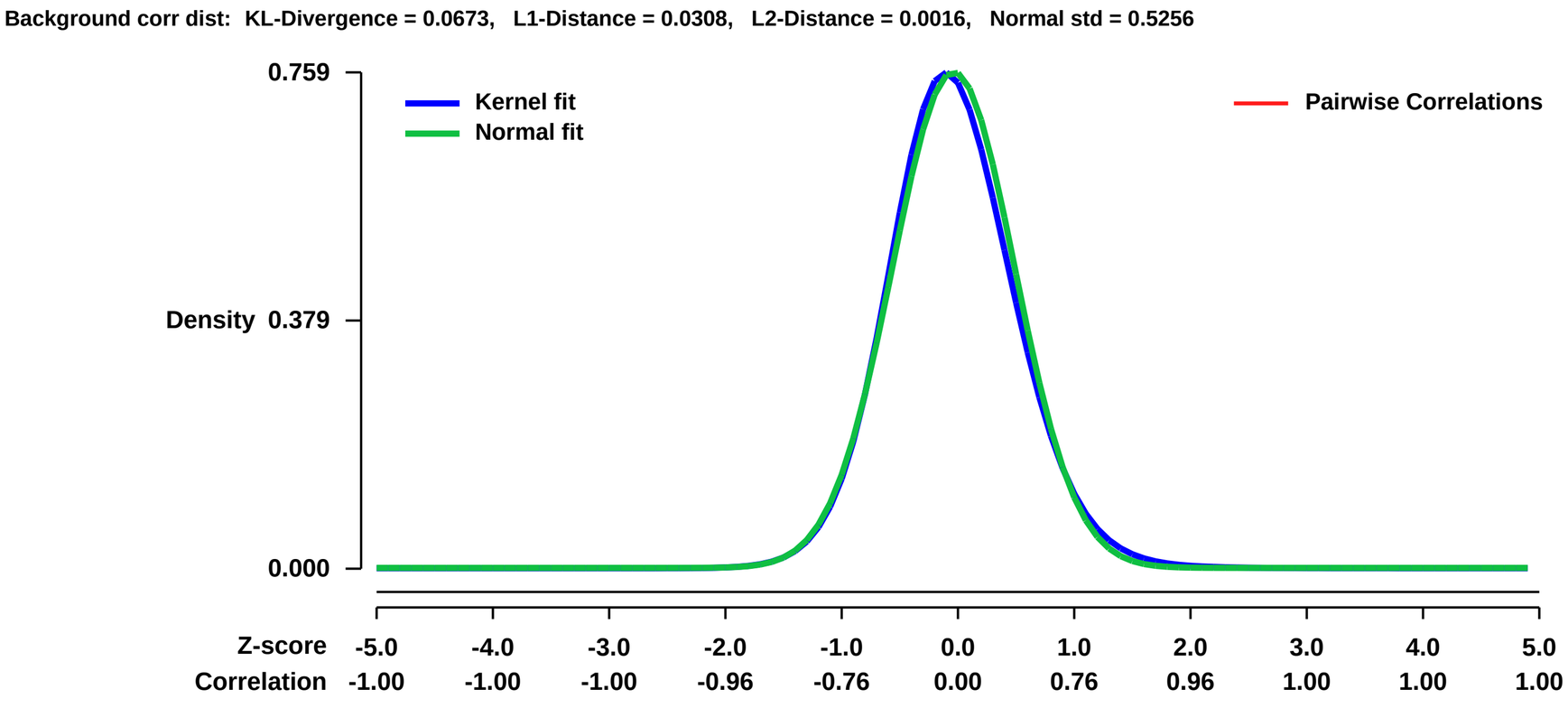

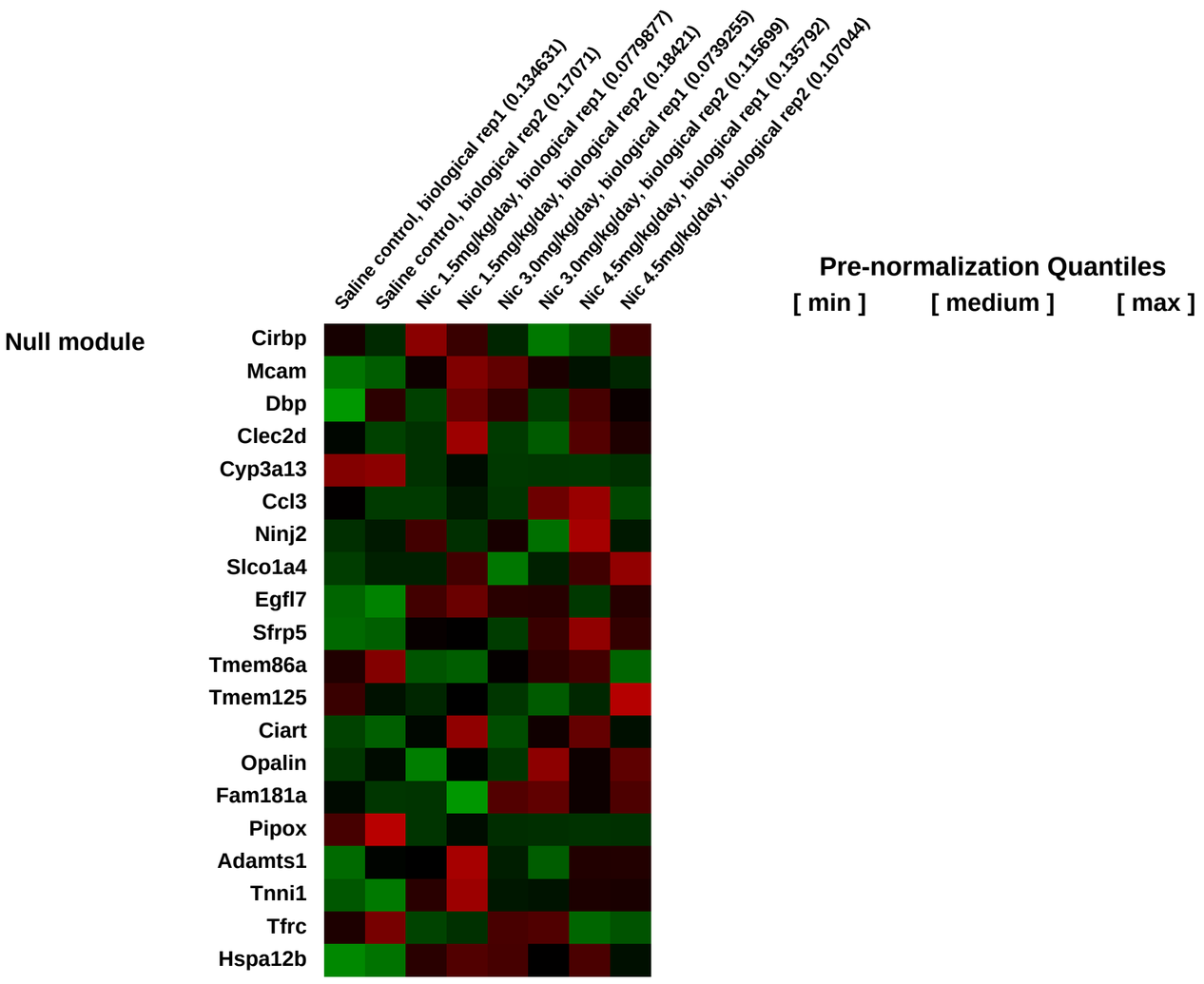

GEO Series "GSE44084" Expression Profiles

Num of samples in this series: 8

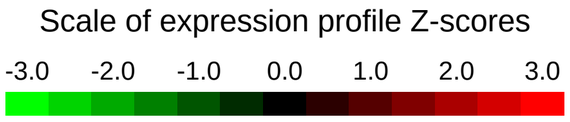

GEO Link:	http://www.ncbi.nlm.nih.gov/geo/query/acc.cgi?acc=GSE44084
Status:	Public on Jun 05 2013
Title:	Expression data from pre-iPSCs with a control, histone methyltransferase or Cbx3 (HP1g) knockdown
Organism:	Mus musculus
Experiment type:	Expression profiling by array
Platform:	GPL1261
Pubmed ID:	23748610
Summary & Design:	**Summary:** Transition from a partially reprogrammed pre-iPSC state to iPSC state can be achieved by modulating levels of histone modifying enzymes or proteins that can bind to histone modifications We used microarrays to determine the gene expression profile of pre-iPSCs depleted for either 3 histone methyltransferases together or the HP1gamma protein **Overall design:** pre-iPSCs were subjected to simultaneous siRNA mediated knockdown of Ehmt1, Ehmt2 and Setdb1- which is the 3XHMT sample that mediate H3k9me2/me3 or Cbx3(HP1gamma) or control siRNA to luciferase

Background corr dist: KL-Divergence = 0.0611, L1-Distance = 0.0178, L2-Distance = 0.0003, Normal std = 0.5259

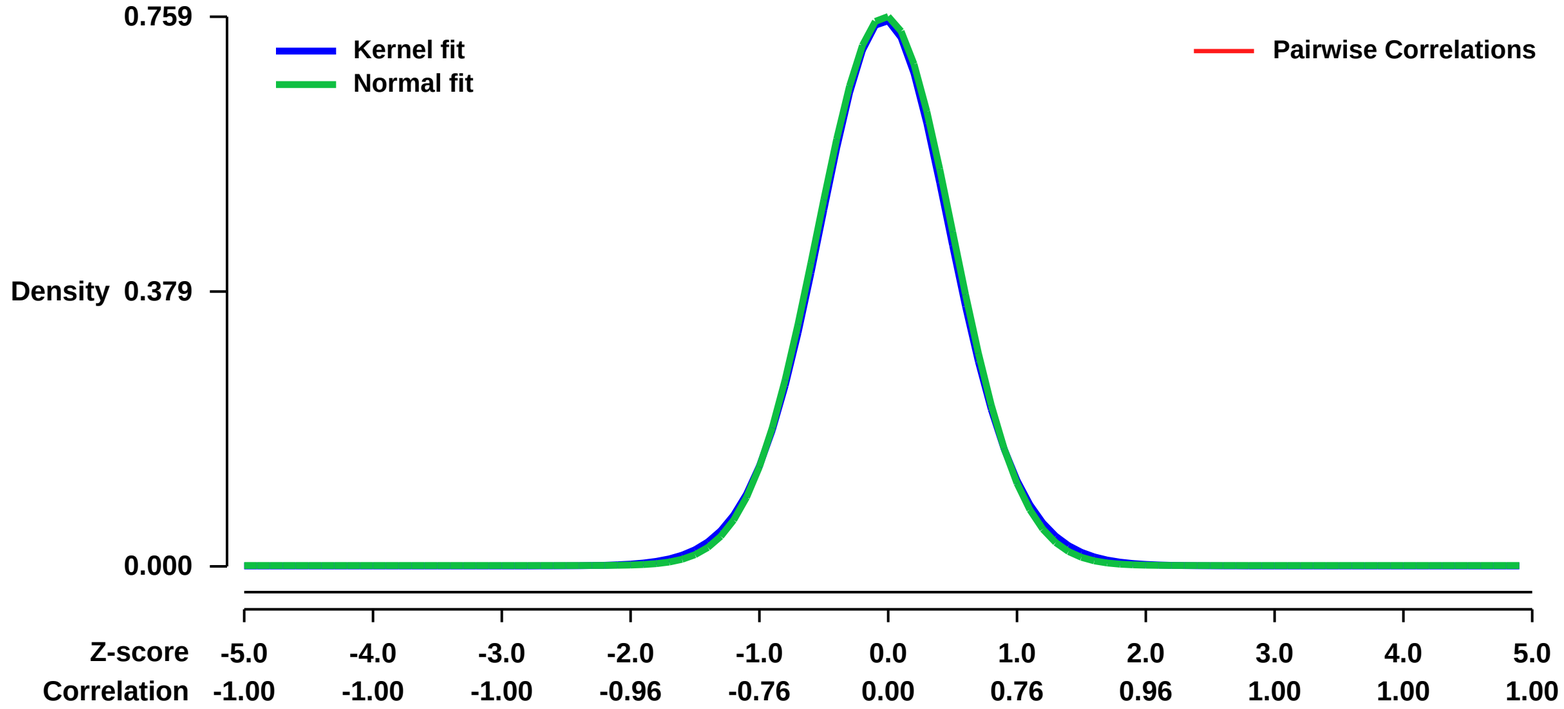

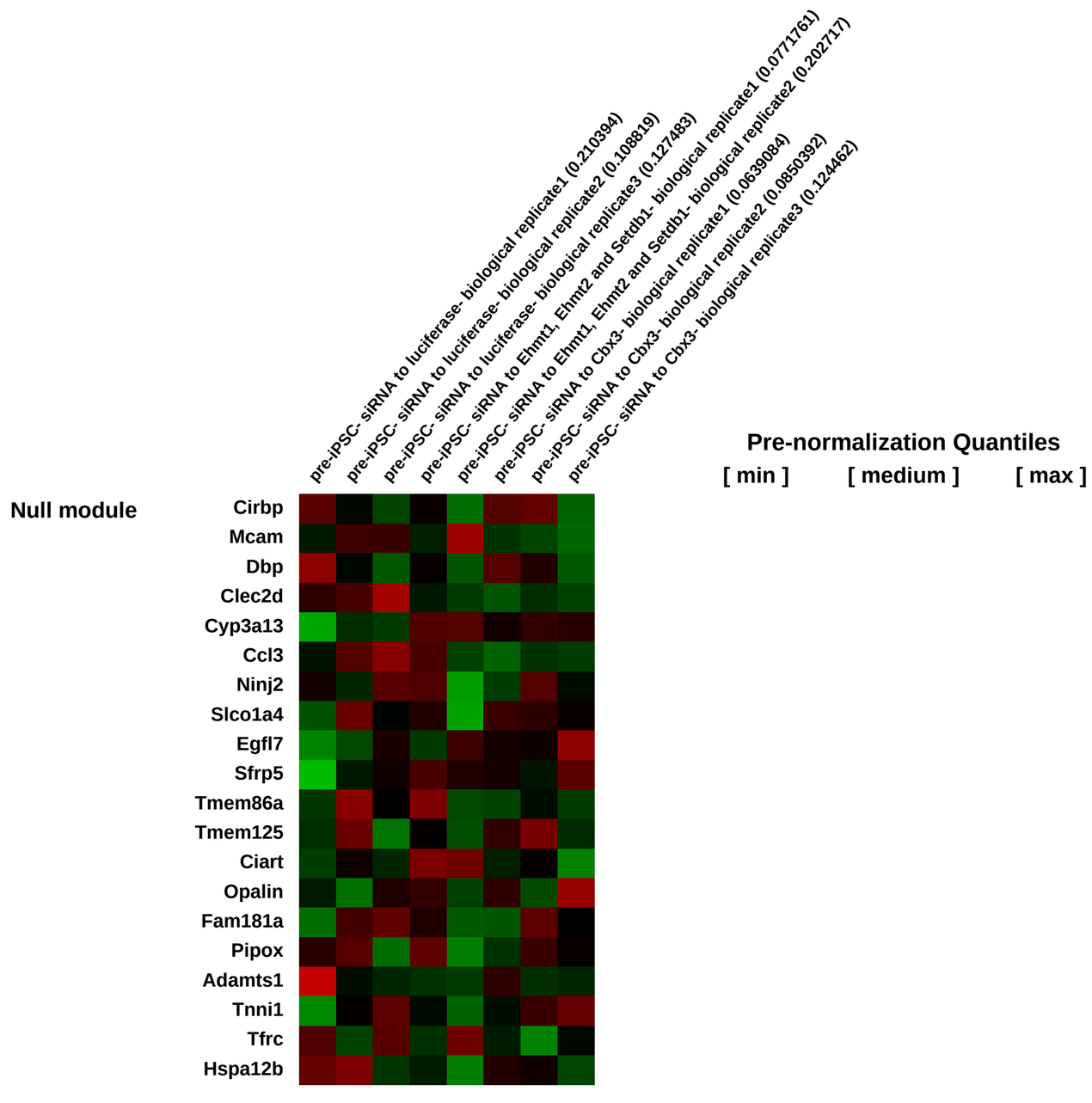

GEO Series "GSE43635" Expression Profiles

Num of samples in this series: 9

Scale of expression profile Z-scores

-3.0 -2.0 -1.0 0.0 1.0 2.0 3.0

GEO Link:	**http://www.ncbi.nlm.nih.gov/geo/query/acc.cgi?acc=GSE43635**
Status:	**Public on Jan 19 2013**
Title:	**Expression data from mouse T cells after CLIP (Crosslinking immunoprecipitation) procedures (mRNA)**
Organism:	**Mus musculus**
Experiment type:	**Expression profiling by array**
Platform:	**GPL1261**
Pubmed ID:	
Summary & Design:	**Summary:** **Molecular networks based on genome-wide mRNA and miRNA expression in activated T cells are interated by co-regulation with miRNA and protein-coding genes during immune responses, however, accurate prediction of miRs and their targets remains a challenge. Furthermore, the specific changes in the expression of miRNAs and/or mRNAs in allogeneic activated T cells during HCT would be distinct from those responding to non-specific stimulation.** **Recently, Ago-CLIP has been demonstrated to provide a robust platform for identification of precise miRNA-mRNA interactions by definitively distinguishing direct from indirect miRNA-target interactions. We utilized CLIP procedure followed by screening with standard microarray platforms for miRNA and mRNA transcripts to demonstrate the miR-mRNA landscape and identify novel molecular targets for modulating T cell responses.** **Overall design:** **Mixed cell culture was performed with T cells in the presence of syngeneic 57BL/6, or allogeneic BALB/c dendritic cells or cultivated with anti-CD3e and anti-CD28 mAB9 for 24 h. Purified T cells were processde for CLIP procedures and followed by RNA isolation (TRIzol LS and miReasy Kit) and hybridization on Affymetrix microarrays and Exiqon 6th generation miRCURY LNA microRNA Arrays . We sought to obtain that the specific changes in the expression of miRNAs and/or mRNAs in allogeneic activated T cells during hematopoietic cells transplantation and that would be distinct from those responding to non-specific stimulation.**

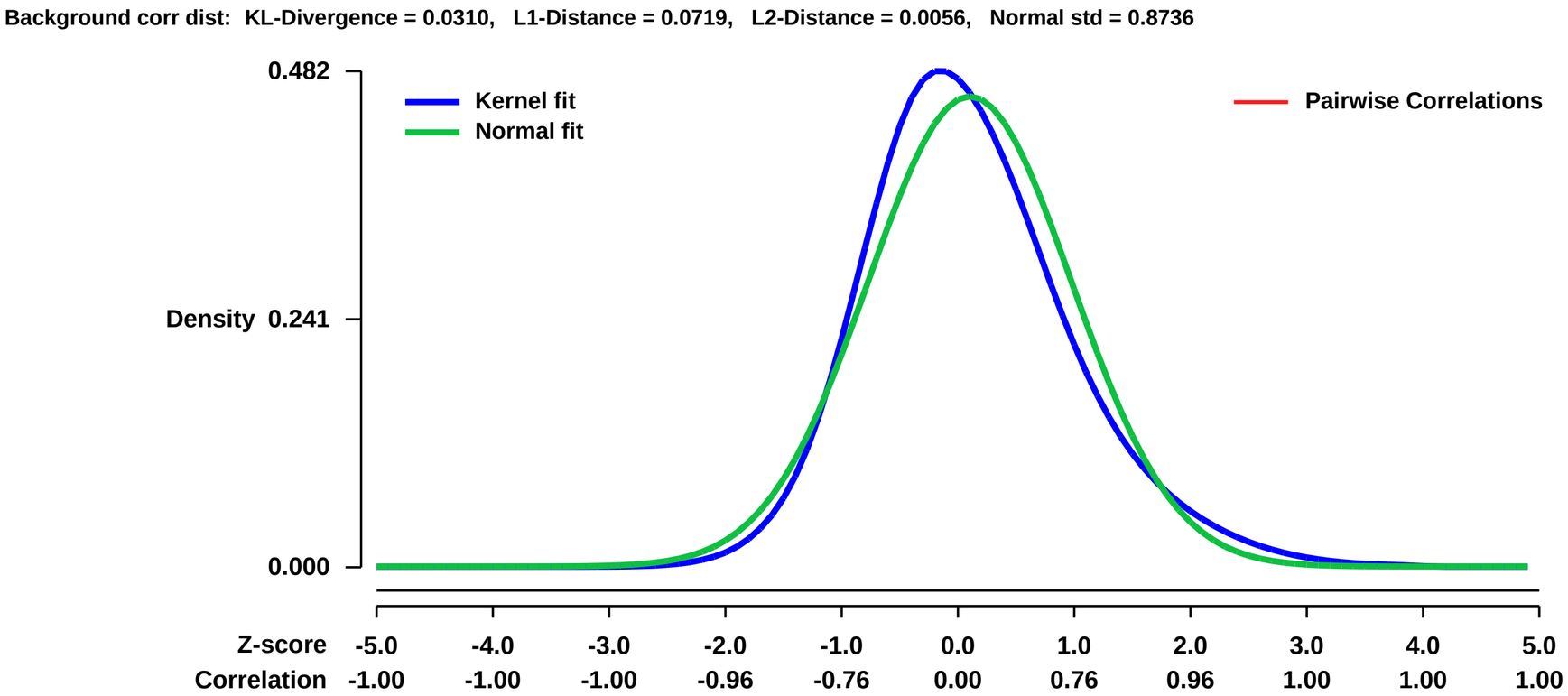

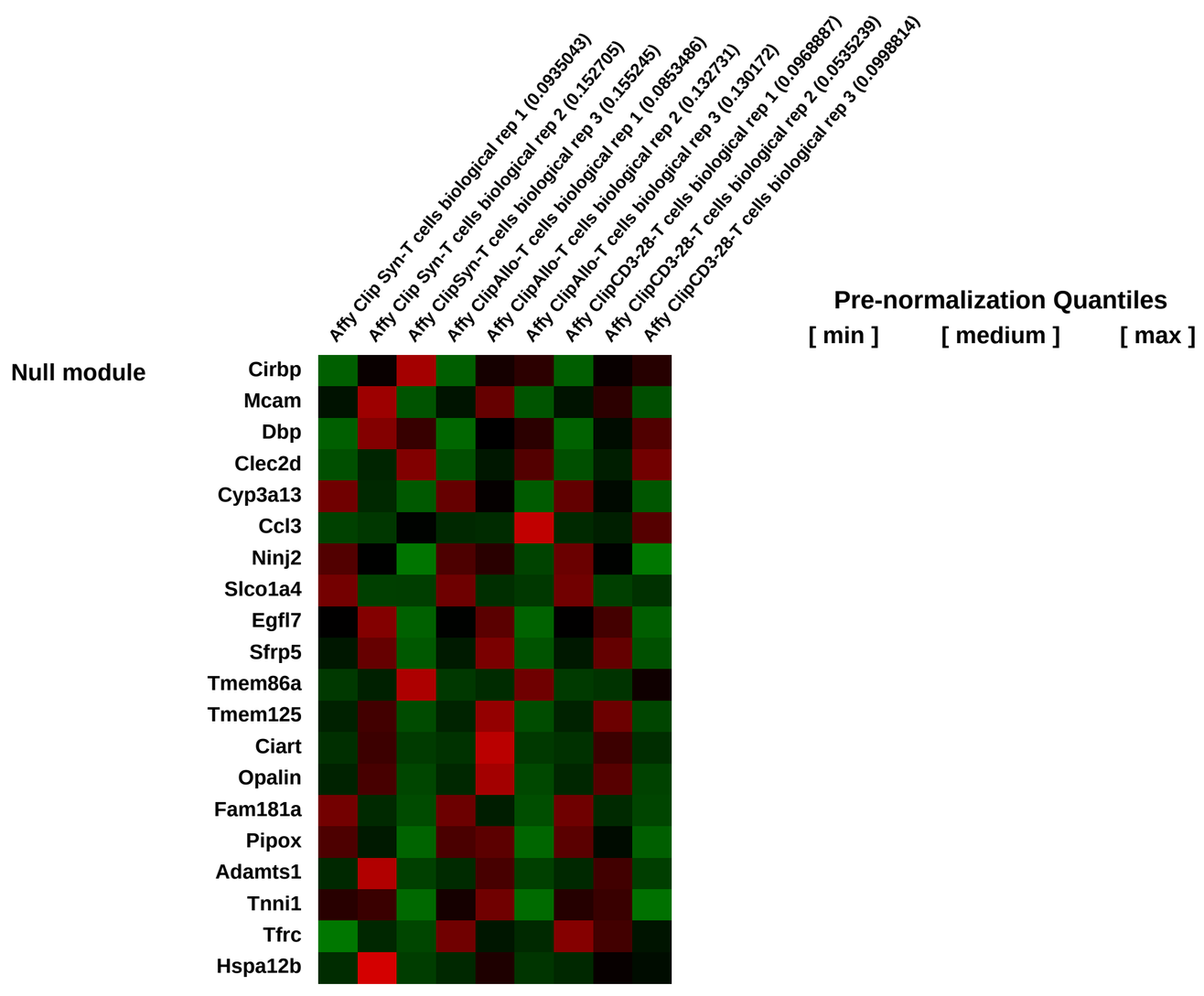

GEO Series "GSE32093" Expression Profiles

Num of samples in this series: 6

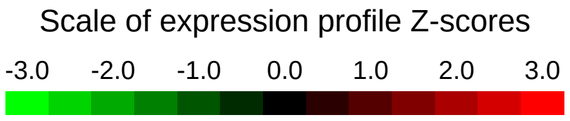

GEO Link:	**http://www.ncbi.nlm.nih.gov/geo/query/acc.cgi?acc=GSE32093**
Status:	**Public on Apr 01 2012**
Title:	**Expression data from E12.5 embryonic kidneys isolated from wild-type and Ret-deficient mice**
Organism:	**Mus musculus**
Experiment type:	**Expression profiling by array**
Platform:	**GPL1261**
Pubmed ID:	
Summary & Design:	**Summary:** **To better understand the signaling and transcriptional events involved in the GDNF-independent emergence of the ureteric bud from the Wolffian duct, microarray expression analysis was performed on embryonic kidneys from wild-type and Ret-deficient mice. Microarray data was used to identify genes and gene networks involved in the GDNF-independent outgrowth of the ureteric bud.** **Overall design:** **Whole embryonic kidneys from E12.5 Ret mutant and wild-type mice were isolated. Isolated kidneys were lysed and RNA was extracted with the Qiagen RNEasy Micro kit. The RNA was amplified using the NuGEn Ovation kit and hybridized to the Affymetrix GeneChip Mouse Whole Genome 430 2.0 microarray. Three biological replicates for Ret-knockout and wild-type kidneys were performed.**

Background corr dist: **KL-Divergence = 0.0400, L1-Distance = 0.0258, L2-Distance = 0.0008, Normal std = 0.6234**

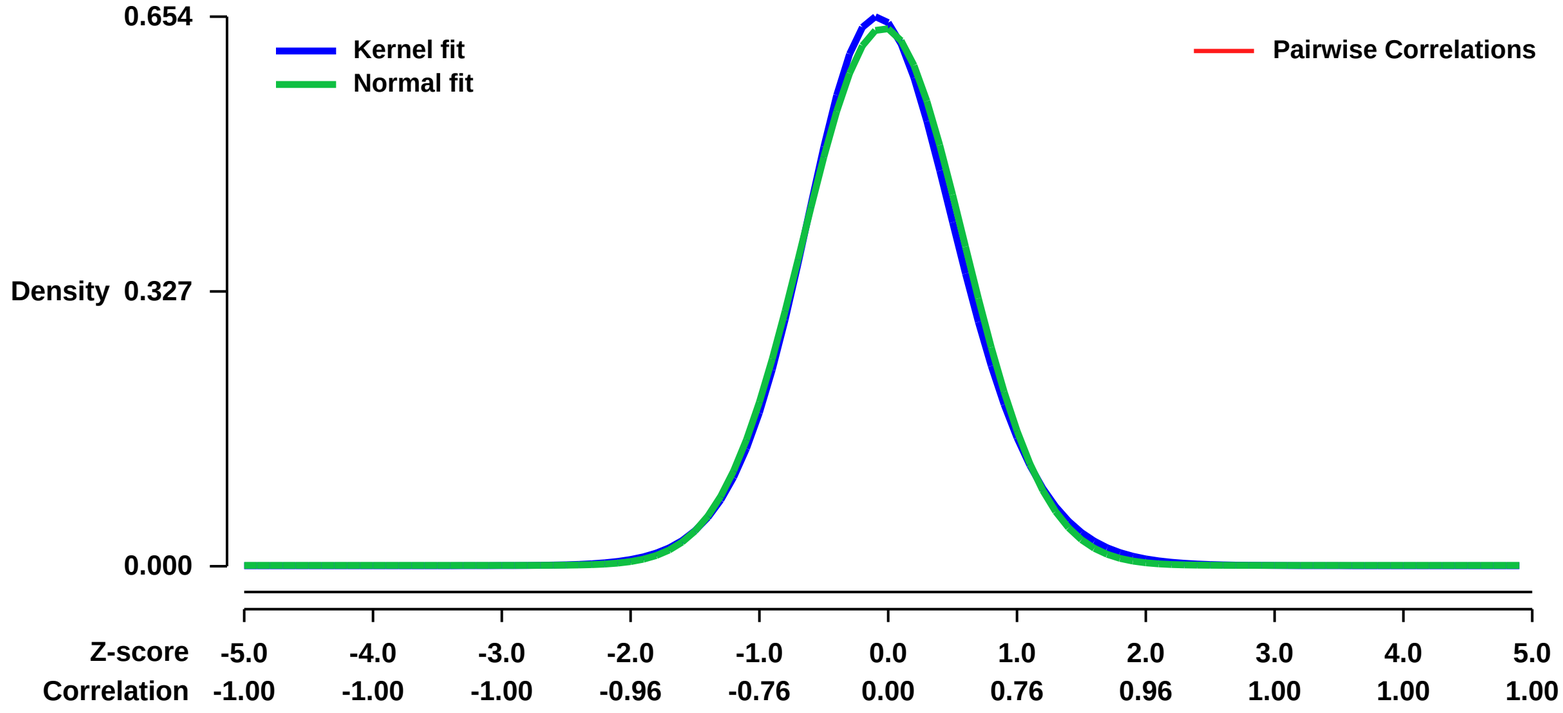

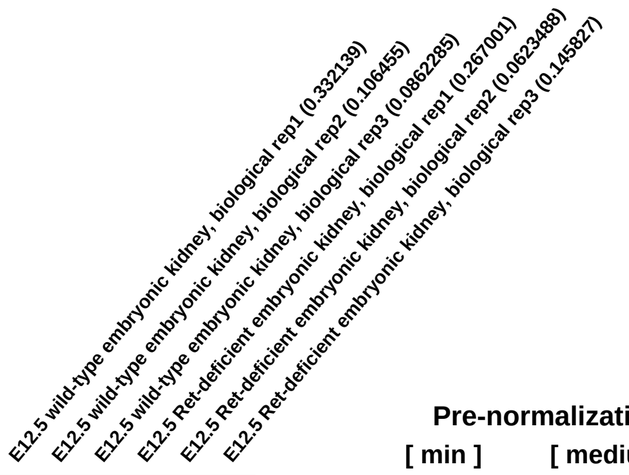

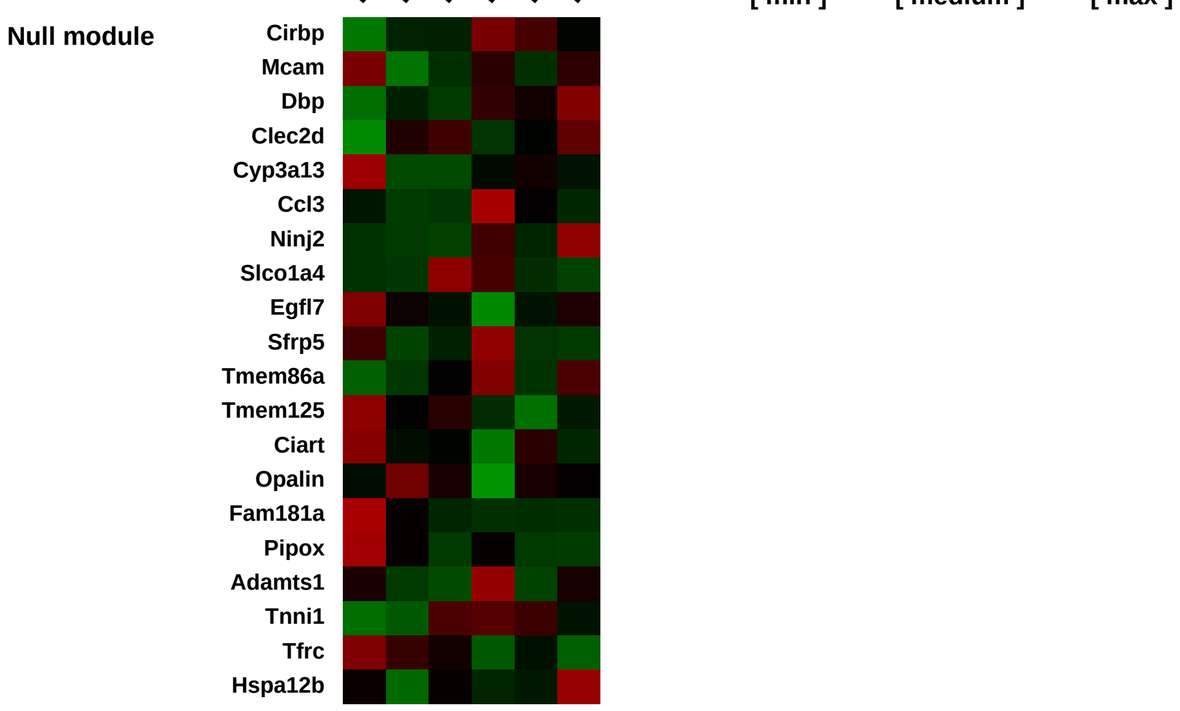

GEO Series "GSE10849" Expression Profiles

Num of samples in this series: 6

Scale of expression profile Z-scores

-3.0 -2.0 -1.0 0.0 1.0 2.0 3.0

GEO Link:	**http://www.ncbi.nlm.nih.gov/geo/query/acc.cgi?acc=GSE10849**
Status:	**Public on Mar 04 2009**
Title:	**Caveolin-1 Knockout Hearts**
Organism:	**Mus musculus**
Experiment type:	**Expression profiling by array**
Platform:	**GPL1261**
Pubmed ID:	**18719368**
Summary & Design:	**Summary:** **Hearts Lacking Caveolin-1 Develop Hypertrophy with Normal Cardiac Substrate Metabolism** **Keywords: gene knockout** **Overall design:** **3 wild types, 3 knockouts**

Background corr dist: **KL-Divergence = 0.0216, L1-Distance = 0.0174, L2-Distance = 0.0003, Normal std = 0.7235**

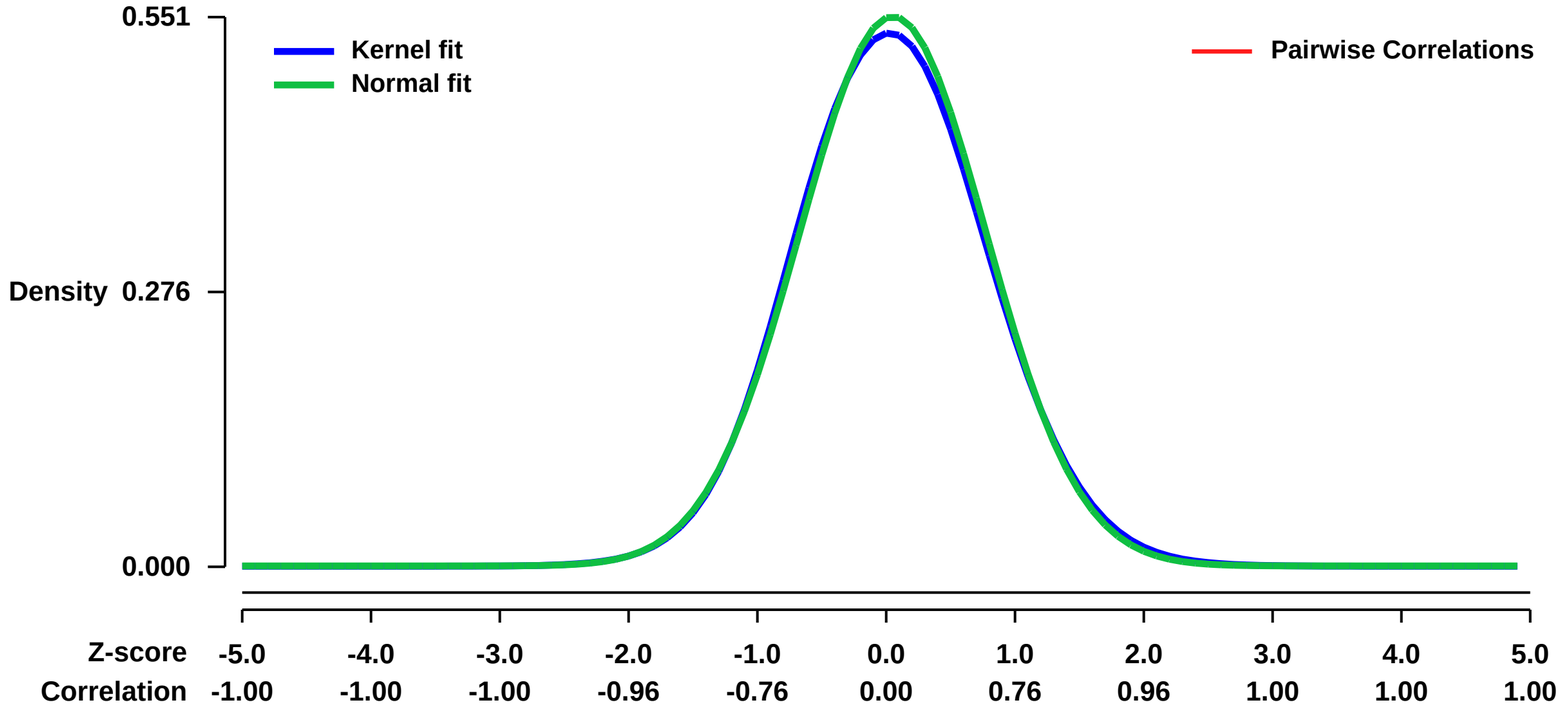

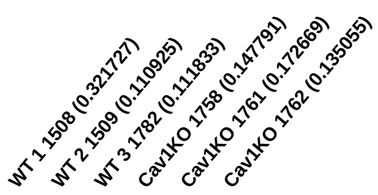

Pre-normalization Quantiles

[min] [medium] [max]

Null module

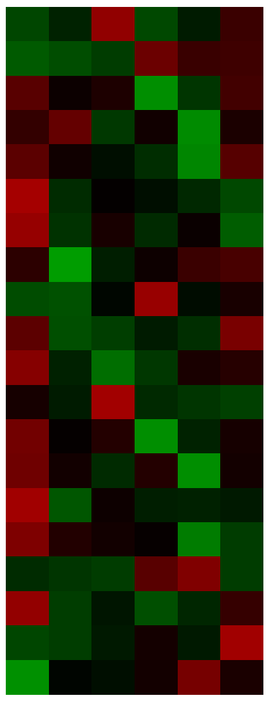

GEO Series "GSE18033" Expression Profiles

Num of samples in this series: 56

Scale of expression profile Z-scores

-3.0 -2.0 -1.0 0.0 1.0 2.0 3.0

GEO Link:	http://www.ncbi.nlm.nih.gov/geo/query/acc.cgi?acc=GSE18033
Status:	Public on Sep 01 2012
Title:	Transcriptomics-based characterization of smoking and cessation effects in mouse muscle
Organism:	Mus musculus
Experiment type:	Expression profiling by array
Platform:	GPL1261
Pubmed ID:	
Summary & Design:	**Summary:** COPD is a disorder characterized by the progressive development of airflow limitation that is not fully reversible. Cigarette smoke has been generally accepted as the most important of many risk factors for the development of COPD. We used microarray technology to perform comprehensive gene expression profiling of smoke exposure and cessation effects in mouse muscle tissue. **Overall design:** Mice received nose-only exposure of 4% mainstream cigarette smoke or air (sham exposure) for 2 hours/day, 5 days/week for 2, 12 or 24 weeks. Mice undergoing smoke cessation received cigarette smoke exposure for 12 weeks, and then sham exposure for 12 weeks.

Background corr dist: KL-Divergence = 0.1917, L1-Distance = 0.0549, L2-Distance = 0.0058, Normal std = 0.3570

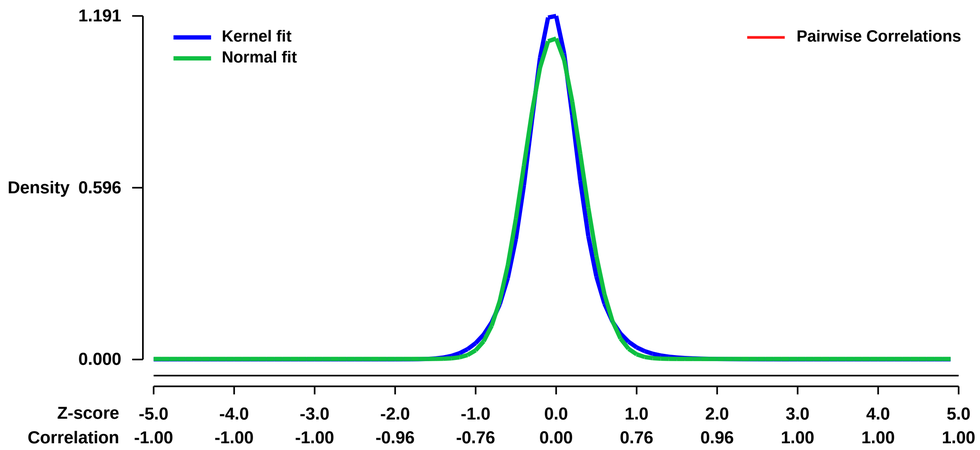

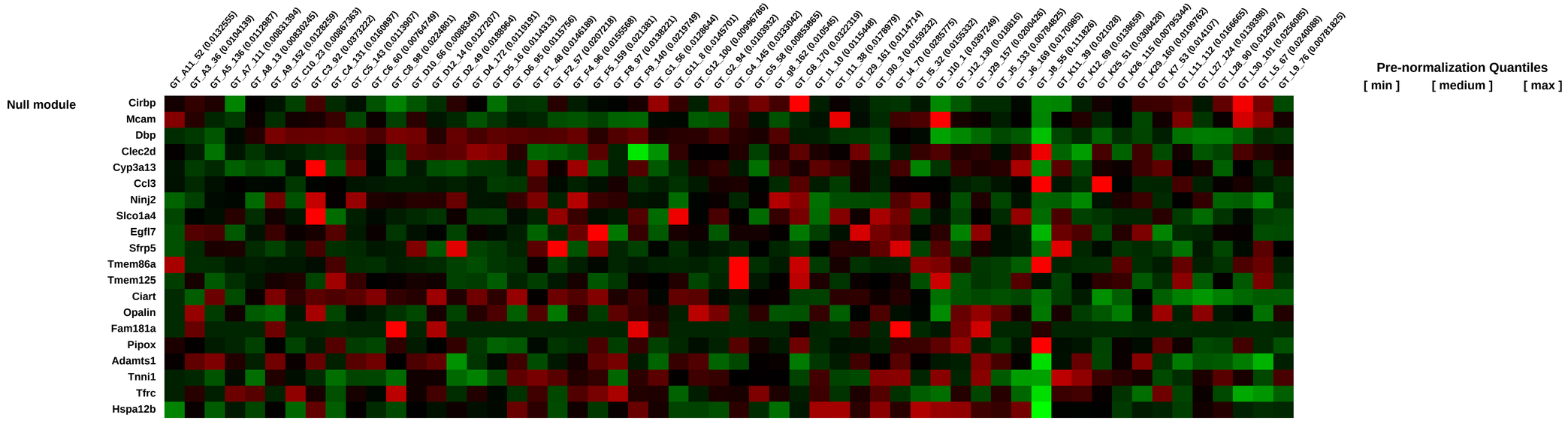

GEO Series "GSE27786" Expression Profiles

Num of samples in this series: 20

Scale of expression profile Z-scores

-3.0 -2.0 -1.0 0.0 1.0 2.0 3.0

GEO Link:	http://www.ncbi.nlm.nih.gov/geo/query/acc.cgi?acc=GSE27786
Status:	Public on May 19 2011
Title:	Gene expression profile of mouse hematopoietic cells
Organism:	Mus musculus
Experiment type:	Expression profiling by array
Platform:	GPL1261
Pubmed ID:	21540074
Summary & Design:	**Summary:** Each fraction of mouse hematopoietic cells was purified by cell sorting from bone marrow of 8-week-old C57BL/6 mice, and its gene expression was analyzed. **Overall design:** Two biological replicates of each fraction were analyzed using a Mouse Genome 430 2.0 array (Affymetrix).

Background corr dist: KL-Divergence = 0.1762, L1-Distance = 0.0498, L2-Distance = 0.0060, Normal std = 0.3706

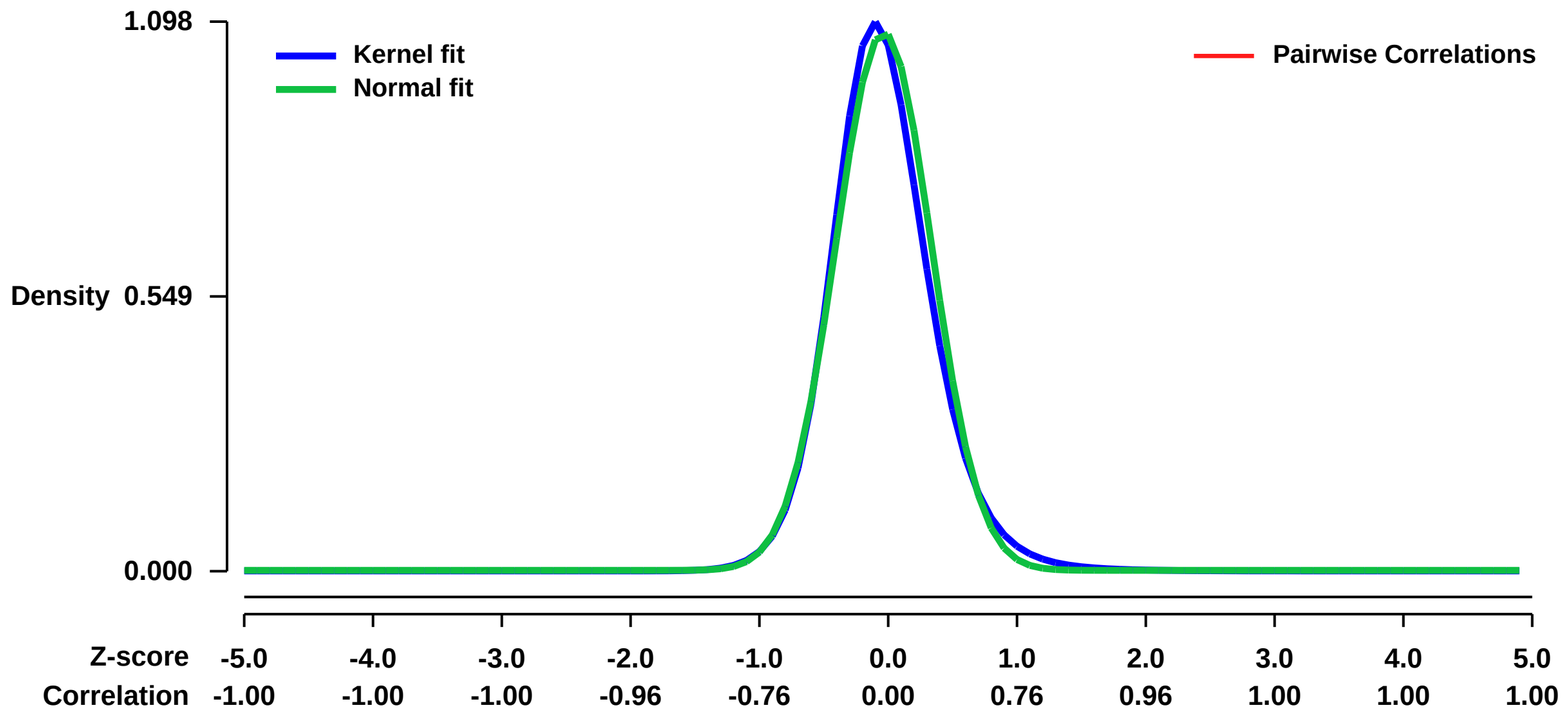

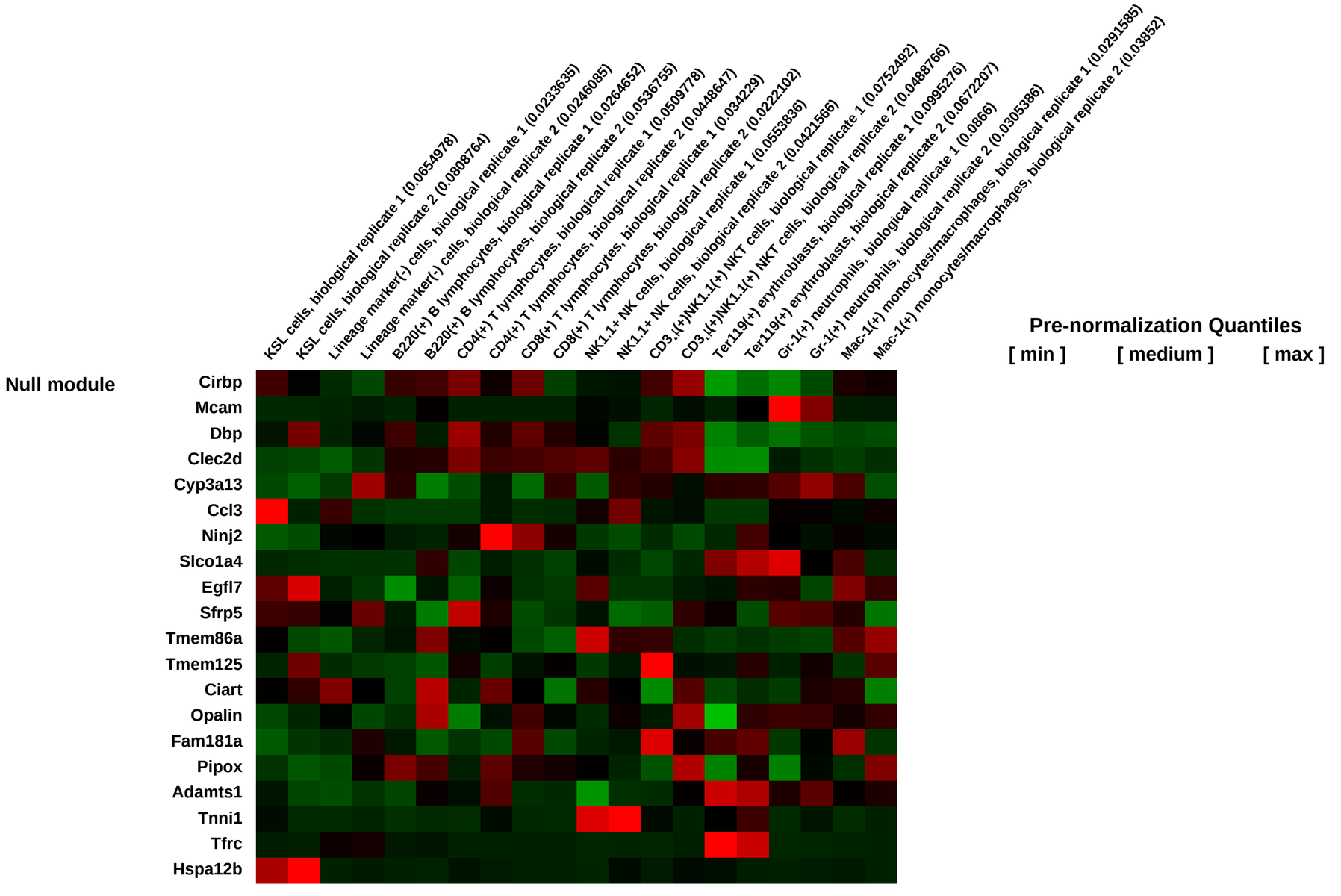

GEO Series "GSE54581" Expression Profiles

Num of samples in this series: 21

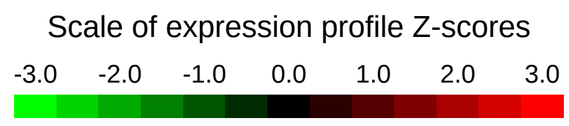

GEO Link:	http://www.ncbi.nlm.nih.gov/geo/query/acc.cgi?acc=GSE54581
Status:	Public on Jun 02 2014
Title:	Selective mRNA translation during eIF2 phosphorylation induces expression of IBTKalpha
Organism:	Mus musculus
Experiment type:	Expression profiling by array
Platform:	GPL1261
Pubmed ID:	24648495
Summary & Design:	**Summary:** **Disruption of protein folding in the endoplasmic reticulum triggers the Unfolded Protein Response (UPR), a transcriptional and translational control network designed to restore protein homeostasis. Central to the UPR is PERK phosphorylation of the alpha subunit of eIF2 (eIF2~P), which represses global translation coincident with preferential translation of mRNAs, such as ATF4 and CHOP, that serve to implement the UPR transcriptional regulation. In this study, we used sucrose gradient ultracentrifugation and a genome-wide microarray approach to measure changes in mRNA translation during ER stress. Our analysis suggests that translational efficiencies vary across a broad range during ER stress, with the majority of transcripts being either repressed or resistant to eIF2~P, while a notable cohort of key regulators are subject to preferential translation. From this latter group, we identify IBTKa as being subject to both translation and transcriptional induction during eIF2~P in both cell lines and a mouse model of ER stress. Translational regulation of IBTKalpha mRNA involves the stress-induced relief of two inhibitory uORFs in the 5'-leader of the transcript. Depletion of IBTKalpha by shRNA reduced viability of cultured cells coincident with increased caspase 3/7 cleavage, suggesting that IBTKalpha is a key regulator in determining cell fate during the UPR.** **We used a genome-wide microarray approach to determine how individual mRNAs were differentially translated during endoplasmic reticulum stress.** **Overall design:** **Please note that the treatment plus fractionation based on association with different numbers of ribosomes did yield different populations of mRNAs, which resulted in considerable variation in normalized data across the samples.**

Background corr dist: KL-Divergence = 0.1148, L1-Distance = 0.0307, L2-Distance = 0.0019, Normal std = 0.4200

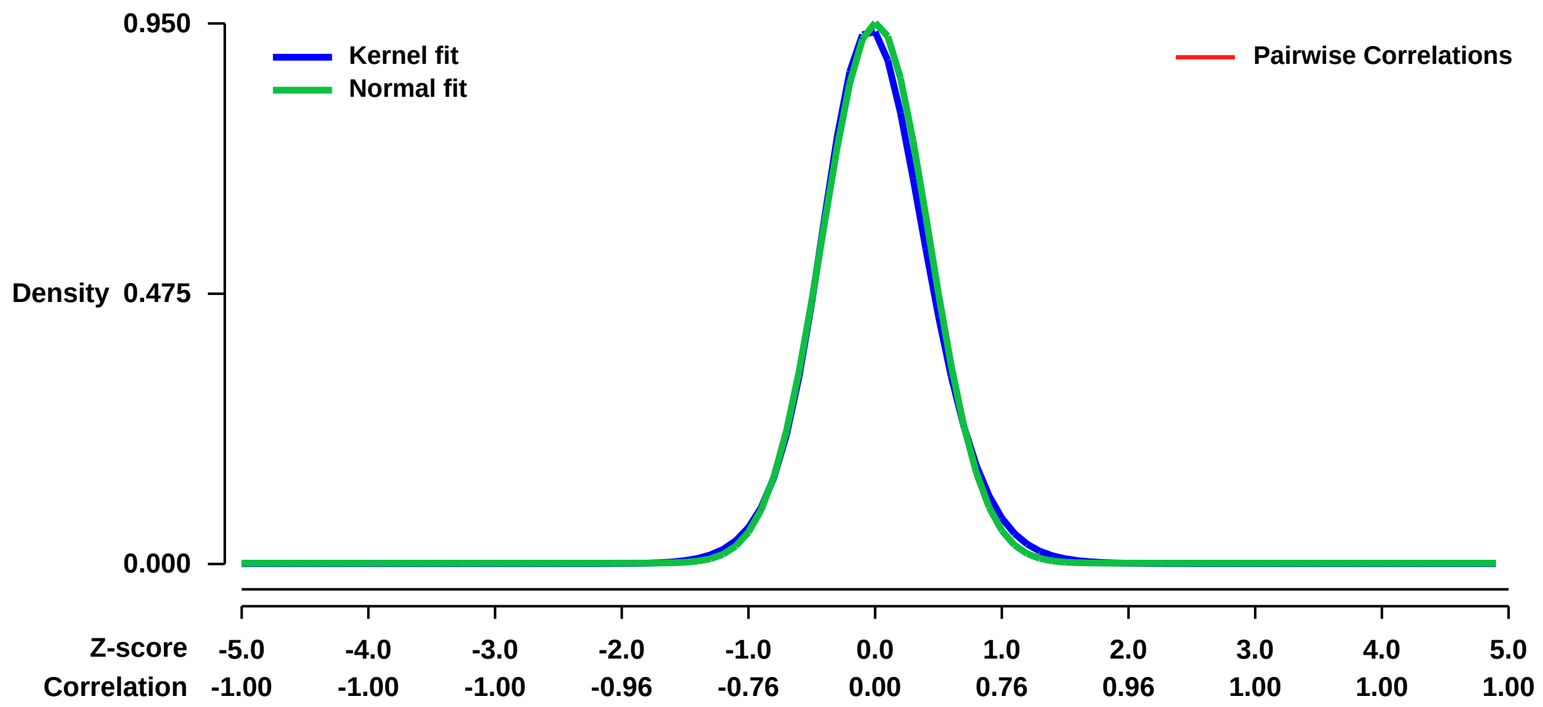

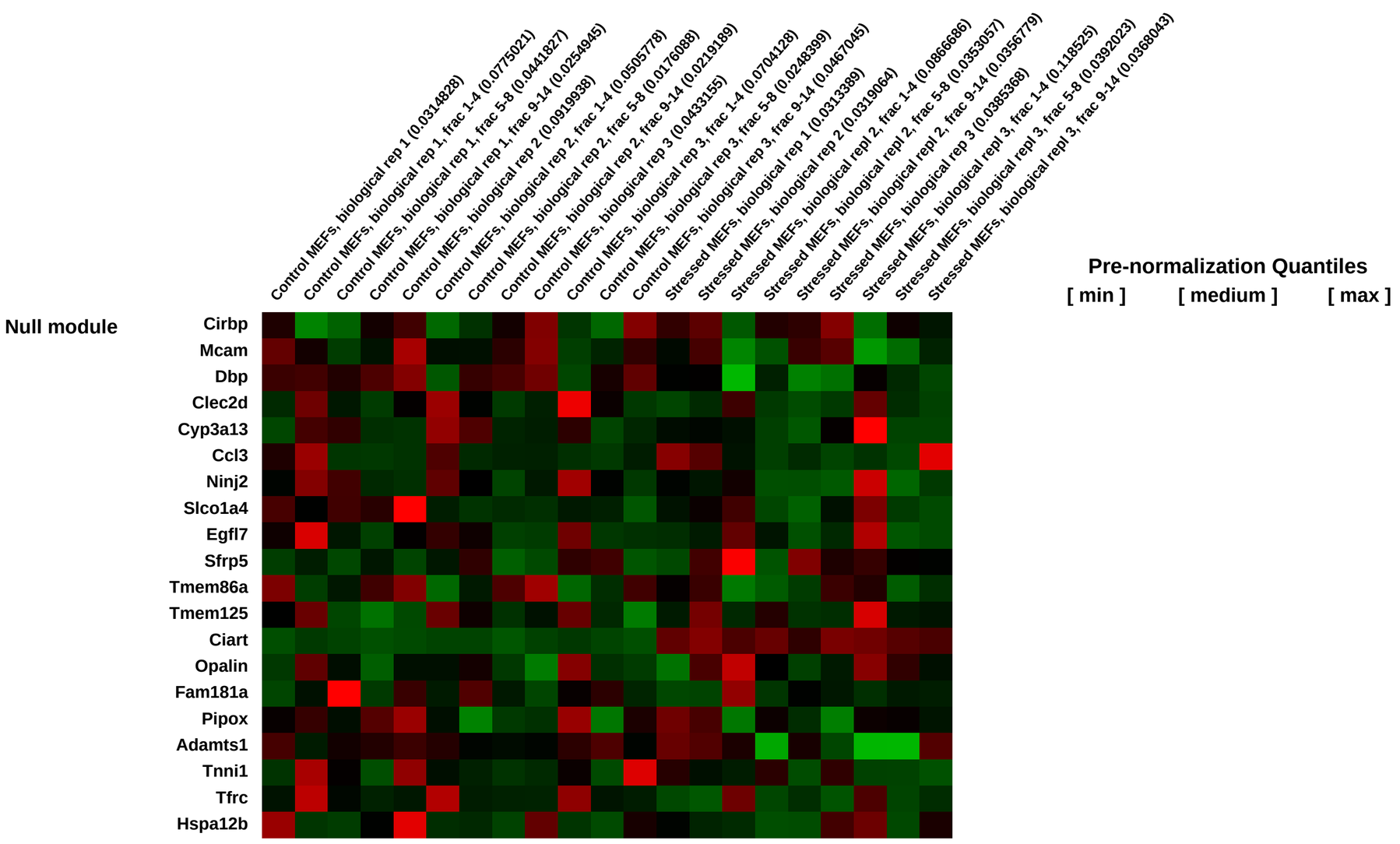

GEO Series "GSE49248" Expression Profiles

Num of samples in this series: 12

Scale of expression profile Z-scores

-3.0 -2.0 -1.0 0.0 1.0 2.0 3.0

GEO Link:	http://www.ncbi.nlm.nih.gov/geo/query/acc.cgi?acc=GSE49248
Status:	Public on Jul 02 2014
Title:	KrasG12D partially compensates for the loss of beta-catenin in MLL-AF9 AML
Organism:	Mus musculus
Experiment type:	Expression profiling by array
Platform:	GPL1261
Pubmed ID:	24189294
Summary & Design:	**Summary:** The Wnt/beta-catenin pathway is required for the development of leukemia stem cells in MLL-AF9 AML. We evaluated the dependance on beta-catenin for KrasG12DMLL-AF9 leukemia. **Overall design:** Lin-Kit+ bone marrow cells obtained from mice transplanted with primary MLL-AF9 leukemia cells and KRasG12DMLL-AF9 leukemia cells were assessed for gene expression in the presence or absence of beta-catenin

Background corr dist: KL-Divergence = 0.1418, L1-Distance = 0.0367, L2-Distance = 0.0025, Normal std = 0.3804

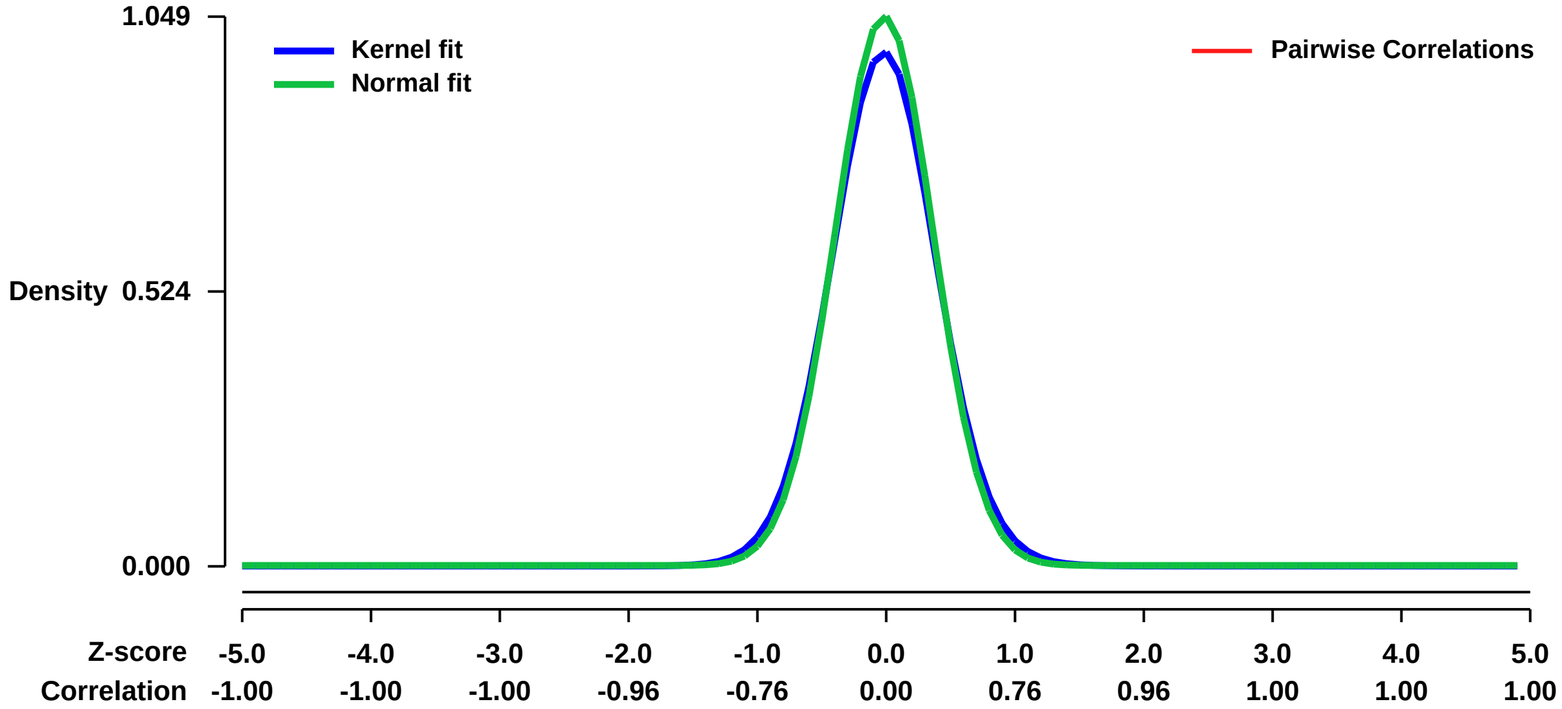

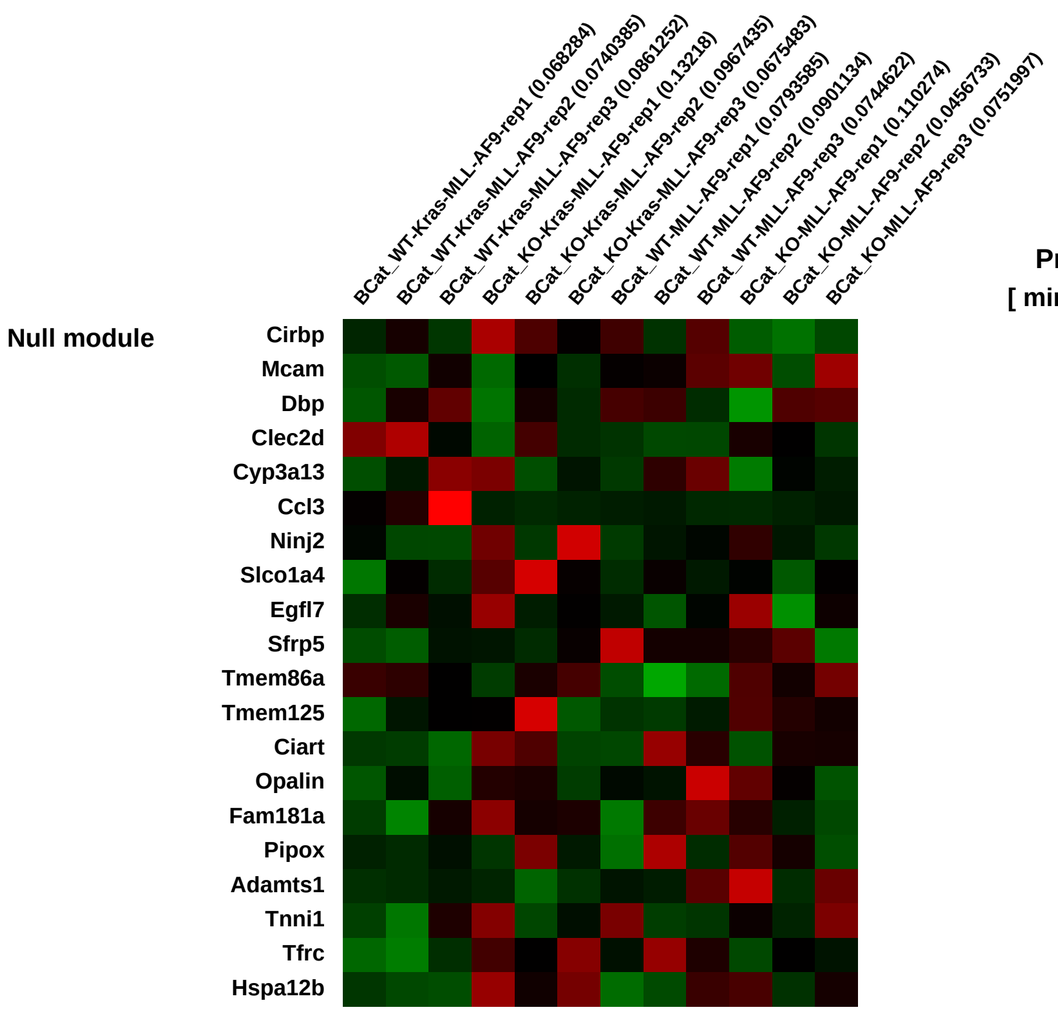

GEO Series "GSE19684" Expression Profiles

Num of samples in this series: 14

Scale of expression profile Z-scores

-3.0 -2.0 -1.0 0.0 1.0 2.0 3.0

GEO Link:	http://www.ncbi.nlm.nih.gov/geo/query/acc.cgi?acc=GSE19684
Status:	Public on Jun 16 2010
Title:	Atoh1 inhibits neuronal differentiation and collaborates with Gli1 to generate medulloblastoma-initiating cells
Organism:	Mus musculus
Experiment type:	Expression profiling by array
Platform:	GPL1261
Pubmed ID:	20516124
Summary & Design:	**Summary:** The morphogen and mitogen, Sonic Hedgehog, activates a Gli1-dependent transcription program that drives proliferation of granule neuron progenitors (GNPs) within the external germinal layer of the postnatally developing cerebellum. Medulloblastomas with mutations activating the Sonic Hedgehog signaling pathway preferentially arise within the external germinal layer, and the tumor cells closely resemble GNPs. Atoh1/Math1, a basic helix-loop-helix transcription factor essential for GNP histogenesis, does not induce medulloblastomas when expressed in primary mouse GNPs that are explanted from the early postnatal cerebellum and transplanted back into the brains of naˆflve mice. However, enforced expression of Atoh1 in primary GNPs enhances the oncogenicity of cells overexpressing Gli1 by almost three orders of magnitude. Unlike Gli1, Atoh1 cannot support GNP proliferation in the absence of Sonic Hedgehog signaling and does not govern expression of canonical cell cycle genes. Instead, Atoh1 maintains GNPs in a Sonic Hedgehog-responsive state by regulating genes that trigger neuronal differentiation, including many expressed in response to bone morphogenic protein-4. Therefore, by targeting multiple genes regulating the differentiation state of GNPs, Atoh1 collaborates with the pro-proliferative Gli1-dependent transcriptional program to influence medulloblastoma development. **Keywords:** disease state analysis **Overall design:** 14 samples, 1 time series, 2 engineered Medulloblastoma tumors

Background corr dist: KL-Divergence = 0.0925, L1-Distance = 0.0252, L2-Distance = 0.0009, Normal std = 0.4558

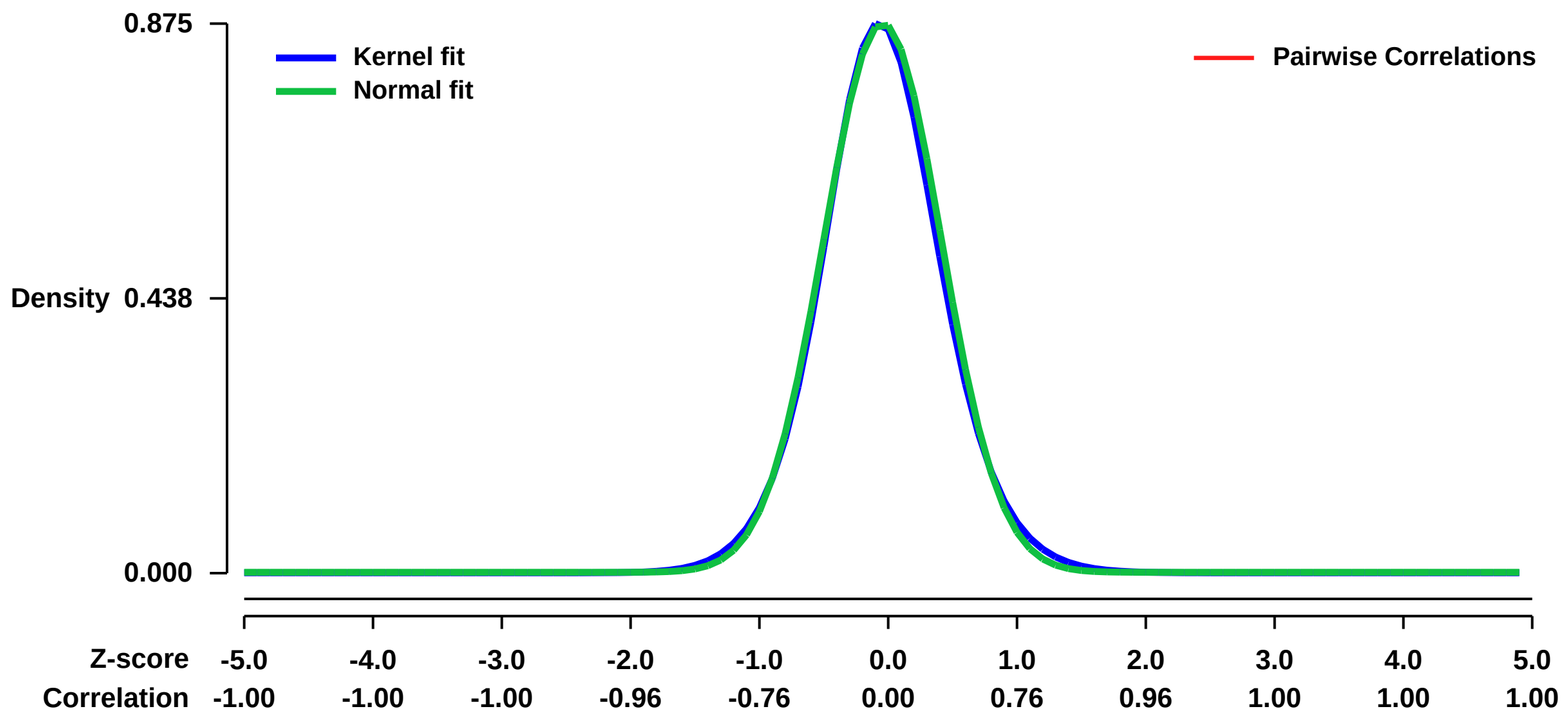

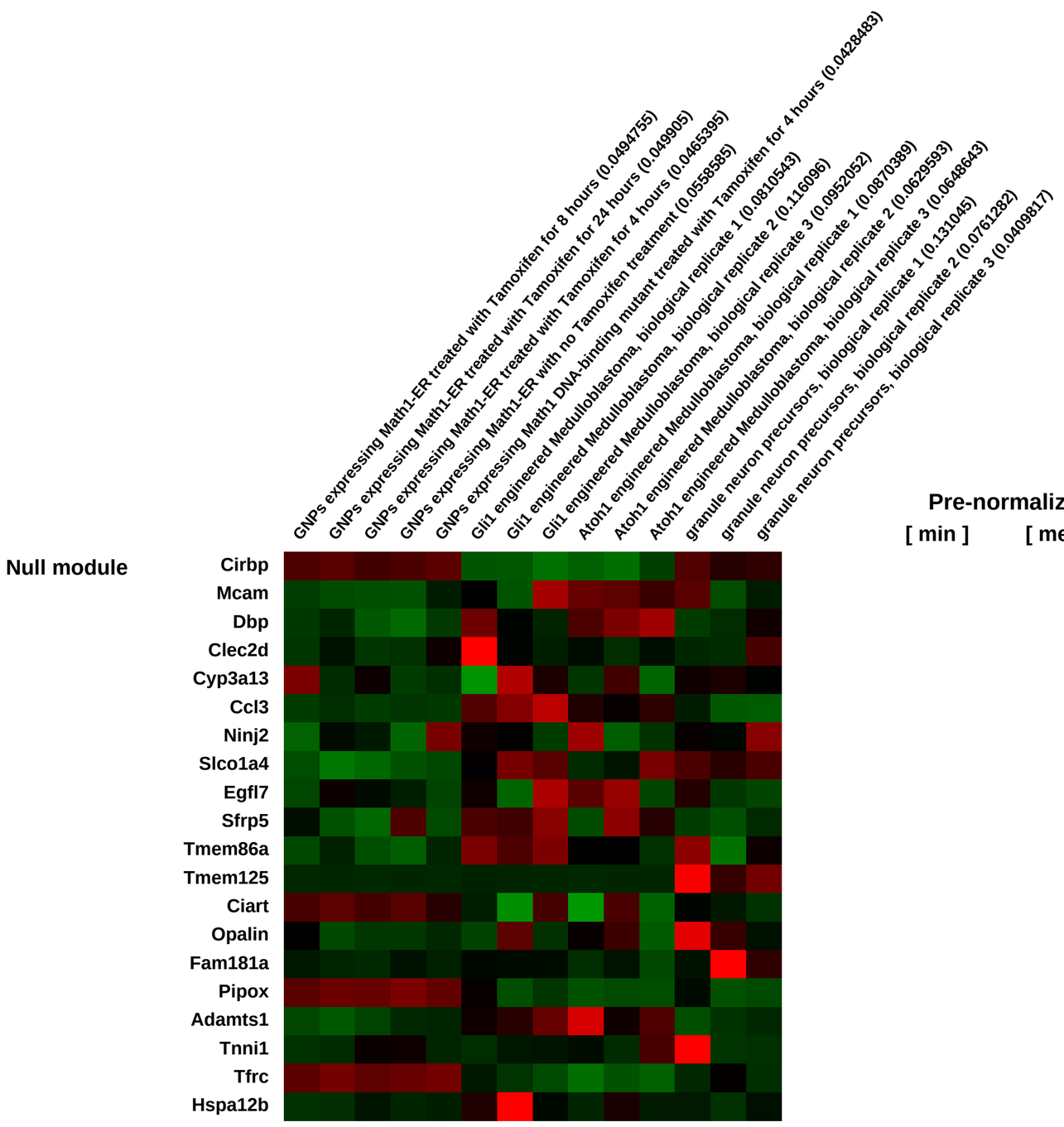

GEO Series "GSE6085" Expression Profiles

Num of samples in this series: 43

Scale of expression profile Z-scores

-3.0 -2.0 -1.0 0.0 1.0 2.0 3.0

GEO Link:	http://www.ncbi.nlm.nih.gov/geo/query/acc.cgi?acc=GSE6085
Status:	Public on Jan 11 2008
Title:	Expression data from Murine T cell in response to IL-2 at 10 time points in 24 hours after IL-2 treatment
Organism:	Mus musculus
Experiment type:	Expression profiling by array
Platform:	GPL1261
Pubmed ID:	21722407
Summary & Design:	**Summary:** The cytokine IL-2 determines T cell fate by controlling T cell proliferation and differentiation, but the expression files of IL-2 regulated genes are not defined Using Affymetrix mouse genome array and mouse T cell line CTLL-2, we analyzed the expression profiles of IL-2 regulated genes over 10 time points in 24 hours after IL-2 treatment. A total of 2,813 genes were differentially expressed (?2-fold change) at least at one time point in response to IL-2 stimulation. Clustering analyses showed that these genes consist of 9 clusters, suggesting that the IL-2 regulated genes in mouse T cells have 9 expression patterns. These genes involve in many biological processes, including immune response, signal transduction, apoptosis, cell cycle, transcription, transport, biosynthesis and various metabolisms. Two supplementary tables are linked to this series: Table 1: IL-2 responsive genes over the first 24 hours post-stimulation Table 2: Newly identified IL-2 regulated genes function in a variety of biological processes Keywords: stress response **Overall design:** Murine cytotoxic T lymphocyte cell line CTLL-2, derived from a C57BL/6 mouse, is an IL-2 dependent cell line. Cells were cultured in D10 medium in an incubator with 5% CO2 at 37oC to mid-log phase (~2 X 105 cells/mL), and collected by centrifugation, washed with phosphate buffered saline (PBS) (Invitrogen), resuspended at 1 X 106 cells/mL in the medium without IL-2 (IL-2 starvation) and cultured for 14 hours (No IL-2 stimulation, T0, 5 reps). After adding human rIL-2 (100 U/mL, Chiron, IL-2 stimulation), cells were collected at time point 0.5, 1, 2, 4, 6, 8, 10, 12, 16 and 24 hours, at least 3 biological replicates were carried out for each time point.Total RNA were extracted from the cells and was hybridized on Affymetrix GeneChip Mouse Genome 430 2.0 Array.

Background corr dist: KL-Divergence = 0.3087, L1-Distance = 0.0479, L2-Distance = 0.0053, Normal std = 0.2794

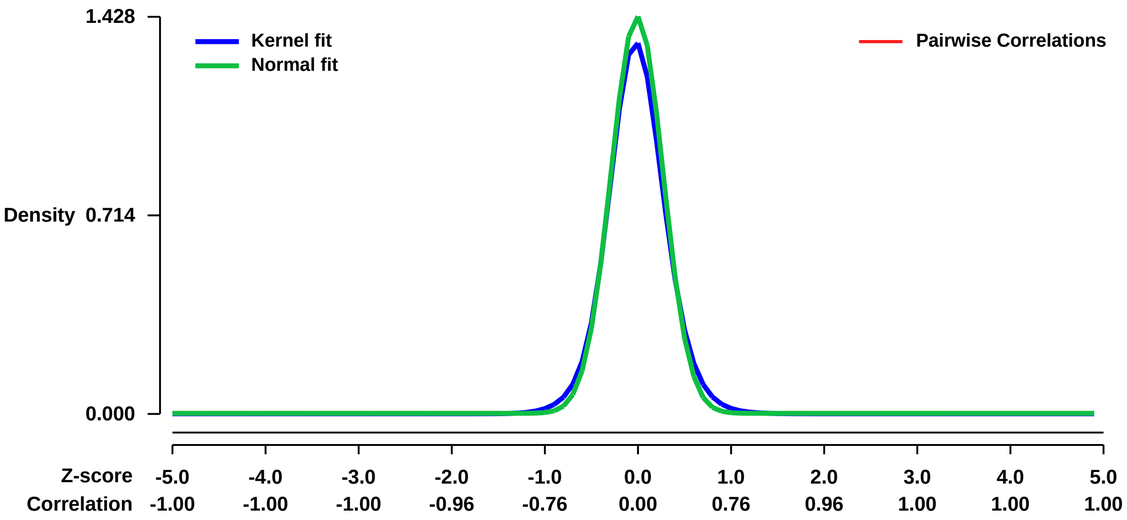

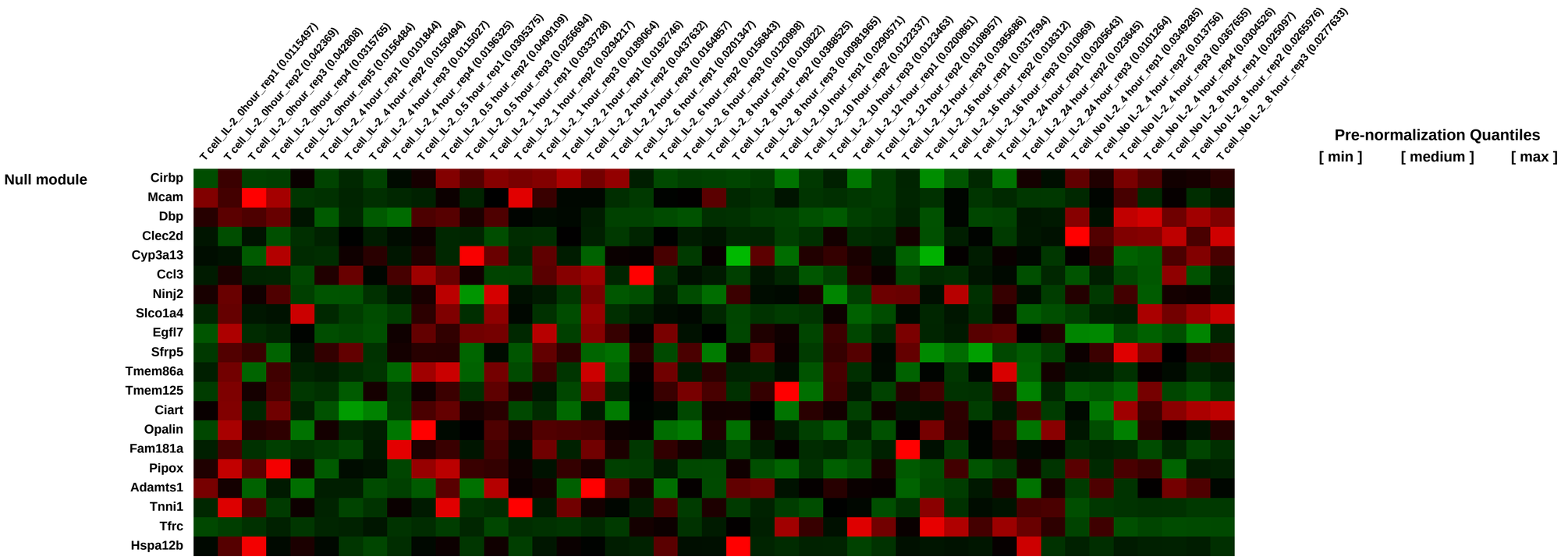

GEO Series "GSE14585" Expression Profiles

Num of samples in this series: 9

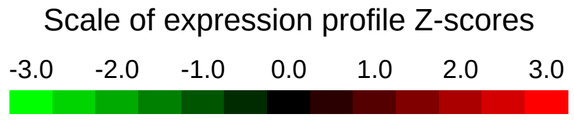

GEO Link:	**http://www.ncbi.nlm.nih.gov/geo/query/acc.cgi?acc=GSE14585**
Status:	**Public on Apr 21 2009**
Title:	**Expression data from mouse normal thymus, thymus tumor, and XIST resistant thymus tumor**
Organism:	**Mus musculus**
Experiment type:	**Expression profiling by array**
Platform:	**GPL1261**
Pubmed ID:	**19386260**
Summary & Design:	**Summary:** **The non-coding Xist RNA triggers silencing of one of the two female X chromosomes during X inactivation in mammals. Gene silencing by Xist is restricted to special developmental contexts found in cells of the early embryo and specific hematopoietic precursors. The absence of critical silencing factors might explain why Xist cannot silence outside these contexts. Here, we show that Xist can also initiate silencing in a lymphoma model. Using the tumor context we identify the special AT rich binding protein SATB1 as an essential silencing factor. We show that loss of SATB1 in tumor cells abrogates the silencing function of Xist. In normal female lymphocytes Xist localizes along SATB1 filaments and, importantly, forced Xist expression can relocalize SATB1 into the Xist cluster. This reciprocal influence on localization suggests a molecular interaction between Xist and SATB1. SATB1 and its close homologue SATB2 are expressed during the initiation window for X inactivation in embryonic stem cells and are recruited to surround the Xist cluster. Furthermore, ectopic expression SATB1 or SATB2 enables gene silencing by Xist in embryonic fibroblasts, which normally do not provide an initiation context. Thus, SATB1 functions as a crucial initiation factor and may act to organize genes for silencing by Xist during the initiation of X inactivation.** **Overall design:** **Normal mouse thymus, tumor, and XIST resistant tumor tissue was hybridized on the Affymetrix Mouse430_2 chip. All groups consist of triplicates.**

Background corr dist: KL-Divergence = 0.0327, L1-Distance = 0.0272, L2-Distance = 0.0010, Normal std = 0.6504

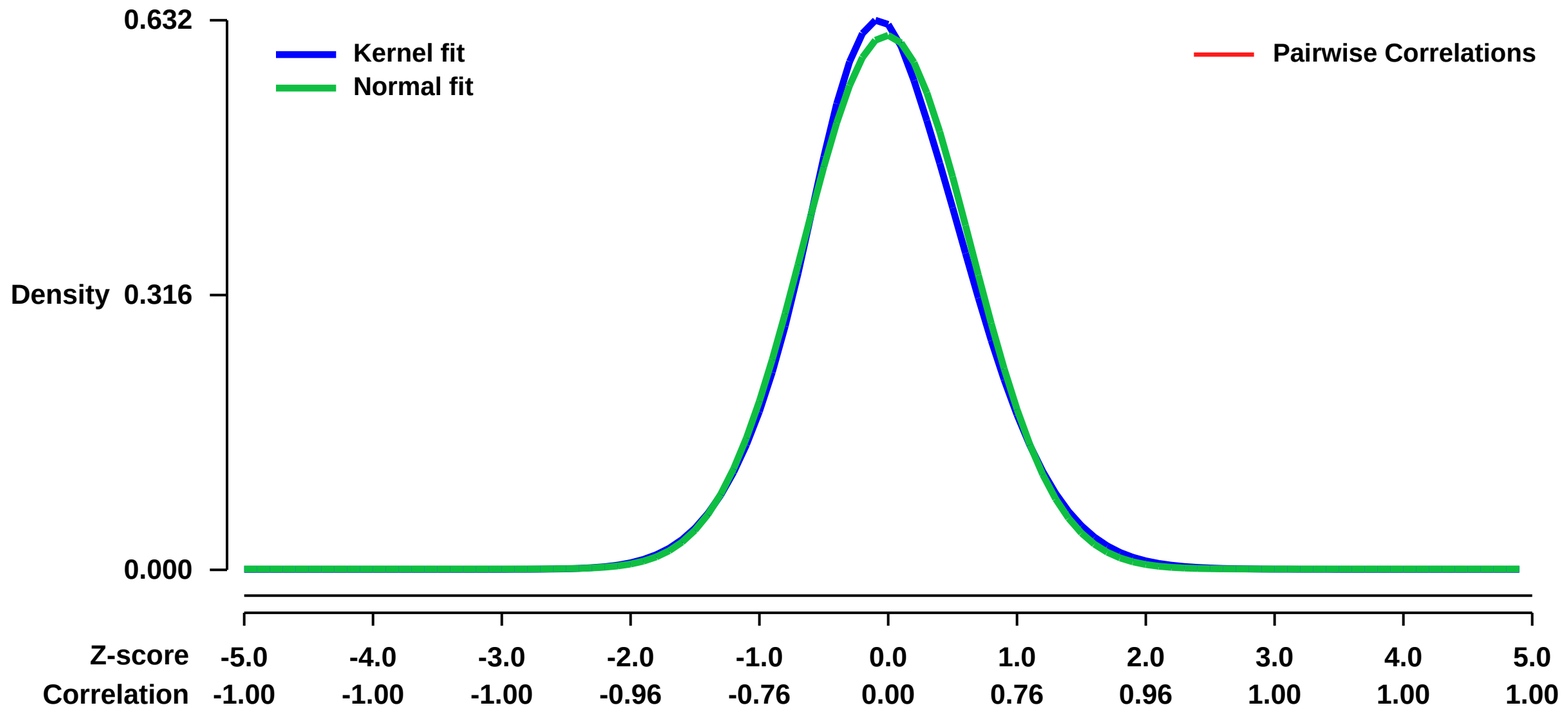

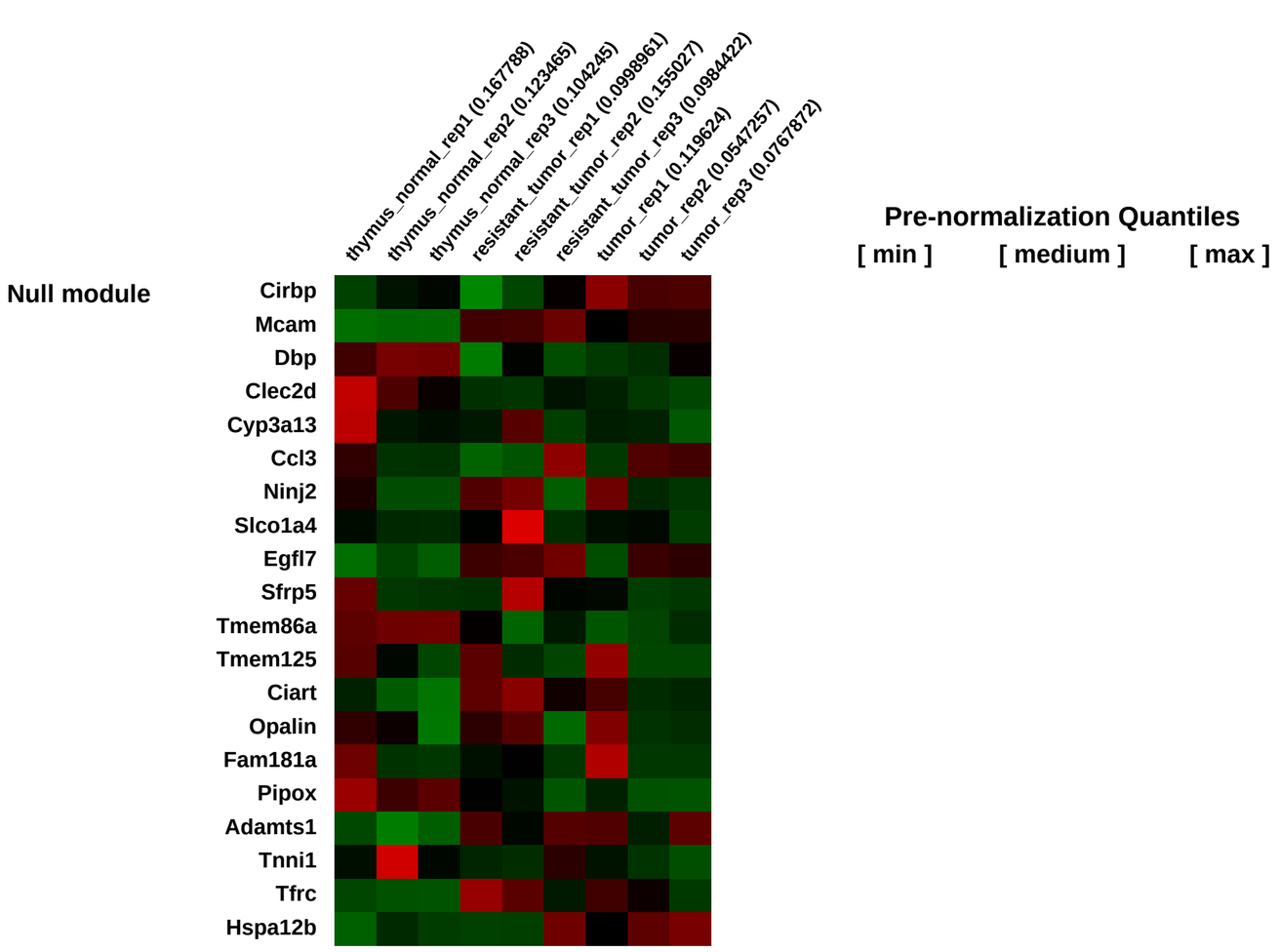

GEO Series "GSE3554" Expression Profiles

Num of samples in this series: 6

Scale of expression profile Z-scores

-3.0 -2.0 -1.0 0.0 1.0 2.0 3.0

GEO Link:	http://www.ncbi.nlm.nih.gov/geo/query/acc.cgi?acc=GSE3554
Status:	Public on Nov 04 2005
Title:	Microarray Analysis of Retinal Gene Expression in the DBA/2J Model of Glaucoma
Organism:	Mus musculus
Experiment type:	Expression profiling by array
Platform:	GPL1261
Pubmed ID:	16505032
Summary & Design:	**Summary:** **Purpose: The DBA/2J mouse is a model for secondary angle-closure glaucoma due to iris atrophy and pigment dispersion, which ultimately leads to increased intraocular pressure (IOP). We sought to correlate changes in retinal gene expression with glaucoma-like pathology by performing microarray analysis of retinal RNA from DBA/2J mice at 3 months before disease onset, and at 8 months, after IOP elevation. Methods: IOP was monitored monthly in DBA/2J animals by Tono-Pen and animals with normal (3 months) or elevated IOP (8 months) were identified. RNA was prepared from 3 individual retinas at each age, and the RNA was amplified and used to generate biotin-labeled probe for high density mouse Affymetrix arrays (U430.2). A subset of genes was selected for confirmation by quantitative RT-PCR using independent retina samples from DBA/2J animals at 3, 5 and 8 months of age, and compared to retinas from C57BL/6J control animals at 3 and 8 months. Results: There were changes in expression of 68 genes, with 32 genes increasing and 36 genes decreasing at 8 months versus 3 months. Upregulated genes were associated with immune response, glial activation, signaling and gene expression, while down-regulated genes included multiple crystallin genes. Significant changes in 9 upregulated genes and 2 downregulated genes were confirmed by quantitative RT-PCR, with some showing changes in expression by 5 months. Conclusions: DBA/2J retina shows evidence for glial activation and an immune-related response following IOP elevation, similar to what has been reported following acute elevation of IOP in other models.** **Keywords: retina, glaucoma, DBA/2J, elevated intraocular pressure** **Overall design:** **IOP was monitored monthly in DBA/2J animals by Tono-Pen and animals with normal (3 months) or elevated IOP (8 months) were identified. RNA was prepared from 3 individual retinas at each age, and the RNA was amplified and used to generate biotin-labeled probe for high density mouse Affymetrix arrays (U430.2). A subset of genes was selected for confirmation by quantitative RT-PCR using independent retina samples from DBA/2J animals at 3, 5 and 8 months of age, and compared to retinas from C57BL/6J control animals at 3 and 8 months.**

Background corr dist: KL-Divergence = 0.0472, L1-Distance = 0.0372, L2-Distance = 0.0019, Normal std = 0.6520

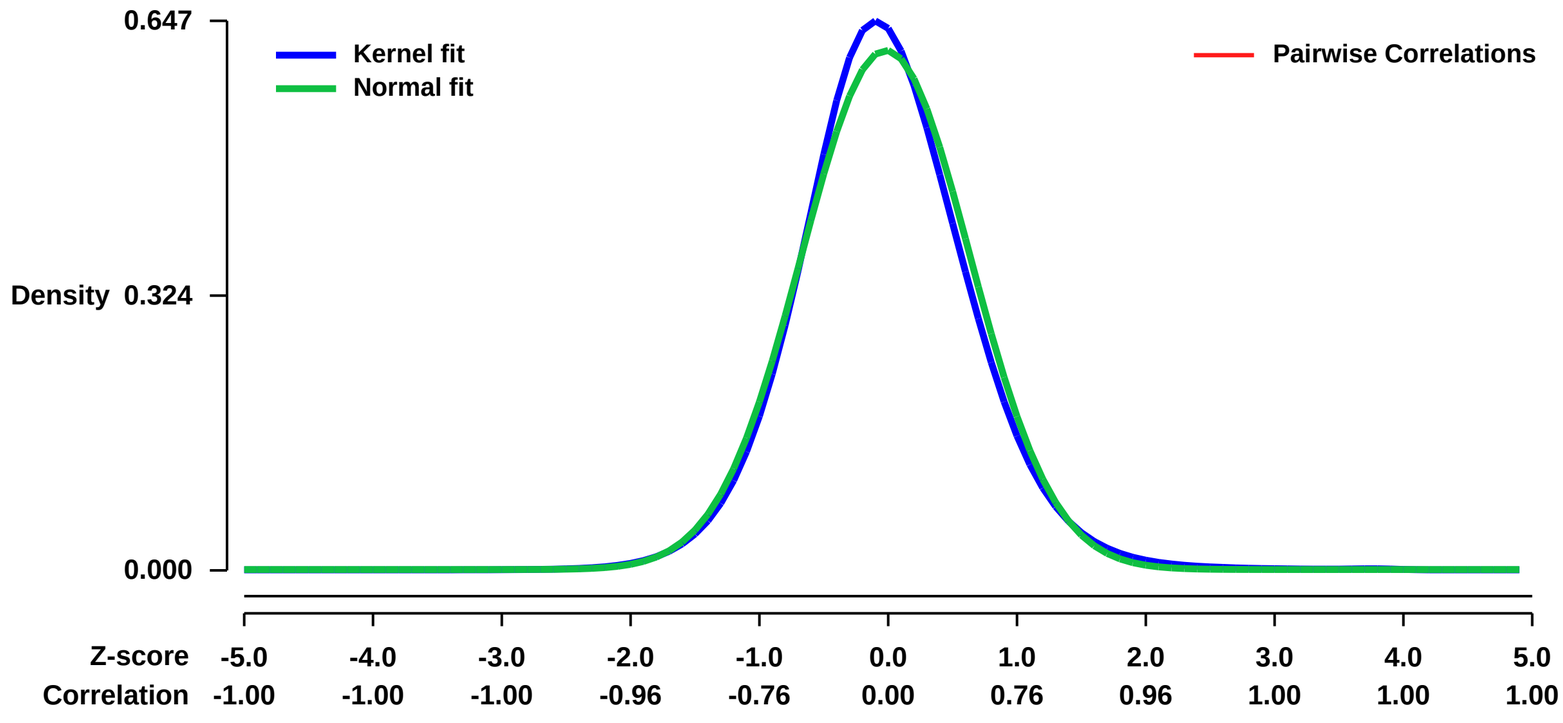

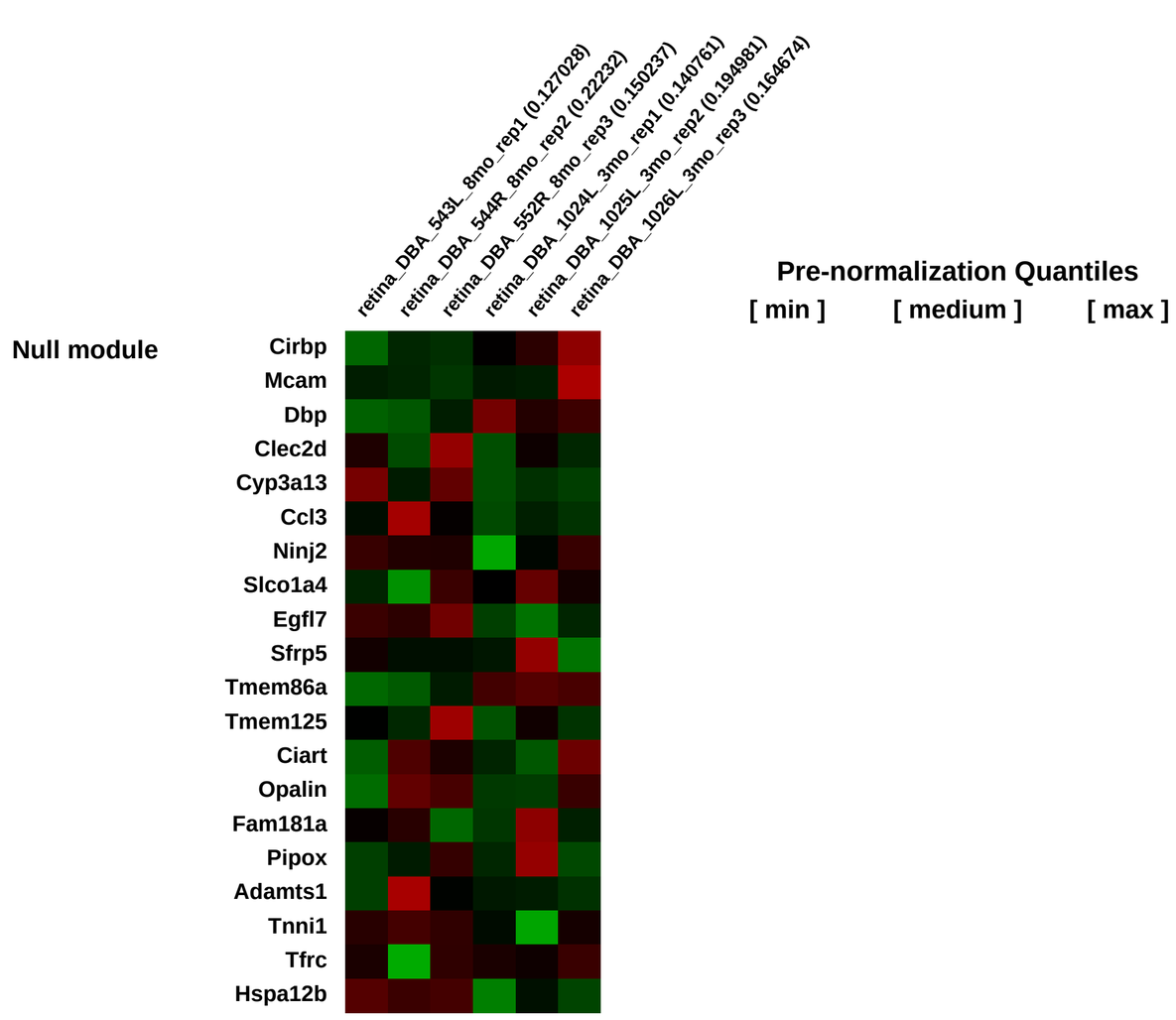

GEO Series "GSE47425" Expression Profiles

Num of samples in this series: 7

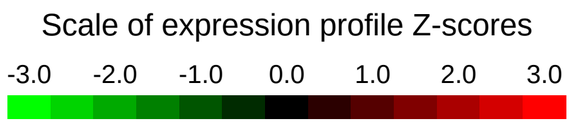

GEO Link:	**http://www.ncbi.nlm.nih.gov/geo/query/acc.cgi?acc=GSE47425**
Status:	**Public on Aug 26 2013**
Title:	**Lung transcript expression profile after Gata5 gene deletion**
Organism:	**Mus musculus**
Experiment type:	**Expression profiling by array**
Platform:	**GPL1261**
Pubmed ID:	**24199649**
Summary & Design:	**Summary:** **Gata5 is a zinc finger transcription factor that is expressed in embryonic pulmonary mesenchyme and becomes upregulated in the lungs, gut, and bladder during postnatal development. We used microarray to comapre gene expression profiles of mouse lung between Gata5 knockout and wild type mice. We hope to identify the differentially expressed genes that affected by Gata5 gene deletion and their functional clusters or pathways.** **The goal of this study is to identify the differentially expressed genes that affected by Gata5 gene deletion and their functional clusters or pathways.** **Overall design:** **Total RNA samples from three Gata5 KO and four wild type control mouse left lungs were extracted from the mouse lungs and profiled using Affymetrix GeneChip Mouse Genome 430 2.0 Array.**

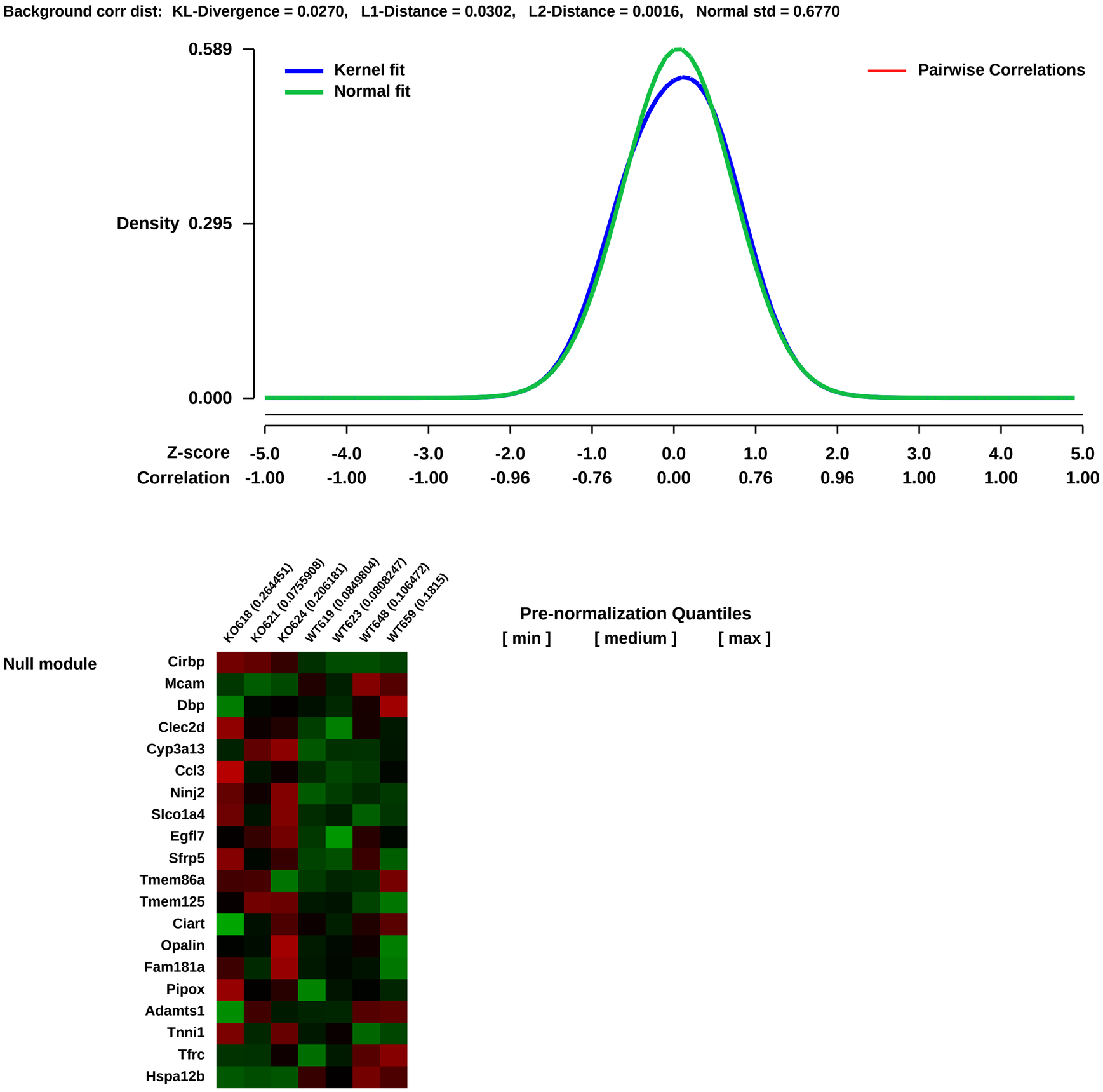

GEO Series "GSE31938" Expression Profiles

Num of samples in this series: 8

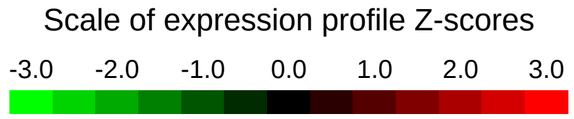

GEO Link:	**http://www.ncbi.nlm.nih.gov/geo/query/acc.cgi?acc=GSE31938**
Status:	**Public on Mar 01 2012**
Title:	**Hypothalamus**
Organism:	**Mus musculus**
Experiment type:	**Expression profiling by array**
Platform:	**GPL1261**
Pubmed ID:	
Summary & Design:	**Summary:** **These arrays contain data from hypthalamus tissue of nestin-Pex5 -/- male mice** **Overall design:** **Gene expression in biological replicates from hypothalamus of 4 wild type mice was compared with 4 NestinPex5-/- mice. In the latter, functional peroxisomes were deleted from all neural cells.**

Background corr dist: **KL-Divergence = 0.0553, L1-Distance = 0.0186, L2-Distance = 0.0004, Normal std = 0.5391**

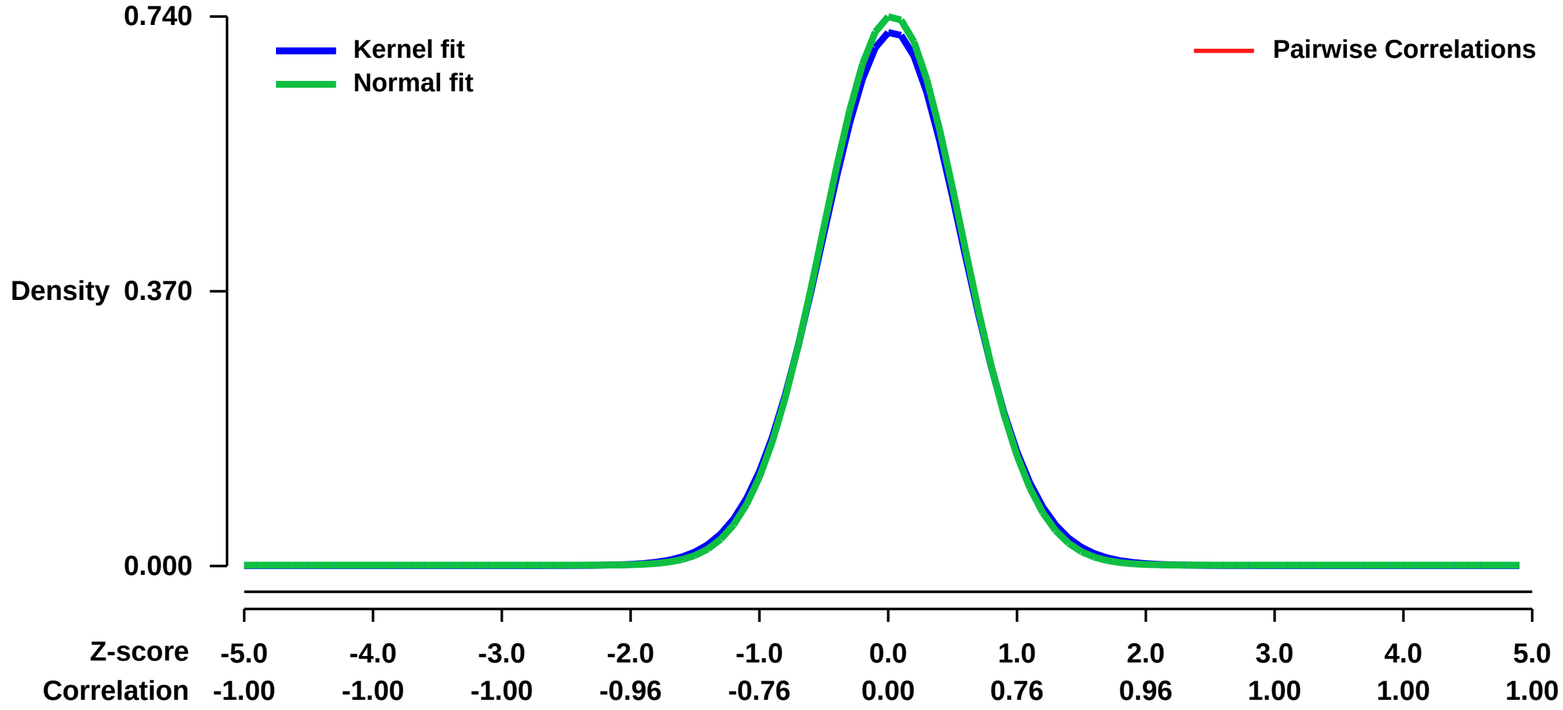

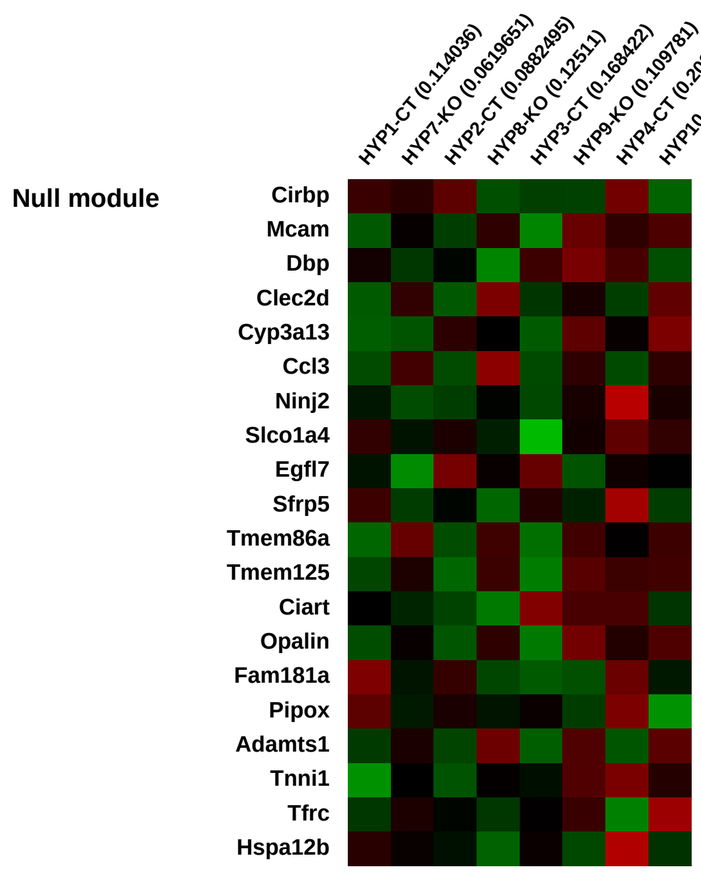

GEO Series "GSE23002" Expression Profiles

Num of samples in this series: 8

Scale of expression profile Z-scores

-3.0 -2.0 -1.0 0.0 1.0 2.0 3.0

GEO Link:	http://www.ncbi.nlm.nih.gov/geo/query/acc.cgi?acc=GSE23002
Status:	Public on Jul 20 2010
Title:	Transcriptional and Phenotypic Reprogramming of Tumors by Host Stroma Deficient in TNF¸– Signaling
Organism:	Mus musculus
Experiment type:	Expression profiling by array
Platform:	GPL1261
Pubmed ID:	
Summary & Design:	**Summary:** **Background: We previously demonstrated that B16F1 melanoma tumors growing in syngeneic germline-deleted TNFR1,2 -/- mice were more sensitive to ionizing radiation (IR) compared to tumors growing in C57BL/6 wild-type mice; however, the mechanisms linked to this difference in radiosensitivity are not fully understood.** **Methodology/ Principal Findings: We used DNA microarrays to identify alterations in the expression of functional gene clusters associated with the radiosensitization of B16F1 tumors growing in TNFR1,2 -/- mice. At the basal level, disruption of host stromal TNF¸– signaling resulted in the over-expression of tumor genes involved in extracellular matrix remodeling and angiogenesis. Phenotypically, these tumors exhibited a reduced vascular density, which induced the expression of oxidative stress signaling pathways and increased levels of tissue hypoxia and necrosis. These alterations were paralleled by the suppression of genes involved in chromosomal stability and key effectors of the ATM-dependent/ non-homologous end-joining pathways including phosphorylated-ATM, BRCA1, and RAD51, which resulted in greater DNA double-strand breaks and caspase 3 activation following IR treatment.** **Conclusions/ Significance: Taken together, these results demonstrate that disruption of TNF¸– signaling in the host stroma mediates transcriptional and phenotypic changes in tumors which may alter tumor radiosensitivity. These results suggest a critical role for TNF¸– in the maintenance of tumor-associated vasculature and radioresistance. They also indicate that TNF¸– signaling blockade in stromal cells may represent a strategy for tumor radiosensitization.** **Overall design:** **To investigate the genes associated with the radiosensitization of B16F1 melanoma tumors in the context of disrupted stromal TNF¸– signaling, we performed expression profiling of B16F1 tumors grown in syngeneic TNFR 1, 2 -/- and wild-type C57BL/6 mice. Tumors were lysed to collect total RNA, pooled by treatment group according to total RNA level, and analyzed in duplicates with Affymetrix GeneChip´fi Mouse Genome 430 2.0 Arrays.**

Background corr dist: KL-Divergence = 0.0476, L1-Distance = 0.0310, L2-Distance = 0.0011, Normal std = 0.5957

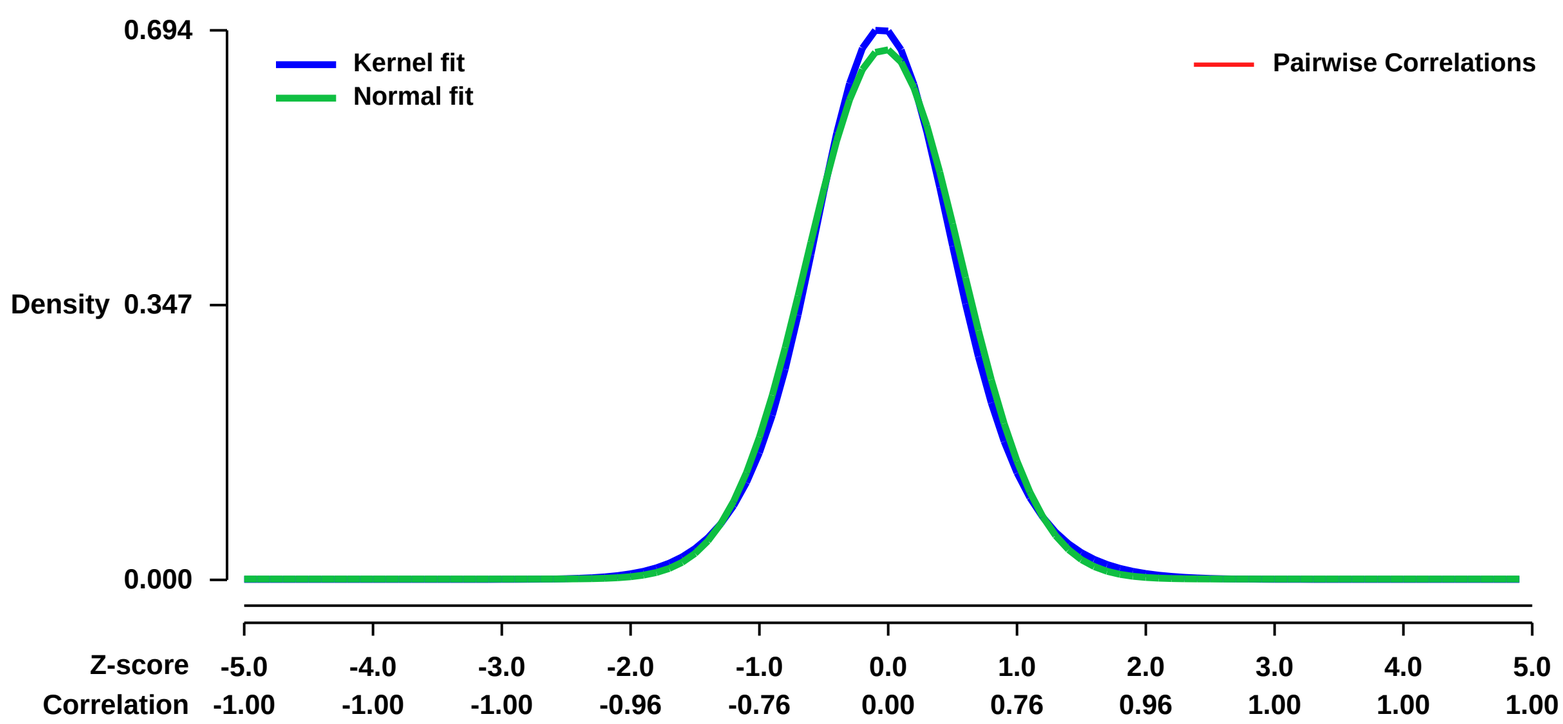

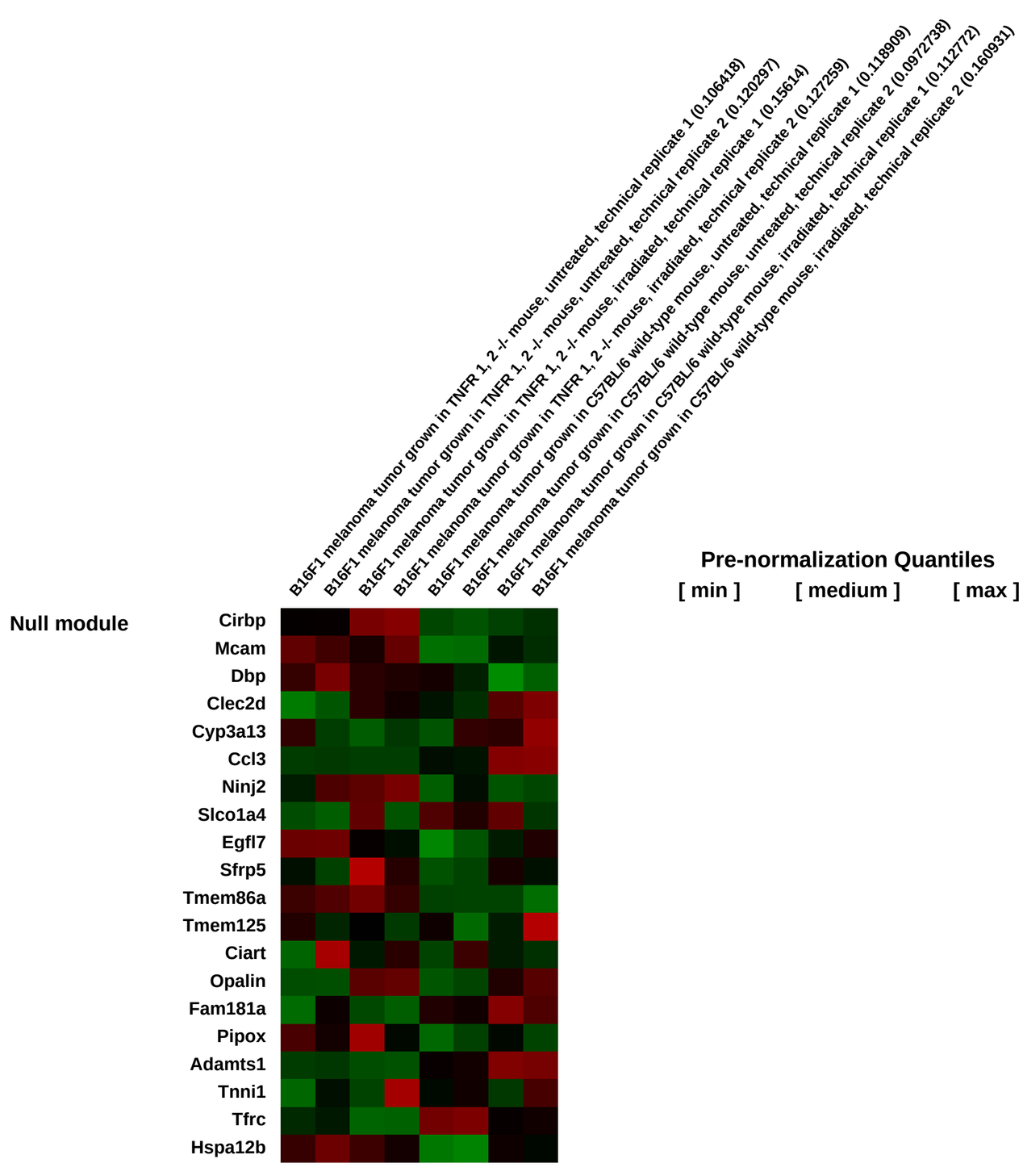

GEO Series "GSE15078" Expression Profiles

Num of samples in this series: 6

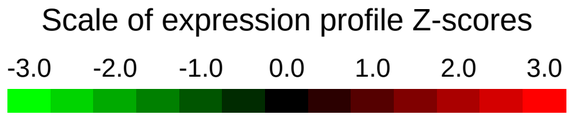

GEO Link:	http://www.ncbi.nlm.nih.gov/geo/query/acc.cgi?acc=GSE15078
Status:	Public on Mar 05 2009
Title:	Fog2 regulation of gene expression in the adult heart
Organism:	Mus musculus
Experiment type:	Expression profiling by array
Platform:	GPL1261
Pubmed ID:	19411759
Summary & Design:	**Summary:** **MHCaCre induced knockout of Fog2flox.** **Aberrant transcriptional regulation contributes to the pathogenesis of both congenital and adult forms of heart disease. While the transcriptional regulator FOG2 is known to be essential for heart morphogenesis and coronary development, its tissue specific function has not been previously investigated. Additionally, little is known about the role of FOG2 in the adult heart. Here we use spatiotemporally regulated inactivation of Fog2 to delineate its function both in embryo and adult heart. Early cardiomyocyte-restricted loss of Fog2 recapitulated the cardiac and coronary defects of the Fog2 germline knockouts. Later cardiomyocyte-restricted loss of Fog2 (Fog2MC) did not result in defects in cardiac structure or coronary vessel formation. However, Fog2MC adult mice had severely depressed ventricular function and died at 8-14 weeks. Fog2MC adult hearts displayed a paucity of coronary vessels. This was associated with myocardial hypoxia, increased cardiomyocyte apoptosis, and cardiac fibrosis. Induced inactivation of Fog2 in adult heart resulted in similar phenotype, as did ablation of FOG2 interaction with the transcription factor GATA4. Loss of FOG2 or FOG2-GATA4 interaction altered expression of a panel of angiogenesis-related genes. Collectively, our data indicated that FOG2 regulates adult heart function and coronary angiogenesis. #!#** **Overall design:** **Fog2flox/delta; MHCaCre (3) compared to Fog2flox/delta; no Cre (3). One heart per sample.**

Background corr dist: KL-Divergence = 0.0396, L1-Distance = 0.0184, L2-Distance = 0.0003, Normal std = 0.6169

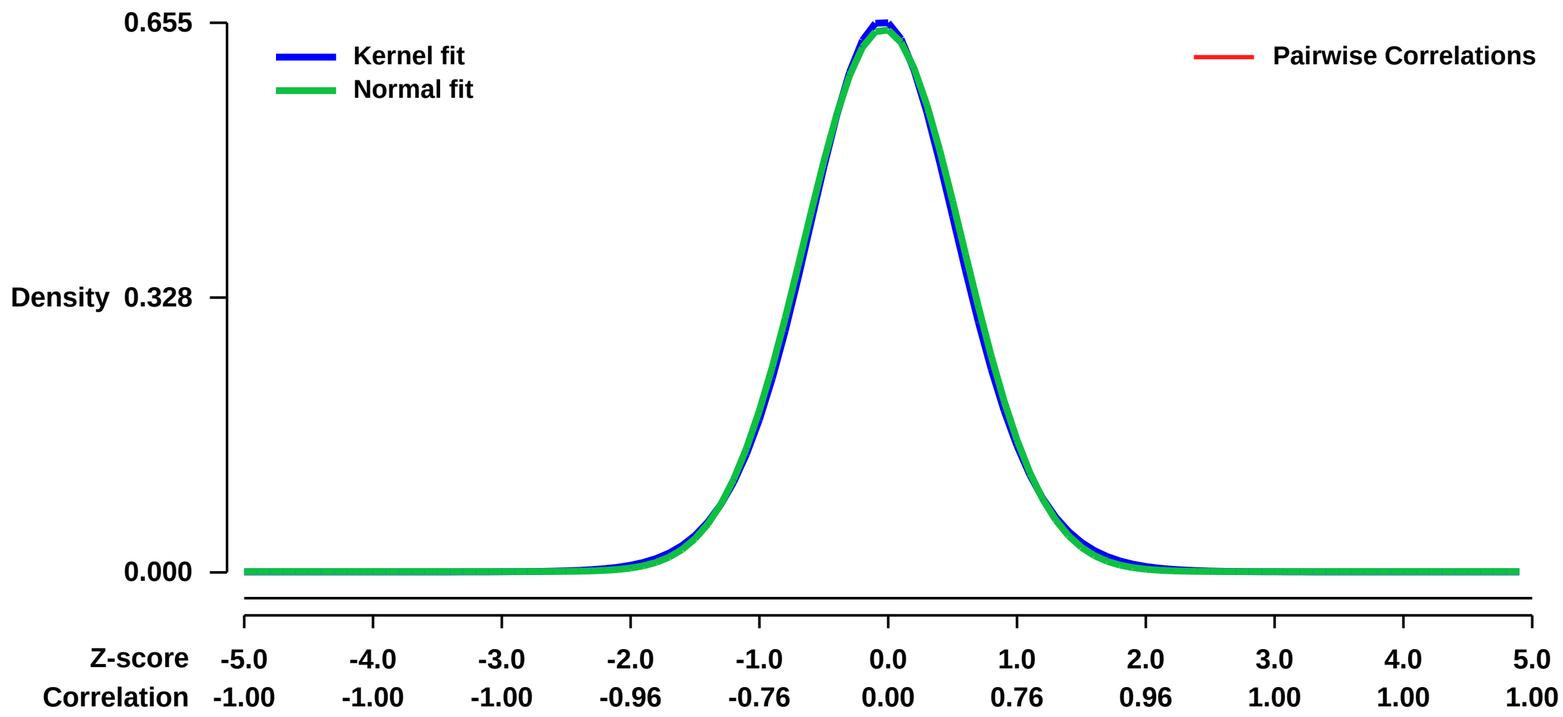

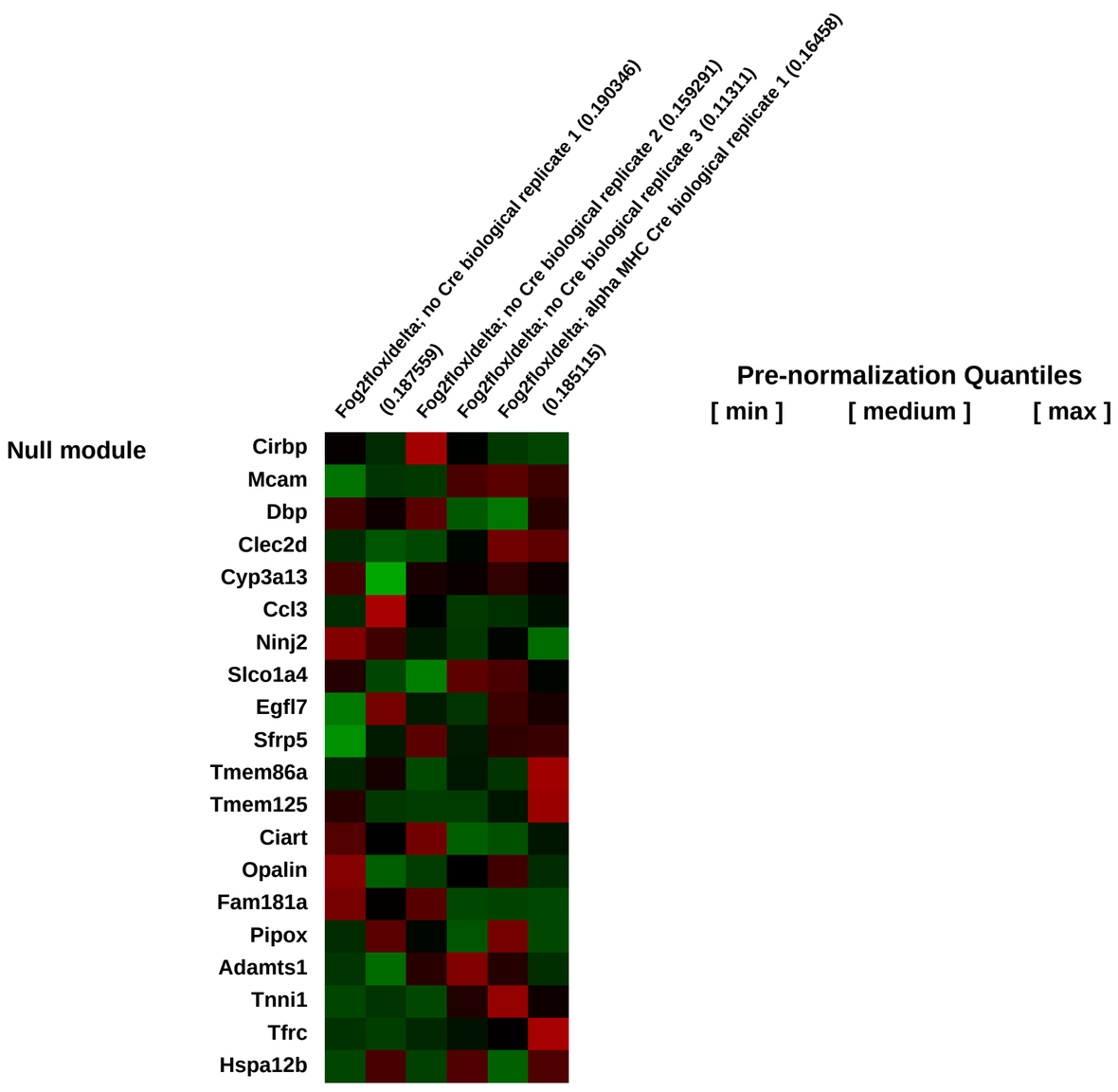

GEO Series "GSE18358" Expression Profiles

Num of samples in this series: 10

Scale of expression profile Z-scores

-3.0 -2.0 -1.0 0.0 1.0 2.0 3.0

GEO Link:	http://www.ncbi.nlm.nih.gov/geo/query/acc.cgi?acc=GSE18358
Status:	Public on Oct 02 2009
Title:	Gene Expression Profiling of Glomeruli from a mouse model of Denys-Drash Syndrome
Organism:	Mus musculus
Experiment type:	Expression profiling by array
Platform:	GPL1261
Pubmed ID:	19797313
Summary & Design:	**Summary:** The Wilms tumor-suppressor gene WT1, a key player in renal development, also has a crucial role in maintenance of the glomerulus in the mature kidney. However, molecular pathways orchestrated by WT1 in podocytes, where it is highly expressed, remain unknown. Their defects are thought to modify the cross-talk between podocytes and other glomerular cells and ultimately lead to glomerular sclerosis, as observed in diffuse mesangial sclerosis (DMS) a nephropathy associated with WT1 mutations. To identify podocyte WT1 targets, we generated a novel DMS mouse line, performed gene expression profiling in isolated glomeruli, and identified excellent candidates that may modify podocyte differentiation and growth factor signalling in glomeruli. Scel, encoding sciellin, a protein of the cornified envelope in the skin, and sulf1, encoding a 6-O endosulfatase, are shown to be expressed in wild type podocytes and to be strongly down-regulated in mutants. Co-expression of Wt1, Scel and Sulf1 was also found in a mesonephric cell line, and siRNA-mediated knockdown of WT1 decreased Scel and Sulf1 mRNAs and proteins. By ChIP we show that Scel and Sulf1 are direct WT1 targets. Cyp26a1, encoding an enzyme involved in the degradation of retinoic acid, is shown to be up-regulated in mutant podocytes. Cyp26a1 may play a role in the development of glomerular lesions but does not seem to be regulated by WT1. These results provide novel clues in our understanding of normal glomerular function and early events involved in glomerulosclerosis. **Overall design:** Isolation of glomeruli from mutant (FVB-N4 Wt1+/R394W) and wild-type (FVB-N4 Wt1+/+) was performed after cardiac Dynabead perfusion. GeneChip analysis of glomeruli from 5 Wt1+/R394W mice and 5 Wt1+/+ littermates (N4-FVB) were performed independently. Animals were unweaned 27-day-old males. The Wt1+/R394W mice used were showing little albuminuria (<3 ug/ul on Coomassie blue stained SDS-PAGE gel) and no evidence of mesangial lesions by light microscopy.

Background corr dist: KL-Divergence = 0.1193, L1-Distance = 0.0302, L2-Distance = 0.0016, Normal std = 0.4090

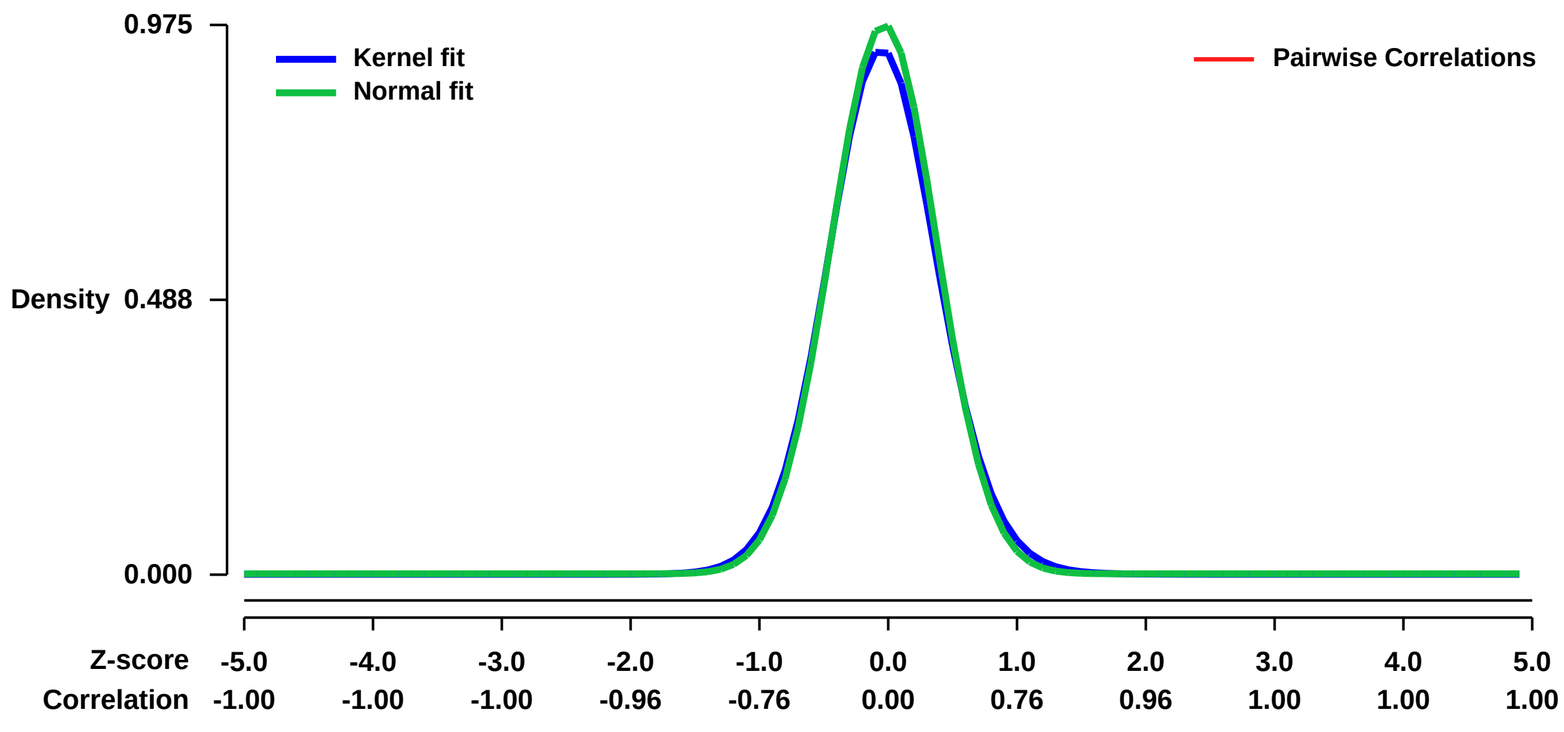

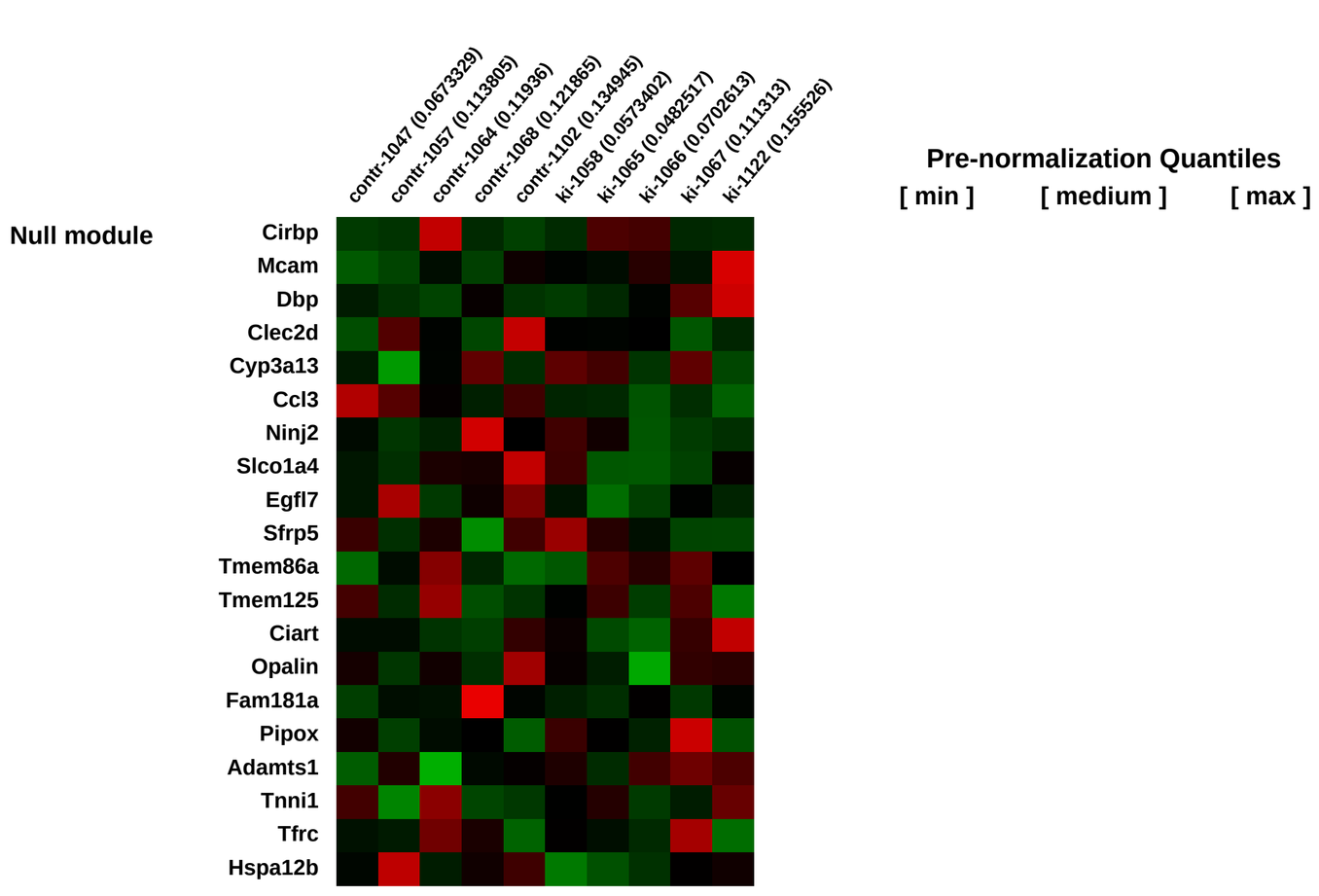

GEO Series "GSE44363" Expression Profiles

Num of samples in this series: 16

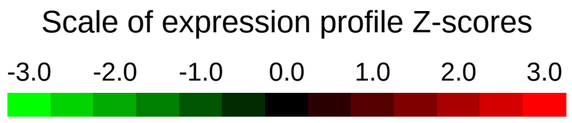

GEO Link:	http://www.ncbi.nlm.nih.gov/geo/query/acc.cgi?acc=GSE44363
Status:	Public on May 01 2013
Title:	Transcriptomic modulation by adenosine 2A receptors in normal and endotoxemic myocardium
Organism:	Mus musculus
Experiment type:	Expression profiling by array
Platform:	GPL1261
Pubmed ID:	
Summary & Design:	**Summary:** Analysis of venticular myocardium from adenosine 2A receptors (A2AR) knockouts following LPS stimulation. Results provide insight into the molecular components of A2AR mediated protection, but also reveal pathogenetic components of endotoxemic myocarditis as a result of LPS exposure. These findings demonstrate that intrinsic A2AR activity exerts limited transcriptional effects in unstressed heart, modifying G-coupled cAMP/PKA signal paths. LPS-dependent injury and dysfunction is associated with profound up-regulation of inflammatory/immune processes, fibrotic and cell death paths, and NF-kB, Erk/MAPK and JAK/Stat signaling, with shifts in multiple determinants of cardiac contraction and survival. Intrinsic A2AR activity modulates key aspects of these inflammatory responses, involving MAPK, JAK/Stat and NF-kB signaling **Overall design:** Total RNA obtained from adenosine 2A receptor knockout or wild-type murine ventricular myocardium that were treated for 24 hours with either saline or lipopolysaccharide (n=4/group).

Background corr dist: KL-Divergence = 0.1147, L1-Distance = 0.0360, L2-Distance = 0.0019, Normal std = 0.4273

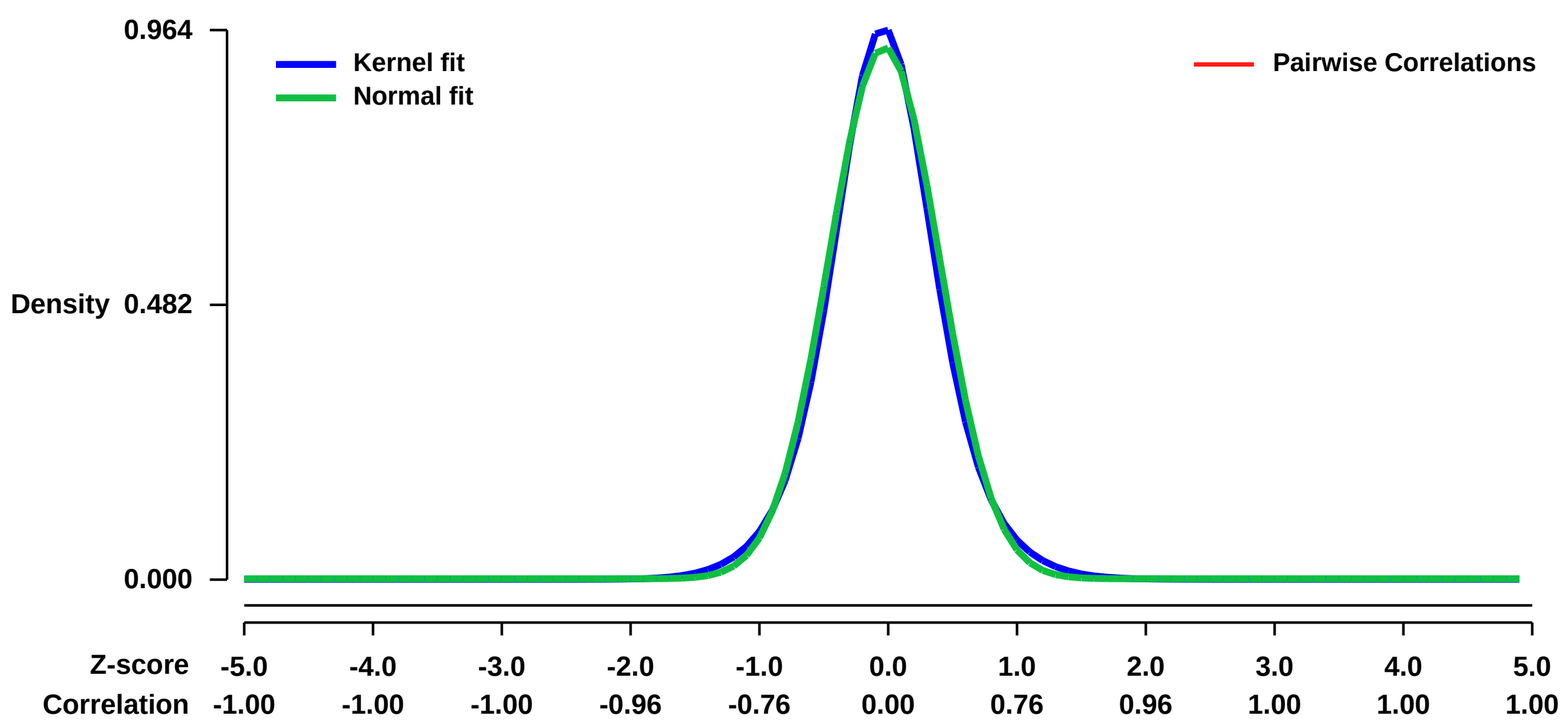

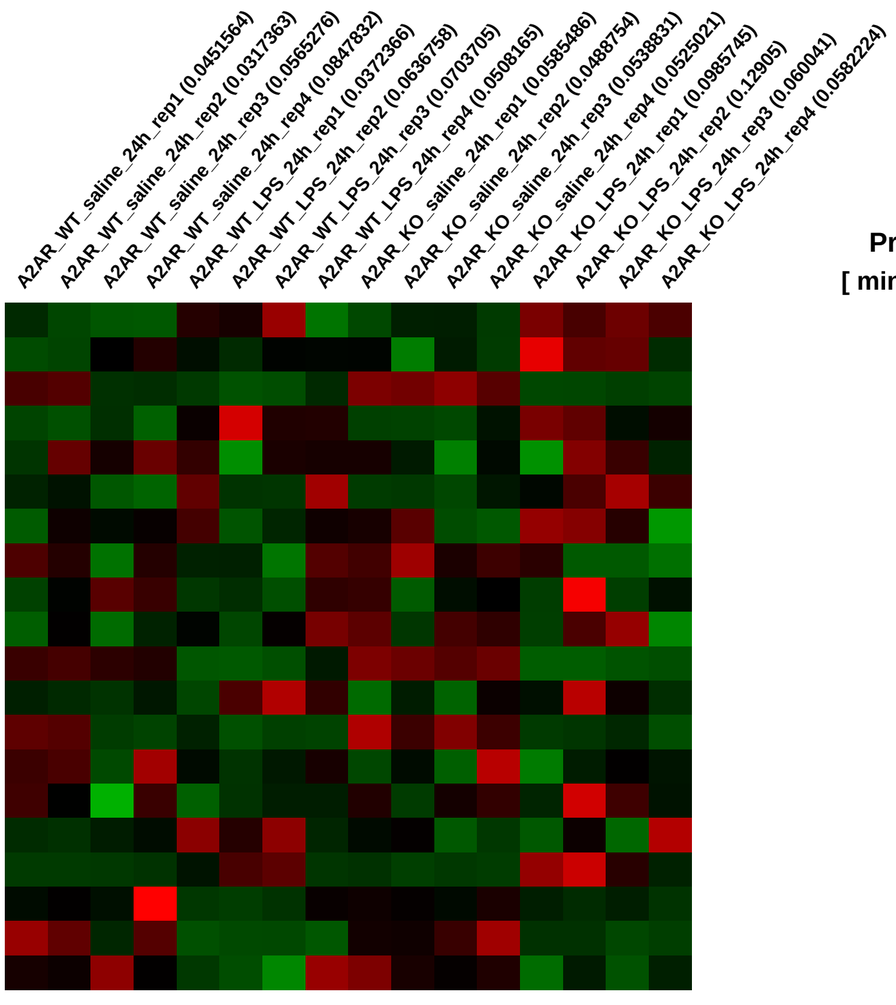

GEO Series "GSE17617" Expression Profiles

Num of samples in this series: 18

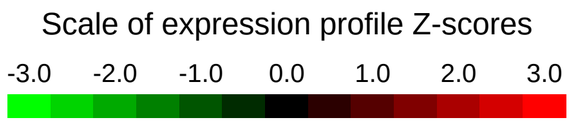

GEO Link:	**http://www.ncbi.nlm.nih.gov/geo/query/acc.cgi?acc=GSE17617**
Status:	**Public on Feb 15 2010**
Title:	**Gene profiling within the orexin-producing neurons**
Organism:	**Mus musculus**
Experiment type:	**Expression profiling by array**
Platform:	**GPL1261**
Pubmed ID:	**20160349**
Summary & Design:	**Summary:** **Narcolepsy is a sleep disorder characterized by excessive daytime sleepiness and attacks of muscle atonia triggered by strong emotions (cataplexy). The best biological marker of narcolepsy is orexin deficiency with dramatic loss in hypothalamic orexin-producing neurons. Together with a tight HLA and T-cell receptor alpha(5) association, narcolepsy is believed to be autoimmune although all attempts to prove it have failed.To characterize orexin specific peptides we produced a transgenic mouse model to access to the orexin neurons transcription profile. We generated BAC-based transgenic mice by replacing the orexin coding sequence by a flag-tagged poly(A) binding protein (Pabp1) cDNA sequence. The basis of this construct is to take advantage of the ability of Pabp1 to bind to the poly(A) tails of mRNAs in vivo. Thus mRNAs from orexin cells are expected to be enriched by cross-linking them to the flag-tagged PABP and then co-immunoprecipitating this complex with a specific anti-flag monoclonal antibody.** **Keywords: cell type comparison** **Overall design:** **Comparison between immunoprecipitated (IP) mRNA (n=9) and whole brain (WB) RNA (n=9) from BAC-based transgenic mice**

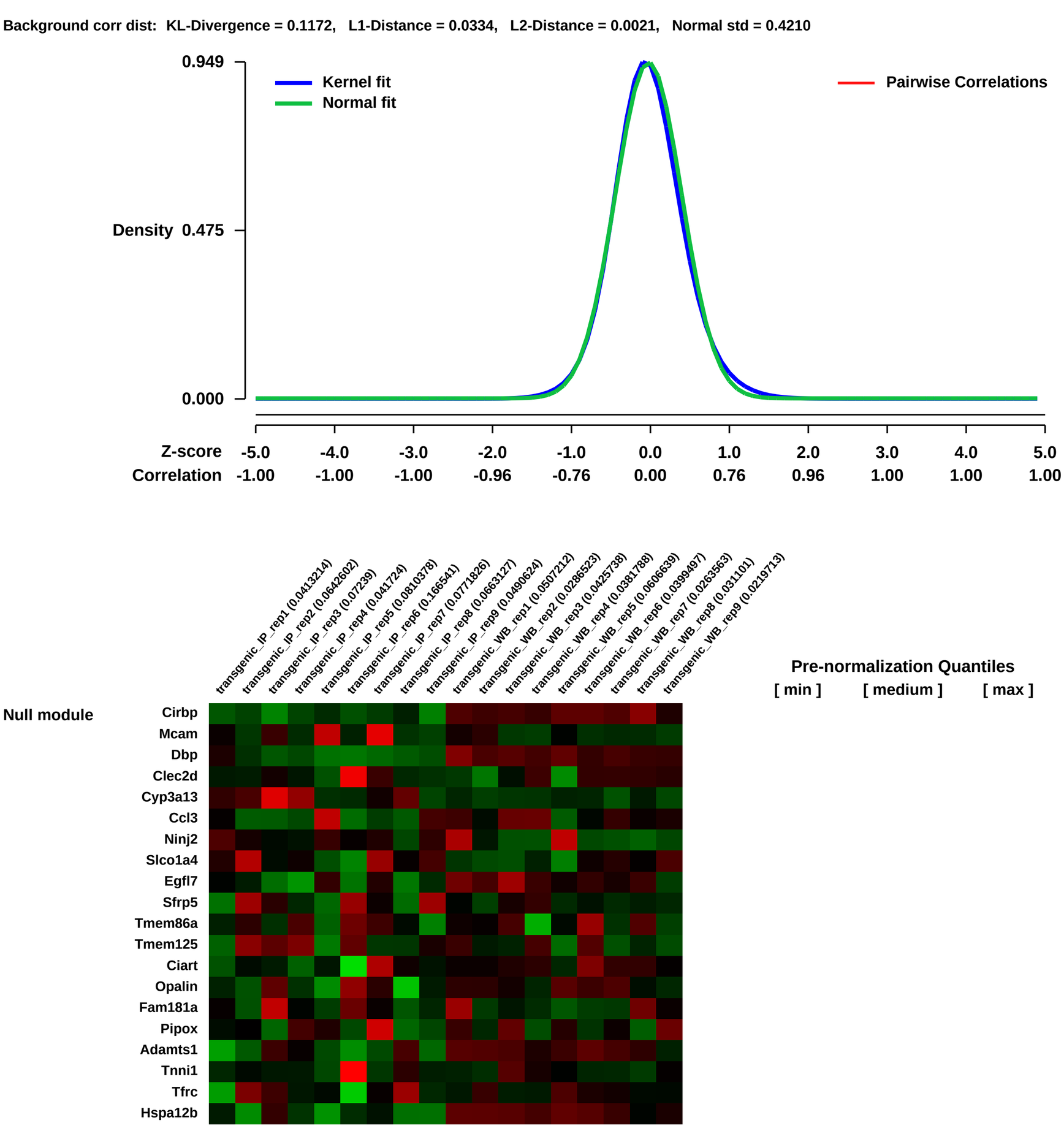

GEO Series "GSE5324" Expression Profiles

Num of samples in this series: 48

Scale of expression profile Z-scores

-3.0 -2.0 -1.0 0.0 1.0 2.0 3.0

GEO Link:	http://www.ncbi.nlm.nih.gov/geo/query/acc.cgi?acc=GSE5324
Status:	Public on Oct 17 2006
Title:	TTP mRNA targets identified by global analysis of stabilized transcripts in TTP-deficient fibroblasts
Organism:	Mus musculus
Experiment type:	Expression profiling by array
Platform:	GPL1261
Pubmed ID:	17030620
Summary & Design:	**Summary:** Tristetraprolin (TTP) is a tandem CCCH zinc finger protein that was identified through its rapid induction by mitogens in fibroblasts. Studies of TTP-deficient mice, and cells derived from them, showed that TTP could bind to certain AU-rich elements in mRNAs, leading to increases in the rates of mRNA deadenylation and destruction. Known physiological target mRNAs for TTP include tumor necrosis factor alpha (TNF), granulocyte macrophage colony stimulating factor (GM-CSF) and interleukin 2 beta (IL2 beta). Here we used microarray analysis of RNA from wild-type and TTP-deficient fibroblast cell lines to identify transcripts with different decay rates, after serum stimulation and actinomycin D treatment. Of 250 mRNAs apparently stabilized in the absence of TTP, 23 contained conserved TTP binding sites; 10 of these were shown by secondary analyses to be stabilized. The most dramatically affected transcript encoded the protein Ier3, recently implicated in the physiological control of blood pressure. The Ier3 transcript contained several conserved TTP binding sites that could bind TTP directly, and conferred TTP sensitivity to the mRNA in cell transfection studies. These studies have identified several new, physiologically relevant TTP target transcripts in fibroblasts; these target mRNAs encode proteins from a variety of functional classes. **Keywords:** mRNA degradation, time course, knockout experiment **Overall design:** 90 min and another sample taken, after which 5 …g/ml actinomycin D was added; samples for RNA analysis were then removed at 30, 60, 90 and 120 min after actinomycin D treatment. In all experiments, each sample represented three combined 100 mm dishes of cells.

Background corr dist: KL-Divergence = 0.1605, L1-Distance = 0.0418, L2-Distance = 0.0041, Normal std = 0.3654

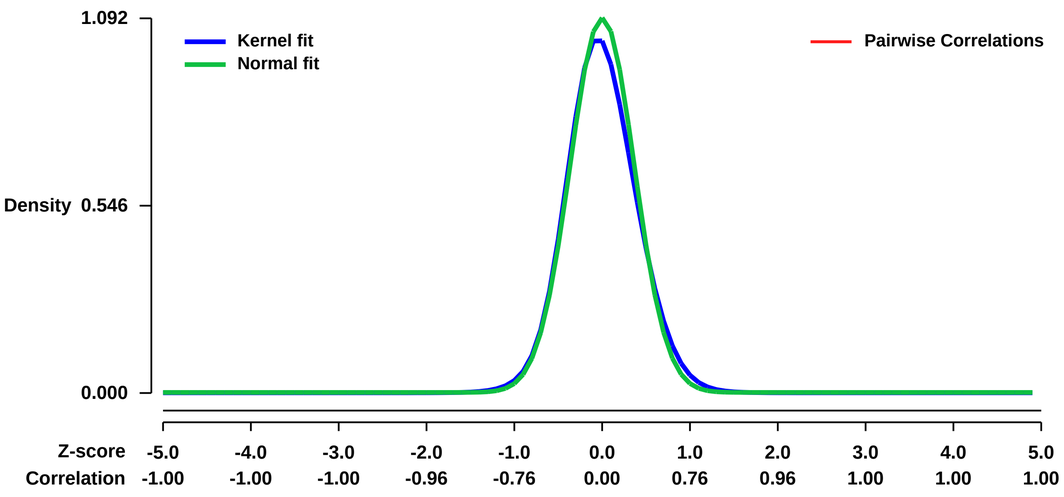

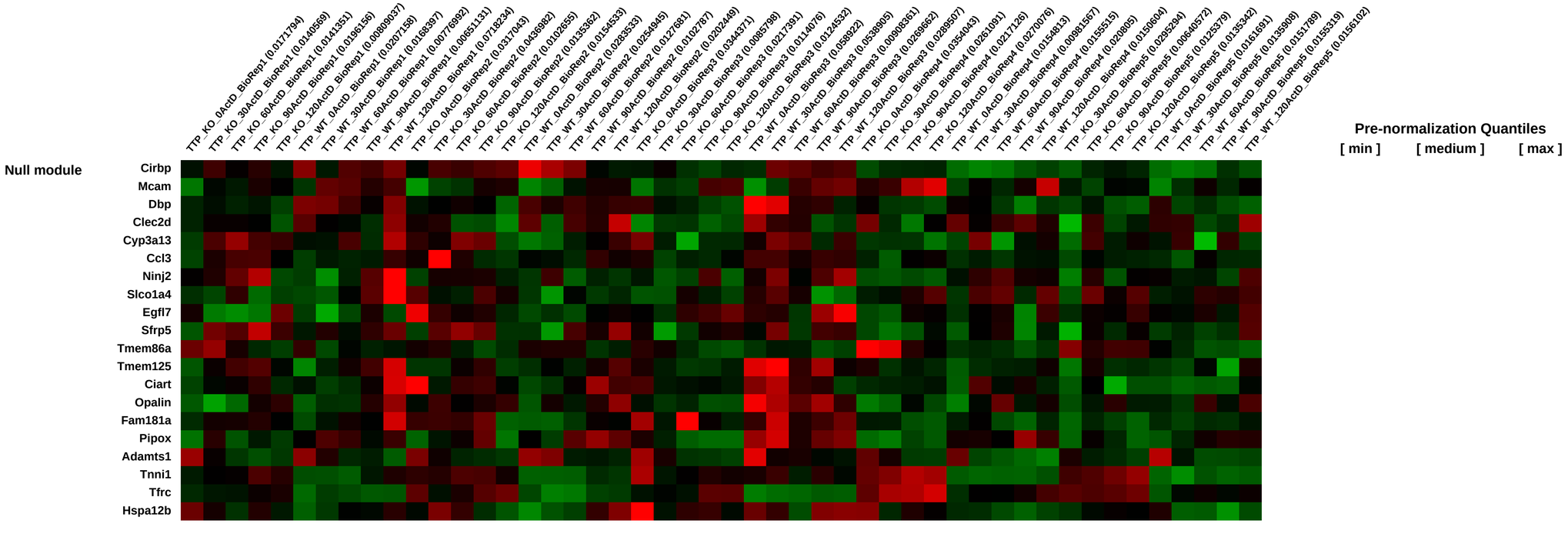

GEO Series "GSE55809" Expression Profiles

Num of samples in this series: 8

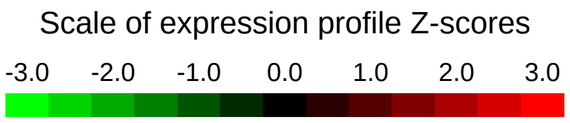

GEO Link:	**http://www.ncbi.nlm.nih.gov/geo/query/acc.cgi?acc=GSE55809**
Status:	**Public on Mar 12 2014**
Title:	**Cell autonomous and non-autonomous interactions of a western-style diet and the vitamin D receptor in intestinal homeostasis and tumorigenesis**
Organism:	**Mus musculus**
Experiment type:	**Expression profiling by array**
Platform:	**GPL1261**
Pubmed ID:	
Summary & Design:	**Summary:** **These data suggest that co-culture with macrophages increases expression of NDRG-1 in epithelial cell lines. The finding is confirmed in 2 human epithelial cell lines, and in tissue derived from mice genetically and dietetically altered to increase macrophage infiltration of the small and large intestinal epithelium. NDRG1 is identified as a potential mediator of macrophage effects on tumorigenesis in the large and small intestine.** **Array data is part of a larger study involving the effects of Vitamin D, in concert with macrophages, on intestinal homeostasis and tumorigenesis.** **Overall design:** **Cells from mouse epithelial cell line CT26 were cultured either alone, or with RAW macrophages in a system which allowed no physical contact but exchange of soluble factors between the cell types. The experiment was peformed twice.**

Background corr dist: **KL-Divergence = 0.0280, L1-Distance = 0.0347, L2-Distance = 0.0014, Normal std = 0.7125**

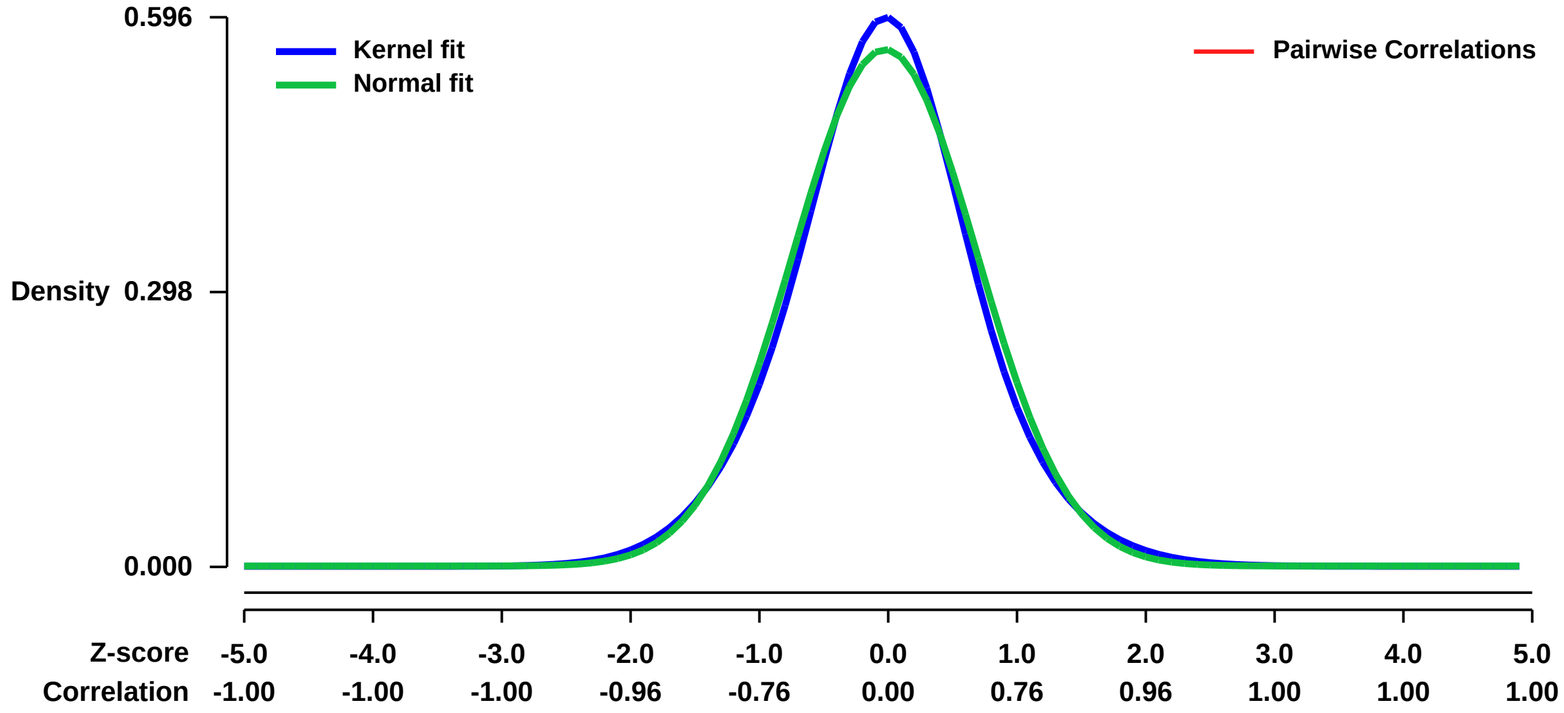

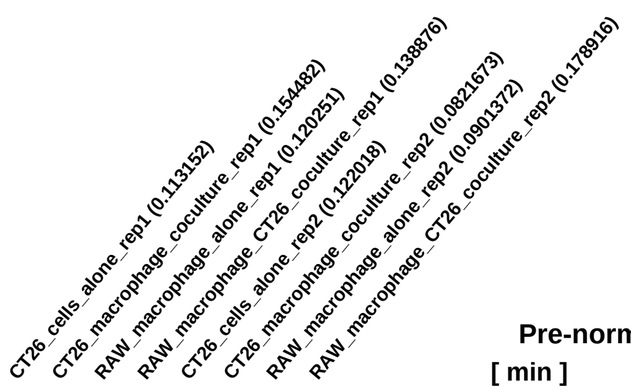

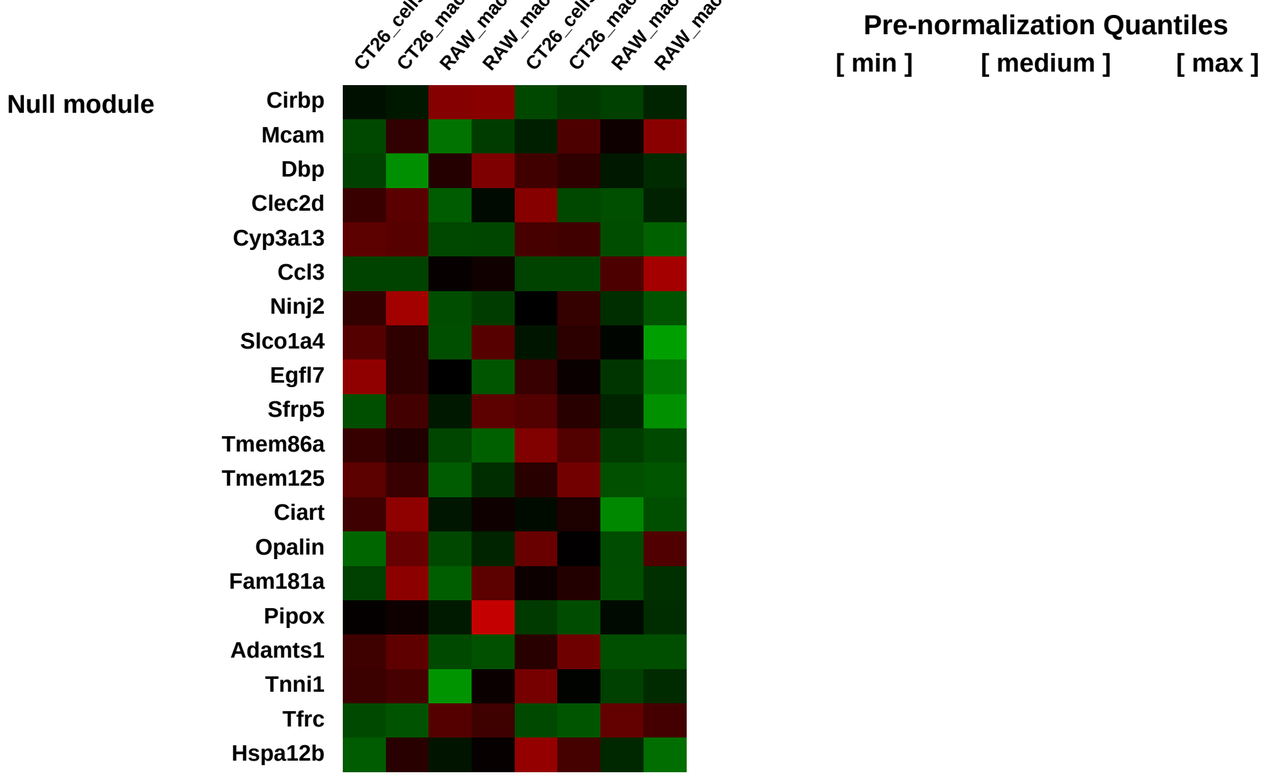

GEO Series "GSE19194" Expression Profiles

Num of samples in this series: 14

Scale of expression profile Z-scores

-3.0 -2.0 -1.0 0.0 1.0 2.0 3.0

GEO Link:	http://www.ncbi.nlm.nih.gov/geo/query/acc.cgi?acc=GSE19194
Status:	Public on Mar 31 2010
Title:	Cbfb/Runx1-repression independent blockage of differentiation and accumulation of Csf2rb expressing cells by Cbfb-MYH11
Organism:	Mus musculus
Experiment type:	Expression profiling by array
Platform:	GPL1261
Pubmed ID:	20007544
Summary & Design:	**Summary:** It is known that CBFB-MYH11, the fusion gene generated by inversion of chromosome 16 in human acute myeloid leukemia, is causative for oncogenic transformation. However, the mechanism by which CBFB-MYH11 initiates leukemogenesis is not clear. Previously published reports showed that CBFB-MYH11 dominantly inhibits RUNX1 and CBFB, and such inhibition has been suggested as the mechanism for leukemogenesis. However, knockin mice expressing Cbfb-MYH11 (Cbfb+/MYH11) showed defects in primitive hematopoiesis not seen in Cbfb null (Cbfb-/-) embryos indicating that Cbfb-MYH11 has repression independent activities as well. To identify gene expression changes associated with this novel activity, we compared the gene expression profile in the blood cells of Cbfb+/MYH11 and Cbfb-/- embryonic day 12.5 (E12.5) embryos with that of their wildtype littermates. **Overall design:** Cbfb-MYH11 chimeras were mated to C57/Bl6 females to generate Cbfb+/MYH11 (Cbfb+/MYH11) and Cbfb+/+ (WT) embryos. Cbfb+/- x Cbfb+/- matings were used to generate Cbfb+/+ (Cbfb+/+) and Cbfb-/- (Cbfb-/-) embryos. Blood from 8-10 E12.5 embryos of the same genotype was pooled, and RNA was isolated, labeled, and hybridized to Affymetrix Genechip mouse microarray (430 2.0) chips. 4 chips were used for both the Cbfb+/MYH11 and littermate control samples. 3 chips were used for the Cbfb-/- samples and littermate control samples.

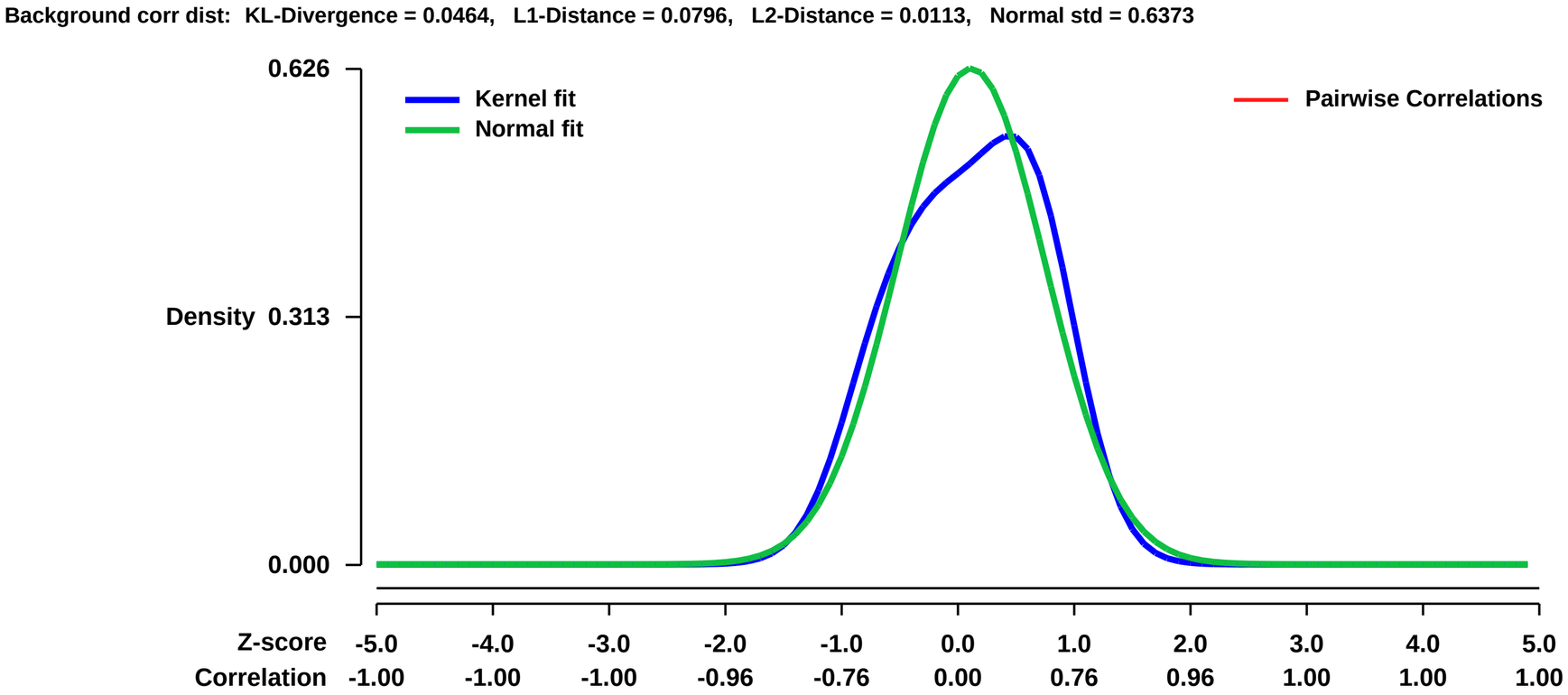

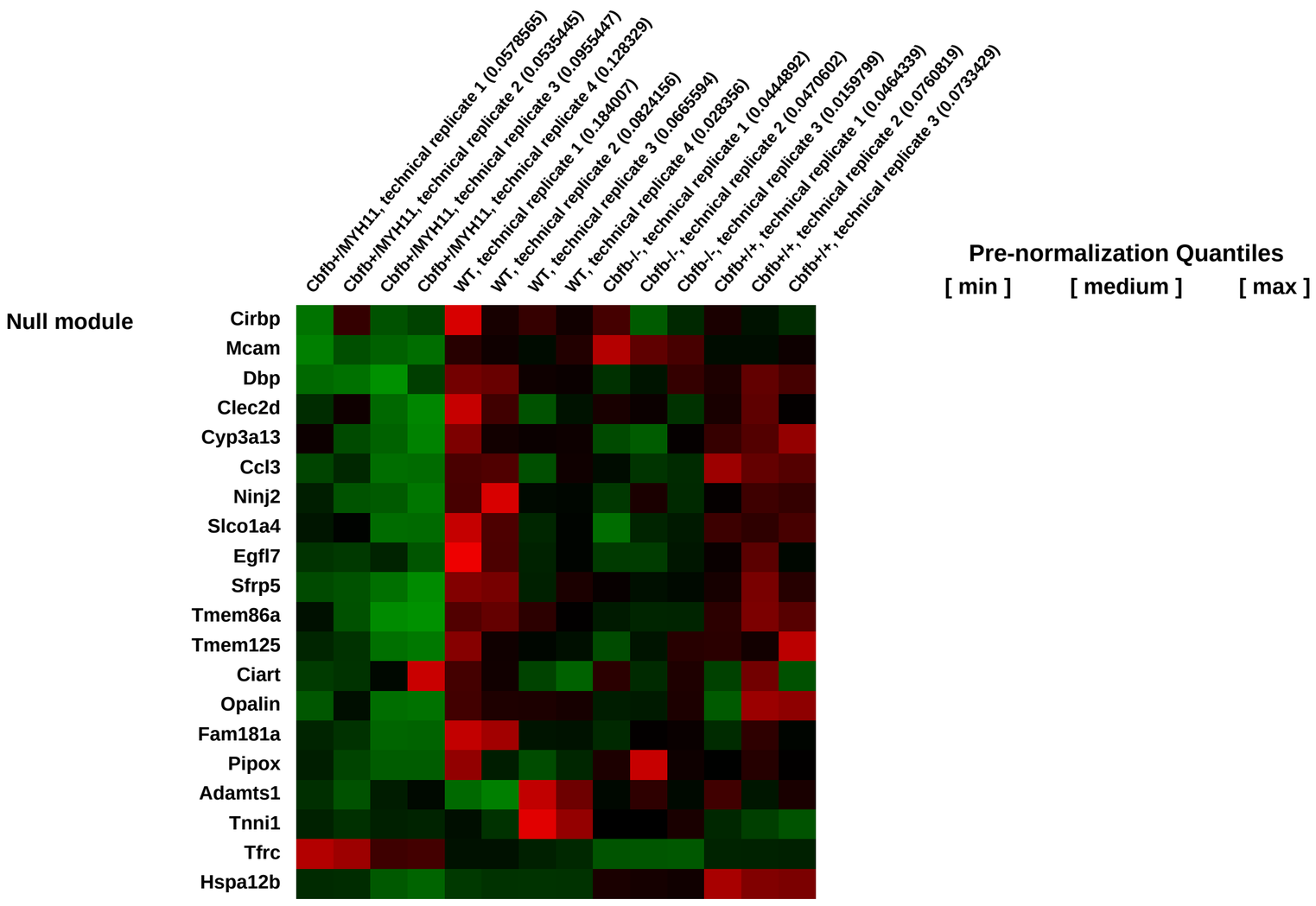

GEO Series "GSE40939" Expression Profiles

Num of samples in this series: 10

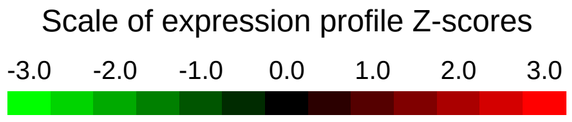

GEO Link:	http://www.ncbi.nlm.nih.gov/geo/query/acc.cgi?acc=GSE40939
Status:	Public on Dec 21 2012
Title:	Leukemogenesis by CDX2 involves KLF4 repression and deregulated PPARgamma signaling.
Organism:	Mus musculus
Experiment type:	Expression profiling by array
Platform:	GPL1261
Pubmed ID:	23202735
Summary & Design:	**Summary:** Aberrant expression of the homeodomain transcription factor CDX2 occurs in most cases of acute myeloid leukemia (AML) and promotes leukemogenesis, making CDX2, in principle, an attractive therapeutic target. Conversely, CDX2 acts as a tumor suppressor in colonic epithelium. The effectors mediating the leukemogenic activity of CDX2 and the mechanism underlying its context-dependent properties are poorly characterized, and strategies for interfering with CDX2 function in AML remain elusive. We report data implicating repression of the transcription factor KLF4 as important for the oncogenic activity of CDX2, and demonstrate that CDX2 differentially regulates KLF4 in AML versus colon cancer cells through a mechanism that involves tissue-specific patterns of promoter binding and epigenetic modifications. Furthermore, we identified deregulation of the PPAR‚Ä‡ signaling pathway as a feature of AML expressing CDX2, and observed that PPAR‚Ä‡ agonists derepress KLF4 and are preferentially toxic to CDX2-positive leukemic cells. These data delineate transcriptional programs associated with CDX2 expression in hematopoietic cells; provide insight into the antagonistic duality of CDX2 function in AML versus colon cancer; and suggest reactivation of KLF4 expression, through modulation of PPAR‚Ä‡ signaling, as a new therapeutic modality in a large proportion of AML patients. **Overall design:** Experiment 2 (Samples 7-10): The transcriptional changes induced by Cdx2 were assessed in vivo in Cdx2-initiated murine leukemias and compared with those of leukemias initiated by 5 different MLL fusion oncogenes (previously published data, available at GSE13690). Bone marrow cells isolated from C57BL/6 mice were transduced with pMSCV-Cdx2-IRES-GFP, and 8x10e5 GFP-positive cells were injected into lethally irradiated syngeneic recipient mice after 48 hours, followed by injection of 1x10e6 spleen cells from primary leukemic animals into sublethally irradiated secondary recipients. Spleen cells from secondary leukemic animals were harvested.

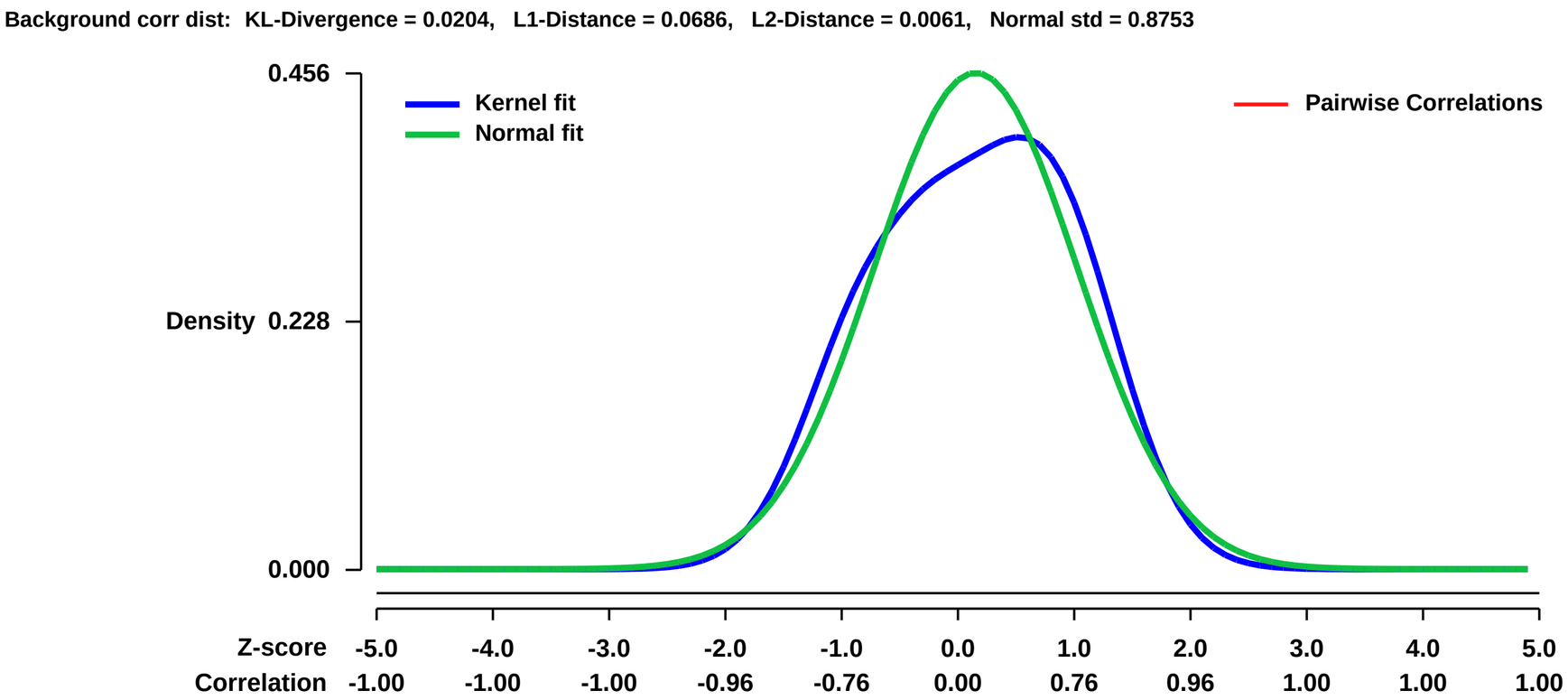

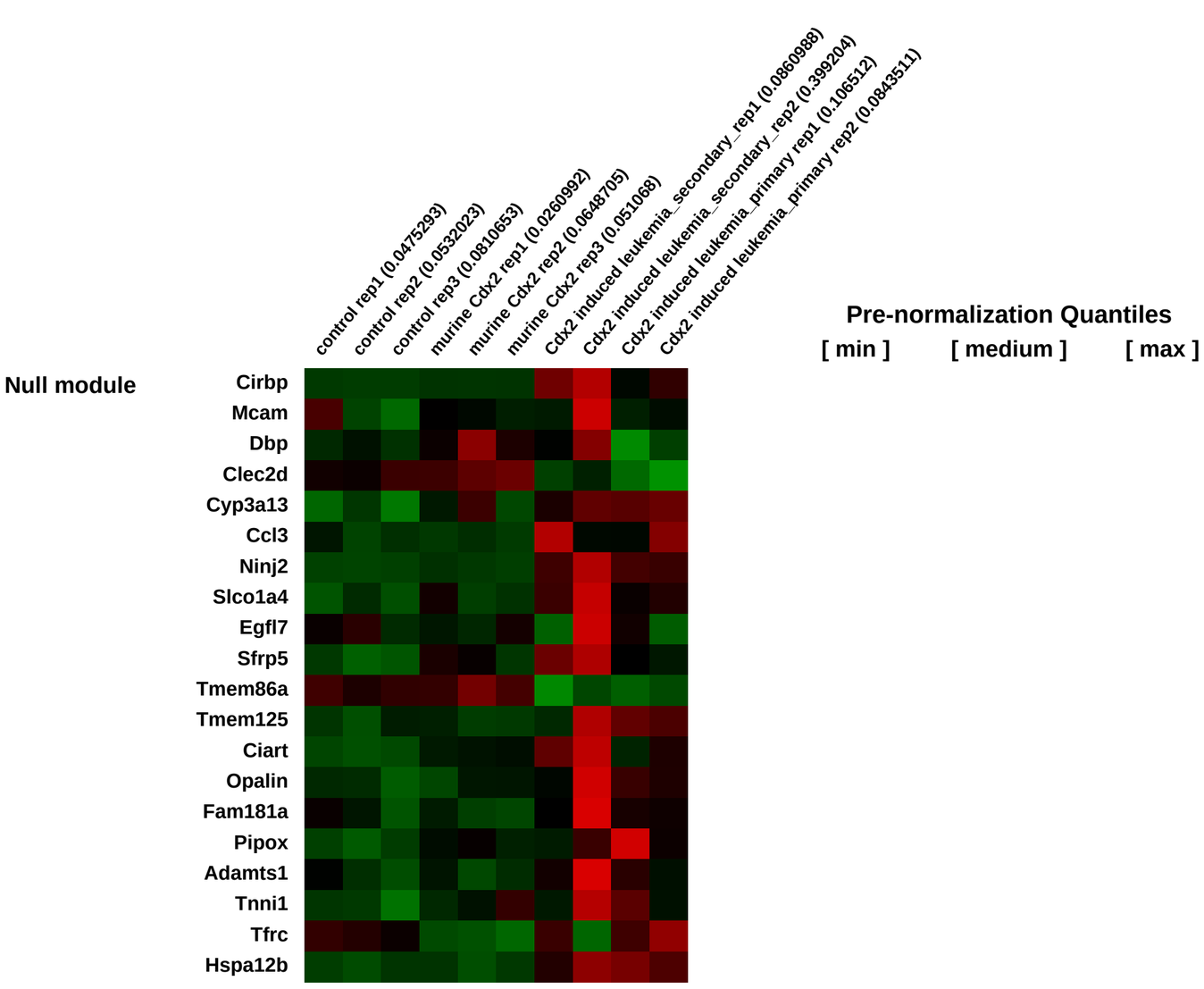

GEO Series "GSE11186" Expression Profiles

Num of samples in this series: 33

Scale of expression profile Z-scores

-3.0 -2.0 -1.0 0.0 1.0 2.0 3.0

GEO Link:	http://www.ncbi.nlm.nih.gov/geo/query/acc.cgi?acc=GSE11186
Status:	Public on Jul 17 2009
Title:	Expression profiling of mouse dorsal skin during hair follicle cycling
Organism:	Mus musculus
Experiment type:	Expression profiling by array
Platform:	GPL1261
Pubmed ID:	19629164
Summary & Design:	**Summary:** Hair follicles undergo recurrent cycling of controlled growth (anagen), regression (catagen), and relative quiescence (telogen) with a defined periodicity. Taking a genomics approach to study gene expression during synchronized mouse hair follicle cycling, we discovered that, in addition to circadian fluctuation, CLOCK-regulated genes are also modulated in phase with the hair growth cycle. During telogen and early anagen, circadian clock genes are prominently expressed in the secondary hair germ, which contains precursor cells for the growing follicle. Analysis of Clock and Bmal1 mutant mice reveals a delay in anagen progression, and the secondary hair germ cells show decreased levels of phosphorylated Rb and lack mitotic cells, suggesting that circadian clock genes regulate anagen progression via their effect on the cell cycle. Consistent with a block at the G1 phase of the cell cycle, we show a significant upregulation of p21 in Bmal1 mutant skin. While circadian clock mechanisms have been implicated in a variety of diurnal biological processes, our findings indicate that circadian clock genes may be utilized to modulate the progression of non-diurnal cyclic processes. **Overall design:** To investigate the molecular control of hair follicle cycling, we profiled mRNA expression in mouse dorsal skin at multiple representative time points in the synchronized second postnatal hair growth cycle and in a depilation-induced hair growth cycle. For profiling of second synchronized and depilation-induced hair growth cycle, the same upper-mid region of dorsal skin was excised from C57BL/6 mice at representative postnatal days (P). The time points for second hair growth cycle are classified into different phases of the hair growth cycle based on established morphological guidelines as follow: early anagen (P23, P25), mid anagen (P27), late anagen (P29, P34), early catagen (P37, P39), mid catagen (P41), and telogen (P44). Depilation-induced hair growth cycle by applying wax/rosin mixture on the dorsal skin of seven-week old mice (all follicles in telogen) was performed on mice. The corresponding phases of the hair growth cycle at number of days following depilation (D) is as follow: early anagen (D3), mid anagen (D5), late anagen (D8, D12), and early catagen (D17). For each time point, multiple biological replicates were profiled, with each mouse dorsal skin separately hybridized to an Affymetrix array.

Background corr dist: KL-Divergence = 0.2054, L1-Distance = 0.0354, L2-Distance = 0.0025, Normal std = 0.3341

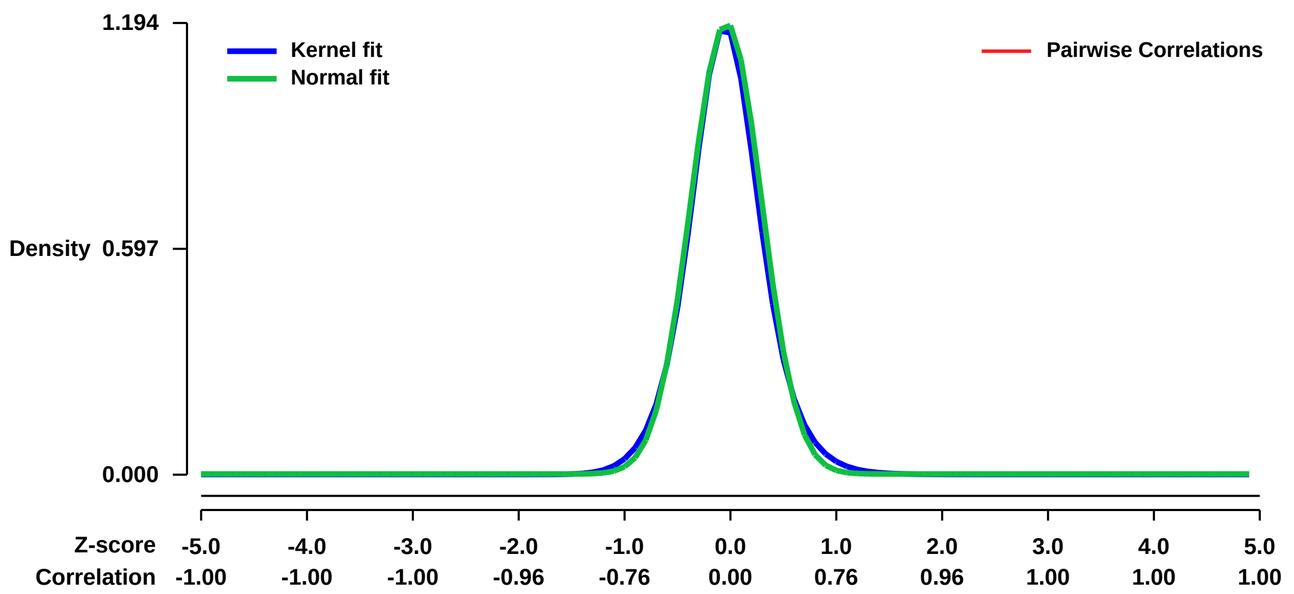

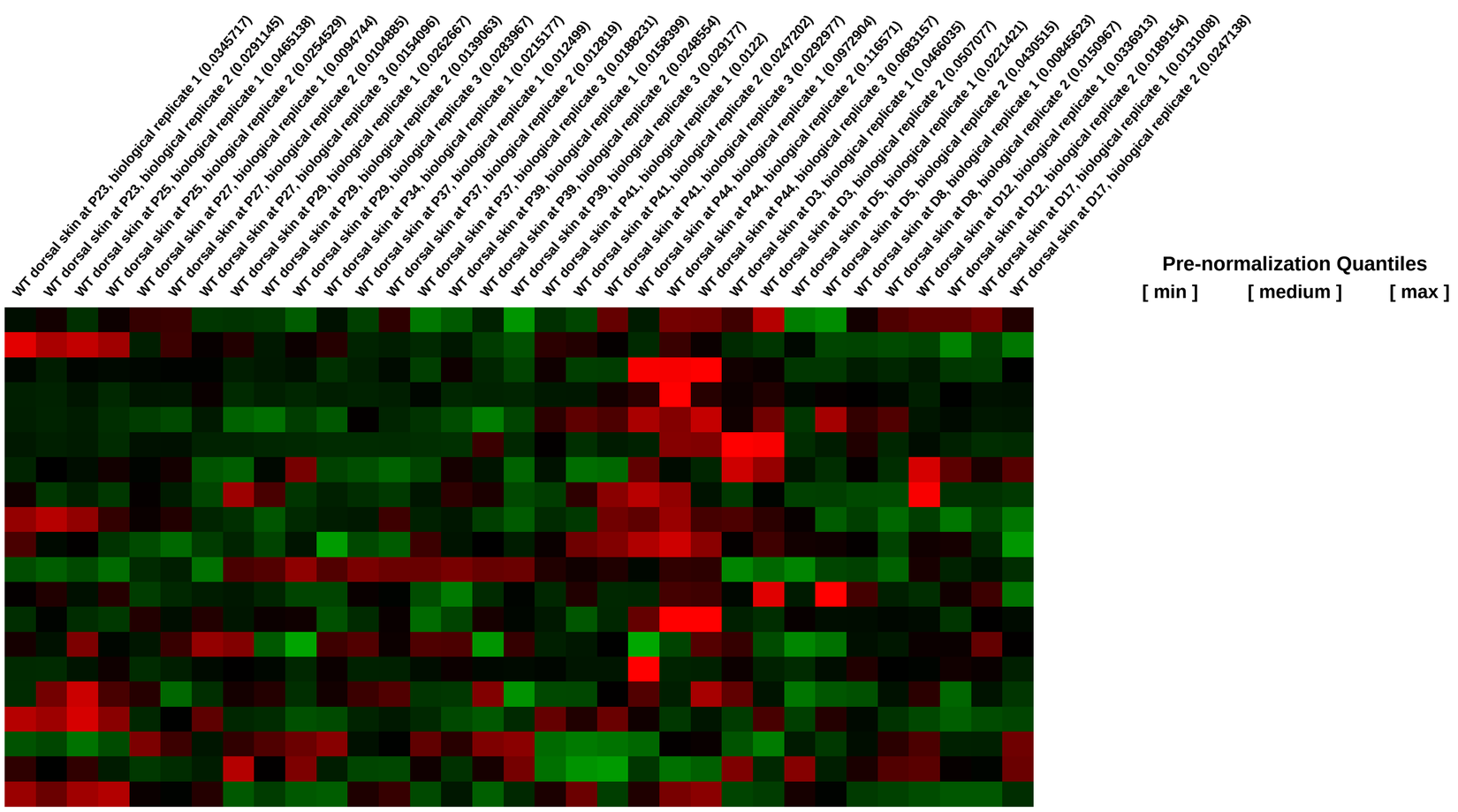

GEO Series "GSE12049" Expression Profiles

Num of samples in this series: 6

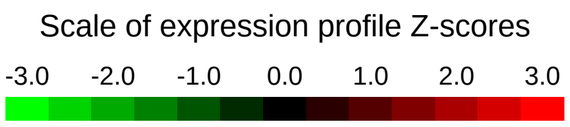

GEO Link:	http://www.ncbi.nlm.nih.gov/geo/query/acc.cgi?acc=GSE12049
Status:	Public on Jul 10 2008
Title:	Expression data from laminin alpha 2 chain deficient mice vs wild type
Organism:	Mus musculus
Experiment type:	Expression profiling by array
Platform:	GPL1261
Pubmed ID:	18611855
Summary & Design:	**Summary:** Mutations in the gene encoding laminin a2 chain cause congenital muscular dystrophy, MDC1A. In skeletal muscle, laminin a2 chain binds at least two receptor complexes; the dystrophin-glycoprotein complex and integrin a7b1. To gain insight into the molecular mechanisms underlying this disorder, we performed gene expression profiling of laminin a2 chain deficient mouse limb muscle. One of the down-regulated genes encodes a protein called calcium and integrin binding protein 2 (Cib2) whose expression and function is unknown. However, the closely related Cib1 has been reported to bind integrin allb and may be involved in outside-in-signaling in platelets. Since Cib2 might be a novel integrin a7b1 binding protein in muscle, we have studied Cib2 expression in the developing and adult mouse. Cib2 mRNA is mainly expressed in the developing central nervous system and in developing and adult skeletal muscle. In skeletal muscle Cib2 colocalizes with integrin a7B subunit at the sarcolemma and at the neuromuscular- and myotendinous junctions. Finally, we demonstrate that Cib2 is a calcium binding protein that interacts with integrin a7Bb1D. Thus, our data suggest a role for Cib2 as a cytoplasmic effector of integrin a7Bb1D signaling in skeletal muscle **Keywords: disese state analysis** **Overall design:** Skeletal muscle (all hind limb skeletal muscle) from 4-weeks old laminin alpha 2 chain deficient mice and 4-weeks old wild type mice were isolated individually and RNA were extracted and hybridized on Affiymetrix microarrys. Three biological replicates from each group were analyzed.

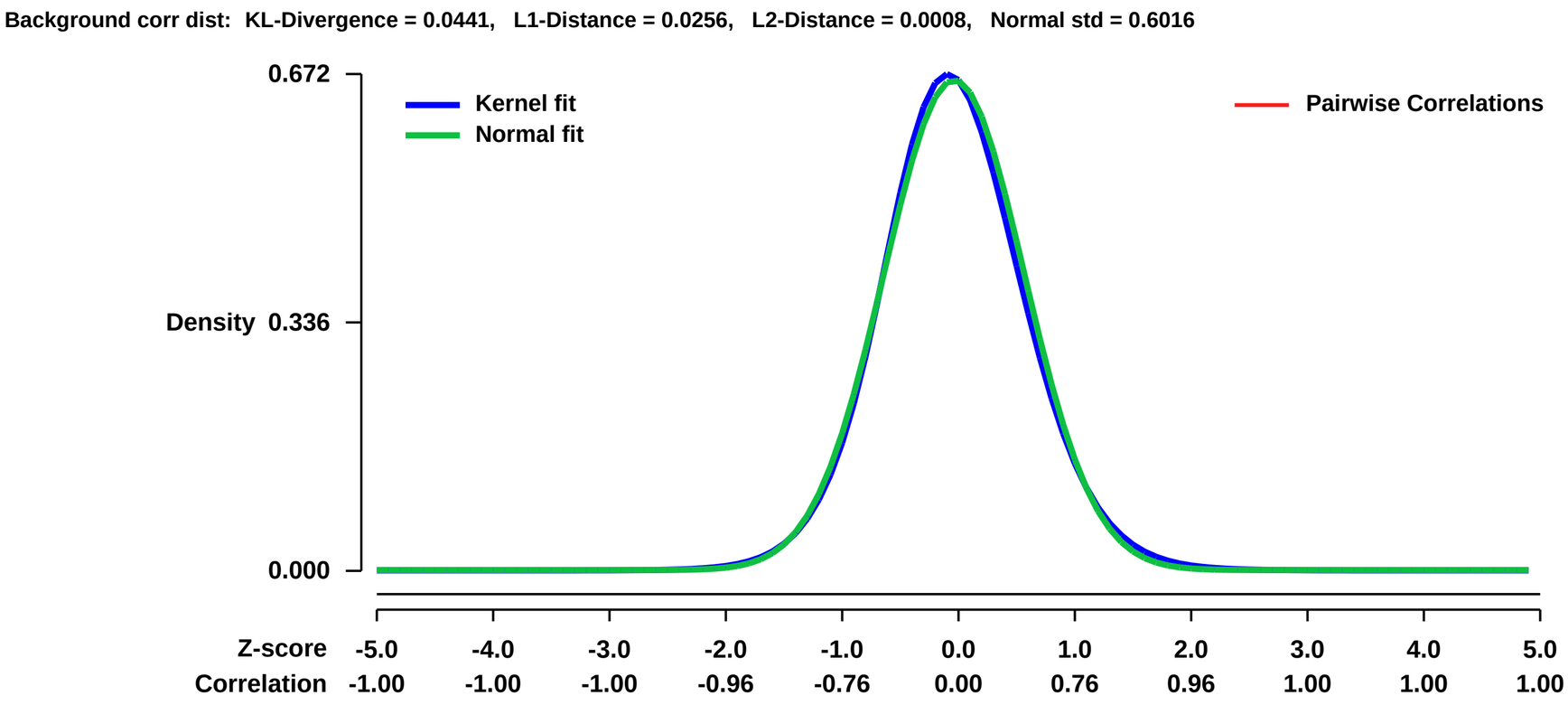

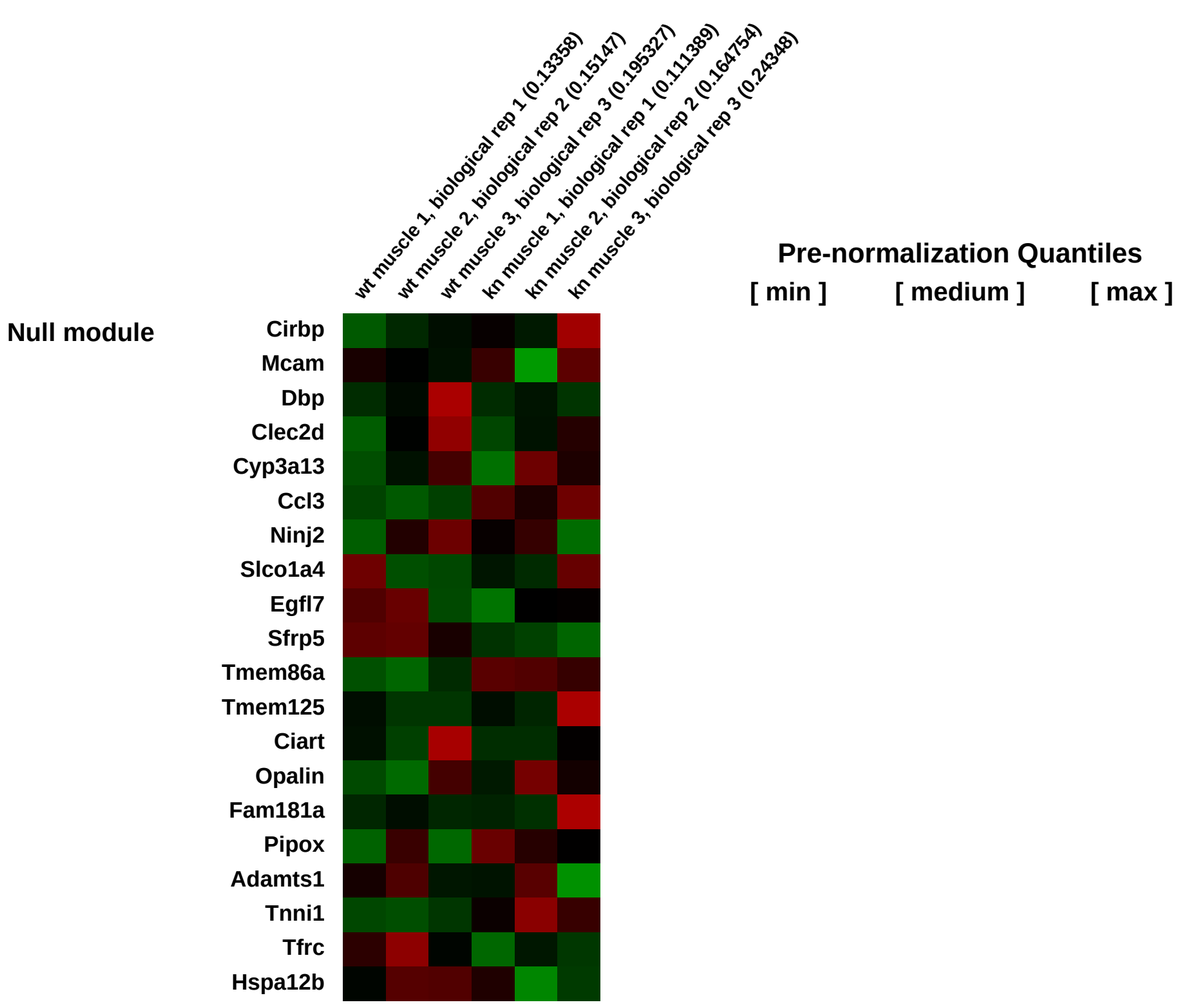

GEO Series "GSE29572" Expression Profiles

Num of samples in this series: 21

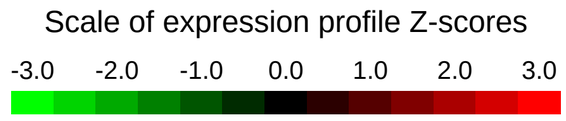

GEO Link:	**http://www.ncbi.nlm.nih.gov/geo/query/acc.cgi?acc=GSE29572**
Status:	**Public on Jul 22 2011**
Title:	**Differential effects of krill oil and fish oil on the hepatic transcriptome in mice**
Organism:	**Mus musculus**
Experiment type:	**Expression profiling by array**
Platform:	**GPL1261**
Pubmed ID:	
Summary & Design:	**Summary:** **Dietary supplementation with ˇ-3 polyunsaturated fatty acids (ˇ-3 PUFAs), specifically the fatty acids docosahexaenoic acid (DHA; 22:6 ˇ-3) and eicosapentaenoic acid (EPA; 20:5 ˇ-3), is known to have beneficial health effects including improvements in glucose and lipid homeostasis and modulation of inflammation. To evaluate the efficacy of two different sources of ˇ-3 PUFAs, we performed gene expression profiling in the liver of mice fed diets supplemented with either fish oil or krill oil. We found that ˇ-3 PUFA supplements derived from a phospholipid krill fraction (krill oil) downregulated the activity of pathways involved in hepatic glucose production as well as lipid and cholesterol synthesis. The data also suggested that krill oil-supplementation increases the activity of the mitochondrial respiratory chain. Surprisingly, an equimolar dose of EPA and DHA derived from fish oil modulated fewer pathways than a krill oil-supplemented diet and did not modulate key metabolic pathways regulated by krill oil, including glucose metabolism, lipid metabolism and the mitochondrial respiratory chain. Moreover, fish oil upregulated the cholesterol synthesis pathway, which was the opposite effect of krill supplementation. Neither diet elicited changes in plasma levels of lipids, glucose or insulin, probably because the mice used in this study were young and were fed a low fat diet. Further studies of krill oil supplementation using animal models of metabolic disorders and/or diets with a higher level of fat may be required to observe these effects.** **Overall design:** **Twenty-one microarrays: three diets (CO, FO, KO) x seven mice per diet x one microarray per mouse**

Background corr dist: KL-Divergence = 0.1248, L1-Distance = 0.0276, L2-Distance = 0.0012, Normal std = 0.4084

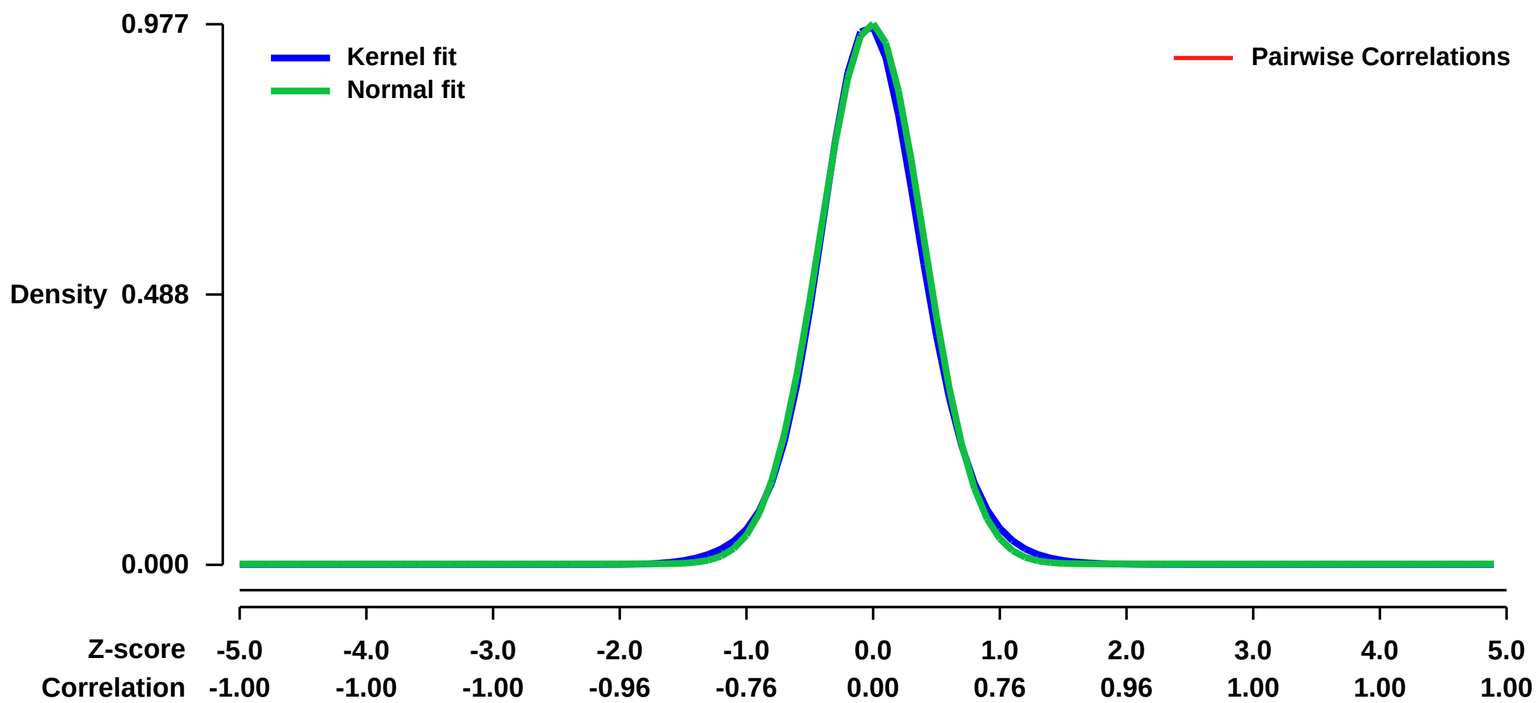

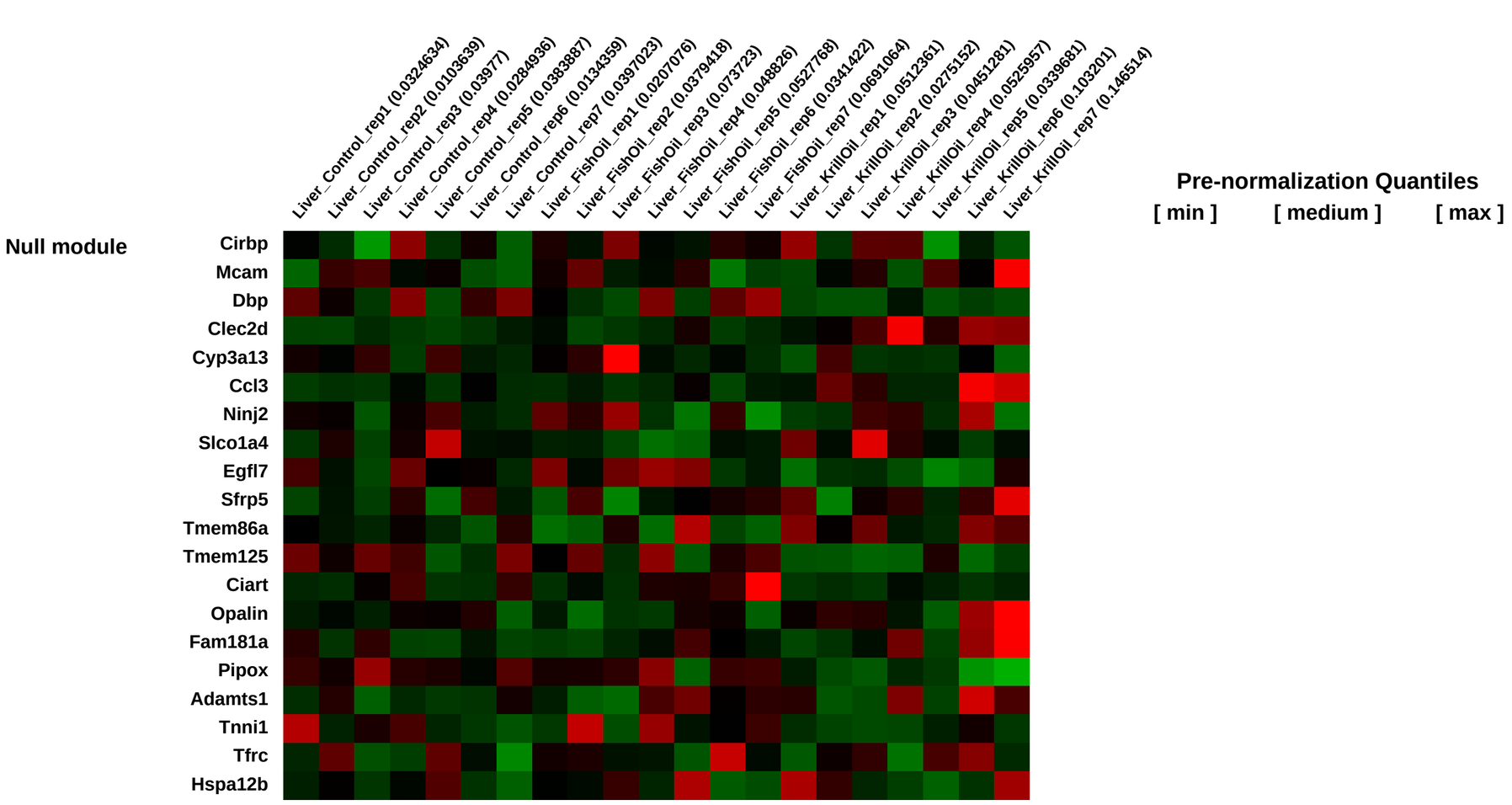

GEO Series "GSE4936" Expression Profiles

Num of samples in this series: 8

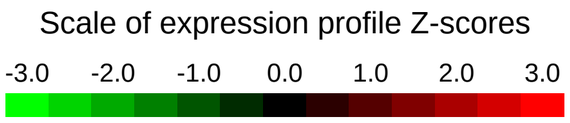

GEO Link:	**http://www.ncbi.nlm.nih.gov/geo/query/acc.cgi?acc=GSE4936**
Status:	**Public on Apr 20 2007**
Title:	**Transcriptional Profiling of Hh-Treated Embryoid Bodies**
Organism:	**Mus musculus**
Experiment type:	**Expression profiling by array**
Platform:	**GPL1261**
Pubmed ID:	**17442700**
Summary & Design:	**Summary:** **This experiment was specifically designed to measure neural targets of Shh signaling, we sought to profile the genes upregulated by Hh signaling in the ventral neural tube to obtain a valid dataset. To obtain ventral-specific markers, we generated retinoic acid-treated EBs grown in the presence or absence of HH-Ag. We did not observe induction of ventral Hh markers in RA-treated constitutive Gli1FLAG EBs and used these for the control, baseline set. The presence of FoxA2, Nkx2.9 and Nkx6.1 amongst the top 10 genes based on expression levels suggests that profiling significantly enriches for Hh-dependent cell types. As expected, the benchmark standard Gli1 was not up-regulated in our array, since it is constitutively expressed in the control as well.** **Keywords: neural progenitors, embryoid bodies, differentiation, Hedgehog, retinoic acid** **Overall design:** **There are a total of 8 samples. Four biological replicates of Retinoic-acid treated EBs (Baseline) and 4 additional biological samples of retinoic acid + Hh-Ag treated EBs (induced sample).**

Background corr dist: KL-Divergence = 0.0856, L1-Distance = 0.0227, L2-Distance = 0.0007, Normal std = 0.4632

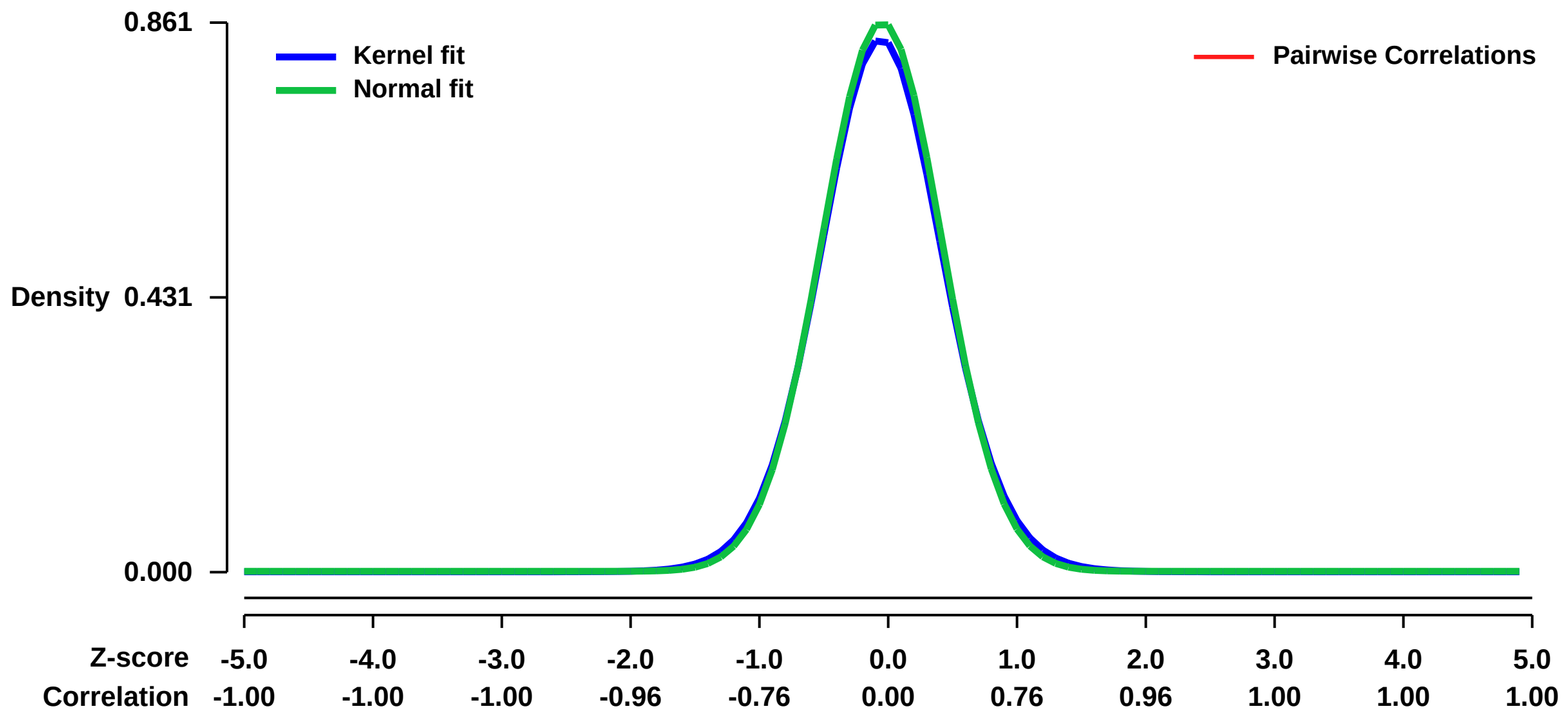

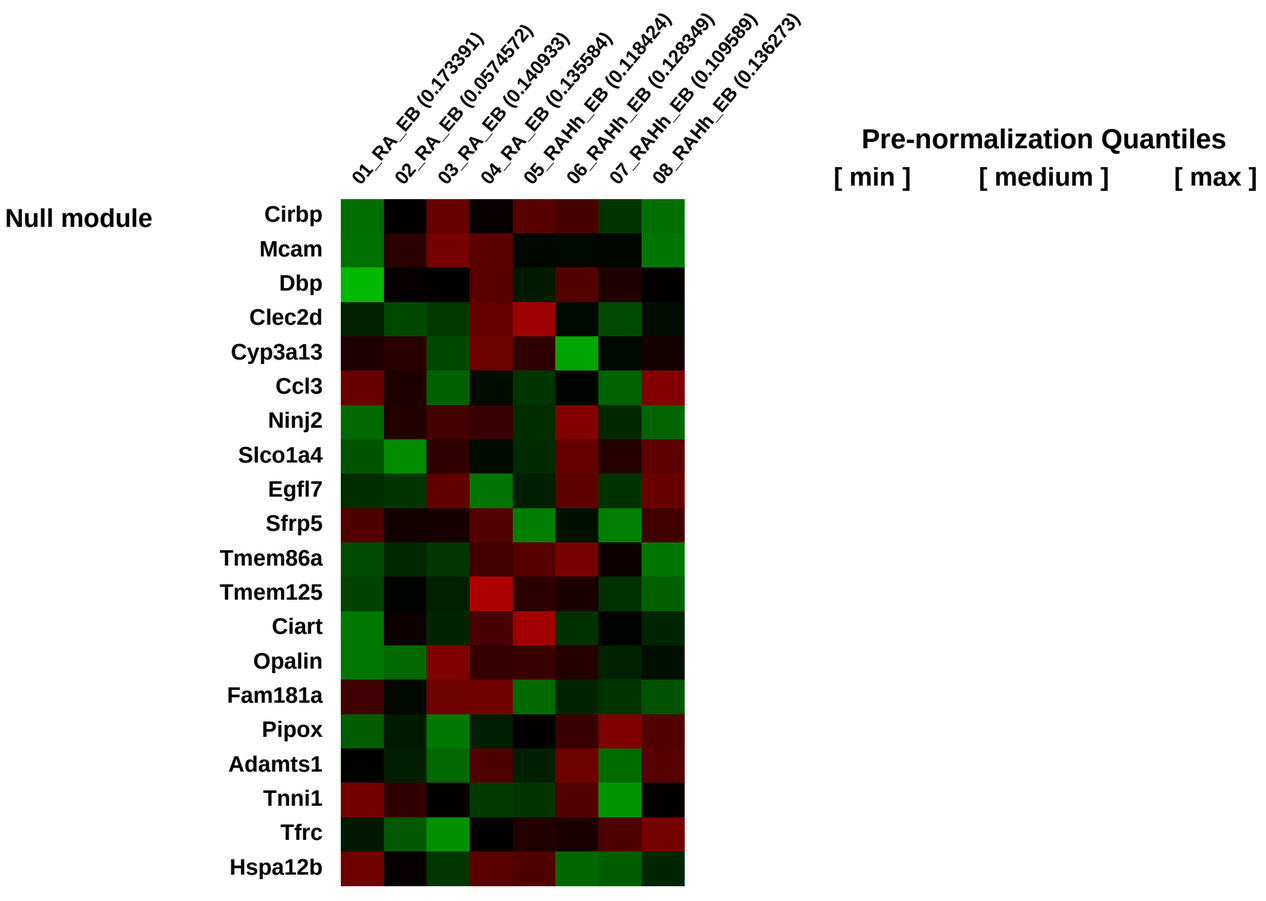

GEO Series "GSE37221" Expression Profiles

Num of samples in this series: 6

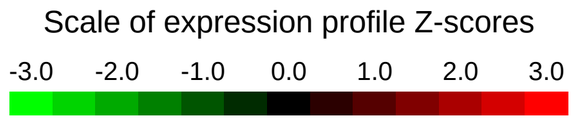

GEO Link:	http://www.ncbi.nlm.nih.gov/geo/query/acc.cgi?acc=GSE37221
Status:	Public on Apr 13 2012
Title:	Fz2-Fz7 double knock-out E8.5 mouse
Organism:	Mus musculus
Experiment type:	Expression profiling by array
Platform:	GPL1261
Pubmed ID:	23095888
Summary & Design:	**Summary:** Fz2Fz7 double knock out mouse microarray (E8.5) **Overall design:** Fz2-Fz7 double KO vs. Fz7 KO

Background corr dist: KL-Divergence = 0.0369, L1-Distance = 0.0220, L2-Distance = 0.0005, Normal std = 0.6370

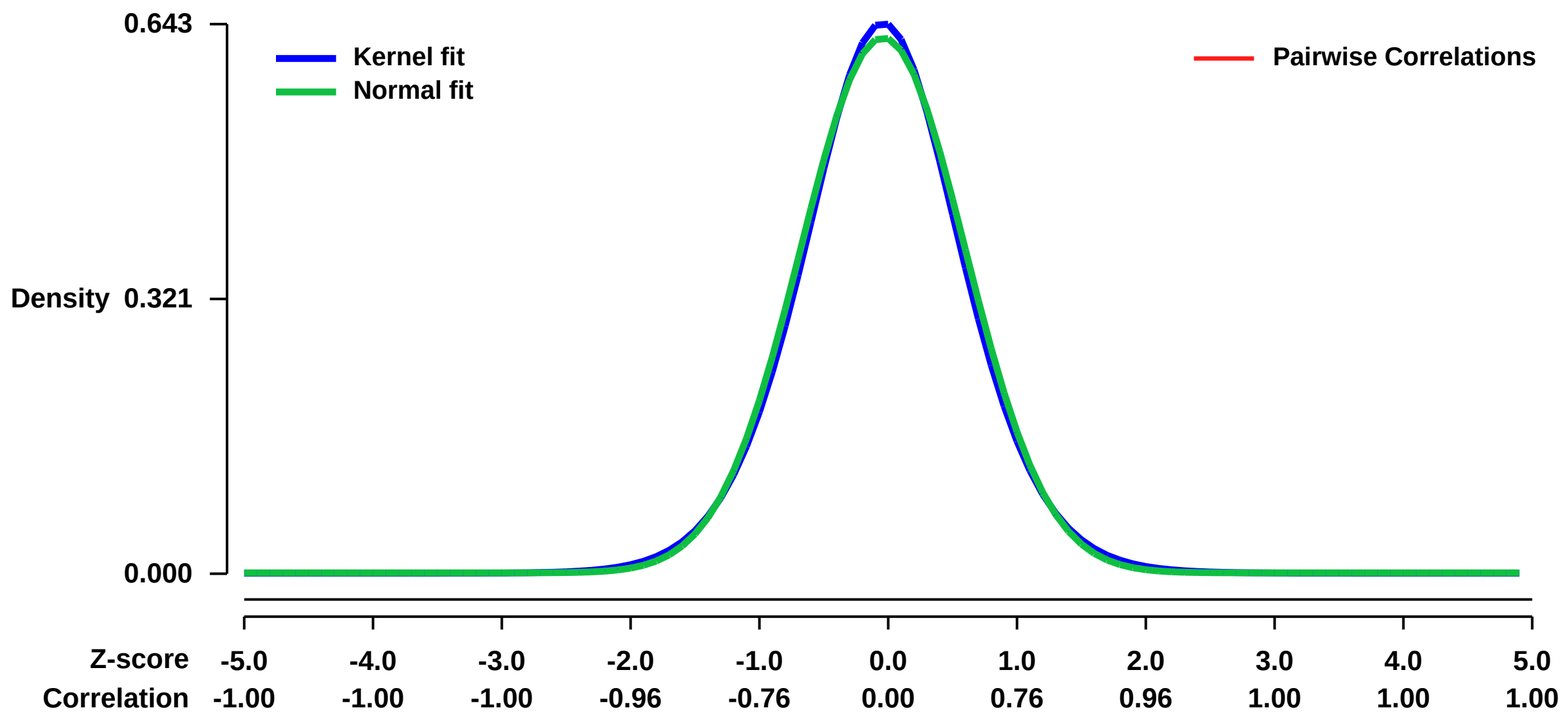

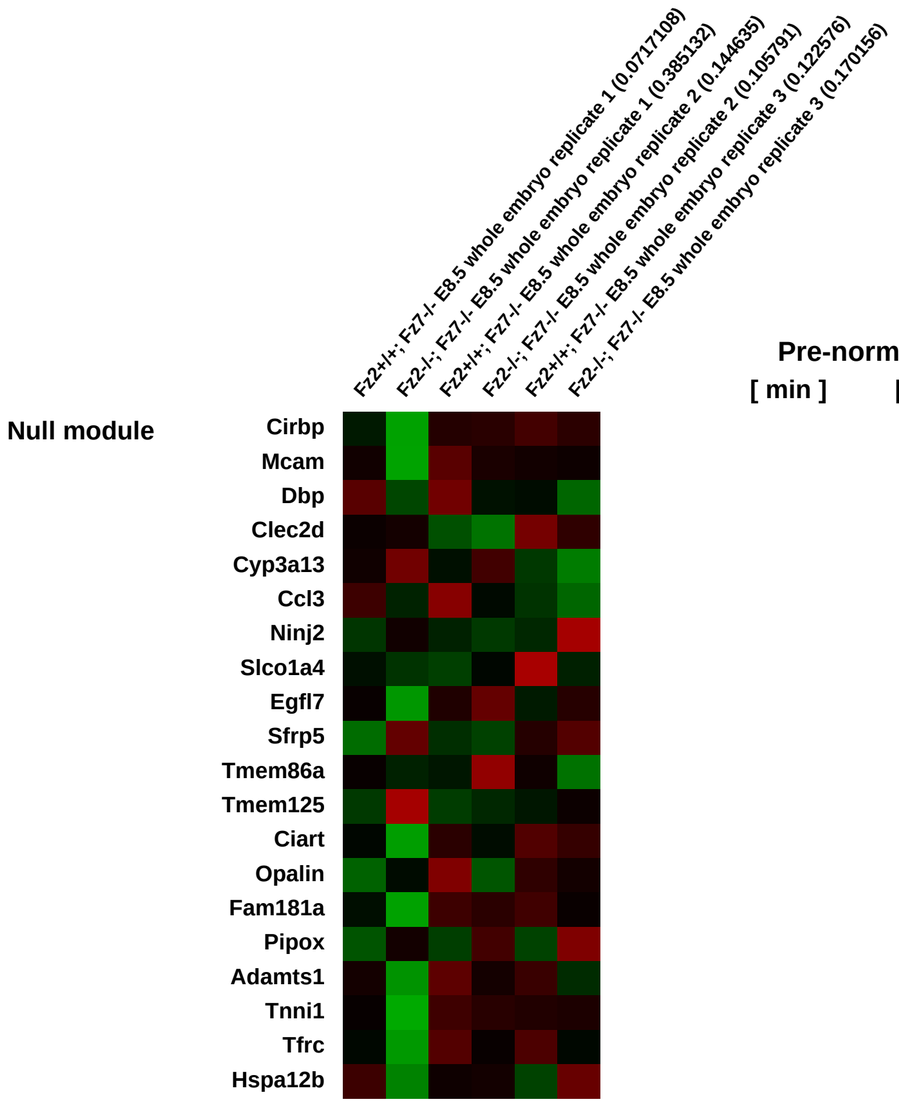

GEO Series "GSE10167" Expression Profiles

Num of samples in this series: 6

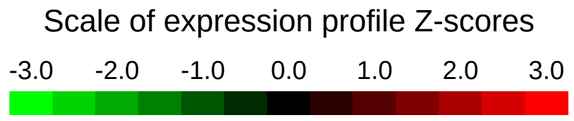

GEO Link:	**http://www.ncbi.nlm.nih.gov/geo/query/acc.cgi?acc=GSE10167**
Status:	**Public on Jan 15 2008**
Title:	**Microarray Analysis of Treacher Collins Syndrome**
Organism:	**Mus musculus**
Experiment type:	**Expression profiling by array**
Platform:	**GPL1261**
Pubmed ID:	**18246078**
Summary & Design:	**Summary:** **The object of this study was to identify genes transcriptionally upregulated and downregulated in response to Tcof1 haploin-sufficiency during mouse embryogensis** **Keywords: mouse embryo, littermates, Tcof1, Treacher Collins sydnrome, comparative hybridisation** **Overall design:** **Total RNA was extracted from 3 E8.5 wild-type and 3 E8.5 Tcof1+/- littermate embryos using the RNeasy Mini Protocol for Isolation of Total RNA from Animal Tissues (Qiagen) according to the manufacturerâ s protocol. RNA quality and quantity was determined using the Bioanalyser. To generate targets for microarray analysis, total RNA (100 ng) from each wild-type and mutant embryo was amplified using Two-Cycle Target Labeling (Affymetrix) according to the manufacturerâ s instructions. Biotinylated target cRNAs (20 ¸…g) from the 3 wild-type and 3 Tcof1+/- embryos were hybridised to separate GeneChip´fi Mouse Genome 430 2.0 arrays (Affymetrix), following standard Affymetrix procedures.**

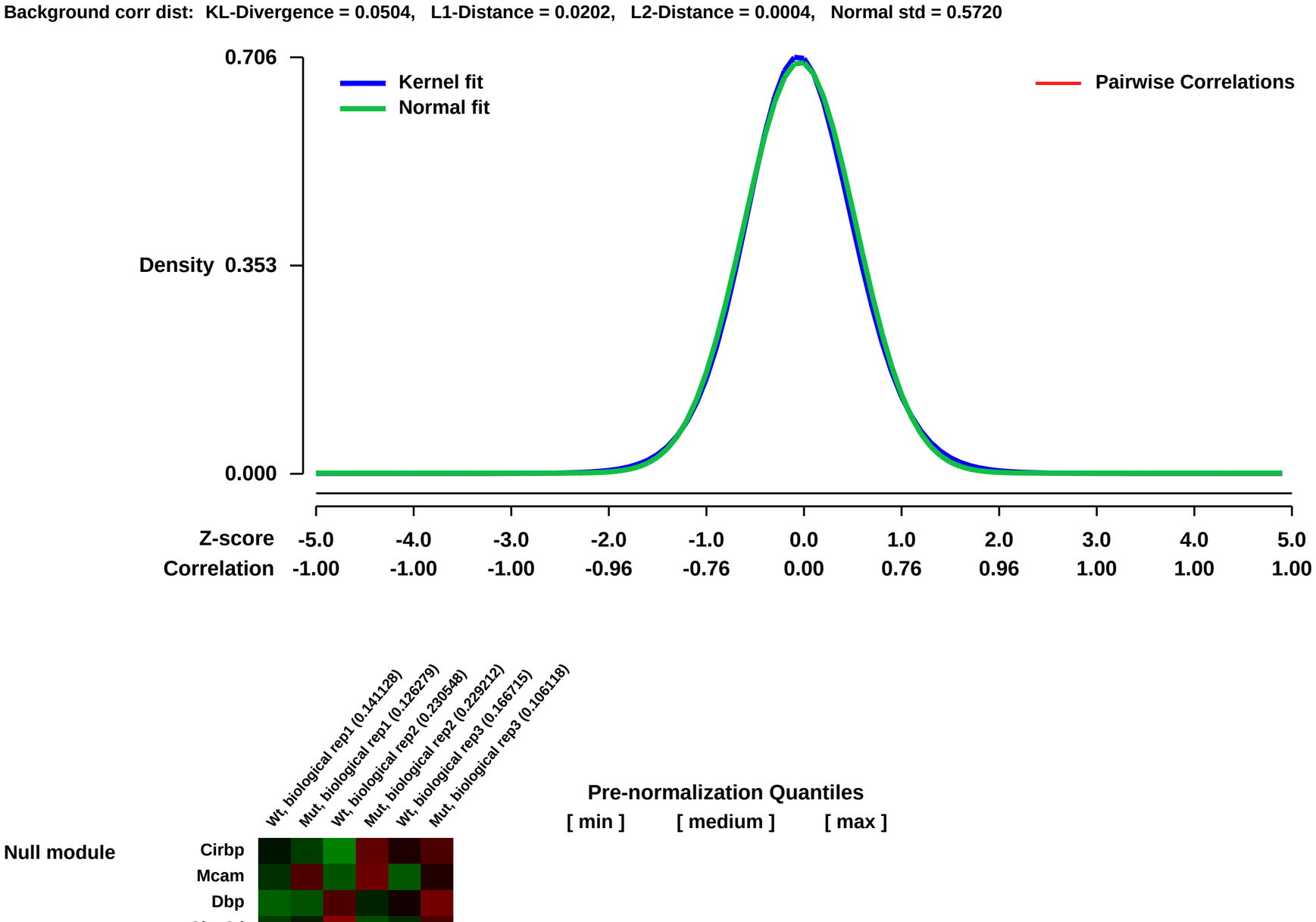

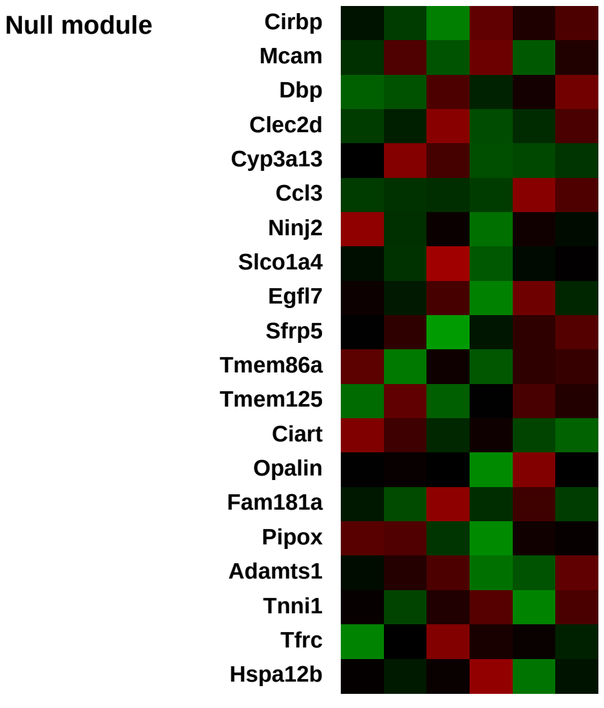

GEO Series "GSE6487" Expression Profiles

Num of samples in this series: 30

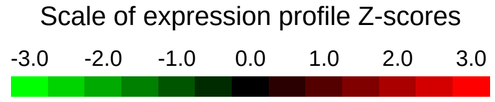

GEO Link:	http://www.ncbi.nlm.nih.gov/geo/query/acc.cgi?acc=GSE6487
Status:	Public on Dec 13 2006
Title:	Myogenesis MyoD
Organism:	Mus musculus
Experiment type:	Expression profiling by array
Platform:	GPL1261
Pubmed ID:	17965412
Summary & Design:	**Summary:** The transcription factor MyoD can coax na?e fibroblasts or otherwise committed cells to adopt the skeletal muscle phenotype by activating the muscle gene expression program. Activation of muscle gene expression occurs in quantal steps with not all the target genes of MyoD being activated at the same time. Some genes are induced in the initial phases, others at later stages despite the fact that MyoD is present throughout the differentiation process. MyoD is post-translationally modified by phosphorylation, ubiquitination, and acetylation. Here, we have employed a model system in which MyoD and its non-acetylatable version were inducibly expressed in mouse embryonic fibroblasts derived from mice to investigate how MyoD acetylation may contribute to differential gene activation. **Keywords: Time-Series** **Overall design:** Mouse embryos fibroblasts (MEFs) obtained from MyoD-/-/Myf5-/- animals will be transduced with retroviruses expressing a estrogen receptor hormone binding domain fused to either mouse MyoD wild type (ER-MyoD wt) or MyoD bearing three point mutations at lysine residues 99, 102, and 104 that render it no longer acetylatable (ER-MyoD RRR). A retrovirus without the ER-MyoD insert was also employed as negative control.</p> Aim 2. We will compare genome-wide expression profiling of MEFs transduced with either ER-MyoD wt or ER-MyoD RRR cultured in the presence of a medium that promotes skeletal muscle differentiation (DM) supplemented with beta-estradiol for 0, 6, 12, and 24 hours, respectively.

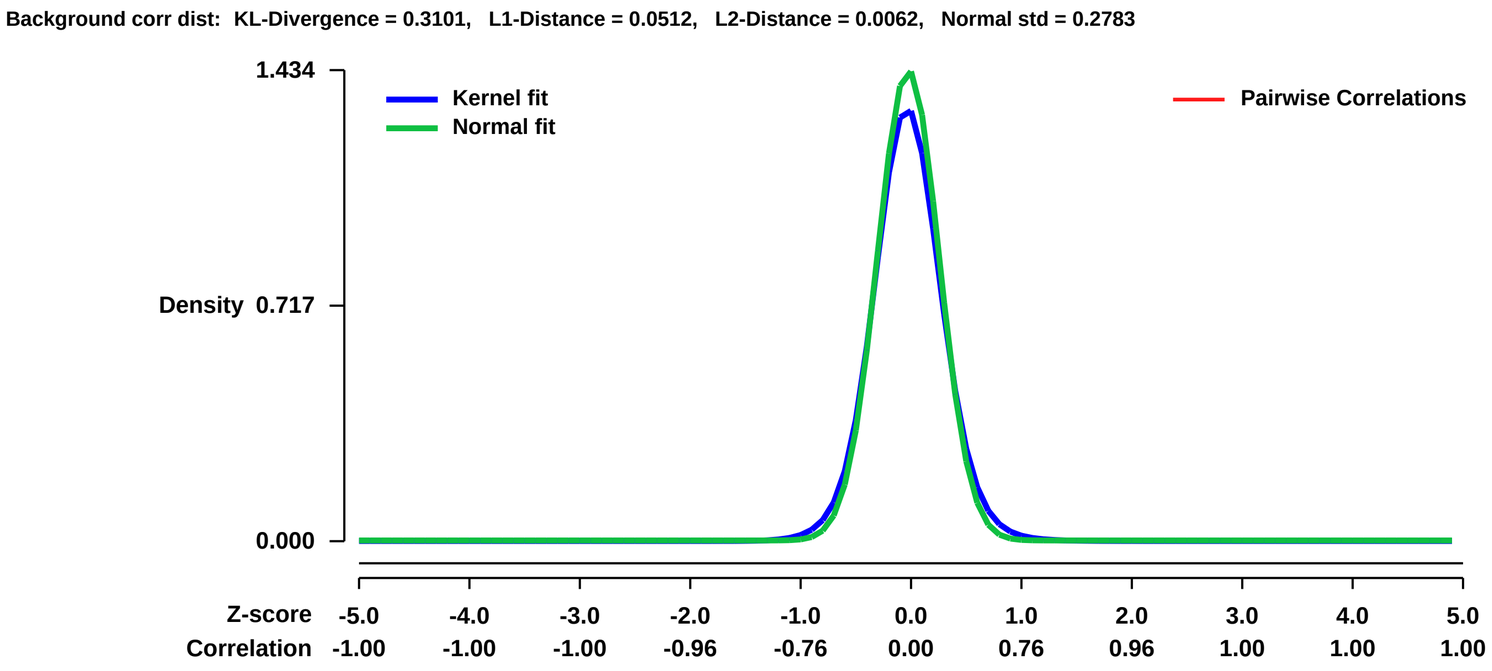

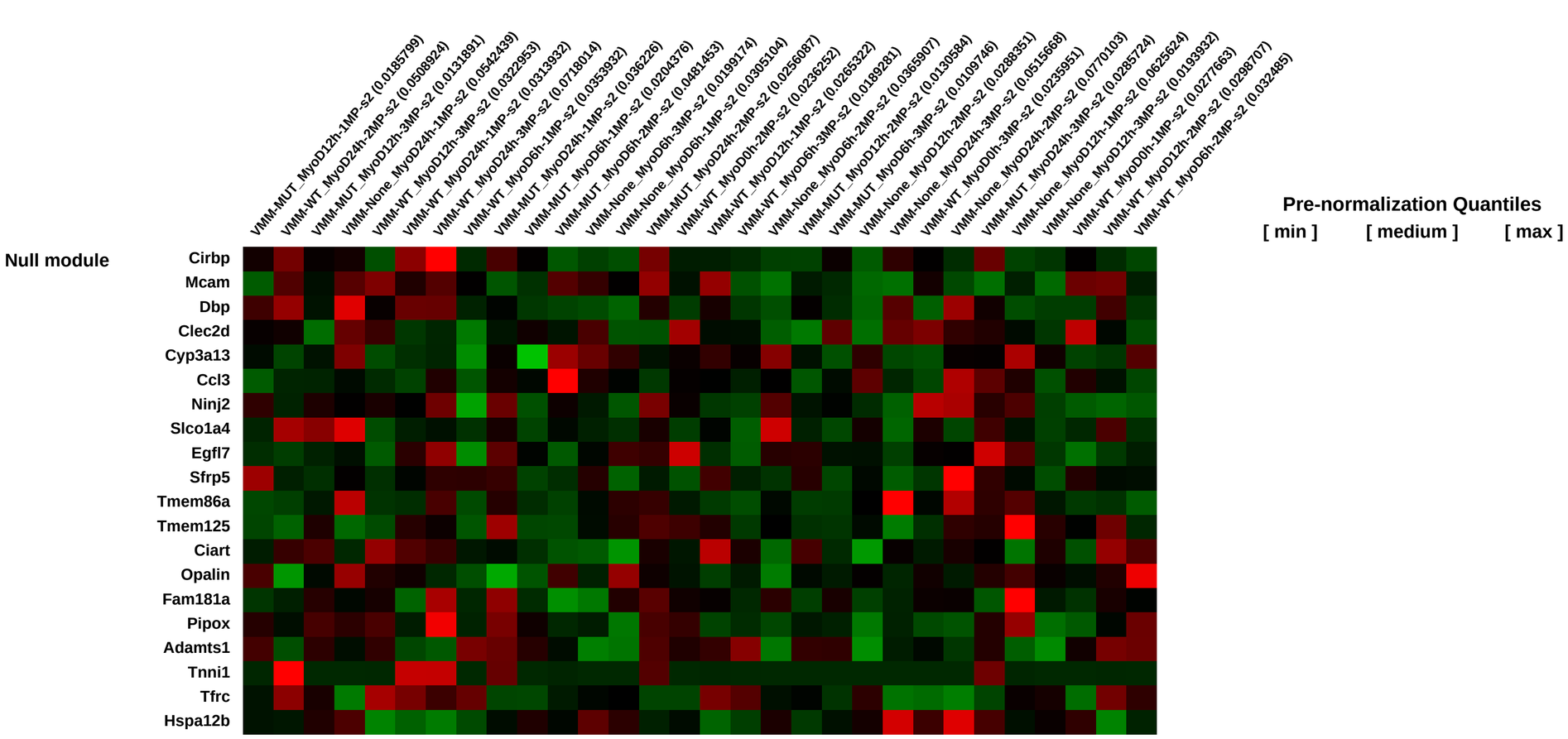

GEO Series "GSE36336" Expression Profiles

Num of samples in this series: 6

Scale of expression profile Z-scores

-3.0 -2.0 -1.0 0.0 1.0 2.0 3.0

GEO Link:	http://www.ncbi.nlm.nih.gov/geo/query/acc.cgi?acc=GSE36336
Status:	Public on Apr 25 2014
Title:	Expression data from kidneys of diabetic WT and T3-/- mice
Organism:	Mus musculus
Experiment type:	Expression profiling by array
Platform:	GPL1261
Pubmed ID:	
Summary & Design:	**Summary:** Activation of A Disintegrin and A Metalloprotease Domain17 (ADAM17) is involved in nephropathy, but the role of this metalloprotease and its inhibitor TIMP3 in diabetic kidney disease is unclear. We used microarray profiling to find genes differentially expressed in the 2 genotypes which could explain the more severe diabetic kidney disease features observed in T3-/- mice compared to the WT littermates. **Overall design:** Total RNA was extracted from 3 WT and 3 Timp3-/- diabetic kidneys

Background corr dist: KL-Divergence = 0.0281, L1-Distance = 0.0112, L2-Distance = 0.0001, Normal std = 0.6704

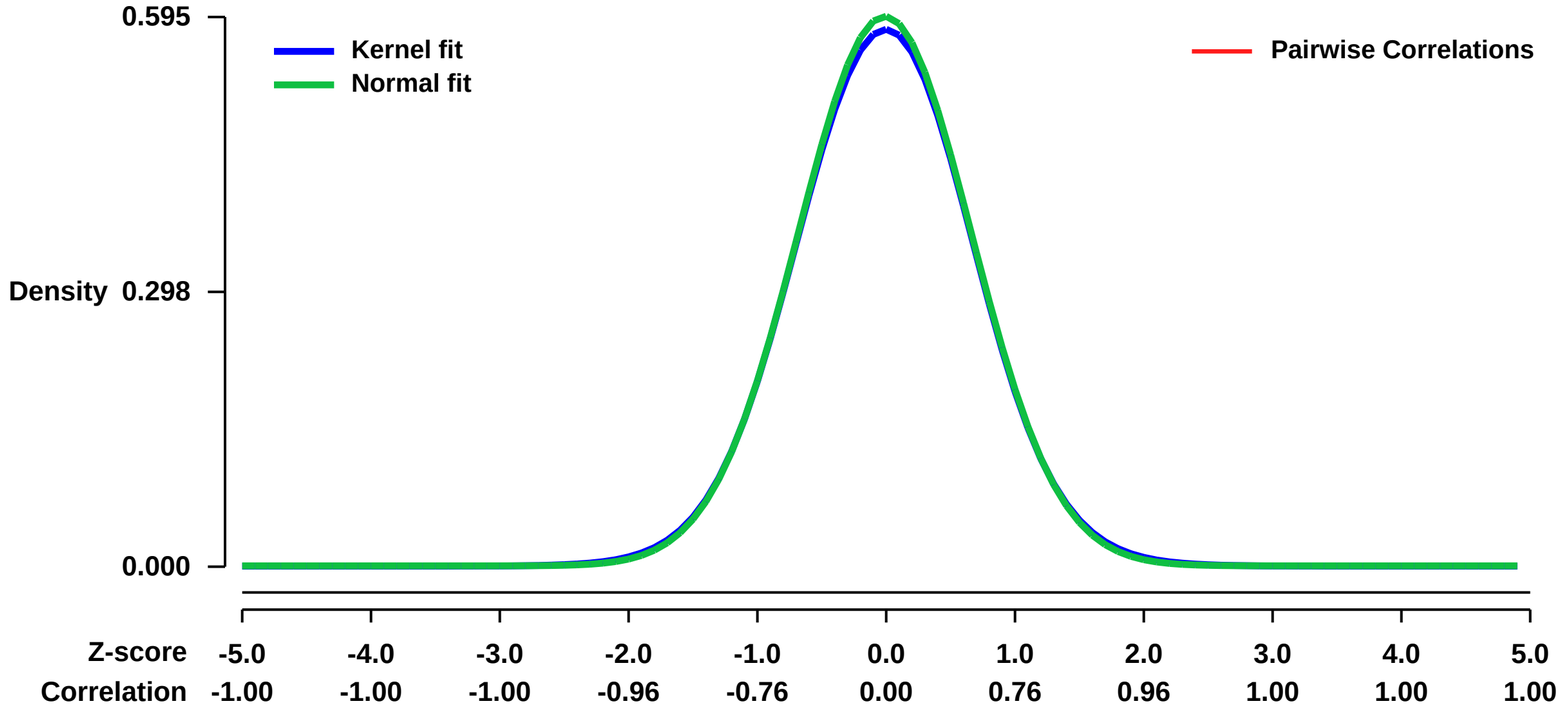

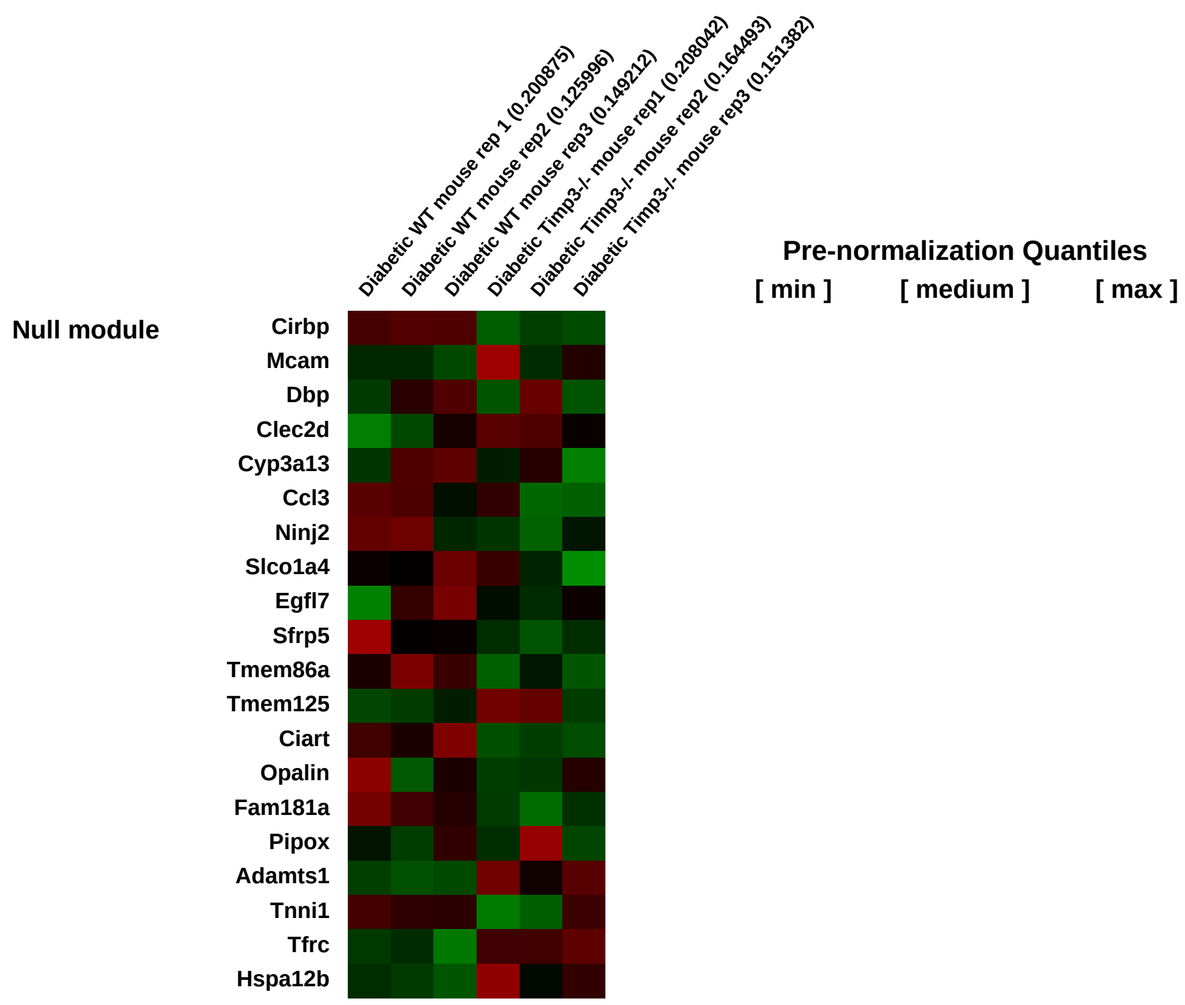

GEO Series "GSE2557" Expression Profiles

Num of samples in this series: 6

Scale of expression profile Z-scores

-3.0 -2.0 -1.0 0.0 1.0 2.0 3.0

GEO Link:	http://www.ncbi.nlm.nih.gov/geo/query/acc.cgi?acc=GSE2557
Status:	Public on Jan 01 2006
Title:	Transcriptome Profiling of High Glucose and Glucosamine-Induced Mouse Mesangial Cells
Organism:	Mus musculus
Experiment type:	Expression profiling by array
Platform:	GPL1261
Pubmed ID:	17178593

Summary & Design:

Summary:
The renal mesangial cells play an important role in the development of diabetic glomerulosclerosis and renal failure. We have previously demonstrated some of the effects of high glucose are mediated via the hexosamine biosynthesis pathway (HBP) in which fructose-6-phosphate is converted to glucosamine-6-phosphate by the rate-limiting enzyme glutamine:fructose-6-phosphate amidotransferase (GFAT). Using Affymetrix murine expression U430 2.0 chips, we examined the global effects of high glucose (HG) and glucosamine (GlcN) on the transcriptomes of a mouse mesangial cell line (MES-13). Of the 34,000 genes on the chip, ~55-60% genes are detected in MES-13 cells. HG induces the expression of ~369 genes at >2-fold where 263 genes are up and 106 genes down regulated. Similarly, GlcN increases the expression of 120 genes and decreases 94 genes. Seventy-two genes are commonly regulated by HG and GlcN, in which 33 genes are up and 39 genes are down. The differential expressions of several genes found in the microarray are also confirmed by quantitative PCR. Significant pathways co-modulated by HG and GlcN are the thioredoxin system (a 20-fold increase in thioredoxin interacting protein expression), endoplasmic reticulum (ER) stress, extracellular matrix and interferon-inducible genes. Furthermore, HG and GlcN target various intracellular pathways including the mitogen-activated protein kinase, TOLL-like receptor, fructose and mannose metabolism, and the biosynthesis of steroids and N-glycans. We conclude from this microarray data and other experimental results that the HBP mediates several effects of high glucose on mesangial cell metabolism, which promotes ER stress, oxidative stress and the interferon-inducible gene expression to cause cell cycle arrest, ECM gene expression and apoptosis.

Cell culture: Stable murine mesangial (MES-13) cells transformed with non-capsid-forming SV-40 virus were obtained from the ATCC, Manassas, VA. These cells display a differentiated mesangial cell phenotype including the typical spindle-like appearance, positive staining for vimentin and desmin, and contraction in response to ANG II and expression of AT1 receptor. The cells were maintained in DMEM and F-12 Nutrient Mixture (Ham's) (4:1 ratio) (GIBCO BRL, Gaithersburg, MD) containing a normal D-glucose concentration of 5.5 mmol/L, 2% FCS, 100 ´µg/ml streptomycin, 100 U/ml penicillin, and 2 mmol/L glutamine (26). The cells were incubated in a humidified incubator of 5% CO2 at 37 ´°C and routinely passaged at confluence every 3 days by trypsinization using 10-cm culture dishes. Approximately 50% confluent monolayers were starved in the above medium without FCS for 1 day and then incubated in the starvation medium with the desired concentrations of glucose and GlcN for 48h (LG, 5.5 mM; HG, 25 mM and GlcN, 1.5 mM + LG).

Total RNA isolation, cDNA and cRNA synthesis and genechip hybridization: Total RNA was isolated using Trizol reagent (Life Technologies, Inc., Massachusetts). cDNA and cRNA synthesis, genechip hybridization, and scanning of the Affymetrix murine expression U430 2.0 chips (the Affymetrix U430 2.0 chip contains 39,000 transcripts targeted at 34,000 well characterized genes) were performed according to the manufacturer's protocol (Affymetrix, Santa Clara, CA). Briefly, 5 mg of RNA (from LG, HG and GlcN treated MES-13 cells) was converted into double-stranded cDNA by reverse transcription using a cDNA synthesis kit (SuperScript Choice, Life Technologies, Inc., MA) with an oligo(dT) 24 primer containing a T7 RNA polymerase promoter site added 3' of the poly(T) (Genset, La Jolla, CA). After second-strand synthesis, labeled cRNA was generated from the cDNA sample by an in vitro transcription reaction supplemented with biotin-11-CTP and biotin-16-UTP (Enzo, Farmingdale, NY). The labeled-cRNAs were purified in RNeasy spin columns (Qiagen, Valencia, CA). Fifteen mg of each cRNA was fragmented at 94 ´°C for 35 min in a fragmentation buffer (40 mM Tris acetate, pH 8.1, 100 mM potassium acetate, 30 mM magnesium acetate). These cRNA fragments were then used to prepare 300 ml of hybridization mixture (100 mM MES, 0.1 mg/ml herring sperm DNA (Promega), 1M sodium chloride, 10 mM Tris, pH 7.6, 0.005% Triton X-100). The solution was equilibrated at 45 ´°C for 5 min and clarified by centrifugation (14,000 x g) at room temperature for 5 min. Aliquots of each sample (10 mg of cRNA in 200 ml of the mater mix) were hybridized to GeneChip Mouse Genome U430 2.0 Array at 45 ´°C for 16 h in a rotisserie oven set at 60 rpm. After the overnight hybridization, the chips were washed with a non-stringent wash buffer (6x saline/sodium phosphate/EDTA) at 25 ´°C, followed by a stringent wash buffer (100 mM MES (pH 6.7), 0.1 M NaCl, 0.01% Tween-20) at 50 ´°C. The GeneChips were then stained with streptavidin-phycoerythrin (Molecular Probe), washed with 6x saline/sodium phosphate/EDTA, incubated with biotinylated anti-streptavidin IgG, followed by a second staining with streptavidin-phycoerythrin. Finally, a third wash with 6x saline/sodium phosphate/EDTA was performed using the GeneChip Fluidics Station 450. The arrays were then scanned in a GeneChip Scanner 3000 (Affymetrix). Each experiment was repeated twice.

Microarray Data analysis: The chips were read with Affymetrix GCOS v1.2, and the probe intensity files were modeled with DChip 1.3 (Harvard School of Public Health) in both PM-only and PM-MM modes. Consensus differentially regulated genes were initially derived from repeat experiments on the bases of a 90% CI of greater than 2-fold change in expression and with p<0.05 of error in paired t-test across repeats. This was further validated through modeling of variance between sample groups (one-way ANOVA) conducted in GeneSpring 6 (Silicon Genetix). The consensus gene-set was clustered in DChip and GeneSpring 6.0, with OntoExpress (Wayne State University) to explore ontological associations. Further ontological and pathway analyses were conducted with the GeneGo software and NIH's DAVID bioinformatics programs (http://appls.niaid.nih.gov/david).

Keywords = glucose

Keywords = glucosamine

Keywords = mesangial cells

Keywords = hexosamine

Keywords: repeat sample

Overall design:

Background corr dist: KL-Divergence = 0.0110, L1-Distance = 0.0200, L2-Distance = 0.0005, Normal std = 0.8500

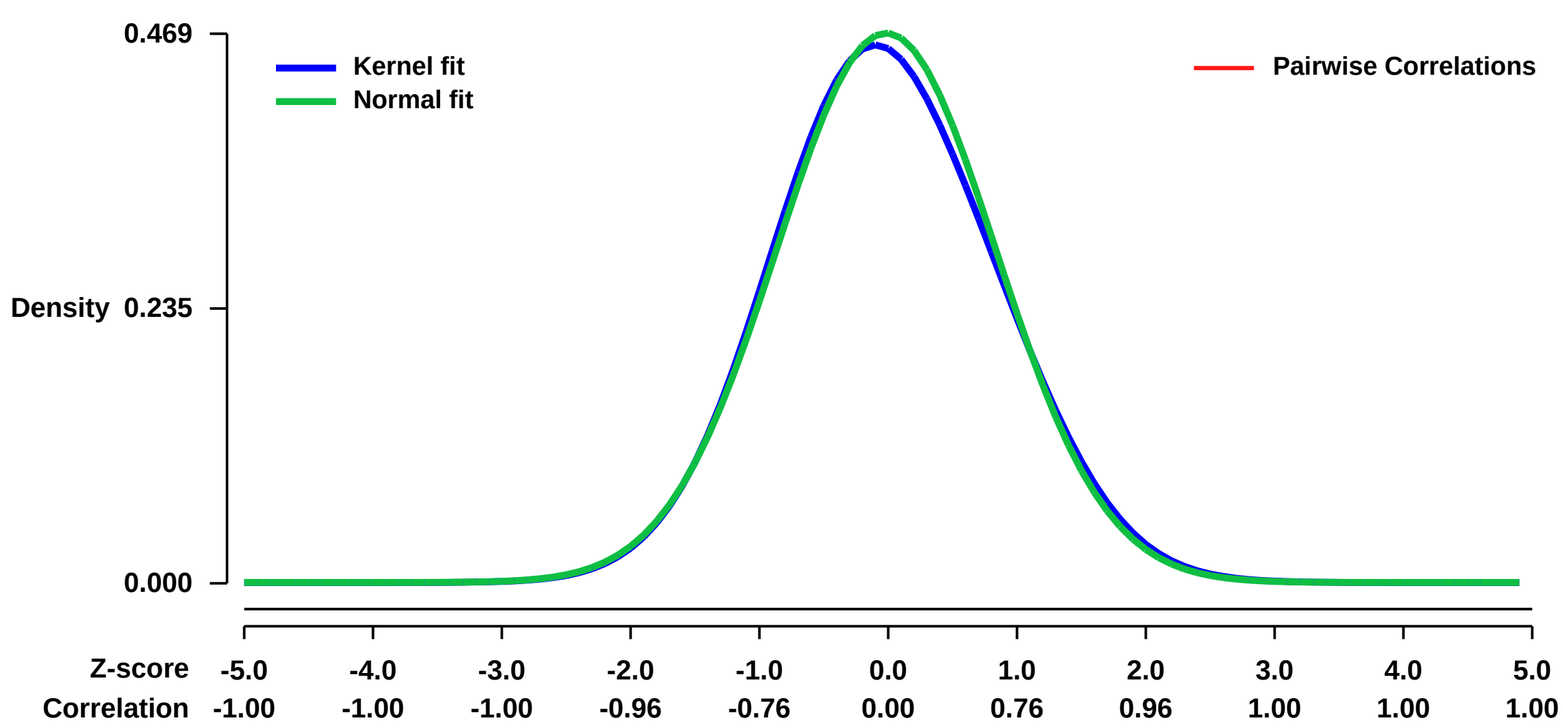

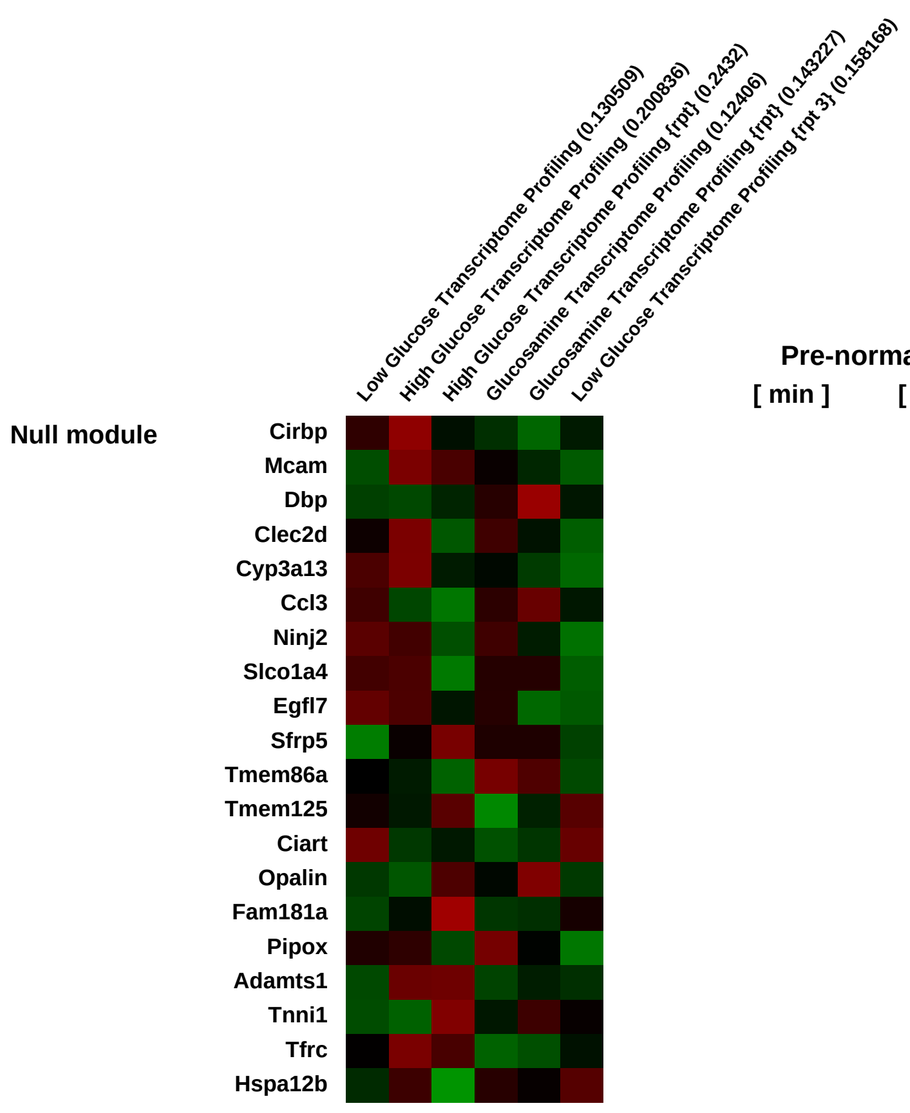

GEO Series "GSE32334" Expression Profiles

Num of samples in this series: 19

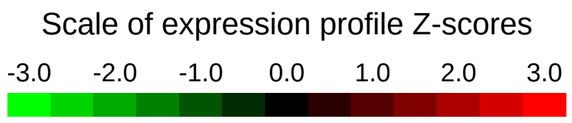

GEO Link:	http://www.ncbi.nlm.nih.gov/geo/query/acc.cgi?acc=GSE32334
Status:	Public on Feb 16 2012
Title:	Developmental timecourse of mouse ocular lens and whole embryo control
Organism:	Mus musculus
Experiment type:	Expression profiling by array
Platform:	GPL1261
Pubmed ID:	22323457
Summary & Design:	**Summary:** Identification of genes involved in ocular birth defects remains a challenge. To facilitate the identification of genes associated with cataract, we developed iSyTE (integrated Systems Tool for Eye gene discovery; http://bioinformatics.udel.edu/Research/iSyTE). iSyTE contains microarray gene expression profiles of the mouse embryonic lens as it transitions from the stage of placode invagination to that of vesicle formation. We identified differentially regulated genes by comparing lens microarray profiles to those representing whole embryonic body (WB) without ocular tissue. These were then utilized to generate a ranked list of lens-genes enrichment, which can be viewed as iSyTE tracks in the UCSC Genome browser to aid identification of genes with lens function. **Overall design:** We microdissected embryonic lens from mice at E10.5, E11.5, and E12.5 (triplicate at each time point). To have a proper control, we also generated gene expression profiles of whole embryonic body (WB) at these time points. For comparative analysis, we also generated gene expression profiles of E13.5 tooth germs tissues, and matched WB. These profiles are used to identify lens and tooth specific gene expression enrichment at these embryonic time points. This dataset is then used to prioritize analysis of candidate cataract associated genes.

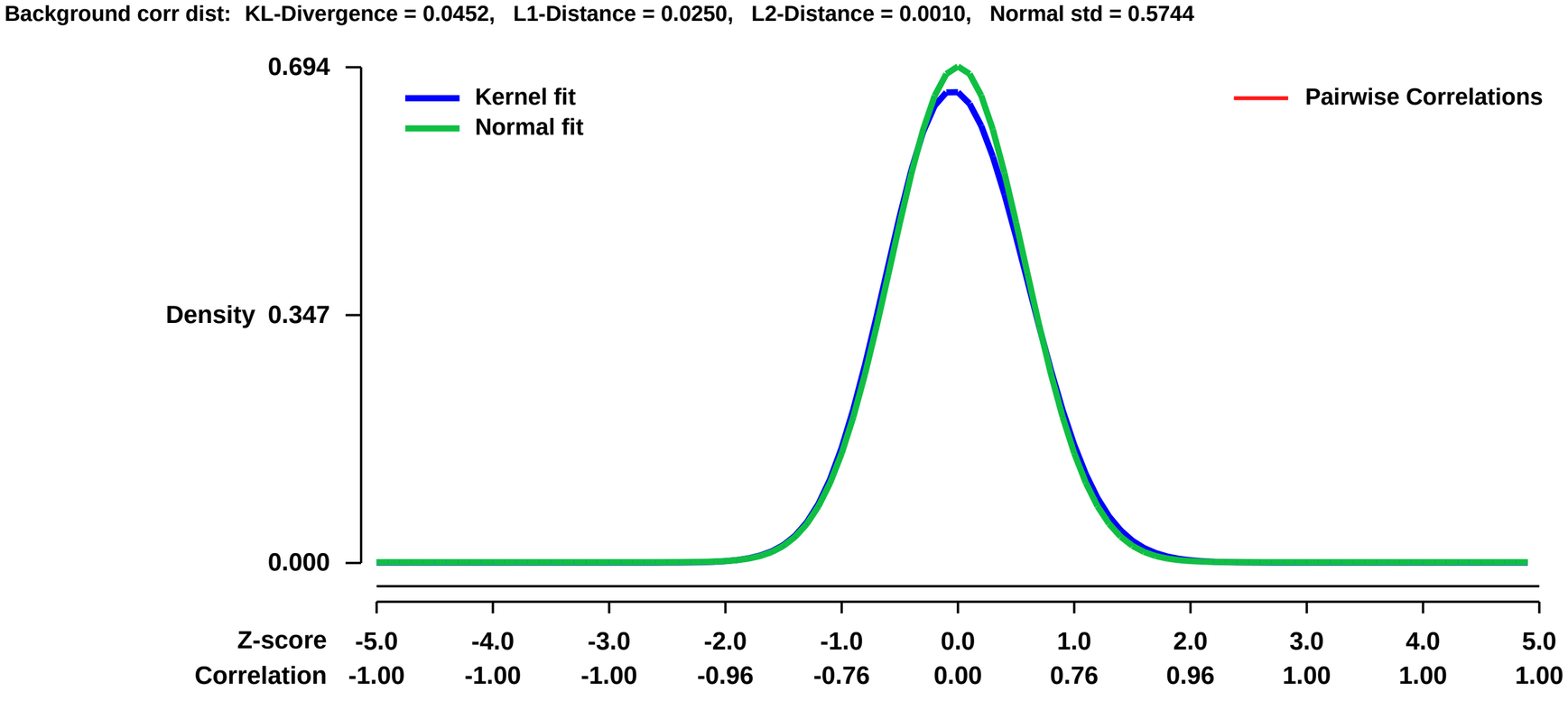

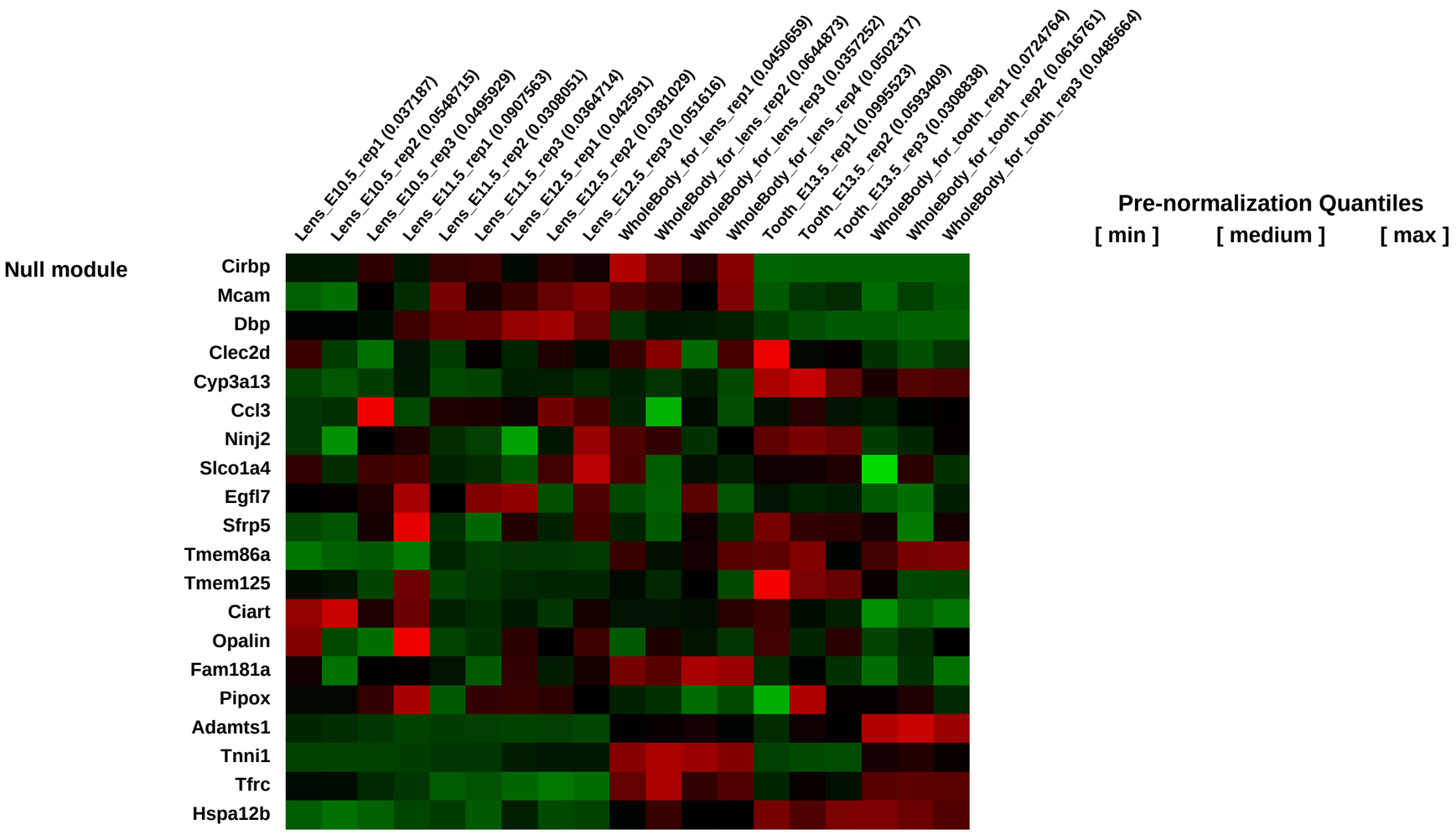

GEO Series "GSE32015" Expression Profiles

Num of samples in this series: 51

Scale of expression profile Z-scores

-3.0 -2.0 -1.0 0.0 1.0 2.0 3.0

GEO Link:	http://www.ncbi.nlm.nih.gov/geo/query/acc.cgi?acc=GSE32015
Status:	Public on Dec 03 2012
Title:	Expression data from inducible ES stable cell lines
Organism:	Mus musculus
Experiment type:	Expression profiling by array
Platform:	GPL1261
Pubmed ID:	23180766
Summary & Design:	**Summary:** In order to identify the effects of the induction of the gene of interest on the mouse ES transcriptome, we performed Affymetrix Gene-Chip hybridization experiments for the different inducible cell lines Transcriptome analysis of the inducible transgenic mouse ES cell lines **Overall design:** For the analysis on the different inducible cell lines, total RNA was extracted from three biological replicates grown in medium deprived of Tetracycline for 17 and 24 hours; RNA extracted from un-induced clones was used as control. Total RNA extracted from parental cell line EBRTcH3 (EB3) was used as additional control.

Background corr dist: KL-Divergence = 0.3818, L1-Distance = 0.0747, L2-Distance = 0.0167, Normal std = 0.2525

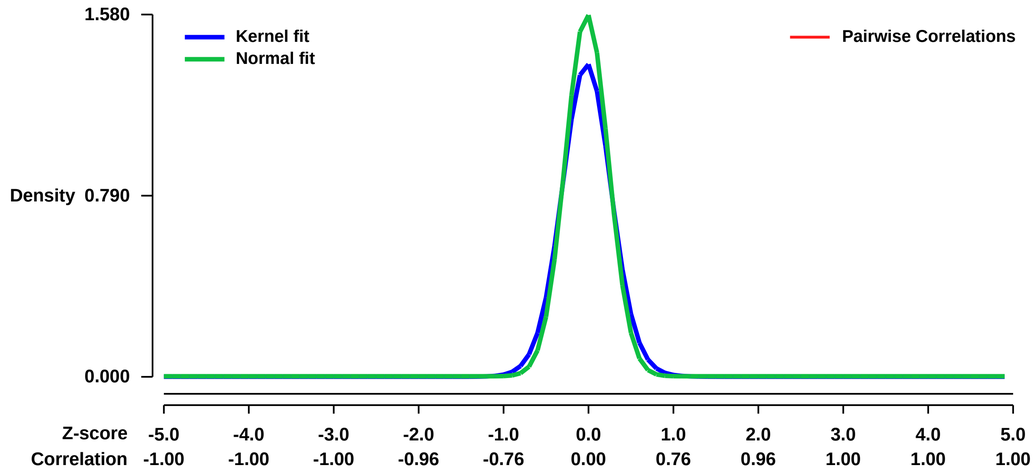

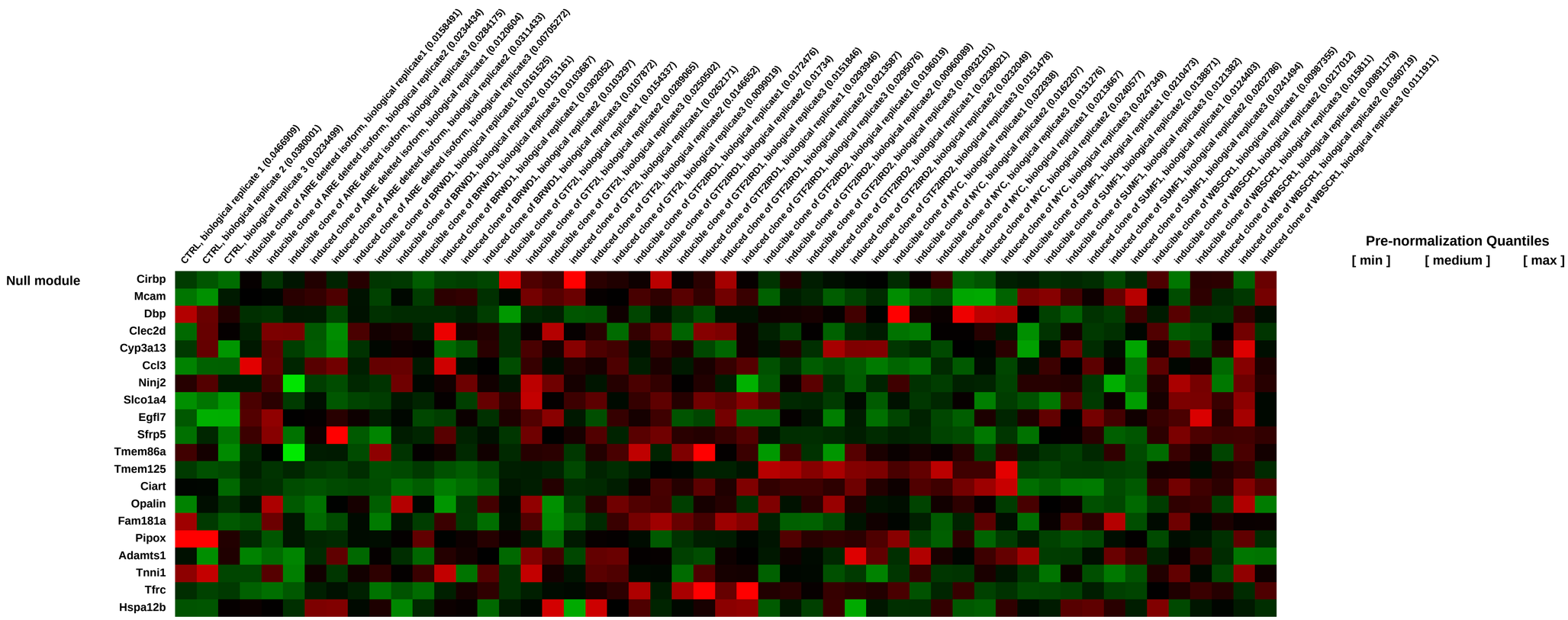

GEO Series "GSE21263" Expression Profiles

Num of samples in this series: 68

Scale of expression profile Z-scores

-3.0 -2.0 -1.0 0.0 1.0 2.0 3.0

GEO Link: http://www.ncbi.nlm.nih.gov/geo/query/acc.cgi?acc=GSE21263

Status: Public on Dec 22 2010

Title: Network Analysis of Skin Tumor Progression Identifies a Rewired Genetic Architecture Affecting Inflammation and Tumor Susceptibility (papillomas)

Organism: Mus musculus

Experiment type: Expression profiling by array

Platform: GPL1261

Pubmed ID: 21244661

Summary & Design:

Summary:
Germline polymorphisms influence gene expression networks in normal mammalian tissues. Analysis of this genetic architecture can identify single genes and whole pathways that influence to complex traits including inflammation and cancer susceptibility. Changes in the genetic architecture during the development of benign and malignant tumours have not been investigated. Here, we document major changes in germline control of gene expression during skin tumour development as a consequence of cell selection, somatic genetic events, and changes in tumour microenvironment. Immune response genes such as Interleukin 18 and Granzyme E are under germline control in tumours but not in normal skin. Gene expression networks linked to tumour susceptibility and hair follicle stem cell markers in normal skin undergo significant reorganization during tumour progression. Our data highlight opposing roles of Interleukin-1 signaling networks in tumour susceptibility and tumour progression and have implications for the development of chemopreventive strategies to reduce cancer incidence.

Overall design:
Skin tumors were induced on dorsal back skin from a Mus spretus / Mus musculus backcross ([SPRET/Ei X FVB/N] X FVB/N) mice by treatment of dorsal back skin with dimethyl benzanthracene (DMBA) and tetradecanoyl-phorbol acetate (TPA). This treatment induced multiple benign papillomas as well as malignant squamous cell carcinomas (SCC) and spindle cell carcinomas. Gene expression analysis was performed on mRNA extracted from 68 papillomas: two papillomas from each of 31 FVBBX mice and a single papilloma from six additional FVBBX mice. Papillomas were harvested when mice were sacrificed due to presence of a carcinoma or termination of the experiment.

Background corr dist: KL-Divergence = 0.4519, L1-Distance = 0.0925, L2-Distance = 0.0279, Normal std = 0.2347

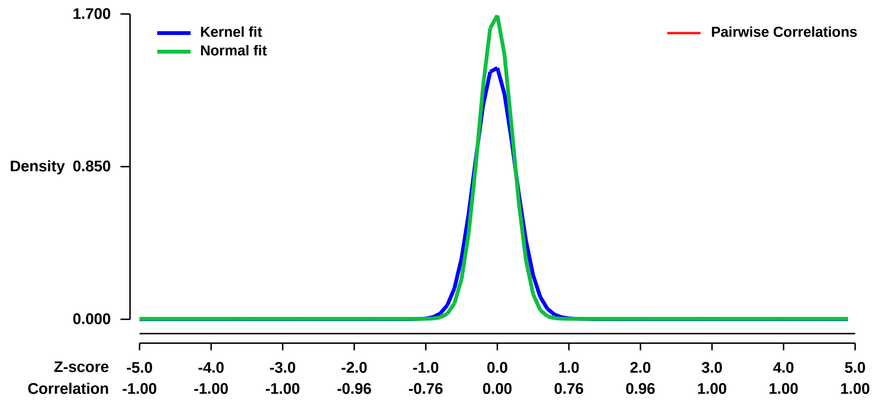

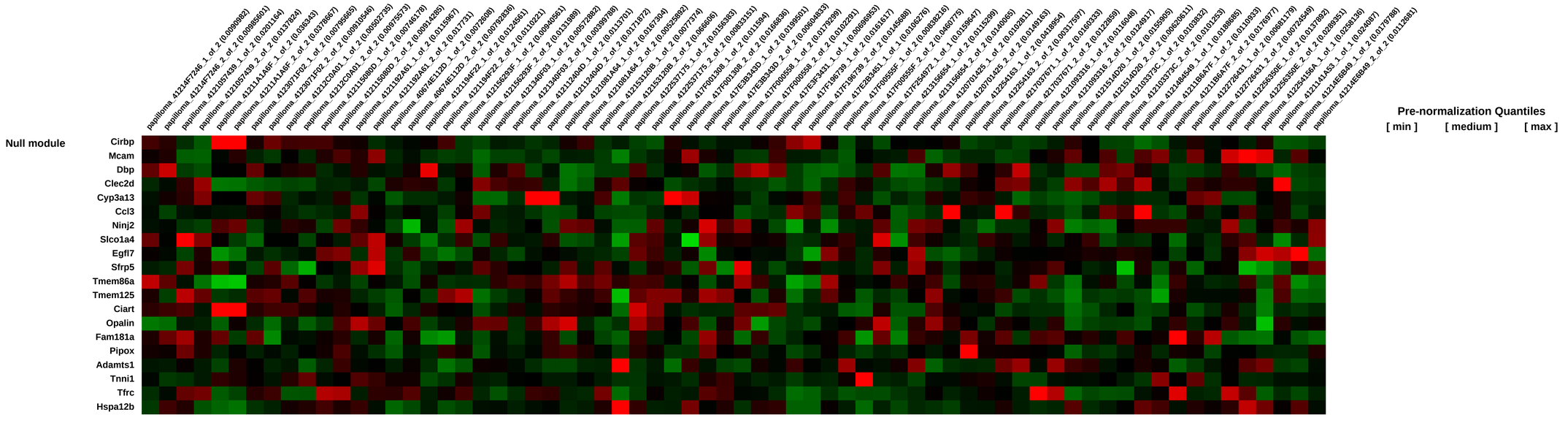

GEO Series "GSE7196" Expression Profiles

Num of samples in this series: 6

Scale of expression profile Z-scores

-3.0 -2.0 -1.0 0.0 1.0 2.0 3.0

GEO Link:	http://www.ncbi.nlm.nih.gov/geo/query/acc.cgi?acc=GSE7196
Status:	Public on Mar 08 2007
Title:	Differential gene expression between WT and ERRa-null hearts
Organism:	Mus musculus
Experiment type:	Expression profiling by array
Platform:	GPL1261
Pubmed ID:	17488637
Summary & Design:	**Summary:** Total RNA was isolated from 3 WT and 3 ERRa null hearts and independent hybridizations were performed using MOE430 2.0 microarrays. Expression profiling was conducted to determine changes in gene expression in hearts lacking ERRa. The expression of genes involved in heart and muscle development, muscle contraction, lipid metabolism, OxPhos, protein metabolism and transcription were affected by the loss of ERRa. **Keywords: microarray and genetic modification** **Overall design:** 3 hearts from WT and 3 hearts from ERRa-null mice were used in the study. The expression of genes in the ERRa KO hearts were compared to the reference WT hearts.

Background corr dist: KL-Divergence = 0.0468, L1-Distance = 0.0226, L2-Distance = 0.0006, Normal std = 0.5889

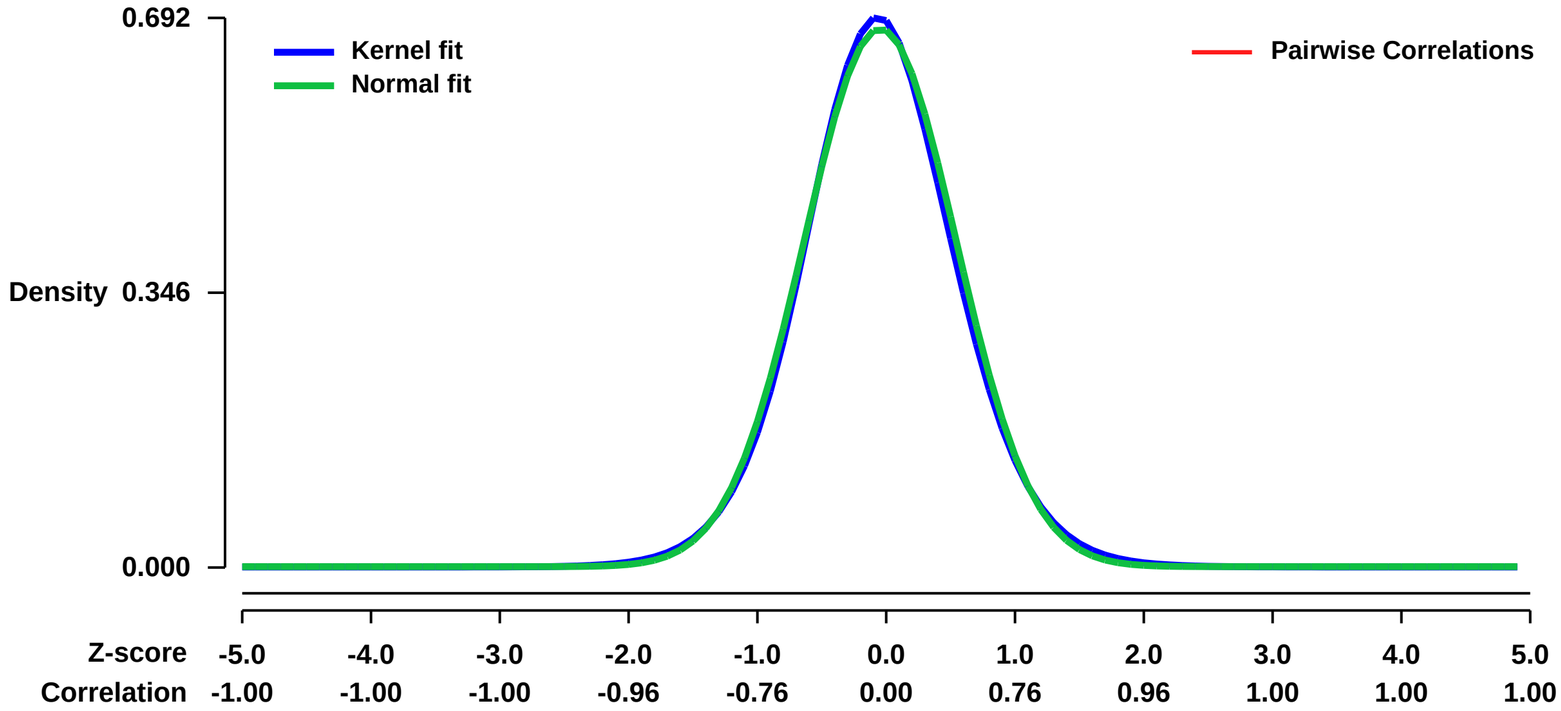

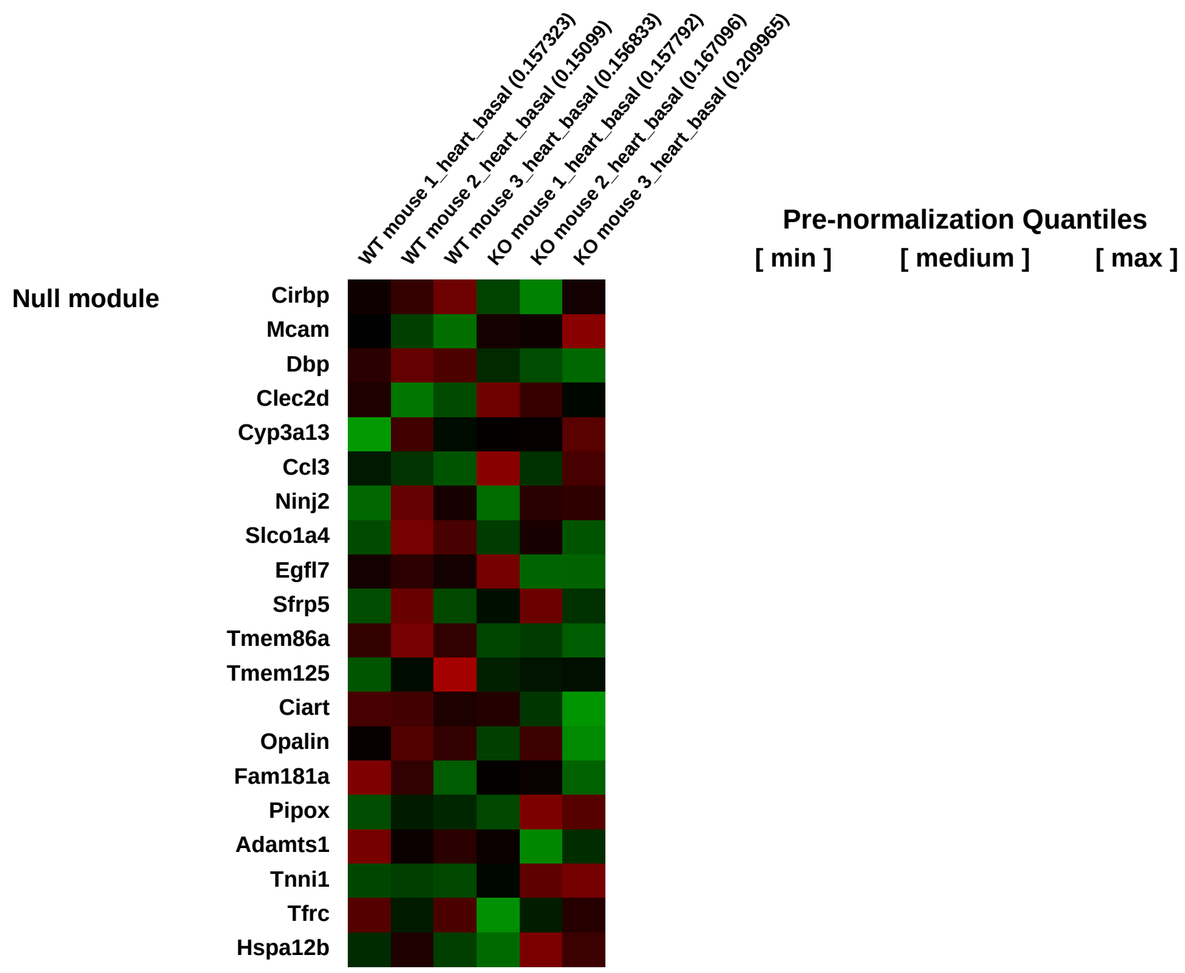

GEO Series "GSE9760" Expression Profiles

Num of samples in this series: 12

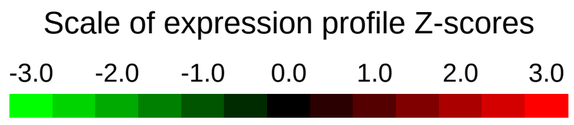

GEO Link:	http://www.ncbi.nlm.nih.gov/geo/query/acc.cgi?acc=GSE9760
Status:	Public on Dec 04 2007
Title:	Embryonic stem cells with expanded CAG repeats (lorin-affy-mouse-501743)
Organism:	Mus musculus
Experiment type:	Expression profiling by array
Platform:	GPL1261
Pubmed ID:	
Summary & Design:	**Summary:** Huntington´ s disease (HD) is a devastating neurodegenerative disease, with out effective treatment. Despite significant advances, our understanding of how an expanded CAG repeat in the amino terminus of the large ubiquitously expressed HD gene product remains incomplete. Augmented adult neurogenesis in response to acute and chronic injury, including Huntington´ s disease, has been demonstrated, but its role development, disease, and recovery is largely unknown, as are the factors controlling it. The HD gene product, huntingtin (htt) is know to interact with a number of transcription factors which subsequently influence gene expression. Understanding the factors involved in controlling neurogenesis in response to disease would bridge a significant knowledge gap and have tremendous therapeutic potential. We propose to identify transcripts responsible for CAG repeat facilitated neurogenesis. Our hypothesis is that expanded CAG repeats in the Huntington´ s disease gene facilitates neurogenesis by altering transcription of genes critical in neurogenesis. We have developed a model in which mouse embryonic stem cells (ESC) with expanded CAG repeats have facilitated neurogenesis. In this model more ESC with expanded CAG repeats transition to neuronal precursors and then develop into mature neurons more rapidly than control ESC. We propose to compare the gene expression profiles between ESC with expanded CAG repeats and control ESCs on days 4 and 6 of neuronal differentiation. Initial studies indicate that key transcriptional differences are occurring at these time points. Control ECS and a an ESC line with150 CAG repeats will be differentiated in triplicate, and RNA isolated form each replicate. It is anticipated that comparison of gene expression between the control and CAG repeat lines at each time point will identify transcripts involved in CAG repeat facilitated neurogenesis. Observed differences at day 4 may be more relevant to the transition from ESC to neuronal precursor whereas differences at day 6 may be more relevant to the neuronal precursor to neuron transition. Keywords: time-course Overall design:

Background corr dist: KL-Divergence = 0.0981, L1-Distance = 0.0297, L2-Distance = 0.0012, Normal std = 0.4524

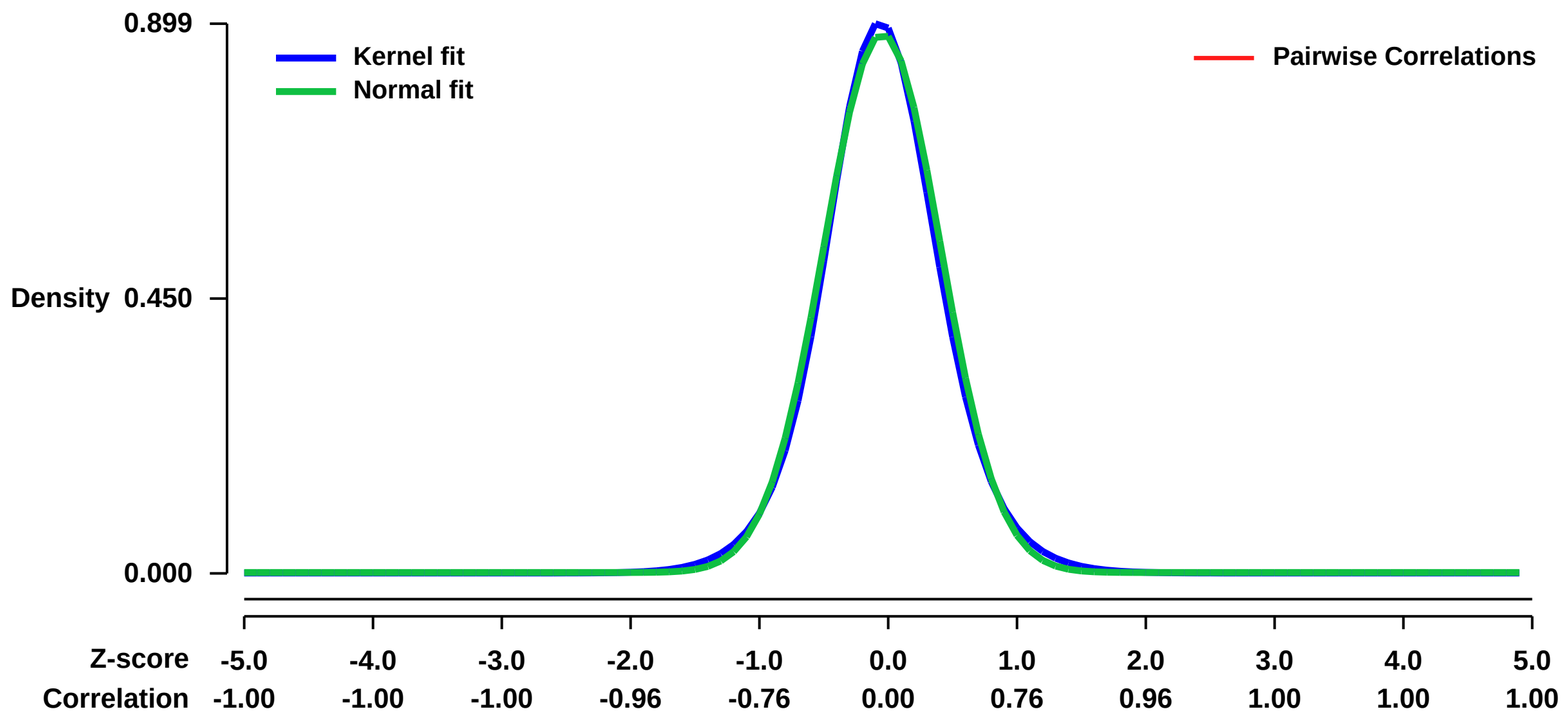

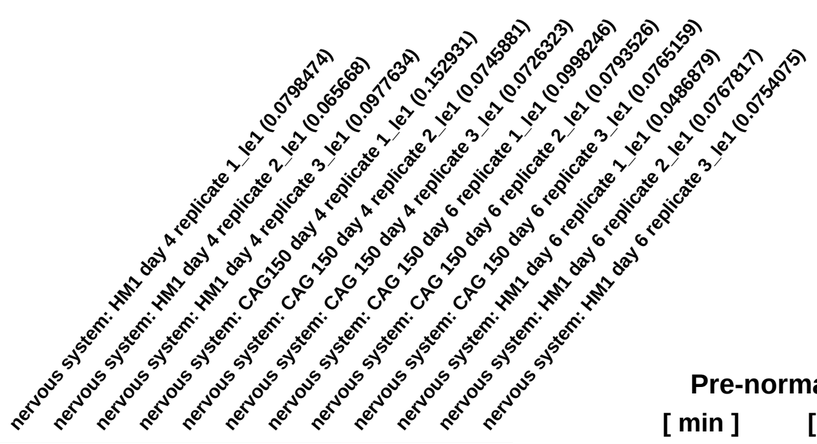

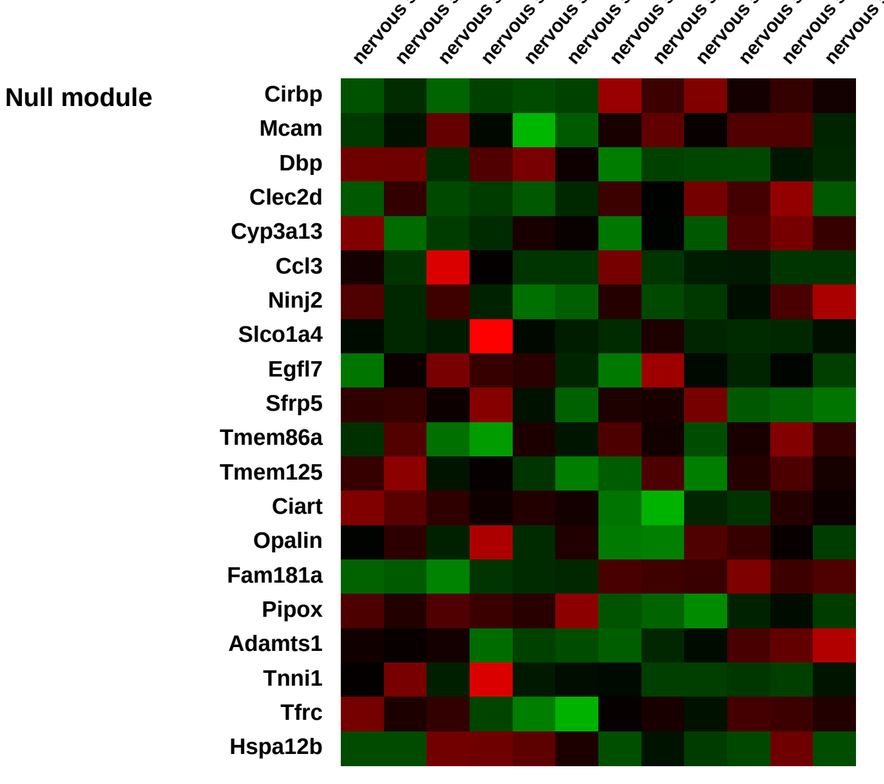

GEO Series "GSE24031" Expression Profiles

Num of samples in this series: 18

Scale of expression profile Z-scores

-3.0 -2.0 -1.0 0.0 1.0 2.0 3.0

GEO Link:	http://www.ncbi.nlm.nih.gov/geo/query/acc.cgi?acc=GSE24031
Status:	Public on Sep 09 2010
Title:	Adipose tissue dysfunction signals progression of hepatic steatosis towards nonalcoholic steatohepatitis in C57Bl/6 mice
Organism:	Mus musculus
Experiment type:	Expression profiling by array
Platform:	GPL1261
Pubmed ID:	20858684
Summary & Design:	**Summary:** **Objective: Nonalcoholic fatty liver disease (NAFLD) is linked to obesity and diabetes, suggesting an important role of adipose tissue in the pathogenesis of NAFLD. Here we aim to investigate the interaction between adipose tissue and liver in NAFLD, and identify potential early plasma markers that predict NASH. Research Design and Methods: C57Bl/6 mice were chronically fed a high fat diet to induce NAFLD and compared with mice fed low fat diet. Extensive histological and phenotypical analyses coupled with a time-course study of plasma proteins using multiplex assay was performed. Results: Mice exhibited pronounced heterogeneity in liver histological scoring, leading to classification into 4 subgroups: LF-low (LFL) responders displaying normal liver morphology, LF-high (LFH) responders showing benign hepatic steatosis, HF-low (HFL) responders displaying pre-NASH with macrovesicular lipid droplets, and HF-high (HFH) responders exhibiting overt NASH characterized by ballooning of hepatocytes, presence of Mallory bodies, and activated inflammatory cells. Compared to HFL responders, HFH mice gained weight more rapidly and exhibited adipose tissue dysfunction characterized by decreased final fat mass, enhanced macrophage infiltration and inflammation, and adipose tissue remodelling. Plasma haptoglobin, IL-1¸†, TIMP-1, adiponectin and leptin were significantly changed in HFH mice. Multivariate analysis indicated that in addition to leptin, plasma CRP, haptoglobin, eotaxin and MIP-1¸– early in the intervention were positively associated with liver triglycerides. Intermediate prognostic markers of liver triglycerides included IL-18, IL-1¸†, MIP-1¸‡ and MIP-2, whereas insulin, TIMP-1, GCP-2 and MPO emerged as late markers. Conclusions: Our data support the existence of a tight relationship between adipose tissue dysfunction and NASH pathogenesis and point to several novel potential predictive biomarkers for NASH.** **Keywords: Expression profiling by array** **Overall design:** **Male wildtype C57Bl/6 mice were fed LFD or HFD for 21 weeks. Mice were divided into 4 groups based on liver histology.**

Background corr dist: KL-Divergence = 0.2859, L1-Distance = 0.0624, L2-Distance = 0.0104, Normal std = 0.2854

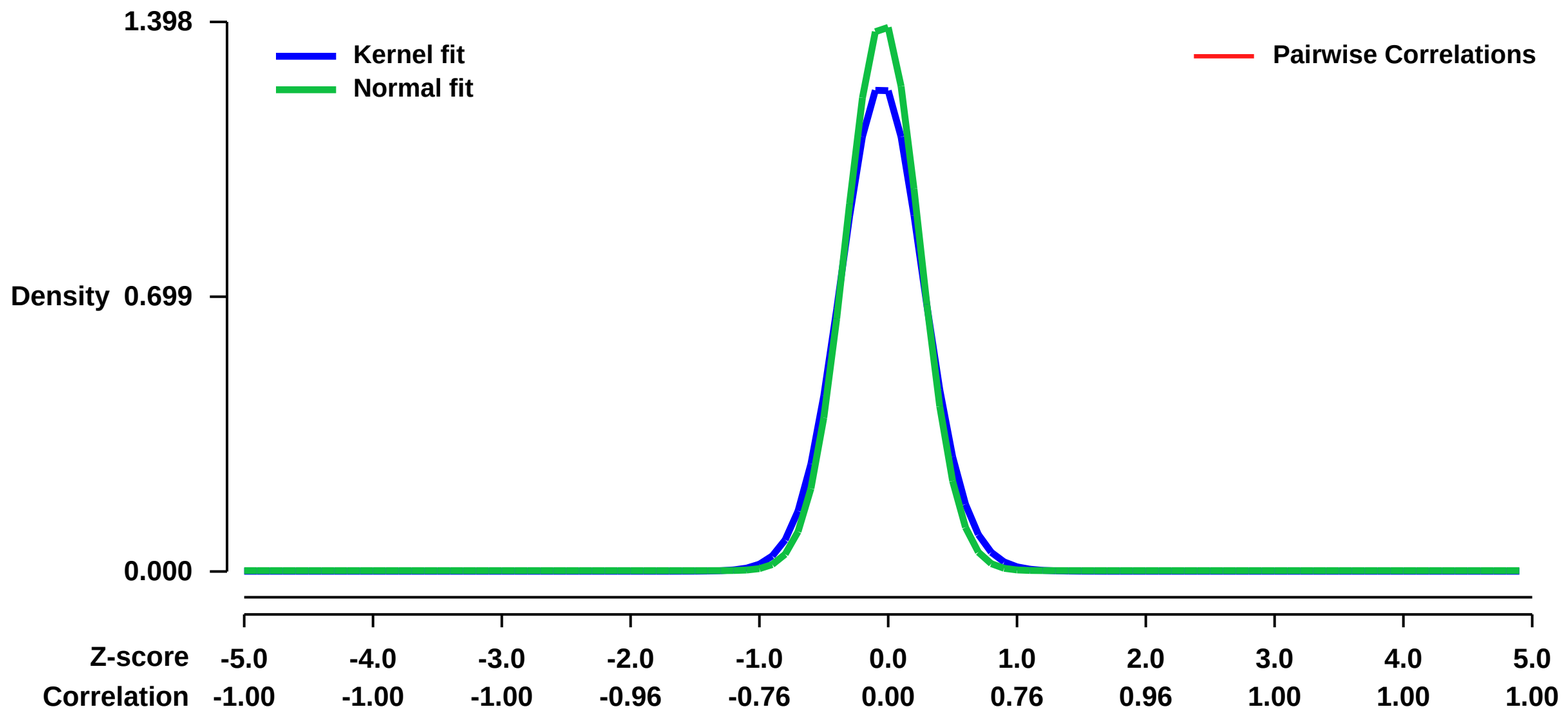

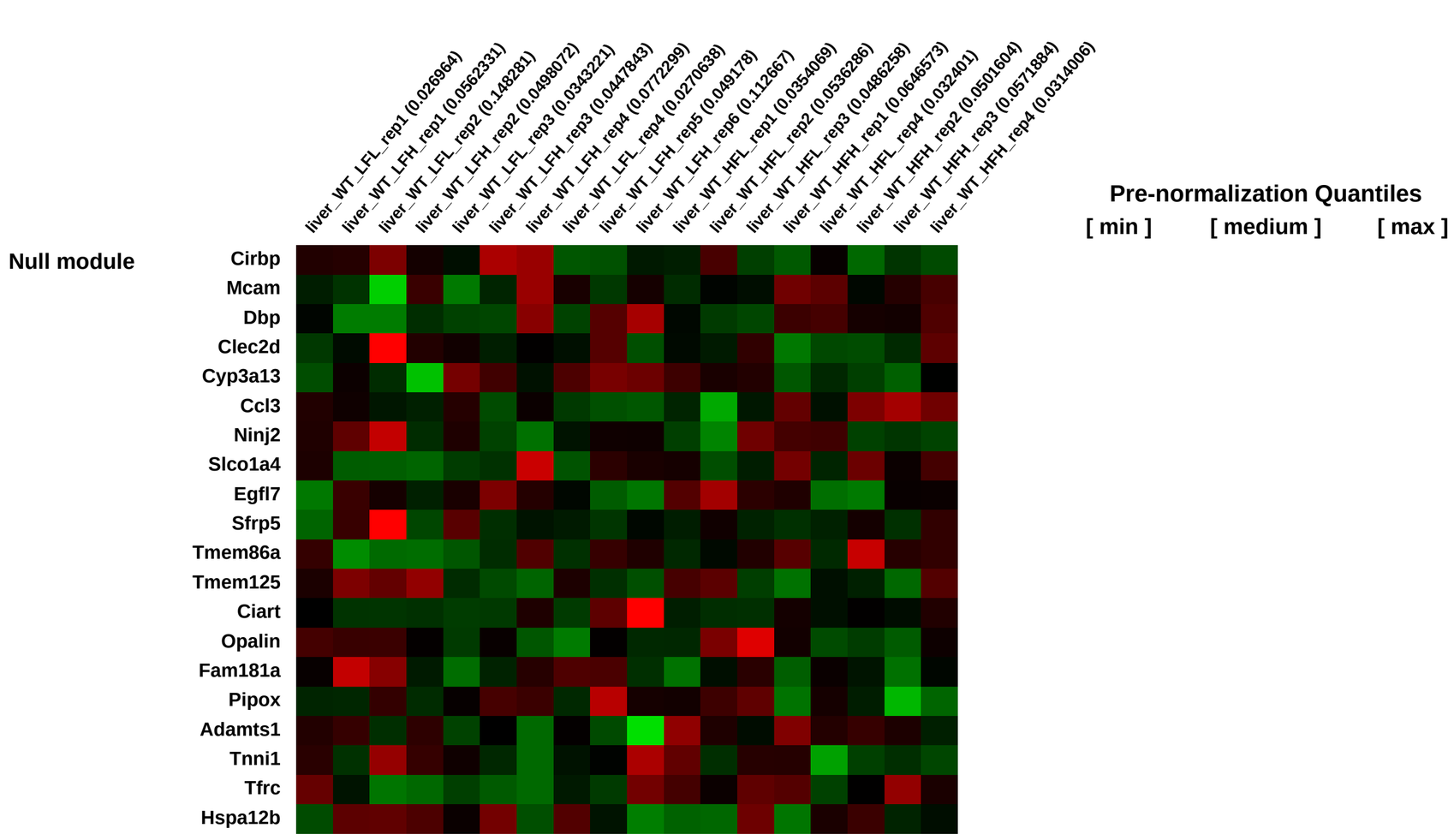

GEO Series "GSE11148" Expression Profiles

Num of samples in this series: 6

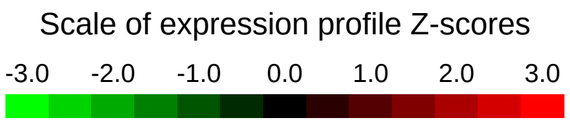

GEO Link:	**http://www.ncbi.nlm.nih.gov/geo/query/acc.cgi?acc=GSE11148**
Status:	**Public on Apr 12 2008**
Title:	**Polytopic protease downregulation effect on the brain (rogae-affy-arabi-492460)**
Organism:	**Mus musculus**
Experiment type:	**Expression profiling by array**
Platform:	**GPL1261**
Pubmed ID:	
Summary & Design:	**Summary:** **Regulation of AD-related genes. Presenilins are intramembrane polytopic proteases. These proteases are critical proteins in pathogenesis of Alzheimer's disease. The function of other polytopic proteases expressed in brains is unknown. Proteins that may potentially interact with PS pathway are of interest to elucidate.** **In this project we will determine gene expression patterns in the brains of mice with altered expression of polytopic protease.** **We hypothesize that family of polytopic proteases expressed in brain may potentially interact with presenilin pathway.** **We will examine 4 RNA samples isolated from brains of mice with significant downregulation of polytopic protease and control animals.** **Total RNA was extracted, purified according to the manufacturer's protocol and stored at -80C.** **Keywords: polytopic protease, brain** **Overall design:**

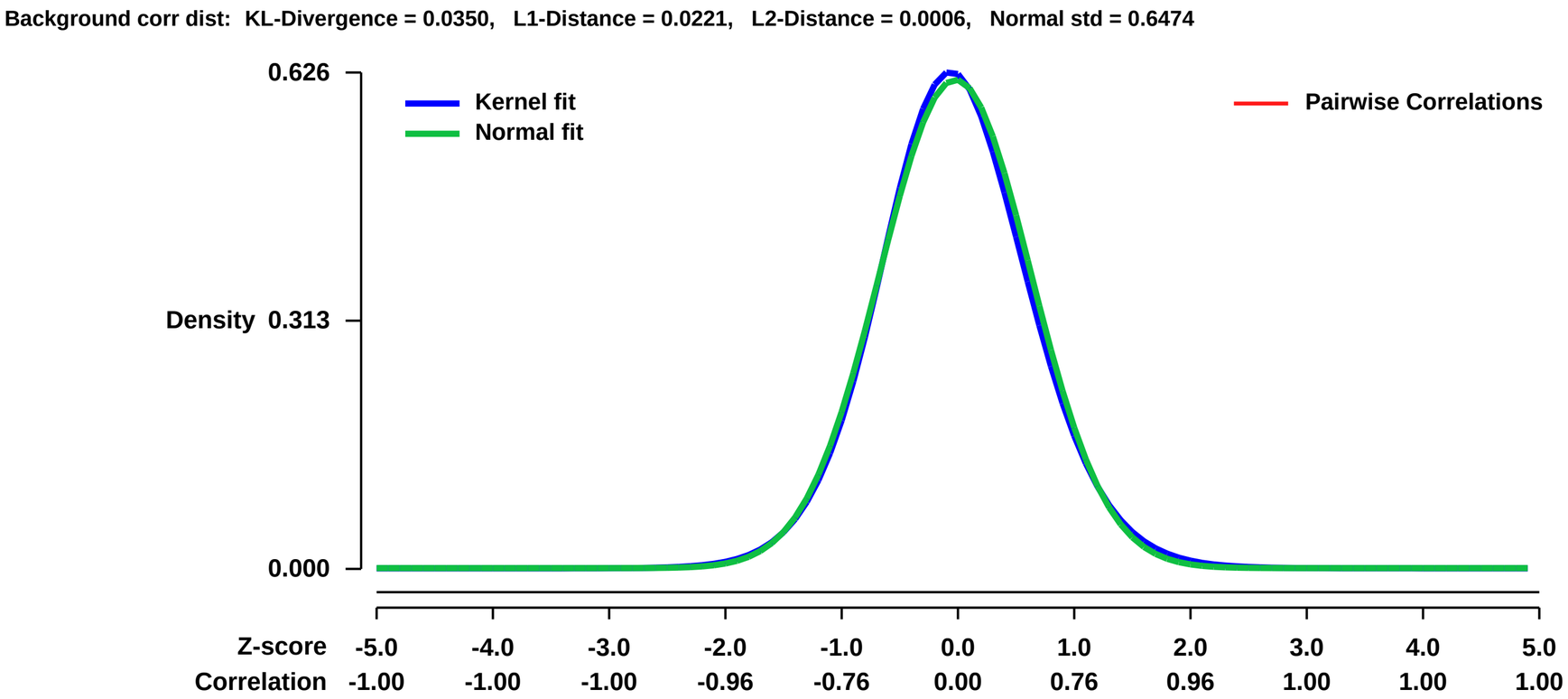

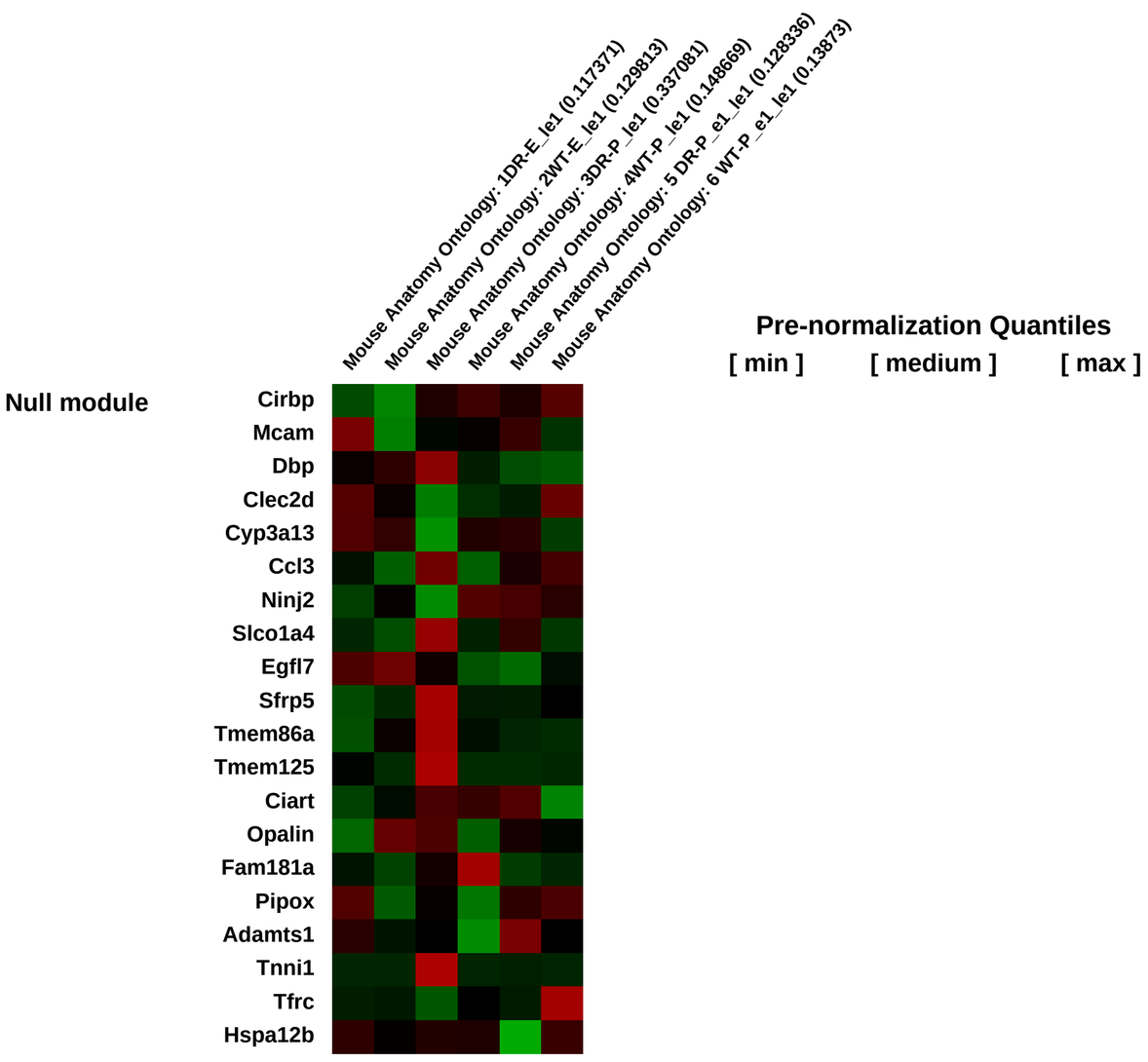

GEO Series "GSE9913" Expression Profiles

Num of samples in this series: 9

Scale of expression profile Z-scores

-3.0 -2.0 -1.0 0.0 1.0 2.0 3.0

GEO Link:	http://www.ncbi.nlm.nih.gov/geo/query/acc.cgi?acc=GSE9913
Status:	Public on Mar 01 2008
Title:	Intestinal gene expression in ENU mutagenesis mouse strains with missense mutations in Muc2 mucin and ER stress
Organism:	Mus musculus
Experiment type:	Expression profiling by array
Platform:	GPL1261
Pubmed ID:	18318598
Summary & Design:	Summary: Background MUC2 mucin produced by intestinal goblet cells is the major component of the intestinal mucus barrier. MUC2 homo-oligomerizes intracellularly into large secreted polymers which give mucus its viscous properties. The inflammatory bowel disease (IBD) ulcerative colitis is characterized by depleted goblet cells and a reduced mucus layer, whereas goblet cells and the mucus layer are increased in the other major inflammatory bowel disease, Crohnâ s disease. Methods and Findings By murine N-ethyl-N-nitrosourea-mutagenesis we identified two distinct non-complementing missense mutations in Muc2 exons encoding N- and C-terminal homo-oligomerization domains causing an ulcerative colitis-like phenotype. Both strains developed mild spontaneous distal intestinal inflammation, chronic diarrhea, rectal bleeding and prolapse, increased susceptibility to acute and chronic colitis induced by a luminal toxin, aberrant Muc2 biosynthesis, smaller goblet cell thecae (less stored mucin) and a diminished mucus barrier. Enhanced local production of IL-1beta, TNF-alpha and IFN-gamma was seen in the distal colon. The number of leukocytes within mesenteric lymph nodes was increased five-fold and leukocytes cultured in vitro produced both Th1 and Th2 cytokines (IFN-gamma, TNF-alpha and IL-13). Intestinal permeability was increased and the luminal bacterial flora were more heavily coated with immunoglobulin as occurs in IBD. This pathology was accompanied by accumulation of the Muc2 precursor and ultrastructural and biochemical evidence of endoplasmic reticulum (ER) stress in goblet cells, activation of the unfolded protein response, and altered intestinal expression of genes involved in ER stress, inflammation, apoptosis and wound repair. Expression of mutated Muc2 oligomerization domains in vitro demonstrated that aberrant Muc2 oligomerization underlies the ER stress. These models show that mutations in Muc2 oligomerization domains can lead to aberrant assembly of the Muc2 complex leading to ER stress, a depleted mucus barrier and intestinal inflammation. In ulcerative colitis we demonstrate similar accumulation of non-glycosylated MUC2 precursor in goblet cells together with ultrastructural and biochemical evidence of ER stress even in non-inflamed intestinal tissue. Conclusions The observations that mucin misfolding and ER stress lead directly to intestinal inflammation and that ER stress and goblet cell pathology occur in ulcerative colitis suggest that ER stress-related mucin depletion could be a fundamental component of the pathogenesis of colitis. Keywords: Single gene, multiple mutant comparison Overall design: 3 individual mice from the Eeyore, Winnie or Wild-type strains were compared as groups. An Affymetrix ID was compared between groups if the ID was Present within two of the three mice within each grouping. IDs were compared by calculating the log2 of Group One average signal divided by Group 2 average signal.

Background corr dist: KL-Divergence = 0.0799, L1-Distance = 0.0215, L2-Distance = 0.0007, Normal std = 0.4781

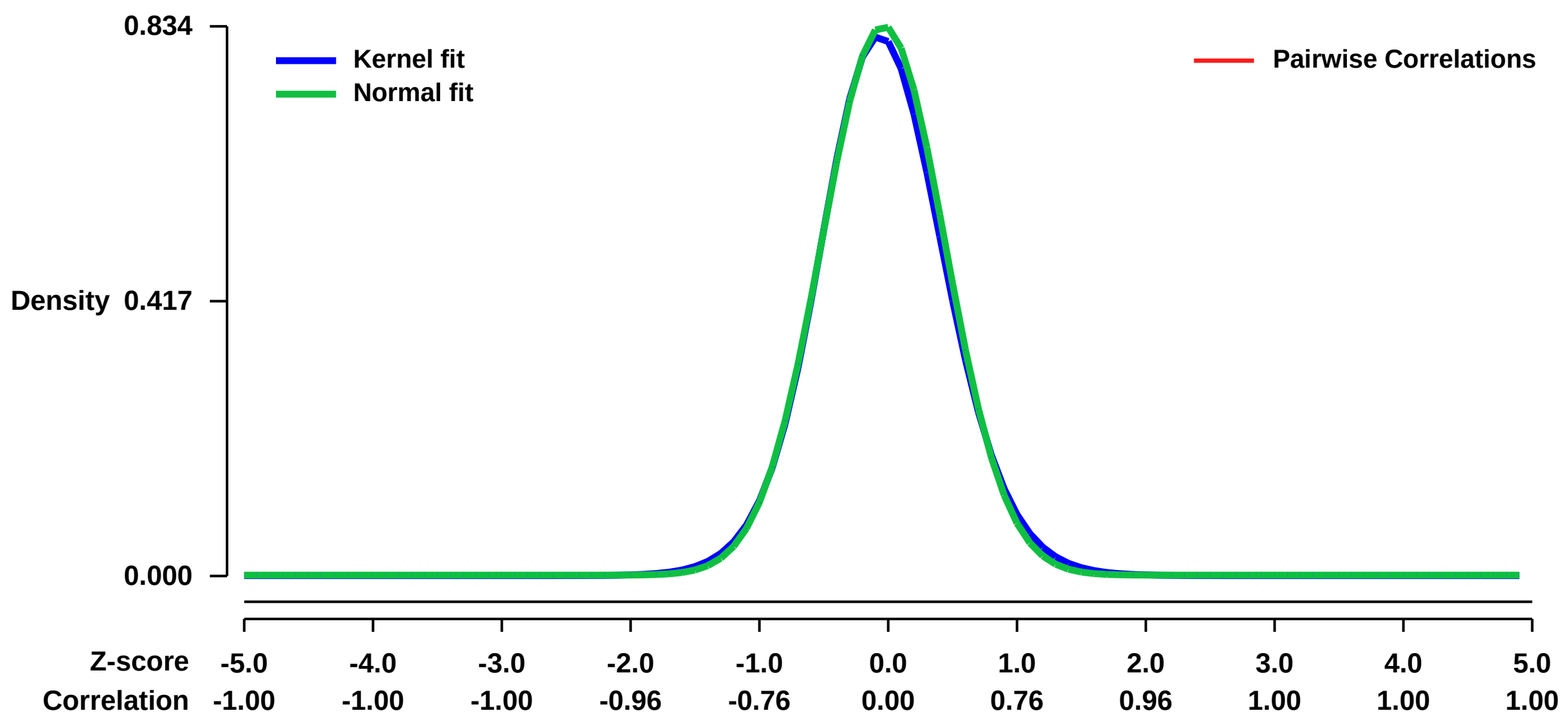

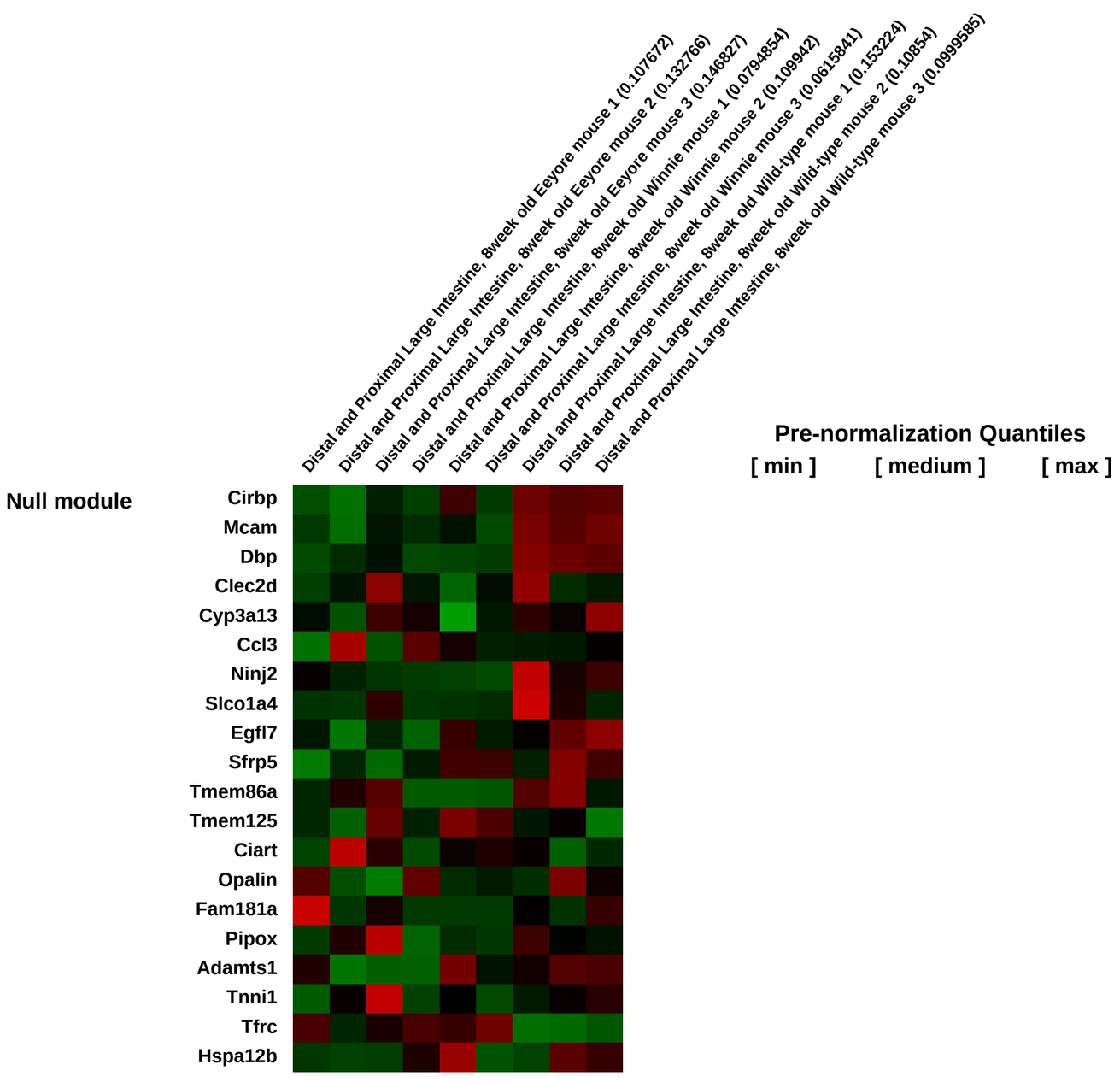

GEO Series "GSE13873" Expression Profiles

Num of samples in this series: 27

Scale of expression profile Z-scores

-3.0 -2.0 -1.0 0.0 1.0 2.0 3.0

GEO Link:	http://www.ncbi.nlm.nih.gov/geo/query/acc.cgi?acc=GSE13873
Status:	Public on Mar 05 2009
Title:	Expression data from murine gastric epithelium
Organism:	Mus musculus
Experiment type:	Expression profiling by array
Platform:	GPL1261
Pubmed ID:	19454706
Summary & Design:	**Summary:** Chronic infection with the bacterial pathogen Helicobacter pylori is a risk factor for the development of gastric cancer, yet remains asymptomatic in a majority of individuals. We report here that the C57Bl6 mouse model of experimental infection with the closely related H. felis recapitulates this wide range in host susceptibility. A majority of infected mice develop premalignant lesions such as gastric atrophy, compensatory epithelial hyperplasia and intestinal metaplasia, whereas a minority is completely protected from preneoplasia. Protection is associated with the failure to mount an IFN-gamma response to the infection and an associated high Helicobacter burden. We demonstrate that IFN-gamma is essential for clearance of Helicobacter, but also mediates the formation of preneoplastic lesions. We further provide evidence that IFN-gamma triggers a specific transcriptional program in murine gastric epithelial cells in vitro and in vivo, and induces their preferential transformation to the hyperplastic phenotype. In summary, our data suggest a dual role for IFN-gamma in Helicobacter pathogenesis that could provide an explanation for the differential susceptibility to H. pylori-induced gastric pathology in the human population. **Keywords: response to in vitro stimulus / comparison of histopathological states** **Overall design:** We chose mice for gene expression profiling that following Helicobacter infection had (a) symptoms of gastritis, but no epithelial changes, (b) atrophic gastritis accompanied by corpus gland hyperplasia or (c) atrophic gastritis accompanied by intestinal metaplasia. An uninfected control group was also included in the analysis, as were two groups of mice that lacked mature T- and B-cells due to a deletion mutation in the rag1 gene (Rag-1-/-) and that were either experimentally infected or served as Rag-1-/- uninfected controls. To see the effects of IFNg on murine gastric epithelial cells we analysed an immortalized murine primary gastric epithelial cell line treated with three different concentrations of IFNg in comparison to an untreated control.

Background corr dist: KL-Divergence = 0.0517, L1-Distance = 0.0400, L2-Distance = 0.0031, Normal std = 0.5764

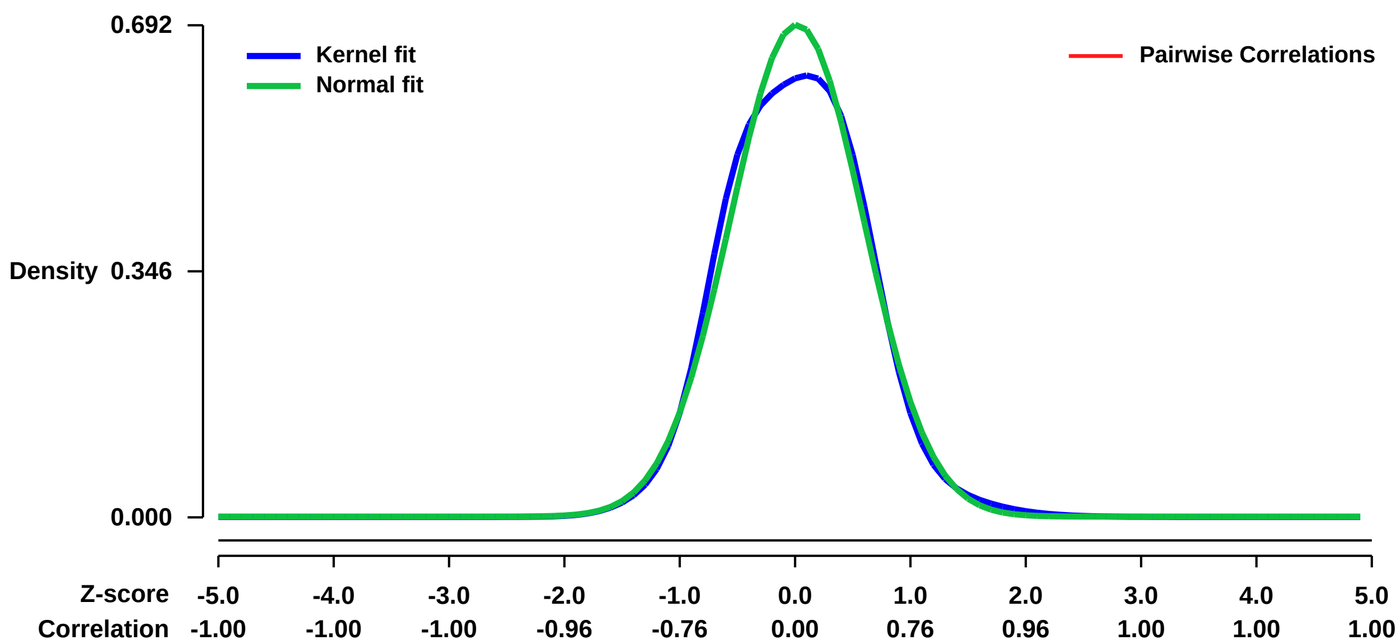

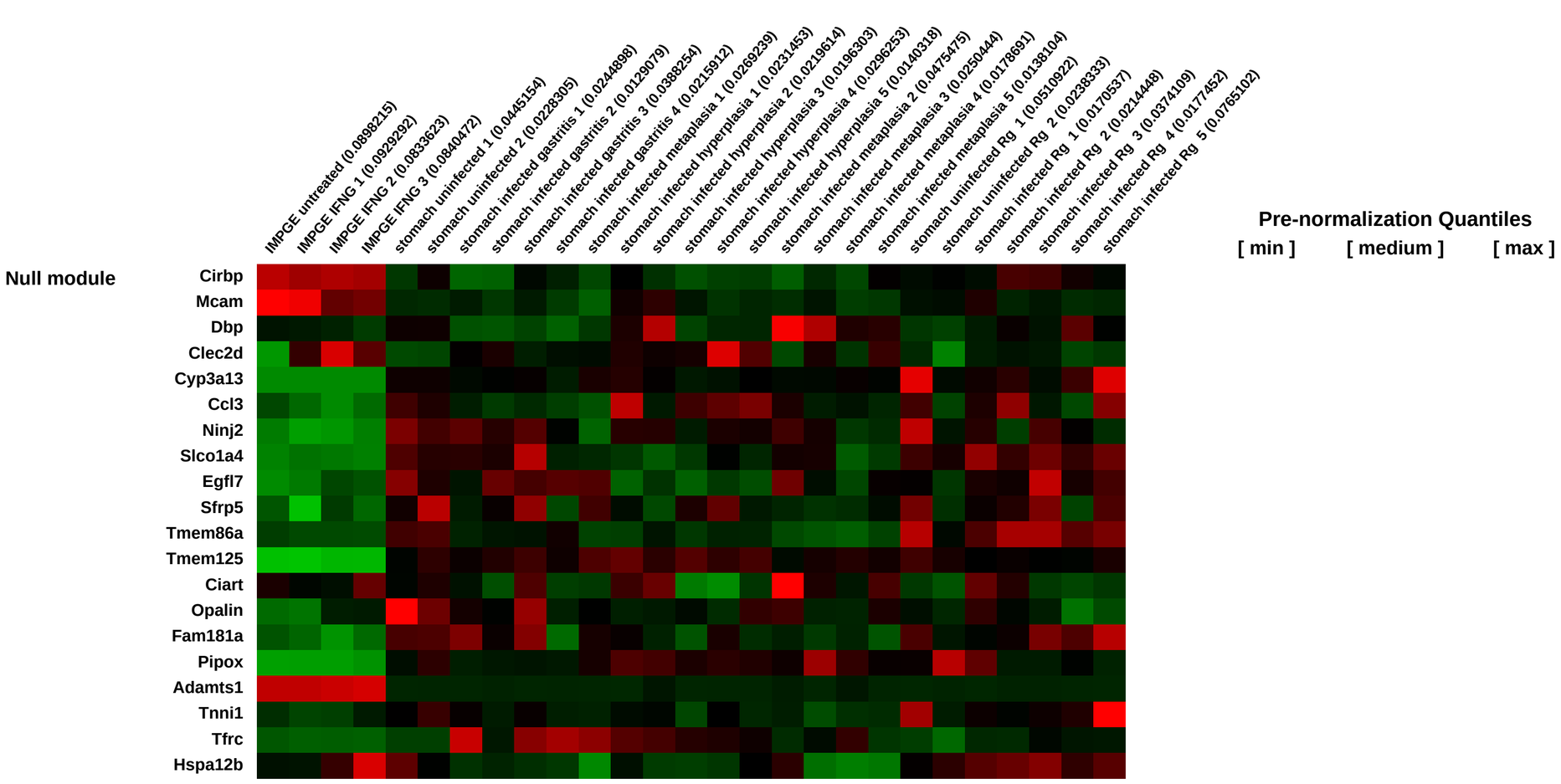

GEO Series "GSE56534" Expression Profiles

Num of samples in this series: 32

Scale of expression profile Z-scores

-3.0 -2.0 -1.0 0.0 1.0 2.0 3.0

GEO Link:	http://www.ncbi.nlm.nih.gov/geo/query/acc.cgi?acc=GSE56534
Status:	Public on Jun 01 2014
Title:	Infection of macrophages by Toxoplasma Progeny from a Type II x Type III cross
Organism:	Mus musculus
Experiment type:	Expression profiling by array
Platform:	GPL1261
Pubmed ID:	
Summary & Design:	**Summary:** Infection of RAW264.7 cells for 24 hours with 32 Toxoplasma Progeny from a Type II x Type III cross To measure changes in gene expression induced in macropahges upon Toxoplasma infection, we infected RAW 264.7 macrophages in cell culture with one of 32 Toxoplasma parasite progeny from a Type II x Type III cross. RNA was harvested 24 hours post infection. **Overall design:** Cells were infected with Toxoplasma parasites, in vitro

Background corr dist: KL-Divergence = 0.1124, L1-Distance = 0.0430, L2-Distance = 0.0039, Normal std = 0.4154

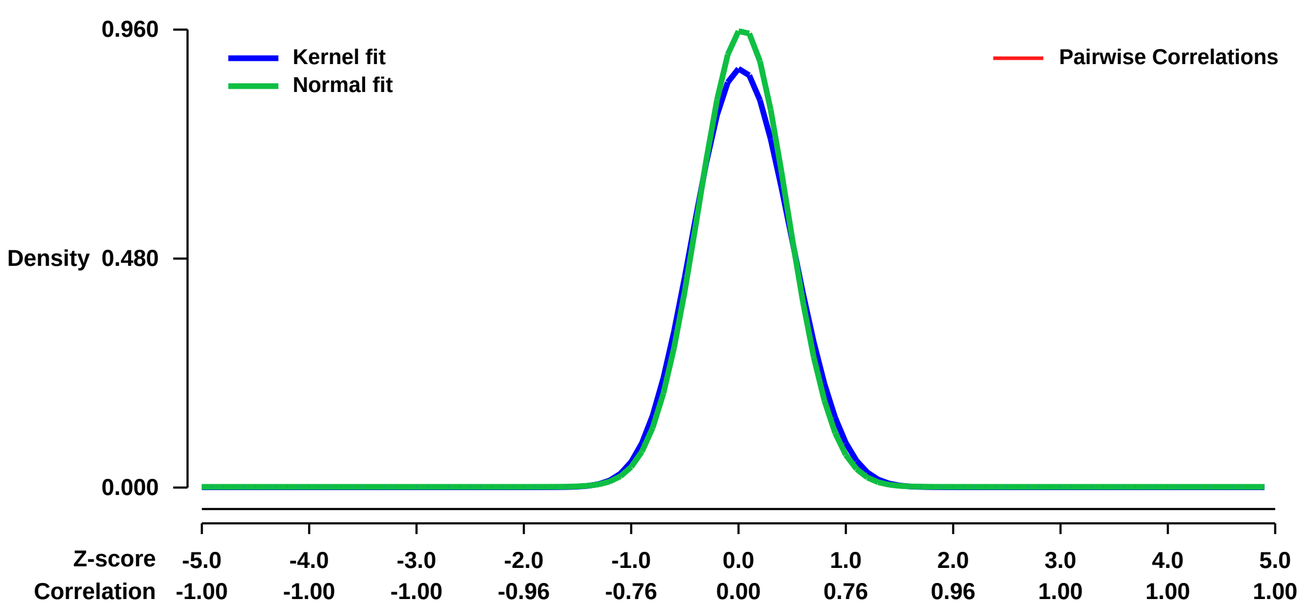

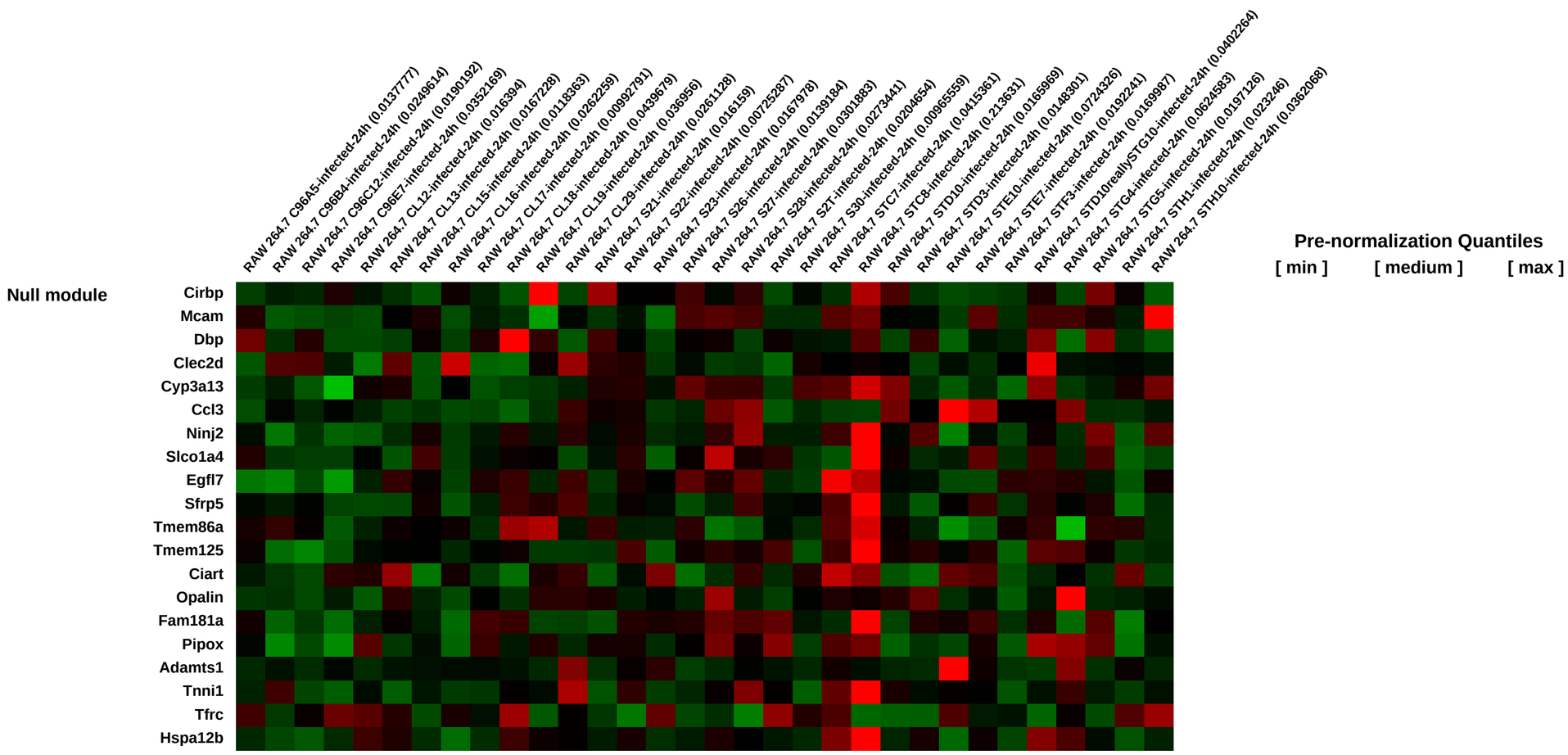

GEO Series "GSE3530" Expression Profiles

Num of samples in this series: 36

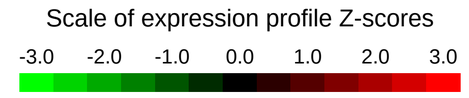

GEO Link:	http://www.ncbi.nlm.nih.gov/geo/query/acc.cgi?acc=GSE3530
Status:	Public on Nov 01 2005
Title:	Distinct Gene Expression Profiles in Adult Mouse Heart Following Targeted MAP Kinase Activation
Organism:	Mus musculus
Experiment type:	Expression profiling by array
Platform:	GPL1261
Pubmed ID:	16368875
Summary & Design:	**Summary:** Three major MAP kinase signaling cascades, ERK, p38 and JNK, play significant roles in the development of cardiac hypertrophy and heart failure in response to external stress and neural/hormonal stimuli. In order to study the specific function of each MAP kinase branch in adult heart, we have generated three transgenic mouse models with cardiac specific and temporally regulated expression of activated mutants of Ras, MKK3 and MKK7, which are selective upstream activators for ERK, p38 and JNK, respectively. Gene expression profiles in transgenic adult hearts were determined using cDNA microarrays at both early (4-7 days) and late (2-4 weeks) time points following transgene induction. From this study, we revealed common changes in gene expression among the three models, particularly involving extracellular matrix remodeling. However, distinct expression patterns characteristic for each pathway were also identified in cell signaling, growth and physiology. In addition, genes with dynamic expression differences between early vs. late stages illustrated primary vs. secondary changes upon MAP kinase activation in adult hearts. These results provide an overview to both short term and long term effects of MAP kinase activation in heart and support some common as well as unique roles for each MAP kinase cascade in the development of heart failure. **Keywords:** MAP Kinase induction comparison, time course **Overall design:** ¸–MHC-floxed-HRas-v12/MKK3bE/MKK7D transgenic mice were bred with ¸–MHC-Mer-Cre-Mer (MCM) mice (from Dr. J. Molkentin, Cincinnati Childrenâ s Hospital)to generate double transgenic animals harboring both floxed transgenes and Mer-Cre-Mer transgene. At 12 weeks of age the double transgenic mice and non-transgenic littermate controls were treated via i.p. injection of tamoxifen at a dosage of 20mg/kgBW once a day for 3 consecutive days as reported. The hearts were harvested at an early (4-7 days post first tamoxifen injection) and a late (2-4 weeks) time point. Left ventricles were dissected and rapidly frozen in liquid nitrogen and stored at -80¸ C prior to protein and RNA analysis.

Background corr dist: KL-Divergence = 0.3192, L1-Distance = 0.0530, L2-Distance = 0.0066, Normal std = 0.2747

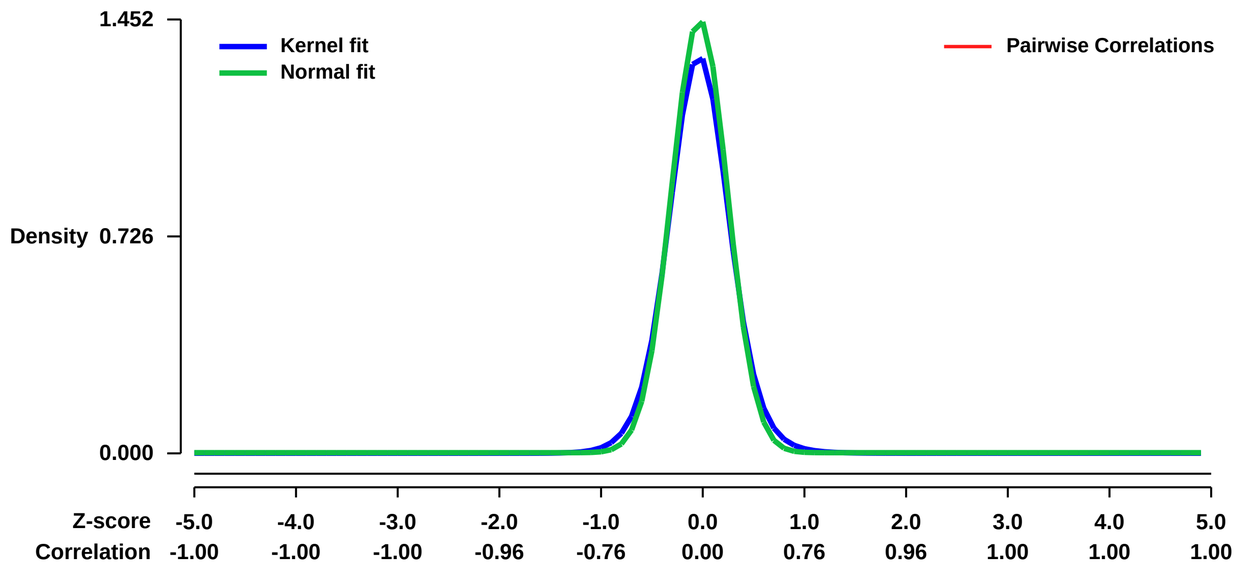

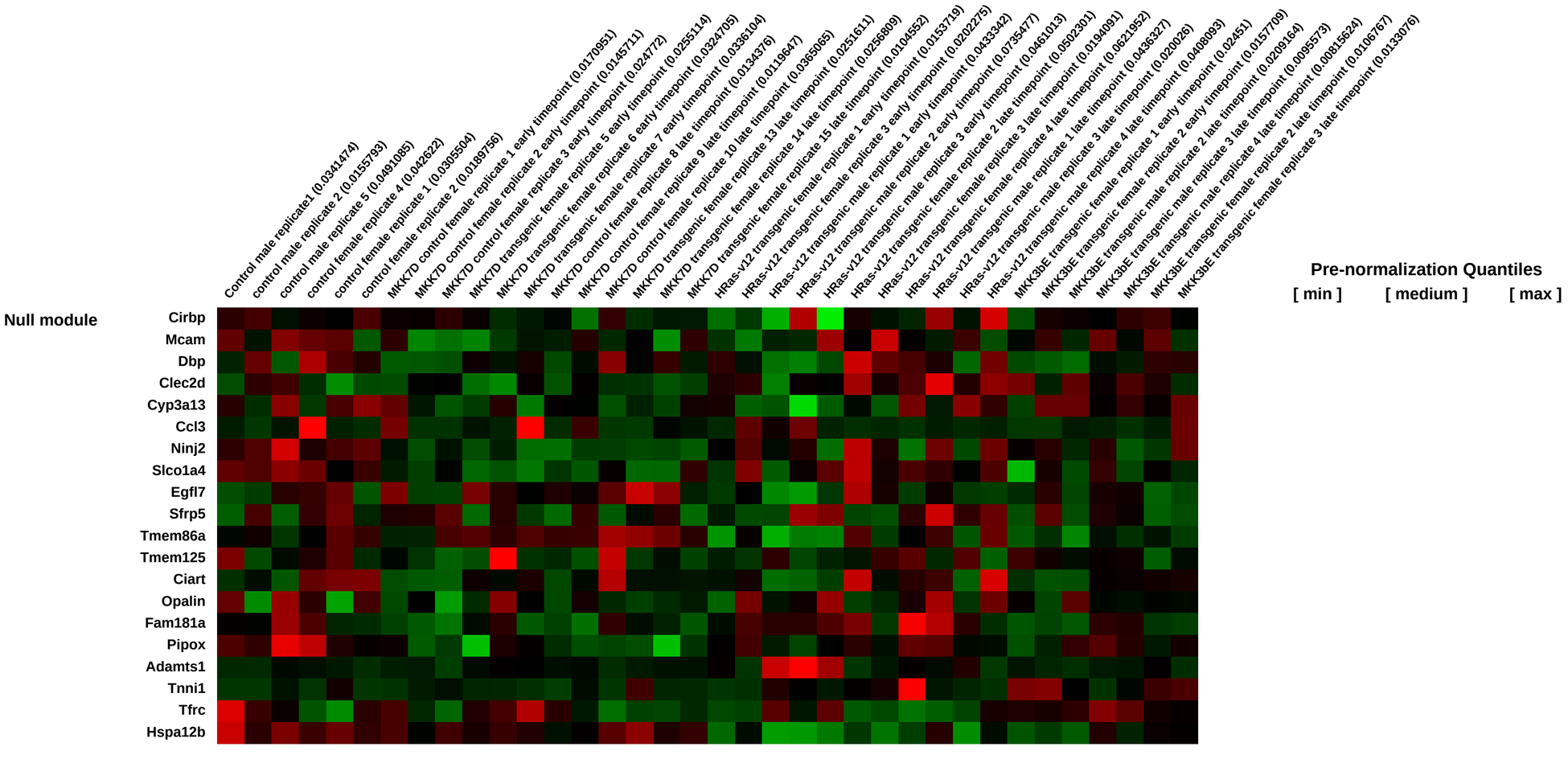

GEO Series "GSE52597" Expression Profiles

Num of samples in this series: 7

Scale of expression profile Z-scores

-3.0 -2.0 -1.0 0.0 1.0 2.0 3.0

GEO Link:	http://www.ncbi.nlm.nih.gov/geo/query/acc.cgi?acc=GSE52597
Status:	Public on Feb 20 2014
Title:	Expression data during plantaris muscle hypertrophy with/without satellite cells induced by synergist ablation in young adult Pax7-DTA mice
Organism:	Mus musculus
Experiment type:	Expression profiling by array
Platform:	GPL1261
Pubmed ID:	24376025
Summary & Design:	**Summary:** Global gene expression patterns were determined from microarray results from sham surgery or following 1 week of plantaris muscle hypertrophy induced by synergist ablation in young adult Pax7-DTA mice (4 months). Vehicle treated mice have their full complement of satellite cells; tamoxifen treated mice have had their satellite cells genetically depleted through Cre-loxP technology **Overall design:** After sham surgery or 1 week of overload, Affymetrix chips (mouse430_2.0) were used with 1 ´µg of total RNA derived from a pooled sample of the right and left plantaris muscles from 11 animals.

Background corr dist: KL-Divergence = 0.0322, L1-Distance = 0.0265, L2-Distance = 0.0008, Normal std = 0.6614

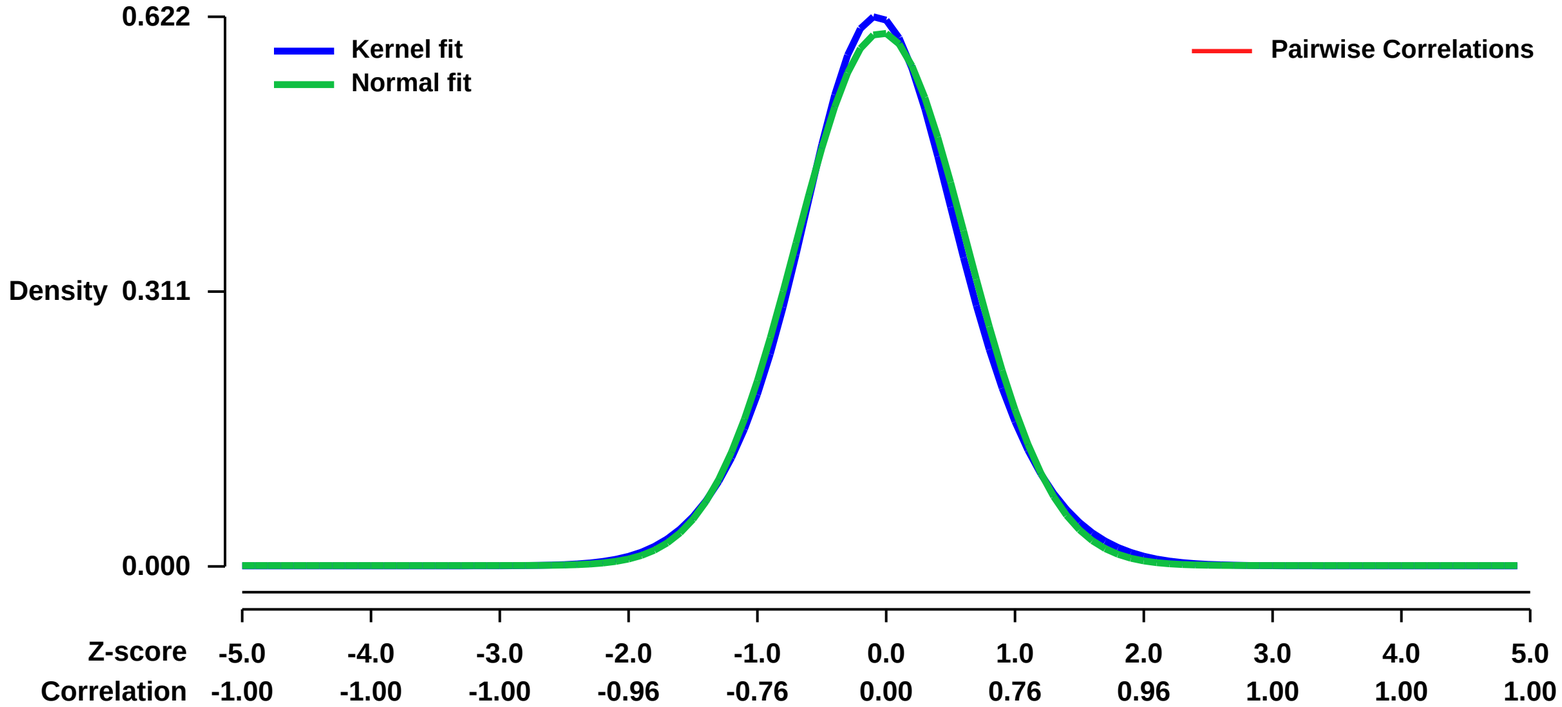

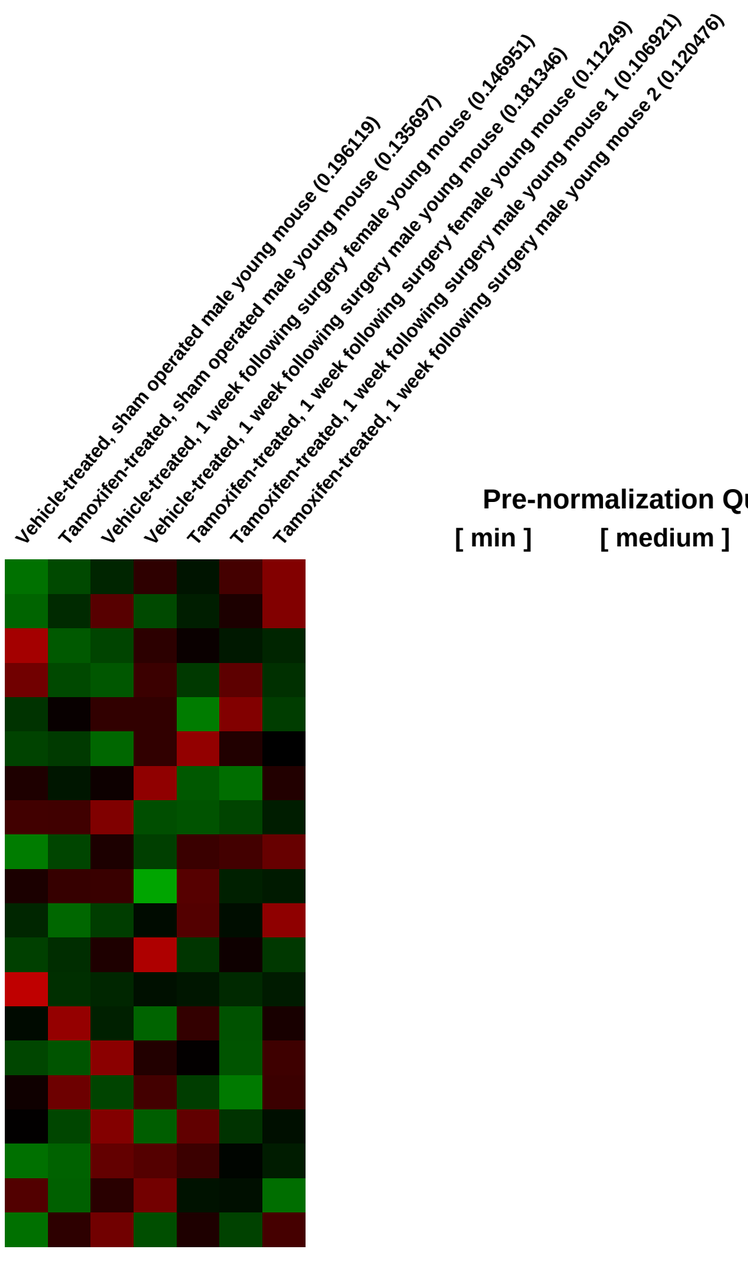

GEO Series "GSE29145" Expression Profiles

Num of samples in this series: 10

Scale of expression profile Z-scores

-3.0 -2.0 -1.0 0.0 1.0 2.0 3.0

GEO Link:	http://www.ncbi.nlm.nih.gov/geo/query/acc.cgi?acc=GSE29145
Status:	Public on Jan 10 2012
Title:	PKCz-mediated Gaq stimulation of the ERK5 pathway is involved in cardiac hypertrophy
Organism:	Mus musculus
Experiment type:	Expression profiling by array
Platform:	GPL1261
Pubmed ID:	22232556
Summary & Design:	**Summary:** **Background: Gq-coupled G protein-coupled receptors (GPCR) mediate the actions of a variety of messengers that are key regulators of cardiovascular function. Enhanced Gaq-mediated signaling plays an important role in cardiac hypertrophy and in the transition to heart failure. We have recently described that Gaq acts as an adaptor protein that facilitates PKCz-mediated activation of ERK5 in epithelial cells. Since the ERK5 cascade is known to be involved in cardiac hypertrophy, we have investigated the potential relevance of this pathway in Gq-dependent signaling in cardiac cells.** **Methodology/Principal Findings: We have explored the mechanisms involved in Gq-coupled GPCR-mediated stimulation of the ERK5 pathway and its functional consequences in cardiac hypertrophy using both cultured cardiac cells and an animal model of angiotensin-dependent induction of cardiac hypertrophy in wild-type and PKCz knockout mice. We find that PKC¸¶ is required for the activation of the ERK5 pathway by Gq-coupled GPCR in cardiomyocytes and in cardiac fibroblasts. Stimulation of ERK5 by angiotensin II is blocked upon pharmacological inhibition or siRNA-mediated silencing of PKCz in primary cultures of cardiac cells and in cardiomyocytes isolated from PKCz-deficient mice. Moreover, these mice do not develop cardiac hypertrophy upon chronic challenge with angiotensin II, as assessed by morphological, biomarker, electrocardiographic and global gene expression pattern analysis.** **Conclusion/Significance: Our data put forward that PKC¸¶ is essential for Gq- dependent ERK5 activation in cardiac cells and indicate a key cardiac physiological role for this recently described Gaq/PKCz/MEK5 signaling axis.** **Overall design:** **Littermate wild-type and PKCz -/- male mice (32 weeks of age) were subjected to continuous infusion of angiotensin II (or PBS as a control) for 14 days, a well established model for the induction of cardiac hypertrohy**

Background corr dist: KL-Divergence = 0.0510, L1-Distance = 0.0437, L2-Distance = 0.0038, Normal std = 0.5596

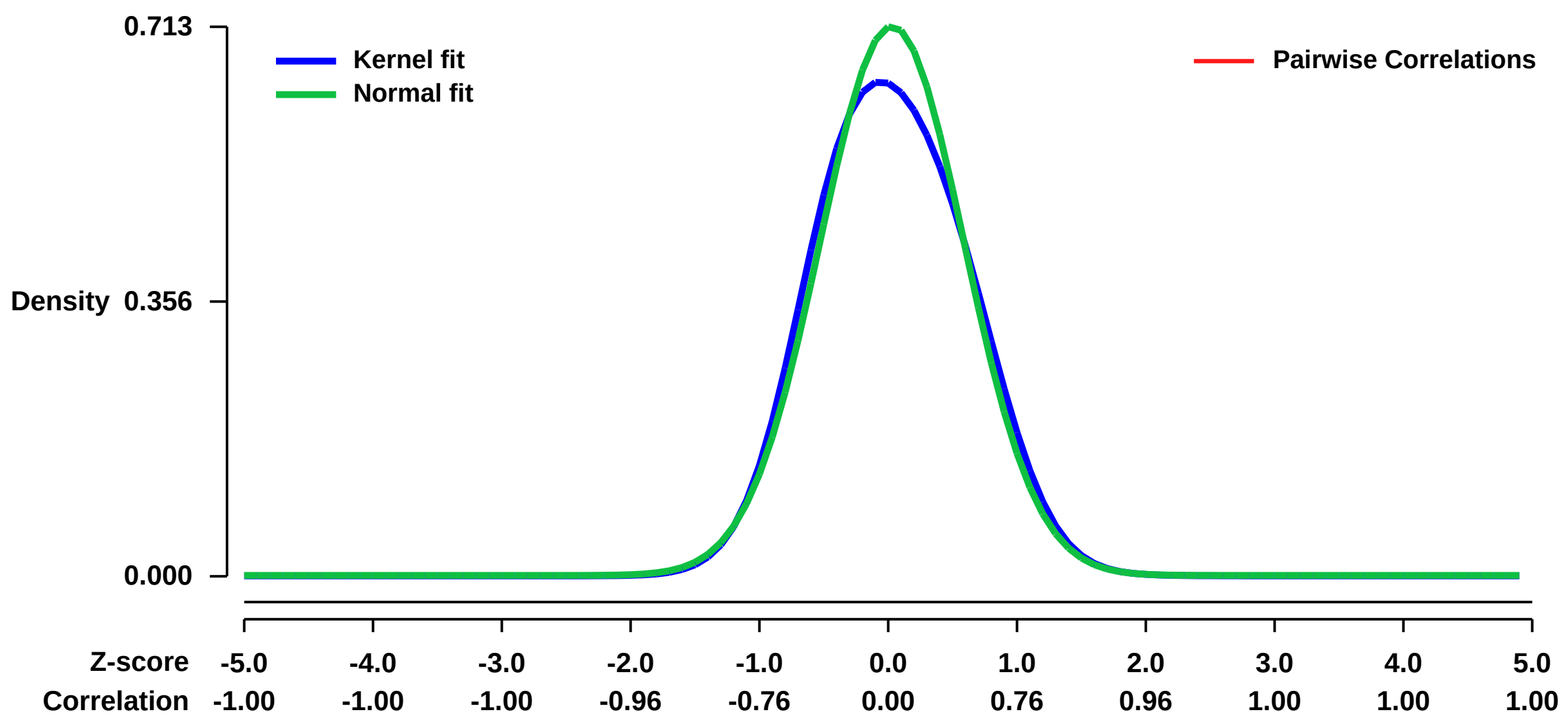

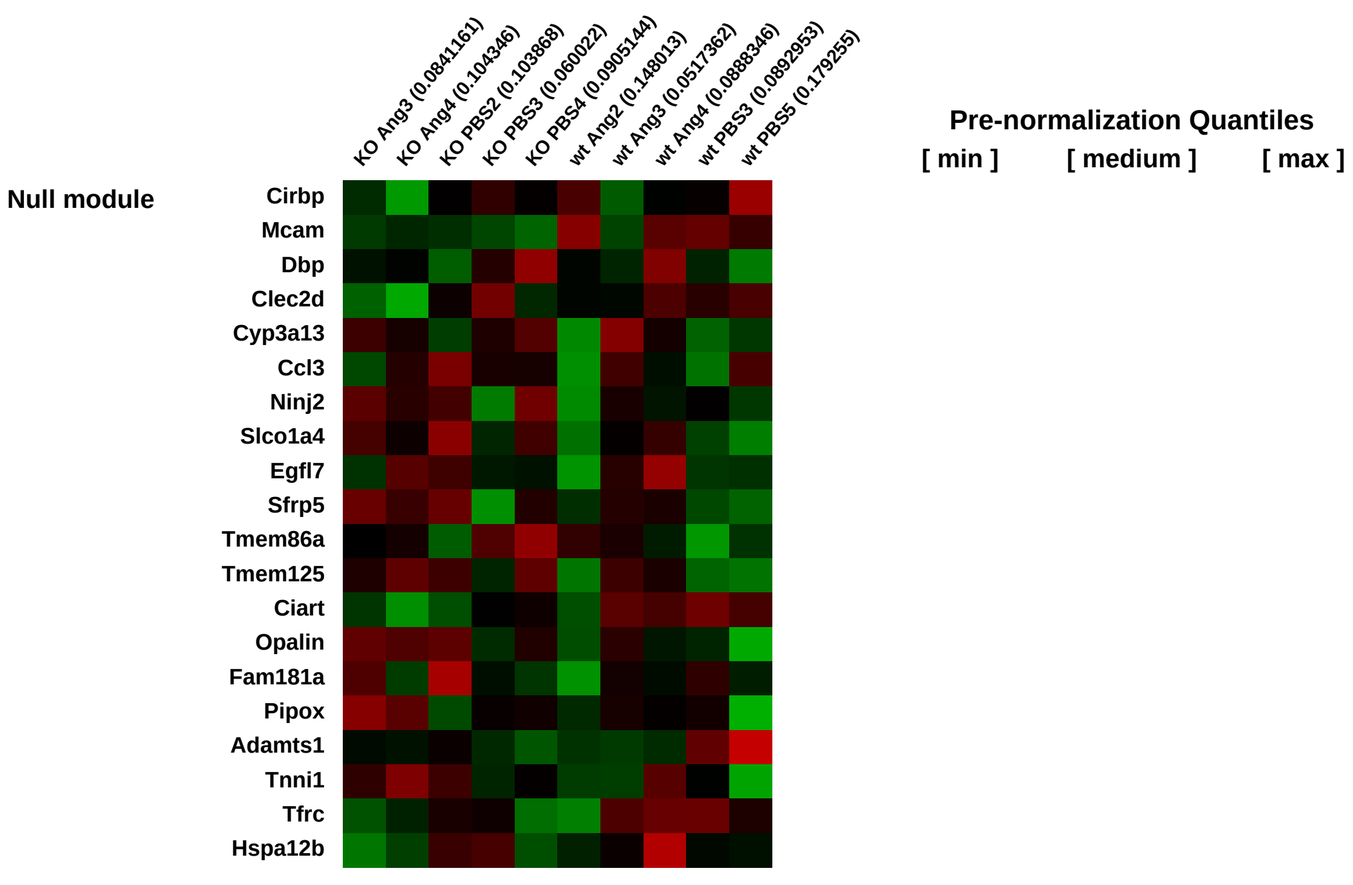

GEO Series "GSE38138" Expression Profiles

Num of samples in this series: 20

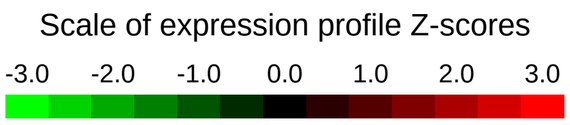

GEO Link:	http://www.ncbi.nlm.nih.gov/geo/query/acc.cgi?acc=GSE38138
Status:	Public on May 30 2012
Title:	Hepatic gene expression in streptozotocin-induced diabetic mice fed a phloridzin diet
Organism:	Mus musculus
Experiment type:	Expression profiling by array
Platform:	GPL1261
Pubmed ID:	19413312
Summary & Design:	**Summary:** Phloridzin is a dihydrochalcone typically contained in apples. A diet containing 0.5 % phloridzin significantly improves hyperglycemia but not hypoinsulinemia and tissue lipid peroxidation in streptozotocin (STZ)-induced diabetic mice after 14 days. The phloridzin diet has no effect on the alteration of hepatic gene expression in STZ-induced diabetic mice. A quantitative RT-PCR analysis showed a reversal of the STZ induction of the sodium/glucose cotransporter gene Sglt1 and the drug-metabolizing enzyme genes Cyp2b10 and Ephx1 in the small intestine of mice fed a 0.5% phloridzin diet. These mice also showed a reversal of the STZ-mediated renal induction of the glucose-regulated facilitated glucose transporter gene Glut2. Dietary phloridzin improved the abnormal elevations in blood glucose level and the overexpression of Sglt1, Cyp2b10 and Ephx1 in the small intestine of STZ-induced diabetic mice. **Overall design:** Six-week-old male mice were divided into 4 groups of 6 mice each, housed in groups of 3 per cage. After 1 week mice were intraperitoneally injected with STZ. Mice (n=6) in the untreated control group did not receive any treatment. After 1 week, 18 mice showing non-fasting blood glucose levels of 330-590 mg/dL were divided into 3 groups: one group was fed with AIN93G only (control group), the others with an AIN93G diet containing 0.1% or 0.5% phloridzin (Funakoshi, Tokyo, Japan) for 2 weeks.

Background corr dist: KL-Divergence = 0.2564, L1-Distance = 0.0474, L2-Distance = 0.0051, Normal std = 0.3007

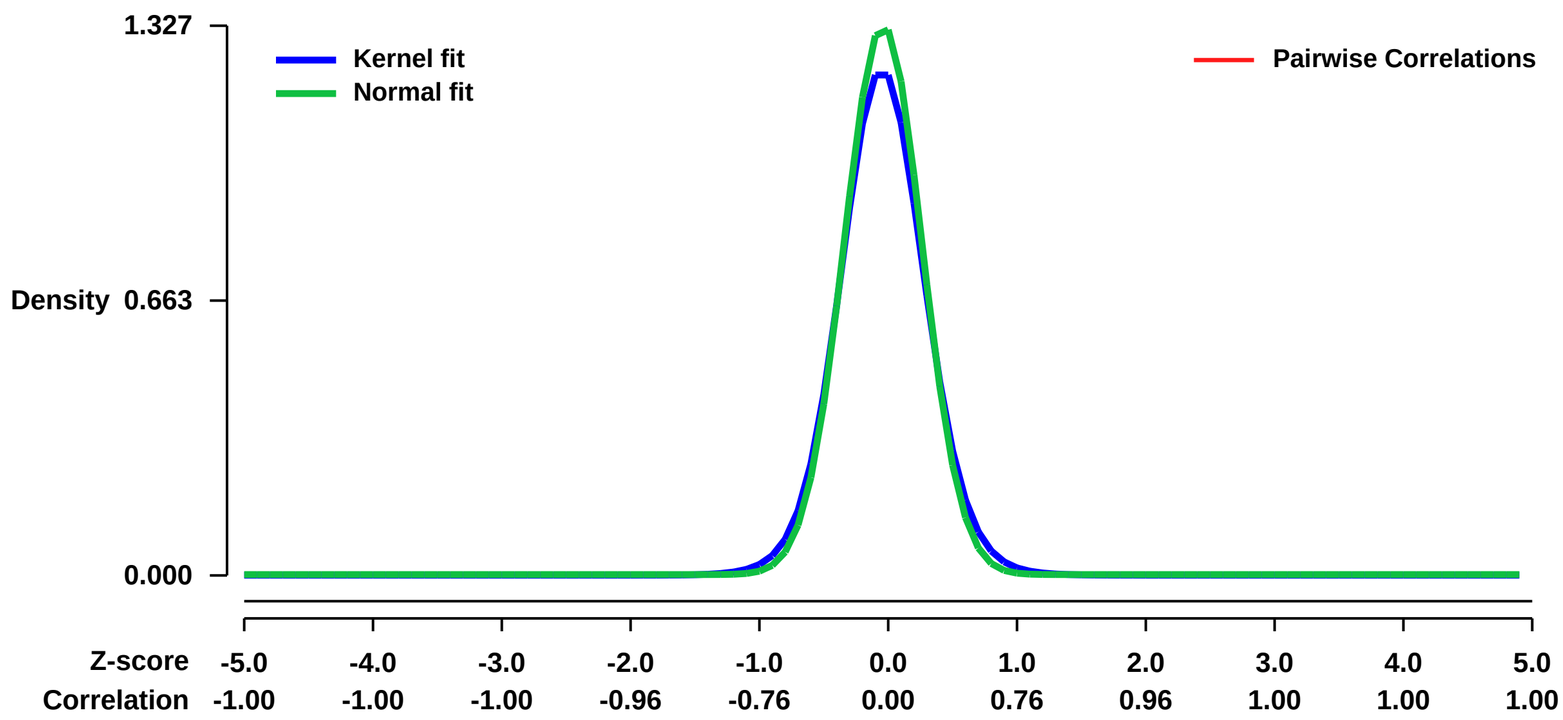

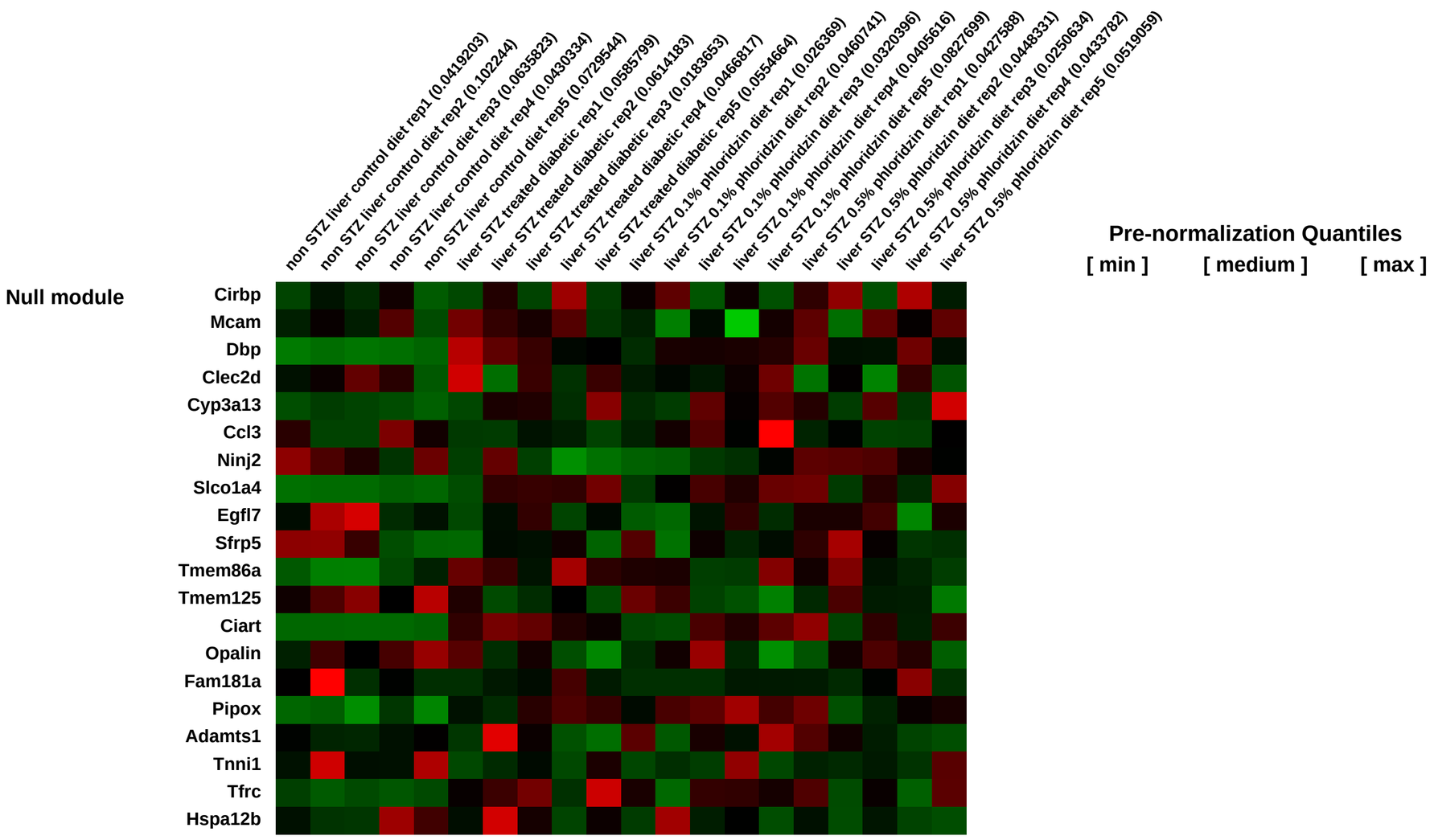

GEO Series "GSE34091" Expression Profiles

Num of samples in this series: 8

Scale of expression profile Z-scores

-3.0 -2.0 -1.0 0.0 1.0 2.0 3.0

GEO Link:	**http://www.ncbi.nlm.nih.gov/geo/query/acc.cgi?acc=GSE34091**
Status:	**Public on Jul 25 2012**
Title:	**Nucleosome dynamics specifies genome-wide binding of the male germ cell gene regulator CTCFL and of CTCF [Mouse430_2 Expression]**
Organism:	**Mus musculus**
Experiment type:	**Expression profiling by array**
Platform:	**GPL1261**
Pubmed ID:	**22709888**
Summary & Design:	**Summary:** **The effect of CTCFL mutation on the transcriptional program in testes** **Overall design:** **Testis RNA extracted from CTCFL wildtype and mutant mice was hybridized on Affymetrix Mouse430_2 arrays**

Background corr dist: **KL-Divergence = 0.0649, L1-Distance = 0.0180, L2-Distance = 0.0003, Normal std = 0.5147**

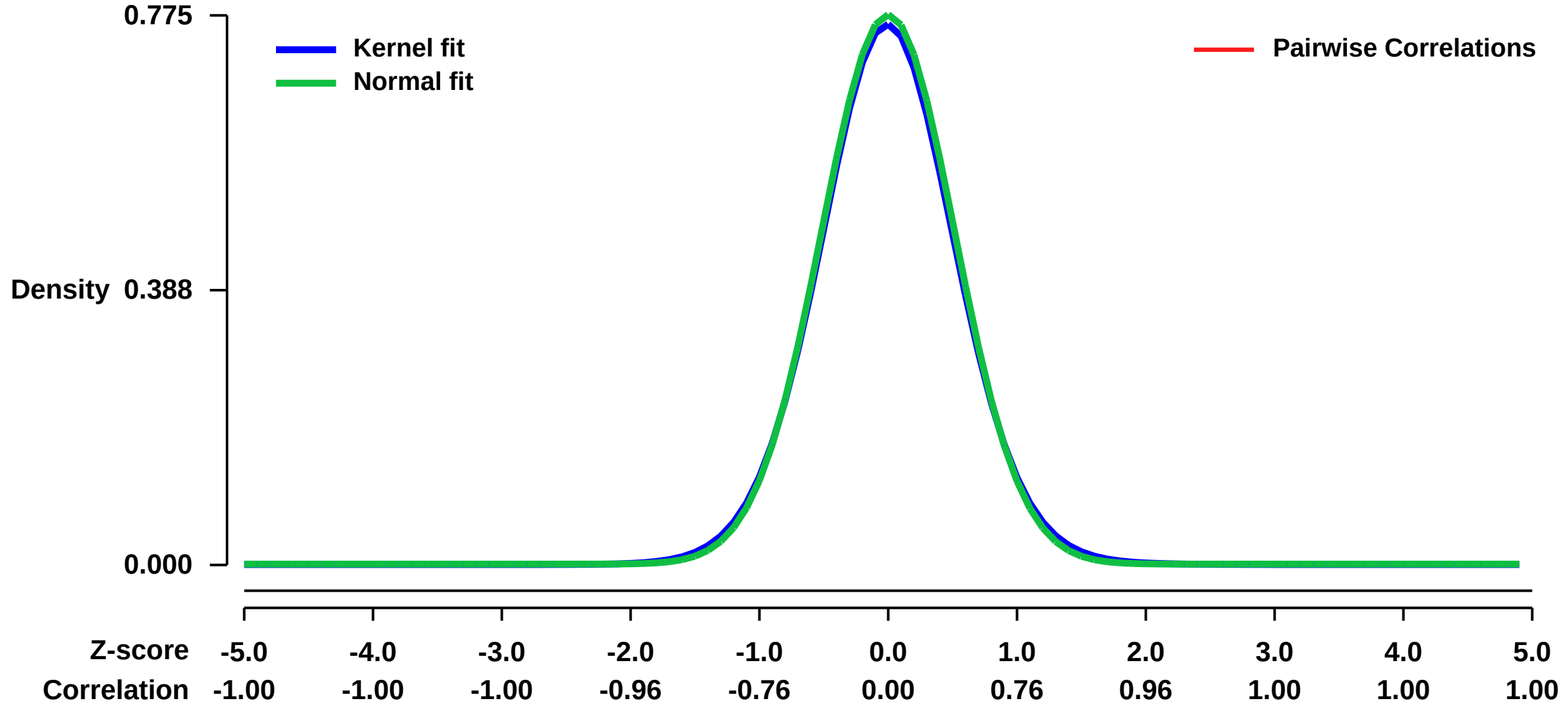

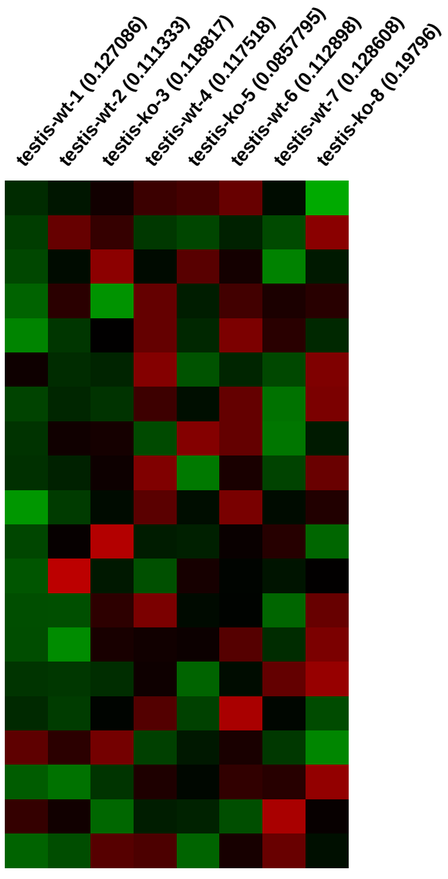

GEO Series "GSE31940" Expression Profiles

Num of samples in this series: 8

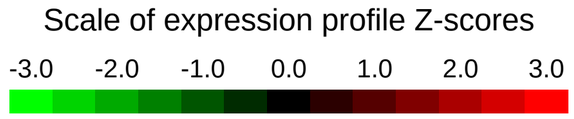

GEO Link:	**http://www.ncbi.nlm.nih.gov/geo/query/acc.cgi?acc=GSE31940**
Status:	**Public on Mar 01 2012**
Title:	**White adipose tissue from aP2-Pex5 knockout and control mice**
Organism:	**Mus musculus**
Experiment type:	**Expression profiling by array**
Platform:	**GPL1261**
Pubmed ID:	
Summary & Design:	**Summary:** **These arrays contain data from gonodal adipose tissue of aP2-Pex5 -/- male mice** **Overall design:** **4 arrays from gonadal adipose tissue from control mice (Swiss background) are compared with 4 arrays from gonadal adipose tissue of aP2-Pex5 knockout mice. The latter lack functional peroxisomes in adipose tissue.**

Background corr dist: **KL-Divergence = 0.0585, L1-Distance = 0.0201, L2-Distance = 0.0006, Normal std = 0.5314**

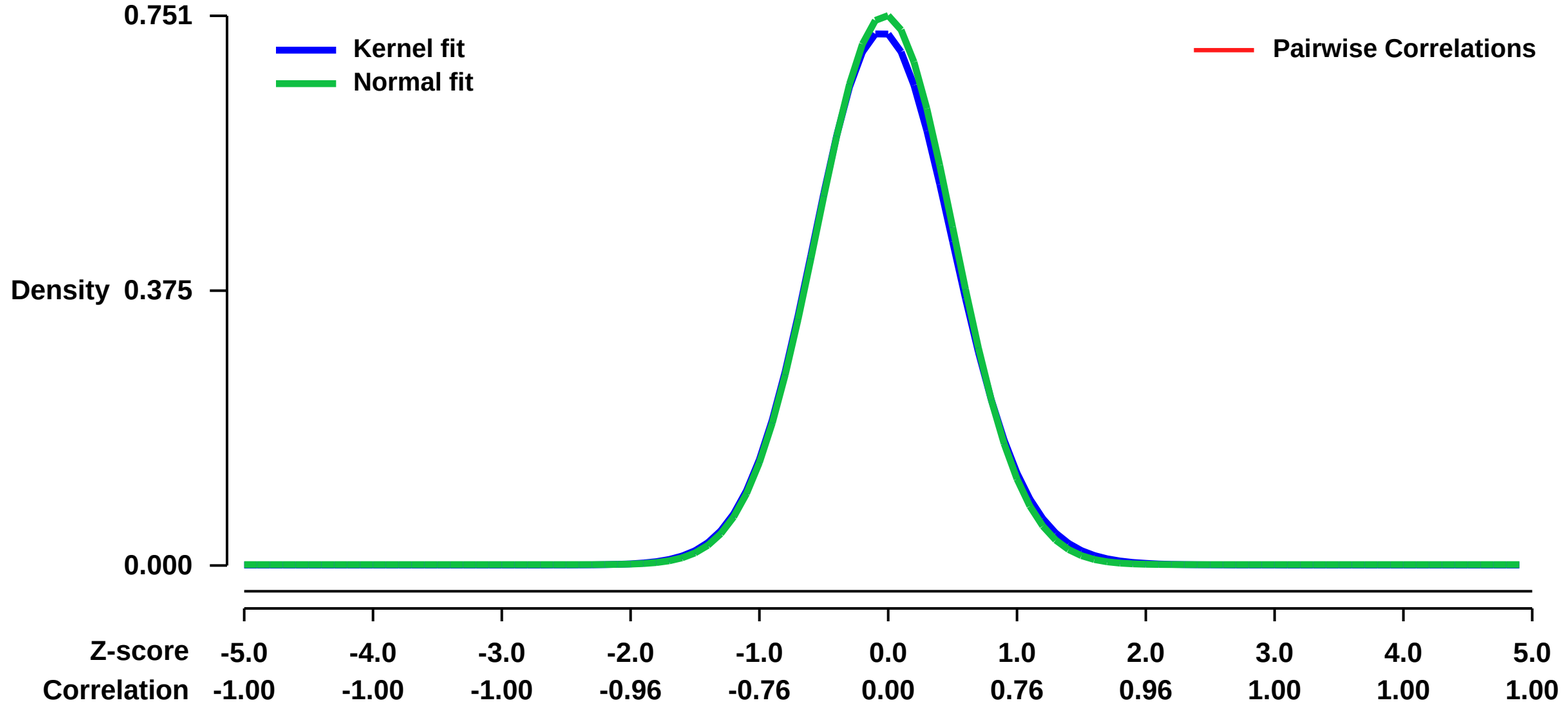

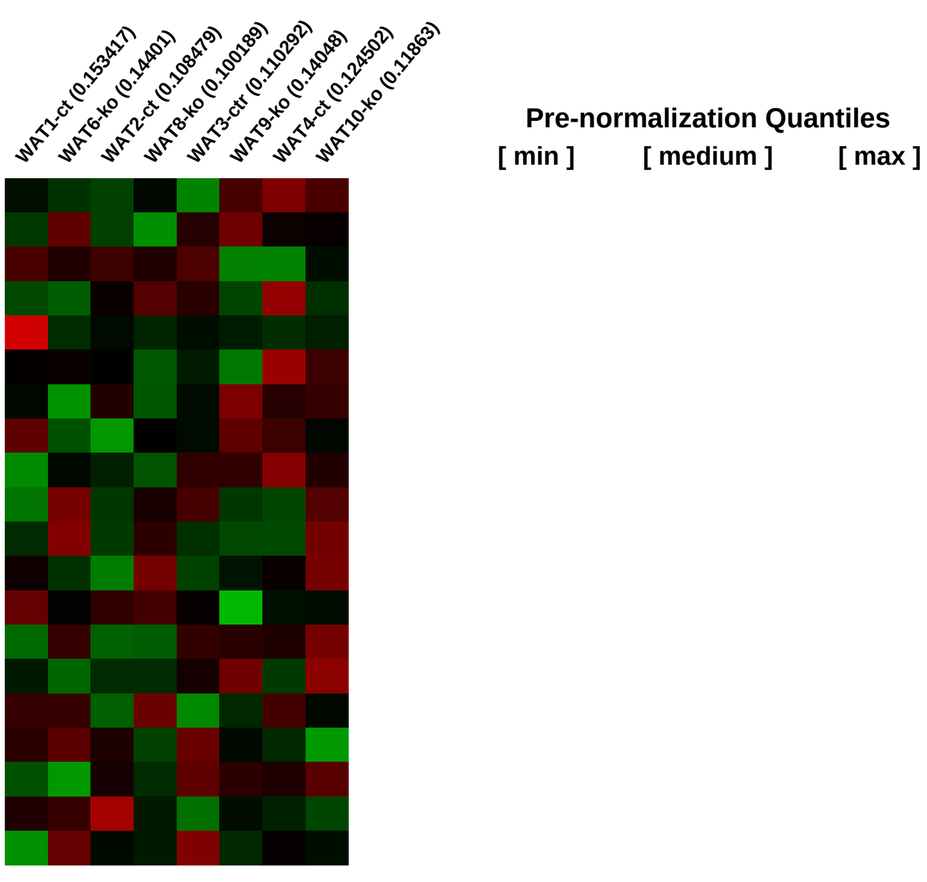

GEO Series "GSE8249" Expression Profiles

Num of samples in this series: 46

Scale of expression profile Z-scores

-3.0 -2.0 -1.0 0.0 1.0 2.0 3.0

GEO Link:	http://www.ncbi.nlm.nih.gov/geo/query/acc.cgi?acc=GSE8249
Status:	Public on Aug 02 2007
Title:	Systematic discovery and classification of ovarian fertility factors.
Organism:	Mus musculus
Experiment type:	Expression profiling by array
Platform:	GPL1261
Pubmed ID:	17660561
Summary & Design:	**Summary:** Female infertility syndromes are among the most prevalent chronic health disorders in women, but their molecular basis remains unknown because of the complexity of oogenesis and uncertainty regarding the number and identity of ovarian factors controlling the assembly, preservation, and maturation of ovarian follicles. To systematically discover such ovarian fertility factors en masse, we employed a mouse model (Foxo3), where follicles are assembled normally but are then synchronously activated. Gene expression profiling of mutant and normal ovaries led to the identification a surprisingly large set of ovarian factors. The set included the vast majority of known ovarian factors, many of which when mutated produce female sterility phenotypes, but most were novel. Subsequent analyses revealed novel classes of ovarian factors and significant overrpresentation on the X chromosome, among other insights into the general properties of oogenesis genes and their patterns of expression. **Keywords: time course, ovarian fertility factors, Foxo3 mutant** **Overall design:** Total ovarian RNA from +/+ and -/- ovaries at PND1, 3, 7, and 14 (n=3 replicates per timepoint and genotype, a total of 24 microarrays) was subjected to linear RNA amplification and hybridized to Affymetrix 430 2.0 mouse whole-genome microarrays, which interrogate >39K transcripts including the vast majority of protein-coding genes. We also profiled 14 somatic tissues. Additionally, to provide more refined views of gene expression, we profiled adult ovaries, adult testis, KitlSl/KitlSl-d testis (devoid of germ cells except for rare spermatogonia) (Shinohara et al., 2000), ES cells, laser-capture microdissected (LCM) primary oocytes, LCM somatic cells (granulosa cells + surrounding stroma), superovulated unfertilized eggs, cumulus granulosa cells, and E11 Foxo3 +/+ and -/- embryos. Each array data set was independently normalized by global median scaling, and the signal strengths were averaged for those samples for which replicates were available (PND1-14).

Background corr dist: KL-Divergence = 0.3733, L1-Distance = 0.0696, L2-Distance = 0.0162, Normal std = 0.2829

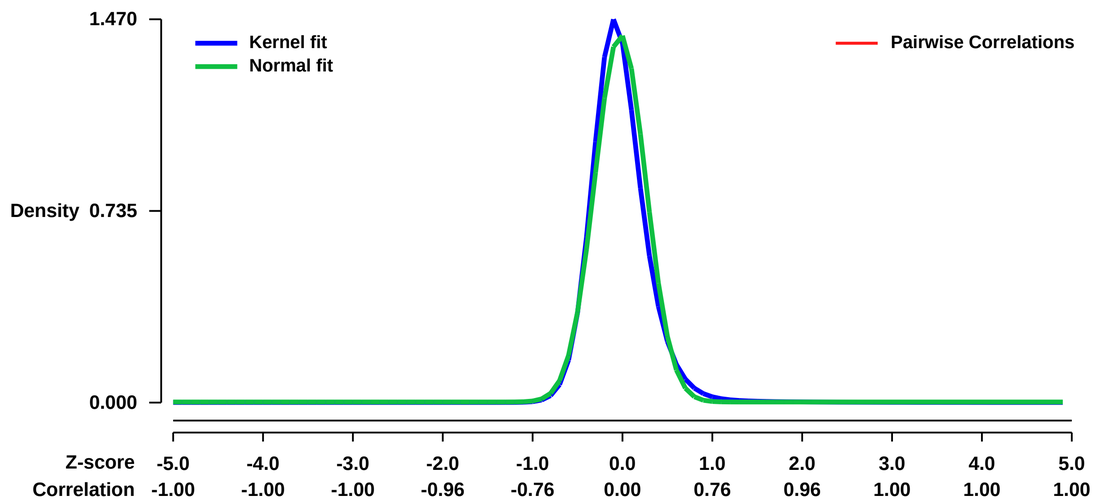

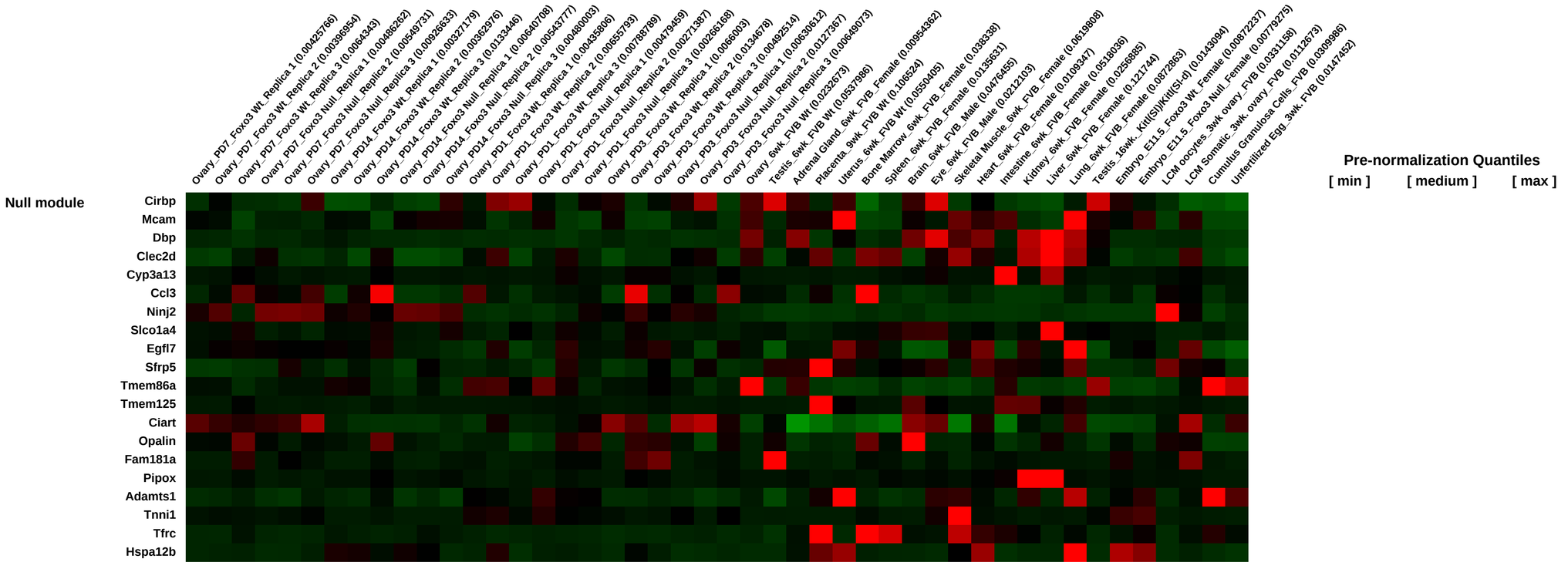

GEO Series "GSE57425" Expression Profiles

Num of samples in this series: 6

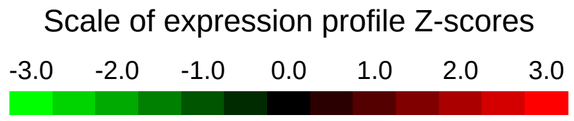

GEO Link:	**http://www.ncbi.nlm.nih.gov/geo/query/acc.cgi?acc=GSE57425**
Status:	**Public on May 09 2014**
Title:	**Gene expression data of livers from C57BL/6 fed a normal diet or high-fat-diet**
Organism:	**Mus musculus**
Experiment type:	**Expression profiling by array**
Platform:	**GPL1261**
Pubmed ID:	
Summary & Design:	**Summary:** **Obesity is tightly associated with an increased risk of nonalcoholic fatty liver disease (NAFLD). However, the molecular mechanisms of obesity-induced fatty liver remain largely unknown.In order to identify genes that are potentially involved in dysfunctional hepatic lipid homeostasis in obesity, we performed a clustering analysis of Affymetrix arrays,which revealed that a number of mRNAs were dys-regulated in the livers of mice fed a high-fat diet (HFD), compared with mice fed a normal chow diet (ND).** **Overall design:** **To identify genes that are potentially involved in dysfunctional hepatic lipid homeostasis in obesity, male C57BL/6 mice aged 8 weeks were fed a normal diet (ND) or high-fat-diet (HFD) containing 60 Kcal% of fat for 12 weeks. Then mice were sacrificed and total RNAs were isoloated from hepatic tissues. Affymetrix array hybridisation and scanning were performed using Mouse Genome 430 2.0 chips.Total RNA samples obtained from six mice per group (ND and HFD) and pooled by each of the two were used for microarray analysis.**

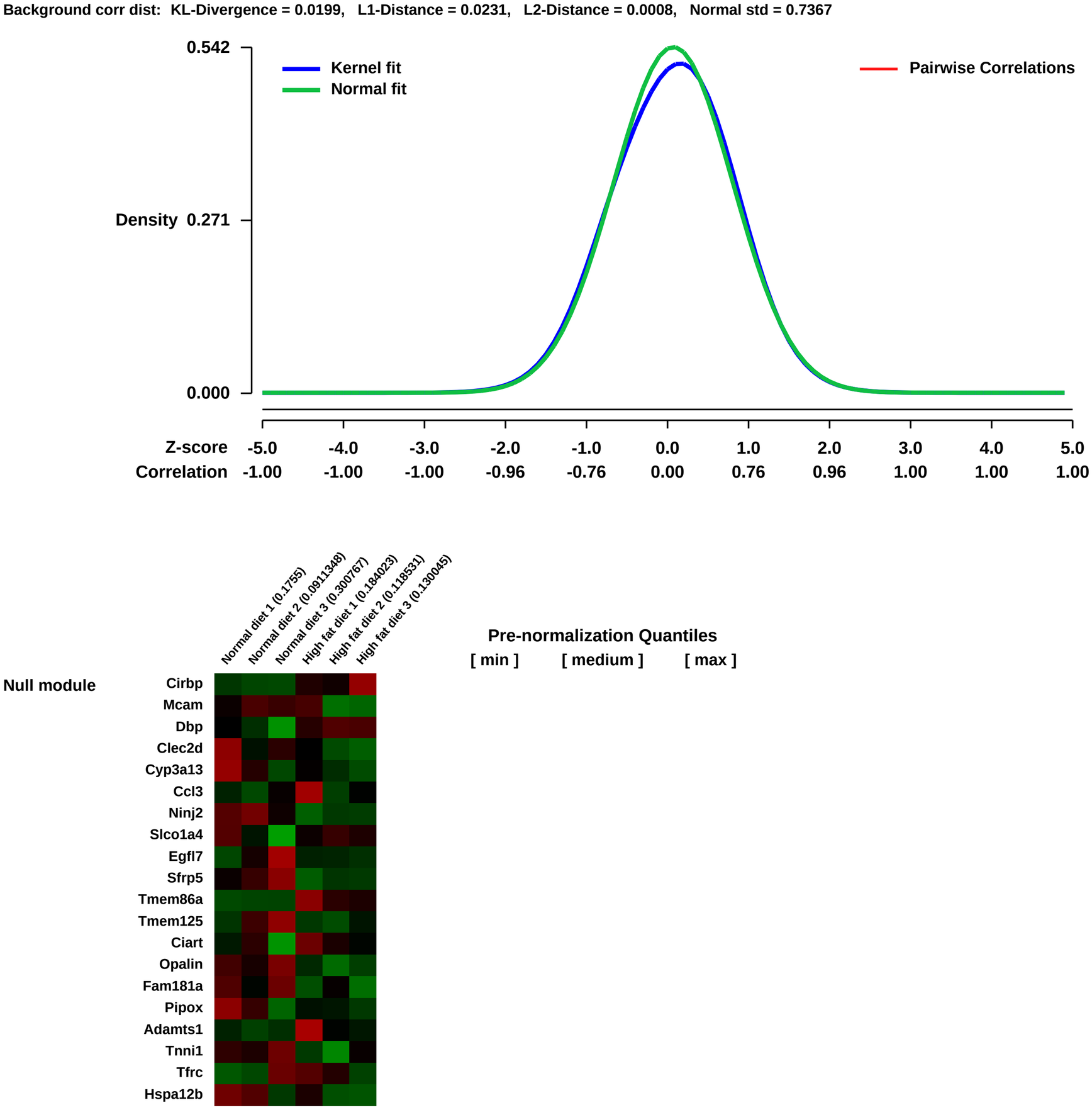

GEO Series "GSE19204" Expression Profiles

Num of samples in this series: 6

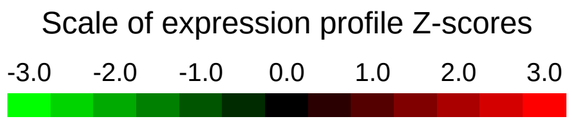

GEO Link:	http://www.ncbi.nlm.nih.gov/geo/query/acc.cgi?acc=GSE19204
Status:	Public on Feb 25 2010
Title:	Foxa2 programs Th2-cell mediated innate immunity in the developing lung.
Organism:	Mus musculus
Experiment type:	Expression profiling by array
Platform:	GPL1261
Pubmed ID:	20483781
Summary & Design:	**Summary:** Deletion of the gene encoding Foxa2, a winged helix transcription factor selectively expressed in respiratory epithelial cells, caused spontaneous pulmonary eosinophilic inflammation and goblet cell metaplasia. Loss of Foxa2 induced the recruitment and activation of myeloid dendritic cells (mDCs) and Th2 cells in the lung, and was associated with the increased production of T helper 2 (Th2) cytokines and chemokines. mRNA microarray analysis demonstrated that deletion of Foxa2 induced the expression of a number of mRNAs regulating pulmonary dendritic cell activation, Th2 mediated inflammation, and goblet cell differentiation. The spontaneous pulmonary inflammation and goblet cell metaplasia caused by loss of Foxa2 was inhibited by treatment of newborn Foxa2â /â mice with monoclonal IL-4Ralpha antibody. Expression of Foxa2 in non-ciliated secretory cells (Clara cells) in vivo inhibited goblet cell differentiation induced by pulmonary allergen exposure. The respiratory epithelium plays a central role in the regulation of Th2-mediated inflammation and innate immunity in the developing lung in a process regulated by Foxa2. **Overall design:** To investigate the role of Foxa2 and its downstream targets associated with the Th2 inflammation and goblet cell hyperplasia, RNAs were isolated from the lungs of Foxa2-/- and control littermates at PN15. Lung cRNA was hybridized to the murine genome MOE430 V2 chips.

Background corr dist: KL-Divergence = 0.0292, L1-Distance = 0.0142, L2-Distance = 0.0002, Normal std = 0.6704

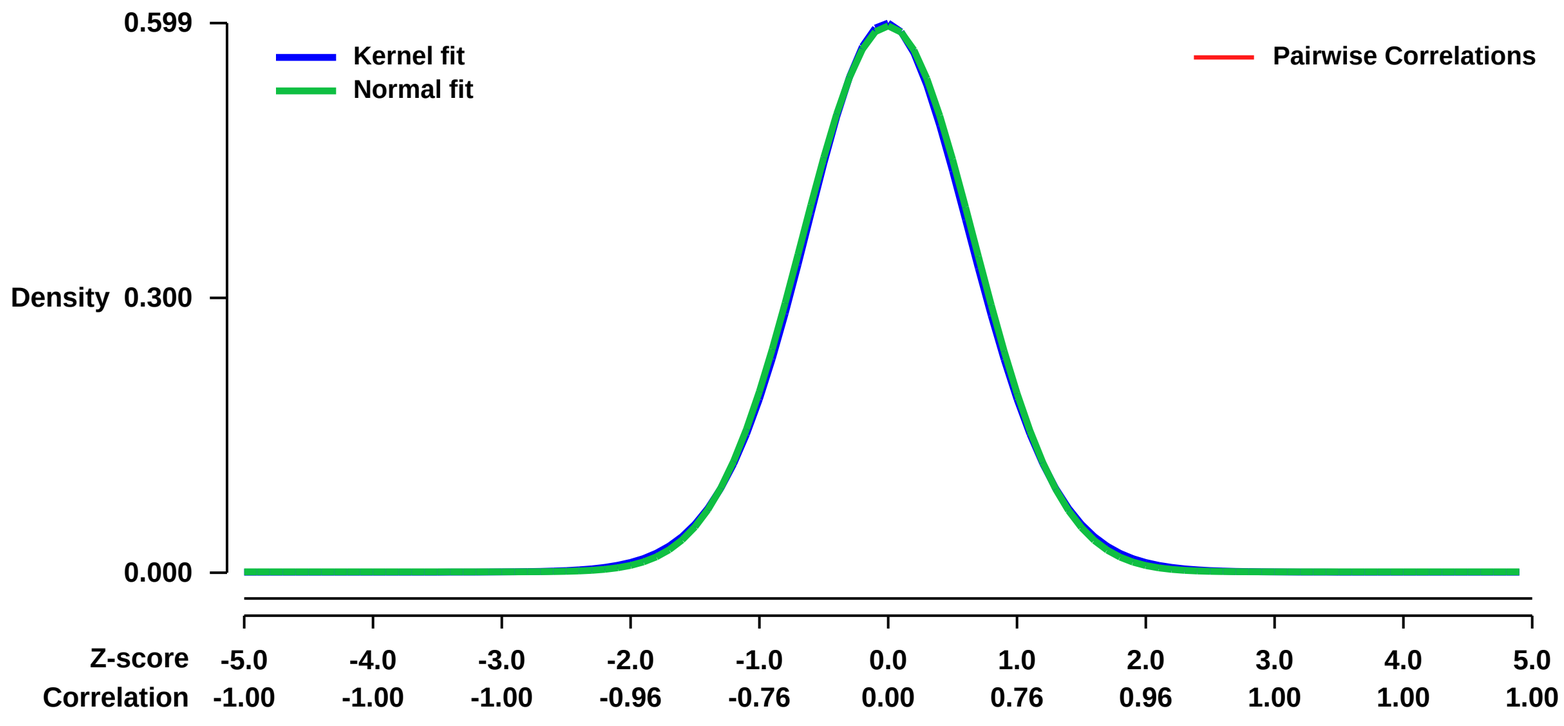

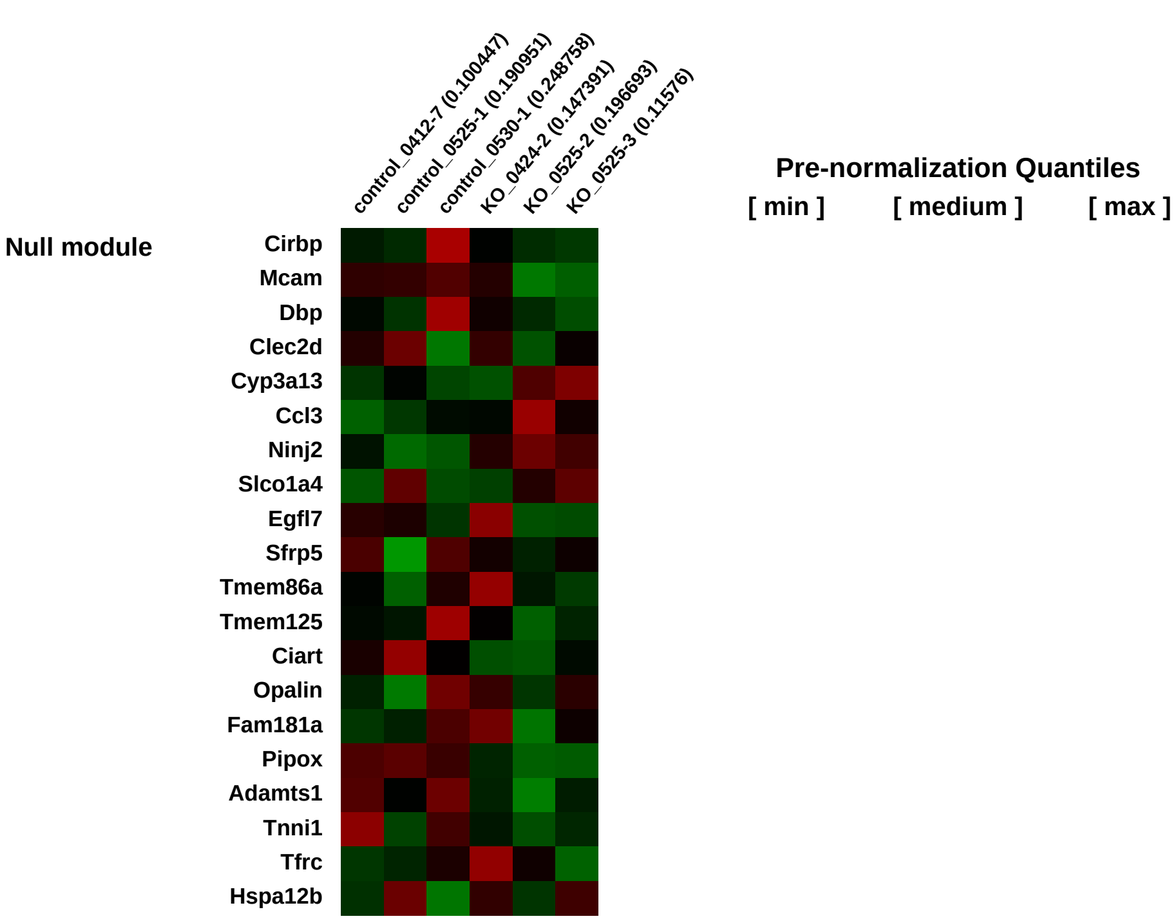

GEO Series "GSE23725" Expression Profiles

Num of samples in this series: 12

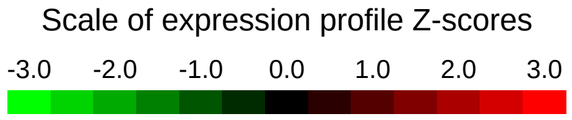

GEO Link:	**http://www.ncbi.nlm.nih.gov/geo/query/acc.cgi?acc=GSE23725**
Status:	**Public on Aug 21 2010**
Title:	**Expression data from mouse neonatal ovarian xenobiotic culture experiments**
Organism:	**Mus musculus**
Experiment type:	**Expression profiling by array**
Platform:	**GPL1261**
Pubmed ID:	**20829426**
Summary & Design:	**Summary:** **Mammalian females are born with a finite number of non-renewing primordial follicles, the majority of which remain in a quiescent state for many years. Due to their non-renewing nature, these â restingâ oocytes are particularly vulnerable to xenobiotic insult, resulting in premature ovarian senescence and the formation of dysfunctional oocytes. In this study we characterised the mechanisms of ovotoxicity for three ovotoxic agents, 4-Vinylcyclohexene Diepoxide (VCD), Methoxychlor (MXC), and Menadione (MEN), all of which target immature follicles. Neonatal mouse ovaries (PND3-4) were cultured in the presence of 4-Vinylcyclohexene Diepoxide (50uM), Methoxychlor (50uM), and Menadione (5uM) for 96 hours to observe their effects on the ovarian transcriptome. This was done in the hopes of gaining a better understanding of the mechanisms underpinning xenobiotic induced pre-antral ovotoxicity.** **Overall design:** **Ovaries from day 3-4 Swiss neonatal mice were cultured in xenobiotic containing media for 96 hours. The ovaries were then collected for RNA extraction and hybridization on Affymetrix microarrays (Mouse 430 version 2.0 GeneChip).**

Background corr dist: **KL-Divergence = 0.0684, L1-Distance = 0.0239, L2-Distance = 0.0011, Normal std = 0.5027**

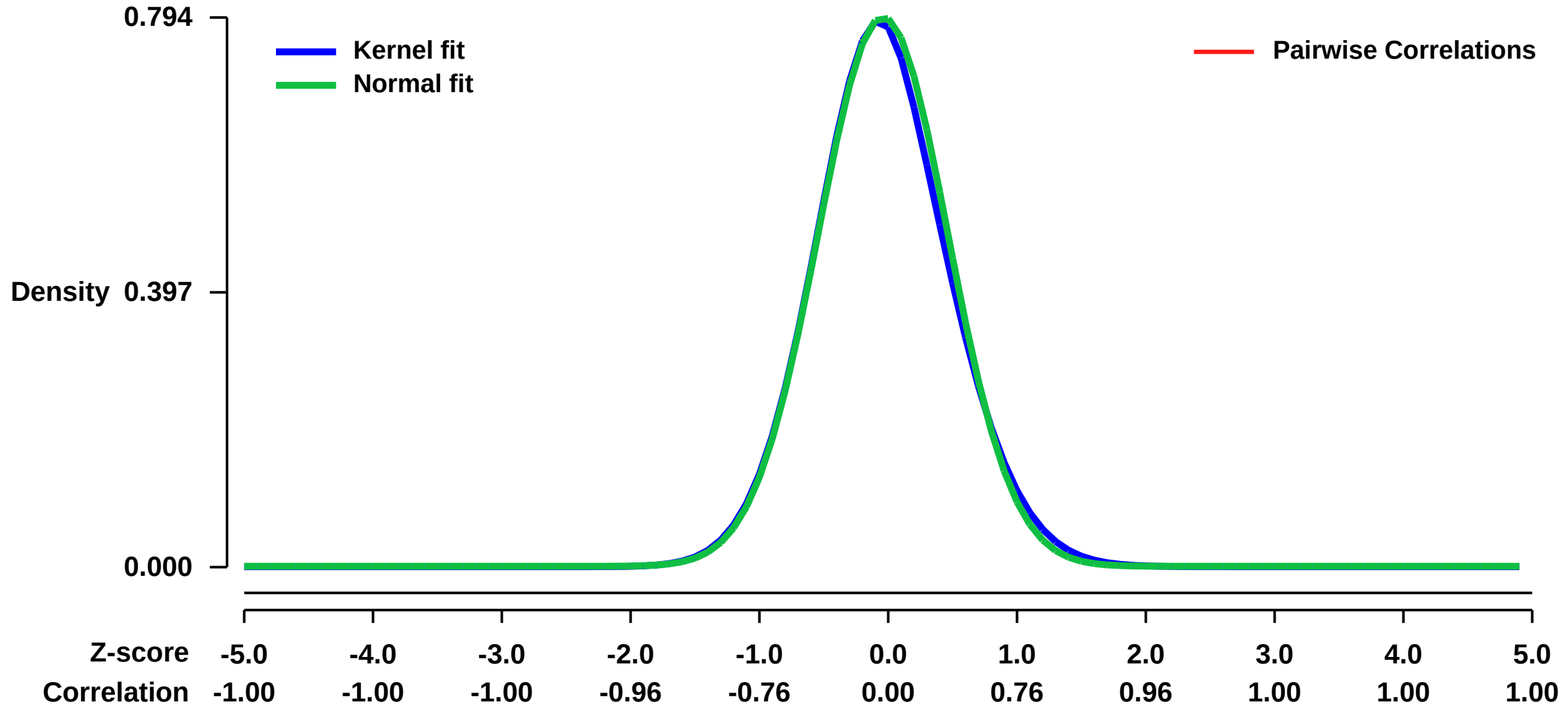

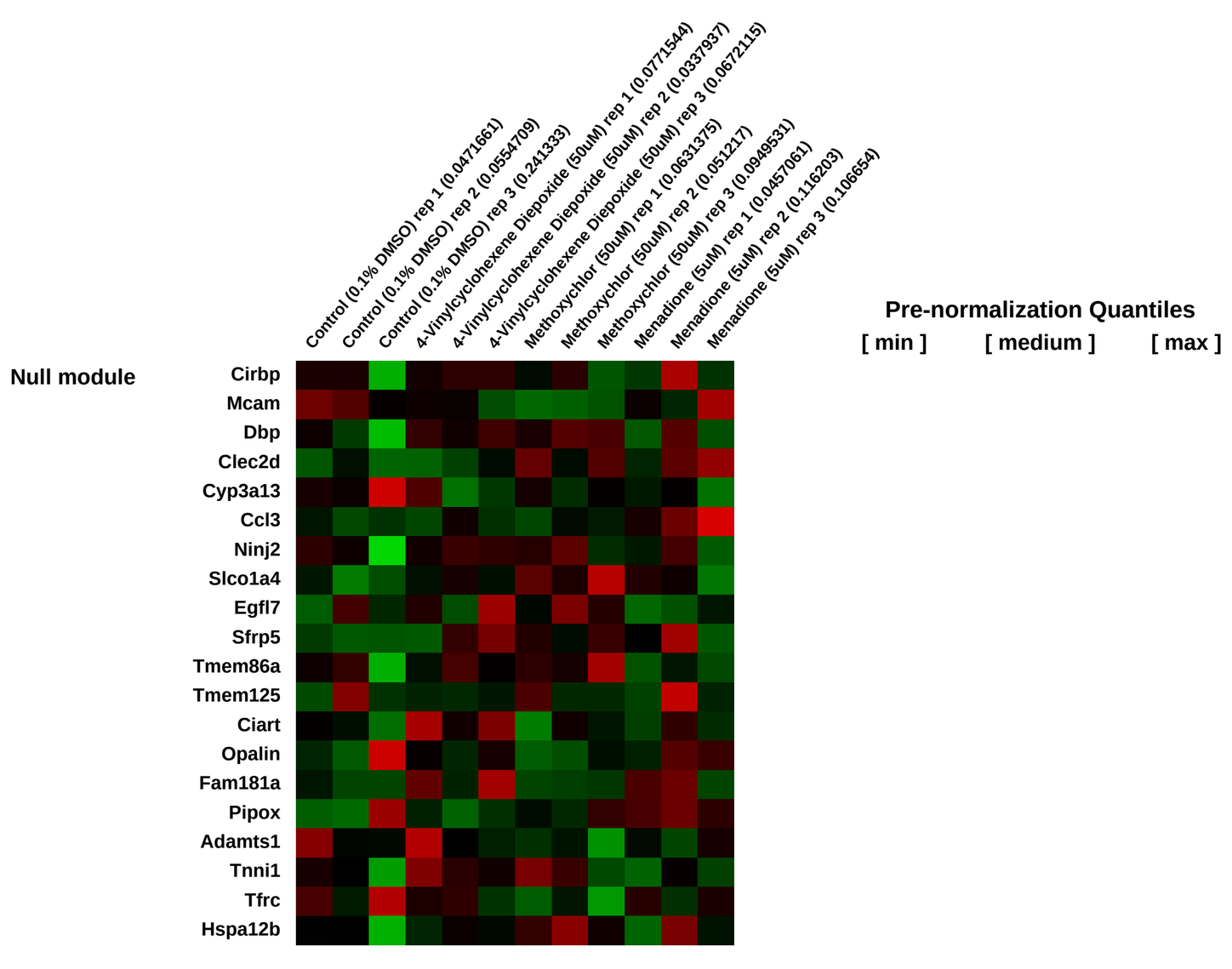

GEO Series "GSE26496" Expression Profiles

Num of samples in this series: 6

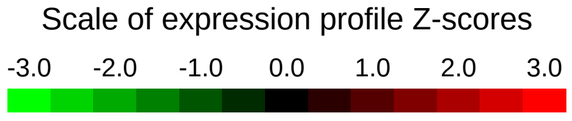

GEO Link:	**http://www.ncbi.nlm.nih.gov/geo/query/acc.cgi?acc=GSE26496**
Status:	**Public on Jan 08 2011**
Title:	**Deletion of Scap in Alveolar Type II Cells Influences Lung Lipid Homeostasis and Identifies a Compensatory Role for Pulmonary Lipofibroblasts**
Organism:	**Mus musculus**
Experiment type:	**Expression profiling by array**
Platform:	**GPL1261**
Pubmed ID:	
Summary & Design:	**Summary:** **Pulmonary function after birth is dependent upon surfactant lipids that reduce surface tension in the alveoli. The sterol-responsive element-binding proteins (SREBPs) are transcription factors regulating expression of genes controlling lipid homeostasis in many tissues. To identify the role of SREBPs in the lung, we conditionally deleted the SREBP cleavage-activating protein gene, Scap, in respiratory epithelial cells (Scapâ /â) in vivo. Prior to birth (E18.5), deletion of Scap decreased the expression of both SREBPs and a number of genes regulating fatty acid and cholesterol metabolism. Nevertheless, Scapâ /â mice survived postnatally, surfactant and lung tissue lipids being substantially normalized in adult Scapâ /â mice. Although phospholipid synthesis was decreased in type II cells from adult Scapâ /â mice, lipid storage, synthesis, and transfer by lung lipofibroblasts were increased. mRNA microarray data indicated that SCAP influenced two major gene networks, one regulating lipid metabolism and the other stress-related responses. Deletion of the SCAP/SREBP pathway in respiratory epithelial cells altered lung lipid homeostasis and induced compensatory lipid accumulation and synthesis in lung lipofibroblasts.** **Overall design:** **To identify the role of SREBPs in the lung, we conditionally deleted the SREBP cleavage-activating protein gene, Scap, in respiratory epithelial cells (Scapâ /â) in vivo.Lung cRNA was hybridized to the murine genome MOE430 V2 chips.**

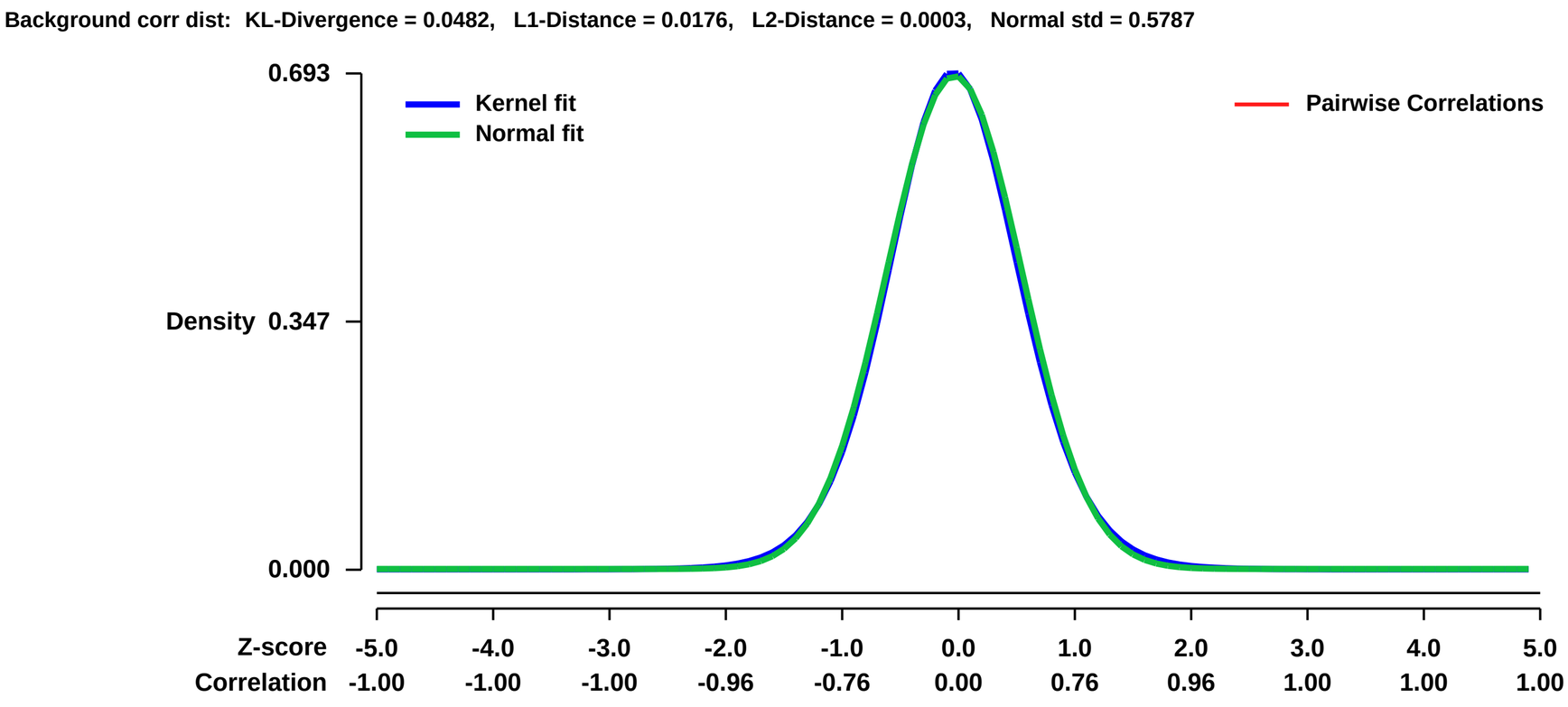

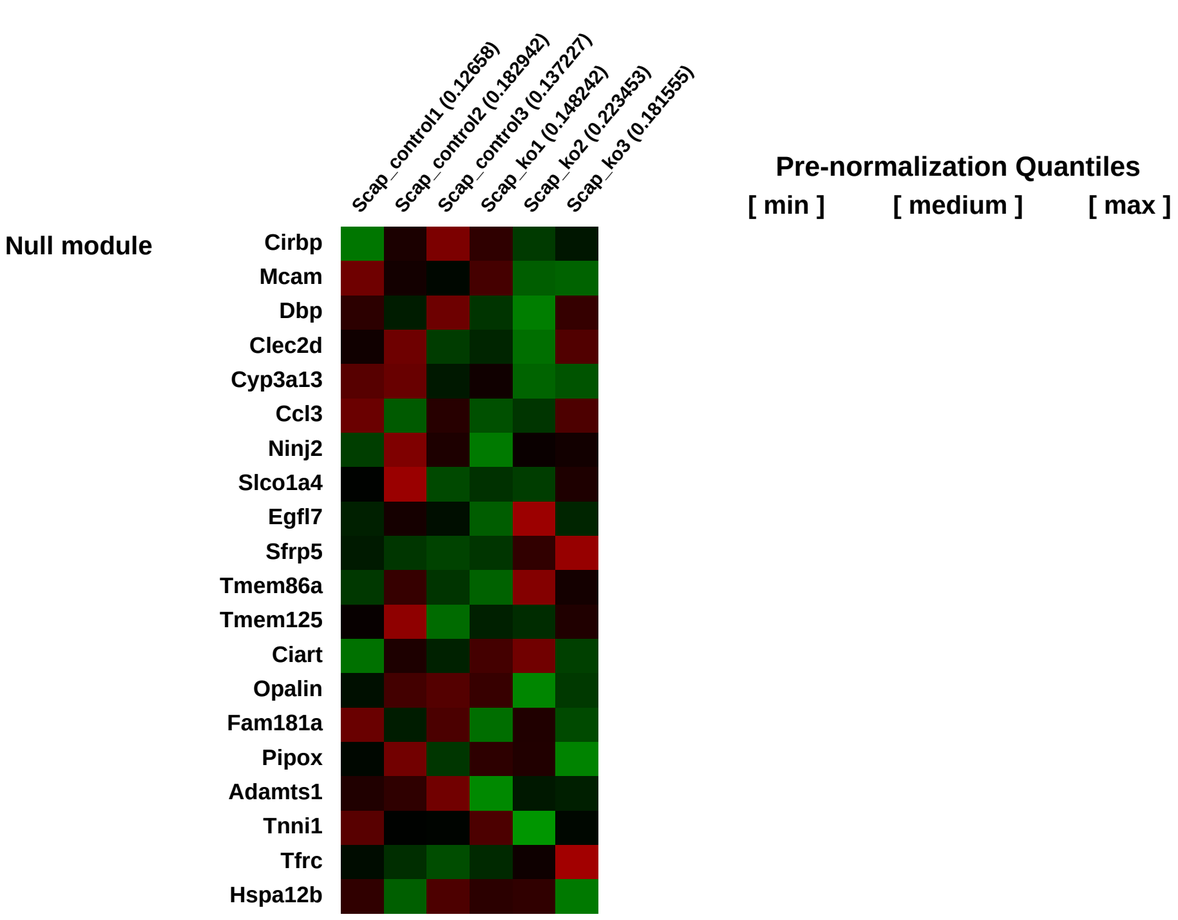

GEO Series "GSE46871" Expression Profiles

Num of samples in this series: 6

Scale of expression profile Z-scores

-3.0 -2.0 -1.0 0.0 1.0 2.0 3.0

GEO Link:	http://www.ncbi.nlm.nih.gov/geo/query/acc.cgi?acc=GSE46871
Status:	Public on May 14 2013
Title:	Hippocampal gene expression profiling of a model of Alzheimer‘s Disease upon treatment with the ACE inhibitor captopril
Organism:	Mus musculus
Experiment type:	Expression profiling by array
Platform:	GPL1261
Pubmed ID:	23959119
Summary & Design:	**Summary:** Extracellular senile plaques of amyloid beta (Abeta) are a pathological hallmark in brain of patients with Alzheimer‘s Disease (AD). Abeta is generated by the amyloidogenic processing of the amyloid precursor protein (APP). Concomitant to Abeta load, AD brain is characterized by an increase in protein level and activity of the angiotensin-converting enzyme (ACE). ACE inhibitors are a widely used class of drugs with established benefits for patients with cardiovascular disease. However, the role of ACE and ACE inhibition in the development of Abeta plaques and the process of AD-related neurodegeneration is not clear since ACE was reported to degrade Abeta. To investigate the effect of ACE inhibition on AD-related pathomechanisms, we used Tg2576 mice with neuron-specific expression of APPSwe as AD model. From 12 months of age, substantial Abeta plaque load accumulates in the hippocampus of Tg2576 mice as a brain region, which is highly vulnerable to AD-related neurodegeneration. The effect of central ACE inhibition was studied by treatment of 12 month-old Tg2576 mice for six months with the brain penetrating ACE inhibitor captopril. At an age of 18 months, hippocampal gene expression profiling was performed of captopril-treated Tg2576 mice relative to untreated 18 month-old Tg2576 controls with high Abeta plaque load. As an additional control, we used 12 month-old Tg2576 mice with low Abeta plaque load. Whole genome microarray gene expression profiling revealed gene expression changes induced by the brain-penetrating ACE inhibitor captopril, which could reflect the neuro-regenerative potential of central ACE inhibition. **Overall design:** Microarray gene expression profiling was performed of hippocampi isolated from aged, 18 month-old Tg2576 (APPSwe-transgenic) AD mice with high Abeta plaque load relative to age-matched Tg2576 mice, which were treated for 6 months with the centrally active ACE inhibitor captopril. Another study group consisted of 12 month-old Tg2576 mice with low Abeta plaque load. In total, three study groups were analyzed, i.e. (i) 18 month-old untreated Tg2576 mice with high Abeta plaque load, (ii) age-matched Tg2576 mice treated for 6 months with the brain-penetrating ACE inhibitor captopril (20 mg/kg body weight/day in drinking water), and (iii) untreated 12 month-old Tg2576 mice with low Abeta plaque load reflecting the time point when captopril treatment was initiated. Two biological replicates were made of each group, and total hippocampal RNA of four mice was pooled for one gene chip.

Background corr dist: KL-Divergence = 0.0289, L1-Distance = 0.0256, L2-Distance = 0.0007, Normal std = 0.6941

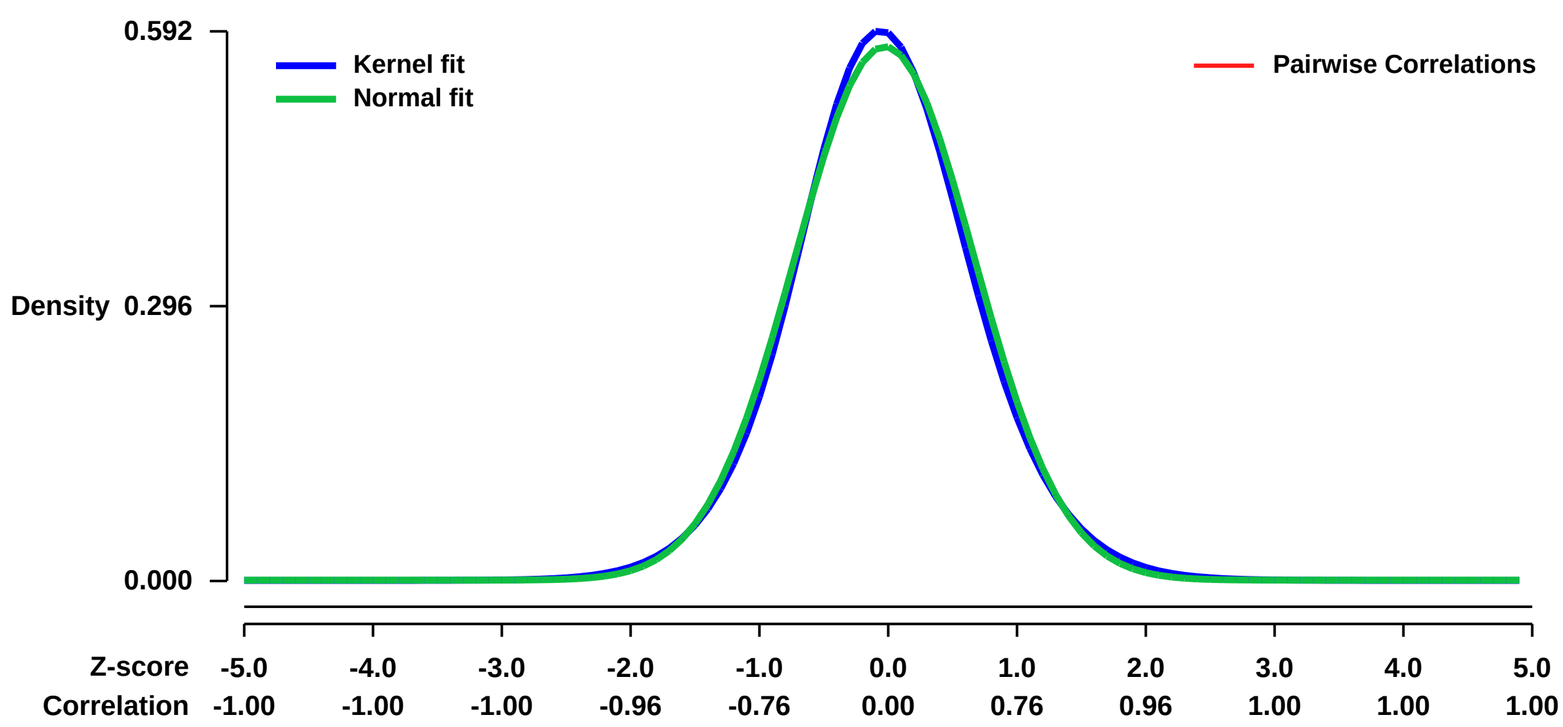

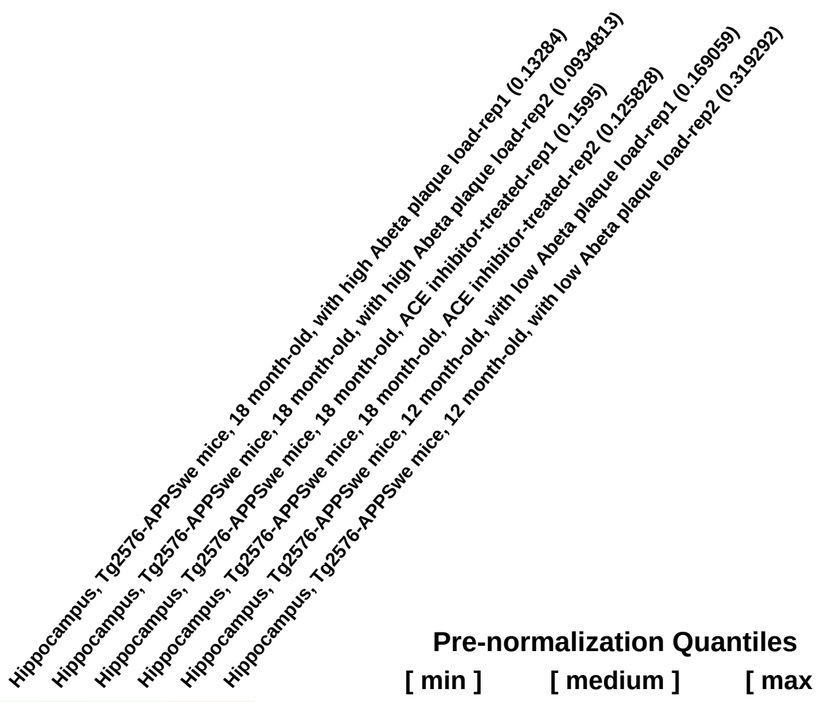

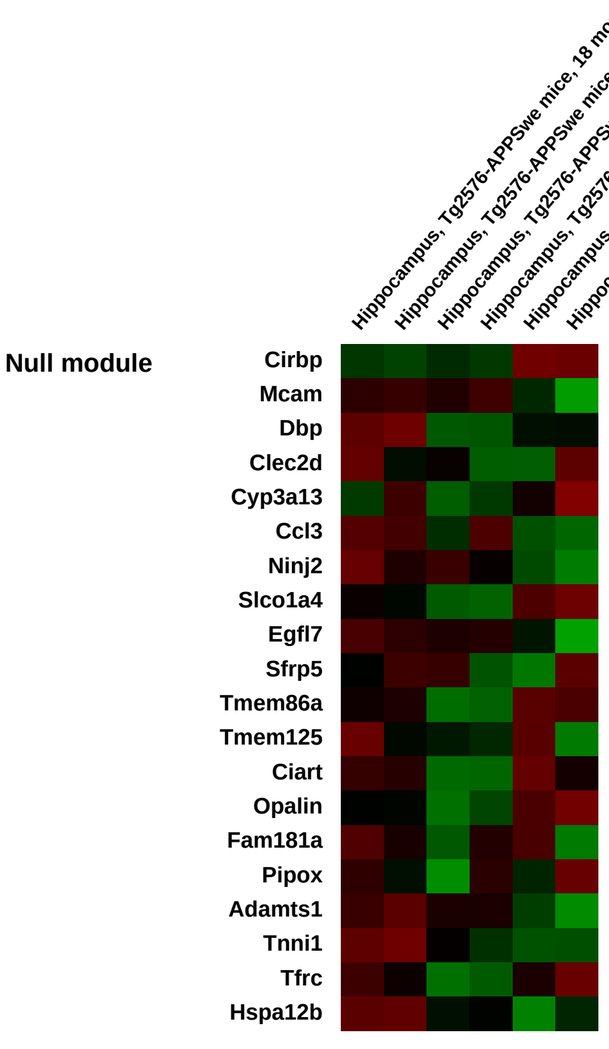

GEO Series "GSE32653" Expression Profiles

Num of samples in this series: 6

Scale of expression profile Z-scores

-3.0 -2.0 -1.0 0.0 1.0 2.0 3.0

GEO Link:	http://www.ncbi.nlm.nih.gov/geo/query/acc.cgi?acc=GSE32653
Status:	Public on Mar 07 2013
Title:	Hlxb9 regulated genes in pancreatic beta cells
Organism:	Mus musculus
Experiment type:	Expression profiling by array
Platform:	GPL1261
Pubmed ID:	23419452
Summary & Design:	**Summary:** Hlxb9 is a differentiation factor important for neuronal, and pancreatic beta cell differentiation. It is a transcription factor that represses transcription. It's target genes are unknown. The mouse pancreatic beta cell line MIN6 was used to assess the expression of genes de-repressed upon Hlxb9 knockdown. **Overall design:** Several independent transfections of MIN6 cells were performed with scrambled negative control siRNA (Qiagen) or with mouse Hlxb9 siRNA (Dharmacon). The cells were processed for RNA isolation and whole cell protein extracts, 72 hours post-transfection. The level of Hlxb9 knockdown was assessed by western blot analysis. RNA preps from those samples that showed more than 75% knockdown were used for microarray analysis.

Background corr dist: KL-Divergence = 0.0259, L1-Distance = 0.0136, L2-Distance = 0.0002, Normal std = 0.6933

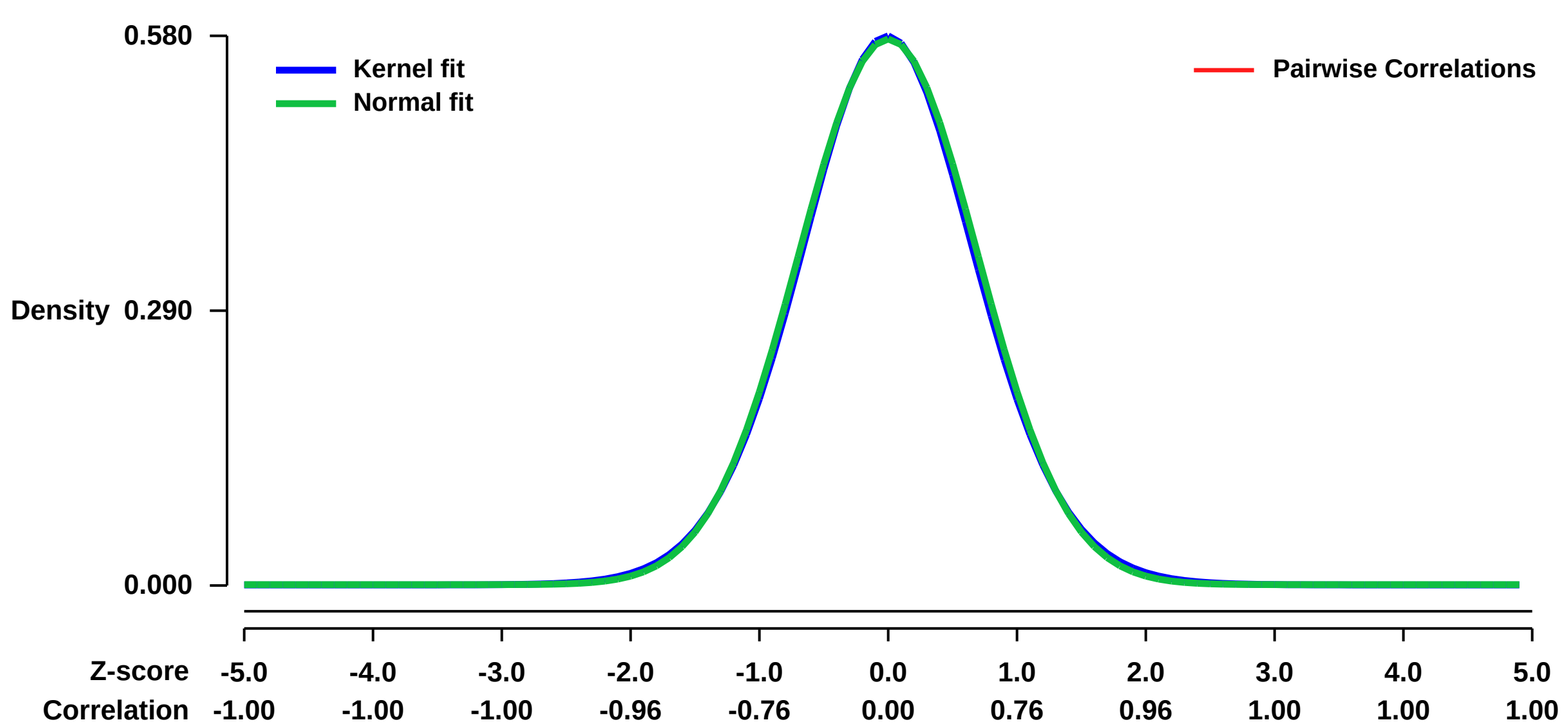

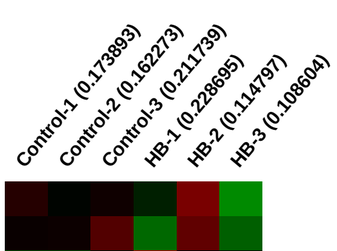

Pre-normalization Quantiles

[min] [medium] [max]

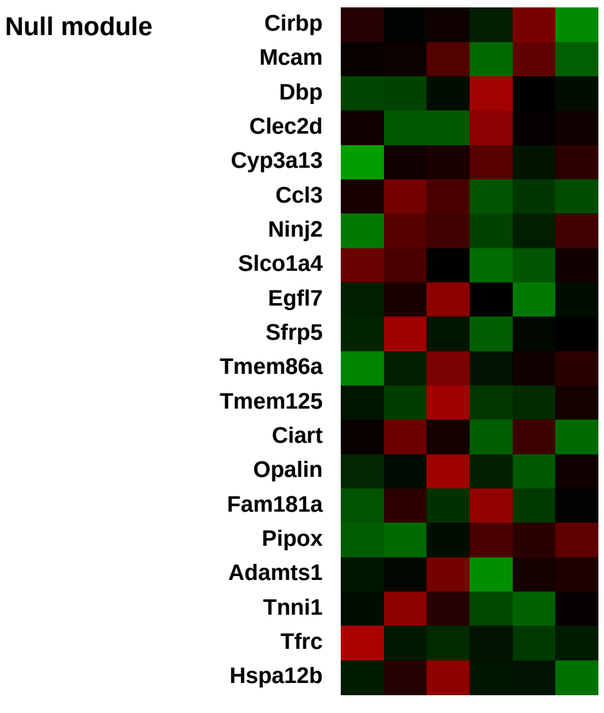

GEO Series "GSE12248" Expression Profiles

Num of samples in this series: 83

Scale of expression profile Z-scores

-3.0 -2.0 -1.0 0.0 1.0 2.0 3.0

GEO Link: http://www.ncbi.nlm.nih.gov/geo/query/acc.cgi?acc=GSE12248
Status: Public on Dec 31 2008
Title: Genetic architecture of murine skin inflammation and tumor susceptibility
Organism: Mus musculus x Mus spretus
Experiment type: Expression profiling by array
Platform: GPL1261
Pubmed ID: 19136944

Summary & Design:

Summary:
Gene expression in self-renewing epithelial tissues is controlled by cis- and trans-activating regulatory factors that mediate responses to exogenous agents capable of causing tissue damage, infection, inflammation, or tumorigenesis. We used network construction methods to analyze the genetic architecture of gene expression in normal mouse skin in a cross between tumor-susceptible Mus musculus and tumor-resistant Mus spretus. We demonstrate that gene expression motifs representing different constituent cell types within the skin such as hair follicle cells, haematopoietic cells, and melanocytes are under separate genetic control. Motifs associated with inflammation, epidermal barrier function and proliferation are differentially regulated in mice susceptible or resistant to tumor development. The intestinal stem cell marker Lgr5 is identified as a candidate master regulator of hair follicle gene expression, and the Vitamin D receptor (Vdr) links epidermal barrier function, inflammation, and tumor susceptibility.

Keywords: Expression Quantitative Trait Loci

Overall design:
A backcross was generated using male Mus spretus and female FVB/N mice; female F1 hybrids were mated with male FVB/N mice. Seventy-one backcross mice (8-12 weeks old) received a single dose of DMBA (25 ´¡g per mouse in 200 ´¡l acetone). Starting one week after the initiation tumors were promoted with TPA (200 ´¡l of 10-4 M solution in acetone) twice weekly for 20 weeks. Initiation and promotion were performed on doral back skin. Normal tail skin was snap frozen when the animals were sacrificed. Tail epidermis from completely untreated Spretus, FVB, and Spretus x FVB F1 mice was also analyzed.

Background corr dist: KL-Divergence = 0.4400, L1-Distance = 0.0894, L2-Distance = 0.0259, Normal std = 0.2378

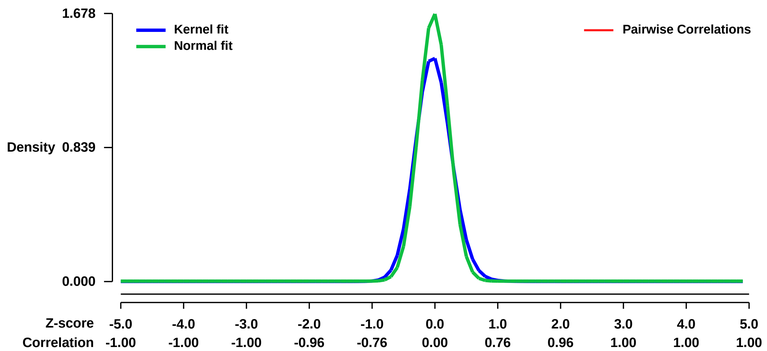

Null module

Pre-normalization Quantiles
[min] [medium] [max]

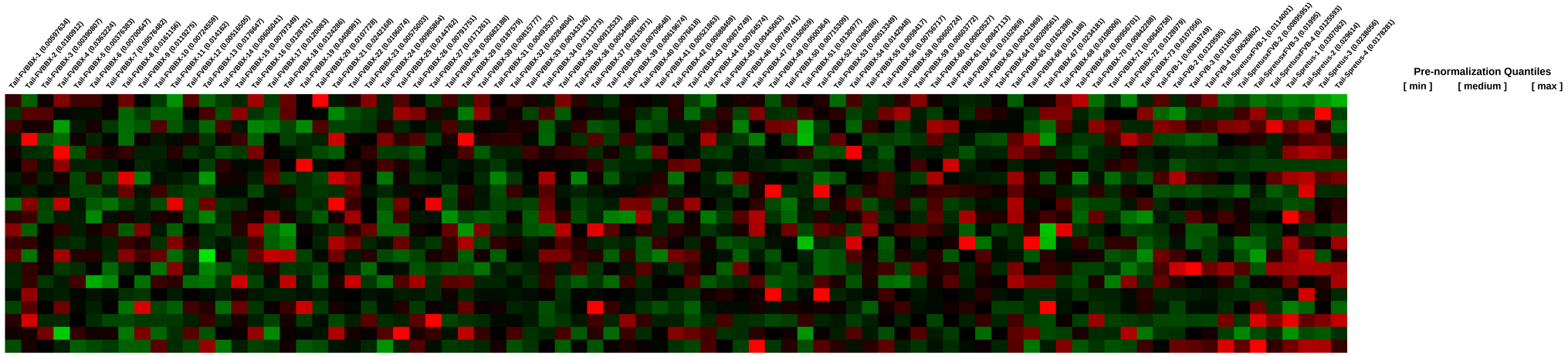

GEO Series "GSE7342" Expression Profiles

Num of samples in this series: 12

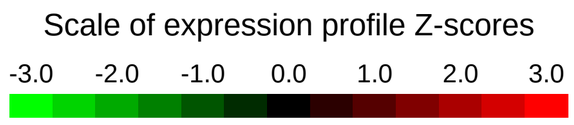

GEO Link:	http://www.ncbi.nlm.nih.gov/geo/query/acc.cgi?acc=GSE7342
Status:	Public on Mar 23 2007
Title:	Expression data from p38 knock out versus wild type fetal liver
Organism:	Mus musculus
Experiment type:	Expression profiling by array
Platform:	GPL1261
Pubmed ID:	17468757
Summary & Design:	**Summary:** The mitogen-activated protein kinase (MAPK) p38alpha controls inflammatory responses and cell proliferation. Using mice carrying conditional p38alpha alleles, we investigated its function in postnatal development and tumorigenesis. When p38alpha is specifically deleted in the mouse embryo, fetuses develop to term but die shortly after birth, likely due to lung dysfunction. Fetal hematopoietic cells and embryonic fibroblasts deficient in p38alpha display increased proliferation, resulting from sustained activation of the c-Jun N-terminal kinase (JNK)/c-Jun pathway. Importantly, in chemical-induced liver cancer development, mice with liver-specific deletion of p38alpha show enhanced hepatocyte proliferation and tumor development that also correlates with JNK/c-Jun upregulation. Furthermore, increased proliferation of p38alpha-deficient hepatocytes and tumor cells is suppressed by inactivation of JNK or c-Jun. These results reveal a novel mechanism whereby p38alpha negatively regulates cell proliferation through antagonizing the JNK/c-Jun pathway in multiple cell types and in liver cancer development. We used microarrays to identifiy differental regulated genes by p38alpha in fetal liver cells **Keywords:** time course **Overall design:** Wild type and p38 deficient fetal liver cell were used for RNA extraction and hybridization on Affymetrix microarrays.

Background corr dist: KL-Divergence = 0.0482, L1-Distance = 0.0409, L2-Distance = 0.0034, Normal std = 0.5674

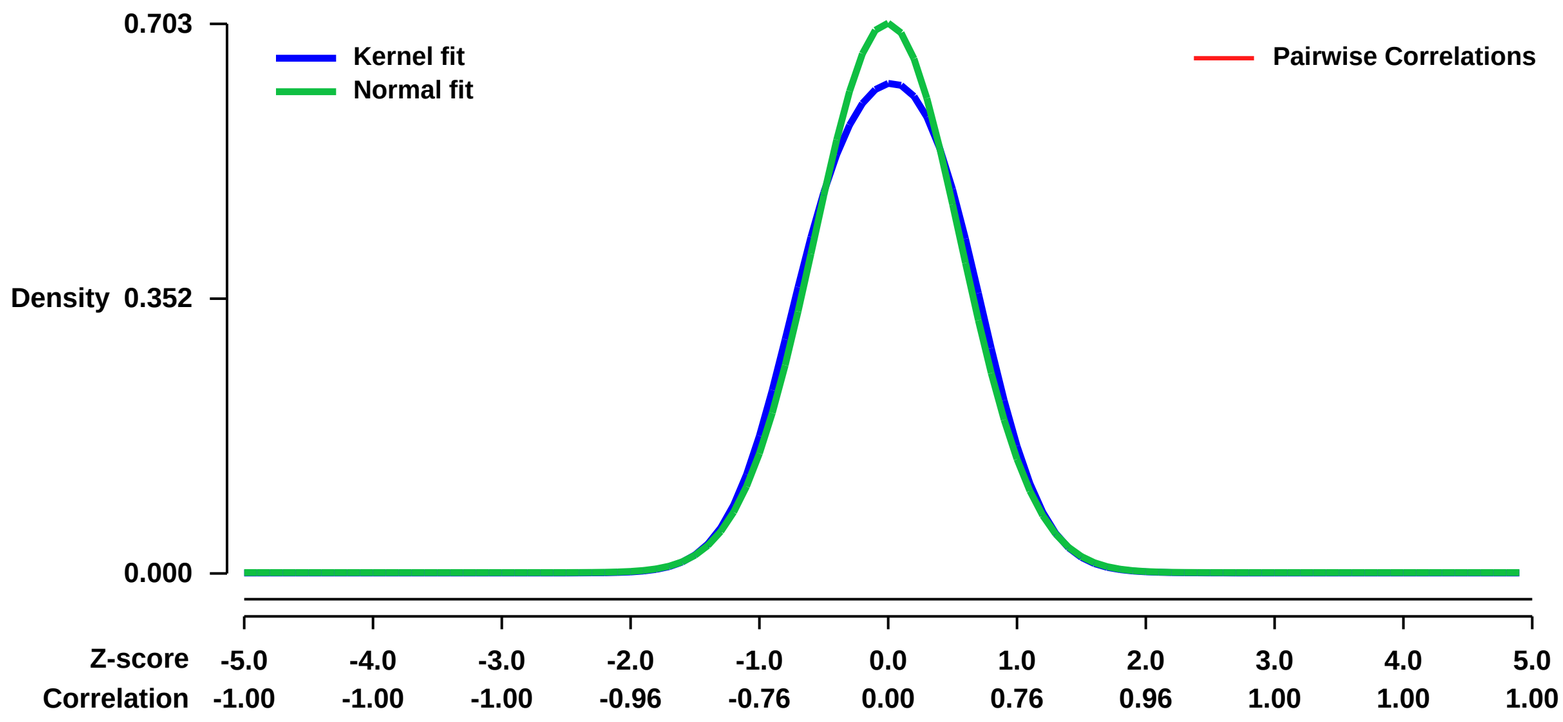

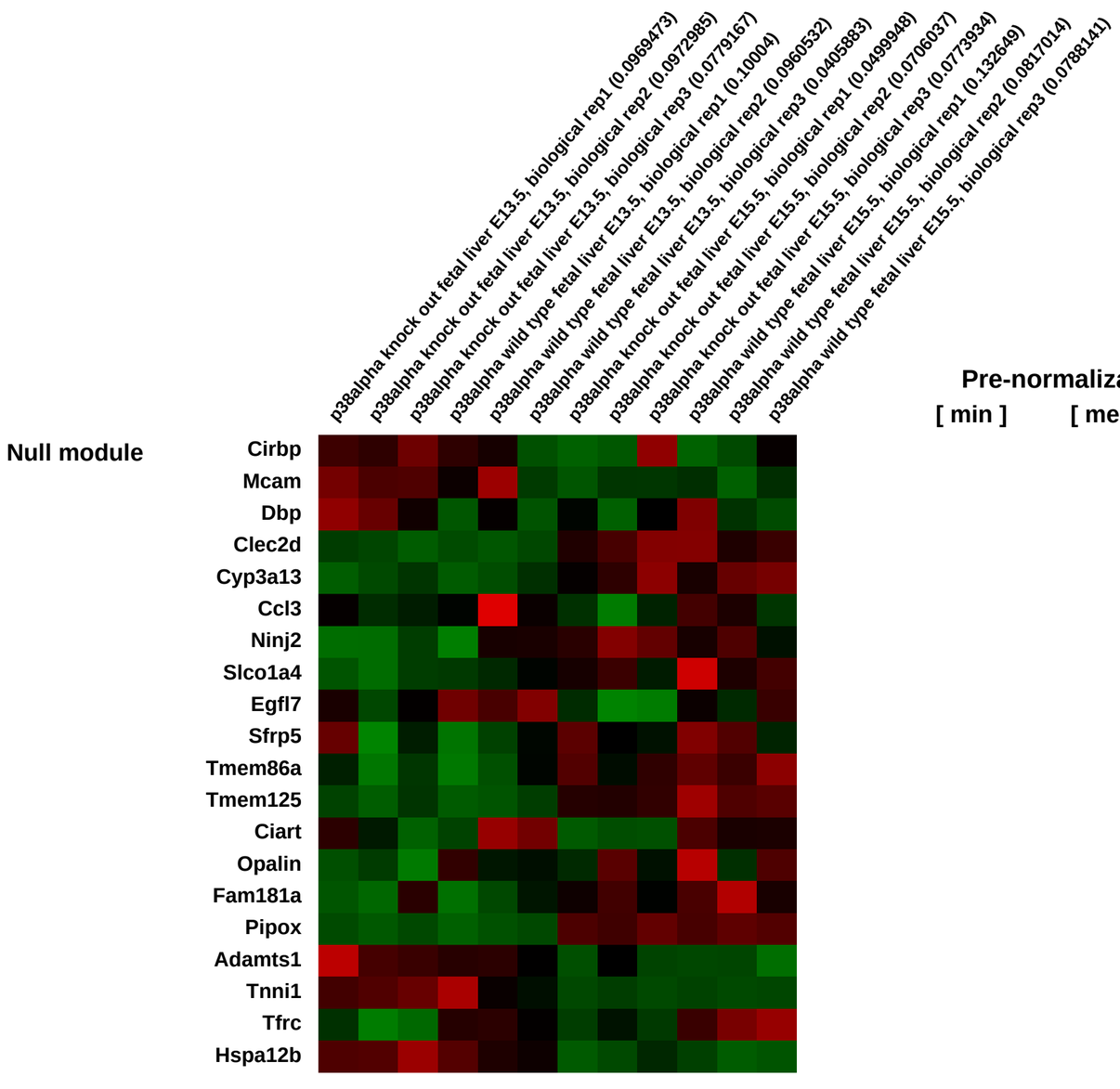

GEO Series "GSE30767" Expression Profiles

Num of samples in this series: 8

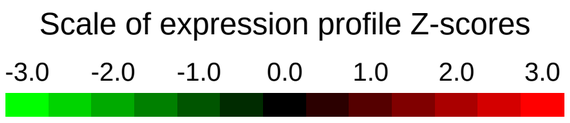

GEO Link:	http://www.ncbi.nlm.nih.gov/geo/query/acc.cgi?acc=GSE30767
Status:	Public on Dec 01 2011
Title:	Vascular endothelial growth factor (VEGF) isoform regulation of early forebrain development
Organism:	Mus musculus
Experiment type:	Expression profiling by array
Platform:	GPL1261
Pubmed ID:	21803034
Summary & Design:	**Summary:** This work was designed to determine the role of the vascular endothelial growth factor A (VEGF) isoforms during early neuroepithelial development in the mammalian central nervous system (CNS), specifically in the forebrain. An emerging model of interdependence between neural and vascular systems includes VEGF, with its dual roles as a potent angiogenesis factor and neural regulator. Although a number of studies have implicated VEGF in CNS development, little is known about the role that the different VEGF isoforms play in early neurogenesis. We used a mouse model of disrupted VEGF isoform expression that eliminates the predominant brain isoform, VEGF164, and expresses only the diffusible form, VEGF120. We tested the hypothesis that VEGF164 plays a key role in controlling neural precursor populations in developing cortex. We used microarray analysis to compare gene expression differences between wild type and VEGF120 mice at E9.5, the primitive stem cell stage of the neuroepithelium. We quantified changes in PHH3-positive nuclei, neural stem cell markers (Pax6 and nestin) and the Tbr2-positive intermediate progenitors at E11.5 when the neural precursor population is expanding rapidly. Absence of VEGF164 (and VEGF188) leads to reduced proliferation without an apparent effect on the number of Tbr2-positive cells. There is a corresponding reduction in the number of mitotic spindles that are oriented parallel to the ventricular surface relative to those with a vertical or oblique angle. These results support a role for the VEGF isoforms in supporting the neural precursor population of the early neuroepithelium. **Overall design:** Four samples each of E9.5 wildtype or VEGF120 mouse forebrain were analyzed with the Mouse 430 2.0 Affymetrix GeneChip

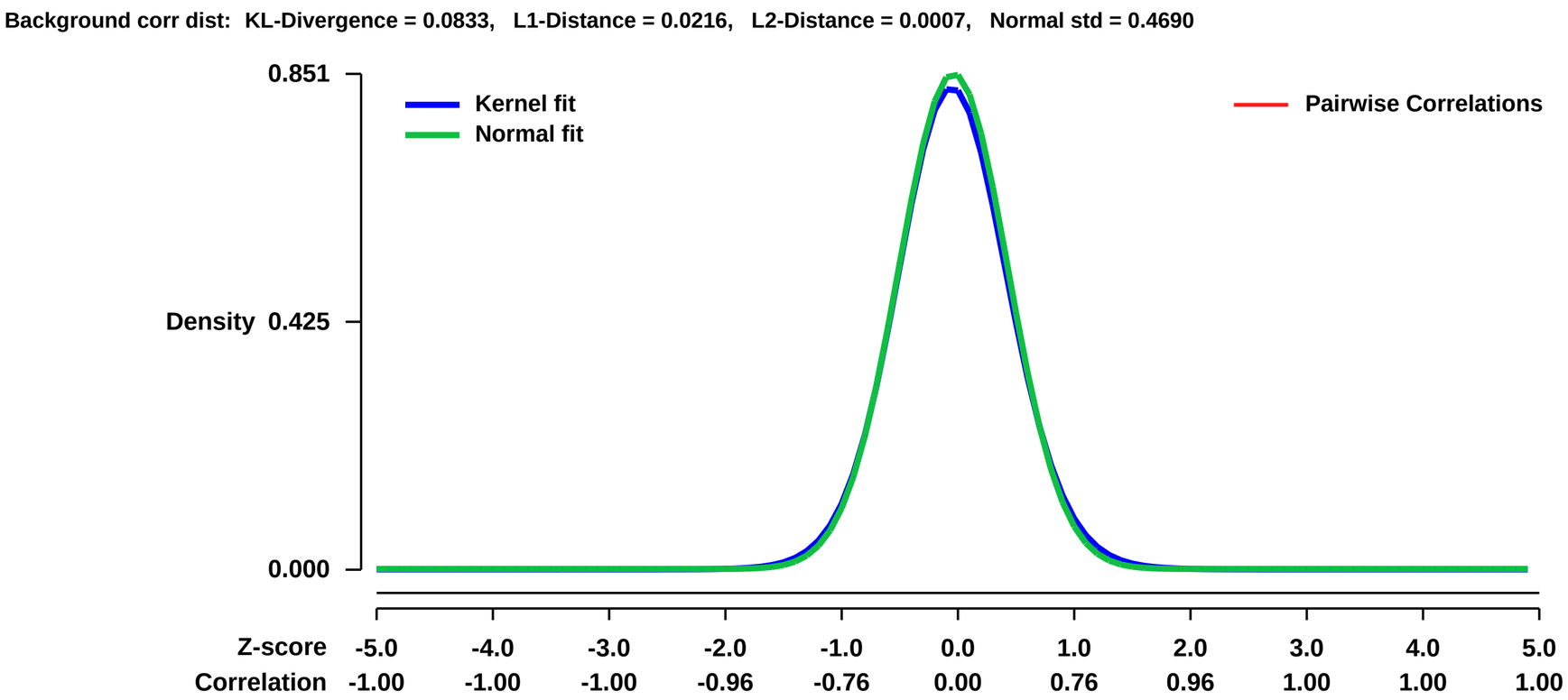

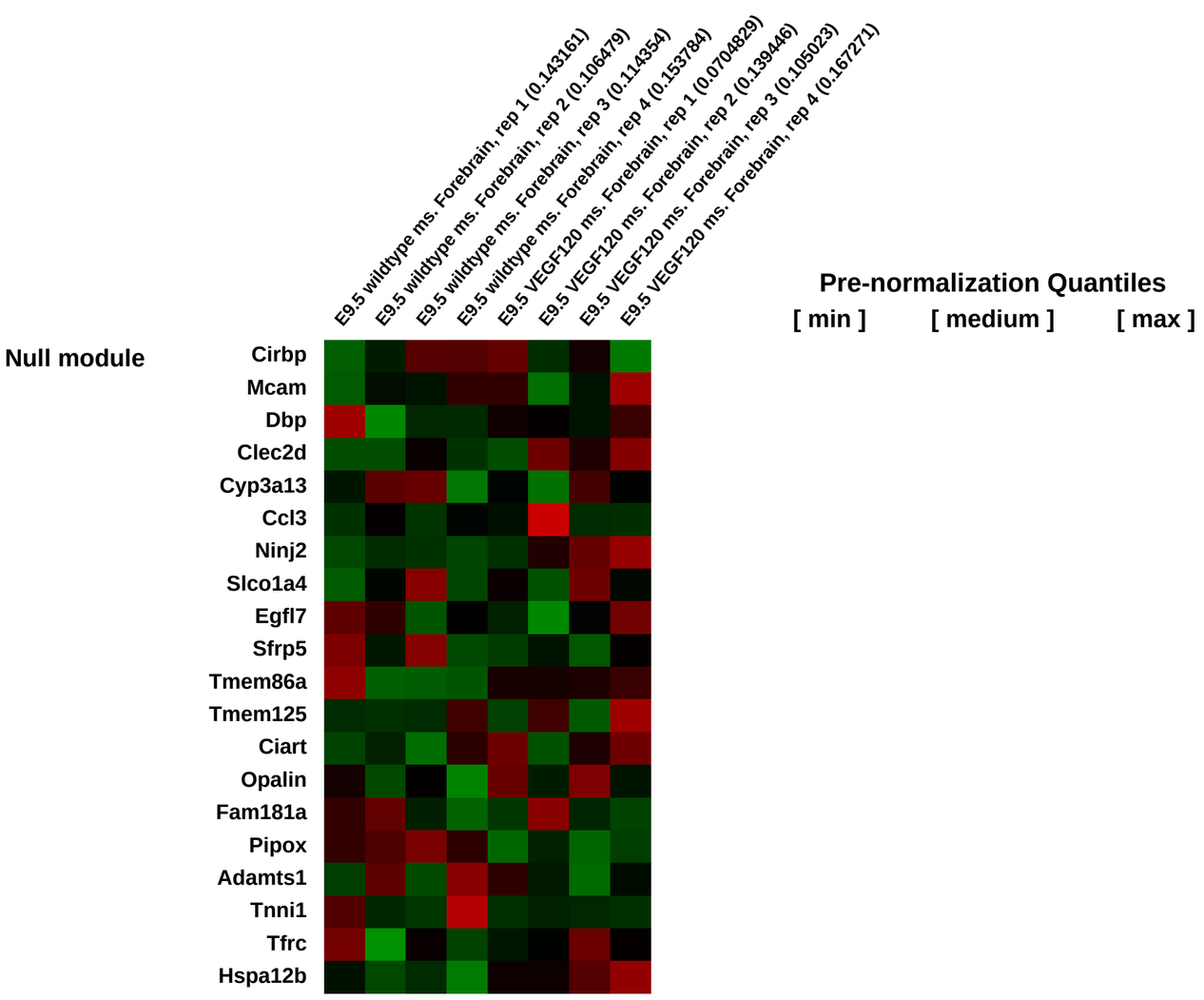

GEO Series "GSE16790" Expression Profiles

Num of samples in this series: 18

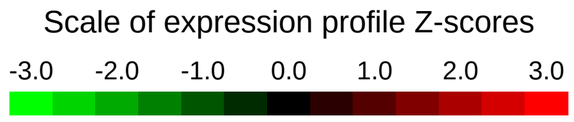

GEO Link:	http://www.ncbi.nlm.nih.gov/geo/query/acc.cgi?acc=GSE16790
Status:	Public on Apr 29 2011
Title:	Caloric Restriction in Leptin Deficiency Worsens Myocardial Steatosis
Organism:	Mus musculus
Experiment type:	Expression profiling by array
Platform:	GPL1261
Pubmed ID:	21427359
Summary & Design:	**Summary:** **Caloric Restriction in Leptin Deficiency Worsens Myocardial Steatosis: Failure to Upregulate PPAR gamma and Thermogenic Glyecrolipid/Fatty Acid Cycling** **Growing evidence supports an anti-lipotoxic role for leptin in preventing inappropriate peripheral tissue lipid deposition. Obese, leptin deficient ob/ob mice develop left ventricular (LV) hypertrophy and myocardial steatosis with increased apoptosis and decreased longevity. Here we investigated the cardiac effects of caloric restriction in leptin deficiency. Echocardiography was performed on C57Bl/6 wild-type mice (WT) and 7-month-old ob/ob mice fed ad lib, leptin-repleted (LR-ob/ob), or calorie-restricted (CR-ob/ob) for four weeks. Ventricular tissue was examined by electron microscopy (EM), mitochondrial coupling assay, and microarray expression profiling. LR and CR-ob/ob mice showed decreased body weight, heart weight, and LV wall thickness compared to ad lib ob/ob mice. LV fractional shortening was decreased in ad lib ob/ob mice, but restored to WT levels in LR and CR groups. However, EM revealed severe cardiac steatosis in the CR-ob/ob group compared to only moderate steatosis in ad lib ob/ob . Despite marked cardiac steatosis, CR (like LR) restored mitochondrial coupling to WT levels. CR up-regulated genes associated with oxidative stress and cell death, changes suggestive of cardiac lipotoxicity. LR, but not CR was shown to induce core genes involved in glycerolipid/free fatty acid cycling, a highly thermogenic pathway that can reduce intracellular lipid stores. LR, but not CR up-regulated and restored PGC1-alpha and PPAR-alpha to wild type levels; CR paradoxically further suppressed cardiac PPAR-alpha. Thus, leptin is essential in protecting the heart from lipotoxicity, and the inability to up-regulate the thermogenic glycerolipid/free fatty acid cycling pathway may impair the response of leptin deficient animals to the lipotoxic stress of calorie restriction.** **Overall design:** **6 month aged ob/ob mice were either leptin repleted with osmotic mini-pumps, calorie restricted to match the caloric intake of the leptin repleted mice, or fed ad lib for one month. 6-8 month C57Bl/6J mice were aged to serve as controls.**

Background corr dist: KL-Divergence = 0.2714, L1-Distance = 0.0612, L2-Distance = 0.0098, Normal std = 0.2917

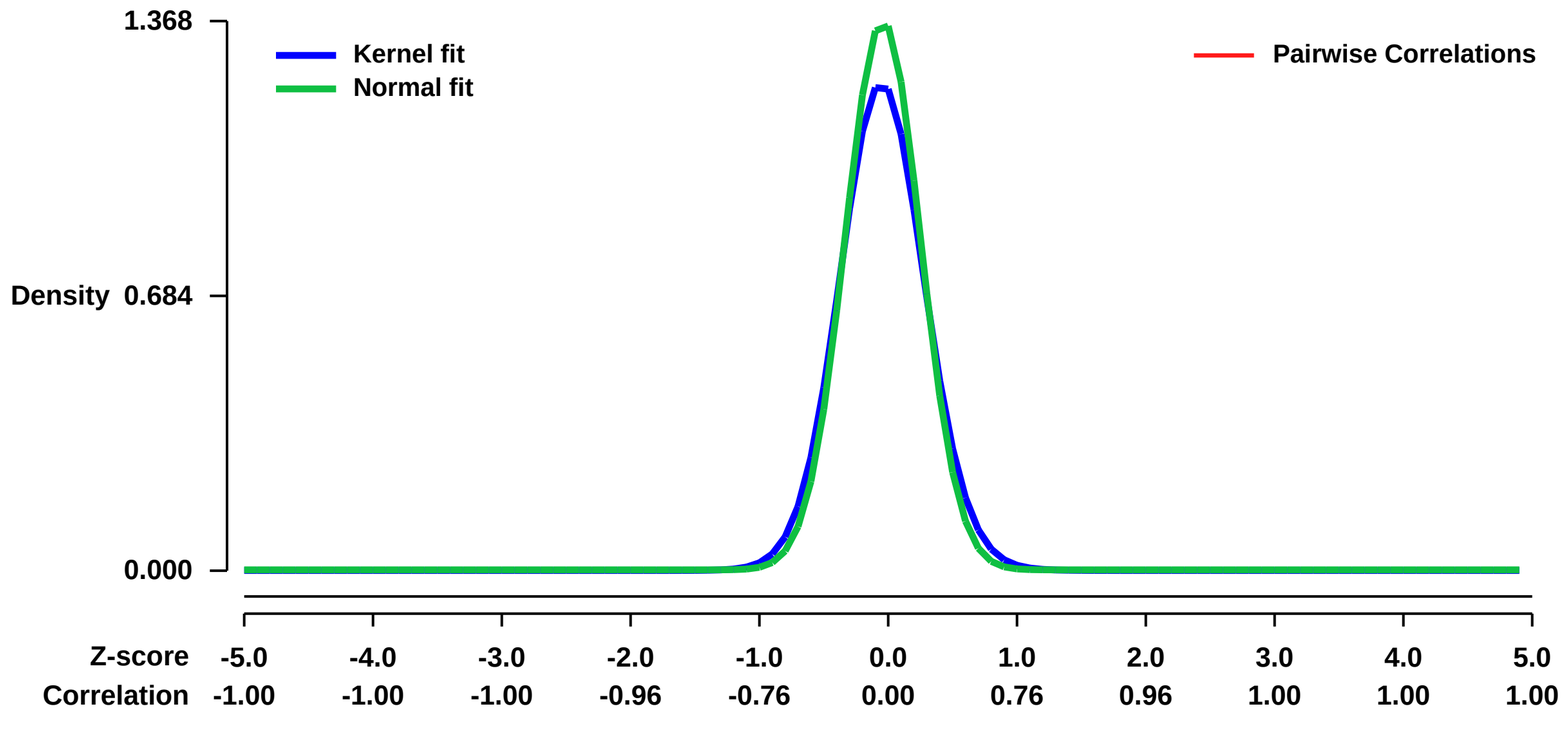

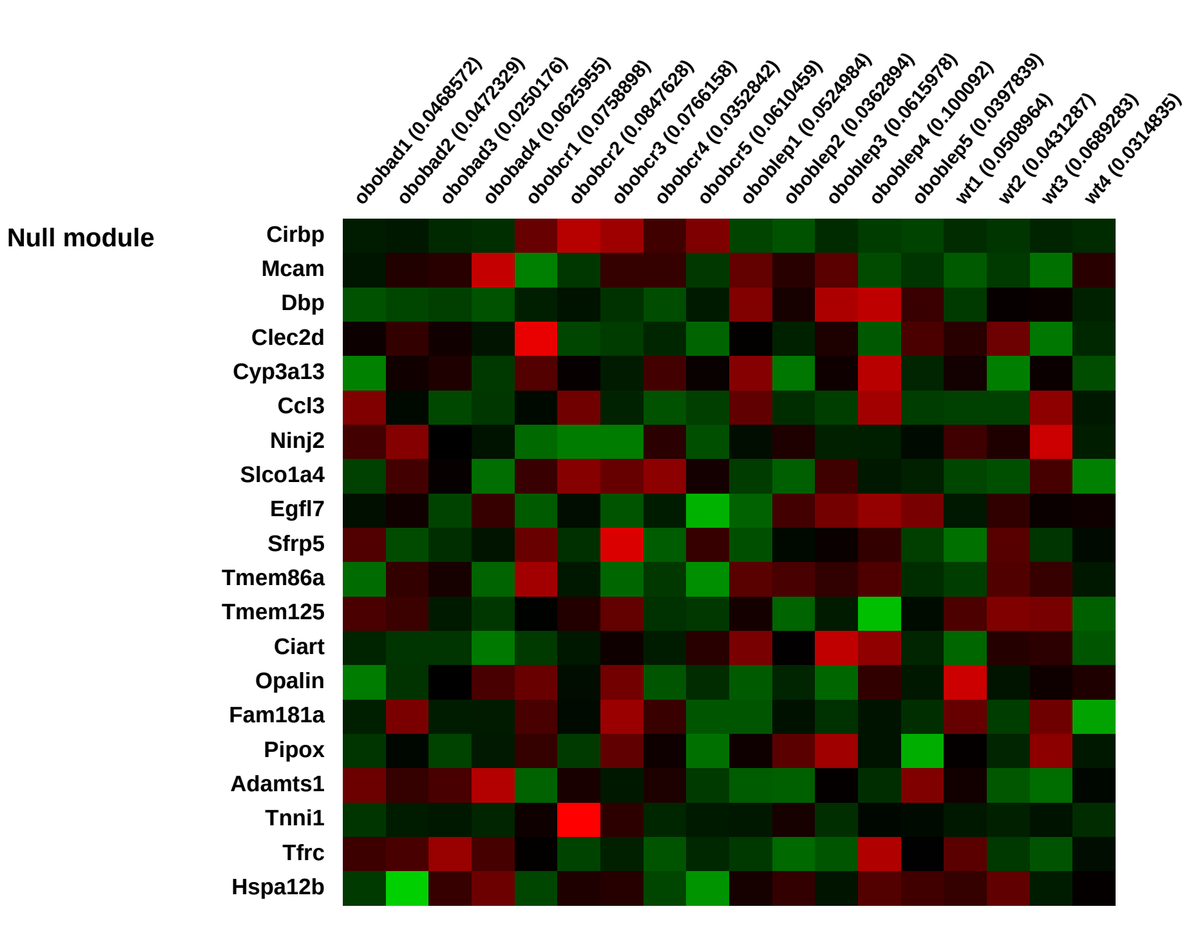

GEO Series "GSE6675" Expression Profiles

Num of samples in this series: 8

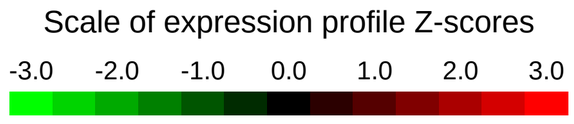

GEO Link:	http://www.ncbi.nlm.nih.gov/geo/query/acc.cgi?acc=GSE6675
Status:	Public on Jan 09 2007
Title:	Astroglial gene expression program elicited by fibroblast growth factor-2 mande-affy-mouse-307080
Organism:	Mus musculus
Experiment type:	Expression profiling by array
Platform:	GPL1261
Pubmed ID:	

Summary & Design:

Summary:
Astroglia, the star-shaped cells found throughout the central nervous system are the most numerous cell type in the brain. The astroglial response to injury, generically termed reactive astrogliosis, is classically defined by cellular hypertrophy and process extension, increased glial filament production, and some degree of proliferation. Astrogliosis and its functional outcomes, glial scar formation and neuroinflammation, are often viewed as detrimental to recovery. However, increasing evidence points to neuroprotective roles of reactive astroglia in the setting of brain injury. Therapeutic modulation of this double-edged sword will require detailed knowledge of mechanisms by which specific signals induce detrimental and beneficial phenotypes.

This proposal is is a logical extension of a published, peer reviewed study (Heffron DS and Mandell JW, Opposing roles of ERK and p38 MAP kinases in FGF2-induced astroglial process extension. Mol Cell Neurosci 2005, 28:779-90). The downstream gene expression changes underlying these pathway-specific responses are largely unknown. The data generated from the proposed project will delineate pathway-specific gene expression responses of astroglia to fibroblast growth factors. This information will allow a rational approach to pharmacological approaches to modulate reactive astrogliosis in brain and spinal cord injury.

Determine the astroglial gene expression program elicited by fibroblast growth factor-2, and dissect specific contributions of the ERK and p38 MAP kinase pathways using highly specific pharmacological inhibitors.

FGF2, acting via two distinct intracellular signaling pathways, ERK- and p38 MAPK, leads to pathway-specific gene expression changes in astrocytes which promote the morphological plasticity (ERK-dependent) and pro-inflammatory properties (p38-dependent) of reactive astroglia.

Cell culture

Neonatal primary astrocyte cultures are prepared exactly as previously described (Heffron and Mandell, 2005), using slight modifications of established protocols (McCarthy and de Vellis, 1980).

Astrocytes prepared with these methods comprised greater than 95% of cell cultures as determined by GFAP staining. Microglia are present as a contaminating cell type at a percentage of 3.6 ´– 0.9% as determined by CD11B staining.

For process induction experiments, cells are trypsinized and replated in DMEM with 1% fetal bovine serum. This low serum concentration is necessary for good adhesion of the cells. Pharmacological inhibitors are dissolved in DMSO and added 2 h later. P38 MAP kinase inhibitors SB202190 (Calbiochem) and the MEK inhibitor U0126 (Promega) are used at 20 ´µM. We previously determined that the inactive analog of SB 202190, SB202474 (Calbiochem) had no effects on pathway activation or astrocyte morphology. Therefore, the inactive drug analog will not be used in the array experiments.

Final DMSO concentration in the drug treatments and vehicle controls is 0.2%. Human recombinant FGF2 (obtained from the National Cancer Institute Preclinical Repository) is used at 25 ng/ml, based on extensive dose/response analyses in our published work.

Keywords: fibroblast growth factor-2 treatment

Overall design:

Background corr dist: **KL-Divergence = 0.0599, L1-Distance = 0.0210, L2-Distance = 0.0005, Normal std = 0.5359**

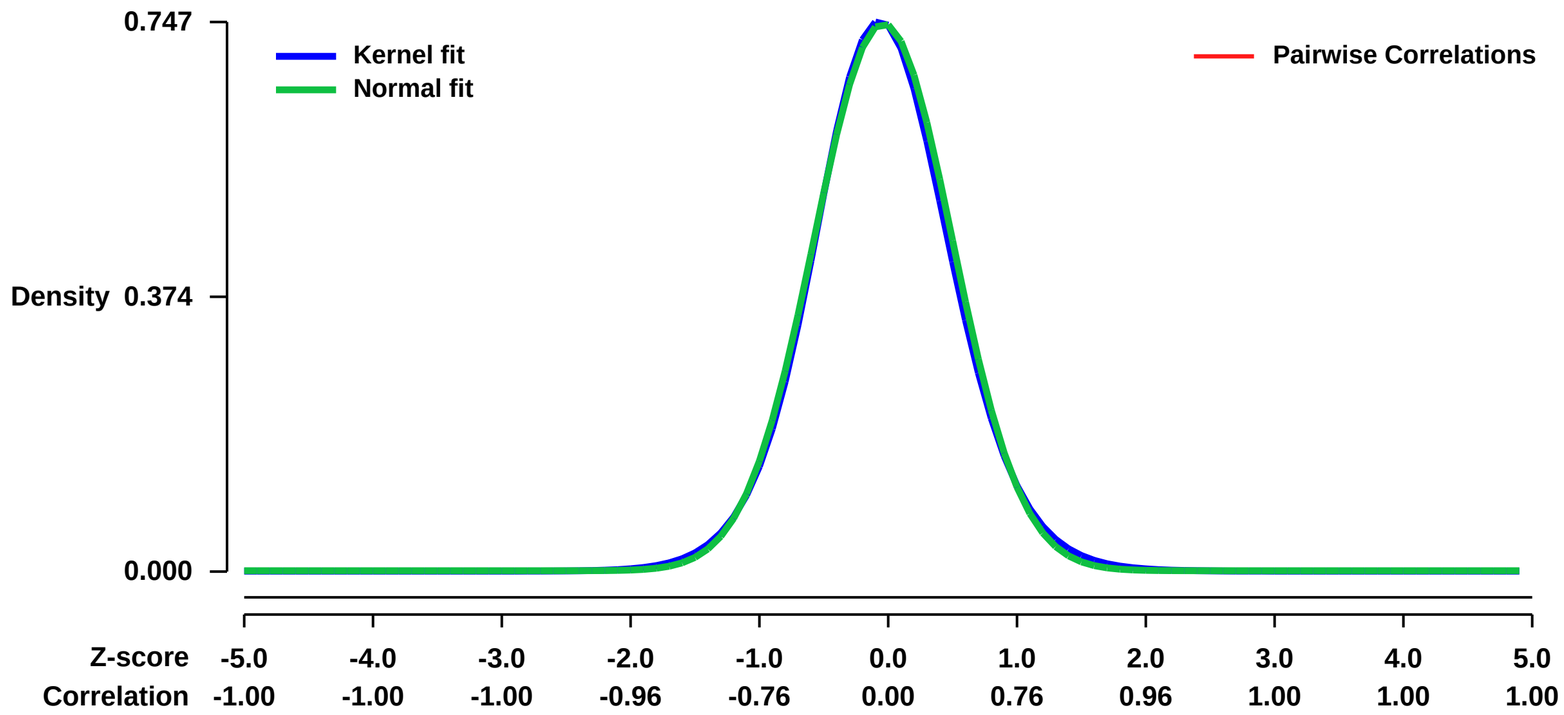

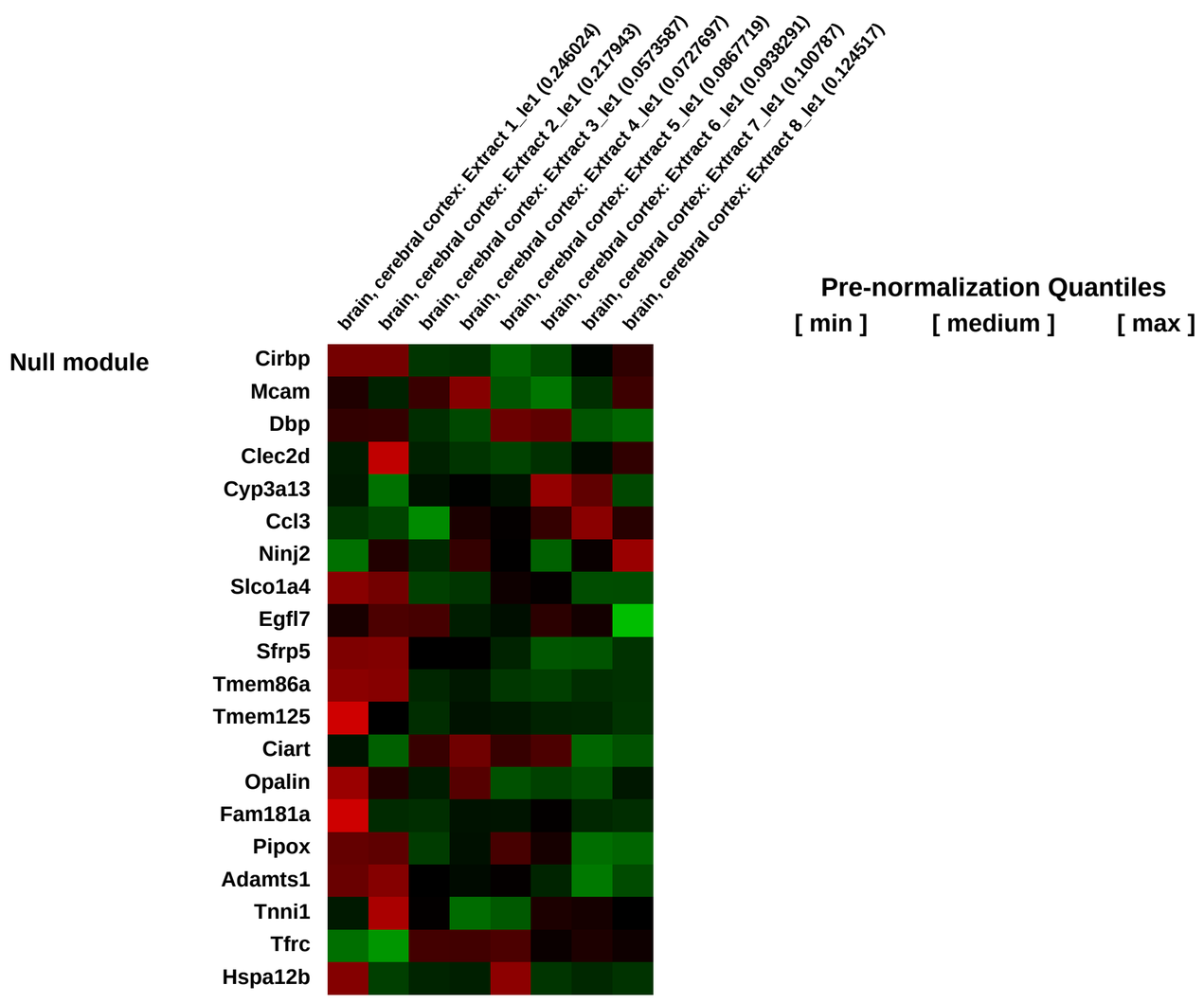

GEO Series "GSE13386" Expression Profiles

Num of samples in this series: 24

Scale of expression profile Z-scores

-3.0 -2.0 -1.0 0.0 1.0 2.0 3.0

GEO Link:	http://www.ncbi.nlm.nih.gov/geo/query/acc.cgi?acc=GSE13386
Status:	Public on Nov 14 2008
Title:	Comparative analysis of Drd1+ Medium Spiny Neurons, Drd2+ Medium Spiny Neurons, cocaine treatment
Organism:	Mus musculus
Experiment type:	Expression profiling by array
Platform:	GPL1261
Pubmed ID:	19013281
Summary & Design:	**Summary:** The cellular heterogeneity of the brain confounds efforts to elucidate the biological properties of distinct neuronal populations. Using Bacterial Artificial Chromosome (BAC) transgenic mice which express EGFP-tagged ribosomal protein L10a in defined cell populations, we have developed a methodology to affinity purify polysomal mRNAs from genetically defined cell populations in the brain. The utility of this approach is illustrated by the comparative analysis of four types of neurons, revealing hundreds of genes that distinguish these four cell populations. We find that even two morphologically indistinguishable, intermixed subclasses of medium spiny neuron display vastly different translational profiles and present examples of the physiological significance of such differences. This genetically targeted Translating Ribosome Affinity Purification (TRAP) methodology is a generalizable method useful for the identification of molecular changes in any genetically defined cell type in response to genetic alterations, disease, or pharmacological perturbations. **Keywords:** Cell Type Comparison **Overall design:** We recommend that only genes where more than one sample has a normalized intensity larger than 16 (4 in log2 scale) should be kept in the analysis.

Background corr dist: KL-Divergence = 0.1843, L1-Distance = 0.0598, L2-Distance = 0.0087, Normal std = 0.3672

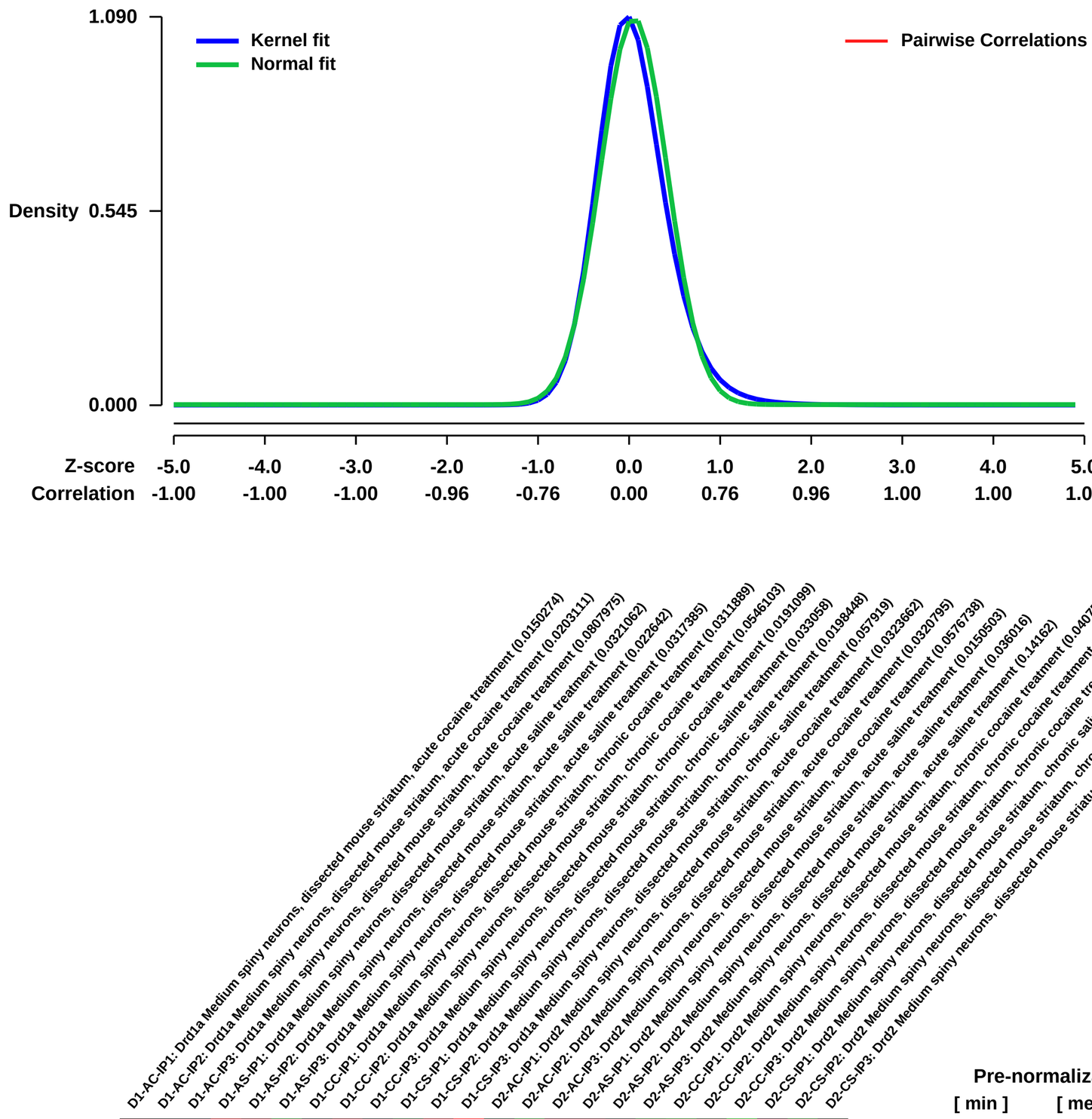

GEO Series "GSE18586" Expression Profiles

Num of samples in this series: 9

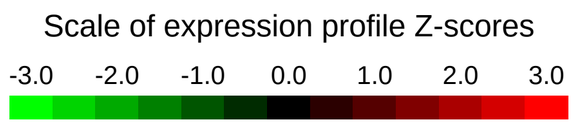

GEO Link:	http://www.ncbi.nlm.nih.gov/geo/query/acc.cgi?acc=GSE18586
Status:	Public on Jun 18 2012
Title:	Saturated fat stimulates obesity and hepatic steatosis and affects gut microbiota composition by an enhanced overflow of dietary fat to the distal intestine
Organism:	Mus musculus
Experiment type:	Expression profiling by array
Platform:	GPL1261
Pubmed ID:	22700822

Summary & Design:

Summary:
We studied the effect of dietary fat type, varying in polyunsaturated/saturated fatty acid ratio's (P/S) on development of metabolic syndrome. C57Bl/6J mice were fed purified high-fat diets (45E% fat) containing palm oil (HF-PO; P/S 0.4), olive oil (HF-OO; P/S 1.1) or safflower oil (HF-SO; P/S 7.8) for 8 weeks. A low-fat palm oil diet (LF-PO; 10E% fat) was used as a reference. Additionally, we analyzed diet-induced changes in gut microbiota composition and mucosal gene expression. The HF-PO diet induced a higher body weight gain and liver triglyceride content compared to the HF-OO, HF-SO or LF-PO diet. In the intestine, the HF-PO diet reduced microbial diversity and increased the Firmicutes/Bacteroidetes ratio. Although this fits a typical obesity profile, our data clearly indicate that an overflow of the HF-PO diet to the distal intestine, rather than obesity itself, is the main trigger for these gut microbiota changes. A HF-PO diet-induced elevation of lipid metabolism-related genes in the distal small intestine confirmed the overflow of palm oil to the distal intestine. Some of these lipid metabolism-related genes were previously already associated with the metabolic syndrome. In conclusion, our data indicate that saturated fat (HF-PO) has a more stimulatory effect on weight gain and hepatic lipid accumulation than unsaturated fat (HF-OO and HF-SO). The overflow of fat to the distal intestine on the HF-PO diet induced changes in gut microbiota composition and mucosal gene expression. We speculate that both are directly or indirectly contributive to the saturated fat-induced development of obesity and hepatic steatosis.

Keywords: Diet intervention study

Overall design:
Nine-week-old C57Bl/6J mice were fed a low-fat diet (LF-PO) and three different types of high-fat diet, based on palm oil (HF-PO; P/S1.0), olive oil (HF-OO; P/S4.6) and safflower oil (HF-SO; P/S10.1) for 8 weeks. Body weight was recorded weekly and after 7 weeks of diet intervention an oral glucose tolerance test was performed. After 2 weeks of diet intervention, 6 mice per high-fat diet group were anaesthetized with a mixture of isofluorane (1.5%), nitrous oxide (70%) and oxygen (30%) and the small intestines were excised. Adhering fat and pancreatic tissue were carefully removed. The small intestines were divided in three equal parts along the proximal to distal axis (SI 1, SI 2 and SI 3) and microarray analysis was performed on mucosal scrapings.

Background corr dist: KL-Divergence = 0.0644, L1-Distance = 0.0264, L2-Distance = 0.0008, Normal std = 0.5278

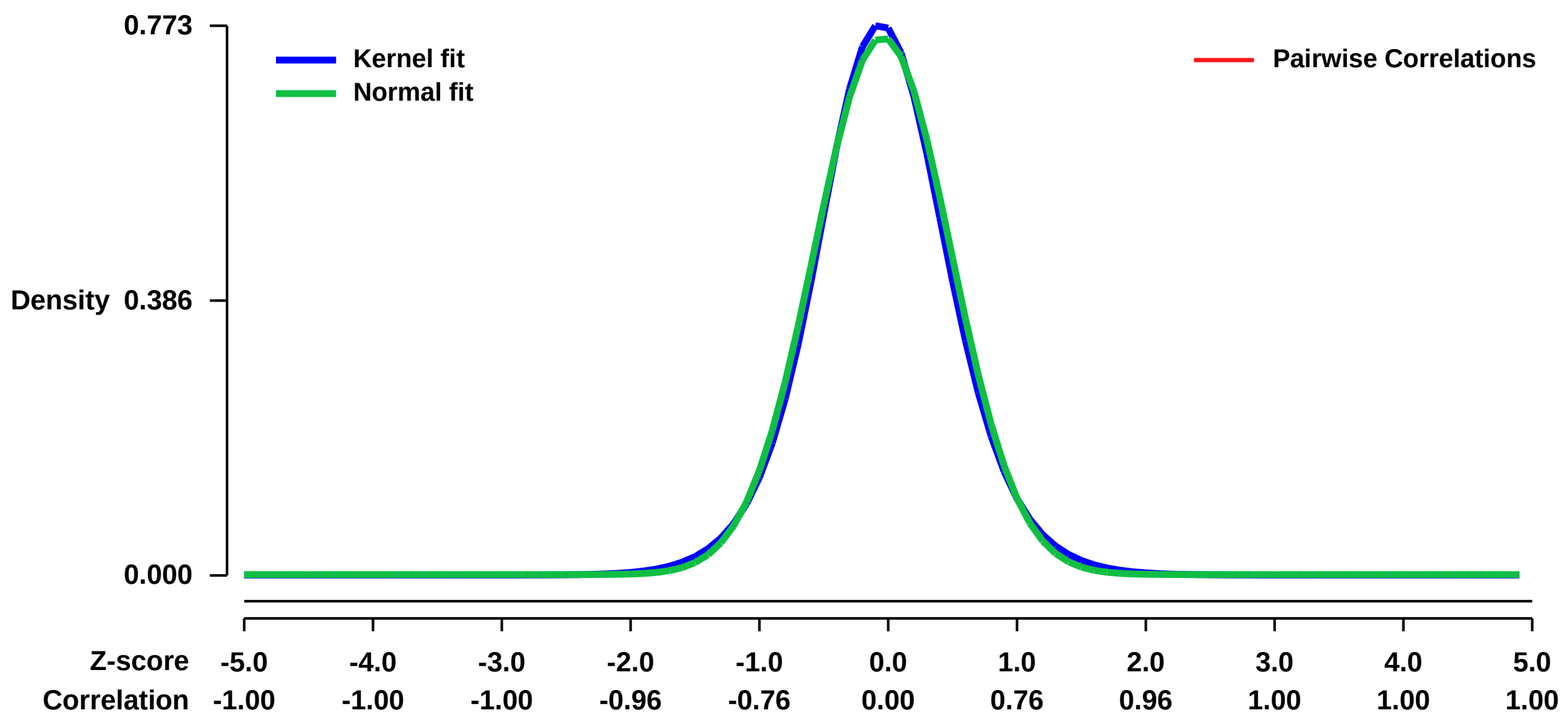

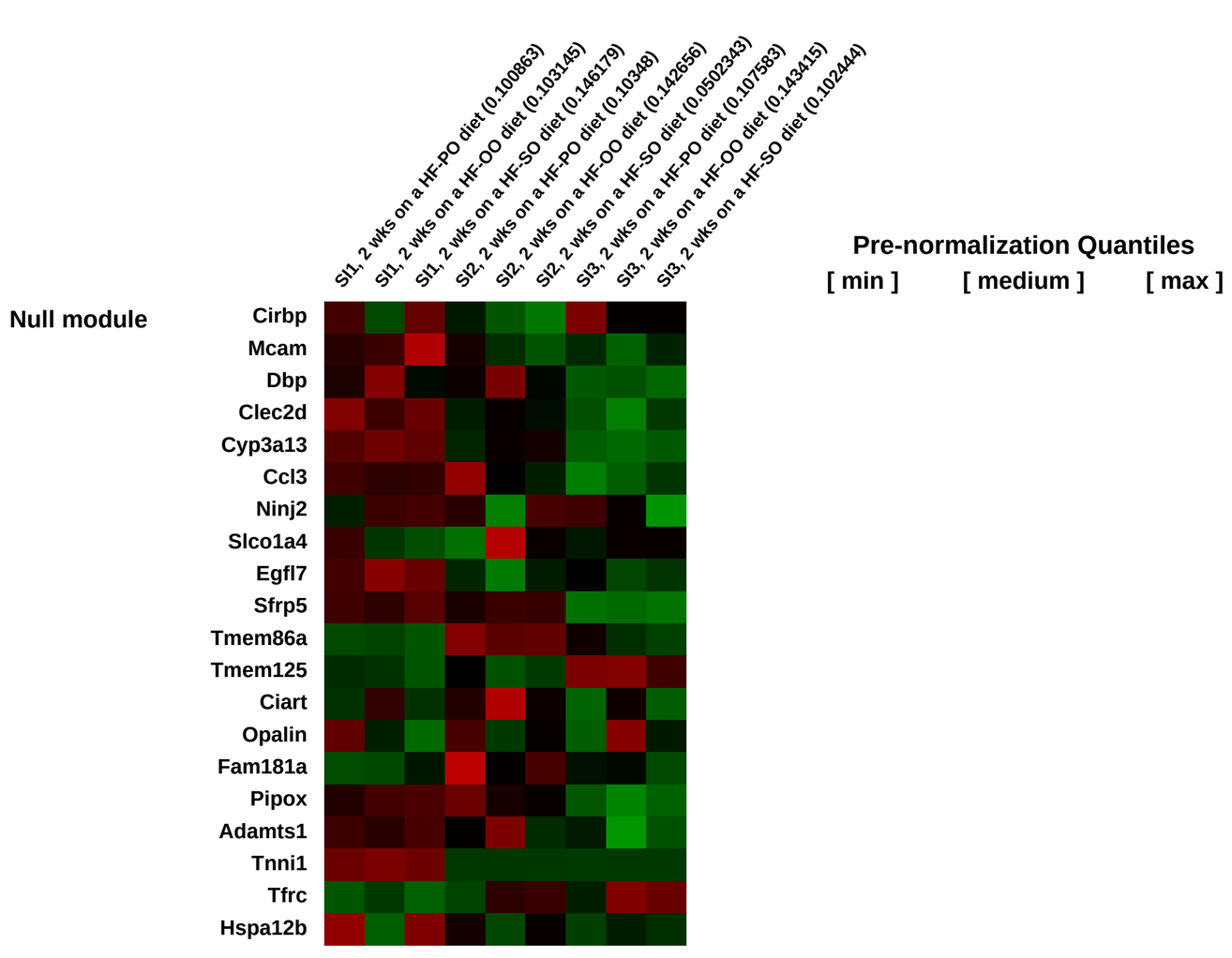

GEO Series "GSE47196" Expression Profiles

Num of samples in this series: 6

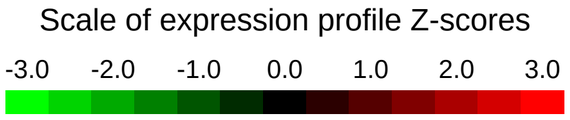

GEO Link:	http://www.ncbi.nlm.nih.gov/geo/query/acc.cgi?acc=GSE47196
Status:	Public on May 23 2013
Title:	Immunoglobulin-like domain receptor 1 mediates fat-stimulated cholecystokinin secretion.
Organism:	Mus musculus
Experiment type:	Expression profiling by array
Platform:	GPL1261
Pubmed ID:	23863714
Summary & Design:	**Summary:** Cholecystokinin (CCK) is a satiety hormone produced by discrete enteroendocrine cells scattered among absorptive cells of the small intestine. CCK is released into blood following a meal; however, the mechanisms inducing hormone secretion are largely unknown. Ingested fat is the major stimulant of CCK secretion. We recently identified a novel member of the lipoprotein remnant receptor family known as immunoglobulin-like domain containing receptor 1 (ILDR1) in intestinal CCK cells and postulated that this receptor conveyed the signal for fat-stimulated CCK secretion. In the intestine, ILDR1 is expressed exclusively in CCK cells. Orogastric administration of fatty acids elevated blood levels of CCK in wild type but not ILDR1-deficient mice, although the CCK secretory response to trypsin inhibitor was retained. The uptake of fluorescently labeled lipoproteins in ILDR1-transfected CHO cells and release of CCK from isolated intestinal cells required a unique combination of fatty acid plus HDL. CCK secretion secondary to ILDR1 activation is associated with increased [Ca2+]i consistent with regulated hormone release. These findings demonstrate that ILDR1 regulates CCK release through a mechanism dependent on fatty acids and lipoproteins and that absorbed fatty acids regulate gastrointestinal hormone secretion. **Overall design:** GFP positive cells from CCK-EGFP transgenic mice were isolated by FACS and the expression profile was compared with an equal number of non-fluorescent intestinal cells.

Background corr dist: KL-Divergence = 0.0167, L1-Distance = 0.0318, L2-Distance = 0.0015, Normal std = 0.7899

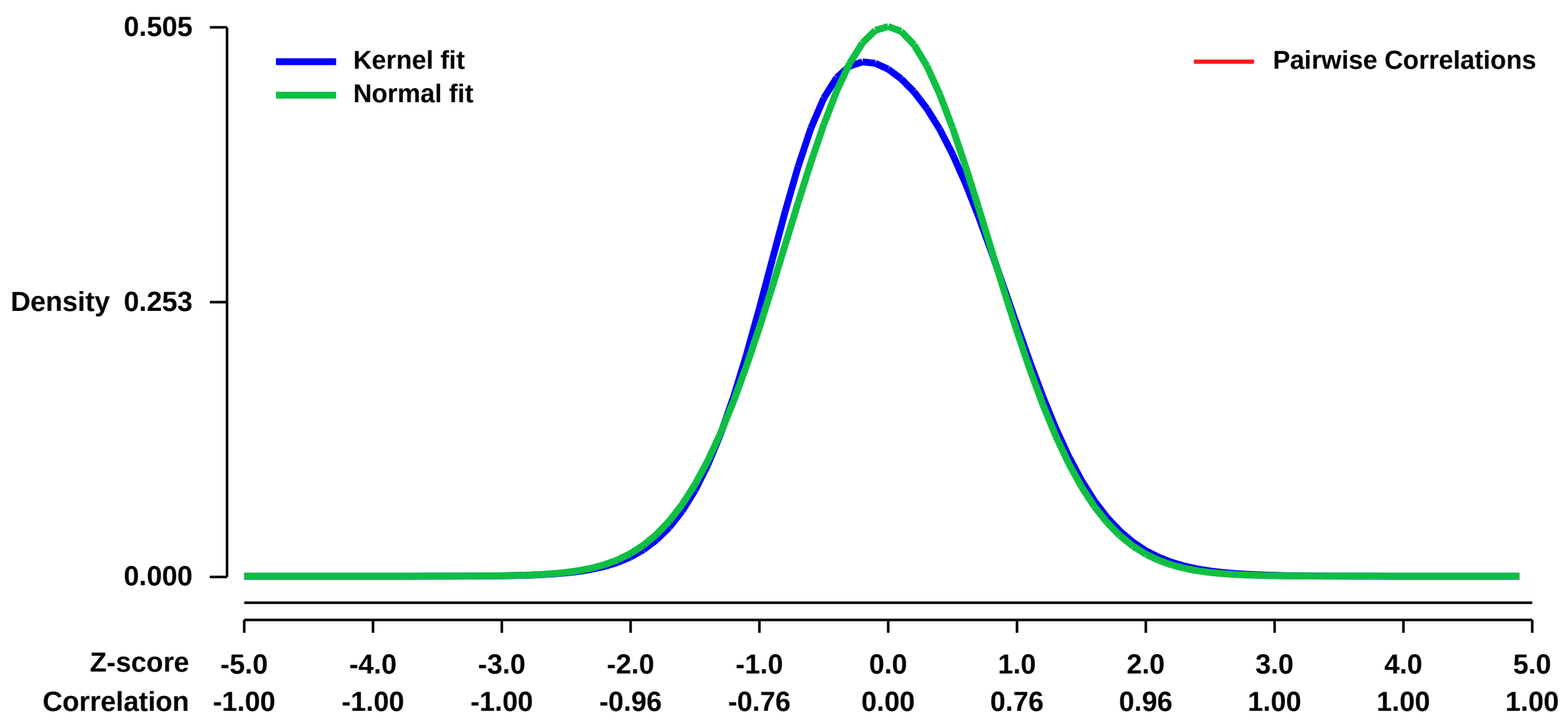

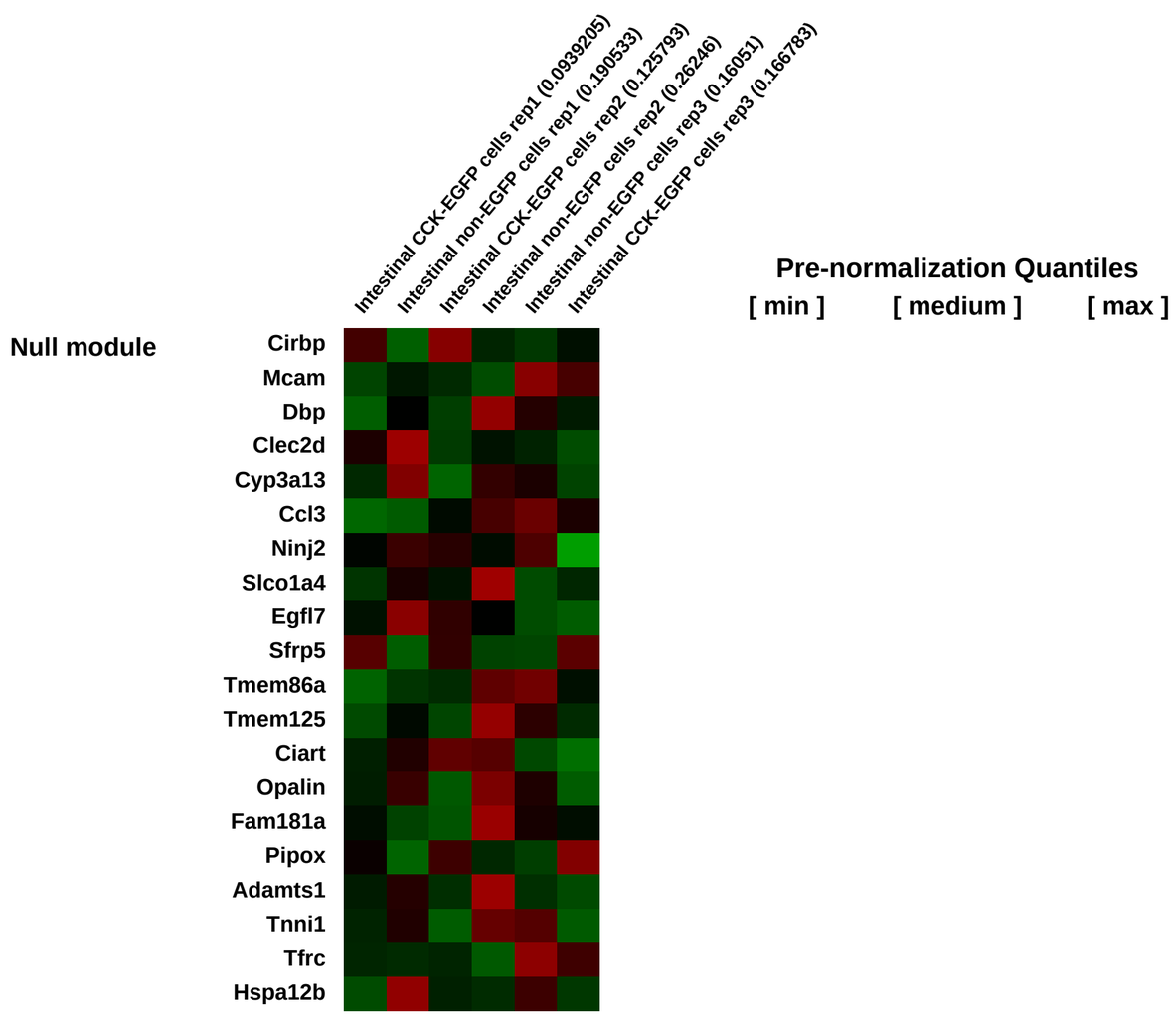

GEO Series "GSE21944" Expression Profiles

Num of samples in this series: 6

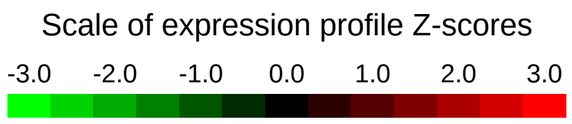

GEO Link:	http://www.ncbi.nlm.nih.gov/geo/query/acc.cgi?acc=GSE21944
Status:	Public on Jul 02 2010
Title:	The orphan nuclear hormone receptor ERR‚† controls rod photoreceptor survival.
Organism:	Mus musculus
Experiment type:	Expression profiling by array
Platform:	GPL1261
Pubmed ID:	20534447
Summary & Design:	**Summary:** Mutation of rod photoreceptor-enriched transcription factors is a major cause of inherited blindness. We identified the orphan nuclear hormone receptor ERR‚† as selectively expressed in rod photoreceptors. Overexpression of ERR‚† induces expression of rod-specific genes in retinas of both wildtype and in Nrl-/- mice, which lack rod photoreceptors. Mutation of ERR‚† results in dysfunction and degeneration of rods, while inverse agonists of ERR‚† trigger rapid rod degeneration, which is rescued by constitutively active mutants of ERR‚†. ERR‚† coordinates expression of multiple genes that are rate-limiting regulators of ATP generation and consumption in photoreceptors. Furthermore, enhancing ERR‚† activity rescues photoreceptor defects that result from loss of the photoreceptor-specific transcription factor Crx. Our findings demonstrate that ERR‚† is a critical regulator of rod photoreceptor function and survival, and suggest that ERR‚† agonists may be useful in the treatment of certain retinal dystrophies. **Overall design:** Affymetrix MOE430 microarrays were used to analyze the expression patterns of P21 mouse retinal tissues. The results were compared across the variable of Genotype, specifically ERR‚† knockout versus wildtype.

Background corr dist: KL-Divergence = 0.0113, L1-Distance = 0.0143, L2-Distance = 0.0002, Normal std = 0.8473

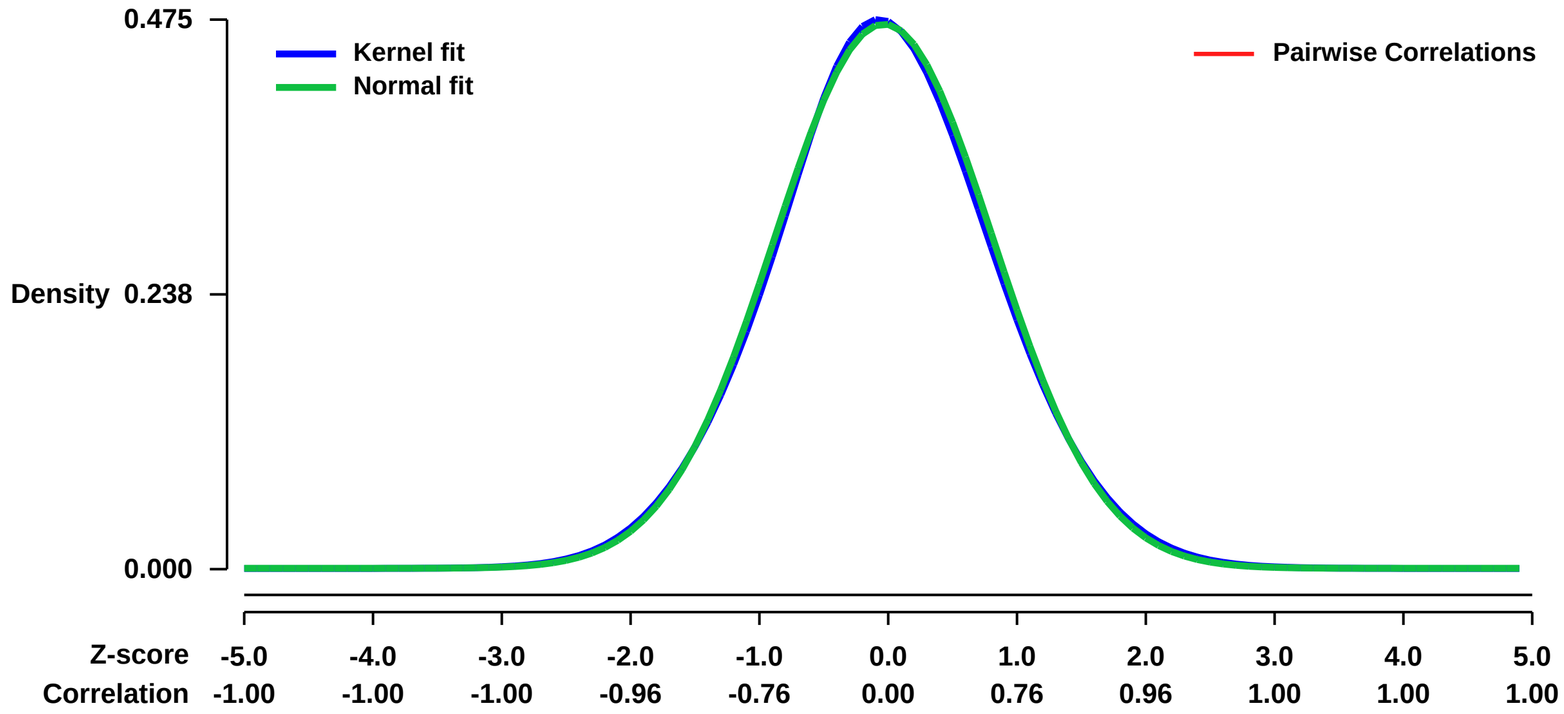

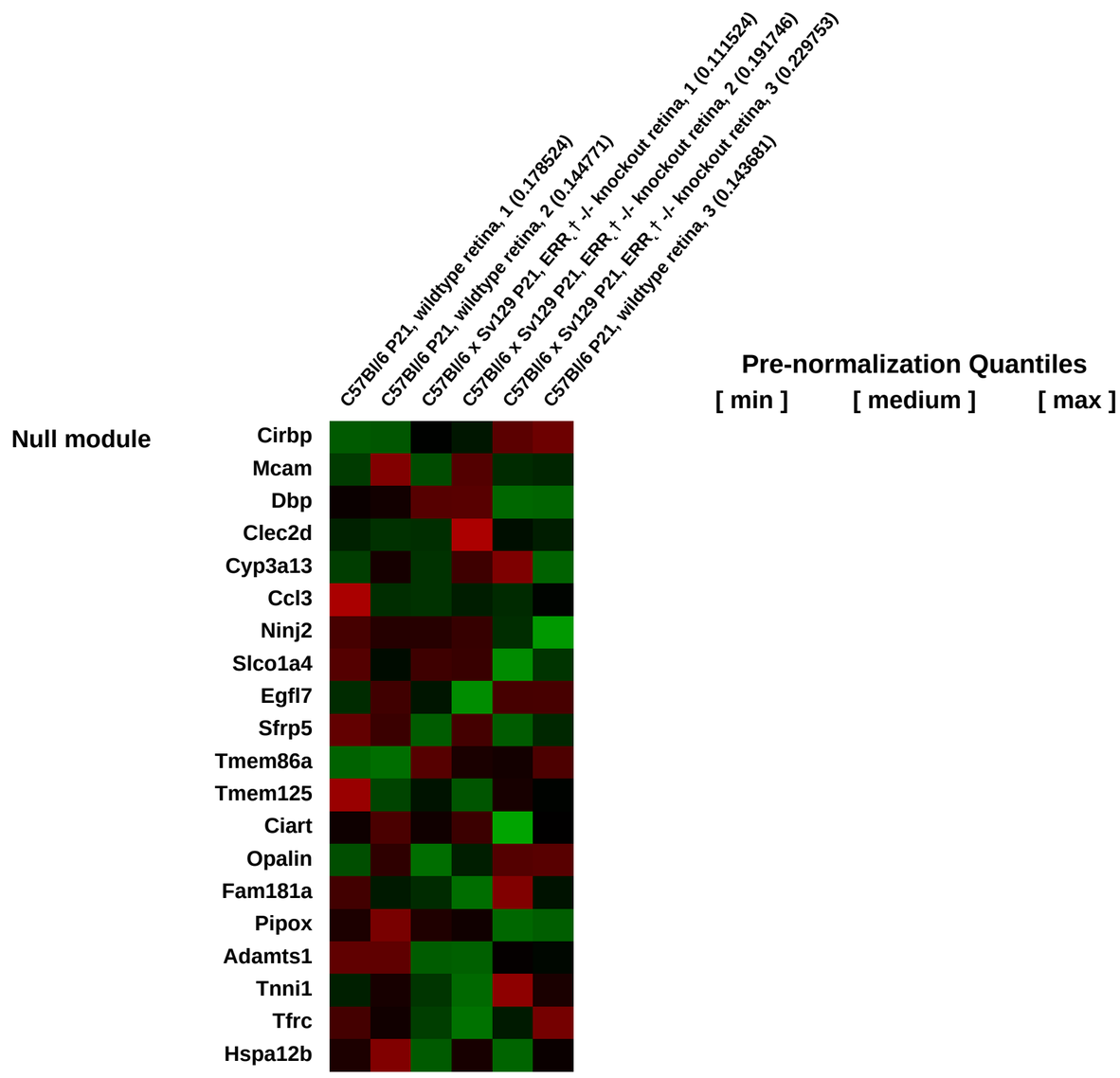

GEO Series "GSE17513" Expression Profiles

Num of samples in this series: 12

Scale of expression profile Z-scores

-3.0 -2.0 -1.0 0.0 1.0 2.0 3.0

GEO Link:	http://www.ncbi.nlm.nih.gov/geo/query/acc.cgi?acc=GSE17513
Status:	Public on Sep 01 2009
Title:	Expression data from murine embryonic stem cell derived cardiac progenitors
Organism:	Mus musculus
Experiment type:	Expression profiling by array
Platform:	GPL1261
Pubmed ID:	19833966
Summary & Design:	**Summary:** Mamamlian cardiogenesis occurs through the development of discreate populations of first and second heart field progenitors. We have used a dual transgenic color reproter system to isolate purified populations of these progenitors. We used microarrays to detail the global programme of gene expression underlying cardiac development in mouse All four populations of cells are derived from embryonic stem cells differentiating in vitro (day 6 of in vitro differentaition). The stem cell line has two transgenic reporters as follows: 1. The second heart field (SHF) specific reporter of the Mef2C gene (E. Dodou, S. M. Xu, B. L. Black, Mech Dev 120, 1021 (Sep, 2003)) driving the expression of dsRed 2. The cardiac specific enhancer (C. L. Lien et al., Development 126, 75 (Jan, 1999)) driving the expression of eGFP. Thus, the red cells are SHF specific, the green cells are cardiac specific, and the red/green are SHF and cardiac specific. These cells are compared to the double negative cells which serve as a control. **Overall design:** Embryonic stem cell derived progenitors were isolated into four distinct populations by FACS purifying these progenitors based on a two color reporter system. Four populations were then compared to each other by transcriptional profiling.

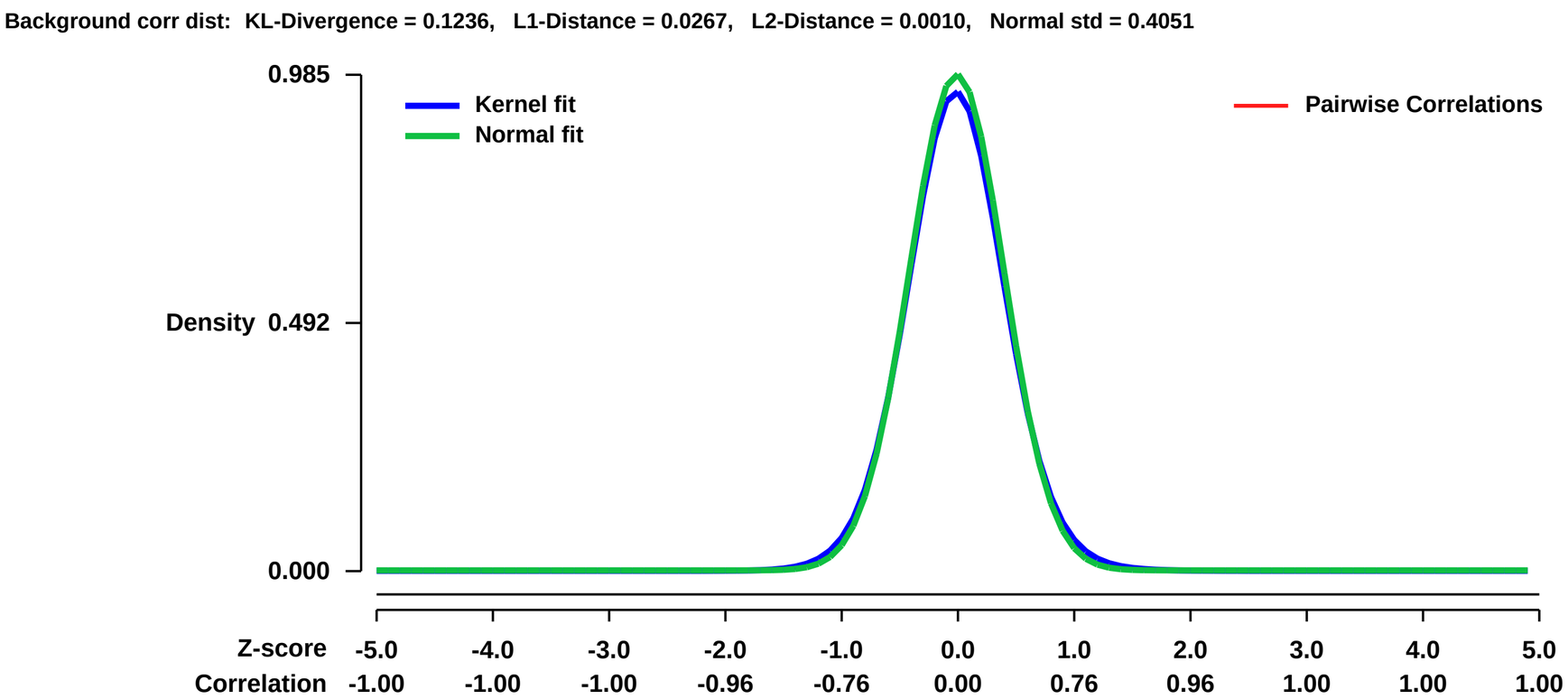

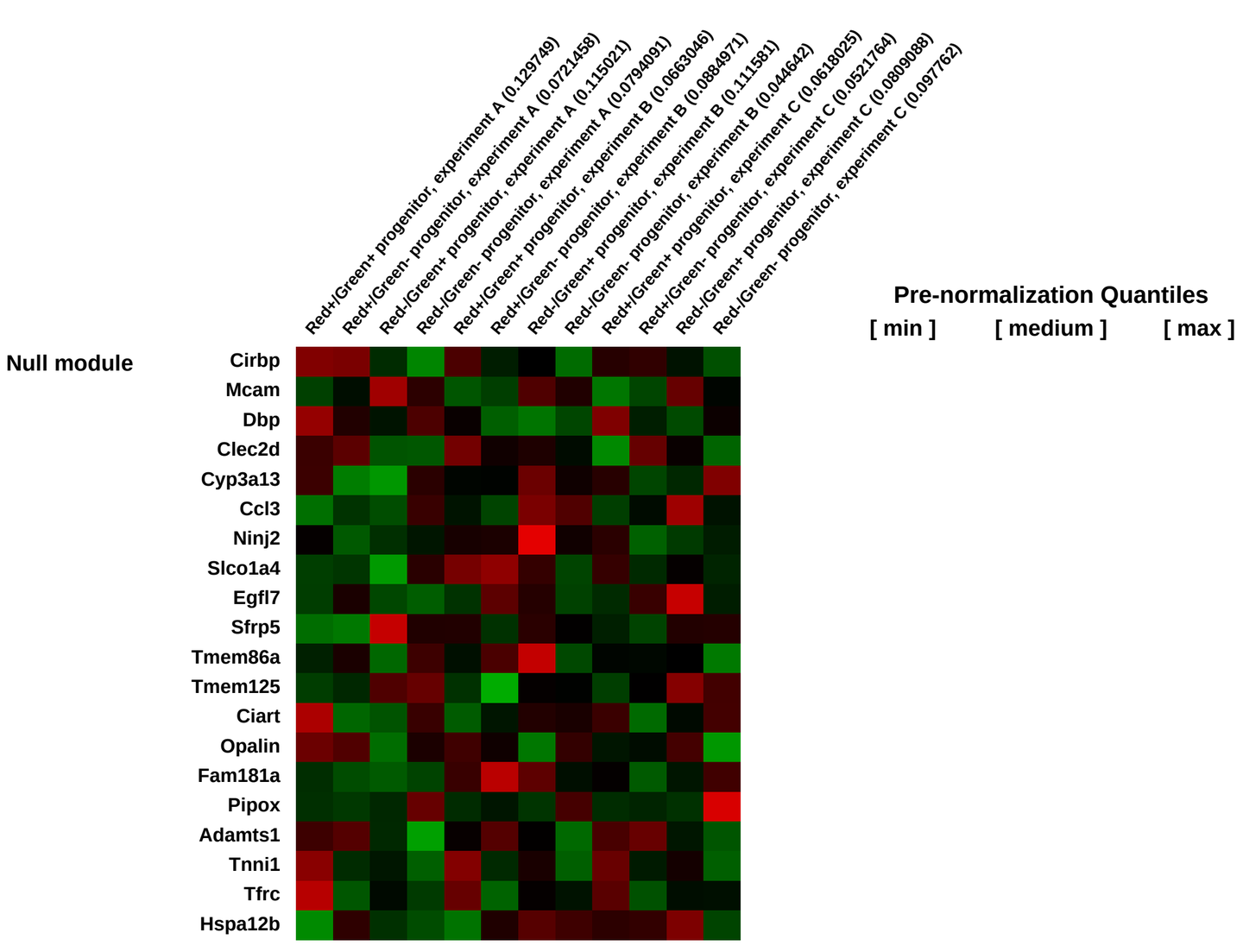

GEO Series "GSE10902" Expression Profiles

Num of samples in this series: 6

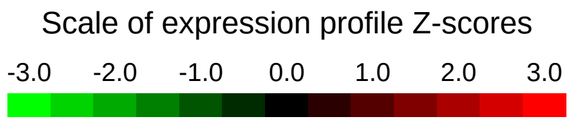

GEO Link:	http://www.ncbi.nlm.nih.gov/geo/query/acc.cgi?acc=GSE10902
Status:	Public on Jun 06 2008
Title:	Differential expression between FHL2-/- and WT MEFs.
Organism:	Mus musculus
Experiment type:	Expression profiling by array
Platform:	GPL1261
Pubmed ID:	19018287
Summary & Design:	**Summary:** The LIM-only protein FHL2 acts as a transcriptional modulator that positively or negatively regulates multiple signaling pathways. We recently reported that FHL2 cooperates with CBP/p300 in the activation of ^-catenin/TCF target gene cyclin D1. In this paper, we demonstrate that FHL2 is associated with the cyclin D1 promoter at the TCF/CRE site, providing evidence that cyclin D1 is a direct target of FHL2. We show that deficiency of FHL2 greatly reduces the proliferative capacity of spontaneously immortalized mouse fibroblasts which is associated with decreased expression of cyclin D1 and p16INK4a, and hypophosphorylation of Rb. Reexpression of FHL2 in FHL2-null fibroblasts efficiently restores cyclin D1 levels and cell proliferative capacity, indicating that FHL2 is critical for cyclin D1 activation and cell growth. Moreover, ectopic cyclin D1 expression is sufficient to override growth inhibition of immortalized FHL2-null fibroblasts. Gene expression profiling revealed that FHL2 deficiency triggers a broad change of the cell cycle program that is associated with downregulation of several G1/S and G2/M cyclins, E2F transcription factors and DNA replication machinery, thus correlating with reduced cell proliferation. This change also involves downregulation of the negative cell cycle regulators, particularly INK4 inhibitors, which could counteract the decreased expression of cyclins, allowing cells to grow. Our study illustrates that FHL2 can act on different aspects of the cell cycle program to finely regulate cell proliferation. **Keywords:** mouse embryonic fibroblasts derived from FHL2-/- and WT mouse embryos (14.5 days) **Overall design:** Two biological genotypes, FHL2-/- and WT MEF cells. Three spontaneously immortalized clones of each genotype were analyzed using Affymetrix arrays.

Background corr dist: KL-Divergence = 0.0204, L1-Distance = 0.0119, L2-Distance = 0.0002, Normal std = 0.7307

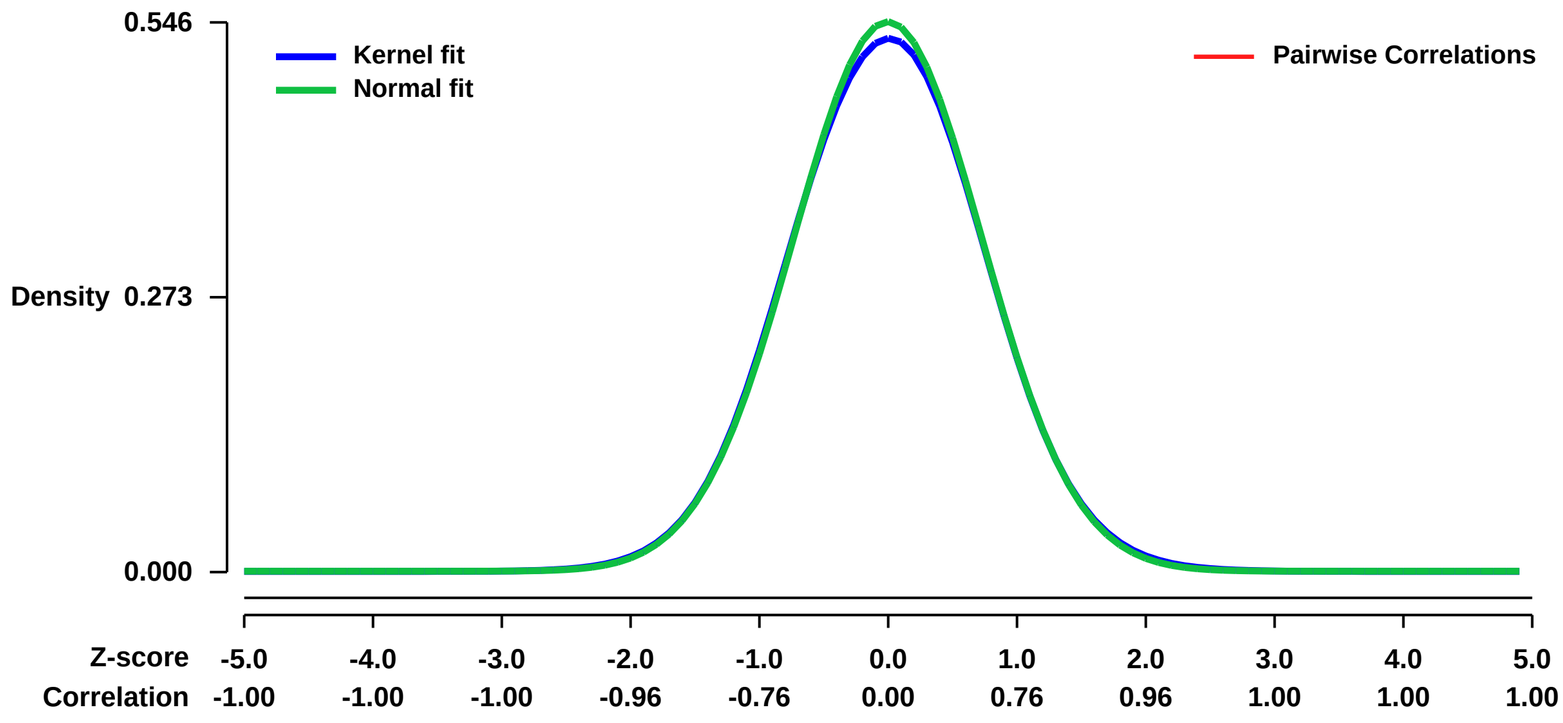

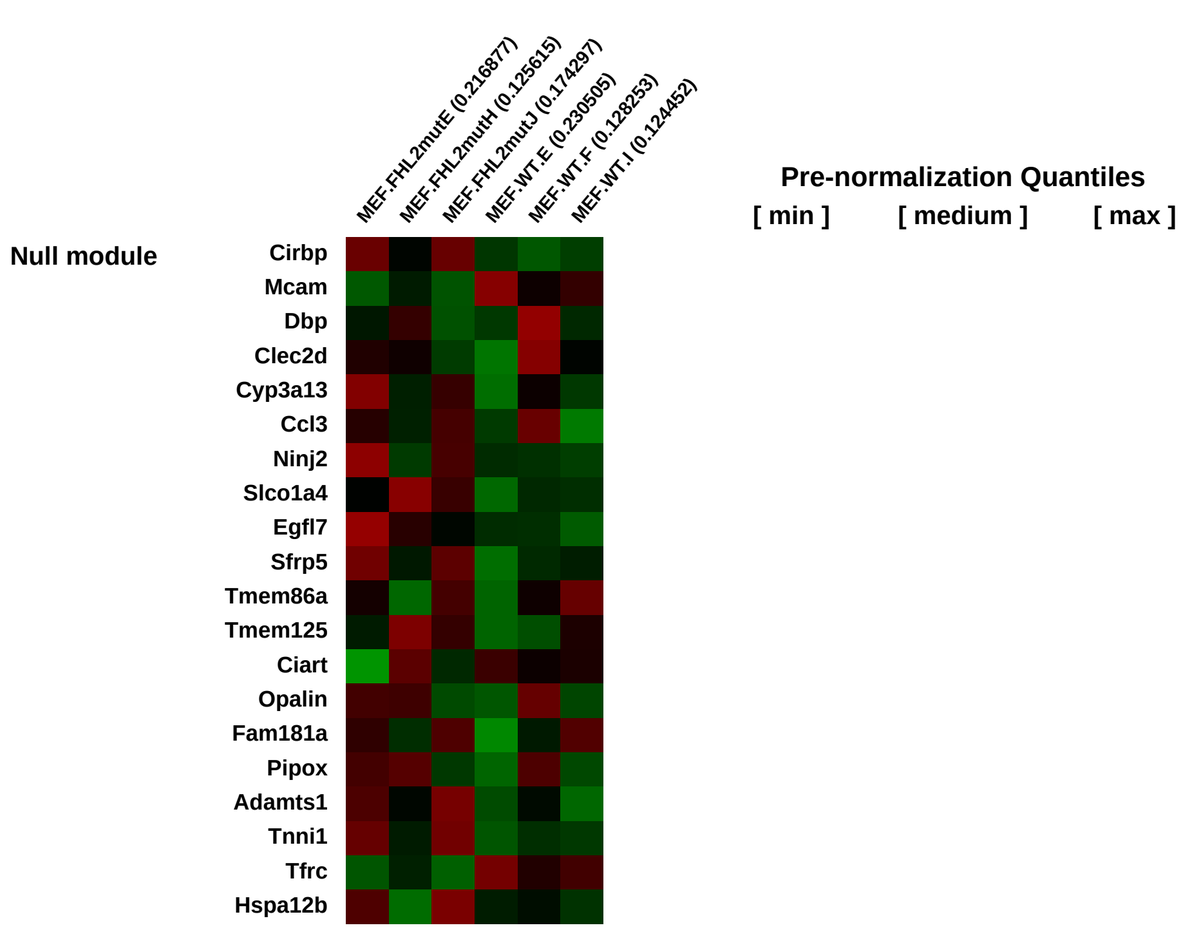

GEO Series "GSE42930" Expression Profiles

Num of samples in this series: 10

Scale of expression profile Z-scores

-3.0 -2.0 -1.0 0.0 1.0 2.0 3.0

GEO Link: http://www.ncbi.nlm.nih.gov/geo/query/acc.cgi?acc=GSE42930

Status: Public on Dec 15 2012

Title: Differential gene expression in APOE3 and APOE4 gene targeted replacement mice

Organism: Mus musculus

Experiment type: Expression profiling by array

Platform: GPL1261

Pubmed ID:

Summary & Design:

Summary:
The aim of the study was to investigate hepatic gene expression profiles differentially regulated by the APOE genotype in gene targeted replacement mice. The APOE4 genotype is associated with increased mortality in the elderly and is an independent risk factor for age-dependent chronic diseases. However, little is known about the underlying mechanisms and molecular targets involved in the APOE4-risk association. As APOE is centrally involved in lipid and cholesterol metabolism and in large part is produced in the liver, we analyzed hepatic RNA profiles of APOE4- and APOE3-expressing mice.

Overall design:
2 groups of 5 animals with 1 liver extract per animal. Mice were homozygous for a human APOE3 or APOE4 gene targeted replacement of the endogenous mouse Apoe gene (B6.129P2-Apoetm2(APOE*3)Mae N8 or B6.129P2-Apoetm3(APOE*4)Mae N8, Taconic Transgenic Modelsâ¢, http://www.taconic.com/wmspage.cfm?parm1=2542), purchased at the age of 6-8 weeks, strain C57BL/6, 3 months old at the performance of the microarray, 6 weeks on a high-fat diet containing 41% energy from milk fat and 2 g/kg cholesterol.

Background corr dist: KL-Divergence = 0.1274, L1-Distance = 0.0331, L2-Distance = 0.0020, Normal std = 0.3974

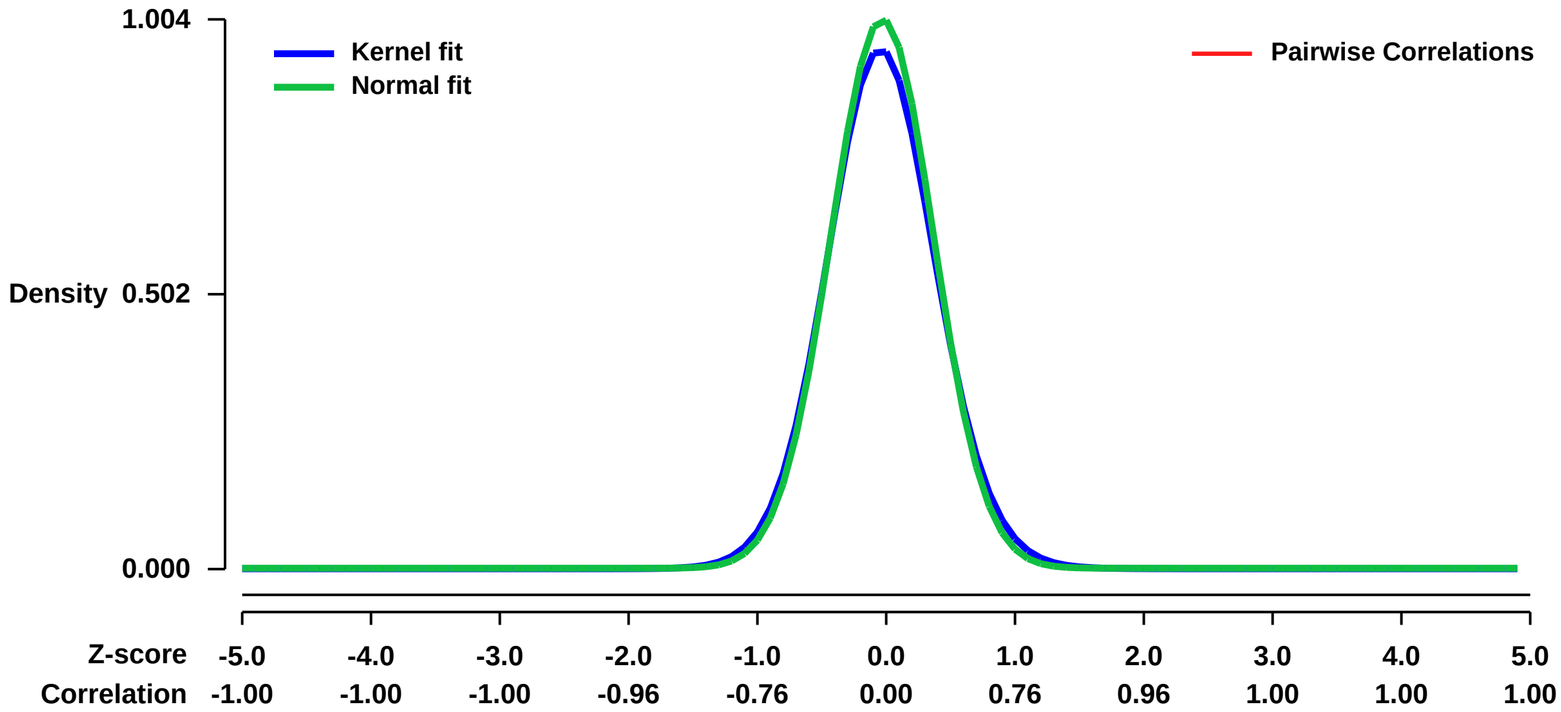

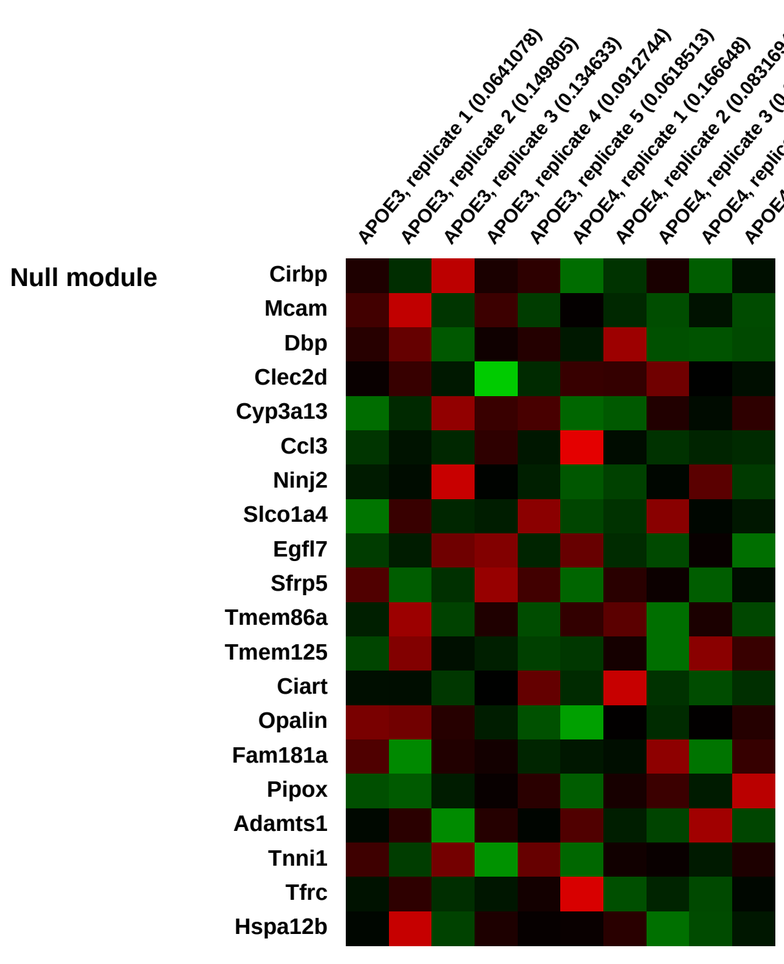

GEO Series "GSE9124" Expression Profiles

Num of samples in this series: 6

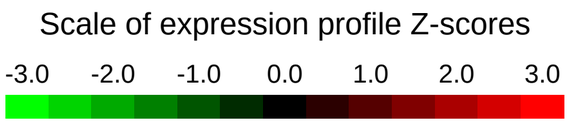

GEO Link:	http://www.ncbi.nlm.nih.gov/geo/query/acc.cgi?acc=GSE9124
Status:	Public on Nov 01 2007
Title:	Gene expression profiling of E12.5 wildtype- and Sp3 null hearts
Organism:	Mus musculus
Experiment type:	Expression profiling by array
Platform:	GPL1261
Pubmed ID:	17923686
Summary & Design:	**Summary:** Mice lacking the zinc finger transcription factor Specificity protein 3 (Sp3) die prenatally in the C57Bl/6 background. To elucidate the cause of mortality we analyzed the potential role of Sp3 in embryonic heart development. Sp3 null hearts display defective looping at E10.5, and at E14.5 the Sp3 null mutants have developed a range of severe cardiac malformations. In an attempt to position Sp3 in the cardiac developmental hierarchy, we analysed the expression patterns of >15 marker genes in Sp3 null hearts. Expression of Cardiac ankyrin repeat protein (Carp) was downregulated prematurely after E12.5, while expression of the other marker genes was not affected. ChIP analysis revealed that Sp3 is bound to the Carp promoter region in vivo. Microarray analysis indicates that small molecule metabolism and cell-cell interactions are the most significantly affected biological processes in E12.5 Sp3 null myocardium. Since the epicardium showed distension from the myocardium, we studied expression of Wt1, a marker for epicardial cells. Wt1 expression was diminished in epicardium-derived cells in the myocardium of Sp3 null hearts. We conclude that Sp3 is required for normal cardiac development, and suggest that it has a crucial role in myocardial differentiation. (**Keywords:** Transcription factors, Sp3, knockout mice, cardiac malformations, E12.5 **Overall design:** Hearts were dissected from E12.5 wildtype (n=3) and Sp3 knockout (n=3) fetuses. Total RNA was isolated from individual hearts; 5¸…g was used for labelling and hybridization to 430 2.0 Gene Chips (a total of 6).

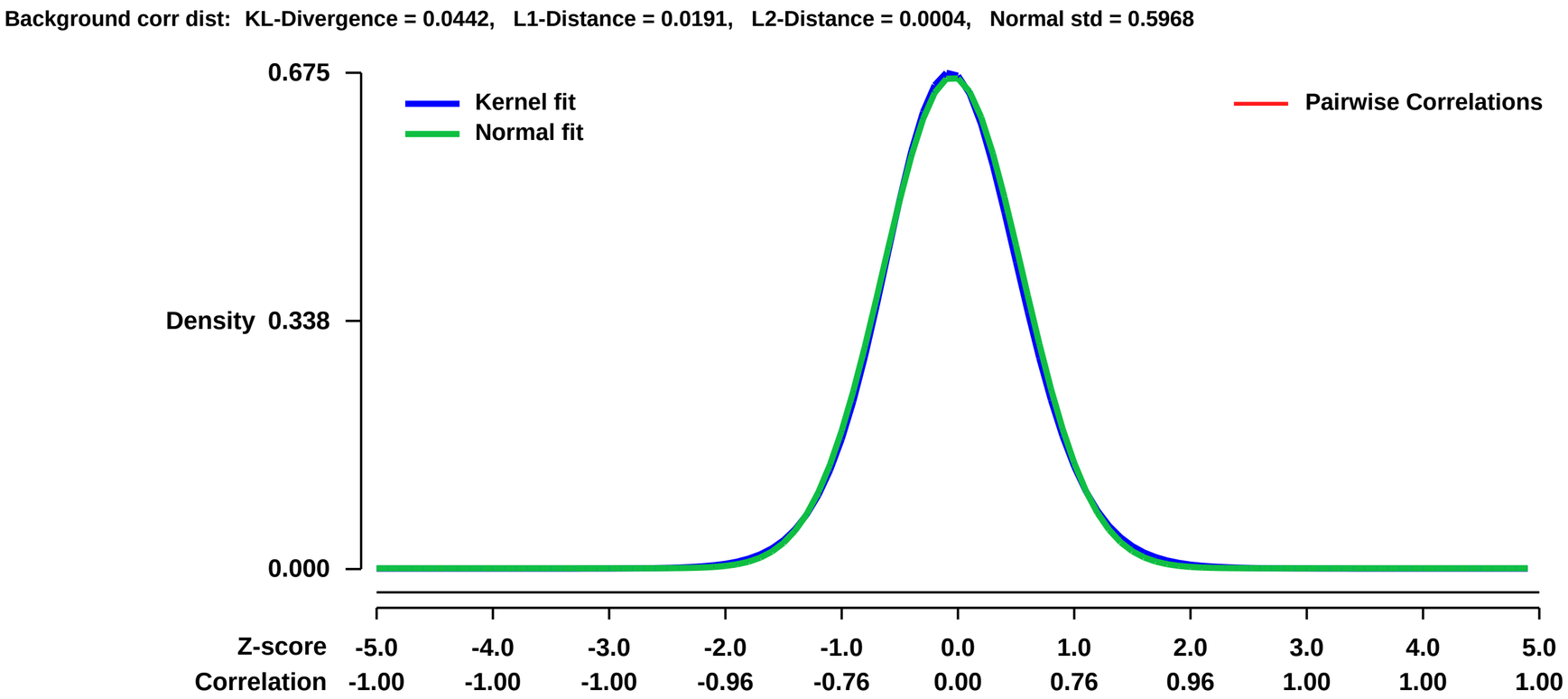

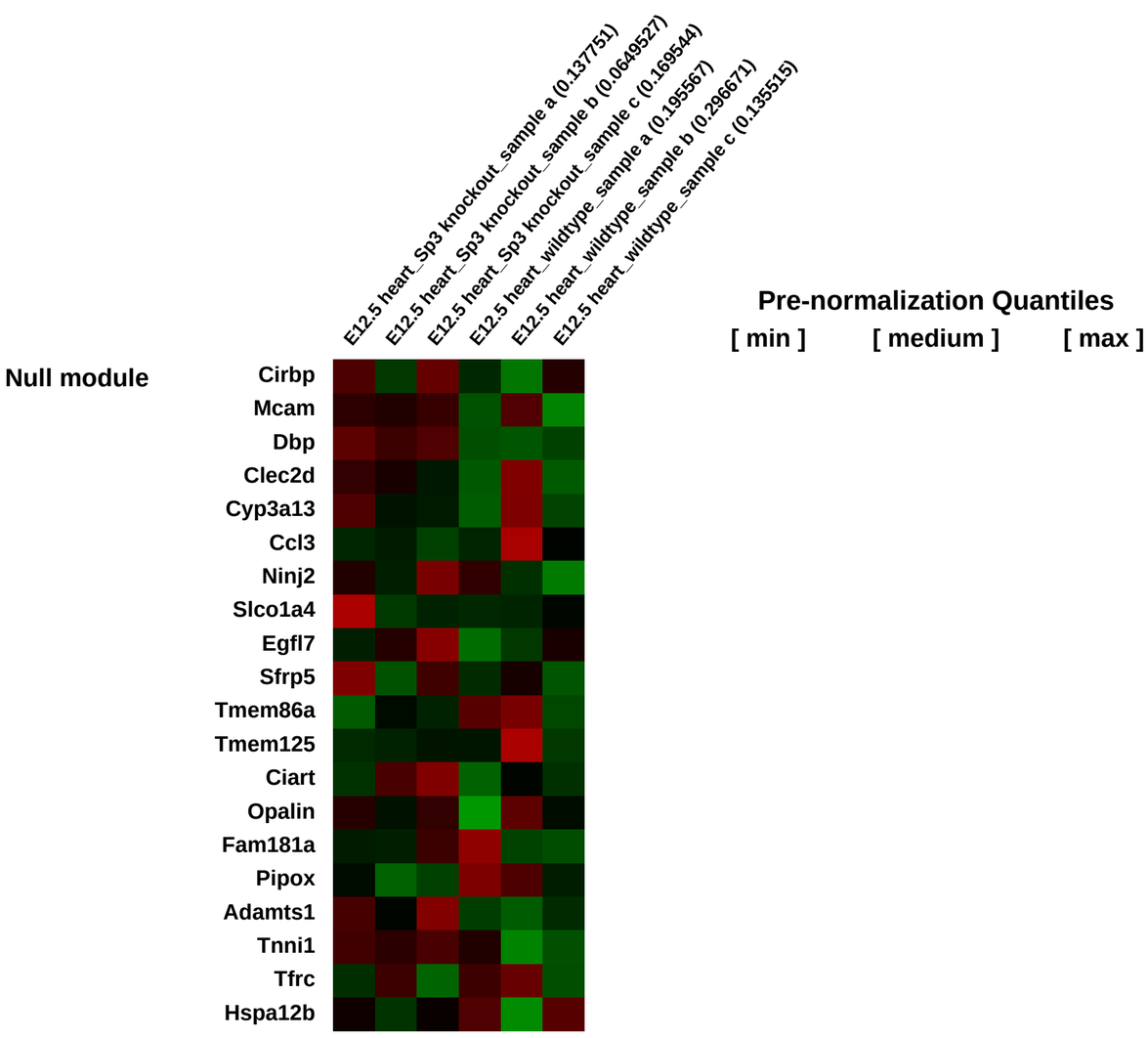

GEO Series "GSE38409" Expression Profiles

Num of samples in this series: 16

Scale of expression profile Z-scores

-3.0 -2.0 -1.0 0.0 1.0 2.0 3.0

GEO Link:	http://www.ncbi.nlm.nih.gov/geo/query/acc.cgi?acc=GSE38409
Status:	Public on Jun 02 2012
Title:	Expression data from mouse lungs, exposed in-utero to second-hand smoke (SHS) and challenged with ovalbumin (OVA) as adults.
Organism:	Mus musculus
Experiment type:	Expression profiling by array
Platform:	GPL1261
Pubmed ID:	23898987
Summary & Design:	**Summary:** SHS exposure during pregnancy has adverse effects on offspring. We used microarrays to characterize the gene expression changes caused by in-utero SHS exposure and adult (19-23 weeks) OVA challenge in 23-week mouse lungs. **Overall design:** Left lungs from Balb/c male and female mice were collected at 23 weeks of age for RNA extraction and hybridization on Affymetrix mouse 430 2.0 microarrays. Based on the gender differences and in-utero exposure status, there are 4 groups of mice, females and males, exposed in-utero to filtered-air or SHS. All were exposure to OVA (19-23 weeks). We extracted RNA from 4 animals from each group for microarray analysis (total N = 16 samples).

Background corr dist: KL-Divergence = 0.0488, L1-Distance = 0.0396, L2-Distance = 0.0021, Normal std = 0.5850

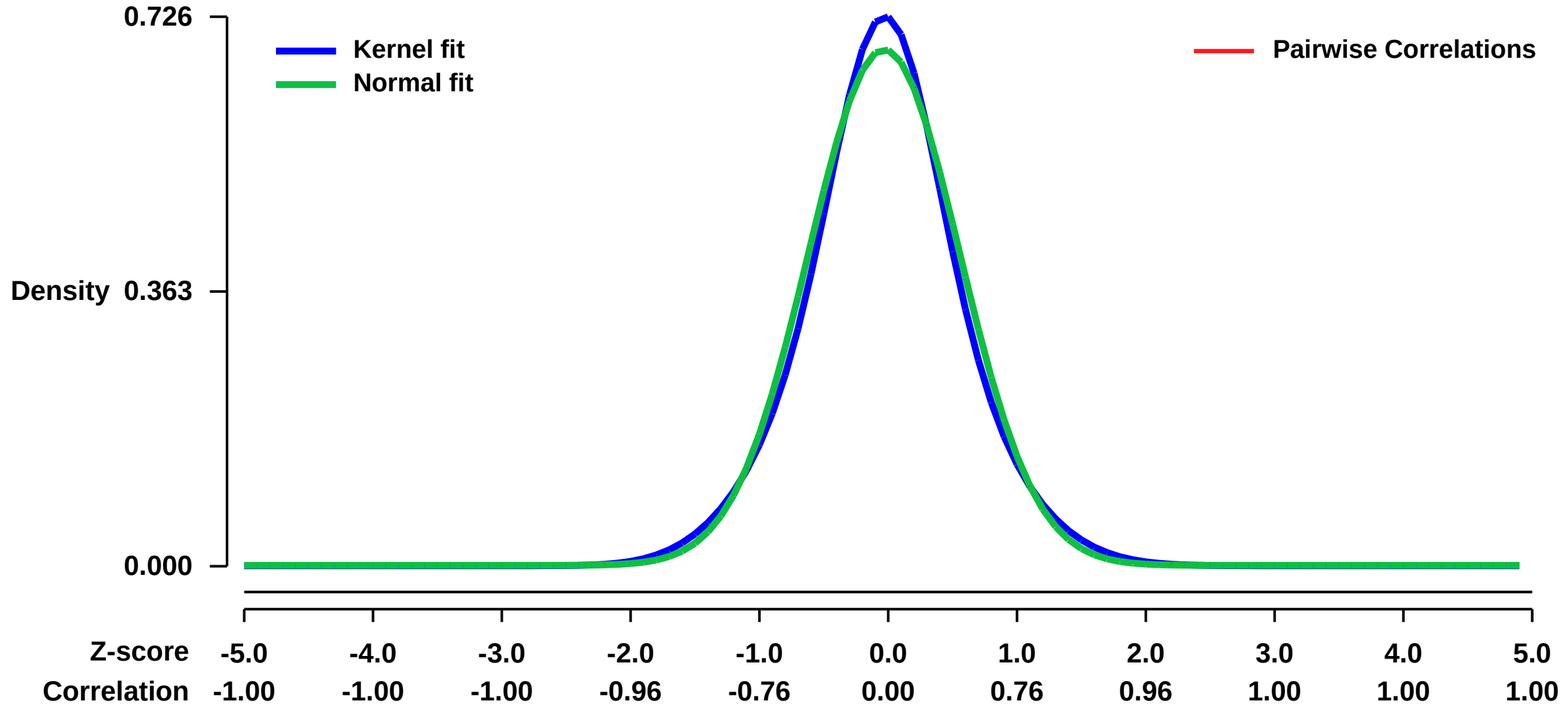

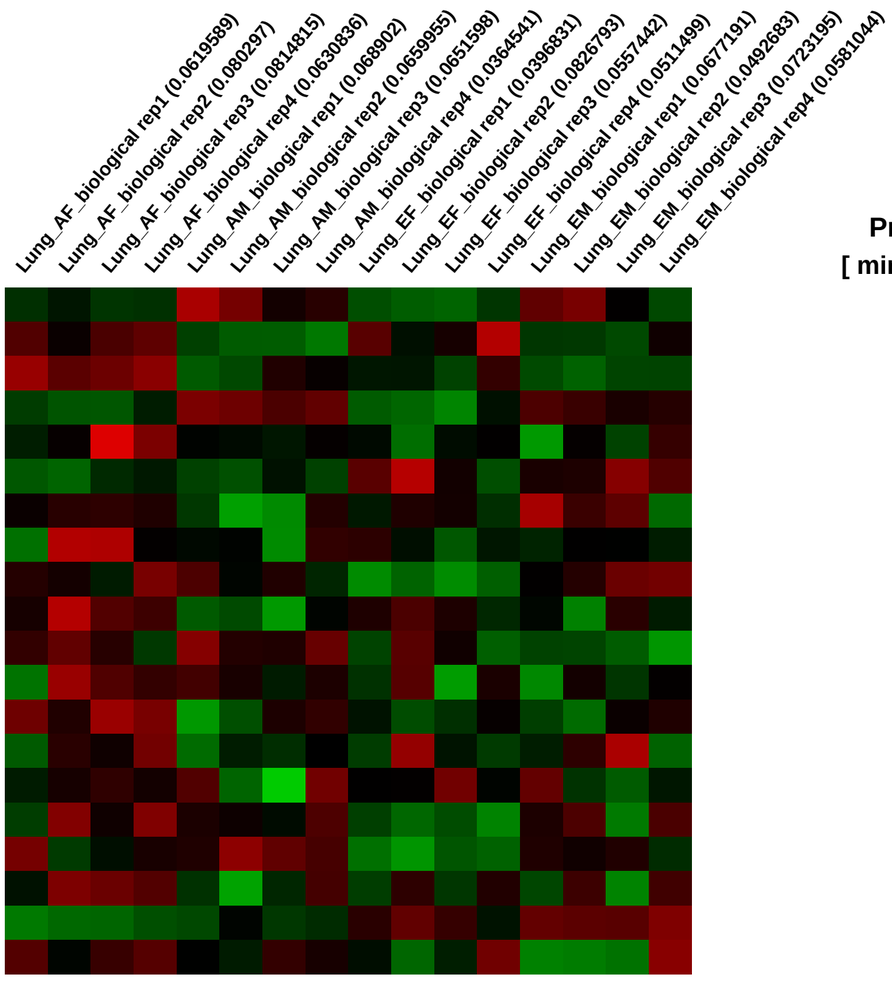

GEO Series "GSE11973" Expression Profiles

Num of samples in this series: 6

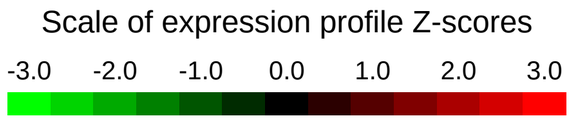

GEO Link:	http://www.ncbi.nlm.nih.gov/geo/query/acc.cgi?acc=GSE11973
Status:	Public on Jul 31 2008
Title:	Wild-type cultured neutrophils versus miR-223 null cultured neutrophils
Organism:	Mus musculus
Experiment type:	Expression profiling by array
Platform:	GPL1261
Pubmed ID:	18668037
Summary & Design:	**Summary:** This array analysis is to study the regulation of target messagesâ expression in in vitro cultured murine neutrophils versus miR-223 null neutrophils. Culture media was SILAC-IMDM for MS analysis. **Overall design:** Wild-type cultured neutrophils versus miR-223 null cultured neutrophils

Background corr dist: KL-Divergence = 0.0336, L1-Distance = 0.0241, L2-Distance = 0.0006, Normal std = 0.6585

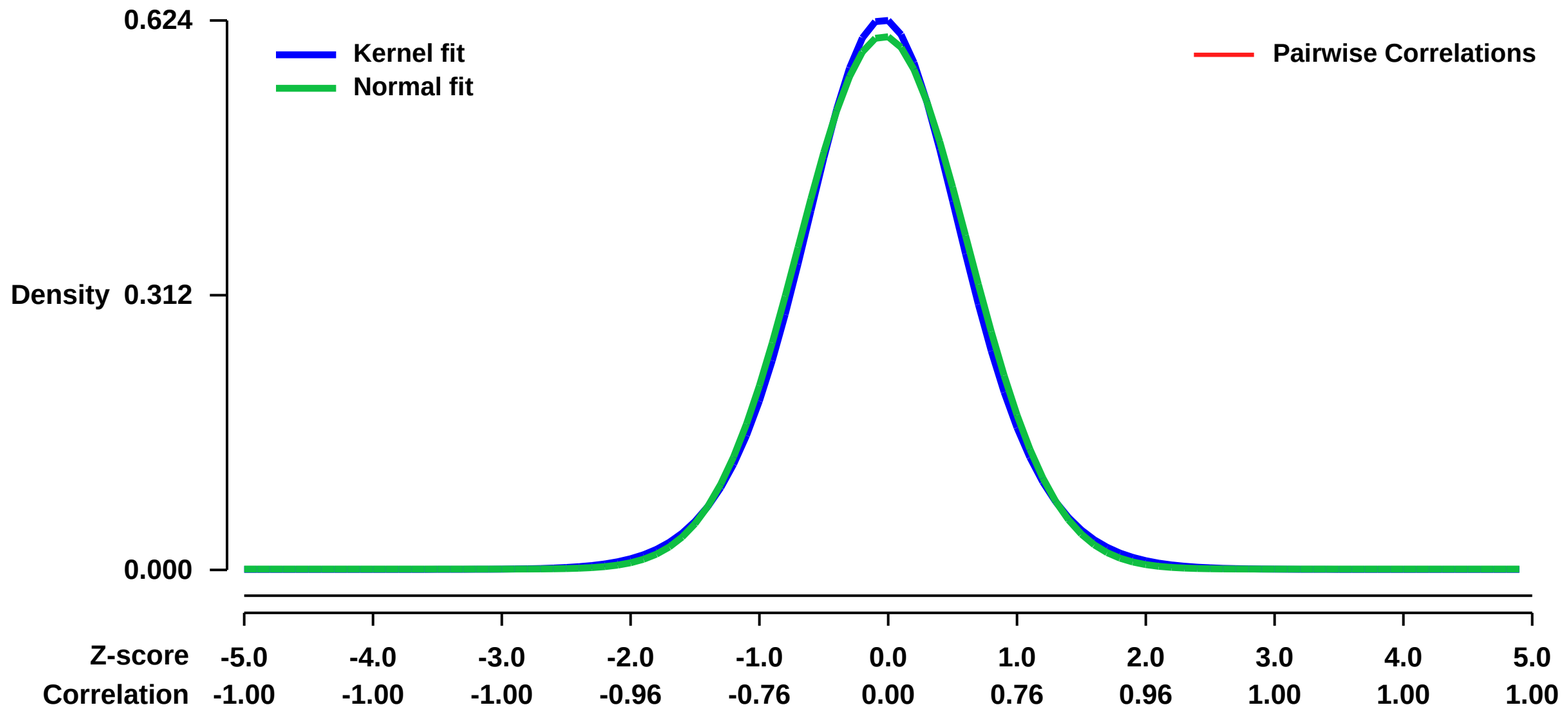

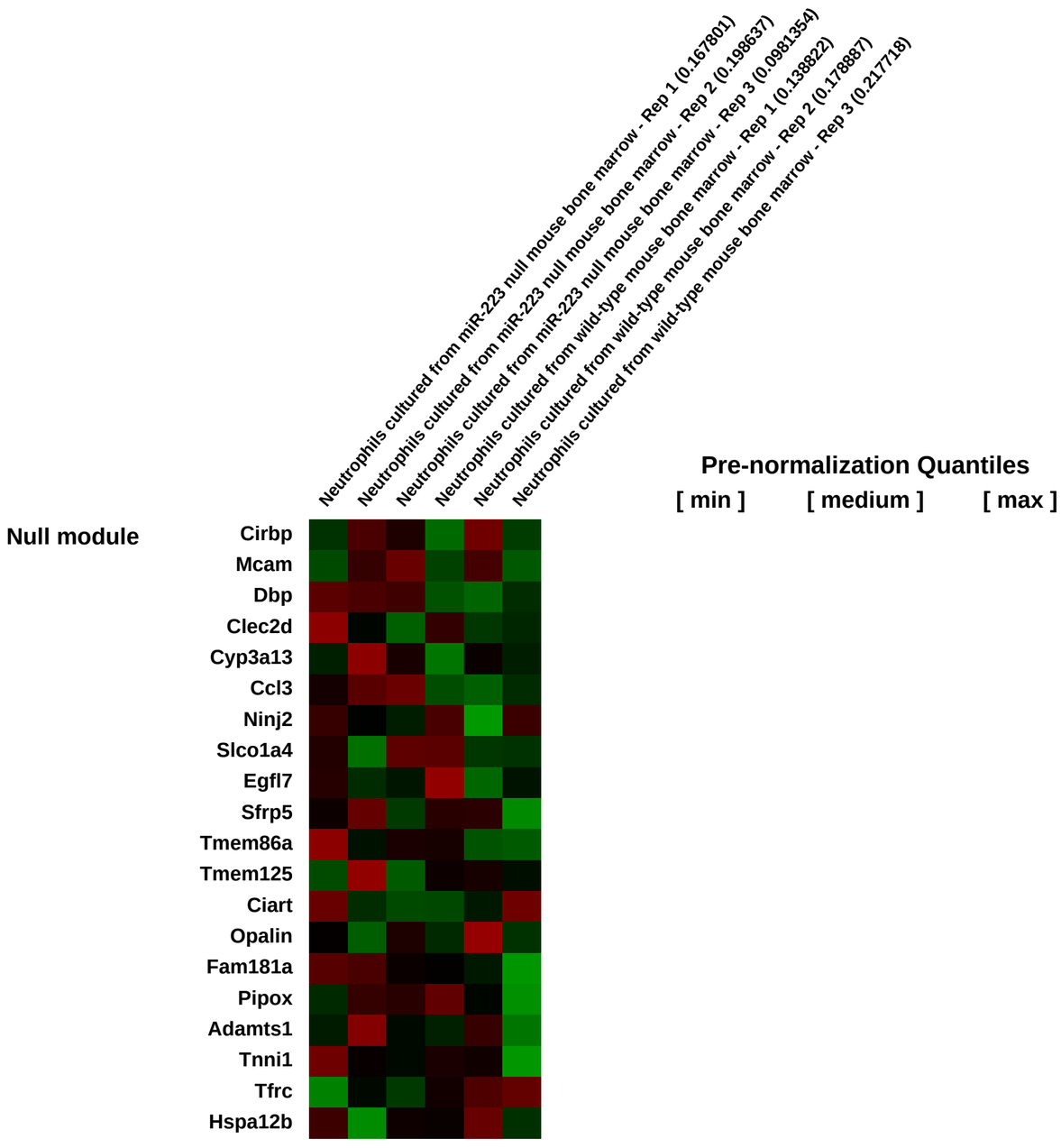

GEO Series "GSE30834" Expression Profiles

Num of samples in this series: 9

Scale of expression profile Z-scores

-3.0 -2.0 -1.0 0.0 1.0 2.0 3.0

GEO Link:	**http://www.ncbi.nlm.nih.gov/geo/query/acc.cgi?acc=GSE30834**
Status:	**Public on Jul 23 2011**
Title:	**Influence of C/EBP¸† 3'UTR on RasV12 induced gene expression**
Organism:	**Mus musculus**
Experiment type:	**Expression profiling by array**
Platform:	**GPL1261**
Pubmed ID:	
Summary & Design:	**Summary:** **C/EBPb is an auto-repressed protein that becomes posttranslationally activated by Ras-MEK-ERK signalling. C/EBPb is required for oncogene-induced senescence (OIS) of primary fibroblasts, but also displays pro-oncogenic functions in many tumour cells. Here, we show that C/EBPb activation by H-RasV12 is suppressed in immortalized/transformed cells, but not in primary cells, by its 30 untranslated region (30UTR). 30UTR sequences inhibited Ras-induced cytostatic activity of C/EBPb, DNA binding, transactivation, phosphorylation, and homodimerization, without significantly affecting protein expression. The 30UTR suppressed induction of senescence-associated C/EBPb target genes, while promoting expression of genes linked to cancers and TGFb signalling. An AU-rich element (ARE) and its cognate RNA-binding protein, HuR, were required for 30UTR inhibition. These components also excluded the Cebpb mRNA from a perinuclear cytoplasmic region that contains activated ERK1/2, indicating that the site of C/EBPb translation controls de-repression by Ras signalling. Notably, 30UTR inhibition and Cebpb mRNA compartmentalization were absent in primary fibroblasts, allowing Ras-induced C/EBPb activation and OIS to proceed. Our findings reveal a novel mechanism whereby non-coding mRNA sequences selectively regulate C/EBPb activity and suppress its anti-oncogenic functions.** **Overall design:** **NIH-3T3 cells were retrovirally infected and selected with appropriate antiobiotics. Equal number of cells were plated and collected 48-72 hours later.**

Background corr dist: KL-Divergence = 0.0581, L1-Distance = 0.0180, L2-Distance = 0.0004, Normal std = 0.5331

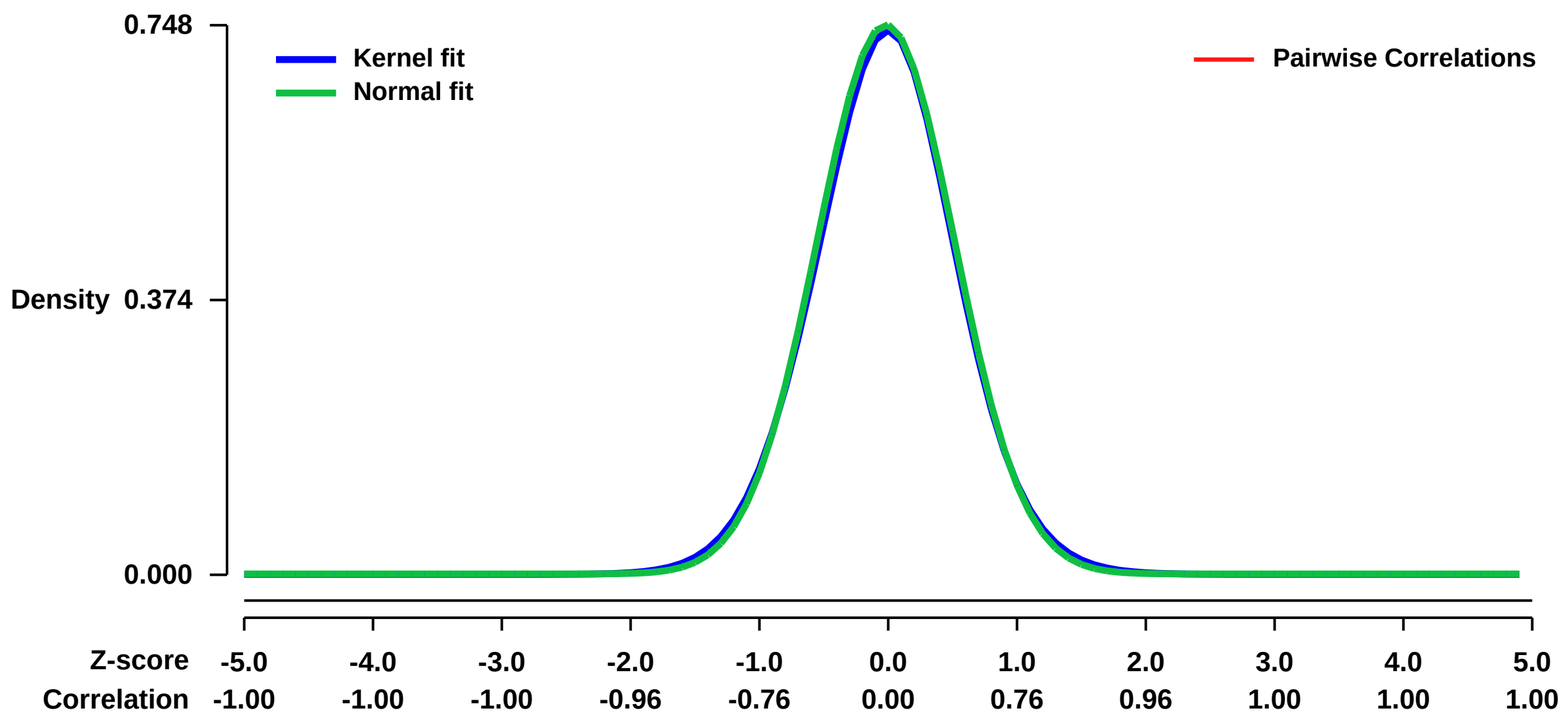

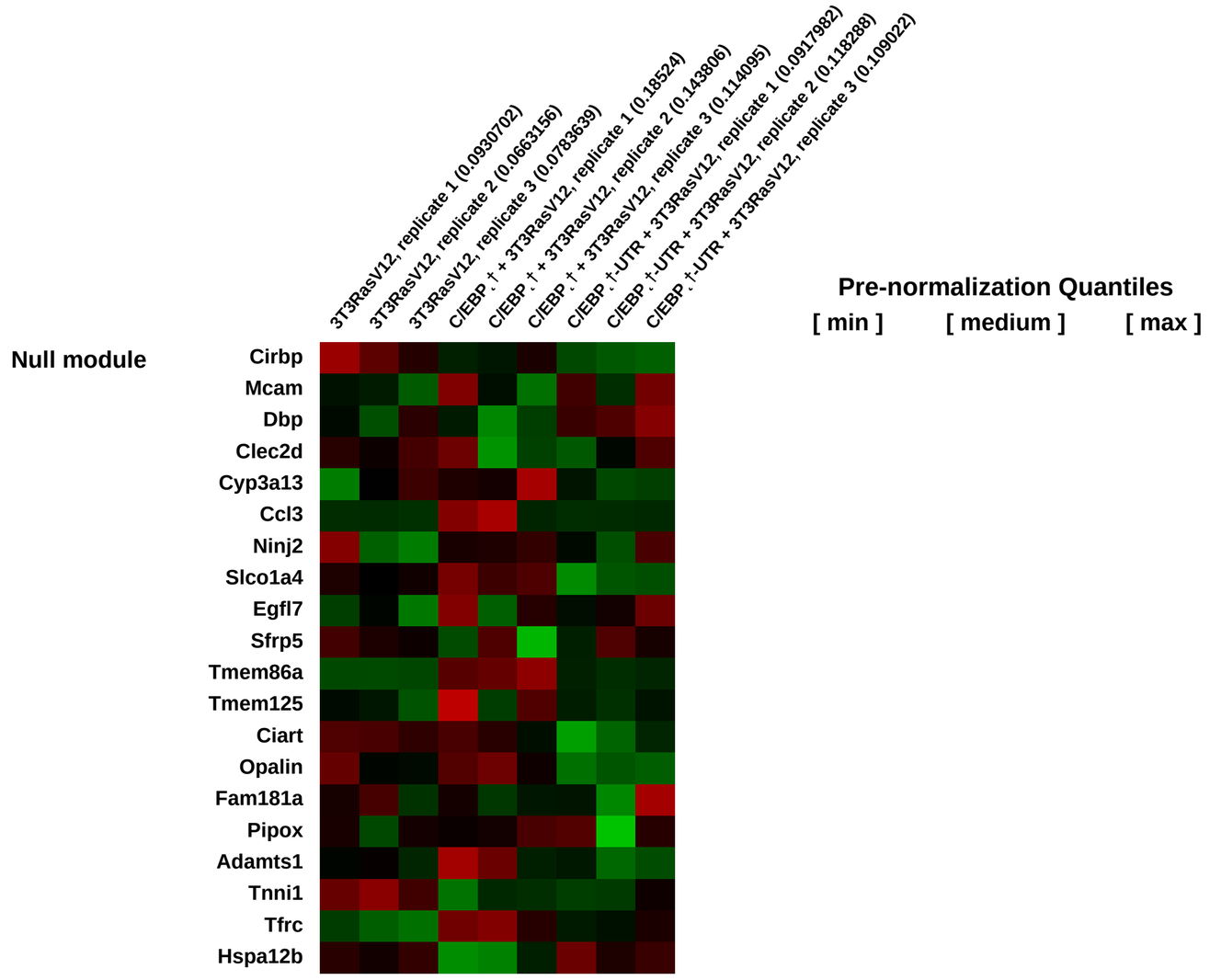

GEO Series "GSE41808" Expression Profiles

Num of samples in this series: 6

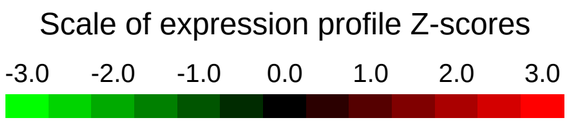

GEO Link:	http://www.ncbi.nlm.nih.gov/geo/query/acc.cgi?acc=GSE41808
Status:	Public on Oct 25 2012
Title:	Expression data from adult (9 month-old) and young (4 month-old) hearts from GRK2 heterozygous C57BL/6J mice.
Organism:	Mus musculus
Experiment type:	Expression profiling by array
Platform:	GPL1261
Pubmed ID:	
Summary & Design:	**Summary:** G protein-coupled receptor kinase 2 (GRK2) has emerged as a key regulator of cardiac function and myocardial structure. Cardiac GRK2 is increased in heart failure and ischemia in humans, whereas genetic inhibition of GRK2 is cardioprotective in animal models of these pathologies. However, the mechanistic basis underlying these effects are not fully understood. We have used adult GRK2 hemizygous mice (GRK2+/-) as a model to assess the effects of a sustained systemic inhibition of GRK2 in heart tissue with age. We used microarrays to determine the global programme of gene expression underlying cardioprotection in GRK2 hemizygous mice with age. **Overall design:** 9 month-old and 4 month-old mice hearts were collected for RNA extraction and hybridization on Affymetrix microarrays.

Background corr dist: KL-Divergence = 0.0467, L1-Distance = 0.0166, L2-Distance = 0.0003, Normal std = 0.5832

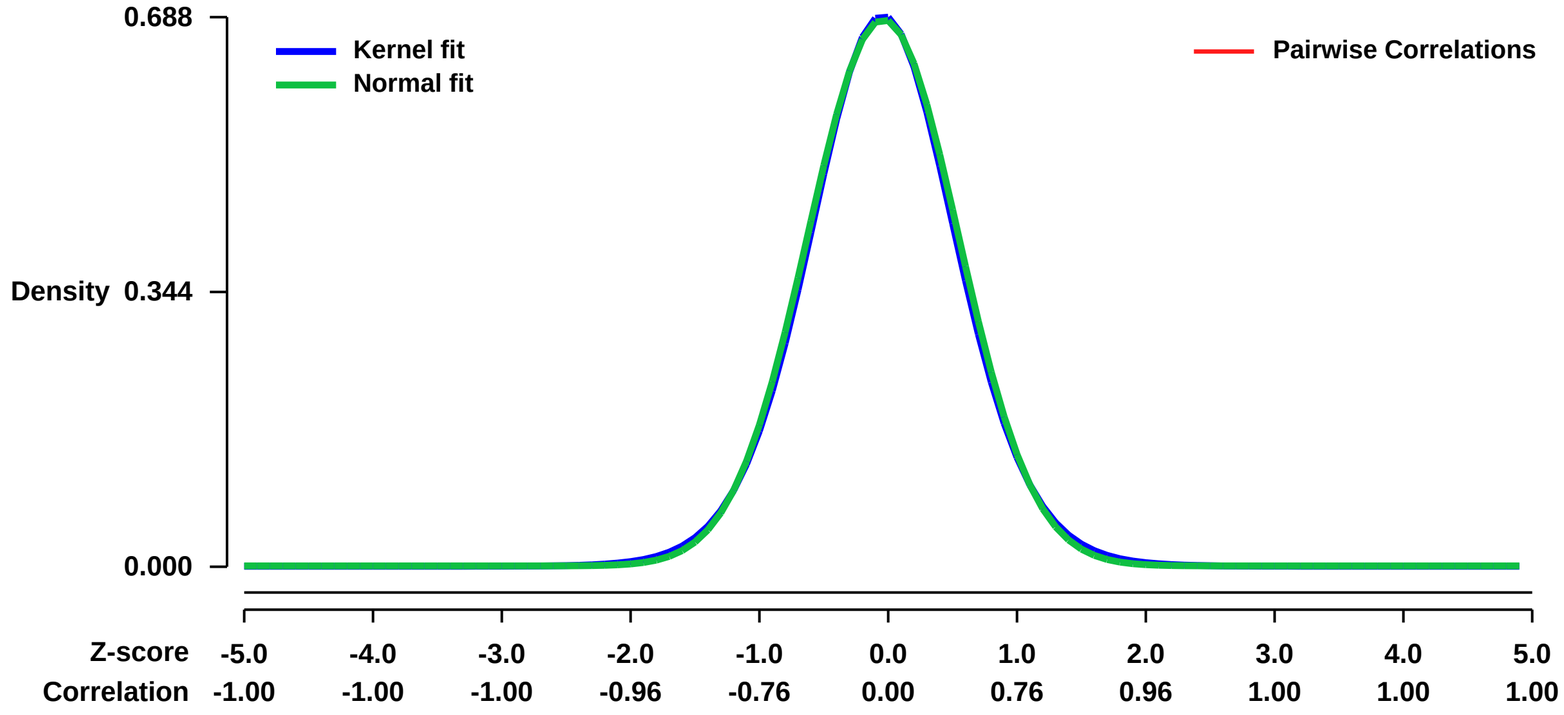

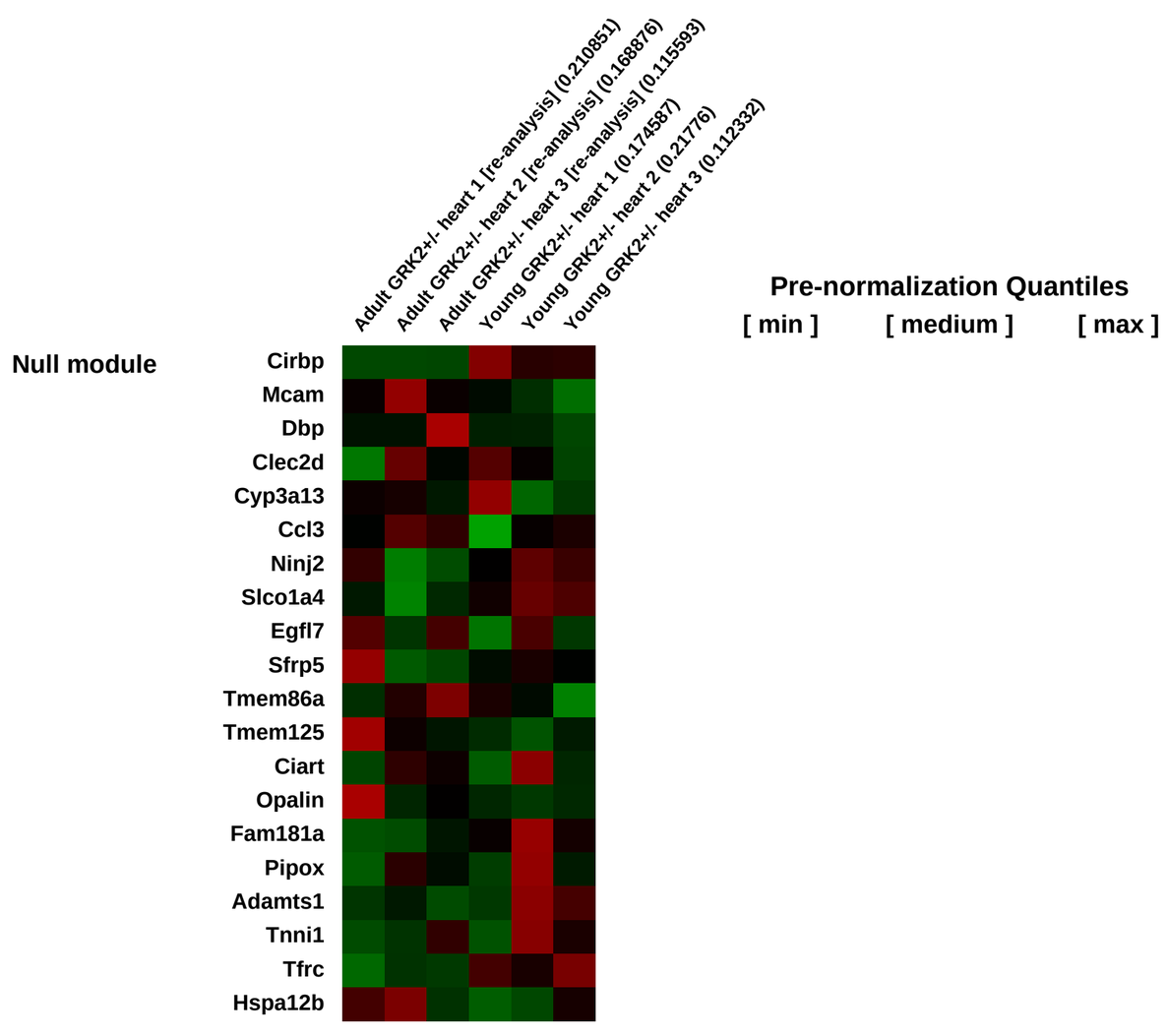

GEO Series "GSE30488" Expression Profiles

Num of samples in this series: 52

Scale of expression profile Z-scores

-3.0 -2.0 -1.0 0.0 1.0 2.0 3.0

GEO Link:	http://www.ncbi.nlm.nih.gov/geo/query/acc.cgi?acc=GSE30488
Status:	Public on Aug 31 2012
Title:	Expression data from E2f7/E2f8/E2f3a null placentas and embryos
Organism:	Mus musculus
Experiment type:	Expression profiling by array
Platform:	GPL1261
Pubmed ID:	22516201
Summary & Design:	**Summary:** To understand the underlying cause and mechanisms of embryonic lethality observed in combined loss of E2f7 and E2f8, we compared global gene expression profiles of wild type, germline deleted and sox2-Cre/Cyp19-Cre deleted embryos and placentas. **Overall design:** RNA was extracted from E10.5 embryos and placentas. Gene deletion in samples confirmed by PCR genotyping of DNA isolated from each sample.

Background corr dist: KL-Divergence = 0.0427, L1-Distance = 0.0236, L2-Distance = 0.0008, Normal std = 0.5868

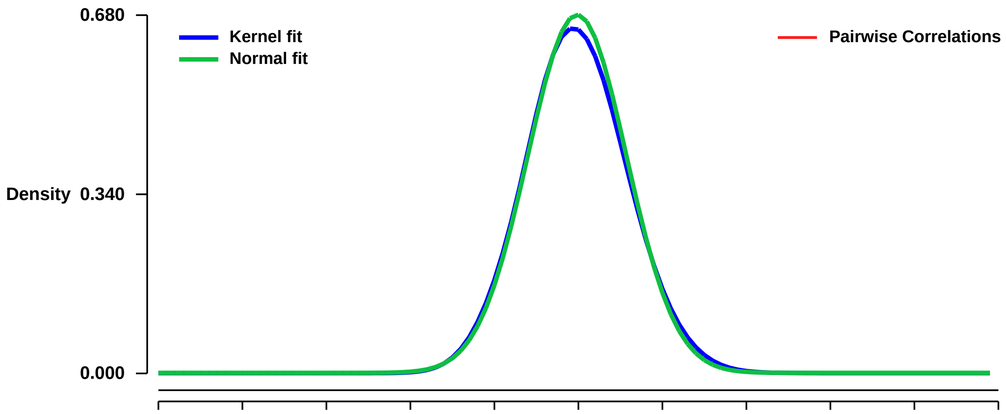

Z-score	-5.0	-4.0	-3.0	-2.0	-1.0	0.0	1.0	2.0	3.0	4.0	5.0
Correlation	-1.00	-1.00	-1.00	-0.96	-0.76	0.00	0.76	0.96	1.00	1.00	1.00

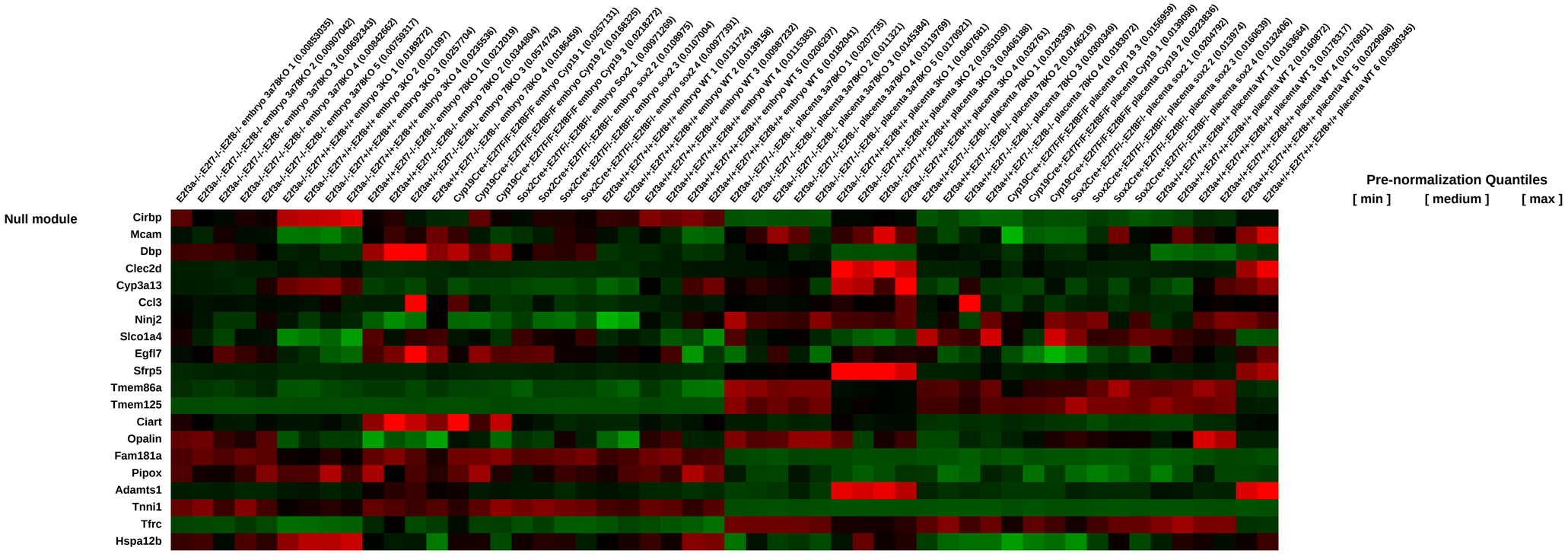

GEO Series "GSE27379" Expression Profiles

Num of samples in this series: 6

Scale of expression profile Z-scores

-3.0 -2.0 -1.0 0.0 1.0 2.0 3.0

GEO Link:	http://www.ncbi.nlm.nih.gov/geo/query/acc.cgi?acc=GSE27379
Status:	Public on Dec 21 2011
Title:	CD8+ T cell mediated lung inflammation
Organism:	Mus musculus
Experiment type:	Expression profiling by array
Platform:	GPL1261
Pubmed ID:	21518973
Summary & Design:	**Summary:** Role for naturally occurring CD4+CD25+Foxp3+ regulatory T cells (nTregs) in counterbalancing this process. Using a transgenic murine model for autoimmune-mediated lung disease, we demonstrated that, despite pulmonary inflammation, lung-specific CD8+ T cells can reside quiescently in close proximity to self-antigen. Whereas self-reactive CD8+ T cells in the inflamed lung and lung-draining lymph nodes down-regulated the expression of effector molecules, those located in the spleen appeared to be partly antigen-experienced and displayed a memory-like phenotype. Since ex vivo-reisolated self-reactive CD8+ T cells were very well capable to respond to the antigen in vitro, we investigated a possible contribution of nTregs to the immune control over autoaggressive CD8+ T cells in the lung. **Overall design:** CD8+ T cell type comparison; lung disease state analysis

Background corr dist: KL-Divergence = 0.0455, L1-Distance = 0.0339, L2-Distance = 0.0016, Normal std = 0.6061

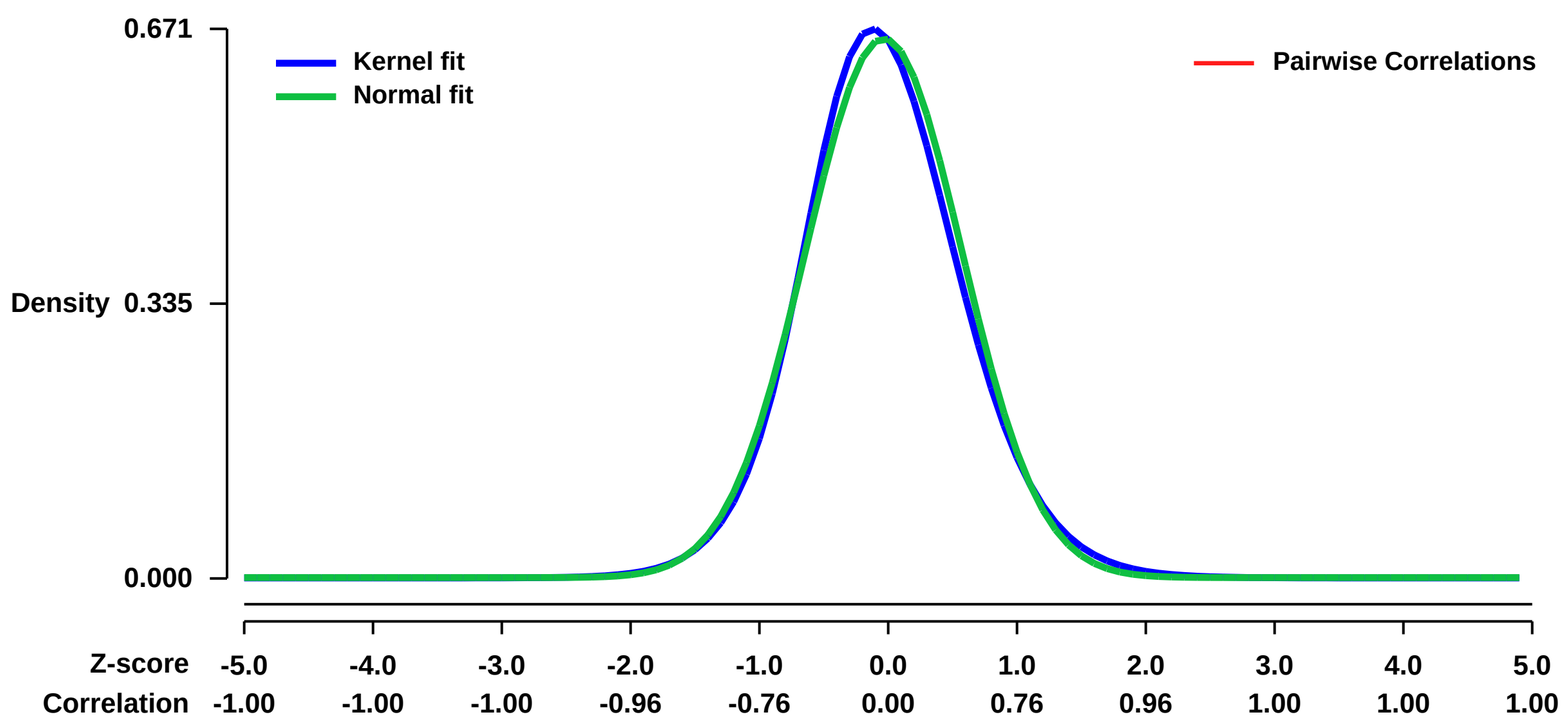

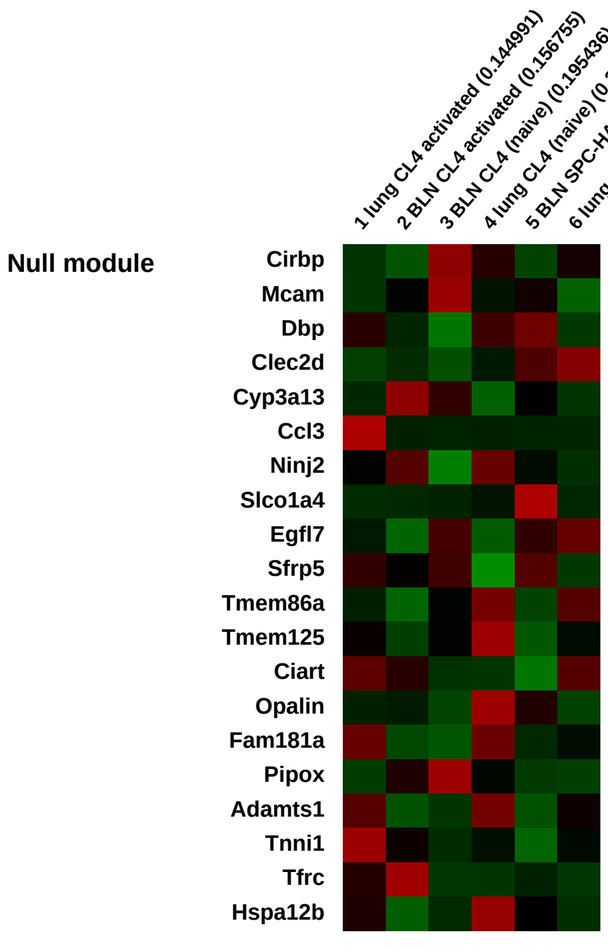

GEO Series "GSE7809" Expression Profiles

Num of samples in this series: 8

Scale of expression profile Z-scores

-3.0 -2.0 -1.0 0.0 1.0 2.0 3.0

GEO Link:	http://www.ncbi.nlm.nih.gov/geo/query/acc.cgi?acc=GSE7809
Status:	Public on Nov 29 2007
Title:	Transcriptional expression of ICC-DMP and ICC-MY in murine small intestine
Organism:	Mus musculus
Experiment type:	Expression profiling by array
Platform:	GPL1261
Pubmed ID:	17895395
Summary & Design:	**Summary:** Interstitial cells of Cajal (ICC) have important functions in regulation of motor activity in the gastrointestinal tract. In murine small intestine ICC are gathered in the region of the myenteric plexus (ICC-MY) and within the deep-muscular plexus near the submucosal surface of the circular muscle layer (ICC-DMP). These two classes of ICC have different physiological functions. ICC-MY are pacemaker cells and generate the slow wave electrical rhythmicity of gastrointestinal organs. ICC-DMP form synaptic connections with the varicose nerve terminals of enteric motor neurons and are involved in reception and transduction of motor neurotransmission. In the present study we used recently developed highly selective techniques to isolate the two classes of ICC from enzymatically dispersed intestinal muscles by fluorescence-activated cell sorting. Transcriptional expression of the two functional classes was investigated using DNA microarray analysis. **Keywords:** comparative transcriptional profiling **Overall design:** ICC-DMP and ICC-MY cells were isolated from the murine small intestinal tissues and their transcriptional expression was compared with that of the tunica muscularis tissues. Transcriptional expression profiles of ICC-DMP and ICC-MY were compared to each other also.

Background corr dist: KL-Divergence = 0.0359, L1-Distance = 0.0622, L2-Distance = 0.0065, Normal std = 0.6724

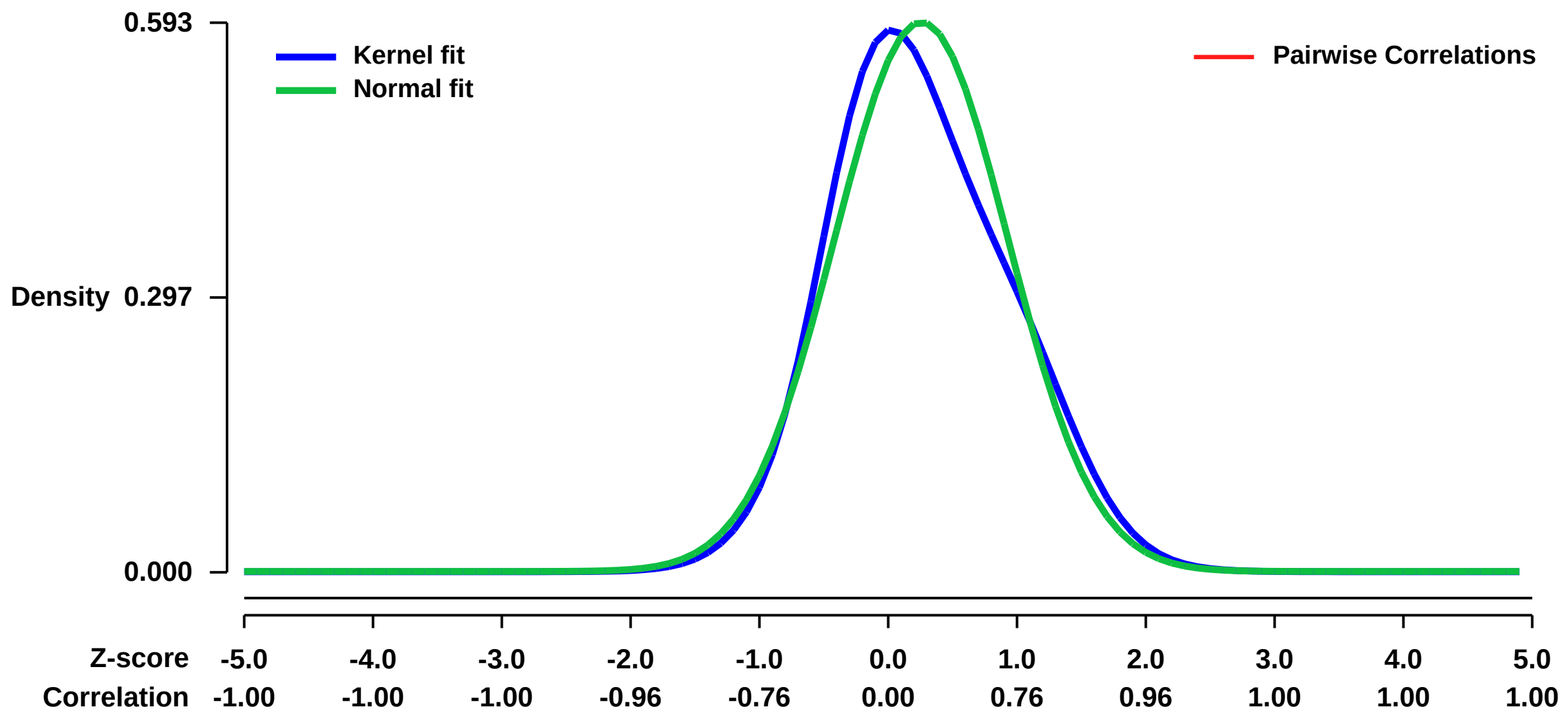

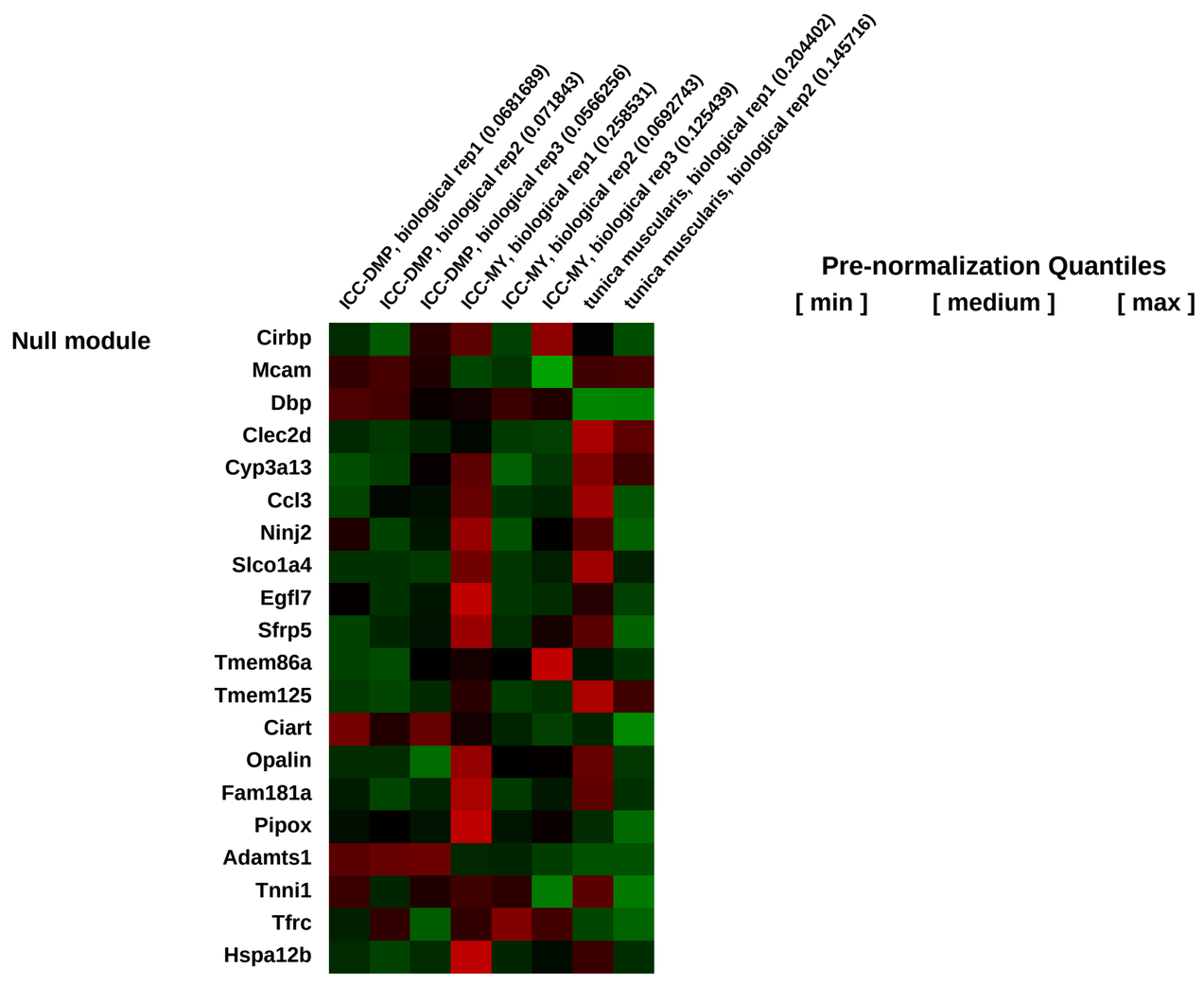

GEO Series "GSE13104" Expression Profiles

Num of samples in this series: 14

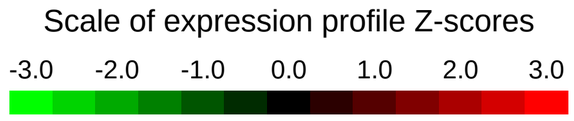

GEO Link:	**http://www.ncbi.nlm.nih.gov/geo/query/acc.cgi?acc=GSE13104**
Status:	**Public on Oct 10 2008**
Title:	**p53+/- mouse osteosarcoma RNA array (with mc3T3 and one RS control)**
Organism:	**Mus musculus**
Experiment type:	**Expression profiling by array**
Platform:	**GPL1261**
Pubmed ID:	
Summary & Design:	**Summary:** **RNA expression profiles from 12 (twelve) osteosarcomas arisen from p53+/- mouse were compared with a mc3T3 osteoblast control, and a rhabdomyosarcoma expression profile which was from a mouse with the same genetic background.** **Overall design:** **Total RNA was extracted from 12 osteosarcomas and 1 rhabdomyosarcoma, both arisen from p53+/- mice. Total RNA was also extracted from a cultured mc3T3 osteoblast cell line as control. RNA microarray was performed on the 14 samples, and expression profiles were compared.**

Background corr dist: **KL-Divergence = 0.1999, L1-Distance = 0.0504, L2-Distance = 0.0061, Normal std = 0.3348**

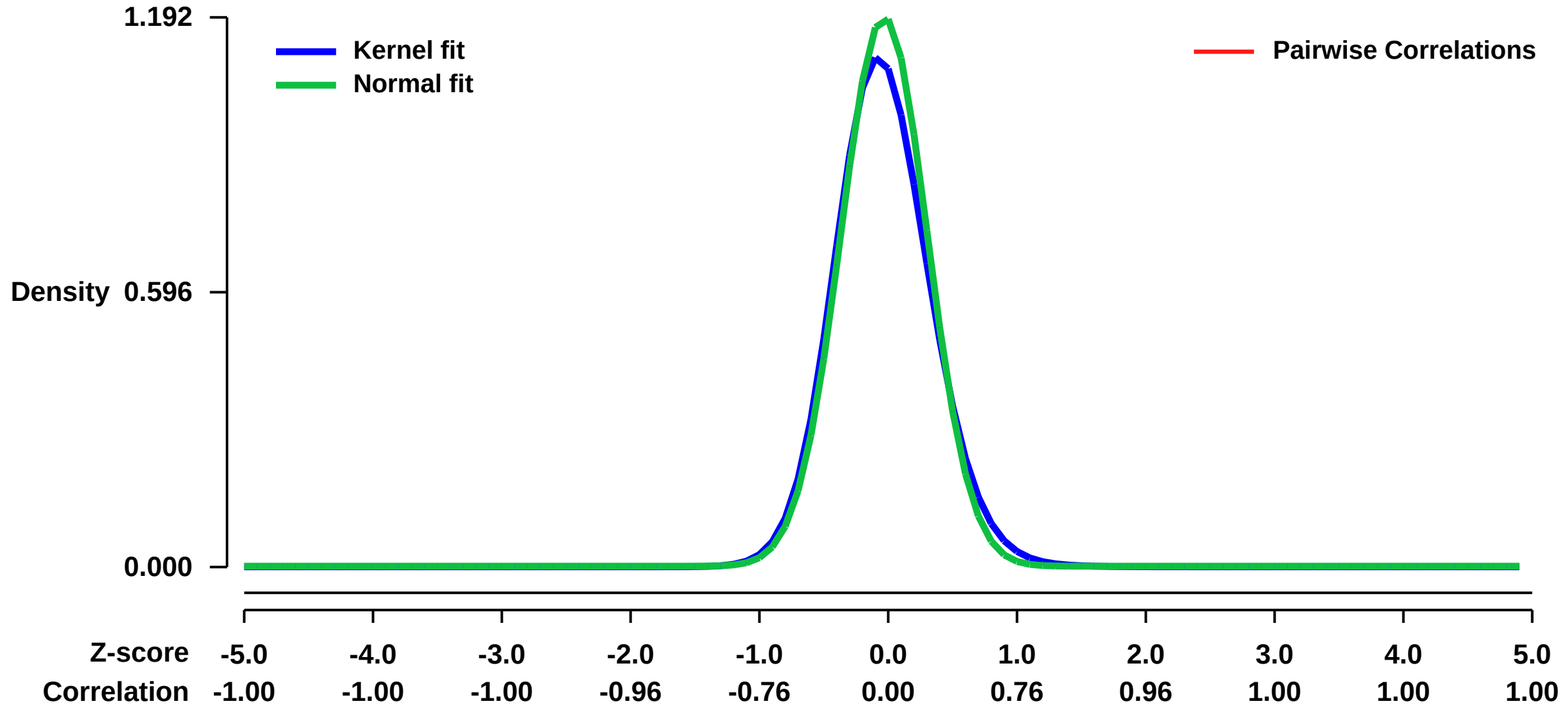

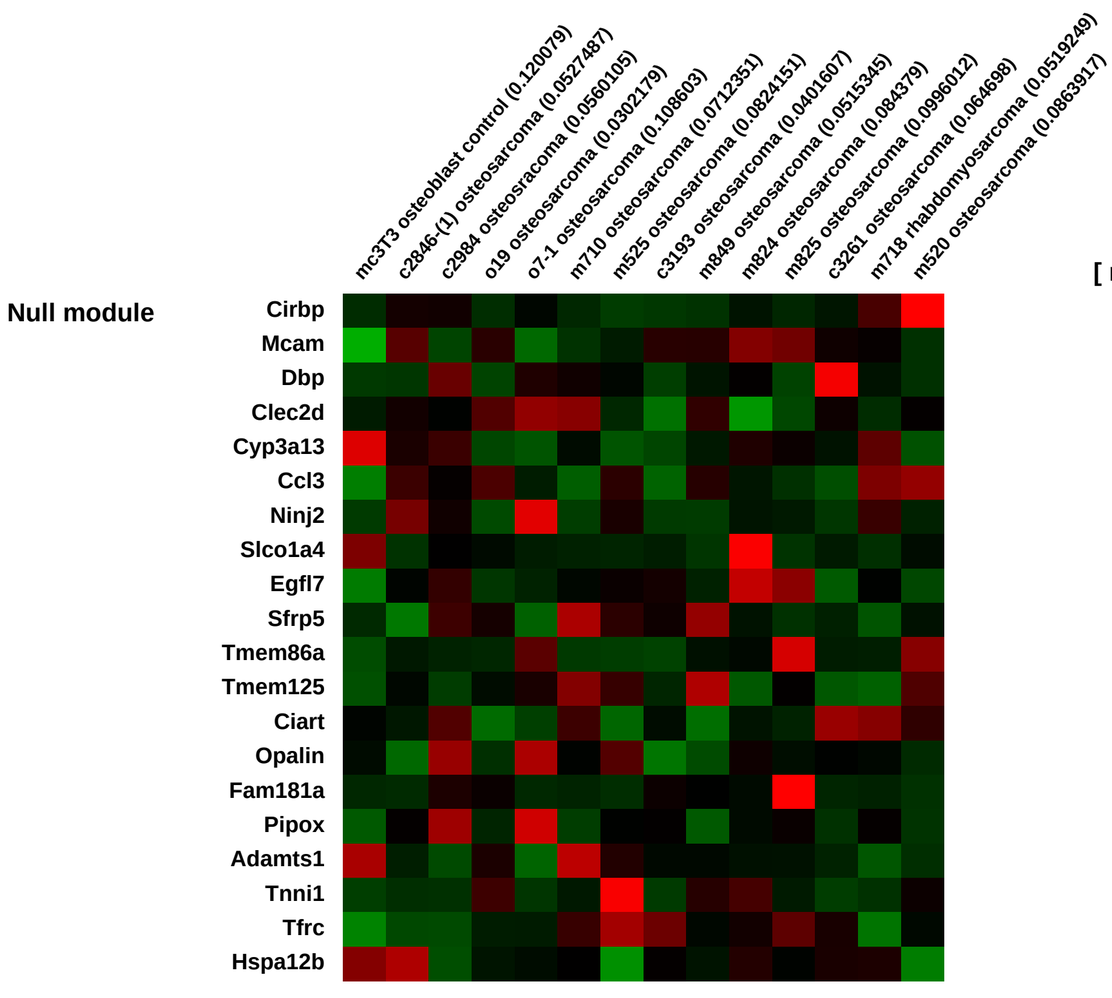

GEO Series "GSE17553" Expression Profiles

Num of samples in this series: 16

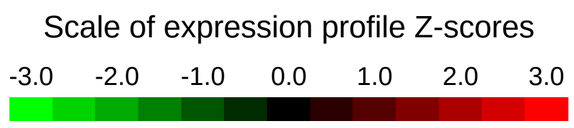

GEO Link:	http://www.ncbi.nlm.nih.gov/geo/query/acc.cgi?acc=GSE17553
Status:	Public on Dec 31 2009
Title:	Estradiol or Testosterone treated efferent duct and caput epididymis
Organism:	Mus musculus
Experiment type:	Expression profiling by array
Platform:	GPL1261
Pubmed ID:	19553595
Summary & Design:	**Summary:** The role of estrogen and testosterone in the regulation of gene expression in the proximal reproductive tract is not completely understood. To address this question, mice were treated with testosterone or estradiol and RNA from the efferent ducts and caput epididymis was processed and hybridized to Affymetrix MOE 430 2.0 microarrays. Analysis of array output identified probe sets in each tissue with altered levels in hormone treated versus control animals. Hormone treatment efficacy was confirmed by determination of serum hormone levels pre- and post-treatment and observed changes in transcript levels of previously reported hormone-responsive genes. Tissue-specific hormone sensitivity was observed with 2867 and 3197 probe sets changing significantly in the efferent ducts after estrogen and testosterone treatment, respectively. In the caput epididymis, 117 and 268 probe sets changed after estrogen and testosterone treatment, respectively, demonstrating a greater response to hormone in the efferent ducts than the caput epididymis. Transcripts sharing similar profiles in the intact and hormone-treated animals compared with castrated controls were also identified. Ontological analysis of probe sets revealed a significant number of hormone-regulated transcripts encode proteins associated with lipid metabolism, transcription and steroid metabolism in both tissues. Real-time RT-PCR was employed to confirm array data and investigate other potential hormone-responsive regulators of proximal reproductive tract function. The results of this work reveal previously unknown responses to estrogen in the caput epididymis and to testosterone in the efferent ducts as well as tissue specific hormone sensitivity in the proximal reproductive tract. **Overall design:** Adult animals were castrated or sham-castrated, allowed to recover for 14 days, and then treated with 0.015 mg estradiol (castrated), 0.015 mg testosterone propionate (castrated), or vehicle (castrated and sham-castrated as biological controls) in duplicate. Efferent duct and caput epididymis was collected from each sample and analyzed. Duplicates are included in the provided data and numbered 1 or 2 for each treatment regimen.

Background corr dist: KL-Divergence = 0.0449, L1-Distance = 0.0261, L2-Distance = 0.0011, Normal std = 0.5797

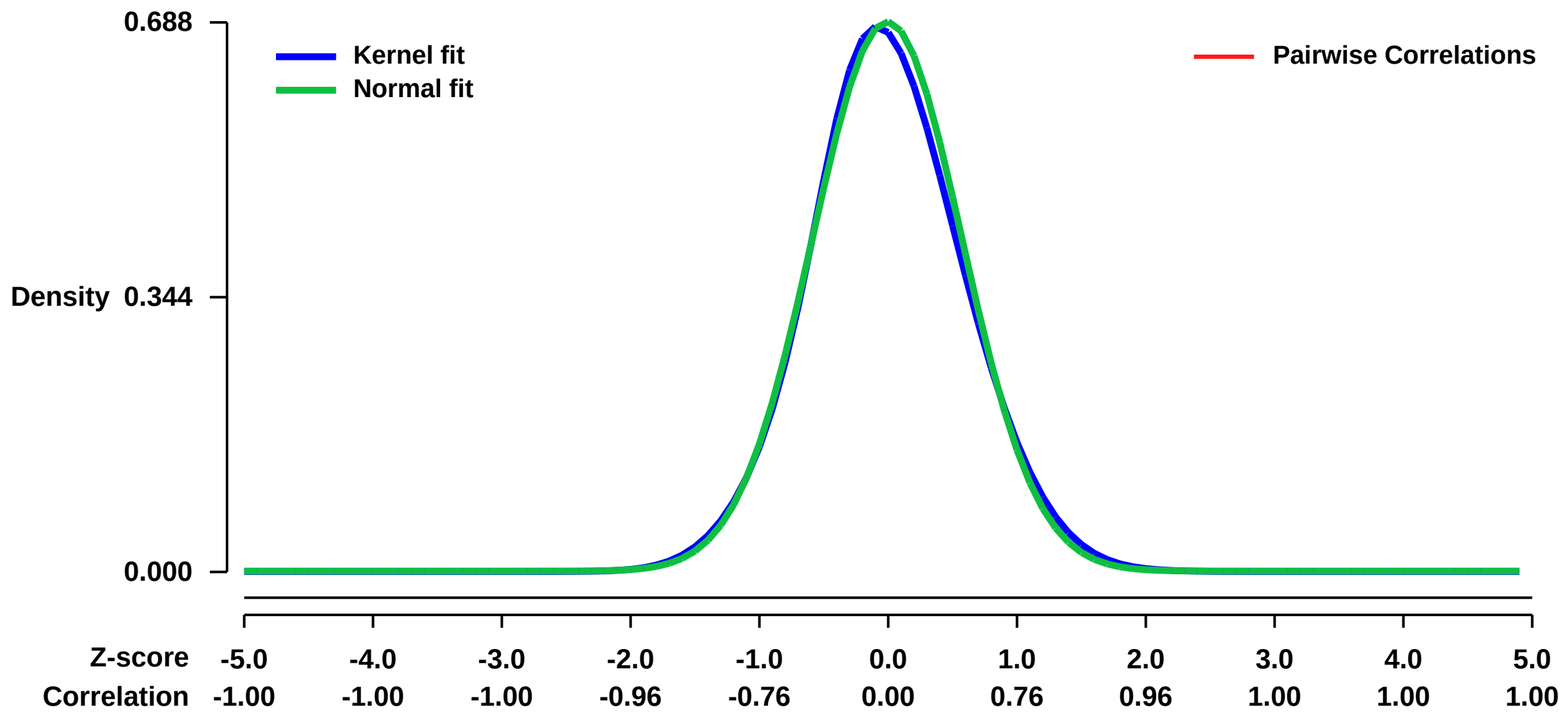

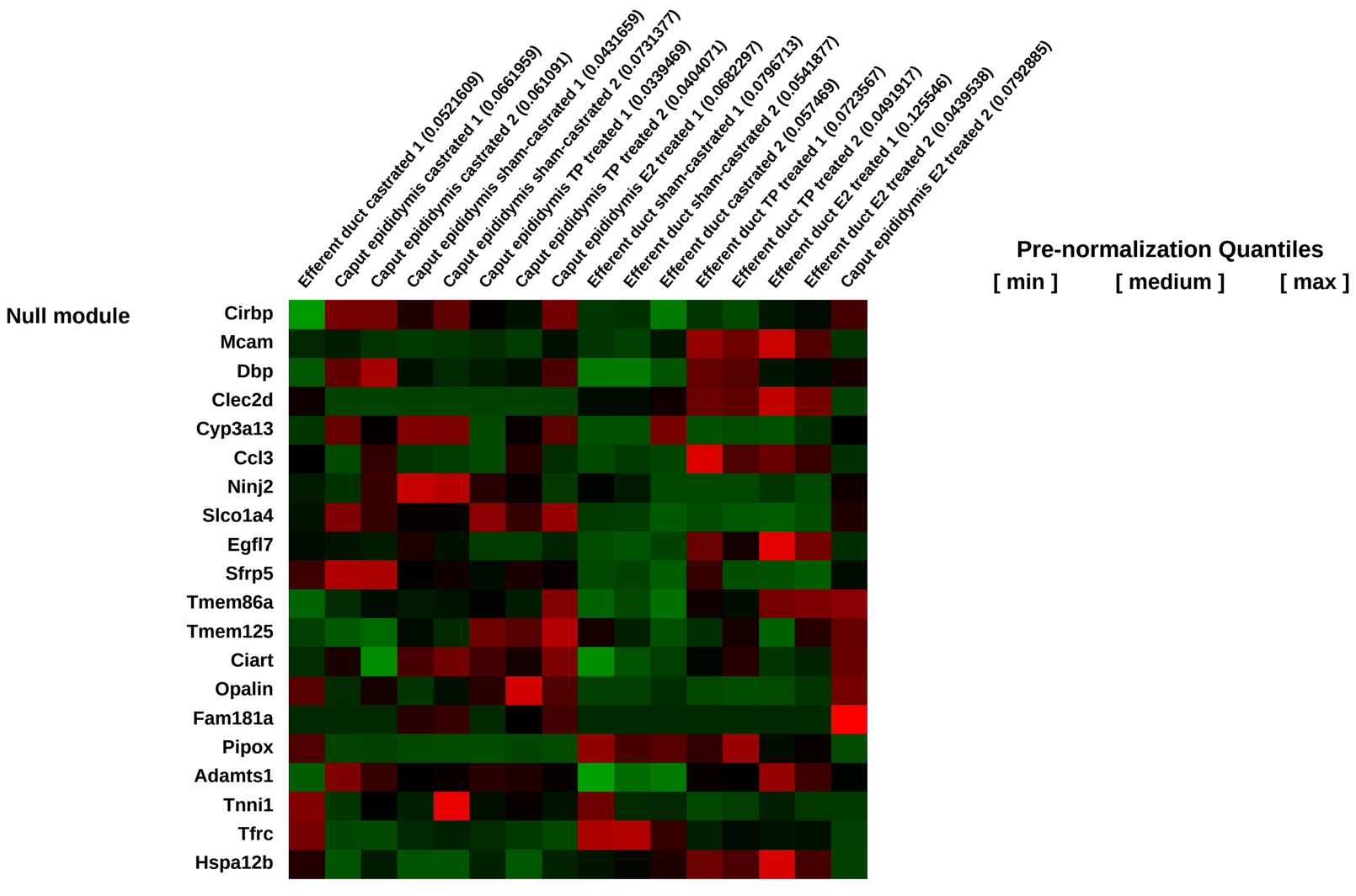

GEO Series "GSE11766" Expression Profiles

Num of samples in this series: 48

Scale of expression profile Z-scores

-3.0 -2.0 -1.0 0.0 1.0 2.0 3.0

GEO Link:	http://www.ncbi.nlm.nih.gov/geo/query/acc.cgi?acc=GSE11766
Status:	Public on Jun 13 2008
Title:	Transcriptional repression of c-Myb and GATA-2 is involved in the effects of C/EBP‚– in p210 BCR/ABL-expressing cells
Organism:	Mus musculus
Experiment type:	Expression profiling by array
Platform:	GPL1261
Pubmed ID:	18550858
Summary & Design:	**Summary:** Levels of C/EBP‚– are low in myeloid blast crisis (BC) of chronic myelogenous leukemia (CML) and its expression in p210BCR/ABL-expressing hematopoietic cells induces granulocytic differentiation, inhibits proliferation and suppresses leukemogenesis. To assess the mechanisms involved in these effects, C/EBP‚– targets were identified by microarray analyses. Upon C/EBP‚– activation, expression of c-Myb and GATA-2 was repressed in 32D-BCR/ABL, K562 and CML-BC primary cells but only c-Myb levels decreased slightly in CD34+ normal progenitors. The role of these two genes for the biological effects of C/EBP‚– was assessed by perturbing their expression in K562 cells. Expression of c-Myb blocked the proliferation inhibition and differentiation-inducing effects of C/EBP‚– while c-Myb siRNA treatment enhanced C/EBP‚–-mediated proliferation inhibition and induced changes in gene expression indicative of monocytic differentiation. GATA-2 expression suppressed the proliferation inhibitory effect of C/EBP‚– but blocked in part the effect on differentiation; GATA-2 siRNA treatment had no effects on C/EBP‚– induction of differentiation but inhibited proliferation of K562 cells, alone or upon C/EBP‚– activation. In summary, the effects of C/EBP‚– in p210BCR/ABL -expressing cells depend, in part, on transcriptional repression of c-Myb and GATA-2. Since perturbation of c-Myb and GATA-2 expression has non identical consequences for proliferation and differentiation of K562 cells, the effects of C/EBP‚– appear to involve different transcription-regulated targets. **Overall design:** 48 samples total. 4-HT-treated 32D-BCR/ABL cells transduced with the MigRI empty vector, MigRI WT C/EBP‚–-ER , MigRI K298E C/EBP‚–-ER (a DNA binding-deficient mutant) or MigRI-delta(177-191) C/EBP‚–-ER (a mutant deficient in CDK2/CDK4 interaction). Total RNA was extracted at 0, 6, 9 and 12h post-4-HT treatment in triplicate and hybridized onto the Affymetrix MOE430 _2 array.

Background corr dist: KL-Divergence = 0.4094, L1-Distance = 0.0458, L2-Distance = 0.0042, Normal std = 0.2511

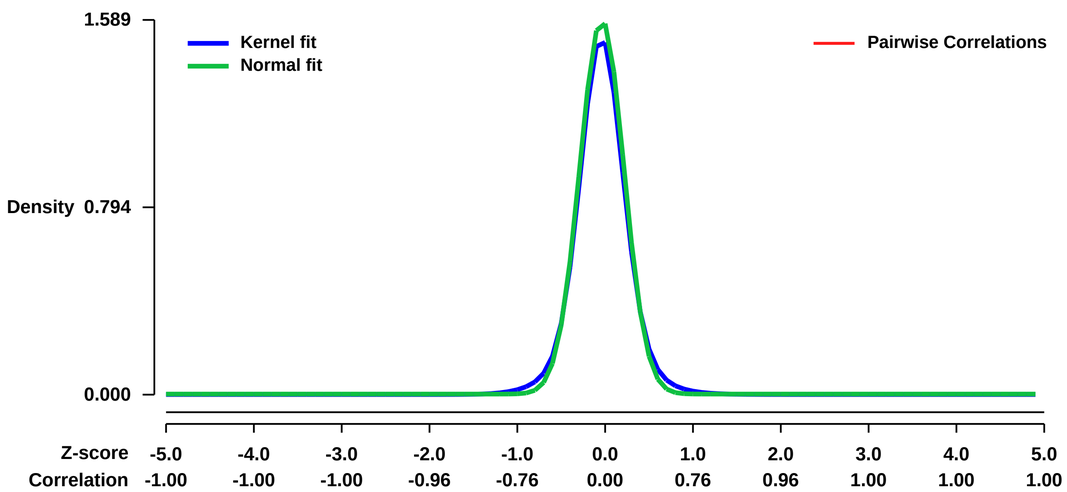

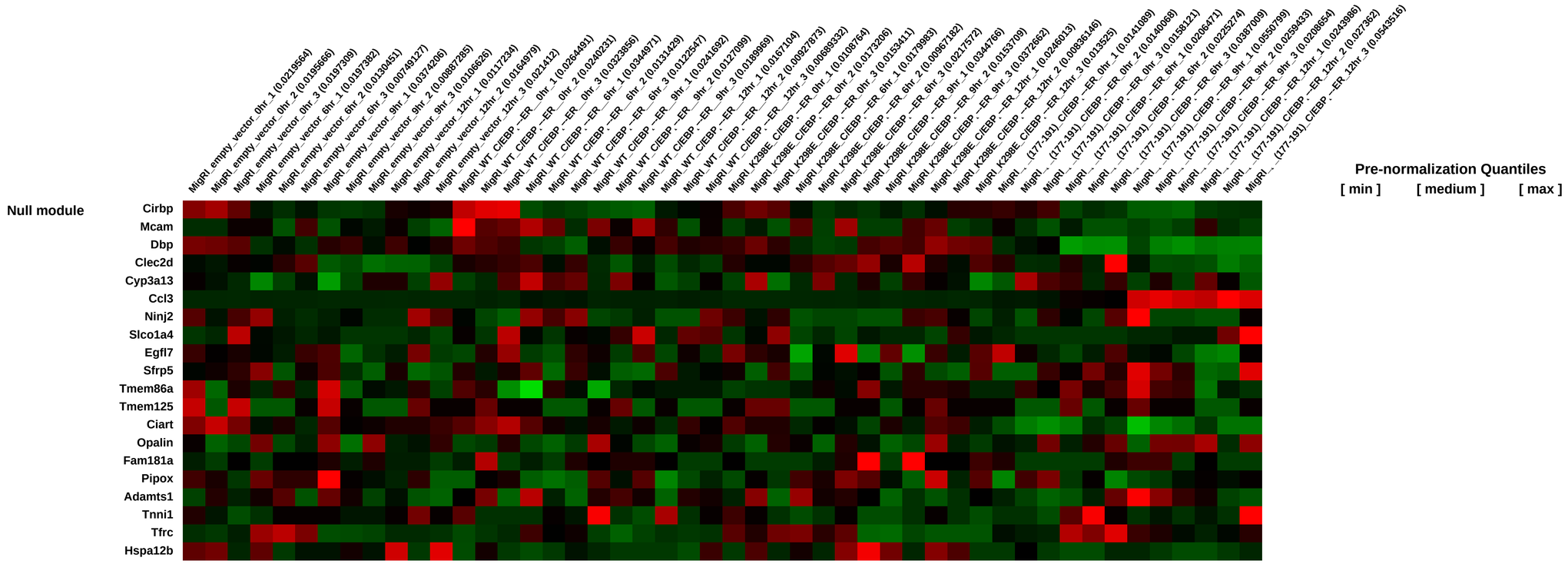

GEO Series "GSE19355" Expression Profiles

Num of samples in this series: 6

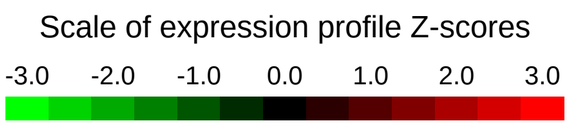

GEO Link:	http://www.ncbi.nlm.nih.gov/geo/query/acc.cgi?acc=GSE19355
Status:	Public on May 03 2010
Title:	Silencing of mrhl non coding RNA in mouse spermatoginial cells GC1-Spg
Organism:	Mus musculus
Experiment type:	Expression profiling by array
Platform:	GPL1261
Pubmed ID:	22665494
Summary & Design:	**Summary:** Mrhl is a non coding RNA identified from mouse chromosome 8. It is a 2.4kb poly adenylated, nuclear restricted RNA expressed in multiple tissues. The 2.4 kb RNA also undergoes a nuclear processing event mediated through Drosha that generates an 80nt intermediate RNA. This study was aimed at understanding the functiion of mrhl by silencing the mrhl RNA in the mouse spermatogonial cells using a pool of siRNAs targeted against the mrhl and analyse the global gene expression change using Affymetrix mouse expression array. The mRNAs that showed significant change in expression in mrhl siRNA treated cells against control were studied further for their biological significance with respect to mrhl silencing. **Overall design:** The mouse spermatogonial cells that were either mock silenced using scrambled siRNA or silenced using siRNAs against mrhl were harvested at 44hrs post transfection. The silencing efficiency was checked by realtime quantitative PCR and was found be almost 80% in all three independent experiments.The total RNA was extracted using Trizol and was taken further for microarray expriment. All the subsequent steps were according to the Affymetrix protocol. Gene expression was profiled for control and mrhl silenced cells.

Background corr dist: KL-Divergence = 0.0351, L1-Distance = 0.0184, L2-Distance = 0.0003, Normal std = 0.6402

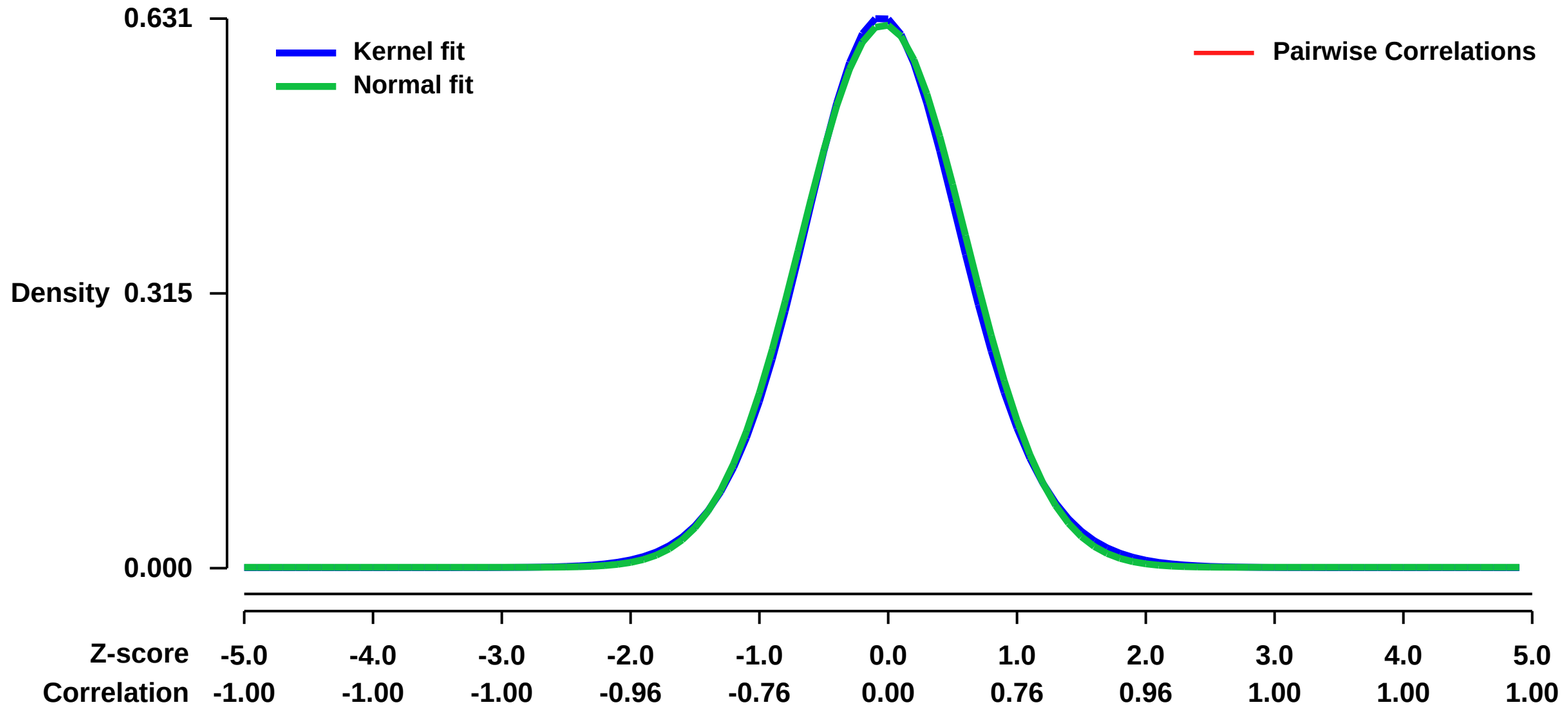

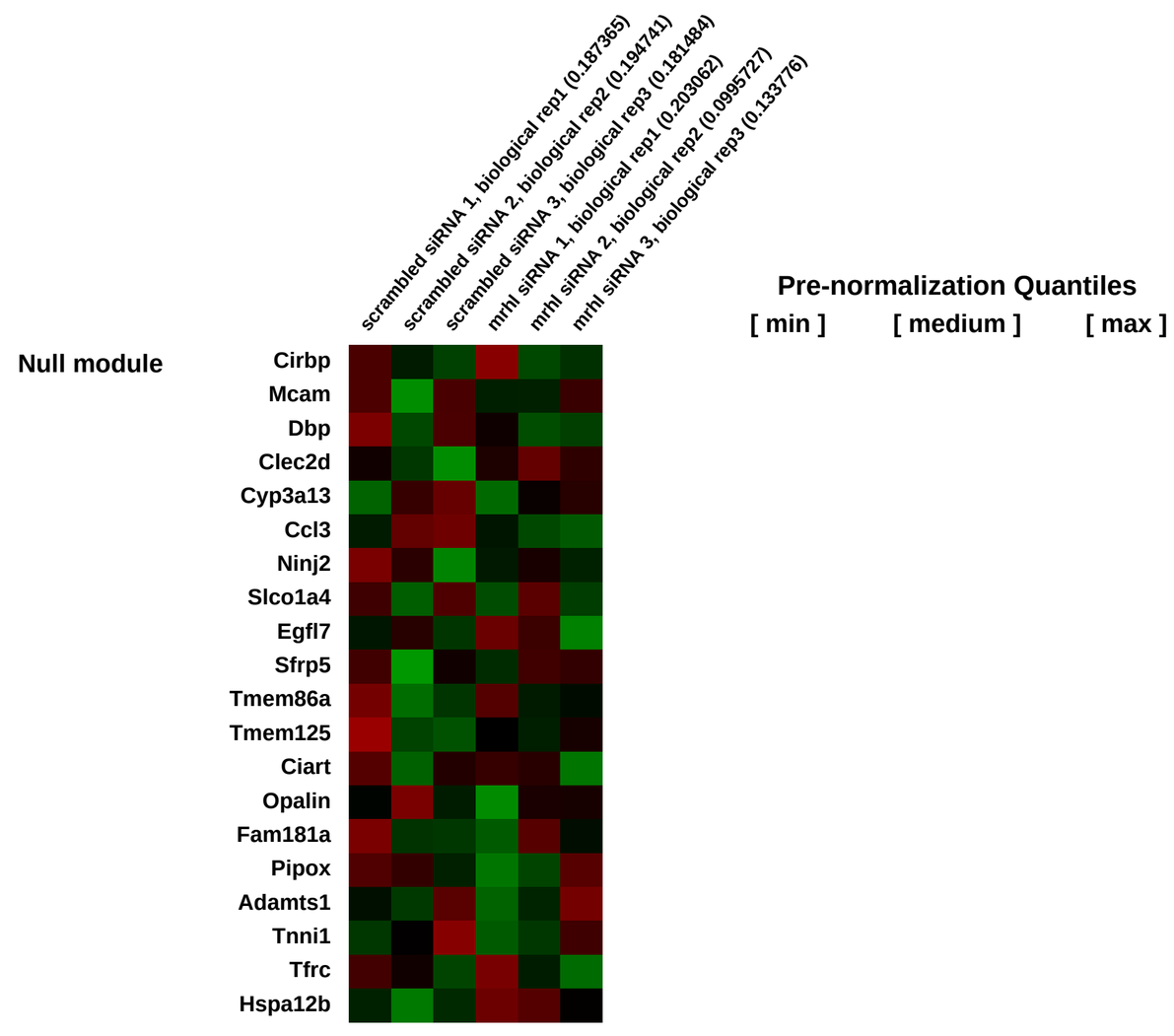

GEO Series "GSE39886" Expression Profiles

Num of samples in this series: 24

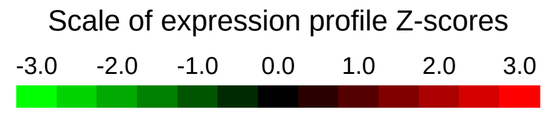

GEO Link:	http://www.ncbi.nlm.nih.gov/geo/query/acc.cgi?acc=GSE39886
Status:	Public on Aug 04 2012
Title:	Selective inhibition of CD4+ T-cell cytokine production and autoimmunity by BET protein and c-Myc inhibitors
Organism:	Mus musculus
Experiment type:	Expression profiling by array
Platform:	GPL1261
Pubmed ID:	22912406
Summary & Design:	**Summary:** Bromodomain-containing proteins bind acetylated lysine residues on histone tails and are involved in the recruitment of additional factors that mediate histone modifications and enable transcription. A compound, I-BET-762, that inhibits binding of an acetylated histone peptide to BRD4 and other proteins of the BET (bromodomain and extra-terminal domain) family, was previously shown to suppress the production of pro-inflammatory proteins by macrophages and block acute inflammation in mice. Here we investigate the effect of I-BET-762 on T cell function. We show that treatment of naˆflve CD4+ T cells with I-BET-762 during early differentiation modulates subsequent cytokine production, and inhibits the ability of Th1-skewed cells to induce autoimmune pathogenesis in a model of experimental autoimmune encephalomyelitis (EAE) in vivo. The suppressive effects of I-BET-762 on T-cell mediated inflammation were not due to inhibition of expression of the pro-inflammatory cytokines, IFN-. or IL-17, but correlated with the ability to suppress GM-CSF production from CNS-infiltrating T cells, resulting in decreased recruitment of macrophages and granulocytes. The effects of I-BET-762 were distinct from those of the fumarate ester, dimethyl fumarate (DMF), a candidate drug for treatment of multiple sclerosis (MS). Our data suggest that I-BET and DMF could have complementary roles in the treatment of MS, and provide a strong rationale for inhibitors of BET-family proteins in the treatment of autoimmune diseases, based on their dual ability to suppress granulocyte and macrophage recruitment by T cells as well as production of pro-inflammatory proteins by macrophages. **Overall design:** RNA from resting or activated CD4+ T cells grown in the presence of a control substance (DMSO or Control-768) or two different concentrations of I-BET-762, was hybridized to the chip. There are 3 biological replicates for a total of 2 (cell states) x 4 (conditions) x 3 (replicates) = 24 samples.

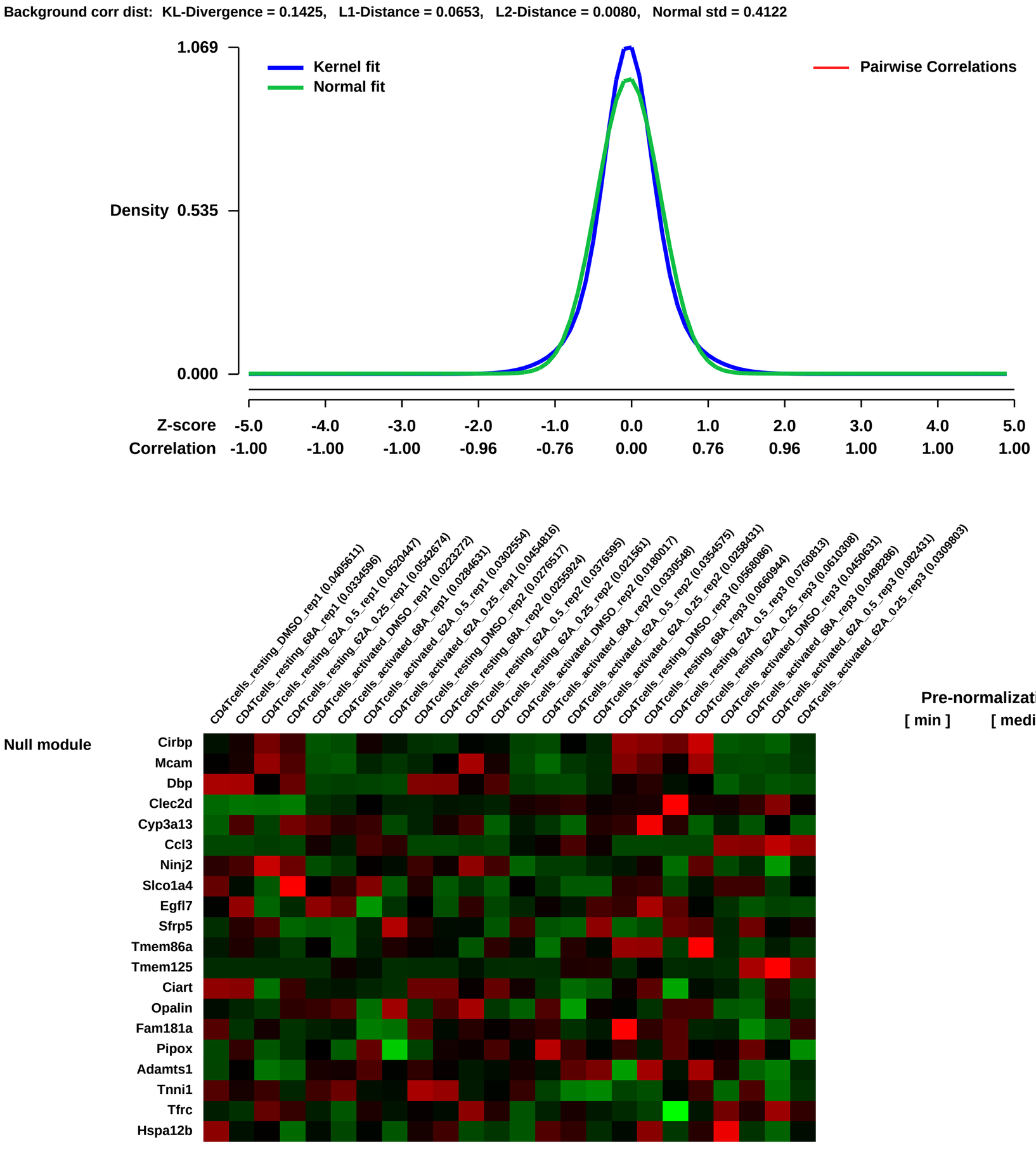

GEO Series "GSE12748" Expression Profiles

Num of samples in this series: 7

Scale of expression profile Z-scores

-3.0 -2.0 -1.0 0.0 1.0 2.0 3.0

GEO Link:	http://www.ncbi.nlm.nih.gov/geo/query/acc.cgi?acc=GSE12748
Status:	Public on Sep 10 2009
Title:	Weighted Gene Coexpression Network Analysis Identifies Biomarkers in Glycerol Kinase Deficient Mice
Organism:	Mus musculus
Experiment type:	Expression profiling by array
Platform:	GPL1261
Pubmed ID:	19546021
Summary & Design:	**Summary:** Symptomatic glycerol kinase deficiency (GKD) is associated with episodic metabolic and central nervous system deterioration. We report here the first application of Weighted Gene Co-Expression Network Analysis (WGCNA) to investigate a knockout (KO) murine model of a human genetic disease. WGCNA identified networks and key hub transcripts from liver mRNA of glycerol kinase (Gyk) KO and wild type (WT) mice. Day of life 1 (dol1) samples from KO mice contained a network module enriched for organic acid metabolism before Gyk KO mice develop organic acidemia and die on dol3-4 and the module containing Gyk was enriched with apoptotic genes. Roles for the highly connected Acot, Psat and Plk3 transcripts were confirmed in cell cultures and subsequently validated by causality testing. We provide evidence that GK may have an apoptotic moonlighting role that is lost in GKD. This systems biology strategy has improved our understanding of GKD pathogenesis and suggests possible treatments. **Overall design:** Male WT and KO mouse pups were sacrificed on day of life (dol) 1 and each liver was harvested. Total RNA from 4 KO and 3 WT livers was isolated individually. Affymetrix mus 430 2.0 GeneChips were used to analyze differences in liver gene expression between KO and WT mice. Dol1 and 3 Gyk KO mice represent different disease states. Dol 1 was chosen because mice are phenotypically asymptomatic with respect to Glycerol Kinase Deficiency (GKD) and allowed us to look at alterations that occur before the overt disease state. Dol 3 mice are phenotypically symptomatic with respect to GKD.

Background corr dist: KL-Divergence = 0.0602, L1-Distance = 0.0183, L2-Distance = 0.0005, Normal std = 0.5298

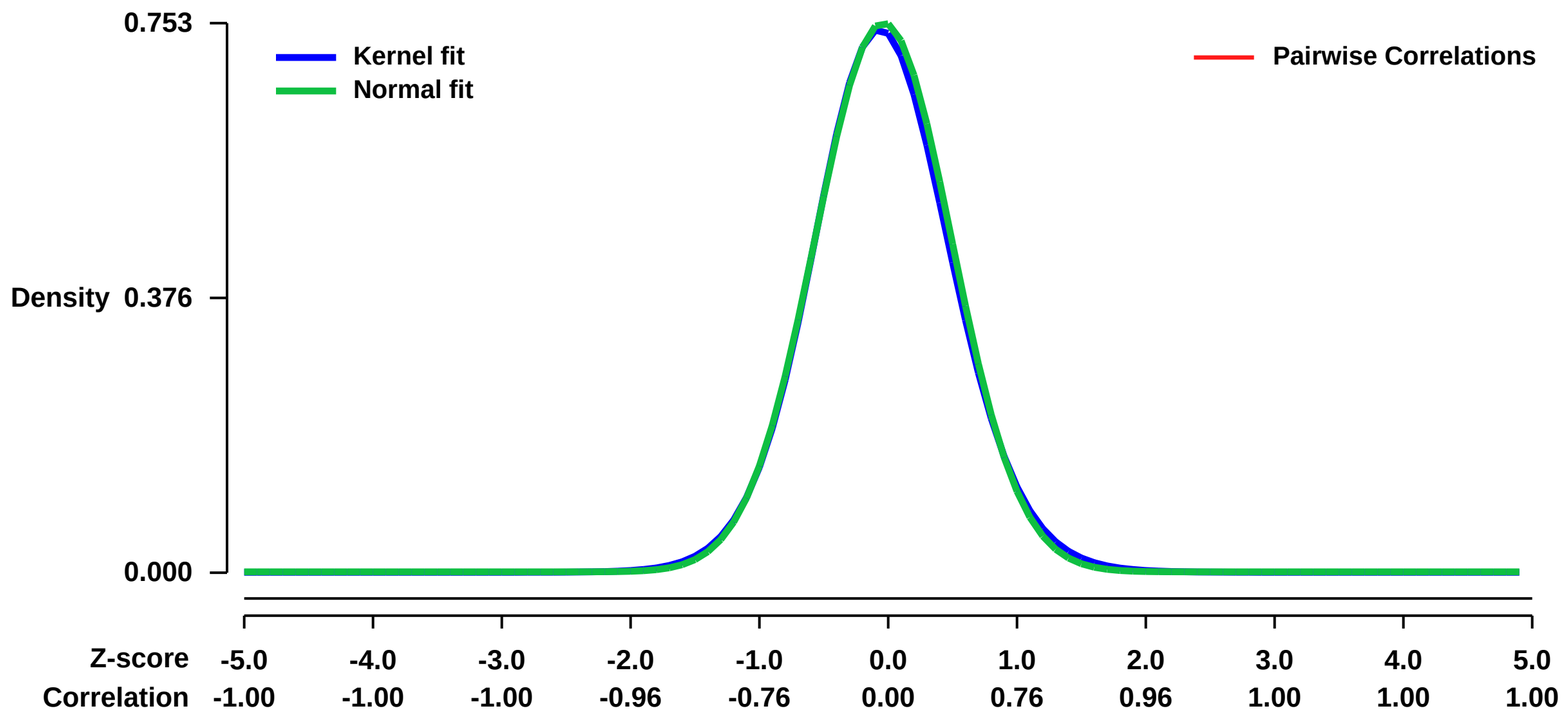

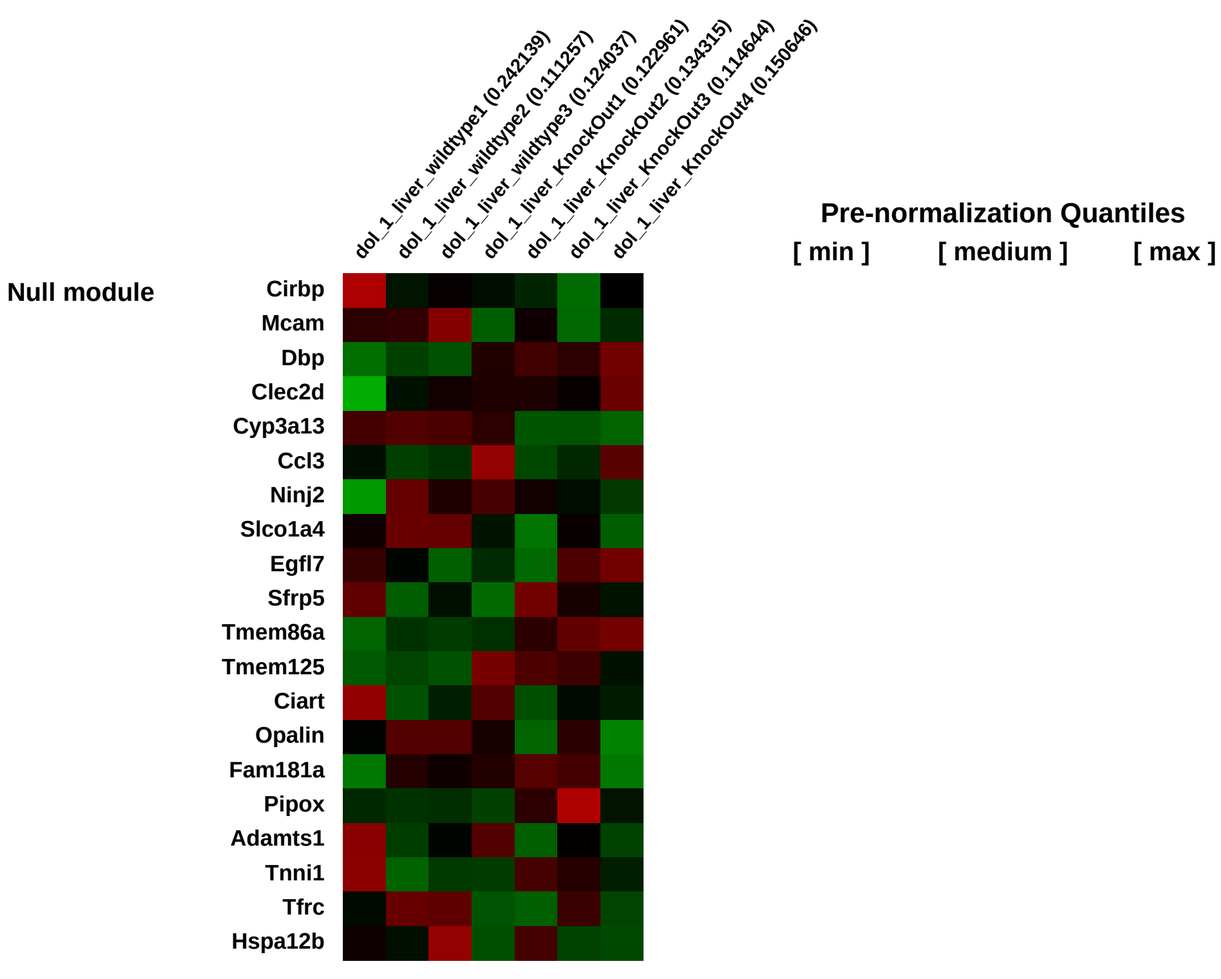

GEO Series "GSE24350" Expression Profiles

Num of samples in this series: 8

Scale of expression profile Z-scores

-3.0 -2.0 -1.0 0.0 1.0 2.0 3.0

GEO Link: http://www.ncbi.nlm.nih.gov/geo/query/acc.cgi?acc=GSE24350

Status: Public on Sep 28 2010

Title: Expression data from peptidoglycan stimulated CD11b+ cells from NOD and NOD.Idd3

Organism: Mus musculus

Experiment type: Expression profiling by array

Platform: GPL1261

Pubmed ID:

Summary & Design:

Summary:
CD11b+ CD11c- cells were isolated by cell sorting from the spleens of NOD and NOD.Idd3 mice. Cells were then either unstimulated or stimulated with peptidoglycan (5ug/ml) for 4 hours at 37 degrees prior to RNA extraction. Peptidoglycan was chosen as a stimulus due to its know ability to stimulate CD11b+ cells through Toll-like receptor 2 and our previous data showing biological differences between NOD and NOD.Idd3-derived CD11b+CD11c- cells after stimulation with peptidoglycan.

Overall design:
CD11b+ cells from NOD and NOD.Idd3 were either unstimulated or stimulated with peptidoglycan(PGN) for 4 hours at 37 degerees prior to RNA extraction.

Background corr dist: KL-Divergence = 0.0550, L1-Distance = 0.0253, L2-Distance = 0.0010, Normal std = 0.5461

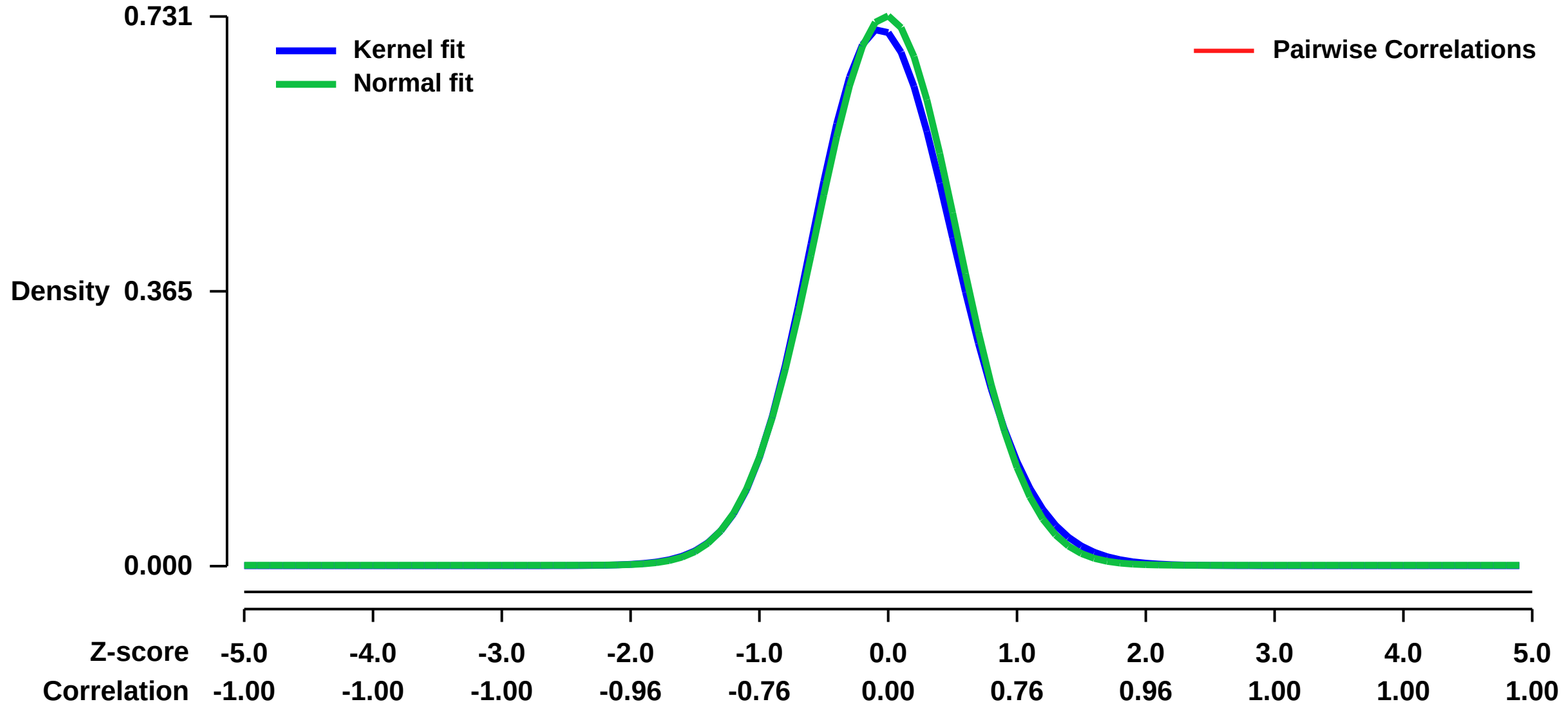

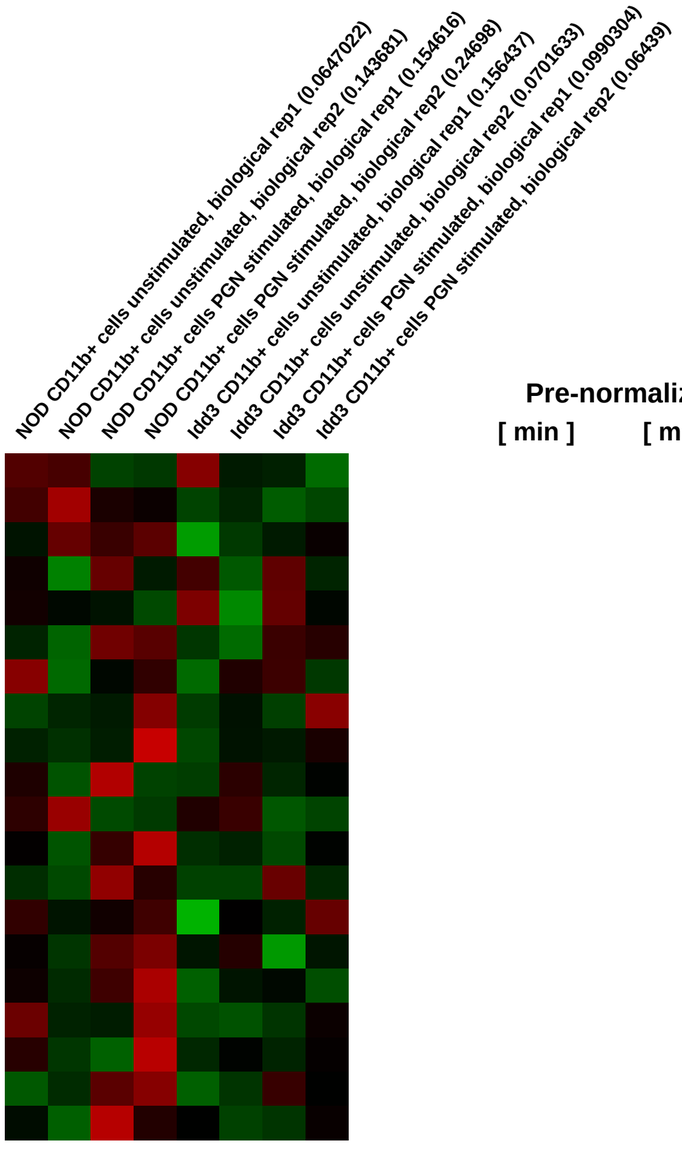

GEO Series "GSE27309" Expression Profiles

Num of samples in this series: 10

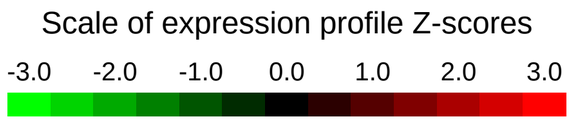

GEO Link:	http://www.ncbi.nlm.nih.gov/geo/query/acc.cgi?acc=GSE27309
Status:	Public on Mar 15 2011
Title:	SIRT3 opposes metabolic reprogramming of cancer cells through HIF1a destabilization
Organism:	Mus musculus
Experiment type:	Expression profiling by array
Platform:	GPL1261
Pubmed ID:	21397863
Summary & Design:	**Summary:** Tumor cells exhibit aberrant metabolism characterized by high glycolysis even in the presence of oxygen. This metabolic reprogramming, known as the Warburg effect, provides tumor cells with the substrates and redox potential required for the generation of biomass. Here, we show that the mitochondrial NAD-dependent deacetylase SIRT3 is a crucial regulator of the Warburg effect. SIRT3 loss promotes a metabolic profile consistent with high glycolysis required for anabolic processes in vivo and in vitro. Mechanistically, SIRT3 mediates metabolic reprogramming independently of mitochondrial oxidative metabolism and through HIF1a, a transcription factor that controls expression of key glycolytic enzymes. SIRT3 loss increases reactive oxygen species production, resulting in enhanced HIF1a stabilization. Strikingly, SIRT3 is deleted in 40% of human breast cancers, and its loss correlates with the upregulation of HIF1a target genes. Finally, we find that SIRT3 overexpression directly represses the Warburg effect in breast cancer cells. In sum, we identify SIRT3 as a regulator of HIF1a and a suppressor of the Warburg effect. **Overall design:** RNA isolated from brown adipose tissue of SIRT3 WT and KO mice. 5 wild-type samples and 5 SIRT3 KO samples

Background corr dist: KL-Divergence = 0.1165, L1-Distance = 0.0301, L2-Distance = 0.0015, Normal std = 0.4112

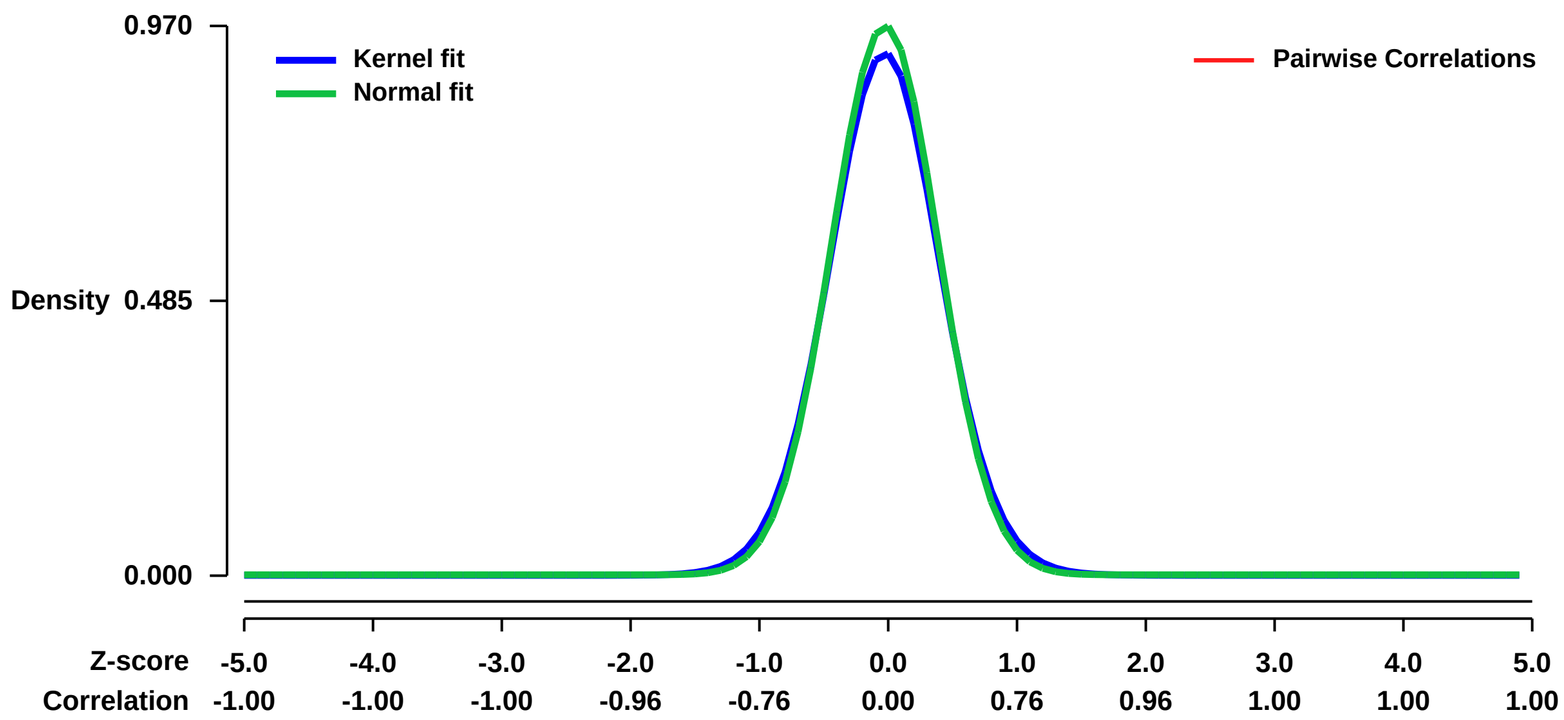

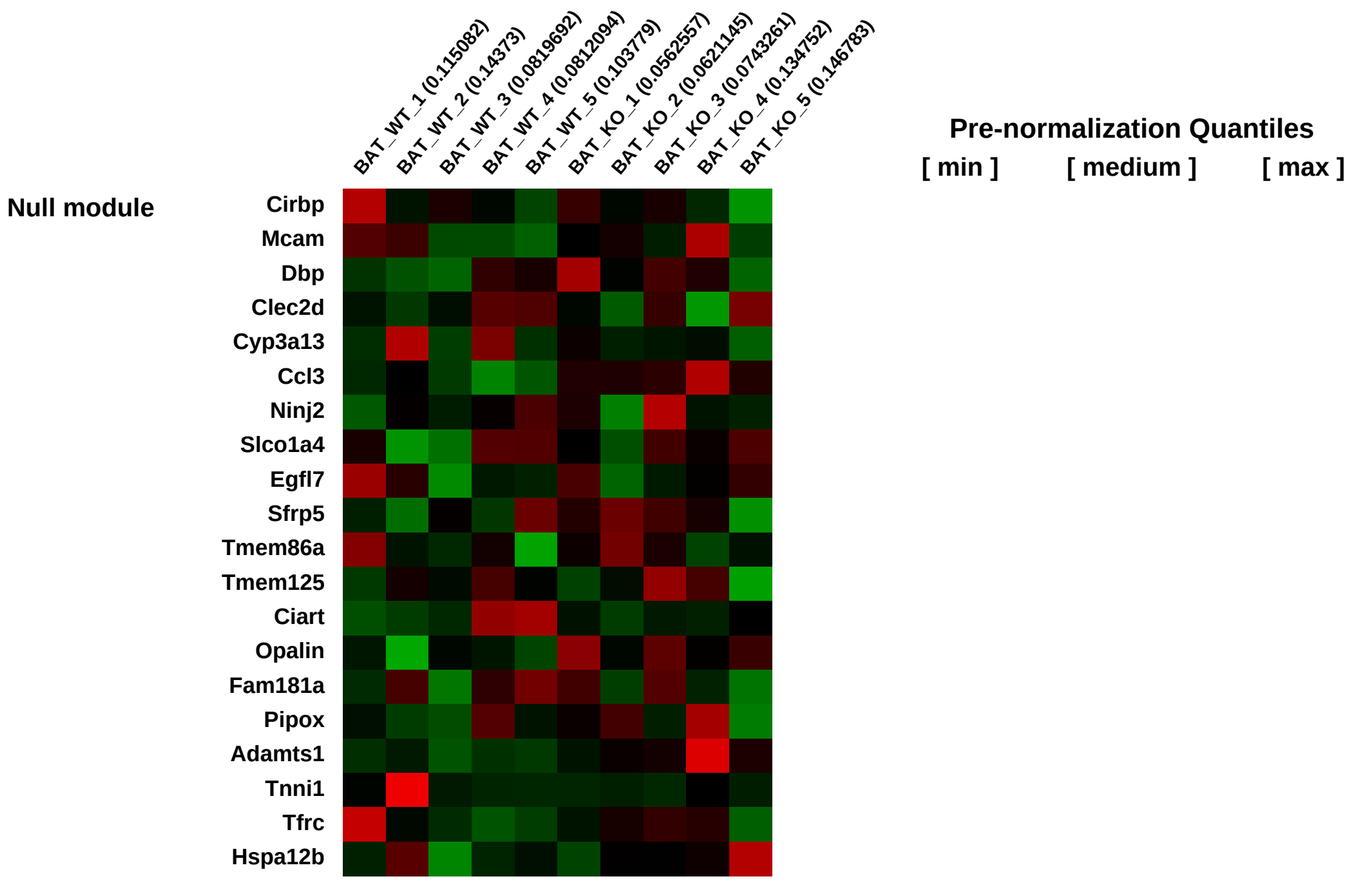

GEO Series "GSE19299" Expression Profiles

Num of samples in this series: 6

Scale of expression profile Z-scores

-3.0 -2.0 -1.0 0.0 1.0 2.0 3.0

GEO Link:	http://www.ncbi.nlm.nih.gov/geo/query/acc.cgi?acc=GSE19299
Status:	Public on Dec 04 2009
Title:	Expression data with mouse osteoblast cell from wild-type and retinoblastoma tumor suppressor(Rb) knock-out.
Organism:	Mus musculus
Experiment type:	Expression profiling by array
Platform:	GPL1261
Pubmed ID:	21085651
Summary & Design:	**Summary:** Here we report the characterization of a novel role for the retinoblastoma protein (pRb) as a regulator of osteoblast adhesion. Abrogation of pRb in osteoblasts resulted in aberrant cadherin expression and loss of adherens junctions. This produced defects suggestive of a transformed phenotype such as impaired cell-to-cell adhesion, loss of contact-dependent growth arrest, and the capacity to evade anoikis. This also resulted in profound abnormalities in bone structure. Consistent with this, microarray analyses showed that pRb regulates a wide repertoire of osteoblast cell adhesion genes. In addition, pRb loss also resulted in altered expression and function of several known regulators of cellular adhesion and adherens junction assembly, such as the Rho GTPase Rac1 and the merlin tumor suppressor. Taken together, our results show that pRb controls cell adhesion by regulating the expression and adherens junction components and by regulating the function of molecules involved in adherens junction assembly and stability. Microarray results helped us to portrait the overall influence on cell adhesion via both individual genes and pathway analysis. **Overall design:** MC3T3 cells were obtained from immortalizing primary cultured mouse osteoblast cells by using 3T3 protocol. There are 3 biological replicates for each group, 6 samples in total were analyzed.

Background corr dist: KL-Divergence = 0.0176, L1-Distance = 0.0417, L2-Distance = 0.0018, Normal std = 0.8480

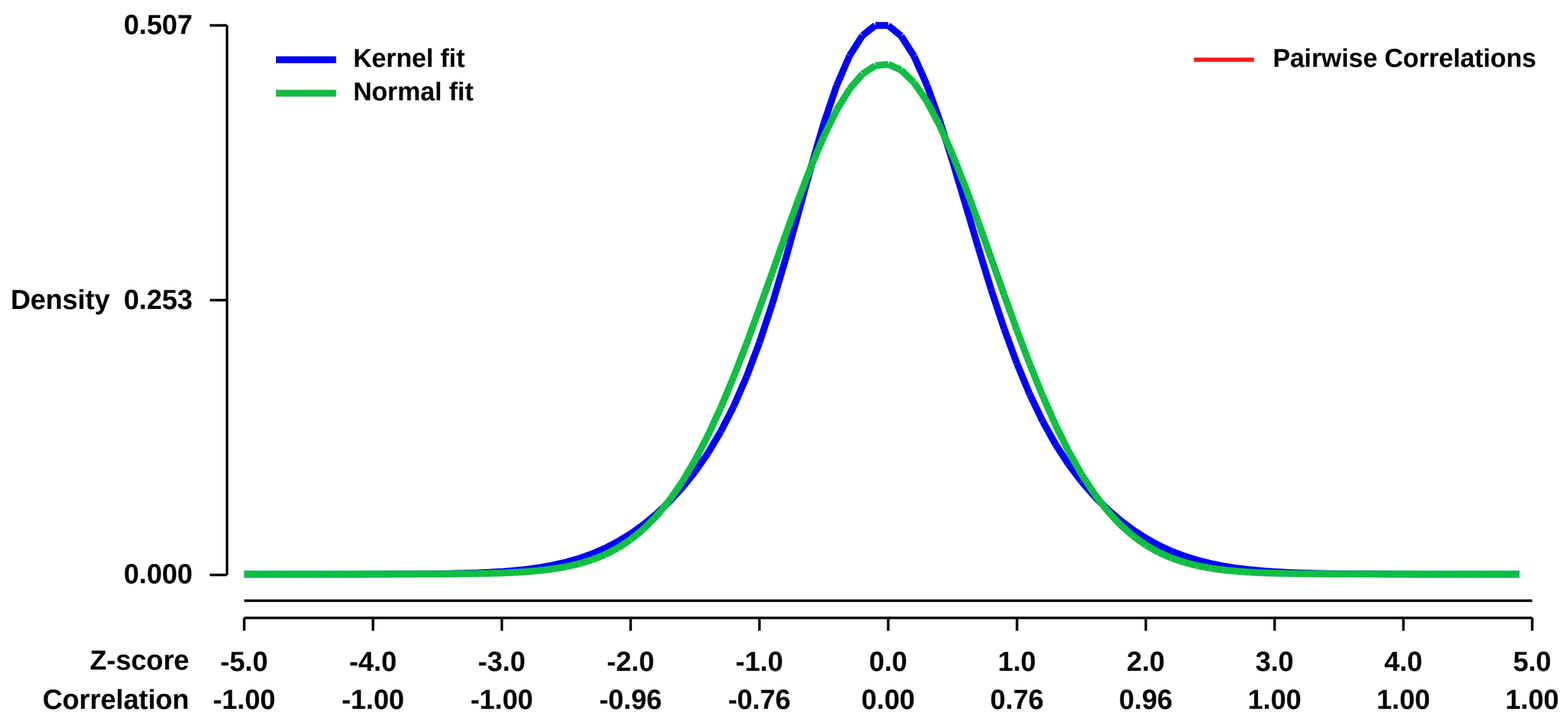

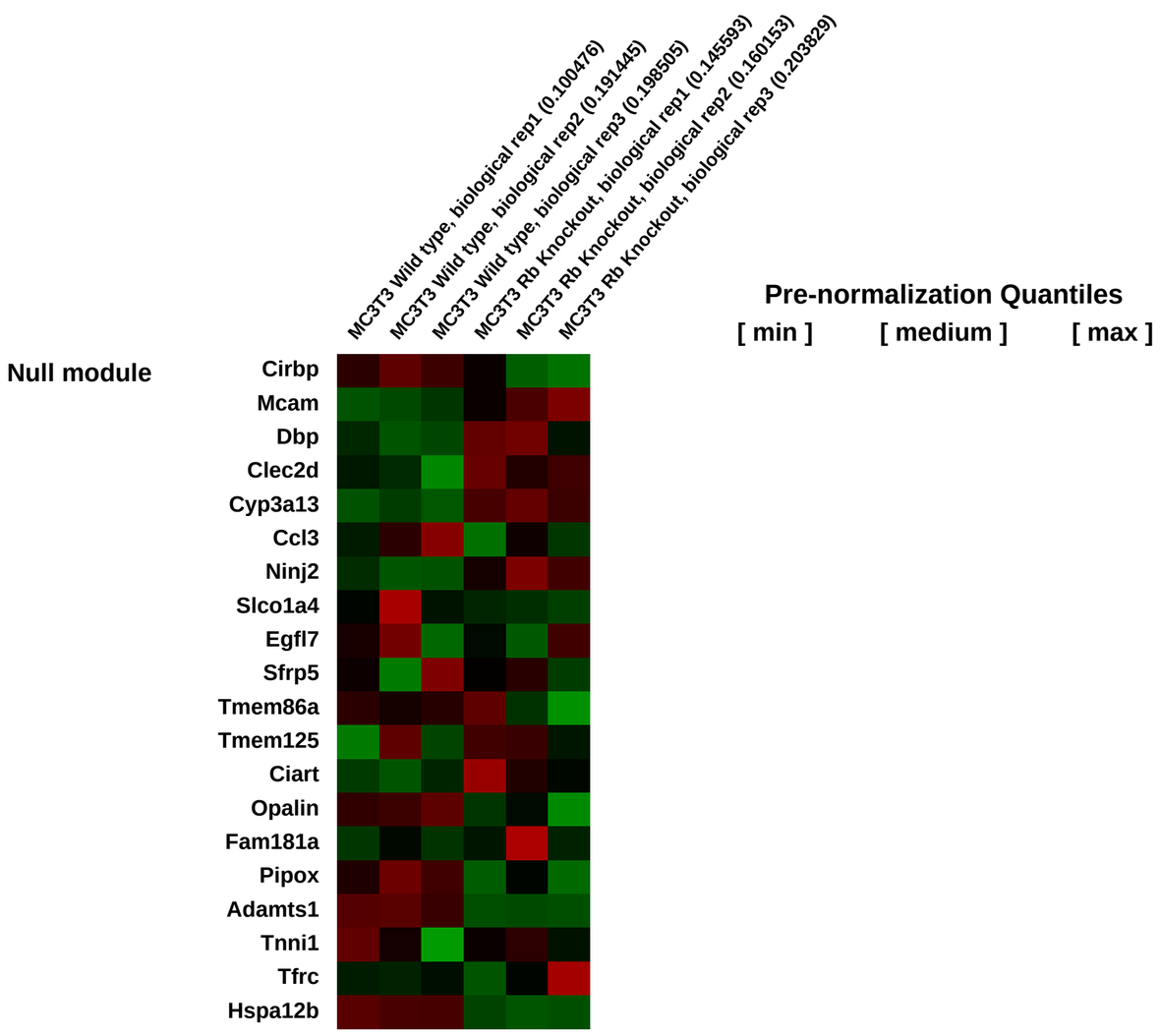

GEO Series "GSE27402" Expression Profiles

Num of samples in this series: 8

Scale of expression profile Z-scores

-3.0 -2.0 -1.0 0.0 1.0 2.0 3.0

GEO Link:	http://www.ncbi.nlm.nih.gov/geo/query/acc.cgi?acc=GSE27402
Status:	Public on Nov 22 2011
Title:	Expression data from WT, HEB-KO and E2A-KO LY6D- CLP cells
Organism:	Mus musculus
Experiment type:	Expression profiling by array
Platform:	GPL1261
Pubmed ID:	21972416
Summary & Design:	**Summary:** The E-protein transcription factors E2A and HEB play important roles at several stages of hematopoiesis. However, the exact mechanism for theire action and the main targets in the LY6D negative common lymphoid progentior (CLP) compartment remains unknown. By adressing this question, we will gain important infromation regarding the early events leading to B-cell specification. **Overall design:** FACS sorted LY6D negative common lymphoid progenitors from WT, HEB-KO and E2A-KO mice were subjected to RNA extraction and hybridization on Affymetrix microarrays. At least two independent sorts were performed per genotype. During each sort, cells were pooled from several bone marrows.

Background corr dist: KL-Divergence = 0.0437, L1-Distance = 0.0309, L2-Distance = 0.0016, Normal std = 0.5853

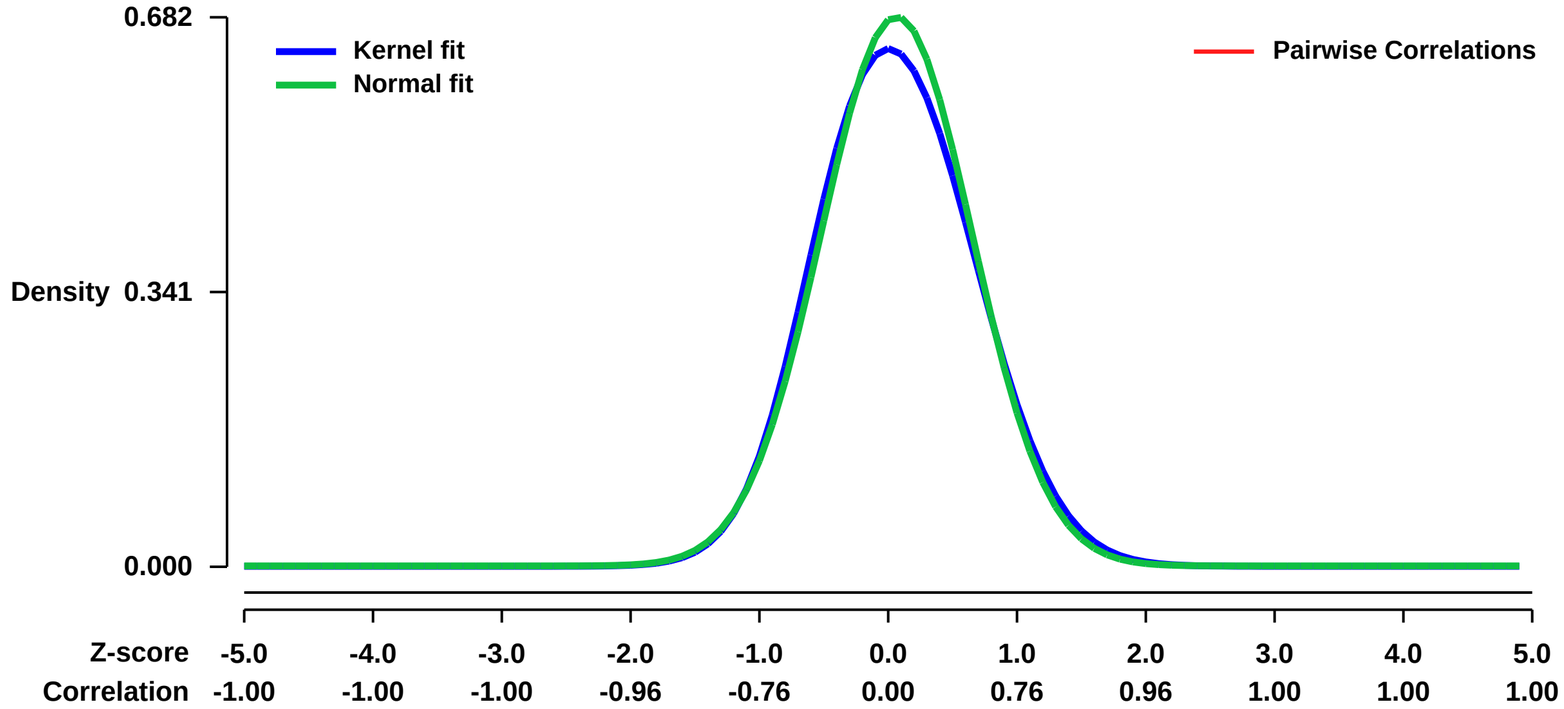

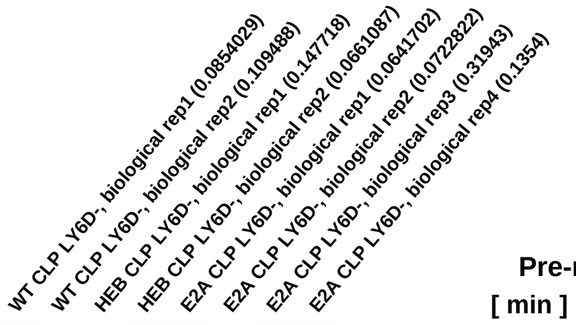

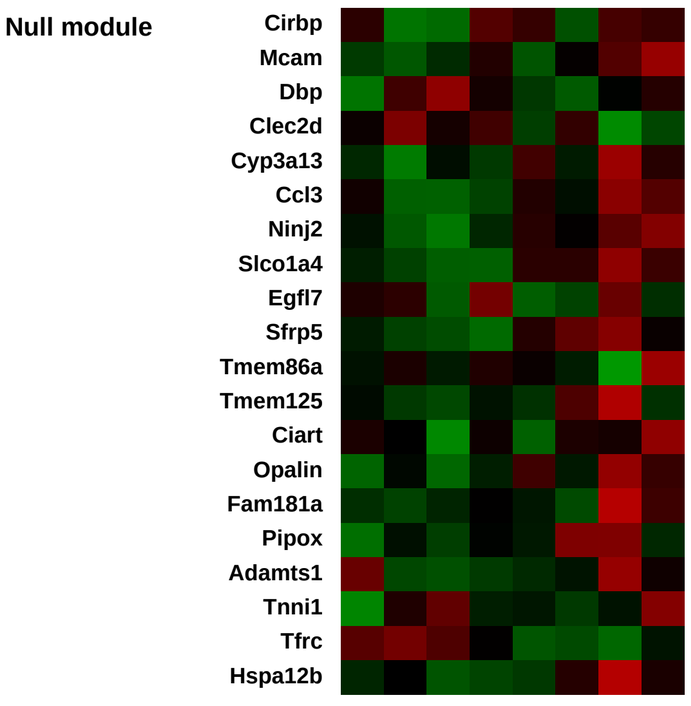

GEO Series "GSE45854" Expression Profiles

Num of samples in this series: 8

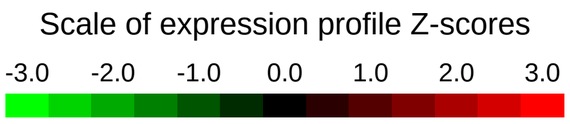

GEO Link:	http://www.ncbi.nlm.nih.gov/geo/query/acc.cgi?acc=GSE45854
Status:	Public on Apr 08 2013
Title:	Expression profiling data of RD and C2C12 cells ectopically expressing DUX4
Organism:	Mus musculus
Experiment type:	Expression profiling by array
Platform:	GPL1261
Pubmed ID:	23717650
Summary & Design:	**Summary:** **Transcriptomic changes induced by DUX4 expression were compared between human and mouse cell lines of muscle lineage.** **We used microarrays to compare transcripts induced in human rhabdmyosarcoma and mouse C2C12 cells ectopically expressing DUX4.** **Overall design:** **Human rhabdomyosarcoma and mouse C2C12 cells were transfected with DUX4 expression vectors (n=4). Cells transfected with insertless vectors were used as controls. Samples were processed for RNA extraction 16 hours following transfection.**

Background corr dist: **KL-Divergence = 0.0776, L1-Distance = 0.0214, L2-Distance = 0.0007, Normal std = 0.4846**

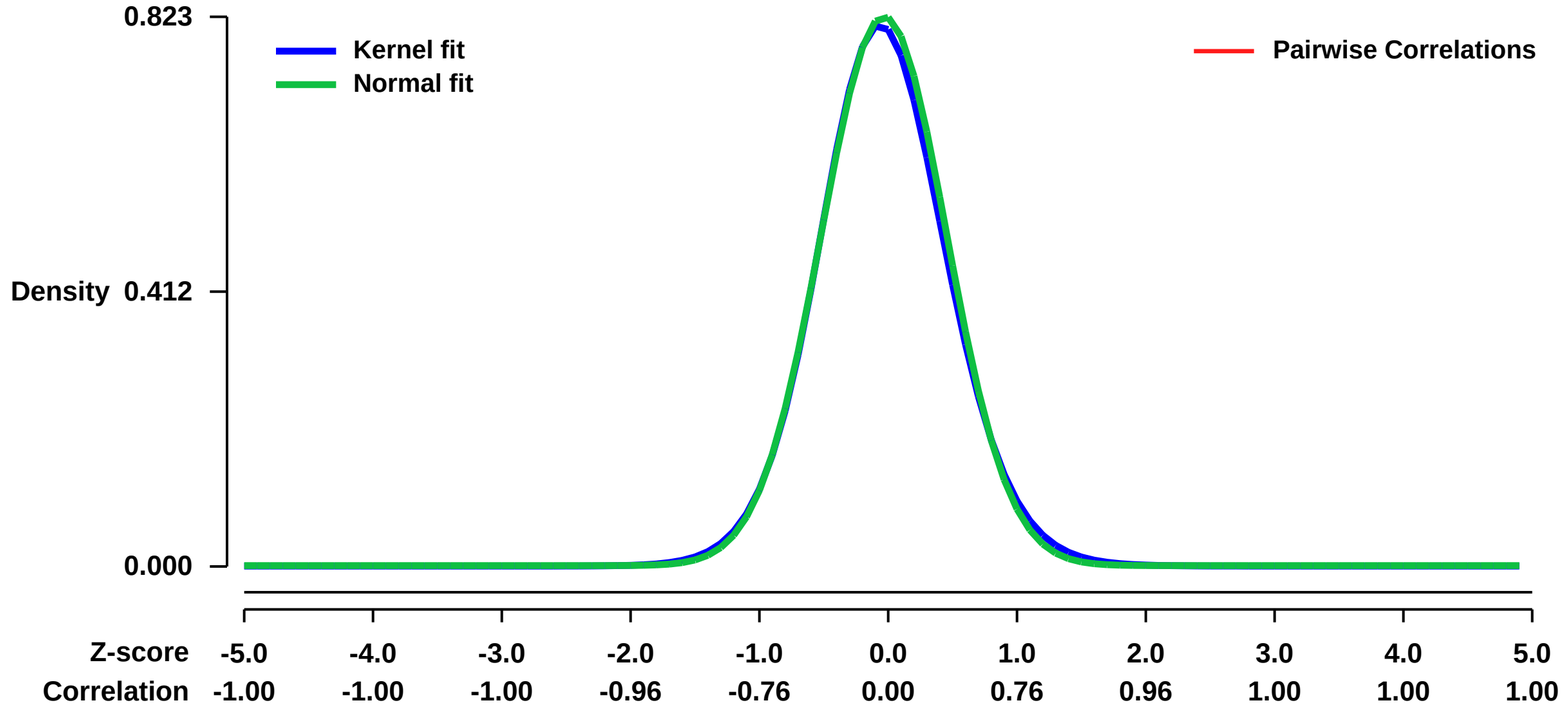

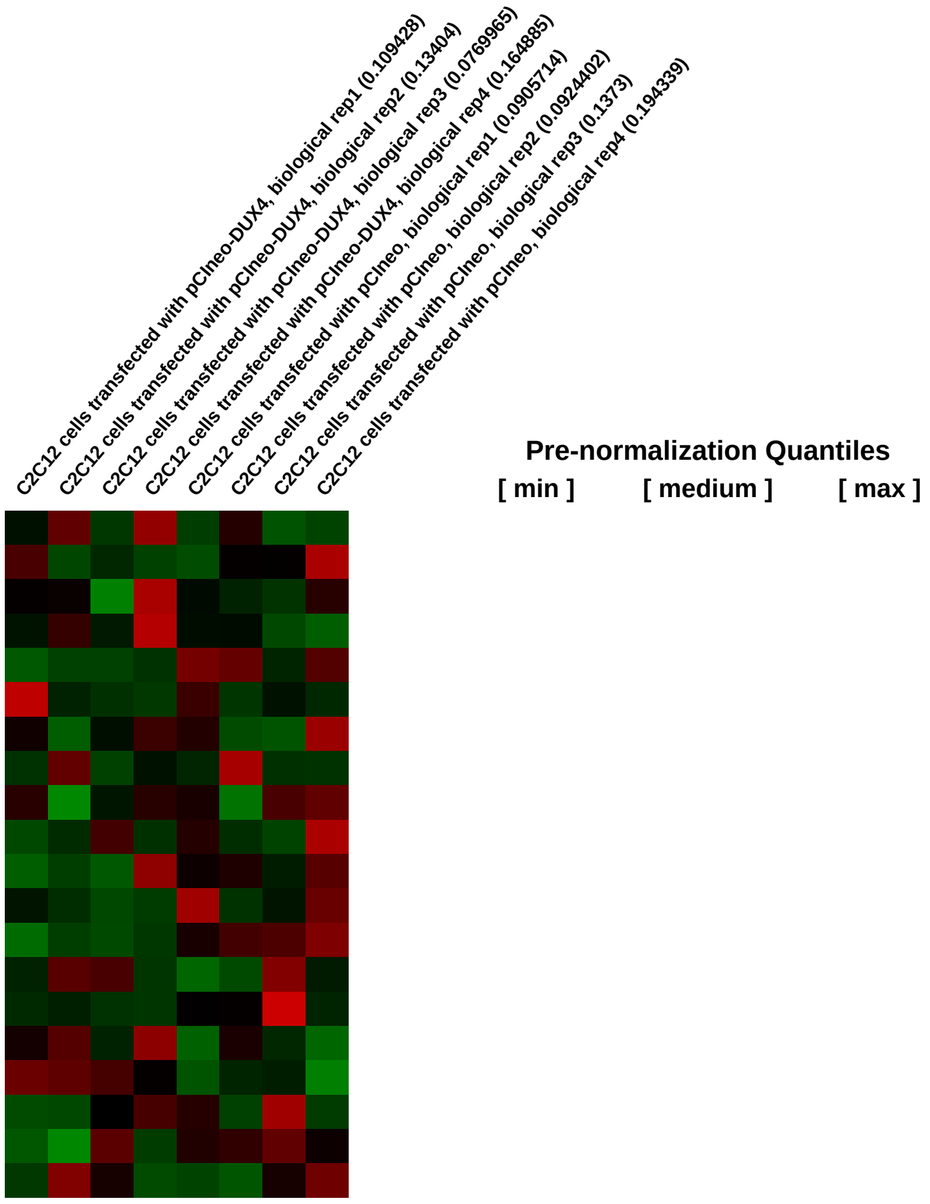

GEO Series "GSE4035" Expression Profiles

Num of samples in this series: 24

Scale of expression profile Z-scores

-3.0 -2.0 -1.0 0.0 1.0 2.0 3.0

GEO Link:	http://www.ncbi.nlm.nih.gov/geo/query/acc.cgi?acc=GSE4035
Status:	Public on Jan 13 2006
Title:	Selection for contextual fear conditioning affects anxiety-like behaviors and gene expression (palme-affy-mouse-84746)
Organism:	Mus musculus
Experiment type:	Expression profiling by array
Platform:	GPL1261
Pubmed ID:	17309658
Summary & Design:	**Summary:** These data are from the brains (amygdala and hippocampus) of mice originally derived from a cross between C57BL/6J and DBA/2J inbred strains. We used short-term selection to produce outbred mouse lines with differences in contextual fear conditioning, which is a measure of fear learning. We selected for a total of 4 generations. Fear learning differed in the selected lines and this difference was stronger with each successive generation of selection. These mice also showed differences for measures of anxiety-like behavior, but were not different for tests of non-fear motivated learning, suggesting that selection altered alleles that are specifically involved in emotional behaviors. We identified several QTLs for the selection response. We used Affymetrix microarrays to identify differentially expressed genes in the amygdala and hippocampus of mice from the final generation of selection. Amygdala and hippocampus samples were rapidly dissected out of experimentally naˆflve mice f rom each selected line. Three samples were pooled and hybridized to each array. Experimentally naˆflve mice were used because the behavior of the mice can be reliably anticipated due to their lineage. Thus, these gene expression differences are not due to the response to human handling, foot shock or fear-inducing conditioned stimuli. We have a second similar study that focuses on a different selected population that was based on C57BL/6J and A/J mice (see GES4034). **Overall design:**

Background corr dist: KL-Divergence = 0.2538, L1-Distance = 0.0389, L2-Distance = 0.0030, Normal std = 0.3049

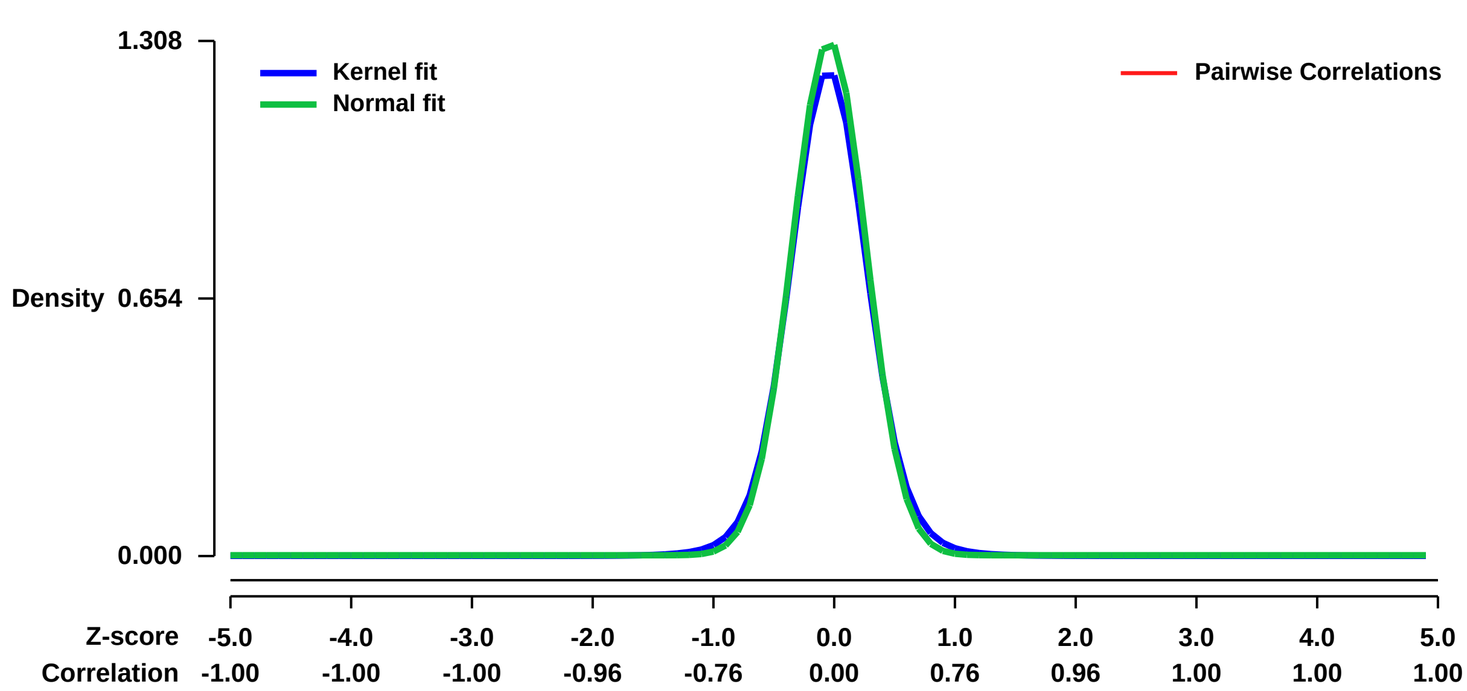

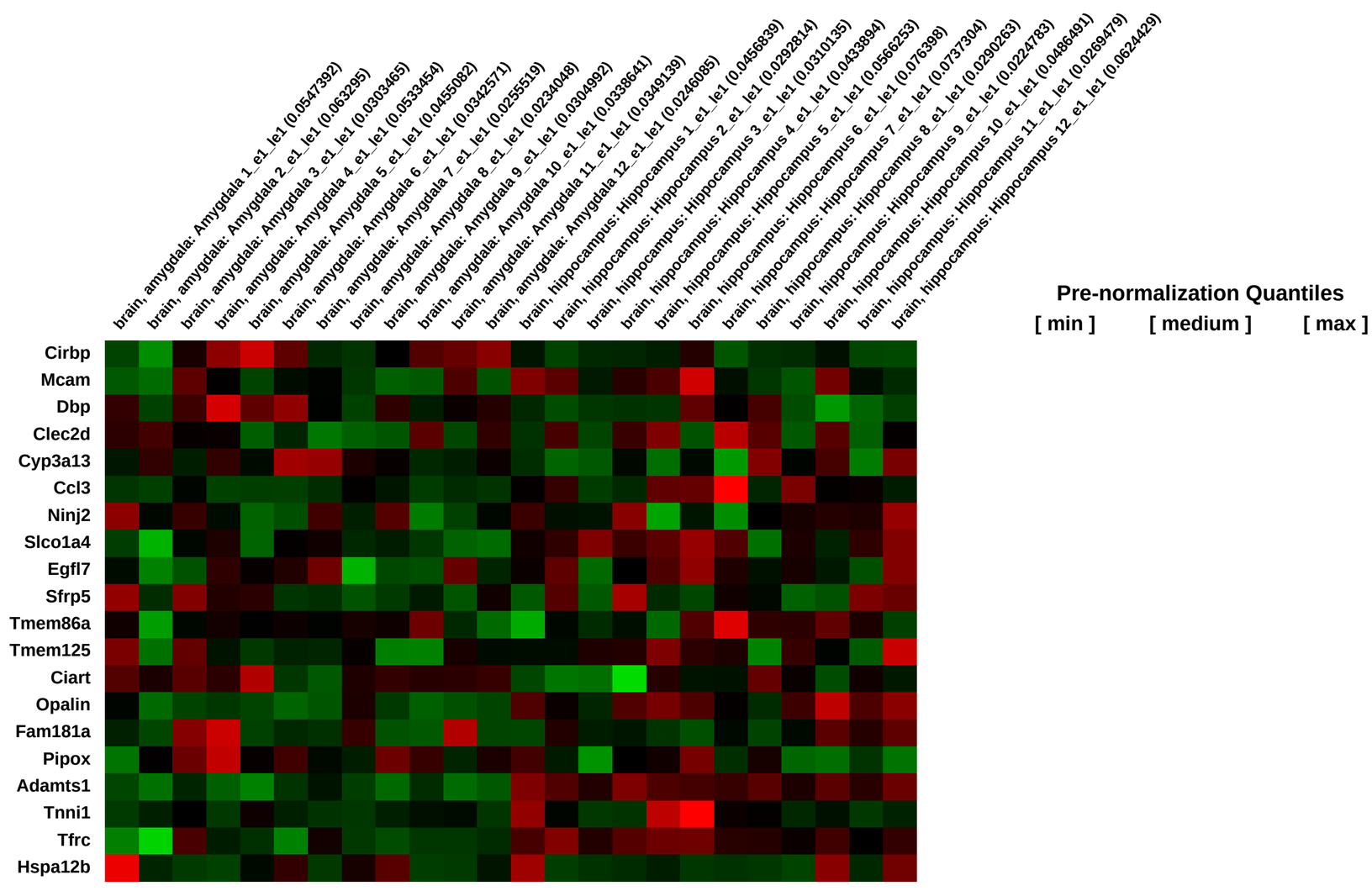

GEO Series "GSE31106" Expression Profiles

Num of samples in this series: 18

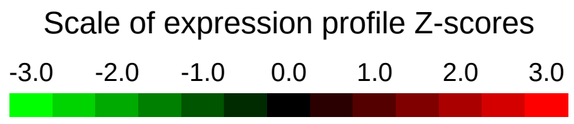

GEO Link:	http://www.ncbi.nlm.nih.gov/geo/query/acc.cgi?acc=GSE31106
Status:	Public on Aug 02 2012
Title:	Expression data for the different phases of ulcerative colitis-associated carcinogenesis in a mouse model
Organism:	Mus musculus
Experiment type:	Expression profiling by array
Platform:	GPL1261
Pubmed ID:	22610167
Summary & Design:	**Summary:** **Nonresolving inflammation is correlated to carcinogenesis. Ulcerative colitis-associated colorectal cancer (UC-CRC), one of the typical carcinoma generated by inflammation that cannot be resolved properly, has been widely believed to involve a multistep process contains â inflammation-dysplasia-cancerâ sequence. The exact molecular mechanisms underlying the step-wise development of UC-CRC is still not fully understood. Detecting the changes in gene expression profiles may help to reveal why and how does the prolonged inflammatory response lead to carcinogenesis, and to characterize potential diagnostic/prognostic markers or additional therapeutic targets for UC-CRC. There for, we performed temporal genome expression profiling analysis using the Affymetrix genome wide microarray system to identify broad scale changes in gene expression associated with the development of colitis-associated cancer, based on an AOM/DSS induced mouse model of UC-CRC.** **Overall design:** **6-week-old male ICR mice were given a single intraperitoneal injection of AOM (10mg/kg) at Day 1, followed by three cycles of DSS administration (cycle 1: 2%, Day 8~14; cycle 2: 1.5%, Day 29~33; cycle 3: 1.5%, Day 50~54) in the drinking water. Instead, control group of mice were given a single intraperitoneal injection of saline (10mg/kg) at Day 1 and distilled water drinking from the beginning to the end without DSS. Colorectal tissues were collected at days 14, 28, 42, 56 and 140 (at the end of the 2nd, 4th, 6th, 8th and 20th week) from the AOM/DSS group and at day 14 from the control group. Pathological changes of each sample were identified under microscope. Samples collected at the end of the 2nd week were inflamed mucosae, the 4th week were low grade dysplasias, the 6th week were high grade dysplasias, the 8th week were high grade dysplasias with active inflammation, the 20th week were carcinomas, and the control sample were normal mucosae. Total RNA were extracted and detected by Affymerix GeneChip Mouse Genome 430 2.0 Array.**

Background corr dist: **KL-Divergence = 0.1191, L1-Distance = 0.0266, L2-Distance = 0.0013, Normal std = 0.4164**

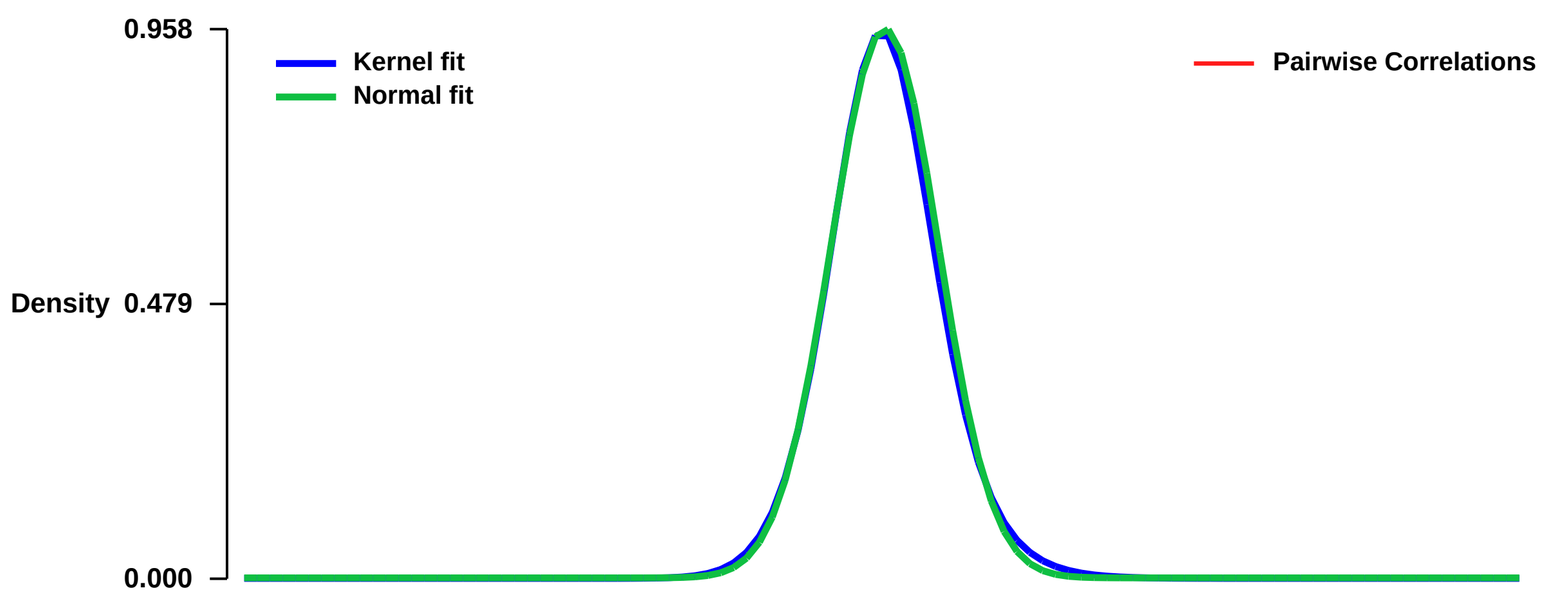

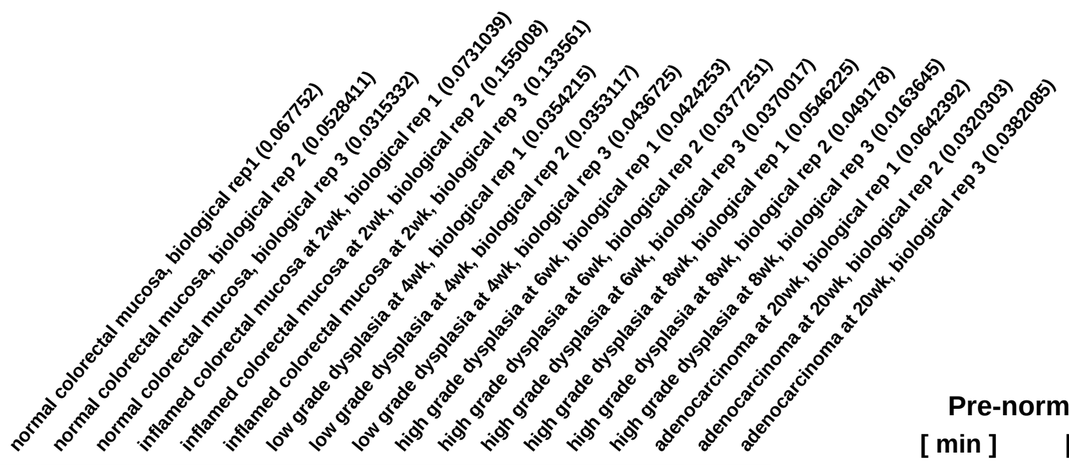

GEO Series "GSE27455" Expression Profiles

Num of samples in this series: 12

Scale of expression profile Z-scores

-3.0 -2.0 -1.0 0.0 1.0 2.0 3.0

GEO Link:	http://www.ncbi.nlm.nih.gov/geo/query/acc.cgi?acc=GSE27455
Status:	Public on Feb 24 2011
Title:	Wnt and Tcf3-mediated regulation of gene expression in mouse embryonic stem cells
Organism:	Mus musculus
Experiment type:	Expression profiling by array
Platform:	GPL1261
Pubmed ID:	21685894
Summary & Design:	**Summary:** The observation that Tcf3 (MGI name: Tcf7l1) bound the same genes as core stem cell transcription factors, Oct4 (MGI name:Pou5f1), Sox2 and Nanog, revealed a potentially important aspect of the poorly understood mechanism whereby Wnts stimulate self renewal of pluripotent mouse embryonic stem (ES) cells. Although the conventional view of Tcf proteins as the ¸†-catenin-binding effectors of Wnt signaling suggested Tcf3 should activate target genes in response to Wnts, here we show that Wnt3a and Tcf3 effectively antagonize each otherâ s effects on gene expression. Genetic ablation of Tcf3 caused similar effects as treating cells with recombinant Wnt3a. Moreover, Tcf3 was not necessary for Wnt3a-stimulation of gene expression as the majority of Wnt3a-stimulated genes exhibited a greater increase in Tcf3-/- ES cells than in Tcf3+/+ ES cells. These expression data, together with genetic experiments, show that Wnt3a stimulates ES cell self renewal by inhibiting Tcf3. **Overall design:** Tcf3+/+ and Tcf3-/- mouse embryonic stem cells were cultured in self renewal conditions containing recombinant Wnt3a for RNA extraction and hybridization on Affymetrix microarrays.

Background corr dist: KL-Divergence = 0.0555, L1-Distance = 0.0185, L2-Distance = 0.0004, Normal std = 0.5419

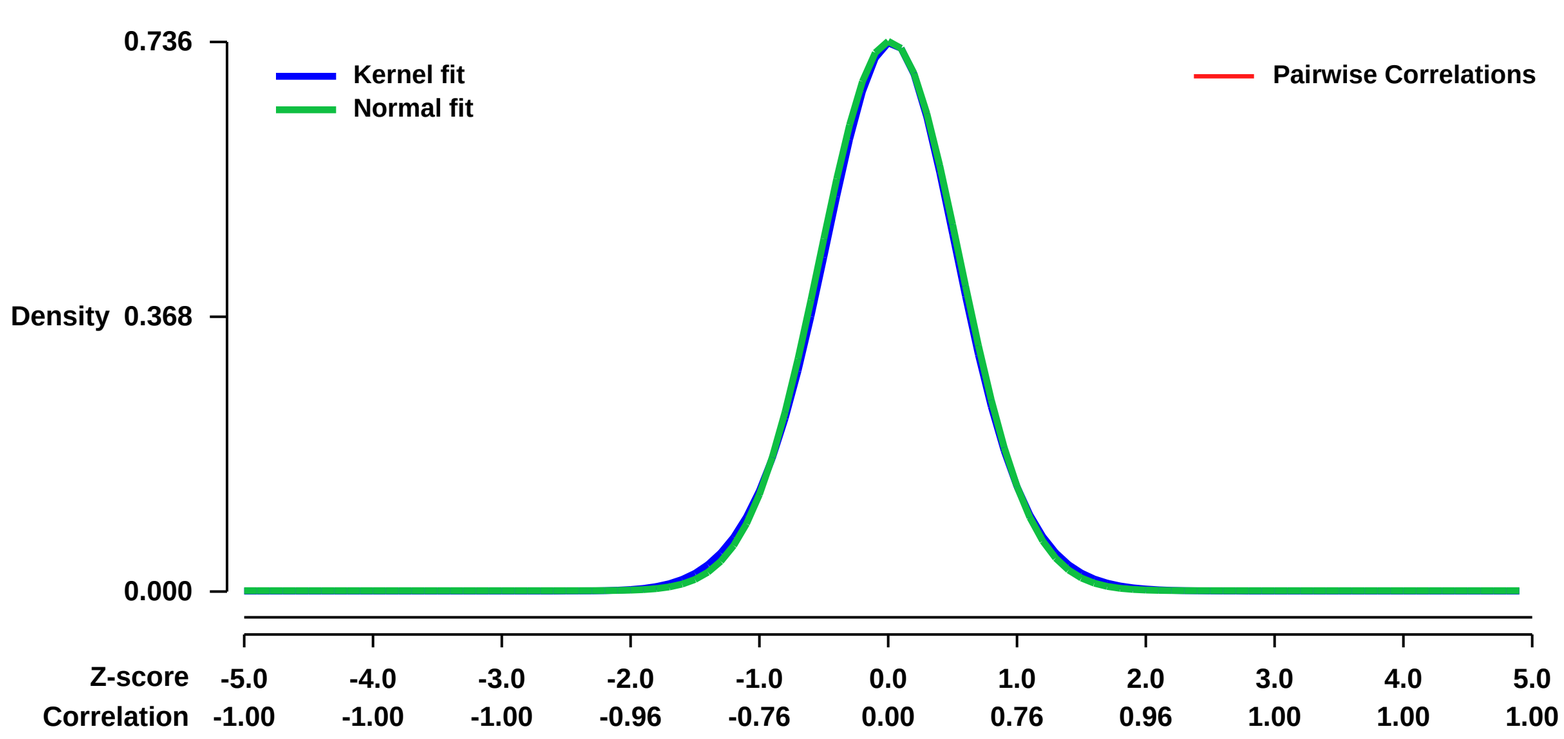

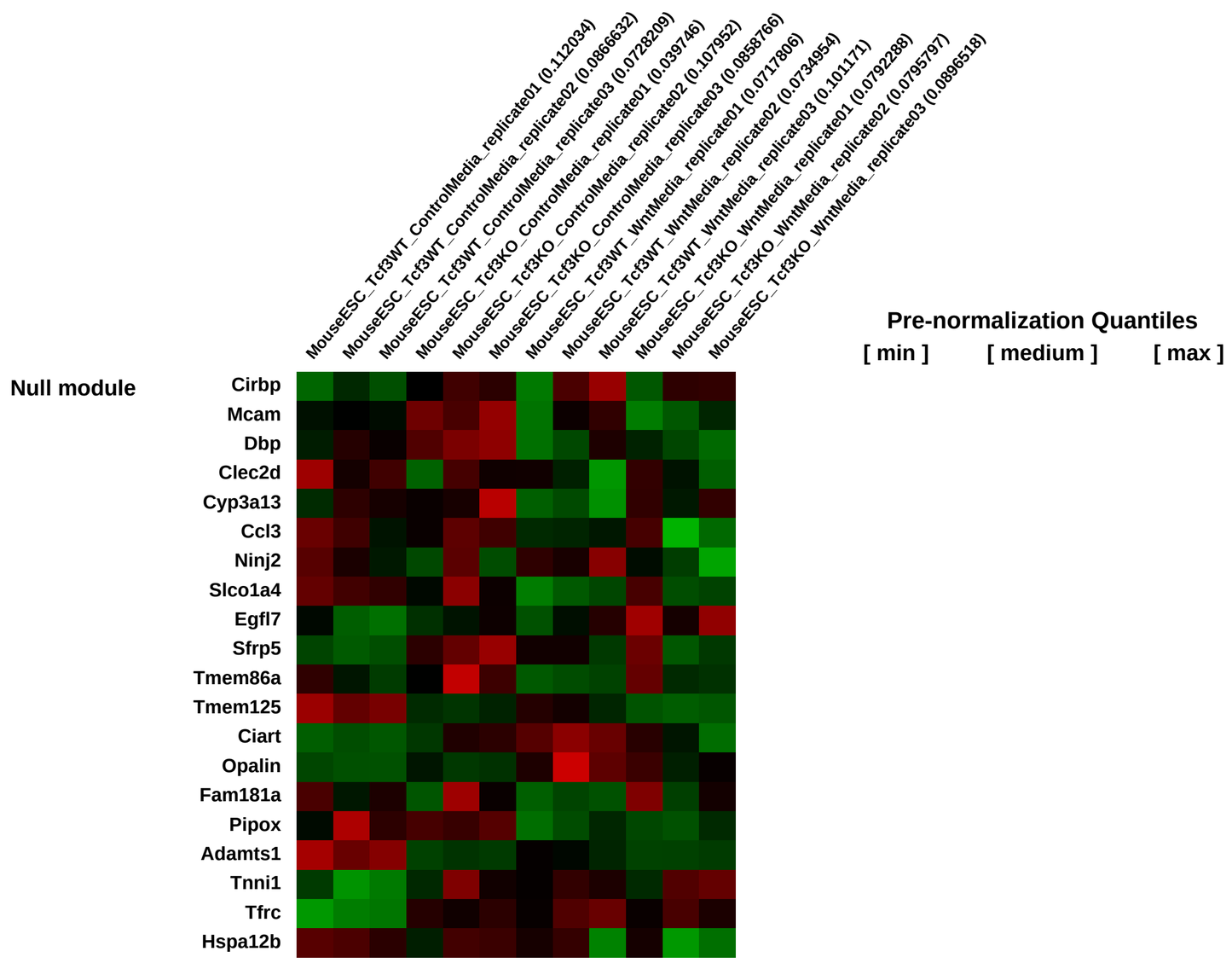

GEO Series "GSE51483" Expression Profiles

Num of samples in this series: 45

Scale of expression profile Z-scores

-3.0 -2.0 -1.0 0.0 1.0 2.0 3.0

GEO Link:	http://www.ncbi.nlm.nih.gov/geo/query/acc.cgi?acc=GSE51483
Status:	Public on May 19 2014
Title:	Transcriptional Atlas of Cardiogenesis Maps Congenital Heart Disease Interactome
Organism:	Mus musculus
Experiment type:	Expression profiling by array
Platform:	GPL1261
Pubmed ID:	24803680
Summary & Design:	**Summary:** Mammalian heart development is built on highly conserved molecular mechanisms with polygenetic perturbations resulting in a spectrum of congenital heart diseases (CHD). However, the transcriptional landscape of cardiogenic ontogeny that regulates proper cardiogenesis remains largely based on candidate-gene approaches. Herein, we designed a time-course transcriptome analysis to investigate the genome-wide expression profile of innate murine cardiogenesis ranging from embryonic stem cells to adult cardiac structures. This comprehensive analysis generated temporal and spatial expression profiles, prioritized stage-specific gene functions, and mapped the dynamic transcriptome of cardiogenesis to curated pathways. Reconciling the bioinformatics of the congenital heart disease interactome, we deconstructed disease-centric regulatory networks encoded within this cardiogenic atlas to reveal stage-specific developmental disturbances clustered on epithelial-to-mesenchymal transition (EMT), BMP regulation, NF-AT signaling, TGFb-dependent induction, and Notch signaling. Therefore, this cardiogenic transcriptional landscape defines the time-dependent expression of cardiac ontogeny and prioritizes regulatory networks at the interface between health and disease. **Overall design:** To interrogate the temporal and spatial expression profiles across the entire genome during mammalian heart development, we designed a time-course microarray experiment using the mouse model at defined stages of cardiogenesis, starting with embryonic stem cells (ESC, R1 stem cell line), early embryonic developmental stages: E7.5 whole embryos, E8.5 heart tubes, left and right ventricle tissues at E9.5, E12.5, E14.5, E18.5 to 3 days after birth (D3) and adult heart (Figure 1A). At each time point, microarray experiments were performed on triplicate biological samples. Starting at E9.5, tissue samples from left ventricles (LV) and right ventricles (RV) were microdissected for RNA purification and microarray analysis to determine spatially differential gene expression between LV and RV during heart development.

Background corr dist: KL-Divergence = 0.0679, L1-Distance = 0.0271, L2-Distance = 0.0013, Normal std = 0.5057

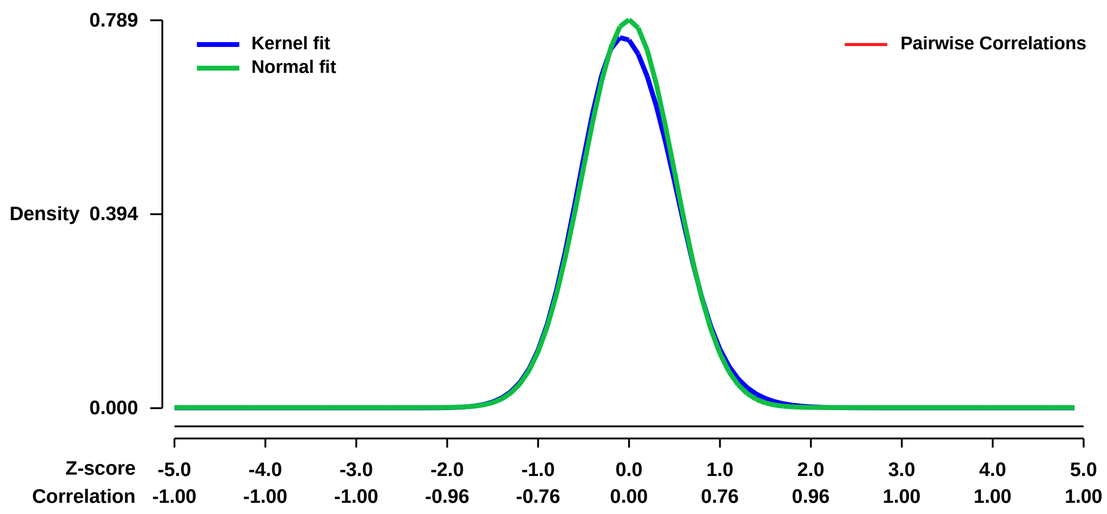

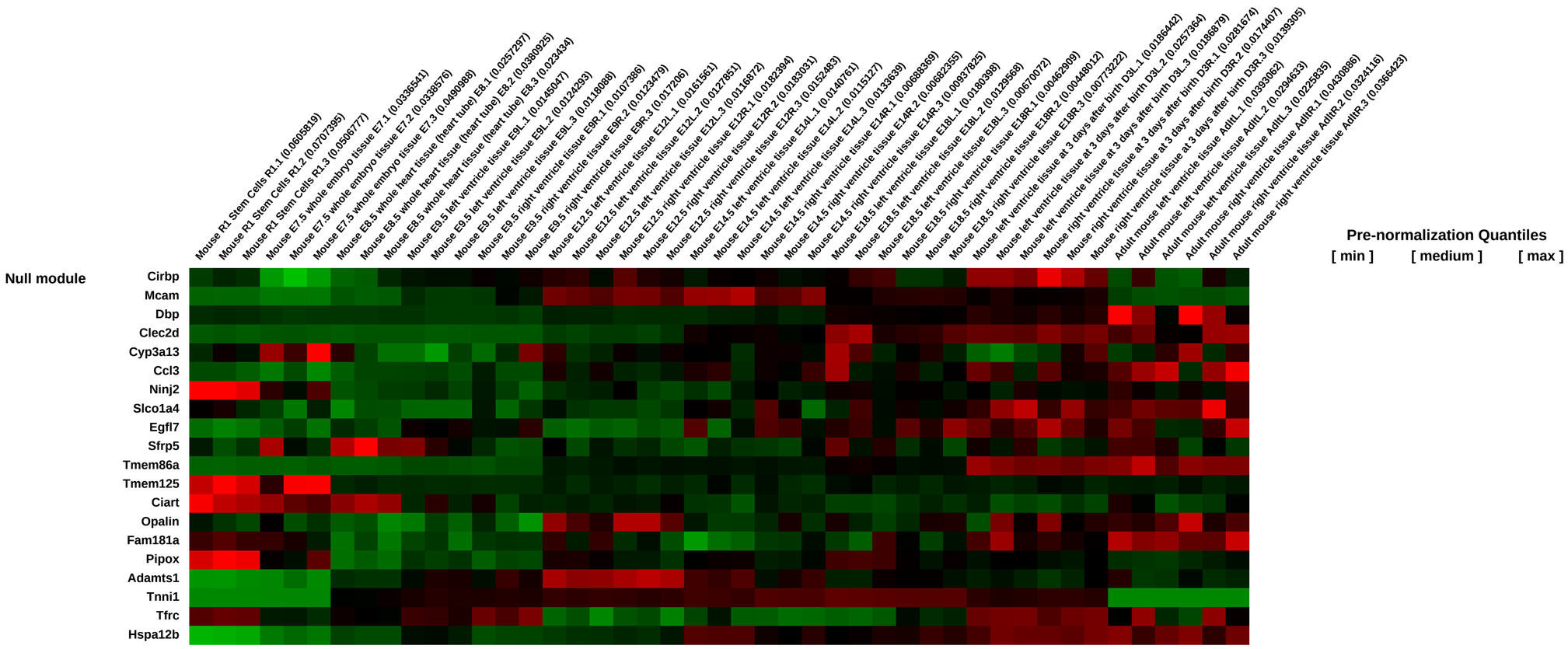

GEO Series "GSE11420" Expression Profiles

Num of samples in this series: 15

Scale of expression profile Z-scores

-3.0 -2.0 -1.0 0.0 1.0 2.0 3.0

GEO Link:	http://www.ncbi.nlm.nih.gov/geo/query/acc.cgi?acc=GSE11420
Status:	Public on Apr 09 2009
Title:	Microarray of Mouse Brain Tumors grown from injections of GL26 cell line
Organism:	Mus musculus
Experiment type:	Expression profiling by array
Platform:	GPL1261
Pubmed ID:	
Summary & Design:	**Summary:** RNA was extracted from the tumors that grew in the brains of mice that were injected with the GL26 cell line. RNA from GL26 cells was also taken. The chip used for all was an affymetrix mouse genome chip (GPL1261). This is the mouse model compliment to a human experiment in which the human chip was used for GBM tumors. **Keywords:** disease state analysis **Overall design:** Samples include GL26 tumors taken from C57BL6 untreated wild type, 10 month Old C57BL6 untreated wild type, C57BL6 Foxline Mutated Nudes, and from C57BL6 wild types that received a dendritic cell vaccine against GL26.

Background corr dist: KL-Divergence = 0.1764, L1-Distance = 0.0413, L2-Distance = 0.0036, Normal std = 0.3495

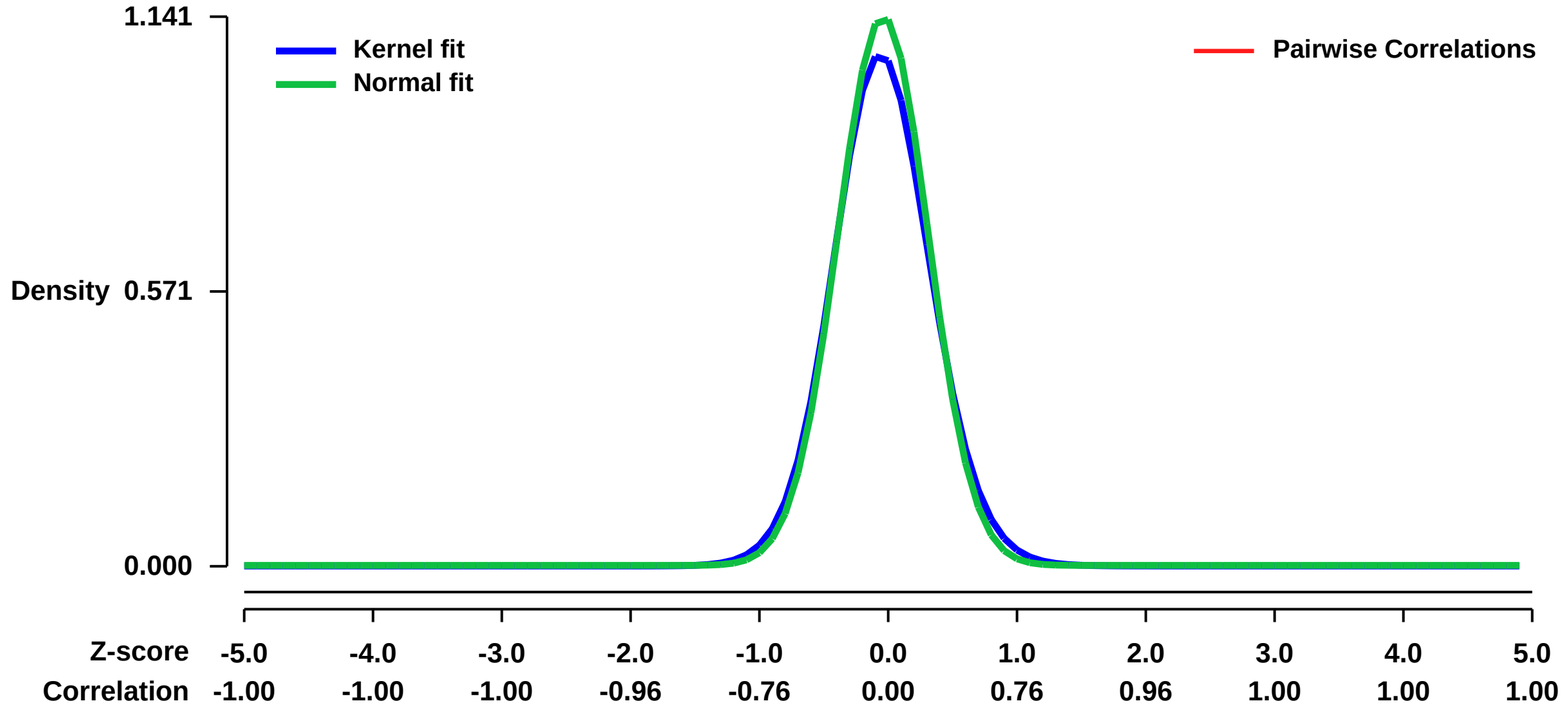

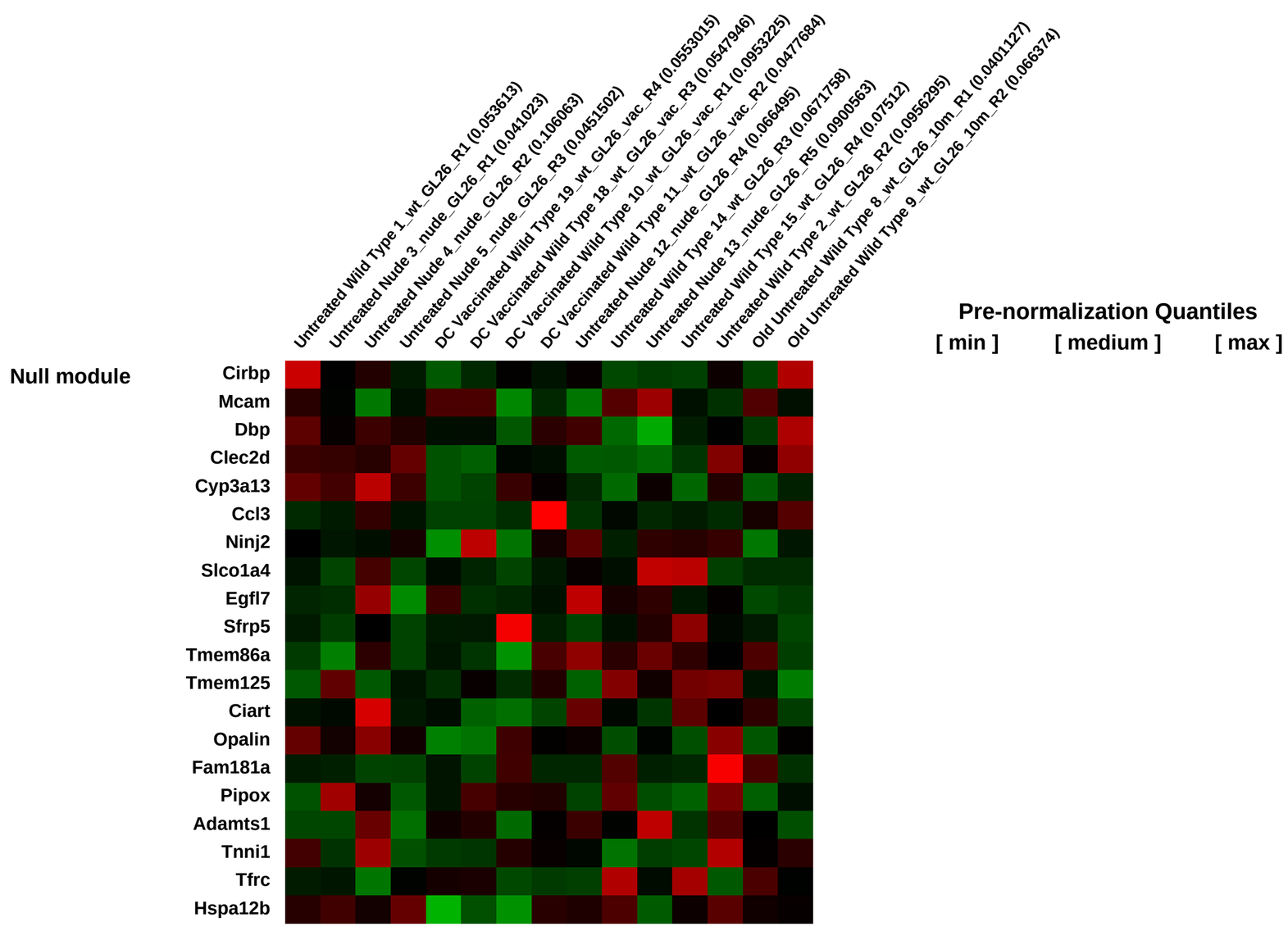

GEO Series "GSE10182" Expression Profiles

Num of samples in this series: 7

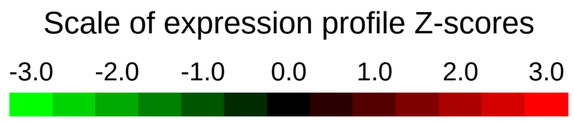

GEO Link:	http://www.ncbi.nlm.nih.gov/geo/query/acc.cgi?acc=GSE10182
Status:	Public on Mar 15 2008
Title:	MDP- and Pam3CSK4-induced genes in naˆflve and tolerant macrophages
Organism:	Mus musculus
Experiment type:	Expression profiling by array
Platform:	GPL1261
Pubmed ID:	18261938
Summary & Design:	**Summary:** Most of the genes were self-tolerized by Pam3CSK4 and MDP but there was no or minimal cross-tolerization. The transcriptome induced via Nod2 stimulation is greatly expanded in TLR2-tolerant macrophages. Keywords: self and cross tolerance by MDP or Pam3CSK4 **Overall design:** Genes induced by Pam3CSK4 or MDP were selected based on a three-fold increase over expression levels in unstimulated macrophages. Tolerized genes are defined as genes downregulated more than 2-fold in tolerant macrophages stimulated with Pam3CSK4 or MDP.

Background corr dist: KL-Divergence = 0.0435, L1-Distance = 0.0246, L2-Distance = 0.0007, Normal std = 0.6065

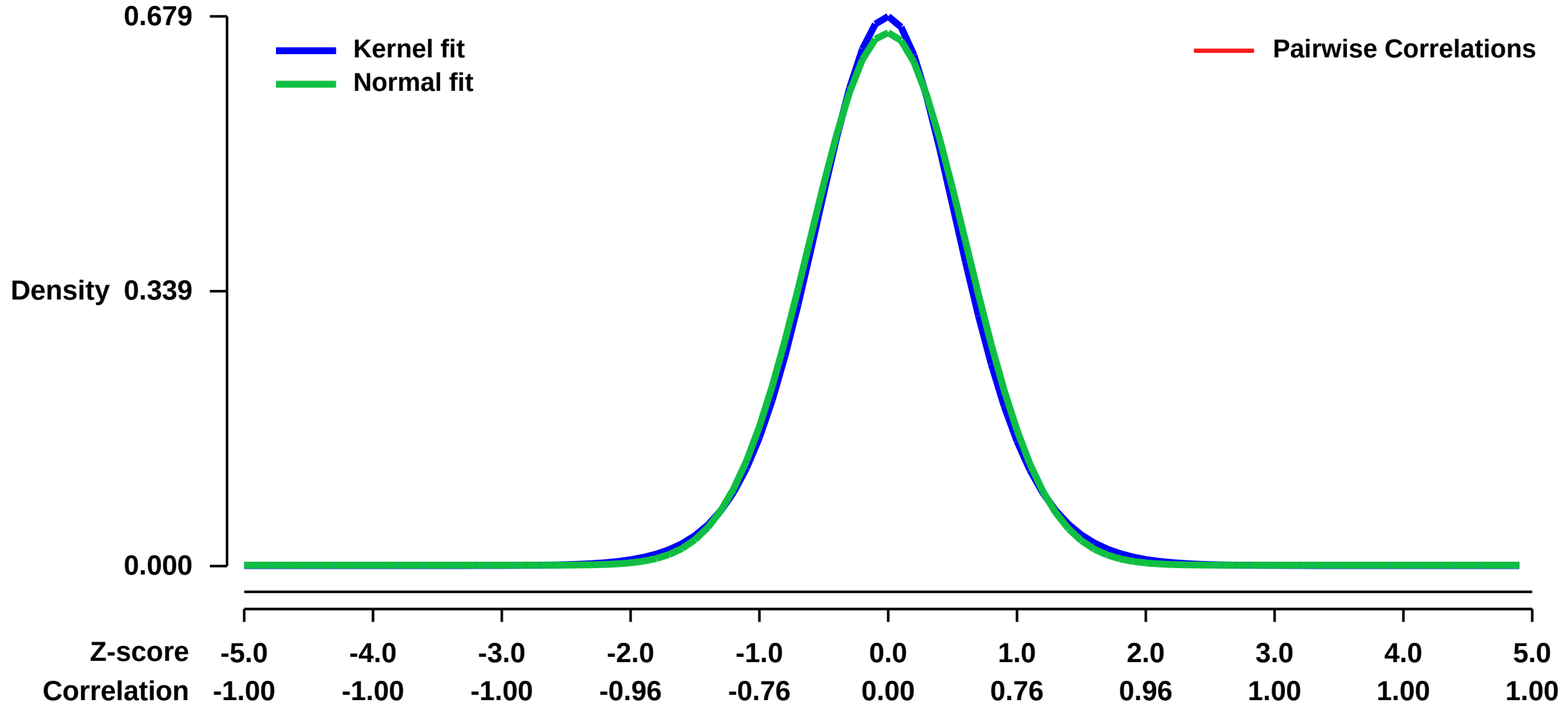

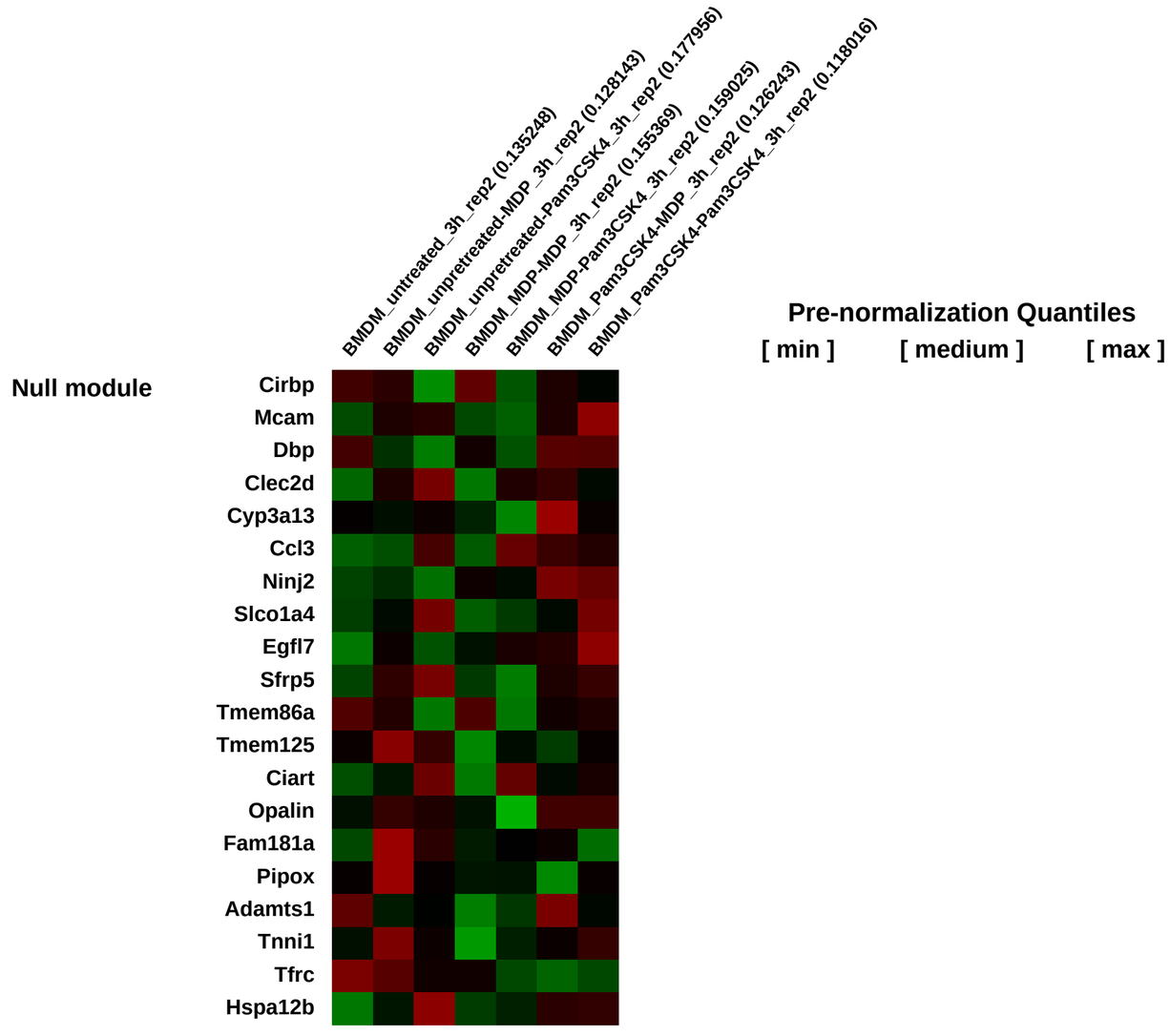

GEO Series "GSE22140" Expression Profiles

Num of samples in this series: 13

Scale of expression profile Z-scores

-3.0 -2.0 -1.0 0.0 1.0 2.0 3.0

GEO Link:	http://www.ncbi.nlm.nih.gov/geo/query/acc.cgi?acc=GSE22140
Status:	Public on Jun 05 2010
Title:	Arthritic KRN T cells and wild type T cells from germ free and specific pathogen free mice
Organism:	Mus musculus
Experiment type:	Expression profiling by array
Platform:	GPL1261
Pubmed ID:	20620945
Summary & Design:	**Summary:** A general defect of GF K/BxN T cell proliferation response toward antigen motivated us to look for the impairment in GF K/BxN T cells that might leads to the low Ab production and reduced disease phenotype seen in GF K/BxN mice. To find the difference between GF and SPF K/BxN T cells in a broad and non-biased fashion, we performed gene-expression profiling of these cells using microarrays. **Overall design:** All gene expression profiles were obtained from highly purified T cell populations sorted by flow cytometry. To reduce variability, cells from multiple mice were pooled for sorting, and triplicates or quadruplates were generated for all groups. Raw data were preprocessed with the RMA algorithm in GenePattern, and averaged expression values were used for analysis.

Background corr dist: KL-Divergence = 0.0478, L1-Distance = 0.0480, L2-Distance = 0.0044, Normal std = 0.5756

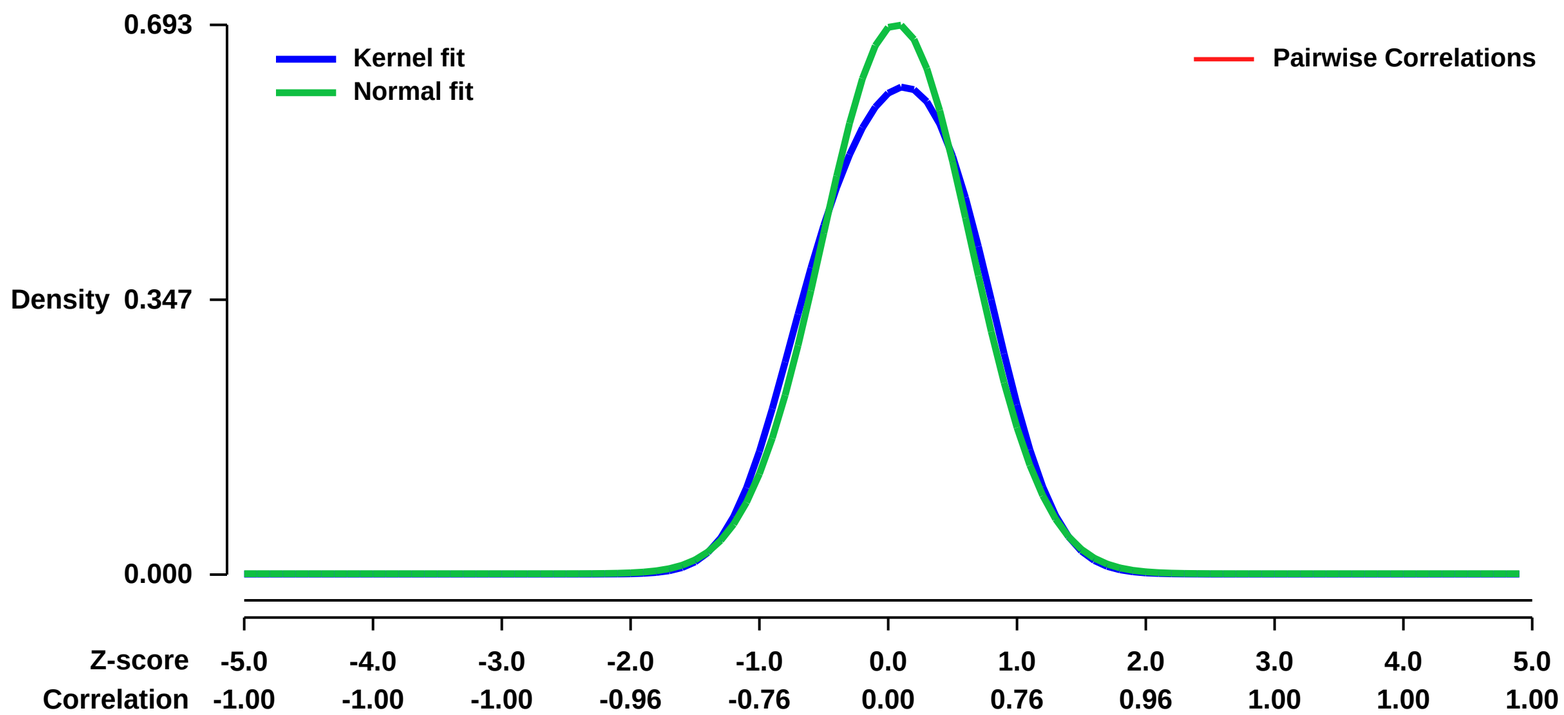

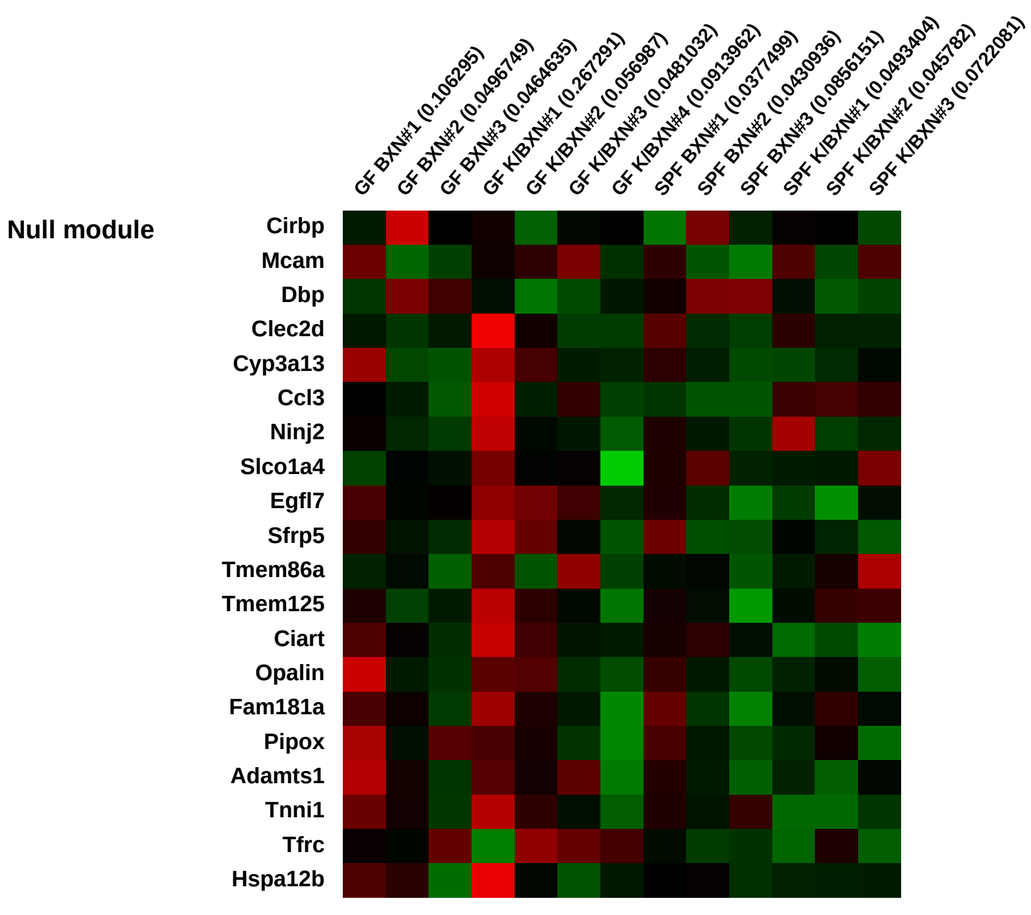

GEO Series "GSE9355" Expression Profiles

Num of samples in this series: 51

Scale of expression profile Z-scores

-3.0 -2.0 -1.0 0.0 1.0 2.0 3.0

GEO Link:	http://www.ncbi.nlm.nih.gov/geo/query/acc.cgi?acc=GSE9355
Status:	Public on Dec 14 2007
Title:	Microarray expression profiles of mammary tumors developed in Wap-Cre;Etv6-NTRK3 mice
Organism:	Mus musculus
Experiment type:	Expression profiling by array
Platform:	GPL1261
Pubmed ID:	18068631
Summary & Design:	**Summary:** We report a mouse model that recapitulates expression of the ETV6-NTRK3 (EN) fusion oncoprotein, the product of the t(12;15)(p13;q25) translocation characteristic of human secretory breast carcinoma. Activation of EN expression in mammary tissues by Whey acidic protein (Wap) promoter-driven Cre leads to fully penetrant, multifocal malignant breast cancer with short latency. We provide genetic evidence that committed bipotent or CD61+ luminal alveolar progenitors, are targets of tumorigenesis. Furthermore, EN transforms these otherwise transient progenitors through activation of the AP1 complex. Given increasing relevance of chromosomal translocations in epithelial cancers, such mice serve as a paradigm for the study of their genetic pathogenesis and cellular origins, and generation of novel preclinical models. In this study, we generated microarray expression profiling data from both genetically marked, FACS-sorted tumor epithelial cells and from unfractionated mammary tumors and normal mammary glands. By using gene set enrichment analysis (GSEA) on these data, we have identified the AP1 transcriptional complex as the major downstream effector of the ETV6-NTRK3 signaling. Keywords: genetic modification, cell type comparison **Overall design:** Take the advantage of the Cre-lox system and a floxed lacZ reporter at the Rosa26 locus (Rosa-Stop-lacZ), we genetically marked mammary epithelial cells in which the conditional Etv6-NTRK3 knockin allele were turned on, and followed them to the hyperplasia and tumor stages. We then sorted lacZ+ hyperplastic mammary epithelial cells and lacZ+ tumor epithelial cells and collected their expression profiles by Affymetrix mouse whole genome MOE430.2 chips. We also collected expression profiles from unfractionated mammary tumors (unsorted tumors) derived from the same mouse model and mammary glands from normal mice.

Background corr dist: KL-Divergence = 0.3099, L1-Distance = 0.0635, L2-Distance = 0.0108, Normal std = 0.2772

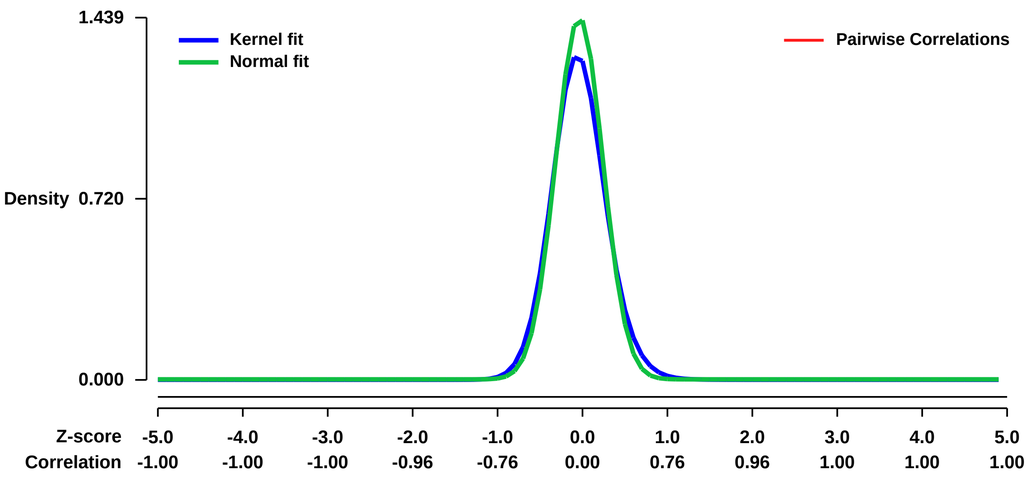

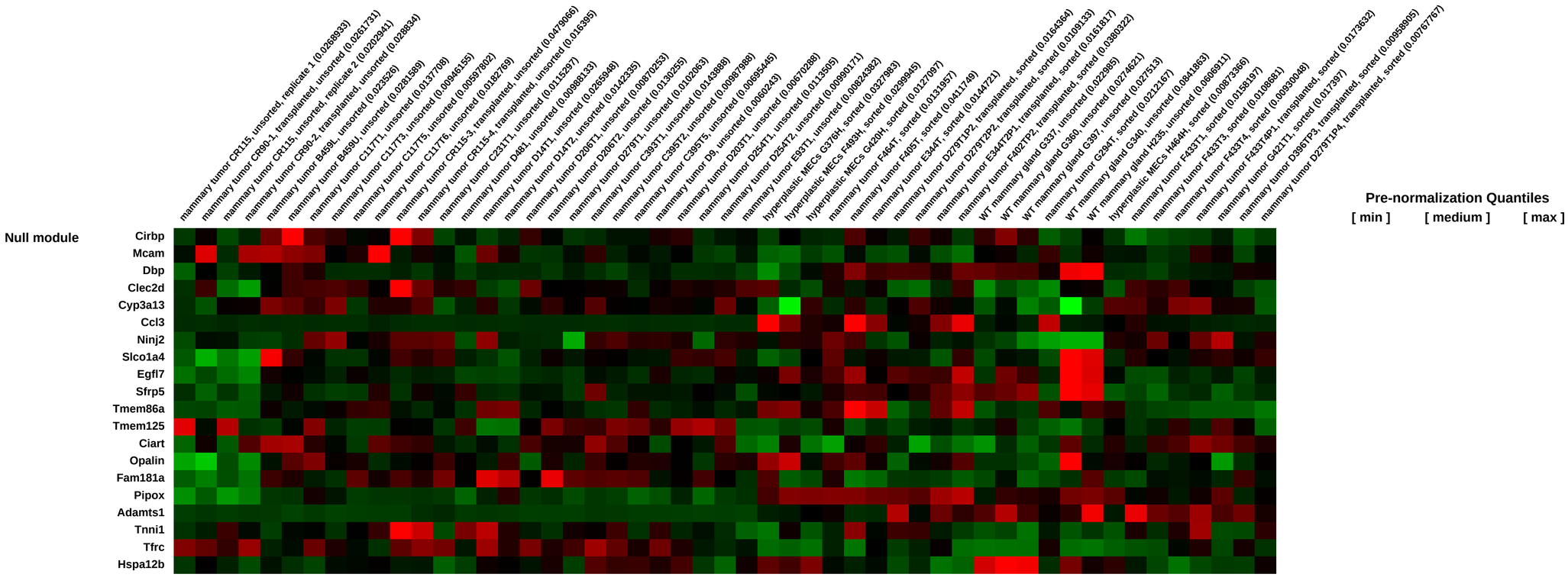

GEO Series "GSE24203" Expression Profiles

Num of samples in this series: 8

Scale of expression profile Z-scores

-3.0 -2.0 -1.0 0.0 1.0 2.0 3.0

GEO Link:	**http://www.ncbi.nlm.nih.gov/geo/query/acc.cgi?acc=GSE24203**
Status:	**Public on Sep 18 2010**
Title:	**A20 Role in Liver regeneration**
Organism:	**Mus musculus**
Experiment type:	**Expression profiling by array**
Platform:	**GPL1261**
Pubmed ID:	
Summary & Design:	**Summary:** **Genome wide transcriptional profiling on liver mRNA retrieved from recombinant adenovirus A20 (rAd.A20) and rAd.bgalactosidase transduced livers, before and 24 hours after 78% extended liver resection. Overexpression of the NF-kB inhibitory protein A20 improves recovery of liver function and mass following extended liver resection and severe liver ischemia reperfusion injury in mice. In this project, we explored effects of A20 using transcriptional profiling on liver mRNA retrieved from recombinant adenovirus A20 (rAd.A20) and rAd.bgalactosidase transduced livers, before and 24 hours after 78% extended liver resection.** **Overall design:** **A20 or beta-galactosidase gene expression in the mouse liver was achieved by penile vein injection of 1x109 pfu of rAd. in 100uL of normal saline, which results in optimal transgene expression 5 days after injection in 30% to 40% of hepatocytes (Longo et al, 2005). Extended (78%) LR, consisting of resection of the lateral, medial, left, and right lobes, was performed 5 days following rAd. administration in 8-week old BALB/c mice weighing 25 to 30 grams (Taconic, Germantown, NY), as described (Longo et al, 2005). RNA was extracted from the resected portion of the liver (before samples) and from the remnant liver 24 hours after resection (after samples). RNA from three animals was pooled per microarray and 2 microarrays per group were performed.**

Background corr dist: KL-Divergence = 0.0548, L1-Distance = 0.0201, L2-Distance = 0.0005, Normal std = 0.5412

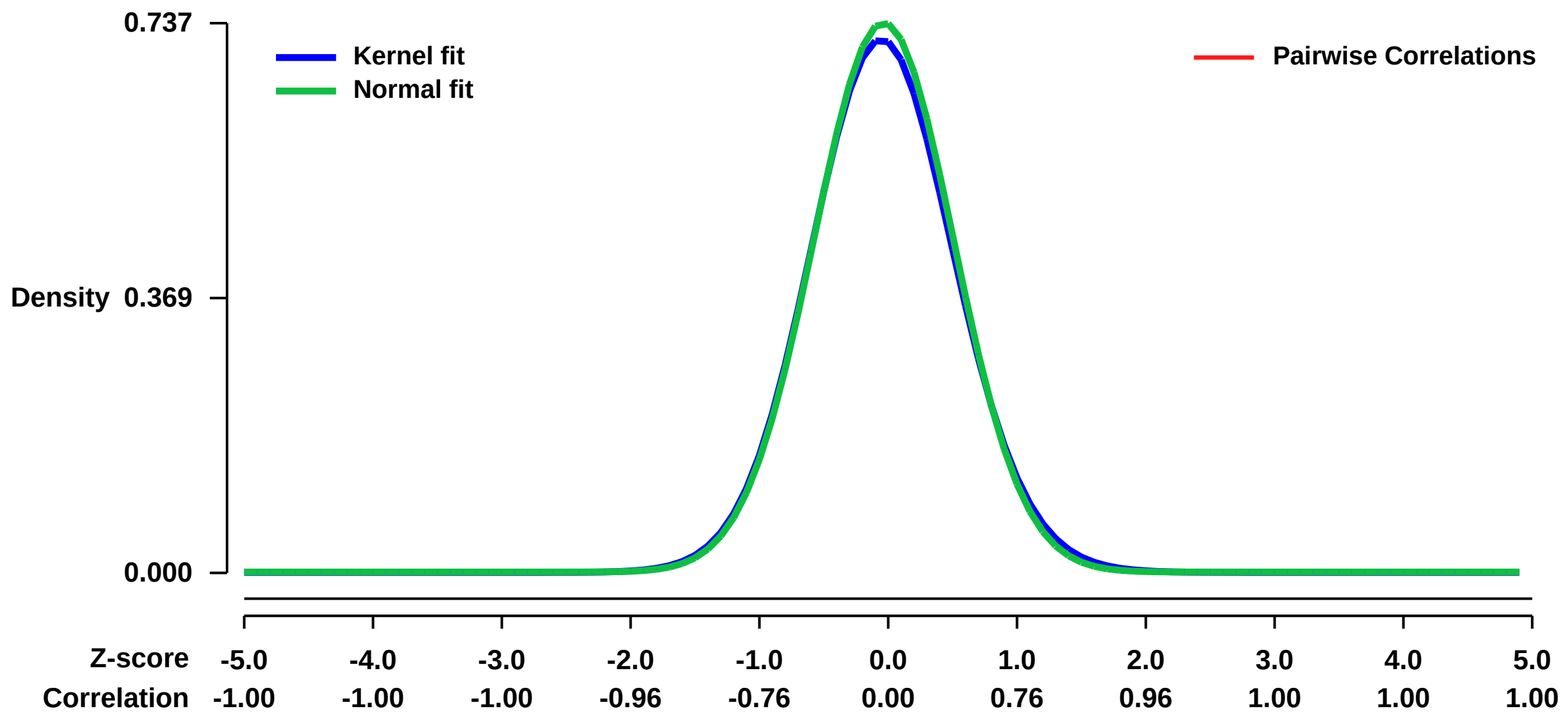

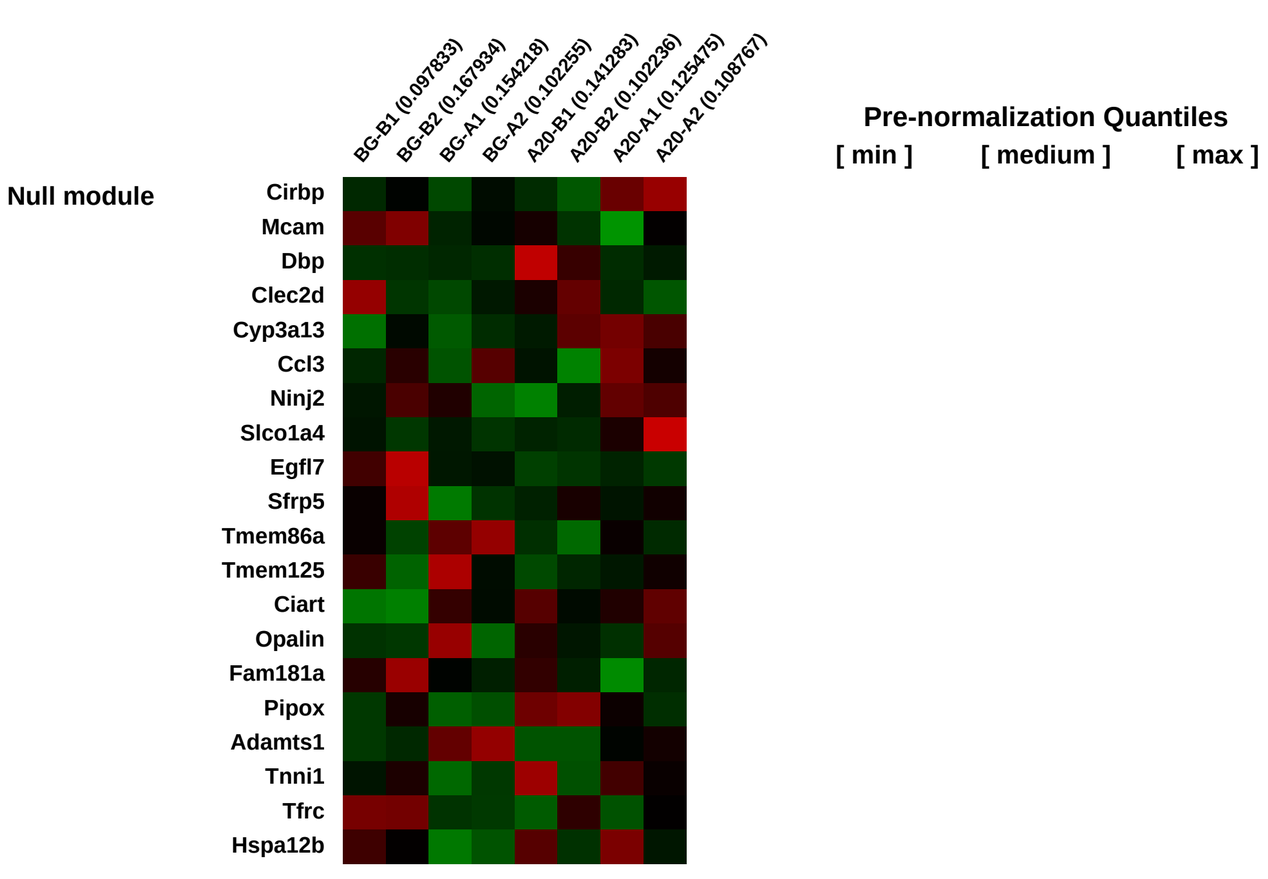

GEO Series "GSE36209" Expression Profiles

Num of samples in this series: 9

Scale of expression profile Z-scores

-3.0 -2.0 -1.0 0.0 1.0 2.0 3.0

GEO Link:	**http://www.ncbi.nlm.nih.gov/geo/query/acc.cgi?acc=GSE36209**
Status:	**Public on Mar 02 2012**
Title:	**Expression data for OVE26 diabetic mouse podocyte**
Organism:	**Mus musculus**
Experiment type:	**Expression profiling by array**
Platform:	**GPL1261**
Pubmed ID:	
Summary & Design:	**Summary:** **Podocytes form filtration barrier through foot process around glomerualar basement membrane and selectively permit permeability of molecular smaller than albumin. Diabetes can cause podocyte pathological changes leading to high urine albumin level. Diabetic mouse model OVE26 has extremly high urine albumin and previously studies indicated its podocyte damaged.** **Here we try to find the key genes change in OVE26 diabetic mouse model podocyte by microarray assay while normal FVB mouse podocyte set as control.** **Overall design:** **Podocyte eGFP transgenic mice were made on FVB background and crossbred to OVE26 diabetic model. Glomeruli isolated from OVE-GFP mice were digested by trypsin into signal cell. Podocytes with GFP were sorting out by FACS.**

Background corr dist: **KL-Divergence = 0.0948, L1-Distance = 0.0240, L2-Distance = 0.0010, Normal std = 0.4481**

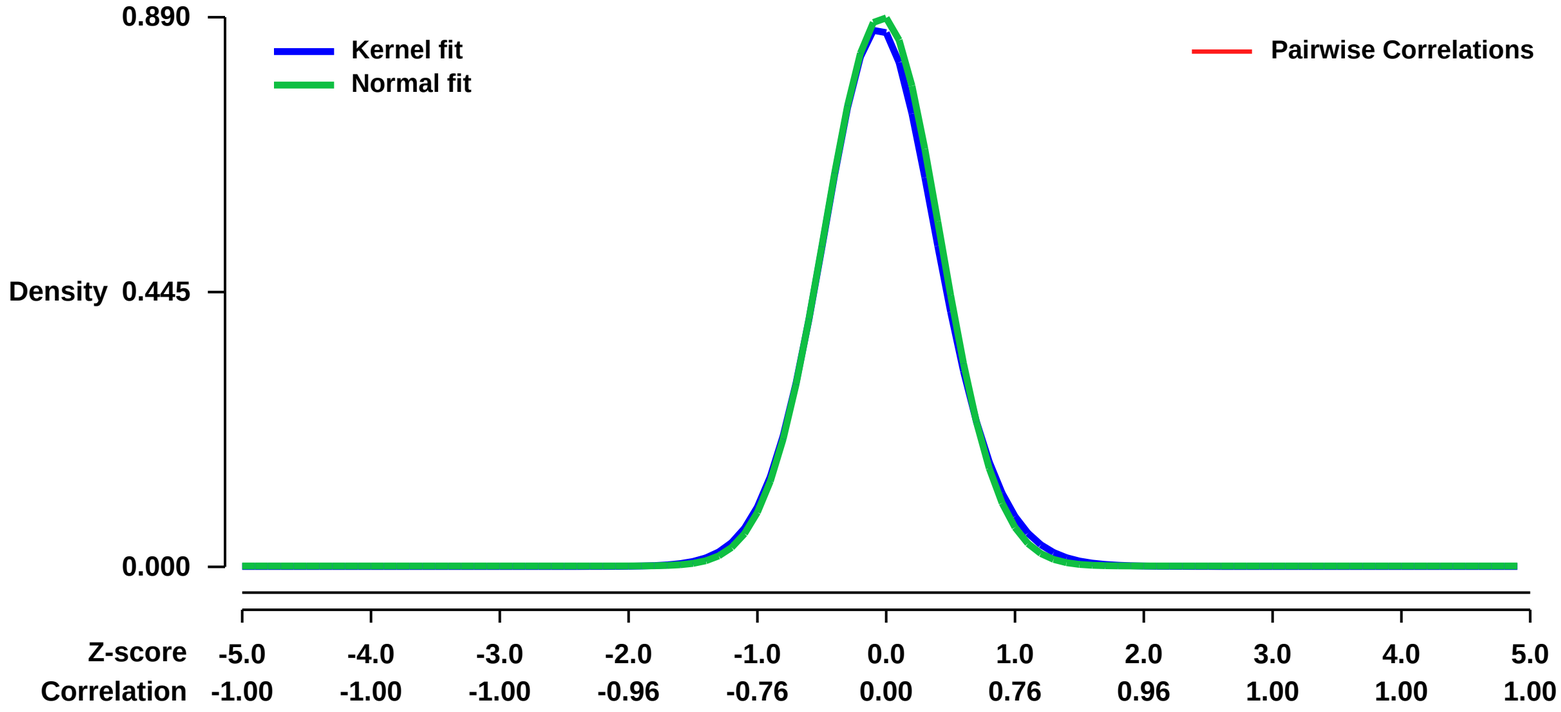

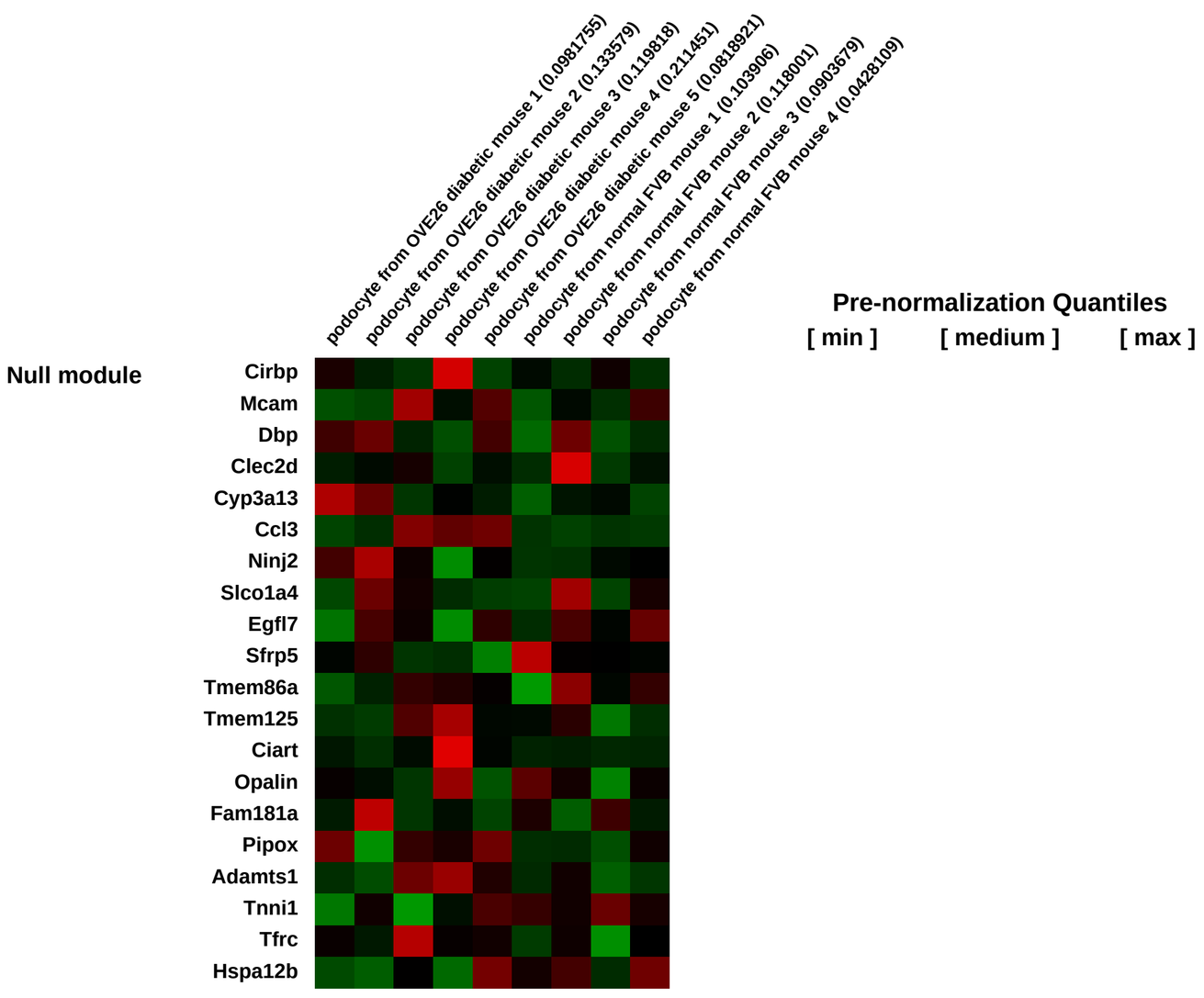

GEO Series "GSE32102" Expression Profiles

Num of samples in this series: 49

Scale of expression profile Z-scores

-3.0 -2.0 -1.0 0.0 1.0 2.0 3.0

GEO Link: http://www.ncbi.nlm.nih.gov/geo/query/acc.cgi?acc=GSE32102
Status: Public on Sep 15 2011
Title: Arsenate Sub-chronic Drinking Water Study
Organism: Mus musculus
Experiment type: Expression profiling by array
Platform: GPL1261
Pubmed ID: 21795629

Summary & Design:

Summary:
Concentration- and time-dependent genomic changes in the mouse urinary bladder following exposure to arsenate in drinking water for up to twelve weeks.

Inorganic arsenic (Asi) is a known human bladder carcinogen. The objective of this study was to examine the concentration dependence of the genomic response to Asi in the urinary bladders of mice. C57BL/6J mice were exposed for 1 or 12 weeks to arsenate in drinking water at concentrations of 0.5, 2, 10, and 50 mg As/L. Urinary bladders were analyzed using gene expression microarrays. A consistent reversal was observed in the direction of gene expression change: from predominantly decreased expression at 1 week to predominantly increased expression at 12 weeks. These results are consistent with evidence from in vitro studies of an acute adaptive response that is suppressed on longer exposure due to down-regulation of Fos. Pathways with the highest enrichment in gene expression changes were associated with epithelial-to-mesenchymal transition, inflammation, and proliferation. Benchmark dose (BMD) analysis determined that the lowest median BMD values for pathways were above 5 mg As/L, despite the fact that pathway enrichment was observed at the 0.5 mg As/L exposure concentration. This disparity may result from the non-monotonic nature of the concentration-responses for the expression changes of a number of genes, as evidenced by the much fewer gene expression changes at 2 mg As/L compared to lower or higher concentrations. Pathway categories with concentration-related gene expression changes included cellular morphogenesis, inflammation, apoptosis/survival, cell cycle control, and DNA damage response. The results of this study provide evidence of a concentration-dependent transition in the mode of action for the subchronic effects of Asi in mouse bladder cells in the vicinity of 2 mg Asi/L.

Overall design:
Female C57Bl/J mice will be exposed to COLD Arsenate in drinking water. One week interium sac on 7/18/06. 100 samples including liver, lung, kidney and bladder. Bladder will be analyzed with microarrays, 24 samples. Twelve week terminal sac on 10/05/06. 75 total samples including lung, kidney, and bladder. Bladdler will be analyzed by microarray, 25 samples. Drinking water containing As will be prepared weekly with monitoring to determine amount used by mice. Following tissues will be available for genomic study: Bladder, liver, lung, and kidney.

Background corr dist: KL-Divergence = 0.4036, L1-Distance = 0.0614, L2-Distance = 0.0095, Normal std = 0.2485

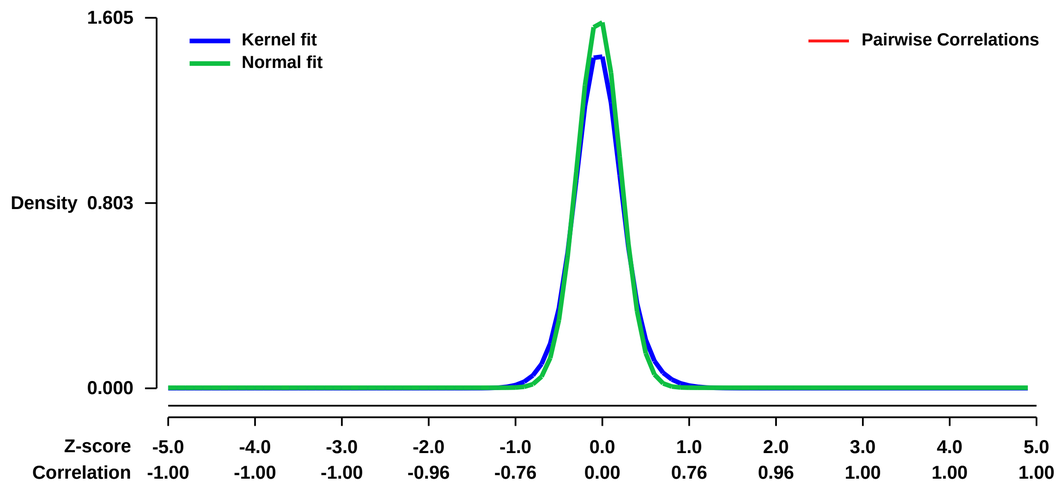

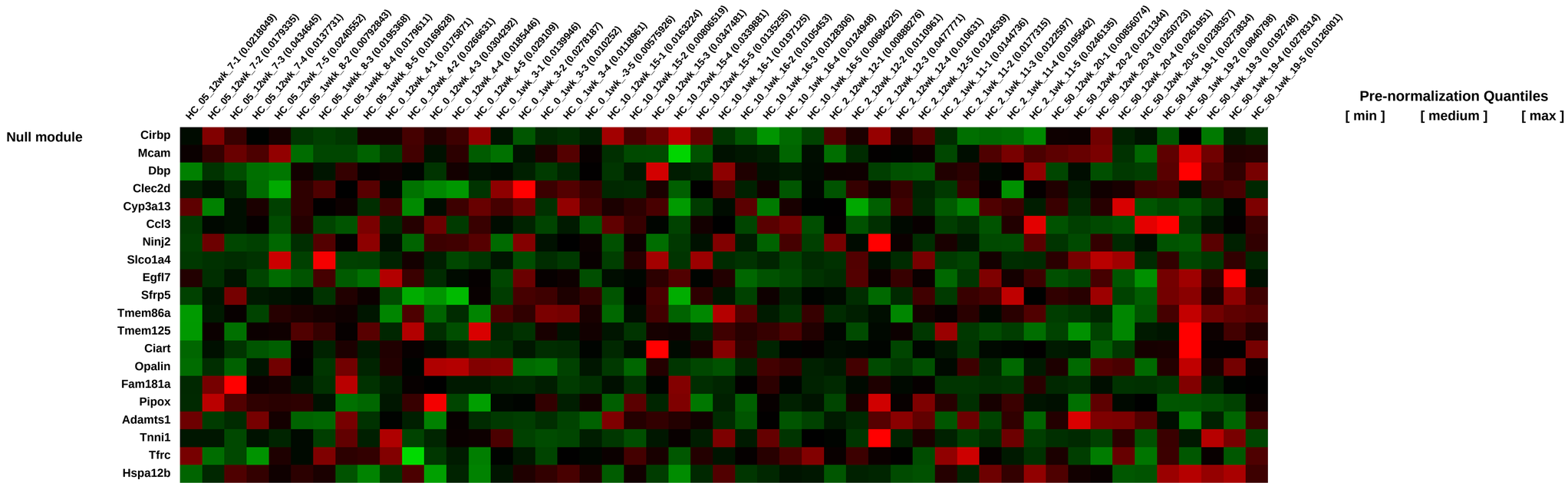

GEO Series "GSE4040" Expression Profiles

Num of samples in this series: 6

Scale of expression profile Z-scores

-3.0 -2.0 -1.0 0.0 1.0 2.0 3.0

GEO Link:	**http://www.ncbi.nlm.nih.gov/geo/query/acc.cgi?acc=GSE4040**
Status:	**Public on Jan 13 2006**
Title:	**sikes-affy-mouse-84486**
Organism:	**Mus musculus**
Experiment type:	**Expression profiling by array**
Platform:	**GPL1261**
Pubmed ID:	
Summary & Design:	**Summary:** **Reversible phosphorylation is a critical step in the control of cellular signaling events. The protein phosphatase 1 (PP1) regulates neuronal proteins by mediating their de-phosphorylation. PP1 selectivity and subcellular localization is conferred via association with a panel of interacting proteins. We have extensively characterized the association of PP1 with inhibitor-1, an interacting protein widely expressed in brain and heart. Inhibitor-1 deletion results in a persistently active PP1 phosphatase in vitro. Inhibitor-1 overexpression results in increased transformation of cultured cells and enhances the rate of learning and memory in mouse models through largely unknown mechanisms. Significantly, inhibitor-1 activation is cAMP-sensitive. The genes regulated by inhibitor-1/PP1 signals have not been characterized. Identification of these genes is expected to provide key insights into the role of inhibitor-1/PP1 escape from cellular homeostasis and regulation of neuronal learning and memory.** **We will determine gene expression patterns in hippocampus of wild-type and inhibitor-1 knock-out mice. The results of these studies of constitutive expression will be used as a baseline for future studies aimed to determine the role cAMP-mediated gene expression in I-1 knock-out mice.** **We hypothesize that the genes regulated by the inhibitor-1/PP1 holoenzyme are critical to cellular growth commitment including resistance to growth arrest and neuronal learning and memory** **We will examine the role of inhibitor-1 in regulating hippocampal gene expression using total RNA isolated from whole hippocampi of inhibitor-1 knockout (I-1-/-) animals and parental C57Bl6 controls under non-stimulated conditions. Animals will be sacrificed by a standard protocol. Hippocampal tissue will be rapidly dissected from several animals, flash frozen within 1 minute of extraction, pooled, and total RNA will be processed immediately using TriZol.** **Keywords: dose response** **Overall design:**

Background corr dist: **KL-Divergence = 0.0489, L1-Distance = 0.0183, L2-Distance = 0.0003, Normal std = 0.5764**

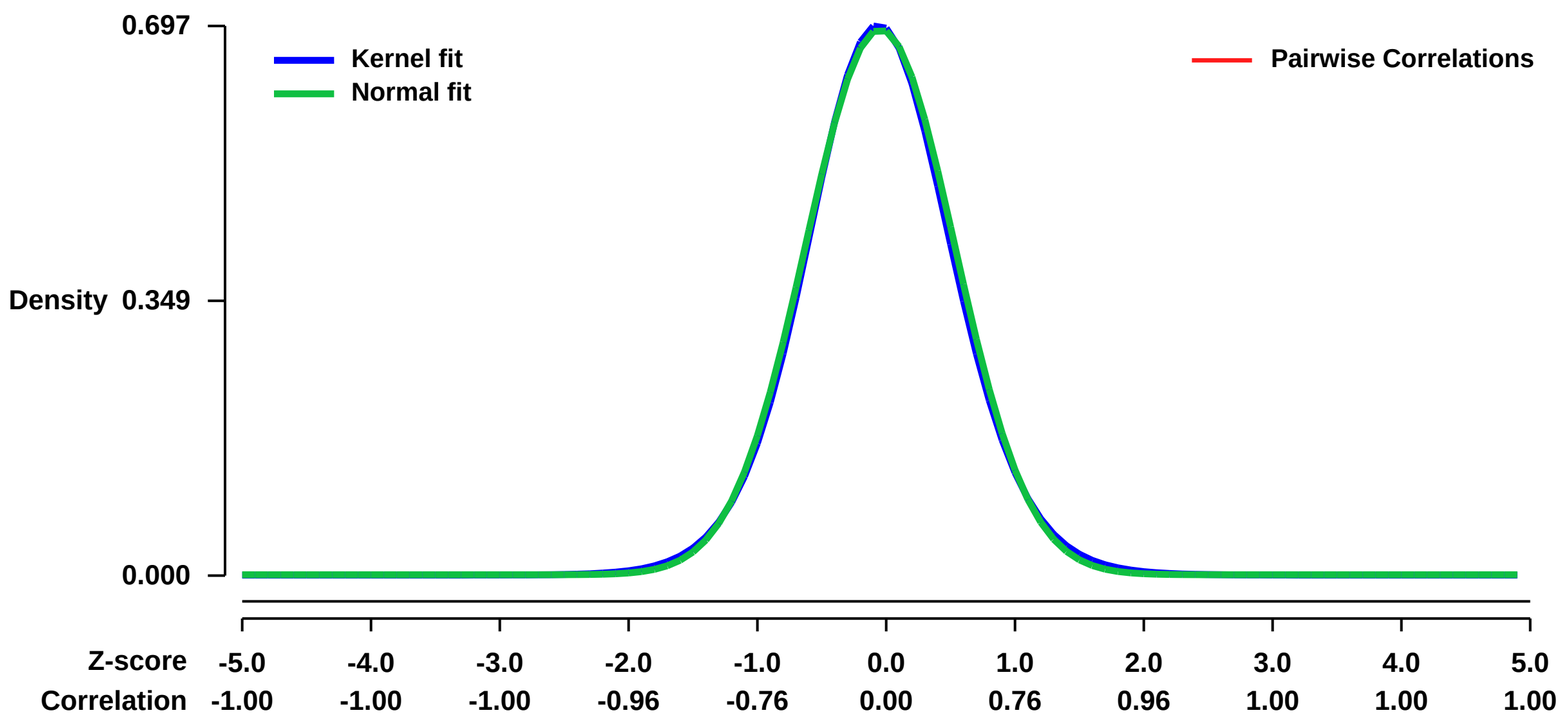

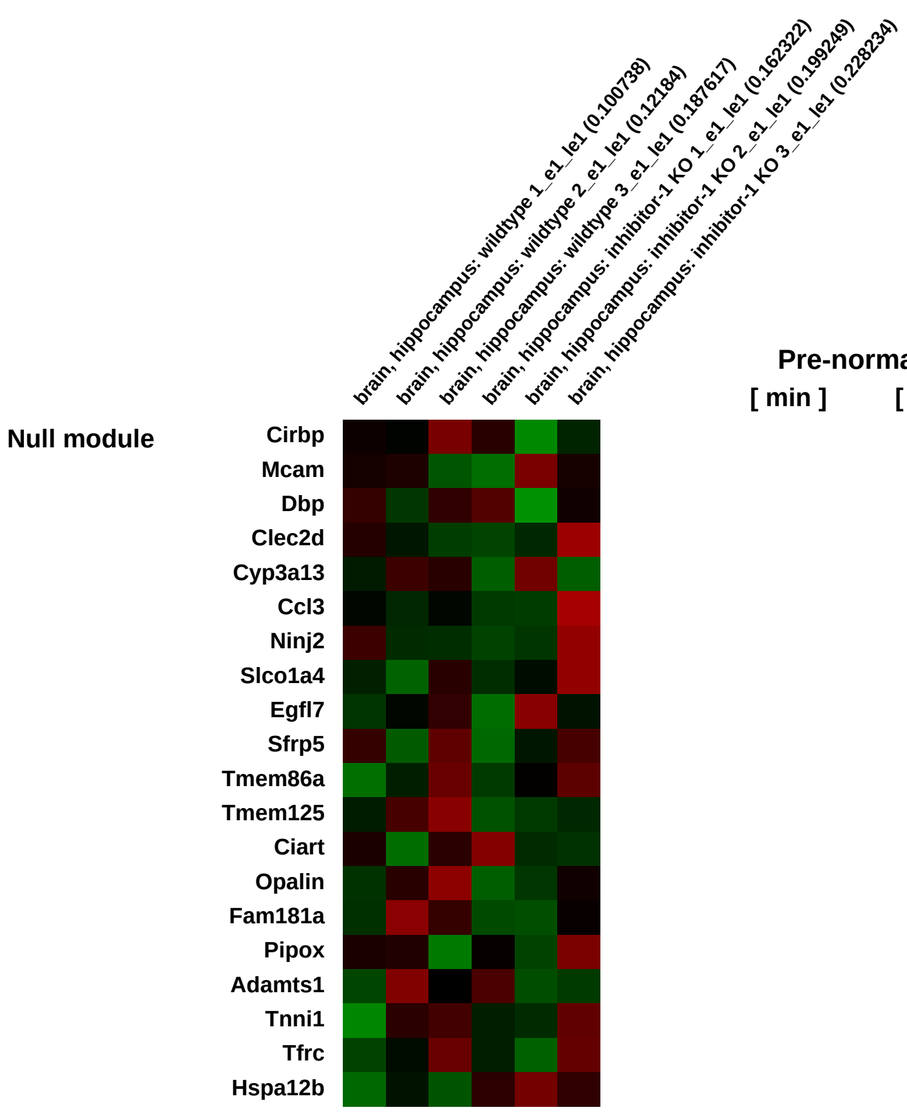

GEO Series "GSE41706" Expression Profiles

Num of samples in this series: 6

Scale of expression profile Z-scores

-3.0 -2.0 -1.0 0.0 1.0 2.0 3.0

GEO Link:	http://www.ncbi.nlm.nih.gov/geo/query/acc.cgi?acc=GSE41706
Status:	Public on Oct 20 2012
Title:	Expression data from adult (9 month-old) hearts from GRK2 heterozygous C57BL/6J mice and its wild type littermates
Organism:	Mus musculus
Experiment type:	Expression profiling by array
Platform:	GPL1261
Pubmed ID:	
Summary & Design:	**Summary:** G protein-coupled receptor kinase 2 (GRK2) has emerged as a key regulator of cardiac function and myocardial structure. Cardiac GRK2 is increased in heart failure and ischemia in humans, whereas genetic inhibition of GRK2 is cardioprotective in animal models of these pathologies. However, the mechanistic basis underlying these effects are not fully understood. We have used adult GRK2 hemizygous mice (GRK2+/-) as a model to assess the effects of a sustained systemic inhibition of GRK2 in heart tissue with age. We used microarrays to determine the global programme of gene expression underlying cardioprotection in GRK2 hemizygous mice. **Overall design:** 9 month-old mice hearts were collected for RNA extraction and hybridization on Affymetrix microarrays.

Background corr dist: KL-Divergence = 0.0396, L1-Distance = 0.0137, L2-Distance = 0.0002, Normal std = 0.6109

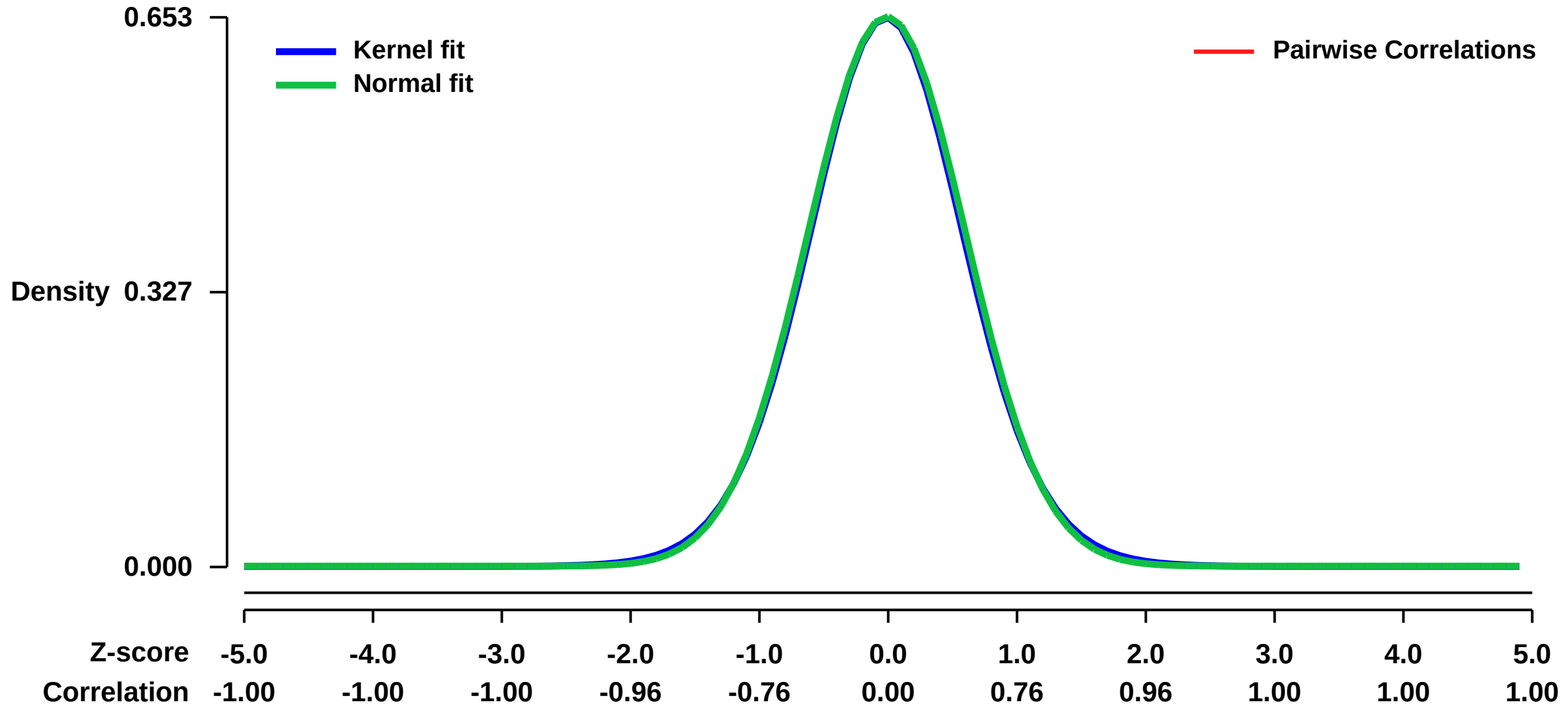

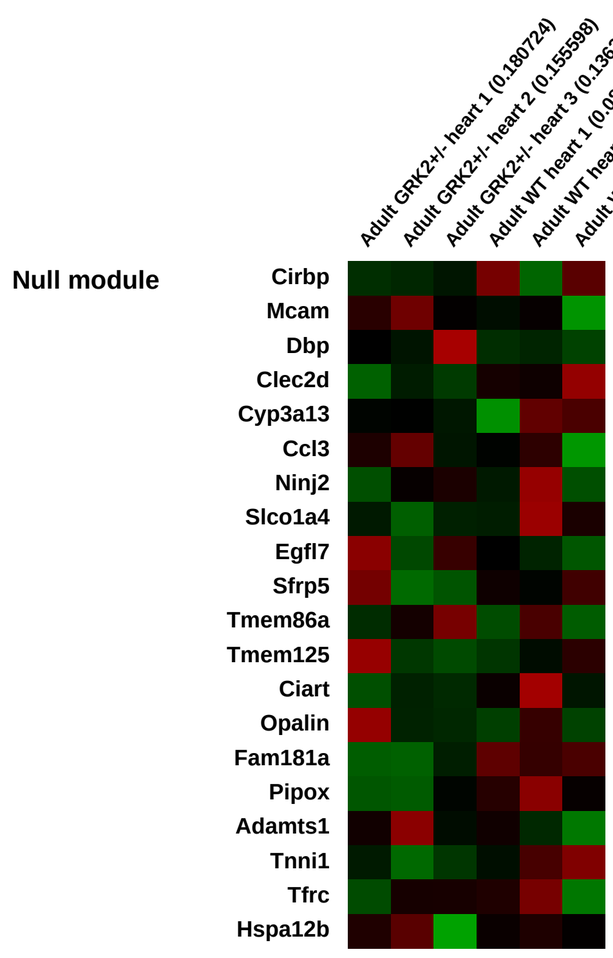

GEO Series "GSE17250" Expression Profiles

Num of samples in this series: 24

Scale of expression profile Z-scores

-3.0 -2.0 -1.0 0.0 1.0 2.0 3.0

GEO Link:	http://www.ncbi.nlm.nih.gov/geo/query/acc.cgi?acc=GSE17250
Status:	Public on Sep 21 2009
Title:	Comparative analysis of gene regulation by the transcription factor PPAR¿–_mouse
Organism:	Mus musculus
Experiment type:	Expression profiling by array
Platform:	GPL1261
Pubmed ID:	22215653
Summary & Design:	**Summary:** Studies in mice have shown that PPAR¿– is an important regulator of hepatic lipid metabolism and the acute phase response. However, little information is available on the role of PPAR¿– in human liver. Here we set out to compare the function of PPAR¿– in mouse and human hepatocytes via analysis of target gene regulation. Primary hepatocytes from 6 human and 6 mouse donors were treated with PPAR¿– agonist Wy14643 and gene expression profiling was performed using Affymetrix GeneChips followed by a systems biology analysis. Baseline PPAR¿– expression was similar in human and mouse hepatocytes. Depending on species and time of exposure, Wy14643 significantly induced the expression of 362-672 genes. Surprisingly minor overlap was observed between the Wy14643-regulated genes from mouse and human, although more substantial overlap was observed at the pathway level. Xenobiotics metabolism and apolipoprotein synthesis were specifically regulated by PPAR¿– in human hepatocytes, whereas glycolysis-gluconeogenesis was regulated specifically in mouse hepatocytes. Most of the genes commonly regulated in mouse and human were involved in lipid metabolism and many represented known PPAR¿– targets, including CPT1A, HMGCS2, FABP, ACSL, and ADFP. Several genes were identified that were specifically induced by PPAR¿– in human (MBL2, ALAS1, CYP1A1, TSKU) or mouse (Fbp2, lgals4, Cd36, Ucp2, Pxmp4). Furthermore, several putative novel PPAR¿– targets were identified that were commonly regulated in both species, including CREB3L3, KLF10, KLF11 and MAP3K8. Our results suggest that PPAR¿– activation has a major impact on gene regulation in human hepatocytes. Importantly, the role of PPAR¿– as master regulator of hepatic lipid metabolism is generally well-conserved between mouse and human. Overall, however, PPAR¿– regulates a mostly divergent set of genes in mouse and human hepatocytes. **Keywords:** Analysis of target gene regulation by using microarrays **Overall design:** Primary hepatocytes from 6 mice from 6 different strains were treated with the PPAR¿– agonist Wy14643 for 6 and 24 hours, and gene expression profiling was performed using Affymetrix GeneChips. Mouse primary hepatocytes were isolated by two-step collagenase perfusion from 6 different strains of mouse; NMRI, SV129, FVB, DBA, BALB/C and C57BL/6J. Cells were plated on collagen-coated six-well plates. Viability was determined by Trypan Blue exclusion, and was at least 75%. Hepatocytes were suspended in William's E medium (Lonza Bioscience, Verviers, Belgium) supplemented with 10% (v/v) fetal calf serum, 20 m-units/mL insulin, 10 nM dexamethasone, 100 U/mL penicillin, 100 ¿…g/mL of streptomycin, 0.25 ¿…g/mL fungizone and 50 ¿…g/mL gentamycin. After four hours the medium was discarded and replaced with fresh medium. The next day, cells were incubated in fresh medium in the presence or absence of Wy14643 (10 microM) dissolved in DMSO for 6 and 24 hours, followed by RNA isolation. A 5-fold lower concentration of Wy14643 was used in mouse primary hepatocytes to take into account the higher affinity of Wy14643 for mouse PPAR¿– compared to human PPAR¿–.

Background corr dist: KL-Divergence = 0.2666, L1-Distance = 0.0531, L2-Distance = 0.0067, Normal std = 0.2952

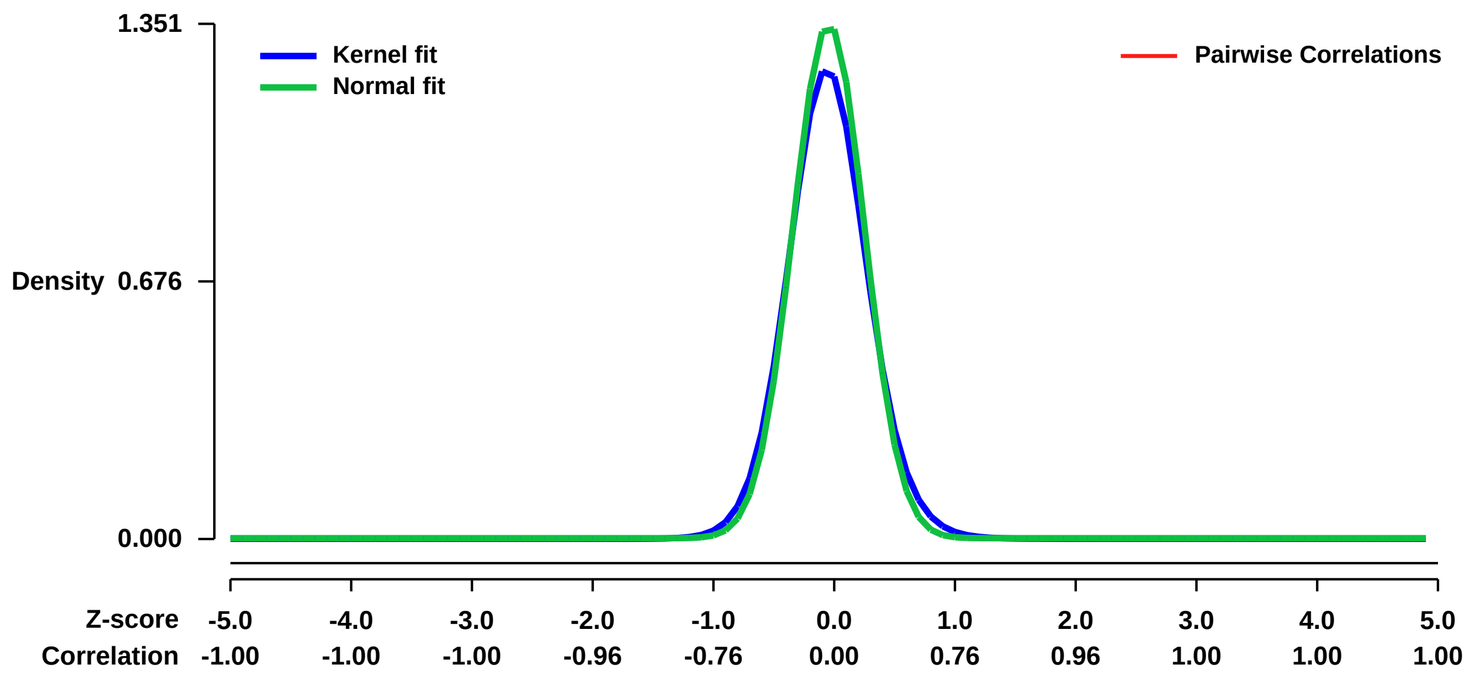

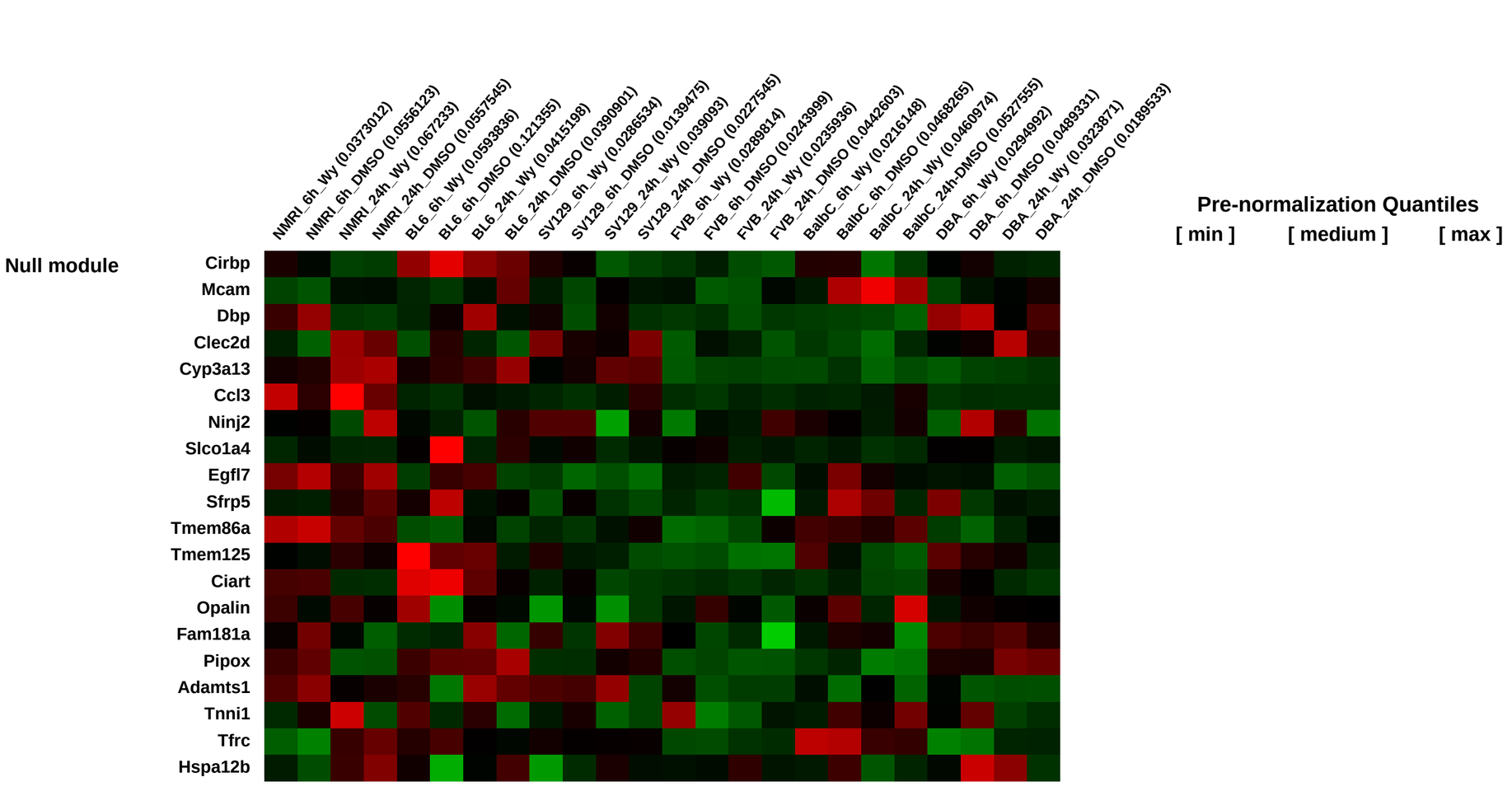

GEO Series "GSE34723" Expression Profiles

Num of samples in this series: 101

Details of this dataset are not shown due to large number of samples and the page size limit.

Find details in http://www.ncbi.nlm.nih.gov/geo/query/acc.cgi?acc=GSE34723

Background corr dist: KL-Divergence = 0.3721, L1-Distance = 0.0718, L2-Distance = 0.0149, Normal std = 0.2563

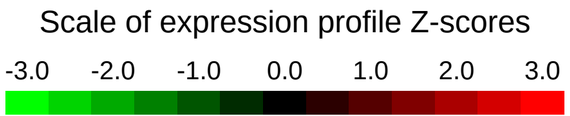

GEO Series "GSE13103" Expression Profiles

Num of samples in this series: 8

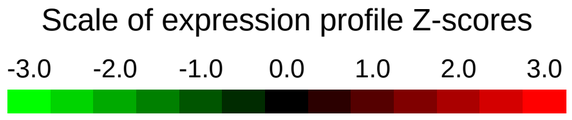

GEO Link:	http://www.ncbi.nlm.nih.gov/geo/query/acc.cgi?acc=GSE13103
Status:	Public on Oct 08 2008
Title:	Expression data from early mouse embryo eye development, specifically optic fissure.
Organism:	Mus musculus
Experiment type:	Expression profiling by array
Platform:	GPL1261
Pubmed ID:	19171890
Summary & Design:	**Summary:** The different stages of the optic fissure can be clearly visualized by making sagittal sections through the mouse eye during early development which represent the optic fissure at open (E10.5), closing (E11.5) and fused (E12.5) states. Laser capture microdissection (LCM) was employed to dissect tissue from the margins of the optic fissure consisting of the outer (presumptive RPE) and inner (presumptive neurosensory retina) layers of the retina. An approximately square-shaped block of optic fissure (50 x 50 mm) was dissected from each side of the fissure. Two rounds of linear amplification were performed on RNA isolated from each of the samples prior to microarray hybridization. Expression data were gathered in biological triplicate at E10.5, E11.5 and duplicate at E12.5, each array representing pooled optic fissure tissue from three embryos from a single litter. Expression signals were ascertained from 45,101 probe sets and normalized across arrays. **Keywords:** Time course **Overall design:** Differential gene expression over the course of three days in laser capture microdissected tissue from wild type mouse embryos.

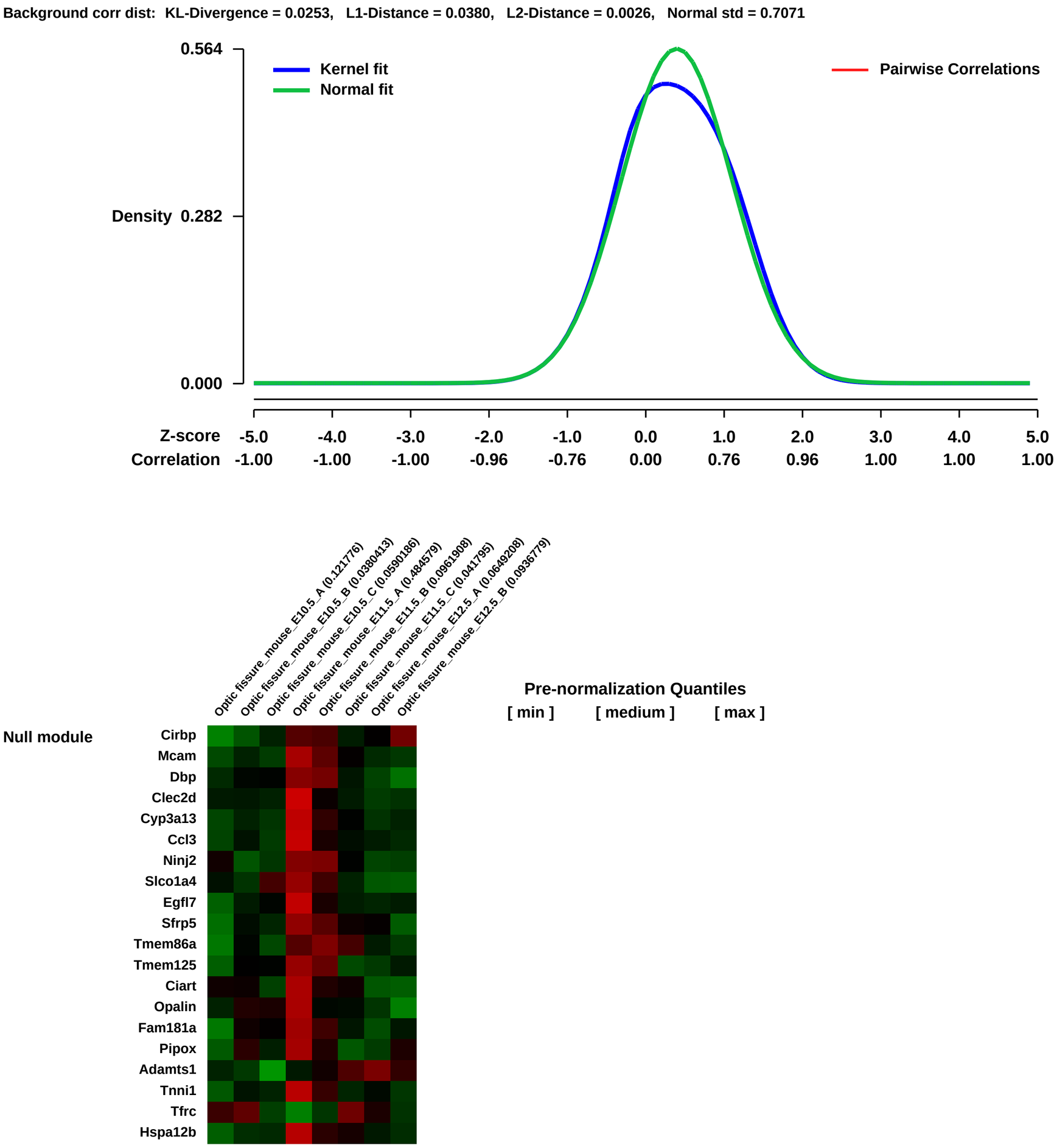

GEO Series "GSE22418" Expression Profiles

Num of samples in this series: 8

Scale of expression profile Z-scores

-3.0 -2.0 -1.0 0.0 1.0 2.0 3.0

GEO Link:	http://www.ncbi.nlm.nih.gov/geo/query/acc.cgi?acc=GSE22418
Status:	Public on Jun 18 2010
Title:	Comparison of gene expression between wild type, Notch1-activated, and RBPJ loss-of-function embryonic mouse yolk sac tissue at E9.5
Organism:	Mus musculus
Experiment type:	Expression profiling by array
Platform:	GPL1261
Pubmed ID:	21352545
Summary & Design:	**Summary:** The signaling cascades that direct the morphological differentiation of the vascular system during early embryogenesis are not well defined. To further understand the role of Notch signaling during endothelial differentiation, this study uses both an in vivo gain-of-function and an in vivo loss-of-function approach. At embryonic day 9.5, embryos with activated Notch1 signaling in the endothelia display a variety of growth and cardiovascular defects, and die soon after E10.5. Most notably, the extra-embryonic vasculature of the yolk sac displays remodeling differentiation defects. In the wild-type yolk sac, the primary vascular network has begun to reorganize, forming the large primary vessels and the smaller capillaries. In the activated Notch1 embryos, remodeling is defective; the vasculature have an enlarged surface with decreased inter-vessel space. Embryos with ablated Notch signaling also display growth and vascular defects at E9.5 similar to the activated Notch1 embryos, however they exhibit a lack of vascular remodeling in the yolk sac, retaining the simple vascular plexus seen at E8.5. These results indicate that Notch signaling plays a critical role in the remodeling of the vasculature in the early embryo, particularly in the extra-embryonic region. **Overall design:** A conditional transgenic system was used in this study to activate Notch signaling. The ubiquitous ROSA26Notch transgene with a Neo/stop cassette flanked by loxP sites, followed by the N1-ICD cDNA, was recombined with a Tie2-CRE mouse, resulting in the removal of the STOP cassette and the subsequent activation of the Notch1 intracellular domain. This allowed for the overexpression and expansion of Notch signaling in all endothelial cells. Male Tie2-Cre mice were mated with female ROSA26Notch mice and the resulting embryos were dissected at embryonic day 9.5. To ablate Notch signaling, Tie2-Cre mice were used in a two-generation cross to obtain Tie2-Cre; Rbpj flox/flox embryos. These embryos lack RBPJ binding activity in the endothelia. In both instances, embryos were used for genotyping and the yolk sac were separated and used to isolate total RNA with an RNeasy mini kit. The RNA was analyzed with the Mouse Genome 430A Array from Affymetrix. Samples were performed in duplicate, and RNA from wild type yolk sac tissues was compared to activated Notch and RBPJ loss-of-function yolk sac tissues.

Background corr dist: KL-Divergence = 0.0384, L1-Distance = 0.0242, L2-Distance = 0.0010, Normal std = 0.6041

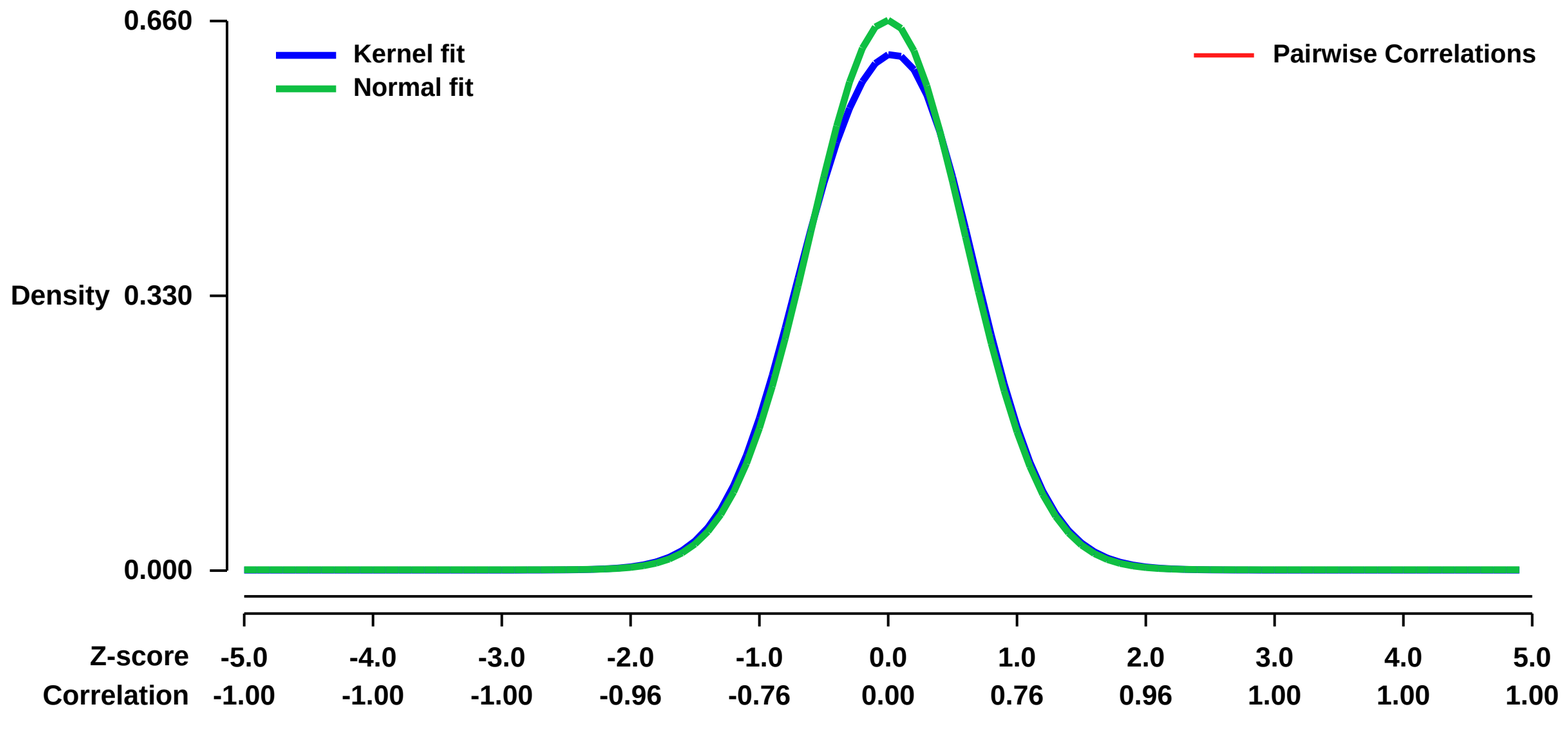

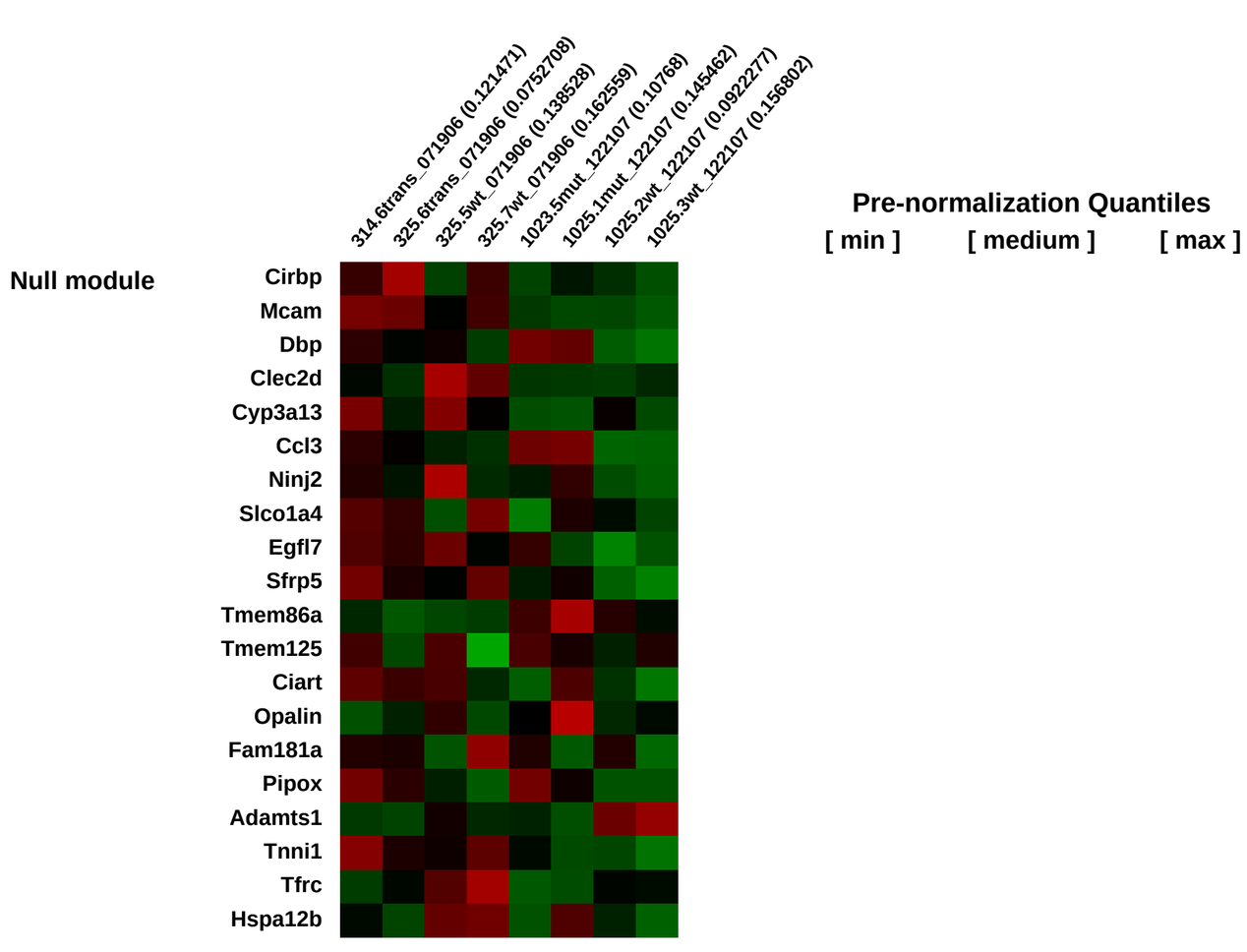

GEO Series "GSE12134" Expression Profiles

Num of samples in this series: 12

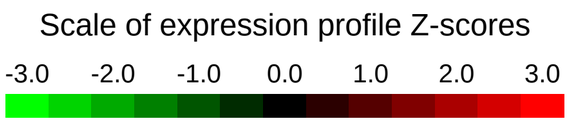

GEO Link:	http://www.ncbi.nlm.nih.gov/geo/query/acc.cgi?acc=GSE12134
Status:	Public on Sep 22 2009
Title:	The transcription factor AP2‚ ‡ regulates the number of basal progenitors
Organism:	Mus musculus
Experiment type:	Expression profiling by array
Platform:	GPL1261
Pubmed ID:	19749747
Summary & Design:	**Summary:** Understanding the mechanisms that specify neuronal subtypes is important to unravel the complex mechanisms of neuronal circuit assembly. Here we have identified a novel role for the transcription factor AP2‚ ‡ in progenitor and neuronal subtype specification in the cerebral cortex. Conditional deletion of AP2‚ ‡ causes misspecification of basal progenitors starting at mid-neurogenesis and gain-of-function experiments show that AP2‚ ‡ directly regulates the expression of several genes characteristic for basal progenitors, such as Math3 and Tbr2. The misspecification of basal progenitors upon loss of AP2‚ ‡ resulted in their increased death and the ultimate reduction of callosal layer II/III projection neurons. This had pronounced effects on visual performance with a strong reduction of visual acuity. Thus, we have identified a novel regulator of basal progenitor fate regulating the number of layer II/III neurons in an area-specific manner and revealing their importance for accurate function of the visual cortex. **Overall design:** We analysed 12 samples from the cortex (rostral and caudal) of AP2gamma k.o. mice and control mice. For each of the 4 groups (caudal ko, caudal wt, rostral ko, rostral wt) three biological replicates were analysed.

Background corr dist: KL-Divergence = 0.1625, L1-Distance = 0.0407, L2-Distance = 0.0034, Normal std = 0.3602

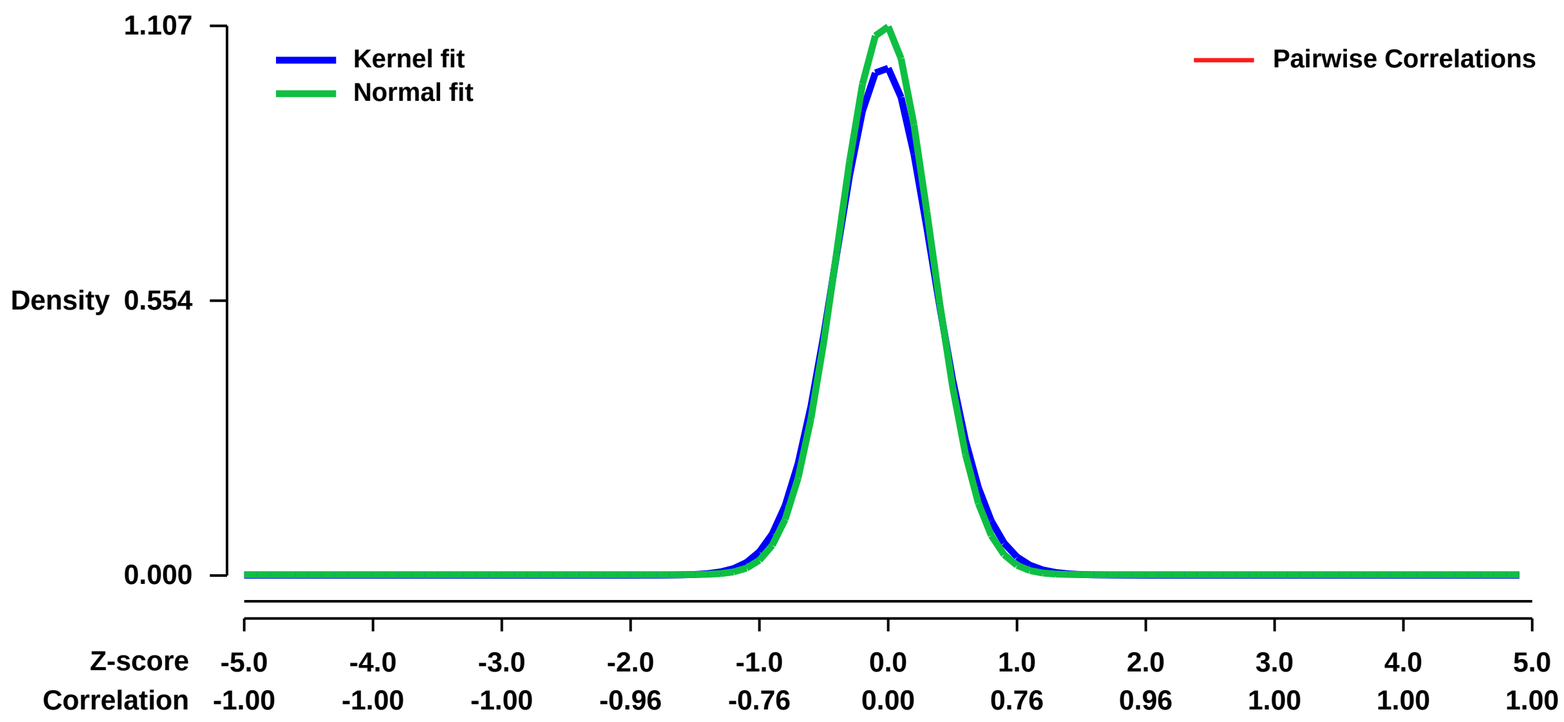

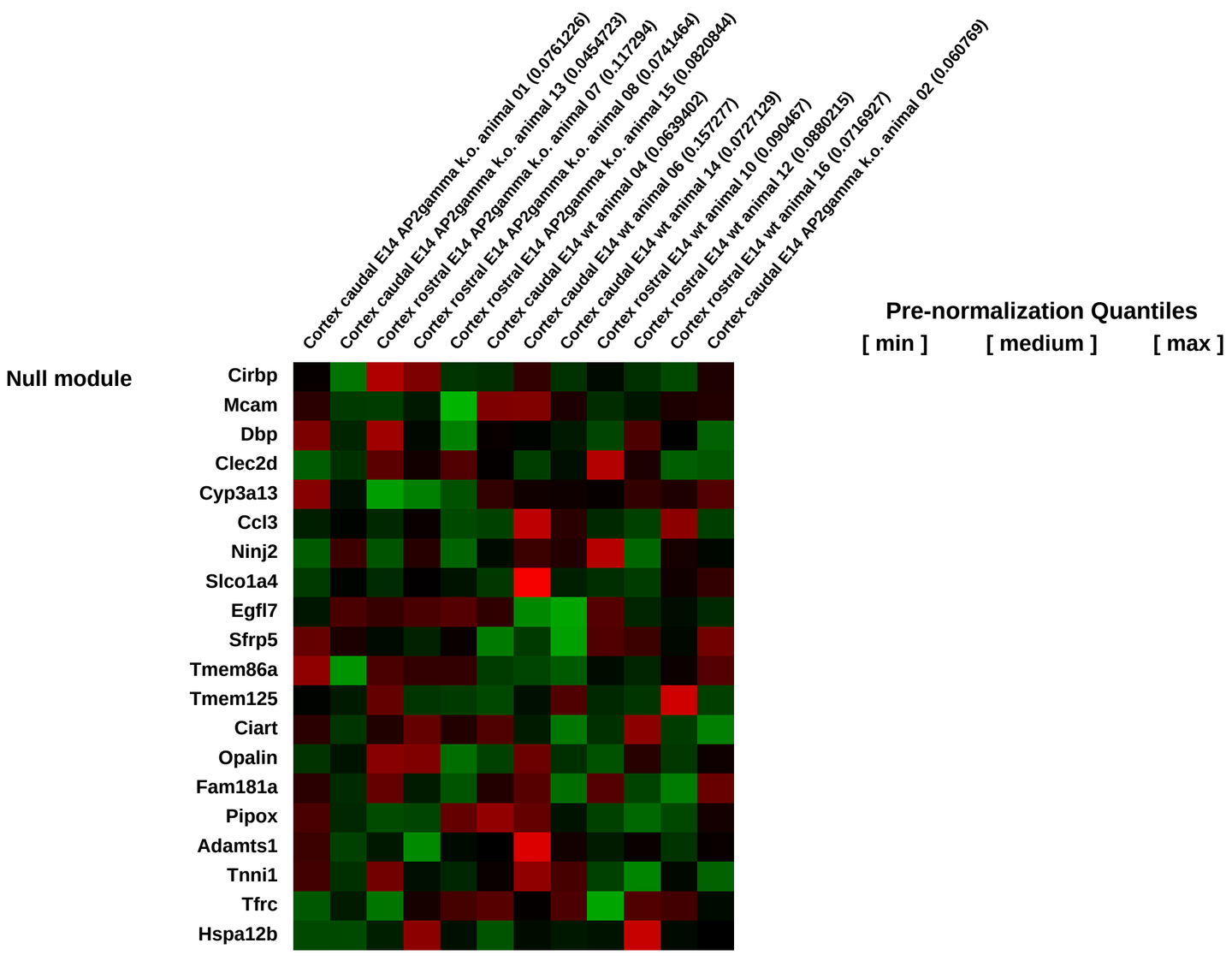

GEO Series "GSE20390" Expression Profiles

Num of samples in this series: 6

Scale of expression profile Z-scores

-3.0 -2.0 -1.0 0.0 1.0 2.0 3.0

GEO Link:	http://www.ncbi.nlm.nih.gov/geo/query/acc.cgi?acc=GSE20390
Status:	Public on Jul 07 2010
Title:	Deficiency in the 15 kDa Selenoprotein Inhibits Tumorigenicity and Metastasis of Colon Cancer Cells
Organism:	Mus musculus
Experiment type:	Expression profiling by array
Platform:	GPL1261
Pubmed ID:	20388823
Summary & Design:	**Summary:** Selenium has cancer preventive activity that is mediated, in part, through selenoproteins. The role of the 15 kDa selenoprotein (Sep15) in colon cancer was assessed by preparing and using mouse colon CT26 cells stably transfected with shRNA constructs targeting Sep15. Metabolic 75Se-labeling and Northern and Western blot analyses revealed that more than 90% of Sep15 was knocked down. Growth of the resulting Sep15-deficient CT26 cells was reduced (p<0.01) and cells formed significantly (p<0.001) fewer colonies in soft agar compared to control CT26 cells. Whereas most (14/15) BALB/c mice injected with control cells developed tumors, few (3/30) mice injected with Sep15 knockdown cells developed tumors (p<0.0001). The ability to form pulmonary metastases had similar results. Mice injected with the plasmid-transfected control cells had >250 lung metastases/mouse; however, mice injected with the Sep15 knockdown cells only had 7.8 +/- 5.4 metastases. To investigate molecular targets affected by Sep15 status, gene expression patterns between control and knockdown CT26 cells were compared. Ingenuity Pathways Analysis was used to analyze the 1045 genes that were significantly (p<0.001) affected by Sep15 deficiency. The highest scored biological functions were cancer and cellular growth and proliferation. Consistent with these observations, subsequent analyses revealed a G2/M cell cycle arrest in Sep15 CT26 knockdown cells. In contrast, to CT26 cells Sep15 knockdown in Lewis Lung Carcinoma (LLC1) cells did not affect anchorage-dependent or â independent cell growth. These data suggest tissue specificity in the cancer protective effects of Sep15 knockdown, which are mediated, at least in part, by influencing the cell cycle. **Overall design:** mRNA was isolated from plasmid-transfected control and shSep15 knockdown CT26 cells (three replicates of each). Microarray analysis was performed on Affymetrix Mouse 430_2 gene chips. Three arrays were analyzed from different mRNA samples for each construct.

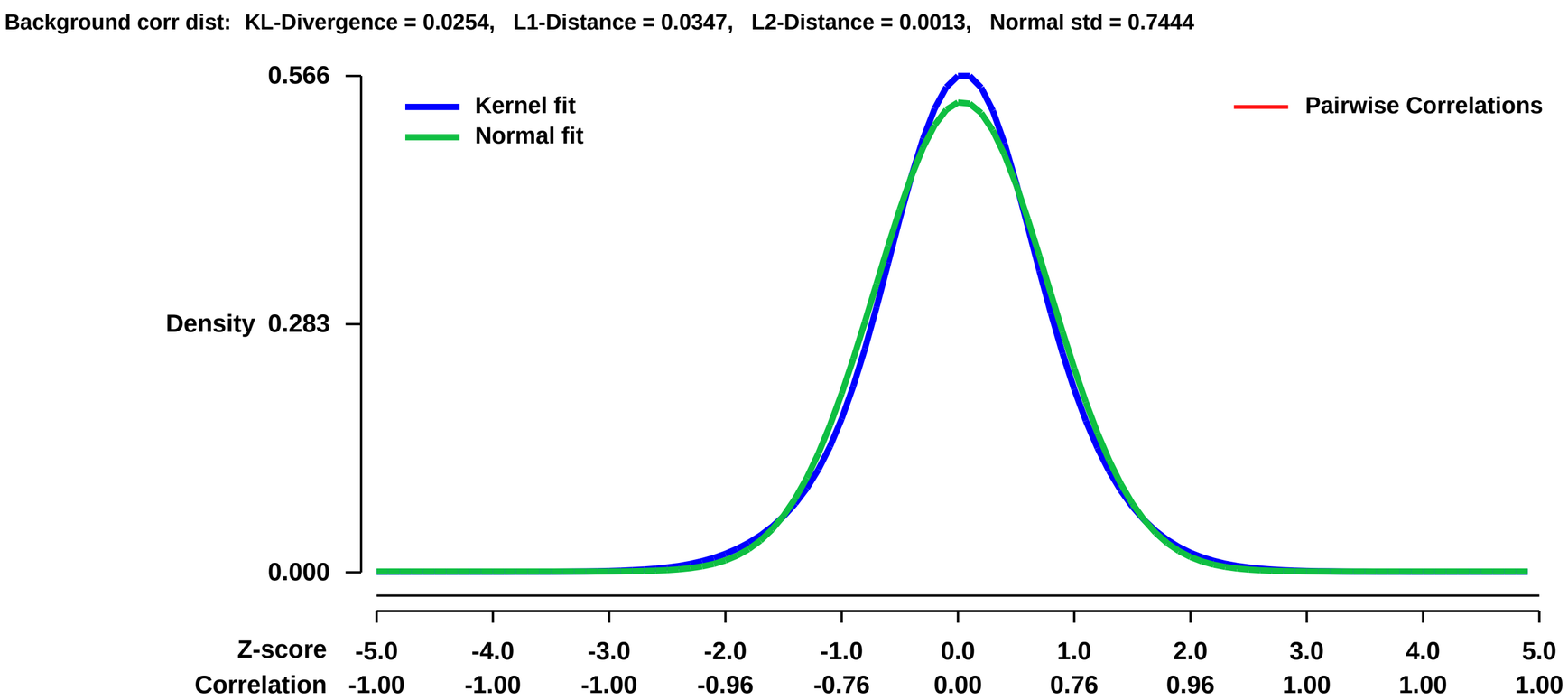

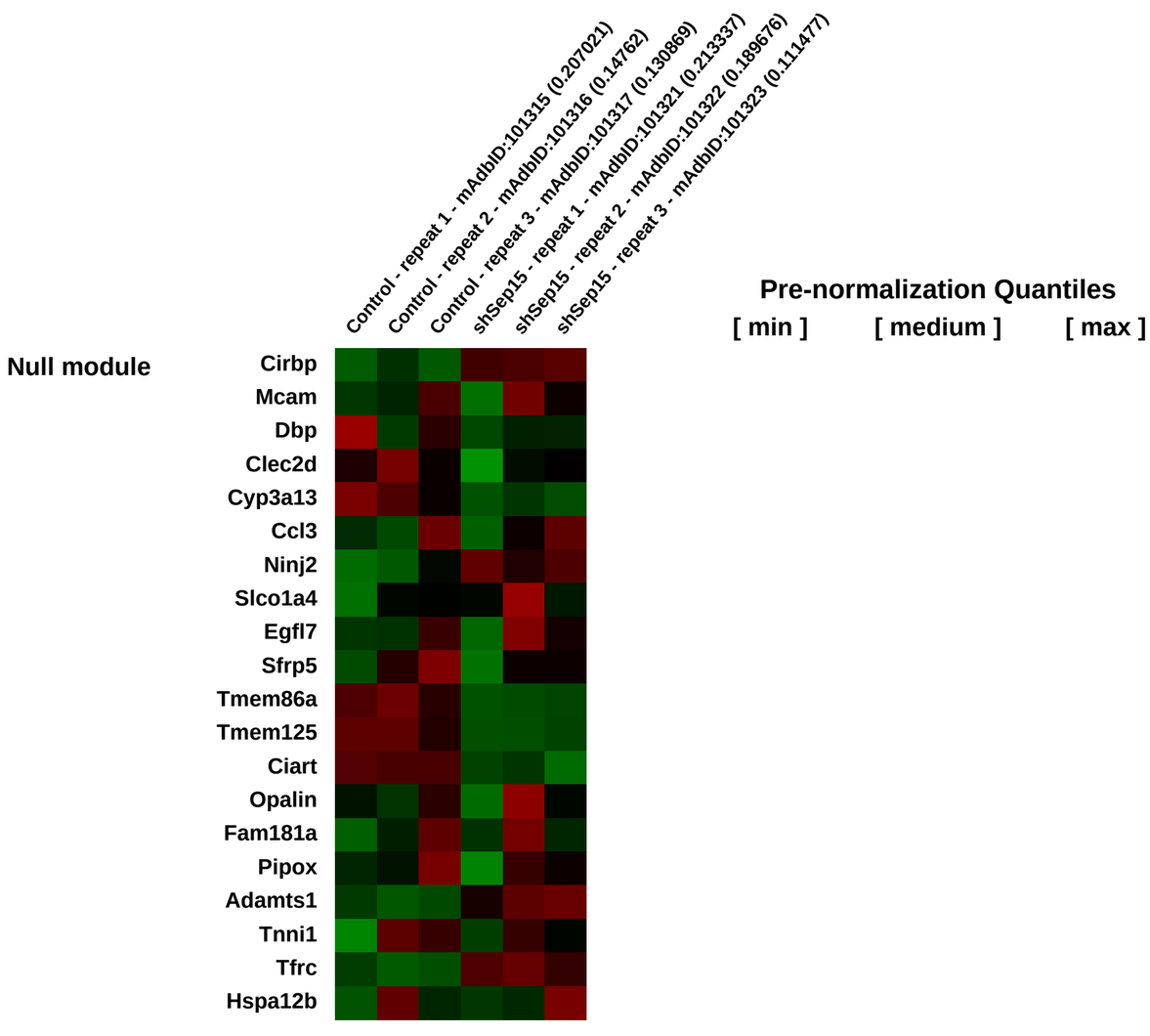

GEO Series "GSE46088" Expression Profiles

Num of samples in this series: 8

Scale of expression profile Z-scores

-3.0 -2.0 -1.0 0.0 1.0 2.0 3.0

GEO Link:	http://www.ncbi.nlm.nih.gov/geo/query/acc.cgi?acc=GSE46088
Status:	Public on Apr 17 2013
Title:	Ikaros responsive genes in the T29 cell line
Organism:	Mus musculus
Experiment type:	Expression profiling by array
Platform:	GPL1261
Pubmed ID:	24643801
Summary & Design:	**Summary:** The mouse Ikaros-deficient thymic lymphoma cell line T29 was transduced with an empty retrovirus (MigR1) or a retrovirus expressing an fusion proein between Ikaros1 and the ligand binding domain of the estrogen receptor. Cells trreated with ethanol or 4-hydroxy-tamoxyfen (4OHT) for 24h were profiled. **Overall design:** We used expression of an inducible ersion of the Ikaros protein in an Ikaros-deficient cell line to identify Ikaros-regulated genes

Background corr dist: KL-Divergence = 0.0639, L1-Distance = 0.0176, L2-Distance = 0.0003, Normal std = 0.5178

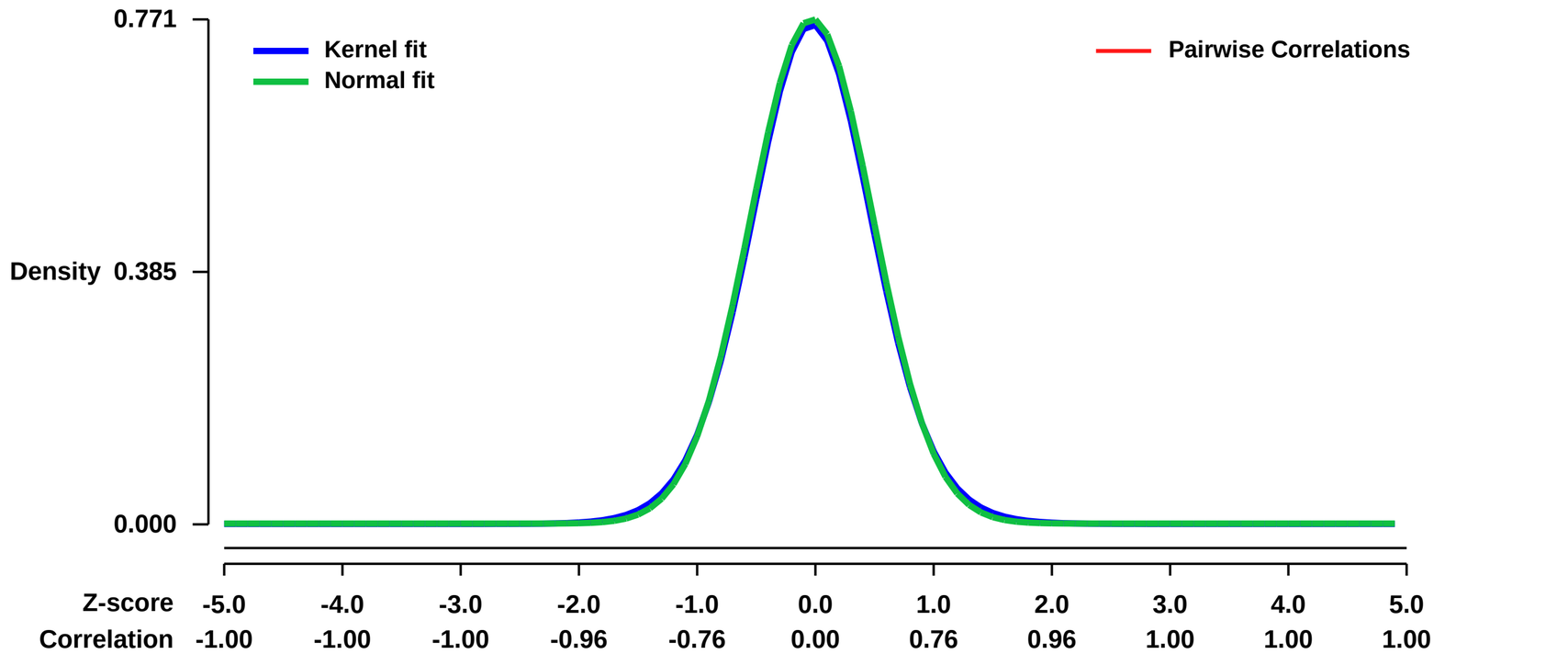

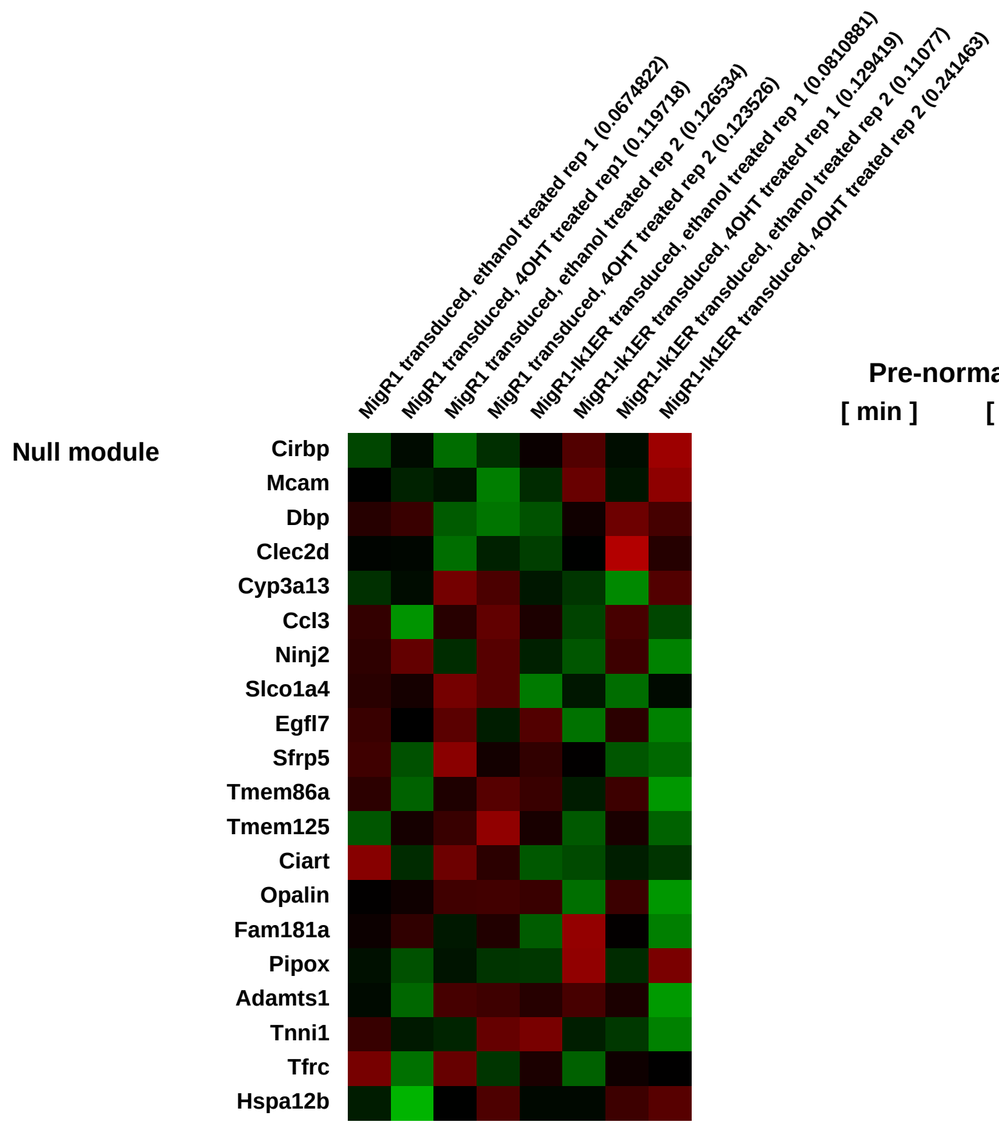

GEO Series "GSE13874" Expression Profiles

Num of samples in this series: 14

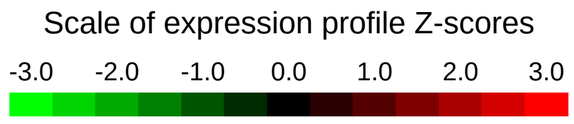

GEO Link:	http://www.ncbi.nlm.nih.gov/geo/query/acc.cgi?acc=GSE13874
Status:	Public on Mar 05 2009
Title:	microRNA-1 negatively regulates expression of the hypertrophy-associated genes calmodulin and Mef2a
Organism:	Mus musculus
Experiment type:	Non-coding RNA profiling by array
Platform:	GPL1261
Pubmed ID:	19188439
Summary & Design:	**Summary:** Calcium signaling is a central regulator of cardiomyocyte growth and function. Calmodulin is a critical mediator of calcium signals. Because the amount of calmodulin within cardiomyocytes is limiting, precise regulation of calmodulin expression may be an important for regulation of calcium signaling. In this study, we show for the first time that calmodulin levels are regulated post-transcriptionally in heart failure. The cardiomyocyte-restricted microRNA miR-1 inhibited translation of calmodulin-encoding mRNAs via highly conserved target sites within their 3â -untranslated regions. In keeping with its effect on calmodulin expression, miR-1 downregulated calcium-calmodulin signaling through the calcineurin to NFAT. miR-1 also negatively regulated expression of Mef2a and Gata4, key transcription factors that mediate calcium-dependent changes in gene expression. Consistent with downregulation of these hypertrophy-associated genes, miR-1 attenuated cardiomyocyte hypertrophy in cultured neonatal rat cardiomyocytes and in the intact adult heart. Our data indicate that miR-1 regulates cardiomyocyte growth responses by negatively regulating the calcium-signaling components calmodulin, Mef2a, and Gata4. **Overall design:** We show that miR-1 is downregulated in a murine heart failure model. miRNAs expression changes were measured in calcineurin transgenic model of heart failure and control mice using a Luminex platform. Reduced miR-1 expression was associated with broad alteration in expression of predicted target genes. To test this, we measured miRs including miR-1 and genome wide transcriptome changes in vivo and in vitro system. Calcineurin transgenic heart was compared to nontransgenic heart (NTg vs. CNTg). We also investigated the gene expression changes during the course of cardiomyocytes differentiation using DMSO treated P19CL6 cell lines. Two time points (day 6 and day 10) were compared to identified the gene expression changes of predicted miR-1 targets (Day 6 vs. Day 10).

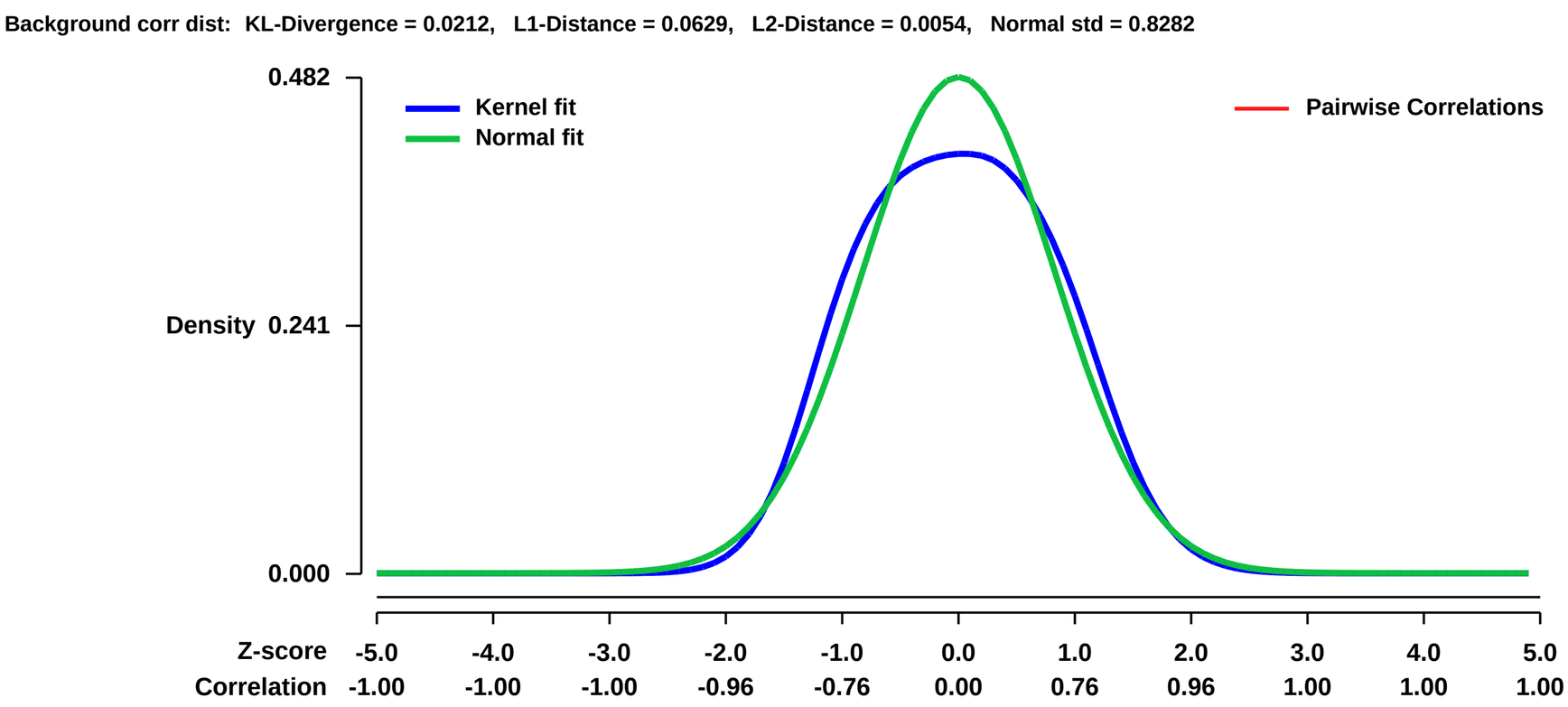

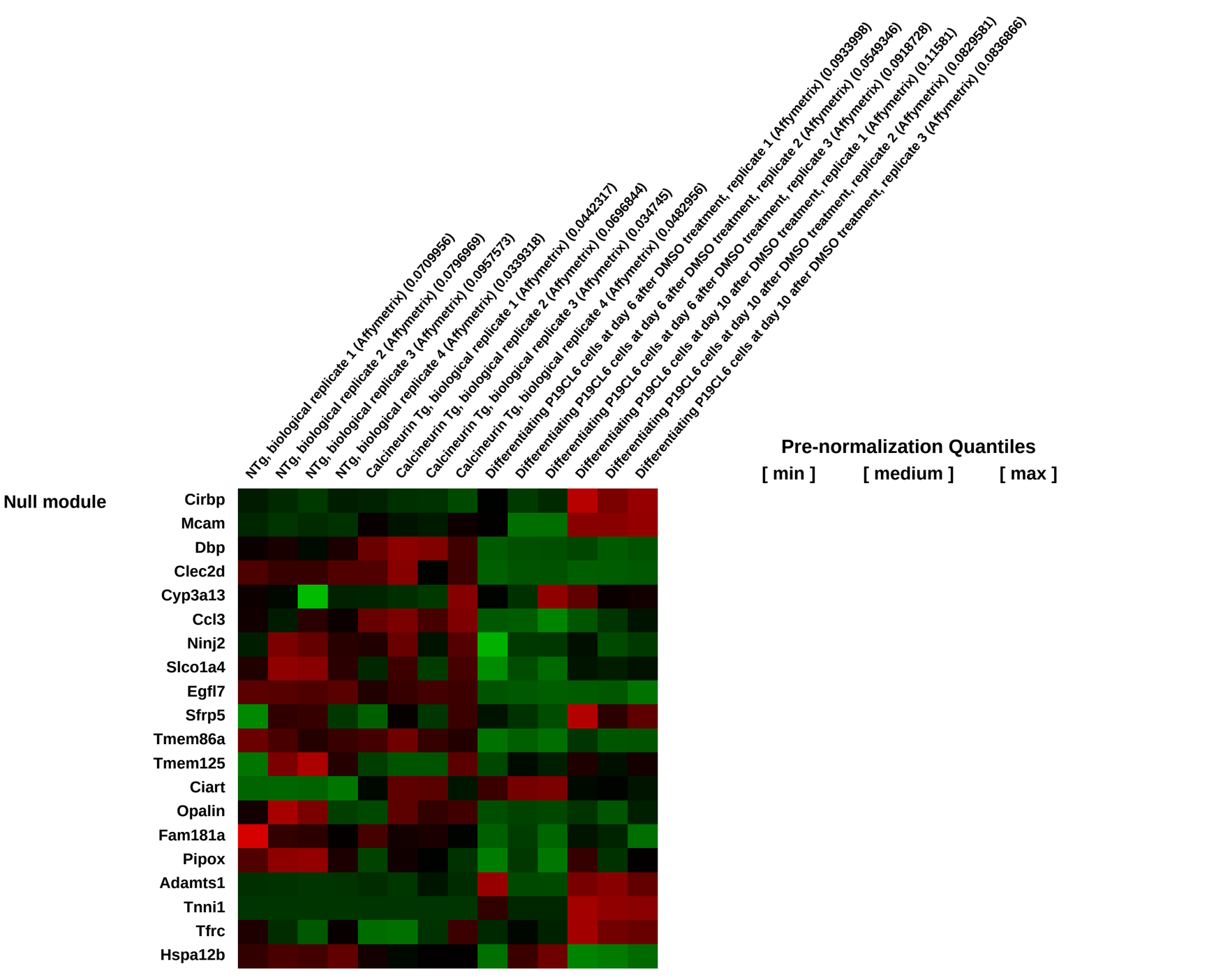

GEO Series "GSE49283" Expression Profiles

Num of samples in this series: 12

Scale of expression profile Z-scores

-3.0 -2.0 -1.0 0.0 1.0 2.0 3.0

GEO Link:	http://www.ncbi.nlm.nih.gov/geo/query/acc.cgi?acc=GSE49283
Status:	Public on Jul 27 2013
Title:	Translational activation of developmental mRNAs during neonatal mouse testis development
Organism:	Mus musculus
Experiment type:	Expression profiling by array
Platform:	GPL1261
Pubmed ID:	23926285
Summary & Design:	**Summary:** The sequence of gene regulatory events that drive neonatal germ cell development in the mammalian testis is not yet clear. We assessed changes in mRNA utilization in the neonatal testis at 1 and 4 dpp, times when the testis contains quiescent gonocytes (1 dpp) and proliferating spermatogonia (4 dpp). There are not thought to be major changes in the nature or number of somatic cells over that interval. We used microarrays to detail the global expression levels of mRNA distribution between non-translating mRNAs and efficiently translating mRNAs during testis development at 1 dpp and 4 dpp **Overall design:** Extracts of mouse testes from 1 dpp and 4 dpp CD-1 mice were fractionated over a sucrose gradient in triplicate. Gradients were fractionated using an ISCO gradient fractionation system equipped with a UA-6 detector. The position of the 80S peak defined the boundary between translating and non-translating mRNAs. Pooled non-polysomal (non-translating; fractions 1-3) and heavy polysomal (efficiently translating, fractions 7-13) RNAs were isolated from sucrose gradient fractions for hybridization on Affymetrix 420 2.0 microarrays.

Background corr dist: KL-Divergence = 0.0491, L1-Distance = 0.0591, L2-Distance = 0.0063, Normal std = 0.5856

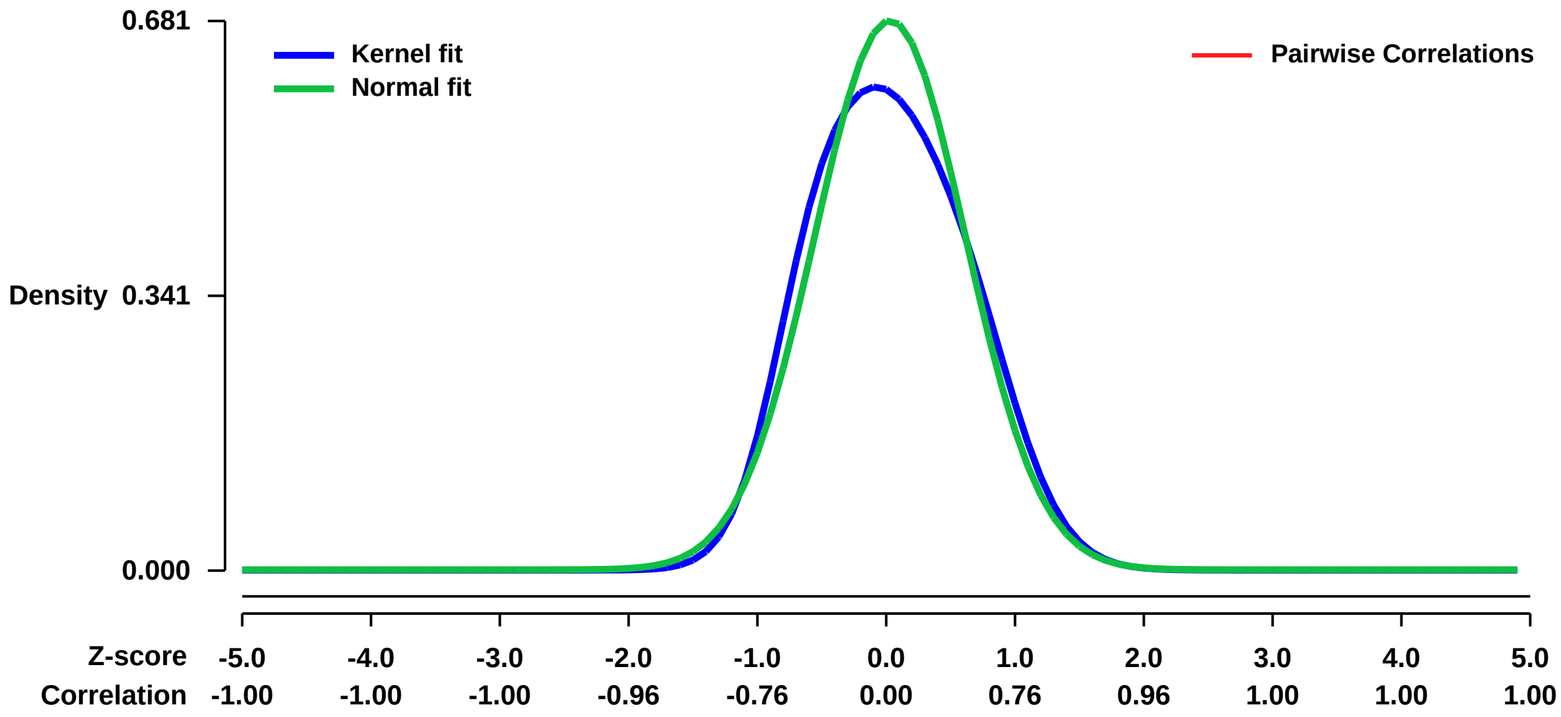

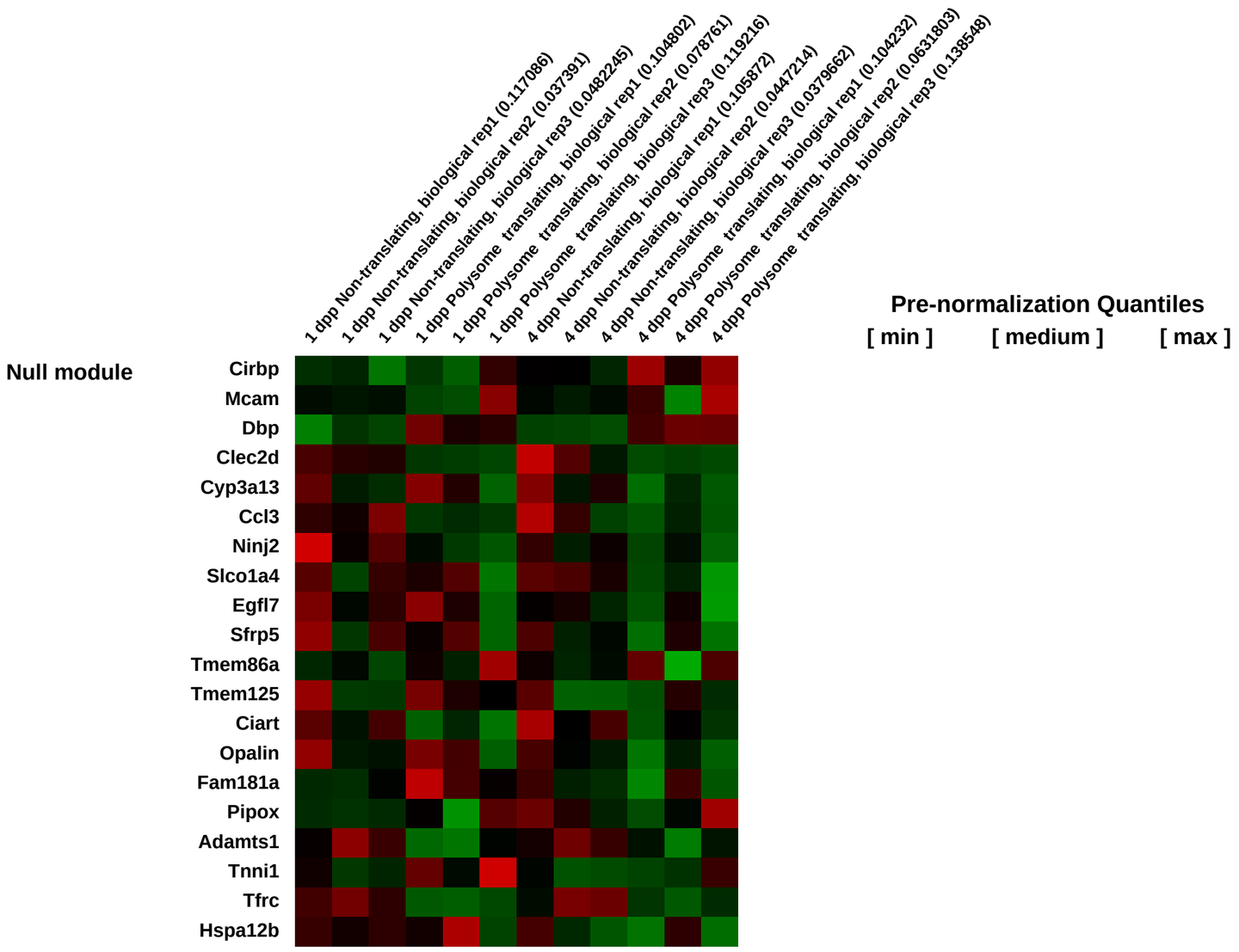

GEO Series "GSE1986" Expression Profiles

Num of samples in this series: 17

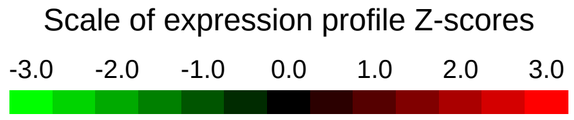

GEO Link:	**http://www.ncbi.nlm.nih.gov/geo/query/acc.cgi?acc=GSE1986**
Status:	**Public on Feb 23 2007**
Title:	**Global gene expression across a range of tissues**
Organism:	**Mus musculus**
Experiment type:	**Expression profiling by array**
Platform:	**GPL1261**
Pubmed ID:	
Summary & Design:	**Summary:** **The aim of this study is to survey global gene expression across a range of mouse tissues. Biotinylated cRNA was synthesized from total RNA, then fragmented and hybridized to Affymetrix Mouse Genome 430 2.0 GeneChip arrays at the Siteman Cancer Center Gene Chip Core Facility (Washington University, St Louis, Missouri) according to manufacturer's protocols. Image files were generated using MicroArray Suite 5.0 (Affymetrix).** **Keywords: other** **Overall design:**

Background corr dist: **KL-Divergence = 0.2441, L1-Distance = 0.0808, L2-Distance = 0.0181, Normal std = 0.3425**

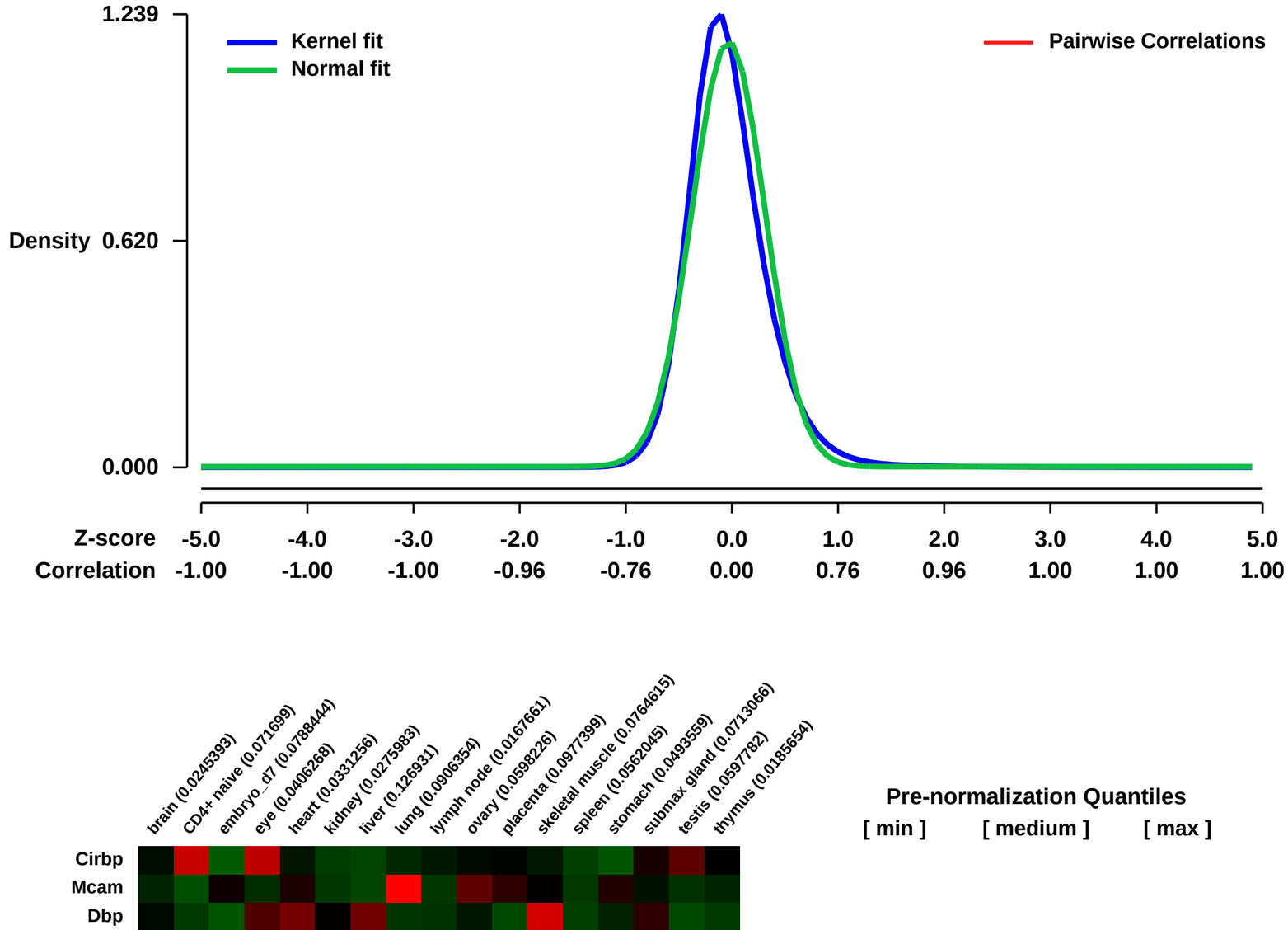

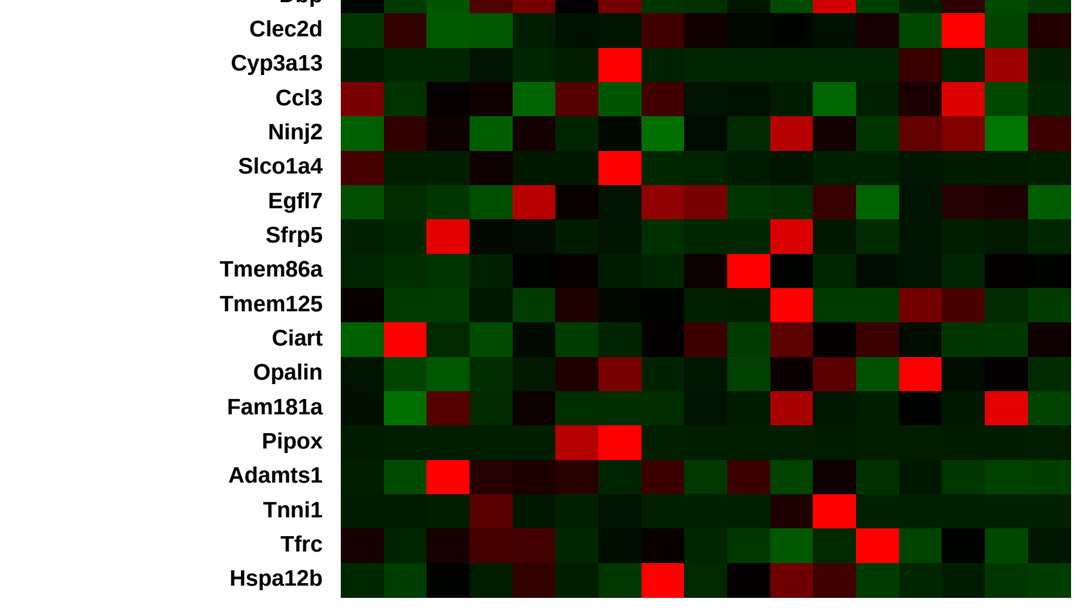

GEO Series "GSE52101" Expression Profiles

Num of samples in this series: 17

Scale of expression profile Z-scores

-3.0 -2.0 -1.0 0.0 1.0 2.0 3.0

GEO Link:	**http://www.ncbi.nlm.nih.gov/geo/query/acc.cgi?acc=GSE52101**
Status:	**Public on Dec 17 2013**
Title:	**Transcript abundance comparison between BALB/c ears inoculated with Leishmania mexicana and Leishmania mexicana plus promastigote secretory gel (PSG)**
Organism:	**Mus musculus**
Experiment type:	**Expression profiling by array**
Platform:	**GPL1261**
Pubmed ID:	
Summary & Design:	**Summary:** **To determine the modulation of gene expression of Leishmania mexicana(M379)-inoculated BALB/c ears in the presence of promastigote secretory gel (PSG)** **Overall design:** **A genome-wide transcriptional analysis was performed by comparing the gene expression profiles of Leishmania mexicana- inoculated BALB/c ears and Leishmania mexicana plus PSG BALB/c ears. Leishmania mexicana amastigotes were purified from mouse cutaneous lesions and transformed in vitro in metacycic promastigotes (MT). After 6, 24 and 48 hours, ears were collected and processed for RNA extraction. Three Biological replicates per condition were run.**

Background corr dist: **KL-Divergence = 0.0239, L1-Distance = 0.0741, L2-Distance = 0.0075, Normal std = 0.9021**

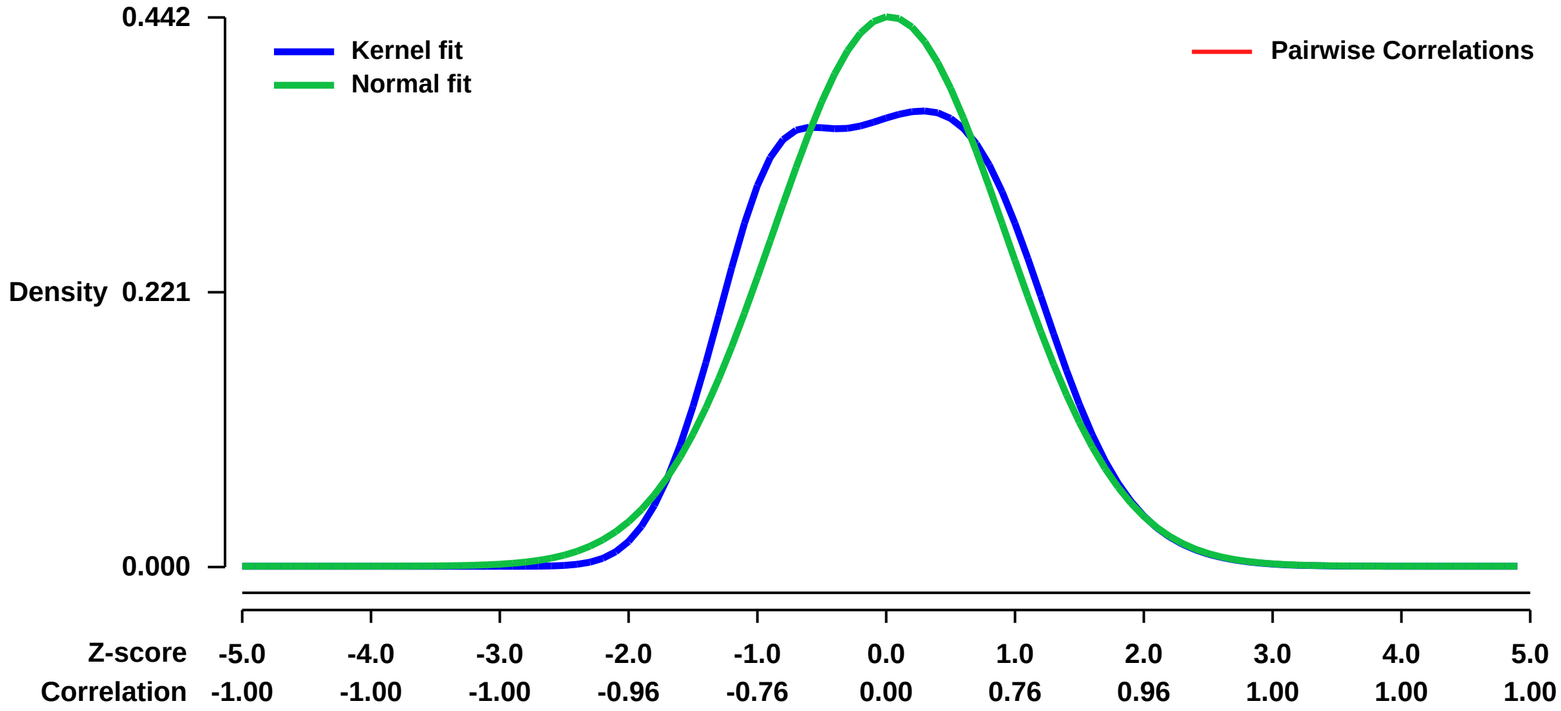

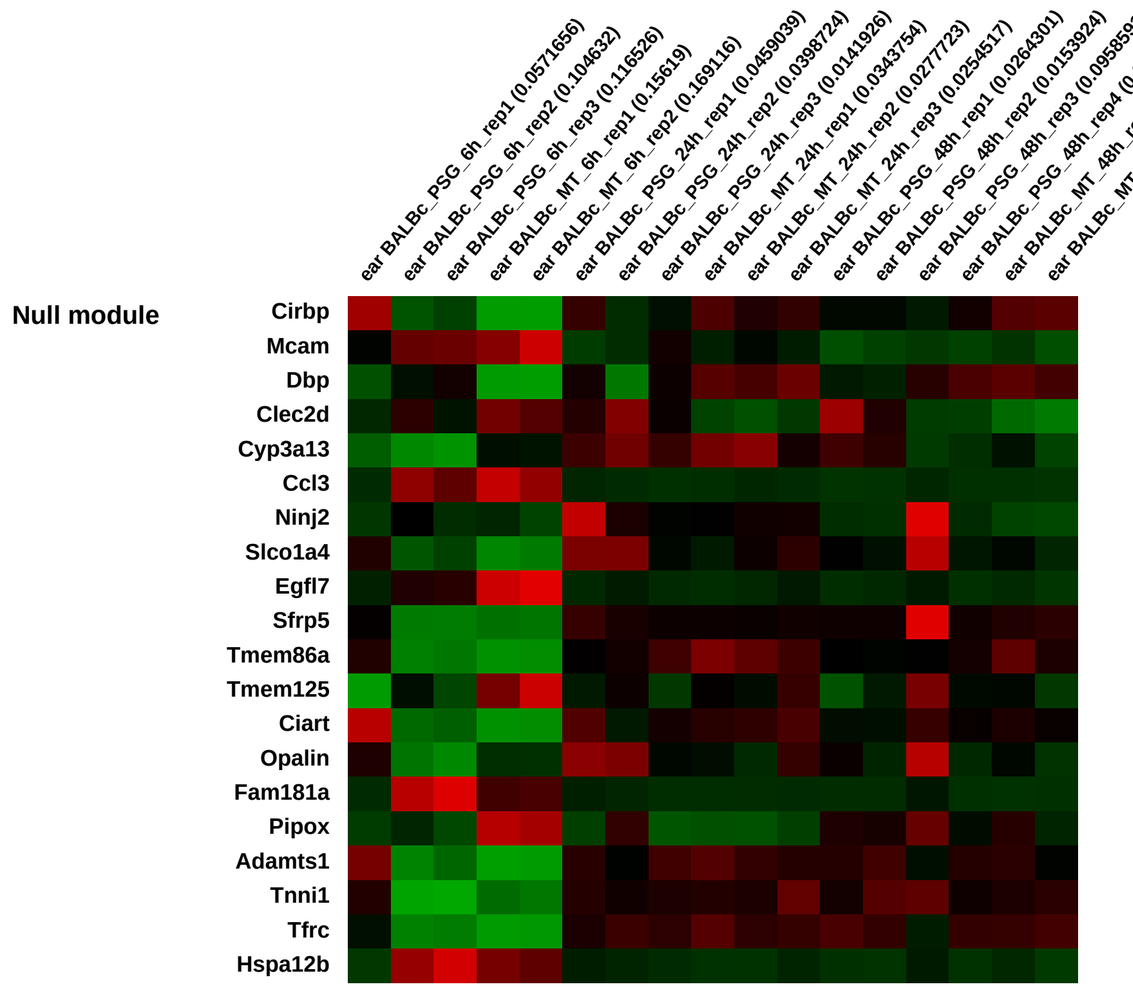

GEO Series "GSE22307" Expression Profiles

Num of samples in this series: 23

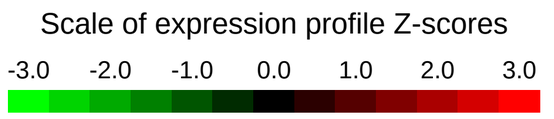

GEO Link:	http://www.ncbi.nlm.nih.gov/geo/query/acc.cgi?acc=GSE22307
Status:	Public on Oct 13 2010
Title:	Expression data from mouse colon tissue response to DSS induction at day 0, 2, 4 and 6
Organism:	Mus musculus
Experiment type:	Expression profiling by array
Platform:	GPL1261
Pubmed ID:	20923862
Summary & Design:	**Summary:** **Temporal genome profiling of DSS colitis** **The DSS induced mouse colitis model is often used to emulate Ulcerative Colitis (UC) in order understand pathophysiological mechanism of inflammatory bowel disease (IBD). Given the progressive nature of IBD, colon tissue gene expression changes during the evolution of disease, and knowing the changes in gene expression profiles could indentify potential diagnostic markers or additional therapeutic targets for colitis. Therefore, we performed temporal genome expression profiling analysis using the Affymetrix genome wide microarray system to identify broad scale changes in gene expression associated with the development of colitis.** **Keywords: Expression time course of mouse colon tissue induced by 3% DSS.** **Overall design:** **C57BL/6J mice were given 3% DSS in the drinking water and tissues from individual cohorts were collected at days 0, 2, 4 and 6. Total RNA were extracted from the colon tissue and detected by Affymerix GeneChip Mouse Genome 430 2.0 Array.**

Background corr dist: **KL-Divergence = 0.2821, L1-Distance = 0.0519, L2-Distance = 0.0064, Normal std = 0.2889**

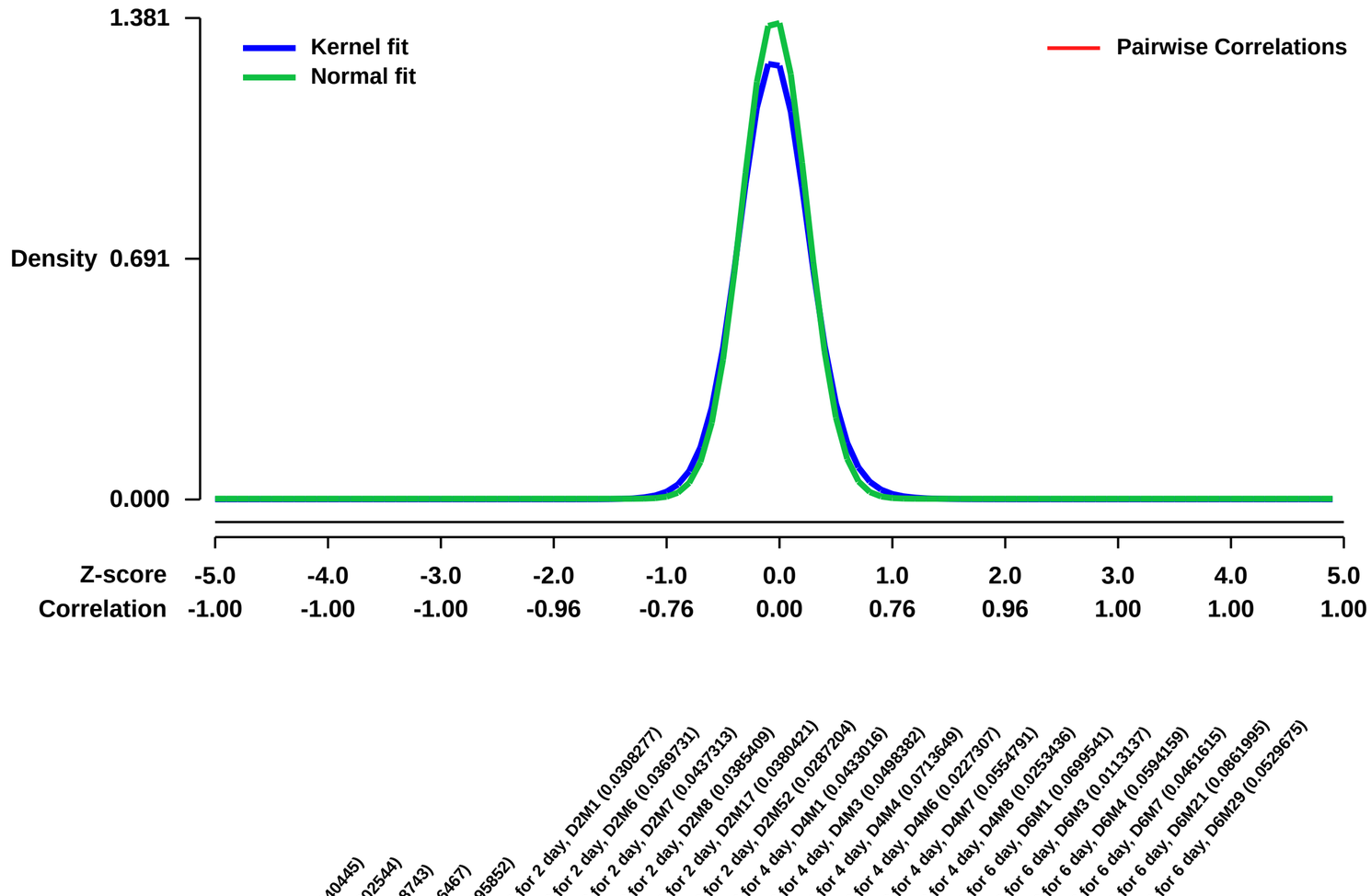

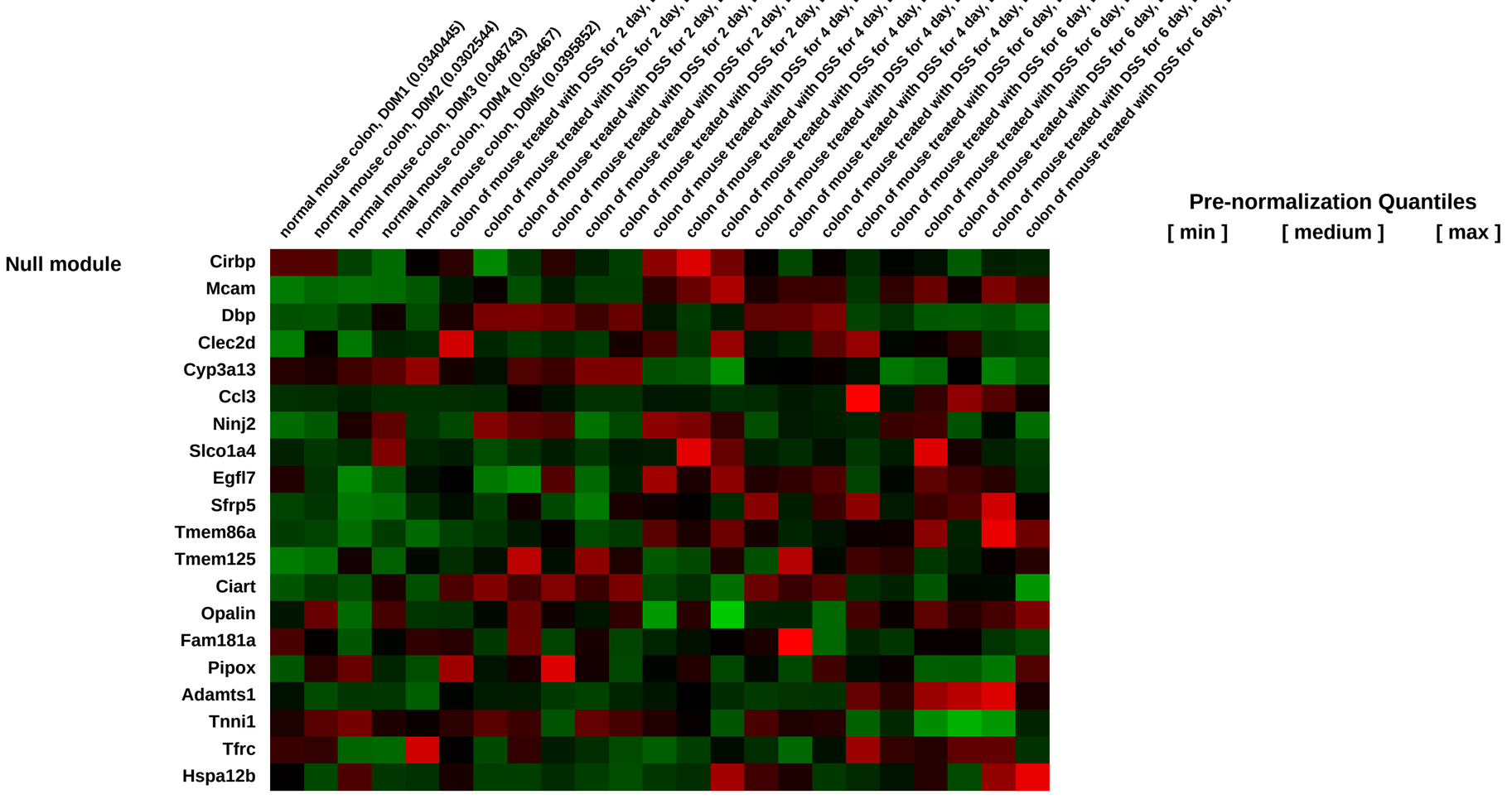

GEO Series "GSE21716" Expression Profiles

Num of samples in this series: 28

Scale of expression profile Z-scores

-3.0 -2.0 -1.0 0.0 1.0 2.0 3.0

GEO Link: http://www.ncbi.nlm.nih.gov/geo/query/acc.cgi?acc=GSE21716

Status: Public on Oct 01 2010

Title: Hepatic xenobiotic metabolizing enzyme gene expression through the life stages of the mouse

Organism: Mus musculus

Experiment type: Expression profiling by array

Platform: GPL1261

Pubmed ID:

Summary & Design:

Summary:
Using full-genome arrays, the expression of all XMEs was examined during fetal (gestation day (GD) 19), neonatal (postnatal day (PND) 7), prepubescent (PND30), middle age (12 mon), and old age (18 and 24 mon) in the C57Bl6/J mouse liver and compared to young adults. Fetal and neonatal life stages had a dramatic effect on XME expression compared to the relatively minor effects of old age. At all life stages except PND30 down-regulated genes outnumbered up-regulated genes. The altered XMEs included those in all of the major metabolic phases including phase I (alcohol and aldehyde dehydrogenase and Cyp genes), phase II (aldo-keto reductase, glutathione-S-transferases, sulfotransferases and UDP-glucuronosyl transferases) and phase III (transporters). We have generated a comprehensive catalog of XME hepatic gene changes through the life stages of the mouse that can be used to predict chemicals and chemical classes different life stages are more sensitive to. Some CEL files used in this study have been submitted through GSE21224.

Keywords: gene expression/microarray

Overall design:
We characterized gene expression changes in the developing mouse liver at gestational days (GD) 19), neonatal (postnatal day (PND) 7), prepubescent (PND30), middle age (12 mon), and old age (18 and 24 mon) in the C57Bl6/J mouse liver using full-genome microarrays and compared these changes to that in the adult liver.. We also compared results to GD19, PND32, and PND67 C3H mice. Total RNA was isolated from liver samples and gene expression analyzed using Affymetrix Mouse 430 2.0 GeneChips. Data from 28 samples, four mice in each of the age groups for C57BL/6 and C3H, were analyzed.

Background corr dist: KL-Divergence = 0.1189, L1-Distance = 0.0776, L2-Distance = 0.0143, Normal std = 0.4578

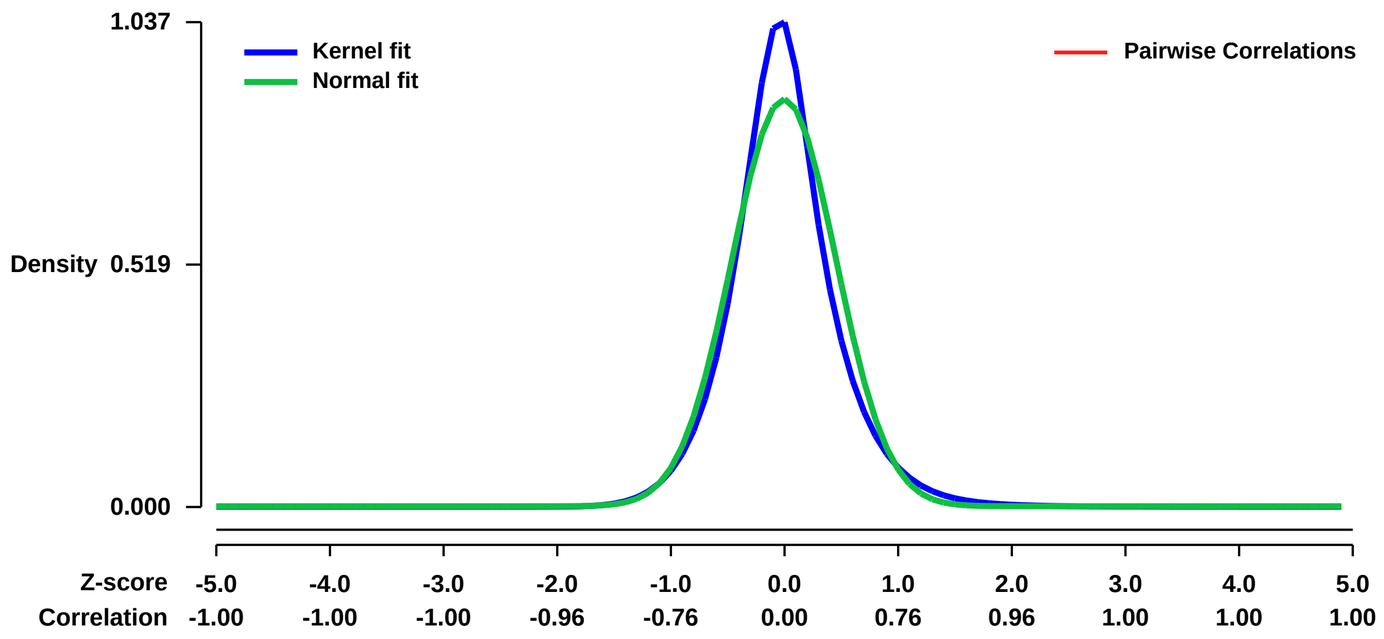

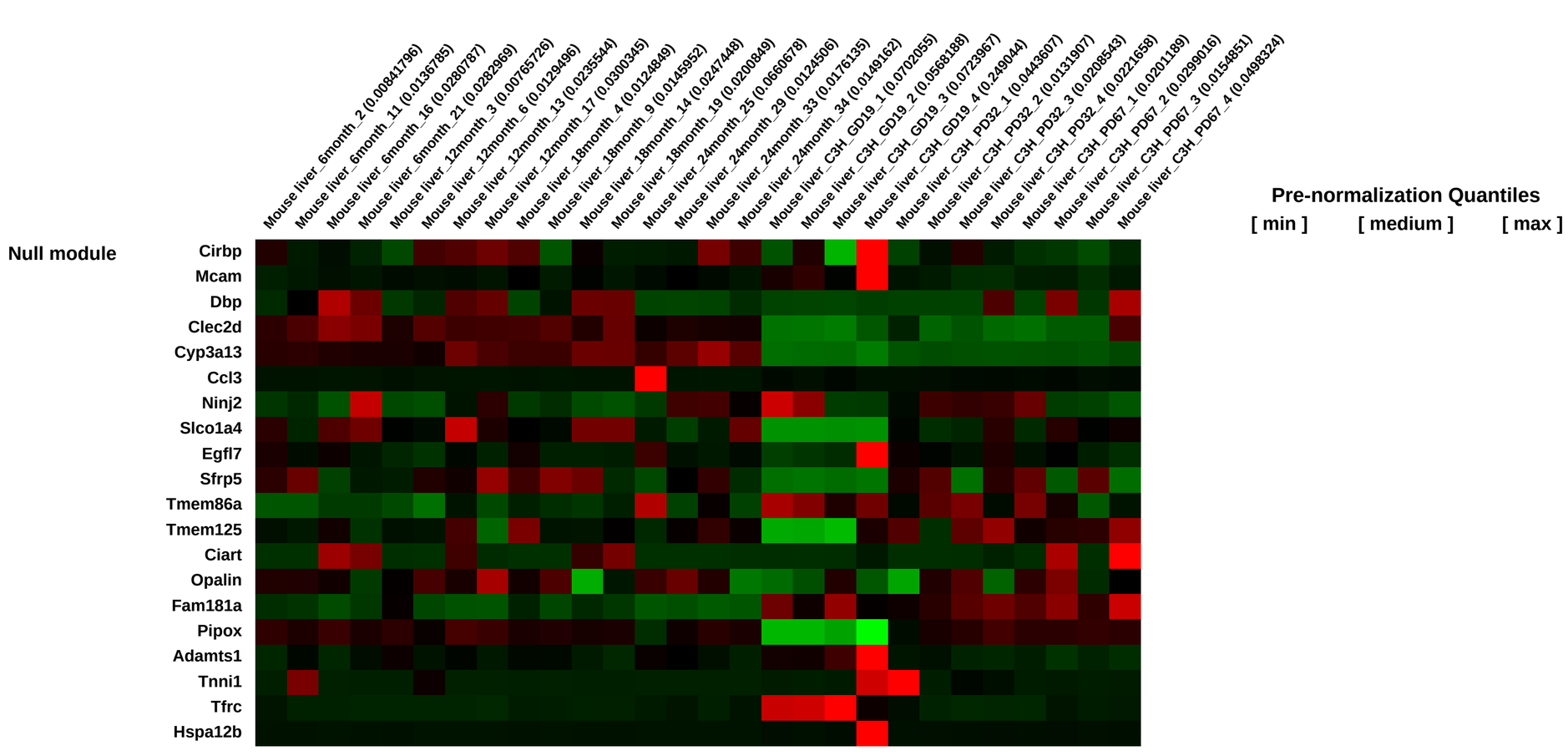

GEO Series "GSE27261" Expression Profiles

Num of samples in this series: 8

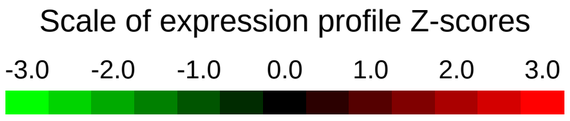

GEO Link:	**http://www.ncbi.nlm.nih.gov/geo/query/acc.cgi?acc=GSE27261**
Status:	**Public on Jul 29 2011**
Title:	**Dmrt1 (doublesex and mab-3 related transcription factor 1) conditional knockout expression analysis of P28 testes**
Organism:	**Mus musculus**
Experiment type:	**Expression profiling by array**
Platform:	**GPL1261**
Pubmed ID:	**21775990**
Summary & Design:	**Summary:** **Dmrt1 (doublesex and mab-3 related transcription factor 1) is a conserved transcriptional regulator of male differentiation required for testicular development in vertebrates. This study examines the result of conditional removal of Dmrt1 from Sertoli cells in P28 testis tissue.** **Overall design:** **Testes from P28 Dmrt1 flox/flox mice were compared to testes from P28 Dmrt1 flox/flox mice with the Sertoli cell-specific Sf1 (Nr5a1; MGI:1346833) or Dhh (MGI:94891) promoters driving Cre expression.**

Background corr dist: **KL-Divergence = 0.0110, L1-Distance = 0.0306, L2-Distance = 0.0011, Normal std = 0.9264**

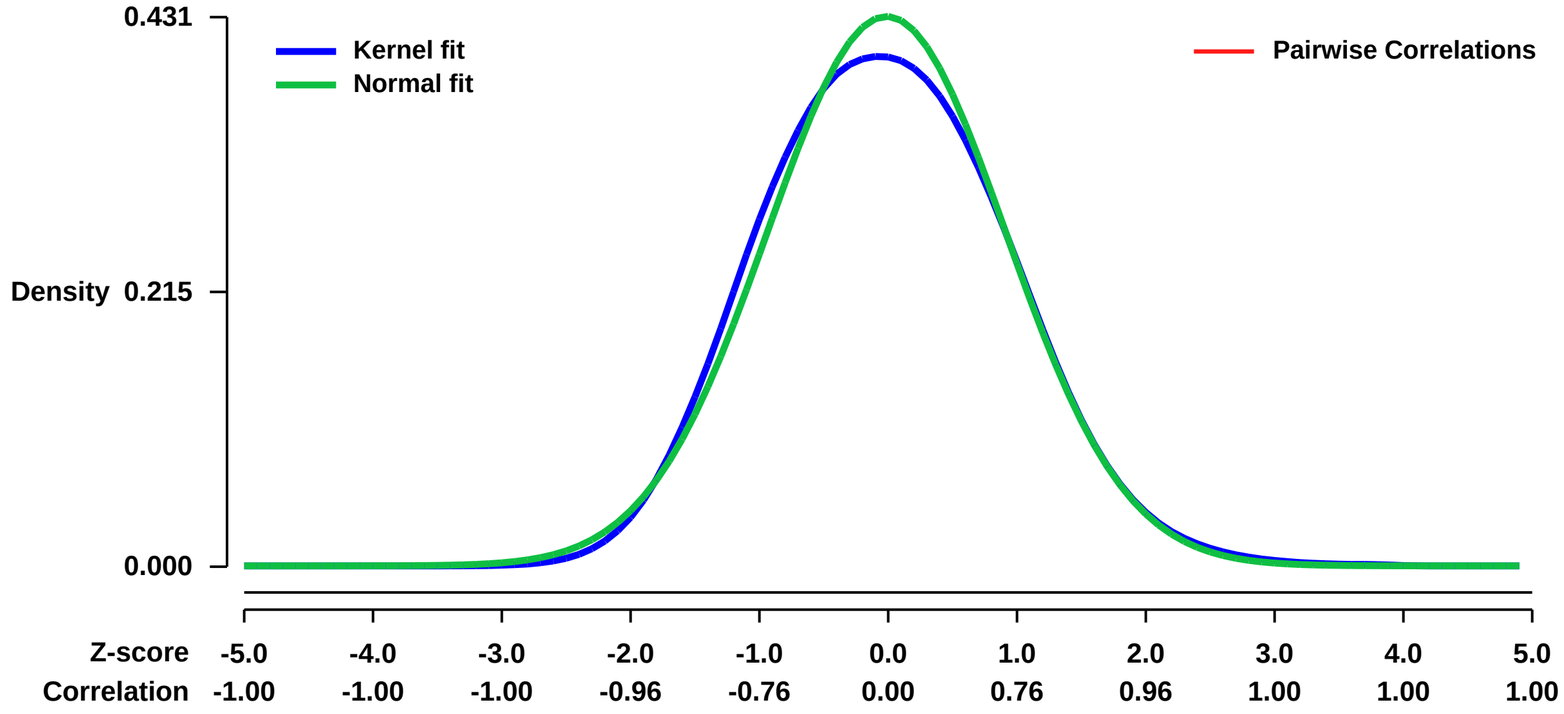

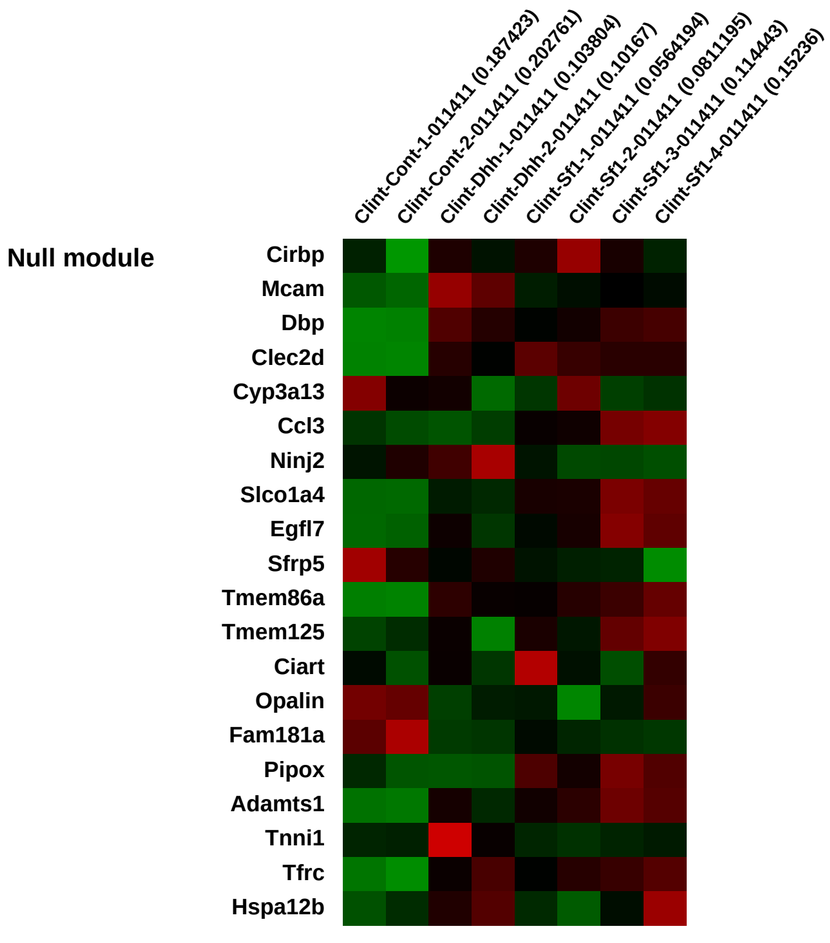

GEO Series "GSE9013" Expression Profiles

Num of samples in this series: 12

Scale of expression profile Z-scores

-3.0 -2.0 -1.0 0.0 1.0 2.0 3.0

GEO Link:	http://www.ncbi.nlm.nih.gov/geo/query/acc.cgi?acc=GSE9013
Status:	Public on Nov 12 2007
Title:	Expression data from side-population sorted putative intestinal stem cells.
Organism:	Mus musculus
Experiment type:	Expression profiling by array
Platform:	GPL1261
Pubmed ID:	18006601
Summary & Design:	**Summary:** While the existence of intestinal epithelial stem cells (IESCs) has been well established, their study has been limited due to the inability to isolate them. Previous work has utilized side population (SP) sorting of the murine small intestinal mucosa to isolate a viable fraction of cells enriched for putative IESCs. We have used microarray analyses to characterize the molecular features of this potential stem cell population. **Keywords: Comparitive gene expression analysis** **Overall design:** Fluorescence activated cell sorting of cells stained with Hoechst 33342 and FITC labeled anti-CD45 antibody was used to isolate CD45-/SP and CD45-/nSP cell fractions from mucosal specimens pooled from 3 mice. Intact jejunum specimens were collected prior to sorting. 4 sorts were completed. Therefore, 3 experimental groups were defined: CD45-/SP, CD45-/nSP and intact jejunum, each with 4 biological replicates. Total RNA was extracted from each experiment group for each sort, resulting in 12 specimens submitted for analysis using Affymetrix 430 2.0 Gene Chips.

Background corr dist: KL-Divergence = 0.0860, L1-Distance = 0.0298, L2-Distance = 0.0017, Normal std = 0.4720

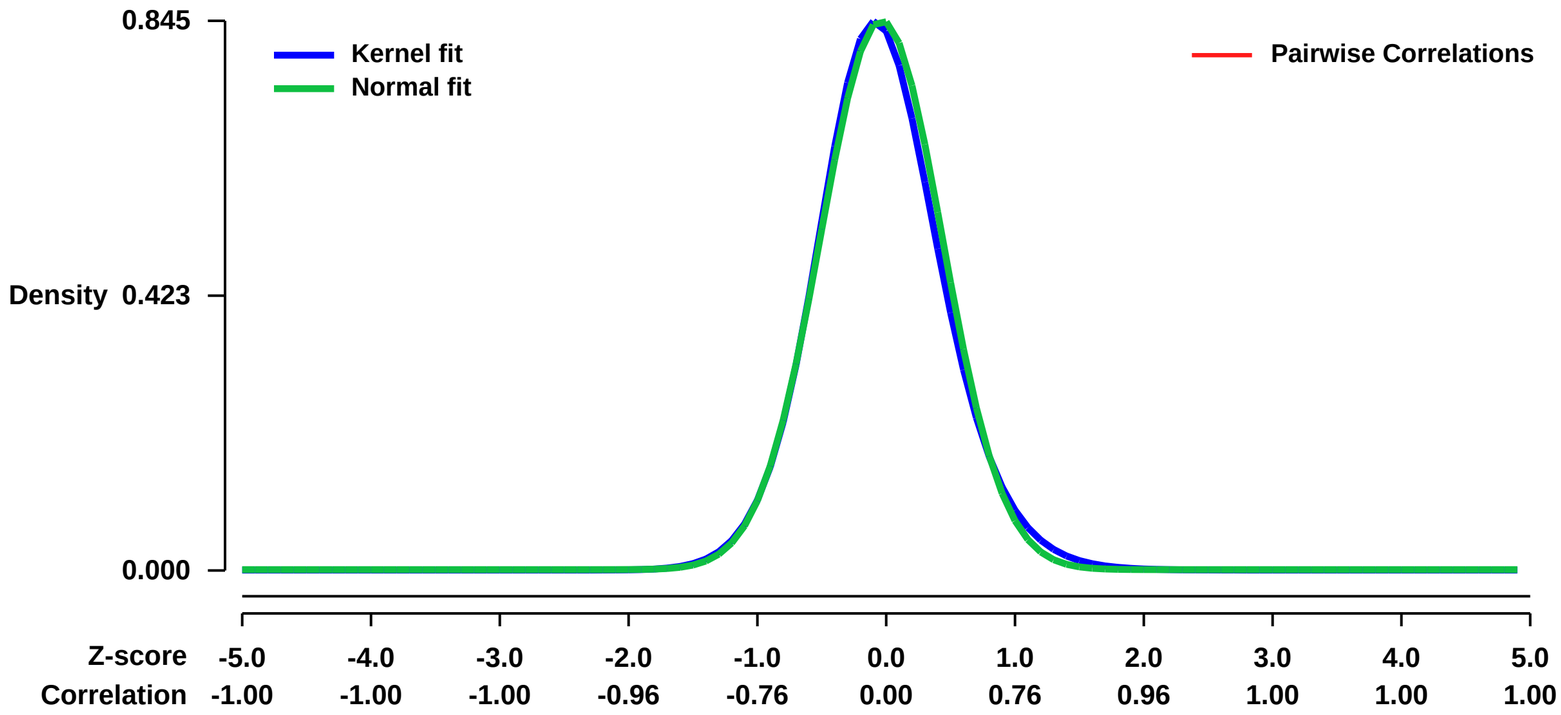

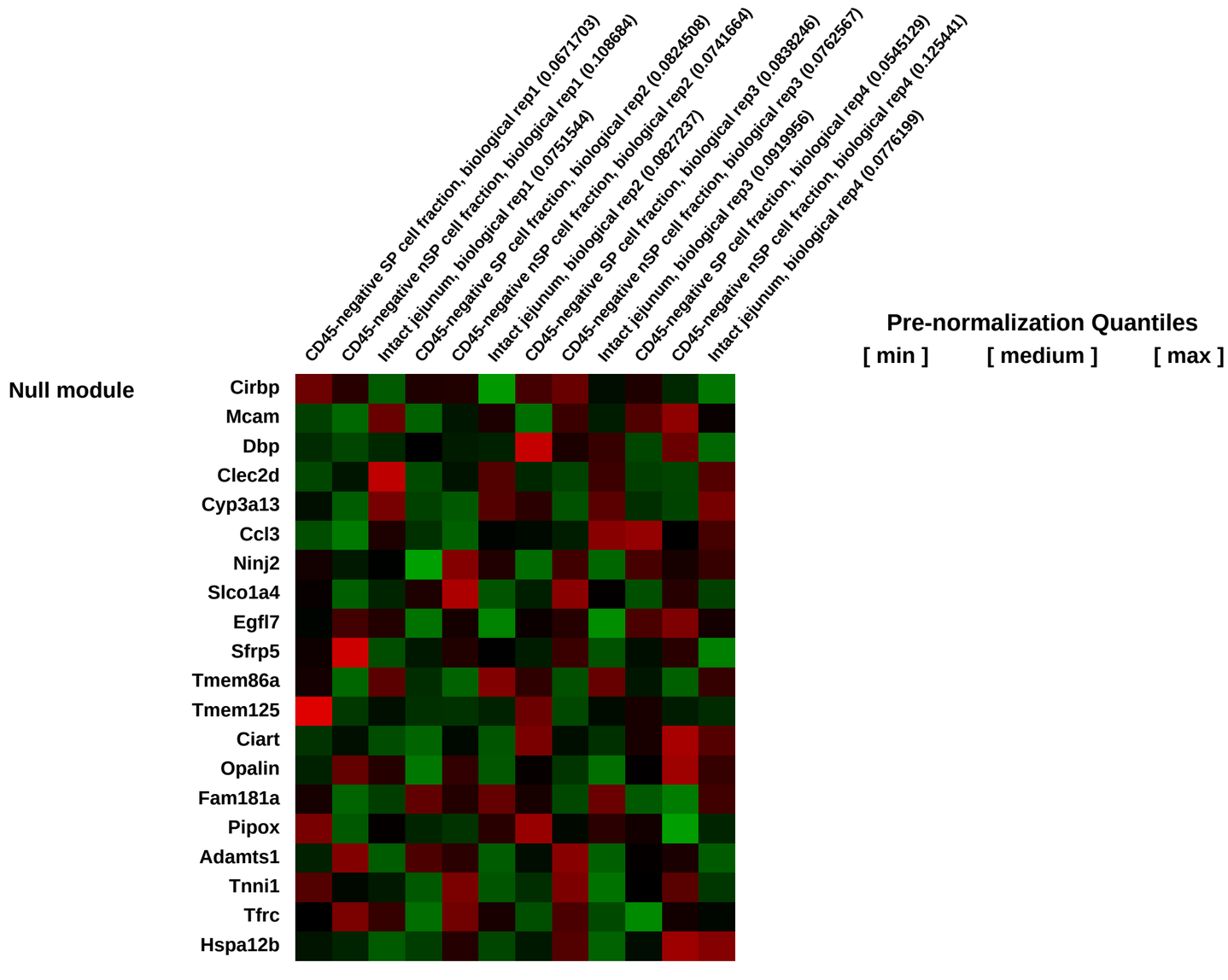

GEO Series "GSE12464" Expression Profiles

Num of samples in this series: 23

Scale of expression profile Z-scores

-3.0 -2.0 -1.0 0.0 1.0 2.0 3.0

GEO Link:	http://www.ncbi.nlm.nih.gov/geo/query/acc.cgi?acc=GSE12464
Status:	Public on May 20 2009
Title:	Transcriptional signatures of Itk-deficiency using CD3+ T-cells
Organism:	Mus musculus
Experiment type:	Expression profiling by array
Platform:	GPL1261
Pubmed ID:	19450280
Summary & Design:	**Summary:** The Tec-family kinase Itk plays an important role during T-cell activation and function, and controls also conventional versus innate-like T-cell development. We have characterized the transcriptome of Itk-deficient CD3+ T-cells, including CD4+ and CD8+ subsets, using Affymetrix microarrays. The largest difference between Itk-/- and Wt CD3+ T-cells was found in unstimulated cells, e.g. for killer cell lectin-like receptors. Compared to anti-CD3-stimulation, anti-CD3/CD28 significantly decreased the number of transcripts suggesting that the CD28 co-stimulatory pathway is mainly independent of Itk. The signatures of CD4+ and CD8+ T-cell subsets identified a greater differential expression than in total CD3+ cells. Cyclosporin (CsA)-treatment had a stronger effect on transcriptional regulation than Itk-deficiency, suggesting that only a fraction of TCR-mediated calcineurin/NFAT-activation is dependent on Itk. Bioinformatic analysis of NFAT-sites of the group of transcripts similarly regulated by Itk-deficiency and CsA-treatment, followed by chromatin-immunoprecipitation, revealed NFATc1-binding to the Bub1, IL7R, Ctla2a, Ctla2b, and Schlafen1 genes. Finally, to identify transcripts that are regulated by Tec-family kinases in general, we compared the expression profile of Itk-deficient T-cells with that of Btk-deficient B-cells and a common set of transcripts was found. Taken together, our study provides a general overview about the global transcriptional changes in the absence of Itk. **Overall design:** CD3+ T-cells from pooled suspensions of spleen and lymph nodes of Wt and Itk knockout mice on C57BL/6 background were isolated after negative depletion. Unstimulated as well as stimulated T-cells were studied. Stimulations were done with anti-CD3 (1 mg/ml) with or without anti-CD28 (3 mg/ml) in the presence or absence of CsA (1 mg/ml) for 24 hrs. For each stimulus, at least duplicate samples were used.

Background corr dist: KL-Divergence = 0.1100, L1-Distance = 0.0376, L2-Distance = 0.0025, Normal std = 0.4333

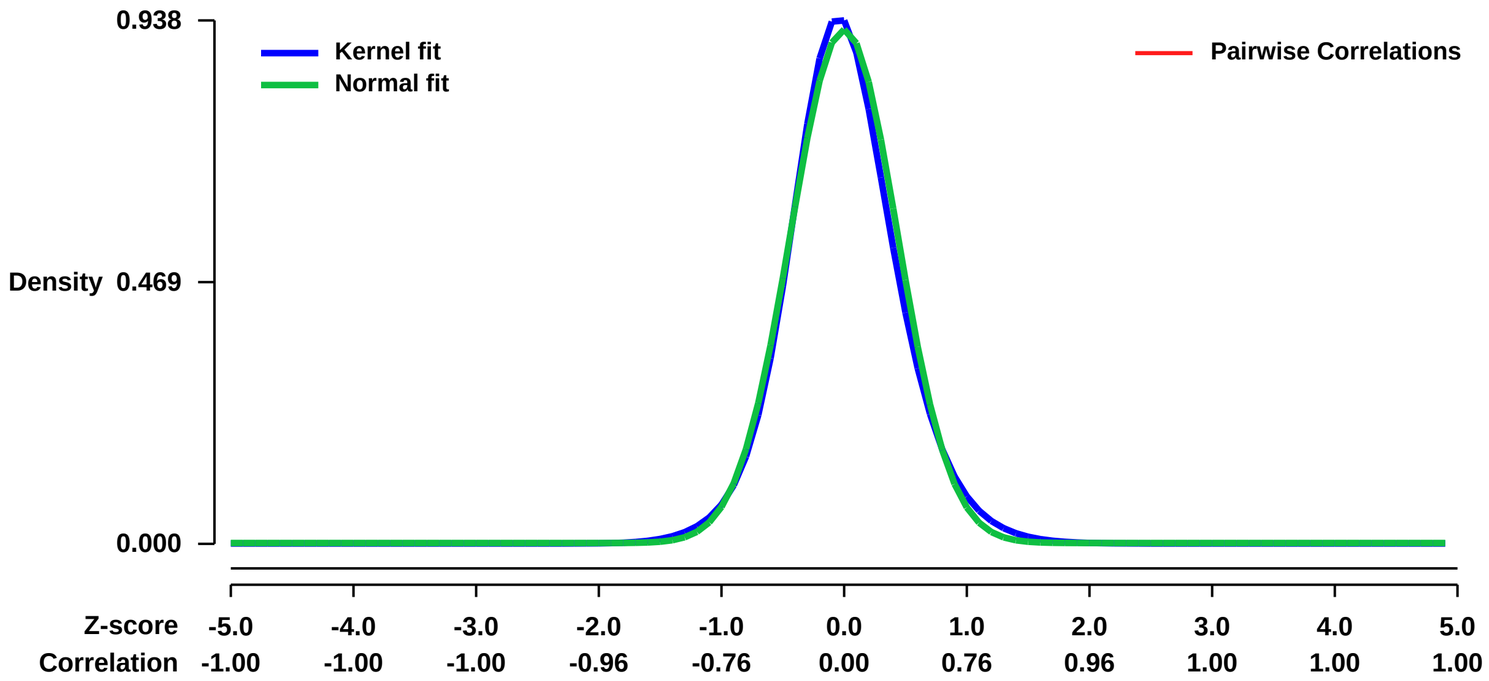

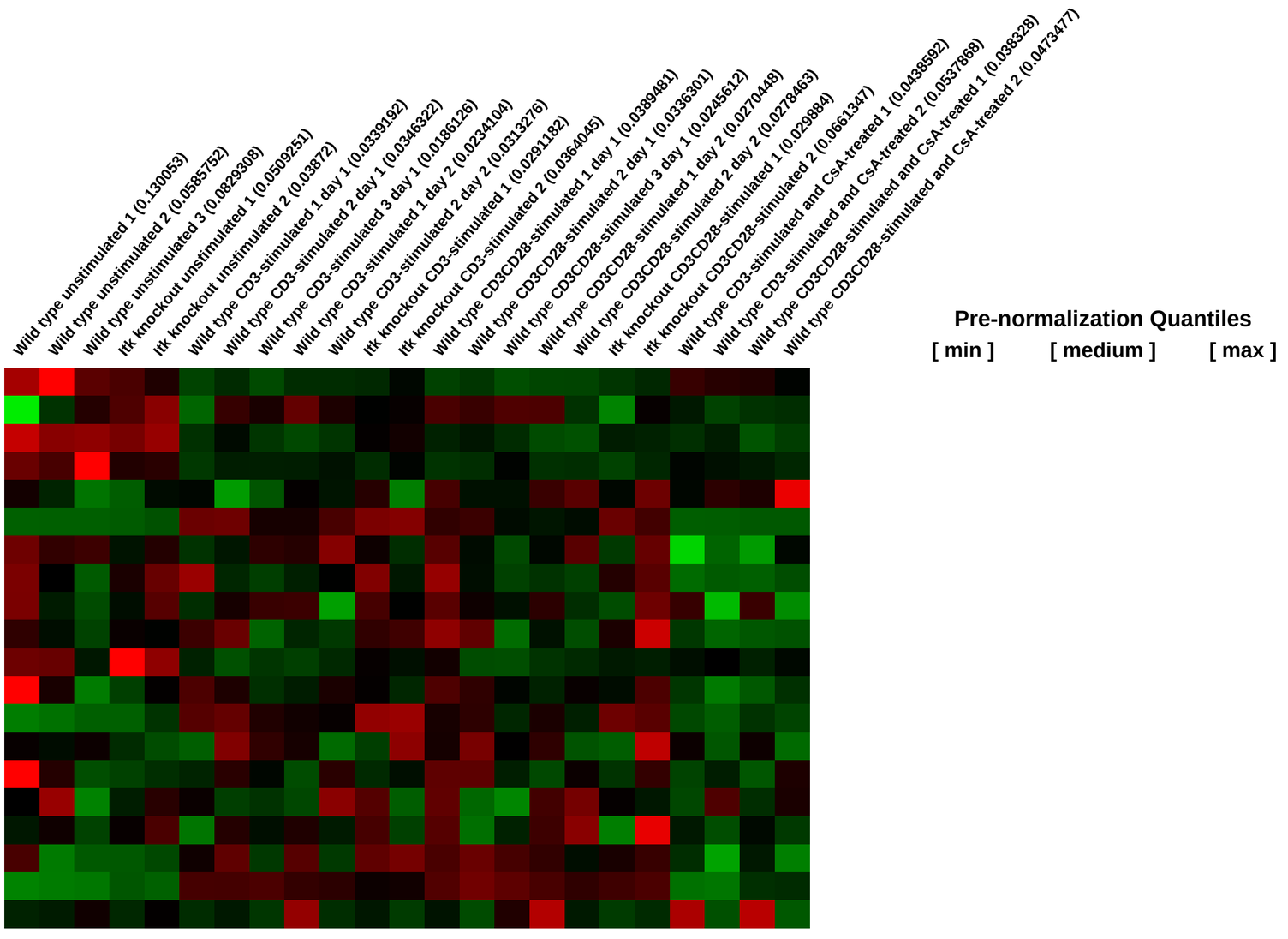

GEO Series "GSE6810" Expression Profiles

Num of samples in this series: 10

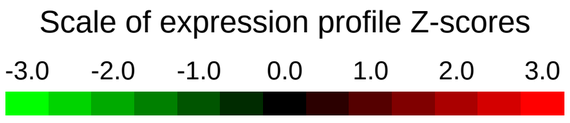

GEO Link:	http://www.ncbi.nlm.nih.gov/geo/query/acc.cgi?acc=GSE6810
Status:	Public on Aug 08 2007
Title:	Response of murine splenocytes to infection with wild type or virB mutant Brucella strains
Organism:	Mus musculus
Experiment type:	Expression profiling by array
Platform:	GPL1261
Pubmed ID:	17441987
Summary & Design:	**Summary:** The virB operon, encoding a Type IV secretion system (T4SS), is essential for intracellular survival and persistent infection of Brucella spp. To better understand the role of the T4SS in evading host defense mechanisms and establishing chronic infection, we compared transcriptional profiles of the host response to infection with wild type Brucella strains and strains that fail to express the virB genes. Analysis of host gene expression profiles three days after inoculation with wild type Brucella strains revealed an inflammatory response dominated by interferon-induced genes. This analysis found that not only the type II but also type I interferon pathway was elicited by Brucella infection. Real time RT-PCR showed that a group of genes from these pathways was induced by day 3 post-infection and declined to baseline levels by day 7. In contrast, neither of the two virB mutant strains elicited expression of interferon-induced genes, demonstrating that the T4SS was required to trigger an inflammatory response early during infection. **Keywords:** analysis of transcriptional responses induced by infection **Overall design:** We performed microarray-based expression analyses of splenocytes from mice infected with two virulent strains (B. abortus 2308 and B. melitensis 16M), and two different B. abortus virB mutants, whose virB operon was either disrupted (BA41) or completely deleted (ADH4.2), to better understand the contribution of the T4SS in establishing infection of the reticuloendothelial system. 3 days after infection of mice, spleens were excised for RNA extraction. For each bacterial strain, RNA from 5 mice was pooled and reverse transcribed for hybridization to an array. Each experiment was performed in duplicate.

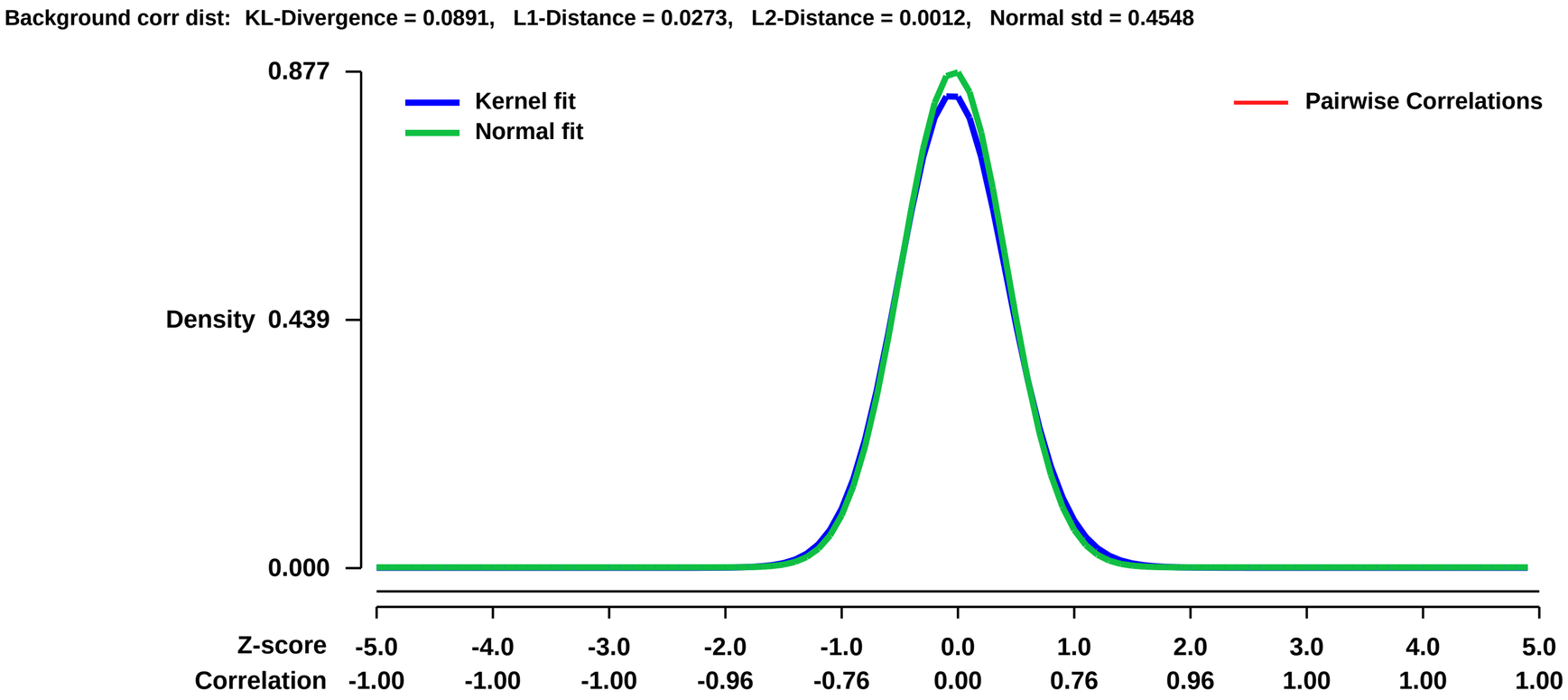

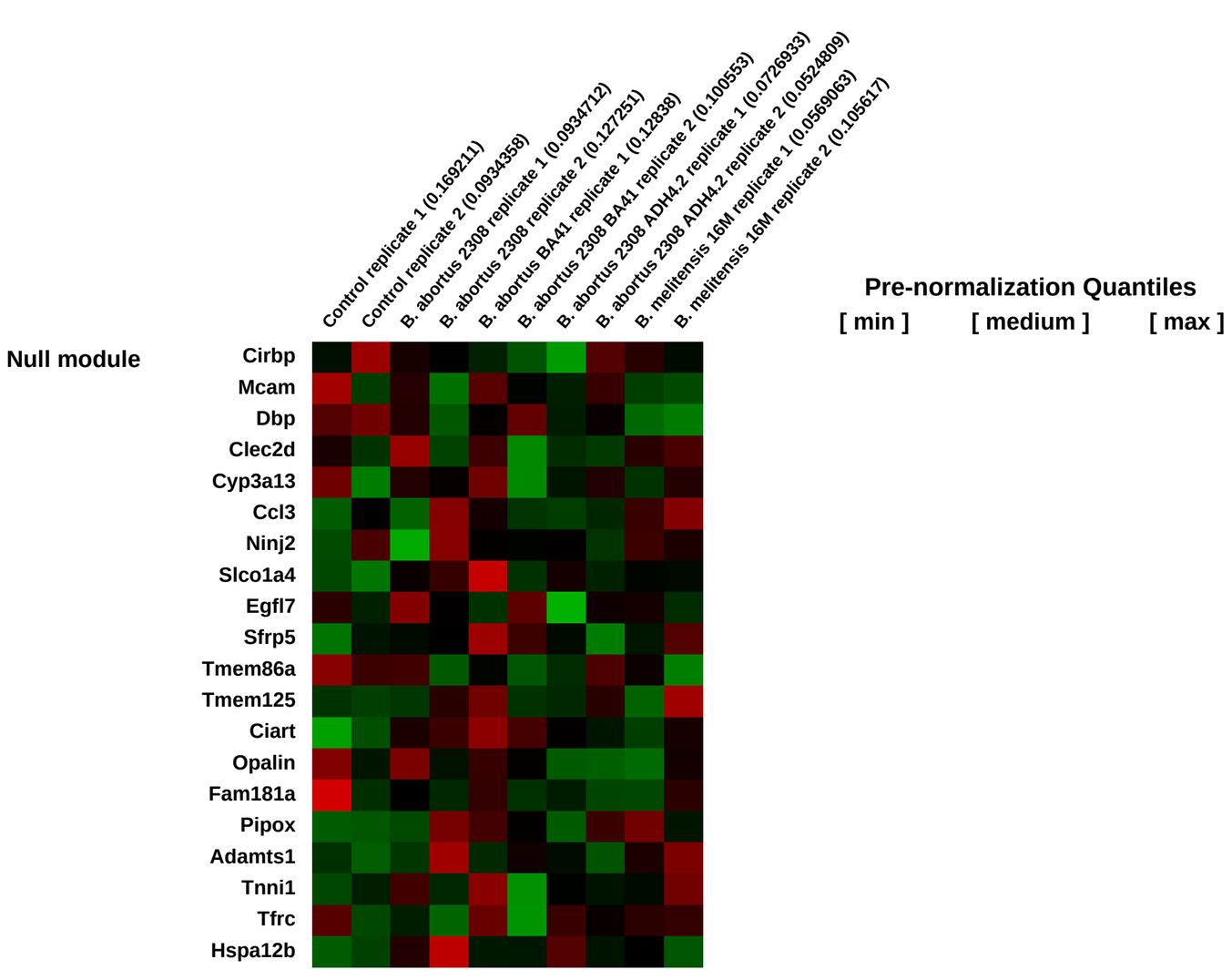

GEO Series "GSE51285" Expression Profiles

Num of samples in this series: 36

Scale of expression profile Z-scores

-3.0 -2.0 -1.0 0.0 1.0 2.0 3.0

GEO Link:	http://www.ncbi.nlm.nih.gov/geo/query/acc.cgi?acc=GSE51285
Status:	Public on Sep 30 2013
Title:	Expression and Metabolic Profiles in a Panel of Five Neural Tube Defect Mouse Models
Organism:	Mus musculus
Experiment type:	Expression profiling by array
Platform:	GPL1261
Pubmed ID:	
Summary & Design:	**Summary:** Neural tube defects (NTDs) are serious birth defects with an estimated worldwide incidence of 1 per 1,000 live births. The multifactorial nature of NTDs in humans has made it difficult to elucidate pathogenesis mechanisms. However, a strong relationship has been established between folate-homocysteine metabolism and NTD risk. Prevention of a substantial proportion of fetal NTDs can be achieved through maternal folic acid (FA) supplementation. However the mechanism by which FA exerts its beneficial effect remains unclear. METHODS: To improve our understanding of the underlying mechanisms of NTD pathogenesis and the ways in which folate exerts its beneficial effect, we analyzed mRNA profiles as well as folate and vitamin B12 levels in five NTD mouse mutants whose response to dietary FA was previously established. RESULTS: Differentially expressed genes representing the effect of each NTD-causing mutation were identified and associated with biologic pathways. Interestingly, the panel of NTD mutants collectively revealed pathways related to two nuclear receptors, retinoid X receptor (RXR) and pregnane X receptor (PXR), suggesting that these pathways may be related to a shared mechanism of NTD development. Moreover, the NTD-causing mutations that were associated with FA responsiveness had expression profiles that were related to folate-homocysteine metabolic pathways. These pathways were not strongly associated with mutants that do not respond to FA supplementation, implying that FA may be beneficial when the NTD mutation affects pathways related to folate-homocysteine metabolism. **Overall design:** 5 groups of NTD mutants were studied. From each mutant group Heterozygous (test) and wild-type (control) female pups were used for this study at 6-8 weeks of age. 4 biological replicates were used for each of the test and control groups of each mutant. All mice used for the experiments were fasted 4-5 hours before dissection. A total of 36 samples were analyzed.

Background corr dist: KL-Divergence = 0.4270, L1-Distance = 0.0761, L2-Distance = 0.0177, Normal std = 0.2414

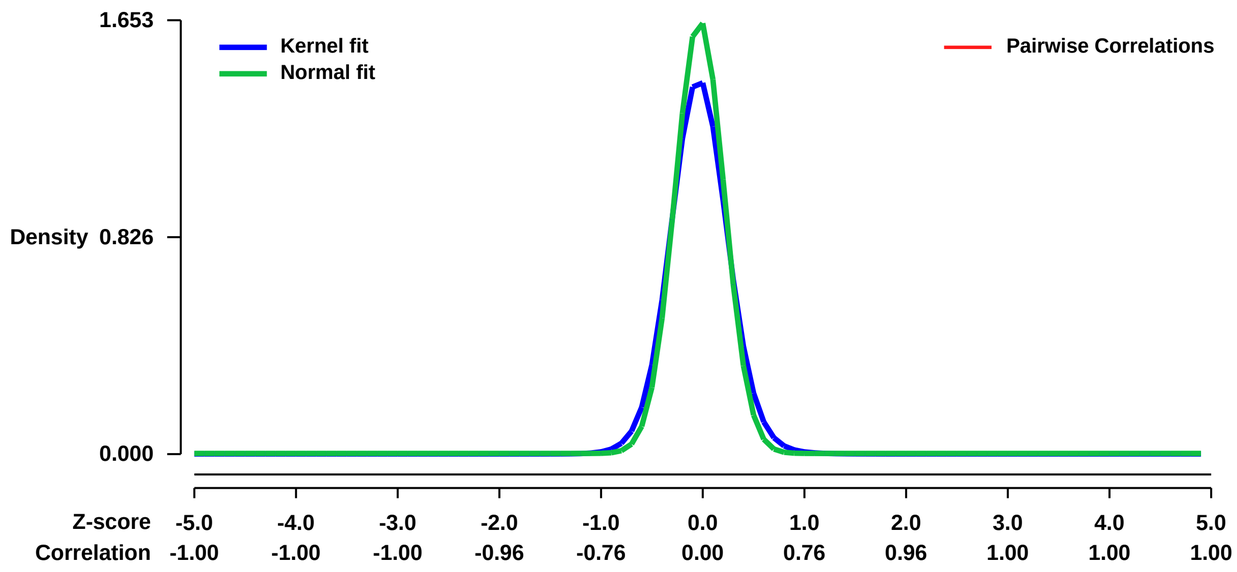

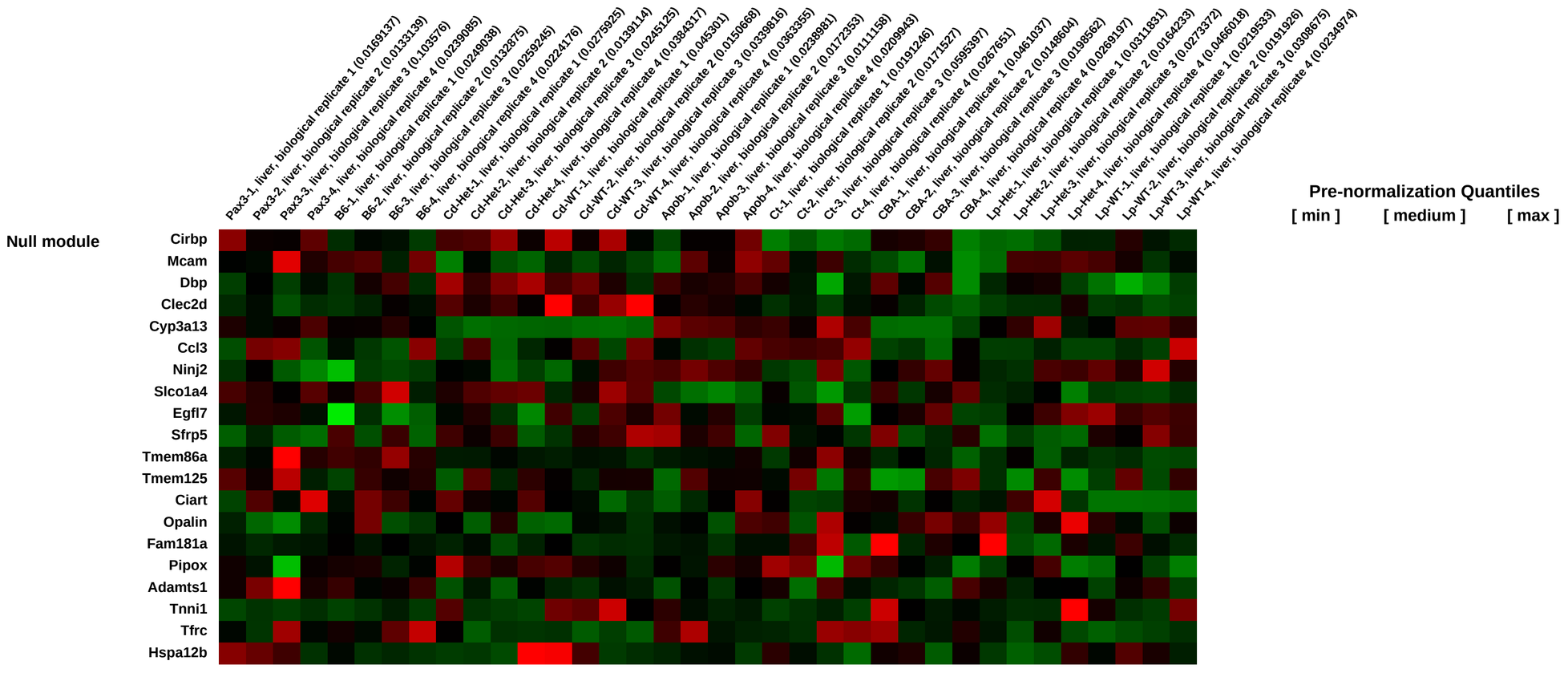

GEO Series "GSE15379" Expression Profiles

Num of samples in this series: 12

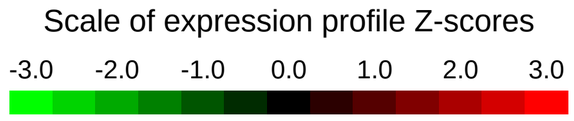

GEO Link:	**http://www.ncbi.nlm.nih.gov/geo/query/acc.cgi?acc=GSE15379**
Status:	**Public on Mar 04 2010**
Title:	**Expression data from lung of septic PPTA knockout mouse**
Organism:	**Mus musculus**
Experiment type:	**Expression profiling by array**
Platform:	**GPL1261**
Pubmed ID:	**20454520**
Summary & Design:	**Summary:** **In this study, we have explored microarray-based differential gene expression profile in mouse lung tissue 8 h after inducing polymicrobial sepsis and the effect of preprotachykinin-A (PPTA) gene deletion. A range of genes differentially expressed (> 2-fold) in microarray analysis was assessed, PPTA-knockout septic mice with their respective sham controls.** **Overall design:** **Lung samples from wild-type or PPTA-knockout mice were selected at 8 h after cecal ligation and puncture (CLP) or sham surgery for RNA extraction and hybridization to Affymetrix microarrays. Triplicates were performed for each condition.**

Background corr dist: **KL-Divergence = 0.1050, L1-Distance = 0.0235, L2-Distance = 0.0008, Normal std = 0.4333**

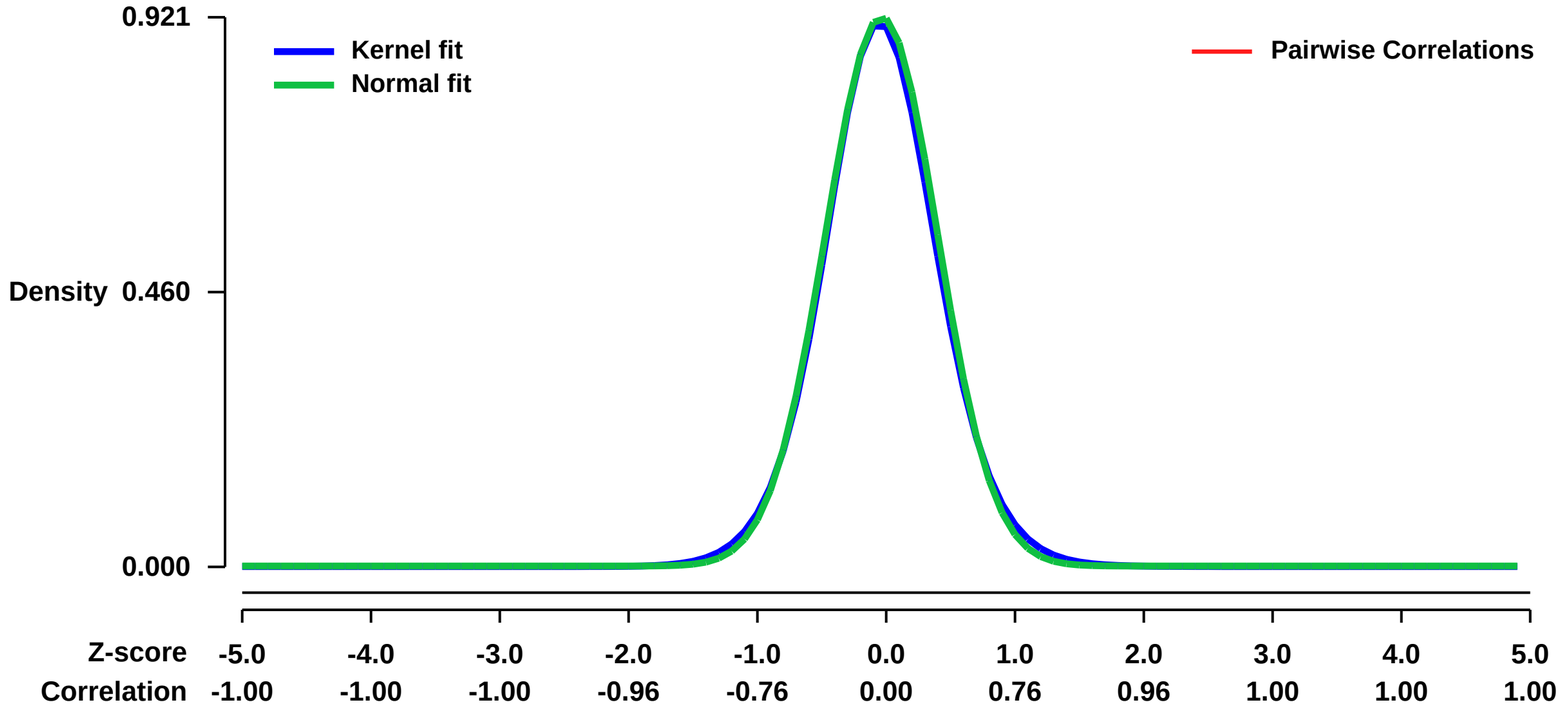

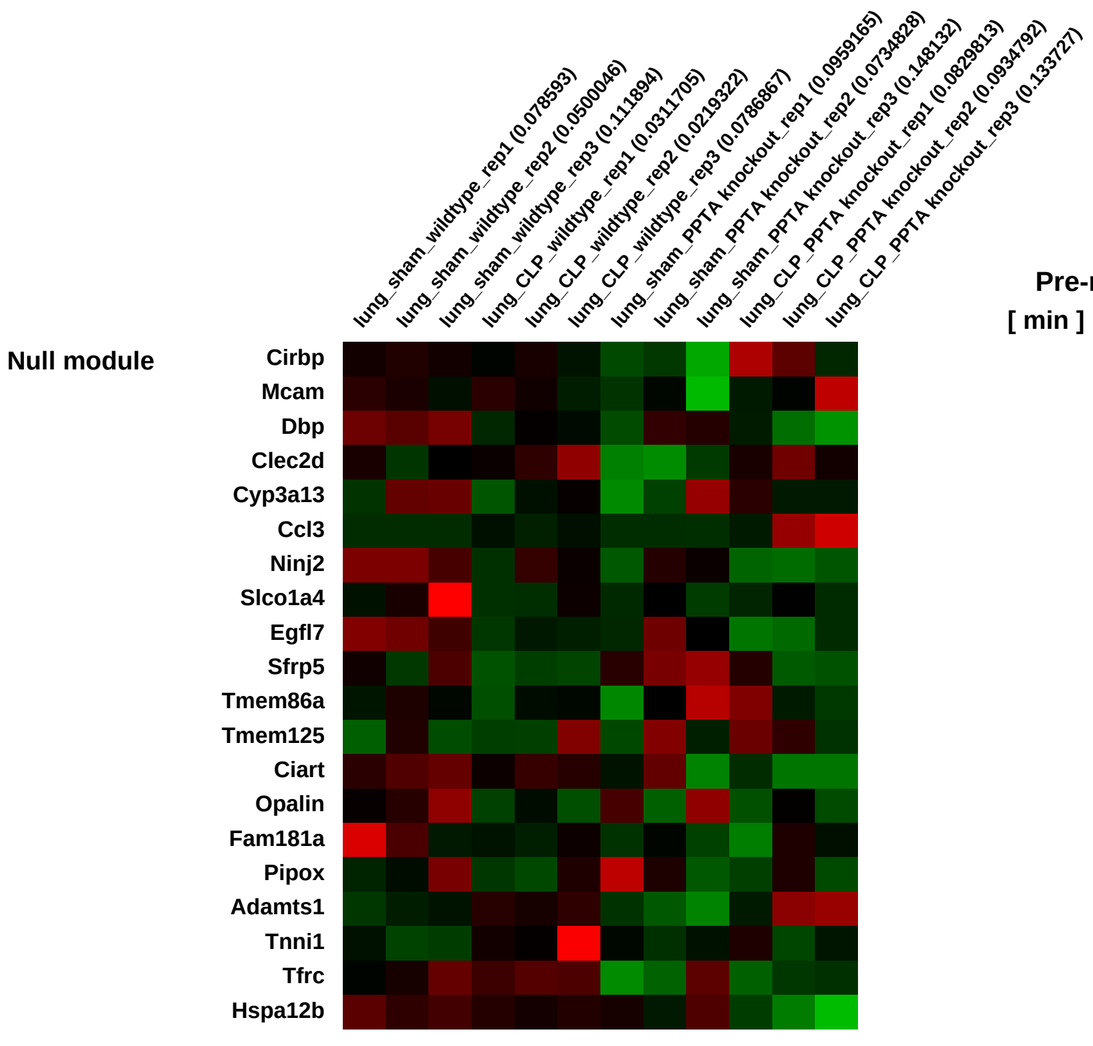

GEO Series "GSE14211" Expression Profiles

Num of samples in this series: 6

Scale of expression profile Z-scores

-3.0 -2.0 -1.0 0.0 1.0 2.0 3.0

GEO Link:	http://www.ncbi.nlm.nih.gov/geo/query/acc.cgi?acc=GSE14211
Status:	Public on Oct 01 2011
Title:	Expression profiling of Noto-GFP+ notochord progenitor cells sorted from E8.5 mouse embryos
Organism:	Mus musculus
Experiment type:	Expression profiling by array
Platform:	GPL1261
Pubmed ID:	22008794
Summary & Design:	**Summary:** Using a combination of cell sorting and microarray analysis, we identified almost 200 genes as having a high level of expression in the notochord. After whole mount in situ hybridization screening, we confirmed approximately one third of these as having a novel notochord expression pattern. Keywords: cell type comparison - embryonic Noto-GFP+ notochord progenitors versus surrounding GFP- comparator cells **Overall design:** 3 biological replicates - each replicate includes an experiment cell population (Noto-GFP positive cell sort) and a comparator population (GFP negative cell sort)

Background corr dist: KL-Divergence = 0.0298, L1-Distance = 0.0329, L2-Distance = 0.0014, Normal std = 0.6893

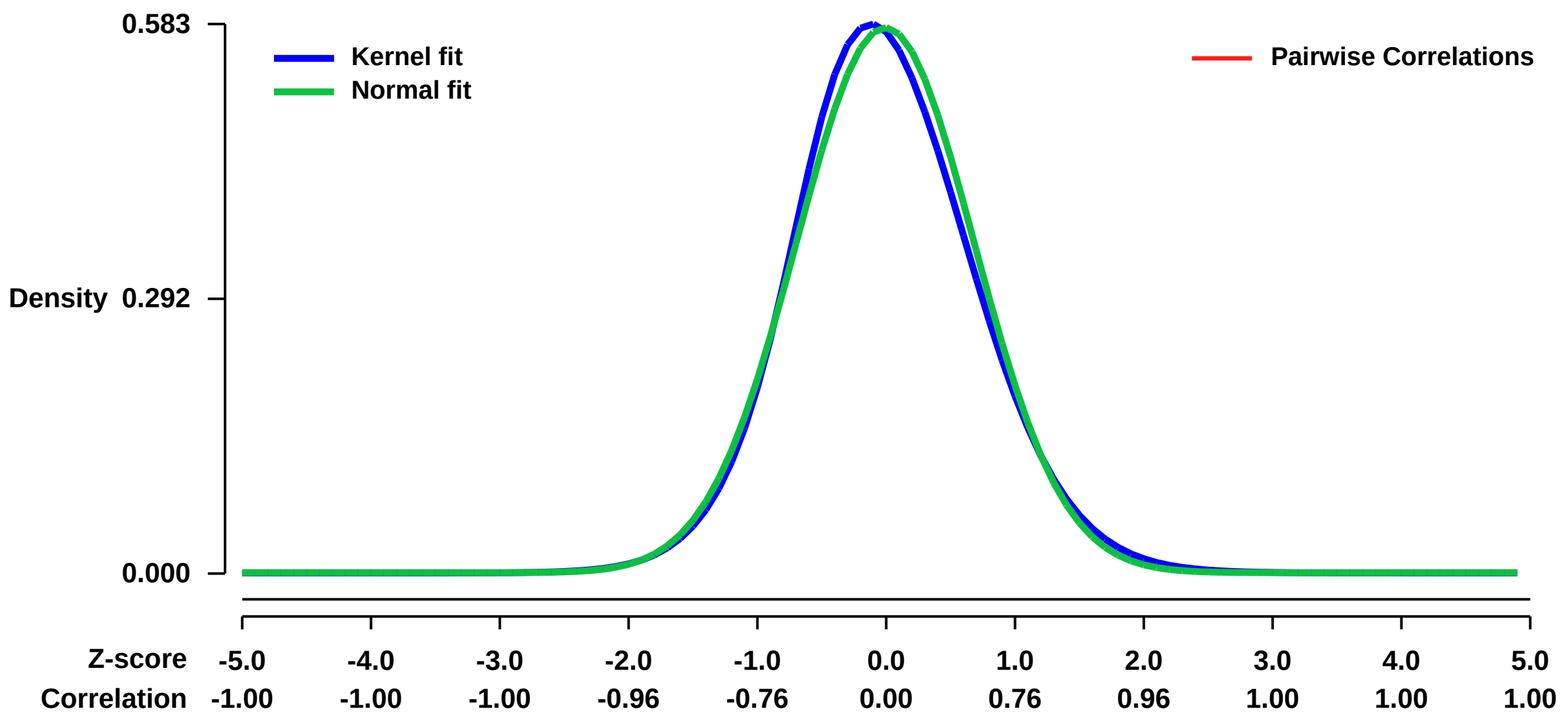

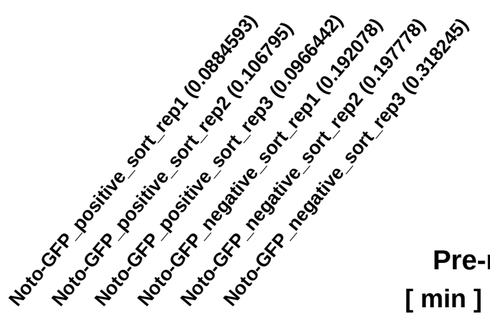

Pre-normalization Quantiles

[min] [medium] [max]

Null module

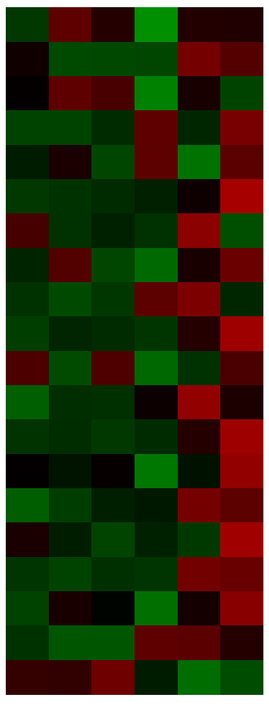

GEO Series "GSE39562" Expression Profiles

Num of samples in this series: 26

Scale of expression profile Z-scores

-3.0 -2.0 -1.0 0.0 1.0 2.0 3.0

GEO Link:	http://www.ncbi.nlm.nih.gov/geo/query/acc.cgi?acc=GSE39562
Status:	Public on Jul 24 2012
Title:	Immortalized clonal brown, beige and white adipose cell lines
Organism:	Mus musculus
Experiment type:	Expression profiling by array
Platform:	GPL1261
Pubmed ID:	22796012
Summary & Design:	**Summary:** Brown fat generates heat via the mitochondrial uncoupling protein UCP1, defending against hypothermia and obesity. Recent data suggest that there are two distinct types of brown fat: classical brown fat derived from a myf-5 cellular lineage and UCP1-positive cells that emerge in white fat from a non-myf-5 lineage. Here, we report the isolation of â beigeâ cells from murine white fat depots. **Overall design:** Microarray analysis of the differentiated clonal inguinal and interscapular adipocytes in the presence of forskolin (10microM). These samples were profiled using Affymetrix mouse 430 2.0 arrays, 26 samples in total.

Background corr dist: KL-Divergence = 0.3735, L1-Distance = 0.0779, L2-Distance = 0.0186, Normal std = 0.2548

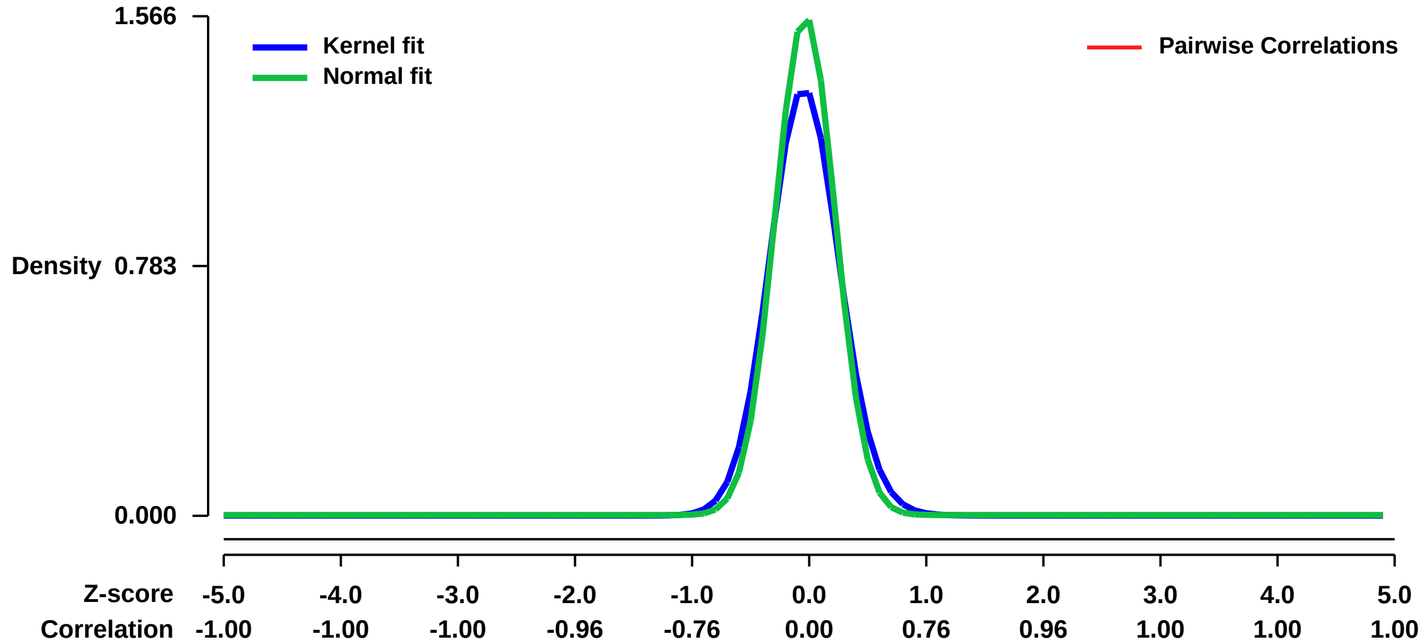

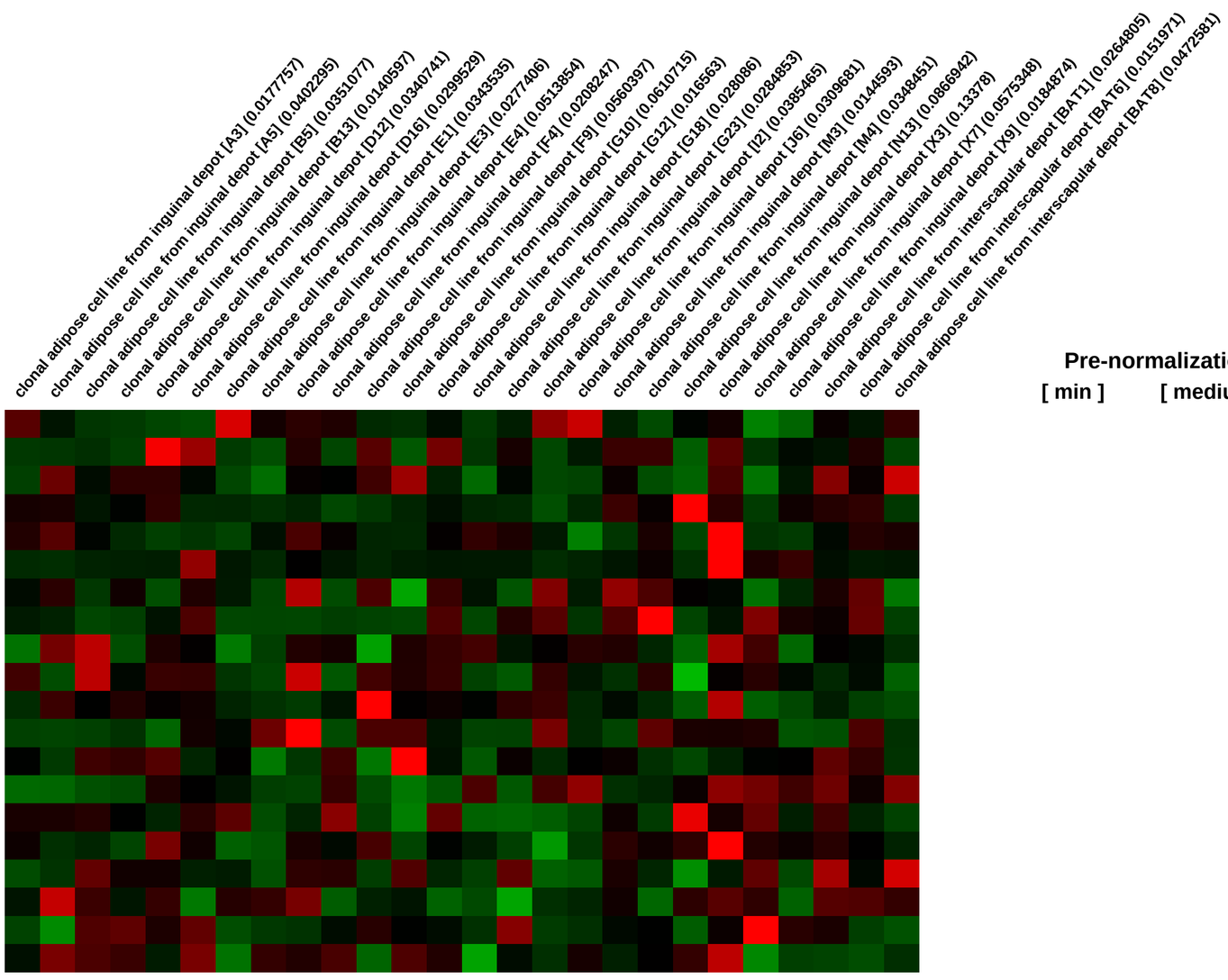

GEO Series "GSE23895" Expression Profiles

Num of samples in this series: 18

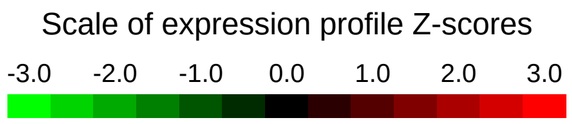

GEO Link:	**http://www.ncbi.nlm.nih.gov/geo/query/acc.cgi?acc=GSE23895**
Status:	**Public on Jan 19 2011**
Title:	**Selenium toxicity but not deficient or super-nutritional selenium status vastly alters the transcriptome in rodents**
Organism:	**Mus musculus**
Experiment type:	**Expression profiling by array**
Platform:	**GPL1261**
Pubmed ID:	**21226930**
Summary & Design:	**Summary:** **Protein and mRNA levels for several selenoproteins, such as glutathione peroxidase-1 (Gpx1), are down-regulated dramatically by selenium (Se) deficiency.** **Selenoprotein levels in rats increase sigmoidally with increasing dietary Se and reach defined plateaus at the Se requirement, making them sensitive biomarkers for Se deficiency, but not high for Se status. Biomarkers for high Se status are needed as super-nutritional Se intakes are associated with beneficial and adverse health outcomes, but conventional biomarkers are not especially useful above the Se requirement. To characterize Se regulation of the transcriptome, we conducted 3 microarray experiments in weanling mice and rats fed Se-deficient diets supplemented with levels of Se up to 5 ´µg Se/g diet.** **Overall design:** **Rats or mice were fed Se-deficient diets supplemented with sodium selenite up to 5 ug Se/g diet for 28 or 35 days. Affymetrix Rat 230 2.0 and Mouse 430 2.0 Genome Arrays were used to analyze gene expression in liver in all studies plus kidney in the mouse study.**

Background corr dist: KL-Divergence = 0.0133, L1-Distance = 0.0509, L2-Distance = 0.0031, Normal std = 0.9121

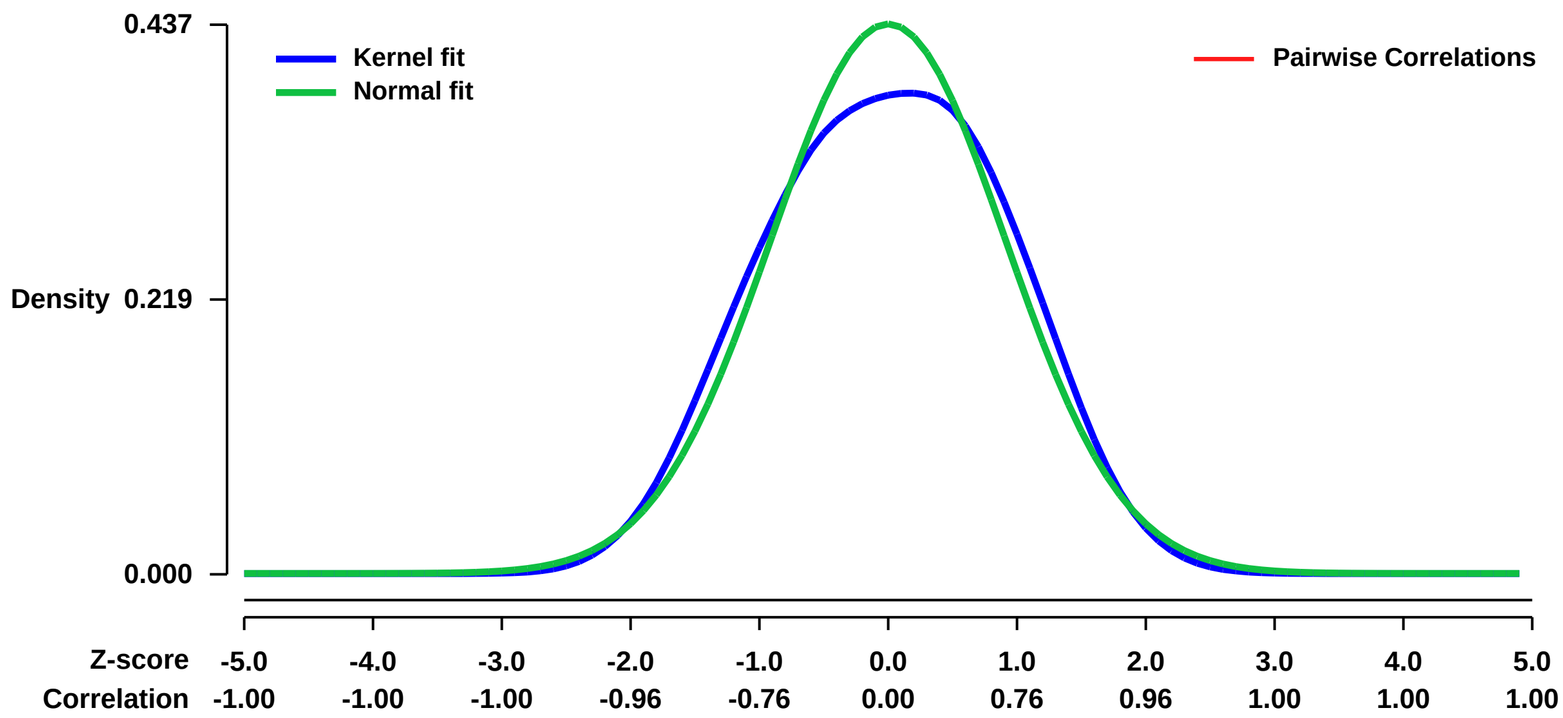

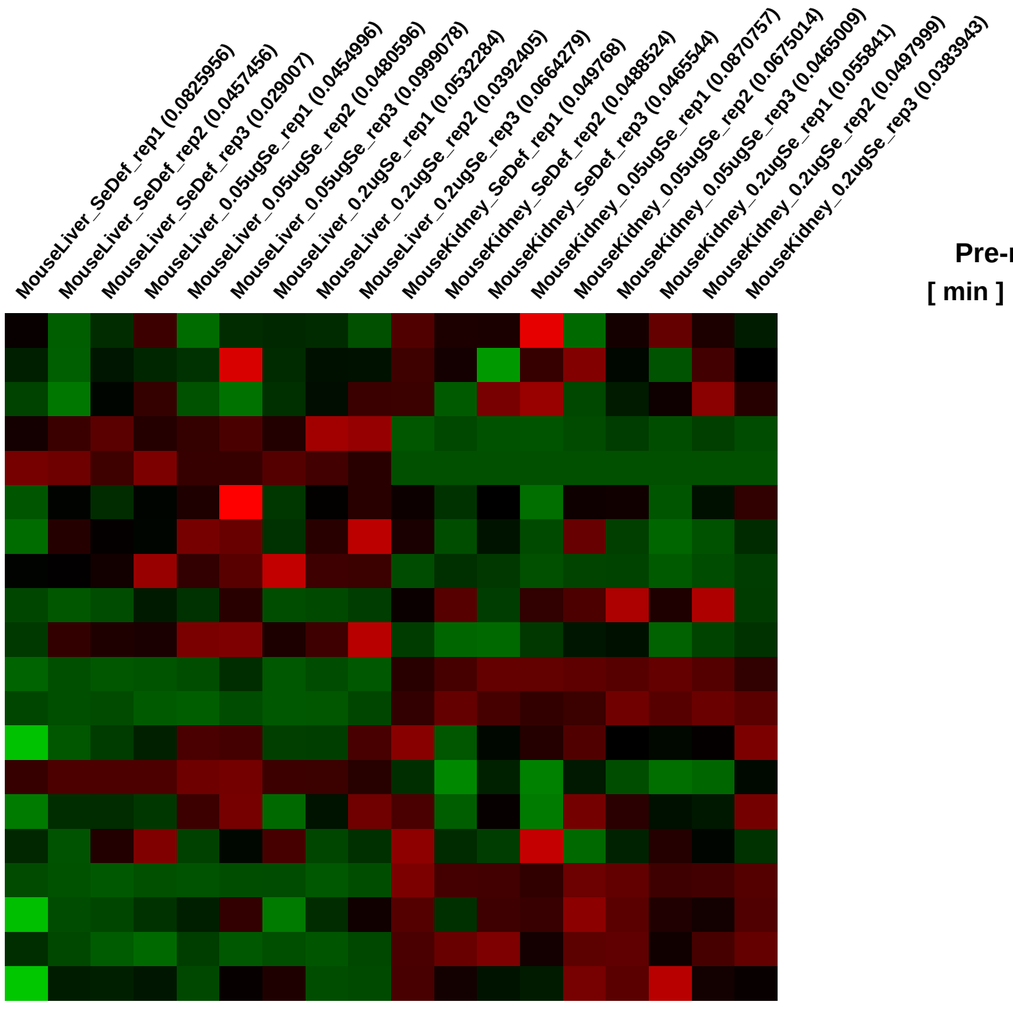

GEO Series "GSE23200" Expression Profiles

Num of samples in this series: 6

Scale of expression profile Z-scores

-3.0 -2.0 -1.0 0.0 1.0 2.0 3.0

GEO Link:	http://www.ncbi.nlm.nih.gov/geo/query/acc.cgi?acc=GSE23200
Status:	Public on Jun 23 2011
Title:	Immunoprotective properties of sertoli cells: potential genes and pathways that confer immune privilege for sertoli cell transplantation and in the testis
Organism:	Mus musculus
Experiment type:	Expression profiling by array
Platform:	GPL1261
Pubmed ID:	21900683
Summary & Design:	**Summary:** Immune privileged Sertoli cells (SC) survive when transplanted across immunological barriers and prolong the survival of co-transplanted allogeneic and xenogeneic cells in rodent models. However, the mechanism for this survival and protection remains unresolved. We have recently identified a mouse Sertoli cell line (MSC-1) that lacks some of the immunoprotective abilities associated with primary SC. The objective of this study was to compare the survival and gene expression profiles of primary SC and MSC-1 cells to identify factors or immune-related pathways potentially important for SC immune privilege. Primary SC or MSC-1 cells were transplanted as allografts to the renal subcapsular area of naˆflve BALB/c mice and cell survival was analyzed by immunohistochemistry. Additionally, transcriptome differences were investigated by microarray and pathway analyses. While primary SC were detected within the grafts with 100% graft survival throughout the 20-day study, MSC-1 cells w ere rejected between 11 and 14 days with 0% graft survival at 20 days post-transplantation. Microarray analysis identified 3198 genes that were differentially expressed with a ´– 4-fold or higher level in primary SC. Cluster and pathway analyses indicate that the mechanism of SC immune privilege is likely complex with multiple immune modulators being involved such as immunosuppressive cytokines and complement inhibitors, lipid mediators for controlling inflammation, and junctional molecules that control leukocyte movement in and out of the immune privileged space. Further study of these immune modulators will increase our understanding of SC immune privilege and in the long-term lead to improvements in transplantation success. **Overall design:** Aggregated 19 to 20-day mice primary Sertoli cells and MSC-1 cell line were used to determine the global transcriptome differences important for the survival and protection of transplanted cells.

Background corr dist: KL-Divergence = 0.0095, L1-Distance = 0.0345, L2-Distance = 0.0013, Normal std = 0.9520

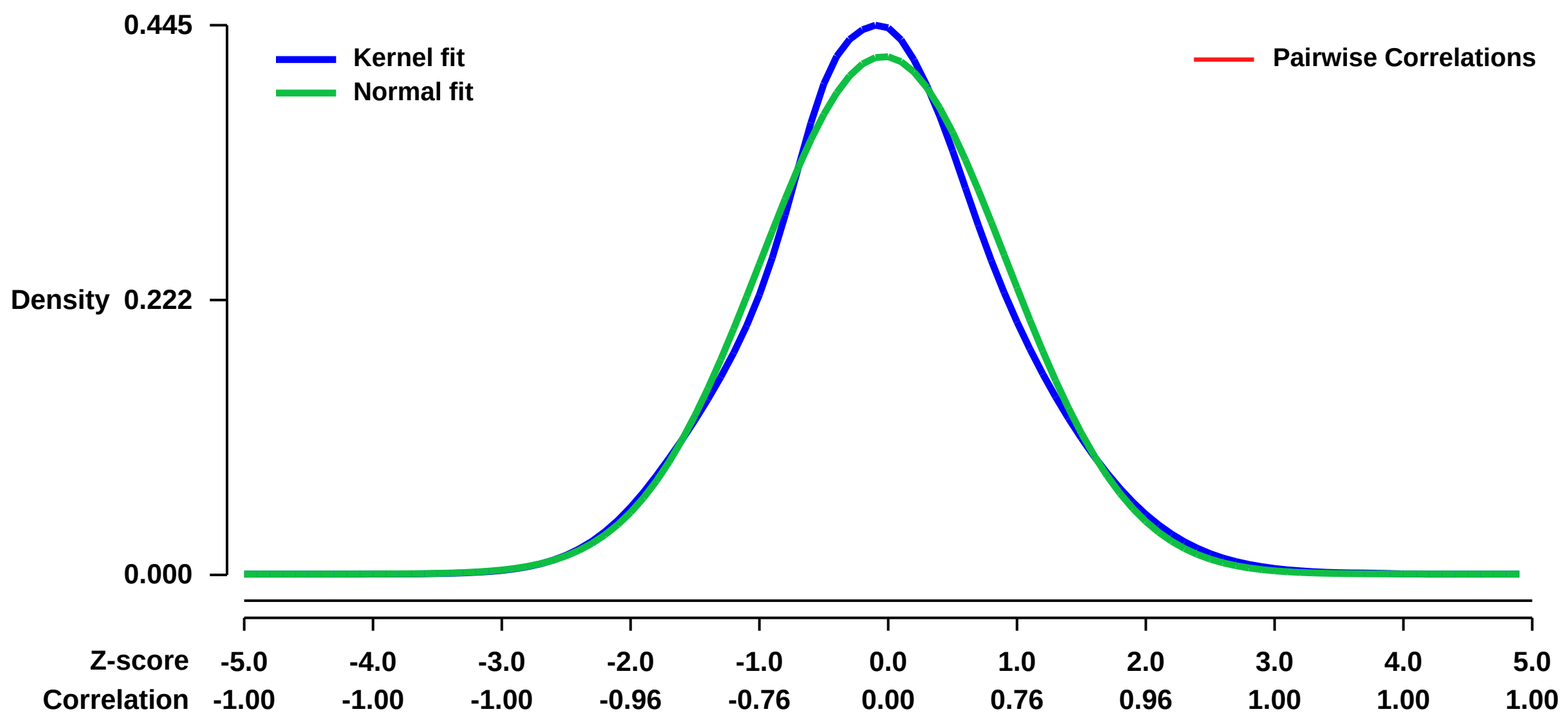

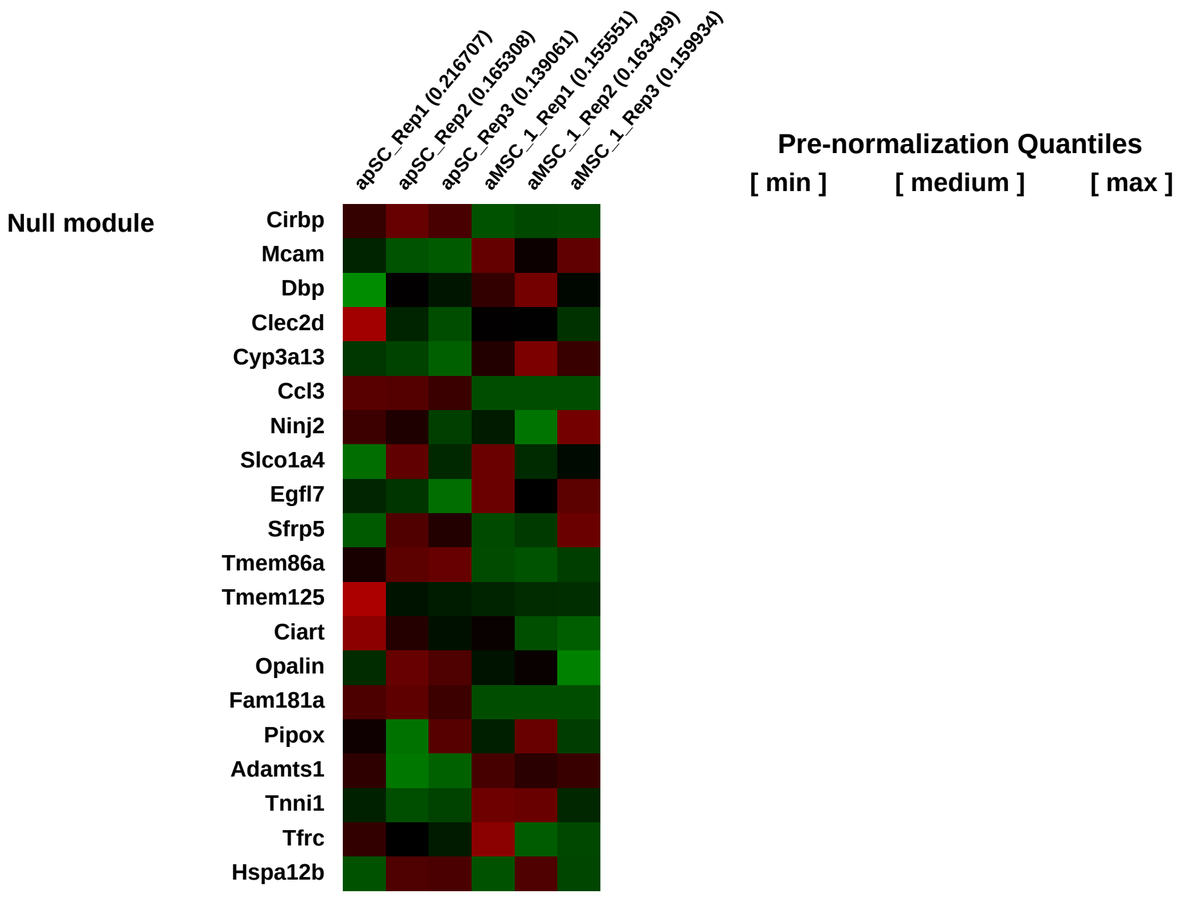

GEO Series "GSE9977" Expression Profiles

Num of samples in this series: 24

Scale of expression profile Z-scores

-3.0 -2.0 -1.0 0.0 1.0 2.0 3.0

GEO Link:	http://www.ncbi.nlm.nih.gov/geo/query/acc.cgi?acc=GSE9977
Status:	Public on Sep 30 2009
Title:	Expression data from NIH-3T3 cells treated with mock, 100 U/ml IFN alpha or 100 U/ml gamma for 1or 3h
Organism:	Mus musculus
Experiment type:	Expression profiling by array
Platform:	GPL1261
Pubmed ID:	18658122
Summary & Design:	**Summary:** Differential gene expression caused by 1h and 3h of IFN alpha or gamma treatment was analyzed in total cellular RNA of NIH-3T3 cells compared to mock We used microarrays to analyze the effects of 1 and 3h of IFNalpha and gamma treatment in total cellular RNA Keywords: time course in total cellular RNA (tc-RNA) **Overall design:** NIH-3T3 cells (5th to 15th passage after thawing) were split from confluent plates 24h before start of the experiment. At the begin of the experiment about 80% confluency was reached. The experiment was started by applying fresh, prewarmed, CO2-equilibrated medium containing either mock, 100U/ml IFN alpha or 100 U/ml IFN gamma. Labeling was either started together with addition of IFN for 60 minutes or for 30 minutes starting 150 minutes after begin of treatment.

Background corr dist: KL-Divergence = 0.0343, L1-Distance = 0.0629, L2-Distance = 0.0042, Normal std = 0.7786

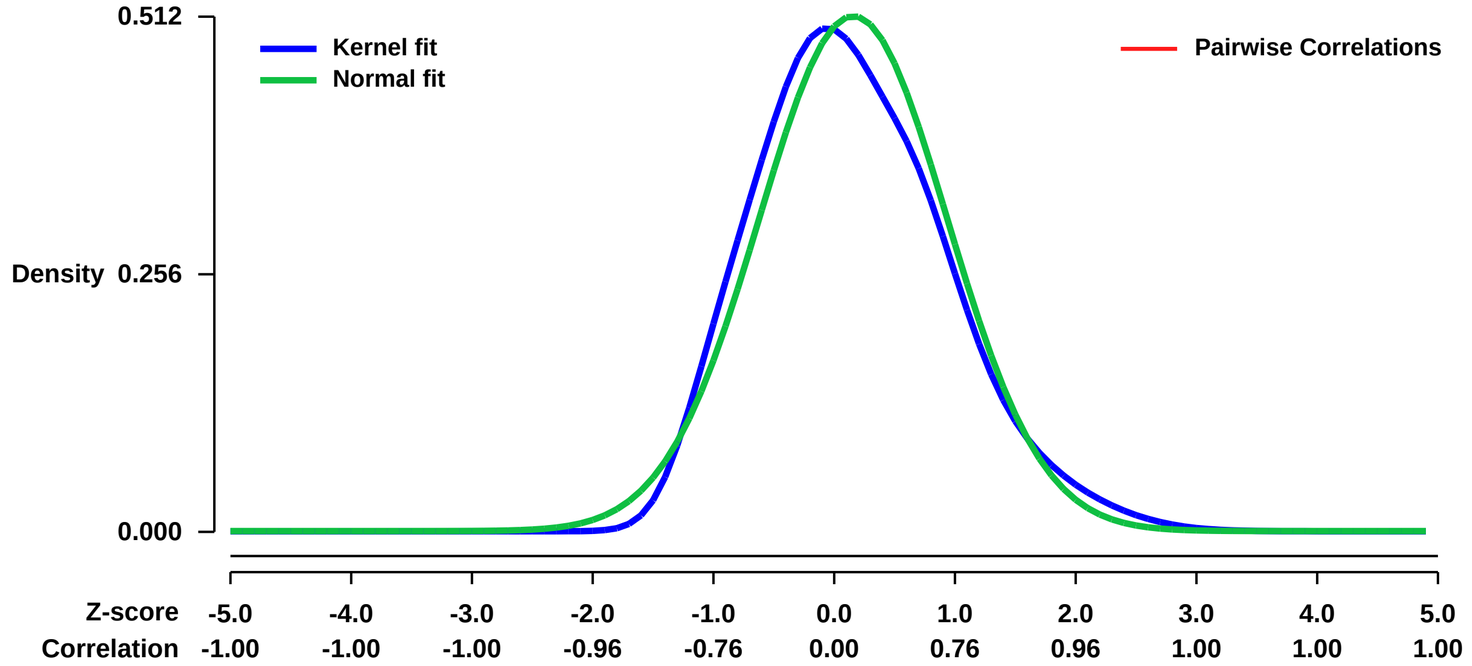

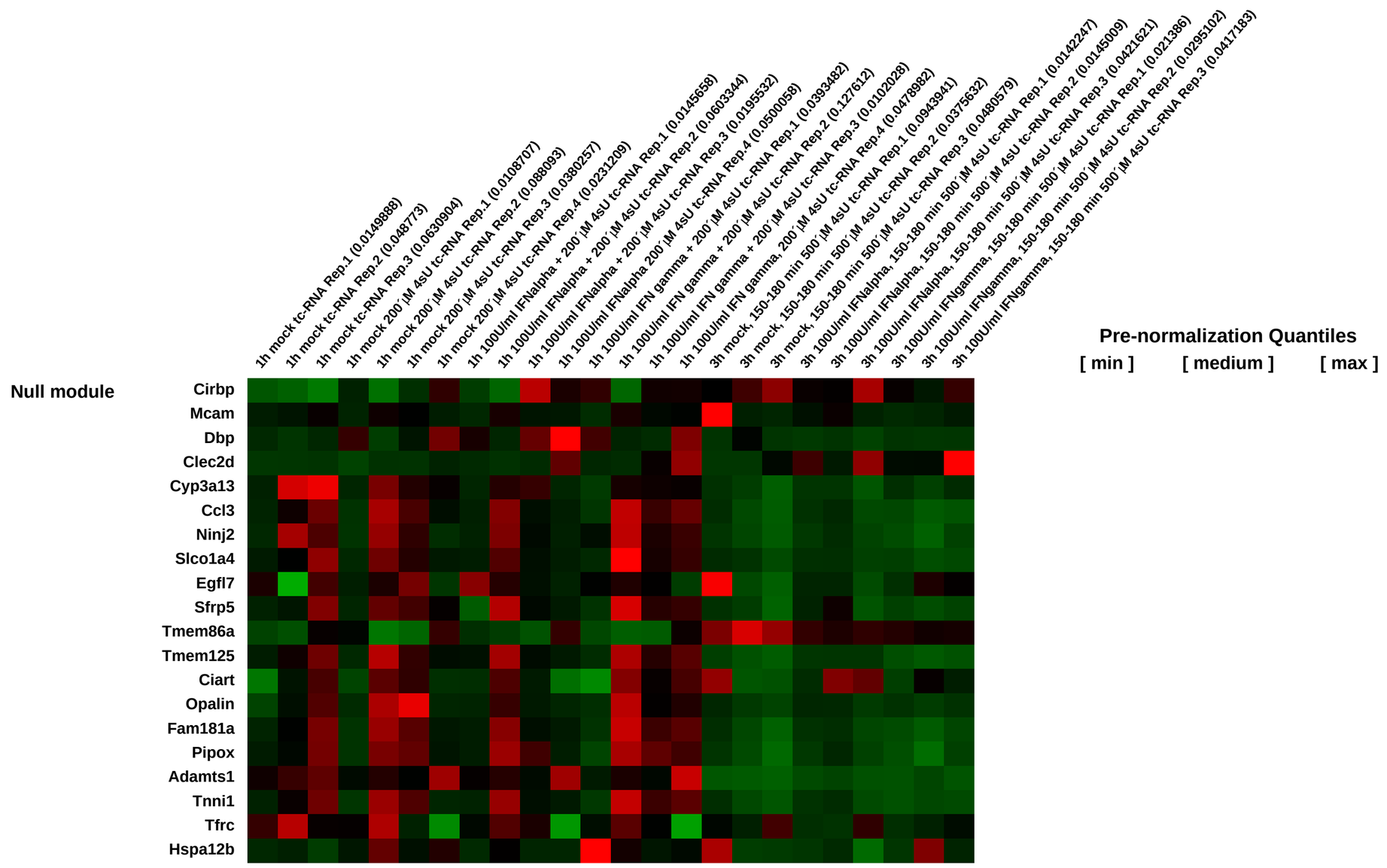

GEO Series "GSE17184" Expression Profiles

Num of samples in this series: 12

Scale of expression profile Z-scores

-3.0 -2.0 -1.0 0.0 1.0 2.0 3.0

GEO Link:	http://www.ncbi.nlm.nih.gov/geo/query/acc.cgi?acc=GSE17184
Status:	Public on Jul 21 2009
Title:	ConA-induced fulminant hepatitis in a mouse model
Organism:	Mus musculus
Experiment type:	Expression profiling by array
Platform:	GPL1261
Pubmed ID:	20398290
Summary & Design:	**Summary:** The goal of this experiment was to investigate the early mechanisms of human fulminant hepatitis through ConA-induced hepatitis model.Early diagnosis and interventions are important for patients with fulminant hepatitis and gene expression may be pivotal in the early diagnosis. Keyword :ConA-induced hepatitis model **Overall design:** ConA was injected through the mouse caudal vein at one of 4 time points (0 hr, 1 hr, 3 hr, 6 hr). The effects of ConA treatment on hepatic gene expression at these time points were analyzed .There are 3 replicates at each timepoint then 4*3=12 samples in all.

Background corr dist: KL-Divergence = 0.1011, L1-Distance = 0.0314, L2-Distance = 0.0014, Normal std = 0.4480

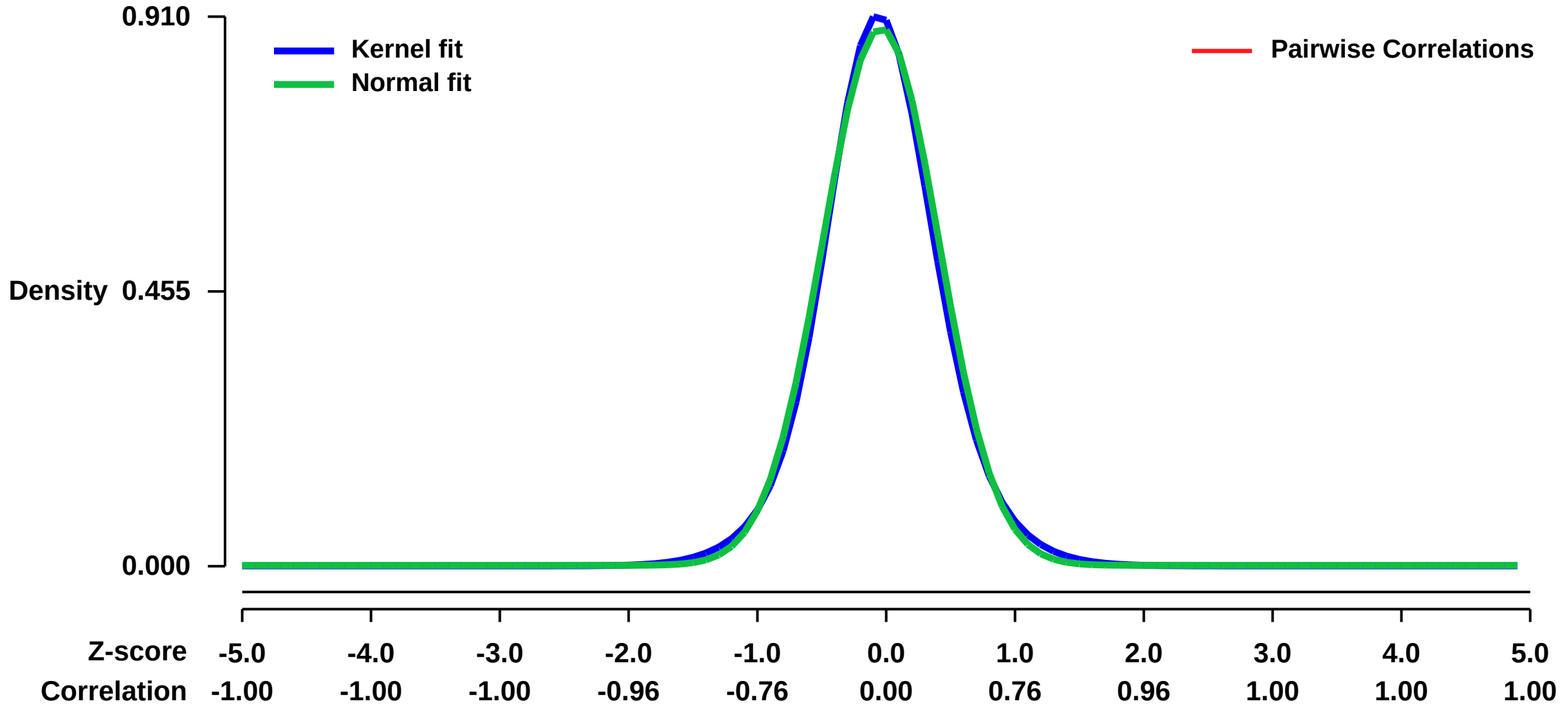

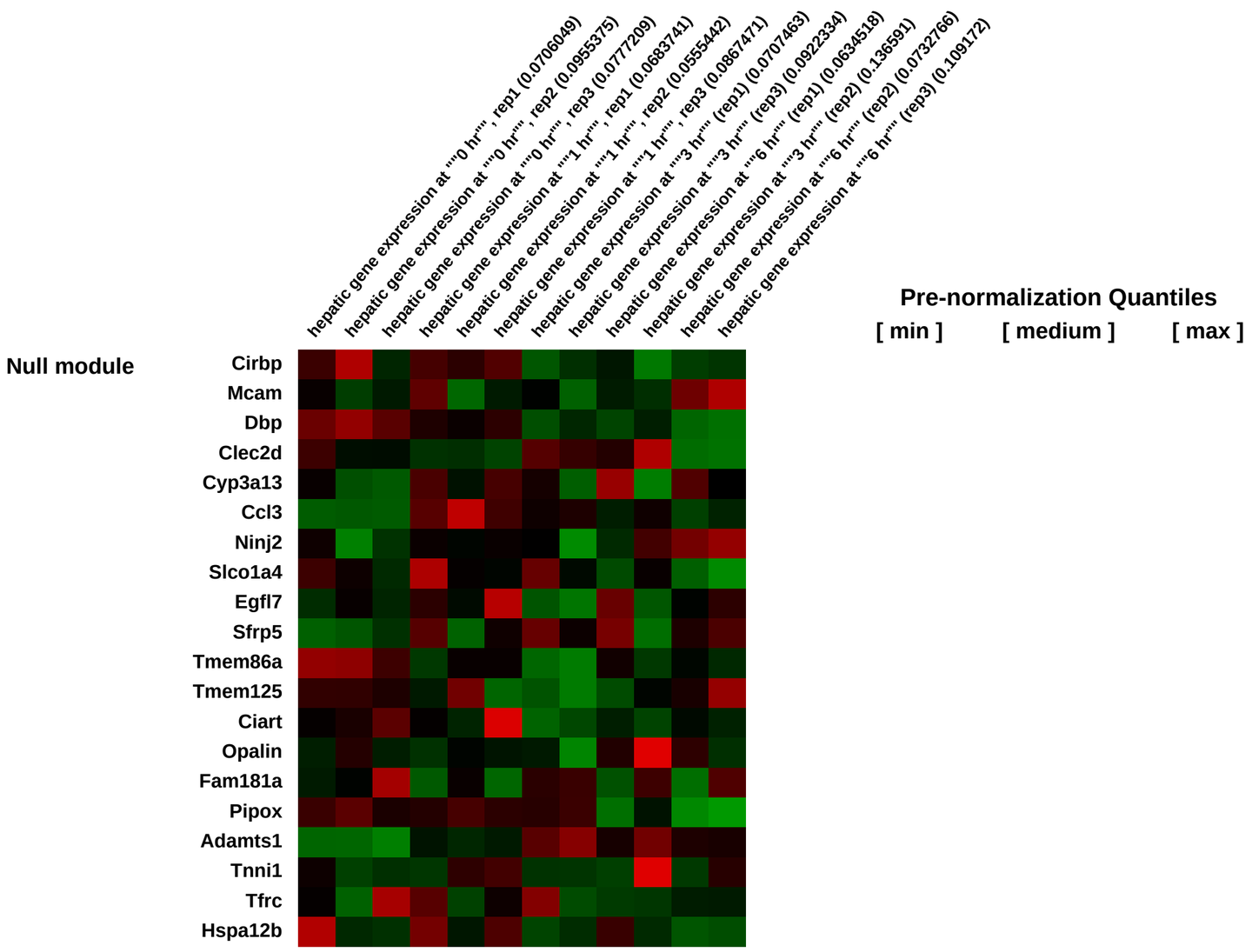

GEO Series "GSE9368" Expression Profiles

Num of samples in this series: 12

Scale of expression profile Z-scores

-3.0 -2.0 -1.0 0.0 1.0 2.0 3.0

GEO Link:	http://www.ncbi.nlm.nih.gov/geo/query/acc.cgi?acc=GSE9368
Status:	Public on Nov 01 2007
Title:	Mouse lung with recombinant human soluble PBEFtreatment and ventilator-induced lung injury: age 8-12wks
Organism:	Mus musculus
Experiment type:	Expression profiling by array
Platform:	GPL1261
Pubmed ID:	18658108
Summary & Design:	**Summary:** We have previously demonstrated that pre-B-cell colony enhancing factor (PBEF) ais a biomarker in sepsis and sepsis-induced acute lung injury (ALI) with genetic variants conferring ALI susceptibility118. In the current study, we explored the mechanistic participation of PBEF in ALI and ventilator-induced associated lung injury (VIALI). Initial in vitro studies and demonstrated rhPBEF aas a direct rat neutrophil chemotactic factor in vitro producing marked in vivo increases in BAL leukocytes (PMNs) in vivo following (intratracheal injection (,IT) in C57B6 mice. These latter changes were accompanied by increased BAL levels of the PMN chemoattractants (, KC and MIP2), and modest changes in lung vascular and but were not associated with significant increasesin alveolar permeability. We next explored the potential synergism between rhPBEF administration (IT) and a mechanical ventilation model of modest VILI lung injury (4 hours, 30 ml/kg tidal volume). We and observed dramatic synergistic increases in BAL PMNs, and both BAL protein and cytokine levels (IL-6, TNF-?, KC). Gene expression profiling Microarray analysis further supported a major role for PBEF in the induction of gene modules associated with ALI and VALI (NFkB pathway, leukocyte extravasation, apoptosis, toll receptor signaling). Finally, we exposed wild type and heterozygous PBEF+/- mice (targeted deletion of a single PBEF allele deletion) to a model of severe VILImechanical ventilation-induced lung injury (4 hours, 40 ml/kg tidal volume). PBEF+/- mice were significantly protected from VIALI-associated increases in BAL protein and BAL IL-6 levels and exhibited significantly reduced expression of ALI-associated gene expression modules. Together, these results indicate that PBEF is a key inflammatory mediator intimately involved in both the development and severity of ventilator-induced ALI. We used microarrays to detail the global programme of gene expression induced by rhPBEF treatment and VALI. Keywords: response to treatment and/or stress **Overall design:** animals were treated by PBS, rhPBEF (IT administration), VILI (4 hours, 30 ml/kg tidal volume), or both.

Background corr dist: KL-Divergence = 0.1051, L1-Distance = 0.0265, L2-Distance = 0.0010, Normal std = 0.4288

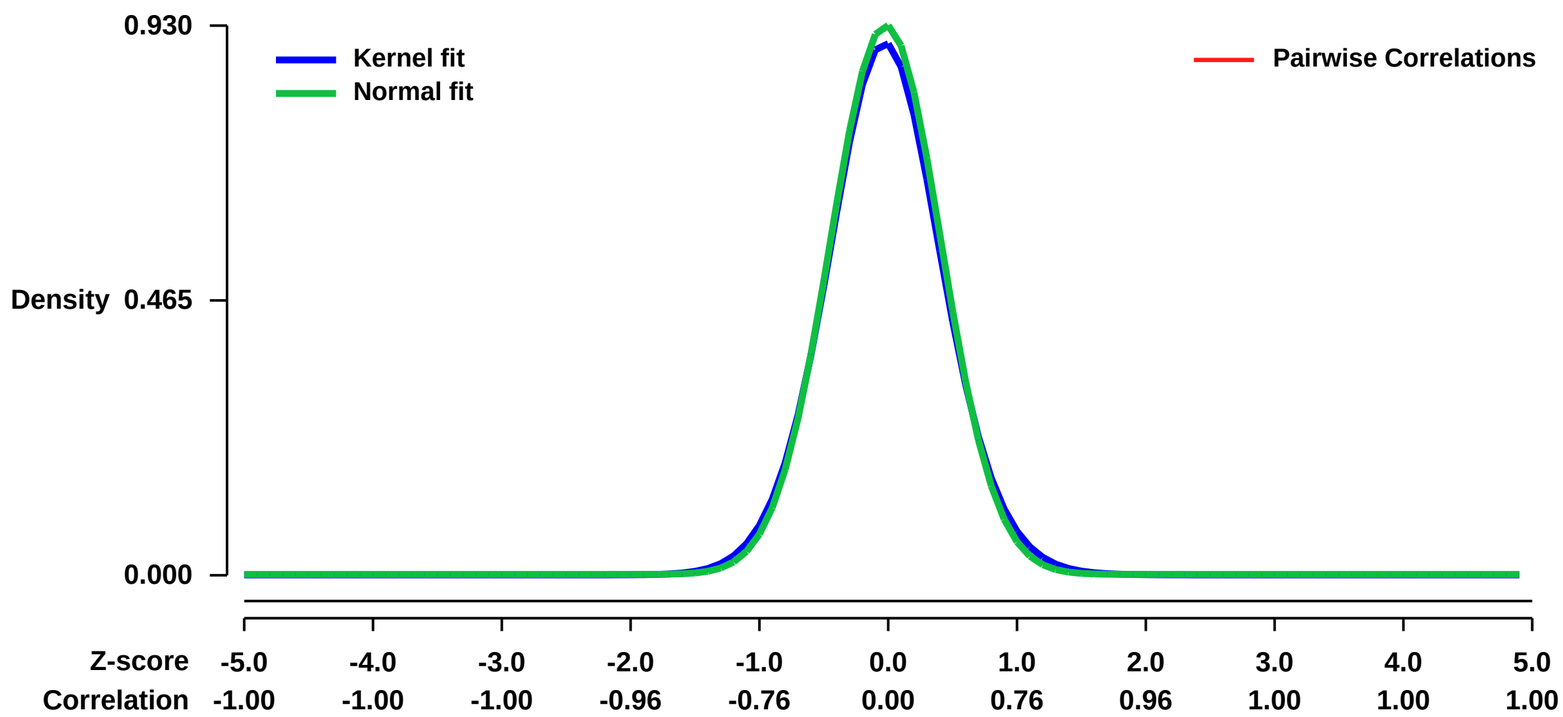

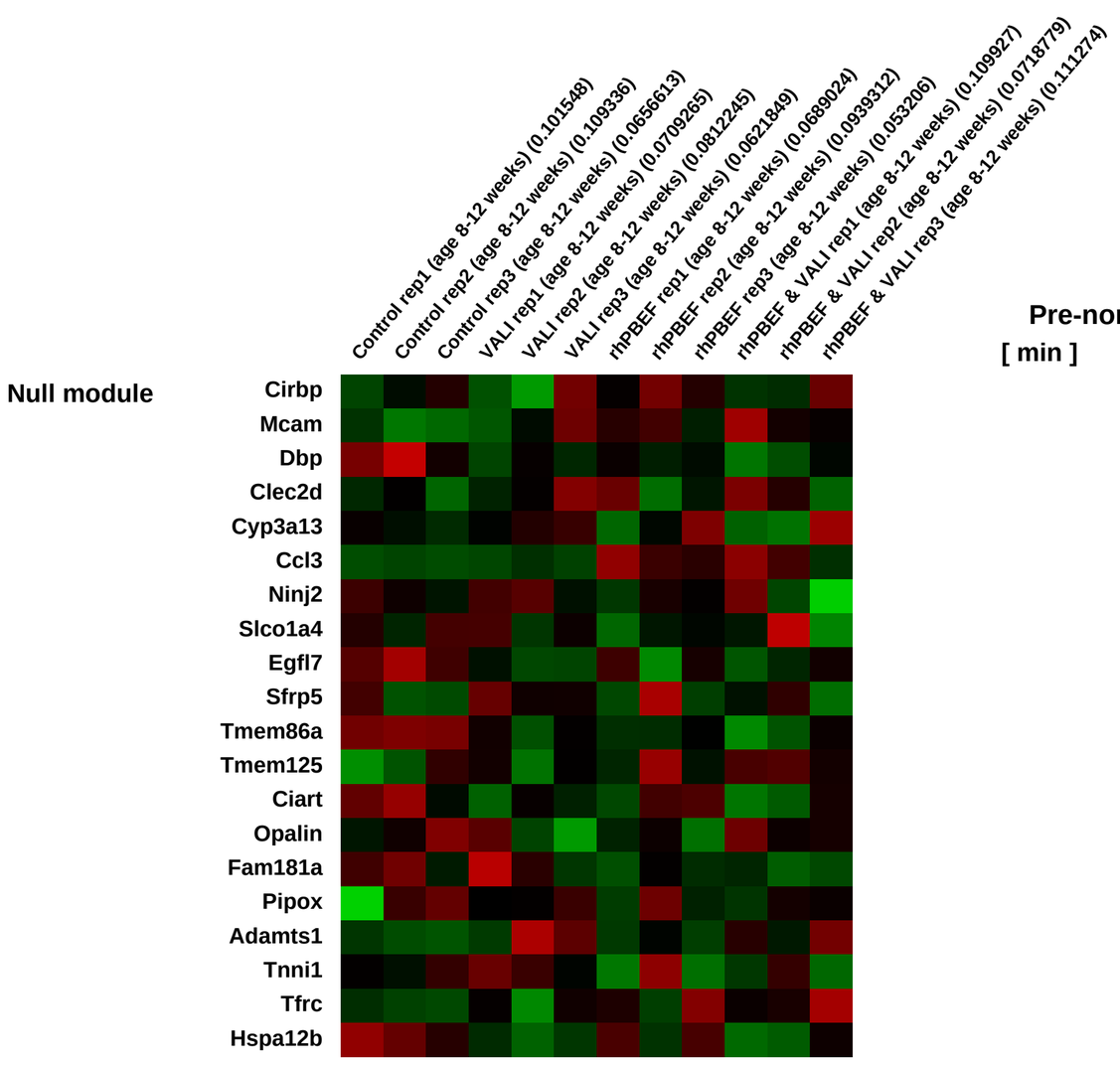

GEO Series "GSE13229" Expression Profiles

Num of samples in this series: 6

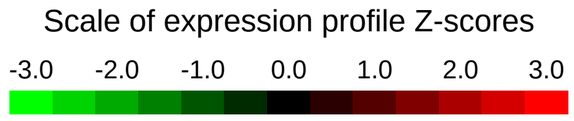

GEO Link:	http://www.ncbi.nlm.nih.gov/geo/query/acc.cgi?acc=GSE13229
Status:	Public on Mar 15 2009
Title:	Comparison of mouse NK cell subsets defined by CD27 and CD11b expression
Organism:	Mus musculus
Experiment type:	Expression profiling by array
Platform:	GPL1261
Pubmed ID:	22267813
Summary & Design:	**Summary:** Previous reports have defined three subsets of mouse NK cells on the basis of the expression of CD27 and CD11b. The developmental relationship between these subsets was unclear. To address this issue, we evaluated the overall proximity between mouse NK cell subsets defined by CD27 and CD11b expression using pangenomic gene expression profiling. The results suggest that CD27+CD11b-, CD27+CD11b+ and CD27-CD11b+ correspond to three different intermediates stages of NK cell development. **Overall design:** Spleen cells from RAG-/- mice have been isolated and stained with anti-NK1.1, anti CD27 and anti CD11b antibodies. NK1.1+ cells were sorted into CD27+ CD11b-, CD27+ CD11b+ and CD27- CD11b+ subsets by flow cytometry. There are two independent replicates for each sample. Total RNA was extracted with the RNeasy microkit (Qiagen) and gene expression profiles were performed according to manufacturer instructions (Affymetrix mouse 430 2.0).

Background corr dist: KL-Divergence = 0.0289, L1-Distance = 0.0175, L2-Distance = 0.0004, Normal std = 0.6674

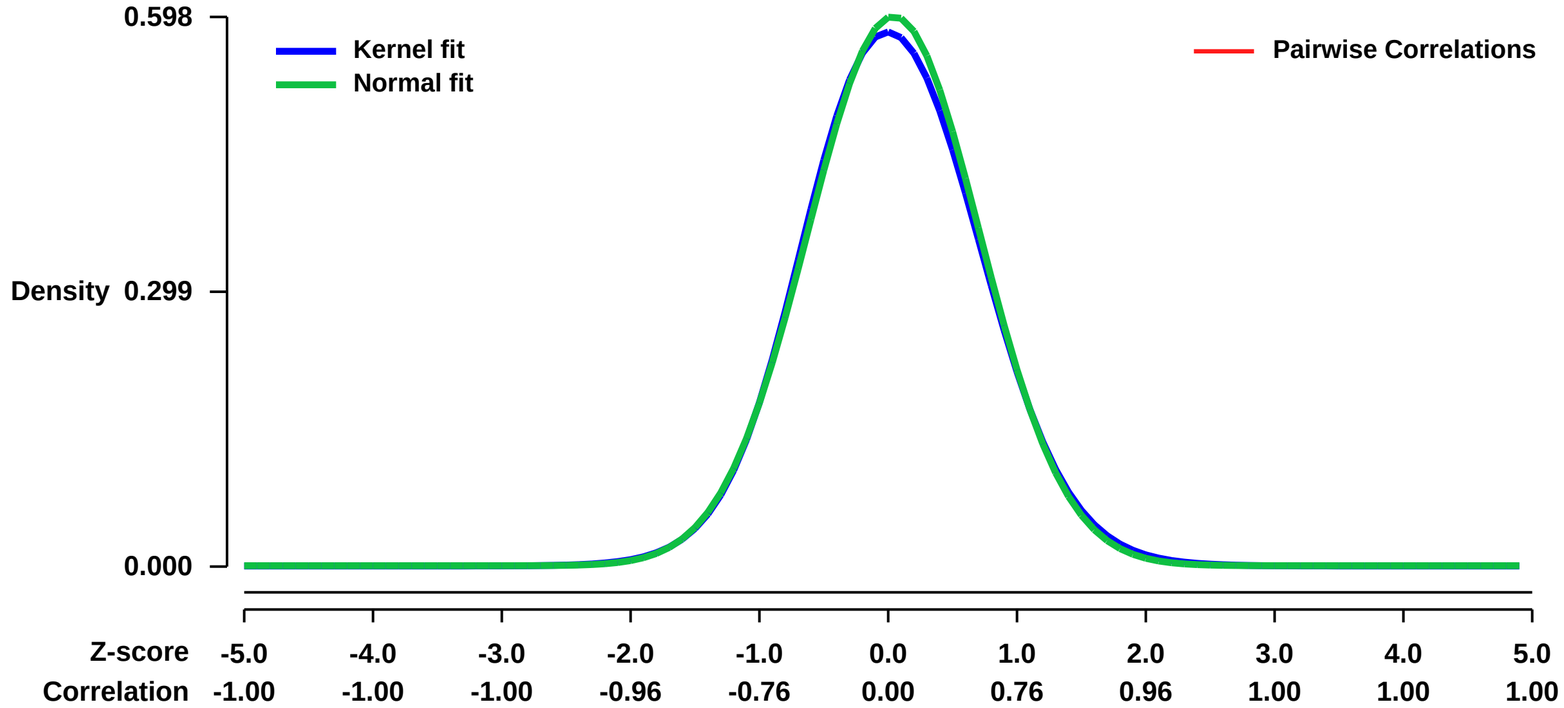

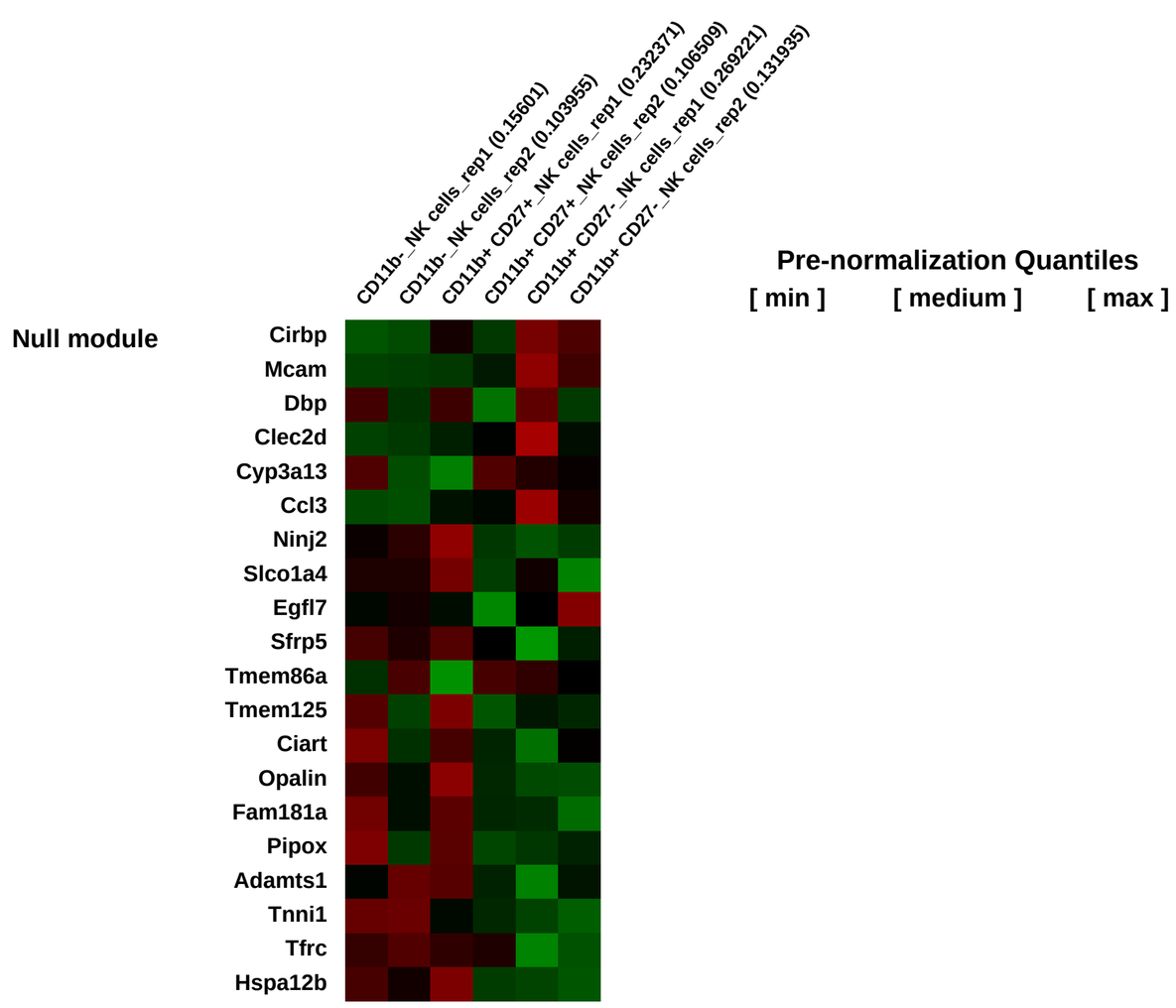

GEO Series "GSE9098" Expression Profiles

Num of samples in this series: 12

Scale of expression profile Z-scores

-3.0 -2.0 -1.0 0.0 1.0 2.0 3.0

GEO Link:	http://www.ncbi.nlm.nih.gov/geo/query/acc.cgi?acc=GSE9098
Status:	Public on Dec 10 2008
Title:	Estrogen-modulated gene expression in c-kit+ stem cells and CD44+ stromal cells
Organism:	Mus musculus
Experiment type:	Expression profiling by array
Platform:	GPL1261
Pubmed ID:	19006456
Summary & Design:	**Summary:** The recent interest in the role of bone marrow derived endothelial progenitor cells in the benefits of estrogen on cardiovascular health brought us to evaluate if estrogen could affect cardiac repair more broadly by regulating biological processes involved in the functional organization of the bone marrow stem cell niche. To assess such possibility, we evaluated gene expression profiles of bone marrow c-kit+ stem cells and CD44+ stromal cells, derived from primary whole bone marrow cultured system, after exposure to a physiological concentration of 17˛†-estradiol (17˛†E). Keywords: estrogen treatment response **Overall design:** 6 samples per cell type (c-kit+ stem cells or CD44+ stromal cells) were analysed. Of these, triplicates of 17˛†E treated and corresponding control non-treated cells are included.

Background corr dist: KL-Divergence = 0.0761, L1-Distance = 0.0377, L2-Distance = 0.0028, Normal std = 0.4812

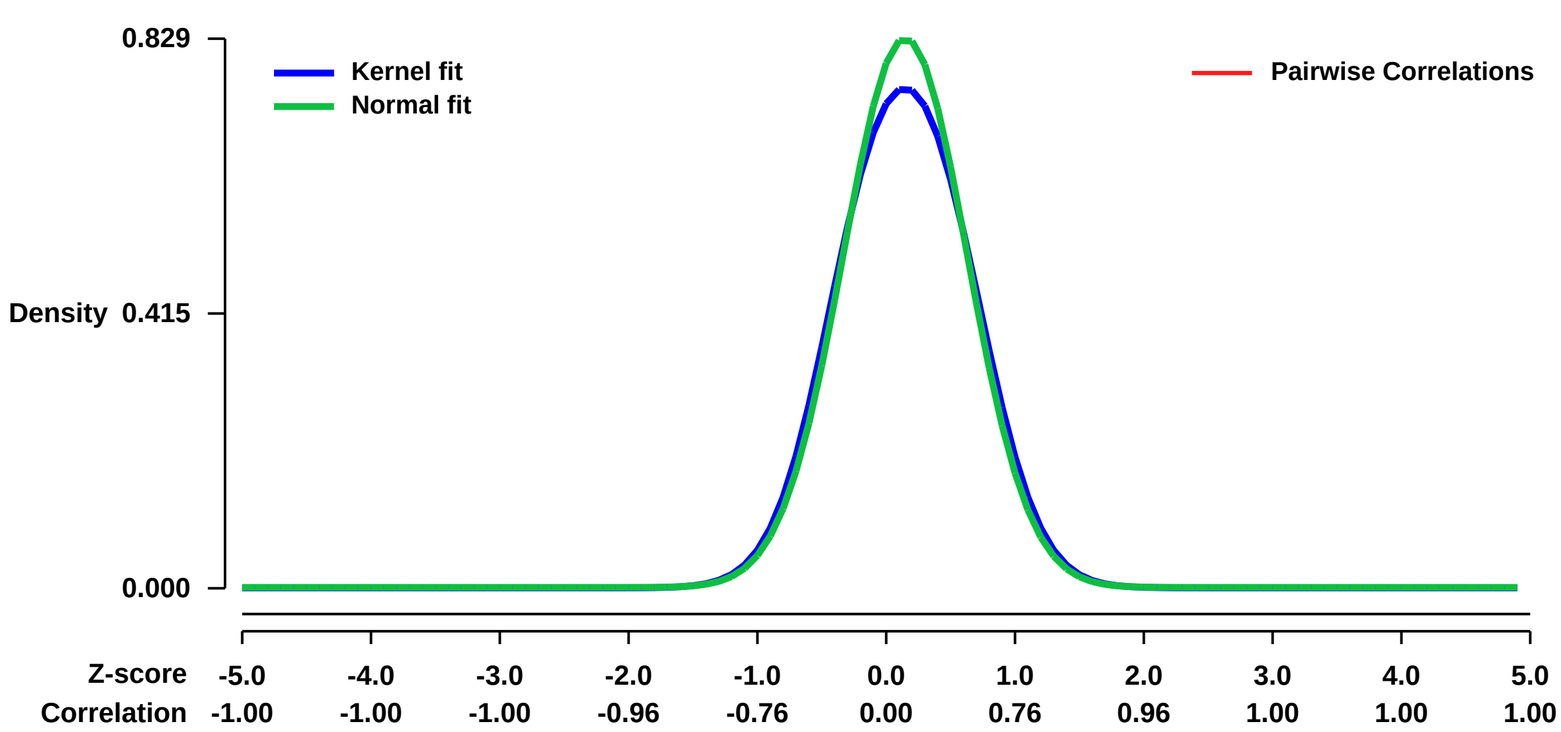

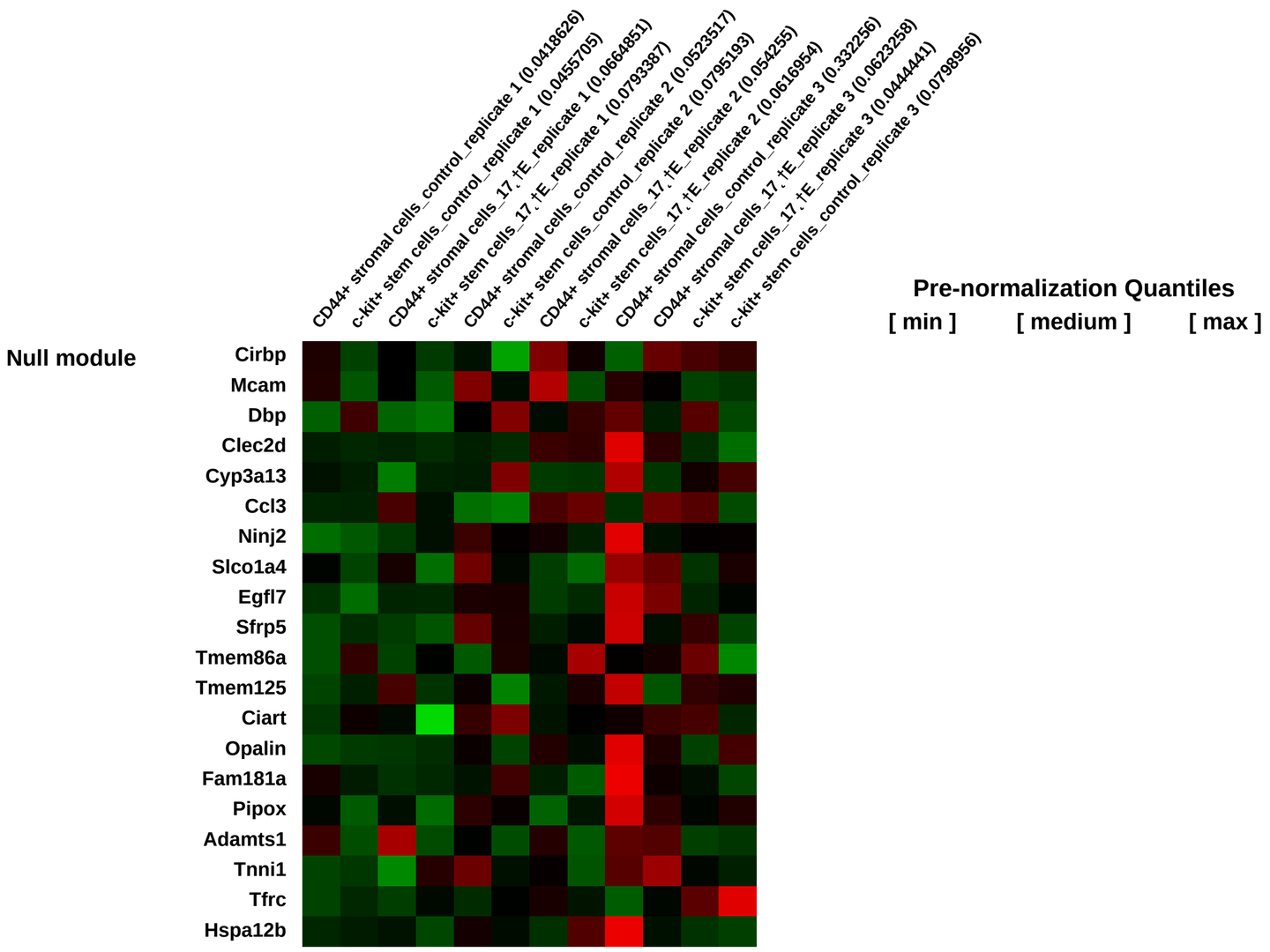

GEO Series "GSE15894" Expression Profiles

Num of samples in this series: 8

Scale of expression profile Z-scores

-3.0 -2.0 -1.0 0.0 1.0 2.0 3.0

GEO Link:	http://www.ncbi.nlm.nih.gov/geo/query/acc.cgi?acc=GSE15894
Status:	Public on Apr 25 2010
Title:	Comparison of gene expression in whole blood of mice subjected to normobaric hypoxia in vivo.
Organism:	Mus musculus
Experiment type:	Expression profiling by array
Platform:	GPL1261
Pubmed ID:	
Summary & Design:	**Summary:** To determine hypoxia mediated changes in whole blood, normal C57Bl/10 mice were gradually exposed to a chronic hypoxic environment, equivalent to an altitude of 6500m, for 2 weeks in vivo. Control, age-matched mice were maintained under normoxic, normobaric conditions by exposing them to ambient air in Philadelphia (c. 50 mts above sea level). #!# **Overall design:** Conclusion: Transcriptome level differences exist in the whole blood of animals subjected to normobaric hypoxia. Our definition of the normobaric hypoxia blood transcriptome provides insight into the functioning and response to hypoxia in whole blood.

Background corr dist: KL-Divergence = 0.0600, L1-Distance = 0.0331, L2-Distance = 0.0018, Normal std = 0.5385

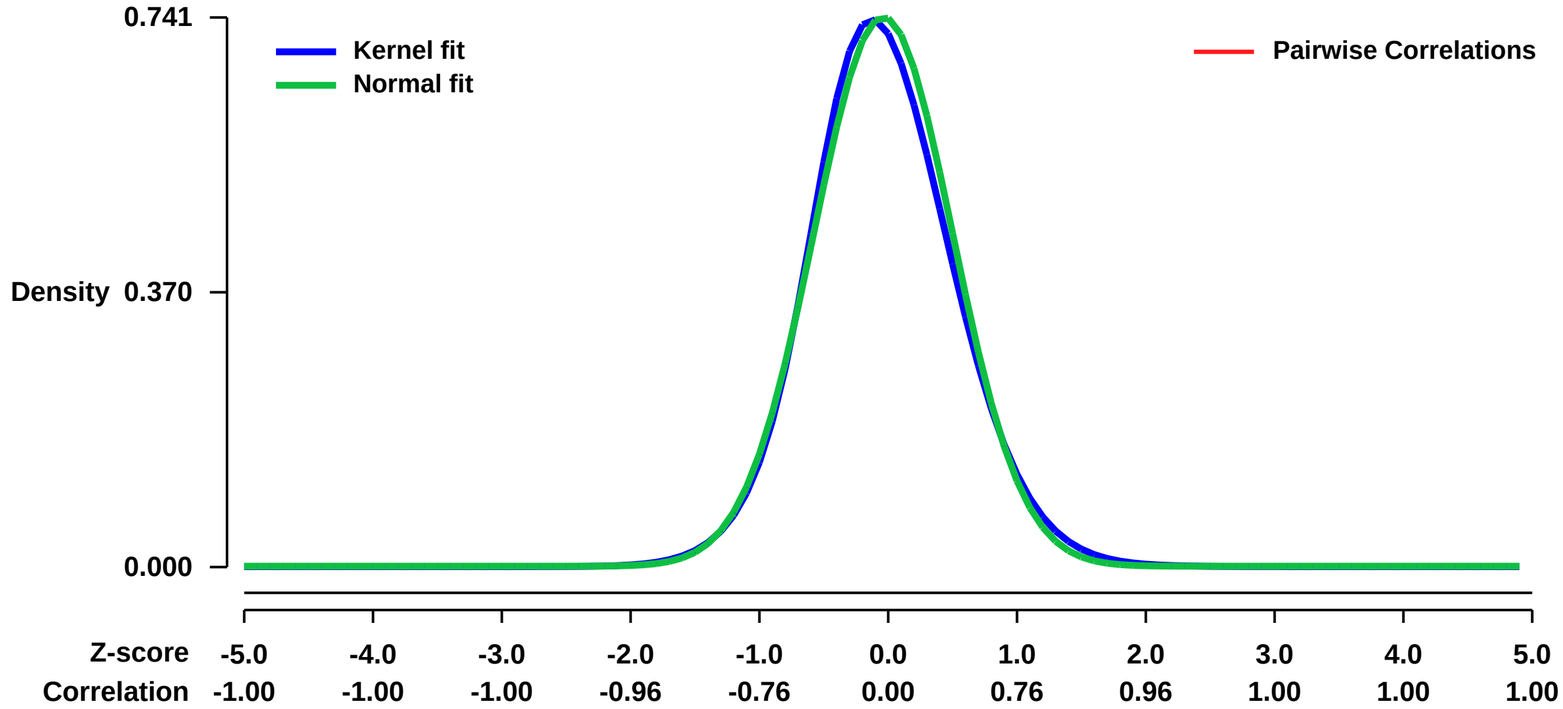

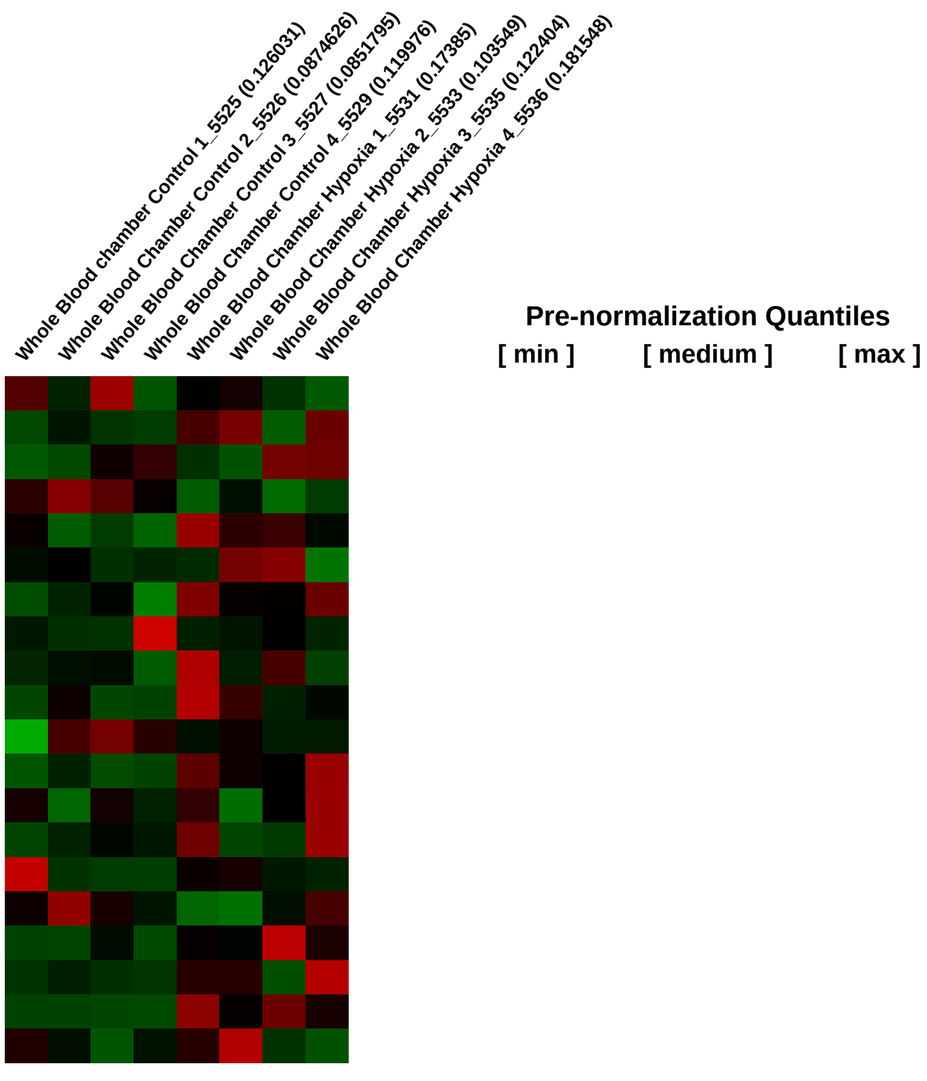

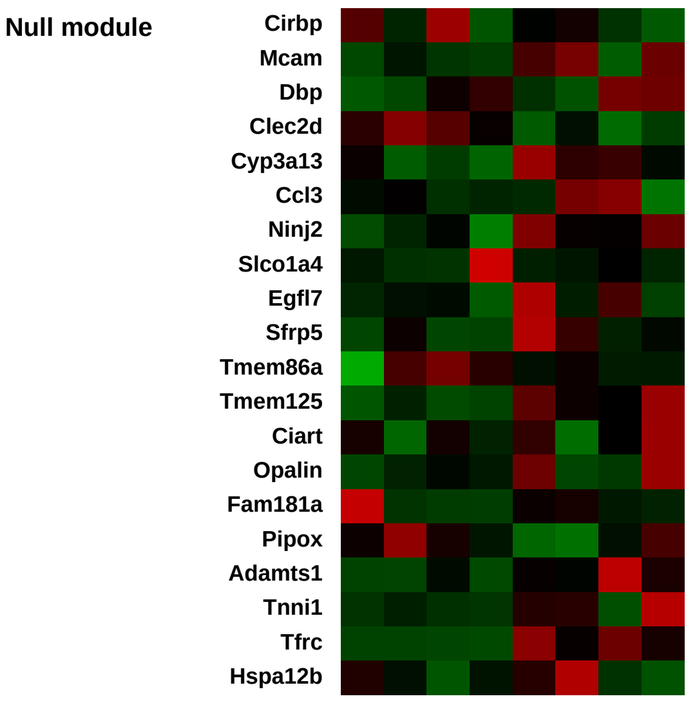

GEO Series "GSE34217" Expression Profiles

Num of samples in this series: 7

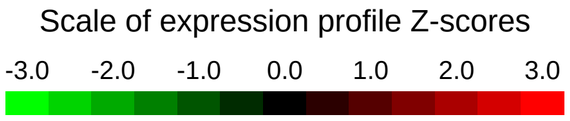

GEO Link:	http://www.ncbi.nlm.nih.gov/geo/query/acc.cgi?acc=GSE34217
Status:	Public on Jun 05 2012
Title:	Expression profile of miR-17-92a-MSCV-IRES-Thy1.1 transduced P14 CD8+ T cells
Organism:	Mus musculus
Experiment type:	Expression profiling by array
Platform:	GPL1261
Pubmed ID:	22665768
Summary & Design:	**Summary:** During acute viral infections, effector CD8+ T cells differentiate into memory precursors or short-lived terminal effectors. miR-17-92a over-expression skews CD8+ effector cells to the terminal differentiation. We used microarray to identify the genes that are differentially expressed caused by miR-17-92a over-expression. **Overall design:** CD8+ T cells from P14 TCR transgenic mice were infected with miR-17-92a-MSCV-IRES-Thy1.1 vector and transfer to C57BL6 recipients. Chimeras were infected with LCMV Armstrong. Thy1.1+ miR-17-92a-MSCV-IRES-Thy1.1 transduced P14 cells and Thy1.1- non-transduced P14 cells were sorted by FACS. RNA was extracted from samples, labeled, and hybridized to Affymetrix microarrays.

Background corr dist: KL-Divergence = 0.0441, L1-Distance = 0.0242, L2-Distance = 0.0007, Normal std = 0.5956

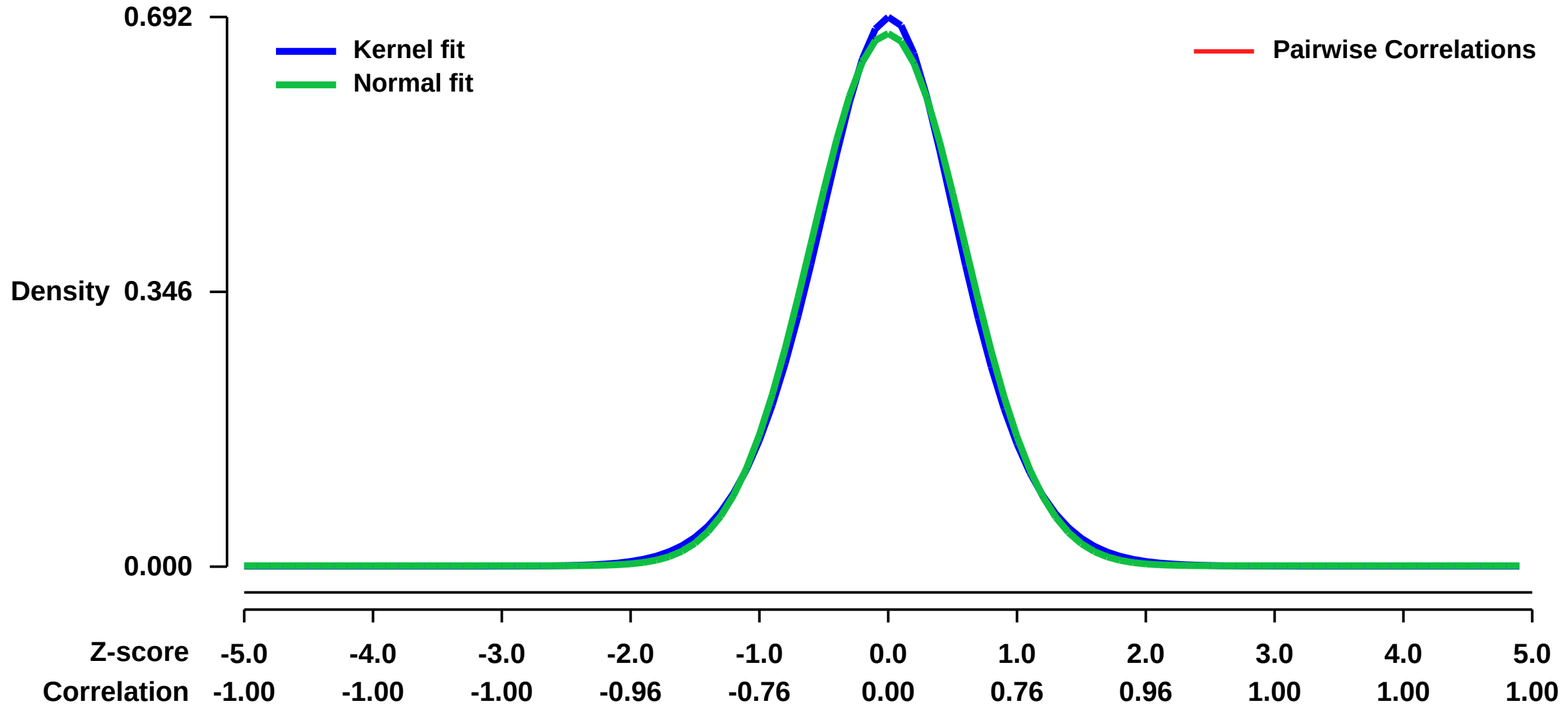

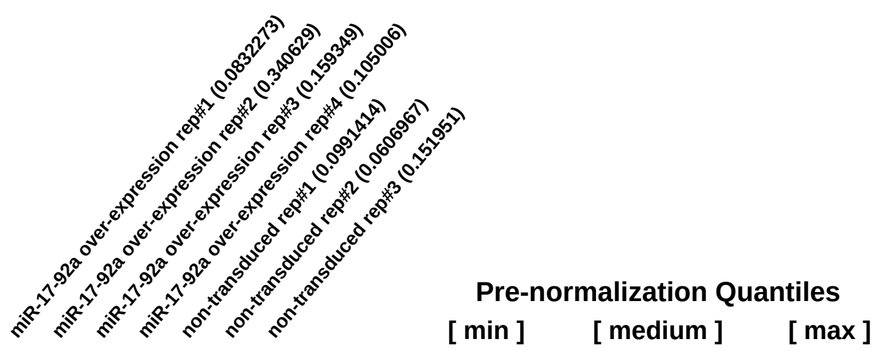

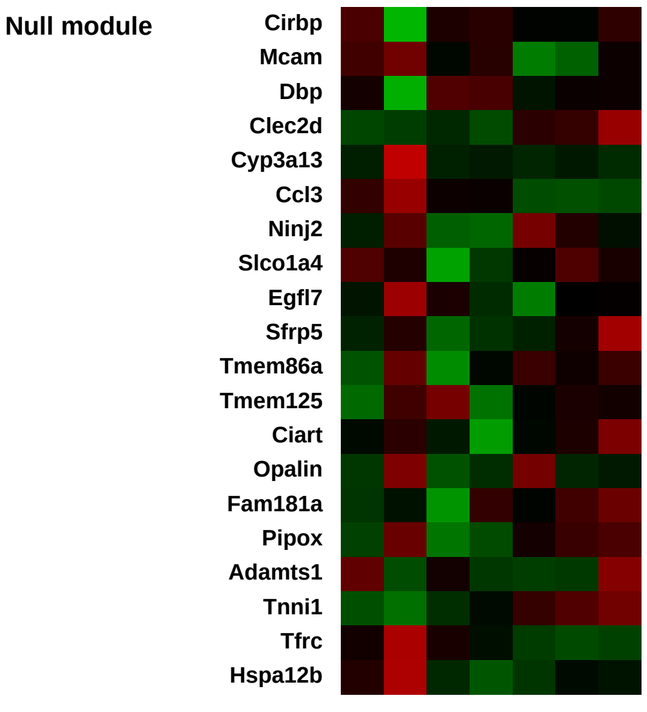

GEO Series "GSE16364" Expression Profiles

Num of samples in this series: 6

Scale of expression profile Z-scores

-3.0 -2.0 -1.0 0.0 1.0 2.0 3.0

GEO Link:	http://www.ncbi.nlm.nih.gov/geo/query/acc.cgi?acc=GSE16364
Status:	Public on Feb 05 2010
Title:	Polycomb-like 2 associates with PRC2 and is required for mouse embryonic stem cell
Organism:	Mus musculus
Experiment type:	Expression profiling by array
Platform:	GPL1261
Pubmed ID:	20144788
Summary & Design:	**Summary:** Polycomb group (PcG) proteins are highly conserved epigenetic transcriptional repressors important for the control of numerous developmental gene expression programs and have recently been implicated in the modulation of embryonic stem cell (ESC) identity. We identified the PcG protein PCL2 (polycomb-like 2) in a genome-wide screen for novel regulators of self-renewal and pluripotency and predicted that it would play an important role in mouse ESC fate determination. Using multiple biochemical strategies, we provide evidence that PCL2 is a novel Polycomb Repressive Complex 2 (PRC2)-associated protein in mouse ESCs. Knockdown of Pcl2 in ESCs resulted in heightened self-renewal characteristics, defects in differentiation and altered patterns of histone methylation. Through integration of global gene expression and promoter occupancy analyses of both PCL2 and PRC2 components EZH2 and SUZ12, we have predicted PCL2 target genes and formulated regulatory networks describing the role of PCL2 both in modulating transcription of ESC self-renewal genes in undifferentiated ESCs as well as developmental regulators during early commitment and differentiation. **Overall design:** Cells were stably expressing Pcl2 shRNA or shRNA mismatch control sequences. Hybridizations of three biological replicates for both the control and Pcl2 shRNA clone were performed.

Background corr dist: KL-Divergence = 0.0389, L1-Distance = 0.0217, L2-Distance = 0.0005, Normal std = 0.6242

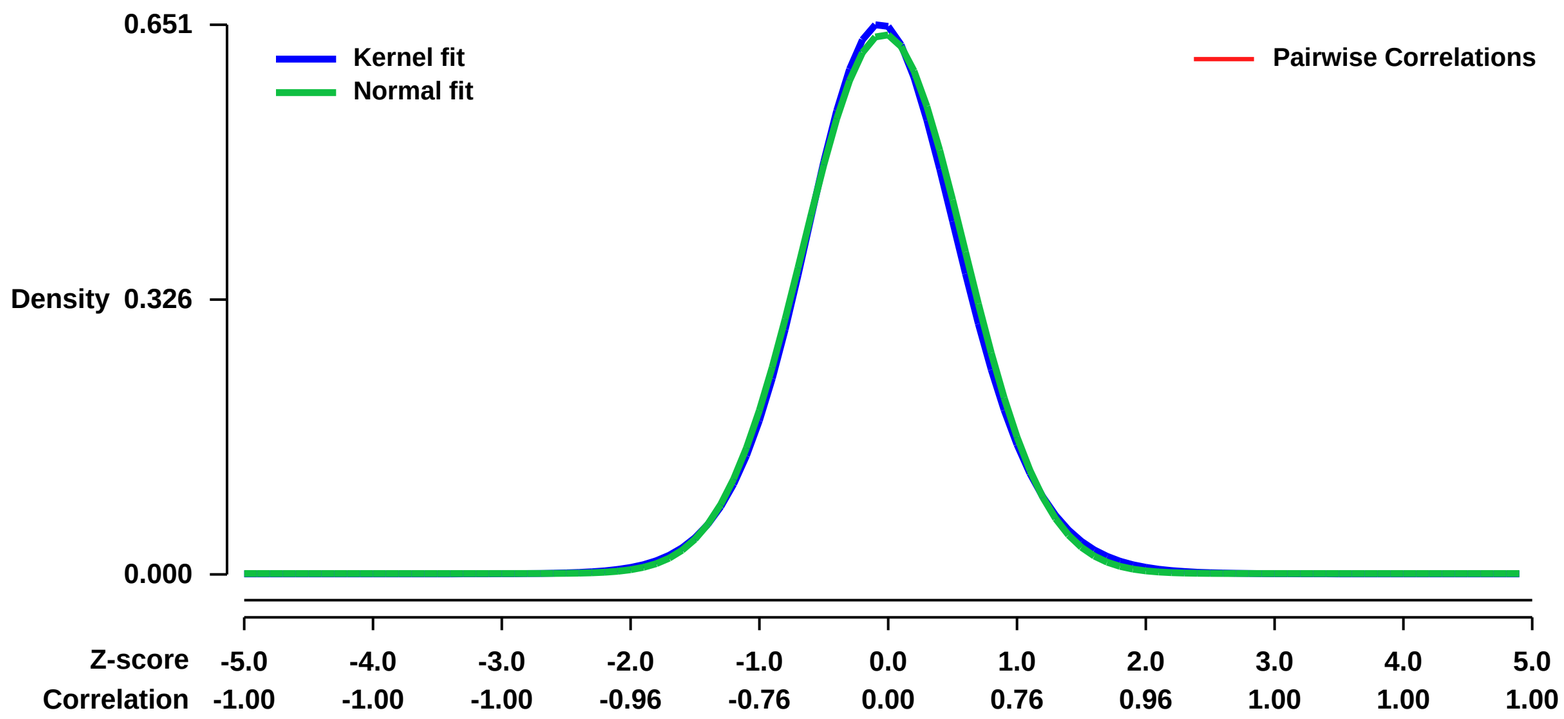

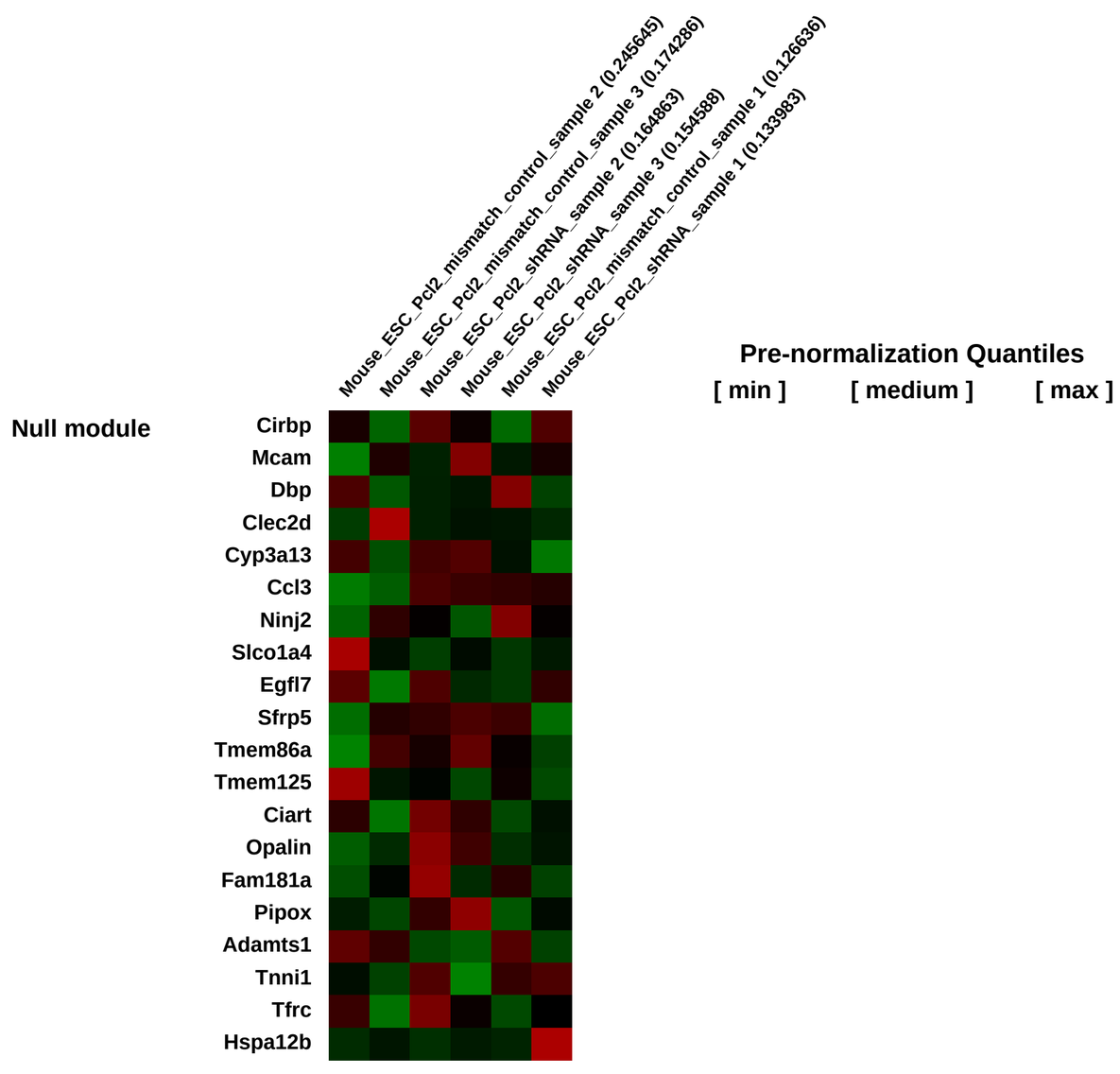

GEO Series "GSE20577" Expression Profiles

Num of samples in this series: 12

Scale of expression profile Z-scores

-3.0 -2.0 -1.0 0.0 1.0 2.0 3.0

GEO Link:	**http://www.ncbi.nlm.nih.gov/geo/query/acc.cgi?acc=GSE20577**
Status:	**Public on Dec 01 2010**
Title:	**Gestational taurine supplementation of mice: effect on offspring gene expression in liver and skeletal muscle**
Organism:	**Mus musculus**
Experiment type:	**Expression profiling by array**
Platform:	**GPL1261**
Pubmed ID:	
Summary & Design:	**Summary:** **Taurine is known to be important for fetal well being and to be able to prevent effects of a low birthweight phenotype when supplemented to pregnant dams.** **We hypothesized that gestational taurine supplementation would affect gene expression level in 4w offspring liver and skeletal muscle.** **Overall design:** **Pregnant mouse dams were subjected to different diet schemes from day 1 of pregnancy until birth. Pups were killed at 4 weeks of age and liver and quadriceps skeletal muscle taken out and frozen at -80C until analysis. Diet schemes: Normal Protein (20% casein; NP), Normal Protein + taurine (1% taurine supplementation in water ad libitum; NP+tau). The liver and muscle samples were normalized separately.**

Background corr dist: **KL-Divergence = 0.0243, L1-Distance = 0.0507, L2-Distance = 0.0039, Normal std = 0.7351**

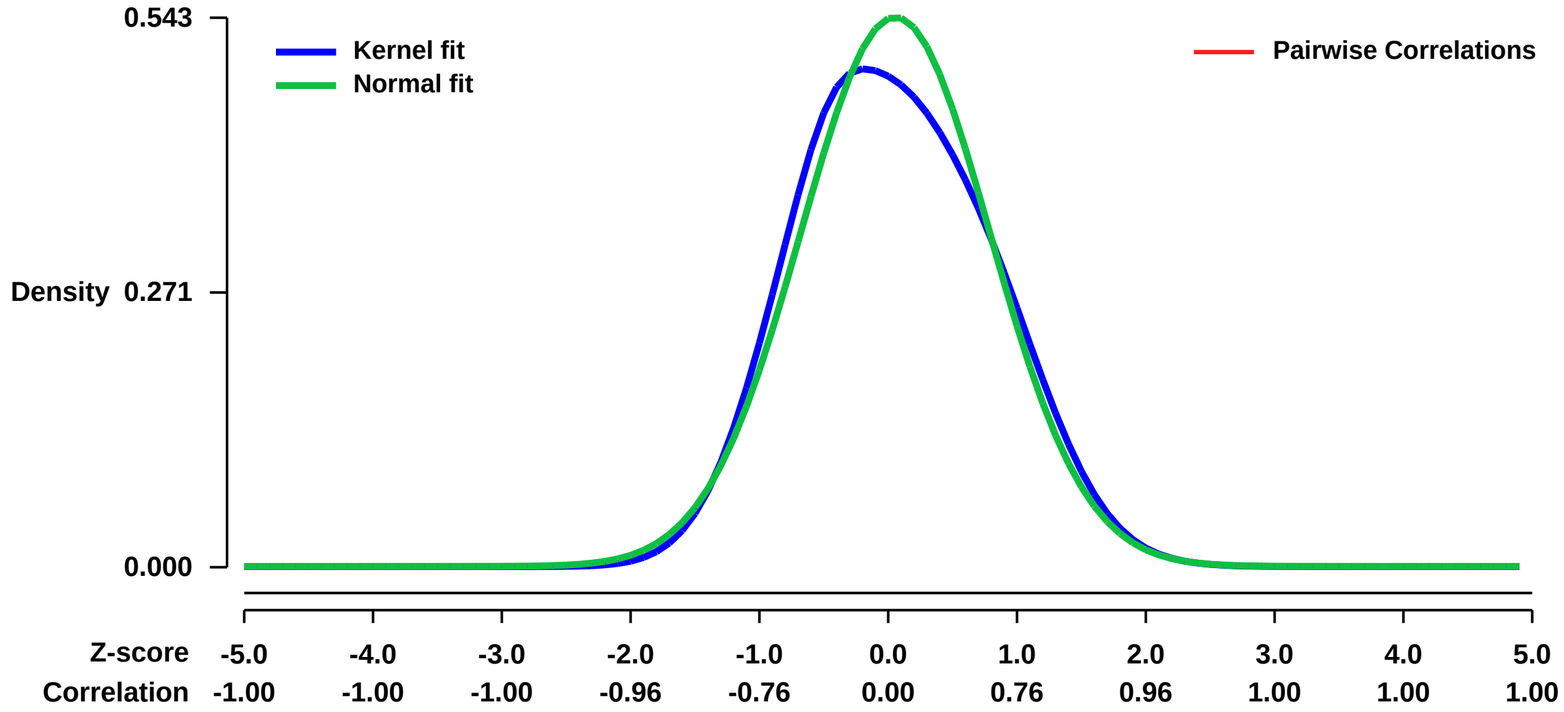

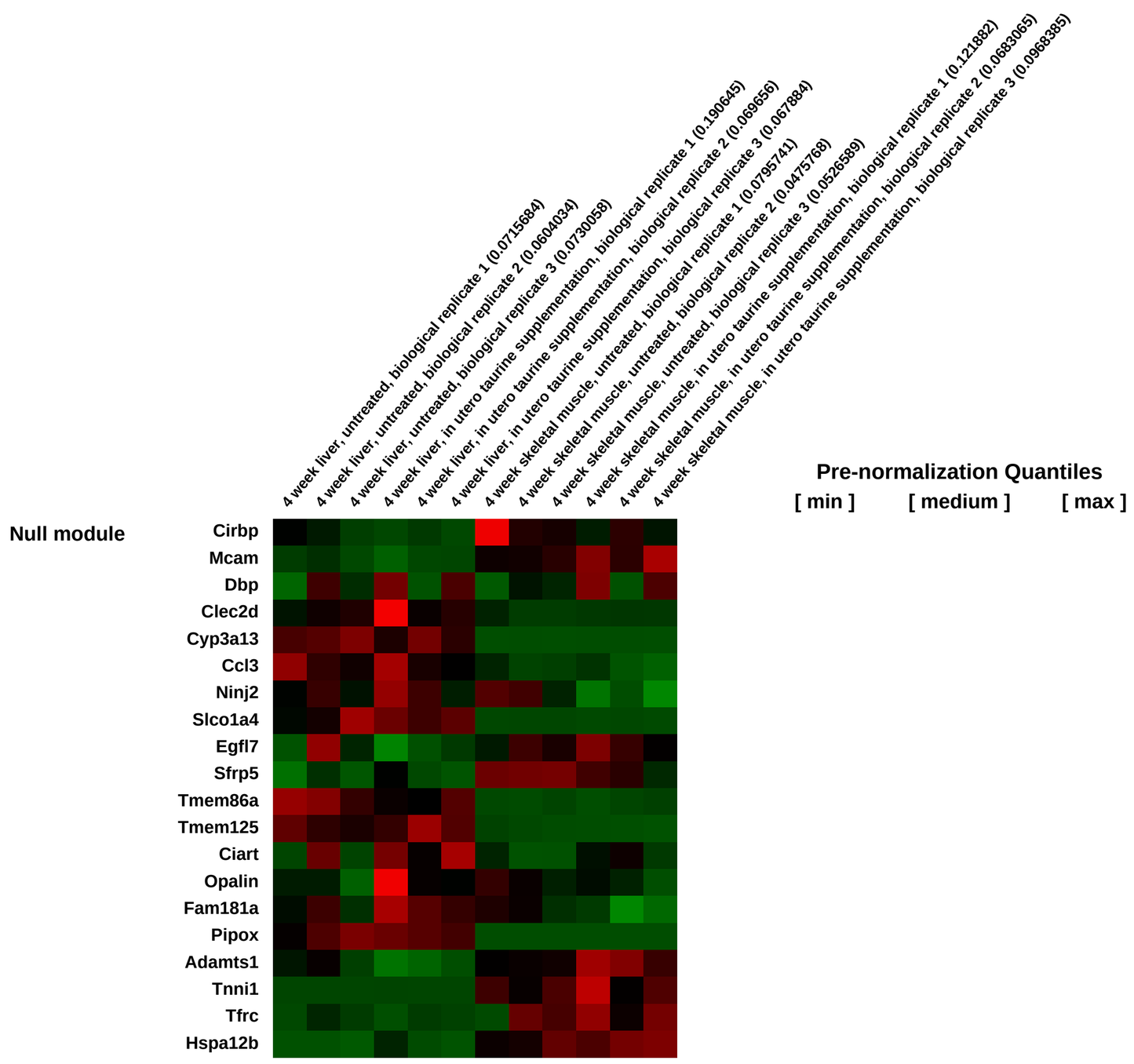

GEO Series "GSE6789" Expression Profiles

Num of samples in this series: 12

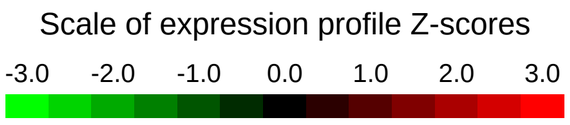

GEO Link:	http://www.ncbi.nlm.nih.gov/geo/query/acc.cgi?acc=GSE6789
Status:	Public on Mar 30 2007
Title:	response to IL-1b of WT and IRAK4 kinase dead mouse embryonic fibroblasts
Organism:	Mus musculus
Experiment type:	Expression profiling by array
Platform:	GPL1261
Pubmed ID:	17337443
Summary & Design:	**Summary:** **IRAK-4 is an essential component of the signal transduction complex downstream of the IL-1- and Toll-like receptors. Though regarded as the first kinase in the signaling cascade, the role of IRAK-4 kinase activity versus its scaffold function is still controversial. In order to investigate the role of IRAK-4 kinase function in vivo, â knock-inâ mice were generated by replacing the wild type IRAK-4 gene with a mutant gene encoding kinase deficient IRAK-4 protein (IRAK-4 KD). Analysis of embryonic fibroblasts and macrophages obtained from IRAK-4 KD mice with a number of experimental techniques demonstrated that they greatly lack responsiveness to stimulation with IL-1b or a Toll-like receptor 7 (TLR7) agonist. One of the techniques used, microarray analysis, identified IRAK-4 kinase-dependent IL-1b response genes in mouse embryonic fibroblasts and revealed that the induction of IL-1b-responsive mRNAs was largely ablated in IRAK-4 KD cells. In summary, our results suggest that IRAK-4 kinase activity plays a critical role in IL-1R/TLR7-mediated induction of inflammatory responses.** **Keywords: genetic modification, strain comparison, cell stimulation, time course, inflammatory response** **Overall design:** **The response of mouse embryonic fibroblasts from WT and IRAK4 kinase dead animals to stimulation with IL-1b at two time points was determined. There were 12 samples in total, 6 from WT and 6 from IRAK4 kinase dead cells; for each strain there were 3 conditions: growth for 4 hours without stimulation (the strain-specific control), growth for 1 hour with stimulation, and growth for 4 hours with stimulation; for each condition there were two biological replicates.**

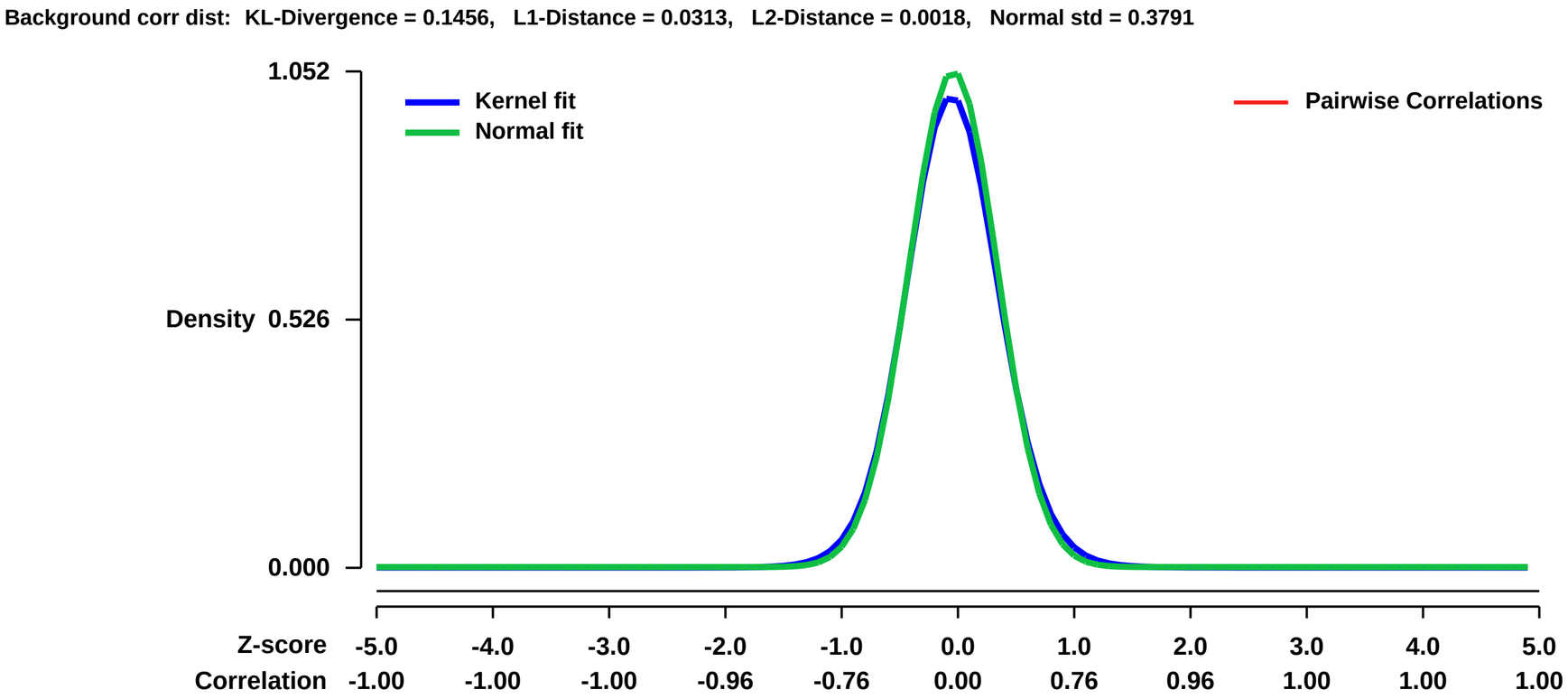

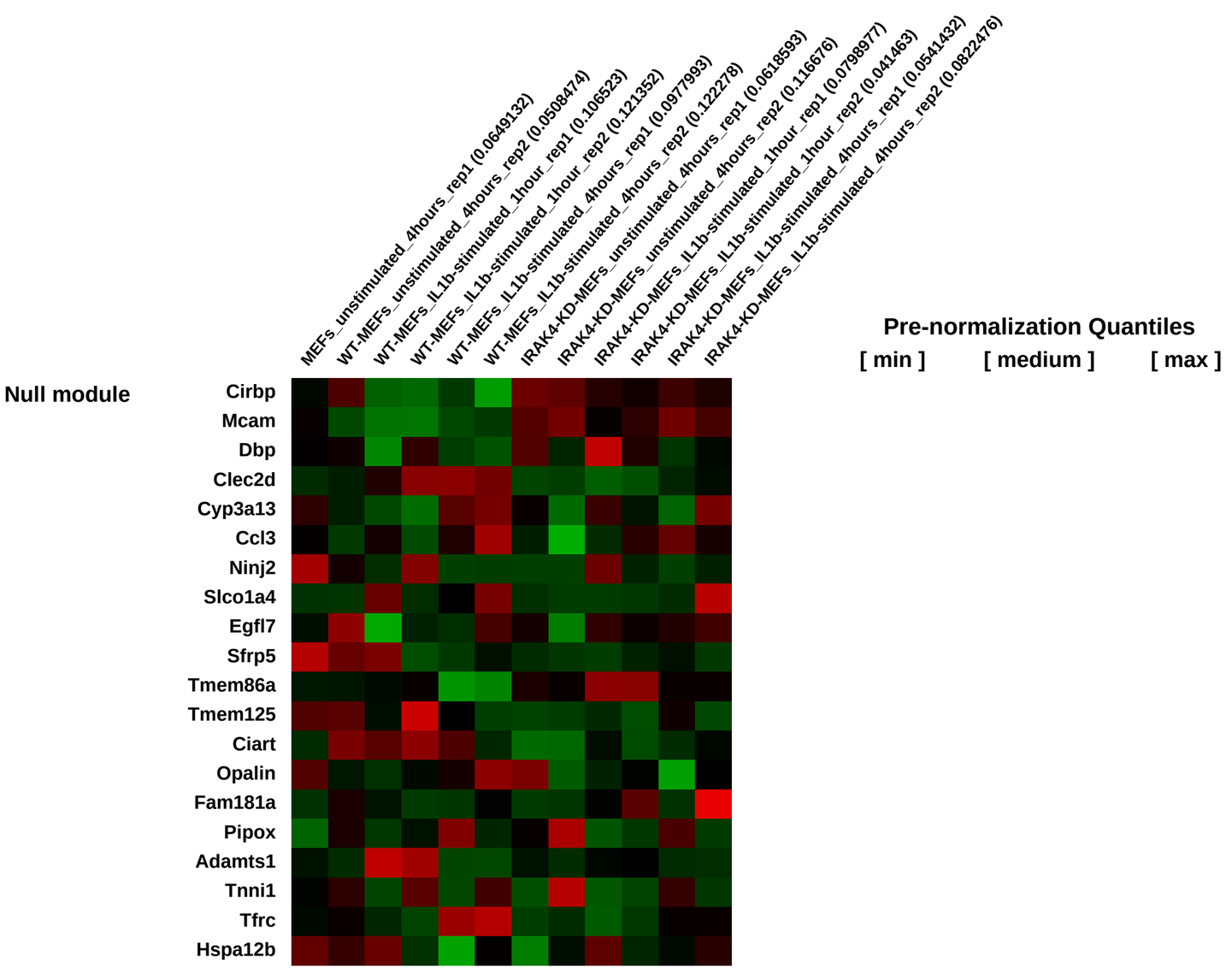

GEO Series "GSE33471" Expression Profiles

Num of samples in this series: 12

Scale of expression profile Z-scores

-3.0 -2.0 -1.0 0.0 1.0 2.0 3.0

GEO Link:	http://www.ncbi.nlm.nih.gov/geo/query/acc.cgi?acc=GSE33471
Status:	Public on Jan 04 2012
Title:	Paracrine TGFˆ Signaling Counterbalances BMP-Mediated Repression in Hair Follicle Stem Cell Activation
Organism:	Mus musculus
Experiment type:	Expression profiling by array
Platform:	GPL1261
Pubmed ID:	22226356
Summary & Design:	**Summary:** Hair follicle (HF) regeneration begins when communication between quiescent epithelial stem cells (SCs) and underlying mesenchymal dermal papillae (DP) generates sufficient activating cues to overcome repressive BMP signals from surrounding niche cells. We uncovered a hitherto unrecognized DP transmitter, TGF‚†2, which activates Smad2/3 transiently in HFSCs concomitant with entry into tissue regeneration. We used microarrays to detect the genes specifically affected by TGFˆ receptor II-deficient mice upon HFSC activation. **Overall design:** Hair follicle stem cells (HFSCs) of hair gem (HG) and bulge, and total skin keratinocytes were FACS-purified from the mouse back skin at 2nd telogen-to-anagen transition stages.

Background corr dist: KL-Divergence = 0.1215, L1-Distance = 0.0369, L2-Distance = 0.0028, Normal std = 0.4111

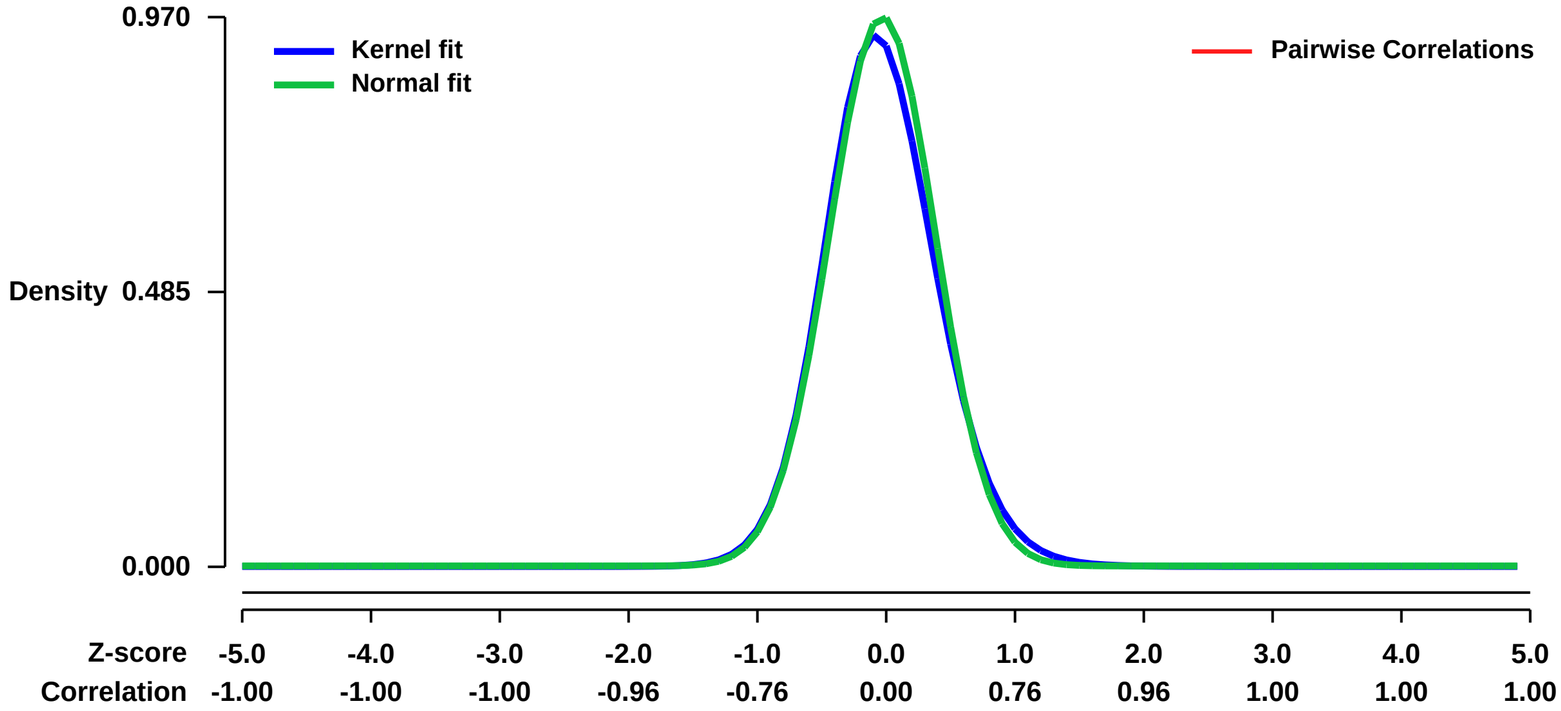

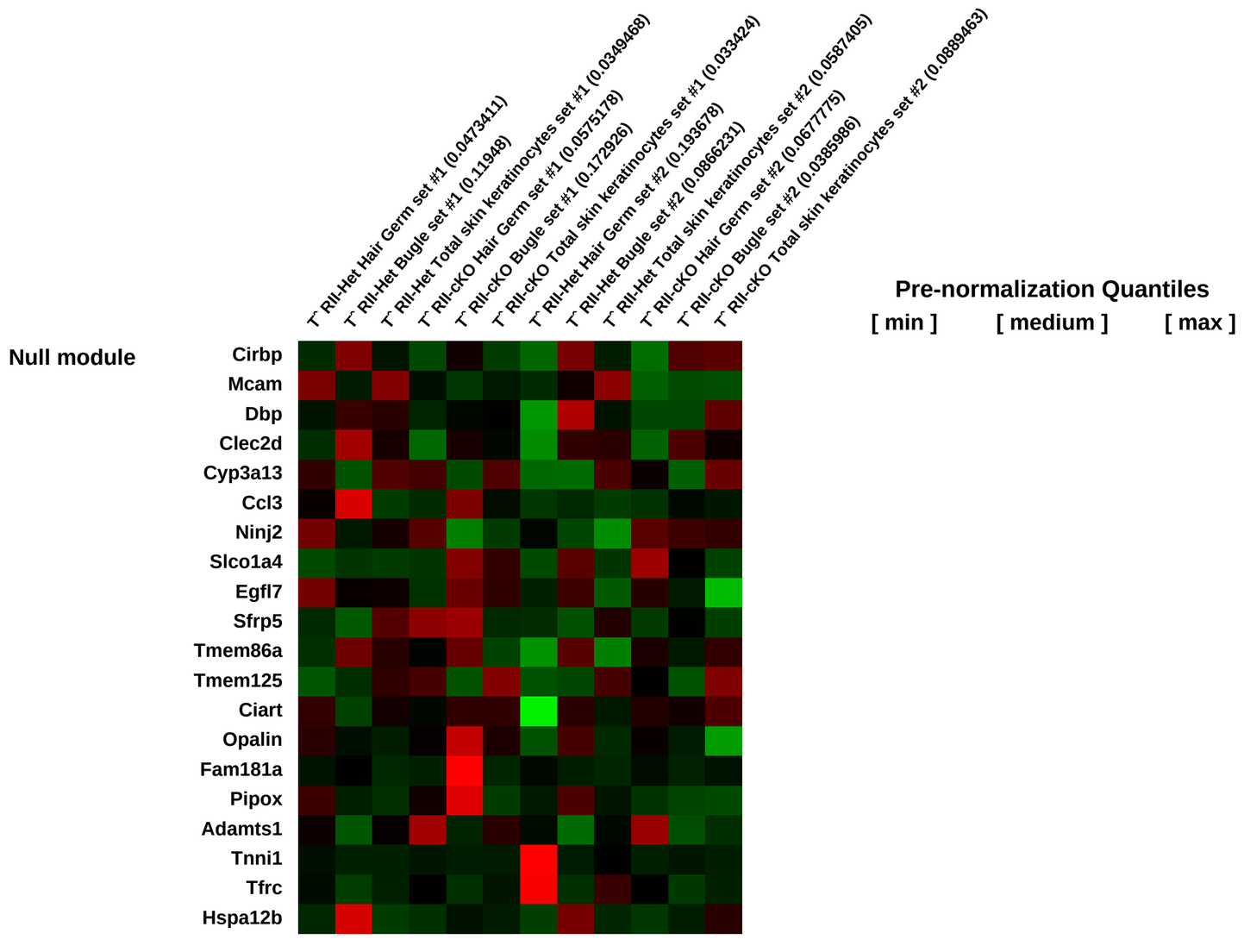

GEO Series "GSE9294" Expression Profiles

Num of samples in this series: 12

Scale of expression profile Z-scores

-3.0 -2.0 -1.0 0.0 1.0 2.0 3.0

GEO Link:	**http://www.ncbi.nlm.nih.gov/geo/query/acc.cgi?acc=GSE9294**
Status:	**Public on Oct 09 2008**
Title:	**EOM and TA Sp cell comparison**
Organism:	**Mus musculus**
Experiment type:	**Expression profiling by array**
Platform:	**GPL1261**
Pubmed ID:	**19116248**
Summary & Design:	**Summary:** **Using Affymetrix GeneChips, we analyzed expression profiles of SP cells from EOM and TA. 348 differentially expressed transcripts defined the EOM-SP transcriptome: 229 upregulated in EOM-SP and 119 in TA-SP.** **Keywords: Expression Profiling** **Overall design:** **Six independently separated EOM and six TA SP cell preparations were used for microarray analysis using the Affymetrix´fi Mouse 430 ver 2.0 GeneChip arrays.**

Background corr dist: **KL-Divergence = 0.0728, L1-Distance = 0.0522, L2-Distance = 0.0052, Normal std = 0.5125**

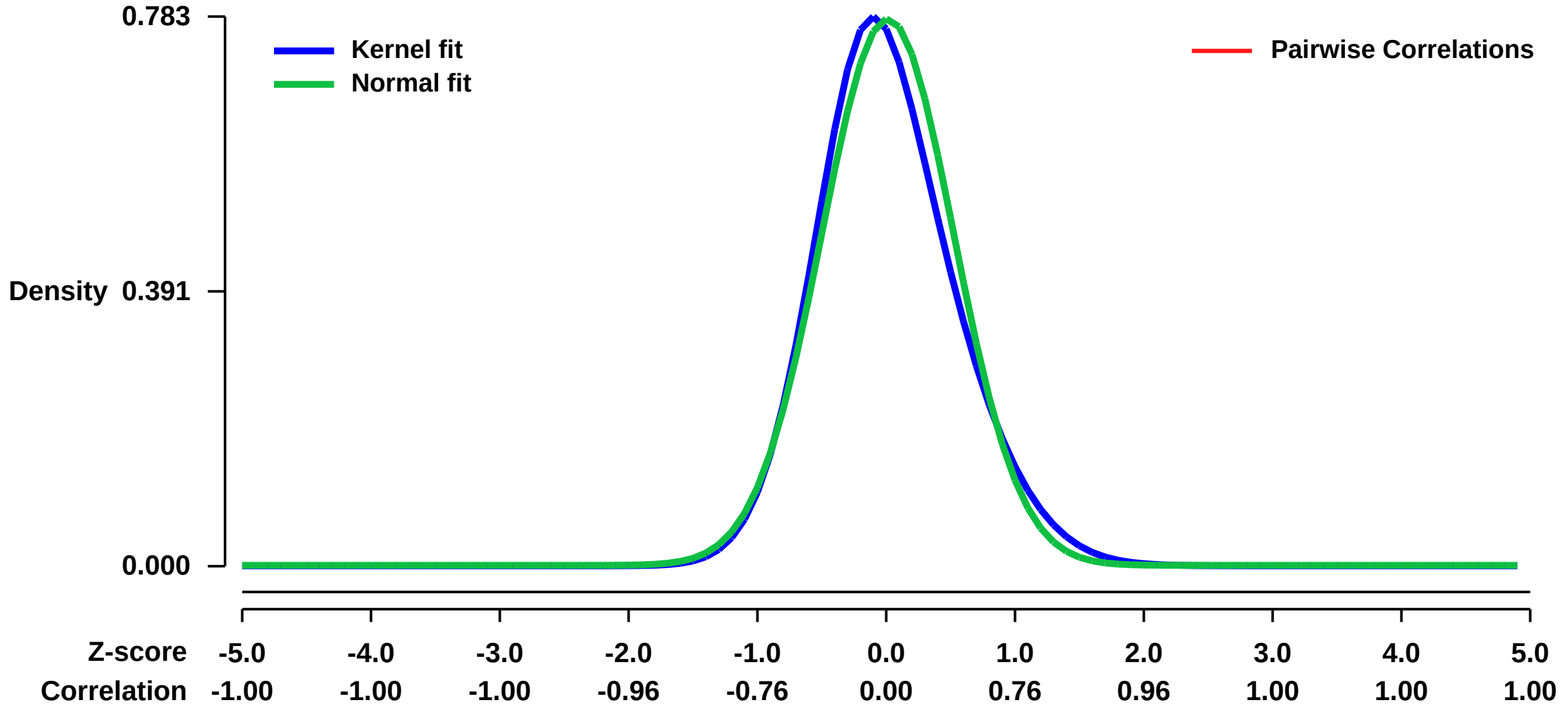

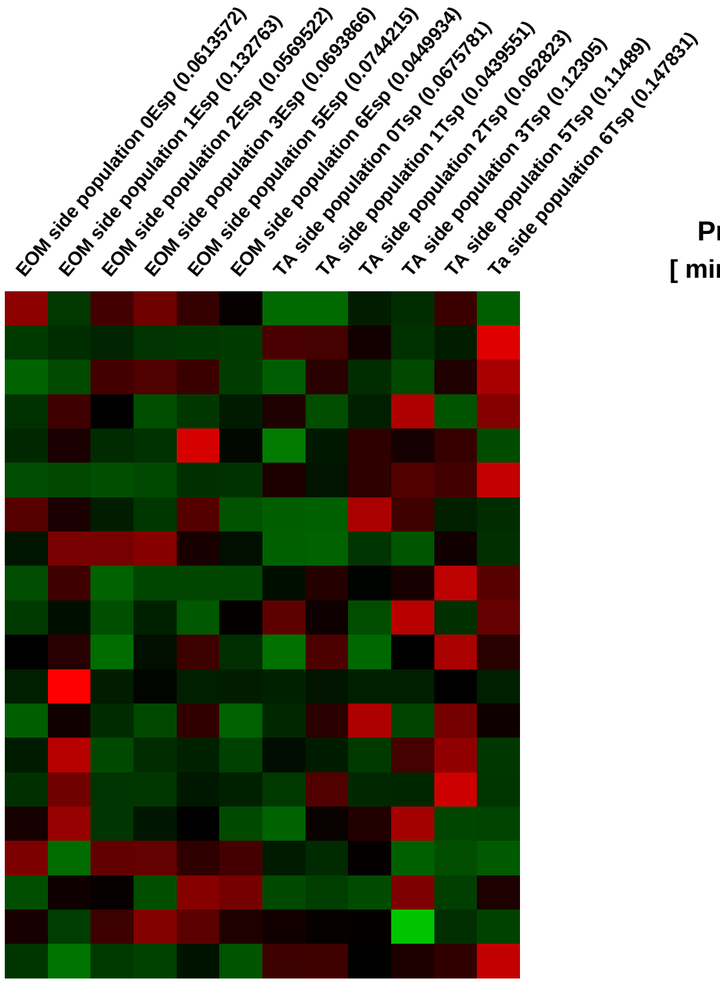

GEO Series "GSE7310" Expression Profiles

Num of samples in this series: 10

Scale of expression profile Z-scores

-3.0 -2.0 -1.0 0.0 1.0 2.0 3.0

GEO Link:	http://www.ncbi.nlm.nih.gov/geo/query/acc.cgi?acc=GSE7310
Status:	Public on Jan 01 2008
Title:	Comparison analysis of 2 week old C57BL6J lung exposed to 2 weeks of cigarette smoke compared to age-matched controls
Organism:	Mus musculus
Experiment type:	Expression profiling by array
Platform:	GPL1261
Pubmed ID:	17975176
Summary & Design:	**Summary:** We hypothesize that gene expression in the cigarette smoke (CS) exposed neonatal lung and age-matched controls will be divergent. CS exposed lung will have divergence of immune response genes and structural genes. The lungs of (6) 2 week old neonatal mice exposed to 2 weeks of CS were compared to the lung of (4) 2 week old age-matched control mice. We utilized microarray analysis to examine transcriptional differences between smoke exposed neonatal lung and age-matched controls. **Keywords: comparative expression profiling** **Overall design:** This study utilizes microarray analysis to test these hypotheses. Six sets of lungs were harvested from CS exposed mice and four sets of lungs were harvested from age-matched control mice. RNA was isolated and used for global gene expression profiling (Affymetrix Mouse 430 2.0 array). Statistically significant gene expression was determined as a minimum 6 counts of 9 pairwise comparisons, minimum 1.5-fold change, and p < 0.05. Further, Absolute | FC - FC SEM | >= 1.5.

Background corr dist: KL-Divergence = 0.0562, L1-Distance = 0.0341, L2-Distance = 0.0021, Normal std = 0.5400

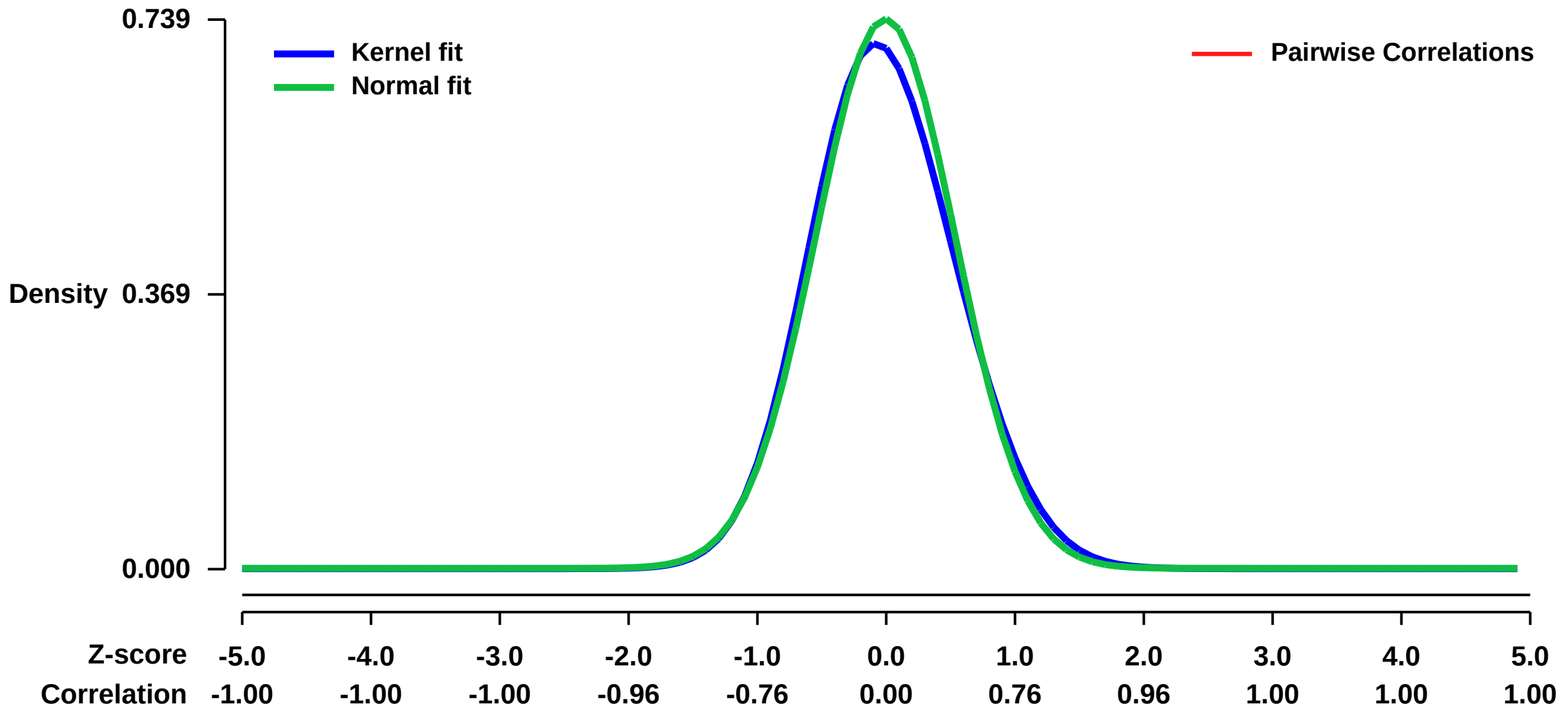

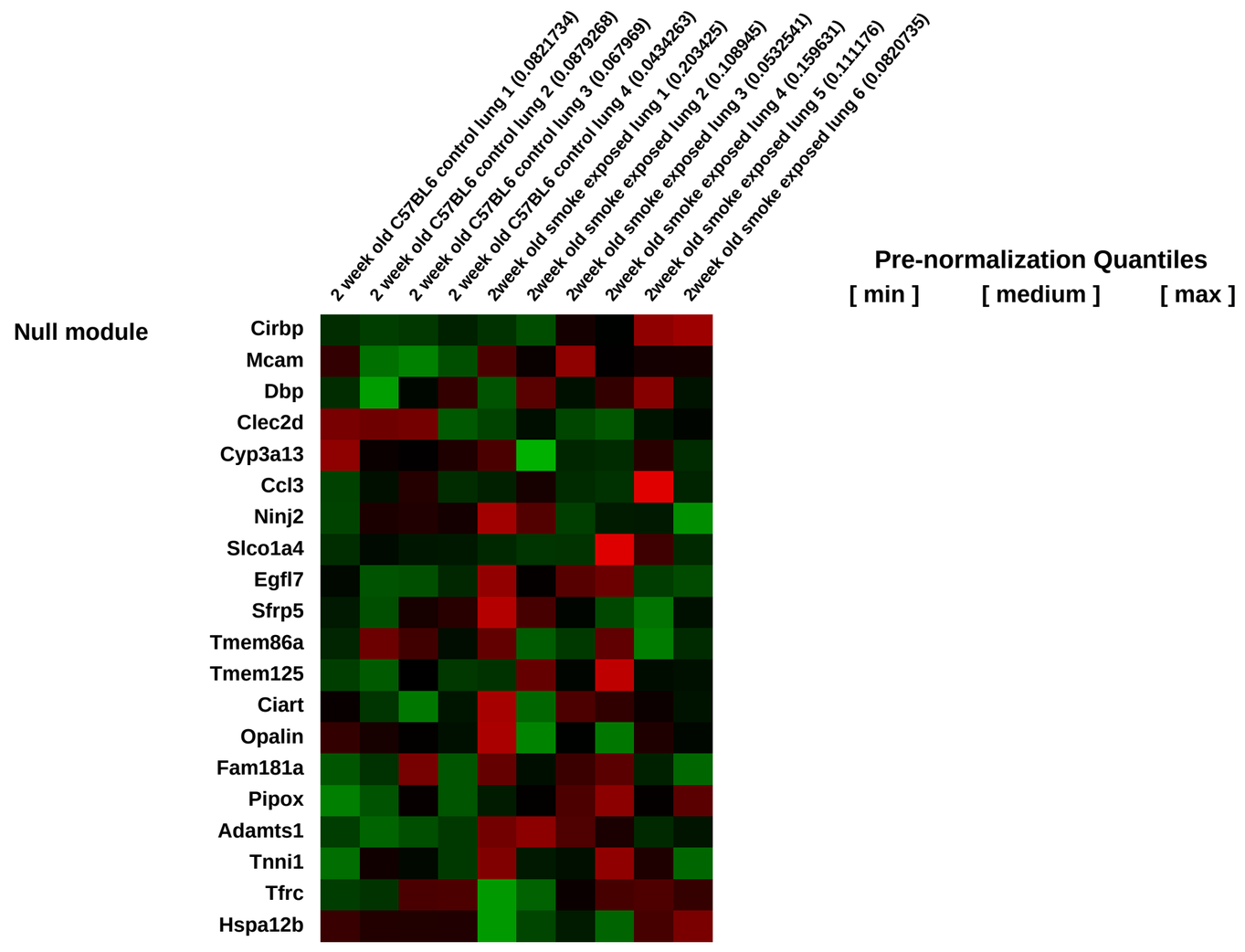

GEO Series "GSE22251" Expression Profiles

Num of samples in this series: 9

Scale of expression profile Z-scores

-3.0 -2.0 -1.0 0.0 1.0 2.0 3.0

GEO Link:	http://www.ncbi.nlm.nih.gov/geo/query/acc.cgi?acc=GSE22251
Status:	Public on Sep 09 2011
Title:	Necdin, a Negative Growth Regulator, is a Novel STAT3 Target Gene Down-Regulated in Human Cancer
Organism:	Mus musculus
Experiment type:	Expression profiling by array
Platform:	GPL1261
Pubmed ID:	22046235
Summary & Design:	**Summary:** We took a broad approach to identify novel STAT3 regulated genes by examining changes in the genome-wide gene expression profile by microarray, using cells expressing constitutively-activated STAT3. Using computational analysis, we were able to define the gene expression profiles of cells containing activated STAT3 and identify candidate target genes with a wide range of biological functions. We demonstrated that STAT3 has an important role in regulating, both positively and negatively, a diverse array of cellular processes, including cell adhesion, cytoskeletal remodeling, nucleotide, lipid and protein metabolism, as well as signal transduction. This suggest that STAT3 coordinates expression of genes involved in multiple metabolic and biosynthetic pathways, integrating signals that lead to global transcriptional changes and oncogenesis. **Overall design:** Balb/c-3T3 mouse fibroblasts, v-Src 3T3 cells and STAT3-C 3T3 cells were grown in DMEM/10% bovine calf serum supplemented with 1% penicillin and streptomycin. At each of 3 passages, cells from the five dishes were pooled and total RNA was extracted.

Background corr dist: KL-Divergence = 0.0448, L1-Distance = 0.0153, L2-Distance = 0.0002, Normal std = 0.5807

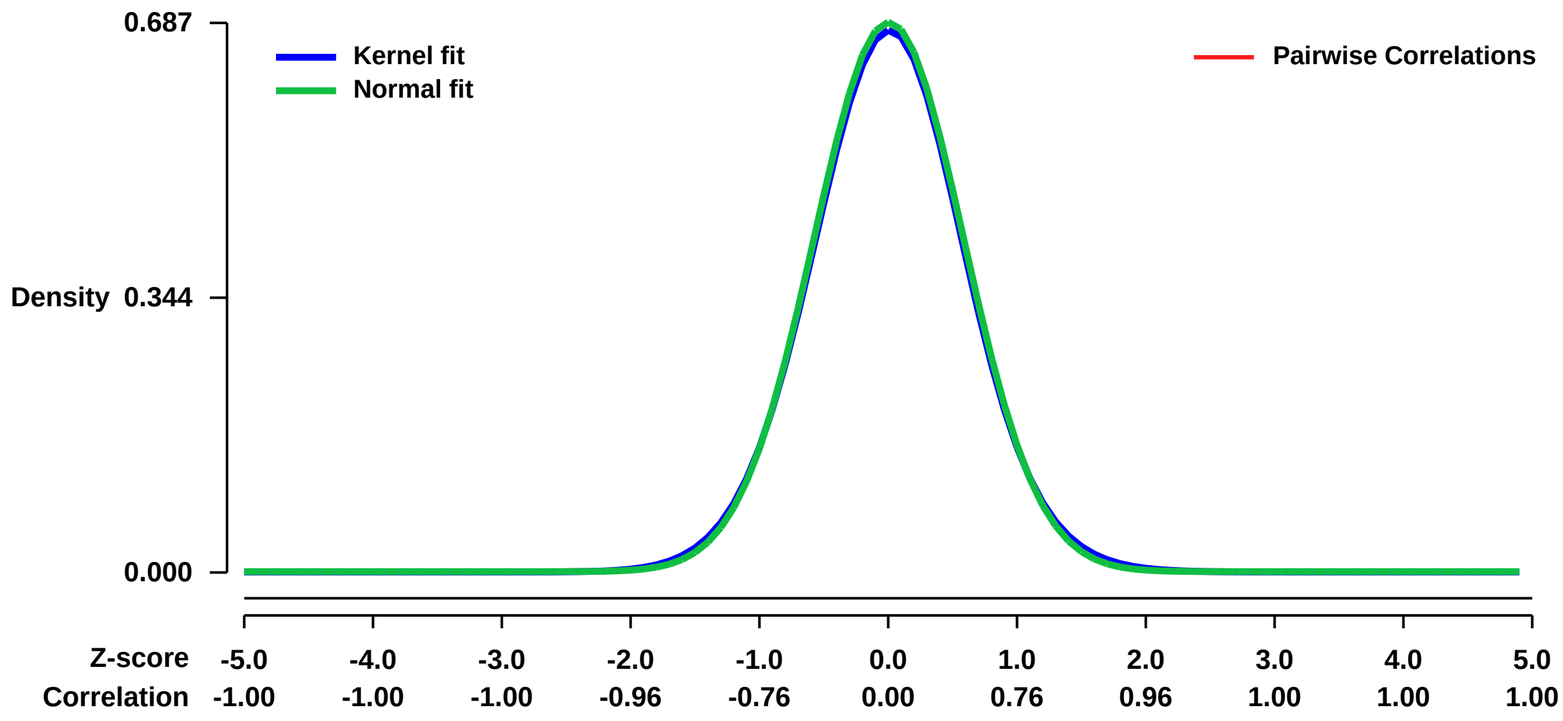

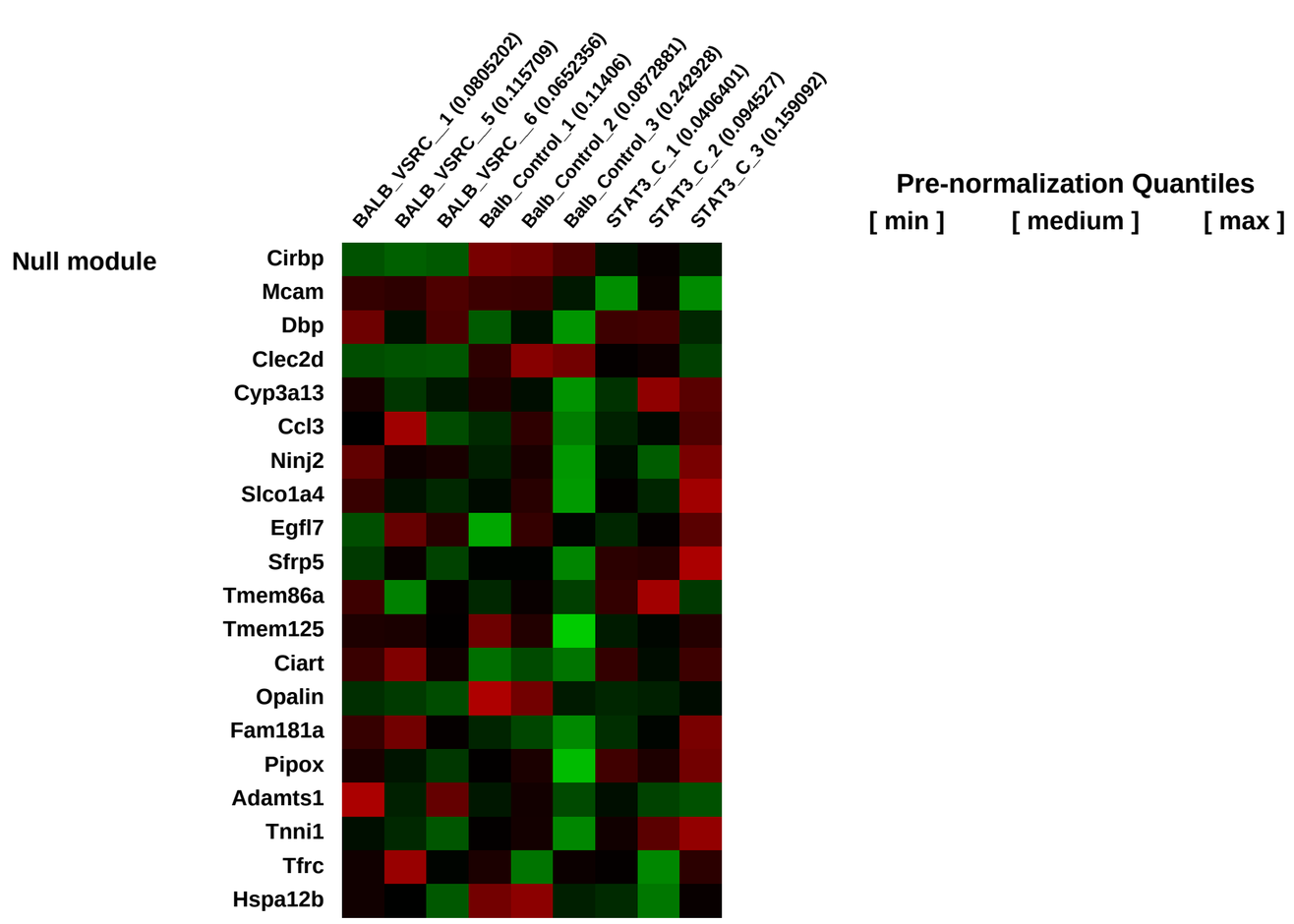

GEO Series "GSE23101" Expression Profiles

Num of samples in this series: 20

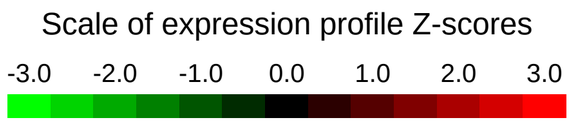

GEO Link:	**http://www.ncbi.nlm.nih.gov/geo/query/acc.cgi?acc=GSE23101**
Status:	**Public on Mar 31 2013**
Title:	**Comparative Effects of Statins on Murine Cardiac Gene Expression Profiles in Normal Mice**
Organism:	**Mus musculus**
Experiment type:	**Expression profiling by array**
Platform:	**GPL1261**
Pubmed ID:	**23524094**
Summary & Design:	**Summary:** **Recent clinical data suggest that the efficacy of statin treatment in patients with heart failure varies depending on the drugs administered. Therefore, the present study was undertaken to compare murine cardiac gene expression following treatment with four different statins.** **Statins directly regulated cardiac gene expression in a drug-specific manner in mice. The influence of each statin on the cardiac mRNA expression of various genes, including several genes that might be involved in the development of cardiac disease, was not a general effect of this class of drugs.** **Overall design:** **Male C57BL/6J mice (n = 20) were treated with or without a statin (pitavastatin calcium, pravastatin sodium, rosuvastatin calcium, or atorvastatin calcium hydrate) (n = 4 in each group) for four weeks. Total RNA was isolated from the left ventricle of each animal. The fragmented and labeled amplified cDNA was hybridized to a GeneChip Mouse Genome 430 2.0 Array (Affymetrix). Data and statistical analysis were performed with GeneSpring GX version 11.0 software (Agilent Technologies).**

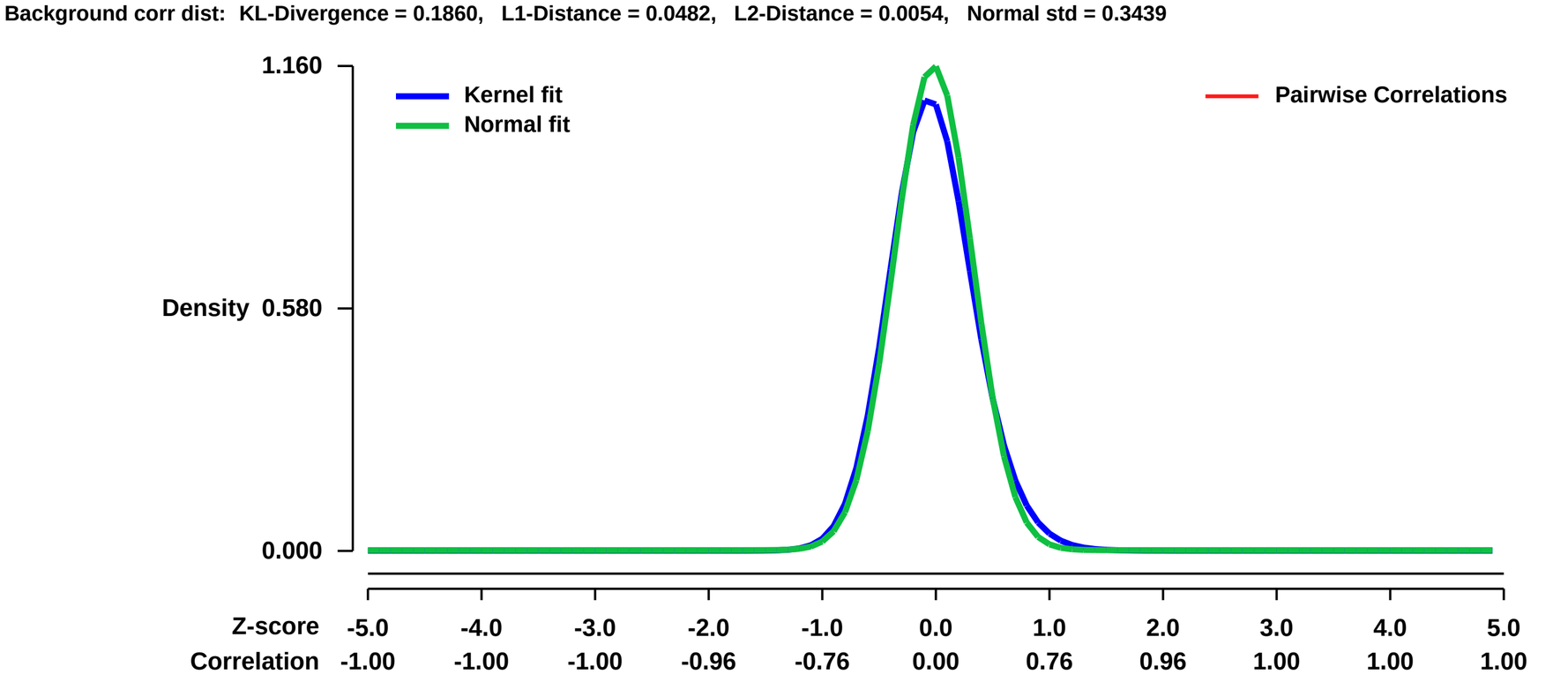

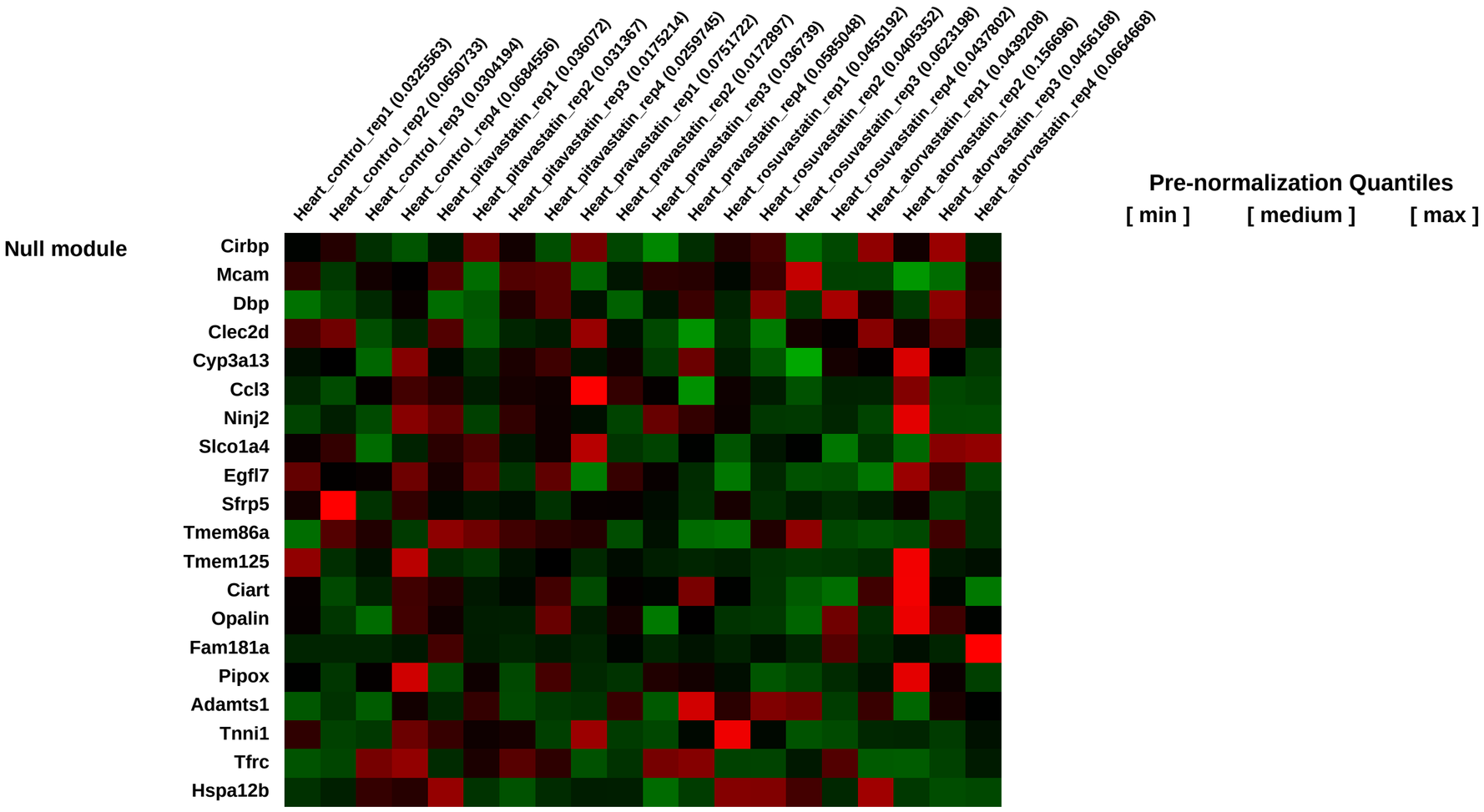

GEO Series "GSE32223" Expression Profiles

Num of samples in this series: 12

Scale of expression profile Z-scores

-3.0 -2.0 -1.0 0.0 1.0 2.0 3.0

GEO Link:	http://www.ncbi.nlm.nih.gov/geo/query/acc.cgi?acc=GSE32223
Status:	Public on Nov 02 2011
Title:	Transcriptional profile of ER71 EYFP positive/negative cells in ER71 WT and MT embryos
Organism:	Mus musculus
Experiment type:	Expression profiling by array
Platform:	GPL1261
Pubmed ID:	21989919
Summary & Design:	**Summary:** ER71 mutant embryos are nonviable and lack hematopoietic and endothelial lineages. To further define the functional role for ER71 in cell lineage decisions, we generated genetically modified mouse models. We engineered an ER71-EYFP transgenic mouse model by fusing the 3.9 kb ER71 promoter to the EYFP reporter gene. Using FACS and transcriptional profiling, we examined the EYFP+ populations of cells in ER71 mutant and wildtype littermates. In the absence of ER71, we observed an increase in the number of EYFP expressing cells, increased expression of the cardiac molecular program and decreased expression of the hemato-endothelial program compared to the wildtype littermate controls. We have also generated a novel ER71-Cre transgenic mouse model using the same 3.9 kb ER71 promoter. Genetic fate mapping studies revealed that the ER71 expressing cells daughter hematopoietic and endothelial lineages in the wildtype background. In the absence of ER71, these cell populations contributed to alternative mesodermal lineages including the cardiac lineage. To extend these analyses, we used an inducible ES/EB system and observed that ER71 overexpression repressed cardiogenesis. Together, these studies identify ER71 as a critical regulator of mesodermal fate decisions, acting to specify the hematopoietic and endothelial lineages at the expense of cardiac lineages. This enhances our understanding of the mechanisms that govern mesodermal fate decisions early during embryogenesis. **Overall design:** 12samples were analyzed, including triplicates of WT; EYFP positive, WT EYFP negative, ER71 MT; EYFP positive and ER71 MT; EYFP negative cells

Background corr dist: KL-Divergence = 0.1330, L1-Distance = 0.0360, L2-Distance = 0.0025, Normal std = 0.3907

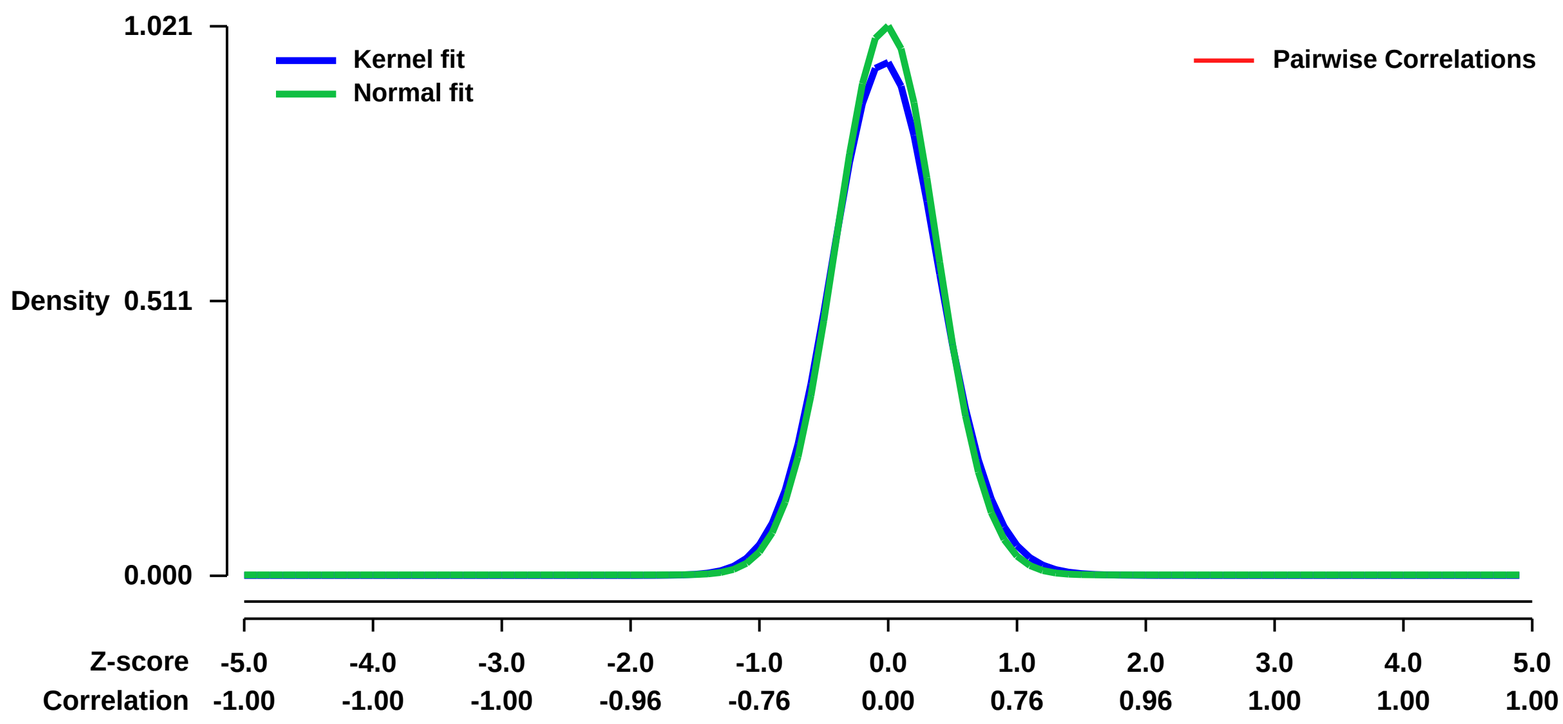

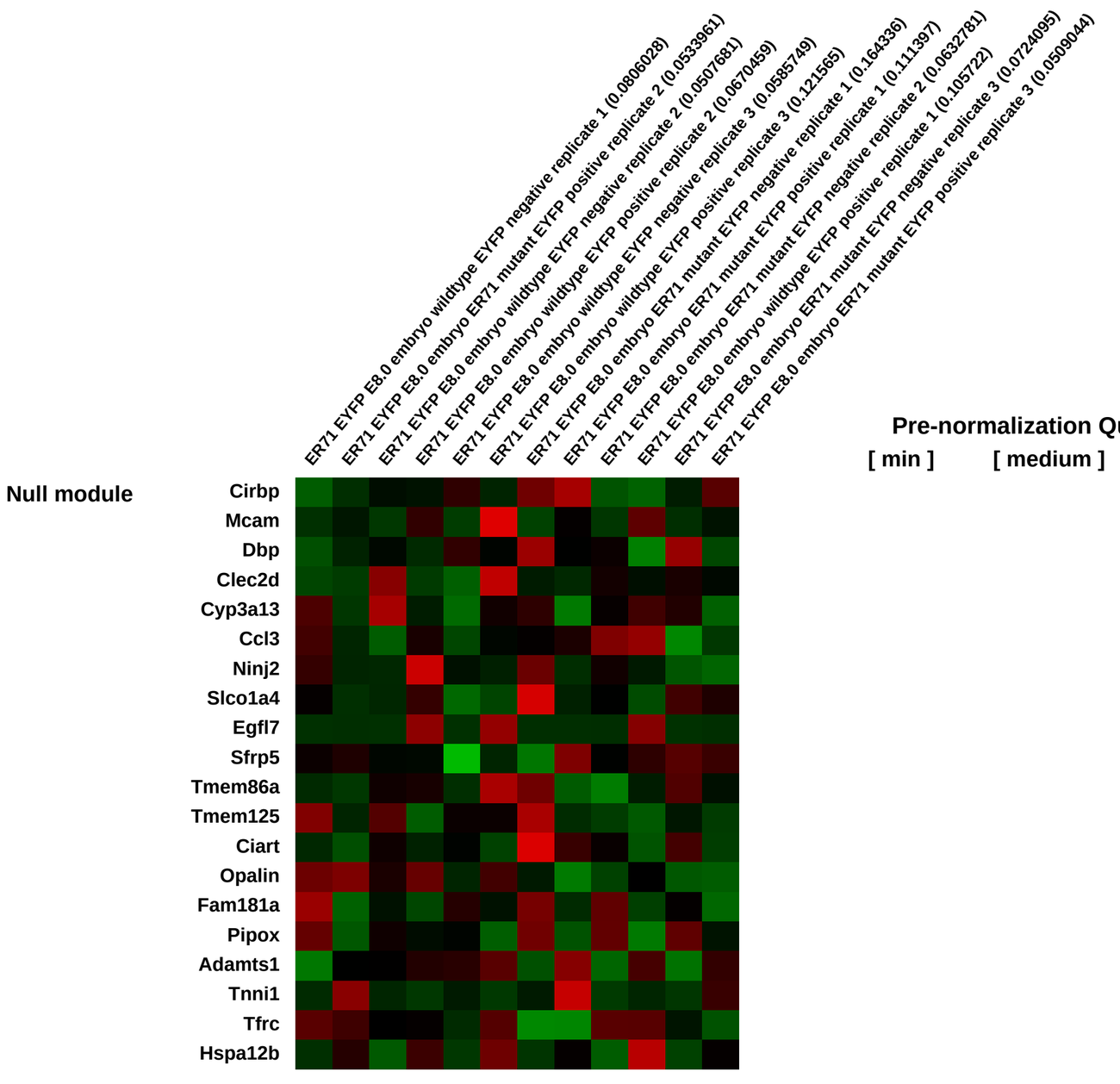

GEO Series "GSE27564" Expression Profiles

Num of samples in this series: 8

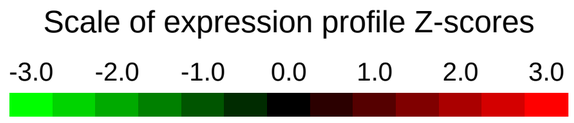

GEO Link:	**http://www.ncbi.nlm.nih.gov/geo/query/acc.cgi?acc=GSE27564**
Status:	**Public on Feb 24 2012**
Title:	**Gene expression profiles of subepithelial myofibroblasts from mouse ileum or colon, implanted together with human cancer cells in mouse xenografts**
Organism:	**Mus musculus**
Experiment type:	**Expression profiling by array**
Platform:	**GPL1261**
Pubmed ID:	
Summary & Design:	**Summary:** **We isolated myofibroblasts from C57BL6/J mouse ileum or colon and analyzed gene expression profiles from the cultured cells. We also isolated human colon cancer cells from xenografts interacting with mouse intestinal subepithelial myofibroblasts (lSEMFs) and analyzed gene expression in sorted human cancer cells.** **We used Affymetrix microarrays to detail the global gene expression prolfiles in mouse fibroblasts and human colon cancer cells and identified distinct biological processes of differentially expressed genes in mouse fibroblasts and interacting human colon cancer cells** **Overall design:** **For mouse SEMFs, we isolated fresh fibroblasts from mouse ileum and colon, confirmed their predicted immunophenotype (alpha SMA positive, vimentin positive, desmin negative), and expanded cells in culture before expression array analysis. We examined gene expression in human cancer cells following their interaction with murine ileal or colonic SEMFs, using flow cytometry to isolate DsRed-expressing Caco2 or T84 cells after 5 weeks of growth in NOD/SCID mice in the presence of GFP-expressing ileal or colonic SEMFs.**

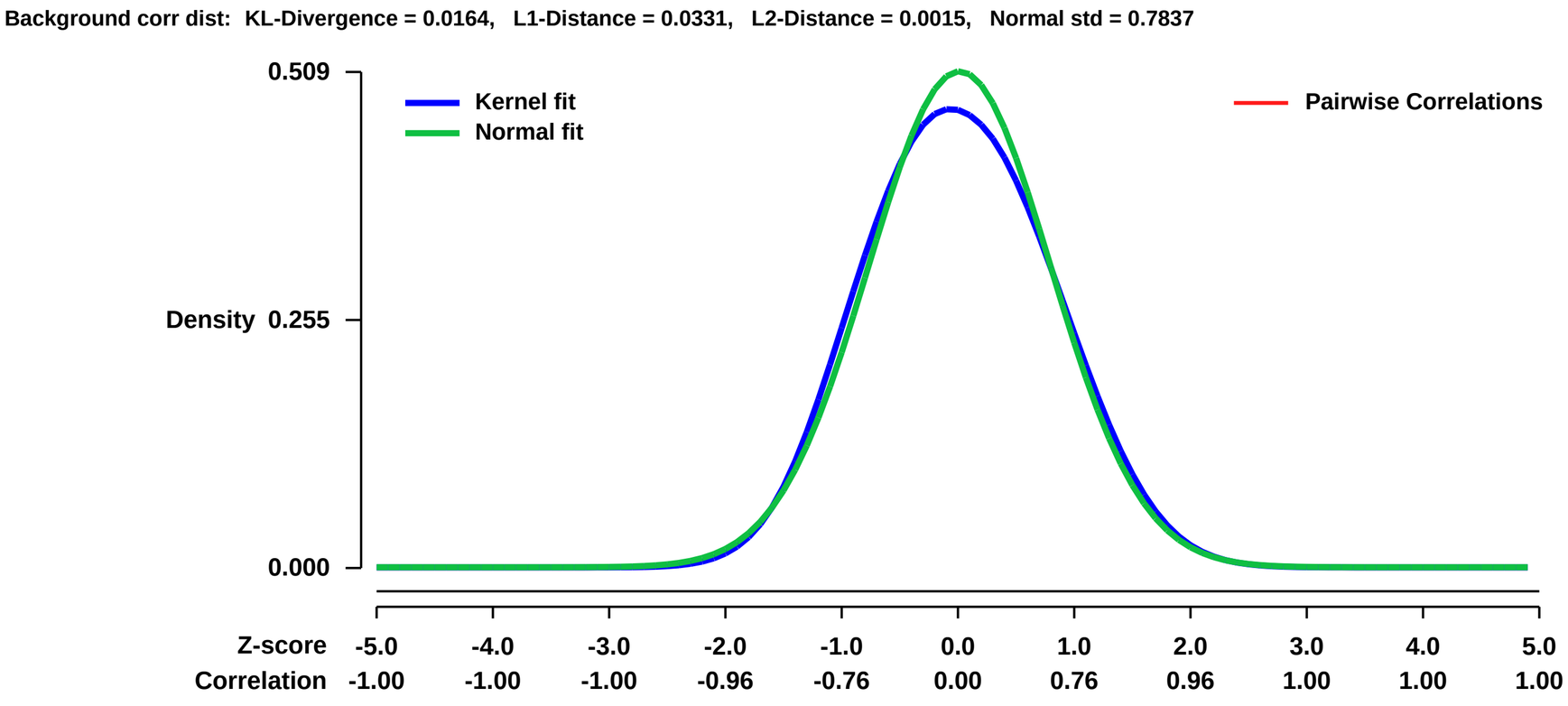

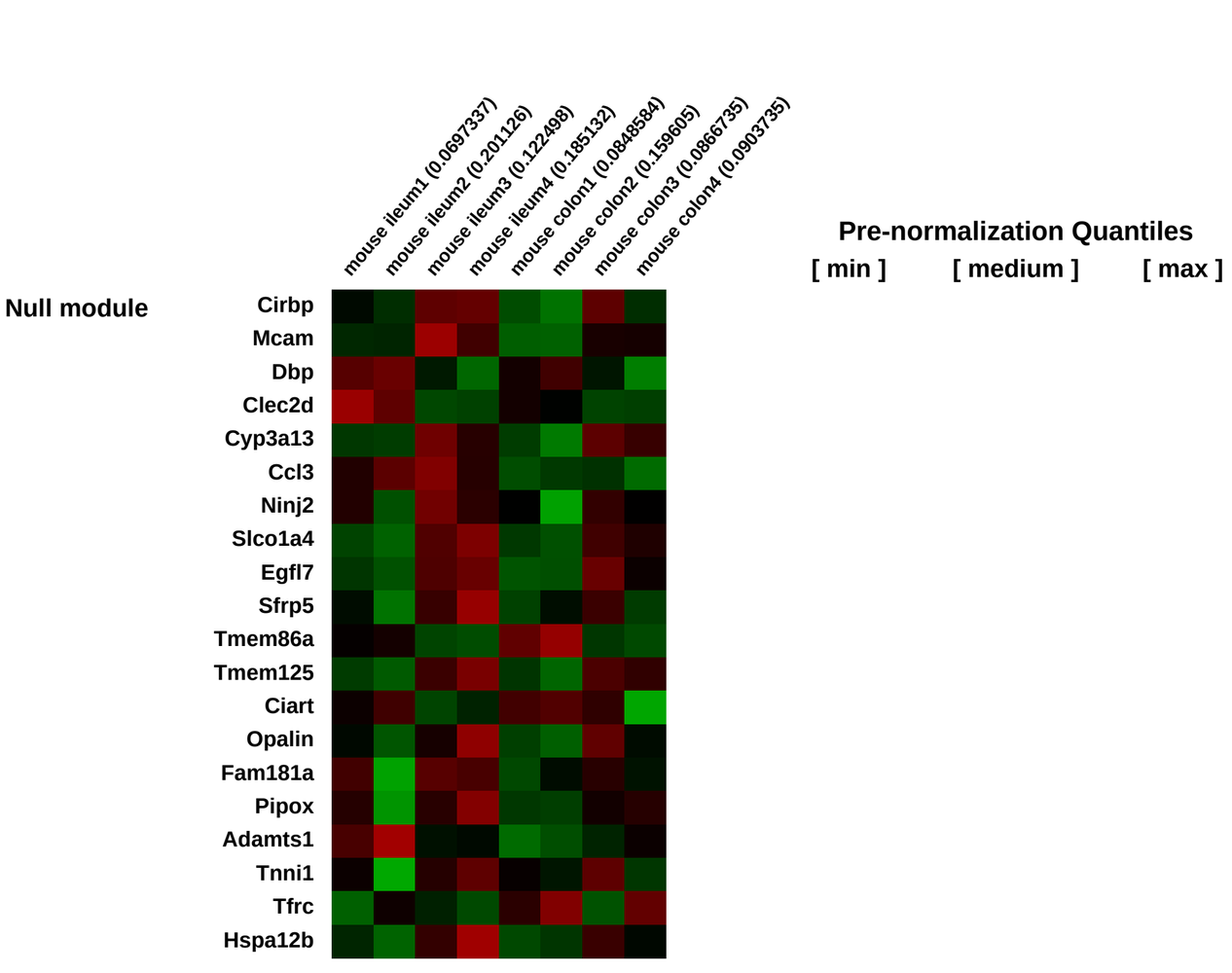

GEO Series "GSE27451" Expression Profiles

Num of samples in this series: 6

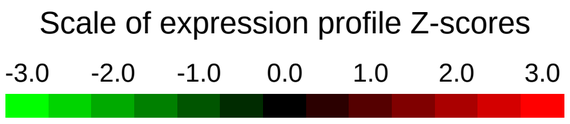

GEO Link:	http://www.ncbi.nlm.nih.gov/geo/query/acc.cgi?acc=GSE27451
Status:	Public on Feb 25 2011
Title:	Functions of HDAC1 and HDAC2 in Schwann cells during postnatal
Organism:	Mus musculus
Experiment type:	Expression profiling by array
Platform:	GPL1261
Pubmed ID:	21423190
Summary & Design:	**Summary:** The aim of our study is to determine the functions of histone deacetylases (HDACs) 1 and 2 in Schwann cells during postnatal development of the peripheral nervous system (PNS). Schwann cells are the myelinating glial cells of the PNS. At birth, mouse sciatic nerves mature in 2 subsequent phases: 1/ big caliber axons get sorted into a 1 to 1 relationship with Schwann cells, 2/ Schwann cells build a myelin sheath around sorted axons. In mice where both HDAC1 & HDAC2 have been specifically knocked out in Schwann cells, both phases are impaired. HDACs are chromatin remodeling enzymes, they can thus alter gene expression directly. We want to identify which genes controlled by HDAC1 and HDAC2 in Schwann cells are necessary for the maturation of sciatic nerves. Because HDAC1 and HDAC2 can compensate for each other loss to some extend, we will first analyze changes of gene expression in HDAC1/HDAC2 double KO animals. We expect to gain critical insights into the molecular mechanisms controlling Schwann cell differentiation and myelination. This knowledge is of key importance for the success of regenerative medicine in peripheral neuropathies, nerve tumors, and transplantation paradigms in non-regenerative CNS lesions and in large PNS injuries. **Overall design:** 3 double knockout mutants for HDAC1 and HDAC2 and 3 control littermates were analyzed. Tissues analyzed: sciatic nerves of 2 day-old mouse pups

Background corr dist: KL-Divergence = 0.0264, L1-Distance = 0.0155, L2-Distance = 0.0002, Normal std = 0.6935

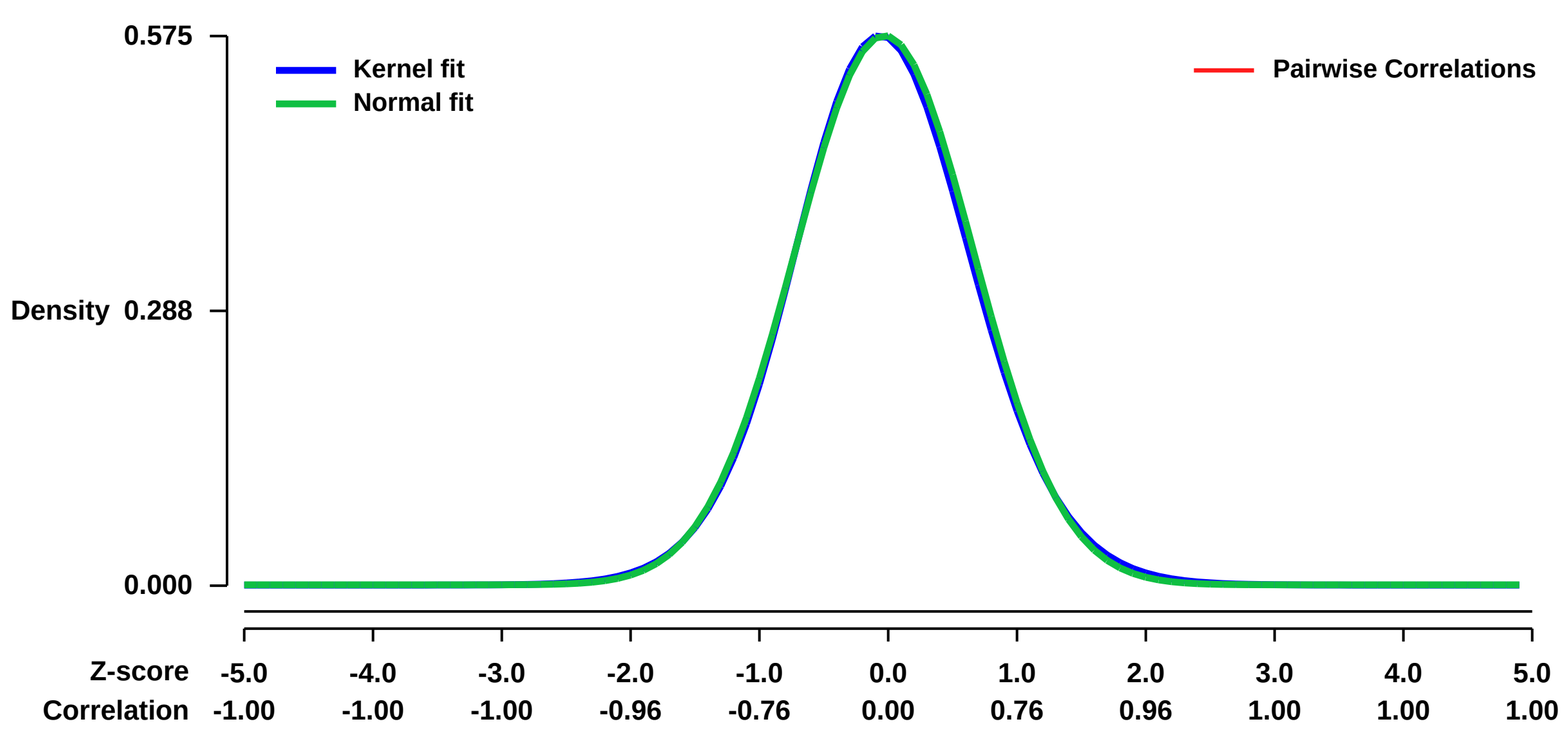

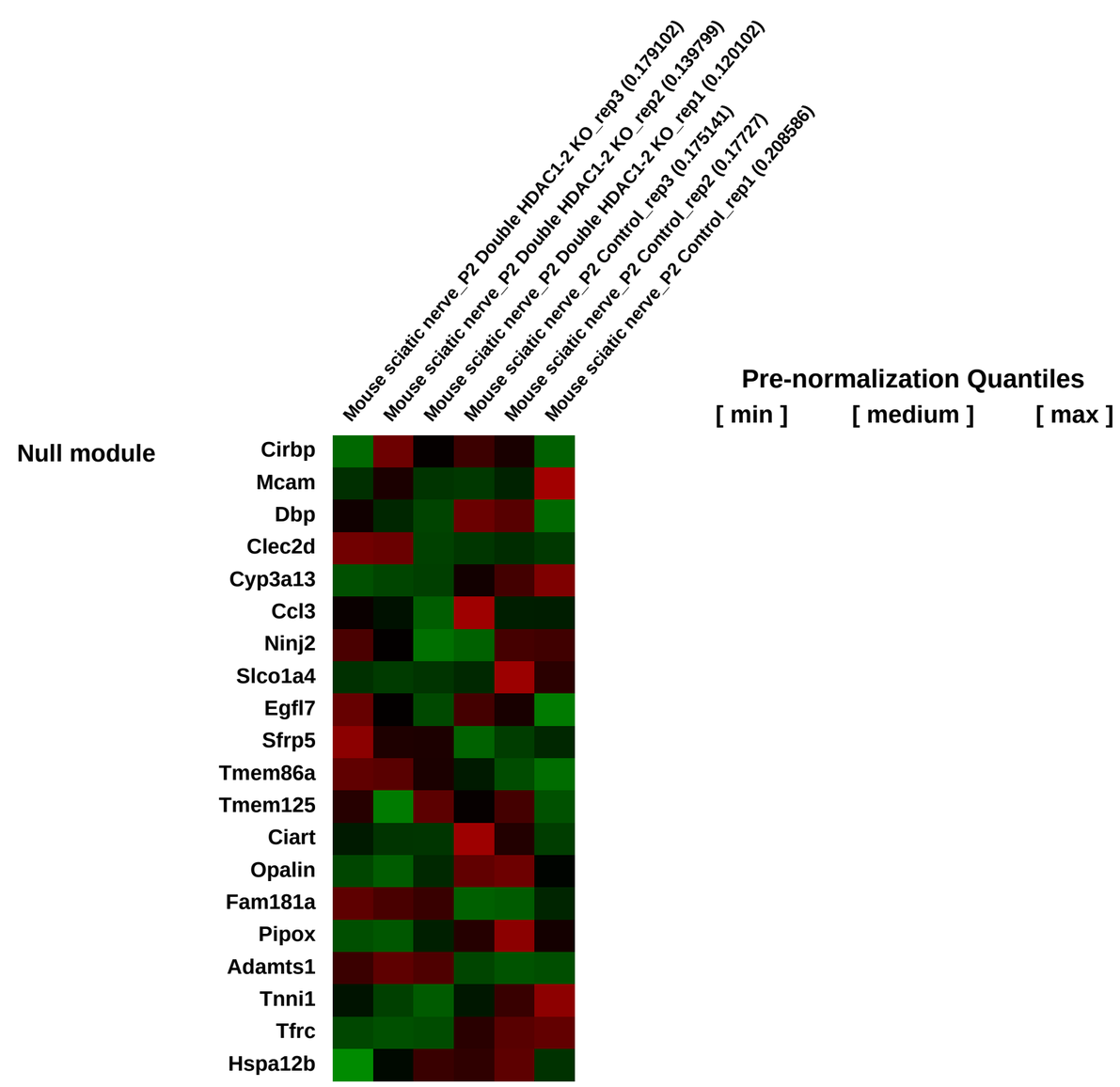

GEO Series "GSE9130" Expression Profiles

Num of samples in this series: 6

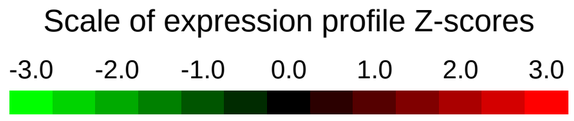

GEO Link:	**http://www.ncbi.nlm.nih.gov/geo/query/acc.cgi?acc=GSE9130**
Status:	**Public on Sep 22 2007**
Title:	**aP2-nSREBP1c_white_Adipose_Tissue_expression_differentials**
Organism:	**Mus musculus**
Experiment type:	**Expression profiling by array**
Platform:	**GPL1261**
Pubmed ID:	**17921248**
Summary & Design:	**Summary:** **Identifying gene expression changes in adipose tissue of lipodystrophic aP2-nSREBP1c trangenic mice** **Keywords: Genetic modification** **Overall design:** **RNA from epididymal white adipose pads of three 10-week-old aP2-nSREBP1c transgenic males and three litter-matched WT controls was analyzed by MOE430v2.0 GeneChipâ¢ arrays, one mouse per array.**

Background corr dist: **KL-Divergence = 0.0222, L1-Distance = 0.0289, L2-Distance = 0.0009, Normal std = 0.7553**

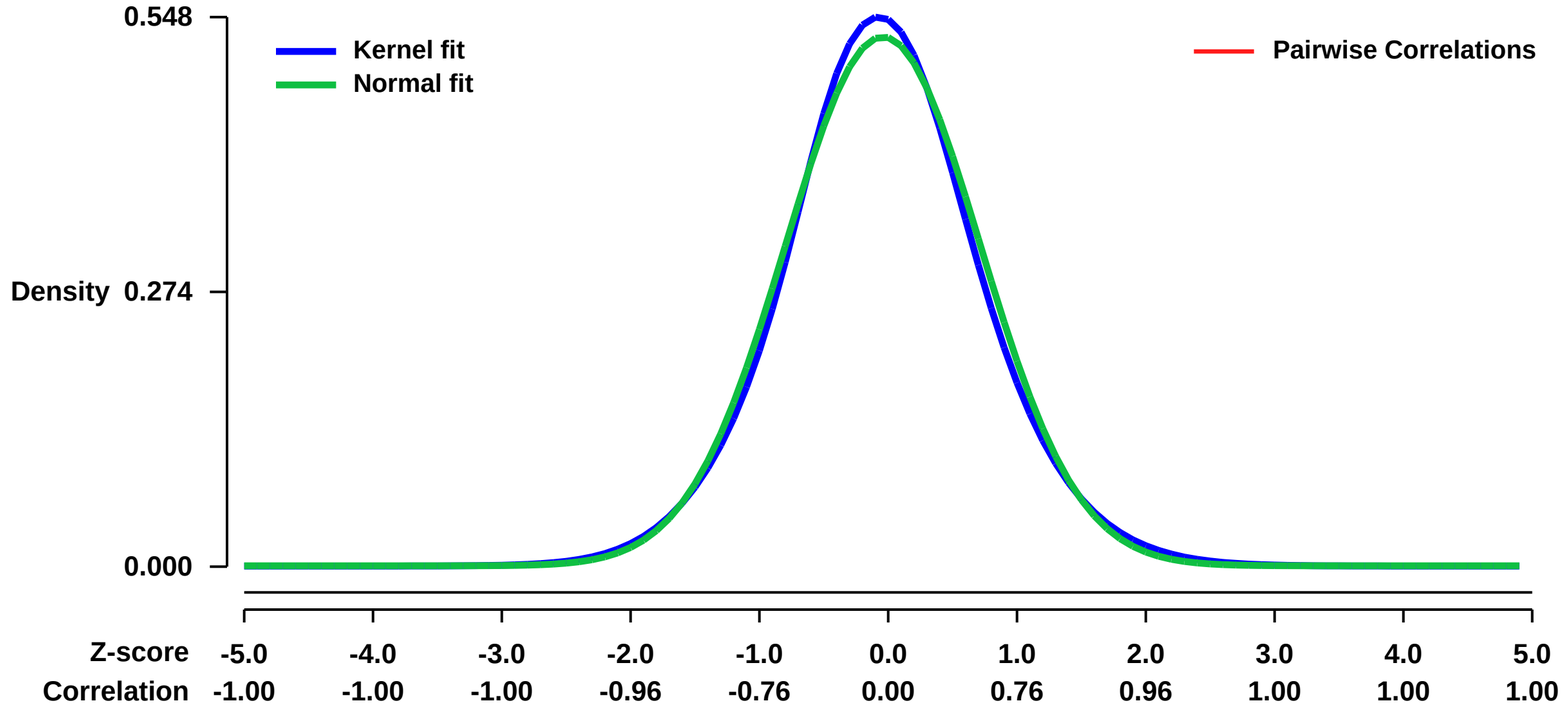

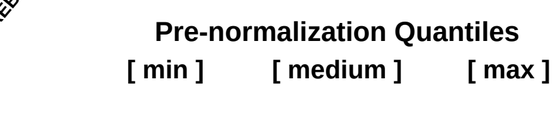

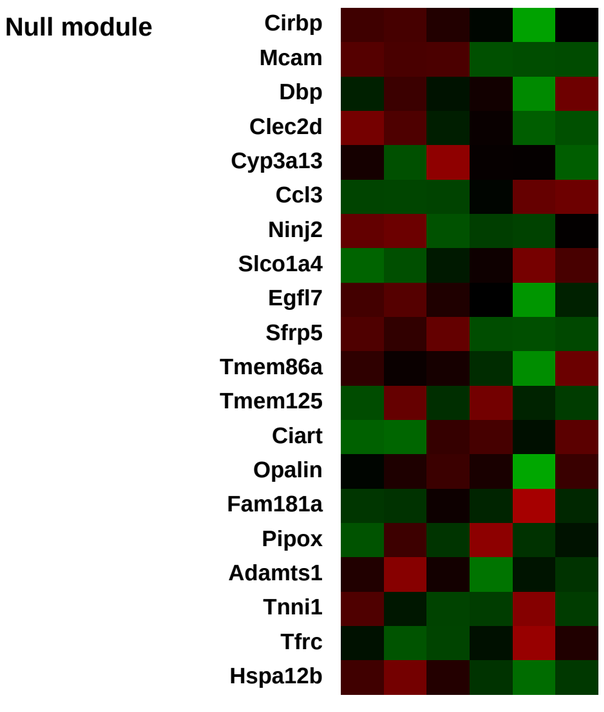

GEO Series "GSE42753" Expression Profiles

Num of samples in this series: 6

Scale of expression profile Z-scores

-3.0 -2.0 -1.0 0.0 1.0 2.0 3.0

GEO Link:	http://www.ncbi.nlm.nih.gov/geo/query/acc.cgi?acc=GSE42753
Status:	Public on Dec 06 2012
Title:	Microarray gene expression profiling of transgenic mice with myocardium-specific expression of RKIP or a GRK-specific peptide inhibitor
Organism:	Mus musculus
Experiment type:	Expression profiling by array
Platform:	GPL1261
Pubmed ID:	23362259
Summary & Design:	**Summary:** The Raf kinase inhibitor protein (RKIP) is a dual inhibitor of the Raf kinase and the G-protein-coupled receptor kinase 2 (GRK2). GRK2 is an indispensable kinase, which exerts a major role in the pathogenesis of heart failure, and inhibition of GRK2 is cardioprotective in experimental models of heart failure. To investigate the cardiac function of RKIP as GRK2 inhibitor, we generated transgenic mice with myocardium-specific expression of RKIP under control of the alpha-MHC promoter. For comparison, mice with myocardium-specific expression of a GRK-specific peptide inhibitor (GRK-Inh) were also generated. Two different transgenic mouse models were established. Transgenic RKIP mice and transgenic GRK-Inh mice were born at Mendelian frequencey and grew to adulthood normally. **Overall design:** Microarray gene expression profiling was performed with heart tissue isolated from three study groups: (i) RKIP-transgenic mice, (ii) GRK-Inh-transgenic mice, and (iii) B6 control mice.

Background corr dist: KL-Divergence = 0.0459, L1-Distance = 0.0191, L2-Distance = 0.0004, Normal std = 0.5905

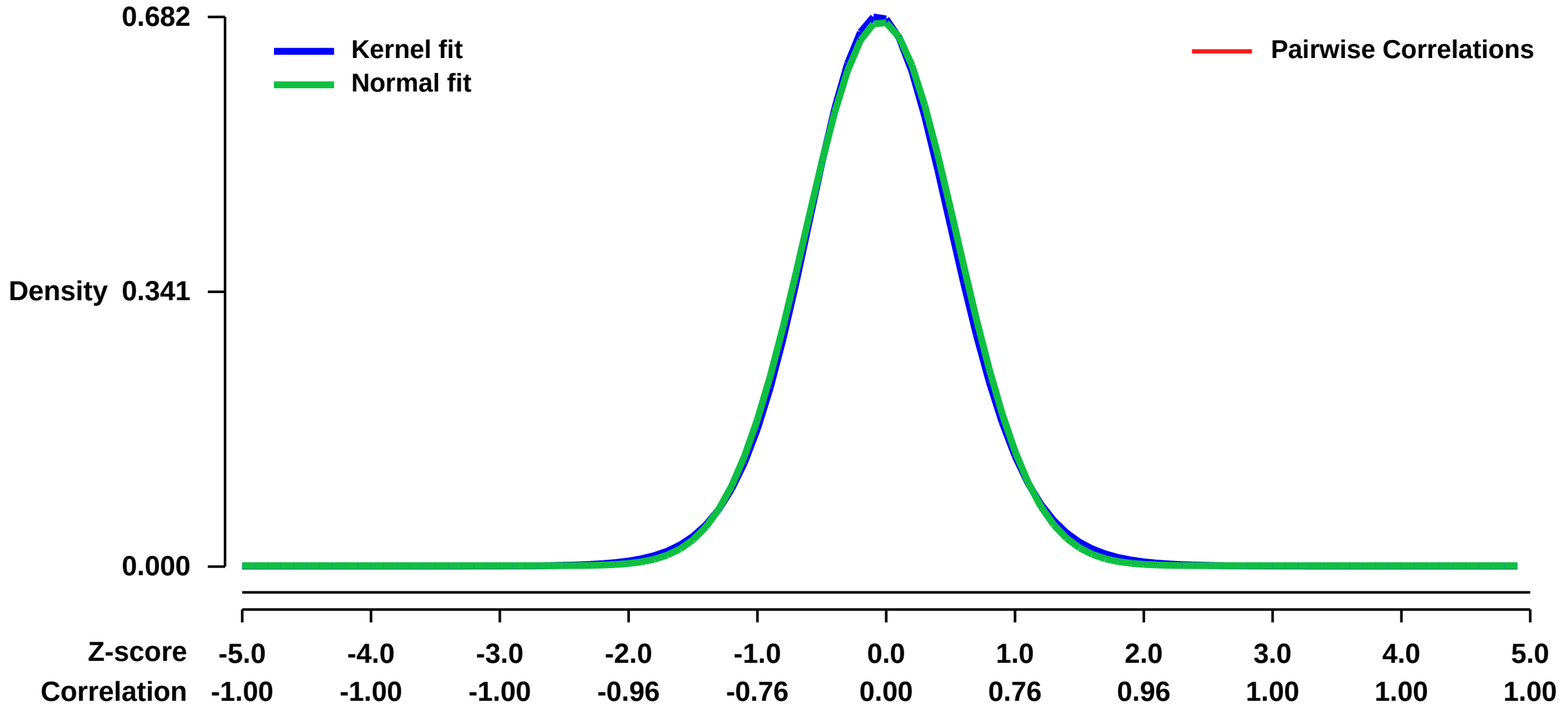

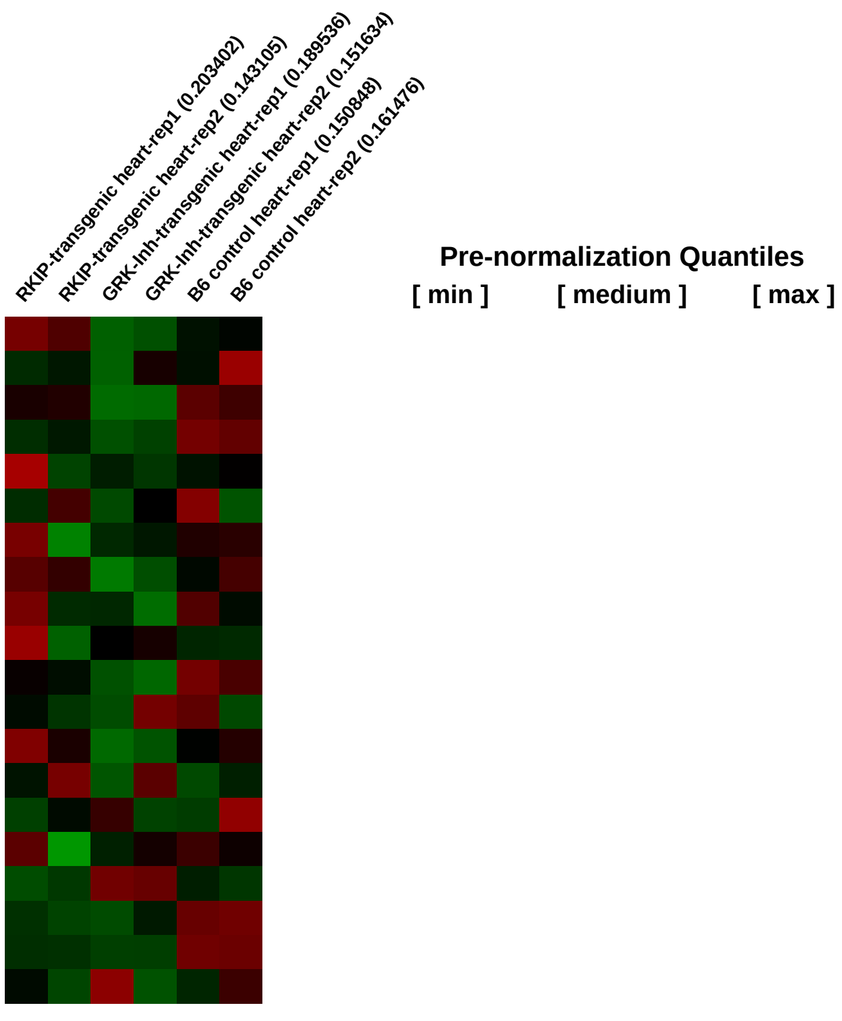

GEO Series "GSE11110" Expression Profiles

Num of samples in this series: 11

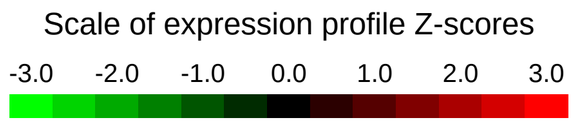

GEO Link:	**http://www.ncbi.nlm.nih.gov/geo/query/acc.cgi?acc=GSE11110**
Status:	**Public on Jun 29 2008**
Title:	**Expression data from bone marrow CLP and B-cell progenitor subfractions.**
Organism:	**Mus musculus**
Experiment type:	**Expression profiling by array**
Platform:	**GPL1261**
Pubmed ID:	
Summary & Design:	**Summary:** **Expression profiling of CLP subfractions (with different potential to develop into T-cells) and B-cell progenitors.** **Keywords: cell type comparison, B-cell progenitor, common lymphoid progenitor cells (CLP)** **Overall design:** **CLP and B-cell progenitor subpopulations were FACS sorted. Subsequently RNA was extracted, labelled and hybridized to Affymetrix microarrays. The CLP subfractions were the target of investigation (B-cell progenitors subpopulations served as references of expression levels for B-cell related transcripts) as we sought to identify expression changes potentially explaining difference in function between the hCD25 positiv and negativ subsets.**

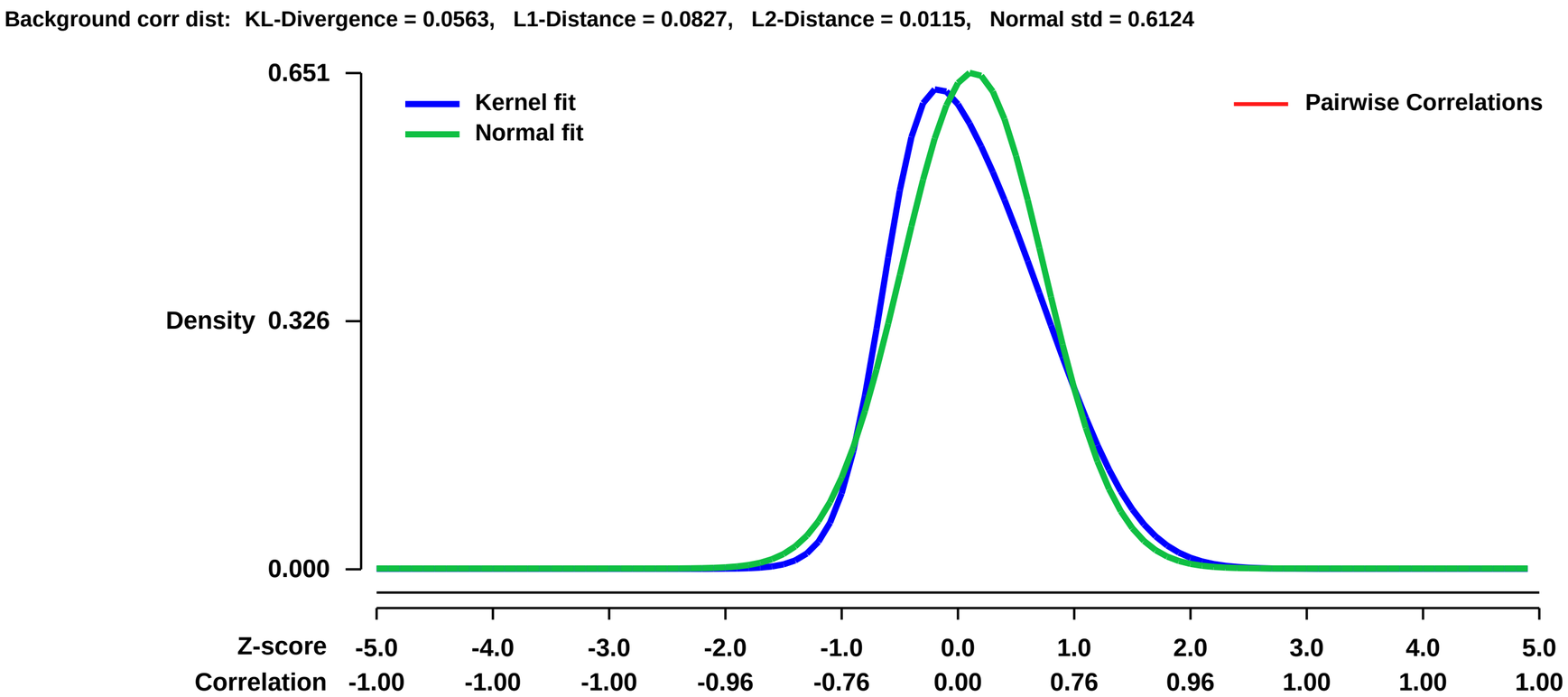

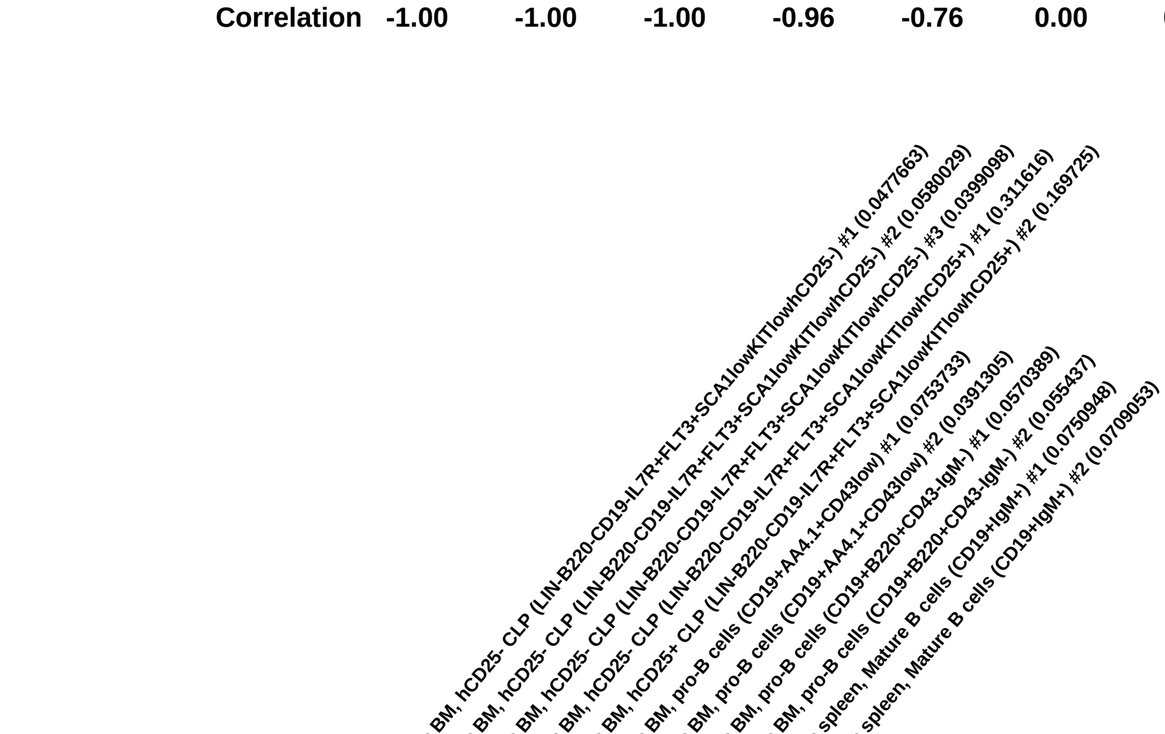

GEO Series "GSE5870" Expression Profiles

Num of samples in this series: 8

Scale of expression profile Z-scores

-3.0 -2.0 -1.0 0.0 1.0 2.0 3.0

GEO Link:	http://www.ncbi.nlm.nih.gov/geo/query/acc.cgi?acc=GSE5870
Status:	Public on Jan 01 2007
Title:	Gnotobiotic mouse cecal epithelium; B.thetaiotaomicron-B. longum mono- versus bi-association, PR chow, NMRI
Organism:	Mus musculus
Experiment type:	Expression profiling by array
Platform:	GPL1261
Pubmed ID:	17132046
Summary & Design:	**Summary:** Laser captured cecal epithelium from gnotobiotic mice colonized with B. thetaiotaomicron or B. longum (mono-association) or B. thetaiotaomicron bi-association with B. longum. Samples were derived from 10d colonizations of NMRI mice fed a standard-chow polysaccharide rich (PR) diet. **Keywords: Germ-free vs. Mono-associations or Bi-association, in vivo** **Overall design:** Total RNA was prepared from laser captured cecal epithelium of 10 day associated gnotobiotic mice, double amplified, and hybridized to 430 2.0 GeneChips or to GlycoGeneChipsv1.

Background corr dist: KL-Divergence = 0.0856, L1-Distance = 0.0338, L2-Distance = 0.0022, Normal std = 0.4715

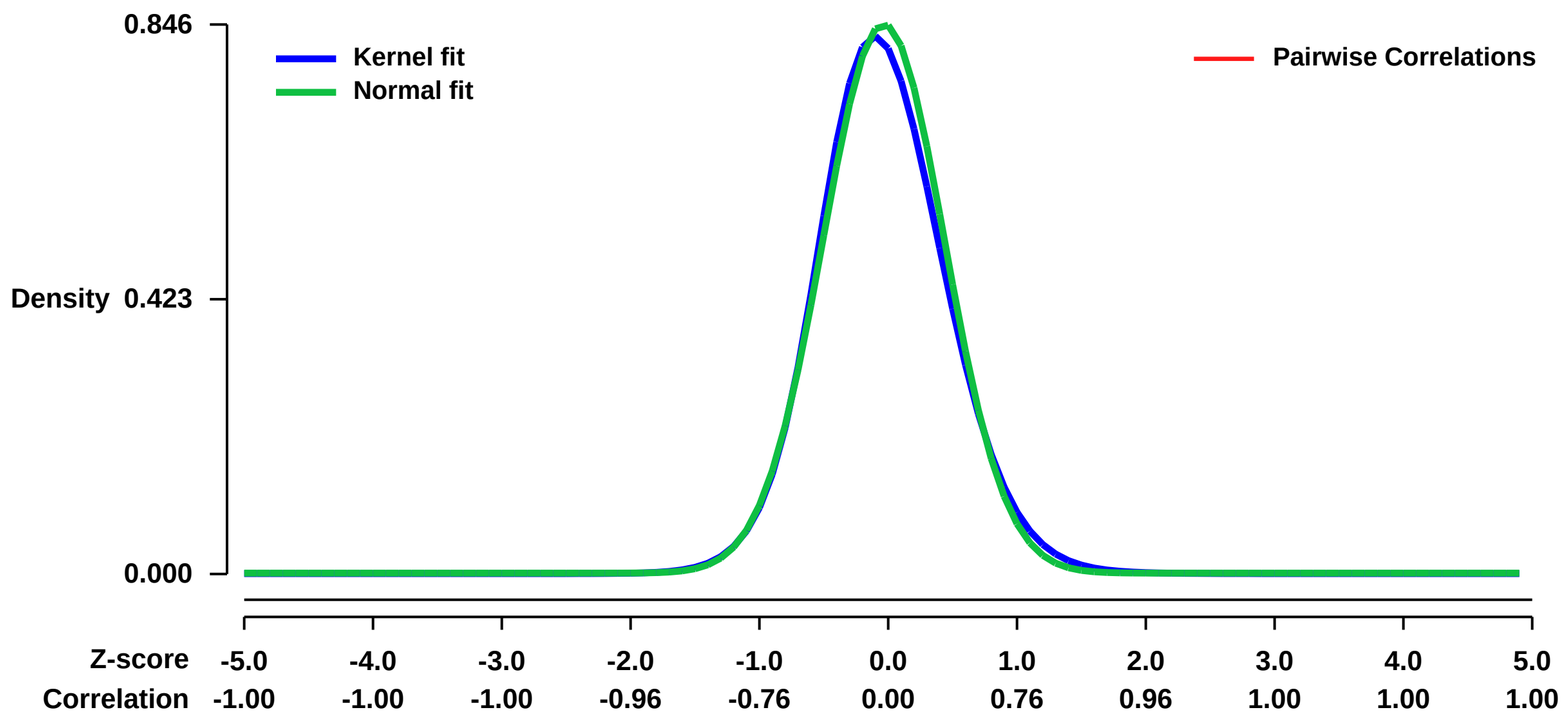

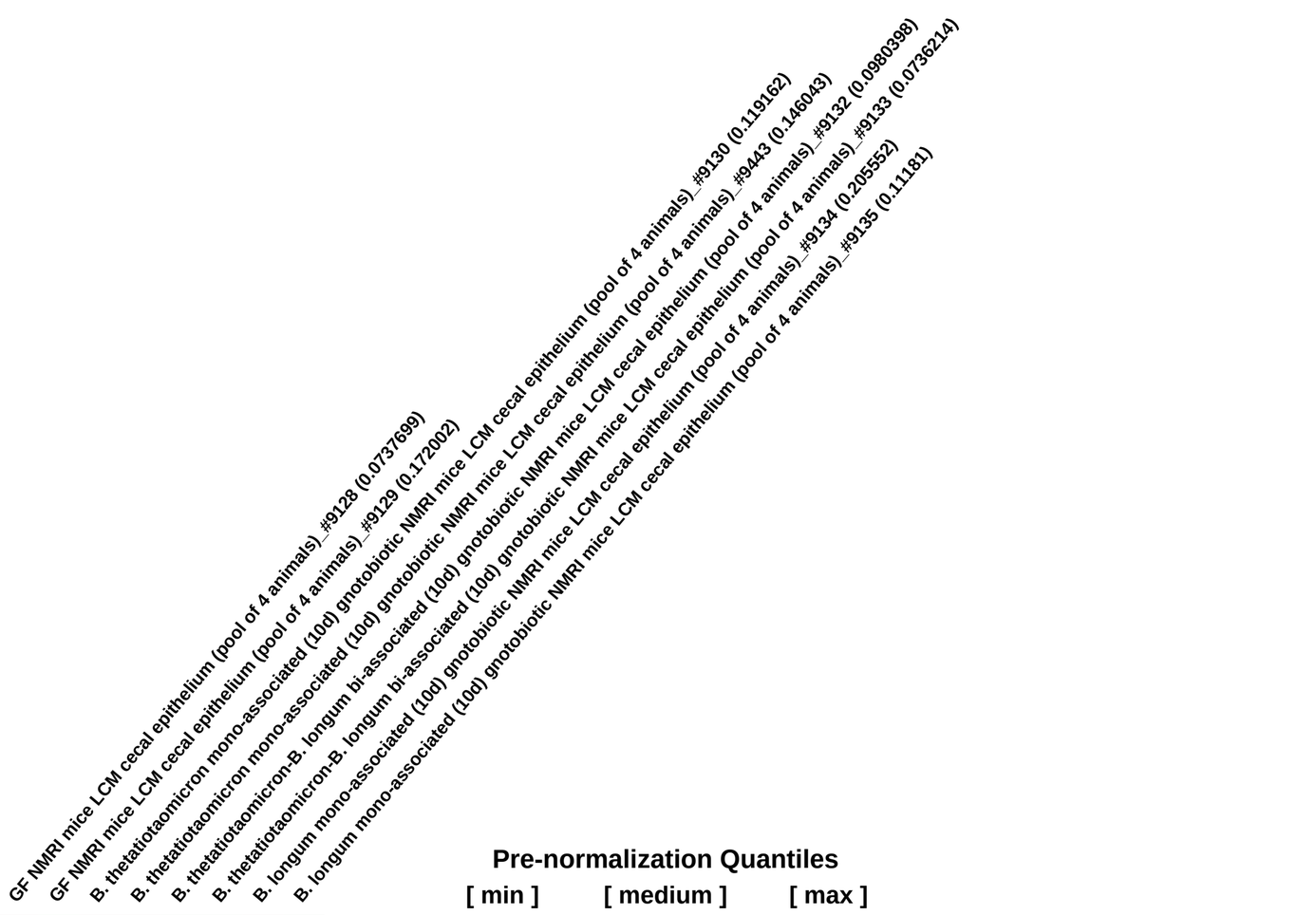

GEO Series "GSE15760" Expression Profiles

Num of samples in this series: 6

Scale of expression profile Z-scores

-3.0 -2.0 -1.0 0.0 1.0 2.0 3.0

GEO Link: http://www.ncbi.nlm.nih.gov/geo/query/acc.cgi?acc=GSE15760

Status: Public on Apr 01 2010

Title: Comparative transcriptional profiling of tumor-associated and normal lymphatic endothelial cells

Organism: Mus musculus

Experiment type: Expression profiling by array

Platform: GPL1261

Pubmed ID:

Summary & Design:

Summary:
In the past decade, the relevance of tumor-induced lymphangiogenesis for the metastatic spread of tumor cells has been demonstrated, thus indicating the potential of targeting tumor lymphangiogenesis to treat cancer. Whereas numerous preclinical studies demonstrated that blocking angiogenesis or lymphangiogenesis could inhibit tumor metastasis, the scarcity of highly selective targeting candidates hampers their translation to the clinic.

We employed a new approach consisting of immuno-laser capture microdissection (i-LCM) and transcriptional profiling by means of microarrays in order to identify novel tumor-specific endothelial markers.

Overall design:
By using short immunostainings prior to microdissection, specific identification of lymphatic (LECs) and blood (BECs) endothelial cells was allowed. For the subsequent gene expression profiling, a single round of the Ribo-Spia amplification method in combination with the Affymterix microarray platform was used. Comparison of gene expression profiles of tumor-associated and normal LECs resulted in the identification of differentially expressed genes in tumor-associated lymphatic vasculature.

Background corr dist: KL-Divergence = 0.0432, L1-Distance = 0.0637, L2-Distance = 0.0065, Normal std = 0.6547

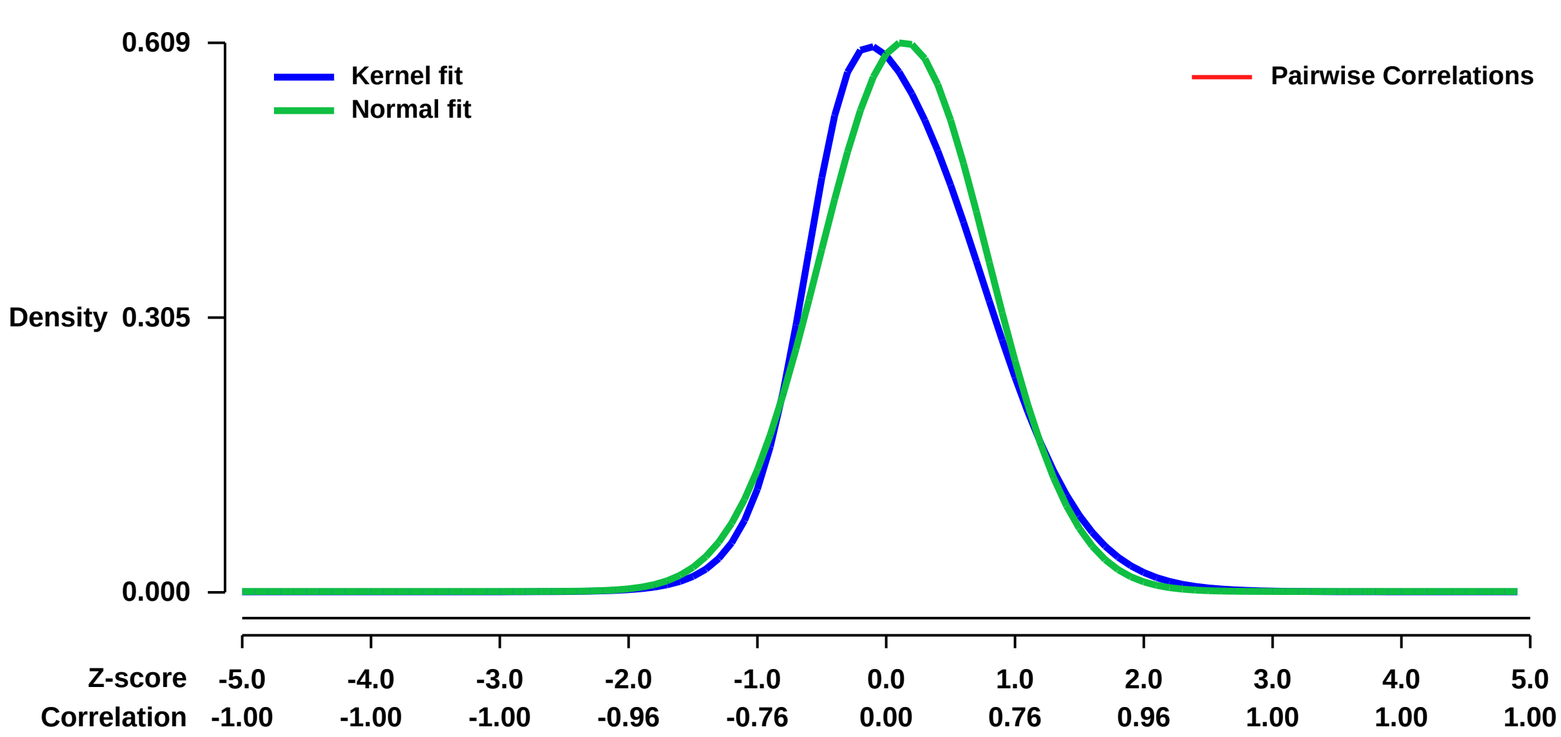

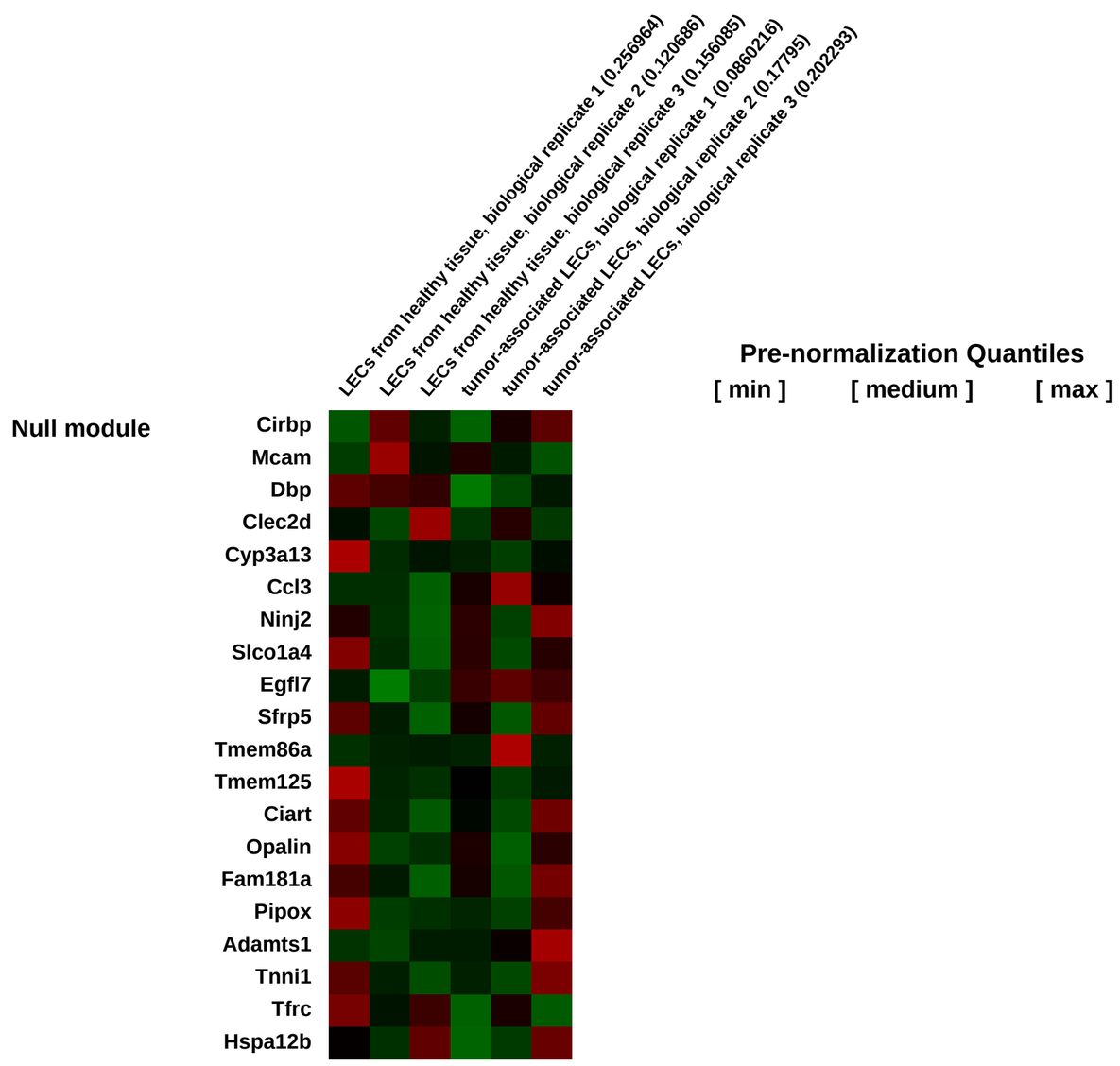

GEO Series "GSE39865" Expression Profiles

Num of samples in this series: 21

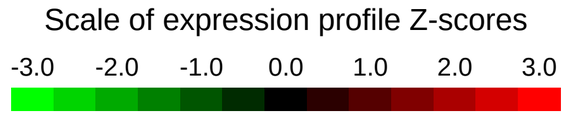

GEO Link:	**http://www.ncbi.nlm.nih.gov/geo/query/acc.cgi?acc=GSE39865**
Status:	**Public on Aug 04 2012**
Title:	**The gene expression analysis of the spinal cord of SBMA (Spinal Bulbar Muscular Atrophy) model mice**
Organism:	**Mus musculus**
Experiment type:	**Expression profiling by array**
Platform:	**GPL1261**
Pubmed ID:	**23023499**
Summary & Design:	**Summary:** **To identify the gene expression changes that are specific to SBMA, we prepared total mRNA samples from the spinal cords of transgenic mice carrying a full-length human AR with 97 CAGs (AR-97Q), transgenic mice bearing a wild-type allele of AR with 24 CAGs (AR-24Q), and the wild-type littermates of the AR-97Q mice (C57BL/6). We used AR-97Q (Line #7-8) male mice because they show progressive muscular atrophy and weakness as well as SBMA-like pathology such as the accumulation of the pathogenic androgen receptor in the nucleus of motor neurons.** **Using microarray analysis, we identified the genes with significantly altered expression among the three types of mice.** **Overall design:** **For each group, we examined the male mice at 7-9, 10-12, and 13-15 weeks of age. These stages were chosen because the AR-97Q mice are generally asymptomatic at 7-9 weeks of age (before-onset stage), present with mild motor impairment at 10-12 weeks (early stage), and are severely weakened with profound muscle atrophy at 13-15 weeks (advanced stage). RNA from the total spinal cord, excluding the dorsal root ganglia, was isolated from three mice of each genotype at each stage. For wild-type, pooled sample for three mice were used in each stage.**

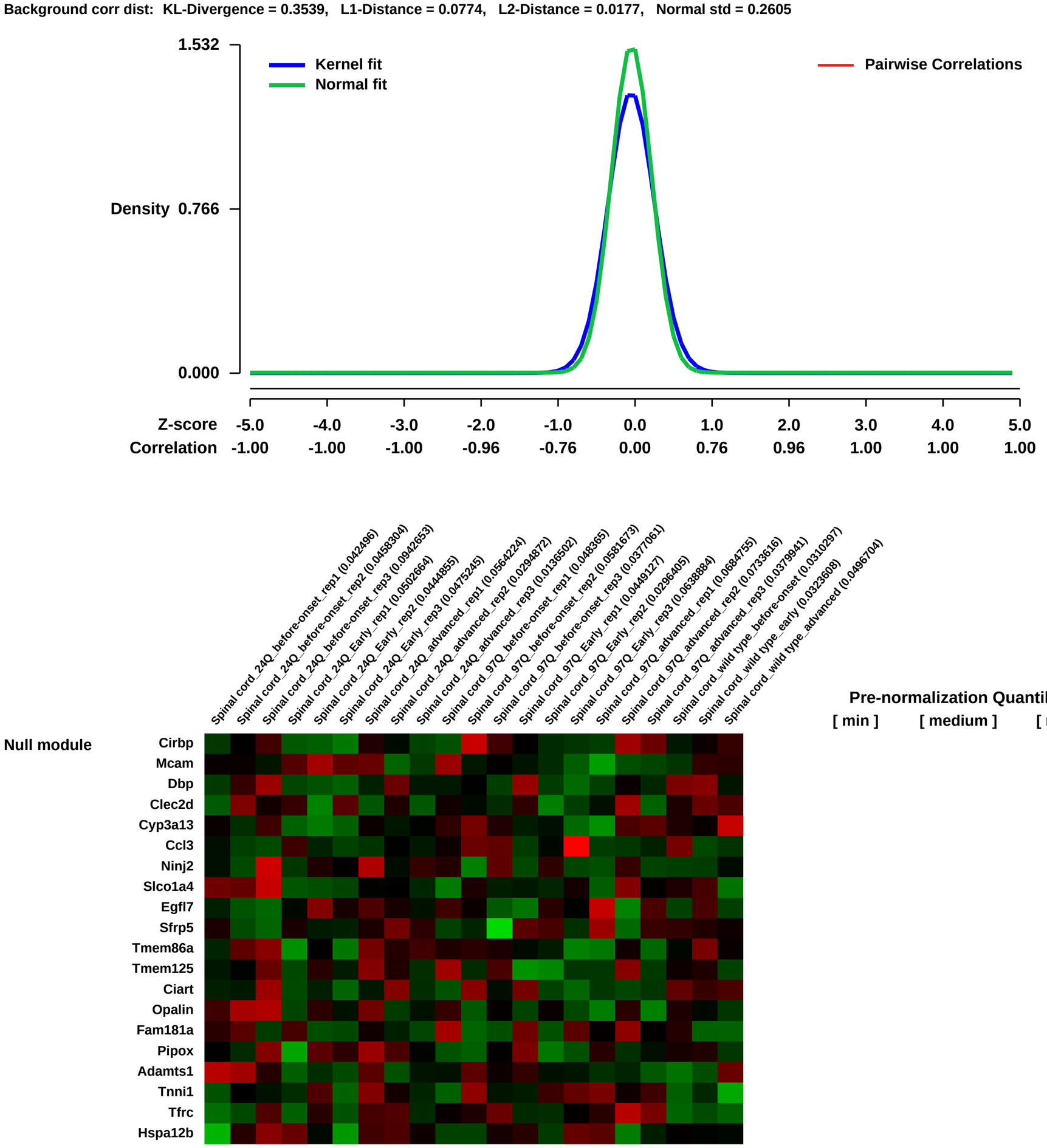

GEO Series "GSE57543" Expression Profiles

Num of samples in this series: 6

Scale of expression profile Z-scores

-3.0 -2.0 -1.0 0.0 1.0 2.0 3.0

GEO Link: http://www.ncbi.nlm.nih.gov/geo/query/acc.cgi?acc=GSE57543
Status: Public on May 13 2014
Title: Expression data from B6 mouse miR-142 KO and WT T cells
Organism: Mus musculus
Experiment type: Expression profiling by array
Platform: GPL1261
Pubmed ID:

Summary & Design:

Summary:
T cells are critical for modulating immune responses. miRNAs are small, noncoding RNAs and play a significant role in T cell responses. miR-142 is a hematopoietic specific miRNA. To explore the potential role of miR-142 in regulating T cell responses, we generated mutant mice bearing a targeted deletion of the miR-142 gene.

We used microarrays to detail the global programme of gene expression underlying the profile changes between miR-142 KO and WT T cell and identified distinct classes of up-regulated genes during this process.

Overall design:
miR-142 KO mice and WT littermates (biological triplicates) matched with age and sex were selected. T cells were purified from spleens by negative selection and processed for RNA isolation and hybridization on Affymetrix microarrays.

Background corr dist: KL-Divergence = 0.0094, L1-Distance = 0.0206, L2-Distance = 0.0006, Normal std = 0.8842

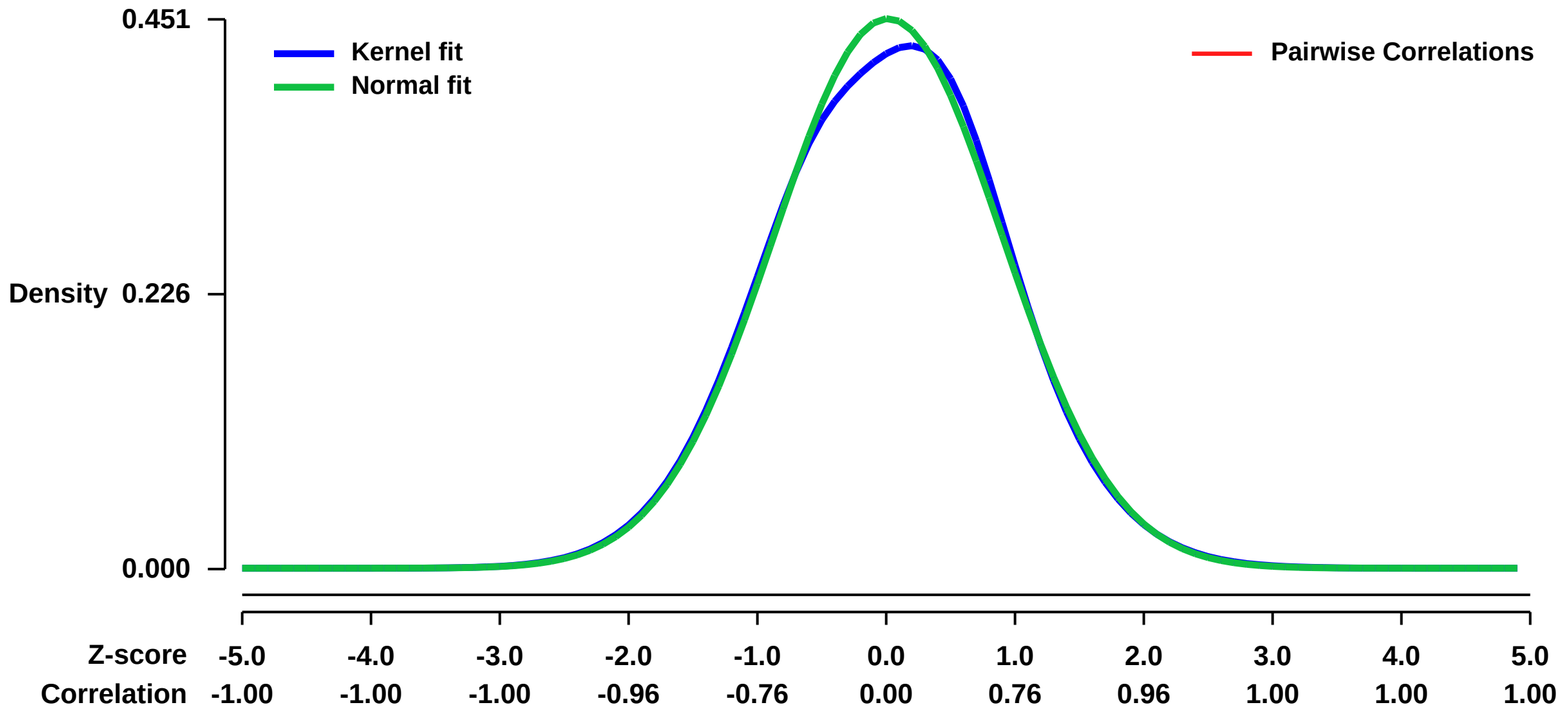

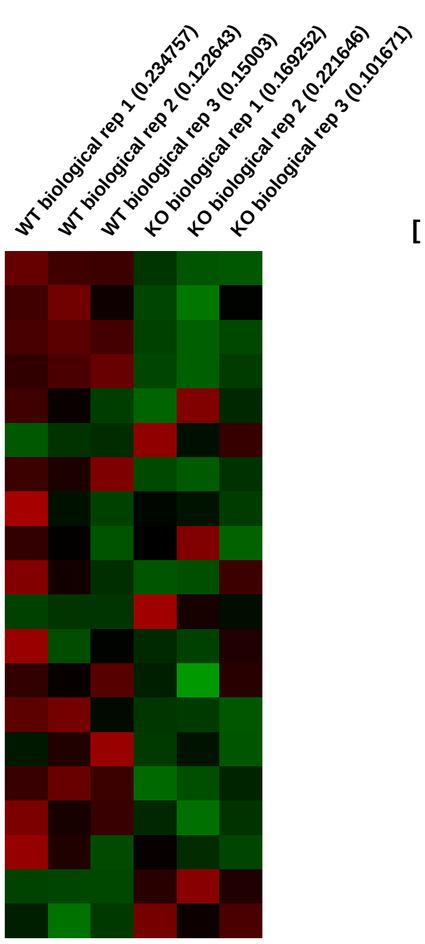

GEO Series "GSE26151" Expression Profiles

Num of samples in this series: 20

Scale of expression profile Z-scores

-3.0 -2.0 -1.0 0.0 1.0 2.0 3.0

GEO Link:	http://www.ncbi.nlm.nih.gov/geo/query/acc.cgi?acc=GSE26151
Status:	Public on Jun 30 2011
Title:	Splitting Function enables Dual Feedback Regulation to Control JAK2/STAT5 Signaling for a Wide Ligand Range
Organism:	Mus musculus
Experiment type:	Expression profiling by array
Platform:	GPL1261
Pubmed ID:	21772264
Summary & Design:	**Summary:** **Cellular signal transduction is governed by multiple feedback mechanisms to elicit robust cellular decisions. We combined mathematical modeling and extensive time-resolved data sets in primary erythroid progenitor cells and dissected the roles of the two transcriptional feedback regulators of the SOCS family, CIS and SOCS3 in JAK2/STAT5 signaling. Our model revealed that both feedbacks are most effective at different ligand concentration ranges.** **To identify the relevant transcriptional feedback regulators that are involved in attenuation of Epo-induced JAK2-STAT5 signaling in addition to CIS, we performed a time-resolved genome-wide expression profiling of murine erythroid progenitor cells at the colony forming unit erythroid (CFU-E) stage up to 24 and 7 hours after EPO stimulation and in control, repectively. The analysis identified SOCS3 as the only further de novo regulated gene upon Epo-induced JAK2-STAT5 signaling. From subsequent mathematical modeling, we calculated the STAT5 response in previously unobserved Epo concentrations, which provided a quantitative link between cell survival and the integrated response of STAT5 in the nucleus. In conclusion, our combined modeling approach revealed novel insights into the orchestrated action of feedback control to regulate STAT5-mediated survival decisions over a broad range of ligand concentrations.** **Overall design:** **Freshly sorted CFU-E cells were starved for 1 h in Panserin 401 supplemented with BSA and 50 ´µM ¸†-Mercaptoethanol. Subsequently, cells were stimulated with 0.5 U/ml Epo or left untreated and RNA was extracted at different time points (0,1,2,3,4,5,6,7,8,14,19,24 hrs after Epo stimulation and at 0,1,2,3,4,5,6,7 hrs without Epo treatment) using the RNeasy Mini Plus Kit (Qiagen, Hilden, Germany).**

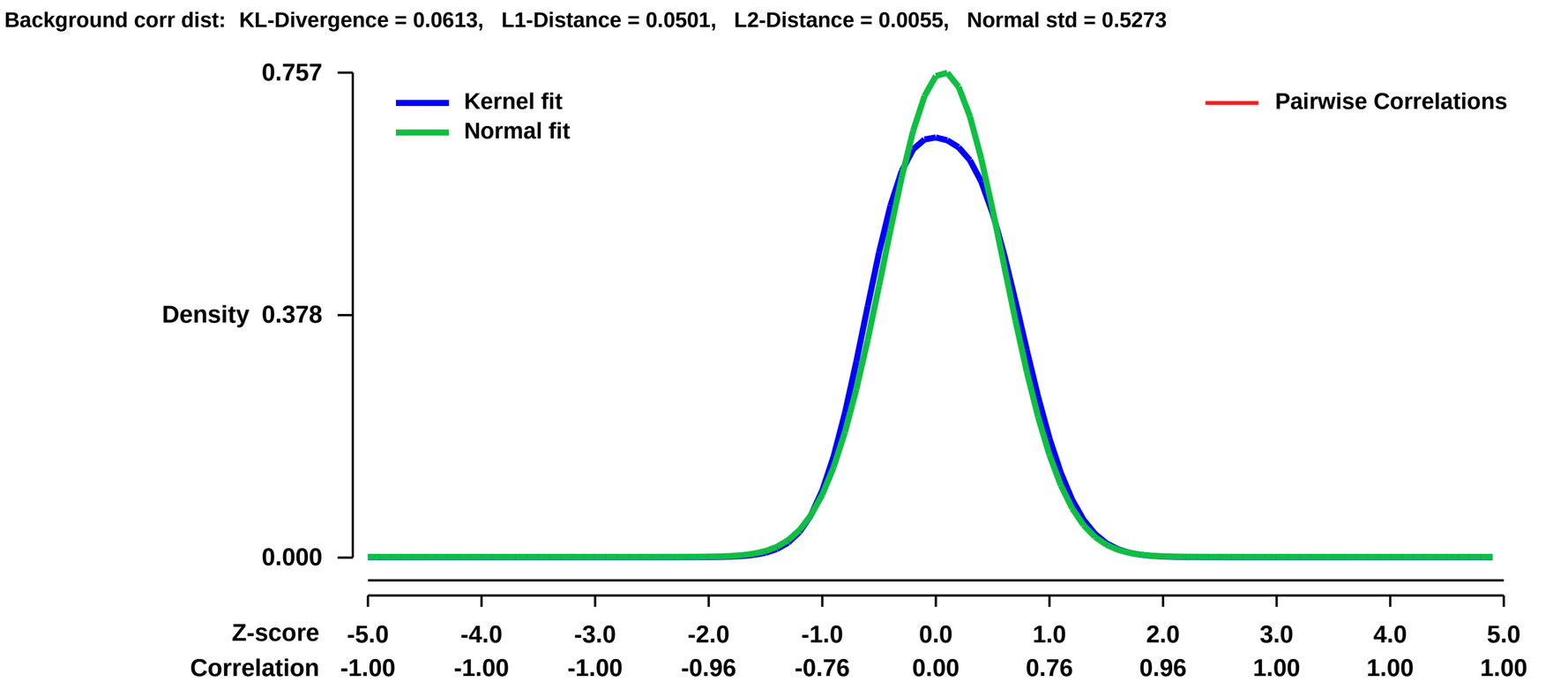

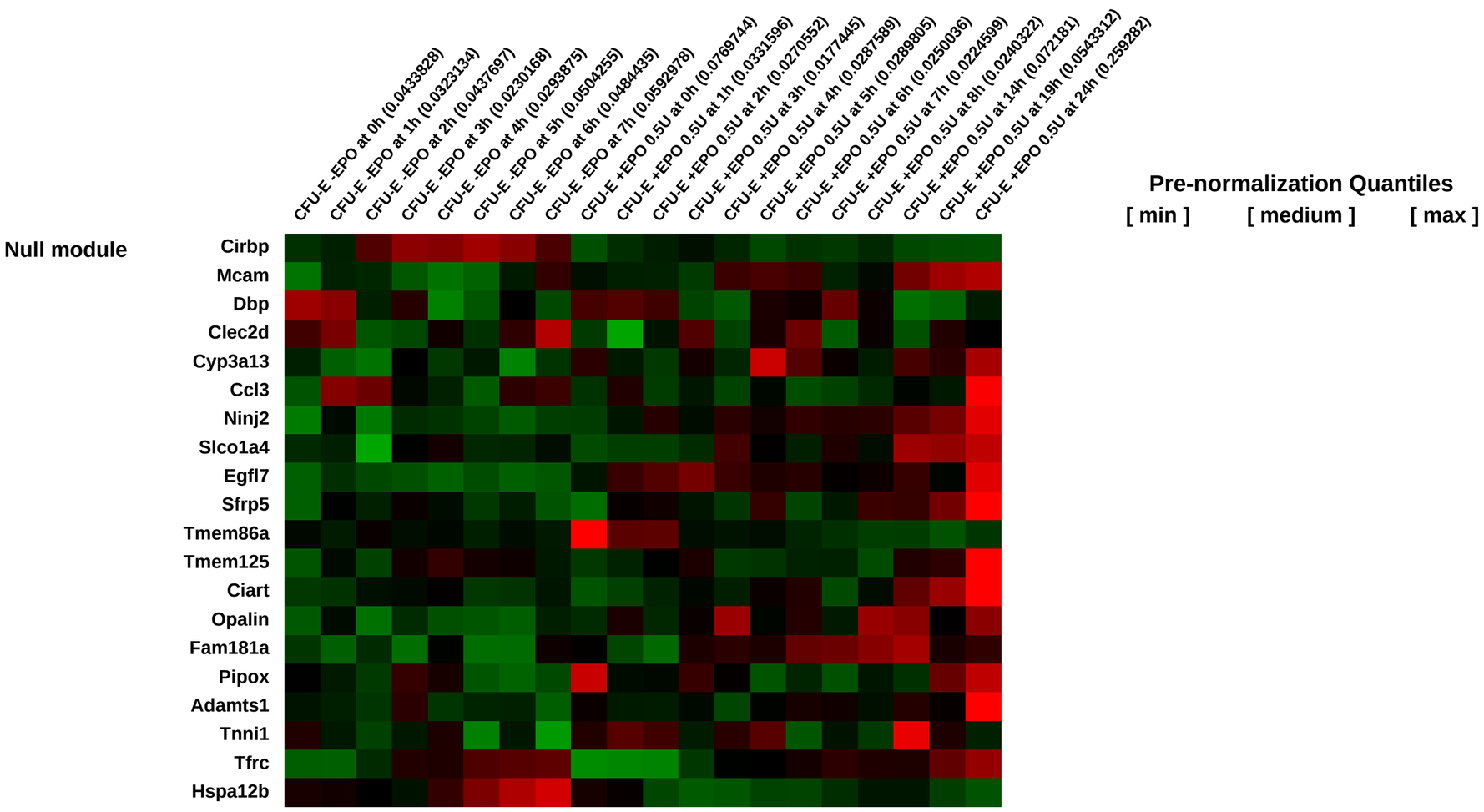

GEO Series "GSE36833" Expression Profiles

Num of samples in this series: 49

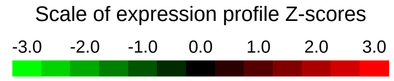

GEO Link:	http://www.ncbi.nlm.nih.gov/geo/query/acc.cgi?acc=GSE36833
Status:	Public on Mar 28 2012
Title:	Gene Expression profiling in DBA/2J glaucoma
Organism:	Mus musculus
Experiment type:	Third-party reanalysis
Platform:	GPL1261
Pubmed ID:	22426214
Summary & Design:	**Summary:** Glaucoma is a common ocular disorder that is a leading cause of blindness worldwide. It is characterized by the dysfunction and loss of retinal ganglion cells (RGCs). Although many studies have implicated various molecules in glaucoma, no mechanism has been shown to be responsible for the earliest detectable damage to RGCs and their axons in the optic nerve. Here, we show that the leukocyte transendothelial migration pathway is activated in the optic nerve head at the earliest stages of disease in an inherited mouse model of glaucoma. This resulted in proinflammatory monocytes entering the optic nerve prior to detectable neuronal damage. A 1-time x-ray treatment prevented monocyte entry and subsequent glaucomatous damage. A single x-ray treatment of an individual eye in young mice provided that eye with long-term protection from glaucoma but had no effect on the contralateral eye. Localized radiation treatment prevented detectable neuronal damage and dysfunction in treated eyes, despite the continued presence of other glaucomatous stresses and signaling pathways. Injection of endothelin-2, a damaging mediator produced by the monocytes, into irradiated eyes, combined with the other glaucomatous stresses, restored neural damage with a topography characteristic of glaucoma. Together, these data support a model of glaucomatous damage involving monocyte entry into the optic nerve. Genome-wide assessment of gene expression changes was performed in DBA/2J-Gpnmb+, DBA/2J mice and irradiated DBA/2J mice at 8.5 and 10.5 months of age. **Overall design:** In this study (Howell et al, JCI, 2012), 50 samples (10 D2-Gpnmb+ control at 8.5 mos, 20 NOE DBA/2J at 8.5 mos, 10 radiation-treated DBA2J at 8.5 mos and 10 radiation-treated DBA/2J at 10.5 mos) were combined with 30 of ONH samples from the GSE26299 study (10 D2-Gpnmb+ and 20 NOE DBA/2J all at 10.5 mos). One D2-Gpnmb+ 8.5mo sample failed QC and was not included in the analysis. Quantile normalization was performed for all optic nerve head samples reported in the study. The complete dataset is linked below as a supplementary file.

Background corr dist: KL-Divergence = 0.4034, L1-Distance = 0.0737, L2-Distance = 0.0161, Normal std = 0.2470

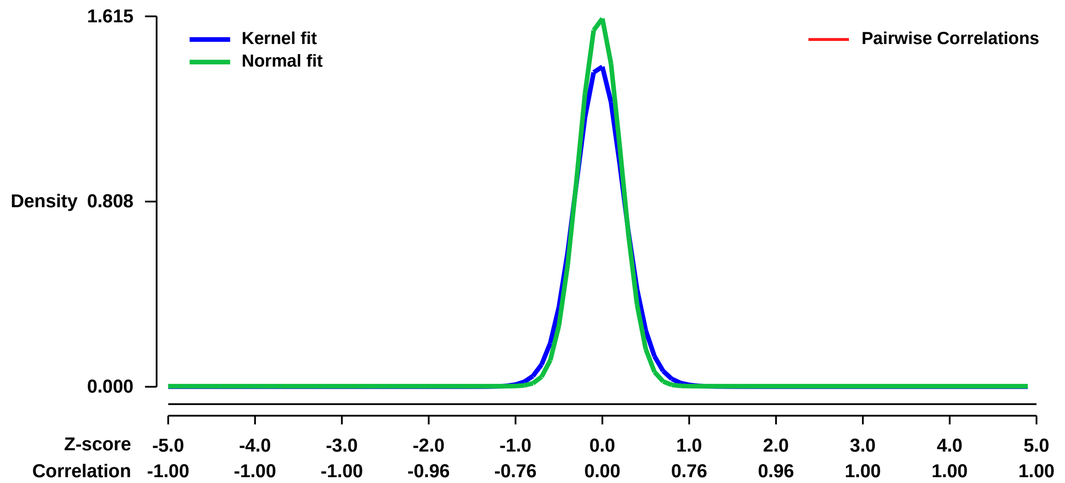

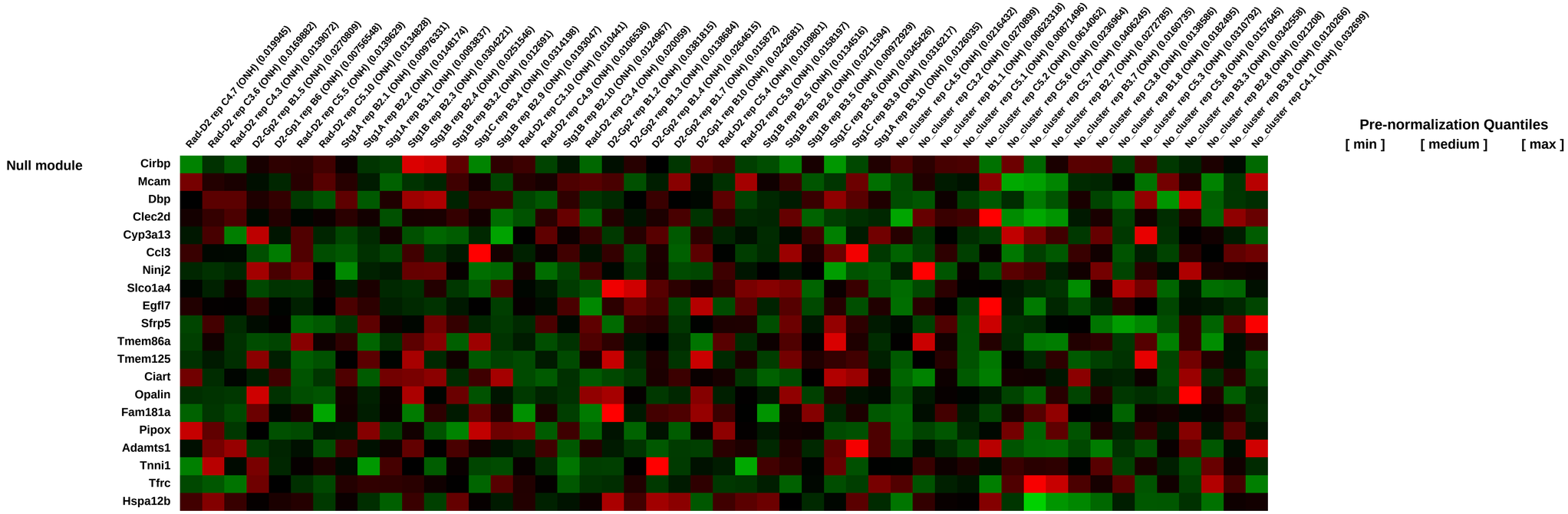

GEO Series "GSE50123" Expression Profiles

Num of samples in this series: 6

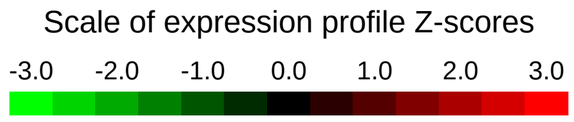

GEO Link:	**http://www.ncbi.nlm.nih.gov/geo/query/acc.cgi?acc=GSE50123**
Status:	**Public on Nov 18 2013**
Title:	**Runx3 function in splenic NK cells**
Organism:	**Mus musculus**
Experiment type:	**Expression profiling by array**
Platform:	**GPL1261**
Pubmed ID:	**24236182**
Summary & Design:	**Summary:** **NK cells are innate immune cells that recognize and kill foreign, virally-infected and tumor cells without the need for prior immunization. NK expansion following viral infection is IL-2 or IL-15-dependent.** **Overall design:** **To identify Runx3 responsive genes, NK cells were isolated from spleen of WT and Runx3-/- mice . Six samples (3 WT and 3 Runx3-/-) of freshly isolated NK cells (resting) were separately obtained from individual mice.**

Background corr dist: **KL-Divergence = 0.0470, L1-Distance = 0.0852, L2-Distance = 0.0114, Normal std = 0.6857**

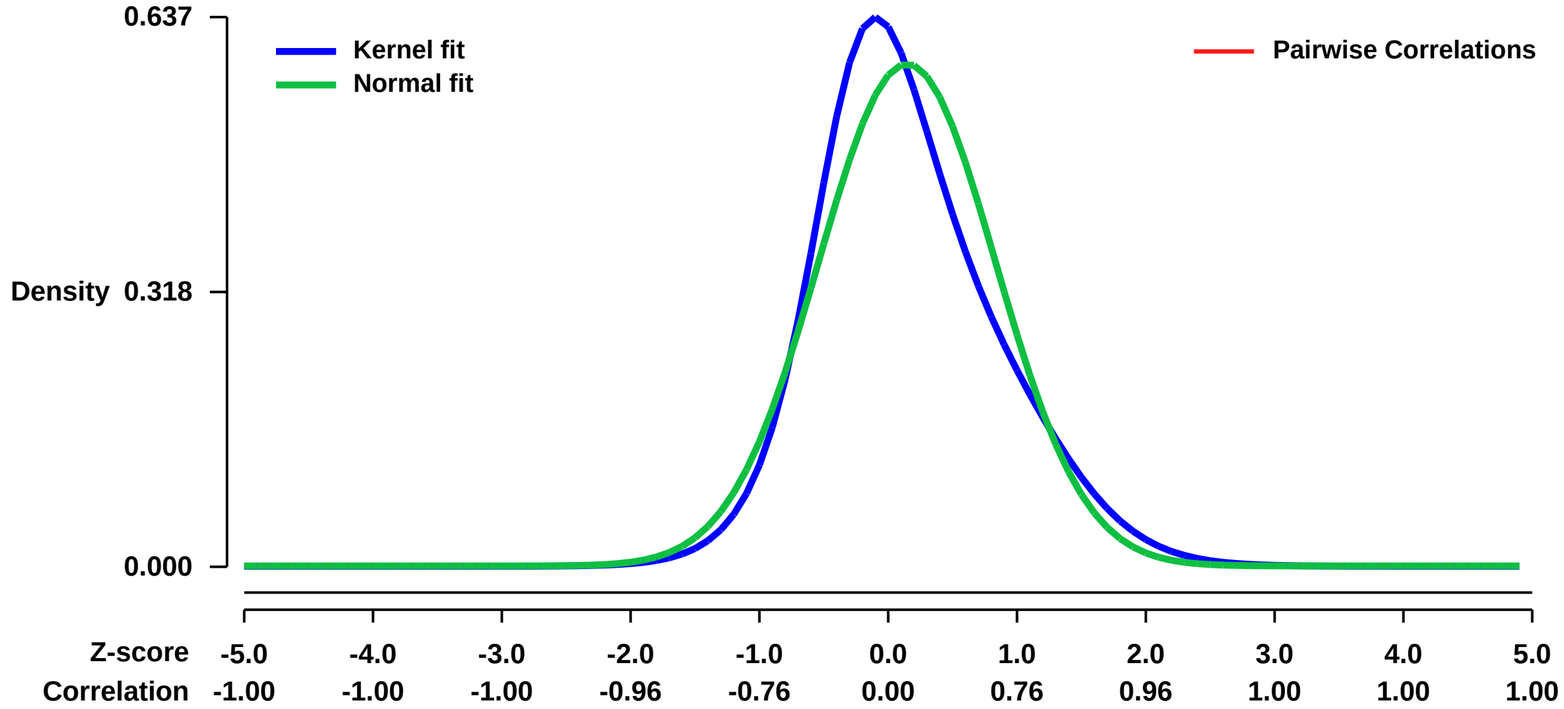

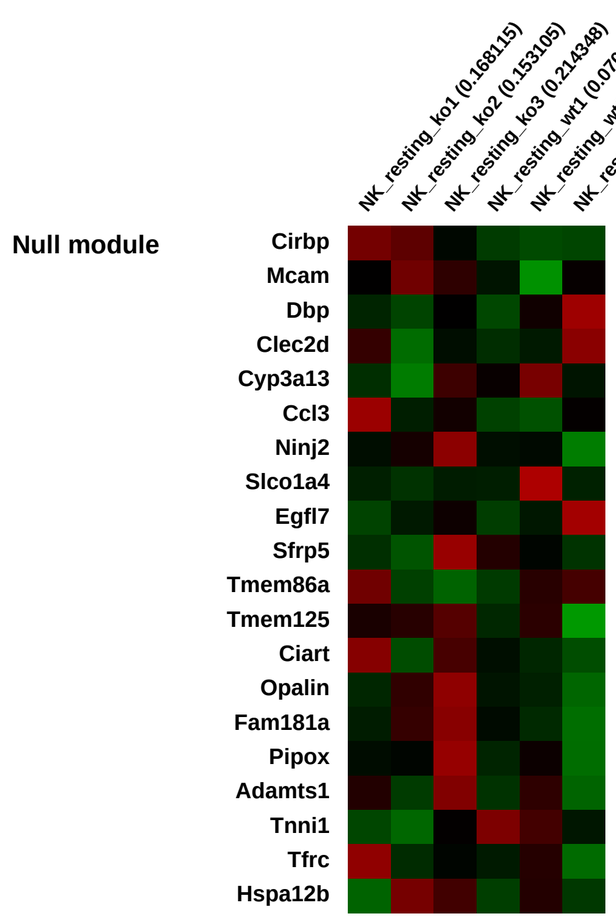

GEO Series "GSE27605" Expression Profiles

Num of samples in this series: 8

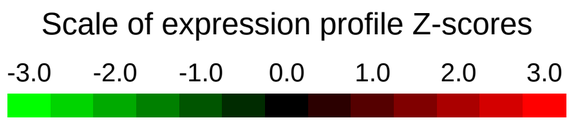

GEO Link:	http://www.ncbi.nlm.nih.gov/geo/query/acc.cgi?acc=GSE27605
Status:	Public on Mar 14 2011
Title:	The intestinal stem cell signature identifies colorectal cancer stem cells and predicts disease relapse
Organism:	Mus musculus
Experiment type:	Expression profiling by array
Platform:	GPL1261
Pubmed ID:	21419747
Summary & Design:	**Summary:** **Using EphB2 or the ISC marker Lgr5, we have FACS-purified and profiled intestinal stem cells (ISCs), crypt proliferative progenitors and late transient amplifying cells to define a gene expression program specific for normal ISCs.** **A frequent complication in colorectal cancer (CRC) is regeneration of the tumor after therapy. The intestinal stem cell signature predicts disease relapse in CRC and identifies a stem cell-like population that displays robust tumor- initiating capacity in immunodeficient mice as well as long-term self-renewal potential.** **Overall design:** **We FACS purified mouse intestinal crypt cells according to their EphB2 or Lgr5 contents. We used Affymetrix chips to hybridize 2 samples from EphB2 high, 2 samples from EphB2 medium and 2 samples from EphB2 low cells (one sample from each group in a first hybridization on February 2009 plus an additional sample from each group on March 2009). Additionally, we hybridized one sample from Lgr5-EGFP high and one sample from Lgr5-EGFP low cells, obtained from Lgr5-EGFP knock-in mice (Barker et al., 2007).**

Background corr dist: KL-Divergence = 0.0298, L1-Distance = 0.0338, L2-Distance = 0.0014, Normal std = 0.6870

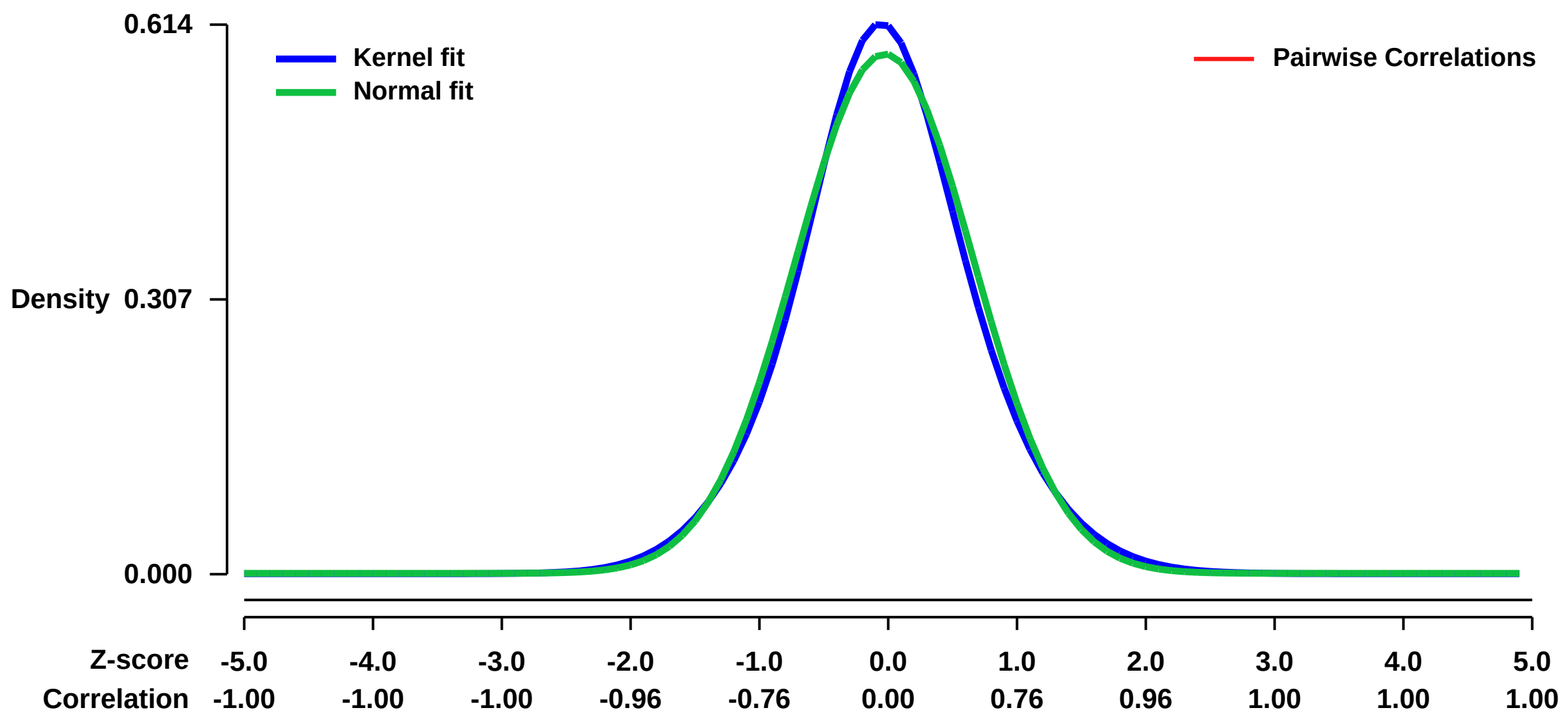

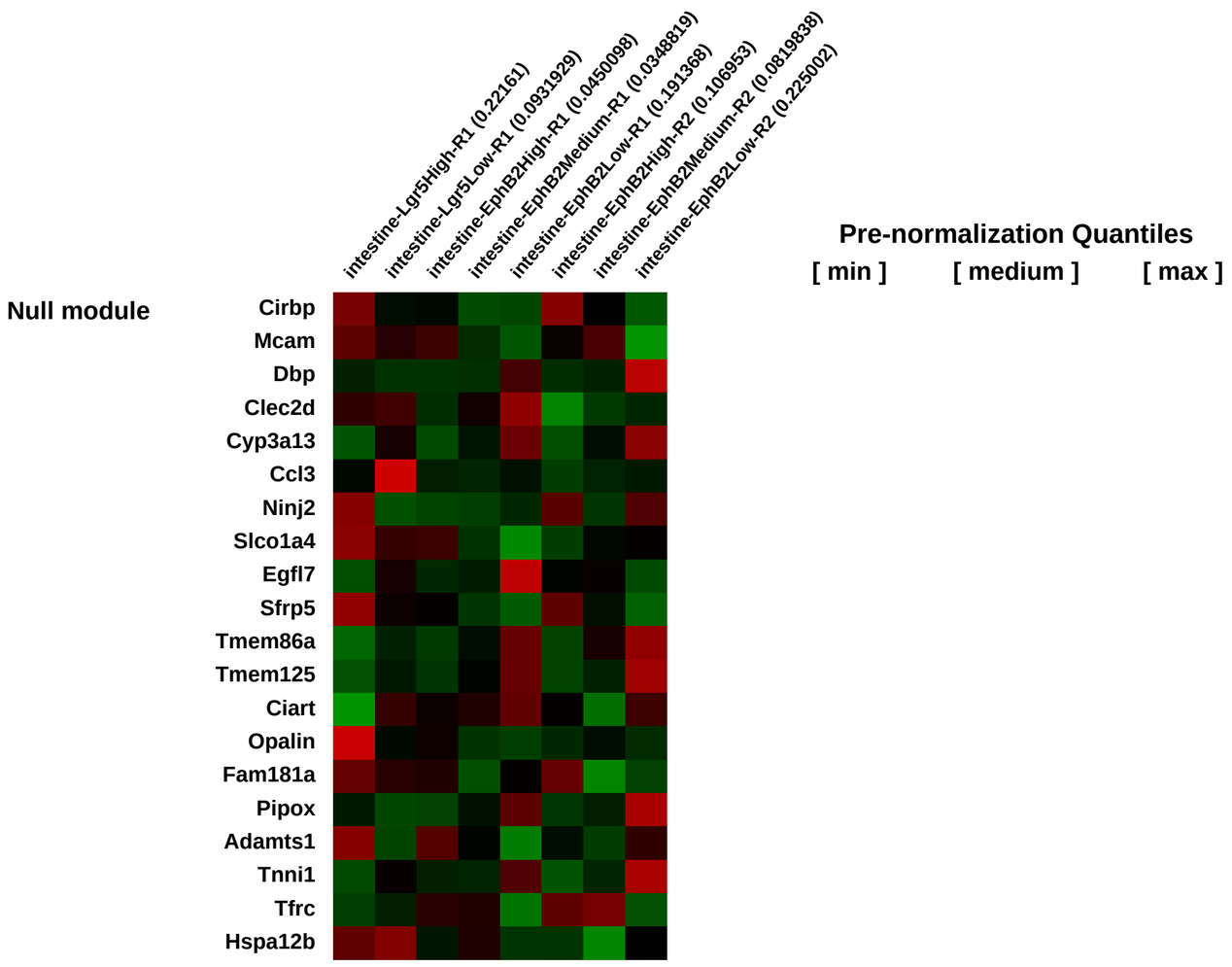

GEO Series "GSE38538" Expression Profiles

Num of samples in this series: 6

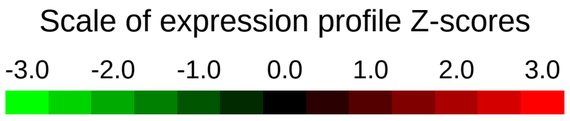

GEO Link:	http://www.ncbi.nlm.nih.gov/geo/query/acc.cgi?acc=GSE38538
Status:	Public on Jun 07 2012
Title:	Expression data from E12.5 NSP cells, CTL v REST shRNA
Organism:	Mus musculus
Experiment type:	Expression profiling by array
Platform:	GPL1261
Pubmed ID:	22791895
Summary & Design:	**Summary:** REST is a master regulator of genes that are involved in the acqusition of neuronal fate. The role of REST is not well understood so we attempted to investigate the role of REST in the development of neural cells by analysing the genes that are upregulated when REST is knocked down via shRNA We used microarrays to assess the genes which were up and down regulated after REST is knocked down **Overall design:** E12.5 NSP cells were infected with either control or REST shRNA expressing lentiviruses and collected after 6 days for RNA extraction

Background corr dist: KL-Divergence = 0.0362, L1-Distance = 0.0235, L2-Distance = 0.0007, Normal std = 0.6399

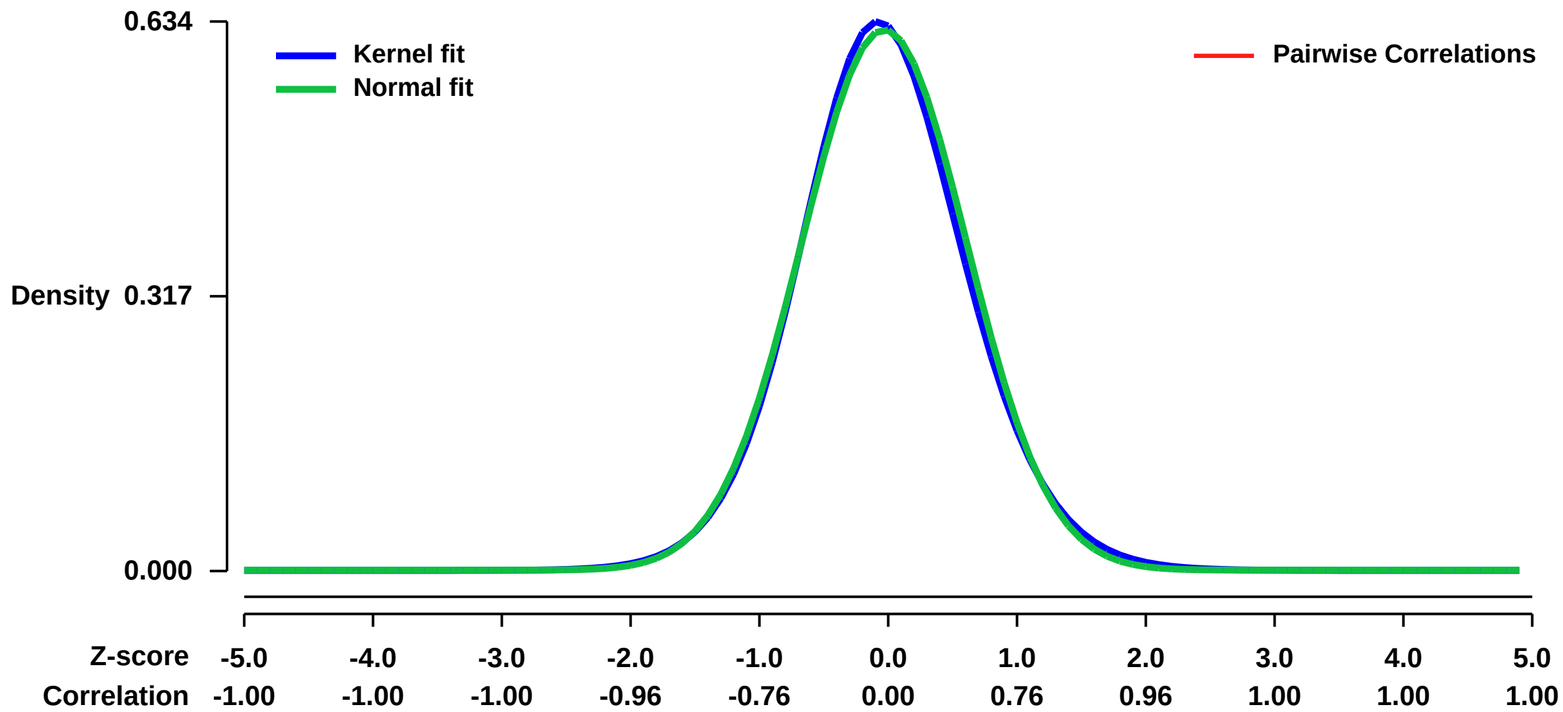

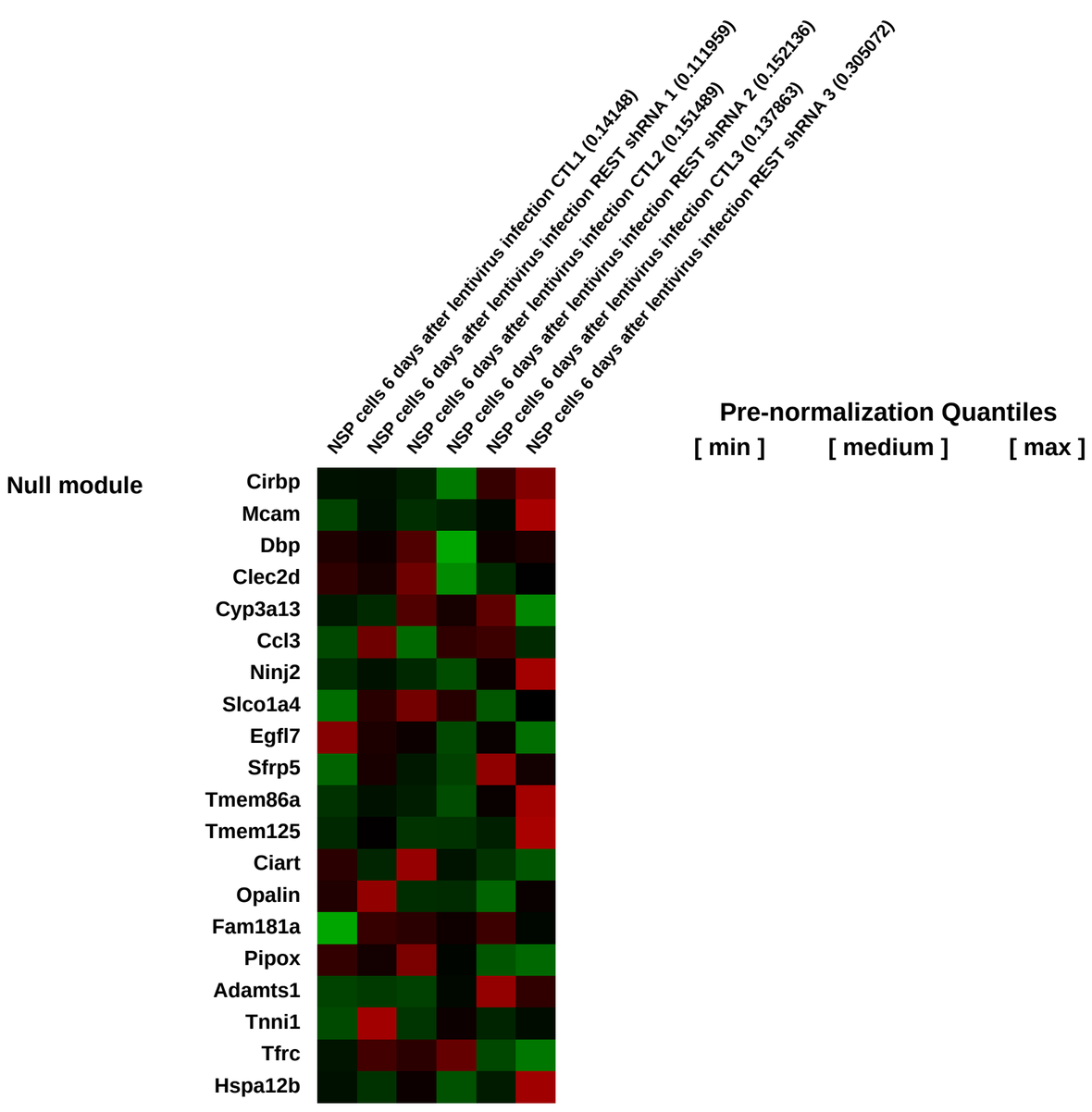

GEO Series "GSE22039" Expression Profiles

Num of samples in this series: 9

Scale of expression profile Z-scores

-3.0 -2.0 -1.0 0.0 1.0 2.0 3.0

GEO Link:	**http://www.ncbi.nlm.nih.gov/geo/query/acc.cgi?acc=GSE22039**
Status:	**Public on Dec 01 2010**
Title:	**Gene expression data from forelimb buds of E10.5 mouse embryos**
Organism:	**Mus musculus**
Experiment type:	**Expression profiling by array**
Platform:	**GPL1261**
Pubmed ID:	
Summary & Design:	**Summary:** **We used microarrays to identify Pax3 targets during myogenesis in the mouse embryo** **Overall design:** **Mouse embryos were genotyped Pax3GFP/+ or Pax3PAX3-FKHR/GFP and dissected at E10.5 under a fluorescent binocular. The forelimb buds were dissected and dissociated and GFP positive cells were then sorted by flow cytometry before RNA extraction and hybridization on Affymetrix microarrays. We also sorted GFP negative cells.**

Background corr dist: **KL-Divergence = 0.0643, L1-Distance = 0.0217, L2-Distance = 0.0007, Normal std = 0.5113**

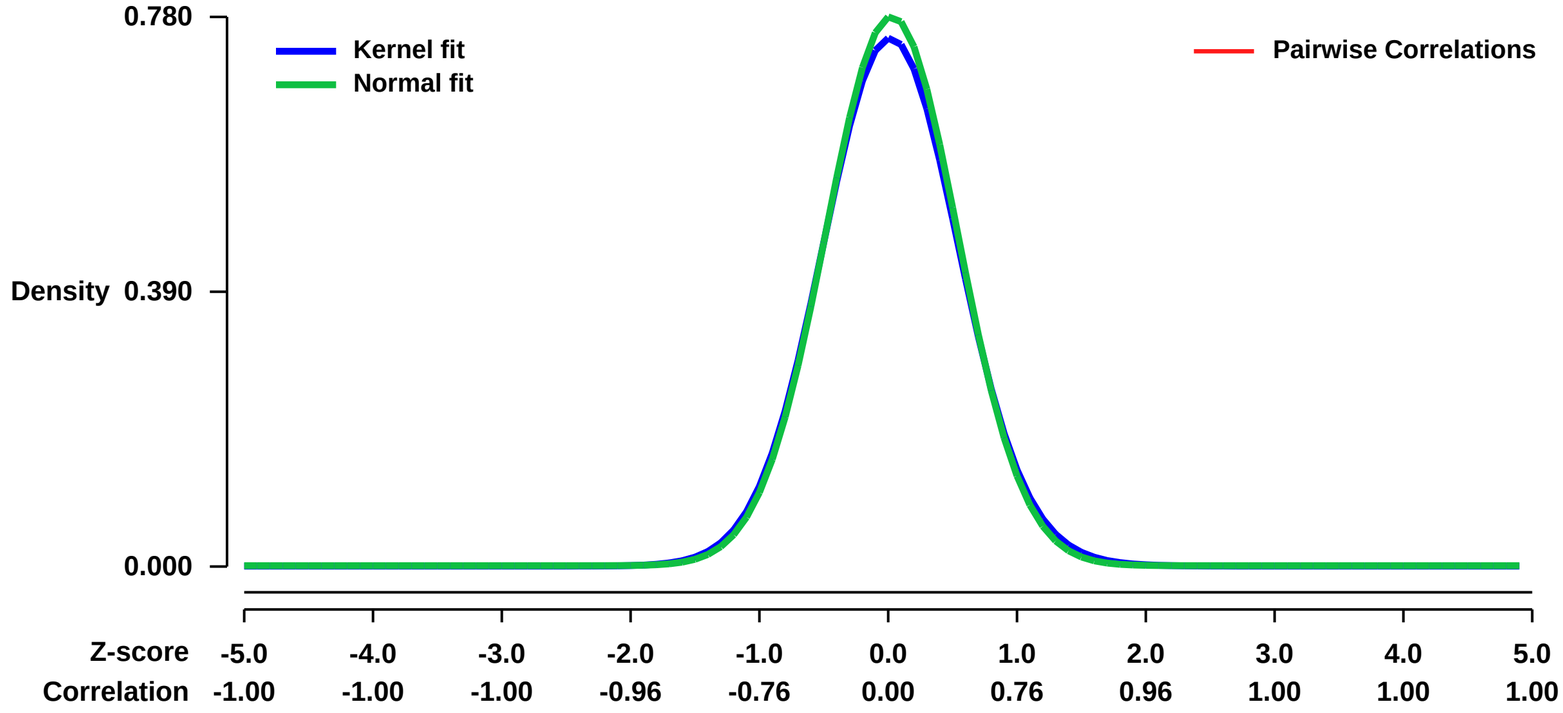

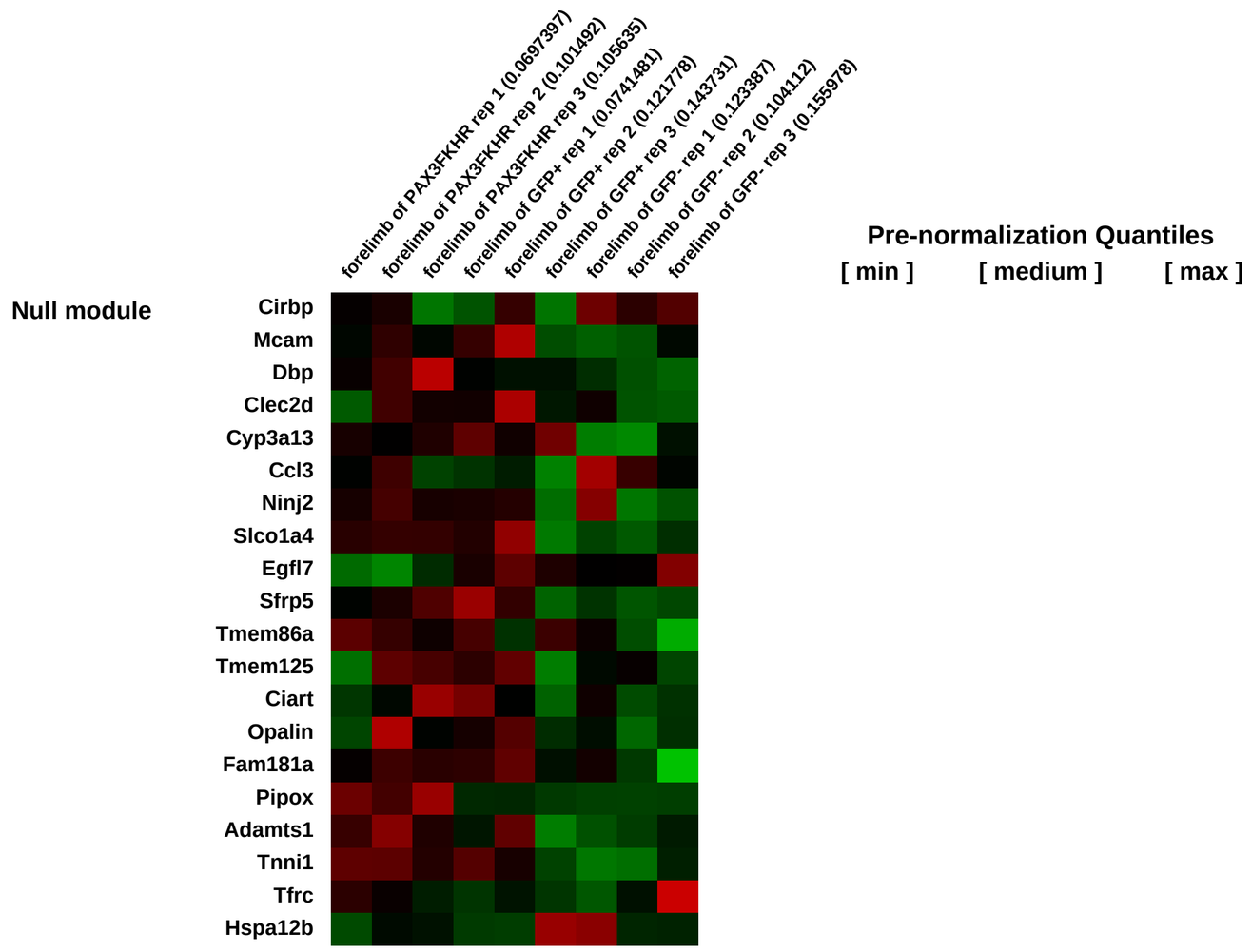

GEO Series "GSE34351" Expression Profiles

Num of samples in this series: 12

Scale of expression profile Z-scores

-3.0 -2.0 -1.0 0.0 1.0 2.0 3.0

GEO Link:	http://www.ncbi.nlm.nih.gov/geo/query/acc.cgi?acc=GSE34351
Status:	Public on Aug 15 2012
Title:	Gene expression profile on ischemic kidneys from wildtype C57BL/10 and TLR4 null C57BL/10ScNJ mice
Organism:	Mus musculus
Experiment type:	Expression profiling by array
Platform:	GPL1261
Pubmed ID:	22895517
Summary & Design:	**Summary:** TLR4 deficiency attenuates kidney injury after ischemic reperfusion as measured by both renal function and morphology. To better understand the role of TLR4 during the acute kidney injury, we used DNA microarray to identify genes that were differentially expressed on kidneys in wildtype B10 mice and TLR4 null mice during the early stage of injury. **Overall design:** A murine ischemic reperfusion injury model was established. After right nephrectomy, the left pedicle was clamped for 23min followed by 4hr reperfusion. Sham mice were used as controls. 6 WT males and 6 TLR4 null males were included with 3 ischemic and 3 shams in each group.

Background corr dist: KL-Divergence = 0.1223, L1-Distance = 0.0249, L2-Distance = 0.0008, Normal std = 0.4083

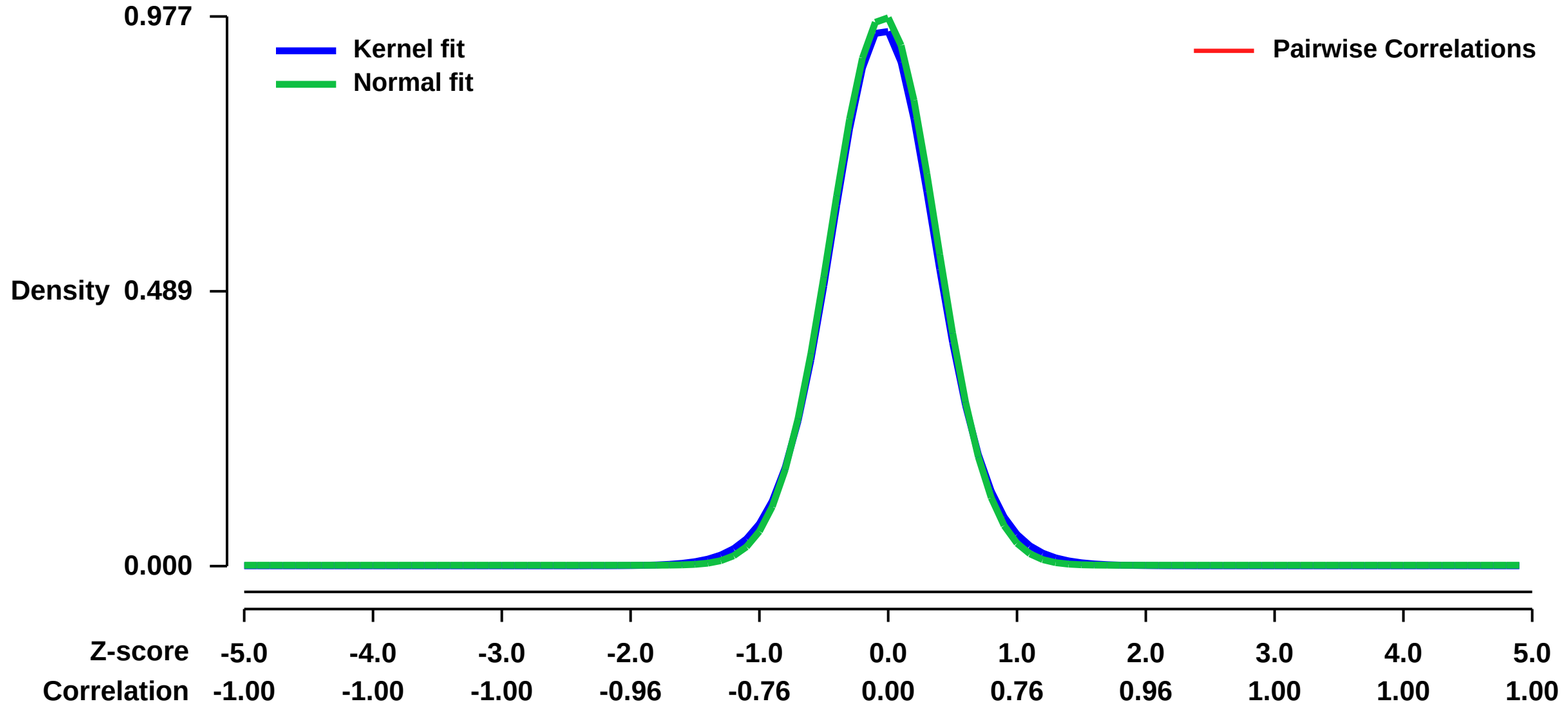

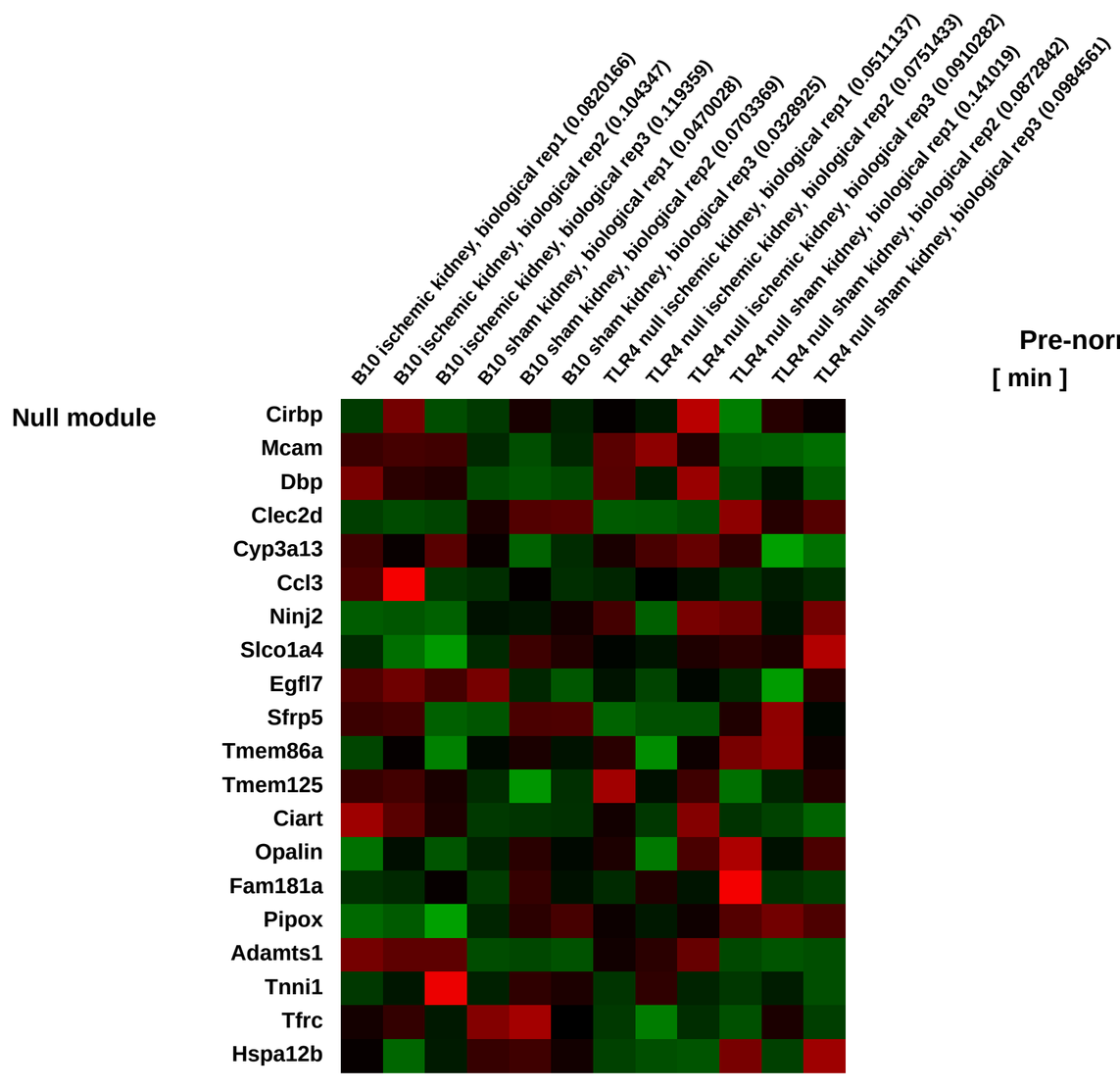

GEO Series "GSE14672" Expression Profiles

Num of samples in this series: 12

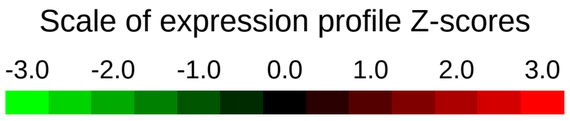

GEO Link:	**http://www.ncbi.nlm.nih.gov/geo/query/acc.cgi?acc=GSE14672**
Status:	**Public on Sep 30 2009**
Title:	**GM-CSF-mediated granulopoiesis is regulated by the transcription factor STAT5A/B**
Organism:	**Mus musculus**
Experiment type:	**Expression profiling by array**
Platform:	**GPL1261**
Pubmed ID:	**19779039**
Summary & Design:	**Summary:** **GM-CSF controls the development of granulocytes but little is known about the contribution of the downstream mediating transcription factor STAT5A/B. To elucidate this pathway, we generated mice lacking the Stat5a and 5b genes in blood cells. Peripheral neutrophils were decreased and administration of 5-FU and GM-CSF failed to induce granulopoiesis in Stat5a/b-mutant mice. GMPs were isolated and cultured with GM-CSF. Both the number and size of STAT5A/B-null colonies were reduced and GM-CSF-induced survival of mature STAT5A/B-null neutrophils was impaired. Time-lapse cinematography and single cell tracking of GMPs revealed that STAT5A/B-null cells were characterized by a longer generation time and an increased cell death. Gene expression profiling experiments suggested that STAT5A/B directs GM-CSF signaling through the regulation of cell survival genes. #!#** **Overall design:** **Mice lacking or with the Stat5a and 5b genes in blood cells, which were treated w/o GMP**

Background corr dist: **KL-Divergence = 0.0805, L1-Distance = 0.0370, L2-Distance = 0.0028, Normal std = 0.4793**

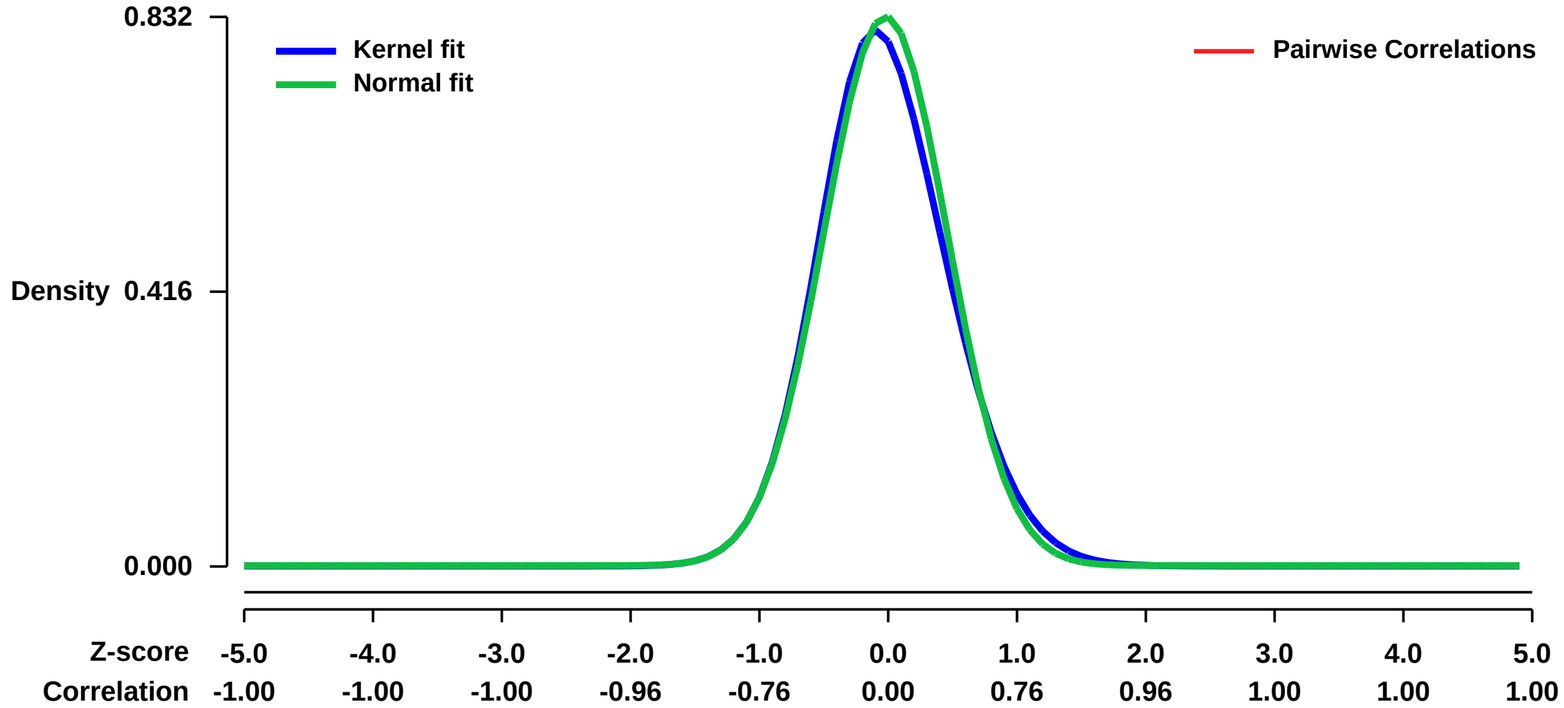

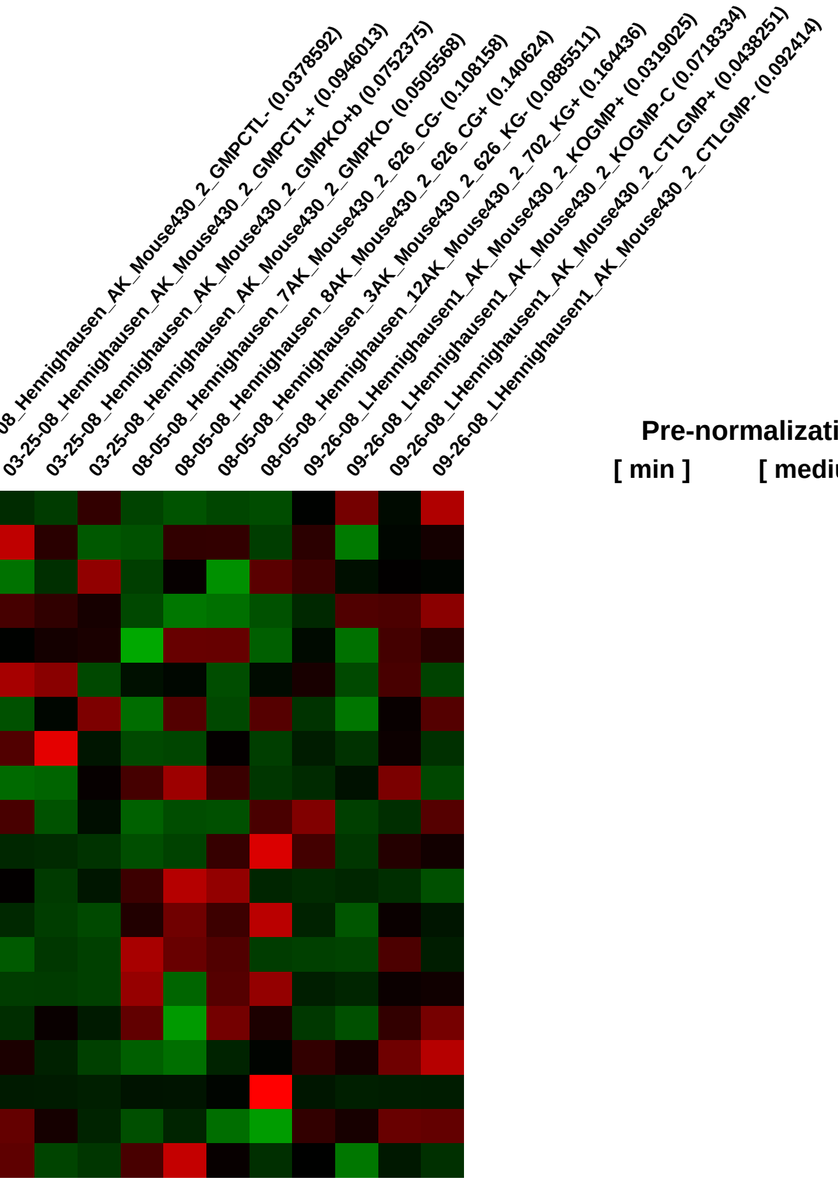

GEO Series "GSE11149" Expression Profiles

Num of samples in this series: 8

Scale of expression profile Z-scores

-3.0 -2.0 -1.0 0.0 1.0 2.0 3.0

GEO Link:	http://www.ncbi.nlm.nih.gov/geo/query/acc.cgi?acc=GSE11149
Status:	Public on May 06 2008
Title:	Cranial neural crest cells of E11.5 wild type and FAK mutants (valle-affy-mouse-480721)
Organism:	Mus musculus
Experiment type:	Expression profiling by array
Platform:	GPL1261
Pubmed ID:	
Summary & Design:	**Summary:** **Cranial neural crest cells (NCC) give rise to the majority of the cartilage, bone, connective tissue, and sensory ganglia in the head, and also participate in the remodeling of the cardiac outflow tract and pharyngeal arch arteries during cardiovascular development. Our preliminary results show that targeted deletion of focal adhesion kinase (FAK) in murine NCC results in cardiovascular and craniofacial alterations, resembling human congenital heart diseases The objective of this project is to elucidate the underlying mechanisms by which FAK mediates NCC function during development.** **Compare gene expression in cranial neural crest cells of E11.5 wild type and FAK mutants.** **FAK is a tyrosine kinase that transduces integrin and growth factor signaling pathways. Abnormal growth factor signaling leads to cardiovascular malformations caused by deficient cardiac NCC function. However, a direct role for FAK in NCC morphogenesis has not been demonstrated. We will test the hypothesis that FAK is a downstream target of essential growth factor signaling in cranial neural crest cells during development.** **1) Generate E11.5 mouse embryos that are either control (FAK+/flox) or NCC specific FAK knockout (Wnt1Cre;FAKflox/flox). 2) Determine genotype by PCR. 3) Dissect head and torax from the different genotypes. 4) Obtain NCC from dissected tissue by magnetic cell sorting using p75 antibody. 5) Prepare total RNA from speciments. We will pool the NCC from 3 different embryos of the same genotype, and send total RNA to TGEN for probe preparation, hybridization and array result analysis.** **Keywords: other** **Overall design:**

Background corr dist: KL-Divergence = 0.0453, L1-Distance = 0.0369, L2-Distance = 0.0019, Normal std = 0.6042

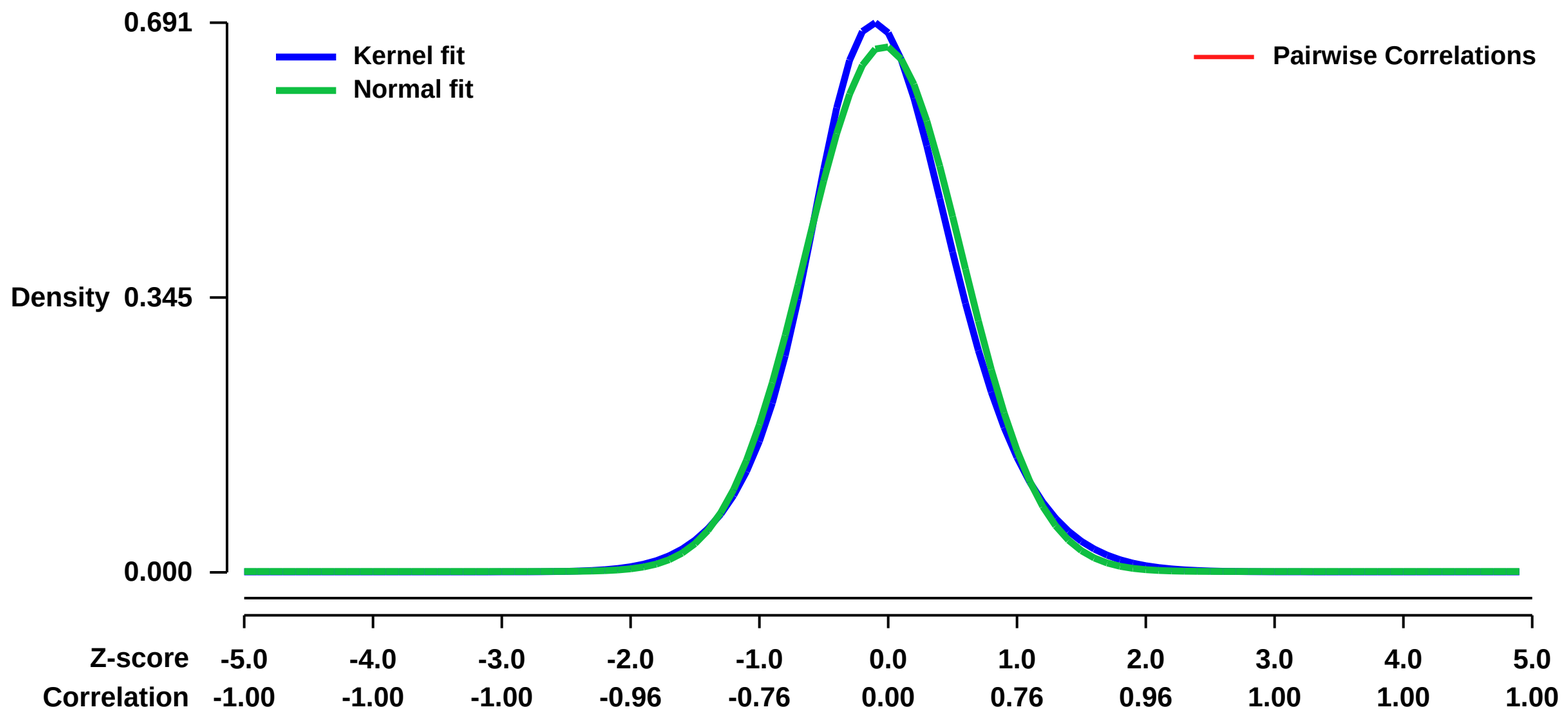

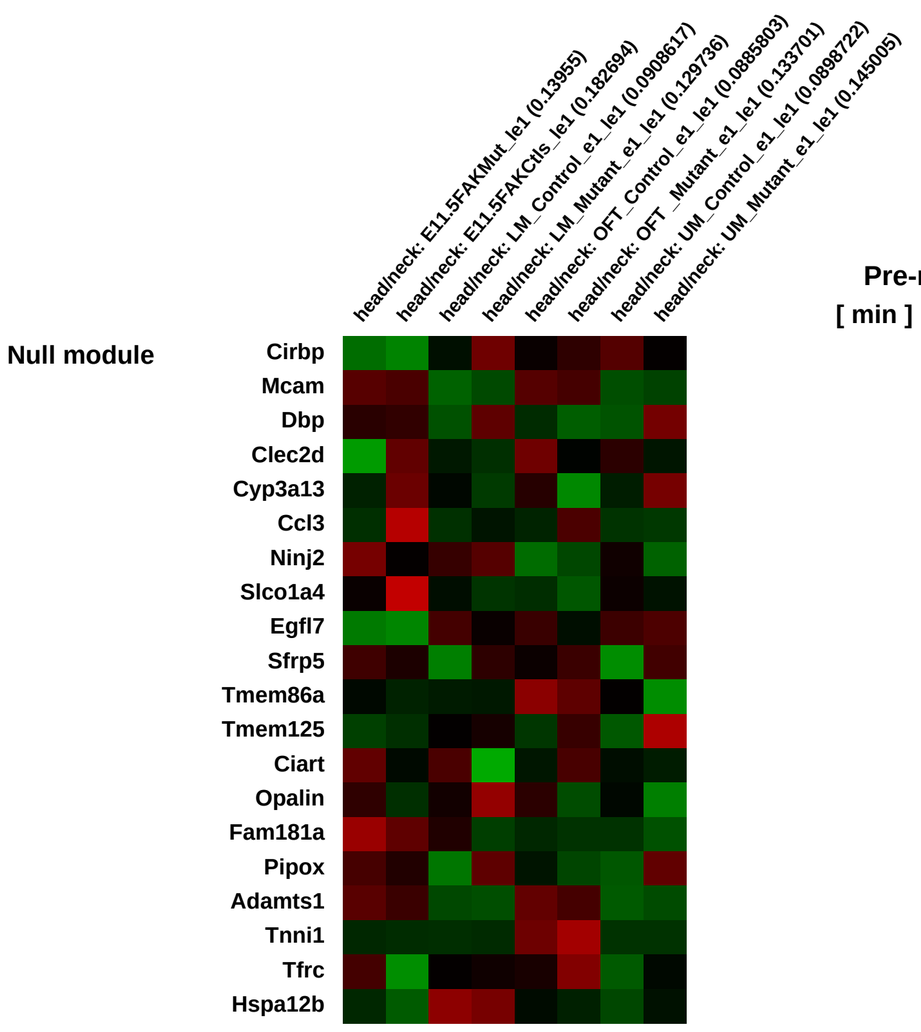

GEO Series "GSE10216" Expression Profiles

Num of samples in this series: 6

Scale of expression profile Z-scores

-3.0 -2.0 -1.0 0.0 1.0 2.0 3.0

GEO Link:	http://www.ncbi.nlm.nih.gov/geo/query/acc.cgi?acc=GSE10216
Status:	Public on Jan 30 2008
Title:	Emx2 knock-out urogenital epithelium
Organism:	Mus musculus
Experiment type:	Expression profiling by array
Platform:	GPL1261
Pubmed ID:	20962046
Summary & Design:	**Summary:** Series of samples studying effect of knock out Emx2 in urogenital epithelium of mouse embryos at E10.5. **Keywords: repeated sample** **Overall design:** The epithelial cells of the gonadal primordium were obtained by Laser Microdissection System. The specimens prepared from three individuals were mixed as one pool. There are three experimental replicates in each genotype, 3-pools of wild-type and 3-pools of Emx2 KO mouse.

Background corr dist: KL-Divergence = 0.0463, L1-Distance = 0.0207, L2-Distance = 0.0005, Normal std = 0.5877

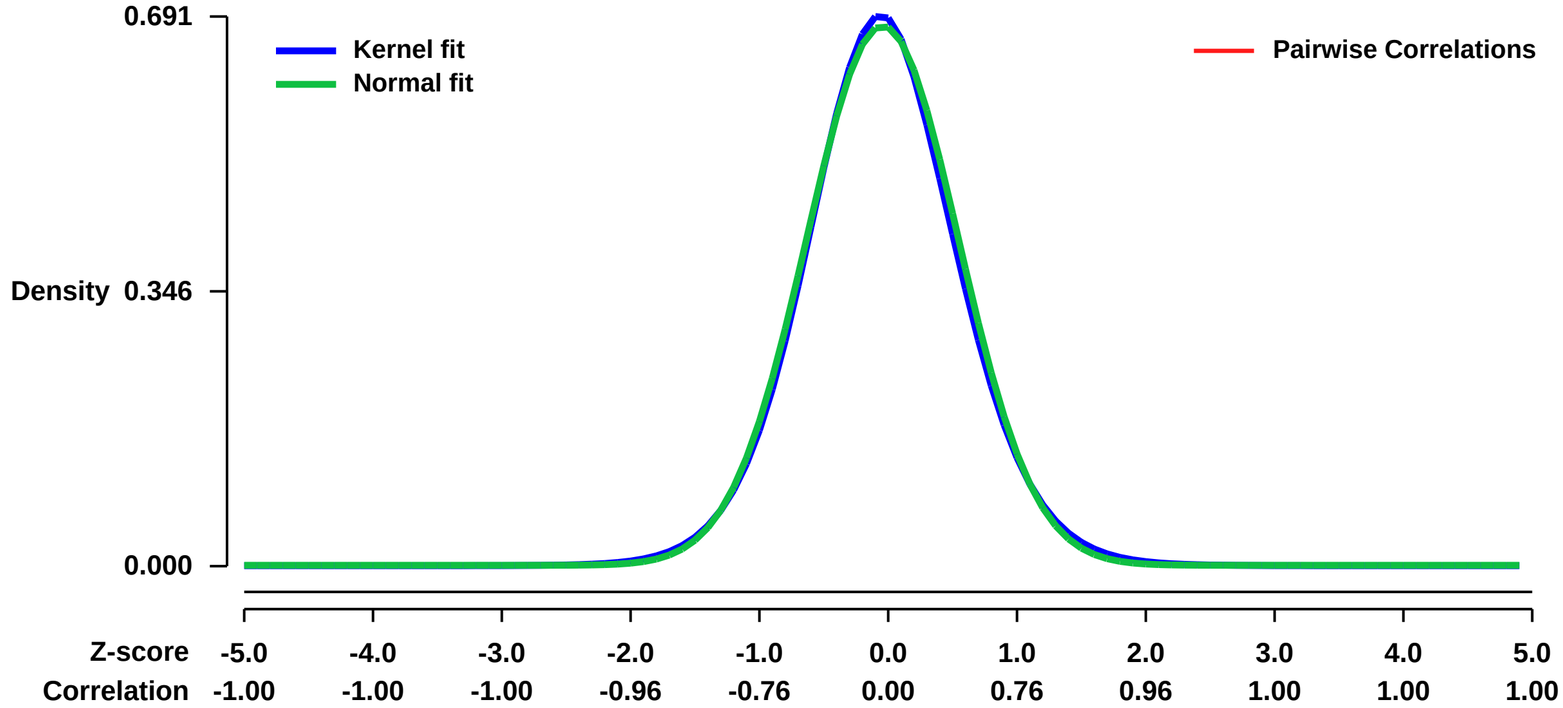

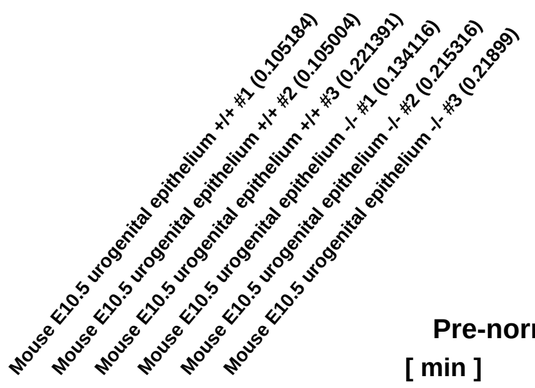

Pre-normalization Quantiles

[min] [medium] [max]

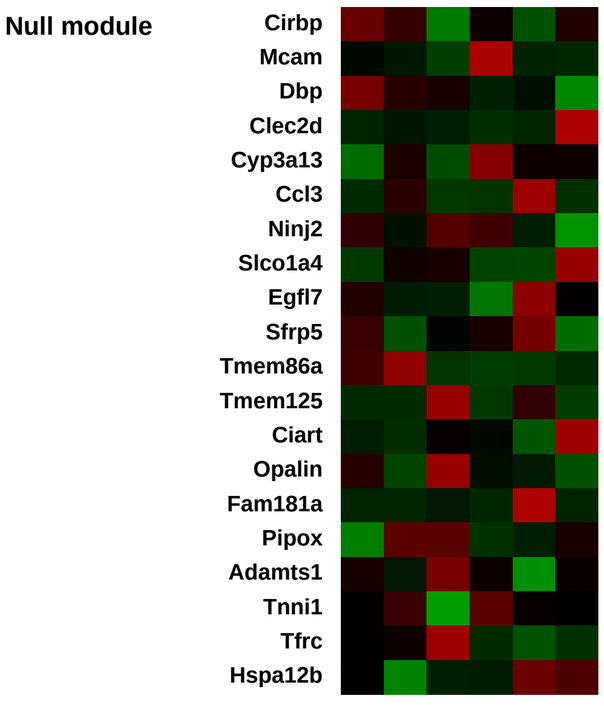

GEO Series "GSE15173" Expression Profiles

Num of samples in this series: 6

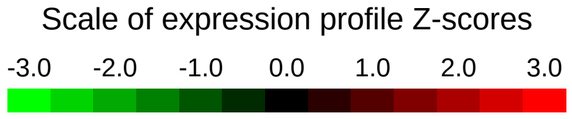

GEO Link:	http://www.ncbi.nlm.nih.gov/geo/query/acc.cgi?acc=GSE15173
Status:	Public on May 01 2009
Title:	Dppa4 is dispensable for embryonic stem cell identity and germ cell development, but essential for embryogenesis
Organism:	Mus musculus
Experiment type:	Expression profiling by array
Platform:	GPL1261
Pubmed ID:	19332562
Summary & Design:	**Summary:** Dppa4 (Developmental pluripotency-associated 4) has been identified in several highprofile screens as a gene that is expressed exclusively in pluripotent cells. It encodes a nuclear protein with a SAP-like domain and appears to be associated preferentially with transcriptionally active chromatin. Its exquisite expression pattern and results of RNA interference experiments have led to speculation that Dppa4, as well as its nearby homolog Dppa2, might play essential roles in embryonic stem cell function and/or germ cell development. To rigorously assess suggested roles, we have generated Dppa4-deficient and Dppa4/Dppa2 double-deficient ES cells, as well as mice lacking Dppa4. Contrary to predictions, we find that Dppa4 is completely dispensable for ES cell identity and germ cell development. Instead, loss of Dppa4 in mice results in late embryonic/peri-natal death and striking skeletal defects with partial penetrance. Thus, surprisingly, Dppa4-deficiency affects tissues, which never transcribed the gene, and at least some loss-of-function defects manifest phenotypically at an embryonic stage long after physiologic Dppa4 expression has ceased. Concomitant with targeted gene inactivation, we have introduced into the Dppa4 locus a red fluorescent marker (tandem-dimer RFP), which is compatible with GFP-based proteins and allows non-invasive visualization of pluripotent cells and reprogramming events. **Overall design:** Comparison of Dppa4 knockout ES cells (CI#243.12) against Dppa4 hemizygous parental ES cell line (CI#84.2). Both cell lines were grown in presence of mouse embrionic fibroblasts as feeder cells

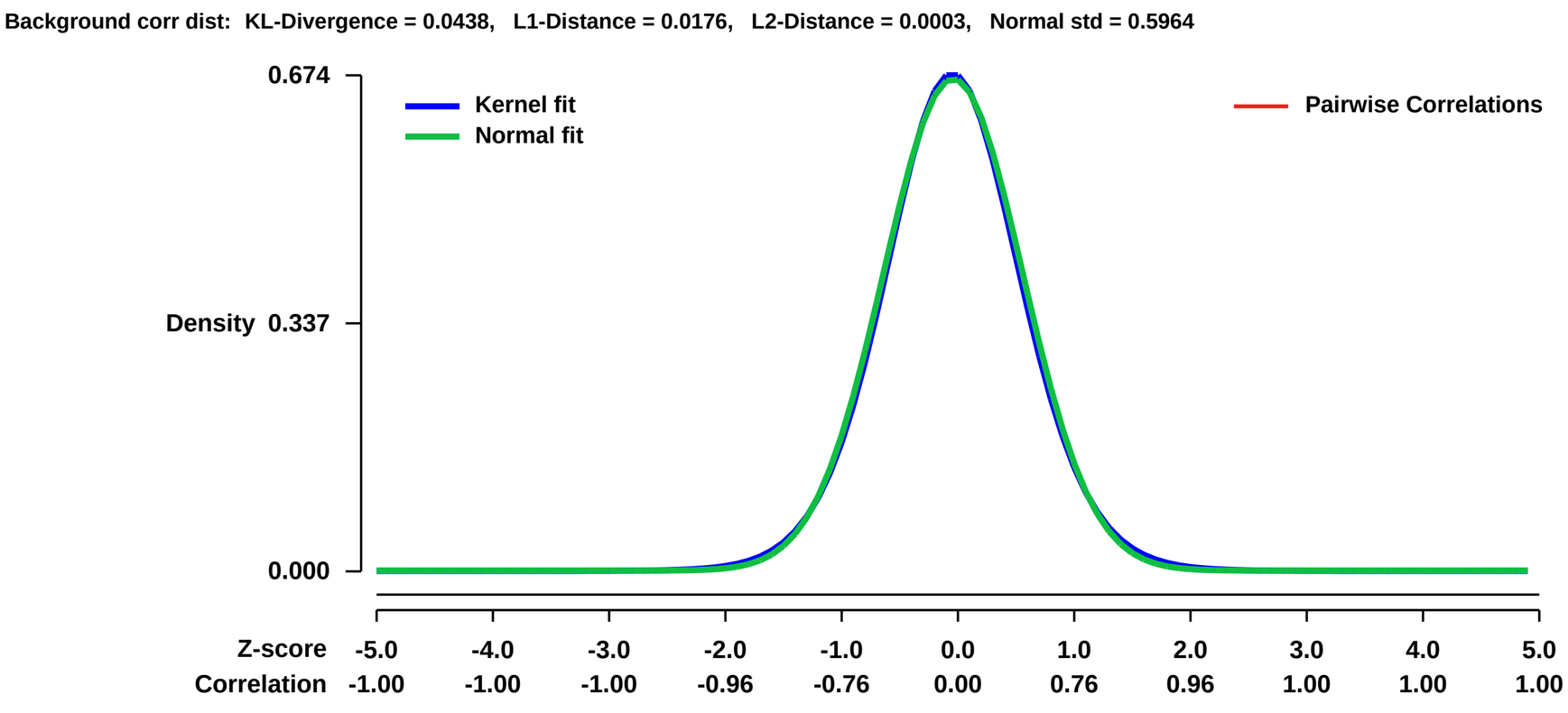

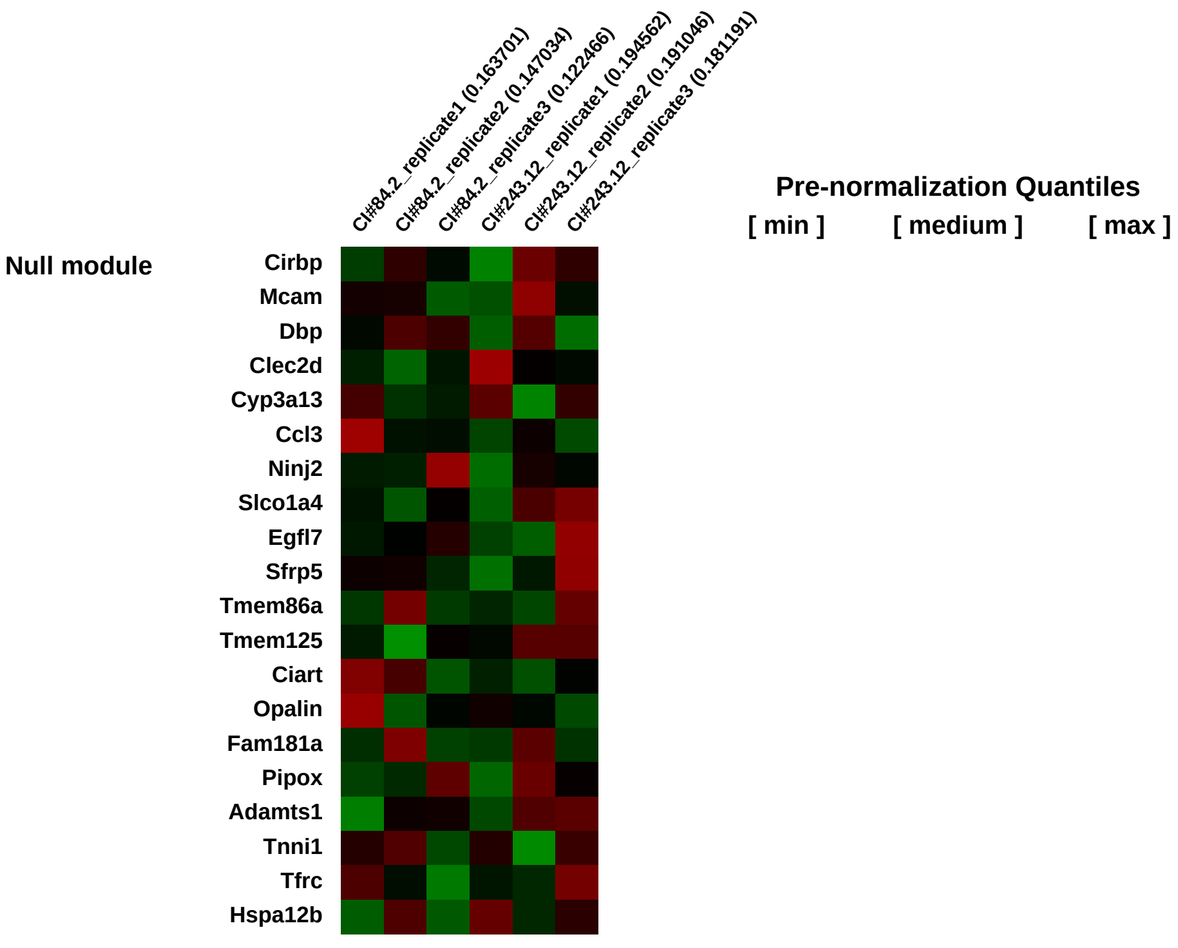

GEO Series "GSE7020" Expression Profiles

Num of samples in this series: 8

Scale of expression profile Z-scores

-3.0 -2.0 -1.0 0.0 1.0 2.0 3.0

GEO Link:	http://www.ncbi.nlm.nih.gov/geo/query/acc.cgi?acc=GSE7020
Status:	Public on Feb 14 2007
Title:	The molecular consequences of Nix ablation on apoptosis and erythropoiesis
Organism:	Mus musculus
Experiment type:	Expression profiling by array
Platform:	GPL1261
Pubmed ID:	17420462
Summary & Design:	**Summary:** Normal erythropoiesis requires a critical balance between proapoptotic and antipaoptotic pathways. Bcl-xl, an antiapoptotic protein is induced at end-stages of differentiation of erythroid precursors in response to erythropoietin. The details of the proapoptotic pathway and the critical proapoptotic proteins inhibited by Bcl-xl in erythropoiesis are not well understood. We employed gene targeting to ablate Nix, a proapoptotic BH3-domain only Bcl2 family protein, which is known to be transcriptionally induced during erythropoiesis. Nix null mice exhibited reticulocytosis and thrombocytosis in the peripheral blood; and profound splenomegaly with erythroblastosis in the spleen and bone marrow despite normal erythropoietin levels and blood oxygen tension. In vivo apoptosis was diminished in erythroblast precursors from Nix null spleens. To define the molecular consequences of Nix ablation on apoptosis and erythropoiesis, we conducted a detailed comparative analysis of gene expression in spleens from 8 week old Nix null mice and wild type controls. Of 45,101 genes analyzed, 514 were significantly upregulated and 386 down-regulated in Nix-/- splenocytes. Functional cluster analysis delineated the ten most highly regulated gene sets, revealing increased levels of cell cycle and erythroid genes, with decreased levels of cell death and B-cell genes. **Keywords: strain comparison** **Overall design:** In the study, we hybridized RNA from 8 week old spleens of wild type (WT) control and Nix null mice (Nix-/-) to Affymetrix MOE430A GeneChip´fi arrays containing 45,101 well characterized mouse genes/ESTs.

Background corr dist: KL-Divergence = 0.0316, L1-Distance = 0.0553, L2-Distance = 0.0034, Normal std = 0.7696

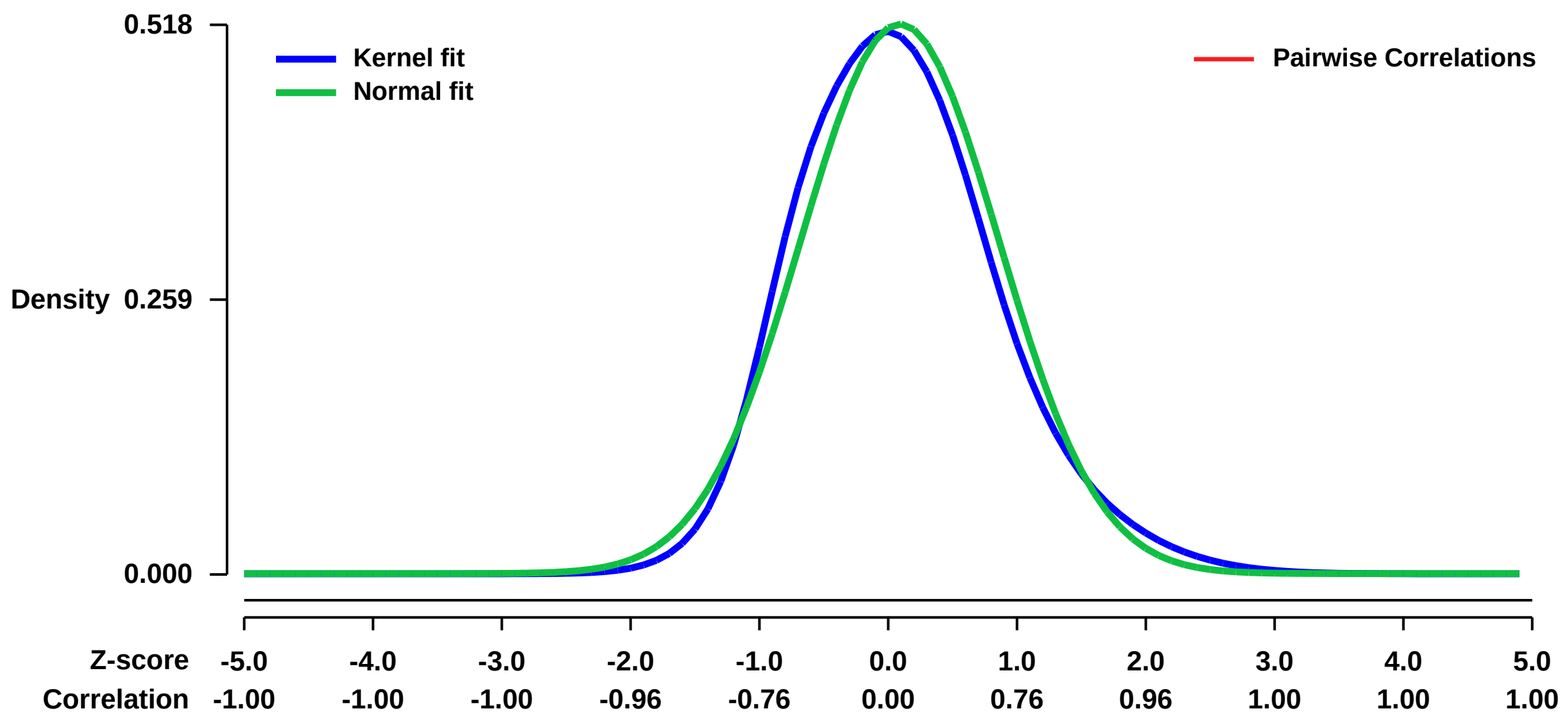

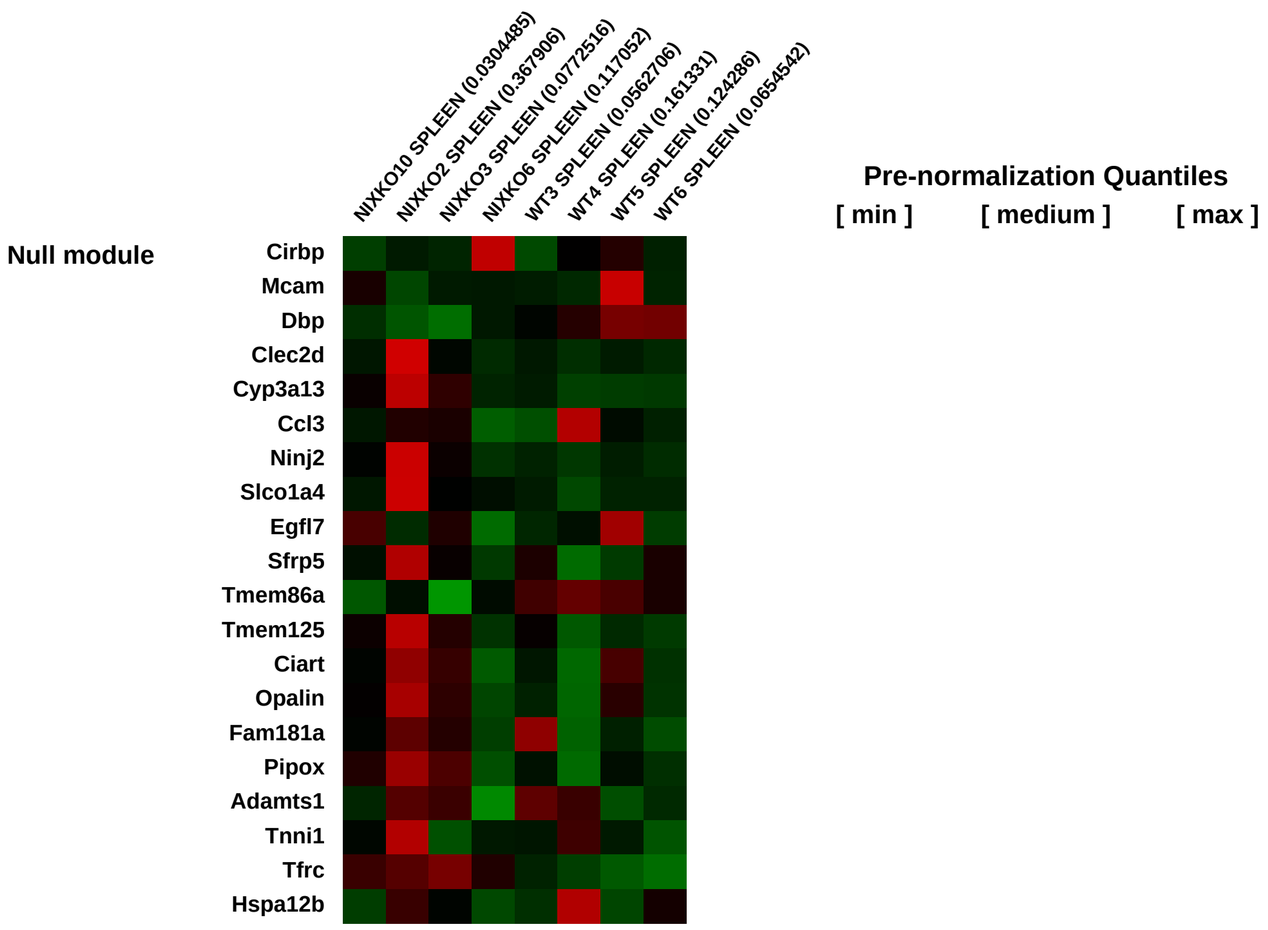

GEO Series "GSE8966" Expression Profiles

Num of samples in this series: 12

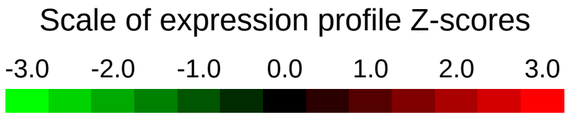

GEO Link:	http://www.ncbi.nlm.nih.gov/geo/query/acc.cgi?acc=GSE8966
Status:	Public on Aug 17 2009
Title:	Liver Transcriptome Profiles Associated with Strain-Specific Ehrlichia chaffeensisâ induced Hepatitis
Organism:	Mus musculus
Experiment type:	Expression profiling by array
Platform:	GPL1261
Pubmed ID:	19001077
Summary & Design:	**Summary:** Infection of humans with Ehrlichia chaffeensis, the etiologic agent of human monocytic ehrlichiosis, can cause hepatitis of varying severity. When the three human isolates of E. chaffeensis, each belongs to different geno-groups, are inoculated into severe combined immunodeficiency mice, the severity of clinical signs and bacterial burden detected in the liver are strain Wakulla>Liberty>Arkansas. Disseminated and granulomatous inflammation is evident in the liver of mice infected with strains Wakulla and Arkansas, respectively, but not in mice infected with strain Liberty. In this paper, we used microarray analysis to define transcriptional profiles characteristic to the histopathological features in the mouse liver. Cytokine and chemokine profiles were strikingly different among three strains of E. chaffeensis: IFN-¿‡, CCL5, CXCL1, CXCL2, CXCL7 and CXCL9 were highly up-regulated with strain Arkansas, TNF-¿–, CCL2, CCL3, CCL5, CCL6, CCL12, CCL20, CXCL2, CXCL7, CXCL9 and CXCL13 were highly up-regulated with strain Wakulla. With strain Liberty, only CXCL13 was highly up-regulated. In the livers infected with the Arkansas strain, monocytes/macrophages and NK cells were enriched in the granulomas and increase of NK cell-marker mRNAs was detected. Livers infected with the Wakulla strain displayed infiltration of significantly more neutrophils and increase of neutrophil-marker mRNAs. Genes up-regulated commonly in the liver infected with the three stains are other host innate immune and inflammatory response genes including several acute phase proteins. Genes down-regulated commonly are related to host physiologic functions. The results suggest that marked modulation of host cytokine and chemokine profiles by E. chaffeensis strains underlie the distinct host liver disease. **Overall design:** Three mice were examined for each of the 4 groups.

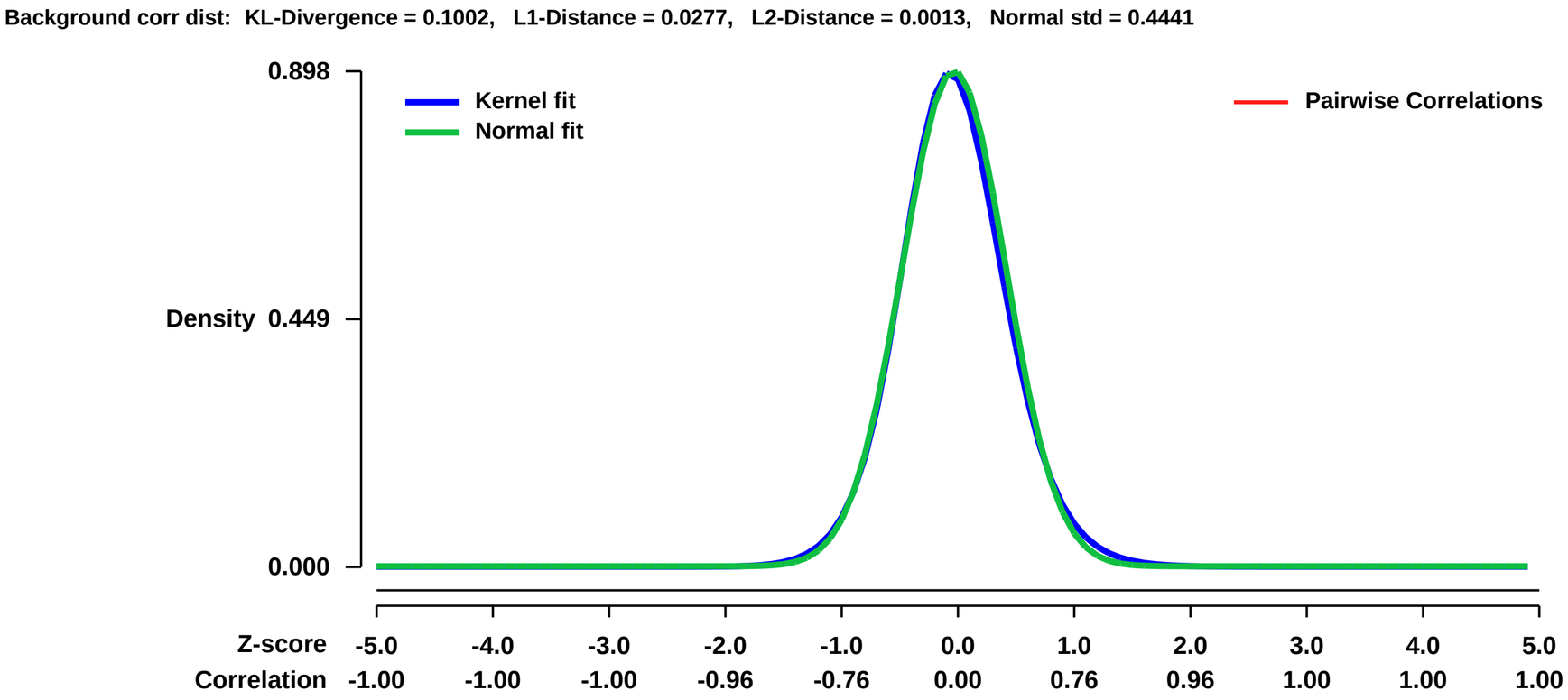

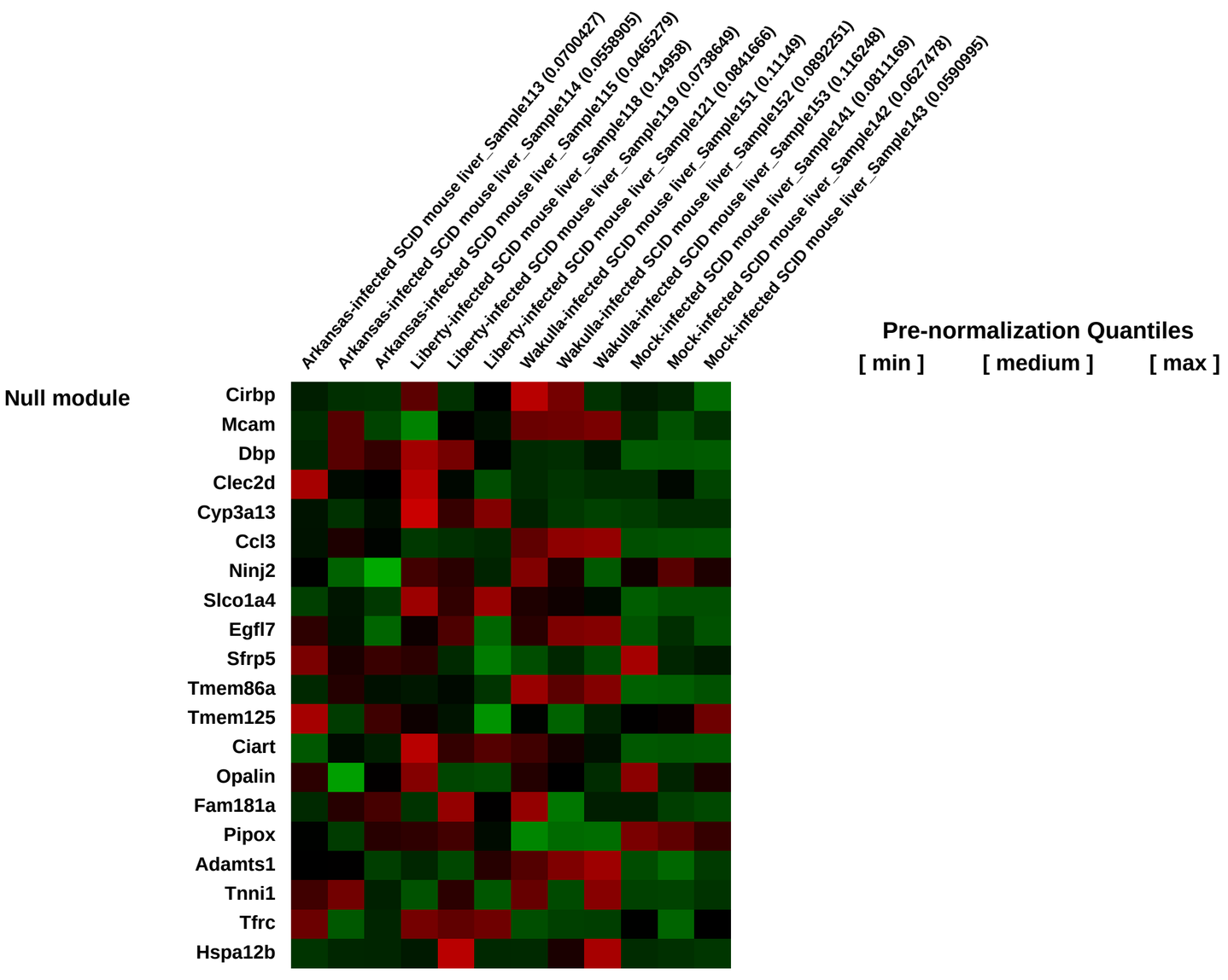

GEO Series "GSE28593" Expression Profiles

Num of samples in this series: 9

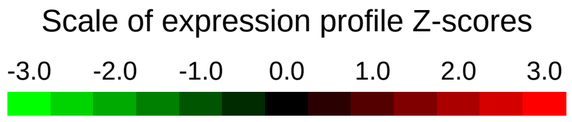

GEO Link:	http://www.ncbi.nlm.nih.gov/geo/query/acc.cgi?acc=GSE28593
Status:	Public on Apr 15 2011
Title:	KMT1E Mediated H3K9 Methylation Is Required for the Maintenance of Embryonic Stem Cells by Repressing Trophectoderm Differentiation
Organism:	Mus musculus
Experiment type:	Expression profiling by array
Platform:	GPL1261
Pubmed ID:	20014010
Summary & Design:	**Summary:** Dynamic regulation of histone methylation by methyltransferases and demethylases plays a central role in regulating the fate of embryonic stem (ES) cells. The histone H3K9 methyltransferase KMT1E, formerly known as ESET or Setdb1, is essential to embryonic development as the ablation of the Setdb1 gene results in peri-implantation lethality and prevents the propagation of ES cells. However, Setdb1- null blastocysts do not display global changes in H3K9 methylation or DNA methylation, arguing against a genome- wide defect. Here we show that conditional deletion of the Setdb1 gene in ES cells results in the upregulation of lineage differentiation markers, especially trophectoderm-specific factors, similar to effects observed upon loss of Oct3/4 expression in ES cells. We demonstrate that KMT1E deficiency in ES cells leads to a decrease in histone H3K9 methylation at and derepression of trophoblast-associated genes such as Cdx2. Furthermore, we find genes that are derepressed upon Setdb1 deletion to overlap with known targets of polycomb mediated repression, suggesting that KMT1E mediated H3K9 methylation acts in concert with polycomb controlled H3K27 methylation. Our studies thus demonstrate an essential role for KMT1E in the control of developmentally regulated gene expression programs in ES cells. **Overall design:** Analysis of KMT1E-deficiency in mouse embryonic stem cells using a Setdb1 conditional allele and tamoxifen-inducible Cre/loxP recombination

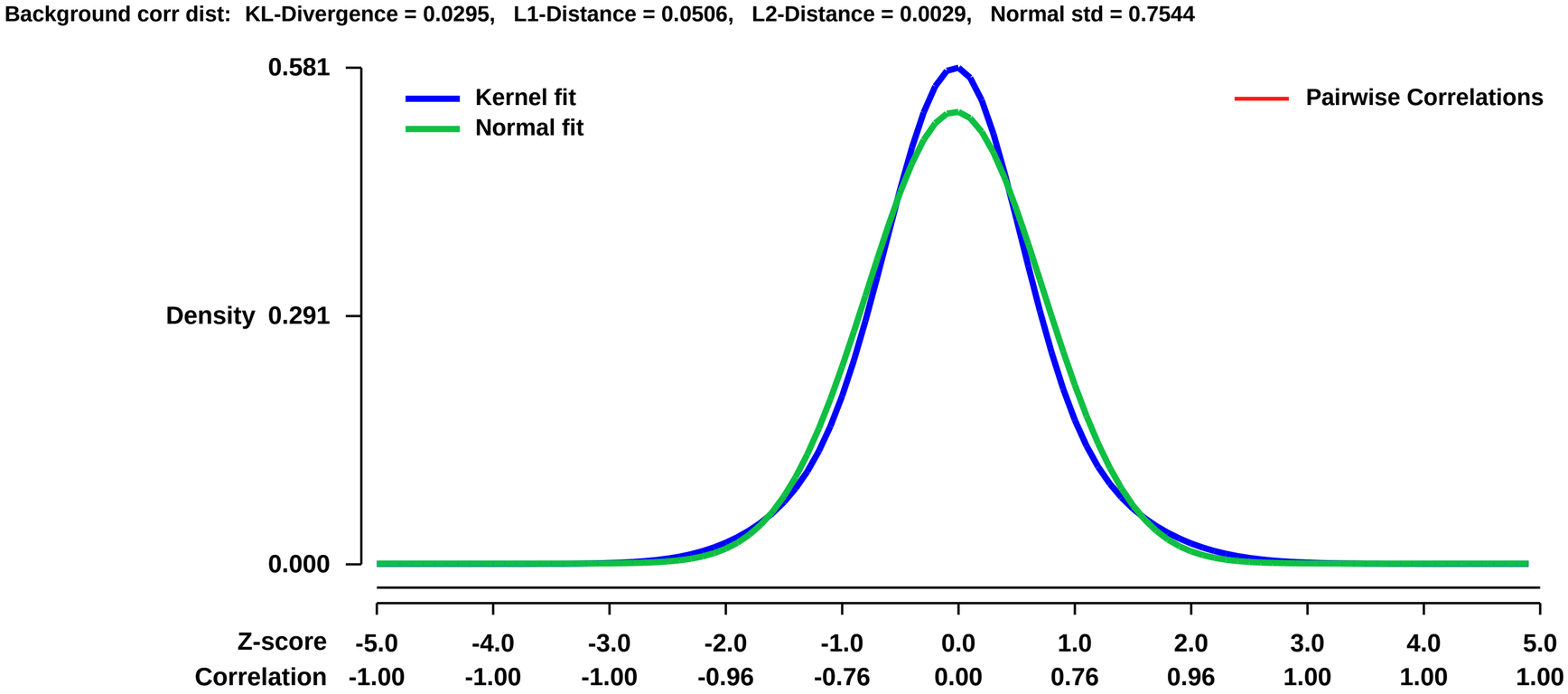

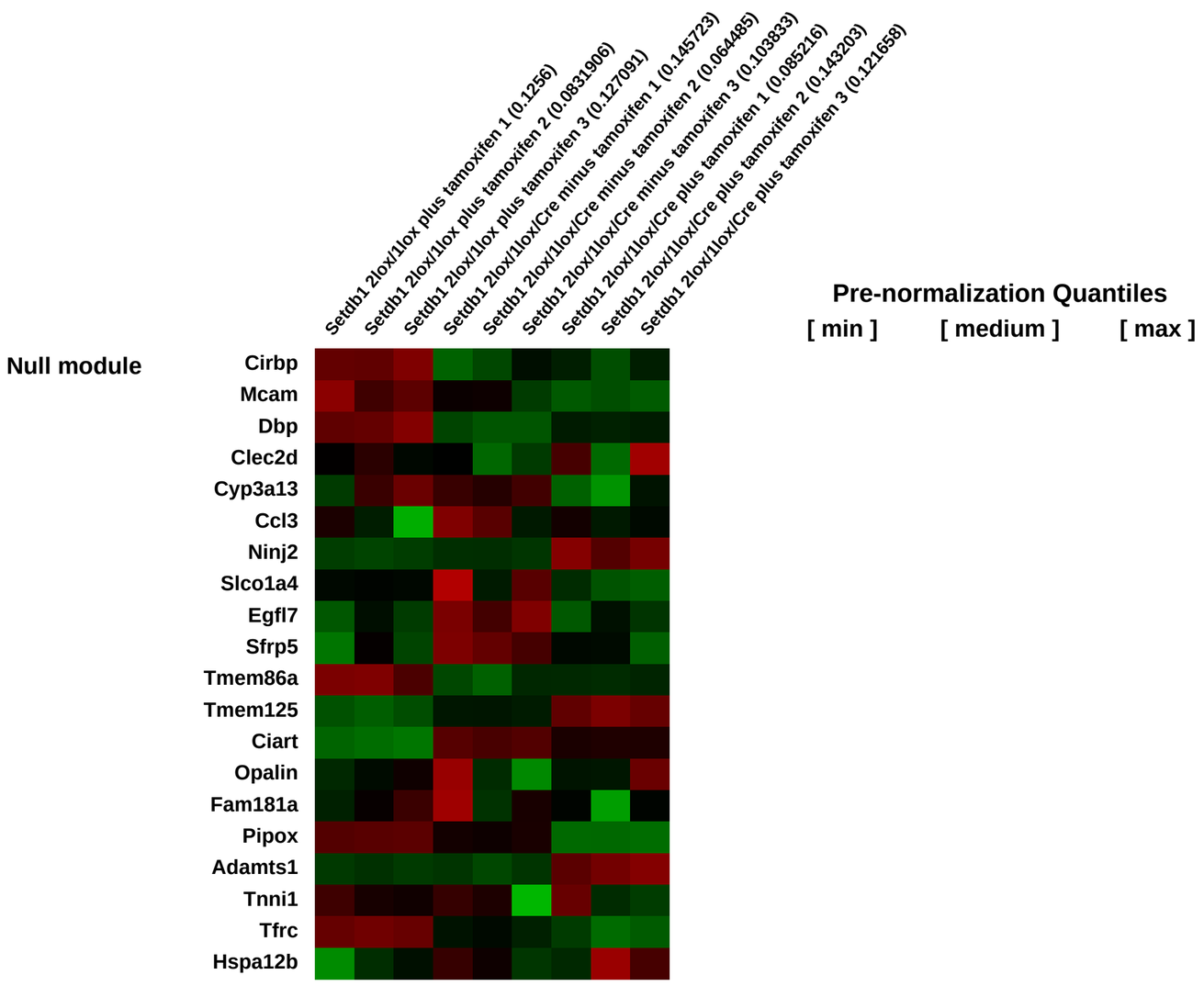

GEO Series "GSE21822" Expression Profiles

Num of samples in this series: 12

Scale of expression profile Z-scores

-3.0 -2.0 -1.0 0.0 1.0 2.0 3.0

GEO Link:	http://www.ncbi.nlm.nih.gov/geo/query/acc.cgi?acc=GSE21822
Status:	Public on Oct 02 2010
Title:	Role of sex chromosome complement in autosomal gene expression
Organism:	Mus musculus
Experiment type:	Expression profiling by array
Platform:	GPL1261
Pubmed ID:	20833369
Summary & Design:	**Summary:** It has generally been assumed that most differences between males and females are due to developmental and hormonal differences between the sexes. Here we investigate the contribution of sex chromosomal complement to such sexual dimorphisms. These genome-wide transcription profiling showed that the expression of hundreds of autosomal genes was sensitive to sex chromosome complement, rather than gender. The existence of such differences between males and females holds important implications for understanding sexual dimorphisms in physiology and disease hitherto attributed solely to gender or hormonal effects. **Overall design:** Thymic total RNA was isolated from 7-8 week old mice, with 3 biological replicates for each of four genotypes with different sex chromosome complements

Background corr dist: KL-Divergence = 0.1577, L1-Distance = 0.0398, L2-Distance = 0.0032, Normal std = 0.3646

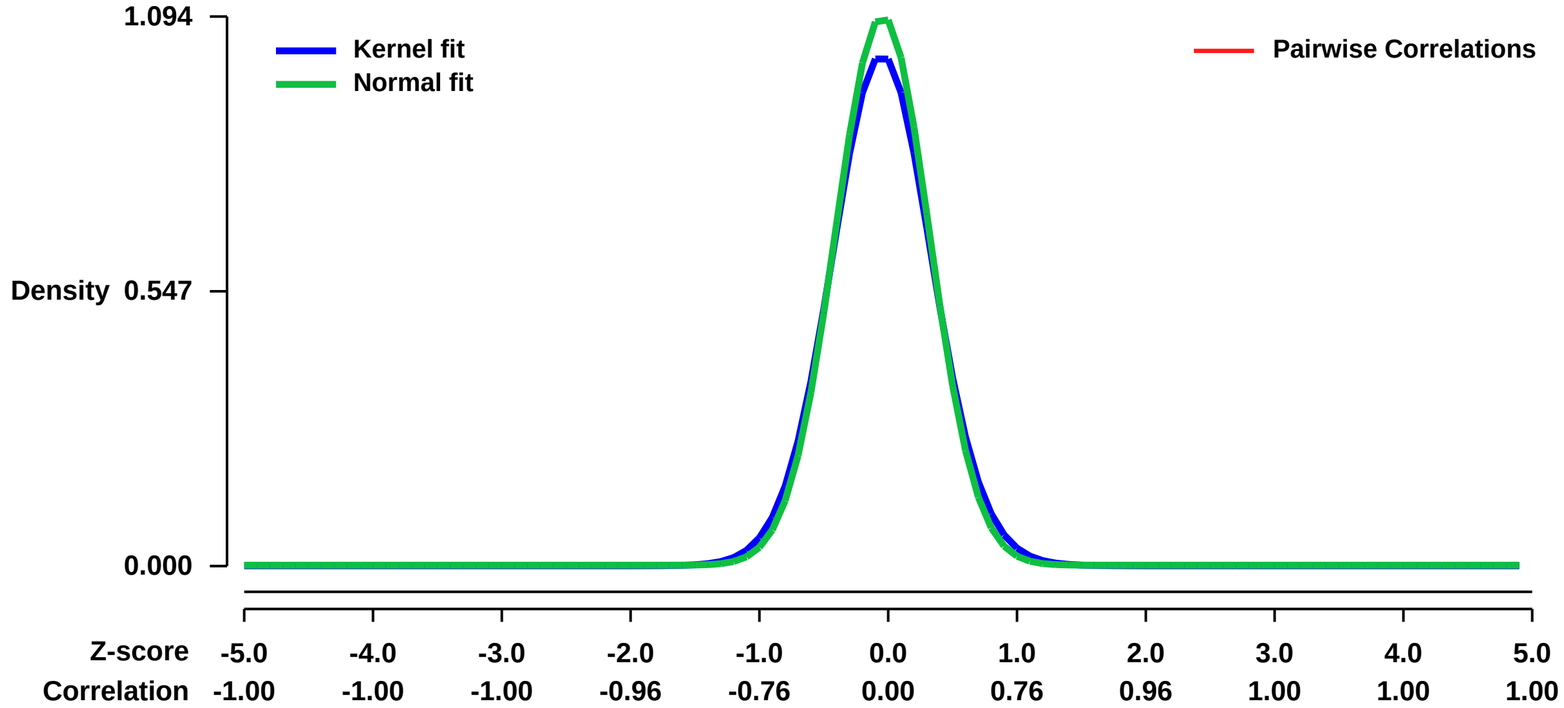

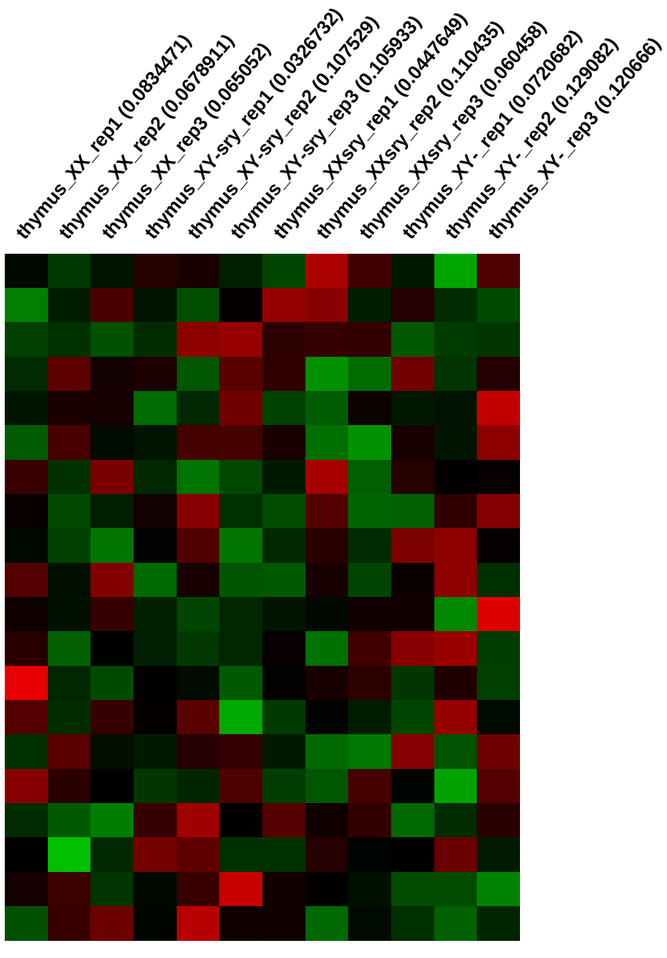

GEO Series "GSE32423" Expression Profiles

Num of samples in this series: 18

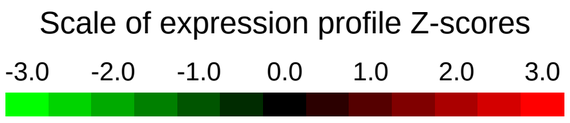

GEO Link:	http://www.ncbi.nlm.nih.gov/geo/query/acc.cgi?acc=GSE32423
Status:	Public on Sep 28 2011
Title:	Expression data from naive and memory CD8 T cells cultured in presence or absence of IL-4
Organism:	Mus musculus
Experiment type:	Expression profiling by array
Platform:	GPL1261
Pubmed ID:	22942430
Summary & Design:	**Summary:** Effects of IL-4 on CD8 T cells functions are largely unknown. IL-4 induces survival and proliferation of CD8 T cells, but several studies suggest that IL-4 could also affect several functions of CD8 T cells such as cytotoxicity. Our team has shown that IL-4 repress the expression of Ccl5 in vitro. To define more precisely the impact of IL-4 on CD8 T cells, we performed a whole genome expression microarray analysis of naive and memory CD8 T cells cultured in presence or absence of IL-4. This approach allowed us to define the IL4-gene-expression signature on CD8 T cells. **Overall design:** In addition, 4 populations of F5 TIM memory CD8 T cells were FACS-sorted: samples from 2 of these populations were incubated 20 hours in presence of IL-7 and/or IL-4, or in medium alone. Thus, 12 â Memoryâ samples were processed.

Background corr dist: KL-Divergence = 0.1166, L1-Distance = 0.0363, L2-Distance = 0.0027, Normal std = 0.4102

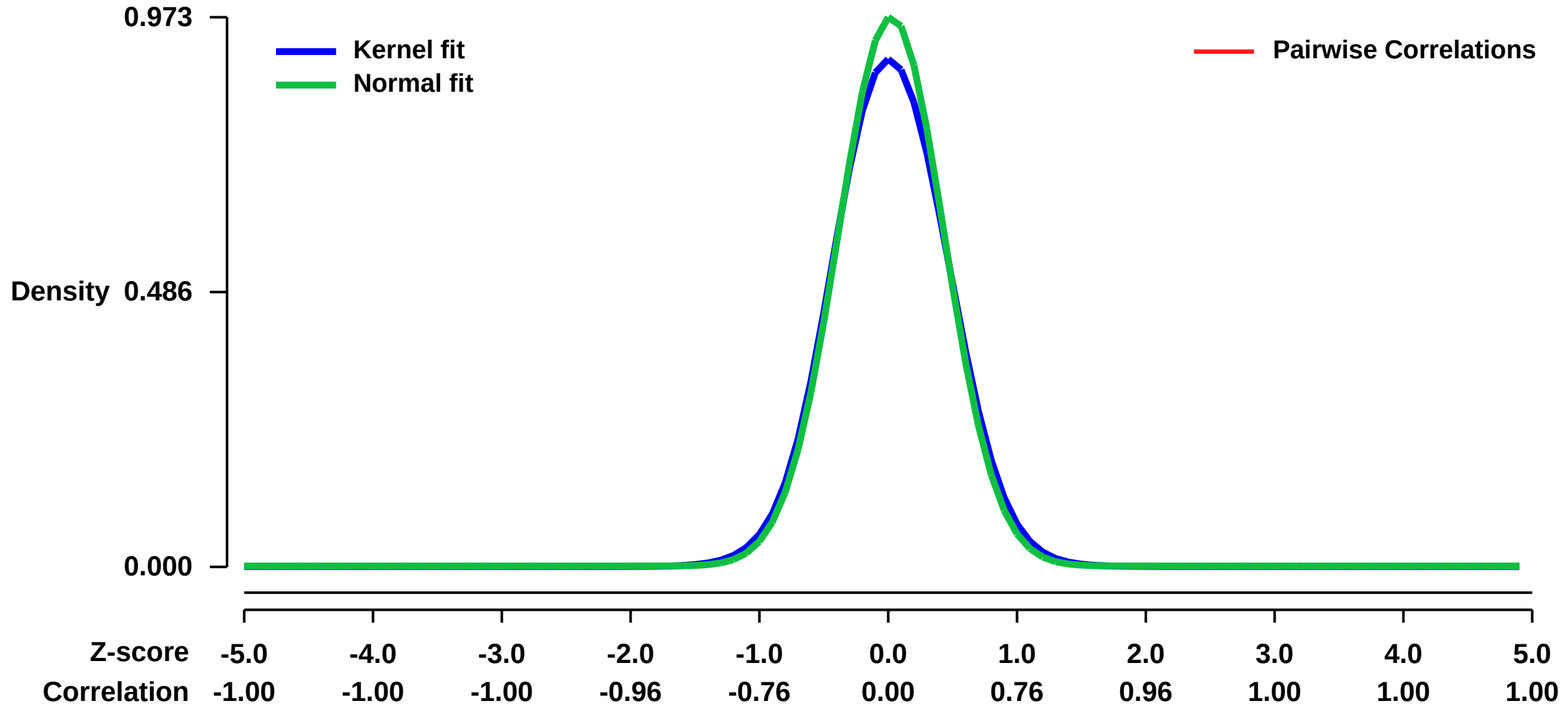

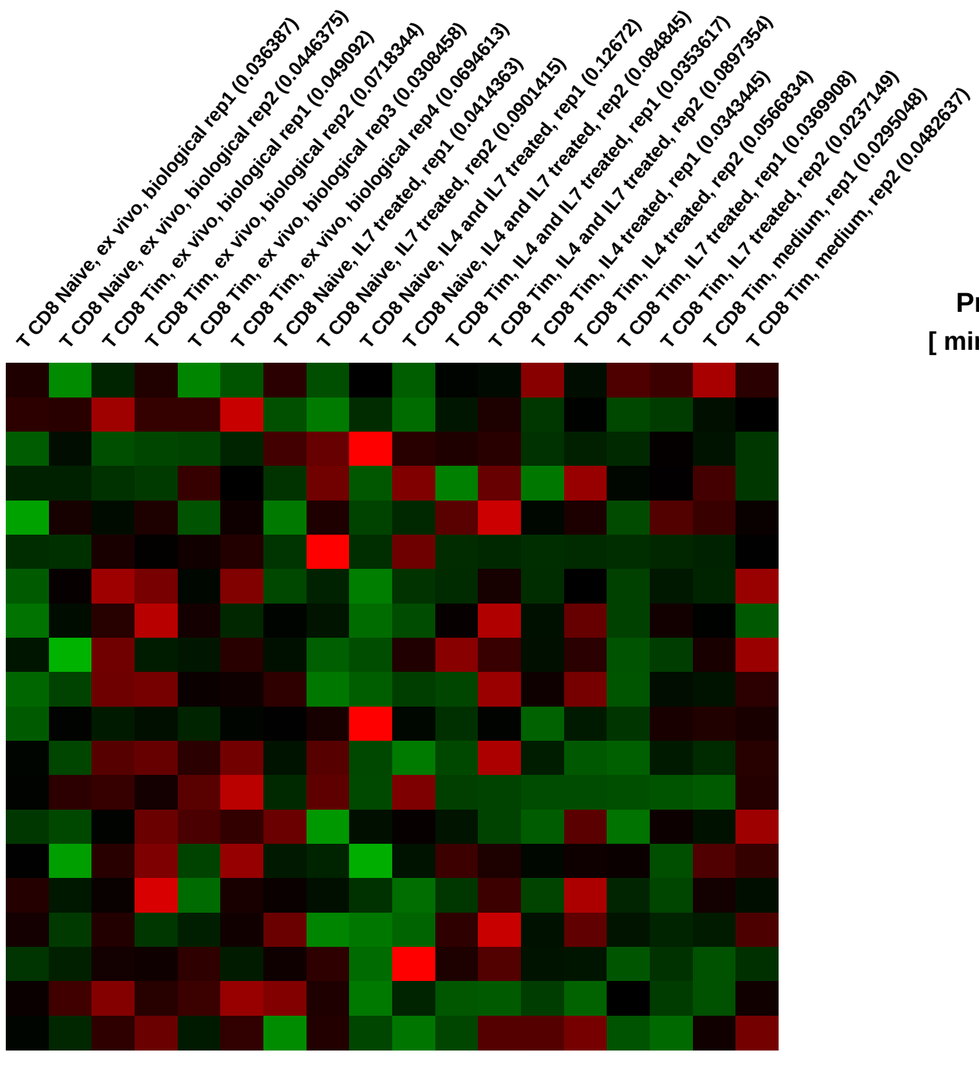

GEO Series "GSE21900" Expression Profiles

Num of samples in this series: 12

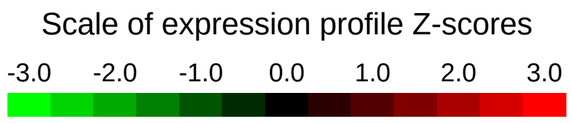

GEO Link:	**http://www.ncbi.nlm.nih.gov/geo/query/acc.cgi?acc=GSE21900**
Status:	**Public on May 18 2011**
Title:	**Expression profiling of the Otx2 CKO retina**
Organism:	**Mus musculus**
Experiment type:	**Expression profiling by array**
Platform:	**GPL1261**
Pubmed ID:	**21602925**
Summary & Design:	**Summary:** **In the vertebrate retina, the Otx2 transcription factor plays a crucial role in the cell fate determination of both rod and cone photoreceptors. Otx2 conditional knockout (CKO) mice exhibited a total absence of rods and cones in the retina due to their cell fate conversion to amacrine-like cells. In order to investigate the entire transcriptome regulated by Otx2 in the developing retina, we performed microarray analysis on the Otx2 CKO retina.** **Overall design:** **In order to clarify the molecular role of Otx2 in transcriptional regulation during development, we investigated the expression profile of the Otx2 CKO retina compared with that of the control retina with the genotype Otx2flox/flox;Crx-cre- using microarrays at two time points, P1 and P12.**

Background corr dist: **KL-Divergence = 0.0680, L1-Distance = 0.0265, L2-Distance = 0.0012, Normal std = 0.5091**

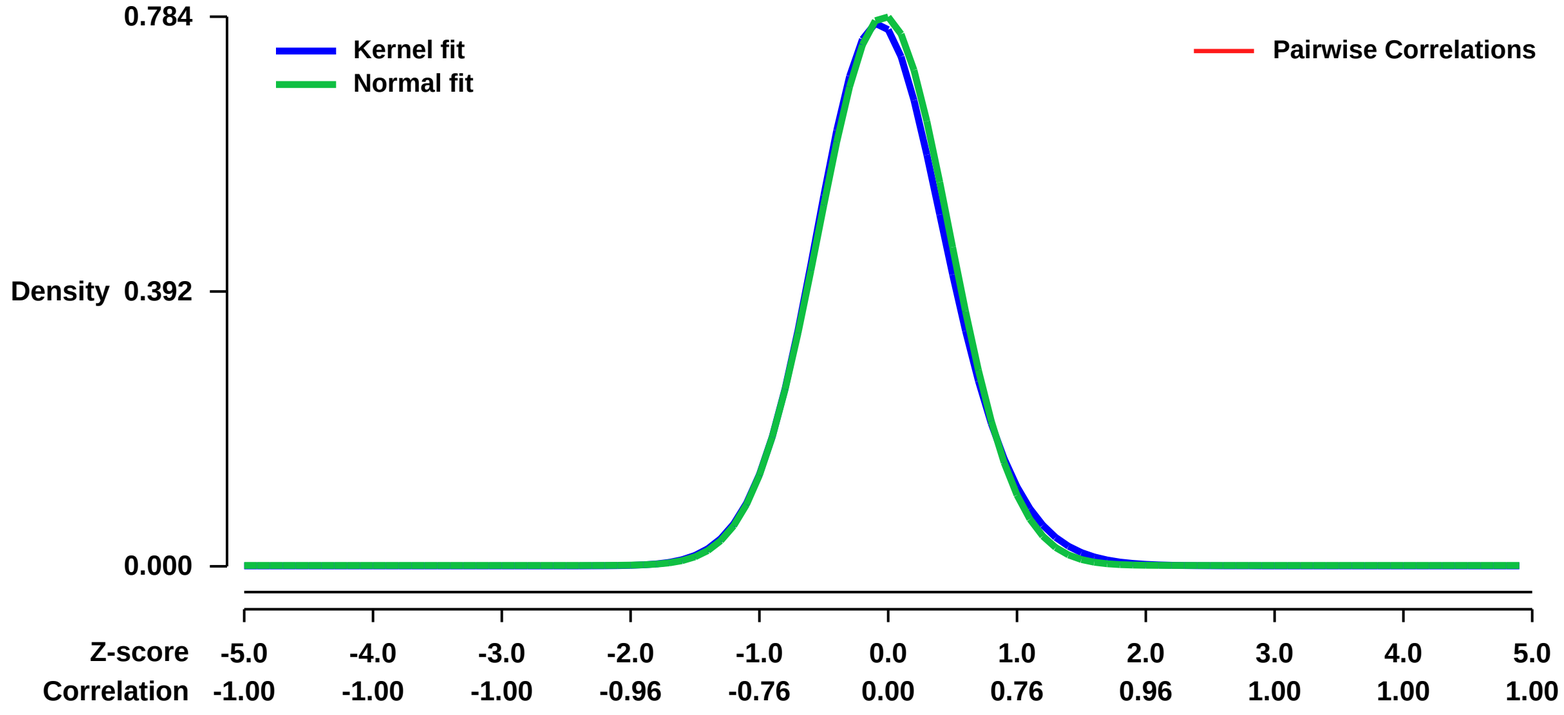

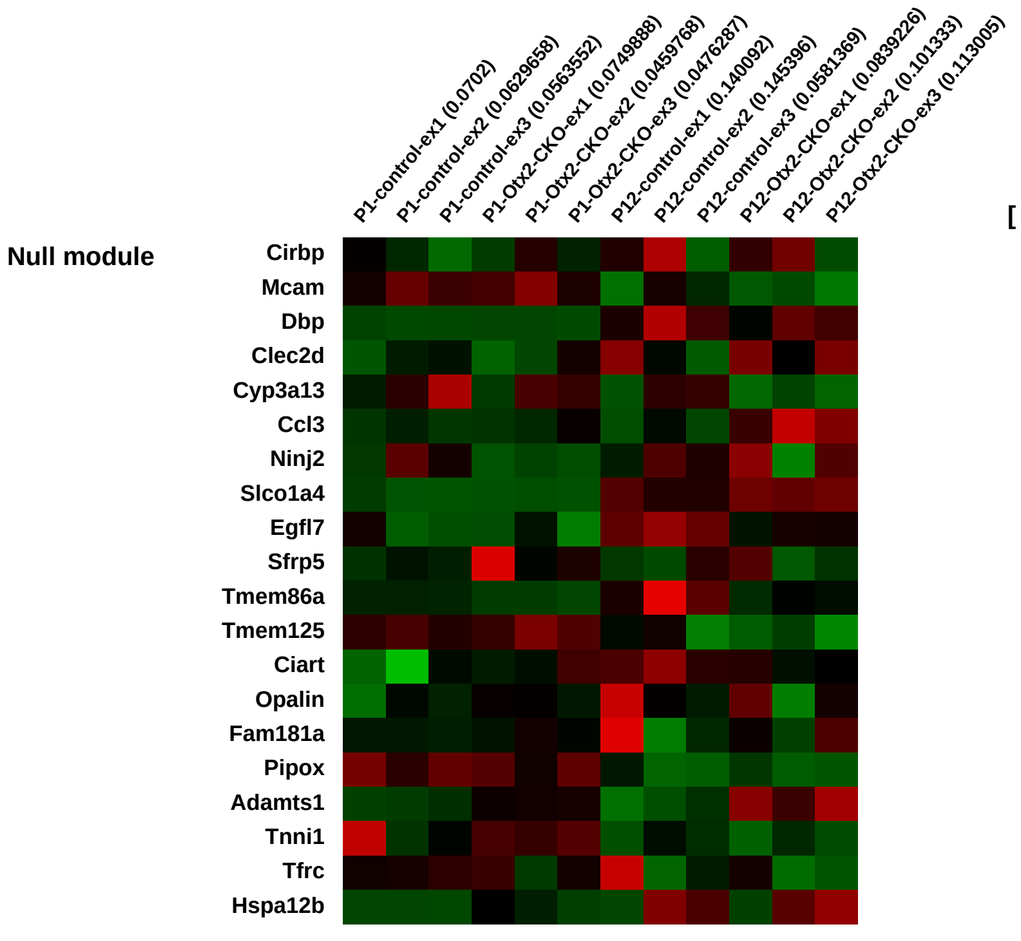

GEO Series "GSE11382" Expression Profiles

Num of samples in this series: 10

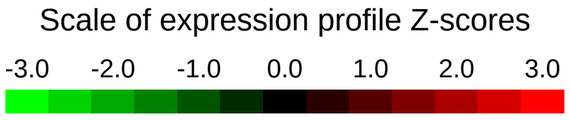

GEO Link:	http://www.ncbi.nlm.nih.gov/geo/query/acc.cgi?acc=GSE11382
Status:	Public on May 09 2008
Title:	Liver and cecum from mice exposed to aflatoxin B1 (AFB1) and/or Helicobacter hepaticus
Organism:	Mus musculus
Experiment type:	Expression profiling by array
Platform:	GPL1261
Pubmed ID:	19850960
Summary & Design:	**Summary:** We evaluated aflatoxin B1-induced liver tumor promotion by H. hepaticus. Microarrays of liver and cecum from female mice were used to evaluate the individual and combined transcriptional effects of AFB1 and H. hepaticus **Keywords: Tumor co-promotion study** **Overall design:** C3H/HeN mice were inoculated with 7 ug/g BW AFB1 or vehicle IP at 10 days of age, and gavaged with H. hepaticus or broth at 3 weeks; necropsied at 40 weeks

Background corr dist: KL-Divergence = 0.0322, L1-Distance = 0.0613, L2-Distance = 0.0051, Normal std = 0.7235

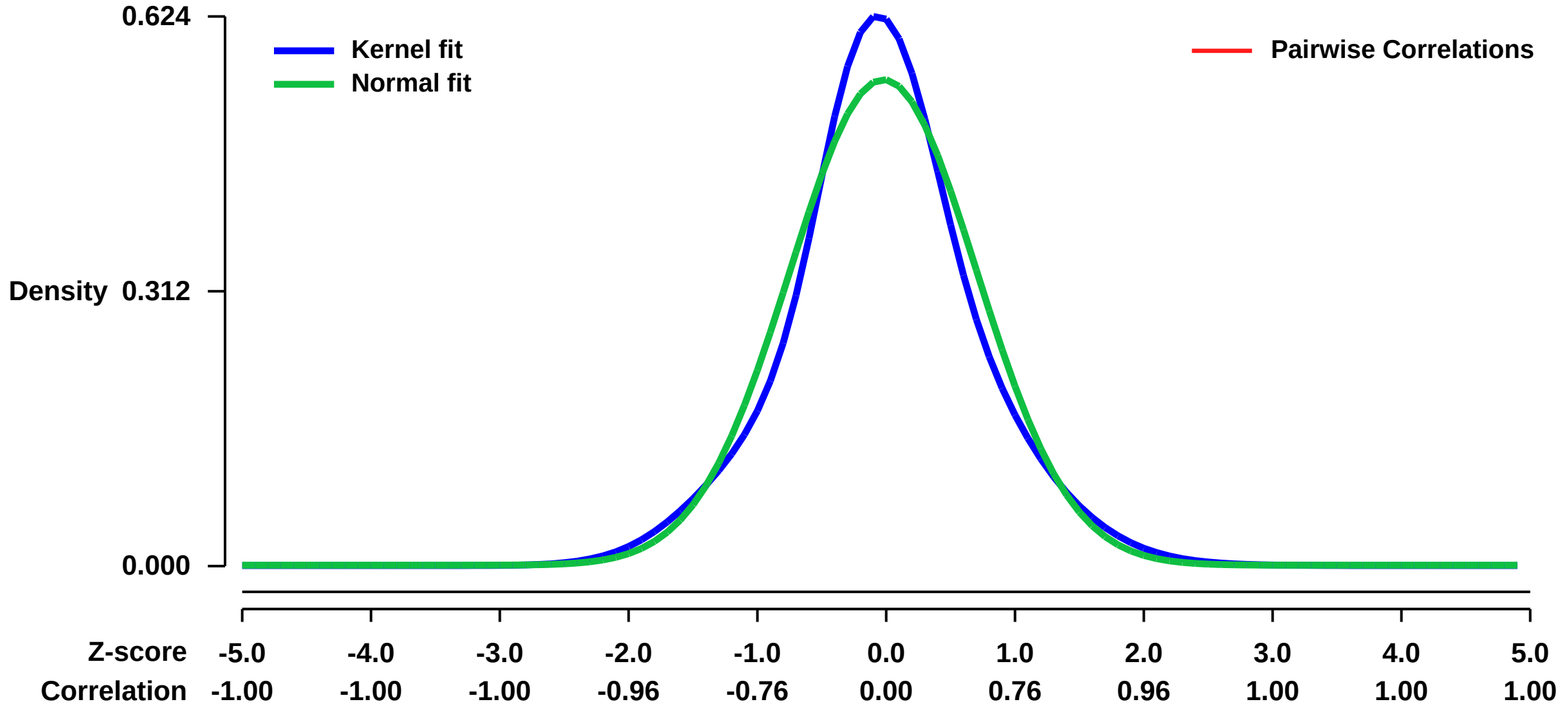

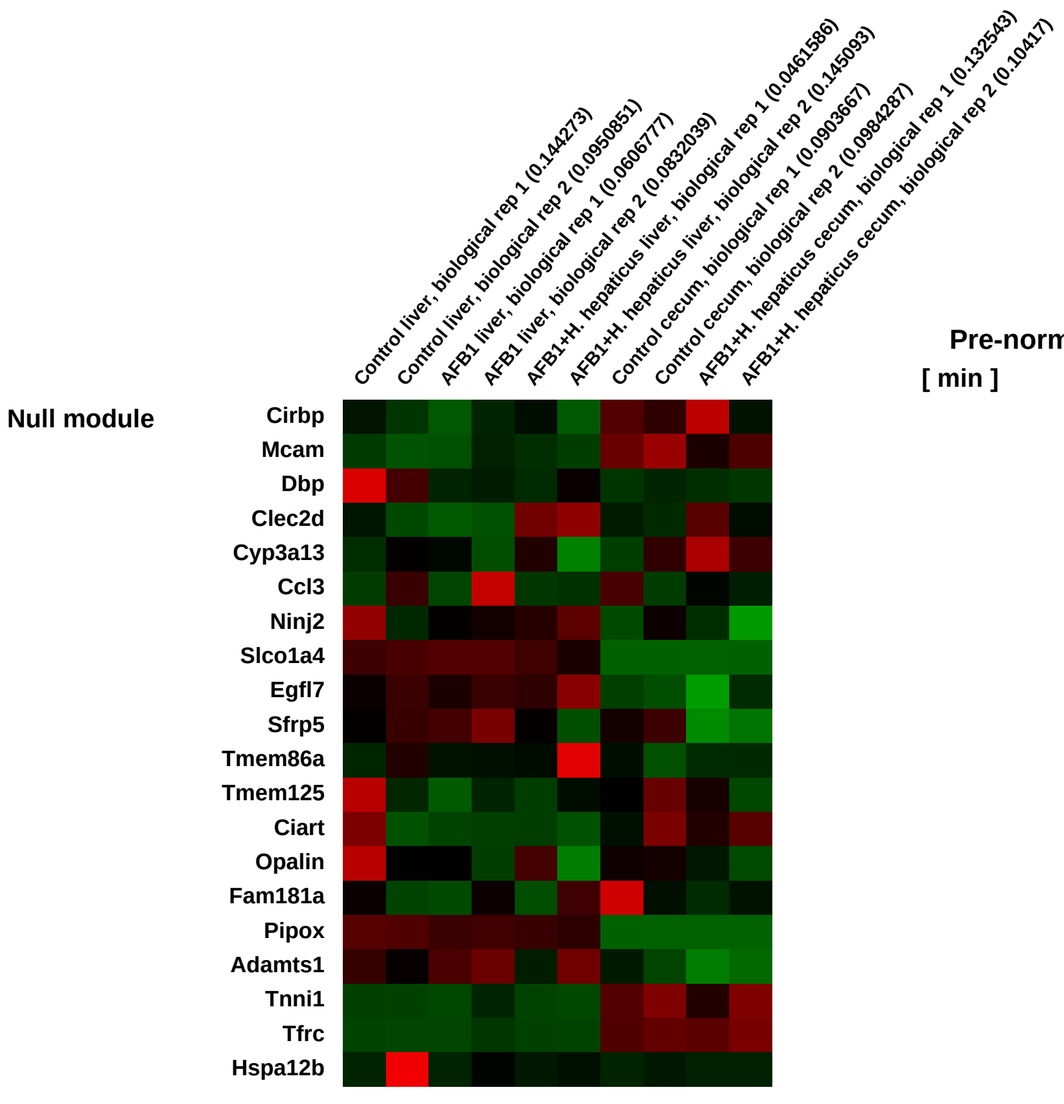

GEO Series "GSE50789" Expression Profiles

Num of samples in this series: 96

Scale of expression profile Z-scores

-3.0 -2.0 -1.0 0.0 1.0 2.0 3.0

GEO Link:	http://www.ncbi.nlm.nih.gov/geo/query/acc.cgi?acc=GSE50789
Status:	Public on Sep 26 2013
Title:	Gene expression in mouse liver in response to short-term calorie restriction
Organism:	Mus musculus
Experiment type:	Expression profiling by array
Platform:	GPL1261
Pubmed ID:	
Summary & Design:	**Summary:** The effect of a short-term calorie restricted diet was evaluated in six strains of mice The dietary intervention was initiated at 8 weeks of age and continued until 22 weeks of age **Overall design:** Tissues were collected from mice at 22 weeks of age; there were 96 microarrays used in total: for each of the 6 strains of mice, there were 8 control-fed mice and 8 calorie restricted mice (one individual mouse per microarray)

Background corr dist: KL-Divergence = 0.2595, L1-Distance = 0.0730, L2-Distance = 0.0155, Normal std = 0.3052

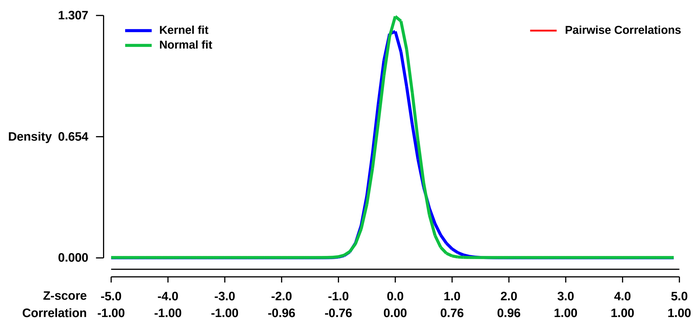

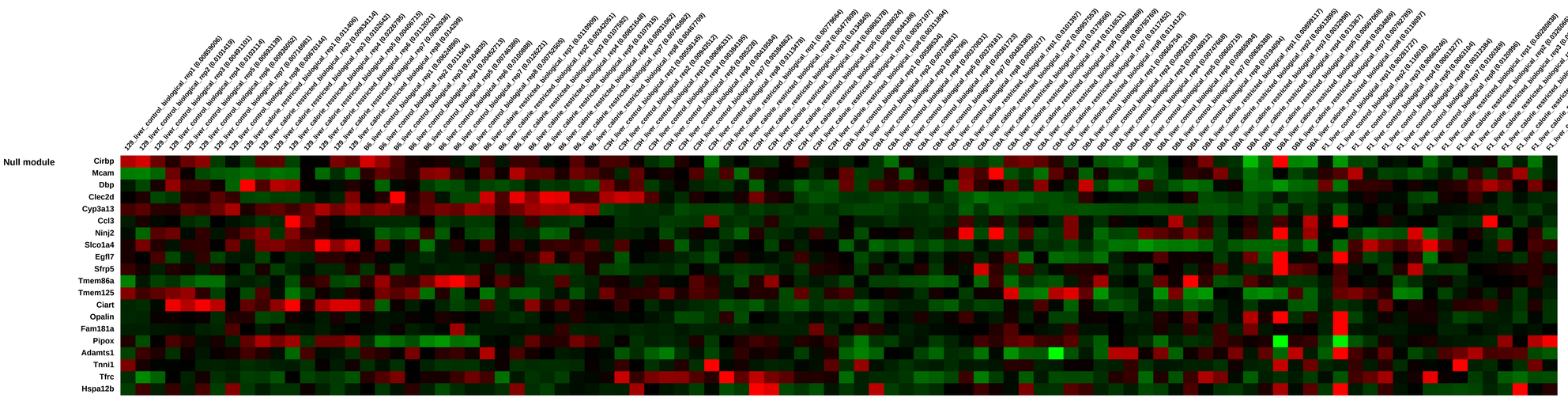

GEO Series "GSE8307" Expression Profiles

Num of samples in this series: 68

Scale of expression profile Z-scores

-3.0 -2.0 -1.0 0.0 1.0 2.0 3.0

GEO Link: http://www.ncbi.nlm.nih.gov/geo/query/acc.cgi?acc=GSE8307

Status: Public on Aug 08 2008

Title: Expression and neurobehavioral analyses in prosaposin deficient mice: Molecular alterations precede neuronal deficits

Organism: Mus musculus

Experiment type: Expression profiling by array

Platform: GPL1261

Pubmed ID: 18673548

Summary & Design:

Summary:
Prosaposin encodes, in tandem, four small acidic activator proteins (saposins) with specificities for glycosphingolipids hydrolases in lysosomes. To explore the molecular mechanism(s) of disease progression, temporal transcriptome microarray analyses of cerebrum and cerebellum tissues were conducted using mRNA from three prosaposin deficiency mouse models: PS-NA (hypomorphic prosaposin deficiency), PS-/- (prosaposin null) and 4L/PS-NA (a V394L/V394L glucocerebrosidase mutation and PS-NA) mice. Our results indicate that regionally specific gene expression abnormalities preceded the histological and behavioral changes and CEBPD is a candidate regulator of brain disease in prosaposin deficiency. The alterations of gene expression are detected at birth and are more profound in cerebellum than cerebrum.

Keywords: disease-state analysis

Overall design:
In order to increase the temporal resolution of expression profile in brain, the disease progression in those models were inverstigated in two regions of brains (cerebellum and cerebrum) at three or four time points according to the genotypes. PS-/-: new born (0d), 10 days (10d), 20 days (20d), 25 days (25d); PS-NA: new born, 4 weeks (4w), 12 weeks (12w), 18 weeks (18w); 4L/PS-NA: 4 weeks (4w), 12 weeks (12w), 18 weeks (18w). The data from those models were analyzed relative to the corresponding wild type at same time point (0d, 10d, 20d, 4w, 12w, 18w).

Background corr dist: KL-Divergence = 0.3045, L1-Distance = 0.0496, L2-Distance = 0.0056, Normal std = 0.2806

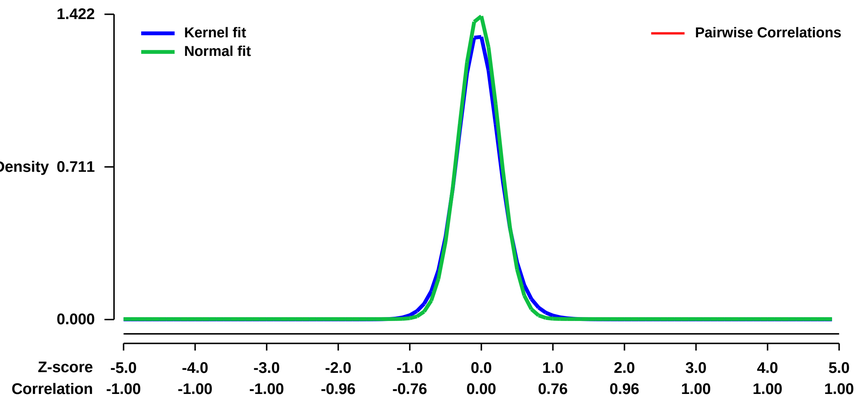

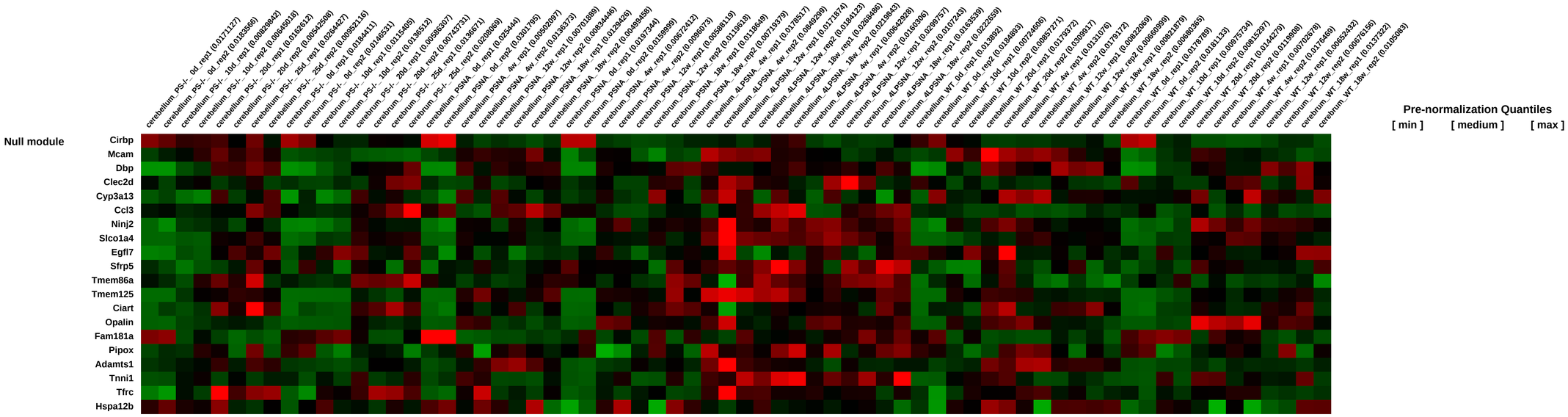

GEO Series "GSE40412" Expression Profiles

Num of samples in this series: 14

Scale of expression profile Z-scores

-3.0 -2.0 -1.0 0.0 1.0 2.0 3.0

GEO Link:	http://www.ncbi.nlm.nih.gov/geo/query/acc.cgi?acc=GSE40412
Status:	Public on Mar 04 2013
Title:	Replication-coupled passive DNA demethylation for the erasure of genome imprints in mice
Organism:	Mus musculus
Experiment type:	Expression profiling by array
Platform:	GPL1261
Pubmed ID:	23241950
Summary & Design:	**Summary:** Genome-wide DNA demethylation, including the erasure of genome imprints, in primordial germ cells (PGCs), is critical as a first step for creating the totipotent epigenome in the germ line. Here, we provide evidence that contrary to the prevailing model involving active DNA demethylation, imprint erasure in mouse PGCs occurs in a manner consistent with replication-coupled passive DNA demethylation: PGCs erase imprints during their rapid proliferation with little de novo as well as maintenance DNA methylation potential and no major chromatin alterations. Our findings necessitate the re-evaluation of and provide novel insights into the mechanism of genome-wide DNA demethylation in PGCs. **Overall design:** We performed expression analysis of primordial germ cells (PGCs) at embryonic days 10.5-13.5. Because the number of PGCs available at these stages were low, cDNAs were amplified by the method that we previously published (Kurimoto et al. 2006, NAR 34: e42 (PMID 16547197)). To include analysis of PGC gene expression at E9.5, we re-normalized the data from our E9.5 PGC samples (GSM744103, GSM744104) from our previous publication (Hayashi et al., 2011, Cell 146: 519-32 (PMD 21820164)) together with the data from this submission.

Background corr dist: KL-Divergence = 0.1317, L1-Distance = 0.0284, L2-Distance = 0.0016, Normal std = 0.3977

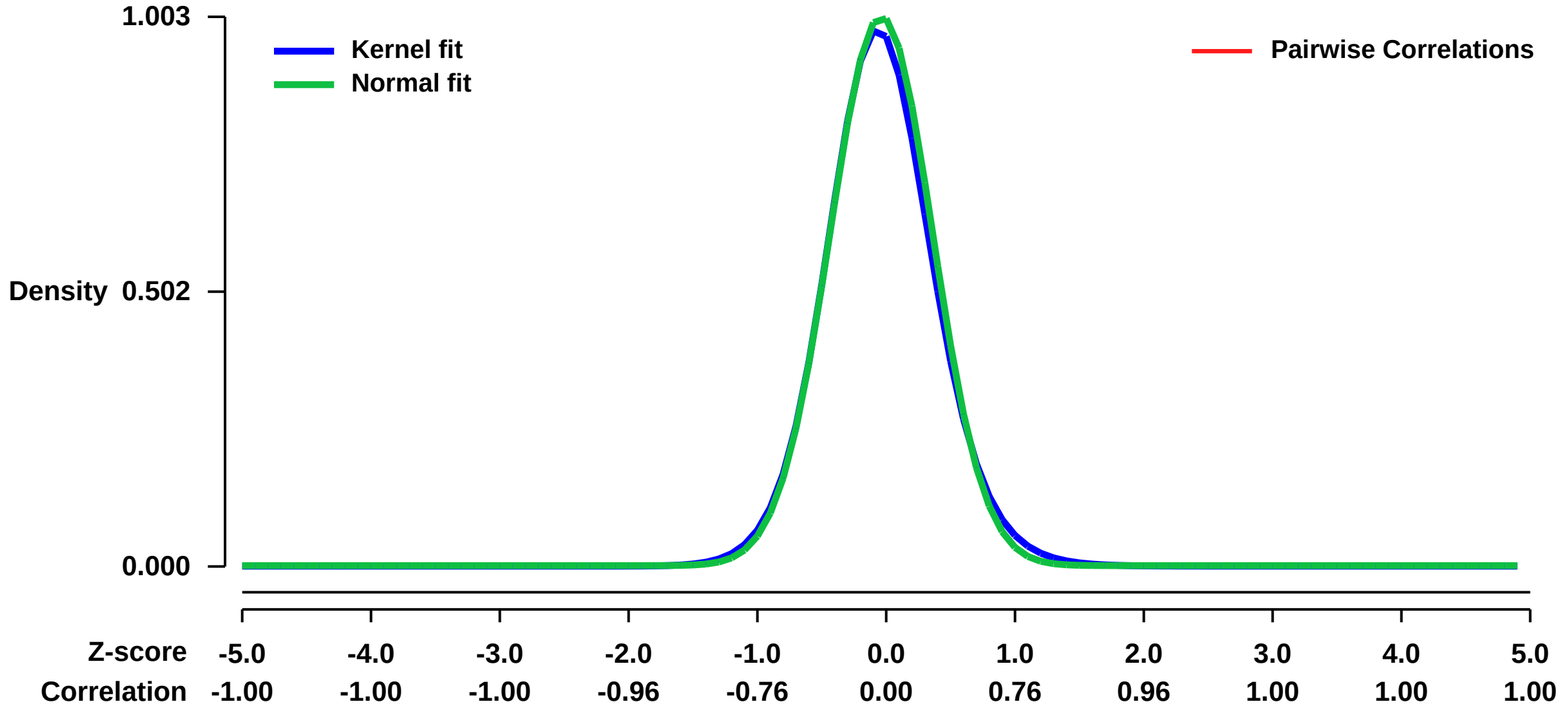

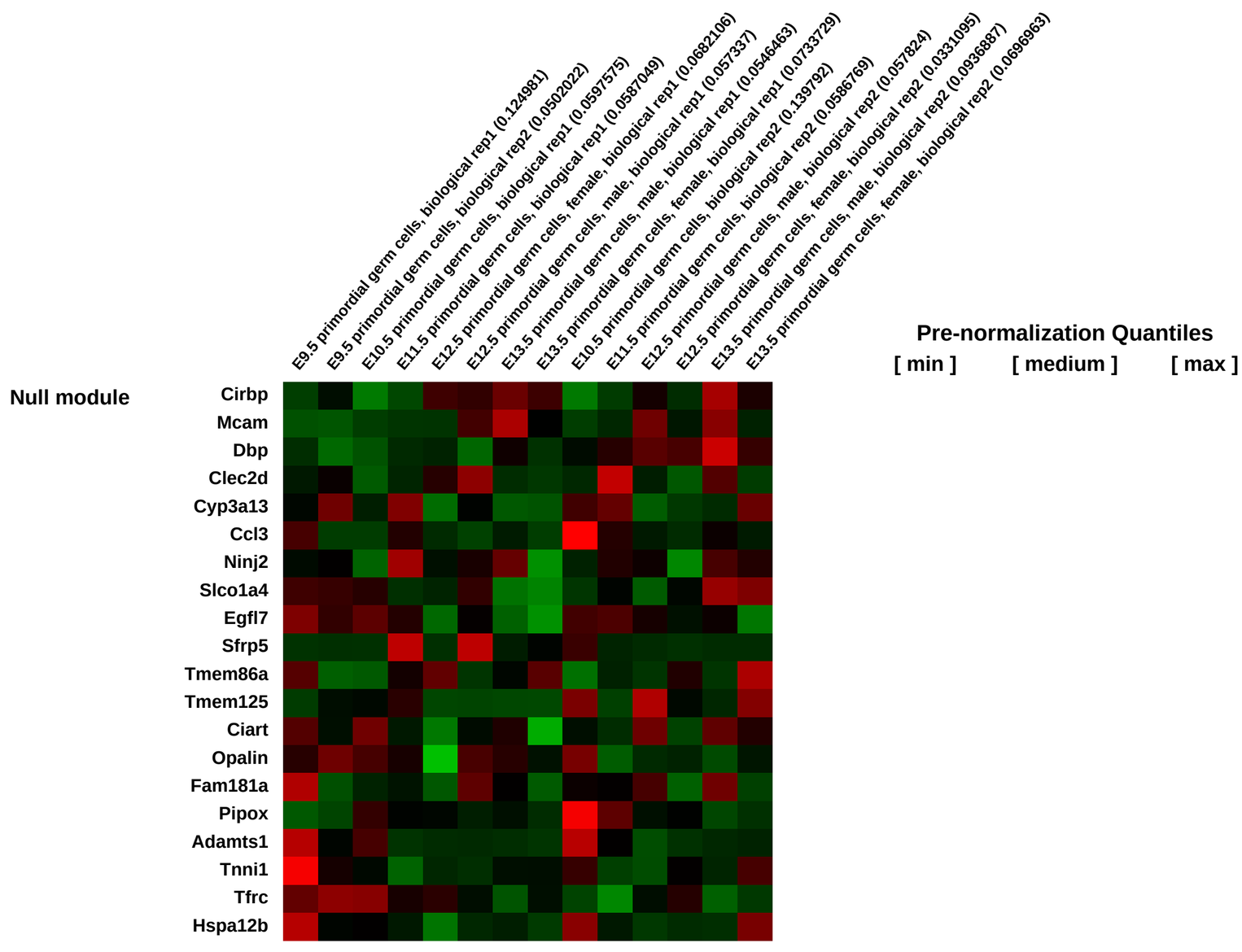

GEO Series "GSE5334" Expression Profiles

Num of samples in this series: 19

Scale of expression profile Z-scores

-3.0 -2.0 -1.0 0.0 1.0 2.0 3.0

GEO Link:	**http://www.ncbi.nlm.nih.gov/geo/query/acc.cgi?acc=GSE5334**
Status:	**Public on Jul 22 2006**
Title:	**Gene expression profiling of whole ovary in embryonic (gestional day 11, 12, 14, 16 & 18) and postnatal day 2 mice. (GUDMAP Series ID: 5)**
Organism:	**Mus musculus**
Experiment type:	**Expression profiling by array**
Platform:	**GPL1261**
Pubmed ID:	
Summary & Design:	**Summary:** **The overall objective of this proposal is to map the temporal and spatial dynamics of gene expression in the fetal mouse testis at key developmental timepoints. Urogenital tract malformations are the most common birth defects in males and their incidence together with other male reproductive health concerns such as reduced fertility and testicular cancer are reportedly on the rise in the human population. To better understand the impact of genetic factors and environmental influences on testicular development, it is important to first understand normal gene expression patterns and signaling cascades within the fetal testis during development. The goal of this study is to identify cell-specific genes that can be used as biomarkers for key differentiation events.** **Keywords: developmental time course** **Overall design:** **Day to day comparison in whole ovary throughout development with triplicates at each time point. Each sample is a pair of ovaries from a single animal and each animal is taken from a different dam (with the exception of gd11 sample numbers 18 and 19 which come from the same dam).**

Background corr dist: **KL-Divergence = 0.1760, L1-Distance = 0.0465, L2-Distance = 0.0050, Normal std = 0.3897**

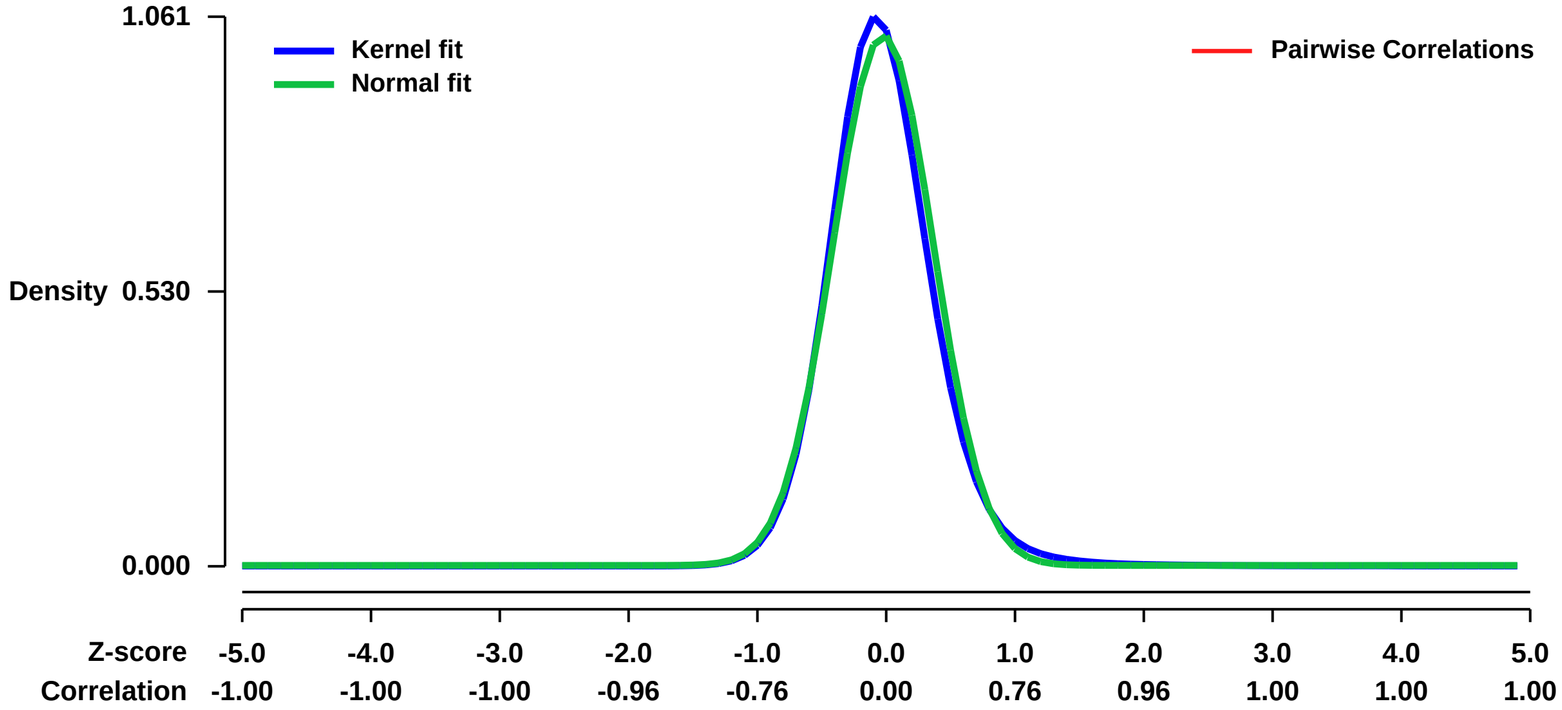

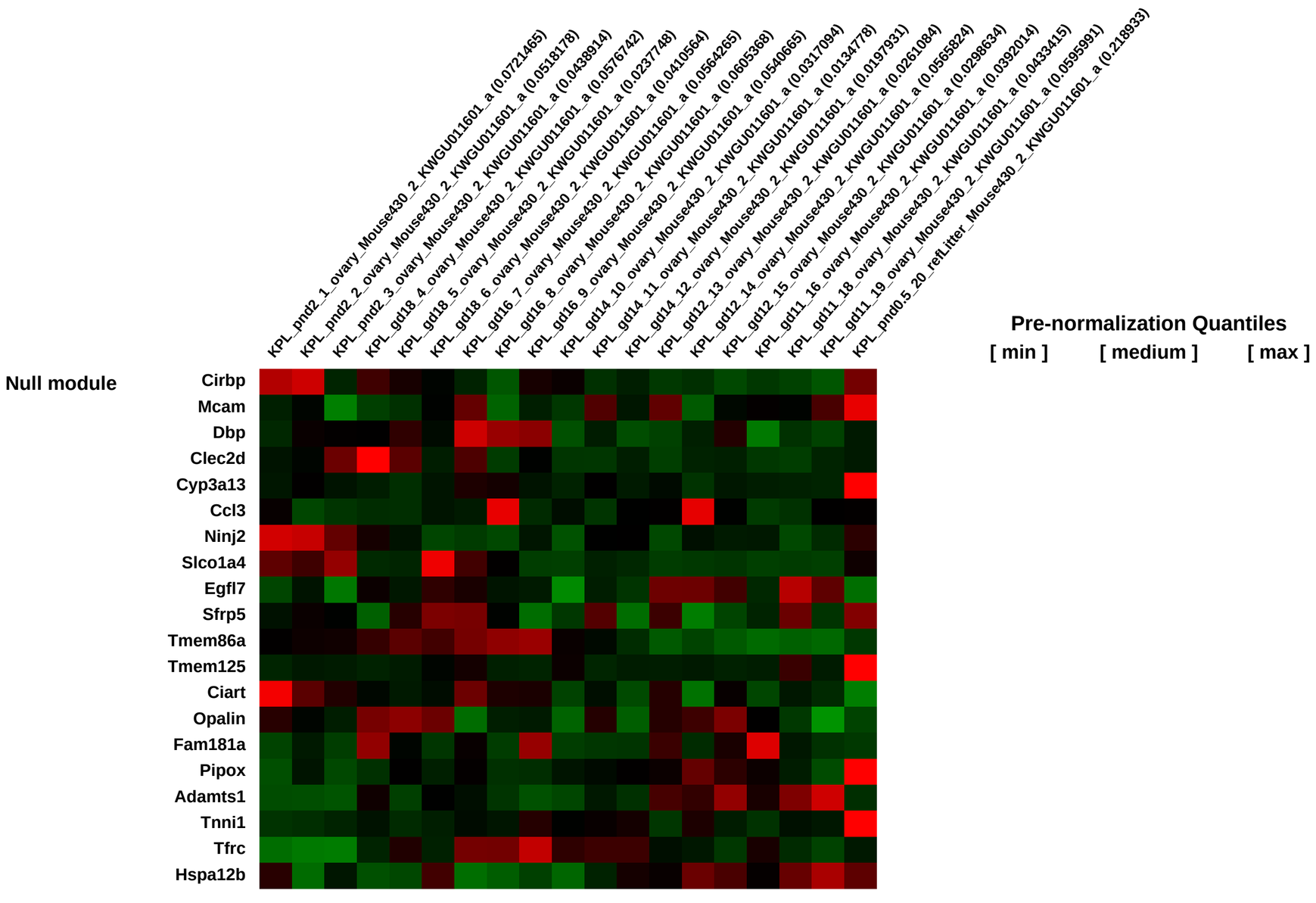

GEO Series "GSE8949" Expression Profiles

Num of samples in this series: 20

Scale of expression profile Z-scores

-3.0 -2.0 -1.0 0.0 1.0 2.0 3.0

GEO Link:	http://www.ncbi.nlm.nih.gov/geo/query/acc.cgi?acc=GSE8949
Status:	Public on Dec 12 2007
Title:	Gene expression changes in mouse aorta during activation of or interference with PPAR gamma signaling.
Organism:	Mus musculus
Experiment type:	Expression profiling by array
Platform:	GPL1261
Pubmed ID:	20018933
Summary & Design:	**Summary:** Ligand-mediated activation of the nuclear hormone receptor PPAR gamma lowers blood pressure and improves glucose tolerance in humans. Two naturally occurring mutations (P467L, V290M) in the ligand binding domain of PPAR gamma have been described in humans that lead to severe insulin resistance and hypertension. Experimental evidence suggests that these mutant versions of PPAR gamma act in a dominant negative fashion. To better understand the molecular mechanisms underlying PPAR gamma action in the vasculature, we determined the gene expression patterns in mouse aorta in response to activation or interference with the PPAR gamma signaling pathway. **Keywords: time course, dose response** **Overall design:** To assess the response to PPAR gamma interference, we used adult mice containing a dominant negative form of PPAR gamma. These mice have a targeted P465L mutation, which is equivalent to the P467L mutant, described in human patients. Wild-type littermates were used as the genetic control. The PPAR gamma signaling pathway was activated by administration of rosiglitazone for either 2 or 14 days to adult mice (C57BL/6J strain) at a dose of 3 or 10 mg/kg/day via the food. Control mice were fed standard mouse chow. For the microarray hybridizations, 2-3 biological replicates from each experimental group were used. Biological replicates were RNA pooled from 8 different mouse aortas. All the microarray procedures were conducted at the University of Iowa DNA Core facility using standard Affymetrix protocols. In brief, approximately 3 ug of total RNA was used as input to a one-step amplification procedure to generate biotin-labeled RNA fragments for hybridization to the Affymetrix GeneChip Mouse Genome 430 2.0 array.

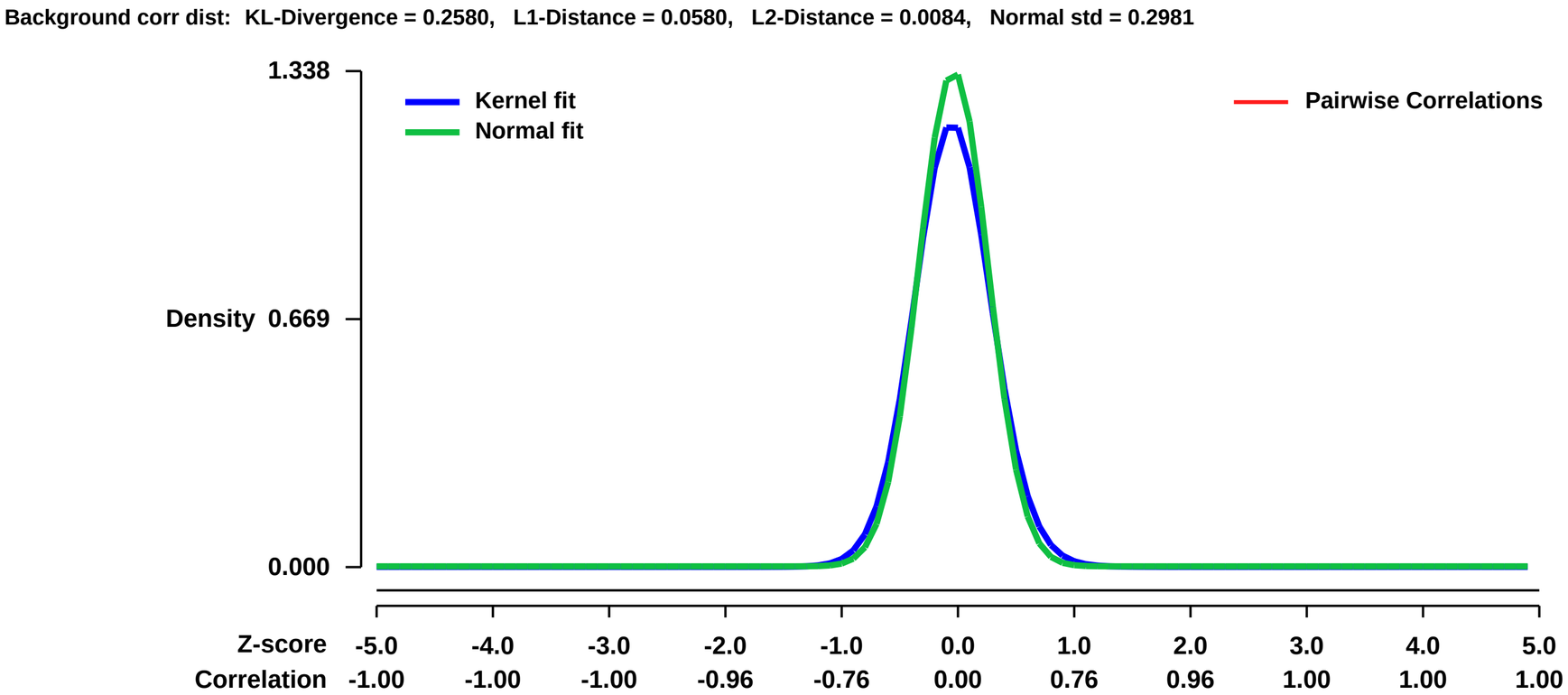

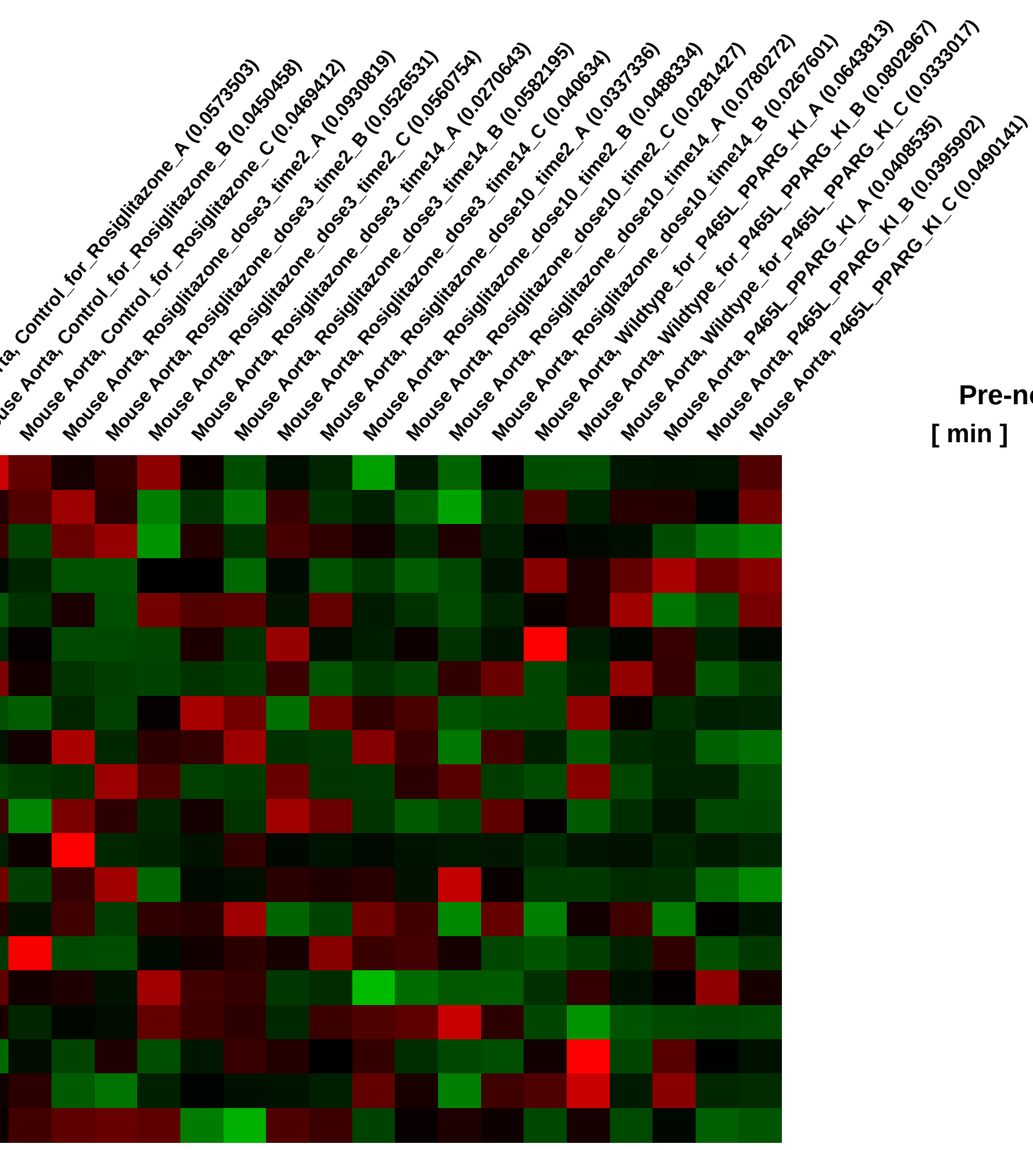

GEO Series "GSE25574" Expression Profiles

Num of samples in this series: 8

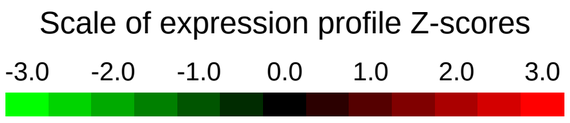

GEO Link:	http://www.ncbi.nlm.nih.gov/geo/query/acc.cgi?acc=GSE25574
Status:	Public on Nov 29 2010
Title:	Hypothalamic transcriptome plasticity in two rodent species reveals divergent differential gene expression but conserved pathways
Organism:	Mus musculus
Experiment type:	Expression profiling by array
Platform:	GPL1261
Pubmed ID:	21070396
Summary & Design:	**Summary:** We have addressed the question of how different rodent species cope with the life-threatening homeostatic challenge of dehydration at the level of transcriptome modulation in the supraoptic nucleus (SON), a specialised hypothalamic neurosecretory apparatus responsible for the production of the antidiuretic peptide hormone arginine vasopressin (AVP). AVP maintains water balance by promoting water conservation at the level of the kidney. Dehydration evokes a massive increase in the regulated release of AVP from SON axon terminals located in the posterior pituitary, and this is accompanied by a plethora of changes in the morphology, electrophysiological properties, biosynthetic and secretory activity of this structure. Microarray analysis was used to generate a definitive catalogue of the genes expressed in the mouse SON, and to describe how the gene expression profile changes in response to dehydration. Comparison of the genes differentially expressed in the mouse SON as a consequence of dehydration with those of the rat has revealed many similarities, pointing to common processes underlying the function-related plasticity in this nucleus. In addition we have identified many genes that are differentially expressed in a species-specific manner. However, in many cases, we have found that the hyperosmotic cue can induce species-specific alterations in the expression of different genes in the same pathway. The same functional end can be served by different means, via differential modulation, in different species, of different molecules in the same pathway. We suggest that pathways, rather than specific genes, should be the focus of integrative physiological studies based on transcriptome data. **Overall design:** Microarray analysis. Separate microarrays (n=4) were probed using independently generated target. For each completely independent replicate, tissue from 1 mouse was used for RNA extraction.

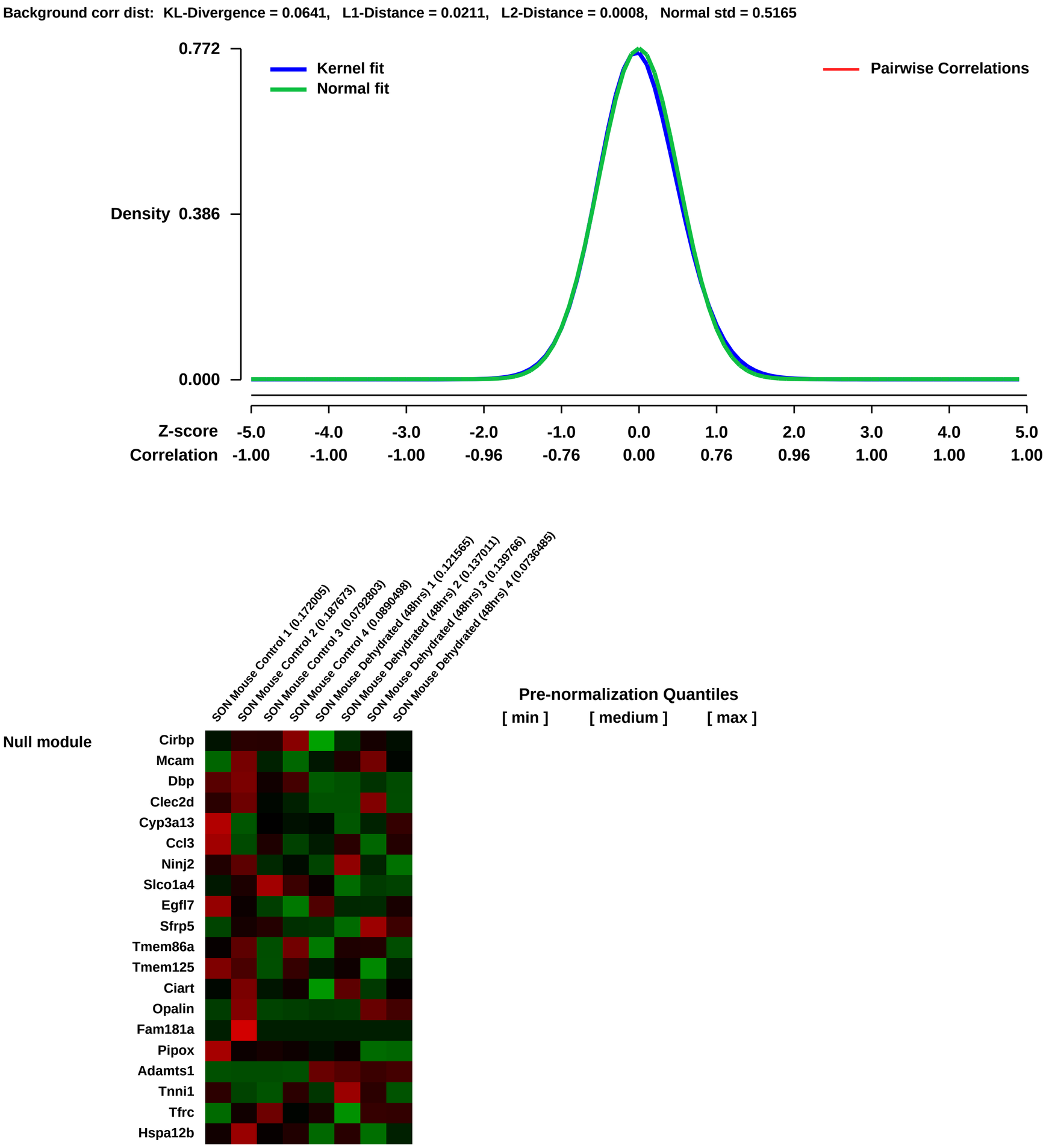

GEO Series "GSE16684" Expression Profiles

Num of samples in this series: 6

Scale of expression profile Z-scores

-3.0 -2.0 -1.0 0.0 1.0 2.0 3.0

GEO Link:	http://www.ncbi.nlm.nih.gov/geo/query/acc.cgi?acc=GSE16684
Status:	Public on Aug 01 2010
Title:	Murine M7 leukemia derived from retroviral insertional mutagenesis of Gata1s fetal progenitors depends on IGF signaling
Organism:	Mus musculus
Experiment type:	Expression profiling by array
Platform:	GPL1261
Pubmed ID:	20679399
Summary & Design:	**Summary:** The goal of this study is to derive a mouse model of human Down Syndrome (DS) megakaryocytic leukemia involving mutations in the hematopoietic transcription factor, GATA1 (called GATA1s mutation). We achieved this through transduction of Gata1s mutant fetal progenitors by MSCV-based retrovirus expressing a GFP marker, followed by in vitro selection (for immortalized cell lines), and then in vivo selection (for transformed cell lines) through transplantation. Here we report one such cell line [T6(6)] that gives rise to megakaryocytic leukemia (M7 leukemia) upon transplantation. We show knockdown of IGF1R in these cells leads to their reduced proliferation. **Overall design:** IGF1R was knocked down in these cells using a tet-regulatable shRNA-based lentiviral system. Cells infected with the empty vector or those infected with shRNA construct against IGF1R but in the absence of Doxycycline were used as controls. The latter cells in the presence of Doxycycline exhibited reduced IGF1R at the RNA level.

Background corr dist: KL-Divergence = 0.0413, L1-Distance = 0.0184, L2-Distance = 0.0003, Normal std = 0.6111

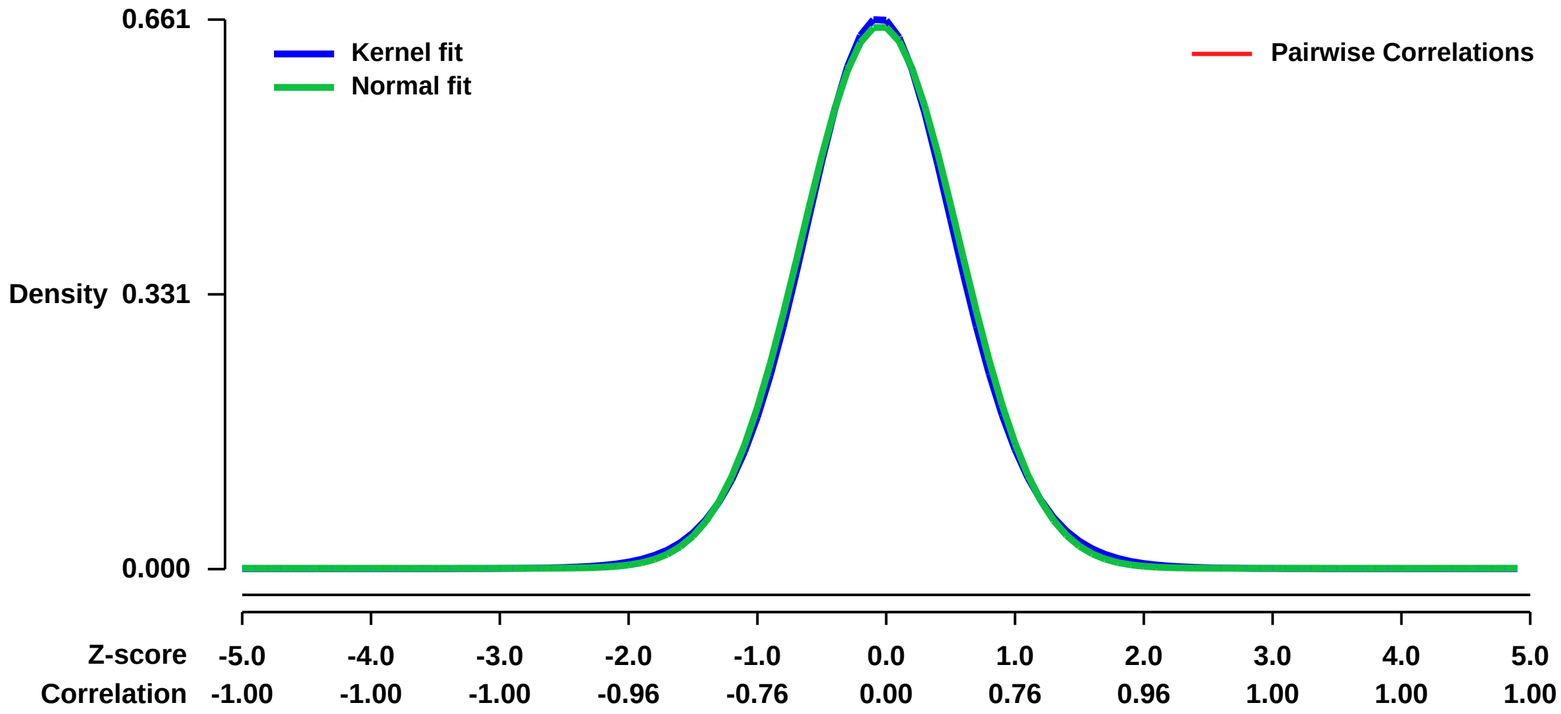

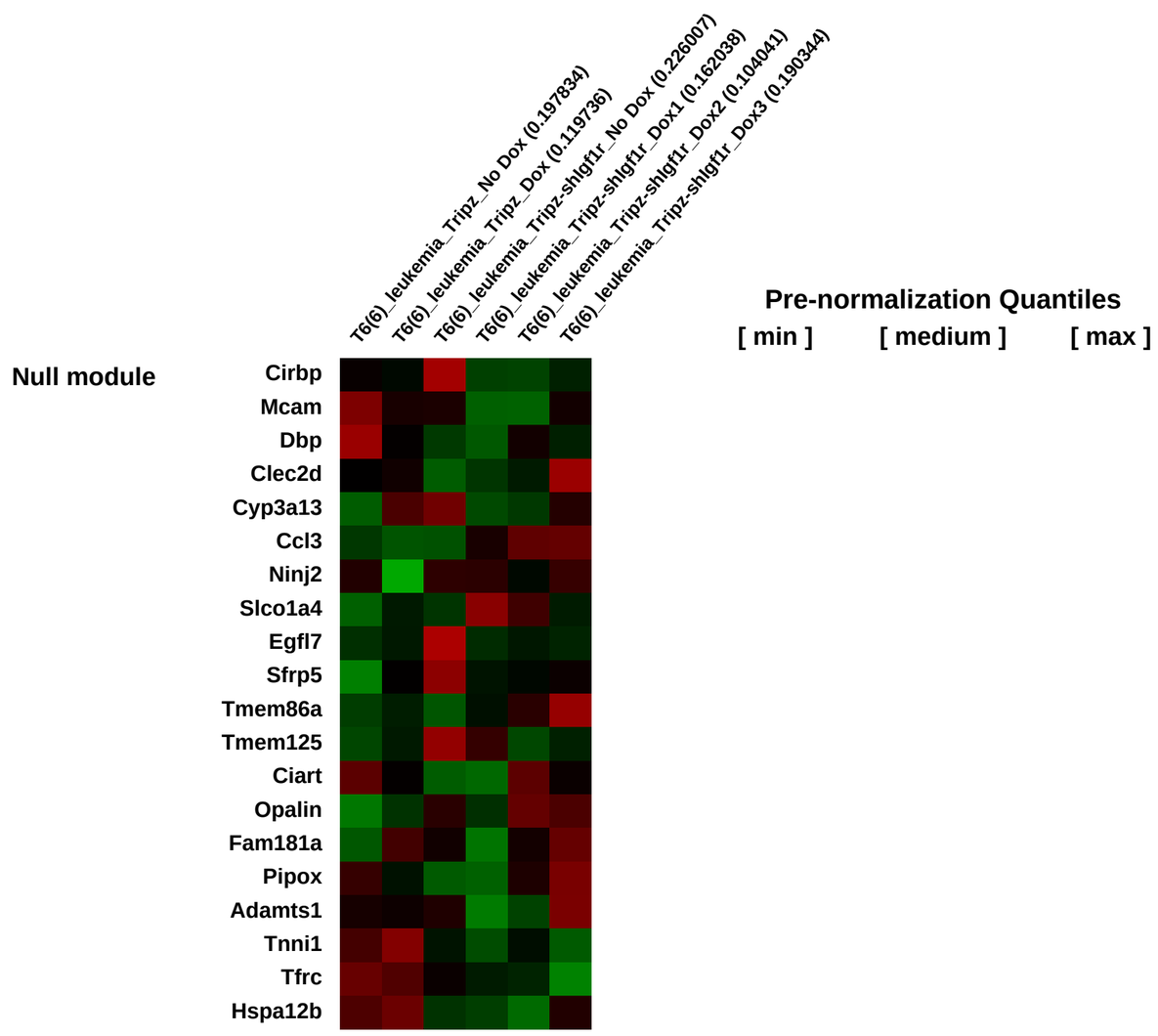

GEO Series "GSE14753" Expression Profiles

Num of samples in this series: 6

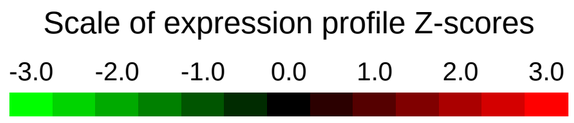

GEO Link:	http://www.ncbi.nlm.nih.gov/geo/query/acc.cgi?acc=GSE14753
Status:	Public on Feb 10 2009
Title:	Mammary tumors from K14-cre; ApcCKO/+ mice vs control mammary glands
Organism:	Mus musculus
Experiment type:	Expression profiling by array
Platform:	GPL1261
Pubmed ID:	19197353
Summary & Design:	**Summary:** Many components of Wnt/¸†-catenin signaling pathway also play critical roles in mammary tumor development. To study the role of Apc in mammary tumorigensis, we introduced conditional Apc mutations specifically into two different mammary epithelial populations using K14-Cre (progenitor) and WAP-cre (lactaing luminal) transgenic mice. Only the K14-cre mediated Apc heterozygosity developed mammary adenocarcinomas demonstrating histological and molecular heterogeneity, suggesting the progenitor cell origin of these tumors. These tumors harbored truncation mutation in a very defined region in the remaining wild-type allele of Apc that would retain some down-regulating activity of ¸†-catenin signaling. Our results suggest that not only the epithelial origin but also a certain Apc mutations are selected to achieve a specific level of ¸†-catenin signaling optimal for mammary tumor development. **Overall design:** We have compared 3 mammary tumors from K14-cre; ApcCKO/+ mice with 3 control mammary glands.

Background corr dist: KL-Divergence = 0.0282, L1-Distance = 0.0235, L2-Distance = 0.0007, Normal std = 0.6907

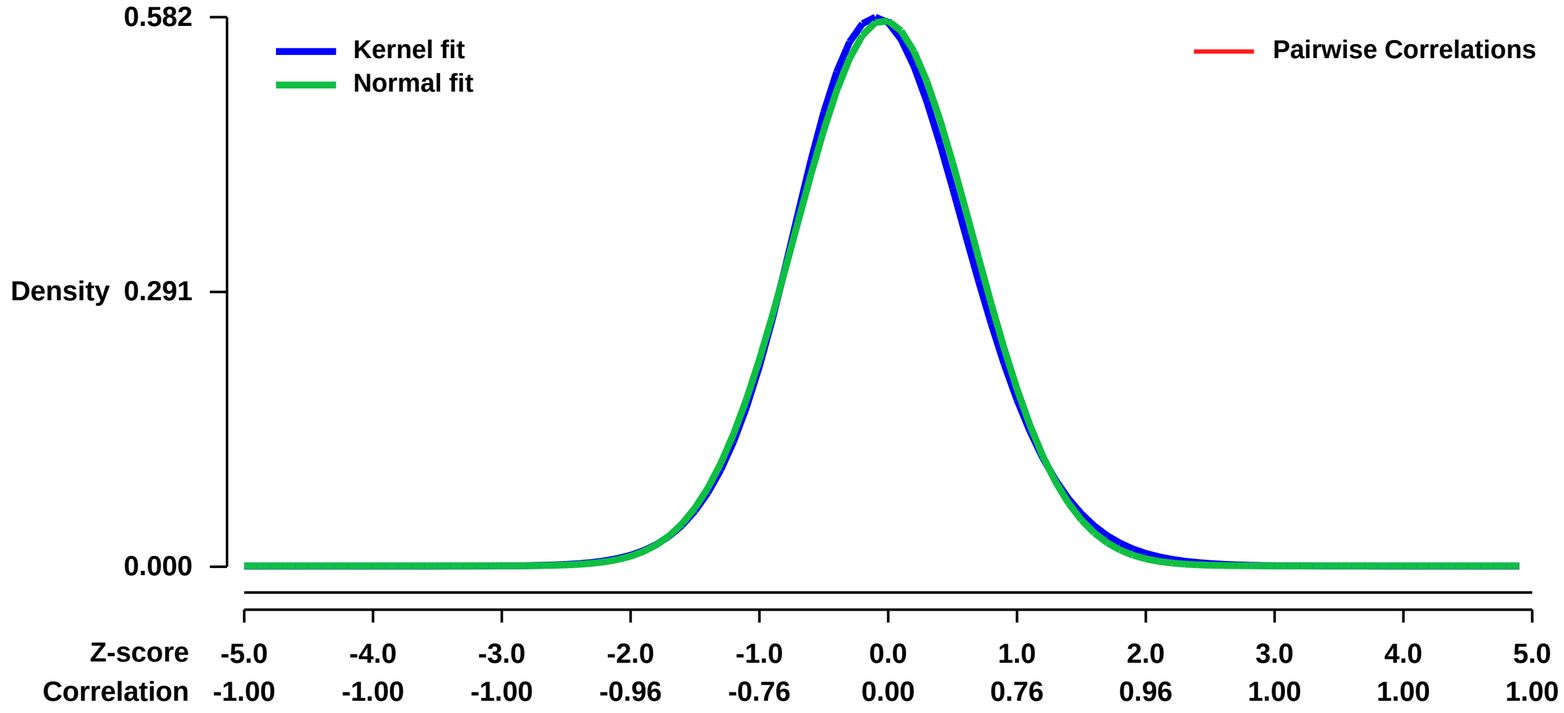

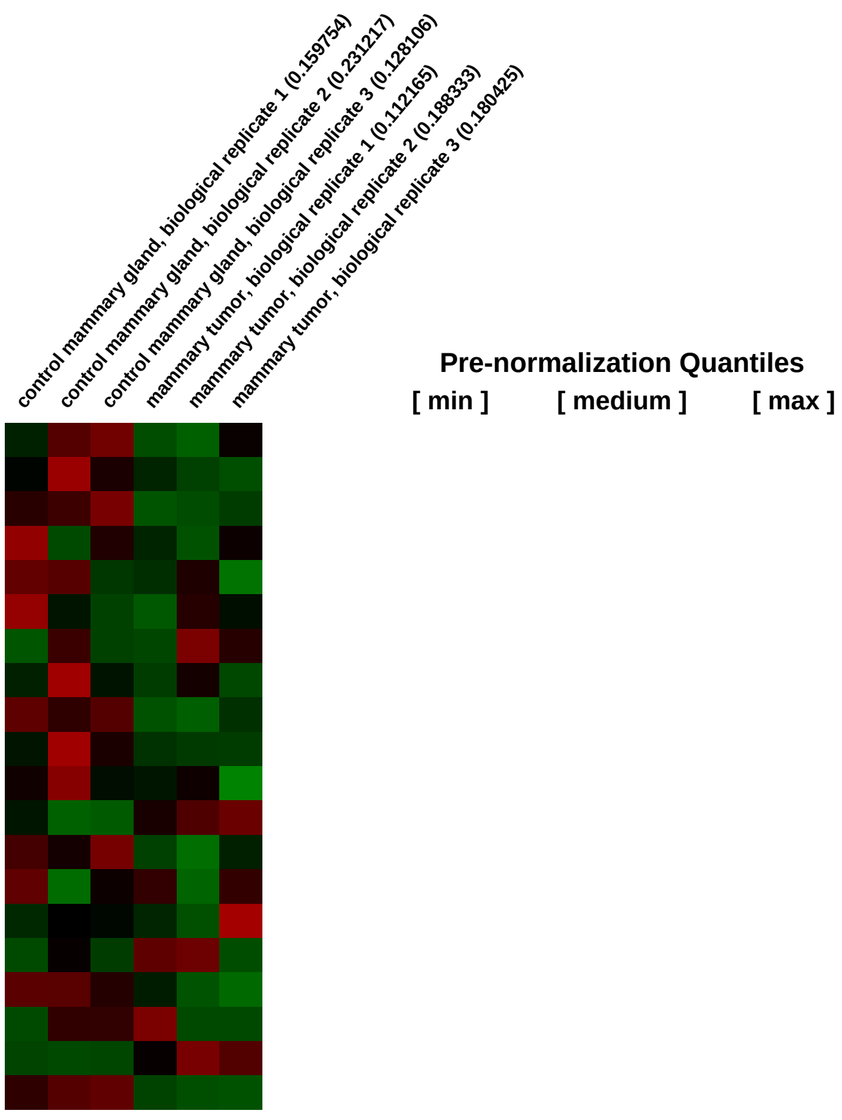

GEO Series "GSE12985" Expression Profiles

Num of samples in this series: 14

Scale of expression profile Z-scores

-3.0 -2.0 -1.0 0.0 1.0 2.0 3.0

GEO Link:	http://www.ncbi.nlm.nih.gov/geo/query/acc.cgi?acc=GSE12985
Status:	Public on Feb 01 2010
Title:	Differentiation time course of trophoblast stem cells
Organism:	Mus musculus
Experiment type:	Expression profiling by array
Platform:	GPL1261
Pubmed ID:	20081188
Summary & Design:	**Summary:** To characterized the changes in gene expression during the differentiation of TS cells. TS cells can be derived from two time point during embryogenesis, cell lines tested were from each of these time points. **Keywords: time course** **Overall design:** TS cells derived from either E3.5 or E6.5 embryos were differentiated over 6 days by withdrawal of FGF4 and feeder conditioned medium. Cell were sampled every 24 hrs and assayed by microarray.

Background corr dist: KL-Divergence = 0.0675, L1-Distance = 0.0263, L2-Distance = 0.0011, Normal std = 0.5003

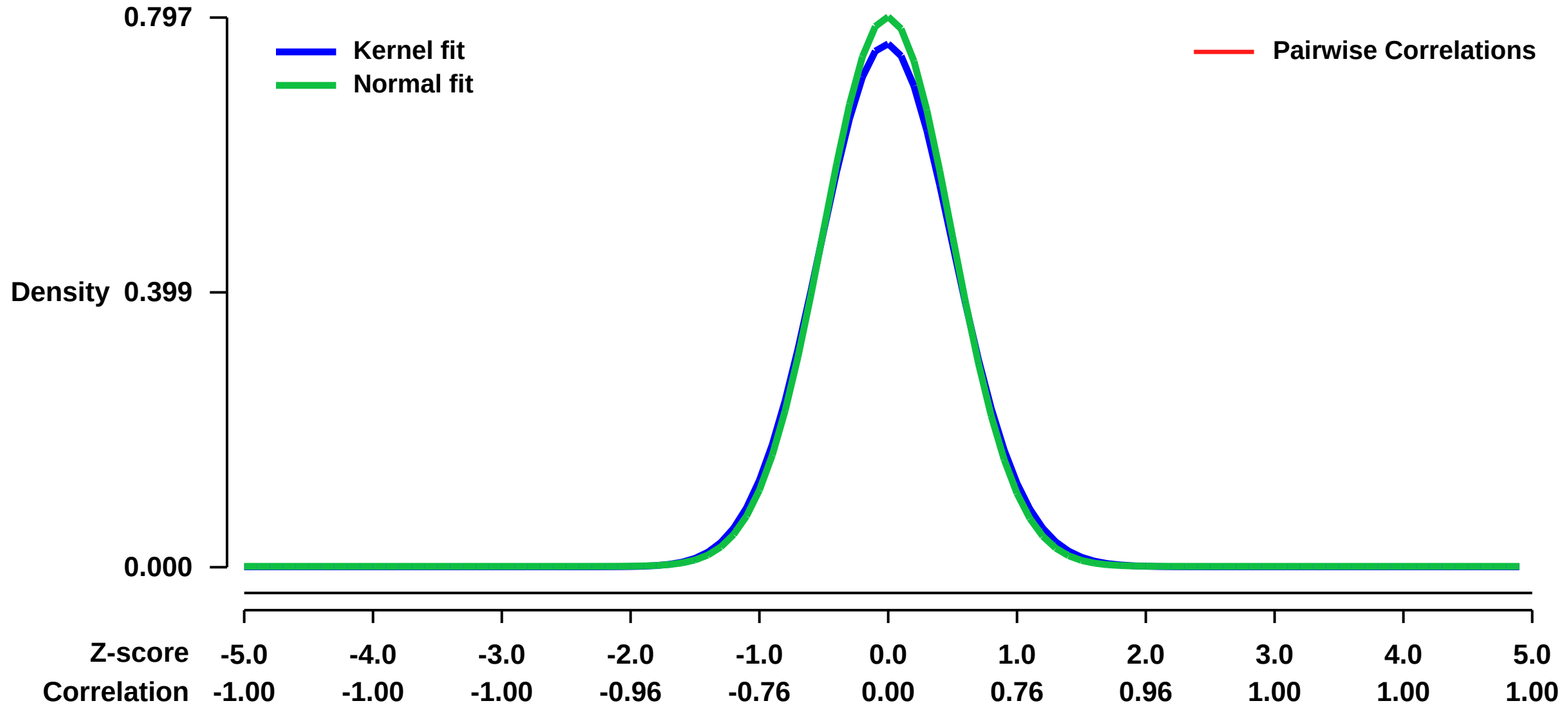

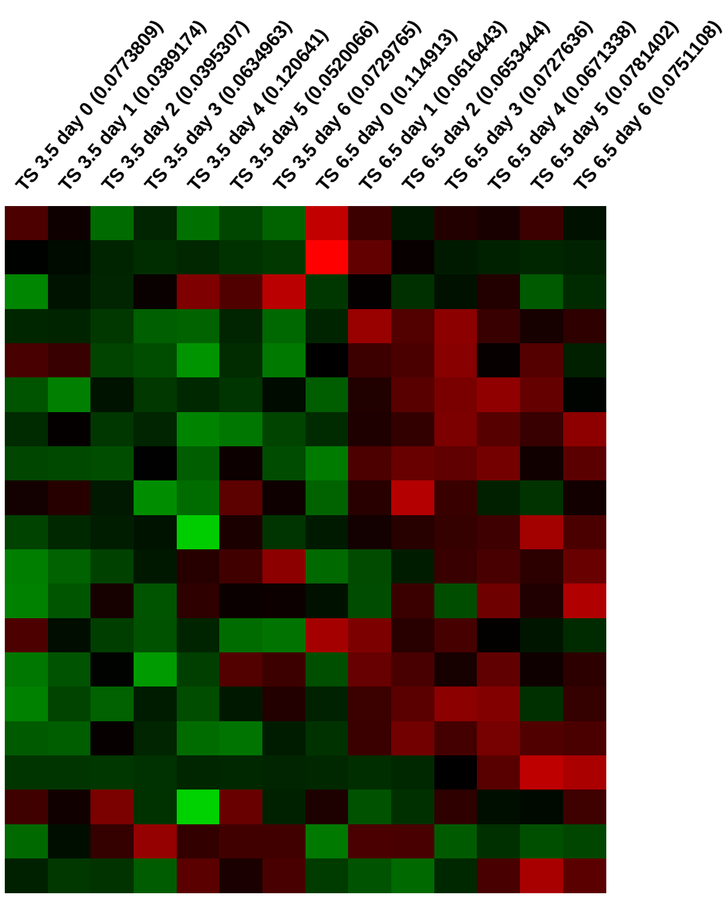

GEO Series "GSE21670" Expression Profiles

Num of samples in this series: 16

Scale of expression profile Z-scores

-3.0 -2.0 -1.0 0.0 1.0 2.0 3.0

GEO Link:	http://www.ncbi.nlm.nih.gov/geo/query/acc.cgi?acc=GSE21670
Status:	Public on May 30 2010
Title:	Diverse Targets of the Transcription Factor STAT3 Contribute to T Cell Pathogenicity and Homeostasis [Affymetrix Expression]
Organism:	Mus musculus
Experiment type:	Expression profiling by array
Platform:	GPL1261
Pubmed ID:	20493732
Summary & Design:	**Summary:** STAT3, an essential transcription factor with pleiotropic functions, plays critical roles in the pathogenesis of autoimmunity. Despite recent data linking STAT3 with inflammatory bowel disease, exactly how it contributes to chronic intestinal inflammation is not known. Using a T cell transfer model of colitis we found that STAT3 expression in T cells was essential for the induction of both colitis and systemic inflammation. STAT3 was critical in modulating the balance of T helper 17 (Th17) and regulatory T (Treg) cells, as well as in promoting CD4+ T cell proliferation. We used chromatin immunoprecipitation and massive parallel sequencing (ChIP-Seq) to define the genome-wide targets of STAT3 in CD4+ T cells. We found that STAT3 bound to multiple genes involved in Th17 cell differentiation, cell activation, proliferation and survival, regulating both expression and epigenetic modifications. Thus, STAT3 orchestrates multiple critical aspects of T cell function in inflammation and homeostasis. **Overall design:** WT and STAT3-deficient CD4+ T cells were activated with anti-CD3 and anti-CD28, in the presence of cytokines (interleukin (IL)-6 and TGFb) or medium alone for three days. RNA was extracted and hybridized to Affymetrix microarray chips.

Background corr dist: KL-Divergence = 0.1042, L1-Distance = 0.0408, L2-Distance = 0.0034, Normal std = 0.4302

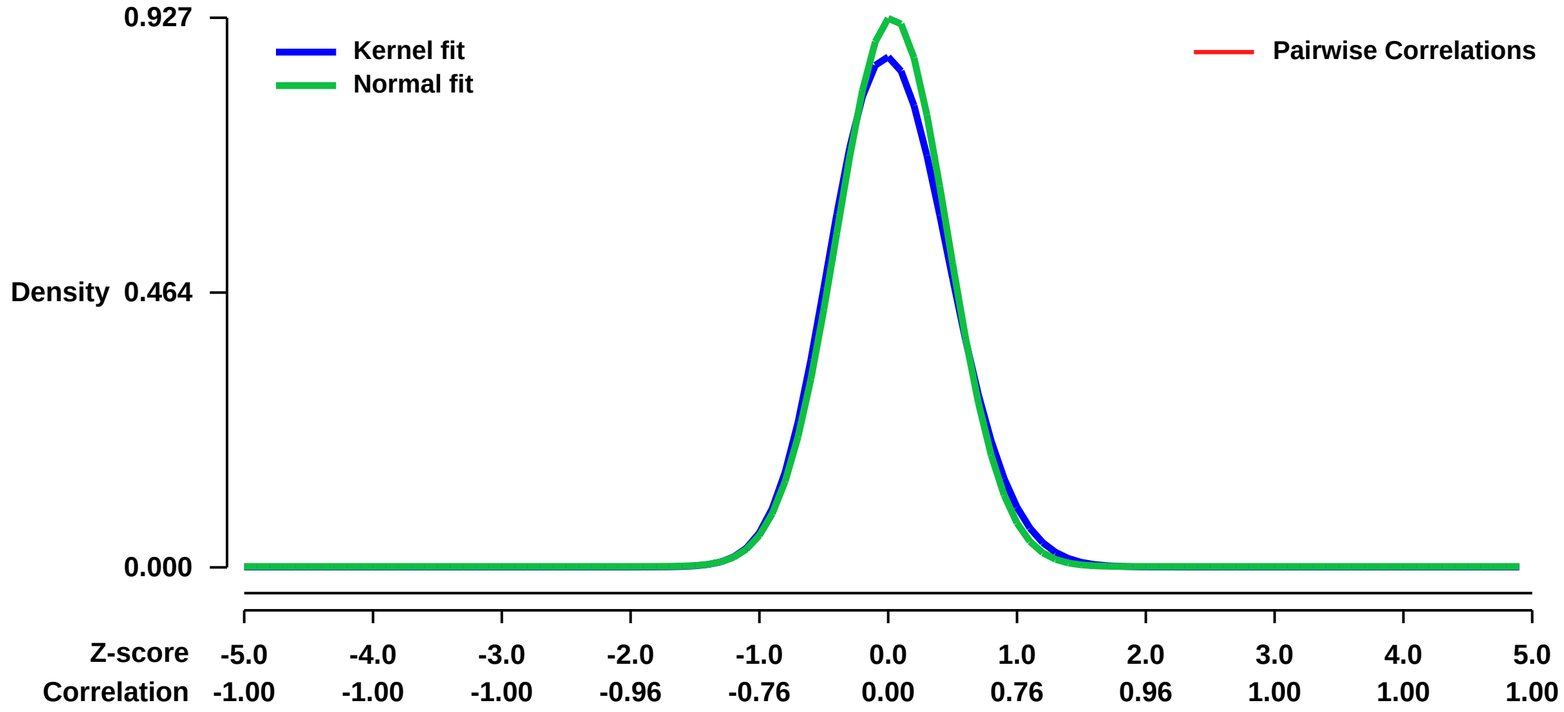

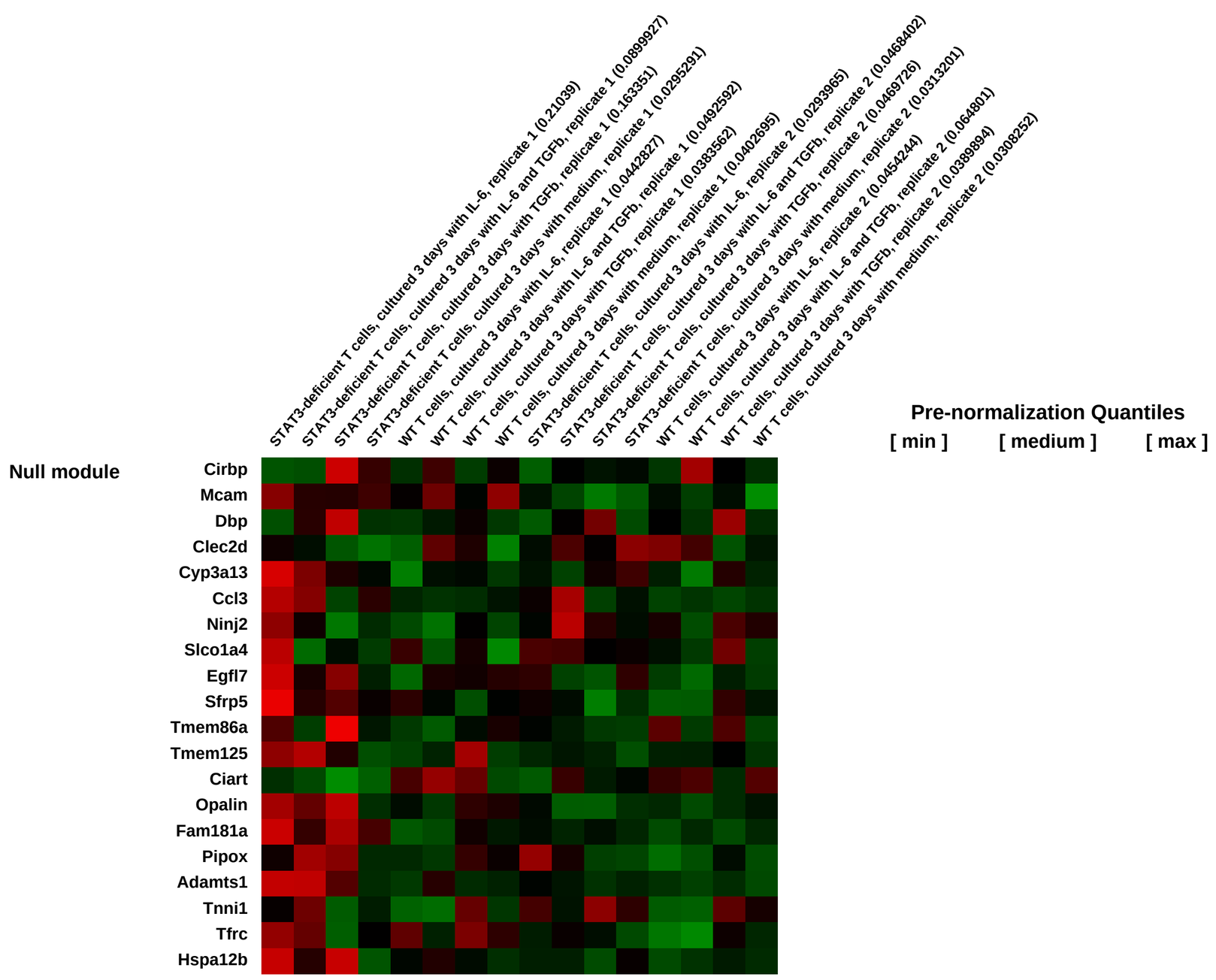

GEO Series "GSE5582" Expression Profiles

Num of samples in this series: 6

Scale of expression profile Z-scores

-3.0 -2.0 -1.0 0.0 1.0 2.0 3.0

GEO Link:	**http://www.ncbi.nlm.nih.gov/geo/query/acc.cgi?acc=GSE5582**
Status:	**Public on Mar 14 2007**
Title:	**Neocortical and cerebellar astrocytes**
Organism:	**Mus musculus**
Experiment type:	**Expression profiling by array**
Platform:	**GPL1261**
Pubmed ID:	**17283119**
Summary & Design:	**Summary:** **Affymetrix Mouse Genome 430 2.0 GeneChip microarrays were used to analyze murine neocortical and cerbellar astrocytes generated from postnatal (PN) day 1 wild-type (ICR) pups.** **Keywords: neocortical astrocyte, cerebellar astrocyte, murine, postnatal day 1** **Overall design:** **Three samples each of murine neocortical and cerebellar astrocytes were analyzed.**

Background corr dist: **KL-Divergence = 0.0397, L1-Distance = 0.0198, L2-Distance = 0.0004, Normal std = 0.6194**

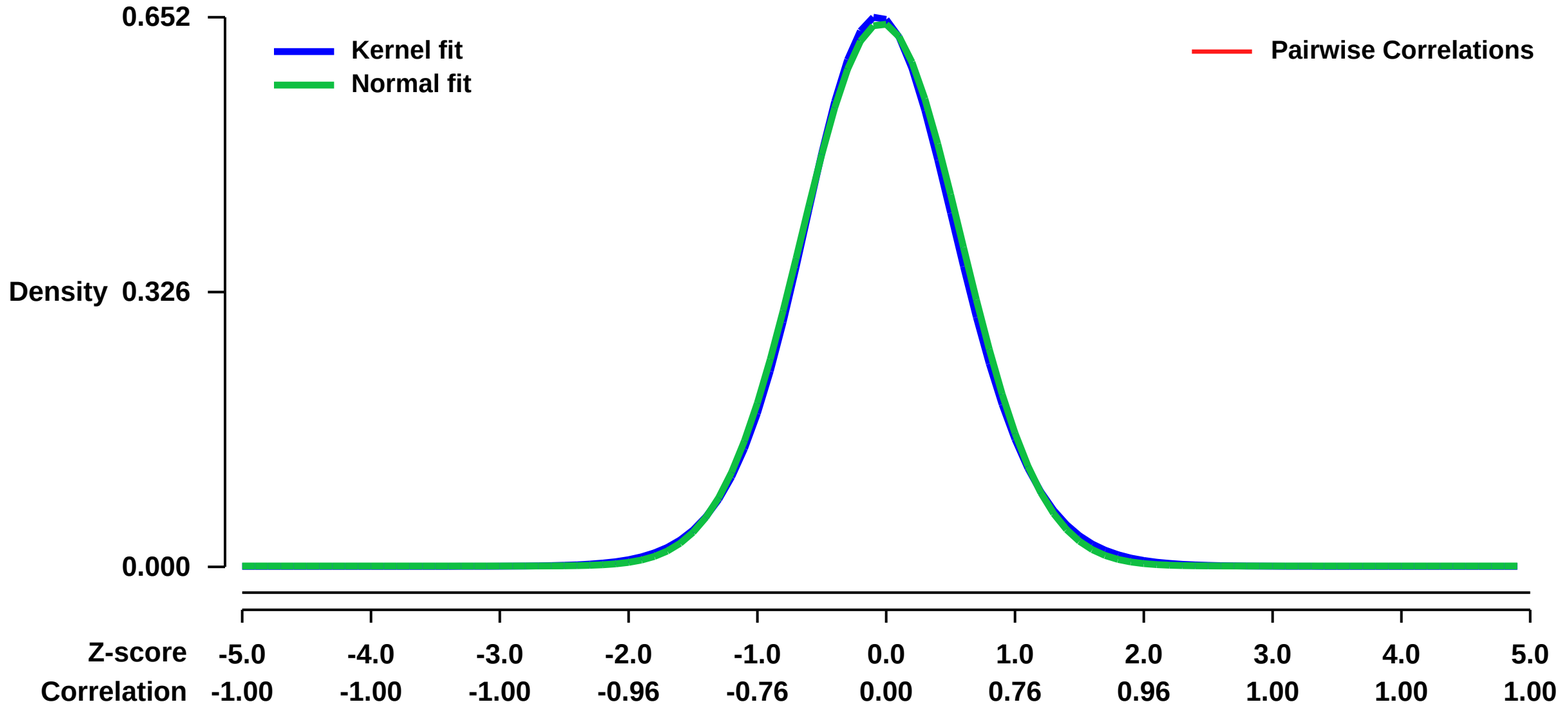

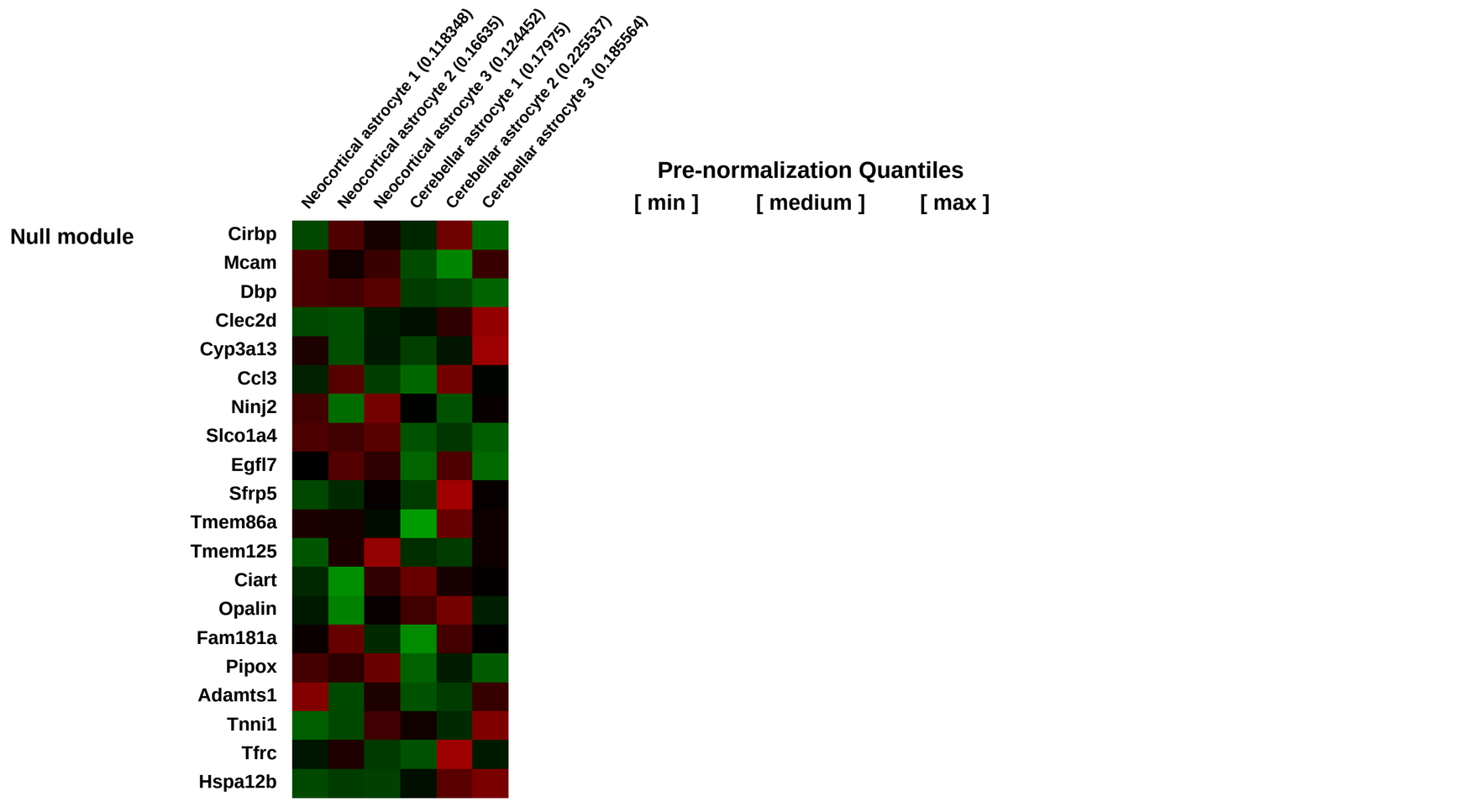

GEO Series "GSE40612" Expression Profiles

Num of samples in this series: 16

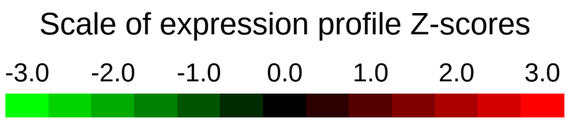

GEO Link:	http://www.ncbi.nlm.nih.gov/geo/query/acc.cgi?acc=GSE40612
Status:	Public on Sep 06 2012
Title:	Transcriptional profiling of SmoM2 expressing IFE cells at different stages of basal cell carcinoma formation
Organism:	Mus musculus
Experiment type:	Expression profiling by array
Platform:	GPL1261
Pubmed ID:	23178882
Summary & Design:	**Summary:** Basal cell carcinoma initiating cells undergo profound and rapid reprogramming into embryonic hair follicle progenitor like fate upon SmoM2 expression. Activation of Wnt/˛†-catenin signaling pathways is required in a cell autonomous manner for the reprogramming of adult IFE progenitors into EHFP-like fate as well as for tumor initiation. We used MA to define the molecular changes that occur in basal cell carcinoma initiating cells form the first oncogenic hit to the development of invasive tumor and further on to investigate the role of Wnt/˛†-catenin signaling activation in molecular changes occurring early during BCC development. **Overall design:** Basal interfollicular cells expressing SmoM2 were FACS isolated at different stages of tumor development and in ˛†-catenin LOF condition for RNA extraction and hybridization on Affymetrix microarrays. By comparing the transcriptional profile of SmoM2 expressing cells with FACS-isolated cells from littermate control mice, we determined a list of genes differentially regulated by SmoM2 expression as specific SmoM2 signature.

Background corr dist: KL-Divergence = 0.1374, L1-Distance = 0.0441, L2-Distance = 0.0043, Normal std = 0.3915

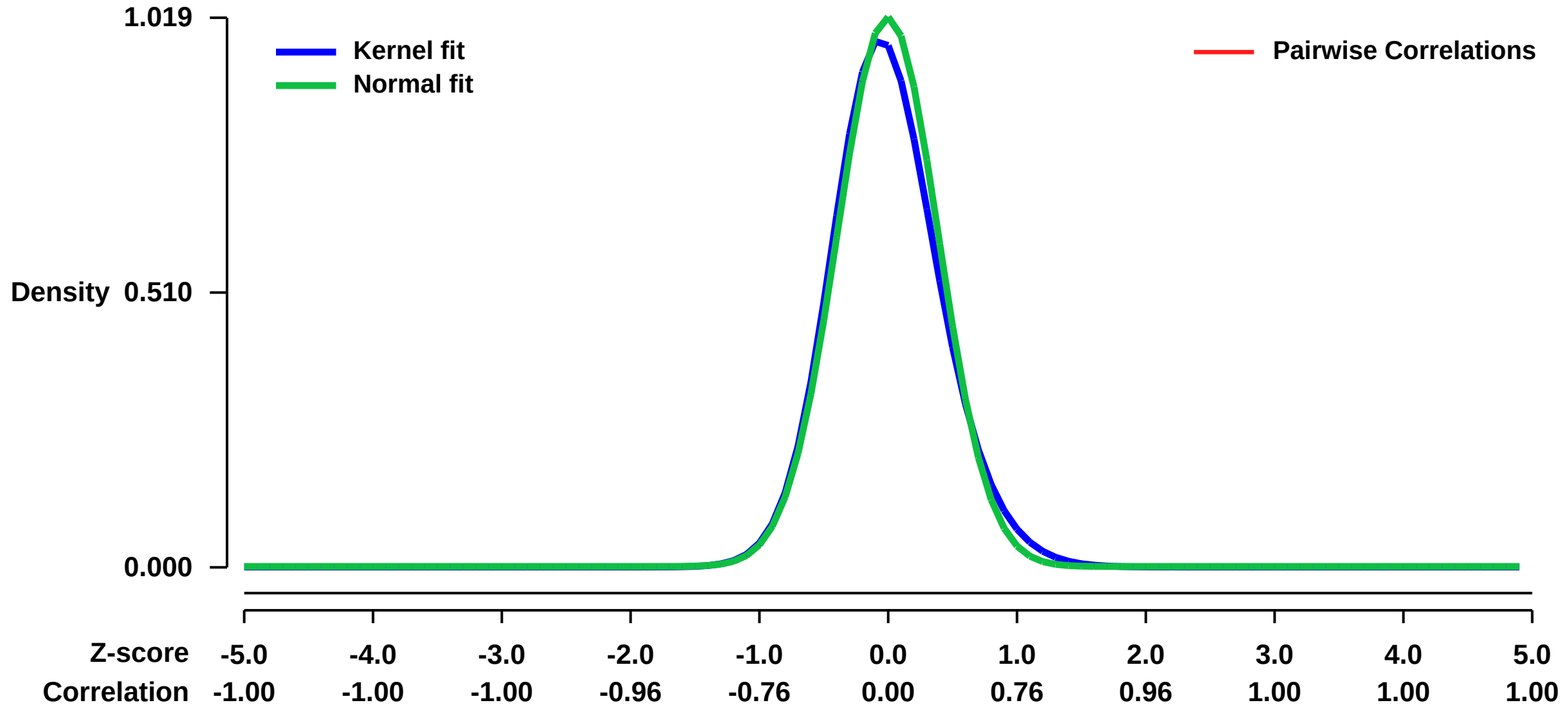

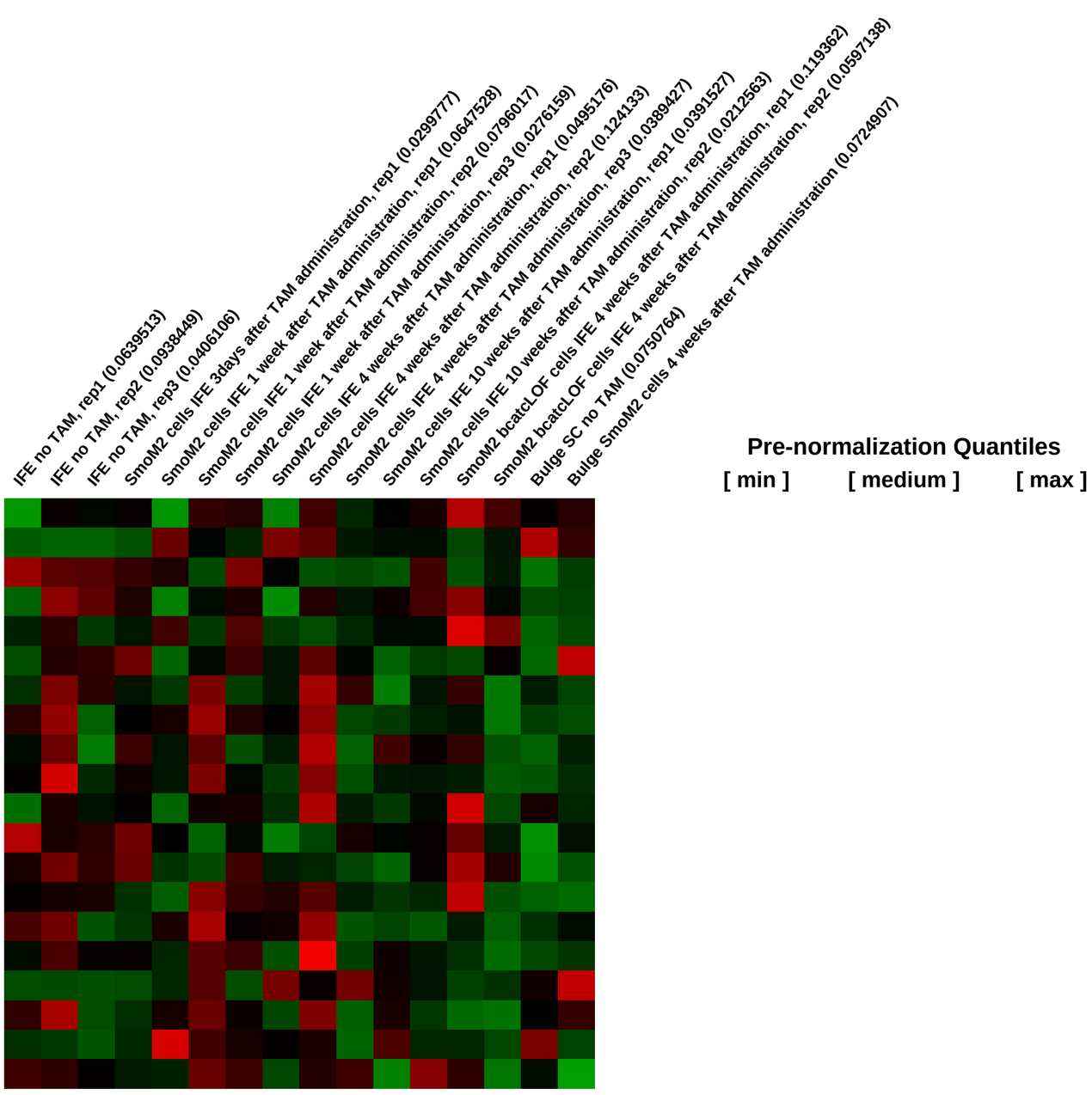

GEO Series "GSE17322" Expression Profiles

Num of samples in this series: 6

Scale of expression profile Z-scores

-3.0 -2.0 -1.0 0.0 1.0 2.0 3.0

GEO Link:	http://www.ncbi.nlm.nih.gov/geo/query/acc.cgi?acc=GSE17322
Status:	Public on Mar 15 2010
Title:	Mouse lung CD103+ and CD11b-high dendritic cell (DC) subsets
Organism:	Mus musculus
Experiment type:	Expression profiling by array
Platform:	GPL1261
Pubmed ID:	20351058
Summary & Design:	**Summary:** Mouse lung CD11c+ dendritic cells are composed of 2 major DC subsets, the CD103+CD11b-low/intermediate DC (CD103+ DC) and the CD11b-highCD103- DC (CD11b-high DC). These 2 subsets are functionally distinct. Comparison of their functions showed CD103+ DC Microarray analysis was performed to compare the gene expression profiles of the 2 lung DC subsets in naˆflve mice. **Overall design:** Perfused lungs from 6-8-week naˆflve BALB/cByJ mice were pooled and digested with collagenase D. CD11c+ cells were selected by anti-CD11c magnetic microbeads (Miltenyi) and stained by fluorochrome-conjugated mAb against I-A, CD103, CD11b, and CD11c plus 7-

Background corr dist: KL-Divergence = 0.0401, L1-Distance = 0.0255, L2-Distance = 0.0008, Normal std = 0.6224

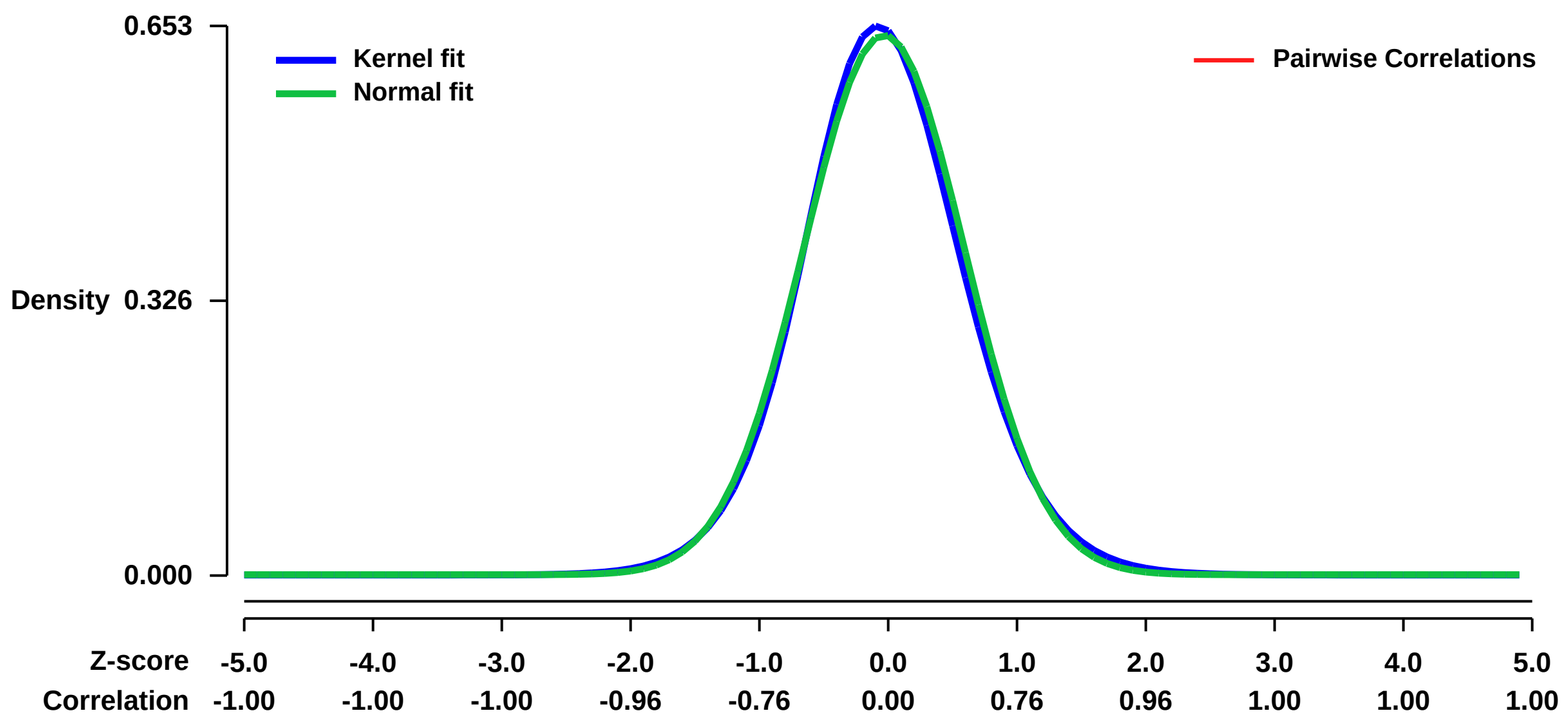

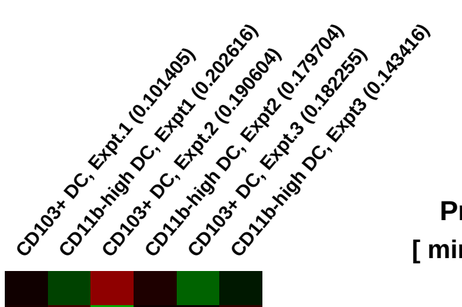

Pre-normalization Quantiles

[min] [medium] [max]

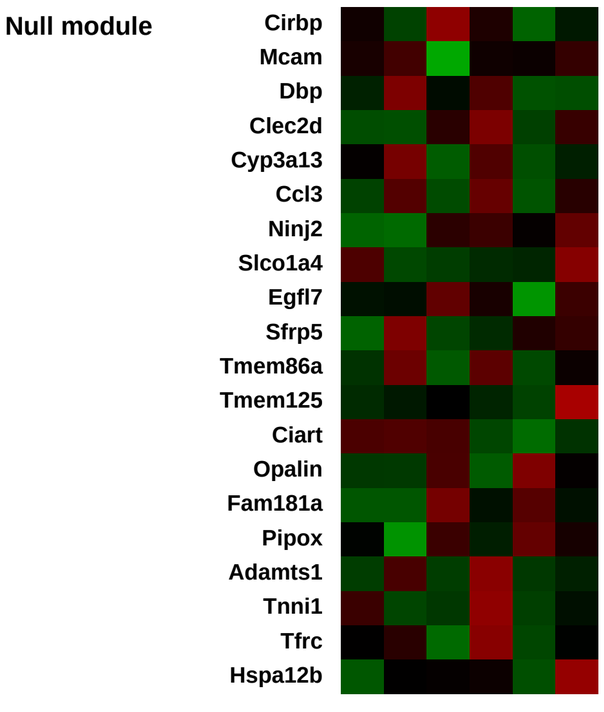

GEO Series "GSE44118" Expression Profiles

Num of samples in this series: 6

Scale of expression profile Z-scores

-3.0 -2.0 -1.0 0.0 1.0 2.0 3.0

GEO Link:	http://www.ncbi.nlm.nih.gov/geo/query/acc.cgi?acc=GSE44118
Status:	Public on Dec 01 2013
Title:	Expression Data from Endothelial Cells as a Consequence of Ets2 Signaling in PyMT Tumor Associated Fibroblasts
Organism:	Mus musculus
Experiment type:	Expression profiling by array
Platform:	GPL1261
Pubmed ID:	23977064
Summary & Design:	**Summary:** Tumor associated fibroblasts are known to play an important role in angiogenesis, however the specific signaling pathways playing an important role in this cross talk remain ill defined. Here, we studied how Ets2 transcrpiton factor signaling in tumor associated fibroblasts effected gene expression in surrounding endothelial cells in the MMTV-PyMT mammary tumor model. Inactivation of Ets2 specifically in fibroblasts using Fsp-cre significantly reduced tumor associated angiogenesis, and was indicated to effect ECM remodeling, cell adhesion and cell chemotaxis processes in neighboring endothelial cells. We have identified Ets2 in fibroblasts as a key signaling molecule to induce tumor associated angiogenesis. Additionally, this function does not rely on the presence of tumor cells, indicating a memory in fibroblasts to induce angiogenesis. **Overall design:** Primary mammary endothelial cells were isolated from mice with or without fibroblast Ets2 in the presence of the PyMT oncogene through sorting with a CD31 antibody. RNA was extracted and samples were submitted for Affymetrix gene expression arrays

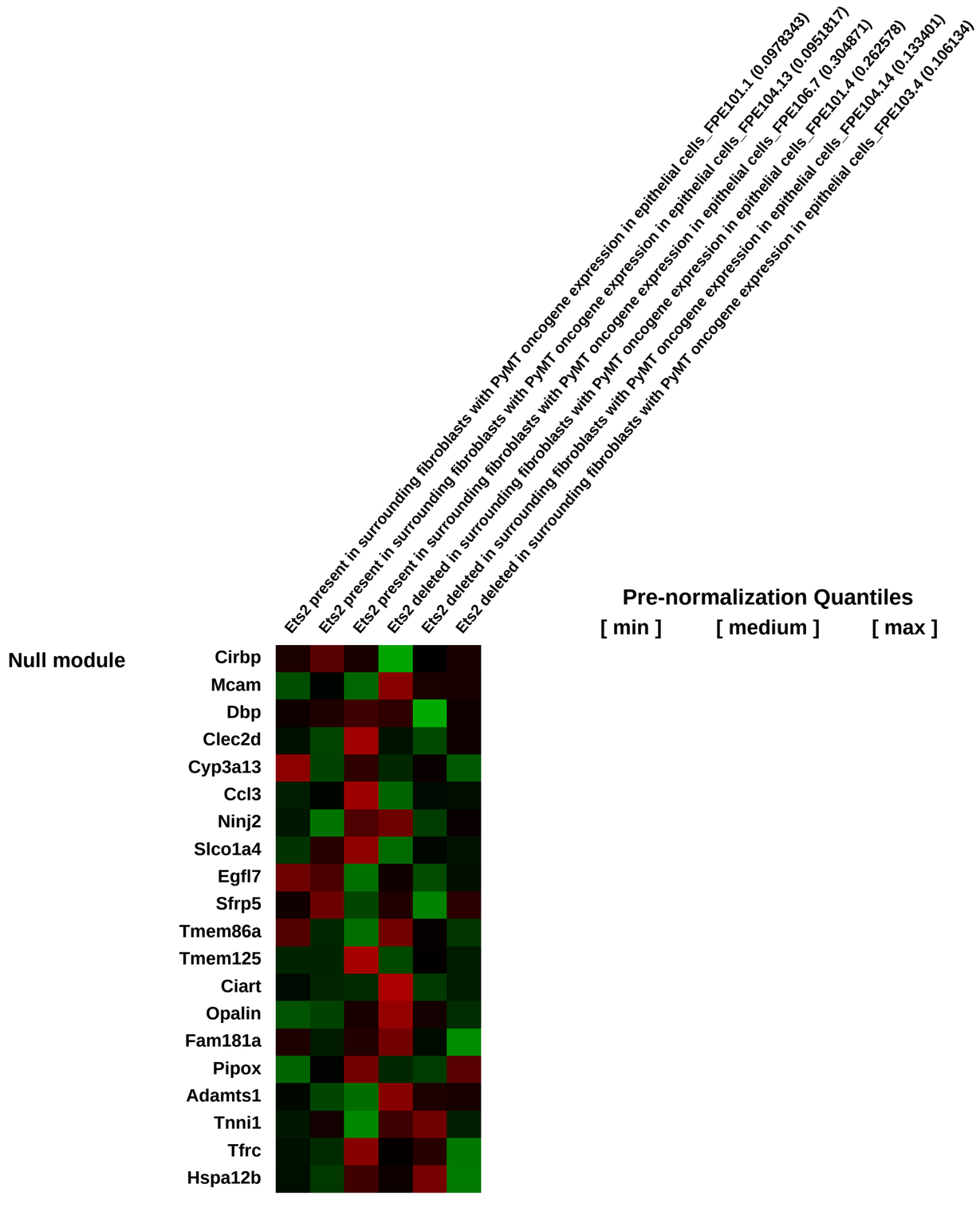

GEO Series "GSE28277" Expression Profiles

Num of samples in this series: 10

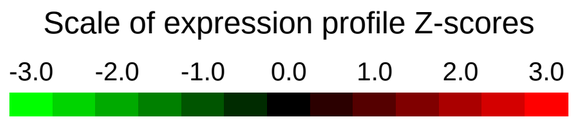

GEO Link:	http://www.ncbi.nlm.nih.gov/geo/query/acc.cgi?acc=GSE28277
Status:	Public on Jun 01 2011
Title:	Altered Gene Expression in Placentae from a Mouse Model of Diabetic Pregnancy
Organism:	Mus musculus
Experiment type:	Expression profiling by array
Platform:	GPL1261
Pubmed ID:	21491160
Summary & Design:	**Summary:** **AIMS/HYPOTHESIS: Pregnancies complicated by diabetes have a higher risk of adverse outcomes for mothers and children, including predisposition to disease later in life, such as metabolic syndrome and hypertension. We hypothesized that adverse outcomes from diabetic pregnancies may be linked to compromised placental function. Our goal in this study was to identify cellular and molecular abnormalities in diabetic placenta.** **METHODS: Using a mouse model of diabetic pregnancy, placental gene expression was assayed at midgestation and cellular composition was analyzed at various stages. Genome-wide expression profiling was validated by quantitative PCR, and tissue localization studies were performed to identify cellular correlates of altered gene expression in diabetic placenta.** **RESULTS: We detected significantly altered gene expression in diabetic placenta for genes expressed in the maternal as well as those in the embryonic compartments. We also found altered cellular composition of the decidual compartment. Furthermore, the junctional and labyrinth layers were reduced in diabetic placenta, accompanied by aberrant differentiation of spongiotrophoblast cells.** **CONCLUSIONS/INTERPRETATION: Diabetes during pregnancy alters transcriptional profiles in the murine placenta, affecting cells of both embryonic and maternal origin, and involving several genes not previously implicated in diabetic pregnancies. The molecular changes and abnormal differentiation of multiple cell types precede impaired growth of junctional zone and labyrinth, and placenta overall. Whether these changes represent direct responses to hyperglycaemia or physiological adaptations, they are likely to play a role in pregnancy complications and outcomes, and have implications for developmental origins of adult disease.** **Overall design:** **The STZ diabetic mouse model was used to investigate gene expression changes in diabetic placentae at E10.5. Placentae were dissected from 5 different FVB dams at embryonic day 10.5 under diabetic conditions and from 5 control dams. Gene expression profiles from five individual placentae from independent pregnancies per group were compared.**

Background corr dist: KL-Divergence = 0.0896, L1-Distance = 0.0222, L2-Distance = 0.0008, Normal std = 0.4569

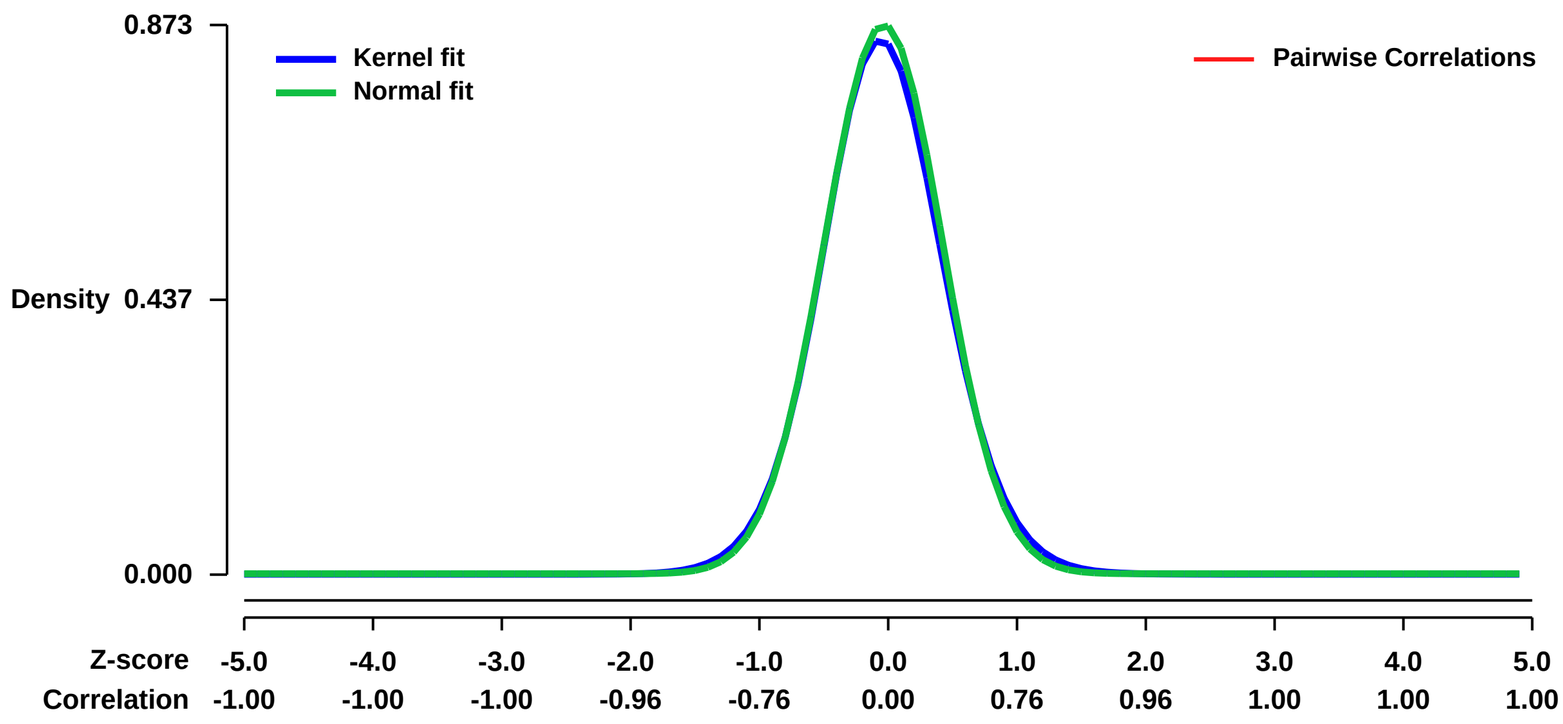

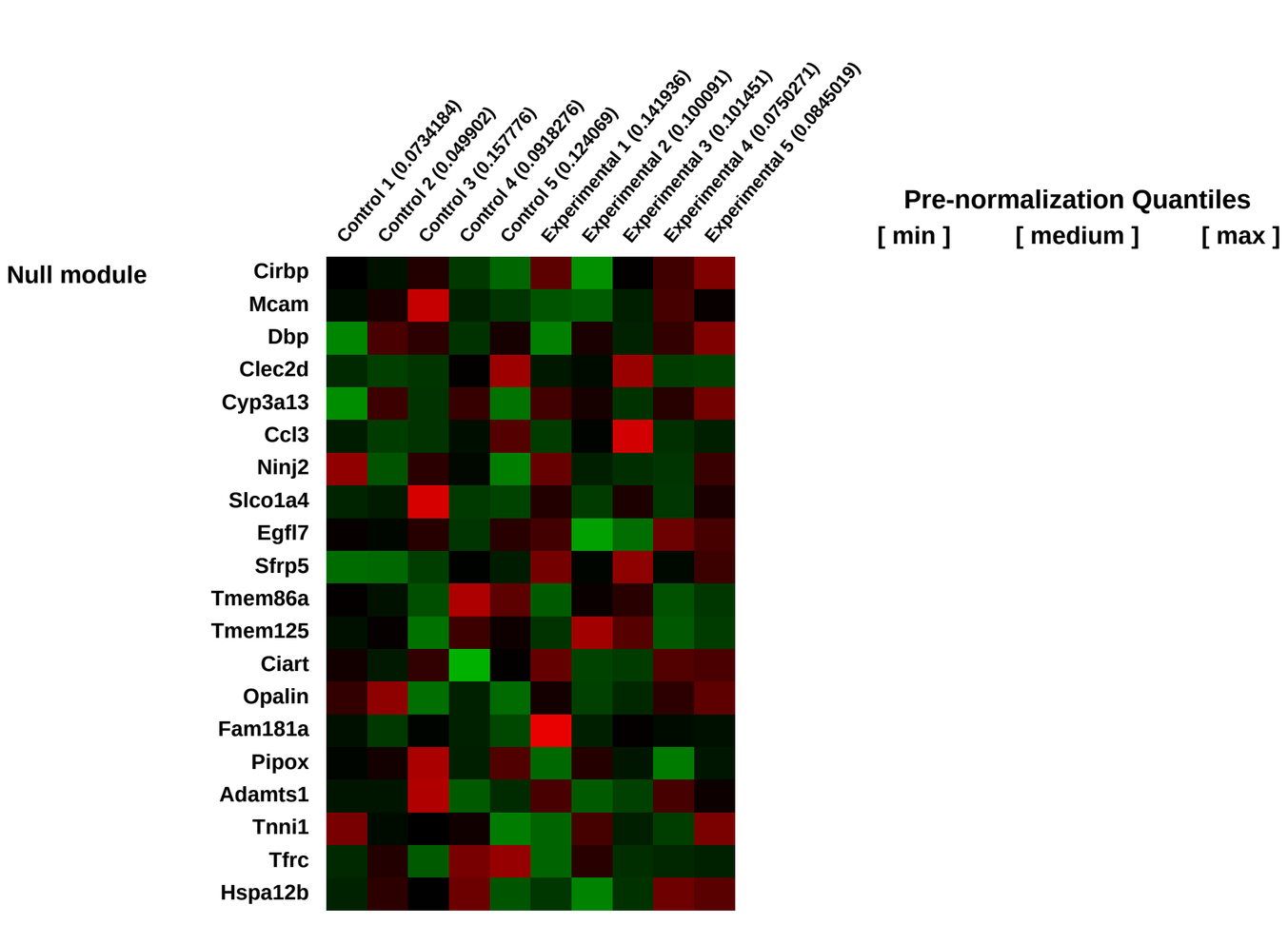

GEO Series "GSE46090" Expression Profiles

Num of samples in this series: 12

Scale of expression profile Z-scores

-3.0 -2.0 -1.0 0.0 1.0 2.0 3.0

GEO Link:	**http://www.ncbi.nlm.nih.gov/geo/query/acc.cgi?acc=GSE46090**
Status:	**Public on Apr 17 2013**
Title:	**Gene expression in WT and Ikaros-deficient DN3, DN4 and DP thymocyte populations**
Organism:	**Mus musculus**
Experiment type:	**Expression profiling by array**
Platform:	**GPL1261**
Pubmed ID:	**24643801**
Summary & Design:	**Summary:** **DN3, DN4 and DP cells were sorted from 3-4 week old WT and mice and subjected to transcriptome analysis** **Overall design:** **Cells from 3 mice were pooled for sorting.**

Background corr dist: **KL-Divergence = 0.0692, L1-Distance = 0.0334, L2-Distance = 0.0015, Normal std = 0.5233**

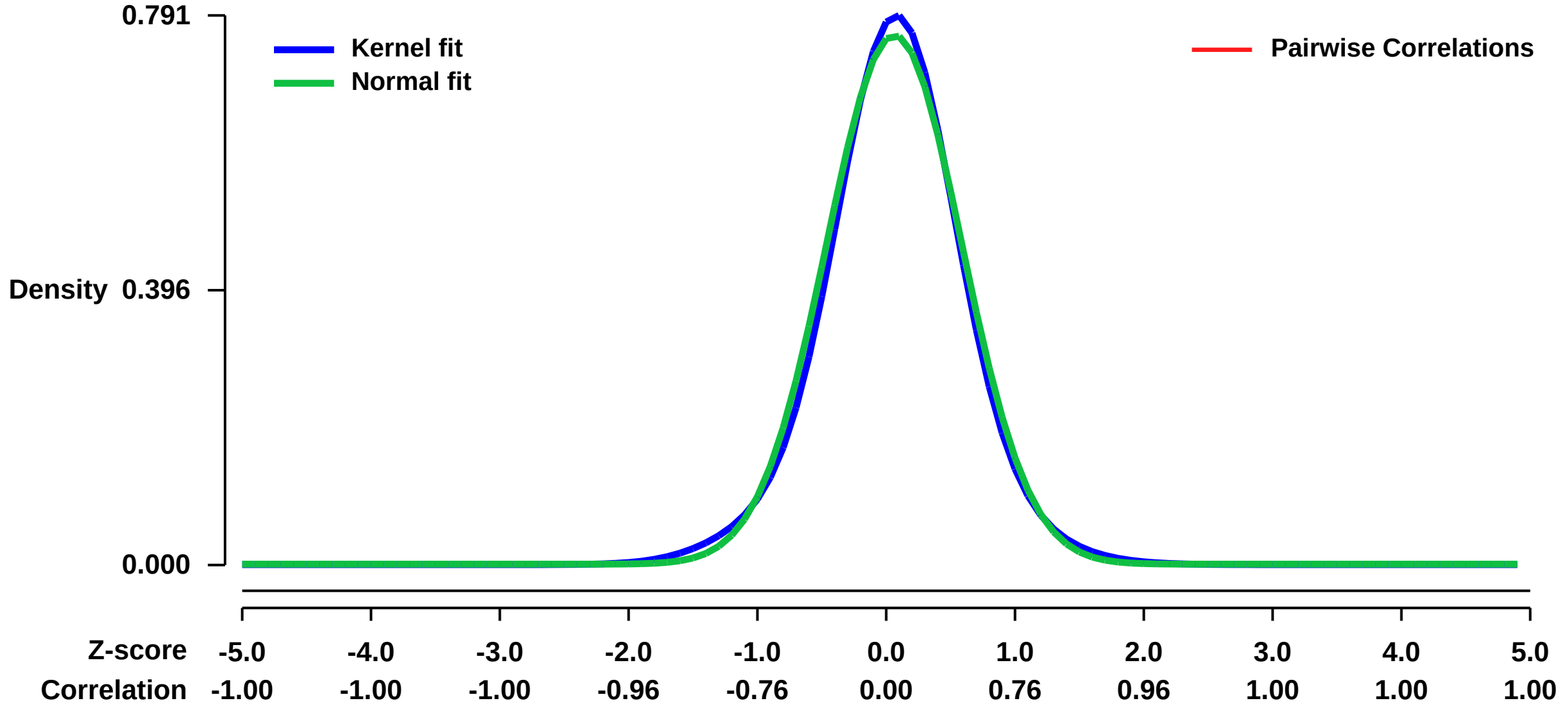

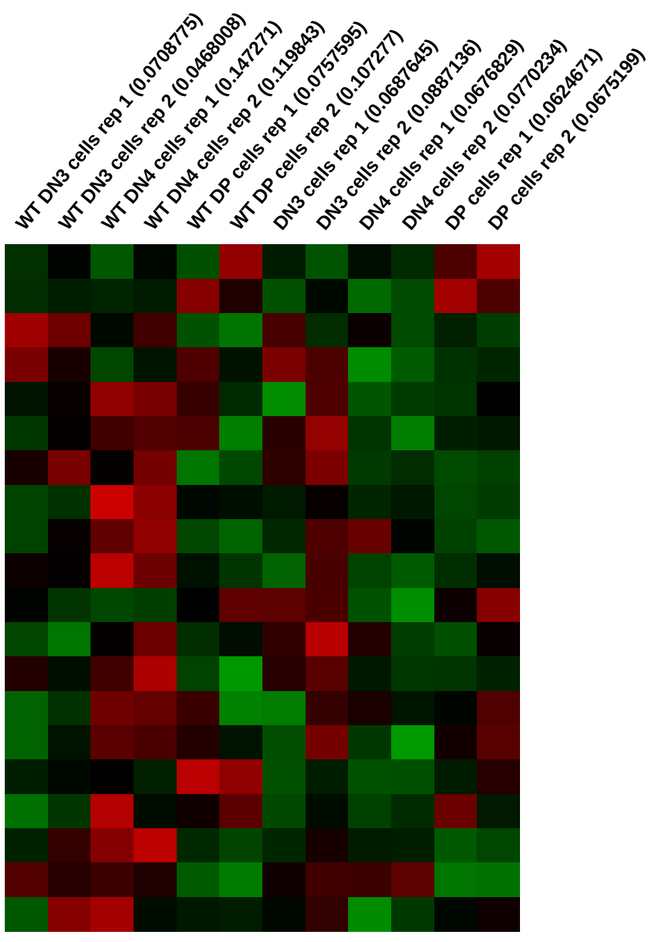

GEO Series "GSE21031" Expression Profiles

Num of samples in this series: 12

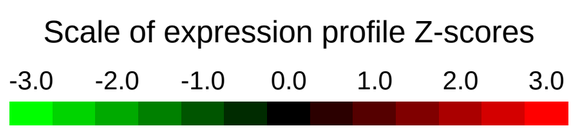

GEO Link:	http://www.ncbi.nlm.nih.gov/geo/query/acc.cgi?acc=GSE21031
Status:	Public on Mar 24 2010
Title:	Time-series of IL-6 stimulated primary mouse hepatocytes
Organism:	Mus musculus
Experiment type:	Expression profiling by array
Platform:	GPL1261
Pubmed ID:	21118515
Summary & Design:	**Summary:** External stimulations of cells by hormones, growth factors or cytokines activate signal transduction pathways that subsequently induce a rearrangement of cellular gene expression. The representation and analysis of changes in the gene response is complicated, and essentially consists of multiple layered temporal responses. In such situations, matrix factorization techniques may provide efficient tools for the detailed temporal analysis. Related methods applied in bioinformatics intentionally do not take prior knowledge into account. In signal processing, factorization techniques incorporating data properties like second-order spatial and temporal structures have shown a robust performance. However, large-scale biological data rarely imply a natural order that allows the definition of an autocorrelation function. We therefore develop the concept of graph-autocorrelation. We encode prior knowledge like transcriptional regulation, protein interactions or metabolic pathways as a weighted directed graph. By linking features along this underlying graph, we introduce a partial ordering of the samples to define an autocorrelation function. Using this framework as constraint to the matrix factorization task allows us to set up the fast and robust graph decorrelation (GraDe) algorithm. To analyze the alterations in the gene response in IL-6 stimulated primary mouse hepatocytes by GraDe, a time-course microarray experiment was performed. Extracted gene expression profiles show that IL-6 activates genes involved in cell cycle progression and cell division in a time-resolved manner. On the contrary, genes linked to metabolic and apoptotic processes are down-regulated indicating that IL-6 mediated priming rendered hepatocytes more responsive towards cell proliferation and reduces expenses for the energy household. **Overall design:** Primary mouse hepatocytes were used in the analysis comprising stimulations with 1 nM IL-6 for 1 h, 2 h, 4 h and an unstimulated control (0 h), each performed in triplicate.

Background corr dist: KL-Divergence = 0.1375, L1-Distance = 0.0314, L2-Distance = 0.0016, Normal std = 0.3866

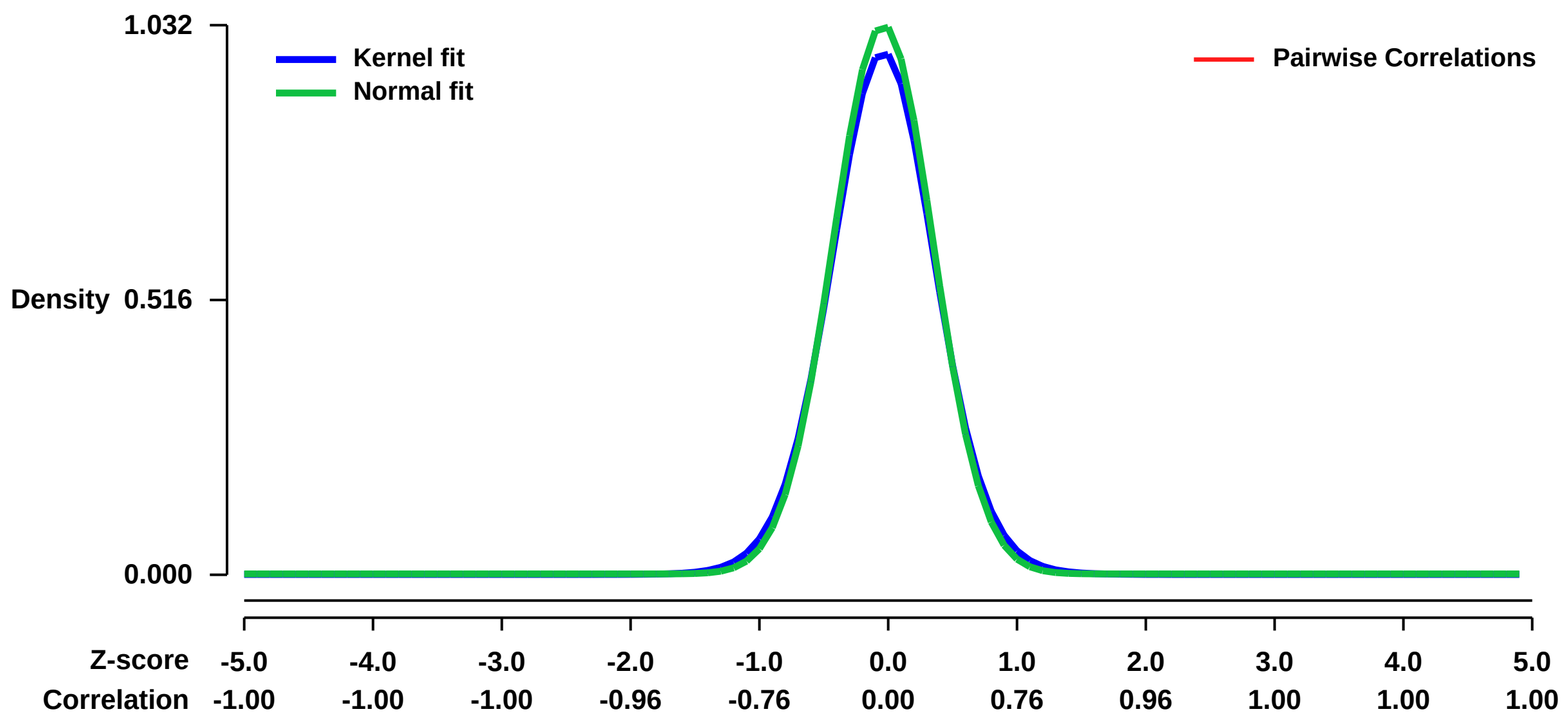

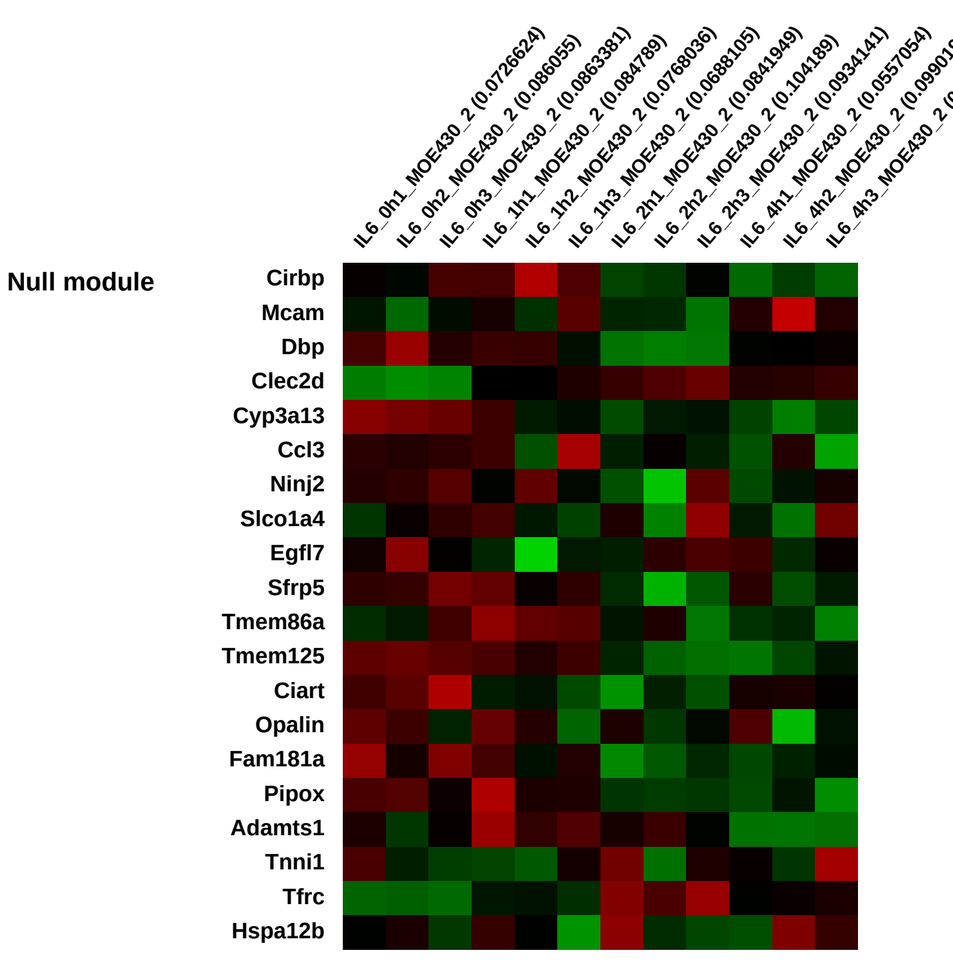

GEO Series "GSE5232" Expression Profiles

Num of samples in this series: 6

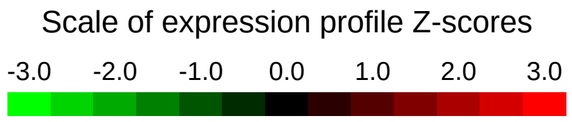

GEO Link:	**http://www.ncbi.nlm.nih.gov/geo/query/acc.cgi?acc=GSE5232**
Status:	**Public on Jul 05 2006**
Title:	**Expression data from Lbeta T2 cells upon activin treatment**
Organism:	**Mus musculus**
Experiment type:	**Expression profiling by array**
Platform:	**GPL1261**
Pubmed ID:	
Summary & Design:	**Summary:** **The primary response of Lbeta T 2cells upon activin treatment at 1hr, 2hr, and 6hr is the significant up-regulation of FSHbeta subunit. Affymetrix genearray missed this important information due to cross-hybridization of its probes with other genes and chromosome segments.** **Activin modulates a network of genes and signaling pathways to exert a variety of functions.** **Keywords: time course** **Overall design:** **Subconfluent Lbeta T2 cells were seeded in cell culture flasks for 16 hours in phenol-free, serum-free medium, and then treated with either vehicle or activin A (30ng/ml). At 1hr, 2hr, or 6hr after treatment, total RNA was isolated using RNeasy Mini Kit. Integrity of RNA was evaluated with an Agilent 2100 Bioanalyzer, and purity/concentration was determined using a GeneSpec III before target preparationi and hybridizations.**

Background corr dist: KL-Divergence = 0.0477, L1-Distance = 0.0179, L2-Distance = 0.0003, Normal std = 0.5807

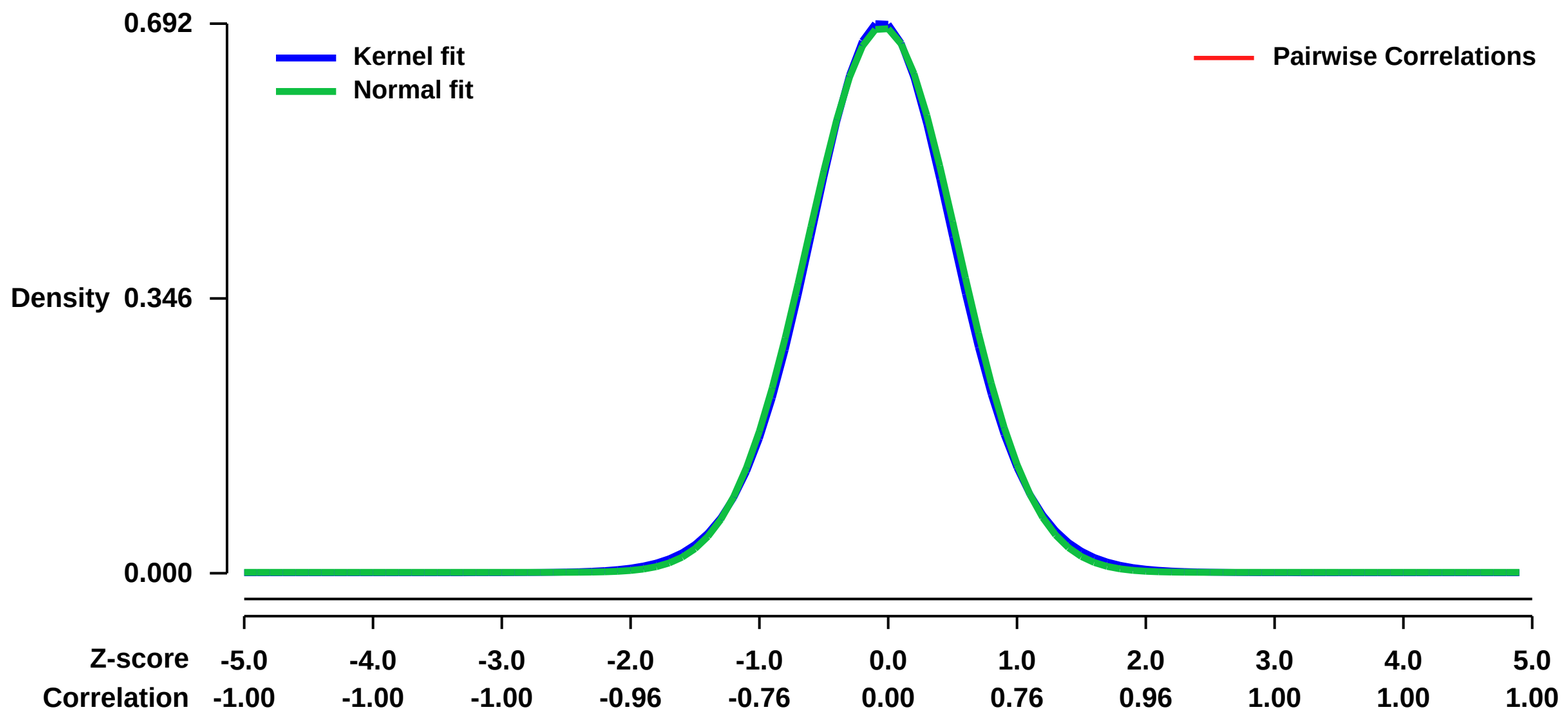

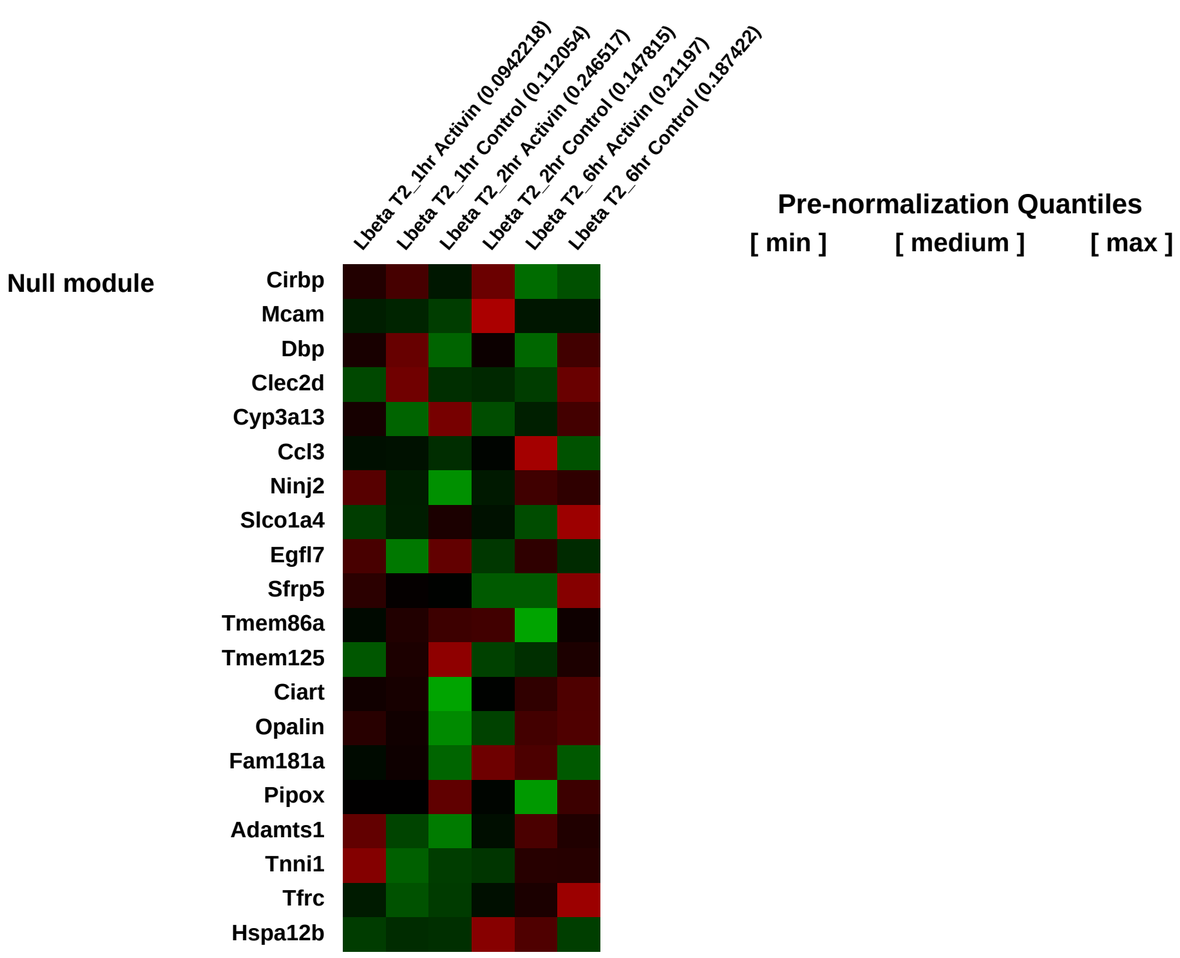

GEO Series "GSE16266" Expression Profiles

Num of samples in this series: 6

Scale of expression profile Z-scores

-3.0 -2.0 -1.0 0.0 1.0 2.0 3.0

GEO Link:	http://www.ncbi.nlm.nih.gov/geo/query/acc.cgi?acc=GSE16266
Status:	Public on Dec 21 2009
Title:	Identification of inflammatory genes suppressed by heat shock
Organism:	Mus musculus
Experiment type:	Expression profiling by array
Platform:	GPL1261
Pubmed ID:	20018623
Summary & Design:	**Summary:** To clarify inflammatory genes whose expression is suppressed at high temperatures, we performed comprehensive analysis of gene expression by using a DNA microarray. Two independent primary cultures of mouse embryo fibroblasts (MEF1 and MEF2) were treated with LPS for 4 hours, or treated with LPS for 4 hours after the pretreatment with heat shock at 42¸ C for 1 hour, and we identified 100 genes that undergo more than a 3-fold increase with LPS treatment. Remarkably, 86 genes (86%) underwent less than a 2-fold increase after combined treatments with heat shock and LPS in MEF1 and MEF2 cells. **Overall design:** Total RNAs were prepared from two primary cultures of mouse embryo fibroblasts (MEF) derived from two independent embryos at embryonic day 15.5 (ICR mice). Cells were maintained at 37¸ C (Control), treated with lipopolysaccharide (LPS, E. coli 0127:B8, Sigma, 1 ¸…g/ml) for 4 hours, or treated with LPS for 4 hours after the pretreatment of heat shock at 42¸ C for 1 hour. Gene expression was analyzed by using GeneChip Mouse Genome 430 2.0 Array (Affymetrix, Santa Clara, CA).

Background corr dist: KL-Divergence = 0.0404, L1-Distance = 0.0284, L2-Distance = 0.0010, Normal std = 0.6266

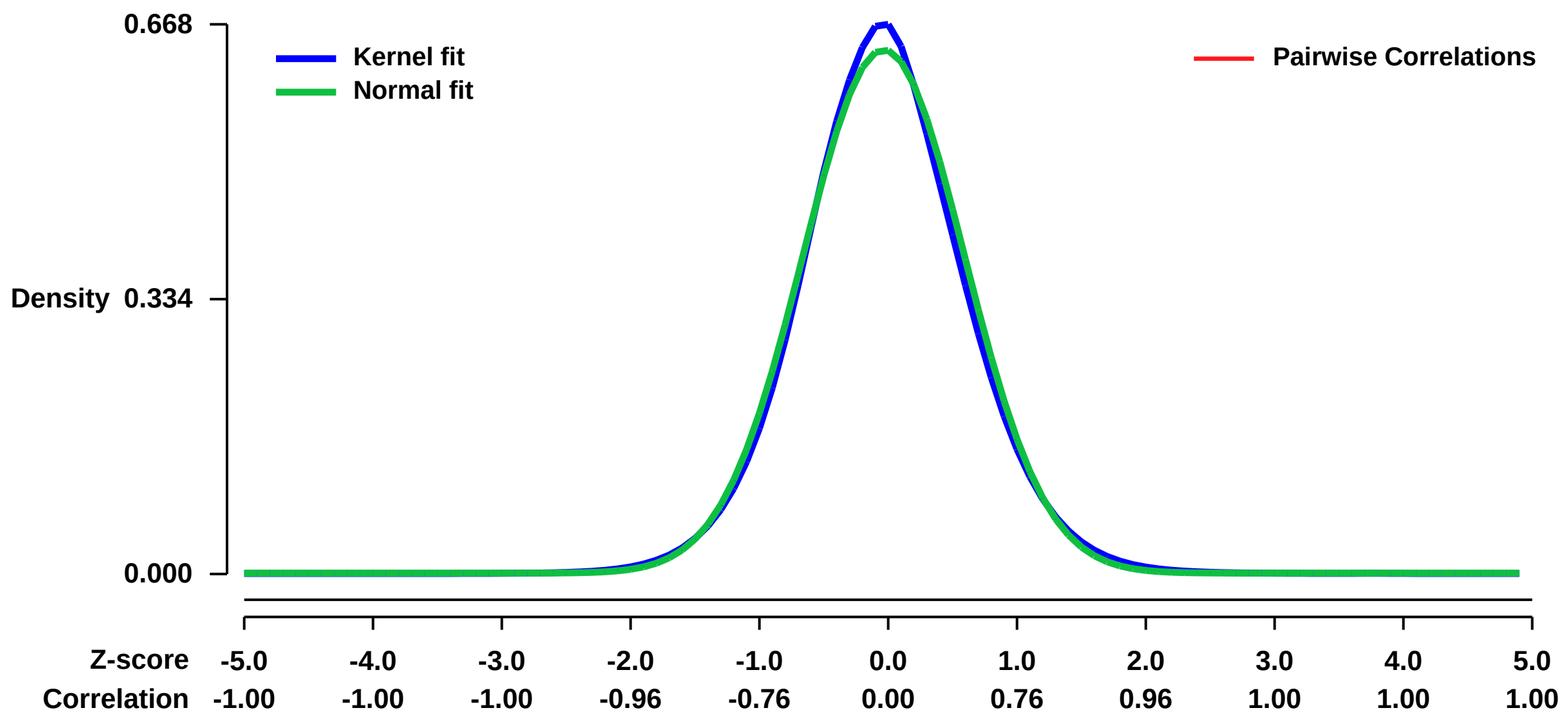

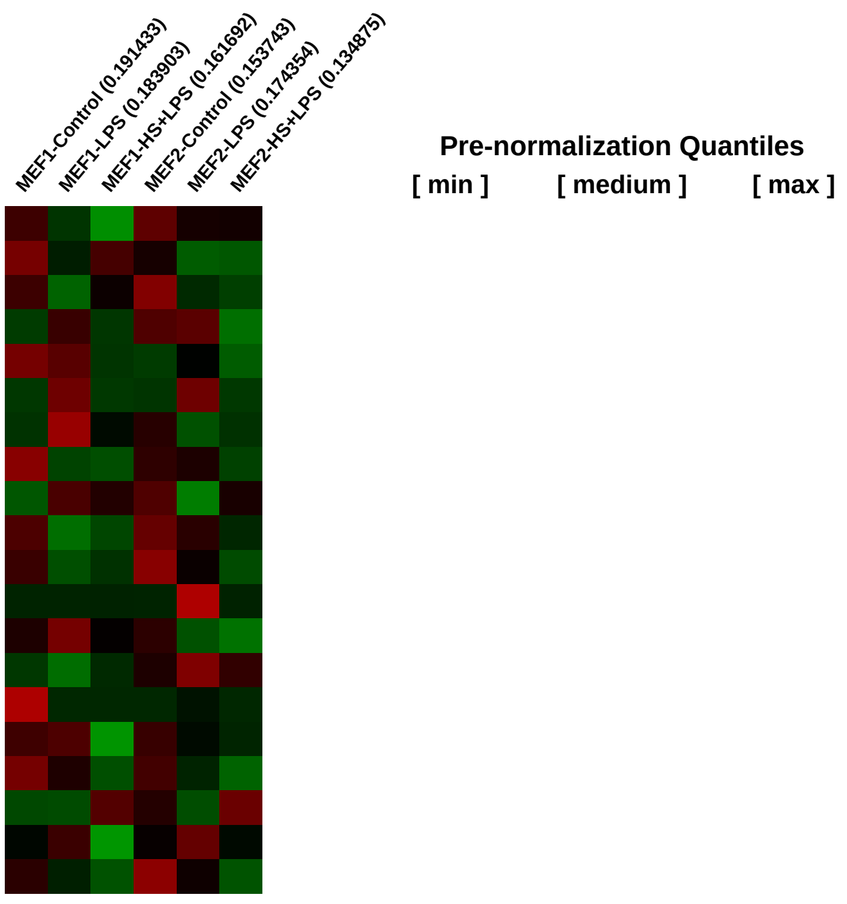

GEO Series "GSE56162" Expression Profiles

Num of samples in this series: 18

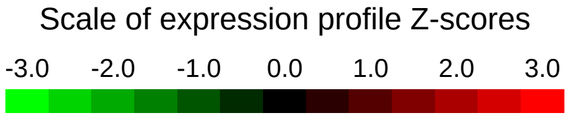

GEO Link:	http://www.ncbi.nlm.nih.gov/geo/query/acc.cgi?acc=GSE56162
Status:	Public on Jun 30 2014
Title:	Differential effects of maternal high protein diets on liver transcriptomes
Organism:	Mus musculus
Experiment type:	Expression profiling by array
Platform:	GPL1261
Pubmed ID:	
Summary & Design:	**Summary:** The objective of this study was to test if maternal high protein diet during pregnancy or lactation, imposes different transient or persistently imprinted effects on the liver transcriptome of offspring **Overall design:** Livers from 4 to 5 animals (one animal per litter) at days 21 and 150 of of each dietary group were combined to 3 pools each, and processed for microarray analysis.

Background corr dist: KL-Divergence = 0.2001, L1-Distance = 0.0369, L2-Distance = 0.0028, Normal std = 0.3341

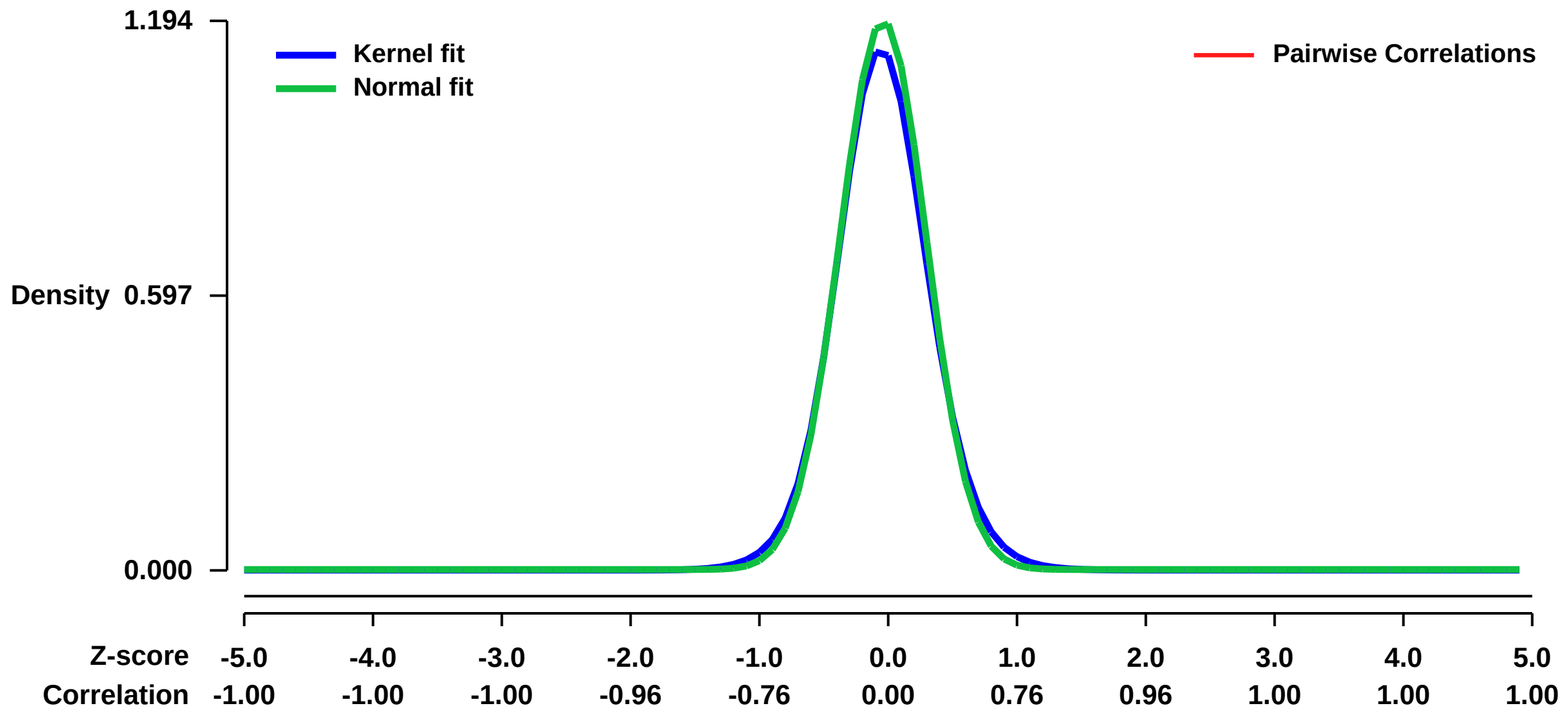

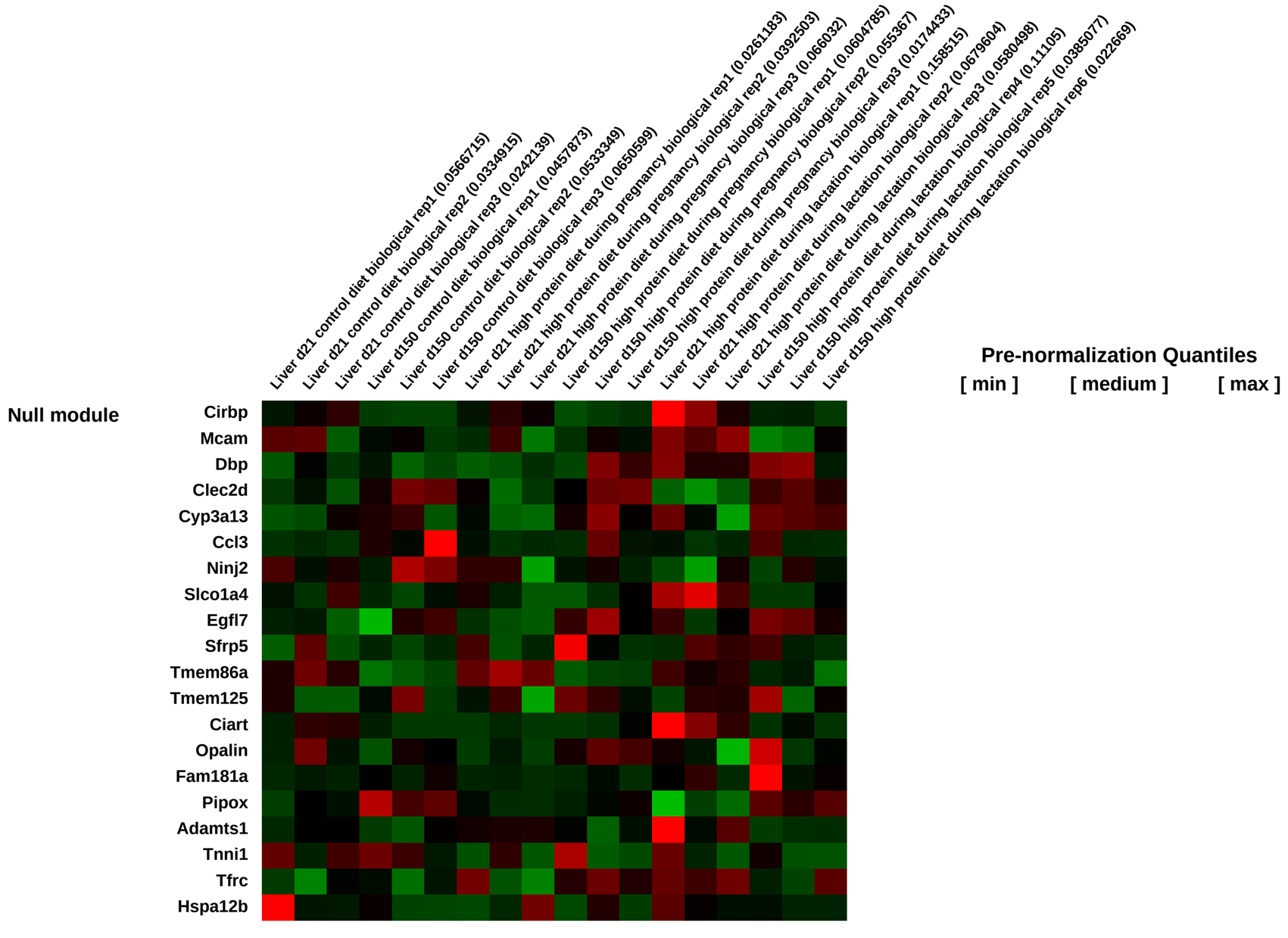

GEO Series "GSE20398" Expression Profiles

Num of samples in this series: 30

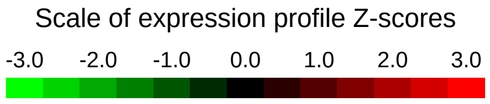

GEO Link:	http://www.ncbi.nlm.nih.gov/geo/query/acc.cgi?acc=GSE20398
Status:	Public on Apr 01 2010
Title:	Regulation of chondrogenesis in early murine limb mesenchyme by BMP signals
Organism:	Mus musculus
Experiment type:	Expression profiling by array
Platform:	GPL1261
Pubmed ID:	20501701
Summary & Design:	**Summary:** Numerous studies have established a critical role for BMP signaling in skeletal development. In the developing axial skeleton, sequential SHH and BMP signals are required for specification of a chondrogenic fate in somitic tissue. A similar paradigm is thought to operate in the limb, but the signals involved are unclear. To investigate the nature of these signals we examined BMP action in mesenchymal populations derived from the early murine limb bud (~ E10.5). These populations exhibited a graded response to BMPs, in which early limb mesenchymal (EL) cells (from the distal hind limb) displayed an anti-chondrogenic response, whereas BMPs promoted chondrogenesis in older cell populations. To better understand the molecular basis of disparate BMP action in these various populations, gene expression profiling with Affymetrix microarrays was employed to identify BMP-regulated genes. These analyses showed that BMPs induced a distinct gene expression pattern in the EL cultures versus later mesenchymal limb populations (IM and LT). **Overall design:** Mouse embryos at gestational age E10.5 were collected and various portions of the limb were micro-dissected. These led to the generation of three populations of cells, early (EL) limb mesenchymal cells from the distal half of the hind limb, an intermediate (IM) population derived from the distal 1/3 of the fore limb, and a later (LT) population from the proximal 2/3 of the fore limb. Mesenchymal cells were isolated and cultured with and without BMP4 treatment. RNA was extracted from cultures at either Day 0,1 or 2, labelled and hybridized to Affymetrix 430 2.0 microarrays. For each time point, RNA was collected from two biological replicates for each treatment condition.

Background corr dist: KL-Divergence = 0.2351, L1-Distance = 0.0379, L2-Distance = 0.0024, Normal std = 0.3143

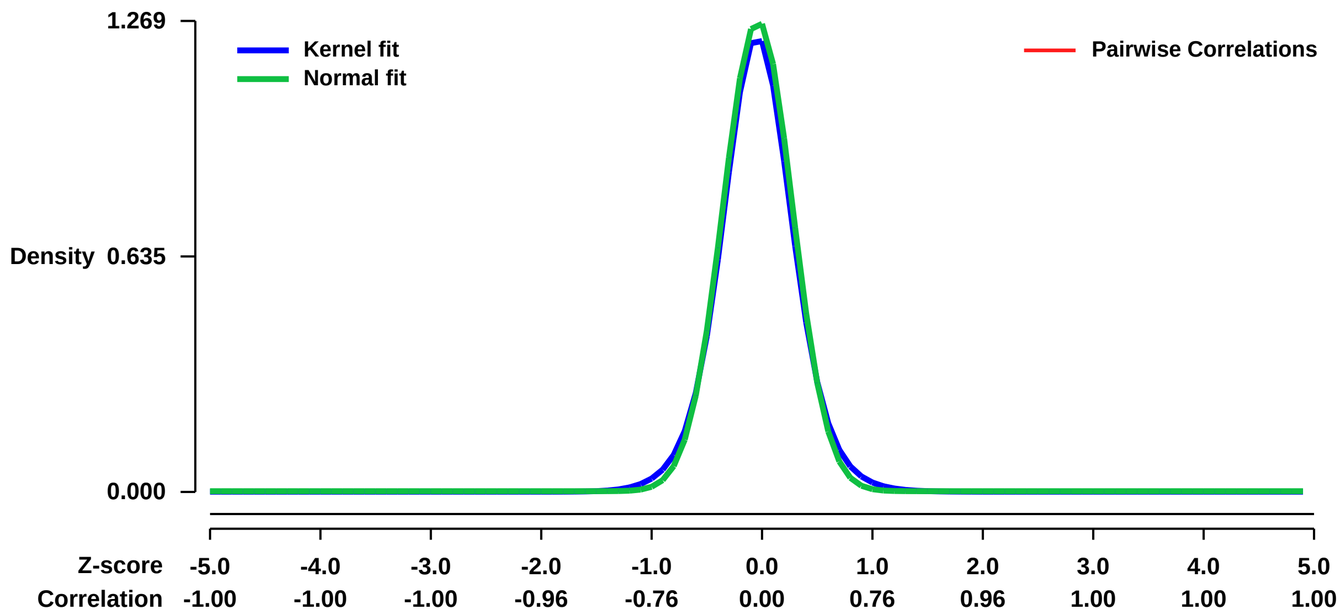

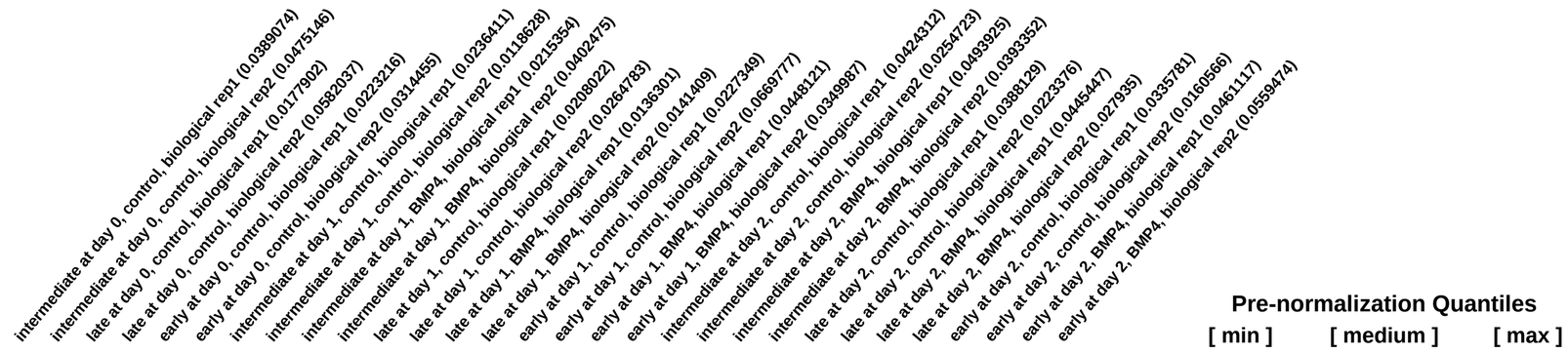

Null module

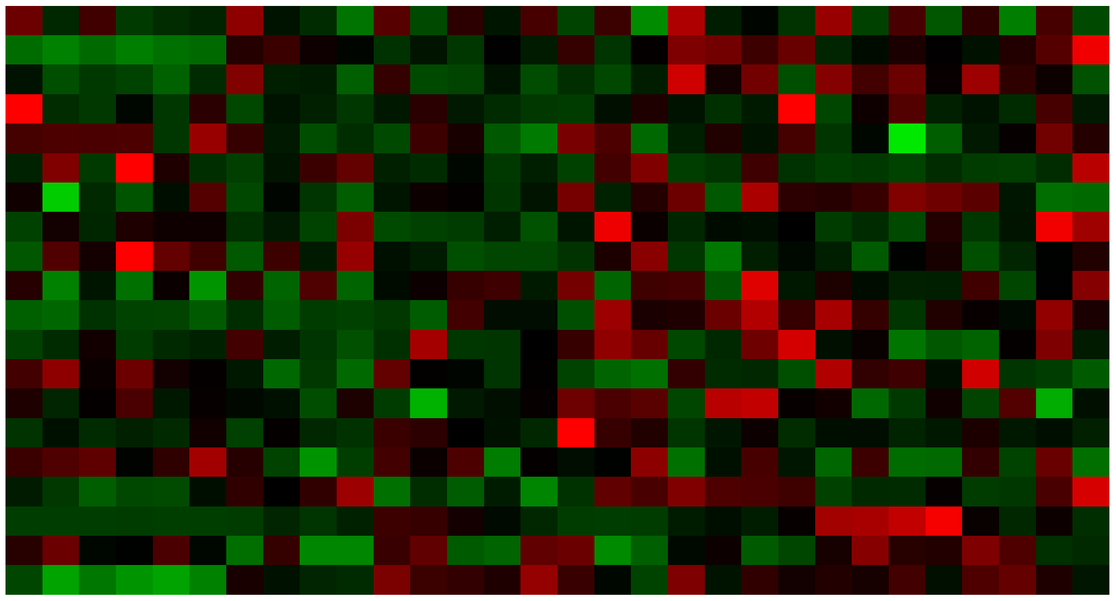

GEO Series "GSE18914" Expression Profiles

Num of samples in this series: 6

Scale of expression profile Z-scores

-3.0 -2.0 -1.0 0.0 1.0 2.0 3.0

GEO Link:	http://www.ncbi.nlm.nih.gov/geo/query/acc.cgi?acc=GSE18914
Status:	Public on Nov 07 2009
Title:	Prepubertal Human Spermatogonia and Mouse Gonocytes Share Conserved Gene Expression of Germline Stem Cell Regulatory
Organism:	Mus musculus
Experiment type:	Expression profiling by array
Platform:	GPL1261
Pubmed ID:	20018717
Summary & Design:	**Summary:** **Full title: Prepubertal Human Spermatogonia and Mouse Gonocytes Share Conserved Gene Expression of Germline Stem Cell Regulatory Molecules** **Oligonucleotide Microarray Analysis Reveals Novel Genes Expressed in Prepubertal Human Spermatogonia and Mouse Gonocytes** **Overall design:** **Oligonucleotide microarray was utilized to identify genes enriched in human and mouse selected germ cell populations and testis somatic cells.**

Background corr dist: **KL-Divergence = 0.0441, L1-Distance = 0.0650, L2-Distance = 0.0066, Normal std = 0.6614**

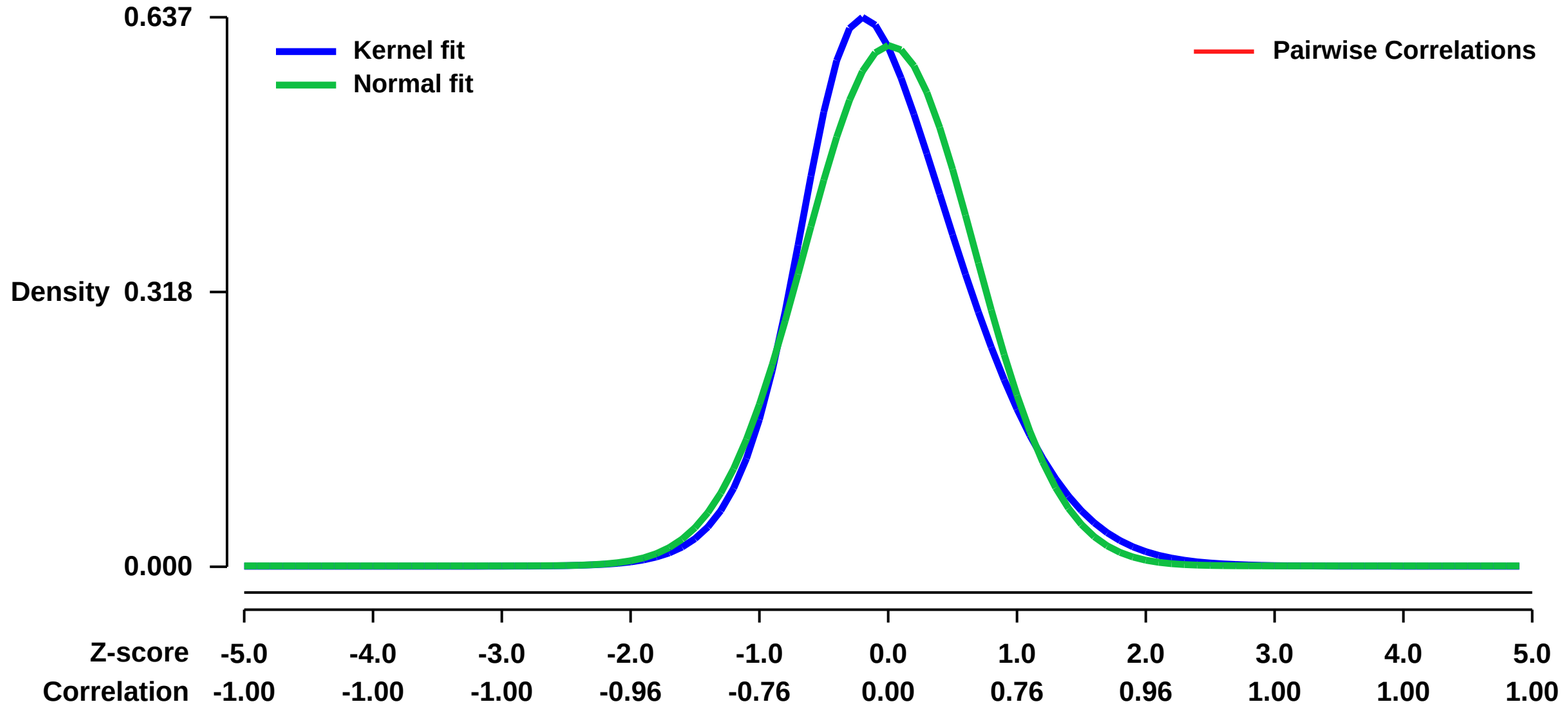

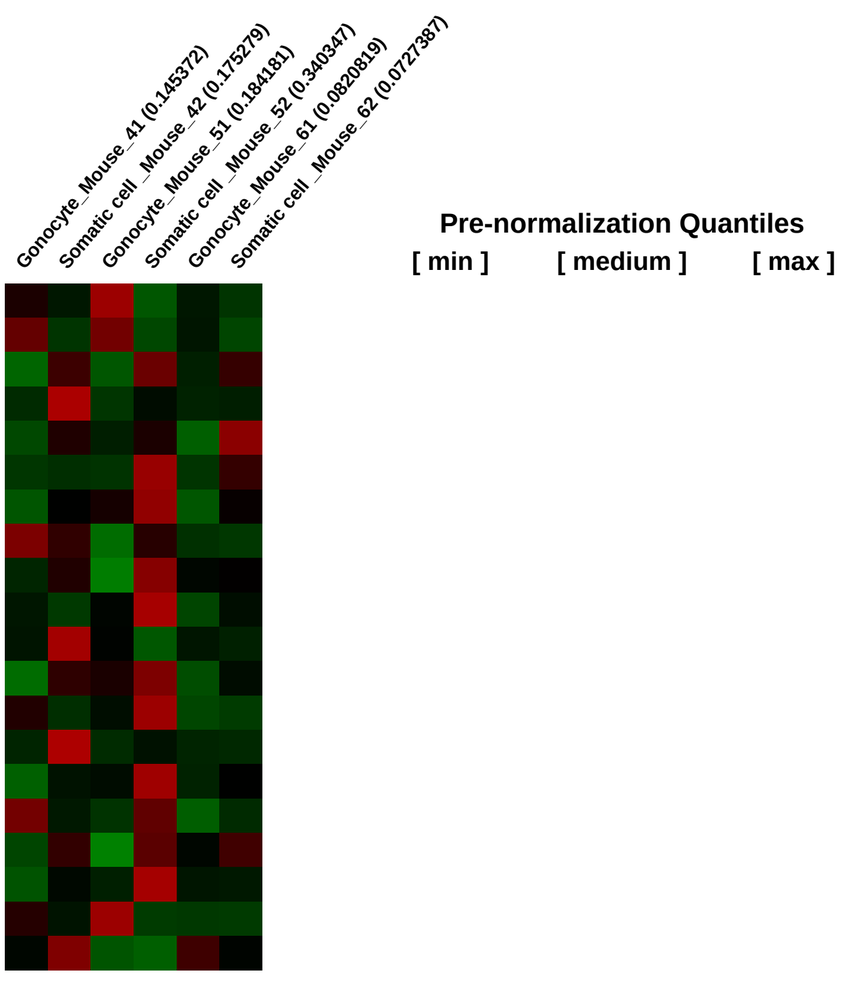

GEO Series "GSE34761" Expression Profiles

Num of samples in this series: 8

Scale of expression profile Z-scores

-3.0 -2.0 -1.0 0.0 1.0 2.0 3.0

GEO Link:	http://www.ncbi.nlm.nih.gov/geo/query/acc.cgi?acc=GSE34761
Status:	Public on Feb 01 2012
Title:	All-iPS cell mice generated from terminally differentiated B cells
Organism:	Mus musculus
Experiment type:	Expression profiling by array
Platform:	GPL1261
Pubmed ID:	22387999
Summary & Design:	**Summary:** The generation of induced pluripotent stem cells (iPSCs) often results in aberrant silencing of the imprinted Dlk1-Dio3 gene cluster, which compromises their ability to generate entirely iPSC-derived mice (â all-iPSC miceâ). Here, we show that reprogramming in the presence of ascorbic acid attenuates hypermethylation of Dlk1-Dio3 by enabling a chromatin configuration at its imprint control region that interferes with abnormal binding of the DNA methyltransferase Dnmt3a. This approach allowed us to generate adult all-iPSC mice from mature B cells, which have thus far failed to support the development of exclusively iPSC-derived postnatal mice. Our data demonstrate that factor-mediated reprogramming can endow a defined, terminally differentiated cell type with a developmental potential equivalent to that of embryonic stem cells. More generally, these findings indicate that the choice of culture conditions used for transcription factor-mediated reprogramming can strongly influence the epigenetic and biological properties of resultant iPSCs. **Overall design:** iPS cells were generated from MEFs of the Col-OKSM reprogrammable mice. In the presence of doxycycline, the reprogramming transcription factors Oct4, Sox2, Klf4, and cMyc were induced in MEFs to derivate iPS cells. Total RNA was isolated from iPS cells derivated in the presence or absence of ascorbic acid in culture medium.

Background corr dist: KL-Divergence = 0.0891, L1-Distance = 0.0231, L2-Distance = 0.0007, Normal std = 0.4564

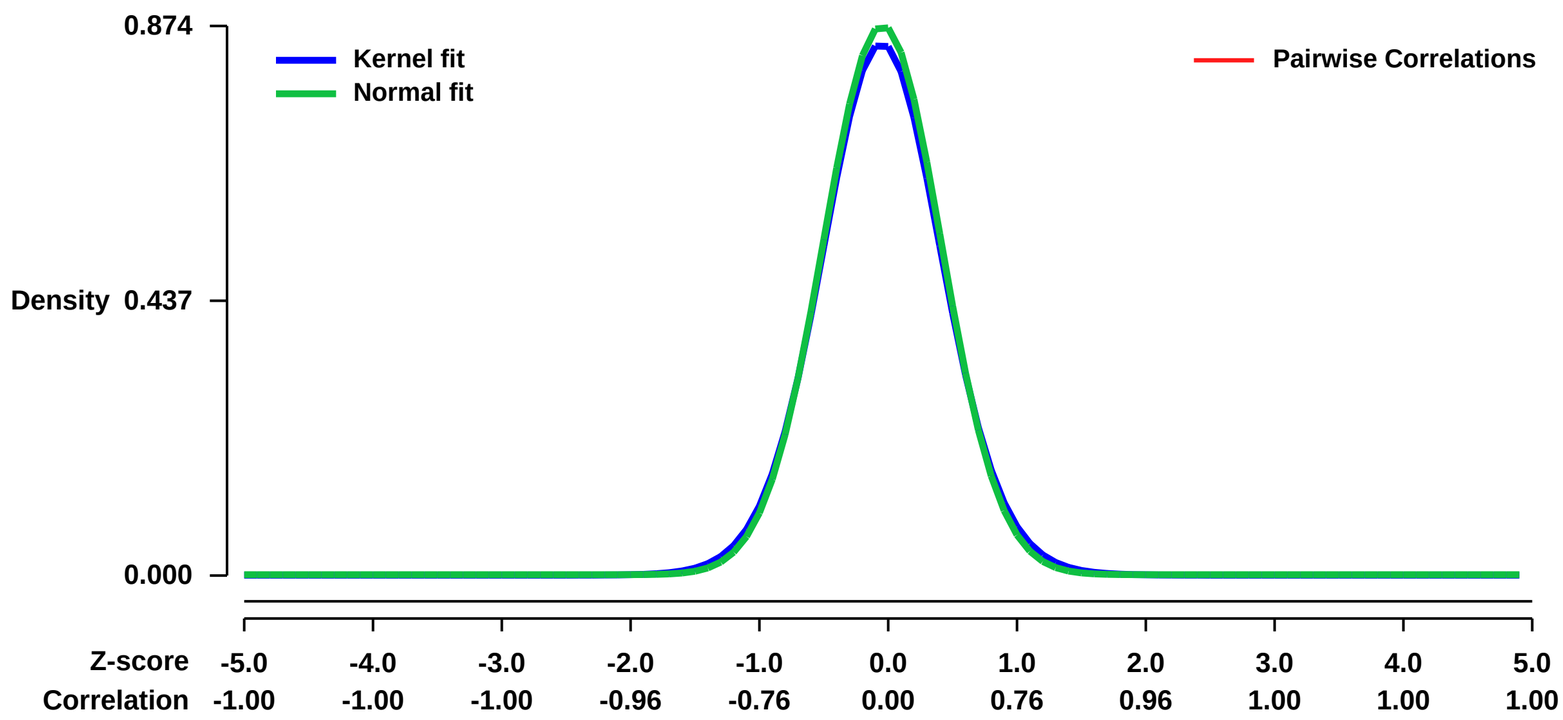

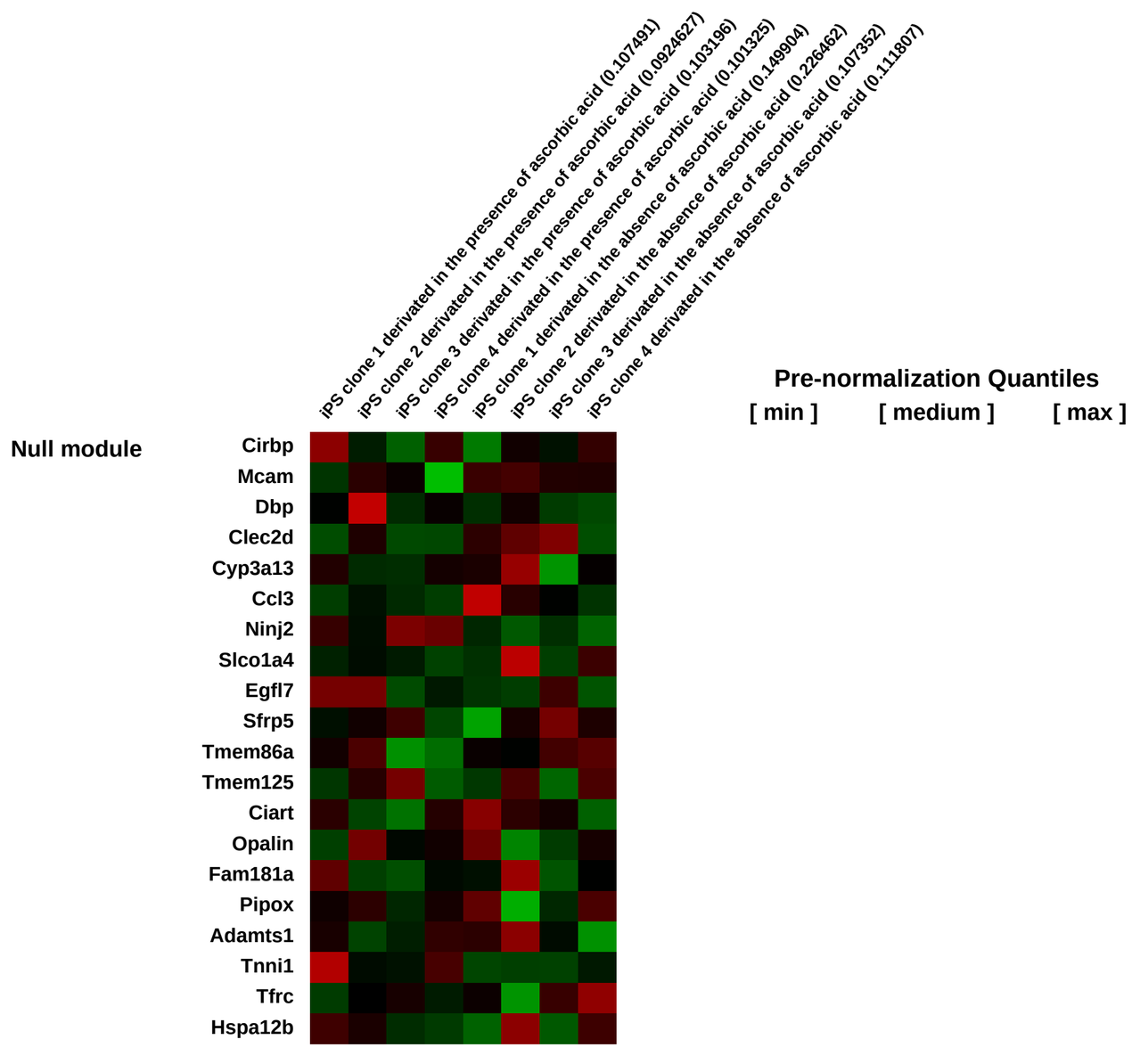

GEO Series "GSE6485" Expression Profiles

Num of samples in this series: 6

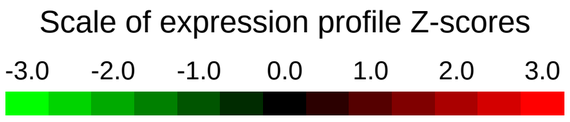

GEO Link:	http://www.ncbi.nlm.nih.gov/geo/query/acc.cgi?acc=GSE6485
Status:	Public on Dec 06 2007
Title:	Expression data from olfactory epithelium of Harlequin mutant mice compared to littermate controls
Organism:	Mus musculus
Experiment type:	Expression profiling by array
Platform:	GPL1261
Pubmed ID:	17868149
Summary & Design:	**Summary:** Microarray analysis of gene expression in the olfactory epithelium of Harlequin mouse as a model of oxidative-stress induced neurodegeneration of olfactory sensory neurons **Keywords: comparison of gene expression level in unperturbed tissue of mutant vs. control mouse** **Overall design:** Olfactory epithelium from Harlequin mutant mice and littermate control mice was microdissected for RNA extraction and hybridization on Affymetrix microarrays. We compared levels of gene expression in 6-month old mice to begin to identify mechanisms of oxidative-stress induced neurodegeneration and to correlate the cellular changes that we observed in the olfactory epithelium by using histology and immunohistochemistry with gene expression changes.

Background corr dist: KL-Divergence = 0.0482, L1-Distance = 0.0186, L2-Distance = 0.0004, Normal std = 0.5794

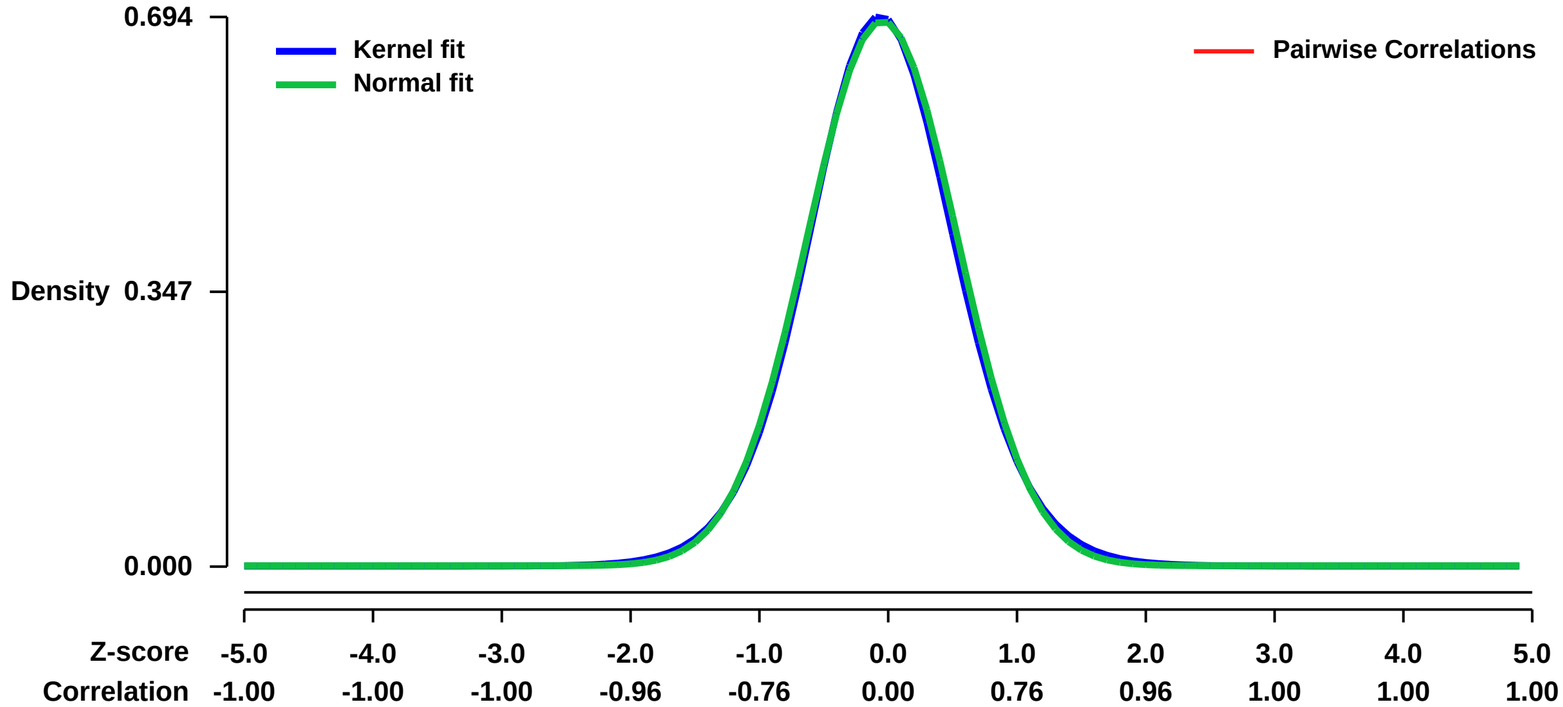

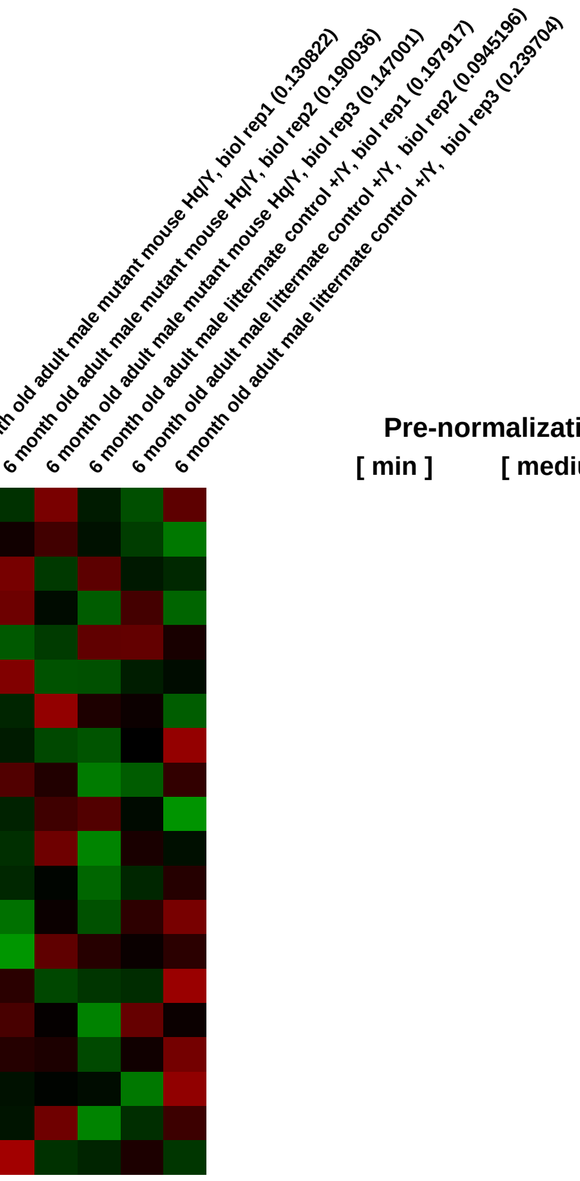

GEO Series "GSE10776" Expression Profiles

Num of samples in this series: 15

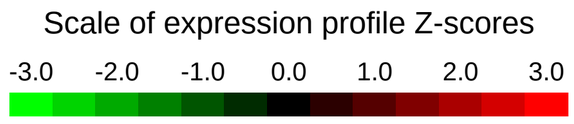

GEO Link:	**http://www.ncbi.nlm.nih.gov/geo/query/acc.cgi?acc=GSE10776**
Status:	**Public on Dec 31 2008**
Title:	**Expression profiles of Embryonic stem cells derived from normal fertilization and parthenogenesis**
Organism:	**Mus musculus**
Experiment type:	**Expression profiling by array**
Platform:	**GPL1261**
Pubmed ID:	
Summary & Design:	**Summary:** **To identify the imprinting loci, we designed microarray analysis on the parthenogenetic embryonic stem cells and normal embryos. We could predict 217 imprinting domains associated with embryo development and maternal imprinting.** **Keywords: Cell type comparison** **Overall design:** **Five embryonic stem (ES) cell lines were derived from two F1 hybrid strains that were produced by mating female C57BL6 mice with male DBA2 or CBA/Ca mice. Two-week-old prepubertal female was used for follicle retrieval. All procedures for animal management, breeding, and surgery followed the standard protocols of Seoul National University, Korea. The Institutional Animal Care and Use Committee Review Board at Seoul National University approved our research proposal in April 2005 (approval number: SNU0050331-02). Three parthonogenetic ES embryo cell lines were established from parthenogenetic activation on naturally ovulated oocytes (OpB6D2-SNU-1) and in vitro-growth oocytes (FpB6CBA-SNU8 and FpB6D2-SNU2). Two normal ES embryo cell lines were derived from mating naturally ovulated female mice in estrus with male mice (NmB6D2-SNU-1) and purchased from ATCC. Detailed procedures, including establishment of ES cell lines can be found elsewhere (FpB6CBA-SNU8, FpB6D2-SNU2 and OpB6D2-SNU-1 for and NmB6D2-SNU-1 and OP1 for manuscript in preparation).**

Background corr dist: KL-Divergence = 0.0921, L1-Distance = 0.0287, L2-Distance = 0.0011, Normal std = 0.4649

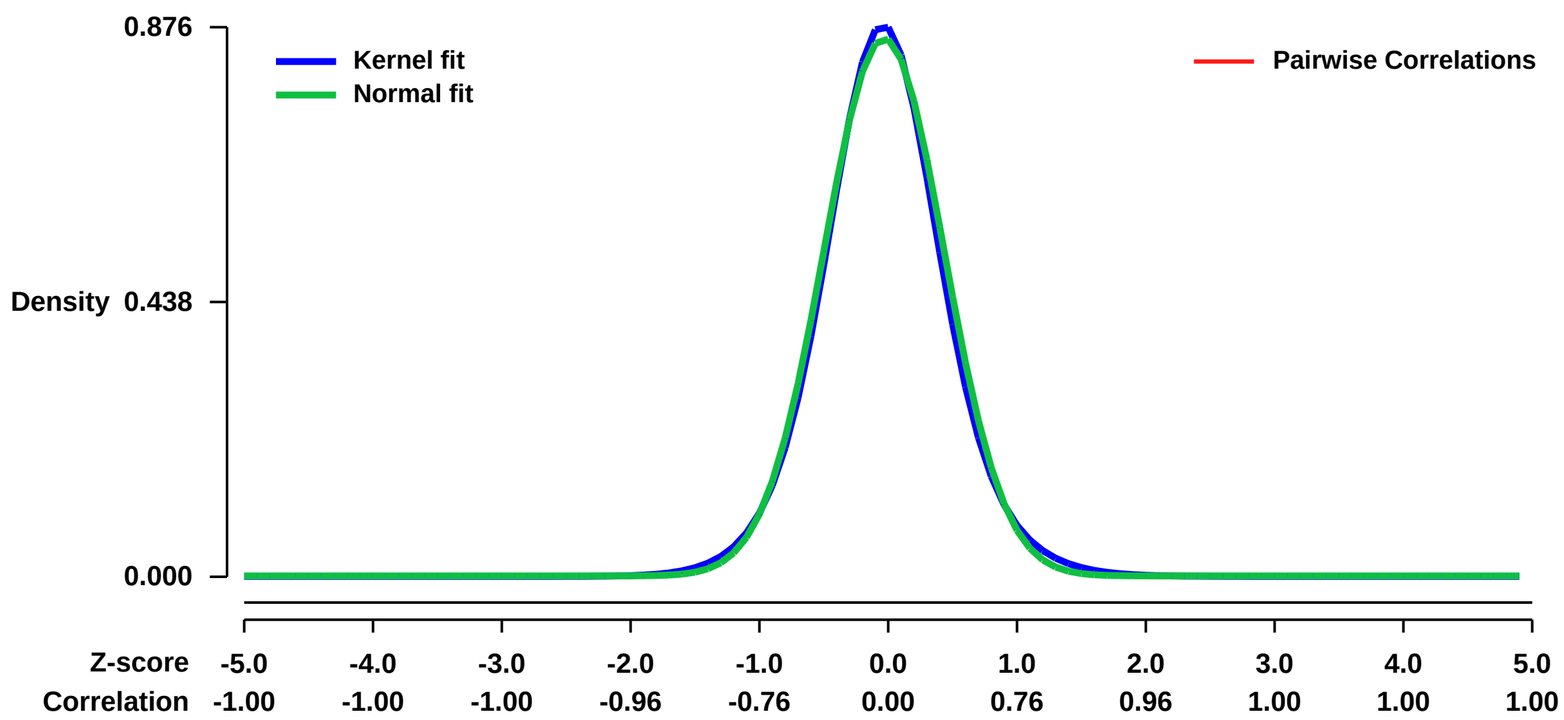

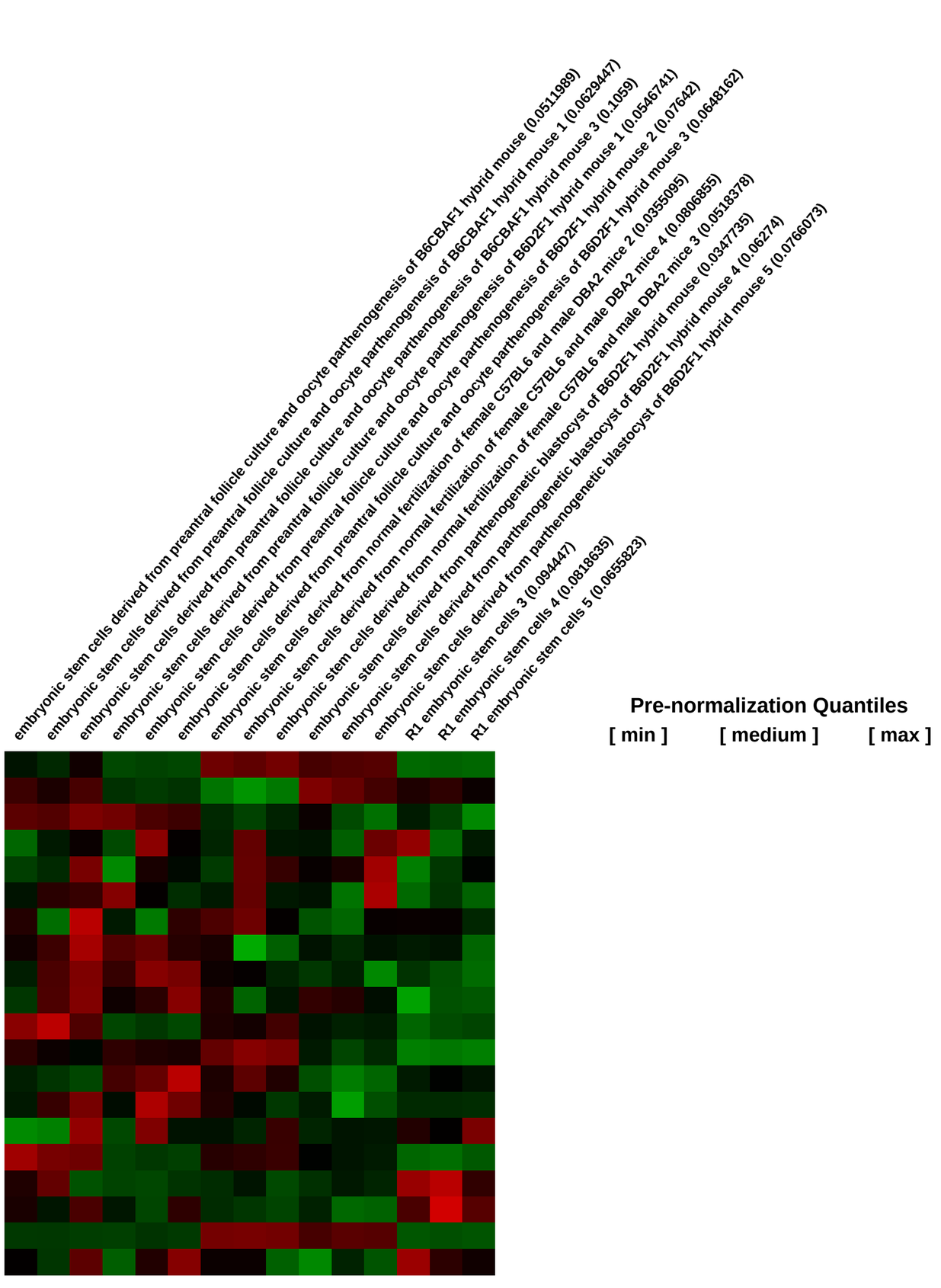

GEO Series "GSE11777" Expression Profiles

Num of samples in this series: 6

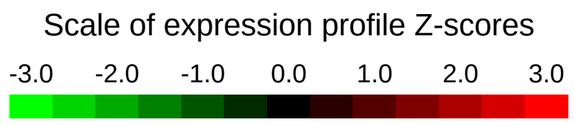

GEO Link:	http://www.ncbi.nlm.nih.gov/geo/query/acc.cgi?acc=GSE11777
Status:	Public on Jun 13 2008
Title:	Microarray data of mouse fetal liver
Organism:	Mus musculus
Experiment type:	Expression profiling by array
Platform:	GPL1261
Pubmed ID:	18552213
Summary & Design:	**Summary:** Iron is essential for all cells but is toxic in excess, so iron absorption and distribution are tightly regulated. Serum iron is bound to transferrin and primarily enters erythroid cells via receptor-mediated endocytosis of the transferrin receptor (Tfr1). Tfr1 is essential for developing erythrocytes and reduced Tfr1 expression is associated with anemia. The transcription factors STAT5A/B are activated by many cytokines, including erythropoietin. Stat5a/b-/- mice are severely anemic and die perinatally, but no link has been made to iron homeostasis. To study the function of STAT5A/B in vivo, we deleted the floxed Stat5a/b locus in hematopoietic cells with a Tie2-Cre transgene. These mice exhibited microcytic, hypochromic anemia, as did lethally irradiated mice transplanted with Stat5a/b-/- fetal liver cells. Flow cytometry and RNA analyses of erythroid cells from mutant mice revealed a 50% reduction in Tfr1 mRNA and protein. We detected STAT5A/B binding sites in the first intron of the Tfr1 gene and found that expression of constitutively active STAT5A in an erythroid cell line increased Tfr1 levels. Chromatin immunoprecipitation experiments confirmed the binding of STAT5A/B to these sites. We conclude that STAT5A/B is an important regulator of erythroid progenitor iron uptake via its control of Tfr1 transcription. **Keywords:** genetic modification **Overall design:** Isolated Ter119-positive fetal liver cells from three to five E14.5 embryos of the same genotype were combined, and total RNA was extracted using TRIzol reagent (Life Technologies) with two additional ethanol precipitations. RNA quality was verified using an Agilent Bioanalyzer (Agilent Technologies). Microarray analyses were performed using Affymetrix Mouse Genome 430 2.0 array GeneChips (Affymetrix). Up- and down-regulated genes were selected based on P values of <0.05 and fold changes of >1.5 or -1.5 as assessed by ANOVA using Partek Pro software (Partek). To determine specific pathways, gene pathway analysis was obtained using the statistically significant gene list (P<0.05) represented on the chip.

Background corr dist: KL-Divergence = 0.0431, L1-Distance = 0.0190, L2-Distance = 0.0004, Normal std = 0.5998

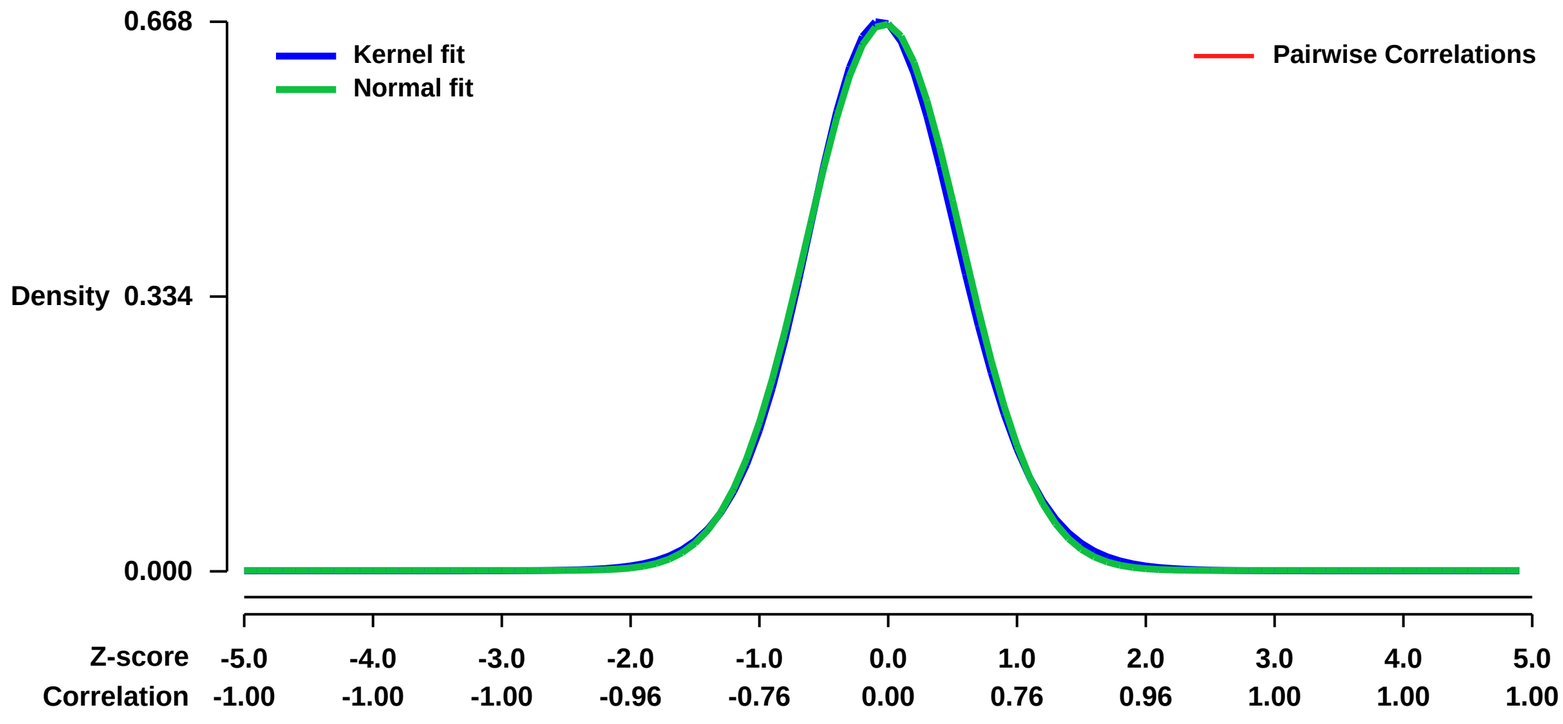

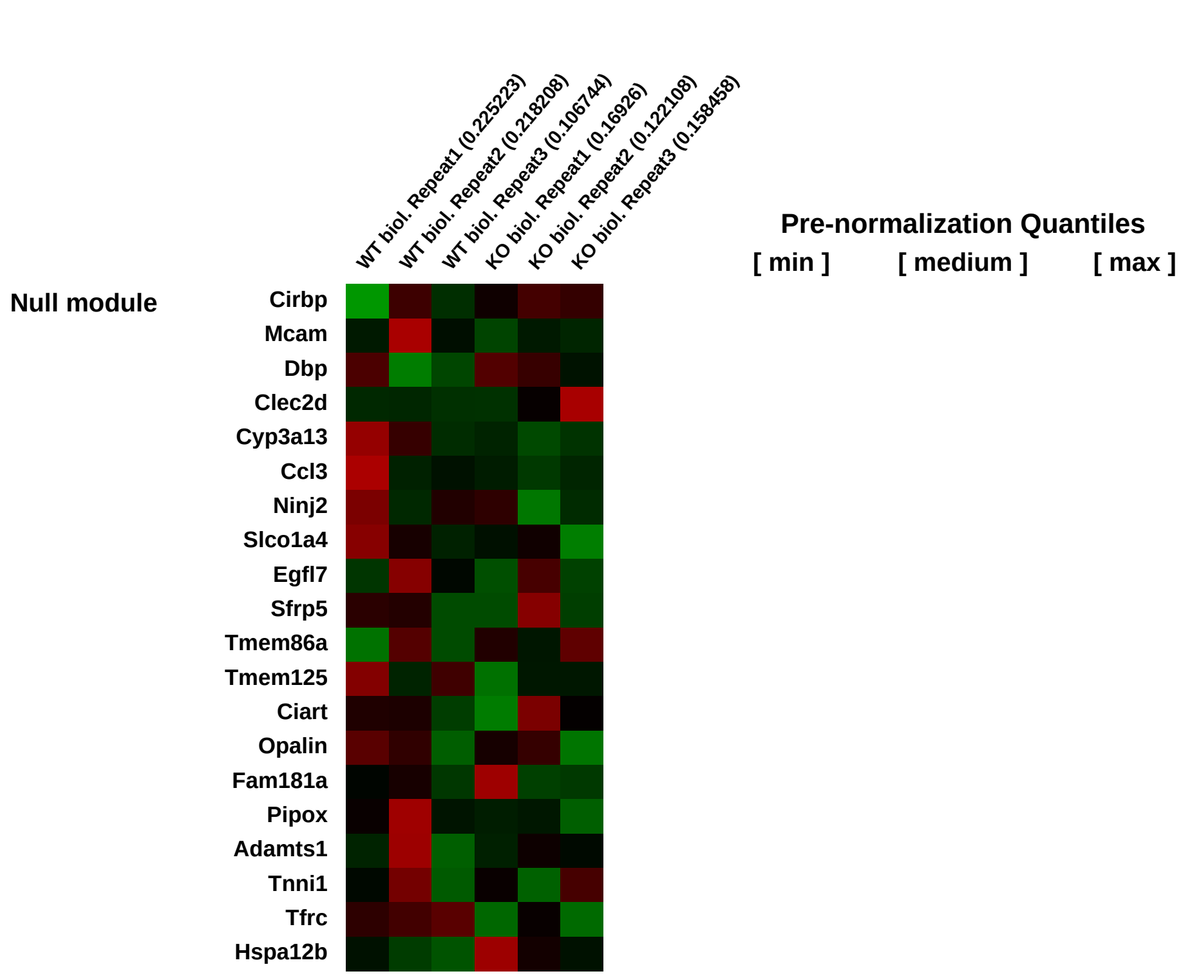

GEO Series "GSE47643" Expression Profiles

Num of samples in this series: 12

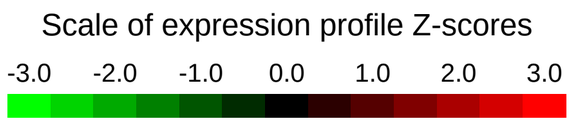

GEO Link:	http://www.ncbi.nlm.nih.gov/geo/query/acc.cgi?acc=GSE47643
Status:	Public on Jun 05 2013
Title:	Gene expression of in vitro cultivated preB cells before and after 8, 16 and 24 hours induction of miR-221
Organism:	Mus musculus
Experiment type:	Expression profiling by array
Platform:	GPL1261
Pubmed ID:	23716169
Summary & Design:	**Summary:** PreB cells were analyzed for differences in gene expression before and after the overexpression of miR-221. In order to dissect possible targets for the miR-221, gene expression profiles of preB cells un-induced or induced for the miR-221 expression after 8, 16 and 24 hours were compared. All induction time-points, e.g. after 8, 16 and 24 hours were compared to un-induced preB cells and to each other group. **Overall design:** After total RNA extraction, reverse transcription, cDNA extraction, the biotinylated cRNA was transcribed, fragmented, and 15 ´µg cRNA hybridized in triplicates for each of the four groups to the 12 GeneChip arrays: Group1, un-induced preB cells, Group2, preB cells induced for miR-221 expression after 8h, Group3, preB cells induced for miR-221 expression after 16h, Group4, preB cells induced for miR-221 expression after 24h.

Background corr dist: KL-Divergence = 0.1416, L1-Distance = 0.0249, L2-Distance = 0.0012, Normal std = 0.3853

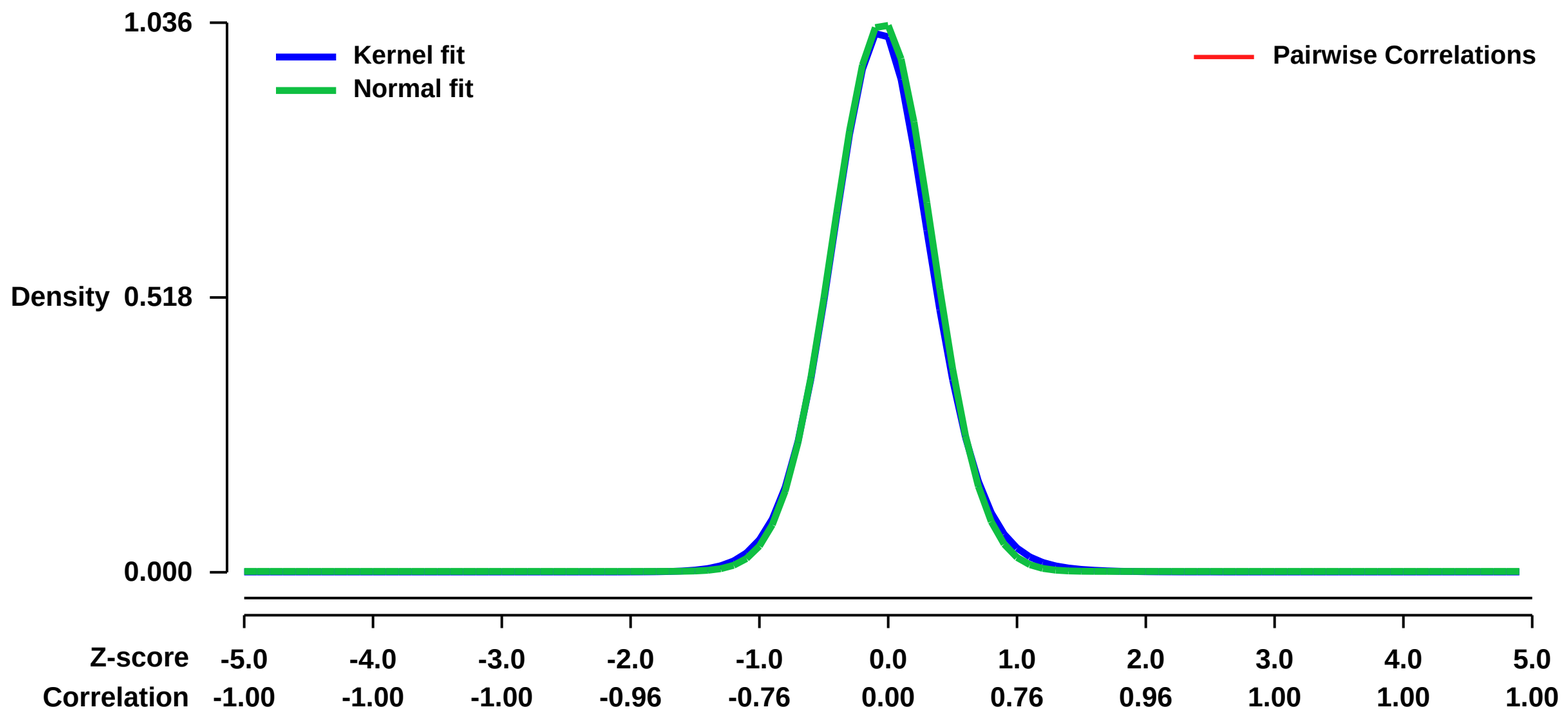

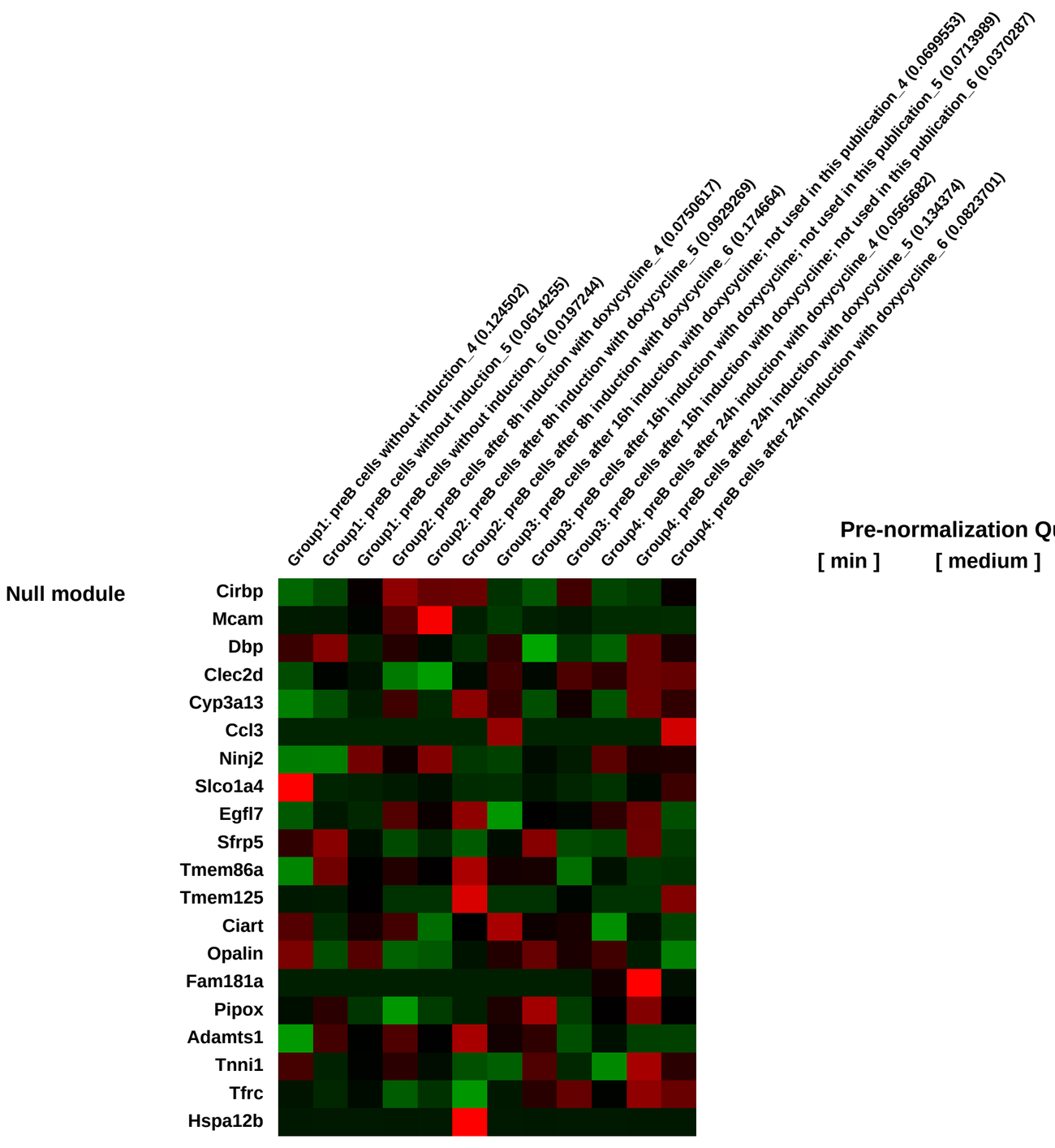

GEO Series "GSE56755" Expression Profiles

Num of samples in this series: 13

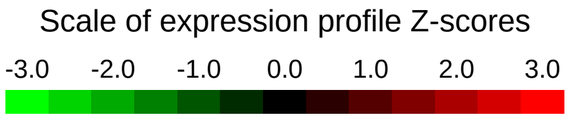

GEO Link:	**http://www.ncbi.nlm.nih.gov/geo/query/acc.cgi?acc=GSE56755**
Status:	**Public on Apr 18 2014**
Title:	**The Cellular and Molecular Origin of Tumor-associated Macrophages**
Organism:	**Mus musculus**
Experiment type:	**Expression profiling by array**
Platform:	**GPL1261**
Pubmed ID:	**24812208**
Summary & Design:	**Summary:** **Long recognized as an evolutionarily ancient cell type involved in tissue homeostasis and immune defense against pathogens, macrophages are being rediscovered as regulators of several diseases including cancer. Here we show that in mice, mammary tumor growth induces the accumulation of tumor-associated macrophages (TAMs) that are phenotypically and functionally distinct from mammary tissue macrophages (MTMs). TAMs express the adhesion molecule Vcam1 and proliferate upon their differentiation from inflammatory monocytes, but do not exhibit an â alternatively activatedâ phenotype. TAM differentiation depends on the transcriptional regulator of Notch signaling, RBPJ; and TAM, but not MTM, depletion restores tumor-infiltrating cytotoxic T cell responses and suppresses tumor growth. These findings reveal the ontogeny of TAMs and a discrete tumor-elicited inflammatory response, which may provide new opportunities for cancer immunotherapy.** **Overall design:** **In the MMTV-PyMT spontaneous mammary tumor model, we found the key Notch transcriptional regulator, RBPJ, to be required for TAM terminal differentiation from inflammatory monocytes. The bulk myeloid cell population that remains in CD11cCreRbpj fl/fl mice (the cells in ""Rbpj KO"" samples), represents monocytes that have begun their differentiation into macrophages, but are unable to terminally differentiate due to the lack of Rbpj.**

Background corr dist: KL-Divergence = 0.0672, L1-Distance = 0.0289, L2-Distance = 0.0015, Normal std = 0.5079

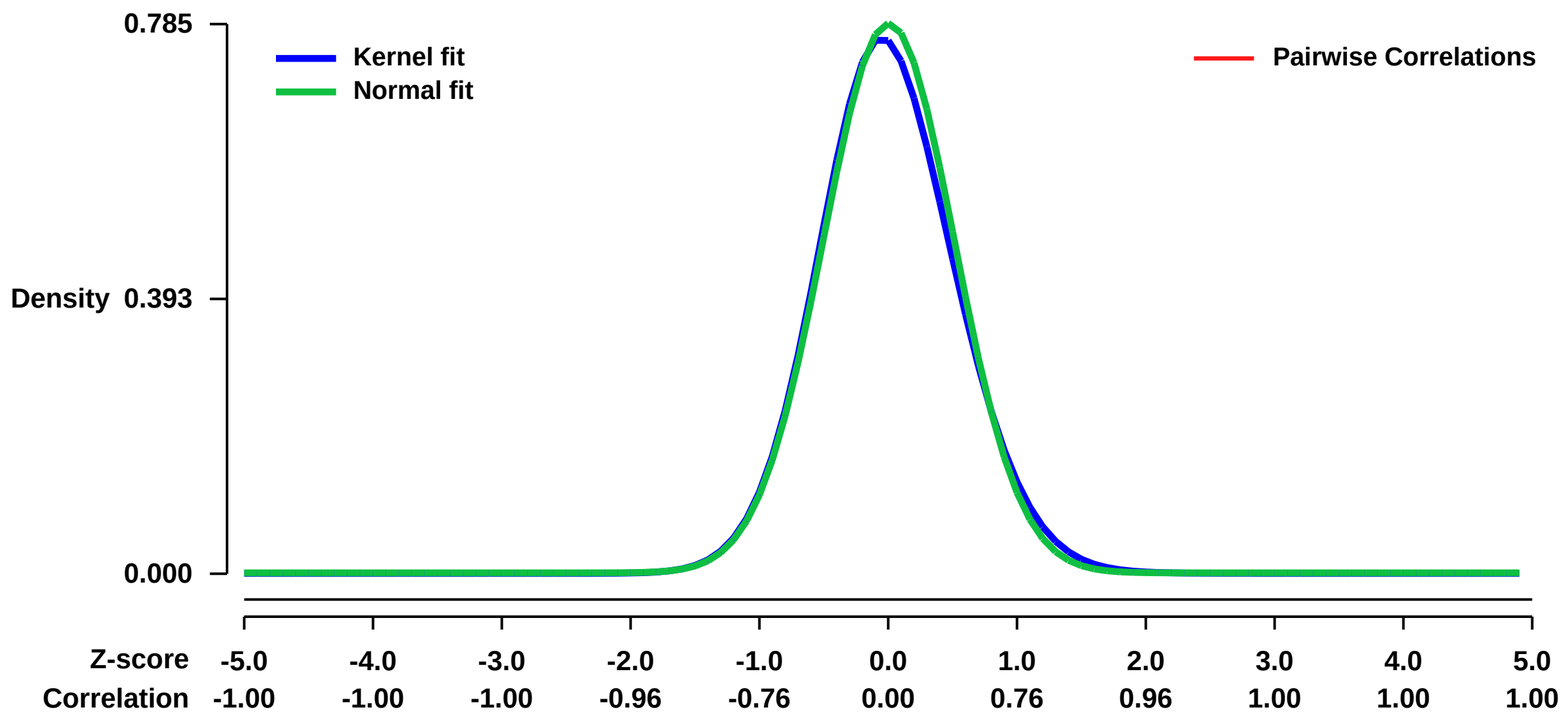

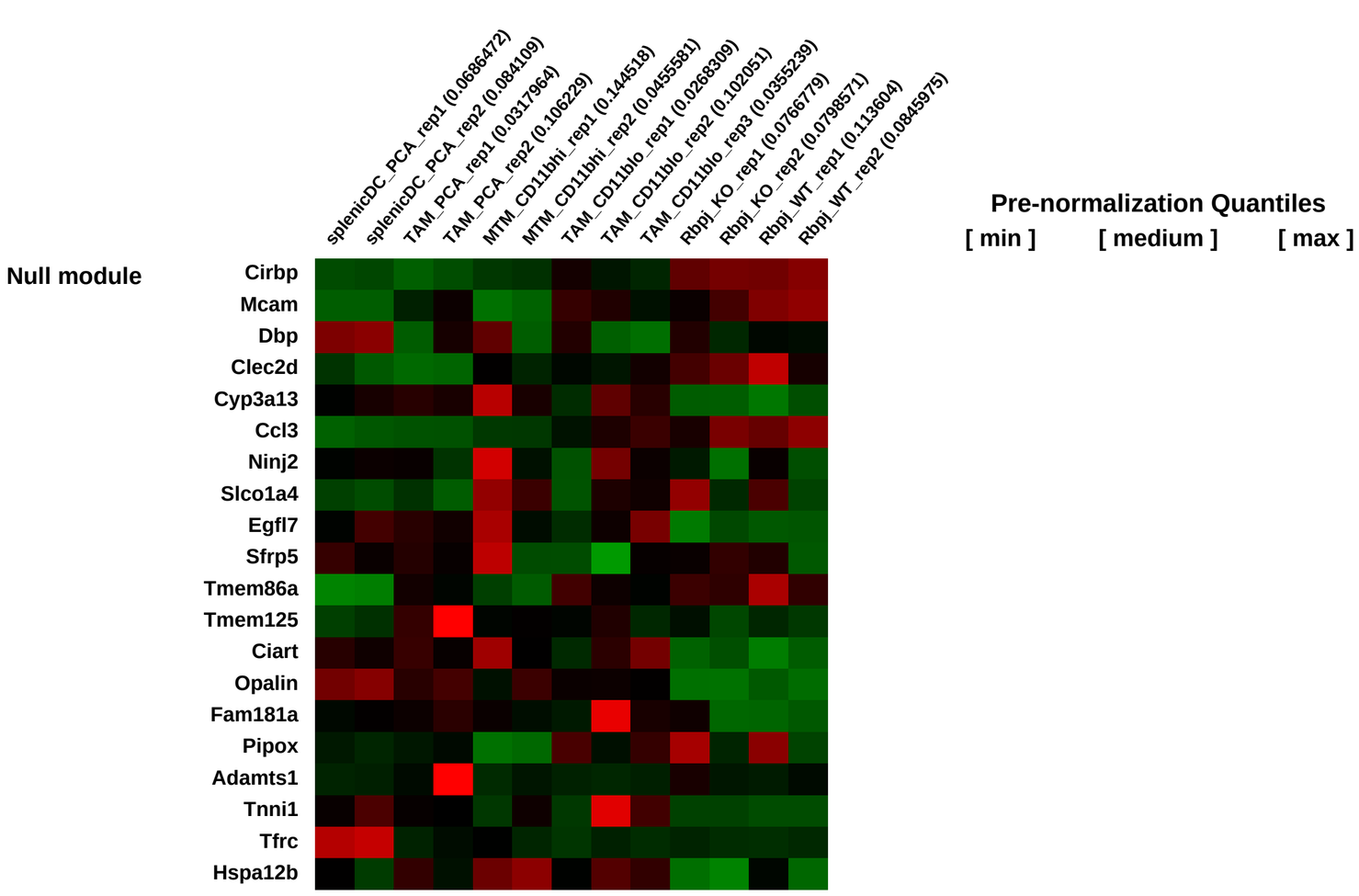

GEO Series "GSE6813" Expression Profiles

Num of samples in this series: 12

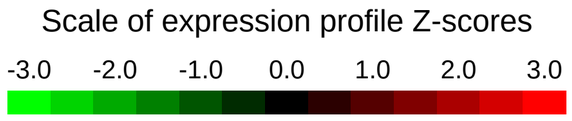

GEO Link:	**http://www.ncbi.nlm.nih.gov/geo/query/acc.cgi?acc=GSE6813**
Status:	**Public on Dec 19 2008**
Title:	**Gene expression profiles of CD4+CD25+ Tregs from NOD and B6.H2g7 mice**
Organism:	**Mus musculus**
Experiment type:	**Expression profiling by array**
Platform:	**GPL1261**
Pubmed ID:	**19073938**
Summary & Design:	**Summary:** **The NOD (nonobese diabetic) mouse strain develops a characteristic autoimmune syndrome that closely resembles human type I diabetes. It has been suggested that NOD mice exhibit both numerical deficiency in CD4+CD25+ regulatory T cells (Treg) and reduced suppressive activity. We compared sorted CD4+CD25+ Tregs from the spleens of 6-7 week-old female NOD and nondiabetic B6.H2g7 mice. Tregs were 93´–2% and 95´–1% Foxp3+ in NOD and B6.H2g7 cells, respectively, on post-sort reanalysis. ""Conventional"" CD4+CD25- T cells (Tconv) are included as reference populations. Surprisingly, Treg ""signature"" is similar between the two strains, with only a few probesets that subtly deviate.** **Keywords: Cell population comparison from two mouse strains.** **Overall design:** **For each strain (NOD and B6.g7), we analyzed two populations: CD4+CD25+ Treg and CD4+CD25- Tconv cells, for a total of four distinct populations. RNA from three mice were pooled for each replicate; there are three independent replicates for each population. After RMA normalization, intensity values were averaged across the three replicates and analyzed. We calculated the ratio of Treg/Tconv intensity values for each strain and compared the results.**

Background corr dist: KL-Divergence = 0.0779, L1-Distance = 0.0343, L2-Distance = 0.0022, Normal std = 0.4767

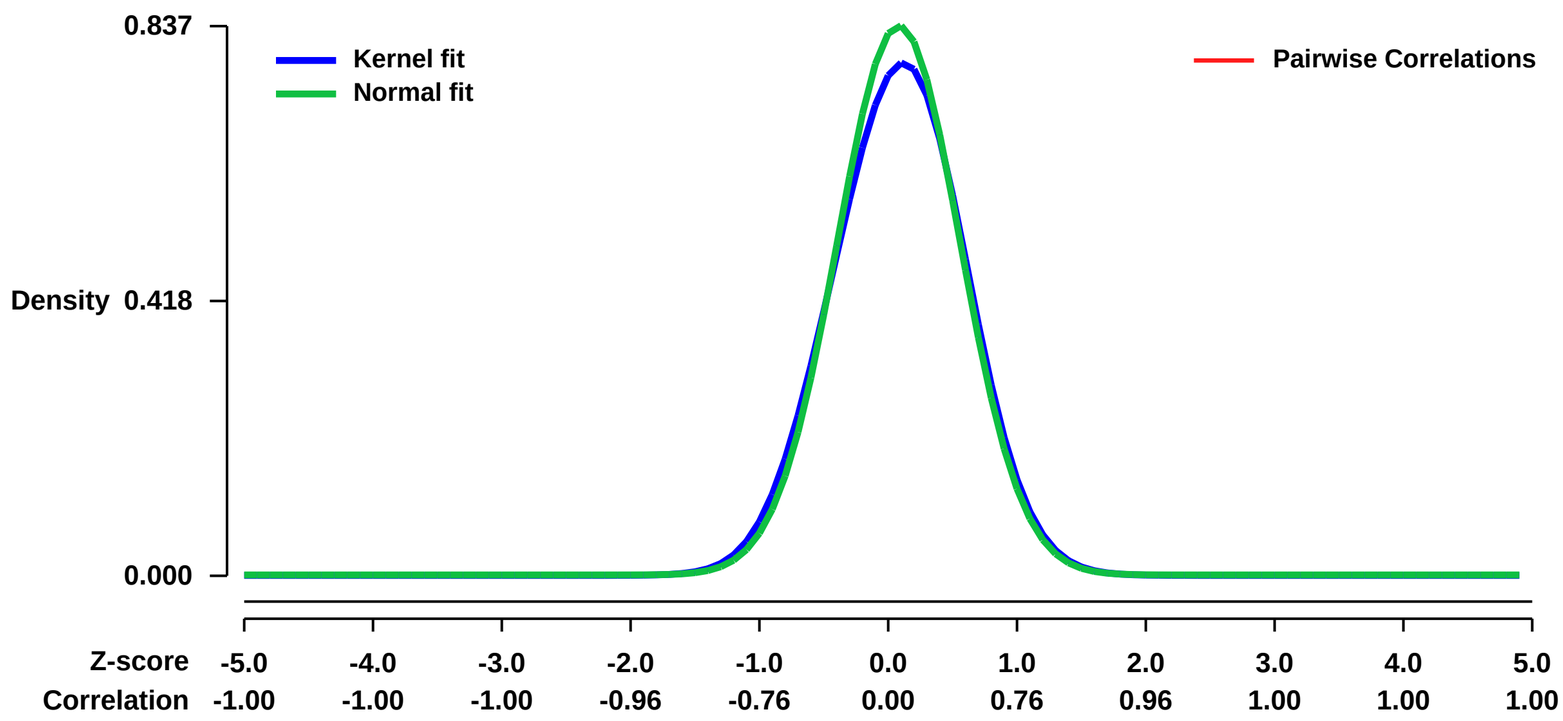

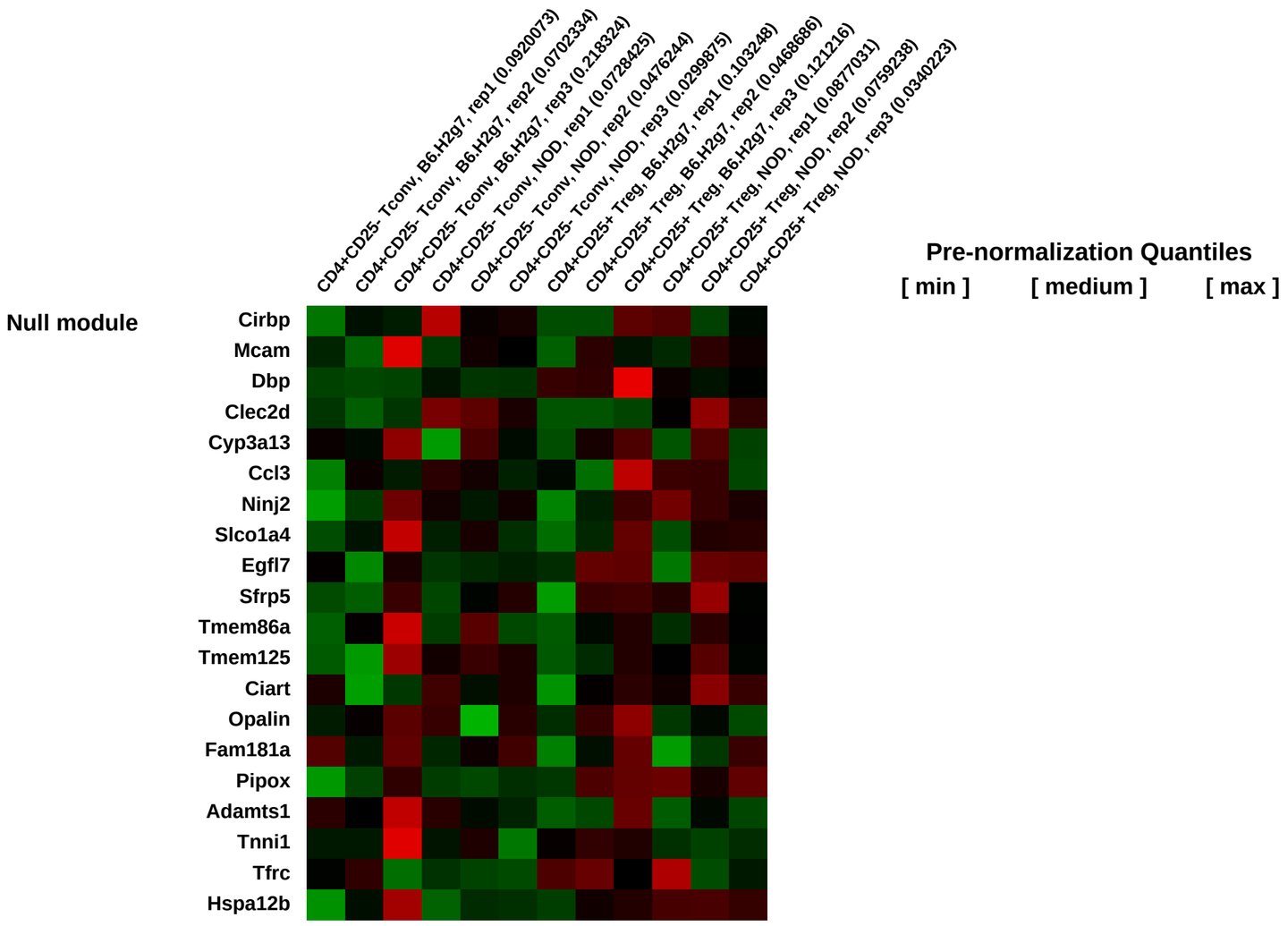

GEO Series "GSE40260" Expression Profiles

Num of samples in this series: 6

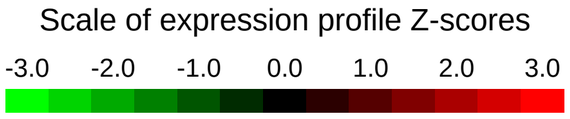

GEO Link:	http://www.ncbi.nlm.nih.gov/geo/query/acc.cgi?acc=GSE40260
Status:	Public on Aug 17 2013
Title:	Microarray using CD31+/CD41-/CD45- cells from E9.5 mouse heart tube, caudal half and yolk sac
Organism:	Mus musculus
Experiment type:	Expression profiling by array
Platform:	GPL1261
Pubmed ID:	23463007
Summary & Design:	**Summary:** Hematopoietic cells arise from spatiotemporally restricted domains in the developing embryo. Although studies of non-mammalian animal and in vitro embryonic stem cell models suggest a close relationship among cardiac, endocardial, and hematopoietic lineages, it remains unknown whether the mammalian heart tube serves as a hemogenic organ akin to the dorsal aorta. Here, we examined the hemogenic activity of the developing endocardium. Mouse heart explants generated myeloid and erythroid colonies in the absence of circulation. Hemogenic activity arose from a subset of endocardial cells in the outflow cushion and atria earlier than in the aorta-gonad-mesonephros region, and was transient and definitive in nature. Interestingly, key cardiac transcription factors, Nkx2-5 and Isl1, were expressed in and required for the hemogenic activity of the endocardium. Together, these data suggest that a subset of endocardial and yolk sac endothelial cells expressing cardiac markers serve as a de novo source for transient definitive hematopoietic progenitors. **Overall design:** Two independent biological duplicates of freshly isolated mouse tissues (caudal half, heart tube, yolk sac) were sorted for CD31+/CD41-/CD45- cells.

Background corr dist: KL-Divergence = 0.0387, L1-Distance = 0.0296, L2-Distance = 0.0012, Normal std = 0.6347

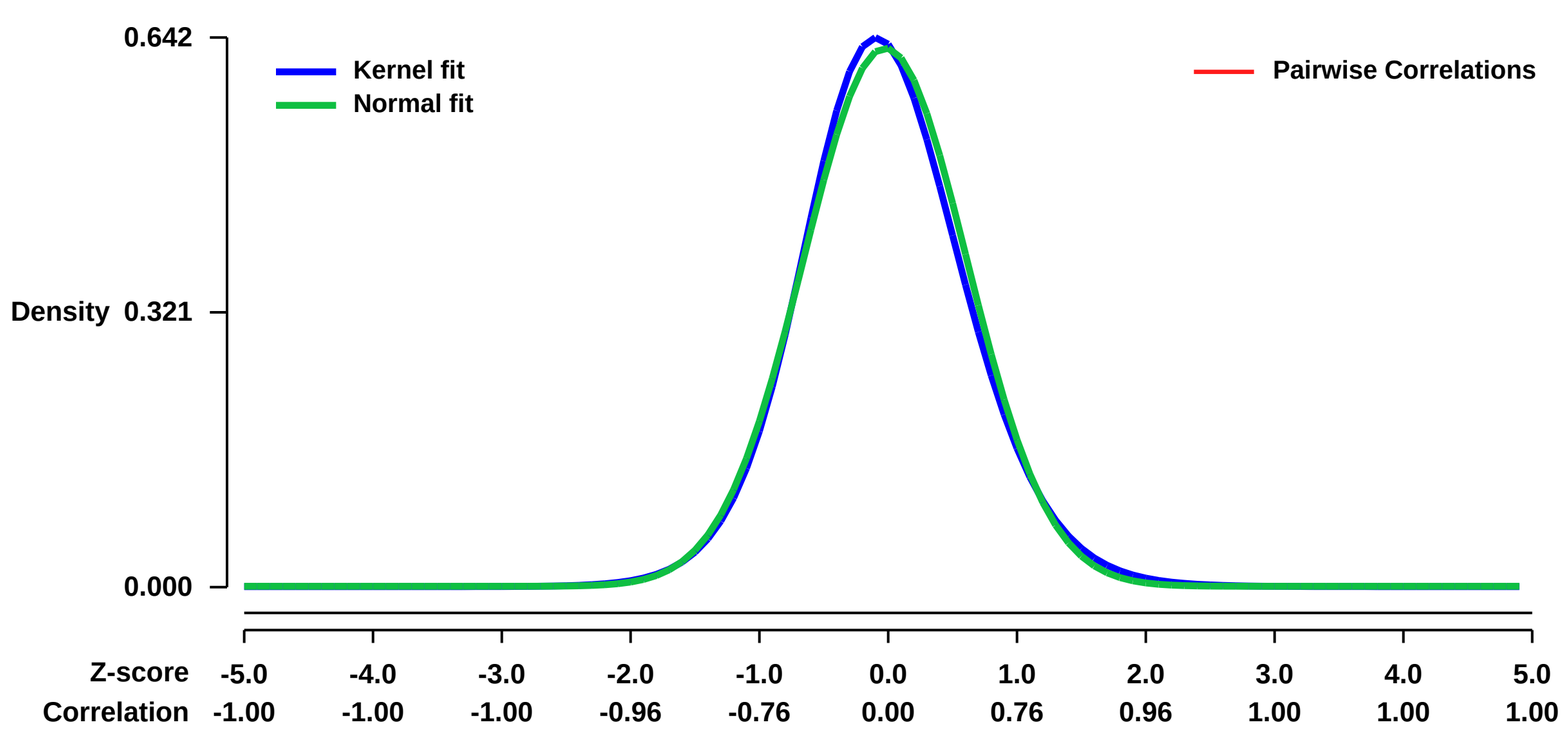

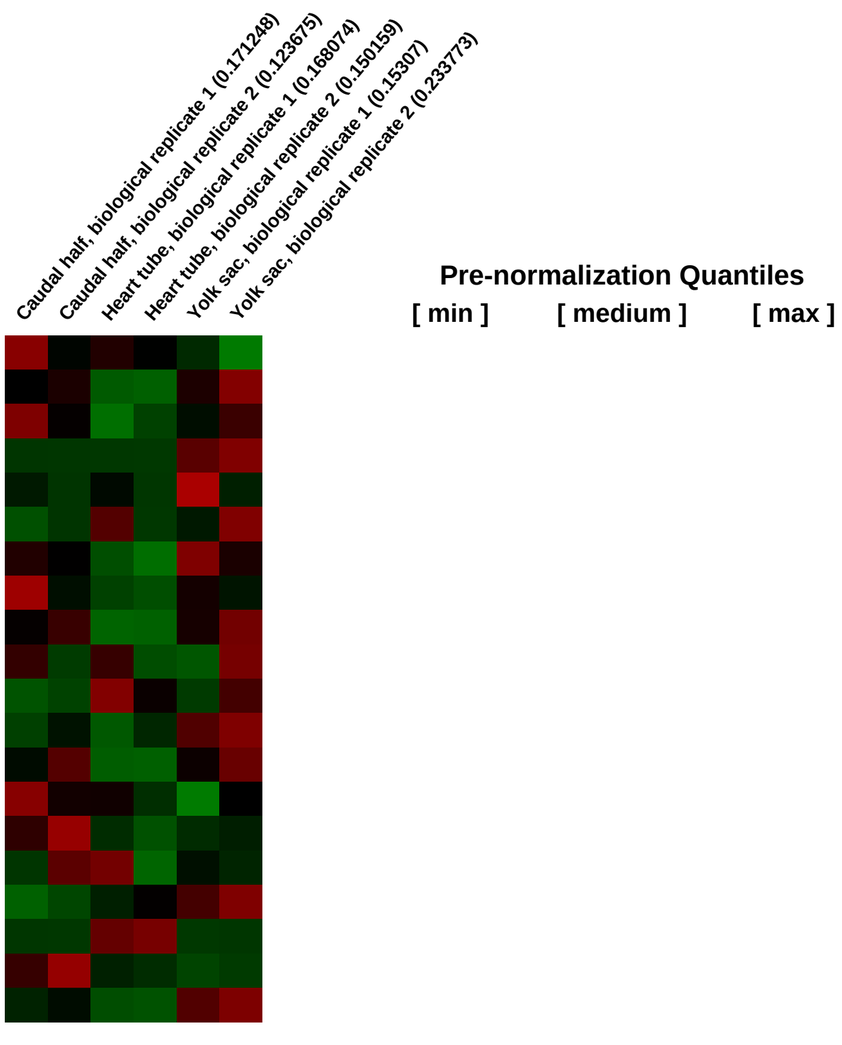

GEO Series "GSE35091" Expression Profiles

Num of samples in this series: 11

Scale of expression profile Z-scores

-3.0 -2.0 -1.0 0.0 1.0 2.0 3.0

GEO Link:	**http://www.ncbi.nlm.nih.gov/geo/query/acc.cgi?acc=GSE35091**
Status:	**Public on Jul 13 2012**
Title:	**Expression data from mandibular arches in mouse embryos**
Organism:	**Mus musculus**
Experiment type:	**Expression profiling by array**
Platform:	**GPL1261**
Pubmed ID:	
Summary & Design:	**Summary:** **Fusion of branchial arch derivatives is an essential event in the development of craniofacial architecture. A unique feature of the mandibular arch development is medial/lateral compartmentalization for the molecular networks. Those networks give rise to multiple region-specific organs, namely teeth, a tongue, salivary glands, and the supporting matrices such as bones and cartilages.** **We aimed to investigate molecular networks that govern the fusion process during mouse mandibular development. To this end, cDNA microarray technology was employed for screening of spatio-temporal gene expression in developing mandibular arch from E9.7 through E14.5.** **Overall design:** **We conducted to divide a mandibular arch medially and laterally to compare both gene expression. From an embryo at E10.5, a medial (M) sample of the mandibular arch was dissected out -at just the distal end of opposed lateral lingual swellings-, and the bulk of remnant lateral region was collected as (L) sample under a stereomicroscope. Forty embryos for each time-point were used to obtain a pool of total RNA.**

Background corr dist: **KL-Divergence = 0.0510, L1-Distance = 0.0439, L2-Distance = 0.0035, Normal std = 0.5824**

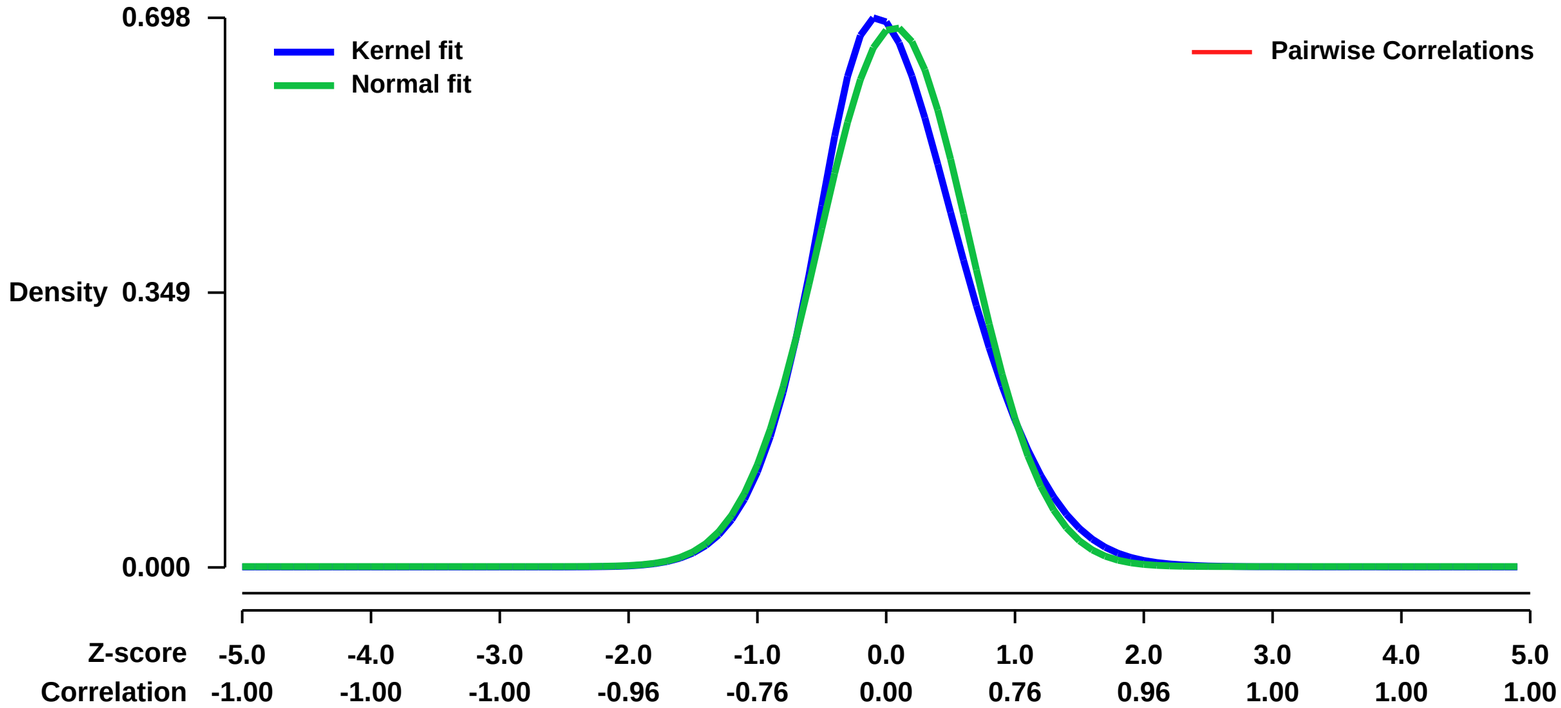

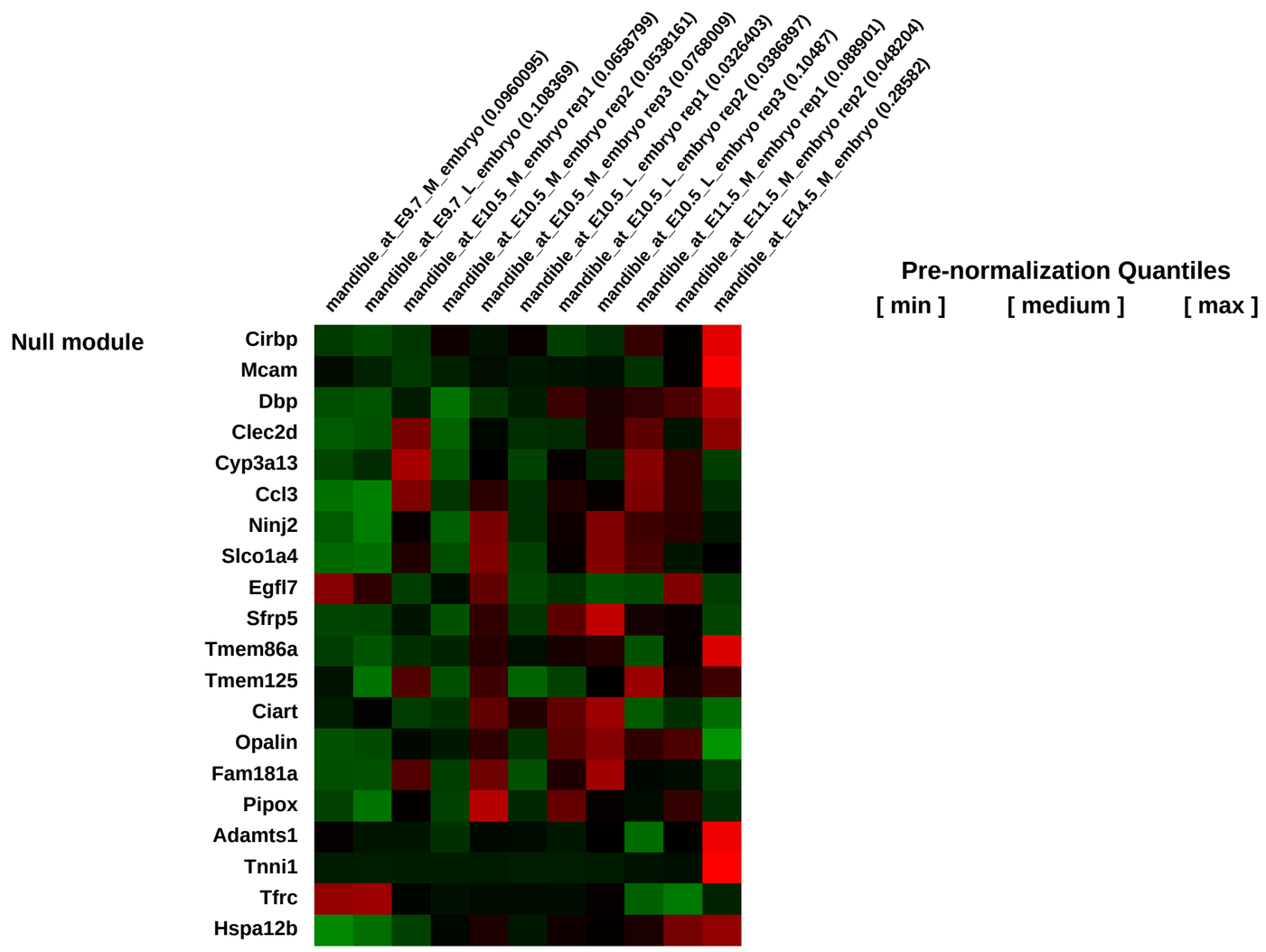

GEO Series "GSE4029" Expression Profiles

Num of samples in this series: 10

Scale of expression profile Z-scores

-3.0 -2.0 -1.0 0.0 1.0 2.0 3.0

GEO Link:	**http://www.ncbi.nlm.nih.gov/geo/query/acc.cgi?acc=GSE4029**
Status:	**Public on May 01 2006**
Title:	**Basonuclin: A novel mammalian maternal effect gene**
Organism:	**Mus musculus**
Experiment type:	**Expression profiling by array**
Platform:	**GPL1261**
Pubmed ID:	**16624857**
Summary & Design:	**Summary:** **Keywords: RNAi knockdown** **Overall design:** **Basonuclin-deficient oocytes were created by a mouse transgenic RNAi approach, which knocks down basonuclin mRNA level specifically in oocytes. Microarray analysis was performed on total RNA from four non-transgenic (control) and six transgenic (basonuclin-deficient) oocyte samples (approximately 50 oocytes per sample).**

Background corr dist: **KL-Divergence = 0.0734, L1-Distance = 0.0871, L2-Distance = 0.0111, Normal std = 0.6253**

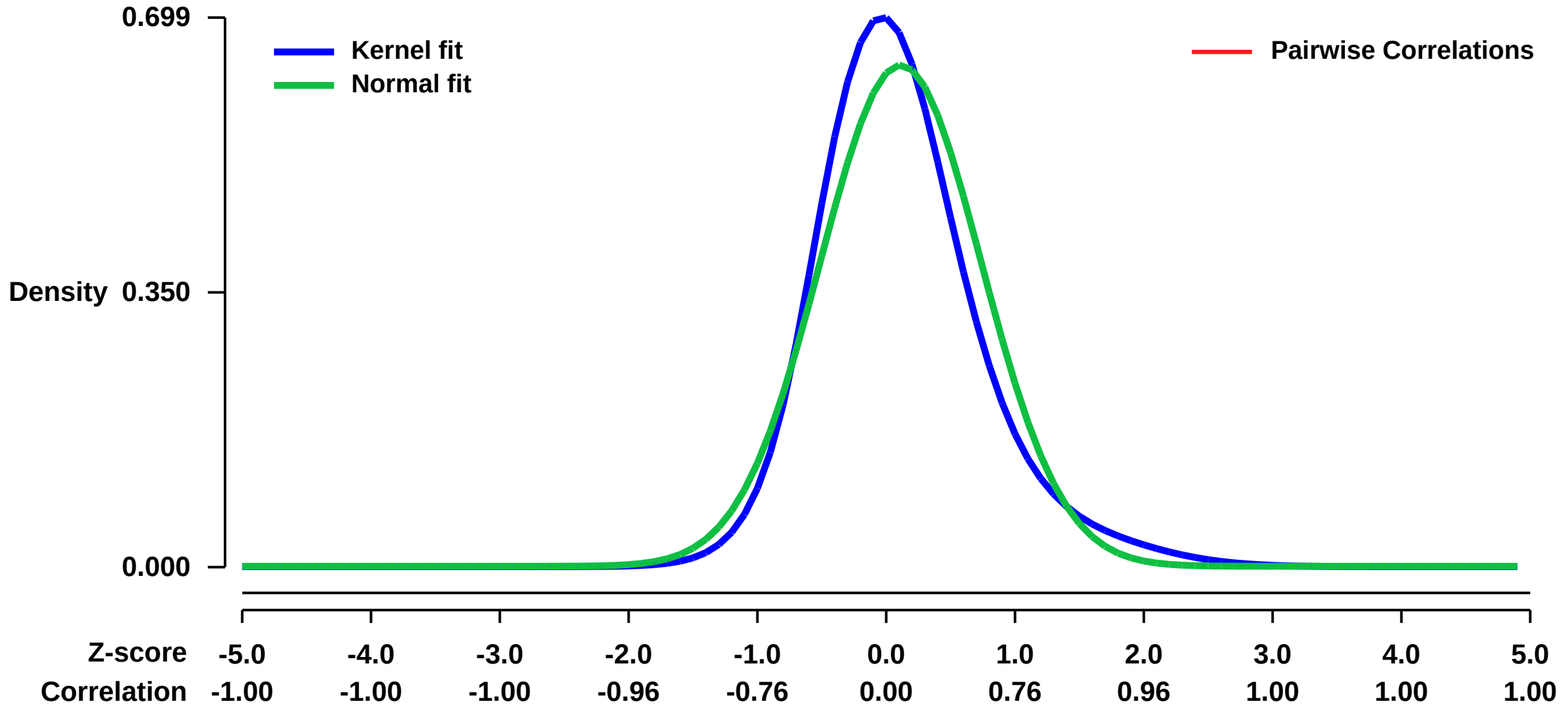

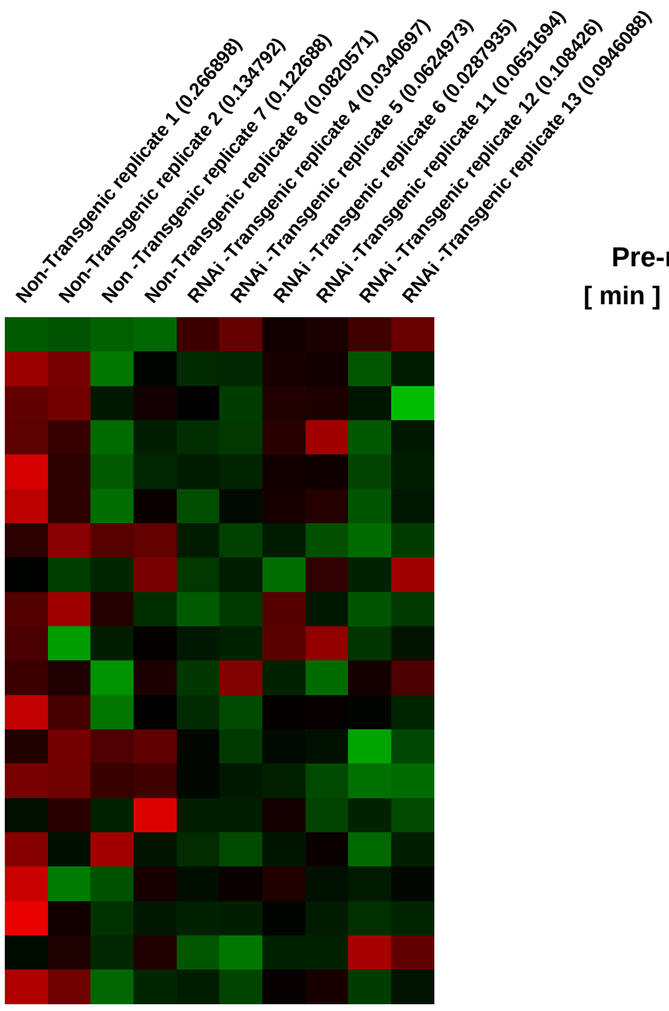

GEO Series "GSE13259" Expression Profiles

Num of samples in this series: 10

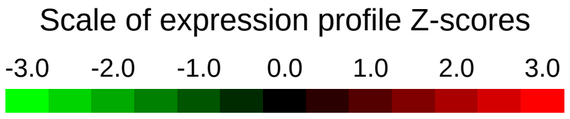

GEO Link:	http://www.ncbi.nlm.nih.gov/geo/query/acc.cgi?acc=GSE13259
Status:	Public on Apr 01 2009
Title:	Comparisons of epithelial and mesenchymal murine breast tumor cell lines
Organism:	Mus musculus
Experiment type:	Expression profiling by array
Platform:	GPL1261
Pubmed ID:	19276366
Summary & Design:	**Summary:** Epithelial tumor cells (E) underwent EMT in vivo in FVB/N mice generating mesenchymal tumors. Mesenchymal cell lines (M1-M4) were each derived from a different mouse. This study compares gene expression between these two different tumor types. **Keywords: cell type comparison** **Overall design:** Two replicates were prepared for each of five cell lines, one epithelial cell line (E) and 4 mesenchymal cell lines M1-M4.

Background corr dist: KL-Divergence = 0.0778, L1-Distance = 0.0460, L2-Distance = 0.0031, Normal std = 0.5332

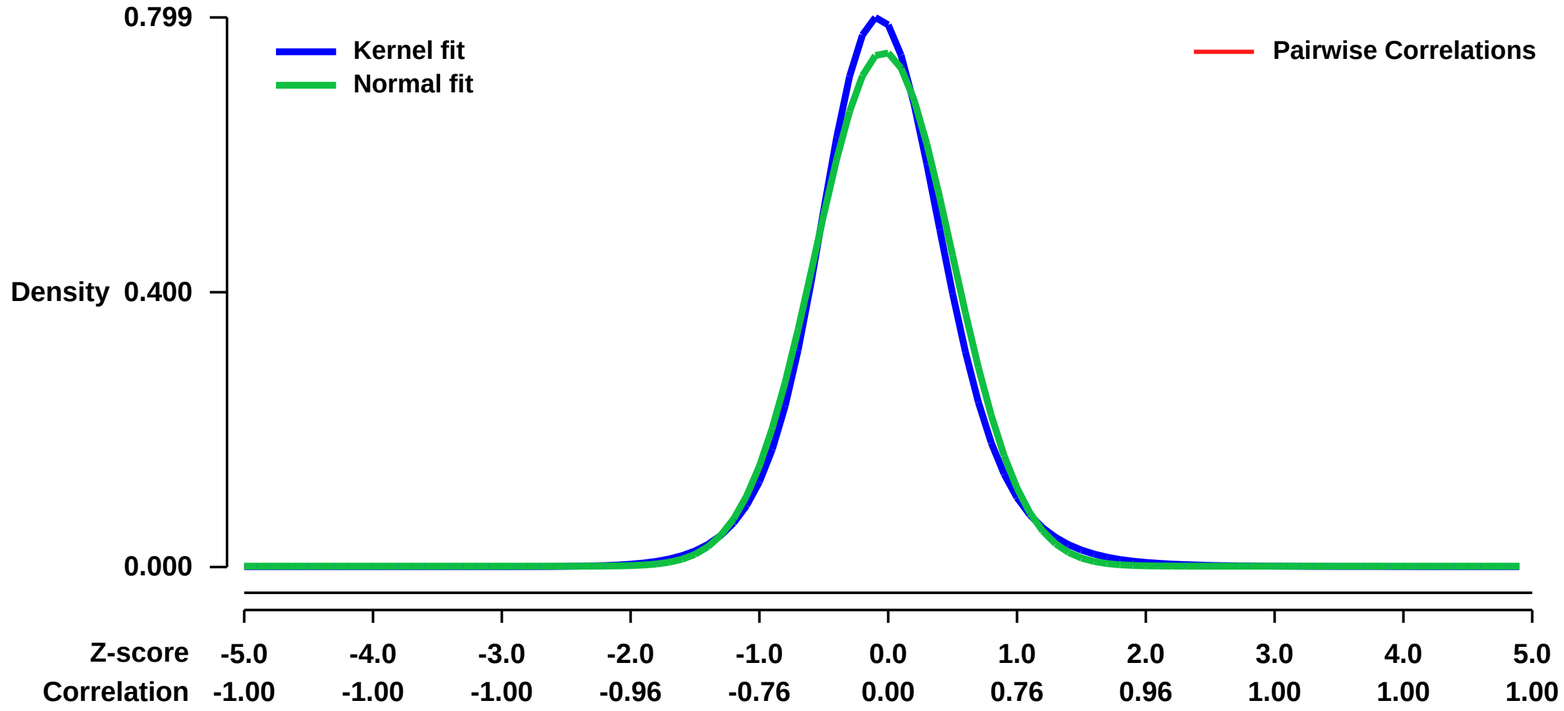

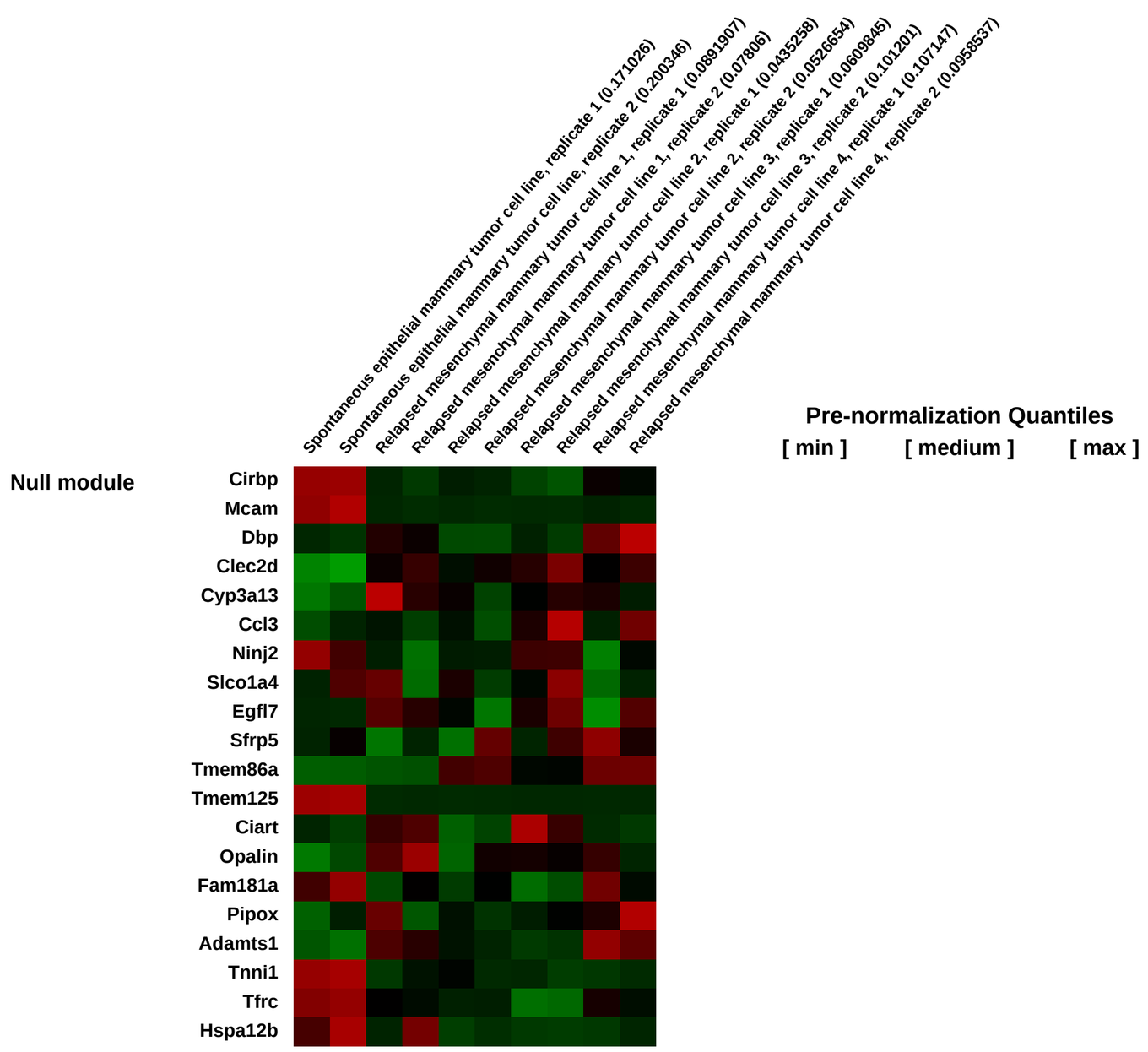

GEO Series "GSE53077" Expression Profiles

Num of samples in this series: 8

Scale of expression profile Z-scores

-3.0 -2.0 -1.0 0.0 1.0 2.0 3.0

GEO Link:	http://www.ncbi.nlm.nih.gov/geo/query/acc.cgi?acc=GSE53077
Status:	Public on Jan 15 2014
Title:	High Runx1 levels promote a reversible more differentiated cell-state in hair follicle stem cells during quiescence
Organism:	Mus musculus
Experiment type:	Expression profiling by array
Platform:	GPL1261
Pubmed ID:	24462289
Summary & Design:	**Summary:** Quiescent hair follicle (HF) bulge stem cells (SCs) differentiate to early progenitor (EP) hair germ (HG) cells, which divide to produce transit-amplifying (TA) matrix cells. EPs can revert to SCs upon injury, but whether this de-differentiation occurs in normal HF homeostasis (hair cycle), and the mechanisms regulating both differentiation and de-differentiation are unclear. Here we use lineage tracing, gain of function, transcriptional profiling, and functional assays to examine the role of observed endogenous Runx1 level changes in the hair cycle. We find that forced Runx1 expression implements hair degeneration (catagen) and simultaneously promotes changes in the quiescent bulge SC transcriptome towards a cell-state resembling the EP HG fate. This cell-state transition is functionally reversible. We propose that SC differentiation and de-differentiation are likely to occur during normal HF degeneration and niche restructuring in response to changes in endogenous Runx1 levels associated with SC location with respect to the niche. **Overall design:** Freshly isolated skin cells were FACS sorted based on K15-GFP+/a6-integrin+/CD34- as hair germ and K15-GFP+/a6-integrin+/CD34+ bulge cells. Duplicate samlpes from mice at PD20 that showed telogen morphology throughout skin were used for RNA prepartion and Affymetrix analysis. Wild and transgenic samples after 1-day of doxycycline treatement were compared.

Background corr dist: KL-Divergence = 0.0588, L1-Distance = 0.0239, L2-Distance = 0.0009, Normal std = 0.5355

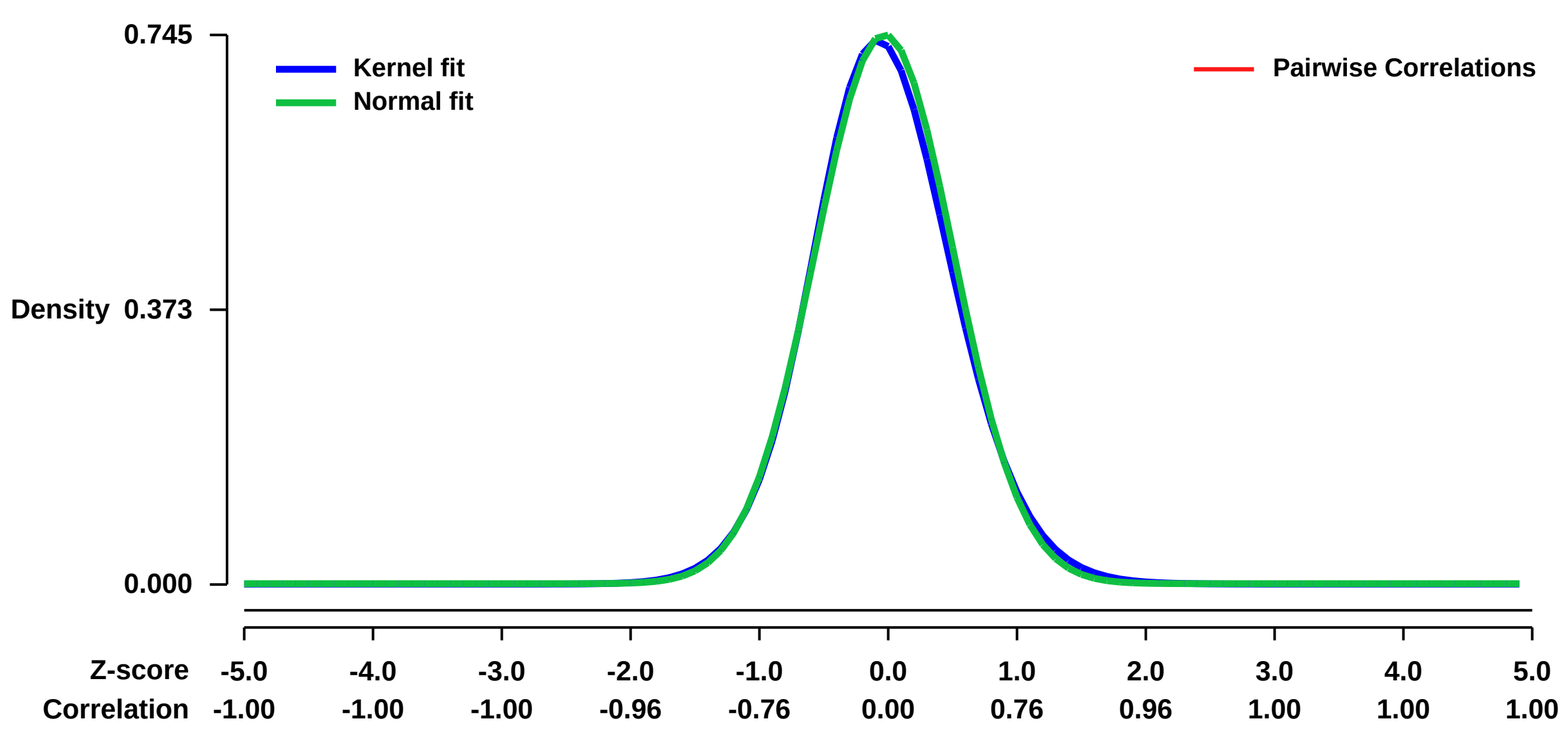

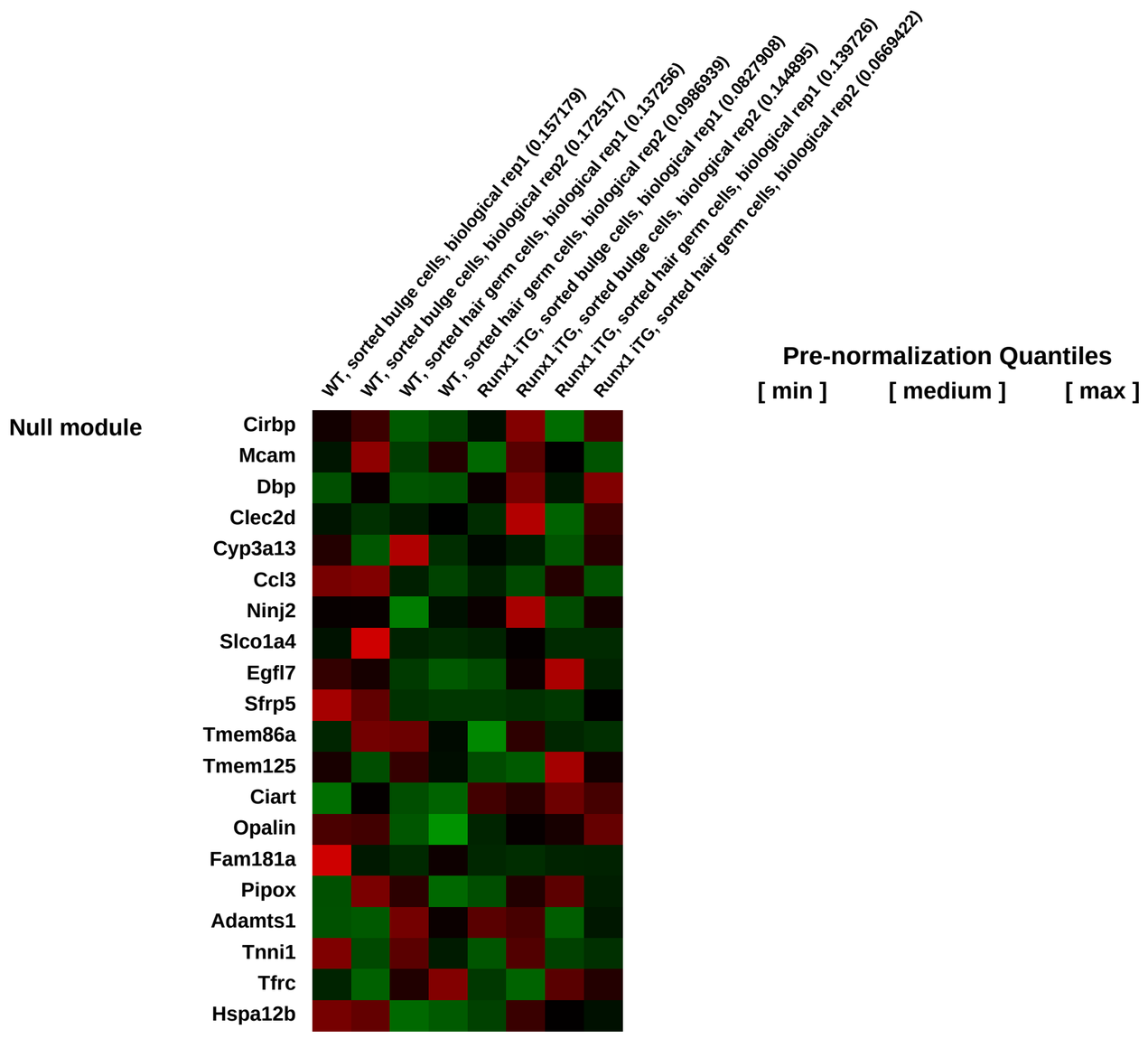

GEO Series "GSE38224" Expression Profiles

Num of samples in this series: 12

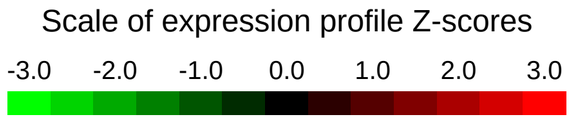

GEO Link:	http://www.ncbi.nlm.nih.gov/geo/query/acc.cgi?acc=GSE38224
Status:	Public on Jun 11 2012
Title:	Expression data from Ring1A(-/-);Ring1B(fl/fl);R26::CreERT2 ES cells expressing either of mock, WT or mutant Ring1B construct before or after OHT treatment
Organism:	Mus musculus
Experiment type:	Expression profiling by array
Platform:	GPL1261
Pubmed ID:	22844243
Summary & Design:	**Summary:** We used microarrays to investigate the restoration of repression of PRC1 target gene expression in Ring1A/B-dKO ES cells stably expressing either of mock, WT or mutant Ring1B construct. **Overall design:** Total RNAs were extracted from the respective ES cells, and were subjected to microarray analysis using Affymetrix GeneChip Mouse Genome 430A 2.0 arrays

Background corr dist: KL-Divergence = 0.1261, L1-Distance = 0.0314, L2-Distance = 0.0017, Normal std = 0.3993

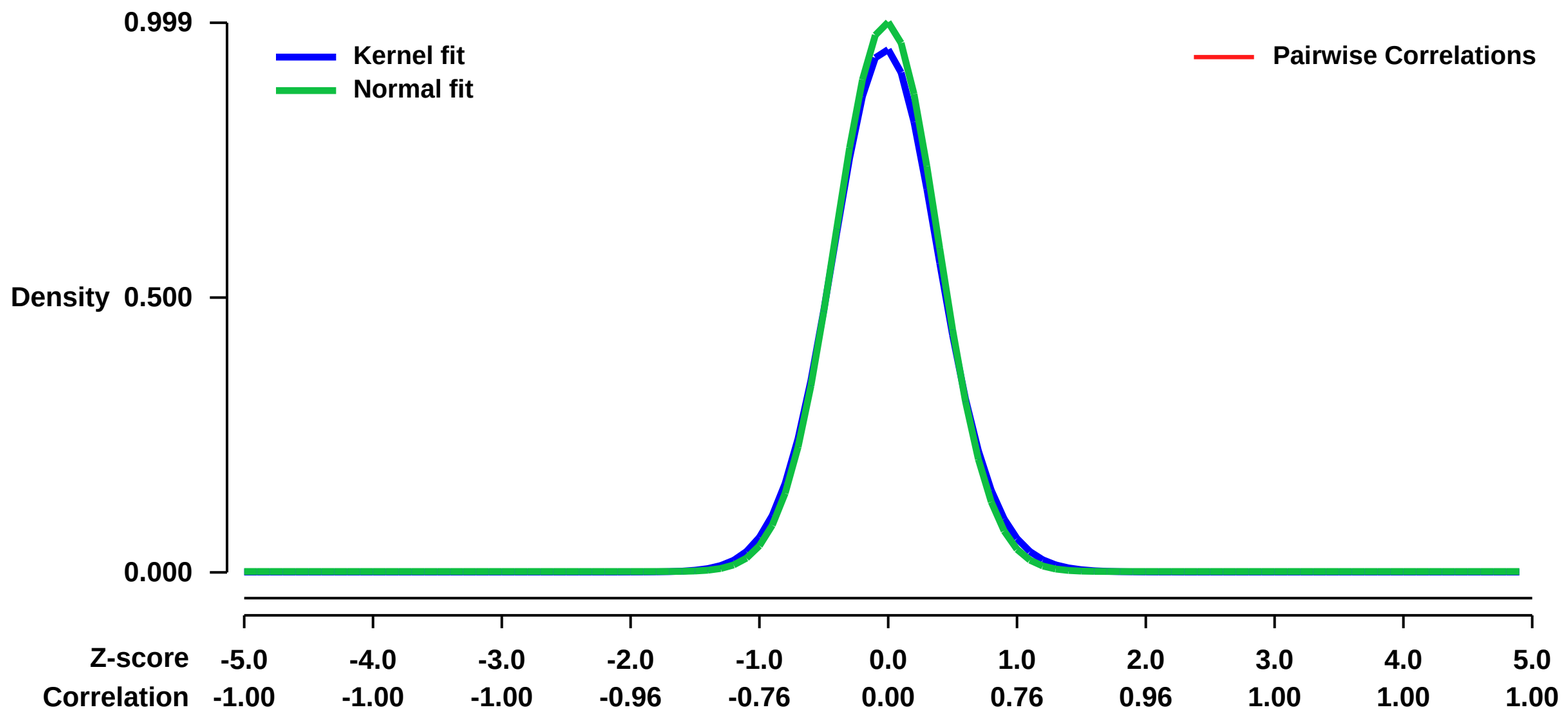

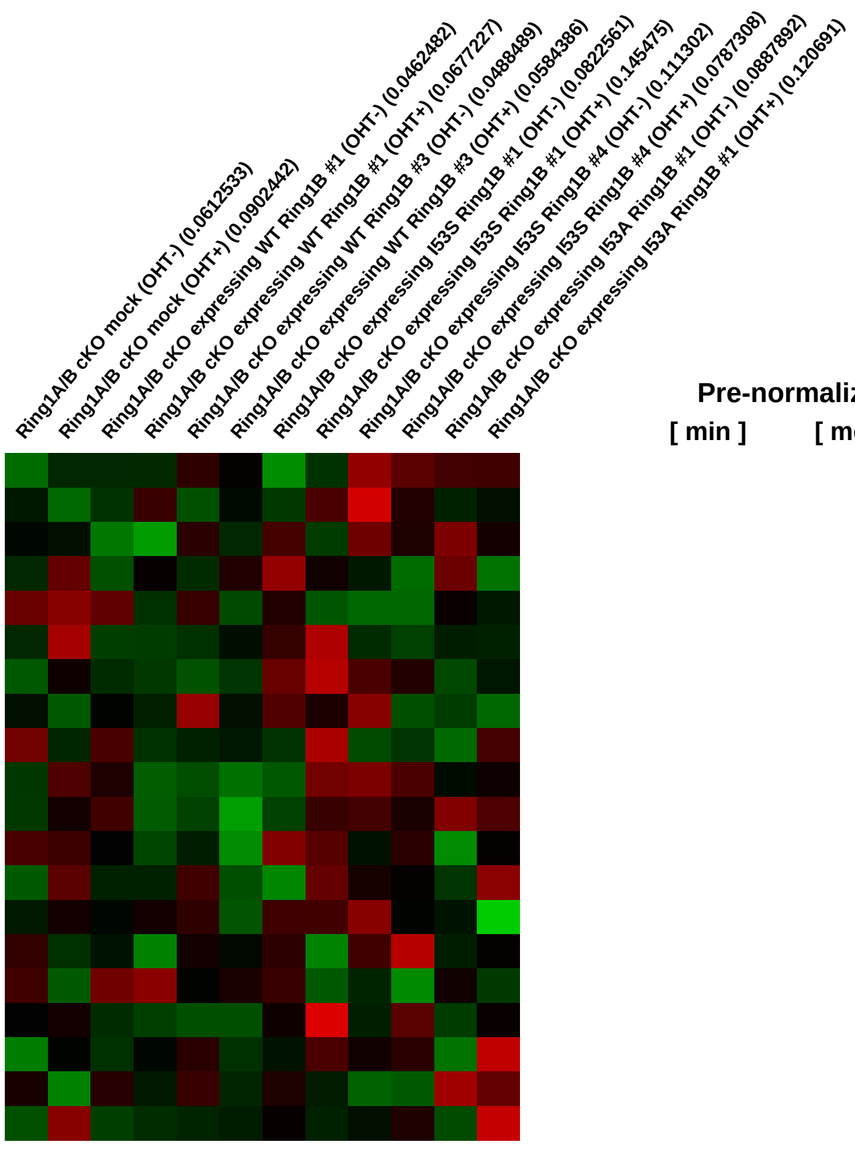

GEO Series "GSE30863" Expression Profiles

Num of samples in this series: 20

Scale of expression profile Z-scores

-3.0 -2.0 -1.0 0.0 1.0 2.0 3.0

GEO Link:	**http://www.ncbi.nlm.nih.gov/geo/query/acc.cgi?acc=GSE30863**
Status:	**Public on Dec 14 2011**
Title:	**Candidate Genes for Panhypopituitarism identified by gene expression profile**
Organism:	**Mus musculus**
Experiment type:	**Expression profiling by array**
Platform:	**GPL1261**
Pubmed ID:	
Summary & Design:	**Summary:** **Prop1 controls the expression of genes besides Pit1 that are important for cell mgration, survival and differentiation in the mouse and human pituitary gland.** **Microarray analysis was used to compare pituitary RNA from newborn Prop1 and Pit1 mutants and their wild type littermates.** **Overall design:** **Total RNA was collected and pooled from Prop1df/df, Porp1+/+, Pit1dw/dw, and Pit+/+ at the age of P1. 5 pools per genotype were hybridized to the Affymetrix Mouse Genome 430 2.0 array.**

Background corr dist: **KL-Divergence = 0.1694, L1-Distance = 0.0448, L2-Distance = 0.0044, Normal std = 0.3551**

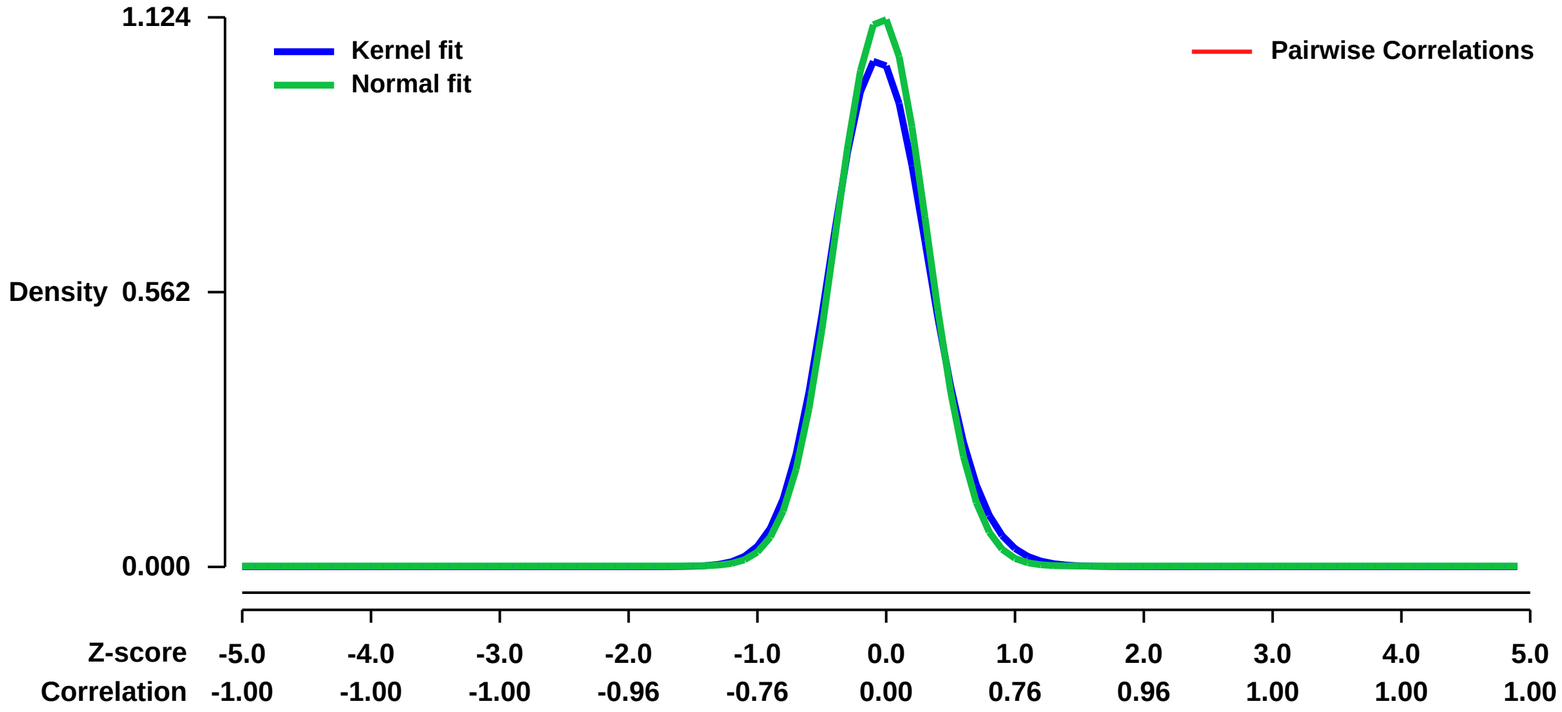

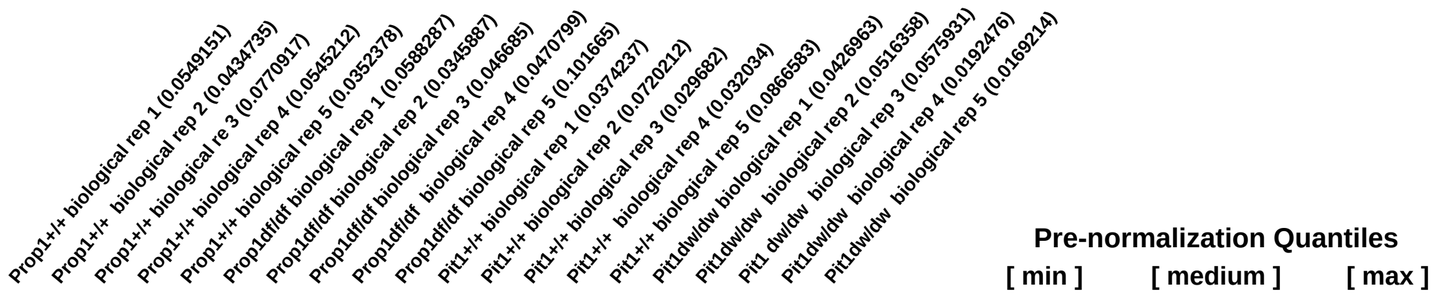

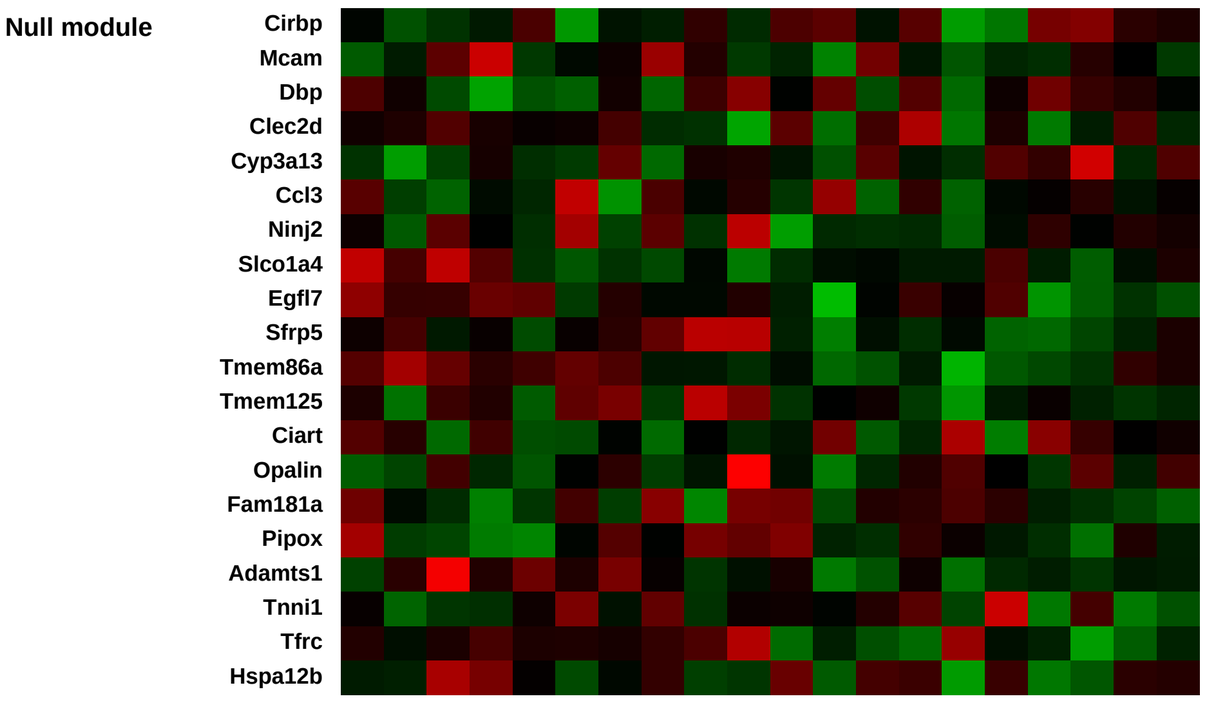

GEO Series "GSE11333" Expression Profiles

Num of samples in this series: 6

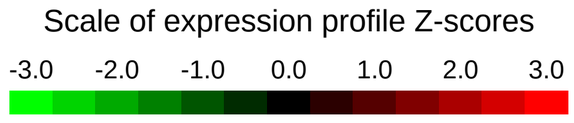

GEO Link:	**http://www.ncbi.nlm.nih.gov/geo/query/acc.cgi?acc=GSE11333**
Status:	**Public on May 06 2008**
Title:	**ELAV-like protein HuD overexpression and pulldown (perro-affy-mouse-482241)**
Organism:	**Mus musculus**
Experiment type:	**Expression profiling by array**
Platform:	**GPL1261**
Pubmed ID:	
Summary & Design:	**Summary:** **Post-transcriptional mechanisms play an important role in the control of gene expression. RNA-binding proteins are key players in the post-transcriptional control of many neural genes and they participate in multiple processes, from RNA splicing and mRNA transport to mRNA stability and translation. Our laboratory has developed the first mouse model overexpressing a RNA-binding protein, the ELAV-like protein HuD, in the CNS under the control of the CaMKinII alpha promoter. Initial behavioral characterization of the mice revealed that they had significant learning deficits together with abnormalities in prepulse inhibition (PPI). At the molecular level, we found that the expression of the growth-associated protein GAP-43, one of the targets of HuD, was increased in the hippocampus of HuD transgenic mice.** **Besides binding and stabilizing the GAP-43 mRNA, HuD was shown to bind in vitro or in vivo the mRNAs of acetylcholinesterase, tau, p21, neuroserpin, and MARCKS among others. To identify additional targets of HuD, we propose to pull down the RNAs bound to myc-tagged HuD in vivo in the brains of HuD transgenic mice, to isolate these bound RNAs and use these to probe DNA microarrays. We will use pull downs using non-immune IgGs as controls.** **To test our hypothesis we propose 2 specific aims:** **1) To identify the targets of HuD in HuD overexpressor mice and** **2) To compare these target mRNAs to those we identified previously as having increased levels of expression in the hippocampus of HuD transgenic mice (see protocol # Perrone-Bizzozero-5R01NS030255-12) and/or those that show increased expression in dentate granule cells of HuD transgenic mice (protocol # perro-affy-mouse-309741)** **Based upon the role of the RNA-binding HuD in neuronal development and synaptic plasticity, we expect that HuD targets will include mRNAs for proteins involved in these processes.** **All mice are in C57BL/6 background and are male approximately 60 days old. To identify target of HuD in our transgenic mice, we will homogenize the homogenize the hippocampi (2 per animal) of 3 transgenic mice and use these protein extracts for immunoprecipitation assays. Briefly, transgenic myc-tagged HuD protein will be immunoprecipitated using myc-tag antibodies and protein-G agarose beads and samples will be sent to T-Gen for RNA isolation, single round amplification and probing of DNA microarrays. We will use non-immune IgG as a negative control.** **Conditions:** **Pooled Extracts from 3 transgenic mice IP with myc-tag antibodies: Triplicates** **Pooled extract from 3 transgenic mice IP with non-immune IgGs (negative control): duplicates** **Keywords: dose response** **Overall design:**

Background corr dist: KL-Divergence = 0.0289, L1-Distance = 0.0352, L2-Distance = 0.0016, Normal std = 0.7007

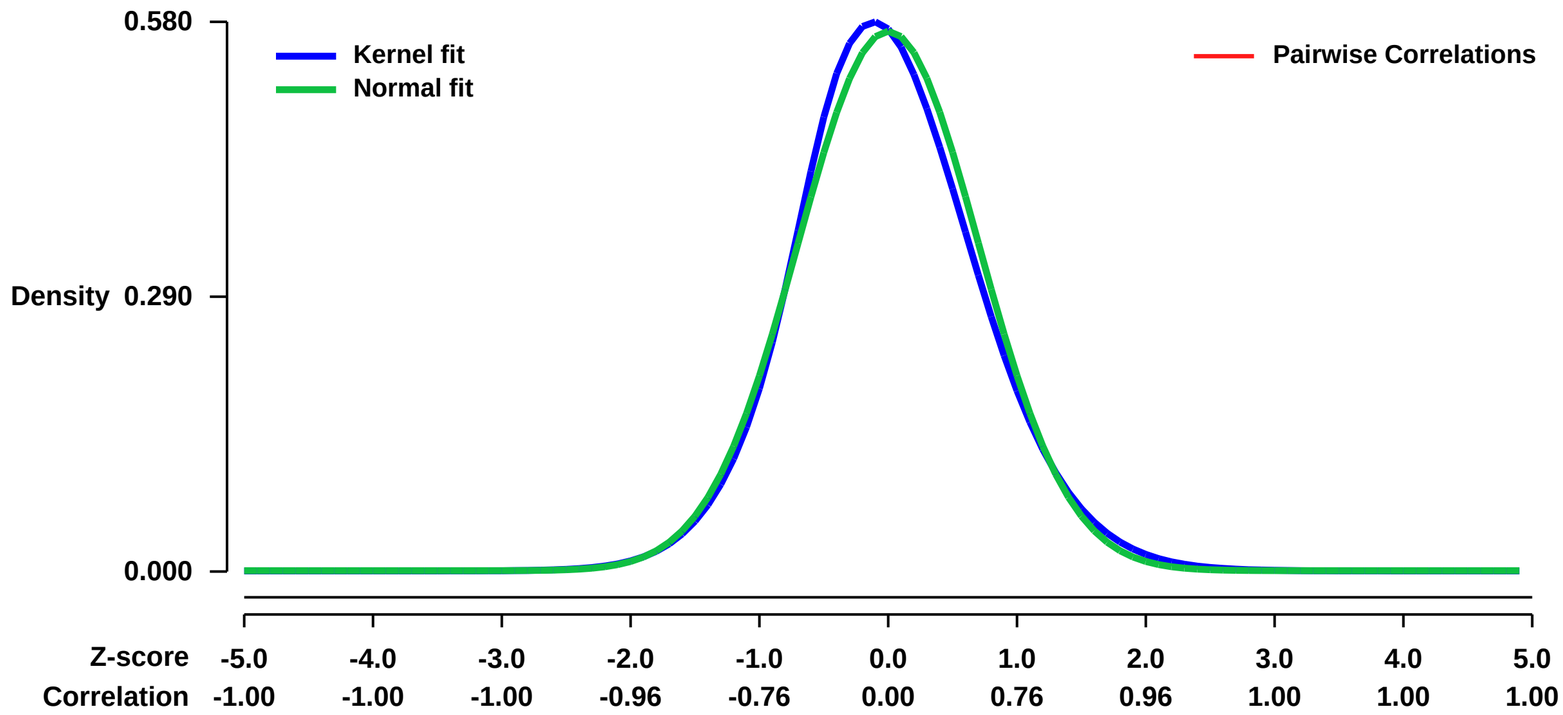

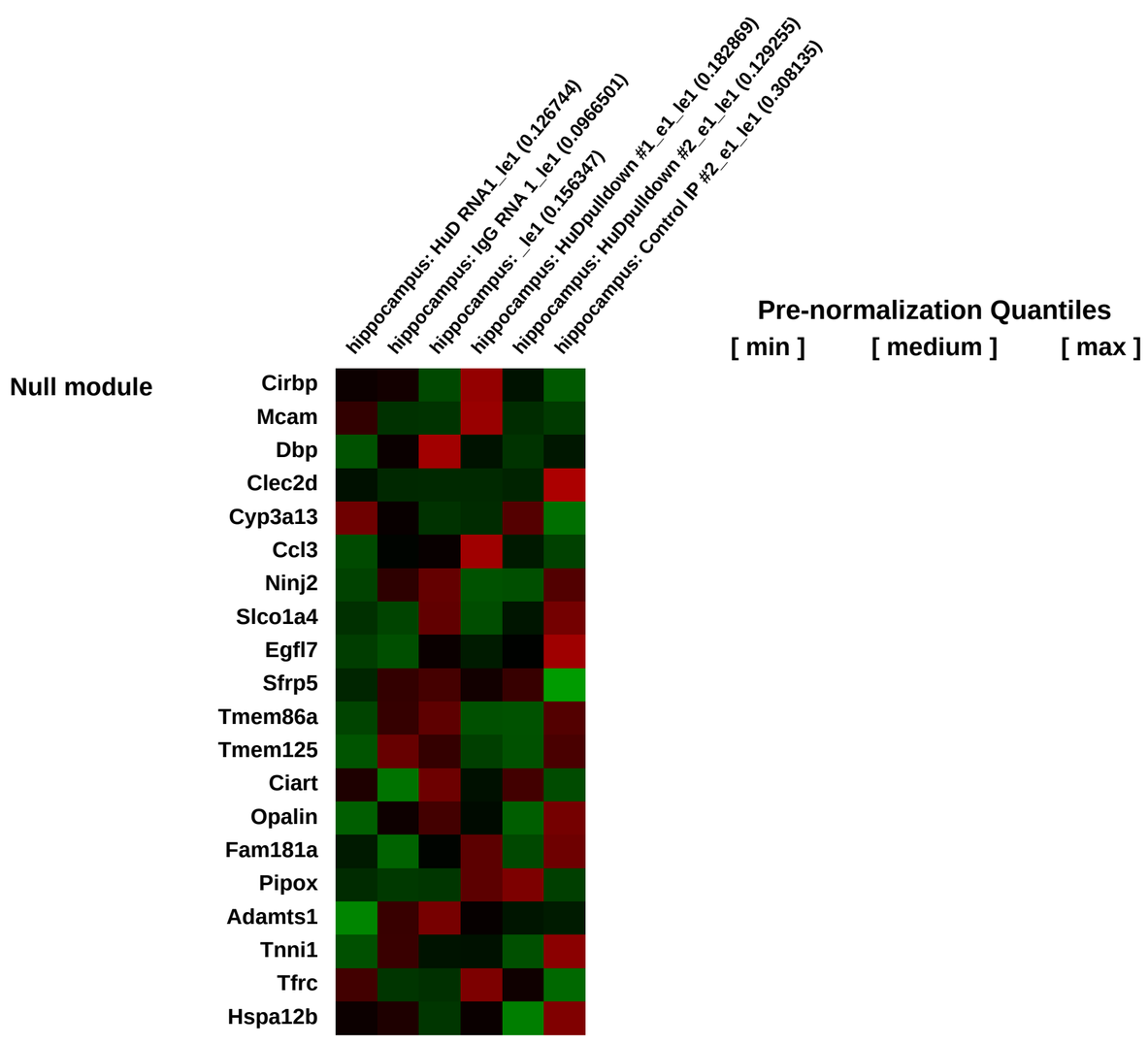

GEO Series "GSE47402" Expression Profiles

Num of samples in this series: 6

Scale of expression profile Z-scores

-3.0 -2.0 -1.0 0.0 1.0 2.0 3.0

GEO Link:	**http://www.ncbi.nlm.nih.gov/geo/query/acc.cgi?acc=GSE47402**
Status:	**Public on Jun 30 2013**
Title:	**Runx1 deficiency effect on MLL-ENL cells**
Organism:	**Mus musculus**
Experiment type:	**Expression profiling by array**
Platform:	**GPL1261**
Pubmed ID:	**23979164**
Summary & Design:	**Summary:** **To identify the target genes of Runx1 in MLL fusion leukemia, we performed microarray analysis using control and Runx1-deficient MLL-ENL leukemia cells.** **Overall design:** **Runx1 intact and excised bone marrow cells were transduced with MLL-ENL and transplanted into congenic mice. Leukemic cells were harvested from moribund mice, and gene expression was compared using 3 independent leukemia cells for each genotype.**

Background corr dist: **KL-Divergence = 0.0413, L1-Distance = 0.0212, L2-Distance = 0.0005, Normal std = 0.6105**

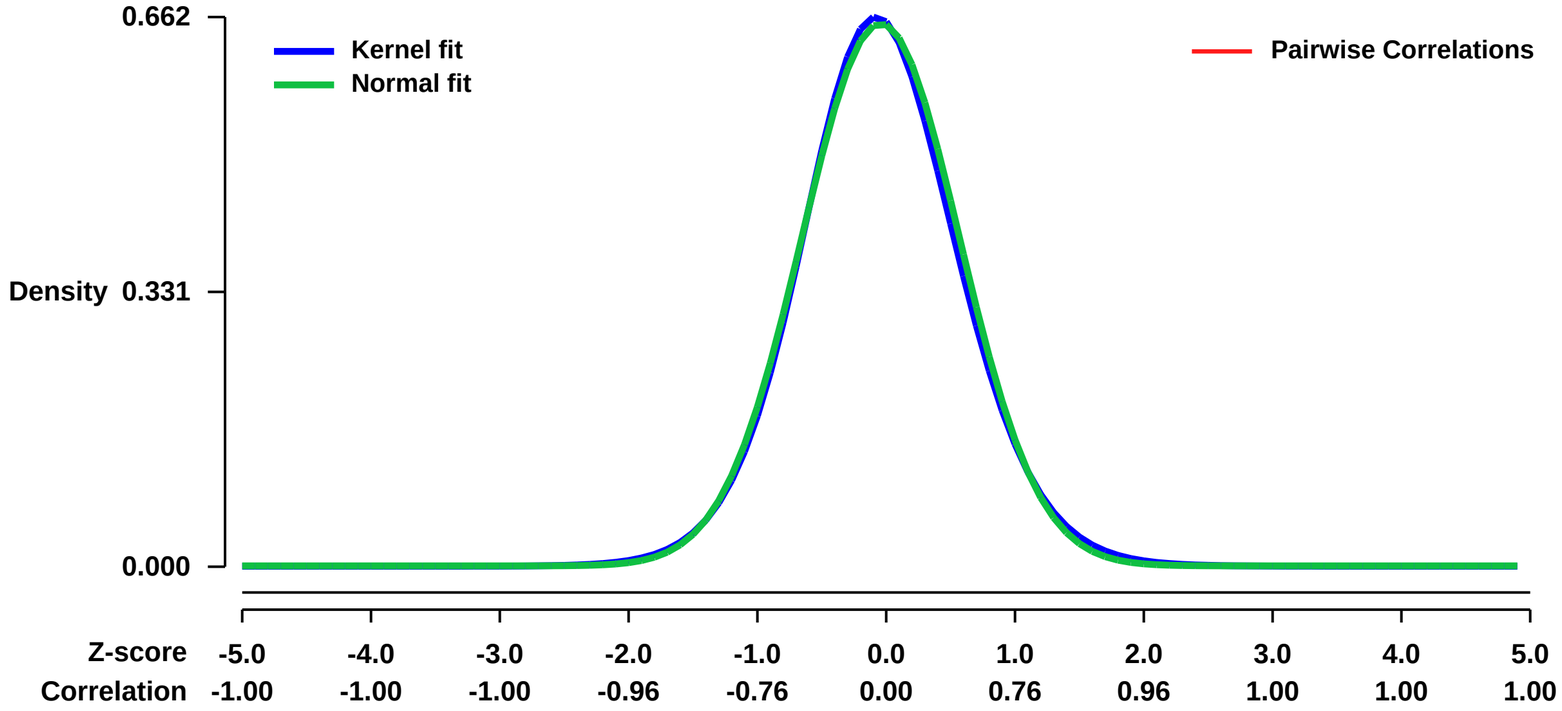

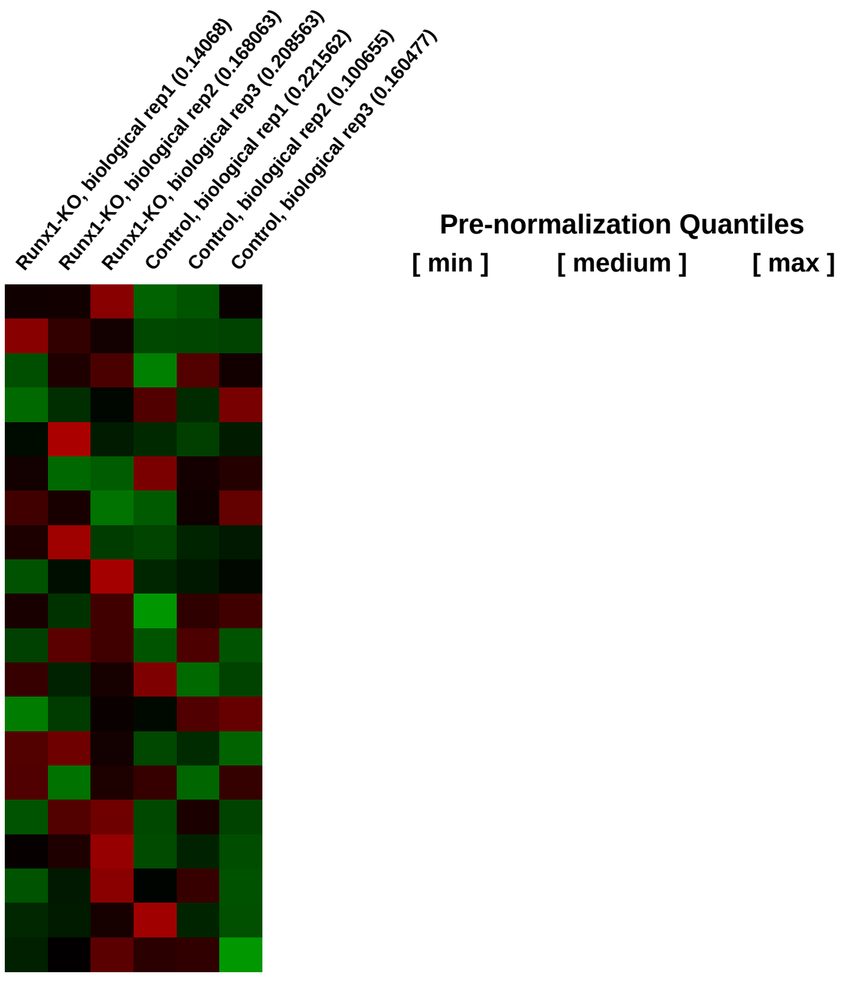

GEO Series "GSE46869" Expression Profiles

Num of samples in this series: 6

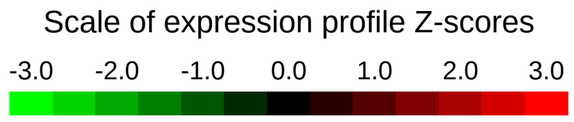

GEO Link:	http://www.ncbi.nlm.nih.gov/geo/query/acc.cgi?acc=GSE46869
Status:	Public on May 02 2014
Title:	Gene expression profiles of PIK3CA knockdown by shRNA in lung cancer cells
Organism:	Mus musculus
Experiment type:	Expression profiling by array
Platform:	GPL1261
Pubmed ID:	24762440
Summary & Design:	**Summary:** To gain insight into EMT-independent biological processes through which PI3K promotes invasion, RNA samples from 344SQ_p110‸–shRNA cells and 344SQ_scr cells were subjected to global transcriptional profiling. **Overall design:** Two group comparison

Background corr dist: KL-Divergence = 0.0368, L1-Distance = 0.0279, L2-Distance = 0.0008, Normal std = 0.6524

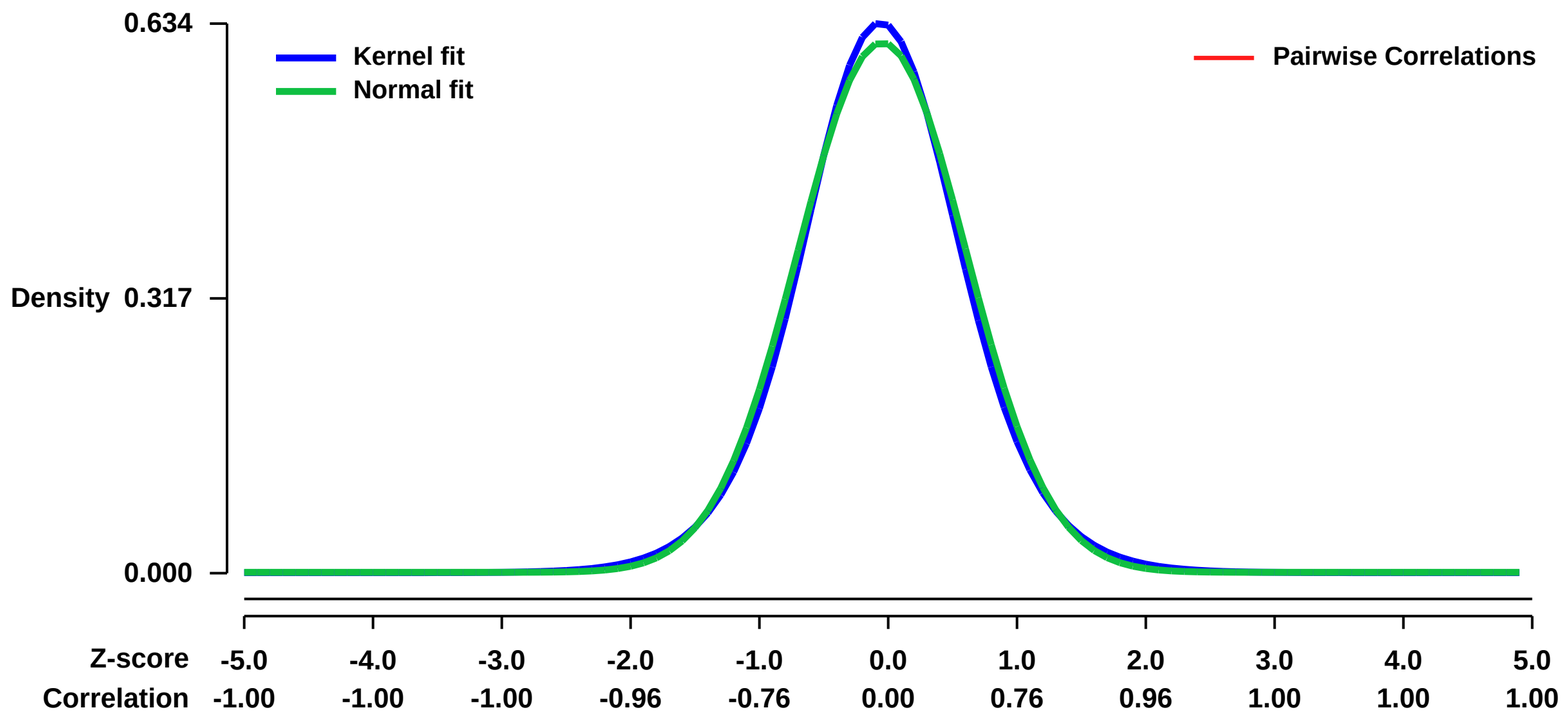

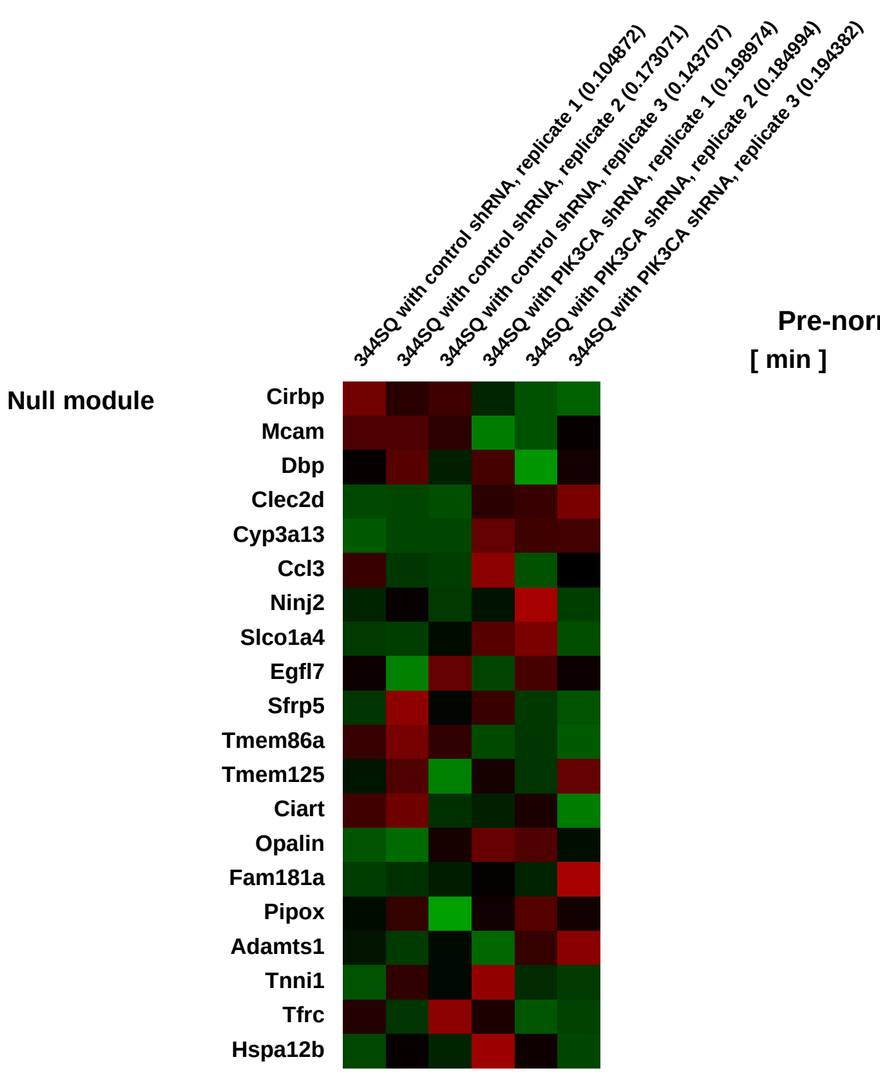

GEO Series "GSE15452" Expression Profiles

Num of samples in this series: 26

Scale of expression profile Z-scores

-3.0 -2.0 -1.0 0.0 1.0 2.0 3.0

GEO Link:	http://www.ncbi.nlm.nih.gov/geo/query/acc.cgi?acc=GSE15452
Status:	Public on Mar 31 2010
Title:	Expression data from lung of mice bearing mutations of FGFR3 and FGFR4
Organism:	Mus musculus
Experiment type:	Expression profiling by array
Platform:	GPL1261
Pubmed ID:	20093646
Summary & Design:	**Summary:** Gene expression profiling of newborn lung tissue revealed few changes in compound FGFR3/FGFR4 deficient mice, consistent with their normal lung morphology at birth, suggesting the sequence of events leading to the phenotype initiates after birth in this model. Profiling of 4 week-old lung tissues revealed an induction of genes related to elastic fiber assembly in compound mutants. **Overall design:** Lung RNA isolated from three animals of each genotype-age group were pooled for each Affymetrix chip (n=3 chips for each, except n=2 for wild type at 4 weeks.

Background corr dist: KL-Divergence = 0.0340, L1-Distance = 0.0512, L2-Distance = 0.0041, Normal std = 0.6581

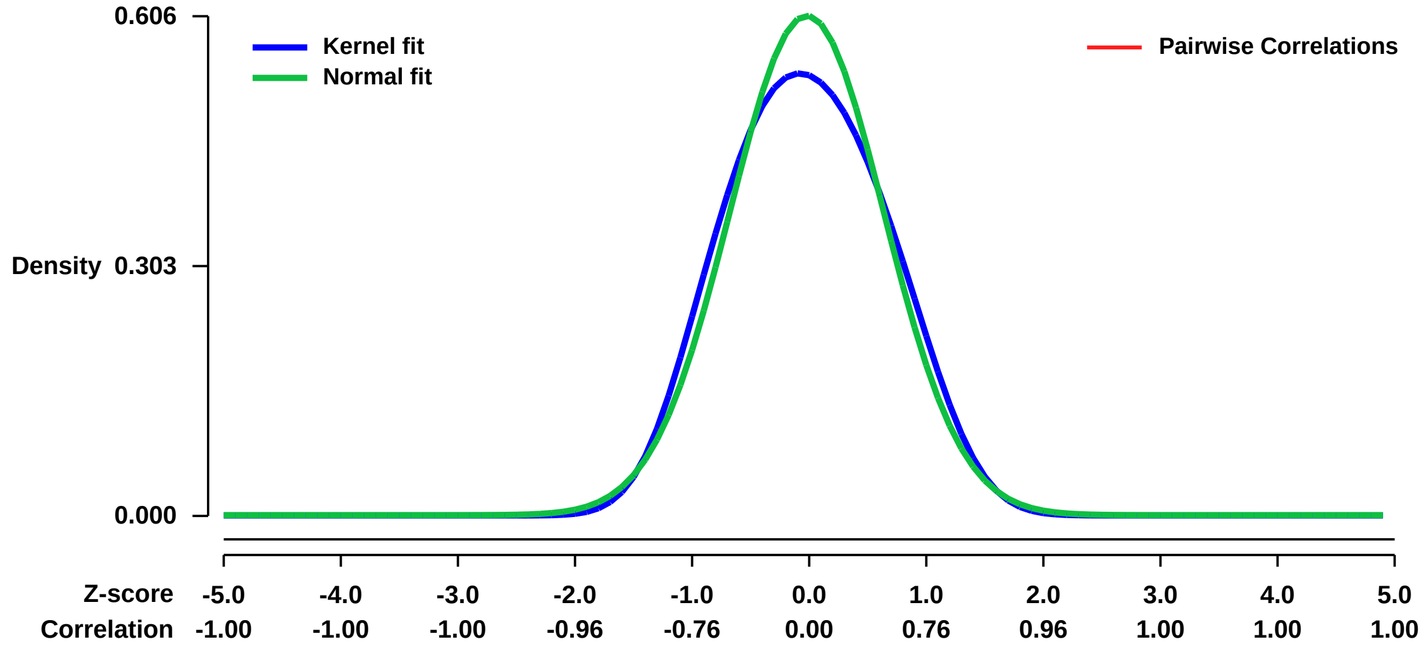

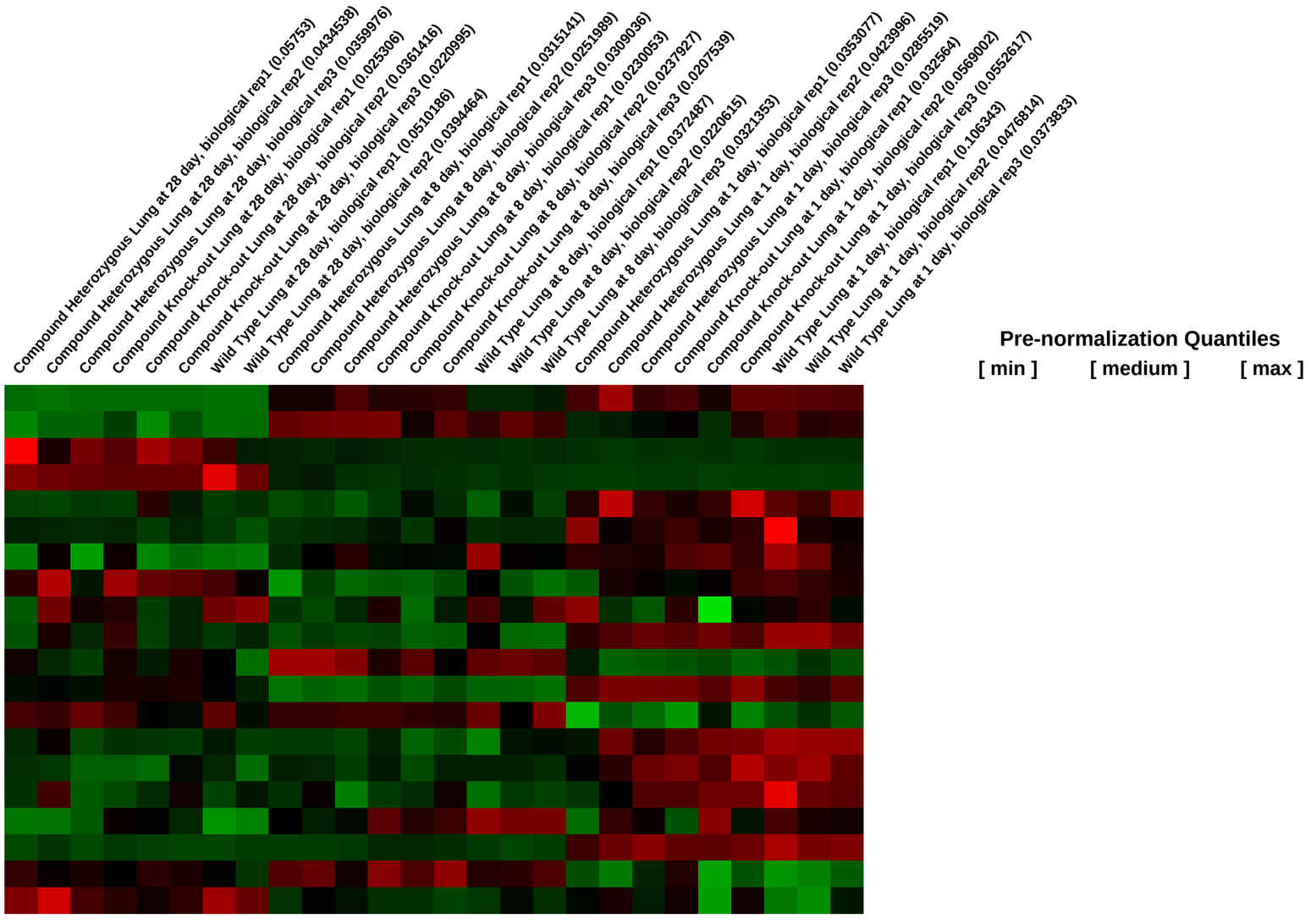

GEO Series "GSE39391" Expression Profiles

Num of samples in this series: 21

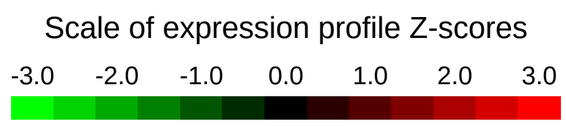

GEO Link:	http://www.ncbi.nlm.nih.gov/geo/query/acc.cgi?acc=GSE39391
Status:	Public on Aug 30 2012
Title:	Gene expression data from ahES cells, ES cells, MEF cells and round sperm
Organism:	Mus musculus
Experiment type:	Expression profiling by array
Platform:	GPL1261
Pubmed ID:	23023130
Summary & Design:	**Summary:** Haploid stem cells offer an easy-to-manipulate genetic system and therefore have great values for studies of recessive phenotypes. Here, we show that mouse androgenetic haploid ES (ahES) cell lines can be established by transferring sperm into enucleated oocyte. The ahES cells maintain haploidy and stable growth over 30 passages, express pluripotent markers, possess the ability to differentiate into all three germ-layers in vitro and in vivo, and contribute to germline of chimeras when injected into blastocysts. Although epigenetically distinct from sperm cells, the ahES cells can produce viable and fertile progenies after intracytoplasmic injection into mature oocytes. The oocyte injection procedure can also produce viable transgenic mice from genetically engineered ahES cells. We used microarrays to compare the global programme of gene expression among ahES cells, normal diploid ES cells, MEF cells and round sperm cells and found that gene expression pattern of ahES cells was highly similar with ES cells but was distinct from MEF cells and round sperms. **Overall design:** Androgenetic haploid ES cells were FACS sorted to harvest the G0/G1 phase haploid cells. Total RNA were extracted from three ahES cell lines (AH129-5, AH129-N1, AH129-NC1, all 129Sv genetic background), two ES cell lines (CS1-1, R1, 129Sv background), MEF cells and round sperm and hybridized with Affymetrix GeneChip 430 2.0 array. Data were collected and analyzed to compare their gene expression pattern.

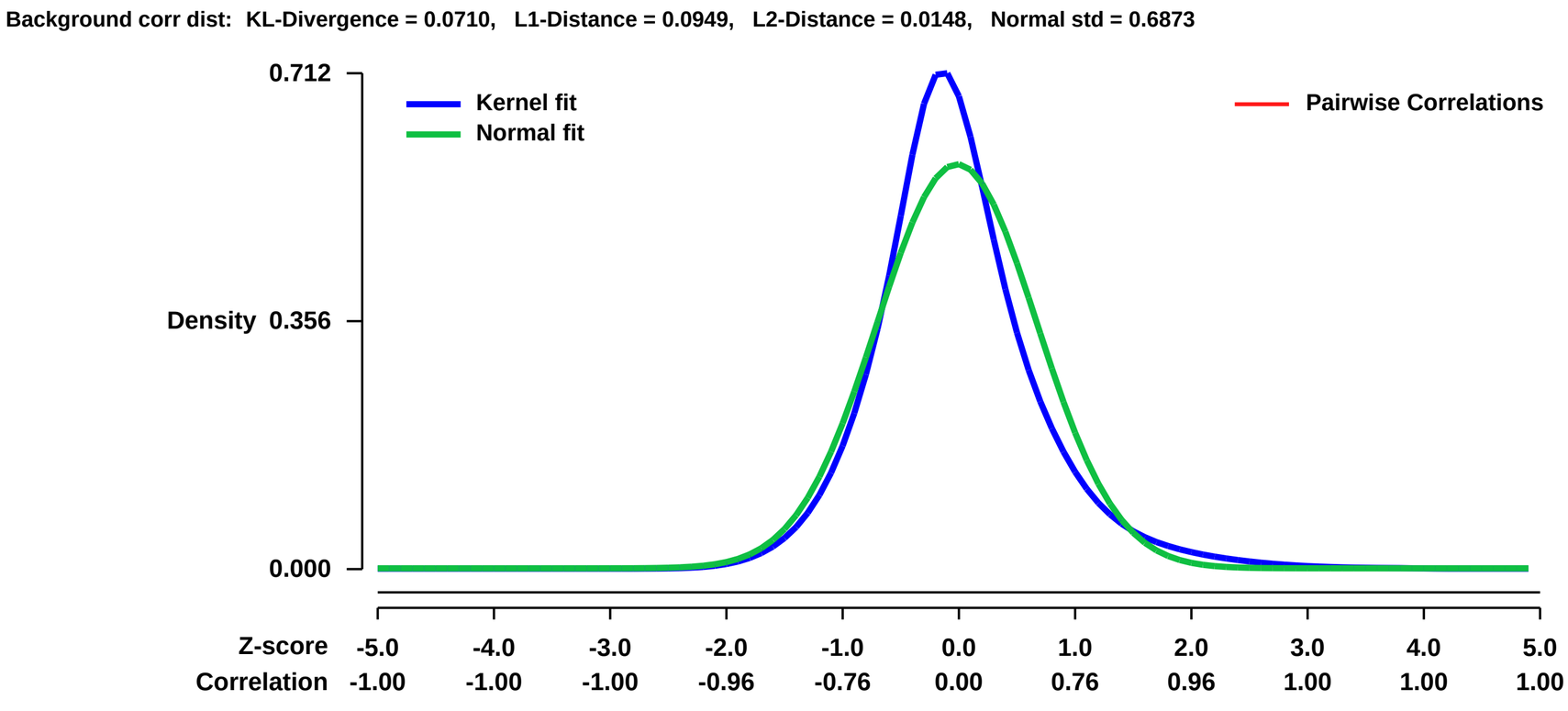

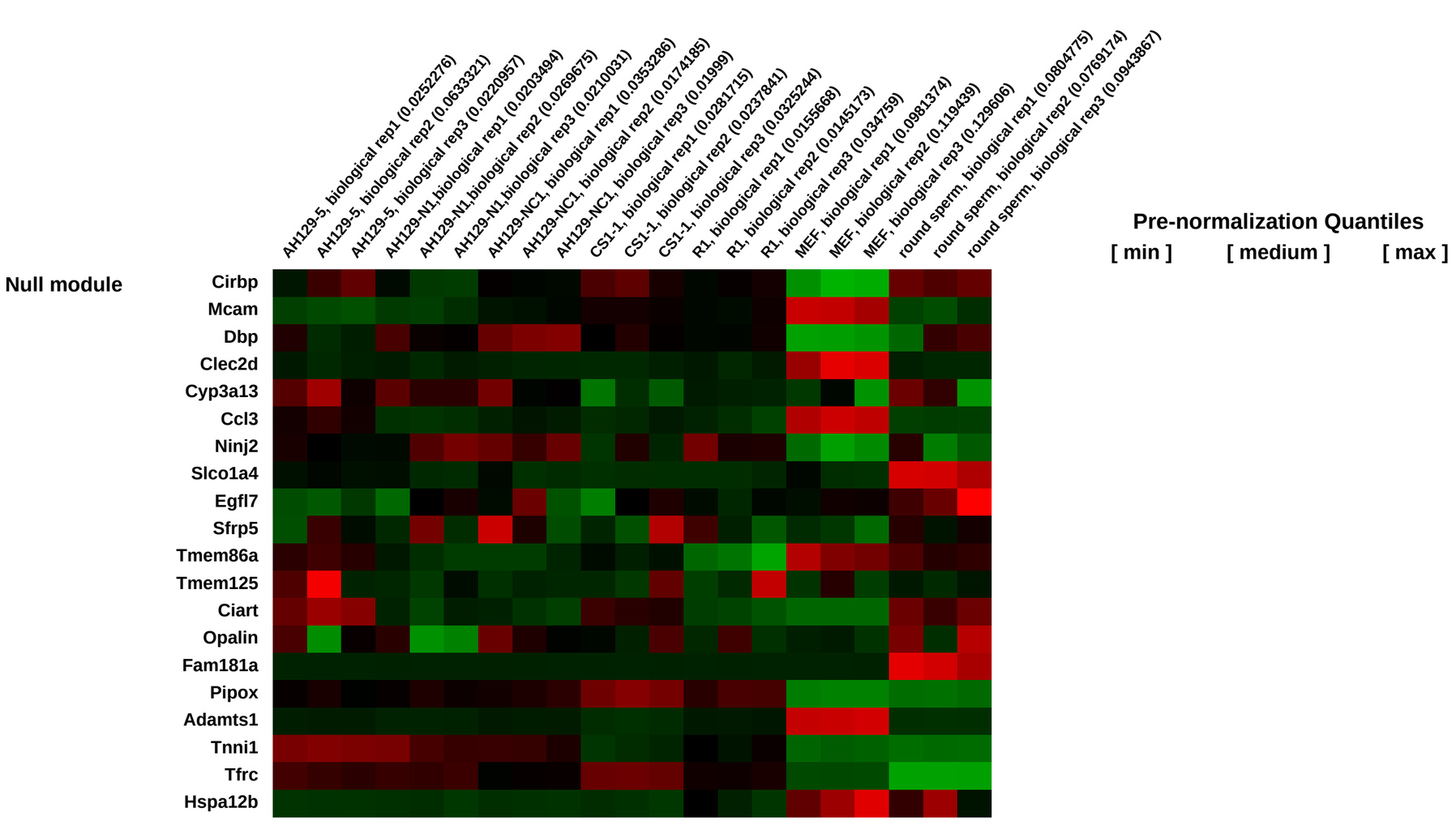

GEO Series "GSE4308" Expression Profiles

Num of samples in this series: 16

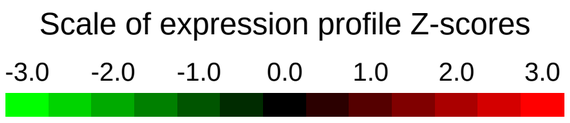

GEO Link:	**http://www.ncbi.nlm.nih.gov/geo/query/acc.cgi?acc=GSE4308**
Status:	**Public on Apr 26 2006**
Title:	**Expression data for validation of single cell cDNA amplification method (V1V3 method)**
Organism:	**Mus musculus**
Experiment type:	**Expression profiling by array**
Platform:	**GPL1261**
Pubmed ID:	**16547197**
Summary & Design:	**Summary:** **A systems-level understanding of a small but essential population of cells in development or adulthood (e.g., somatic stem cells) requires accurate quantitative monitoring of genome-wide gene expression, ideally from single cells. We report here a strategy to globally amplify mRNAs from single cells for highly quantitative high-density oligonucleotide microarray analysis that combines a small number of directional PCR cycles with subsequent linear amplification. Using this strategy, both the representation of gene expression profiles and reproducibility between individual experiments are unambiguously improved from the original method, along with high coverage and accuracy.** **Keywords: Method validation** **Overall design:** **To verify the ability of the developed method, we prepared total RNA from ES cells and diluted it to the single-cell level (10 pg). Eight array data from the cDNA samples amplified independently from the 10 pg RNA (amplified samples) were compared to each other, and to eight array data from the undiluted 5 ug RNA (nonamplified controls). Since all the materials were the same, all of the observed variations were attributable to the methodogoly.**

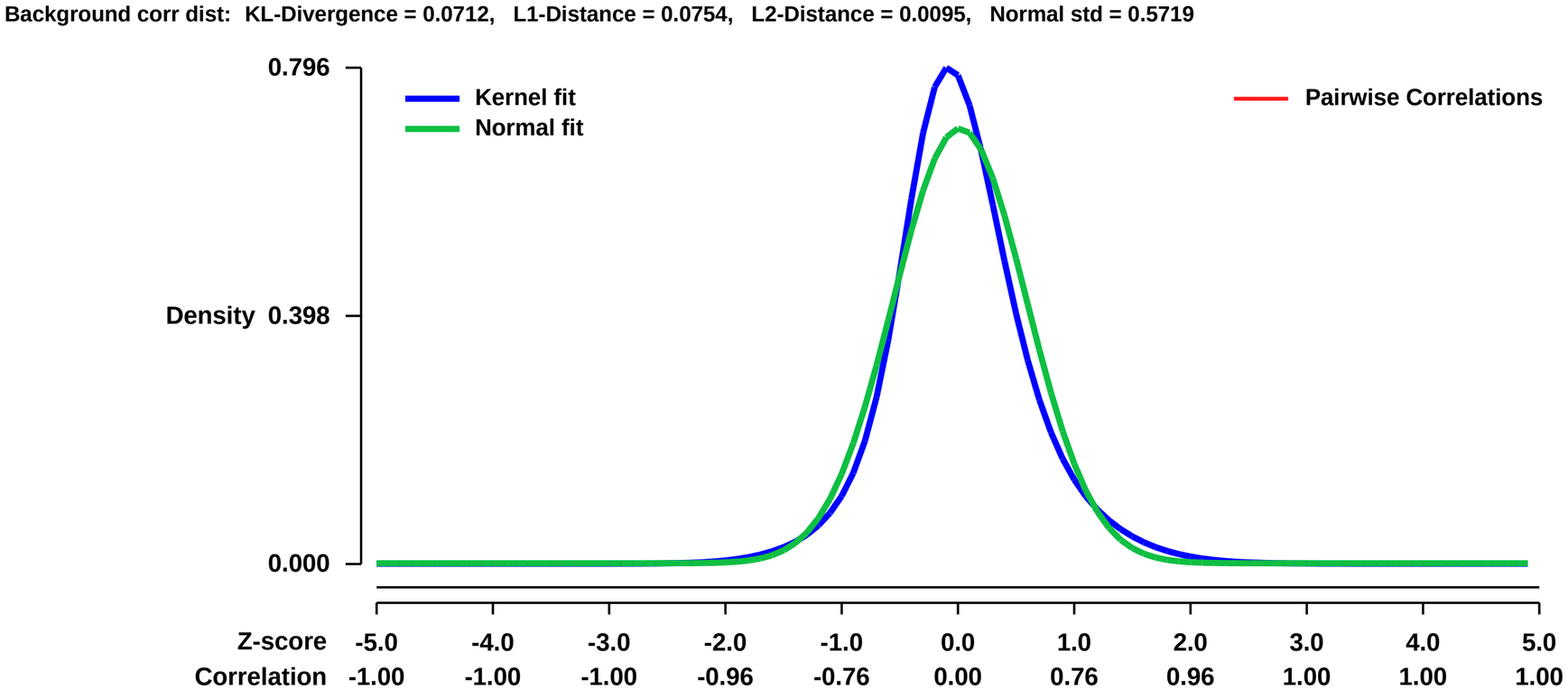

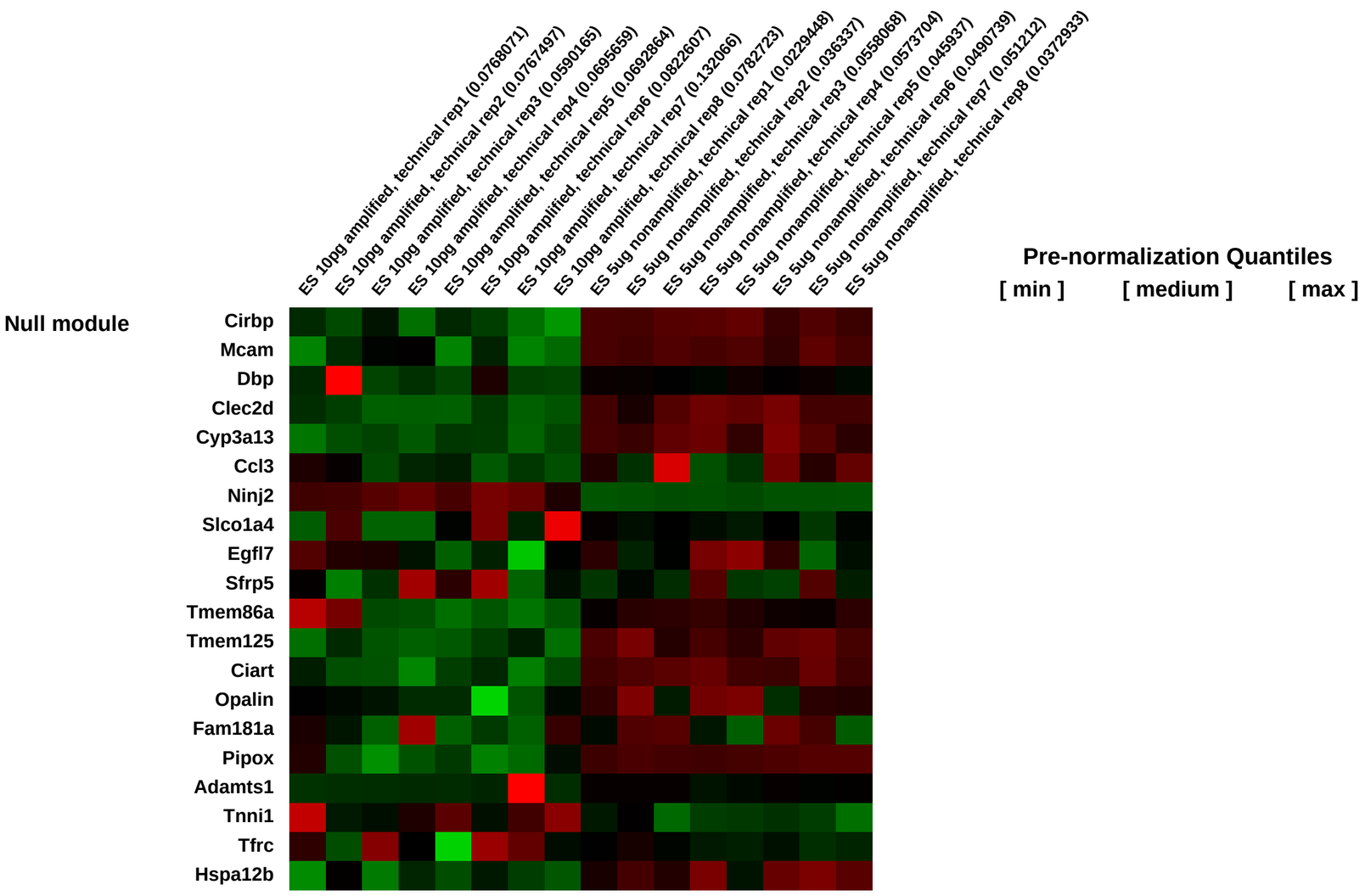

GEO Series "GSE8555" Expression Profiles

Num of samples in this series: 8

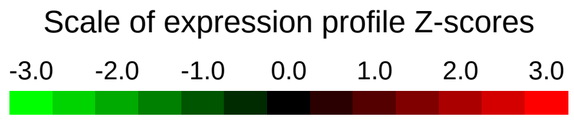

GEO Link:	http://www.ncbi.nlm.nih.gov/geo/query/acc.cgi?acc=GSE8555
Status:	Public on Jul 25 2007
Title:	Genome-wide analysis of Phgdh inactivation in murine embryonic head
Organism:	Mus musculus
Experiment type:	Expression profiling by array
Platform:	GPL1261
Pubmed ID:	18228065
Summary & Design:	**Summary:** **D-3-Phosphoglycerate dehydrogenase (Phgdh; EC 1.1.1.95) is a necessary enzyme for de novo L-serine biosynthesis via the phosphorylated pathway. We demonstrated previously that Phgdh is expressed exclusively by neuroepithelium and radial glia in developing mouse brain and later mainly by astrocytes. Mutations in the human PHGDH gene cause serine deficiency disorders (SDD) associated with severe neurological symptoms such as congenital microcephaly, psychomotor retardation, and intractable seizures. We recently demonstrated that genetically engineered mice, in which the gene for Phgdh has been disrupted, have significantly decreased levels of serine and glycine, and exhibit malformation of brain such as microcephaly. The Phgdh null (KO) embryos exhibit lethal phenotype after gestational day 14, indicating that the phosphorylated pathway is essential for embryogenesis, especially for brain development. It is worth noting that the Phgdh knockout (KO) embryos primarily displayed microcephaly, which is the most conspicuous phenotype of patients with SDD. Thus, Phgdh KO mice are a useful animal model for studying the effect of diminished L-serine levels on development of the central nervous system and other organs. To better understand the mechanism underlying the molecular pathogenesis of SDD, we sought to examine whether gene expression is altered in the Phgdh KO mouse model. We identify genes that have altered expression in the head of the Phgdh KO embryos using the GeneChip array. Some of the genes identified by this method belong in functional categories that are relevant to the biochemical and morphological aberrations of the Phgdh deletion.** **Keywords: genetic modification** **Overall design:** **RNA of 4 biological replicates was hybridized to Affymetrix Mouse Genome 430 2.0 arrays. Five microgram total RNA was labelled according to the ENZO-protocol, fragmented and hybridized according to Affymetrix's protocols.**

Background corr dist: **KL-Divergence = 0.0229, L1-Distance = 0.0165, L2-Distance = 0.0003, Normal std = 0.6997**

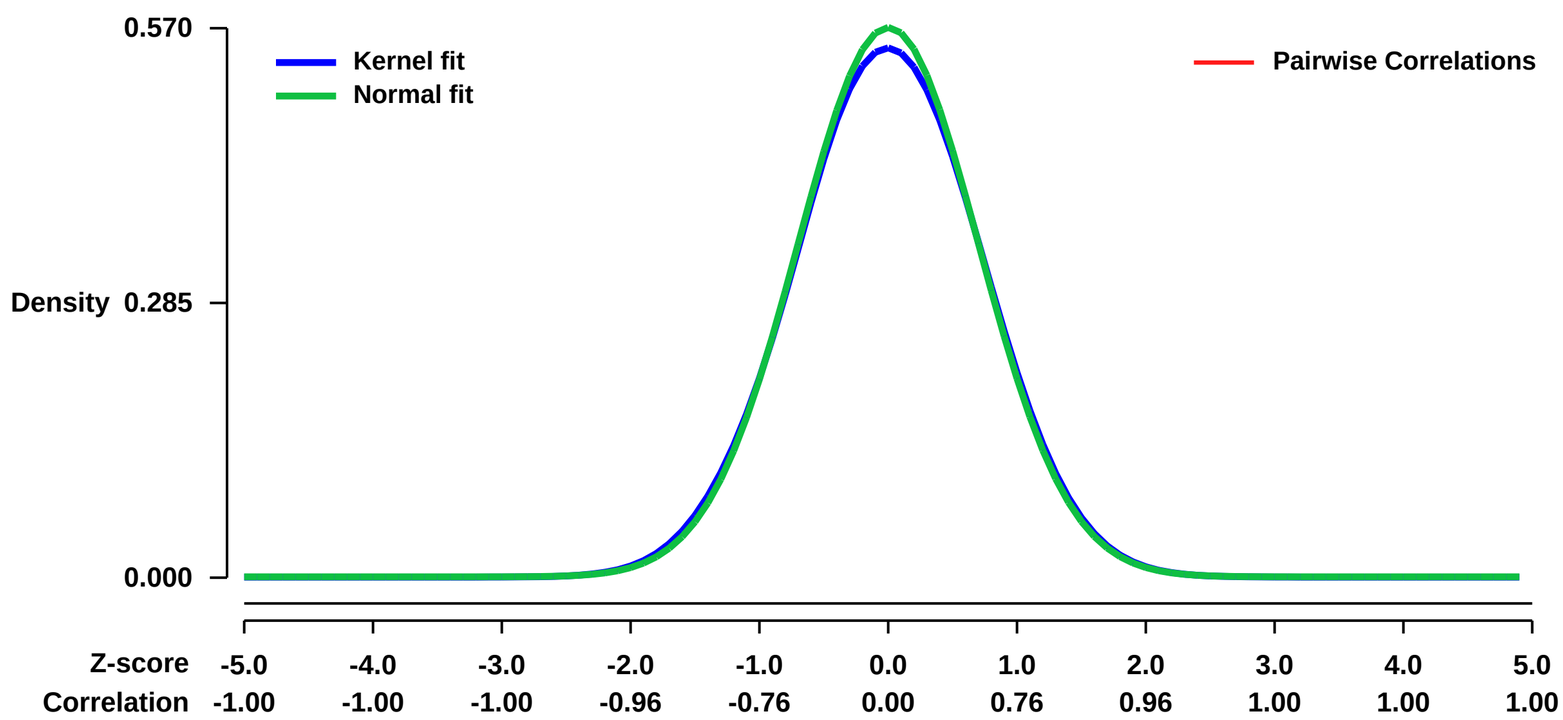

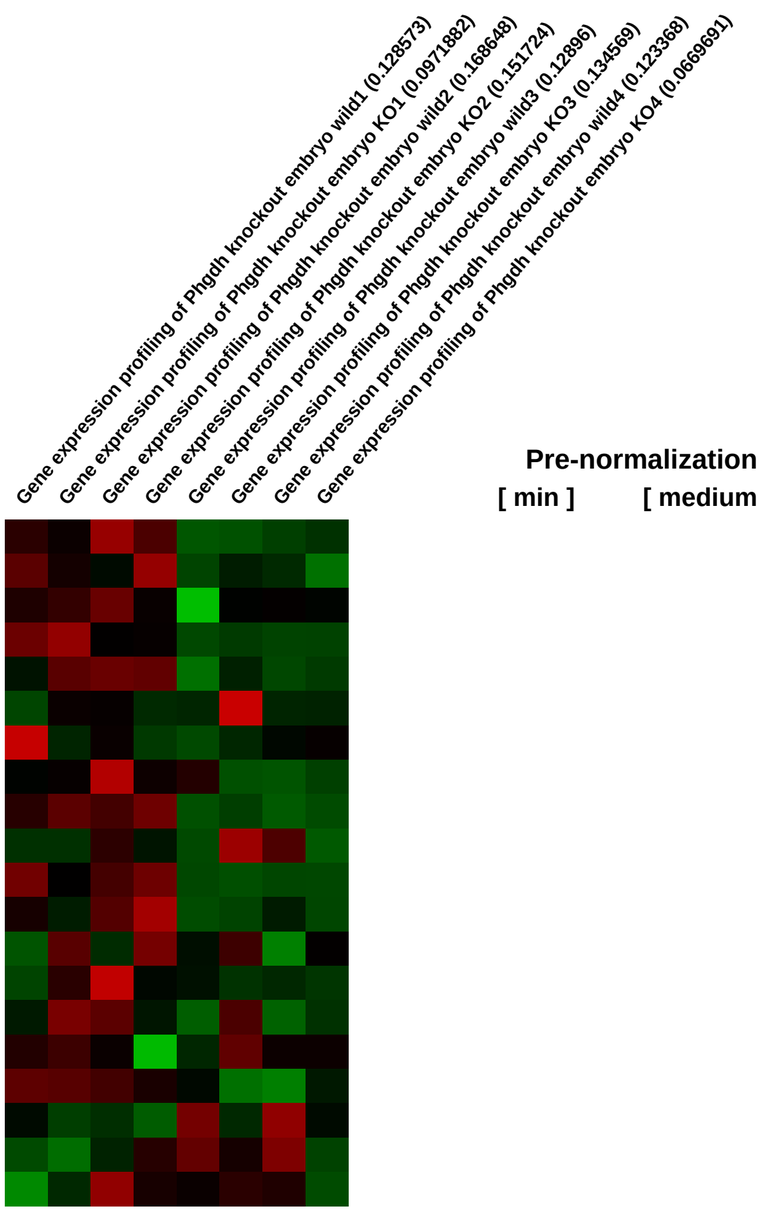

GEO Series "GSE31752" Expression Profiles

Num of samples in this series: 6

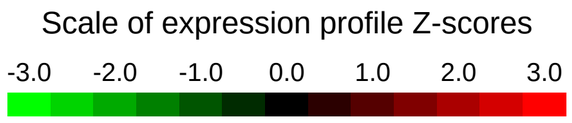

GEO Link:	**http://www.ncbi.nlm.nih.gov/geo/query/acc.cgi?acc=GSE31752**
Status:	**Public on Aug 31 2011**
Title:	**Mig-6 plays a critical role in the regulation of cholesterol homeostasis and bile acid synthesis.**
Organism:	**Mus musculus**
Experiment type:	**Expression profiling by array**
Platform:	**GPL1261**
Pubmed ID:	
Summary & Design:	**Summary:** **The disruption of cholesterol homeostasis leads to an increase in cholesterol levels which results in the development of cardiovascular disease. Mitogen Inducible Gene 6 (Mig-6) is an immediate early response gene that can be induced by various mitogens, stresses, and hormones. To identify the metabolic role of Mig-6 in the liver, we conditionally ablated Mig-6 in the liver using the Albumin-Cre mouse model (Albcre/+Mig-6f/f; Mig-6d/d). Mig-6d/d mice exhibit hepatomegaly and fatty liver. Serum levels of total, LDL, and HDL cholesterol and hepatic lipid were significantly increased in the Mig-6d/d mice. The daily excretion of fecal bile acids was significantly decreased in the Mig-6d/d mice. DNA microarray analysis of mRNA isolated from the livers of these mice showed alterations in genes that regulate lipid metabolism, bile acid, and cholesterol synthesis, while the expression of genes that regulate biliary excretion of bile acid and triglyceride synthesis showed no difference in the Mig-6d/d mice compared to Mig-6f/f controls. These results indicate that Mig-6 plays an important role in cholesterol homeostasis and bile acid synthesis. Mice with liver specific conditional ablation of Mig-6 develop hepatomegaly and increased intrahepatic lipid and provide a novel model system to investigate the genetic and molecular events involved in the regulation of cholesterol homeostasis and bile acid synthesis. Defining the molecular mechanisms by which Mig-6 regulates cholesterol homeostasis will provide new insights into the development of more effective ways for the treatment and prevention of cardiovascular disease.** **Overall design:** **Eight week old Mig-6f/f vs Mig-6d/d male mice after undergoing a 24 hour fast**

Background corr dist: KL-Divergence = 0.0256, L1-Distance = 0.0139, L2-Distance = 0.0002, Normal std = 0.6931

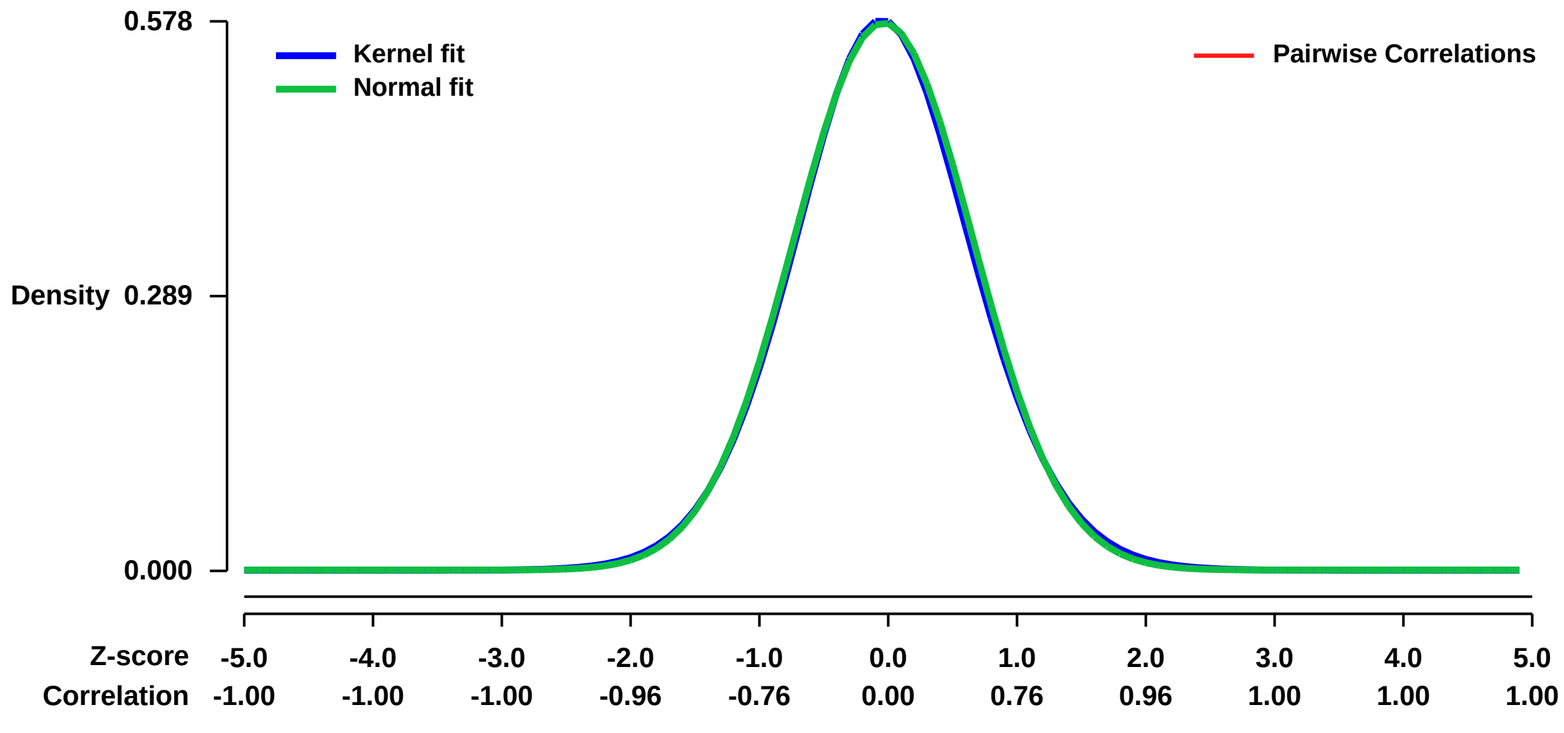

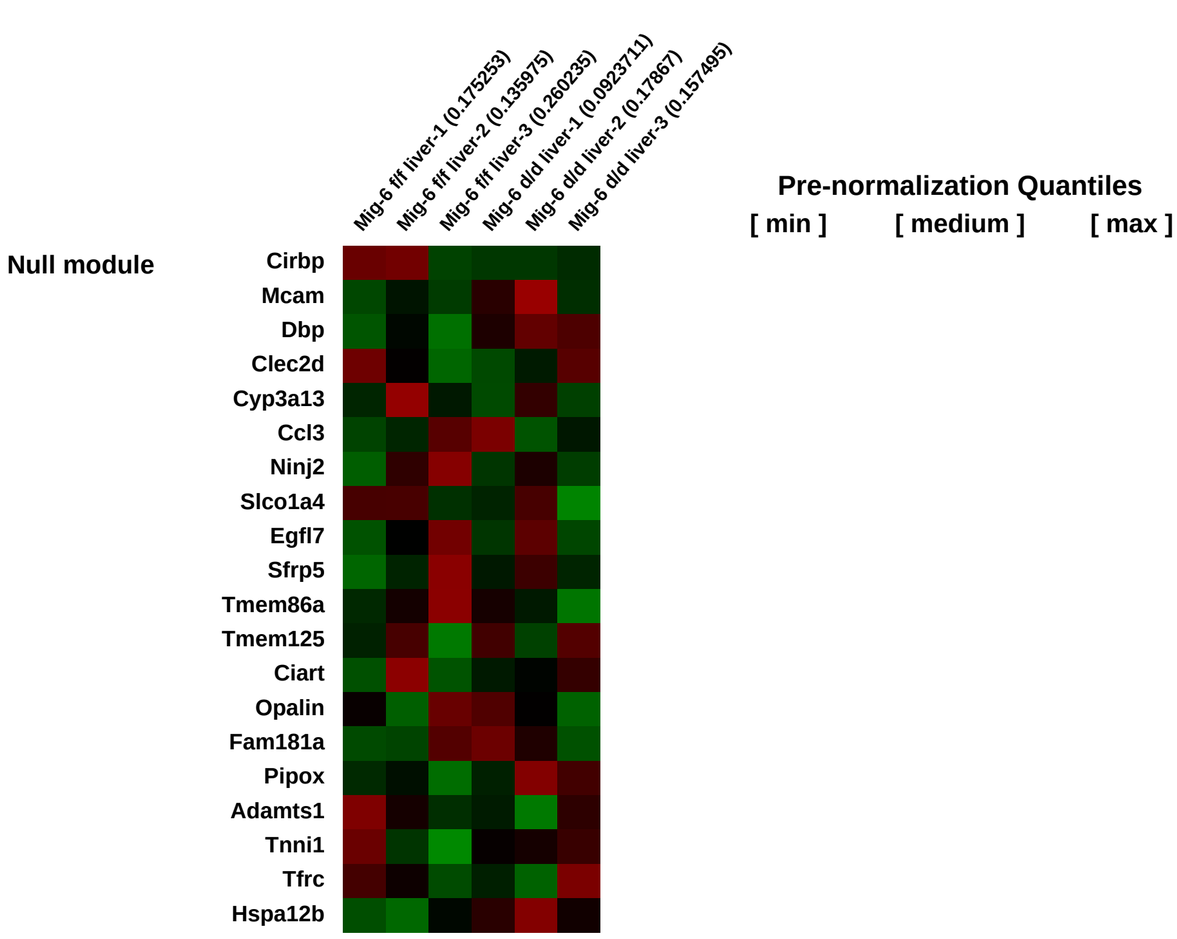

GEO Series "GSE52474" Expression Profiles

Num of samples in this series: 154

Details of this dataset are not shown due to large number of samples and the page size limit.

Find details in http://www.ncbi.nlm.nih.gov/geo/query/acc.cgi?acc=GSE52474

Background corr dist: KL-Divergence = 0.1954, L1-Distance = 0.0793, L2-Distance = 0.0167, Normal std = 0.3721

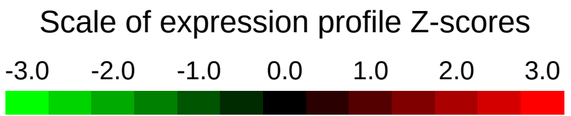

GEO Series "GSE46724" Expression Profiles

Num of samples in this series: 6

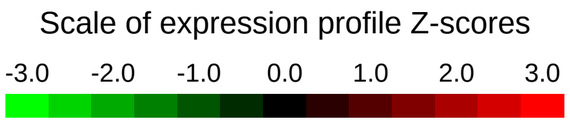

GEO Link:	http://www.ncbi.nlm.nih.gov/geo/query/acc.cgi?acc=GSE46724
Status:	Public on Jul 01 2013
Title:	Expression data from adult Myeloerythroid Progenitors (MP) ICN2 positive and adult Myeloerythroid Progenitors (MP) ICN2 negative
Organism:	Mus musculus
Experiment type:	Expression profiling by array
Platform:	GPL1261
Pubmed ID:	23791481
Summary & Design:	**Summary:** Notch signaling defines a conserved, fundamental pathway, responsible for determination in metazoan development and is widely recognized as an essential component of lineage specific differentiation and stem cell self-renewal in many tissues including the hematopoietic system. Until recently, the majority of studies in the hematopoietic system focused on Notch signaling in lymphocyte differentiation and knowledge of individual Notch receptor roles in early hematopoiesis has been limited due to a paucity of genetic tools available To fate-map Notch receptor expression and pathway activity in the hematopoietic system we used tamoxifen-inducible CreER knock-in mice for individual Notch receptors in combination to a novel Notch reporter strain (Hes1GFP) and a conditional gain of function allele of Notch2 receptor (Rosa-lsl-ICN2). **Overall design:** Bone marrow lineage negative, cKit+, Sca1- cells were sorted from Rosa-lsl-ICN2 Mx1-cre+ mice or Mx1-cre+ littermates for RNA extraction and hybridization on Affymetrix microarrays

Background corr dist: KL-Divergence = 0.0317, L1-Distance = 0.0230, L2-Distance = 0.0005, Normal std = 0.6657

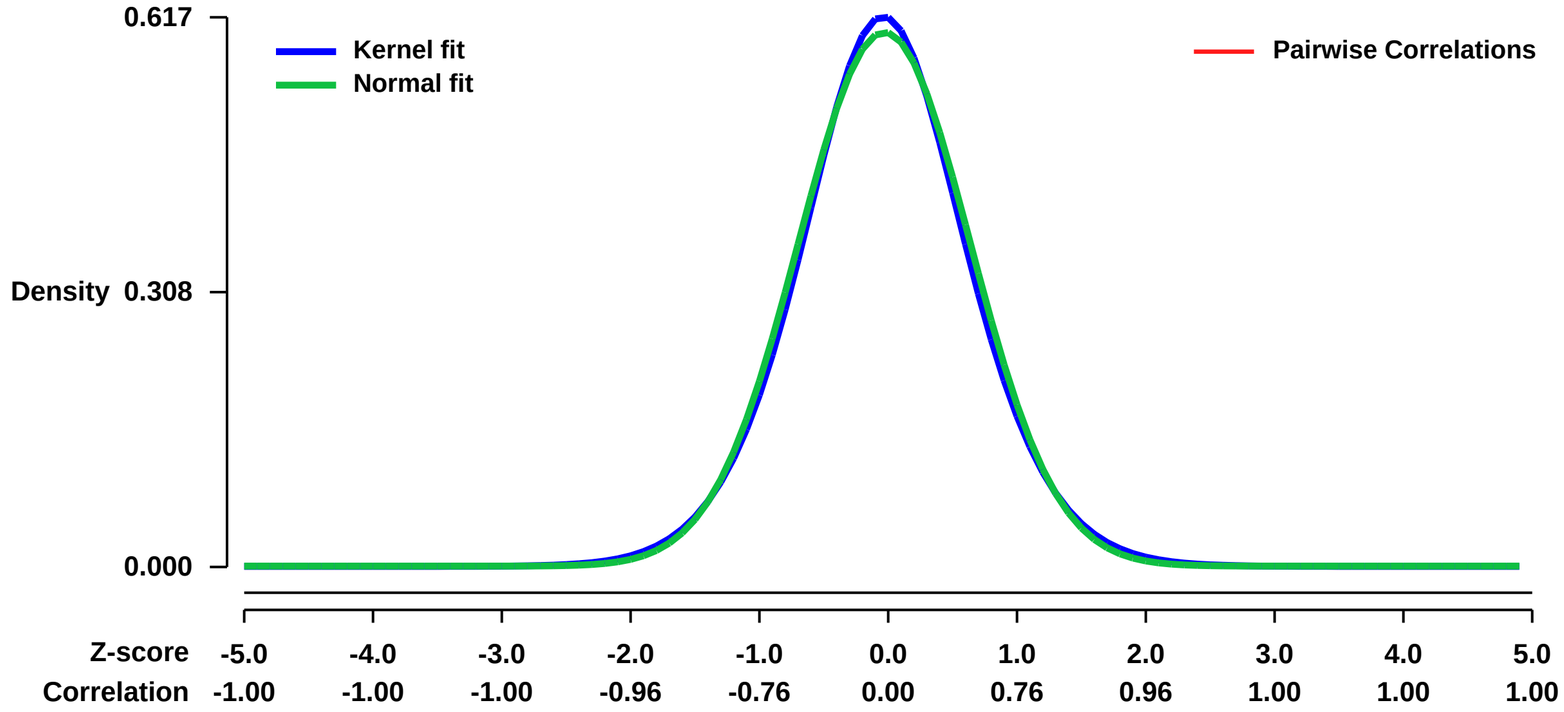

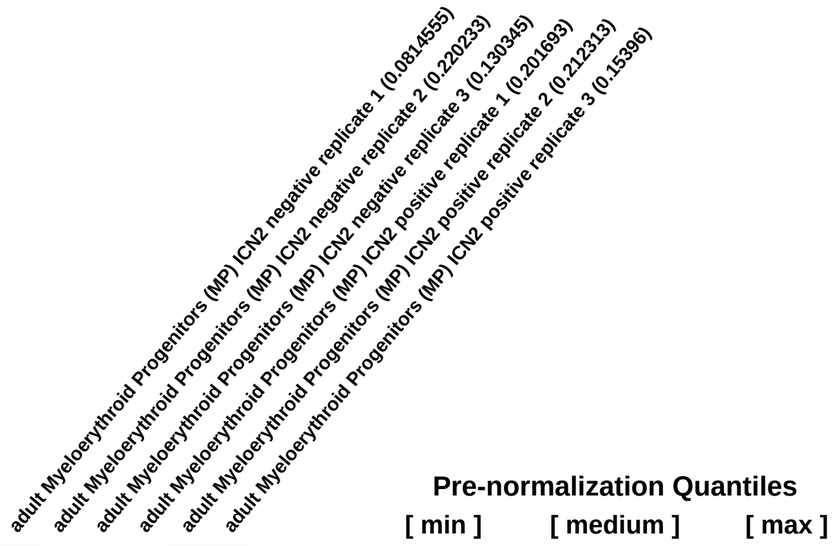

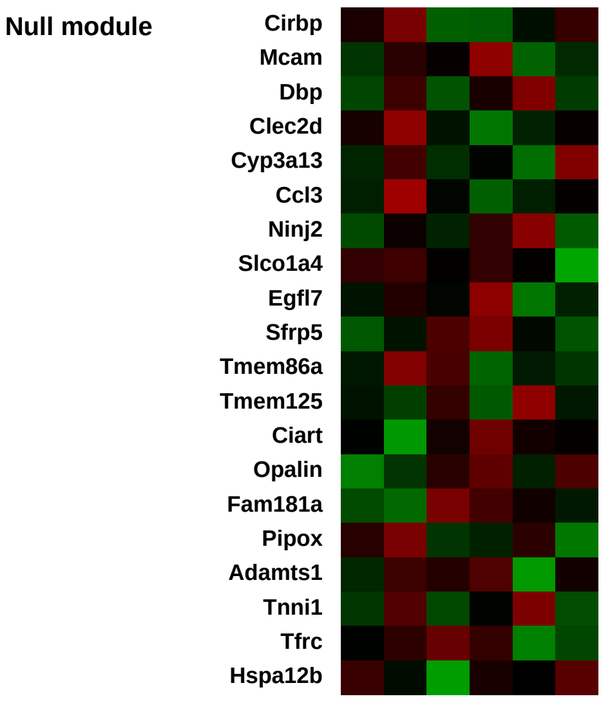

GEO Series "GSE45807" Expression Profiles

Num of samples in this series: 11

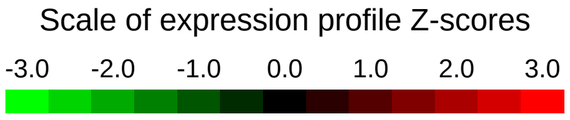

GEO Link:	http://www.ncbi.nlm.nih.gov/geo/query/acc.cgi?acc=GSE45807
Status:	Public on Oct 01 2013
Title:	Phrenic neuronal determinants screen in M.Musculus [1]
Organism:	Mus musculus
Experiment type:	Expression profiling by array
Platform:	GPL1261
Pubmed ID:	24496616
Summary & Design:	**Summary:** **Expression response after induction of putative phrenic neuronal determinants in ES cells was compared to a pre-determined list of genes over-expressed in FACS-sorted phrenic cells.** **Transcription factor Pou3f1 was identified as a major determinant of phrenic identity.** **Overall design:** **Cells type individually compared to the overall expression to identify differentially expressed genes patterns**

Background corr dist: **KL-Divergence = 0.0948, L1-Distance = 0.0318, L2-Distance = 0.0018, Normal std = 0.4452**

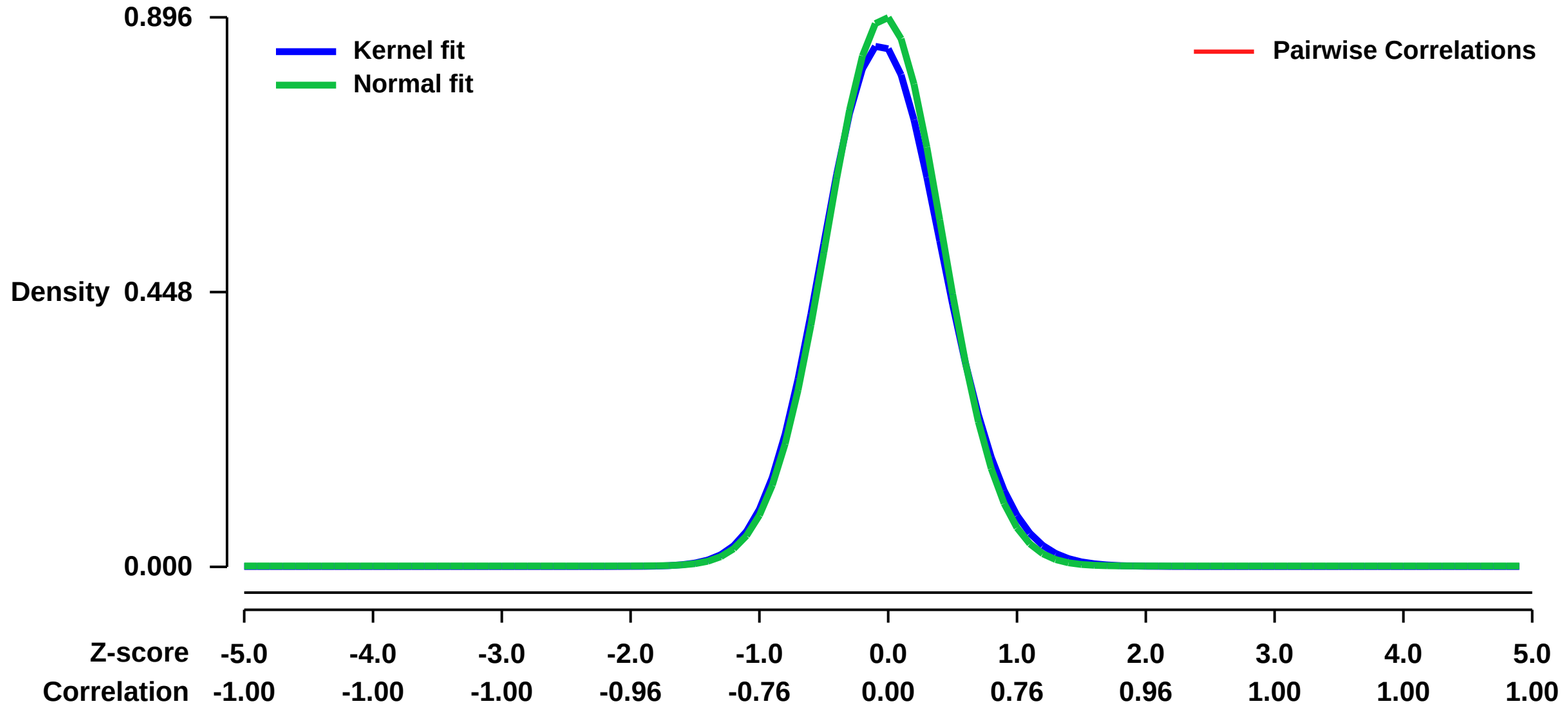

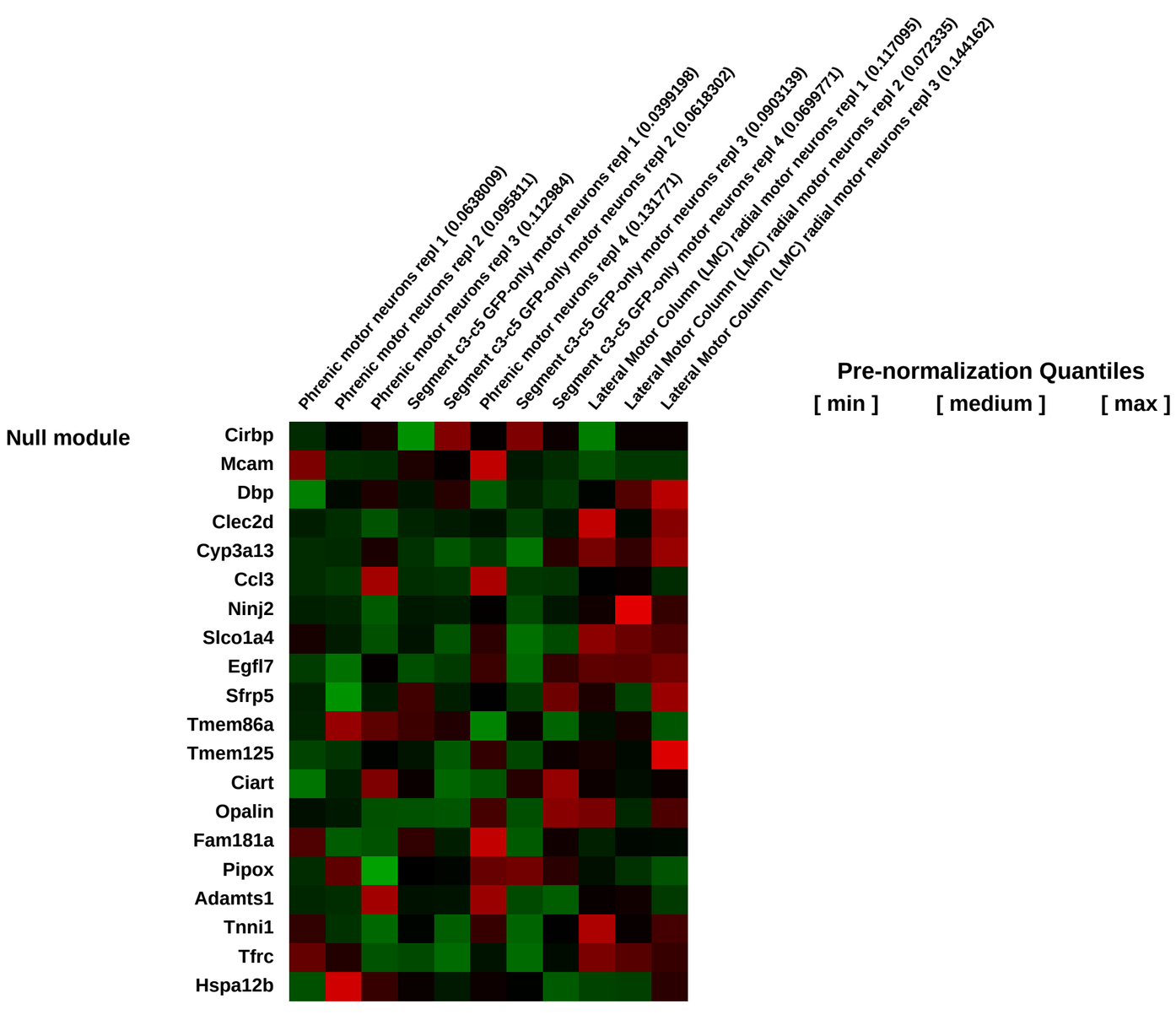

GEO Series "GSE31797" Expression Profiles

Num of samples in this series: 6

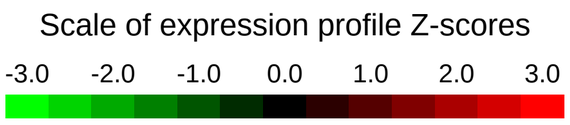

GEO Link:	http://www.ncbi.nlm.nih.gov/geo/query/acc.cgi?acc=GSE31797
Status:	Public on Mar 01 2012
Title:	Activation of SREBP in Alveolar Type II Cells Enhances Lipogenesis Causing Pulmonary Lipotoxicity
Organism:	Mus musculus
Experiment type:	Expression profiling by array
Platform:	GPL1261
Pubmed ID:	22267724
Summary & Design:	**Summary:** **Background: Lung function is dependent upon the precise regulation of the synthesis, storage, and catabolism of tissue and alveolar lipids.** **Results: Activation of SREBP (Sterol Response Element Binding Protein) induced lipogenesis in alveolar epithelial cells, causing neutral lipid accumulation, lung inflammation, and tissue remodeling.** **Conclusions: The accumulation of neutral lipids in type II epithelial cells and alveolar macrophages caused lung inflammation, consistent with findings in lipid storage disorders.** **Significance: Pulmonary lipotoxicity may contribute to the pathogenesis of lung dysfunction associated with diabetes, obesity, and other metabolic disorders.** **Overall design:** **Genome-wide transcription profiling comparison between doxycycline-exposed SFTPC-rtTAWT/Tg/(tetO)7CMV-CreWT/Tg/Insig1flox/flox/Insig2-/- mice (i.e., Insig1/2â /â) and Insig1flox/flox/Insig2-/- . Three independent pooled RNA from isolated lung type 2 cells of each genotype were used.**

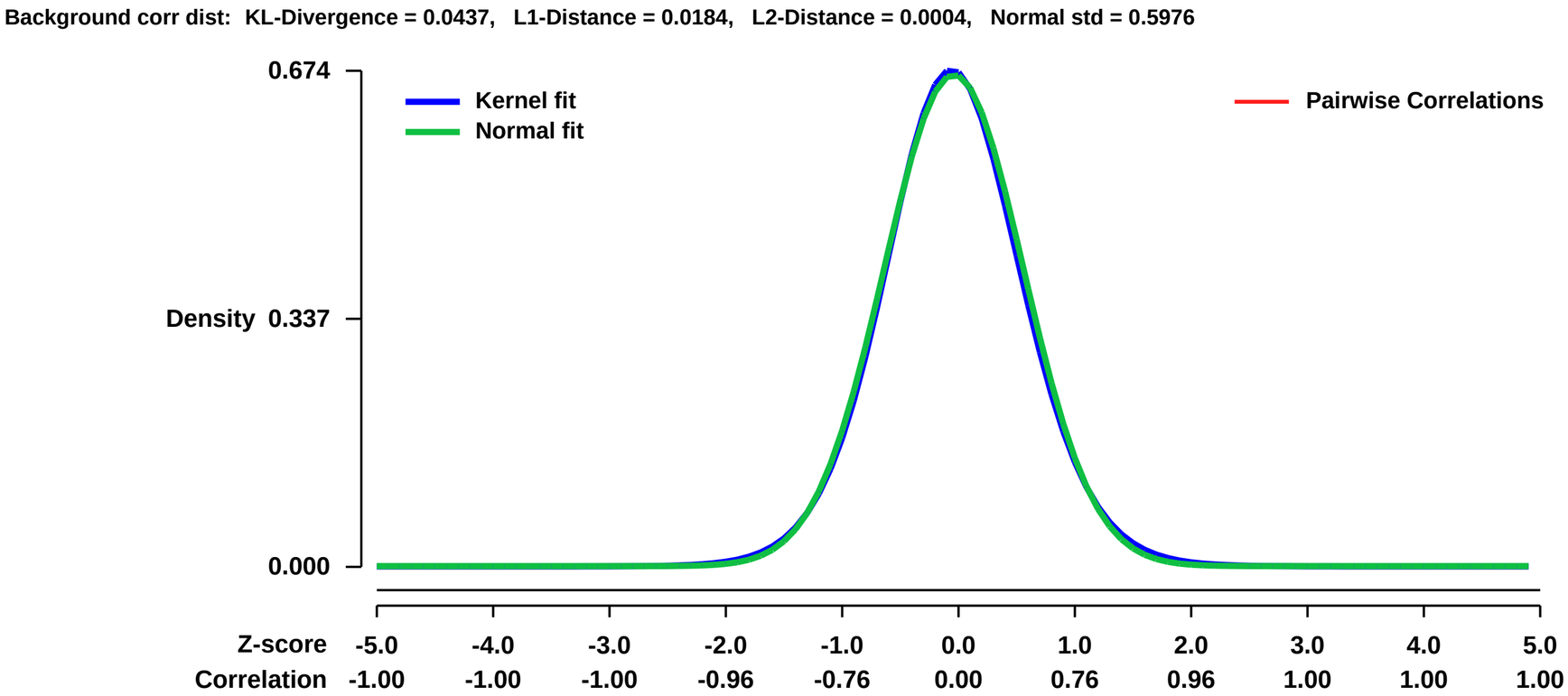

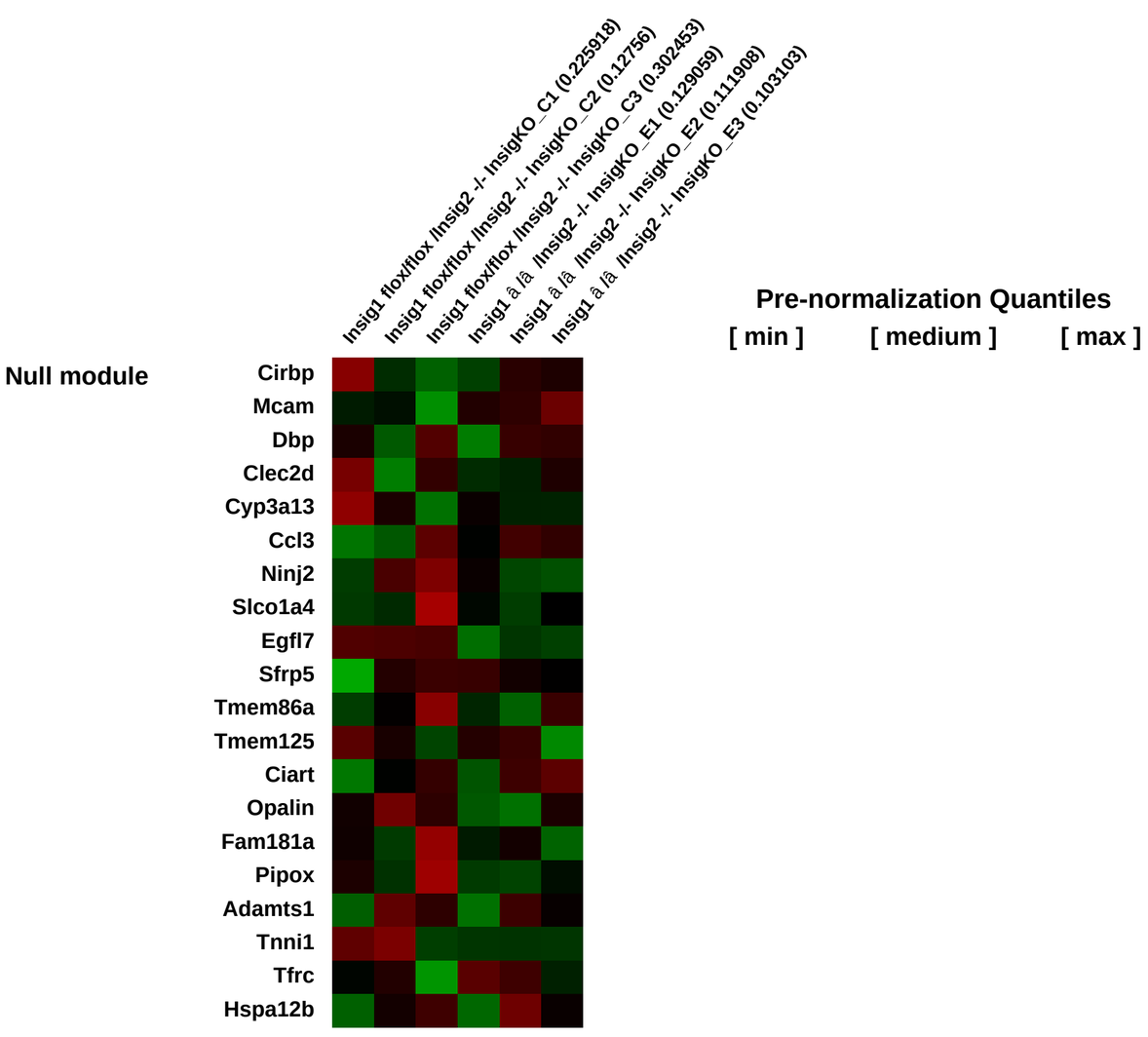

GEO Series "GSE42260" Expression Profiles

Num of samples in this series: 6

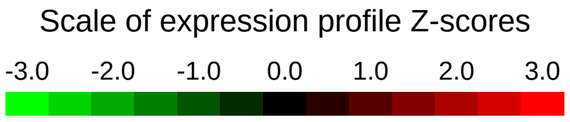

GEO Link:	http://www.ncbi.nlm.nih.gov/geo/query/acc.cgi?acc=GSE42260
Status:	Public on Jan 18 2013
Title:	Notch Pathway Activation Targets AML Cell Homeostasis and Differentiation: MLL-AF9 transformed LGMP
Organism:	Mus musculus
Experiment type:	Expression profiling by array
Platform:	GPL1261
Pubmed ID:	23359070
Summary & Design:	**Summary:** To determine role of Notch signaling in AML leukemia initiating cells we used a conditional mouse knock-in model of Notch1-IC to induce Notch1-IC expression in MLL-AF9 transformed LGMP. WT and Notch1-IC+ LGMP were analyzed to determined genes controlled by Notch signaling. **Overall design:** 12 weeks old wt lethaly irradiated mice were transplanted with 50000 cKit+ MLL-AF9-IRES-YFP infected cells from MLL-AF9 EF1 wt/wt ROSAwt/CreERT2 or MLL-AF9 EF1 wt/lsl-N1-IC ROSAwt/CreERT2 mice + 250000 support wt total bone marrow cells. 4 weeks after transplant mice were injected 2 times with tamoxifen (0.2mg/g body weight) every other day. Mice were sacrificed and analyzed 6 days after last injection. LGMP were flow purified for RNA extraction and hybridization on Affymetrix microarrays.

Background corr dist: KL-Divergence = 0.0405, L1-Distance = 0.0182, L2-Distance = 0.0004, Normal std = 0.6118

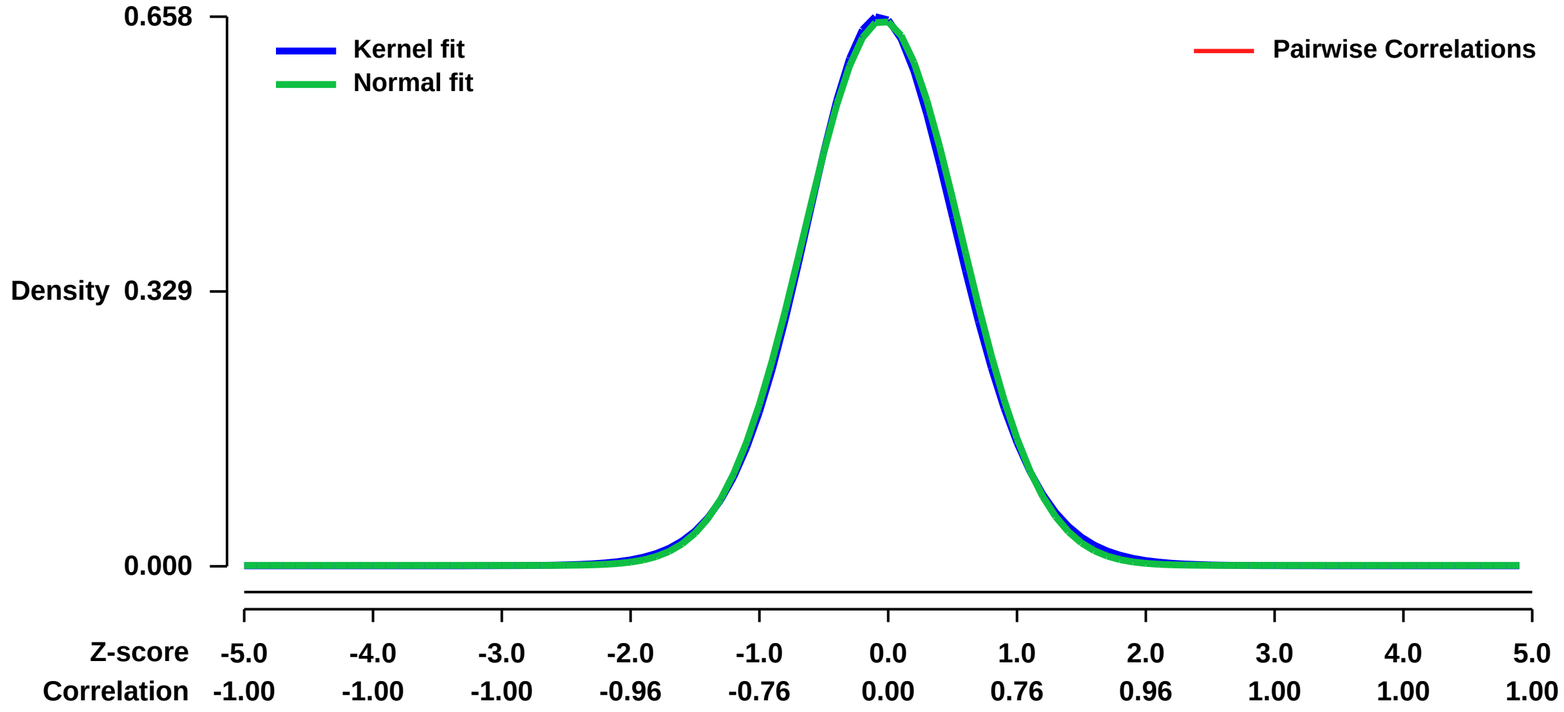

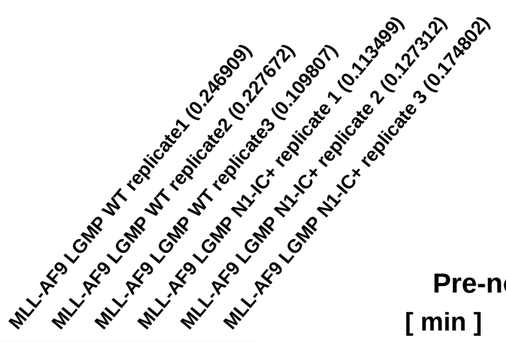

Pre-normalization Quantiles

[min] [medium] [max]

Null module

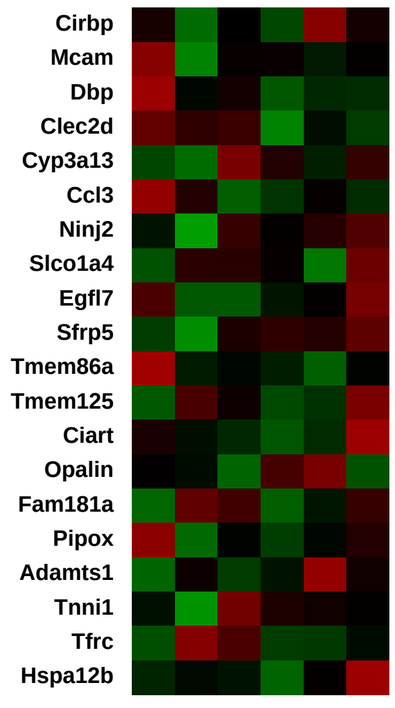

GEO Series "GSE8091" Expression Profiles

Num of samples in this series: 16

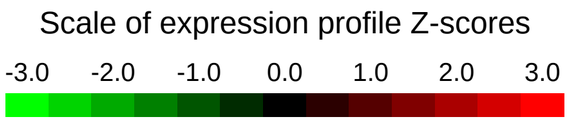

GEO Link:	http://www.ncbi.nlm.nih.gov/geo/query/acc.cgi?acc=GSE8091
Status:	Public on May 29 2008
Title:	Transcriptome and proteome analysis of early embryonic mouse brain development
Organism:	Mus musculus
Experiment type:	Expression profiling by array
Platform:	GPL1261
Pubmed ID:	18283662
Summary & Design:	**Summary:** Embryonic mouse brain development involves a sequential differentiation of multipotent progenitor cells into neurons and glia. Using microarrays and large 2-D electrophoresis, we investigated the transcriptome and proteome of mouse brains at embryonic days 9.5, 11.5 and 13.5. During this developmental period, neural progenitor cells shift from proliferation to neuronal differentiation. As expected, we detected numerous expression changes between the time points investigated but interestingly, the rate of alteration was about 10% to 13% of all proteins and mRNAs during every two days of development. Furthermore, up- and downregulation was balanced. This was confirmed for two additional stages of development, embryonic day 16 and 18. We hypothesize that during embryonic development, the rate of protein expression alteration is rather constant due to a limitation of cellular resources such as energy, space and free water. The similar complexity found at the transcriptome and proteome level at all stages suggests, that changes in relative concentration of gene products rather than an increased number of gene products dominate throughout cellular differentiation. We found that metabolism and cell cycle related gene products were downregulated in expression when precursor cells switched from proliferation to neuronal differentiation (day 9.5 to 11.5), whereas neuron specific gene products were upregulated. A detailed analysis revealed their implication in differentiation related processes such as rearrangement of the actin cytoskeleton as well as Notch and Wnt signaling pathways. **Keywords: time course, development, transcriptome, proteome** **Overall design:** E13.5: 6 biological replicates

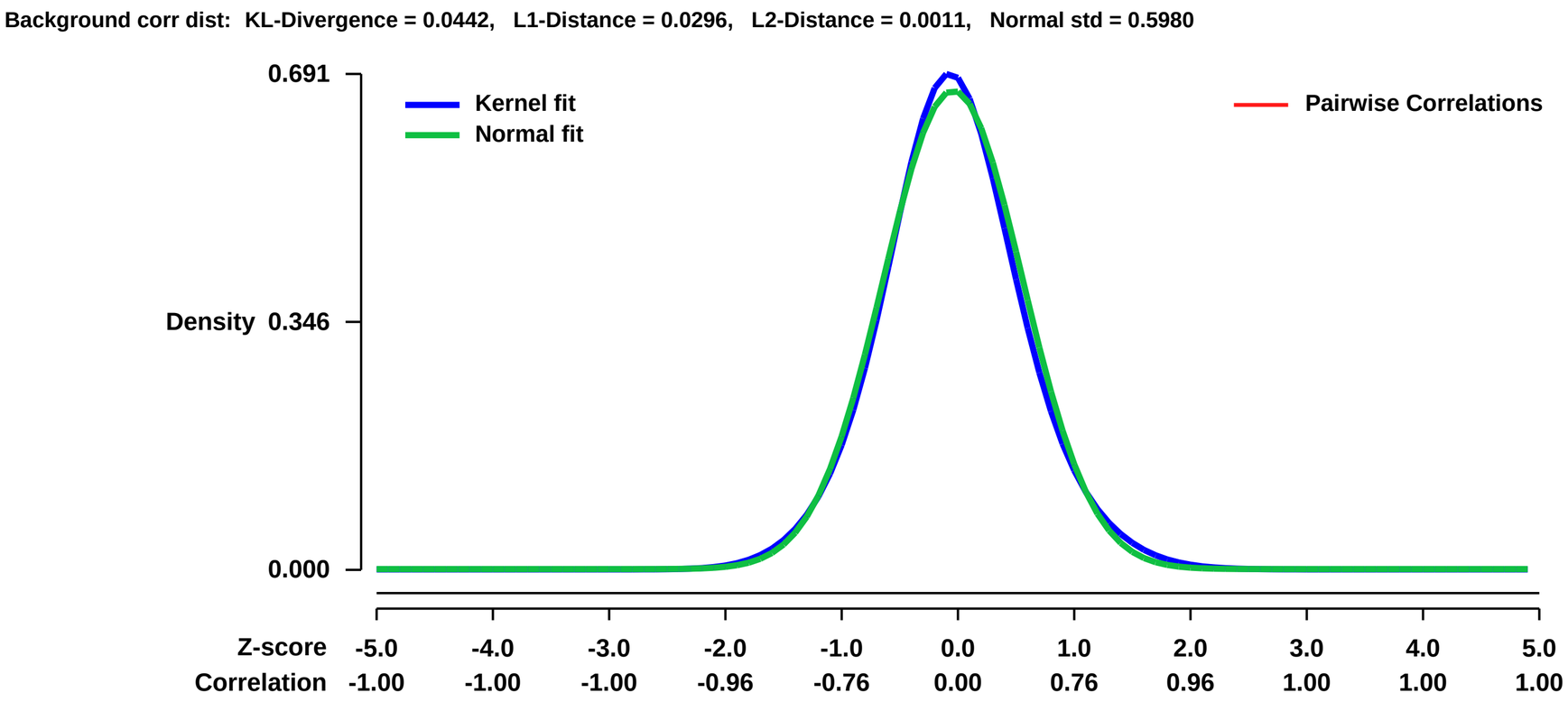

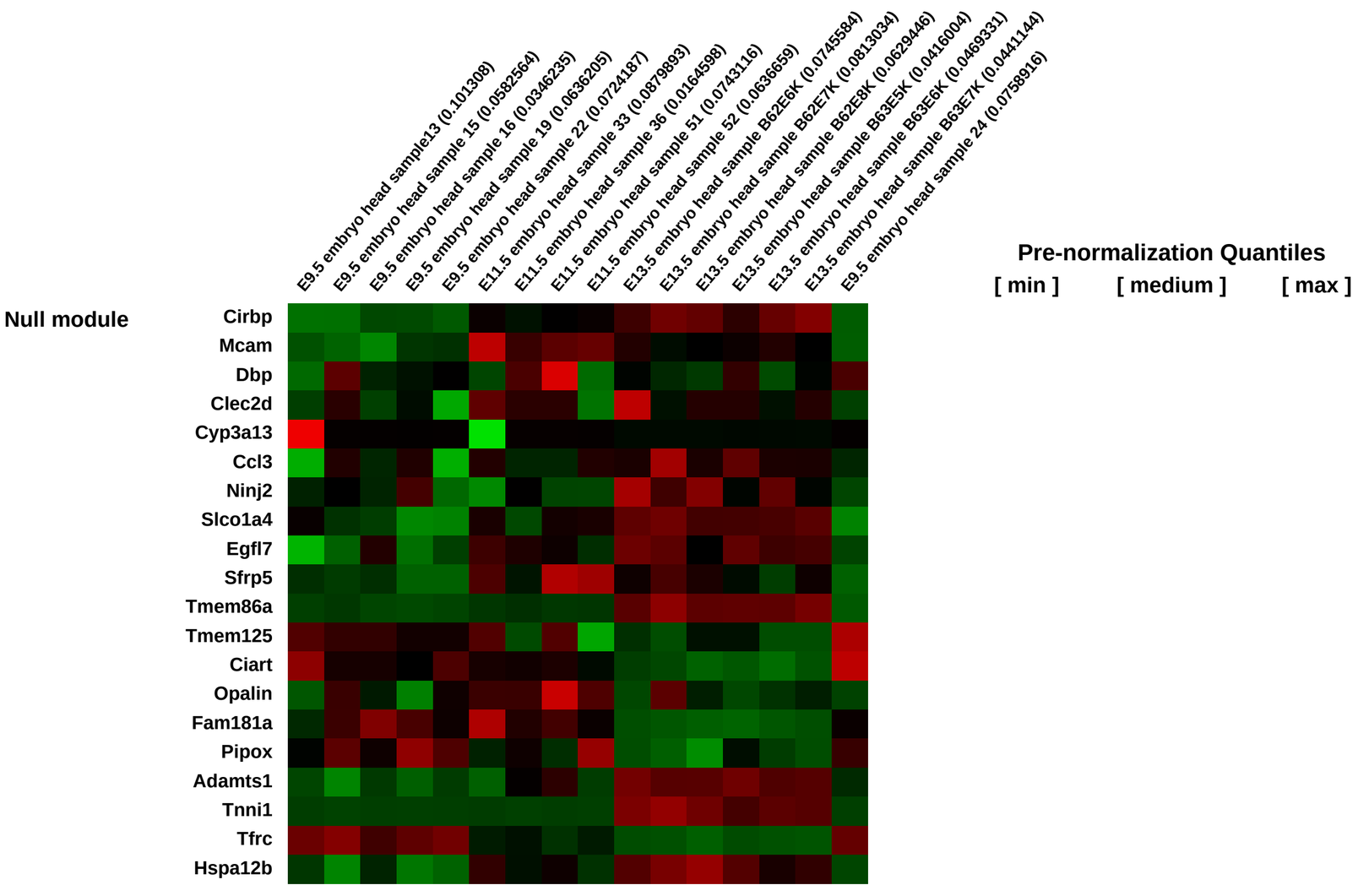

GEO Series "GSE30745" Expression Profiles

Num of samples in this series: 12

Scale of expression profile Z-scores

-3.0 -2.0 -1.0 0.0 1.0 2.0 3.0

GEO Link:	http://www.ncbi.nlm.nih.gov/geo/query/acc.cgi?acc=GSE30745
Status:	Public on Aug 05 2011
Title:	Expression data from murine acute myeloid leukemia (AML) cells following shRNA-mediated suppression of Myb
Organism:	Mus musculus
Experiment type:	Expression profiling by array
Platform:	GPL1261
Pubmed ID:	21828272
Summary & Design:	**Summary:** Using an integrative approach combining a Tet-off conditional AML mouse model, global expression profiling following suppression of the driving MLL-AF9 oncogene, and a new Tet-on conditional shRNA expression system we have identified Myb as critical mediator of addiction to MLL-AF9. Suppression of Myb in established AML in vivo terminates aberrant self-renewal and triggers a terminal myeloid differentiation program that precisely phenocopies the effects of suppressing MLL-AF9. Remarkably, suppressing Myb effectively eradicates aggressive and chemotherapy resistant AML. To further investigate Myb dependent transcriptional programs involved in mediating aberrant self-renewal in leukemia, we globally surveyed gene expression changes following acute shRNA-induced suppression of Myb in an established Tet-on competent model of MLL-AF9;NrasG12D-induced AML. **Overall design:** To enable regulatable suppression of Myb in AML, we retrovirally transduced established Tet-on competent MLL-AF9;NrasG12D induced AML cells with TRMPV-Neo vectors (Zuber et al., Nature Biotech, 2010) harboring shRNAs targeting Myb (shMyb.2572 and shMyb.2652), a control shRNA targeting Renilla Luciferase (shRen.713), or an empty miR30 cassette of the recipient cloning vector (Rec). Following drug selection, shRNA expression was induced by doxycycline treatment and total RNA was isolated from sorted shRNA expressing (Venus+/dsRed+) leukemia cells after 3 days of dox treatment, and subjected to Affymetrix microarray expression analysis. Expression profiles following expression of two independent Myb shRNAs were compared to those observed after induction in shRen.713- and Rec-expressing control samples (each in 3 biological replicates).

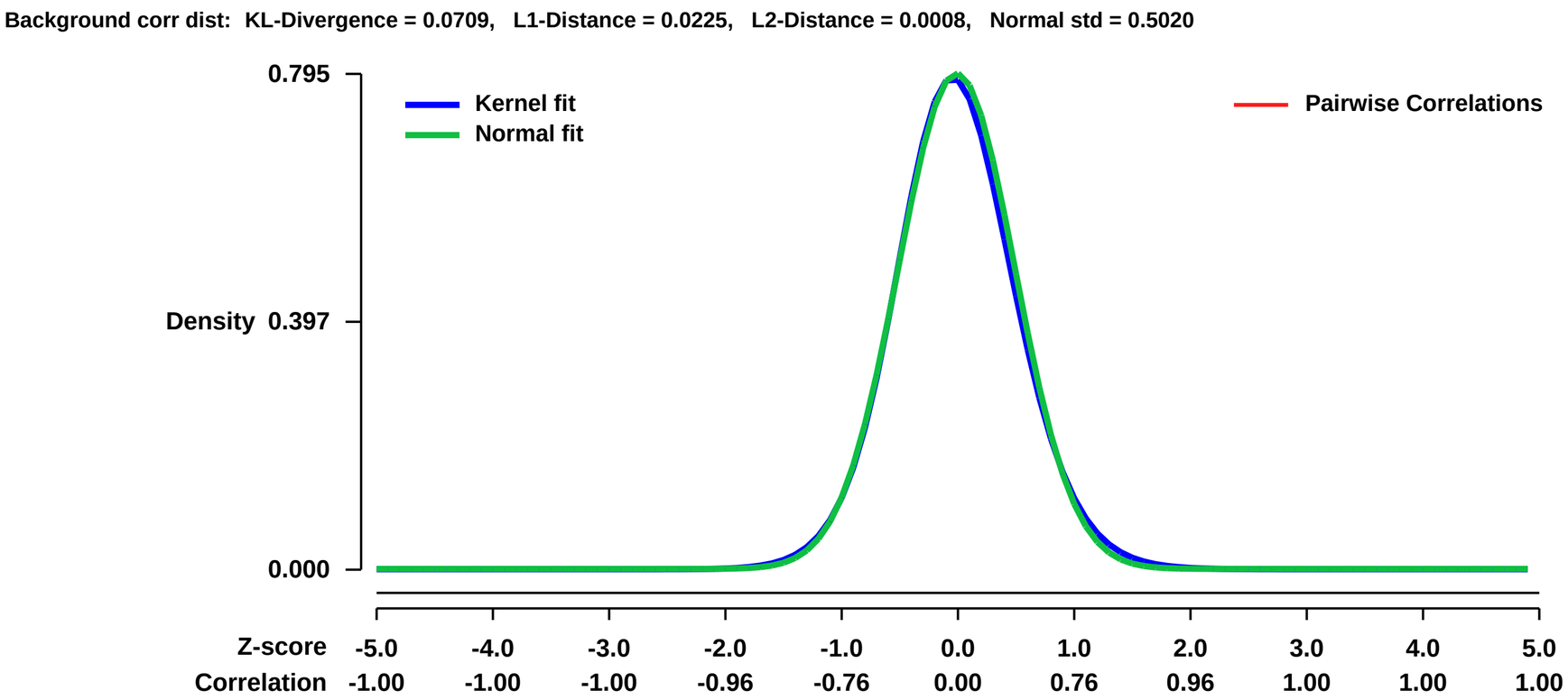

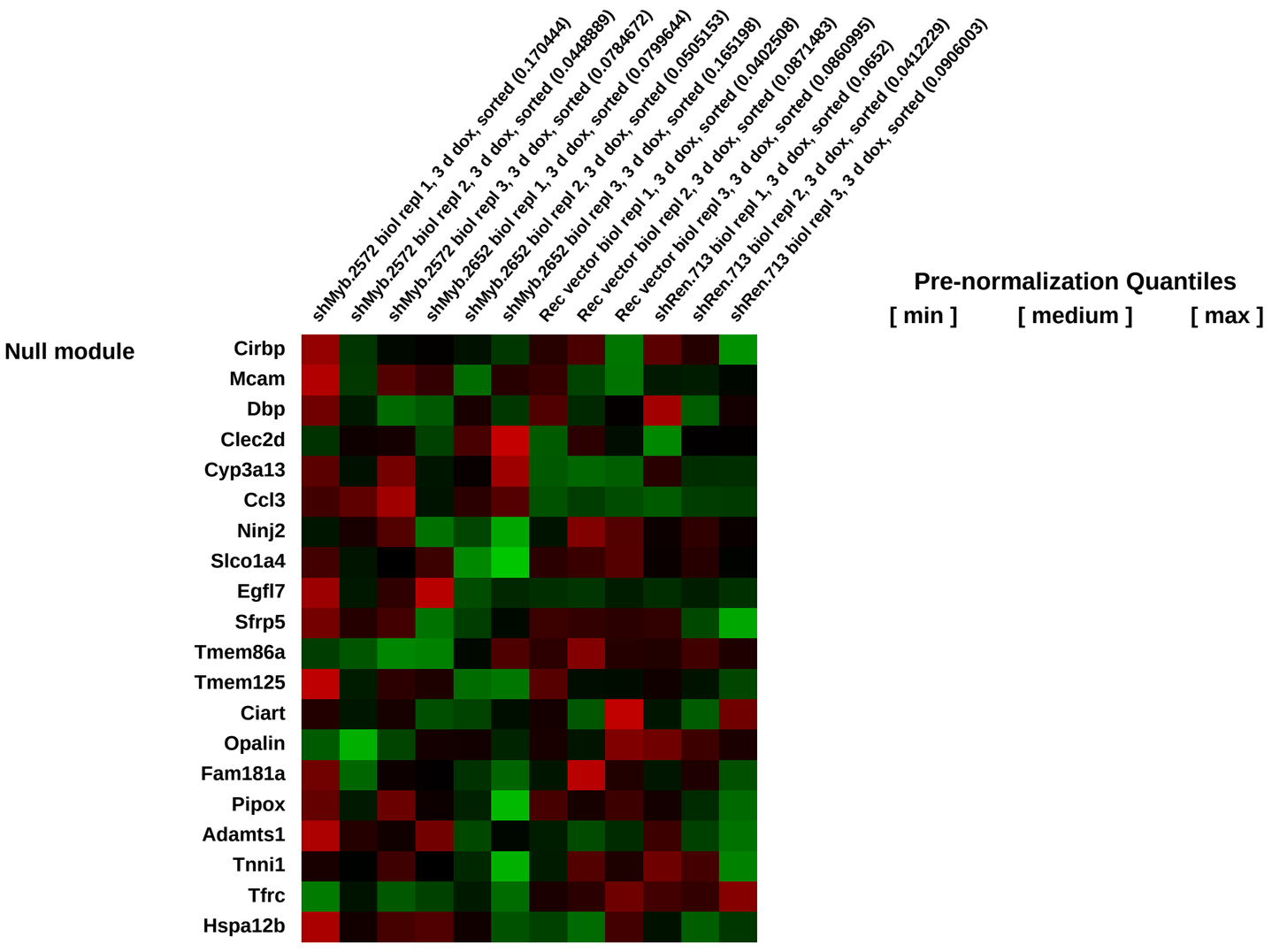

GEO Series "GSE9743" Expression Profiles

Num of samples in this series: 12

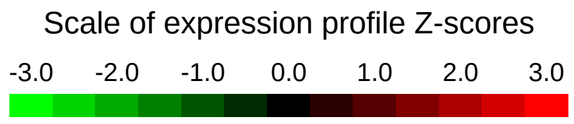

GEO Link:	http://www.ncbi.nlm.nih.gov/geo/query/acc.cgi?acc=GSE9743
Status:	Public on May 30 2008
Title:	The in vivo effect of actin cytoskeletal abnormalities on gene expression
Organism:	Mus musculus
Experiment type:	Expression profiling by array
Platform:	GPL1261
Pubmed ID:	18381839
Summary & Design:	**Summary:** Remodeling of the actin cytoskeleton through actin dynamics (assembly and disassembly of filamentous actin) is known to be essential for numerous basic biological processes. In addition, recent in vitro studies provided evidence that actin dynamics participate in the control of gene expression. A spontaneous mouse mutant, corneal disease 1 (corn1), is deficient for a regulator of actin dynamics, destrin (DSTN; also known as actin depolymerizing factor or ADF), and develops epithelial hyperproliferation and neovascularization in the cornea. Dstncorn1 mice exhibit the actin dynamics defect in the corneal epithelial cells as evidenced by increased filamentous actin, offering an in vivo model to investigate the physiological significance of the transcriptional regulation by actin dynamics. To examine the effect of the Dstncorn1 mutation on gene expression, we performed a microarray analysis using the cornea from Dstncorn1 and wild-type control mice. A dramatic alteration of gene expression was observed in the Dstncorn1 cornea, with 1,226 annotated genes differentially expressed. Functional annotation of these genes revealed that most significantly enriched functional categories are associated with actin and/or cytoskeleton. Among genes that belong to these categories, a considerable number of serum response factor (SRF) target genes were found, indicating the existence of the actin-SRF pathway of transcriptional regulation in vivo. A comparative study using an allelic mutant strain, Dstncorn1-2J, with milder corneal phenotypes also suggested that the severity of the actin dynamics defect correlates with the level of gene expression changes. Our study provides evidence that actin dynamics have a strong impact on gene expression in vivo. **Keywords:** Comparative gene expression **Overall design:** Microarray analysis was performed in triplicate with RNA from each genotype, A. BY H2bc H2-T18f/SnJ (A. BY wild-type), A. BY H2bc H2-T18f/SnJ-Dstncorn1/J (Dstncorn1), C57BL/6J (B6 wild-type), C57BL/6JSmn-Dstncorn1-2J/J (Dstncorn1-2J), and C.129S2(B6)-Il8rbtm1Mwm/J (Il8rb-/-), hybridized to three Affymetrix MG 430 2.0 arrays.

Background corr dist: KL-Divergence = 0.0655, L1-Distance = 0.0932, L2-Distance = 0.0099, Normal std = 0.8050

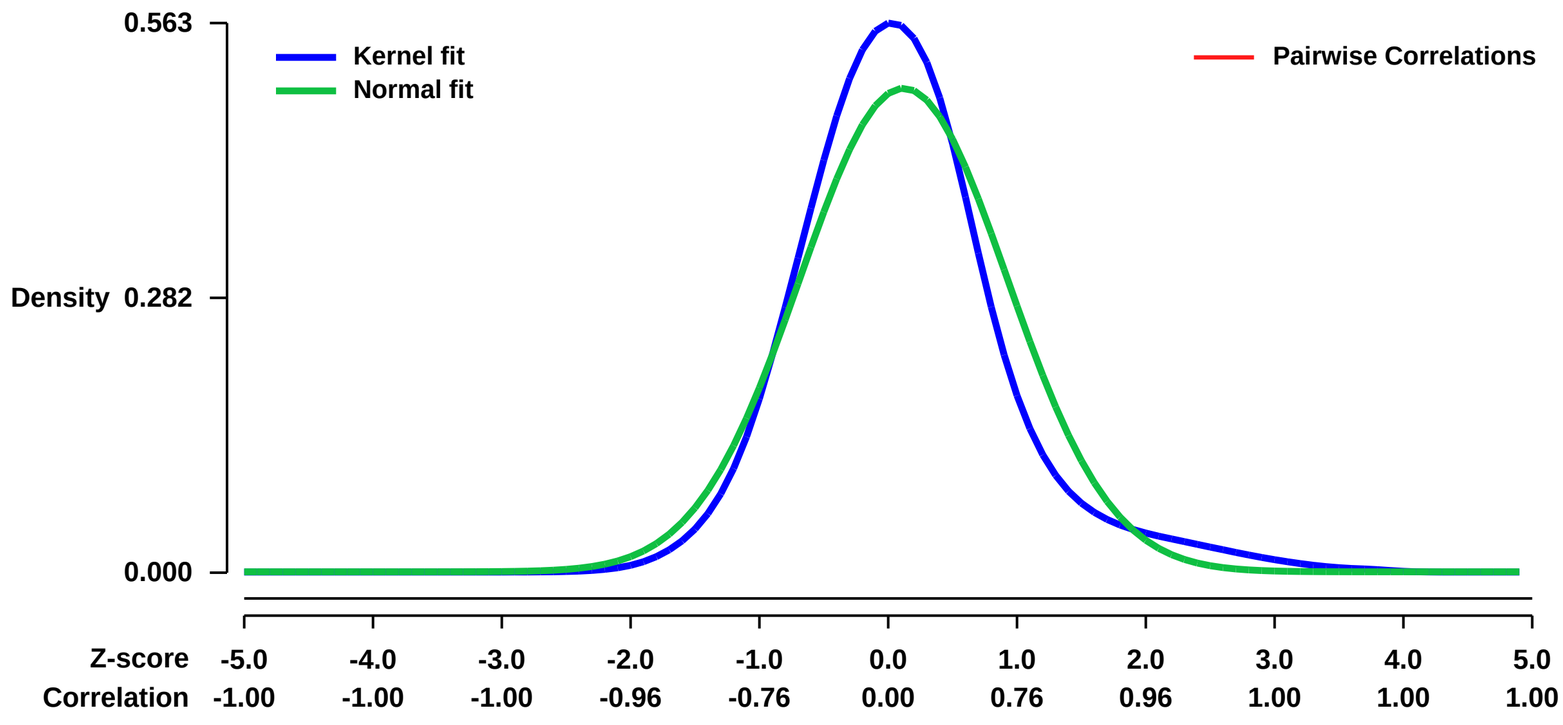

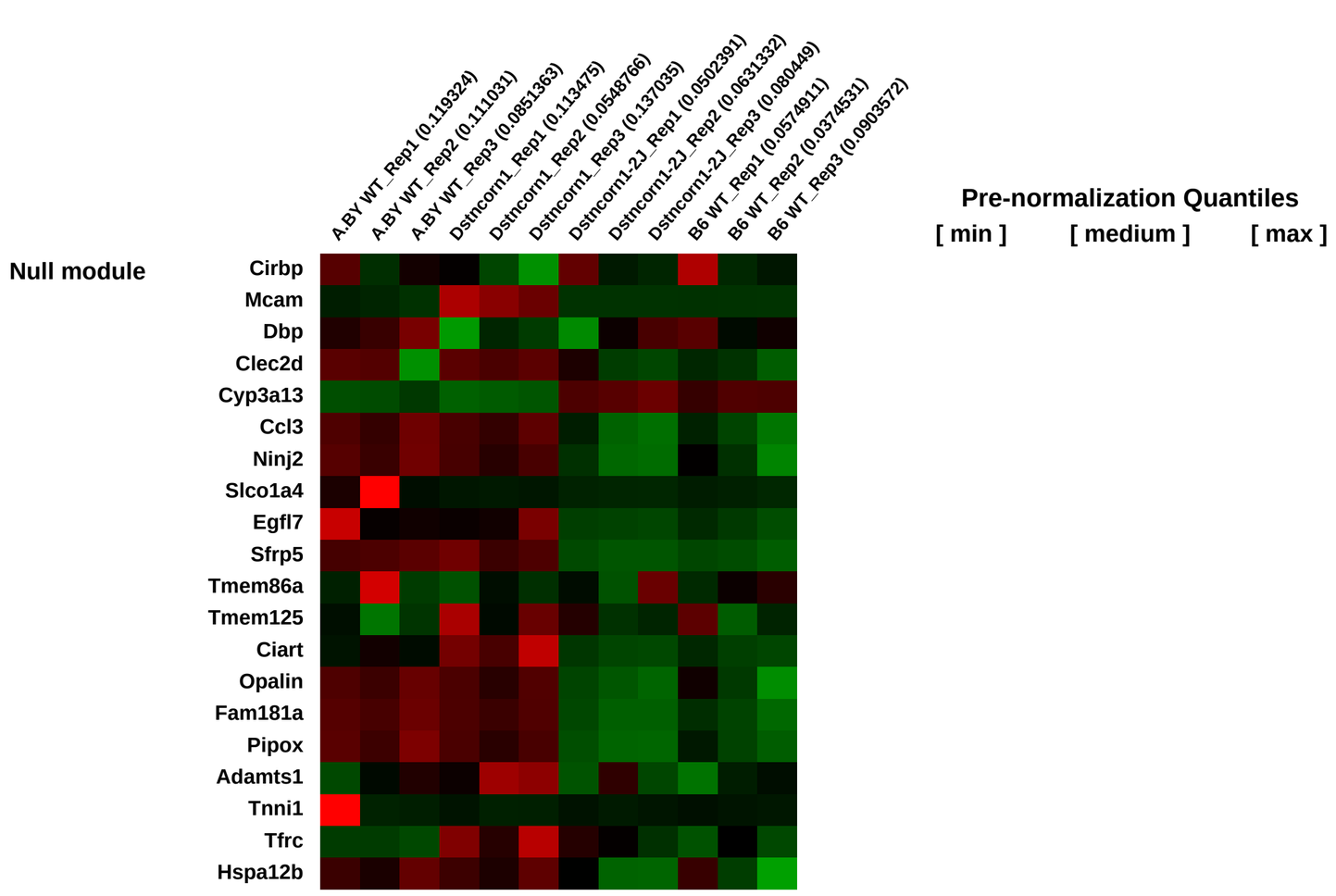

GEO Series "GSE19512" Expression Profiles

Num of samples in this series: 6

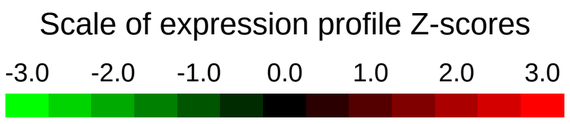

GEO Link:	http://www.ncbi.nlm.nih.gov/geo/query/acc.cgi?acc=GSE19512
Status:	Public on Jun 30 2011
Title:	Gene expression profiling of in vivo derived induced and natural FOXP3+ regulatory T cells in the mouse
Organism:	Mus musculus
Experiment type:	Expression profiling by array
Platform:	GPL1261
Pubmed ID:	21723159
Summary & Design:	**Summary:** The relative contribution of induced and natural Foxp3+ regulatory T cells (iTreg and nTreg cells, respectively) to the maintenance of tolerance is unknown. We examined their respective roles by in vivo adoptive transfer immunotherapy of newborn Foxp3-deficient BALB/c mice. Survival, weight gain, tissue infiltration, T cell activation, and the concentration of proinflammatory cytokines were used as outcome measurements. Treatment with iTreg cells alone was not successful. While effective in preventing death, treatment with nTreg cells alone was associated with chronic inflammation and autoimmunity. Outcomes markedly improved when conventional T (Tconv) cells were transferred together with the nTreg cells, where 10% of the peripheral Treg cell pool was derived by in-situ conversion. This enhancement depended upon the capacity of Tconv cells to express Foxp3. The gene expression profile of in vivo derived iTreg cells was similar to the established nTreg cell genetic signature. These results identify iTreg cells as an essential regulatory subset that supplements tolerance maintained by nTreg cells. **Overall design:** In vitro derived iTreg cells 72 hours after Foxp3 induction: GSM360147 - GSM360151

Background corr dist: KL-Divergence = 0.0200, L1-Distance = 0.0212, L2-Distance = 0.0007, Normal std = 0.7342

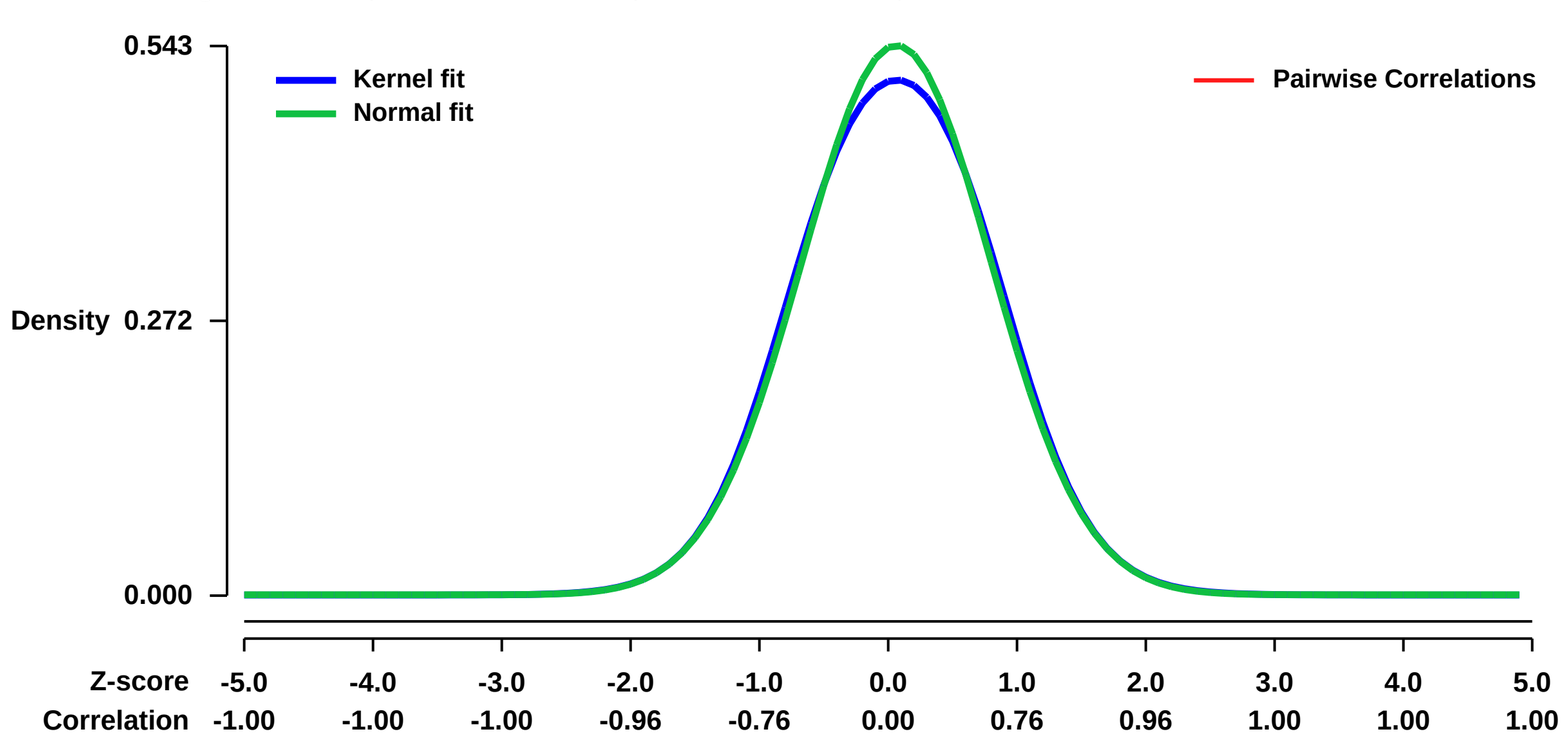

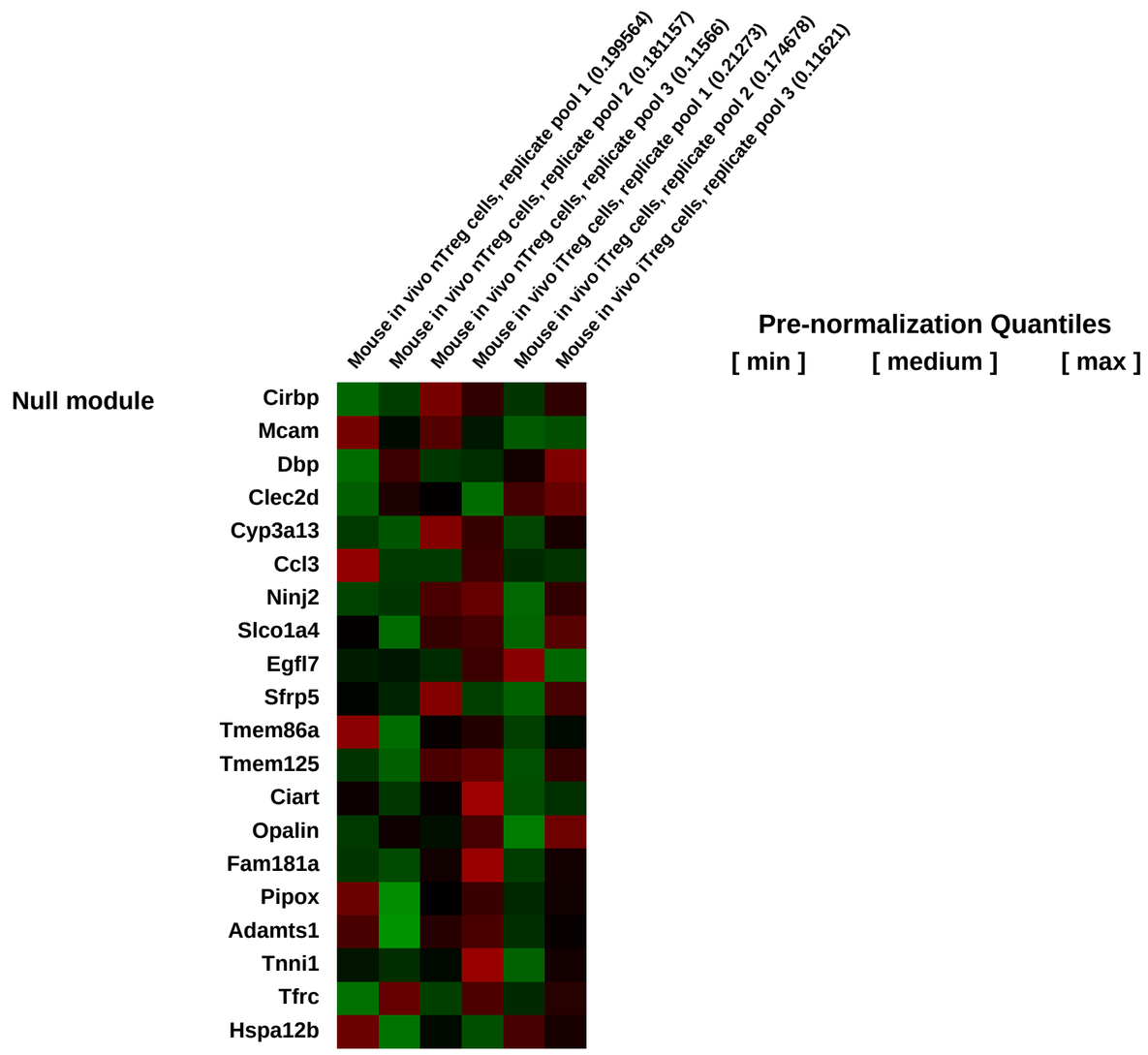

GEO Series "GSE35260" Expression Profiles

Num of samples in this series: 21

Scale of expression profile Z-scores

-3.0 -2.0 -1.0 0.0 1.0 2.0 3.0

GEO Link:	http://www.ncbi.nlm.nih.gov/geo/query/acc.cgi?acc=GSE35260
Status:	Public on Mar 19 2013
Title:	Functional dissection of the Paired domain of Pax6 â distinct roles of subdomains in neurogenesis and proliferation
Organism:	Mus musculus
Experiment type:	Expression profiling by array
Platform:	GPL1261
Pubmed ID:	23404109
Summary & Design:	**Summary:** The transcription factor Pax6 acts as a key developmental regulator in various organs. In the developing brain Pax6 regulates patterning, neurogenesis and proliferation, but how these diverse effects are mediated at the molecular level is not well understood. As Pax6 regulates forebrain development including neurogenesis, proliferation and patterning, almost exclusively by one of its DNA-binding domains, the bipartite paired domain, we examined the role of its respective DNA-binding subdomains (PAI and RED). Using mice with point mutations in the PAI (Pax6Leca4, N50K) and RED (Pax6Leca2, R128C) subdomains we unravelled opposing roles of mutations in these subdomains in regulating genes that control proliferation in the developing cerebral cortex. Mutation of the PAI domain reduced proliferation of both apical and basal progenitors, while the RED domain mutation significantly increased proliferation. Conversely, neurogenesis was affected only by the PAI domain mutation phenocopying the neurogenic defects observed in full Pax6 mutants. Genome-wide expression analysis supported the molecularly distinct signature upon mutation of these subdomains unravelling the key neurogenic signature mediated by the PAI domain. The altered expression of genes identified as direct Pax6 targets by chromatin immunoprecipitation allowed to further identify regulatory elements whose function was impaired by each individual Pax6 mutated protein. Thus, Pax6 achieves its key roles in the developing forebrain by utilizing distinct subdomains to regulate neurogenesis and exert opposing effects on proliferation, while Pax6-target genes involved in patterning tolerate either subdomain mutation. **Overall design:** We performed gene expression microarray analysis of Pax6 mutant mice (Leca2, Leca4, Sey) and control mice

Background corr dist: KL-Divergence = 0.0555, L1-Distance = 0.0286, L2-Distance = 0.0013, Normal std = 0.5344

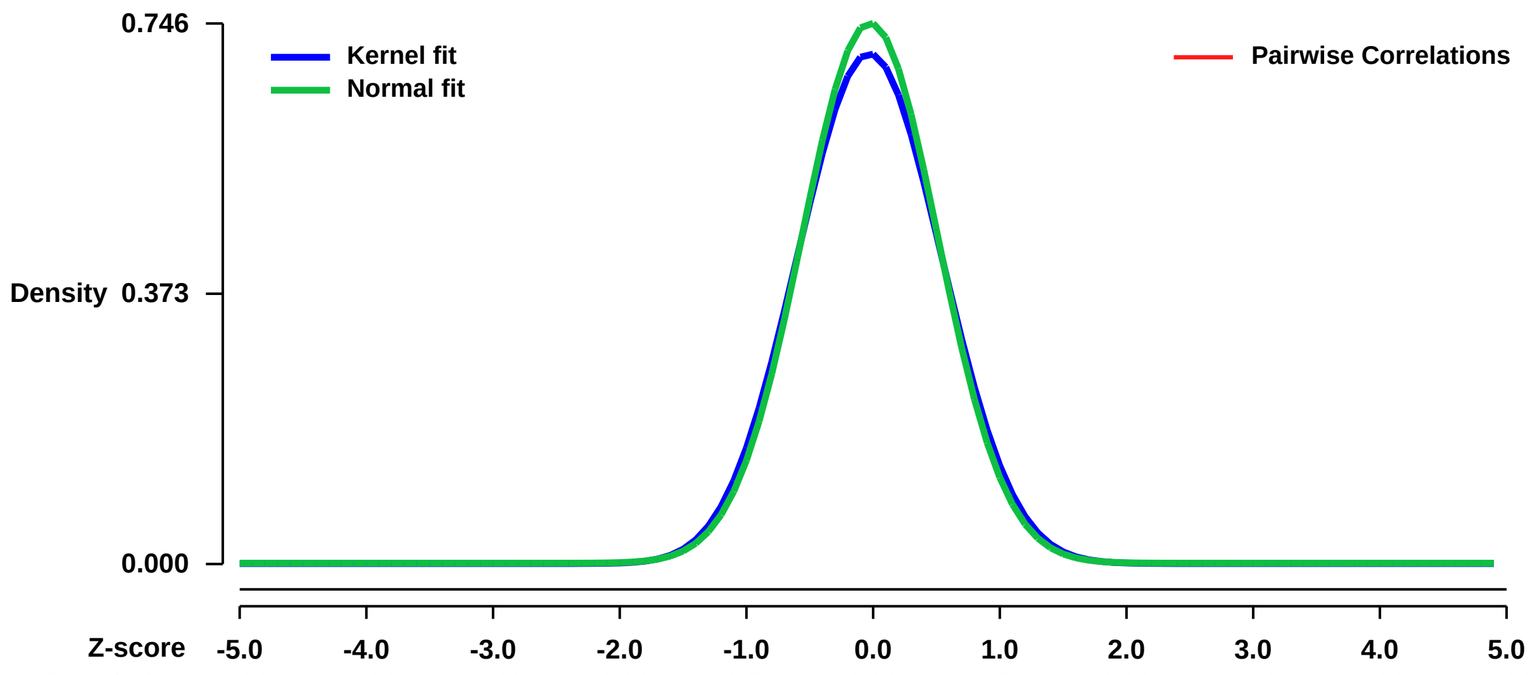

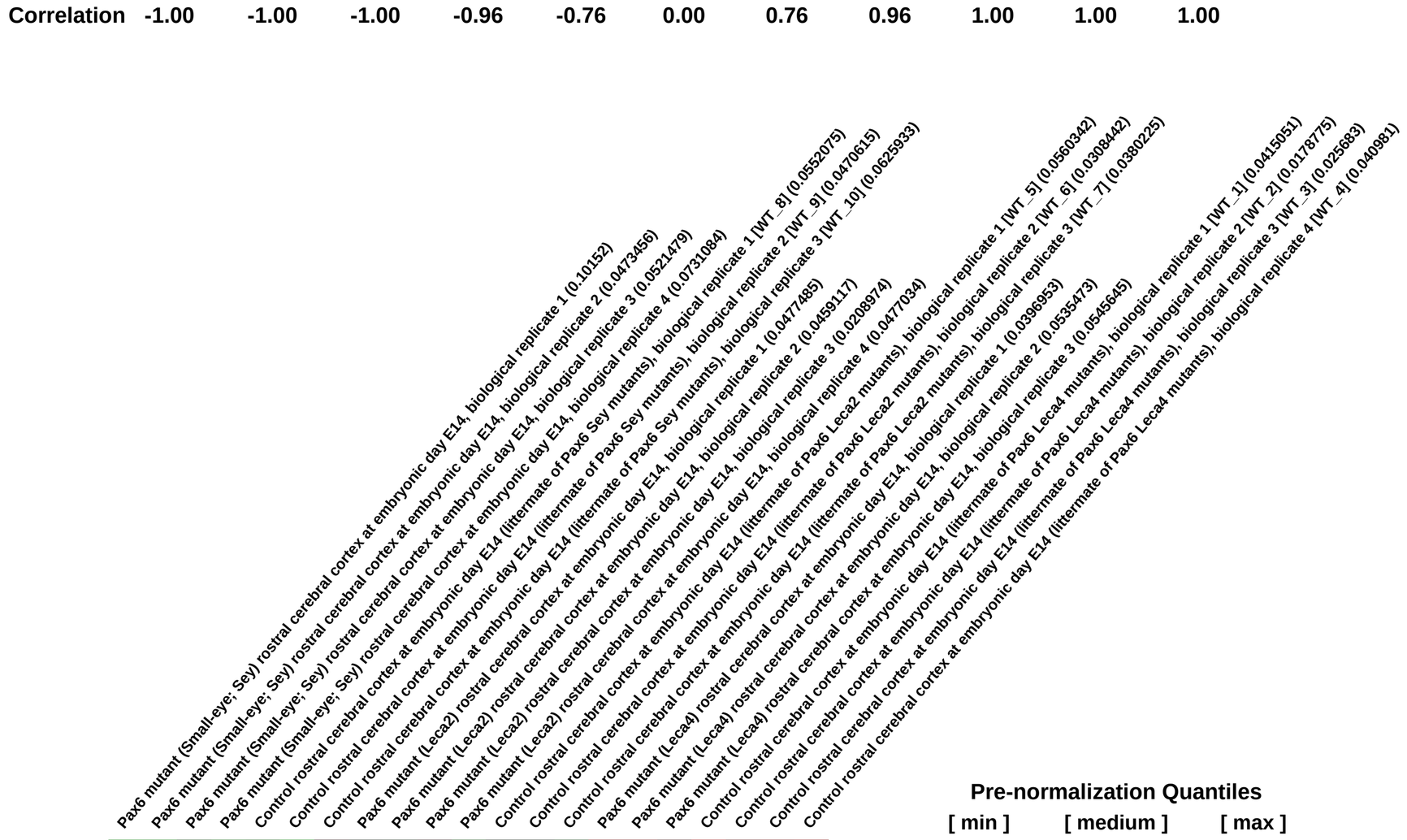

Pre-normalization Quantiles

[min] [medium] [max]

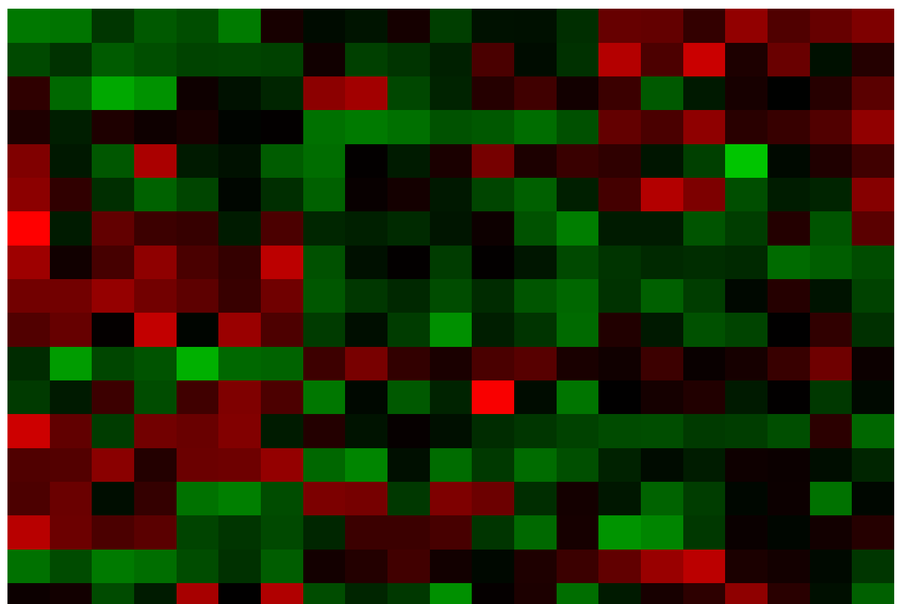

GEO Series "GSE32265" Expression Profiles

Num of samples in this series: 6

Scale of expression profile Z-scores

-3.0 -2.0 -1.0 0.0 1.0 2.0 3.0

GEO Link:	http://www.ncbi.nlm.nih.gov/geo/query/acc.cgi?acc=GSE32265
Status:	Public on Sep 19 2012
Title:	Gene-expression changes resulting from loss of the mTORC1 component Raptor in murine hematopoietic stem and progenitor cell-enriched populations (HSPC)
Organism:	Mus musculus
Experiment type:	Expression profiling by array
Platform:	GPL1261
Pubmed ID:	22958934
Summary & Design:	**Summary:** We investigated the role of mTORC1 in murine hematopoiesis by conditionally deleting the Raptor gene in murine hematopoietic stem cells. We observed mutliple alterations evoked by Raptor loss in hematopoiesis and profiled gene-expression alterations induced by raptor loss in Flt3-Lin-Sca1+cKit+ hematopoietic stem and progenitor enriched cell populations, 5 weeks post Raptor deletion. **Overall design:** Flt3-Lin-Sca1+cKit+ cells were flow sorted from mice containing homozygous floxed alleles for exon 6 of the Raptor gene in the presence (MT group) or absence (WT group) of the MxCre transgene, which was induced with injections of mice with pIpC 5 weeks before cell isolation.

Background corr dist: KL-Divergence = 0.0270, L1-Distance = 0.0296, L2-Distance = 0.0012, Normal std = 0.6994

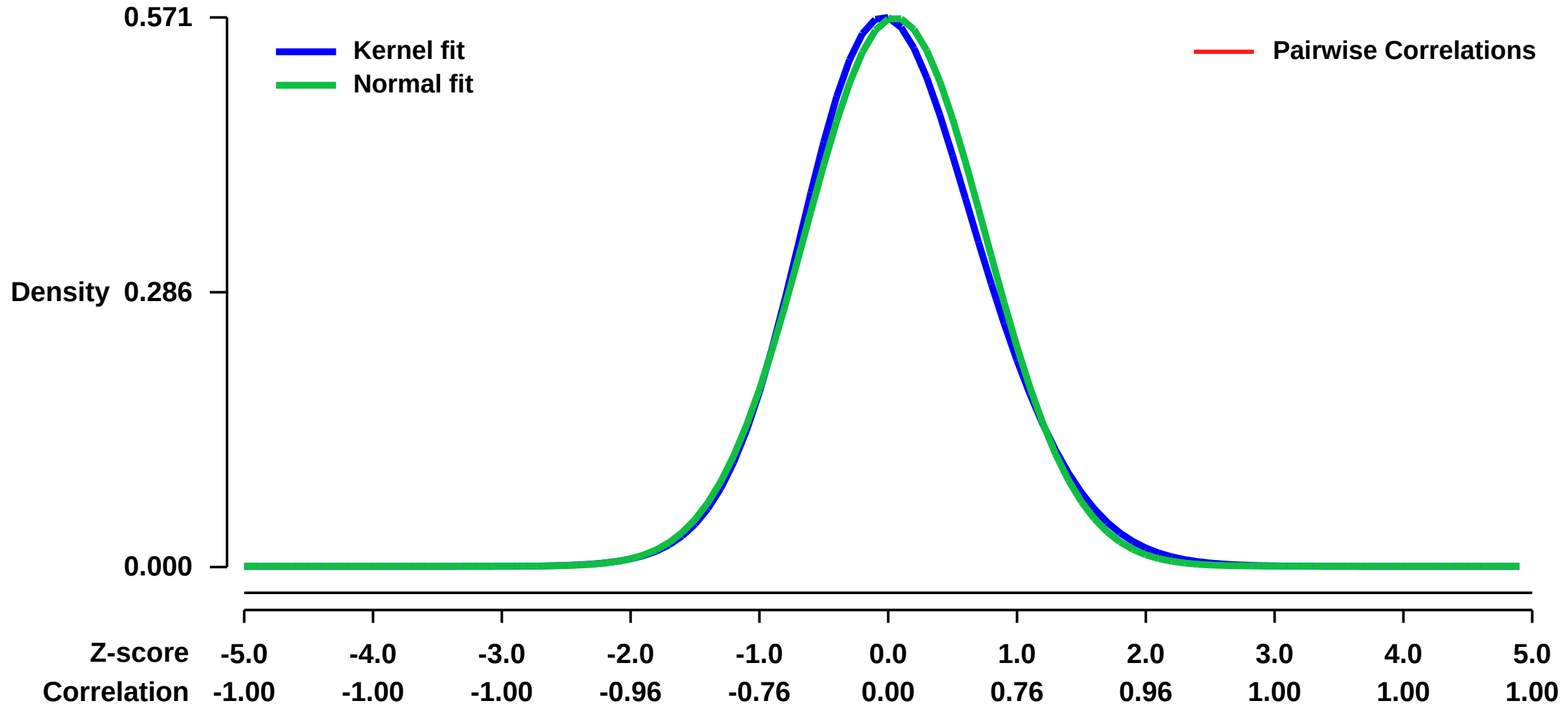

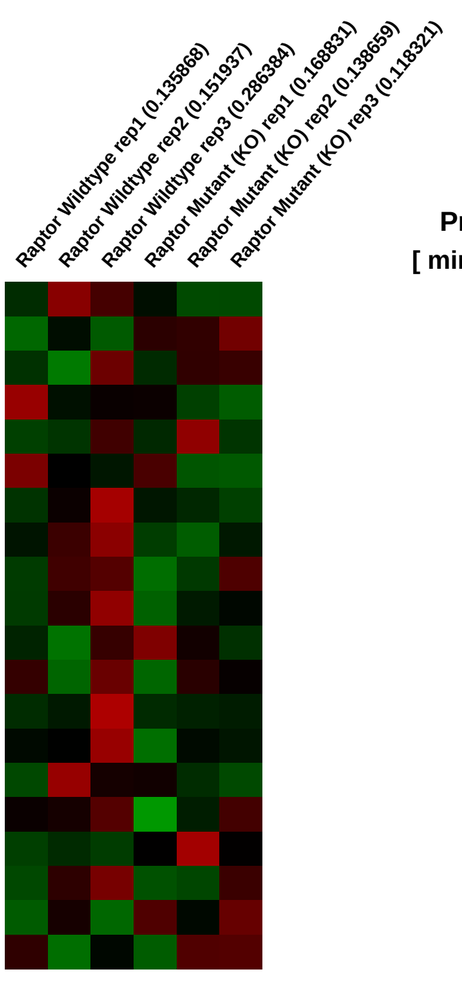

GEO Series "GSE13635" Expression Profiles

Num of samples in this series: 6

Scale of expression profile Z-scores

-3.0 -2.0 -1.0 0.0 1.0 2.0 3.0

GEO Link:	http://www.ncbi.nlm.nih.gov/geo/query/acc.cgi?acc=GSE13635
Status:	Public on Jan 29 2010
Title:	Gene expression change in cyclin D1 -/- retinas in comparison to wildtype.
Organism:	Mus musculus
Experiment type:	Expression profiling by array
Platform:	GPL1261
Pubmed ID:	20090754
Summary & Design:	**Summary:** Cyclin D1 belongs to the core cell cycle machinery1, and it is frequently overexpressed in human cancers2. The full repertoire of cyclin D1 functions in normal development and in cancer cells is currently unknown. To address this question, here we introduce a novel approach that allows one to determine the set of cyclin D1-interacting proteins (D1 â interactomeâ) and cyclin D1-bound genomic fragments (D1 â cistromeâ) in essentially any mouse organ, at any point of development or at any stage of cancer progression. Using this approach, we detected several novel tissue-specific interactors of cyclin D1. A significant number of these partners represent proteins involved in transcription. We show, using genome-wide location analysis3, that cyclin D1 occupies promoters of a very large number of genes in the developing mouse, where it binds in close proximity to transcription start sites. Bioinformatics analyses of cyclin D1-bound genomic segments in the developing embryo revealed DNA recognition sequences for several transcription factors. By querying SAGE libraries4, promoter CpG content5 and gene expression profiles of cyclin D1-null organs, we demonstrate that cyclin D1 binds promoters of highly expressed genes, and that it functions to activate or to repress gene expression in vivo. Analyses of cyclin D1 transcriptional targets reveal that cyclin D1 contributes to cell proliferation by upregulating genes required for S-phase entry and progression. Hence, cyclin D1 plays a broad transcriptional regulatory function in vivo during normal mouse development. **Overall design:** We wished to determine whether cyclin D1 functioned to positively or negatively regulate transcription of the target genes (identified by chip-on-chip) in vivo. To address this question, we asked how expression of cyclin D1-bound genes changes when cyclin D1 has been knocked-out. We dissected retinas from eyes of cyclin D1-/- or wild-type neonates, isolated RNA and hybridized it onto Affymetrix expression arrays.

Background corr dist: KL-Divergence = 0.0303, L1-Distance = 0.0162, L2-Distance = 0.0003, Normal std = 0.6631

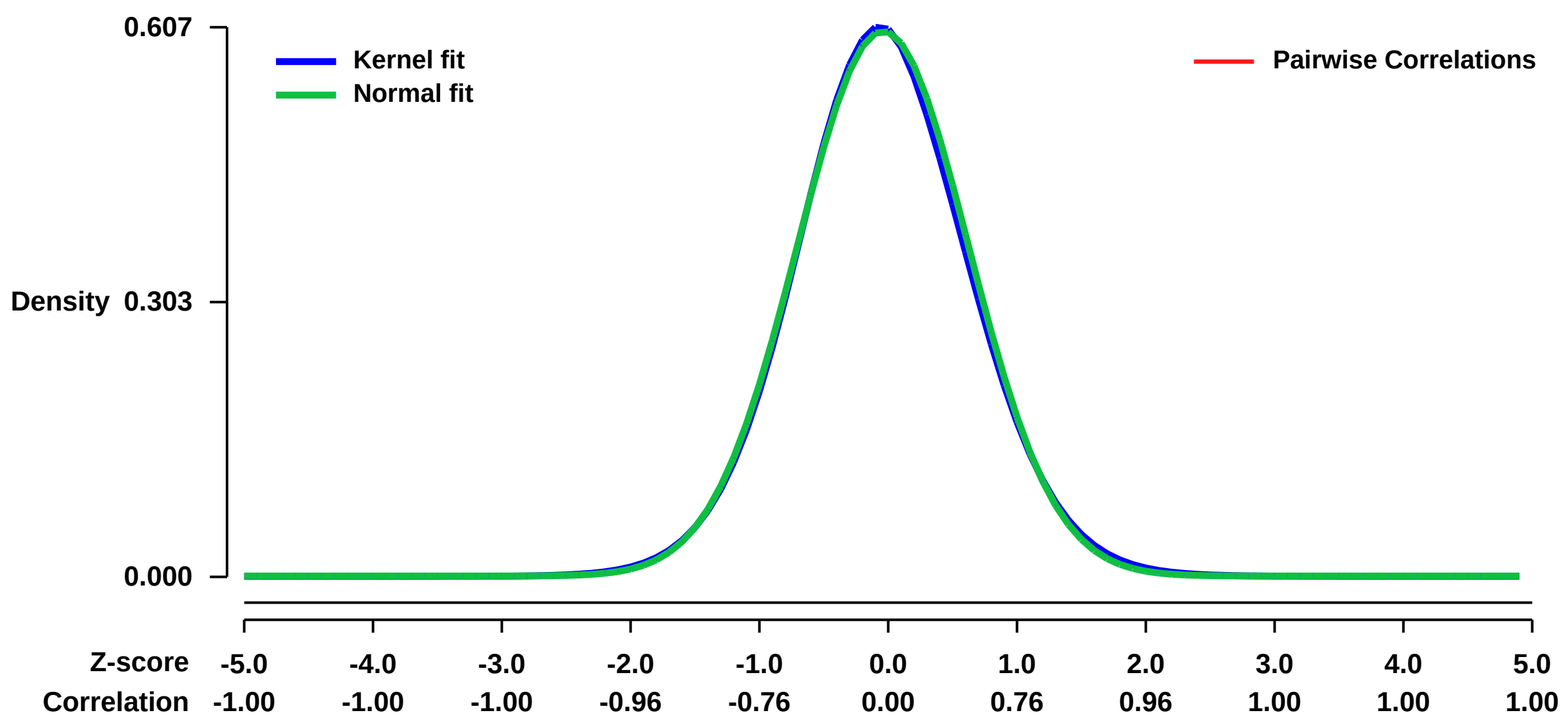

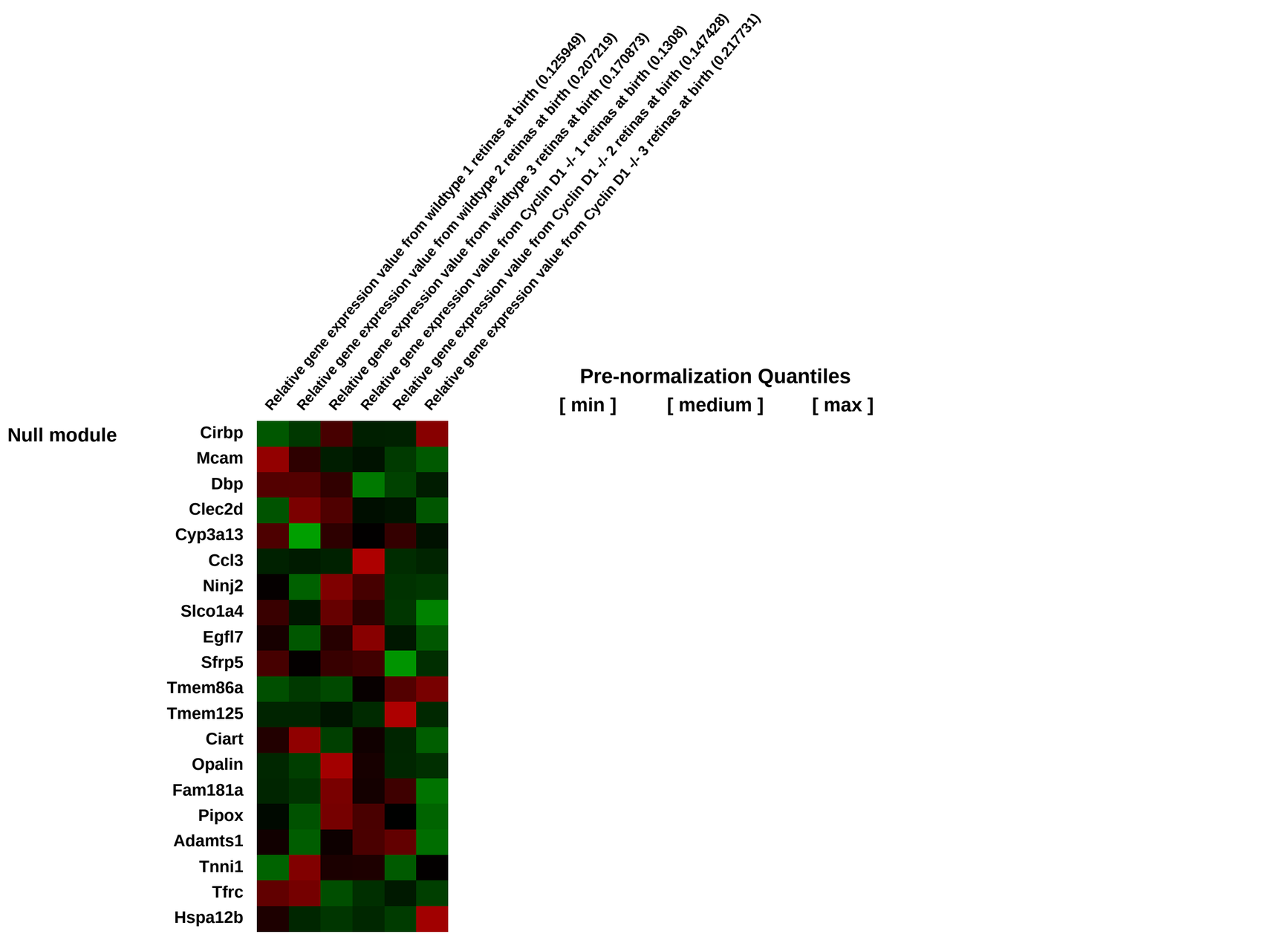

GEO Series "GSE13547" Expression Profiles

Num of samples in this series: 12

Scale of expression profile Z-scores

-3.0 -2.0 -1.0 0.0 1.0 2.0 3.0

GEO Link:	http://www.ncbi.nlm.nih.gov/geo/query/acc.cgi?acc=GSE13547
Status:	Public on Apr 17 2009
Title:	Zfx controls BCR-induced proliferation and survival of B lymphocytes
Organism:	Mus musculus
Experiment type:	Expression profiling by array
Platform:	GPL1261
Pubmed ID:	19329779
Summary & Design:	**Summary:** The development, homeostasis and function of B lymphocytes involve multiple rounds of B cell receptor (BCR)-controlled proliferation and prolonged maintenance. We analyzed the role of transcription factor Zfx, a recently identified regulator of stem cell maintenance, in B cell development and homeostasis. Conditional Zfx deletion in the bone marrow blocked B cell development at the pre-BCR selection checkpoint. Zfx deficiency in peripheral B cells caused impaired generation of the B-1 cell lineage, accelerated B cell turnover, depletion of mature recirculating cells, and delayed T-dependent antibody responses. Zfx-deficient B cells showed normal proximal BCR signaling, but impaired BCR-induced proliferation and survival. This was accompanied by aberrantly enhanced and prolonged integrated stress response, and delayed induction of Cyclin D2 and Bcl-xL proteins. Thus, Zfx restrains the stress response and couples antigen receptor signaling to B cell expansion and maintenance during development and peripheral homeostasis. **Keywords:** Expression profiling by array **Overall design:** For global gene expression analysis, 2.5 x 105 flow-sorted follicular B cells (B220+ AA4.1- CD23hi CD21int) were cultured in 200 ¸…L B cell media containing 10 ¸…g/mL ¸–-IgM for 0, 2, and 12 hrs. Cells were harvested in Trizol (Invitrogen). Total RNA was isolated using Trizol (Invitrogen), and 100 ng of each RNA sample were used for reverse transcription and two rounds of linear antisense RNA amplification/labeling (Ambion). The aRNA was amplified without labeling in the first round, and then labeled with Biotin-16-UTP(Roche Applied Sciences) and Biotin-11-CTP (PerkinElmer Life Sciences) in the second round. Labeled aRNA was fragmented in RNA Fragmentation Buffer (QIAGEN) prior to hybridization. Labeled RNA samples (10 ug/array) were hybridized in duplicate to Mouse Genome 430 2.0 arrays (Affymetrix) at the Columbia University Microarray Project core facility according to the manufacturer's instructions. Quality control and normalization were performed using positive and negative hybridization controls (Affymetrix) spiked into the RNA prior to labeling. Linear amplification of RNA was confirmed for every sample. Array scanning and raw data processing were done using GCOS 1.4 software (Affymetrix).

Background corr dist: KL-Divergence = 0.0888, L1-Distance = 0.0336, L2-Distance = 0.0016, Normal std = 0.4757

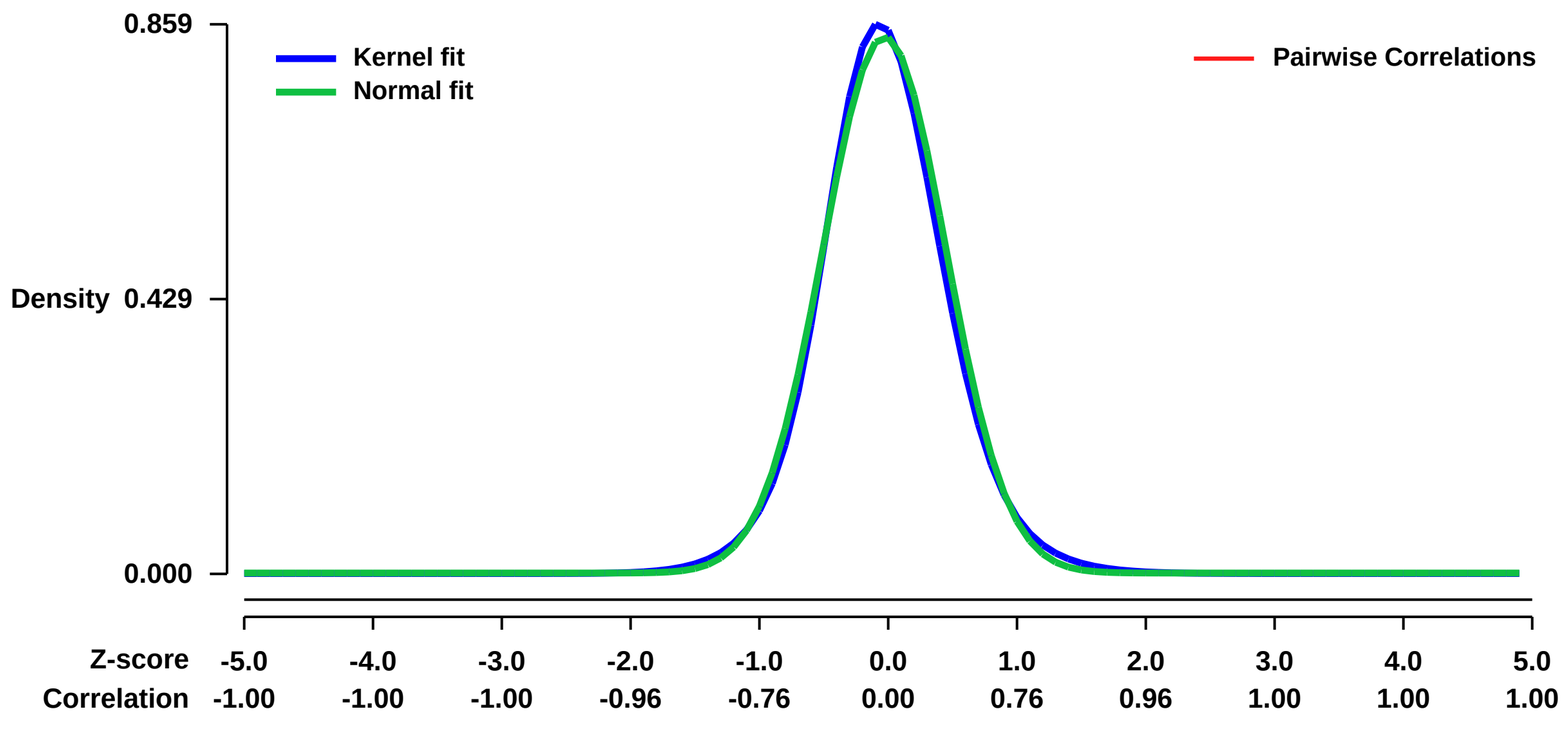

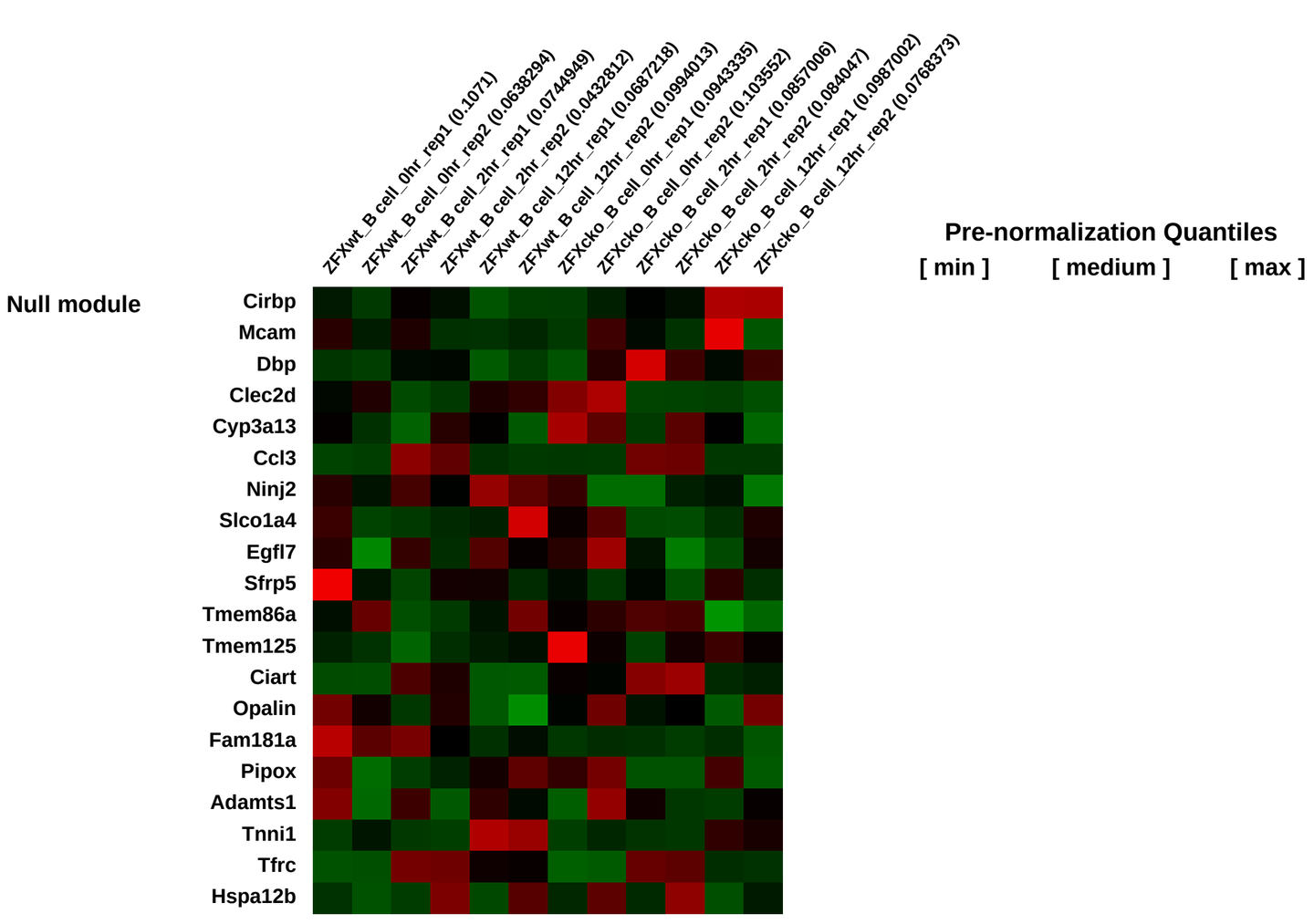

GEO Series "GSE4739" Expression Profiles

Num of samples in this series: 19

Scale of expression profile Z-scores

-3.0 -2.0 -1.0 0.0 1.0 2.0 3.0

GEO Link:	http://www.ncbi.nlm.nih.gov/geo/query/acc.cgi?acc=GSE4739
Status:	Public on Jun 15 2006
Title:	Temporal control of gene expression by ERK MAP kinase during cell cycle progression from G0/G1 to S phase
Organism:	Mus musculus
Experiment type:	Expression profiling by array
Platform:	GPL1261
Pubmed ID:	19160492
Summary & Design:	**Summary:** The ERK family of MAP kinase plays a critical role in growth factor-stimulated cell cycle progression from G0/G1 to S phase. But, how sustained activation of ERK promotes G1 progression has remained unclear. Here, our systematic analysis on the temporal program of ERK-dependent gene expression shows that sustained activation of ERK is required for induction and maintenance of the decreased expression levels of a set of genes. Moreover, our cell biological analysis reveals that these ERK-dependent downregulated genes have the ability to block S phase entry. Cessation of ERK activation at mid or late G1 leads to a rapid increase of these anti-proliferative genes and results in the inhibition of S phase entry. These findings uncover an important mechanism by which the duration of ERK activation regulates cell cycle progression through dynamic changes in gene expression, and identify novel ERK target genes crucial for the regulation of cell cycle progression. **Keywords:** time course **Overall design:** time points: 0h, 1h, 4h, 7h, 12h

Background corr dist: KL-Divergence = 0.2379, L1-Distance = 0.0474, L2-Distance = 0.0052, Normal std = 0.3097

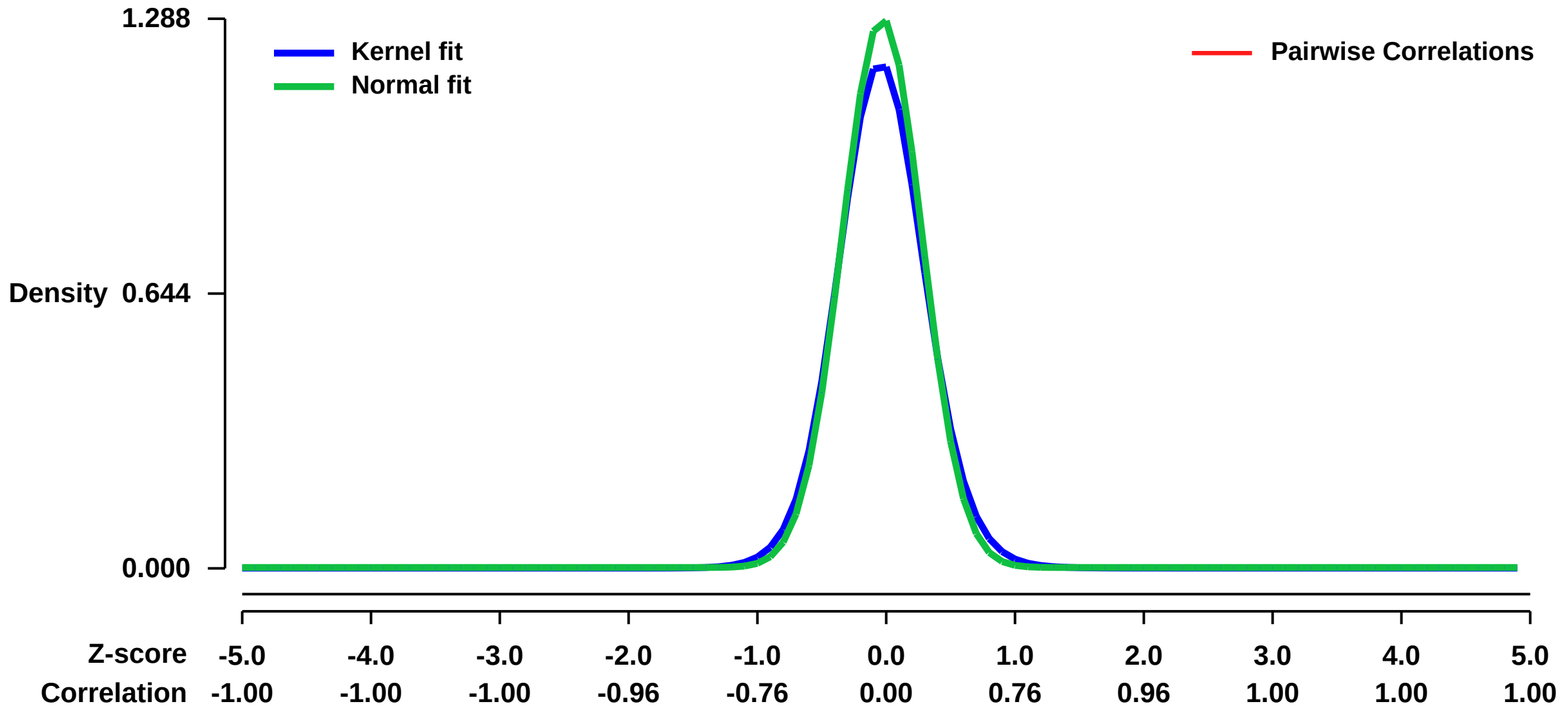

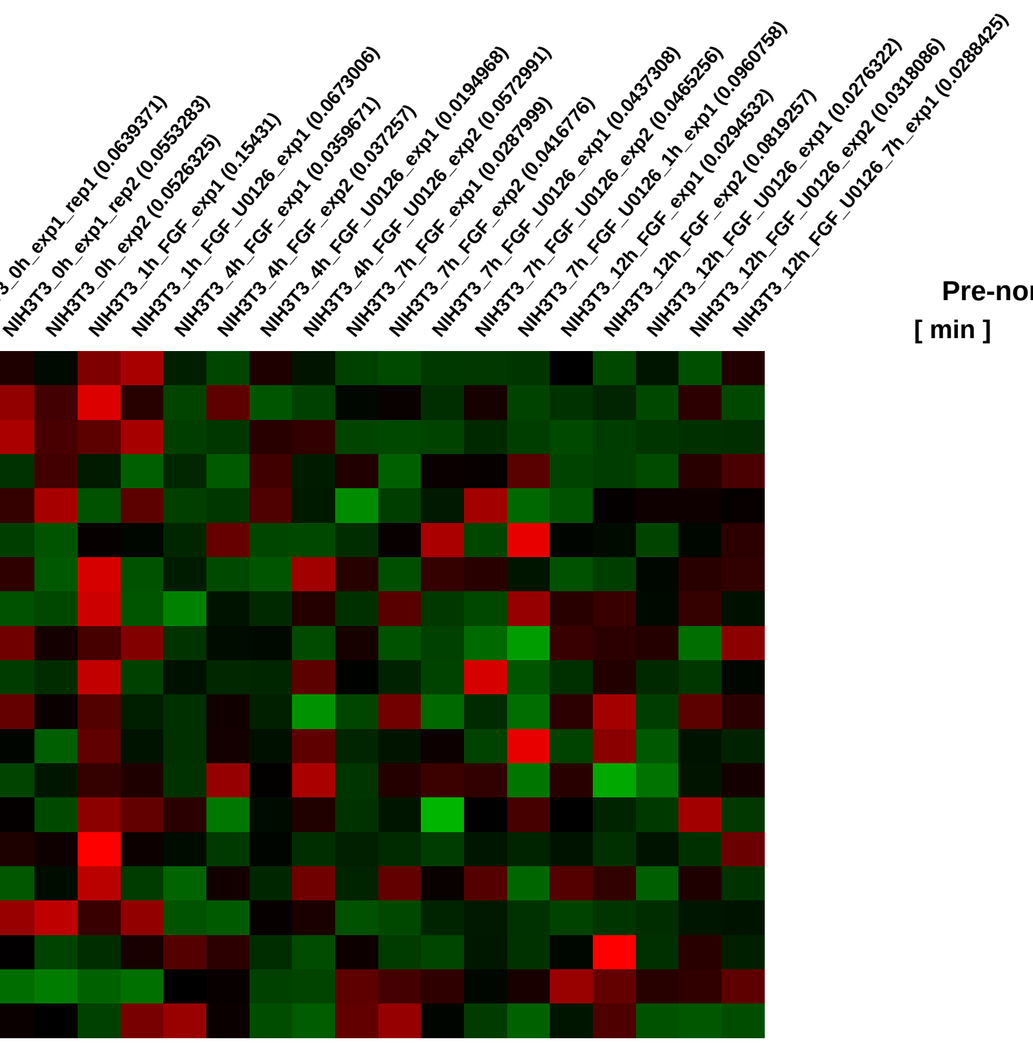

GEO Series "GSE49122" Expression Profiles

Num of samples in this series: 14

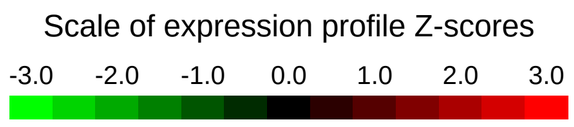

GEO Link:	http://www.ncbi.nlm.nih.gov/geo/query/acc.cgi?acc=GSE49122
Status:	Public on Jul 23 2013
Title:	Otitis Media Impact on Inner Ear
Organism:	Mus musculus
Experiment type:	Expression profiling by array
Platform:	GPL1261
Pubmed ID:	24124478

Summary & Design:

Summary:
Objective: Otitis media is known to alter expression of cytokine and other genes in the mouse middle ear and inner ear. However, whole mouse genome studies of gene expression in otitis media have not previously been undertaken. Ninety-nine percent of mouse genes are shared in the human, so these studies are relevant to the human condition.

Methods: To assess inflammation-driven processes in the mouse ear, gene chip analyses were conducted on mice treated with trans-tympanic heat-killed Hemophilus influenza using untreated mice as controls. Middle and inner ear tissues were separately harvested at 6 hours, RNA extracted, and samples for each treatment processed on the Affymetrix 430 2.0 Gene Chip for expression of its 34,000 genes.

Results: Statistical analysis of gene expression compared to control mice showed significant alteration of gene expression in 2,355 genes, 11% of the genes tested and 8% of the mouse genome. Significant middle and inner ear upregulation (fold change >1.5, p<0.05) was seen in 1,081 and 599 genes respectively. Significant middle and inner ear downregulation (fold change <0.67, p<0.05) was seen in 978 and 287 genes respectively. While otitis media is widely believed to be an exclusively middle ear process with little impact on the inner ear, the inner ear changes noted in this study were numerous and discrete from the middle ear responses. This suggests that the inner ear does indeed respond to otitis media and that its response is a distinctive process. Numerous new genes, previously not studied, are found to be affected by inflammation in the ear.

Conclusion: Whole genome analysis via gene chip allows simultaneous examination of expression of hundreds of gene families influenced by inflammation in the middle ear. Discovery of new gene families affected by inflammation may lead to new approaches to the study and treatment of otitis media.

Overall design:
There are 6 control samples and 8 samples trans-tympanically injected with H flu 10e9 for 6 hours. Each sample is a pool of 4 animals

Background corr dist: KL-Divergence = 0.0179, L1-Distance = 0.0166, L2-Distance = 0.0003, Normal std = 0.7467

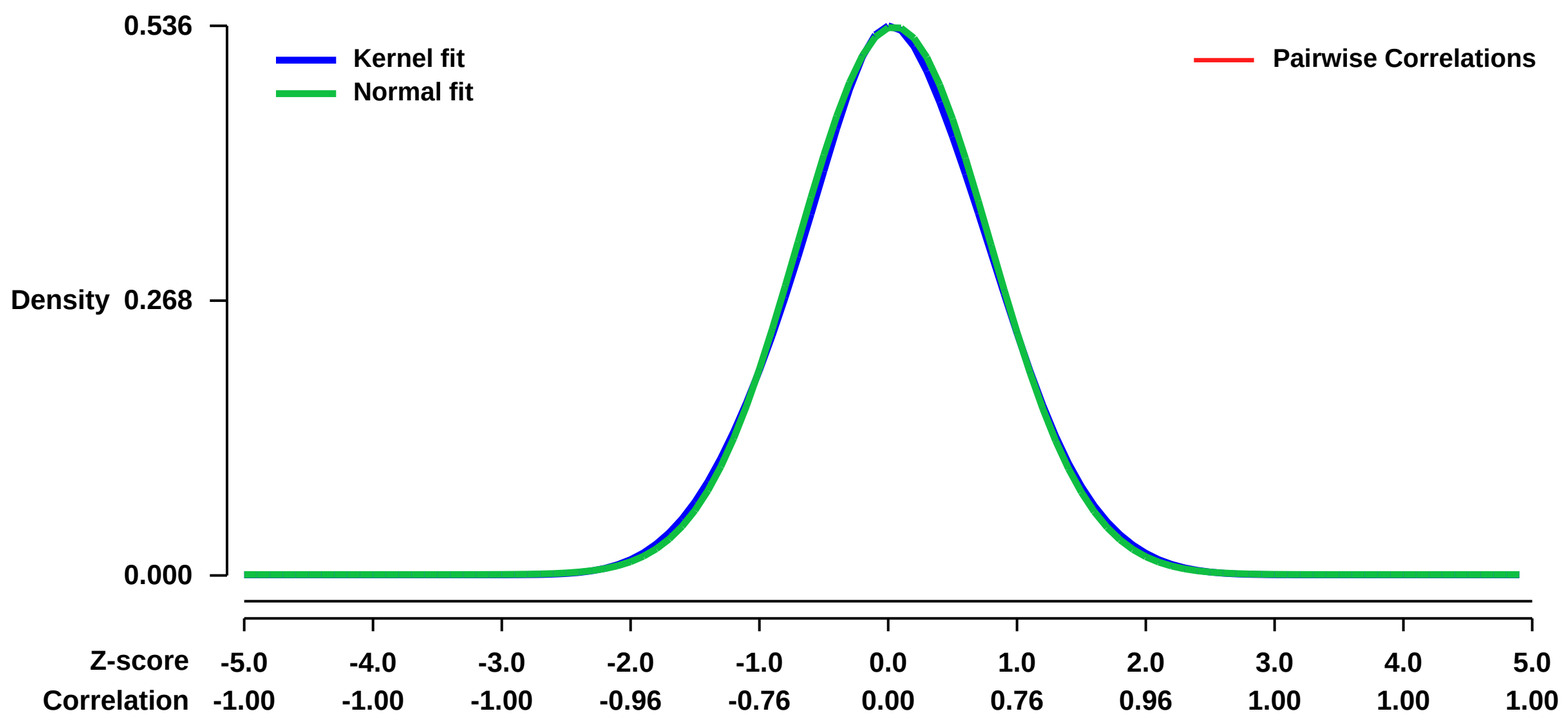

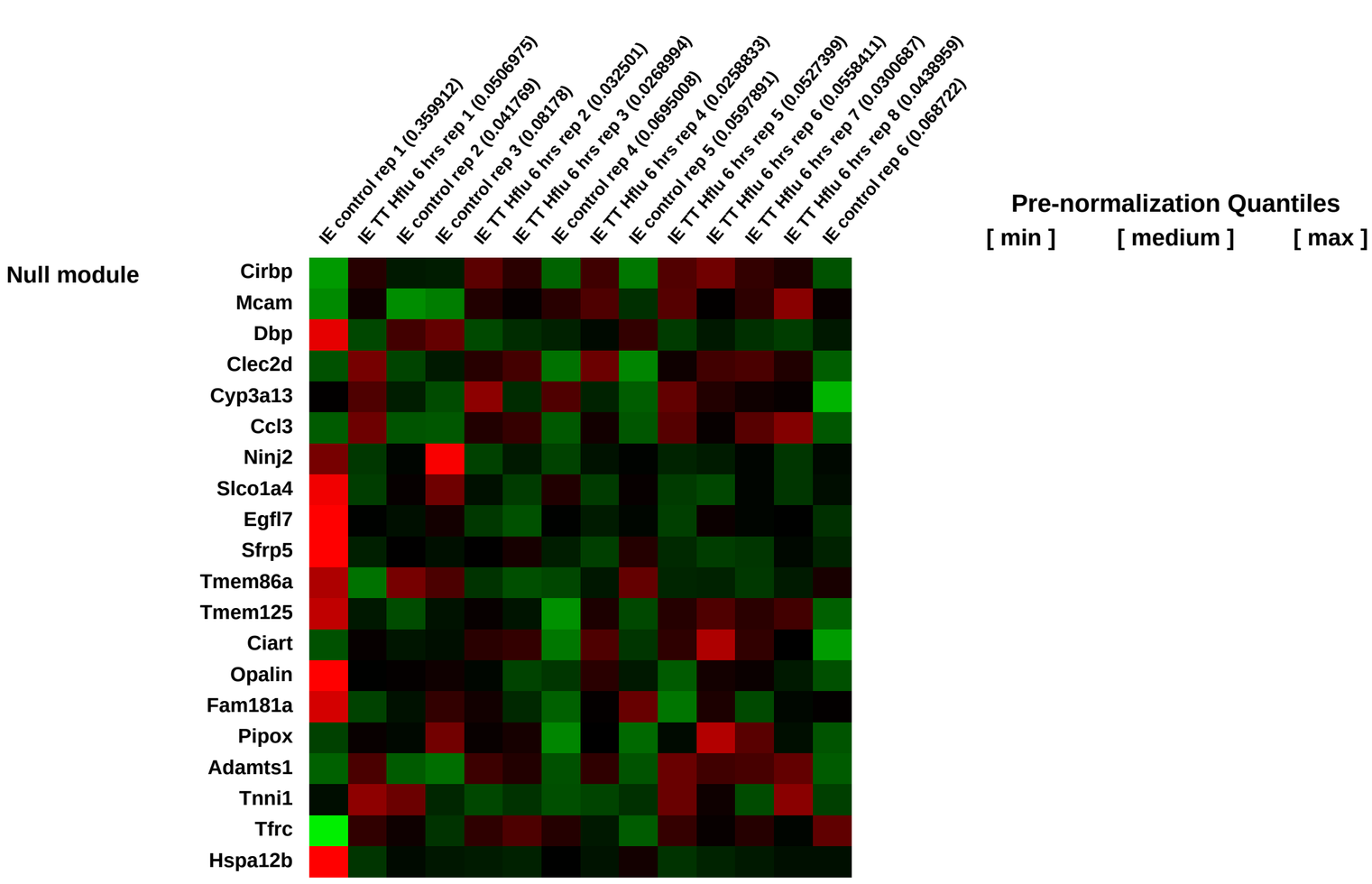

GEO Series "GSE7707" Expression Profiles

Num of samples in this series: 18

Scale of expression profile Z-scores

-3.0 -2.0 -1.0 0.0 1.0 2.0 3.0

GEO Link:	**http://www.ncbi.nlm.nih.gov/geo/query/acc.cgi?acc=GSE7707**
Status:	**Public on Oct 21 2008**
Title:	**Gene expression changes in multiple brain regions of a mouse MPTP model of Parkinson’s disease**
Organism:	**Mus musculus**
Experiment type:	**Expression profiling by array**
Platform:	**GPL1261**
Pubmed ID:	
Summary & Design:	**Summary:** **In Parkinsonâ s disease (PD), the progressive loss of substantia nigra dopamine cells has been associated with their vulnerability to oxidative stress, inflammation, and mitochondrial dysfunction. To identify multiple gene transcription alterations that may potentially underlie early stages of related degenerative processes in brain, we used the subcrhonic MPTP mouse model of PD and microarray analysis at 4 days post-MPTP when neurotoxic activity is maximal. Since PD results in gene changes throughout the brain, we assessed MPTP’s effects in multiple regions: frontal cortex, striatum and midbrain.** **Keywords: neurotoxic response** **Overall design:** **Mus musculus adults were randomly assigned to either MPTP or saline treatment groups. Brain regions of interest (frontal cortex, striatum and midbrain) were dissected from both groups for RNA extraction and hybridization on Affymetrix microarrays.**

Background corr dist: **KL-Divergence = 0.0895, L1-Distance = 0.0433, L2-Distance = 0.0027, Normal std = 0.4809**

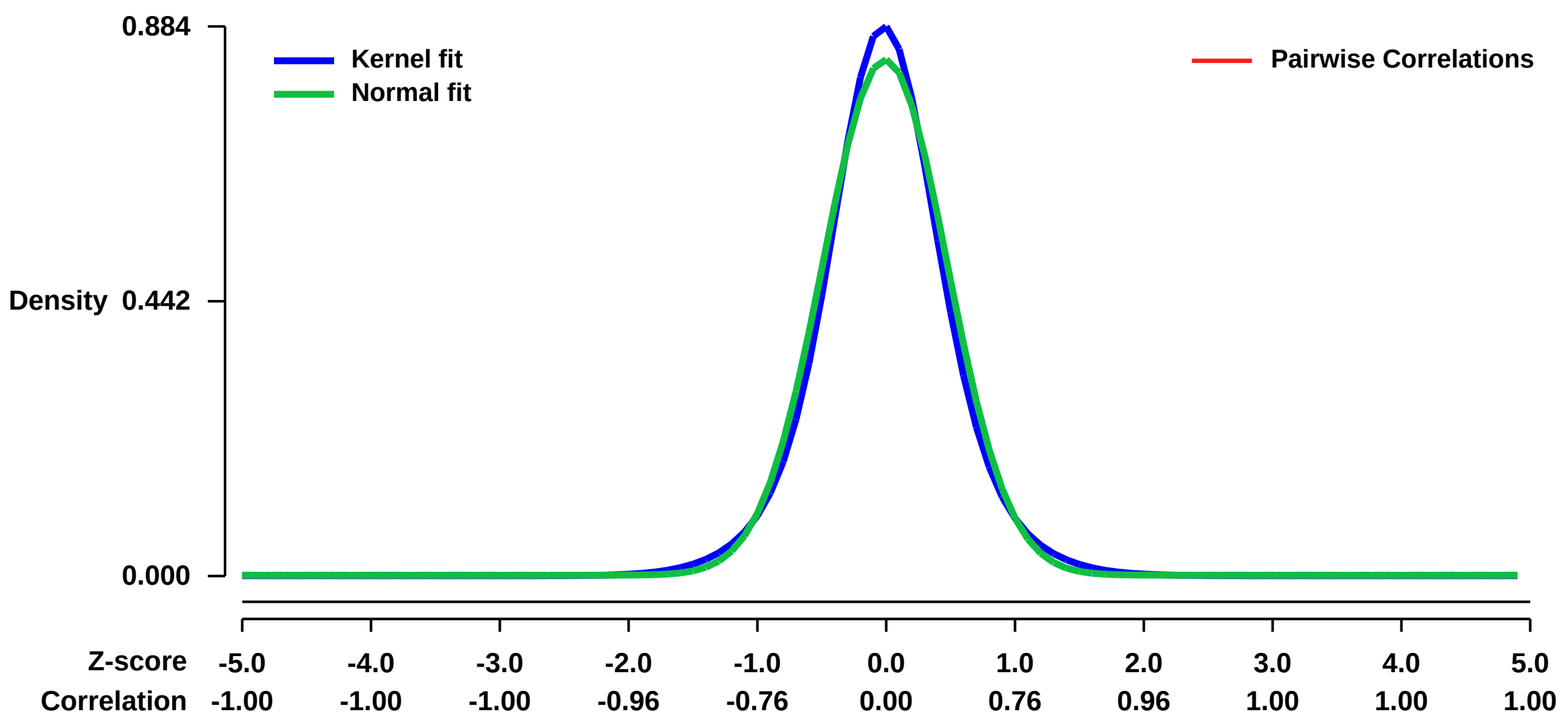

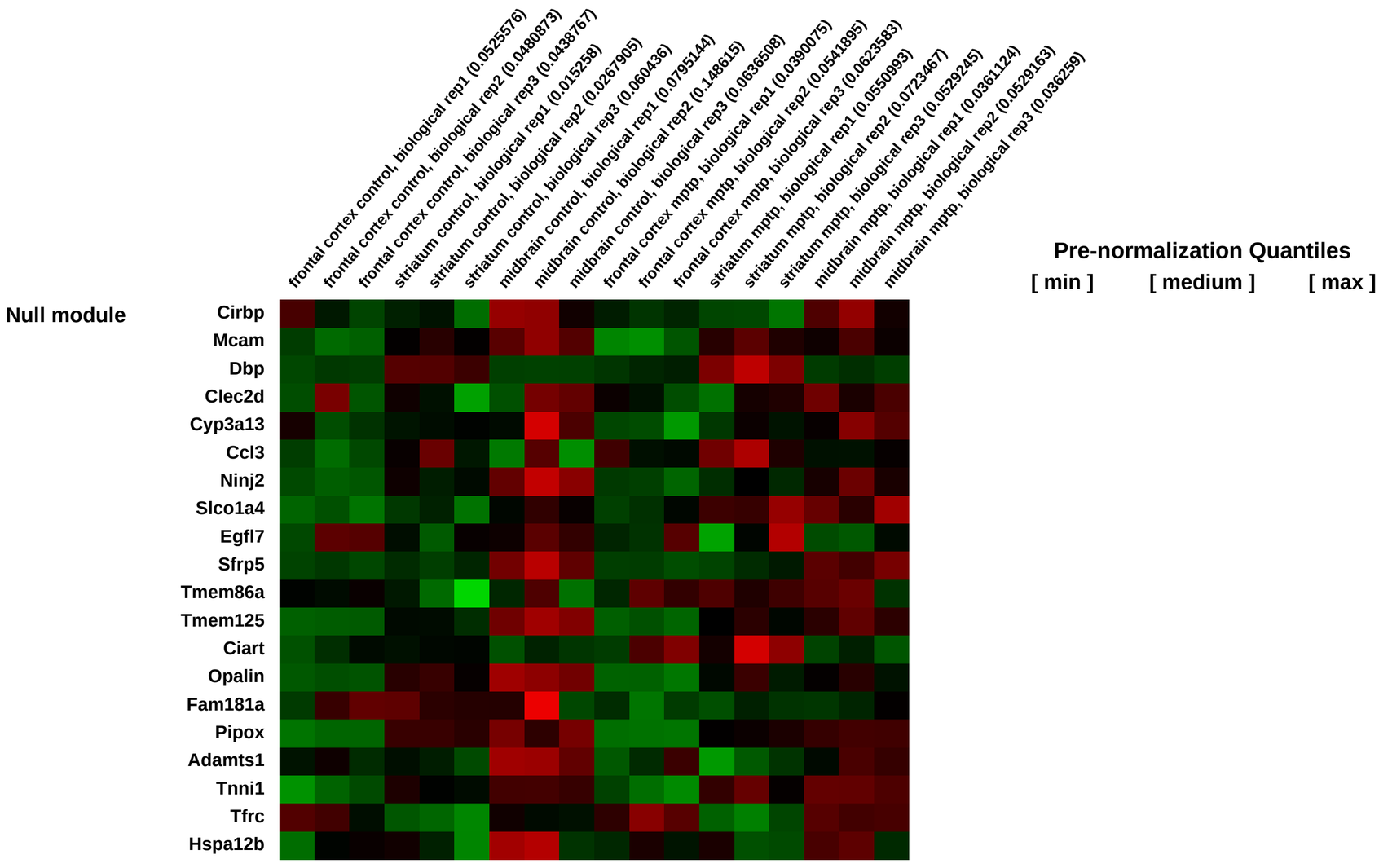

GEO Series "GSE8715" Expression Profiles

Num of samples in this series: 6

Scale of expression profile Z-scores

-3.0 -2.0 -1.0 0.0 1.0 2.0 3.0

GEO Link:	http://www.ncbi.nlm.nih.gov/geo/query/acc.cgi?acc=GSE8715
Status:	Public on Aug 09 2007
Title:	Transcriptional Profiling of the Megabladder Mouse - A Unique Model of Bladder Dysmorphogenesis
Organism:	Mus musculus
Experiment type:	Expression profiling by array
Platform:	GPL1261
Pubmed ID:	
Summary & Design:	**Summary:** Recent studies in our lab have identified a mutant mouse model of obstructive nephropathy designated mgb for megabladder. Homozygotic mgb mice (mgb-/-) develop lower urinary tract obstruction in utero due to a lack of bladder smooth muscle differentiation. This defect is the result of a random transgene insertion into chromosome 16 followed by a translocation of this fragment into chromosome 11. In an effort to identify potential gene targets affected in mgb mice, we performed transcriptional profiling on embryonic day 15 (E15) mgb-/- bladders using both a Chromosome 11/16 Custom GeneChip Array and the Affymetrix Mouse Genome 430 2.0 GeneChip. This analysis identified no definitive mis-expressed gene targets on chromosome 11. In contrast, mgb-/- mice significantly over-expressed a cluster of gene products located on the translocated fragment of chromosome 16 including urotensin II-related peptide (Urp), which was shown to be preferentially over-expressed in developing mgb-/- bladders. Immunohistochemical studies indicated that the spatial distribution of Urp was altered in mgb-/- bladders, while biochemical studies suggested a potential role for Urp in modifying smooth muscle cell phenotype in vitro. Pathway analysis of mgb microarray data showed dysregulation of at least 60 gene products associated with the differentiation of smooth muscle. In conclusion, the results of this study indicate that the molecular pathways controlling normal smooth muscle development are severely altered in mgb-/- bladders, and provide the first evidence that Urp may play a critical role in bladder smooth muscle development. **Keywords:** mgb mutant bladders **Overall design:** Gene expression profiling was performed on two separate study groups. First, total cellular RNA was isolated from wildtype (n=2; 1 female/1 male), mgb+/- (n=2; 1 female/1 male), and mgb-/- (n=2; 1 female/1 male) E15 whole embryos. Second, total cellular RNA was isolated from the bladders of E15 wildtype (n=7; 3 female/4 male), mgb+/- mice (n=7; 3 female/4 male), and mgb-/- mice (n=11; 7 females/4 males).

Background corr dist: KL-Divergence = 0.0433, L1-Distance = 0.0337, L2-Distance = 0.0016, Normal std = 0.6128

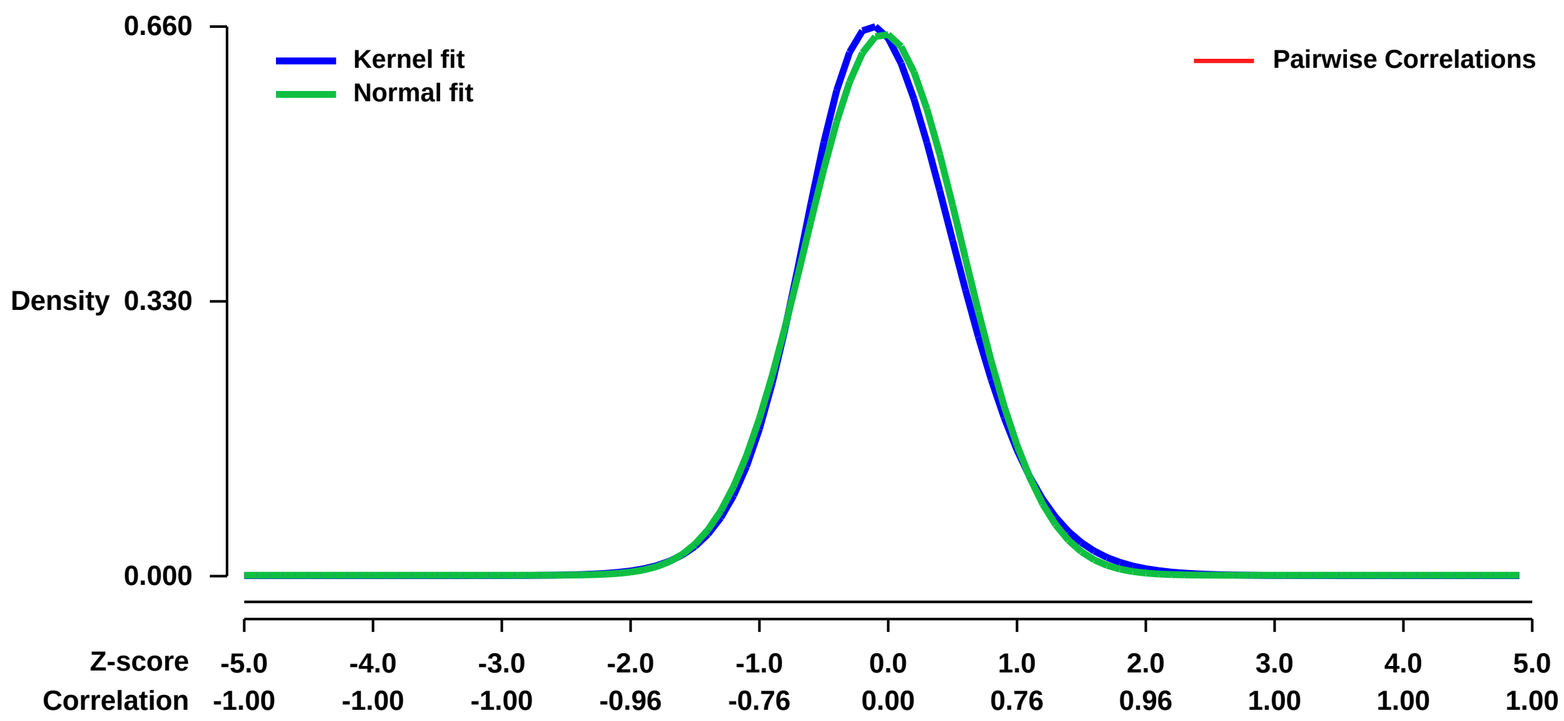

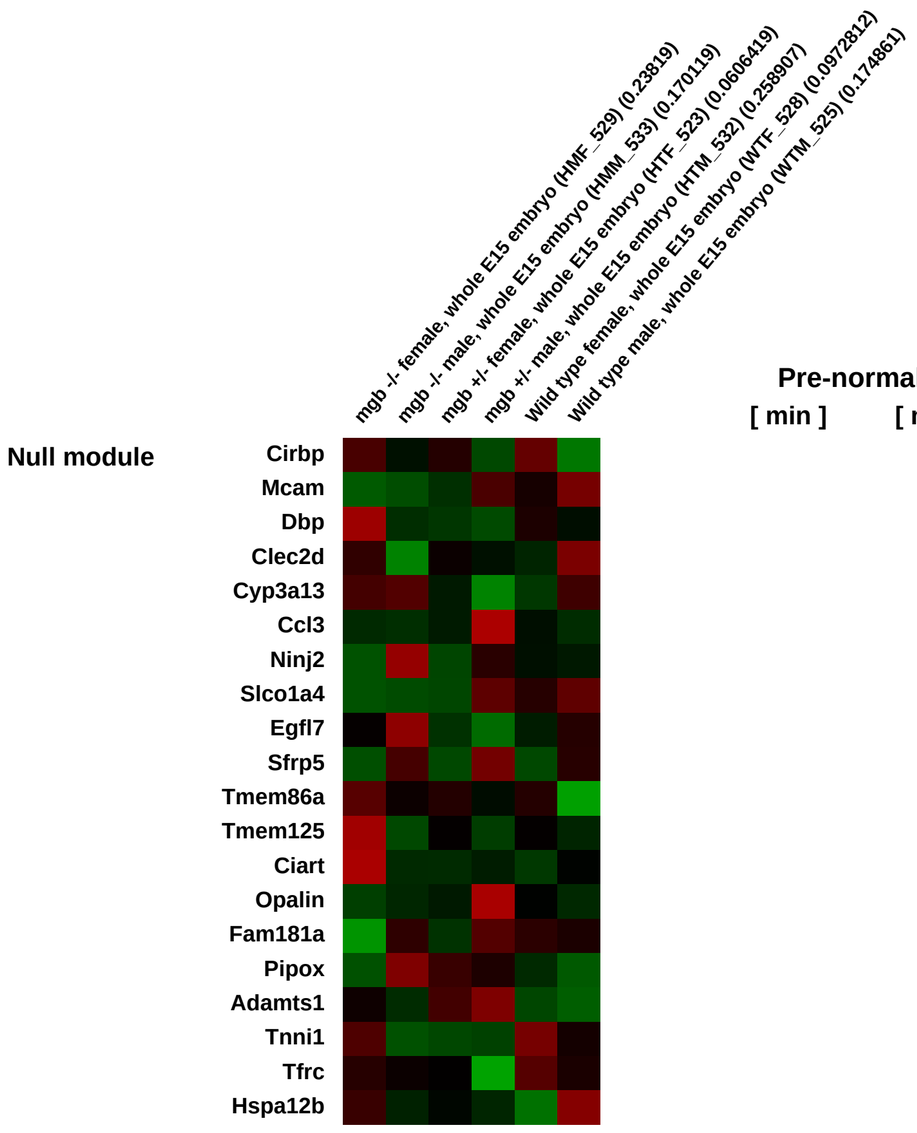

GEO Series "GSE12518" Expression Profiles

Num of samples in this series: 6

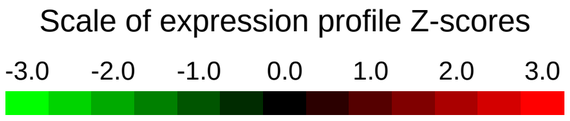

GEO Link:	http://www.ncbi.nlm.nih.gov/geo/query/acc.cgi?acc=GSE12518
Status:	Public on Apr 15 2009
Title:	Differential expression profile between MNV-1 infected and mock-infected RAW 264.7 cells.
Organism:	Mus musculus
Experiment type:	Expression profiling by array
Platform:	GPL1261
Pubmed ID:	19211757
Summary & Design:	**Summary:** Noroviruses have been widely recognized for their importance as causative agents of non-bacterial gastroenteritis. Mouse norovirus is the only representative of the norovirus genus, family Caliciviridae, able to grow in cell culture. The aim of this study is to describe the differences in the expression profiles of MNV-1 and mock-infected macrophages (RAW 264.7 cells), in order to better understand the response of the host cell to norovirus infection. **Overall design:** This study compares two type of samples (MNV-infected and mock-infected RAW cells) in biological triplicates respectively. The MNV stock used for infection was obtained in the same cell line, and purified with a sucrose cushion in order to account for expression changes caused by virus infection only.

Background corr dist: KL-Divergence = 0.0217, L1-Distance = 0.0741, L2-Distance = 0.0057, Normal std = 0.9739

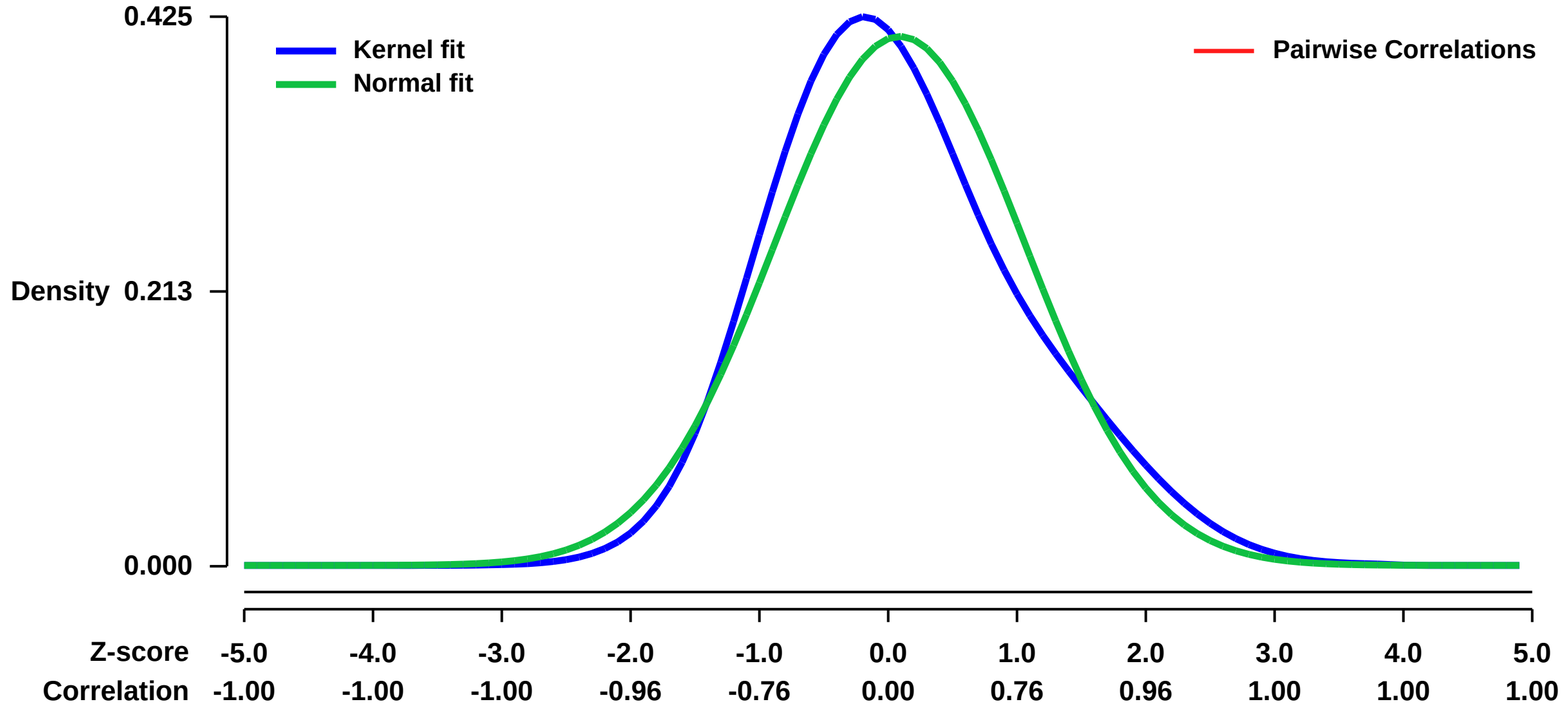

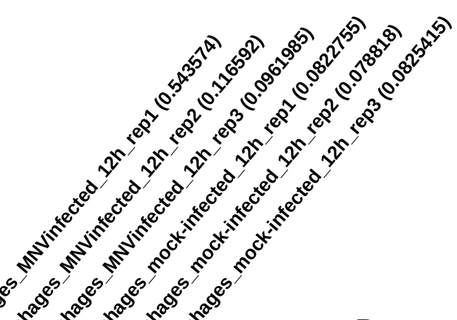

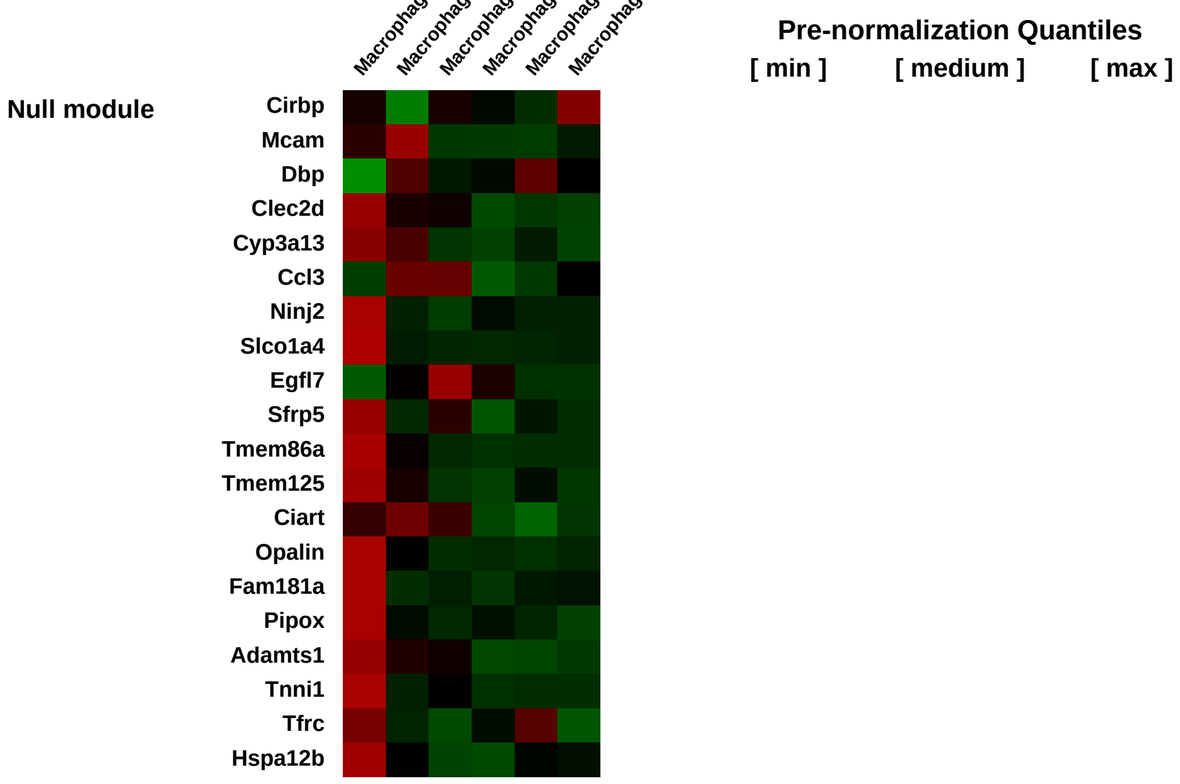

GEO Series "GSE25088" Expression Profiles

Num of samples in this series: 24

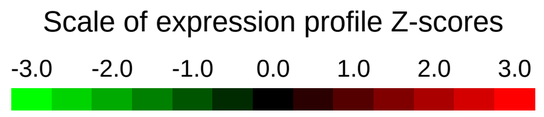

GEO Link:	http://www.ncbi.nlm.nih.gov/geo/query/acc.cgi?acc=GSE25088
Status:	Public on Nov 18 2010
Title:	PPARg and IL-4-induced gene expression data from wild-type and STAT6 knockout mouse bone marrow-derived macrophages
Organism:	Mus musculus
Experiment type:	Expression profiling by array
Platform:	GPL1261
Pubmed ID:	21093321
Summary & Design:	**Summary:** C57Bl/6 wild-type and STAT6 KO mice were used to study PPARg and IL-4 signaling. Bone marrow of 3 mice per group was isolated and differentiated to macrophages with M-CSF (20 ng/ml). 20 ng/ml IL-4 was used to induce alternative macrophage activation and 1 uM Rosiglitazone (RSG) was used to activate PPARg. From each mouse 4 samples were generated: 1. M-CSF, 2. M-CSF+RSG, 3. IL-4 and 4. IL-4+RSG. All compounds were added throughout the whole differentiation process, and frech media was added every other day. Control cells were treated with vehicle (DMSO:ethanol). After 10 days, RNA was isolated and gene expression profiles were analyzed using Mouse Genome 430 2.0 microarrays from Affymetrix. **Overall design:** 3 C57Bl/6 wild-type and 3 STAT6 KO mice were used to isolate bone marrow and from each macrophages were differentiated with or without IL-4 and simultaneously treated with vehicle or RSG. Altogether we analyzed 24 samples with 3 biological replicates as below.

Background corr dist: KL-Divergence = 0.2287, L1-Distance = 0.0913, L2-Distance = 0.0220, Normal std = 0.3531

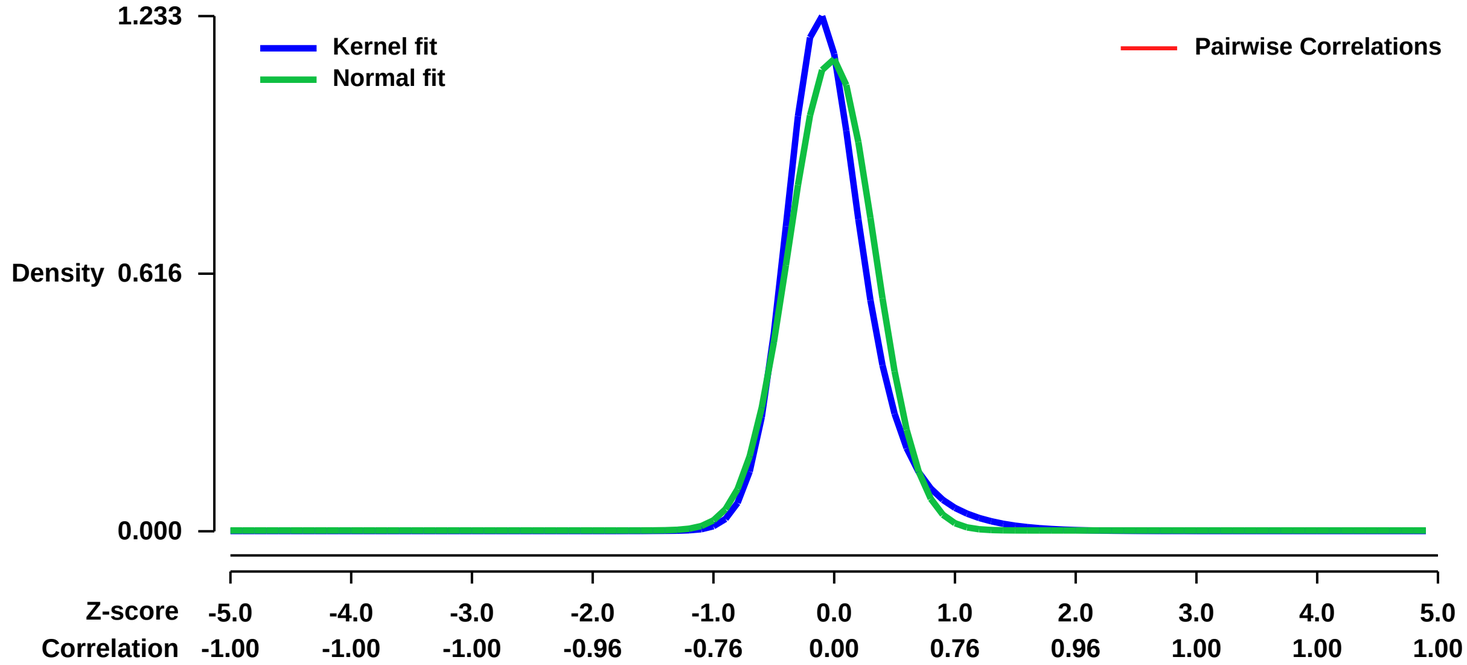

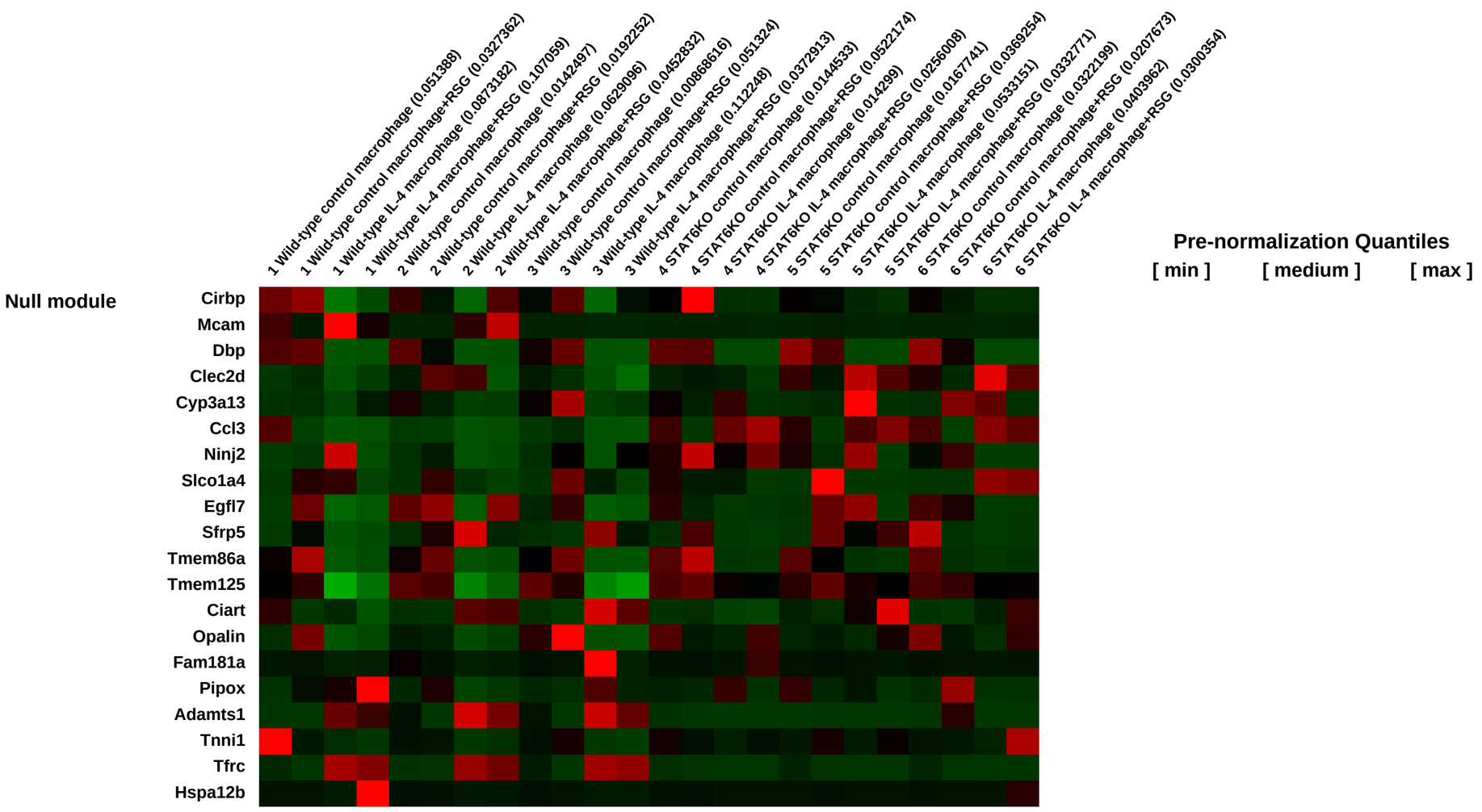

GEO Series "GSE46875" Expression Profiles

Num of samples in this series: 10

Scale of expression profile Z-scores

-3.0 -2.0 -1.0 0.0 1.0 2.0 3.0

GEO Link:	http://www.ncbi.nlm.nih.gov/geo/query/acc.cgi?acc=GSE46875
Status:	Public on Nov 06 2013
Title:	Association of maternal mRNA with the spindle in mouse oocytes
Organism:	Mus musculus
Experiment type:	Other
Platform:	GPL1261
Pubmed ID:	23852387
Summary & Design:	**Summary:** The oocytes of many species, both invertebrate and vertebrate, contain a large collection of localized determinants in the form of proteins and translationally inactive maternal mRNAs. However, it is unknown whether mouse oocytes contain localized MmRNA determinants and what mechanisms might be responsible for their control. We collected intact MII oocytes, enucleated MII oocyte cytoplasts (with the spindle removed), and spindle-chromosome complexes which had been microsurgically removed. RNA was extracted, amplified, labeled, and applied to microarrays to determine if any MmRNA determinants were localized to the SCC. **Overall design:** We used microarrays to determine whether maternal mRNAs in mouse oocytes are enriched in the meiotic spindle

Background corr dist: KL-Divergence = 0.0689, L1-Distance = 0.0509, L2-Distance = 0.0052, Normal std = 0.5144

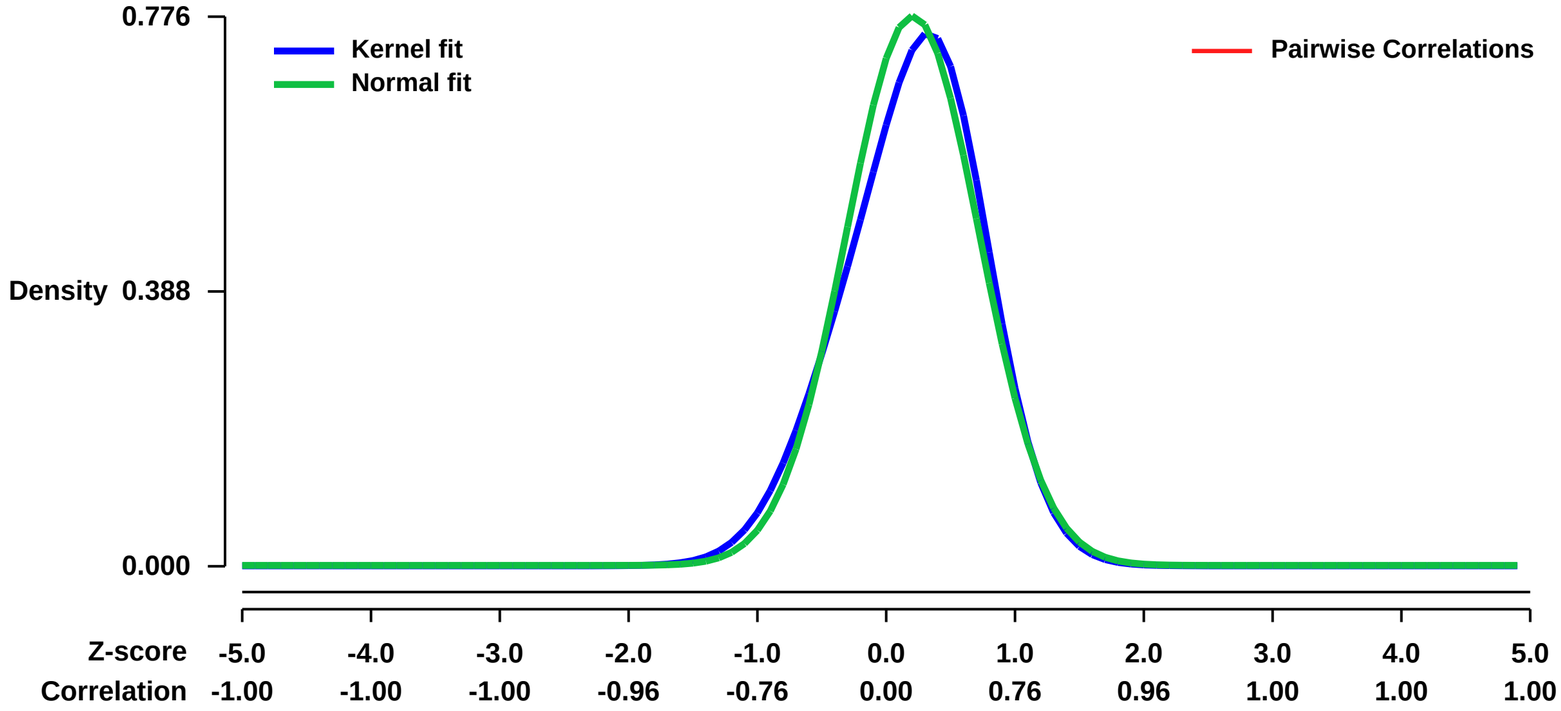

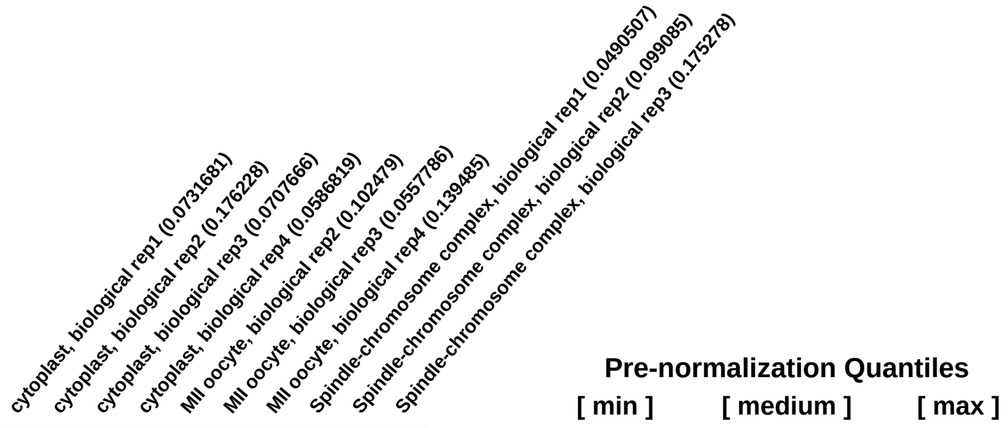

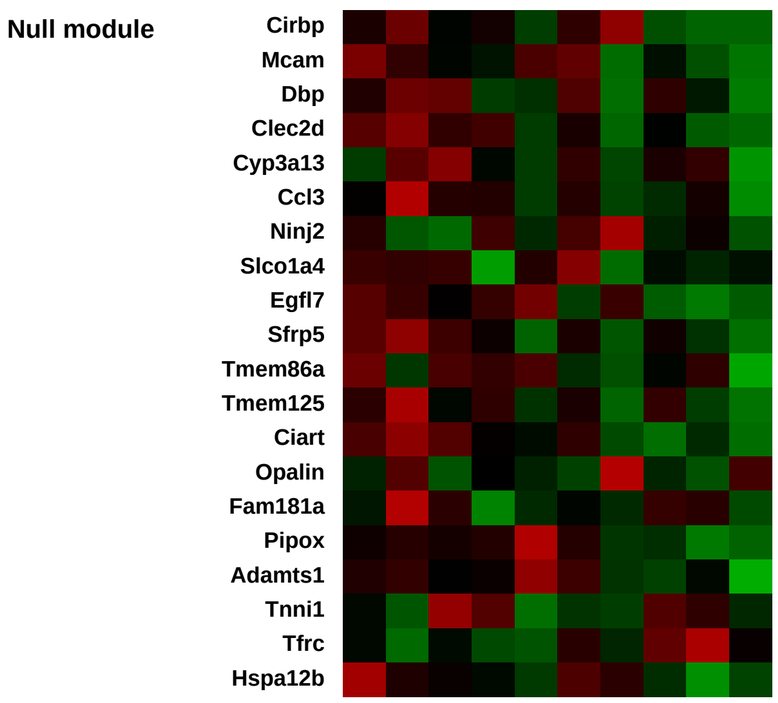

GEO Series "GSE10202" Expression Profiles

Num of samples in this series: 8

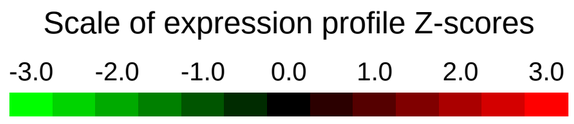

GEO Link:	http://www.ncbi.nlm.nih.gov/geo/query/acc.cgi?acc=GSE10202
Status:	Public on Jan 25 2008
Title:	Striatal gene expression data from 22-month-old CHL2 mice and control mice.
Organism:	Mus musculus
Experiment type:	Expression profiling by array
Platform:	GPL1261
Pubmed ID:	17519223
Summary & Design:	**Summary:** Achieving a mechanistic understanding of disease and initiating preclinical therapeutic trials necessitate the study of huntingtin toxicity and its remedy in model systems. To allow the engagement of appropriate experimental paradigms, Huntingtonâ s disease (HD) models need to be validated in terms of how they recapitulate a particular aspect of human disease. In order to examine transcriptome-related effects of mutant huntingtin, we compared striatal mRNA profiles from seven genetic mouse models of disease to that of postmortem human HD caudate using microarray analysis. Transgenic models expressing short N-terminal fragments of mutant huntingtin (R6/1 and R6/2 mice) exhibited the most rapid effects on gene expression, consistent with previous studies. Although changes in the brains of knock-in models of HD took longer to appear, 15-month and 22-month CHL2Q150/Q150, 18-month HdhQ92/Q92 and 2-year-old YAC128 animals also exhibited significant HD-like mRNA signatures. When the affected genes were compared across models, a robust concordance was observed. Importantly, changes concordant across multiple lines mice were also in excellent agreement with the mRNA changes seen in human HD caudate. Although it was expected that the expression of full-length huntingtin transprotein might result in unique gene expression changes compared to those caused by expression of an N-terminal huntingtin fragment, no discernable differences between full-length and fragment models were detected. There was, however, an overall concordance between transcriptomic signature and disease stage. We thus conclude that the transcriptional changes of HD can be modelled in several available lines of transgenic mice, comprising lines expressing both N-terminal and full-length mutant huntingtin proteins. The combined analysis of mouse and human HD transcriptomes provides an important chronology of mutant huntingtin's gene expression effects. **Keywords:** genetic modification **Overall design:** Striatal samples from 4 CHL2 Q150/Q150 mutant mice and 4 age-matched wild-type mice.

Background corr dist: KL-Divergence = 0.0644, L1-Distance = 0.0182, L2-Distance = 0.0003, Normal std = 0.5164

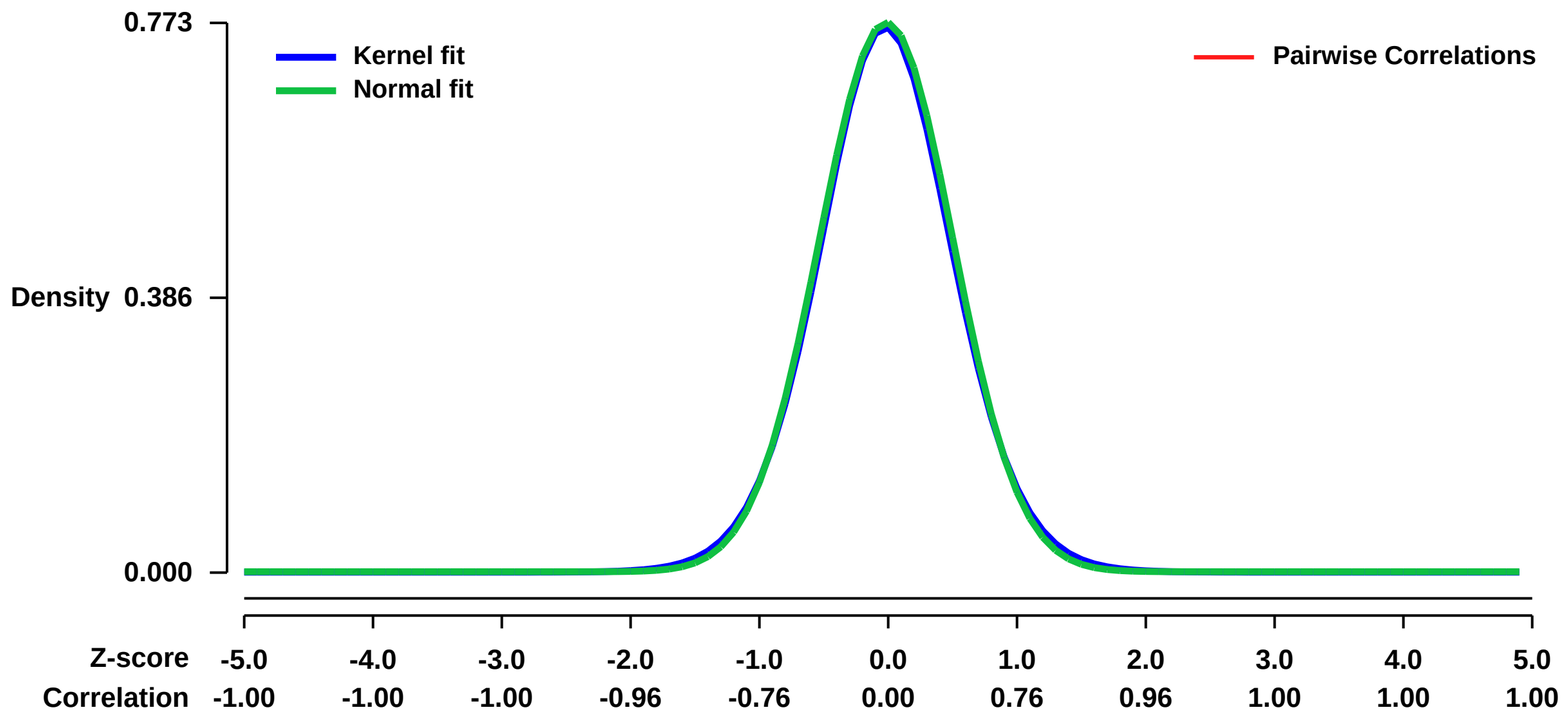

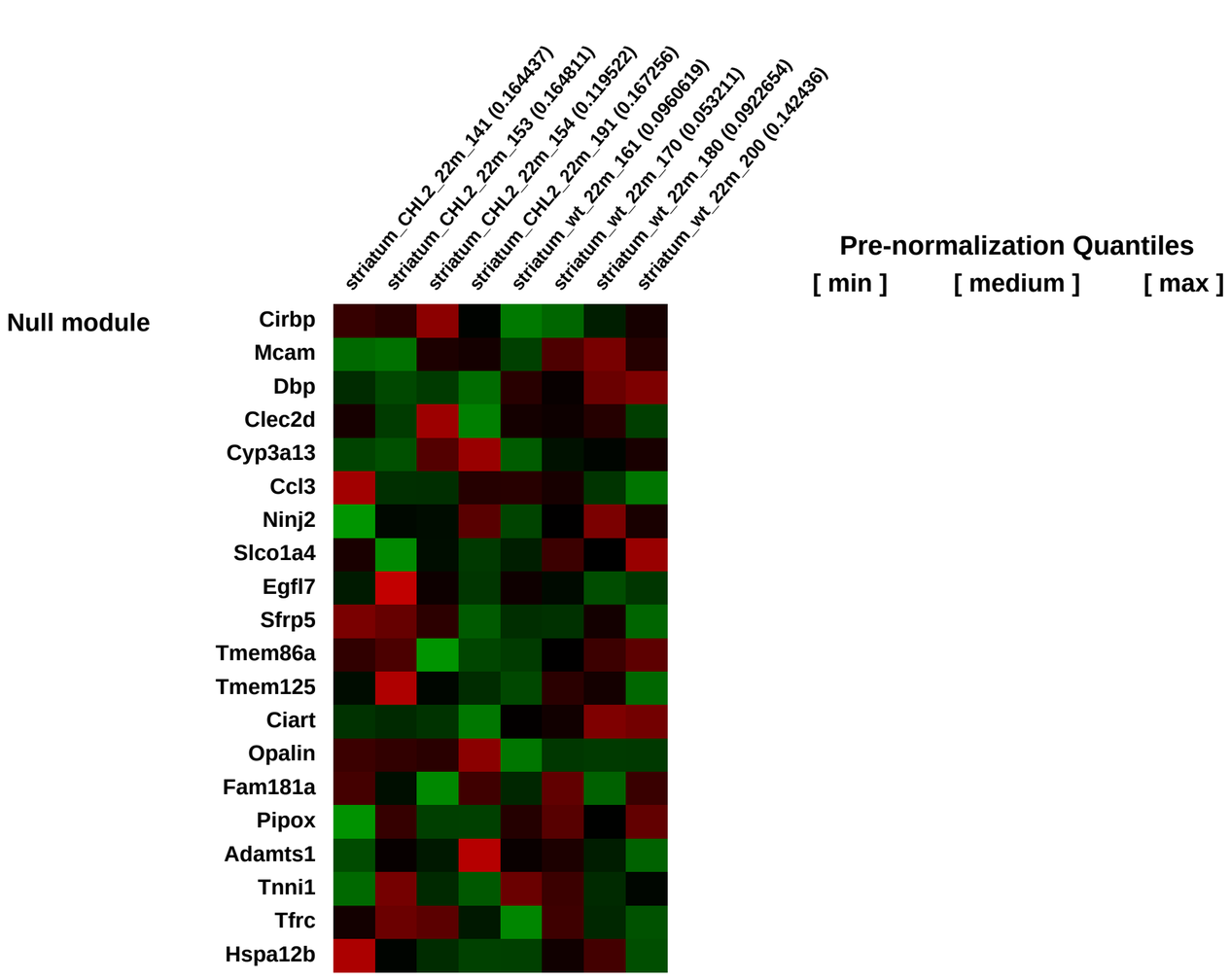

GEO Series "GSE24207" Expression Profiles

Num of samples in this series: 73

Scale of expression profile Z-scores

-3.0 -2.0 -1.0 0.0 1.0 2.0 3.0

GEO Link:	http://www.ncbi.nlm.nih.gov/geo/query/acc.cgi?acc=GSE24207
Status:	Public on Nov 18 2010
Title:	mRNA analysis in different mouse tissues
Organism:	Mus musculus
Experiment type:	Third-party reanalysis
Platform:	GPL1261
Pubmed ID:	21088282
Summary & Design:	**Summary:** The functioning of a specific tissue depends on the expression pattern of the different genes. We used microarrays to compare gene expression across different murine tissues, to get a better understanding in the expression pattern and functioning of the different tissues. With this analysis, we were not only able to identify genes that were specifically expressed in a spicific tissue but, as important, we also identified genes that were specifically repressed in a tissue, compared to al the other analysed tissues. **Overall design:** For every tissue, at least 3 biological replicates were used.

Background corr dist: KL-Divergence = 0.3994, L1-Distance = 0.0931, L2-Distance = 0.0289, Normal std = 0.2840

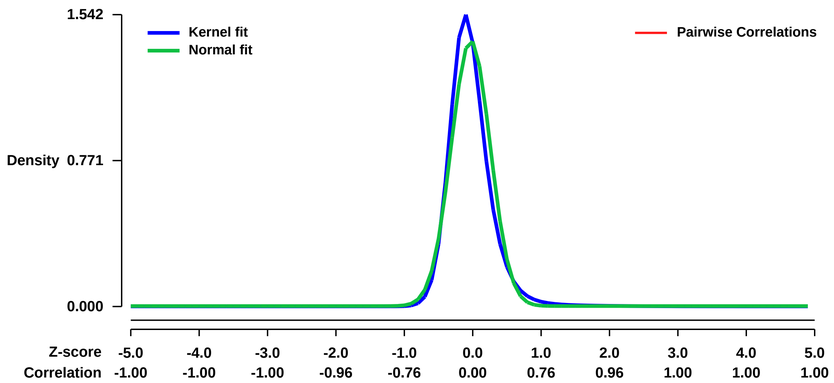

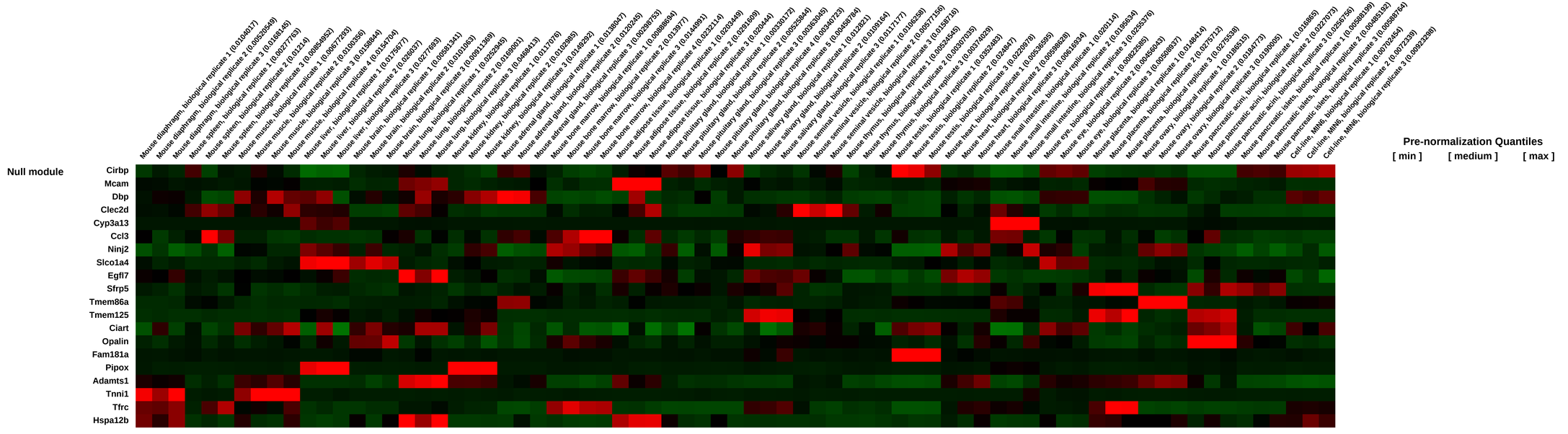

GEO Series "GSE11796" Expression Profiles

Num of samples in this series: 18

Scale of expression profile Z-scores

-3.0 -2.0 -1.0 0.0 1.0 2.0 3.0

GEO Link:	http://www.ncbi.nlm.nih.gov/geo/query/acc.cgi?acc=GSE11796
Status:	Public on Apr 17 2009
Title:	ligand-activated and -unactivated AHR in wiltype and mutant hepatoma cells
Organism:	Mus musculus
Experiment type:	Expression profiling by array
Platform:	GPL1261
Pubmed ID:	19654925
Summary & Design:	**Summary:** Starting with our early global expression analyses of TCDD-treated human hepatoma cells {Puga, 2000 4679 /id}, the AHR transcriptional induction profile has been extensively studied, whether activated by TCDD, B[a]P or in the absence of exogenous ligands (reviewed in {Frericks, 2007 5618 /id}). In addition to using prior knowledge to integrate expression profiles into the AHR gene target network, we performed a new set of expression profile analyses of wild type Hepa-1c1c7 and c35 cell lines and compared the responses in naˆflve cells with responses in TCDD or B[a]P exposed cells for 8 hours. Results of our expression array studies are in close agreement with current knowledge. **Overall design:** Three biological replicates were each performed for wildype naˆflve cells (DMSO), TCDD activated cells, and B[a]P activated cells, and for c35 (AHR mutant) naˆflve cells (DMSO), TCDD activated cells, and B[a]P activated cells.

Background corr dist: KL-Divergence = 0.0767, L1-Distance = 0.0883, L2-Distance = 0.0132, Normal std = 0.5635

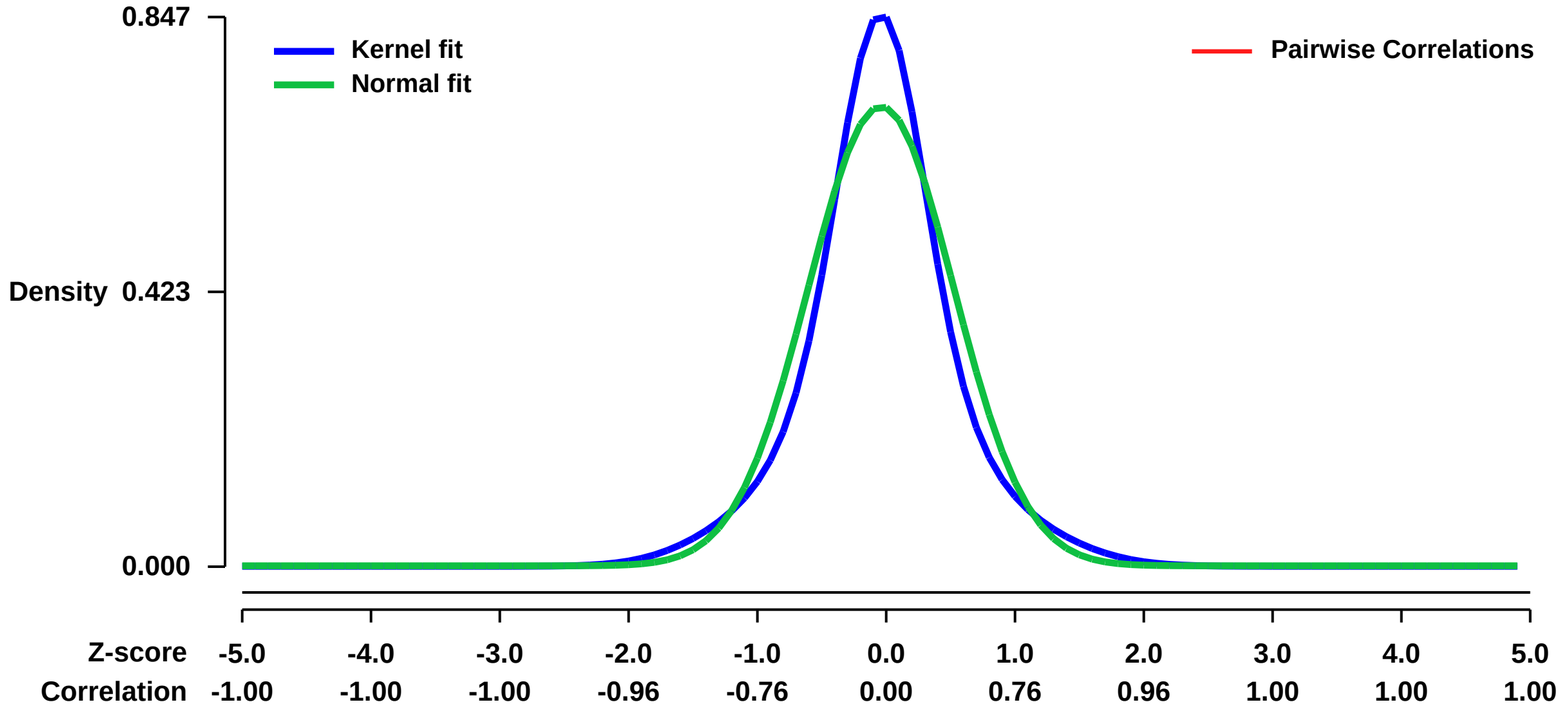

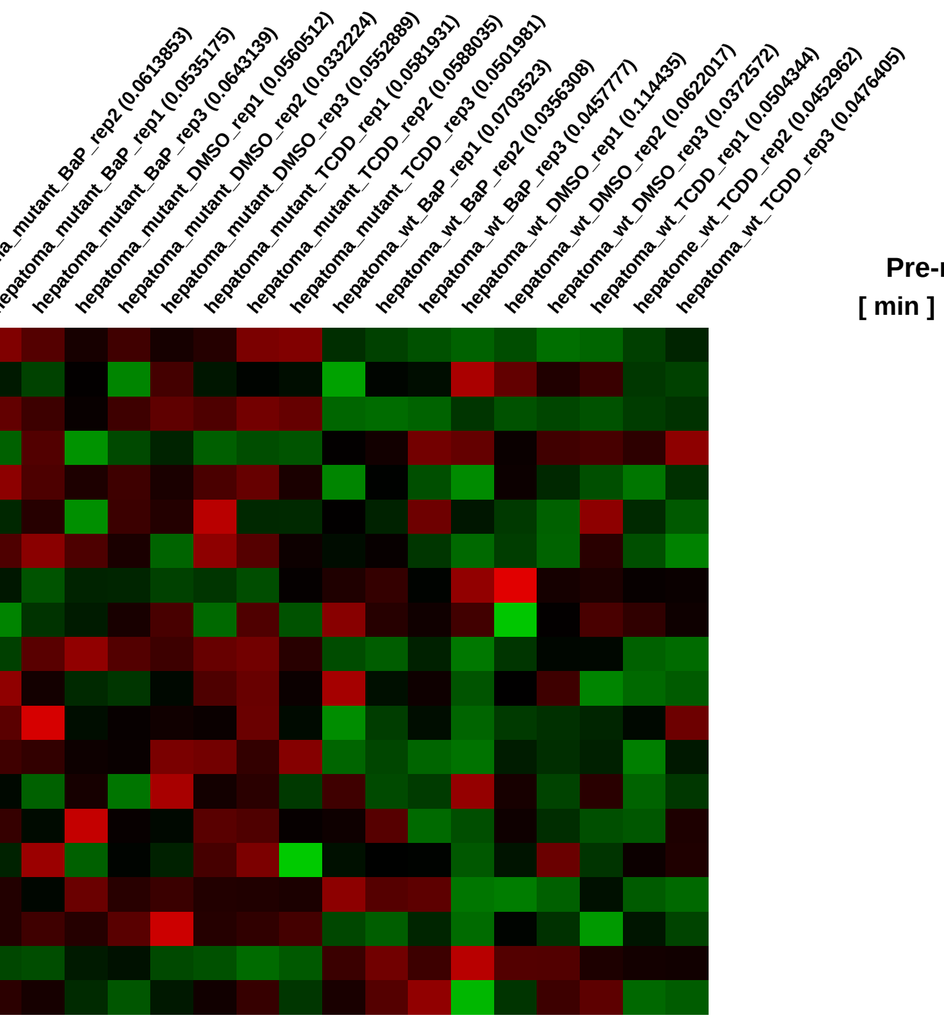

Pre-normalization Quantiles

[min] [medium] [max]

GEO Series "GSE16389" Expression Profiles

Num of samples in this series: 18

Scale of expression profile Z-scores

-3.0 -2.0 -1.0 0.0 1.0 2.0 3.0

GEO Link:	http://www.ncbi.nlm.nih.gov/geo/query/acc.cgi?acc=GSE16389
Status:	Public on Sep 01 2009
Title:	Global analysis of gene expression by SV40 T antigen in the mouse small intestine epithelium
Organism:	Mus musculus
Experiment type:	Expression profiling by array
Platform:	GPL1261
Pubmed ID:	19570859
Summary & Design:	**Summary:** SV40 large T antigen (TAg) contributes to cell transformation, in part, by targeting two well characterized tumor suppressors, pRb and p53. TAg expression affects the transcriptional circuits controlled by Rb and by p53. We have performed a microarray analysis to examine the global change in gene expression induced by wild-type TAg and TAg-mutants, in an effort to link changes in gene expression to specific transforming functions. For this analysis we have used enterocytes from the mouse small intestine expressing TAg. Expression of TAg in the mouse intestine results in hyperplasia and dysplasia. Our analysis indicates that practically all gene expression regulated by TAg in enterocytes is dependent upon its binding and inactivation of the Rb-family proteins. **Overall design:** Laser capture microdissection (LCM) was used to isolate villus enterocytes from three independent non-transgenic mice, four wild-type TAg transgenic mice, five N136 transgenic mice, three D44N transgenic mice and three 3213 transgenic mice. Total RNA was extracted from the enterocytes with the Pico Pure kit and amplified twice with the Ribo Amp kit (Arcturus). Amplified RNA was processed by the Genomics and Proteomics Core Laboratories at the University of Pittsburgh and hybridized to the Affymetrix GeneChip Mouse Genome 430 2.0 array. MAS 5.0 was used to obtain the present/absent calls and CEL files were normalized by RMA to obtain log2 expression values.

Background corr dist: KL-Divergence = 0.1739, L1-Distance = 0.0469, L2-Distance = 0.0050, Normal std = 0.3505

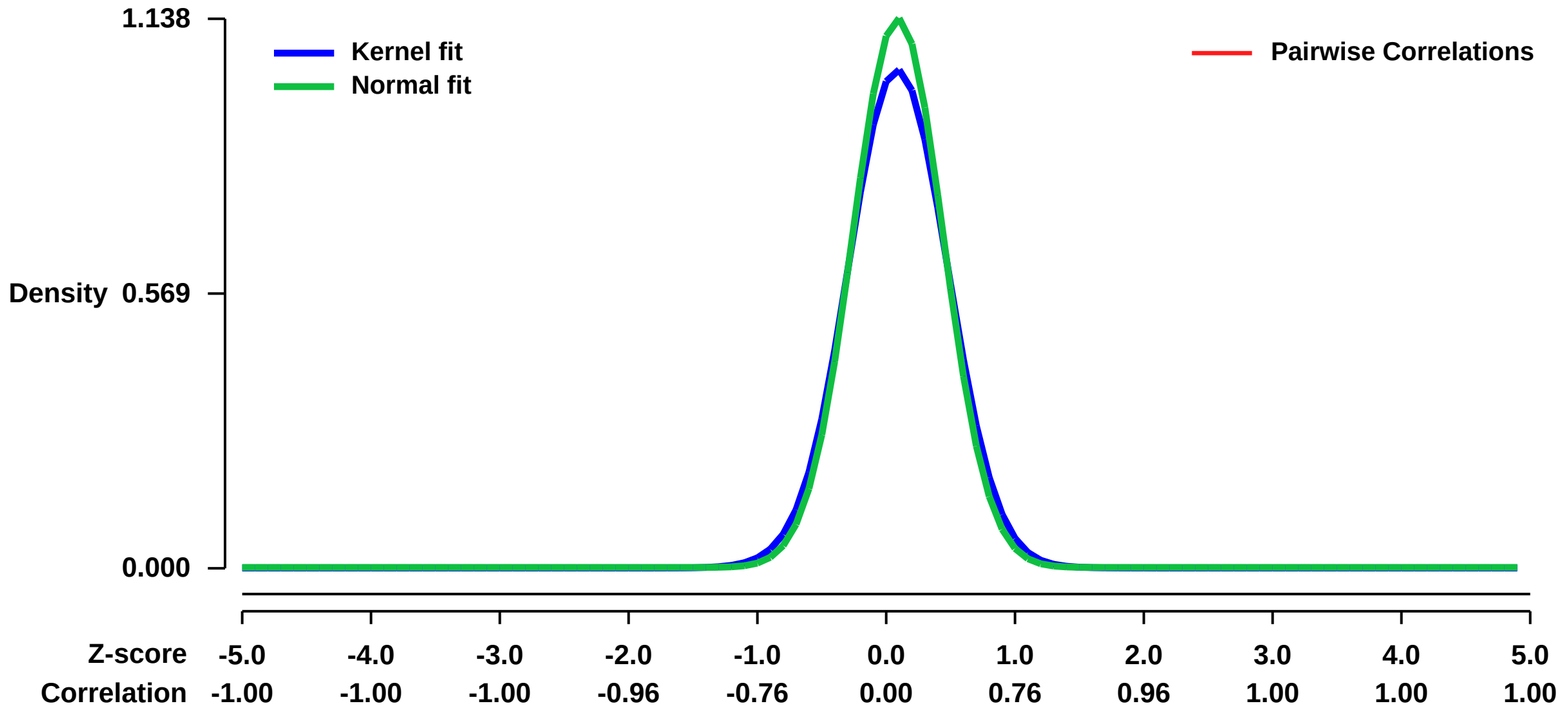

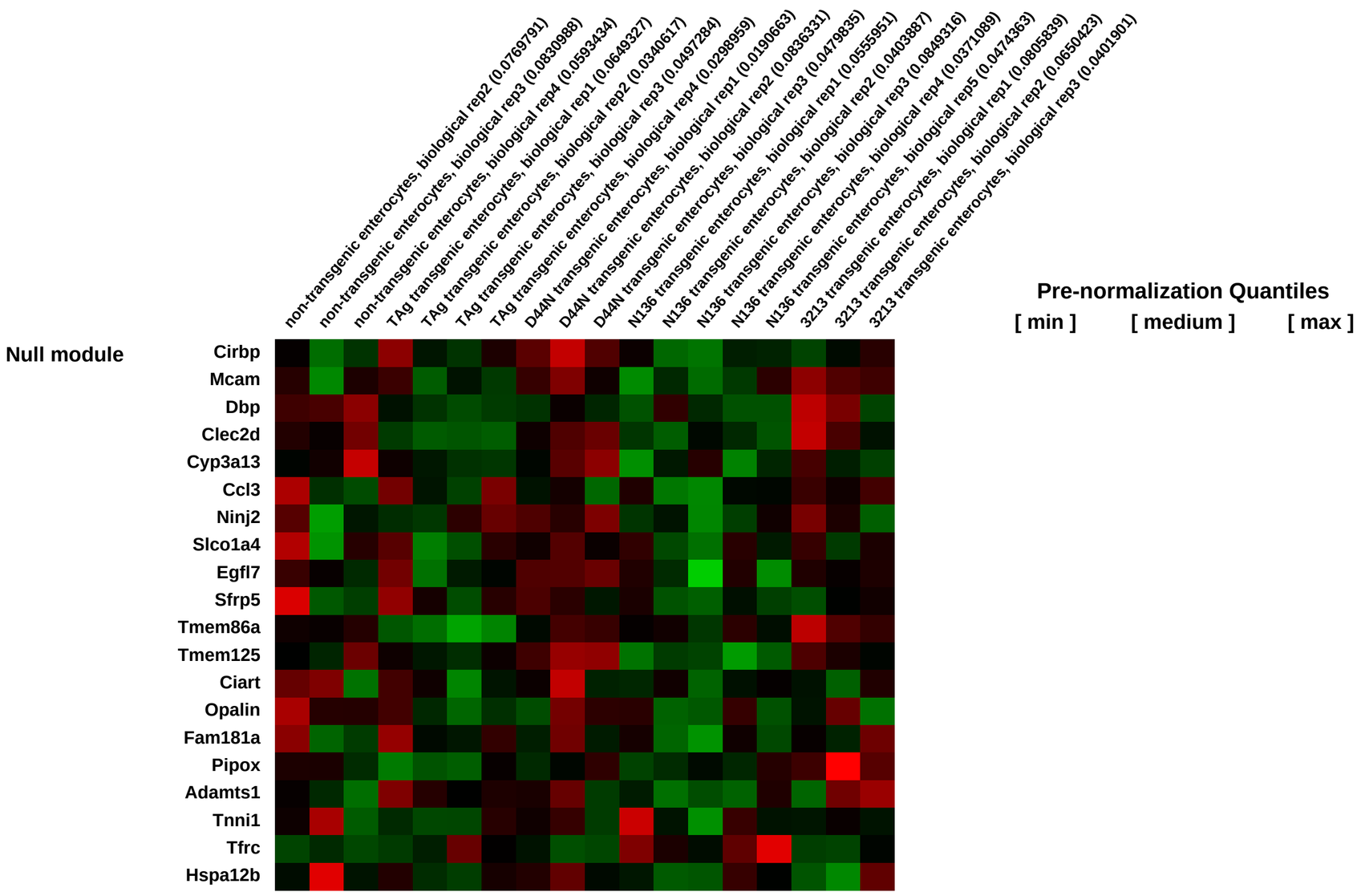

GEO Series "GSE27848" Expression Profiles

Num of samples in this series: 16

Scale of expression profile Z-scores

-3.0 -2.0 -1.0 0.0 1.0 2.0 3.0

GEO Link:	http://www.ncbi.nlm.nih.gov/geo/query/acc.cgi?acc=GSE27848
Status:	Public on Oct 02 2011
Title:	Dietary heme stimulates epithelial cell turnover by downregulating feedback inhibitors of proliferation in murine colon (part 2)
Organism:	Mus musculus
Experiment type:	Expression profiling by array
Platform:	GPL1261
Pubmed ID:	23239972
Summary & Design:	**Summary:** The risk for colon cancer is associated with nutrition, especially high fat and low calcium diets high in red meat. Red meat contains the iron porphyrin pigment heme, which induces cytotoxicity of the colon contents and epithelial hyperproliferation. Using a mouse model, we showed that heme caused damage to the colonic surface epithelium and induced compensatory hyperproliferation. Expression levels of heme- and stress-related genes show that heme affects surface cells and not directly crypt cells. Therefore, injured surface cells should signal to crypt TA cells to induce compensatory hyperproliferation. Surface-specific downregulated inhibitors of proliferation were Wnt inhibitory factor 1, Indian Hedgehog, Bone morphogenic protein 2 and possibly Interleukin-15. Heme also upregulated Amphiregulin, Epiregulin and Cyclooxygenase-2 mRNA in the surface cells, however, their protein/metabolite levels were not increased as heme induced surface-specific translation repression by increasing 4E-BP1. Therefore, we conclude that heme induced colonic hyperproliferation and hyperplasia by repressing feedback inhibition of proliferation. **Overall design:** C57BL/6 mice received a Westernized high fat and low calcium diet with or without heme (the polyporphyrin pigment of red meat). Mice received control or heme diet for 14 days. After 14 days, mice were sacrificed and colons were taken out. RNA was isolated from colon scrapings and subjected to gene expression profiling (n=7 control mice and n=9 heme-fed mice).

Background corr dist: KL-Divergence = 0.1483, L1-Distance = 0.0281, L2-Distance = 0.0012, Normal std = 0.3797

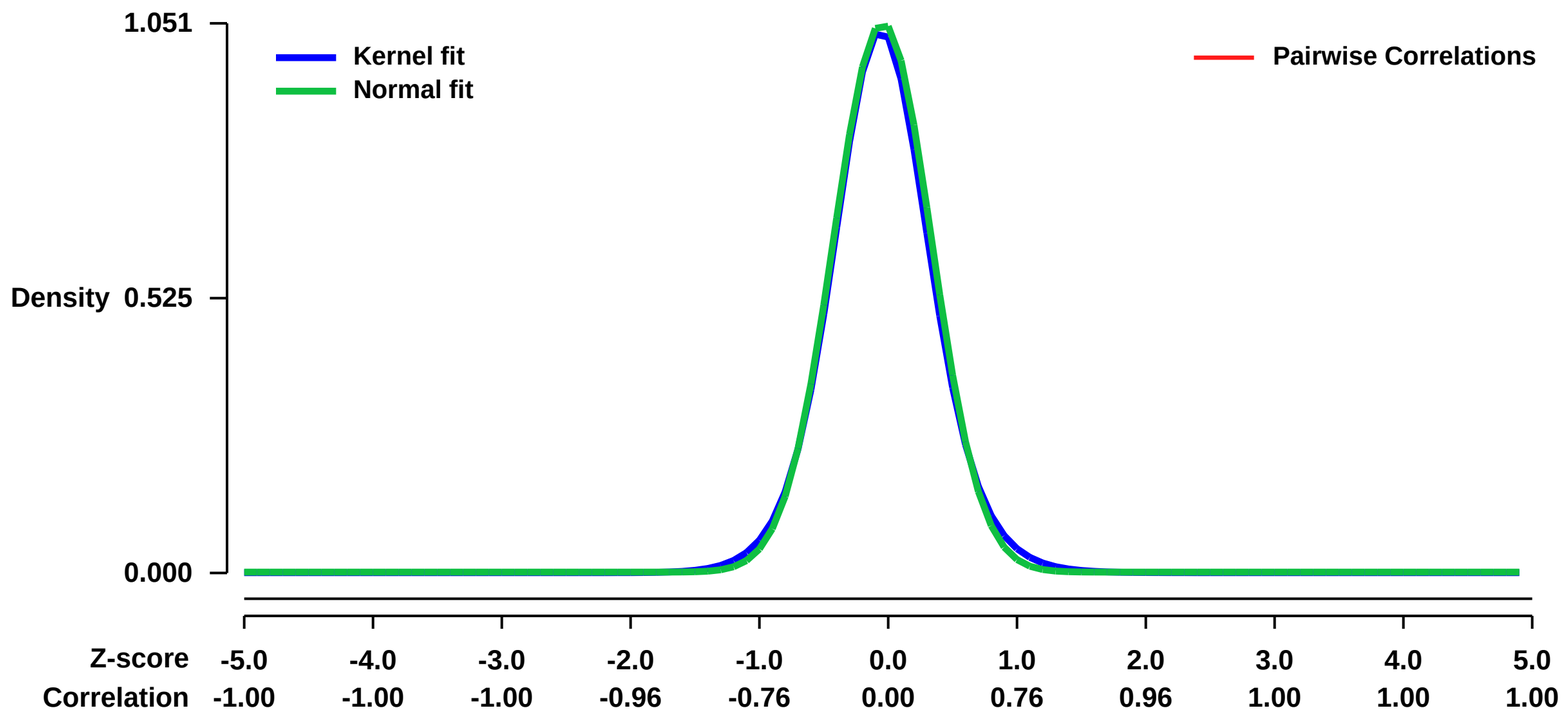

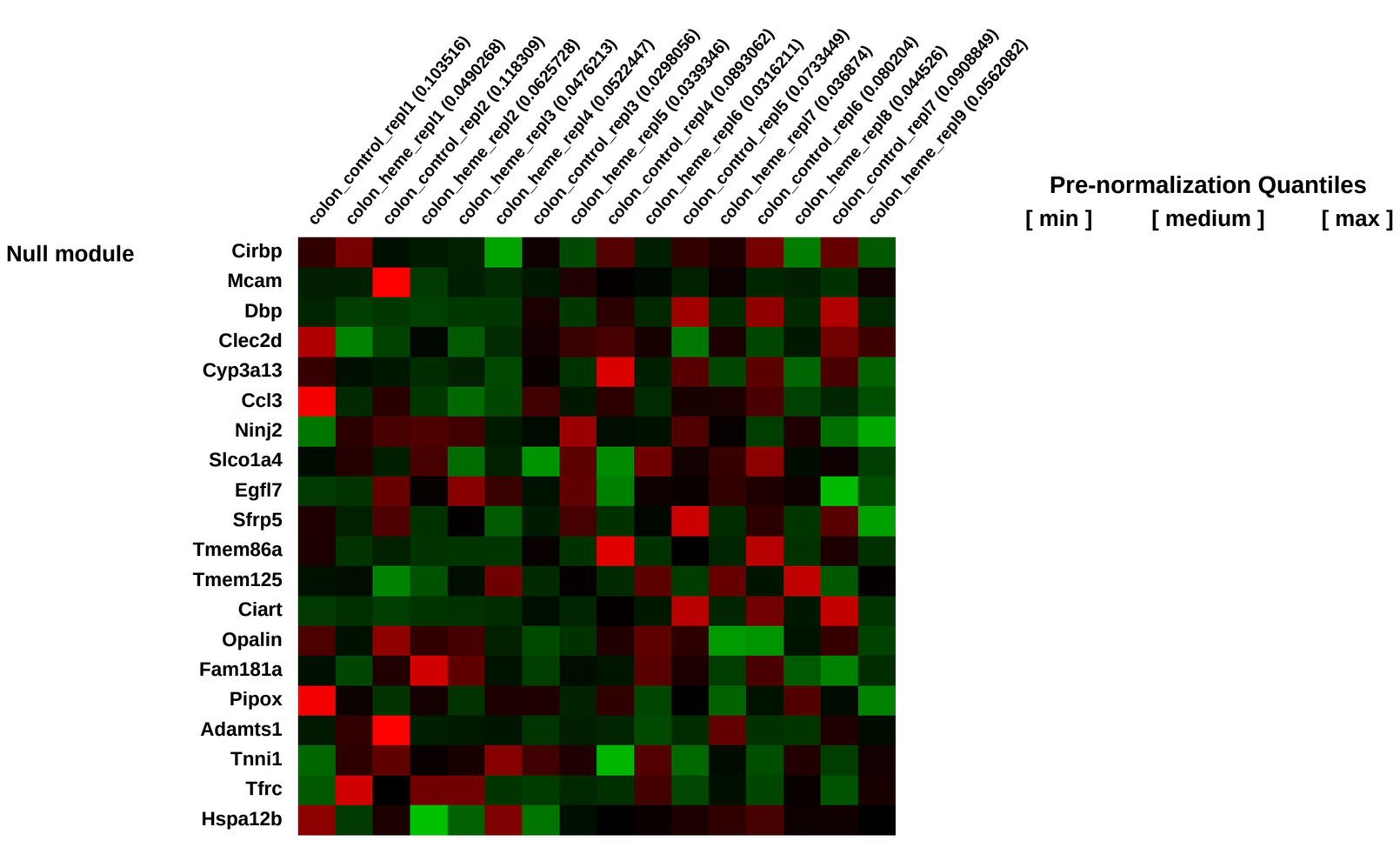

GEO Series "GSE9146" Expression Profiles

Num of samples in this series: 27

Scale of expression profile Z-scores

-3.0 -2.0 -1.0 0.0 1.0 2.0 3.0

GEO Link:	http://www.ncbi.nlm.nih.gov/geo/query/acc.cgi?acc=GSE9146
Status:	Public on Apr 04 2008
Title:	Irradiation response in PKBalpha MEF
Organism:	Mus musculus
Experiment type:	Expression profiling by array
Platform:	GPL1261
Pubmed ID:	18439899
Summary & Design:	**Summary:** MEF proficient or deficient in PKBalpha, or PKBalpha knockout MEF where PKBalpha expression was reconstituted by stable transfection were subjected to 10Gy gamma-IR treatment. 4 or 24 hours after treatment, gene expression changes were analyzed. **Keywords: genotype0-specific stress response in PKBalpha MEF** **Overall design:** three biological replicates were included in the experiment for each condition analyzed. overall, 27 samples were included in the study. the reference samples were untreated MEF of each respective genotype.

Background corr dist: KL-Divergence = 0.2065, L1-Distance = 0.0377, L2-Distance = 0.0026, Normal std = 0.3367

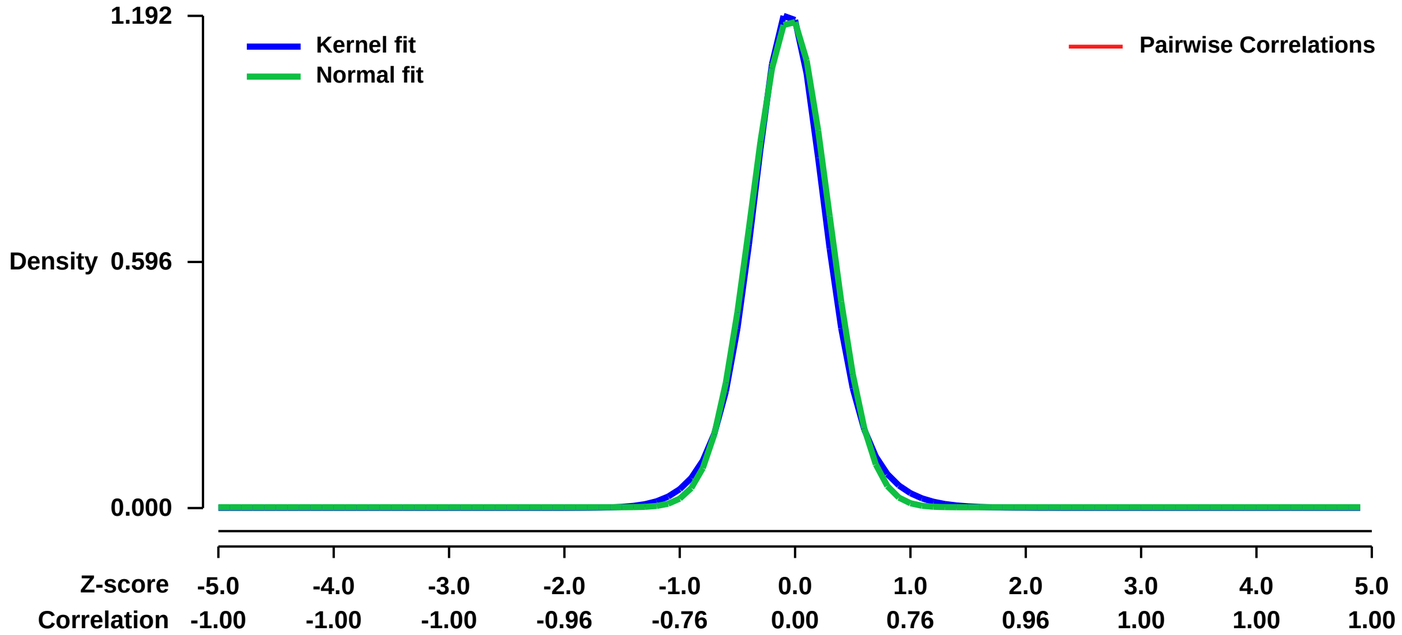

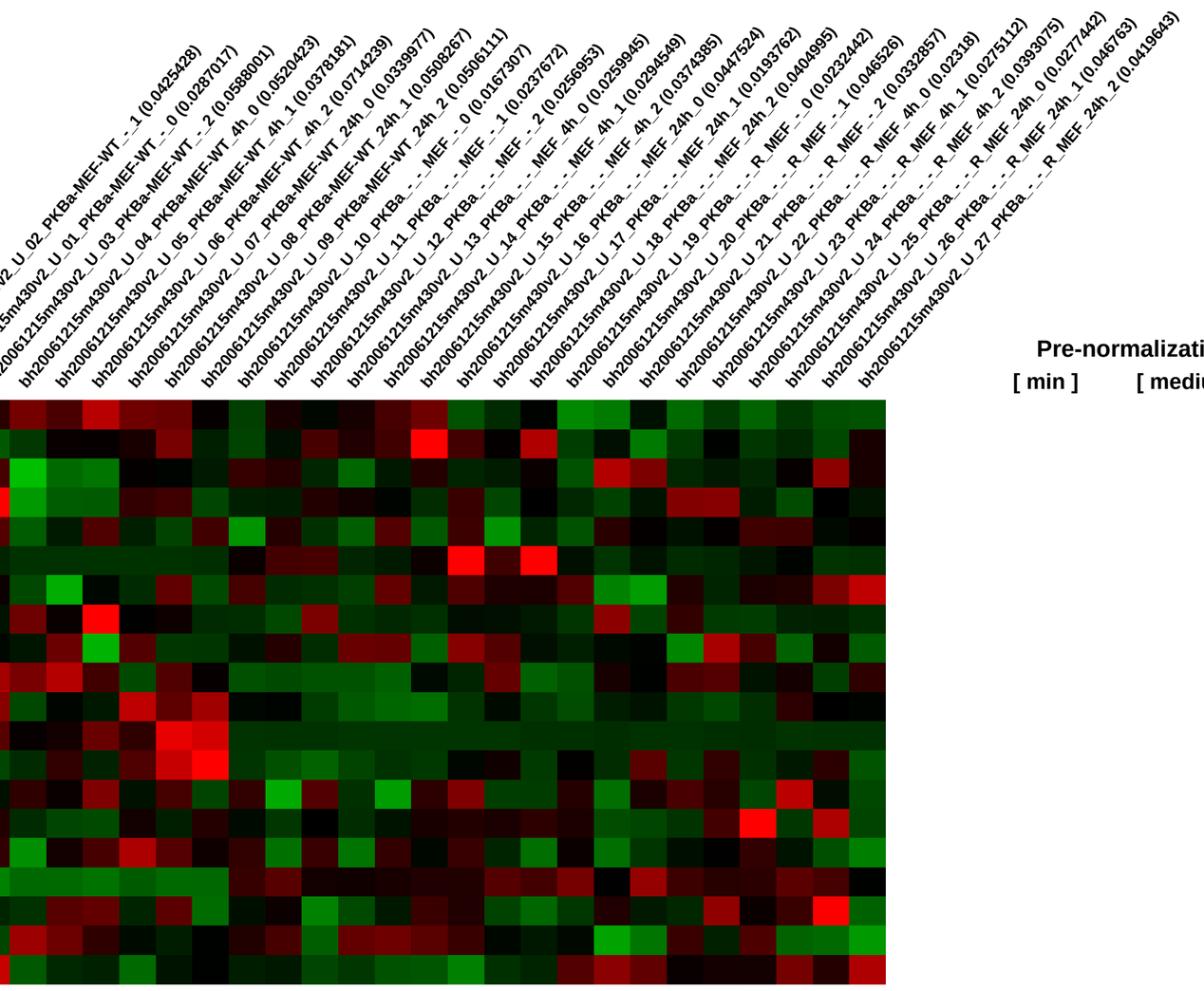

GEO Series "GSE27568" Expression Profiles

Num of samples in this series: 16

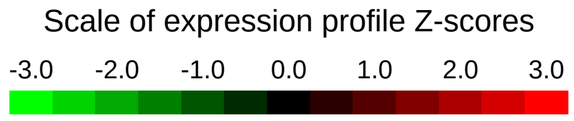

GEO Link:	**http://www.ncbi.nlm.nih.gov/geo/query/acc.cgi?acc=GSE27568**
Status:	**Public on Feb 28 2011**
Title:	**Ubb Knockout Mouse Testis**
Organism:	**Mus musculus**
Experiment type:	**Expression profiling by array**
Platform:	**GPL1261**
Pubmed ID:	**21542049**
Summary & Design:	**Summary:** **Analysis of Ubb knockout mouse testes at 7, 4, 21, and 28 dpp. Ubiquitin (Ub) is an essential protein found in all eukaryotic cells and plays important roles in a variety of cellular functions including germ cell development. Targeted disruption of the polyubiquitin gene Ubb results in male and female infertility in mice with germ cells arrested at meiotic prophase I.** **Overall design:** **Whole testes from wild-type (WT) and Ubbâ /â (KO) mice were harvested at 7, 14, 21, and 28 days postpartum. Total RNA was extracted and hybridized to Affymetrix Mouse Genome 430 2.0 arrays.**

Background corr dist: **KL-Divergence = 0.0537, L1-Distance = 0.0652, L2-Distance = 0.0066, Normal std = 0.6280**

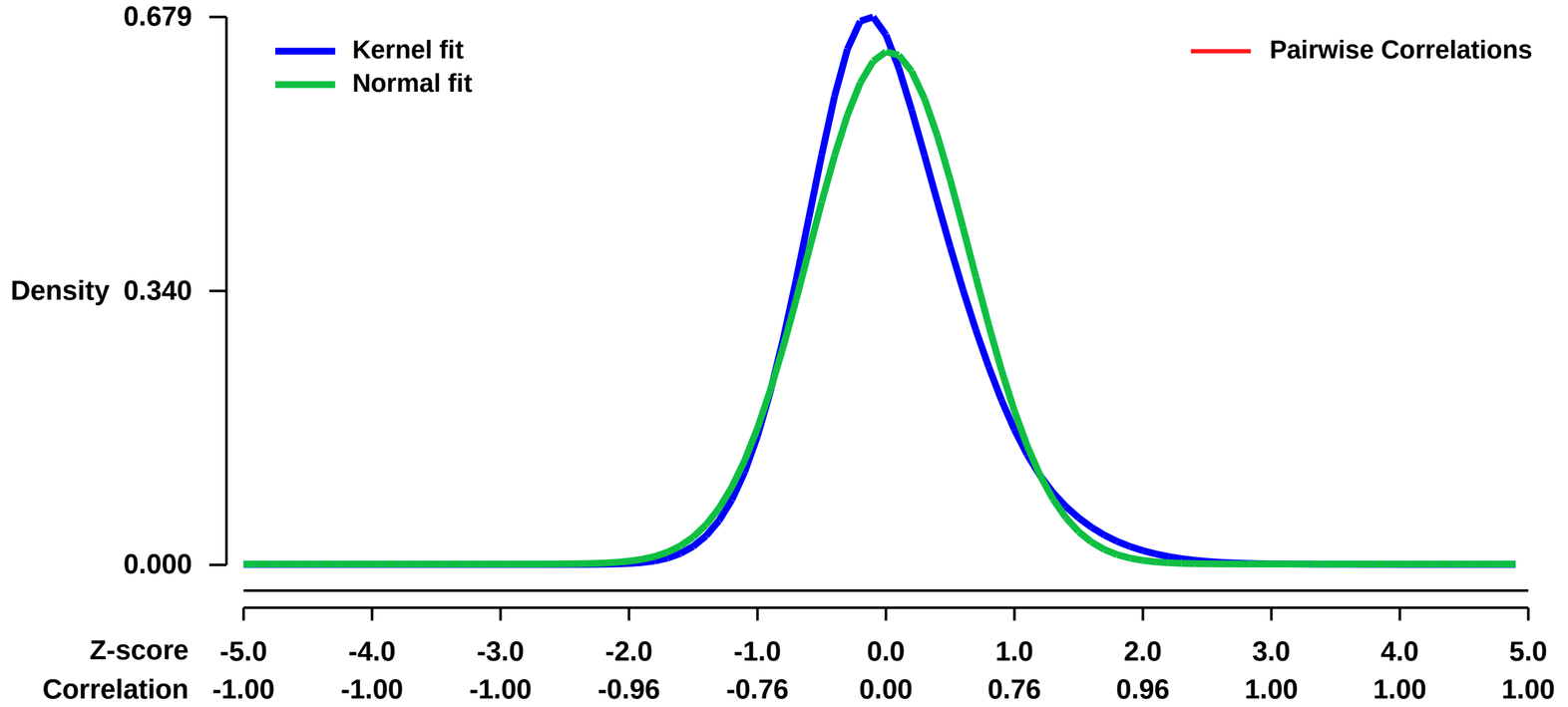

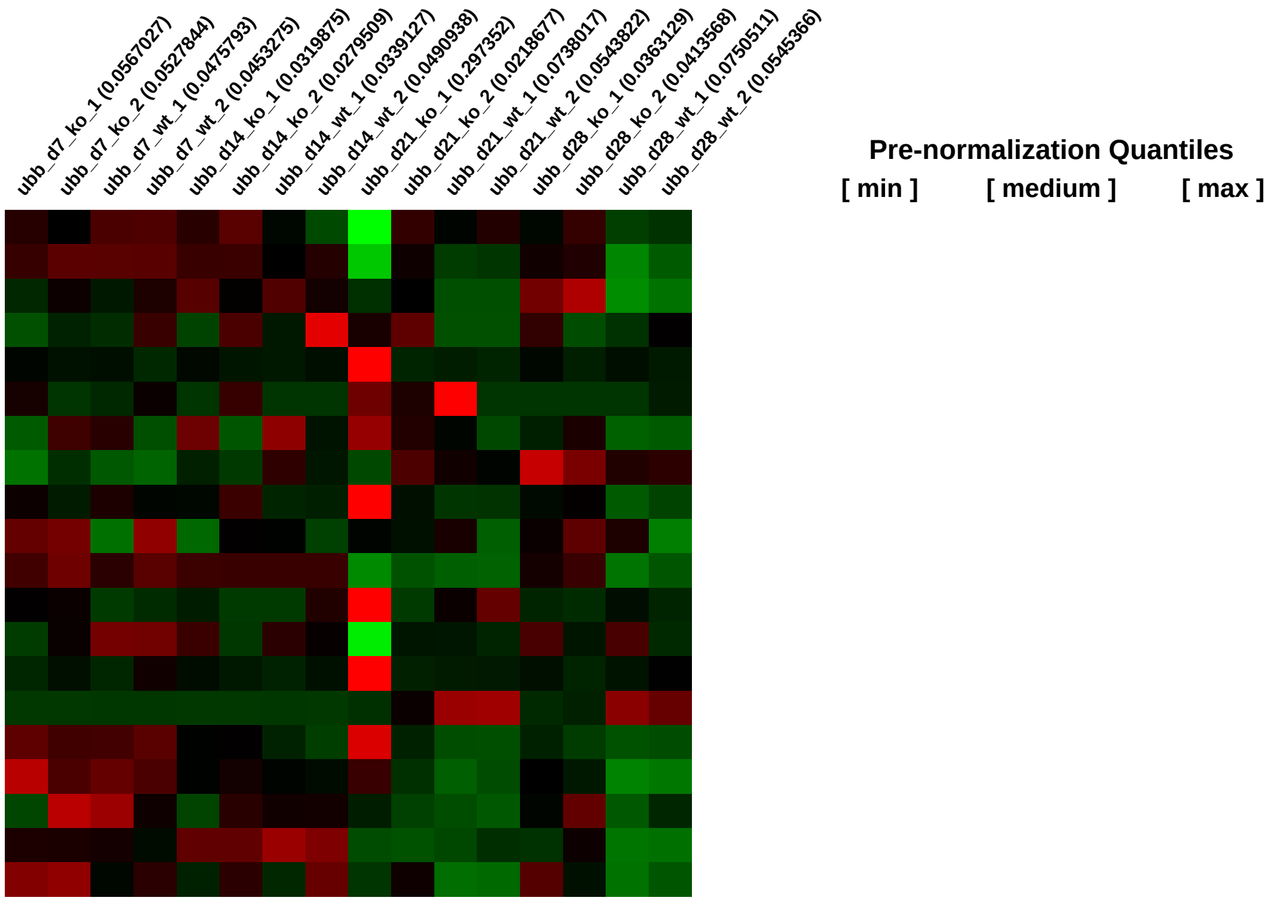

GEO Series "GSE15770" Expression Profiles

Num of samples in this series: 8

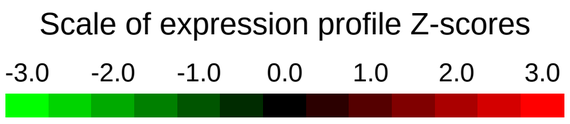

GEO Link:	**http://www.ncbi.nlm.nih.gov/geo/query/acc.cgi?acc=GSE15770**
Status:	**Public on May 20 2009**
Title:	**WT and Get1 +/- Bladder Time Course**
Organism:	**Mus musculus**
Experiment type:	**Expression profiling by array**
Platform:	**GPL1261**
Pubmed ID:	**19494835**
Summary & Design:	**Summary:** **Skin and bladder epithelia form effective permeability barriers through the activation of distinct differentiation gene programs. Employing a genome-wide gene expression study, we identified transcription regulators whose expression correlates highly with that of differentiation markers both in bladder and skin, including the Grainyhead factor Get1/Grhl3, already known to be important for epidermal barrier formation. In the bladder, Get1 is most highly expressed in the differentiated umbrella cells and its mutation in mice leads to a defective bladder epithelial barrier formation due to failure of apical membrane specialization. Genes encoding components of the specialized urothelial membrane, the uroplakins, were downregulated in Get1-/- mice. At least one of these genes, Uroplakin II, is a direct target of Get1. The urothelial-specific activation of the Uroplakin II gene is due to selective binding of Get1 to the Uroplakin II promoter in urothelial cells, most likely regulated by histone modifications. These results demonstrate a key role for Get1 in urothelial differentiation and barrier formation.** **Overall design:** **To gain insights into common and unique transcriptional regulatory programs during bladder differentiation, we profiled global gene expression in whole mouse bladder at E14.5, E16.5, and E18.5.**

Background corr dist: KL-Divergence = 0.0667, L1-Distance = 0.0219, L2-Distance = 0.0008, Normal std = 0.5100

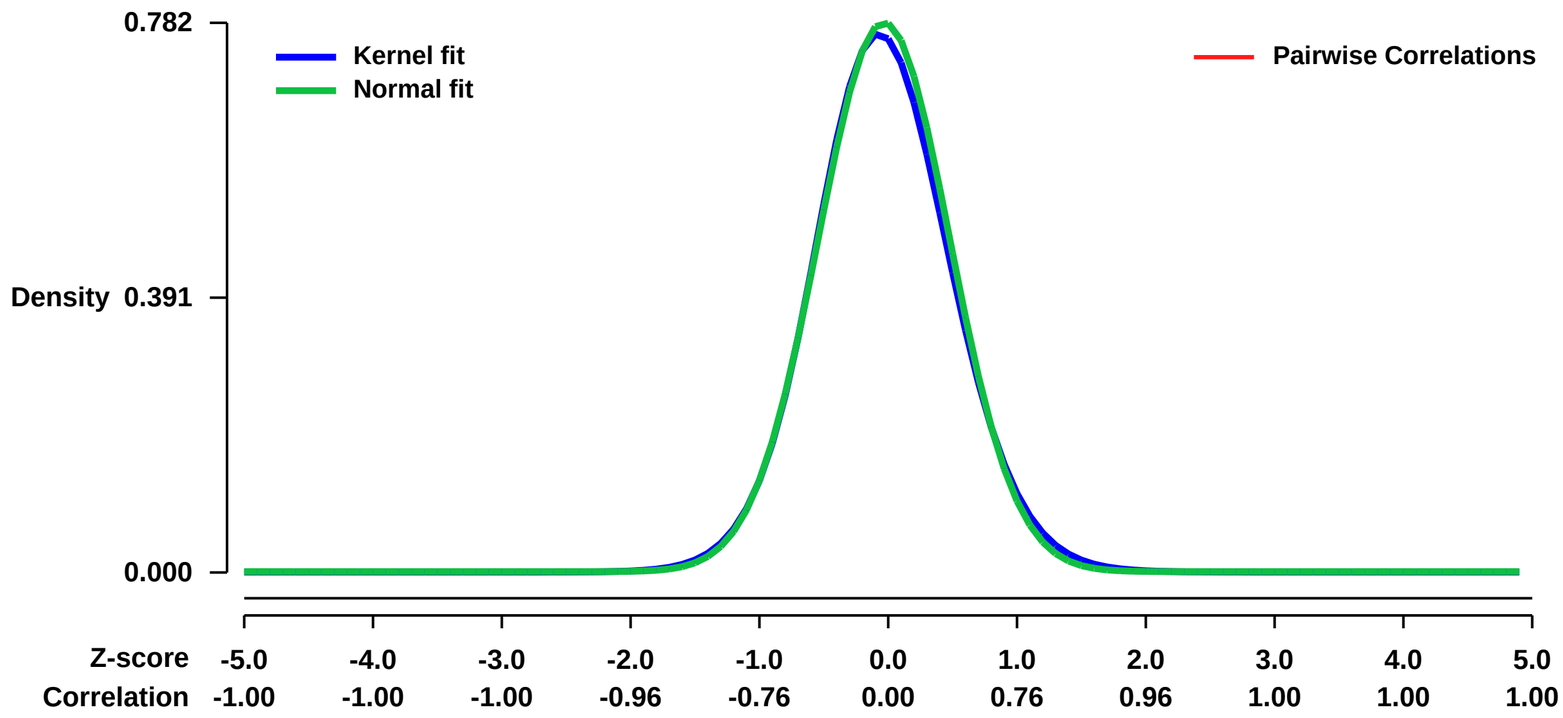

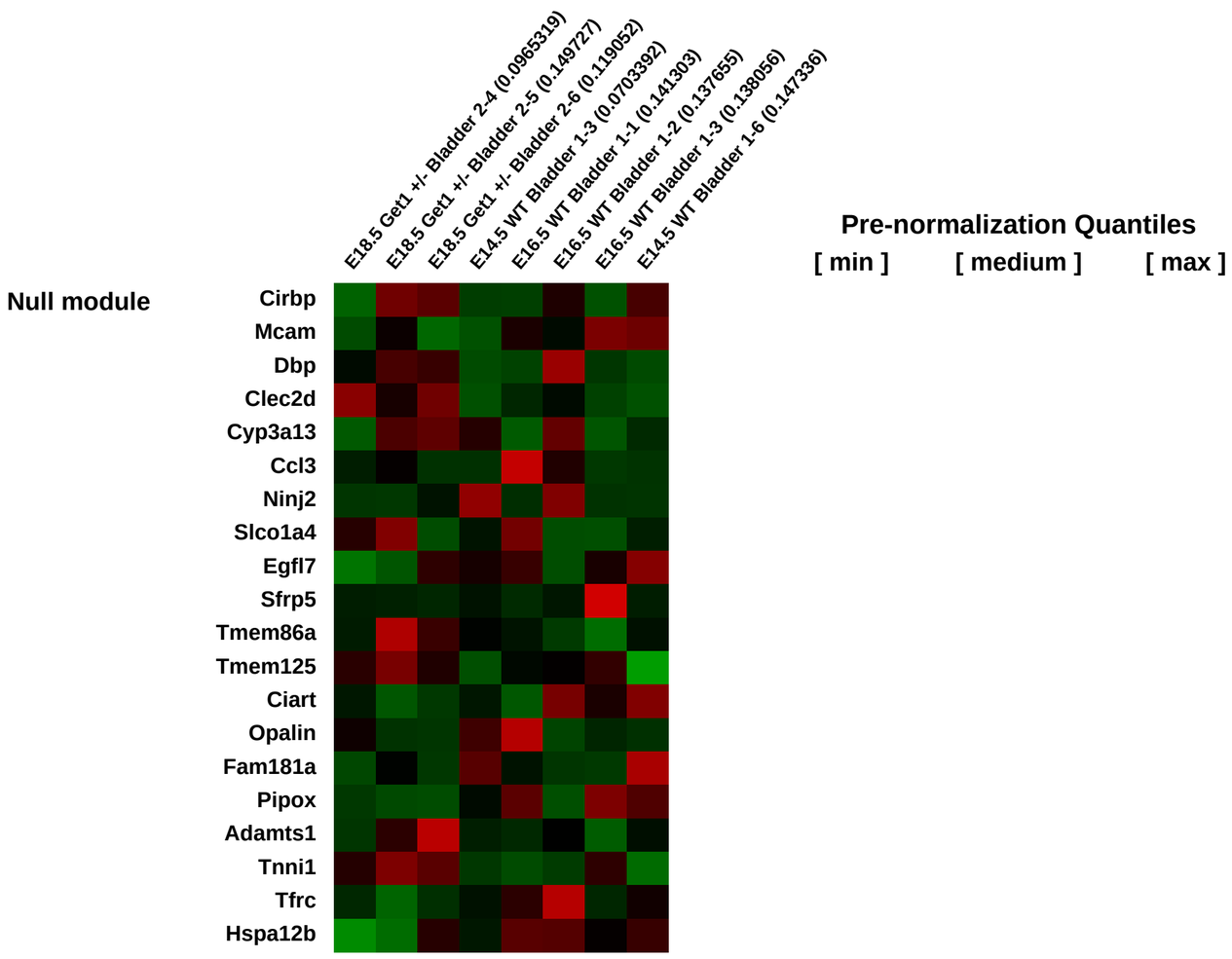

GEO Series "GSE45044" Expression Profiles

Num of samples in this series: 12

Scale of expression profile Z-scores

-3.0 -2.0 -1.0 0.0 1.0 2.0 3.0

GEO Link:	http://www.ncbi.nlm.nih.gov/geo/query/acc.cgi?acc=GSE45044
Status:	Public on May 29 2013
Title:	Age-mediated transcriptomic changes in adult mouse brain ventral tegmental area
Organism:	Mus musculus
Experiment type:	Expression profiling by array
Platform:	GPL1261
Pubmed ID:	23638090
Summary & Design:	**Summary:** Substantia nigra pars compacta (SNpc) is highly sensitive to normal aging and selectively degenerates in Parkinson's disease. However, ventral tegmental area (VTA), a region adjacent to SNpc, is less affected in PD. Until now, molecular mechanisms behind VTA aging have not been fully investigated using high throughput techniques. Here, aging-associated early changes in transcriptome of VTA were investigated comparing late middle-aged (18 months old) to young (2 months old) mice. **Overall design:** Three age groups of C57 wild type mice were used in microarray analysis: young (2 months old), middle aged (10 months old), and late-middle aged (18 months old) mice. Four replicates were included in each age group and each replicate was pooled from 5 mice (5 mice/replicate x 4 replicates x 3 age groups). Total RNA was isolated from VTA for hybridization on Affymetrix microarrays.

Background corr dist: KL-Divergence = 0.0452, L1-Distance = 0.0543, L2-Distance = 0.0056, Normal std = 0.5948

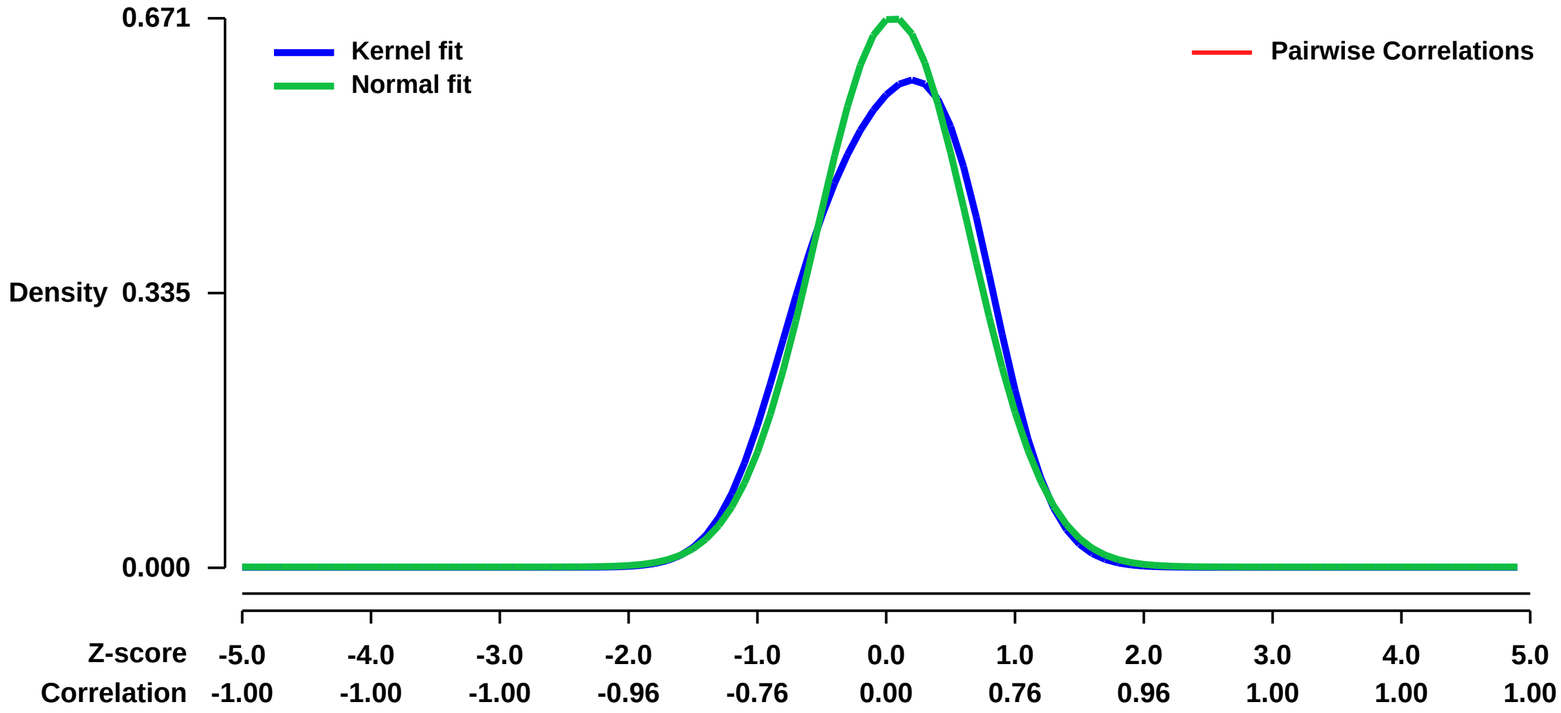

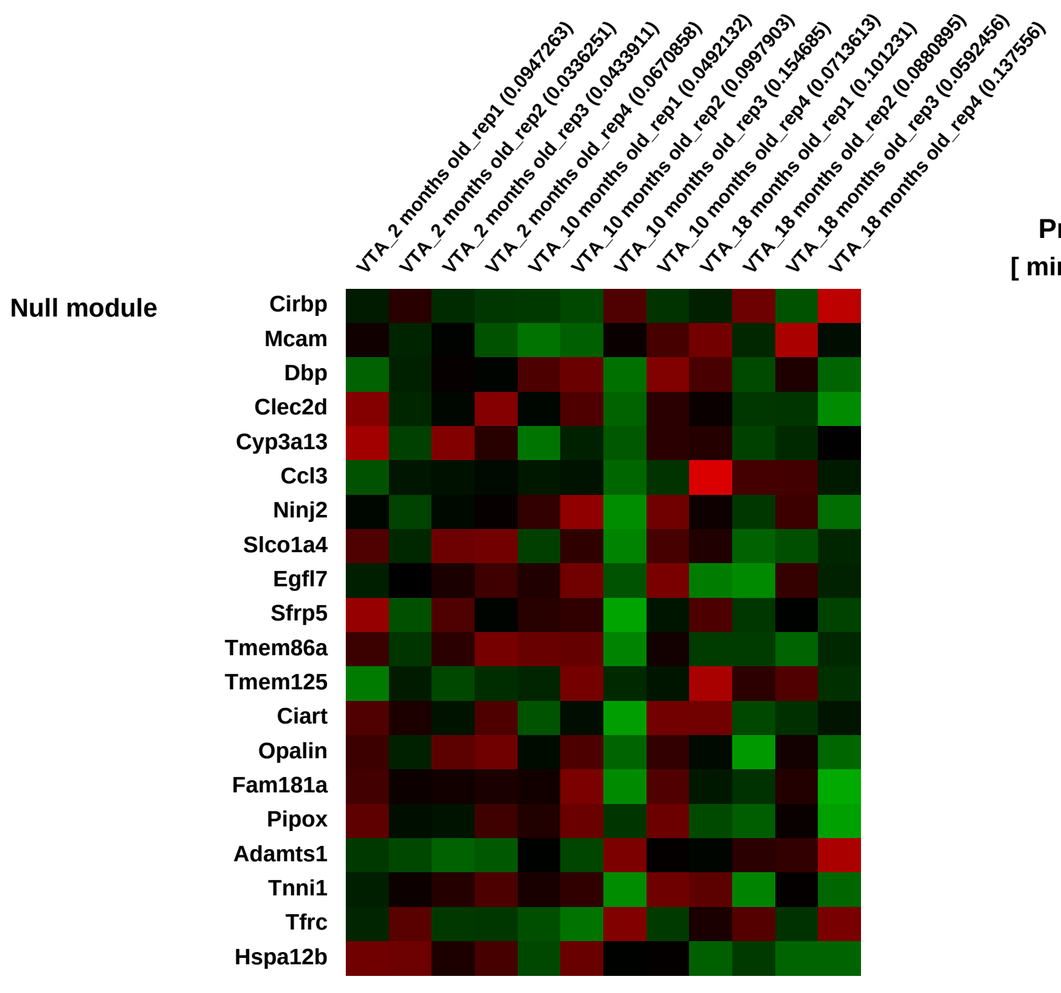

GEO Series "GSE21309" Expression Profiles

Num of samples in this series: 9

Scale of expression profile Z-scores

-3.0 -2.0 -1.0 0.0 1.0 2.0 3.0

GEO Link:	http://www.ncbi.nlm.nih.gov/geo/query/acc.cgi?acc=GSE21309
Status:	Public on Apr 13 2010
Title:	Differential gene expression patterns in lung carcinogenesis mediated by loss of mouse tumor supressor Gprc5a
Organism:	Mus musculus
Experiment type:	Expression profiling by array
Platform:	GPL1261
Pubmed ID:	20686609
Summary & Design:	**Summary:** Increasing the understanding of the impact of changes in oncogenes and tumor suppressor genes is essential for improving the management of lung cancer. Recently, we identified a new mouse lung-specific tumor suppressor - the G-protein coupled receptor 5A (Gprc5a). We sought to understand the molecular consequences of Gprc5a loss and towards this we performed microarray analysis of the transcriptomes of lung epithelial cells cultured from normal tracheas of Gprc5a knockout and wild-type mice to define a loss-of-Gprc5a gene signature. Moreover, we analyzed differential gene expression patterns between Gprc5a knockout normal lung epithelial cells as well as lung adenocarcinoma cells isolated and cultured from tumors of NNK-exposed Gprc5a knockout mice. **Overall design:** Gprc5a wild type cells (WT-NLE) and Gprc5a knockout cells (NULL-NLE) were isolated and cultured from trachea of three week old Gprc5a wild type and knockout mice, respectively. MDA-F471 mouse lung adenocarcinoma cells were derived de novo from an adenocarcinoma that was found in the lung of a female Gprc5a-knockout mouse sacrificed 16 months after NNK tobacco carcinogen i.p. injection based on a protocol approved by the M.D. Anderson Cancer Center Institutional Animal Care and Use Committee. Following RNA extraction and purification, the transcriptome of the Gprc5a wild type and knockout cells were analyzed by microarray analysis using the Affymetrix MG-430 2.0 murine array platform.

Background corr dist: KL-Divergence = 0.0371, L1-Distance = 0.0368, L2-Distance = 0.0016, Normal std = 0.6593

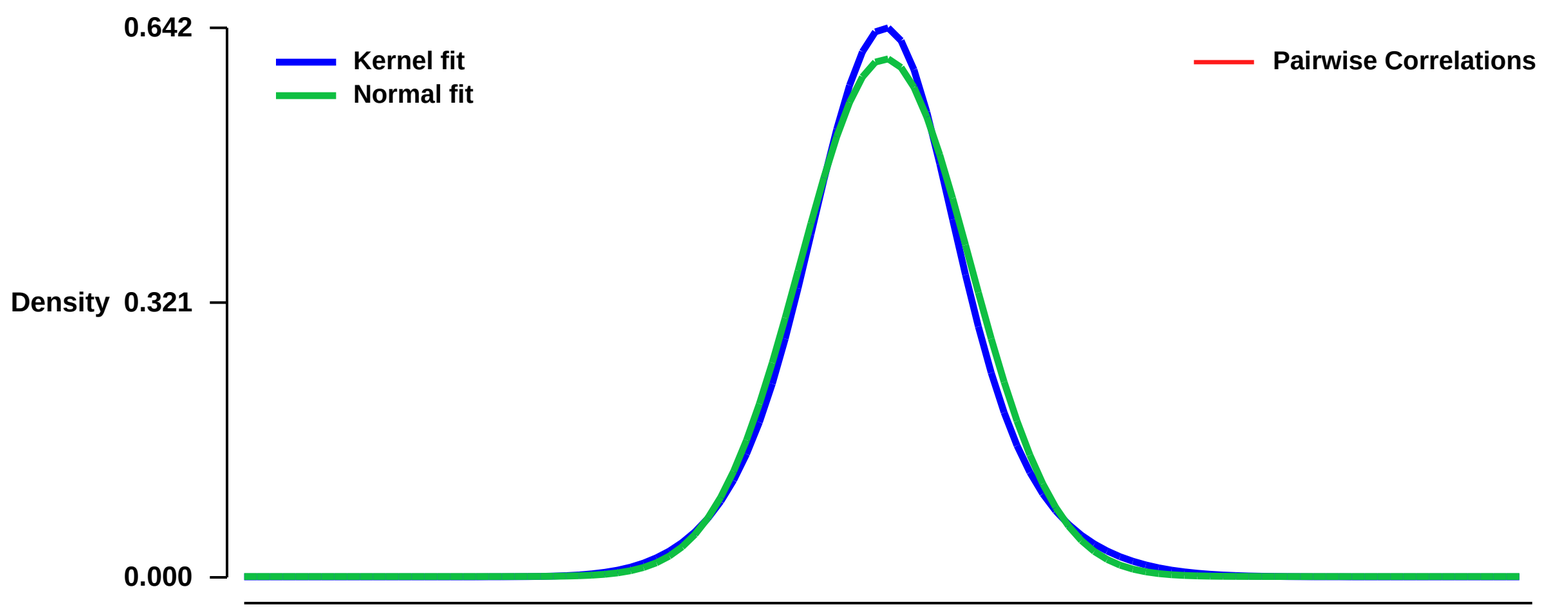

Z-score	-5.0	-4.0	-3.0	-2.0	-1.0	0.0	1.0	2.0	3.0	4.0	5.0
Correlation	-1.00	-1.00	-1.00	-0.96	-0.76	0.00	0.76	0.96	1.00	1.00	1.00

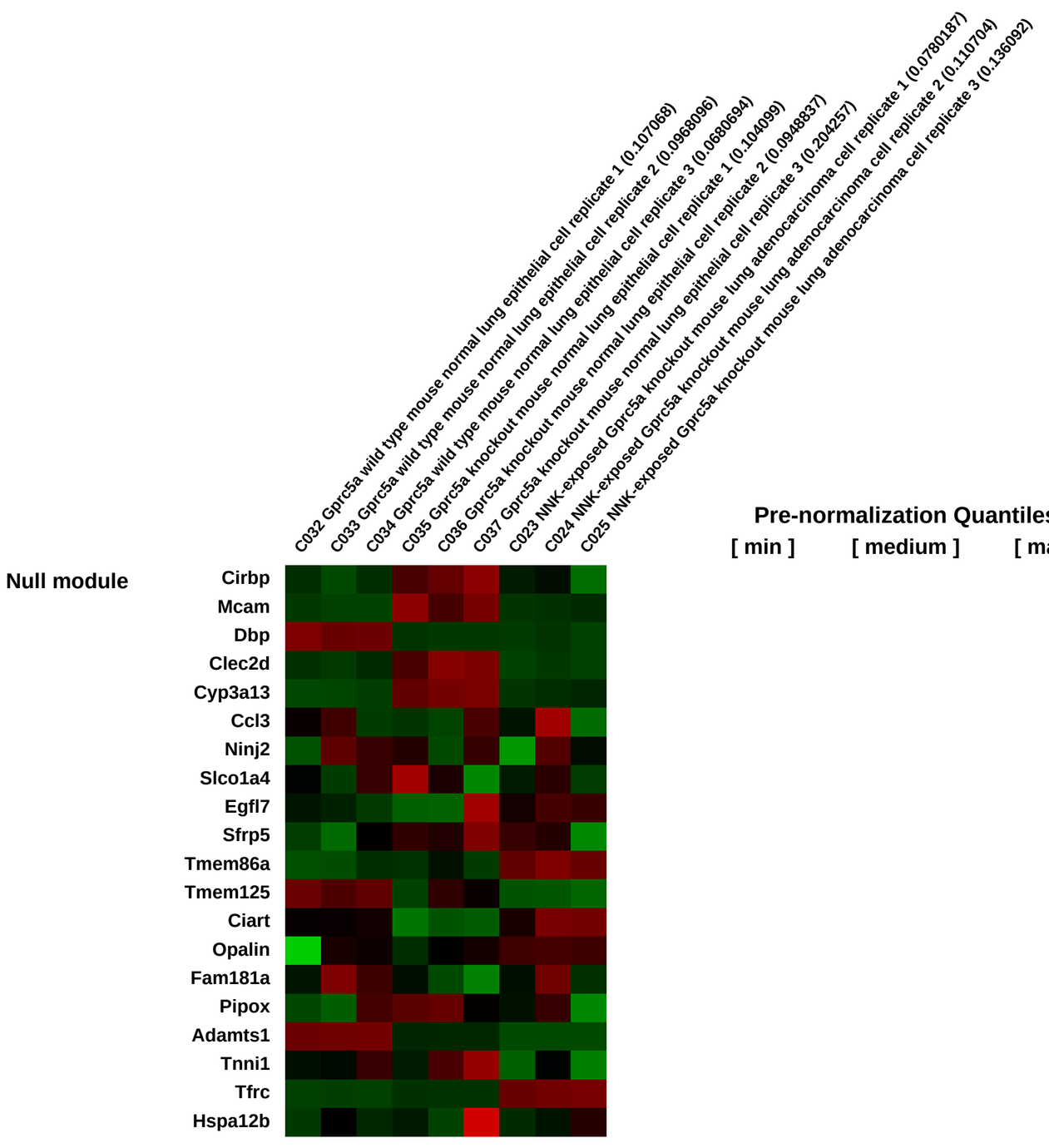

GEO Series "GSE41925" Expression Profiles

Num of samples in this series: 8

Scale of expression profile Z-scores

-3.0 -2.0 -1.0 0.0 1.0 2.0 3.0

GEO Link:	http://www.ncbi.nlm.nih.gov/geo/query/acc.cgi?acc=GSE41925
Status:	Public on Dec 01 2012
Title:	Transcription factor AP-2 gamma is a core regulator of tight junction biogenesis and cavity formation during mouse early embryogenesis
Organism:	Mus musculus
Experiment type:	Expression profiling by array
Platform:	GPL1261
Pubmed ID:	23136388
Summary & Design:	**Summary:** We characterzised global changes in gene expresseion between 8 cell embryos and blastocysts to identify potential genes required for blastocyst formation. **Overall design:** Expression data from mouse 8-cell embryos and blastocysts. Eight-cell embryos and blastocysts were obatained from B6D2F1 female X B6D2F1 male. We analyzed a total of four samples at both stages.

Background corr dist: KL-Divergence = 0.0169, L1-Distance = 0.0482, L2-Distance = 0.0027, Normal std = 0.8501

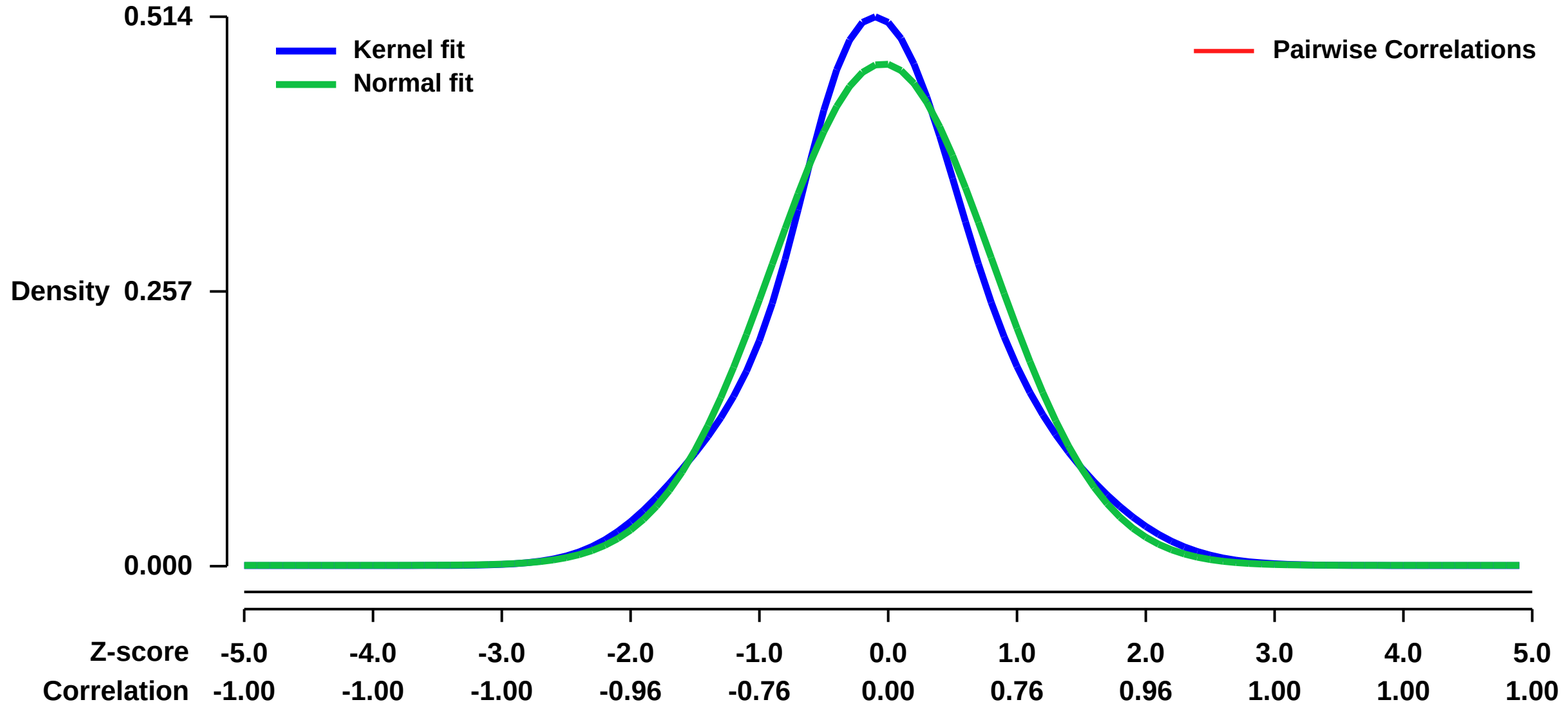

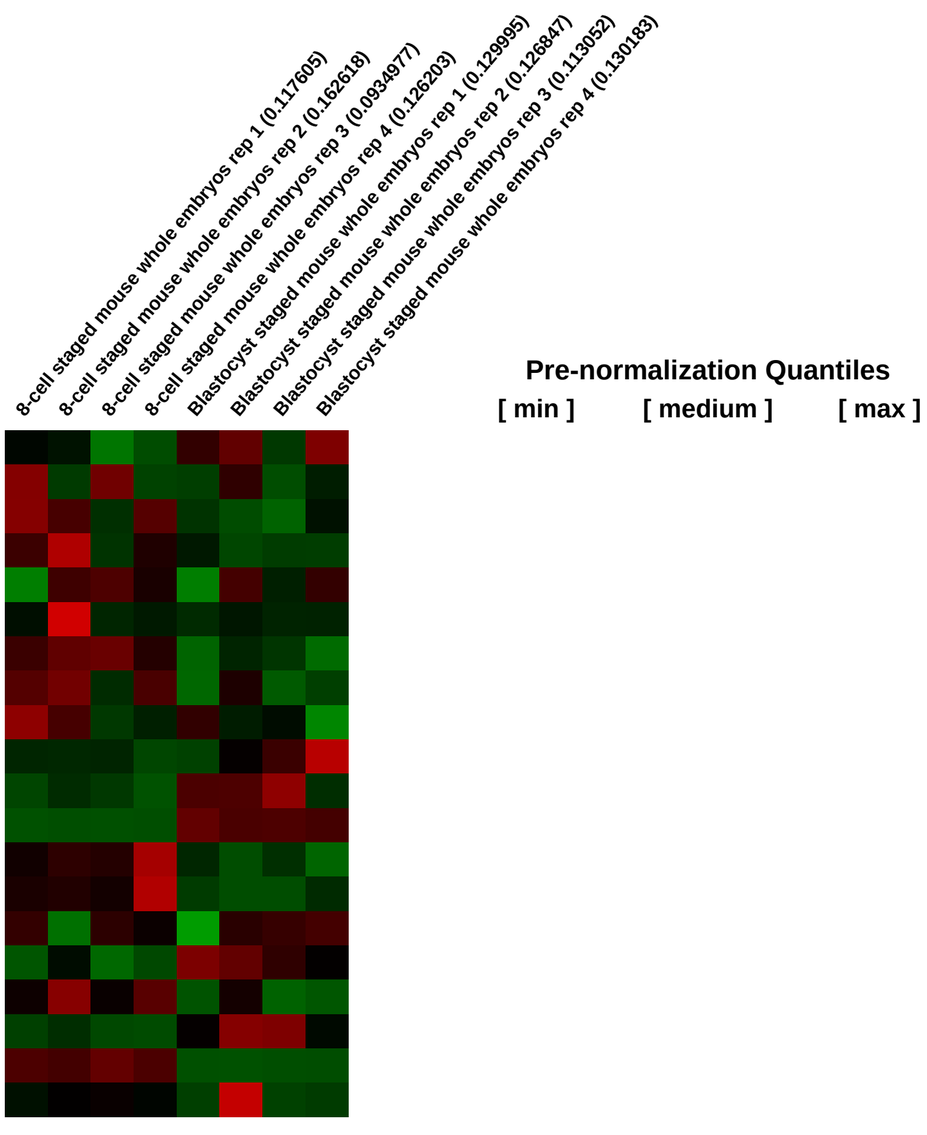

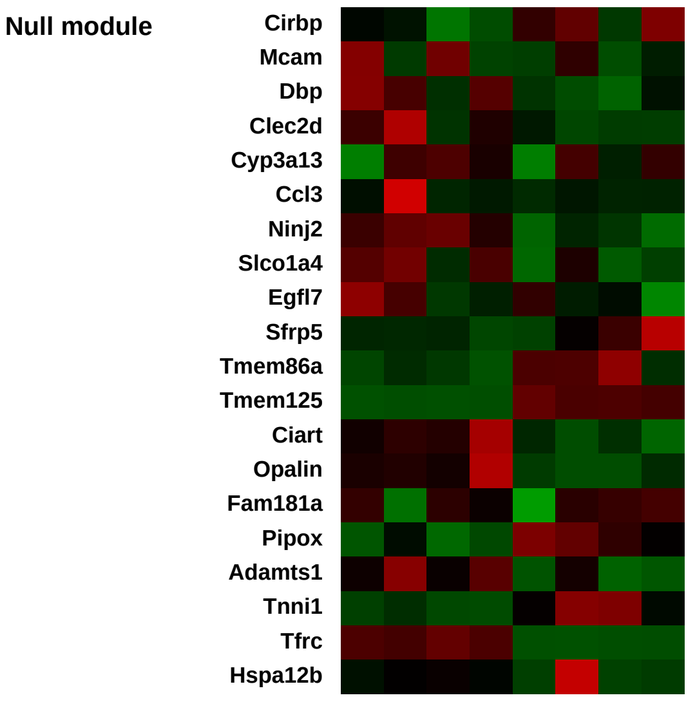

GEO Series "GSE22005" Expression Profiles

Num of samples in this series: 23

Scale of expression profile Z-scores

-3.0 -2.0 -1.0 0.0 1.0 2.0 3.0

GEO Link:	**http://www.ncbi.nlm.nih.gov/geo/query/acc.cgi?acc=GSE22005**
Status:	**Public on Sep 29 2010**
Title:	**Medulloblastoma tumors derived from Ptch+/-HIC+/- transgenic mouse allografted in nude mice**
Organism:	**Mus musculus**
Experiment type:	**Expression profiling by array**
Platform:	**GPL1261**
Pubmed ID:	
Summary & Design:	**Summary:** **Nude mice were allografted with medulloblastoma tumors derived from Ptch+/-HIC+/- transgenic mouse and treated with vehicle or NVP-LDE225.** **Overall design:** **RNA was prepared from tumours from vehicle or NVP-LDE225 treated nude mice allografted with medulloblastoma tumors derived from Ptch+/-HIC+/- transgenic mouse and hybridized on the Affymetrix Mouse Genome 430A 2.0 RNA expression microarray.**

Background corr dist: **KL-Divergence = 0.1856, L1-Distance = 0.0392, L2-Distance = 0.0027, Normal std = 0.3550**

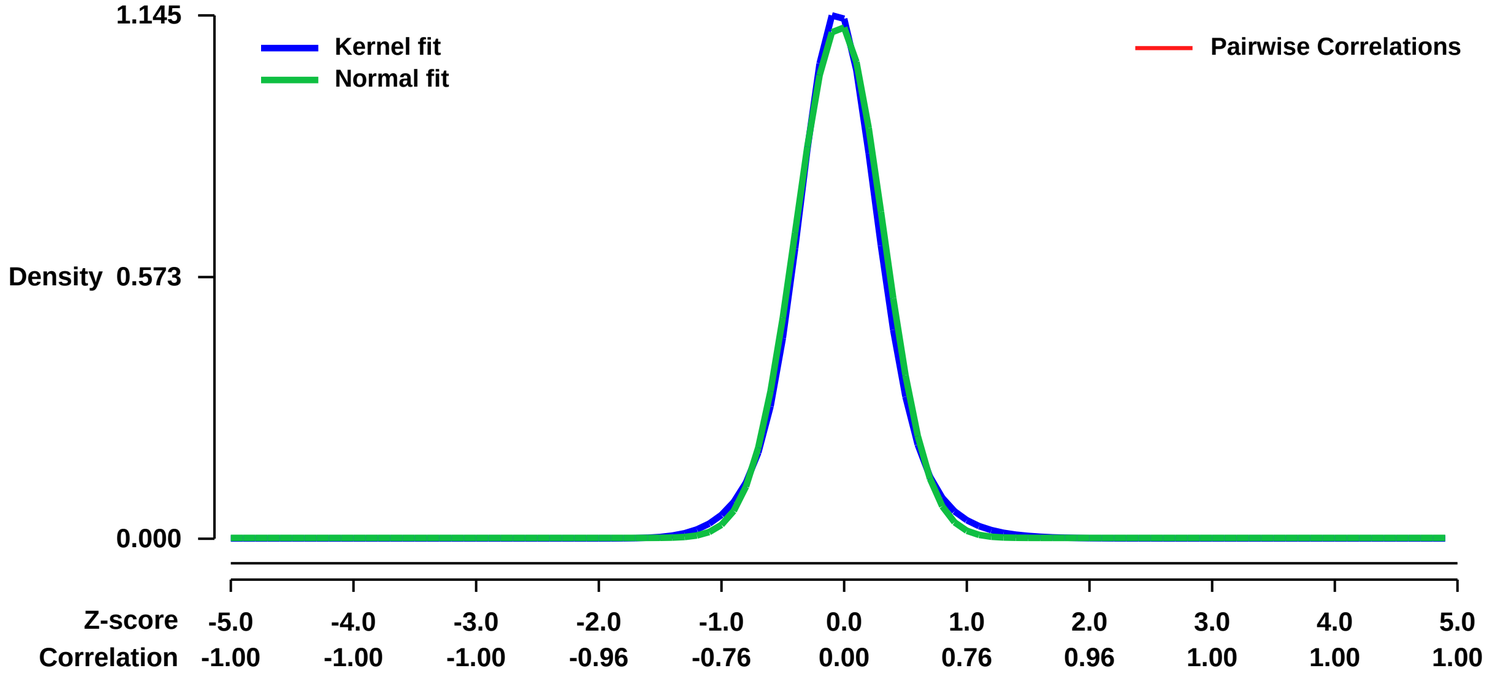

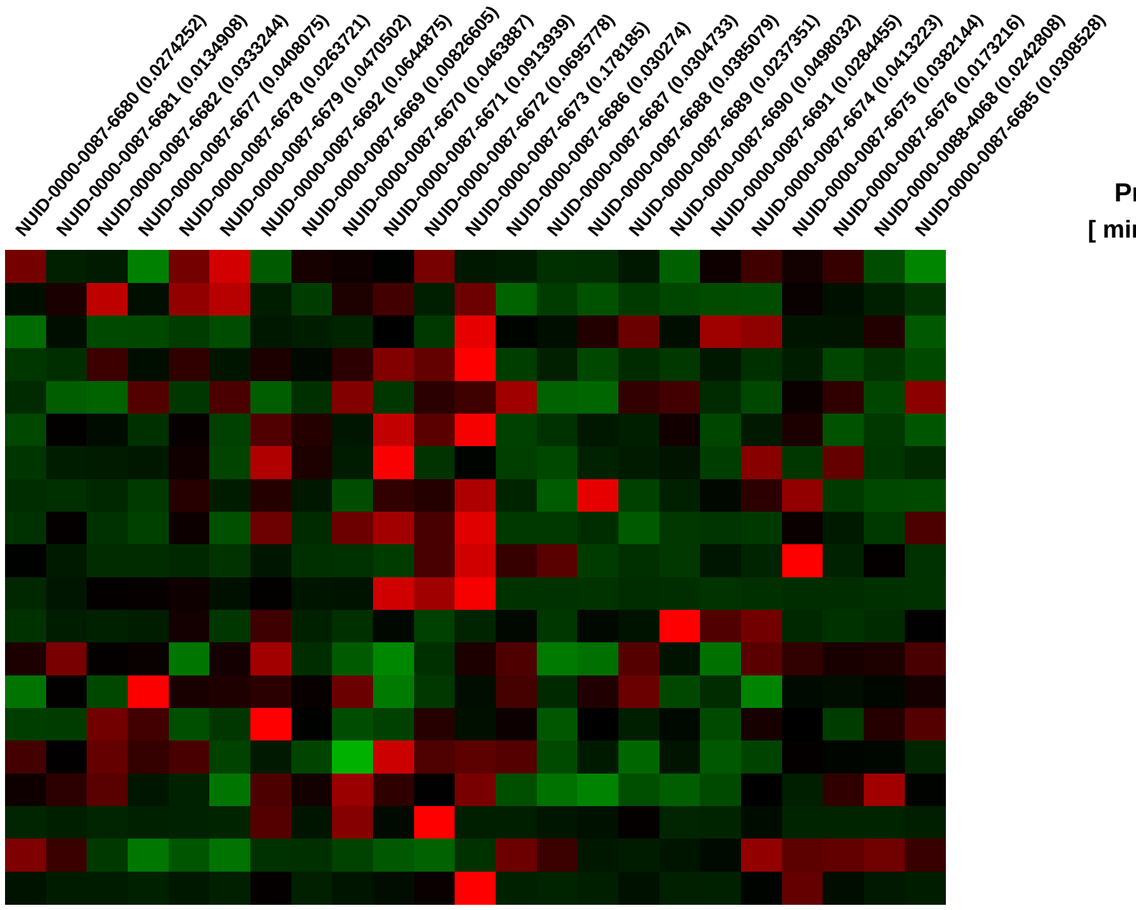

GEO Series "GSE39442" Expression Profiles

Num of samples in this series: 11

Scale of expression profile Z-scores

-3.0 -2.0 -1.0 0.0 1.0 2.0 3.0

GEO Link:	http://www.ncbi.nlm.nih.gov/geo/query/acc.cgi?acc=GSE39442
Status:	Public on Jan 01 2014
Title:	Gene expression profiling in the developing neural tube
Organism:	Mus musculus
Experiment type:	Expression profiling by array
Platform:	GPL1261
Pubmed ID:	
Summary & Design:	**Summary:** At an incidence of approximately 1/1000 births, neural tube defects (NTDs) comprise one of the most common and devastating congenital disorders. In an attempt to enhance and expand our understanding of neural tube closure, we undertook a high-throughput gene expression analysis of the neural tube as it was forming in the mouse embryo. Open and closed sections of the developing neural tube were micro-dissected from mouse embryos, and hybridized to Affymetrix mouse expression arrays. Clustering of genes differentially regulated in open and closed sections of the developing neural tube highlighted molecular processes previously recognized to be involved in neural tube closure and neurogenesis. Analysis of the genes in these categories identified potential candidates underlying neural tube closure. In addition, we identified approximately 25 novel genes, of unknown function, that were significantly up-regulated in the closed neural tube. Based on their expression patterns in the developing neural tube, five novel genes are proposed as interesting candidates for involvement in neurogenesis. The high-throughput expression analysis of the neural tube as it forms allows for better characterization of pathways involved in neural tube closure and neurogenesis, and hopefully will strengthen the foundation for further research along the pathways dictating neural tube development. **Overall design:** Embryos were dissected at days E8.5 and E9.5, and the neuroepithelium/ neural tube were mechanically detached from underlying tissues, and then separated into two regions: 1) â open neuroepitheliumâ : neuroepithelial tissue caudal to the open/closed junction, and 2) â closed neural tubeâ , extending from a somiteâ s breadth rostral to the open/closed junction, up to the level of the fifth- or sixth-to-last somite. Samples consisted of biological triplicates of RNA extract from the above tissues (pooled by litter, and representing a total of 111 embryos): E8.5 open neuroepithelium, E8.5 closed neural tube, E9.5 open neuroepithelium, and E9.5 closed neural tube. Thus, a total of 12 samples (representing 111 embryos) were hybridized to the GeneChip Mouse Genome 430 2.0 Array (Affymetrix Inc., Santa Clara, CA, USA). One of the samples (06, closed E8.5) deviated significantly from the others in quality assessment and was therefore removed from subsequent analysis and not submitted to GEO.

Background corr dist: KL-Divergence = 0.0778, L1-Distance = 0.0273, L2-Distance = 0.0012, Normal std = 0.4764

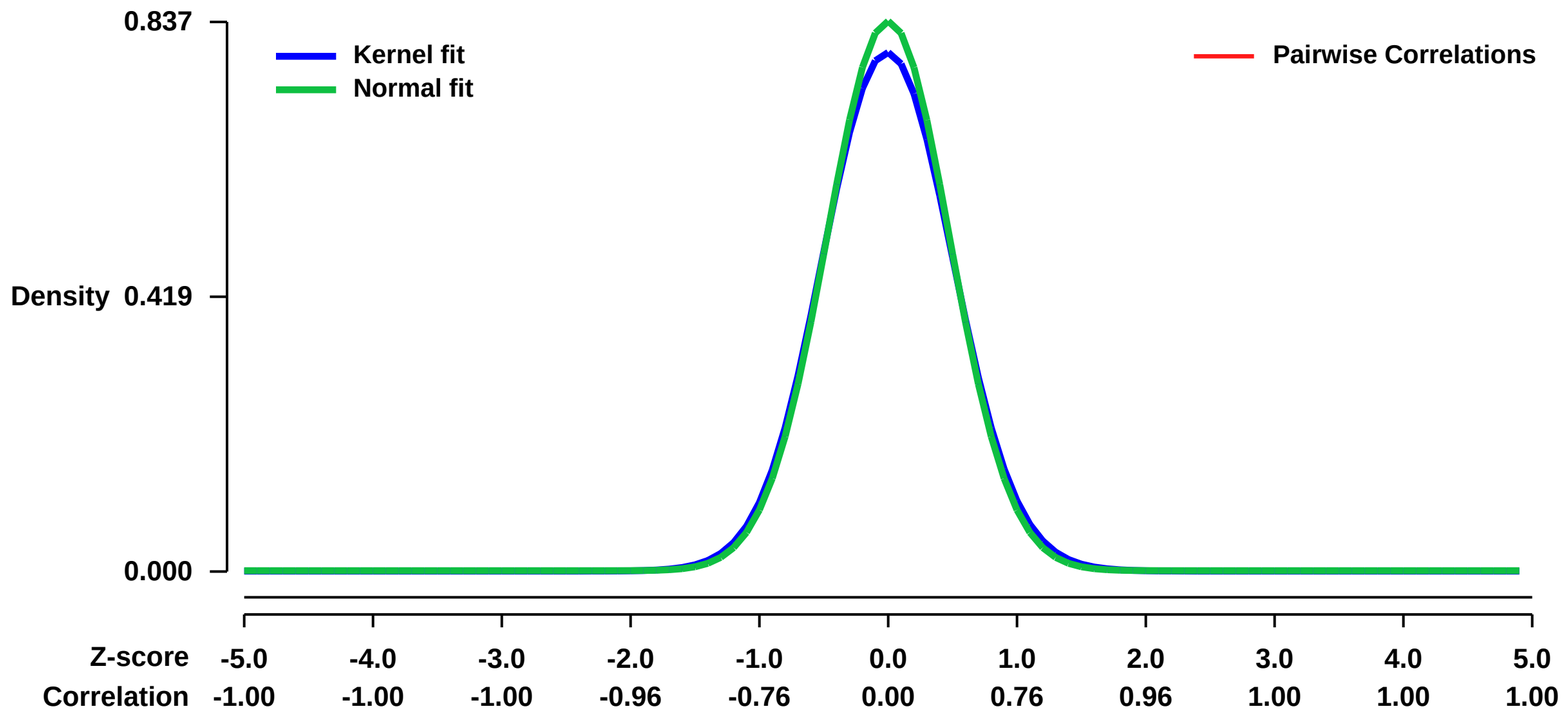

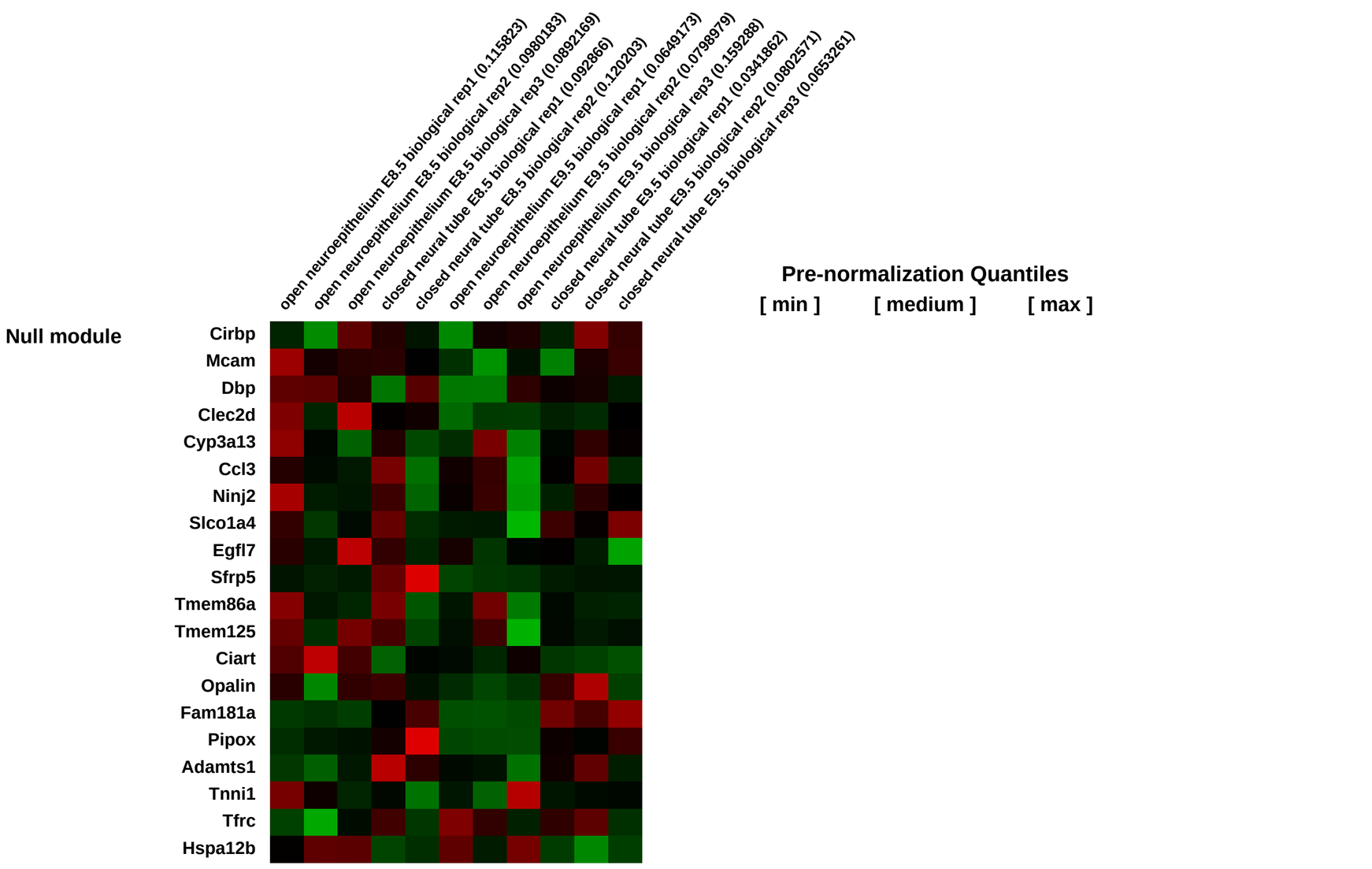

GEO Series "GSE17373" Expression Profiles

Num of samples in this series: 24

Scale of expression profile Z-scores

-3.0 -2.0 -1.0 0.0 1.0 2.0 3.0

GEO Link:	http://www.ncbi.nlm.nih.gov/geo/query/acc.cgi?acc=GSE17373
Status:	Public on Dec 01 2009
Title:	Expression data from EGFR mutant transgenic mice
Organism:	Mus musculus
Experiment type:	Expression profiling by array
Platform:	GPL1261
Pubmed ID:	19759520
Summary & Design:	**Summary:** We performed mRNA expression profiling of lung tumors from C/L858R, C/T790M, and C/L+T mice and from corresponding normal lung tissue. **Overall design:** mRNA was extracted from pulverized lung samples using Trizol (Invitrogen) and then hybridized to MOE 430 2.0 chips (Affymetrix) using standard hybridization techniques.

Background corr dist: KL-Divergence = 0.1056, L1-Distance = 0.0255, L2-Distance = 0.0009, Normal std = 0.4309

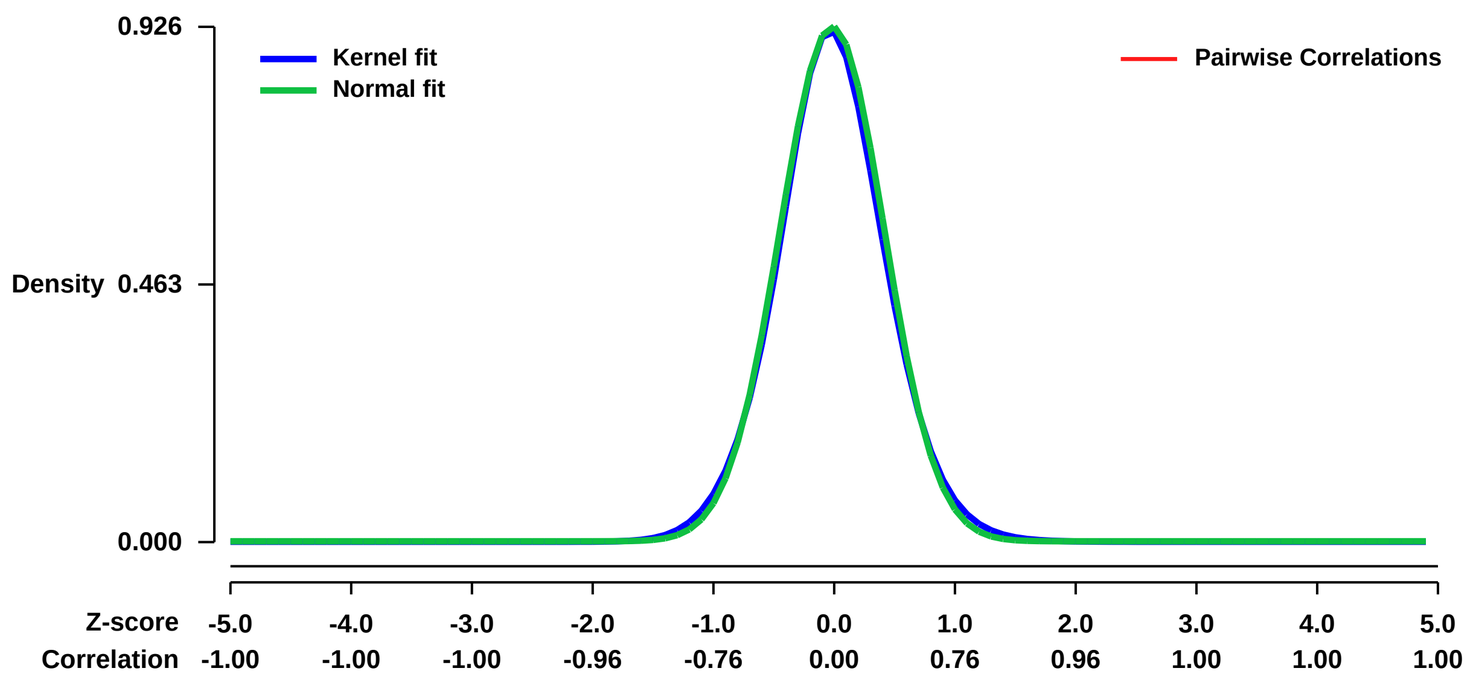

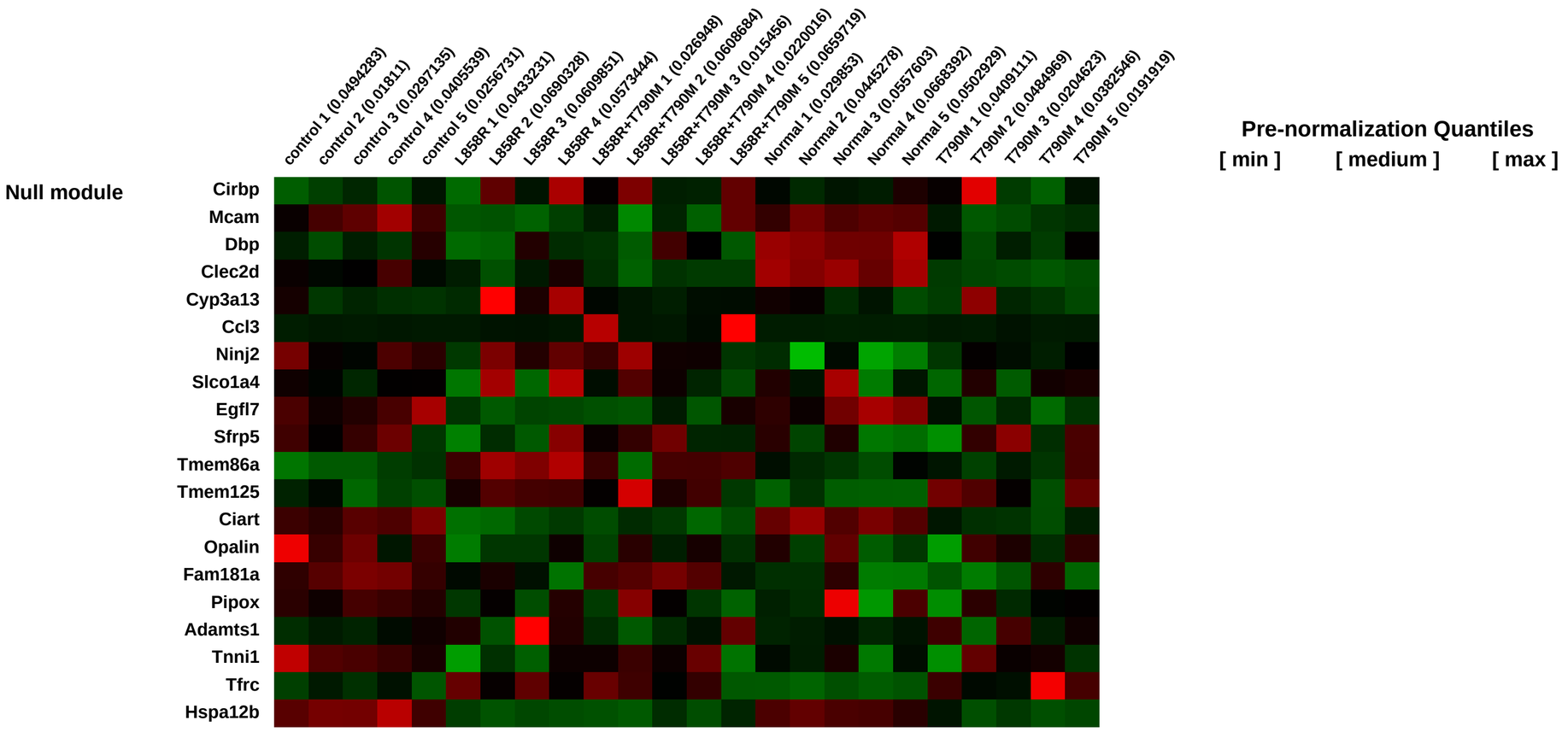

GEO Series "GSE12730" Expression Profiles

Num of samples in this series: 24

Scale of expression profile Z-scores

-3.0 -2.0 -1.0 0.0 1.0 2.0 3.0

GEO Link:	http://www.ncbi.nlm.nih.gov/geo/query/acc.cgi?acc=GSE12730
Status:	Public on Nov 07 2009
Title:	Mouse gestational protein restriction: Newborn offspring liver and hindleg muscle
Organism:	Mus musculus
Experiment type:	Expression profiling by array
Platform:	GPL1261
Pubmed ID:	19823102
Summary & Design:	**Summary:** Gestational protein restriction is a model for low birth size. We hypothesized that taurine supplementation would protect against changes in newborn liver and muscle caused by a maternal low protein diet. **Overall design:** The liver and muscle samples were normalized separately.

Background corr dist: KL-Divergence = 0.0311, L1-Distance = 0.0319, L2-Distance = 0.0015, Normal std = 0.6489

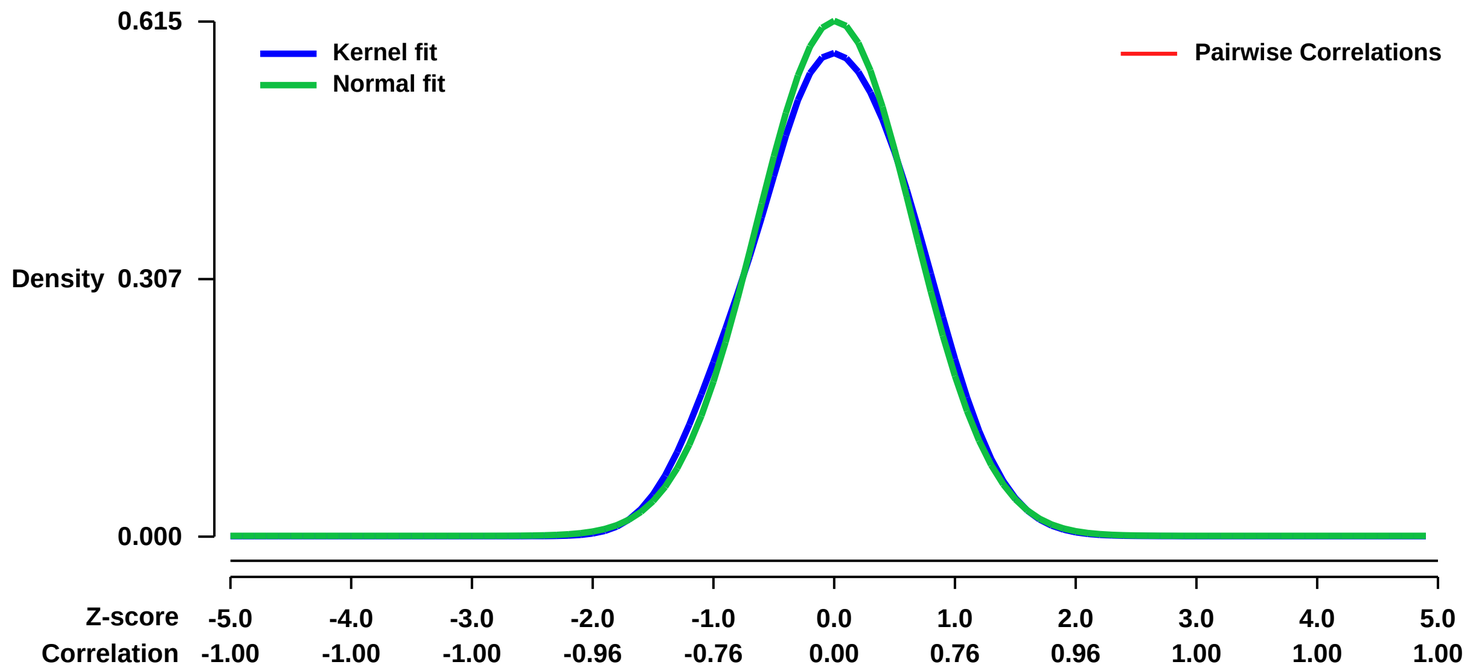

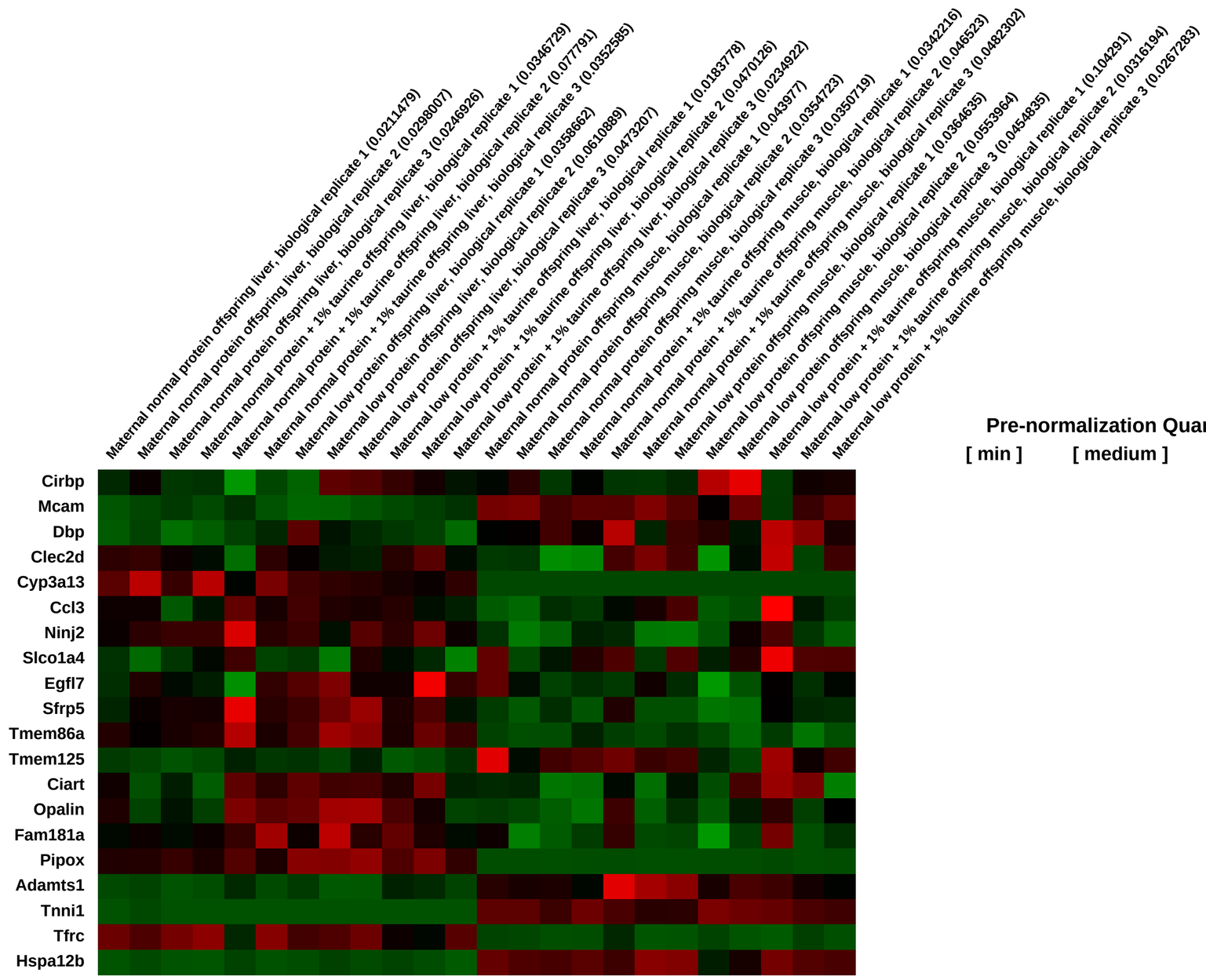

GEO Series "GSE10285" Expression Profiles

Num of samples in this series: 8

Scale of expression profile Z-scores

-3.0 -2.0 -1.0 0.0 1.0 2.0 3.0

GEO Link:	http://www.ncbi.nlm.nih.gov/geo/query/acc.cgi?acc=GSE10285
Status:	Public on Feb 24 2009
Title:	Role of Transglutaminase 2 in Liver Injury via Crosslinking and Silencing of Transcription Factor, Sp1
Organism:	Mus musculus
Experiment type:	Expression profiling by array
Platform:	GPL1261
Pubmed ID:	19208340
Summary & Design:	**Summary:** Gene expression of Ethanol-treated hepatocytes from WT and transglutaminase 2 knockout mice **Keywords: transglutmianse 2** **Overall design:** 8 of Samples were analysed (its replicates are included)

Background corr dist: KL-Divergence = 0.0486, L1-Distance = 0.0293, L2-Distance = 0.0012, Normal std = 0.5776

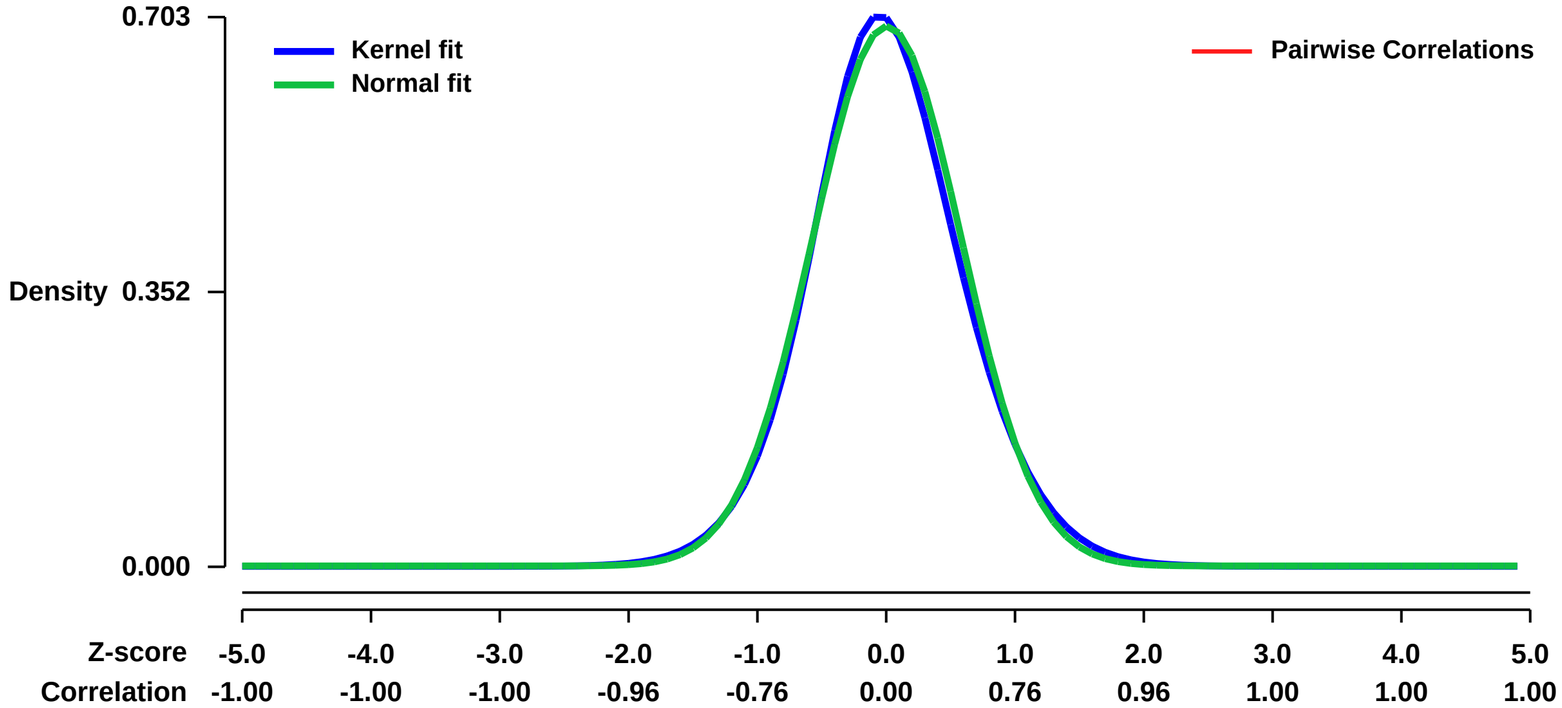

Pre-normalization Quantiles

[min] [medium] [max]

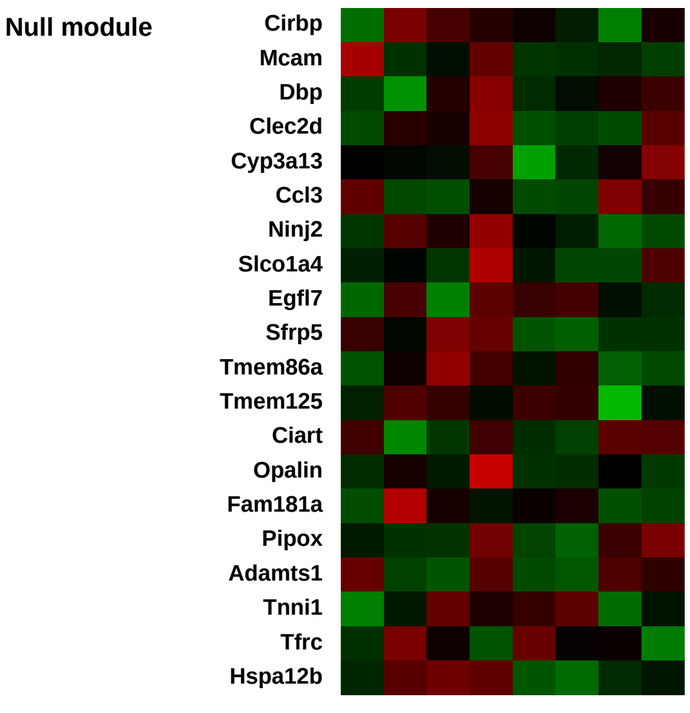

GEO Series "GSE4002" Expression Profiles

Num of samples in this series: 13

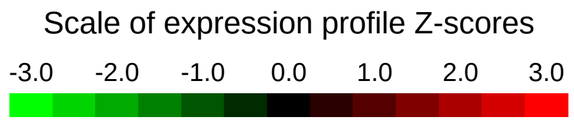

GEO Link:	**http://www.ncbi.nlm.nih.gov/geo/query/acc.cgi?acc=GSE4002**
Status:	**Public on Dec 01 2007**
Title:	**Global gene expression profile of interspecies pregnant implantation sites between rat and mouse**
Organism:	**Mus musculus**
Experiment type:	**Expression profiling by array**
Platform:	**GPL1261**
Pubmed ID:	
Summary & Design:	**Summary:** **In present, interspecies cloning and interspecies-pregnancy were studied for endangered species rescue. However, the low implantation and survival ratio, spontaneous abortion, and unknown reason embryos absorption are the common and difficult problems of interspecies-pregnancy. In order to discover the mechanism of interspecies-pregnant failure and find ways to overcome the xeon-pregnant obstacles, we chosen the rat embryos pregnant in mouse uterus as a interspecies-pregnancy model. Three groups were set, mouse embryos to mouse recipients (MM) as control group, rat embryos to mouse recipients (RM), and rat and mouse embryos to mouse recipients together (RMM) as experiment groups. The former studies showed that rat embryos live no longer than day 7 of mouse pregnancy (D7). Our results showed that rat embryos survived to D7, and still existed to day 9 of mouse pregnancy (D9) in RM group. Surprisingly, the rat embryos survived to day 13 of the mouse gestation (D13) in RMM group. Microarray analysis was used to detect the global-gene expression profile changes of the whole implantation sites among the three groups at D7 and D9. By this way, we screened out the genes promoting the implanted rat embryos development in a mouse uterus which helped the rat embryos survive to D13 in RMM group compared with RM group, and the genes hindering the rat embryos development in a mouse uterus which prevented rat embryos living longer than D7 in RM group and D13 in RMM group compared with MM group. These findings provide insights into the mechanism of interspecies pregnant failure and new idea for interspecies pregnant studies.** **Keywords: time course, pregnancy day** **Overall design:** **totally 6 samples were analyzed, each samples two replications (one of them had three replications).**

Background corr dist: **KL-Divergence = 0.1131, L1-Distance = 0.0258, L2-Distance = 0.0011, Normal std = 0.4189**

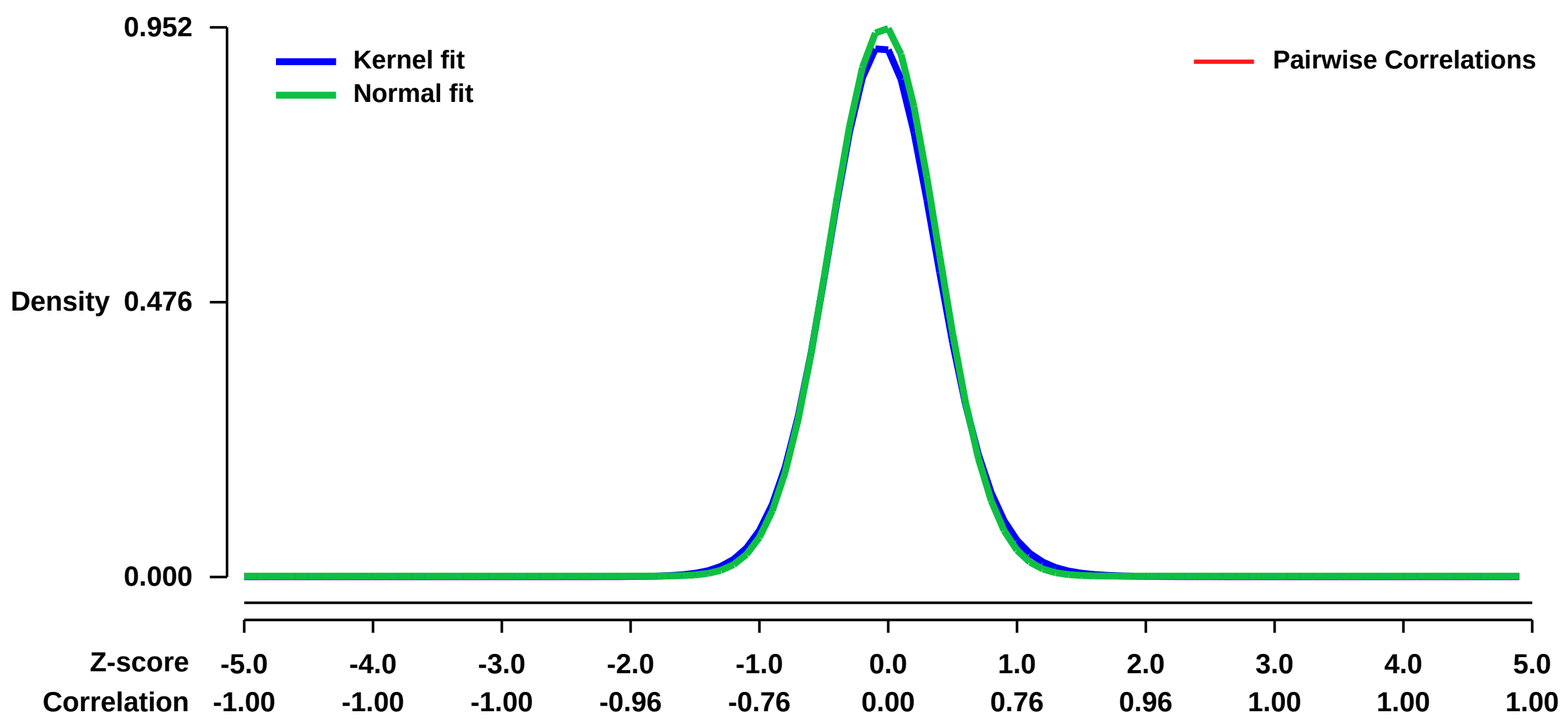

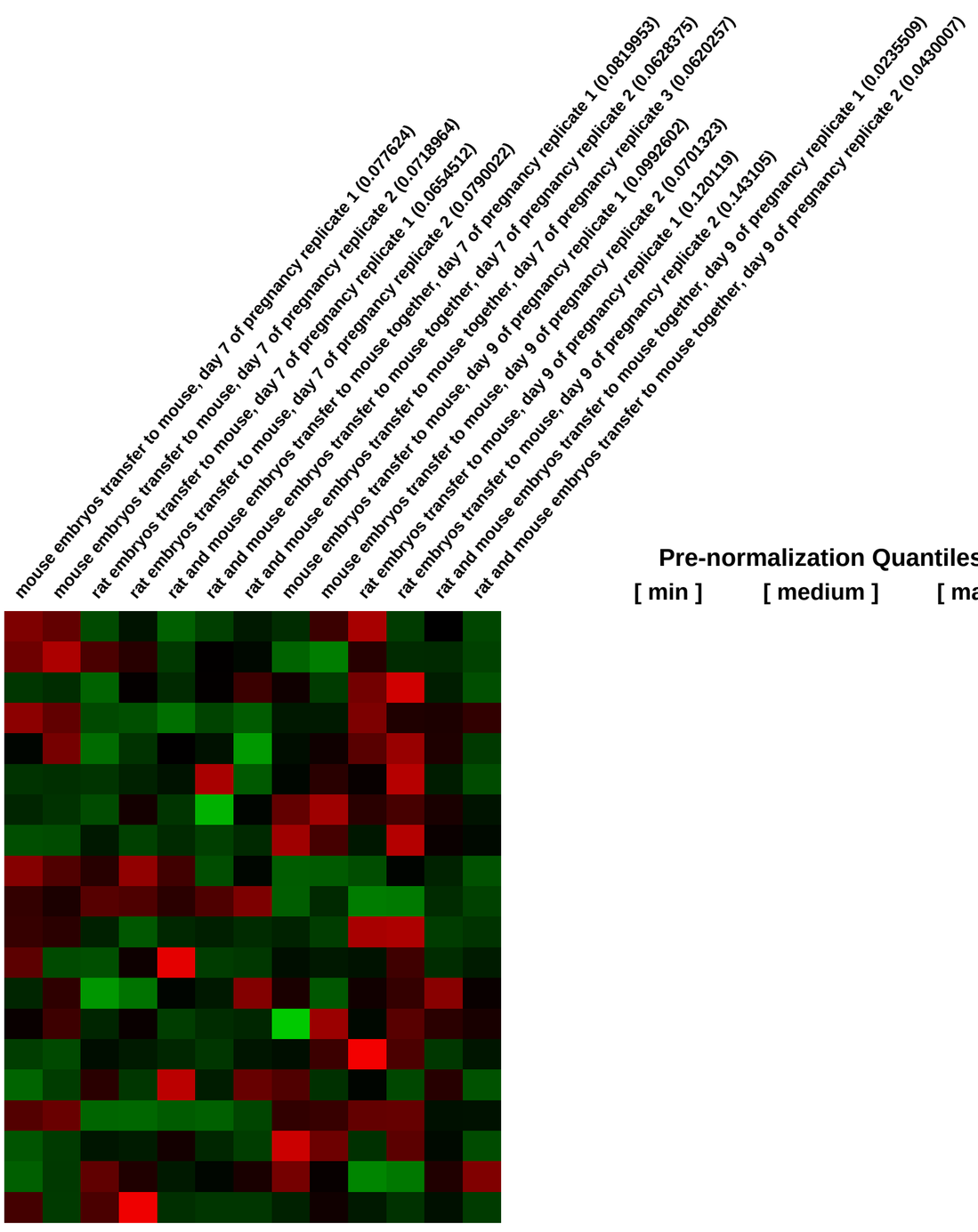

Null module

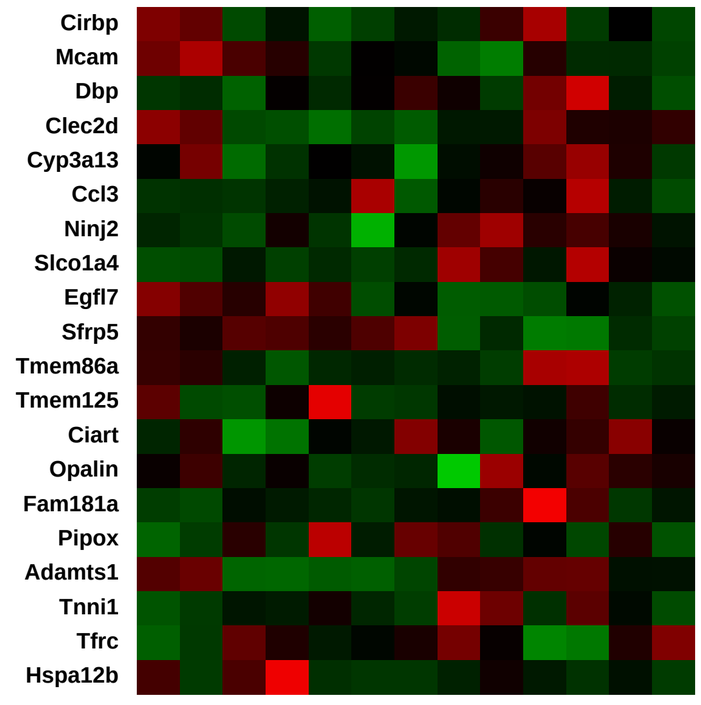

GEO Series "GSE7275" Expression Profiles

Num of samples in this series: 8

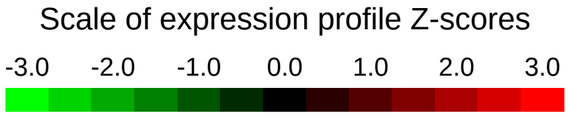

GEO Link:	**http://www.ncbi.nlm.nih.gov/geo/query/acc.cgi?acc=GSE7275**
Status:	**Public on Sep 05 2007**
Title:	**Evaluation of murine mast cells derived exosomal RNA versus their parental cells MC/9.**
Organism:	**Mus musculus**
Experiment type:	**Expression profiling by array**
Platform:	**GPL1261**
Pubmed ID:	**17486113**
Summary & Design:	**Summary:** **Exosomes are vesicles of endocytic origin released by many types of cells into the extracellular environment. In an attempt to further examine the exosome-mediated cellular communication, we show that exosomes from a mouse mast cell line (MC/9), exosomes from primary bone marrow derived mast cells, and exosomes from a human mast cell line (HMC-1) contain RNA but not DNA.** **Microarray assessments of exosome-derived RNA revealed that these vesicles contain mRNA from approximately 1200 genes, many of which are unique and not present in the cytoplasmic RNA pool in the donor cell.** **Keywords: Exosomal RNA versus their parental cells, MC/9** **Overall design:** **Exosomes were prepared from the supernatant of MC/9 cells by differential centrifugations and filtration. RNA was isolated from the exosomes and their parental cells using Trizo. The microarray experiments were performed by SweGene (www.swegene.org/) according to Affymetrix microarray DNA chip analysis. The experiment was performed in quadruple samples. ExoRNA1, ExoRNA2, ExoRNA3, and ExoRNA4 for the exosomes samples and Mast_cells1, Mast_cells2, Mast_cells3, and Mast_cells4 for the MC/9 cells.**

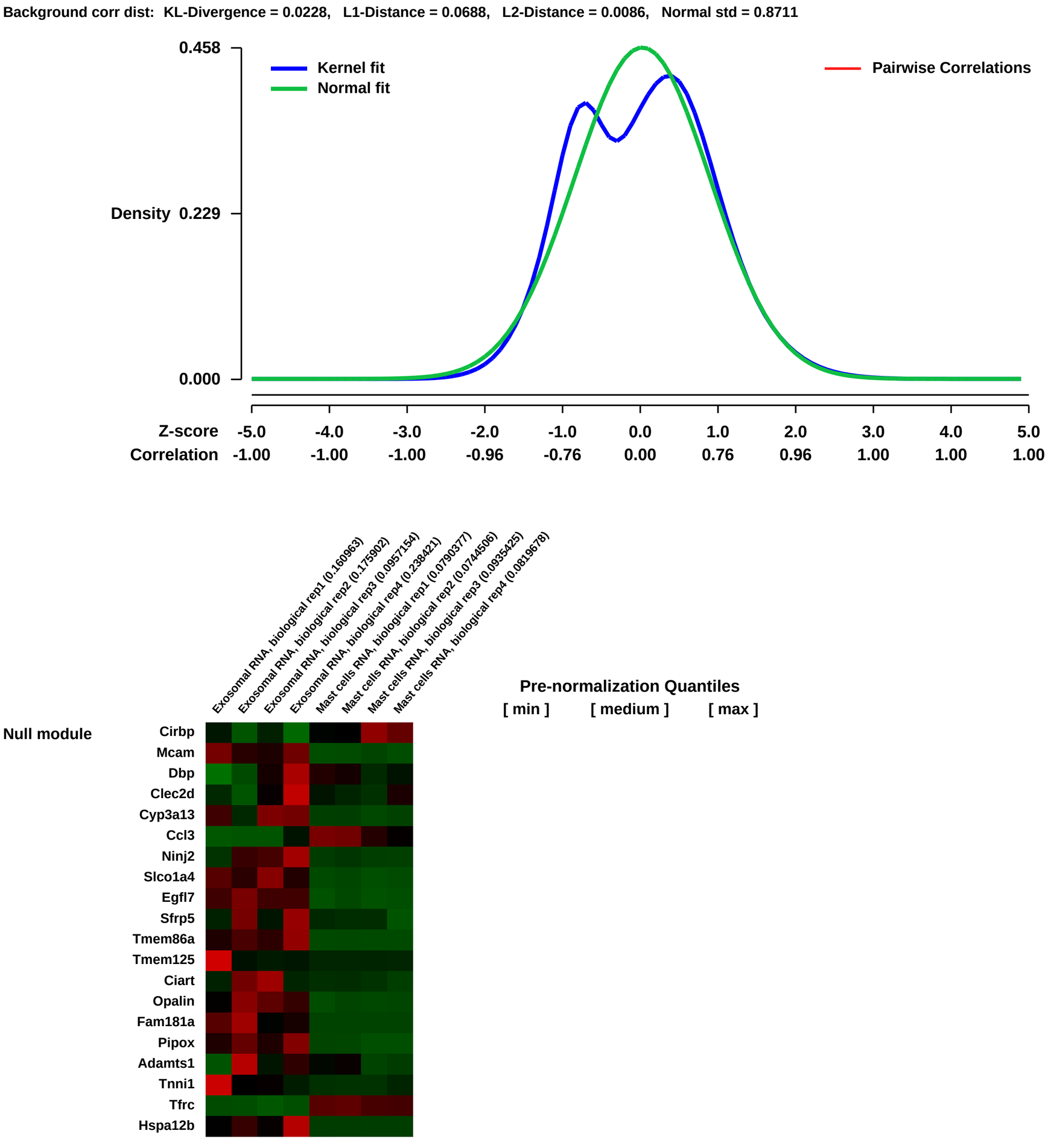

GEO Series "GSE33101" Expression Profiles

Num of samples in this series: 8

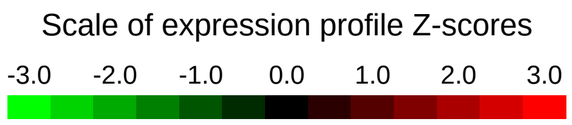

GEO Link:	**http://www.ncbi.nlm.nih.gov/geo/query/acc.cgi?acc=GSE33101**
Status:	**Public on Dec 01 2011**
Title:	**Gene expression profiles in Sirt1/PPARalpha bigenic mice**
Organism:	**Mus musculus**
Experiment type:	**Expression profiling by array**
Platform:	**GPL1261**
Pubmed ID:	**22055503**
Summary & Design:	**Summary:** **Cardiac-specific PPARalpha transgenic (Tg-PPARalpha) mice show mild cardiac hypertrophy and systolic dysfunction. The failing heart phenotypes observed in Tg-PPARalpha are exacerbated by crossing with cardiac-specific Sirt1 transgenic (Tg-Sirt1) mice, whereas Tg-Sirt1 mice themselves do not show any cardiac hypertrophy or systolic dysfunction. To investigate the mechanism leading to the failing heart phenotypes in TgPPARalpha/Tg-Sirt1 bigenic mice, microarray analyses were performed. The microarray analyses revealed that many ERR target genes were downregulated in Tg-PPARalpha and in Tg-Sirt1, and they were further downregulated in the Tg-PPARalpha/Tg-Sirt1 bigenic mice.** **Overall design:** **Four groups of cardiac-specific transgenic mice were used for the study, i.e., control, PPARalpha, Sirt1 and PPARalpha/Sirt1. Hearts were dissected after 10-11 weeks of male FVB background transgenic mice. Total RNA was prepared from the hearts to conduct the microarray analyses.**

Background corr dist: **KL-Divergence = 0.0486, L1-Distance = 0.0164, L2-Distance = 0.0003, Normal std = 0.5638**

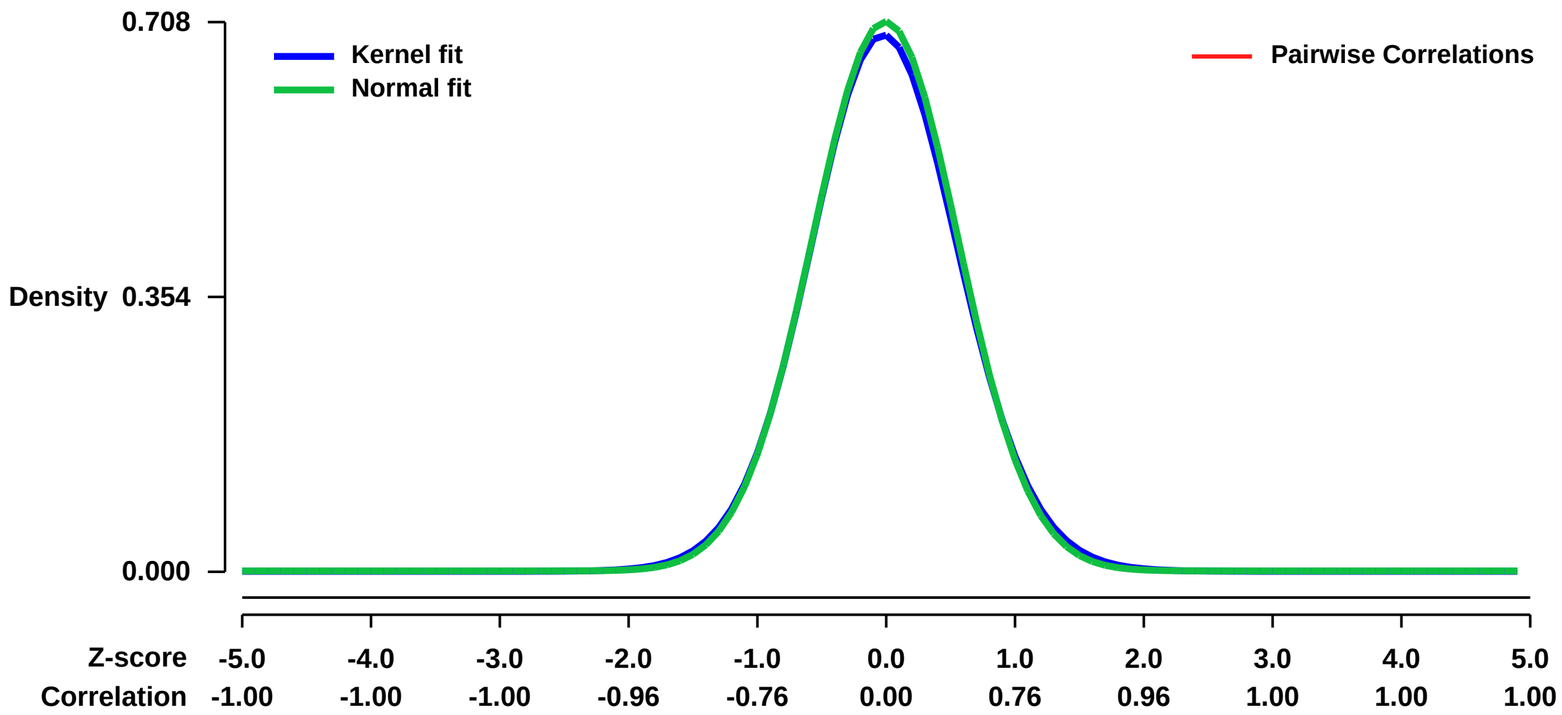

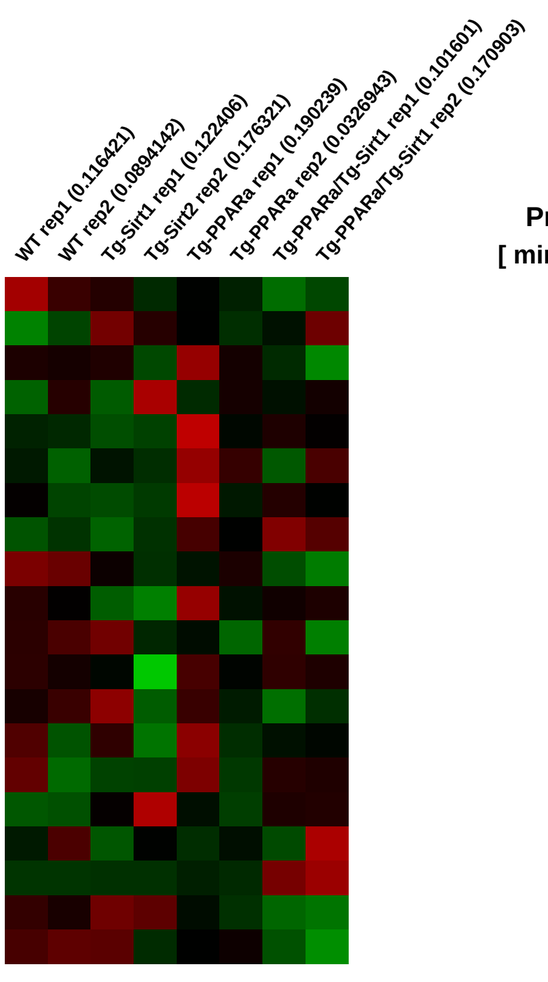

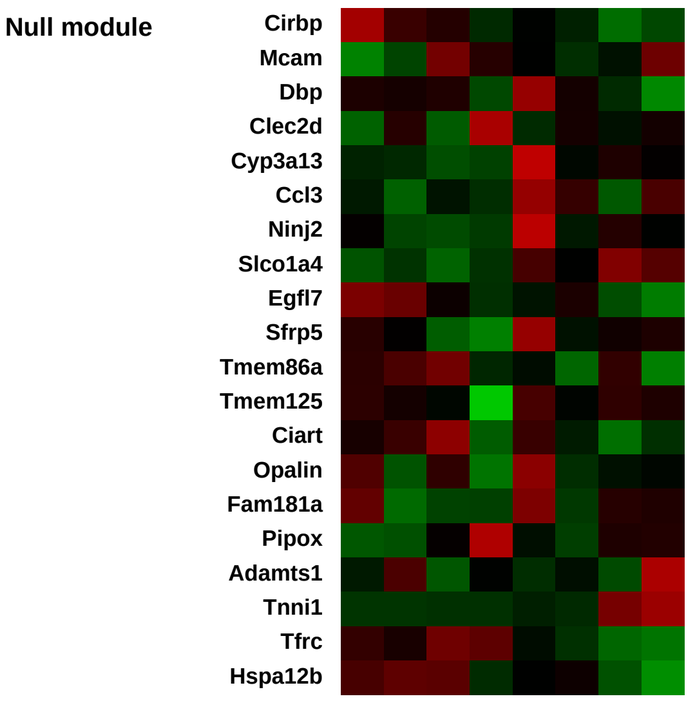

GEO Series "GSE8150" Expression Profiles

Num of samples in this series: 20

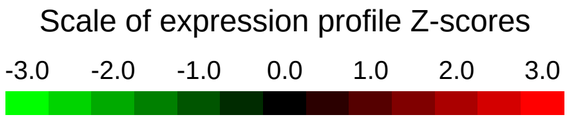

GEO Link:	http://www.ncbi.nlm.nih.gov/geo/query/acc.cgi?acc=GSE8150
Status:	Public on Aug 31 2007
Title:	Age-related transcriptional changes and the effect of dietary supplementation of vitamin E in the mouse brain
Organism:	Mus musculus
Experiment type:	Expression profiling by array
Platform:	GPL1261
Pubmed ID:	17316780
Summary & Design:	**Summary:** We established the transcriptional profile of brain aging and examine the global effects of vitamin E supplementation on age-related alterations in expression in the aged mouse brain. **Keywords: expression profiling** **Overall design:** Gene expression profiles were obtained from the neocortex tissues of 5-month-old controls, 30-month-old controls and 30-month old B6C3F1 mice with middle age-onset supplementation of ¸–-tocopherol or a mixture of ¸–- and ¸‡-tocopherol (500mg/kg of each tocopherol).

Background corr dist: KL-Divergence = 0.2537, L1-Distance = 0.0569, L2-Distance = 0.0081, Normal std = 0.3000

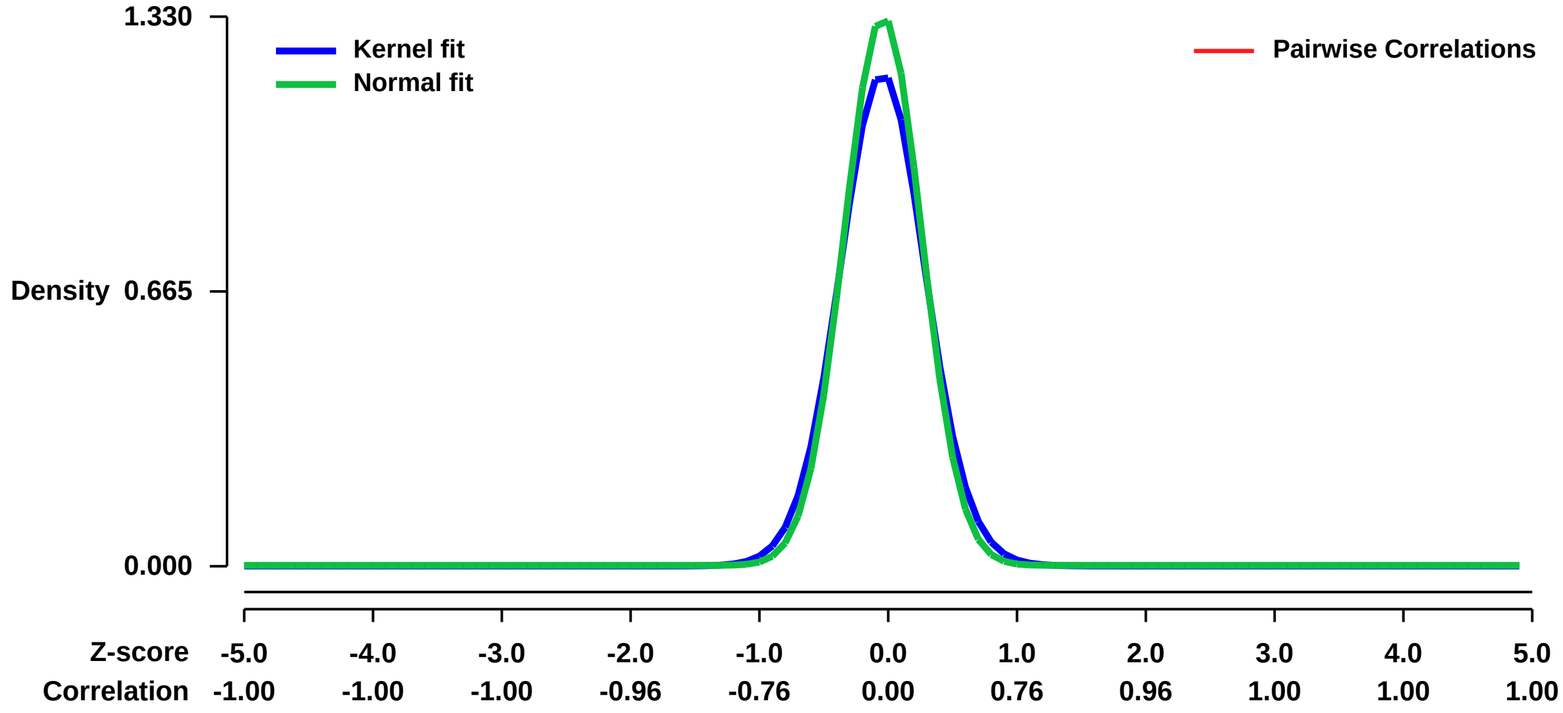

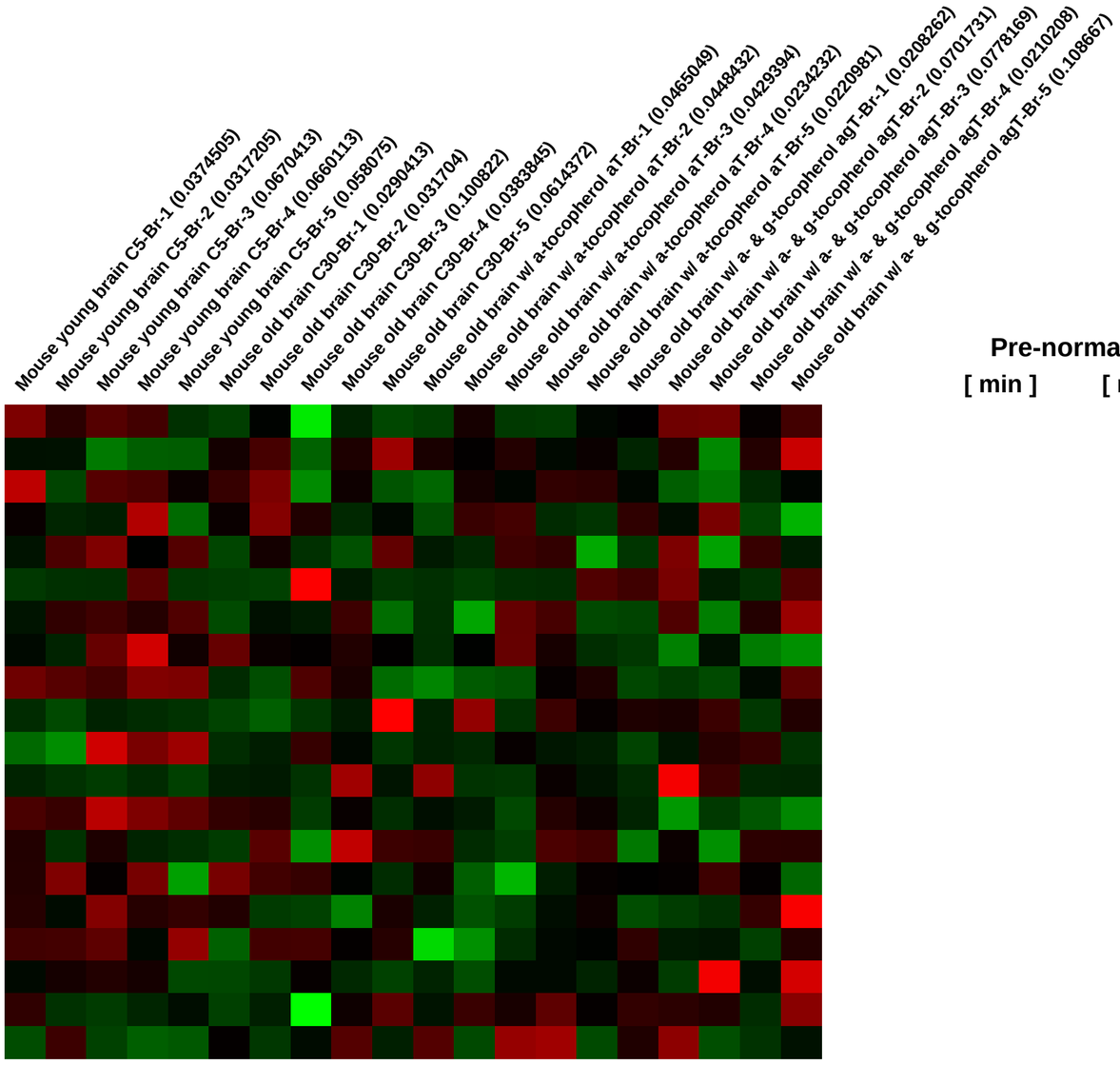

GEO Series "GSE23161" Expression Profiles

Num of samples in this series: 8

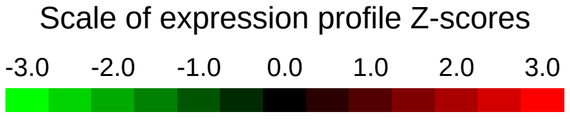

GEO Link:	http://www.ncbi.nlm.nih.gov/geo/query/acc.cgi?acc=GSE23161
Status:	Public on Jun 30 2011
Title:	Beta cell overexpression of HSD11B1 in high fat fed mice
Organism:	Mus musculus
Experiment type:	Expression profiling by array
Platform:	GPL1261
Pubmed ID:	22315313
Summary & Design:	**Summary:** To model the potential diabetogenic effects of higher level of HSD11B1 in b-cells of the pancreas in vivo, we created a transgenic model overexpressing HSD11B1 under the mouse insulin I promoter (MIP-HSD1) in diabetes-prone C57Bl/KsJ mice. KsJ wild type and MIP-HSD1 heterozygous mice have been high fat fed for 12 weeks. Pancreata have been perfused with collagenase and islets isolated by hand picking. Isolated islets (around 500) coming from at least 3 mice (around 200/mice) have been directly lysed in Trizol. Total RNA have been extracted by Trizol plus RNA Purification Kit (invitrogen). **Overall design:** Four biological replicates per group: Wild type KsJ mice on High Fat diet (KsJ1, KsJ2, KsJ3, KsJ4) and MIP-HSD1 transgenic mice on High Fat diet (MIP1, MIP2, MIP3, MIP4) were used to prepare RNA for microarray analysis.

Background corr dist: KL-Divergence = 0.0157, L1-Distance = 0.0347, L2-Distance = 0.0013, Normal std = 0.8338

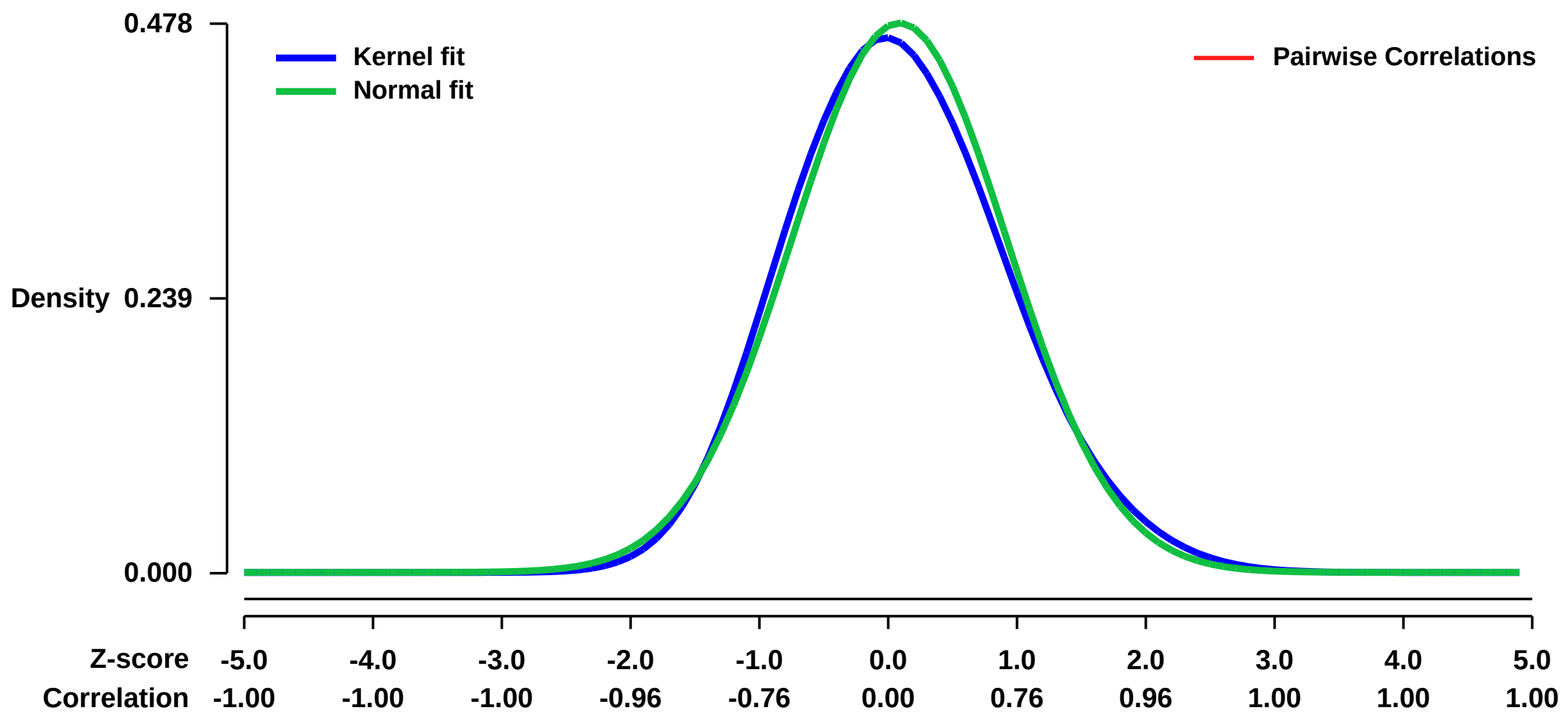

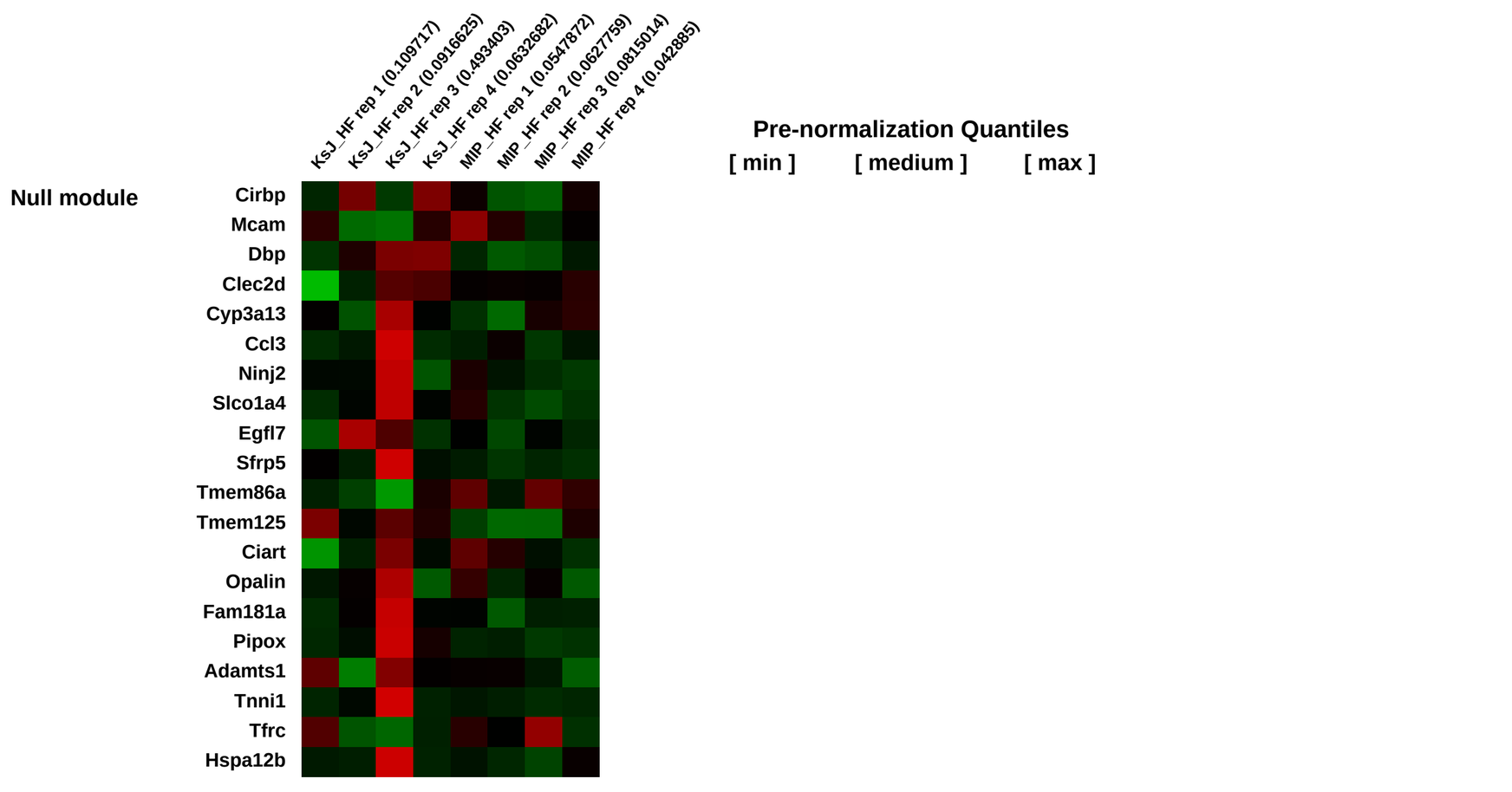

GEO Series "GSE49351" Expression Profiles

Num of samples in this series: 6

Scale of expression profile Z-scores

-3.0 -2.0 -1.0 0.0 1.0 2.0 3.0

GEO Link:	http://www.ncbi.nlm.nih.gov/geo/query/acc.cgi?acc=GSE49351
Status:	Public on Jul 31 2013
Title:	Microarray gene expression profiling of transgenic mice with myocardium-specific over-expression of fatty acid synthase (FASN)
Organism:	Mus musculus
Experiment type:	Expression profiling by array
Platform:	GPL1261
Pubmed ID:	
Summary & Design:	**Summary:** The fatty acid synthase (FASN) is the major fat synthesizing enzyme. FASN is an indispensable enzyme because mice with genetic deletion of Fasn are not viable. Apart from its physiological function, previous studies indicated that FASN could also exert a pathophysiological role, in the heart, because patients with heart failure showed up-reguation of FASN. To investigate the in vivo function of FASN up-regulation in the heart, we generated mice with myocardium-specific expression of FASN under control of the alpha-MHC promoter. Two different founder lines were generated with high and low FASN over-expression. Microarray gene expression profiling of heart tissue was performed of heart tissue from transgenic mice with high and low FASN expression **Overall design:** Microarray gene expression profiling was performed with heart tissue isolated from three study groups: (i) Transgenic mice with high cardiac FASN expression, (ii) transgenic mice with low cardiac FASN expression, and (iii) B6 control mice.

Background corr dist: KL-Divergence = 0.0393, L1-Distance = 0.0214, L2-Distance = 0.0005, Normal std = 0.6240

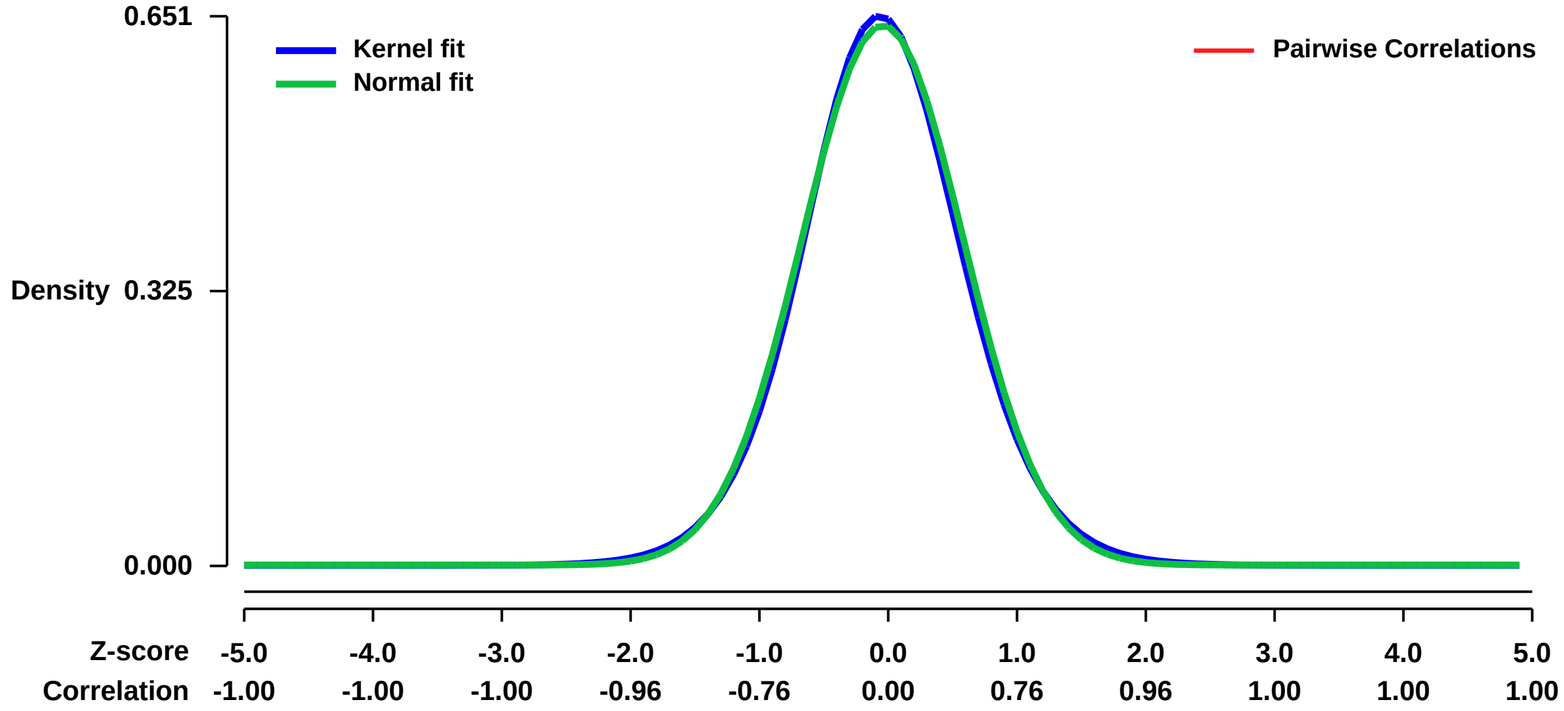

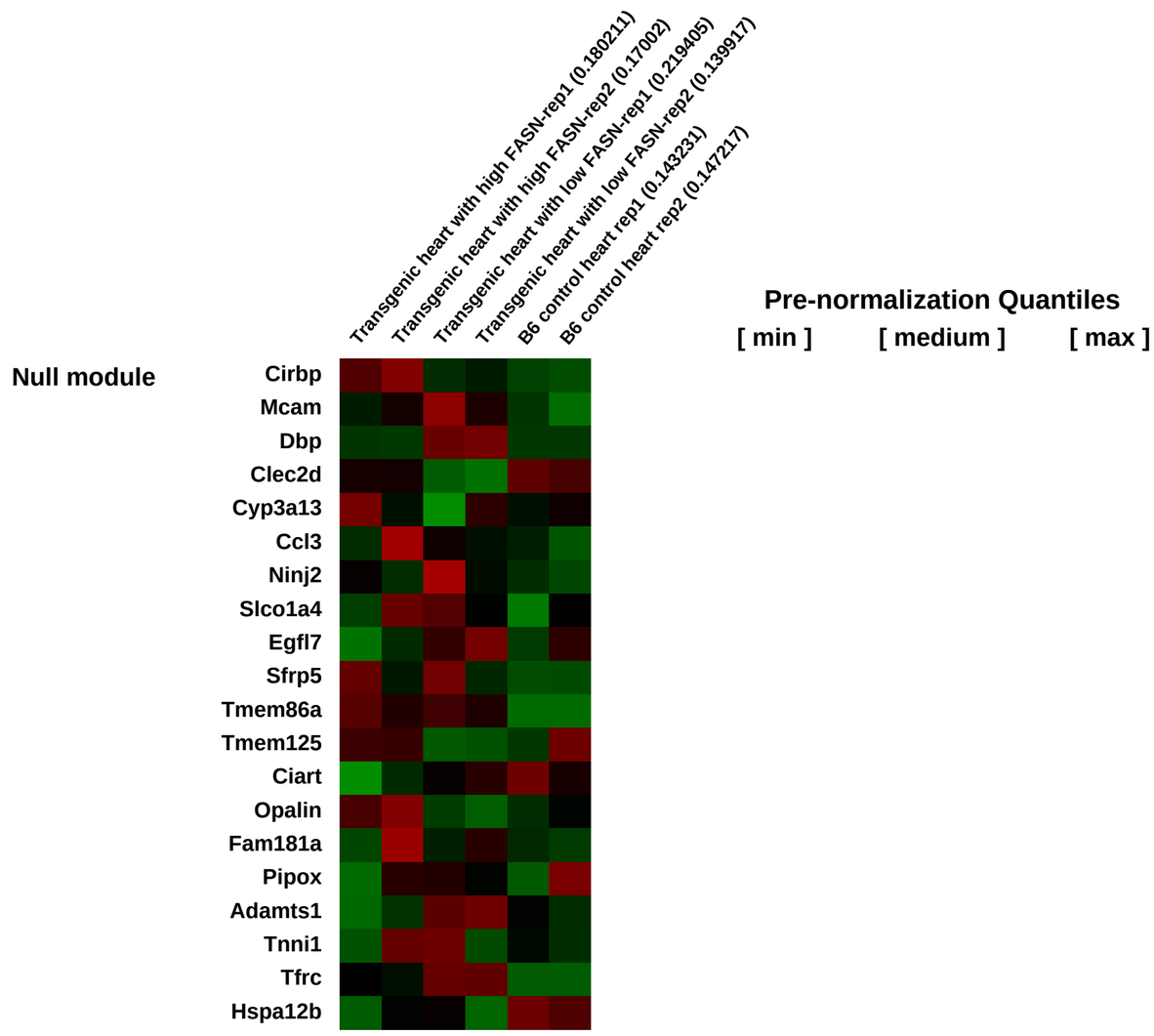

GEO Series "GSE27114" Expression Profiles

Num of samples in this series: 6

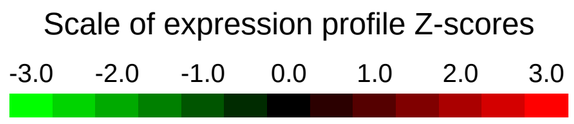

GEO Link:	http://www.ncbi.nlm.nih.gov/geo/query/acc.cgi?acc=GSE27114
Status:	Public on Sep 04 2012
Title:	Expression data from REST knock-out versus REST wild type cells during in vitro neurogenesis
Organism:	Mus musculus
Experiment type:	Expression profiling by array
Platform:	GPL1261
Pubmed ID:	22964890
Summary & Design:	**Summary:** While changes in chromatin are integral to transcriptional reprogramming during cellular differentiation, it is currently unclear how chromatin modifications are targeted to specific loci. We developed a computational model on the premise that transcription factors (TFs) direct dynamic chromatin changes during cell fate decisions. When applied to a neurogenesis paradigm, this approach predicted the TF REST as a determinant of gain of Polycomb-mediated H3K27me3 in neuronal progenitor cells. We prove this prediction experimentally by showing that the absence of REST causes loss of H3K27me3 at target promoters in trans at the same cellular state. Moreover, promoter fragments containing a REST binding site are sufficient to recruit H3K27me3 in cis, while deletion of their REST site results in loss of H3K27me3. These findings illustrate that computational modeling can systematically identify TFs that regulate chromatin dynamics genome-wide. Local determination of Polycomb activity by REST exemplifies such TF based regulation of chromatin. **Overall design:** Expression profiling of REST knock-out (RESTko) versus REST wildtype (RESTwt) or REST heterozygous knock-out (RESThet) cells at three stages of in vitro neuronal differentiation. RESTko and RESTwt/RESThet embryonic stem (ES) cells were differentiated to terminal neurons (TN) via a defined neuronal progenitor (NP) state. Three biological replicates (suffixes a to c).

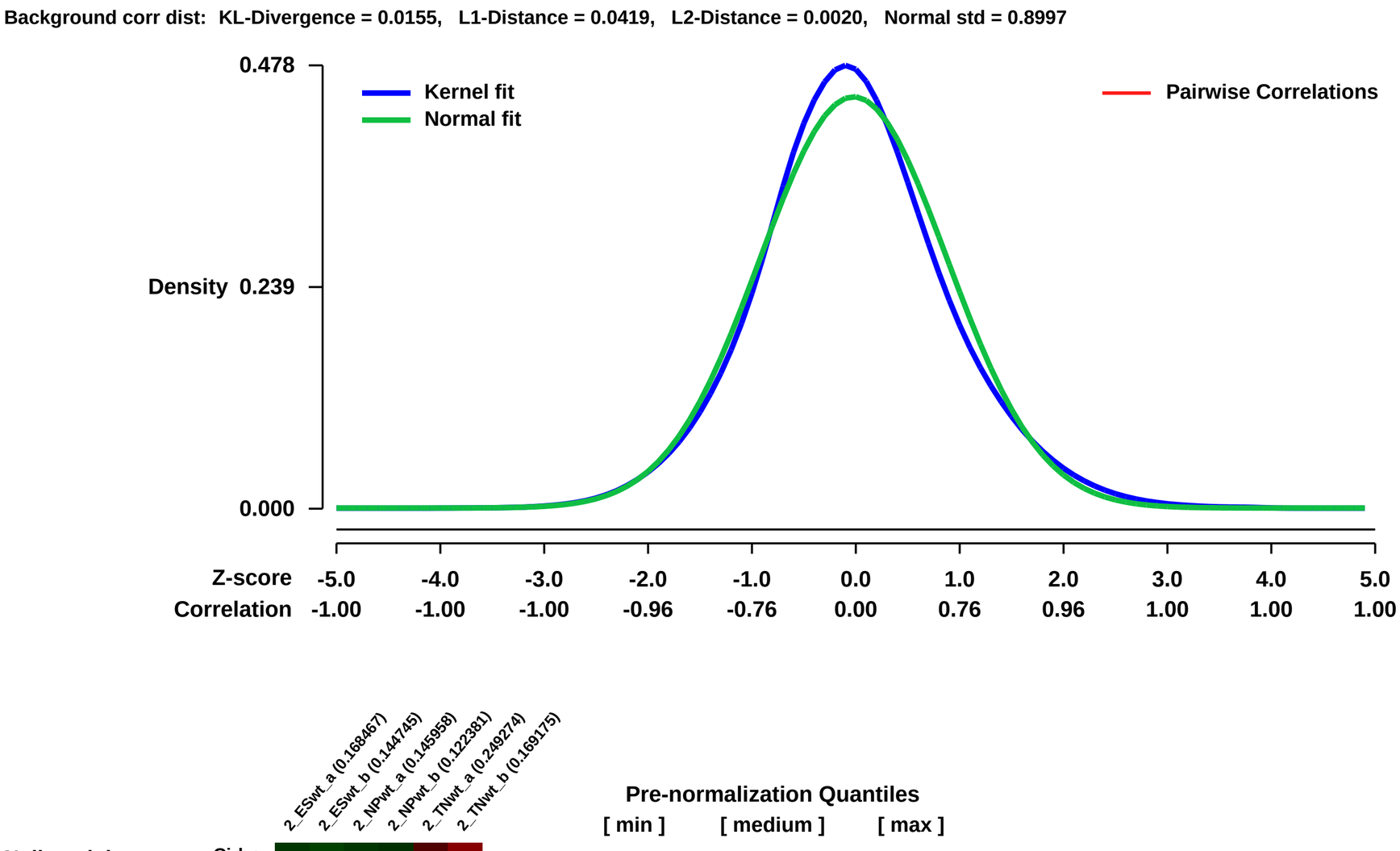

GEO Series "GSE48932" Expression Profiles

Num of samples in this series: 12

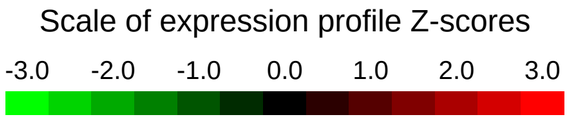

GEO Link:	**http://www.ncbi.nlm.nih.gov/geo/query/acc.cgi?acc=GSE48932**
Status:	**Public on Sep 04 2013**
Title:	**Analysis of gene expression changes induced in wild-type or Atf6a-/- mice by treatment with tunicamycin for 8h**
Organism:	**Mus musculus**
Experiment type:	**Expression profiling by array**
Platform:	**GPL1261**
Pubmed ID:	**24069029**
Summary & Design:	**Summary:** **Protein misfolding stress in the endoplasmic reticulum (ER) leads to dysregulation of lipid metabolism in the liver, and ER stress is associated with human diseases that are accompanied by hepatic lipid accumulation, including obesity, alcoholism, and viral hepatitis; yet the pathways leading from ER stress to the regulation of lipid metabolism are poorly understood. Working exclusively in vivo, we used a â bottom-upâ approach to infer pathways in the genetic regulation of lipid metabolism by the UPR.** **We used a functional genomics to link gene expression patterns taken from microarray data to the severity and persistence of ER stress, using mice lacking the UPR signaling molecule ATF6¸–. This approach revealed that functionally related genes clustered into a small number of distinct expression profiles, and that lipid oxidation and efflux were targets for coordinated transcriptional suppression during ER stress.Our results establish a framework for hepatic gene regulation during ER stress.** **Overall design:** **Atf6a-/- or +/+ mice of variable age and gender were injected intraperitoneally with 2 mg/kg tunicamycin or vehicle. 3 separate mice were used in each group. 8h after injection, mice were sacrificed and total RNA was prepared from resected livers.**

Background corr dist: KL-Divergence = 0.0464, L1-Distance = 0.0564, L2-Distance = 0.0064, Normal std = 0.5923

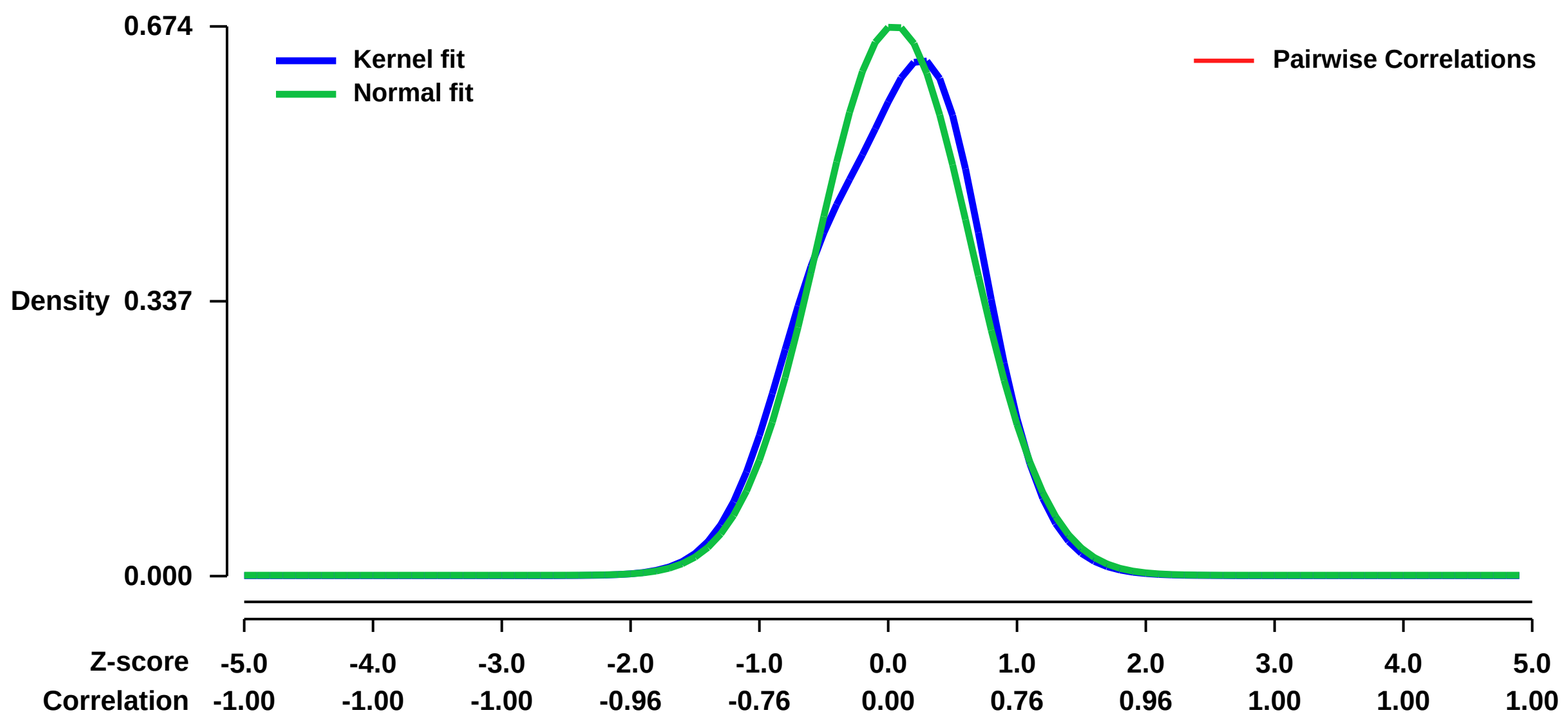

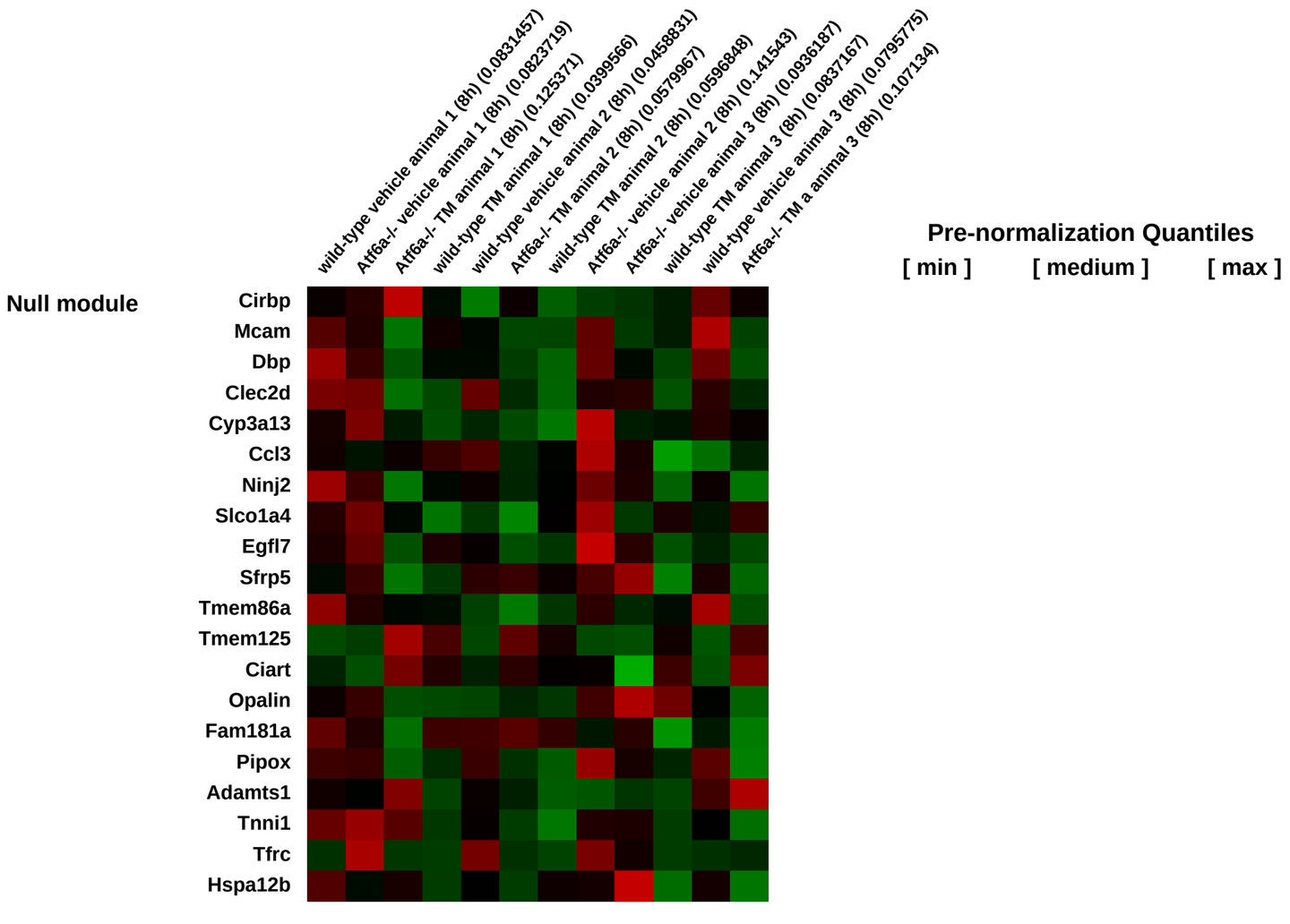

GEO Series "GSE17297" Expression Profiles

Num of samples in this series: 32

Scale of expression profile Z-scores

-3.0 -2.0 -1.0 0.0 1.0 2.0 3.0

GEO Link:	http://www.ncbi.nlm.nih.gov/geo/query/acc.cgi?acc=GSE17297
Status:	Public on Jul 24 2009
Title:	Mndal, a new interferon-inducible family member, suppresses cell growth and may modify plasmacytoma susceptibility
Organism:	Mus musculus
Experiment type:	Expression profiling by array
Platform:	GPL1261
Pubmed ID:	19654412
Summary & Design:	**Summary:** Mndal, a new interferon-inducible family member, is highly polymorphic, suppresses cell growth and may modify plasmacytoma susceptibility. The human HIN-200 gene cluster and its mouse counterpart, the Interferon inducible-200 (Ifi200) family, both on Chr 1, are associated with several diseases, including solid tumors and lupus. Our study was initiated to identify the modifier gene(s) encoded by the Pctm locus, in which mouse B cell plasmacytomas induced by pristane are associated with heterozygosity of Chr 1 genes near the Ifi200 cluster. A screen for differentially expressed genes in granulomatous tissues induced by pristane in resistant and susceptible strains identified a new Ifi200 member whose expression was 1000-fold higher in the strain carrying the resistant allele of Pctm, and was the most highly expressed Ifi200 gene. The gene, designated Mndal (for MNDA-like, myeloid nuclear differentiation antigen like), was absent in the susceptible genome, as were genomic sequences upstream of Ifi203, the gene adjacent to Mndal. Ectopic expression of MNDAL suppressed cell growth, which, together with the disease susceptibility of heterozygotes at the Pctm locus, suggests that Mndal, perhaps with Ifi203, acts as a tumor suppressor and display(s) haplo-insufficiency. Mndal is highly polymorphic among inbred mouse strains, as it is absent in 10/24 strains. This polymorphism may have implications for other disease modifiers mapping to the same region. **Overall design:** Using institutionally approved animal protocols, mice were given 0.5 ml TMPD intraperitoneally. Three and 18 days later, total RNA was extracted from mesentery of experimental/control animals, using TRIzol (Invitrogen). Labeled aRNA prepared from 1 ´¡g of RNA (MessageAmpII aRNA Amplification kit, Ambion protocols) was hybridized to mouse genome 430 2.0 array chips, processed on Workstation 450, and analyzed with Gene Chip Operating Software (GCOS; Affymetrix). Differential expression was assessed by ANOVA (Partek Genomics Suite).

Background corr dist: KL-Divergence = 0.1512, L1-Distance = 0.0349, L2-Distance = 0.0026, Normal std = 0.3805

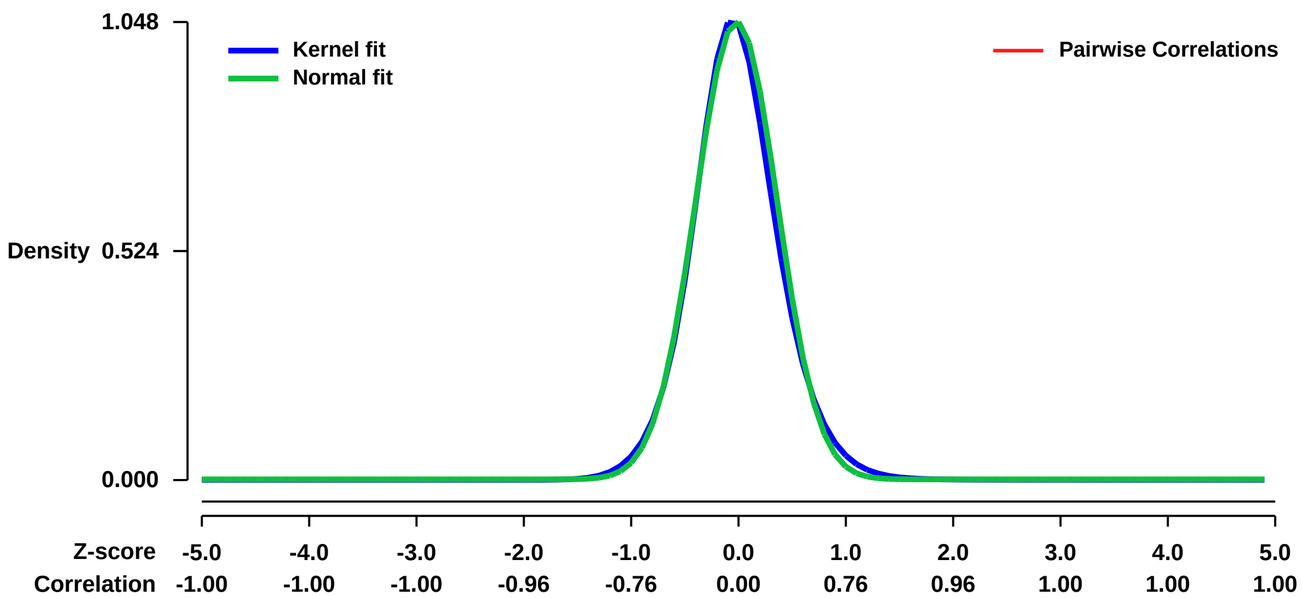

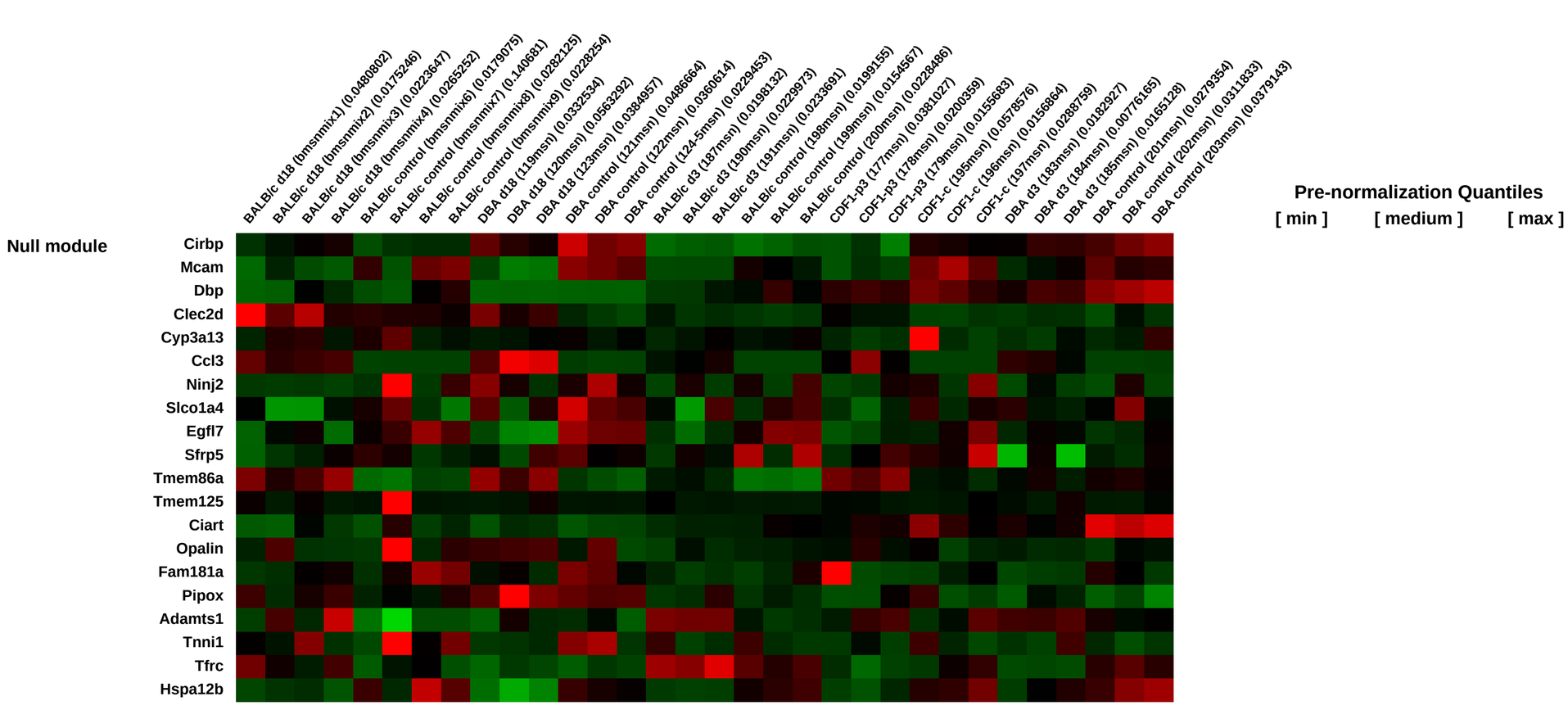

GEO Series "GSE4142" Expression Profiles

Num of samples in this series: 14

Scale of expression profile Z-scores

-3.0 -2.0 -1.0 0.0 1.0 2.0 3.0

GEO Link:	http://www.ncbi.nlm.nih.gov/geo/query/acc.cgi?acc=GSE4142
Status:	Public on Feb 02 2006
Title:	Molecular Analysis of antigen-specific B cell responses
Organism:	Mus musculus
Experiment type:	Expression profiling by array
Platform:	GPL1261
Pubmed ID:	16492737
Summary & Design:	**Summary:** In order to better understand the factors that regulate B cell differentiation upon exposure to antigen, we compares global gene expression profiles from naive B cells with antigen-specific plasma, germinal center, and memory B cells after immunization with the T-dependent antigen, NP-CGG. The memory B cell-enriched transcripts were then compared with memory T cell-enriched and hematopoietic stem cell-enriched transcripts in order to generate a transcriptional profile of self-renewal within the hematopoietic system. **Keywords: Cell Type Comparison** **Overall design:** Naive B cells were FACS sorted from unimmunized mice, while plasma, germinal center, and memory B cells were sorted from NP-CGG-immunized mice at 1, 2, or 10 weeks after immunization, respectively, using a combination of cell surface markers. RNA was extracted, amplified, and hybridized to Affymetrix microarrays.

Background corr dist: KL-Divergence = 0.0855, L1-Distance = 0.0388, L2-Distance = 0.0032, Normal std = 0.4621

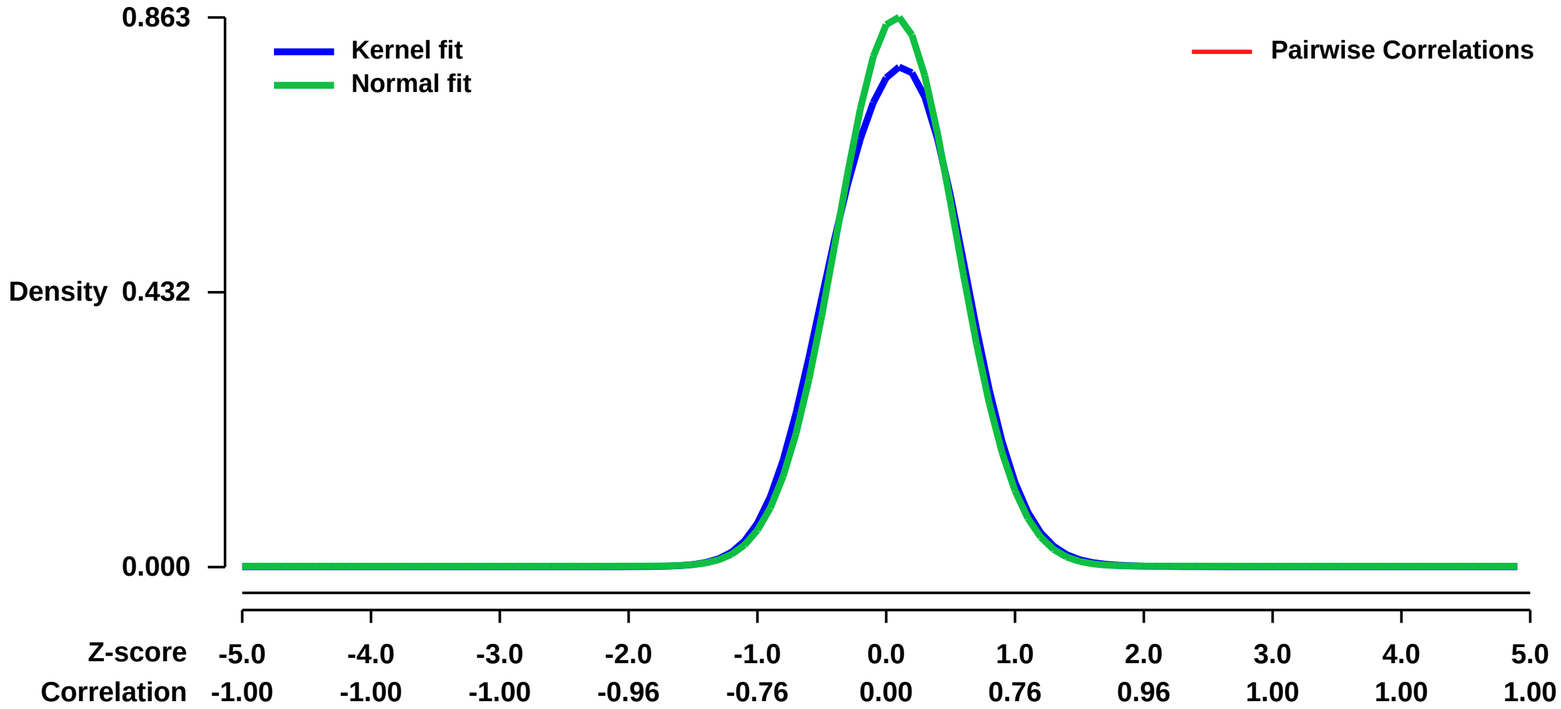

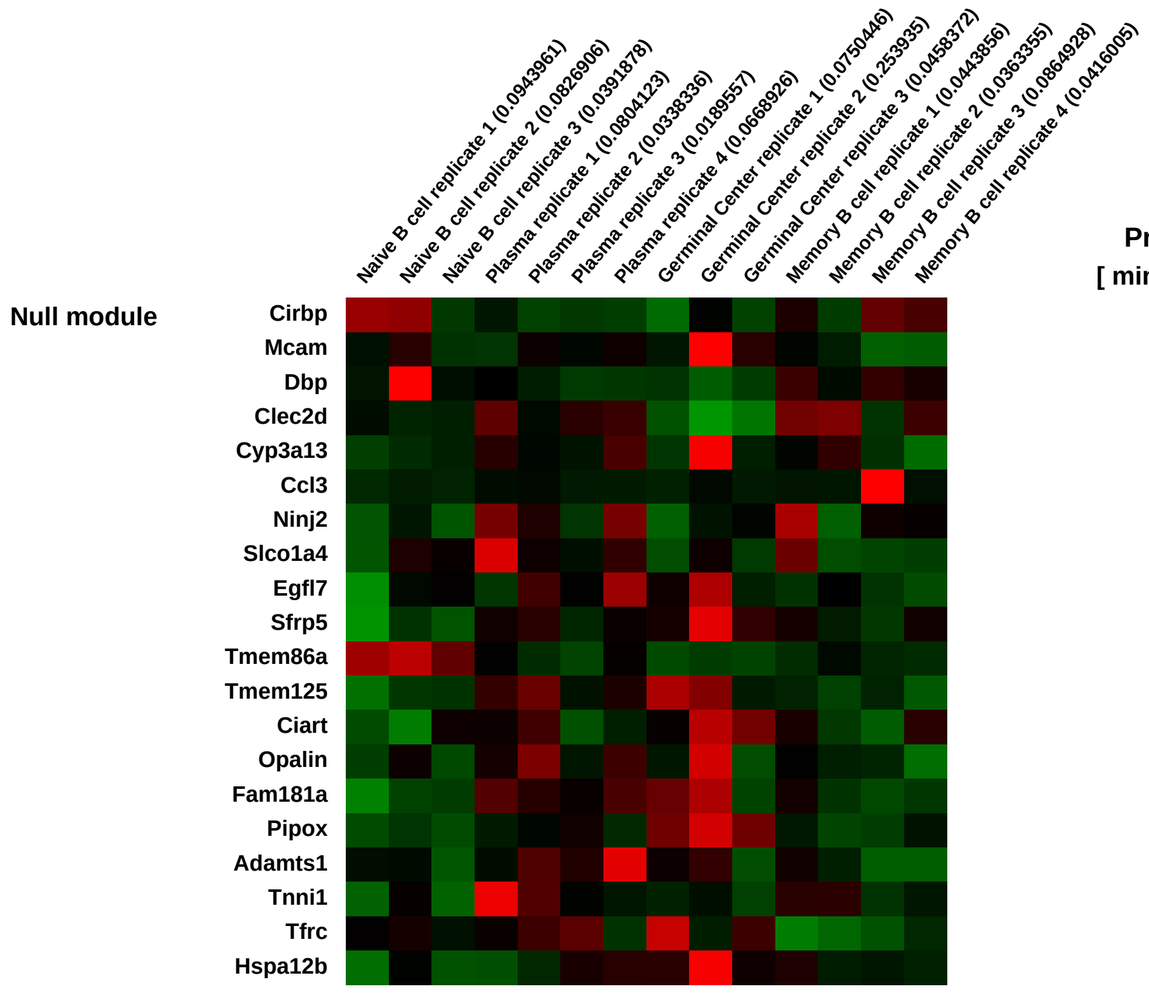

GEO Series "GSE31086" Expression Profiles

Num of samples in this series: 6

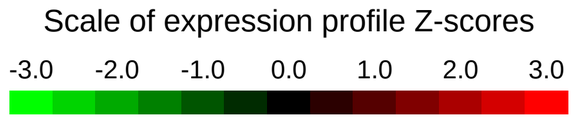

GEO Link:	http://www.ncbi.nlm.nih.gov/geo/query/acc.cgi?acc=GSE31086
Status:	Public on Feb 08 2012
Title:	Expression data from Bmi1-null common myeloid progenitor (CMP)
Organism:	Mus musculus
Experiment type:	Expression profiling by array
Platform:	GPL1261
Pubmed ID:	22351929
Summary & Design:	**Summary:** Bmi1 is a component of polycomb repressive complex 1 and its role in the inheritance of the stemness of adult somatic stem cells has been well characterized. Bmi1 maintains the self-renewal capacity of adult stem cells, at least partially, by repressing the Ink4a/Arf locus that encodes a cyclin-dependent kinase inhibitor, p16Ink4a, and a tumor suppressor, p19Arf 14. Deletion of both Ink4a and Arf in Bmi1-deficient mice substantially restored the defective self-renewal capacity of HSCs and neural stem cells. **Overall design:** Purified CMP from BM of recipient mice repopulated with wild-type, Ink4a-/-Arf-/-, and Bmi1-/- Ink4a-/-Arf-/- BM cells were subjected to RNA extraction and hybridization on Affymetrix microarrays.

Background corr dist: KL-Divergence = 0.0491, L1-Distance = 0.0270, L2-Distance = 0.0010, Normal std = 0.5869

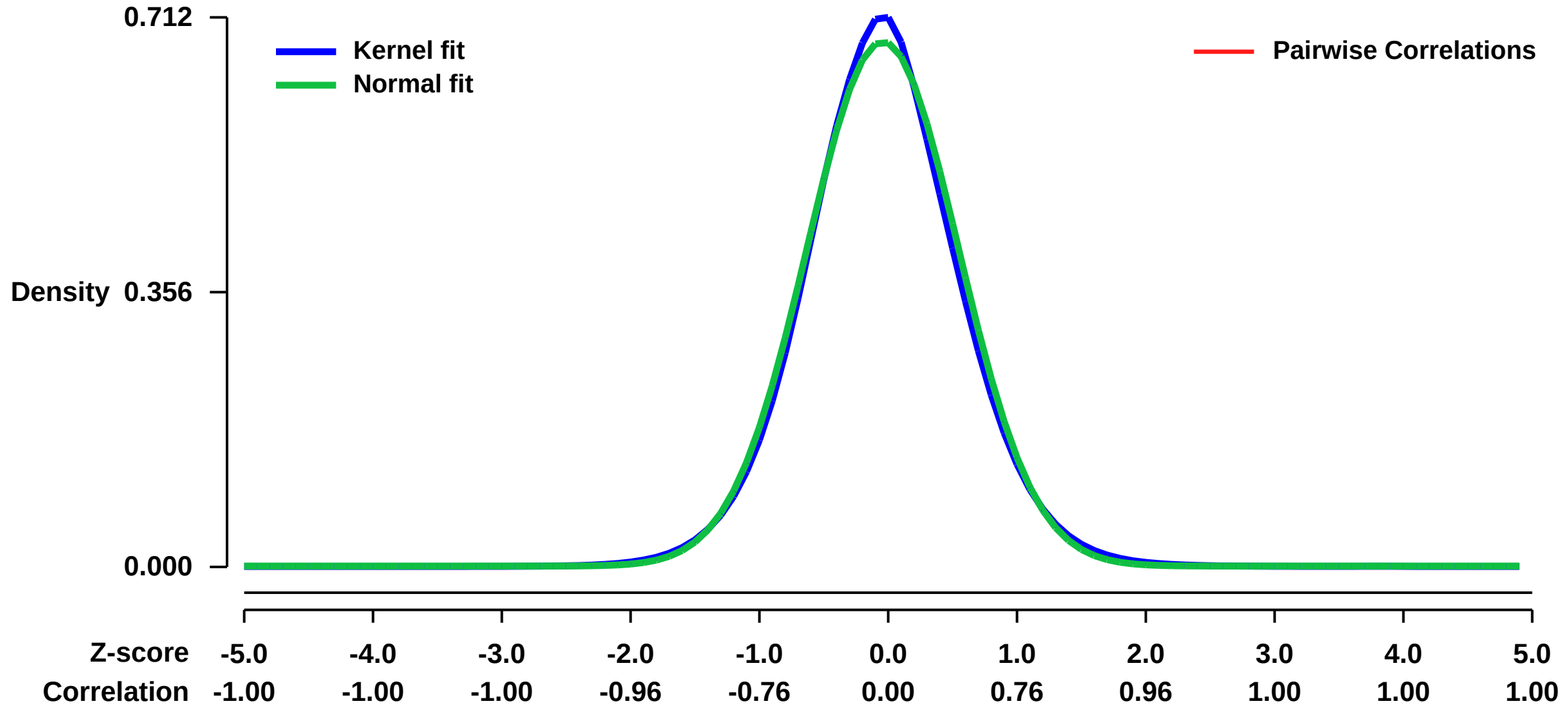

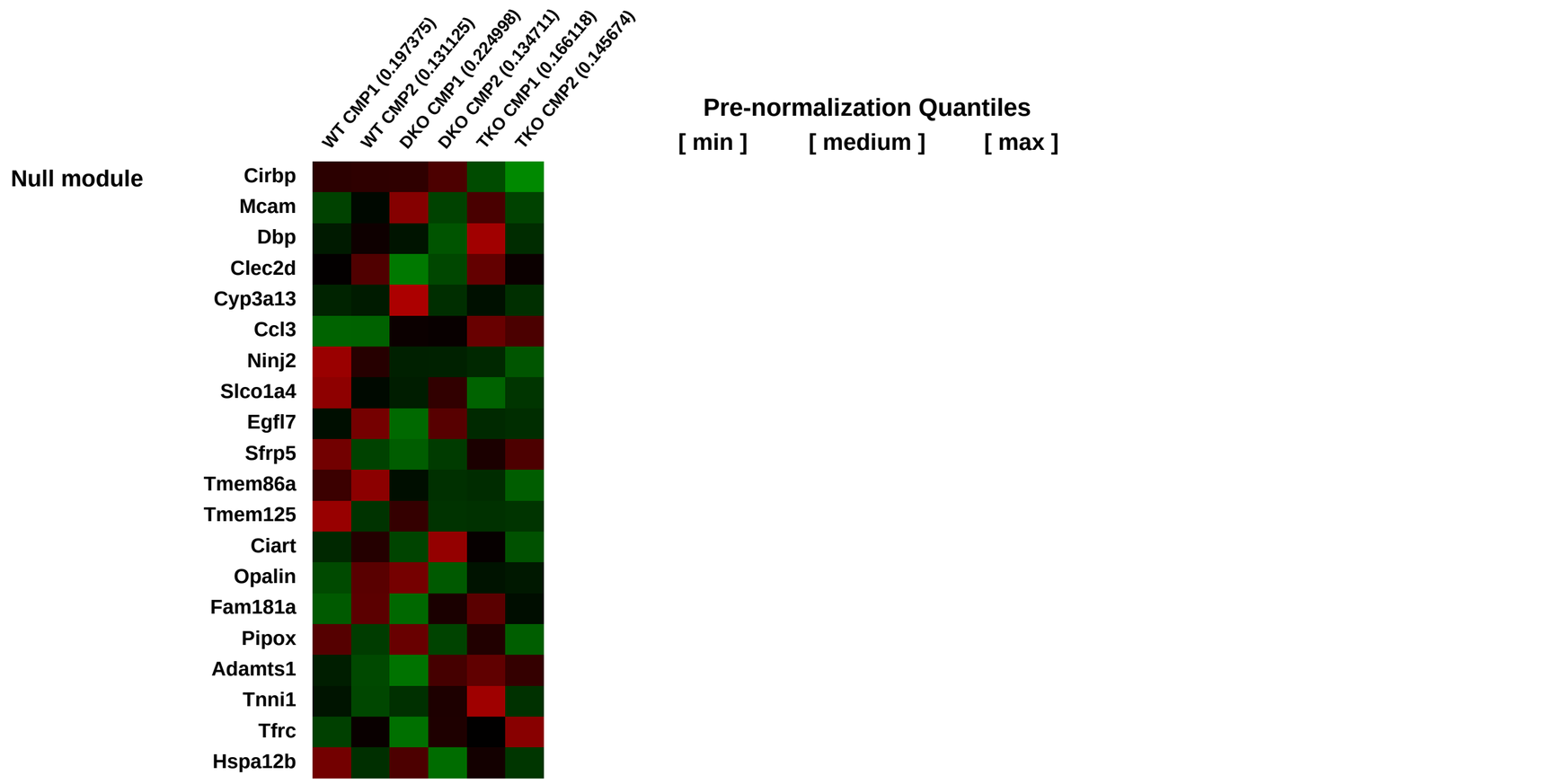

GEO Series "GSE5497" Expression Profiles

Num of samples in this series: 6

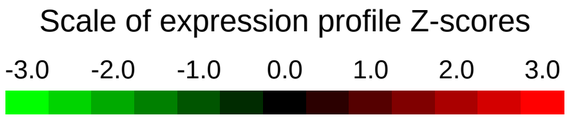

GEO Link:	http://www.ncbi.nlm.nih.gov/geo/query/acc.cgi?acc=GSE5497
Status:	Public on Aug 12 2006
Title:	Pyruvate induces mitochondrial biogenesis by a PGC-1alpha independent mechanism
Organism:	Mus musculus
Experiment type:	Expression profiling by array
Platform:	GPL1261
Pubmed ID:	17182725
Summary & Design:	**Summary:** The present study examines the impact of altering energy provision on mitochondrial biogenesis in muscle cells. C2C12 myoblasts were chronically treated with supraphysiological levels of sodium pyruvate for 72 hr. Treated cells exhibited increased mitochondrial protein expression, basal respiratory rate and maximal oxidative capacity. The increase in mitochondrial biogenesis was independent of increases in PGC-1alpha and PGC-1alpha mRNA expression. To further assess whether PGC-1alpha expression was necessary for pyruvate action, cells were infected with adenovirus containing shRNA for PGC-1alpha prior to treatment with pyruvate. Despite a 70% reduction in PGC-1alpha mRNA the effect of pyruvate was preserved. Furthermore, pyruvate induced mitochondrial biogenesis in primary myoblasts from PGC-1alpha null mice. These data suggest that regulation of mitochondrial biogenesis by pyruvate in myoblasts is independent of PGC-1alpha, suggesting the existence of a novel energy-sensing pathway regulating oxidative capacity. **Keywords:** basal state versus treatment at one time point **Overall design:** C2C12 myoblasts were incubated with either basal media or basal media supplemented with 50 mM sodium pyruvate for 72 hr. Total RNA was extracted using TRIzol and GeneChip experiment was conducted using Gene Chip Mouse Genome 430 2.0 Expression Array. A Gene Chip analysis for each condition was performed in triplicate.

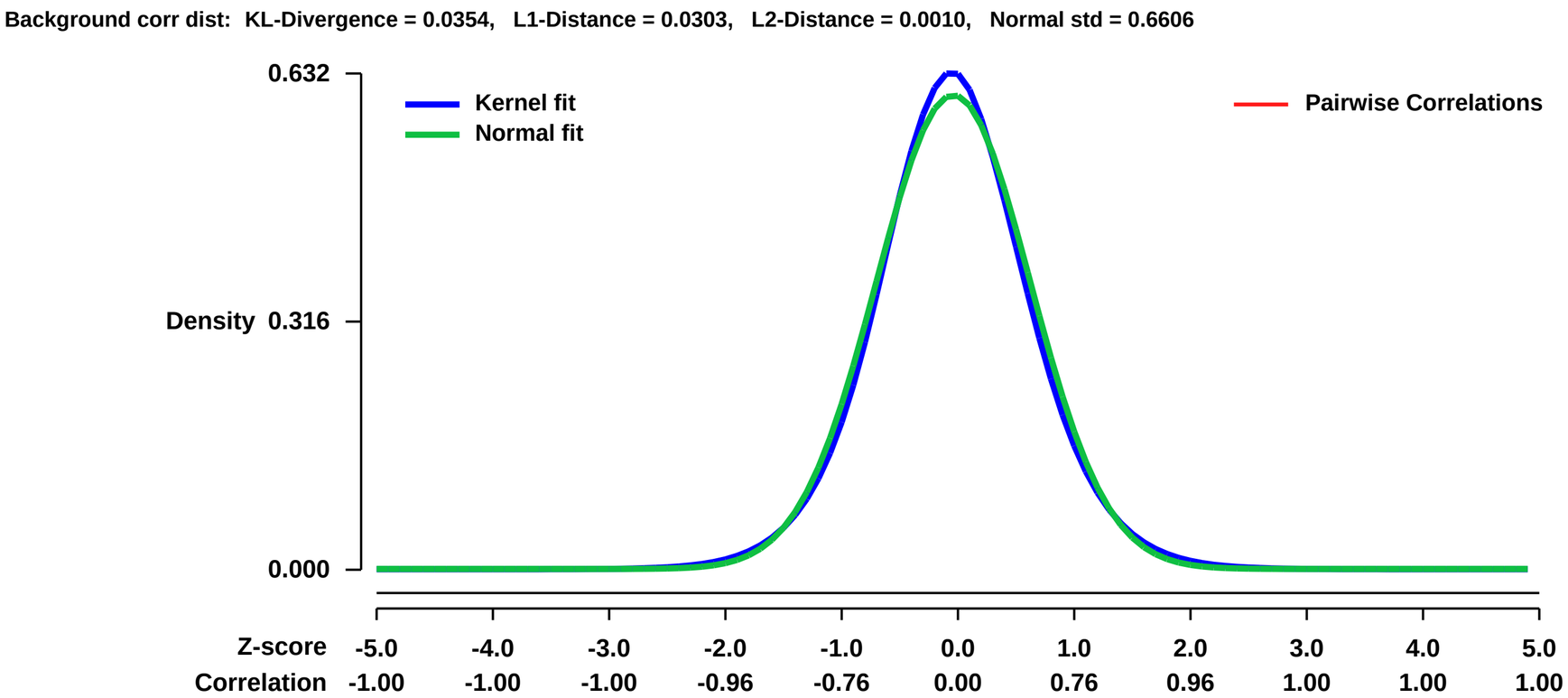

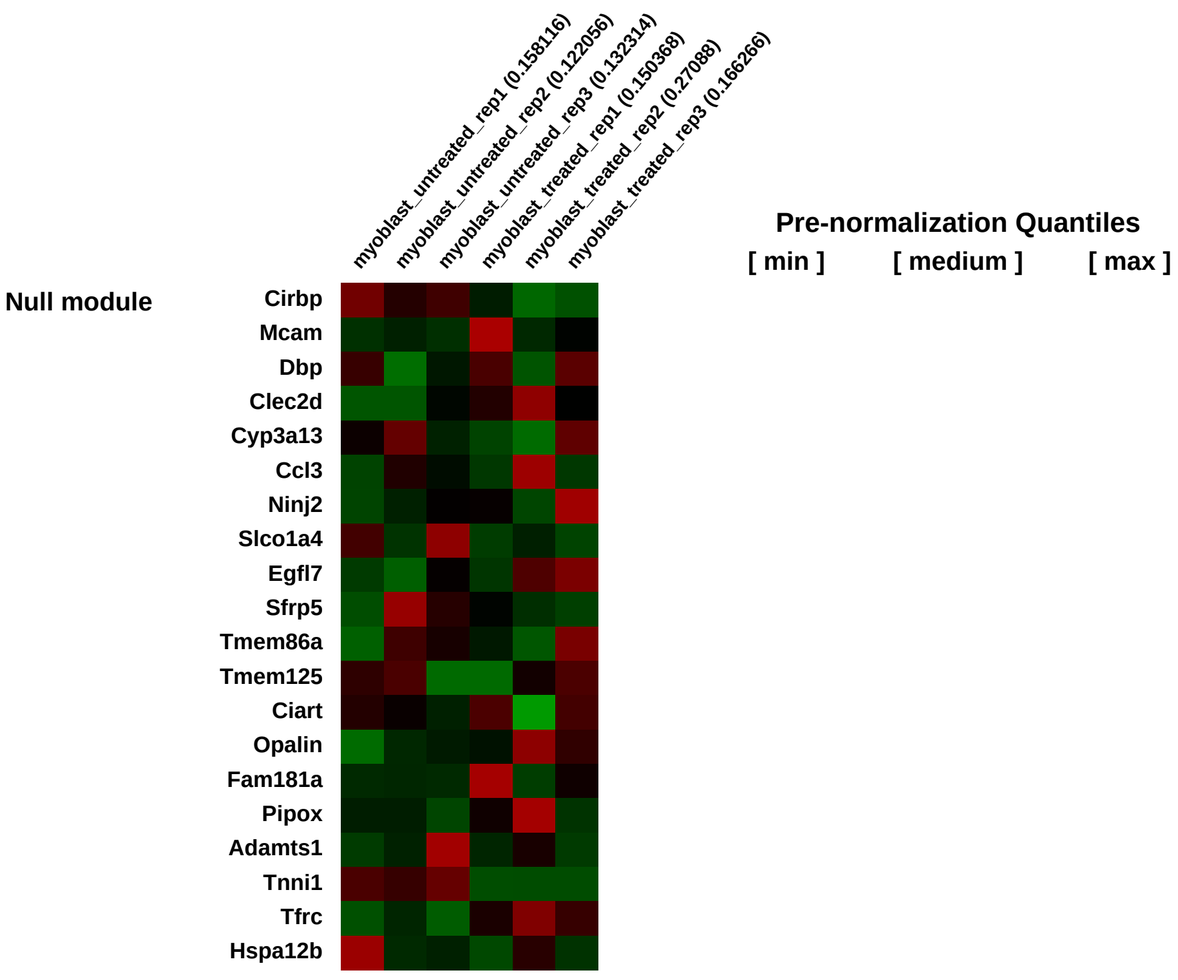

GEO Series "GSE13753" Expression Profiles

Num of samples in this series: 10

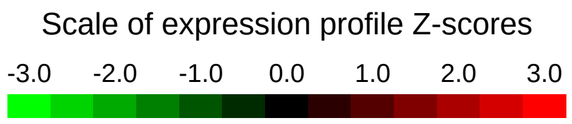

GEO Link: http://www.ncbi.nlm.nih.gov/geo/query/acc.cgi?acc=GSE13753

Status: Public on Jun 08 2009

Title: E2F4 cooperates with pRB in the development of extra-embryonic, not embryonic, tissues

Organism: Mus musculus

Experiment type: Expression profiling by array

Platform: GPL1261

Pubmed ID:

Summary & Design:

Summary:
Homozygous mutation of the murine retinoblastoma tumor suppressor gene, Rb, results in embryonic lethality between E13.5 and E15.5 with defects in cellular proliferation, differentiation and apoptosis. Many of these defects are suppressed by mutation of an activating E2F, E2f1 or E2f3, indicating that they are key downstream targets of the retinoblastoma protein, pRB. In this study, we assess how E2F4 contributes to the developmental consequences of pRb-loss. In stark contrast to the activating E2Fs, the homozygous mutation of E2f4 shortened the lifespan of Rb-/- embryos. This resulted from an exacerbation of the placental defect of the Rb-/- mice indicating that E2F4 and pRB cooperate in the development of this tissue. Further analyses indicated that this defect reflects an increase in trophectoderm-like cells. Under conditions where the placenta was wild-type but the embryo mutant for E2f4 and pRb embryos survived to birth and exhibited all of the defects that were observed in the E2f4 and Rb single mutant embryos. Thus, while pRB and E2F4 cooperate in placental development, they play largely non-overlapping roles the development of many embryonic tissues.

Keywords: genetically modified tissue comparison

Overall design:
In one experiment, embryonic Day 13.5 placentas from wild-type and Rb -/- knock-out mice were compared. In the second experiment, embronic day 11.5 placentas from wild-type and Rb -/-;E2f4 -/- double knock-out mice were compared.

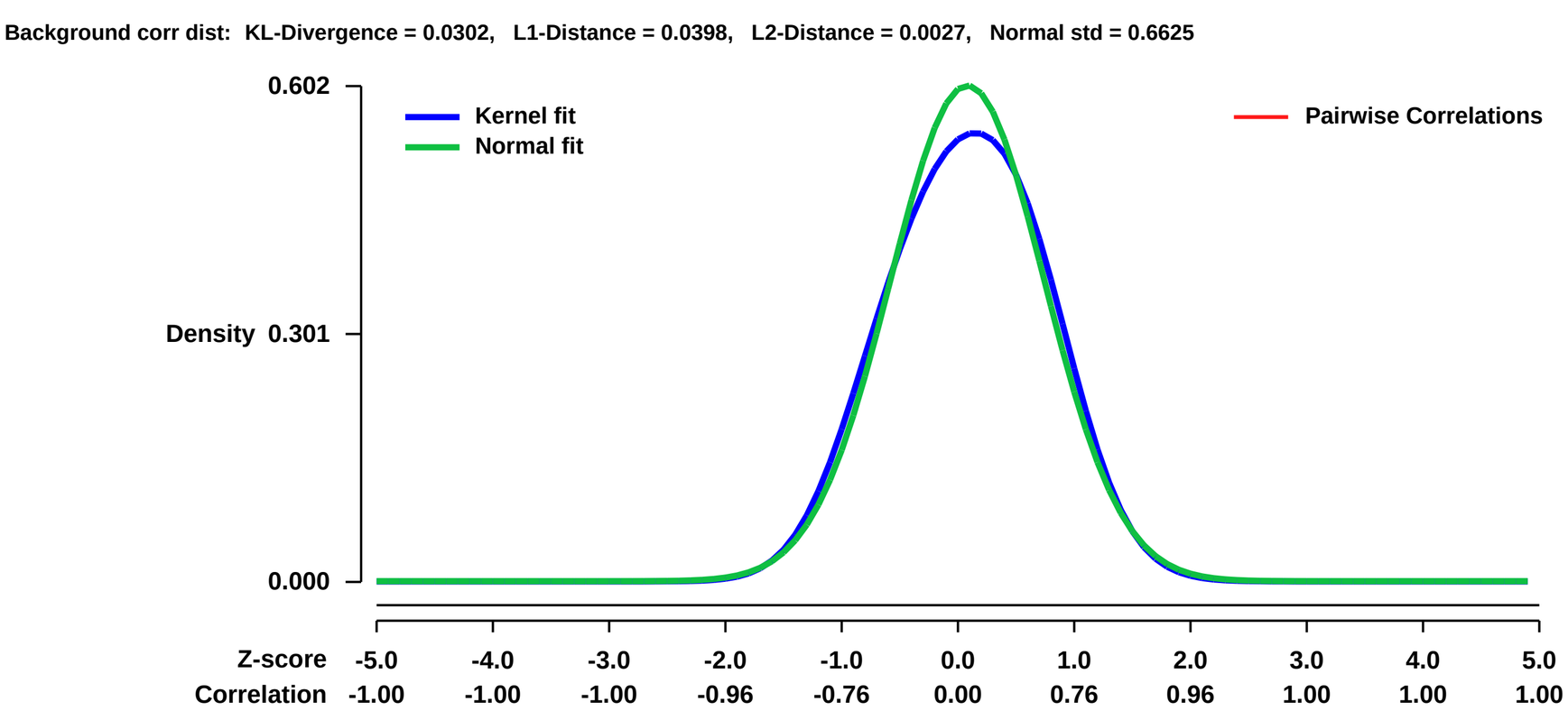

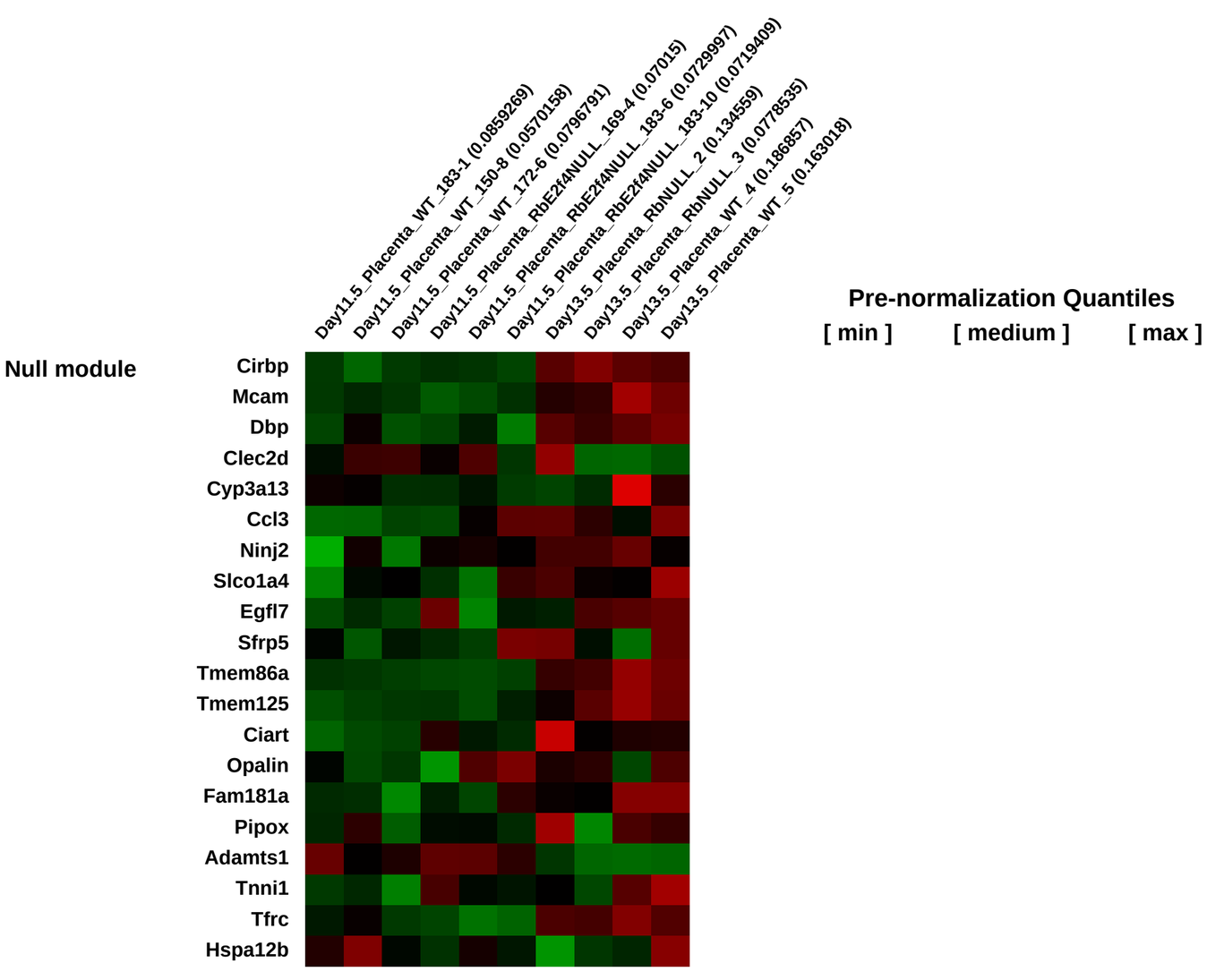

GEO Series "GSE54207" Expression Profiles

Num of samples in this series: 9

Scale of expression profile Z-scores

-3.0 -2.0 -1.0 0.0 1.0 2.0 3.0

GEO Link: http://www.ncbi.nlm.nih.gov/geo/query/acc.cgi?acc=GSE54207
Status: Public on Jan 18 2014
Title: Expression data from mouse limb tendon cells during development.
Organism: Mus musculus
Experiment type: Expression profiling by array
Platform: GPL1261
Pubmed ID:

Summary & Design:

Summary:
We have undertaken a screen of mouse limb tendon cells in order to identify molecular pathways involved in tendon development. Mouse limb tendon cells were isolated based on Scleraxis (Scx) expression at different stages of development: E11.5, E12.5 and E14.5

Microarray comparisons were carried out between tendon progenitor and differentiated stages.

Overall design:
Forelimbs from E11.5, E12.5 and E14.5 Scx-GFP embryos were collected and dissociated with trypsin to obtain cell suspensions. Scx-positive tendon cells were isolated by FACS. RNA was extracted and Fragmented biotin-labelled cRNA samples were hybridized on Affymetrix Gene Chip Mouse Genome 430 2.0 arrays.

Background corr dist: KL-Divergence = 0.0661, L1-Distance = 0.0279, L2-Distance = 0.0010, Normal std = 0.5212

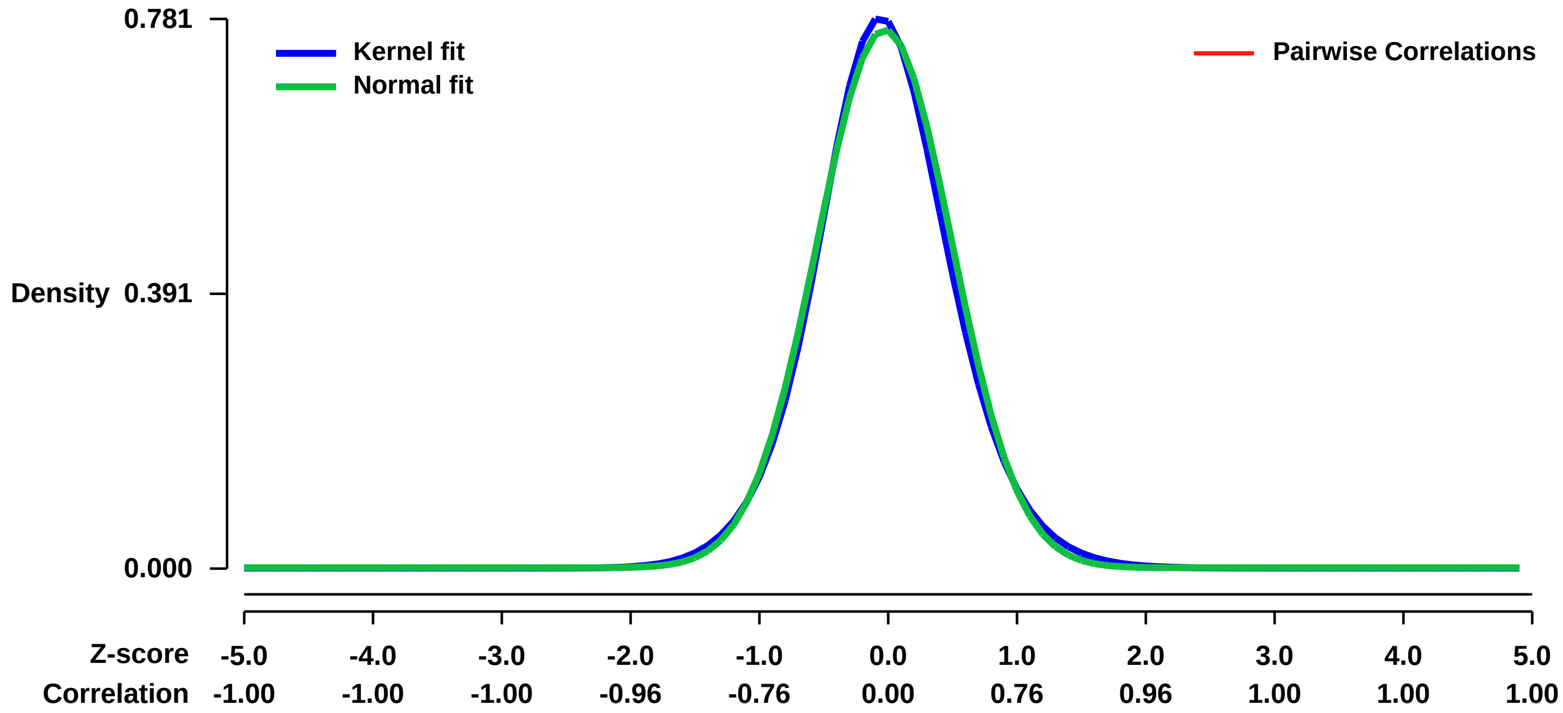

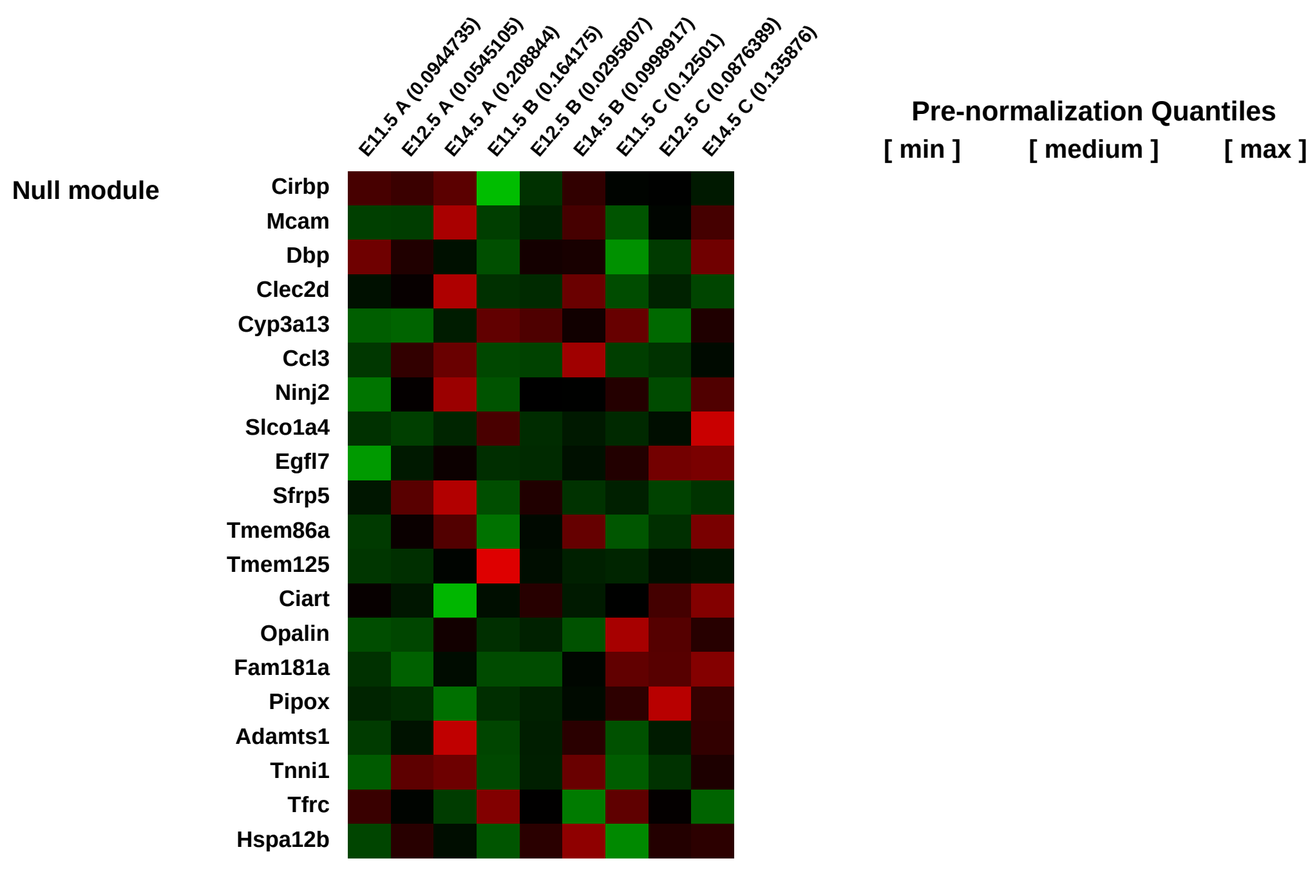

GEO Series "GSE19436" Expression Profiles

Num of samples in this series: 8

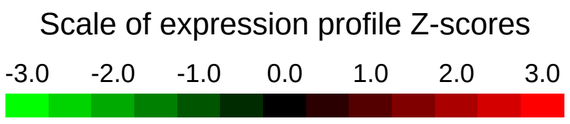

GEO Link:	http://www.ncbi.nlm.nih.gov/geo/query/acc.cgi?acc=GSE19436
Status:	Public on Apr 01 2010
Title:	Transcriptional alterations in cycling neural stem cells underlying alcohol use disorders
Organism:	Mus musculus
Experiment type:	Expression profiling by array
Platform:	GPL1261
Pubmed ID:	23095216
Summary & Design:	**Summary:** Ethanol inhibits the proliferation of neural stem cells in the fetal, adolescent, and adult brain. The consequences are cognitive deficits associated with fetal alcohol spectrum disorder and alcohol use disorder. We tested the hypothesis that ethanol affects progression through cell cycle checkpoints by differentially modifying transcriptional processes. Monolayer cultures of NS-5 neural stem cells were treated for 48 hr with the mitogenic agent FGF2 or the anti-mitogenic TGF¸†1 in the absence or presence of ethanol. Cell cycle elongation was induced by a global down-regulation of genes involved in cell cycle progression, including the cyclin E system. Checkpoint regulation occurred downstream of p21 and Jun-oncogene signaling cascades. Thus, ethanol can affect cell cycle progression by altering transcript expression of strategic genes downstream of the G1/S checkpoint. **Overall design:** NS5 neural stem cells were grown in Euromed Media supplemented with N2 and glutamine. Cells were plated on poly-ornathine and laminin in the presence of FGF2 (10 ng/ul) and EGF (10 ng/ul) for 24 hrs. Media was removed, cells were rinsed, and placed in growth factor free conditions for 4 hrs. NS5 cells were then exposed to one of four treatment for 48 hrs: FGF2 (10 ng/ul) only, FGF2 (10 ng/ul) and ethanol (400 mg/dl), TGF-beta1 (10 ng/ul) only, or TGF-beta1 (10 ng/ul) and ethanol (400 mg/dl). Total RNA was collected immediately following treatment.

Background corr dist: KL-Divergence = 0.0738, L1-Distance = 0.0276, L2-Distance = 0.0013, Normal std = 0.4934

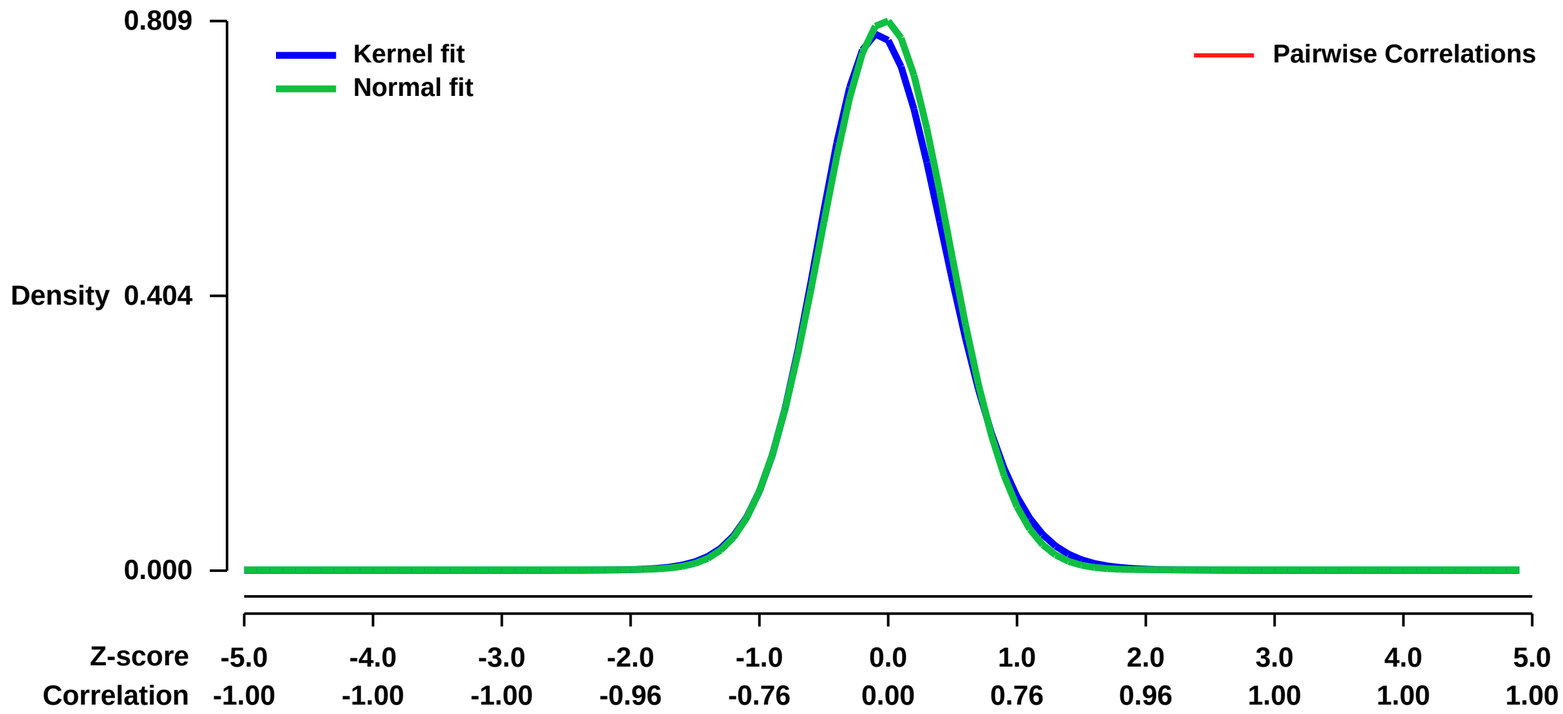

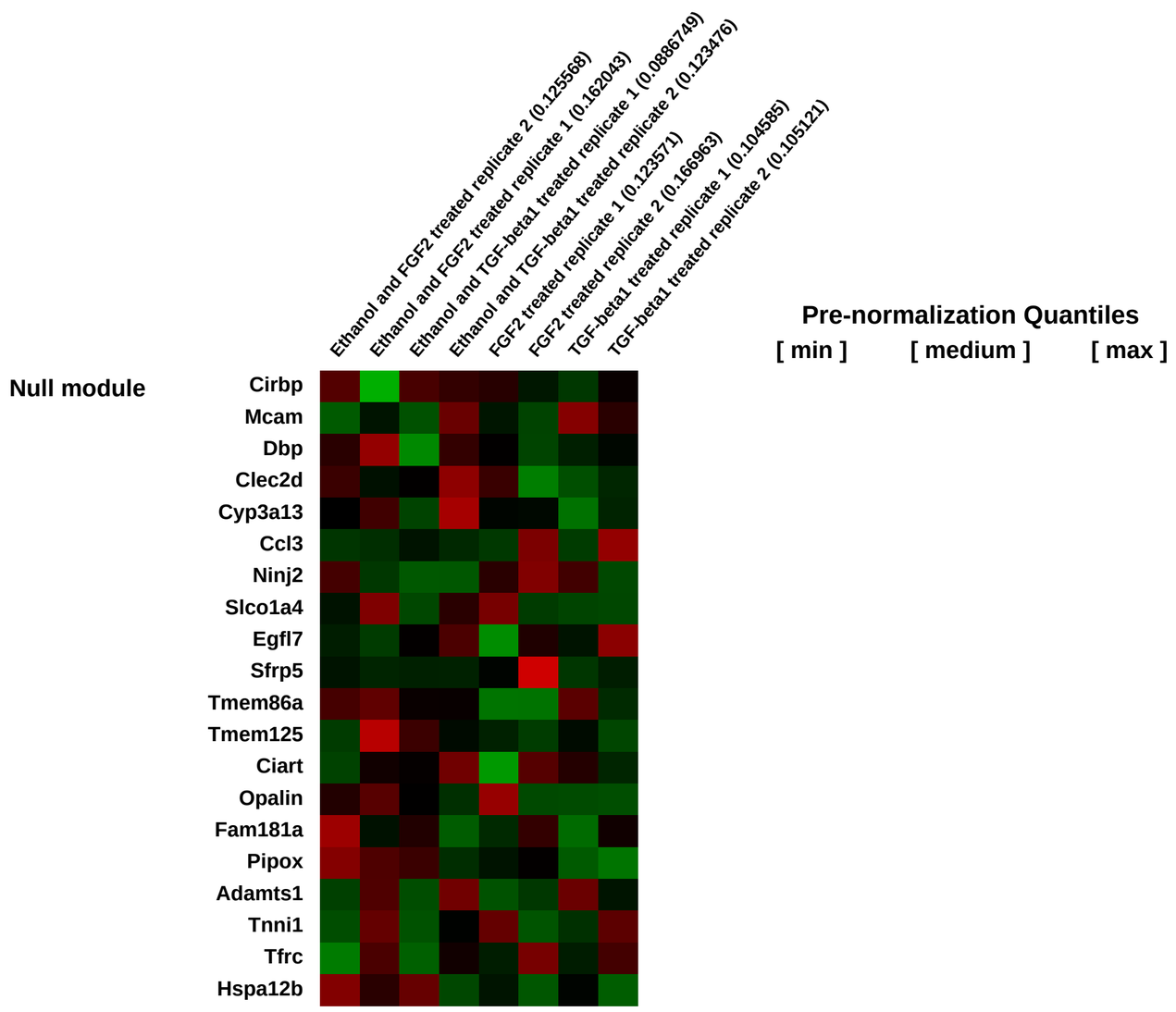

GEO Series "GSE41896" Expression Profiles

Num of samples in this series: 6

Scale of expression profile Z-scores

-3.0 -2.0 -1.0 0.0 1.0 2.0 3.0

GEO Link:	http://www.ncbi.nlm.nih.gov/geo/query/acc.cgi?acc=GSE41896
Status:	Public on Jan 01 2014
Title:	Dmrt1 (doublesex and mab-3 related transcription factor 1) conditional knockout expression analysis of E15.5 ovaries.
Organism:	Mus musculus
Experiment type:	Expression profiling by array
Platform:	GPL1261
Pubmed ID:	
Summary & Design:	**Summary:** Dmrt1 (doublesex and mab-3 related transcription factor 1) is a conserved transcriptional regulator of male differentiation required for testicular development in vertebrates. This study examines the result of conditional removal of Dmrt1 in E15.5 ovaries. **Overall design:** This study examines the result of conditional removal of Dmrt1 in E15.5 ovaries.

Background corr dist: KL-Divergence = 0.0396, L1-Distance = 0.0172, L2-Distance = 0.0003, Normal std = 0.6145

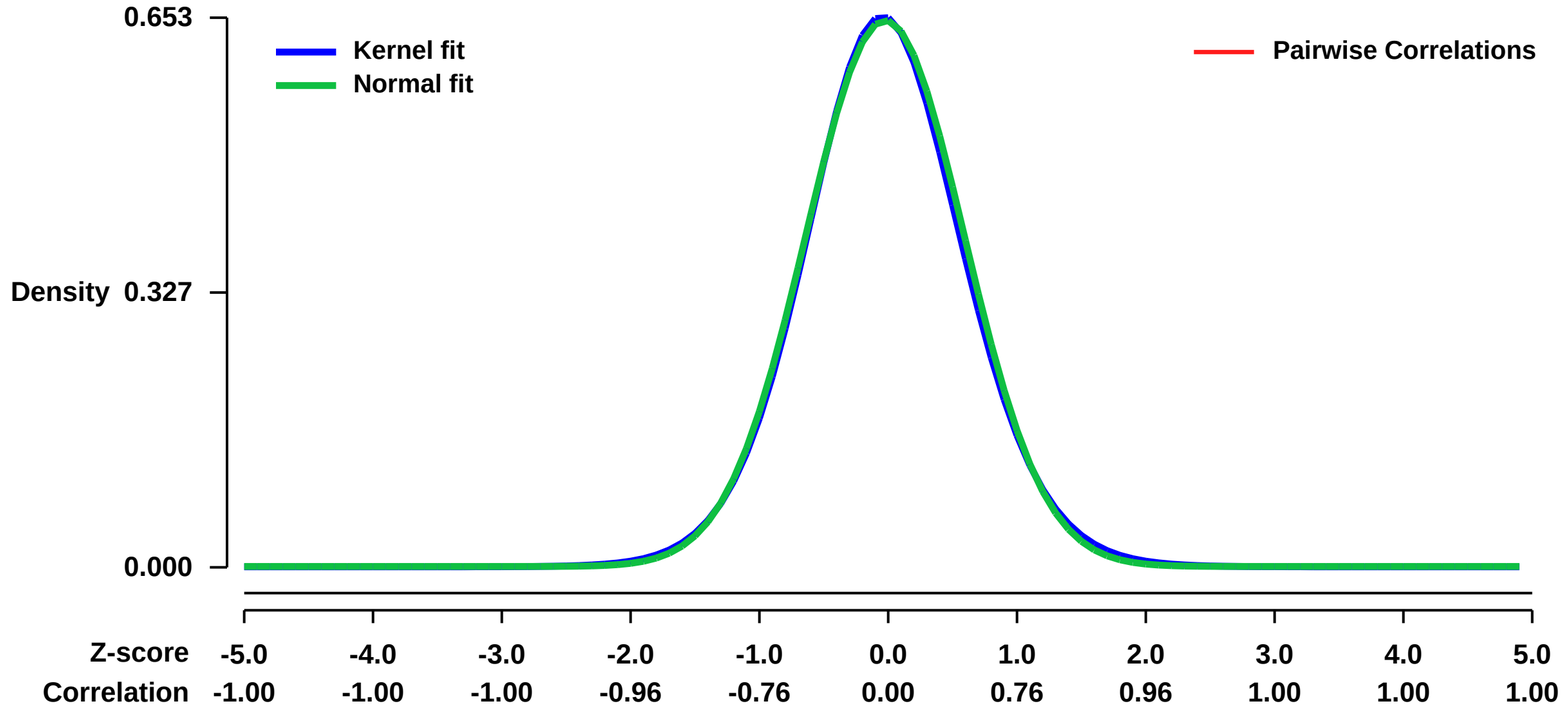

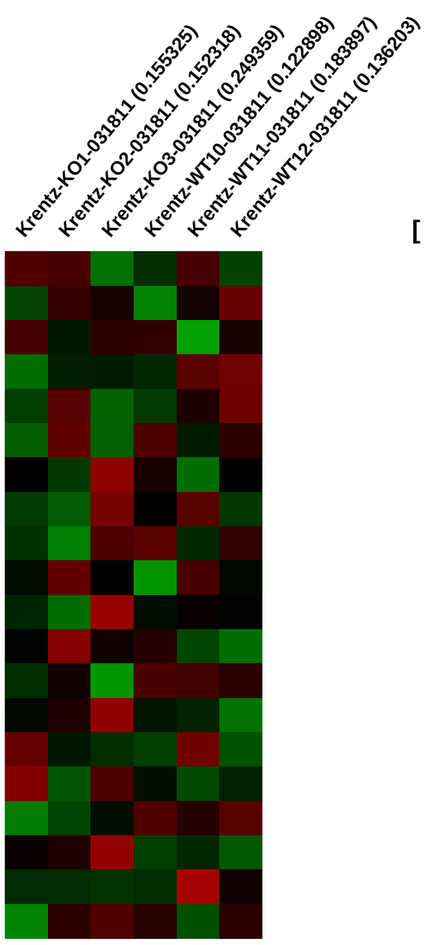

GEO Series "GSE13490" Expression Profiles

Num of samples in this series: 15

Scale of expression profile Z-scores

-3.0 -2.0 -1.0 0.0 1.0 2.0 3.0

GEO Link:	http://www.ncbi.nlm.nih.gov/geo/query/acc.cgi?acc=GSE13490
Status:	Public on Dec 15 2008
Title:	Cancer Stem Cells Are Enriched In The Side-Population Cells In A Mouse Model Of Glioma
Organism:	Mus musculus
Experiment type:	Expression profiling by array
Platform:	GPL1261
Pubmed ID:	19074870
Summary & Design:	**Summary:** The recent identification of cancer stem cells (CSCs) in multiple human cancers provides a new inroad to understanding tumorigenesis at the cellular level. CSCs are defined by their characteristics of self-renewal, multipotentiality, and tumor initiation upon transplantation. By testing for these defining characteristics, we provide evidence for the existence of CSCs in a transgenic mouse model of glioma, S100^ -verbB;Trp53. In this glioma model, CSCs are enriched in the side-population (SP) cells. These SP cells have enhanced tumor-initiating capacity, self-renewal, and multipotentiality compared to non-SP cells from the same tumors. Furthermore, gene expression analysis comparing FACS-sorted cancer SP cells to non-SP cancer cells and normal neural SP cells identified 45 candidate genes that are differentially expressed in glioma stem cells. We validated the expression of two genes from this list (S100a4 and S100a6) in primary mouse gliomas and human glioma samples. Analyses of xenografted human GBM (glioblatoma multiforme) cell lines and primary human glioma tissues show that S100A4 and S100A6 are expressed in a small subset of cancer cells and that their abundance is positively correlated to tumor grade. In conclusion, this study shows that CSCs exist in a mouse glioma model, suggesting that this model can be used to study the molecular and cellular characteristics of CSCs in vivo and to further test the cancer stem cell hypothesis. **Overall design:** This study features two factors, injected cell origin (either tumorsphere or neurosphere) and FACS cell population (either side population or non-side population cells). There were two different tumorspheres, labeled 3447 and 4346 that were isolated from brain tumors in S100beta-verbB;p53-/- or S100beta-verbB;p53+/- mice. The tumorspheres were injected separately into the brains of NOD.Cg-Prkdc<scid>Il2rg<tm1Wjl>/SzJ mice to generate biological triplicates of each primary tumor. Tumorspheres were isolated and cultured before FACS sorting to obtain side population and non-side population cells. As a control, untransformed neurospheres from three independent S100beta-verbB;p53-/- or S100beta-verbB;p53+/- mice were isolated, cultured, and FACS sorted to obtain side population and non-side population cells. Side population and non-side population cells cultured from three mice injected with the 3447 cultured tumorspheres were assayed for gene expression (six samples). Side-population stem cells cultured from three mice injected with the 4346 cultured tumorspheres were assayed for gene expression (three samples). Side-population and non-side population cells cultured from three mice injected with the neurospheres were assayed for gene expression (six samples).

Background corr dist: KL-Divergence = 0.1517, L1-Distance = 0.0400, L2-Distance = 0.0037, Normal std = 0.3801

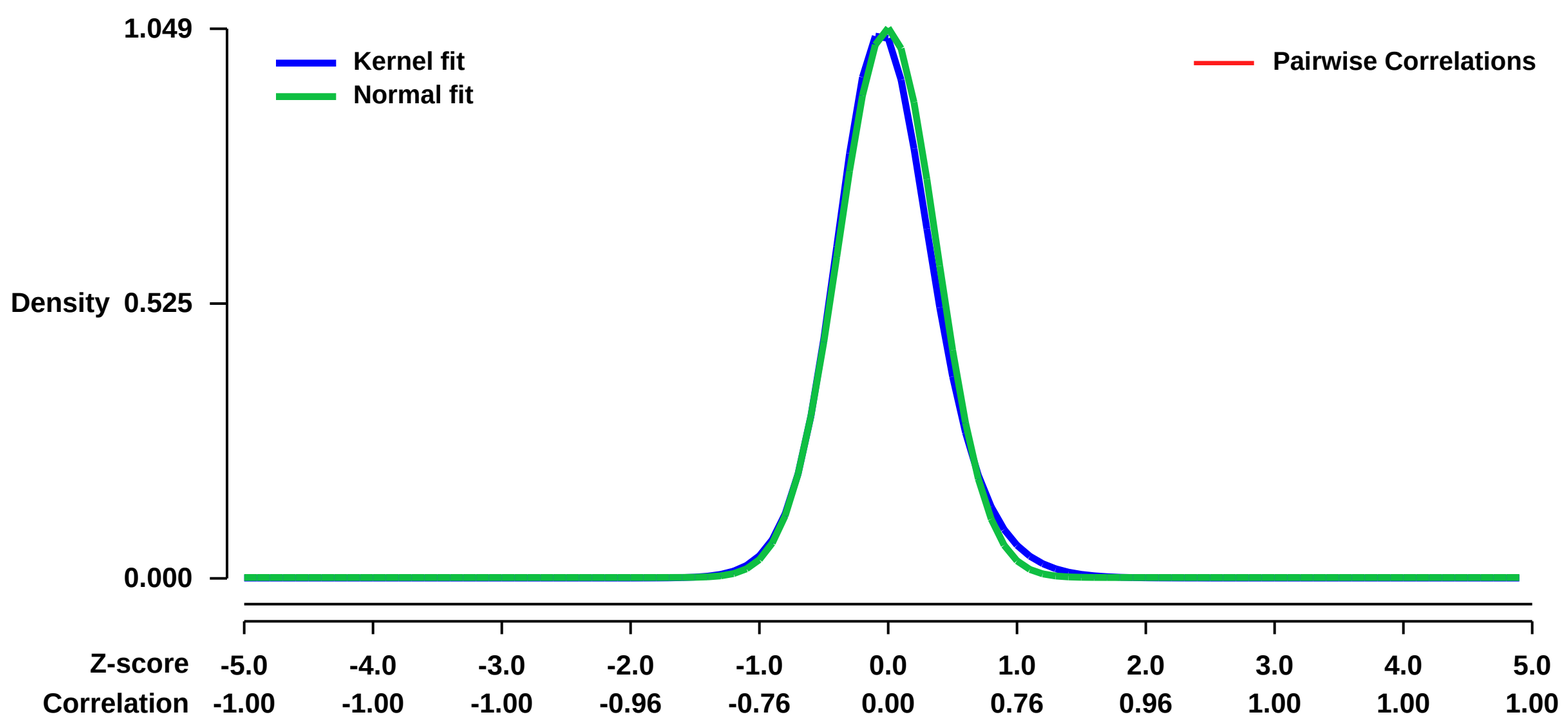

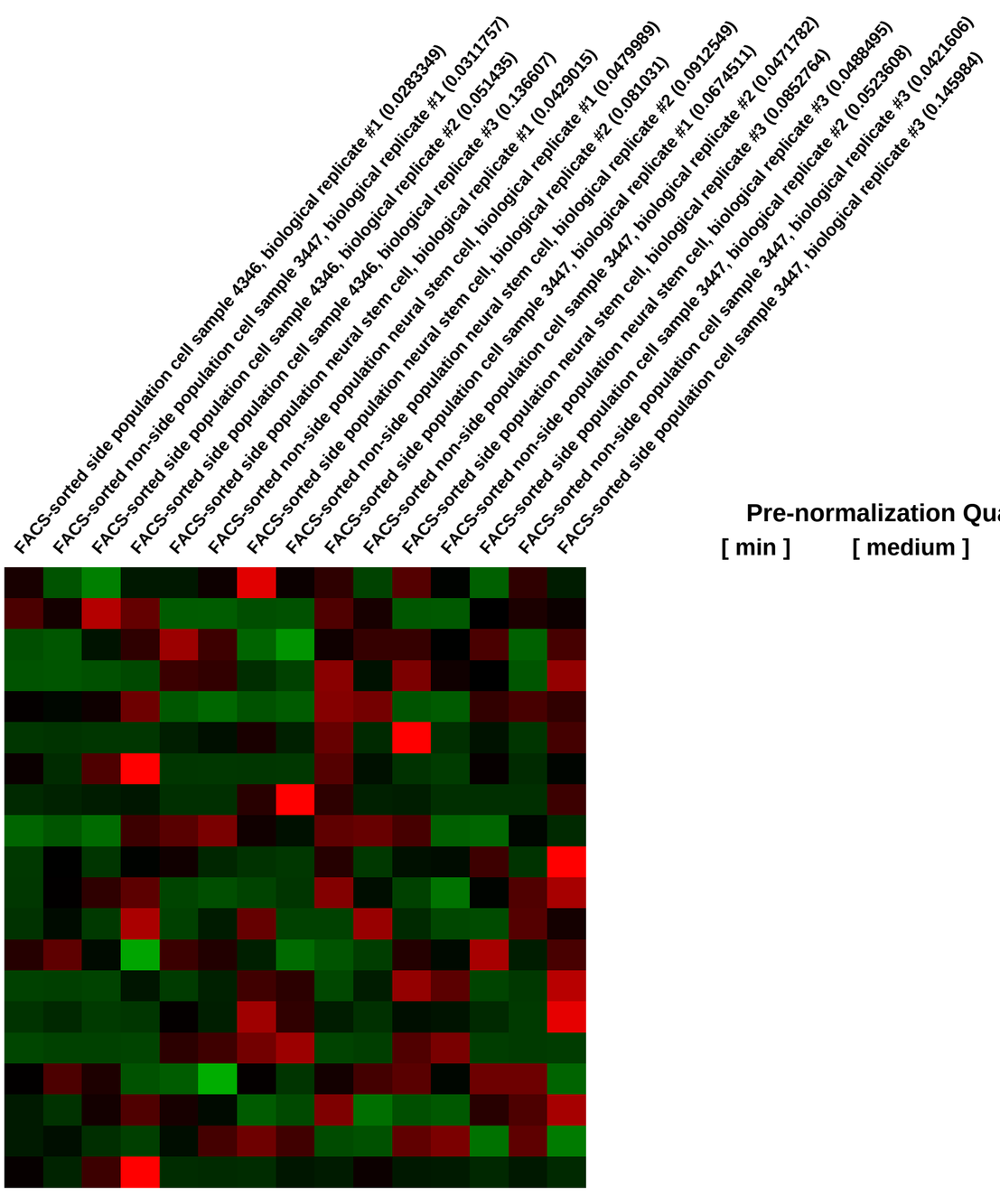

GEO Series "GSE19778" Expression Profiles

Num of samples in this series: 6

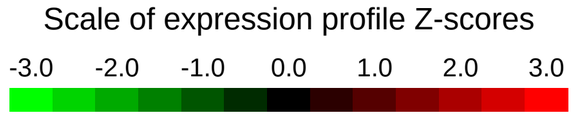

GEO Link:	http://www.ncbi.nlm.nih.gov/geo/query/acc.cgi?acc=GSE19778
Status:	Public on Jan 01 2011
Title:	The soluble intracellular domain of megalin does not affect renal proximal tubular function in vivo
Organism:	Mus musculus
Experiment type:	Expression profiling by array
Platform:	GPL1261
Pubmed ID:	20531455
Summary & Design:	**Summary:** The endocytic receptor megalin constitutes the main pathway for clearance of plasma proteins from the glomerular filtrate in the proximal tubules. However, little is know about the mechanisms that control receptor activity. A widely discussed hypothesis states that the intracellular domain (ICD) of megalin, released upon ligand binding, acts as a transcription regulator to suppress receptor expression - a mechanism proposed to safeguard the proximal tubules from protein overload. Here, we have put this hypothesis to the test by generating a mouse model co-expressing the soluble ICD and the full-length receptor. Despite pronounced expression in the proximal tubules, the ICD failed to exert any effects on renal proximal tubular function such as megalin expression, protein retrieval, or renal gene transcription. Thus, our data argue that the ICD does not play a role in regulation of megalin activity in vivo in the proximal tubules. We used microarrays to compare gene expression profile in adult kidney from a new mouse model expressing the intracellular domain of megalin with wildtype. **Overall design:** 10 week old mice were collected for RNA extraction and hybridization on Affymetrix microarrays. Three individuals for each genotype were analyzed comparing heterozygous animals for the intracellular domain of megalin with littermates controls.

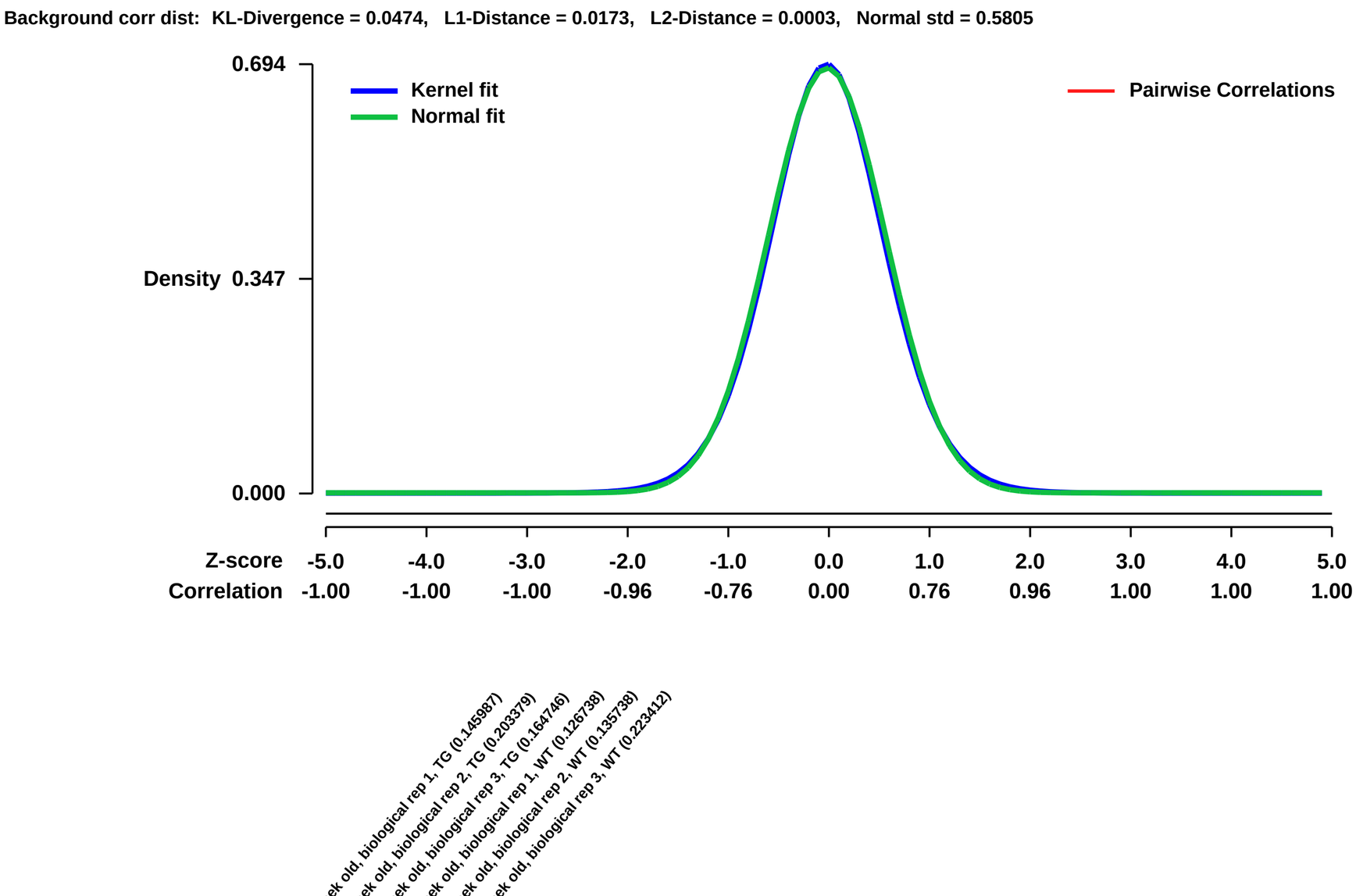

GEO Series "GSE39984" Expression Profiles

Num of samples in this series: 18

Scale of expression profile Z-scores

-3.0 -2.0 -1.0 0.0 1.0 2.0 3.0

GEO Link:	http://www.ncbi.nlm.nih.gov/geo/query/acc.cgi?acc=GSE39984
Status:	Public on Aug 09 2012
Title:	Comparison of the genetic extinction of NRAS to pharmacological MEK inhibition in an inducible mouse model of melanoma
Organism:	Mus musculus
Experiment type:	Expression profiling by array
Platform:	GPL1261
Pubmed ID:	22983396
Summary & Design:	**Summary:** Since direct pharmacological inhibition of RAS has thus far been unsuccessful, we explored system biology approaches to identify synergistic drug combination(s) that can mimic direct RAS inhibition. Leveraging an inducible mouse model of NRAS-mutant melanoma, we compare pharmacological MEK inhibition to complete NRAS-Q61K extinction in vivo. NRAS-Q61K extinction leads to a complete and durable tumor regression by enhancing both apoptosis and cell cycle arrest. By contrast, MEK inhibition only produces tumor stasis at best and we find that it robustly activates apoptosis but does not significantly impede proliferation. We used microarrays to determine which transcripts were affected by NRAS-Q61K extinction but insufficiently by MEK inhibition. We selected a single comparative timepoint, 4 days post-treatment. Downstream analyses included GSEA and TRAP algorithms, leading to the identification of a differentially affected CDK4-driven proliferation network. Immune genes were also identified as significant, but control experiments determined these to be largely the off-target effects of doxycycline and not of NRAS-Q61K extinction. **Overall design:** The iNRAS-475 mouse melanoma cell line was injected intradermally into nude mice which were fed 2mg/ml doxycycline water. Tumors were allowed to reach 200-500mm3 after 6 weeks. Mice were then treated with vehicle or 100mg/kg of the AZD6244 MEK inhibitor, or doxycyline was withdrawn from the diet. Each sample represents a distinct tumor and thus provide six biological, not technical replicates per cohort.

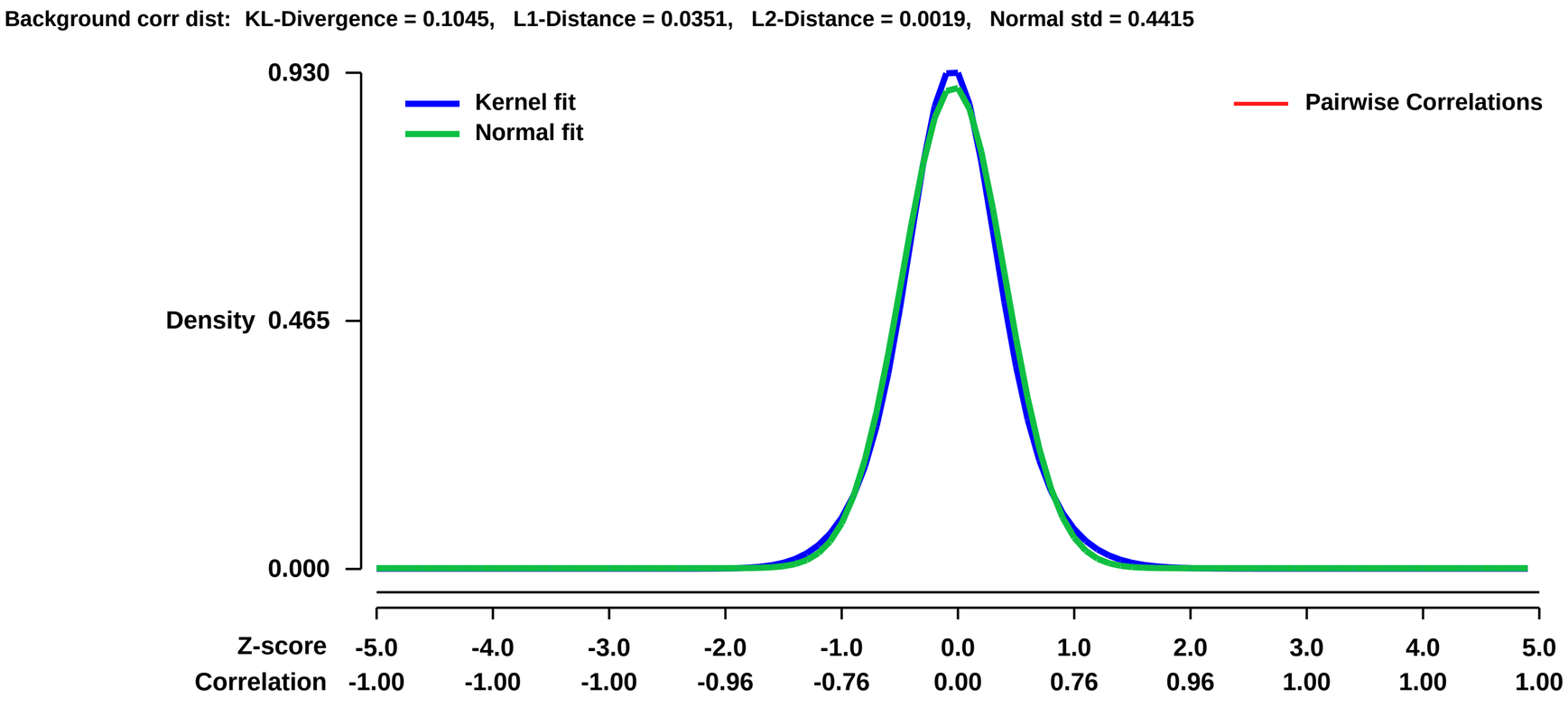

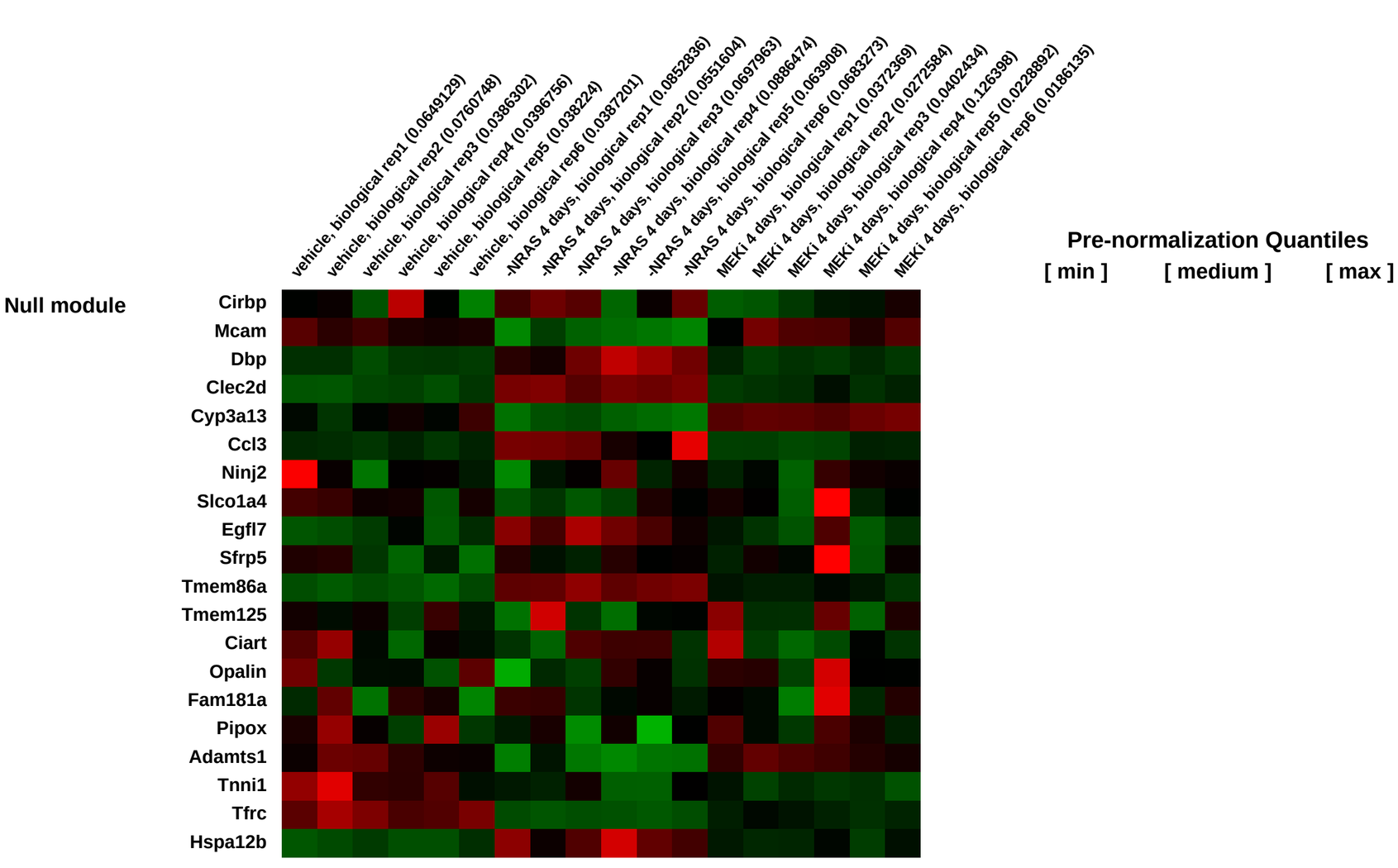

GEO Series "GSE5500" Expression Profiles

Num of samples in this series: 21

Scale of expression profile Z-scores

-3.0 -2.0 -1.0 0.0 1.0 2.0 3.0

GEO Link:	http://www.ncbi.nlm.nih.gov/geo/query/acc.cgi?acc=GSE5500
Status:	Public on Aug 12 2006
Title:	Gata4 is required for postnatal cardiac function and protection from pressure overload-induced heart failure
Organism:	Mus musculus
Experiment type:	Expression profiling by array
Platform:	GPL1261
Pubmed ID:	16983087
Summary & Design:	**Summary:** An important event in the pathogenesis of heart failure is the development of pathological cardiac hypertrophy. In cultured cardiac cardiomyocytes, the transcription factor Gata4 is required for agonist-induced cardiomyocyte hypertrophy. We hypothesized that in the intact organism Gata4 is an important regulator of postnatal heart function and of the hypertrophic response of the heart to pathological stress. To test this hypothesis, we studied mice heterozygous for deletion of the second exon of Gata4 (G4D). At baseline, G4D mice had mild systolic and diastolic dysfunction associated with reduced heart weight and decreased cardiomyocyte number. After transverse aortic constriction (TAC), G4D mice developed overt heart failure and eccentric cardiac hypertrophy, associated with significantly increased fibrosis and cardiomyocyte apoptosis. Inhibition of apoptosis by overexpression of the insulin-like growth factor 1 receptor prevented TAC-induced heart failure in G4D mice. Unlike WT-TAC controls, G4D-TAC cardiomyocytes hypertrophied by increasing in length more than width. Gene expression profiling revealed upregulation of genes associated with apoptosis and fibrosis, including members of the TGF? pathway. Our data demonstrate that Gata4 is essential for cardiac function in the postnatal heart. After pressure overload, Gata4 regulates the pattern of cardiomyocyte hypertrophy and protects the heart from load-induced failure. **Keywords:** genetic modification, pressure overload stress response **Overall design:** overload.

Background corr dist: KL-Divergence = 0.1638, L1-Distance = 0.0479, L2-Distance = 0.0053, Normal std = 0.3620

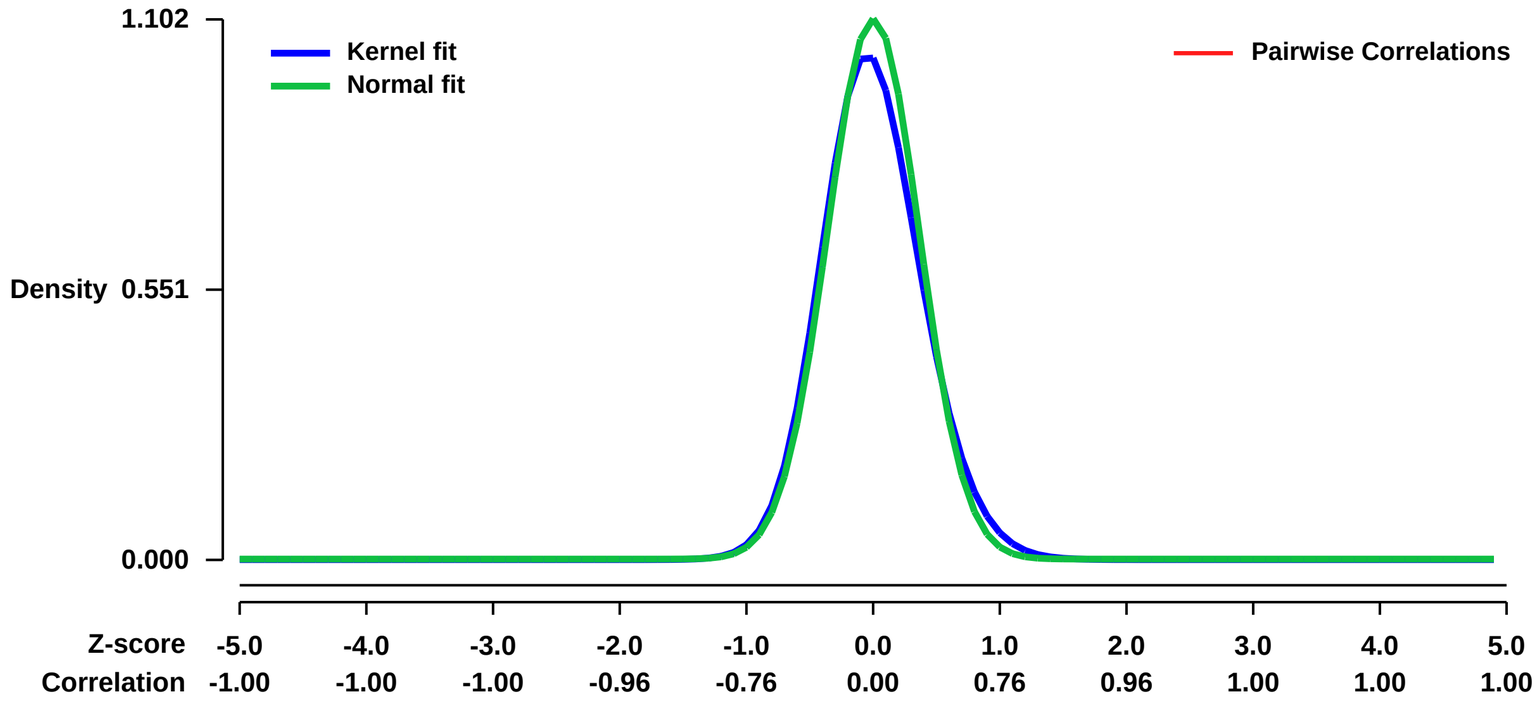

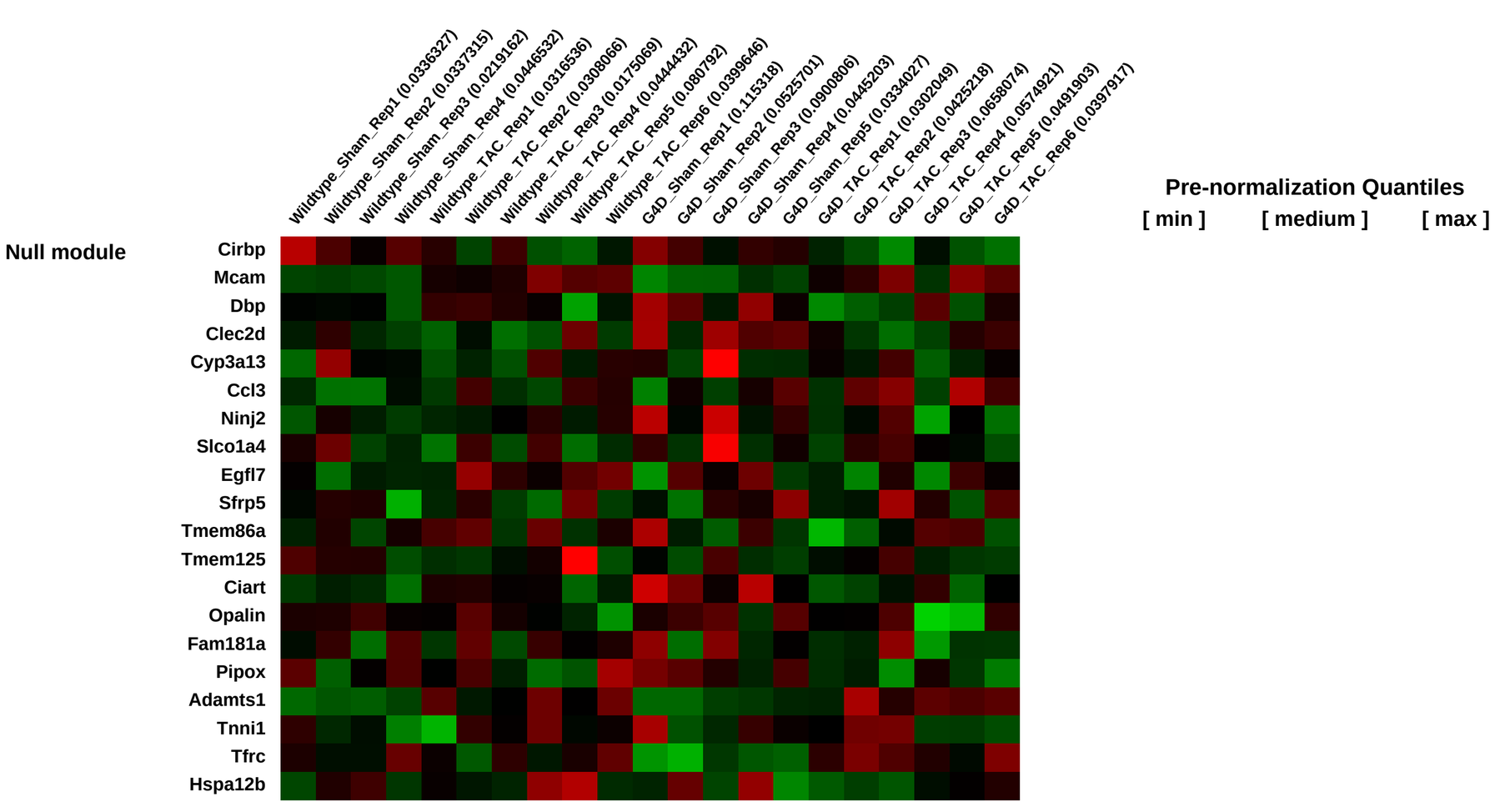

GEO Series "GSE55003" Expression Profiles

Num of samples in this series: 12

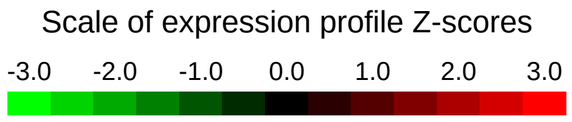

GEO Link:	**http://www.ncbi.nlm.nih.gov/geo/query/acc.cgi?acc=GSE55003**
Status:	**Public on Feb 18 2014**
Title:	**Expression profiling by array in livers of Nrf2 null mice administered CDDO-IM**
Organism:	**Mus musculus**
Experiment type:	**Expression profiling by array**
Platform:	**GPL1261**
Pubmed ID:	
Summary & Design:	**Summary:** **Nrf2 null mice administered CDDO-IM** **Overall design:** **Nrf2 null mice treated with CDDO-IM**

Background corr dist: **KL-Divergence = 0.0863, L1-Distance = 0.0388, L2-Distance = 0.0031, Normal std = 0.4590**

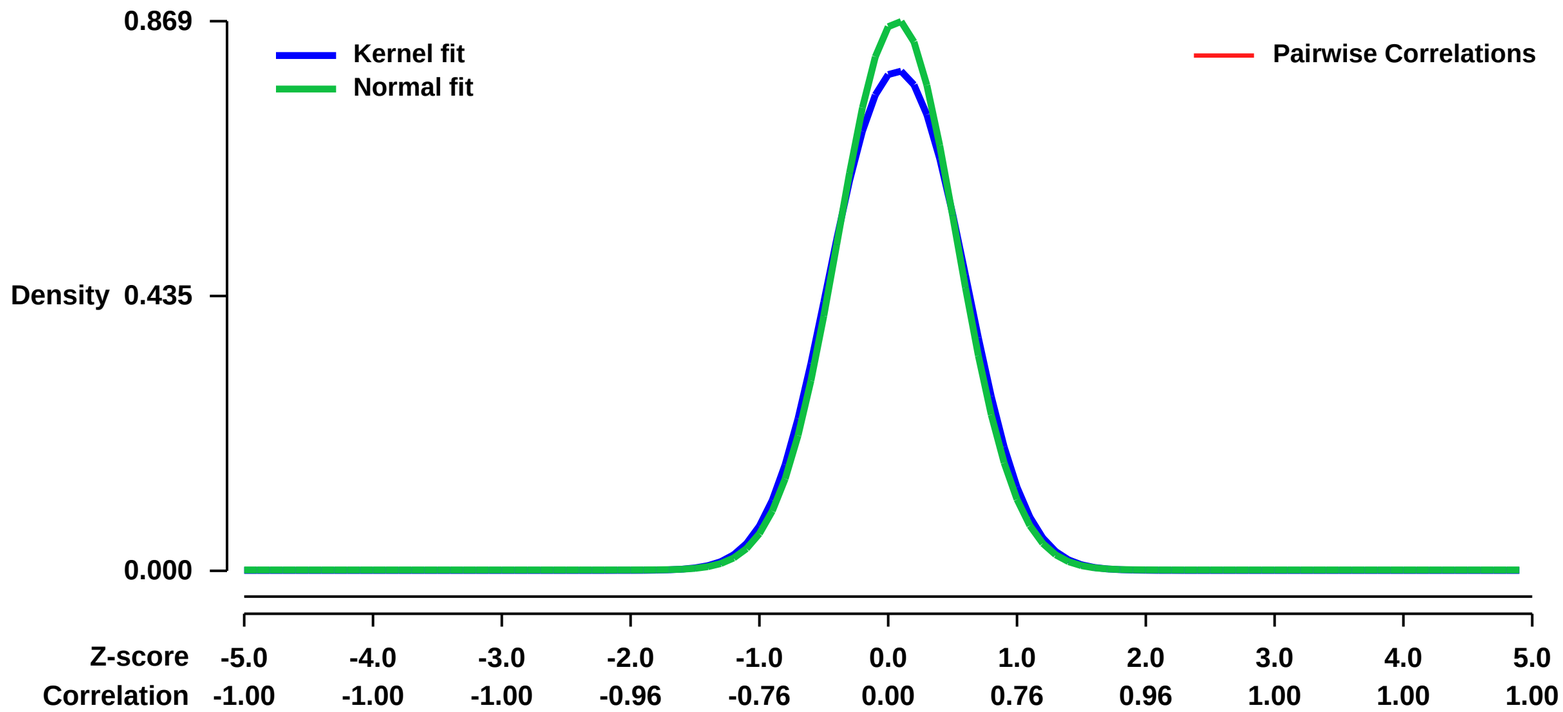

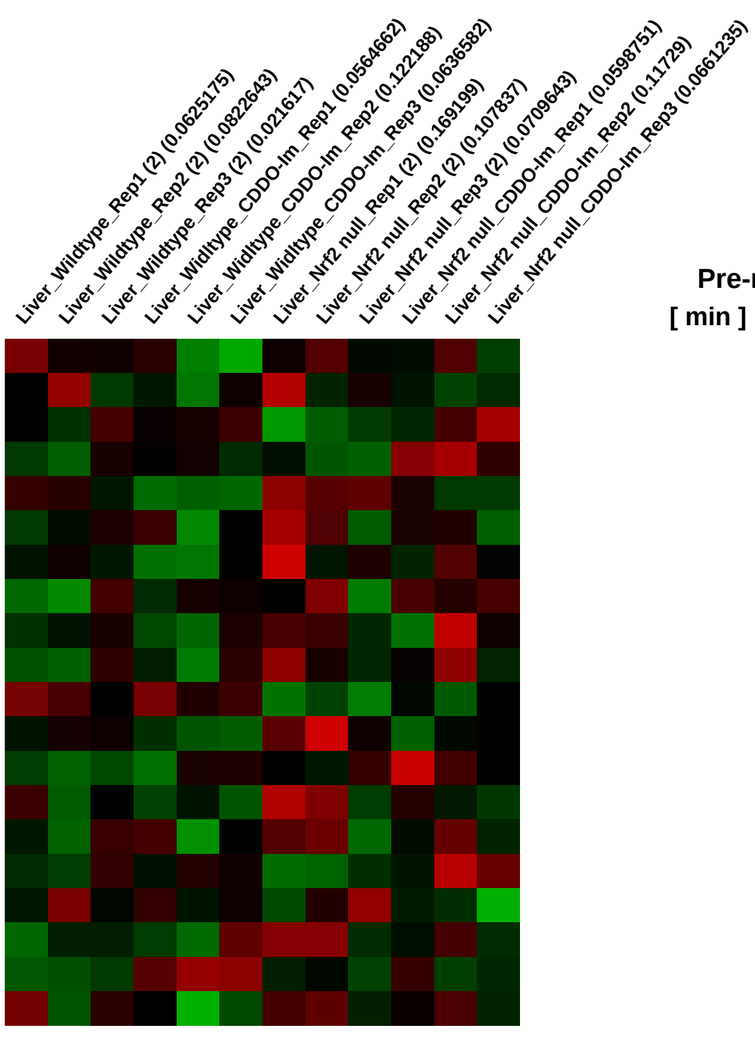

GEO Series "GSE14308" Expression Profiles

Num of samples in this series: 12

Scale of expression profile Z-scores

-3.0 -2.0 -1.0 0.0 1.0 2.0 3.0

GEO Link:	http://www.ncbi.nlm.nih.gov/geo/query/acc.cgi?acc=GSE14308
Status:	Public on Jan 08 2009
Title:	Epigenetic Mechanisms Underlie T Cell Plasticity
Organism:	Mus musculus
Experiment type:	Expression profiling by array
Platform:	GPL1261
Pubmed ID:	19144320
Summary & Design:	**Summary:** Multipotential naˆflve CD4+ T cells differentiate into distinct lineages including T helper 1 (Th1), Th2, Th17, and inducible T regulatory (iTreg) cells. The remarkable diversity of CD4+ T cells begs the question whether the observed changes reflect terminal differentiation with heritable epigenetic modifications or plasticity in T cell responses. We generated genome-wide histone H3 lysine 4 (H3K4) and lysine 27 (H3K27) trimethylation maps in naˆflve, Th1, Th2, Th17, iTreg, and natural (n)Treg cells. We found that although modifications of signature cytokine genes (Ifng, Il4, and Il17) partially conform to the expectation of lineage commitment, critical transcription factors such as Tbx21 exhibit a broad spectrum of epigenetic states, consistent with our demonstration of T-bet and IFN-gamma induction in nTreg cells. Our data suggest an epigenetic mechanism underlying the specificity and plasticity of effector and regulatory T cells and also provide a framework for understanding complexity of CD4+ T helper cell differentiation. **Overall design:** Different T helper subsets are profiled for mRNA expression.

Background corr dist: KL-Divergence = 0.0943, L1-Distance = 0.0377, L2-Distance = 0.0025, Normal std = 0.4622

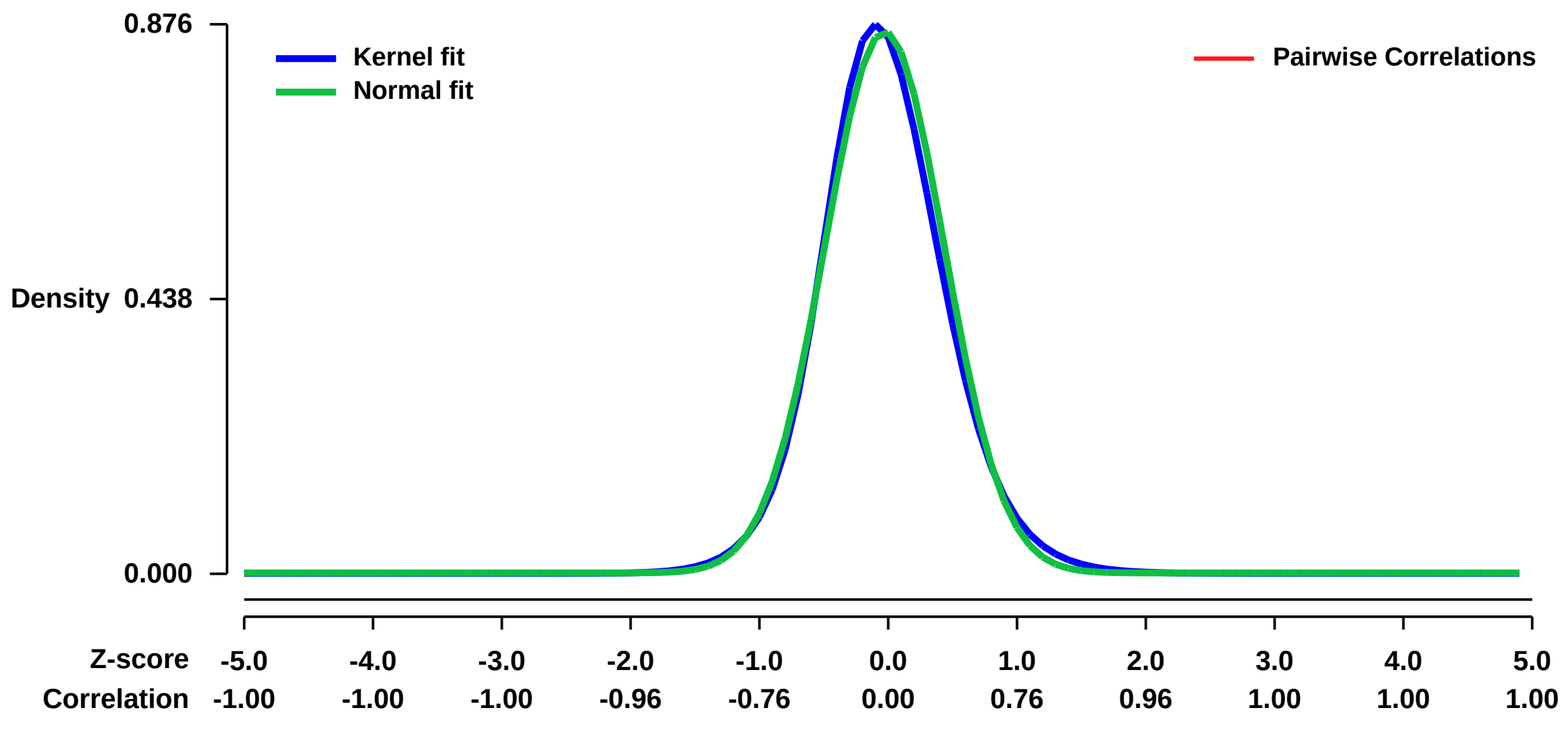

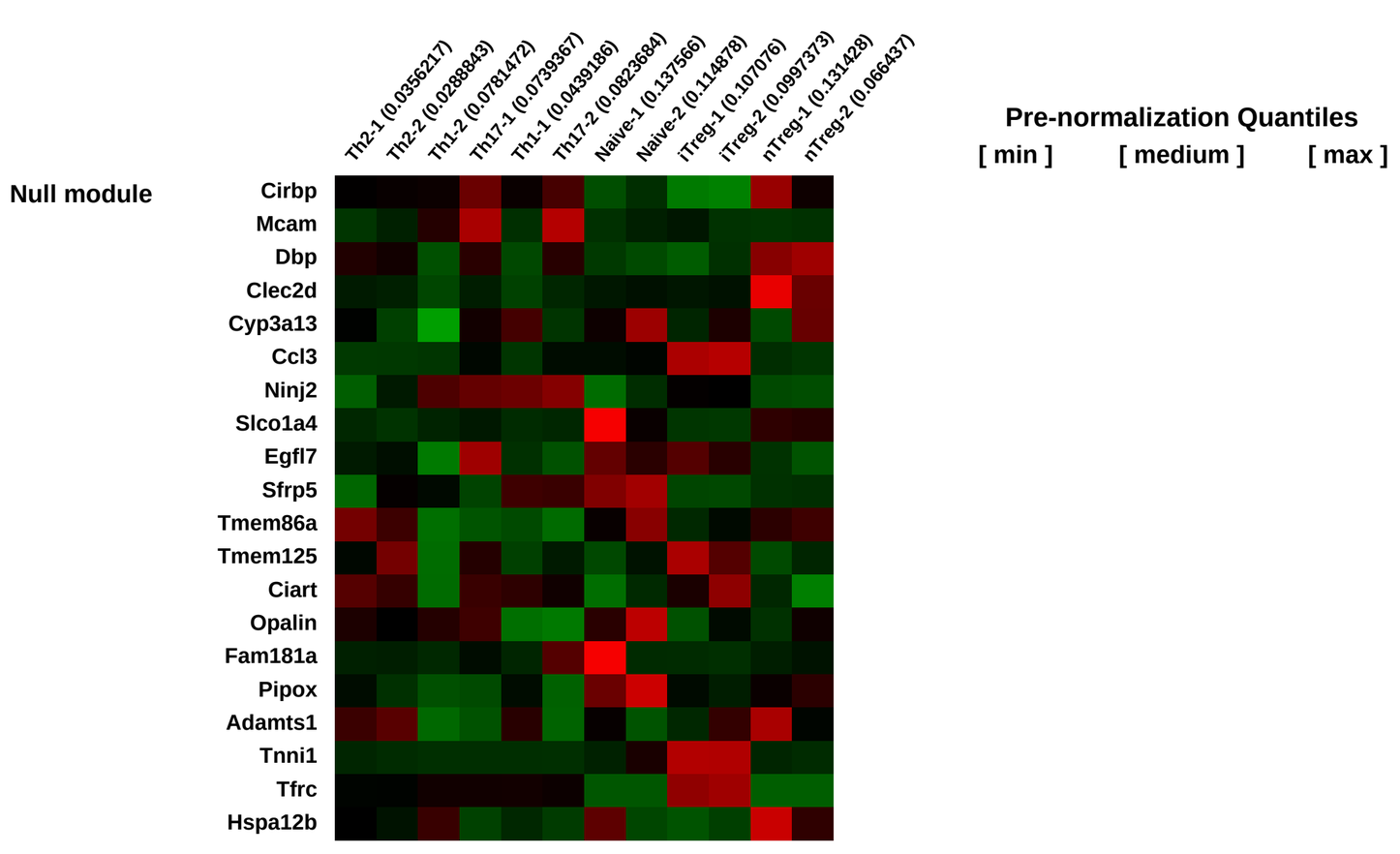

GEO Series "GSE52542" Expression Profiles

Num of samples in this series: 9

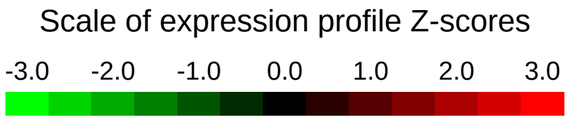

GEO Link:	http://www.ncbi.nlm.nih.gov/geo/query/acc.cgi?acc=GSE52542
Status:	Public on Nov 21 2013
Title:	VEGF Isoform Transcriptome Changes in the E9.5 Murine Forebrain
Organism:	Mus musculus
Experiment type:	Third-party reanalysis
Platform:	GPL1261
Pubmed ID:	24124161
Summary & Design:	**Summary:** Regulation of neural stem cell (NSC) fate decisions is critical during the transition from a multicellular mammalian forebrain neuroepithelium to the multilayered neocortex. Forebrain development requires coordinated vascular investment alongside NSC differentiation. Vascular endothelial growth factor A (Vegf) has proven to be a pleiotrophic gene whose multiple protein isoforms regulate a broad range of effects in neurovascular systems. To test the hypothesis that the Vegf isoforms (120, 164, and 188) are required for normal forebrain development, we analyzed the forebrain transcriptome of mice expressing specific Vegf isoforms, Vegf120, VegfF188, or a combination of Vegf120/188. Transcriptome analysis identified differentially expressed genes in embryonic day (E) 9.5 forebrain, a time point preceding dramatic neuroepithelial expansion and vascular investment in the telencephalon. Meta-analysis identified gene pathways linked to chromosome-level modifications, cell fate regulation, and neurogenesis that were altered in Vegf isoform mice. **Overall design:** This study comprises of new samples and reanalysis of Samples from GSE30767 and GSE8091.

Background corr dist: KL-Divergence = 0.0176, L1-Distance = 0.0390, L2-Distance = 0.0022, Normal std = 0.7805

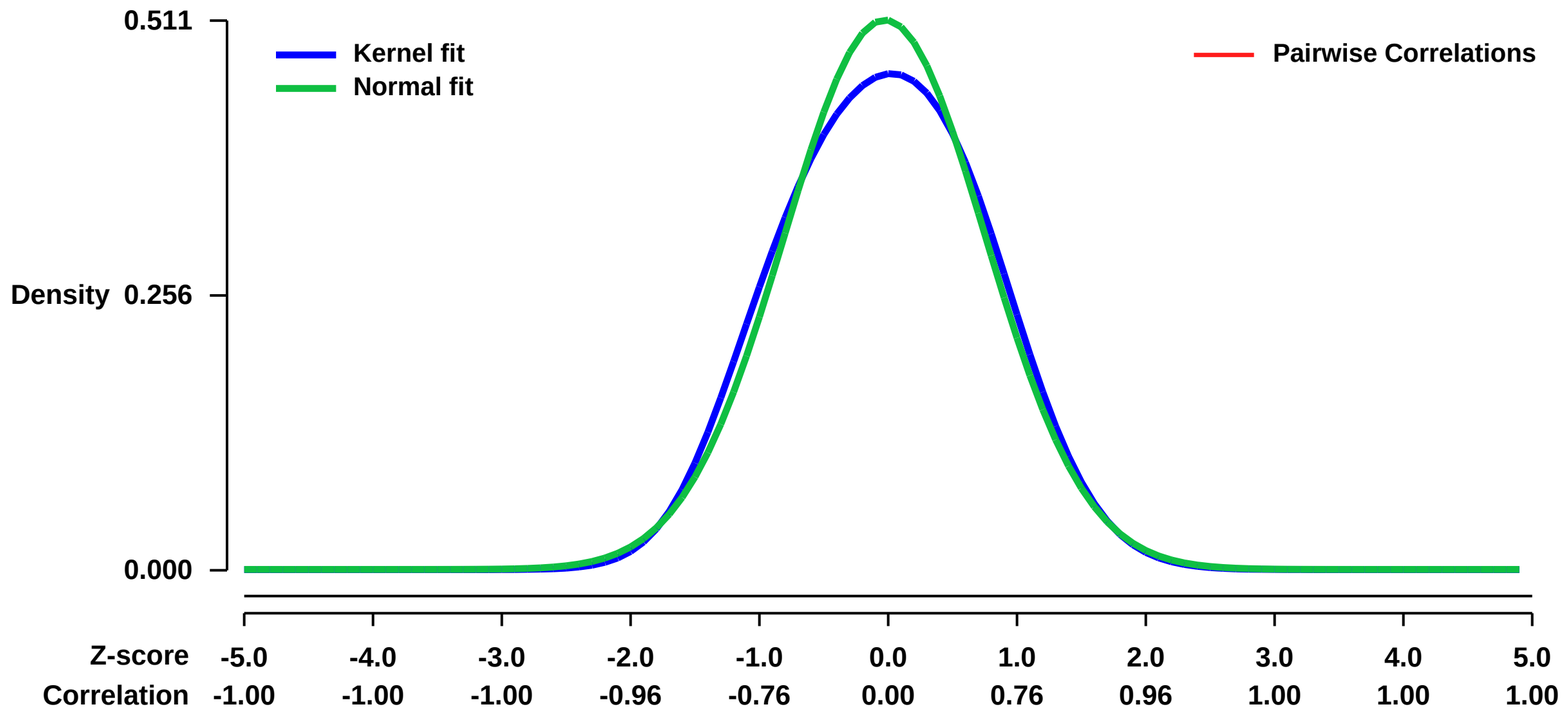

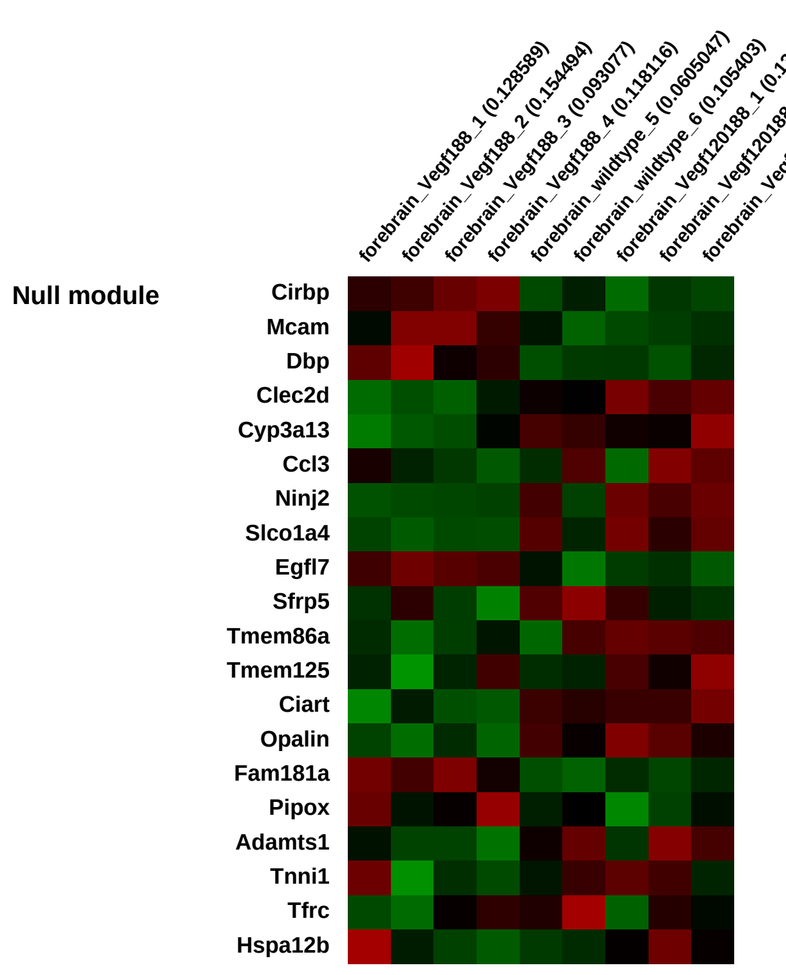

Pre-normalization Quantiles

[min] [medium] [max]

GEO Series "GSE55756" Expression Profiles

Num of samples in this series: 47

Scale of expression profile Z-scores

-3.0 -2.0 -1.0 0.0 1.0 2.0 3.0

GEO Link:	http://www.ncbi.nlm.nih.gov/geo/query/acc.cgi?acc=GSE55756
Status:	Public on Mar 17 2014
Title:	Transcription profiling of mouse liver by array
Organism:	Mus musculus
Experiment type:	Expression profiling by array
Platform:	GPL1261
Pubmed ID:	
Summary & Design:	**Summary:** PPARα−-null and wild-type male mice treated with PFHxS or PFNA **Overall design:** PPARα−-null and wild-type male mice at 6-9 months of age were dosed by gavage for 7 consecutive days with either 0, 3, or 10 mg/kg´ PFHxS, or 1 or 3 mg/kg PFNA (#394459, Sigma-Aldrich, St, Louis, MO) in water.´ PFHxS was kindly provided by 3M Corp (St. Paul, MN).´ Four biological replicates consisting of individual animals were included in each dose group.´ Dose levels reflected exposures that produce hepatomegaly in adult mice without inducing overt toxicity.

Background corr dist: KL-Divergence = 0.3832, L1-Distance = 0.0705, L2-Distance = 0.0143, Normal std = 0.2527

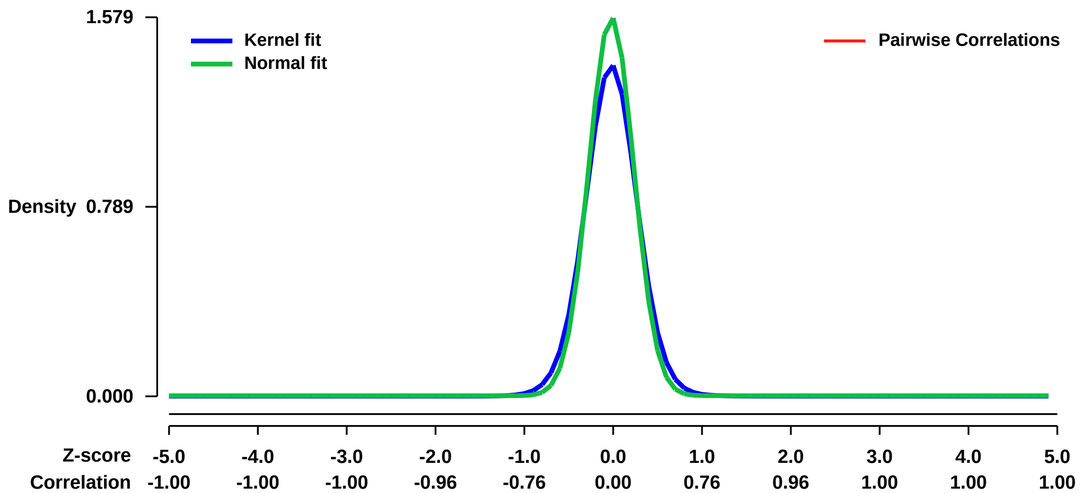

Z-score	-5.0	-4.0	-3.0	-2.0	-1.0	0.0	1.0	2.0	3.0	4.0	5.0
Correlation	-1.00	-1.00	-1.00	-0.96	-0.76	0.00	0.76	0.96	1.00	1.00	1.00

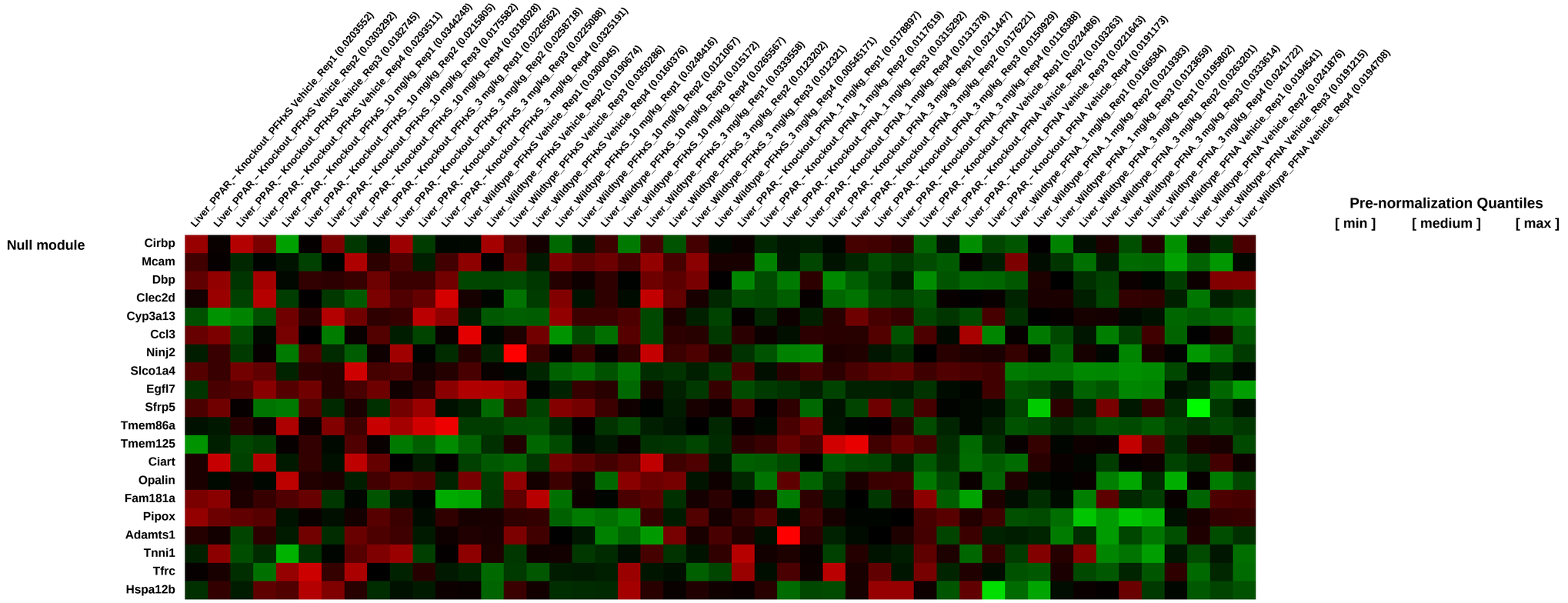

GEO Series "GSE11982" Expression Profiles

Num of samples in this series: 6

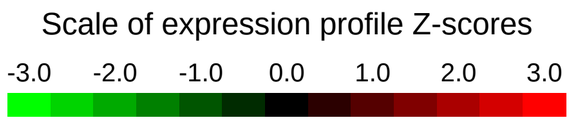

GEO Link:	http://www.ncbi.nlm.nih.gov/geo/query/acc.cgi?acc=GSE11982
Status:	Public on Aug 31 2008
Title:	Expression data from WT and E2A-KO bone marrow stem and progenitor cell subfractions.
Organism:	Mus musculus
Experiment type:	Expression profiling by array
Platform:	GPL1261
Pubmed ID:	
Summary & Design:	**Summary:** Expression profiling of WT and E2A-KO LSK FLT3- and LMPP protenitor cells. **Overall design:** LSK FLT3- and LMPP stem/progenitor cells from WT and E2A-KO mice were FACS sorted. Subsequently RNA was extracted, labelled and hybridized to Affymetrix microarrays. Goal of experiment was to investigate expression changes between WT and KO LMPP cells.

Background corr dist: KL-Divergence = 0.0196, L1-Distance = 0.0664, L2-Distance = 0.0066, Normal std = 0.8601

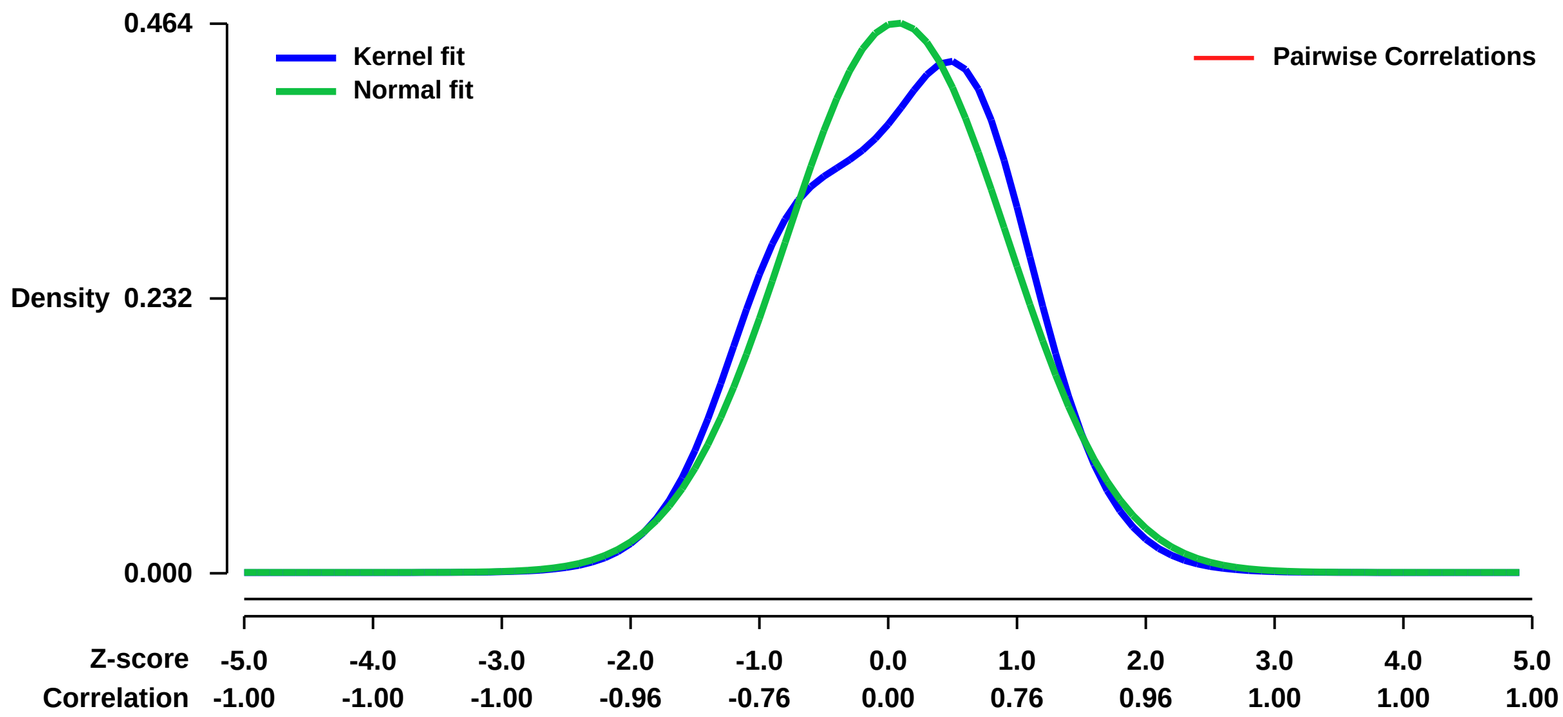

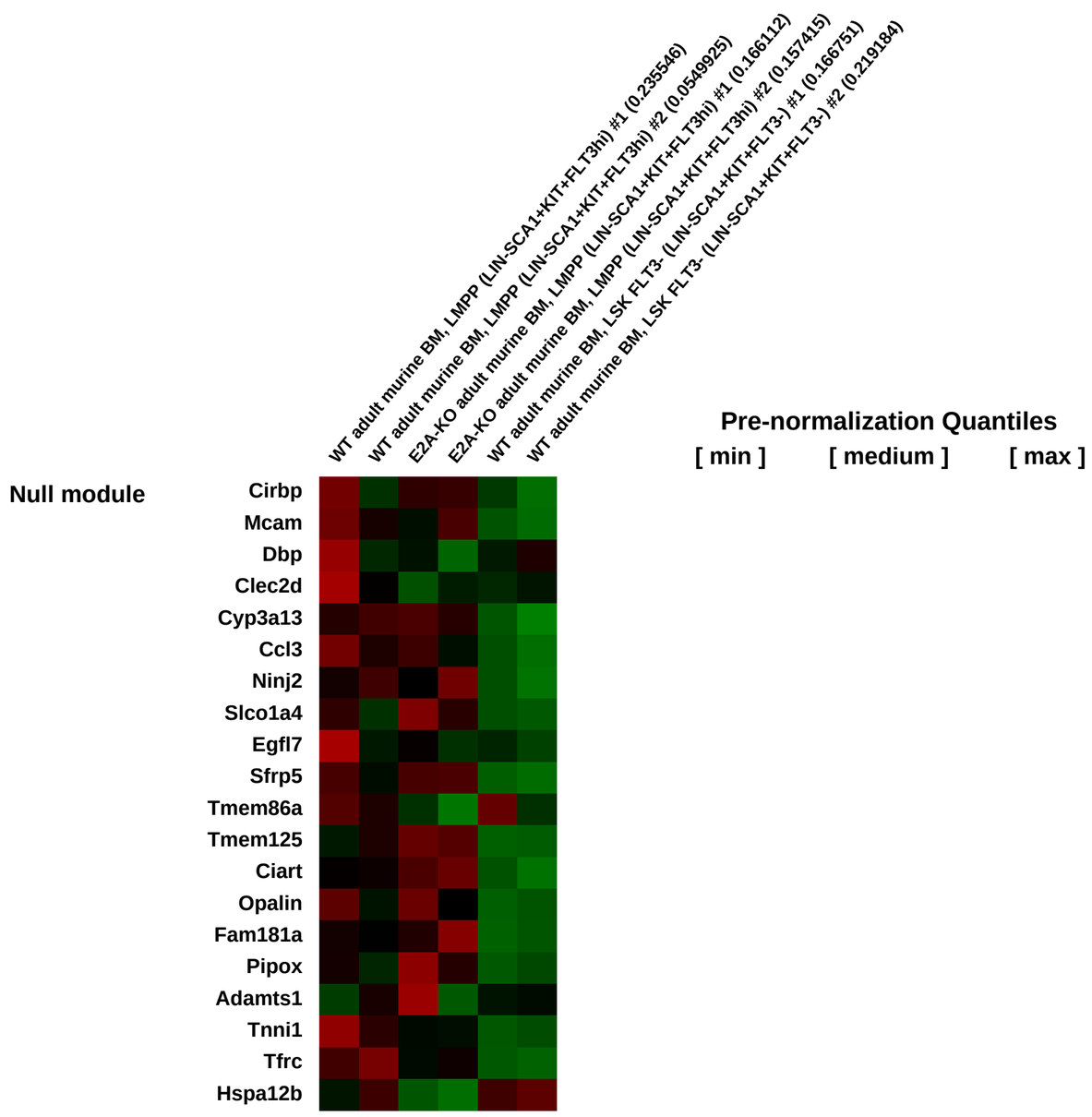

GEO Series "GSE15146" Expression Profiles

Num of samples in this series: 10

Scale of expression profile Z-scores

-3.0 -2.0 -1.0 0.0 1.0 2.0 3.0

GEO Link:	http://www.ncbi.nlm.nih.gov/geo/query/acc.cgi?acc=GSE15146
Status:	Public on Aug 06 2009
Title:	mRNA expression in Zfp36L2 knockout E14.5 fetal liver
Organism:	Mus musculus
Experiment type:	Expression profiling by array
Platform:	GPL1261
Pubmed ID:	19633199
Summary & Design:	**Summary:** ZFP36L2, zinc finger protein 36, C3H type-like 2 (also known as Brf2, Erf2, Tis11D) is a member of the tristetraprolin (TTP; Zfp36) family of tandem CCCH zinc finger proteins that can bind to AU-rich elements (AREs) in the 3'-untranslated region of mRNAs, leading to their deadenylation and subsequent degradation. We have generated Zfp36l2 knockout mice. Knockout mice were born at the expected Mendelian frequency, but within several weeks of birth they died rather suddenly with pallor and frequent intestinal hemorrhage. These mice exhibited pancytopenia, decreased hematopoietic progenitor cells from fetal liver and yolk sac, and ineffective hematopoietic stem cells. Since ZFP26L2 is likely to function as an ARE-containing mRNA destabilizing protein, we were interested in identifying any abnormally stabilized transcripts in fetal livers from the Zfp36l2 knockout mice whose protein product may directly or indirectly affect hematopoietic stem cell function. **Overall design:** Total RNA was isolated from individual embryonic day 14.5 fetal livers. Five wild type and five knockout fetal livers were used to generate 5 wild type replicates and 5 knockout replicates. RNA expression from knockout fetal livers was compared to wild type fetal livers.

Background corr dist: KL-Divergence = 0.1379, L1-Distance = 0.0224, L2-Distance = 0.0011, Normal std = 0.3872

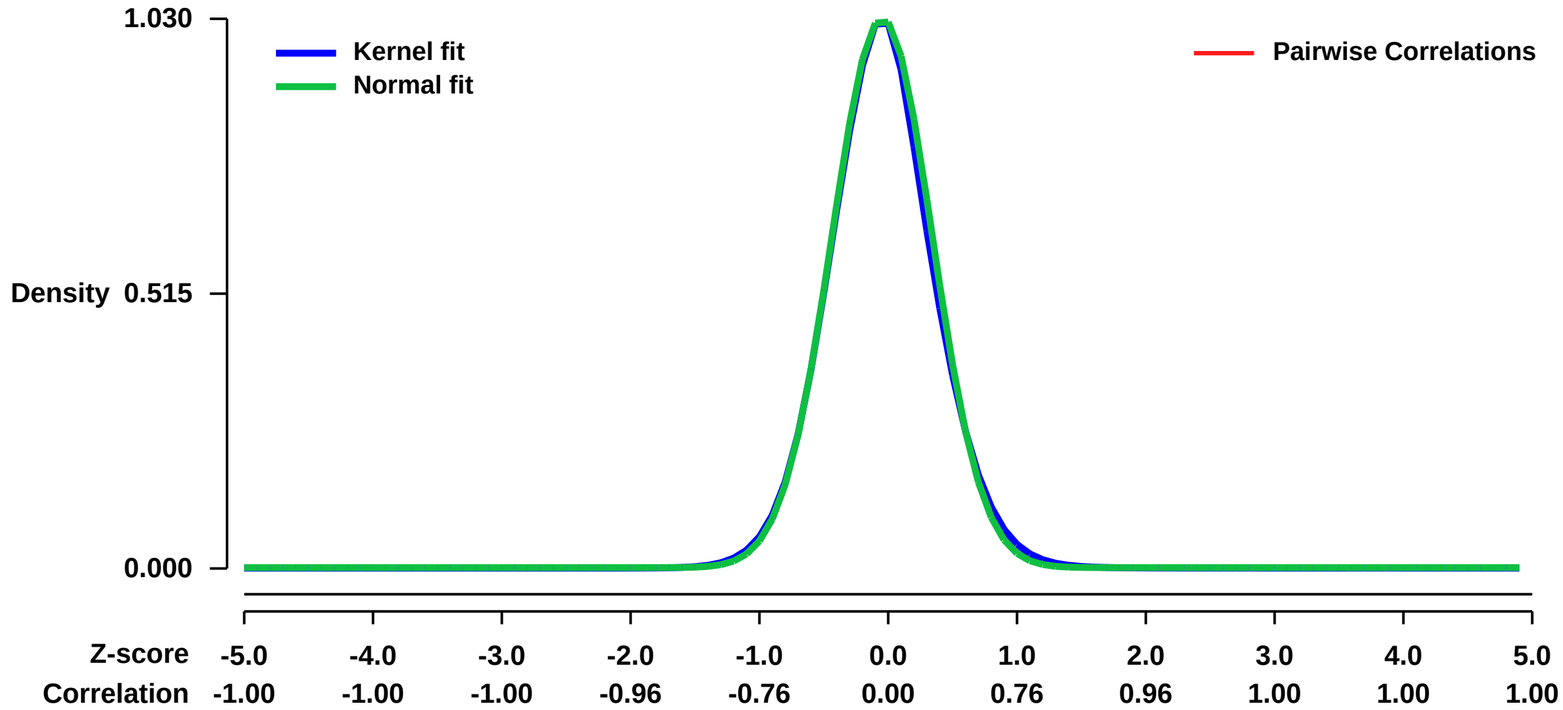

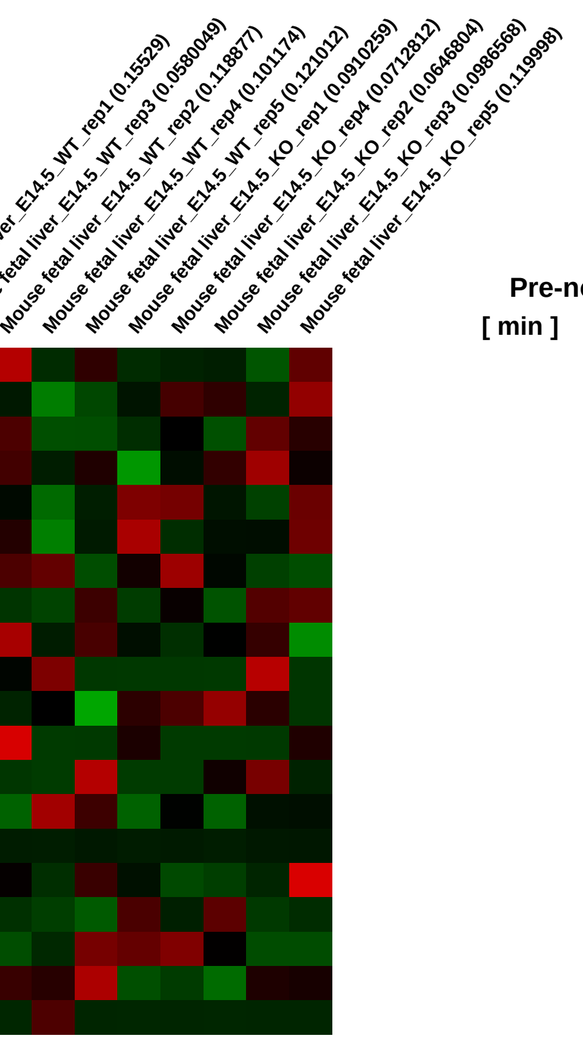

GEO Series "GSE32354" Expression Profiles

Num of samples in this series: 35

Scale of expression profile Z-scores

-3.0 -2.0 -1.0 0.0 1.0 2.0 3.0

GEO Link:	http://www.ncbi.nlm.nih.gov/geo/query/acc.cgi?acc=GSE32354
Status:	Public on Aug 31 2012
Title:	Expression data from E2f7/E2f8 and E2f1/E2f2/E2f3 null liver (Affymetrix)
Organism:	Mus musculus
Experiment type:	Expression profiling by array
Platform:	GPL1261
Pubmed ID:	23064266
Summary & Design:	**Summary:** To understand the underlying cause and mechanisms of changes in hepatocyte ploidy upon Albumin-Cre mediated deletion of E2f7&8 and Mx1-Cre mediated deletion of E2f1,2&3, we analysed global gene expression of 6 weeks and 2 months liver tissues. **Overall design:** RNA was extracted from liver tissues. Gene deletion in samples confirmed by PCR genotyping of DNA isolated from each sample.

Background corr dist: KL-Divergence = 0.0592, L1-Distance = 0.0367, L2-Distance = 0.0023, Normal std = 0.5299

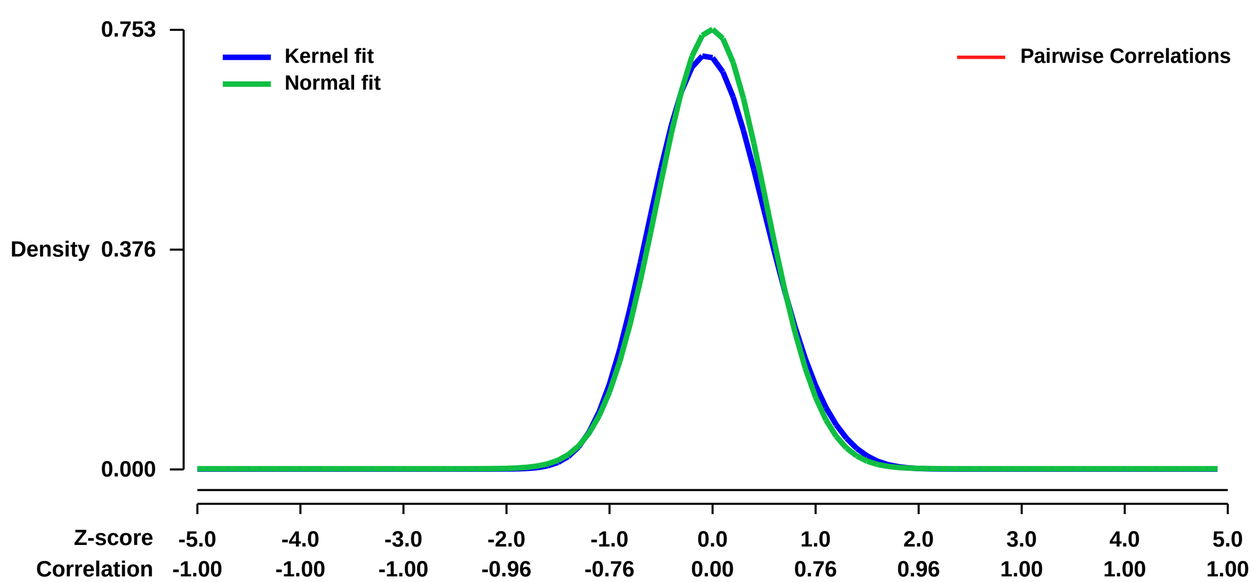

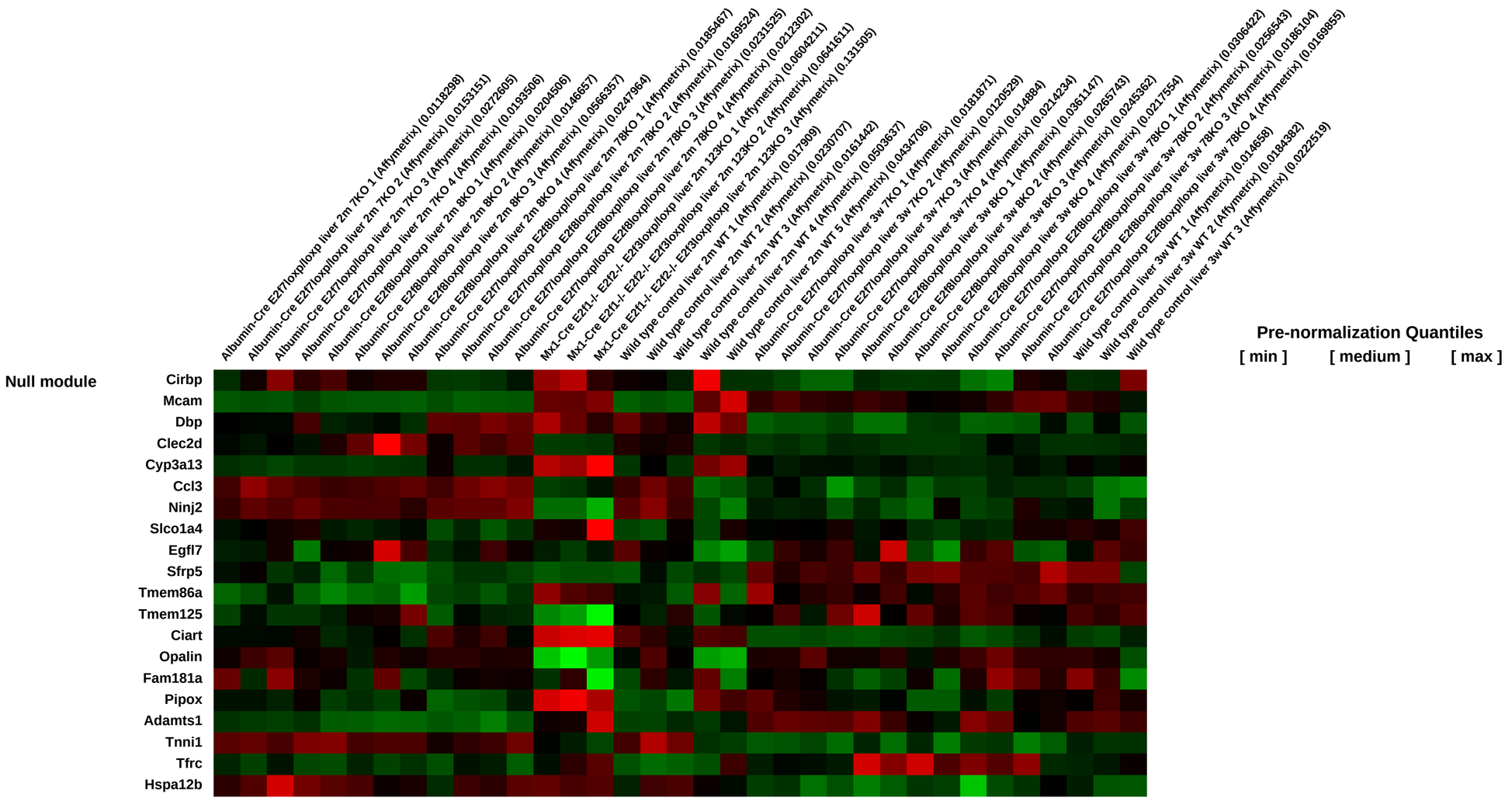

GEO Series "GSE8044" Expression Profiles

Num of samples in this series: 6

Scale of expression profile Z-scores

-3.0 -2.0 -1.0 0.0 1.0 2.0 3.0

GEO Link:	**http://www.ncbi.nlm.nih.gov/geo/query/acc.cgi?acc=GSE8044**
Status:	**Public on Jun 08 2007**
Title:	**Brown versus white tissue adipose selective genes**
Organism:	**Mus musculus**
Experiment type:	**Expression profiling by array**
Platform:	**GPL1261**
Pubmed ID:	**17618855**
Summary & Design:	**Summary:** **The aim of this study was to identify genes expressed selectively in brown adipose tissue as compared to white adipose tissue from the same animals. This analysis provides a gene set that is brown and white adipose selective.** **Keywords: tissue comparison from mice** **Overall design:** **Interscapular brown adipose tissue and epididymal white adipose tissue was carefully dissected from 3 male C57Bl/6 mice. These samples were profiled independently using Affymetrix mouse 430_2 gene arrays, representing 3 biological replicates for each brown and white adipose tissues.**

Background corr dist: **KL-Divergence = 0.0069, L1-Distance = 0.0138, L2-Distance = 0.0002, Normal std = 0.9444**

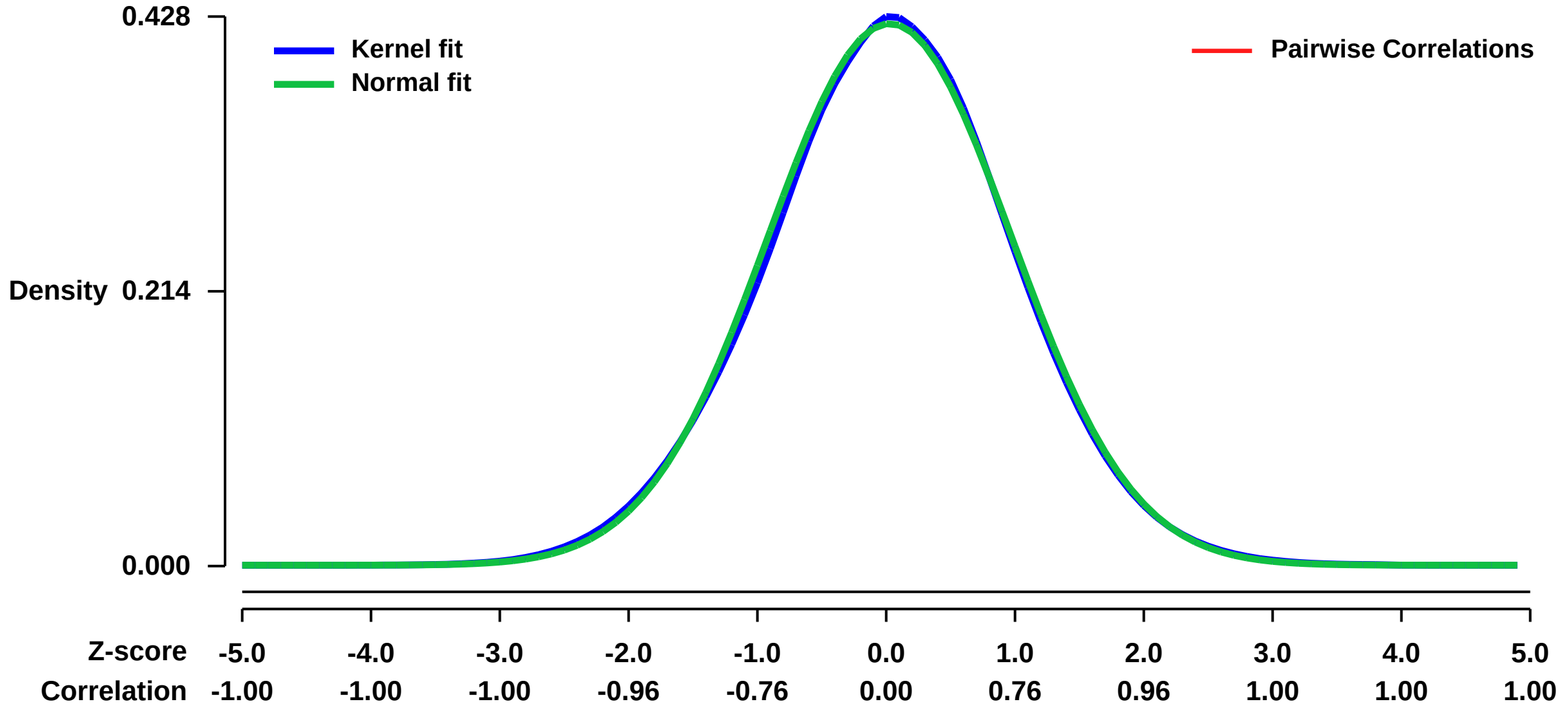

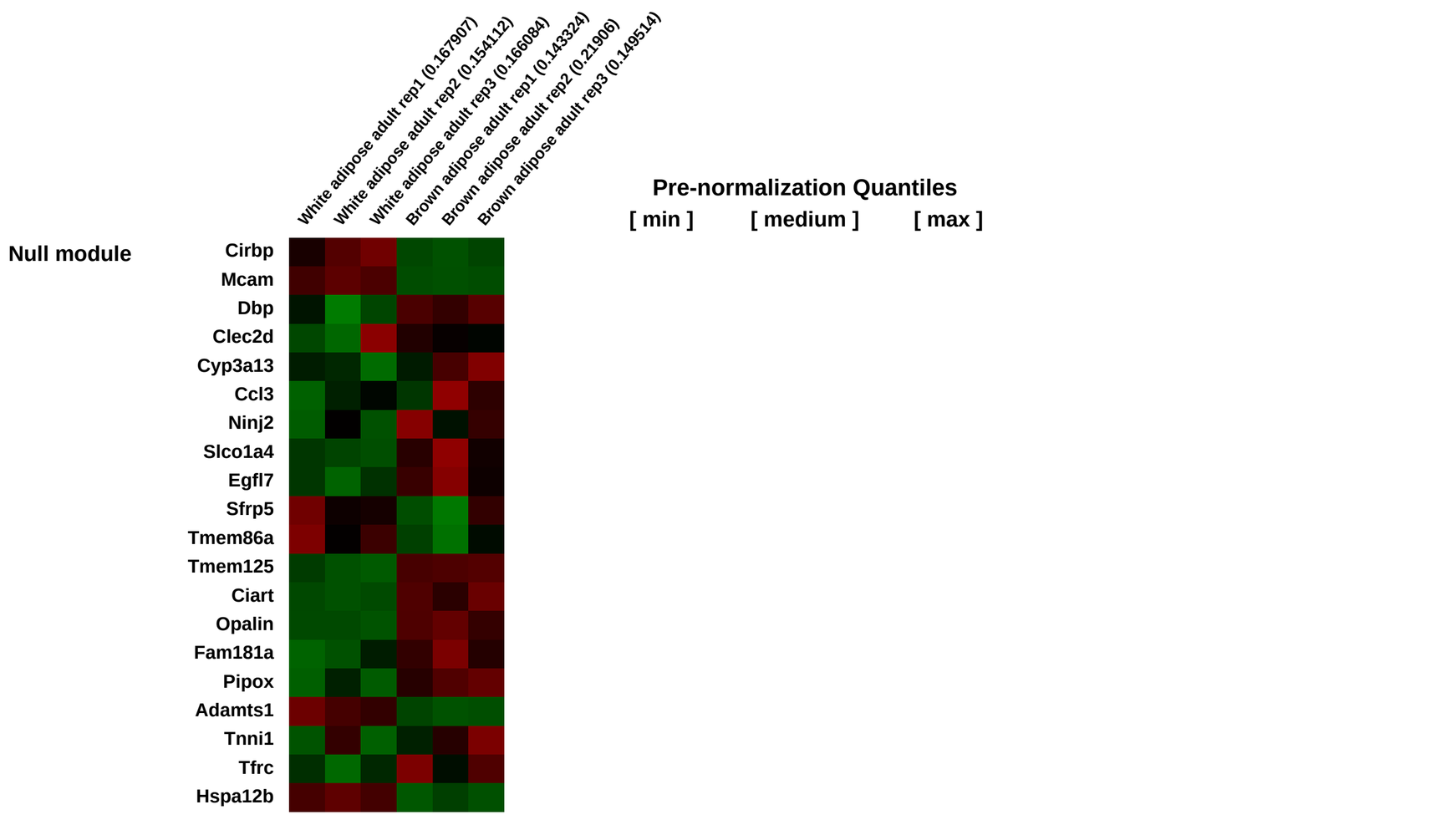

GEO Series "GSE11818" Expression Profiles

Num of samples in this series: 6

Scale of expression profile Z-scores

-3.0 -2.0 -1.0 0.0 1.0 2.0 3.0

GEO Link:	http://www.ncbi.nlm.nih.gov/geo/query/acc.cgi?acc=GSE11818
Status:	Public on Jun 20 2008
Title:	Selective miRNA disruption in Tregs leads to uncontrolled autoimmunity
Organism:	Mus musculus
Experiment type:	Expression profiling by array
Platform:	GPL1261
Pubmed ID:	18725525
Summary & Design:	**Summary:** A new Treg-specific, FoxP3-GFP-hCre BAC transgenic was crossed to a conditional Dicer knock-out mouse strain to analyze the role of microRNAs (miRNA) in the development and function of regulatory T cells (Tregs). Although thymic Tregs developed normally in this setting, the cells showed evidence of altered differentiation and dysfunction in the periphery. Dicer-deficient Treg lineage cells failed to remain stable as a subset of cells down-regulated the Treg-specific transcription factor, FoxP3, while the majority expressed altered levels of multiple genes and proteins (including Neuropilin 1, GITR and CTLA-4) associated with the Treg fingerprint. In fact, a significant percentage of the Treg lineage cells took on a Th memory phenotype including increased levels of CD127, IL-4, and interferon-g. Importantly, Dicer-deficient Tregs lost suppression activity in vivo; the mice rapidly developed fatal systemic autoimmune disease resembling the FoxP3 knockout phenotype. These results support a central role for miRNAs in maintaining the stability of differentiated Treg function in vivo and homeostasis of the adaptive immune system. **Overall design:** Lymph node CD4+YFP+ T cells from FoxP3-GFP-hCre x ROSA26R-YFP Dicerwt/lox (Het) and FoxP3-GFP-hCre x ROSA26R-YFP Dicerlox/lox (KO) mice were isolated by flow cytometry. Triplicate GeneChips were used for each T cell population.

Background corr dist: KL-Divergence = 0.0337, L1-Distance = 0.0497, L2-Distance = 0.0029, Normal std = 0.7485

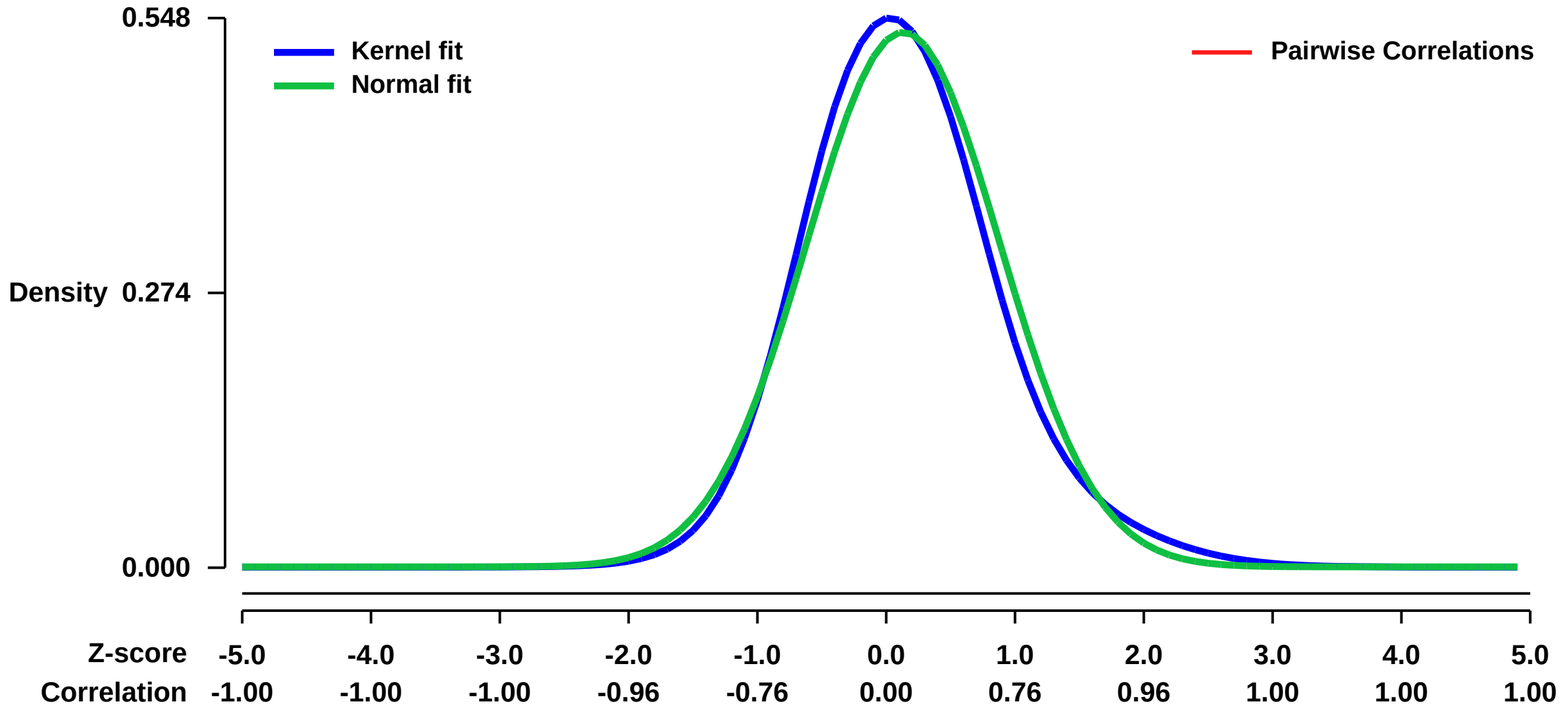

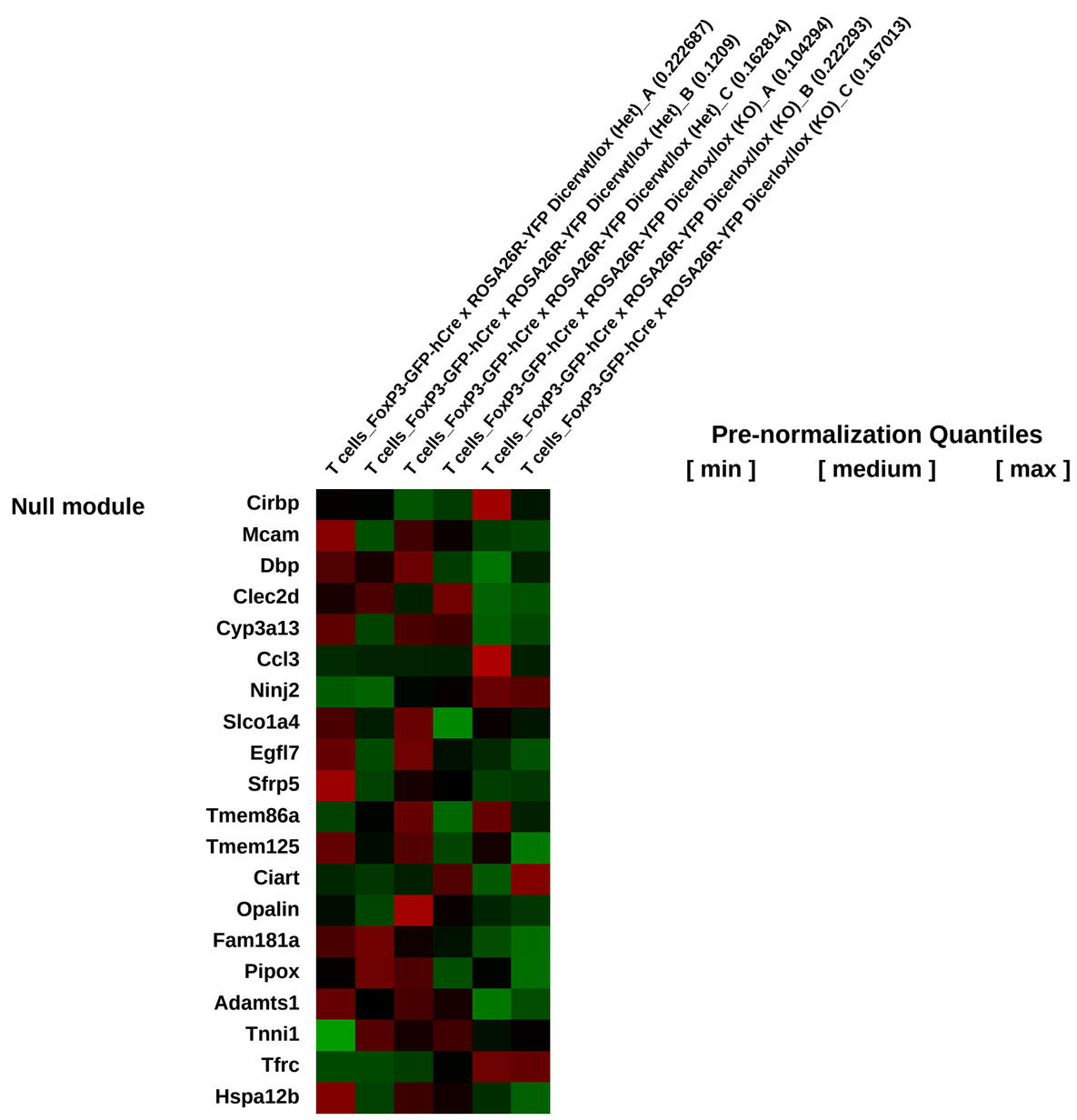

GEO Series "GSE11018" Expression Profiles

Num of samples in this series: 6

Scale of expression profile Z-scores

-3.0 -2.0 -1.0 0.0 1.0 2.0 3.0

GEO Link:	http://www.ncbi.nlm.nih.gov/geo/query/acc.cgi?acc=GSE11018
Status:	Public on Jun 01 2008
Title:	Effect of BMPR2-R899X mutation in lung with and without elevated RVSP
Organism:	Mus musculus
Experiment type:	Expression profiling by array
Platform:	GPL1261
Pubmed ID:	18723761
Summary & Design:	**Summary:** Familial pulmonary arterial hypertension (fPAH) is associated with mutations in BMPR2. Many of these mutations occur in the BMPR2 tail domain, leaving the SMAD functions intact. In order to determine the in vivo consequences of BMPR2 tail domain mutation, we created a smooth-muscle specific doxycycline inducible BMPR2 mutation with an arginine to termination mutation at amino acid 899. When these SM22-rtTA x TetO7-BMPR2R899X mice had transgene induced for 9 weeks, starting at 4 weeks of age, they universally developed pulmonary vascular pruning as assessed by fluorescent microangiography. Approximately half the time the induced animals developed elevated right ventricular systolic pressures (RVSP), associated with extensive pruning, muscularization of small pulmonary vessels, and development of large structural pulmonary vascular changes. These lesions included large numbers of macrophages and T-cells in their adventitial compartment, as well as CD133 positive cells in the lumen. Small vessels filled with CD45 positive and sometimes CD3 positive cells were a common feature in all SM22-rtTA x TetO7-BMPR2R899X mice. Gene array experiments show changes in stress response, muscle organization and function, proliferation and apoptosis, and developmental pathways before RVSP increases. Our results show that the primary phenotypic result of BMPR2 tail domain mutation in smooth muscle is pulmonary vascular pruning leading to elevated RVSP, associated with early dysregulation in multiple pathways with clear relevance to PAH. This model should be useful to the research community in examining early molecular and physical events in the development of PAH, and as a platform to validate potential treatments. **Keywords:** Disease state analysis **Overall design:** Each array is an individual female mouse, age-matched, with two mice & arrays used for each of controls (transactivator only), BMPR2-R899X with normal RVSP, and BMPR2-R899X with high RVSP.

Background corr dist: KL-Divergence = 0.0448, L1-Distance = 0.0170, L2-Distance = 0.0003, Normal std = 0.5915

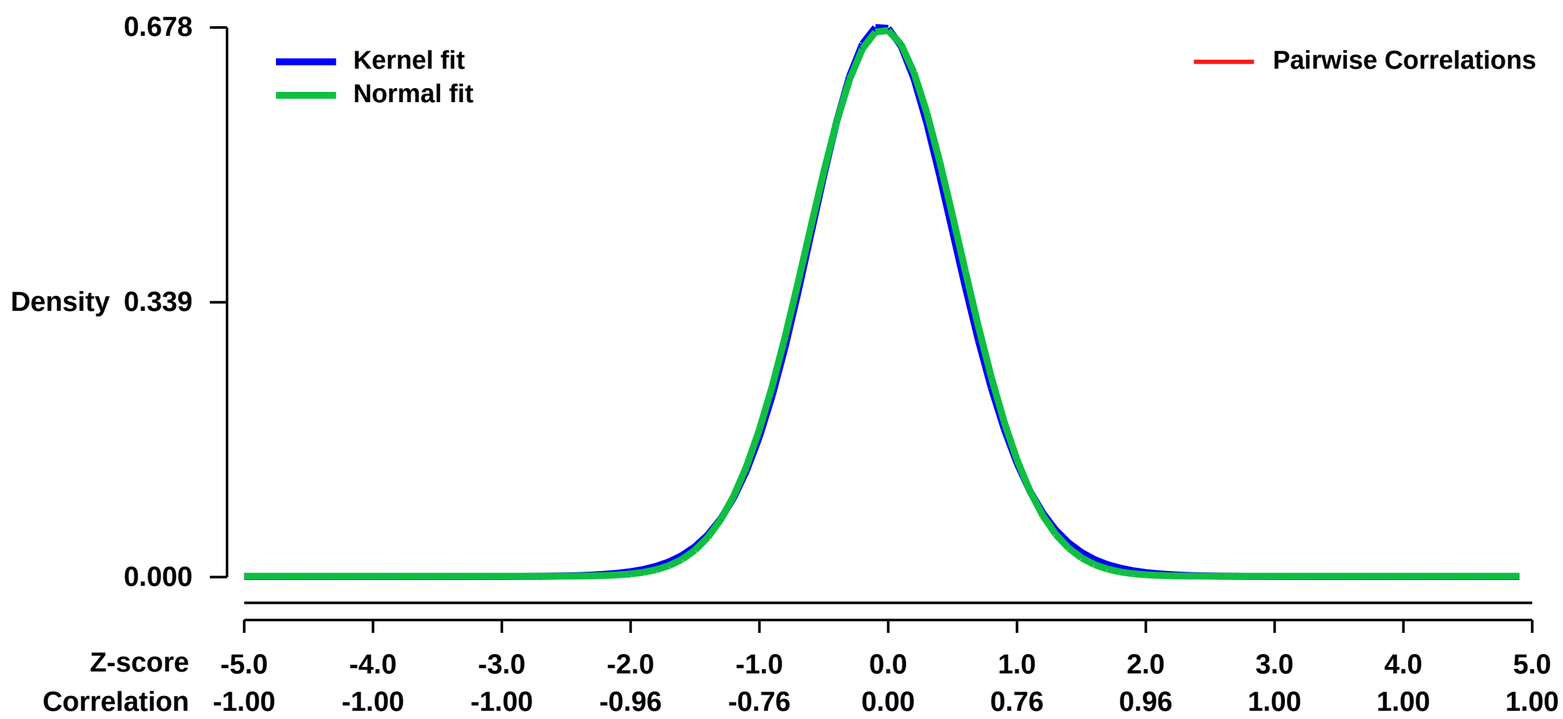

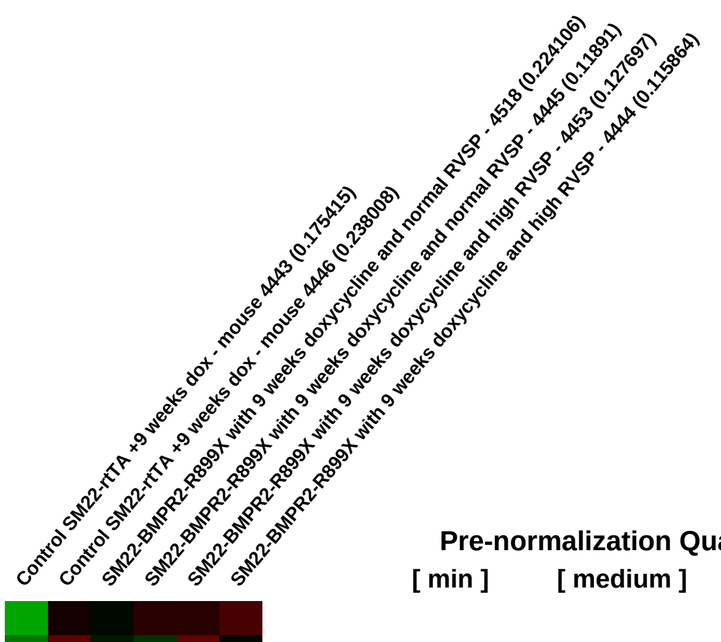

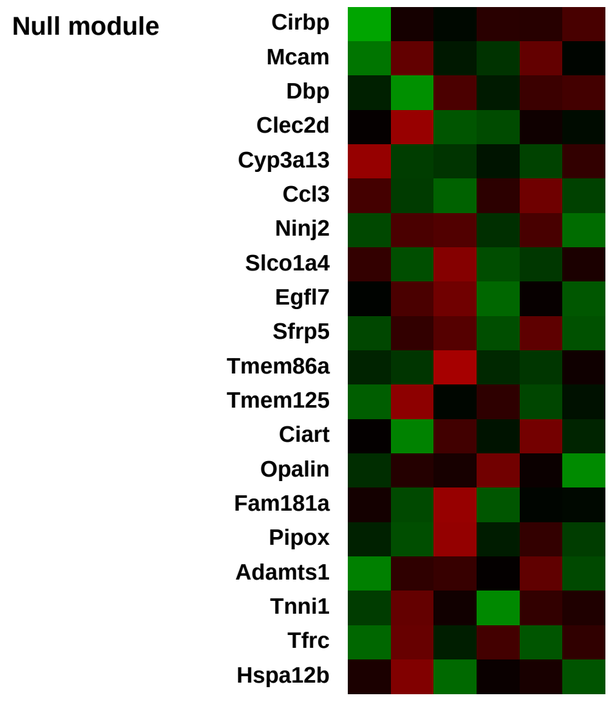

GEO Series "GSE37055" Expression Profiles

Num of samples in this series: 42

Scale of expression profile Z-scores

-3.0 -2.0 -1.0 0.0 1.0 2.0 3.0

GEO Link: http://www.ncbi.nlm.nih.gov/geo/query/acc.cgi?acc=GSE37055
Status: Public on Jul 20 2012
Title: Cell-type specific postnatal developmental expression data from mouse cerebellar Purkinje and Stellate/Basket cells
Organism: Mus musculus
Experiment type: Expression profiling by array
Platform: GPL1261
Pubmed ID: 22754500

Summary & Design:

Summary:
The assembly of neural circuits involves multiple sequential steps such as the specification of cell types, their migration to proper brain locations, morphological and physiological differentiation, and the formation and maturation of synaptic connections. This intricate and often prolonged process is guided by elaborate genetic mechanisms that regulate each developmental event. Evidence from numerous systems suggests that each cell type, once specified, is endowed with a genetic program that directs its subsequent development. This cell intrinsic program unfolds in respond to, and is regulated by, extrinsic signals, including cell-cell and synaptic interactions. To a large extent, the execution of this genetic program is achieved by the expression of specific sets of genes that support distinct developmental processes. Therefore, a comprehensive analysis of the developmental progression of gene expression in synaptic partners of neurons may provide a basis for exploring the genetic mechanisms regulating circuit assembly.

Here we examined the developmental gene expression profiles in well defined cell types in a stereotyped microcircuit of the cerebellar cortex.

Overall design:
Manually sorted pure populations of Purkinje cells and Stellate/Basket cells, 3 biological replicates, from Gad67-GFP bac-transgenic (G42) mice were profiled during postnatal developmental stages P3, P7, P14, P21, P28, P35 and P56 using Affymetrix MOE430.2 expression array

Background corr dist: KL-Divergence = 0.1175, L1-Distance = 0.0758, L2-Distance = 0.0135, Normal std = 0.4253

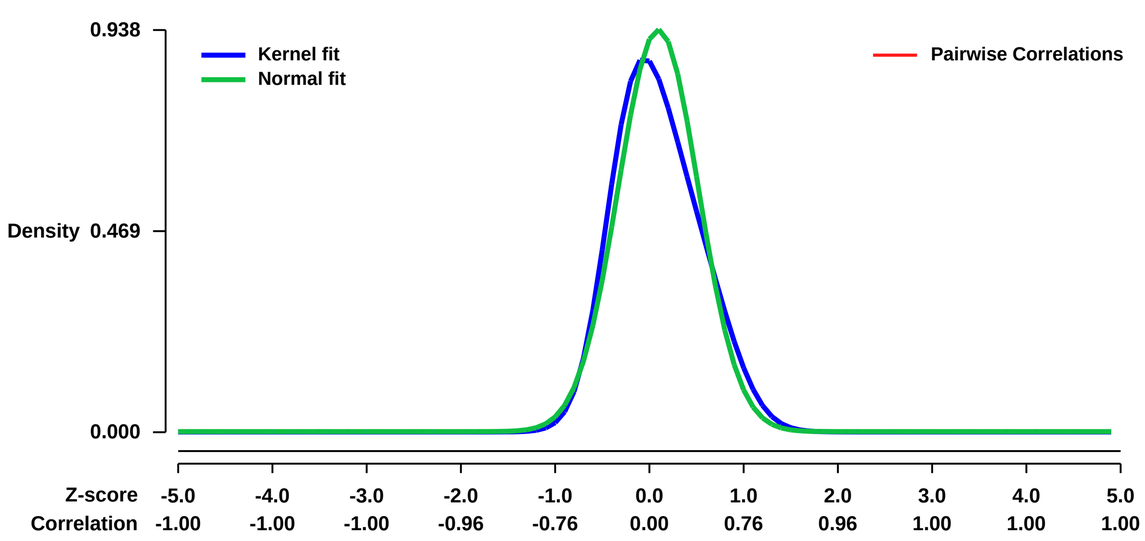

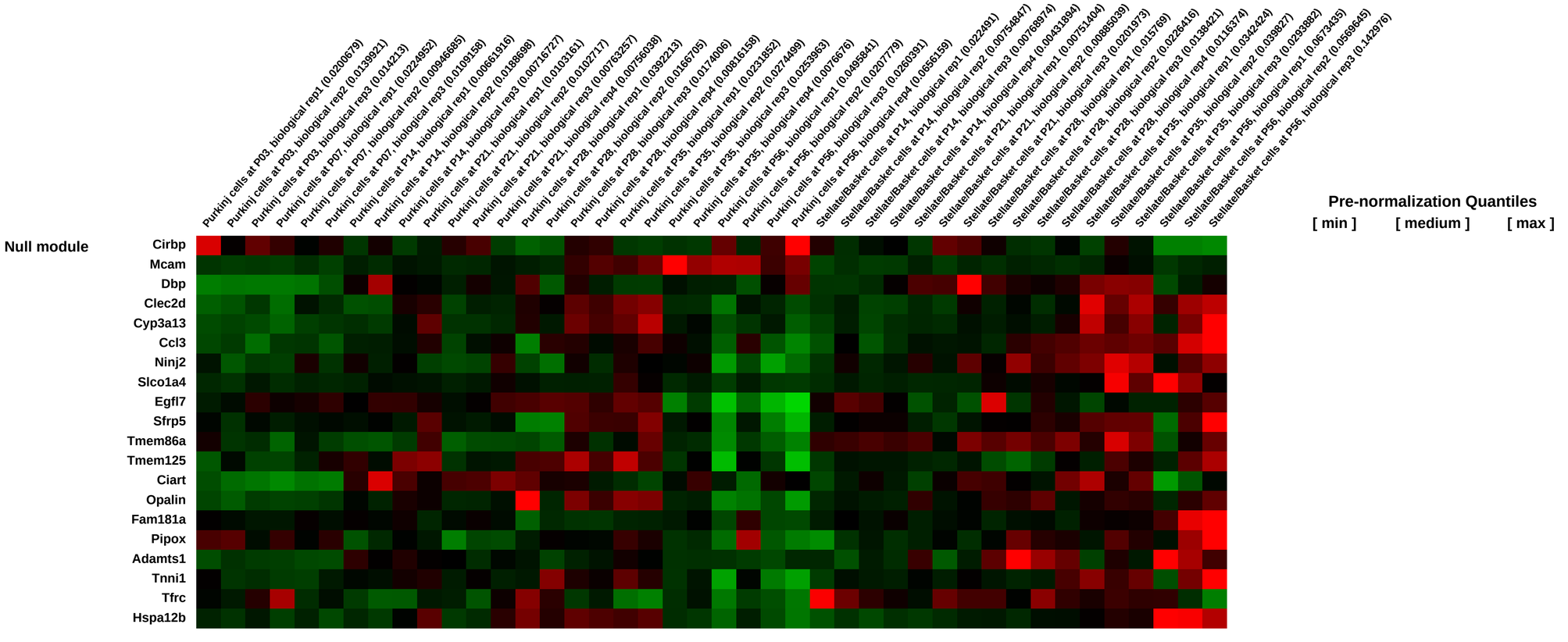

GEO Series "GSE29995" Expression Profiles

Num of samples in this series: 6

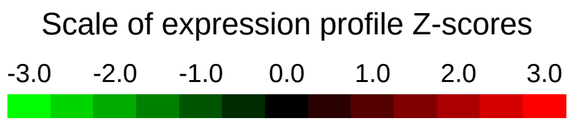

GEO Link:	http://www.ncbi.nlm.nih.gov/geo/query/acc.cgi?acc=GSE29995
Status:	Public on Jun 30 2011
Title:	Expression data from the node and primitive streak (NPS) regions from WT and Wnt3a null embryos
Organism:	Mus musculus
Experiment type:	Expression profiling by array
Platform:	GPL1261
Pubmed ID:	21750544
Summary & Design:	**Summary:** The goal of this project was to elucidate the target genes and transcriptional networks activated by Wnt3a during gastrulation, a complex morphogenetic process in which the embryonic germ layers are formed and the vertebrate body plan is established. **Overall design:** To identify downstream targets of Wnt3a, transcriptional profiling was performed using Affymetrix GeneChips on both wildtype and Wnt3a null embryos at embryonic days (E) 7.75-8. In order to maximize the likelihood of identifying direct target genes of Wnt3a, RNA was isolated from the node and primitive streak (NPS) region, an area where Wnt3a is highly expressed and at a time 12-18 hours before the morpholical phenotype of Wnt3a mutants becomes apparent.

Background corr dist: KL-Divergence = 0.0464, L1-Distance = 0.0222, L2-Distance = 0.0006, Normal std = 0.5907

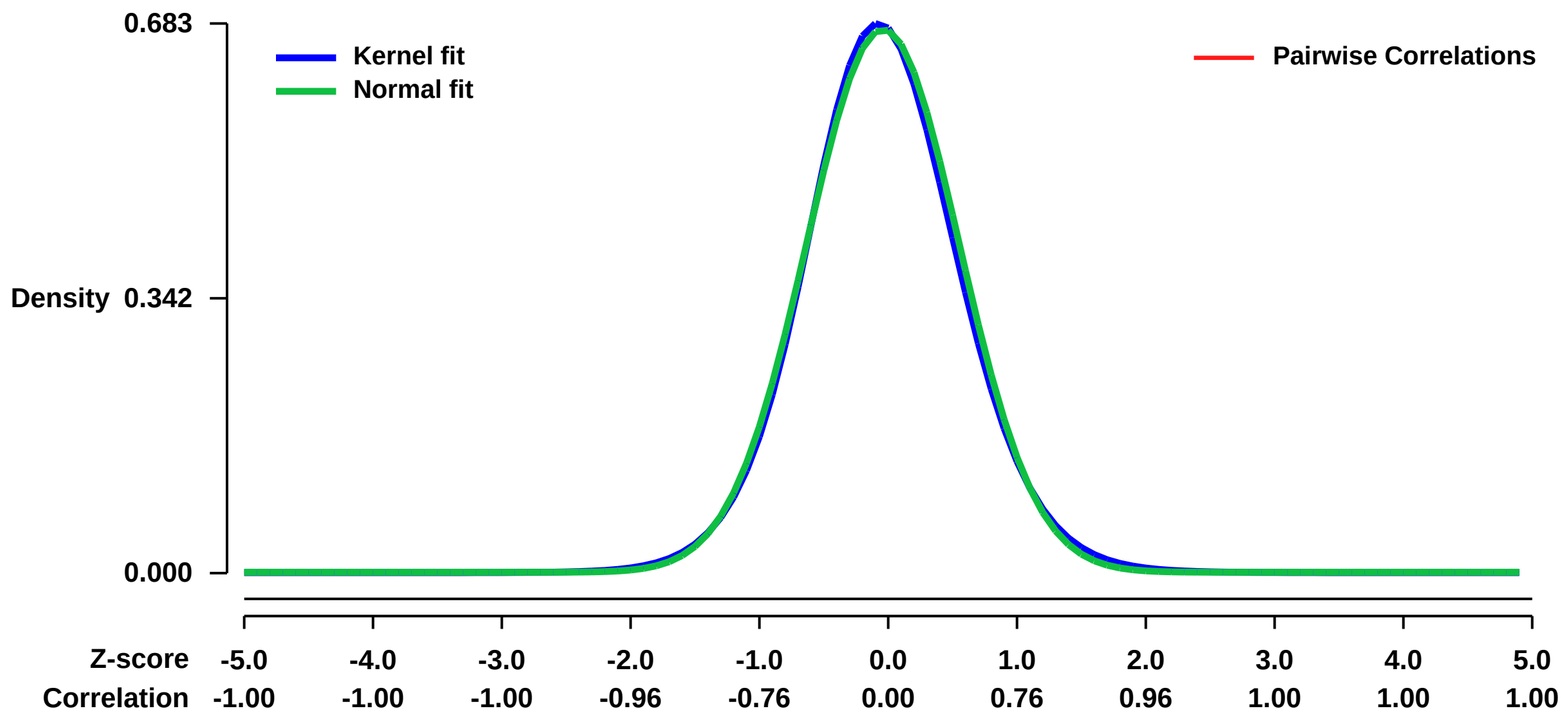

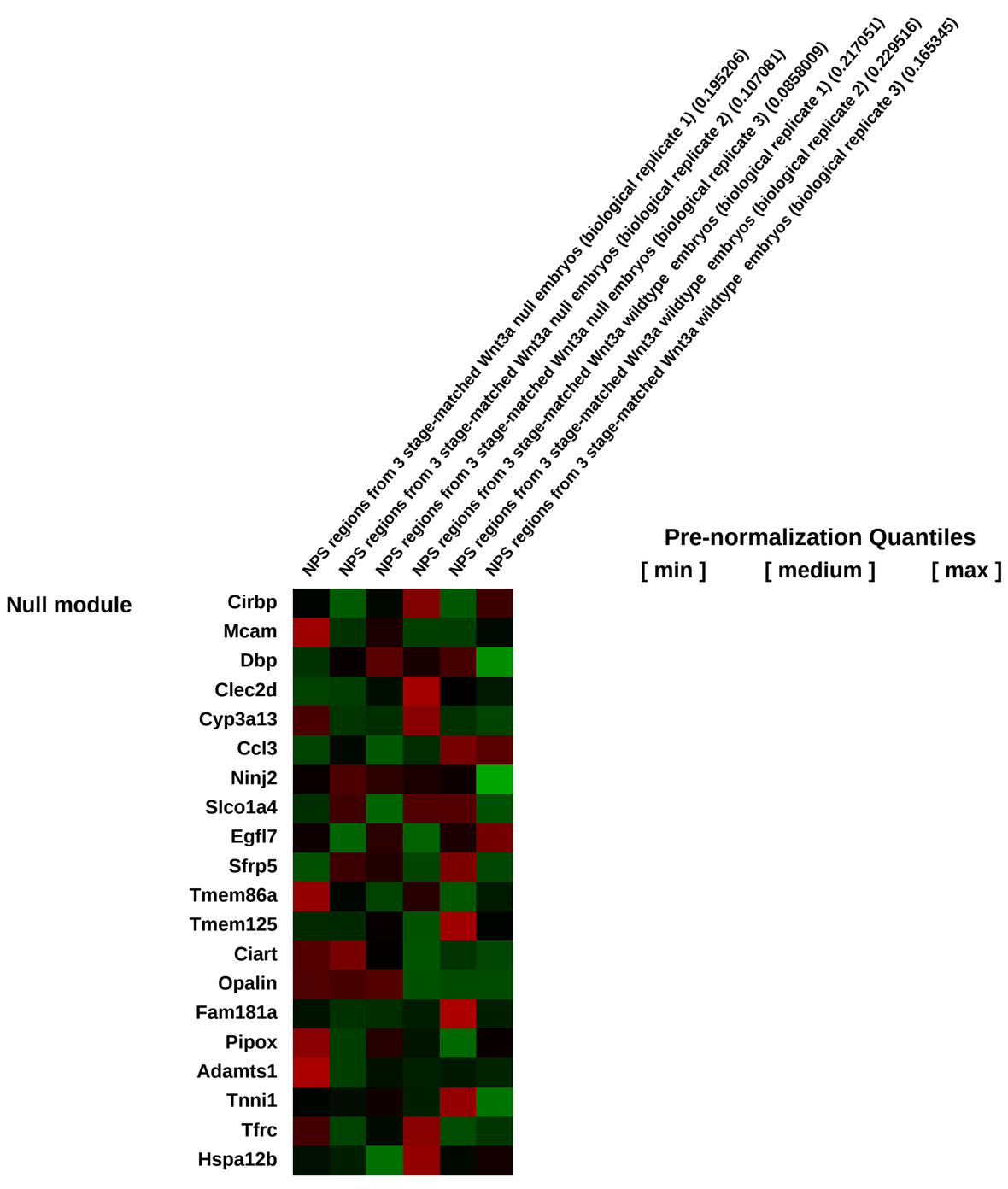

GEO Series "GSE4098" Expression Profiles

Num of samples in this series: 16

Scale of expression profile Z-scores

-3.0 -2.0 -1.0 0.0 1.0 2.0 3.0

GEO Link:	http://www.ncbi.nlm.nih.gov/geo/query/acc.cgi?acc=GSE4098
Status:	Public on Jan 27 2006
Title:	Mouse limbal epithelial basal cells vs. corneal epithelial basal cell gene expression profile
Organism:	Mus musculus
Experiment type:	Expression profiling by array
Platform:	GPL1261
Pubmed ID:	16675456
Summary & Design:	**Summary:** Limbal vs. corneal epithelial basal cell gene expression patterns were identified and compared **Keywords: repeat** **Overall design:** 8 limbal and 8 corneal epithelial basal cells samples from 8 mice were dissected and mRNAs were isolated and amplified for microarray analysis

Background corr dist: KL-Divergence = 0.1724, L1-Distance = 0.0608, L2-Distance = 0.0095, Normal std = 0.3604

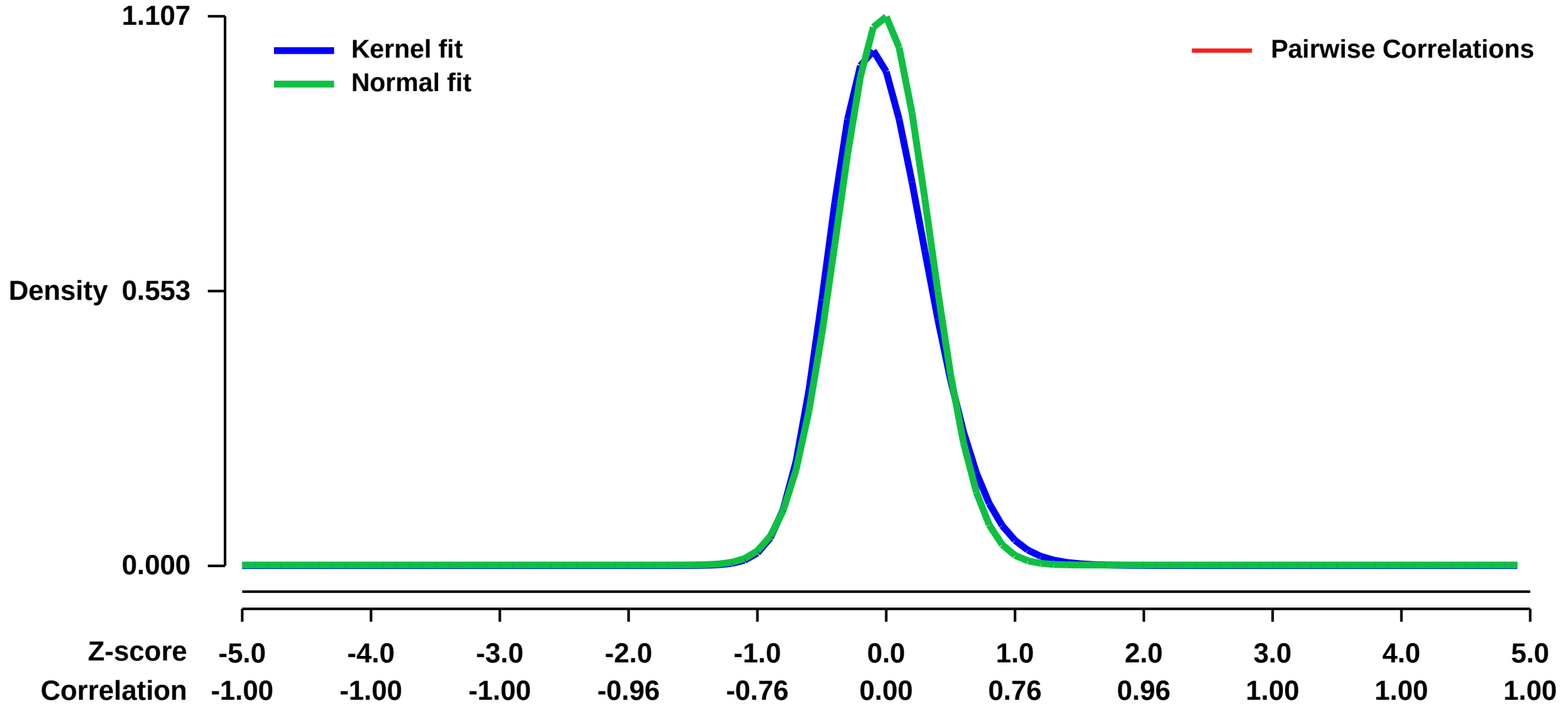

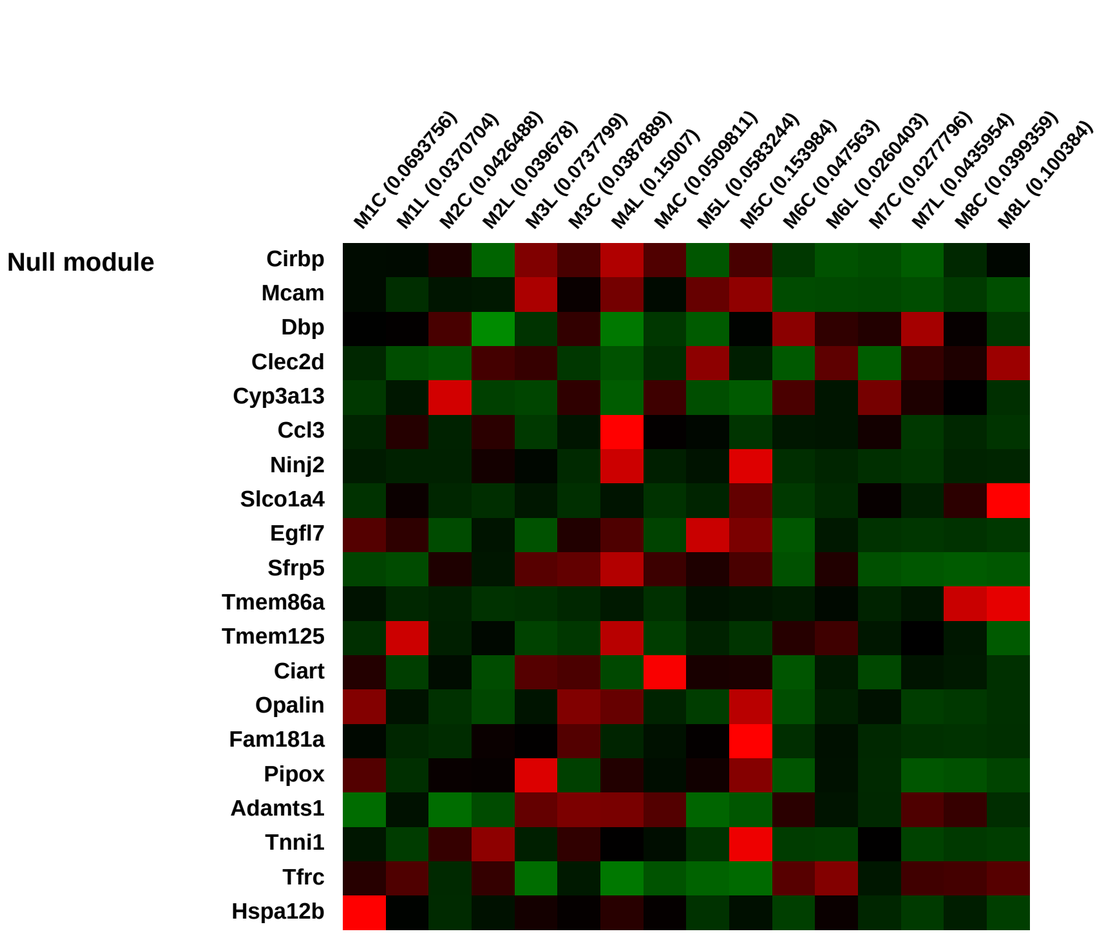

GEO Series "GSE14354" Expression Profiles

Num of samples in this series: 6

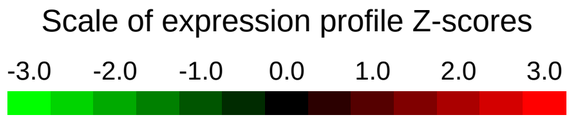

GEO Link:	http://www.ncbi.nlm.nih.gov/geo/query/acc.cgi?acc=GSE14354
Status:	Public on Jan 13 2009
Title:	Testicular germ cell tumor susceptibility genes from the consomic 129.MOLF-Chr19 mouse strain
Organism:	Mus musculus
Experiment type:	Expression profiling by array
Platform:	GPL1261
Pubmed ID:	17671812
Summary & Design:	**Summary:** Chromosome substitution strains (CSS or consomic strains) are useful for mapping phenotypes to chromosomes. However, huge efforts are needed to identify the gene(s) responsible for the phenotype in the complex context of the chromosome. Here, we report the identification of candidate disease genes from a CSS using a combination of genetic and genomic approaches as well as by using knowledge about the germ cell tumor disease etiology. We utilized the CSS, 129.MOLF-Chr 19 chromosome substitution strain (or M19), in which males develop germ cell tumors of the testes at an extremely high rate. We are able to identify 3 protein-coding genes and 1 microRNA on chromosome 19 that have previously not been implicated to be testicular tumor susceptibility genes. Our findings suggest that changes in gene expression levels in the gonadal tissues of multiple genes from Chr 19 likely contribute to the high TGCT incidence of the M19 strain. Our data advances the use of CSS to identify disease susceptibility genes and demonstrates that the 129.MOLF-Chr 19 strain serves as a useful model to elucidate the genetics and biology of germ cell transformation and tumor development. **Overall design:** By analyzing the data of differentially expressed genes present in the 3 samples, as well as selecting those that map to Chr 19, we were able to exclude a majority of the genes but found 3 genes in common. The 3 genes map to Chr 19 and were found to be downregulated in the M19 strain E13.5 and PN1 gonads as well as E13.5 embryos. These are Zfp162, D19Bwg1357e and Cox15. These 3 genes have not been previously implicated in testicular tumorigenesis and are novel TGCT candidate susceptibility genes.

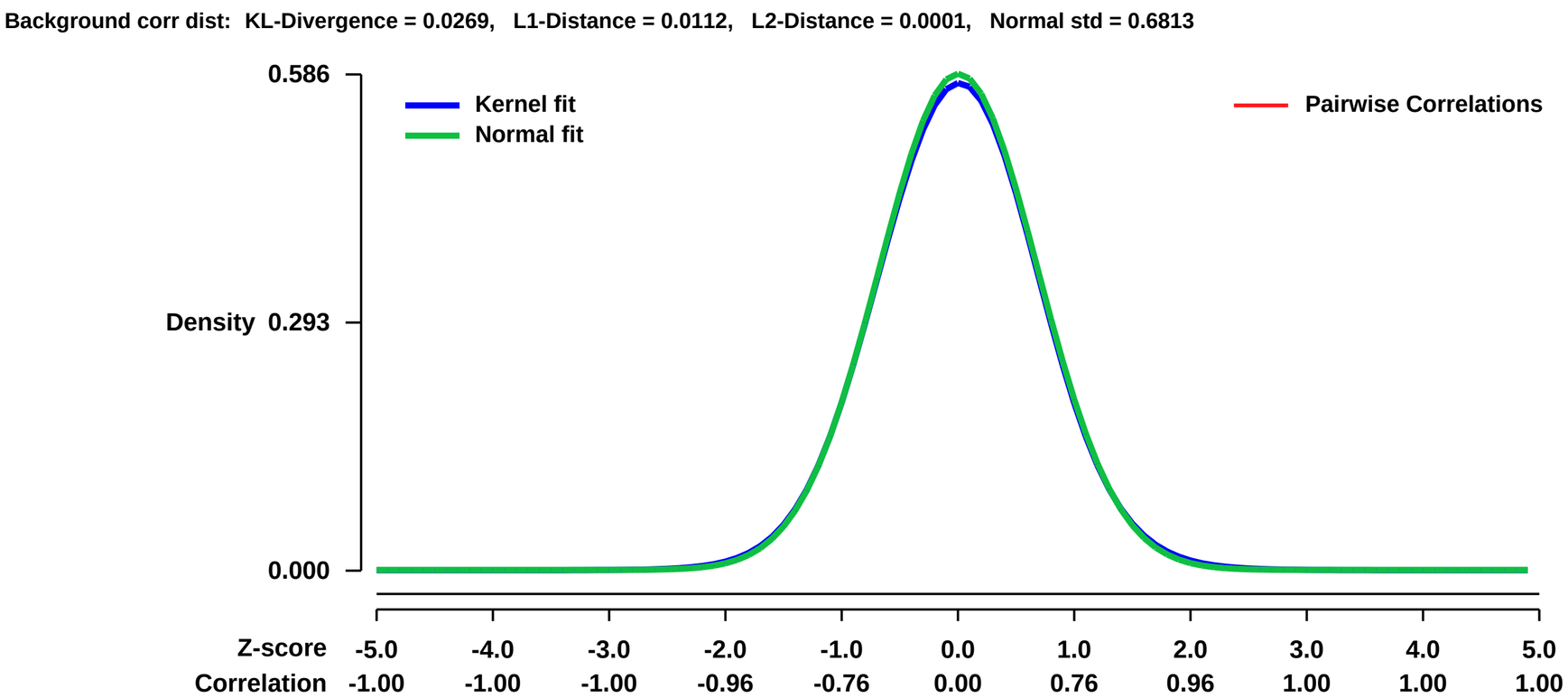

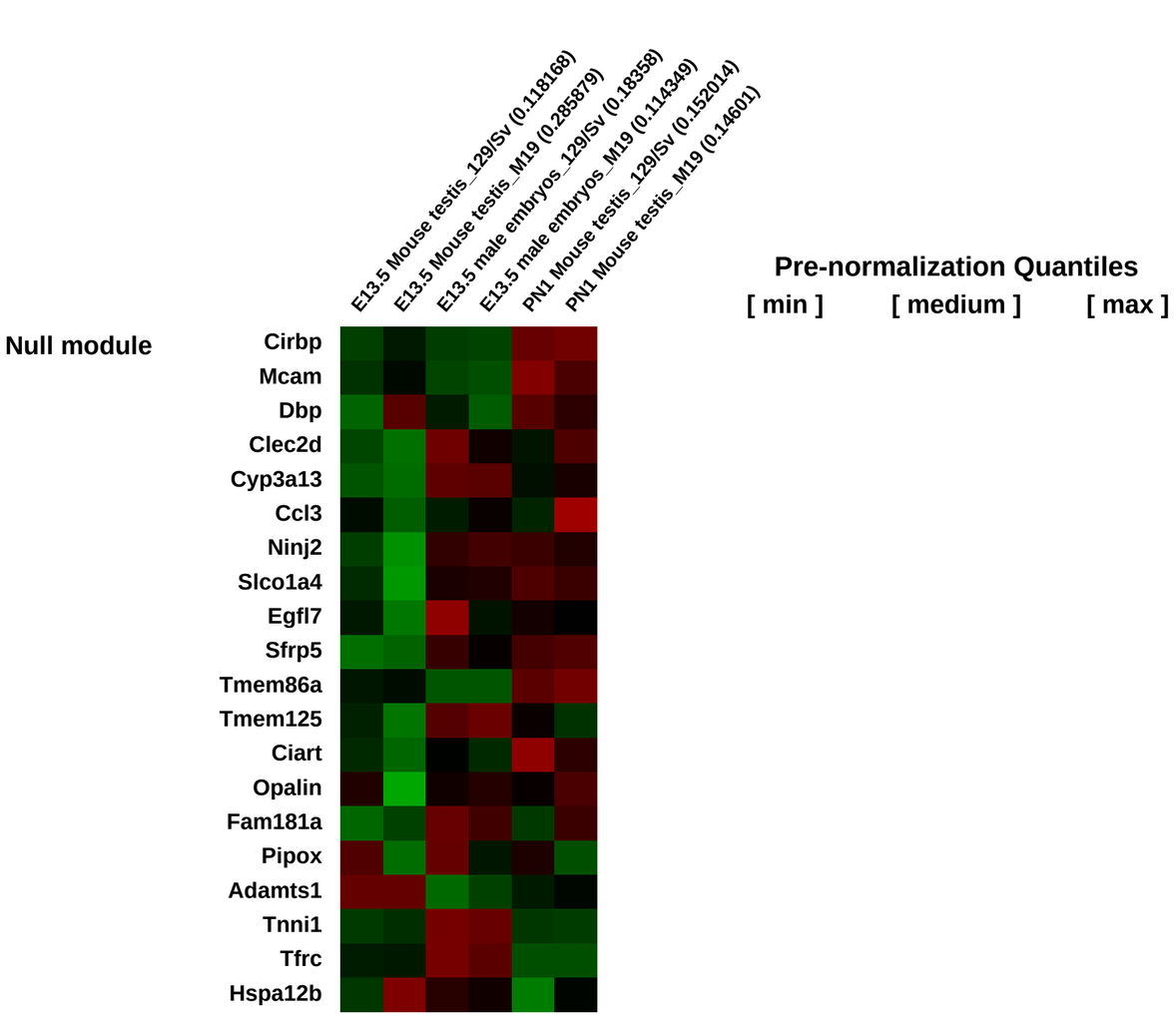

GEO Series "GSE44563" Expression Profiles

Num of samples in this series: 6

Scale of expression profile Z-scores

-3.0 -2.0 -1.0 0.0 1.0 2.0 3.0

GEO Link:	http://www.ncbi.nlm.nih.gov/geo/query/acc.cgi?acc=GSE44563
Status:	Public on Dec 22 2013
Title:	Expression data from C2C12 myotubes infected with RML prions
Organism:	Mus musculus
Experiment type:	Expression profiling by array
Platform:	GPL1261
Pubmed ID:	24244171
Summary & Design:	**Summary:** Prion infection in animals results in neurodegeneration and eventually death. To examine the cellular impact of Prion disease, we profiled non-proliferative fully differentiated C2C12 cells, which can replicate prions to high levels. Results suggest that accumulation of high levels of PrPSc in C2C12 myotubes does not cause any overt cellular dysfunction or molecular pathology. **Overall design:** C2C12 cells were differentiated into confluent myotubes. Cells were infected or not with 100ul of 10% brain homogenate obtained from a C57BL/6 mouse clinically affected with RML prions. 16 days after infection, cells were collected by scraping and RML was purified.

Background corr dist: KL-Divergence = 0.0415, L1-Distance = 0.0144, L2-Distance = 0.0002, Normal std = 0.6034

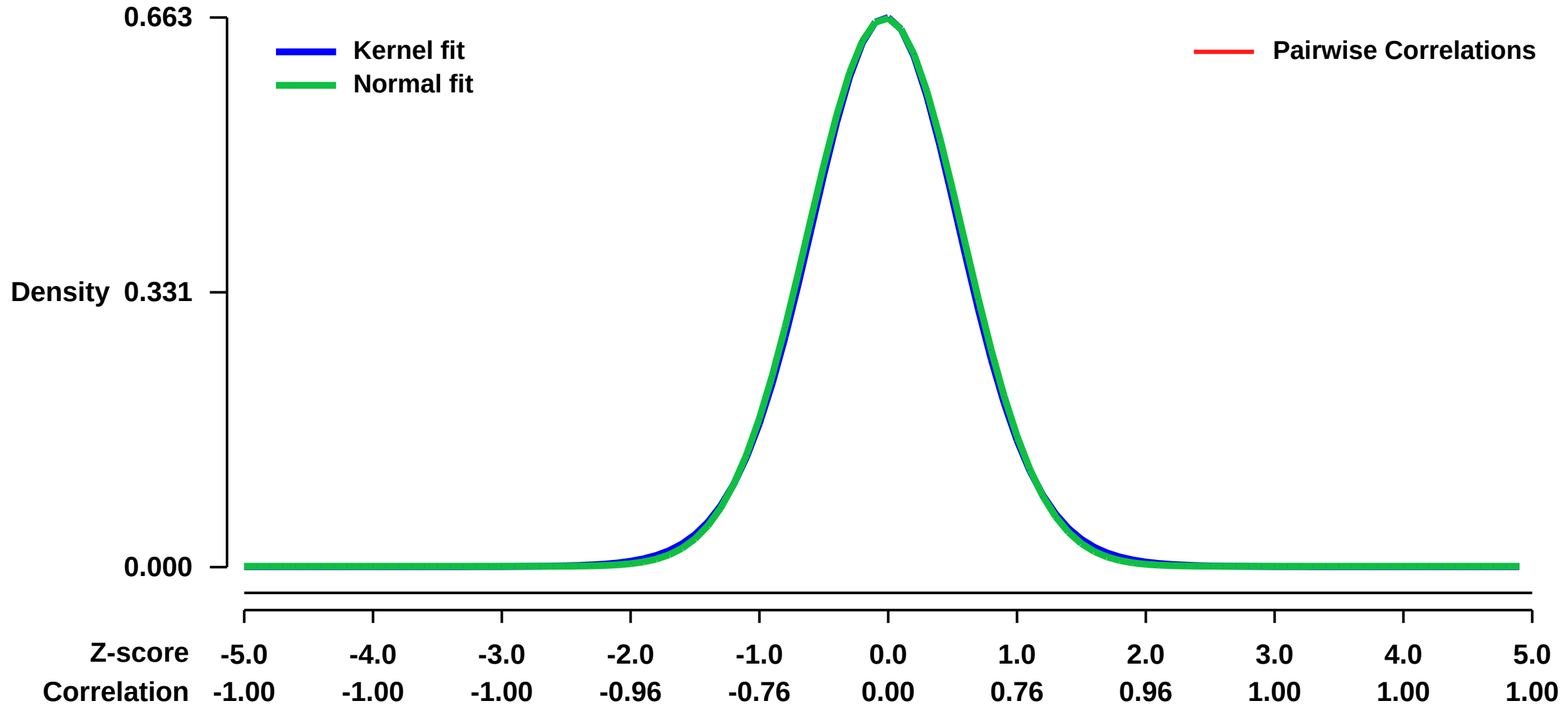

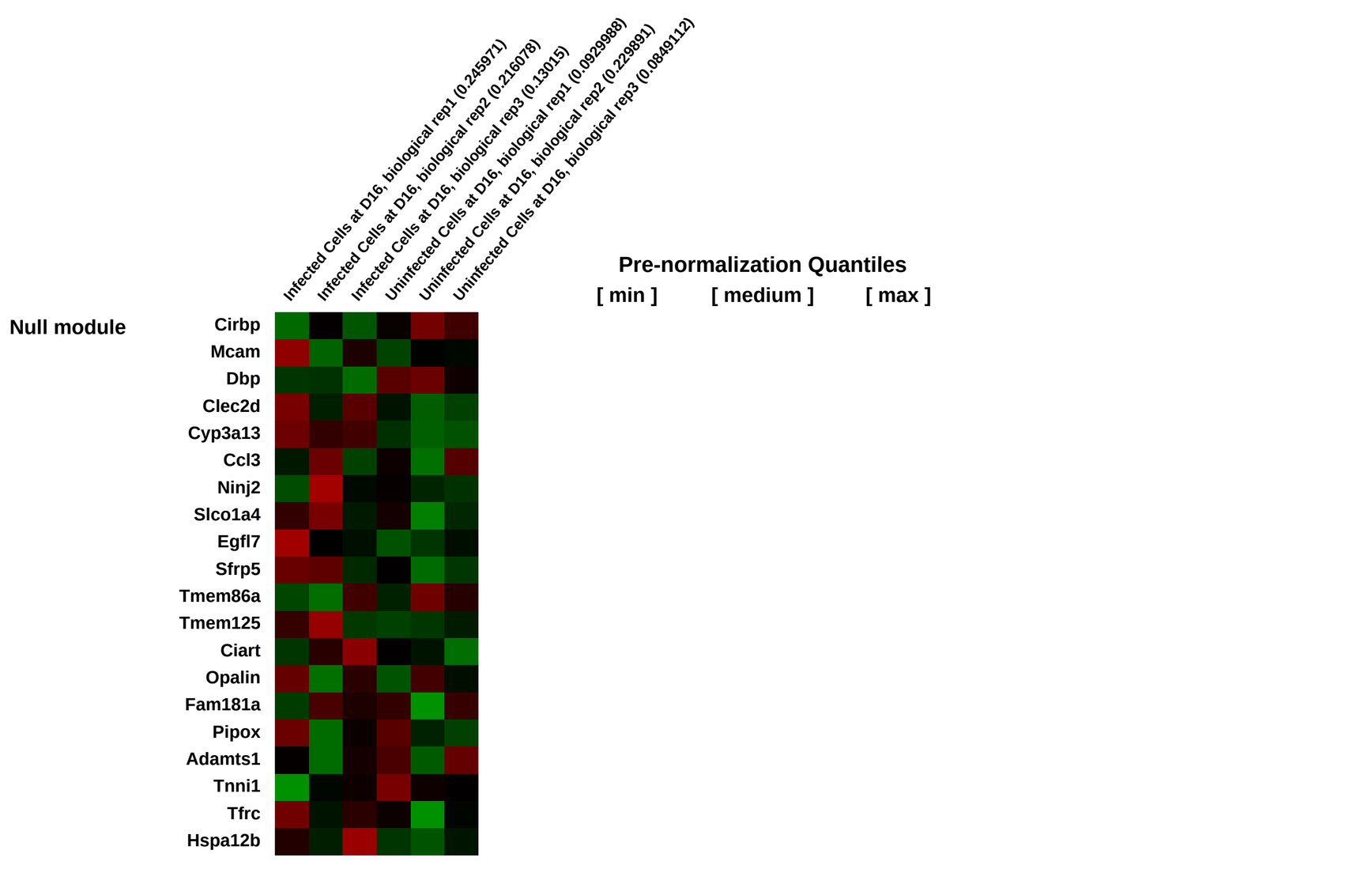

GEO Series "GSE16992" Expression Profiles

Num of samples in this series: 48

Scale of expression profile Z-scores

-3.0 -2.0 -1.0 0.0 1.0 2.0 3.0

GEO Link:	http://www.ncbi.nlm.nih.gov/geo/query/acc.cgi?acc=GSE16992
Status:	Public on Mar 21 2012
Title:	Expression Profiling of Early Myogenesis - Affymetrix Dataset
Organism:	Mus musculus
Experiment type:	Expression profiling by array
Platform:	GPL1261
Pubmed ID:	22147266
Summary & Design:	**Summary:** **Analysis of Early Myogenesis Reveals an Extensive Set of Transcriptional Regulators Whose Knock-down Can Inhibit Differentiation** **Myogenesis is a tightly controlled process involving the transcriptional activation and repression of thousands of genes. Although many components of the transcriptional network are known for the later phases of myogenesis, relatively little work has described the transcriptional landscape within the first 24 hours, when myoblasts commit to differentiate. Through dense temporal sampling of differentiating C2C12 myoblasts, we identify 266 transcriptional regulators (TRs) whose expression is altered within the first 12 hours of myogenesis. A high-content shRNA screen of 76 TRs involving 427 stable lines identified 48 genes whose knockdown significantly inhibits differentiation of C2C12 myoblasts. These include known regulators of myogenesis (Myod1, Myog and Myf5), as well as 26 regulators not previously associated with the process. Of the TRs differentially expressed within the first 24 hours, two-thirds inhibited differentiation when knocked down. Surprisingly, a similar proportion (67%) of shRNAs targeting TRs whose expression did not change during differentiation also inhibited myogenesis, suggesting that both stably and differentially expressed TRs are essential for this complex differentiation program. This implies that microarray-based approaches that concentrate functional validation studies on differentially-expressed genes will fail to identify many genes that are critically implicated in complex biological processes.** **Overall design:** **C2C12 myoblasts were differentiated into myotubes and sampled at various timepoints for gene expression measurement on MOE-430v2 chips. Cells grown in separate plates were harvested at 14 different timepoints: t_-24h, t_0h, t_0.5h, t_1h, t_1.5h, t_2h, t_3h, t_6h, t_9h, t_12h, t_24h, t_48h, t_96h, t_144h. Cells were also pre-treated with 50uM cycloheximide 1 hour prior to inducing differentiation and harvested at two timepoints: t_chx_1h, t_chx_3h. All harvests were performed in triplicate using growths from successive passages.**

Background corr dist: KL-Divergence = 0.1939, L1-Distance = 0.0505, L2-Distance = 0.0065, Normal std = 0.3363

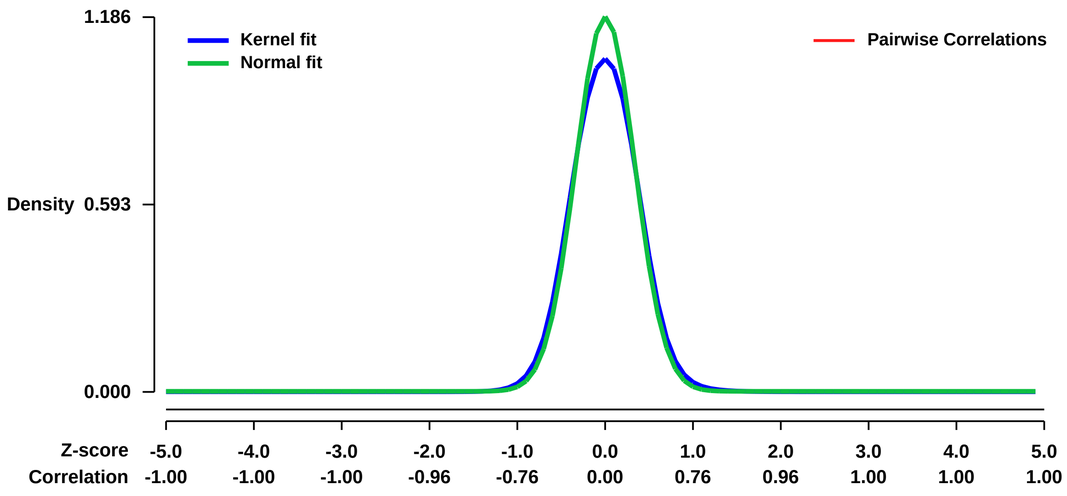

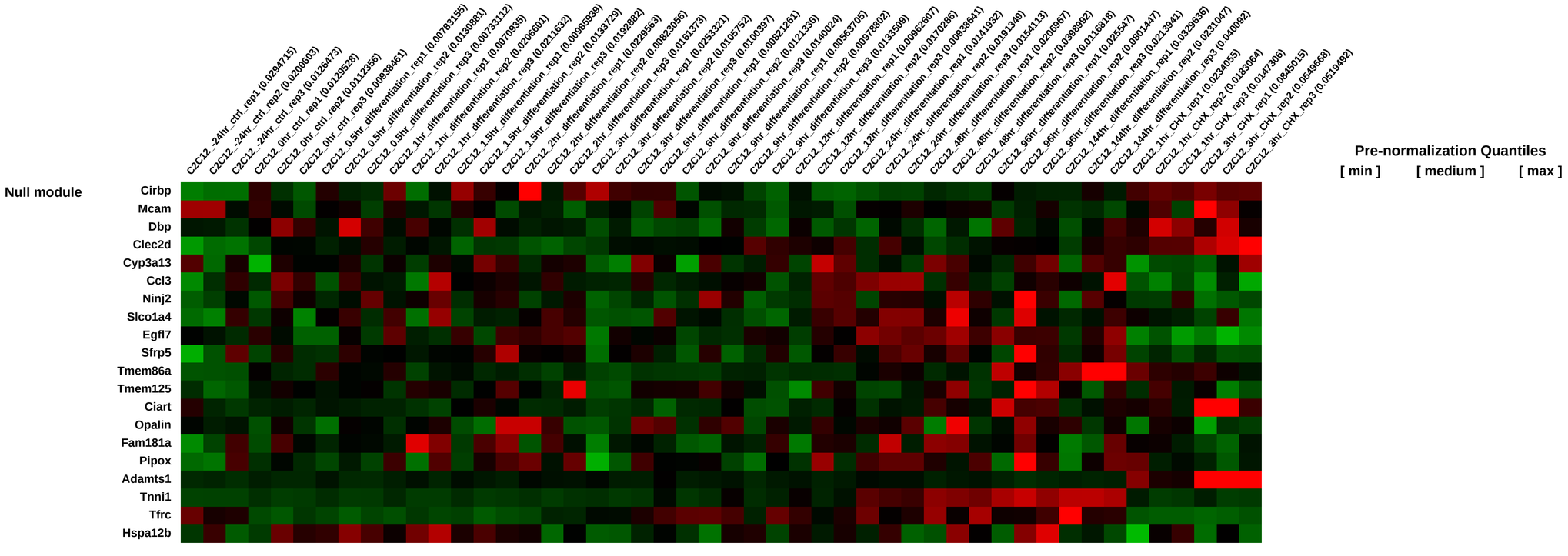

GEO Series "GSE22925" Expression Profiles

Num of samples in this series: 14

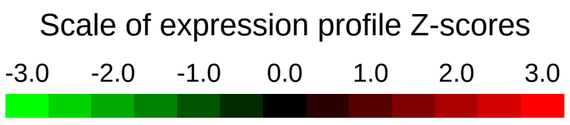

GEO Link:	http://www.ncbi.nlm.nih.gov/geo/query/acc.cgi?acc=GSE22925
Status:	Public on Jul 14 2010
Title:	Murine Bone Marrow Stromal Cell Response to Granulocyte Colony-Stimulating Factor
Organism:	Mus musculus
Experiment type:	Expression profiling by array
Platform:	GPL1261
Pubmed ID:	20516641
Summary & Design:	**Summary:** Neutrophil homeostasis is maintained, in part, by the regulated release of neutrophils from the bone marrow. Constitutive expression of the chemokine CXCL12 by bone marrow stromal cells provides a key retention signal for neutrophils in the bone marrow through activation of its receptor CXCR4. Herein, we show that the ELR chemokines CXCL1 and CXCL2 are constitutively expressed by bone marrow endothelial cells and osteoblasts, and CXCL2 expression is induced in endothelial cells during granulocyte colony-stimulating factor (G-CSF)-induced neutrophil mobilization. Neutrophils lacking CXCR2, the receptor for CXCL1 and CXCL2, are preferentially retained in the bone marrow, reproducing a myelokathexis phenotype. Transient disruption of CXCR4 failed to mobilize CXCR2 neutrophils. However, doubly deficient neutrophils (CXCR2-/- CXCR4-/-) displayed constitutive mobilization, showing that CXCR4 plays a dominant role. Collectively, these data suggest that CXCR2 signaling is a second chemokine axis that interacts antagonistically with CXCR4 to regulate neutrophil release from the bone marrow. We used gene expression microarrays to determine the changes in osteoblasts and bone marrow endothelial cells after G-CSF treatment. **Overall design:** 3 untreated and G-CSF-treated osteoblast samples and 4 untreated and G-CSF-treated endothelial samples.

Background corr dist: KL-Divergence = 0.1124, L1-Distance = 0.0289, L2-Distance = 0.0014, Normal std = 0.4248

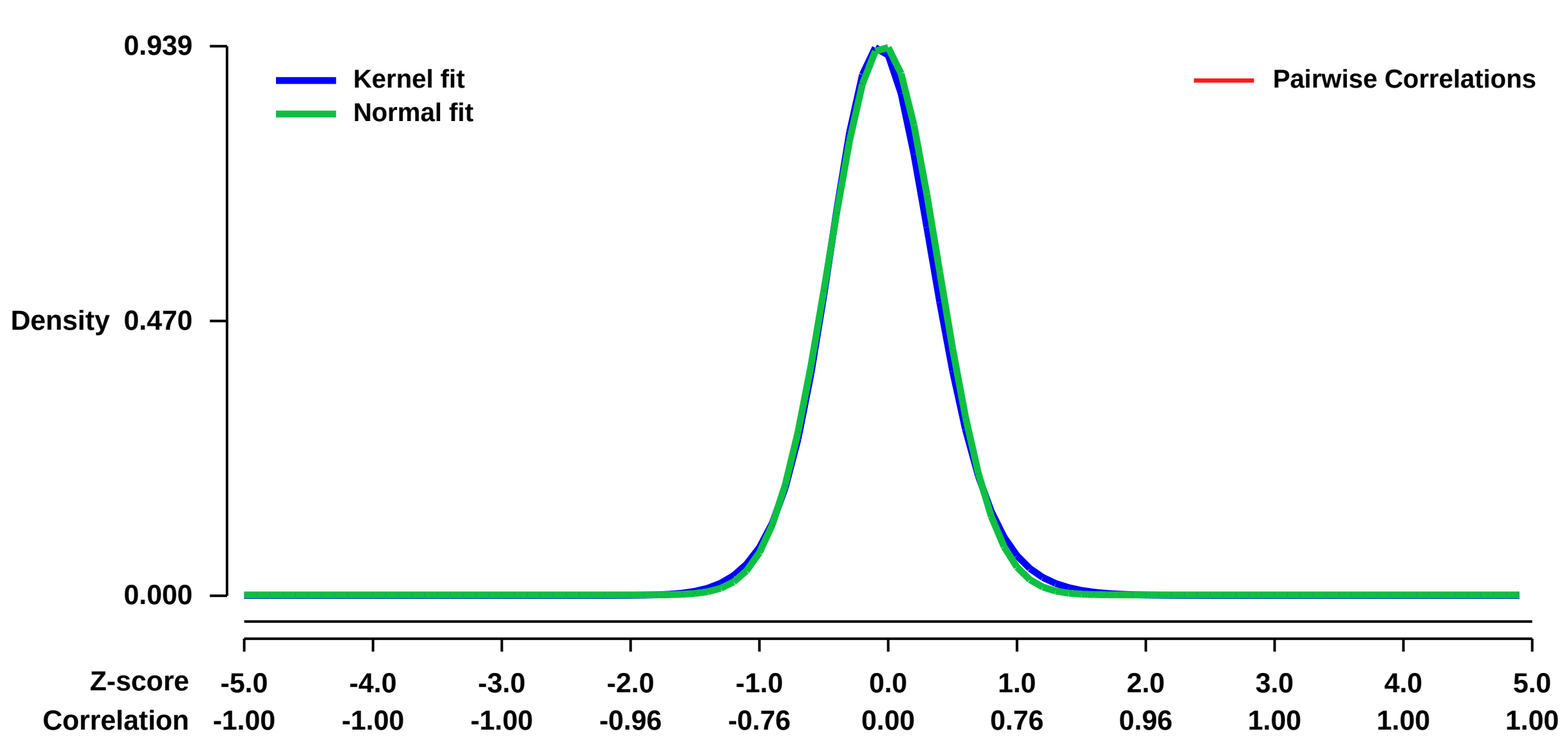

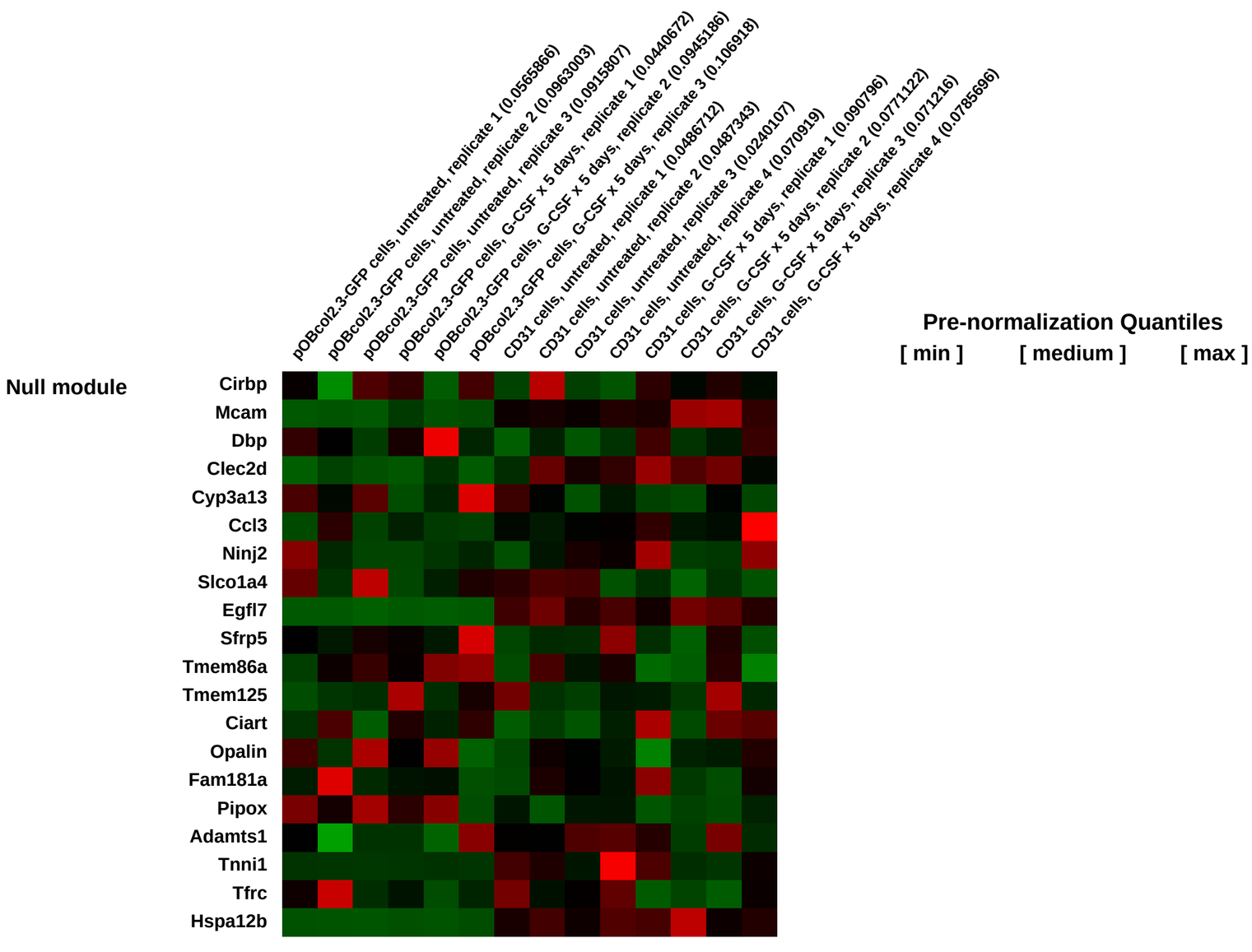

GEO Series "GSE23598" Expression Profiles

Num of samples in this series: 8

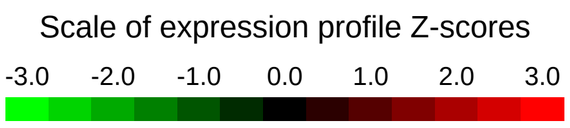

GEO Link:	**http://www.ncbi.nlm.nih.gov/geo/query/acc.cgi?acc=GSE23598**
Status:	**Public on Aug 10 2013**
Title:	**Global gene expression profiles of MT knockout and wild-type mice in the condition of doxorubicin-induced cardiomyopathy**
Organism:	**Mus musculus**
Experiment type:	**Expression profiling by array**
Platform:	**GPL1261**
Pubmed ID:	
Summary & Design:	**Summary:** **The present study was designed using MT knockout mice in concert with genomic approaches to explore the possible molecular and cellular mechanisms involved in the protective effects of MT against DOX cardiotoxicity. MT-â /â¡ null (MT-/-) mice and corresponding wild-type mice (MT+/+) were administrated with a single dose of DOX (15 mg/kg, i.p.) or an equal volume of saline. Animals were sacrificed on the 4th day after DOX administration and samples were collected for further analyses. Global gene expression profiles of cardiac mRNA from two genotype mice revealed that 381 characteristically MT-responsive genes were identified between MT+/+ mice and MT-/- mice in response to DOX, including fos, ucp3, car3, atf3, map3k6, etc.. Functional analysis implied MAPK signaling pathway, p53 signaling pathway, Jak-STAT signaling pathway, PPAR signaling pathway, Wnt signaling pathway, etc. might be involved to mediate the protection of DOX cardiomyopathy by MT. Results from the present study not only validated the previously reported possible mechanisms of MT protection against DOX toxicity, but also provided new clues into the molecular mechanisms involved in this process.** **Overall design:** **Male MT+/+ & MT-/- mice (6-8 weeks old) were randomly assigned to treatment or control groups and administrated with a single dose of DOX (15 mg/kg, i.p.) or an equal volume of normal saline solution (NS) respectively. Animals were sacrificed on the 4th day after DOX injection, and samples were collected for further microarray analyses.**

Background corr dist: **KL-Divergence = 0.0554, L1-Distance = 0.0180, L2-Distance = 0.0004, Normal std = 0.5396**

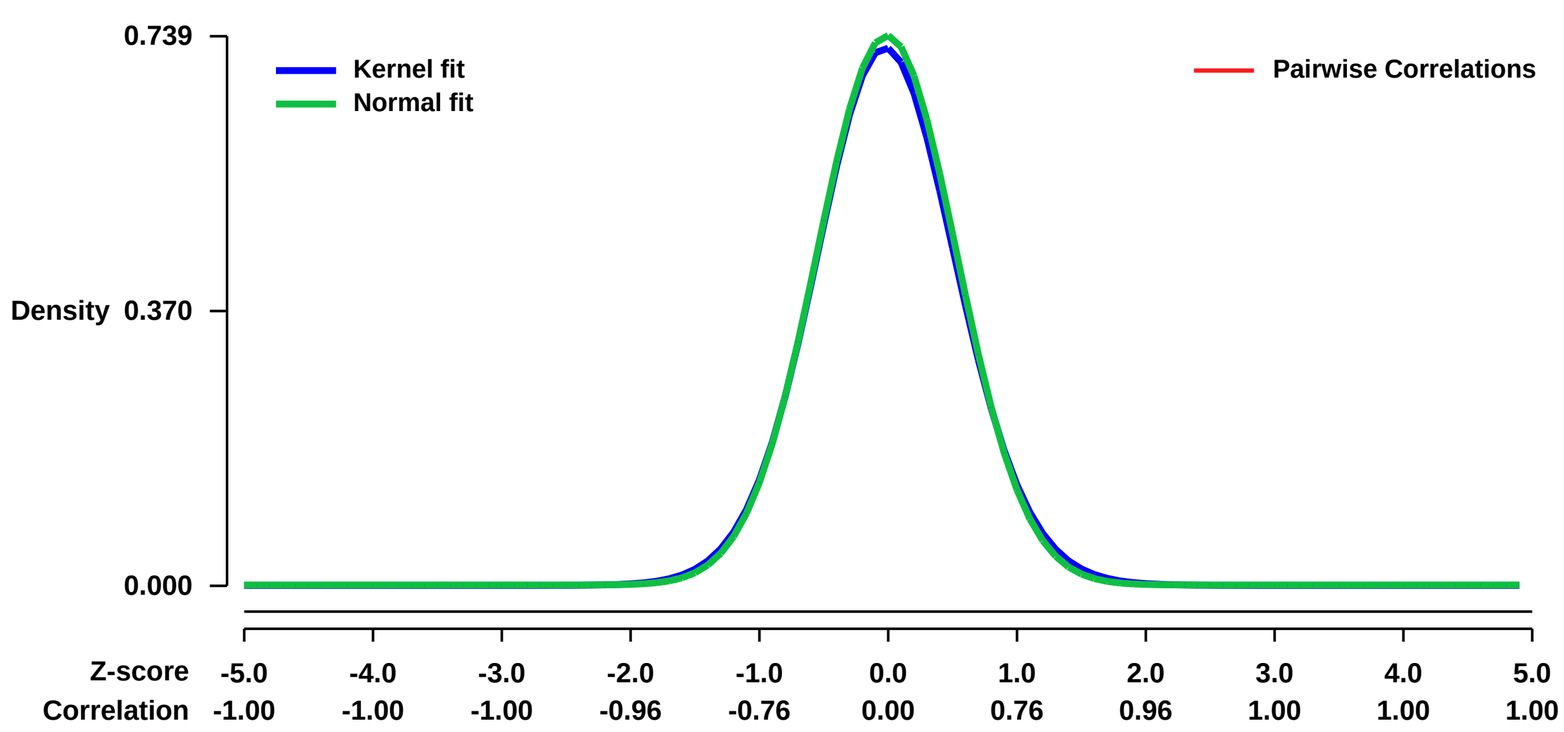

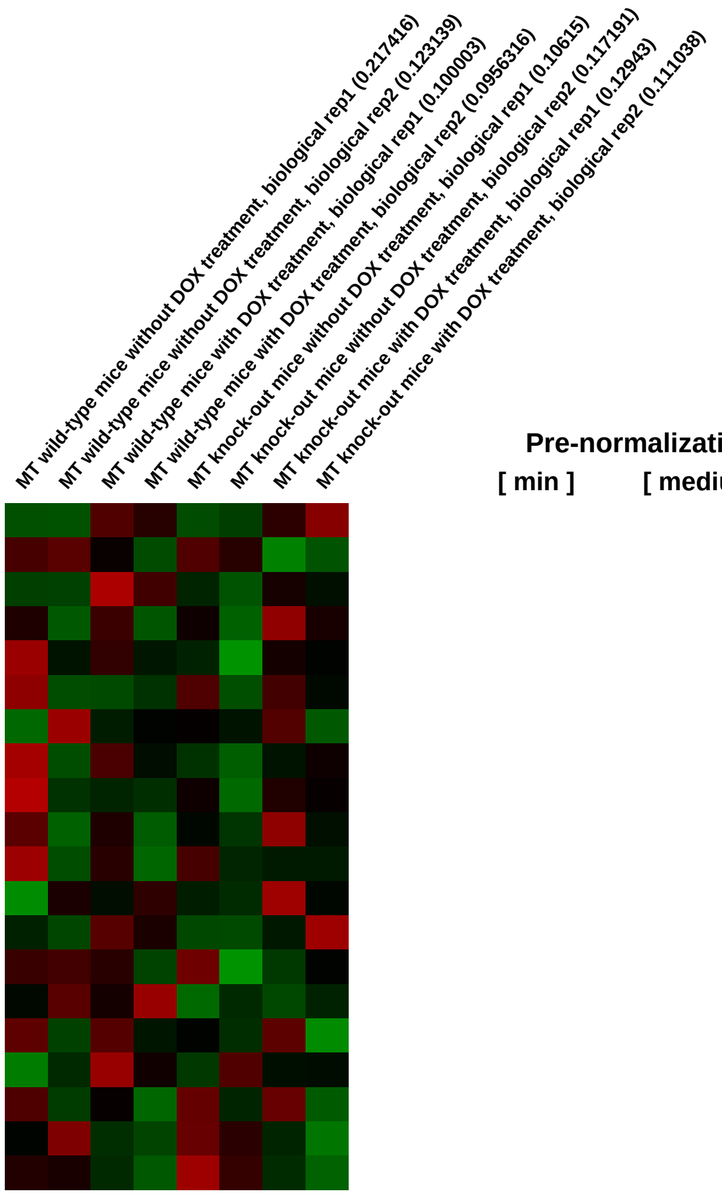

GEO Series "GSE15999" Expression Profiles

Num of samples in this series: 8

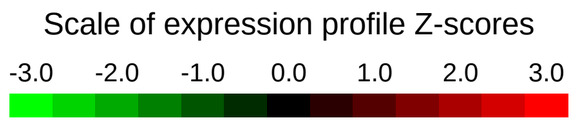

GEO Link:	http://www.ncbi.nlm.nih.gov/geo/query/acc.cgi?acc=GSE15999
Status:	Public on May 08 2009
Title:	Mesenchymal signature of post-pneumonectomy lung regeneration in adult mice
Organism:	Mus musculus
Experiment type:	Expression profiling by array
Platform:	GPL1261
Pubmed ID:	19804646
Summary & Design:	**Summary:** The adult human lung has a very limited capacity to regenerate functional alveoli. In contrast, adult mice have a remarkable capacity for neoalveolarization following either lung resection or injury. The molecular basis for this unique capability to regenerate lung tissue in mice is largely unknown. We examined the transcriptomic responses to single lung pneumonectomy in adult mice in order to elucidate prospective molecular signaling used in this species during lung regeneration. Unilateral left pneumonectomy or sham thoracotomy was performed under general anesthesia (n = 8 mice per group for each of the four time points). Total RNA was isolated from the remaining lung tissue at four time points post-surgery (6 hours, 1 day, 3 days, 7 days) and analyzed using microarray technology. The observed transcriptomic patterns revealed mesenchymal cell signaling, including up-regulation of genes previously associated with activated fibroblasts (Tnfrsf12a, Tnc, Eln, Col3A1), as well as modulation of Igf1-mediated signaling. The data set also revealed early down-regulation of pro-inflammatory cytokine transcripts, up-regulation of genes involved in T cell development and function, but few similarities to transcriptomic patterns observed during embryonic or post-natal lung development. Immunohistochemical analysis suggests that early fibroblast but not myofibroblast proliferation is important during lung regeneration and may explain the preponderance of mesenchymal-associated genes that are over-expressed in this model. This appears to differ from embryonic alveologenesis. These data suggest that modulation of mesenchymal cell signaling and proliferation may act in concert with immunomodulation to control inflammation during post-pneumonectomy lung regeneration in adult mice. **Overall design:** For each of the four time points (6 hr, 1 day, 3 day, 7 day), the mice were divided into two groups: (1) pneumonectomy (PNY) and (2) sham operated (SHAM - thoracotomy without lung resection), with eight animals in each group. One microarray was performed on pooled lung tissue from these 8 animals for each time point. Analysis of expression in PNY vs SHAM animals was performed in two ways: using all four microarrays as replicates in a time-independent analysis, as well as analysis of each time point separately (time-dependent) without replicates.

Background corr dist: KL-Divergence = 0.0531, L1-Distance = 0.0180, L2-Distance = 0.0004, Normal std = 0.5463

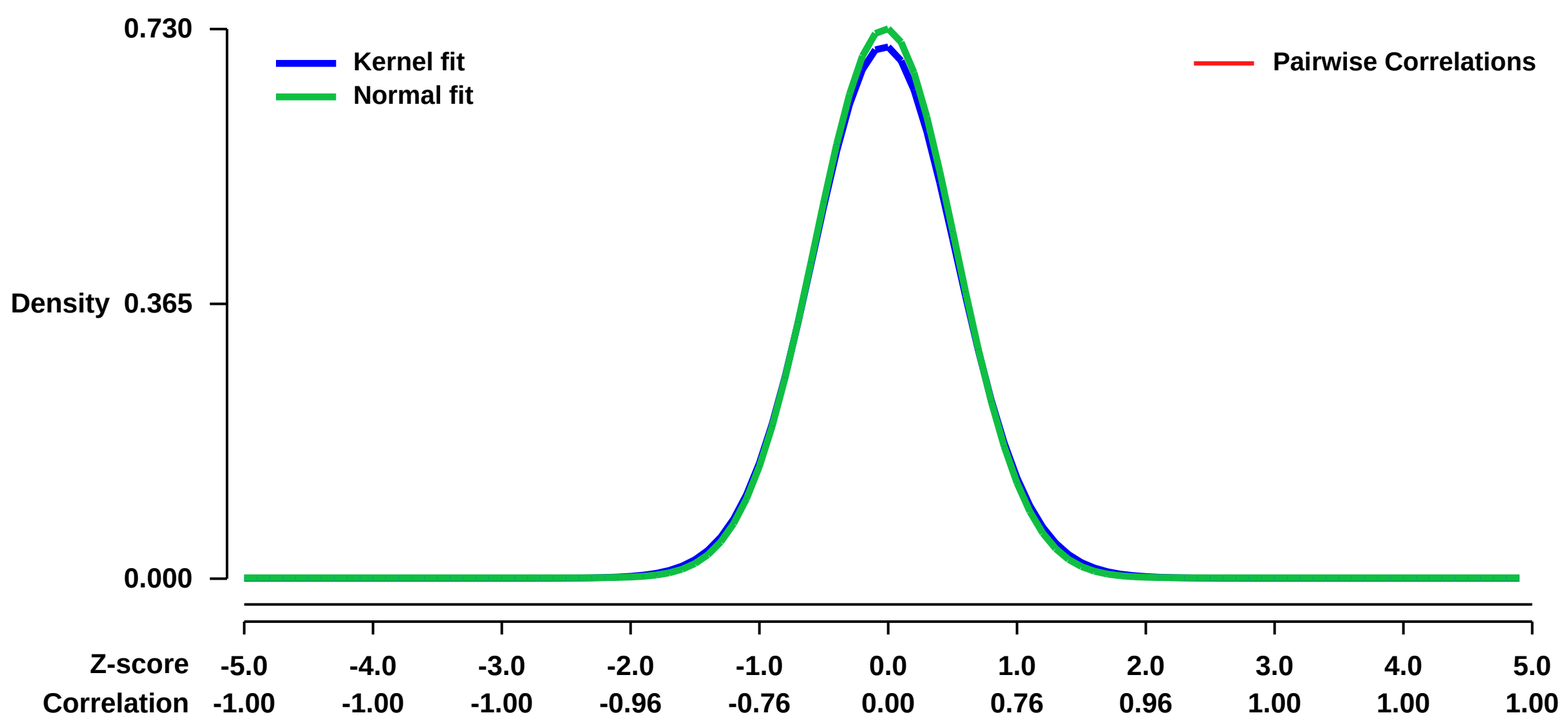

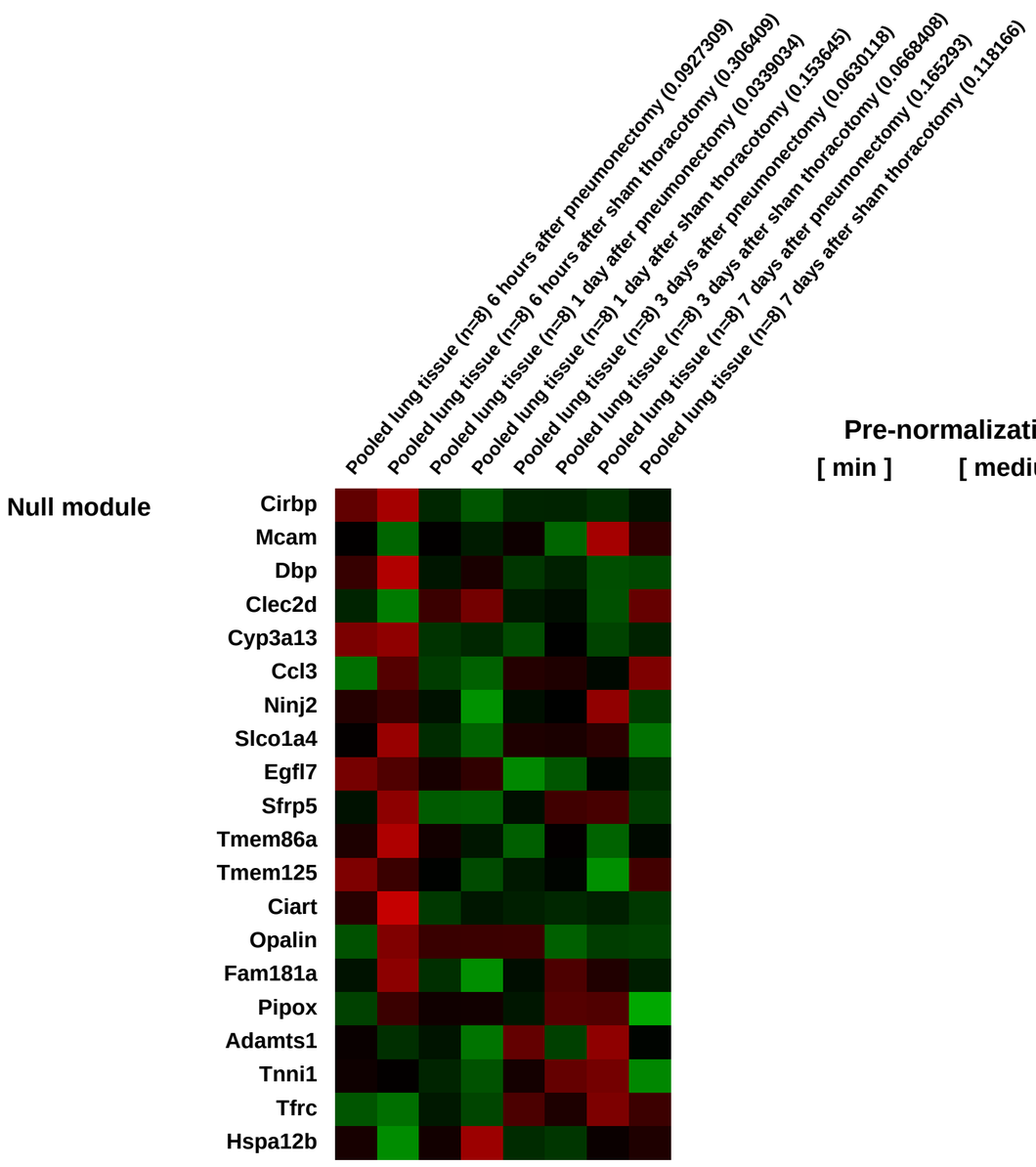

GEO Series "GSE7309" Expression Profiles

Num of samples in this series: 12

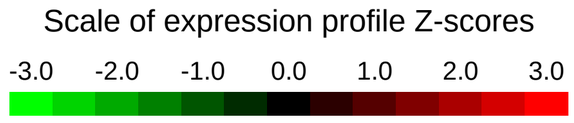

GEO Link:	http://www.ncbi.nlm.nih.gov/geo/query/acc.cgi?acc=GSE7309
Status:	Public on Jun 04 2007
Title:	Requirement for ERK MAP kinase in mouse preimplantation development
Organism:	Mus musculus
Experiment type:	Expression profiling by array
Platform:	GPL1261
Pubmed ID:	17611221

Summary & Design:

Summary:
Preimplantation development is a crucial step for successful implantation and pregnancy. Although both compaction and blastocyst formation have been extensively studied, mechanisms regulating early cell division stages before compaction have remained unclear. Here, we show that ERK MAP kinase function is required for early embryonic cell division and normal cell-cell adhesion before compaction. Our analysis demonstrates that inhibition of ERK activation in the late 2-cell stage embryos leads to a reversible arrest in G2 phase in the 4-cell stage. The G2 arrested, 4-cell stage embryos show weakened cell-cell adhesion as compared to control embryos. Remarkably, microarray analyses show that most of the programmed changes of upregulated and downregulated gene expression during the 4- to 8-cell stages normally proceed in the 4-cell stage-arrested embryos, except for a portion of the genes whose expression profiles closely parallel the stages of embryonic development when arrested in G2 and released to resume development. These parallel genes include the genes encoding intercellular adhesion molecules, whose expression is found to be positively regulated by the ERK pathway. We also show that while ERK inactivation in the 8-cell stage embryos does not lead to cell division arrest, it does cause cell division arrest when cadherin-mediated cell-cell adhesion is disrupted. These results demonstrate an essential role of ERK function in the G2/M transition and the expression of adhesion molecules during the 2-cell to 8-cell stage embryos, and suggest a loose parallelism between the gene expression programs and the developmental stages before compaction.

Keywords: preimplantation development

Overall design:
We examined expression profiles of genes during early cell division stages in mouse preimplantation development. We performed the genome-wide analysis by using Affymetrix GeneChip oligonucleotide microarrays, and examined the effect of the ERK pathway inhibitor U0126 on the expression profiles. Two independent experiments were carried out. We collected embryos at six points as follows; control embryos at day 1.5 (cont. 1.5, 2-cell stage), day 2.5 (cont. 2.5, 4- to 8-cell), and day 3.5 (cont. 3.5, morula to blastocyst), and the U0126-treated embryos at day 2.5 (U2.5, 4-cell arrested), embryos released from the U0126-induced arrest at day 3.5 (U3.5, 8-cell) and at day 4.5 (U4.5, morula to blastocyst). Hybridization was carried out with the Mouse Genome 430 2.0 array following Affymetrix instructions. Hybridized arrays were scanned using an Affymetrix GeneChip Scanner. Expression analysis was performed using GeneChip Operating Software v. 1.2 (GCOS) and GeneSpring 7.3.

Background corr dist: KL-Divergence = 0.1006, L1-Distance = 0.0712, L2-Distance = 0.0102, Normal std = 0.4923

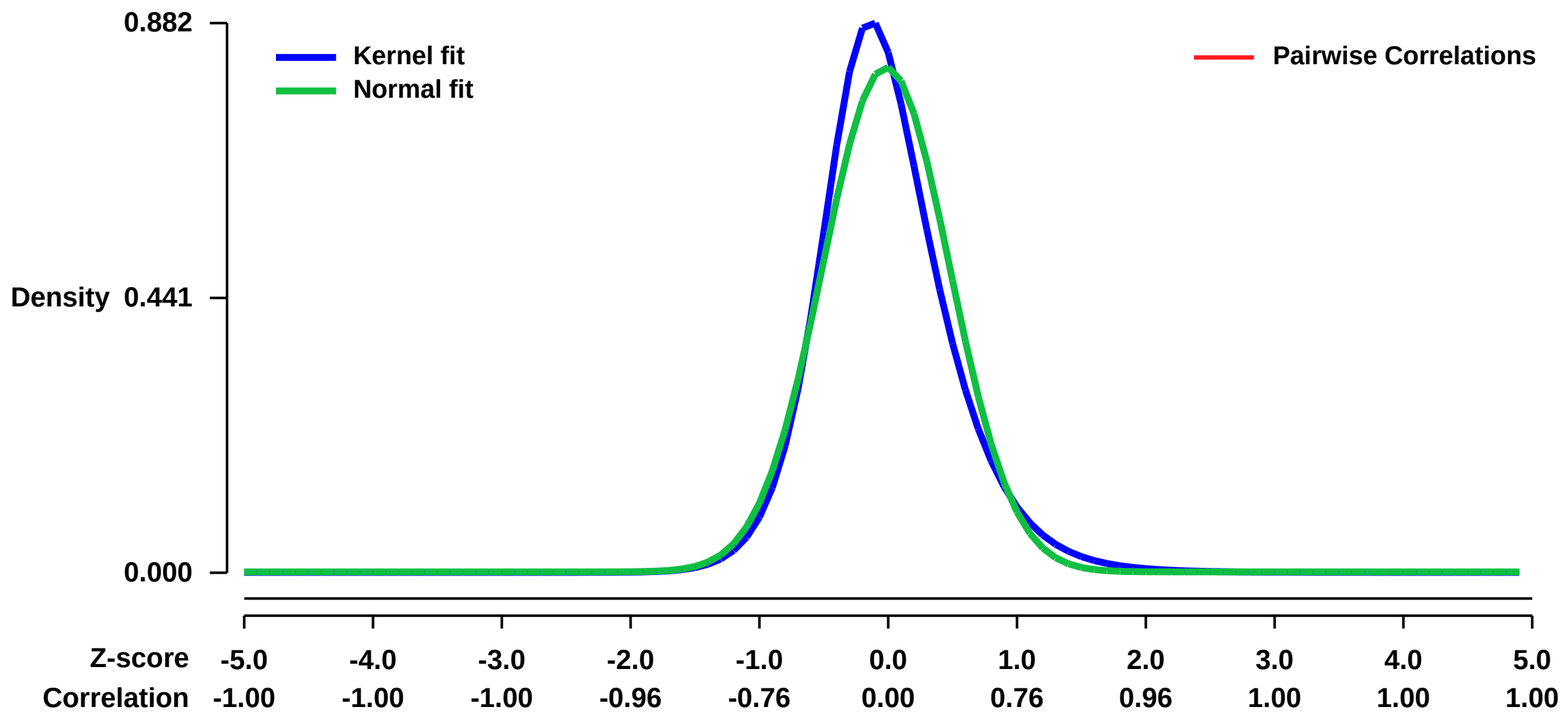

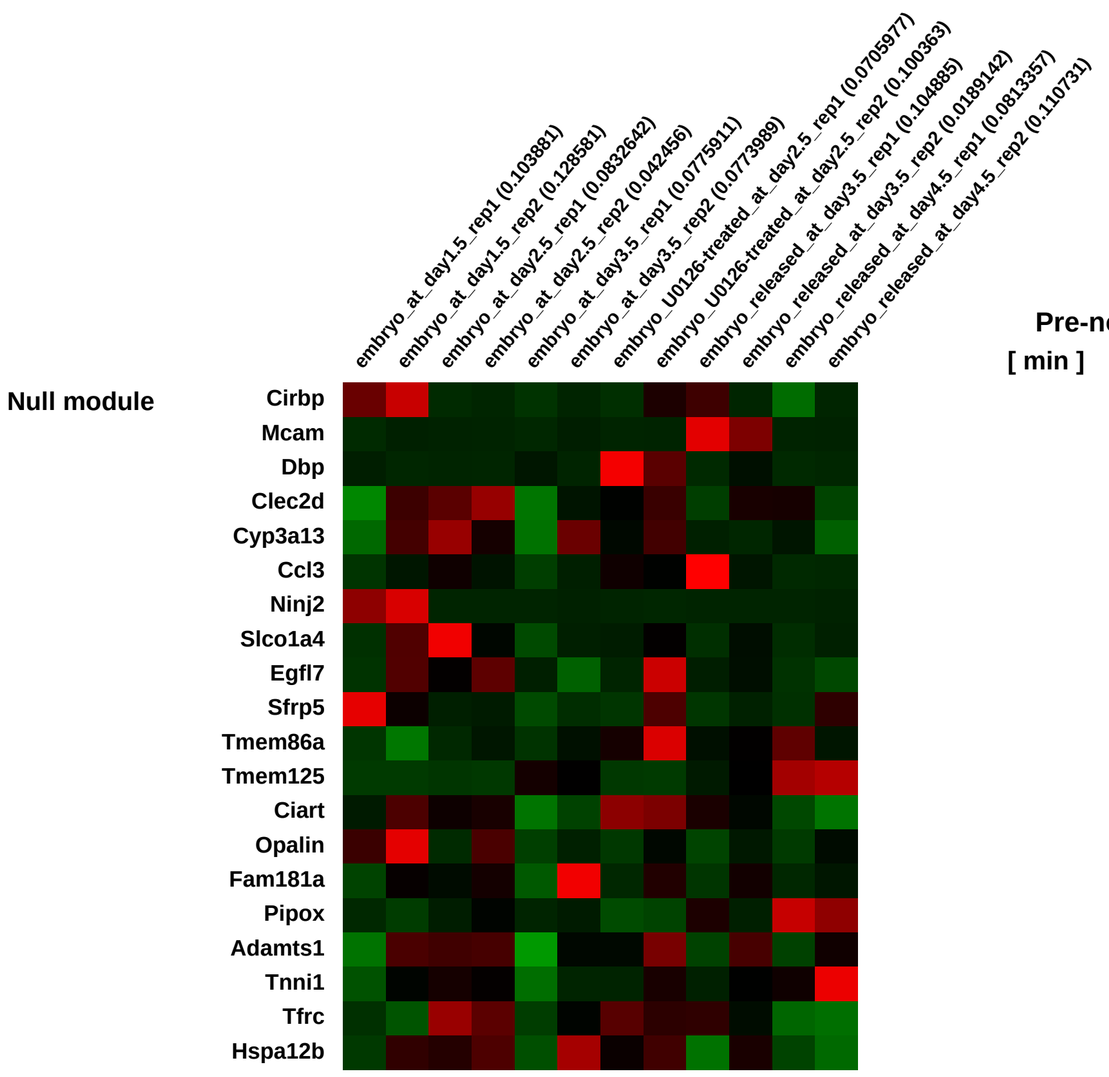

GEO Series "GSE5763" Expression Profiles

Num of samples in this series: 9

Scale of expression profile Z-scores

-3.0 -2.0 -1.0 0.0 1.0 2.0 3.0

GEO Link:	http://www.ncbi.nlm.nih.gov/geo/query/acc.cgi?acc=GSE5763
Status:	Public on Sep 10 2006
Title:	Expression data from mouse brain region bed nucleus of the stria terminalis, nucleus accumbens, and dorsal striatum.
Organism:	Mus musculus
Experiment type:	Expression profiling by array
Platform:	GPL1261
Pubmed ID:	17911379
Summary & Design:	**Summary:** To identify distinct transcriptional patterns between the major subcortical dopamine targets commonly studied in addiction we studied differences in gene expression between the bed nucleus of the stria terminalis (BNST), nucleus accumbens (NAc), and dorsal striatum (dStr) using microarray analysis. We first tested for differences in expression of genes encoding transcripts for common neurotransmitter systems as well as calcium binding proteins routinely used in neuroanatomical delineation of brain regions. This a priori method revealed differential expression of corticotropin releasing hormone (Crh), the GABA transporter (Slc6a1), and prodynorphin (Pdyn) mRNAs as well as several others. Using a gene ontology tool, functional scoring analysis, and Ingenuity Pathway Analysis, we further identified several physiological pathways that were distinct among these brain regions. These two different analyses both identified calcium signaling, G15 coupled protein receptor signaling, and adenylate cyclase-related signaling as significantly different among the BNST, NAc, and dStr. These types of signaling pathways play important roles in, amongst other things, synaptic plasticity. Investigation of differential gene expression revealed several instances that may provide insight into reported differences in synaptic plasticity between these brain regions. The results support other studies suggesting that crucial pathways involved in neurotransmission are distinct among the BNST, NAc, and dStr, and provide insight into the potential use of pharmacological agents that may target region-specific signaling pathways. Further, these studies provide a framework for future mouse-mouse comparisons of transcriptional profiles after behavioral/pharmacological manipulation. **Keywords:** Tissue type comparison **Overall design:** The genome-wide geen expression of mouse brain region bed nucleus of the stria terminalis, nucleus accumbens, and dorsal striatum were analyzed by Affymetrix Mouse430_2 chip. The expression and functional profiles were compared between these 3 tissues and cross-validated from independant data published before.

Background corr dist: KL-Divergence = 0.0578, L1-Distance = 0.0190, L2-Distance = 0.0004, Normal std = 0.5281

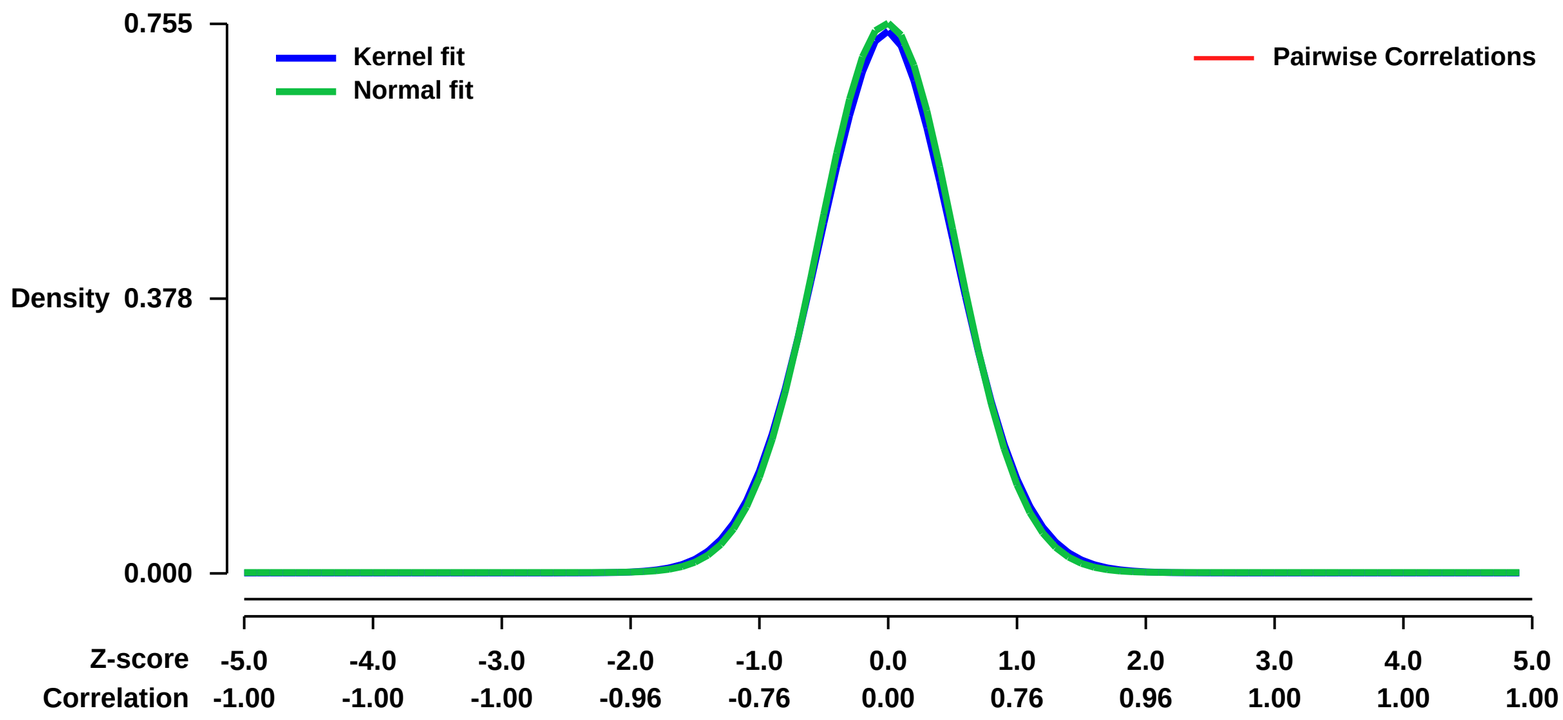

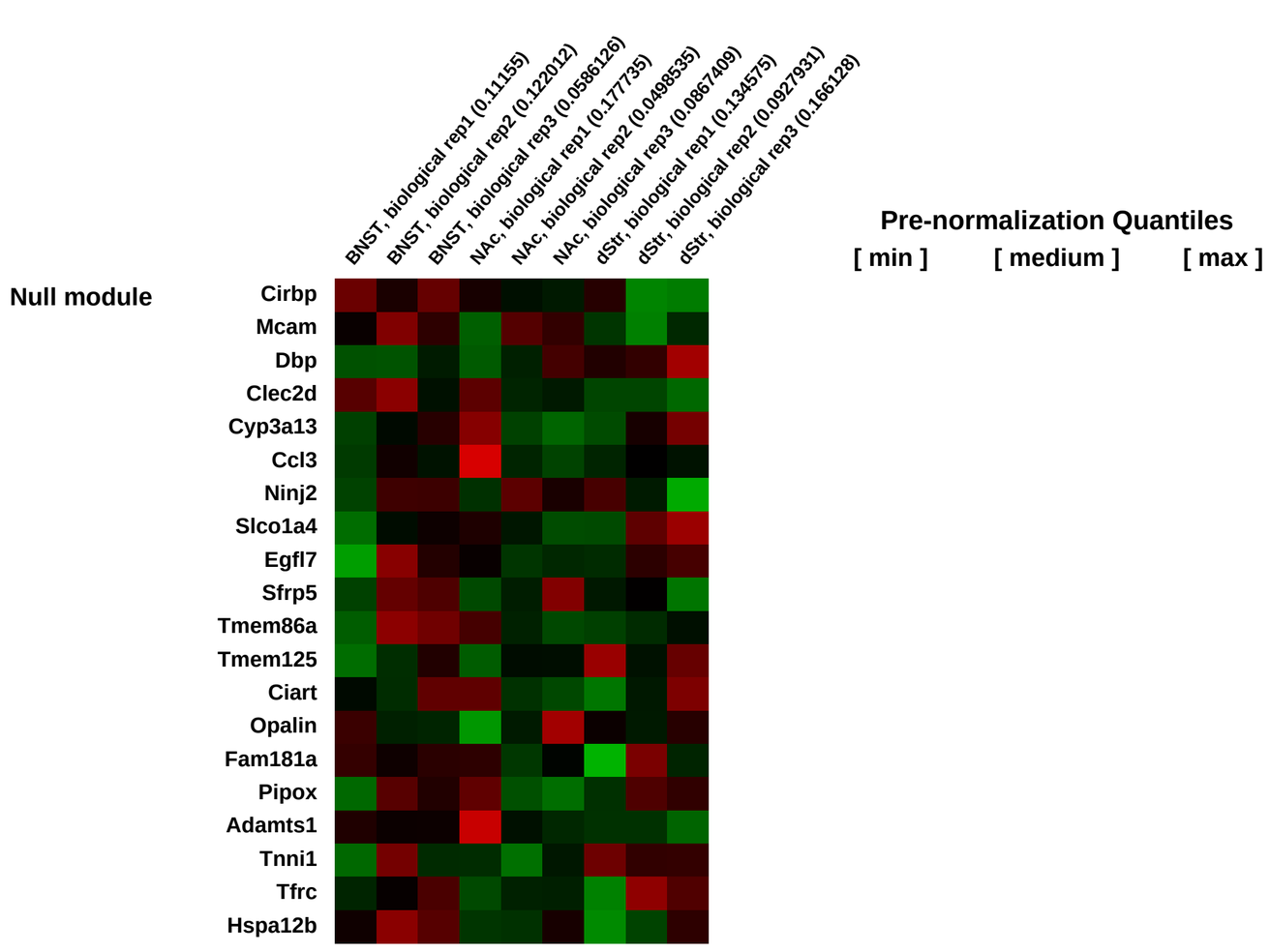

GEO Series "GSE7111" Expression Profiles

Num of samples in this series: 6

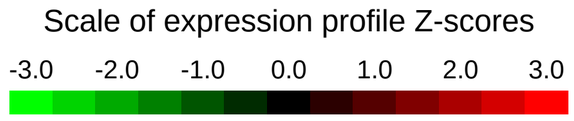

GEO Link:	**http://www.ncbi.nlm.nih.gov/geo/query/acc.cgi?acc=GSE7111**
Status:	**Public on Dec 25 2012**
Title:	**Resveratrol treatment of 3T3-L1 cells**
Organism:	**Mus musculus**
Experiment type:	**Expression profiling by array**
Platform:	**GPL1261**
Pubmed ID:	
Summary & Design:	**Summary:** **Murine 3T3-L1 progenitor adipocytes cell cultures, treated and untreated (Control) with resveratrol before the induction of differentiation and the effects on adipogenesis and insulin signaling was investigated.** **Keywords: Treatment response** **Overall design:** **3 Replicates of treated and untreated (Control) cell cultures**

Background corr dist: **KL-Divergence = 0.0438, L1-Distance = 0.0219, L2-Distance = 0.0005, Normal std = 0.6019**

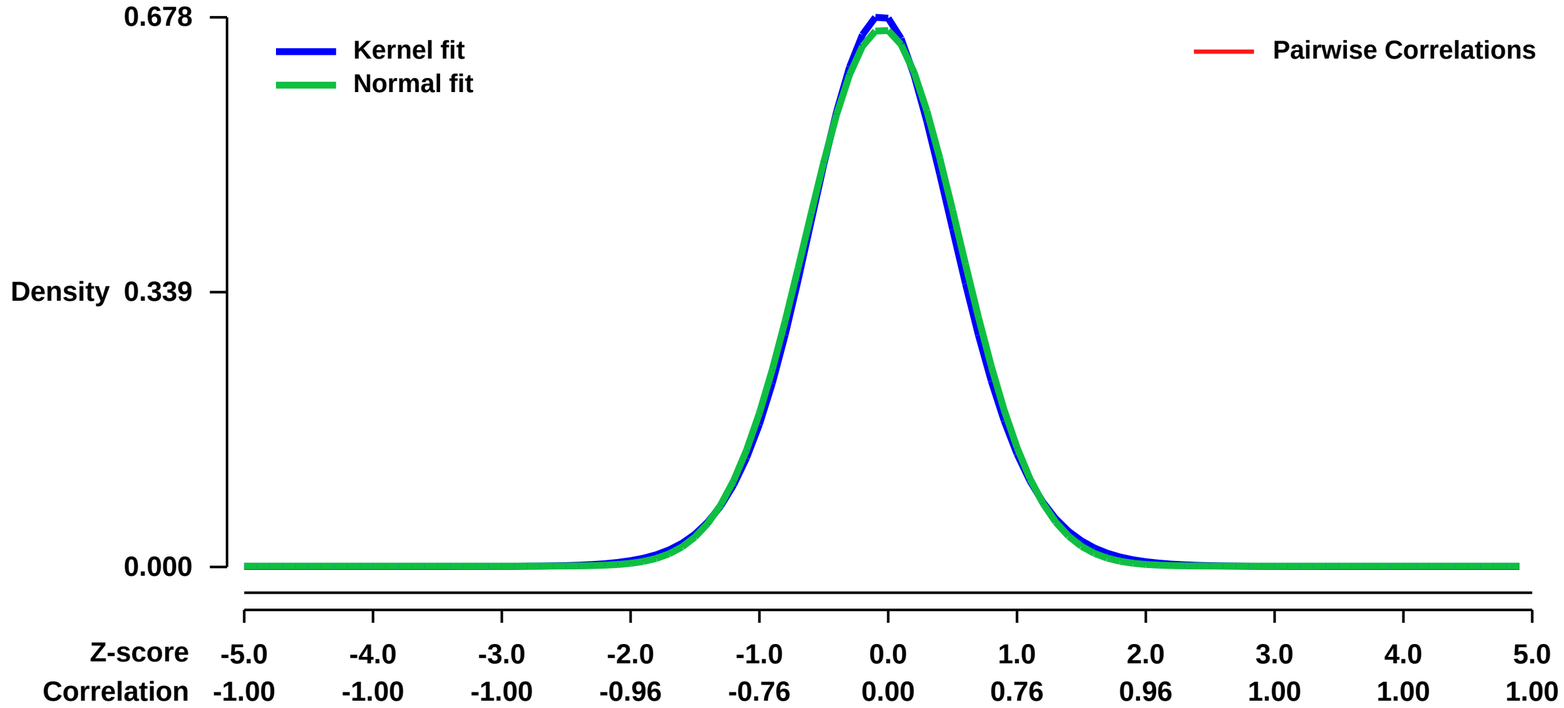

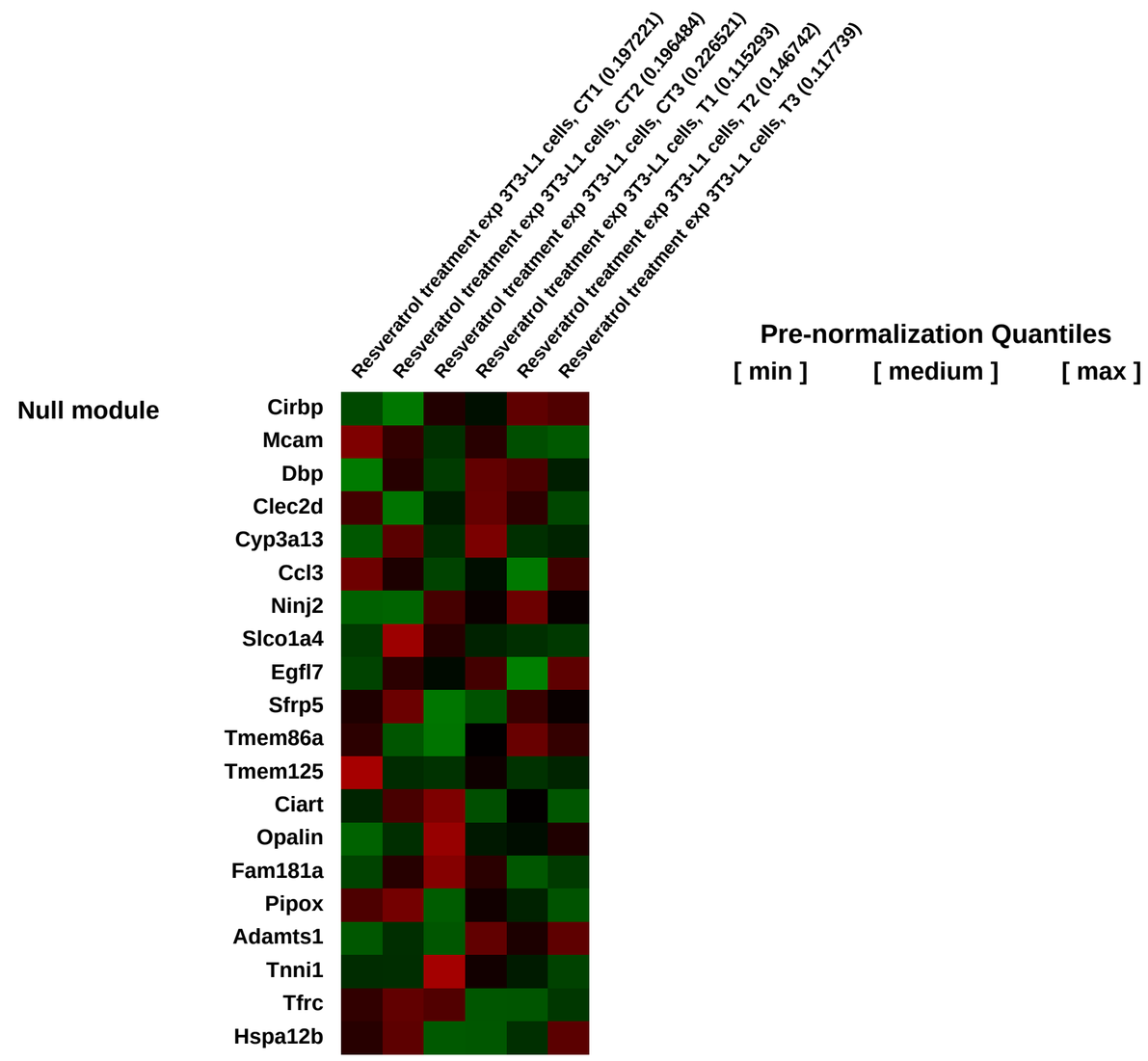

GEO Series "GSE35805" Expression Profiles

Num of samples in this series: 8

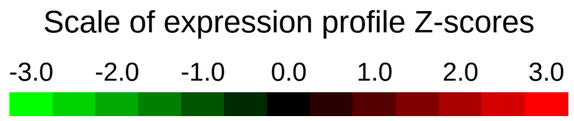

GEO Link:	**http://www.ncbi.nlm.nih.gov/geo/query/acc.cgi?acc=GSE35805**
Status:	**Public on May 16 2014**
Title:	**Gene expression analysis of WT and Flt3-ITD multipotent progenitors**
Organism:	**Mus musculus**
Experiment type:	**Expression profiling by array**
Platform:	**GPL1261**
Pubmed ID:	**23727242**
Summary & Design:	**Summary:** **FLT3-ITDs Introduce a Myeloid Differentiation and Transformation Bias in Lympho-myeloid Multipotent Progenitors** **Overall design:** **WT multipotent progenitors were compared with FLT3-ITD multipotent progenitors**

Background corr dist: **KL-Divergence = 0.0862, L1-Distance = 0.0236, L2-Distance = 0.0010, Normal std = 0.4654**

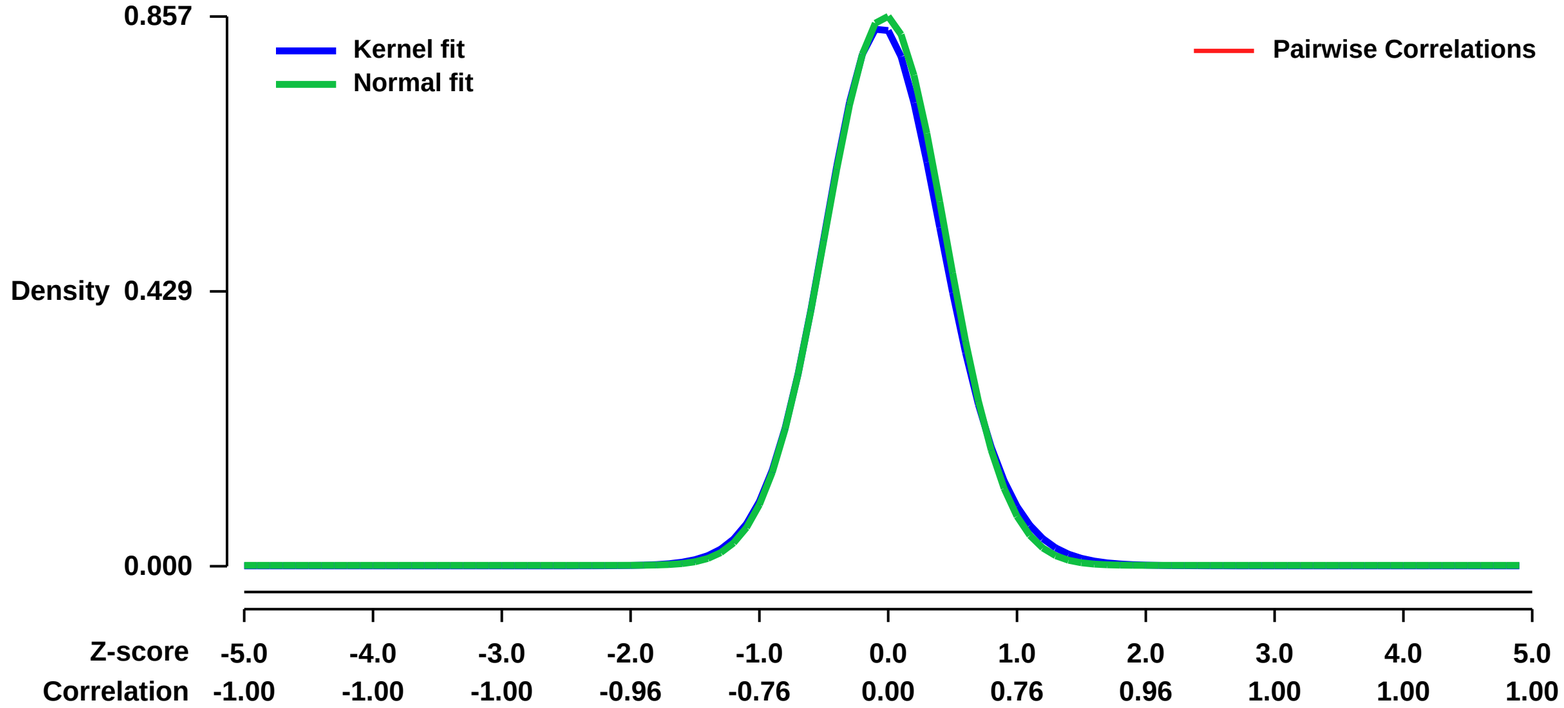

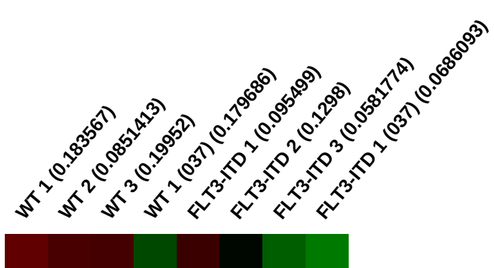

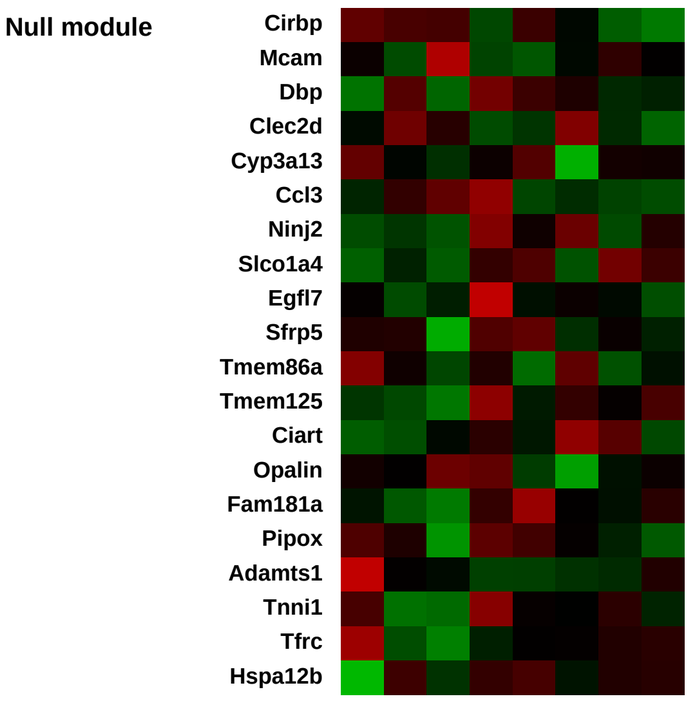

GEO Series "GSE6030" Expression Profiles

Num of samples in this series: 6

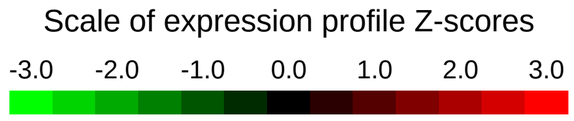

GEO Link:	**http://www.ncbi.nlm.nih.gov/geo/query/acc.cgi?acc=GSE6030**
Status:	**Public on Oct 13 2007**
Title:	**Pineal gland gene expression of 129 Wt P0 mice versus NeuroD1 pineal gene expression at P0**
Organism:	**Mus musculus**
Experiment type:	**Expression profiling by array**
Platform:	**GPL1261**
Pubmed ID:	**17630985**
Summary & Design:	**Summary:** **This study determines pineal gland gene expression levels in the NeuroD1 knockout mouse at postnatal day zero.** **Comparison was performed against pineal gland gene expression levels in 129 wildtype mice also disected at P0.** **Keywords: Comparison of wildtype versus transgenic pineal gland gene expression** **Overall design:** **Triplicate arrays were run for wildtype and the homozygous animals.**

Background corr dist: **KL-Divergence = 0.0386, L1-Distance = 0.0276, L2-Distance = 0.0010, Normal std = 0.6292**

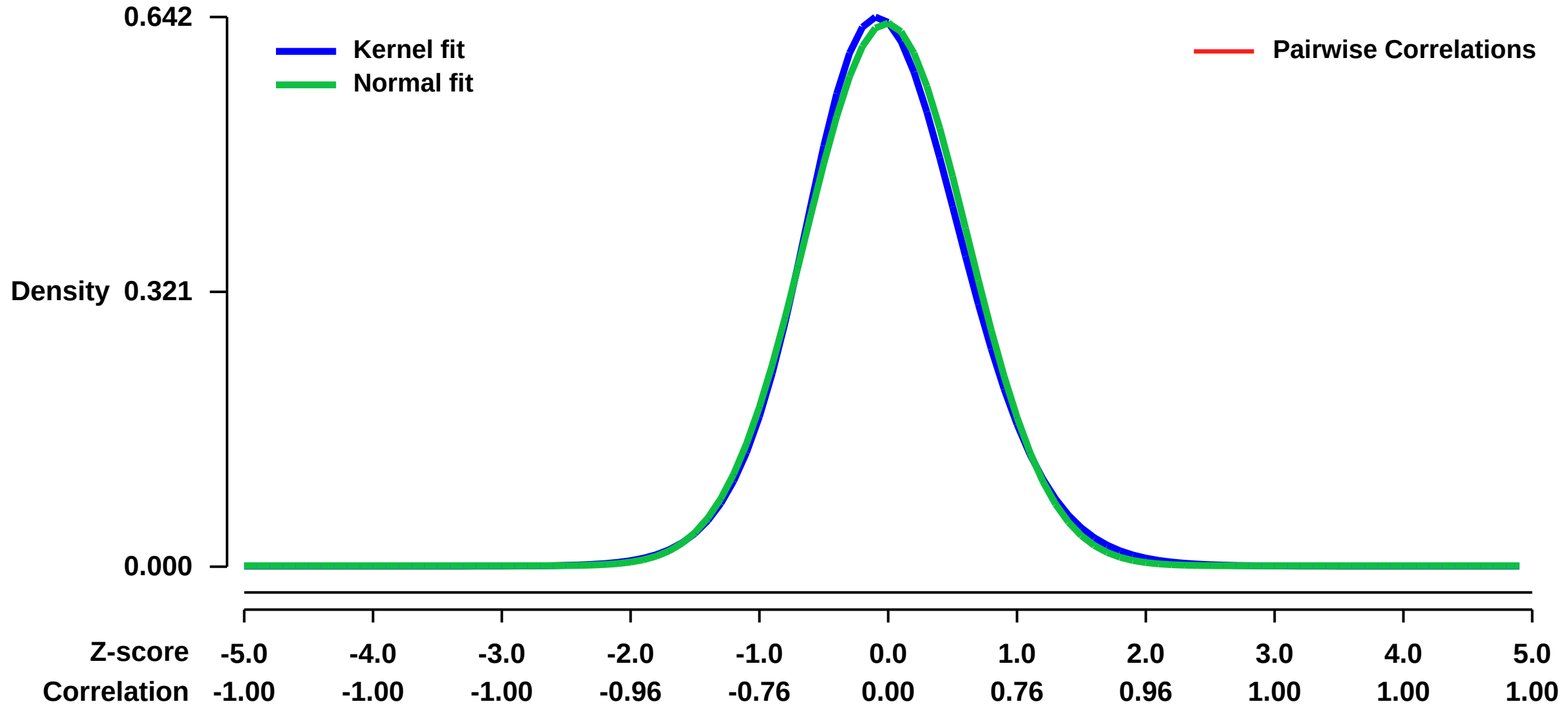

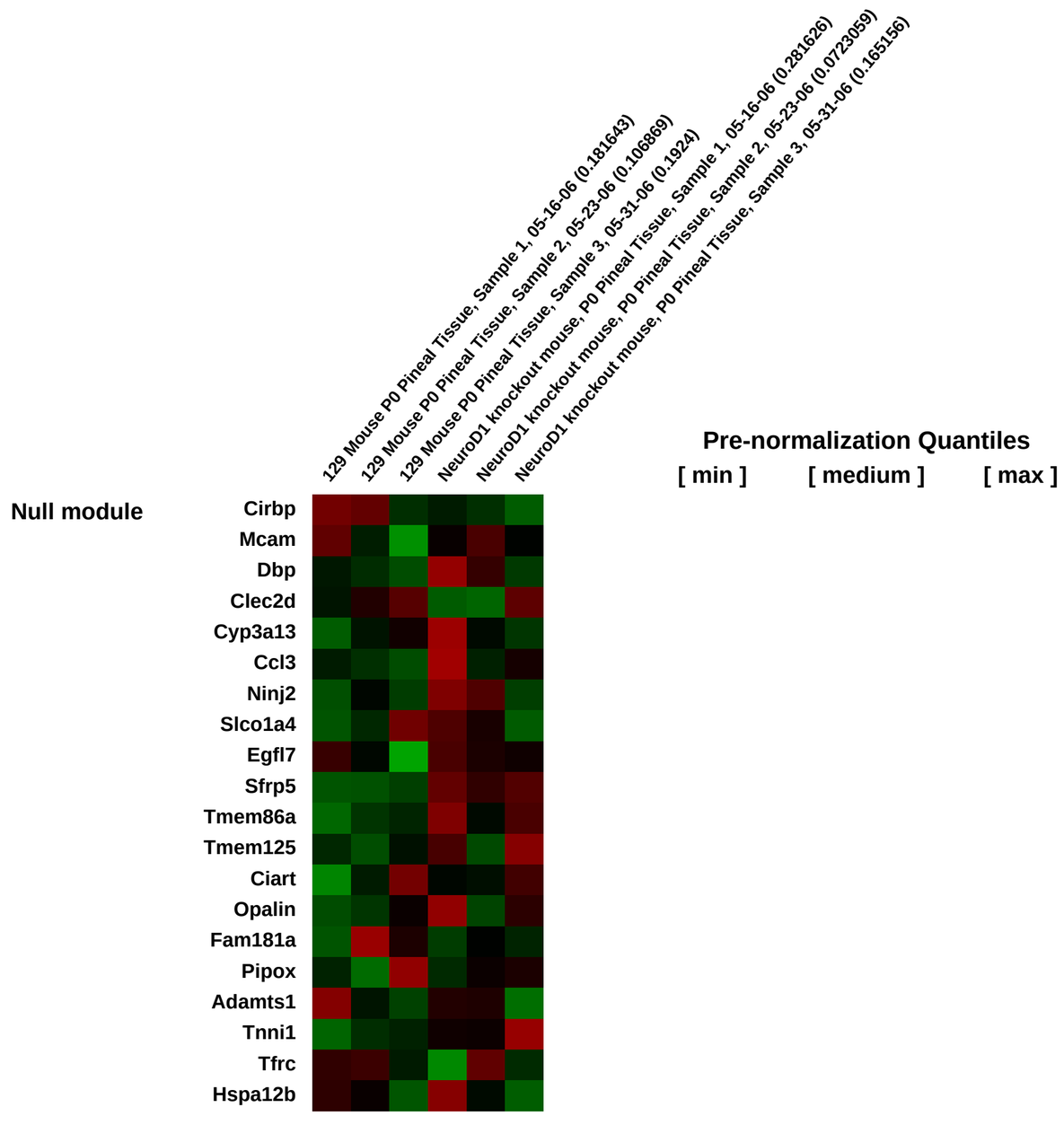

GEO Series "GSE8488" Expression Profiles

Num of samples in this series: 15

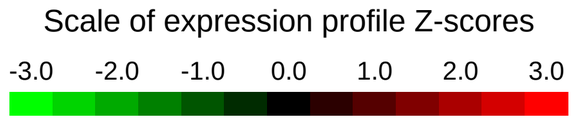

GEO Link:	http://www.ncbi.nlm.nih.gov/geo/query/acc.cgi?acc=GSE8488
Status:	Public on Jan 31 2008
Title:	Inhibitor Trials
Organism:	Mus musculus
Experiment type:	Expression profiling by array
Platform:	GPL1261
Pubmed ID:	20111593
Summary & Design:	**Summary:** **Objectives: To identify similarities and differences in gene expression data in the MEK/ERK and PI3K pathways and to determine how histone modification affects these same pathways.** **Goal: To identify and functionally characterize novel targets of these signaling pathways in the context of chondrocyte differentiation.** **Keywords: Teatment, signaling, one-colour array, signaling pathway comparison** **Overall design:** **A total of 15 genechips were analyzed between 4 treatments and the vehicle (DMSO) control. Three biological replicates per treatment were executed.**

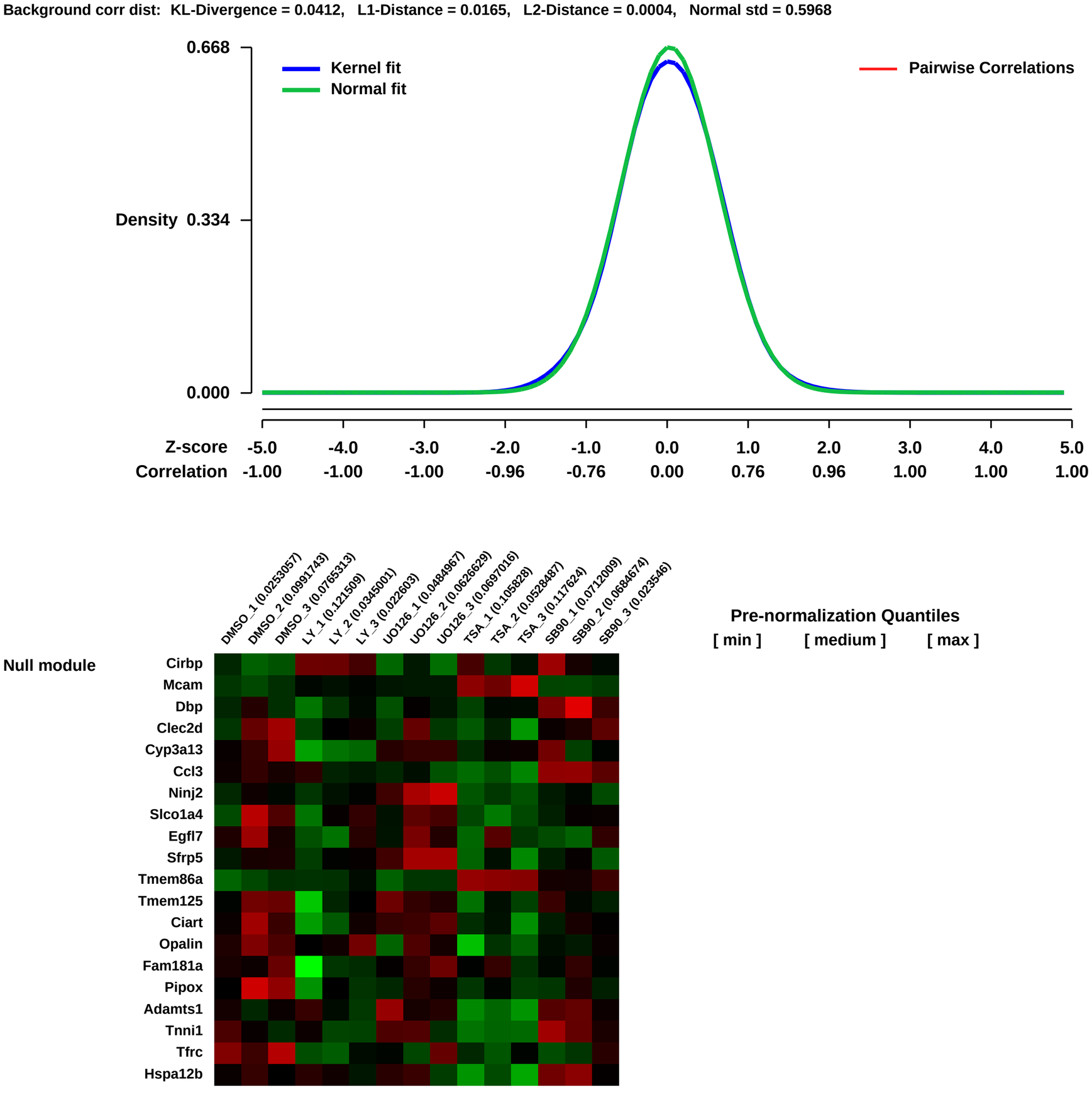

GEO Series "GSE20726" Expression Profiles

Num of samples in this series: 9

Scale of expression profile Z-scores

-3.0 -2.0 -1.0 0.0 1.0 2.0 3.0

GEO Link:	**http://www.ncbi.nlm.nih.gov/geo/query/acc.cgi?acc=GSE20726**
Status:	**Public on Mar 10 2011**
Title:	**Gene expression analysis of mouse ear samples treated with chemical allergen**
Organism:	**Mus musculus**
Experiment type:	**Expression profiling by array**
Platform:	**GPL1261**
Pubmed ID:	**22974541**
Summary & Design:	**Summary:** **Identification of chemical allergen inducible genes in mouse skin.** **Ear samples were isolated from CL57BL/6 mice 6 hours after topical application of a prototypic chemical allergen, a skin irritant or vehicle alone.** **Overall design:** **Total RNA were extracted from ear skin samples treated with a chemical allergen, a skin irritant, or vehicle alone for 6 hours.**

Background corr dist: **KL-Divergence = 0.0921, L1-Distance = 0.0243, L2-Distance = 0.0009, Normal std = 0.4511**

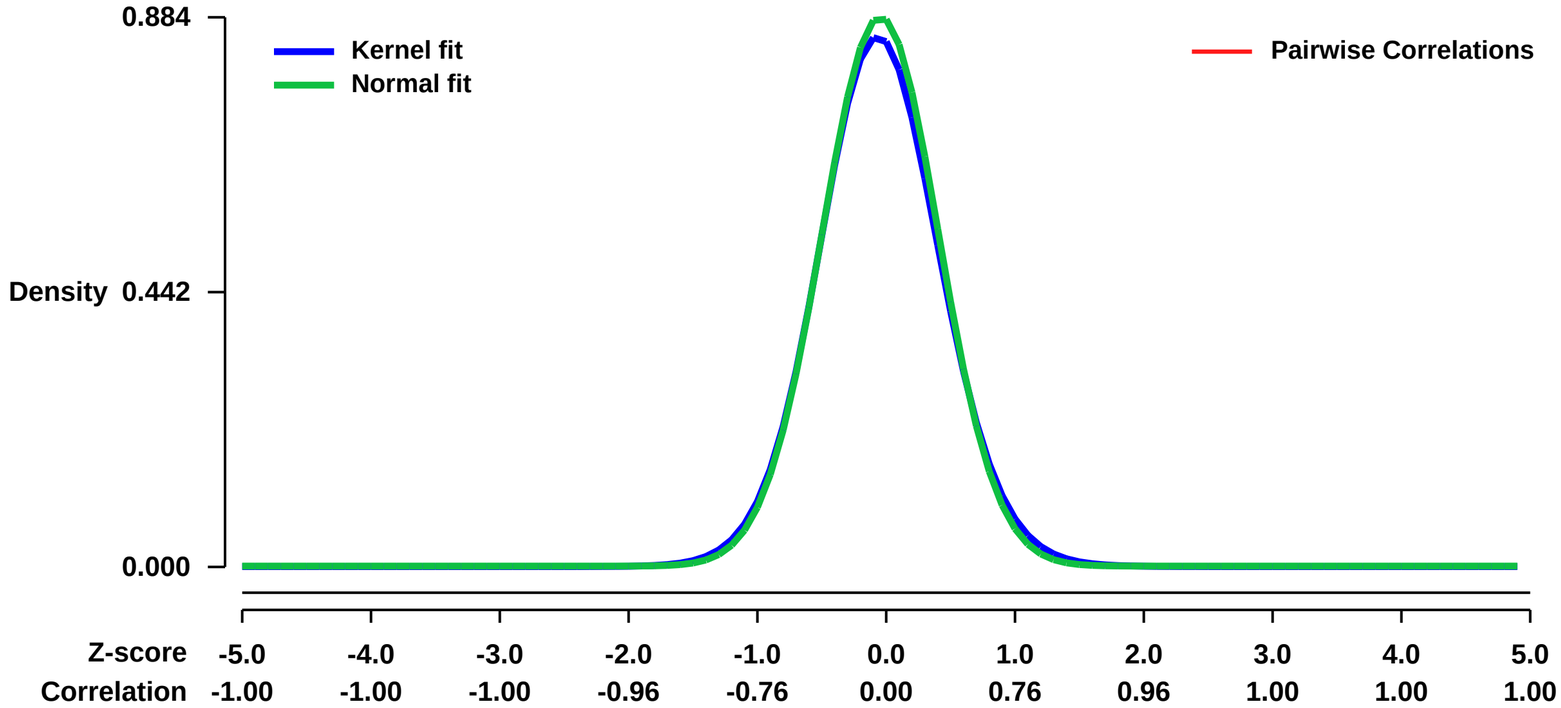

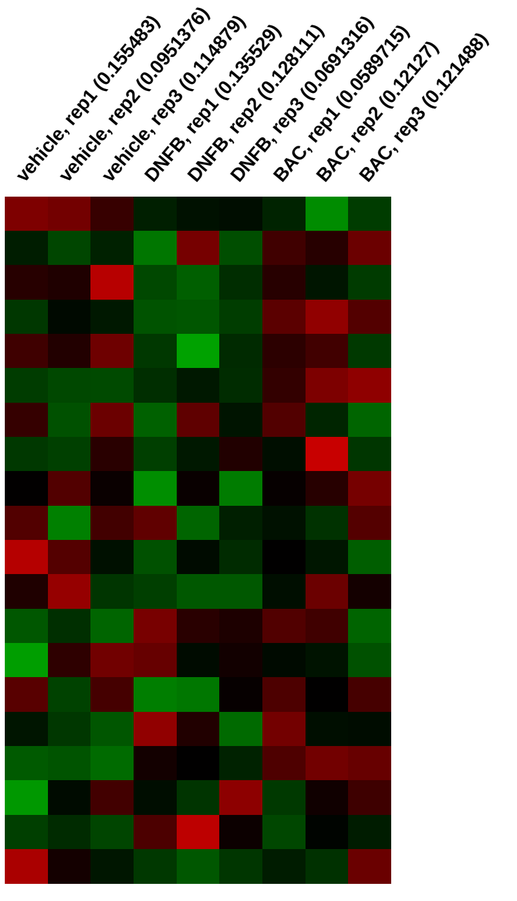

GEO Series "GSE20411" Expression Profiles

Num of samples in this series: 20

Scale of expression profile Z-scores

-3.0 -2.0 -1.0 0.0 1.0 2.0 3.0

GEO Link:	http://www.ncbi.nlm.nih.gov/geo/query/acc.cgi?acc=GSE20411
Status:	Public on Jan 01 2011
Title:	The effects of aging vs. alpha7 nAChR subunit deficiency on the mouse brain transcriptome
Organism:	Mus musculus
Experiment type:	Expression profiling by array
Platform:	GPL1261
Pubmed ID:	20526689
Summary & Design:	**Summary:** Aging is accompanied by expression changes in multiple genes and the brain is one of the tissues most vulnerable to aging. Since the alpha7 nicotinic acetylcholine receptor (nAChR) subunit has been associated with neurodevelopmental disorders and cognitive decline during aging, we hypothesized that its absence might affect gene expression profiles in aged brains. To study whether transcriptional changes occur due to aging, alpha7 deficiency or both, we analyzed whole brain transcriptomes of young (8 week) and aged (2 year) alpha7 deficient and wild-type control mice, using Mouse Genome 430 2.0 microarray. Highly significant expression changes were detected in 47 and 1543 genes (after Bonferroni and FDR correction) in the brains of aged mice compared to young mice, regardless of their genotype. These included genes involved in immune system function and ribosome structure, as well as genes that were previously demonstrated as differentially expressed in aging human brains. Genotype-dependent changes were detected in only 3 genes, Chrna7 which encodes the alpha7 nAChR subunit, and two closely linked genes, likely due to a mouse background effect. Expression changes dependent on age-genotype interaction were detected in 207 genes (with a low significance threshold). Age-dependent differential expression levels were approved in all nine genes that were chosen for validation by real-time RT-PCR. Our results suggest that the robust effect of aging on brain transcription clearly overcomes the almost negligible effect of alpha7 nAChR subunit deletion, and that germline deficiency of this subunit has a minor effect on brain expression profile in aged mice. **Overall design:** Total of 20 samples. 10 from young adult mice (8 weeks) and 10 from aged mice (2 years). In each age group, 5 were wild-type control mice and 5 alpha7 nAChR subunit defecient mice

Background corr dist: KL-Divergence = 0.2632, L1-Distance = 0.0538, L2-Distance = 0.0070, Normal std = 0.2961

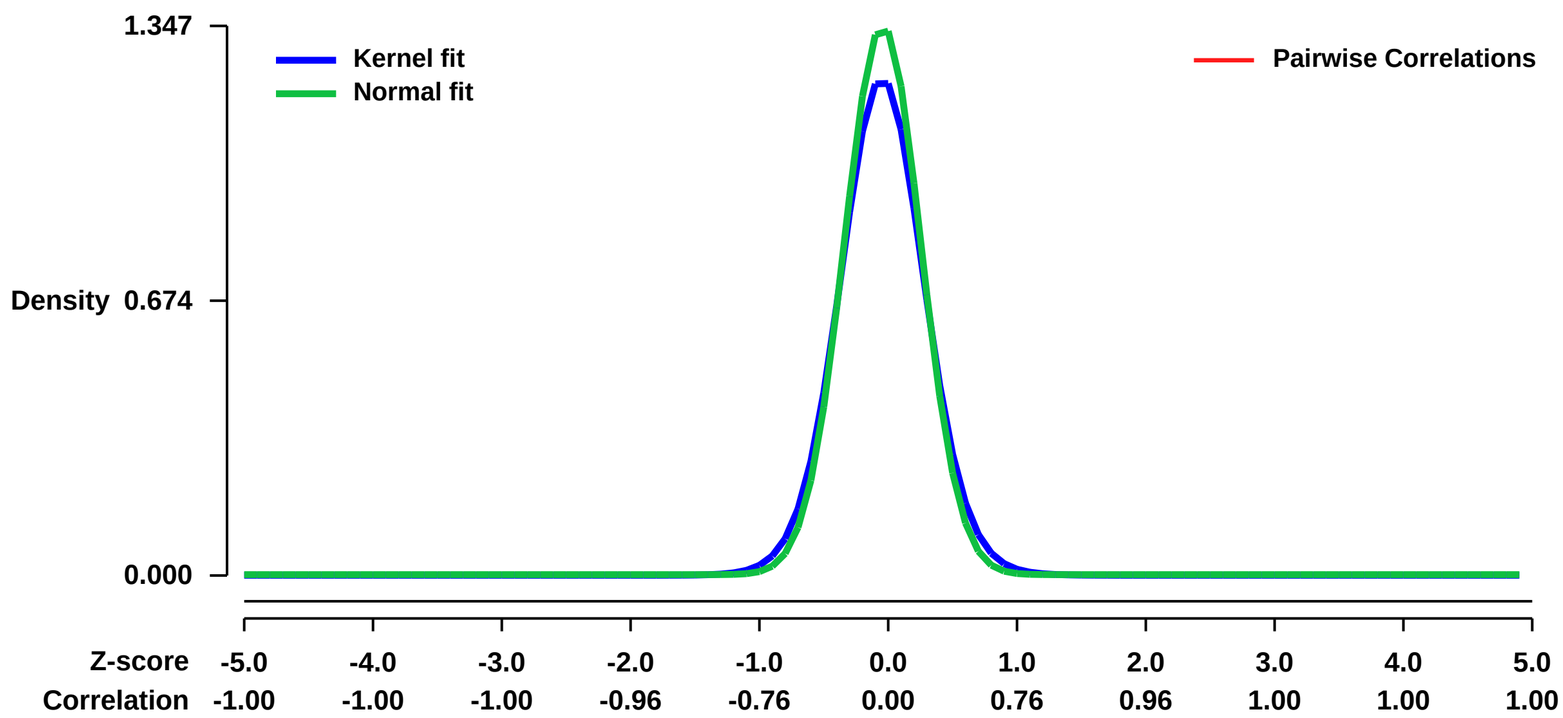

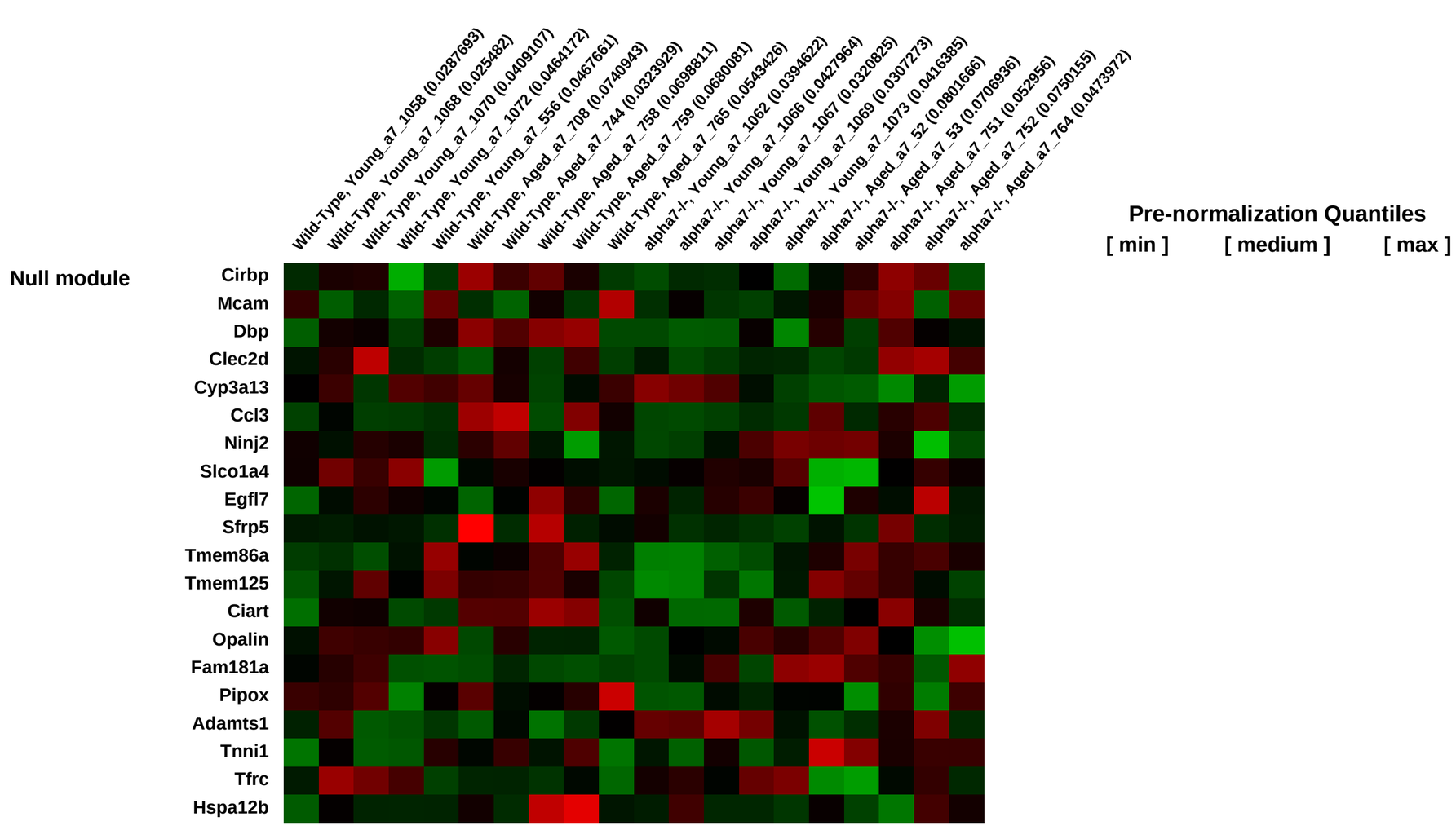

GEO Series "GSE17797" Expression Profiles

Num of samples in this series: 19

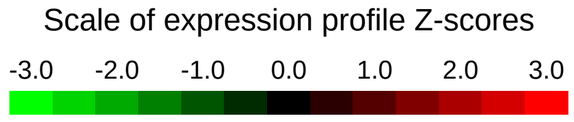

GEO Link:	http://www.ncbi.nlm.nih.gov/geo/query/acc.cgi?acc=GSE17797
Status:	Public on Aug 29 2010
Title:	UGE and UGM Reveal Novel Signaling Pathways and Ligand-Receptor Interactions in the Primitive Prostate Stem Cell Niche
Organism:	Mus musculus
Experiment type:	Expression profiling by array
Platform:	GPL1261
Pubmed ID:	20941365
Summary & Design:	**Summary:** We isolated fetal murine urogenital sinus epithelium and urogenital sinus mesenchyme and determined their global gene expression profiles to define their differentially expressed regulators. To distinguish gene expression patterns that are shared by other developing epithelial/mesenchymal compartments in the embryo from those that pertain to the prostate stem cell niche, we also determine the global gene expression of epidermis and dermis of the same embryos. We identified a distinctive core of transcripts that were differentially regulated in the prostate stem cell niche. Our analysis indicates that several of the key transcriptional components that are likely to be active in the embryonic prostate stem cell niche regulate processes such as self-renewal (e.g., E2f and Ap2), lipid metabolism (e.g., Serbp1) and cell migration (e.g., Areb6 and Rreb1). Several of the promoter binding motifs that are enriched in the profiles are shared between the prostate epithelial/mesenchymal compartments and their epidermis/dermis counterparts, indicating their likely relevance in epithelial/mesenchymal signaling in primitive cellular compartments. We also focused on defining ligand-receptor interactions that may be relevant in controlling signals in the stem cell niche and identified the Wnt/beta-catenin, ephrin, Notch, sonic hedgehog, FGF, TGF-beta and bone morphogenic signaling pathways as being of likely relevance in the prostate stem cell niches. Members of the integrins family including those that bind extracellular matrix proteins such as laminin and activate latent TGF-beta are also expressed in the prostate niche.development. **Keywords:** Differential gene expression **Overall design:** Six biological replicate experiments were performed for UGE. Five biological replicate experiments were performed for UGM. Four biological replicate experiments were performed for Epidermis. Four biological replicate experiments were performed for Dermis.

Background corr dist: KL-Divergence = 0.0825, L1-Distance = 0.0284, L2-Distance = 0.0013, Normal std = 0.4742

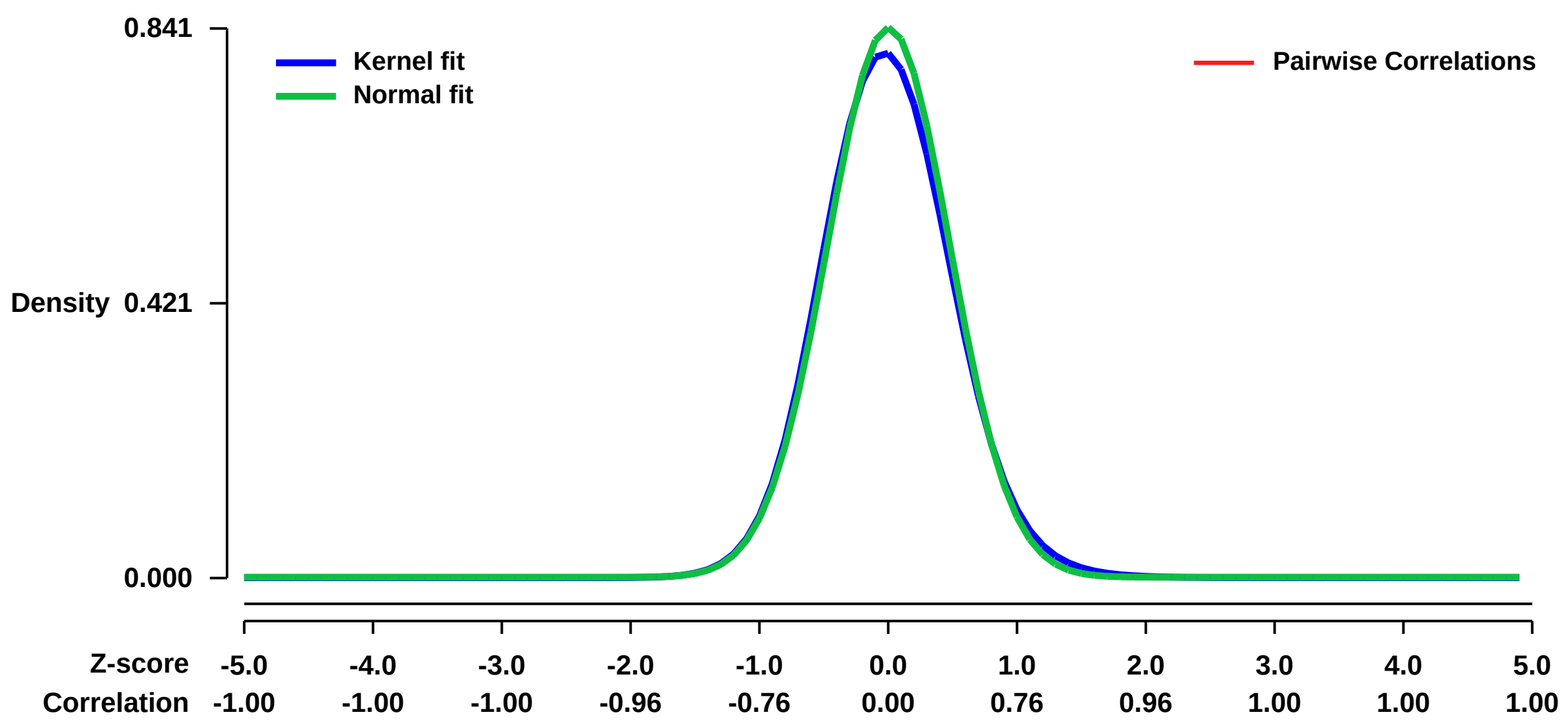

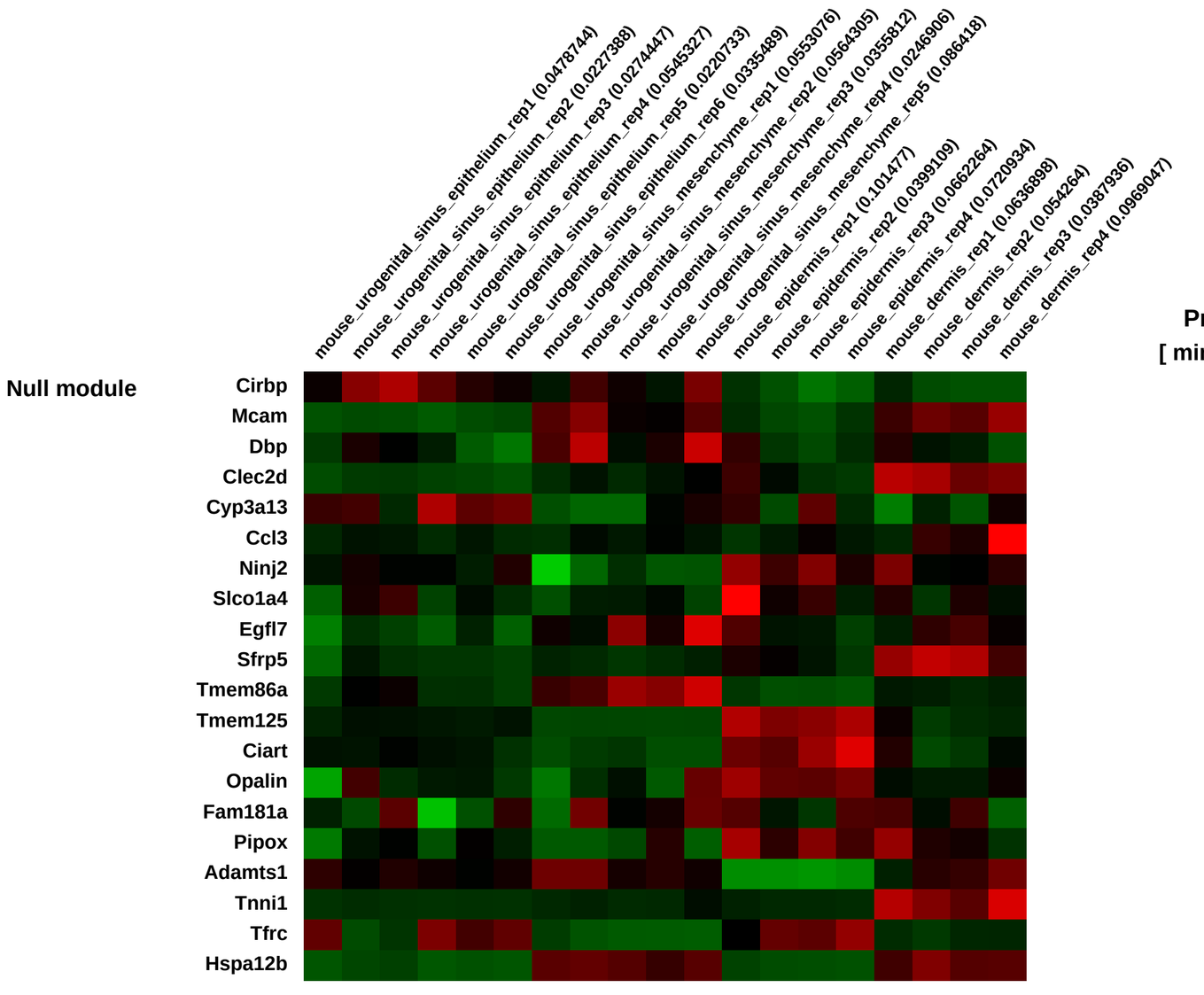

GEO Series "GSE21905" Expression Profiles

Num of samples in this series: 6

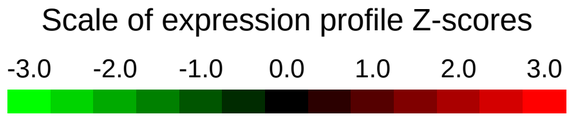

GEO Link:	**http://www.ncbi.nlm.nih.gov/geo/query/acc.cgi?acc=GSE21905**
Status:	**Public on May 21 2010**
Title:	**Gene expression in Lineage negative bone marrow cells of C57B/L6 and B.D(Chr5) mice**
Organism:	**Mus musculus**
Experiment type:	**Expression profiling by array**
Platform:	**GPL1261**
Pubmed ID:	
Summary & Design:	**Summary:** **These mouse strains differ in absolute numbers of hematopoietic stem cells but differ genetically only at the Chr 5 congenic locus.** **We used microarray analysis to identify candidate regulators of hematopoietic stem cells based on differential gene expression patterns.** **Overall design:** **Triplicate RNA samples were isolated from 500,00-800,000 Lineage negative bone marrow cells from each strain. Each of the six samples were analyzed on 6 separate MG 430 2.0 Affymetrix Microarray Chips.**

Background corr dist: **KL-Divergence = 0.0472, L1-Distance = 0.0190, L2-Distance = 0.0004, Normal std = 0.5846**

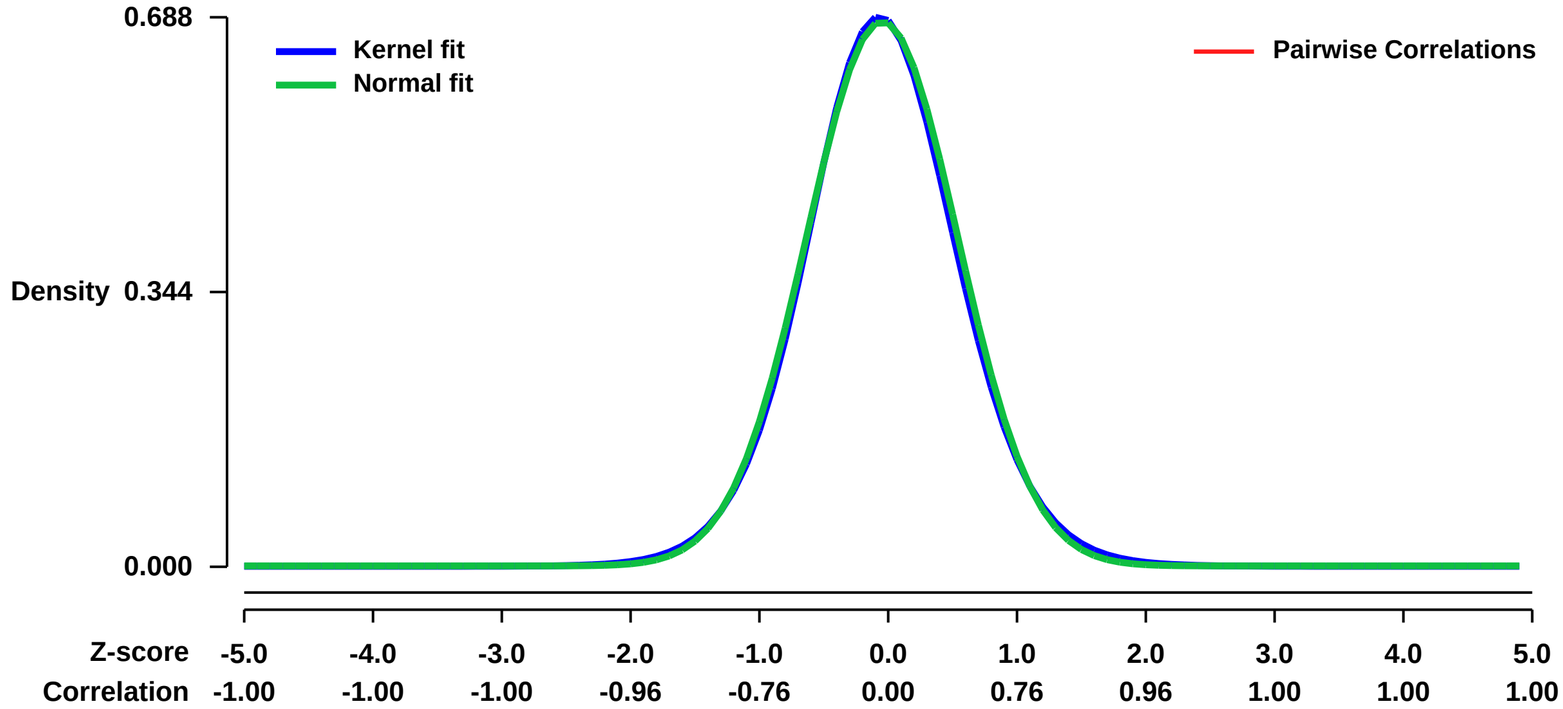

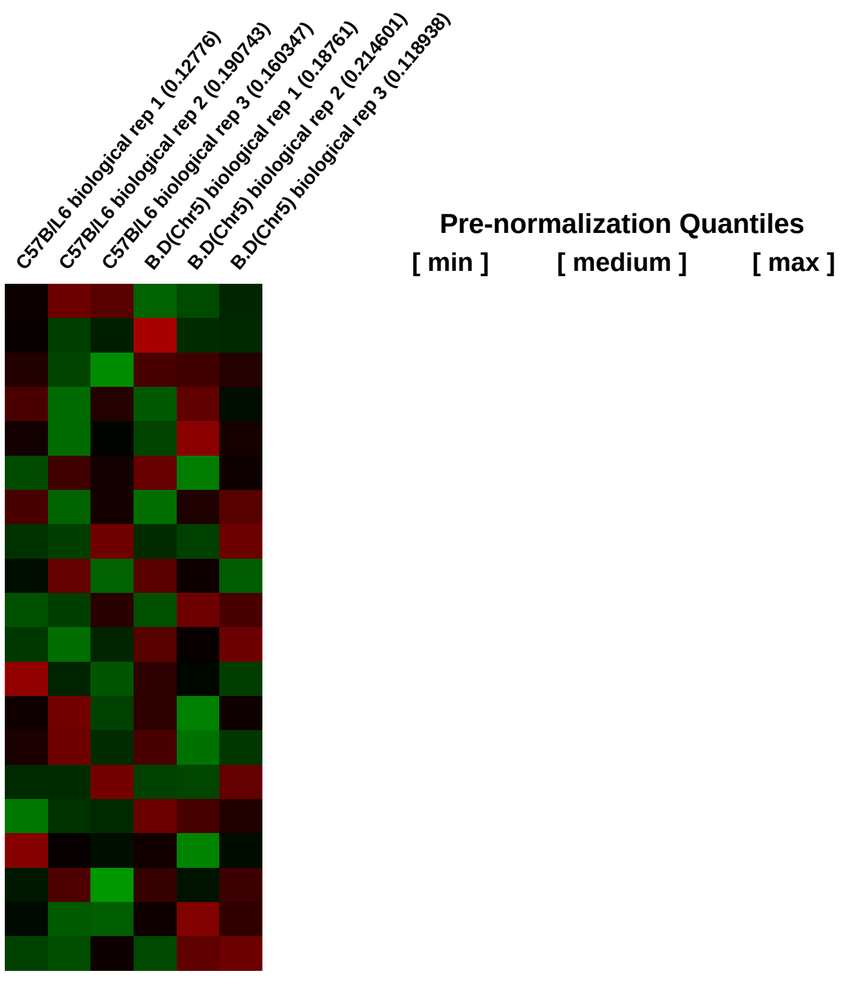

GEO Series "GSE5127" Expression Profiles

Num of samples in this series: 18

Scale of expression profile Z-scores

-3.0 -2.0 -1.0 0.0 1.0 2.0 3.0

GEO Link:	http://www.ncbi.nlm.nih.gov/geo/query/acc.cgi?acc=GSE5127
Status:	Public on Sep 01 2006
Title:	Gene Expression Biomarkers for Predicting Lung Tumors in Two-Year Rodent Bioassays
Organism:	Mus musculus
Experiment type:	Expression profiling by array
Platform:	GPL1261
Pubmed ID:	17114358
Summary & Design:	**Summary:** Two-year rodent bioassays play a central role in evaluating both the carcinogenic potential of a chemical and generating quantitative information on the dose-response behavior for chemical risk assessments. The bioassays involved are expensive and time-consuming, requiring nearly lifetime exposures (two years) in mice and rats and costing $2 to $4 million per chemical. Since there are approximately 80,000 chemicals registered for commercial use in the United States and 2,000 more are added each year, applying animal bioassays to all chemicals of concern is clearly impossible. To efficiently and economically identify carcinogens prior to widespread use and human exposure, alternatives to the two-year rodent bioassay must be developed. In this study, animals were exposed for 13 weeks to two chemicals that were positive for lung tumors in the two-year rodent bioassay, two chemicals that were negative for tumors, and two vehicle controls. Gene expression analysis was performed on the lungs of the animals to assess the potential for identifying gene expression biomarkers that can predict tumor formation in a two-year bioassay following a 13 week exposure. **Keywords:** toxicology, chemical carcinogenesis, lung **Overall design:** Five week old female B6C3F1 mice were exposed for 13 weeks to the following treatments: 1) 1,5-Naphthalenediamine, CAS No. 2243-62-1, feed, 2000 ppm, positive lung carcinogen; 2) 2,3-Benzofuran, CAS No. 271-89-6, gavage, 240 mg/kg, positive lung carcinogen; 3) N-(1-naphthyl)ethylenediamine dihydrochloride, CAS No. 1465-25-4, feed, 2000 ppm, negative lung carcinogen; 4) Pentachloronitrobenzene, CAS No. 82-68-8, feed, 8187 ppm, negative lung carcinogen; 5) Feed control; 6) Corn oil gavage control. Feed animals were exposed 7 days/week and gavage animals were exposed 5 days/week (5 ml/kg). Microarray analysis was performed on the lungs of three mice per treatment group.

Background corr dist: KL-Divergence = 0.1443, L1-Distance = 0.0395, L2-Distance = 0.0032, Normal std = 0.3779

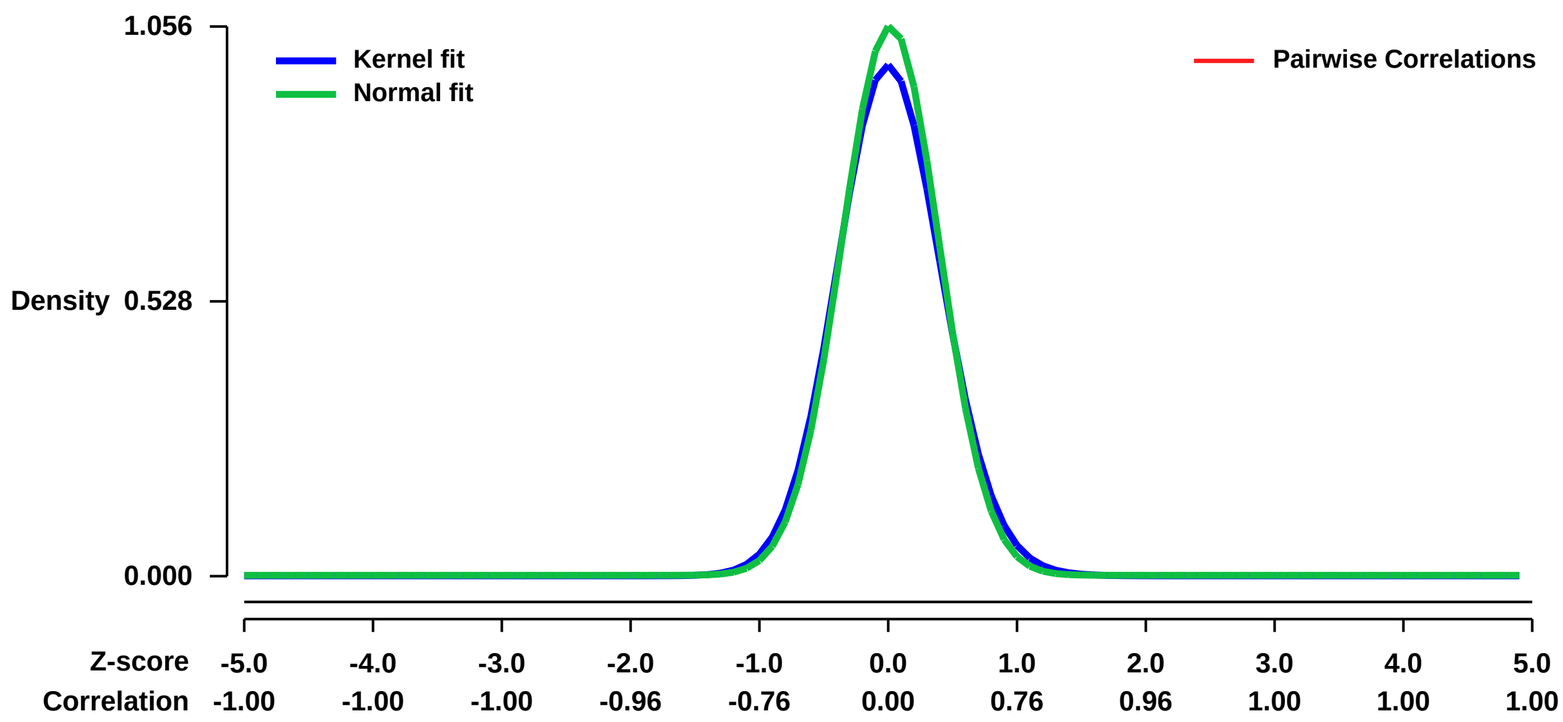

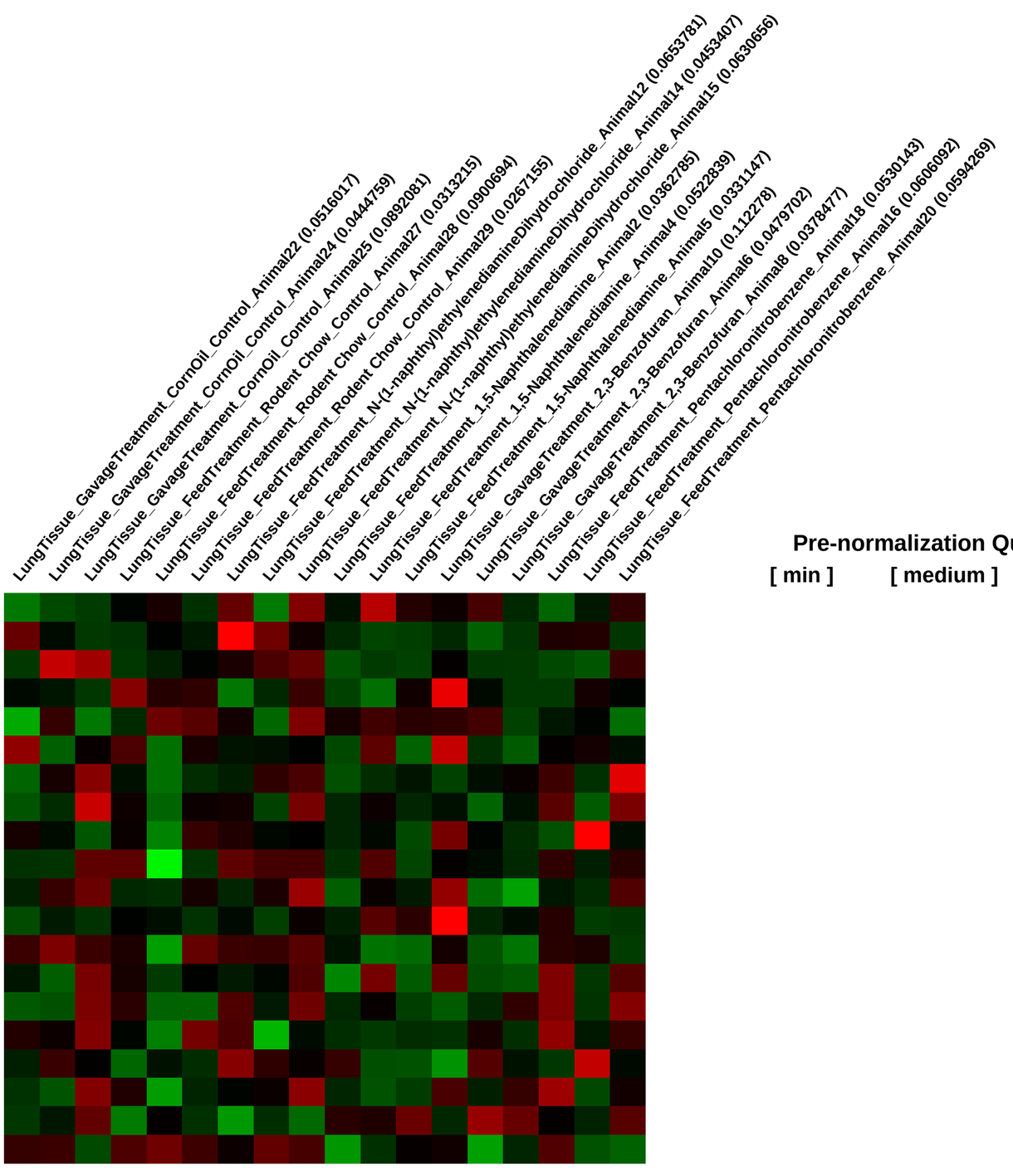

Null module

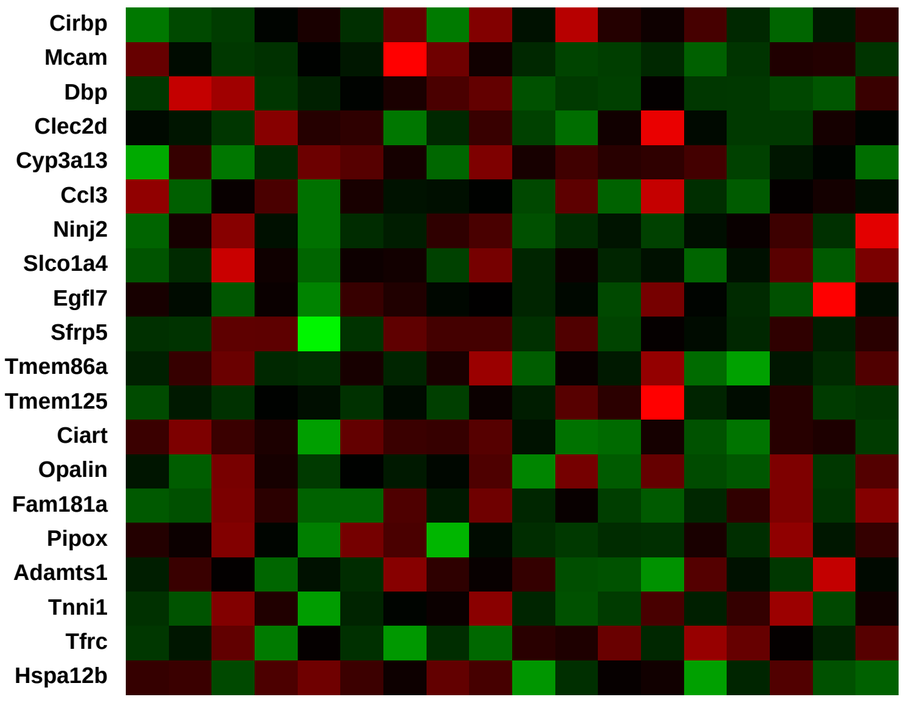

GEO Series "GSE19954" Expression Profiles

Num of samples in this series: 8

Scale of expression profile Z-scores

-3.0 -2.0 -1.0 0.0 1.0 2.0 3.0

GEO Link:	http://www.ncbi.nlm.nih.gov/geo/query/acc.cgi?acc=GSE19954
Status:	Public on Jan 23 2010
Title:	Telmisartan Improves Insulin Resistance with Modulating Adipose Tissue Macrophage Polarization in High Fat-fed Mice
Organism:	Mus musculus
Experiment type:	Expression profiling by array
Platform:	GPL1261
Pubmed ID:	21427223
Summary & Design:	**Summary:** Diet-induced obesity is reported to induce a phenotypic switch in adipose tissue macrophages from an antiinflammatory M2 state to a proinflammatory M1 state. Telmisartan, an angiotensin II type 1 receptor antagonist and a peroxisome proliferator-activated receptor-gamma (PPAR-gamma) agonist, reportedly has beneficial effects on insulin sensitivity. We studied the effects of telmisartan on the adipose tissue macrophage phenotype in high fat-fed mice. Telmisartan was administered for 5 weeks to high fat-fed C57BL/6 mice. Insulin sensitivity, macrophage infiltration, and the gene expressions of M1 and M2 markers in epididymal fat tissues were examined. Insulin- or a glucose-tolerance test showed that telmisartan treatment improved insulin resistance, decreasing the body weight gain, visceral fat weight and adipocyte size without affecting the amount of food intake. Telmisartan treatment reduced the number of CD11c-positive cells and crown-like structures. Telmisartan reduced the mRNA expressions of M1 macrophage markers, such as TNF-alpha and IL-6, and increased the expression of M2 markers, such as IL-10 and Mgl2. The reduction of M1 macrophage markers, as well as the increased gene expression of M2 markers especially IL-10, is a possible mechanism for the improvement of insulin sensitivity by telmisartan. **Overall design:** Six-week-old male C57BL/6J mice were purchased from CLEA Japan. The mice were fed a chow that contained 10% of its calories from fat (control) or a high-fat diet (HFD) that contained 30% of its calories from fat for 24 weeks. The high fat-fed mice were randomized to 3 groups. Either telmisartan (~3 mg/kg/day) in drinking water (HFD+Tel), candesartan (~3 mg/kg/day) in drinking water (HFD+Can), or a HFD without any drugs (HFD) was administered for the next 5 weeks. Two mice were treated per group. Epididymal adipose tissues were rapidly removed from each mouse. Gene expression in epididymal fat tissue was analyzed using a GeneChip´fi system with the Mouse Genome 430 2.0 Array, which was spotted with 45,101 probe sets (Affymetrix, Santa Clara, CA, USA). Sample preparation for the array hybridization was performed according to the manufacturerâ s instructions. In short, 5 ¸…g of total RNA was used to synthesize double-stranded cDNA using the GeneChip´fi Expression 3â†-Amplification Reagents One-Cycle cDNA Synthesis Kit (Affymetrix). Biotin-labeled cRNA was then synthesized from the cDNA using GeneChip´fi Expression 3â†-Amplification Reagents for IVT Labeling (Affymetrix). After fragmentation, the biotinylated cRNA was hybridized to arrays at 45 ´℃ for 16 h. The arrays were washed, stained with streptavidin-phycoerythrin, and scanned using a probe array scanner. The scanned chip was analyzed using the GeneChip Analysis Suite software (Affymetrix). Hybridization intensity data were converted into a presence/absence call for each gene, and changes in gene expression between experiments were detected by a comparison analysis. Data was shown as the fold change relative to the expression level of normal chow-fed mice.

Background corr dist: KL-Divergence = 0.0652, L1-Distance = 0.0185, L2-Distance = 0.0004, Normal std = 0.5155

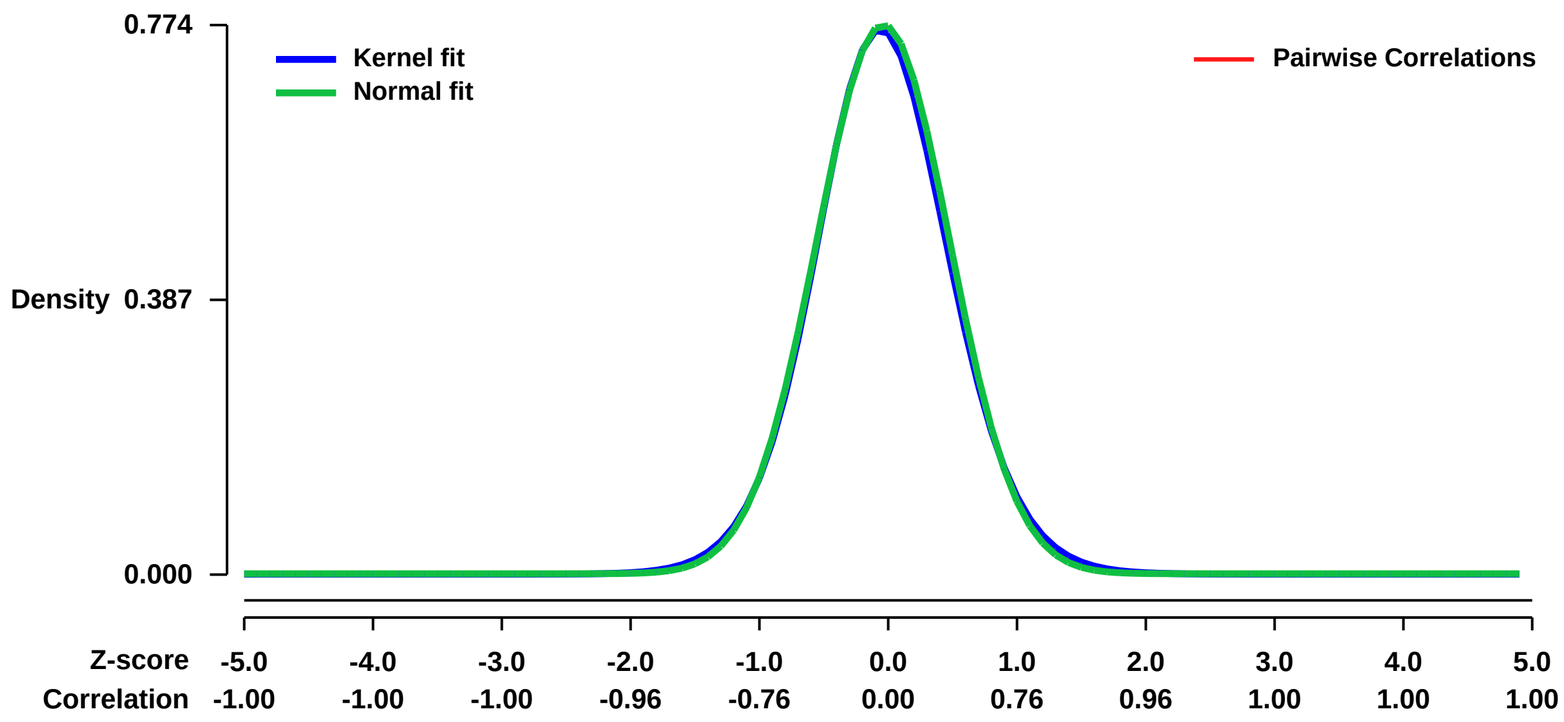

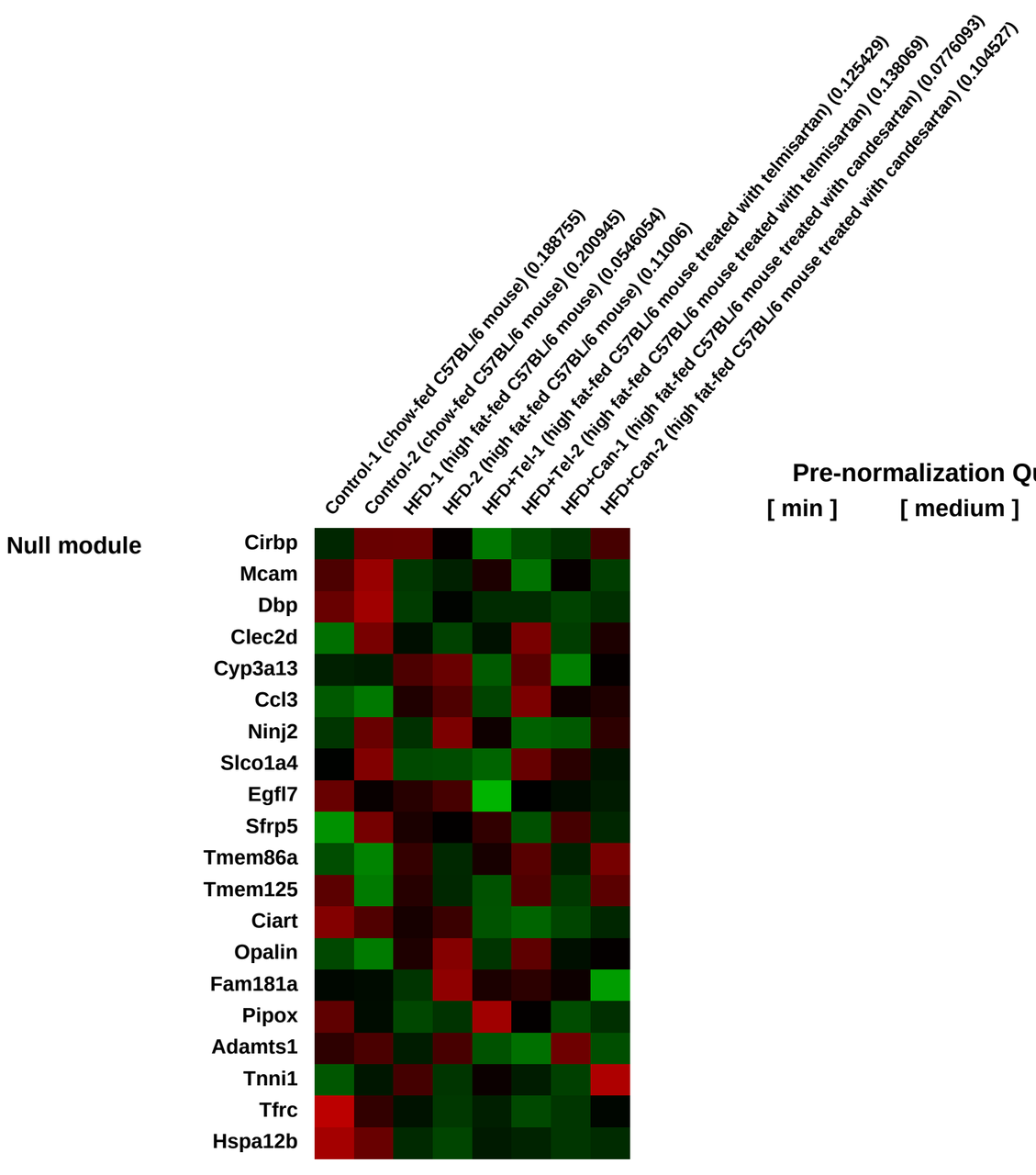

GEO Series "GSE34961" Expression Profiles

Num of samples in this series: 9

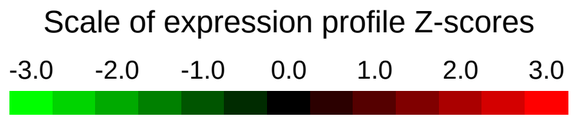

GEO Link:	http://www.ncbi.nlm.nih.gov/geo/query/acc.cgi?acc=GSE34961
Status:	Public on Feb 22 2012
Title:	Expression profiling of secondary wild type (WT) and Ezh2-null murine MLL-AF9 AML
Organism:	Mus musculus
Experiment type:	Expression profiling by array
Platform:	GPL1261
Pubmed ID:	22396593
Summary & Design:	**Summary:** We evaluated gene expression changes in secondary recipient murine leukemia caused by retroviral overexpression of MLL-AF9. We compared wild-type (WT) leukemia cells with mutant leukemia cells after cre-mediated inactivation of a homozygous conditional allele for Ezh2, a component of the Polycomb Repressive Complex2. **Overall design:** For WT cells, 4 biological replicates were hybridized. For Ezh2-null cells, 5 biological replicates were hybridized.

Background corr dist: KL-Divergence = 0.0622, L1-Distance = 0.0284, L2-Distance = 0.0014, Normal std = 0.5159

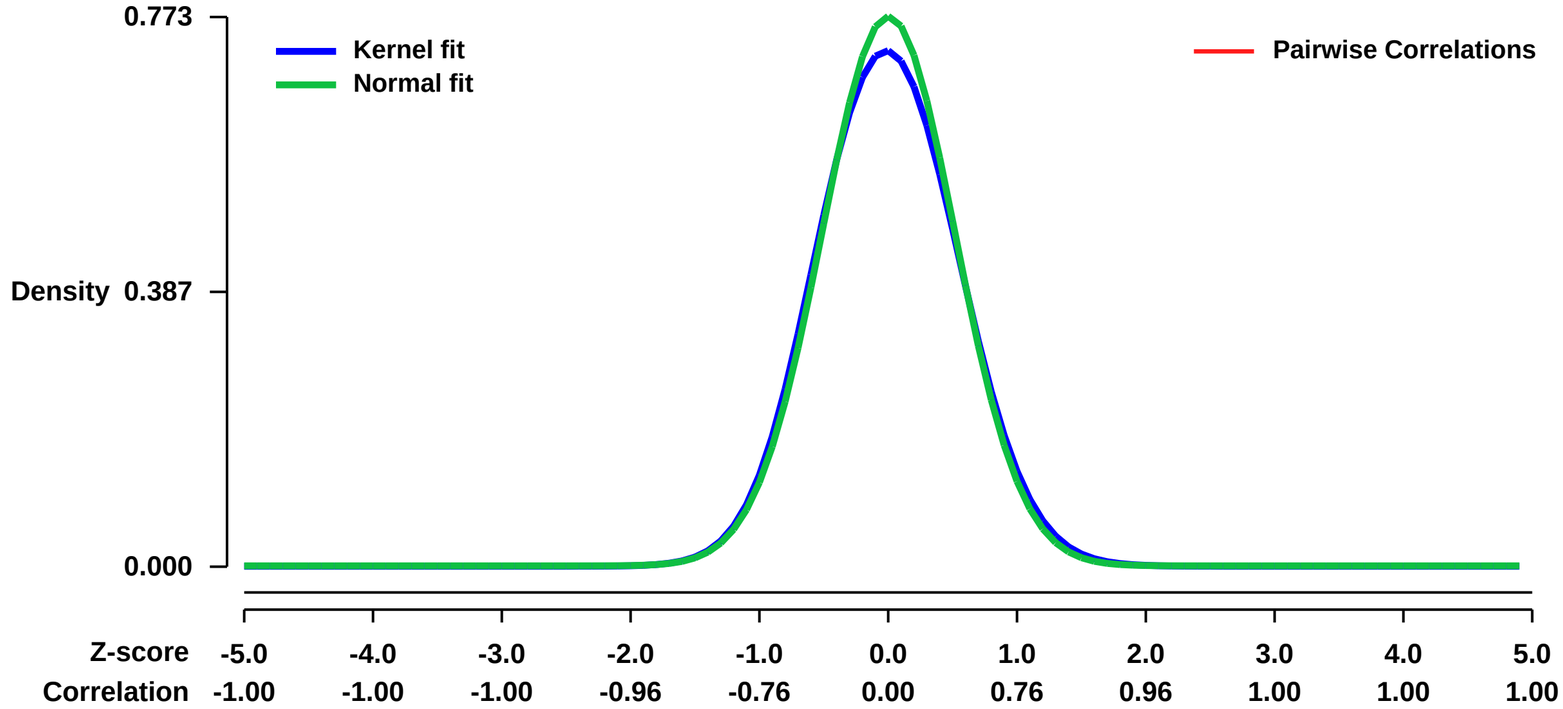

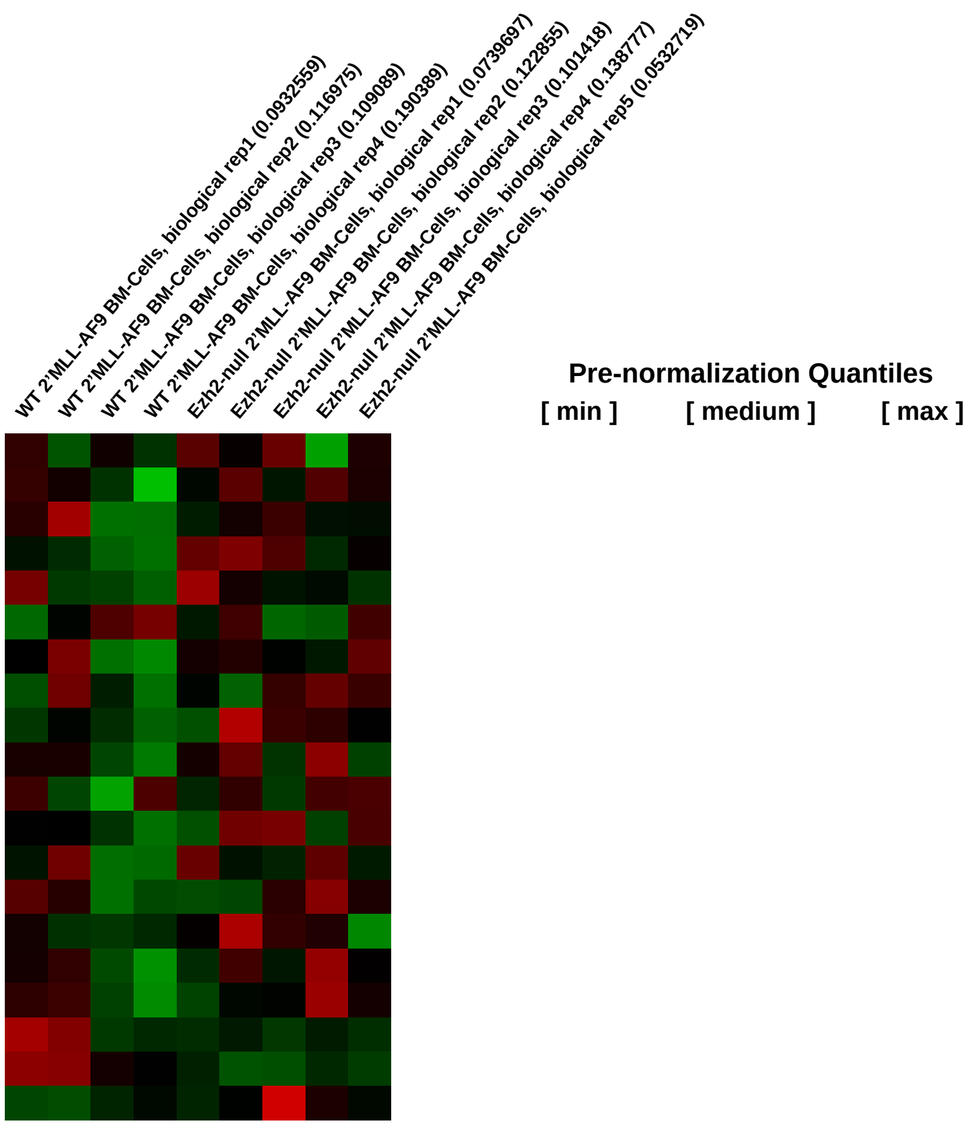

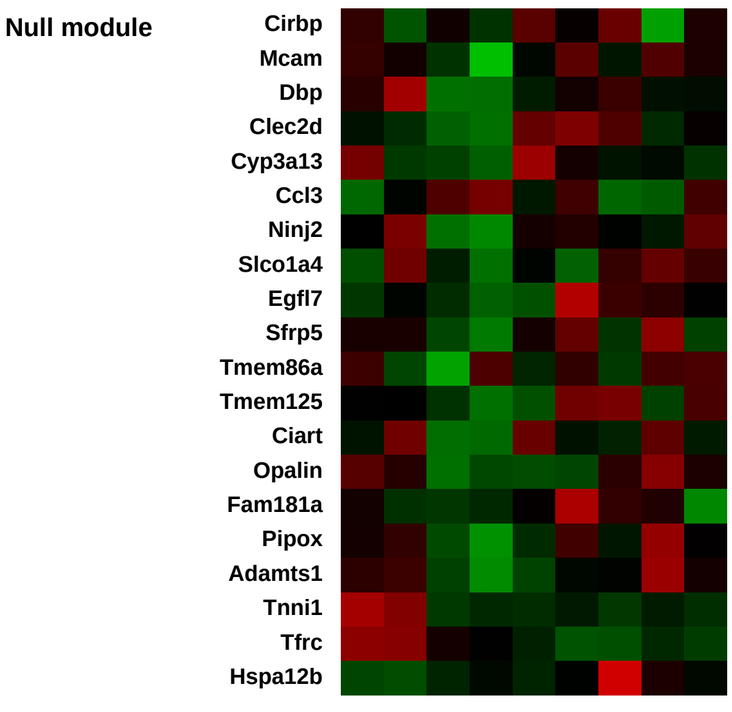

GEO Series "GSE12432" Expression Profiles

Num of samples in this series: 15

Scale of expression profile Z-scores

-3.0 -2.0 -1.0 0.0 1.0 2.0 3.0

GEO Link:	**http://www.ncbi.nlm.nih.gov/geo/query/acc.cgi?acc=GSE12432**
Status:	**Public on Jul 12 2010**
Title:	**Microarray data of prepubertal, peripubertal, and adult oocytes, and from GV and MII oocytes matured in vivo or in vitro**
Organism:	**Mus musculus**
Experiment type:	**Expression profiling by array**
Platform:	**GPL1261**
Pubmed ID:	
Summary & Design:	**Summary:** **Expression data from prepubertal, peripubertal, and adult derived mouse oocytes, and from germinal vesicle (GV), in vivo matured, and in vitro matured mouse oocytes.** **Oocytes derived from prepubertal females, or oocytes matured in vitro, are less developmentally competent compared to adult derived, or in vivo matured, oocytes, indicated by decreased embryonic development. One potential mechanism for decreased developmental potetential in prepubertal or in vitro matured oocytes is inadequate or inappropriate RNA degradation during oocyte maturation (progression from GV to MII).** **To investigate mechanisms involved in establishing oocyte cytoplasmic maturation and developmental competence, Affymetrix GeneChip microarrays were used.** **Keywords: Oocyte developmental competence** **Overall design:** **The study encompassed three experimental designs using female B6D2F1 mice: 1) In vitro matured oocytes were obtained from d20 (prepubertal), d26 (peripubertal), and 7-8 wk old (adult) mice; 2) in vivo and in vitro matured oocytes were obtained from d26 mice; and 3) GV, in vivo matured, and in vitro matured oocytes were obtained from 7-8 wk old mice. RNA was extracted from pools of 150 oocytes and hybridized onto the Affymetrix microarrays.**

Background corr dist: KL-Divergence = 0.1390, L1-Distance = 0.0842, L2-Distance = 0.0153, Normal std = 0.4490

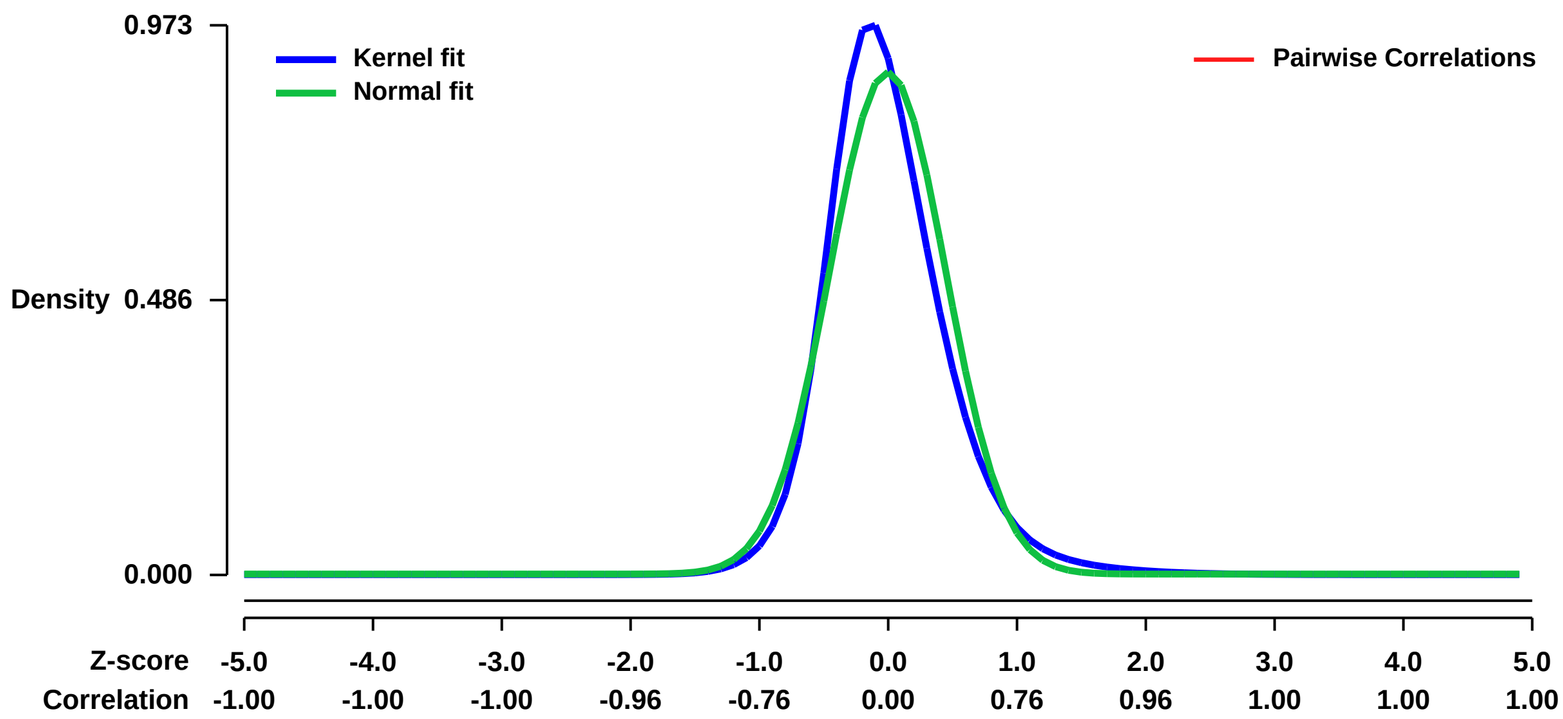

GEO Series "GSE11287" Expression Profiles

Num of samples in this series: 6

Scale of expression profile Z-scores

-3.0 -2.0 -1.0 0.0 1.0 2.0 3.0

GEO Link:	http://www.ncbi.nlm.nih.gov/geo/query/acc.cgi?acc=GSE11287
Status:	Public on May 01 2008
Title:	Keap1-dependent gene expression determined in the liver using conditional Keap1 knockout mice vs. genetic control mice
Organism:	Mus musculus
Experiment type:	Expression profiling by array
Platform:	GPL1261
Pubmed ID:	18417483
Summary & Design:	**Summary:** To compare hepatic gene expression in conditional Keap1 knockout (Alb-Cre:Keap1(flox/-)) and genetic control mice. Disruption of Keap1-mediated repression of Nrf2 signaling was expected to result in increased expression of Nrf2-regulated genes. **Keywords: comparative expression profiling** **Overall design:** Hepatic gene expression was compared in conditional Keap1 knockout and genetic control mice (Alb-Cre:Keap1(flox/+)) mice. Male 9 week old mice were used, n=3/group.

Background corr dist: KL-Divergence = 0.0460, L1-Distance = 0.0177, L2-Distance = 0.0003, Normal std = 0.5880

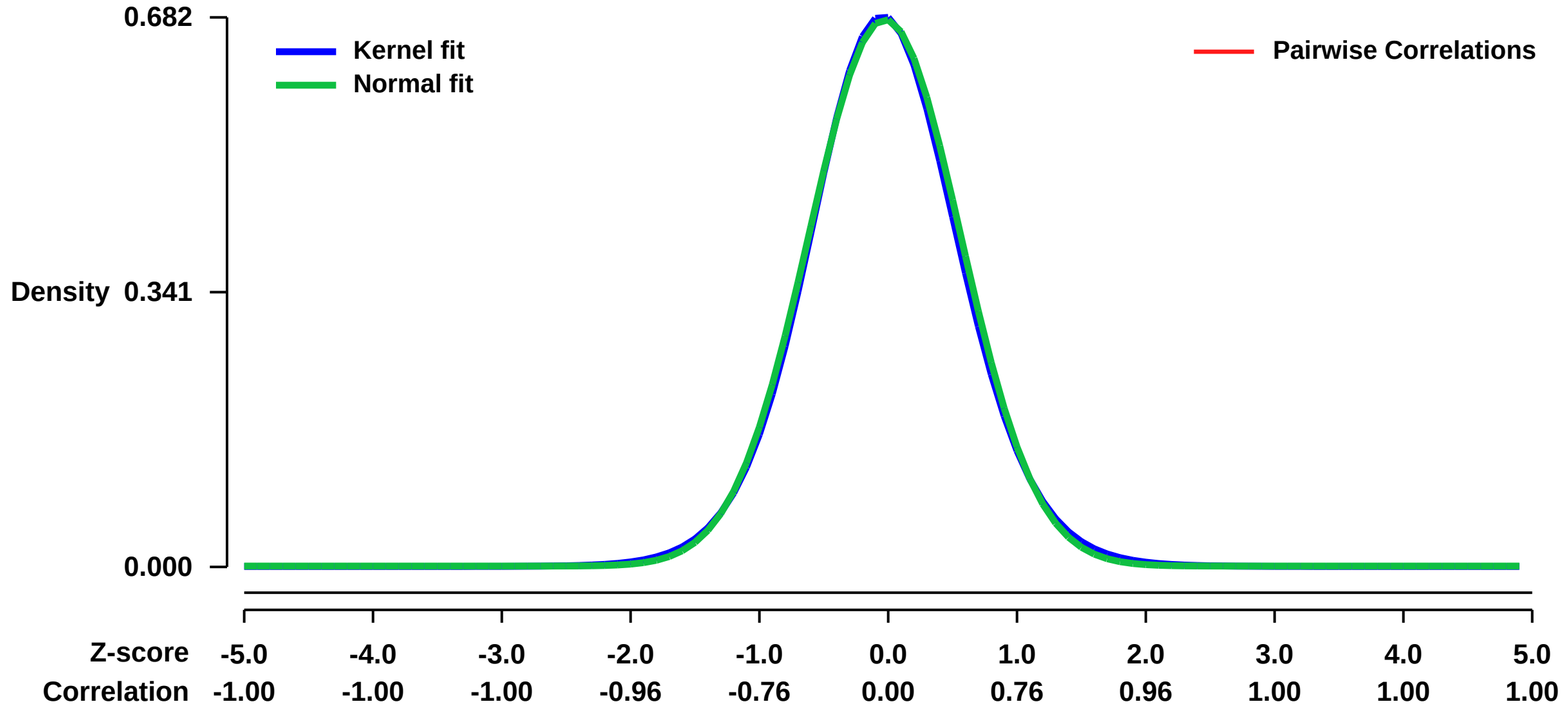

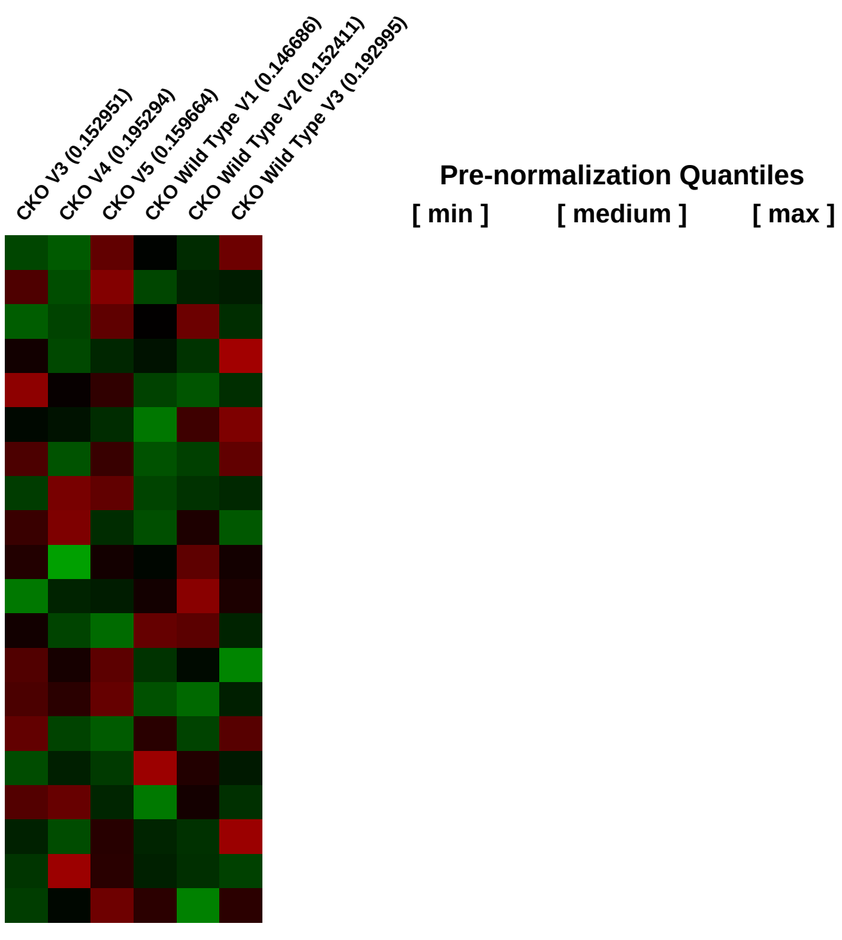

GEO Series "GSE41307" Expression Profiles

Num of samples in this series: 8

Scale of expression profile Z-scores

-3.0 -2.0 -1.0 0.0 1.0 2.0 3.0

GEO Link:	**http://www.ncbi.nlm.nih.gov/geo/query/acc.cgi?acc=GSE41307**
Status:	**Public on Aug 13 2013**
Title:	**Gene expression microarray analysis on hippocampus of Schnurri-2 knockout and wild-type control mice**
Organism:	**Mus musculus**
Experiment type:	**Expression profiling by array**
Platform:	**GPL1261**
Pubmed ID:	**23389689**
Summary & Design:	**Summary:** **Schnurri-2 (Shn-2), an NF-kappa B site-binding protein, tightly binds to the enhancers of major histocompatibility complex (MHC) class I genes and inflammatory cytokines, which have been shown to harbor common variant single nucleotide polymorphisms associated with schizophrenia. Shn-2 knockout mice show behavioral abnormalities that strongly resemble those of schizophrenics. We performed gene expression microarray analysis of hippocampi from Shn-2 knockout and wild-type control mice.** **Overall design:** **Hippocampal RNA isolated from four Shn-2 knockout and four control wild-type mice were compared.**

Background corr dist: **KL-Divergence = 0.0637, L1-Distance = 0.0203, L2-Distance = 0.0005, Normal std = 0.5131**

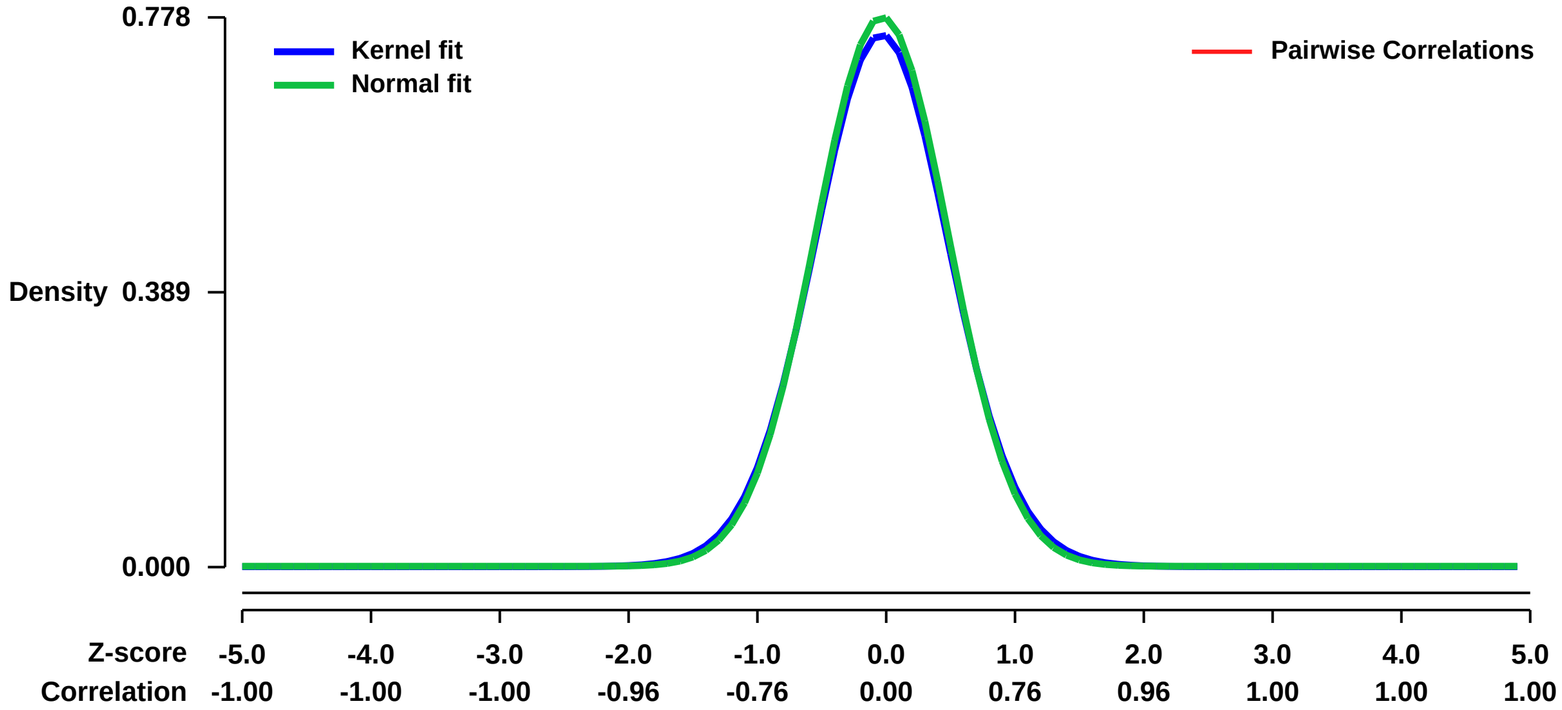

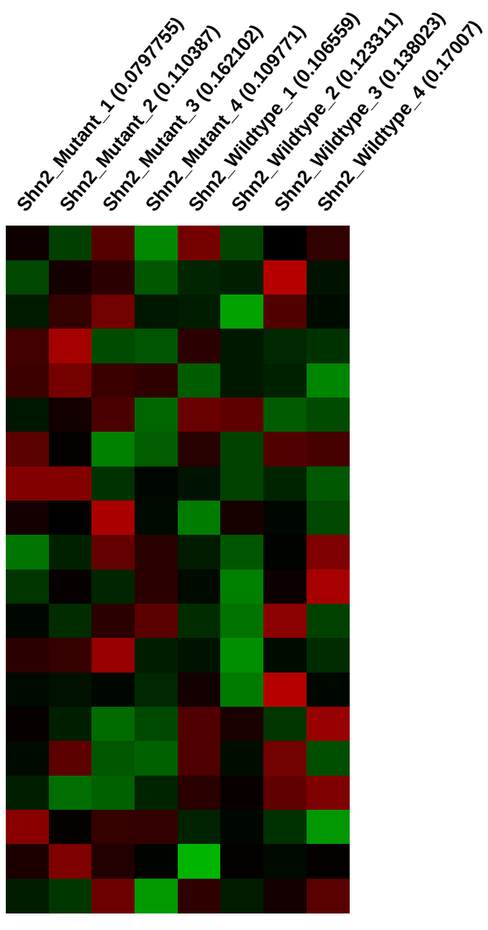

GEO Series "GSE54490" Expression Profiles

Num of samples in this series: 12

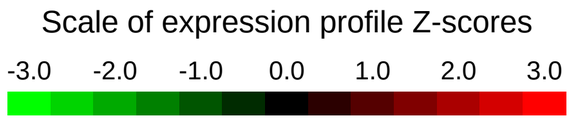

GEO Link:	http://www.ncbi.nlm.nih.gov/geo/query/acc.cgi?acc=GSE54490
Status:	Public on Feb 16 2014
Title:	FoxA1 directs the lineage and immunosuppressive properties of FoxA1+ regulatory T cells in EAE and MS
Organism:	Mus musculus
Experiment type:	Expression profiling by array
Platform:	GPL1261
Pubmed ID:	24531377
Summary & Design:	**Summary:** Affymetrix gene expression analysis was carried out to investigate the differences in gene profile of MBP89-101-reactive encephalitogenic T cells before and after co-culture with cerebellar granular neurons (CGNs). Co-culture of MBP89-101-reactive encephalitogenic T cells with CGNs leads to generation of T cells with regulatory T cells phenotype (CD4+CD25+membrane bound TGF-b+ T cells) or a new regulatory phenotype (CD4highPD-L1high T cells). CGN-induced CD4+CD25+membrane bound TGF-b+ T regulatory cells, CD4highPD-L1high T cells were purified by FACSAria. IFN-beta induced T lymphocytes (CD4highPD-L1high T cells) were also FACSAria purified. All these populations were compared to MBP89-101-reactive encephalitogenic T cells. Samples were prepared from biological triplicates for each FACSAria sorted population. **Overall design:** There are four different cell types, as determined by cell surface markers, in triplicate in the experiment.

Background corr dist: KL-Divergence = 0.0239, L1-Distance = 0.0546, L2-Distance = 0.0040, Normal std = 0.7910

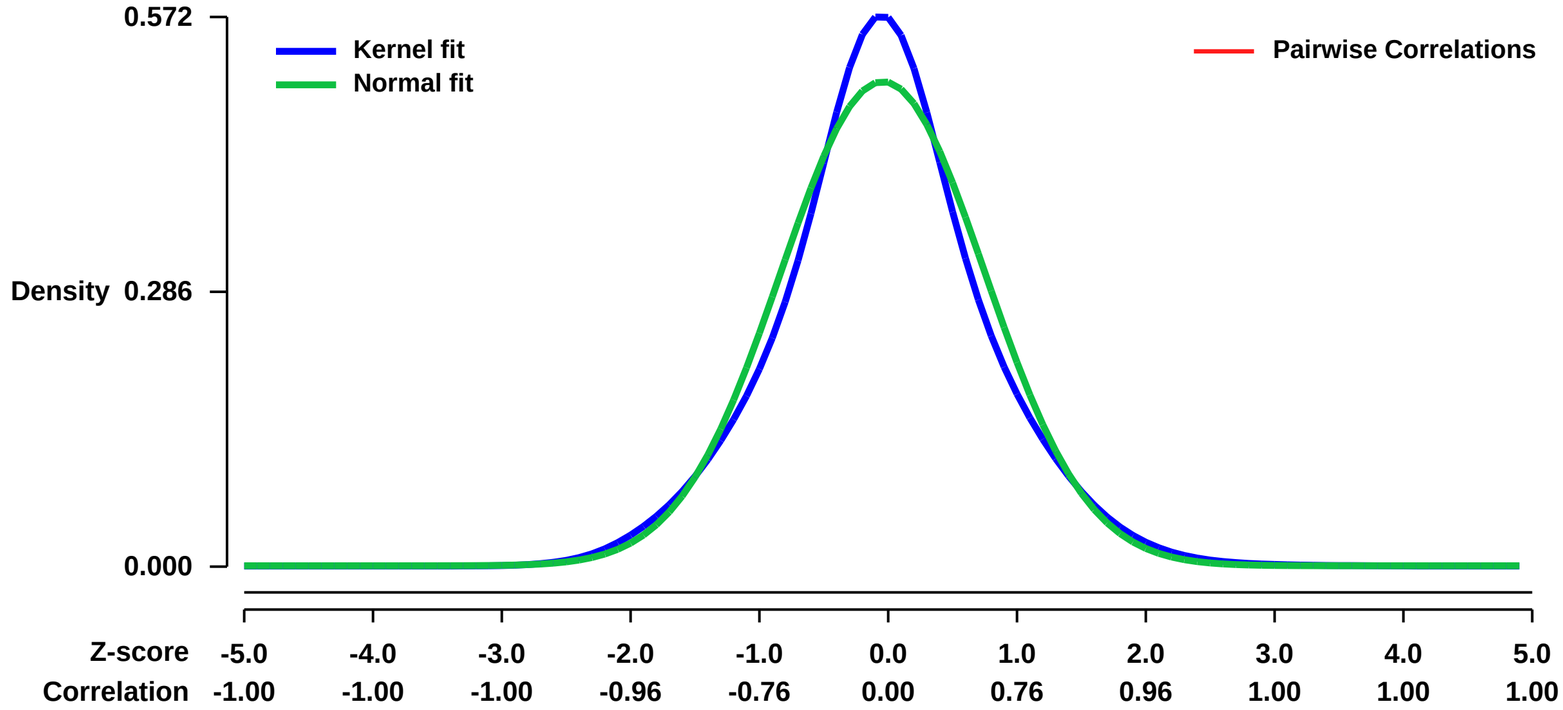

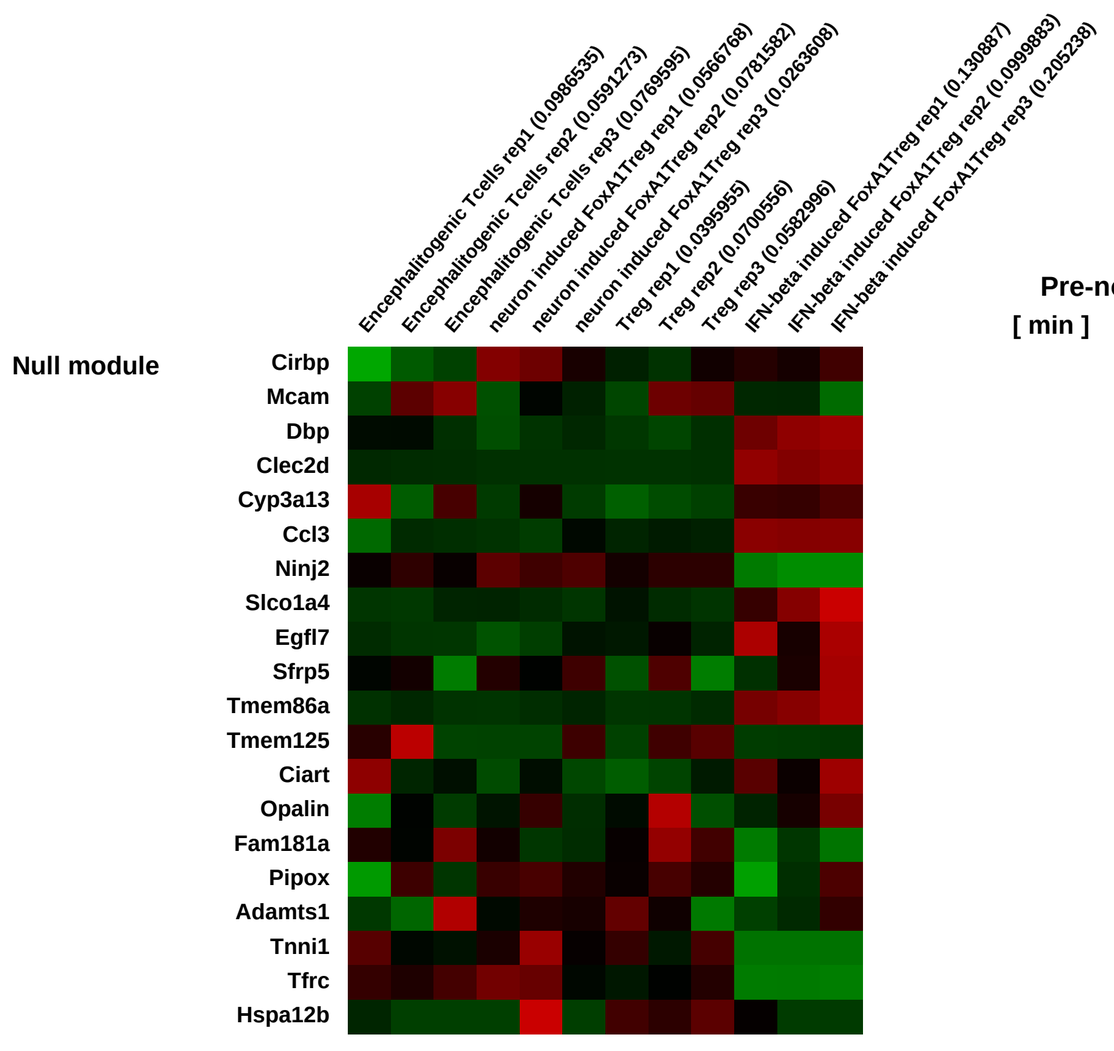

GEO Series "GSE16703" Expression Profiles

Num of samples in this series: 15

Scale of expression profile Z-scores

-3.0 -2.0 -1.0 0.0 1.0 2.0 3.0

GEO Link:	http://www.ncbi.nlm.nih.gov/geo/query/acc.cgi?acc=GSE16703
Status:	Public on Oct 01 2009
Title:	Long-term effect on the transcriptome of a decrement in Norrin/Frizzled4/Lrp signaling in retinal endothelial cells
Organism:	Mus musculus
Experiment type:	Expression profiling by array
Platform:	GPL1261
Pubmed ID:	19837032
Summary & Design:	**Summary:** To characterize the long-term effect on the transcriptome of a decrement in Norrin/Fz4/Lrp signaling, microarray hybridization was performed with RNA from acutely dissociated and anti-PECAM immunoaffinity-purified adult WT, Fz4-/-, Lrp5-/-, and Norrin- retinal vascular cells. **Overall design:** Retinal endothelial cells from 5-10 adult mice were pooled for each sample, the cell immuno-purification procedure follows that described by Matsubara et al. (2000) and Su et al. (2003). 3 replicates of each mutant and 6 replicates of control wild type animals were analyzed.

Background corr dist: KL-Divergence = 0.1043, L1-Distance = 0.0376, L2-Distance = 0.0029, Normal std = 0.4339

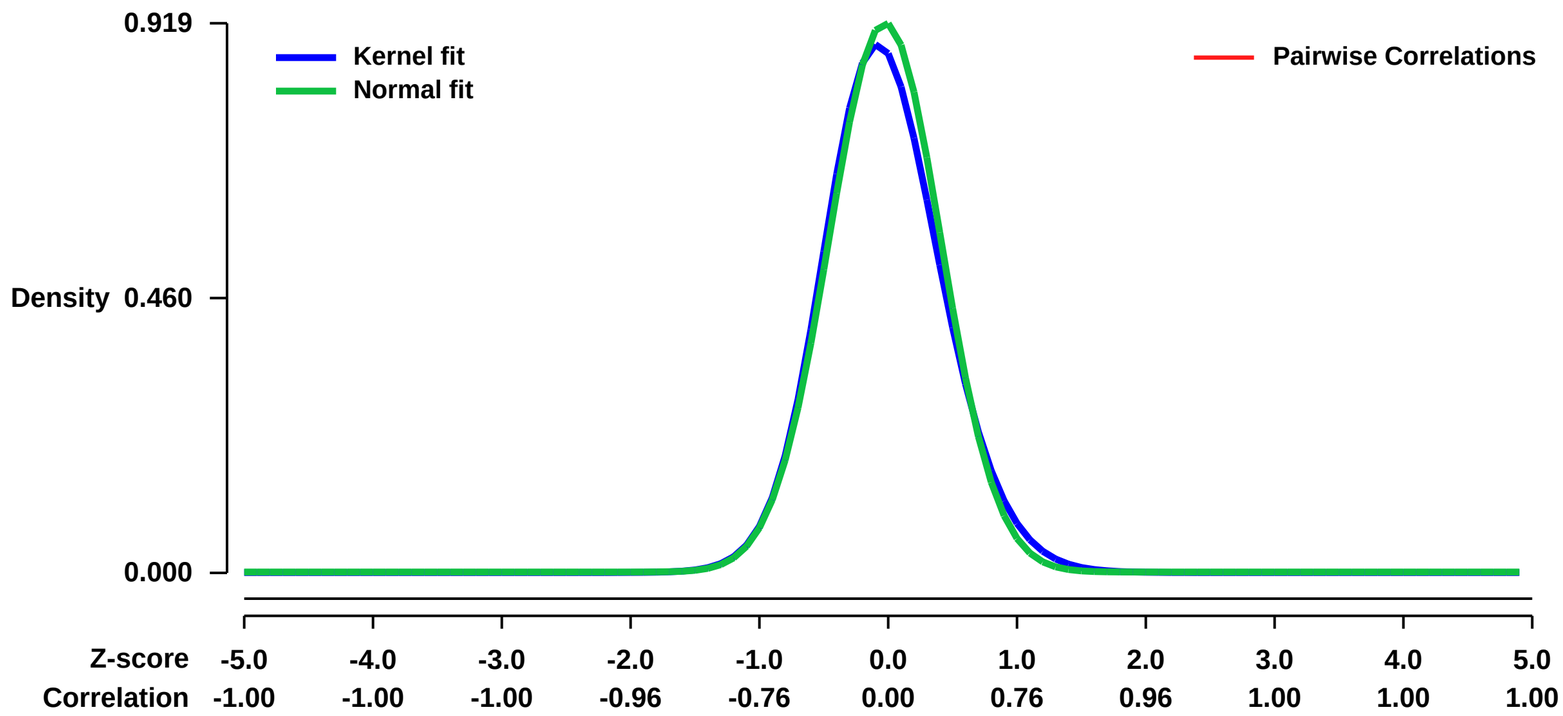

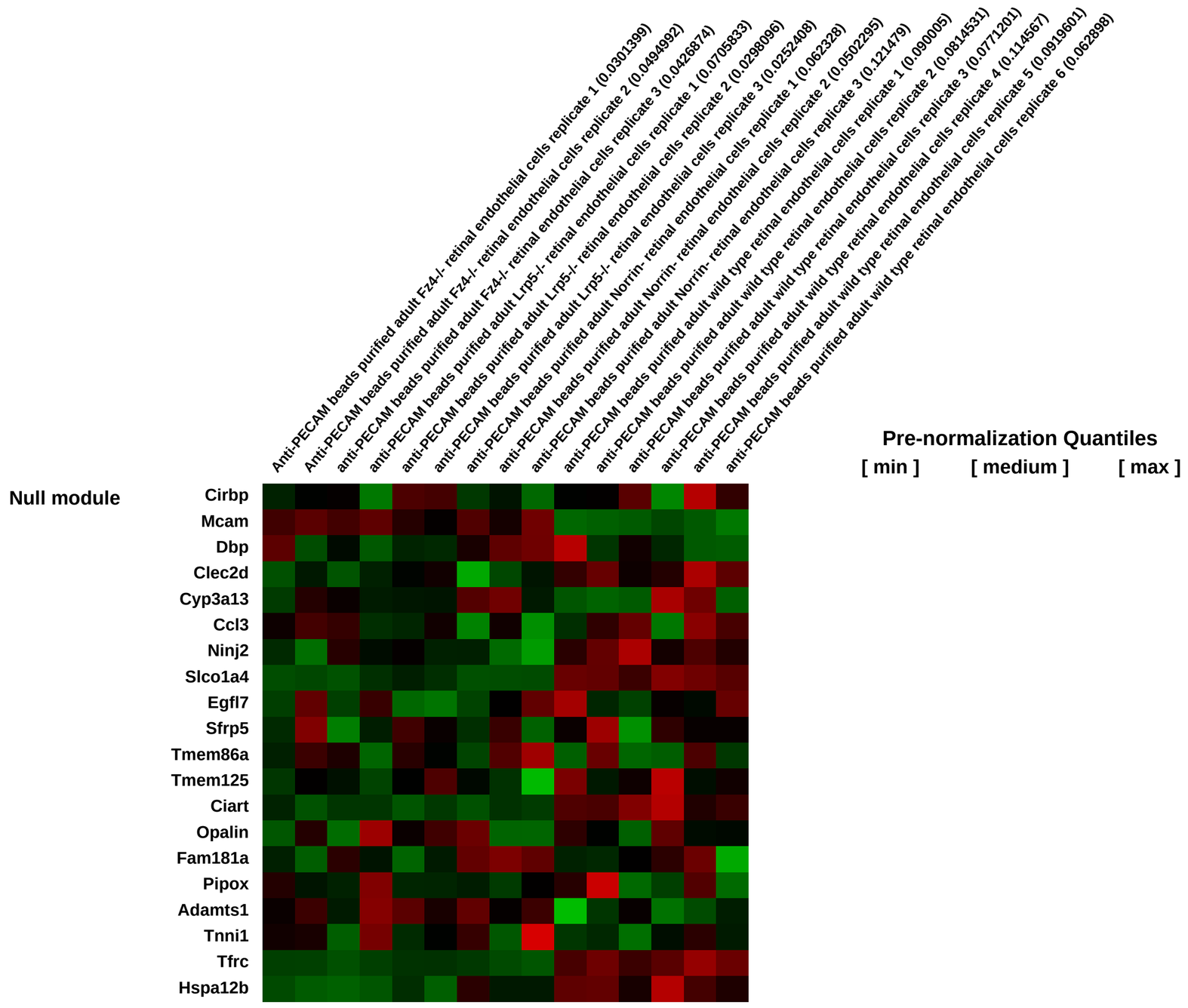

GEO Series "GSE27038" Expression Profiles

Num of samples in this series: 12

Scale of expression profile Z-scores

-3.0 -2.0 -1.0 0.0 1.0 2.0 3.0

GEO Link:	http://www.ncbi.nlm.nih.gov/geo/query/acc.cgi?acc=GSE27038
Status:	Public on Feb 03 2011
Title:	Expression data from the Ire1$_{c}$– null and control murine livers in the absence or presence of ER stress
Organism:	Mus musculus
Experiment type:	Expression profiling by array
Platform:	GPL1261
Pubmed ID:	21407177
Summary & Design:	**Summary:** **Ire1$_{c}$– conditional null or control mice of 3-months old were injected intraperitoneally with TM or vehicle.** **At 8 hours after the injection, total RNA was isolated from murine liver tissue and subjected to Affymetrix microarray analysis.** **Overall design:** **We used microarrays to profile the global programme of gene expression in the livers of Ire1$_{c}$– null and control mice in the absence or presence of ER stress.**

Background corr dist: **KL-Divergence = 0.1000, L1-Distance = 0.0233, L2-Distance = 0.0009, Normal std = 0.4442**

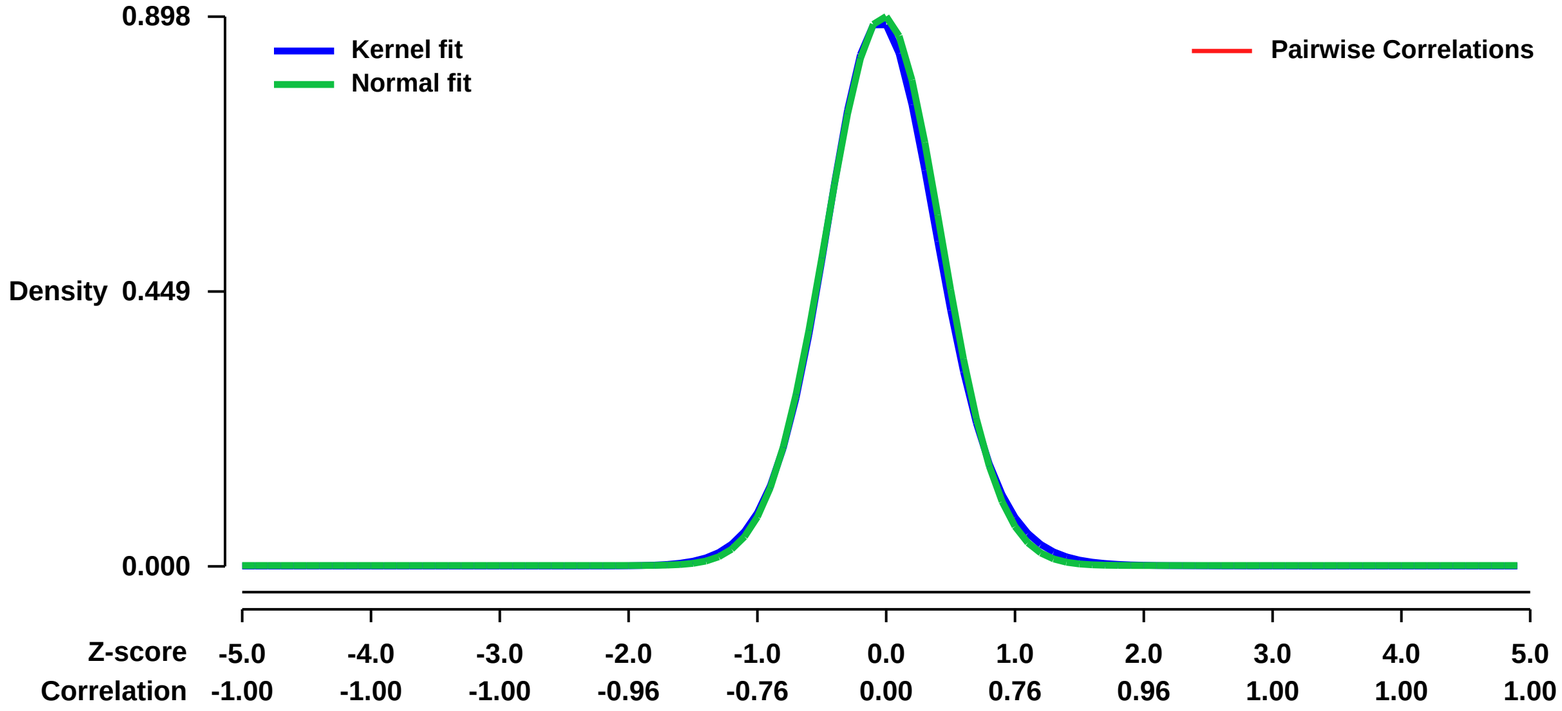

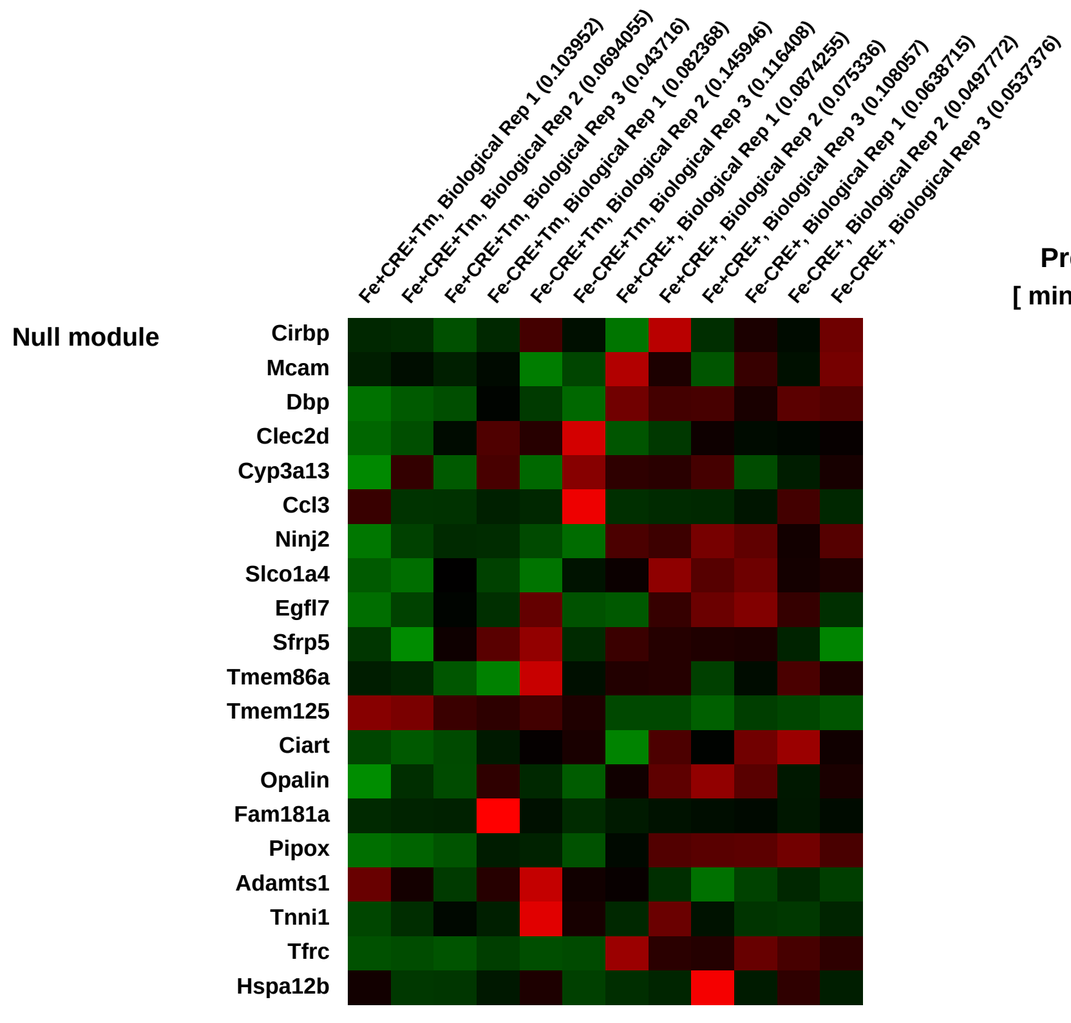

GEO Series "GSE3822" Expression Profiles

Num of samples in this series: 16

Scale of expression profile Z-scores

-3.0 -2.0 -1.0 0.0 1.0 2.0 3.0

GEO Link:	http://www.ncbi.nlm.nih.gov/geo/query/acc.cgi?acc=GSE3822
Status:	Public on May 01 2006
Title:	Complete embryonic E11.5 metanephric kidney analysis of wild type and Hoxa11, Hoxd11 null targeted mice
Organism:	Mus musculus
Experiment type:	Expression profiling by array
Platform:	GPL1261
Pubmed ID:	16581055
Summary & Design:	**Summary:** E11.5 metanephric mesenchyme and ureteric bud were dissected from the E11.5 kidney rudiment using fine manual microdissection (ureteric bud only) or both fine manual microdissection and laser capture microdissection (metanephric mesenchyme) to define the gene expression profiles of these structures. Additionally, HoxA11, HoxD11 compound null E11.5 metanephric mesenchyme was obtained through laser capture microdissection allowing analysis of possible Hox targets in kidney development. Targets from multiple biological replicates of each were generated and the expression profiles were determined using Affymetrix MOE430_v2 arrays. **Keywords:** embryonic metanephric kidney, kidney development, Hoxa11, Hoxd11, compound null targeted mice **Overall design:** Using microdissection techniques, ureteric bud and metanephric mesenchyme were dissected from E11.5 kidney rudiments allowing the identificated genes specifically regulated in either structure. In addition, Hoxa11, Hoxd11 compound null E11.5 metanephric mesenchyme were normalized to wild type embryonic controls allowing the identification of potential Hox targets in normal kidney development. Each structure/genotype were represented in biological (seperate embryo) replicate.

Background corr dist: KL-Divergence = 0.1851, L1-Distance = 0.0434, L2-Distance = 0.0043, Normal std = 0.3462

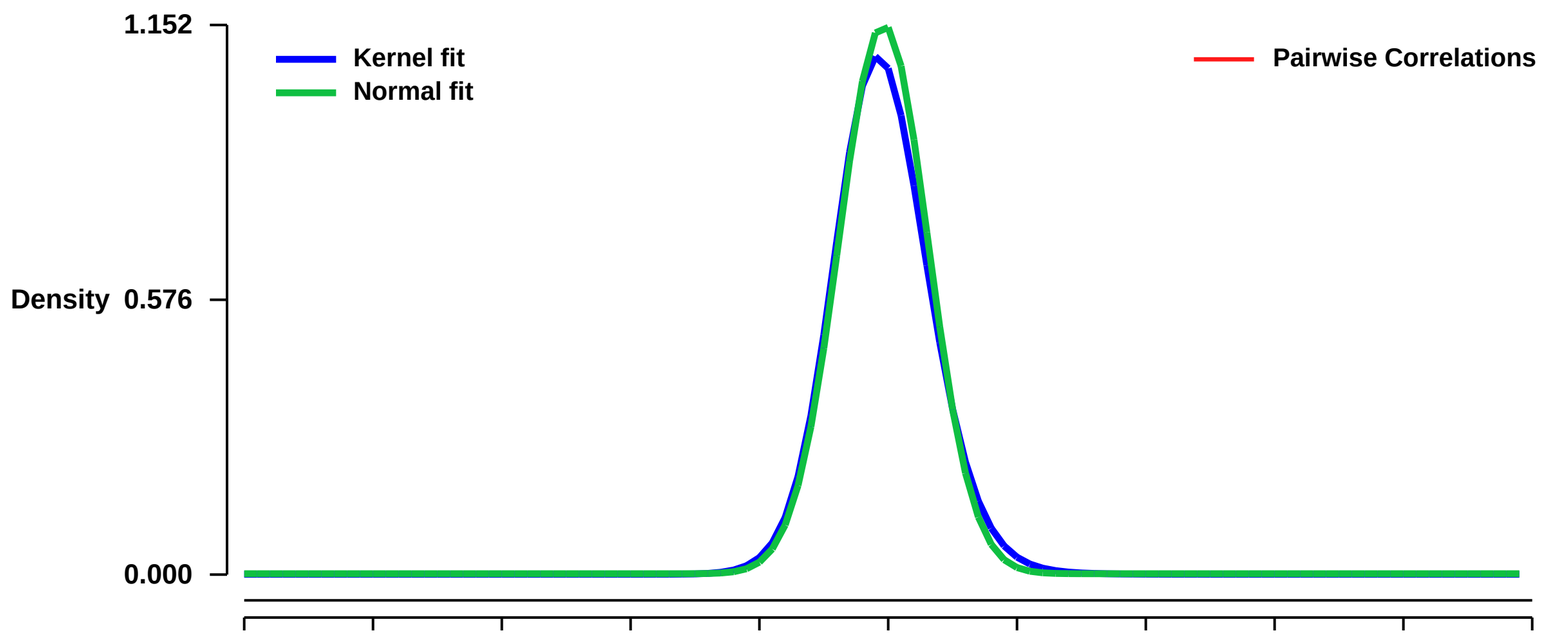

Z-score	-5.0	-4.0	-3.0	-2.0	-1.0	0.0	1.0	2.0	3.0	4.0	5.0
Correlation	-1.00	-1.00	-1.00	-0.96	-0.76	0.00	0.76	0.96	1.00	1.00	1.00

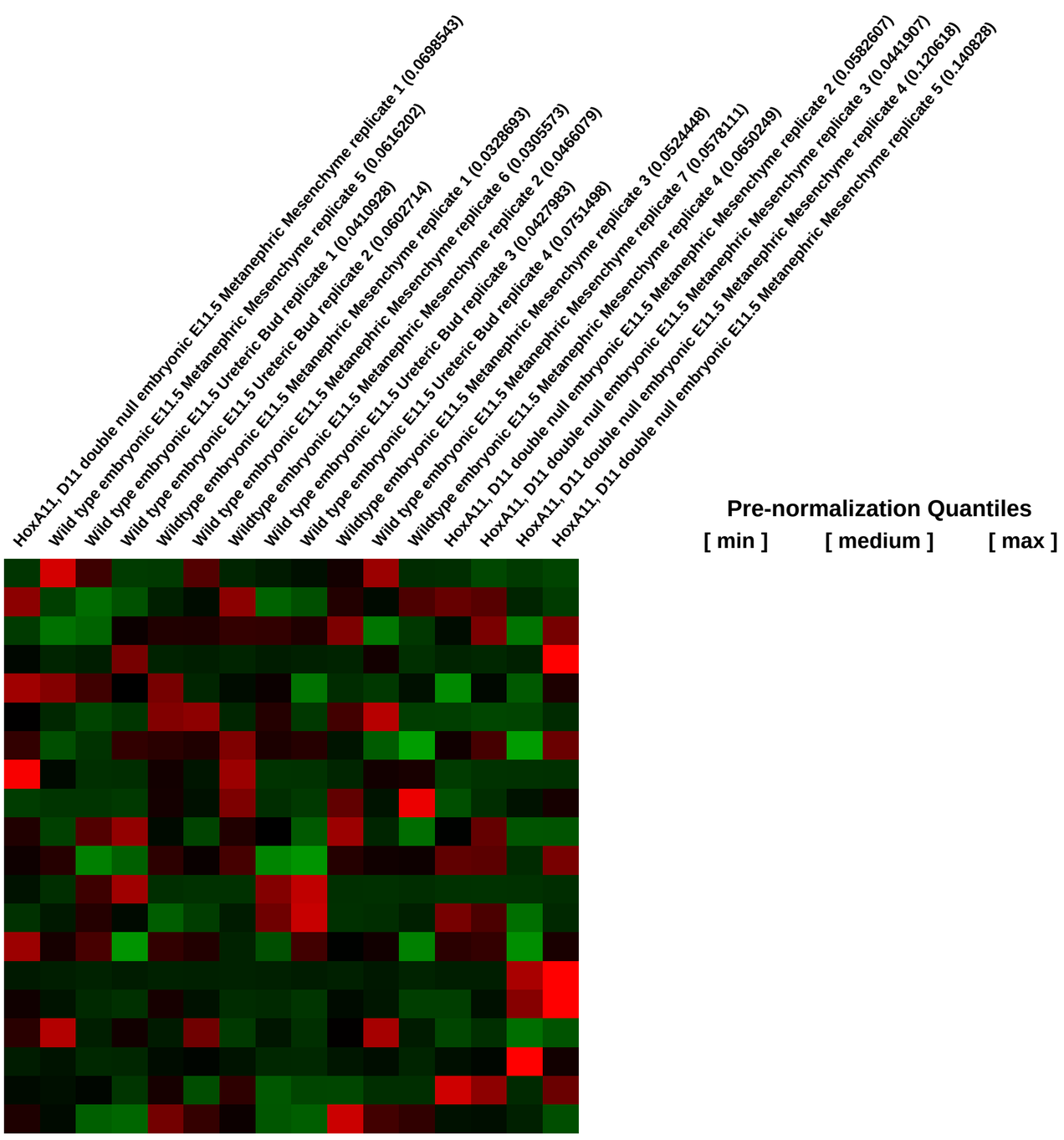

GEO Series "GSE9199" Expression Profiles

Num of samples in this series: 50

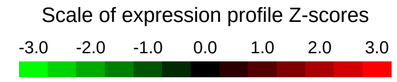

GEO Link:	http://www.ncbi.nlm.nih.gov/geo/query/acc.cgi?acc=GSE9199
Status:	Public on May 25 2008
Title:	Synergistic response to oncogenic mutations defines gene class critical to cancer phenotype
Organism:	Mus musculus
Experiment type:	Expression profiling by array
Platform:	GPL1261
Pubmed ID:	18500333

Summary & Design:

Summary:
Understanding the molecular underpinnings of cancer is of critical importance to developing targeted intervention strategies. Identification of such targets, however, is notoriously difficult and unpredictable. Malignant cell transformation requires the cooperation of a few oncogenic mutations that cause substantial reorganization of many cell features and induce complex changes in gene expression patterns. Genes critical to this multi-faceted cellular phenotype thus only have been identified following signaling pathway analysis or on an ad hoc basis. Our observations that cell transformation by cooperating oncogenic lesions depends on synergistic modulation of downstream signaling circuitry suggest that malignant transformation is a highly cooperative process, involving synergy at multiple levels of regulation, including gene expression. Here we show that a large proportion of genes controlled synergistically by loss-of-function p53 and Ras activation are critical to the malignant state. Remarkably, 14 among 24 such 'cooperation response genes' (CRGs) were found to contribute to tumor formation in gene perturbation experiments. In contrast, only one in 14 perturbations of genes responding in a non-synergistic manner had a similar effect. Synergistic control of gene expression by oncogenic mutations thus emerges as an underlying key to malignancy and provides an attractive rationale for identifying intervention targets in gene networks downstream of oncogenic gain and loss-of-function mutations.

Keywords: Oncogenic mutation-specific comparison

Overall design:
Contains 50 samples total, 10 replicates each of parental cell line YAMC, plus bleo/Neo vector control, mp53-expressing, Ras-expressing and mp53/Ras cells. Polysomal RNA from each sample was run on Affymetrix GeneChip´fi Mouse Genome 430 2.0 Arrays.

Background corr dist: KL-Divergence = 0.2322, L1-Distance = 0.0535, L2-Distance = 0.0068, Normal std = 0.3114

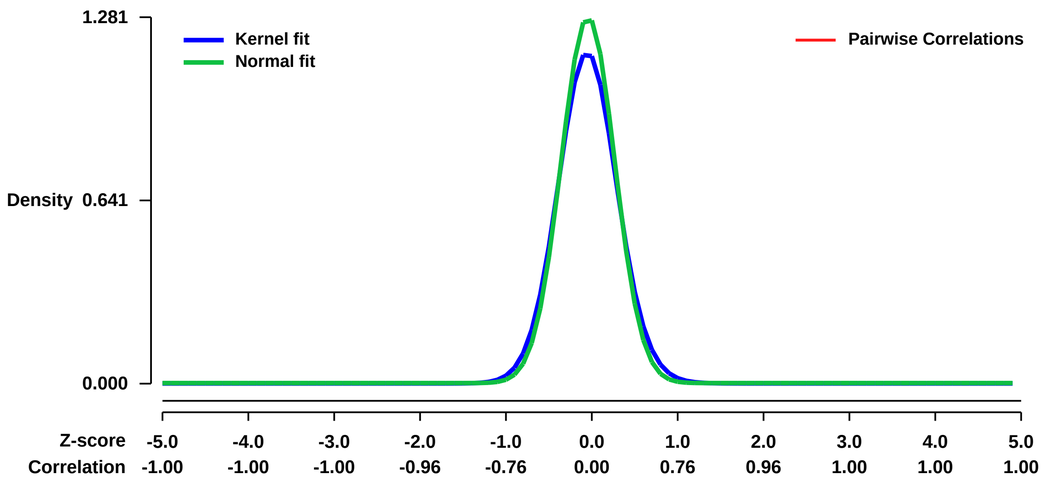

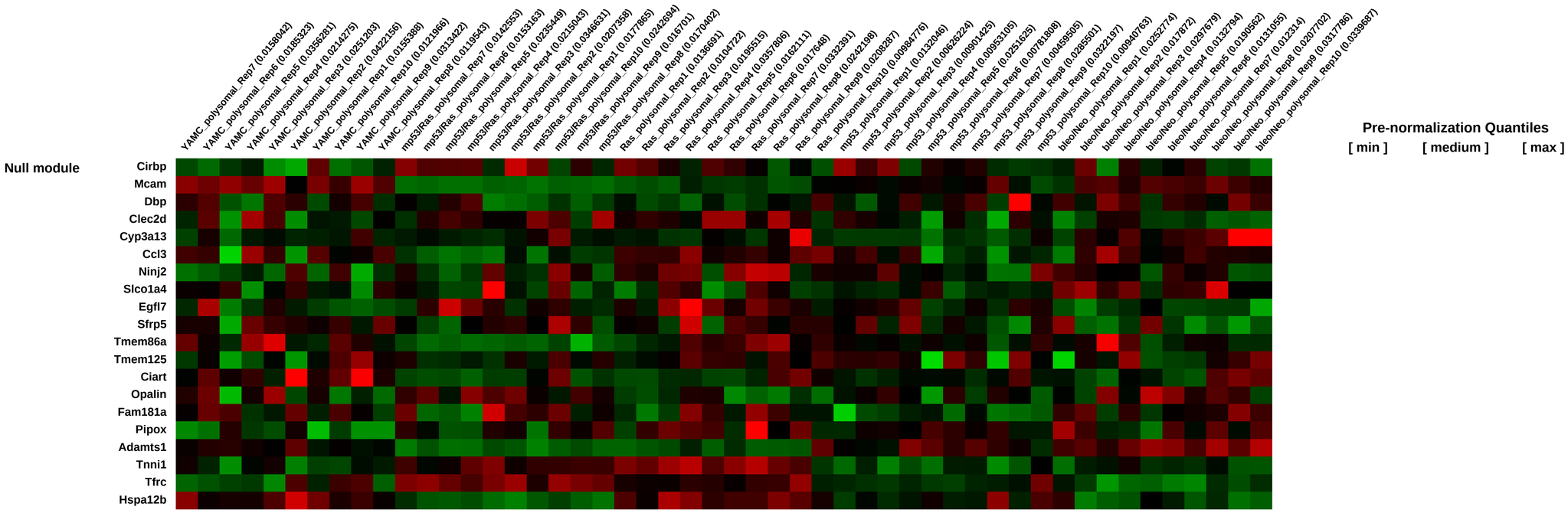

GEO Series "GSE31792" Expression Profiles

Num of samples in this series: 18

Scale of expression profile Z-scores

-3.0 -2.0 -1.0 0.0 1.0 2.0 3.0

GEO Link:	http://www.ncbi.nlm.nih.gov/geo/query/acc.cgi?acc=GSE31792
Status:	Public on Jul 01 2012
Title:	Distinct and Overlapping Gene Regulatory Networks in BMP- and HDAC-Controlled Cell Fate Determination in the Embryonic Forebrain
Organism:	Mus musculus
Experiment type:	Expression profiling by array
Platform:	GPL1261
Pubmed ID:	22748179
Summary & Design:	**Summary:** Both bone morphogenetic proteins (BMPs) and histone deacetylases (HDACs) have previously been established to play a role in the development of the three major cell types of the central nervous system: neurons, astrocytes, and oligodendrocytes. We have previously established a connection between these two protein families, showing that HDACs suppress BMP-promoted astrogliogenesis in the embryonic striatum. Since HDACs act in the nucleus to effect changes in transcription, an unbiased analysis of their transcriptional targets could shed light on their downstream effects on BMP-signaling. Using neurospheres from the embryonic striatum as an in vitro system to analyze this phenomenon, we have performed microarray expression profiling on BMP2- and trichostatin A (TSA)-treated cultures, followed by validation of the findings with quantitative RT-PCR and protein analysis. **Overall design:** Neurospheres from the embryonic striatum were used to analyze cellular differentiation into neurons and astrocytes in vitro. To analyze the role of BMP2 and the HDAC-inhibitor TSA in this system, neurospheres were treated with TSA or BMP2 for 24 h, and mRNA was extracted after 6 and 24 h of the respective treatment.

Background corr dist: KL-Divergence = 0.1556, L1-Distance = 0.0355, L2-Distance = 0.0026, Normal std = 0.3698

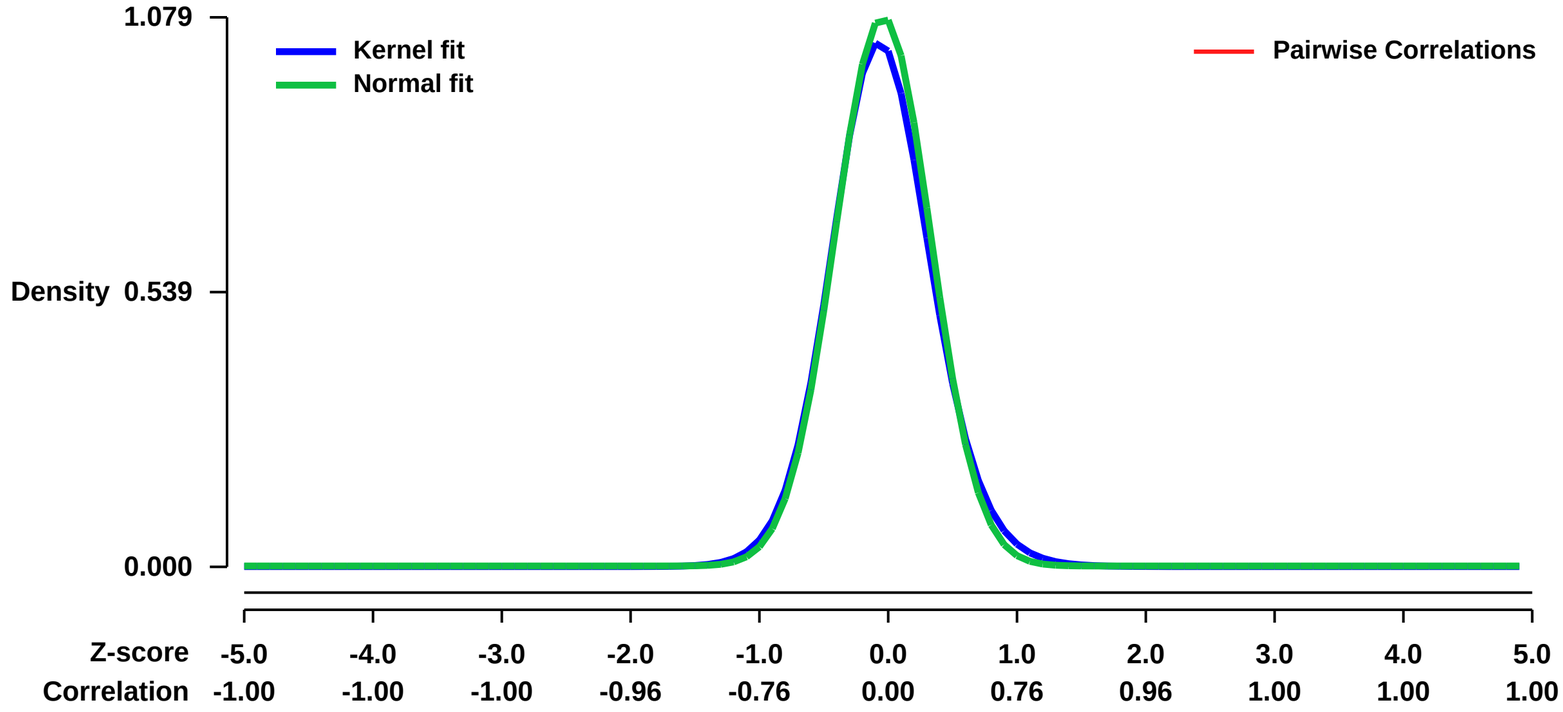

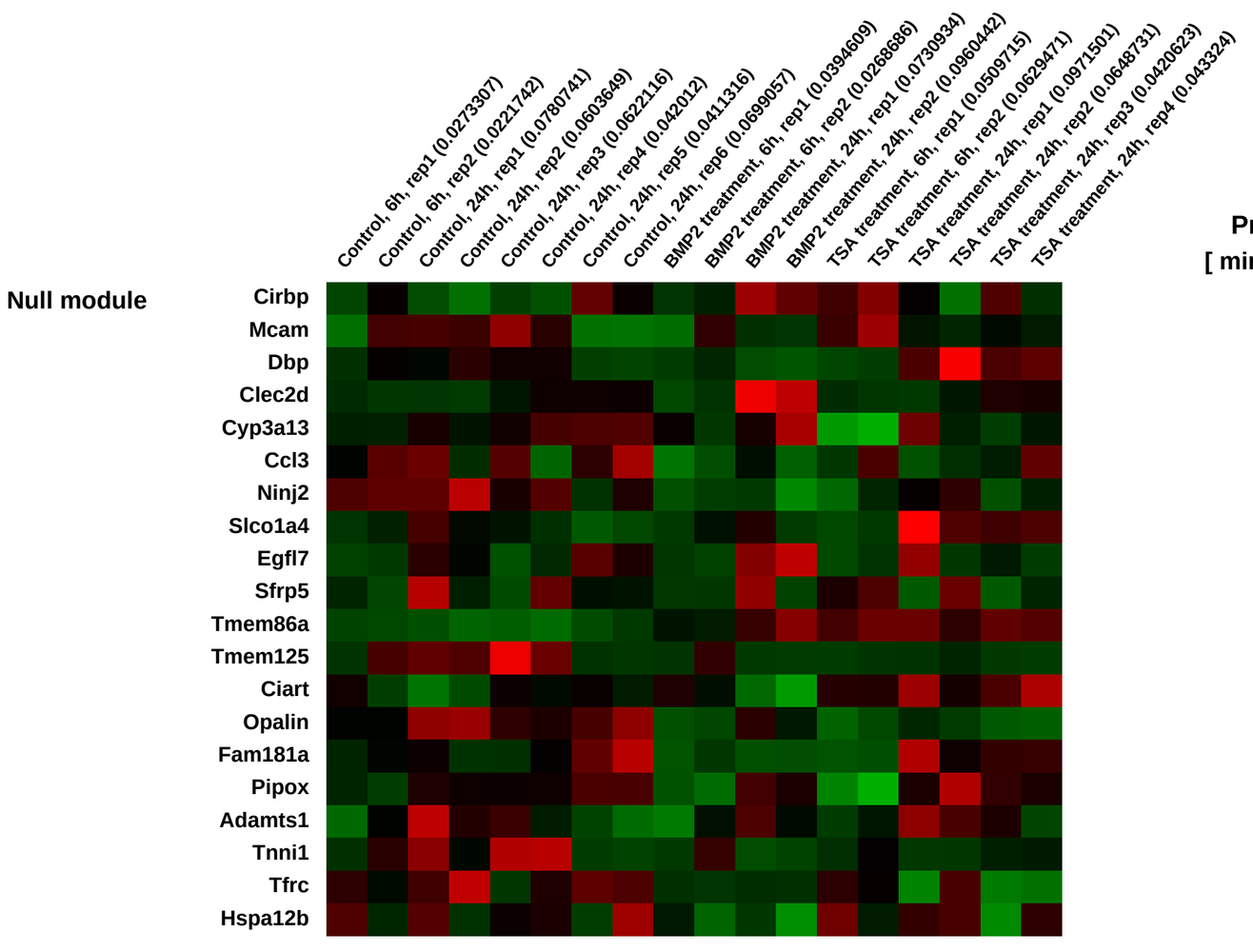

GEO Series "GSE8065" Expression Profiles

Num of samples in this series: 18

Scale of expression profile Z-scores

-3.0 -2.0 -1.0 0.0 1.0 2.0 3.0

GEO Link:	http://www.ncbi.nlm.nih.gov/geo/query/acc.cgi?acc=GSE8065
Status:	Public on Jun 12 2007
Title:	Gene expression during early postnatal development of the small intestine
Organism:	Mus musculus
Experiment type:	Expression profiling by array
Platform:	GPL1261
Pubmed ID:	18388184
Summary & Design:	**Summary:** It was the purpose to analyse the changes in gene expression which occur in the mouse small intestine from the pre-weaning to the post-weaning stage. The gene expression was accordingly followed from postnatal day 4 to postnatal day 32. **Keywords: Time-course** **Overall design:** 6 time-points were defined corresponding to postnatal day 4, 7, 9, 11, 24 and 32. Ileal samples were taken from individual mice at each time-point. All layers of the small intestine were included in the sample. Three samples from individual mice were analysed by hybridization to Affymetrix GeneChips.

Background corr dist: KL-Divergence = 0.0658, L1-Distance = 0.0198, L2-Distance = 0.0006, Normal std = 0.5101

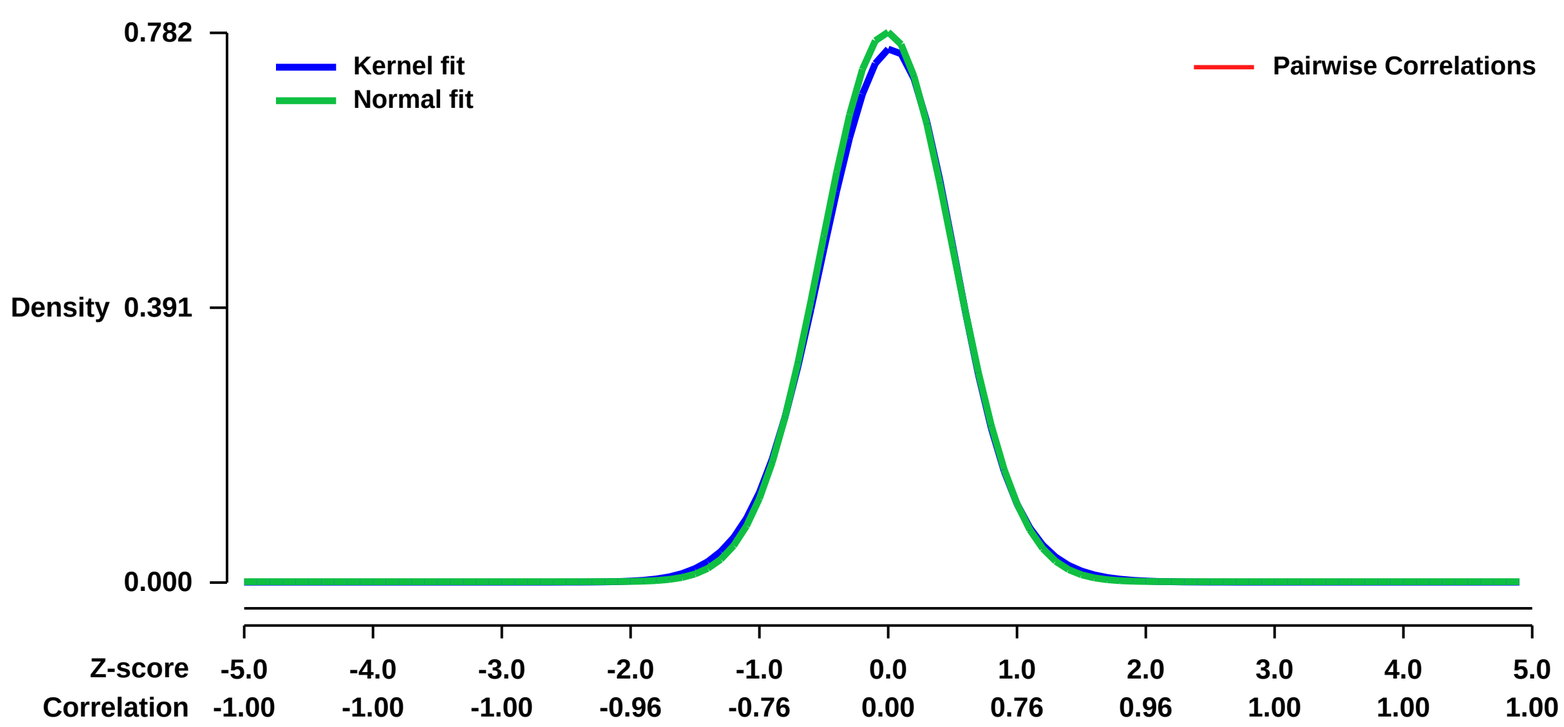

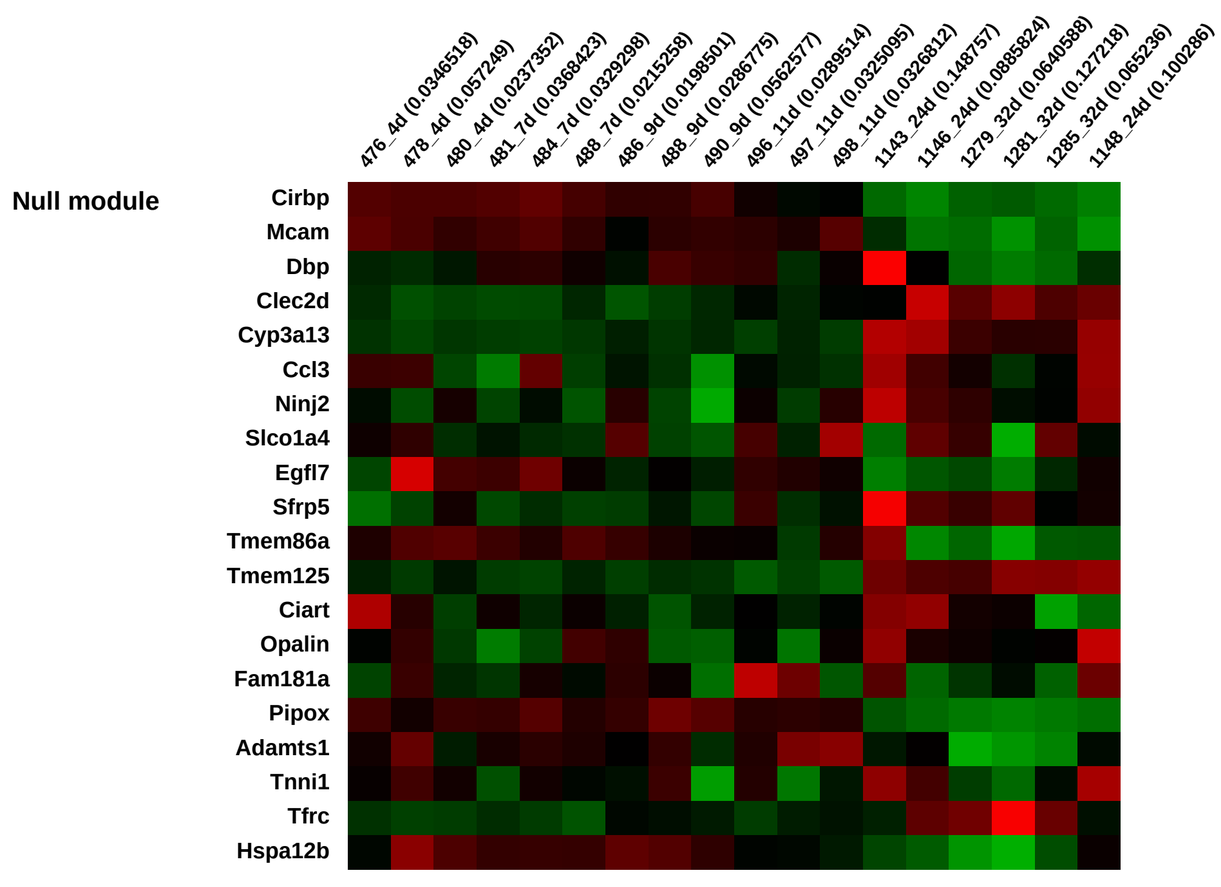

GEO Series "GSE25252" Expression Profiles

Num of samples in this series: 10

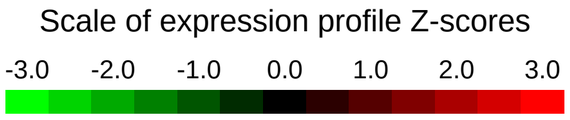

GEO Link:	http://www.ncbi.nlm.nih.gov/geo/query/acc.cgi?acc=GSE25252
Status:	Public on Nov 05 2012
Title:	Comparison of expression profiles of Foxp3(+)epigenetics(-) T cells, Foxp3(-)epigenetics(+) T cells, and Foxp3(+)epigenetics(+) T cells
Organism:	Mus musculus
Experiment type:	Expression profiling by array
Platform:	GPL1261
Pubmed ID:	23123060
Summary & Design:	**Summary:** Analysis of Foxp3(+)epigenetics(-) T cells, Foxp3(-)epigenetics(+) T cells, and Foxp3(+)epigenetics(+) T cells. Results indicate regulatory T cell (Treg) ontogenesis requires two independent processes, expression of the transcription factor Foxp3 and establishment of Treg epigenetic programs induced by T cell receptor (TCR) stimulation. **Overall design:** GFP+CD4+ and GFP-CD4+ splenocytes were sorted from DEREG and DEREG/Scurfy mice. These cells were activated with anti-CD3/CD28 antibodies, and then transduced with Foxp3-expressing retrovirus (pGCSamIN, NGFR marker). NGFR+ T cells sorted were subjected to microarray analysis (Affymetrix, mouse genome 430 2.0 array). To normalize the experimental conditions, Tregs (GFP+ T cells from DEREG) and Tconv (GFP- T cells from DEREG) were also activated and transduced with empty vector. Two replicates each.

Background corr dist: KL-Divergence = 0.1185, L1-Distance = 0.0335, L2-Distance = 0.0023, Normal std = 0.4128

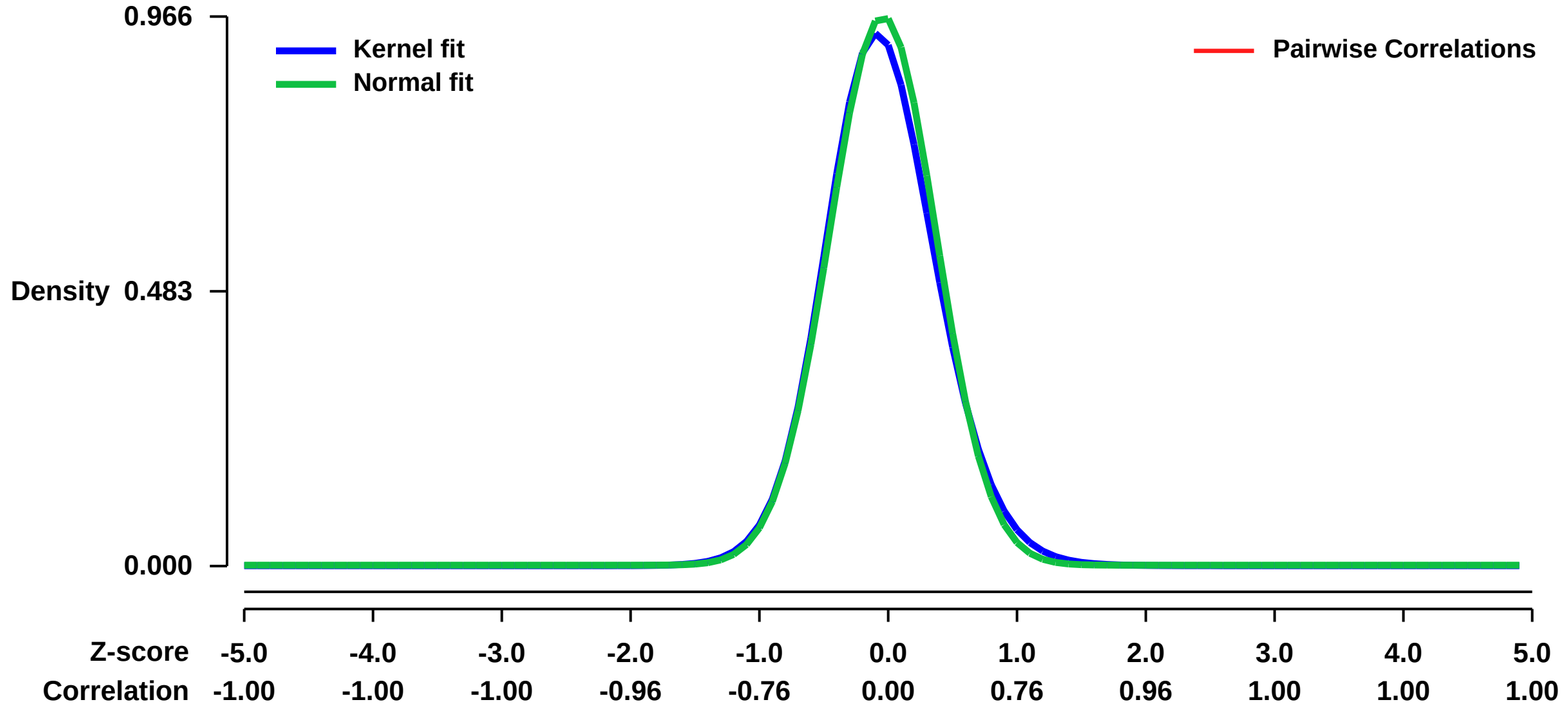

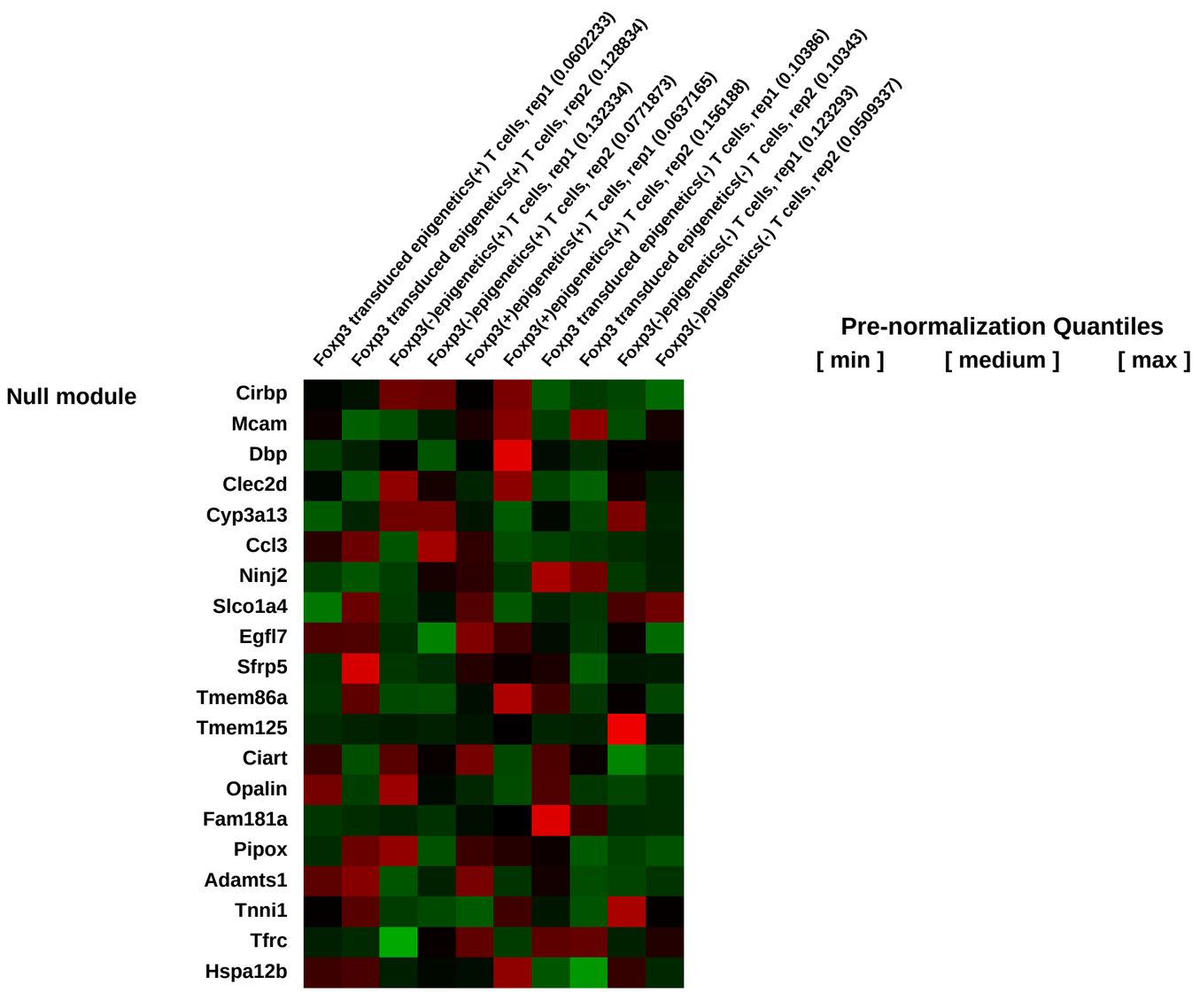

GEO Series "GSE20523" Expression Profiles

Num of samples in this series: 17

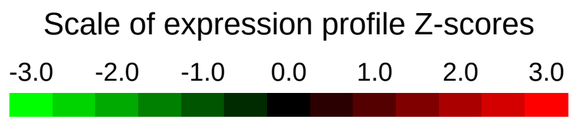

GEO Link:	**http://www.ncbi.nlm.nih.gov/geo/query/acc.cgi?acc=GSE20523**
Status:	**Public on Jun 21 2010**
Title:	**Immunoregulatory actions of T cell PPAR g at the colonic mucosa**
Organism:	**Mus musculus**
Experiment type:	**Expression profiling by array**
Platform:	**GPL1261**
Pubmed ID:	**20537136**

Summary & Design:

Summary:
BACKGROUND: Peroxisome proliferator-activated receptor g (PPAR g) is a nuclear receptor whose activation has been shown to modulate macrophage and epithelial cell-mediated inflammation. The objective of this study was to use a systems approach for investigating the mechanism by which the deletion of PPAR g in T cells modulates the severity of dextran-sodium sulfate (DSS)-induced colitis, immune cell distribution and global gene expression.

METHODS: Wild-type (WT) or PPAR g flfl; CD4 Cre+ (CD4cre) mice in a C57BL/6 background were challenged with 2.5% DSS in their drinking water for 0, 2, or 7 days. Mice were scored on disease severity both clinically and histopathologically. Flow cytometry was used to assess lymphocyte and macrophage populations in the blood, spleen, and mesenteric lymph nodes (MLN). Global gene expression in colonic mucosa was profiled using Affymetrix microarrays.

RESULTS: Both disease severity and inflammation-related body weight loss were accelerated by the deficiency of PPAR g in T cells. Examination of colon histopathology revealed significantly greater epithelial erosion, leukocyte infiltration, and mucosal thickening in the CD4cre mice on day 7. CD4cre mice had more CD8+ T cells than wt mice and fewer CD4+FoxP3+ regulatory T cells (Treg) and IL10+CD4+ T cells in blood and MLN, respectively. Transcriptomic profiling revealed around 3000 genes being transcriptionally altered as a result of DSS challenge in CD4cre mice. These included up-regulated adhesion molecules on day 7 and proinflammatory cytokines interleukin-6 (IL-6) and IL-1b, and suppressor of cytokine signaling 3 (SOCS-3) mRNA expression.

CONCLUSIONS: These findings suggest that T cell PPAR g down-regulates inflammation during DSS colitis by inhibiting colonic expression of inflammatory mediators and increasing MLN Treg.

Overall design:
Colonic mucosa from wt and CD4cre mice were sampled at 0 (no DSS), 2, and 7 days of DSS-induced experimental colitis

Background corr dist: **KL-Divergence = 0.1498, L1-Distance = 0.0988, L2-Distance = 0.0202, Normal std = 0.4522**

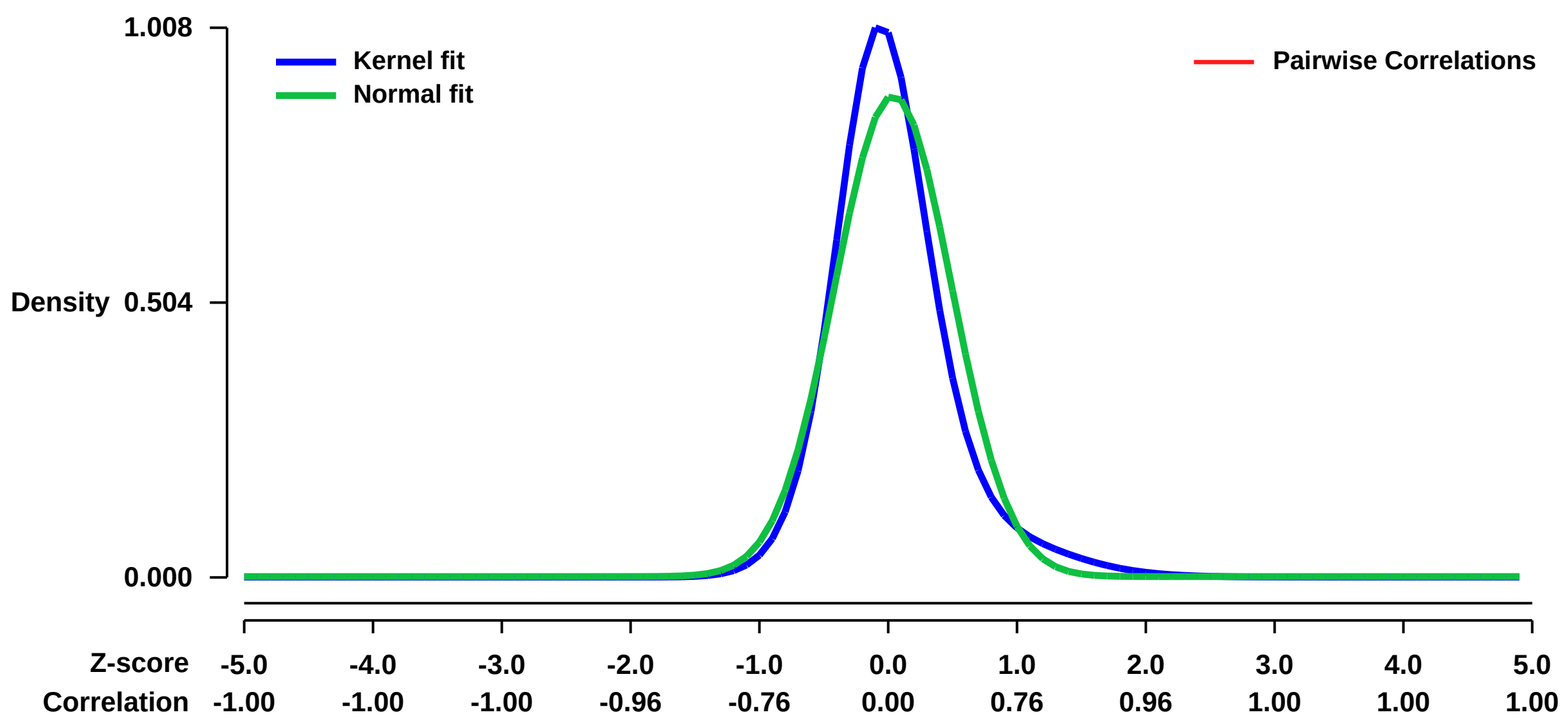

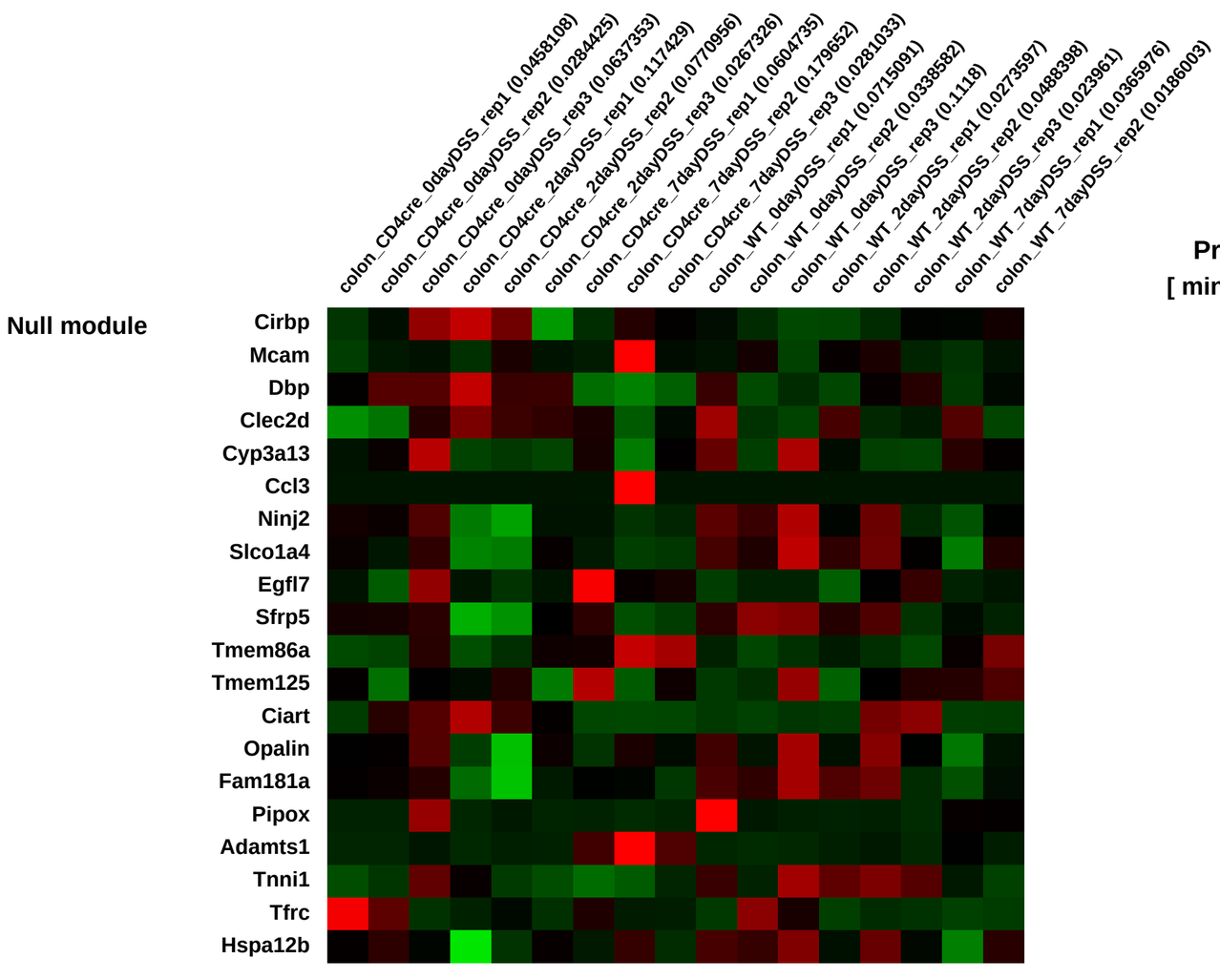

GEO Series "GSE19073" Expression Profiles

Num of samples in this series: 6

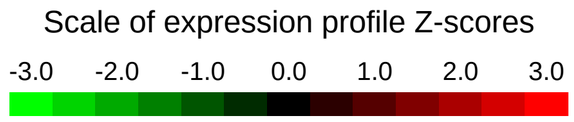

GEO Link:	**http://www.ncbi.nlm.nih.gov/geo/query/acc.cgi?acc=GSE19073**
Status:	**Public on Dec 01 2009**
Title:	**An Experimentally Derived Metastasis Gene Expression Profile Predicts Recurrence and Death in Colon Cancer Patients**
Organism:	**Mus musculus**
Experiment type:	**Expression profiling by array**
Platform:	**GPL1261**
Pubmed ID:	**22115830**
Summary & Design:	**Summary:** **Functional genomics approach to metastatic colon cancer** **Mouse model translated to human colon cancer** **Overall design:** **Gene expression array differences between highly invasive mouse colon cancer cells and non-invasive colon cancer cells**

Background corr dist: **KL-Divergence = 0.0203, L1-Distance = 0.0183, L2-Distance = 0.0003, Normal std = 0.7524**

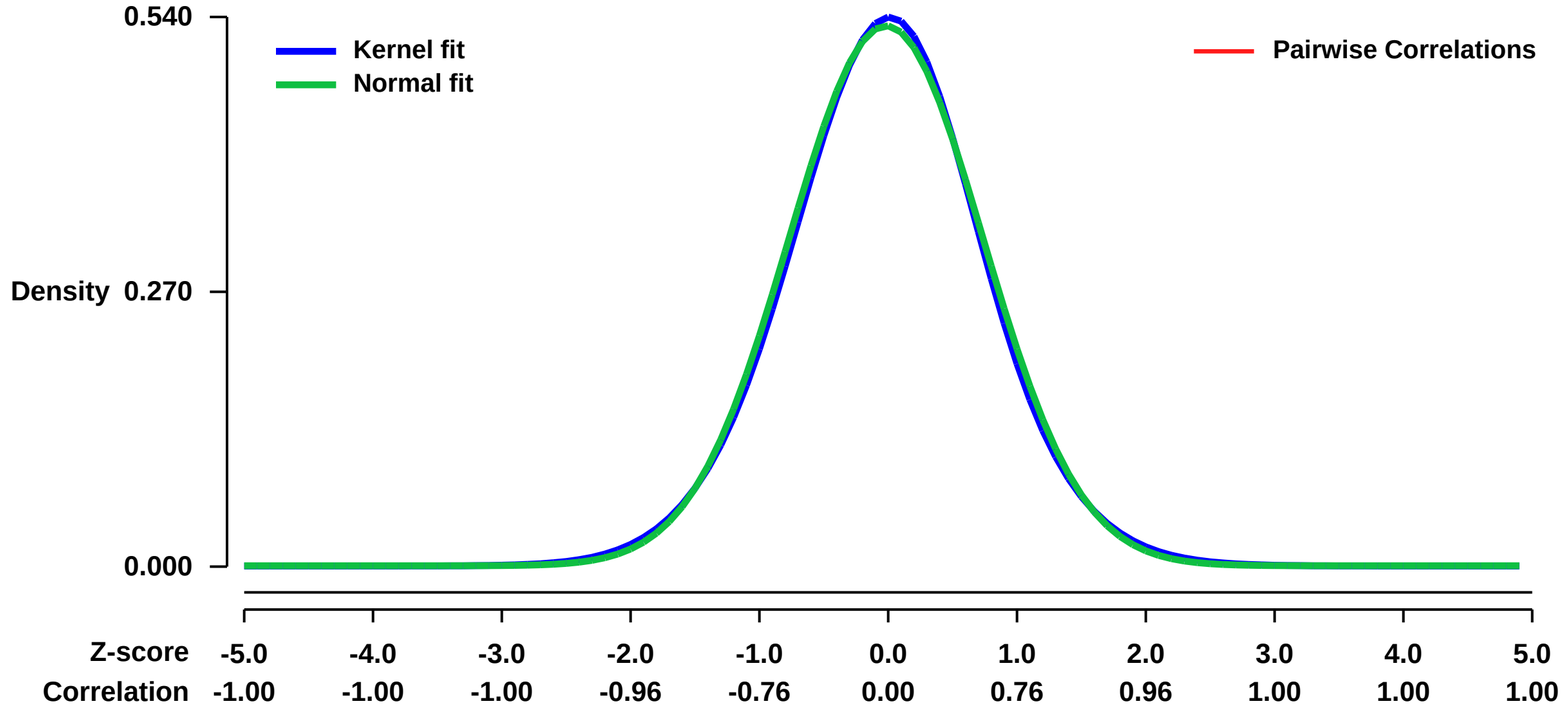

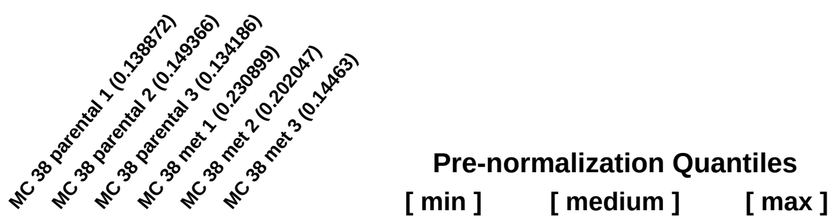

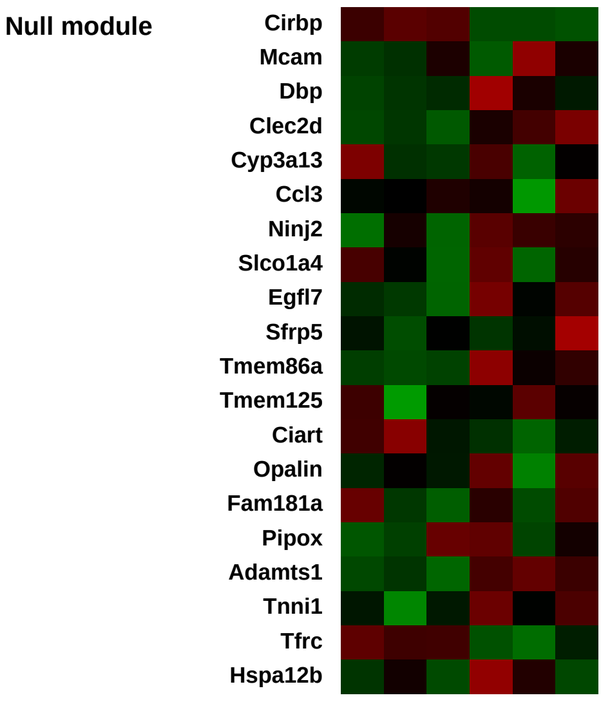

GEO Series "GSE42548" Expression Profiles

Num of samples in this series: 29

Scale of expression profile Z-scores

-3.0 -2.0 -1.0 0.0 1.0 2.0 3.0

GEO Link:	http://www.ncbi.nlm.nih.gov/geo/query/acc.cgi?acc=GSE42548
Status:	Public on May 22 2013
Title:	TH-MYCN Mice with Caspase-8 Deficiency Develop Advanced Neuroblastoma with Bone Marrow Metastasis
Organism:	Mus musculus
Experiment type:	Expression profiling by array
Platform:	GPL1261
Pubmed ID:	23536557
Summary & Design:	**Summary:** Neuroblastoma, the most common extracranial pediatric solid tumor, is responsible for 15% of all childhood cancer deaths. Patients frequently present at diagnosis with metastatic disease, particularly to the bone marrow. Advances in therapy and understanding of the metastatic process have been limited due in part, to the lack of animal models harboring bone marrow disease. The widely employed transgenic model, the TH-MYCN mouse, exhibits limited metastasis to this site. Here we establish the first genetic immunocompetent mouse model for metastatic neuroblastoma with enhanced secondary tumors in the bone marrow. This model recapitulates two frequent alterations in metastatic neuroblasoma, over-expression of MYCN and loss of caspase-8 expression. In this model, the mouse caspase-8 gene was deleted in neural crest lineage cells by crossing a TH-Cre transgenic mouse with a caspase-8 conditional knockout mouse. This mouse was then crossed with the neuroblastoma prone TH-MYCN mouse. While over-expression of MYCN by itself rarely caused bone marrow metastasis (5% average incidence), combining MYCN overexpression and caspase-8 deletion significantly increased bone marrow metastasis (37% average incidence). Loss of caspase-8 expression did not alter the site, incidence, or latency of the primary tumors. However, secondary tumors were detected in the bone marrow of these mice as early as week 9-10. The mouse model described in this work is a valuable tool to enhance our understanding of metastatic neuroblastoma and treatment options and underscores the role of caspase-8 in neuroblastoma progression. **Overall design:** Survey of spontateous 24 NB tumors and 5 bone marrow samples in wt and transgenic mice.

Background corr dist: KL-Divergence = 0.0350, L1-Distance = 0.0336, L2-Distance = 0.0021, Normal std = 0.6306

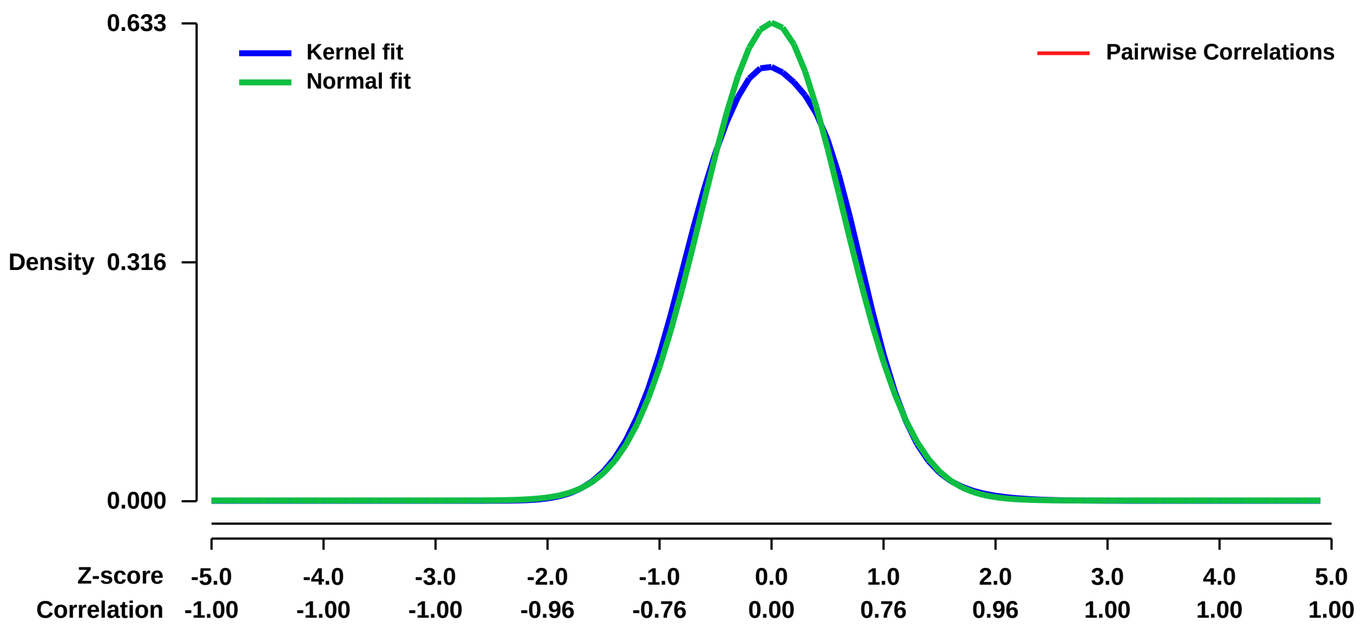

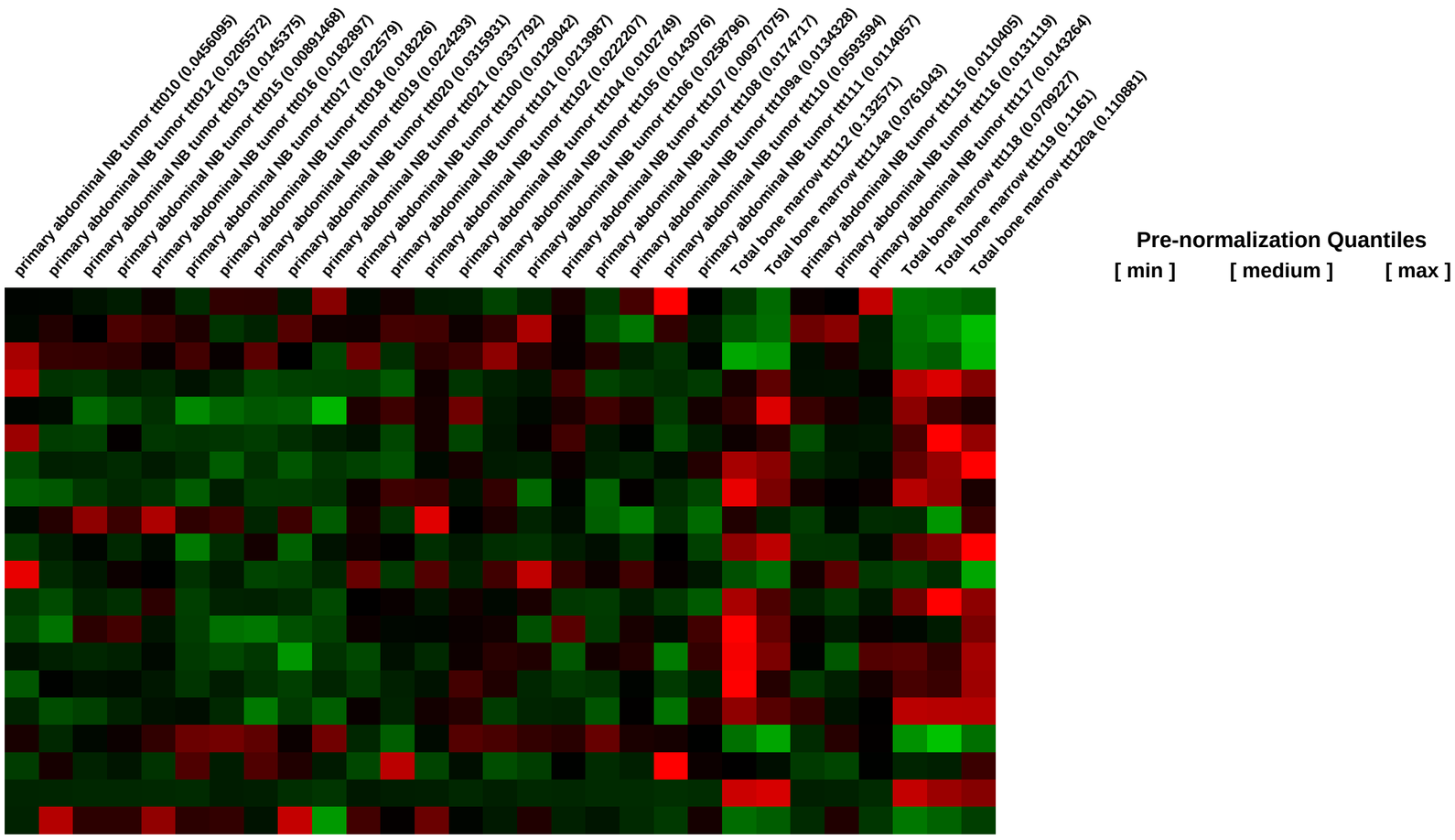

GEO Series "GSE46091" Expression Profiles

Num of samples in this series: 8

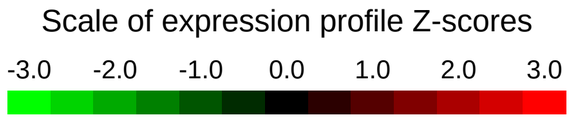

GEO Link:	http://www.ncbi.nlm.nih.gov/geo/query/acc.cgi?acc=GSE46091
Status:	Public on Apr 17 2013
Title:	Genes regulated by the gamma secretase inhibitor in WT and Ikaros deficient DN3 cells
Organism:	Mus musculus
Experiment type:	Expression profiling by array
Platform:	GPL1261
Pubmed ID:	24643801
Summary & Design:	**Summary:** Lineage-negative thymocytes were cultured on OP9-DL1 stromal cells for 16h in the presence of DMSO or the gamma secretase inhibitor MRK-003. DN3 cells cells were then sorted and their transcriptome analyzed. **Overall design:** 8 samples

Background corr dist: KL-Divergence = 0.0511, L1-Distance = 0.0209, L2-Distance = 0.0005, Normal std = 0.5665

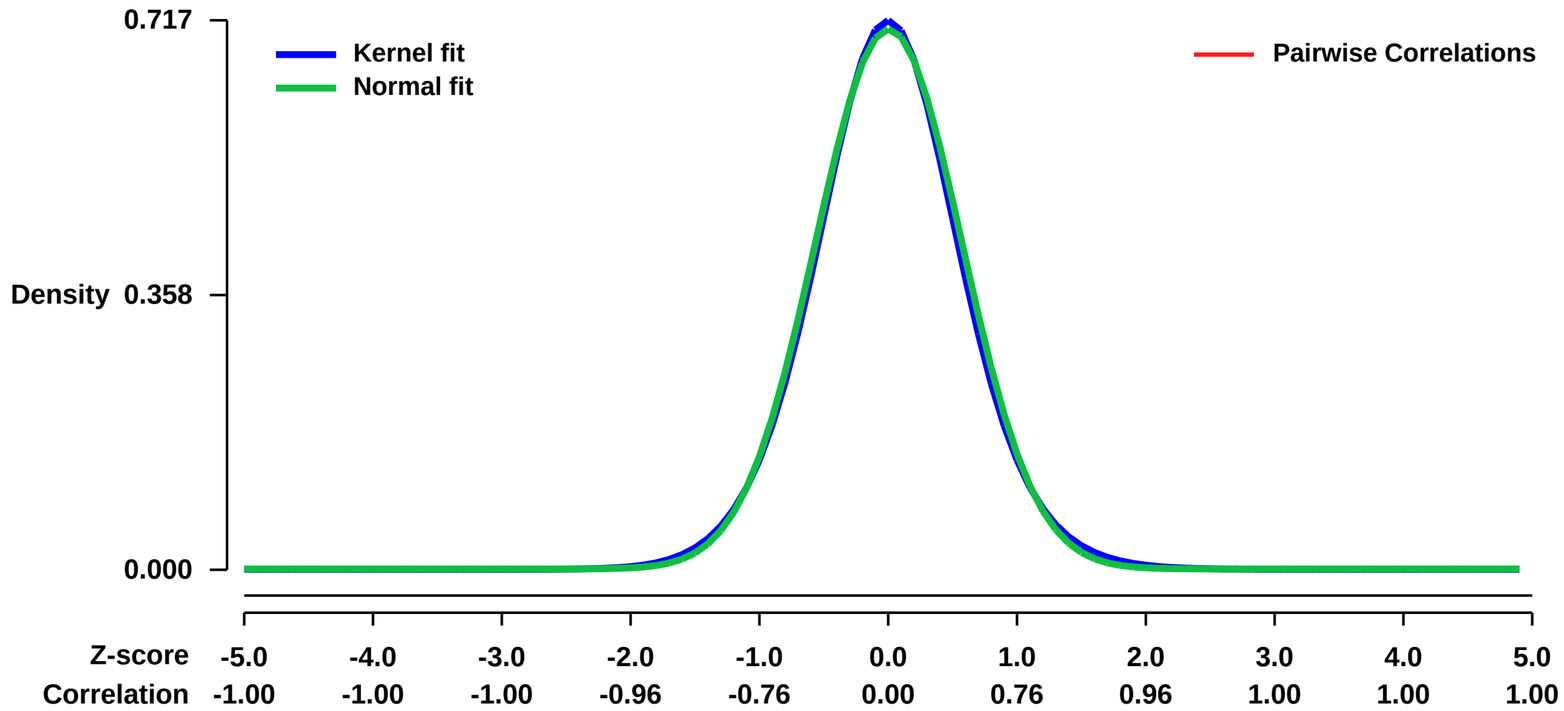

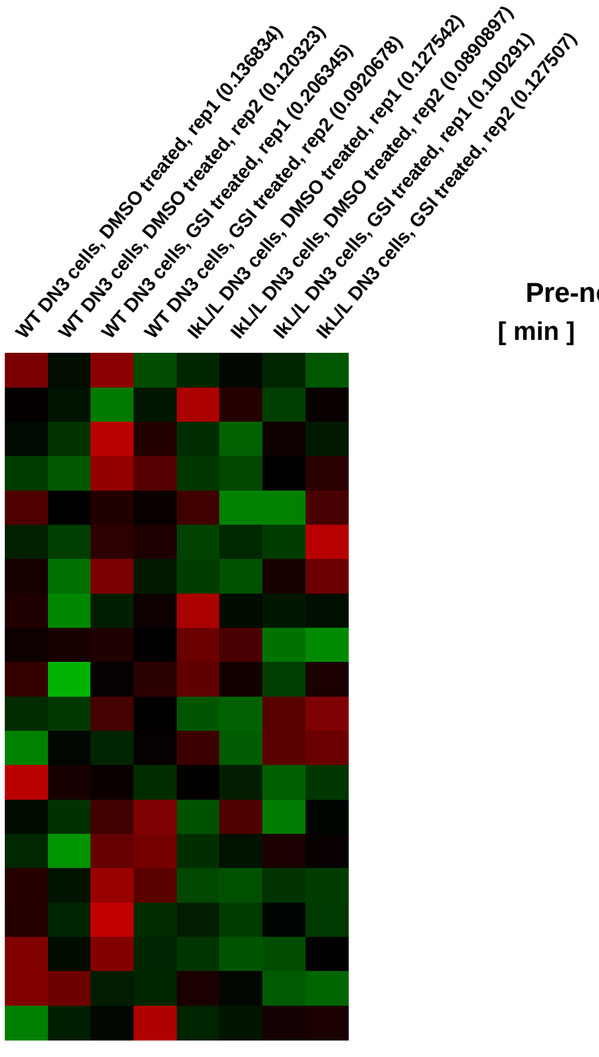

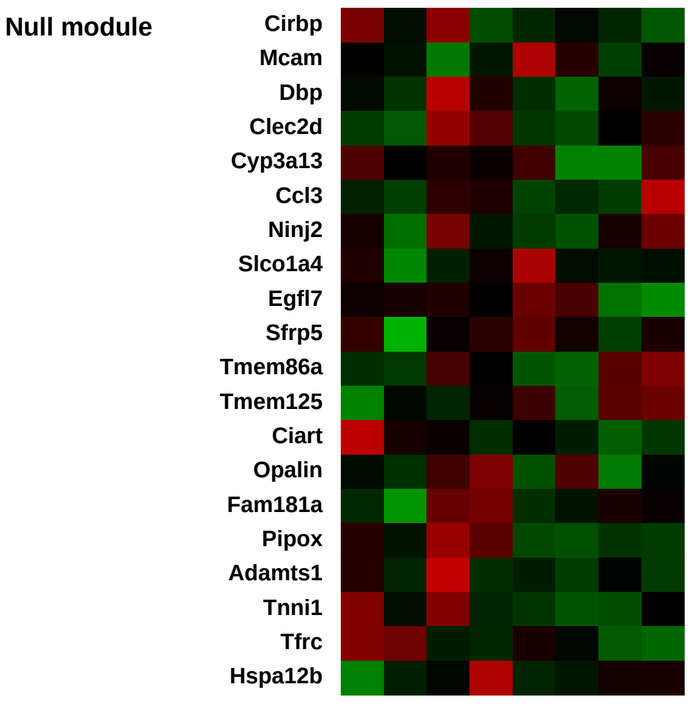

GEO Series "GSE1566" Expression Profiles

Num of samples in this series: 6

Scale of expression profile Z-scores

-3.0 -2.0 -1.0 0.0 1.0 2.0 3.0

GEO Link:	**http://www.ncbi.nlm.nih.gov/geo/query/acc.cgi?acc=GSE1566**
Status:	**Public on Sep 01 2005**
Title:	**Ezh2 deficient T-cell**
Organism:	**Mus musculus**
Experiment type:	**Expression profiling by array**
Platform:	**GPL1261**
Pubmed ID:	**15882624**
Summary & Design:	**Summary:** **Lymph node T cells isolated from Ezh2fl/fl or Ezh2 deficient mice** **Keywords: repeat sample** **Overall design:**

Background corr dist: **KL-Divergence = 0.0471, L1-Distance = 0.0176, L2-Distance = 0.0003, Normal std = 0.5824**

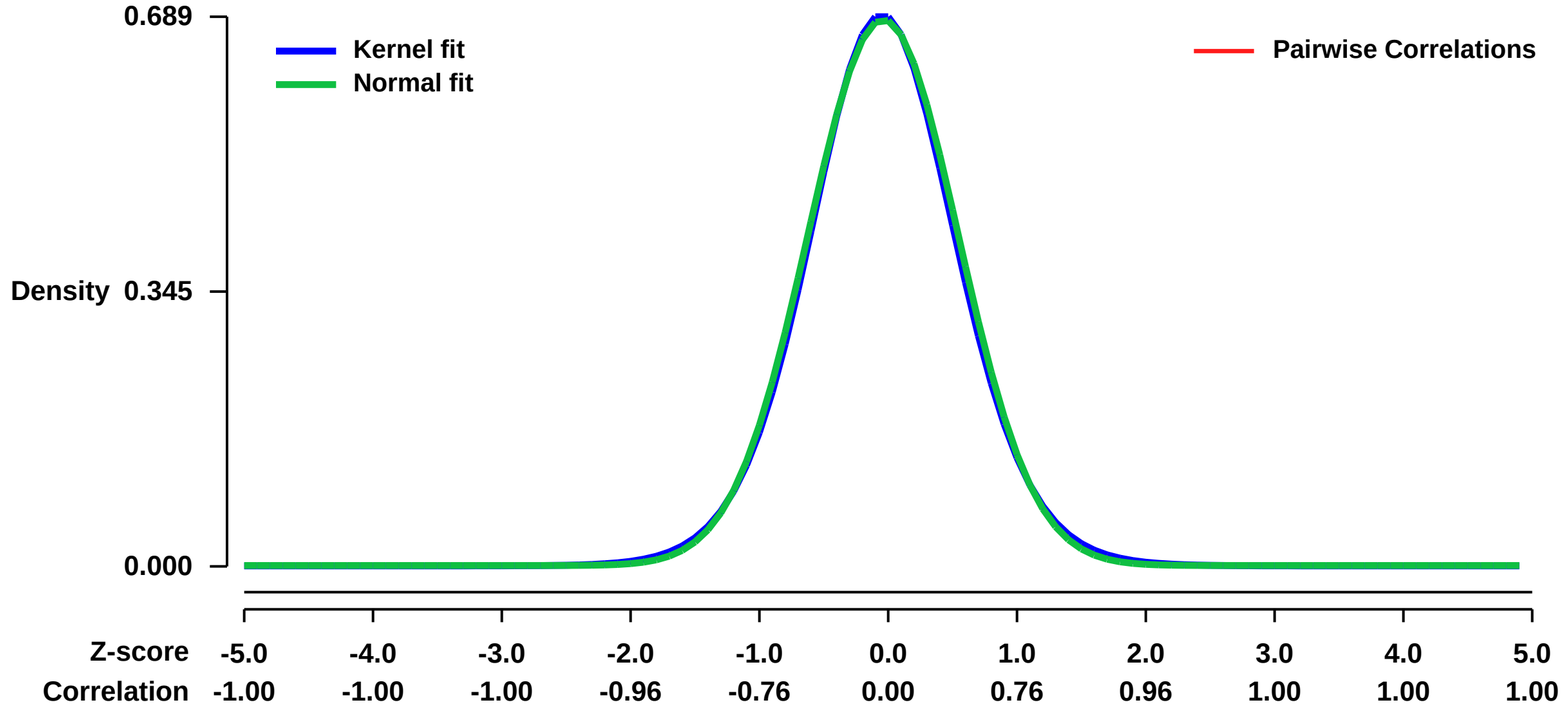

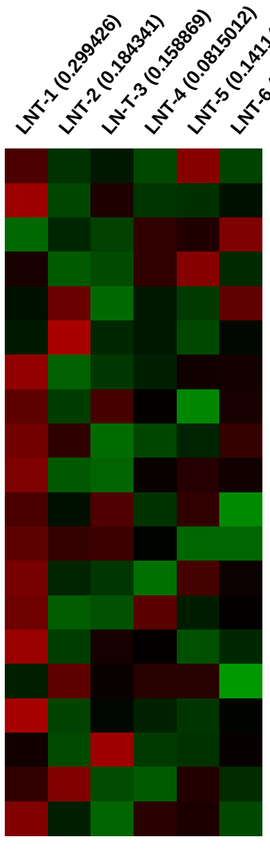

GEO Series "GSE51927" Expression Profiles

Num of samples in this series: 59

Scale of expression profile Z-scores

-3.0 -2.0 -1.0 0.0 1.0 2.0 3.0

GEO Link:	http://www.ncbi.nlm.nih.gov/geo/query/acc.cgi?acc=GSE51927
Status:	Public on Oct 30 2013
Title:	Expression analysis of murine primary and derived orthotopic SEOC tumors
Organism:	Mus musculus
Experiment type:	Expression profiling by array
Platform:	GPL1261
Pubmed ID:	24748377
Summary & Design:	**Summary:** We previously generated genetically engineered mouse (GEM) models based on perturbation of Tp53, Rb with or without Brca1 or Brca2 that develop serous epithelial ovarian cancer (SEOC) closely resembling the human disease on histologic and molecular levels. We have adapted these GEM models to orthotopic allografts that uniformly develop tumors with short latency in immunocompetent recipients and are ideally suited for routine preclinical studies. To monitor passaged tumors at the molecular level, we analyzed transcriptional profiles of a set of primary SEOC and matching derived passaged tumors. We have merged this dataset with previously published (doi: 10.1158/0008-5472.CAN-11-3834; PMID 22617326) dataset of murine primary ovarian tumors from our GEM models (GSE46169) and merged and compared them to expression profiles of human dataset published previously (doi: 10.1038/nature10166). The high mortality rate from ovarian cancers can be attributed to late-stage diagnosis and lack of effective treatment. Despite enormous effort to develop better targeted therapies, platinum-based chemotherapy still remains the standard of care for ovarian cancer patients, and resistance occurs at a high rate. One of the rate limiting factors for translation of new drug discoveries into clinical treatments has been the lack of suitable preclinical cancer models with high predictive value. We previously generated genetically engineered mouse (GEM) models based on perturbation of Tp53, Rb with or without Brca1 or Brca2 that develop serous epithelial ovarian cancer (SEOC) closely resembling the human disease on histologic and molecular levels. Here, we describe an adaptation of these GEM models to orthotopic allografts that uniformly develop tumors with short latency and are ideally suited for routine preclinical studies. **Overall design:** RNA was isolated from flash frozen ovarian tumors using Trizol and Qiagen RNeasy columns

Background corr dist: KL-Divergence = 0.3139, L1-Distance = 0.0666, L2-Distance = 0.0122, Normal std = 0.2763

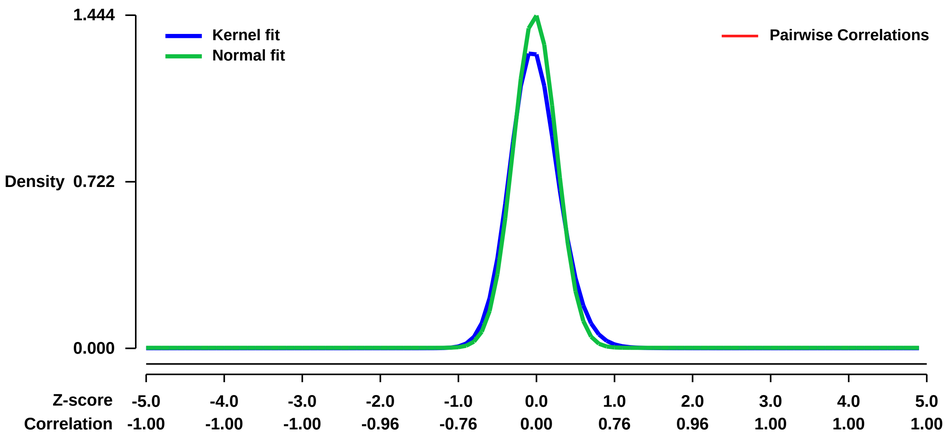

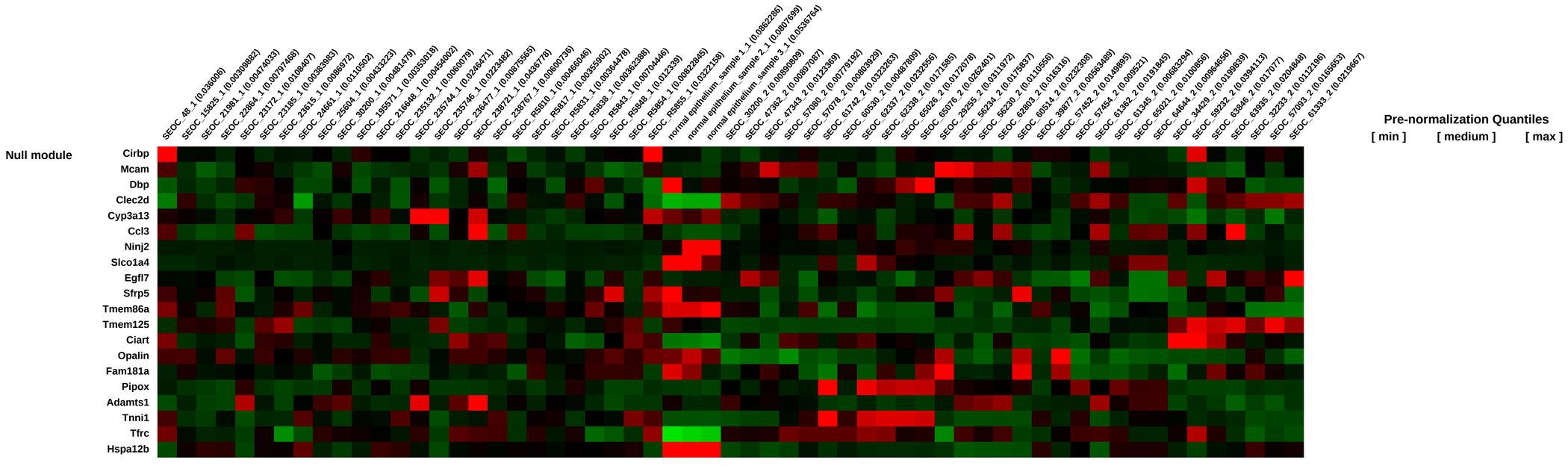

GEO Series "GSE35979" Expression Profiles

Num of samples in this series: 6

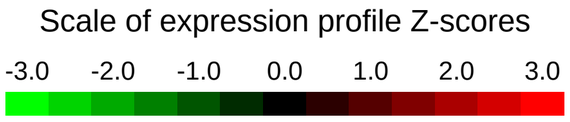

GEO Link:	http://www.ncbi.nlm.nih.gov/geo/query/acc.cgi?acc=GSE35979
Status:	Public on Feb 23 2012
Title:	Gene expression data from IL13-induced allergic airway inflammation of mice lungs
Organism:	Mus musculus
Experiment type:	Expression profiling by array
Platform:	GPL1261
Pubmed ID:	22611474
Summary & Design:	**Summary:** Asthma is a common chronic inflammatory airway condition with a strong genetic and inheritability component, as siblings and first-degree relatives of those with the disease are often affected. For our studies, we used a well-characterized transgenic mouse model of allergic airway inflammation induced by IL13. In this model, IL13 is conditionally overexpressed in the mouse lung when treated with doxycycline. Upon IL13 induction, these mice showed inflammatory cell infiltration, pronounced emphysema, increased pulmonary compliance, lung volume enlargement, mucus metaplasia, and increased expression of matrix metalloproteinases and cathepsins in the lung. We performed gene expression microarray to examine the changes in gene expression during IL13-induced allergic airway inflammation. **Overall design:** The CC10-rtTA-IL13 transgenic (TG) and wildtype (WT) mice were treated with doxycycline for seven days. Mice were euthanized and the left upper lobes from all mice were removed for RNA extraction using the TRIzol method.

Background corr dist: KL-Divergence = 0.0277, L1-Distance = 0.0161, L2-Distance = 0.0003, Normal std = 0.6879

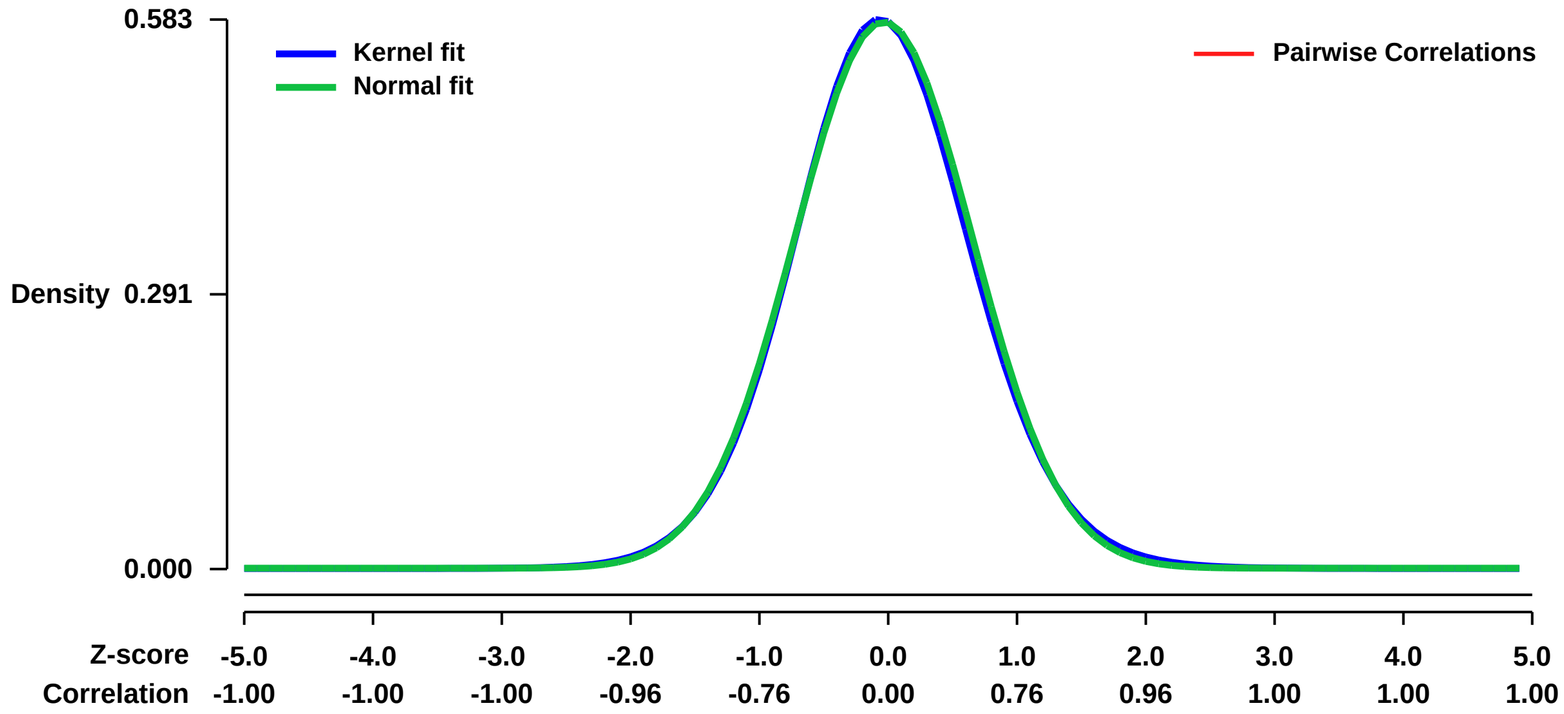

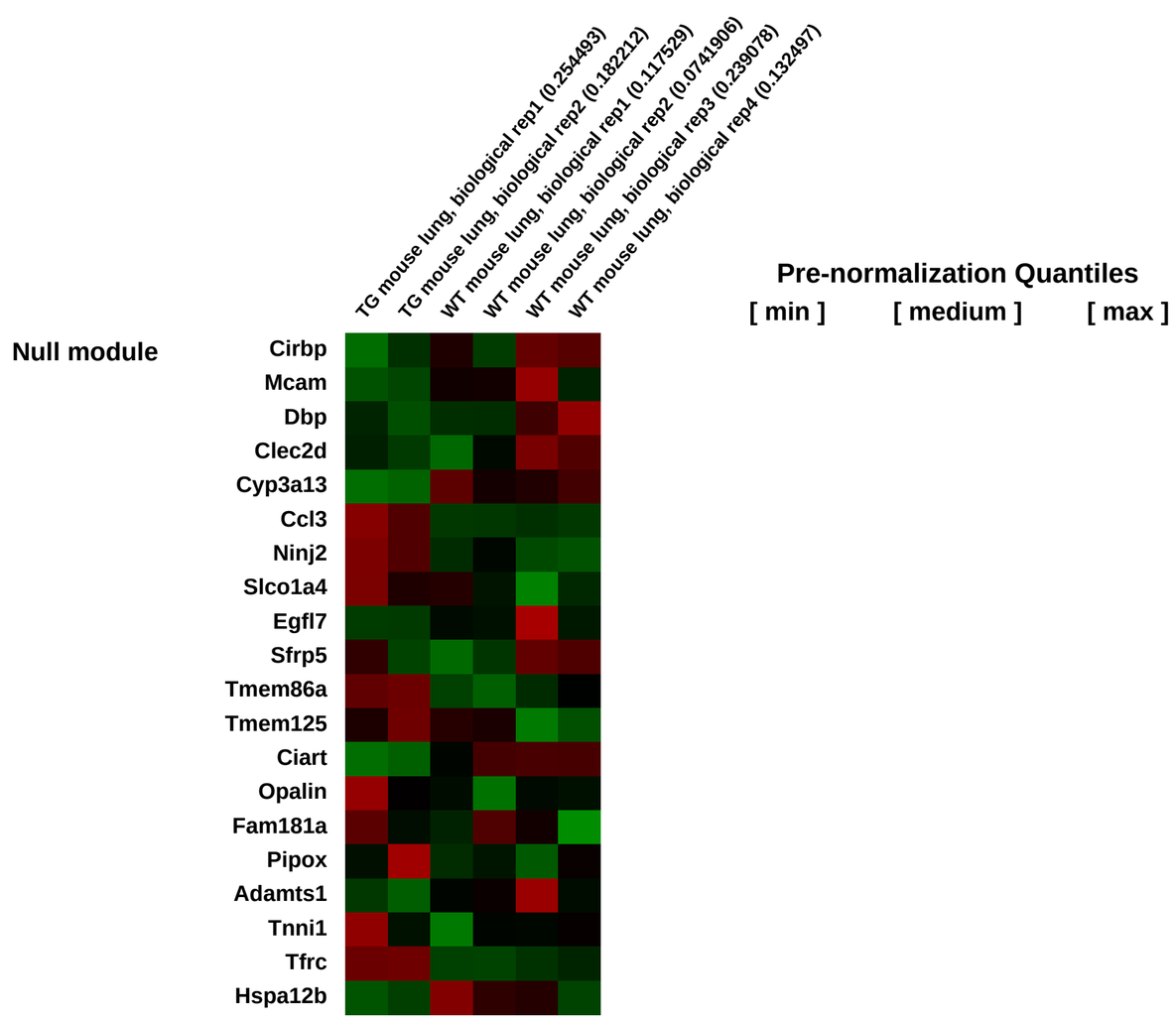

GEO Series "GSE23006" Expression Profiles

Num of samples in this series: 48

Scale of expression profile Z-scores

-3.0 -2.0 -1.0 0.0 1.0 2.0 3.0

GEO Link:	http://www.ncbi.nlm.nih.gov/geo/query/acc.cgi?acc=GSE23006
Status:	Public on Jul 20 2010
Title:	Transcriptional profiling of a wound healing process in skin and oral mucosa
Organism:	Mus musculus
Experiment type:	Expression profiling by array
Platform:	GPL1261
Pubmed ID:	20704739
Summary & Design:	**Summary:** When compared to skin, oral mucosal wounds heal rapidly and with reduced scar formation. This study used an Affymetrix microarray platform to compare the transcriptomes of oral mucosa and skin wounds in order to identify critical differences in the healing response at these two sites. **Overall design:** Using microarrays, we explored the differences in gene expression in skin and oral mucosal wound healing in a murine model of paired equivalent-sized wounds. Samples were examined from day 0 to day 10 and spanned all stages of the wound healing process. Unwounded matched tissue was used as a control. Tissue samples collected at each post-wounding time point, as well as control samples, were represented by 3 biological replicates.

Background corr dist: KL-Divergence = 0.1559, L1-Distance = 0.0300, L2-Distance = 0.0016, Normal std = 0.3721

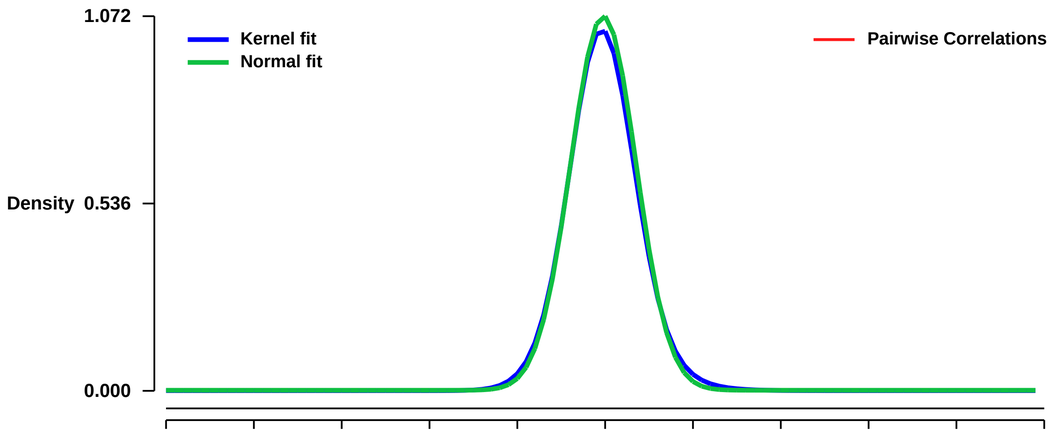

Z-score	-5.0	-4.0	-3.0	-2.0	-1.0	0.0	1.0	2.0	3.0	4.0	5.0
Correlation	-1.00	-1.00	-1.00	-0.96	-0.76	0.00	0.76	0.96	1.00	1.00	1.00

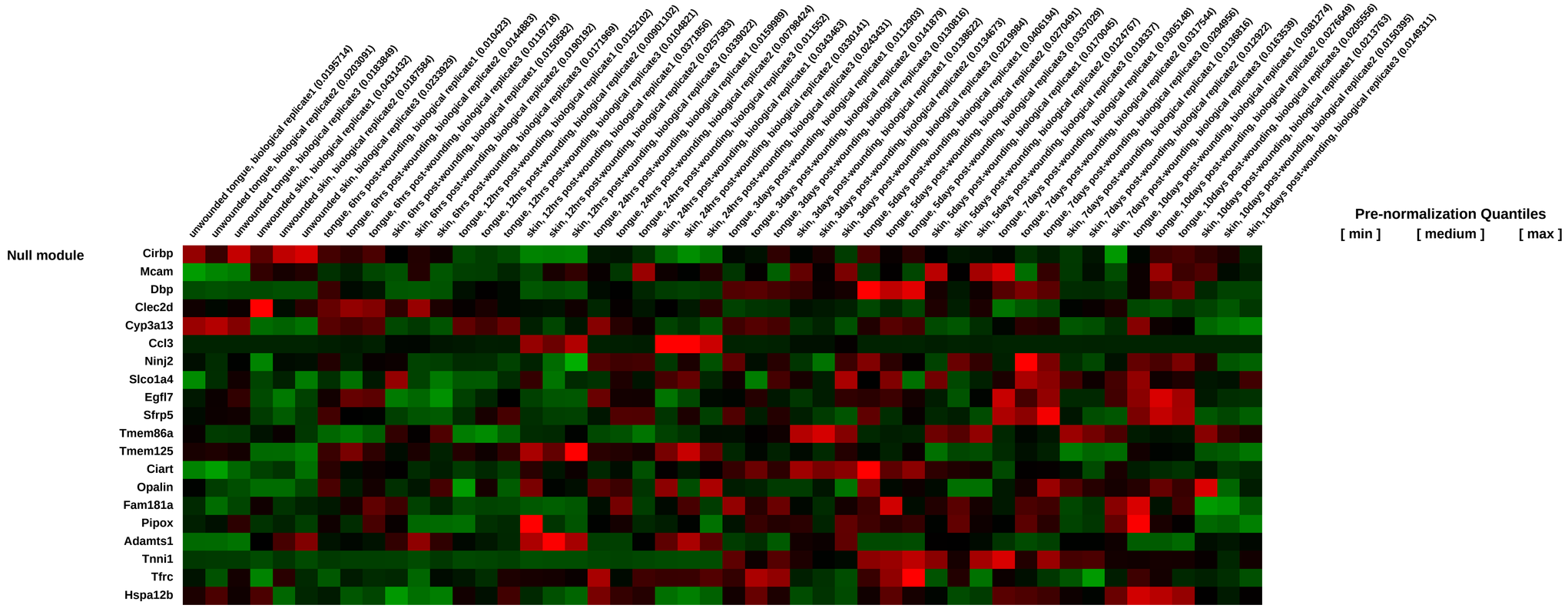

GEO Series "GSE7487" Expression Profiles

Num of samples in this series: 24

Scale of expression profile Z-scores

-3.0 -2.0 -1.0 0.0 1.0 2.0 3.0

GEO Link:	http://www.ncbi.nlm.nih.gov/geo/query/acc.cgi?acc=GSE7487
Status:	Public on Mar 08 2010
Title:	Gene profiling of pathological cardiac hypertrophy vs physiological hypertrophy
Organism:	Mus musculus
Experiment type:	Expression profiling by array
Platform:	GPL1261
Pubmed ID:	20237330
Summary & Design:	**Summary:** Cardiac hypertrophy can lead to heart failure, and is induced either by physiological stimuli eg postnatal development, chronic exercise training or pathological stimuli eg pressure or volume overload. Majority of new therapies for heart failure has mixed outcomes. A combined mouse model and oligo-array approach are used to examine whether phosphoinositide 3-kinase (p110-alpha isoform) activity is critical for maintenance of cardiac function and long-term survival in a setting of heart failure. The significance and expected outcome are to recognise genes involved in models of heart failure ie pathological- vs physiology-hypertrophy, and examine the molecular mechanisms responsible for such activity. Growth of the heart can be induced by physiological stimuli e.g., postnatal development, chronic exercise training, or pathological stimuli e.g., pressure or volume overload. Physiological hypertrophy (â goodâ) is characterised by a normal organisation of cardiac structure, and normal or enhanced cardiac function. In comparison, pathological hypertrophy (â badâ) is associated with fibrosis, cardiac dysfunction, and increased morbidity and mortality. The mechanistic process which allows the heart to enlarge in response to physiological stimuli while maintaining normal or enhanced function is of great clinical relevance because one potential therapeutic strategy is to inhibit the pathological growth process while augmenting the physiological growth process. One of the major process that regulate heart size is by phosphoinositide 3-kinase (PI3K). Thus the end goal of this project is to determine whether the p110 alpha isoform of PI3K could be a potential tool for augmenting physiological growth and improving cardiac function of the failing diseased heart, and to examine the underlying mechanisms responsible. **Keywords:** Disease progression analysis **Overall design:** Multiple comparison normalised to Ntg sham.

Background corr dist: KL-Divergence = 0.3605, L1-Distance = 0.0706, L2-Distance = 0.0146, Normal std = 0.2593

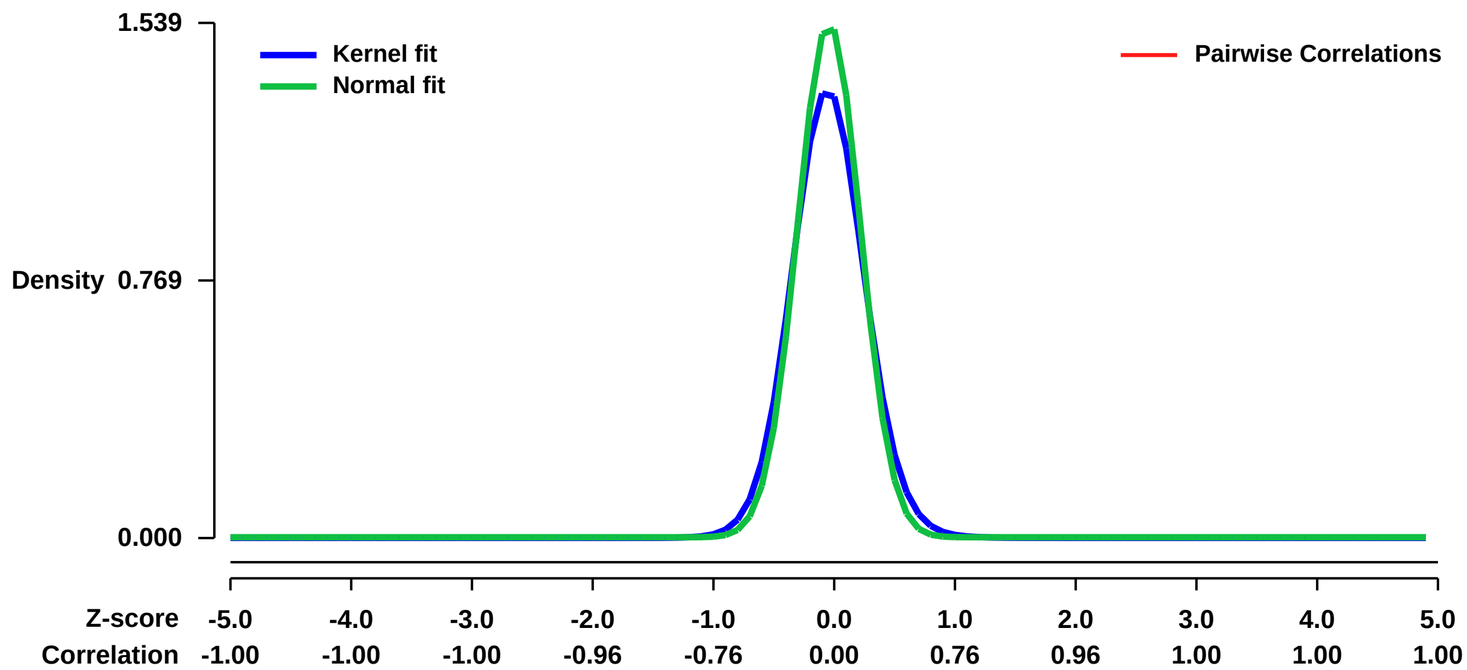

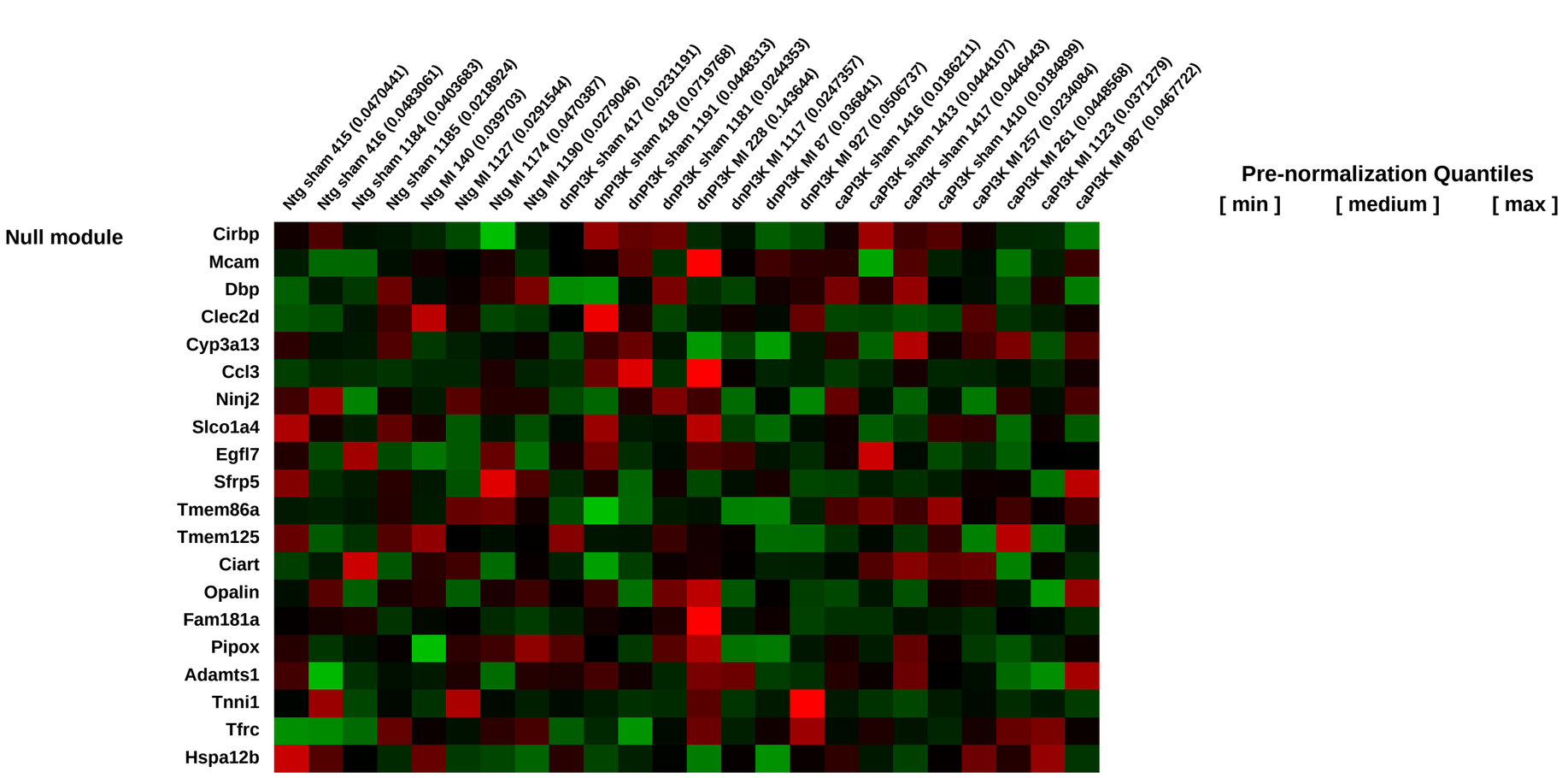

GEO Series "GSE18551" Expression Profiles

Num of samples in this series: 18

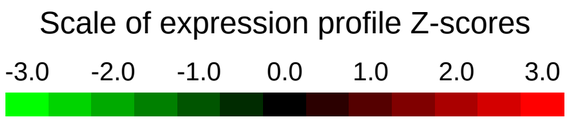

GEO Link:	http://www.ncbi.nlm.nih.gov/geo/query/acc.cgi?acc=GSE18551
Status:	Public on Jan 31 2010
Title:	Striatum of Huntington's disease model mice [Affymetrix data]
Organism:	Mus musculus
Experiment type:	Expression profiling by array
Platform:	GPL1261
Pubmed ID:	20089533
Summary & Design:	**Summary:** Evaluation of transcriptional changes in the striatum may be an effective approach to understanding the natural history of changes in expression contributing to the pathogenesis of Huntington disease (HD). We have performed genome-wide expression profiling of the YAC128 transgenic mouse model of HD at 12 and 24 months of age using two platforms in parallel; Affymetrix and Illumina. We performed gene expression profiling on the same striatal mRNA across both platforms. **Overall design:** Transgenic mice expressing human HD huntingtin with 120 CAG repeats (YAC128) and wildtype littermates were used for the described experiments. The mice were group housed in polystyrene cages under a normal light-dark cycle (6 am to 8 pm) in a clean facility and with free access to water and standard rodent chow. All experiments were performed in accordance with the University of British Columbia animal care committee. Striatal tissue was collected from 12 and 24 month old YAC128 mice and wildtype littermates.

Background corr dist: KL-Divergence = 0.0476, L1-Distance = 0.0999, L2-Distance = 0.0151, Normal std = 0.7151

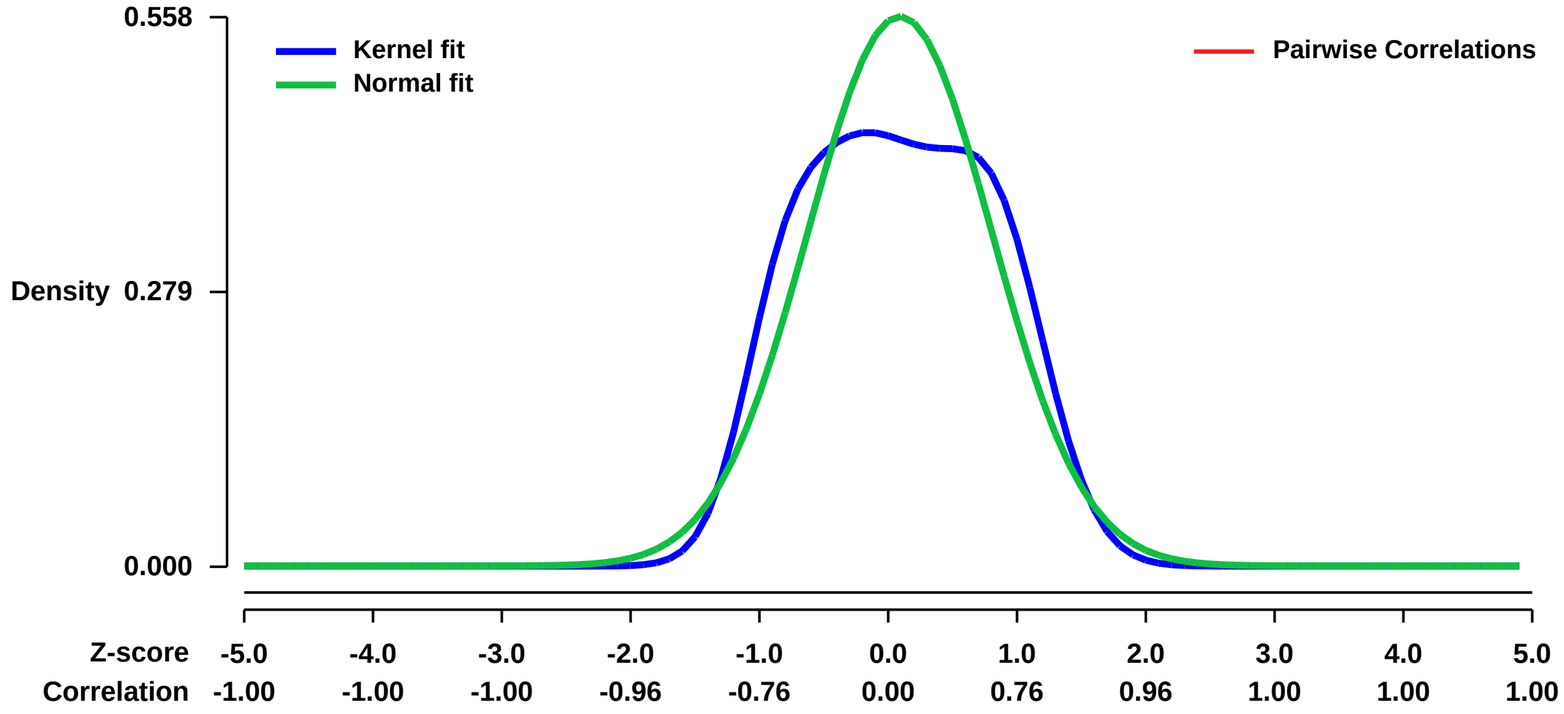

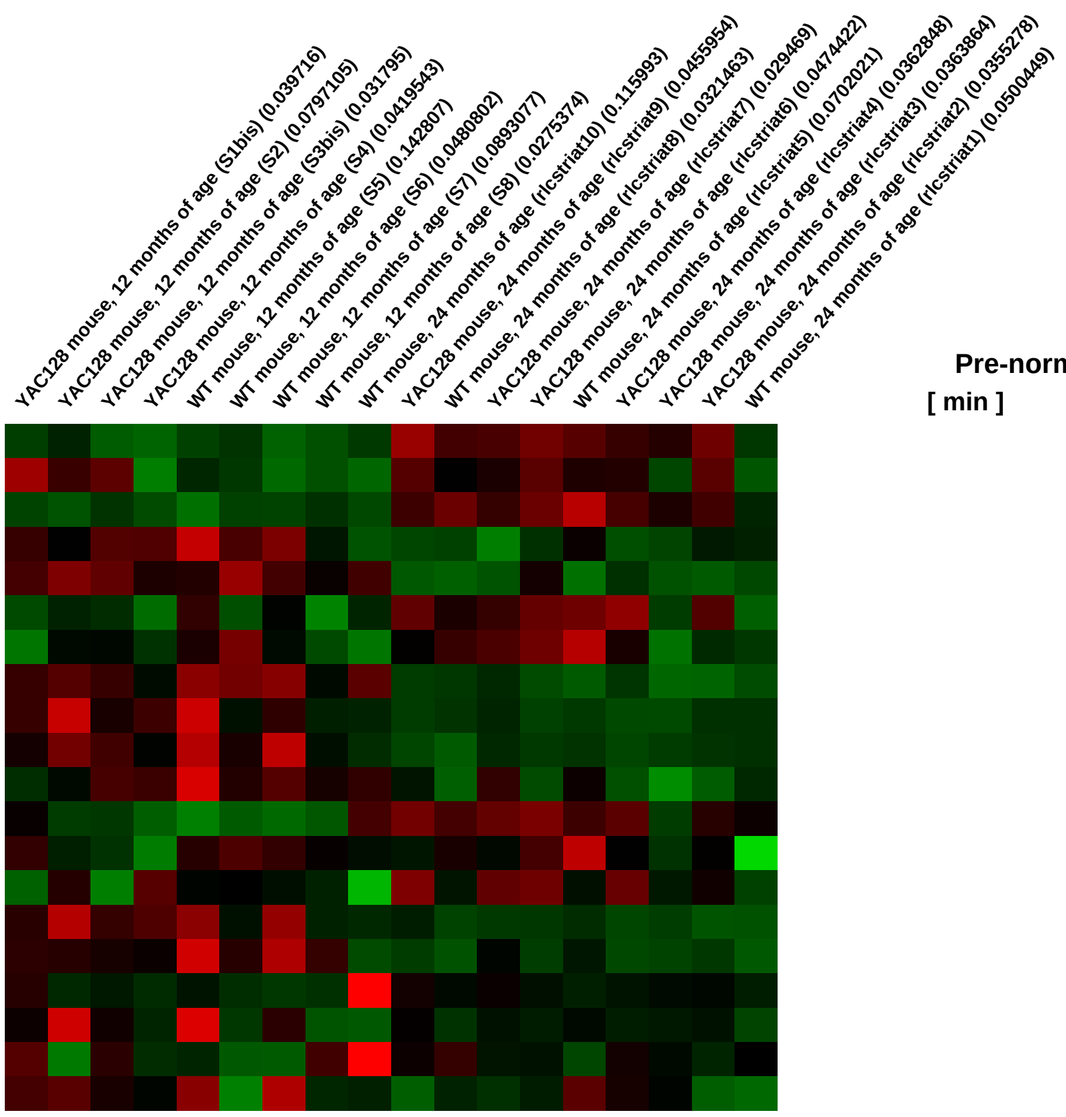

GEO Series "GSE44734" Expression Profiles

Num of samples in this series: 12

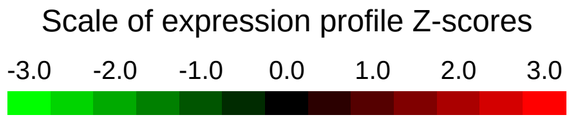

GEO Link:	http://www.ncbi.nlm.nih.gov/geo/query/acc.cgi?acc=GSE44734
Status:	Public on Feb 28 2013
Title:	Expression data from neurotrophin transgenic mice
Organism:	Mus musculus
Experiment type:	Expression profiling by array
Platform:	GPL1261
Pubmed ID:	24378336
Summary & Design:	**Summary:** A limited number of growth factors are capable of regulating numerous developmental processes, but how they accomplish this is unclear. In the gustatory system, brain-derived neurotrophic factor (BDNF) and neurotrophin-4 (NT4) have different developmental roles but exert their effects through the same receptors (TrkB and p75). Using genome wide expression analysis, we determined that BDNF and NT4 also regulate the expression of different sets of genes downstream of receptor signaling in geniculate ganglion. These differences in gene expression likely determine their different roles. BDNF and NT4 could function differently because of temporal or spatial differences of expression or the activation of different signaling pathways. **Overall design:** BDNF and NT4 regulate cell death, axonal growth and axonal guidance by altering gene expression. Because many of these functions of the two neurotrophins differ in taste development, each likely alters gene expression in a unique way. To determine if removal of BDNF and NT4 alters gene expression in different ways, I will compare microarray gene expression profiles in the geniculate ganglion among BDNF knockout, Nt4 knockout, and wild type mice during development.

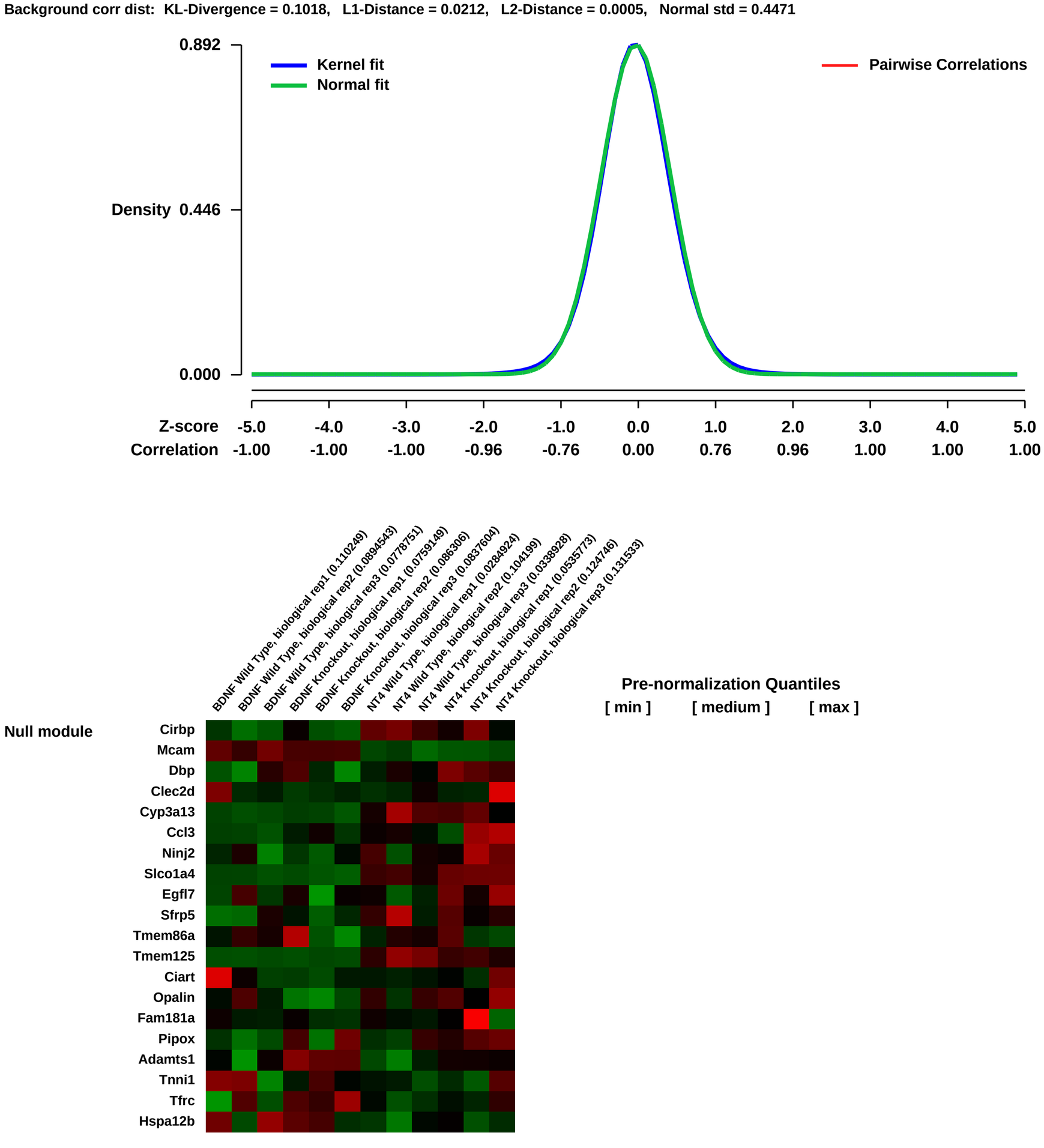

GEO Series "GSE42565" Expression Profiles

Num of samples in this series: 6

Scale of expression profile Z-scores

-3.0 -2.0 -1.0 0.0 1.0 2.0 3.0

GEO Link:	http://www.ncbi.nlm.nih.gov/geo/query/acc.cgi?acc=GSE42565
Status:	Public on Dec 15 2012
Title:	Transcriptional responses to Sonic Hedgehog pathway stimulation in in vitro derived neural progenitors
Organism:	Mus musculus
Experiment type:	Expression profiling by array
Platform:	GPL1261
Pubmed ID:	23249739
Summary & Design:	**Summary:** **The objective of this study was to identify genes regulated by Sonic Hedgehog pathway stimulation in neural progenitors.** **Overall design:** **Paired (parallel culture) triplicates of neuralized embryoid body cultures with and without Shh pathway stimulation (Ag1.3-treatment)**

Background corr dist: **KL-Divergence = 0.0382, L1-Distance = 0.0221, L2-Distance = 0.0005, Normal std = 0.6291**

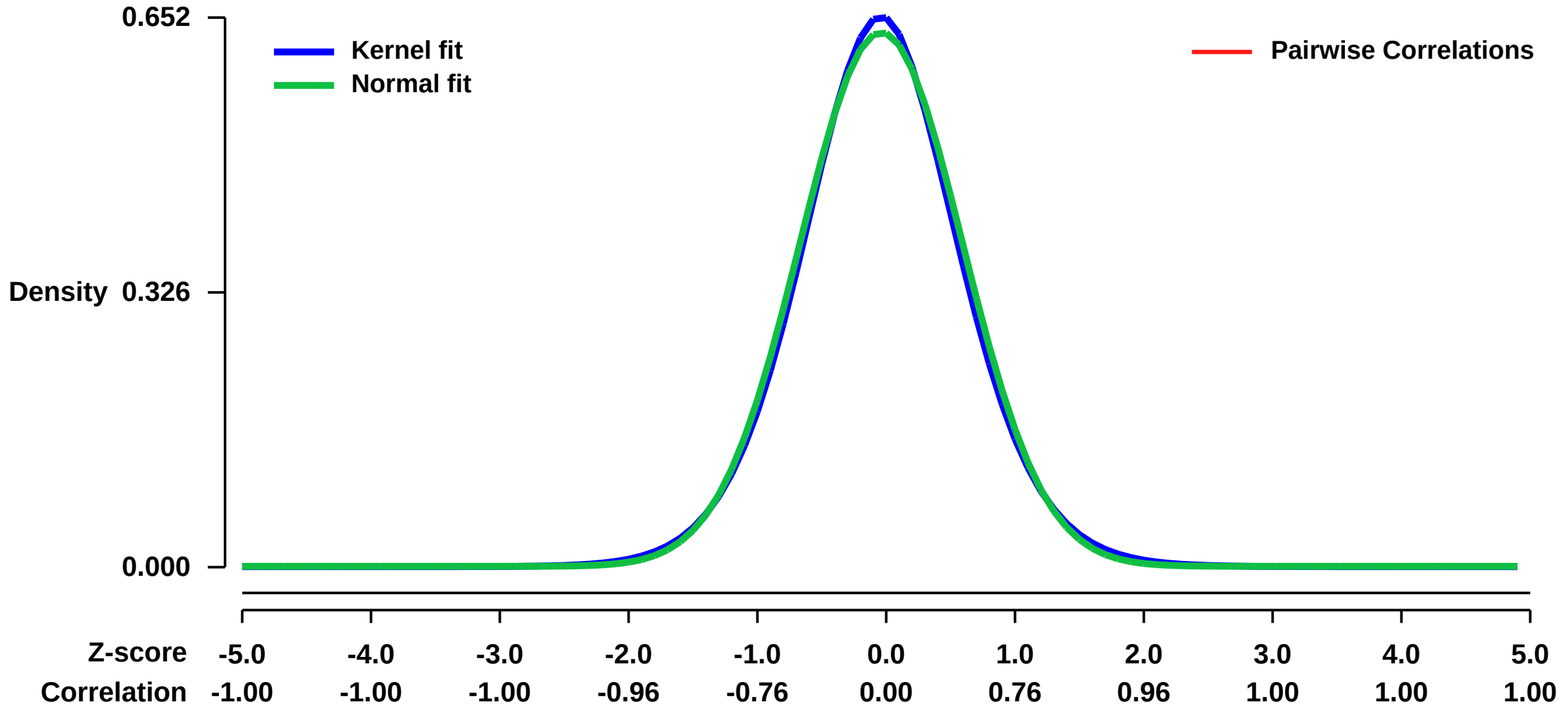

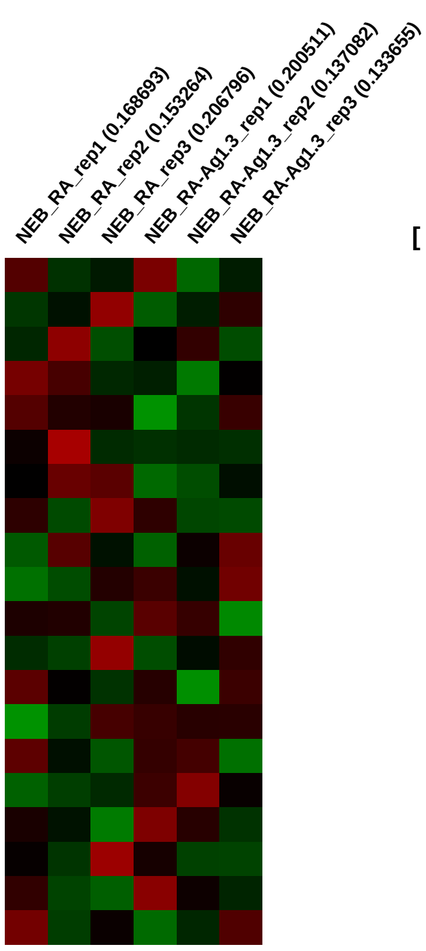

GEO Series "GSE18740" Expression Profiles

Num of samples in this series: 12

Scale of expression profile Z-scores

-3.0 -2.0 -1.0 0.0 1.0 2.0 3.0

GEO Link:	http://www.ncbi.nlm.nih.gov/geo/query/acc.cgi?acc=GSE18740
Status:	Public on Jan 19 2010
Title:	Luteolin has anti-inflammatory and neurotrophic effects on microglia
Organism:	Mus musculus
Experiment type:	Expression profiling by array
Platform:	GPL1261
Pubmed ID:	20074346
Summary & Design:	**Summary:** Our aim was to identify genes that were differentially expressed in microglia stimulated with Lipopolysaccharide, Luteolin, or both. Affymetrix microarrays were used to analyze RNA samples **Overall design:** RNA from control BV-2 cells, and cells treated for 24h with LPS, Luteolin, or LPS+Luteolin was analyzed with Affymetrix GeneChip Mouse Genome 430 2.0 Arrays. Biological triplicates were analyzed for each condition

Background corr dist: KL-Divergence = 0.1095, L1-Distance = 0.0333, L2-Distance = 0.0020, Normal std = 0.4207

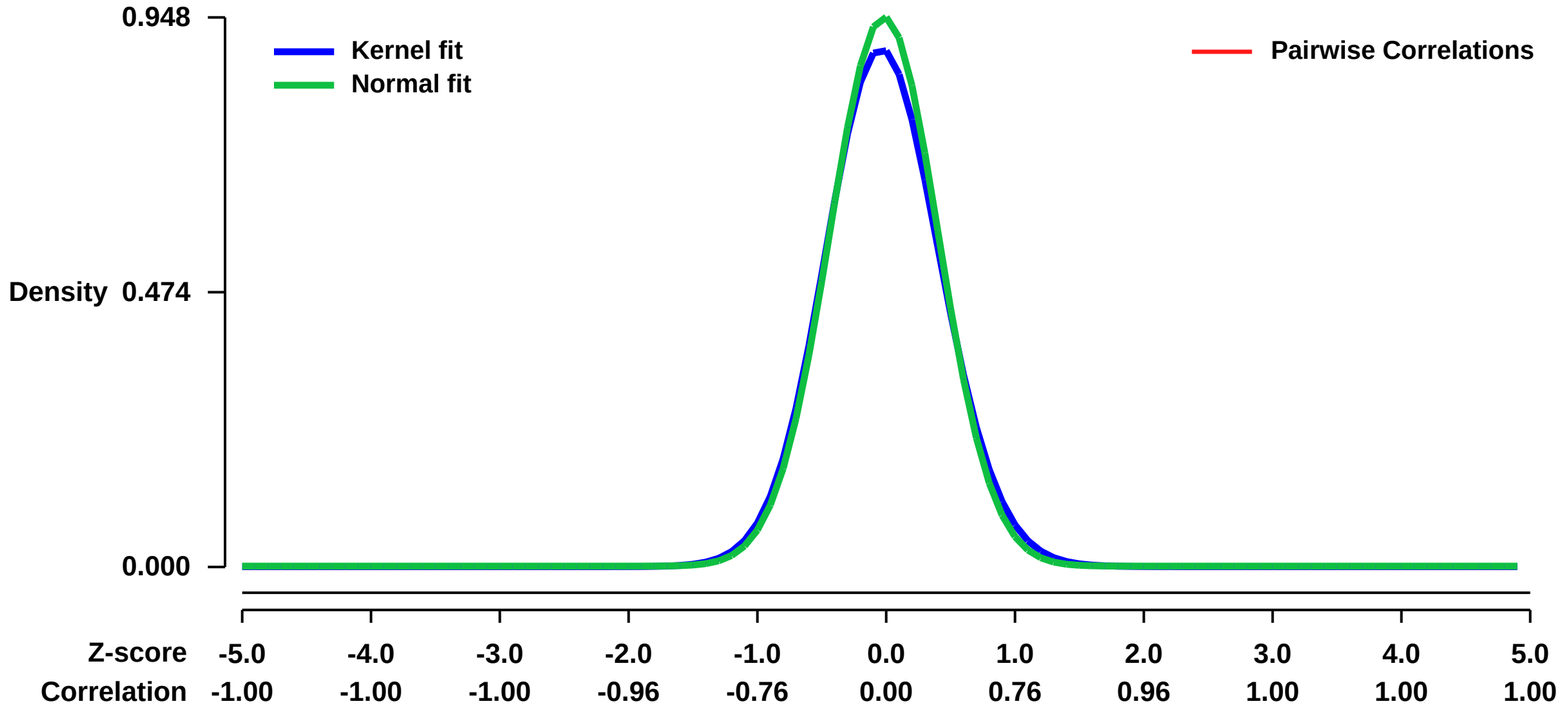

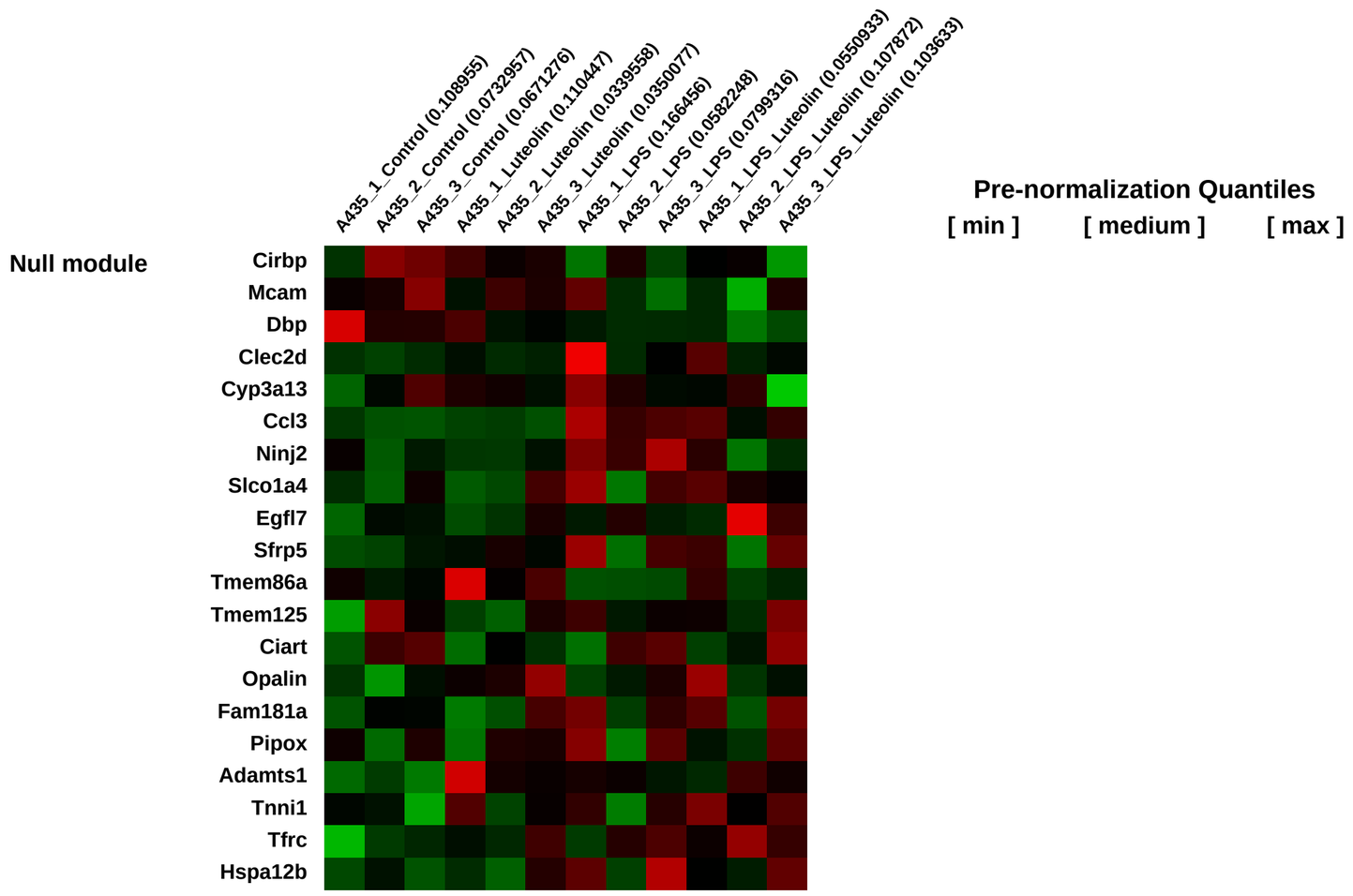

GEO Series "GSE27675" Expression Profiles

Num of samples in this series: 14

Scale of expression profile Z-scores

-3.0 -2.0 -1.0 0.0 1.0 2.0 3.0

GEO Link:	http://www.ncbi.nlm.nih.gov/geo/query/acc.cgi?acc=GSE27675
Status:	Public on Sep 15 2011
Title:	Expression data from lung tumor and stromal cells of KrasTgfbr2 -/- mouse model
Organism:	Mus musculus
Experiment type:	Expression profiling by array
Platform:	GPL1261
Pubmed ID:	21911454
Summary & Design:	**Summary:** Recent data suggests that repression of the Type II TGF-B Receptor (Tgfr2) repression in human lung adenocarcinoma is important for progression from noninvasive to invasive adenocarcinoma. To test this hypothesis in a animal model of non-invasive lung cancer, we generated an inducible, lung specific Tgfbr2 knockout model in the oncogenic Kras mouse. LSL-KrasG12D positive mice were simultaneously backcrossed to C57/Bl6 mice and to the Tgfbr2 flox/flox mice. To induce tumors, 100 ul of saline containing 3x10e10 particles of an adenovirus containing the Cre recombinase (Ad.Cre) was administered to each LSL-KrasG12D mouse intra-nasally. **Overall design:** We evaluated the tumor microenvironment response to Tgfbr2 deficient tumor cells. We compared lung tumor cell and stromal cell transcriptional profiles from five-week KrasTgfbr2 -/- and nine-week KrasTgfbr2 WT mice. We used mice at these time points to allow comparison of the stromal compartment of similarly advanced tumors.

Background corr dist: KL-Divergence = 0.0947, L1-Distance = 0.0412, L2-Distance = 0.0035, Normal std = 0.4458

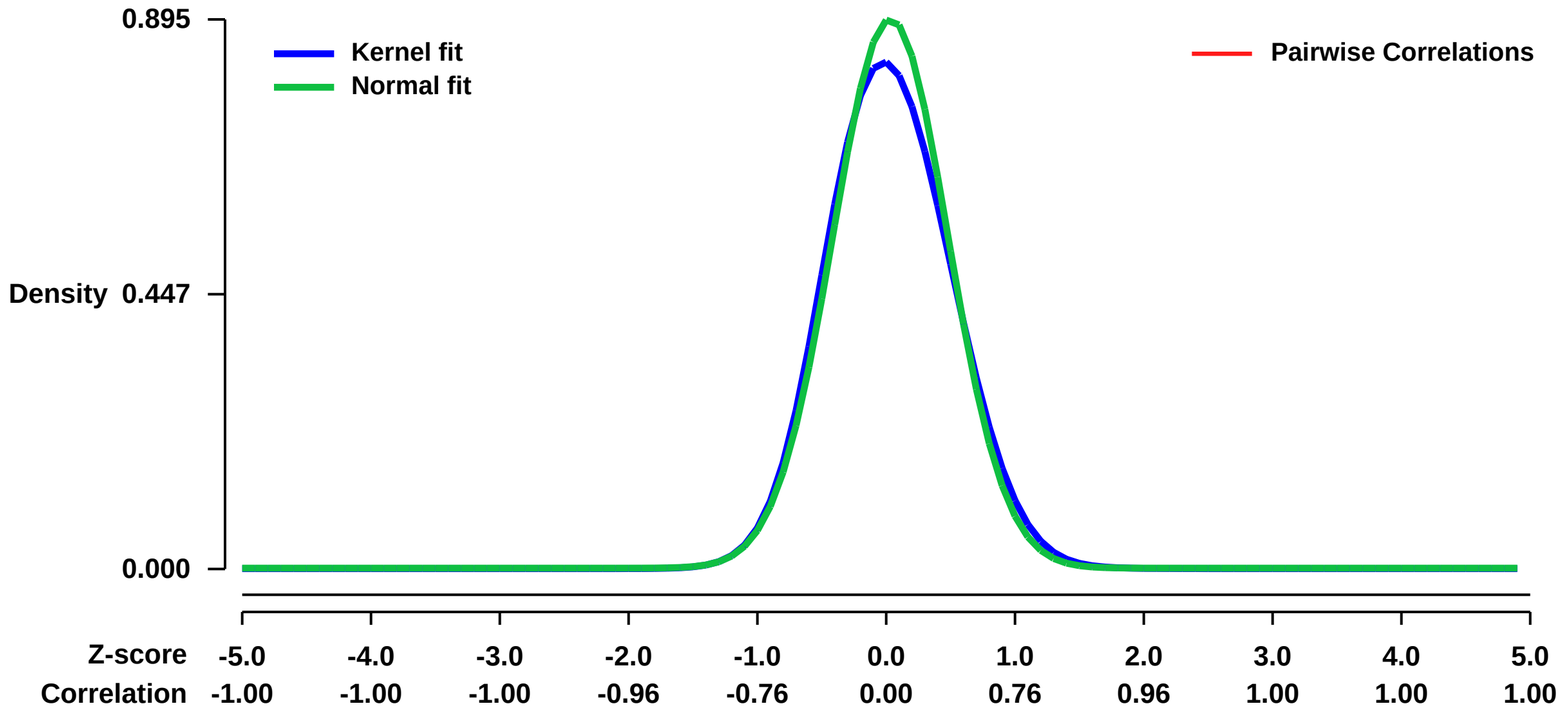

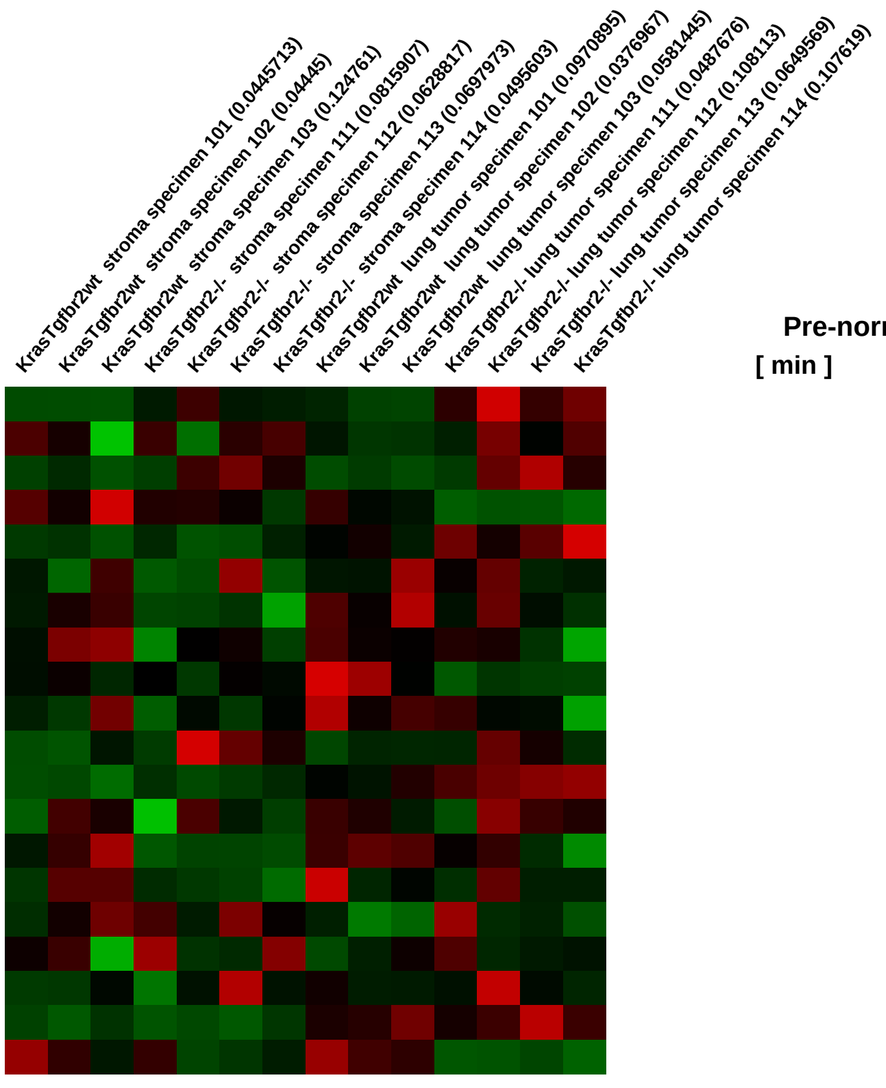

GEO Series "GSE30056" Expression Profiles

Num of samples in this series: 24

Scale of expression profile Z-scores

-3.0 -2.0 -1.0 0.0 1.0 2.0 3.0

GEO Link:	http://www.ncbi.nlm.nih.gov/geo/query/acc.cgi?acc=GSE30056
Status:	Public on Aug 05 2011
Title:	Reconstitution of the mouse germ-cell specification pathway in culture by pluripotent stem cells
Organism:	Mus musculus
Experiment type:	Expression profiling by array
Platform:	GPL1261
Pubmed ID:	21820164
Summary & Design:	**Summary:** The generation of properly functioning gametes in vitro, a key goal in developmental/reproductive biology, requires multi-step reconstitutions of complex germ cell development. Based on the logic of primordial germ cell (PGC)-specification, we demonstrate here the generation of PGC-like cells (PGCLCs) in mice with robust capacity for spermatogenesis from embryonic stem cells (ESCs) and induced pluripotent stem cells (iPSCs) through epiblast-like cells (EpiLCs), a cellular state highly similar to pre-gastrulating epiblasts, but distinct from epiblast stem cells (EpiSCs). The global transcription profiles, epigenetic reprogramming, and cellular dynamics during PGCLC induction from EpiLCs are a meticulous capture of those associated with PGC specification from the epiblasts. Furthermore, we identify Integrin-beta 3 and SSEA1 as markers that purify PGCLCs with spermatogenic capacity free from tumorigenic undifferentiated cells. With the reconstitution of PGC specification pathway from the naive inner cell mass state, our study defines a paradigm for the essential step of in vitro gametogenesis. **Overall design:** We performed this analysis to reveal the characters of the cells that we created in this study, epiblast-like cells (EpiLCs) and primordial germ cells-like cells (PGCLCs). Because EpiLCs were induced from embryonic stem cells (ESCs), and equivalent to pre-gastrulating epiblast (embryonic day [E] 5.5-6.0) in vivo (embryo), ESCs and epiblast were included in this analysis. Epiblast stem cells (EpiSCs) are a culture cell type derived from epiblast, and were also included. PGCLCs were supposed to be equivalent to E9.5 PGCs based on reporter fluorescent transgene expressions and epigenetic properties, and therefore E9.5 PGCs were also inckuded in this analysis. Because epiblast and E9.5 PGCs are of a small number of cells in embryos (a few hundred to thousand cells), cDNAs were amplified with a quantitative global PCR method (Kurimoto et al., 2006, Nucleic Acids Research) for microarray analyses. We took two biological replicate for each cell type.

Background corr dist: KL-Divergence = 0.1263, L1-Distance = 0.0348, L2-Distance = 0.0025, Normal std = 0.4002

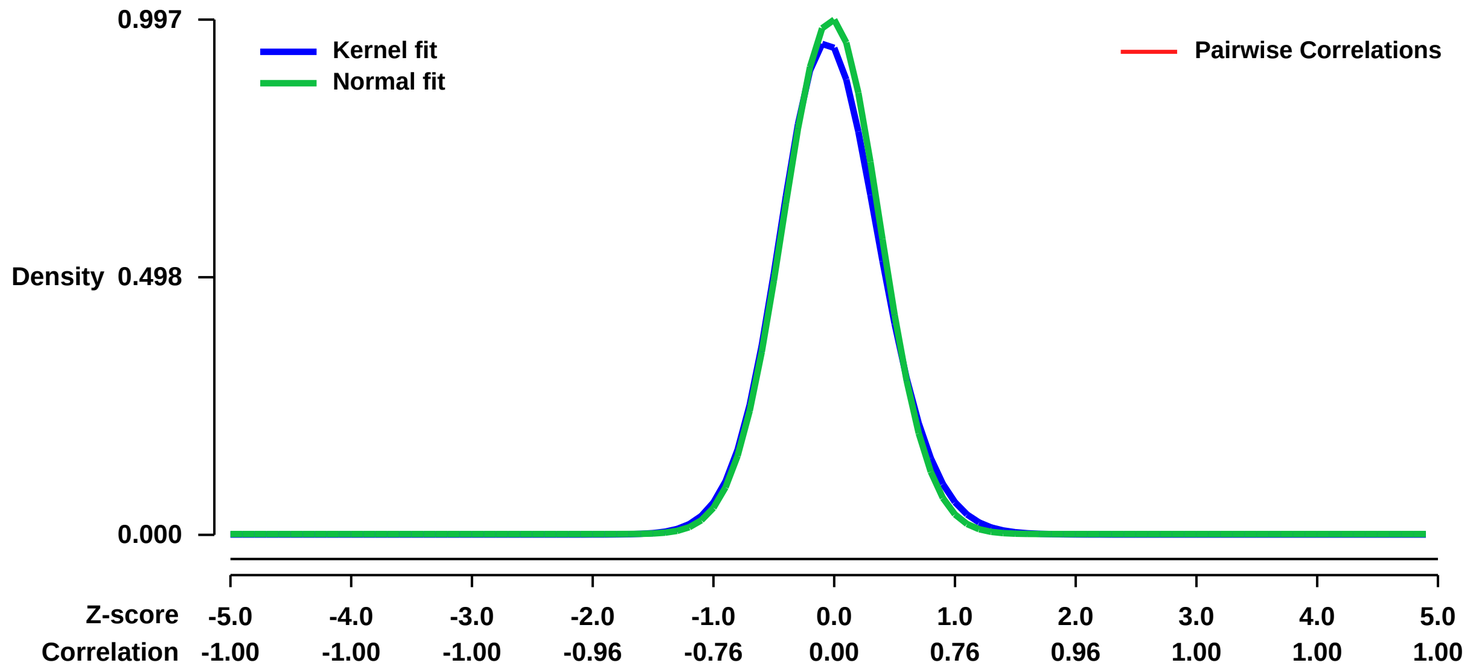

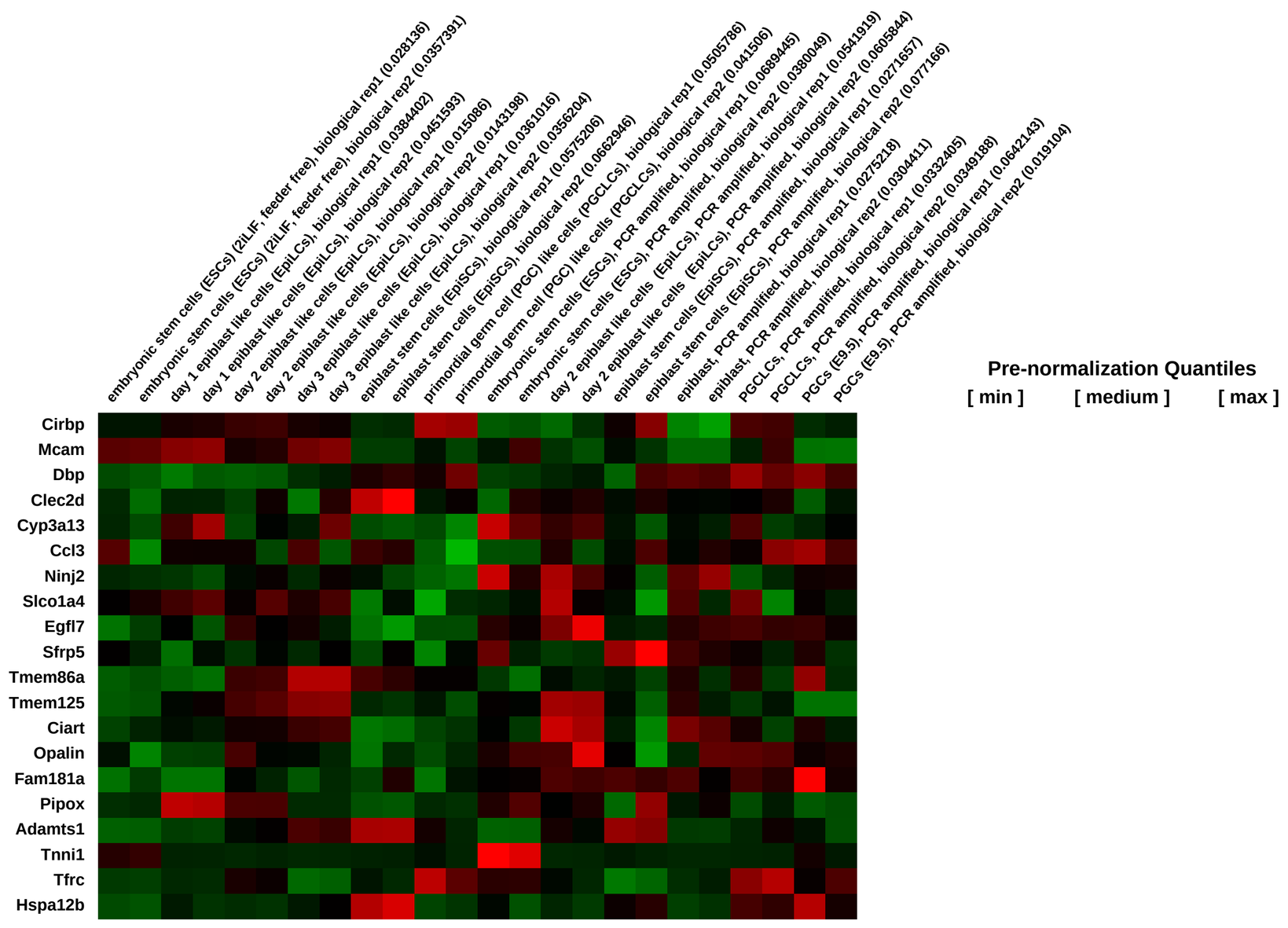

GEO Series "GSE8024" Expression Profiles

Num of samples in this series: 8

Scale of expression profile Z-scores

-3.0 -2.0 -1.0 0.0 1.0 2.0 3.0

GEO Link:	http://www.ncbi.nlm.nih.gov/geo/query/acc.cgi?acc=GSE8024
Status:	Public on Jun 25 2007
Title:	Murine ES cells, neural precursor cells and embryonic fibroblasts
Organism:	Mus musculus
Experiment type:	Expression profiling by array
Platform:	GPL1261
Pubmed ID:	17603471
Summary & Design:	**Summary:** Expression profiles for isogenic (129SvJae x C57BL/6) murine embryonic stem (ES) cells, neural precursors (NPC) obtained through in vitro differentiation of the ES cells, and embryonic fibroblasts (MEF) obtained at day 13.5. **Keywords: cell type comparison** **Overall design:** 3 replicates of wt ES cells, 3 replicates of wt NPCs obtained by in vitro differentiation, 2 replicated of primary MEFs

Background corr dist: KL-Divergence = 0.0402, L1-Distance = 0.0576, L2-Distance = 0.0045, Normal std = 0.7004

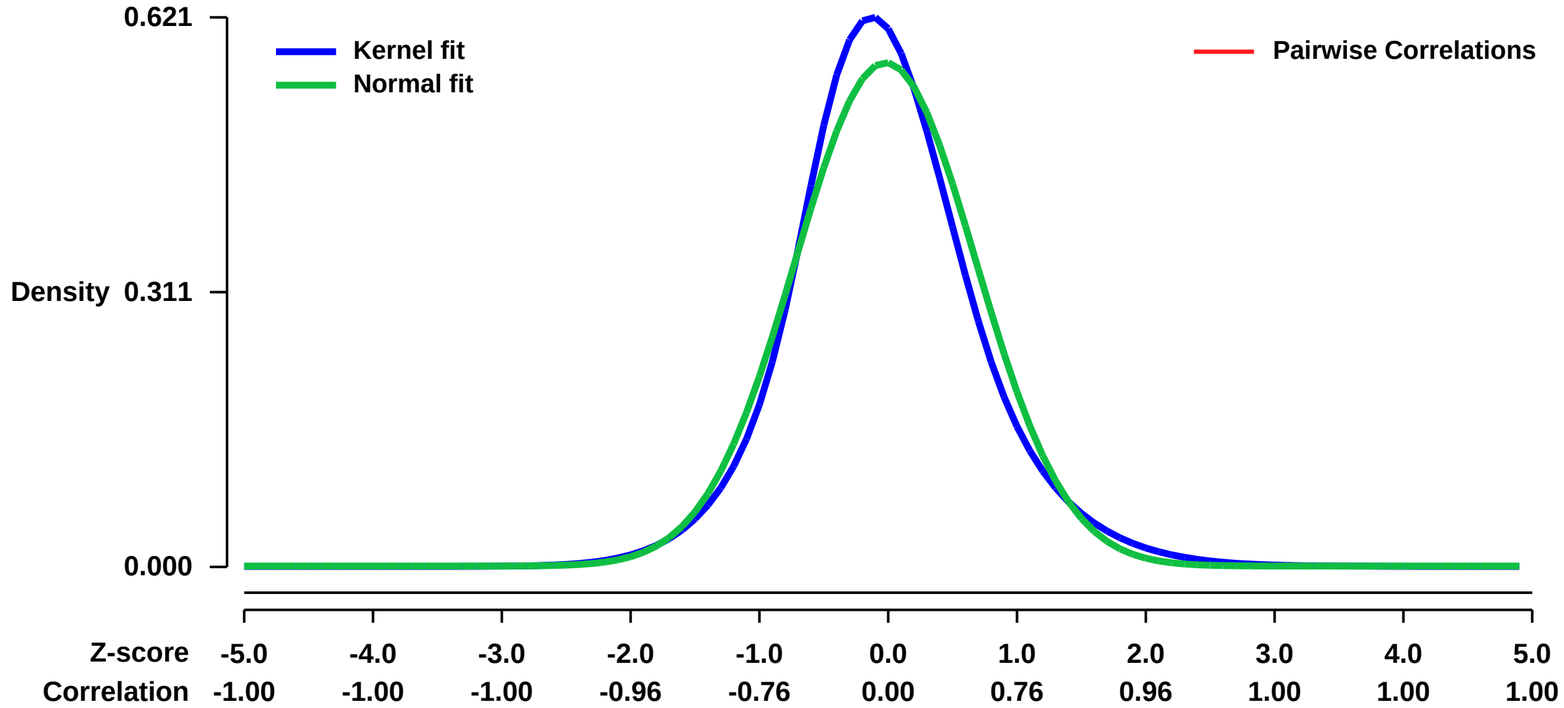

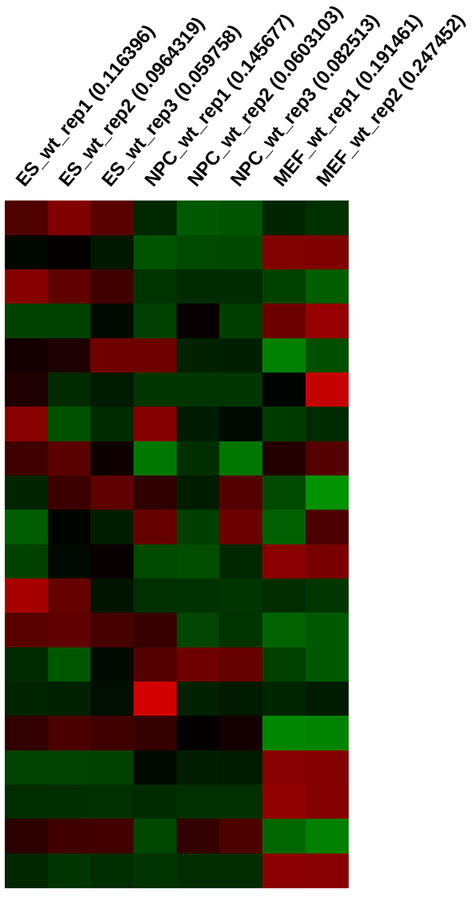

GEO Series "GSE3861" Expression Profiles

Num of samples in this series: 6

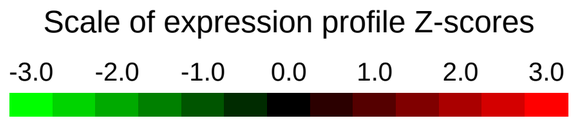

GEO Link:	http://www.ncbi.nlm.nih.gov/geo/query/acc.cgi?acc=GSE3861
Status:	Public on Mar 20 2006
Title:	Distinct hematopoietic cell fates regulated by graded expression of HOXA10
Organism:	Mus musculus
Experiment type:	Expression profiling by array
Platform:	GPL1261
Pubmed ID:	

Summary & Design:

Summary:
The homeobox (Hox) transcription factor HOXA10 has been implicated in regulation of hematopoietic cell fate. Here, using a transgenic mouse model where expression of HOXA10 is tightly regulated in a graded, doxycyclin-dependent manner we demonstrate that several key commitment steps in hematopoietic differentiation have distinctly different outcomes depending on the expression level of HOXA10. Similarly, HOXA10 regulates hematopoietic stem cell (HSC) proliferation in a dose dependent manner, since intermediate levels of HOXA10 generated a 4.5-fold increase in long-term repopulating capacity after 13 days of liquid culture, whereas high levels reduced proliferation of HSCs. Interestingly, the effects on HSC proliferation were associated with altered expression of several known regulators of stem cell self-renewal. Taken together, our findings reveal entirely novel functional and molecular aspects of HOXA10 in regulation of hematopoiesis and emphasize the need for tightly regulated production of HOX proteins in possible future applications of stem cell expansion.

Keywords: Affymetrix

Overall design:
LSK cells were sorted from rtTA-HA10 and cultured for 72 hours in complete serum free medium in three different concentrations of doxycycline (0, 0.1 and 0.5 ´¡g/ml doxycycline). RNA was extracted using RNeasy Mini kit, Qiagen, labeled and amplified according to AffymetrixTM Two Cycle Target Labeling Protocol. Hybridization and washing was performed according to AffymetrixTM GeneChip Expression protocol. Chips were scanned using an AffymetrixTM GeneChip Scanner 3000. The Affymetrix software GCOS was used to generate cell intensity data files (CEL) from two independent experiments. The CEL file data was then imported into the GeneSpring´fi software version 7.2 (Silicon Genetics, Redwood City, CA). The GC-RMA method was used for normalization and data was processed as follows: values below 0.01 were set to 0.01. All of the genes in each sample were divided by the median of the specified list of 100 positive control genes present on the MOE430 v2 chip. All samples were then normalized against the median of the untreated control samples. Each measurement for each gene in the treated samples was divided by the median of that gene's measurements in the corresponding control samples. We judged genes to be differentially expressed when the difference in expression between two conditions was at least 2-fold.

Background corr dist: KL-Divergence = 0.0353, L1-Distance = 0.0186, L2-Distance = 0.0004, Normal std = 0.6391

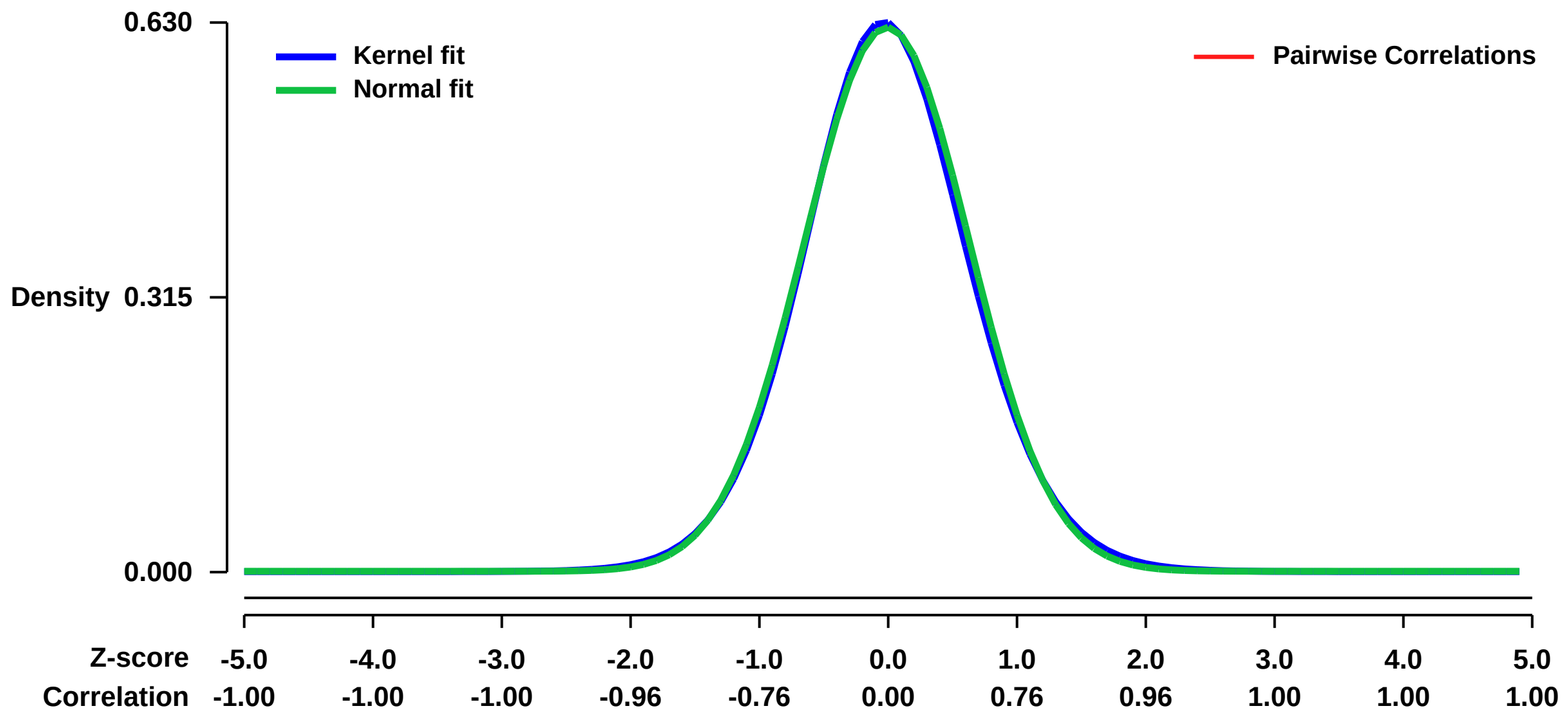

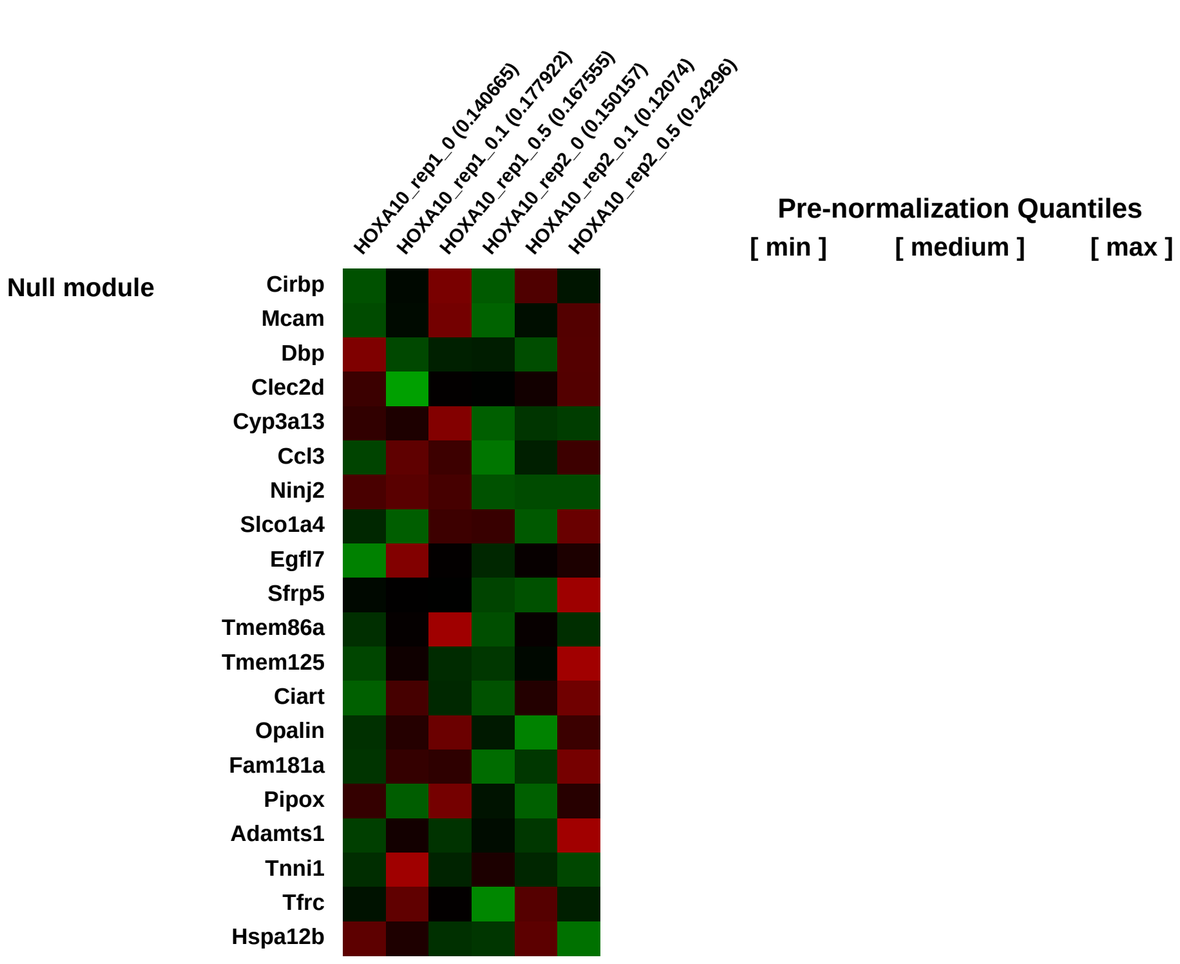

GEO Series "GSE21491" Expression Profiles

Num of samples in this series: 9

Scale of expression profile Z-scores

-3.0 -2.0 -1.0 0.0 1.0 2.0 3.0

GEO Link:	http://www.ncbi.nlm.nih.gov/geo/query/acc.cgi?acc=GSE21491
Status:	Public on Oct 17 2012
Title:	Analysis of early dendritic cell, natural killer cell and B lymphocyte responses to murine cytomegalovirus (MCMV) infection by genome-wide expression profiling
Organism:	Mus musculus
Experiment type:	Third-party reanalysis
Platform:	GPL1261
Pubmed ID:	23084923
Summary & Design:	**Summary:** Dendritic cells (DCs) are a complex group of cells which play a critical role in vertebrate immunity. They are subdivided into conventional DC (cDC) subsets (CD11b and CD8alpha in mouse) and plasmacytoid DCs (pDCs). Natural killer cells are innate lymphocytes involved in the recognition and killing of abnormal self cells, including virally infected cells or tumor cells. DCs and NK cells are activated very early upon viral infections and regulate one another. However, the global responses of DC and NK cells early after viral infection in vivo and their molecular regulation are not entirely characterized. The goal of this experiment was to use global gene expression profiling to assess the global genetic reprogramming of DC and NK cells during a viral infection in vivo, as compared to B lymphocytes, and to investigate the underlying molecular mechanisms This study includes data from cell sort purified DCs, NK cells and B cells isolated from the spleen of MCMV-infected mice. 2 independent replicates were made for each cell type except B cells. The control dataset for cells isolated from uninfected control animals has been previously published and is available in the GEO database as GSE9810. The complete dataset representing: (1) the infected Samples and (2) the uninfected control Samples from Series GSE9810 (re-processed using RMA), is linked below as a supplementary file. **Overall design:** Comparison of the gene expression programs of wild-type spleen leukocyte subsets, including plasmacytoid DCs, CD8alpha conventional DCs, CD11b conventional DCs and NK cells, isolated from MCMV-infected versus control animals.

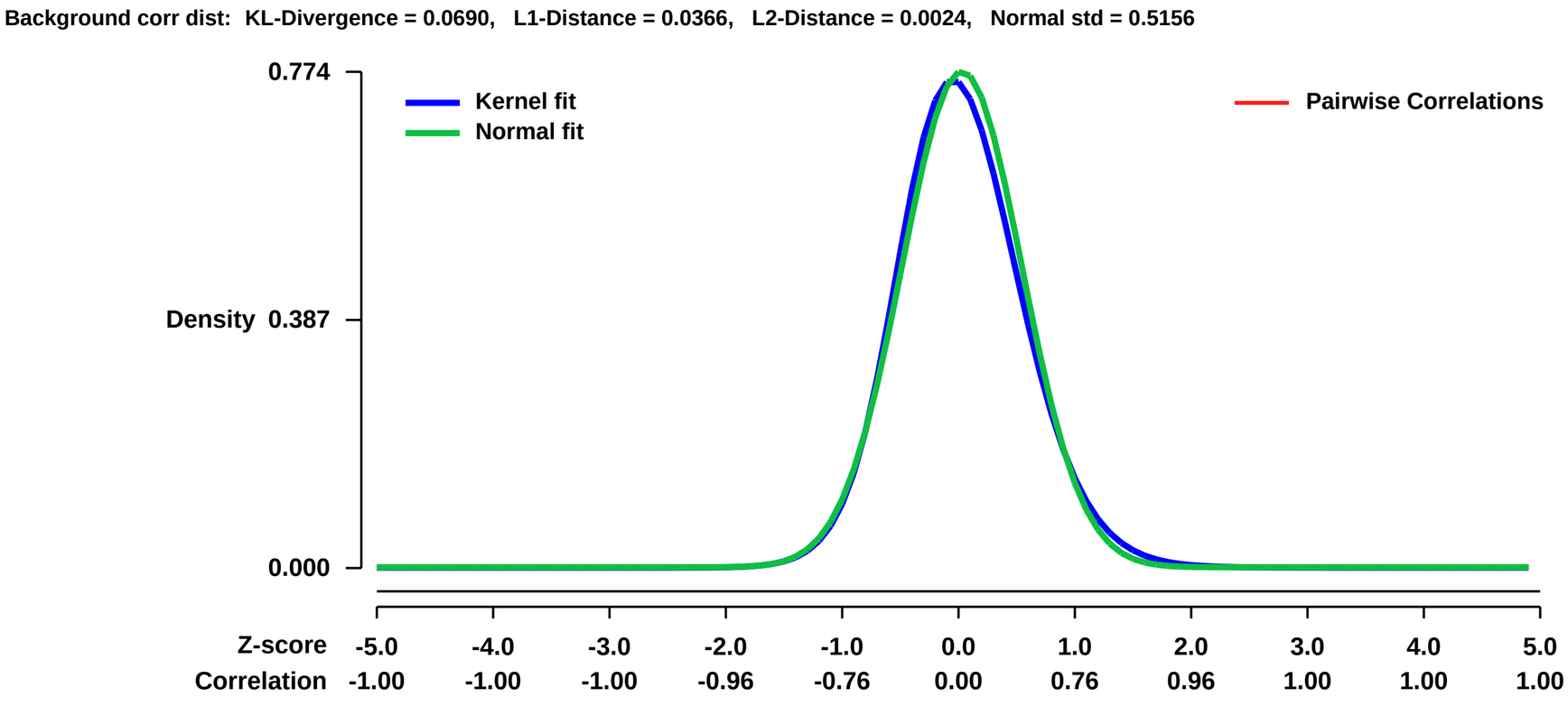

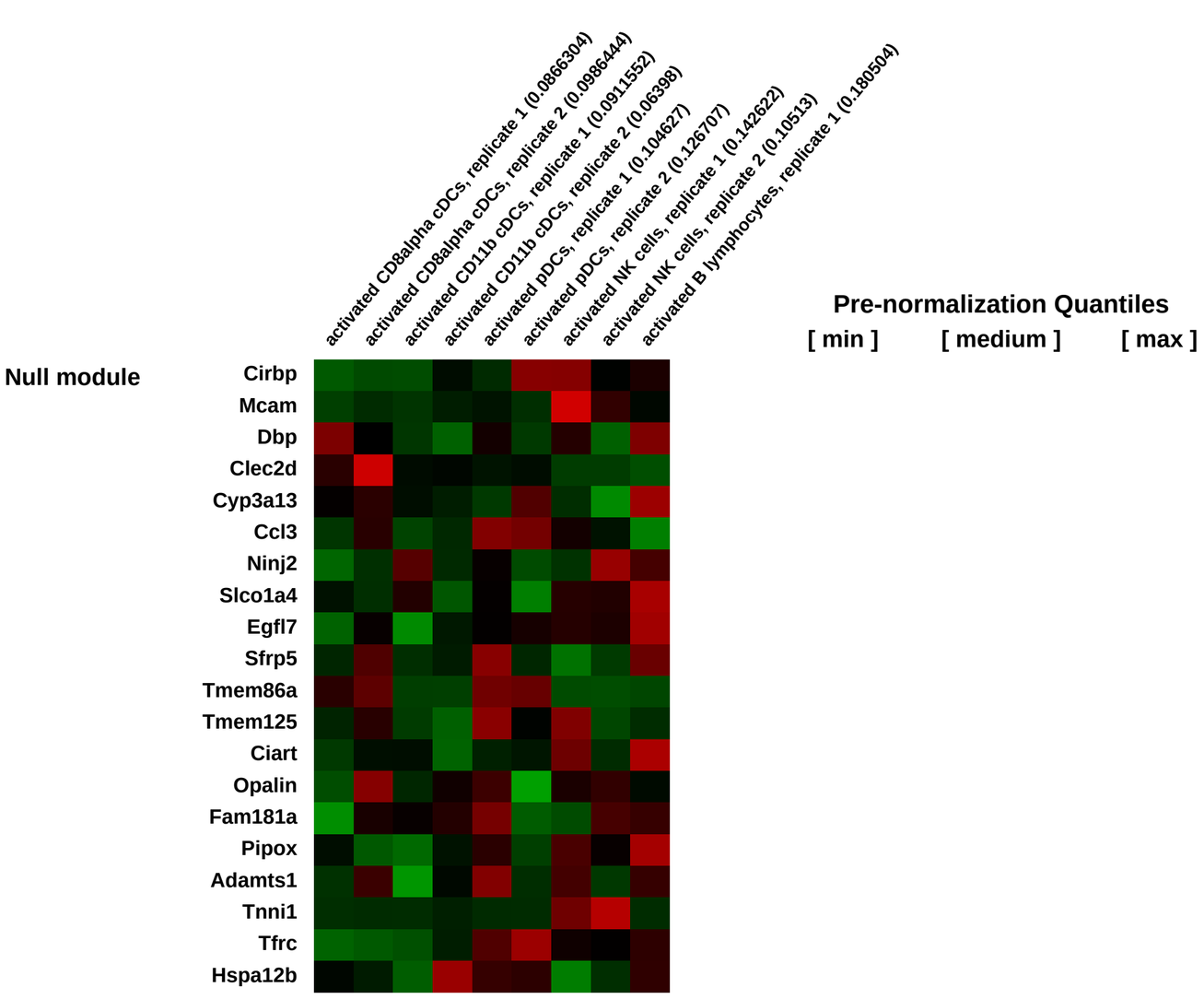

GEO Series "GSE18322" Expression Profiles

Num of samples in this series: 12

Scale of expression profile Z-scores

-3.0 -2.0 -1.0 0.0 1.0 2.0 3.0

GEO Link:	http://www.ncbi.nlm.nih.gov/geo/query/acc.cgi?acc=GSE18322
Status:	Public on Mar 01 2010
Title:	Gene Expression Analysis of Ara-C Resistance in AML
Organism:	Mus musculus
Experiment type:	Expression profiling by array
Platform:	GPL1261
Pubmed ID:	20508618
Summary & Design:	**Summary:** Using two independently derived murine BXH2 cell lines, Ara-C resistant derivatives were developed by exposure to increasing concentrations of Ara-C. Microarray analysis comparing the Ara-C resistant cells to their Ara-C sensitive parental cell lines identified potential genes involved in Ara-C resistance. **Overall design:** Two highly Ara-C-resistant cell lines, B117H and B140H, were derived from Ara-C-sensitive parental cell lines, B117P and B140P. Variations in gene expression between these Ara-C-resistant and -sensitive sets were studied. Three replicates per cell line.

Background corr dist: KL-Divergence = 0.0797, L1-Distance = 0.0246, L2-Distance = 0.0008, Normal std = 0.4839

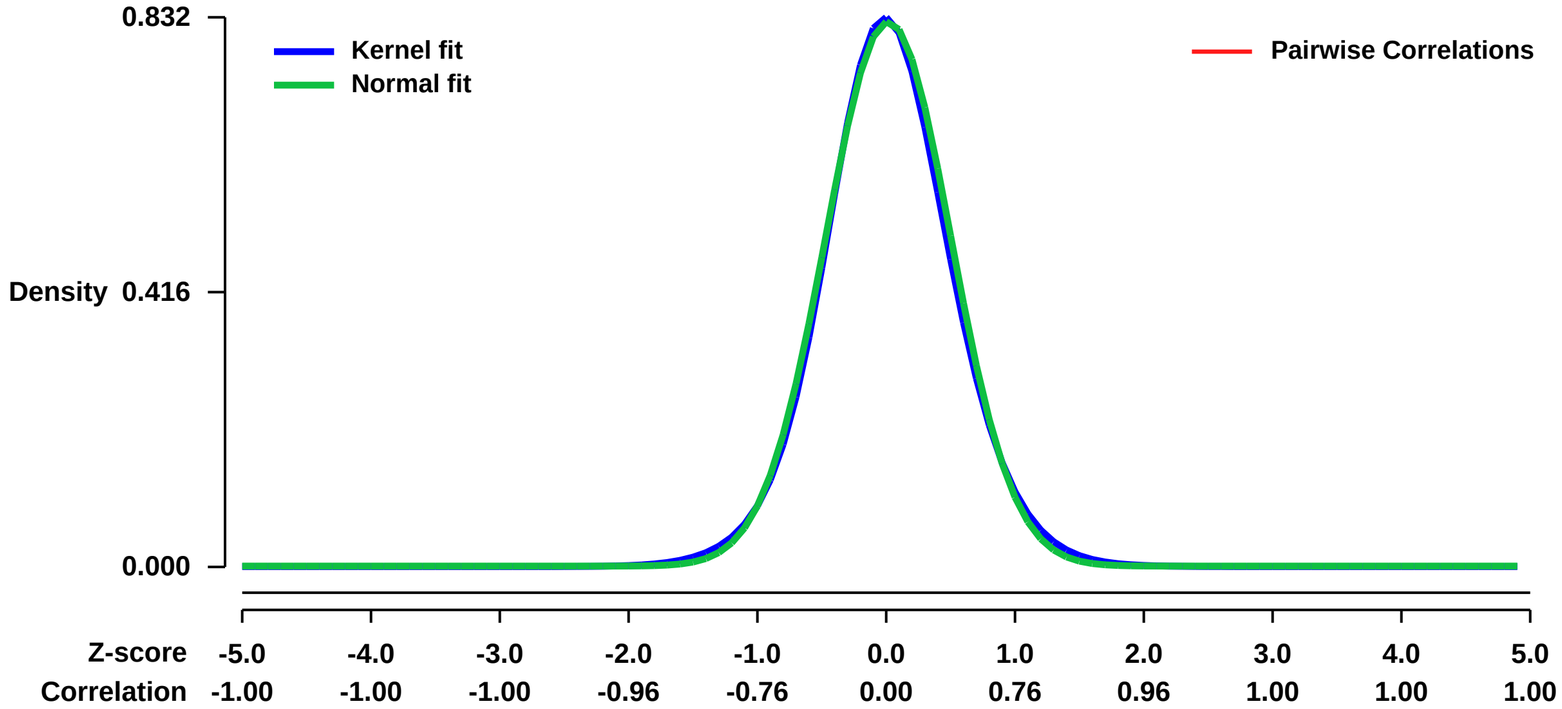

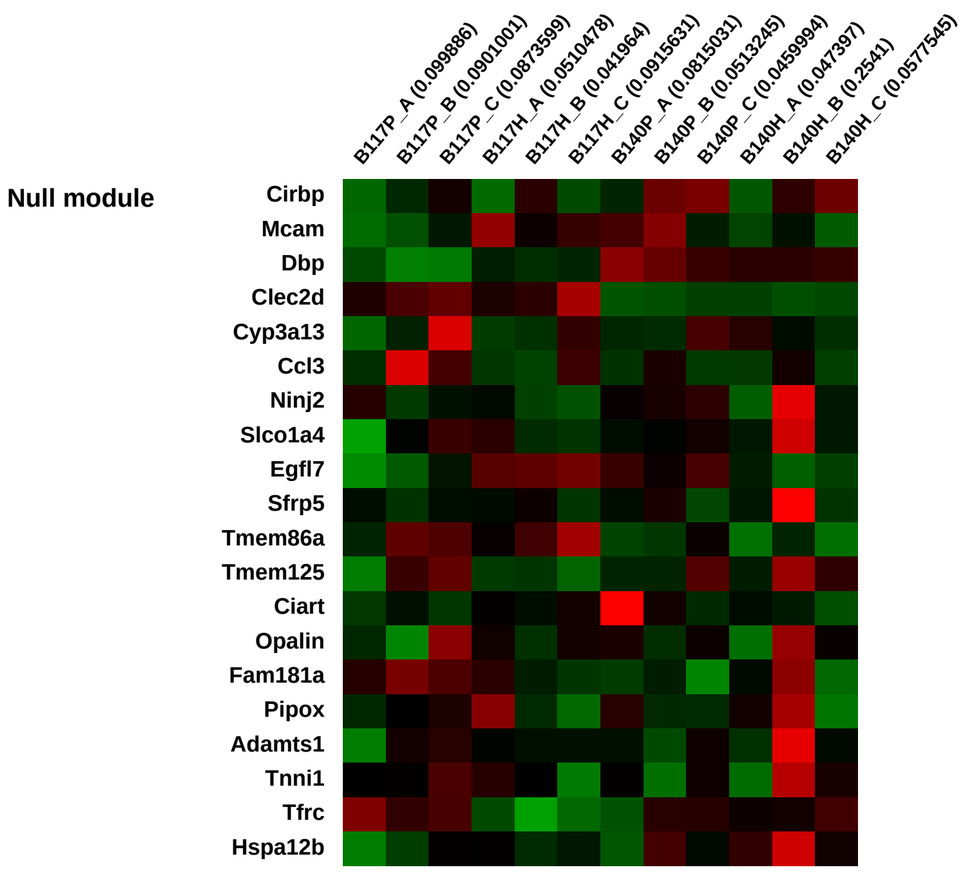

GEO Series "GSE52357" Expression Profiles

Num of samples in this series: 8

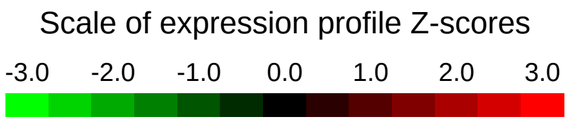

GEO Link:	**http://www.ncbi.nlm.nih.gov/geo/query/acc.cgi?acc=GSE52357**
Status:	**Public on Jun 18 2014**
Title:	**Gene expression profiling of the mandibular arch from Alk5 mutant mouse models**
Organism:	**Mus musculus**
Experiment type:	**Expression profiling by array**
Platform:	**GPL1261**
Pubmed ID:	
Summary & Design:	**Summary:** **The overall goal of this project is to investigate the role of TGF-beta signaling in tissue-tissue interactions between myogenic precursors of craniofacial muscles and cranial neural crest cells (CNCCs). Here, we conducted gene expression profiling of the mandibular arch from mice at embryonic day E11.5 with a CNCC-specific conditional inactivation of the TGF-beta receptor type 1 gene Alk5. These mice provide a model of microglossia as well as disrupted extraocular and masticatory muscle development, which are congenital birth defects commonly observed in several syndromic conditions.** **Overall design:** **To investigate the adverse effects of dysfunctional TGF-beta signaling on tissue-tissue interactions between CNCCs and myogenic precursors of craniofacial muscles, we analyzed mandibular arch tissue of mice with a CNCC-specific conditional inactivation of Alk5 (Wnt1-Cre; Alk5 fl/fl). We performed microarray analyses of the mandibular arch of Alk5 fl/fl control mice and Wnt1-Cre; Alk5 fl/fl mutant mice, collected at embryonic day E11.5 (n=4 per group).**

Background corr dist: **KL-Divergence = 0.0293, L1-Distance = 0.0380, L2-Distance = 0.0021, Normal std = 0.6790**

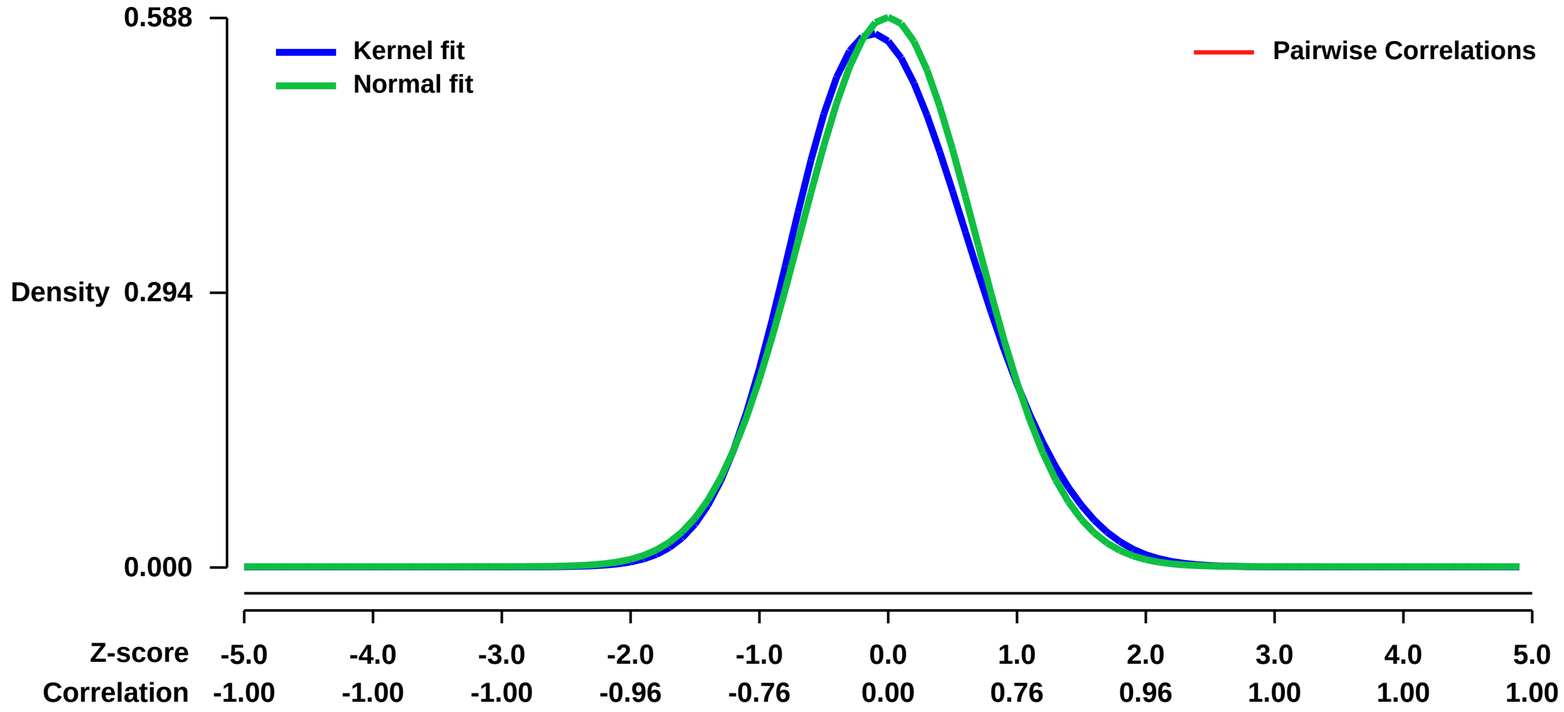

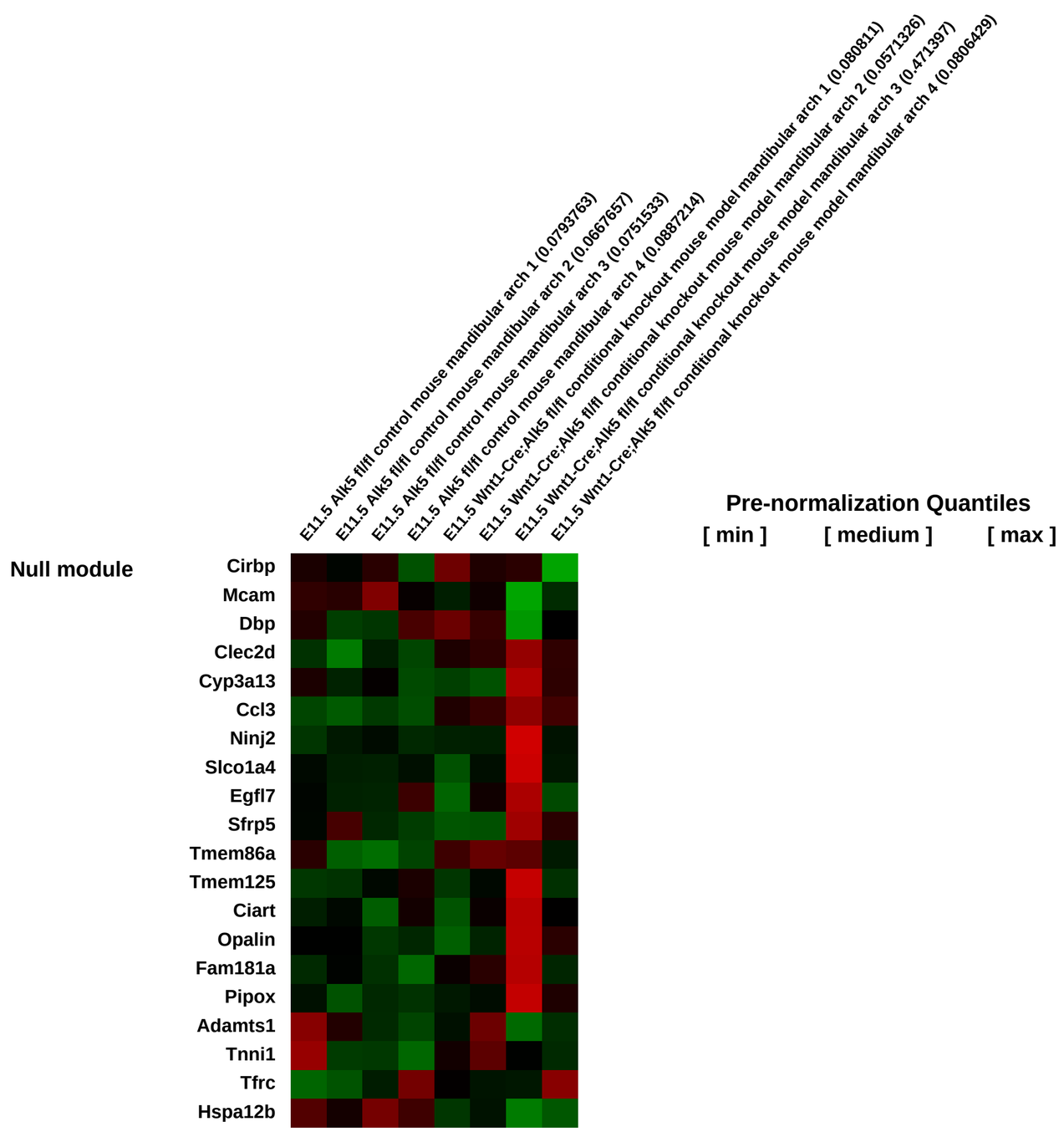

GEO Series "GSE35332" Expression Profiles

Num of samples in this series: 12

Scale of expression profile Z-scores

-3.0 -2.0 -1.0 0.0 1.0 2.0 3.0

GEO Link:	http://www.ncbi.nlm.nih.gov/geo/query/acc.cgi?acc=GSE35332
Status:	Public on May 02 2012
Title:	Stem cell factor programs the mast cell activation phenotype
Organism:	Mus musculus
Experiment type:	Expression profiling by array
Platform:	GPL1261
Pubmed ID:	22529299
Summary & Design:	**Summary:** Mast cells, activated by antigen via the high affinity receptor for IgE (Fc$_\epsilon$RI), release an array of pro-inflammatory mediators that contribute to allergic disorders such as asthma and anaphylaxis. The KIT ligand, stem cell factor (SCF), is critical for mast cell expansion, differentiation and survival, and, under acute conditions, enhances mast cell activation. However, extended SCF exposure in vivo conversely protects against fatal antigen-mediated anaphylaxis. In investigating this dichotomy, we identified a novel mode of regulation of the mast cell activation phenotype through SCF-mediated programming. We found that mouse bone marrow-derived mast cells chronically exposed to SCF displayed a marked attenuation of Fc$_\epsilon$RI-mediated degranulation and cytokine production. The hypo-responsive phenotype was not a consequence of altered signals regulating calcium flux or protein kinase C, but of ineffective cytoskeletal reorganization, with evidence implicating a down-regulation of expression of the Src kinase Hck. Collectively, these findings demonstrate a major role for SCF in the homeostatic control of mast cell activation with potential relevance to mast cell-driven disease and the development of novel approaches for the treatment of allergic disorders. **Overall design:** Mouse bone marrow-derived mast cells were treated with IL3 or IL3+SCF. Six replicates each.

Background corr dist: KL-Divergence = 0.1206, L1-Distance = 0.0248, L2-Distance = 0.0008, Normal std = 0.4115

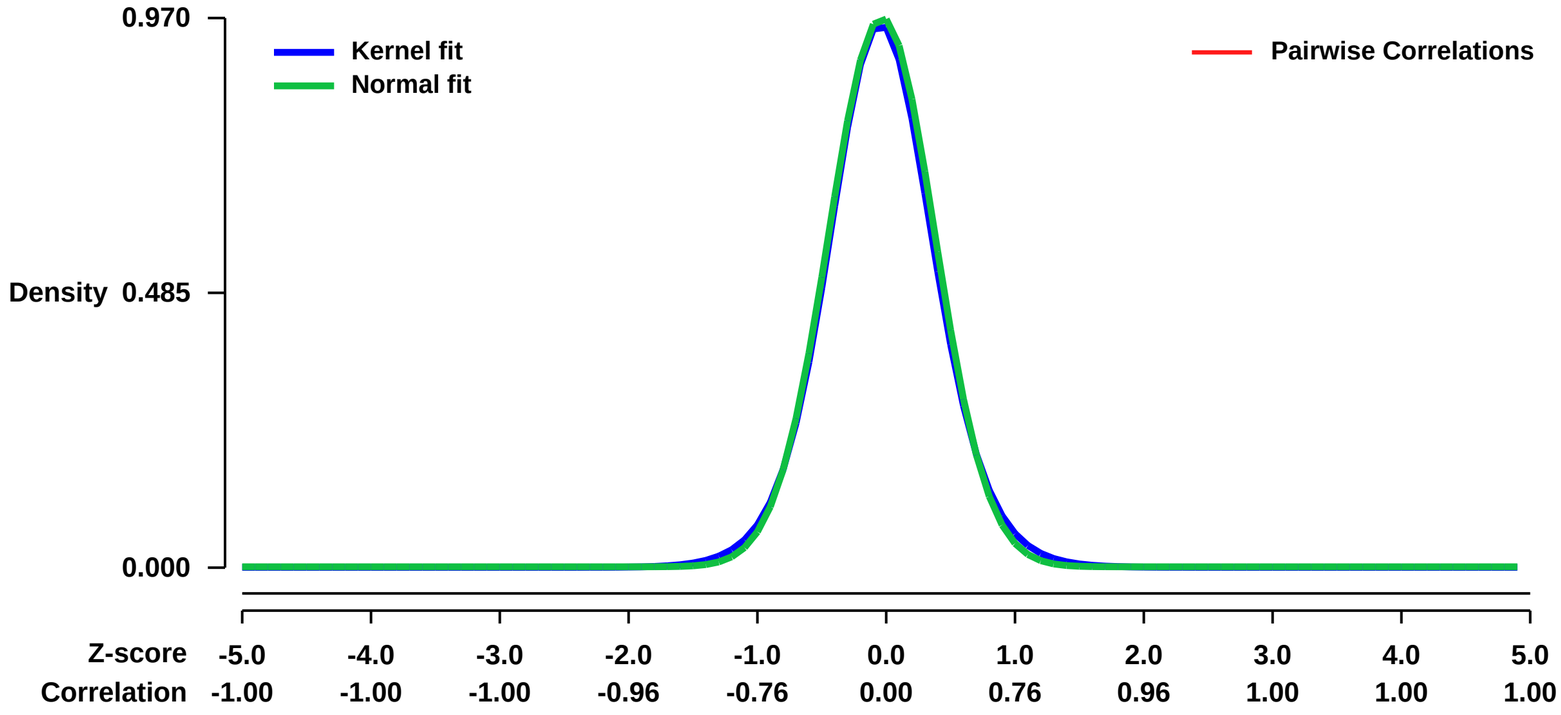

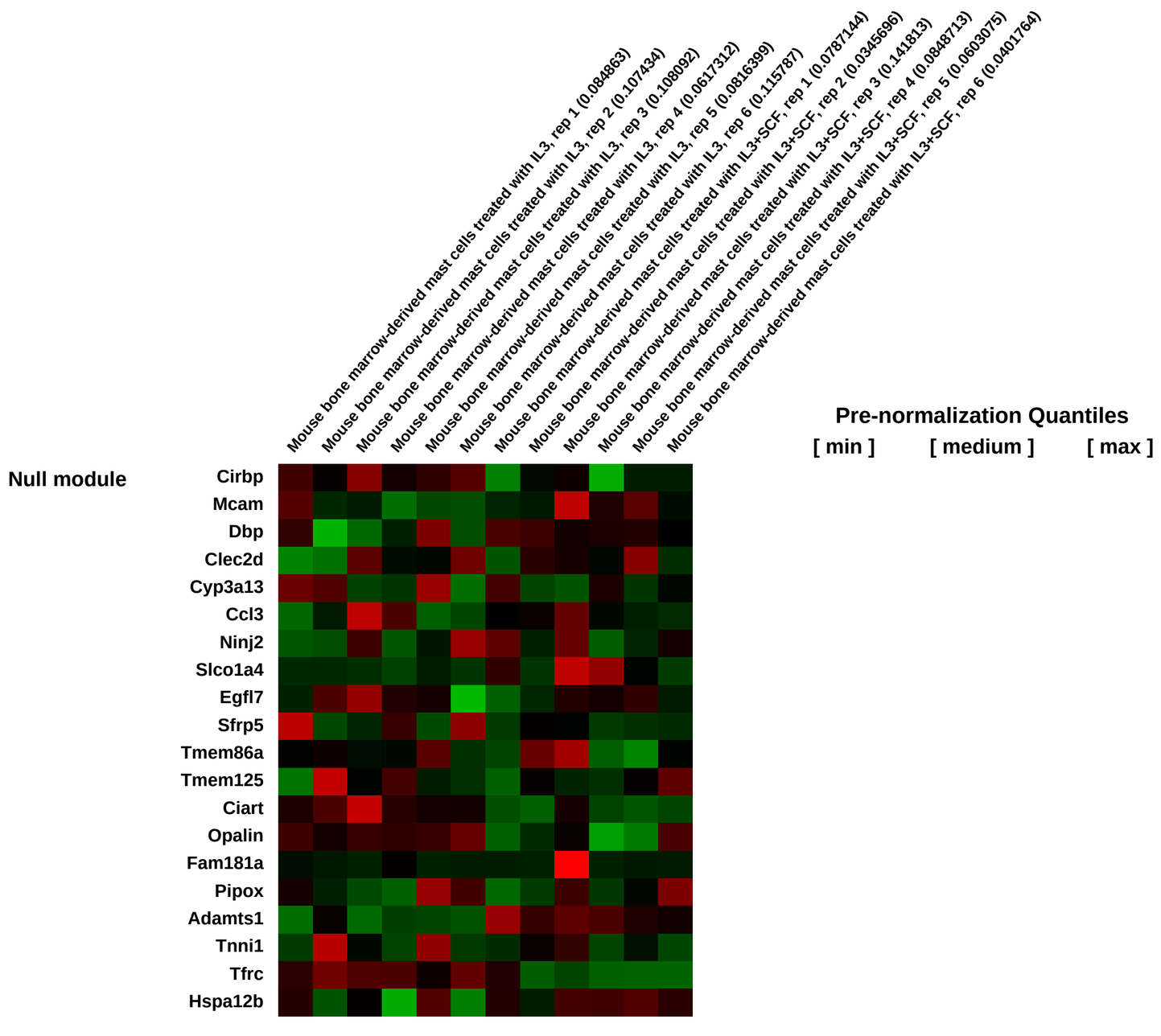

GEO Series "GSE42047" Expression Profiles

Num of samples in this series: 24

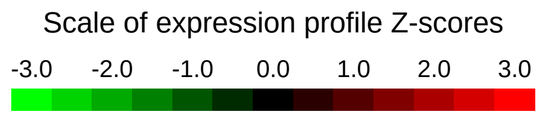

GEO Link:	http://www.ncbi.nlm.nih.gov/geo/query/acc.cgi?acc=GSE42047
Status:	Public on Oct 04 2013
Title:	TWEAK-treated time course in Pan02 cells
Organism:	Mus musculus
Experiment type:	Expression profiling by array
Platform:	GPL1261
Pubmed ID:	23974006
Summary & Design:	**Summary:** Tumor necrosis factor-related weak inducer of apoptosis, TWEAK, is a TNF superfamily member that mediates signaling through its receptor fibroblast growth factor inducible-14, Fn14. In tumor cell lines, TWEAK induces proliferation, survival and NF-kappaB signaling and gene expression that promote tumor growth and suppress antitumor immune responses. Anti-TWEAK antibody, RG7212, inhibits tumor growth in vivo with decreases in pathway activation markers and modulation of tumor, blood and spleen immune cell composition. Candidate response prediction markers, including Fn14, have been identified in mouse models. Phase I pharmacodynamic data from patients are consistent with preclinical results. TWEAK:Fn14 signaling is upregulated in human cancer and pathway activation induces tumor proliferation and survival signaling. Blockade with anti-TWEAK mAb, RG7212, inhibits tumor growth in multiple models in mice. TWEAK induces changes that suppress anti-tumor immune responses and RG7212 blocks these effects resulting in changes in tumor immune cell composition and decreases in cytokines that promote immunosuppression. Antitumor efficacy in mice was observed in a range of Fn14 expressing models with pathway activation and expressing either wild-type or mutant p53, BRAF or KRAS suggesting both a patient selection strategy and potential broad clinical applicability. Preclinical mechanism of action hypotheses are supported by Phase I clinical data, with decreases in proliferation markers and increased tumor T cell infiltration. **Overall design:** Pan02 cells untreated or treated with 1090-TW (TWEAK) for 4 hours, 8 hours, or 24 hours. Four replicates for each condition were performed.

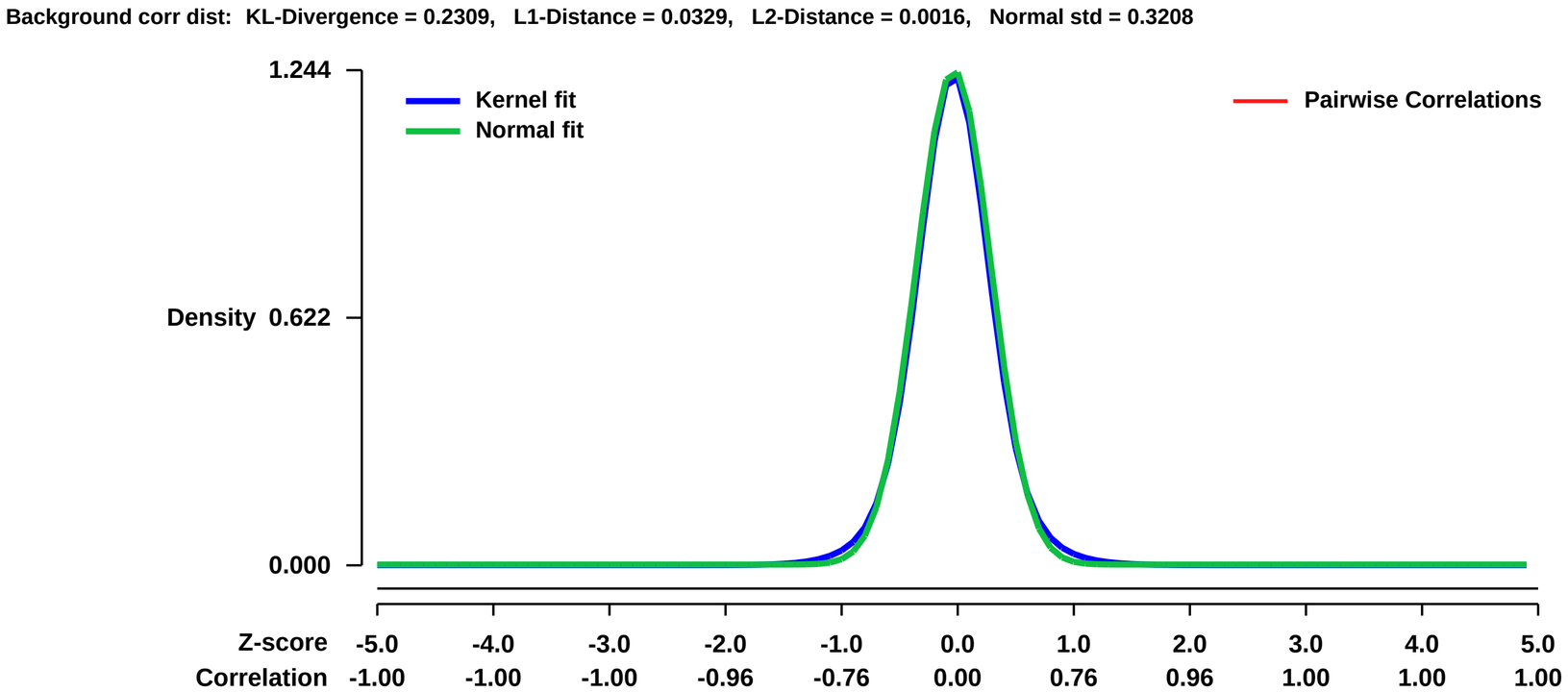

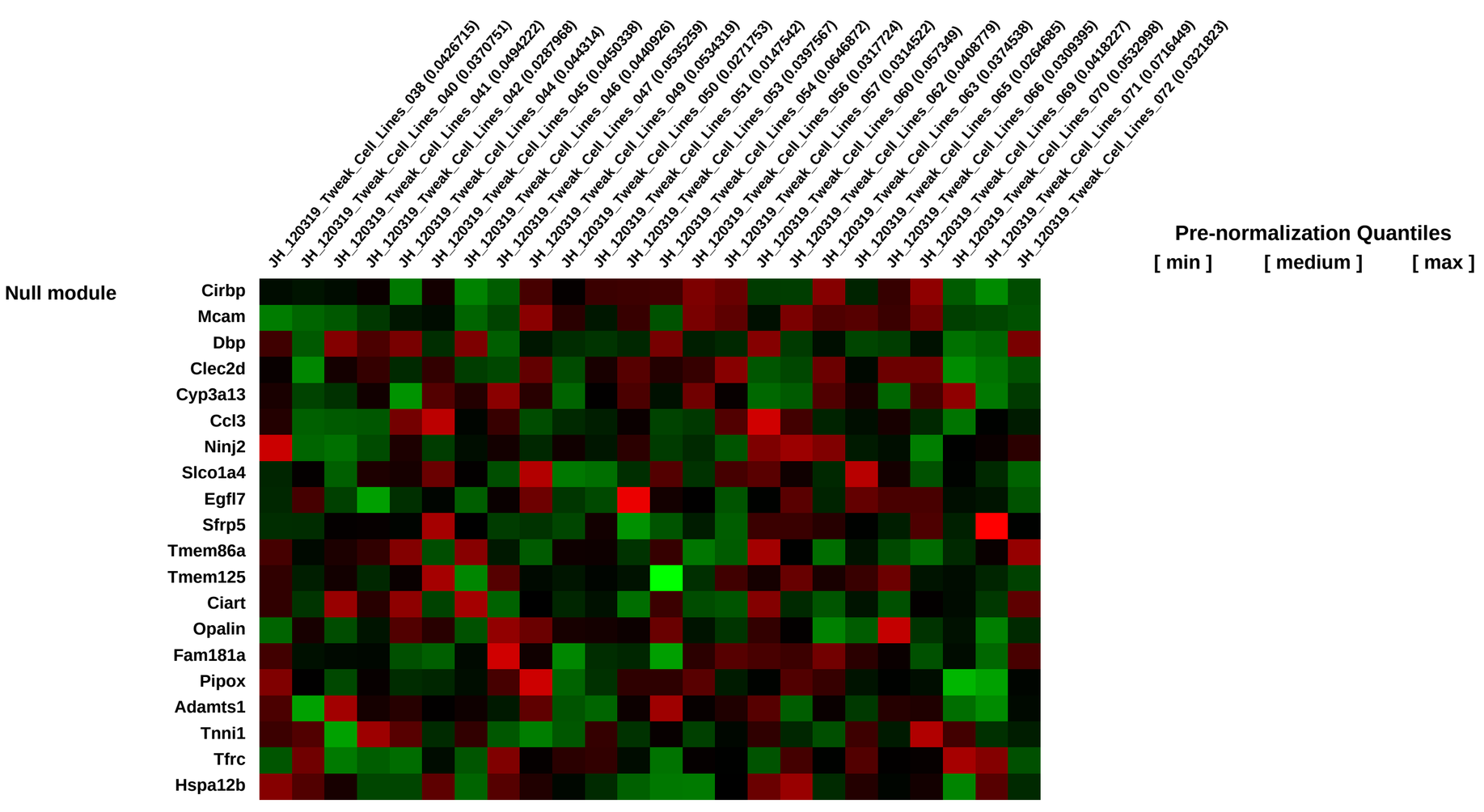

GEO Series "GSE47205" Expression Profiles

Num of samples in this series: 10

Scale of expression profile Z-scores

-3.0 -2.0 -1.0 0.0 1.0 2.0 3.0

GEO Link:	http://www.ncbi.nlm.nih.gov/geo/query/acc.cgi?acc=GSE47205
Status:	Public on May 24 2013
Title:	MLL regulated genes in LSK/CD48- hematopoietic stem cells
Organism:	Mus musculus
Experiment type:	Expression profiling by array
Platform:	GPL1261
Pubmed ID:	23744037
Summary & Design:	**Summary:** The histone methyltransferase mixed lineage leukemia (MLL) is essential to maintain hematopoietic stem cells and is a leukemia protooncogene. Although Hox genes are well-characterized targets of MLL and MLL fusion oncoproteins, the range of Mll-regulated genes in normal hematopoietic cells remains unknown. Here we identify and characterize part of the Mll-transcriptional network in hematopoietic stem cells with an integrated approach by using conditional loss-of-function models, genomewide expression analyses, chromatin immunoprecipitation, and functional rescue assays. The Mll-dependent transcriptional network extends well beyond the previously appreciated Hox targets, is comprised of many characterized regulators of self-renewal, and contains target genes that are both dependent and independent of the MLL cofactor, Menin. Interestingly, Prdm16 emerged as a target gene that is uniquely effective at partially rescuing Mll-deficient hematopoietic stem and progenitor cells. This work highlights the tissue-specific nature of regulatory networks under the control of MLL/Trithorax family members and provides insight into the distinctions between the participation of MLL in normal hematopoiesis and in leukemia. We used microarrays to determine the gene expression profiles of HSCs upon conditional deletion of Mll. **Overall design:** LSK/CD48- HSCs were sorted from 5 pI:pC injected MllF/F control mice or 5 pI:pC injected Mx1-cre;MllF/F mice 6 days after the initial injection. Total RNA was purified from 1,500 to 10,000 sorted cells, amplified, labeled, fragmented and hybridized to GeneChip Mouse Genome 430 2.0 arrays from Affymetrix.

Background corr dist: KL-Divergence = 0.1093, L1-Distance = 0.0348, L2-Distance = 0.0024, Normal std = 0.4249

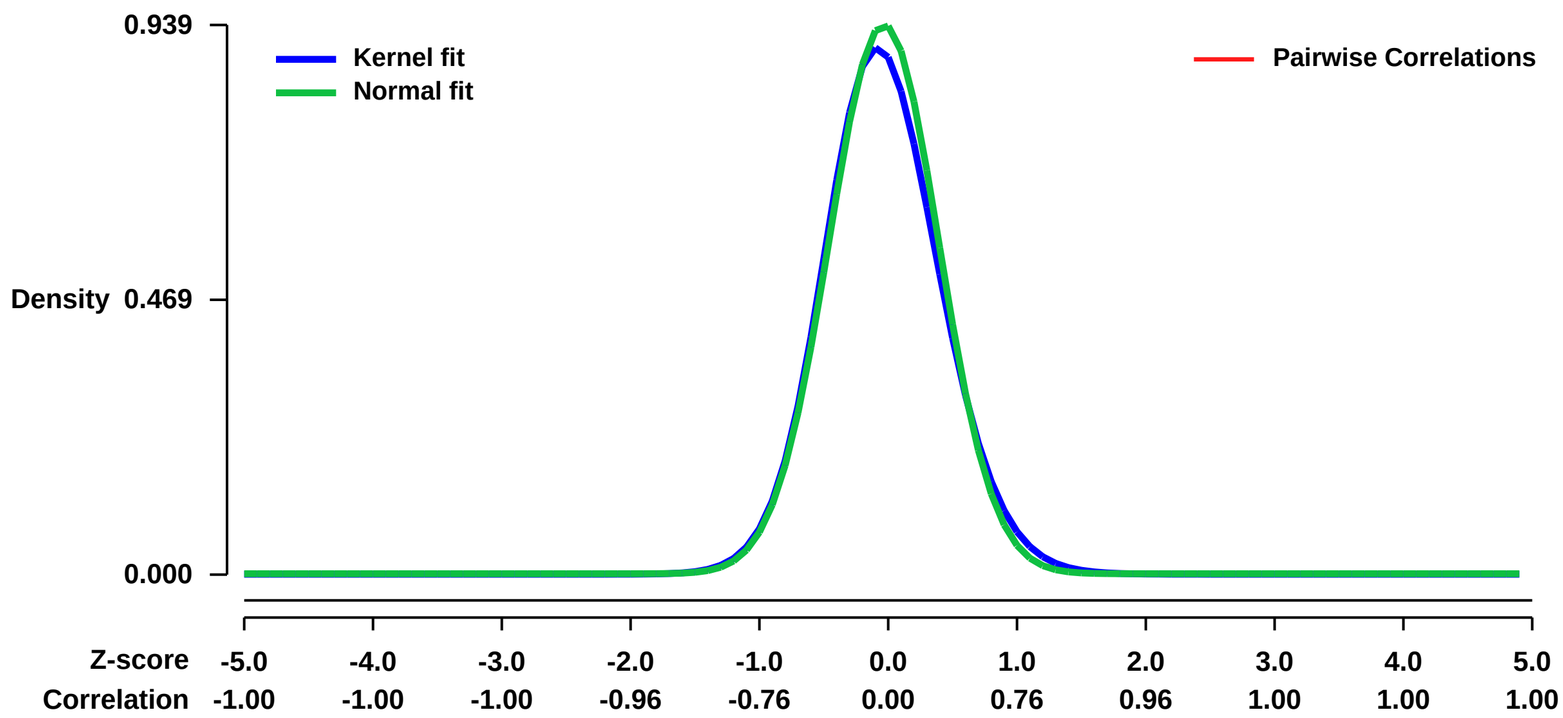

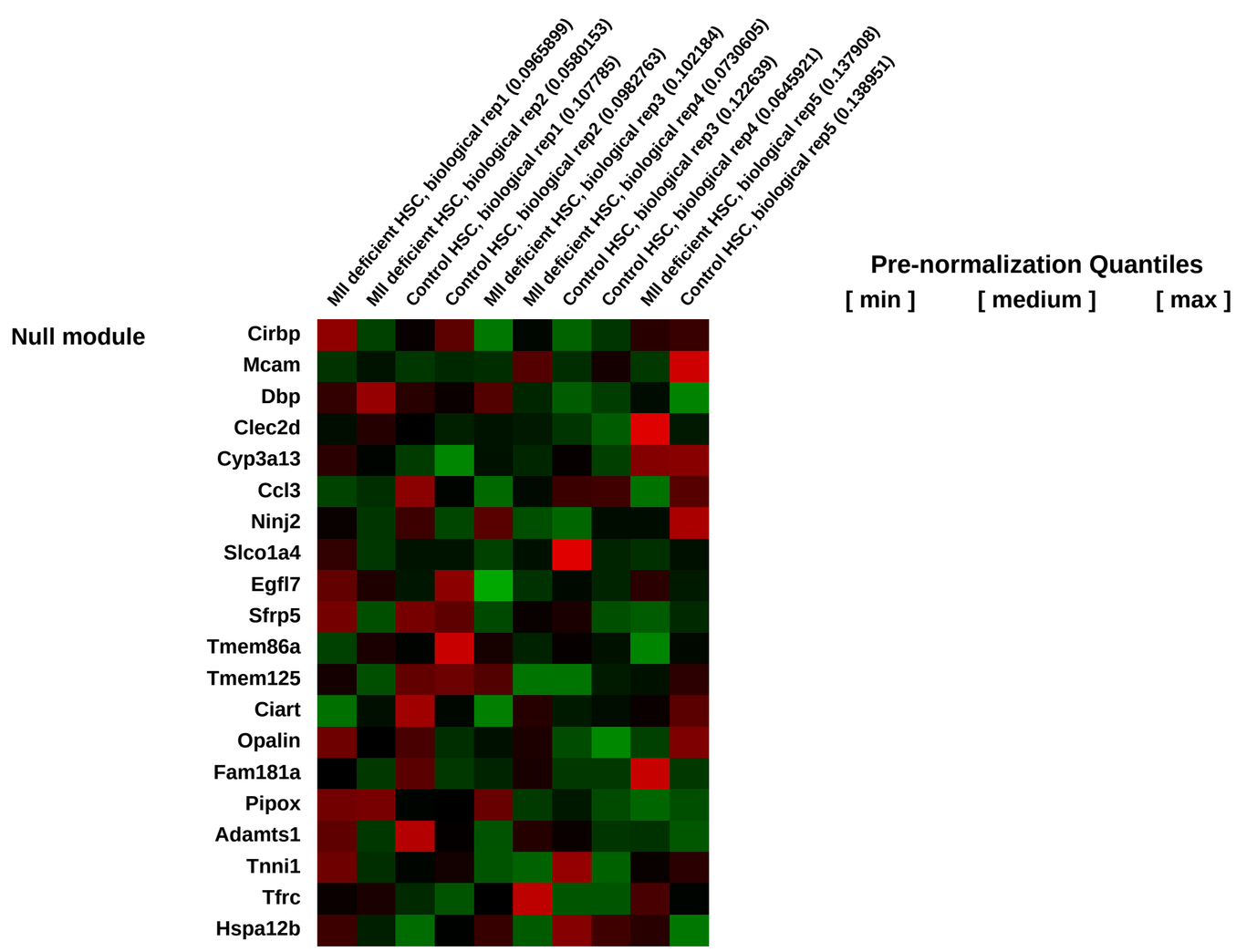

GEO Series "GSE5891" Expression Profiles

Num of samples in this series: 6

Scale of expression profile Z-scores

-3.0 -2.0 -1.0 0.0 1.0 2.0 3.0

GEO Link:	http://www.ncbi.nlm.nih.gov/geo/query/acc.cgi?acc=GSE5891
Status:	Public on Sep 22 2006
Title:	Nuclear organization of active and inactive chromatin domains revealed by 4C technology
Organism:	Mus musculus
Experiment type:	Other
Platform:	GPL1261
Pubmed ID:	17033623
Summary & Design:	**Summary:** The spatial organization of DNA in the cell nucleus is an emerging key contributor to genomic function. We have developed 4C technology, or 3C-on-chip, which allows for an unbiased genome-wide search for DNA loci that contact a given locus in the nuclear space. We demonstrate here that active and inactive genes are engaged in many long-range intrachromosomal interactions and can also form interchromosomal contacts. The active b-globin locus in fetal liver contacts mostly transcribed, but not necessarily tissue-specific, loci elsewhere on chromosome 7, while the inactive locus in fetal brain contacts different, transcriptionally silent, loci. A housekeeping gene in a gene dense region on chromosome 8 forms long-range contacts predominantly with other active gene clusters, both in cis and in trans, and many of these intra- and interchromosomal interactions are conserved between the tissues analyzed. Our data demonstrate that chromosomes fold into areas of active chromatin and areas of inactive chromatin and establish 4C technology as a powerful tool to study nuclear architecture. **Keywords:** 4C technology **Overall design:** Gene expression arrays were performed in triplicate, according to standard procedures (Affymetrix). 4C experiments were performed in duplo (biologically independent samples), dye swap was included. Hybriisation was performed on dedicated micro-arrays. Probes (60-mers) were selected from the sequences 100 bp up â and downstream of HindIII sites. To prevent cross-hybridization, probes that had any similarity with highly abundant repeats (RepBase 10.09) were removed from the probeset. In addition, probes that gave more than two BLAST hits in the genome were also removed from the probeset. Sequence alignments were performed using MegaBLAST using the standard settings. A hit was defined as an alignment of 30 nt or longer.

Background corr dist: KL-Divergence = 0.0158, L1-Distance = 0.0653, L2-Distance = 0.0070, Normal std = 0.9745

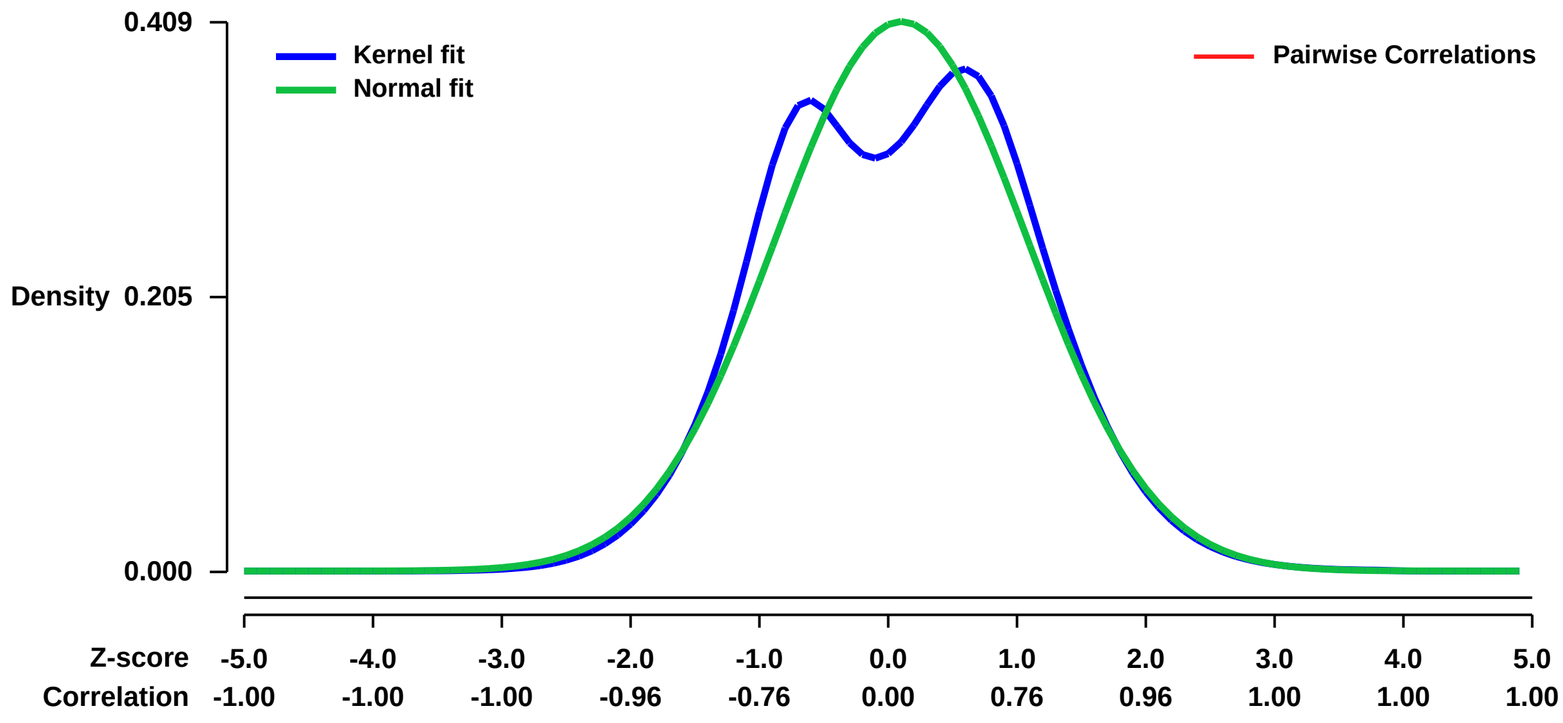

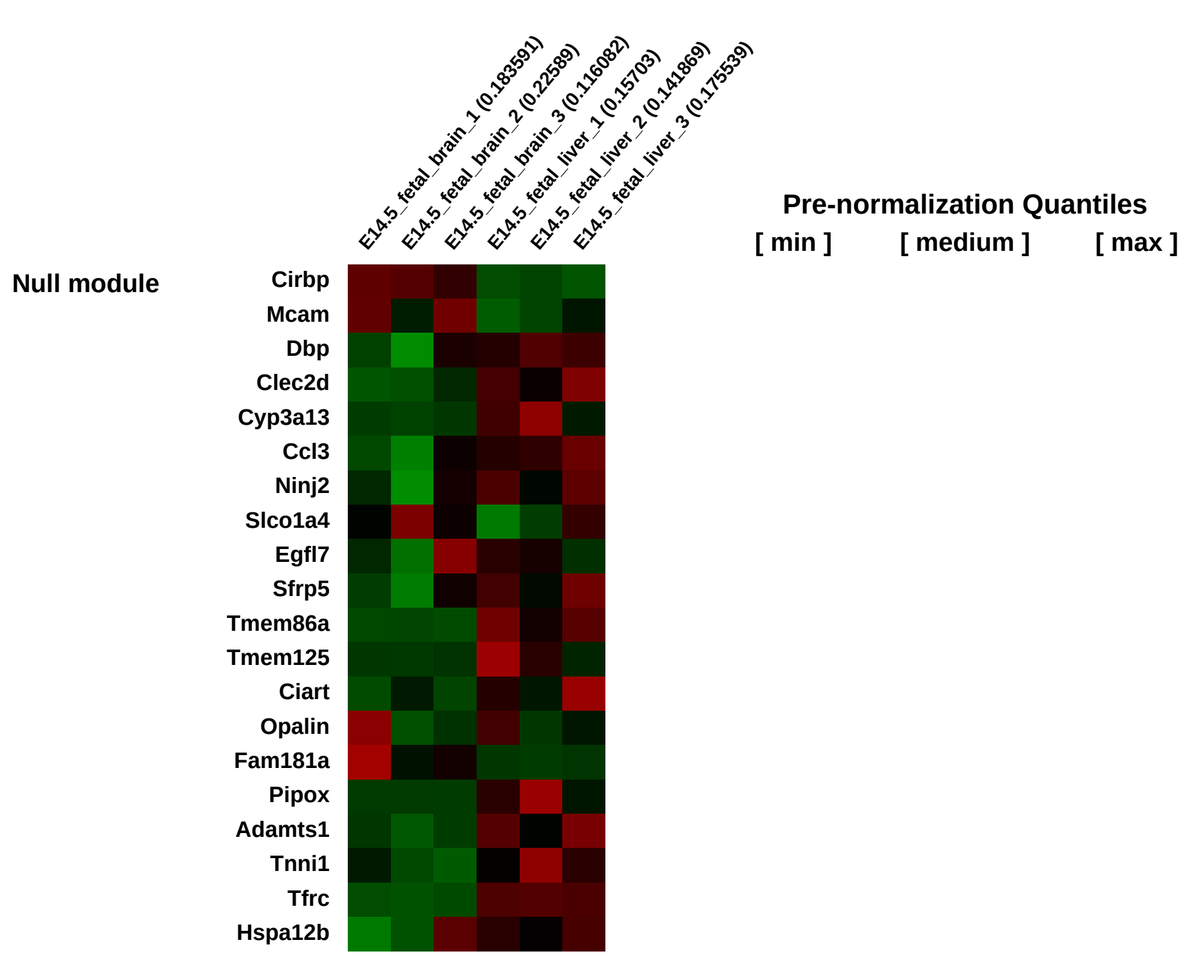

GEO Series "GSE12498" Expression Profiles

Num of samples in this series: 12

Scale of expression profile Z-scores

-3.0 -2.0 -1.0 0.0 1.0 2.0 3.0

GEO Link:	http://www.ncbi.nlm.nih.gov/geo/query/acc.cgi?acc=GSE12498
Status:	Public on Nov 21 2008
Title:	Gene expression profiles regulated by Tead2 mutants, Yap, and cell density in NIH3T3 cells
Organism:	Mus musculus
Experiment type:	Expression profiling by array
Platform:	GPL1261
Pubmed ID:	19004856
Summary & Design:	**Summary:** Regulation of organ size is important for development and tissue homeostasis. In Drosophila, Hippo signaling controls organ size by regulating the activity of a TEAD transcription factor, Scalloped, through modulation of its coactivator protein Yki. The role of mammalian Tead proteins in growth regulation, however, remains unknown. Here we examined the role of mouse Tead proteins in growth regulation. In NIH3T3 cells, cell density and Hippo signaling regulated the activity of Tead proteins by modulating nuclear localization of a Yki homologue, Yap, and the resulting change in Tead activity altered cell proliferation. Tead2-VP16 mimicked Yap overexpression, including increased cell proliferation, reduced cell death, promotion of EMT, lack of cell contact inhibition, and promotion of tumor formation. Growth promoting activities of various Yap mutants correlated with their Tead-coactivator activities. Tead2-VP16 and Yap regulated largely overlapping sets of genes. However, only a few of the Tead/Yapregulated genes in NIH3T3 cells were affected in Tead1-/-;Tead2-/- or Yap-/- embryos. Most of the previously identified Yap-regulated genes were not affected in NIH3T3 cells or mutant mice. In embryos, levels of nuclear Yap and Tead1 varied depending on cell types. Strong nuclear accumulation of Yap and Tead1 were seen in myocardium, correlating with requirements of Tead1 for proliferation. However, their distribution did not always correlate with proliferation. Taken together, mammalian Tead proteins regulate cell proliferation and contact inhibition as a transcriptional mediator of Hippo signaling, but the mechanisms by which Tead/Yap regulate cell proliferation differ depending on cell types, and Tead, Yap and Hippo signaling may play multiple roles in mouse embryos. We used microarrays to know the gene expression profiles regurated by Tead2-VP16, Tead2-EnR, Yap, and cell density in NIH3T3 cells. **Keywords:** Cell density, genetic modification **Overall design:** Tead2-VP16-, Tead2-EnR-, Yap- and control vector-expressing cells were cultured at low or high density for RNA extraction and hybridization on Affymetrix microarrays.

Background corr dist: KL-Divergence = 0.0711, L1-Distance = 0.0551, L2-Distance = 0.0045, Normal std = 0.5445

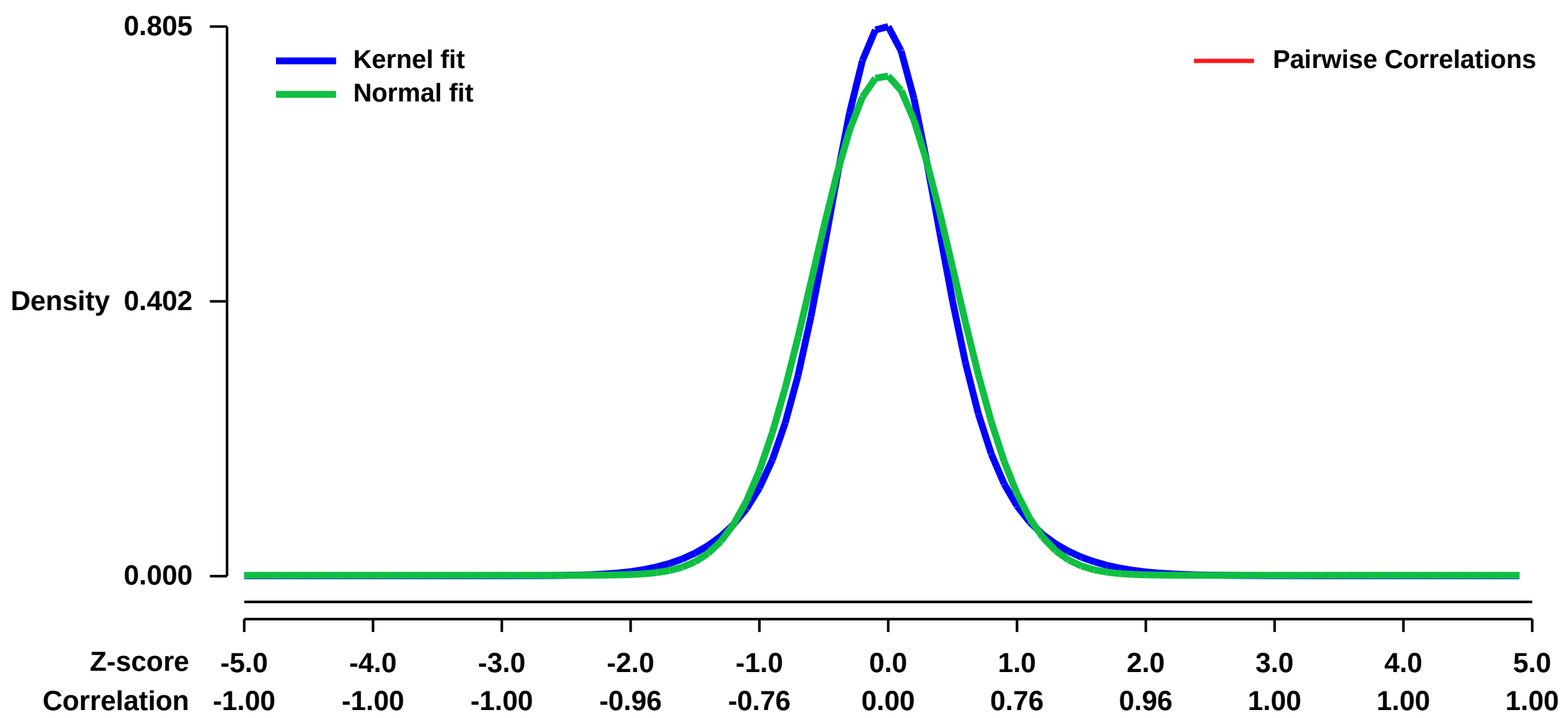

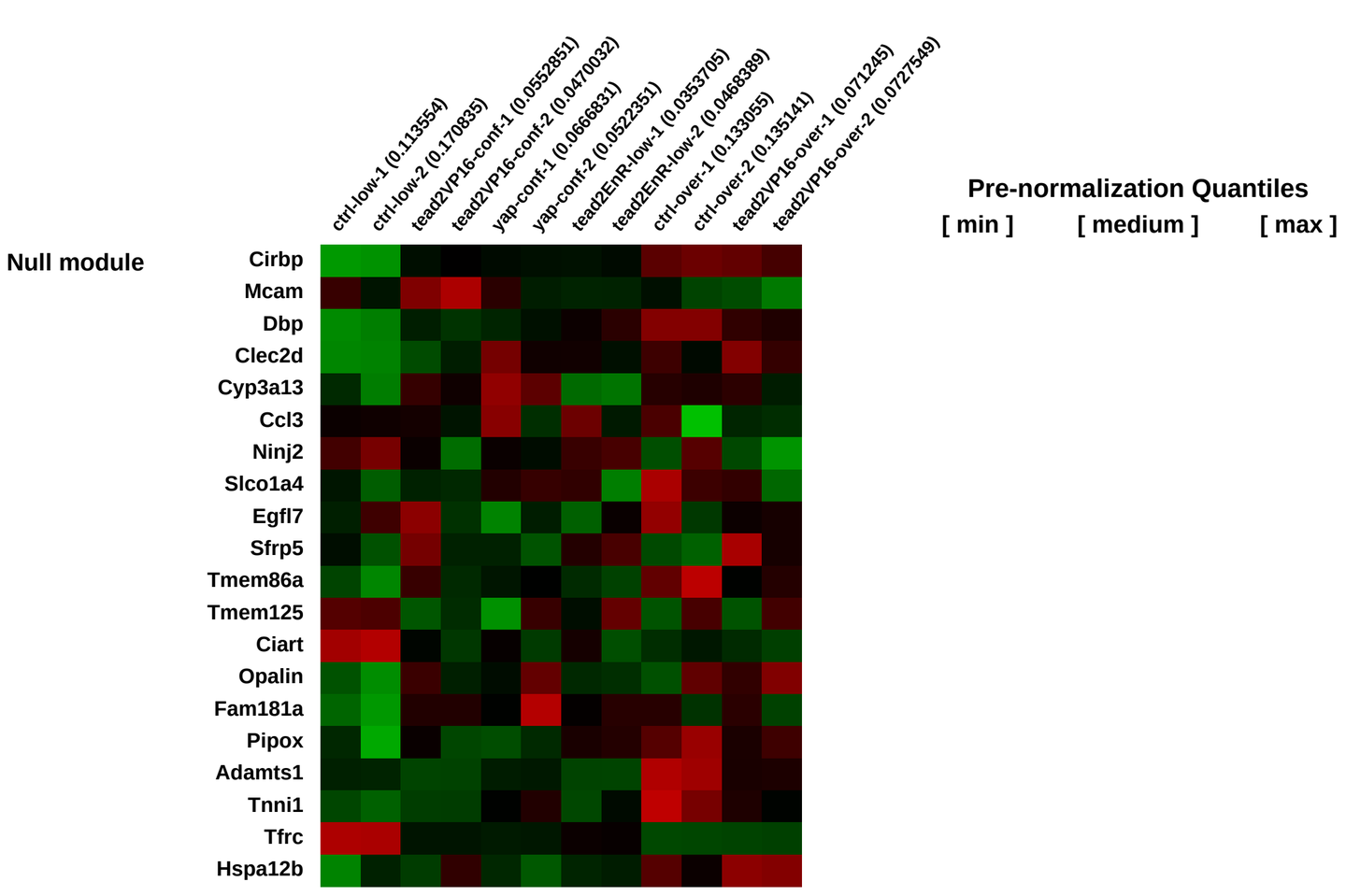

GEO Series "GSE43181" Expression Profiles

Num of samples in this series: 10

Scale of expression profile Z-scores

-3.0 -2.0 -1.0 0.0 1.0 2.0 3.0

GEO Link:	**http://www.ncbi.nlm.nih.gov/geo/query/acc.cgi?acc=GSE43181**
Status:	**Public on Jan 31 2013**
Title:	**Expression data of mouse preoptic region 5 h after LPS-administration comparing wt and mPGES-1 KO mice.**
Organism:	**Mus musculus**
Experiment type:	**Expression profiling by array**
Platform:	**GPL1261**
Pubmed ID:	
Summary & Design:	**Summary:** **WT mice and mPGES-1 KO mice were treated with 120 mikrogram/kg LPS and sacrificed 5 h later.** **The preoptic region was dissected by LCM and analyzed using GeneChip Mouse Genome 430 2.0 arrays (Affymetrix).** **Overall design:** **Groups: WT LPS-treated versus mPGES-1 KO LPS-treated mice.**

Background corr dist: **KL-Divergence = 0.1163, L1-Distance = 0.0361, L2-Distance = 0.0027, Normal std = 0.4143**

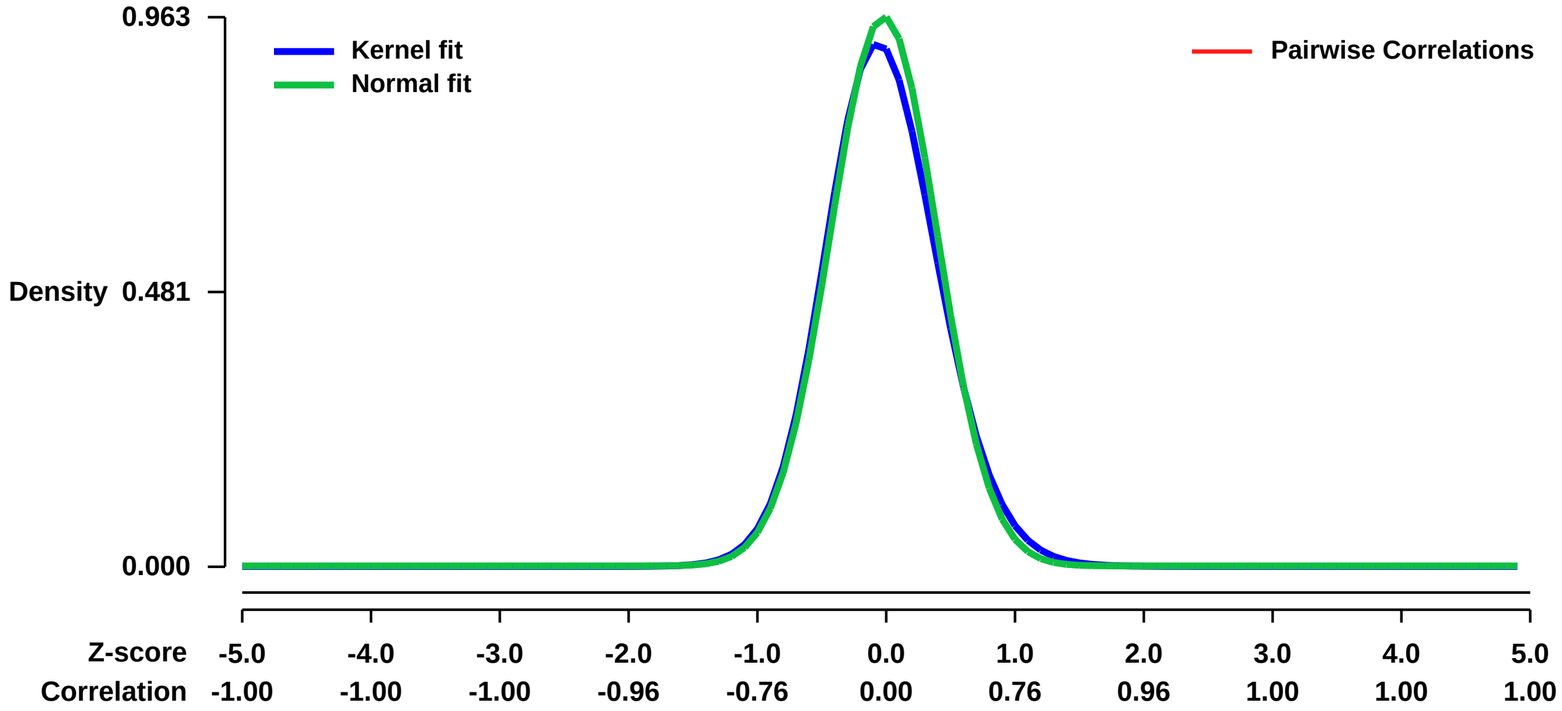

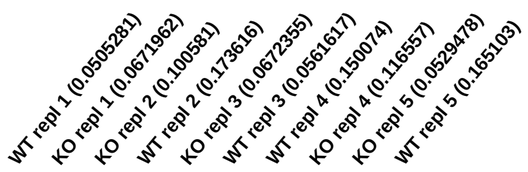

Pre-normalization Quantiles

[min] [medium] [max]

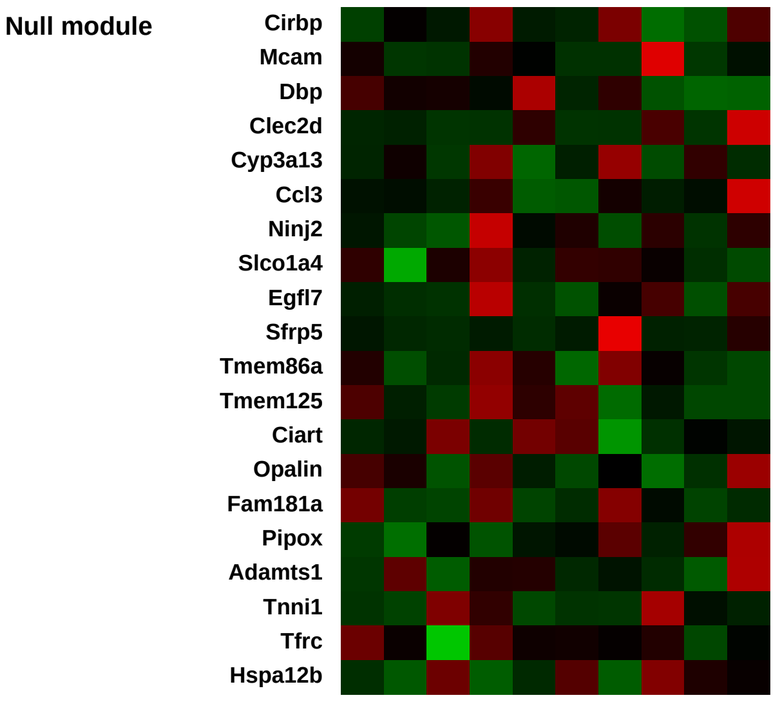

GEO Series "GSE31359" Expression Profiles

Num of samples in this series: 8

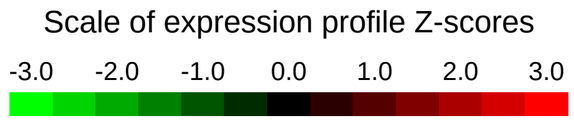

GEO Link:	**http://www.ncbi.nlm.nih.gov/geo/query/acc.cgi?acc=GSE31359**
Status:	**Public on Aug 13 2011**
Title:	**Expression data from mouse EMT-induced and non-induced cells**
Organism:	**Mus musculus**
Experiment type:	**Expression profiling by array**
Platform:	**GPL1261**
Pubmed ID:	
Summary & Design:	**Summary:** **The conversion of an epithelial cell to a mesenchymal cell is critical to vertebrate embryogenesis and a defining structural feature of organ development, such as forming fibroblasts in injured tissues, or in initiating metastases in epithelial cancer. From a general perspective, EMT is about disaggregating epithelial units and reshaping epithelia for movement. This phenotypic conversion requires the molecular reprogramming of epithelia with new biochemical instructions. It is known that commonly used molecular markers for EMT include increased expression of N-cadherin and vimentin, nuclear localization of beta-catenin, and increased production of the transcription factors such as Snail, Twist, and SIP1/ZEB2. Much of this conversion, however, has been studied during experiments that expose new transduction and signaling pathways in epithelia, and more recently in fibrogenic tissues. It is not yet clear whether the fibroblast transition of EMT is an expected middle phase of transdifferentiating epithelia, or whether EMT producing fibroblasts is an arrested form of transdifferentiation. EMT is easily engaged by a combination of cytokines associated with proteolytic digestion of basement membranes upon which epithelia reside. We analyzed PCA and hierarchical clustering method of the gene expression pattern of the renal tubular cells and mammary gland cells. We then identified the genes which discriminate between the renal tubular and the mammary gland epithelial cells (PC1), or EMT-induced and non-induced cells (PC3). Undergoing EMT identifies the genes that discriminate between the renal tubular and the mammary gland epithelial cells(PC1), or EMT-induced and non-induced cells (PC3).** **Overall design:** **Affymetrix GeneChip Mouse Genome 430 2.0 Array was used to transcriptionally profile to compare mouse EMT-induced cells and non-induced cells.**

Background corr dist: KL-Divergence = 0.0562, L1-Distance = 0.0330, L2-Distance = 0.0017, Normal std = 0.5554

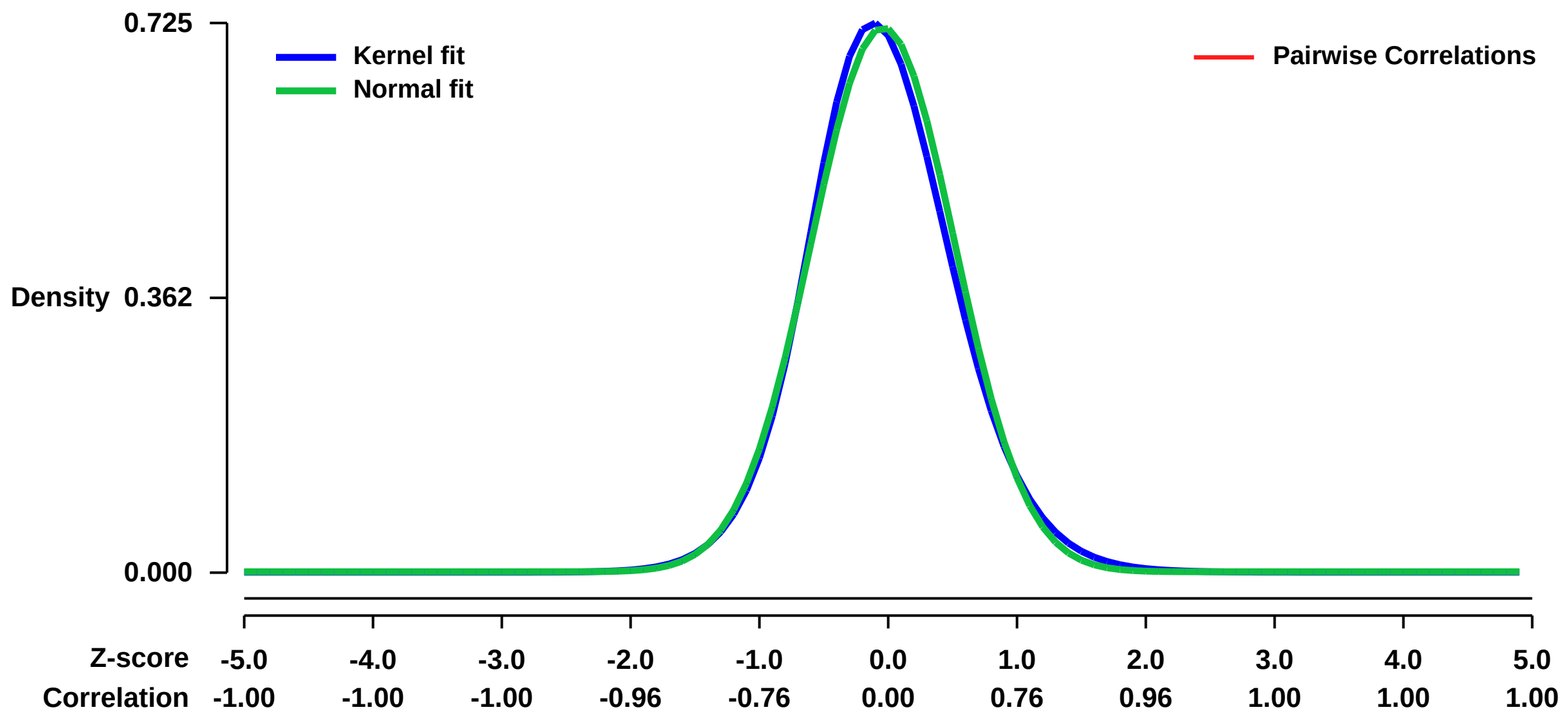

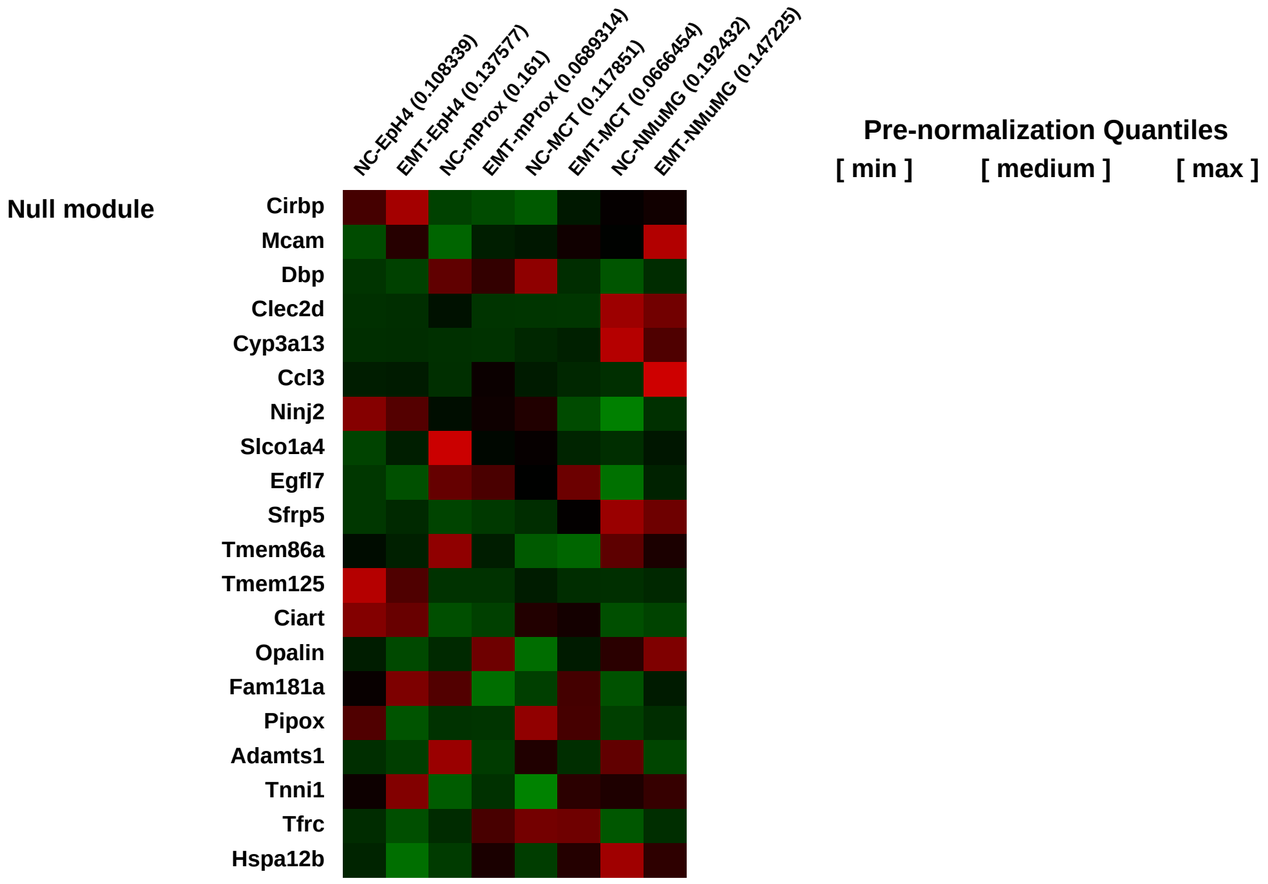

GEO Series "GSE4926" Expression Profiles

Num of samples in this series: 12

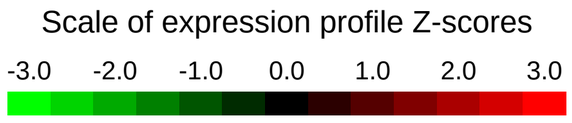

GEO Link:	http://www.ncbi.nlm.nih.gov/geo/query/acc.cgi?acc=GSE4926
Status:	Public on Mar 01 2008
Title:	Gene expression profiling of a mouse model of islet dysmorphogenesis
Organism:	Mus musculus
Experiment type:	Expression profiling by array
Platform:	GPL1261
Pubmed ID:	18297134
Summary & Design:	**Summary:** In the past decade, several transcription factors critical for pancreas development have been identified. Despite this success, many of the cell surface and extracellular factors necessary for proper islet morphogenesis and function remain uncharacterized. Previous studies have shown that transgenic over-expression of the transcription factor HNF6 specifically in the pancreatic endocrine cell lineage resulted in the disruption of islet morphogenesis, including dysfunctional endocrine cell sorting, increased islet size, and failure of islets to migrate away from the ductal epithelium. We exploited the dysmorphic islets in pdx1PBHnf6 animals as a tool to identify factors important for islet morphogenesis. Genome-wide microarray analysis was used to identify differences in the gene expression profiles of late gestation and early postnatal pancreas tissue from wild type and pdx1PBHnf6 animals. We report the identification of genes with an altered expression in HNF6 Tg animals and highlight factors with potential importance in islet morphogenesis. **Keywords:** disease state analysis, developmental stage analysis **Overall design:** Whole genome microarray analysis was used to identify differences in the gene expression profiles of late gestation and early postnatal pancreas tissue from wild type (WT) animals and HNF6 transgenic animals at a time when the events of normal islet morphogenesis are occurring (e18.5 and postnatal day 1). RNA was isolated from individual pancreata at the appropriate developmental stage. Highly pure samples were pooled according to their genotype (3-5 animals per pool) in order to obtain an adequate quantity of RNA for Affymetrix GeneChip analysis. Twelve samples were run in total, 3 replicates each of 4 groups: embryonic day 18.5, wild type mouse; embryonic day 18.5, HNF6 Transgenic mouse; post-natal day 1, wild type mouse; post-natal day 1, HNF6 Transgenic mouse.

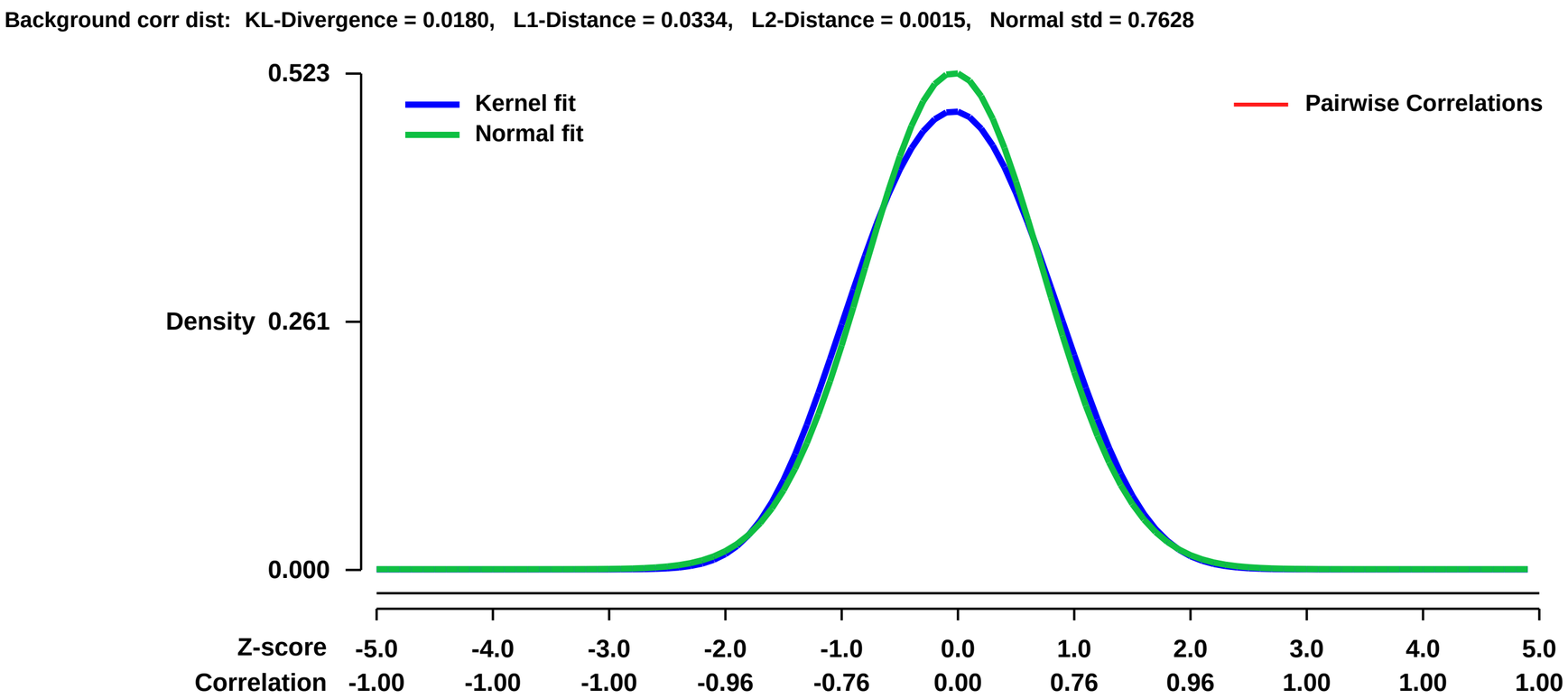

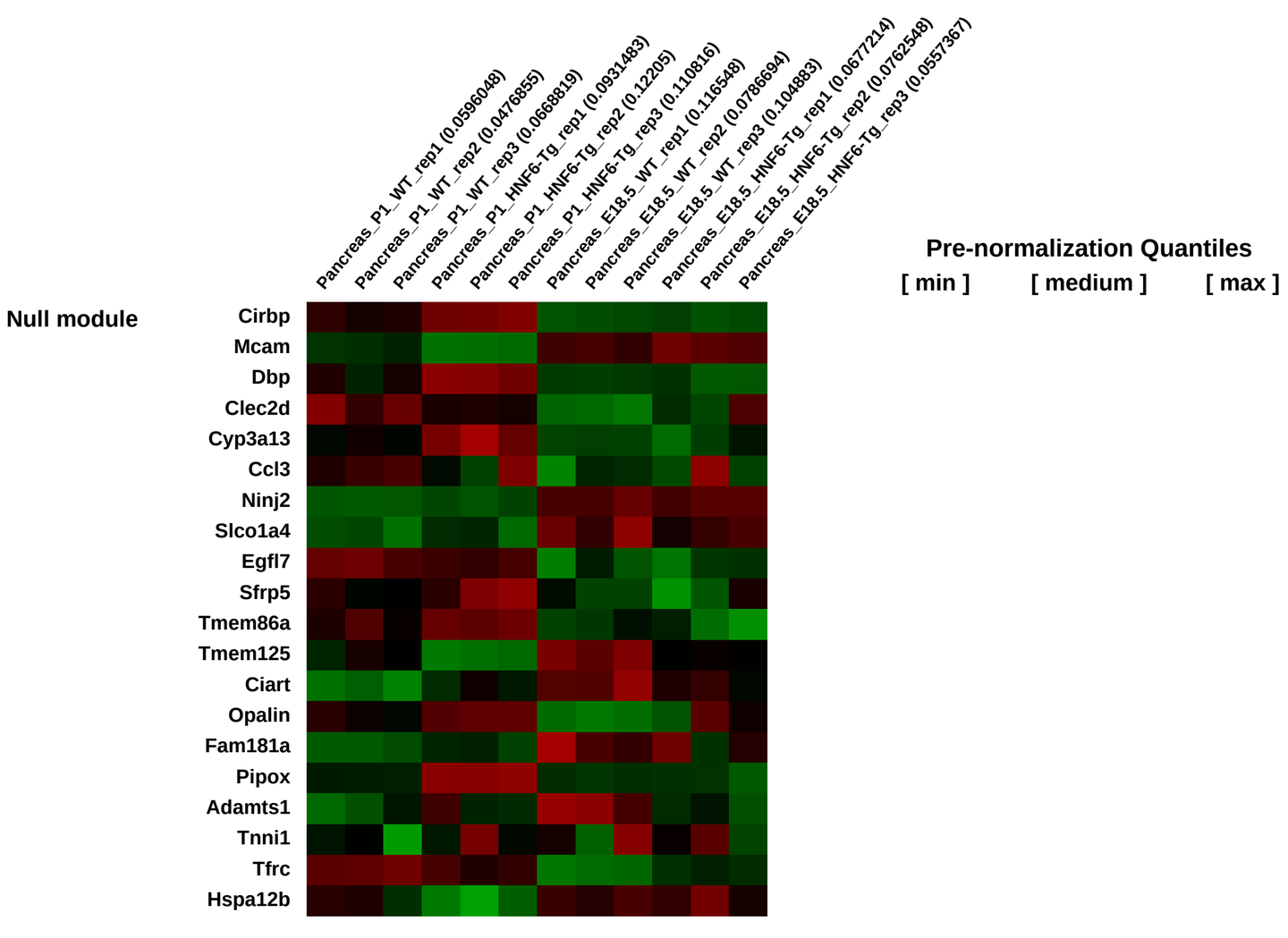

GEO Series "GSE17647" Expression Profiles

Num of samples in this series: 24

Scale of expression profile Z-scores

-3.0 -2.0 -1.0 0.0 1.0 2.0 3.0

GEO Link:	**http://www.ncbi.nlm.nih.gov/geo/query/acc.cgi?acc=GSE17647**
Status:	**Public on Aug 15 2009**
Title:	**Involvement of 4E-BP1 in the protection induced by HDLs on pancreatic beta cells**
Organism:	**Mus musculus**
Experiment type:	**Expression profiling by array**
Platform:	**GPL1261**
Pubmed ID:	**19574449**
Summary & Design:	**Summary:** **High-density lipoproteins (HDLs) protect pancreatic ¸† cells against apoptosis. This property might be related to the increased risk to develop diabetes in patients with low HDL blood levels. However, the mechanisms by which HDLs protect ¸† cells are poorly characterized. Here we use a transcriptomic approach to identify genes differentially modulated by HDLs in ¸† cells subjected to apoptotic stimuli.** **Overall design:** **Starvation medium + HDL (prep. HDL GSK3 or HDL GSK4) [HDL.S]**

Background corr dist: **KL-Divergence = 0.3267, L1-Distance = 0.0543, L2-Distance = 0.0075, Normal std = 0.2719**

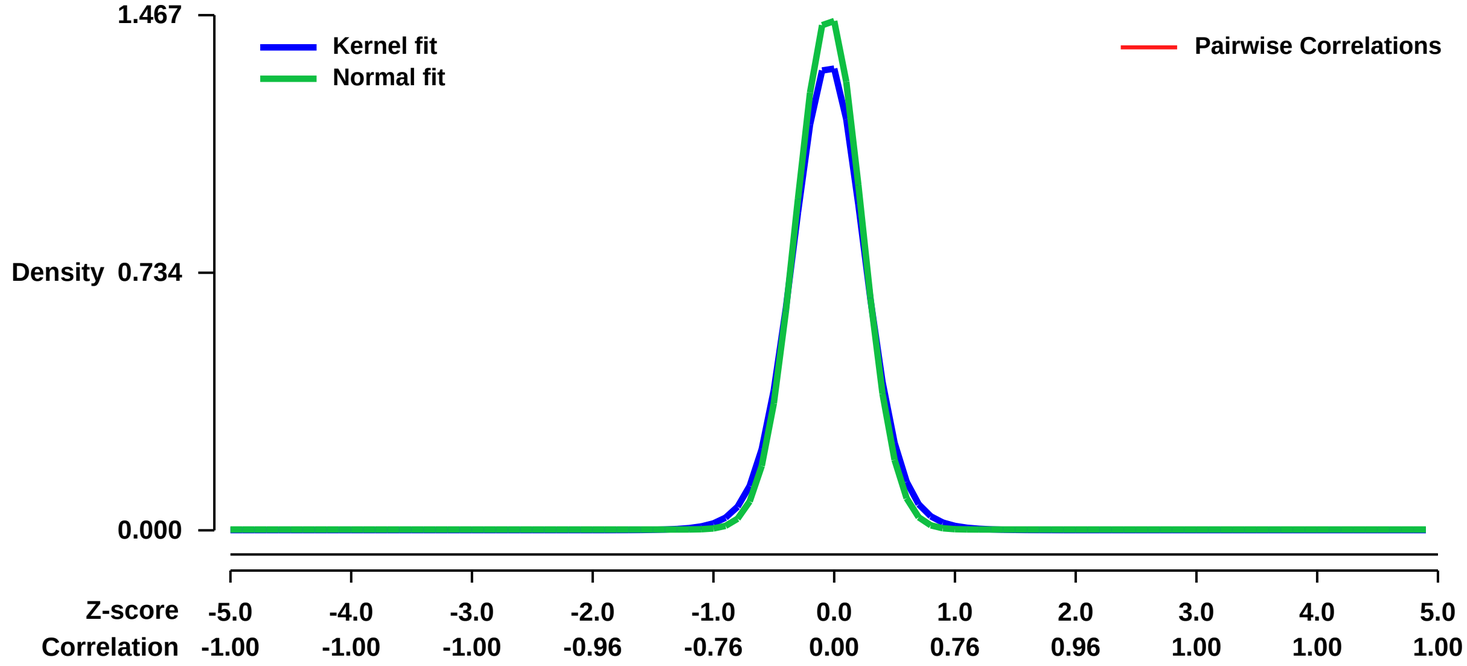

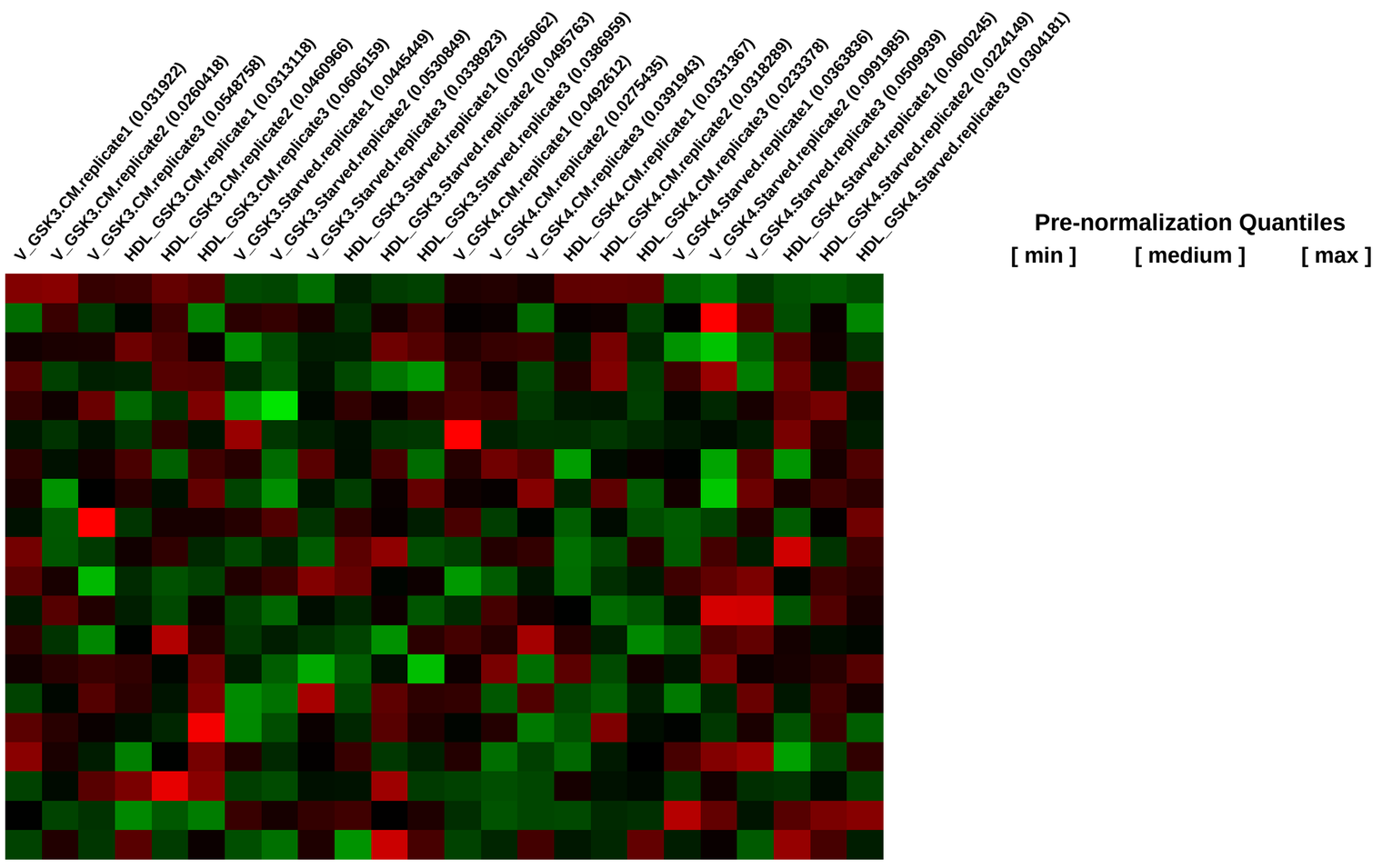

GEO Series "GSE17709" Expression Profiles

Num of samples in this series: 18

Scale of expression profile Z-scores

-3.0 -2.0 -1.0 0.0 1.0 2.0 3.0

GEO Link:	http://www.ncbi.nlm.nih.gov/geo/query/acc.cgi?acc=GSE17709
Status:	Public on Aug 19 2009
Title:	Gene expression analysis of a podocyte specific PTIP deletion in mouse glomerular preparations at 1 month of age
Organism:	Mus musculus
Experiment type:	Expression profiling by array
Platform:	GPL1261
Pubmed ID:	21060806
Summary & Design:	**Summary:** Glomerular RNA comparison between wild-type and podocyte specific deletion of the PTIP gene in 1 month old kidneys. The PTIP gene was deleted using a floxed allele and a Podocin-Cre driver strain. These mice develop protein urea by 3 months of age. This study was designed to find gene expression differences prior to the onset of the phenotype. **Overall design:** Kidneys were excised at 1 month of age. Glomeruli enriched fractions were generated by sieving of the tissue homogenates. RNA was prepared from glomerular enriched fractions.

Background corr dist: KL-Divergence = 0.0391, L1-Distance = 0.0385, L2-Distance = 0.0021, Normal std = 0.6195

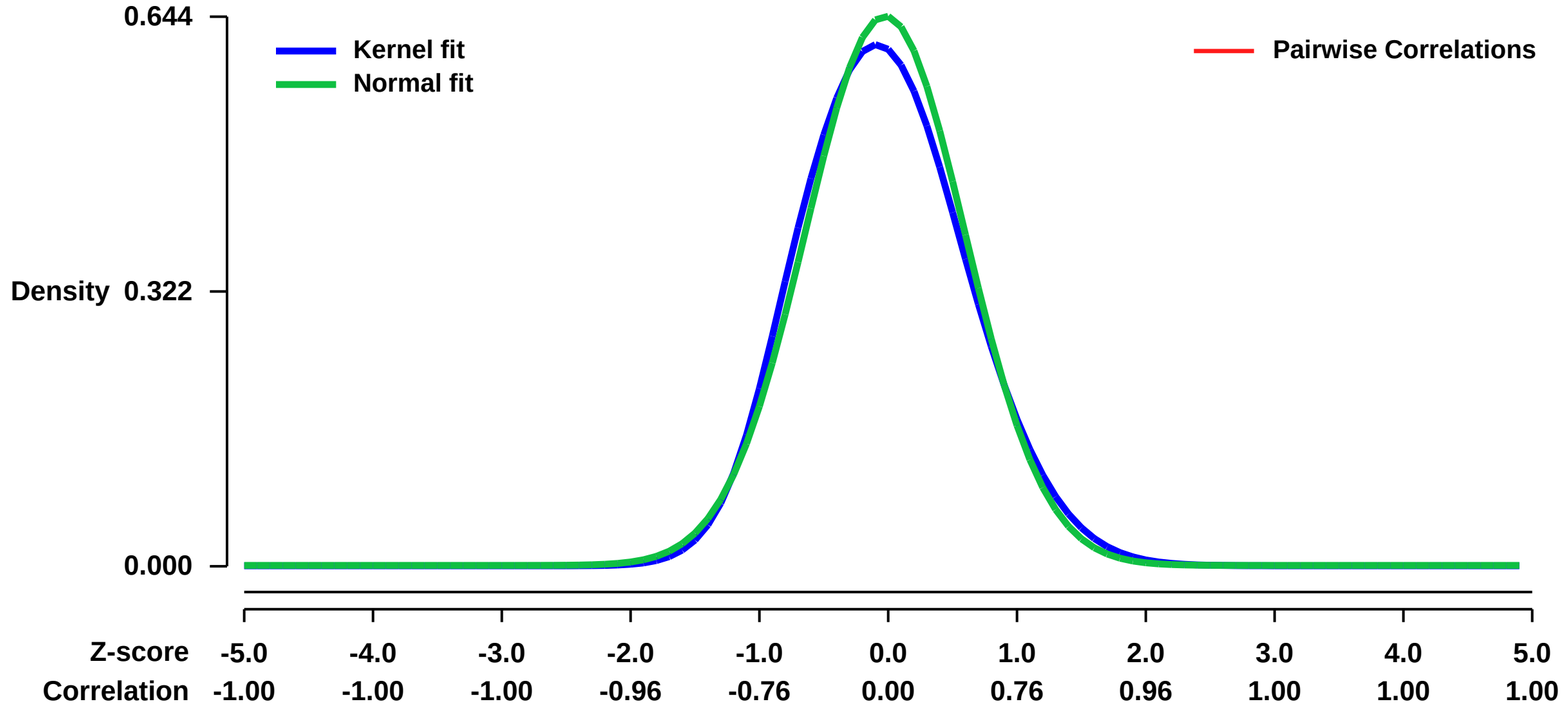

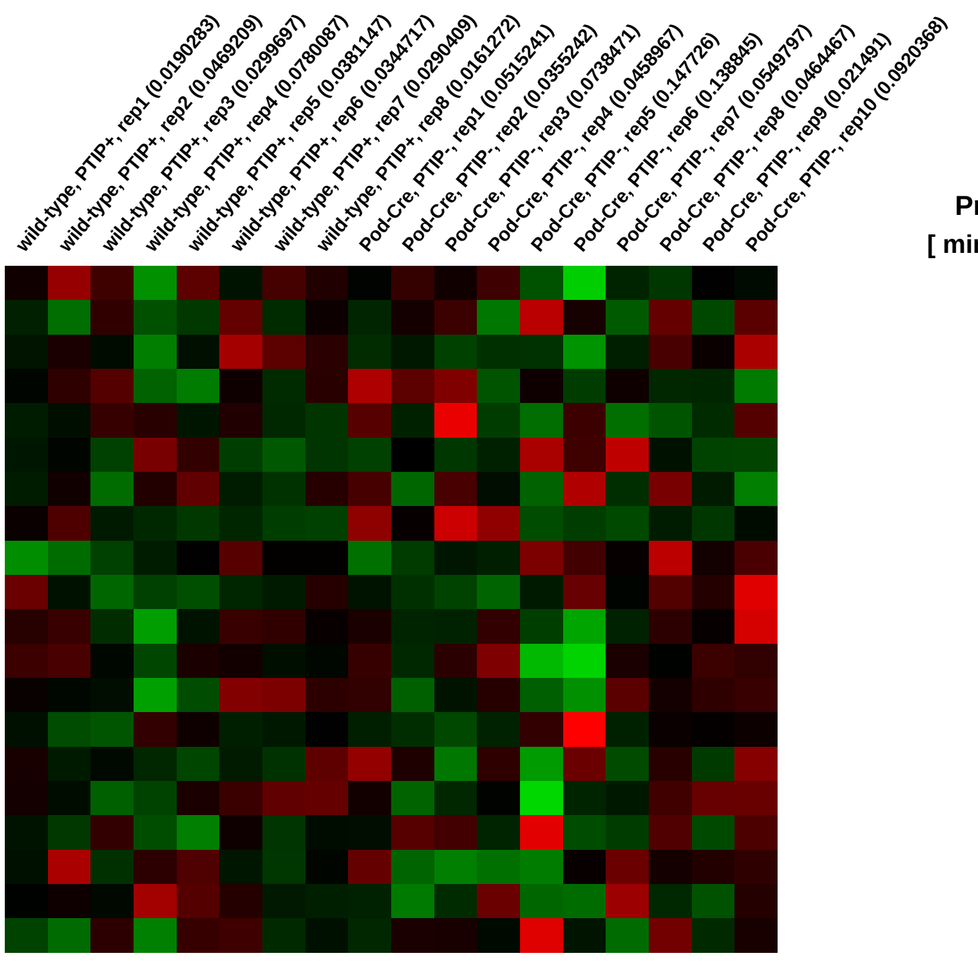

GEO Series "GSE4694" Expression Profiles

Num of samples in this series: 6

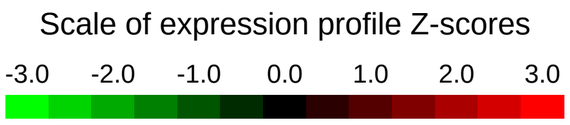

GEO Link:	http://www.ncbi.nlm.nih.gov/geo/query/acc.cgi?acc=GSE4694
Status:	Public on Apr 30 2006
Title:	Expression data from myogenesis
Organism:	Mus musculus
Experiment type:	Expression profiling by array
Platform:	GPL1261
Pubmed ID:	17062158
Summary & Design:	**Summary:** During muscle differentiation, myogenesis sepcific genes are differentially regulated, including Lamins that function at least in maintenance of nuclear architecture and regulation of gene expression. We used microarrays to detail the global changes of gene expression in lamins and nuclear envelope assoicated proteins during myogenesis. Keywords: comparative, myogenesis **Overall design:** C2C12 were cultured either in 20% serum (undifferentiated) or in 2% horse serum (differentiated). Differentiated C2C12 cells were harvested on day 6 after induction of myogenesis in low serum. Affymetirx microarray raw data were further processed by GCRMA to globally normalized signal values and then subjected to analysis of Bayesian regularized t-test. Gene expression, that has a p-value less than 0.05 in the t-test and has more than 1.5 fold change, was considered siginificant.

Background corr dist: KL-Divergence = 0.0380, L1-Distance = 0.0307, L2-Distance = 0.0010, Normal std = 0.6550

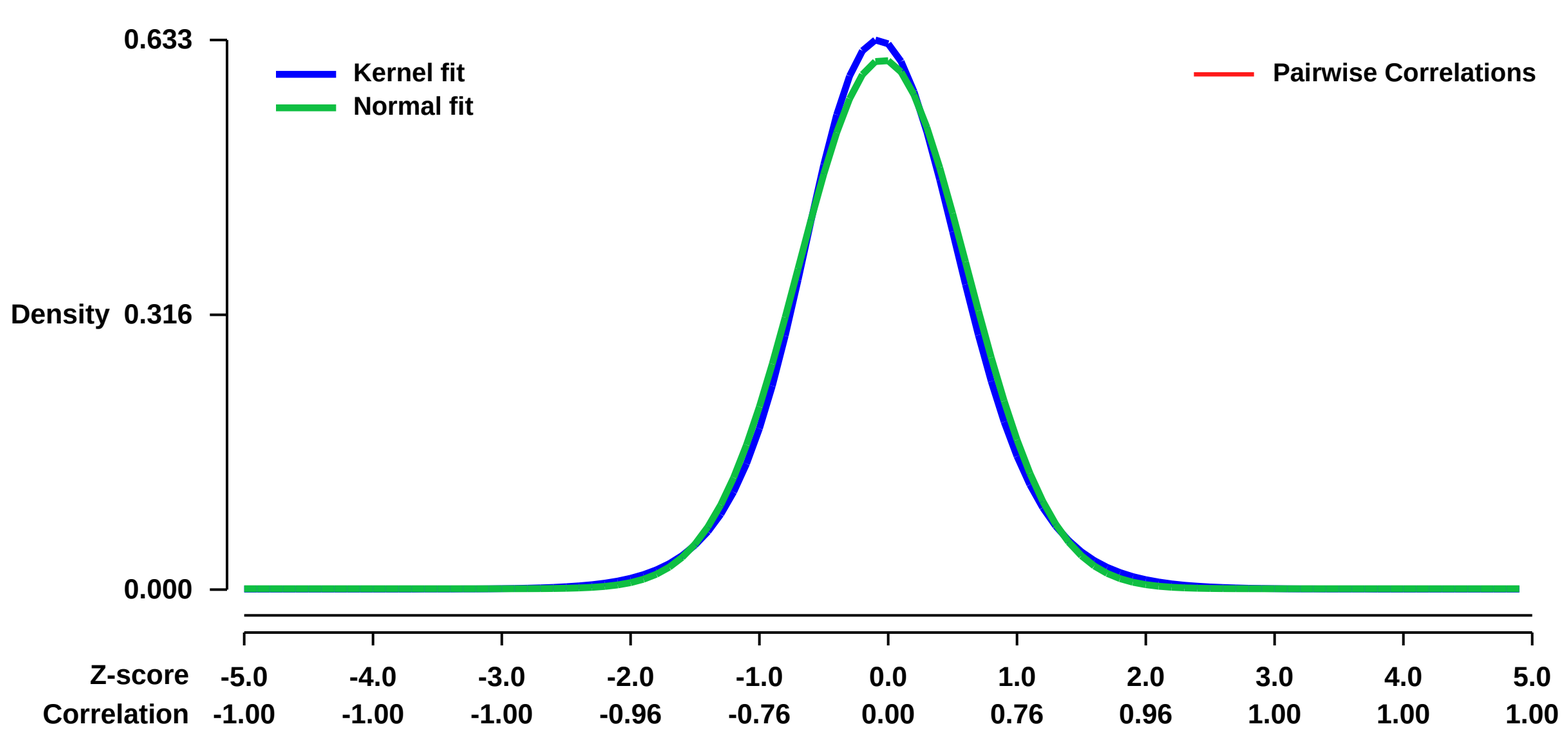

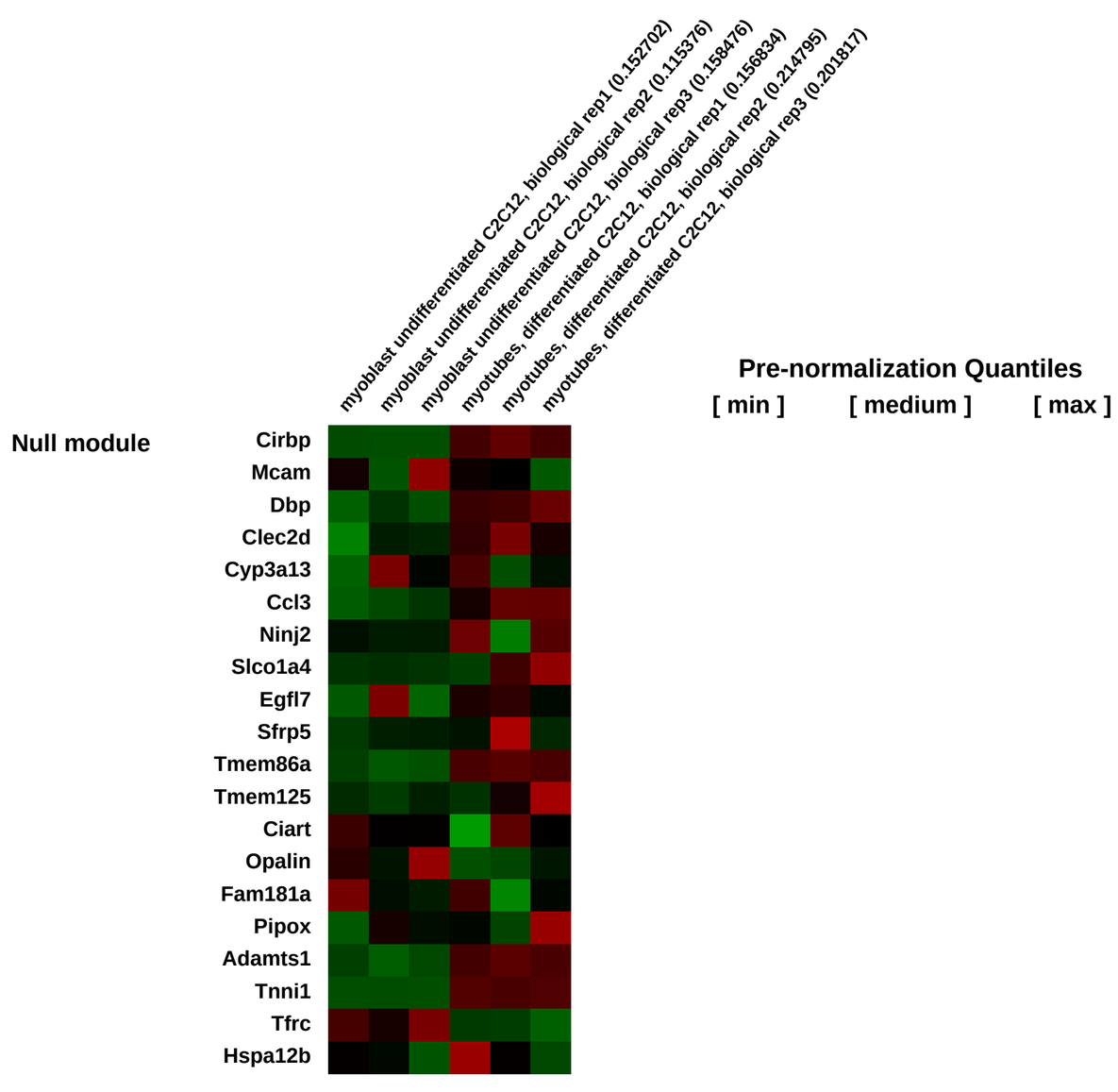

GEO Series "GSE12810" Expression Profiles

Num of samples in this series: 6

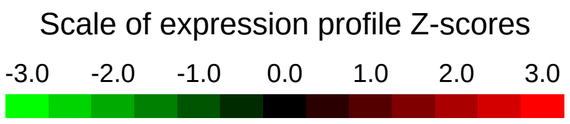

GEO Link:	http://www.ncbi.nlm.nih.gov/geo/query/acc.cgi?acc=GSE12810
Status:	Public on Sep 16 2009
Title:	Expression of Wnt Receptors in Adult Spiral Ganglion Neurons: Fzd 9 Located at Growth Cones of Regenerating Neurites
Organism:	Mus musculus
Experiment type:	Expression profiling by array
Platform:	GPL1261
Pubmed ID:	19716861
Summary & Design:	**Summary:** The fidelity of sound transmission by cochlear implants in patients with sensorineural hearing loss could be greatly improved by increasing the number of frequency channels. This could be achieved by stimulating and guiding neurite outgrowth to reduce the distance between the implant’s electrodes and the remnants of the spiral ganglion neurons. However, little is known about signaling pathways, besides those of neurotrophic factors, that are operational in the adult spiral ganglion. To systematically identify neuronal receptors for guidance cues in the adult cochlea, we conducted a genome-wide cDNA microarray screen with two-month-old CBA/CaJ mice. A meta-analysis of our data and those from older mice in two other studies revealed the presence of neuronal transmembrane receptors that represent all four established guidance pathwaysâ ephrin, netrin, semaphorin, and slitâ in the mature cochlea as late as 15 months. In addition, we observed the expression of all known receptors for the Wnt morphogens, whose neuronal guidance function has only recently been recognized. In situ hybridizations located the mRNAs of the Wnt receptors frizzled 1, 4, 6, 9, and 10 specifically in adult spiral ganglion neurons. Finally, frizzled 9 protein was found in the growth cones of adult spiral ganglion neurons that were regenerating neurites in culture. We conclude from our results that adult spiral ganglion neurons are poised to respond to neurite damage, owing to the constitutive expression of a large and diverse collection of guidance receptors. Wnt signaling, in particular, emerges as a candidate pathway for guiding neurite outgrowth towards a cochlear implant after sensorineural hearing loss. **Overall design:** GSE12810_Meta_GO_Eset_tTests.xls: Meta-analysis of neuronal transmembrane receptors in our study (GSE12810) and two previous studies by Someya and colleagues (GSE4786 & GSE4866) to estimate absolute expression levels in adult cochlea

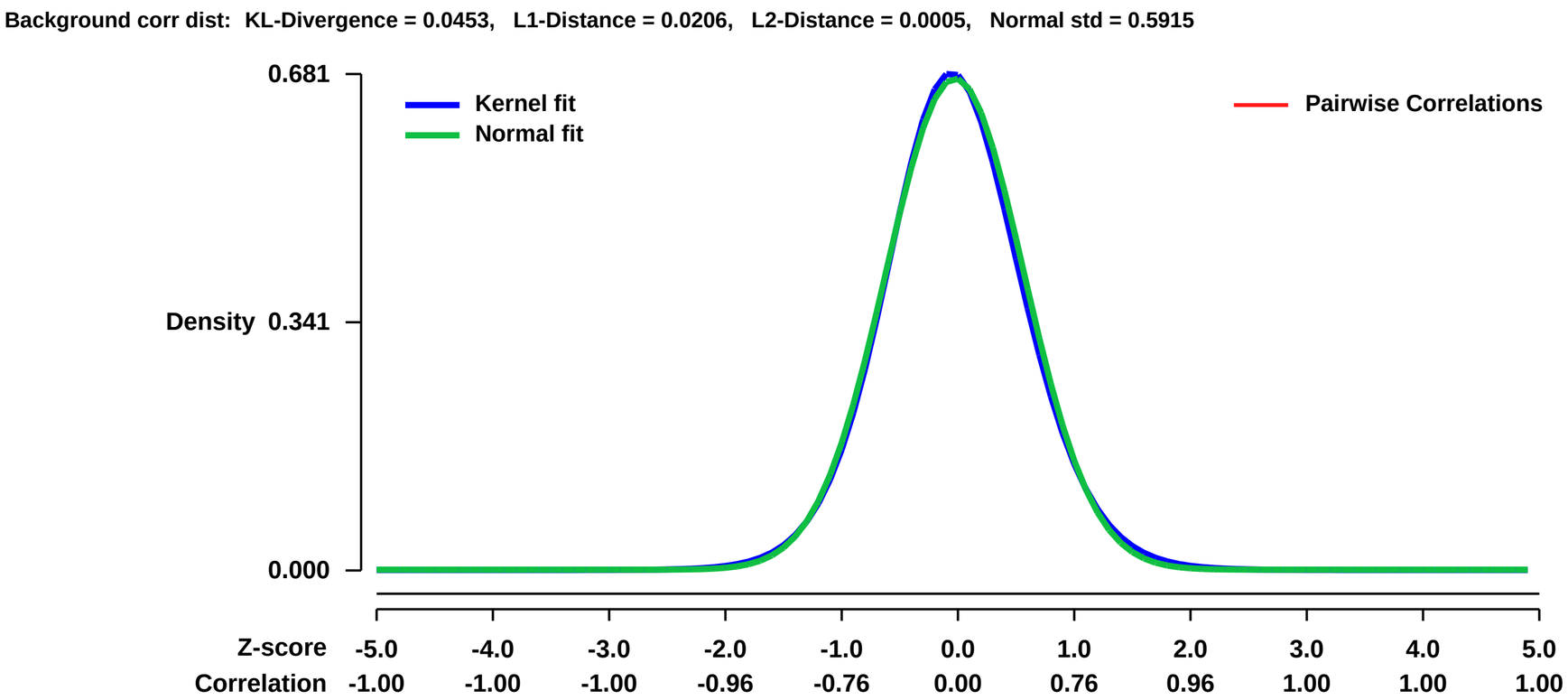

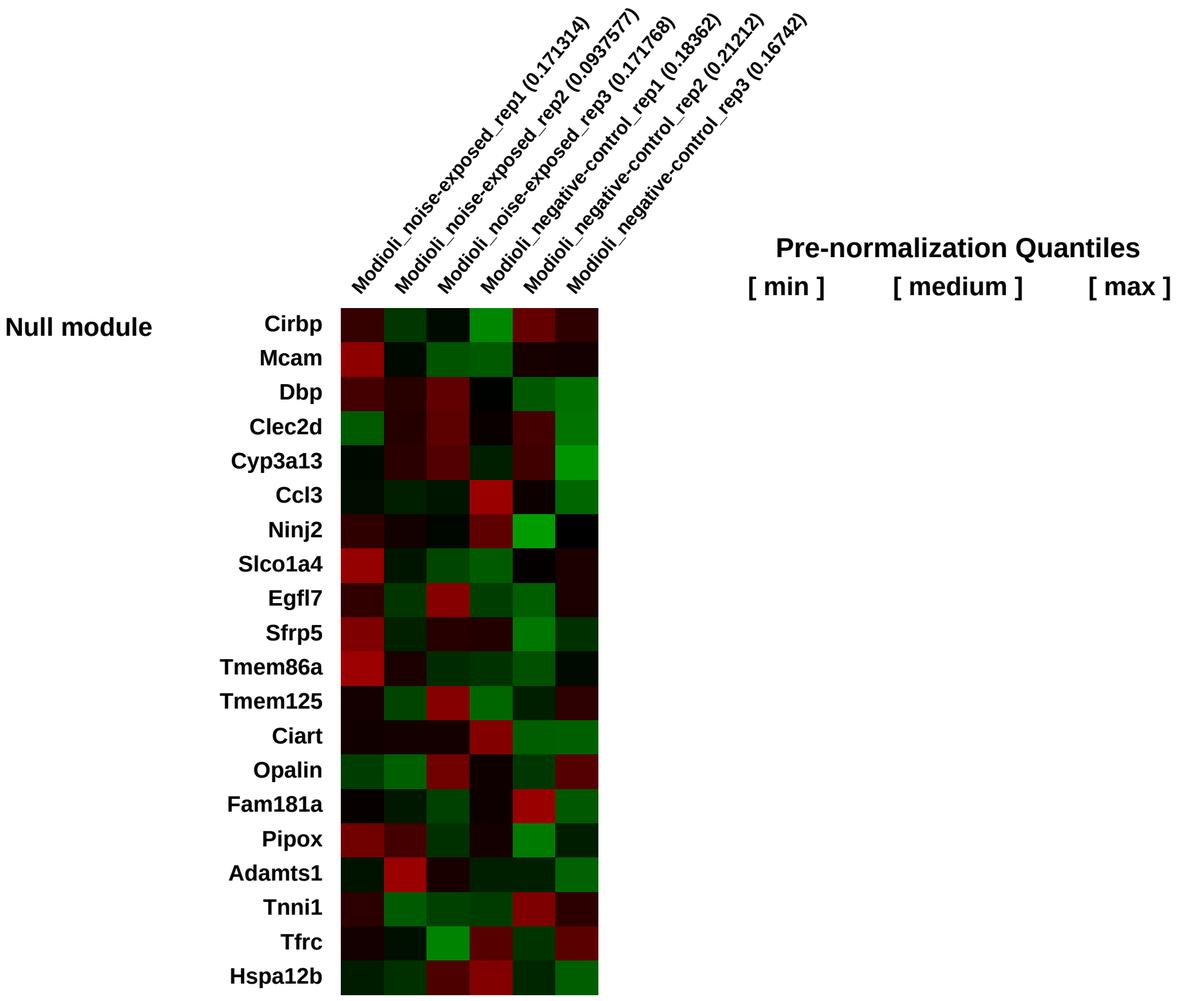

GEO Series "GSE7475" Expression Profiles

Num of samples in this series: 16

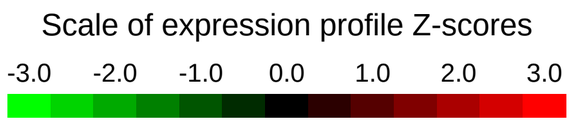

GEO Link:	http://www.ncbi.nlm.nih.gov/geo/query/acc.cgi?acc=GSE7475
Status:	Public on Jun 30 2007
Title:	Inflammatory response to titanium dioxide particles exposure is enhanced during pregnancy
Organism:	Mus musculus
Experiment type:	Expression profiling by array
Platform:	GPL1261
Pubmed ID:	17656681
Summary & Design:	**Summary:** **Rationale: Maternal immune responses can promote allergy development in offspring. Pilot data show that neonates of mother mice exposed during pregnancy to air pollution particles have increased allergic susceptibility. Objective: We investigated whether inflammatory response to titanium dioxide (TiO2) particles earlier considered immunologically â inertâ is enhanced during pregnancy. Methods: Pregnant BALB/c mice (or non-pregnant controls) received particle suspensions intranasally at day 14 of pregnancy. Lung inflammatory responses were evaluated 19 and 48 h after exposure. Results: Pregnant mice showed robust and persistent acute inflammatory responses after exposure to TiO2, while non-pregnant females had the expected minimal responses. Genomic profiling identified genes differentially expressed in pregnant lungs exposed to TiO2. Neonates of mothers exposed to TiO2 (but not PBS) developed increased susceptibility to allergens. Conclusion: Pregnancy enhances lung inflammatory responses to otherwise relatively innocuous inert particles.** **Keywords: Particles exposure, pregnancy vs normal** **Overall design:** **4 samples were analyzed in each of 4 groups: Normal PBS, Normal TiO2, Pregnant PBS and Pregnant TiO2, for a total of 16 samples.**

Background corr dist: KL-Divergence = 0.2293, L1-Distance = 0.0543, L2-Distance = 0.0071, Normal std = 0.3130

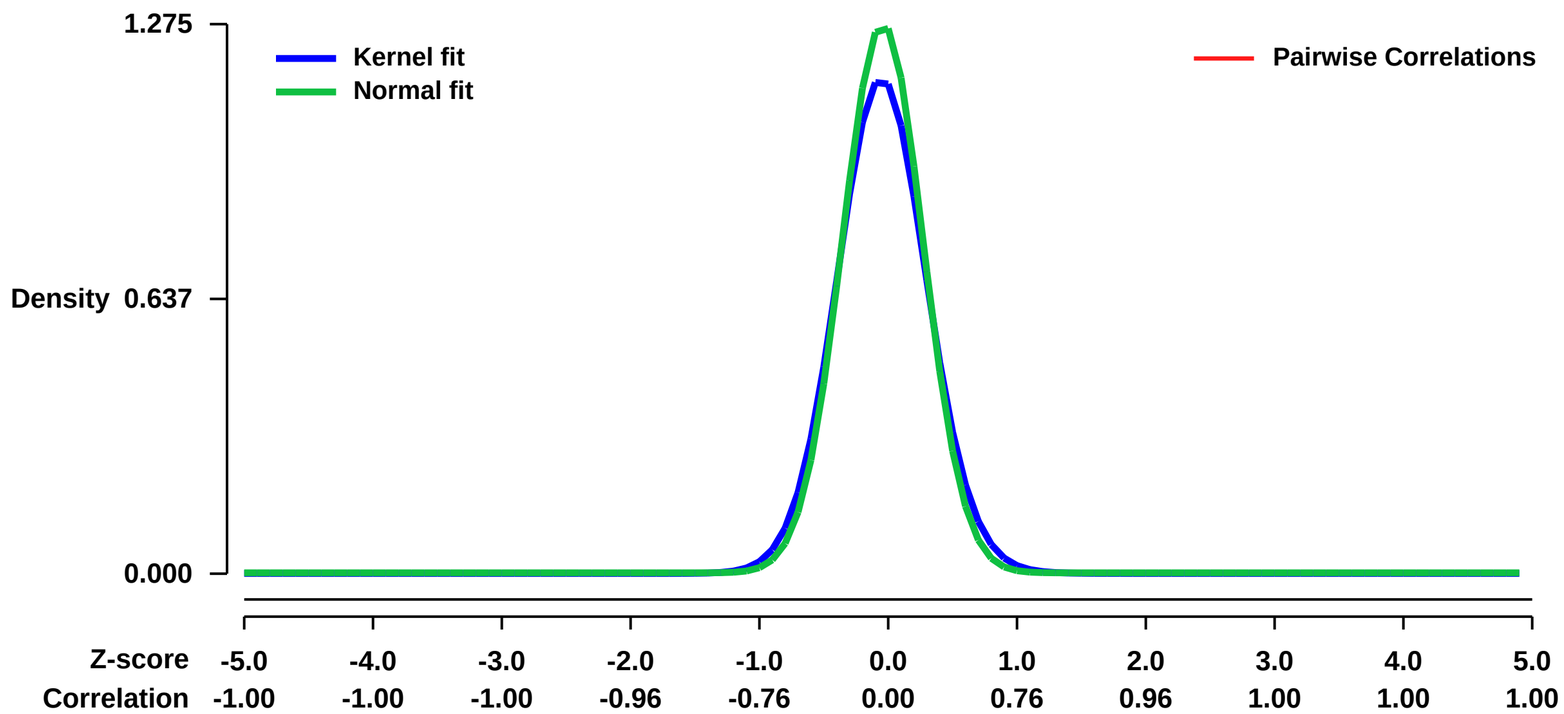

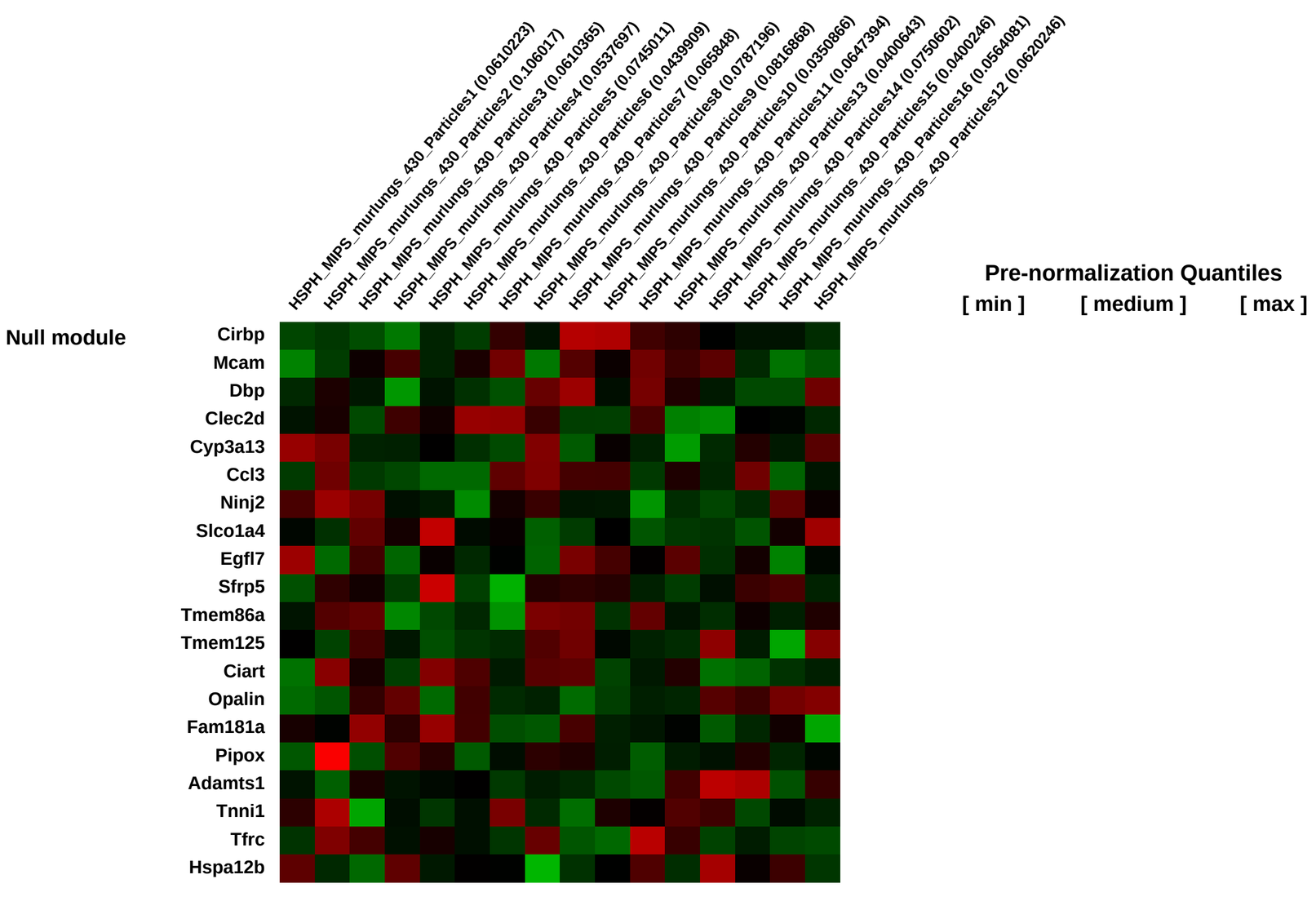

GEO Series "GSE26308" Expression Profiles

Num of samples in this series: 12

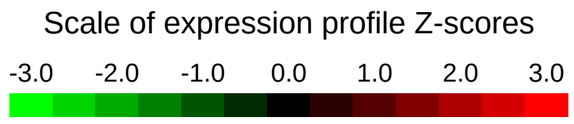

GEO Link:	http://www.ncbi.nlm.nih.gov/geo/query/acc.cgi?acc=GSE26308
Status:	Public on Mar 15 2012
Title:	Dissection of cancer cell and stromal cell-derived signals in melanoma xenografts following treatment with the stromal-targeting agent DMXAA
Organism:	Mus musculus
Experiment type:	Expression profiling by array
Platform:	GPL1261
Pubmed ID:	22415295
Summary & Design:	**Summary:** **5,6-Dimethylxanthenone-4-acetic acid (DMXAA), a tumor vascular disrupting agent, is shown here to have substantial activity as a single agent against human A375 melanoma xenografts in nude mice (94 % hemorrhagic necrosis after 24 h, and 26 days growth delay following single dose at 25 mg/kg). CD45+ cells in tumor tissue increased 5-fold over the first 3 days after treatment, which was due largely to an influx of CD11b+ Ly6G+ neutrophils. Using murine and human multiplex cytokine assays to dissect the cytokines produced by host stromal cells or by the melanoma cells, it was shown that both the stromal cells and the A375 melanoma cells produced cytokines capable of attracting neutrophils into the tumor. The same xenografts were also analyzed using human and mouse Affymetrix microarrays to separately identify tumor cell-specific (human) and stromal cell-specific (mouse) gene expression changes. DMXAA induced numerous stromal cytokine mRNAs, including IP-10, IL-6, MIP-1¸–/¸†, MIP-2, KC, RANTES, MIG, MCP-1 and IL-1¸†, many of which were also elevated at the protein level. Numerous human cytokine mRNAs were also induced including MCP-1, IL-8, GRO, VEGF, GM-CSF and IL-6, which again was in line with our protein data. Pathway analysis indicated that significant numbers of the stromal mRNAs induced by DMXAA are regulated downstream of TNF-¸–, interferon-¸† and NF¸”B. Our results suggest that DMXAA may have utility in combination therapy for human melanoma through the activation of pro-inflammatory signalling pathways and cytokine expression from both stromal and tumor cells, leading to haemorrhagic necrosis, neutrophil influx and growth inhibition.** **Overall design:** **Microarrays were used to identify separately the abundance of tumour cell and stromal cell RNA in A375 melanoma xenografts, with and without treatment by the stromal targetting drug DMXAA.**

Background corr dist: KL-Divergence = 0.0238, L1-Distance = 0.0471, L2-Distance = 0.0035, Normal std = 0.7420

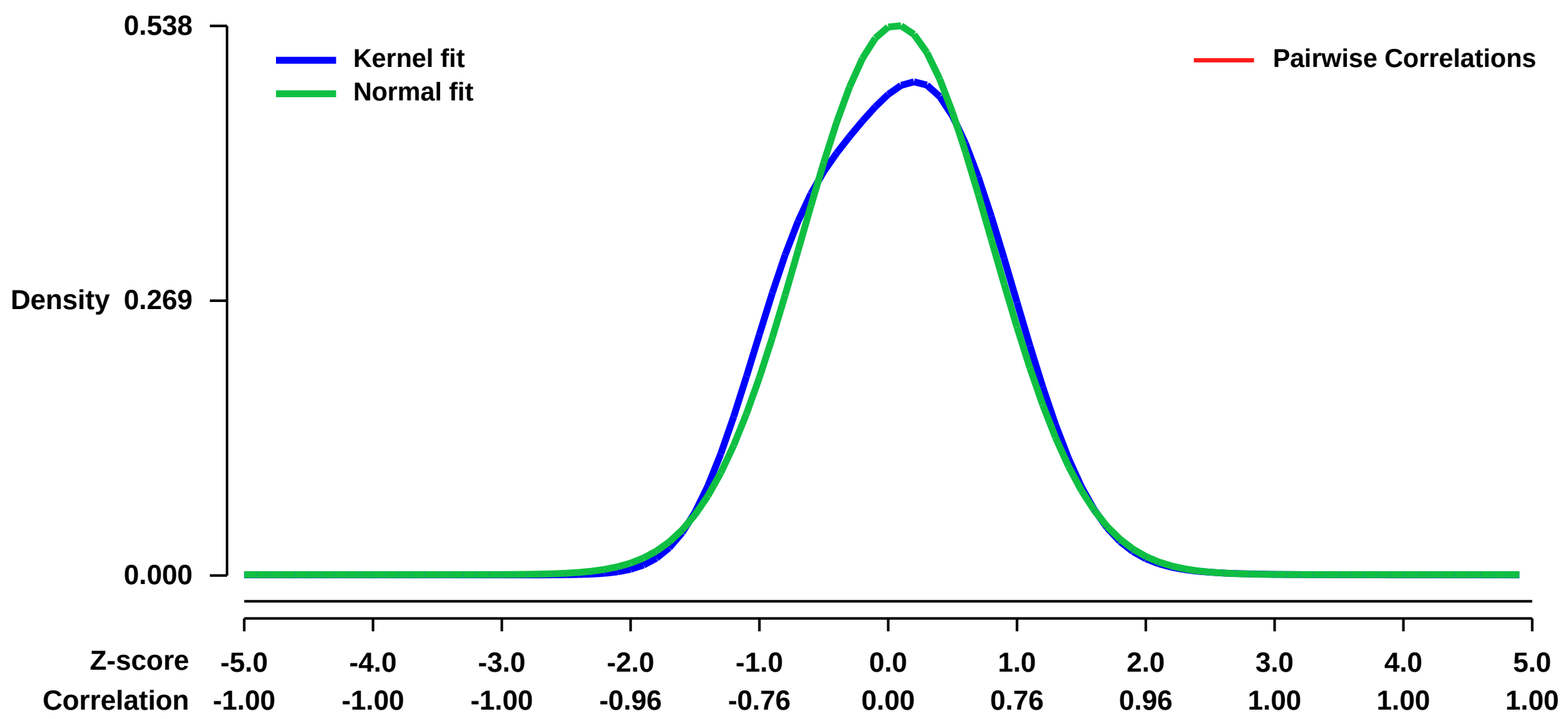

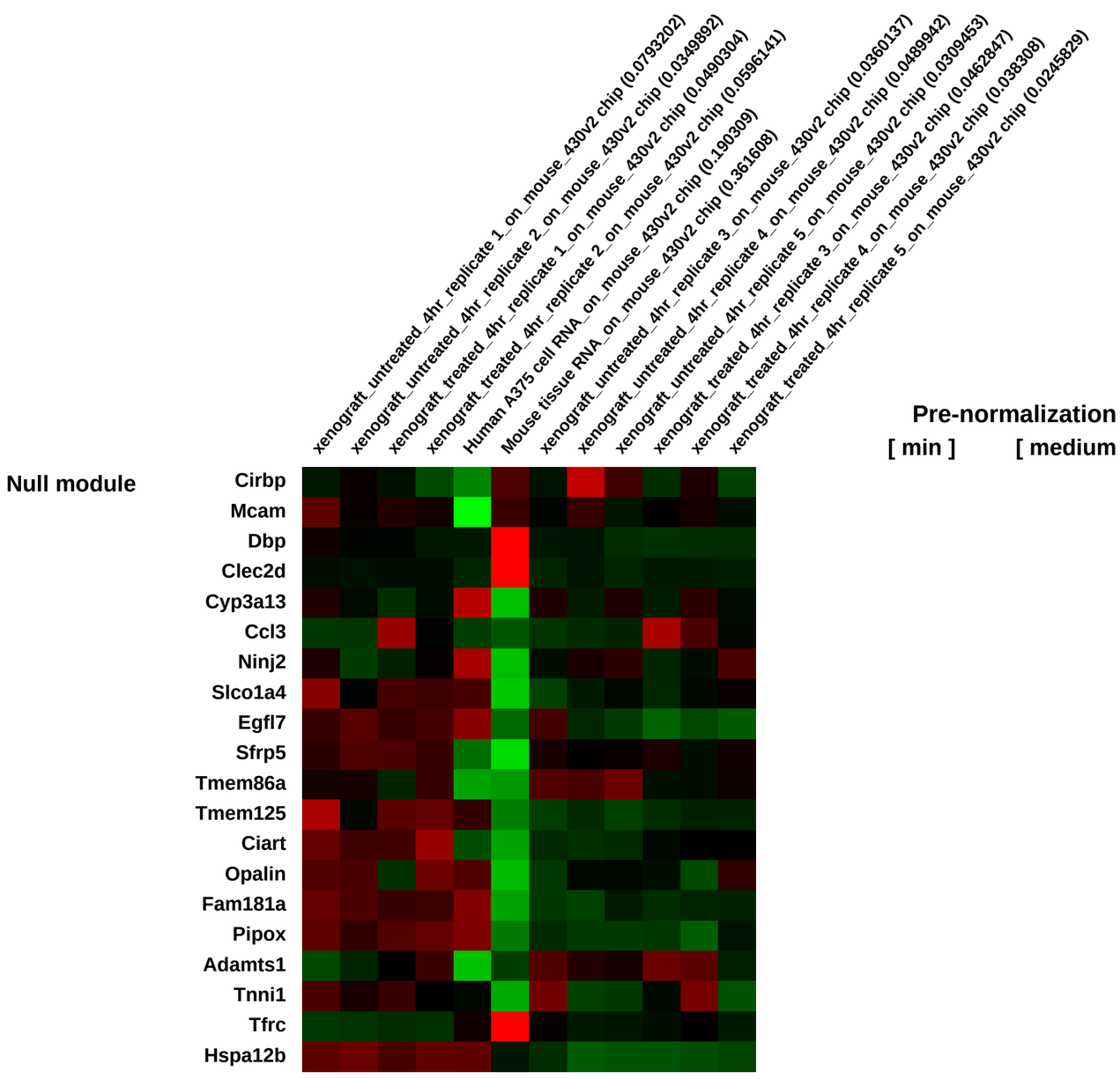

GEO Series "GSE28830" Expression Profiles

Num of samples in this series: 9

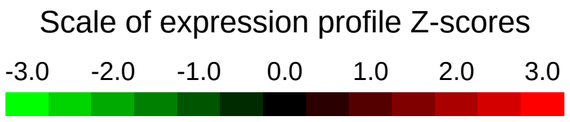

GEO Link:	**http://www.ncbi.nlm.nih.gov/geo/query/acc.cgi?acc=GSE28830**
Status:	**Public on Dec 01 2013**
Title:	**Differential gene expression in CD11b+ splenocytes from mice subject to social threat vs. control (II)**
Organism:	**Mus musculus**
Experiment type:	**Expression profiling by array**
Platform:	**GPL1261**
Pubmed ID:	
Summary & Design:	**Summary:** **Gene expression profiling was carried out on splenocyte mRNA samples collected from 6 animals subject to repeated social threat and 6 animals subject to non-threatening control conditions (pooled into 3 groups of 2). The primary research question is whether gene expression differs in CD11b+ splenocytes from animals exposed to social threat vs non-threatening control conditions.** **Keywords: Risk prediction** **Overall design:** **This study provides an additional body of data from the same general protocol used in Series GSE16661, and will support more extensive analyses than the original study.**

Background corr dist: **KL-Divergence = 0.0554, L1-Distance = 0.0377, L2-Distance = 0.0018, Normal std = 0.5796**

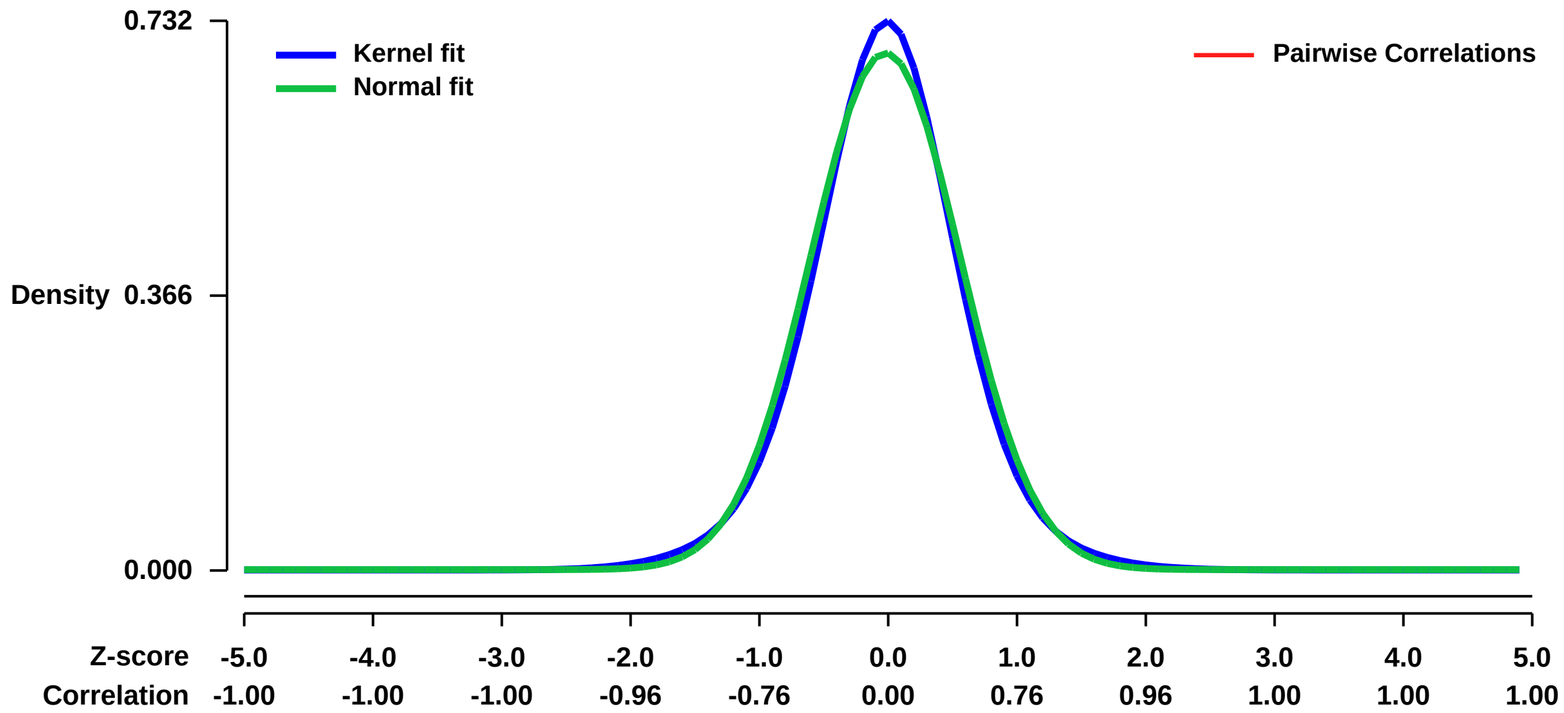

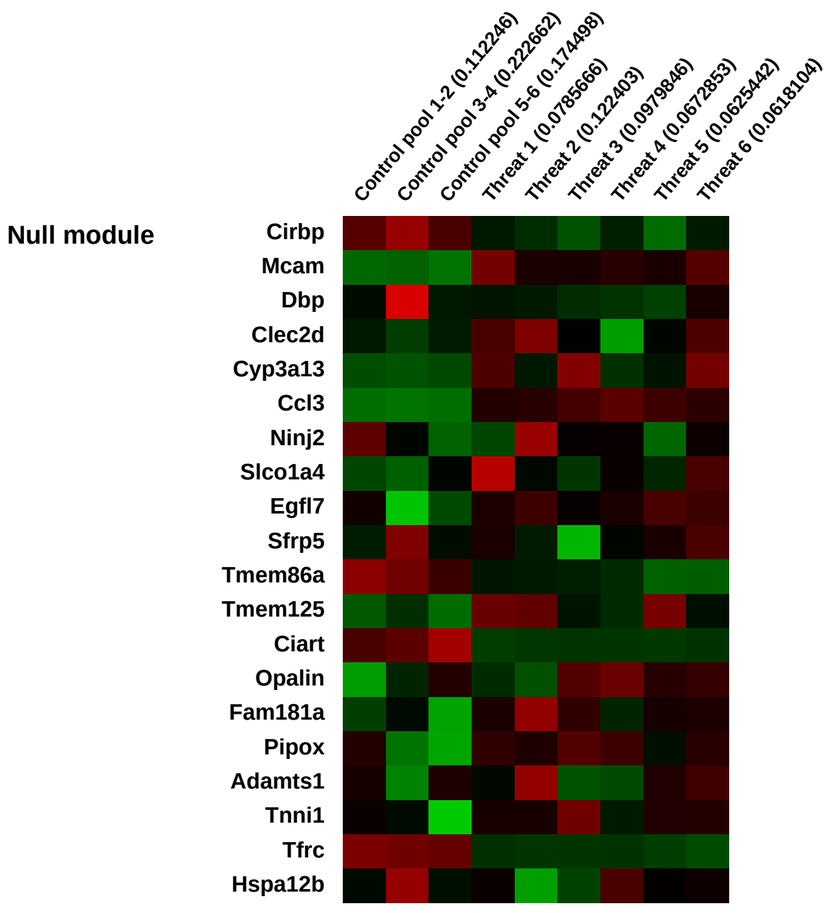

GEO Series "GSE16623" Expression Profiles

Num of samples in this series: 6

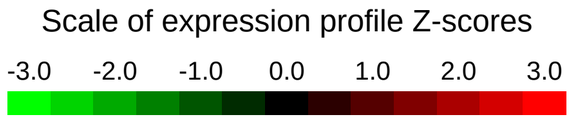

GEO Link:	http://www.ncbi.nlm.nih.gov/geo/query/acc.cgi?acc=GSE16623
Status:	Public on Apr 11 2010
Title:	Differential gene expression between ERRa KO and WT mouse kidneys
Organism:	Mus musculus
Experiment type:	Expression profiling by array
Platform:	GPL1261
Pubmed ID:	19901197
Summary & Design:	**Summary:** Estrogen-related receptor (ERR) alpha is an orphan nuclear receptor highly expressed in the kidneys. ERRalpha is implicated in renal sodium and potassium homeostasis and blood pressure regulation. We used microarray analysis to identify differentially expressed genes in ERR alpha knockout mice kidneys versus wild-type. The results provide insight on the roles of ERRalpha in the kidney. **Overall design:** Three biological replicates of WT and ERRaKO were performed, for a total of 6 samples. 2-3 month old males of each genotype were used.

Background corr dist: KL-Divergence = 0.0447, L1-Distance = 0.0165, L2-Distance = 0.0003, Normal std = 0.5914

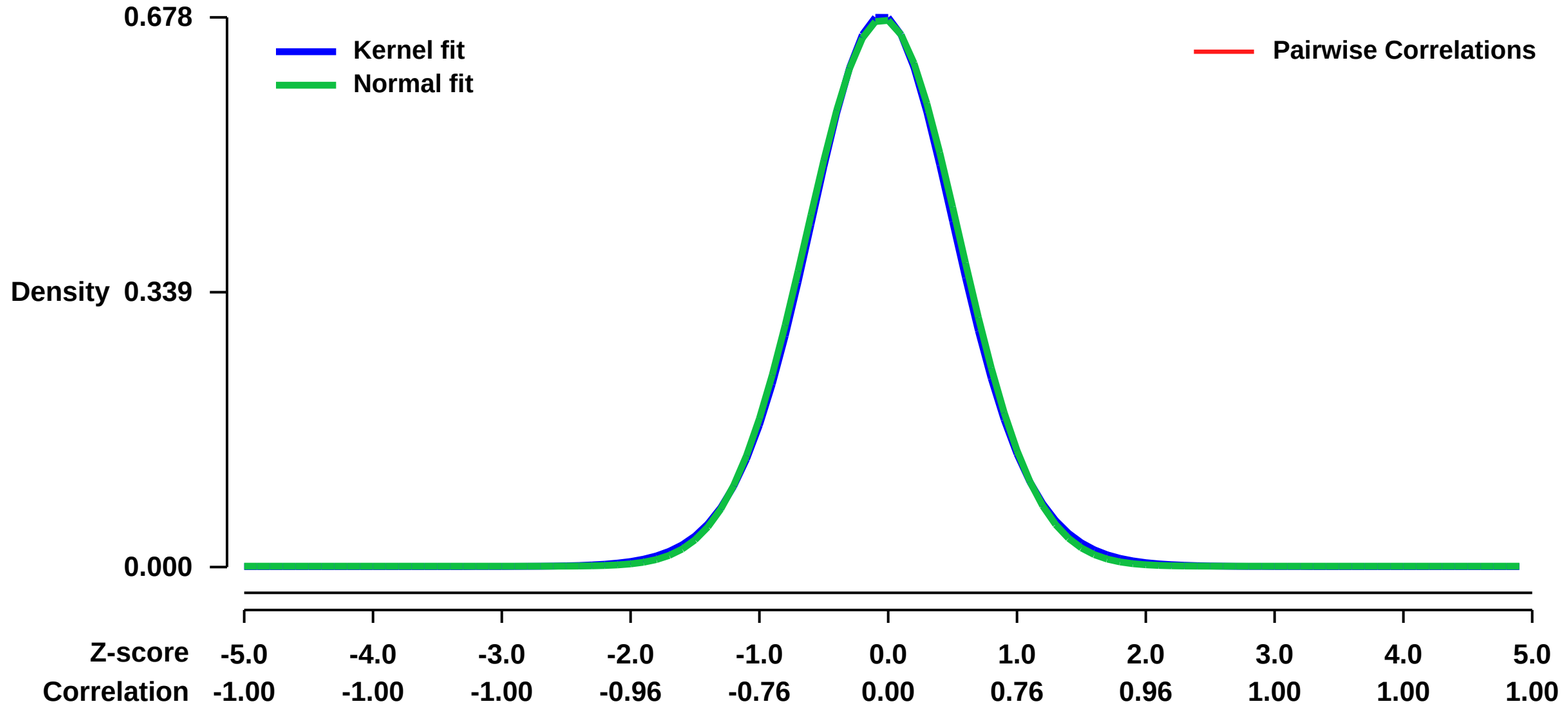

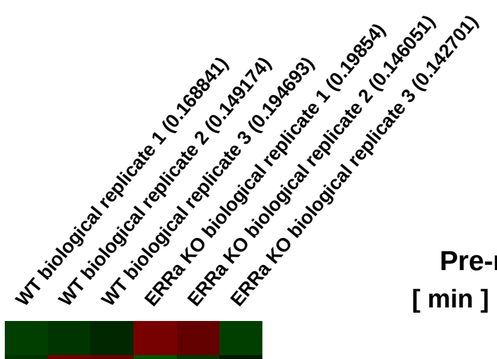

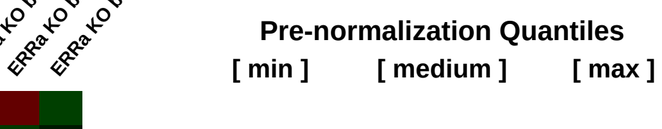

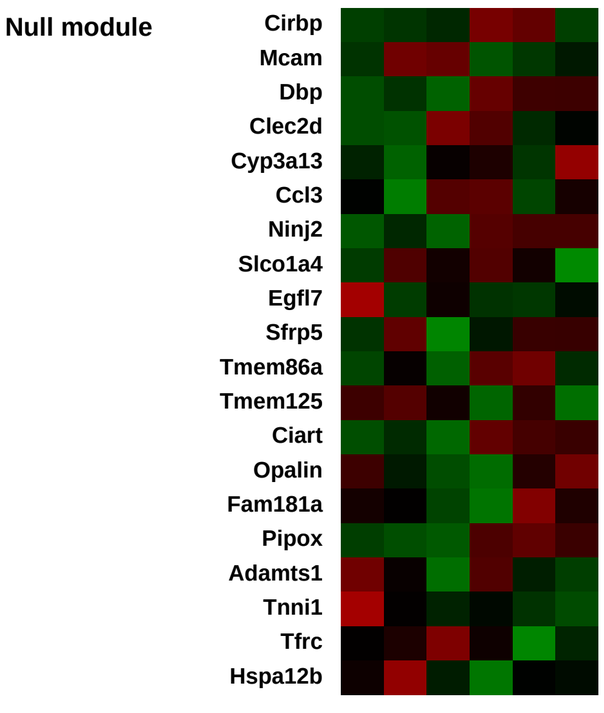

GEO Series "GSE30861" Expression Profiles

Num of samples in this series: 35

Scale of expression profile Z-scores

-3.0 -2.0 -1.0 0.0 1.0 2.0 3.0

GEO Link:	http://www.ncbi.nlm.nih.gov/geo/query/acc.cgi?acc=GSE30861
Status:	Public on Aug 01 2011
Title:	Pathways identified by toxicogenomics analysis reveal the size and dose independency of silica particles-induced toxicity in mice.
Organism:	Mus musculus
Experiment type:	Expression profiling by array
Platform:	GPL1261
Pubmed ID:	
Summary & Design:	**Summary:** Understanding the interactions of nanostructures with biological systems is essential to nanotoxicological research. Using a microarray-based toxicogenomics approach at early stage, this study investigated the relationship between particle size and toxicity of silica particles (SP) with diameters of 30, 70, and 300 nm (SP30, SP70, and SP300) as well as the mechanism of injury in mice. **Overall design:** Two experiments with SiO2 particles of different sizes were considered in mice. One was aimed to investigate the dose-response relationship of SP70 toxicity at a dose of 10, 20, or 40 mg/kg (experiment 1), and the other set to study the size-response relationship of SP-induced toxicity using SP30, SP70, or SP300 (experiment 2). In experiment 2, two dosages each of SP30, SP70, and SP300 were performed. One was 10 mg/kg at three particle sizes, and the other was toxic doses of the three particle sizes, i.e., 10 mg/kg for SP30, 40 mg/kg for SP70, and 200 mg/kg for SP300. The toxic doses of the three particle sizes of SP were decided on the basis of the results of histopathological examinations and serum biochemical analysis in our previous study.n = 5

Background corr dist: KL-Divergence = 0.3288, L1-Distance = 0.0438, L2-Distance = 0.0037, Normal std = 0.2739

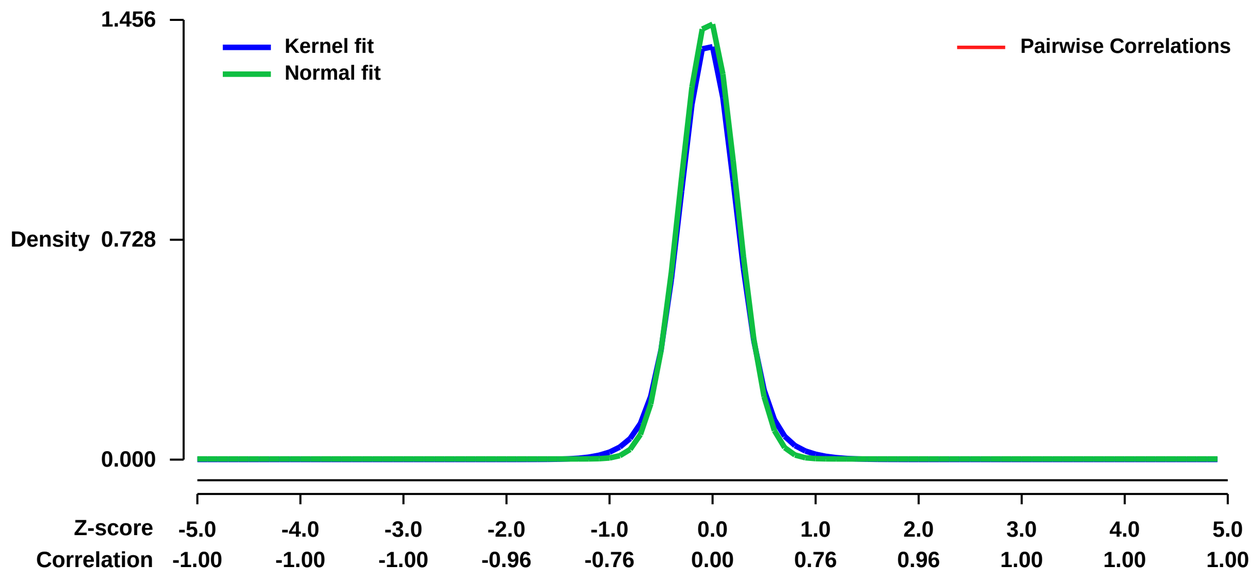

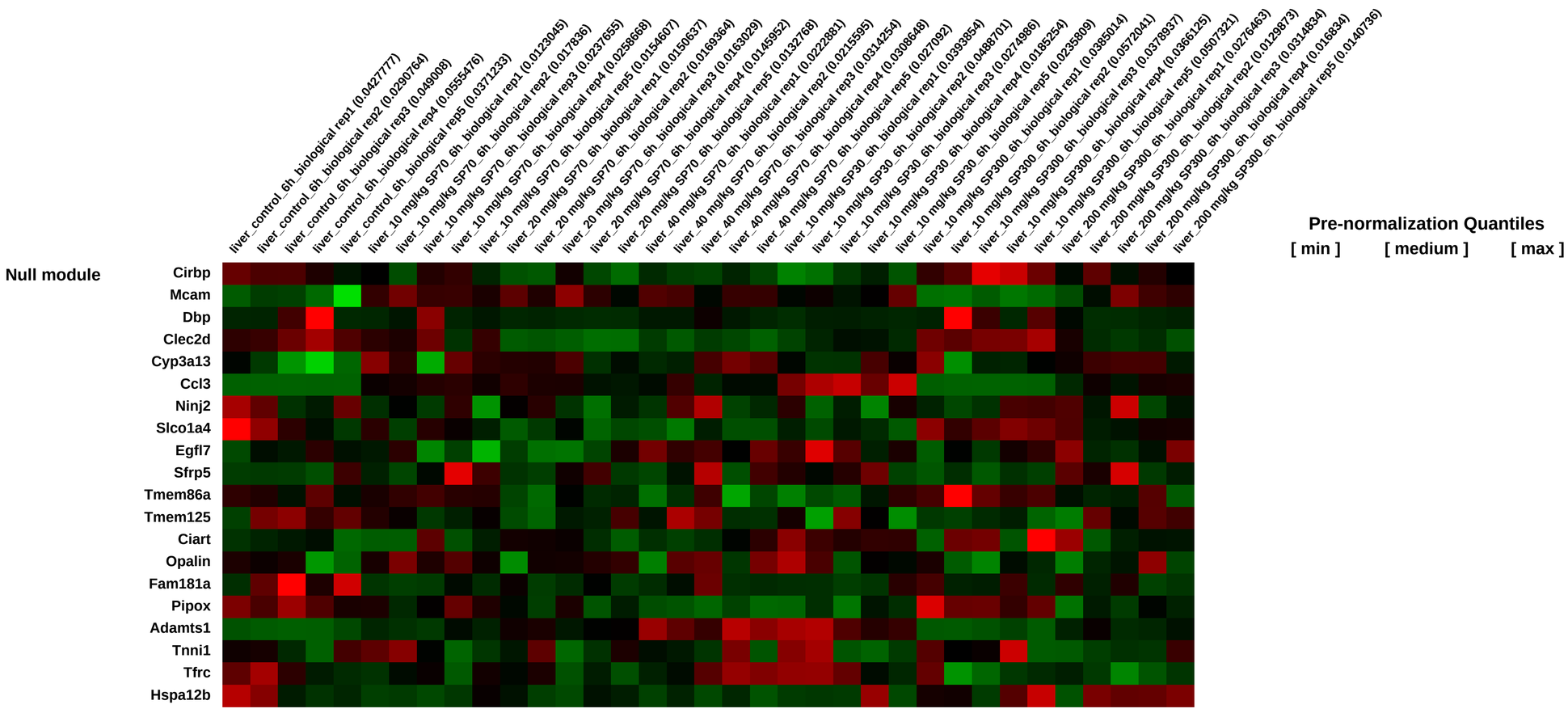

GEO Series "GSE19369" Expression Profiles

Num of samples in this series: 8

Scale of expression profile Z-scores

-3.0 -2.0 -1.0 0.0 1.0 2.0 3.0

GEO Link:	**http://www.ncbi.nlm.nih.gov/geo/query/acc.cgi?acc=GSE19369**
Status:	**Public on Sep 13 2010**
Title:	**Stimulatory effect of Echinacea purpurea extract on trafficking activity in mouse dendritic cells**
Organism:	**Mus musculus**
Experiment type:	**Expression profiling by array**
Platform:	**GPL1261**
Pubmed ID:	
Summary & Design:	**Summary:** **To seek scientific evidence supporting therapeutic use of Echinacea, the transcriptomic effects of Echinacea purpurea extract on mouse bone marrow-derived dendritic cells (BMDCs) were analyzed using primary cultures. Affymetrix DNA microarray and bioinformatics analyses of genes differentially expressed in DCs treated with [BF/S+L/Ep] for 4 or 12 h revealed that the majority of responsive genes were related to cell adhesion or motility (Cdh10, Itga6, Cdh1, Gja1 and Mmp8), or were chemokines (Cxcl2, Cxcl7) or signaling molecules (Nrxn1, Pkce and Acss1).** **Overall design:** **BMDCs from mice were treated with [BF/S+L/Ep] or DMSO for 4 h or 12 h in duplicates.**

Background corr dist: **KL-Divergence = 0.0782, L1-Distance = 0.0197, L2-Distance = 0.0006, Normal std = 0.4830**

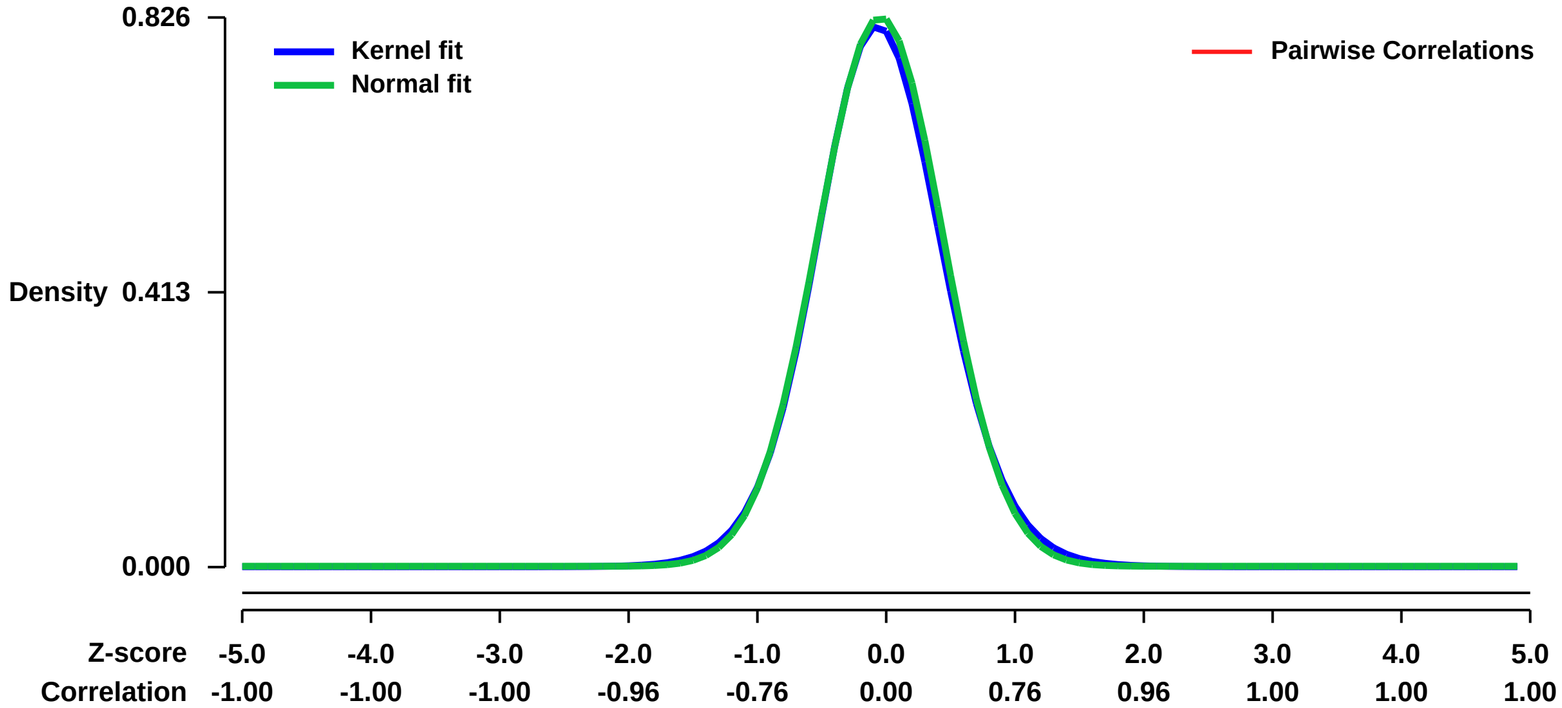

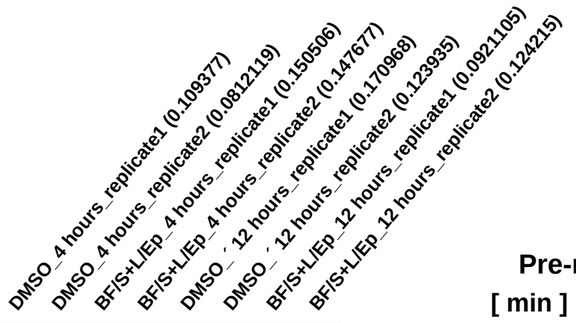

Pre-normalization Quantiles

[min] [medium] [max]

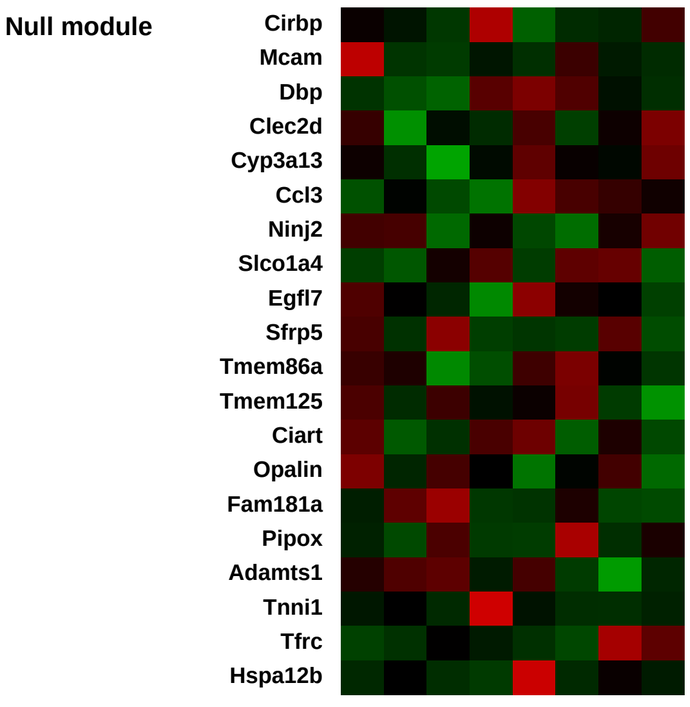

GEO Series "GSE25423" Expression Profiles

Num of samples in this series: 10

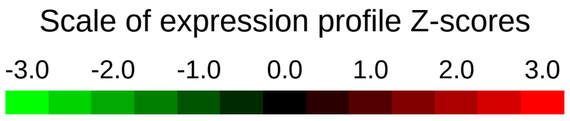

GEO Link:	http://www.ncbi.nlm.nih.gov/geo/query/acc.cgi?acc=GSE25423
Status:	Public on Dec 31 2013
Title:	LSD1 knockdown in 3T3-L1 preadipocytes
Organism:	Mus musculus
Experiment type:	Expression profiling by array
Platform:	GPL1261
Pubmed ID:	23595969
Summary & Design:	**Summary:** Obesity is often associated with a low-grade systemic inflammation state that contributes to the development of insulin resistance and atherosclerotic complications. This is usually coupled with increased macrophage infiltration in the adipose tissue and a defect in adipocyte differentiation that results in accumulation of hypertrophic fat cells characterized by a deregulated pattern of adipokine expression. Here we show that knockdown of histone demethylase lsd1 in 3T3-L1 preadipocytes results in defective adipogenesis and derepression of an inflammatory program in these cells. **Overall design:** The 24h sample groups (siC.24h and siLsd1.24h) consist of two biological replicate samples; the 48h sample groups (siC.48h and siLsd1.48h) consist of three biological replicate samples. Each sample was hybridized to a separate array, for a total of ten arrays.

Background corr dist: KL-Divergence = 0.0685, L1-Distance = 0.0356, L2-Distance = 0.0017, Normal std = 0.5250

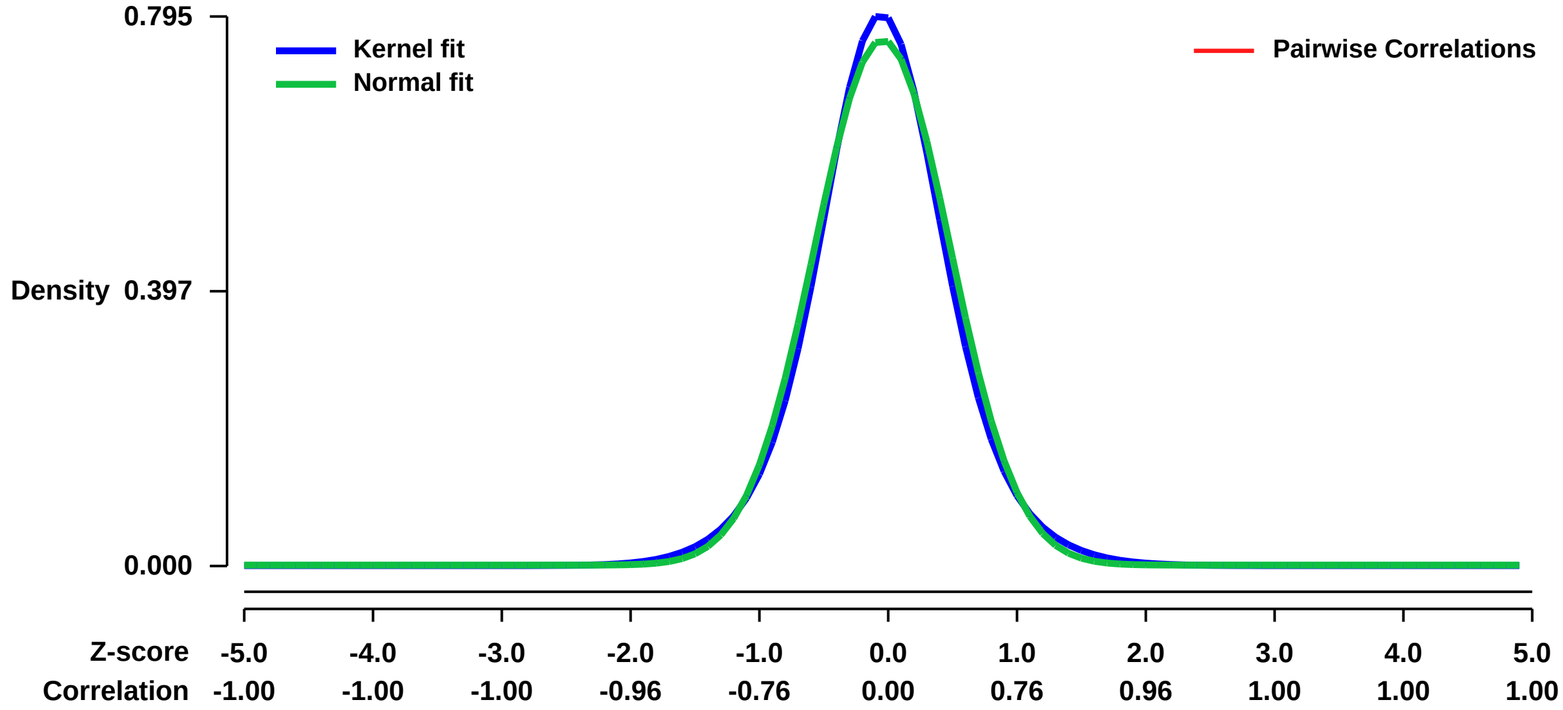

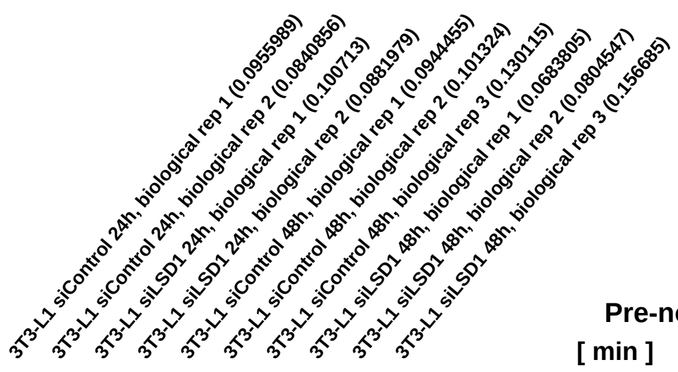

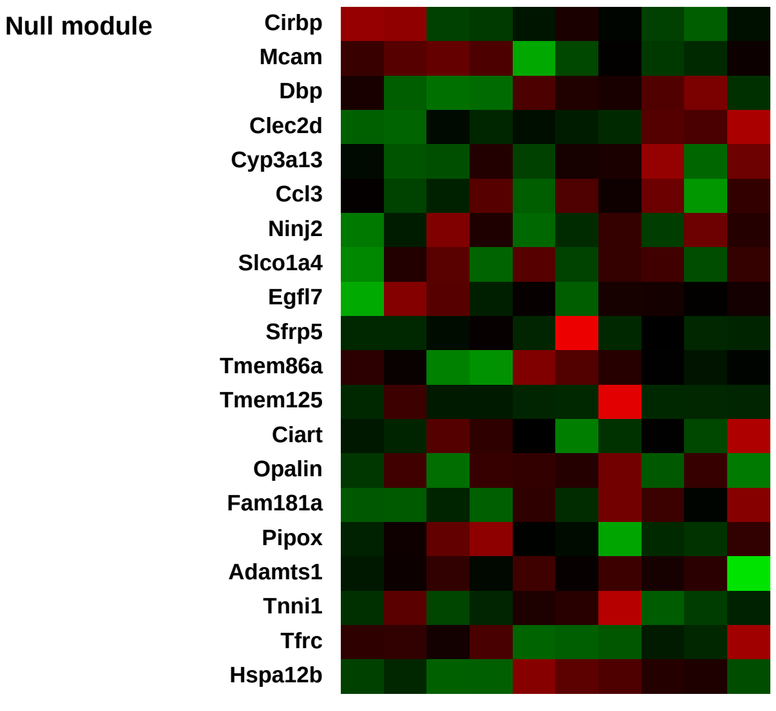

GEO Series "GSE11147" Expression Profiles

Num of samples in this series: 6

Scale of expression profile Z-scores

-3.0 -2.0 -1.0 0.0 1.0 2.0 3.0

GEO Link:	http://www.ncbi.nlm.nih.gov/geo/query/acc.cgi?acc=GSE11147
Status:	Public on Apr 12 2008
Title:	Hippocampus of HuD overexpressor mice (perro-affy-mouse-309741)
Organism:	Mus musculus
Experiment type:	Expression profiling by array
Platform:	GPL1261
Pubmed ID:	
Summary & Design:	**Summary:** Post-transcriptional mechanisms play an important role in the control of gene expression. RNA-binding proteins are key players in the post-transcriptional control of many neural genes and they participate in multiple processes, from RNA splicing and mRNA transport to mRNA stability and translation. Our laboratory has developed the first mouse model overexpressing a RNA-binding protein, the ELAV-like protein HuD, in the CNS under the control of the CaMKinII alpha promoter. Initial behavioral characterization of the mice revealed that they had significant learning deficits together with abnormalities in prepulse inhibition (PPI). At the molecular level, we found that the expression of the growth-associated protein GAP-43, one of the targets of HuD, was increased in the hippocampus of HuD transgenic mice. To characterize these mice further and to evaluate the utility of these animals in understanding human diseases, we propose to use DNA microarray methods. To characterize the pattern of gene expression in the hippocampus of HuD overexpressor mice Based on the behavioral and molecular properties of our HuD transgenic mice we hypothesize that these animals may be good models for the studying the basis of learning disabilities and of diseases that show deficits in PPI such as fetal alcohol syndrome and schizophrenia. All mice are in C57BL/6 background and are male approximately 30 days old. Animals are bred and sacrificed according to our approved animal protocol. Brains will be rapidly dissected on ice, quickly frozen and stored at -80C until analysis. Frozen brains will be embedded in OCT and shipped to the DNA microarray facility at Duke University where LCM was performed. Dentate granule cells from control and HuD transgenic mice will be isolated by Susan Su, who will also perform RNA isolation and the first round of RNA amplification. For our first experiment, we want to examine the pattern of gene expression in the hippocampus of 2 transgenic mice and 2 non-transgenic littermates. Keywords: HuD, hippocampus Overall design:

Background corr dist: KL-Divergence = 0.0495, L1-Distance = 0.0217, L2-Distance = 0.0005, Normal std = 0.5777

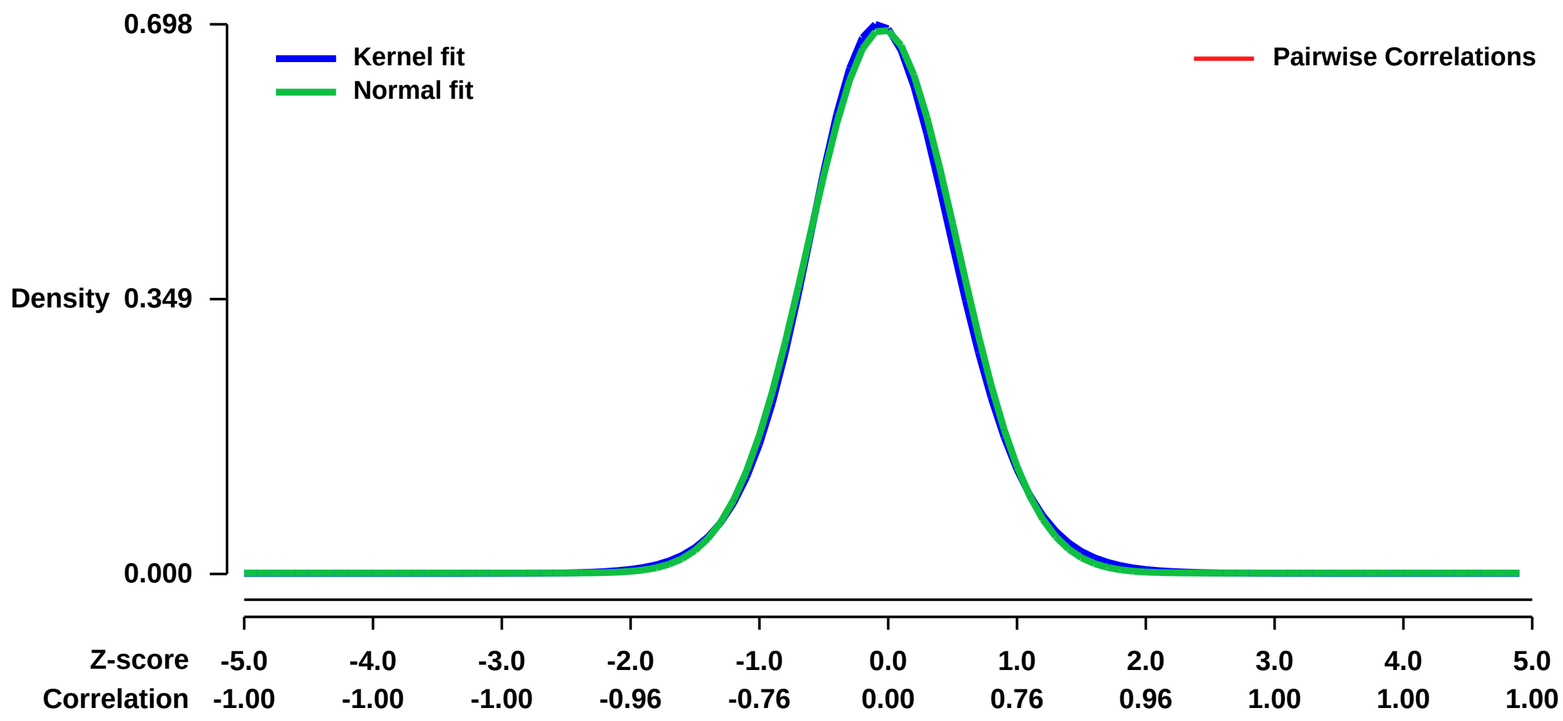

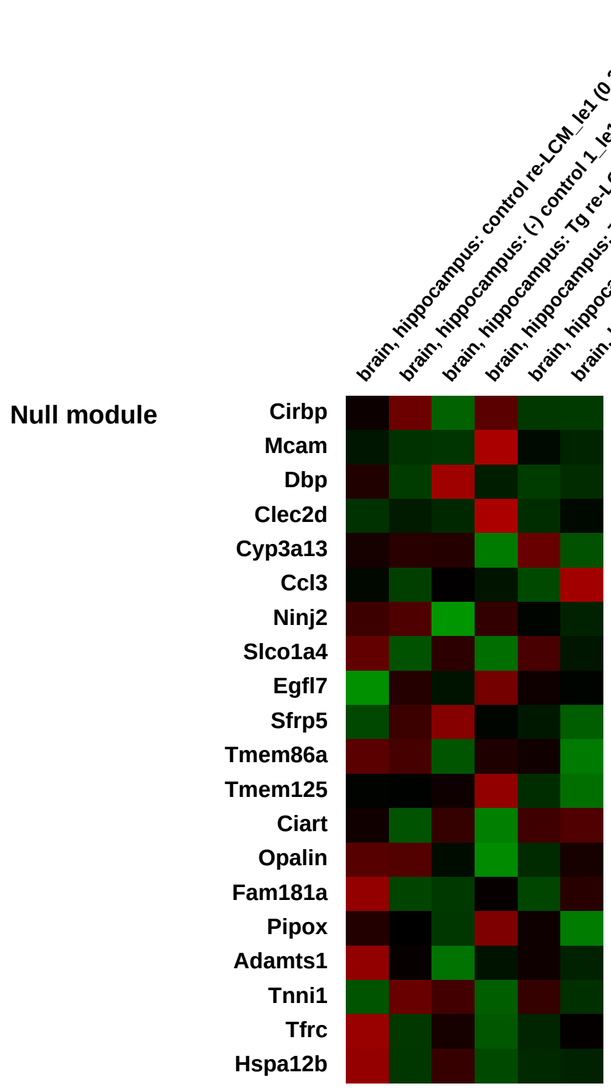

GEO Series "GSE30503" Expression Profiles

Num of samples in this series: 23

Scale of expression profile Z-scores

-3.0 -2.0 -1.0 0.0 1.0 2.0 3.0

GEO Link:	http://www.ncbi.nlm.nih.gov/geo/query/acc.cgi?acc=GSE30503
Status:	Public on May 10 2012
Title:	Integrin alpha-6 (CD49f) defines a novel and distinct subset of CD4+ regulatory T cells with potent suppression activity.
Organism:	Mus musculus
Experiment type:	Expression profiling by array
Platform:	GPL1261
Pubmed ID:	
Summary & Design:	**Summary:** A common method used both in vitro and in vivo, to identify Tregs in CD4+ T cells is through the characterization of surface marker CD25. Although CD25 expression is well correlated with regulatory activity in vitro, CD4+CD25+ T cells are not the only regulatory CD4+ T cells in vivo. Studies suggest that in many situations, CD4+CD25â T cells are as effective as CD4+CD25+ T cells in controlling T cell mediated disease. Therefore, CD25 is not a uniquely specific cell surface marker for the identification of Tregs. CD49f is an ¸–6-integrin subunit which dimerizes with either the ¸†1 or ¸†4 subunit to form receptors for various laminin isoforms. We found that CD4+ T cells from NOD mice express CD49f, and old non-diabetic NOD mice had an increase of CD4+CD49f+ T cells in the spleen and peripheral lymph node when compared to both young and diabetic mice. This study was conducted to further characterize CD4+CD49f+ Treg cell subpopulation in NOD mice. It was found that CD4+CD49f+T cells possess suppressive ability and only one third of CD4+CD49f+ T cells expressing CD25. Based on the expression of CD49f and CD25, CD4+ T cells was divided into four populations , CD25+CD49f+ ,CD25+CD49f- ,CD25-CD49f+ but CD25-CD49f- are of suppressive ability, and we further found that Foxp3 expression was highly correlated with the suppressive ability of these three Treg populations. In conclusion our data indicate that CD49f marks a CD4+ CD25+ Treg subset with more potent suppression activity and identifies a CD25-CD4+ T cell population with suppression function in a Foxp3+ expression dependent manner. **Overall design:** We divided CD4+ T cells into four populations: CD25+CD49f+, CD25+CD49f-, CD25-CD49f+, CD25-CD49f-; Microarray technology was used to determine gene expression differences among these four groups.

Background corr dist: KL-Divergence = 0.0996, L1-Distance = 0.0482, L2-Distance = 0.0053, Normal std = 0.4363

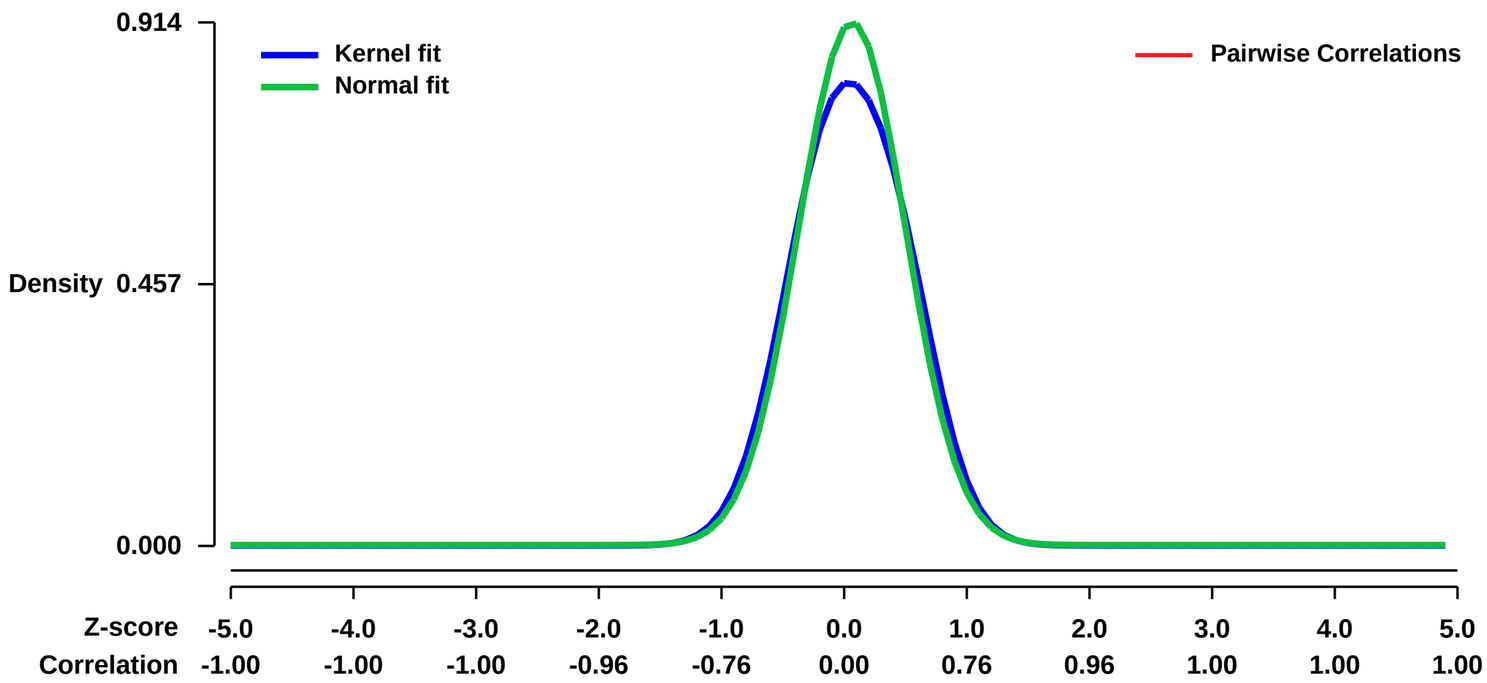

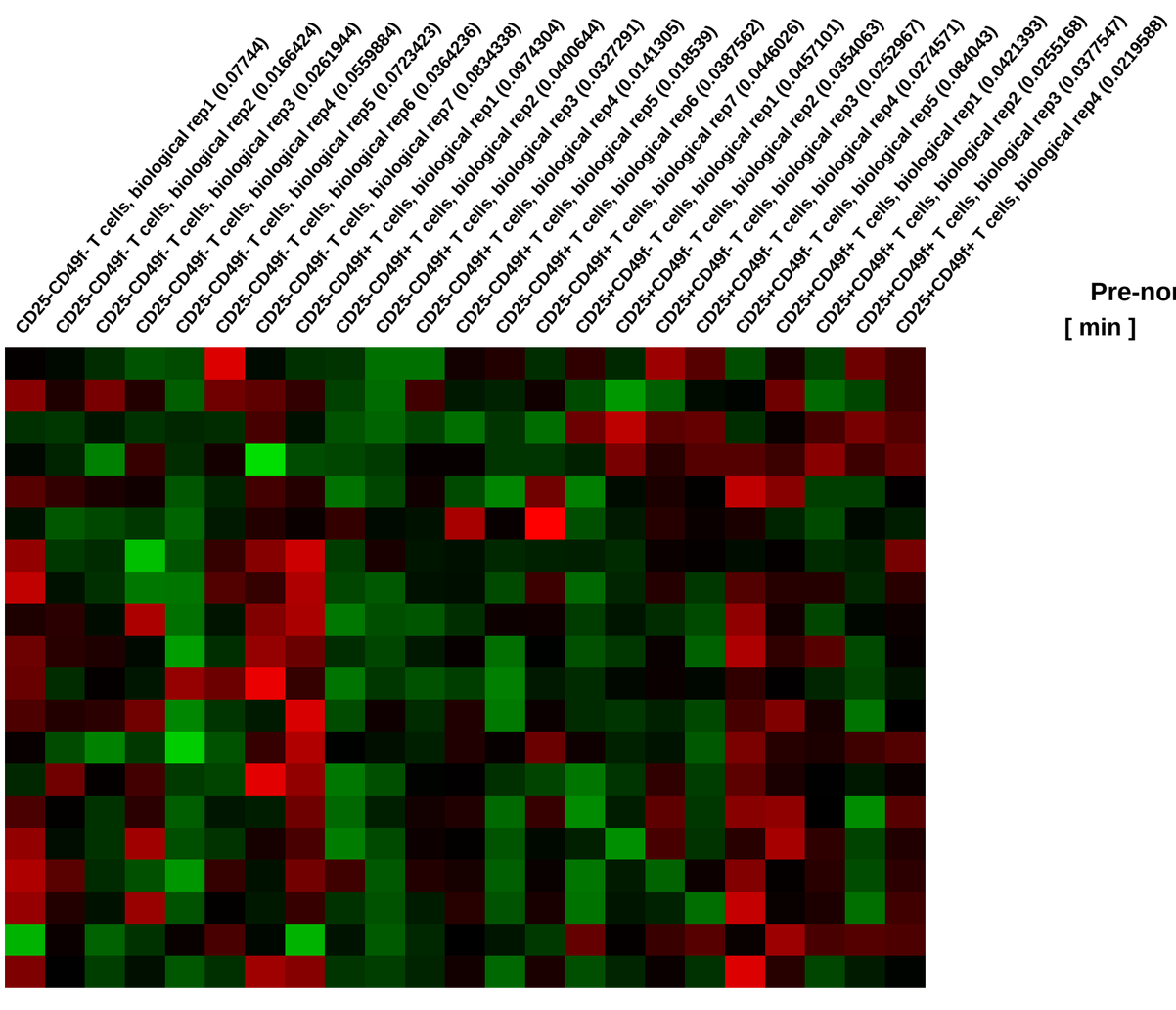

GEO Series "GSE55705" Expression Profiles

Num of samples in this series: 10

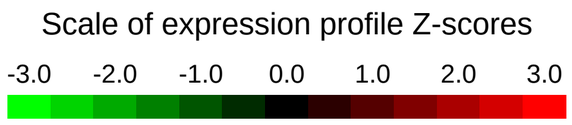

GEO Link:	**http://www.ncbi.nlm.nih.gov/geo/query/acc.cgi?acc=GSE55705**
Status:	**Public on Apr 12 2014**
Title:	**Inflammation induced repression of Foxp3-bound chromatin in regulatory T cells [microarray]**
Organism:	**Mus musculus**
Experiment type:	**Expression profiling by array**
Platform:	**GPL1261**
Pubmed ID:	
Summary & Design:	**Summary:** **The transcription factor Foxp3 is indispensable for the ability of regulatory T (Treg) cells to suppress fatal inflammation. Here, we characterized the role of Foxp3 in chromatin remodeling and regulation of gene expression in actively suppressing Treg cells in an inflammatory setting. Although genome-wide Foxp3 occupancy of DNA regulatory elements was similar in resting and in vivo activated Treg cells, Foxp3-bound enhancers were poised for repression only in activated Treg cells. Following activation, Foxp3-bound sites showed reduced chromatin accessibility and selective H3K27 tri-methylation, which was associated with Ezh2 recruitment and downregulation of nearby gene expression. Thus, Foxp3 poises its targets for repression by facilitating formation of repressive chromatin in regulatory T cells upon their activation in response to inflammatory cues.** **The supplementary file GSE55705_dt_expr.txt is a matrix for Treg expression data from platform GPL1261 that includes co-normalized data from GSE40685.** **Overall design:** **array expression**

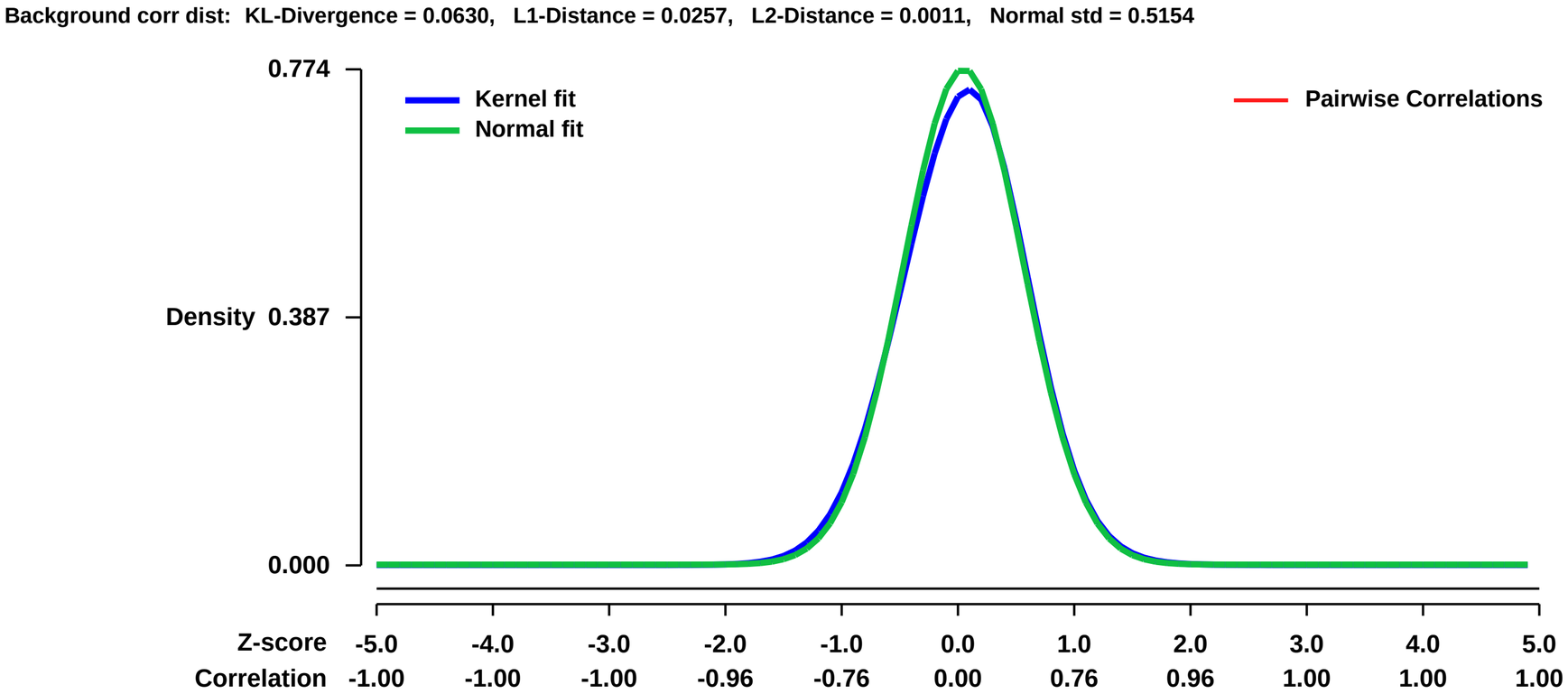

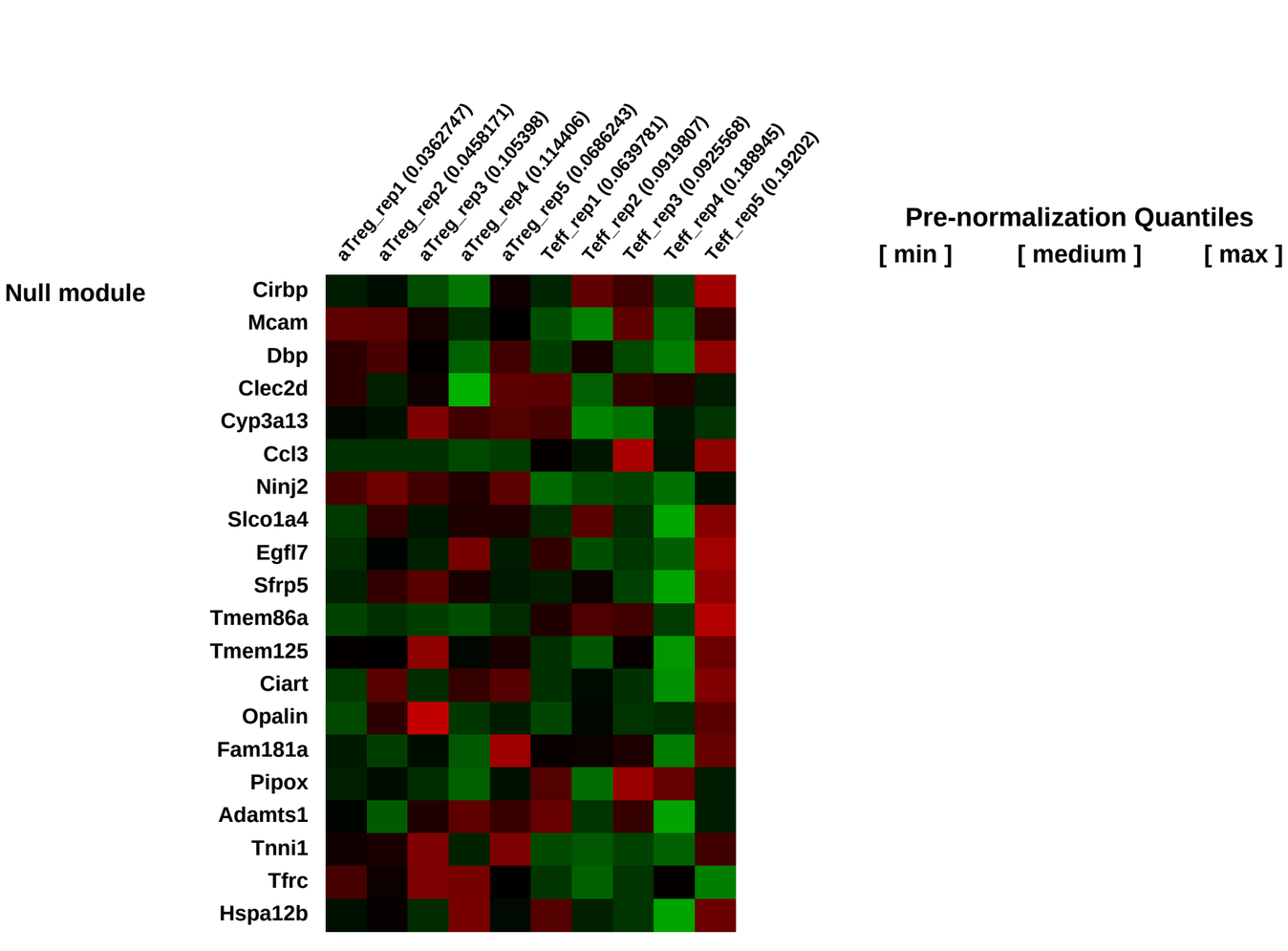

GEO Series "GSE29766" Expression Profiles

Num of samples in this series: 40

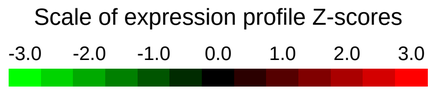

GEO Link:	http://www.ncbi.nlm.nih.gov/geo/query/acc.cgi?acc=GSE29766
Status:	Public on Jul 15 2011
Title:	Developmental profiling of spiral ganglion neurons reveals insights into auditory circuit assembly
Organism:	Mus musculus
Experiment type:	Expression profiling by array
Platform:	GPL1261
Pubmed ID:	21795542
Summary & Design:	**Summary:** The sense of hearing depends on the faithful transmission of sound information from the ear to the brain by spiral ganglion (SG) neurons. However, how SG neurons develop the connections and properties that underlie auditory processing is largely unknown. We catalogued gene expression in mouse SG neurons at six developmental stages, ranging from embryonic day 12 (E12), when SG neurons first extend projections, up until postnatal day 15 (P15), after the onset of hearing. For comparison, we also analyzed the closely-related vestibular ganglion (VG) at the same time points. **Overall design:** To identify genes involved in SG axon guidance and branching, target selection, synaptogenesis, synaptic refinement, and synaptic function, we collected SG at E12 and E13, E16, P0, P6, and P15. We also collected VG at the same time points. For E12 and E13 time points, SG and VG were microdissected from Rnx-cre; Z/EG embryos, which express GFP in the VG. E16-P15 VG was also isolated by microdissection from Rnx-cre; Z/EG animals. E16-P15 SG neurons were isolated by FACS sorting dissociated cochlea from Mafb-GFP animals.

Background corr dist: KL-Divergence = 0.1581, L1-Distance = 0.0337, L2-Distance = 0.0023, Normal std = 0.3675

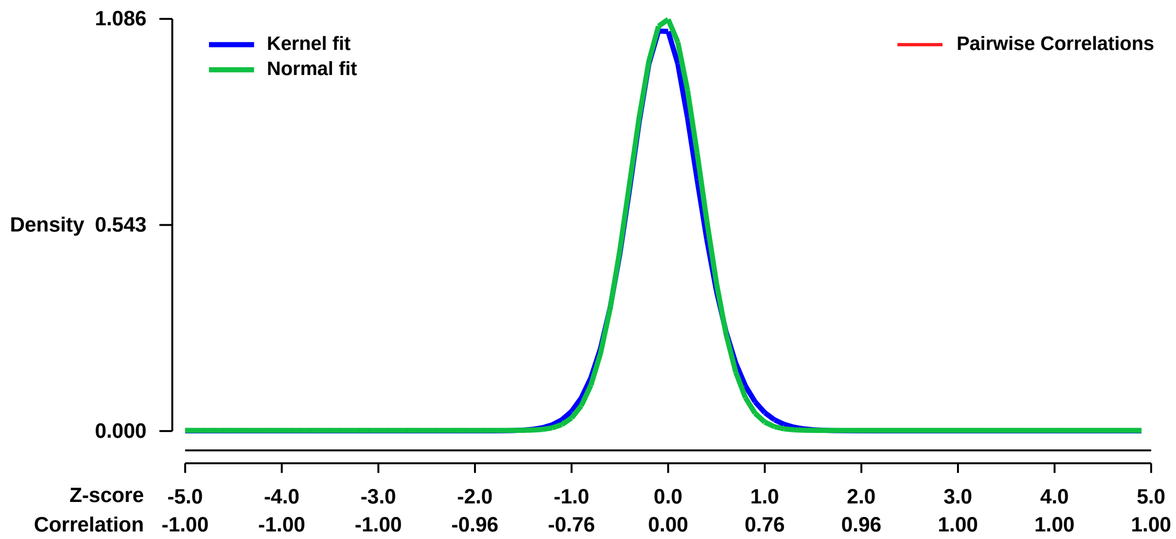

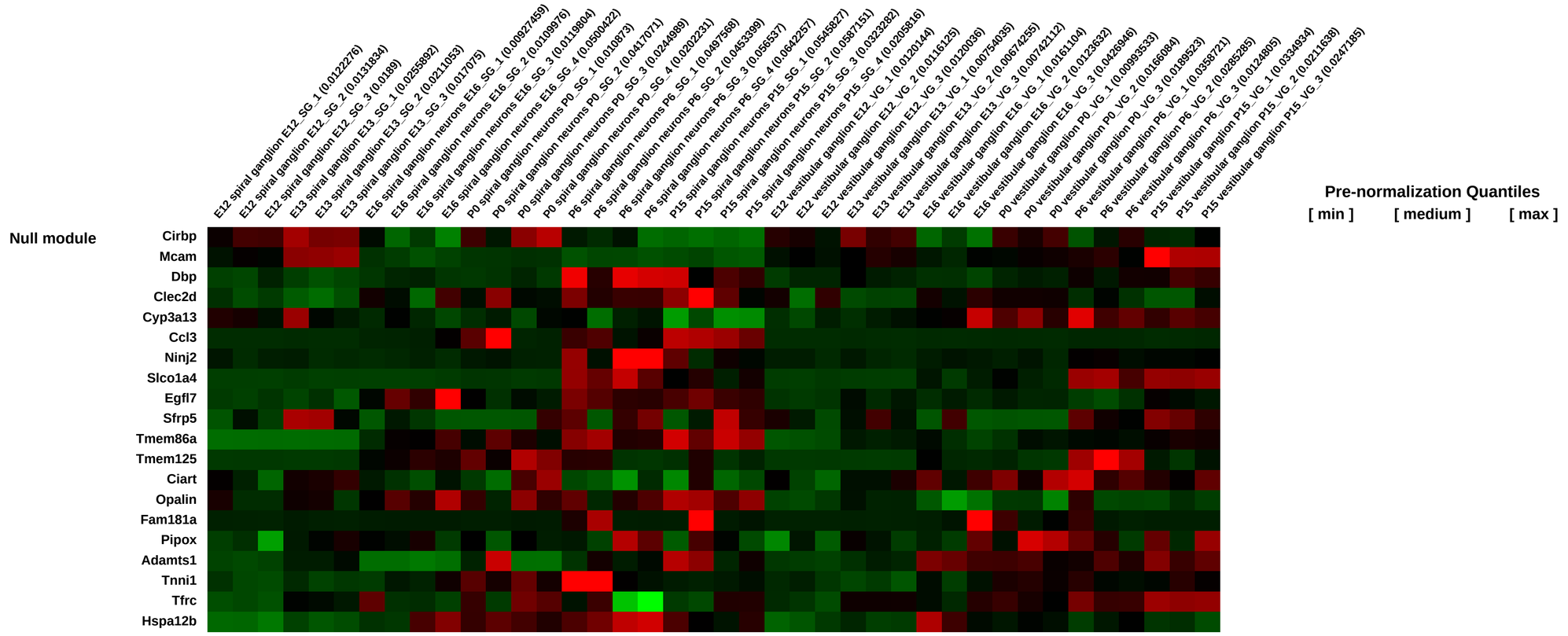

GEO Series "GSE47798" Expression Profiles

Num of samples in this series: 30

Scale of expression profile Z-scores

-3.0 -2.0 -1.0 0.0 1.0 2.0 3.0

GEO Link:	http://www.ncbi.nlm.nih.gov/geo/query/acc.cgi?acc=GSE47798
Status:	Public on Jun 07 2014
Title:	Perinatal-Estrogen-Induced Changes in Gene Expression Related to Brain Sexual Differentiation in Mice
Organism:	Mus musculus
Experiment type:	Expression profiling by array
Platform:	GPL1261
Pubmed ID:	
Summary & Design:	**Summary:** Sexual dimorphism of the behaviors or physiological functions in mammals is mainly due to the sex difference of the brain. The goal of this study is to identify genes mediating sexaul dimorphism of the brain. The large-scale analysis with microarray in the present study is an attempt to obtain the candidate gene(s) mediating the perinatal estrogen effect causing the brain sexual differentiation. **Overall design:** Thirty female mice were injected with estradiol benzoate (EB) or vehicle on the day of birth, and the hypothalamus was collected at either 1, 3, 6, 12, or 24 h after the EB injection.

Background corr dist: KL-Divergence = 0.4219, L1-Distance = 0.0807, L2-Distance = 0.0200, Normal std = 0.2420

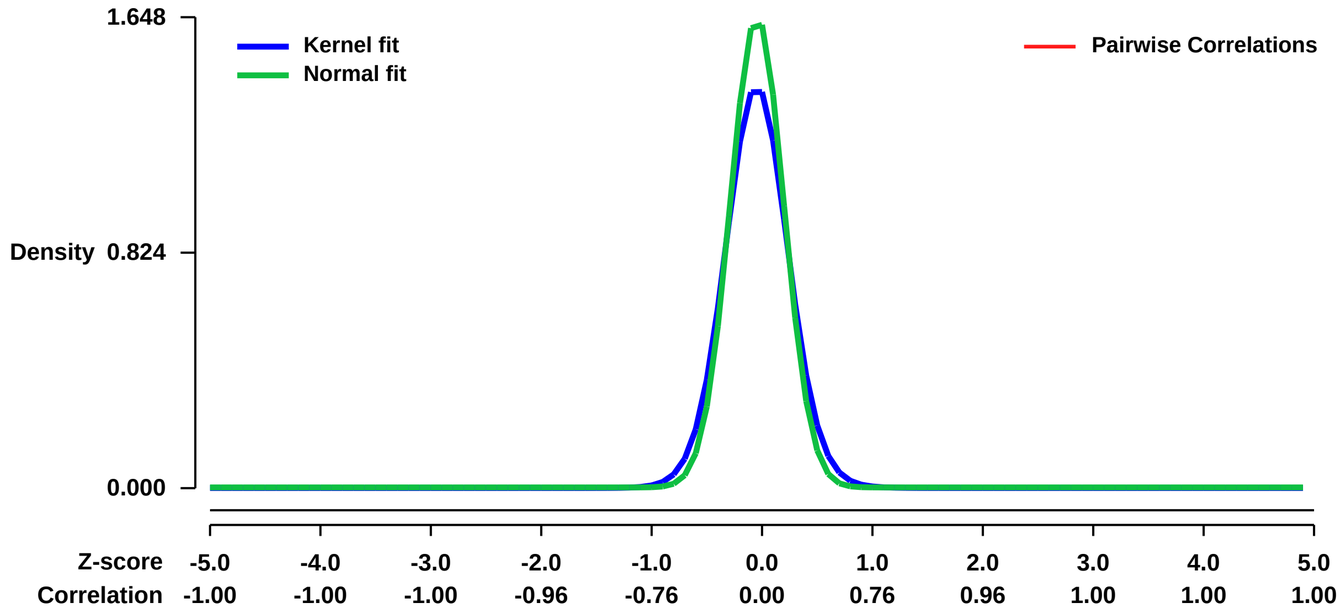

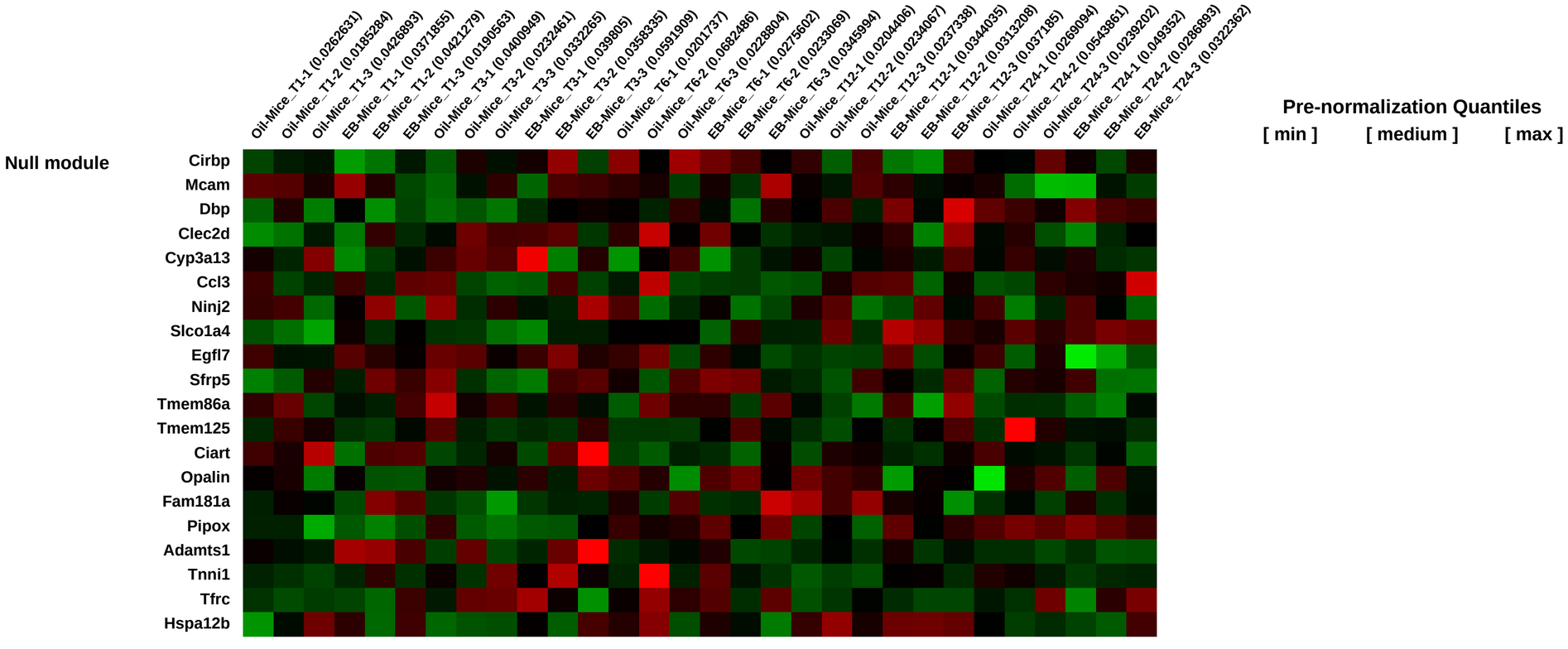

GEO Series "GSE45668" Expression Profiles

Num of samples in this series: 6

Scale of expression profile Z-scores

-3.0 -2.0 -1.0 0.0 1.0 2.0 3.0

GEO Link: http://www.ncbi.nlm.nih.gov/geo/query/acc.cgi?acc=GSE45668

Status: Public on Apr 02 2013

Title: The presence of the Y-chromosome, not the absence of the second X-chromosome, alters the mRNA levels stored in the fully grown XY mouse oocyte

Organism: Mus musculus

Experiment type: Expression profiling by array

Platform: GPL1261

Pubmed ID:

Summary & Design:

Summary:
The oocytes of B6.Y(TIR) sex-reversed female mouse mature in culture but fail to develop after fertilization because of their cytoplasmic defects. To identify the defective components, we compared the gene expression profiles between the fully-grown oocytes of B6.Y(TIR) (XY) females and those of their XX littermates by cDNA microarray. 173 genes were found to be higher and 485 genes were lower in XY oocytes than in XX oocytes by at least 2-fold. We compared the transcript levels of selected genes by RT-PCR in XY and XX oocytes, as well as in XO oocytes missing paternal X-chromosomes. All genes tested showed comparable transcript levels between XX and XO oocytes, indicating that mRNA accumulation is well adjusted in XO oocytes. By contrast, in addition to Y-encoded genes, many genes showed significantly different transcript levels in XY oocytes. We speculate that the presence of the Y-chromosome, rather than the absence of the second X-chromosome, caused dramatic changes in the gene expression profile in the XY fully-grown oocyte.

Overall design:
Mouse GV oocytes of B6.Y(TIR) were collected for RNA extraction and hybridization to Affymetrix microarray. We sought to extract the differentially expressed genes in the XY oocytes.

Background corr dist: KL-Divergence = 0.0297, L1-Distance = 0.0151, L2-Distance = 0.0002, Normal std = 0.6671

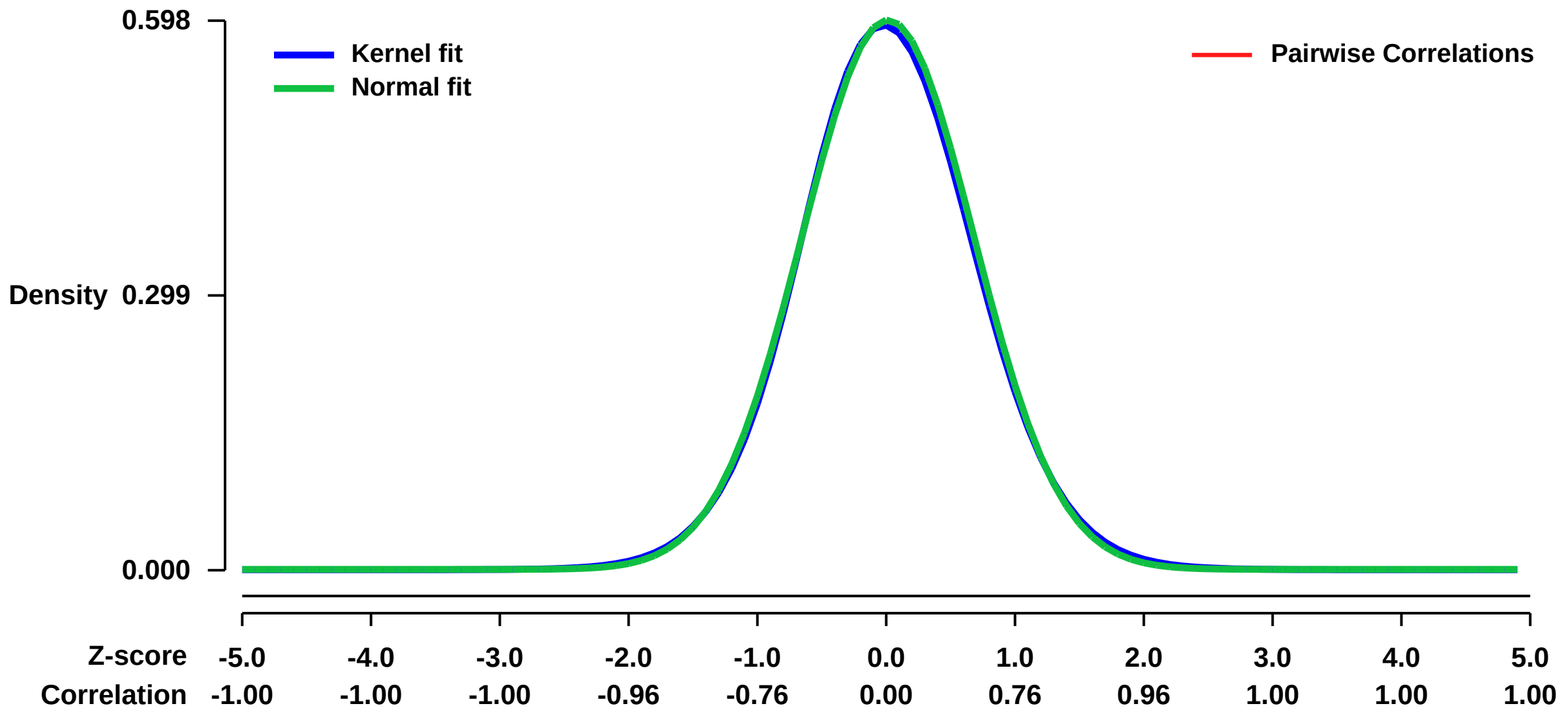

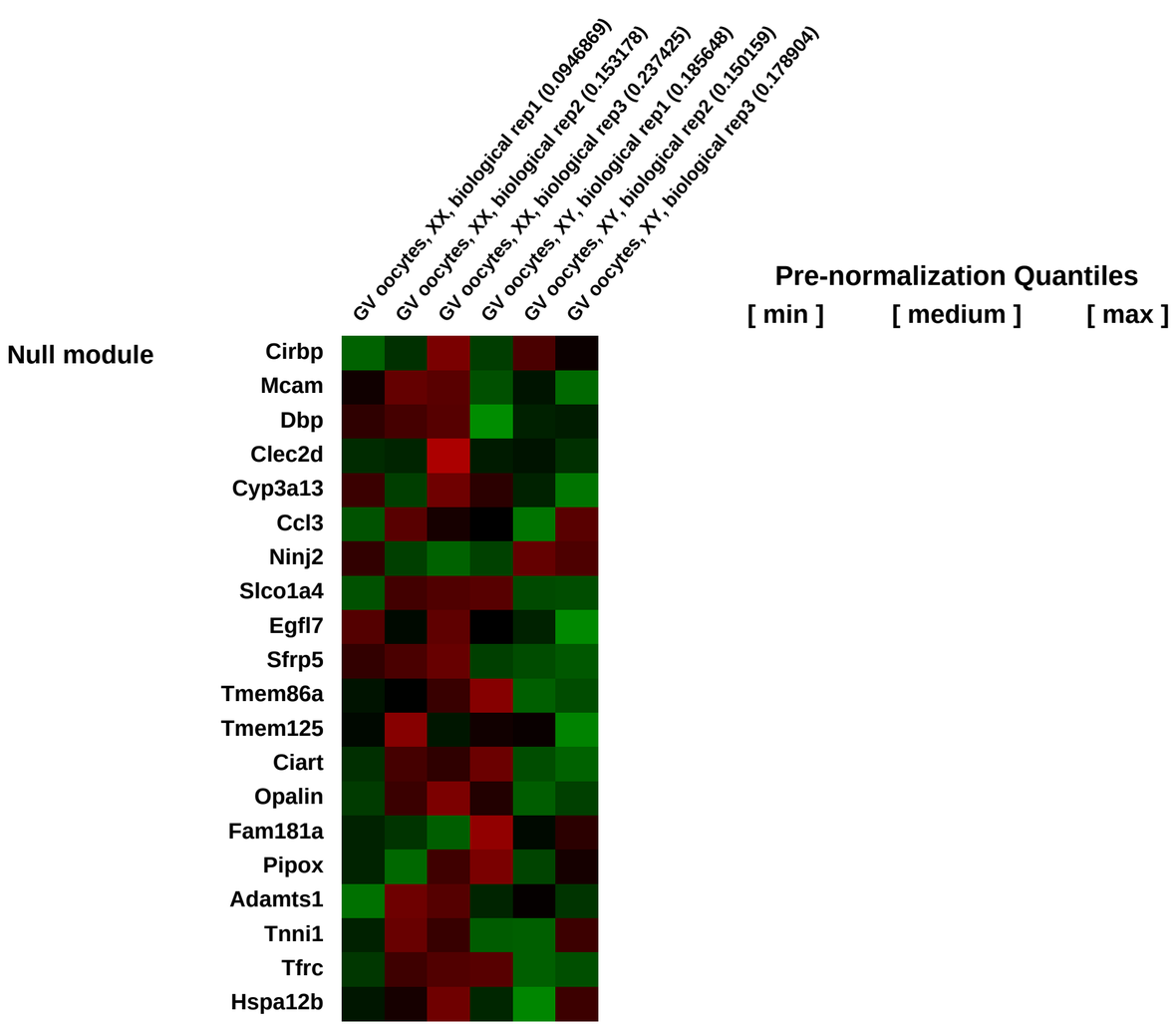

GEO Series "GSE23505" Expression Profiles

Num of samples in this series: 10

Scale of expression profile Z-scores

-3.0 -2.0 -1.0 0.0 1.0 2.0 3.0

GEO Link:	http://www.ncbi.nlm.nih.gov/geo/query/acc.cgi?acc=GSE23505
Status:	Public on Aug 31 2010
Title:	Enhanced Pathogenicity of Th17 cells Generated in the Absence of Transforming Growth Factor-¸† Signaling
Organism:	Mus musculus
Experiment type:	Expression profiling by array
Platform:	GPL1261
Pubmed ID:	20962846
Summary & Design:	**Summary:** CD4+ T cells that selectively produce interleukin (IL)-17, are critical for host defense and autoimmunity1-4. Crucial for T helper17 (Th17) cells in vivo5,6, IL-23 has been thought to be incapable of driving initial differentiation. Rather, IL-6 and transforming growth factor (TGF)-¸†1 have been argued to be the factors responsible for initiating specification7-10. Herein, we show that Th17 differentiation occurs in the absence of TGF-¸† signaling. Neither IL-6 nor IL-23 alone efficiently generated Th17 cells; however, these cytokines in combination with IL-1¸† effectively induced IL-17 production in naˆflve precursors, independently of TGF-¸†. Epigenetic modification of the Il17a/Il17f and Rorc promoters proceeded without TGF-¸†1, allowing the generation of cells that co-expressed Ror¸‡t and T-bet. T-bet+Ror¸‡t+ Th17 cells are generated in vivo during experimental allergic encephalomyelitis (EAE), and adoptively transferred Th17 cells generated with IL-23 in the absence of TGF-¸†1 were more pathogenic in this experimental disease. These data suggest a new model for Th17 differentiation. Consistent with genetic data linking the IL23R with autoimmunity, our findings re-emphasize the role of IL-23 and therefore have important implications for the development of new therapies. **Overall design:** Mouse T helper 17 cell differentiation with or without TGFB

Background corr dist: KL-Divergence = 0.0691, L1-Distance = 0.0488, L2-Distance = 0.0040, Normal std = 0.5469

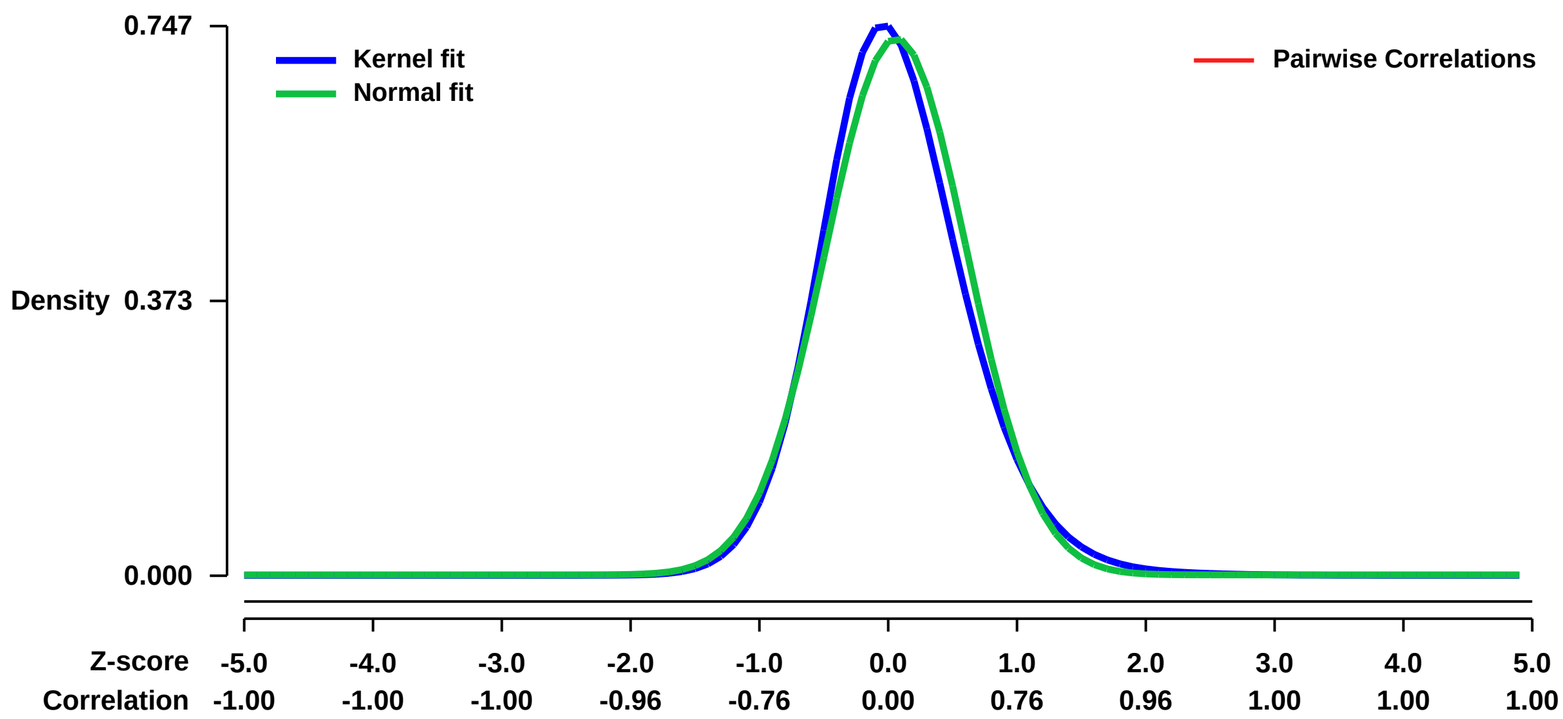

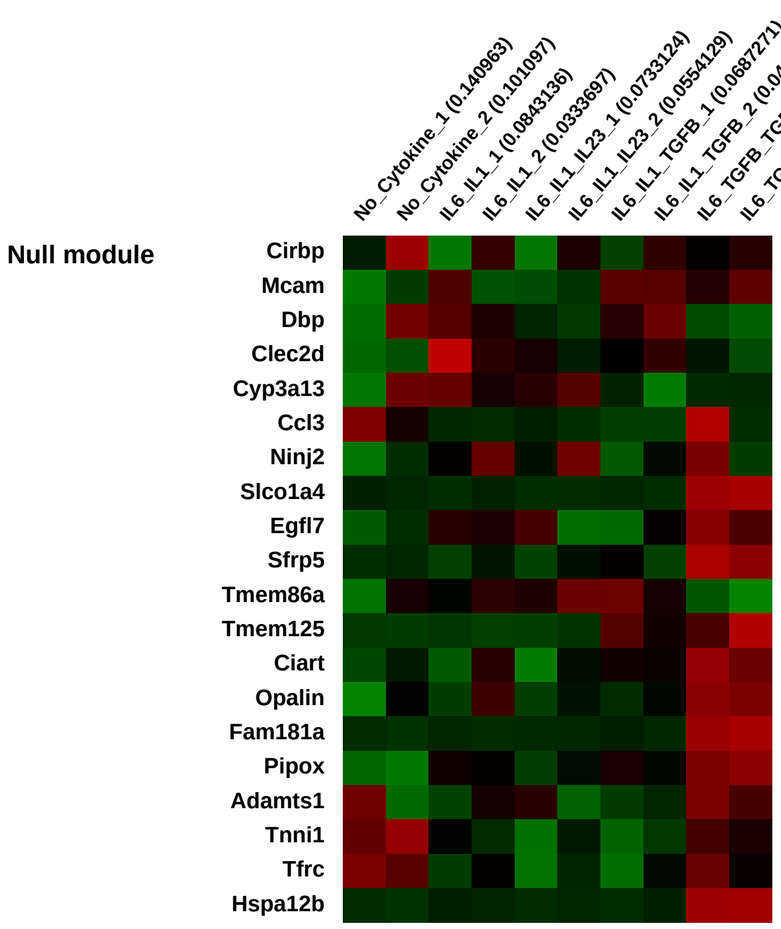

Pre-normalization Quantiles

[min] [medium] [max]

GEO Series "GSE19657" Expression Profiles

Num of samples in this series: 21

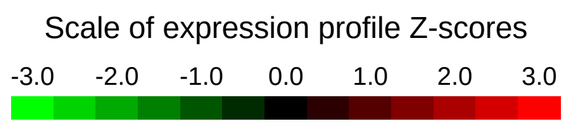

GEO Link:	http://www.ncbi.nlm.nih.gov/geo/query/acc.cgi?acc=GSE19657
Status:	Public on Sep 29 2010
Title:	Targeting resistance to Smoothened antagonists by inhibiting the PI3K pathway
Organism:	Mus musculus
Experiment type:	Genome variation profiling by genome tiling array
Platform:	GPL1261
Pubmed ID:	20881279
Summary & Design:	**Summary:** Mutations in Hedgehog (Hh) pathway genes, leading to constitutive activation of Smoothened (Smo), occur in sporadic medulloblastoma, the most common brain cancer in children. Antagonists of Smo induce tumor regression in mouse models of medulloblastoma and hold great promise for targeted therapy for this tumor. However, acquired resistance has emerged as one of the major challenges of targeted cancer therapy. Here, we describe novel mechanisms of acquired resistance to Smo antagonists in medulloblastoma. NVP-LDE225, a potent and selective Smo antagonist, inhibits Hh signaling and induces tumor regressions in allograft models of medulloblastoma that are driven by mutations of Patched (Ptch), a tumor suppressor in the Hh pathway. However, after long-term treatment, evidence of acquired resistance was observed. Genome-wide profiling of resistant tumors revealed distinct mechanisms to evade the inhibitory effects of Smo antagonists. Chromosomal amplification of Gli2, a downstream effector of Hh signaling, reactivated Hh signaling and restored tumor growth. Analysis of pathway gene-expression signatures selectively deregulated in resistant tumors identified increased phosphoinositide-3-kinase (PI3K) signaling as another potential resistance mechanism. Probing the functional relevance of increased PI3K signaling, we showed that the combination of NVP-LDE225 with the dual PI3K/mTOR inhibitor NVP-BEZ235 markedly delayed the development of resistance. Our findings have important clinical implications for future treatment strategies in medulloblastoma. **Overall design:** aCGH: DNA was prepared from tumors from vehicle or NVP-LDE225 treated nude mice allografted with medulloblastoma tumors derived from Ptch+/-p53-/- transgenic mouse and hybridized on Agilent mouse CGH 244K Array.

Background corr dist: KL-Divergence = 0.1859, L1-Distance = 0.0351, L2-Distance = 0.0028, Normal std = 0.3529

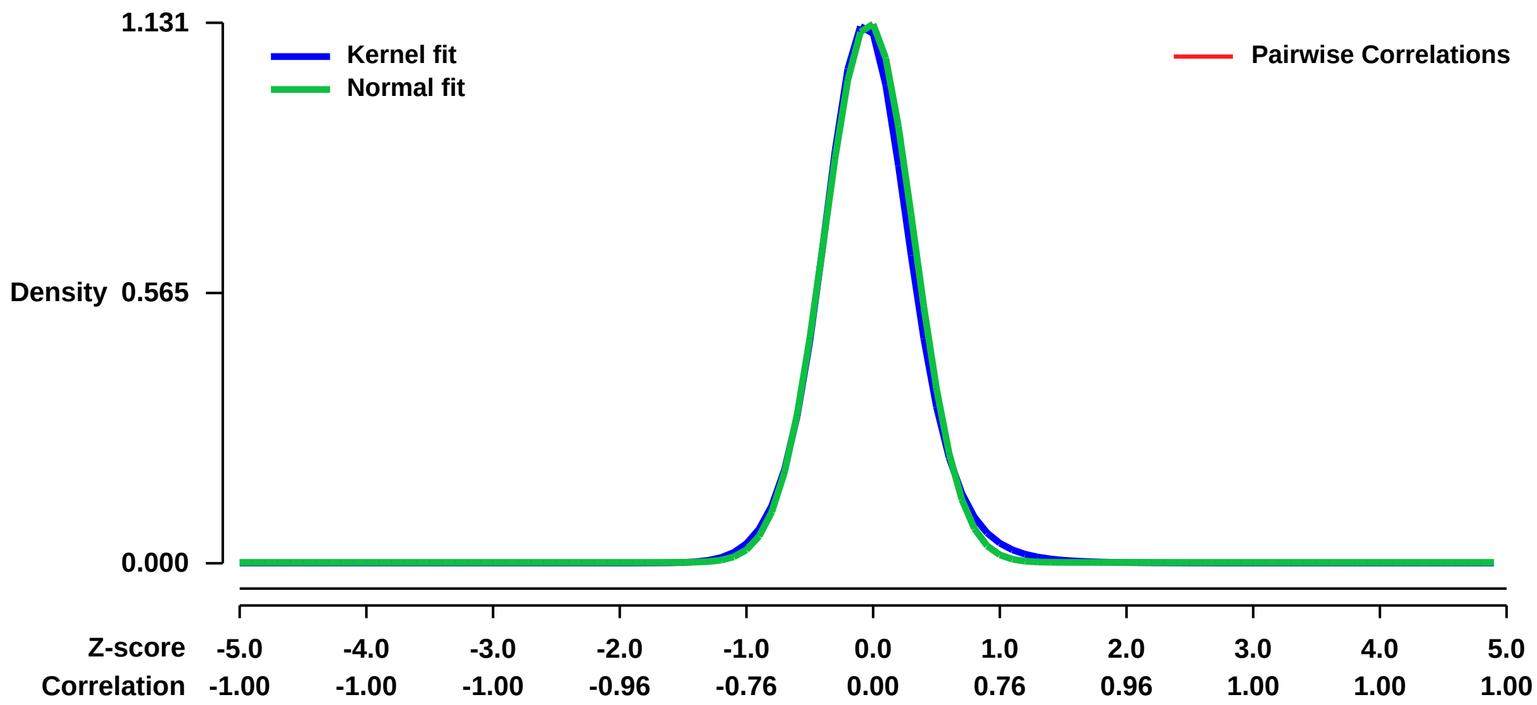

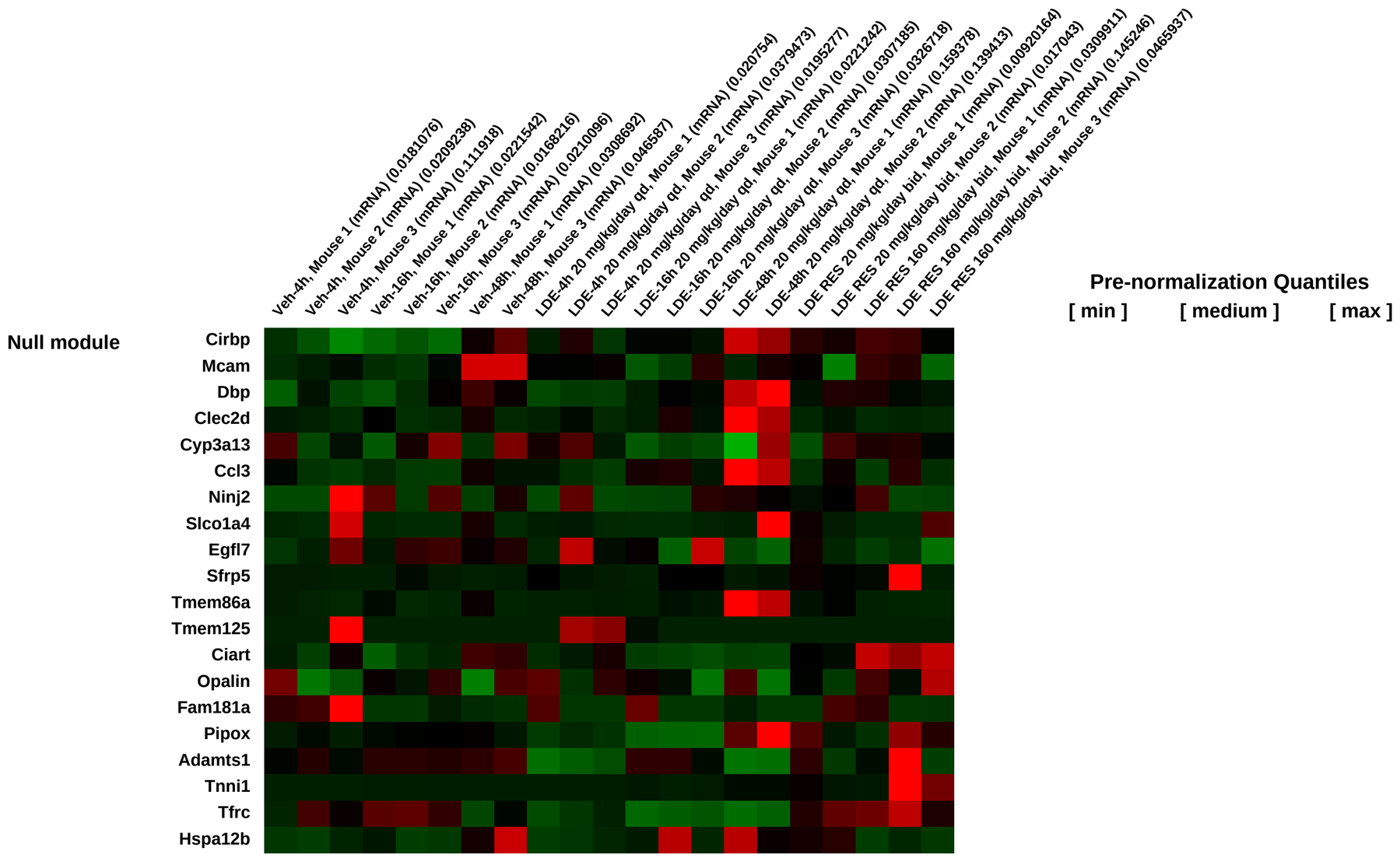

GEO Series "GSE18597" Expression Profiles

Num of samples in this series: 42

Scale of expression profile Z-scores

-3.0 -2.0 -1.0 0.0 1.0 2.0 3.0

GEO Link: http://www.ncbi.nlm.nih.gov/geo/query/acc.cgi?acc=GSE18597
Status: Public on Oct 17 2009
Title: Expression data from mutant SOD1(G93A) transgenic mice
Organism: Mus musculus
Experiment type: Expression profiling by array
Platform: GPL1261
Pubmed ID:
Summary & Design:

Summary:
Expression profiling of spinal cord from SOD1(G93A) mice and age matched controls at ages 28, 42, 56, 70,98,112, and 126 days of age.

We used microarrays to determine differential gene expression throughout disease progression in the spinal cord of mutant SOD1(G93A) model of ALS.

Overall design:
Samples were collected from male B6SJL SOD1(G93A) and age matched controls. 3 samples were collected representing each genotype and age group for RNA extraction and hybridization on Affymetrix microarrays.

Background corr dist: KL-Divergence = 0.1456, L1-Distance = 0.0525, L2-Distance = 0.0067, Normal std = 0.3801

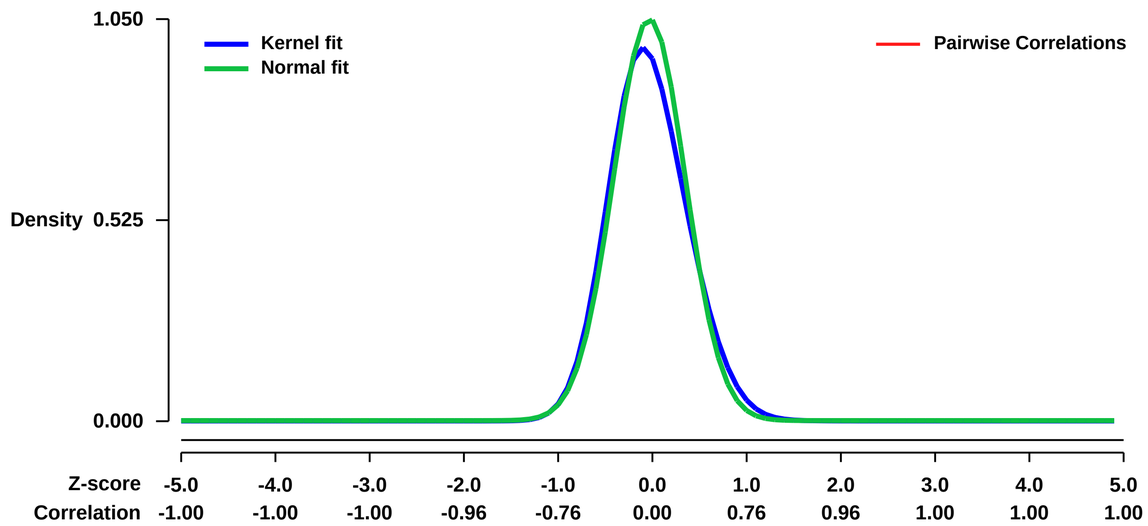

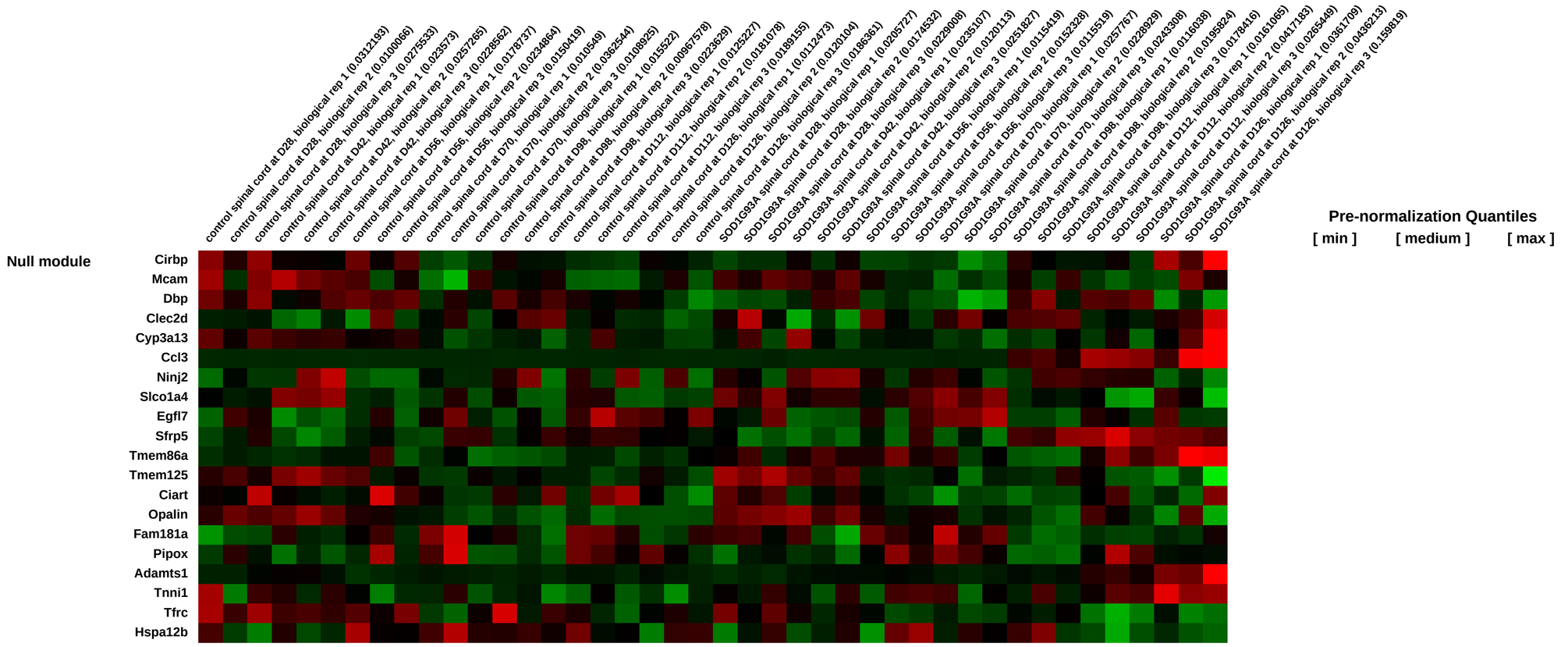

GEO Series "GSE30498" Expression Profiles

Num of samples in this series: 12

Scale of expression profile Z-scores

-3.0 -2.0 -1.0 0.0 1.0 2.0 3.0

GEO Link:	**http://www.ncbi.nlm.nih.gov/geo/query/acc.cgi?acc=GSE30498**
Status:	**Public on Jul 07 2012**
Title:	**Expression data from superior cervical ganglion cultured cells and whole tissue**
Organism:	**Mus musculus**
Experiment type:	**Expression profiling by array**
Platform:	**GPL1261**
Pubmed ID:	
Summary & Design:	**Summary:** **A transcriptomic expression comparison was done among superior cervical ganglion (SCG) cells cultured on 2D substrates, 3D porous polystyrene scaffolds, and in freshly dissected tissue (in vivo surrogate), with the goal of assessing the feasibility of establishing the meaning of 3D and associated physiological relevance at the molecular level** **Overall design:** **SCG cells were cultured on 2D surfaces and in 3D scaffolds. Chemical cues are controlled by coating. Only spacial properties of the culture systems were compared. Cells from freshly dissected tissue were used as in vivo surrogates for positive control of 3D cells.**

Background corr dist: KL-Divergence = 0.0255, L1-Distance = 0.0692, L2-Distance = 0.0061, Normal std = 0.8184

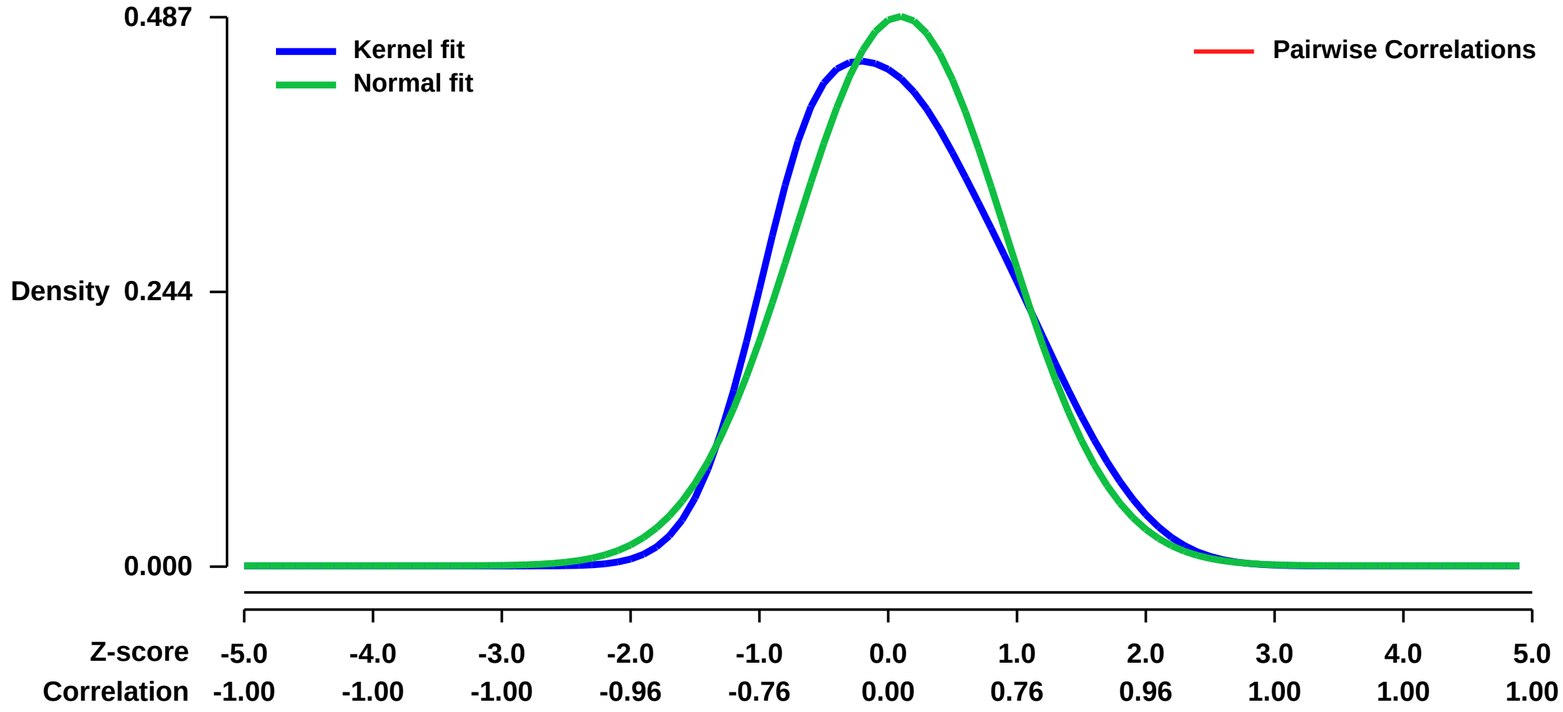

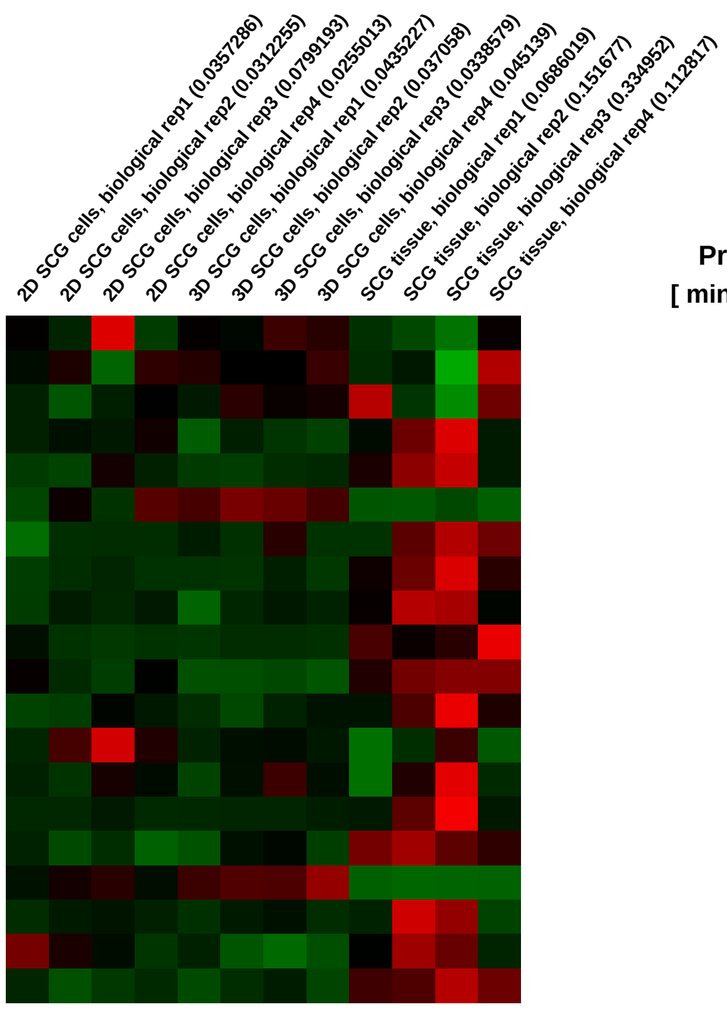

GEO Series "GSE56135" Expression Profiles

Num of samples in this series: 8

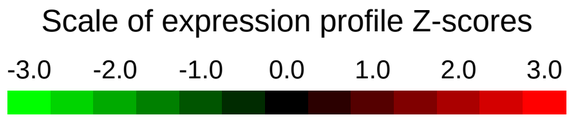

GEO Link:	**http://www.ncbi.nlm.nih.gov/geo/query/acc.cgi?acc=GSE56135**
Status:	**Public on Jun 15 2014**
Title:	**Intrinsic differences between oral and skin keratinocytes**
Organism:	**Mus musculus**
Experiment type:	**Expression profiling by array**
Platform:	**GPL1261**
Pubmed ID:	
Summary & Design:	**Summary:** **The morphology and the behavior of skin and oral tissue keratinocytes are different. One significant dissimilarity between the two sites is the response to injury. Oral and skin keratinocytes have intrinsic differences in the response to injury and such differences are reflected in gene expression profiles.** **We used microarrays to investigate differences in global gene expression patterns between baseline skin and oral epithelium sheets without their underlying connective tissue.** **Overall design:** **Paired skin and oral epithelium was separated from the dermis for RNA extraction and hybridization on Affymetrix microarrays. Skin epidermal tissues were obtained from the tail of mice and oral epidermal tissues were obtained from the hard palate. Enzymatically isolated epithelium was used for analysis.**

Background corr dist: **KL-Divergence = 0.0201, L1-Distance = 0.0140, L2-Distance = 0.0002, Normal std = 0.7354**

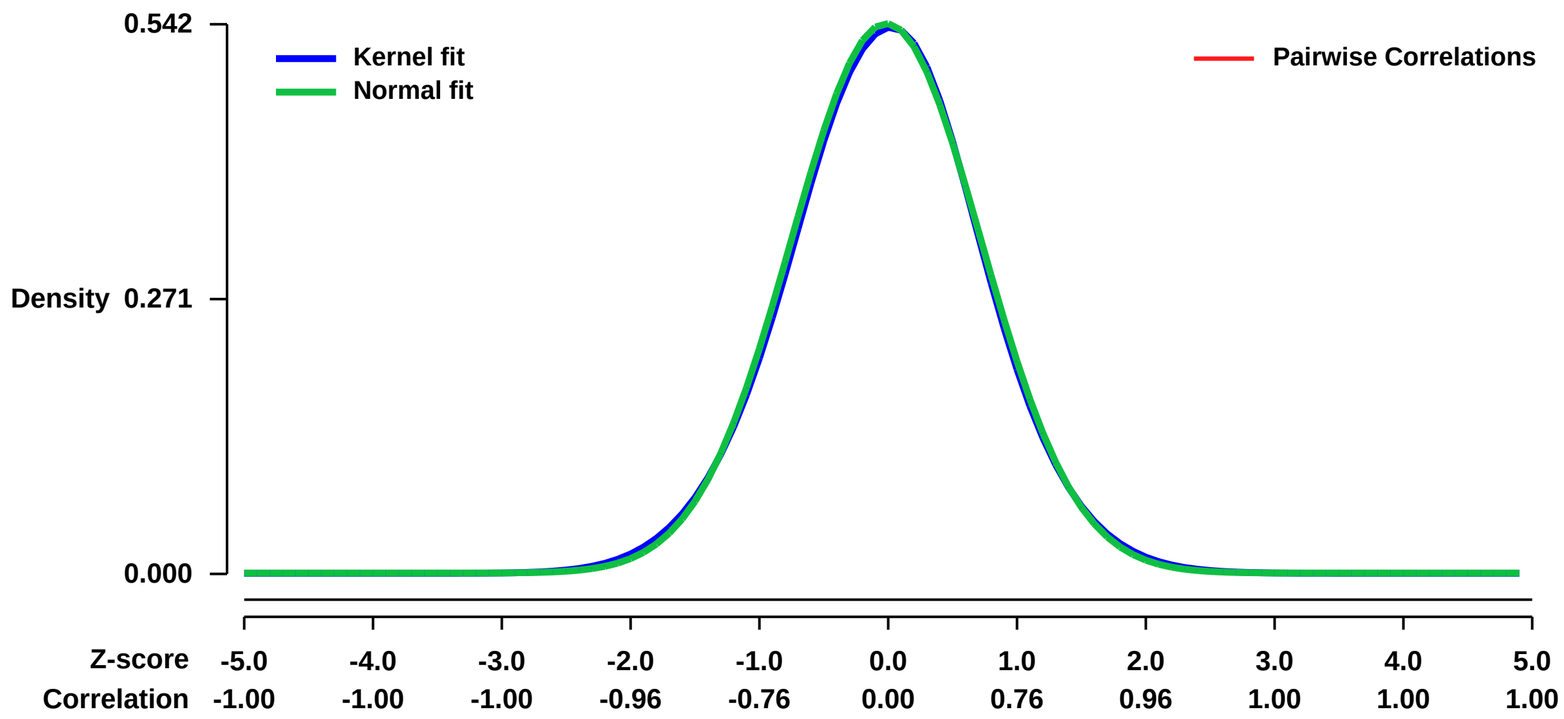

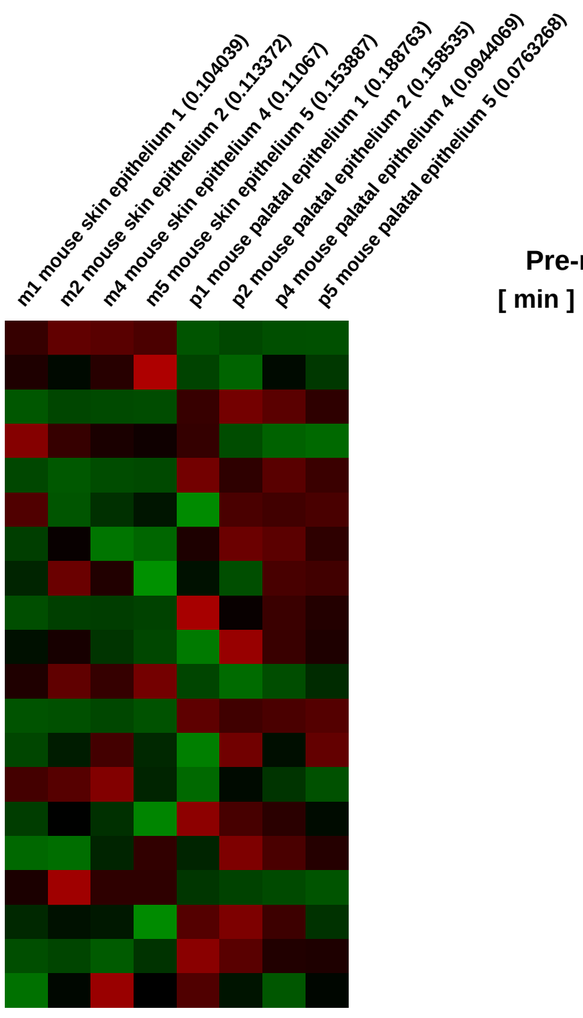

GEO Series "GSE36437" Expression Profiles

Num of samples in this series: 6

Scale of expression profile Z-scores

-3.0 -2.0 -1.0 0.0 1.0 2.0 3.0

GEO Link:	http://www.ncbi.nlm.nih.gov/geo/query/acc.cgi?acc=GSE36437
Status:	Public on Mar 31 2012
Title:	Expression data from caudal artery of Notch3WT and Notch3KO mice
Organism:	Mus musculus
Experiment type:	Expression profiling by array
Platform:	GPL1261
Pubmed ID:	23117660
Summary & Design:	**Summary:** Notch3 is a transmembrane receptor which is critically important for the structure and myogenic response of distal arteries, particularly cerebral arteries. After activation of the receptor, the intracellular domain translocates in the nucleus to activate target genes transcription. In order to identify Notch3 target genes, we used microarrays to compare gene expression from caudal arteries (Notch3+/+ vs Notch3-/-) and selected down-regulated genes in Notch3-/- arteries. **Overall design:** Caudal arteries were dissected from 1 month old Notch3+/+ and Notch3-/- mice. RNA was prepared with arteries pooled from three (AJ_N3WT_3, AJ_N3WT_4) or four (AJ_N3WT_1, AJ_N3KO_1, AJ_N3KO_2, AJ_N3KO_4) mice and hybridized on Mouse MOE430.2 Affymetrix chips. For each group (Notch3+/+ and Notch3-/-), three biological replicates were performed.

Background corr dist: KL-Divergence = 0.0378, L1-Distance = 0.0194, L2-Distance = 0.0004, Normal std = 0.6262

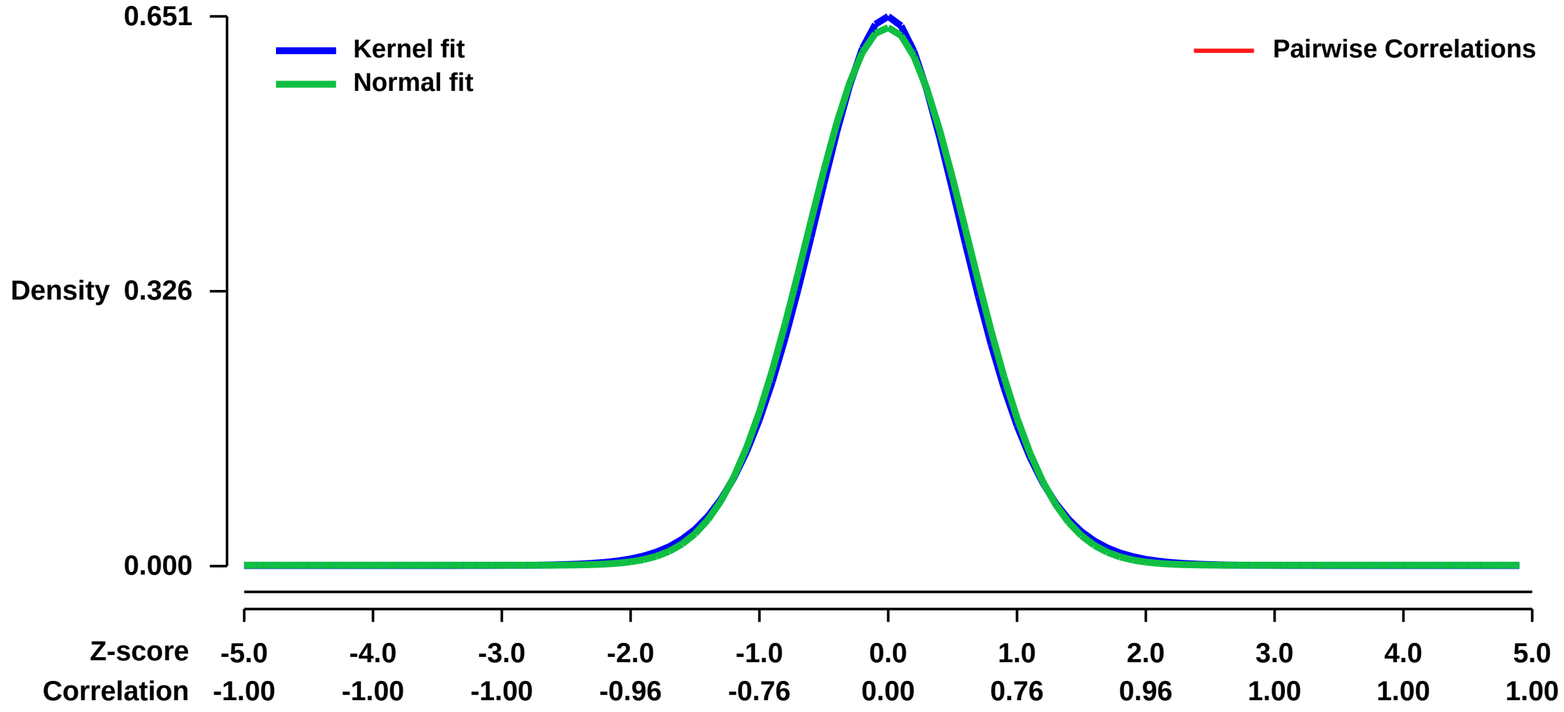

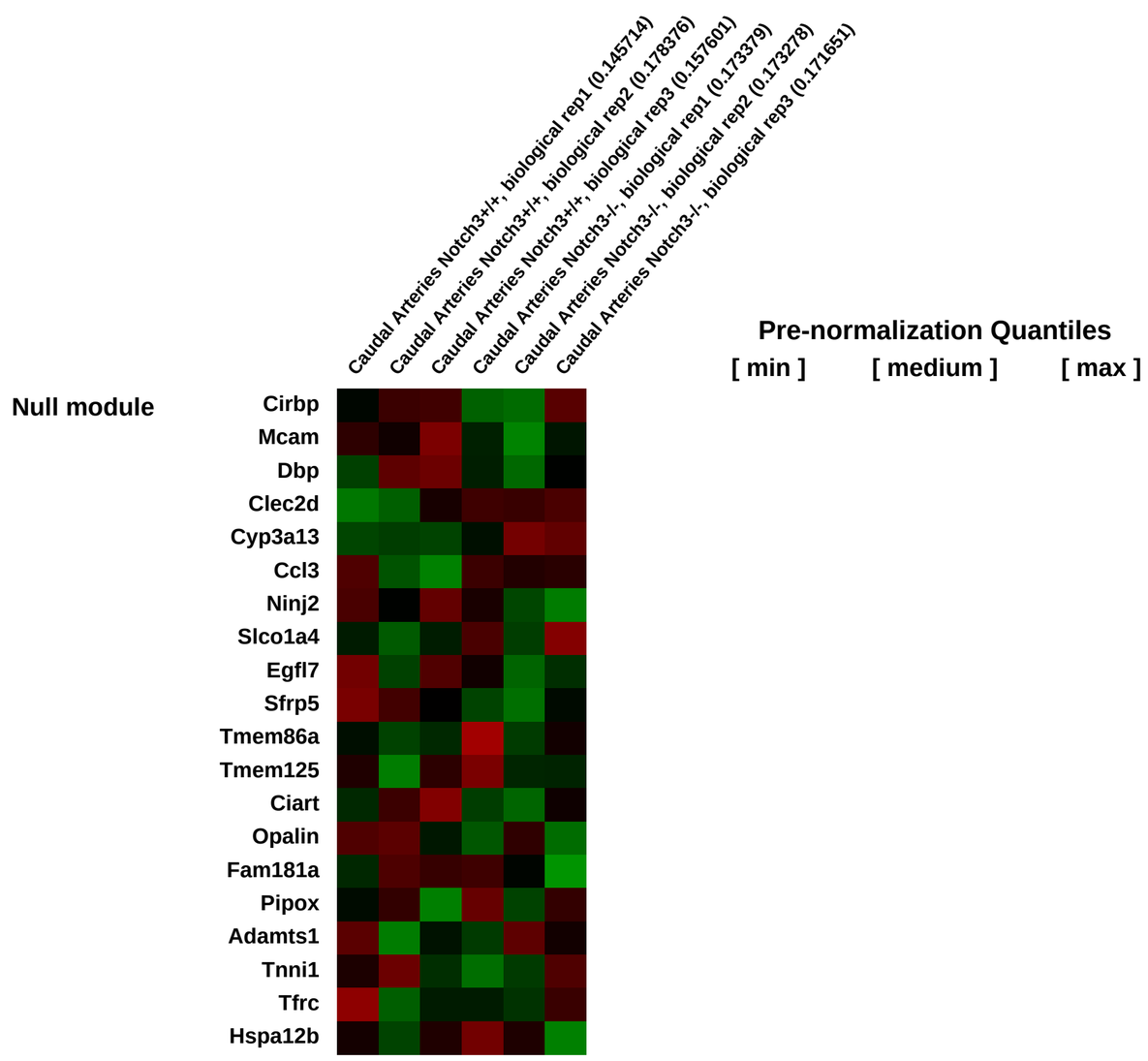

GEO Series "GSE6134" Expression Profiles

Num of samples in this series: 7

Scale of expression profile Z-scores

-3.0 -2.0 -1.0 0.0 1.0 2.0 3.0

GEO Link:	http://www.ncbi.nlm.nih.gov/geo/query/acc.cgi?acc=GSE6134
Status:	Public on Aug 08 2007
Title:	Offsprings of crosses between hypercholesterolemic and normocholesterolemic parents LUMC-HKG-ApoE-Atherosclerosis
Organism:	Mus musculus
Experiment type:	Expression profiling by array
Platform:	GPL1261
Pubmed ID:	17656671
Summary & Design:	**Summary:** Enhanced prenatal fatty streak formation in human fetuses has been associated with maternal hypercholesterolemia. However, the possible roles of maternal genetic background and in utero environment on development of atherosclerosis in adult life have not been unraveled. We generated genetically identical heterozygous apoE-deficient mice offspring with a different maternal background to study the intrauterine effect of maternal genotype and associated hypercholesterolemia on the developing vascular system. As read out for increased atherosclerosis development in adult life, a constrictive collar was placed around the carotid artery to induce lesion formation. A significant increase in endothelial cell activation and damage was detected in the carotid arteries of heterozygous apoE-deficient fetuses with apoE-deficient mothers compared with offspring from wild type mothers, but no fatty streak formation was observed. Postnatally, all carotid arteries revealed normal morphology. In adult offspring with maternal apoE-deficiency, the constrictive collar resulted in severe lesion (9/10) development compared with no to only minor lesions (2/10) in offspring of wild type mothers. Microarray analysis showed no effect of maternal apoE-deficiency on gene expression in adult offspring. We conclude that maternal apoE-deficiency not only affects fetal arteries, but also increases the susceptibility for development of collar-induced atherosclerosis in adult life. **Keywords: Atheroslcersosis development** **Overall design:** Crossing of hypercholesterolemic female with normocholesterolemic male and vice versa, determination of susceptabilioty to atherosclerosis in offspring

Background corr dist: KL-Divergence = 0.0638, L1-Distance = 0.0198, L2-Distance = 0.0006, Normal std = 0.5205

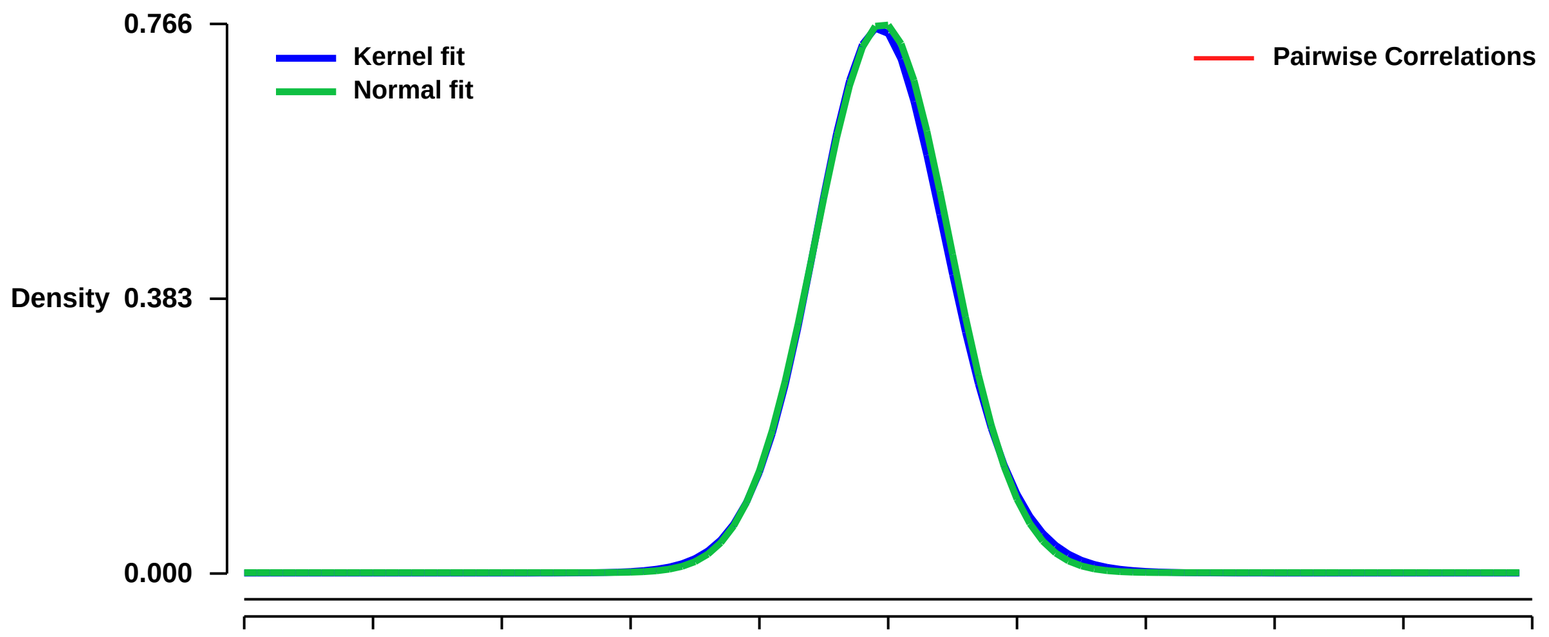

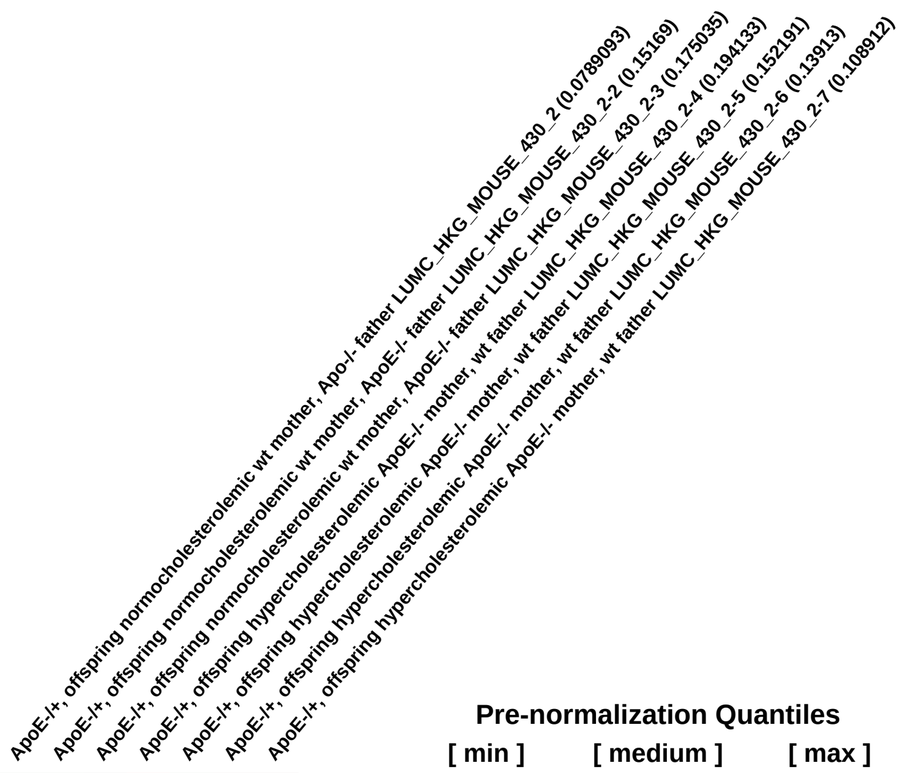

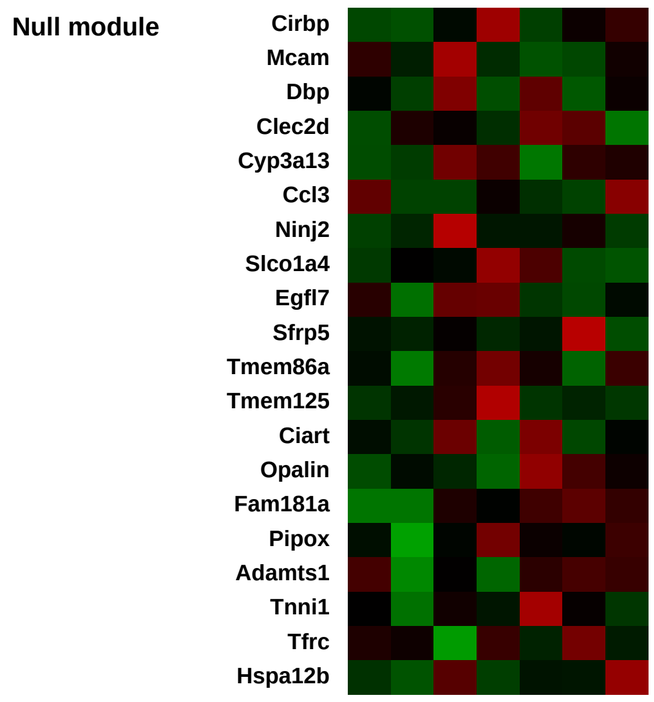

GEO Series "GSE14769" Expression Profiles

Num of samples in this series: 24

Scale of expression profile Z-scores

-3.0 -2.0 -1.0 0.0 1.0 2.0 3.0

GEO Link:	**http://www.ncbi.nlm.nih.gov/geo/query/acc.cgi?acc=GSE14769**
Status:	**Public on Mar 27 2009**
Title:	**Time course of bone marrow-derived macrophages simulated with LPS**
Organism:	**Mus musculus**
Experiment type:	**Expression profiling by array**
Platform:	**GPL1261**
Pubmed ID:	**19270711**
Summary & Design:	**Summary:** **The innate immune system is a two-edged sword; it is absolutely required for host defense against infection, but if left uncontrolled can trigger a plethora of inflammatory diseases. Here we used systems biology approaches to predict and validate a gene regulatory network involving a dynamic interplay between the transcription factors NF-¸”B, C/EBP¸·, and ATF3 that controls inflammatory responses. We mathematically modeled transcriptional regulation of Il6 and Cebpd genes and experimentally validated the prediction that the combination of an initiator (NF-¸”B), an amplifier (C/EBP¸·) and an attenuator (ATF3) forms a regulatory circuit that discriminates between transient and persistent Toll-like receptor 4-induced signals. Our results suggest a mechanism that enables the innate immune system to detect the duration of infection and to respond appropriately.** **Overall design:** **Bone marrow-derived macrophages stimulated with LPS for 0, 20, 40, 60, 80, 120, 240 and 360 minutes.**

Background corr dist: **KL-Divergence = 0.0950, L1-Distance = 0.0642, L2-Distance = 0.0069, Normal std = 0.4890**

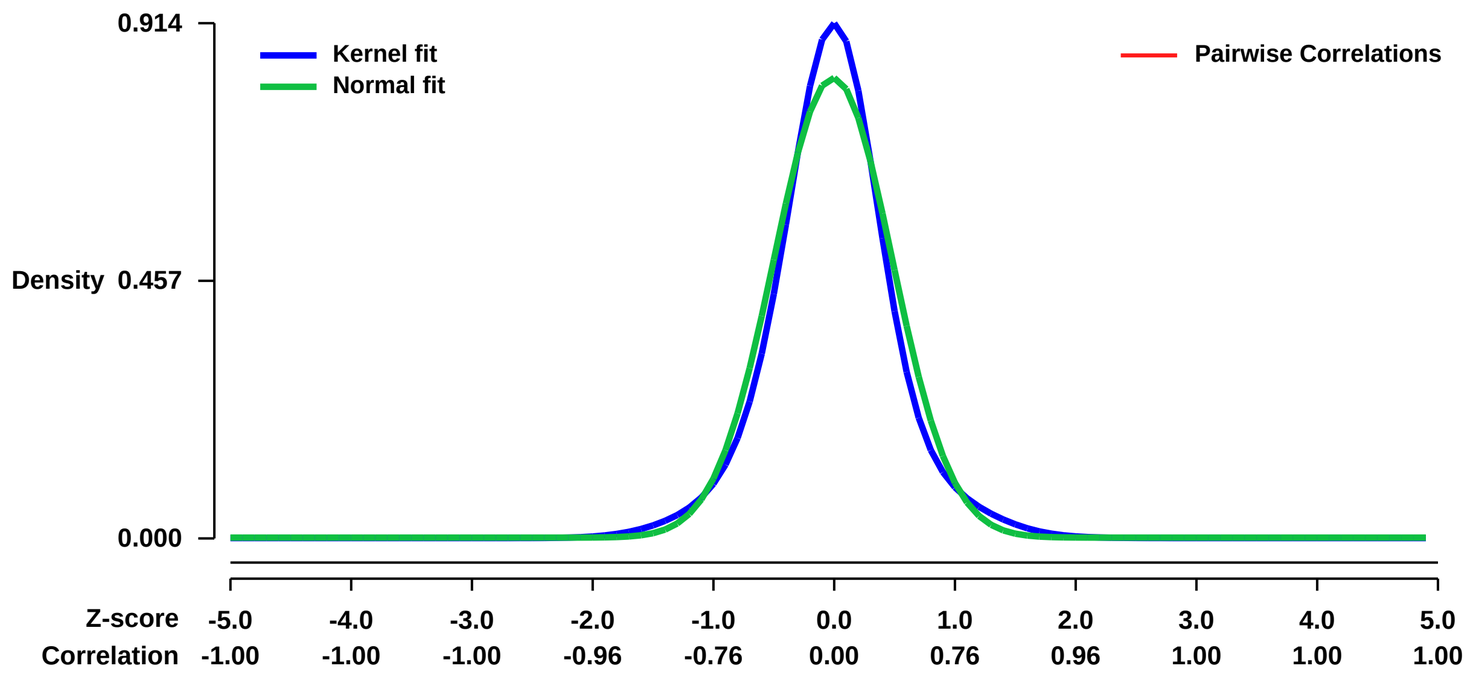

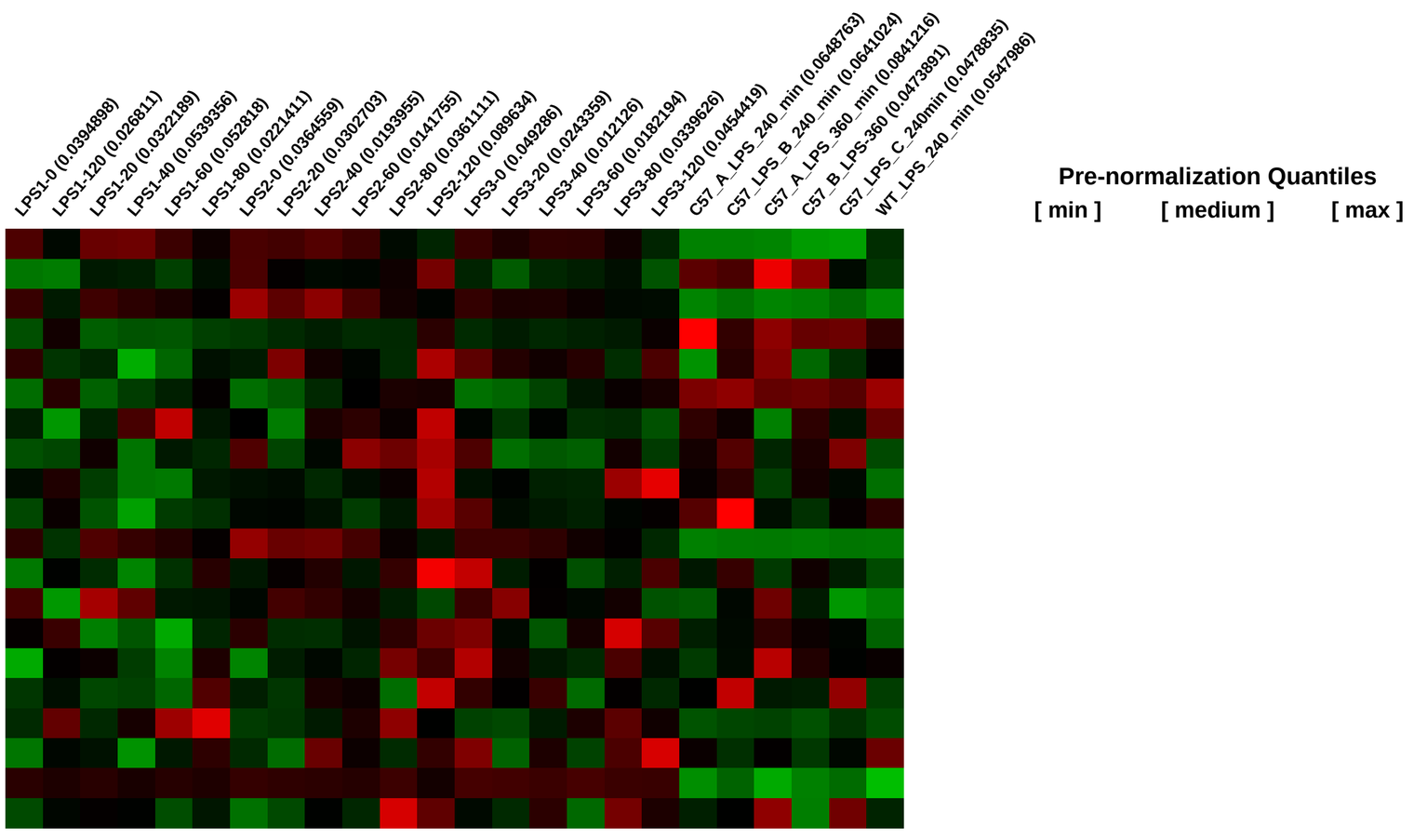

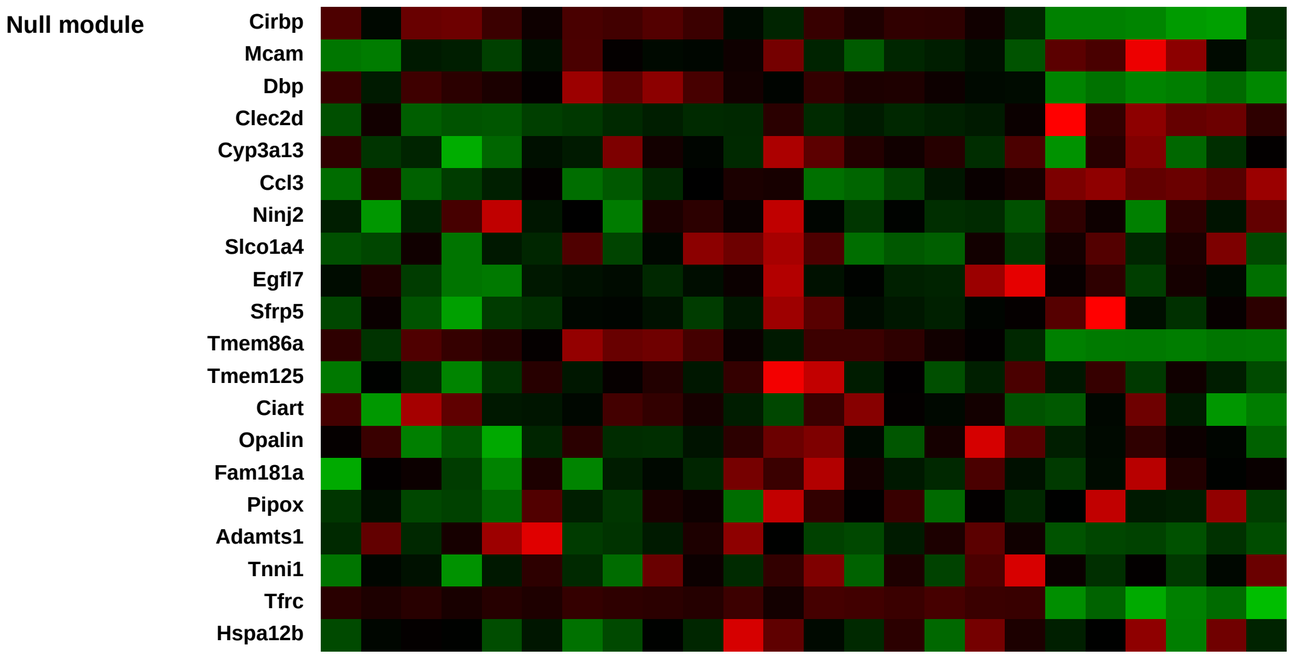

GEO Series "GSE48004" Expression Profiles

Num of samples in this series: 6

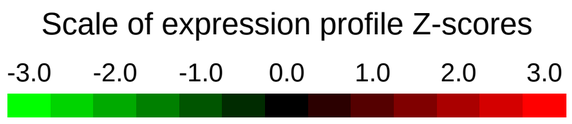

GEO Link:	http://www.ncbi.nlm.nih.gov/geo/query/acc.cgi?acc=GSE48004
Status:	Public on Aug 21 2013
Title:	Targeted disruption of Hotair leads to homeotic transformation and de-repression of imprinted genes [Microarray Analysis]
Organism:	Mus musculus
Experiment type:	Expression profiling by array
Platform:	GPL1261
Pubmed ID:	24075995
Summary & Design:	**Summary:** Long noncoding RNAs (lncRNAs) are thought to be prevalent regulators of gene expression, but the consequences of lncRNA inactivation in vivo are mostly unknown. Here we show that targeted deletion of mouse Hotair lncRNA leads to de-repression of hundreds of genes, resulting in homeotic transformation of the spine and malformation of metacarpal-carpal bones. RNA-seq and conditional inactivation reveal an ongoing requirement of Hotair to repress HoxD genes and multiple imprinted loci such as Dlk1-Meg3 and Igf2-H19. Hotair binds to both Polycomb repressive complex 2 that methylates histone H3 at lysine 27 (H3K27) and Lsd1 complex that demethylates histone H3 at lysine 4 (H3K4) in vivo. Hotair inactivation causes coordinate H3K27me3 loss and H3K4me3 gain at select target genes throughout the genome. These results reveal a shared regulatory mechanism to enforce silent chromatin state at Hox and imprinted genes via Hotair lncRNA. **Overall design:** Microarray analysis was performed on triplicate samples with Affymetrix GeneChip Mouse Genome 430 2.0 Array for both wildtype and Hotair Knockout.

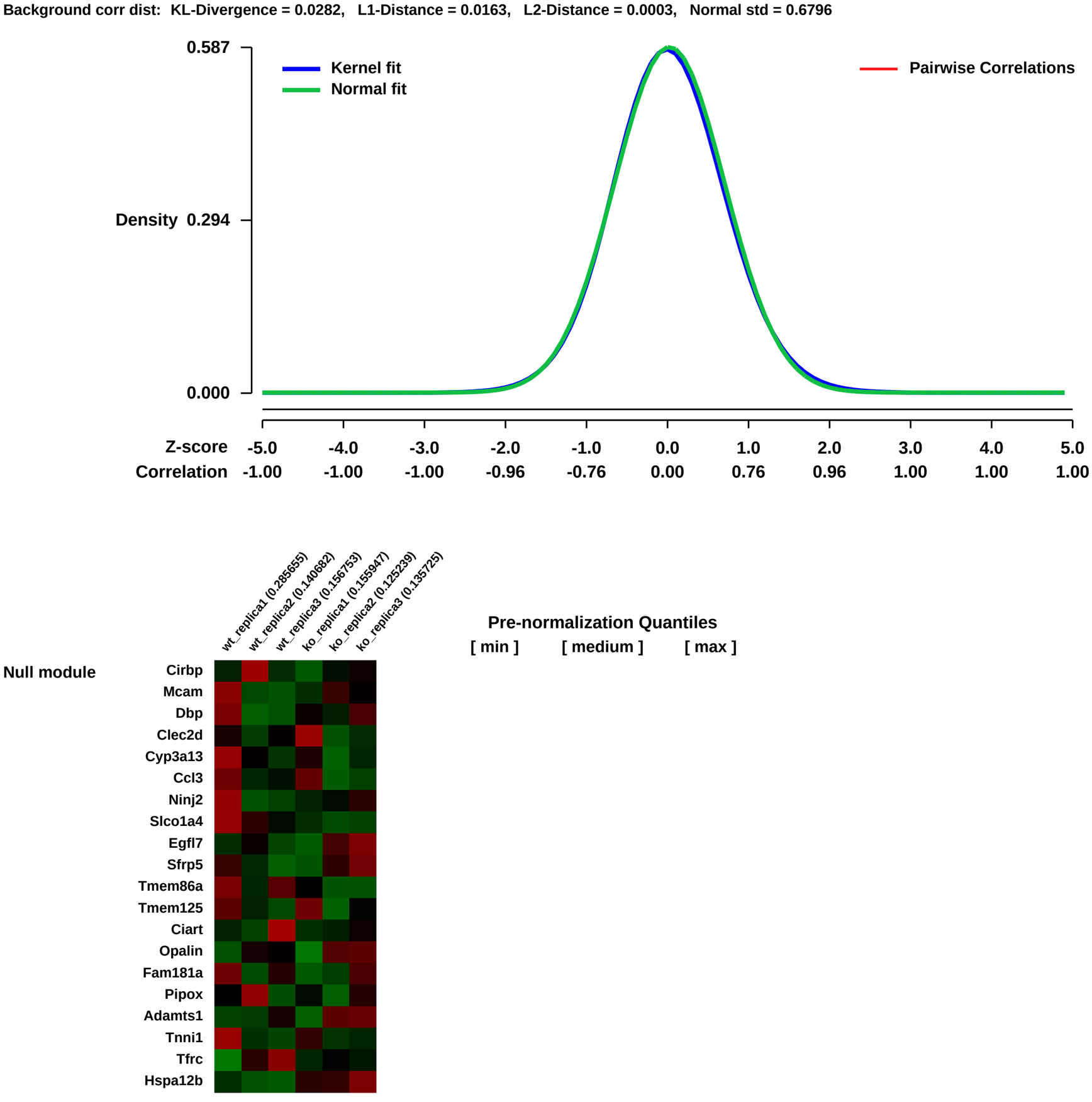

GEO Series "GSE24726" Expression Profiles

Num of samples in this series: 8

Scale of expression profile Z-scores

-3.0 -2.0 -1.0 0.0 1.0 2.0 3.0

GEO Link:	http://www.ncbi.nlm.nih.gov/geo/query/acc.cgi?acc=GSE24726
Status:	Public on Dec 21 2010
Title:	Gene expression profile of mature plasmacytoid dendritic cells (PDC) after the deletion of transcription factor E2-2
Organism:	Mus musculus
Experiment type:	Expression profiling by array
Platform:	GPL1261
Pubmed ID:	21145760
Summary & Design:	**Summary:** The interferon-producing plasmacytoid dendritic cells (PDC) share common progenitors with antigen-presenting classical dendritic cells (cDC), yet they possess distinct morphology and molecular features resembling those of lymphocytes. It is unclear whether the unique cell fate of PDC is actively maintained in the steady state. We report that the deletion of transcription factor E2-2 from mature peripheral PDC caused their spontaneous differentiation into cells with cDC properties. This included the loss of PDC markers, increase in MHC class II expression and T cell priming capacity, acquisition of dendritic morphology and induction of cDC signature genes. Genome-wide chromatin immunoprecipitation revealed direct binding of E2-2 to key PDC-specific and lymphoid genes, as well as to certain genes enriched in cDC. Thus, E2-2 actively maintains the cell fate of mature PDC and opposes the â defaultâ cDC fate, in part through direct regulation of lineage-specific gene expression programs. **Overall design:** Inducible deletion of E2-2 (Tcf4) has been performed by administering tamoxifen to conditional E2-2flox/flox Rosa26-CreER+ mice or to E2-2flox/flox Rosa26-CreER- control littermates. Four or six days later total splenocytes were isolated, pooled from 2-3 mice and PDC (CD11b- B220+ CD11clow Bst2+) were isolated by sorting. Global gene expression profiles of E2-2-deficient (null) and control (Ctrl) PDC were compared using Affymetrix microarrays (GPL1261).

Background corr dist: KL-Divergence = 0.0689, L1-Distance = 0.0375, L2-Distance = 0.0025, Normal std = 0.5200

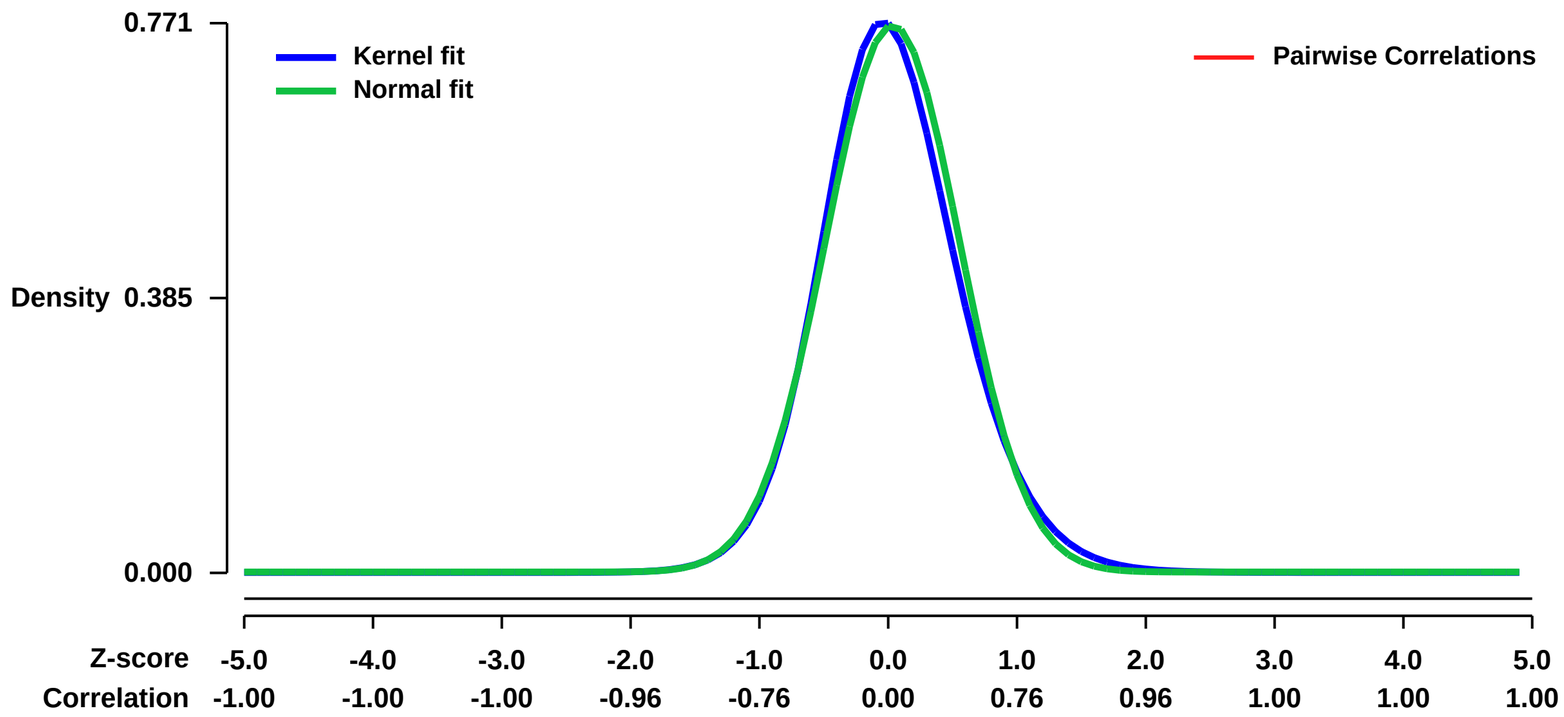

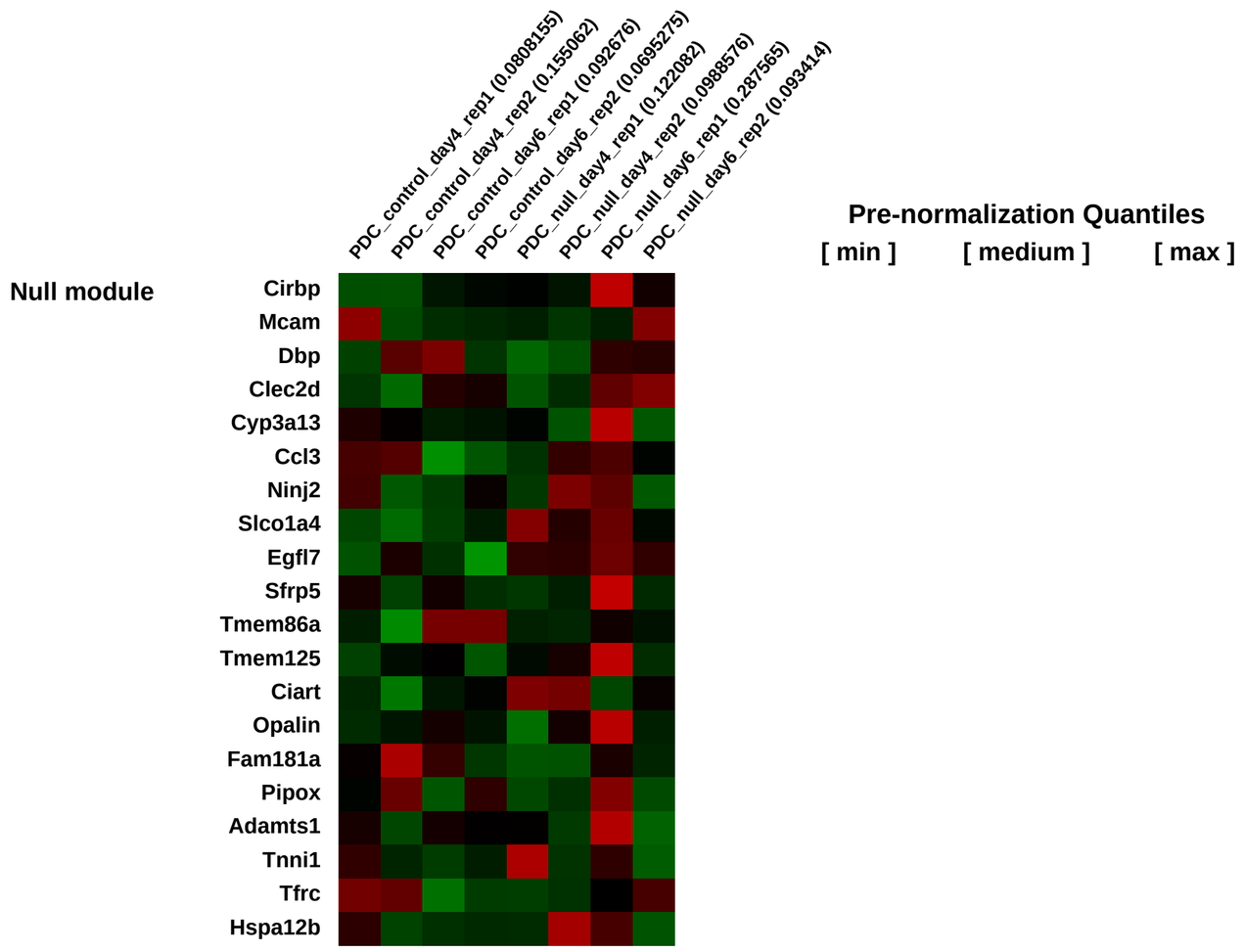

GEO Series "GSE14024" Expression Profiles

Num of samples in this series: 12

Scale of expression profile Z-scores

-3.0 -2.0 -1.0 0.0 1.0 2.0 3.0

GEO Link:	http://www.ncbi.nlm.nih.gov/geo/query/acc.cgi?acc=GSE14024
Status:	Public on May 27 2009
Title:	Reversal of oncogene transformation and suppression of tumor growth by the novel IGF1R kinase inhibitor A-928605.
Organism:	Mus musculus
Experiment type:	Expression profiling by array
Platform:	GPL1261
Pubmed ID:	19732452
Summary & Design:	**Summary:** The insulin-like growth factor (IGF) axis is an important signaling pathway in the growth and survival of many cell types and has been implicated in multiple aspects of cancer progression from tumorigenesis to metastasis. The multiple roles of IGF signaling in cancer suggest that selective inhibition of the pathway might yield clinically effective therapeutics. Here we describe A-928605, a novel small molecule inhibitor of the receptor tyrosine kinase responsible for IGF signal transduction. This small molecule is able to abrogate activation of the pathway as shown by effects on the target and downstream effectors and is shown to be effective at inhibiting the proliferation of an oncogene addicted tumor model cell line (CD8-IGF1R 3T3) both in vitro and in vivo. **Keywords:** Treatment Response **Overall design:** CD8-IGF1R 3T3 cells and 3T3 Vector control treated for 24 h with vehicle or IGF1R inhibitor A-928605, all with 3 replicates.

Background corr dist: KL-Divergence = 0.0597, L1-Distance = 0.0249, L2-Distance = 0.0008, Normal std = 0.5420

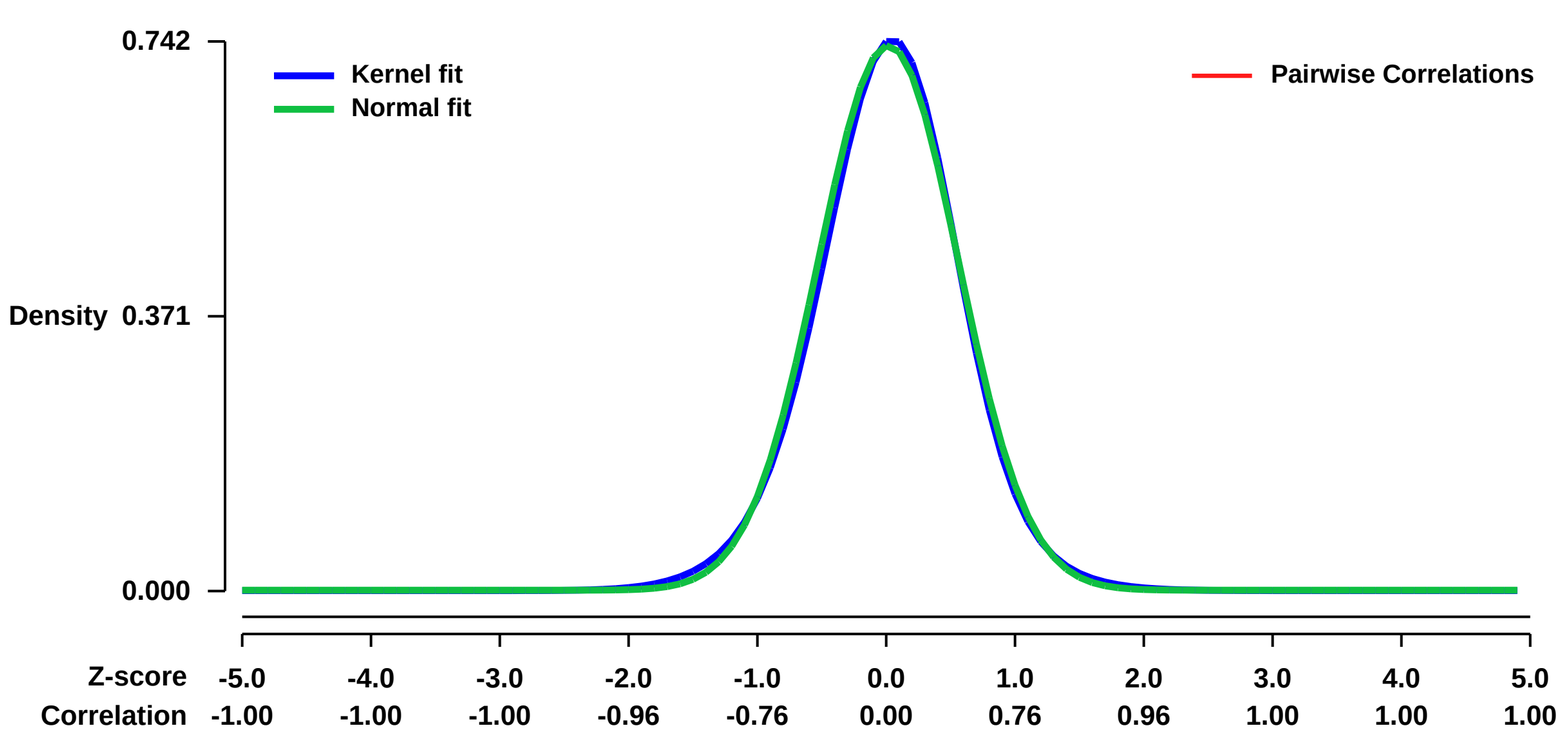

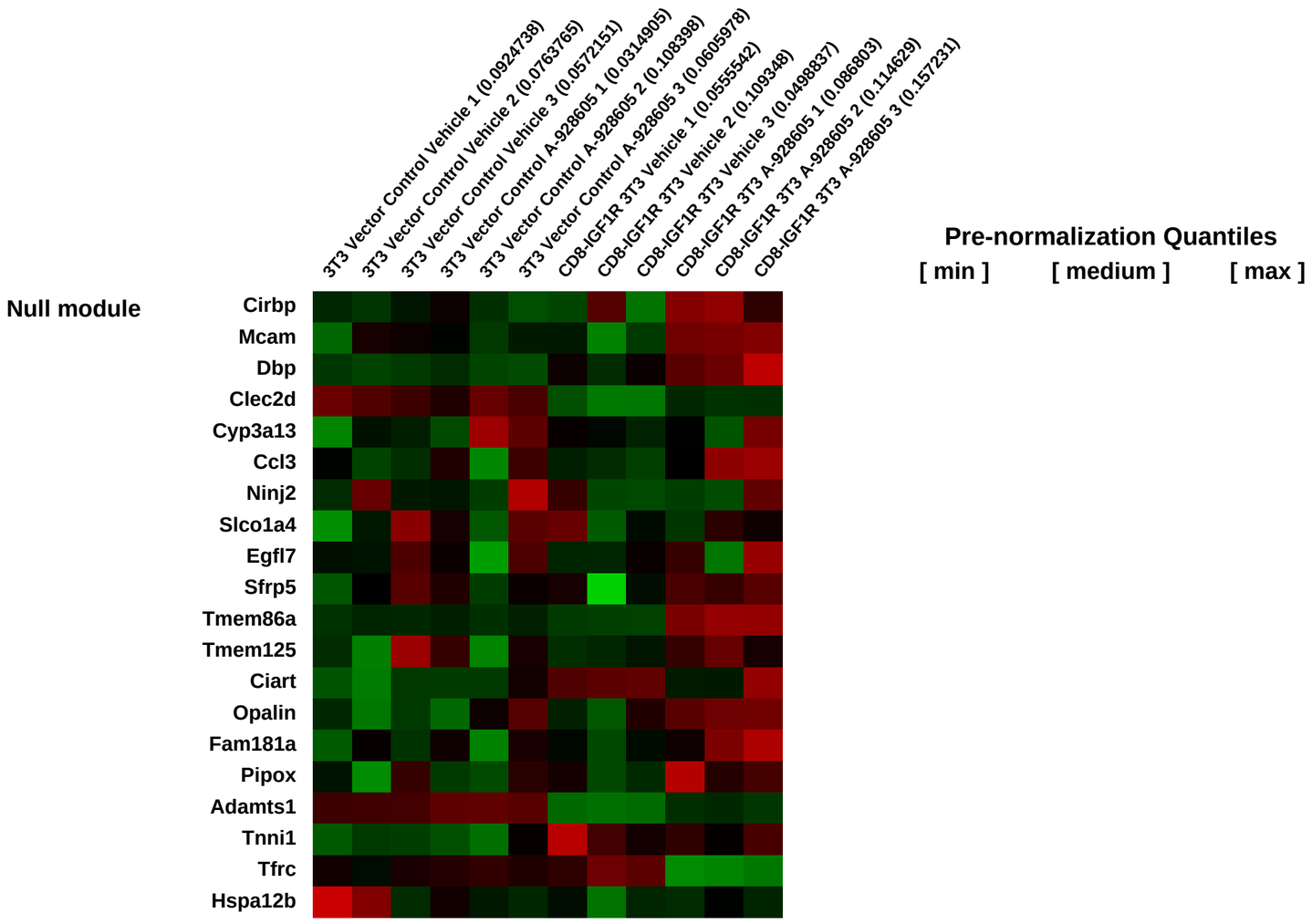

GEO Series "GSE5140" Expression Profiles

Num of samples in this series: 13

Scale of expression profile Z-scores

-3.0 -2.0 -1.0 0.0 1.0 2.0 3.0

GEO Link:	**http://www.ncbi.nlm.nih.gov/geo/query/acc.cgi?acc=GSE5140**
Status:	**Public on Jun 13 2007**
Title:	**Creatine increases health and life span in mice**
Organism:	**Mus musculus**
Experiment type:	**Expression profiling by array**
Platform:	**GPL1261**
Pubmed ID:	**17416441**
Summary & Design:	**Summary:** **Here we show that oral creatine (Cr) supplementation leads to increased life span in mice. Treated mice showed improved neurobehavioral performance, decreased accumulation of the aging pigment lipofuscin and upregulation of â anti-agingâ genes in brain. As Cr is virtually free of adverse effects, it may be a promising food supplement for healthy aging in man.** **Keywords: creatine, life span, neurobehavioural performance, microarray, oxidative stress, aging** **Overall design:** **6 biological replicates for creatine-treated mice, 7 biological replicates for untreated mice.**

Background corr dist: **KL-Divergence = 0.1947, L1-Distance = 0.0477, L2-Distance = 0.0052, Normal std = 0.3346**

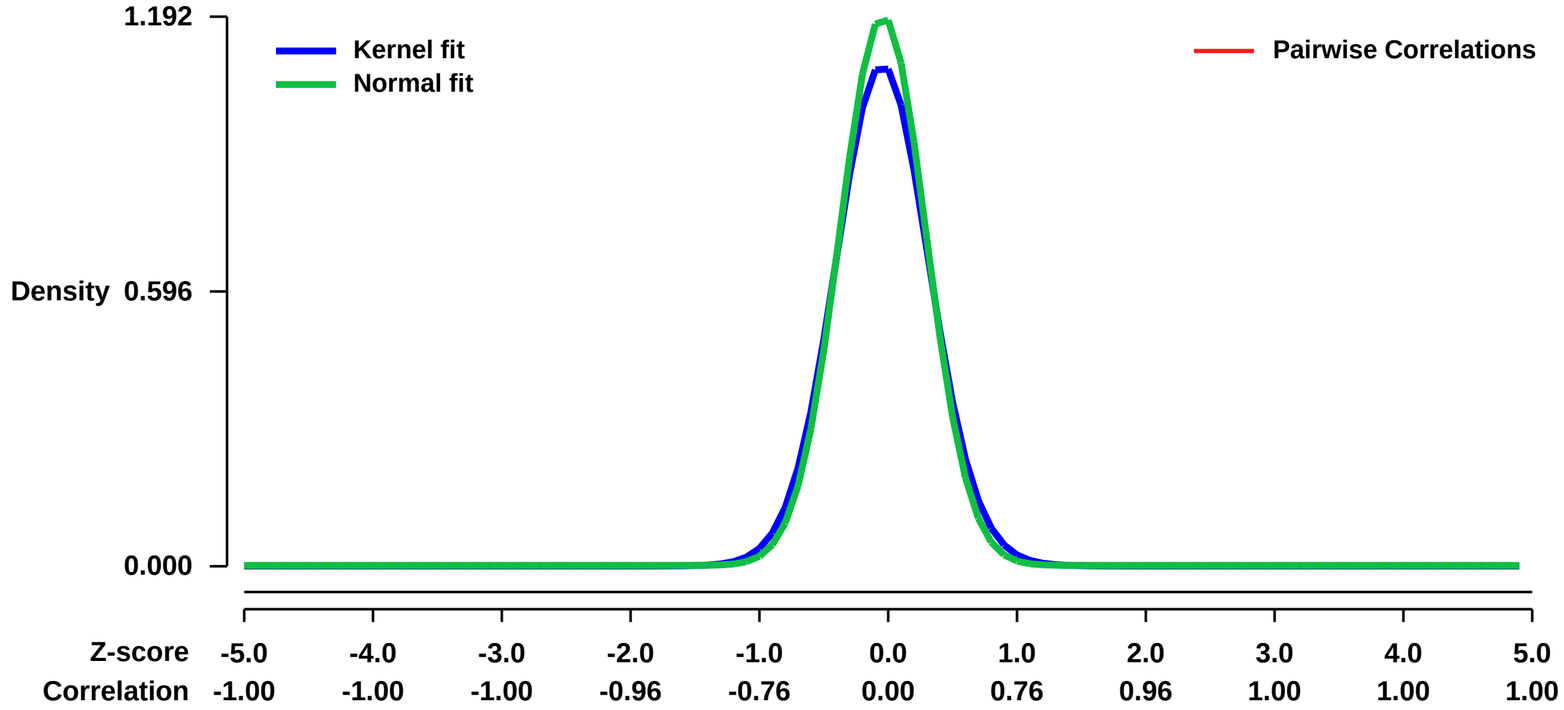

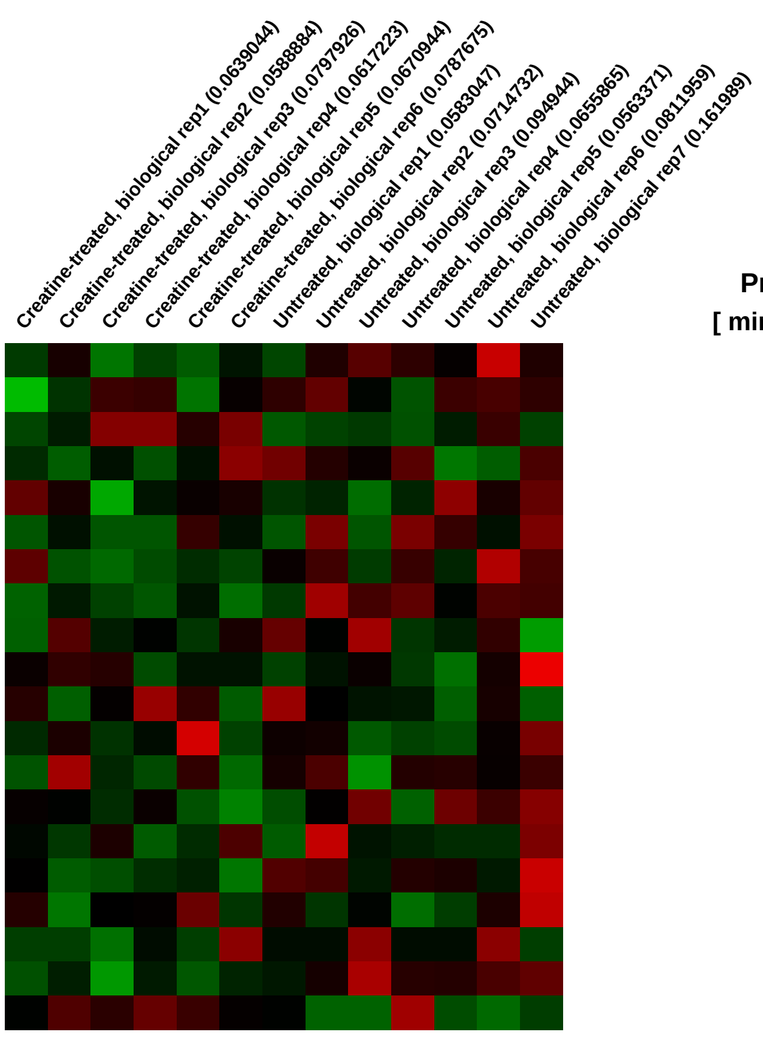

GEO Series "GSE51108" Expression Profiles

Num of samples in this series: 6

Scale of expression profile Z-scores

-3.0 -2.0 -1.0 0.0 1.0 2.0 3.0

GEO Link:	http://www.ncbi.nlm.nih.gov/geo/query/acc.cgi?acc=GSE51108
Status:	Public on Nov 18 2013
Title:	Gene expression in liver tissue from Ghrh-KO and normal (wild-type) mice
Organism:	Mus musculus
Experiment type:	Expression profiling by array
Platform:	GPL1261
Pubmed ID:	24175087
Summary & Design:	**Summary:** The hypothalamus has recently emerged as a key regulator of metabolism and aging in mammals. We have examined the impact of targeted disruption of hypothalamic hypophysiotropic peptide: Growth Hormone-releasing Hormone (GHRH) in mice on longevity, and the putative mechanisms of delayed aging. GHRH knockout (KO) mice are remarkably long-lived and in comparison to genetically normal (wild type) animals exhibiting major shifts in the expression of genes related to xenobiotic detoxification, stress resistance, and insulin signaling. These mutant mice also have increased adiponectin levels and alterations in glucose homeostasis consistent with the removal of the counter-insulin effects of GH. While these effects overlap with those of caloric restriction (CR), we show that effects of CR and the GHRH mutation are additive, with lifespan of GHRH-KO mutants further increased by CR. We conclude that GHRH-KO mice feature perturbations in a network of signaling pathways related to stress resistance, metabolic control and inflammation, and therefore provide a new model that can be used to explore links between GHRH repression, downregulation of the somatotropic axis, and extended longevity. **Overall design:** Hepatic tissue was obtained from 3 Ghrh-KO mice and 3 control (wild-type) mice (males). Expression in each sample was profiled using Affymetrix Mouse Genome 430 2.0 arrays.

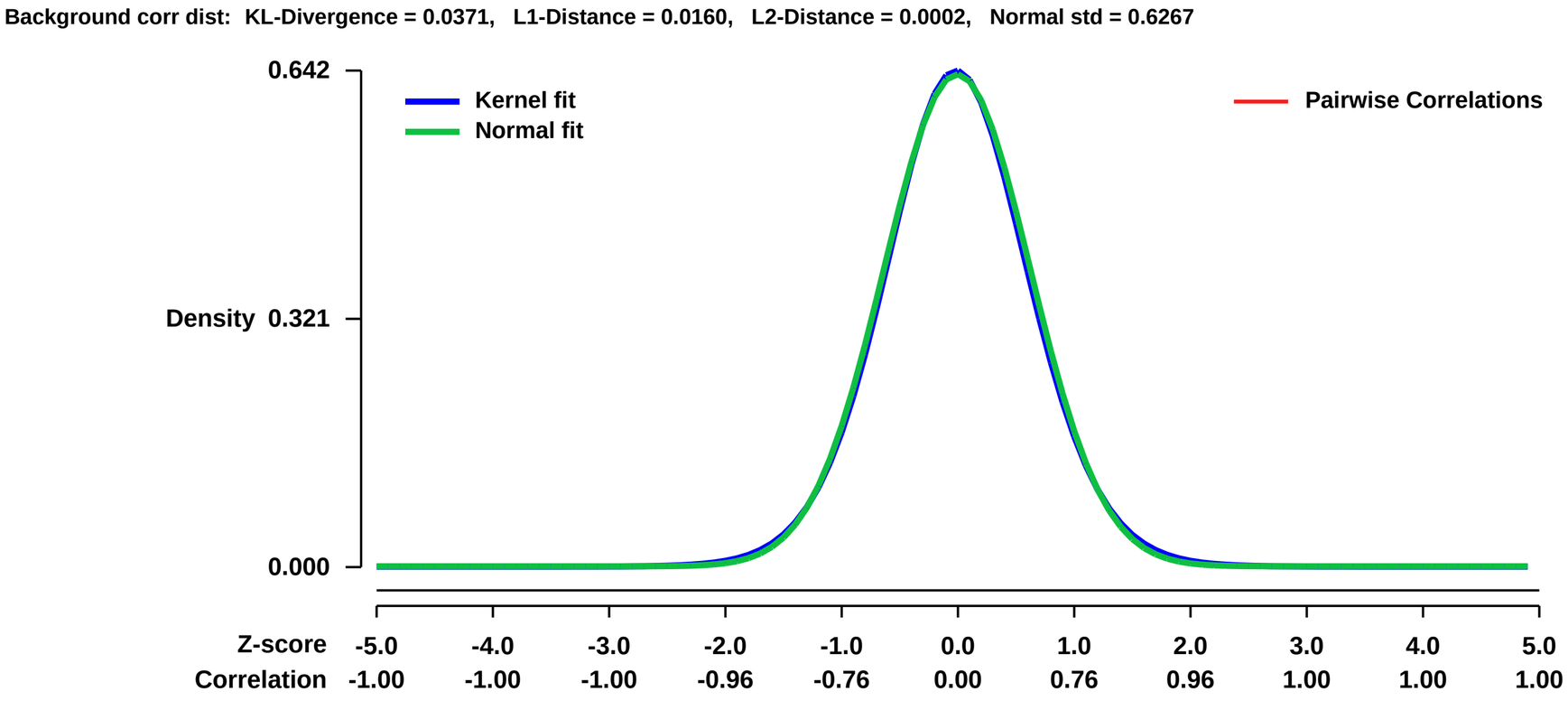

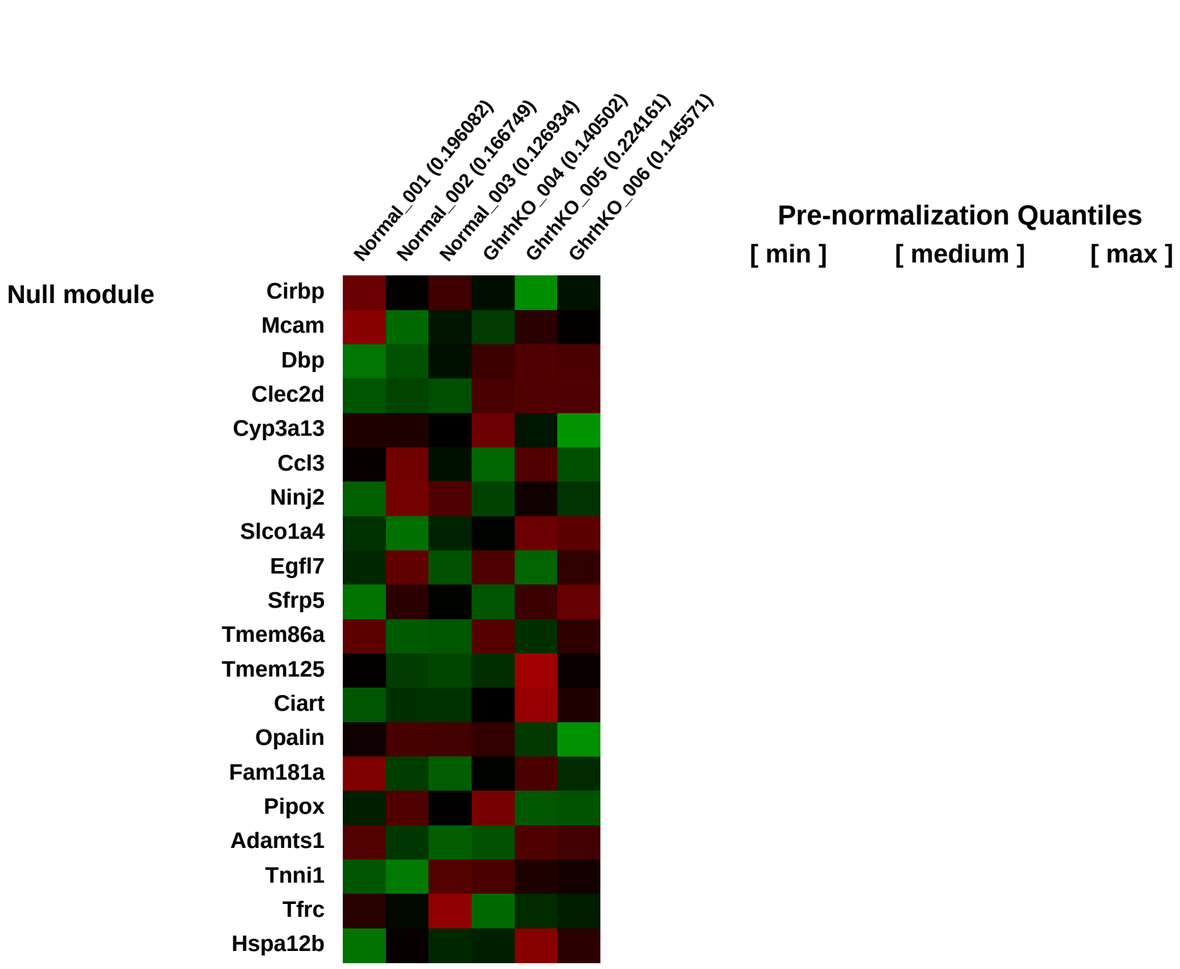

GEO Series "GSE8828" Expression Profiles

Num of samples in this series: 6

Scale of expression profile Z-scores

-3.0 -2.0 -1.0 0.0 1.0 2.0 3.0

GEO Link:	http://www.ncbi.nlm.nih.gov/geo/query/acc.cgi?acc=GSE8828
Status:	Public on Nov 19 2007
Title:	Isolation and molecular characterization of cancer stem cells in MMTVWnt-1 murine breast tumors
Organism:	Mus musculus
Experiment type:	Expression profiling by array
Platform:	GPL1261
Pubmed ID:	17975224
Summary & Design:	**Summary:** In human breast cancers, a phenotypically distinct minority population of tumorigenic cancer (TG) cells (sometimes referred to as cancer stem cells) drives tumor growth when transplanted into immunodeficient mice. Our objective was to identify a mouse model of breast cancer stem cells that could have relevance to studying human breast cancer. To do so, we utilized breast tumors of the MMTVWnt-1 mice. MMTV-Wnt-1 breast tumors were harvested, dissociated into single cell suspensions, and FACS sorted on Thy1, CD24, and CD45. FACS sorted cells were then injected into recipient background FBV/NJ female mice. Thy1+CD24+ cancer cells, which constitute approximately 1-4% of tumor cells were highly enriched for cells capable of regenerating new tumors when compared to cells of the tumor that did not fit this profile (â Not Thy1+CD24+â). Resultant tumors were of the same phenotypic diversity as the original tumor and behaved in a similar manner when passaged. Microarray analysis comparing Thy1+CD24+ tumor cells to â Not Thy1+CD24+â cells identified a list of differentially expressed genes. Orthologs of these differentially expressed genes predicted survival of human breast cancer patients from two different study groups. These studies suggest that there is a cancer stem cell compartment in the MMTV-Wnt-1 murine breast tumor and that there is a clinical utility of this model for the study of cancer stem cells. **Keywords: cell type comparison** **Overall design:** Expression profling were performed on 3 tumorigenic and 3 non tumorigenic samples of MMTV-Wnt-1 breast tumors. A gene signature was derived by comparing the gene expressions of 3 tumorigenic samples with 3 nontumorigenic samples

Background corr dist: KL-Divergence = 0.0509, L1-Distance = 0.0366, L2-Distance = 0.0020, Normal std = 0.5926

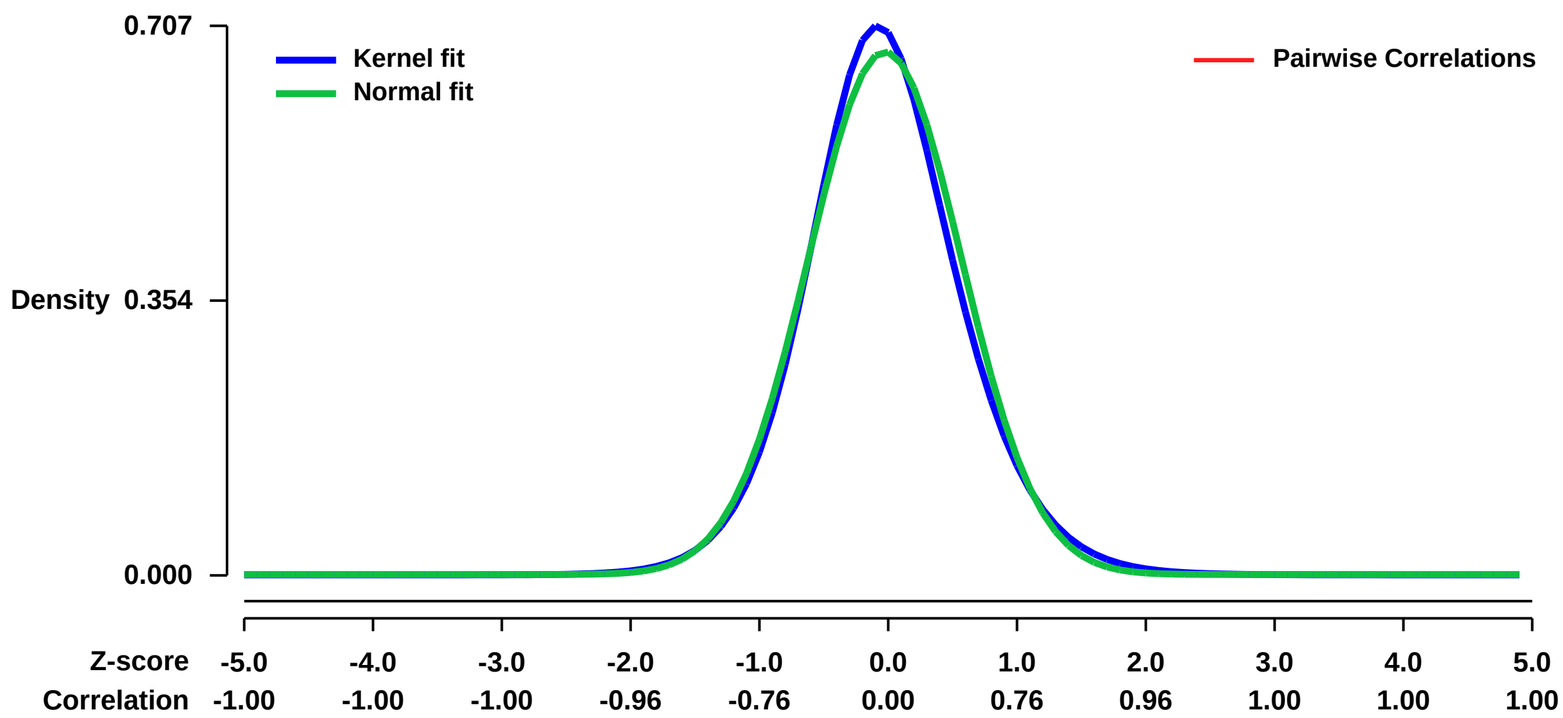

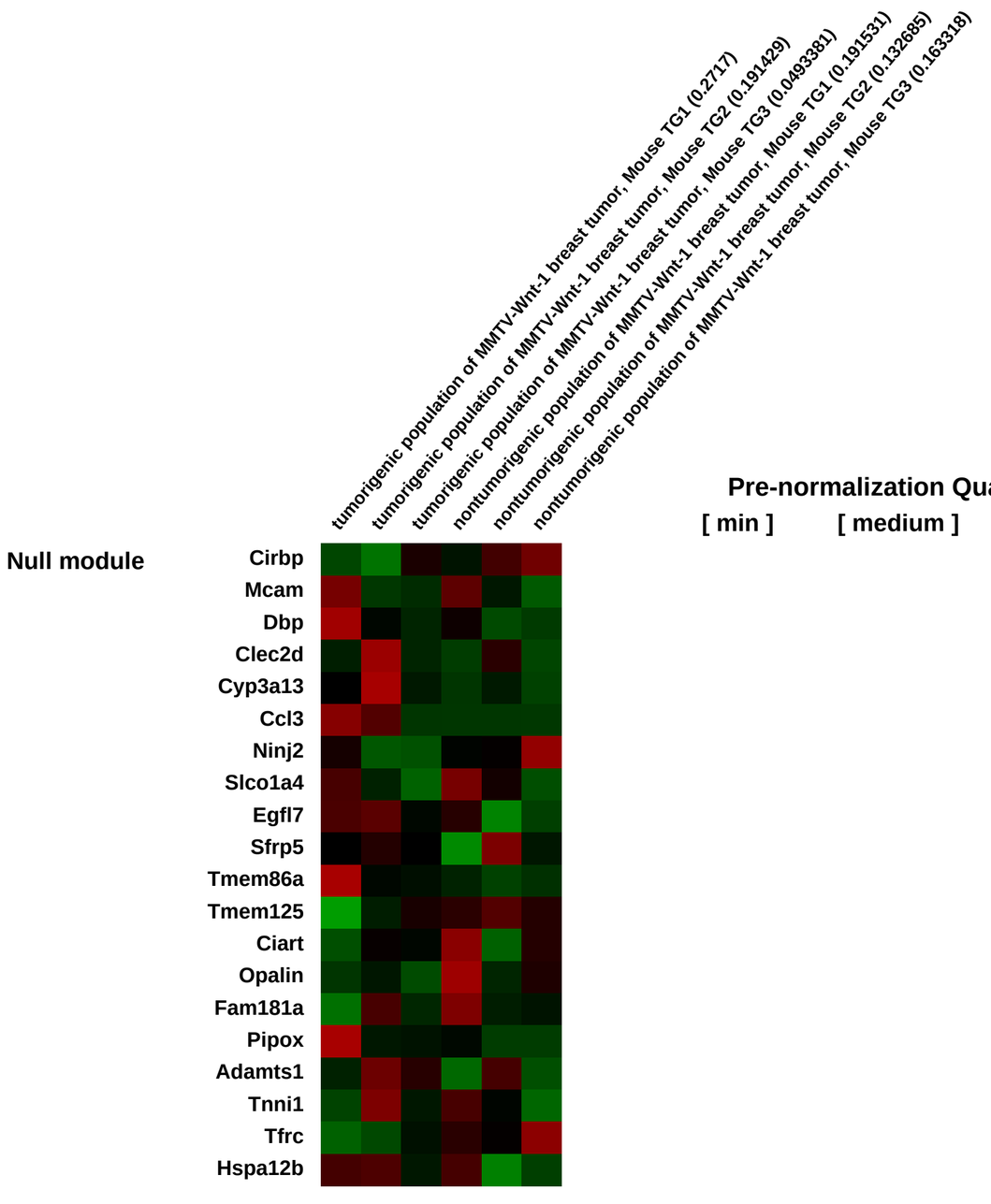

GEO Series "GSE45369" Expression Profiles

Num of samples in this series: 14

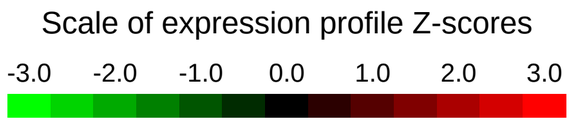

GEO Link:	**http://www.ncbi.nlm.nih.gov/geo/query/acc.cgi?acc=GSE45369**
Status:	**Public on Mar 22 2013**
Title:	**Mouse lung transcriptional response to flagellin stimulation**
Organism:	**Mus musculus**
Experiment type:	**Expression profiling by array**
Platform:	**GPL1261**
Pubmed ID:	
Summary & Design:	**Summary:** **Vaccine adjuvants enhance adaptive immunity to co-administered antigens. Whereas the modes of action are multiple, the activation of antigen-presenting cells (APC) like dendritic cells by adjuvants is a prerequisite. Detection of microbial signals by innate sensors like Toll-like receptors (TLR) is a major mechanism of APC activation. Most candidate or licensed vaccines assume that adjuvant activity of TLR agonists depends on direct effect on APCs. This study addressed whether TLR stimulation of non-hematopoietic cells could contribute to the adjuvant effect. Nasal administration of flagellin enhanced T´ cell- and antibody-mediated immunity to co-administered antigens in a TLR5-dependent but inflammasome-independent manner. We found that lung radioresistant cells were sufficient to promote immunity, thereby suggesting that direct TLR5-mediated APC stimulation is dispensable to adjuvant activity. Consistent with this, radioresistant compartment is essential to stimulate the swift TLR5-dependent transcription. The transcriptional response was restricted to the epithelial compartment and was associated to the production of a narrow set of mediators including the chemokine CCL20, known to promote APC recruitment in mucosal tissues. Besides, flagellin was rapidly degraded in lower airways and was not transported into lung parenchyma or peripheral tissues. This study therefore suggests an unexpected mechanism for how TLR agonists act as adjuvant and how epithelium is instrumental to sense and integrate microbial signals to promote adaptive immunity. In conclusion, the immune-enhancing effect of adjuvants on epithelial cells can be harnessed for improving vaccines.** **Overall design:** **1 ´µg of flagellin was instillated intranasally to LPS-unresponsive C3H/HeJ mice. Total lung RNA was extracted 1h later and prepare for hybridization on Affymetrix microarrays.**

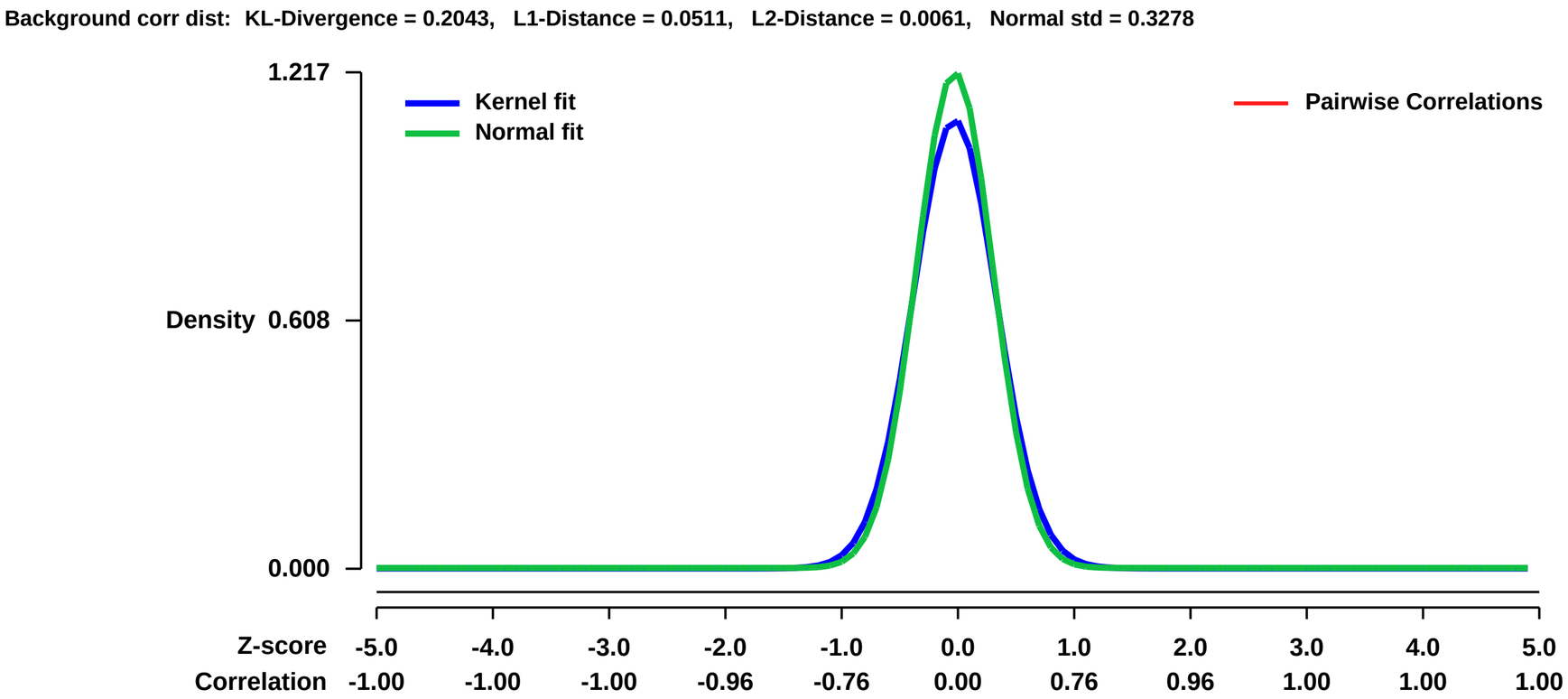

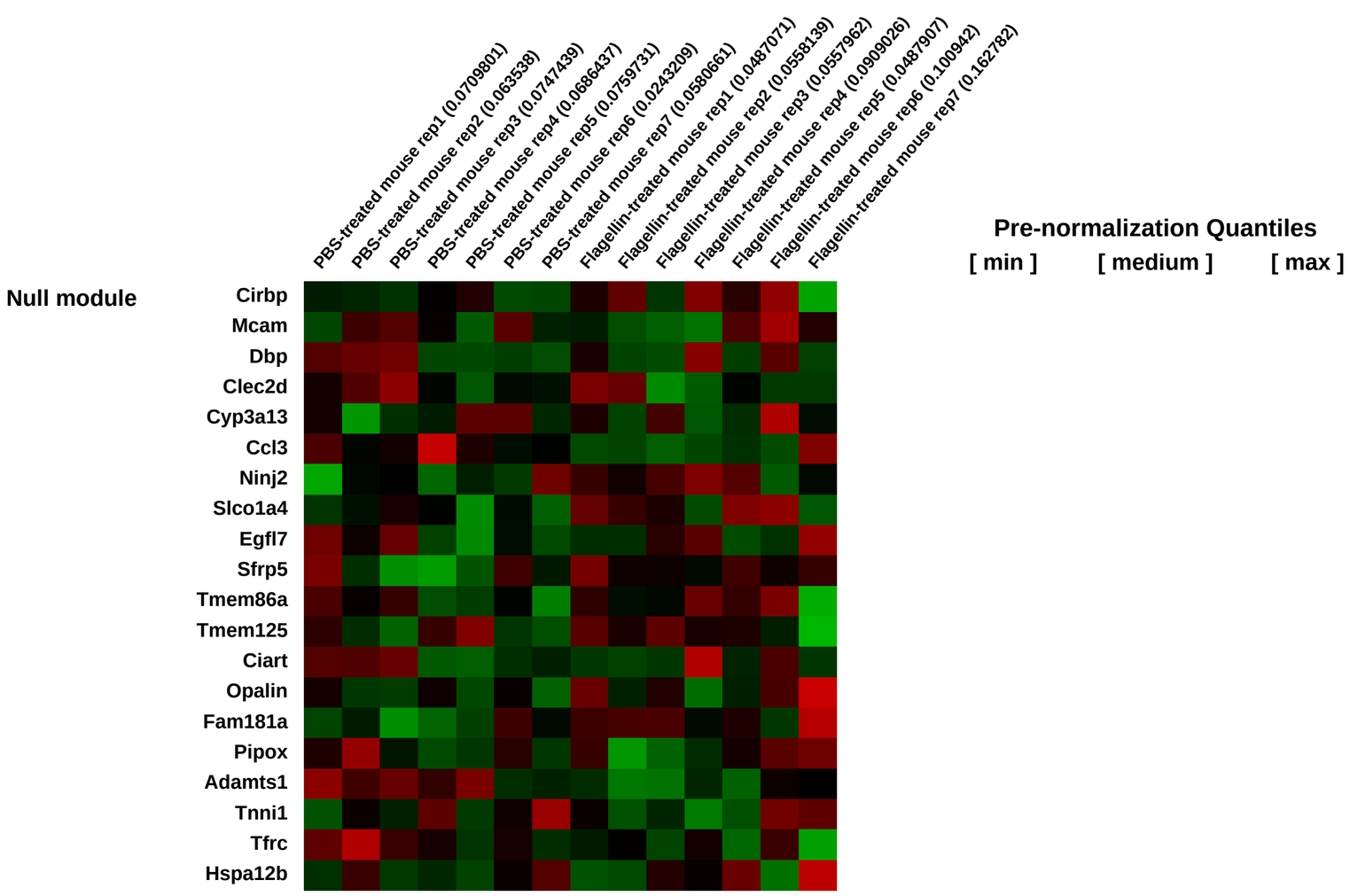

GEO Series "GSE3440" Expression Profiles

Num of samples in this series: 15

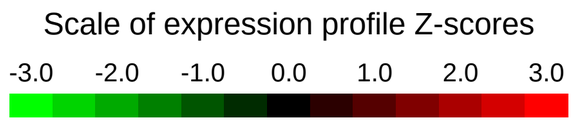

GEO Link:	http://www.ncbi.nlm.nih.gov/geo/query/acc.cgi?acc=GSE3440
Status:	Public on Nov 01 2005
Title:	Effect of aldosterone on gene expression in the heart
Organism:	Mus musculus
Experiment type:	Expression profiling by array
Platform:	GPL1261
Pubmed ID:	16601137

Summary & Design:

Summary:
Aldosterone is known to have a number of direct adverse effects on the heart, including fibrosis and myocardial inflammation. However, genetic mechanisms of aldosterone action on the heart remain unclear.

This experiment investigated of temporal changes in gene expression profile of the whole heart induced by acute administration of a physiologic dose of aldosterone in the mouse. mRNA levels of 34,000 known mouse genes were measured at eight time points after aldosterone administration using oligonucleotide microarrays and compared to those of the control animals who underwent a sham injection. A novel software tool (CAGED) designed for analysis of temporal microarray experiments using a Bayesian approach was used to identify genes differentially expressed between the aldosterone-injected and control group.

CAGED analysis identified twelve genes as having significant differences in their temporal profiles between aldosterone-injected and control groups. All of these genes exhibited a decrease in expression level 1-3 hours after aldosterone injection followed by a brief rebound and a return to baseline. These findings were validated by quantitative RT-PCR. The differentially expressed genes included phosphatases, regulators of steroid biosynthesis, inactivators of reactive oxygen species, and structural proteins. Several of these genes are known to functionally mediate biochemical phenomena previously observed to be triggered by aldosterone administration, such as phosphorylation of ERK1/2. These results provide the first description of cardiac genetic response to aldosterone and identify several potential mediators of known biochemical sequelae of aldosterone administration in the heart.

Methods:

Male C57BL6 mice were injected with aldosterone 10 mcg/kg (experimental group) or vehicle (control group) at time 0. Five animals were sacrificed at each of the following time points in each group: 0, 0.5, 1, 2, 3, 4, 5, and 12 hours from injection. Hearts were removed and total RNA extracted from the hearts of all five animals at each time point / experimental condition was pooled for gene expression analysis.

Keywords: time series

Overall design:
Time series of effect of aldosterone on gene expression in the mouse heart

Background corr dist: **KL-Divergence = 0.1782, L1-Distance = 0.0443, L2-Distance = 0.0043, Normal std = 0.3474**

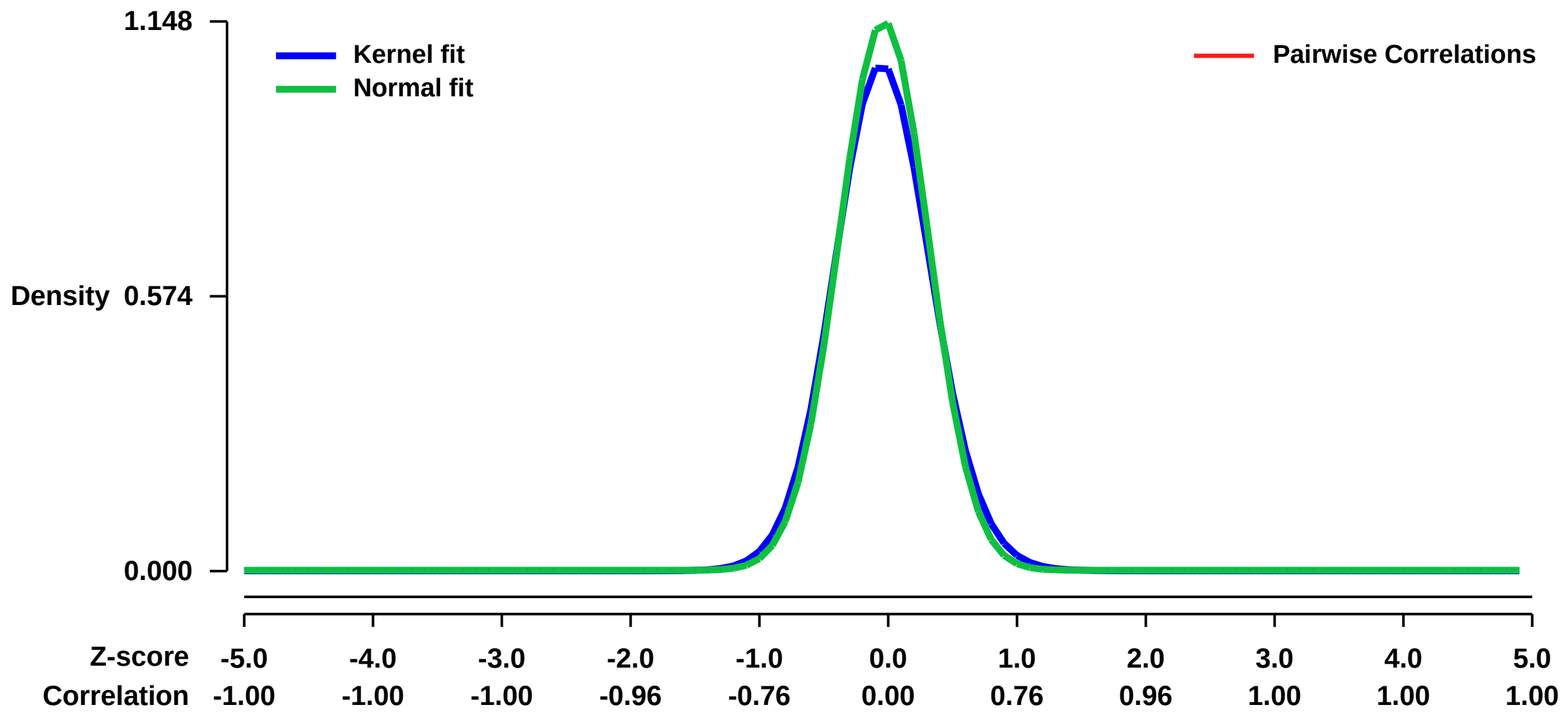

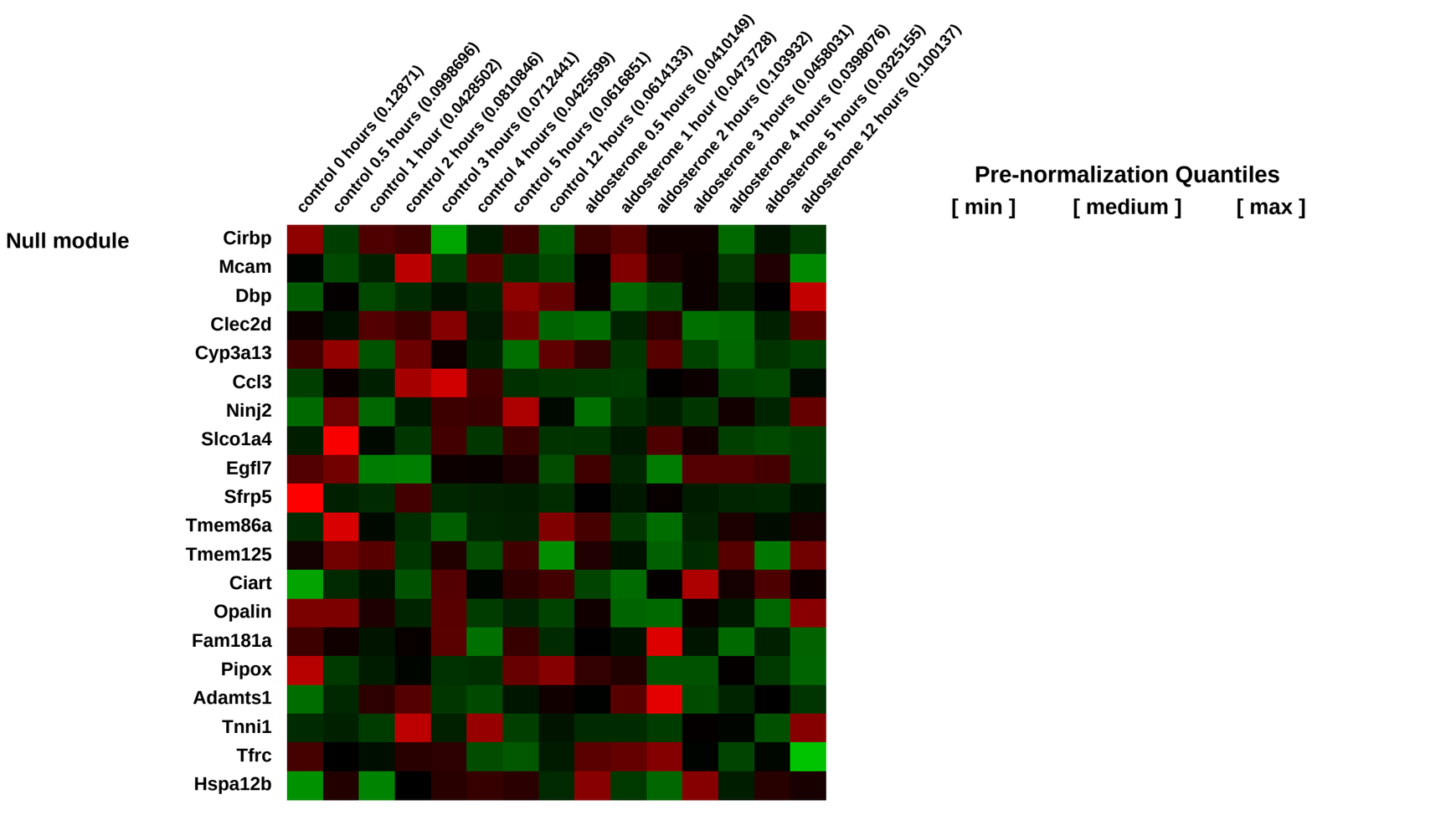

GEO Series "GSE54215" Expression Profiles

Num of samples in this series: 13

Scale of expression profile Z-scores

-3.0 -2.0 -1.0 0.0 1.0 2.0 3.0

GEO Link:	http://www.ncbi.nlm.nih.gov/geo/query/acc.cgi?acc=GSE54215
Status:	Public on Mar 02 2014
Title:	Comparison of gene expression profiles of naˆflve and in vitro effector CD8+ T cells from wild-type and BATF-/- mice
Organism:	Mus musculus
Experiment type:	Expression profiling by array
Platform:	GPL1261
Pubmed ID:	24584090
Summary & Design:	**Summary:** The transcription factor BATF is required for Th17 and TFH differentiation. Here, we show that BATF also has a fundamental role in regulating effector CD8+ T cell differentiation. BATF-deficient CD8+ T cells show profound defects in effector expansion and undergo proliferative and metabolic catastrophe early after antigen encounter. BATF, together with IRF4 and Jun proteins, binds to and promotes early expression of genes encoding lineage-specific transcription-factors (T-bet and Blimp-1) and cytokine receptors, while paradoxically repressing genes encoding effector molecules (IFNg and granzyme B). Thus, BATF amplifies TCR-dependent transcription factor expression and augments inflammatory signal propagation but restrains effector gene expression. This checkpoint prevents irreversible commitment to an effector fate until a critical threshold of downstream transcriptional activity has been achieved. **Overall design:** P14 TCR transgenic CD8+ T cells from wild-type or BATF-/- mice were examined either as naˆflve cells or after 3 days of in vitro stimulation with antibodies to CD3 and CD28 in the presence of IL-2

Background corr dist: KL-Divergence = 0.0486, L1-Distance = 0.0713, L2-Distance = 0.0070, Normal std = 0.6584

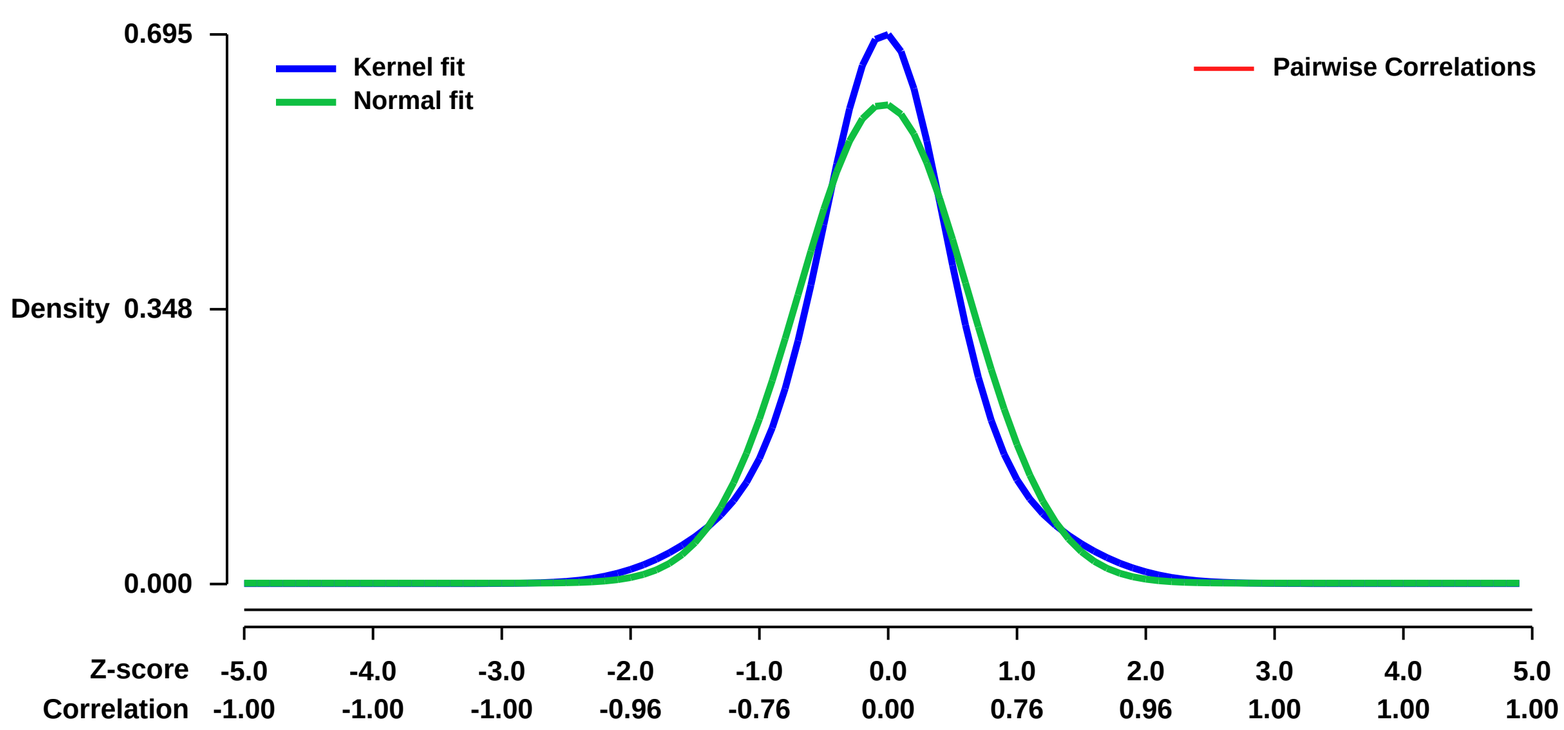

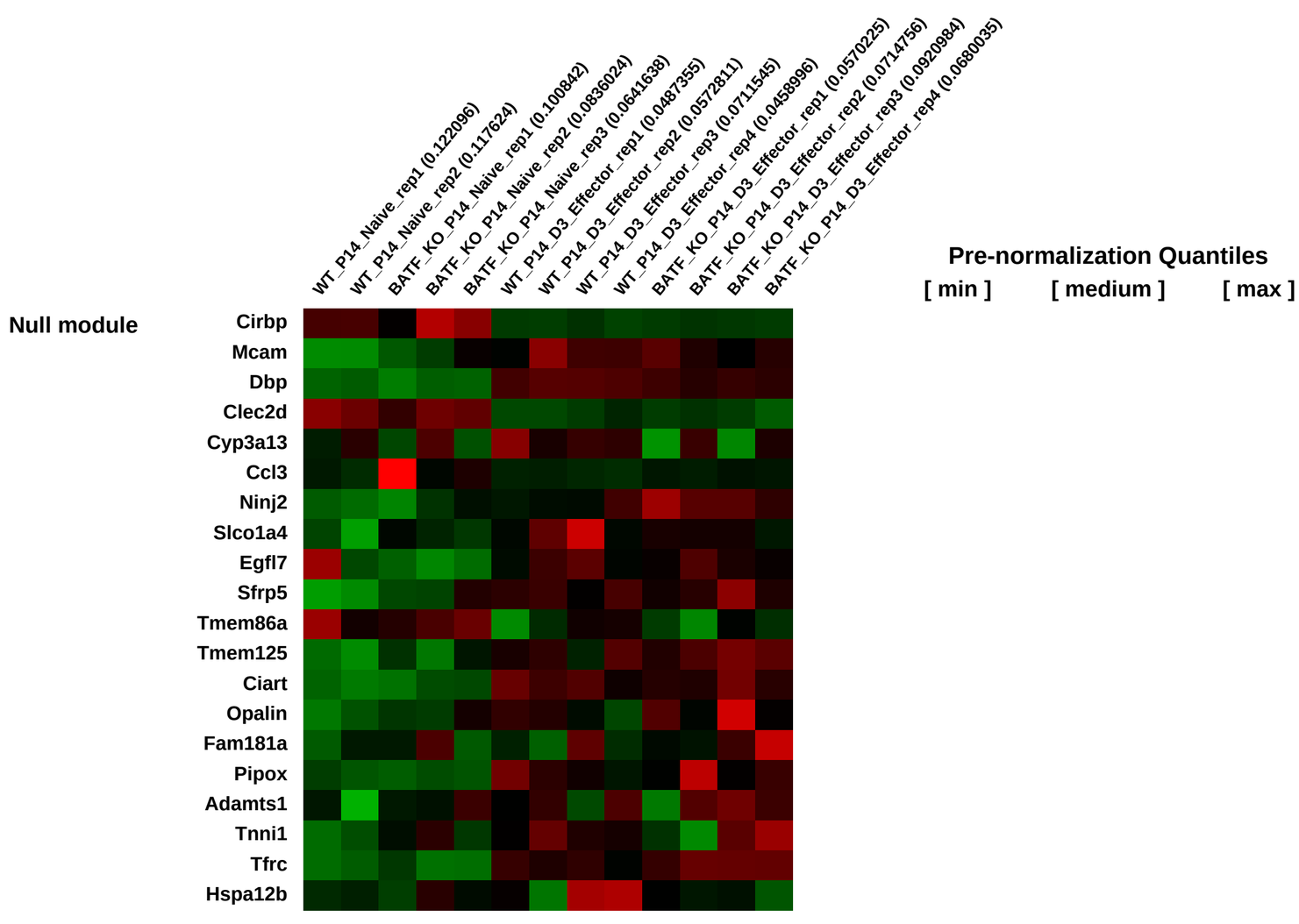

GEO Series "GSE9652" Expression Profiles

Num of samples in this series: 11

Scale of expression profile Z-scores

-3.0 -2.0 -1.0 0.0 1.0 2.0 3.0

GEO Link:	http://www.ncbi.nlm.nih.gov/geo/query/acc.cgi?acc=GSE9652
Status:	Public on Jul 01 2008
Title:	GATA4 is a direct activator of Cyclin D2 and is required for proliferation in 2nd heart field-derived myocardium
Organism:	Mus musculus
Experiment type:	Expression profiling by array
Platform:	GPL1261
Pubmed ID:	18591257
Summary & Design:	**Summary:** The second heart field (SHF) comprises a population of mesodermal progenitor cells that are added to the nascent linear heart to give rise to the majority of the right ventricle, interventricular septum, and outflow tract of mammals and birds. The zinc finger transcription factor GATA4 functions as an integral member of the cardiac transcription factor network in the SHF and its derivatives. In addition to its role in cardiac differentiation, GATA4 is also required for cardiomyocyte replication, although the transcriptional targets of GATA4 required for proliferation have not been previously identified. In the present study, we disrupted Gata4 function exclusively in the SHF and its derivatives. Gata4 SHF knockout mice die by embryonic day 13.5 and exhibit hypoplasia of the right ventricular myocardium and interventricular septum and display profound ventricular septal defects. Loss of Gata4 function in the SHF results in decreased myocyte proliferation in the right ventricle, and we identify numerous cell cycle genes that are dependent on Gata4 by microarray analysis. We show that Gata4 is required for Cyclin D2 expression in the right ventricle and that the Cyclin D2 promoter is bound and activated by GATA4 via three consensus GATA binding sites. These findings establish Cyclin D2 as a direct transcriptional target of GATA4 and support a model in which GATA4 controls cardiomyocyte proliferation by coordinately regulating numerous cell cycle genes. **Keywords:** genetic modification **Overall design:** 170 n=3), and Gata4flox/flox; Nkx2-5Cre/+ (Gata4 CKONkx, n=5).

Background corr dist: KL-Divergence = 0.1111, L1-Distance = 0.0276, L2-Distance = 0.0013, Normal std = 0.4203

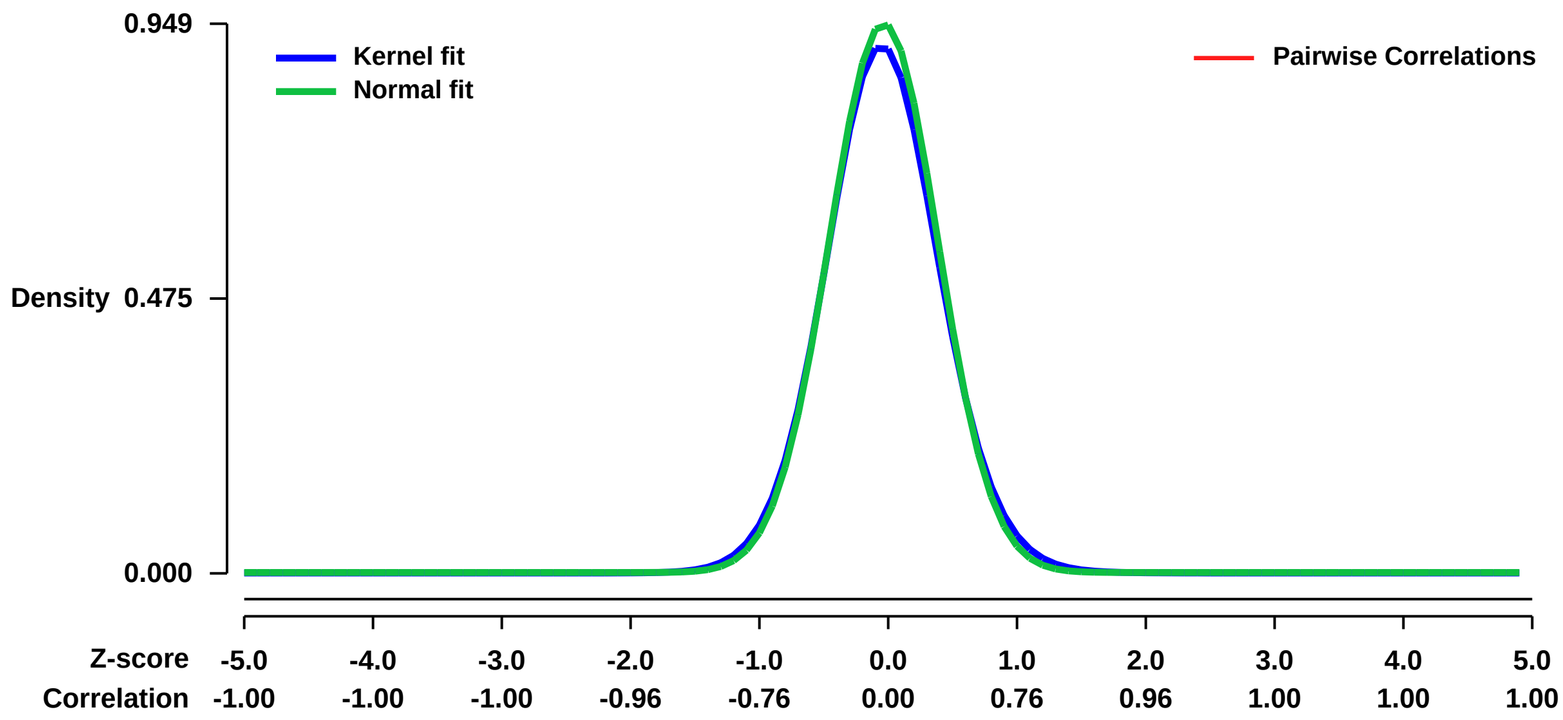

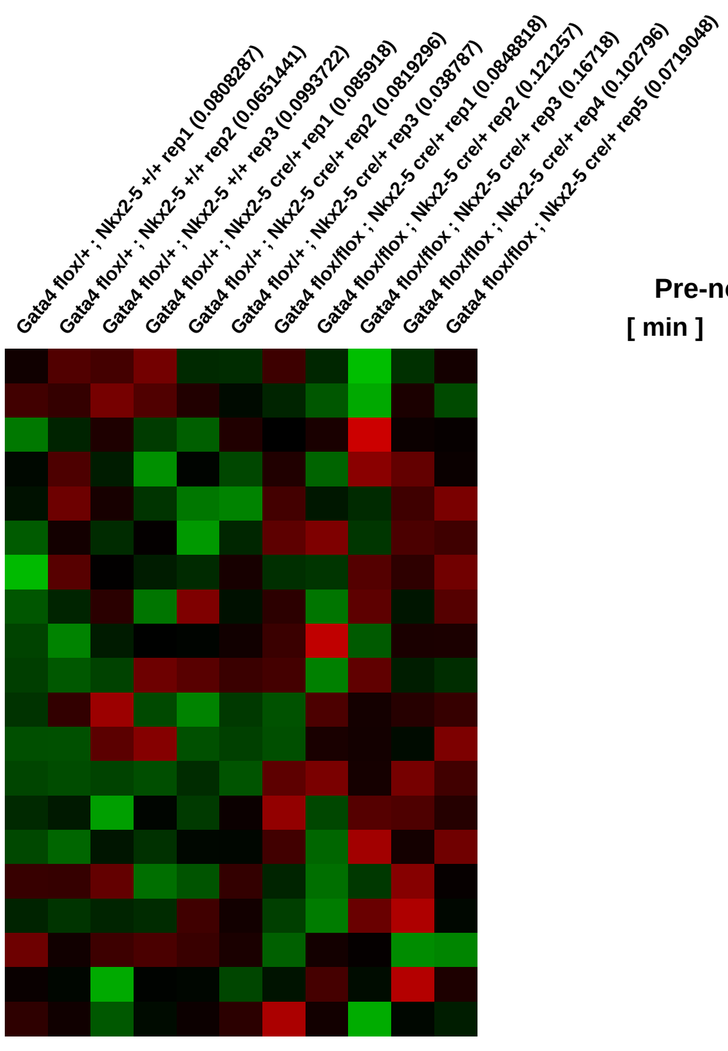

GEO Series "GSE39621" Expression Profiles

Num of samples in this series: 51

Scale of expression profile Z-scores

-3.0 -2.0 -1.0 0.0 1.0 2.0 3.0

GEO Link:	http://www.ncbi.nlm.nih.gov/geo/query/acc.cgi?acc=GSE39621
Status:	Public on Dec 27 2012
Title:	Expression data from brain, liver and spleen of Npc1-/- mice
Organism:	Mus musculus
Experiment type:	Expression profiling by array
Platform:	GPL1261
Pubmed ID:	23094108
Summary & Design:	**Summary:** Niemann-Pick Type C (NPC) disease is a rare, genetic, lysosomal disorder with progressive neurodegeneration. Poor understanding of the pathophysiology and lack of blood-based diagnostic markers are major hurdles in the treatment and management of NPC and several additional neurological, lysosomal disorders. To identify disease severity correlates, we undertook whole genome expression profiling of sentinel organs, brain, liver, and spleen of Balb/c Npc1-/- mice (Npc1nih)relative to Npc1+/- at an asymptomatic stage, as well as early- and late-symptomatic stages. Unexpectedly, we found prominent up regulation of innate immunity genes with age-dependent change in their expression, in all three organs. We shortlisted a set of 12 secretory genes whose expression steadily increased with age in both brain and liver, as potential plasma correlates for the neurological disease. Ten were innate immune genes with eight ascribed to lysosomes. Several are known to be elevated in diseased organs of murine models of other lysosomal diseases including Gaucherâ s disease, Sandhoff disease and MPSIIIB. We validated the top candidate lysozyme, in the plasma of Npc1-/- as well as Balb/c Npc1nmf164 mice (bearing a point mutation closer to human disease mutants) and show its reduction in response to an emerging therapeutic. We further established elevation of innate immunity in Npc1-/- mice through multiple functional assays including inhibition of bacterial infection as well as cellular analysis and immunohistochemistry. We used microarrays on the diseased organs, brain, liver and spleen of the Npc1-/- mice to unserstand the molecular changes occur during the progression of NPC diseases. From the data, we have identified 12 potential genes which can be potentially developed as blood-based biomarker. We have also discovered up regulation of innate iimunity genes in all three organs of Npc1-/- mice and functionally validated them in liver and spleen. **Overall design:** Brain from 11 female Npc1â /â and 16 control female mice (Npc1+/+ and Npc1+/â) from 6 age groups (20-25, 37-40, 54-55, 59-62, 67-71 and 81-84 days) were surgically harvested. Liver and spleen from 6 Npc1-/- and 6 Npc1+/- female mice from three age group (20-25, 54-55 and 67-71 days) were surgically harvested. Organs were kept in RNA later and stored at -20 ´°C until used. RNA was isolated and Affymetrix mouse 430 2.0 array hybridizations were performed by â UCLA Clinical Microarray Coreâ , UCLA, Los Angeles, CA, USA. Subsequent raw data were analyzed using DNA-Chip Analyzer (D-Chip) with the .CEL files obtained from AGCC. Data from Npc1-/- mice from all age groups were compared to control mice (Npc1+/- and/or Npc1-/- mice) from all age groups separately for brain, liver and spleen. 'Matrix Table1' corrsponds for brain, 'Matrix Table2' corresponds for liver and 'Matrix Table3' corresponds for spleen. Thresholds for selecting significant genes were set at a relative difference ´‡1.5-fold, absolute difference ´‡100 signal intensity units and p<0.05. Genes that met all three criteria simultaneously were considered as significant change.

Background corr dist: KL-Divergence = 0.0594, L1-Distance = 0.0598, L2-Distance = 0.0057, Normal std = 0.5712

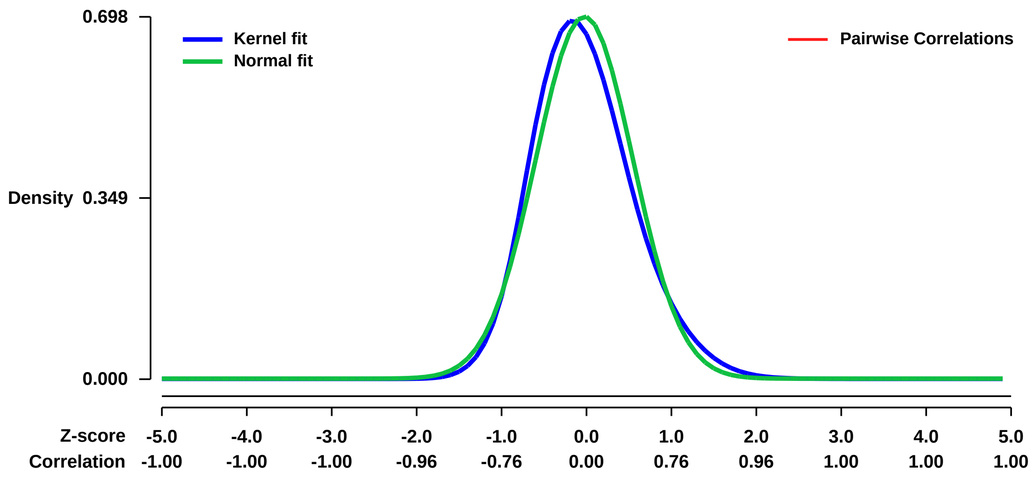

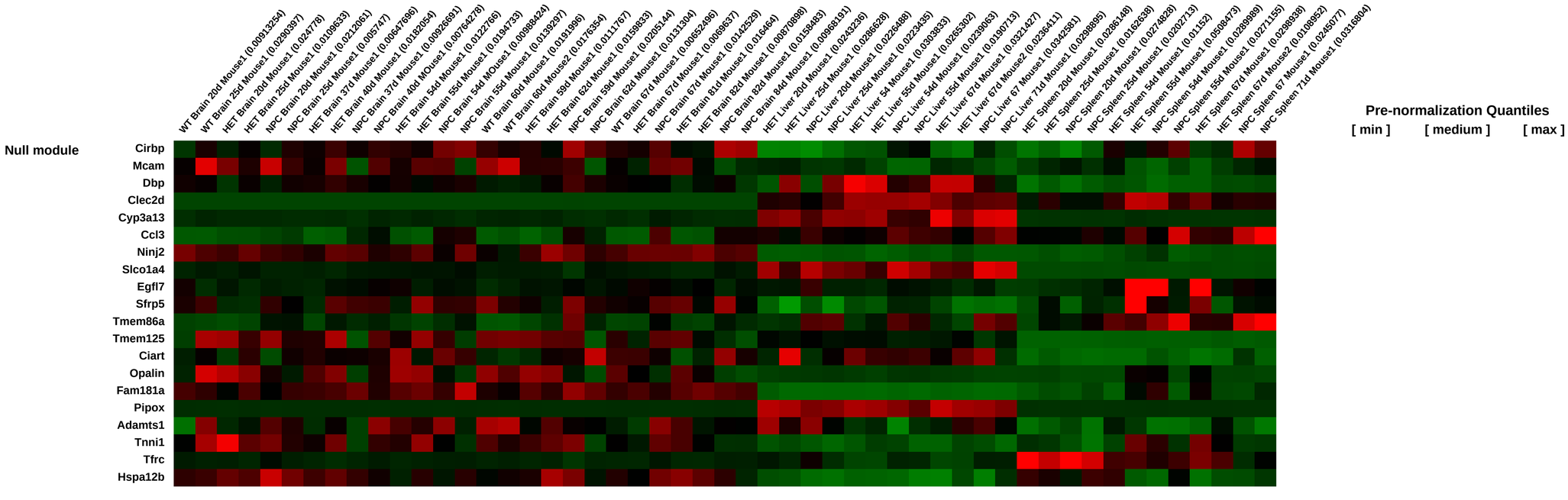

GEO Series "GSE51385" Expression Profiles

Num of samples in this series: 8

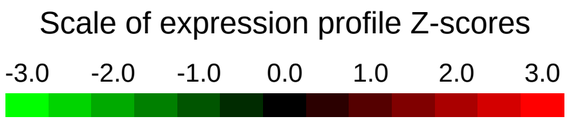

GEO Link:	http://www.ncbi.nlm.nih.gov/geo/query/acc.cgi?acc=GSE51385
Status:	Public on Oct 18 2013
Title:	Expression profiling of ProB and PreB cells in Ebf1 heterozygous mouse bone marrow
Organism:	Mus musculus
Experiment type:	Expression profiling by array
Platform:	GPL1261
Pubmed ID:	24078629
Summary & Design:	**Summary:** Loss of one allele of Ebf1 impairs pre-B cell (B220+CD19+CD43low/negIgM-) expansion. In order to better understand the underlying cause of the reduced pre-B cell compartment in Ebf1+/- mice, we sorted pro-B (B220+CD19+CD43highIgM-) as well as pre-B cells from Wt and Ebf1 heterozygote mutant mice and performed Affymetrix based microarray gene expression analysis. While the overall gene expression patterns as well as Pax5 expression in Wt and Ebf1 pro-B cells were similar, gene set enrichment (GSE) analysis of the microarray data suggested a reduced expression of cell division (p<0.001) and mitosis (p<0.001) genes in the Ebf1+/- pre-B cells as compared to their Wt counterparts. This in combination with rather normal expression of B-lineage genes in Ebf1+/- pre-B cells opens for the possibility that the phenotypic loss of pre-B cells in Ebf1+/- mice could be a result of reduced expansion of progenitors rather than by a differentiation block. **Overall design:** RNA was extracted from 20,000 or 25000 purified adult bone marrow cells using the RNAeasy microkit. RNA was labeled and amplified by dual amplification and hybridized to Affymetrix microarray MOE430_2, according to AffymetrixTM GeneChip Expression Analysis Technical Manual. Probe level expression values were calculated using the RMA algorithm.

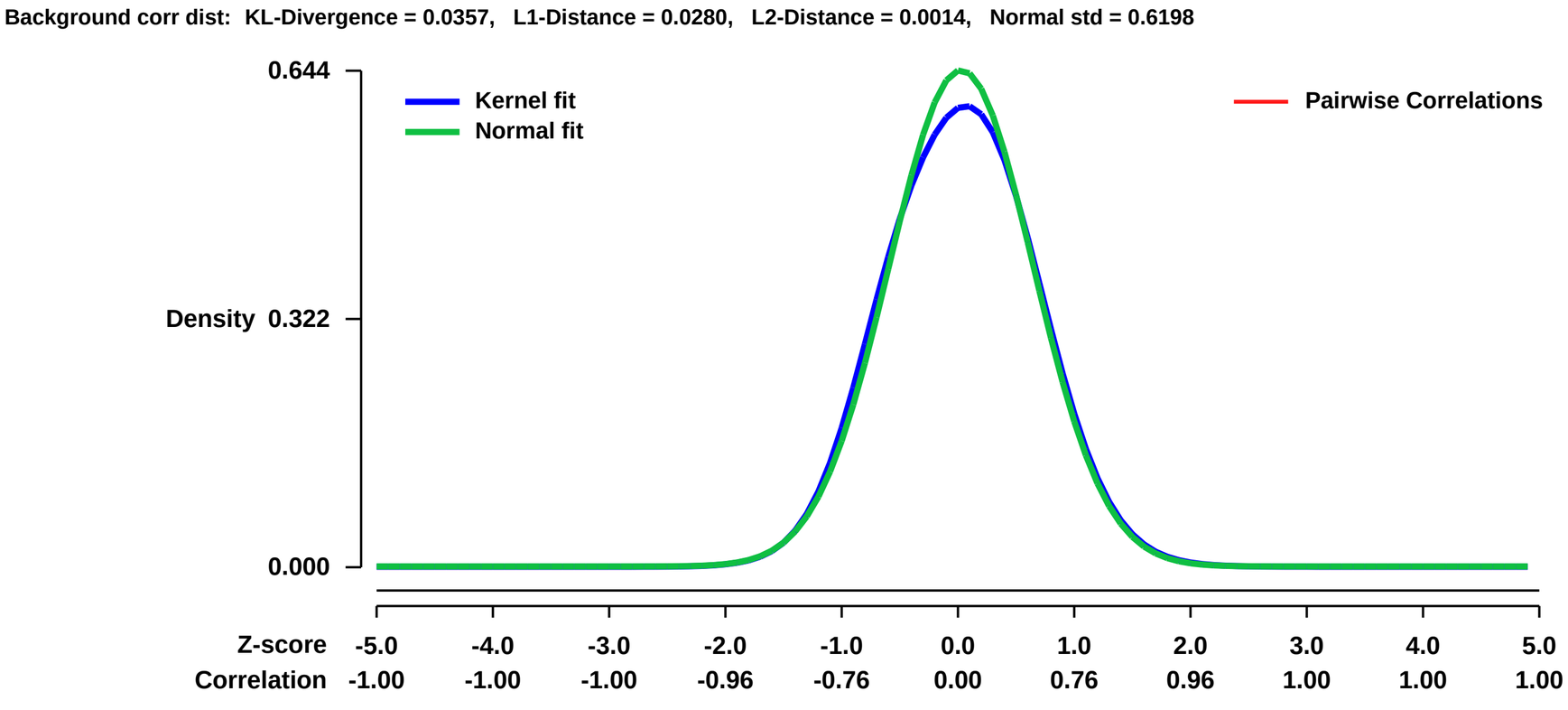

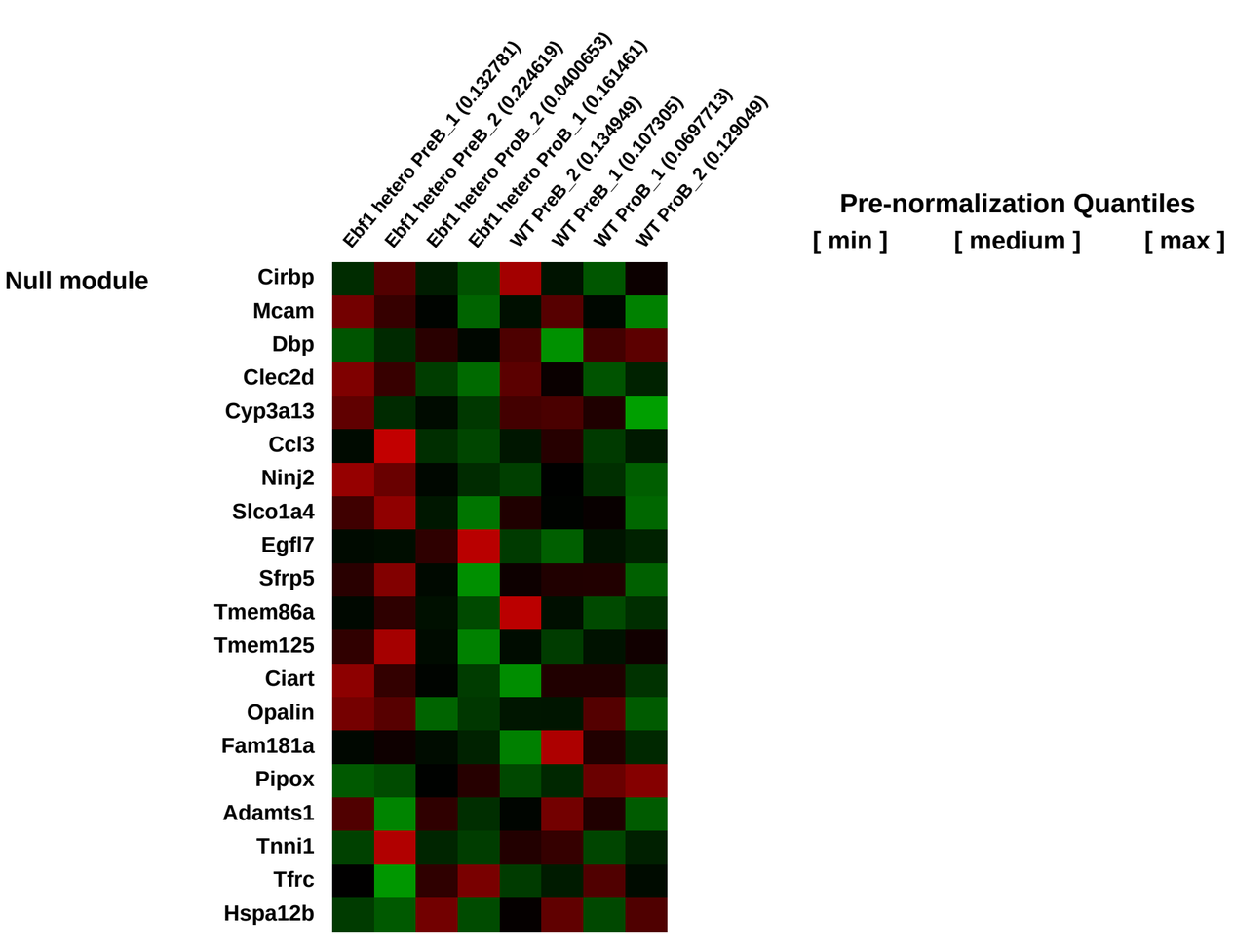

GEO Series "GSE17869" Expression Profiles

Num of samples in this series: 18

Scale of expression profile Z-scores

-3.0 -2.0 -1.0 0.0 1.0 2.0 3.0

GEO Link:	**http://www.ncbi.nlm.nih.gov/geo/query/acc.cgi?acc=GSE17869**
Status:	**Public on Aug 29 2009**
Title:	**Evaluation of Estrogen receptor related gene expression in C57BL/6 vs ERKO-alpha and ERKO-beta mice**
Organism:	**Mus musculus**
Experiment type:	**Expression profiling by array**
Platform:	**GPL1261**
Pubmed ID:	
Summary & Design:	**Summary:** **These samples are part of the MMRRC study conducted at UAlbany** **Keywords: strain comparison** **Overall design:** **Whole brains from C57BL/6 mice were compared to those from estrogen receptor knockout mice on the same background. Six samples (3 male and 3 female) from each strain (wild type B6, ERalphaKO, ERbetaKO) were compared in this study. These were processed on Affymetrix Mouse 430 plus 2.0 arrays to obtain expression data for each cell ine.**

Background corr dist: **KL-Divergence = 0.2224, L1-Distance = 0.0531, L2-Distance = 0.0067, Normal std = 0.3168**

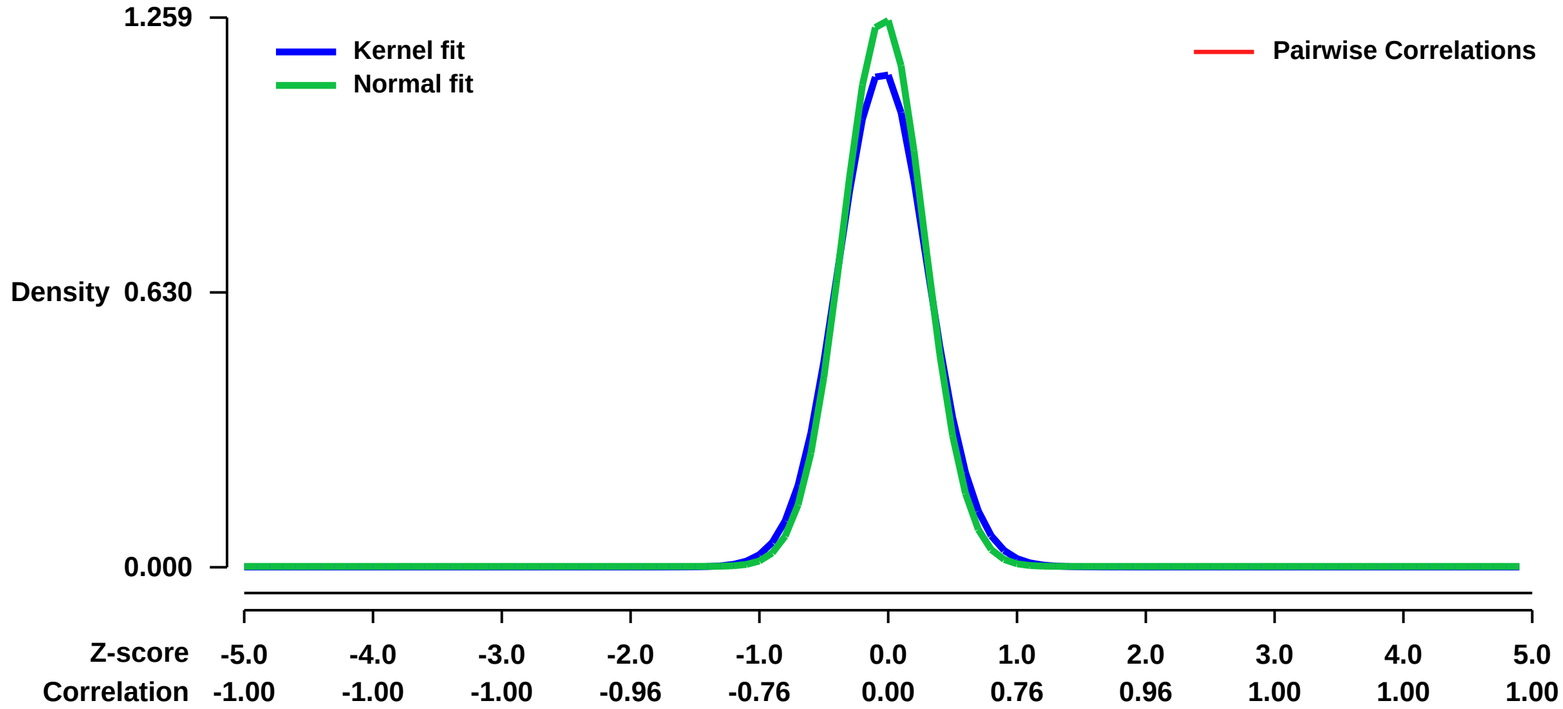

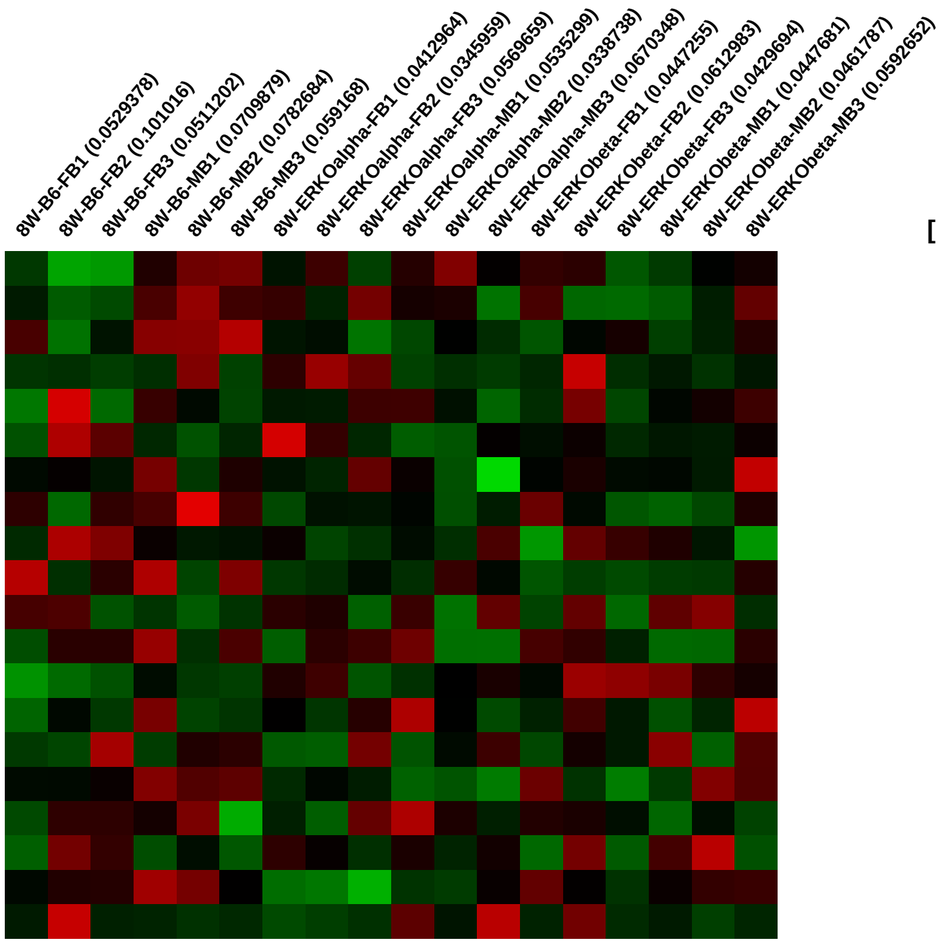

GEO Series "GSE26830" Expression Profiles

Num of samples in this series: 12

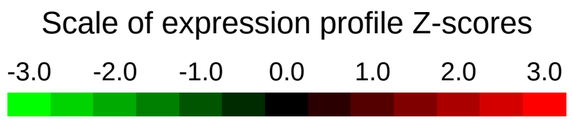

GEO Link:	http://www.ncbi.nlm.nih.gov/geo/query/acc.cgi?acc=GSE26830
Status:	Public on Mar 30 2011
Title:	Dual functions of Tet1 in transcriptional regulation in mouse embryonic stem cells (mRNA)
Organism:	Mus musculus
Experiment type:	Expression profiling by array
Platform:	GPL1261
Pubmed ID:	21460036
Summary & Design:	**Summary:** Epigenetic modification of the mammalian genome by DNA methylation (5-methylcytosine) has a profound impact on chromatin structure, gene expression and maintenance of cellular identity. Recent demonstration that members of the Ten-eleven translocation (Tet) family proteins can convert 5-methylcytosine (5mC) to 5-hydroxymethylcytosine (5hmC) raised the possibility that Tet proteins are capable of establishing a distinct epigenetic state. We have recently demonstrated that Tet1 is specifically expressed in murine embryonic stem (ES) cells and is required for ES cell self-renewal and maintenance. Using chromatin immunoprecipitation coupled with high-throughput DNA sequencing (ChIP-seq), here we show that Tet1 is preferentially bound to CpG-rich sequences at promoters of both transcriptionally active and Polycomb-repressed genes. Despite a general increase in levels of DNA methylation at Tet1 binding-sites, Tet1 depletion does not lead to down-regulation of all the Tet1 targets. Interestingly, while Tet1-mediated promoter hypomethylation is required for maintaining the expression of a group of transcriptionally active genes, it is also required for repression of Polycomb-targeted developmental regulators. Tet1 contributes to silencing of this group of genes by facilitating recruitment of PRC2 to CpG-rich gene promoters. Thus, our study not only establishes a role for Tet1 in modulating DNA methylation levels at CpG-rich promoters, but also reveals a dual function of Tet1 in promoting transcription of pluripotency factors as well as participating in the repression of Polycomb-targeted developmental regulators. **Overall design:** Mouse ES cells infected with control knockdown (KD) or Tet1 KD lentiviruses were FACS-sorted for RNA extraction and hybridization on Affymetrix microarrays. We also investigated the effect of Nanog overexpression (OE) in Tet1 KD mouse ES cells on dys-regulated Tet1 targets. We have collected four biologically independent replicates for each treatment.

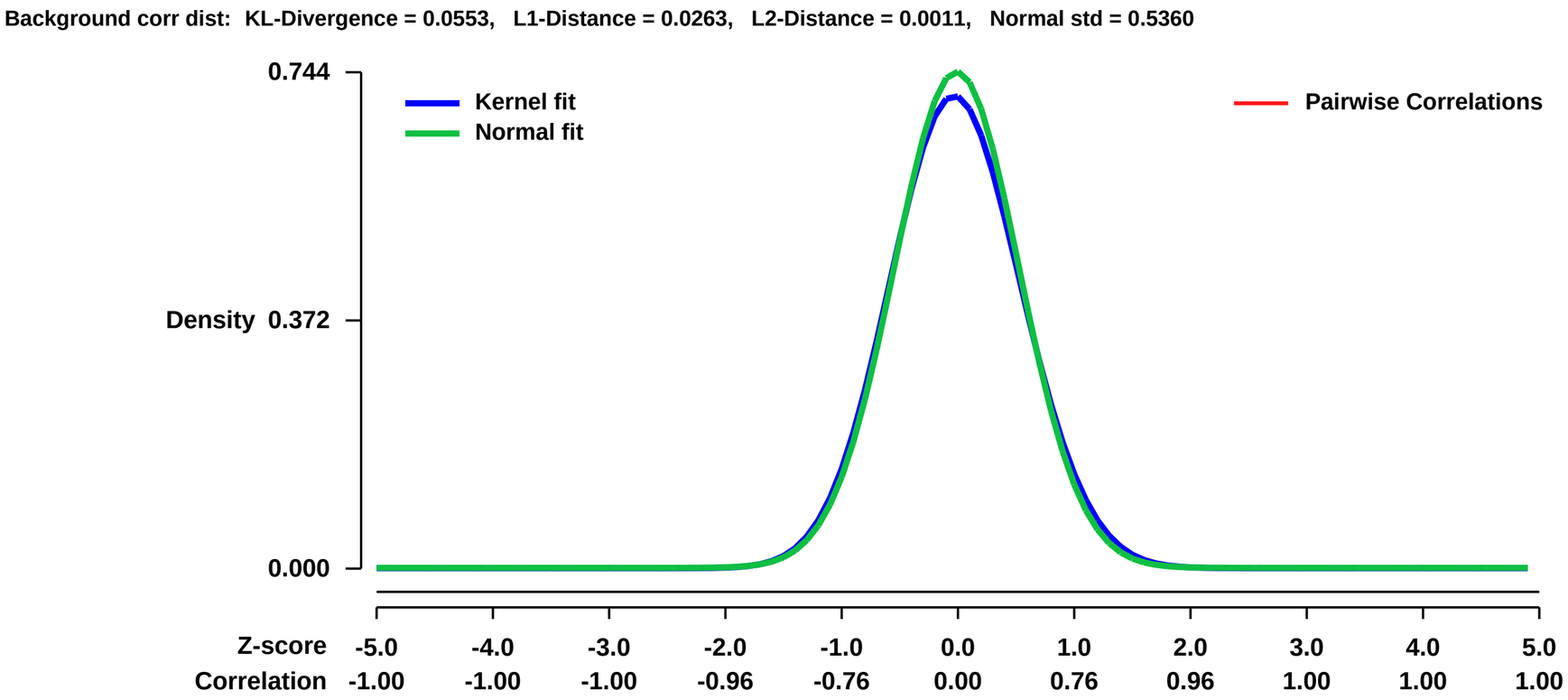

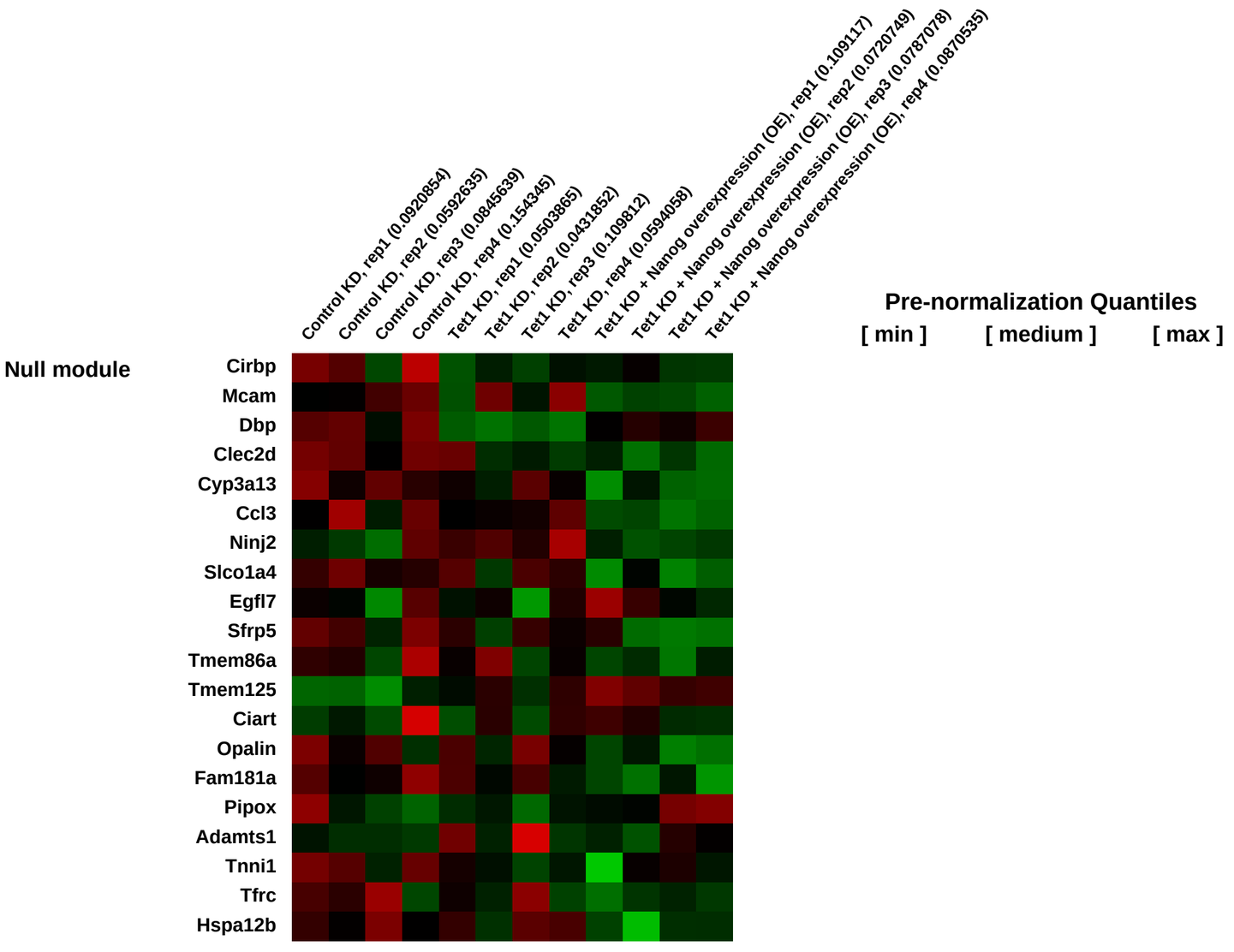

GEO Series "GSE30083" Expression Profiles

Num of samples in this series: 12

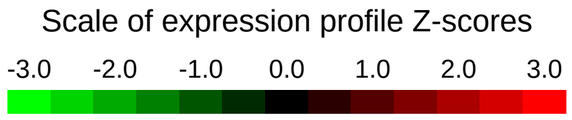

GEO Link:	http://www.ncbi.nlm.nih.gov/geo/query/acc.cgi?acc=GSE30083
Status:	Public on Feb 13 2012
Title:	Expression data from CD4 single positive thymocyte subsets from C57BL/6 mice of 6-8 wks of age
Organism:	Mus musculus
Experiment type:	Expression profiling by array
Platform:	GPL1261
Pubmed ID:	22022412
Summary & Design:	**Summary:** After positive selection in the thymus, the newly generated single positive (SP) thymocytes are phenotypically and functionally immature and undergo apoptosis upon antigen stimulation. In the thymic medullary microenvironment, SP cells progressively acquire immunocompetence. Negative selection to remove autoreactive T cells also occur at this stage. We have defined four subsets of CD4 SP, namely, SP1, SP2, SP3, and SP4 that follow a functional maturation program and a sequential emergence during mouse ontogeny. We used microarray to detail the global programm of gene expression during the maturation of murine CD4 single positive thymocytes **Overall design:** Four subsets of CD4+CD8-CD25-NK1.1- thymocytes from C57BL/6 mice of 6-8 wks of age were purified for RNA extraction and hybridization on Affymetrix microarrays, namely, SP1 (Qa-2-6C10+CD69+), SP2 (Qa-2-6C10-CD69+), SP3 (Qa-2-6C10-CD69-), SP4 (Qa-2+6C10-CD69-).

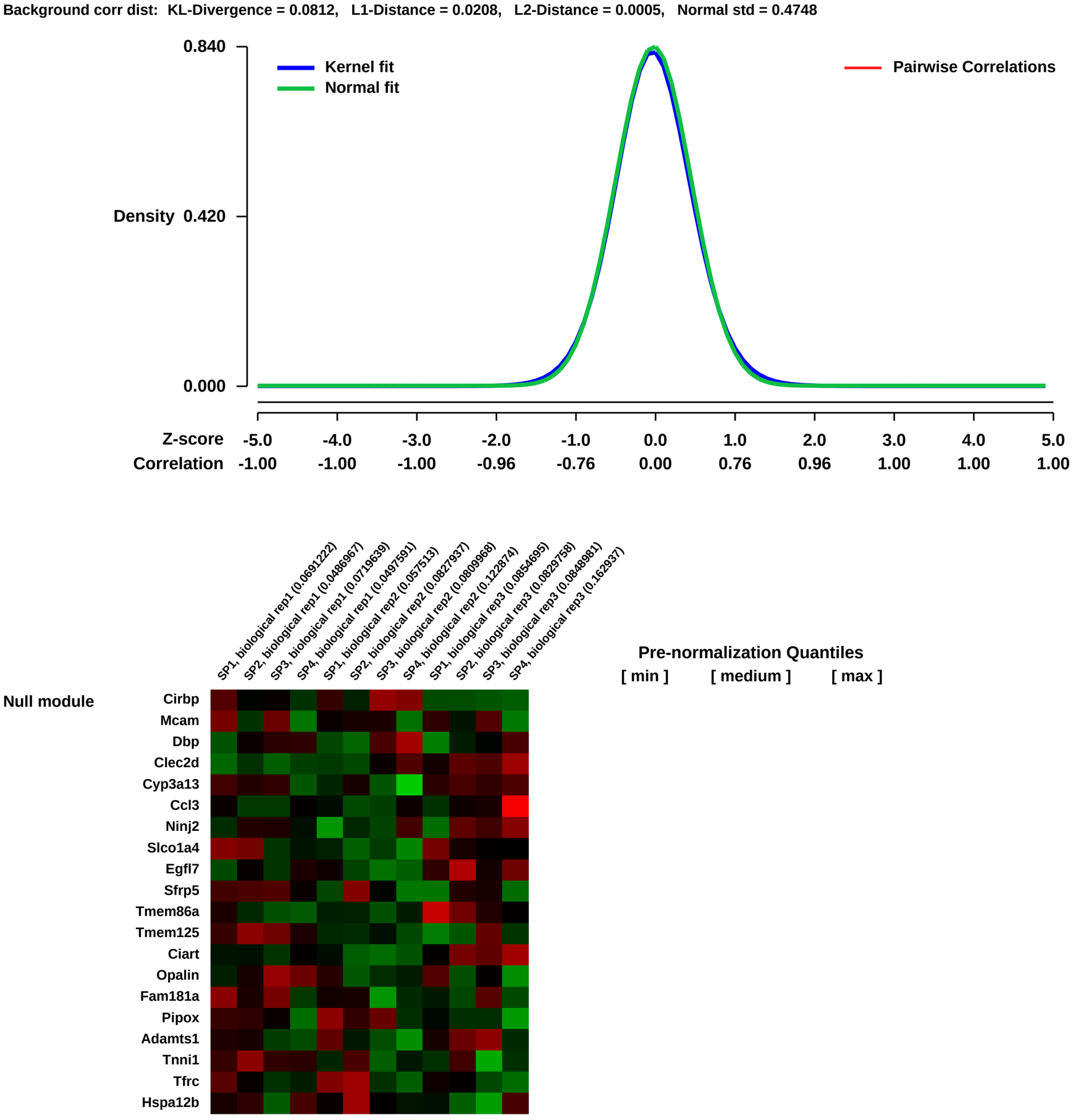

GEO Series "GSE38141" Expression Profiles

Num of samples in this series: 18

Scale of expression profile Z-scores

-3.0 -2.0 -1.0 0.0 1.0 2.0 3.0

GEO Link:	http://www.ncbi.nlm.nih.gov/geo/query/acc.cgi?acc=GSE38141
Status:	Public on May 30 2012
Title:	Chronic dietary intake of quercetin alleviates hepatic fat accumulation associated with consumption of a Western-style diet in C57/BL6J mice
Organism:	Mus musculus
Experiment type:	Expression profiling by array
Platform:	GPL1261
Pubmed ID:	21462320
Summary & Design:	**Summary:** To determine the effect of consumption of a quercetin-rich diet on obesity and dysregulated hepatic gene expression, C56BL/6J mice were fed for 20 weeks on control or a Western diet high in fat, cholesterol and sucrose, both with or without 0.05% quercetin. Chronic dietary intake of quercetin reduced body weight gain and visceral and liver fat accumulation, and improved hyperglyceamia, hyperinsulinaemia, dyslipidaemia in mice fed a Western-style diet. Feeding a Western-style diet altered expression of genes related to inflammatory responses, lipid metabolism and oxidative phosphorylation in C57BL/6J mice after 20 weeks. The results from exhaustive gene expression analysis showed that quercetin minimally influenced hepatic gene expression in mice fed the Western diet. The gene screening results (GSEA) were consistent with the notion that it did improve mitochondrial function to some extent. Quantitative RT-PCR analysis indicated that quercetin did influence important regulators of fat accumulation and metabolic disorders. Our results suggest that quercetin reduces fat accumulation presumably through decreasing oxidative stress and increasing PPAR¸– expression, and the following improvement of gene expression related to steatosis in the liver. **Overall design:** C56BL/6J mice were fed for 20 weeks on AIN93G (con) or a Western diet high in fat, cholesterol and sucrose, both with or without 0.05% quercetin for 20 weeks.

Background corr dist: KL-Divergence = 0.2400, L1-Distance = 0.0510, L2-Distance = 0.0061, Normal std = 0.3079

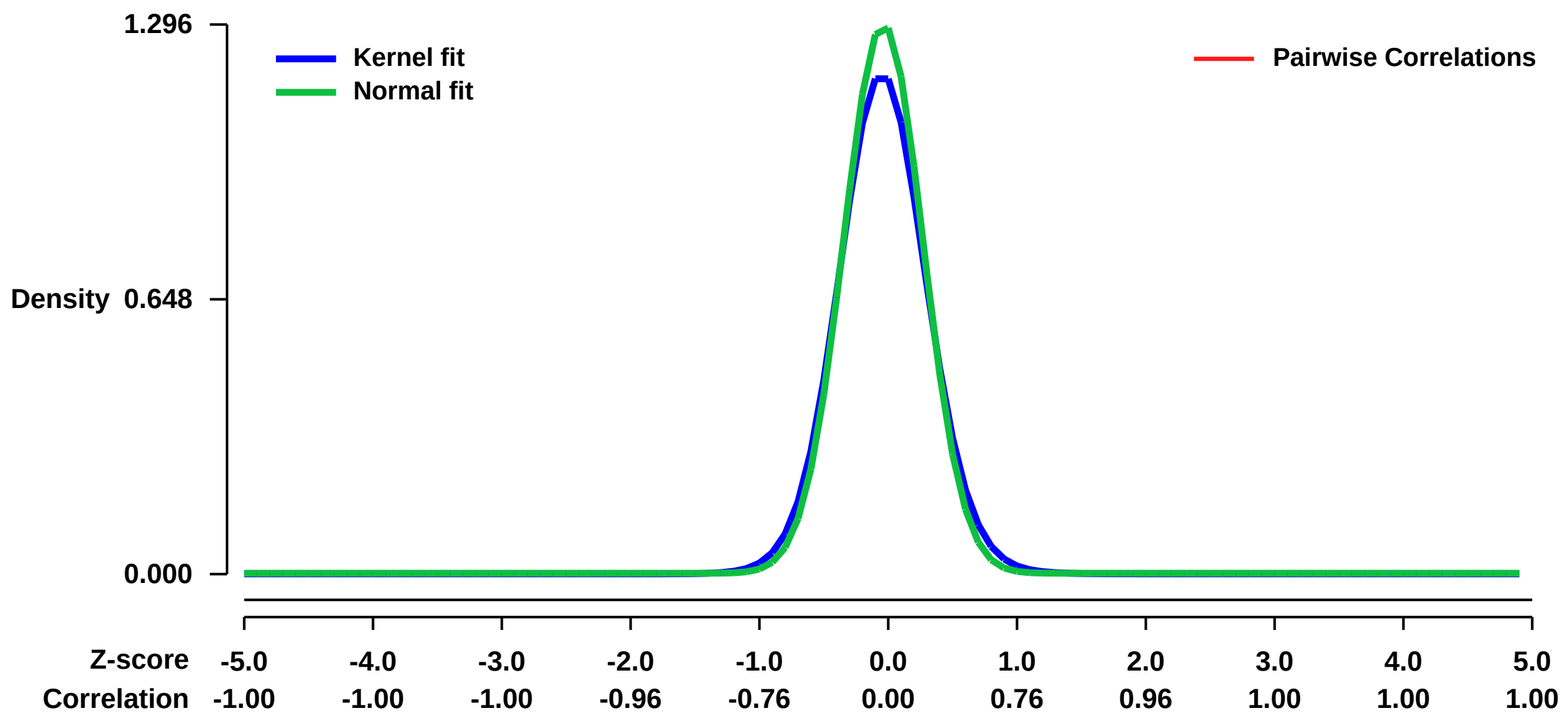

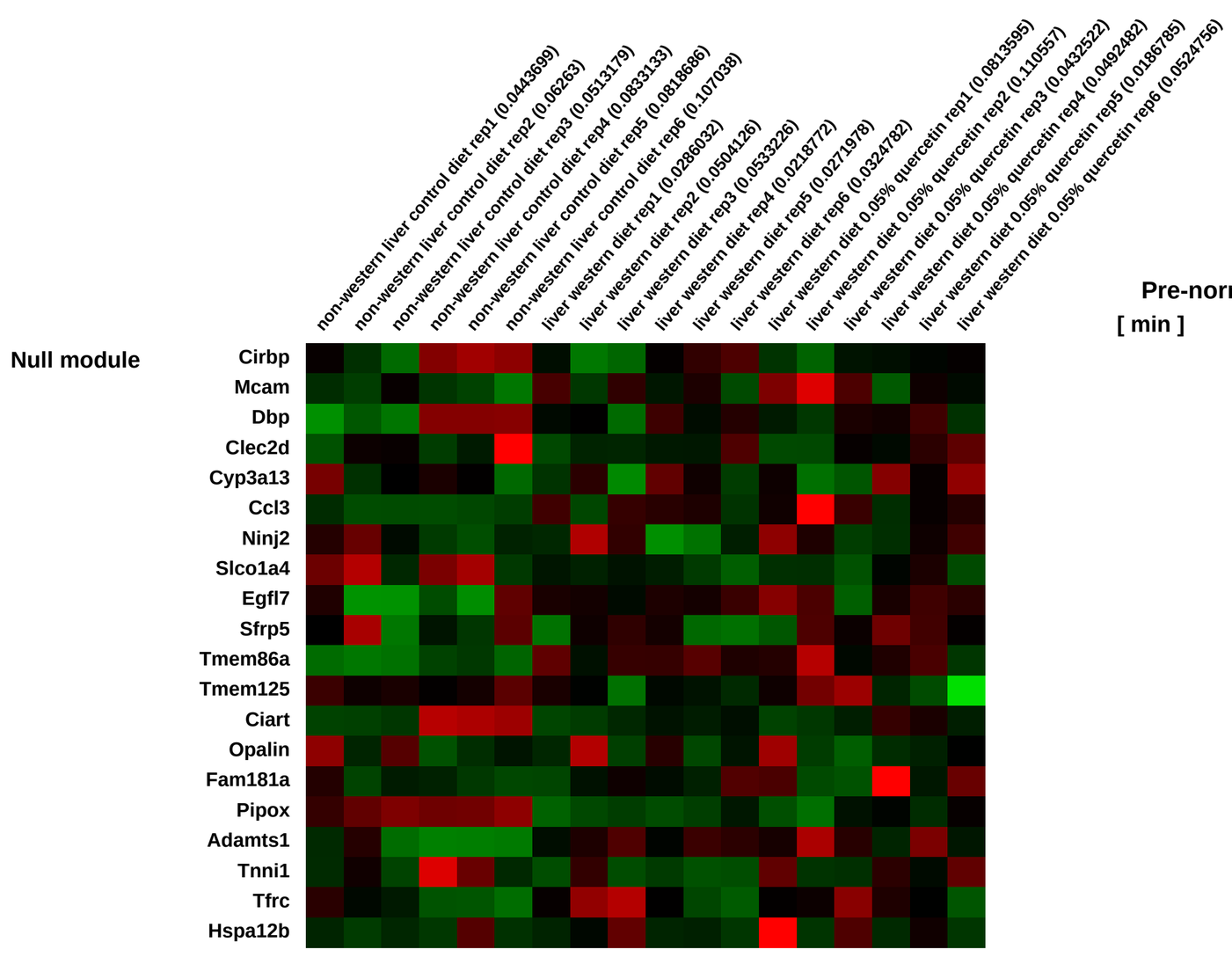

GEO Series "GSE18115" Expression Profiles

Num of samples in this series: 8

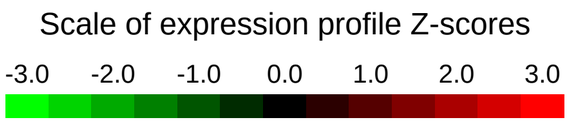

GEO Link:	**http://www.ncbi.nlm.nih.gov/geo/query/acc.cgi?acc=GSE18115**
Status:	**Public on Dec 31 2010**
Title:	**Dendritic cells and stress translation**
Organism:	**Mus musculus**
Experiment type:	**Expression profiling by array**
Platform:	**GPL1261**
Pubmed ID:	
Summary & Design:	**Summary:** **In response to inflammatory stimulation, dendritic cells (DCs) have a remarkable pattern of differentiation that exhibits specific mechanisms to control the immune response. Here we show that in response to polyriboinosinic:polyribocytidylic acid (poly I:C), DCs mount a specific transcription program during which the growth arrest and DNA damage-inducible protein 34 (GADD34/MyD116), a phosphatase 1 (PP1) cofactor, is expressed. Together with its constitutively active counterpart CReP, GADD34 promotes an extensive dephosphorylation of the translation initiation factor eIF2-alfa in activated DCs. In turn, dephosphorylation of eIF2-alfa prevents the translation inhibition normally associated with cellular stress or detection of cytoplasmic double-stranded RNA. These observations have important implications in linking pathogen detection with the integrated stress responses molecular machinery. The importance of this regulation for DC function is exemplified by the alteration of IFN-beta production or the induction of caspase-3 cleavage upon inhibition of PP1 activity. #!#** **Overall design:** **LPS-activated murine bone-marrow derived dendritic cells were transfected or pulsed with pIC and incubated for 4h or 16h. Cells were harvested, total RNA was extracted and analysed by Affymetrix microarrays analysis.**

Background corr dist: KL-Divergence = 0.0630, L1-Distance = 0.0416, L2-Distance = 0.0028, Normal std = 0.5410

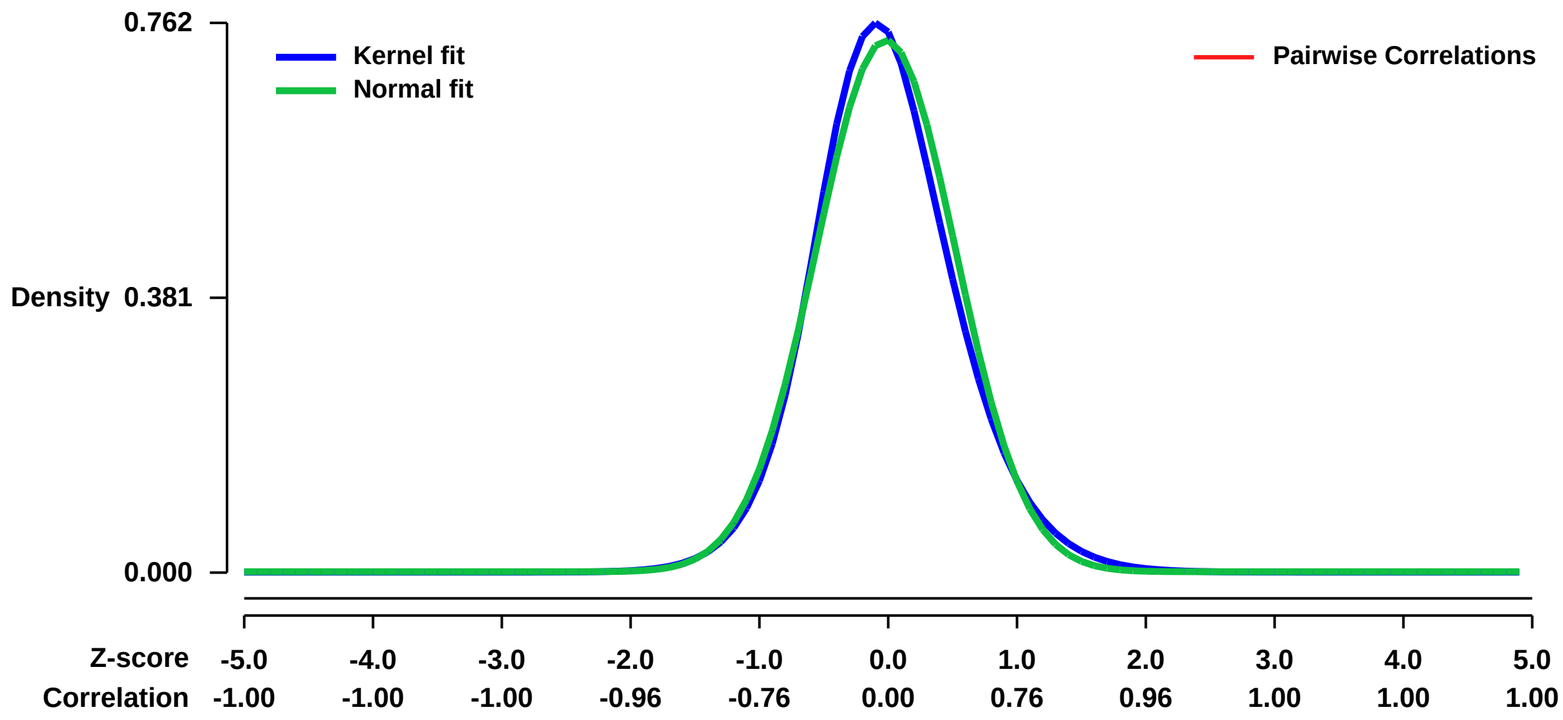

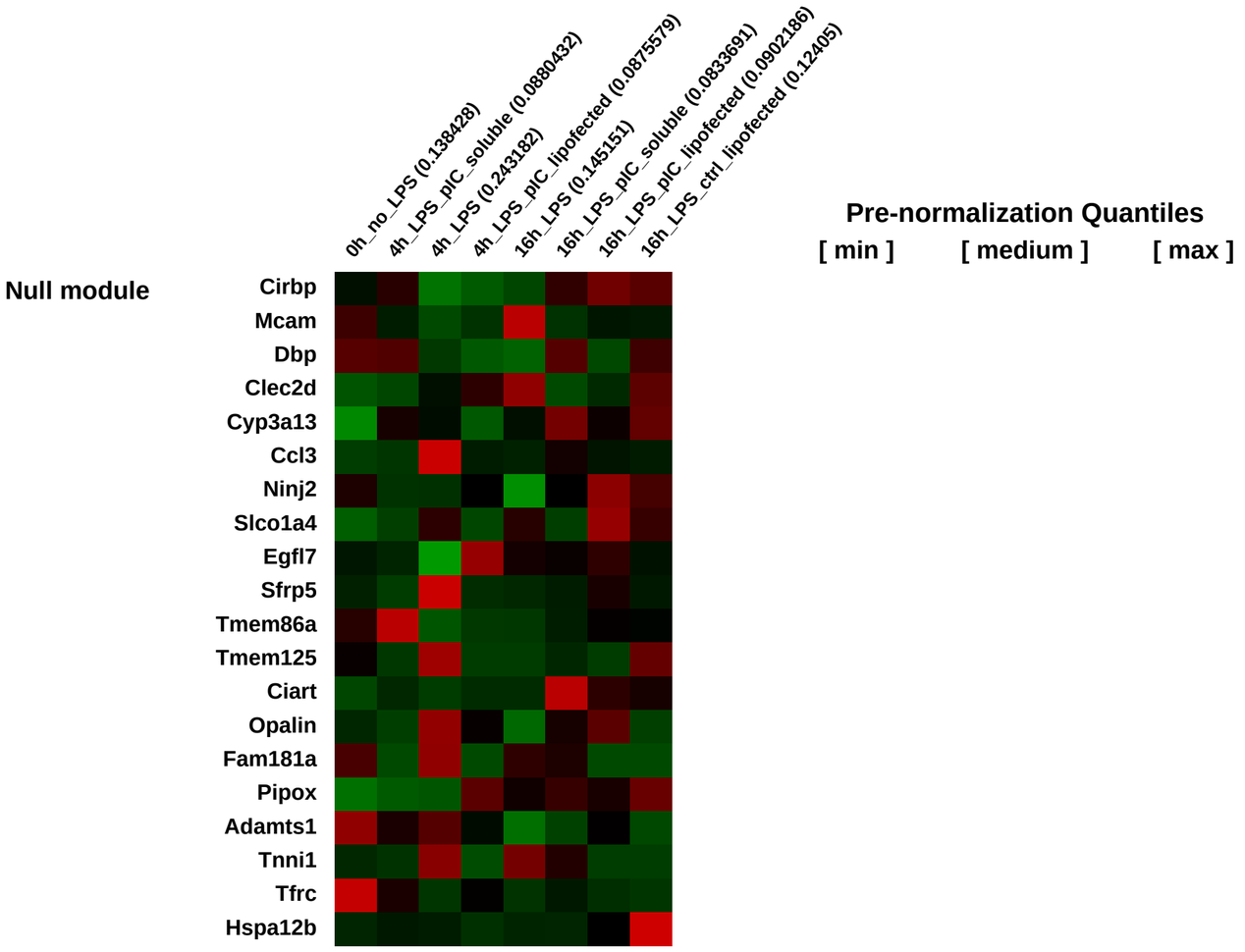

GEO Series "GSE10262" Expression Profiles

Num of samples in this series: 18

Scale of expression profile Z-scores

-3.0 -2.0 -1.0 0.0 1.0 2.0 3.0

GEO Link:	http://www.ncbi.nlm.nih.gov/geo/query/acc.cgi?acc=GSE10262
Status:	Public on Feb 22 2008
Title:	Expression data from Helicobacter pylori-infected mouse gastric epithelial progenitor and non-progenitor cells.
Organism:	Mus musculus
Experiment type:	Expression profiling by array
Platform:	GPL1261
Pubmed ID:	18332421
Summary & Design:	**Summary:** Helicobacter pylori clinical isolates can establish themselves in gastric epithelial stem cells and this interaction may have implications for gastric tumorigenesis. Mouse gastric epithelial progenitor cells (mGEPs) and non-progenitor gastric epithelial cells (npGECs) were infected for 24hrs with Helicobacter pylori clinical isolates Kx1 and Kx2. Kx1 was isolated from a patient with chronic atrophic gastritis (ChAG) and Kx2 from the same patient 4 years later, when he progressed to gastric adenocarcinoma. **Keywords: RNA Expression Array** **Overall design:** mGEPs and npGECs were seeded and grown to 70% confluency in RPMI1640 medium supplemented with 10% FBS before being infected with H. pylori strains Kx1 or Kx2 that had been grown to log phase. After 24h, media and non-attached bacteria were washed off and the cells harvested by trypsinization. RNA was prepared from triplicate cultures of mGEP cells infected with Kx1 or Kx2, npGECs infected with Kx1 or Kx2 and uninfected mGEPs and npGECs that served as controls.

Background corr dist: KL-Divergence = 0.1493, L1-Distance = 0.0336, L2-Distance = 0.0022, Normal std = 0.3829

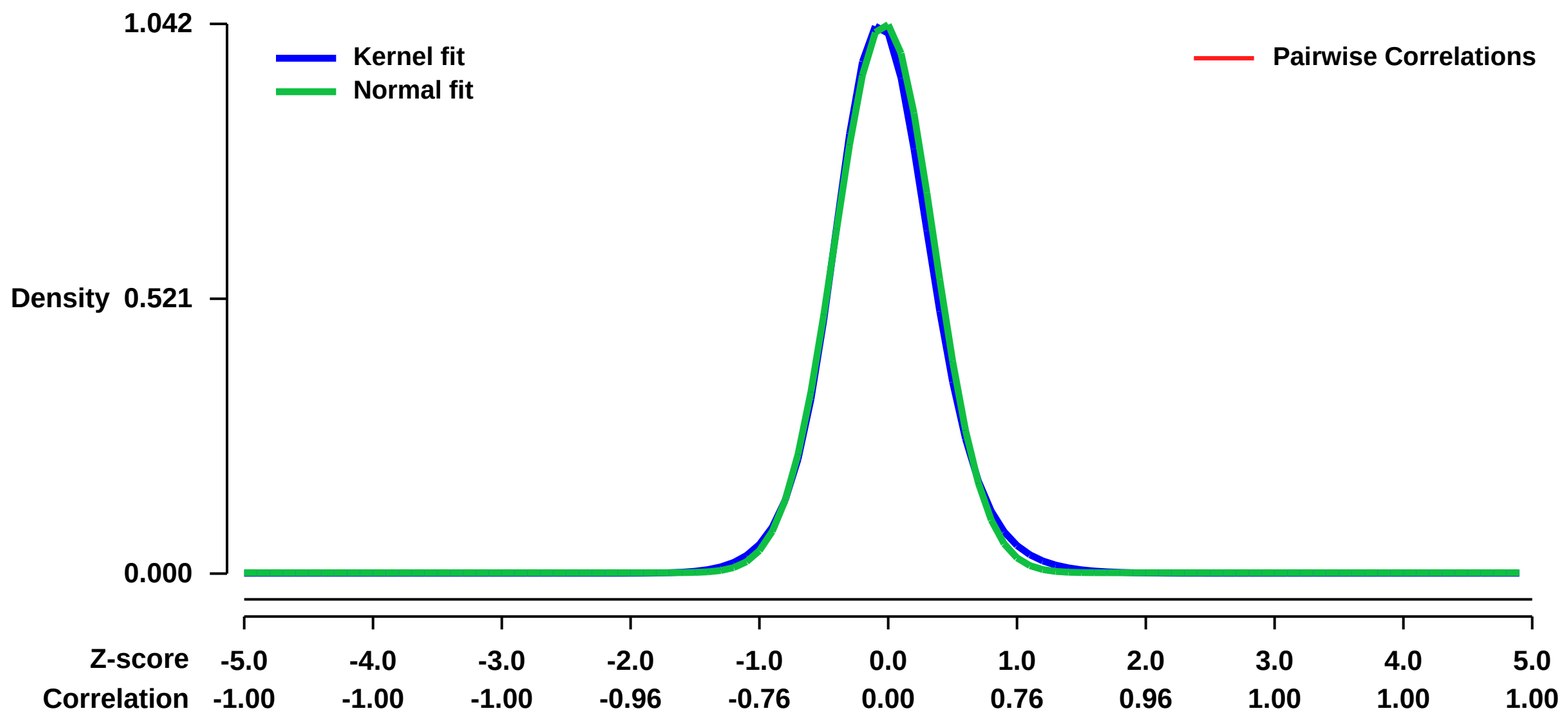

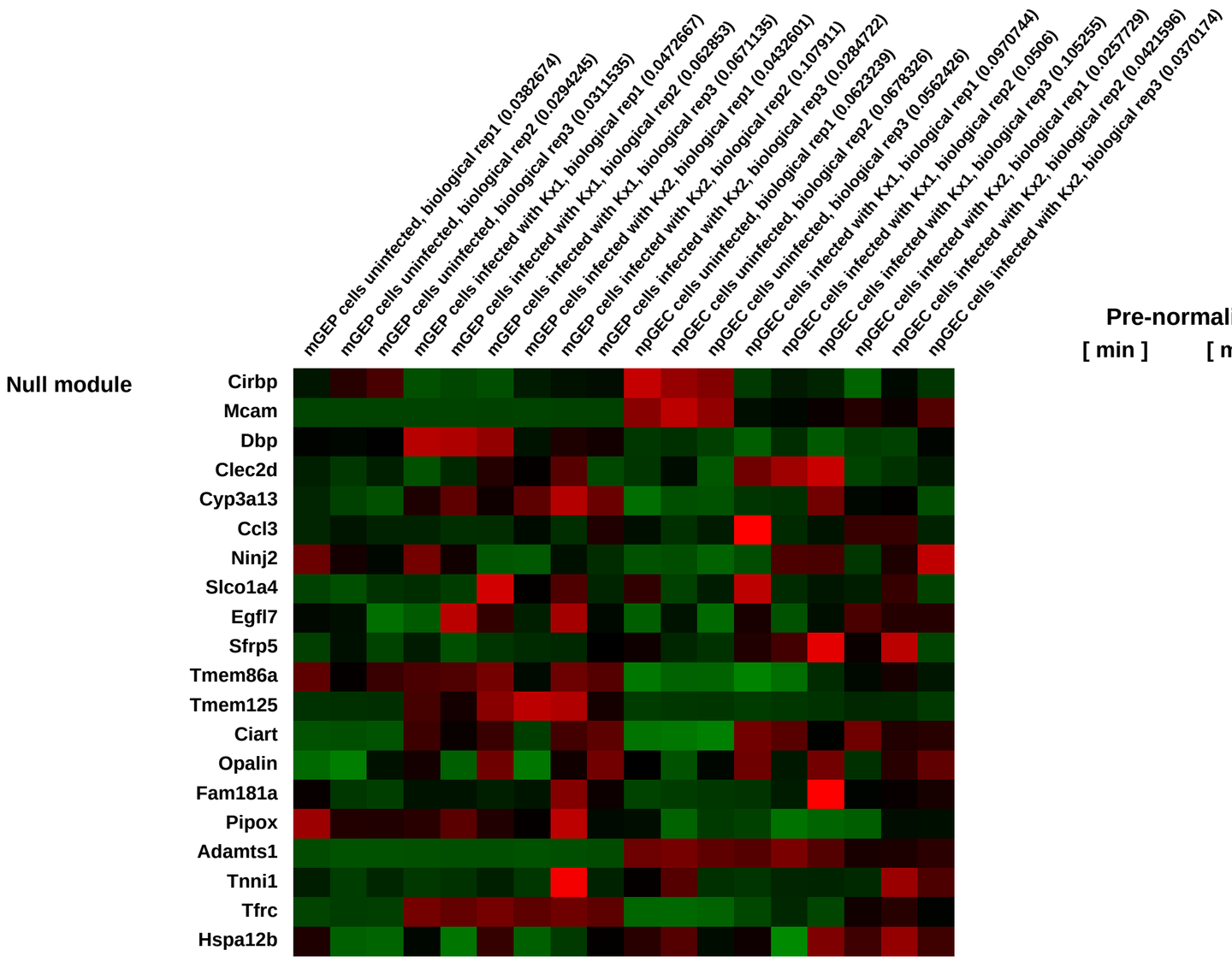

GEO Series "GSE41085" Expression Profiles

Num of samples in this series: 6

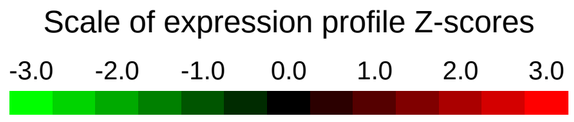

GEO Link:	http://www.ncbi.nlm.nih.gov/geo/query/acc.cgi?acc=GSE41085
Status:	Public on Jul 01 2013
Title:	Expression data after irradiating mMSCs for 2 hours with single frequency terahertz laser source
Organism:	Mus musculus
Experiment type:	Expression profiling by array
Platform:	GPL1261
Pubmed ID:	23378916
Summary & Design:	**Summary:** We report that terahertz (THz) irradiation of mouse mesenchymal stem cells with a pulsed broadband (centered at 10 THz) source, or a single-frequency, 2.52 THz, (SF) laser source, both with weak average power (<1mW/cm2), results in specific heterogenic changes in gene expression. The insignificant differential expression of heat shock and stress related genes as well as our temperature measurements imply a non-thermal response. The microarray survey and RT-PCR experiments demonstrate that at different irradiation conditions distinct groups of genes are activated. Stem cells irradiated for 12 hours with the broadband THz source exhibit an accelerated differentiation toward adipose phenotype, while the 2-hour (broadband or SF) irradiation affects genes transcriptionally active in pluripotent stem cells. Phenotypic and gene expression differences suggest that the THz effect depends on irradiation parameters such as duration and type of THz source, and on the level of stem cell differentiation. Computer simulations of the core promoters of two pluripotency markers reveal association between gene upregulation and propensity for DNA breathing. We propose that THz radiation has potential for non-contact control of cellular gene expression. **Overall design:** Growing in petri dish mouse mesenchymal stem cell cultures are irradiated for 2 hours with a single-frequency (2.52 THz) CW laser source. Three independent biological experiments were conducted. In each experiment, a control mMSC culture was placed adjacent to the irradiated sample, and the temperature was kept at 26-27´"C for both the control and the irradiated sample. Immediately after completing the irradiation, total RNA was extracted from the irradiated sample and the control, and microarrays were used to identify differential changes in gene expression between the irradiated sample and its respective control. In each experiment, the mMSC cultures were synchronized to be at the same differentiation time point immediately before the irradiation.

Background corr dist: KL-Divergence = 0.0484, L1-Distance = 0.0181, L2-Distance = 0.0003, Normal std = 0.5774

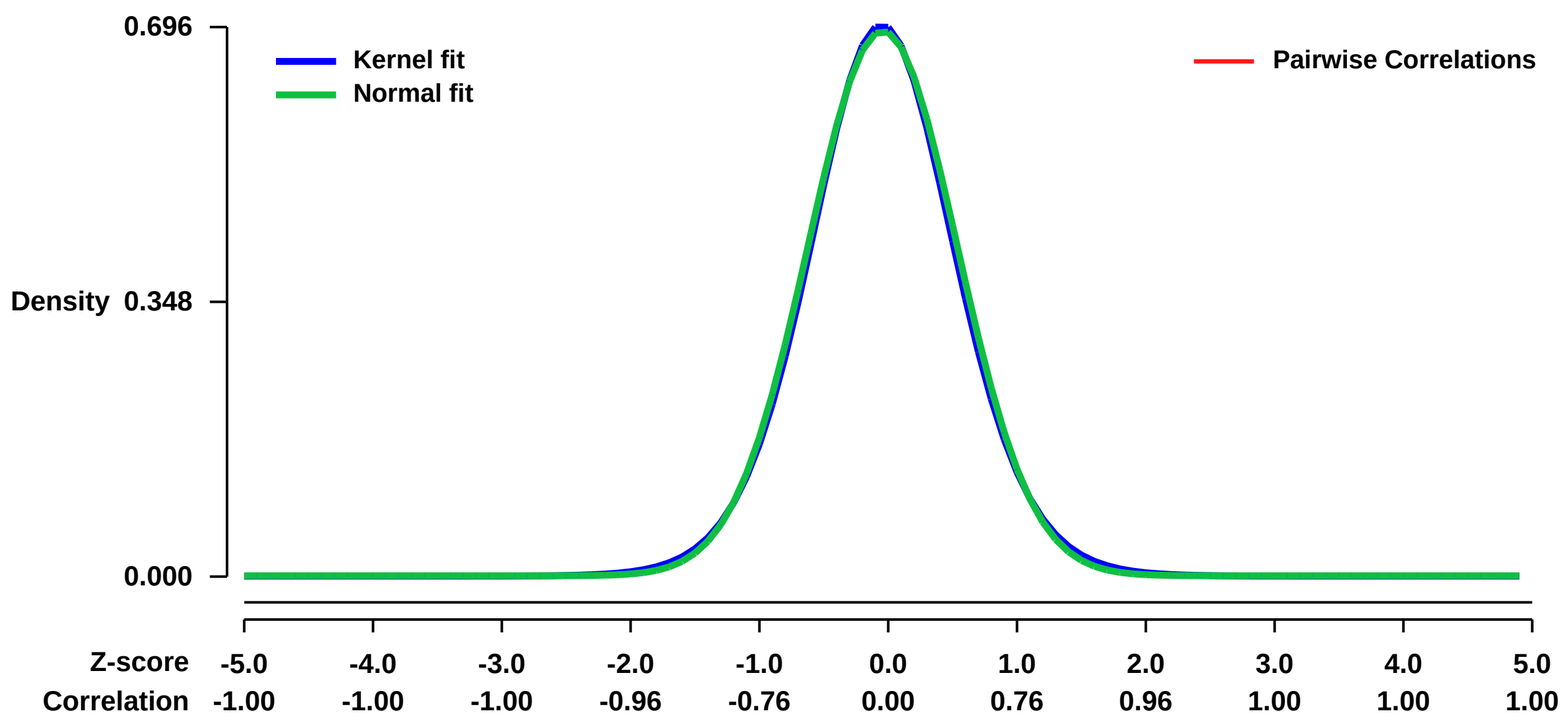

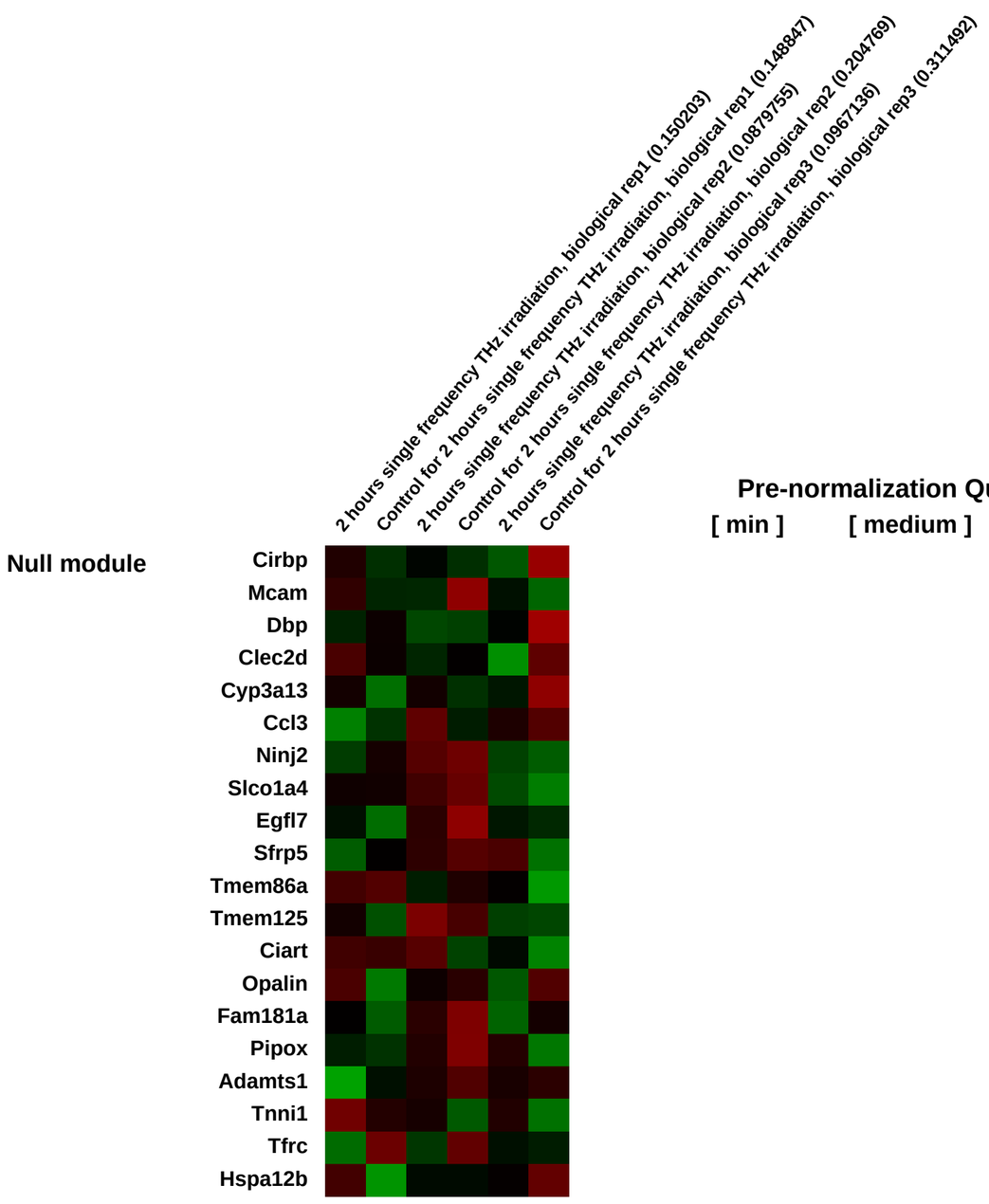

GEO Series "GSE9161" Expression Profiles

Num of samples in this series: 9

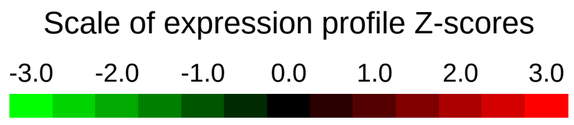

GEO Link:	http://www.ncbi.nlm.nih.gov/geo/query/acc.cgi?acc=GSE9161
Status:	Public on Jan 07 2008
Title:	Expression profiling of cyclin D1 splice variants cyclin D1a and D1b in mouse 3T3 cells.
Organism:	Mus musculus
Experiment type:	Expression profiling by array
Platform:	GPL1261
Pubmed ID:	18180298
Summary & Design:	**Summary:** Cyclin D1 is an important cell cycle regulator but in cancer its overexpression also increases cellular migration mediated by p27KIP1 stabilization and RhoA inhibition. Recently, a common polymorphism at the exon 4-intron 4 boundary of the human cyclin D1 gene within a splice donor region was associated with an altered risk of developing cancer. Altered RNA splicing caused by this polymorphism gives rise to a variant cyclin D1 isoform termed cyclin D1b, which has the same N-terminus as the canonical cyclin D1a isoform but a distinct C-terminus. Analysis was performed of mouse cyclin D1 knockout 3T3 cells infected with splice variants of cyclin D1. 3T3 cells transduced with retroviral vectors expressing each cyclin D1 isoform were processed for expression analysis. **Keywords: Cancer associated risk factor** **Overall design:** Three Mouse Embryonic Fibroblasts cell lines obtained from littermate cyclin D1 knockout E14 embyos were serial passaged to obtain cyclin D1 knockout (D1KO) 3T3 cells. Each of the D1KO 3T3 cell lines were infected using the Murine Stem Cell Virus (MSCV) expressing splice variants of cyclin D1; cyclin D1a/ cyclin D1b or GFP control to give triplicate sample sets. 7 days post infection total RNA from each sample was extracted using Trizol and further purified using Qiagenâ s RNeasy Kit. Preparation of biotinylated cRNA and hybridization to oligonucleotide arrays (Affymetrix mouse genome genechip 430 2.0) were performed in conjuction with Pestell lab and the Nucleic Acid Core Facility at Thomas Jefferson University. Mouse 430 2.0 genechip contains 39,000 transcripts. Gene chips were scanned and analyzed using Robust Multi-array Average (RMA) algorithm.

Background corr dist: KL-Divergence = 0.0683, L1-Distance = 0.0192, L2-Distance = 0.0006, Normal std = 0.5072

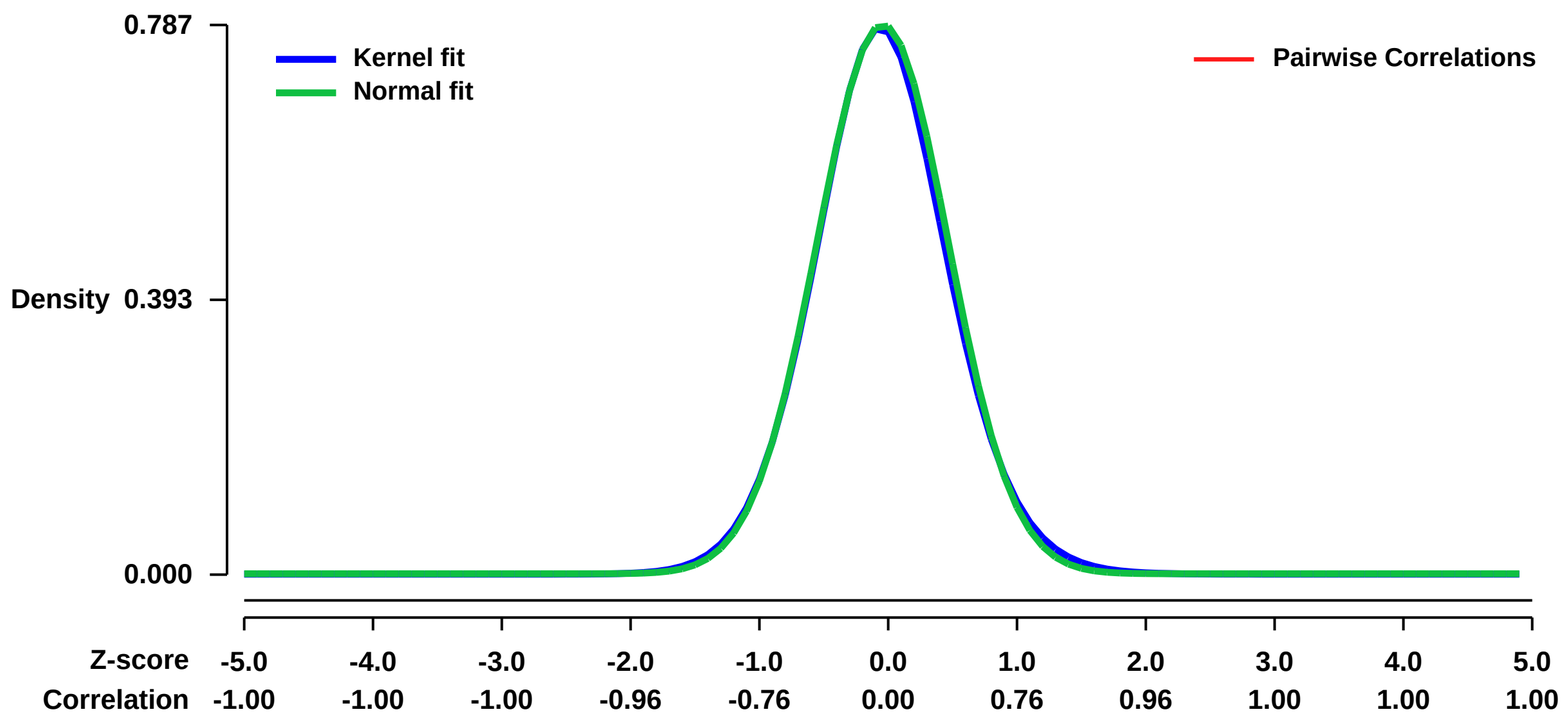

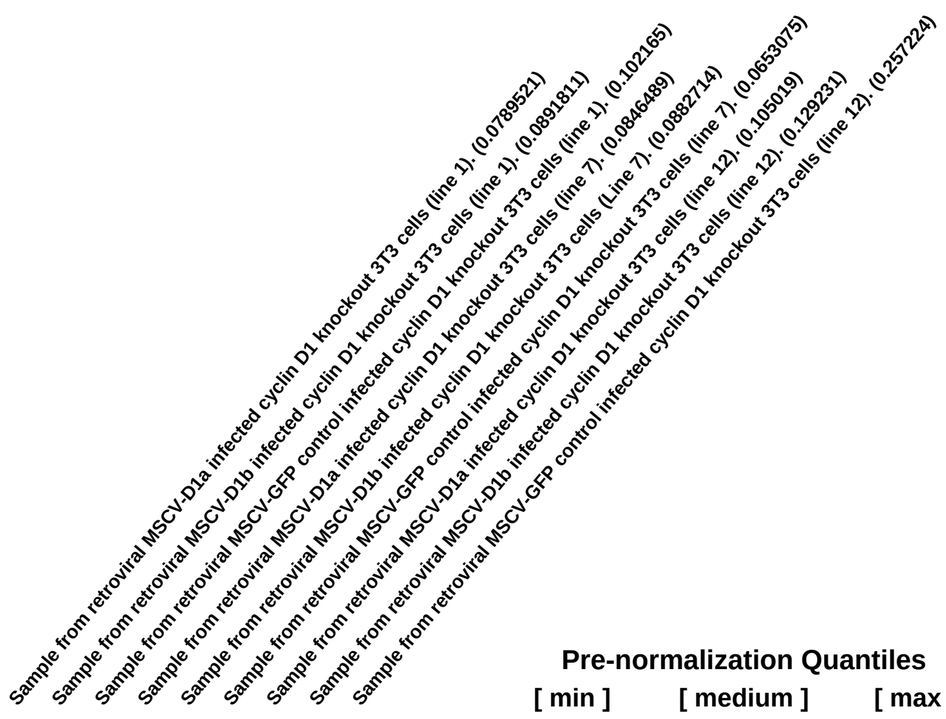

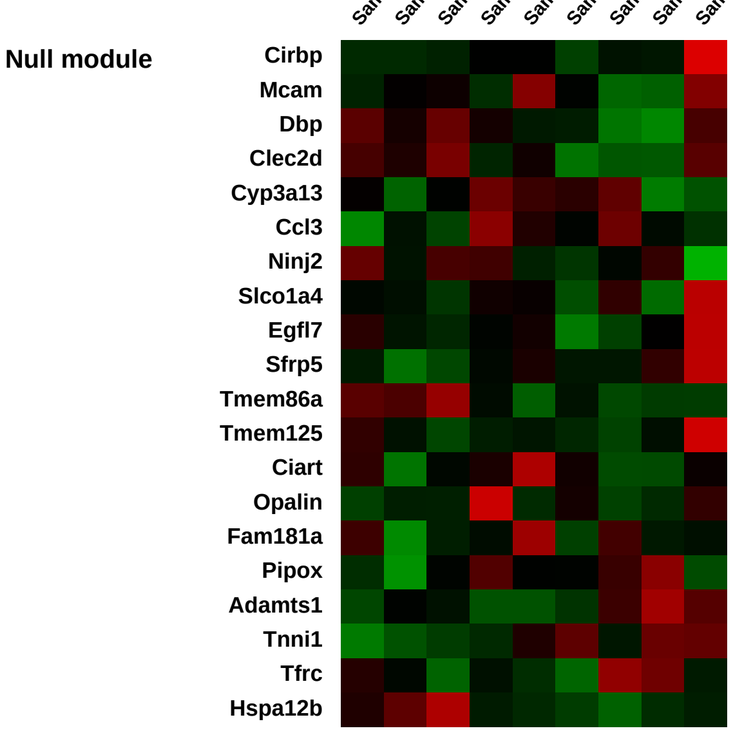

GEO Series "GSE19793" Expression Profiles

Num of samples in this series: 32

Scale of expression profile Z-scores

-3.0 -2.0 -1.0 0.0 1.0 2.0 3.0

GEO Link:	http://www.ncbi.nlm.nih.gov/geo/query/acc.cgi?acc=GSE19793
Status:	Public on Jun 24 2010
Title:	MyD88-mediated signaling prevents development of adenocarcinomas of the colon via interleukin-18
Organism:	Mus musculus
Experiment type:	Expression profiling by array
Platform:	GPL1261
Pubmed ID:	
Summary & Design:	**Summary:** Inflammation has pleiotropic effects on carcinogenesis and tumor progression. Signaling through the adaptor protein MyD88 promotes carcinogenesis in several chemically induced cancer models. Interestingly, we observed a protective role for MyD88 in the development of AOM/DSS colitis-associated cancer. The inability of Myd88-/- mice to heal ulcers generated upon injury creates an inflammatory environment that increases the frequency of mutations and results in a dramatic increase in adenoma formation and cancer progression. Susceptibility to colitis development and enhanced polyp formation were also observed in Il18-/- mice upon AOM/DSS treatment, suggesting that the phenotype of MyD88 knockouts is in part due to their inability to signal through the IL-18 receptor. This study revealed a previously unknown level of complexity surrounding MyD88 activities downstream of different receptors that differentially impact tissue homeostasis and carcinogenesis. **Overall design:** The Myd88 knockout mice were backcrossed to obtain at least 98% congenicity to B6NCr background. As control groups, wild type mice of identical background were used. Ten biological repeats were performed for the treated wild type and Myd88 samples. Six biological repeats were performed for the untreated wild type and Myd88 samples.

Background corr dist: KL-Divergence = 0.3306, L1-Distance = 0.0446, L2-Distance = 0.0044, Normal std = 0.2690

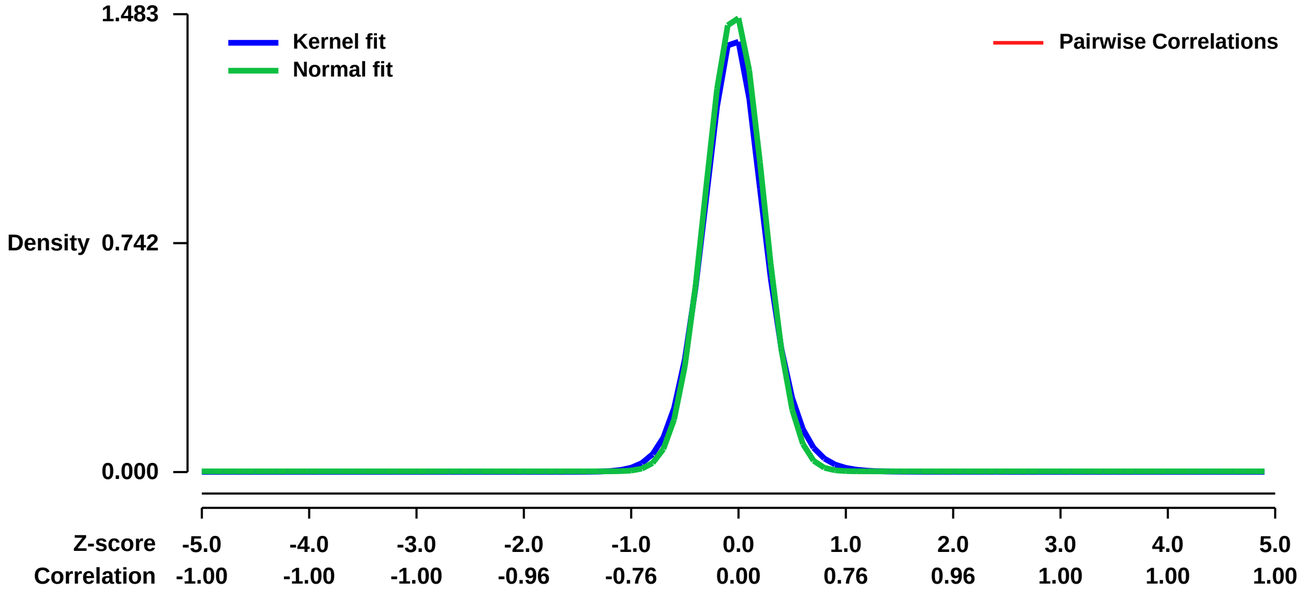

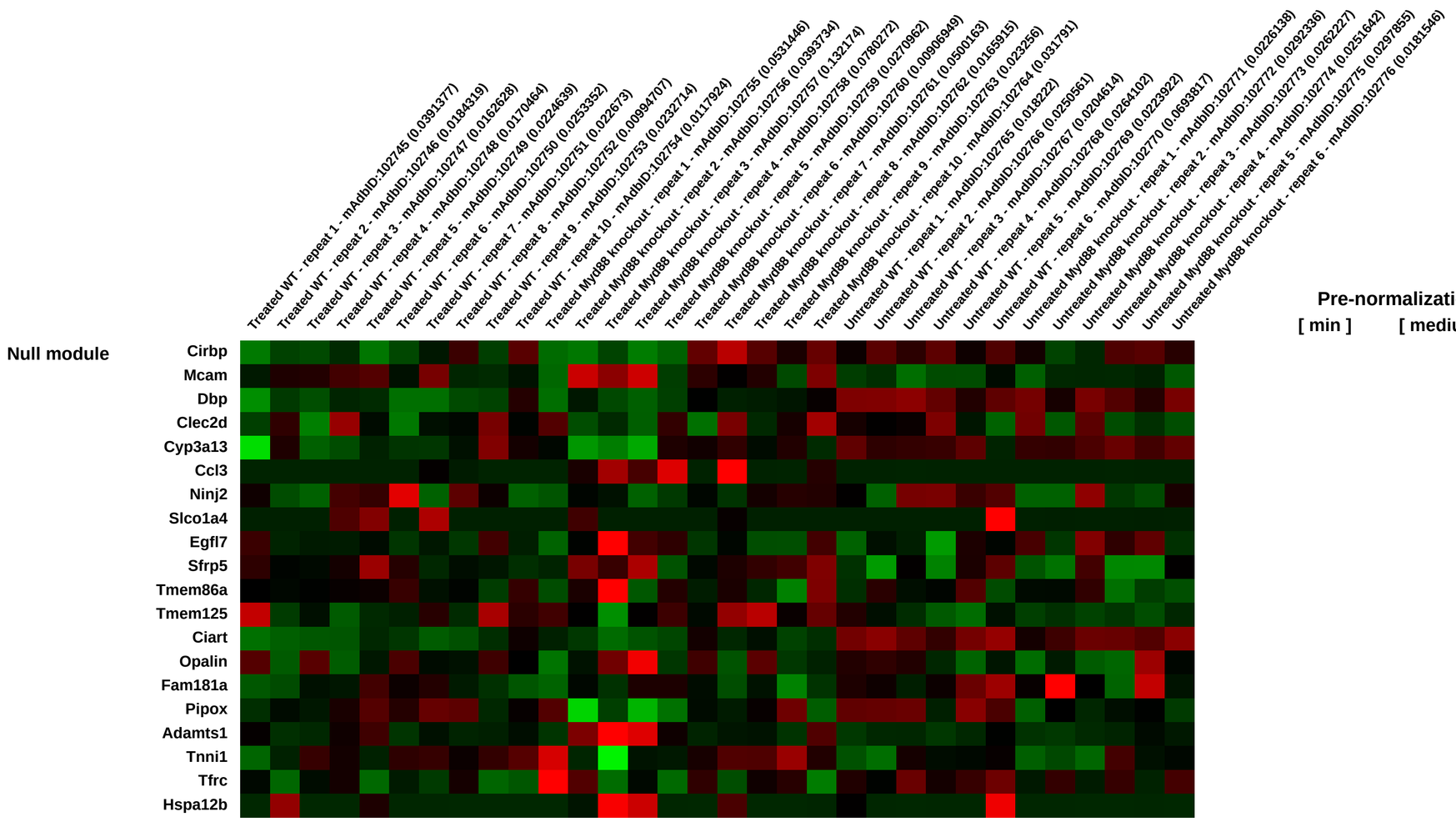

GEO Series "GSE55002" Expression Profiles

Num of samples in this series: 6

Scale of expression profile Z-scores

-3.0 -2.0 -1.0 0.0 1.0 2.0 3.0

GEO Link:	http://www.ncbi.nlm.nih.gov/geo/query/acc.cgi?acc=GSE55002
Status:	Public on Feb 14 2014
Title:	Transcription array by profiling in WT and SRC-2 null mouse liver
Organism:	Mus musculus
Experiment type:	Expression profiling by array
Platform:	GPL1261
Pubmed ID:	16423883
Summary & Design:	**Summary:** The molecular targets of SRC-2 regulation in the murine liver stimulate fatty acid degradation and glycolytic pathway while fatty acid, cholesterol, and steroid biosynthetic pathways are down-regulated. **Overall design:** A genomic approach using microarray analysis was employed to identify the subsets of genes that are altered in the liver of SRC-2-/- mice.

Background corr dist: KL-Divergence = 0.0418, L1-Distance = 0.0178, L2-Distance = 0.0003, Normal std = 0.6064

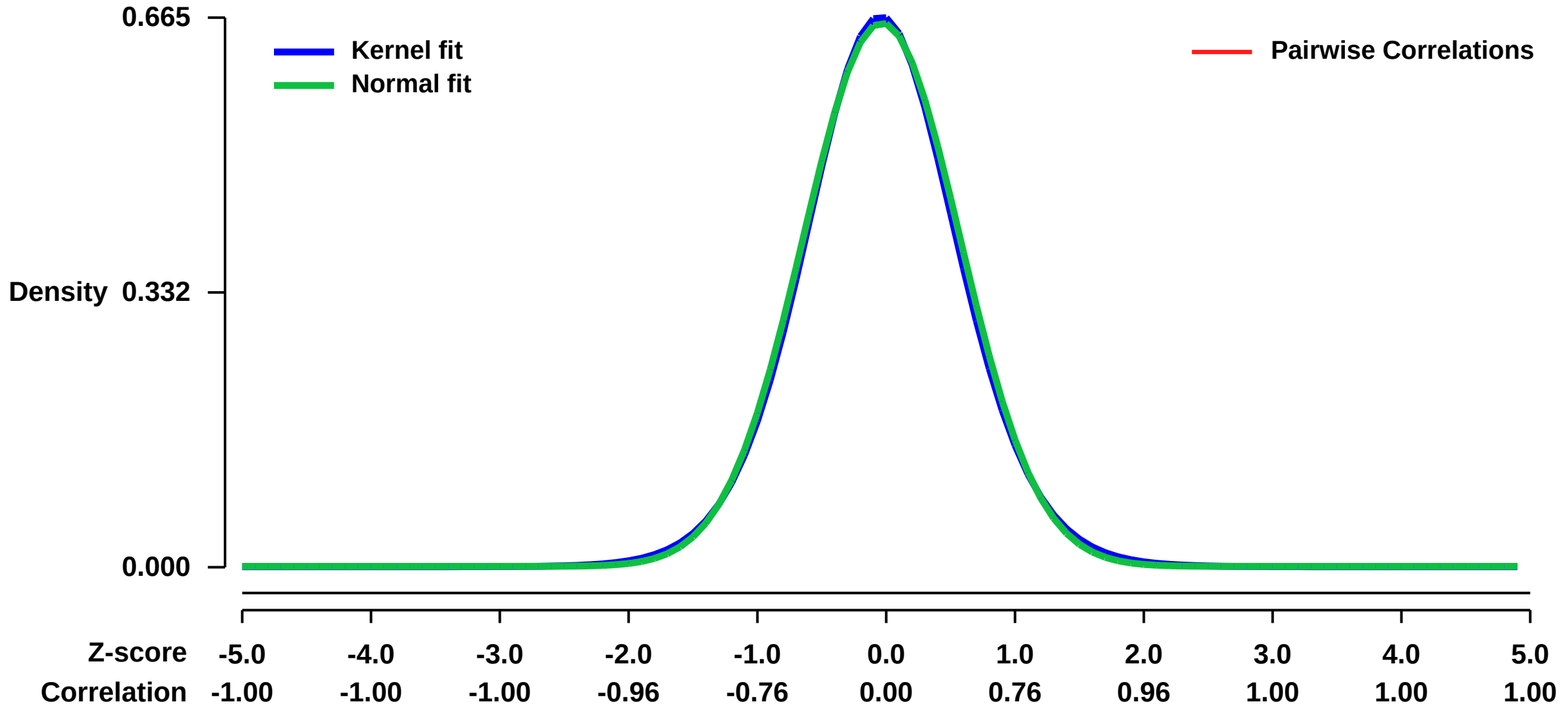

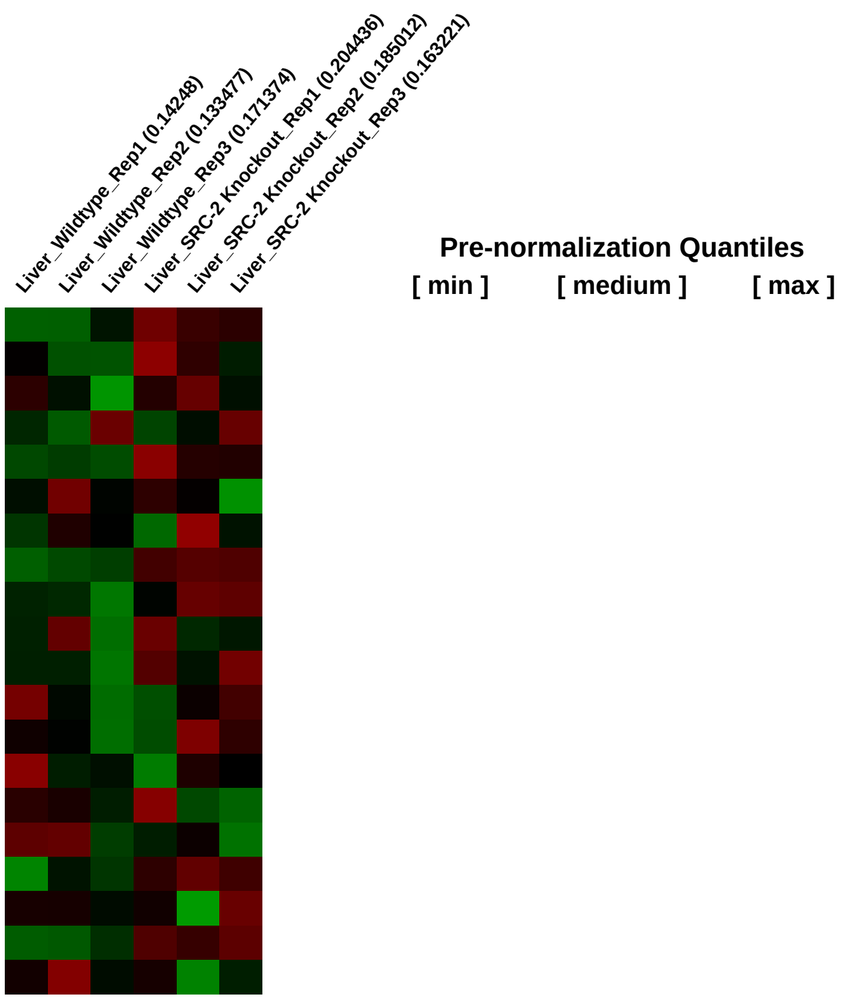

GEO Series "GSE8295" Expression Profiles

Num of samples in this series: 16

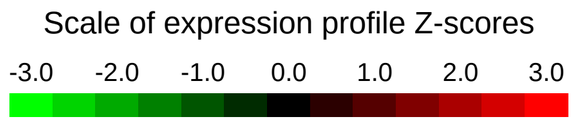

GEO Link:	http://www.ncbi.nlm.nih.gov/geo/query/acc.cgi?acc=GSE8295
Status:	Public on Jul 24 2007
Title:	Comprehensive analysis of PPARα--dependent regulation of hepatic lipid metabolism by expression profiling - 4
Organism:	Mus musculus
Experiment type:	Expression profiling by array
Platform:	GPL1261
Pubmed ID:	18288265
Summary & Design:	**Summary:** PPARα– is a ligand-activated transcription factor involved in the regulation of nutrient metabolism and inflammation. Although much is already known about the function of PPARα– in hepatic lipid metabolism, many PPARα--dependent pathways and genes have yet to be discovered. In order to obtain an overview of PPARα--regulated genes relevant to lipid metabolism, and to probe for novel candidate PPARα– target genes, livers from several animal studies in which PPARα– was activated and/or disabled were analyzed by Affymetrix GeneChips. Numerous novel PPARα--regulated genes relevant to lipid metabolism were identified. Out of this set of genes, eight genes were singled out for study of PPARα--dependent regulation in mouse liver and in mouse, rat, and human primary hepatocytes, including thioredoxin interacting protein (Txnip), electron-transferring-flavoprotein α† polypeptide (Etfb), electron-transferring-flavoprotein dehydrogenase (Etfdh), phosphatidylcholine transfer protein (Pctp), endothelial lipase (EL, Lipg), adipose triglyceride lipase (Pnpla2), hormone-sensitive lipase (Lipe), and monoglyceride lipase (Mgll). Using an in silico screening approach, one or more PPAR response elements (PPREs) were identified in each of these genes. Since Pnpla2, Lipe, and Mgll contribute to hepatic triglyceride hydrolysis, gene regulation was studied under conditions of elevated hepatic lipids. In wild-type mice fed a high fat diet, the decrease in hepatic lipids following treatment with the PPARα– agonist Wy14643 was paralleled by significant up-regulation of Pnpla2, Lipe, and Mgll, suggesting that induction of triglyceride hydrolysis may contribute to the anti-steatotic role of PPARα–. Our study illustrates the power of transcriptional profiling to uncover novel PPARα--regulated genes and pathways in liver. **Keywords:** identification of target genes **Overall design:** Five microgram total RNA was labelled according to the ENZO-protocol, fragmented and hybridized according to Affymetrix's protocols.

Background corr dist: KL-Divergence = 0.1374, L1-Distance = 0.0285, L2-Distance = 0.0011, Normal std = 0.4050

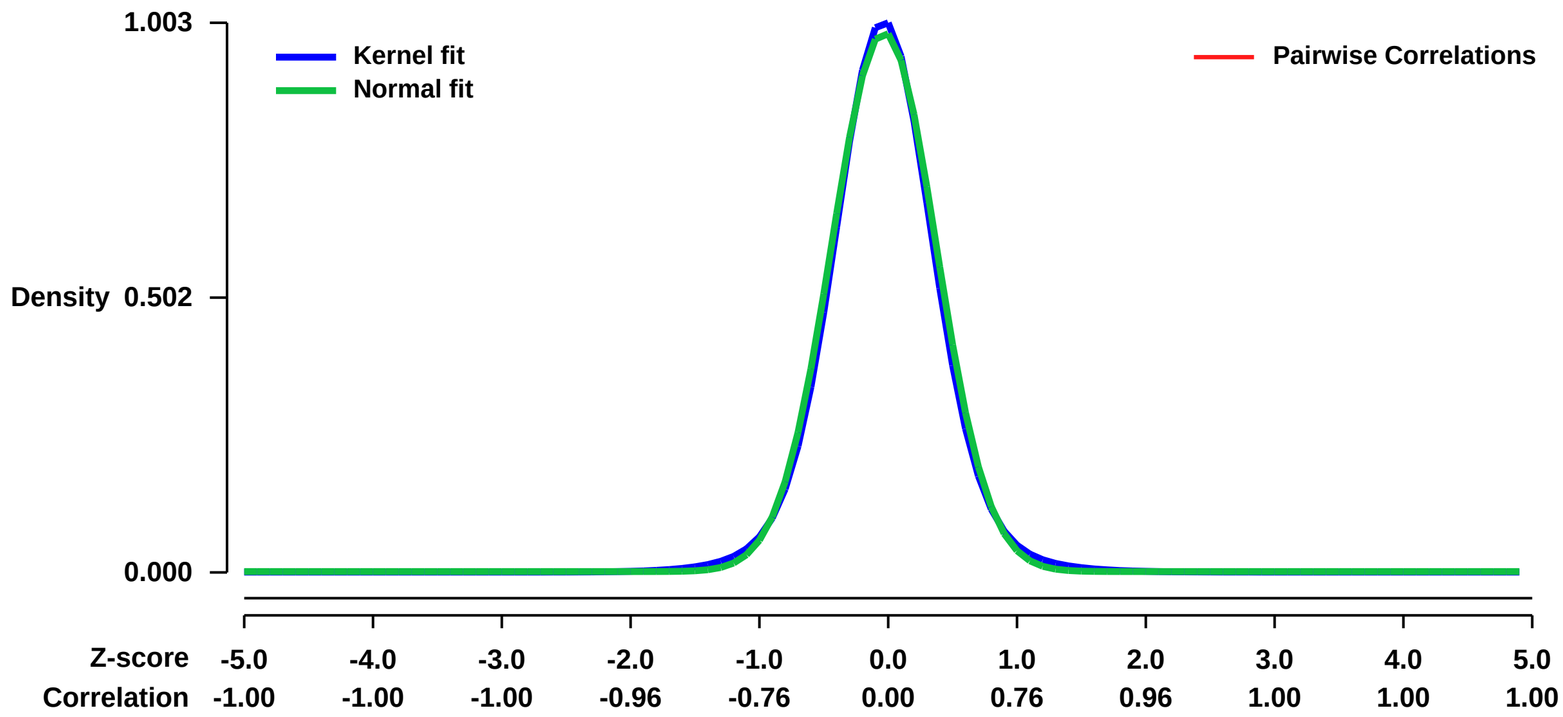

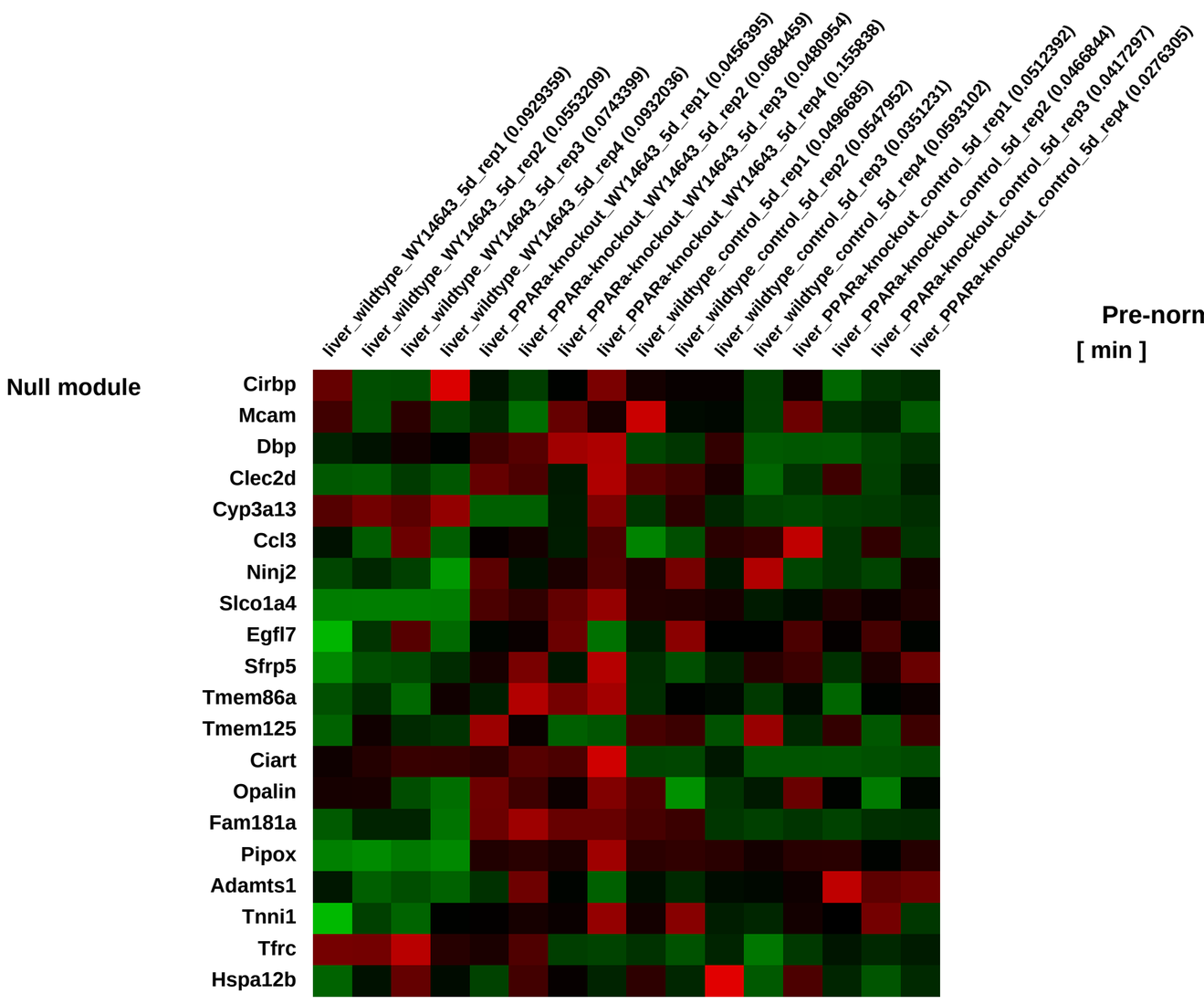

GEO Series "GSE42264" Expression Profiles

Num of samples in this series: 26

Scale of expression profile Z-scores

-3.0 -2.0 -1.0 0.0 1.0 2.0 3.0

GEO Link:	http://www.ncbi.nlm.nih.gov/geo/query/acc.cgi?acc=GSE42264
Status:	Public on Nov 14 2012
Title:	Hsp70 and a Novel Axis of Type 1 Interferon-Dependent Antiviral Immunity in the Measles Virus-Infected Brain
Organism:	Mus musculus
Experiment type:	Expression profiling by array
Platform:	GPL1261
Pubmed ID:	23135720
Summary & Design:	**Summary:** The major inducible 70 kDa heat shock protein (hsp70) is host protective in a mouse model of measles virus (MeV) brain infection. Transgenic constitutive expression of hsp70 in neurons, the primary target of MeV infection, abrogates neurovirulence in neonatal H-2d congenic C57BL/6 mice. A significant level of protection is retained after depletion of T lymphocytes, implicating innate immune mechanisms. Focus of the present work was to elucidate the basis for hsp70-dependent innate immunity using this model. Transcriptome analysis of brains from transgenic (TG) and non-transgenic (NT) mice 5 days after infection identified type 1 interferon (IFN) signaling and macrophage activation/antigen presentation as the main differences linked to survival. The pivotal role for type 1 IFN in hsp70-mediated protection was demonstrated in mice with a genetically disrupted type 1 IFN receptor (IFNAR-/-), where IFNAR-/- eliminated the difference in survival between TG and NT mice. Brain macrophages, not neurons, are the predominant source of type 1 IFN in the virus-infected brain, and in vitro studies provided a mechanistic basis by which MeV-infected neurons can induce IFN-¿† in uninfected microglia in an hsp70-dependent manner. MeV infection induced extracellular release of hsp70 from mouse neuronal cells that constitutively express hsp70, and extracellular hsp70 induced IFN-¿† transcription in mouse microglial cells through Toll-like receptors 2 and 4. Collectively, results support a novel axis of type 1 IFN-dependent antiviral immunity in the virus-infected brain that is driven by hsp70. **Overall design:** Hsp70-overexpressing transgenic (TG) and non-transgenic (NT) mice were infected with MeV intracranially, and total brain mRNA harvested at 5 and 10 days post infection (d.p.i.) was analyzed, sampling the hemisphere opposite the side of viral inoculation. Analysis includes 6 groups: infected TG at 5 d.p.i. (n=4), infected TG at 10 d.p.i. (n=5), infected NT at 5 d.p.i. (n=4), infected NT at 10 d.p.i. (n=5), uninfected TG at 5 d.p.i. (n=4), and uninfected NT at 5 d.p.i. (n=4).

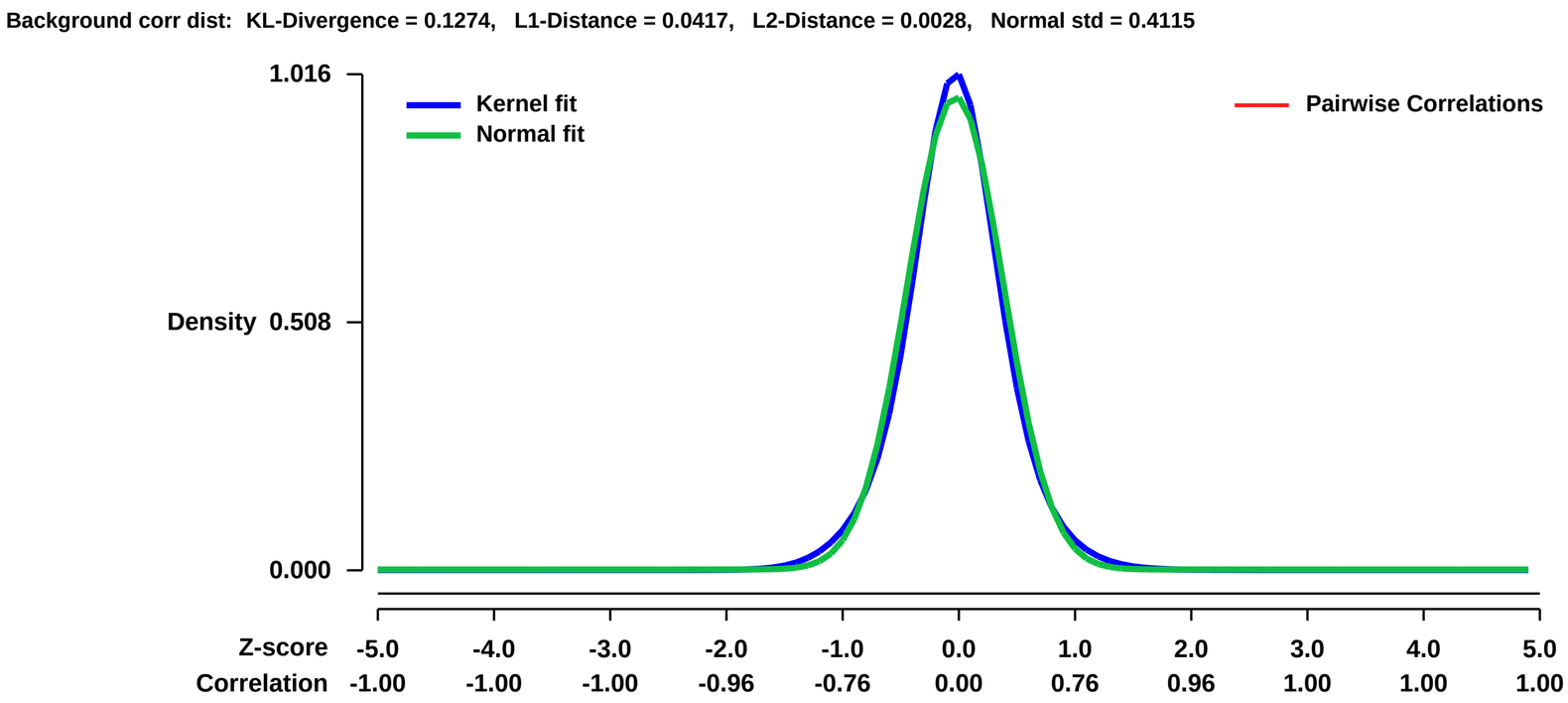

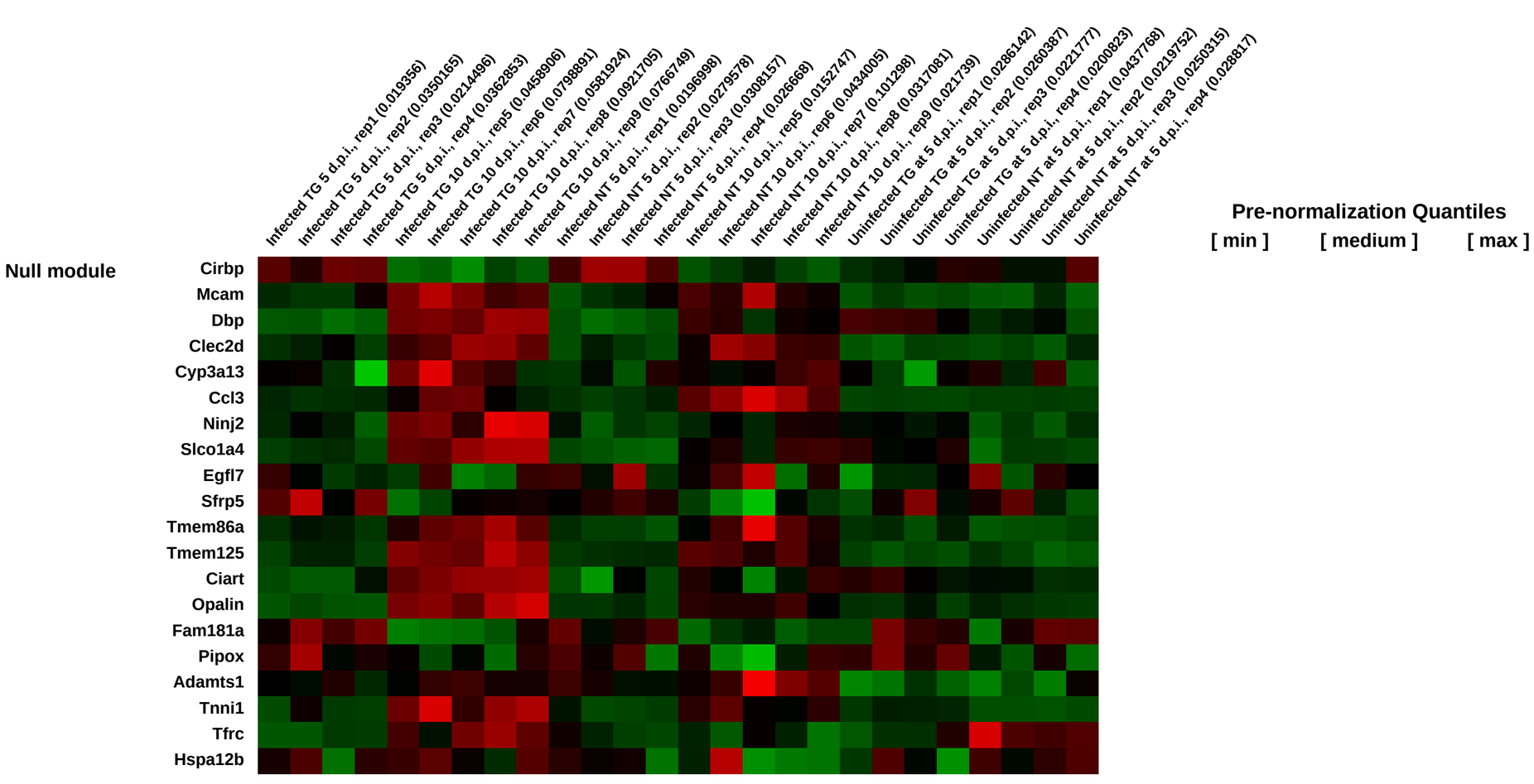

GEO Series "GSE48338" Expression Profiles

Num of samples in this series: 8

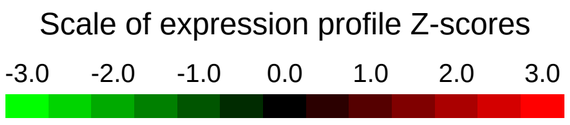

GEO Link:	http://www.ncbi.nlm.nih.gov/geo/query/acc.cgi?acc=GSE48338
Status:	Public on Jun 03 2014
Title:	Tpl2 promotes chemokine/chemokine receptor expression and macrophage migration during acute inflammation
Organism:	Mus musculus
Experiment type:	Expression profiling by array
Platform:	GPL1261
Pubmed ID:	24713702
Summary & Design:	**Summary:** In autoimmune diseases, accumulation of activated leukocytes correlates with inflammation and disease progression, and therefore, disruption of leukocyte trafficking is an active area of research. The protein kinase Tpl2 (MAP3K8) regulates leukocyte inflammatory responses and is also being investigated for therapeutic inhibition during autoimmunity. Herein, we addressed the contribution of Tpl2 to the regulation of macrophage chemokine and chemokine receptor expression and subsequent migration in vivo using a mouse model of Tpl2 ablation. We found that gene expression of the chemokine ligands CCL2, CCL7, CXCL2, and CXCL3 as well as the chemokine receptors CCR1 and CCR5 were reduced in macrophages from the bone marrow and peritoneal cavities of tpl2-/- mice following stimulation with LPS. LPS stimulation repressed chemokine receptor expression of CCR1, CCR2 and CCR5. Notably, LPS-induced repression of CCR1 and CCR5 was significantly enhanced in Tpl2-deficient macrophages and was observed to be dependent upon Erk activation and independent of PI3K and mTOR signaling. Consistent with alterations in chemokine and chemokine receptor expression, tpl2-/- macrophages were defective in trafficking to the peritoneal cavity following thioglycollate-induced inflammation. Overall, this study demonstrates a Tpl2-dependent mechanism for macrophage expression of both chemokine receptors and their ligands and provides further insight into how Tpl2 inhibition may disrupt inflammatory networks in vivo. **Overall design:** microarray was used to profile the genome-wide expression patterns in Tpl2 wild-type and deficient macrophage.

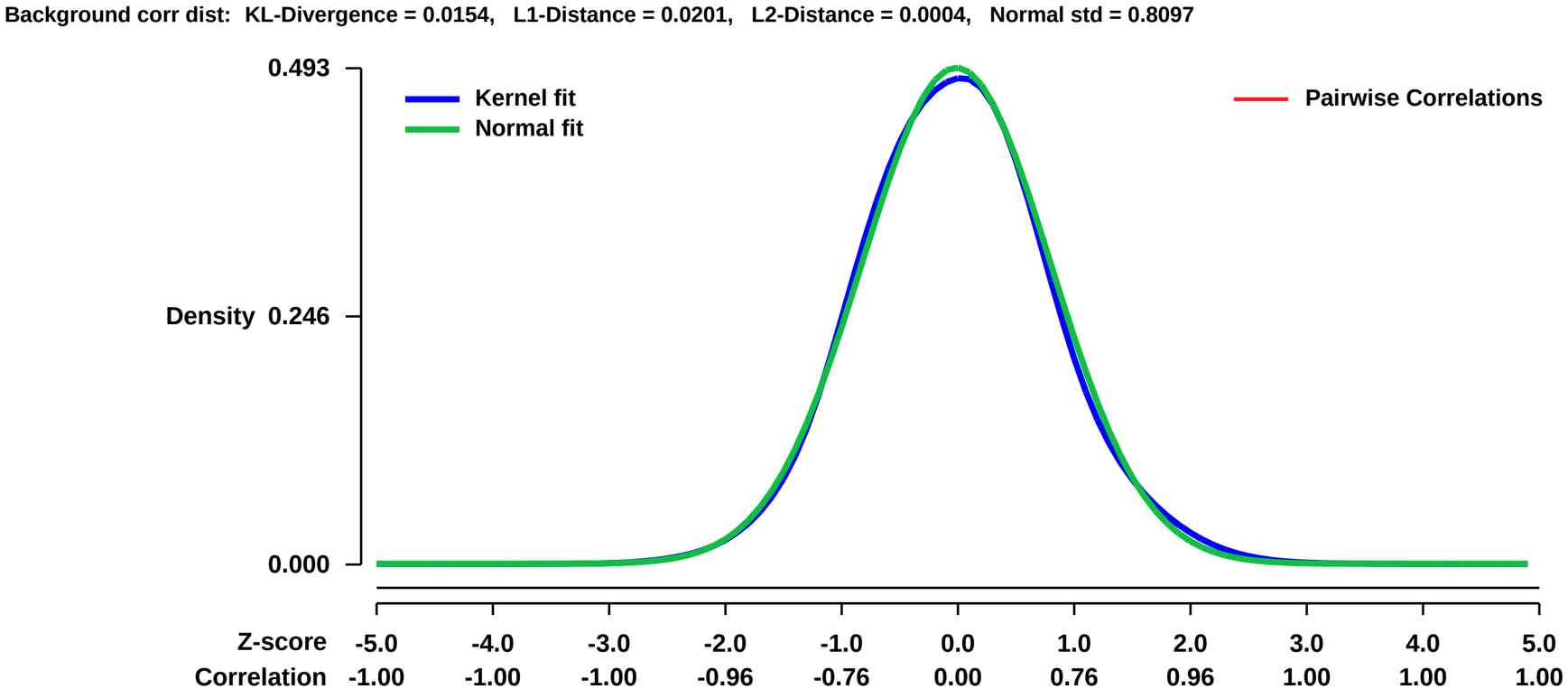

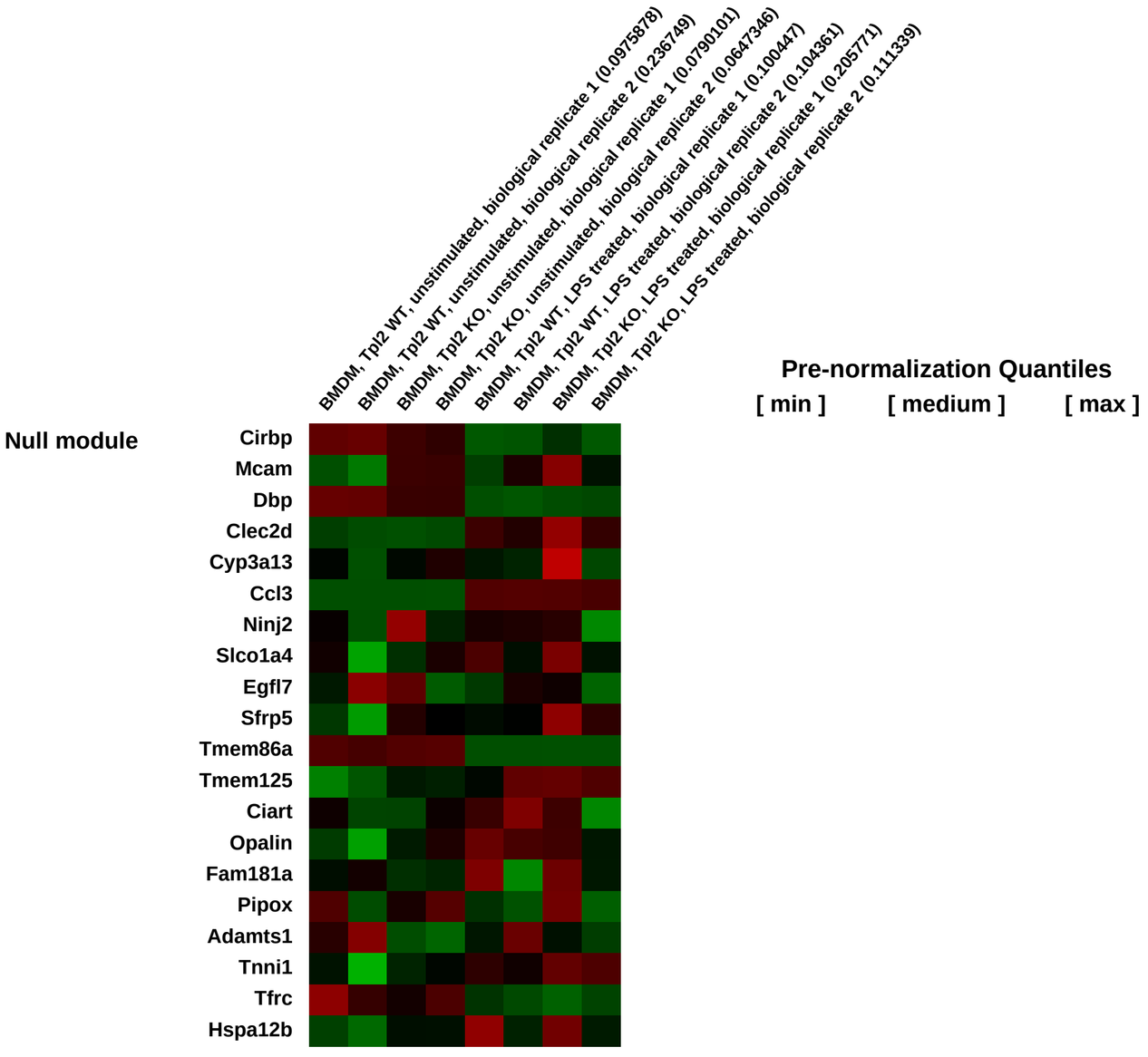

GEO Series "GSE12772" Expression Profiles

Num of samples in this series: 8

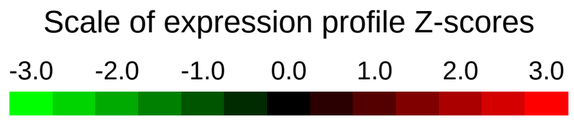

GEO Link:	**http://www.ncbi.nlm.nih.gov/geo/query/acc.cgi?acc=GSE12772**
Status:	**Public on Dec 07 2008**
Title:	**Hematopoietic stem cell (HSC) expression alteration in an ADAR1 mouse model**
Organism:	**Mus musculus**
Experiment type:	**Expression profiling by array**
Platform:	**GPL1261**
Pubmed ID:	**19060901**
Summary & Design:	**Summary:** **Hematopoietic stem cells purified from +/+, +/- and -/- ADAR1 mice were compared with global gene expression analysis.** **Overall design:** **Each sample was purified from one mouse.**

Background corr dist: **KL-Divergence = 0.0542, L1-Distance = 0.0688, L2-Distance = 0.0083, Normal std = 0.5963**

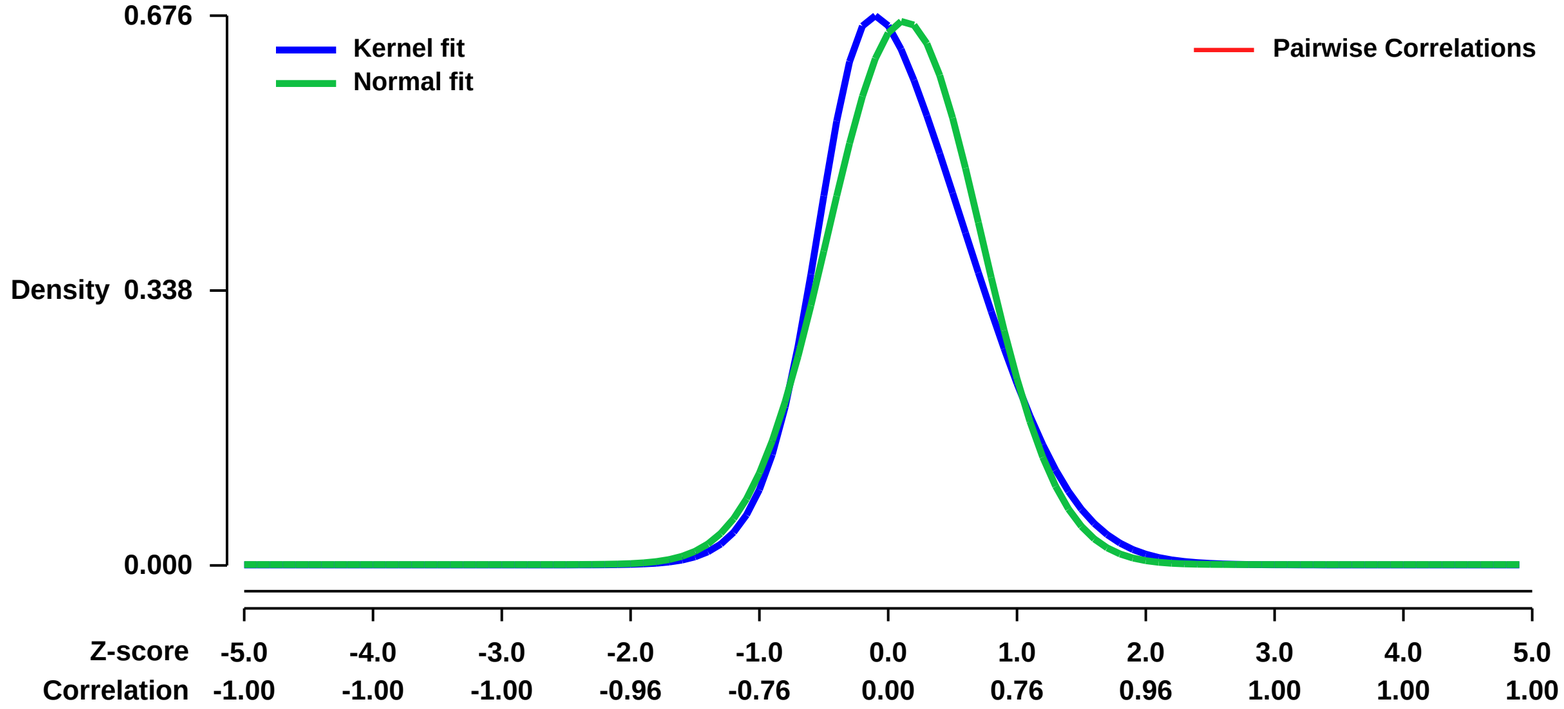

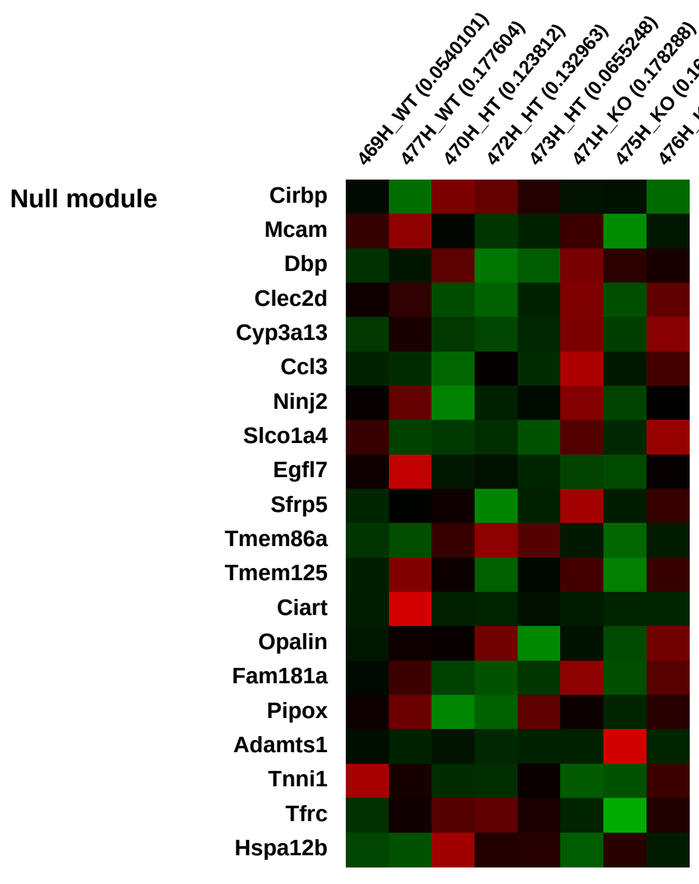

GEO Series "GSE22086" Expression Profiles

Num of samples in this series: 6

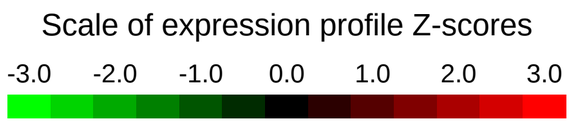

GEO Link:	http://www.ncbi.nlm.nih.gov/geo/query/acc.cgi?acc=GSE22086
Status:	Public on Sep 19 2011
Title:	Expression data from quadriceps muscle of WT and ERRgamma transgenic mice
Organism:	Mus musculus
Experiment type:	Expression profiling by array
Platform:	GPL1261
Pubmed ID:	21356518
Summary & Design:	**Summary:** We show that the orphan nuclear receptor ERRg is expressed at high levels in type I muscle and when transgenically expressed in anaerobic type II muscles (ERRGO mice) or cultured cells, powerfully regulates VEGF expression, angiogenesis and vascular supply in absence of exercise. ERRGO mice show increased expression of genes promoting fat metabolism, mitochondrial respiration and type I fiber specification. In parallel, the type II muscle in ERRGO mice display an activated angiogenic program marked by myofibrillar induction and secretion of pro-angiogenic factors, frank neo-vascularization and a 100% increase in running endurance. Surprisingly, the induction of VEGF and type I muscle properties by ERRg does not involve the transcriptional co-activator PGC1a. Instead, ERRg genetically activates the energy sensor AMPK which is typically inactive in absence of exercise. Therefore, ERRg and AMPK, known regulators of mitochondrial function and metabolism, together control a novel angiogenic pathway that anatomically synchronizes vascular arborization to oxidative metabolism revealing an exercise-independent mechanism for matching supply and demand. **Keywords:** ERRgamma overexpression compared to wild-type **Overall design:** Comparison of gene expression from quadriceps muscles isolated from wild type and alpha-skeletal actin-ERRgamma-transgenic mice.

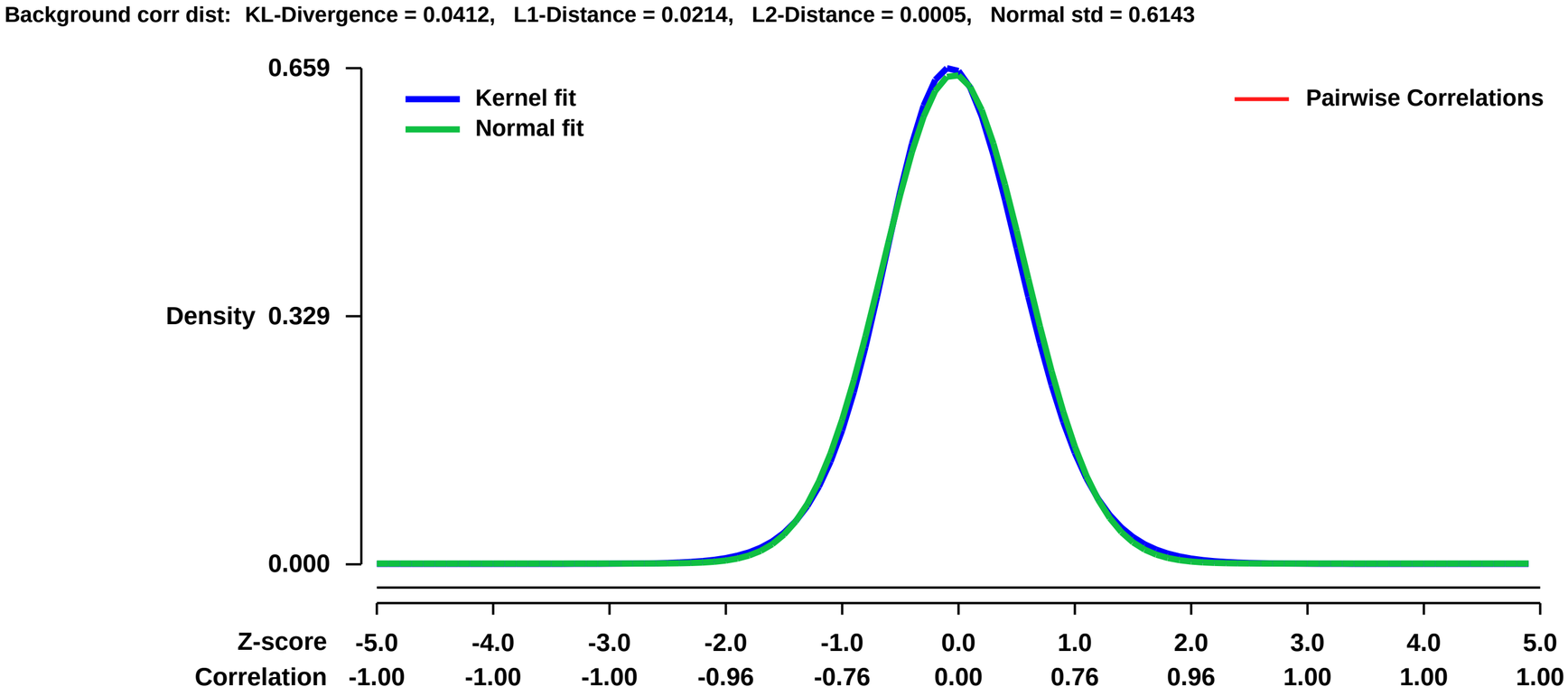

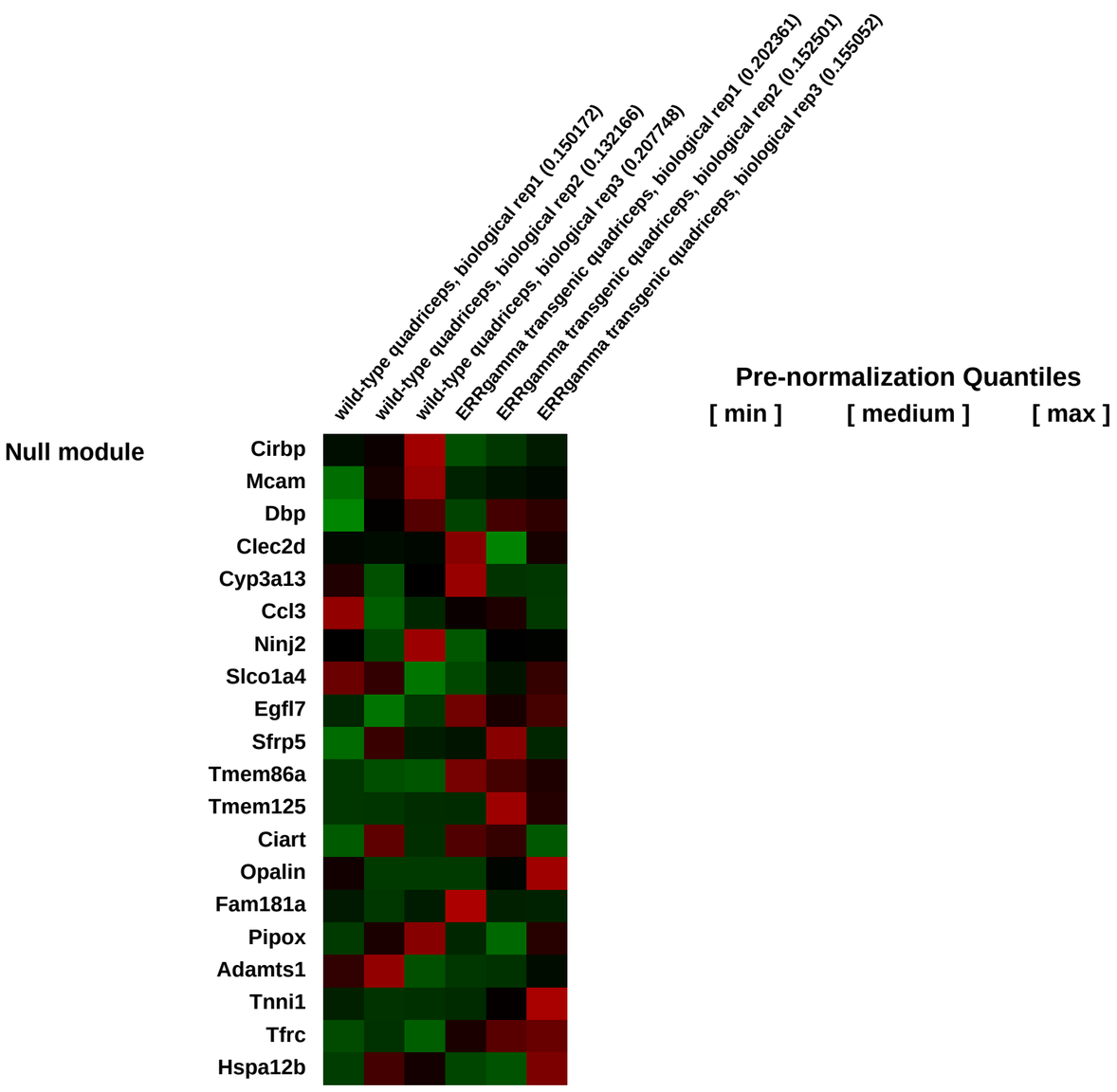

GEO Series "GSE9287" Expression Profiles

Num of samples in this series: 8

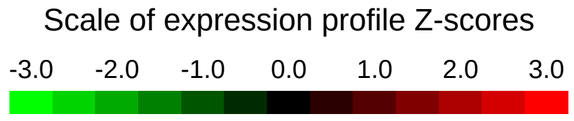

GEO Link: http://www.ncbi.nlm.nih.gov/geo/query/acc.cgi?acc=GSE9287

Status: Public on Dec 15 2009

Title: Differential gene expression in wild-type versus Yaa mutant mouse spleen cells

Organism: Mus musculus

Experiment type: Expression profiling by array

Platform: GPL1261

Pubmed ID:

Summary & Design:

Summary:
T cells from many patients with systemic lupus erythematosus are hypoproliferative in response to TCR ligation. This defect is mediated, at least in part, through down regulation of the TCR zeta chain. Investigation of this phenomenon in lupus-prone mice revealed that the hypoproliferative T cell phenotype apparent in BXSB males is mediated

in part by the Yaa locus. The BXSB model of lupus is a recombinant inbred strain that was originally derived from a cross between a male SB/LE mouse and a female C57BL/6 mouse. BXSB is unique among lupus-prone mouse strains, in that males carry an autoimmune accelerating factor on the Y chromosome, termed Yaa, which accelerates disease onset in male BXSB mice so that fatal glomerulonephritis occurs around 6 months of age. It was recently reported that the Yaa locus is a translocation of a short stretch of genes including that encoding Toll-like

receptor 7 (Tlr-7) from the X to the Y chromosome, leading to a two-fold over expression of a subset of these genes, including Tlr-7, and hypersensitivity of Yaa+ cells to TLR-7 agonists.

To more fully understand the functional significance of the Yaa gene and how it plays a part in the modulation of CD4+ T cell responses, we performed microarray analysis using Affymetrix 430 2.0 arrays on spleens from B6 male B6.Yaa male samples. The analysis revealed an enhanced signature of innate immunity, including increased expression not only of Tlr7 and Tlr8, in line with reports that the Yaa locus leads to a duplication of the murine Tlr7 and Tlr8 genes , but also of Tlr2, Tlr5, Cd14, Lbp, C2, C3 and genes for several heat-shock proteins. T cells from B6.Yaa mice also displayed decreased TCR¸¶ expression. Interestingly, cell surface levels of the inhibitory molecule B7-H1 were increased on B6.Yaa B cells and monocytes/macrophages. In line with increased TLR-7 expression reported in B6.Yaa mice, the TLR-7 agonist imiquimod increased B7-H1 expression on normal B cells. Restoration of proliferation in co-cultures of B6 T cells and B6.Yaa APC with B7-H1 blocking Ab demonstrated a mechanistic contribution of B7-H1 up-regulation to Yaa-mediated APC-dependent T cell hypoproliferation. In addition, T cell hypoproliferation was induced in normal B6 T cells in vitro by the application of imiquimod. However, this defect was not mediated by B7-H1 or secreted factors but was independent of APC and mediated through direct imiquimod stimulation of T cells themselves. We postulate that excessive TLR-7 stimulation in Yaa+ mice mediates T cell hypoproliferation in part through up-regulation of B7-H1 and possibly also through direct T cell-mediated effects.

Keywords: differential gene expression, RNA, spleen, C57Bl/6J, B6.SB-Yaa/J, male, wild type, Yaa

Overall design:
RNA was separately extracted, labeled, and hybridized from each animal.

Background corr dist: KL-Divergence = 0.0581, L1-Distance = 0.0301, L2-Distance = 0.0011, Normal std = 0.5502

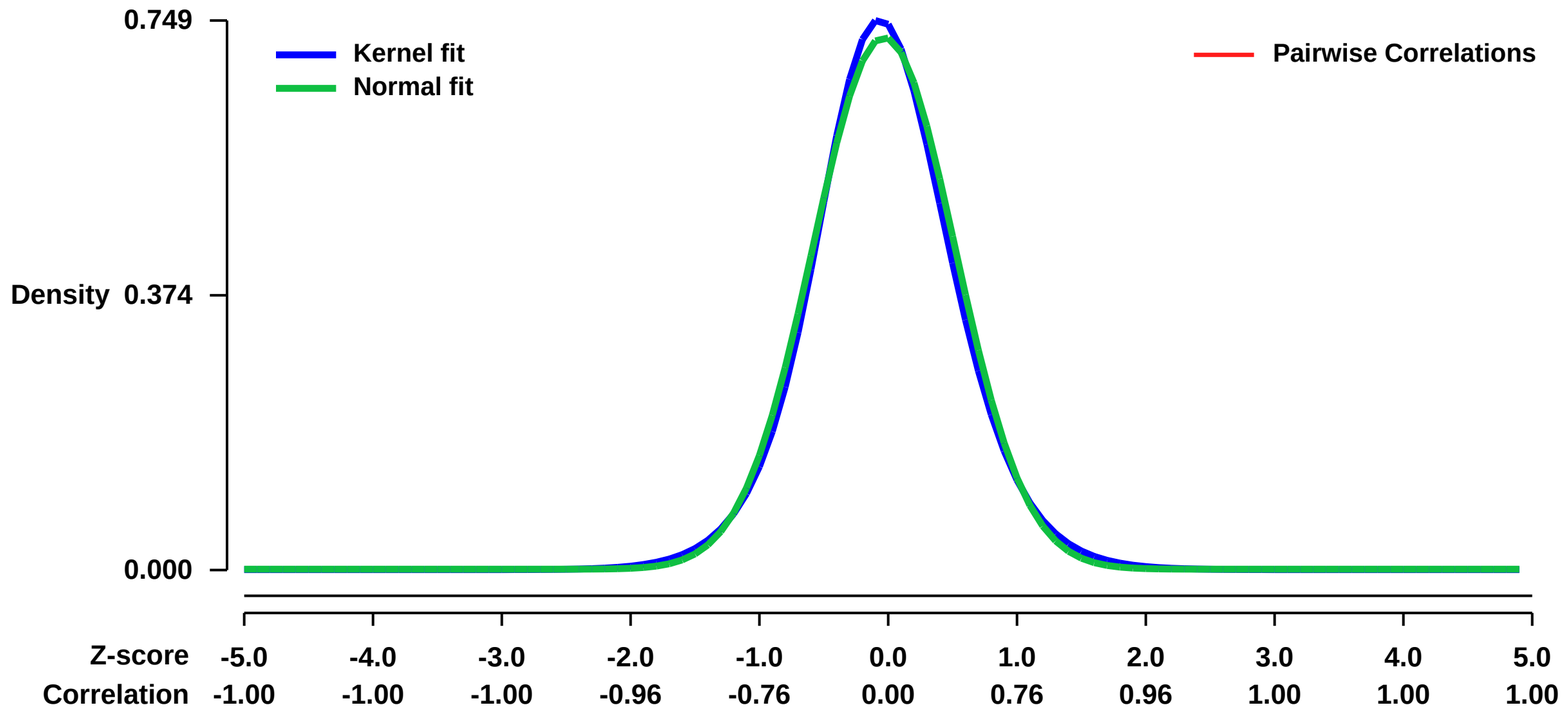

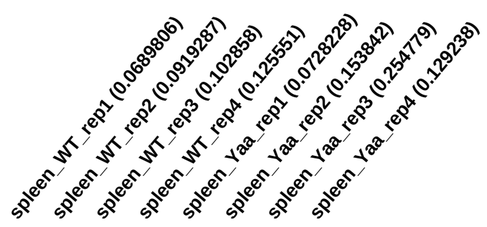

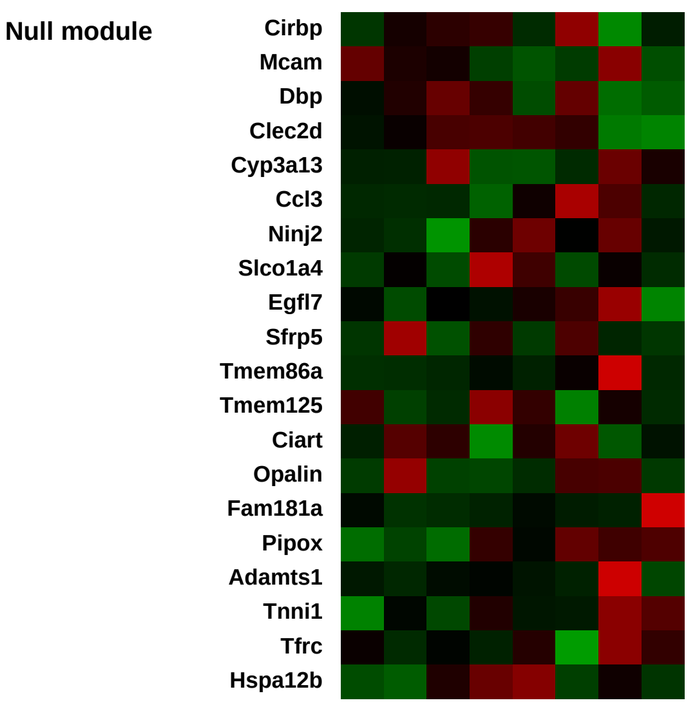

GEO Series "GSE56542" Expression Profiles

Num of samples in this series: 8

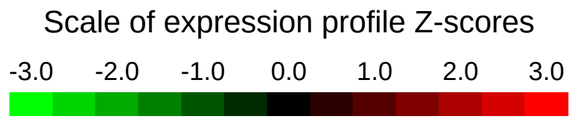

GEO Link:	**http://www.ncbi.nlm.nih.gov/geo/query/acc.cgi?acc=GSE56542**
Status:	**Public on Apr 07 2014**
Title:	**Expression data from CD4+ T cells of germ free mice, SPF IQI mice and SPF C57BL/6 mice depletd with Uhrf1 (by Cd4Cre-Uhrf1flox/flox)**
Organism:	**Mus musculus**
Experiment type:	**Expression profiling by array**
Platform:	**GPL1261**
Pubmed ID:	
Summary & Design:	**Summary:** **Commensal bacteria shapes gut immune system. Colonization bacteria increase the frequency of regulatory T cells, however, the molecular mechanisms has not yet been unknown. To reveal the mechanism, we isolated Treg cells and Non-Treg cells and performed the global expression analysis.** **Overall design:** **Colonic lamina propria cells were isolated from mice described above. Treg cells and Non-Treg cells (also called as Tconv cells) were sorted by FACS AriaIII**

Background corr dist: **KL-Divergence = 0.0404, L1-Distance = 0.0306, L2-Distance = 0.0014, Normal std = 0.6162**

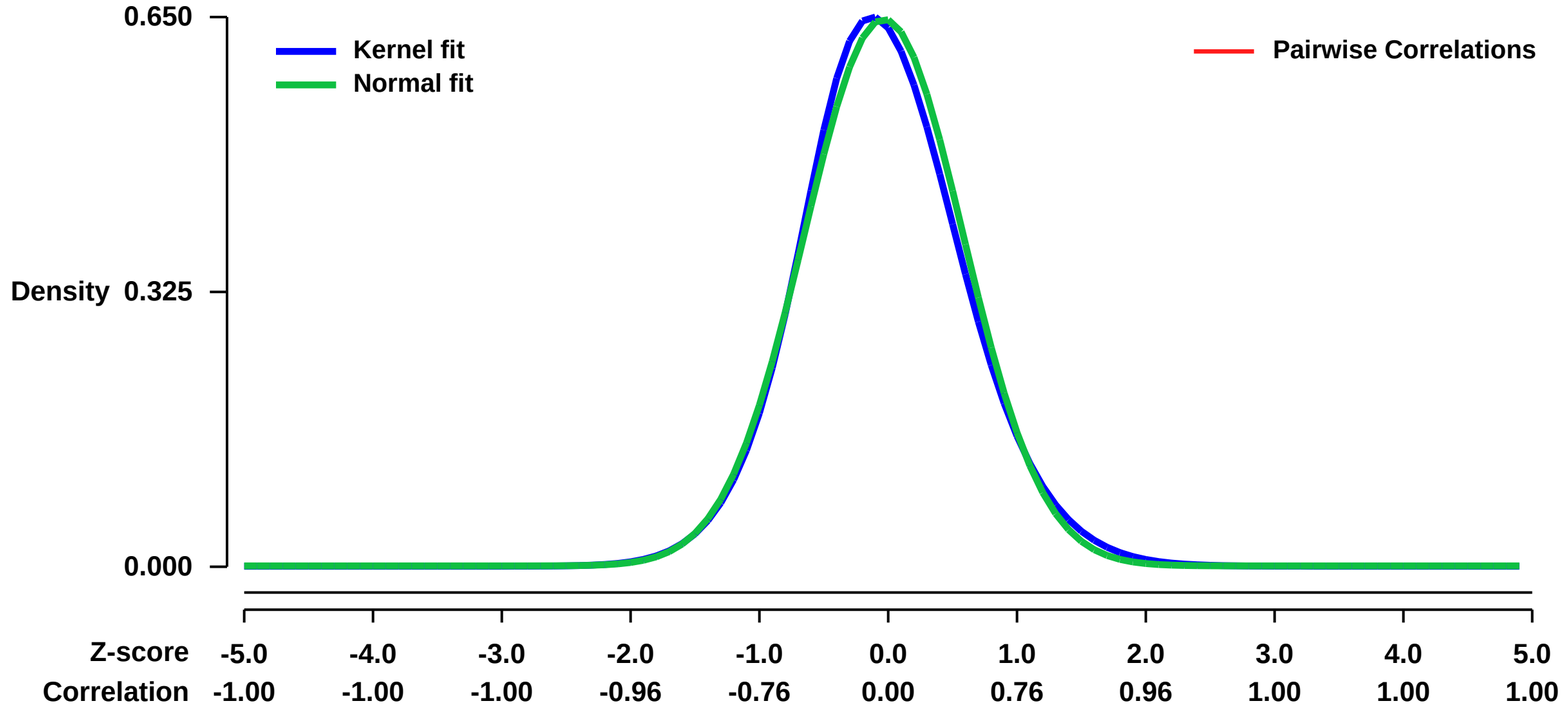

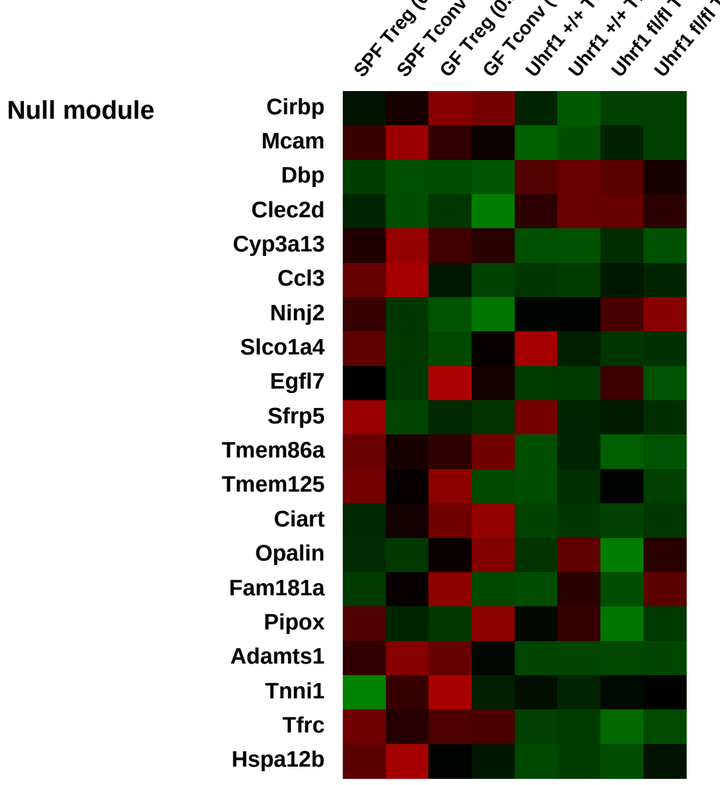

GEO Series "GSE37907" Expression Profiles

Num of samples in this series: 24

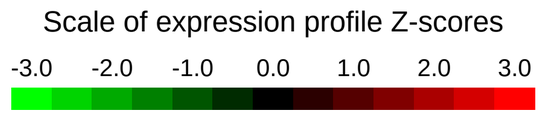

GEO Link:	http://www.ncbi.nlm.nih.gov/geo/query/acc.cgi?acc=GSE37907
Status:	Public on May 11 2012
Title:	Expression data from murine hematopoietic cells expressing BCR-ABL alone, NUP98-HOXA9 alone, BCR-ABL and NUP98-HOXA9, or null for both oncogenes
Organism:	Mus musculus
Experiment type:	Expression profiling by array
Platform:	GPL1261
Pubmed ID:	22863534
Summary & Design:	**Summary:** Leukemia is a complex malignancy with hundreds of distinct mutations associated with disease development. Studies have shown that oncogenes cooperate to promote leukemia transformation, however, the downstream effectors of this cooperation are largely unknown. Using a genetically defined mouse model of acute leuekmia, we investigated the regulated of genes downstream of the cooperative oncogenic interaction between BCR-ABL and NUP98-HOXA9 and identified a unique gene signature abberrantly expression in leukemia. **Overall design:** Total RNA was isolated from hematopoietic cells transduced with BCR-ABL and Nup98-HOXA9 retroviruses and transplanted into recipient mice. Bone marrow cells were purified by GFP (BCR-ABL) and YFP (NUP98-HOXA9) using FACS.

Background corr dist: KL-Divergence = 0.1944, L1-Distance = 0.0342, L2-Distance = 0.0020, Normal std = 0.3407

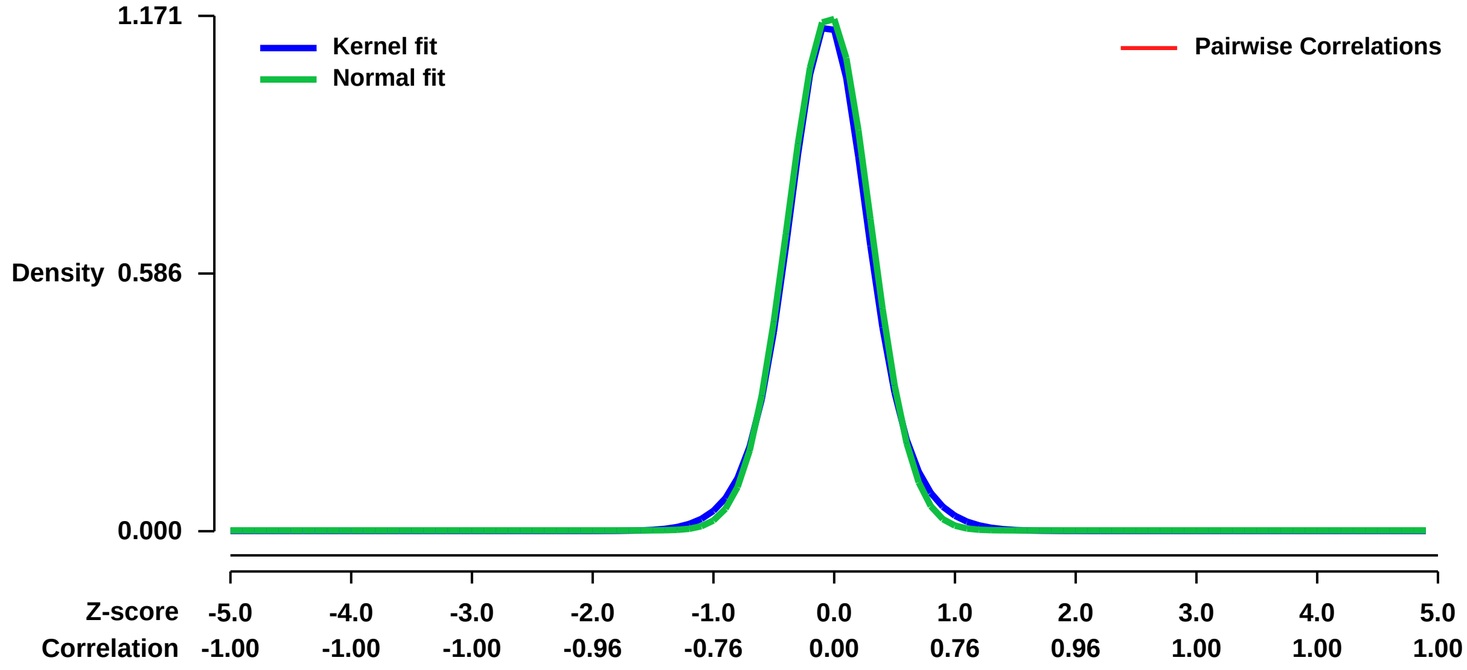

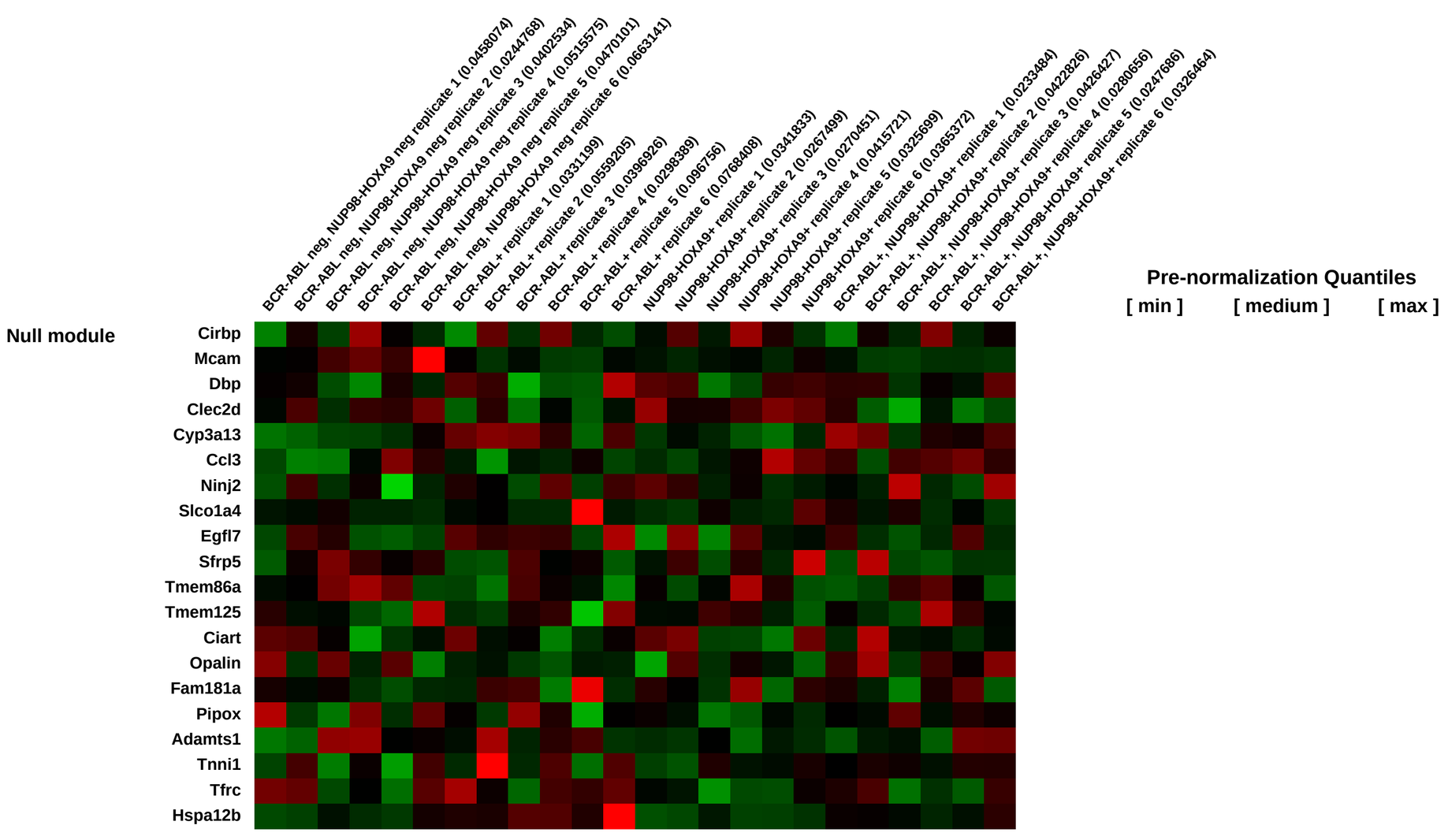

GEO Series "GSE30868" Expression Profiles

Num of samples in this series: 8

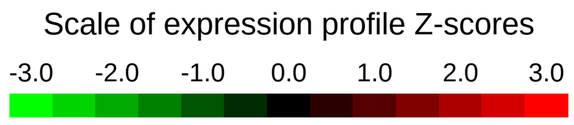

GEO Link:	http://www.ncbi.nlm.nih.gov/geo/query/acc.cgi?acc=GSE30868
Status:	Public on Feb 23 2013
Title:	Parthenogenetic stem cells for tissue-engineered heart repair
Organism:	Mus musculus
Experiment type:	Expression profiling by array
Platform:	GPL1261
Pubmed ID:	23434590
Summary & Design:	**Summary:** Uniparental parthenotes are considered an unwanted byproduct of in vitro fertilization. In utero parthenote development is severely compromised by defective organogenesis and in particular by defective cardiogenesis. Although developmentally compromised, apparently pluripotent stem cells can be derived from parthenogenetic blastocysts. Here we hypothesized that nonembryonic parthenogenetic stem cells (PSCs) can be directed toward the cardiac lineage and applied to tissue-engineered heart repair. We first confirmed similar fundamental properties in murine PSCs and embryonic stem cells (ESCs), despite notable differences in genetic (allelic variability) and epigenetic (differential imprinting) characteristics. Haploidentity of major histocompatibility complexes (MHCs) in PSCs is particularly attractive for allogeneic cell-based therapies. Accordingly, we confirmed acceptance of PSCs in MHC-matched allotransplantation. Cardiomyocyte derivation from PSCs and ESCs was equally effective. The use of cardiomyocyte-restricted GFP enabled cell sorting and documentation of advanced structural and functional maturation in vitro and in vivo. This included seamless electrical integration of PSC-derived cardiomyocytes into recipient myocardium. Finally, we enriched cardiomyocytes to facilitate engineering of force-generating myocardium and demonstrated the utility of this technique in enhancing regional myocardial function after myocardial infarction. Collectively, our data demonstrate pluripotency, with unrestricted cardiogenicity in PSCs, and introduce this unique cell type as an attractive source for tissue-engineered heart repair. **Overall design:** - ESC_3

Background corr dist: KL-Divergence = 0.0306, L1-Distance = 0.0233, L2-Distance = 0.0006, Normal std = 0.6786

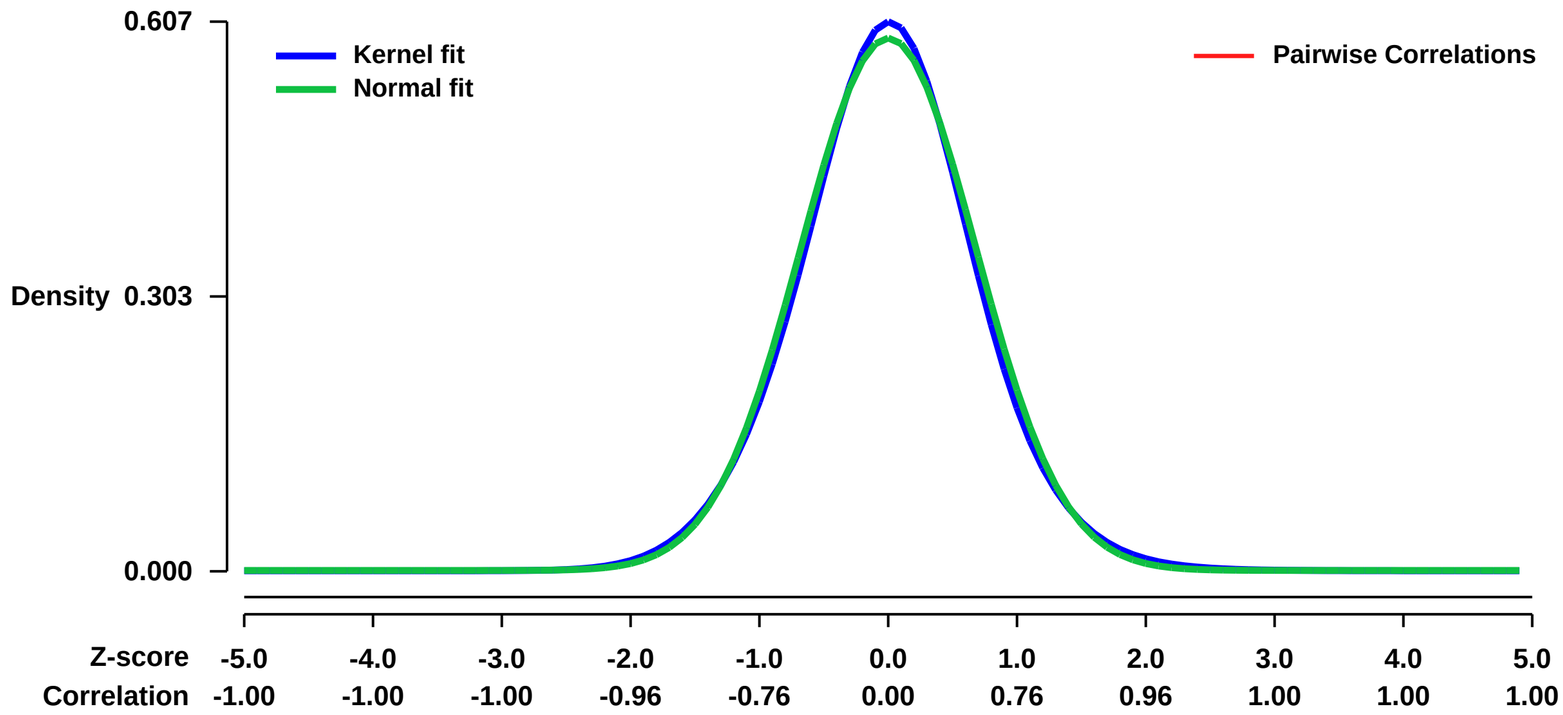

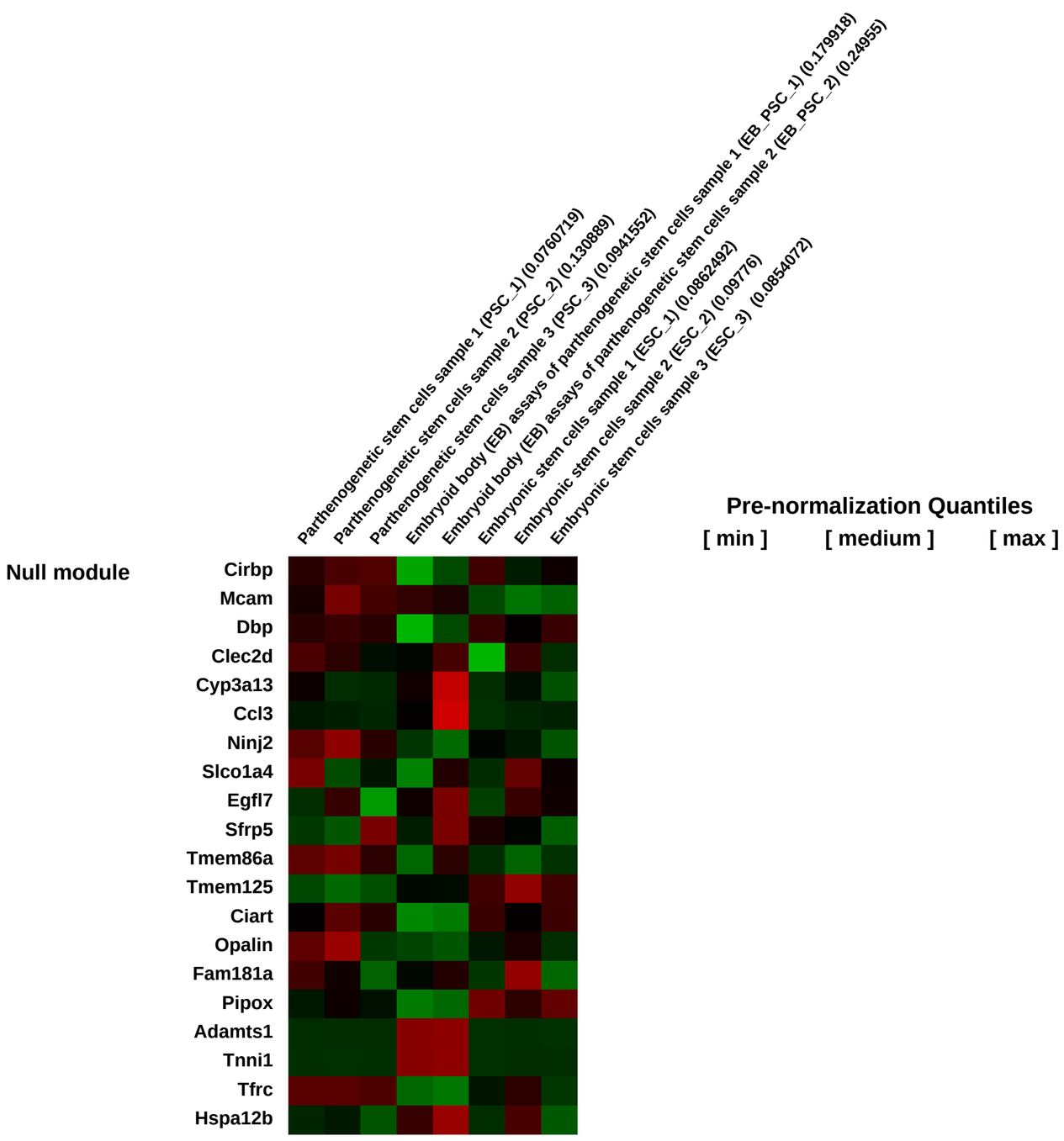

GEO Series "GSE34114" Expression Profiles

Num of samples in this series: 12

Scale of expression profile Z-scores

-3.0 -2.0 -1.0 0.0 1.0 2.0 3.0

GEO Link:	**http://www.ncbi.nlm.nih.gov/geo/query/acc.cgi?acc=GSE34114**
Status:	**Public on Dec 30 2012**
Title:	**Temporal response of mouse peritoneal cells to a non-pathogenic E. coli infection**
Organism:	**Mus musculus**
Experiment type:	**Expression profiling by array**
Platform:	**GPL1261**
Pubmed ID:	
Summary & Design:	**Summary:** **Analysis of early and late changes in the mouse peritoneal cells in response to E. coli induced sepis. Result provide an insight into the molecular function and pathways expressed at these different time points.** **Overall design:** **The mice were divided in two groups; the first group of mice were not treated with E. coli and was referred to as the naive group. Each mouse of the second group was injected with 2 X108 cells of a non- pathogenic isolate of E. coli suspended in a phosphate buffered saline (PBS) solution. After 1h, 2h and 18h of E. coli administration, peritoneal lavage fluid was obtained from two mice each for E. coli treated group at 1 and 2h and three mice of both groups (control and E. coli treated) at 18h. A common naive group of 2 mice harvested at 2h served as a control for both 1h and 2h.**

Background corr dist: **KL-Divergence = 0.0819, L1-Distance = 0.0275, L2-Distance = 0.0011, Normal std = 0.4862**

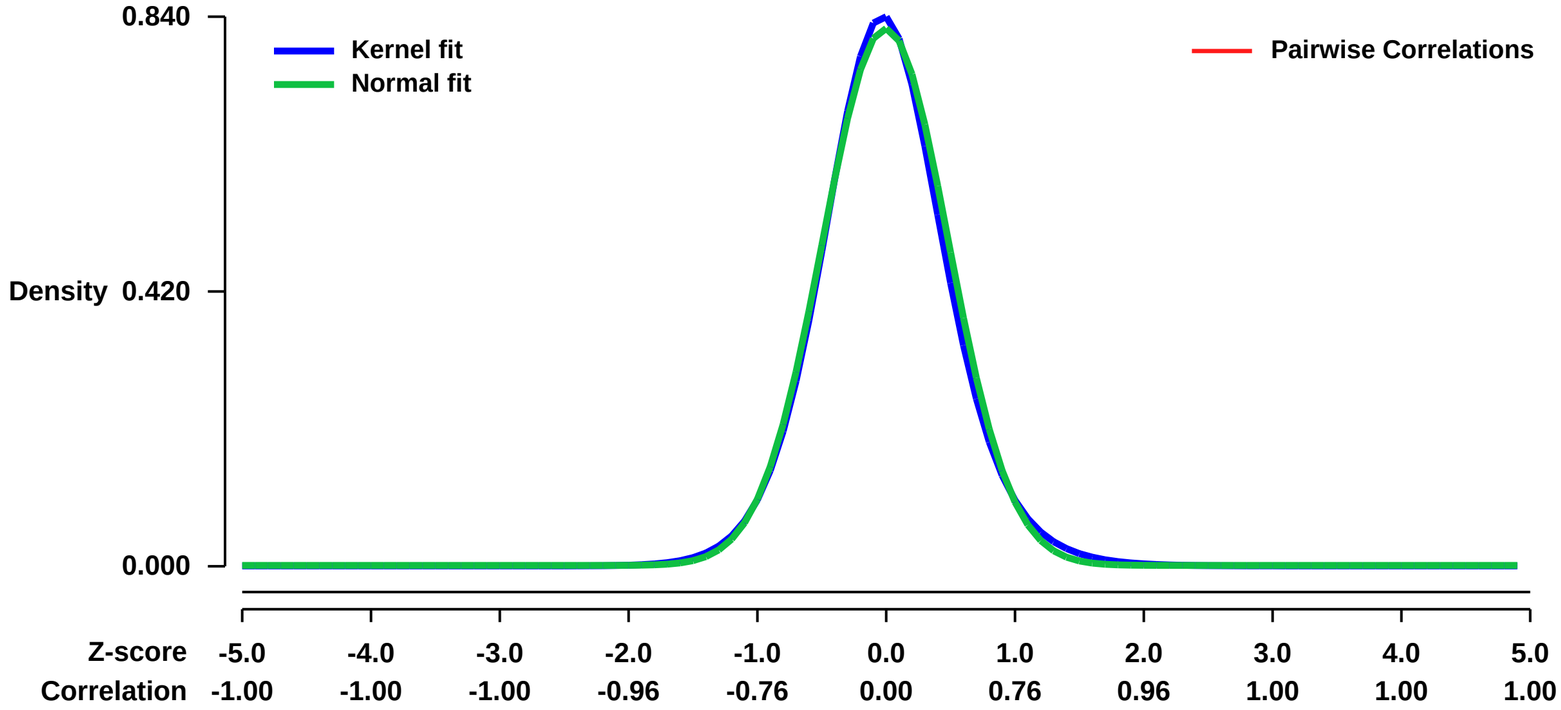

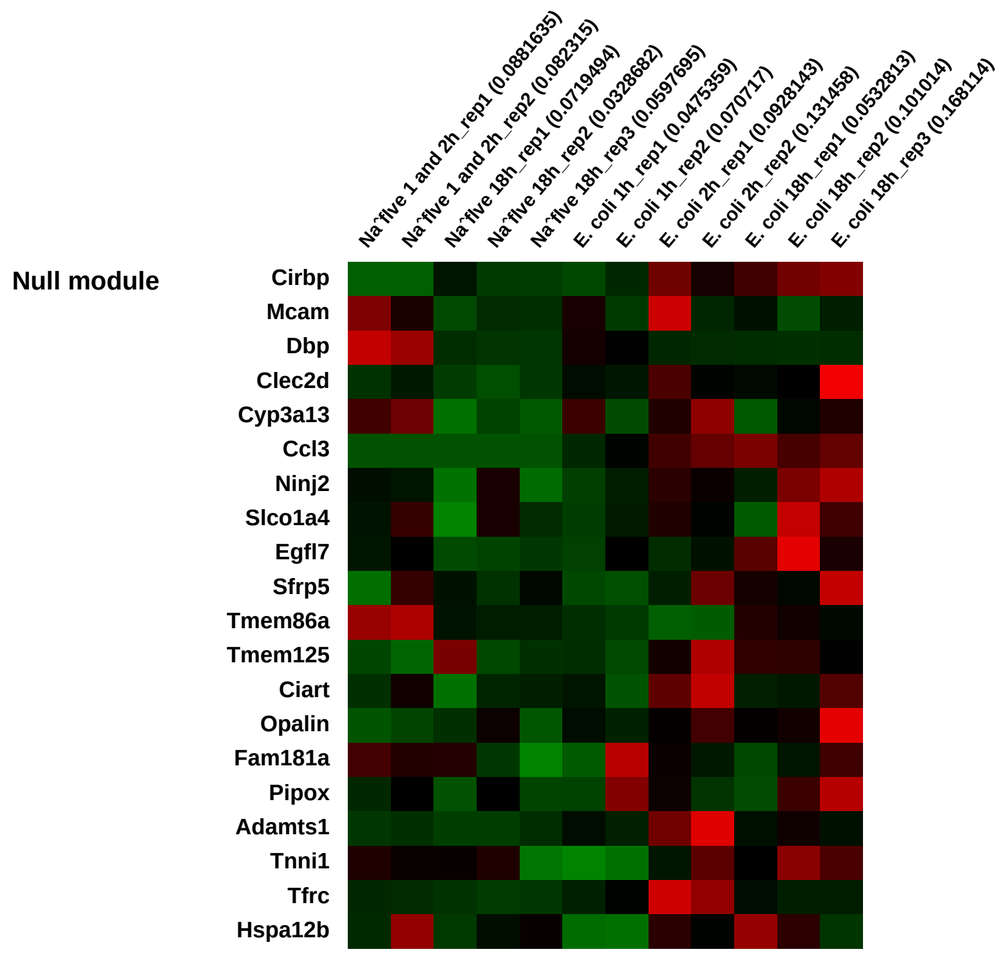

GEO Series "GSE23600" Expression Profiles

Num of samples in this series: 10

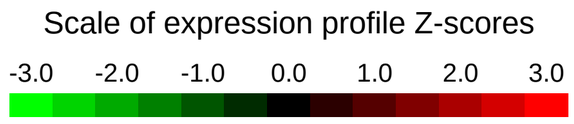

GEO Link:	http://www.ncbi.nlm.nih.gov/geo/query/acc.cgi?acc=GSE23600
Status:	Public on Aug 13 2010
Title:	Expression data from sorted Treg cells from WT or motheaten mice
Organism:	Mus musculus
Experiment type:	Expression profiling by array
Platform:	GPL1261
Pubmed ID:	20952680
Summary & Design:	**Summary:** **The importance of regulatory T cells (Treg) for immune tolerance is well recognized, yet the signaling molecules influencing their suppressive activity are relatively poorly understood. We identified the cytoplasmic tyrosine phosphatase SHP-1 as a novel â endogenous brakeâ and modifier of the suppressive ability of Treg cells; consistent with this notion, loss of SHP-1 expression strongly augments the ability of Treg cells to suppress inflammation in a mouse model. Specific harmacological inhibition of SHP-1 enzymatic activity via the cancer drug sodium stibogluconate (SSG) potently augmented Treg cell suppressor activity both in vivo and ex vivo.** **We evaluated the gene expression profiles of sorted T reg cells (CD4+CD25+) from wild type (wt) mice and mice that were heterozygous (he) or homozygous (me) for SHP-1 knockout (motheaten phenotype).** **Overall design:** **T reg (CD4+CD25+) cells were isolated form wild type (WT) mice and that were heterozygous (he) or homozygous (me) for SHP-1 knockout (motheaten phenotype); totalRNA was isolated using Arcturus reagents; aRNA was generated and amplified using Arcturus reagents; and labeled product was hybridized to Affymetrix chips to asses gene expression patterns.**

Background corr dist: KL-Divergence = 0.0252, L1-Distance = 0.0859, L2-Distance = 0.0097, Normal std = 0.9258

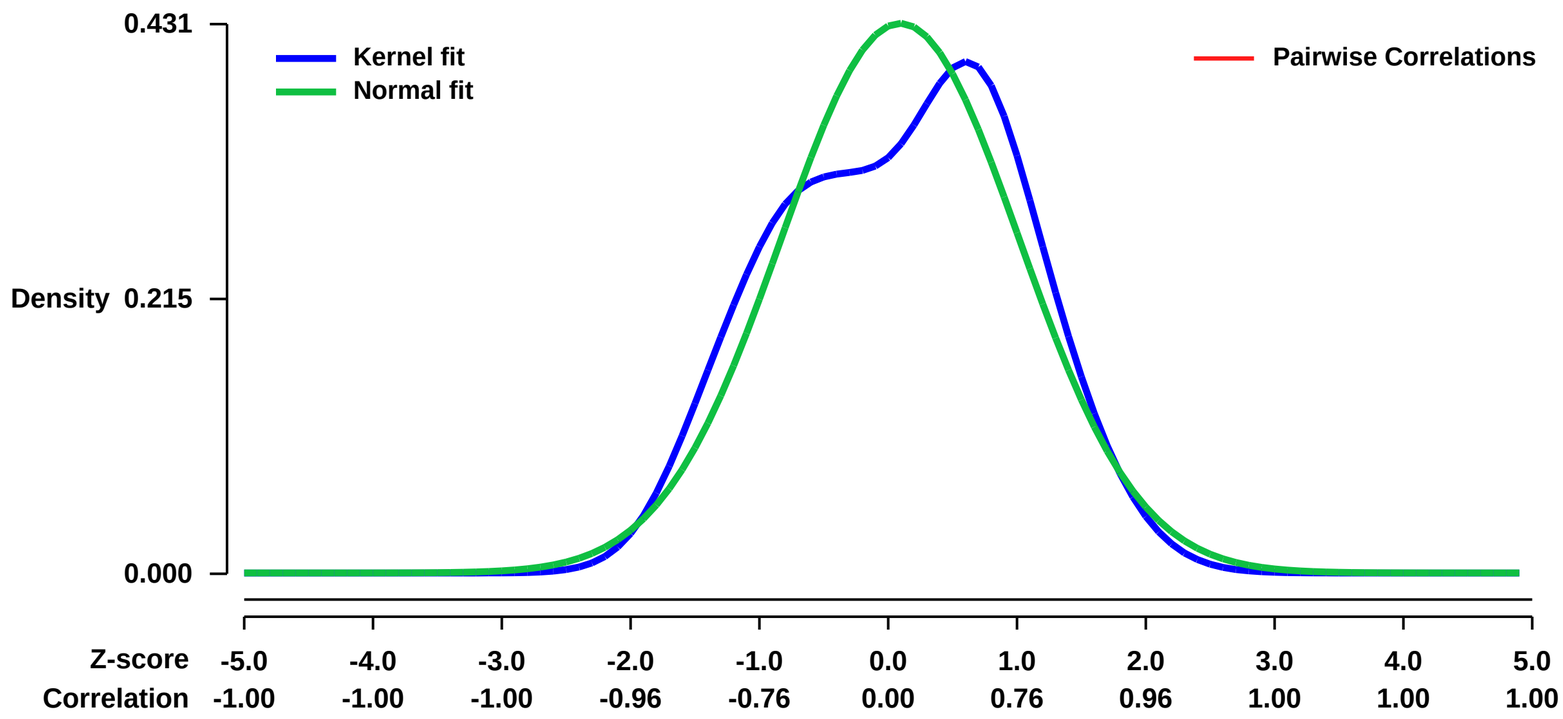

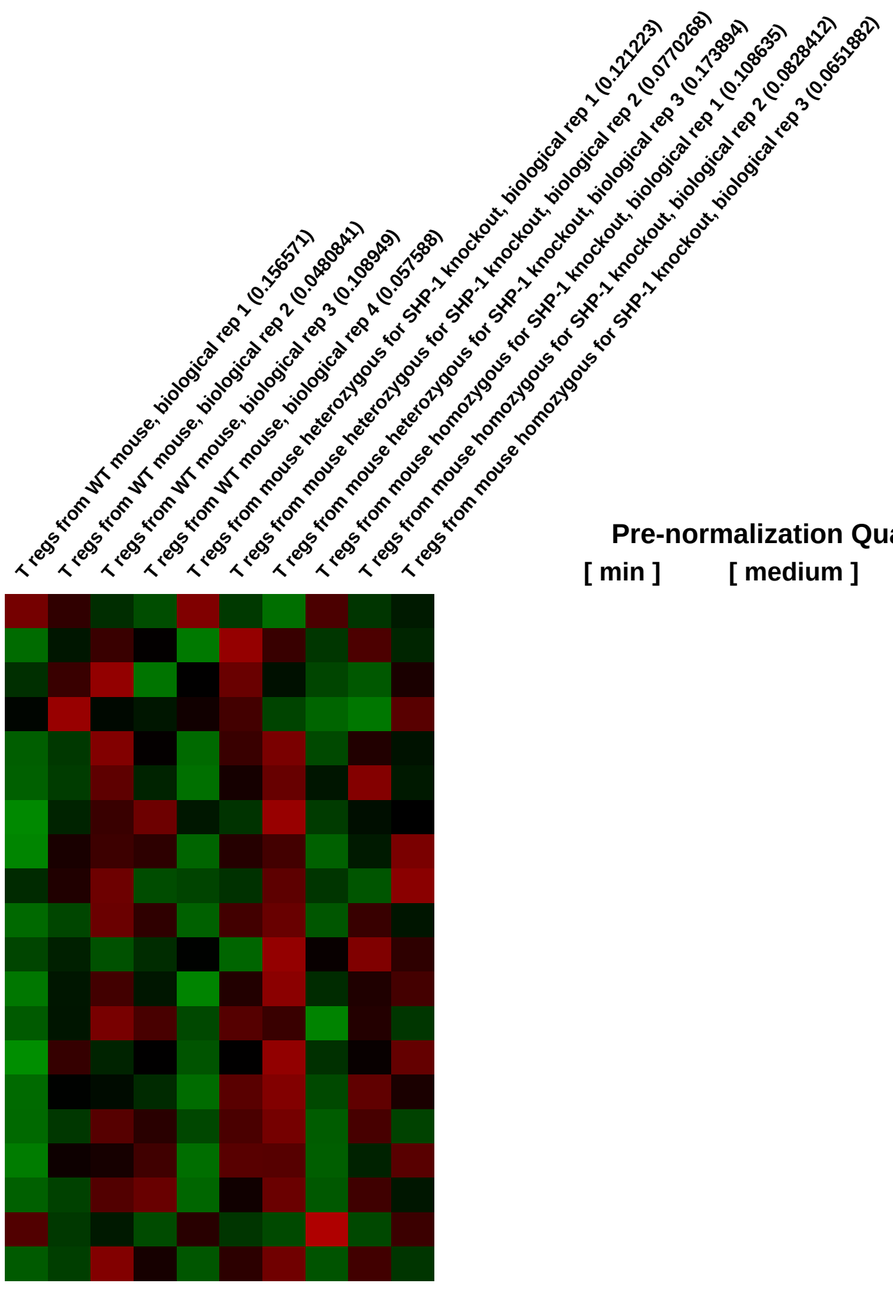

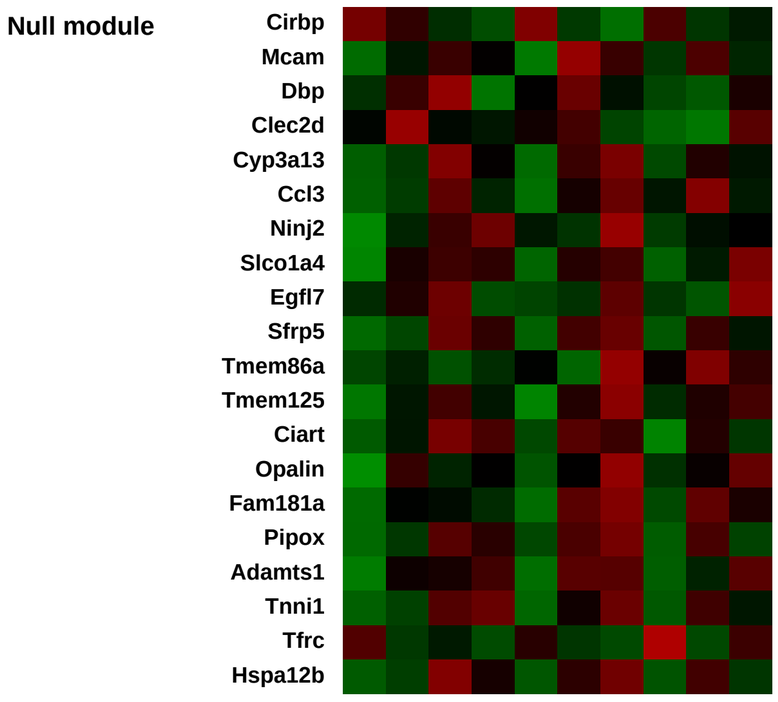

GEO Series "GSE36569" Expression Profiles

Num of samples in this series: 6

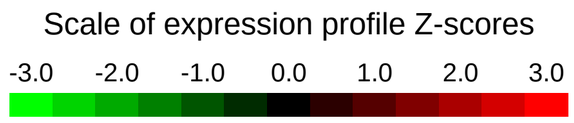

GEO Link:	**http://www.ncbi.nlm.nih.gov/geo/query/acc.cgi?acc=GSE36569**
Status:	**Public on Aug 25 2013**
Title:	**SCFA receptor response**
Organism:	**Mus musculus**
Experiment type:	**Expression profiling by array**
Platform:	**GPL1261**
Pubmed ID:	**23665276**
Summary & Design:	**Summary:** **The purpose of this study was to determine the gene expression patterns of the colon of GPR41 KO and GPR43 KO mice in response to ETOH treatment** **Overall design:** **The mice were treated with rectal injection of ETOH. 24 hours later, the colon tissues were harvested and total RNA was isolated for array experiments.**

Background corr dist: **KL-Divergence = 0.0439, L1-Distance = 0.0213, L2-Distance = 0.0005, Normal std = 0.6022**

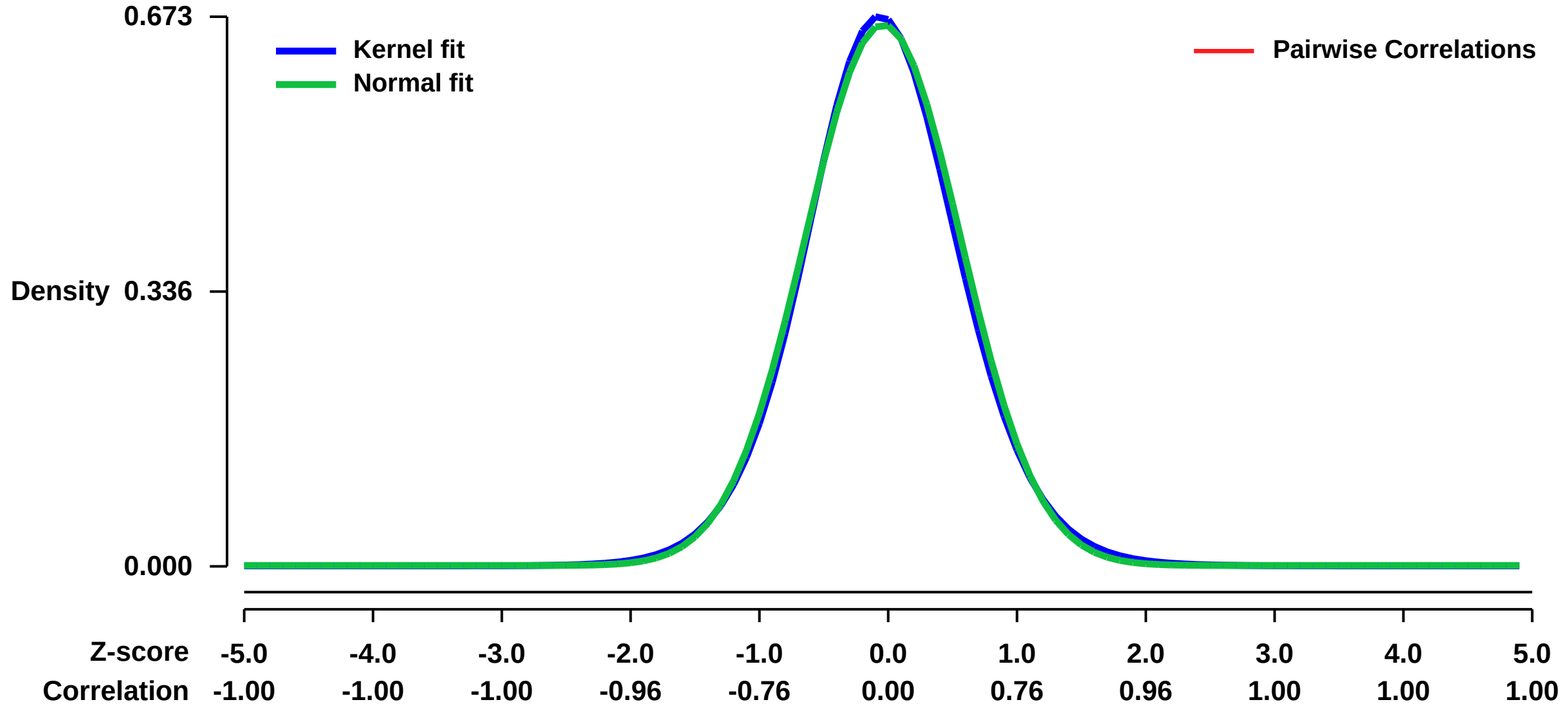

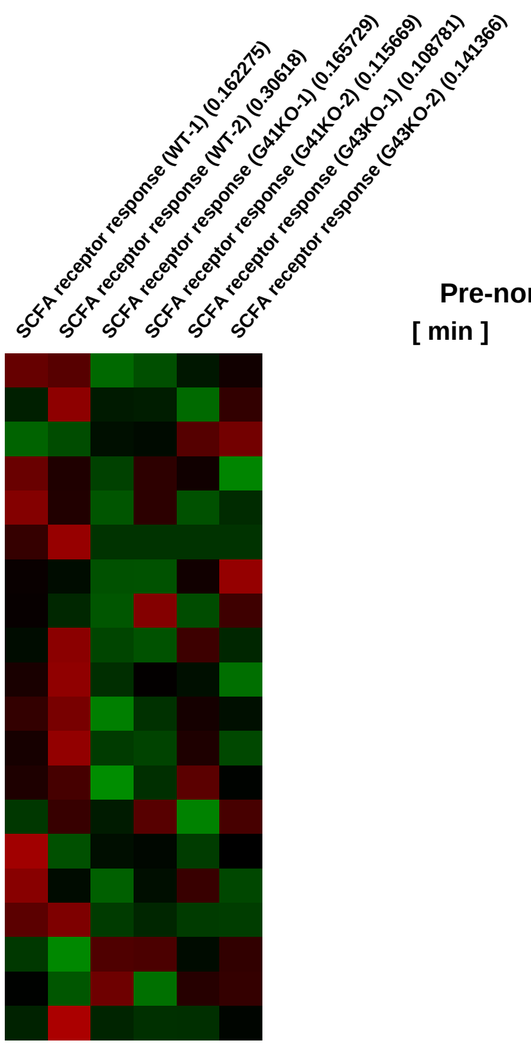

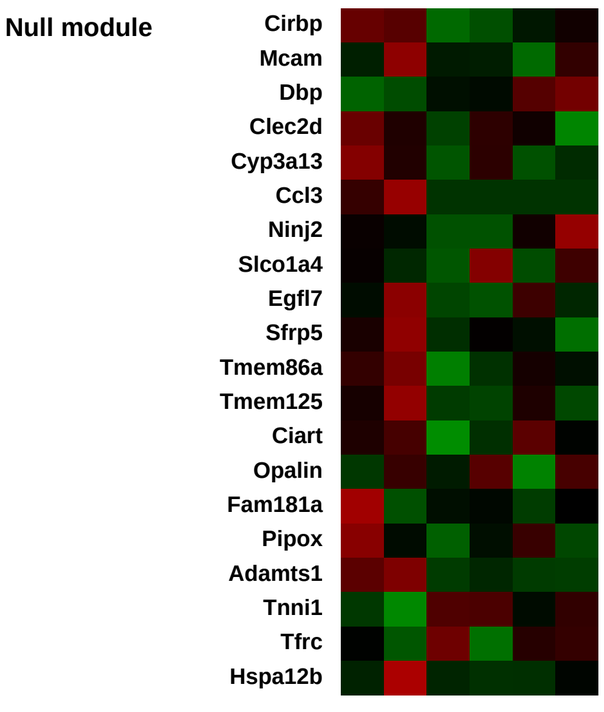

GEO Series "GSE9012" Expression Profiles

Num of samples in this series: 10

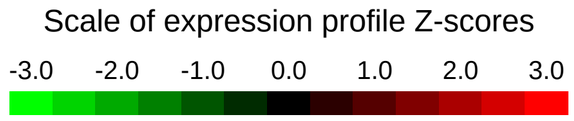

GEO Link:	**http://www.ncbi.nlm.nih.gov/geo/query/acc.cgi?acc=GSE9012**
Status:	**Public on Nov 19 2007**
Title:	**Expression data from spontaneous liver tumors of Trim24/TIF1a-null mice.**
Organism:	**Mus musculus**
Experiment type:	**Expression profiling by array**
Platform:	**GPL1261**
Pubmed ID:	**18026104**
Summary & Design:	**Summary:** **The transcriptional coregulator Trim24 (formerly known as TIF1a) functions in mice as a liver-specific tumor suppressor. Mice carrying a null mutation in the Trim24 gene all develop hepatocellular carcinoma (HCC).** **We used microarrays to identify the alterations in gene expression patterns associated with loss of Trim24 and consequent HCC development.** **Keywords: normal-tumor comparison** **Overall design:** **Five independent liver tumor (HCC) samples taken from five Trim24 knockout (KO) mice and five normal liver tissue samples taken from wild-type (WT) littermate controls were used for RNA extraction and hybridization on Affymetrix microarrays.**

Background corr dist: KL-Divergence = 0.0885, L1-Distance = 0.0298, L2-Distance = 0.0017, Normal std = 0.4668

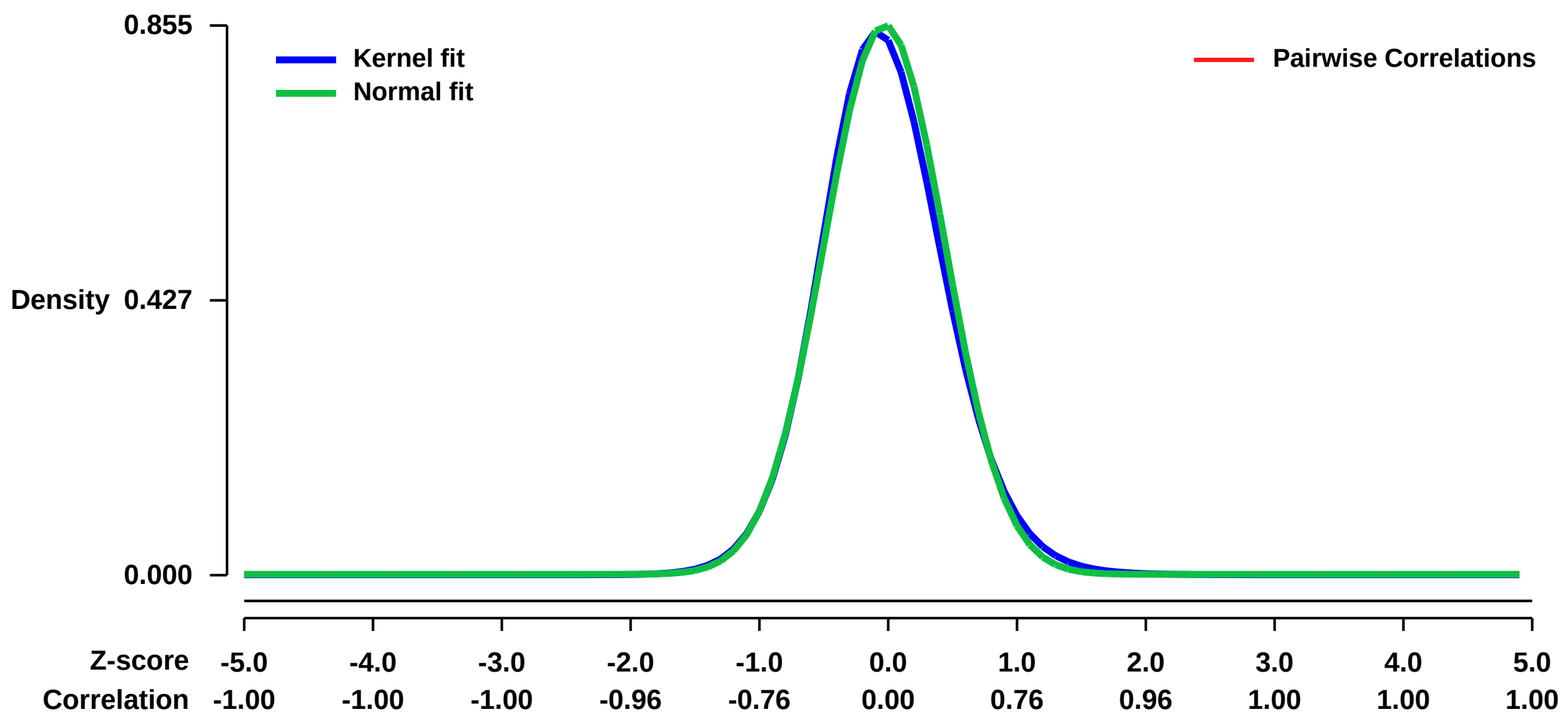

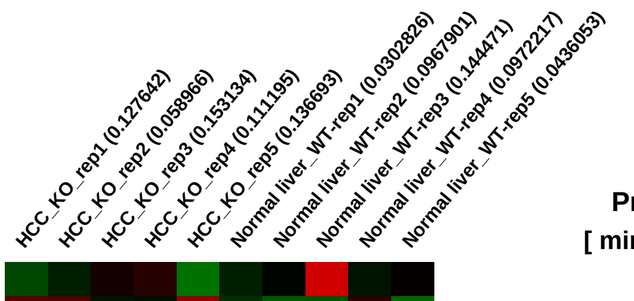

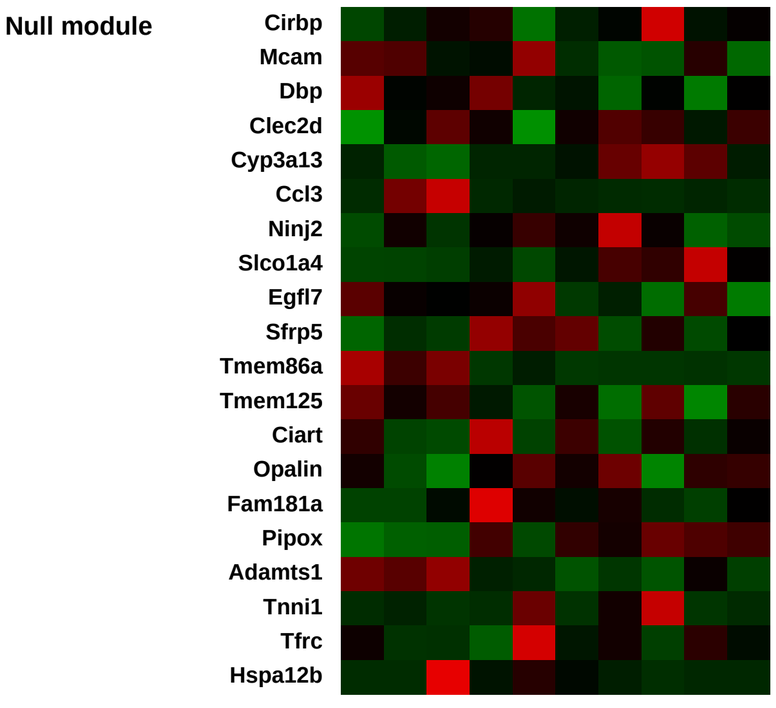

GEO Series "GSE49128" Expression Profiles

Num of samples in this series: 17

Scale of expression profile Z-scores

-3.0 -2.0 -1.0 0.0 1.0 2.0 3.0

GEO Link:	http://www.ncbi.nlm.nih.gov/geo/query/acc.cgi?acc=GSE49128
Status:	Public on Jul 23 2013
Title:	Otitis Media Impact on Middle Ear
Organism:	Mus musculus
Experiment type:	Expression profiling by array
Platform:	GPL1261
Pubmed ID:	24124478
Summary & Design:	**Summary:** **Objective: Otitis media is known to alter expression of cytokine and other genes in the mouse middle ear and inner ear. However, whole mouse genome studies of gene expression in otitis media have not previously been undertaken. Ninety-nine percent of mouse genes are shared in the human, so these studies are relevant to the human condition.** **Methods: To assess inflammation-driven processes in the mouse ear, gene chip analyses were conducted on mice treated with trans-tympanic heat-killed Hemophilus influenza using untreated mice as controls. Middle and inner ear tissues were separately harvested at 6 hours, RNA extracted, and samples for each treatment processed on the Affymetrix 430 2.0 Gene Chip for expression of its 34,000 genes.** **Results: Statistical analysis of gene expression compared to control mice showed significant alteration of gene expression in 2,355 genes, 11% of the genes tested and 8% of the mouse genome. Significant middle and inner ear upregulation (fold change >1.5, p<0.05) was seen in 1,081 and 599 genes respectively. Significant middle and inner ear downregulation (fold change <0.67, p<0.05) was seen in 978 and 287 genes respectively. While otitis media is widely believed to be an exclusively middle ear process with little impact on the inner ear, the inner ear changes noted in this study were numerous and discrete from the middle ear responses. This suggests that the inner ear does indeed respond to otitis media and that its response is a distinctive process. Numerous new genes, previously not studied, are found to be affected by inflammation in the ear.** **Conclusion: Whole genome analysis via gene chip allows simultaneous examination of expression of hundreds of gene families influenced by inflammation in the middle ear. Discovery of new gene families affected by inflammation may lead to new approaches to the study and treatment of otitis media.** **Overall design:** **There are 8 control samples and 9 samples trans-tympanically injected with H flu 10e9 for 6 hours. Each sample is from a single animal.**

Background corr dist: KL-Divergence = 0.1073, L1-Distance = 0.0314, L2-Distance = 0.0014, Normal std = 0.4348

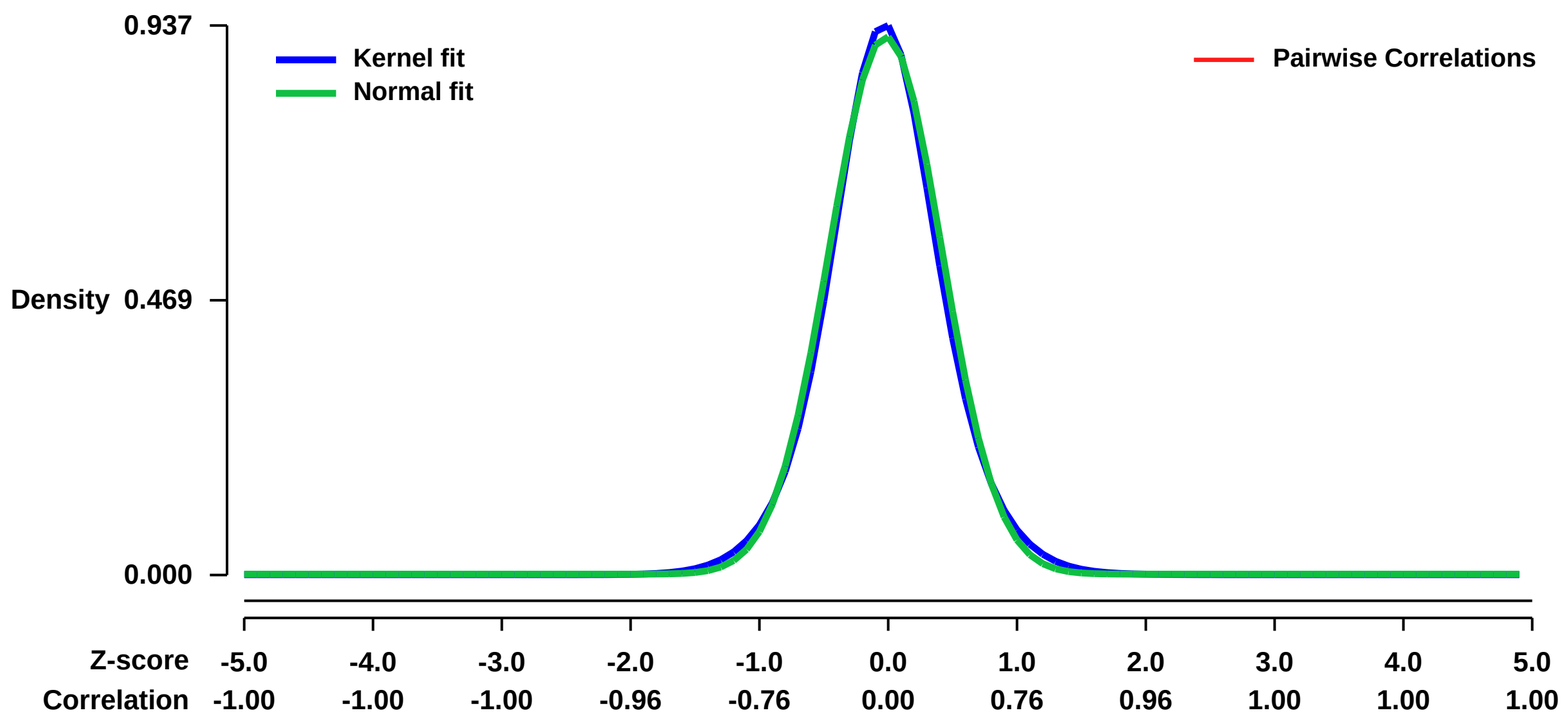

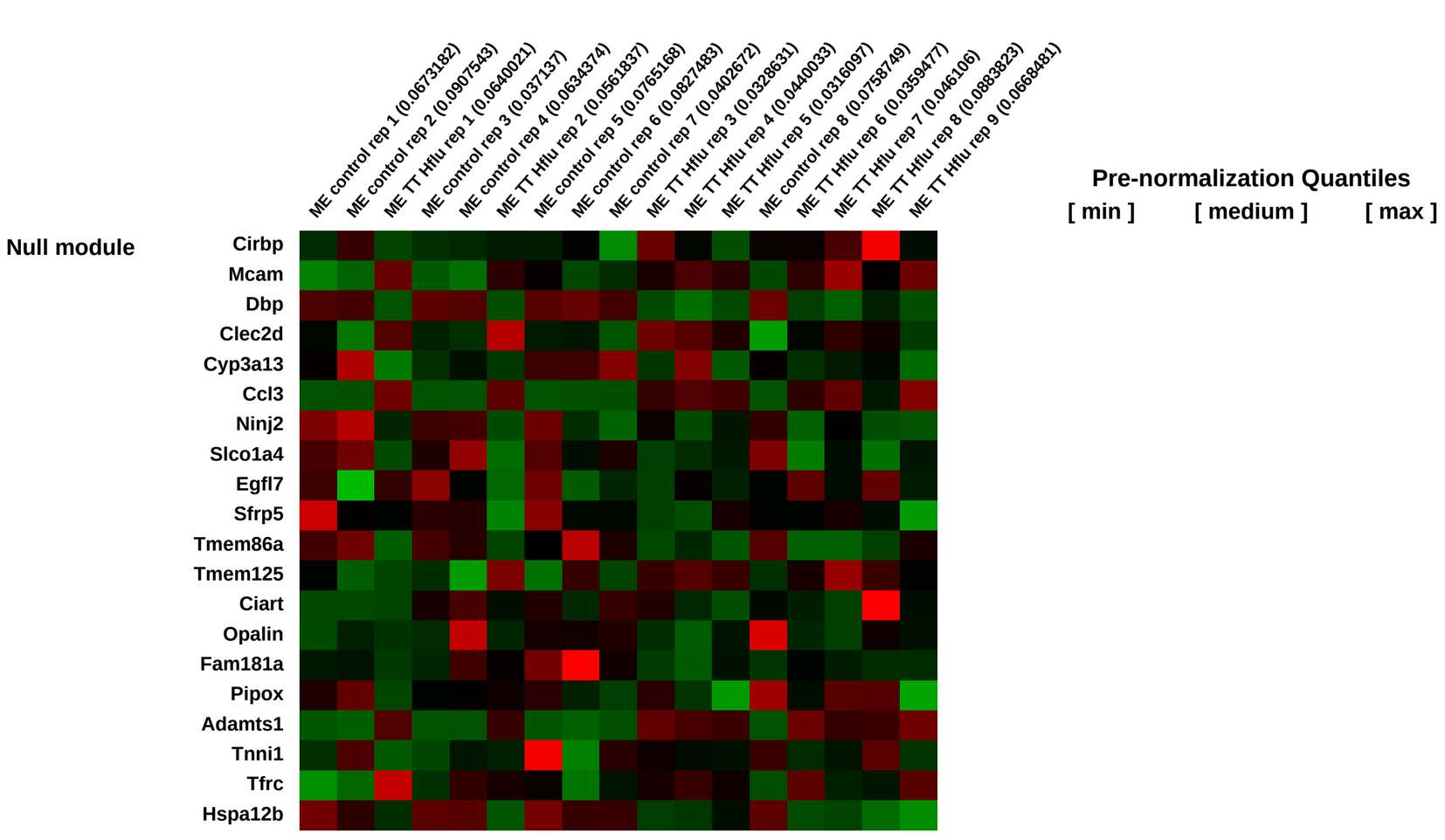

GEO Series "GSE35998" Expression Profiles

Num of samples in this series: 20

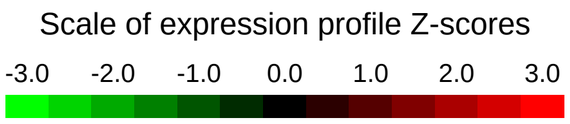

GEO Link:	http://www.ncbi.nlm.nih.gov/geo/query/acc.cgi?acc=GSE35998
Status:	Public on Feb 24 2014
Title:	Gene expression of murine B cells activated via TLR4 or TLR4 + CD40: Group1 naˆflve B cells, Group2 LPS activated B cells 24h, Group3 LPS + anti-CD40 activated B cells
Organism:	Mus musculus
Experiment type:	Expression profiling by array
Platform:	GPL1261
Pubmed ID:	24572363
Summary & Design:	**Summary:** Murine B cells can be activated via the surface receptors TLR4 and CD40. For a global assessment of differences in gene expression between these two different modes of B cell activation a genome wide transcriptome analysis was performed. In order to dissect different gene expression profiles of B cells, activation was induced by LPS or LPS + anti-CD40 for 24h and 72h. Both activation states were compared to each other but also to naˆflve B cells. **Overall design:** All chips were imported into BioRetis (http://www.bioretis-analysis.de) and are open to the community now. If you want to obtain one or more lists of HPCDA significant genes you should click on a link of single chips (e.g. GSM879034) to get a description how to manage this.

Background corr dist: KL-Divergence = 0.1716, L1-Distance = 0.0412, L2-Distance = 0.0039, Normal std = 0.3566

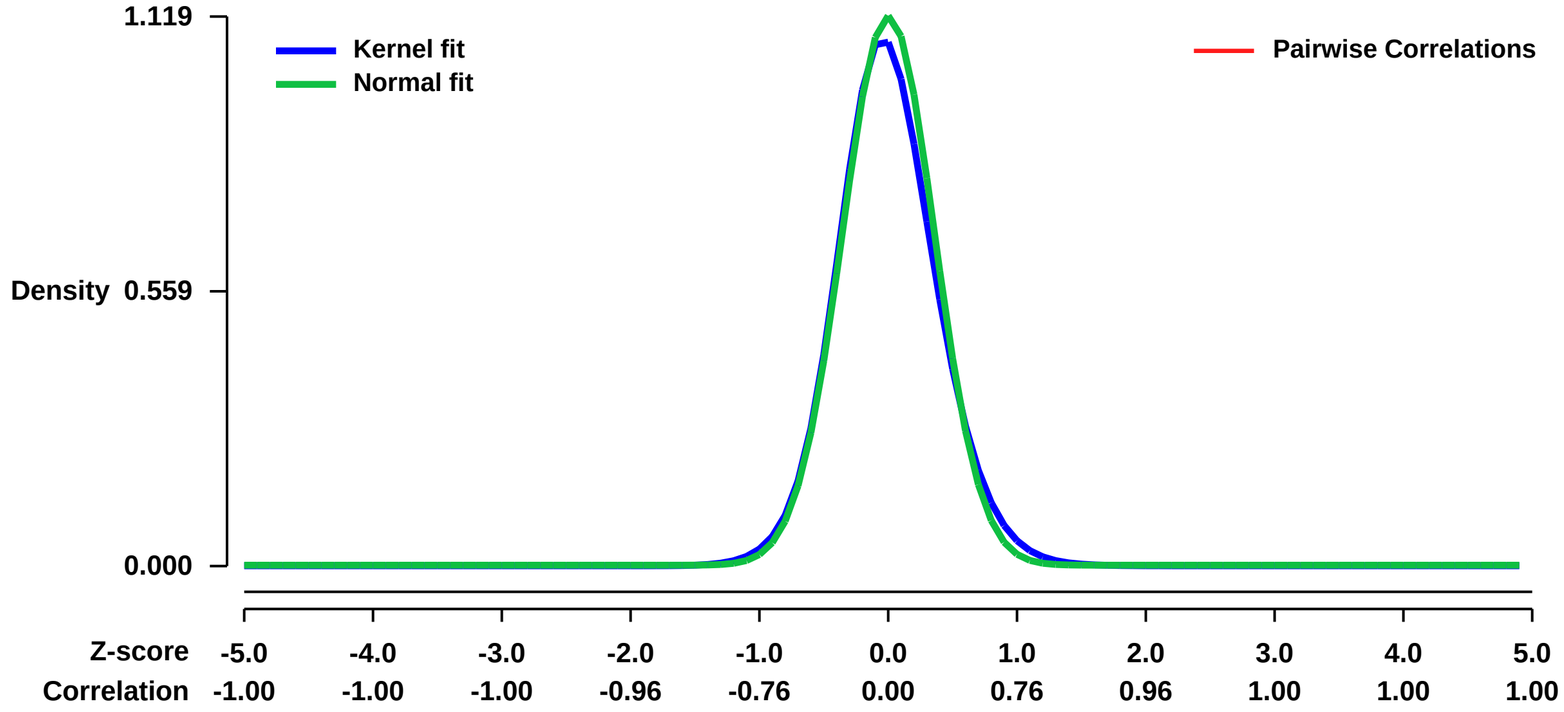

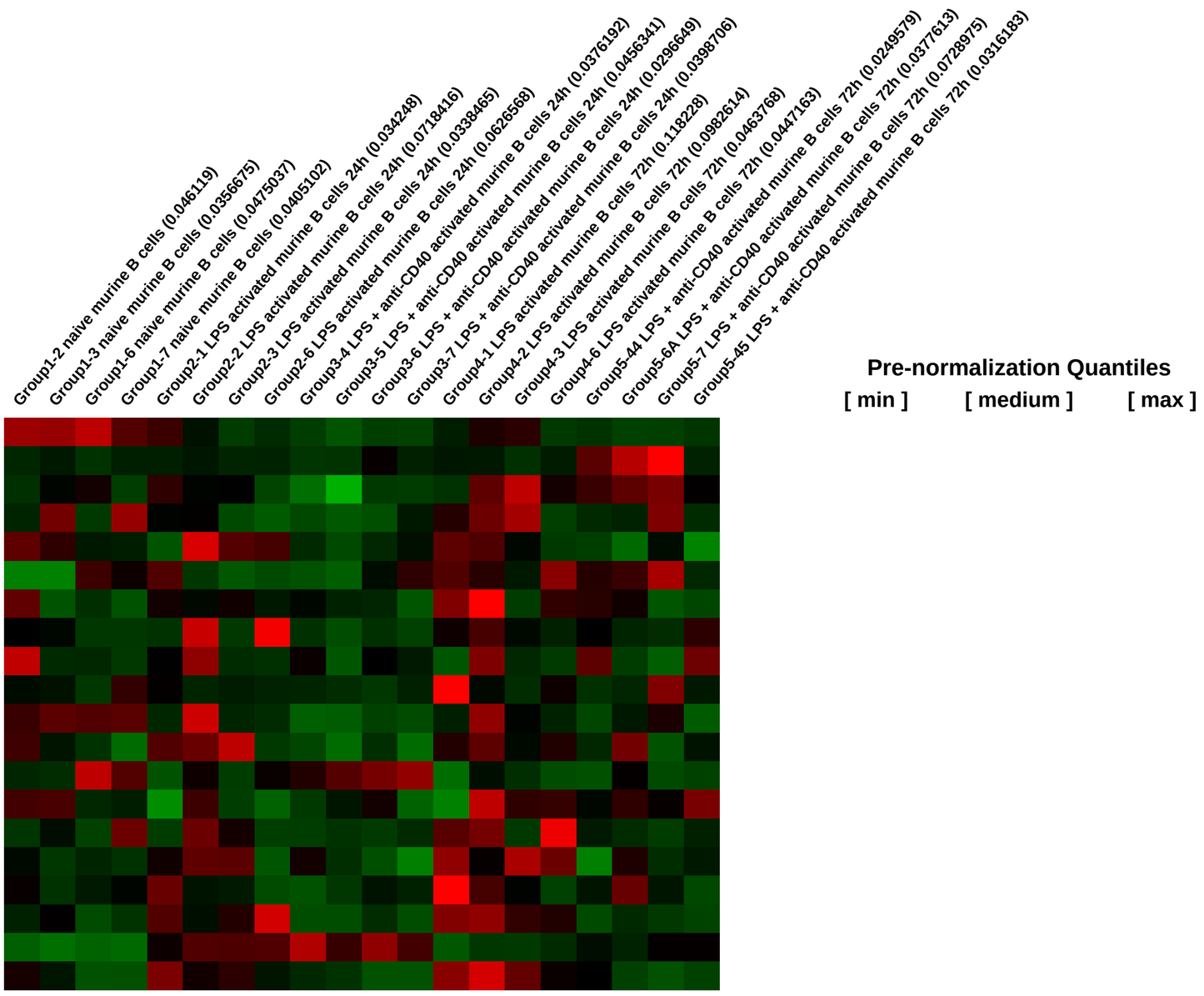

GEO Series "GSE15433" Expression Profiles

Num of samples in this series: 9

Scale of expression profile Z-scores

-3.0 -2.0 -1.0 0.0 1.0 2.0 3.0

GEO Link:	http://www.ncbi.nlm.nih.gov/geo/query/acc.cgi?acc=GSE15433
Status:	Public on Mar 27 2009
Title:	The PPARg2 A/B-domain plays a gene specific role in transactivation and co-factor recruitment
Organism:	Mus musculus
Experiment type:	Expression profiling by array
Platform:	GPL1261
Pubmed ID:	19282365
Summary & Design:	**Summary:** We have previously shown that adenoviral expression of peroxisome proliferator-activated receptors (PPARs) leads to rapid establishment of transcriptionally active complexes and activation of target gene expression within 5-8 h following transduction. Here we have used the adenoviral delivery system combined with expression array analysis to identify novel putative PPARgamma target genes in murine fibroblasts and to determine the role of the A/B-domain in PPARgamma mediated transactivation of genomic target genes. Of the 257 genes found to be induced by PPARgamma2 expression, only 25 displayed A/B-domain dependency, i.e. significantly reduced induction in the cells expressing the truncated PPARgamma lacking the A/B-domain (PPARgammaCDE). Nine of the 25 A/B-domain dependent genes were involved in lipid storage and in line with this, triglyceride accumulation was considerably decreased in the cells expressing PPARgammaCDE compared to cells expressing full length PPARgamma2. Using chromatin immunoprecipitation (ChIP) we demonstrate that PPARgamma binding to genomic target sites and recruitment of the mediator component TRAP220/MED1/PBP/DRIP205 is not affected by the deletion of the A/B-domain. By contrast, the PPARgamma-mediated CBP and p300 recruitment to A/B-domain dependent target genes is abolished by deletion of the A/B-domain. These results indicate that the A/B-domain of PPARgamma2 is specifically involved in the recruitment or stabilization of CBP and p300 containing co-factor complexes to a subset of target genes. **Overall design:** Total RNA samples were obtained from three individual experiments in which NIH-CAR (i.e. a clonal cell line of NIH-3T3 fibroblasts stably expressing the coxsackie-adenovirus receptor (CAR$_{\zeta}$ 1)) cells were transduced with adenovirus containing empty vector (AdEmpty) followed by addition of vehicle (DMSO) or transduced with adenovirus encoding either full length HA-tagged PPARg2 or A/B-domain deleted HA-PPARgCDE and treated with rosiglitazone.

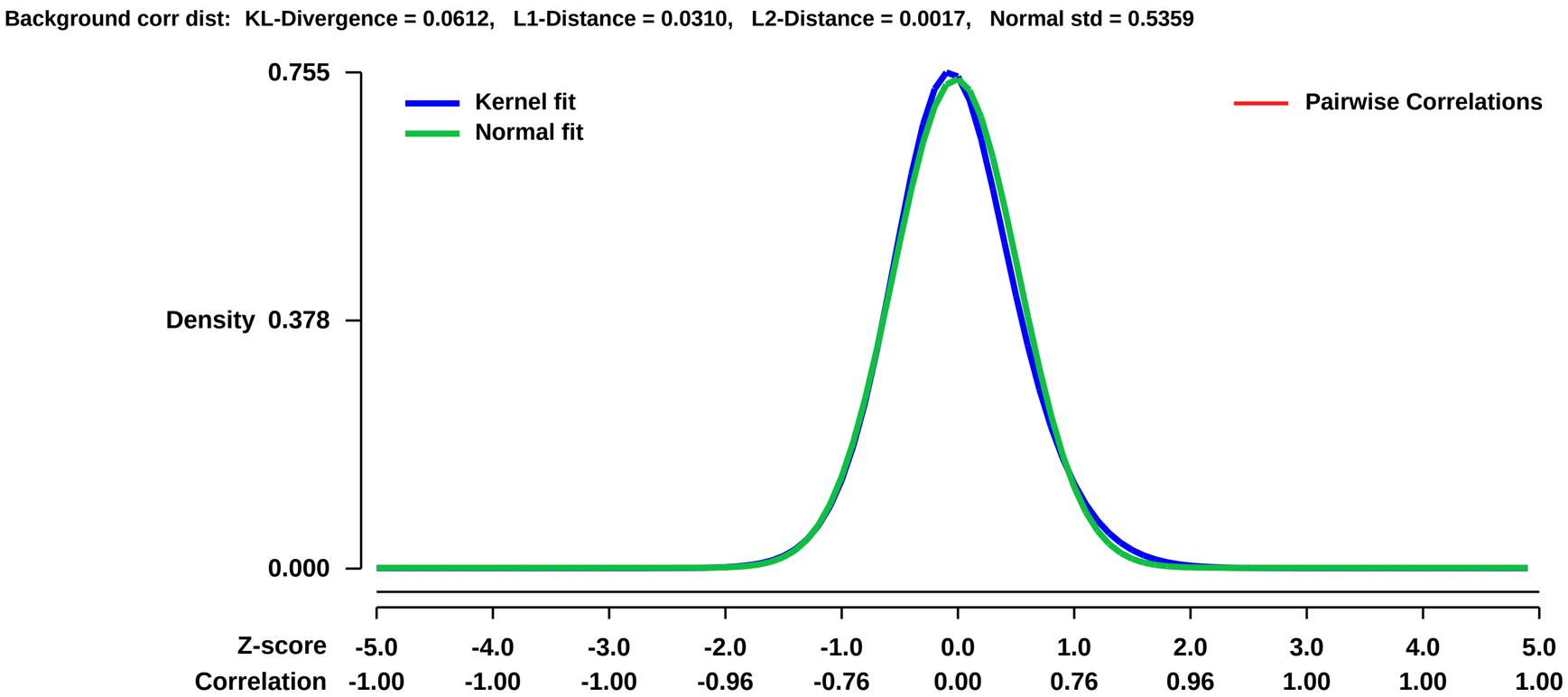

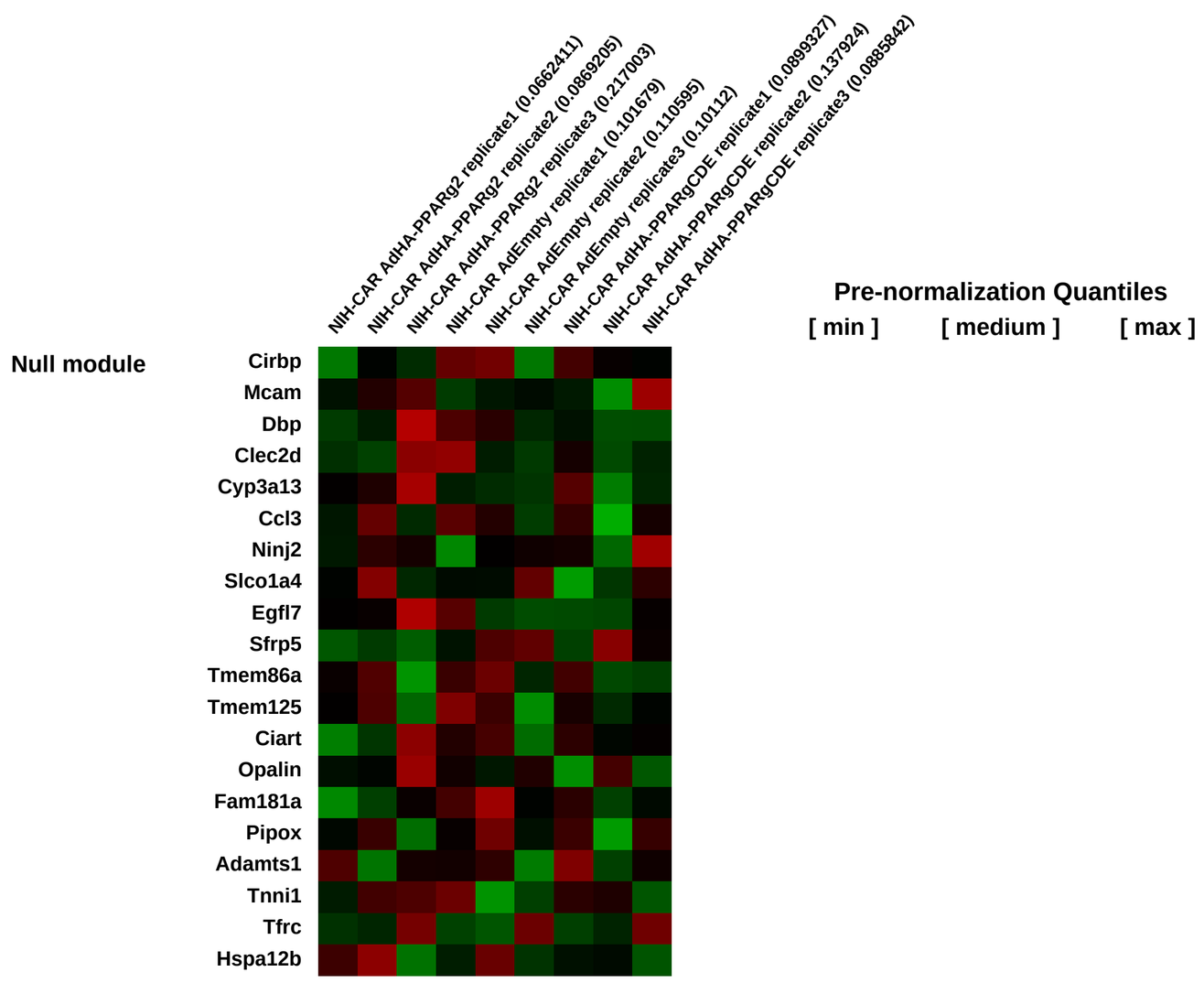

GEO Series "GSE16104" Expression Profiles

Num of samples in this series: 24

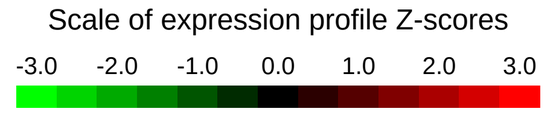

GEO Link:	**http://www.ncbi.nlm.nih.gov/geo/query/acc.cgi?acc=GSE16104**
Status:	**Public on Jul 01 2009**
Title:	**IL-1b responses in receptor-reconstituted AcP-deficient neurons**
Organism:	**Mus musculus**
Experiment type:	**Expression profiling by array**
Platform:	**GPL1261**
Pubmed ID:	**19481478**
Summary & Design:	**Summary:** **The purpose was to determine AcP- and AcPb-dependent gene responses to IL-1 by virally-reconstituting AcP-deficient mouse embryonic cortical neurons with CD25 (control), full length AcP, AcPb or the combination of both. A control population was transduced with a CD25-expressing virus. Half the samples were stimulated with IL-1-beta for four hours, RNA was analyzed by microarray.** **Overall design:** **Each in triplicate: CD25 cells, AcP cells, AcPb cells, AcP+AcPb cells. Cultures stimulated with IL-1b (10 ng/ml) for 4 hours then RNA was collected for processing and microarray analysis.**

Background corr dist: **KL-Divergence = 0.2710, L1-Distance = 0.0353, L2-Distance = 0.0030, Normal std = 0.2886**

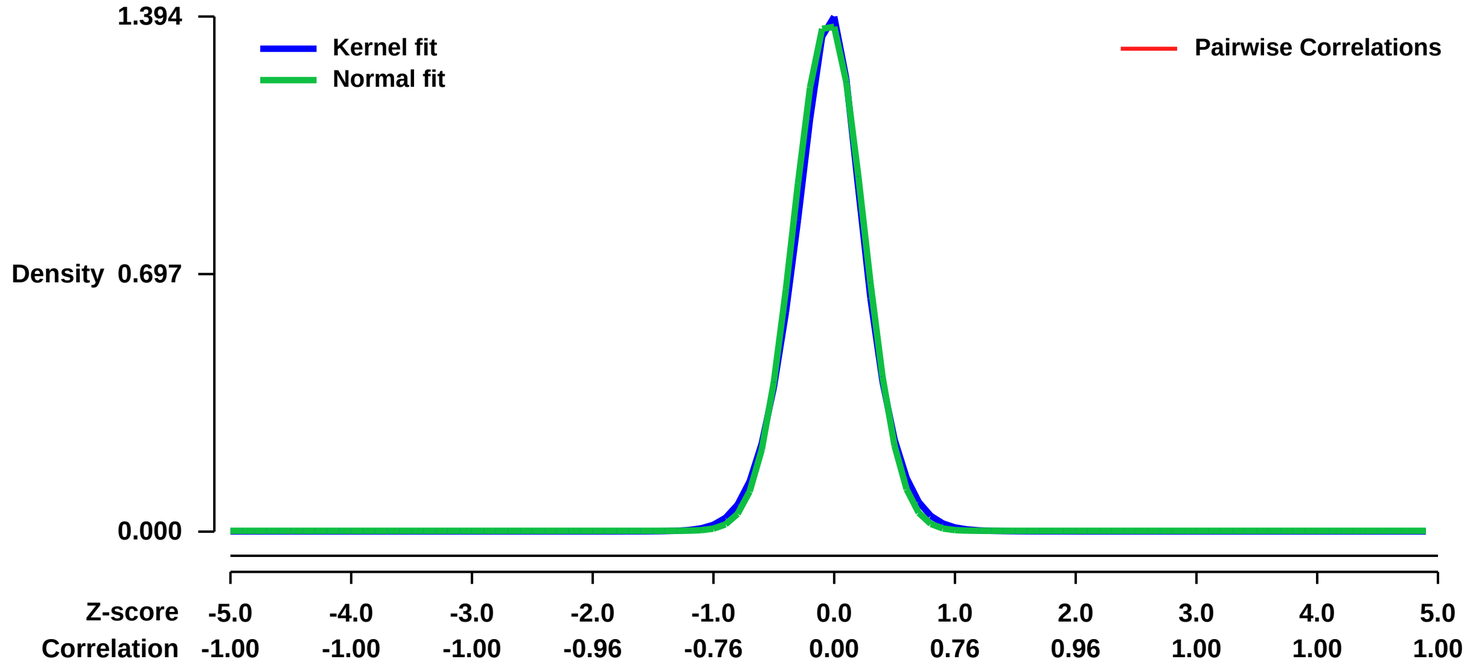

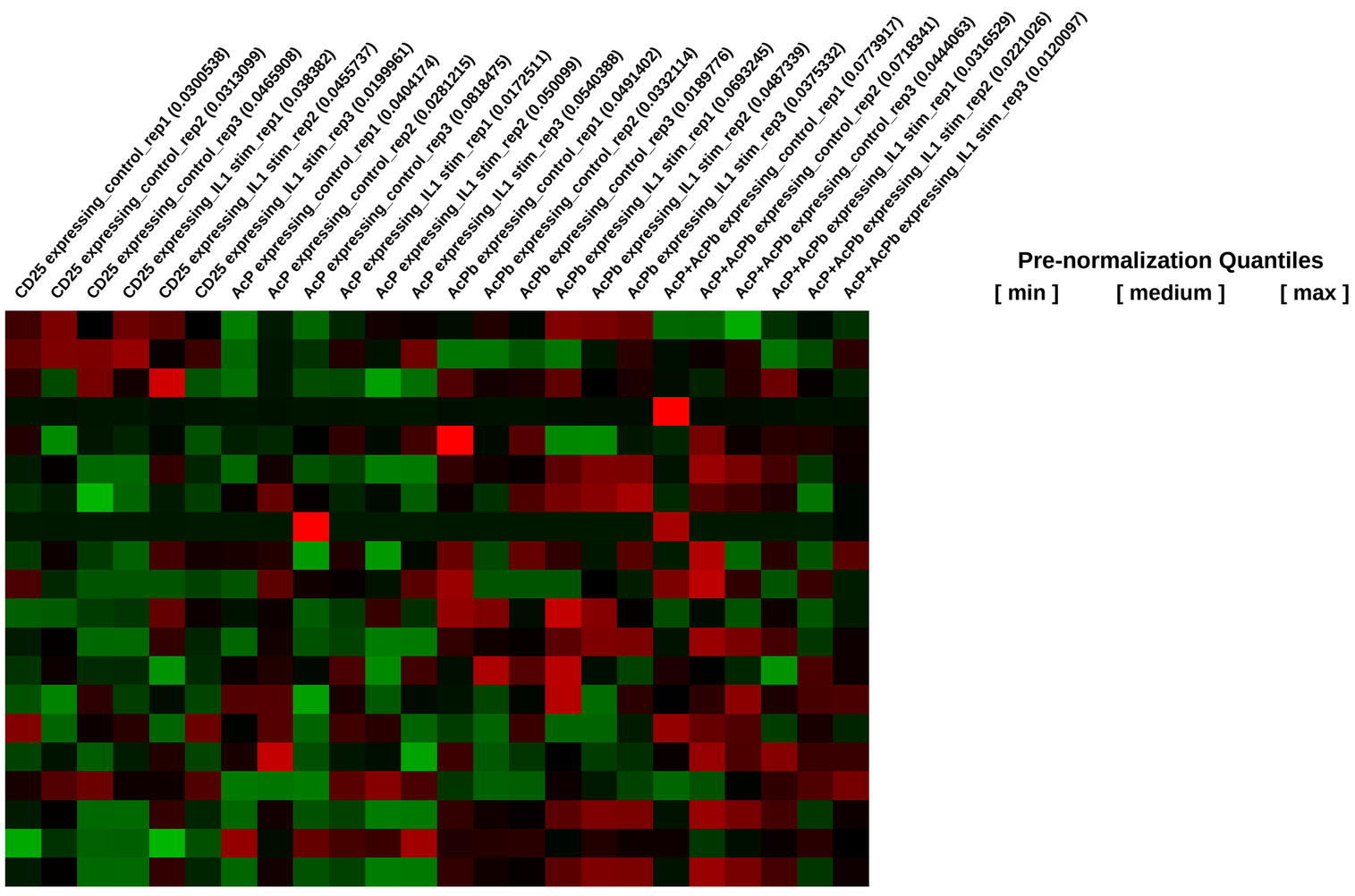

GEO Series "GSE11870" Expression Profiles

Num of samples in this series: 6

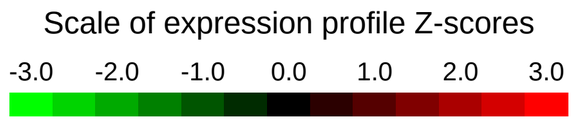

GEO Link:	http://www.ncbi.nlm.nih.gov/geo/query/acc.cgi?acc=GSE11870
Status:	Public on Jul 23 2008
Title:	Gene expression changes in primary aortic endothelial cells during expression of dominant negative PPAR gamma (V290M).
Organism:	Mus musculus
Experiment type:	Expression profiling by array
Platform:	GPL1261
Pubmed ID:	18676352
Summary & Design:	**Summary:** Ligand-mediated activation of the nuclear hormone receptor PPAR gamma lowers blood pressure and improves glucose tolerance in humans. Two naturally occurring mutations (P467L, V290M) in the ligand binding domain of PPAR gamma have been described in humans that lead to severe insulin resistance and hypertension. Experimental evidence suggests that these mutant versions of PPAR gamma act in a dominant negative fashion. To better understand the molecular mechanisms underlying PPAR gamma action in the vasculature, we determined the global gene expression profile in primary aortic endothelial cells in response to endothelial cell specific expression of a dominant negative isoform of PPAR gamma (V290M). **Overall design:** We generated transgenic mice specifically targeting expression of dominant negative human PPAR gamma to the endothelium using an endothelial-specific promoter (vascular endothelial cadherin or CDH5). Primary aortic endothelial cells were isolated from 10 non-transgenic and 10 EC-DN mice by Dominion Pharmakine (http://www.pharmakine.com/). For each group, 5 cultures of cells were established. Each culture was derived from 2 mice and remained separate from the other cultures. Cellular RNA was prepared using conventional methods and quality was assessed using the Bioanalyzer 2100 (Agilent Technologies). For the microarray hybridizations, RNA from 3 of the cultures in each group was used. All the microarray procedures were conducted at the University of Iowa DNA Core facility using standard Affymetrix protocols. In brief, approximately 50 ng of total RNA was used as input to a two-step amplification procedure (NuGen, http://www.nugeninc.com/) to generate biotin-labeled RNA fragments for hybridization to the Affymetrix GeneChip Mouse Genome 430 2.0 array.

Background corr dist: KL-Divergence = 0.0338, L1-Distance = 0.0226, L2-Distance = 0.0006, Normal std = 0.6536

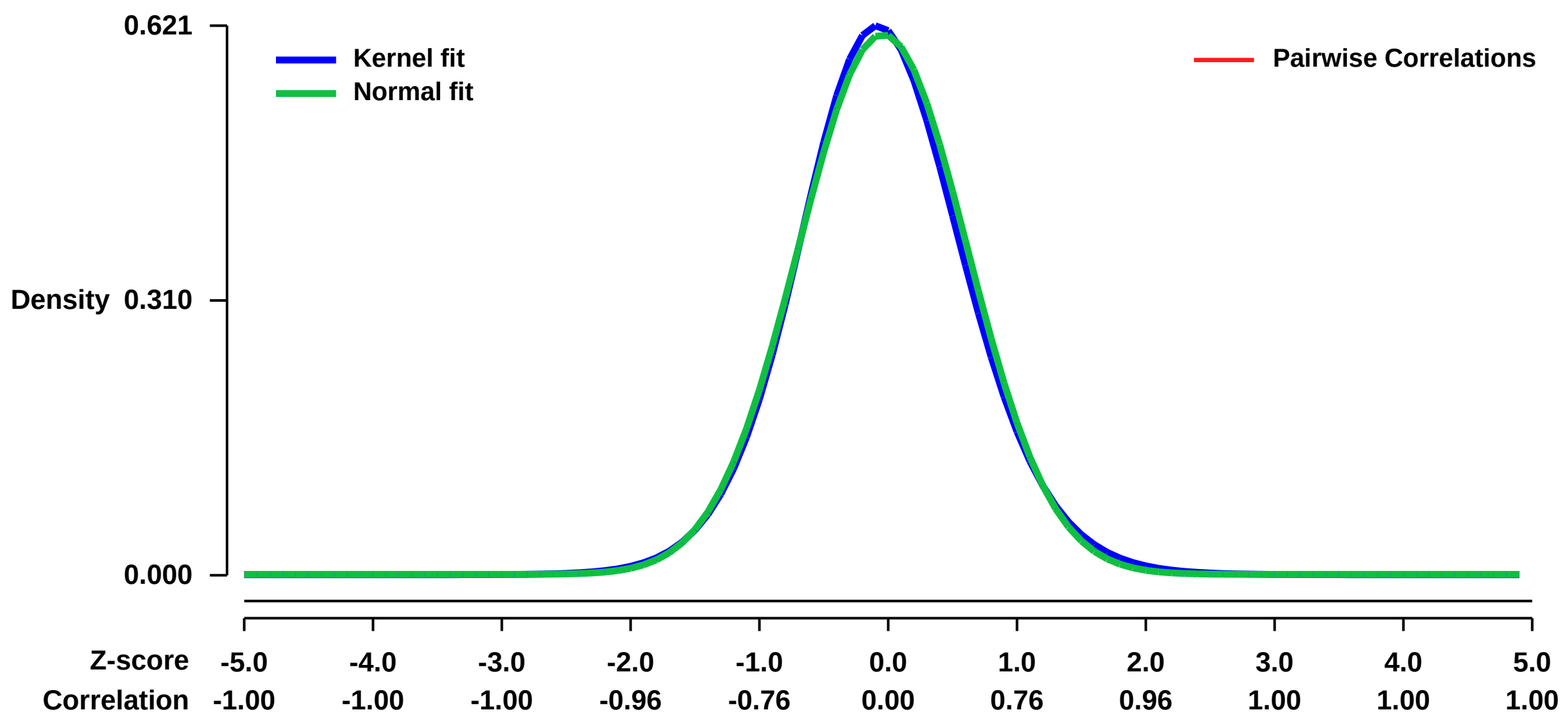

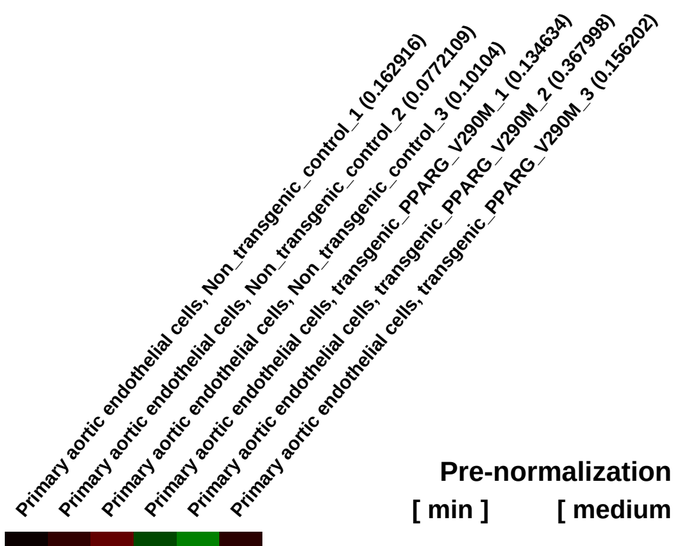

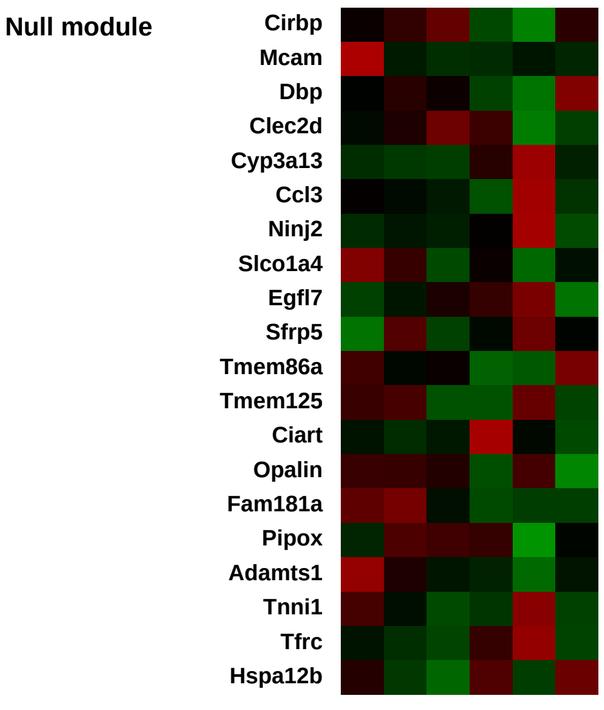

GEO Series "GSE11698" Expression Profiles

Num of samples in this series: 6

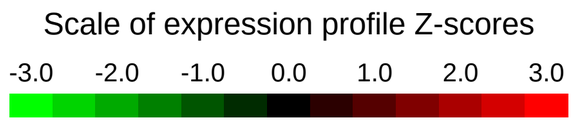

GEO Link:	http://www.ncbi.nlm.nih.gov/geo/query/acc.cgi?acc=GSE11698
Status:	Public on Aug 22 2008
Title:	Microarray of Trex1 WT and Trex1 KO hearts on RAG2KO background
Organism:	Mus musculus
Experiment type:	Expression profiling by array
Platform:	GPL1261
Pubmed ID:	18724932
Summary & Design:	**Summary:** Heart ventricle tissue was harvested from Trex1/RAG2 DKO mice and from Trex1WT/RAG2KO littermate controls. RNA was extracted, and an Affymetrix Mouse 430 2.0 gene chip analysis was performed. **Overall design:** Three pairs of littermates are included: 779/780, 4184/4185, and 4192/4193.

Background corr dist: KL-Divergence = 0.0476, L1-Distance = 0.0187, L2-Distance = 0.0004, Normal std = 0.5822

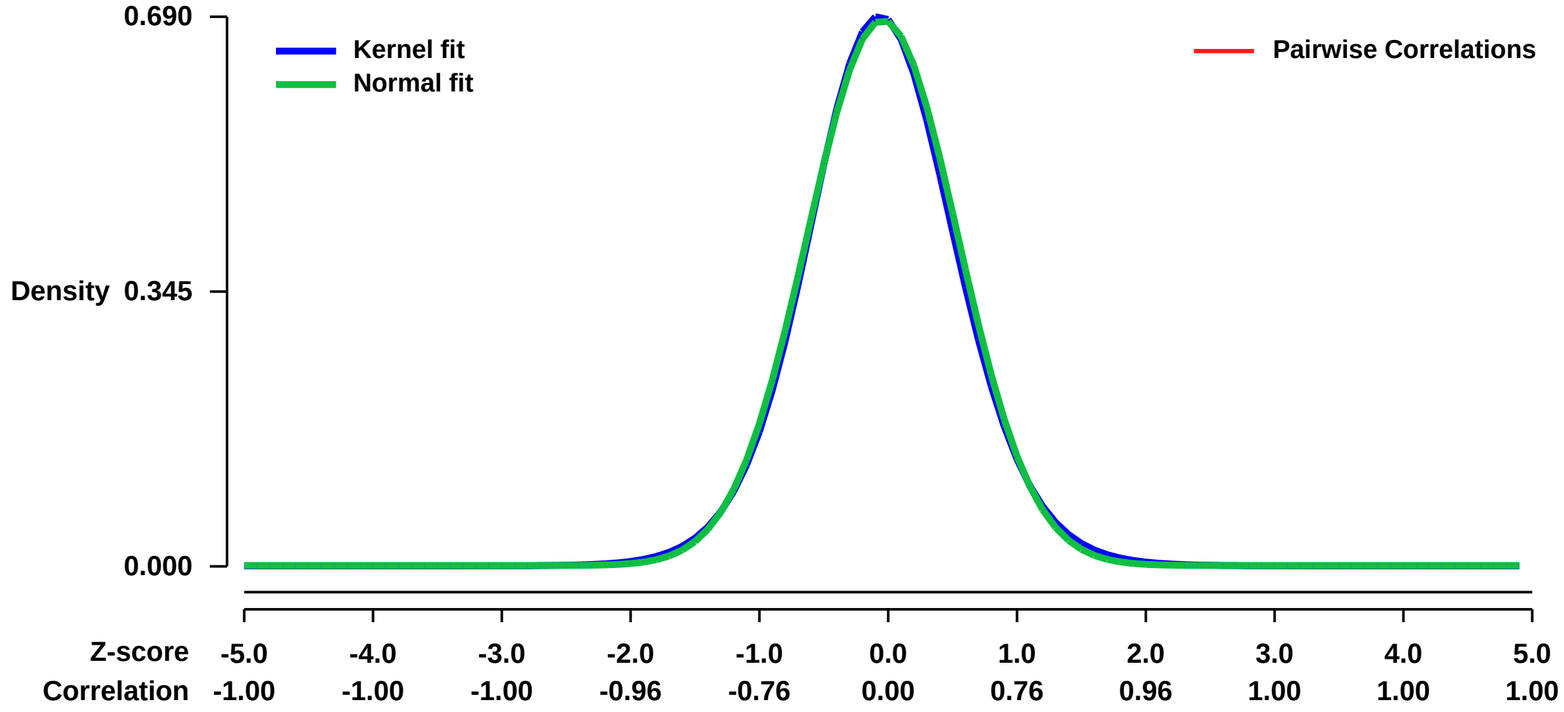

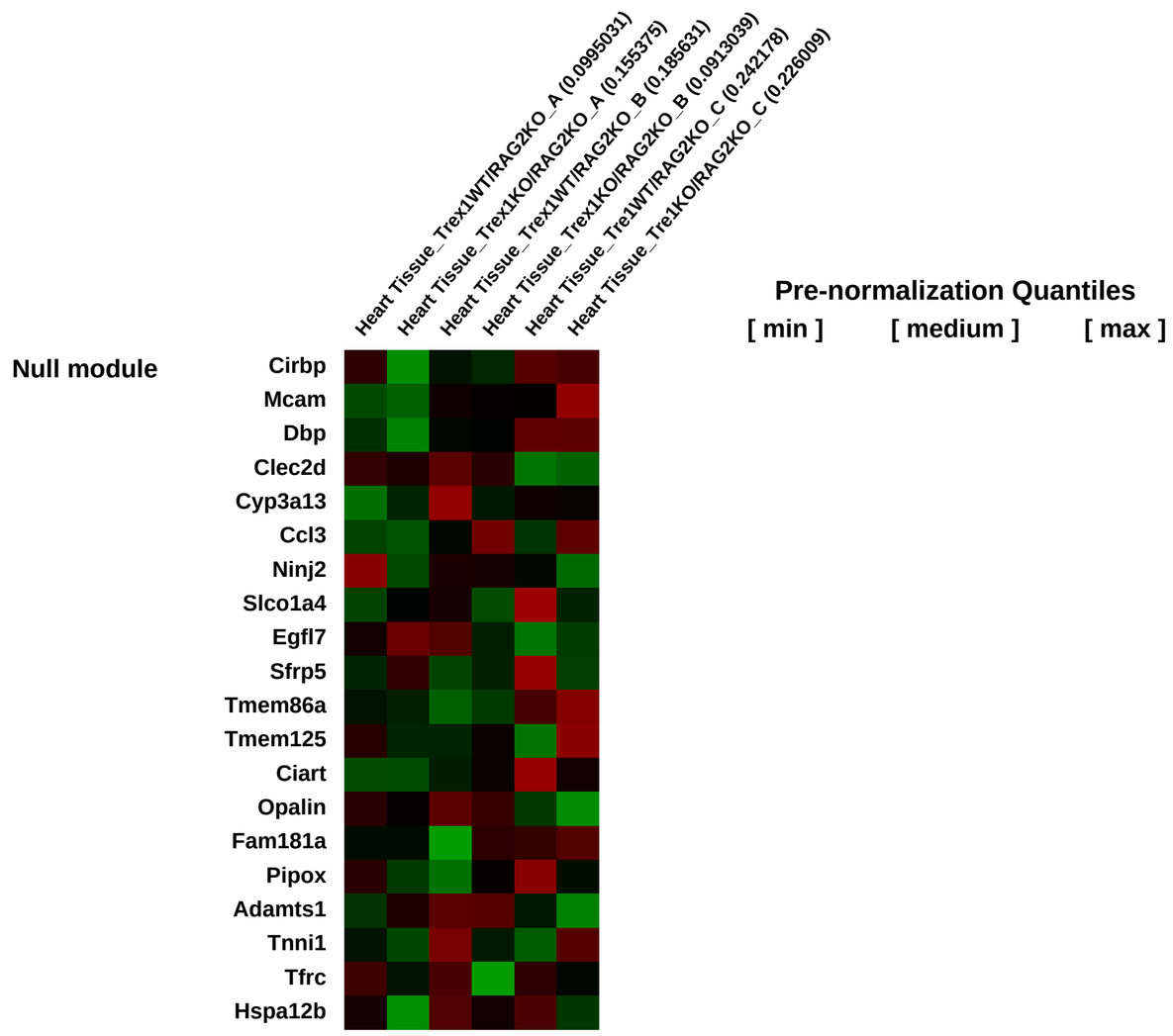

GEO Series "GSE50729" Expression Profiles

Num of samples in this series: 6

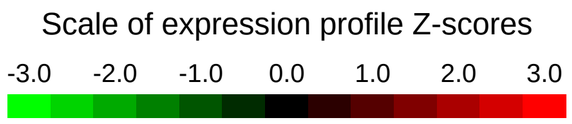

GEO Link:	http://www.ncbi.nlm.nih.gov/geo/query/acc.cgi?acc=GSE50729
Status:	Public on Sep 11 2013
Title:	The polycomb protein Ezh2 regulates differentiation and plasticity of CD4 T helper type-1 and type-2 cells.
Organism:	Mus musculus
Experiment type:	Expression profiling by array
Platform:	GPL1261
Pubmed ID:	24238339
Summary & Design:	**Summary:** Following antigen encounter by CD4 T cells, polarizing cytokines induce the expression of master regulators that control differentiation. Inactivation of the histone methyltransferase Ezh2 was found to specifically enhance T-helper (Th)1 and Th2 cell differentiation and plasticity. Ezh2 directly bound and facilitated correct expression of Tbx21 and Gata3 in differentiating Th1 and Th2 cells, accompanied by substantial tri-methylation at lysine 27 of histone 3 (H3K27-Me3). In addition, Ezh2 deficiency resulted in spontaneous generation of discrete IFN-¿‡ and Th2 cytokine-producing populations in non-polarizing cultures, and under these conditions IFN-¿‡ expression was largely dependent on enhanced expression of the transcription factor Eomesodermin. In vivo, Loss of Ezh2 caused increased pathology in a model of allergic asthma and resulted in progressive accumulation of memory phenotype Th2 cells. This study establishes a functional link between Ezh2 and transcriptional regulation of lineage-specifying genes in terminally differentiated CD4 T cells. **Overall design:** Wild type and Ezh2 knock out unpolarized Th cells, Th1 cells and Th2 cells are profiled for mRNA expression

Background corr dist: KL-Divergence = 0.0344, L1-Distance = 0.0254, L2-Distance = 0.0007, Normal std = 0.6569

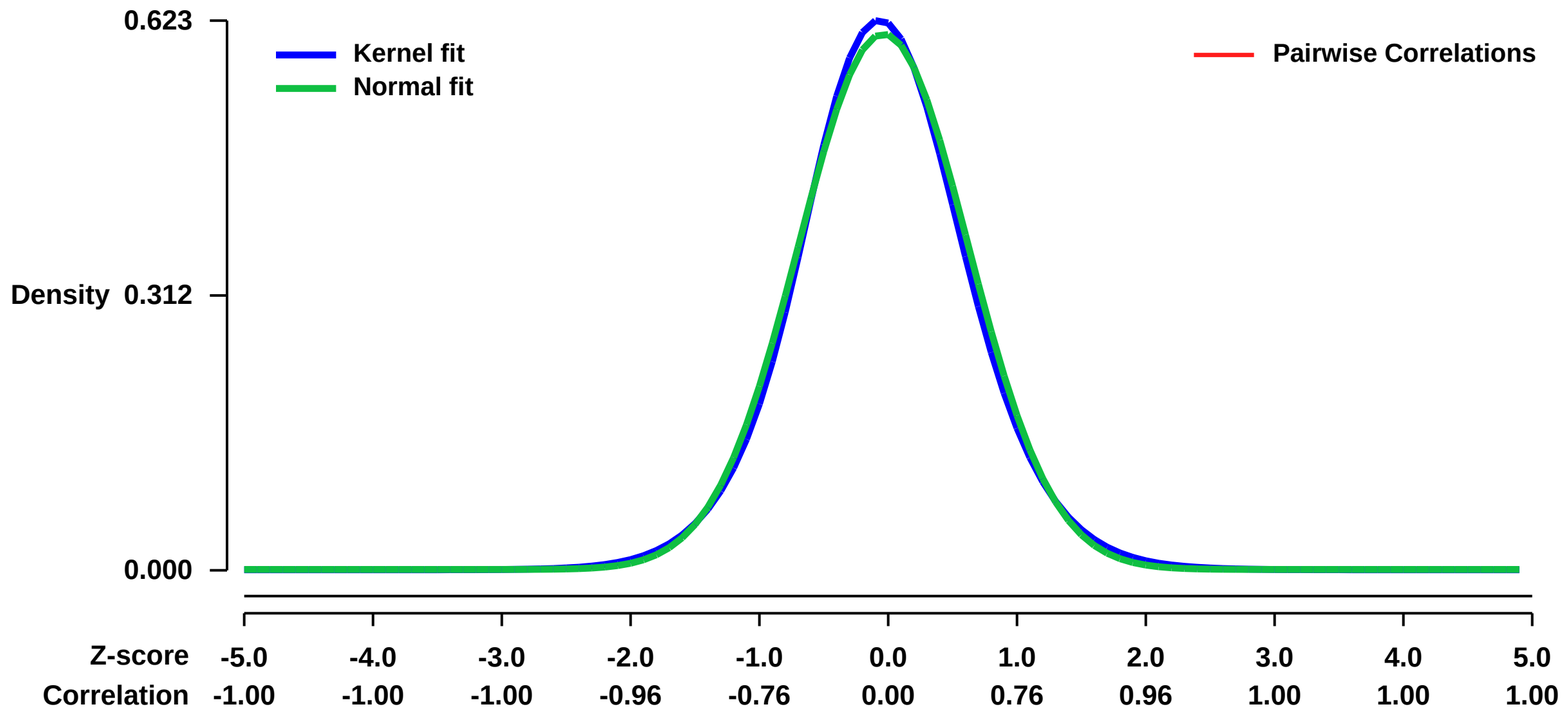

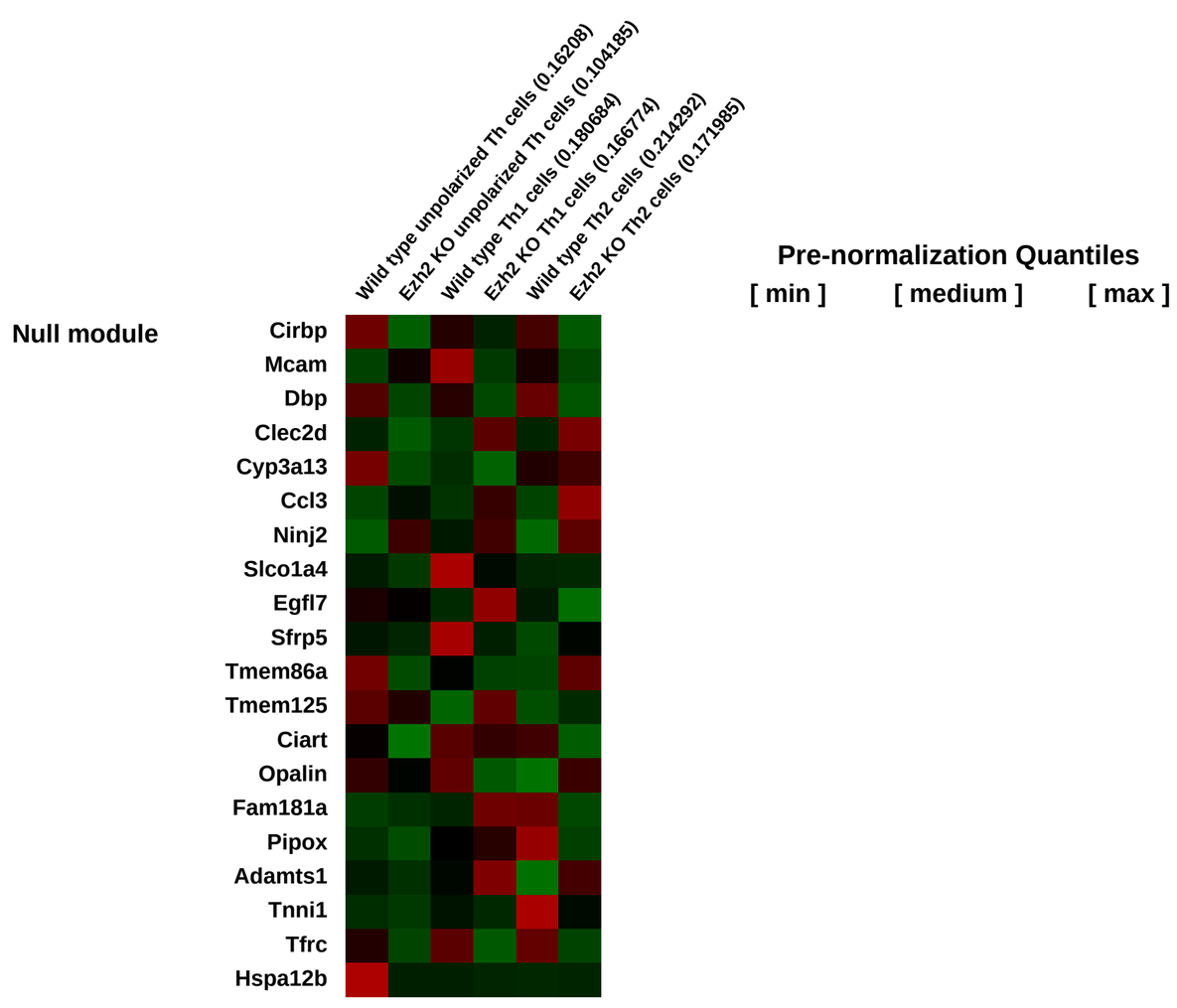

GEO Series "GSE43197" Expression Profiles

Num of samples in this series: 27

Scale of expression profile Z-scores

-3.0 -2.0 -1.0 0.0 1.0 2.0 3.0

GEO Link:	http://www.ncbi.nlm.nih.gov/geo/query/acc.cgi?acc=GSE43197
Status:	Public on Sep 23 2013
Title:	Natural cardiogenesis-based template predicts cardiogenic potential of induced pluripotent stem cell lines
Organism:	Mus musculus
Experiment type:	Expression profiling by array
Platform:	GPL1261
Pubmed ID:	24036272
Summary & Design:	**Summary:** **Rationale: Cardiac development is a complex process that results in the first integrated, multi-lineage embryonic tissue. Imperfect developmental progression leads to congenital heart disease, the most common birth defect with developmental corruption affecting more than 1% of all live births. Interrogation of individual genes has provided the backbone for cardiac developmental biology, yet a comprehensive transcriptome derived from natural cardiogenesis is required to establish an unbiased roadmap to gauge innate developmental milestones necessary for stem cell-based differentiation and in vitro disease modeling.** **Objective: Apply the contextual expression database of spatial-temporal cardiac structures (published in another manuscript by Li X. from the same group) to diagnose and predict cardiogenic outcomes from individual pluripotent stem cell lines.** **Methods and Results: Stage-specific cardiac structures were dissected from eight distinctive embryonic time points to produce a genome-wide expressome analysis across the spectrum of early to late cardiogenesis. Hierarchical clustering of the time course dataset demonstrated discrete gene expression profiles during natural embryonic development. In reference to the native cardiogenic expression roadmap, disruptive iPSC-derived cardiac expression profiles were revealed from pro-cardiogenic 3-factor (SOX2, OCT4, KLF4) compared to non-cardiogenic 4-factor (addition of c-MYC) reprogramming regimens upon stage-specific differentiation. Expression of cardiac-related genes from 3F-iPSC differentiated in vitro at day 0, 5, and 11 recapitulated expression of natural embryos at days 0, E7.5-E8.5, and E14.5-E18.5, respectively. In contrast, 4F-iPSC demonstrated variable gastrulation gene expression profiles beginning at day 5 of differentiation. Differential gene expression within the pluripotent ground state between the archetypical high cardiogenic potential of embryonic stem cells recapitulated in 3F-iPSC vs. the low cardiogenic potential of 4F-iPSC revealed 23 distinguishing candidate genes. Upon subsequent differentiation, cell line-specific gene expression differences were magnified to 399 genes at day 5 and 726 genes at day 11. A confirmed panel of 20 genes, differentially expressed between high and low cardiogenic cell lines, was transformed into a predictive score that was sufficient to correctly rank independent iPSC lines according to cardiogenic potential.** **Conclusions: Transcriptome analysis attuned to the embryonic developing heart provides a robust platform to probe coordinated cardiac specification and maturation from stem cell-based cardiogenesis model systems. Based on this genome-wide expressome roadmap, a panel of pre-cardiac genes was extracted that allowed differential prognosis of cardiogenic competency from individual reprogrammed cell lines at the pluripotent state.** **Overall design:** **4F-iPSC (19BL-iPSCs): Day0 undifferentiated - 3 biological replicates, Differentiated for 5 days (Day5) - 3 biological replicates, Differentiated for 11 days (Day11) - 3 biological replicates.**

Background corr dist: KL-Divergence = 0.0587, L1-Distance = 0.0360, L2-Distance = 0.0023, Normal std = 0.5299

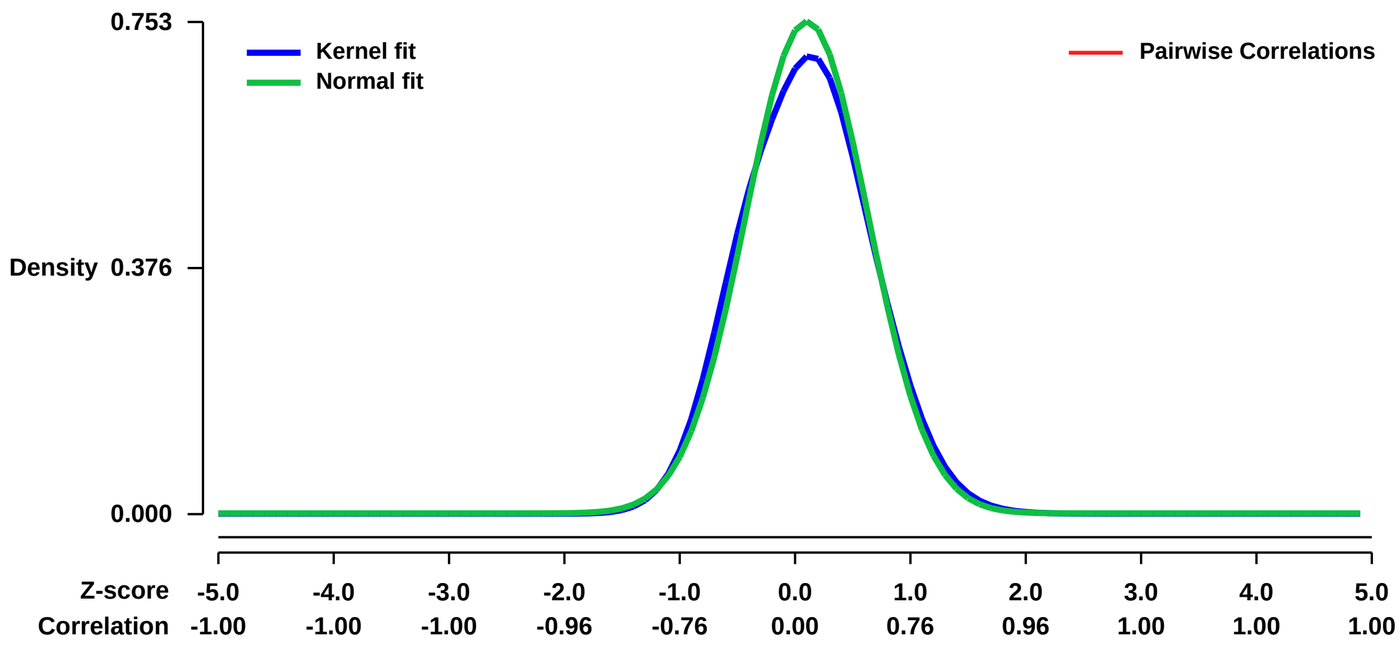

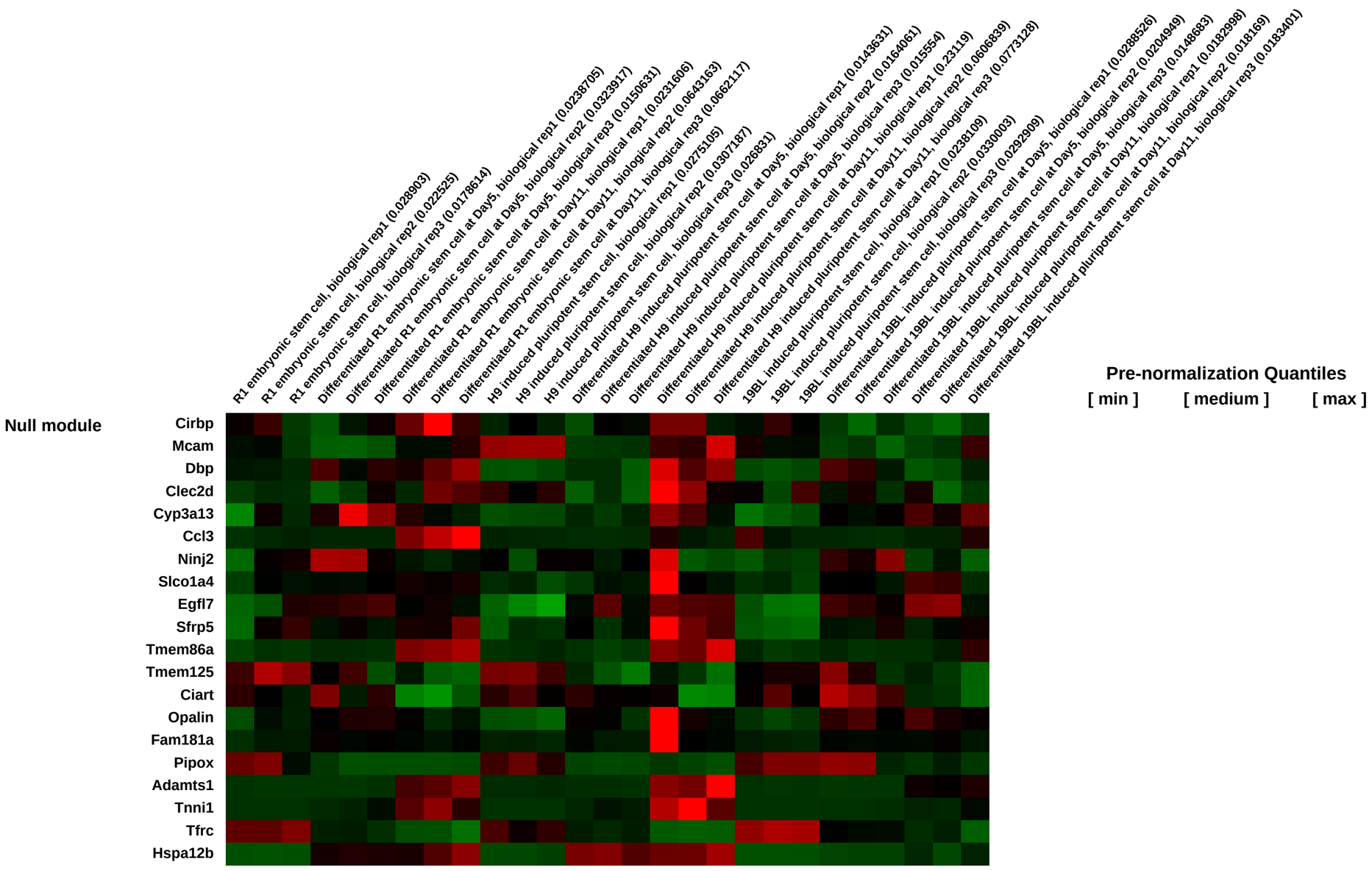

Null module

GEO Series "GSE27378" Expression Profiles

Num of samples in this series: 8

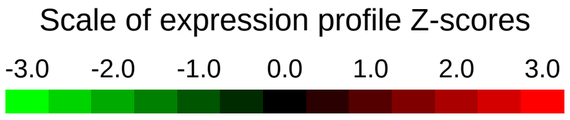

GEO Link:	http://www.ncbi.nlm.nih.gov/geo/query/acc.cgi?acc=GSE27378
Status:	Public on Dec 01 2011
Title:	Differential effects of inhibition of bone morphogenic protein (BMP) signalling on T-cell activation and differentiation
Organism:	Mus musculus
Experiment type:	Expression profiling by array
Platform:	GPL1261
Pubmed ID:	22144105
Summary & Design:	**Summary:** Dorsomorphin is a small molecule inhibitor of type I bone morphogenic protein receptors (BMPRs). We have found that dorsomorphin affects a wide range of T cell function. In order to obtain the bigger picture of the effects of DM in T cell activation. transcriptomic analysis was performed using mouse primary CD25-CD4+ T cells with either DM (4 ¸…M) or vehicle in the presence or absence of stimulation by anti-CD3 and -CD28 antibodies. **Overall design:** Mouse CD4+ T cells were prepared and cultured with or without stimulation by plate bound anti-CD3 mAb and soluble anti-CD28 mAb for 1 hour. Subsequently, 4 ¸…M DM or DMSO was added and cells were incubated for 6 hours. Total RNA was isolated using Qiagen RNeasy mini kits.

Background corr dist: KL-Divergence = 0.0595, L1-Distance = 0.0472, L2-Distance = 0.0033, Normal std = 0.5727

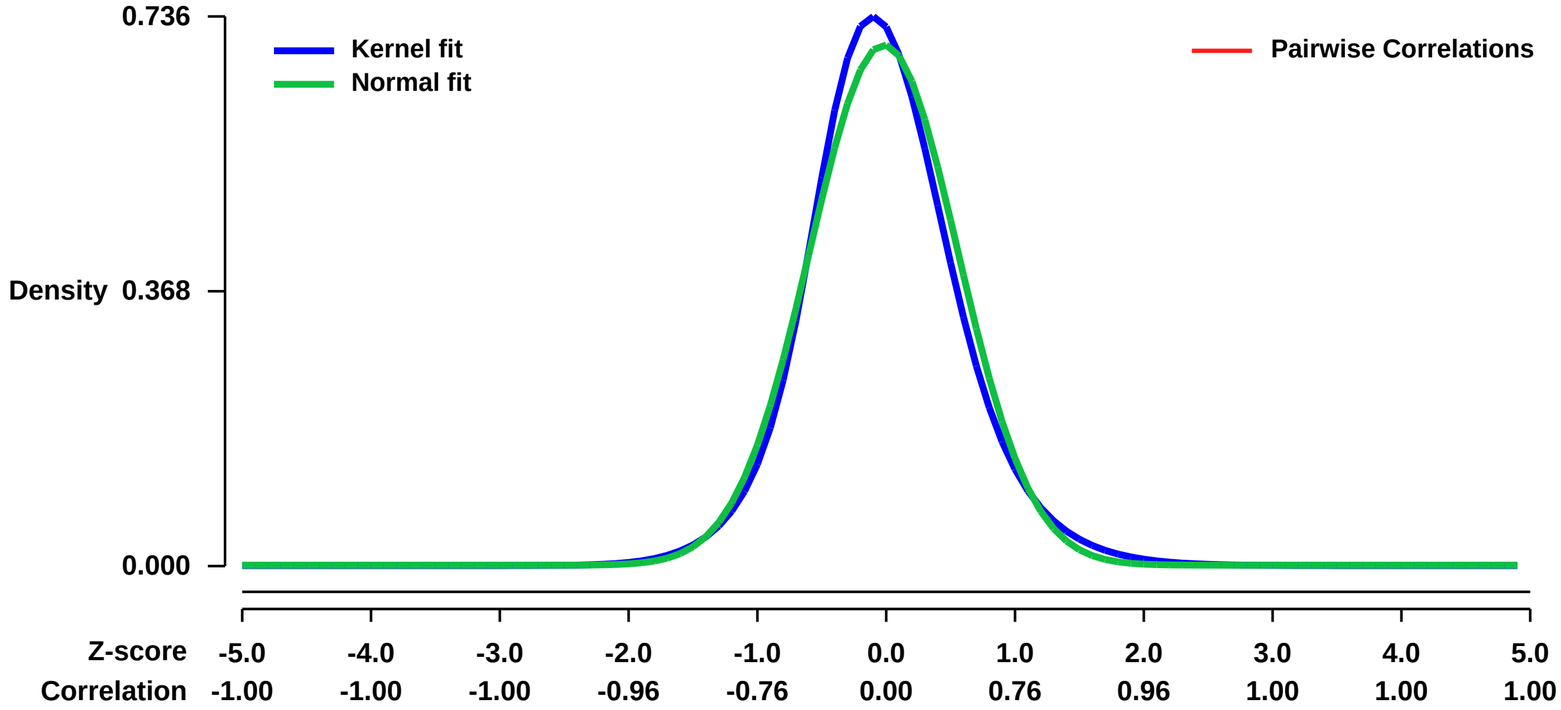

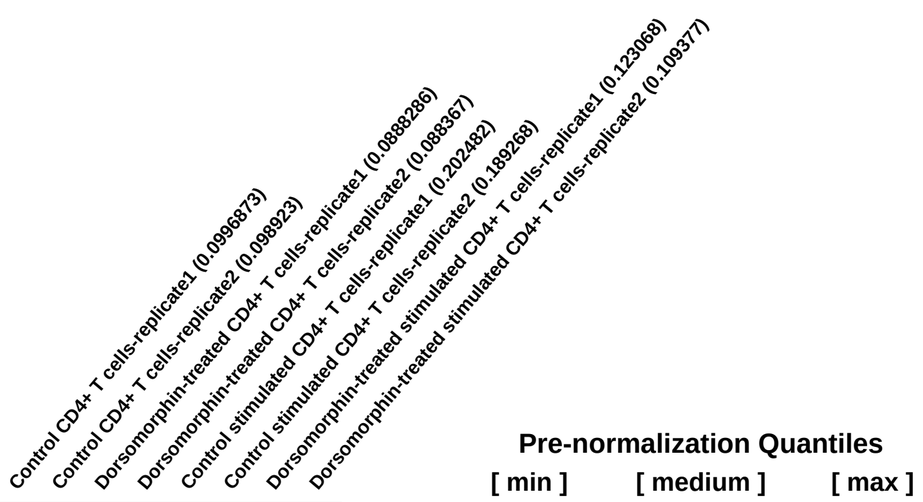

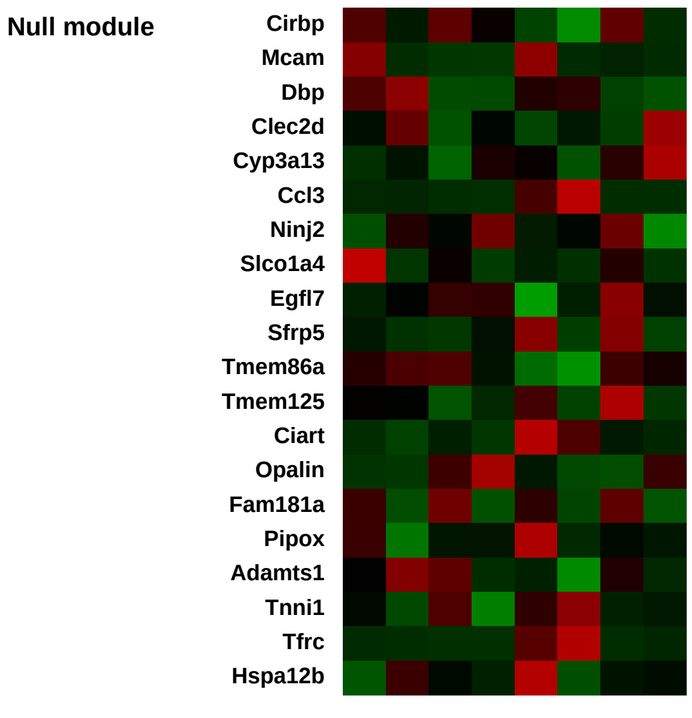

GEO Series "GSE22073" Expression Profiles

Num of samples in this series: 6

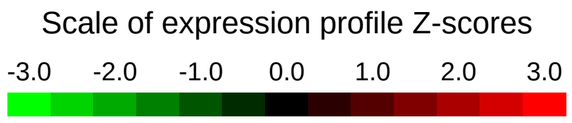

GEO Link:	http://www.ncbi.nlm.nih.gov/geo/query/acc.cgi?acc=GSE22073
Status:	Public on Jun 02 2010
Title:	Testis samples from Alkbh1 wild-type and KO mice
Organism:	Mus musculus
Experiment type:	Expression profiling by array
Platform:	GPL1261
Pubmed ID:	21072209
Summary & Design:	**Summary:** The aim of the study was to elucidate the role of Alkbh1 by targeted deletion in C57/BL6 mice. Alkb deficiency results in sex-ratio distortion of offspring and apoptosis in adult testes, most likely caused by defects in the pachytene stage during spermatogenesis. Due to the pivotal role of Alkbh1 in mouse survival and potentially in germ cells, we searched for Alkbh1-regulated genes in adult testes. **Overall design:** Testes from 12 week old mice were selected for RNA extraction and hybridization on Affymetrix microarrays. We used testes from 3 wild type mice and 3 KO mice

Background corr dist: KL-Divergence = 0.0352, L1-Distance = 0.0146, L2-Distance = 0.0002, Normal std = 0.6347

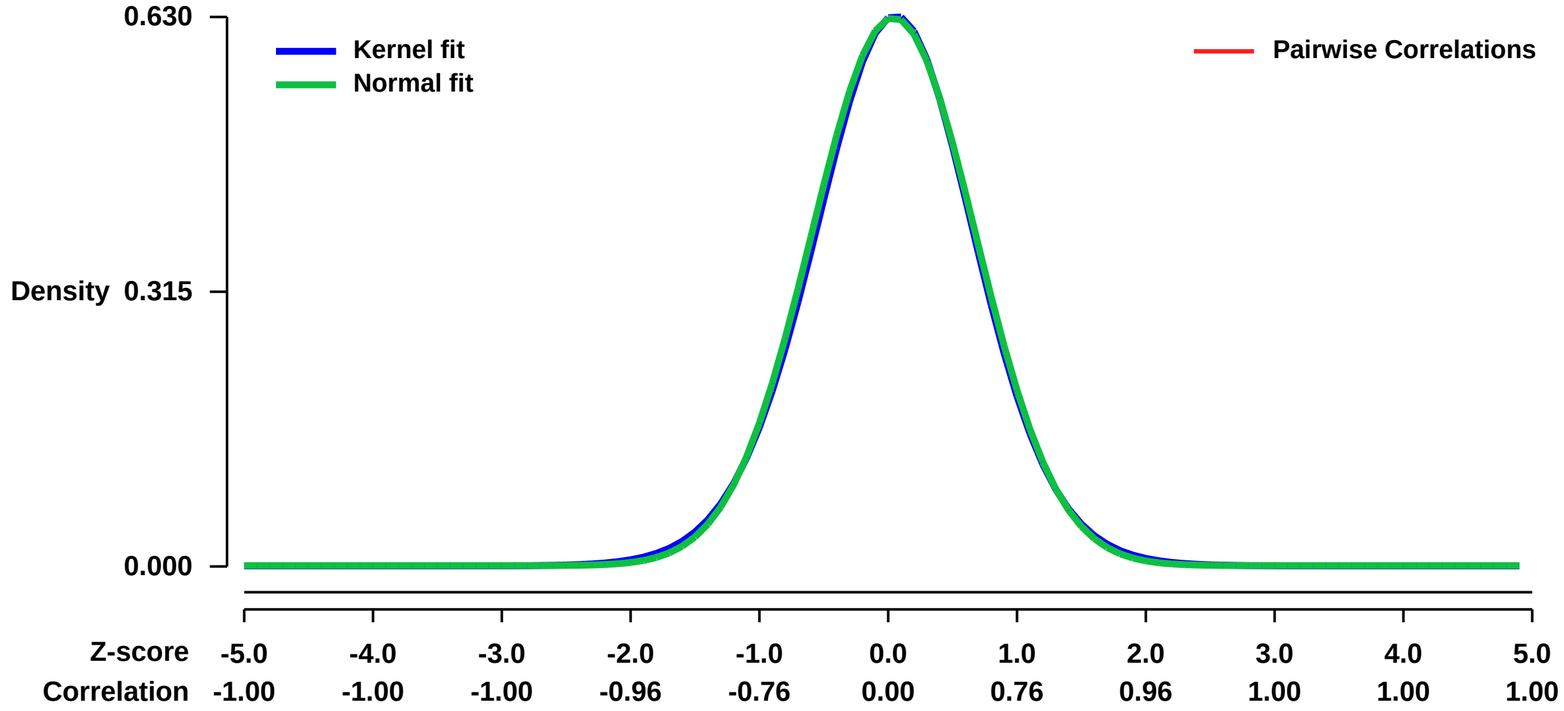

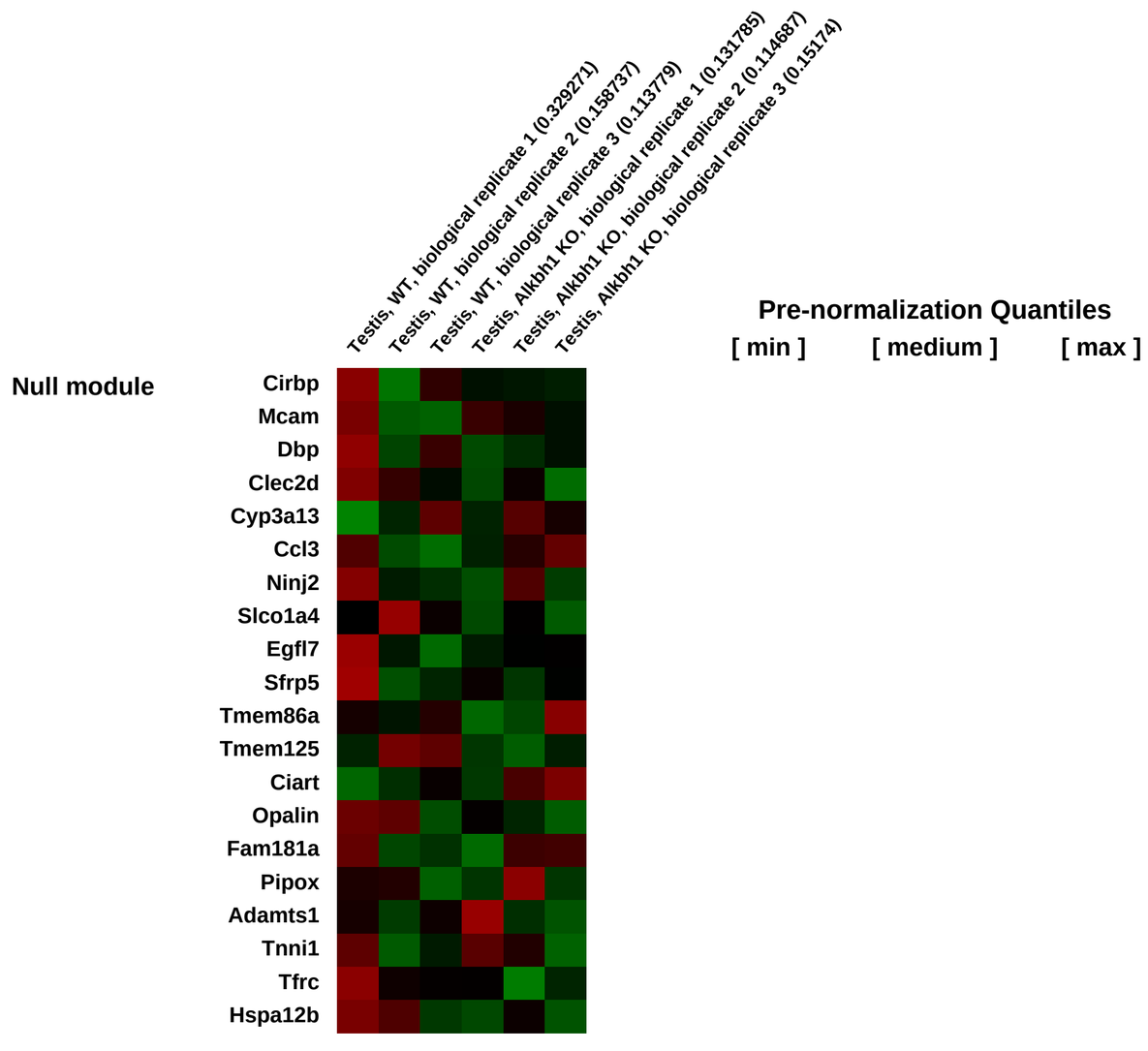

GEO Series "GSE15871" Expression Profiles

Num of samples in this series: 18

Scale of expression profile Z-scores

-3.0 -2.0 -1.0 0.0 1.0 2.0 3.0

GEO Link:	http://www.ncbi.nlm.nih.gov/geo/query/acc.cgi?acc=GSE15871
Status:	Public on Nov 05 2009
Title:	Expression data from NFI-C knock out embryonic fibroblasts
Organism:	Mus musculus
Experiment type:	Expression profiling by array
Platform:	GPL1261
Pubmed ID:	23402308
Summary & Design:	**Summary:** The Nuclear Factor I C (NFI-C) transcription factor has been implicated in TGF-¸† signaling, extracellular matrix deposition and skin appendage pathologies. We performed a global gene expression analysis in NFI-C-/- and wild-type embryonic primary murine fibroblasts. This indicated that NFI-C acts mostly to repress gene expression in response to TGF-¸†1. Misregulated genes featured a prominent over-representation of regulators of connective tissue inflammation and repair. **Overall design:** mRNAs were isolated from embryonic fibroblasts obtained from 3 wild-type and 3 NFI-C knock-out mice, and their levels were probed using microarrays. Prior to RNA extraction, fibroblast cultures were treated or not with TGF-¸†1 for 1 hour to examine the immediate response to the growth factor, or treated for 10 hours to assess the delayed response.

Background corr dist: KL-Divergence = 0.1186, L1-Distance = 0.0278, L2-Distance = 0.0011, Normal std = 0.4192

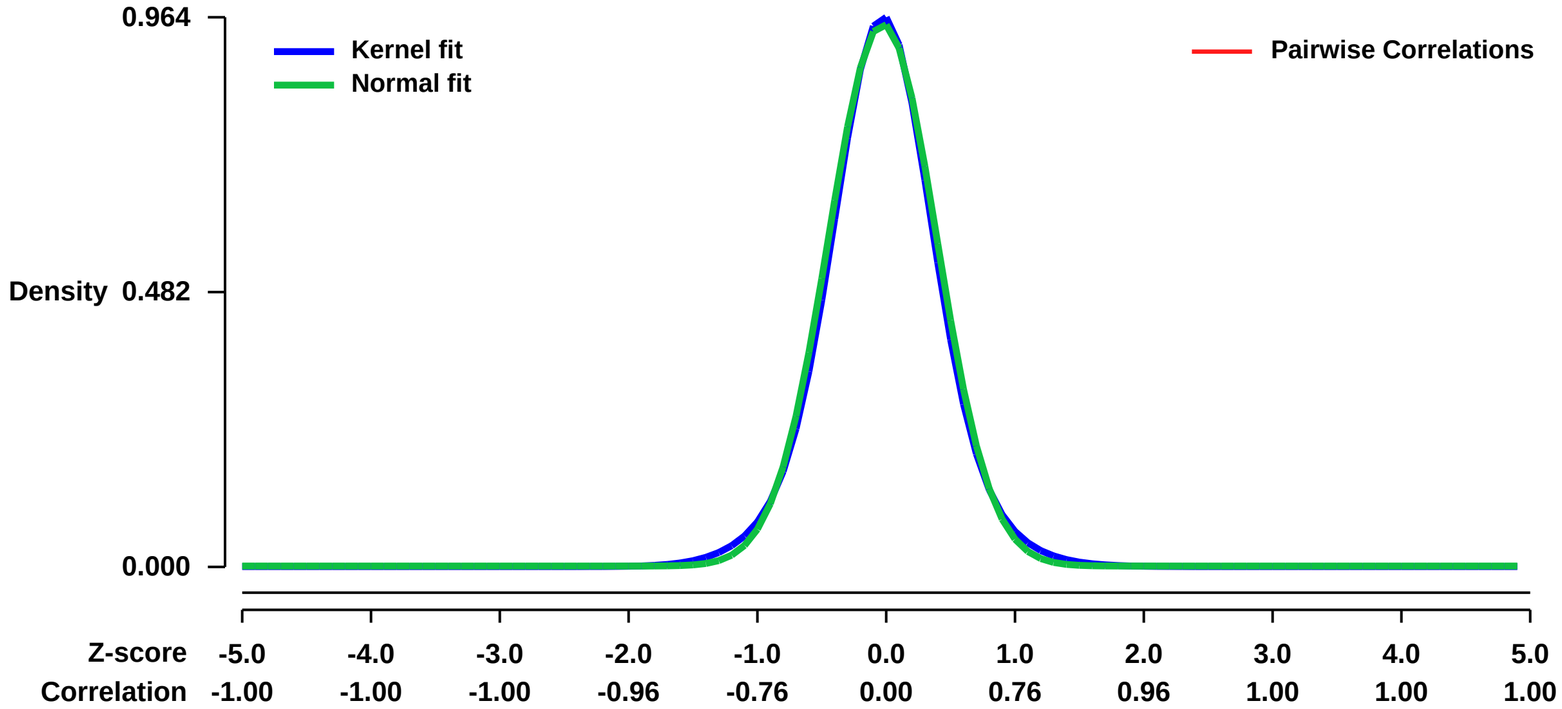

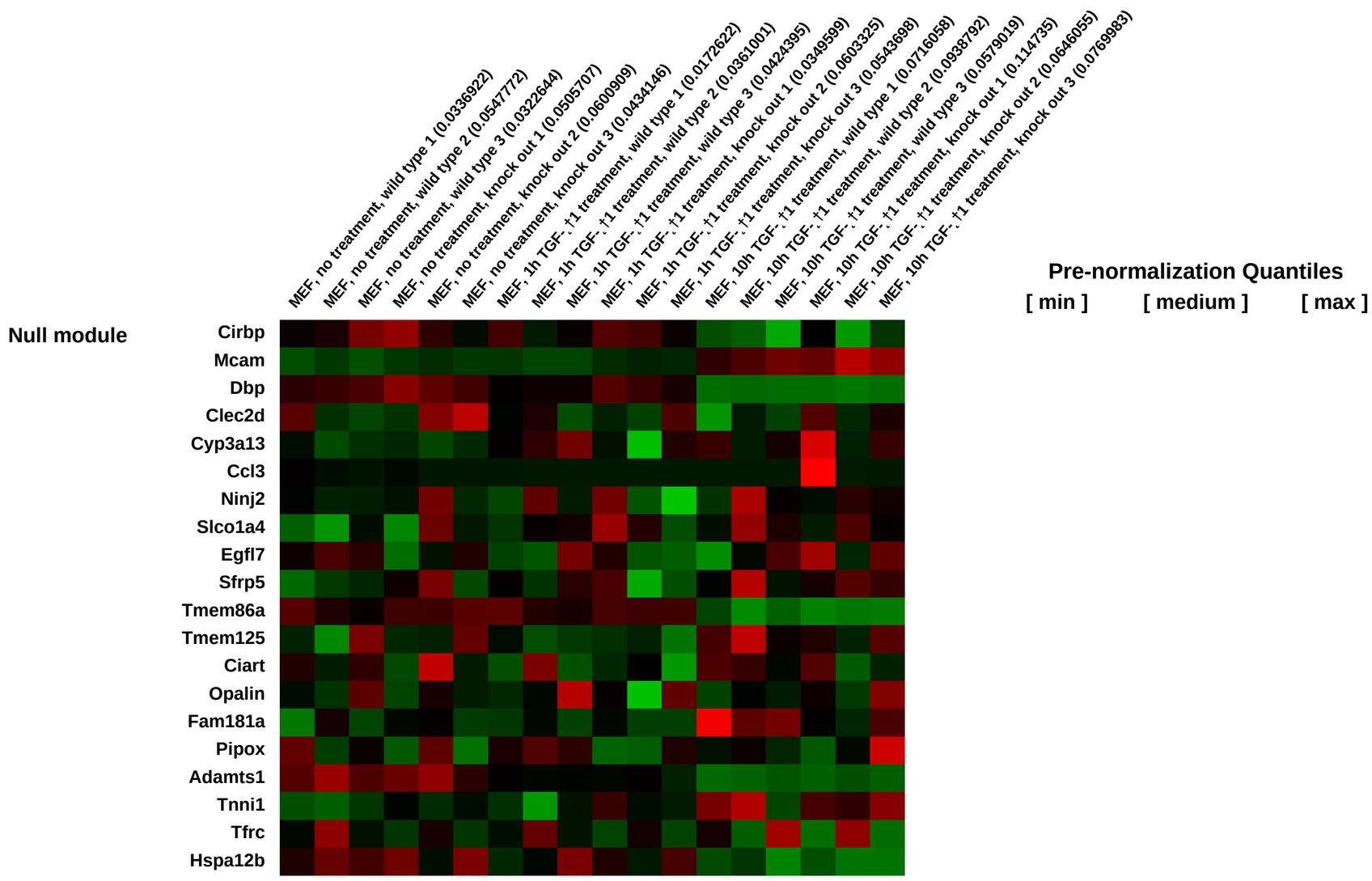

GEO Series "GSE32615" Expression Profiles

Num of samples in this series: 10

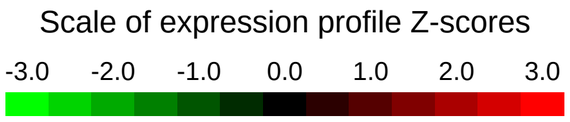

GEO Link:	**http://www.ncbi.nlm.nih.gov/geo/query/acc.cgi?acc=GSE32615**
Status:	**Public on Jun 30 2014**
Title:	**Expression data of mouse Ewing's sarcoma**
Organism:	**Mus musculus**
Experiment type:	**Expression profiling by array**
Platform:	**GPL1261**
Pubmed ID:	
Summary & Design:	**Summary:** **Ewingâ s sarcoma is highly malignant bone tumor that involves childhood and adolescent, and its nature has not been well understood. To clarify its cellular origin and the mechanisms of tumorigenesis, we used ex vivo approach to create a murine model for Ewingâ s sarcoma. The osteochondrogenic progenitors derived from the facial zone (FZ) of murine long bones at late gestation were purified by microdissection, introduced with EWS-FLI1 or EWS-ERG retroviruses and transplanted into nude mice. Ewingâ s sarcoma-like small round cell sarcoma developed at 100% penetrance, whereas tumor induction was less effective when growth place (GP)-derived cells were used. The different response of gene expression to EWS-FLI1 between FZ and GP cells suggests importance of the specific cellular context for EWS-FLI1 to induce Ewingâ s sarcoma. The Wnt/˛†-catenin pathway was involved in close relationship to the cellular context, with Dkk2 and Wipf1 as important downstream modulators. Furthermore, gene expression profiling revealed similarity between our models and human Ewingâ s sarcoma. These results indicate that Ewingâ s sarcoma originates from the embryonic osteochondrogenic progenitor.** **Overall design:** **For comparing with human Ewing's sarcoma, we used expression databases E-MEXP-533 (Henderson SR et al, Genome Biol 6:R76, 2005) and E-MEXP-1142 (Schaefer KL et al, Eur J Cancer 44:699, 2008). In addition, the data sets for other sarcomas that include GSE6481 (Nakayama R et al, Mod Pathol 20:749, 2007), GSE7529 (Albino D et al, Cancer 113:1412, 2008) and GSE21122 (Barretina J et al, Nat Genet 42:715, 2010) were used for clustering analysis.**

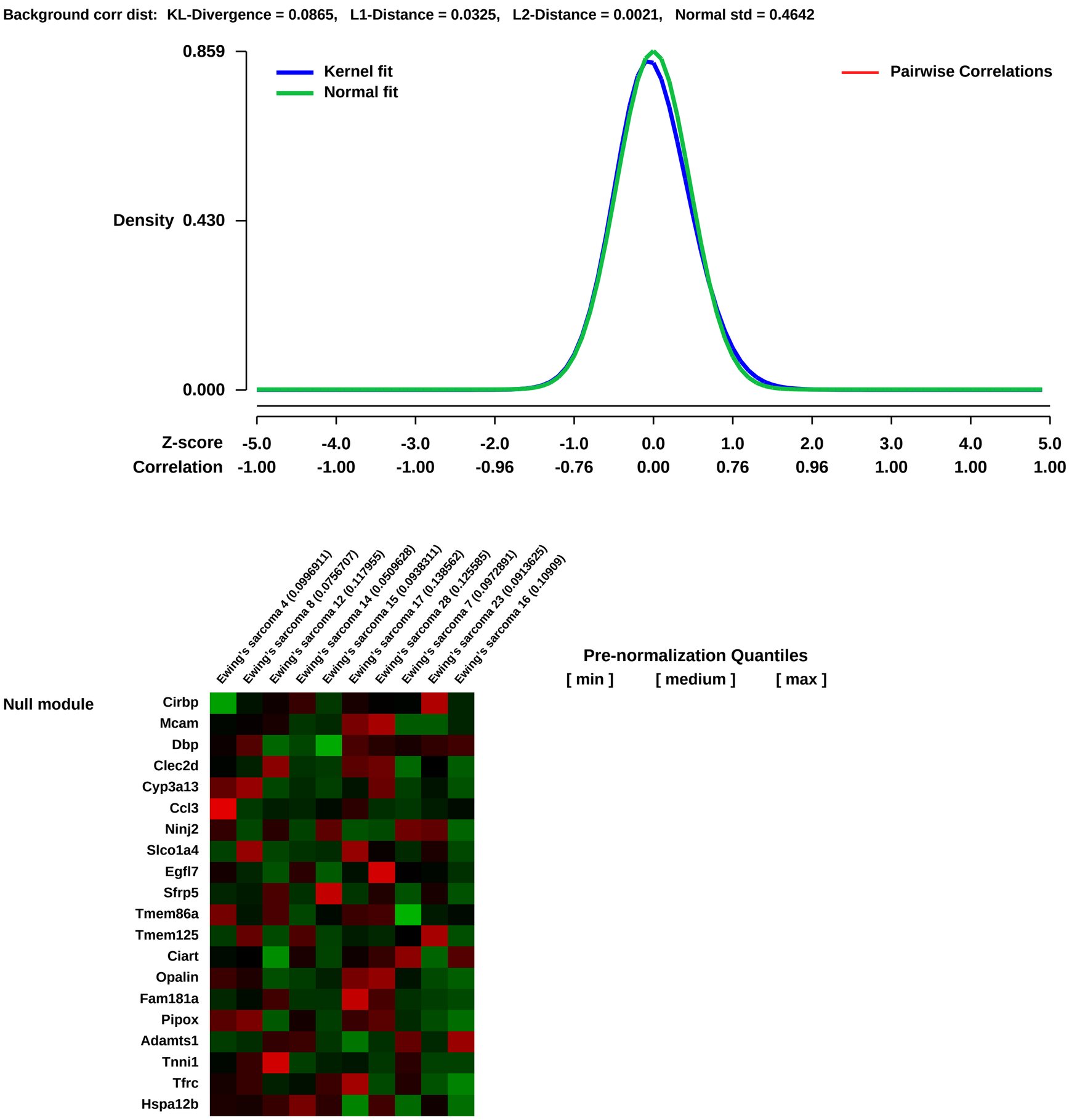

GEO Series "GSE6903" Expression Profiles

Num of samples in this series: 6

Scale of expression profile Z-scores

-3.0 -2.0 -1.0 0.0 1.0 2.0 3.0

GEO Link:	**http://www.ncbi.nlm.nih.gov/geo/query/acc.cgi?acc=GSE6903**
Status:	**Public on Aug 03 2007**
Title:	**Expression data from high-fat diet feeded WT and LIGHT Tg mice**
Organism:	**Mus musculus**
Experiment type:	**Expression profiling by array**
Platform:	**GPL1261**
Pubmed ID:	**17431181**
Summary & Design:	**Summary:** **effect of over-expression LIGHT on T cells for the liver gene expression** **We used microarrays to detail the global programme of gene expression underlying WT and LIGHT Tg liver** **Keywords: genetic difference** **Overall design:** **mice were selected at 4-8 wks old after 2 weeks HFD feeding for RNA extraction and hybridization on Affymetrix microarrays. The total liver were used.**

Background corr dist: KL-Divergence = 0.0282, L1-Distance = 0.0173, L2-Distance = 0.0003, Normal std = 0.6803

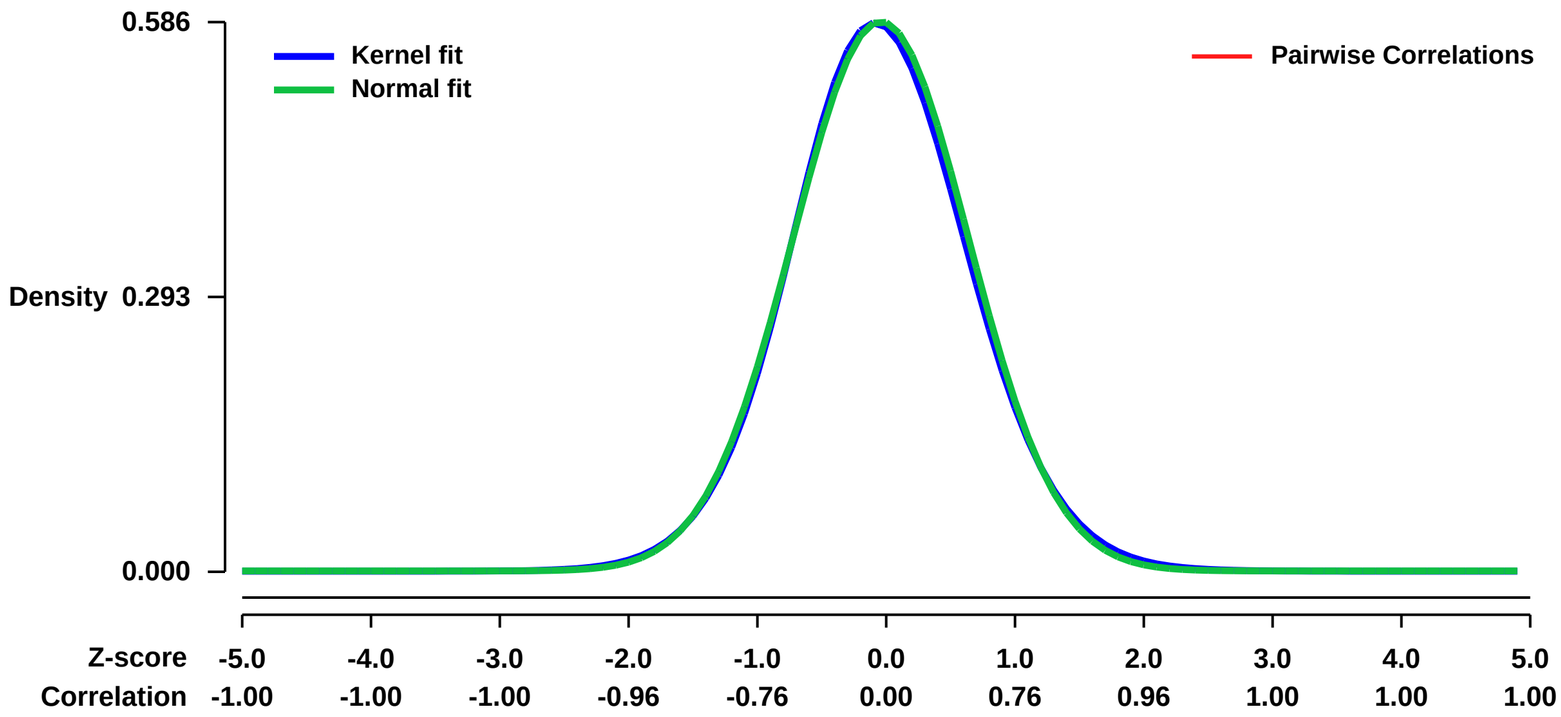

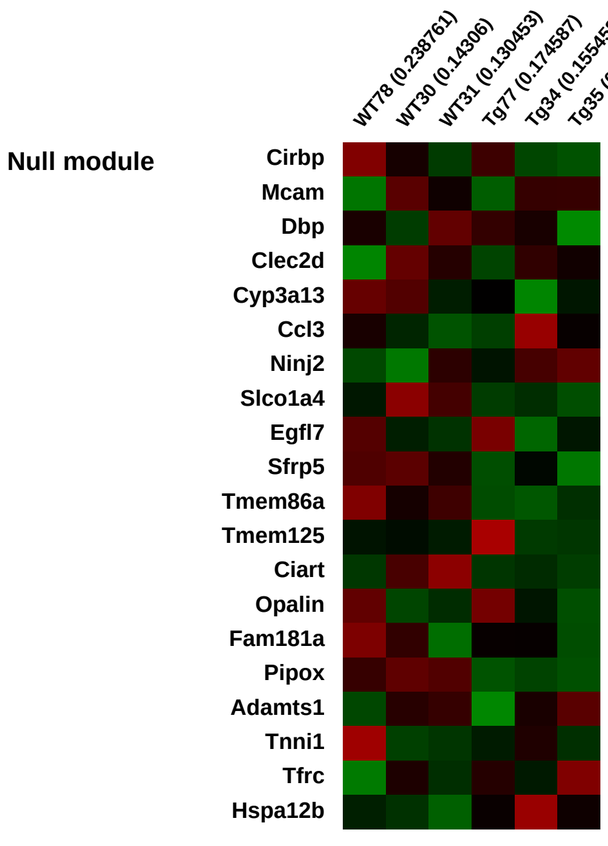

GEO Series "GSE15767" Expression Profiles

Num of samples in this series: 6

Scale of expression profile Z-scores

-3.0 -2.0 -1.0 0.0 1.0 2.0 3.0

GEO Link:	http://www.ncbi.nlm.nih.gov/geo/query/acc.cgi?acc=GSE15767
Status:	Public on Jun 05 2009
Title:	Heterogeneity of LN resident macrophage
Organism:	Mus musculus
Experiment type:	Expression profiling by array
Platform:	GPL1261
Pubmed ID:	19503106
Summary & Design:	**Summary:** **LN resident macrophages lining the lymphatic sinuses play critical roles in antigen capture and presentation as well as degradation.** **We used microarray to examine global gene expression profiles to compare SCS and med macrophages to determine the underlying molecular basis of their differential handling of antigens.** **Overall design:** **Primary SCS and med macrophages were isolated and purified from LNs by flourescence-activated cell sorting and RNA extracted, amplified and hybridized for Affymetrix analysis.**

Background corr dist: **KL-Divergence = 0.0309, L1-Distance = 0.0215, L2-Distance = 0.0005, Normal std = 0.6738**

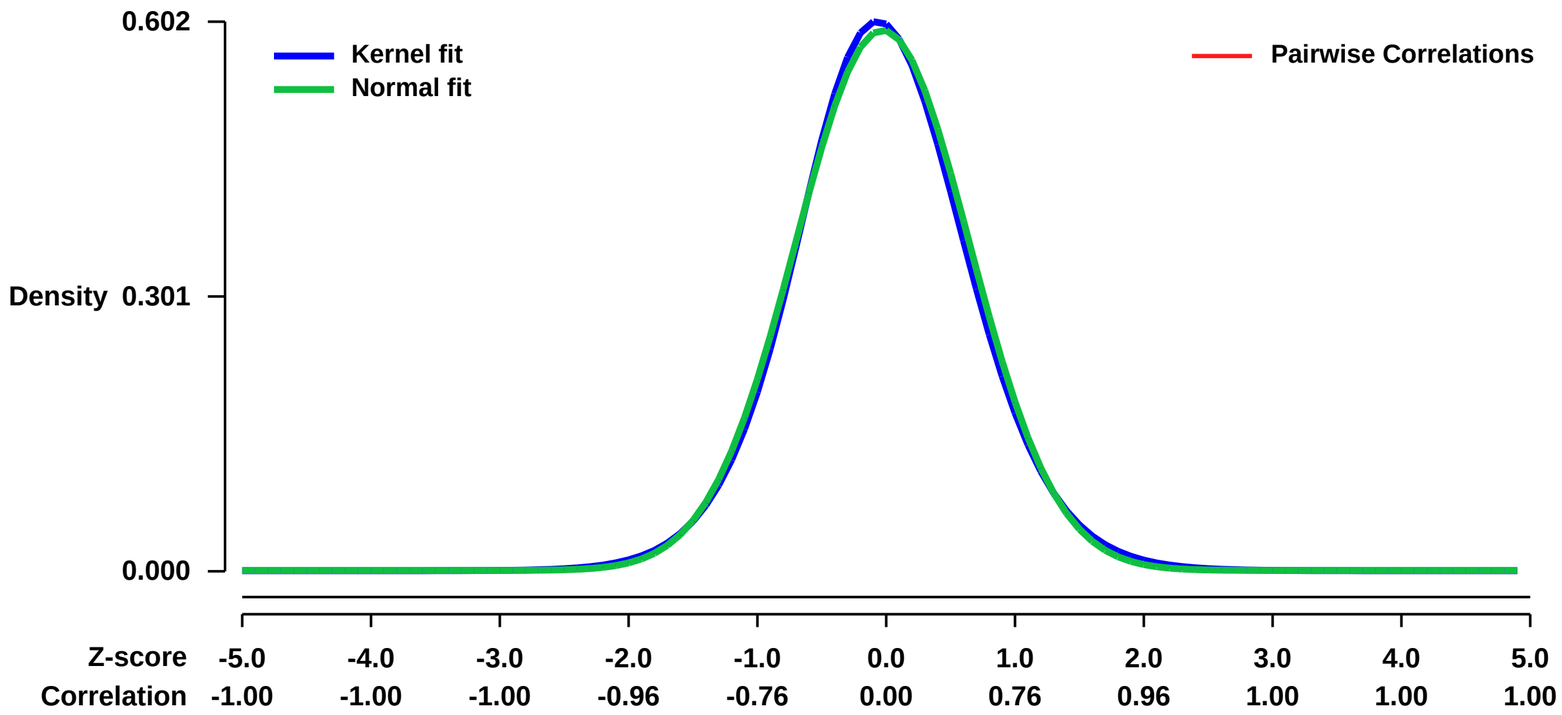

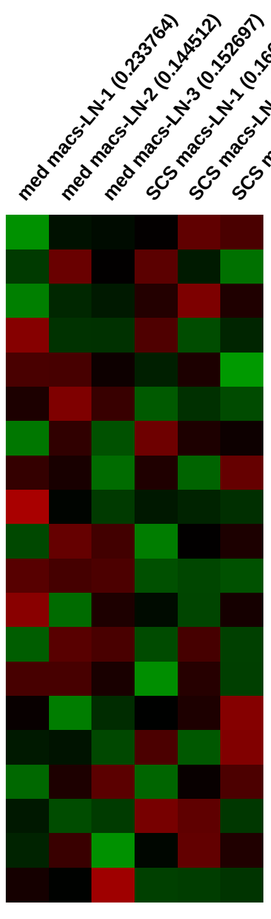

GEO Series "GSE35338" Expression Profiles

Num of samples in this series: 30

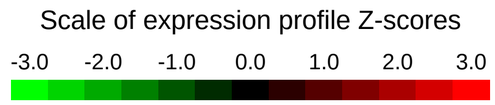

GEO Link:	http://www.ncbi.nlm.nih.gov/geo/query/acc.cgi?acc=GSE35338
Status:	Public on May 02 2012
Title:	Expression data from reactive astrocytes acutely purified from young adult mouse brains
Organism:	Mus musculus
Experiment type:	Expression profiling by array
Platform:	GPL1261
Pubmed ID:	22553043
Summary & Design:	**Summary:** Reactive astrogliosis is characterized by a profound change in astrocyte phenotype in response to all CNS injuries and diseases. To better understand the reactive astrocyte state, we used Affymetrix GeneChip arrays to profile gene expression in populations of reactive astrocytes isolated at various time points after induction using two different mouse injury models, ischemic stroke and neuroinflammation. **Overall design:** Young adult male mice underwent middle cerebral artery occlusion (MCAO) to produce ischemic stroke or control sham surgery. Young adult mice were injected intraperitoneally with 5 mg/kg lipopolysaccharide (LPS) to produce neuroinflammation or saline for control. Astrocytes were acutely purified from control and injured brains at 1 day after injury for LPS/saline injection and 1, 3 days and 7 days after MCAO/sham surgeries.
Background corr dist:	KL-Divergence = 0.1320, L1-Distance = 0.0498, L2-Distance = 0.0057, Normal std = 0.3941

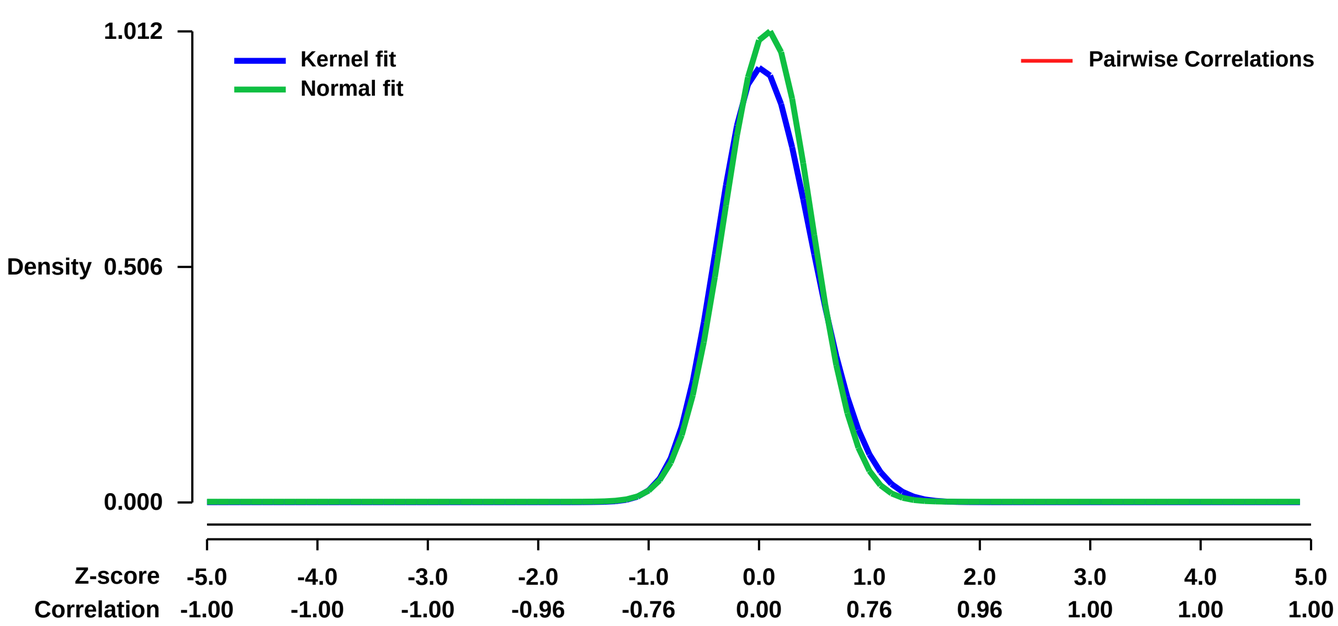

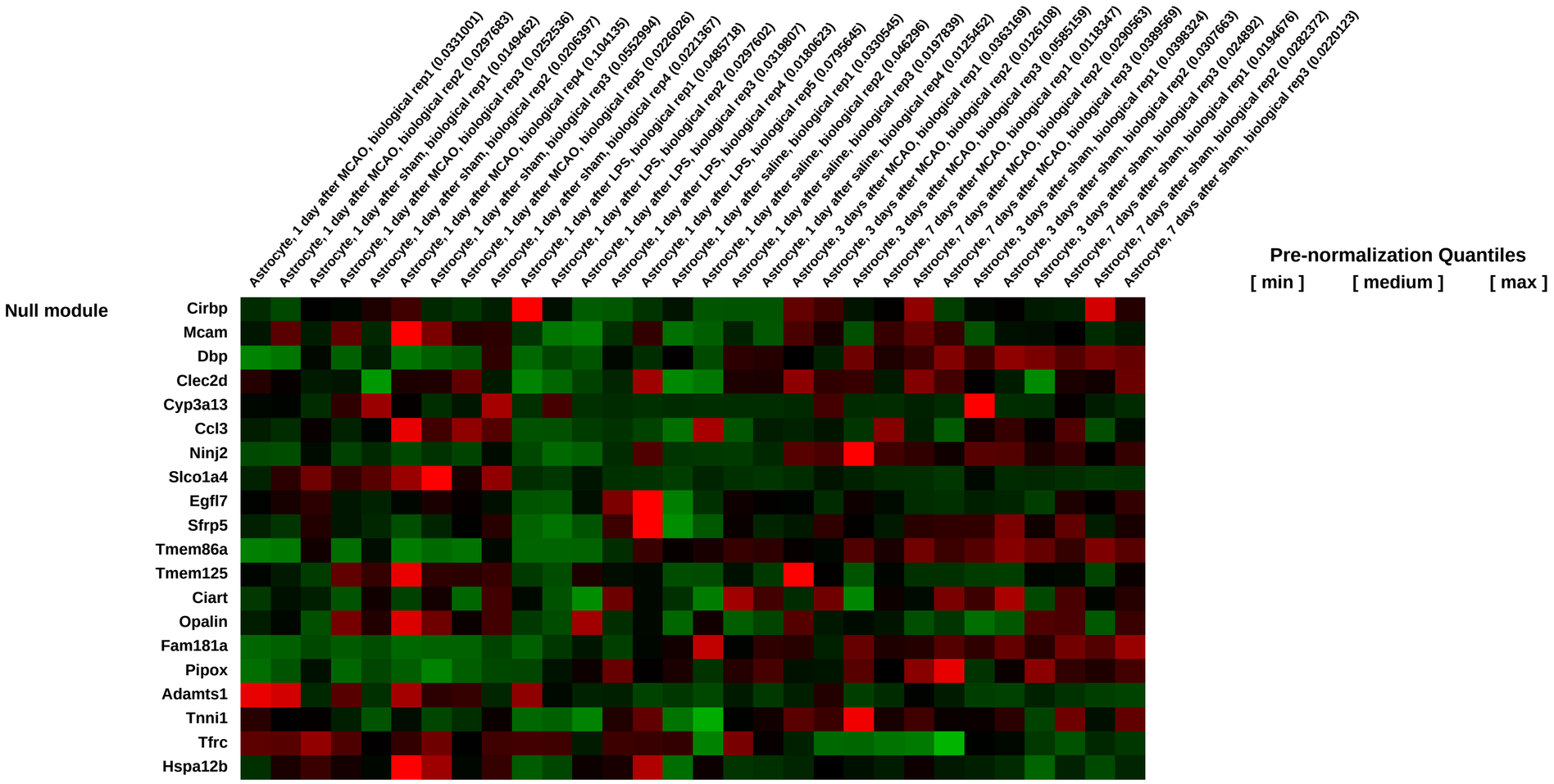

GEO Series "GSE17316" Expression Profiles

Num of samples in this series: 12

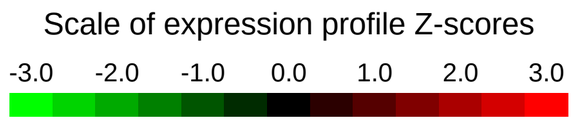

GEO Link:	http://www.ncbi.nlm.nih.gov/geo/query/acc.cgi?acc=GSE17316
Status:	Public on Nov 23 2009
Title:	Reprogramming of a B cell line into macrophages
Organism:	Mus musculus
Experiment type:	Expression profiling by array
Platform:	GPL1261
Pubmed ID:	19896445
Summary & Design:	**Summary:** Transcription factor induced reprogramming of one specialized cell type into another is a promising approach for regenerative medicine. However, the process still remains poorly understood, in large part because of the lack of adequate experimental models. Here we describe a robust cell reprogramming system consisting of a B cell line with an inducible form of C/EBPa that can be converted into macrophages with essentially 100% efficiency in only 2 to 3 days. The conversion involves reciprocal changes in cell surface antigen expression, increase in cell granularity and size, alterations in cellular structures, formation of membrane extensions, acquisition of phagocytic capacity and an increased inflammatory responsiveness as well as migratory activity. Analysis of the transcriptome shows complex reciprocal regulation of B cell and macrophage genes, including transcription factors required for the formation of the two lineages. The fact that the cells become irreversibly committed to a macrophage fate within 1 to 2 days after activation of C/EBPa show that they are truly reprogrammed. The system should be useful to study epigenetic and cell biological mechanisms of transcription factor induced cell reprogramming. **Overall design:** time points: vehicle control, 3h, 12h, 24h, 48h.

Background corr dist: KL-Divergence = 0.0922, L1-Distance = 0.0474, L2-Distance = 0.0035, Normal std = 0.4812

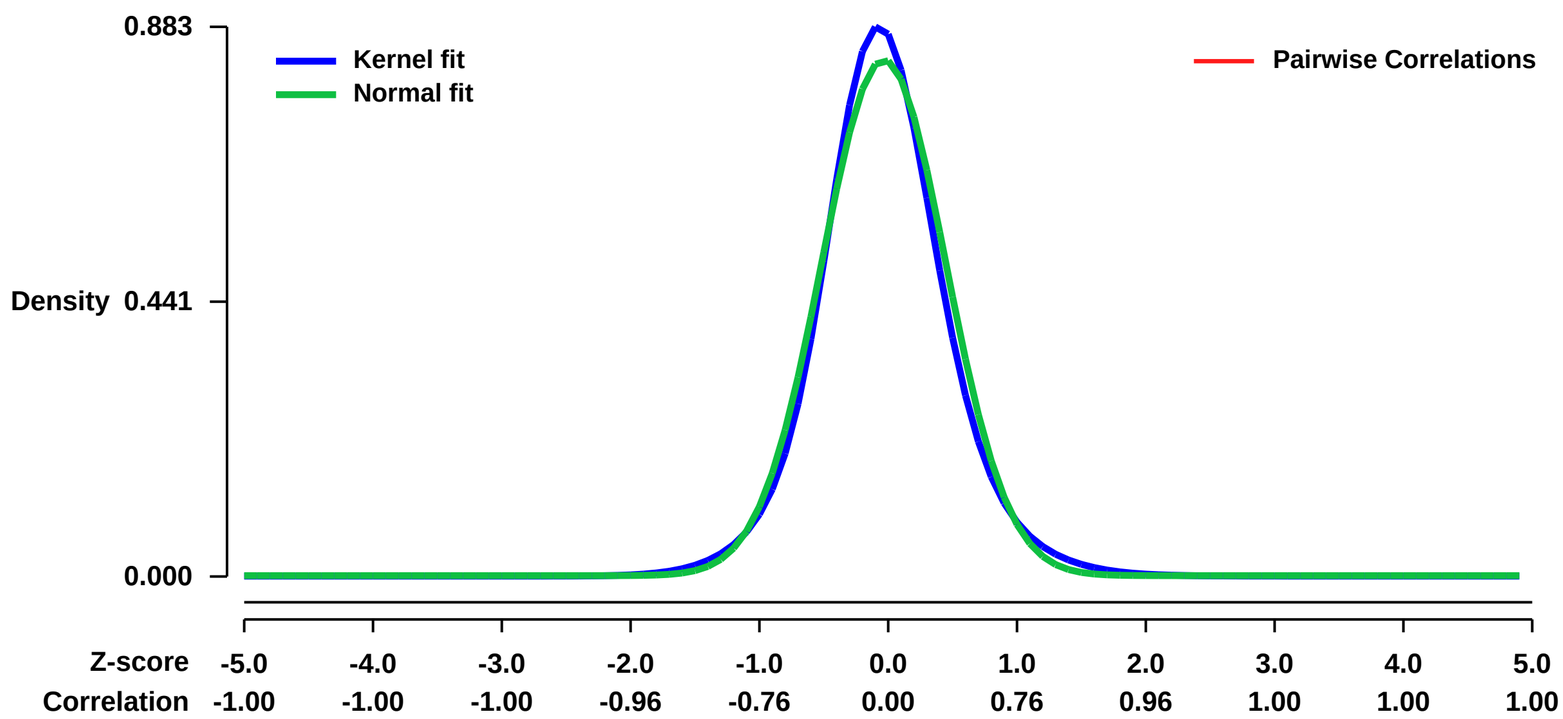

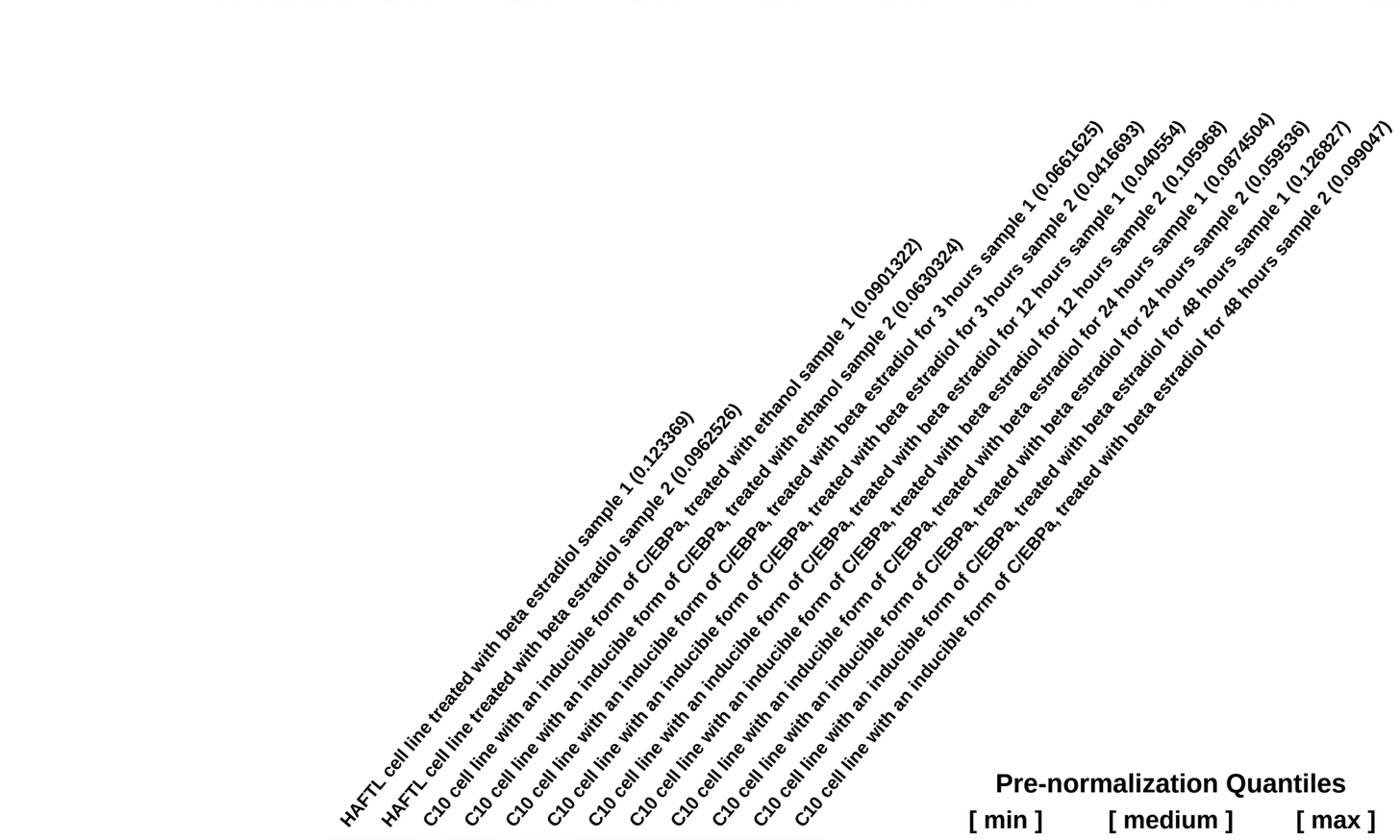

GEO Series "GSE44599" Expression Profiles

Num of samples in this series: 18

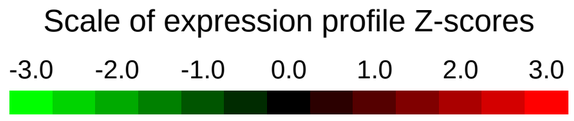

GEO Link:	**http://www.ncbi.nlm.nih.gov/geo/query/acc.cgi?acc=GSE44599**
Status:	**Public on Aug 01 2013**
Title:	**ZNF365 promotes stability of fragile sites and telomeres**
Organism:	**Mus musculus**
Experiment type:	**Expression profiling by array**
Platform:	**GPL1261**
Pubmed ID:	**23776040**
Summary & Design:	**Summary:** **Critically short telomeres activate cellular senescence or apoptosis, as mediated by the tumor suppressor p53, but in the absence of this checkpoint response, telomere dysfunction engenders chromosomal aberrations and cancer. Here, analysis of p53-regulated genes activated in the setting of telomere dysfunction identified Zfp365 (ZNF365 in humans) as a direct p53 target that promotes genome stability. Germline polymorphisms in the ZNF365 locus are associated with increased cancer risk, including those associated with telomere dysfunction. On the mechanistic level, ZNF365 suppresses expression of a subset of common fragile sites (CFS) including telomeres. In the absence of ZNF365, defective telomeres engage in aberrant recombination of telomere ends, leading to increased telomere sister chromatid exchange (T-SCE) and formation of anaphase DNA bridges, including ultra-fine DNA bridges (UFB), and ultimately increased cytokinesis failure and aneuploidy. Thus, the p53-ZNF365 axis contributes to genomic stability in the setting of telomere dysfunction.** **Overall design:** **We expressed an inducible p53 allele encoding a p53-estrogen receptor fusion protein (p53ER) that becomes functional upon addition of 4-hydroxytamoxifen (4-OHT) in TKO cells. We chose a time point of 4 hours post-4-OHT induction to catalog potential direct targets.**

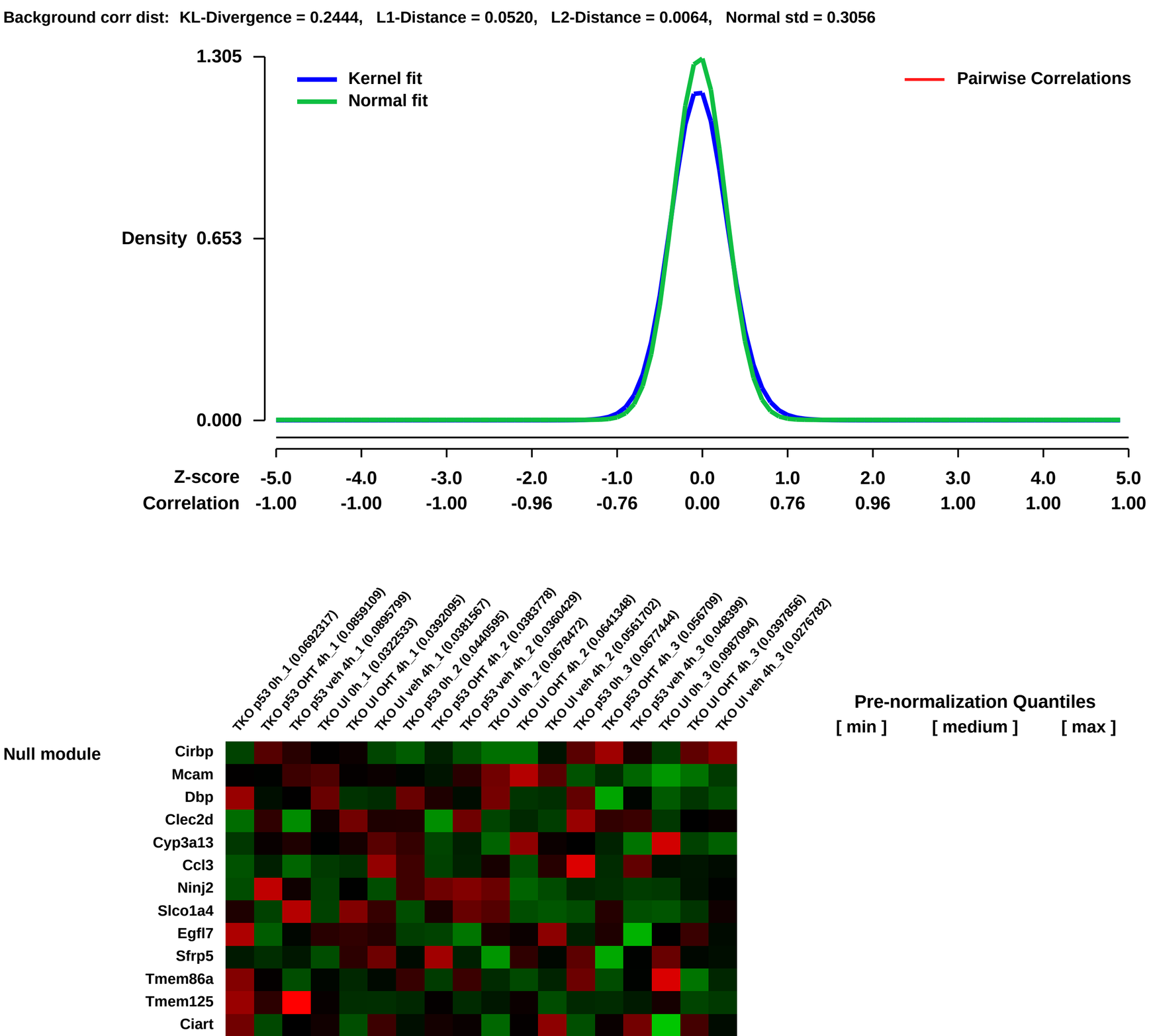

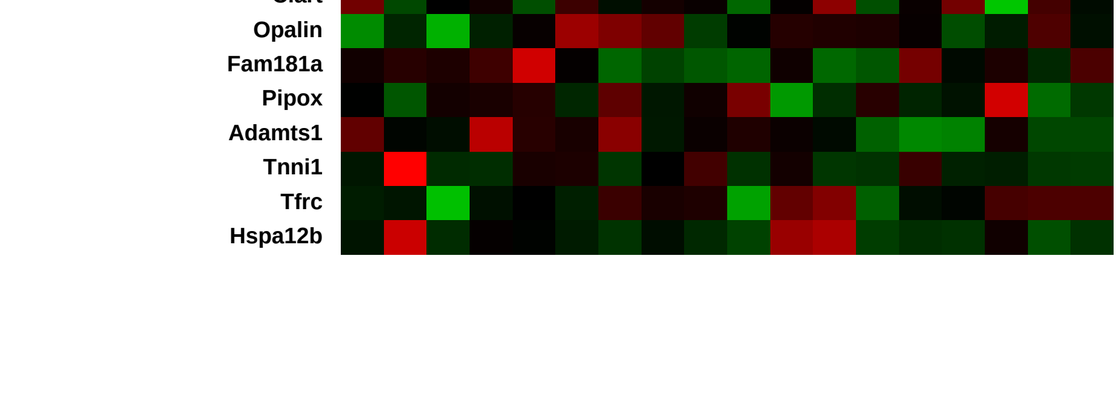

GEO Series "GSE31166" Expression Profiles

Num of samples in this series: 6

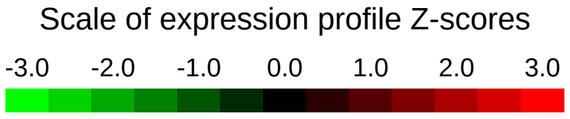

GEO Link:	**http://www.ncbi.nlm.nih.gov/geo/query/acc.cgi?acc=GSE31166**
Status:	**Public on Dec 13 2012**
Title:	**Expression data from inducible ES stable cell line**
Organism:	**Mus musculus**
Experiment type:	**Expression profiling by array**
Platform:	**GPL1261**
Pubmed ID:	**23180766**
Summary & Design:	**Summary:** **In order to identify the effects of the induction of the gene of interest on the mouse ES transcriptome, we performed Affymetrix Gene-Chip hybridization experiments for the inducible not-tagged cell line.** **Transcriptome analysis of the inducible transgenic mouse ES cell line.** **The E13 inducible cell lines derived from parental EB3 cell line. The cell line EB3 was obtained from the laboratory of Dr Hitoshi Niwa as previously described in (Masui S et al., 2005).** **Tthe specific mouse gene is E130012A19Rik.** **Overall design:** **For the analysis on the inducible not-tagged cell line, total RNA was extracted from three biological replicates grown in medium deprived of Tetracycline for 48 hours; RNA extracted from un-induced clones was used as control.**

Background corr dist: KL-Divergence = 0.0196, L1-Distance = 0.0228, L2-Distance = 0.0005, Normal std = 0.7644

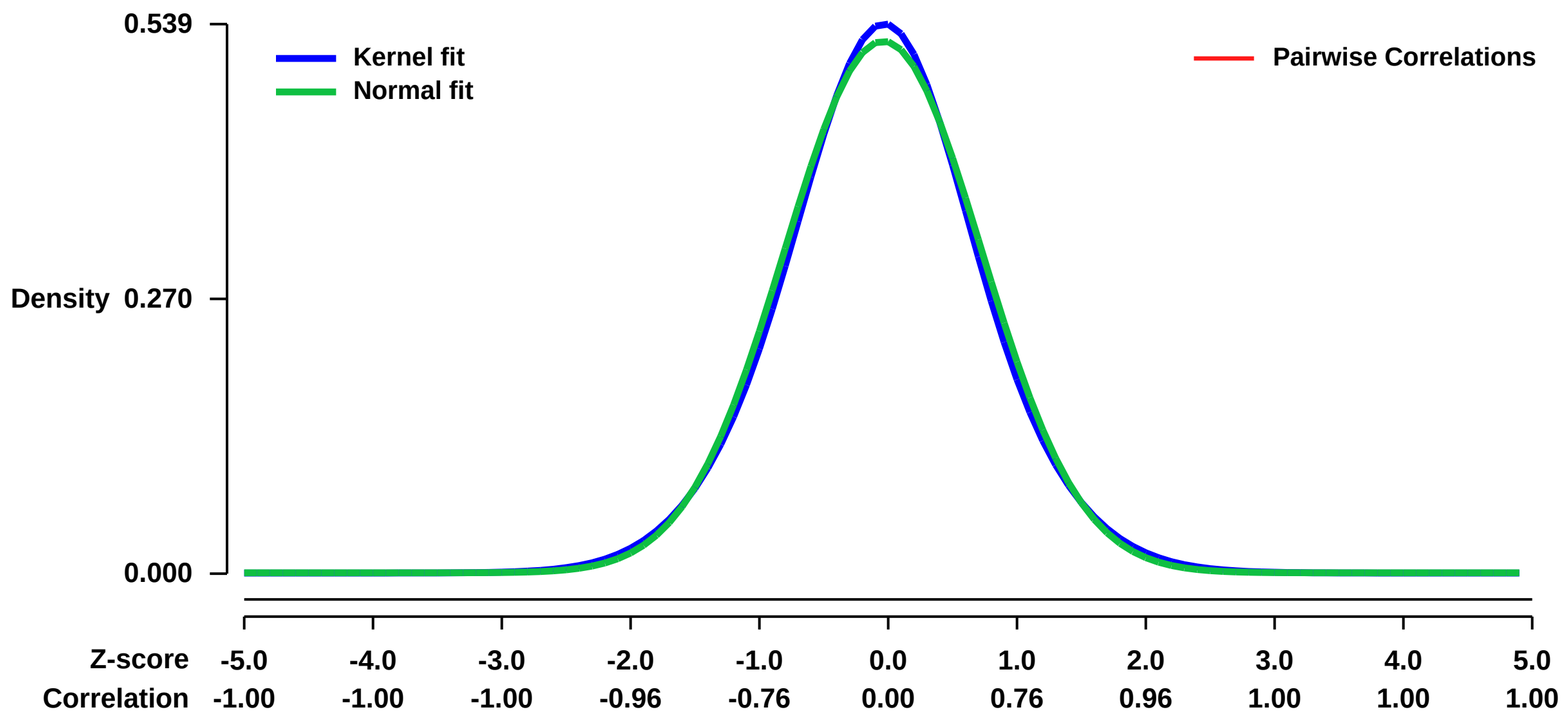

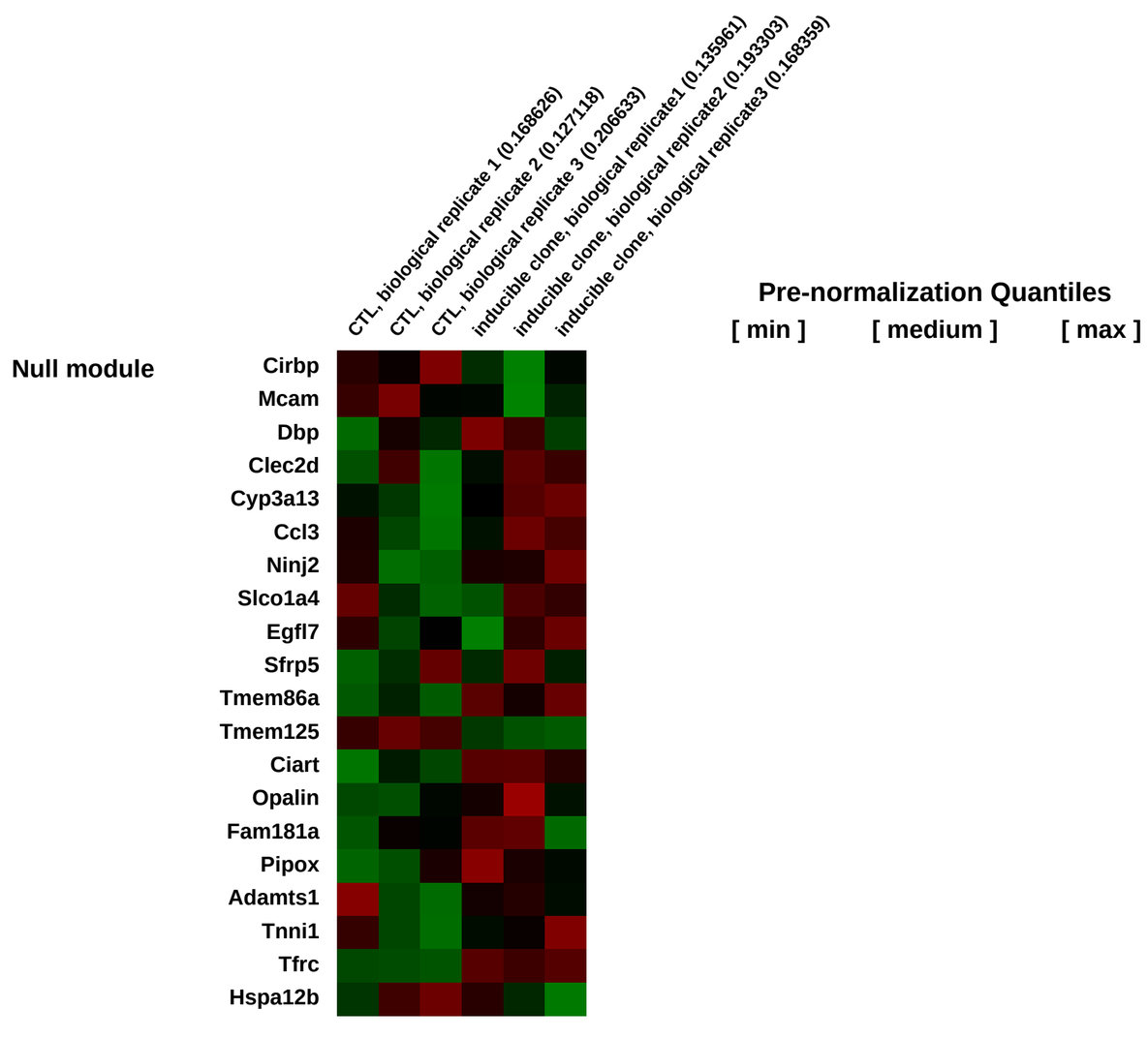

GEO Series "GSE12499" Expression Profiles

Num of samples in this series: 10

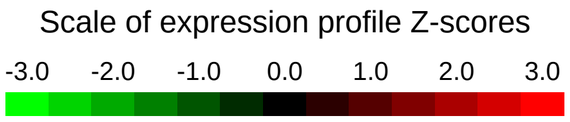

GEO Link:	http://www.ncbi.nlm.nih.gov/geo/query/acc.cgi?acc=GSE12499
Status:	Public on Feb 01 2009
Title:	Oct4-Induced Pluripotency in Adult Neural Stem Cells
Organism:	Mus musculus
Experiment type:	Expression profiling by array
Platform:	GPL1261
Pubmed ID:	19203577
Summary & Design:	**Summary:** The four transcription factors Oct4, Sox2, Klf4, and c-Myc can induce pluripotency in mouse and human fibroblasts. We previously described direct reprogramming of adult mouse neural stem cells (NSCs) by Oct4 and either Klf4 or c-Myc. NSCs endogenously express Sox2, c-Myc, and Klf4 as well as several intermediate reprogramming markers. Here we report that exogenous expression of the germline-specific transcription factor Oct4 is sufficient to generate pluripotent stem cells from adult mouse NSCs. These one-factor induced pluripotent stem (1F iPS) cells are similar to embryonic stem cells in vitro and in vivo. Not only can these cells be efficiently differentiated into NSCs, cardiomyocytes and germ cells in vitro, but they are also capable of teratoma formation and germline transmission in vivo. Our results demonstrate that Oct4 is required and sufficient to directly reprogram NSCs to pluripotency. **Overall design:** - NSC_4

Background corr dist: KL-Divergence = 0.0125, L1-Distance = 0.0370, L2-Distance = 0.0023, Normal std = 0.8572

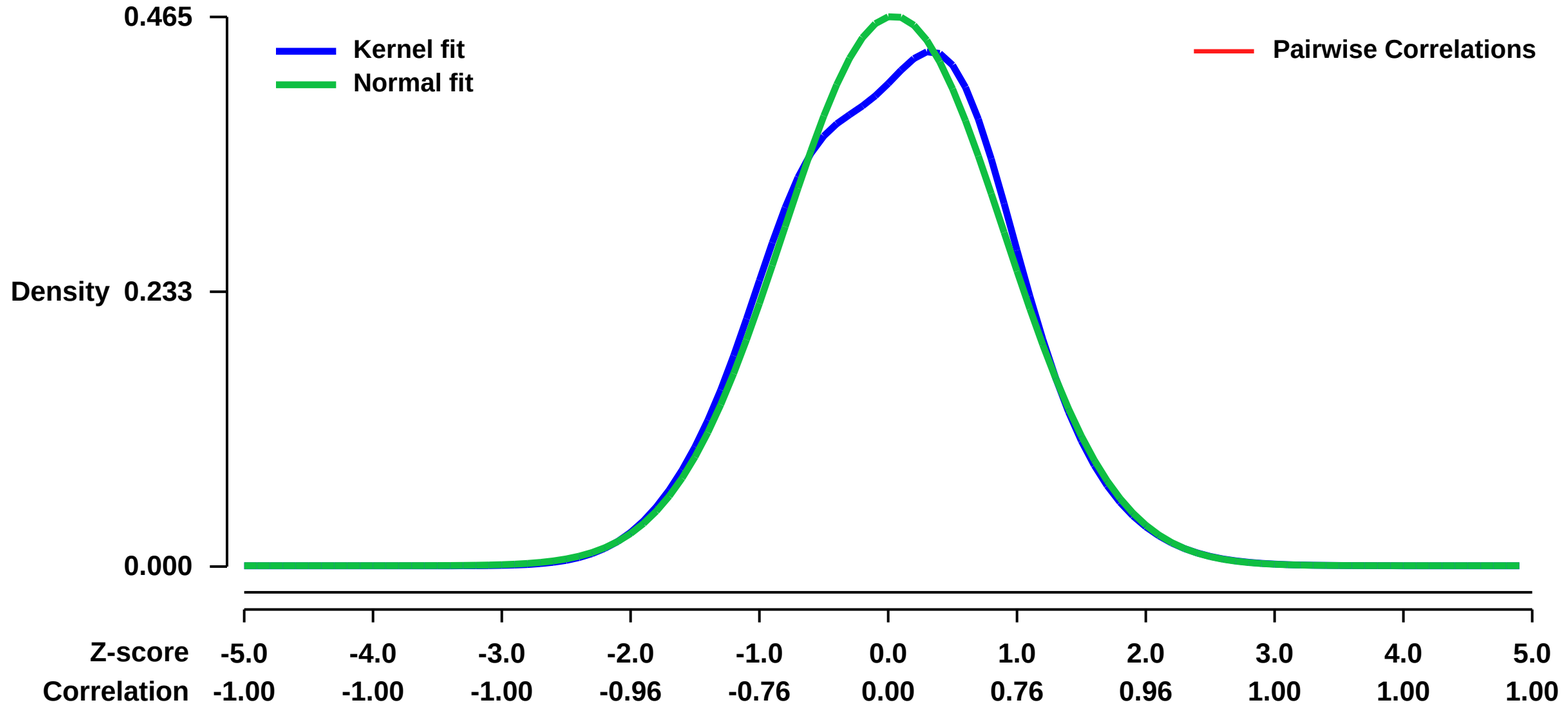

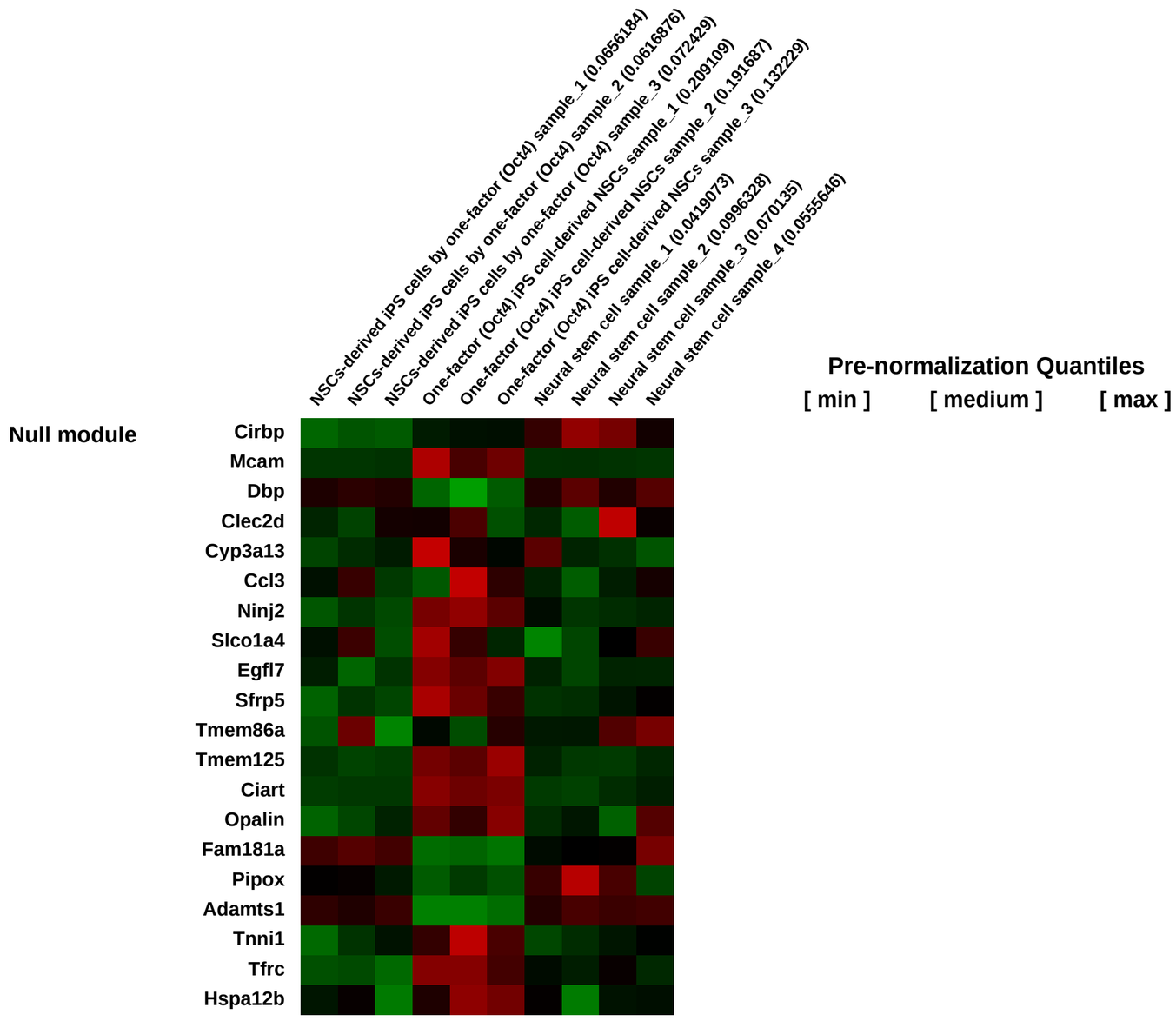

GEO Series "GSE35226" Expression Profiles

Num of samples in this series: 12

Scale of expression profile Z-scores

-3.0 -2.0 -1.0 0.0 1.0 2.0 3.0

GEO Link:	http://www.ncbi.nlm.nih.gov/geo/query/acc.cgi?acc=GSE35226
Status:	Public on Feb 01 2012
Title:	Systems approach identifies HIPK2 as a critical regulator of kidney tubulointerstitial fibrosis
Organism:	Mus musculus
Experiment type:	Expression profiling by array
Platform:	GPL1261
Pubmed ID:	22406746
Summary & Design:	**Summary:** We used an integrated computational/experimental systems biology approach to identify upstream protein kinases that regulate gene expression changes in kidneys of HIV-1 transgenic mice (Tg26), which have significant tubulo-interstitial fibrosis (TIF) and glomerulosclerosis (GS). We identified the homeo-domain interacting protein kinase 2 (HIPK2) as a key regulator of TIF and GS. HIPK2 was upregulated in kidneys of Tg26 and patients with various kidney diseases. HIV infection increased the protein level of HIPK2 by promoting oxidative stress, which inhibited Siah1-mediated proteasomal degradation of HIPK2. The data contain two sets: kidney corticies from WT and Tg26 mice and HEK293 transfected with HIPK2, HIPK2-DN and wild type. **Overall design:** Gene expression comparison between kidney cortecies of Tg26 HIV mouse model and wild type. Gene expression comparison between 293 HEK cells with HIPK-DN, HIPK-KO and normal.

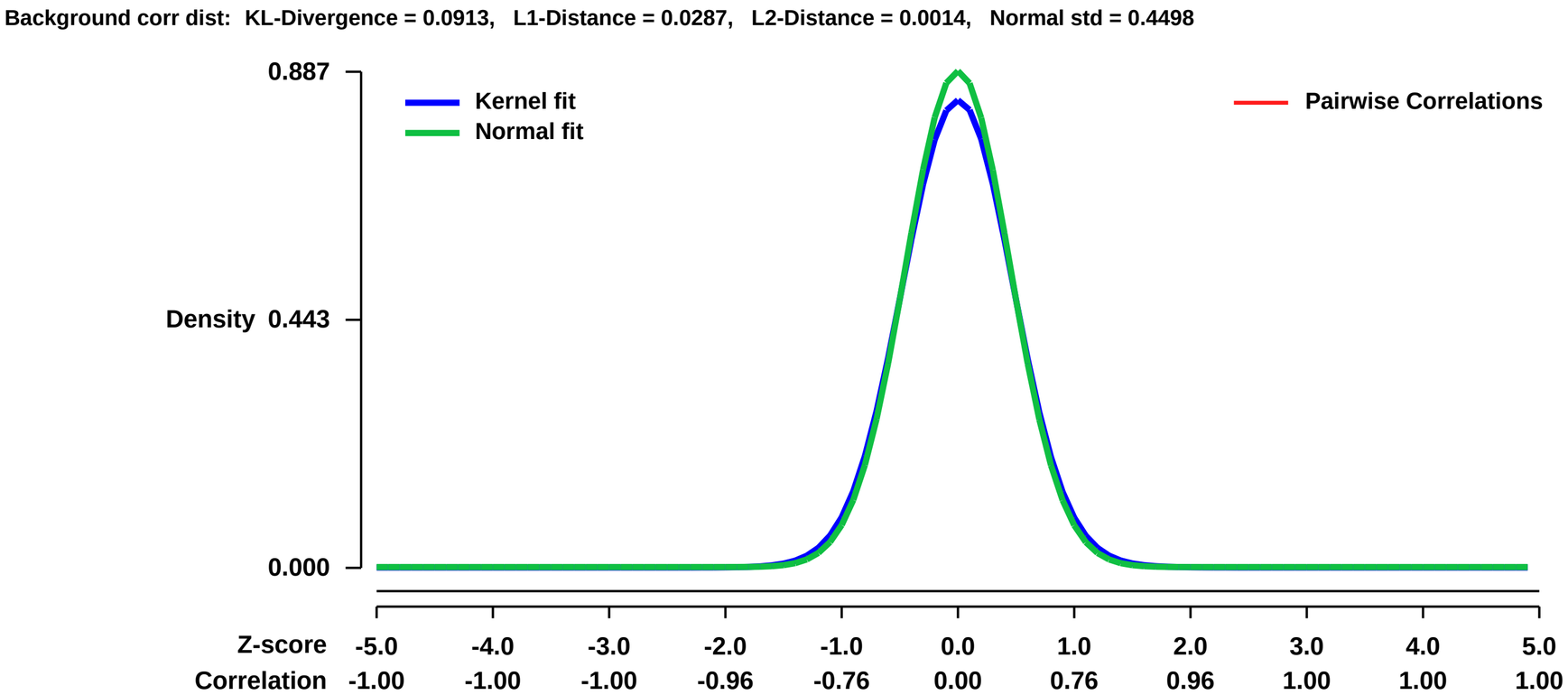

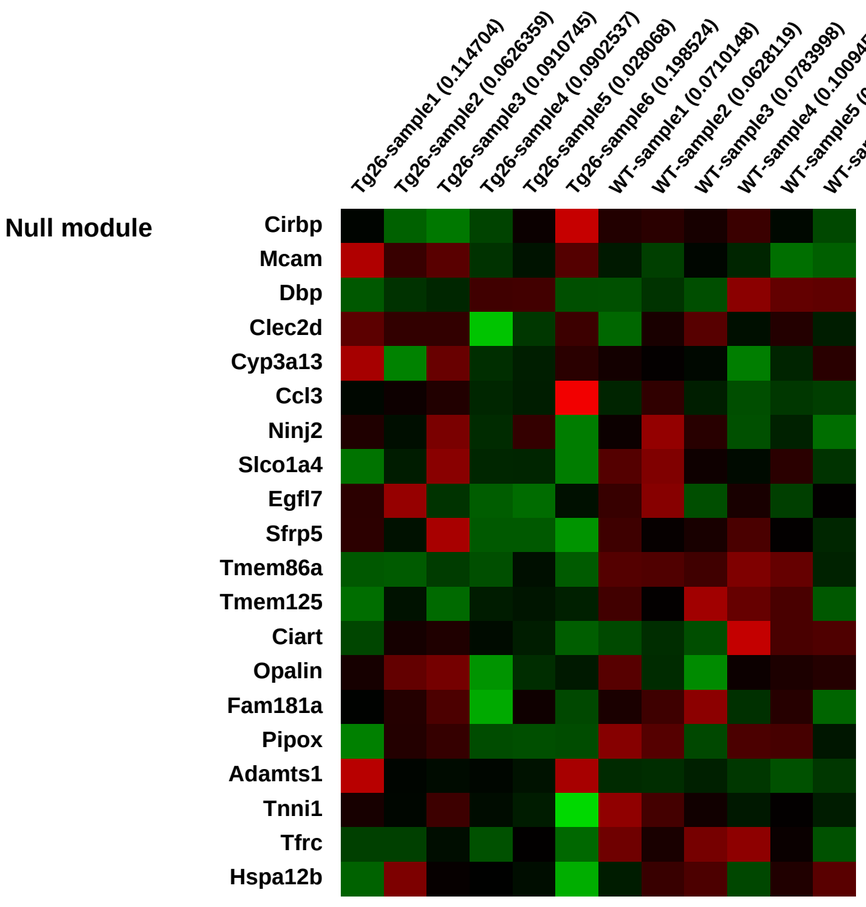

GEO Series "GSE6055" Expression Profiles

Num of samples in this series: 8

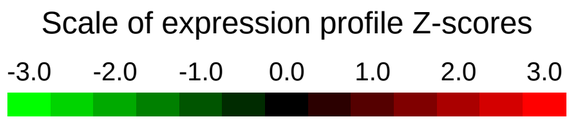

GEO Link:	http://www.ncbi.nlm.nih.gov/geo/query/acc.cgi?acc=GSE6055
Status:	Public on Dec 14 2006
Title:	Gene Expression Profiling Reveals Unique Pathways Associated with Differential Severity of Lyme Arthritis
Organism:	Mus musculus
Experiment type:	Expression profiling by array
Platform:	GPL1261
Pubmed ID:	17114465
Summary & Design:	**Summary:** **Keywords: disease state analysis, time course** **Overall design:** **Expression profiling of ankle tissues of C3H, C57BL/6, and C57BL/6-IL10-/- mice infected with B. burgdorfer (0, 1, 2, and 4 weeks post-infection)**

Background corr dist: **KL-Divergence = 0.0594, L1-Distance = 0.0221, L2-Distance = 0.0005, Normal std = 0.5419**

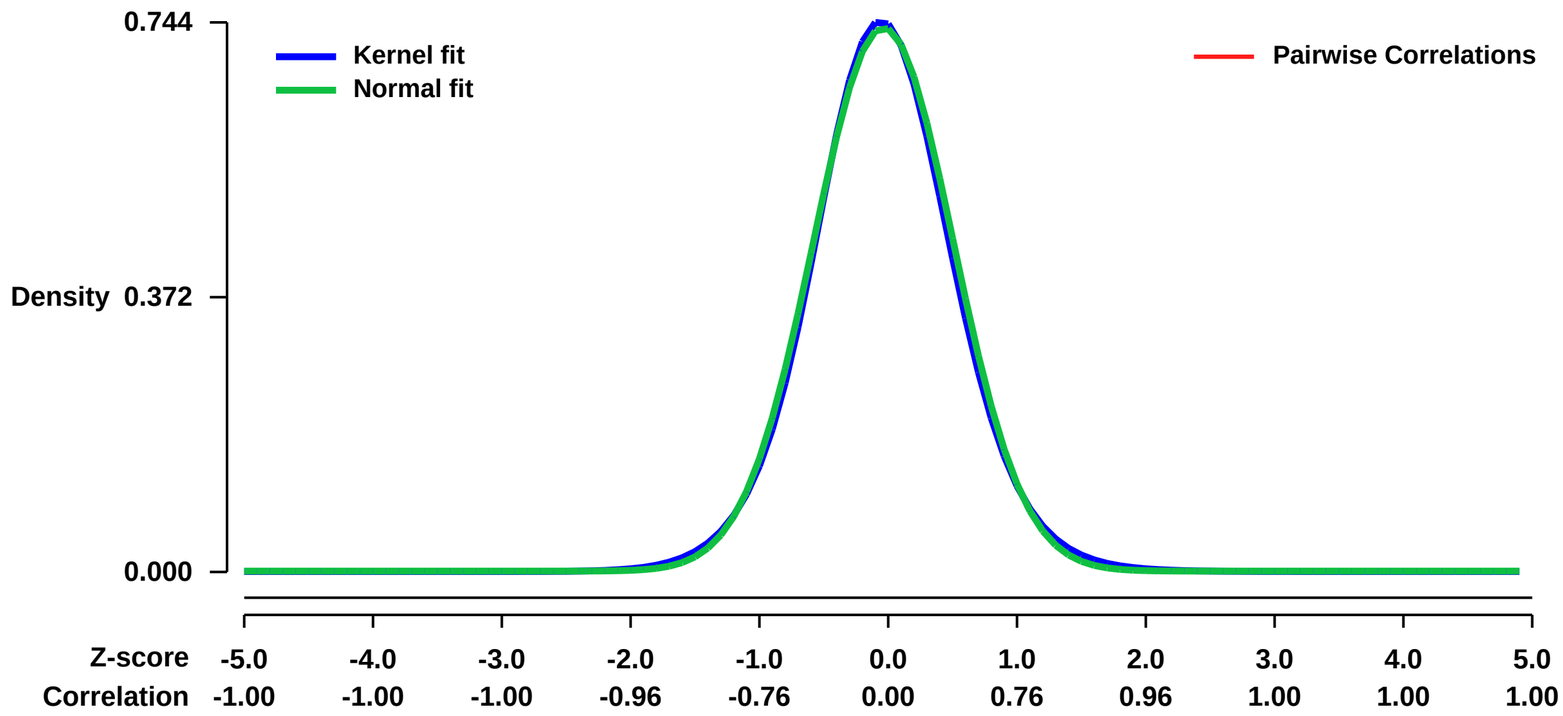

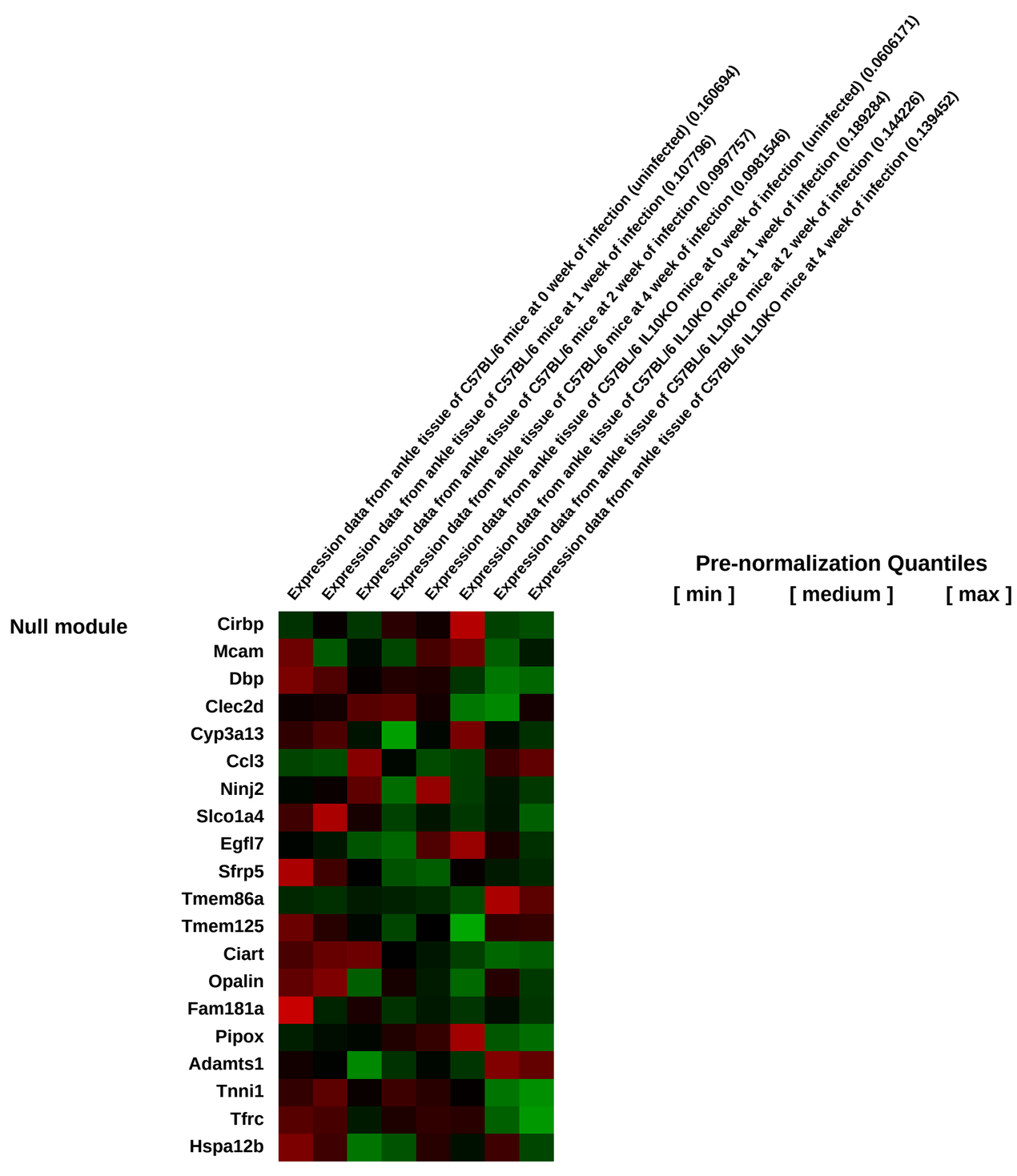

GEO Series "GSE4043" Expression Profiles

Num of samples in this series: 6

Scale of expression profile Z-scores

-3.0 -2.0 -1.0 0.0 1.0 2.0 3.0

GEO Link:	http://www.ncbi.nlm.nih.gov/geo/query/acc.cgi?acc=GSE4043
Status:	Public on Mar 07 2006
Title:	Gene profiling analysis of Src chemical rescue
Organism:	Mus musculus
Experiment type:	Expression profiling by array
Platform:	GPL1261
Pubmed ID:	16513984
Summary & Design:	**Summary:** The restoration of catalytic activity to mutant enzymes by small molecules is well-established for in vitro systems. Here we show that the protein tyrosine kinase Src R388A mutant can be rescued in live cells using the small molecule imidazole. Cellular rescue of a v-Src homolog was rapid and reversible and conferred predicted oncogenic properties. Using chemical rescue in combination with mass spectrometry, six known Src kinase substrates were confirmed, and several new protein targets identified. Chemical rescue data suggests that c-Src is active under basal conditions. Rescue of R388A c-Src also allowed contributions of Src to the MAP kinase pathway to be clarified. This chemical rescue approach is likely to be of broad utility in cell signaling. We were also interested in examining the impact of Src rescue on the kinetics of gene expression. Chronic gene expression changes in v-Src transformed colon cancer and NIH3T3 cells have been reported, but the chemical rescue method permits insights into rapid kinetic changes. We used gene microarray analysis of imidazole activated Src, 1 h after imidazole treatment of 8A7F cells as well as 6N7F control cells, a set of several genes show increases (>1.7-fold) at 1 h in the 8A7F cells and another set show decreases (>1.7-fold) at 1 h with minimal changes in 6N7F control cells. Thirteen of these genes were further analyzed using real-time RT-PCR and most of the genes tested showed similar changes using both techniques. These gene changes were not reported in cells chronically transformed with v-Src or rapidly stimulated with growth factors suggesting that rapid initiation of Src-mediated tyrosine phosphorylation may induce a specialized pattern of gene expression changes. However, these earlier experiments were done under different conditions which may also contribute to gene effects. **Keywords:** time course, cell type comparison **Overall design:** using Murine Genome MOE430 2.0 GeneChips as described in the Affymetrix website.

Background corr dist: KL-Divergence = 0.0386, L1-Distance = 0.0241, L2-Distance = 0.0006, Normal std = 0.6315

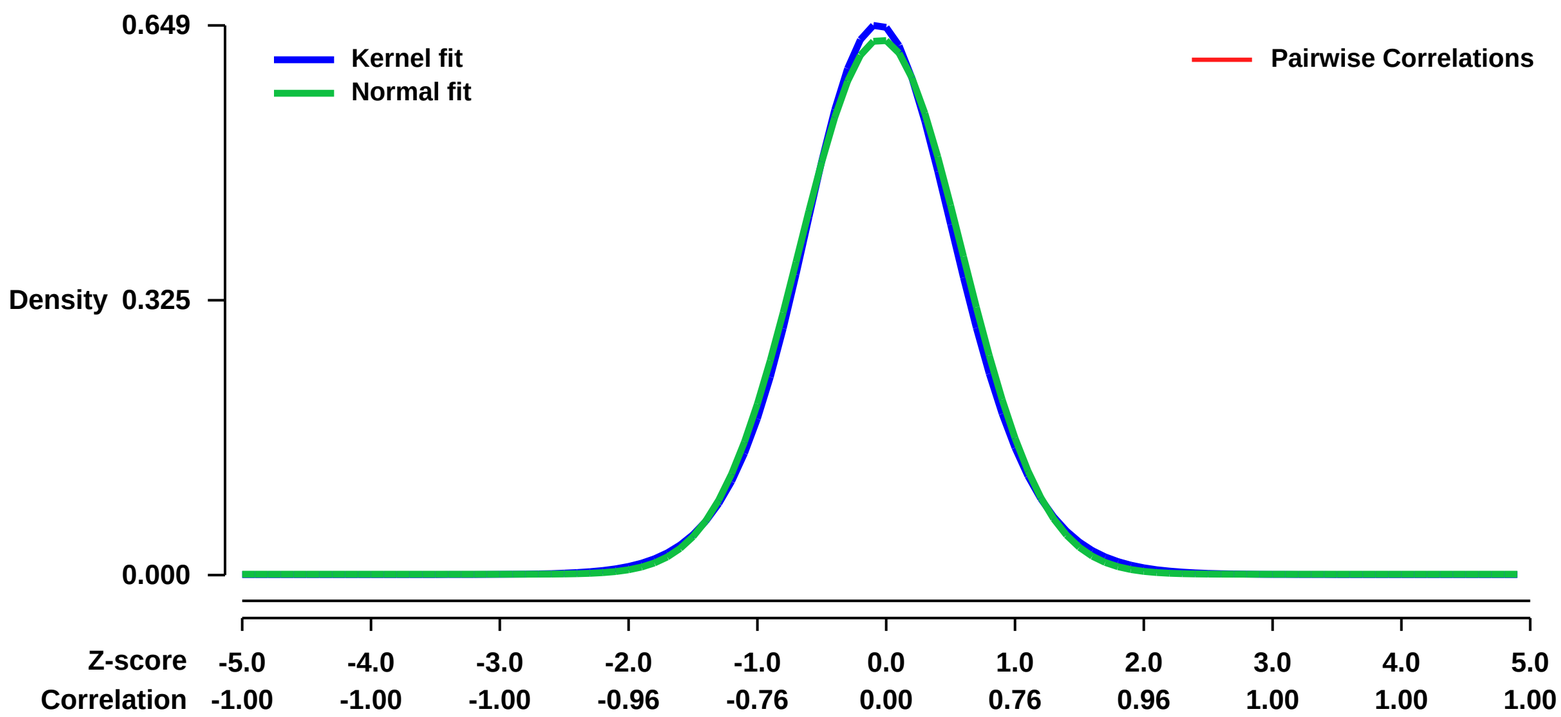

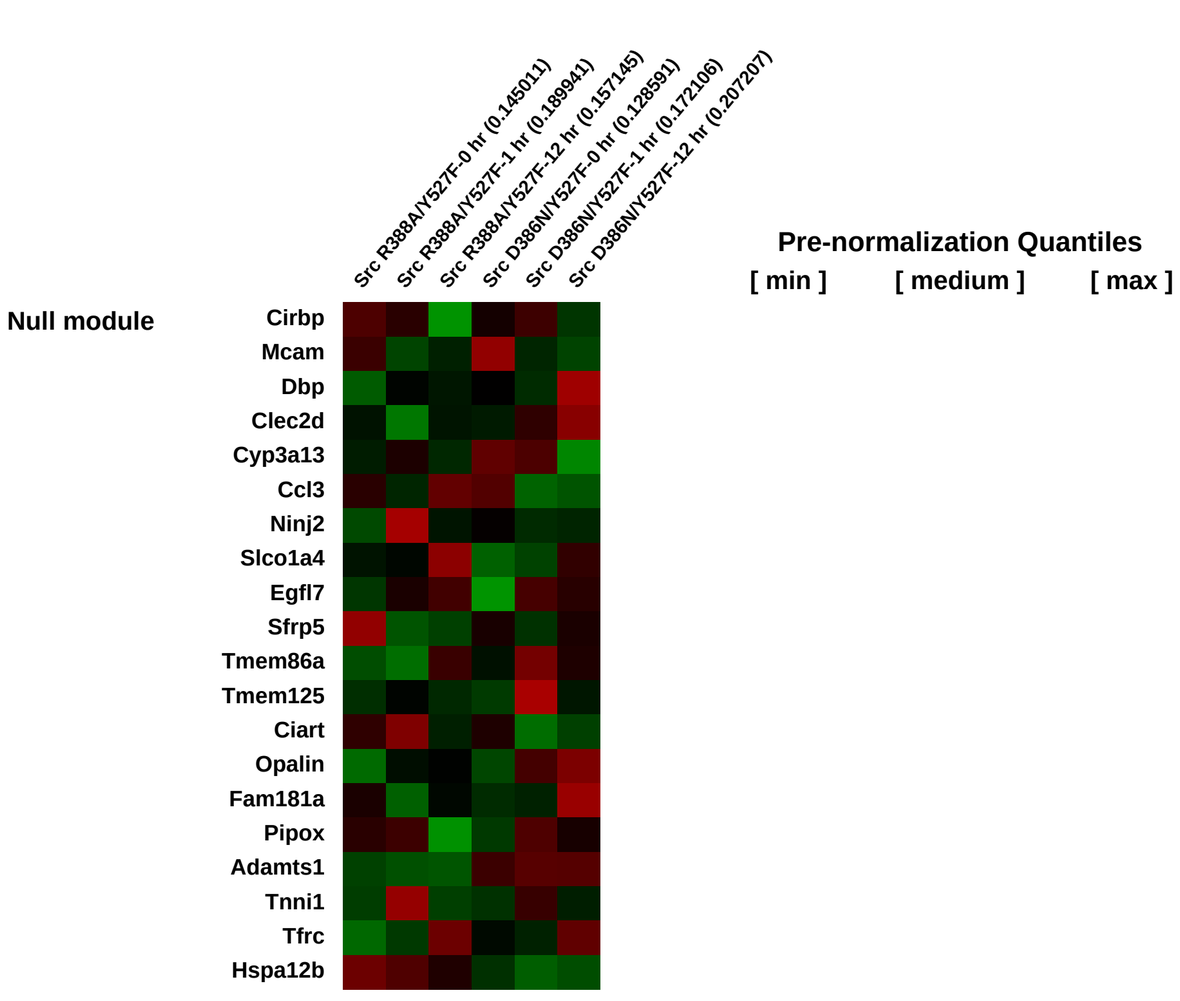

GEO Series "GSE6084" Expression Profiles

Num of samples in this series: 12

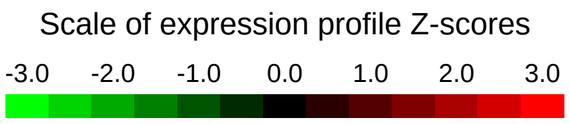

GEO Link:	**http://www.ncbi.nlm.nih.gov/geo/query/acc.cgi?acc=GSE6084**
Status:	**Public on Jan 10 2009**
Title:	**Expression data from Murine T cell in response to cycloheximide treatment**
Organism:	**Mus musculus**
Experiment type:	**Expression profiling by array**
Platform:	**GPL1261**
Pubmed ID:	
Summary & Design:	**Summary:** **Cycloheximide has been used for inhibiting protein synthesis in order to identify IL-2 direct targeted genes in T cells, but the effects of cycloheximide itself on genomewide genes are not well defined** **We conducted a global analysis of cycloheximide regulated genes in mouse T cell line CTLL-2 using Affymetrix mouse genome array, and identified 213 genes differentially expressed (?1.5-fold change) in response to cycloheximide 30min after adding cylcoheximide to T cells cultured without IL-2 for 14 hours. These genes involve in a number biological processes.** **Keywords: stress response** **Overall design:** **Murine cytotoxic T lymphocyte cell line CTLL-2, derived from a C57BL/6 mouse, is an IL-2 dependent cell line. Cells were cultured in D10 medium in an incubator with 5% CO2 at 37oC to mid-log phase (~2 X 105 cells/mL), and collected by centrifugation, washed with phosphate buffered saline (PBS) (Invitrogen), resuspended at 1 X 106 cells/mL in the medium without IL-2 (IL-2 starvation) and cultured for 14 hours (No IL-2 stimulation, T0, 5 reps), followed by adding cycloheximide (20 ?g/mL) for 30min (T4-CHX, 4 reps). Total RNA were extracted from the cells and was hybridized on Affymetrix GeneChip Mouse Genome 430 2.0 Array.**

Background corr dist: KL-Divergence = 0.1175, L1-Distance = 0.0721, L2-Distance = 0.0097, Normal std = 0.5089

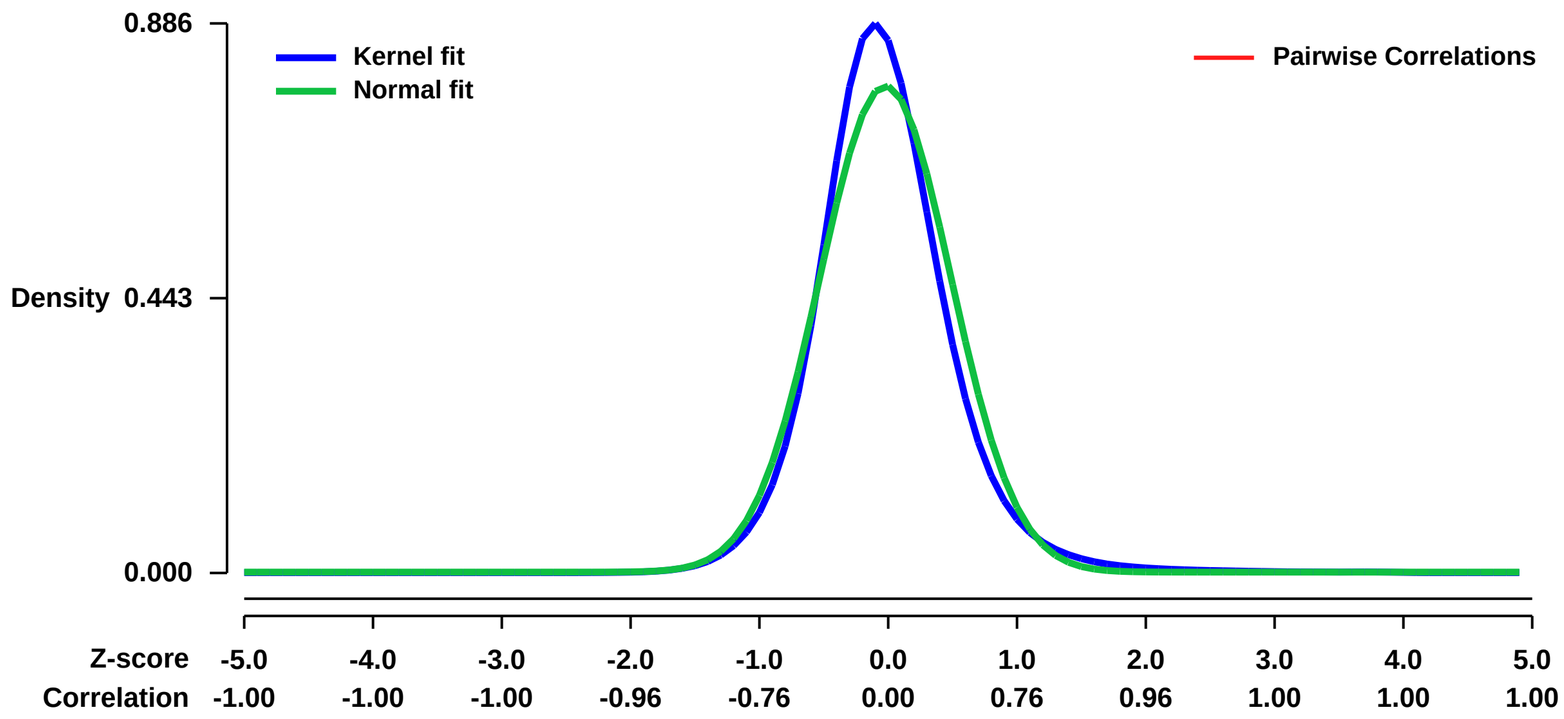

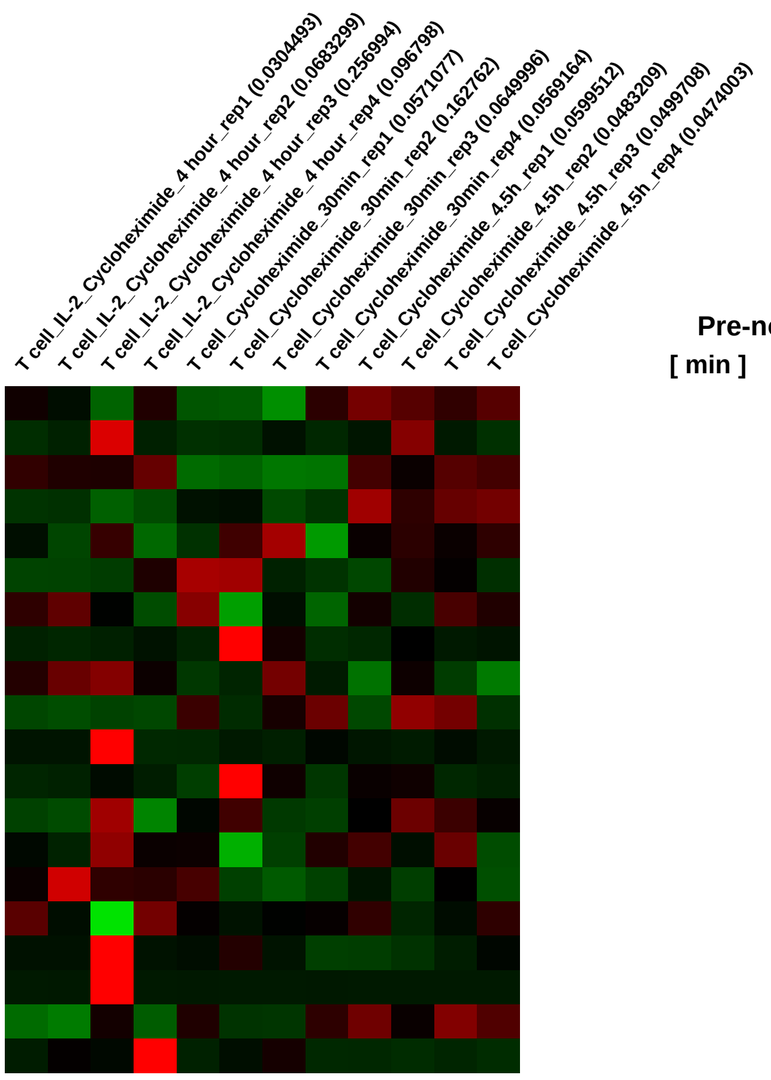

GEO Series "GSE9892" Expression Profiles

Num of samples in this series: 12

Scale of expression profile Z-scores

-3.0 -2.0 -1.0 0.0 1.0 2.0 3.0

GEO Link:	http://www.ncbi.nlm.nih.gov/geo/query/acc.cgi?acc=GSE9892
Status:	Public on Feb 28 2009
Title:	Gene expression profiling in acute murine autoimmune hepatitis
Organism:	Mus musculus
Experiment type:	Expression profiling by array
Platform:	GPL1261
Pubmed ID:	19490417
Summary & Design:	**Summary:** The etiology of autoimmune hepatitis is poorly understood but likely involves Th1 cells producing IFN-¸‡. BALB/c background TGF-¸†1-/- mice rapidly develop fulminant Th1-mediated autoimmune hepatitis. Our aims are to profile liver gene expression in TGF-¸†1-/- mice, to identify gene expression pathways dependent on IFN-¸‡ as possible targets for rational therapy, and to test potential targets directly in vivo in mice. **Keywords: Comparative analysis of gene expression in livers of WT, TGFB1 & IFN knockout mice** **Overall design:** DNA microarray analyses were applied to liver RNA from TGF-¸†1-/- mice, TGF-¸†1-/- /IFN-¸‡-/- mice, and TGF-¸†1+/+ littermate controls. 3 mice from each group were analyzed in this study.

Background corr dist: KL-Divergence = 0.0984, L1-Distance = 0.0375, L2-Distance = 0.0025, Normal std = 0.4545

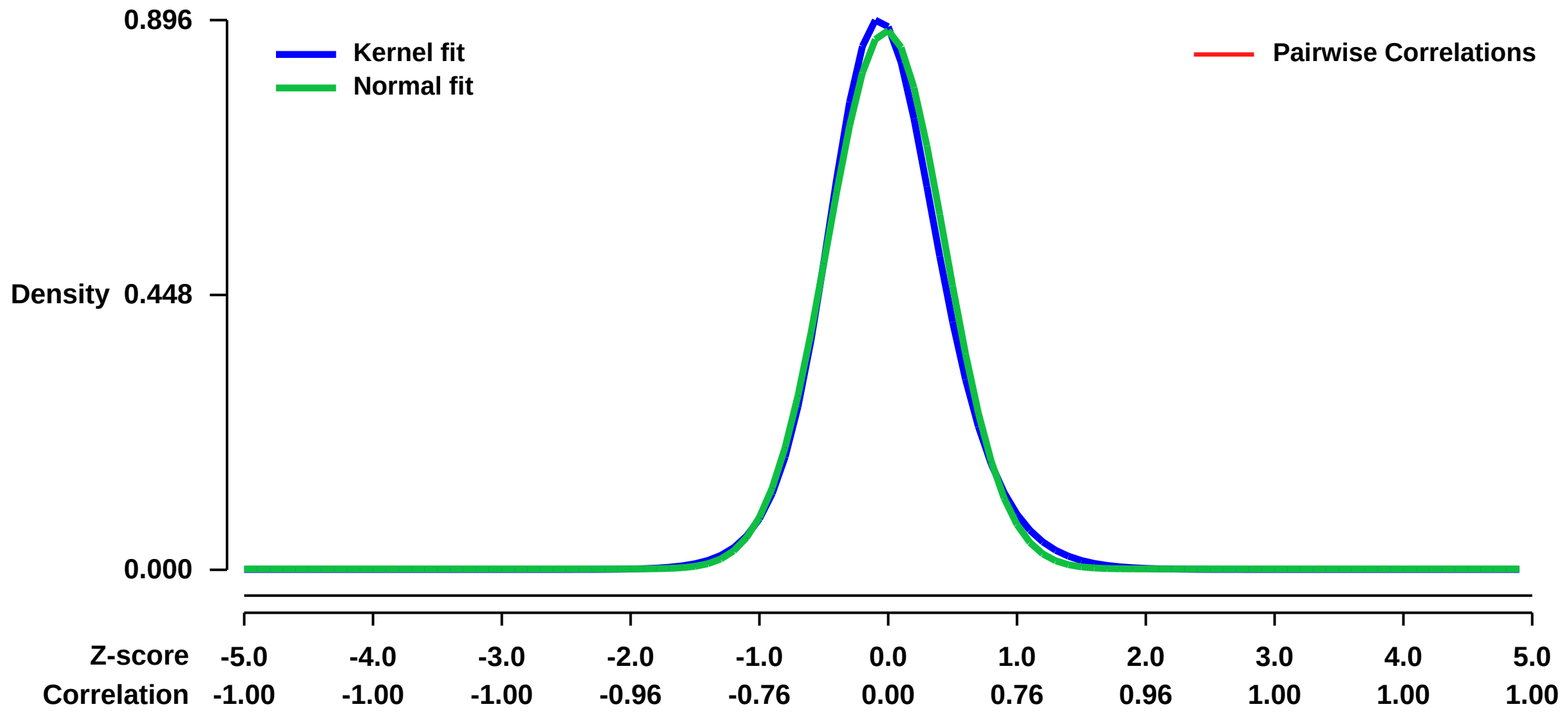

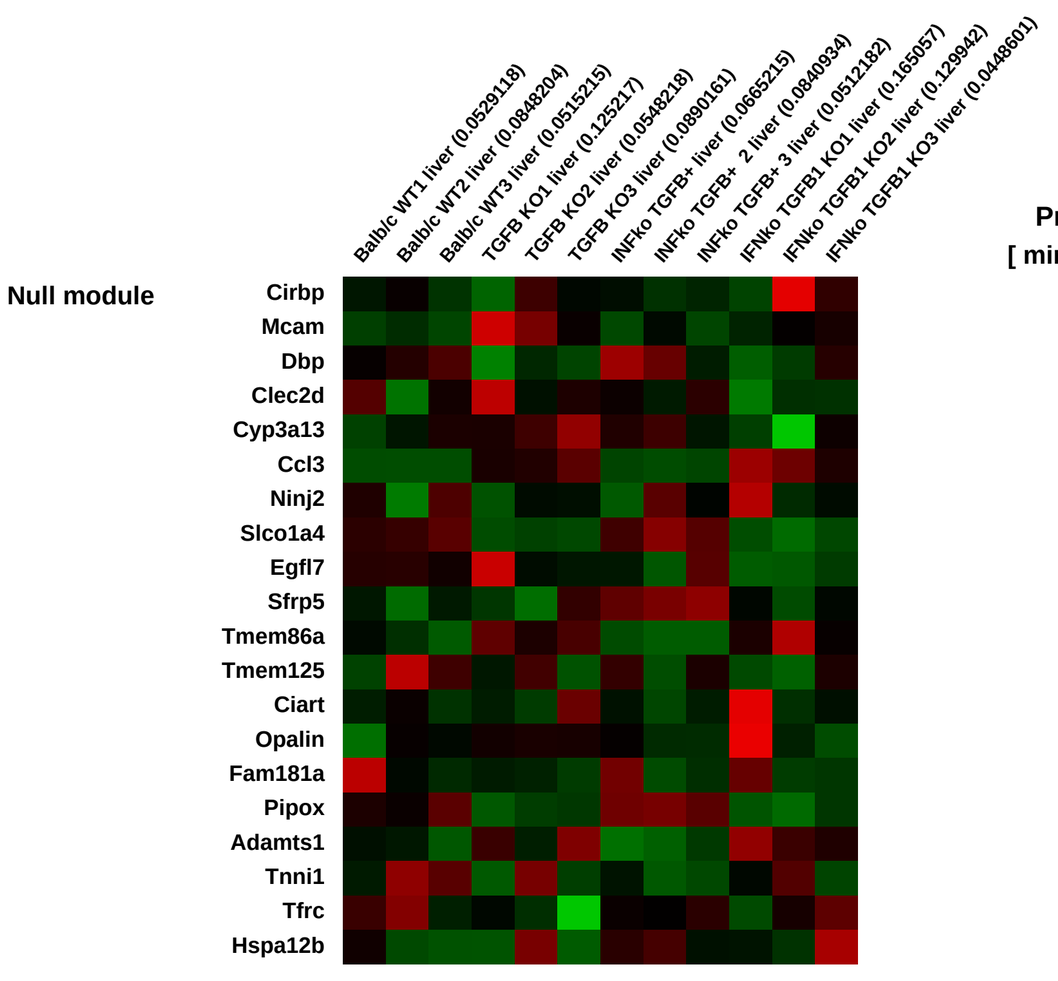

GEO Series "GSE33770" Expression Profiles

Num of samples in this series: 8

Scale of expression profile Z-scores

-3.0 -2.0 -1.0 0.0 1.0 2.0 3.0

GEO Link:	**http://www.ncbi.nlm.nih.gov/geo/query/acc.cgi?acc=GSE33770**
Status:	**Public on Nov 12 2013**
Title:	**Microarray Studies on the STAT5A MUTANT.**
Organism:	**Mus musculus**
Experiment type:	**Expression profiling by array**
Platform:	**GPL1261**
Pubmed ID:	
Summary & Design:	**Summary:** **Stat5+/- mice were bred into the C57BL/6 background. Stat5+/- mice were intercrossed and mouse embryonic fibroblasts (MEFs) were isolated from 12.5-13.5-day WT or Stat5-/- fetuses. The retroviral-expression vector carrying a DNA binding domain mutant Stat5A (E437/E438?AA) or tyrosine-phosphorylated Stat5A Y694F mutation based on an MSCV-IRES-GFP backbone (gift from Richard Moriggl, Ludwig-Boltzmann Institute, Vienna, Austria) was infected into Stat5-/- MEFs. FACS was used to select GFP+ cells. After 5 hours starvation in serum free medium with 0.1% of BSA, MEFs were treated with growth hormone for 2 hours. Total cellular RNA from each group of the MEFs was extracted with TRIzol reagent (Invitrogen) according to the manufacturer's instructions. Microarray analyses were performed using Affymetrix Mouse Genome 430 2.0 GeneChips (Affymetrix, Santa Clara, CA) (four groups, biological replicates for each group). Expression values were determined with GeneChip Operating Software (GCOS) v1.1.1 software. RMA signals were summarized using GeneSpring GX 10.0.1 (Agilent) and normalized by quantile normalization. All data analysis was performed with GeneSpring software GX 10.01.** **Overall design:** **Total 4 groups (EA, EA_GH, YF, YF_GH), biological duplicate replication for each group**

Background corr dist: KL-Divergence = 0.0380, L1-Distance = 0.0916, L2-Distance = 0.0110, Normal std = 0.7913

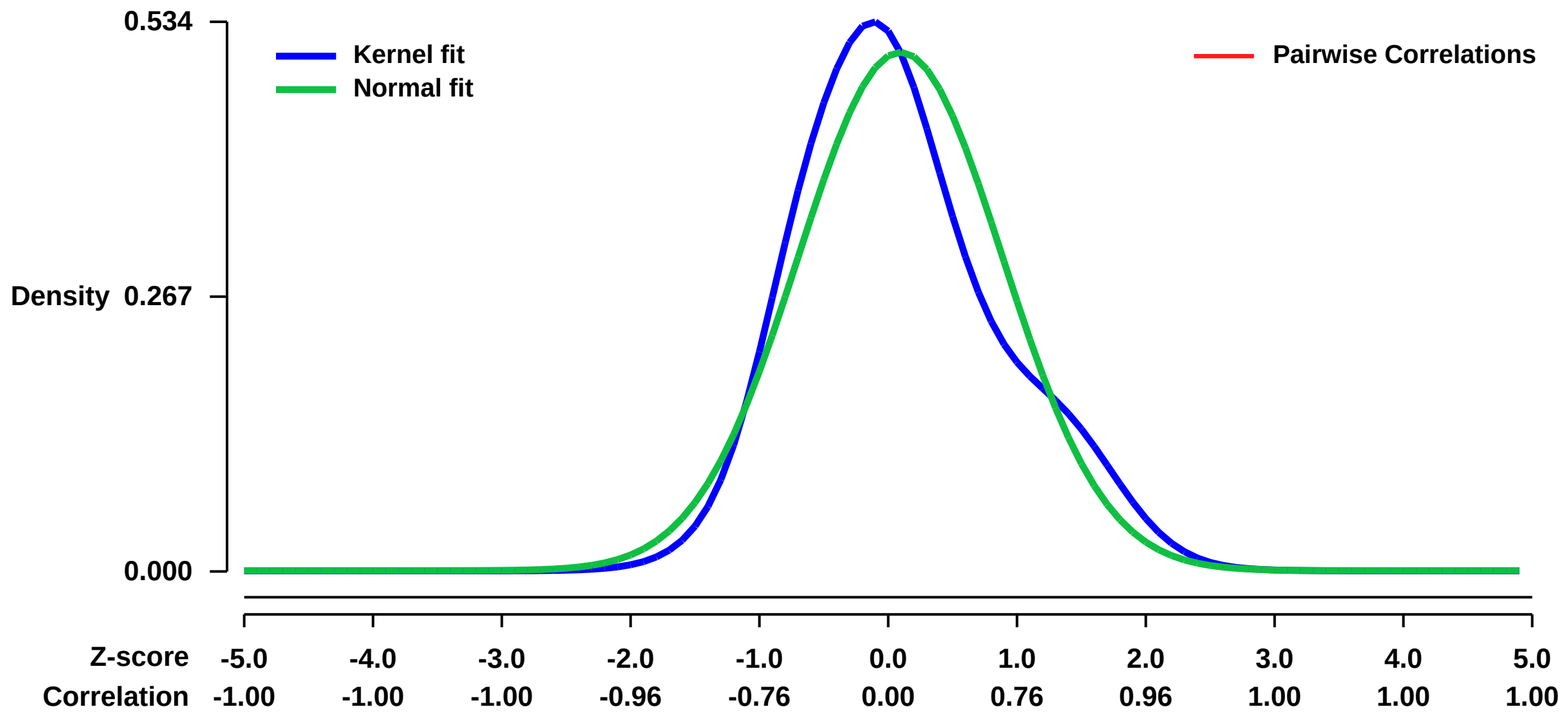

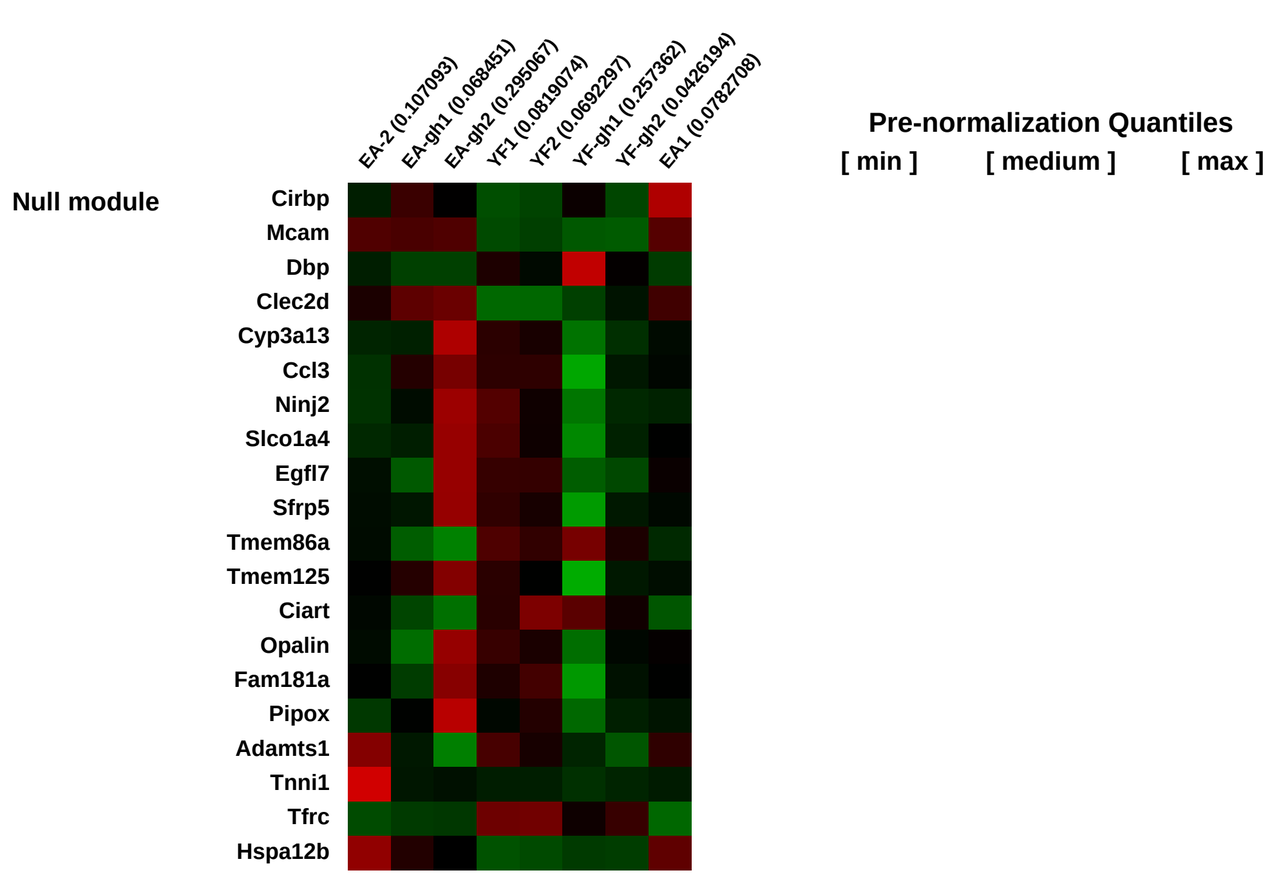

GEO Series "GSE43059" Expression Profiles

Num of samples in this series: 8

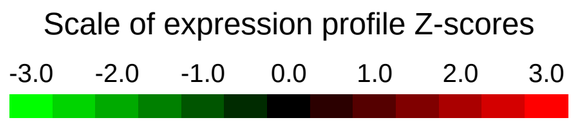

GEO Link:	**http://www.ncbi.nlm.nih.gov/geo/query/acc.cgi?acc=GSE43059**
Status:	**Public on Dec 01 2013**
Title:	**Role of Jmjd2b and Jmjd2c in mESCs identity**
Organism:	**Mus musculus**
Experiment type:	**Expression profiling by array**
Platform:	**GPL1261**
Pubmed ID:	**24361252**
Summary & Design:	**Summary:** **We used microarray to determine the changes in gene expression profile after KD of Jmjd2b and Jmjd2c compared to Anti-GFP KD from mES cells** **Overall design:** **Mouse ES cells were infected with AntiGFP, Jmjd2b and Jmjd2c shRNAs lentivirus, puromycin selected, passage them 2-3 times, collected for RNA isolation and gene expression**

Background corr dist: **KL-Divergence = 0.0472, L1-Distance = 0.0195, L2-Distance = 0.0004, Normal std = 0.5768**

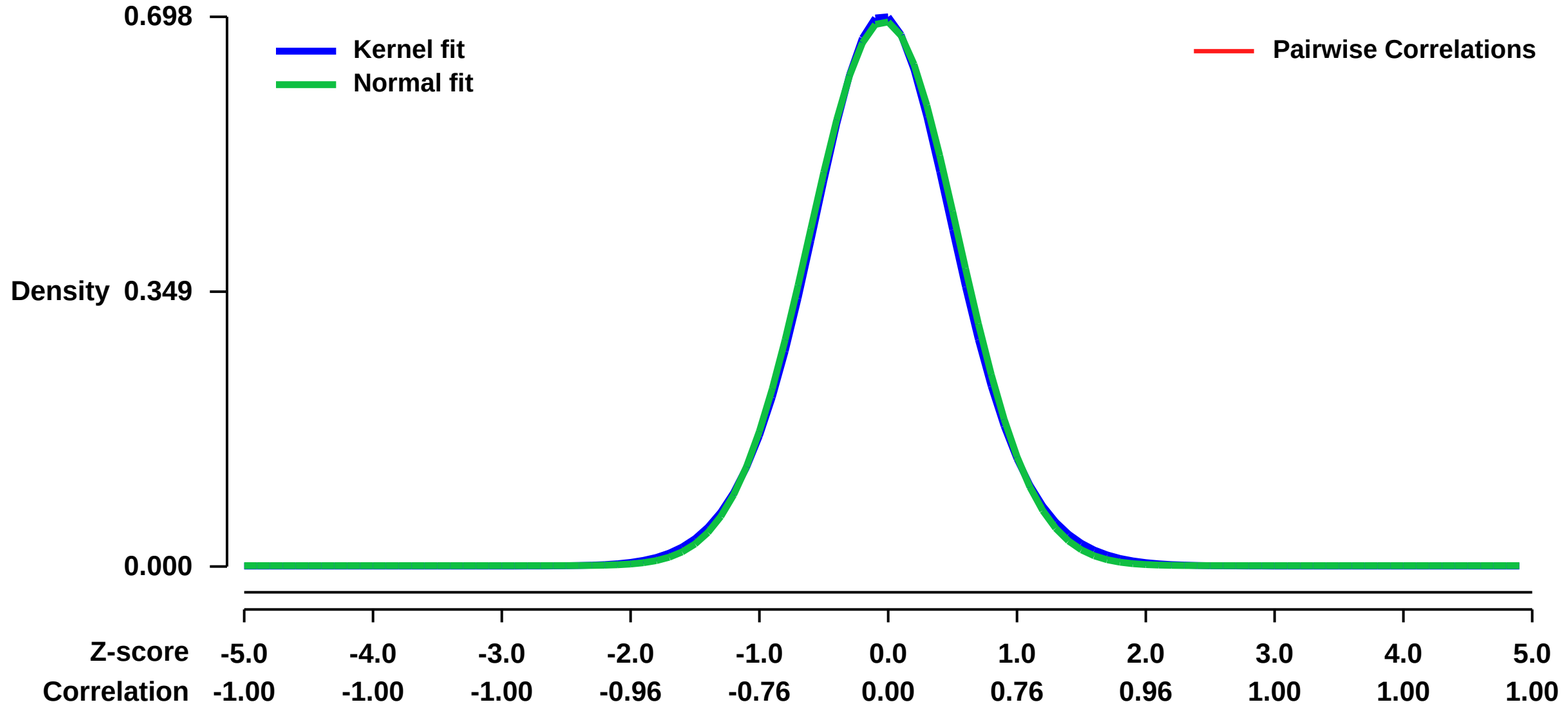

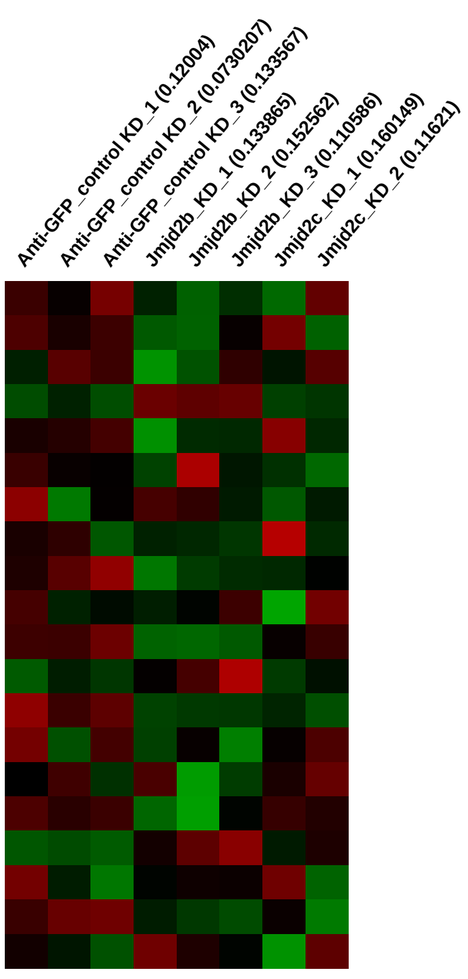

GEO Series "GSE5332" Expression Profiles

Num of samples in this series: 12

Scale of expression profile Z-scores

-3.0 -2.0 -1.0 0.0 1.0 2.0 3.0

GEO Link:	http://www.ncbi.nlm.nih.gov/geo/query/acc.cgi?acc=GSE5332
Status:	Public on Dec 01 2007
Title:	mTOR pathway controls mitochondrial gene expression and respiration through the YY1/PGC-1alpha transcriptional complex
Organism:	Mus musculus
Experiment type:	Expression profiling by array
Platform:	GPL1261
Pubmed ID:	18046414
Summary & Design:	**Summary:** Mitochondrial oxidative function is tightly controlled to maintain energy homeostasis in response to nutrient and hormonal signals. An important cellular component in the energy sensing response is the target of rapamycin (TOR) kinase pathway; however whether and how mTOR controls mitochondrial oxidative activity is unknown. Here, we show that mTOR kinase activity stimulates mitochondrial gene expression and oxidative function. In skeletal muscle cells and TSC2-/- MEFs, the mTOR inhibitor rapamycin largely decreased gene expression of mitochondrial transcriptional regulators such as PGC-1alpha and the transcription factors ERRalpha and NRFs. As a consequence, mitochondrial gene expression and oxygen consumption were reduced upon mTOR inhibition. Using computational genomics, we identified the transcription factor YY1 as a common target of mTOR and PGC-1alpha that controls mitochondrial gene expression. Inhibition of mTOR resulted in a failure of YY1 to interact and be coactivated by PGC-1alpha. Notably, knock-down of YY1 in skeletal muscle cells caused a significant decrease in mRNAs of mitochondrial regulators and mitochondrial genes that resulted in a decrease in respiration. Moreover, YY1 was required for rapamycin-dependent repression of mitochondrial genes. Thus, we have identified a novel mechanism in which a nutrient sensor (mTOR) balances energy metabolism via transcriptional control of mitochondrial oxidative function. These results have important implications for our understanding of how these pathways might be altered in metabolic diseases and cancer. **Keywords:** comparative genomics, drug treatment response **Overall design:** Data were analyzed by RMA (with default settings) in BioConductor 1.2 -- one batch for the Rapamycin vs. Vehicle, and another batch for the PGC vs GFP.

Background corr dist: KL-Divergence = 0.0285, L1-Distance = 0.0213, L2-Distance = 0.0006, Normal std = 0.6590

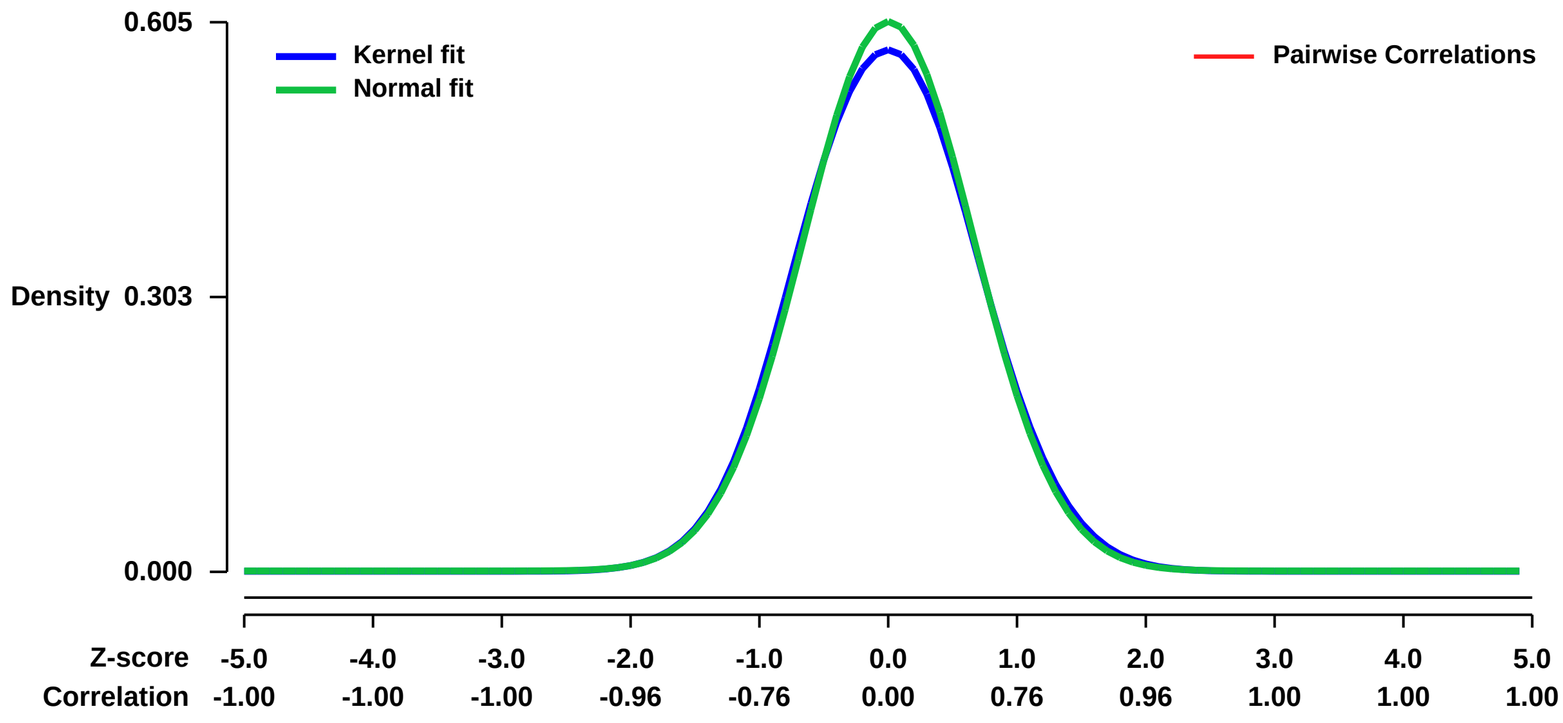

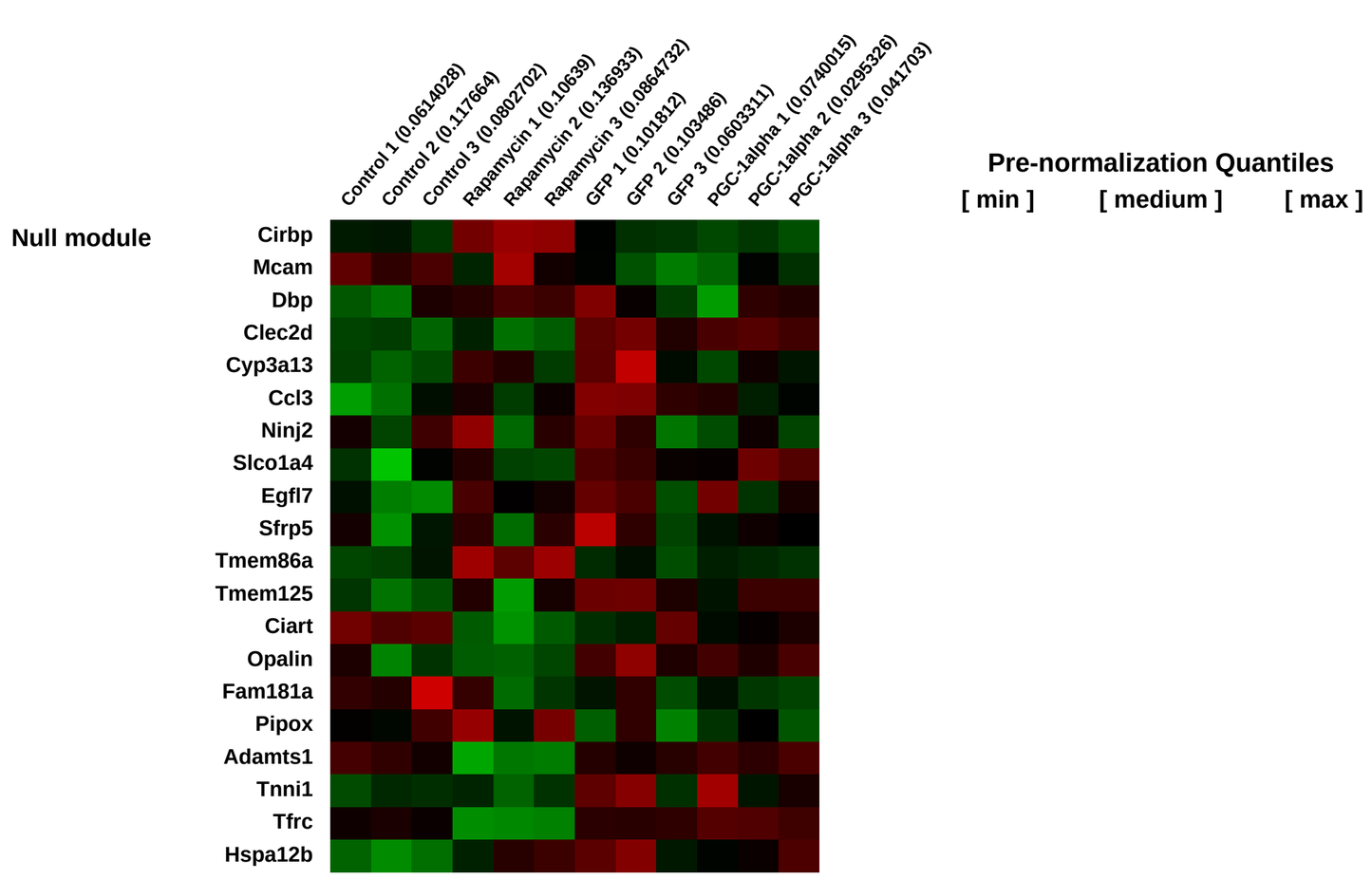

GEO Series "GSE34324" Expression Profiles

Num of samples in this series: 12

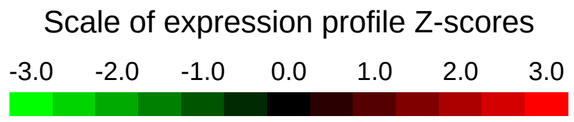

GEO Link:	**http://www.ncbi.nlm.nih.gov/geo/query/acc.cgi?acc=GSE34324**
Status:	**Public on Feb 26 2013**
Title:	**Gene expression by Retinoic Acid in mouse Dendritic Cells**
Organism:	**Mus musculus**
Experiment type:	**Expression profiling by array**
Platform:	**GPL1261**
Pubmed ID:	**23322377**
Summary & Design:	**Summary:** **The purpose of this study was to determine and clarify the retinoic effect on the gene expression profile for mouse dendritic cells.** **Overall design:**

Background corr dist: **KL-Divergence = 0.0982, L1-Distance = 0.0355, L2-Distance = 0.0026, Normal std = 0.4484**

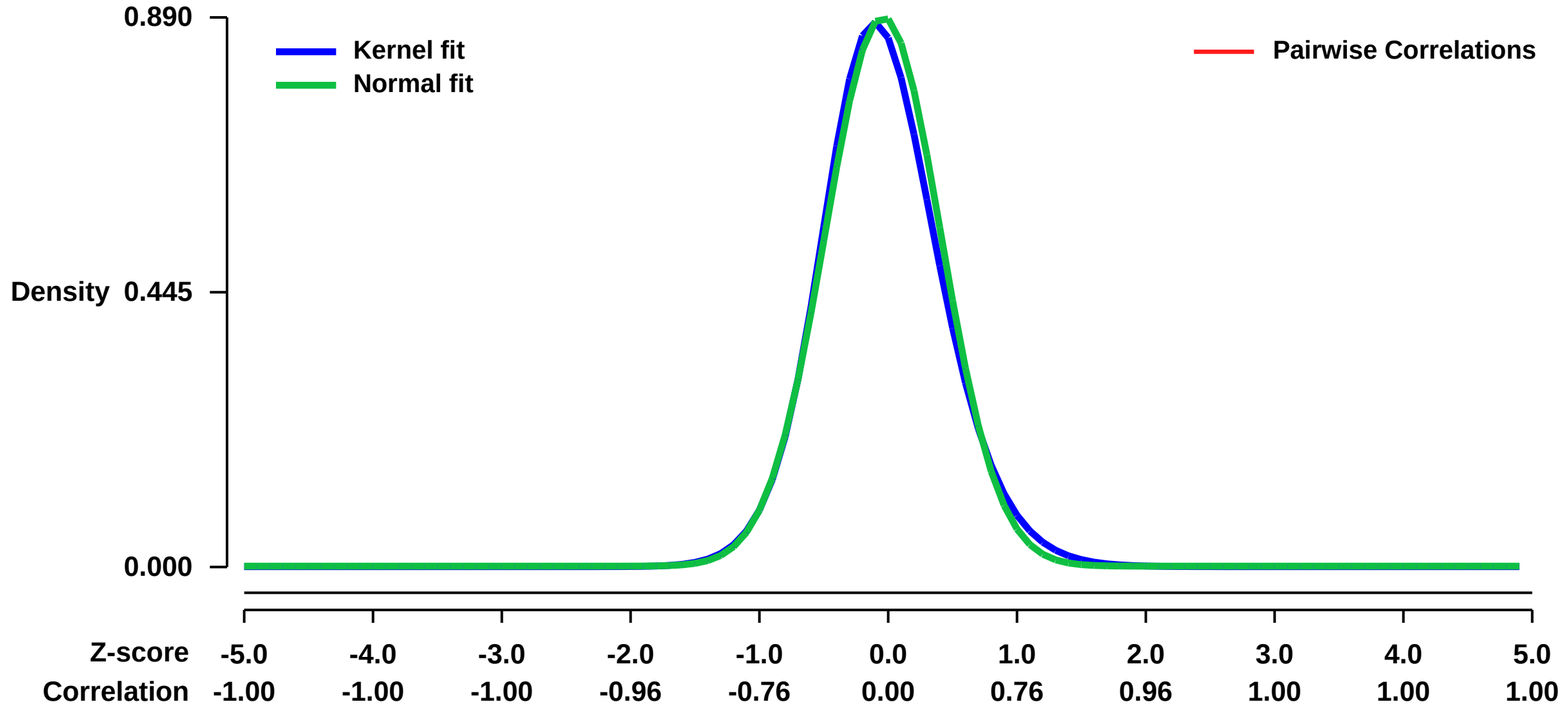

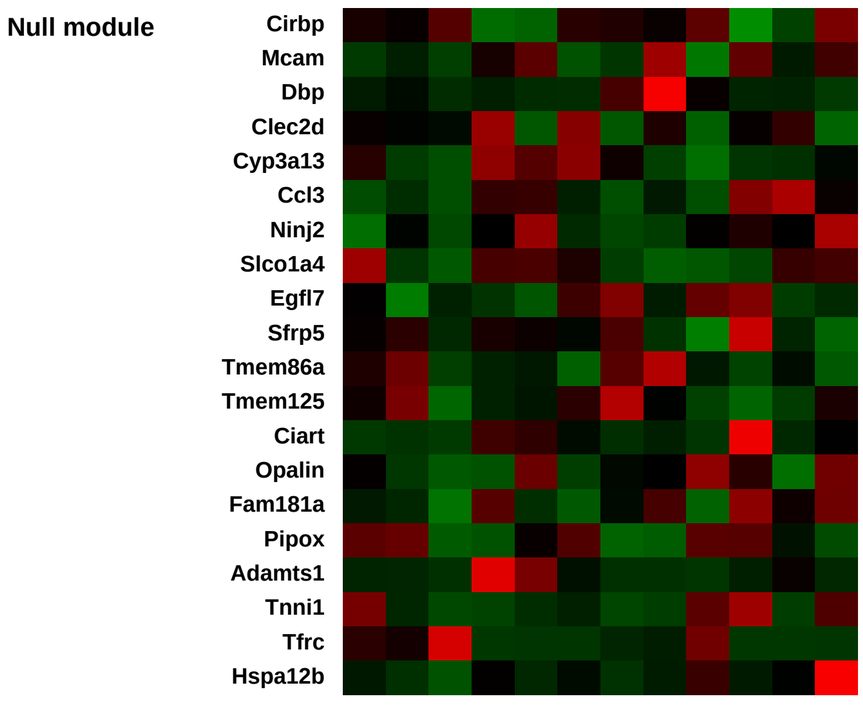

GEO Series "GSE24437" Expression Profiles

Num of samples in this series: 6

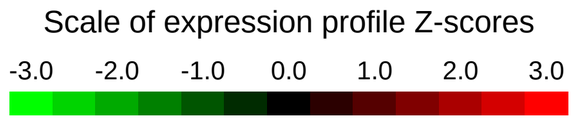

GEO Link:	http://www.ncbi.nlm.nih.gov/geo/query/acc.cgi?acc=GSE24437
Status:	Public on Sep 30 2010
Title:	Persistence of effector memory Th1 cells is regulated by the homeobox only protein Group1 Hopx-/-, Group2 Hopx+/-, Group3 Hopx+/+
Organism:	Mus musculus
Experiment type:	Expression profiling by array
Platform:	GPL1261
Pubmed ID:	19265543
Summary & Design:	**Summary:** Hopx appears to be needed for persistence of Th1 effector memory cells. IFN-gamma-producing Th cells are significantly reduced in Hopx-deficient mice compared to Hopx-expressing littermates and Hopx-deficient Th1 cells show a defective persistence upon adoptive transfer. Moreover, Hopx protects Th1 cells from Fas-mediated cell death in vitro. To further dissect the role of Hopx and to identify target genes of Hopx, we have performed transcriptome analysis to compare gene expression in Hopx-deficient versus Hopx-competent Th1 cells. In agreement with the role of Hopx in supporting survival of Th1 effector memory cells, anti-apoptotic cells were up-regulated and pro-apoptotic genes were down-regulated in Hopx-competent compared to Hopx-deficient Th1 cells. **Overall design:** Gene expression profiles of Hopx-/- versus Hopx+/- and Hopx+/+ Th1 cells, respectively. Naˆflve Th cells were isolated from Hopx+/+, Hopx+/- and Hopx-/- OT2 mice and activated in vitro with their cognate antigen (OVA) under Th1 polarizing conditions. On day 6, viable cells were repeatedly activated. On day 12, viable cells were harvested and compared using Affymetrix 430A Version 2 GeneChip arrays. After total RNA extraction, reverse transcription, cDNA extraction, the biotinylated cRNA was transcribed, fragmented, and 15 ´µg cRNA hybridized in duplicates for each of the three groups to the GeneChip arrays. Group1: Hopx-/-, Group2: Hopx+/-, Group3: Hopx+/+. Lists of differentially regulated genes were created using High Performance Chip Data Analysis (HPCDA) with Bioretis database (http://www.bioretis-analysis.de). Worldwide data sharing is possible via Bioretis, please ask the authors.

Background corr dist: KL-Divergence = 0.0490, L1-Distance = 0.0373, L2-Distance = 0.0024, Normal std = 0.5962

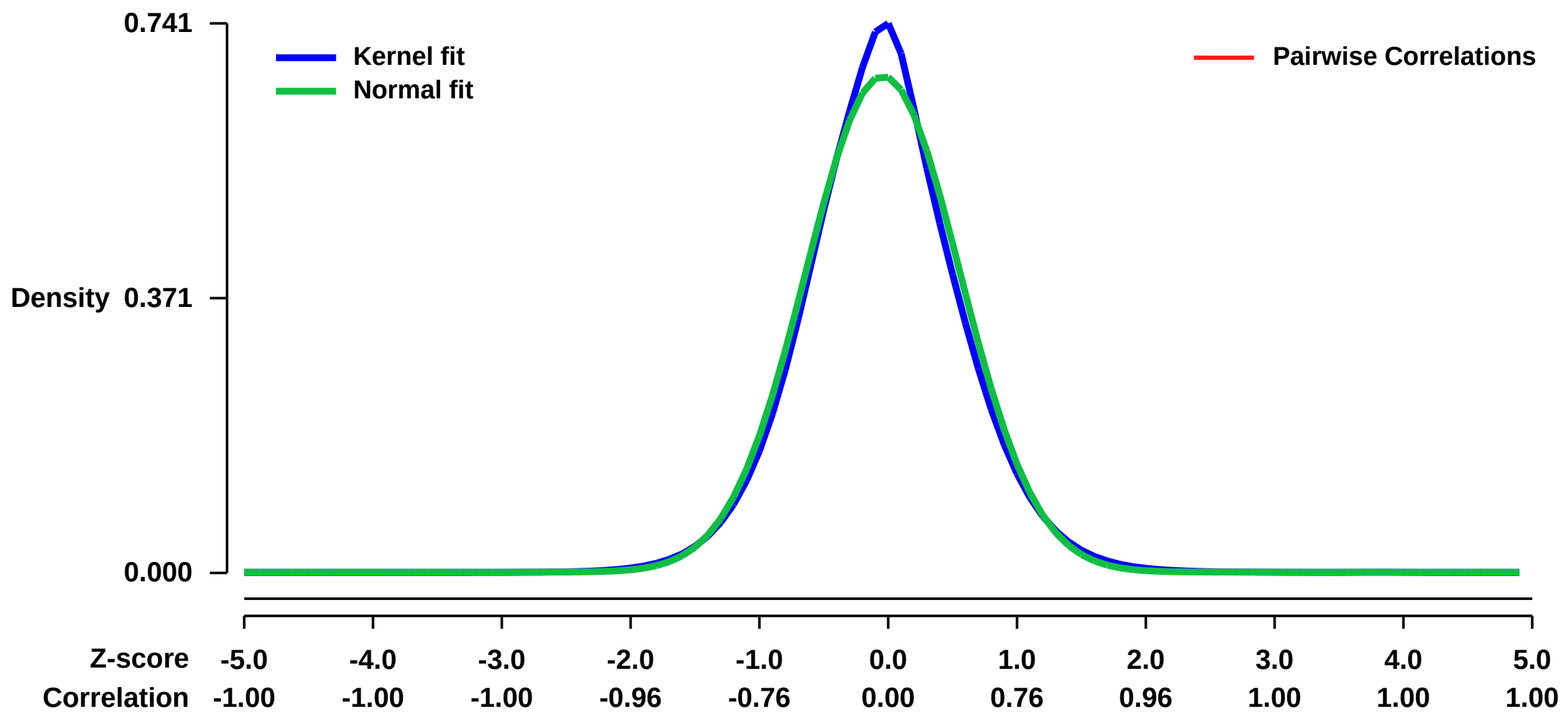

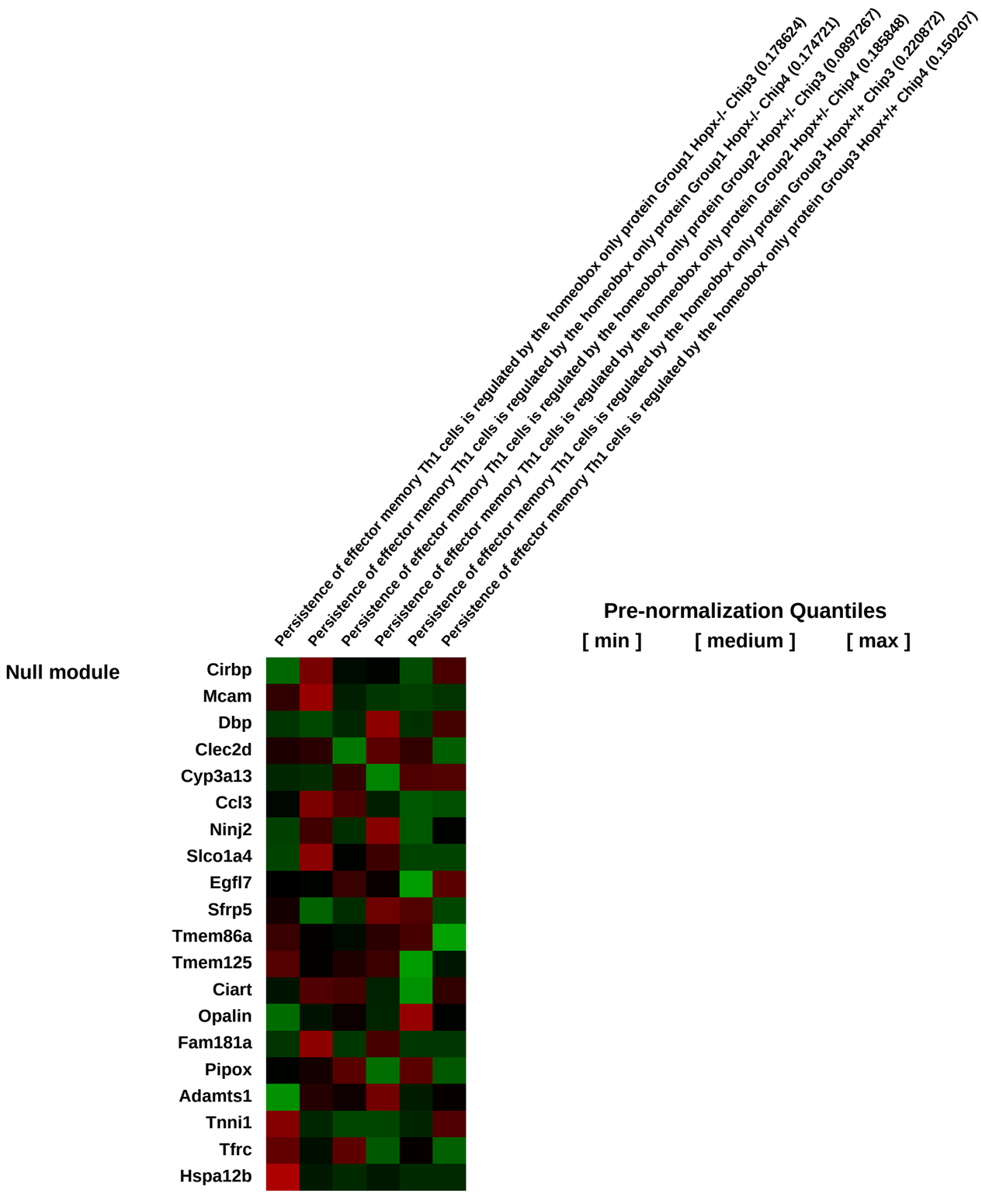

GEO Series "GSE5333" Expression Profiles

Num of samples in this series: 16

Scale of expression profile Z-scores

-3.0 -2.0 -1.0 0.0 1.0 2.0 3.0

GEO Link: http://www.ncbi.nlm.nih.gov/geo/query/acc.cgi?acc=GSE5333

Status: Public on Jul 22 2006

Title: Gene expression profiling of whole epididymis in embryonic (gestational day 12, 14, 16 & 18) and postnatal day 2 mice. (GUDMAP Series ID: 4)

Organism: Mus musculus

Experiment type: Expression profiling by array

Platform: GPL1261

Pubmed ID:

Summary & Design:

Summary:
The overall objective of this proposal is to map the temporal and spatial dynamics of gene expression in the fetal mouse testis at key developmental timepoints. Urogenital tract malformations are the most common birth defects in males and their incidence together with other male reproductive health concerns such as reduced fertility and testicular cancer are reportedly on the rise in the human population. To better understand the impact of genetic factors and environmental influences on testicular development, it is important to first understand normal gene expression patterns and signaling cascades within the fetal testis during development. The goal of this study is to identify cell-specific genes that can be used as biomarkers for key differentiation events.

Keywords: developmental time course

Overall design:
Day to day comparison in whole epididymus throughout development with triplicates at each time point. Each sample is a pair of epididymus from a single animal and each animal is taken from a different dam.

Background corr dist: KL-Divergence = 0.1487, L1-Distance = 0.0469, L2-Distance = 0.0047, Normal std = 0.4166

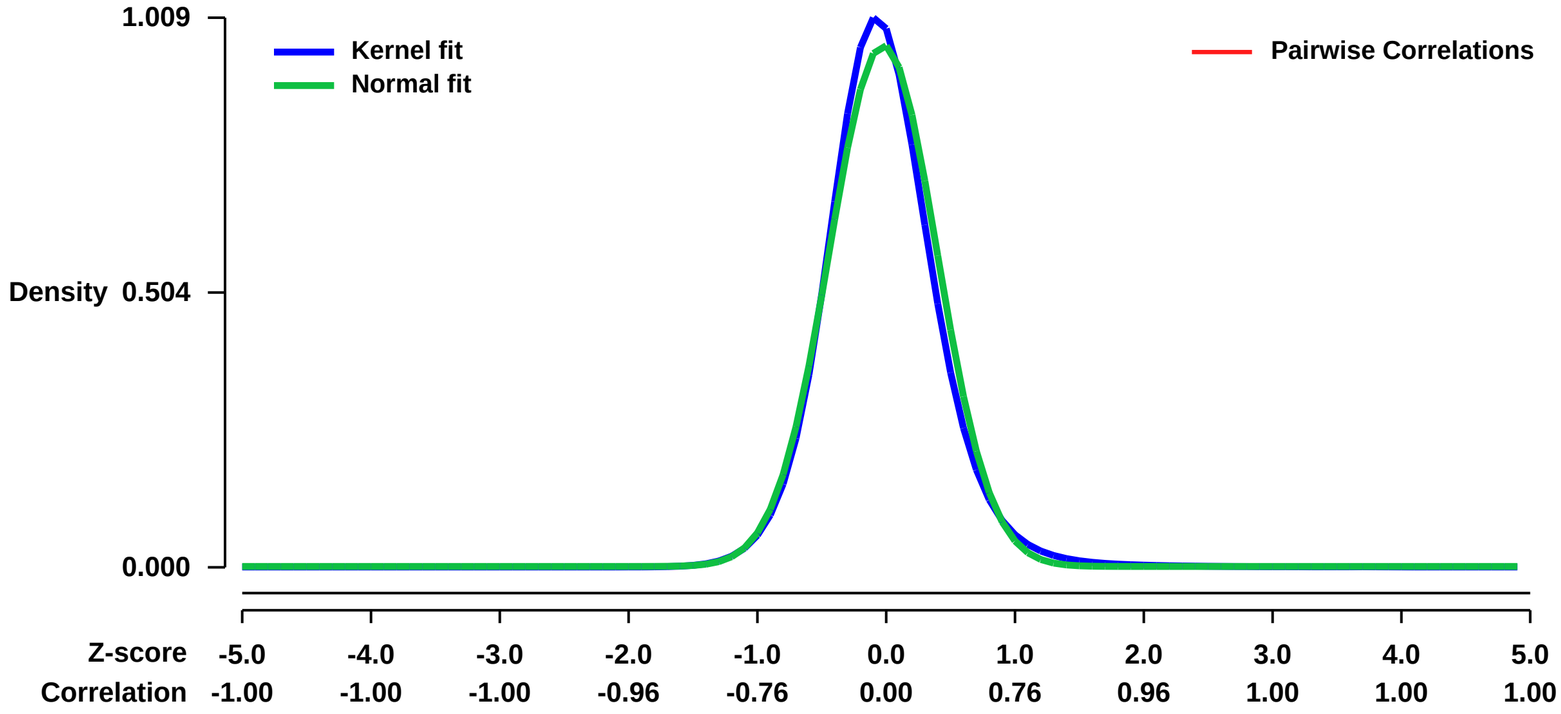

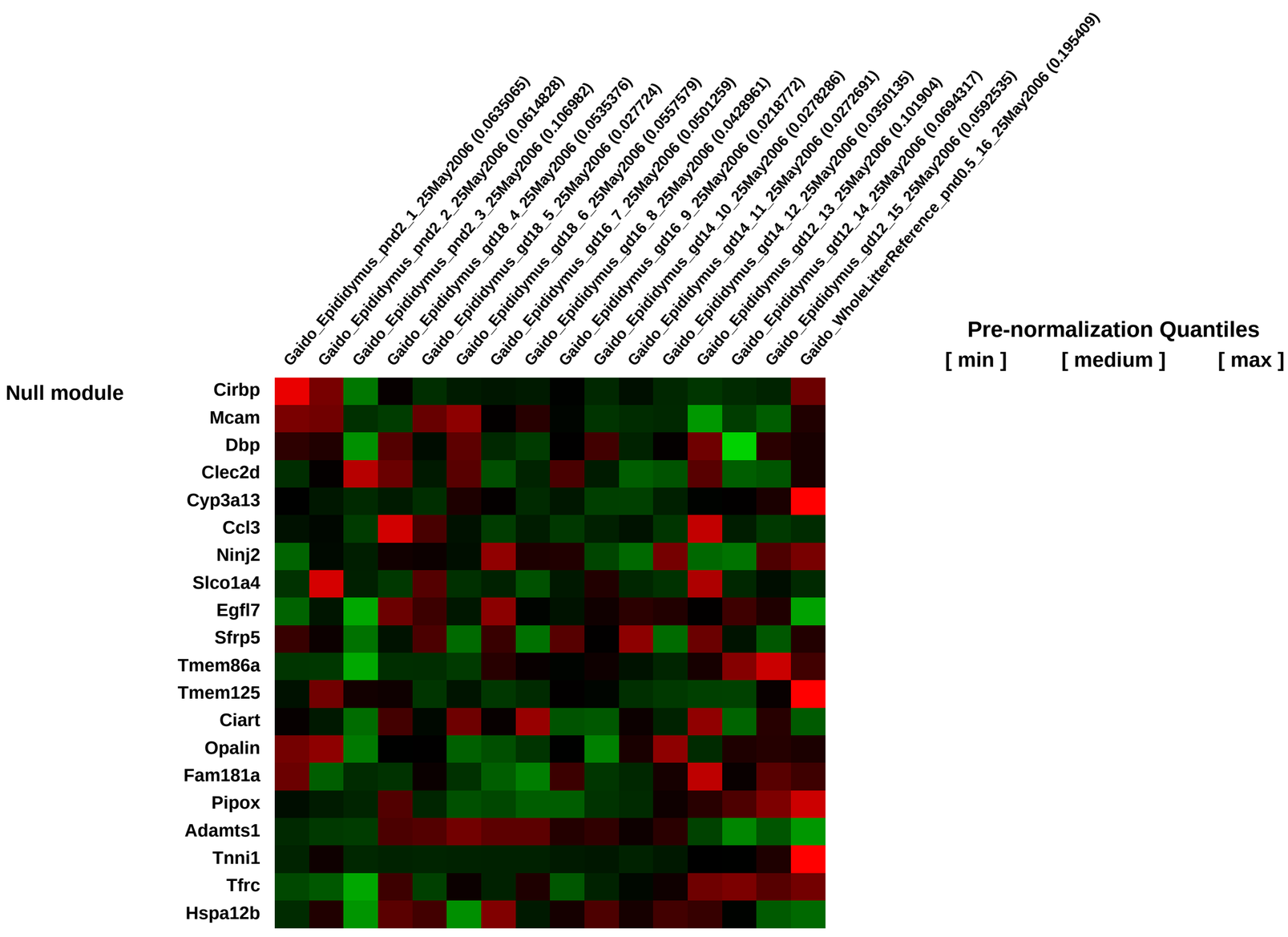

GEO Series "GSE46500" Expression Profiles

Num of samples in this series: 6

Scale of expression profile Z-scores

-3.0 -2.0 -1.0 0.0 1.0 2.0 3.0

GEO Link:	http://www.ncbi.nlm.nih.gov/geo/query/acc.cgi?acc=GSE46500
Status:	Public on May 01 2013
Title:	Gene expression data for three mouse auditory brainstem nuclei at two times of development
Organism:	Mus musculus
Experiment type:	Expression profiling by array
Platform:	GPL1261
Pubmed ID:	23708139
Summary & Design:	**Summary:** Genome-wide gene expression was obtained in three auditory brainstem nuclei (defined below), at two different ages in mice, postnatal day (P)3 and P14. The primary aim was to identify genes which are differentially expressed between the medial nucleus of the trapezoid body (MNTB) and the superior olive (LSO), at both age groups. **Overall design:** Tissue samples from the ventral cochlear nucleus (VCN), the medial nucleus of the trapezoid body (MNTB) and the lateral superior olive (LSO) were collected from 200 ¸…m thick fresh transverse mouse brainstem slices prepared with a vibratome tissue slicer. Individual brainstem nuclei were dissected out with fine forceps under optical control with a binocular. For each nucleus (VCN, MNTB, and LSO), the tissue from six male C57Bl6 mice at postnatal day (P) 3, and from three male C57Bl6 mice at P14 was pooled. The RNA was isolated with the RNeasy Micro kit (Qiagen); RNA samples were amplified using a WT ovation Pico RNA amplification (Nugen, CA, USA). The cDNA was hybridized onto mouse Affymetrix microarrays 430 2.0 (Affymetrix, Santa Clara, USA).

Background corr dist: KL-Divergence = 0.0190, L1-Distance = 0.0101, L2-Distance = 0.0001, Normal std = 0.7487

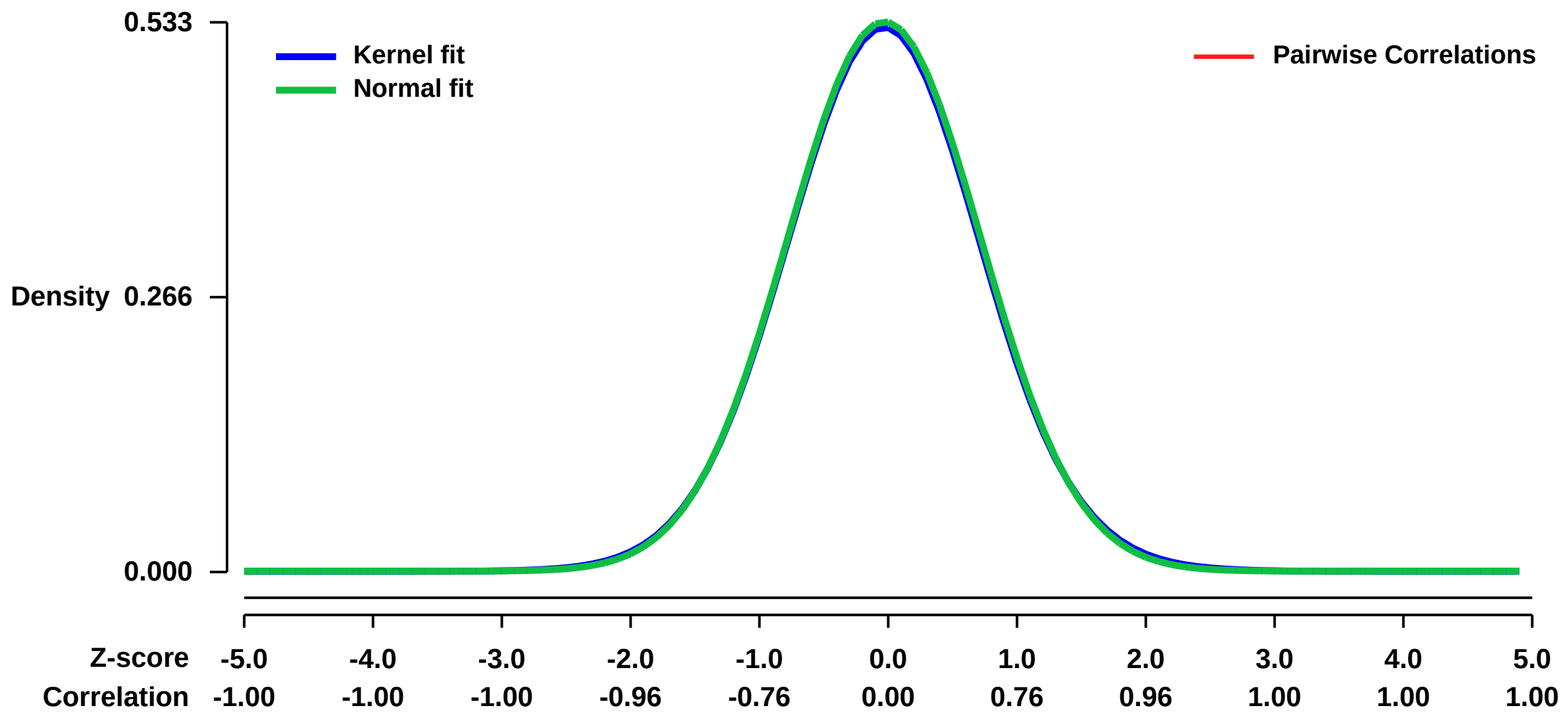

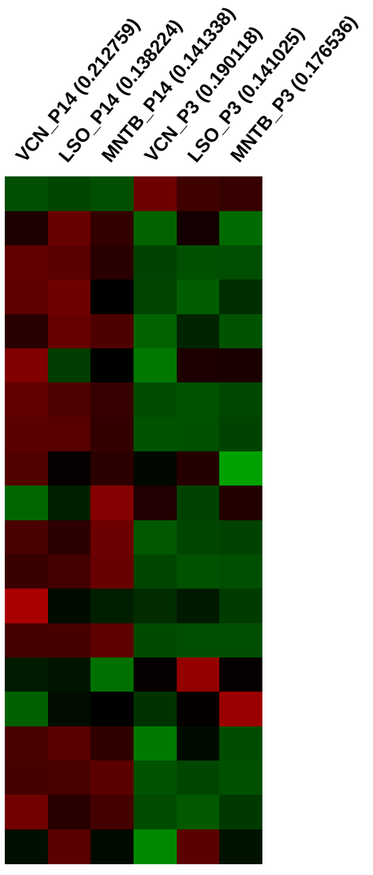

GEO Series "GSE26568" Expression Profiles

Num of samples in this series: 6

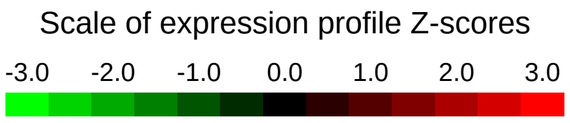

GEO Link:	**http://www.ncbi.nlm.nih.gov/geo/query/acc.cgi?acc=GSE26568**
Status:	**Public on May 31 2013**
Title:	**Impact of KLF2 expression on T cell genetic program**
Organism:	**Mus musculus**
Experiment type:	**Expression profiling by array**
Platform:	**GPL1261**
Pubmed ID:	**24155966**
Summary & Design:	**Summary:** **On triggering of the T cell receptor CD8 T lymphocytes downregulate expression of the transcription factor KLF2. KLF2 expression remains low as these cells differentiate to Cytotoxic T lymphocytes (CTL) but may be re-expressed depending on the local environmental signals.** **We used retroviral transduction to enforce KLF2 expression in CTL to determine the impact of it re-expression on the CTL genetic program.** **Overall design:** **T lymphocytes with a transgenic T cell receptor (P14 LCMV) isolated from murine spleens were activated with gp33-41 peptide for 2 days and transduced with empty vector (evGFP) or GFP-KLF2. After differentiation to CTL in culture with Interleukin-2 for 2 further days, cells positive for GFP were isolated by Fluorescence Activated Cell Sorting and the RNA extracted for microarray analysis.**

Background corr dist: **KL-Divergence = 0.0293, L1-Distance = 0.0215, L2-Distance = 0.0005, Normal std = 0.6816**

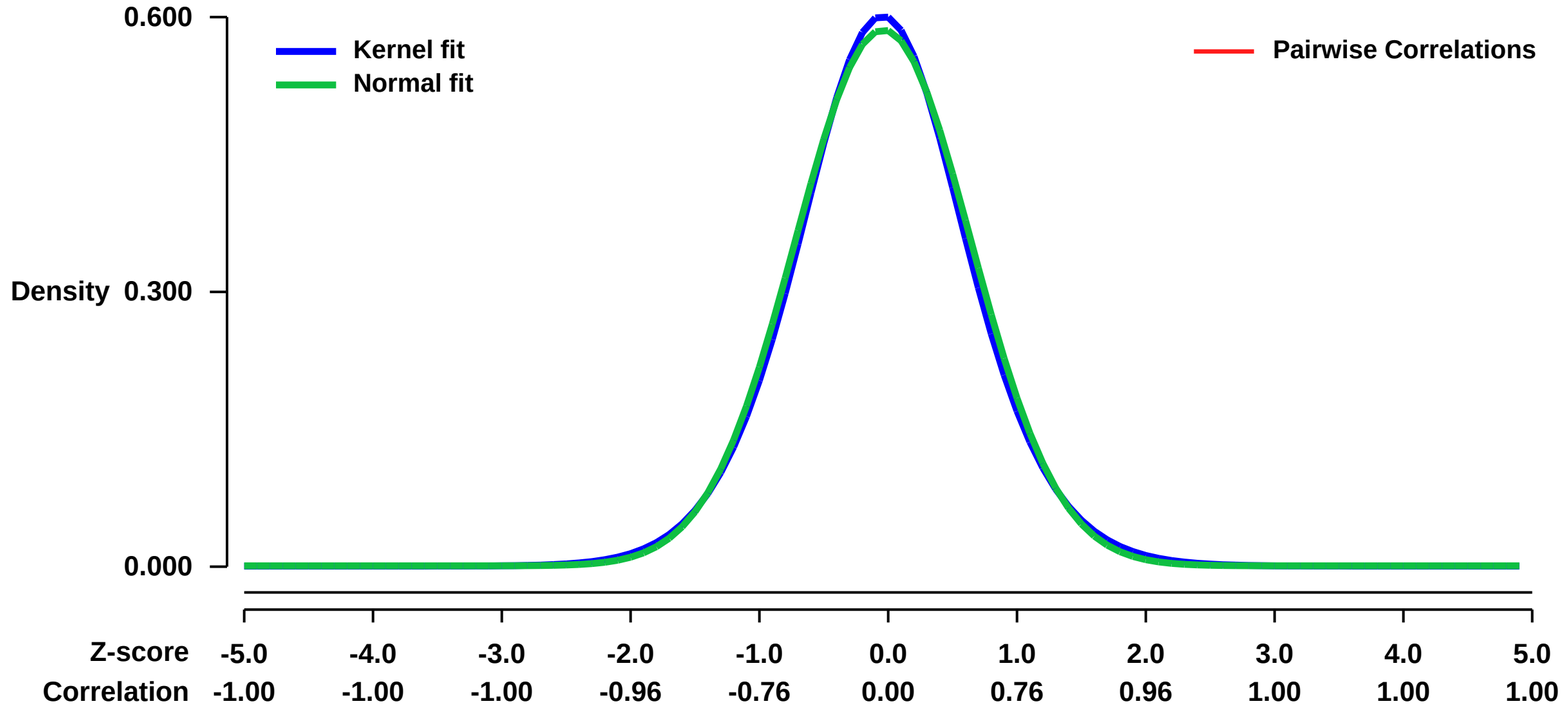

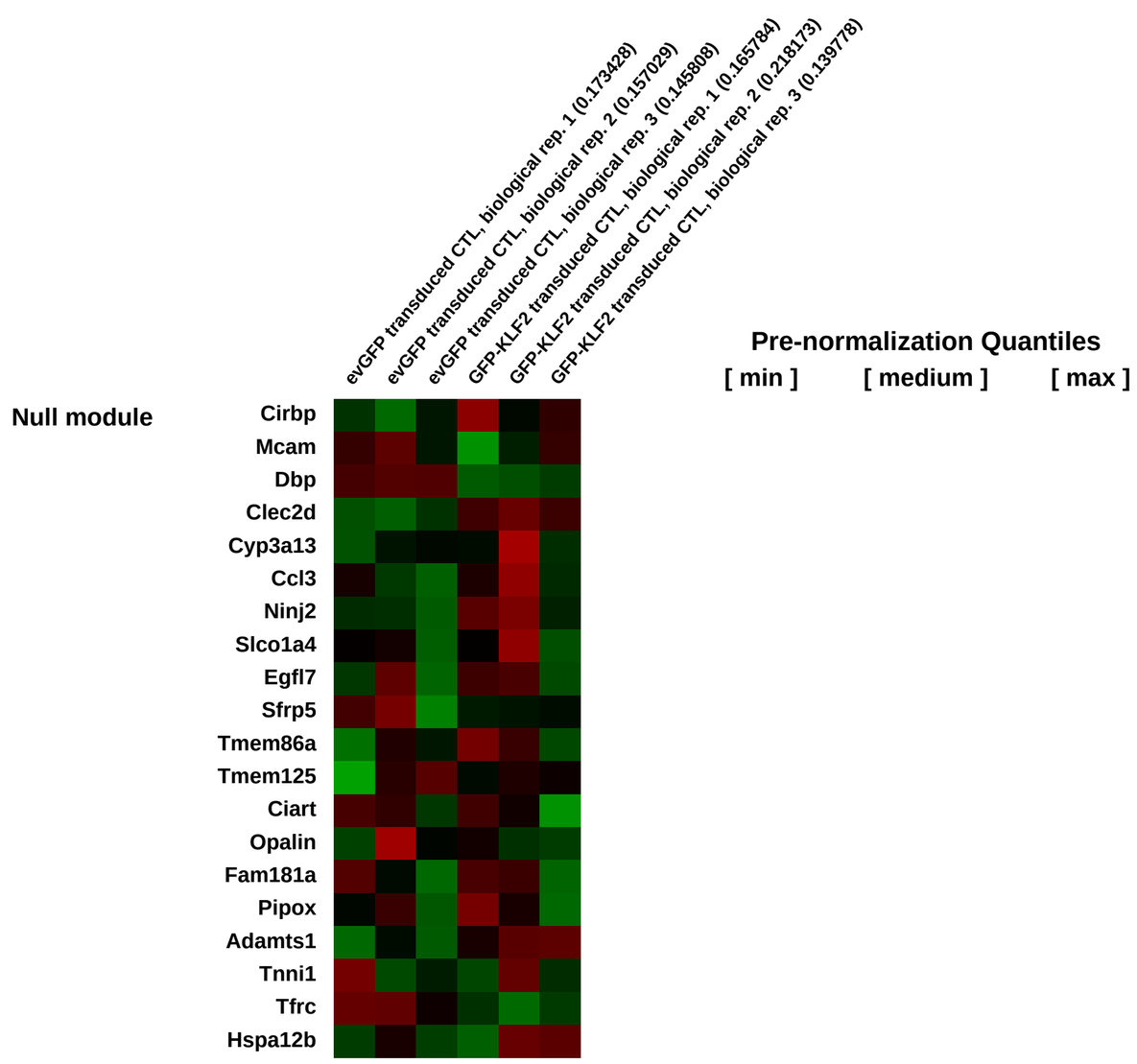

GEO Series "GSE40685" Expression Profiles

Num of samples in this series: 11

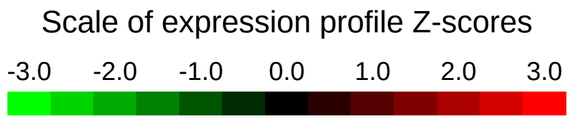

GEO Link:	**http://www.ncbi.nlm.nih.gov/geo/query/acc.cgi?acc=GSE40685**
Status:	**Public on Sep 28 2012**
Title:	**Foxp3 exploits a preexistent enhancer landscape for regulatory T cell lineage specification [Expression]**
Organism:	**Mus musculus**
Experiment type:	**Expression profiling by array**
Platform:	**GPL1261**
Pubmed ID:	**23021222**
Summary & Design:	**Summary:** **Regulatory T (Treg) cells, whose identity and function are defined by the transcription factor Foxp3, are indispensable for immune homeostasis. It is unclear whether Foxp3 exerts its Treg lineage specification function through active modification of the chromatin landscape and establishment of new enhancers or by exploiting a pre-existing enhancer landscape. Analysis of the chromatin accessibility of Foxp3-bound enhancers in Treg and Foxp3-negative T cells showed that Foxp3 was bound overwhelmingly to pre-accessible enhancers occupied by its cofactors in precursor cells or a structurally related predecessor. Furthermore, the bulk of Foxp3-bound Treg cell enhancers inaccessible in Foxp3- CD4+ cells became accessible upon T cell receptor activation prior to Foxp3 expression with only a small subset associated with several functionally important genes being exclusively Treg cell-specific. Thus, in a late cellular differentiation process Foxp3 defines Treg cell functionality in an â opportunisticâ manner by largely exploiting the preformed enhancer network instead of establishing a new enhancer landscape.** **Overall design:** **Array expression. Three cell types with 3-5 replicates each.**

Background corr dist: KL-Divergence = 0.0865, L1-Distance = 0.0219, L2-Distance = 0.0007, Normal std = 0.4629

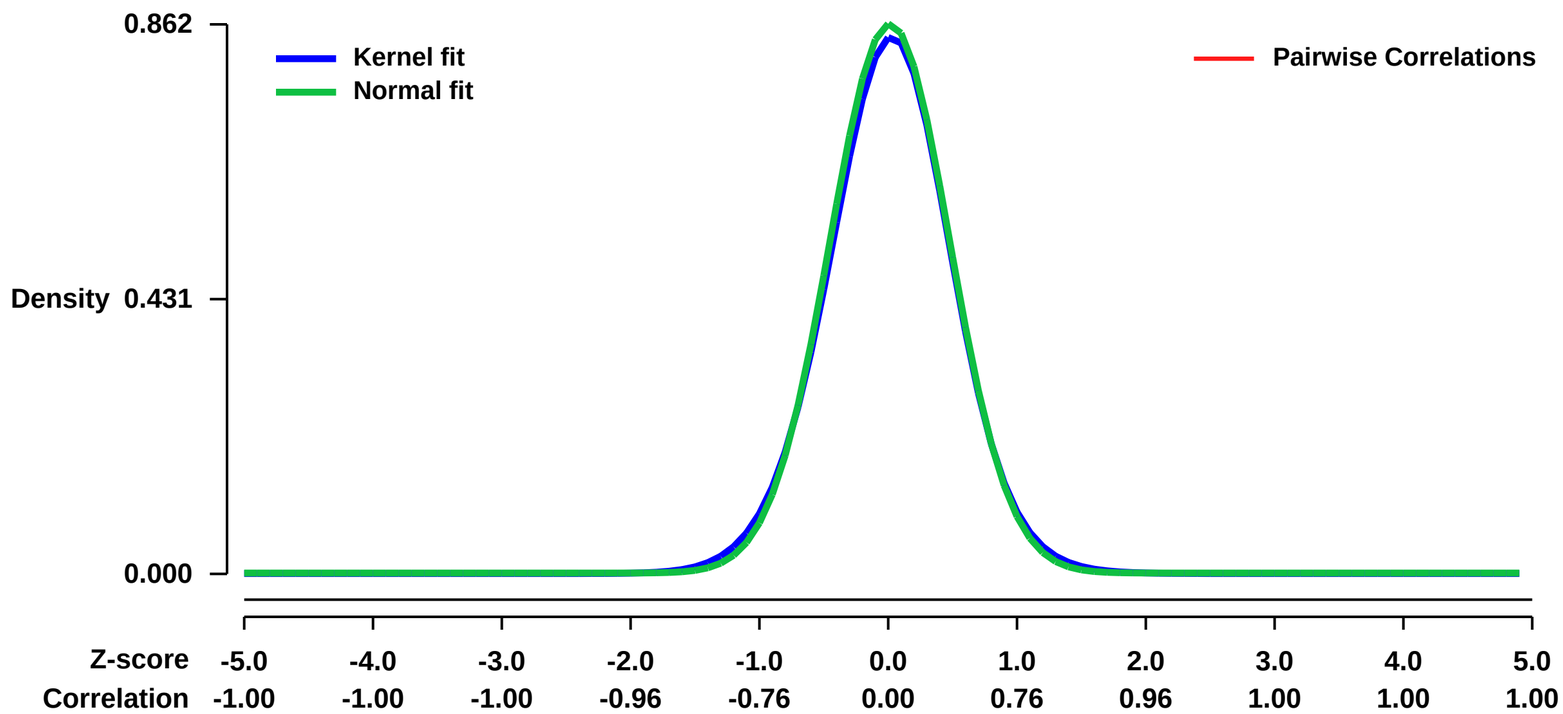

Pre-normalization Quantiles

[min] [medium] [max]

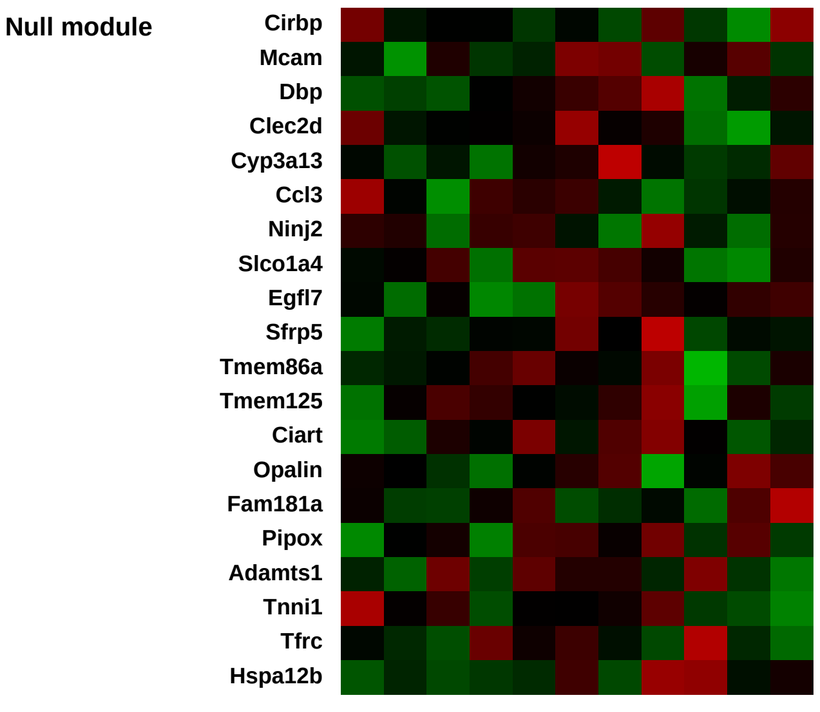

GEO Series "GSE17263" Expression Profiles

Num of samples in this series: 6

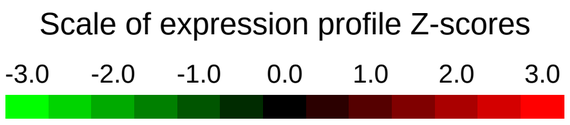

GEO Link:	http://www.ncbi.nlm.nih.gov/geo/query/acc.cgi?acc=GSE17263
Status:	Public on Apr 13 2010
Title:	Gene expression profiling of constitutive activation of Smoothened in the mouse uterus
Organism:	Mus musculus
Experiment type:	Expression profiling by array
Platform:	GPL1261
Pubmed ID:	20130264
Summary & Design:	**Summary:** In order to gain a better understanding of Ihh action during embryo implantation, we constitutively activated Smo in the murine uterus using the PRcre mouse model (PRcre/+SmoM2+; SmoM2). Female SmoM2 mice were infertile. They exhibited normal serum progesterone levels and normal ovulation, but ova failed to be fertilized in vivo and the uterus failed to undergo the artificially induced decidual response. SmoM2 mice exhibited uterine hypertrophy. The endometrium had a reduced number of uterine glands and the endometrial stroma lost its normal morphologic characteristics. Microarray analysis of 3 month old SmoM2 uteri demonstrated a chondrocytic signature and confirmed that constitutive activation of SmoM2 increased extracellular matrix production. Thus, constitutive activation of Smo in the mouse uterus alters the extracellular matrix which interferes with early pregnancy. **Keywords:** two group comparison **Overall design:** We constitutively activated Hh signaling in the uterus by the expression of a mutant SmoM2 allele. We crossed these mice to the PRcre mouse model to constitutively activate Smo in the murine uterus (PRcre/+SmoM2+; SmoM2). High density DNA microarray analysis was performed on 3 month old control and SmoM2 uteri.

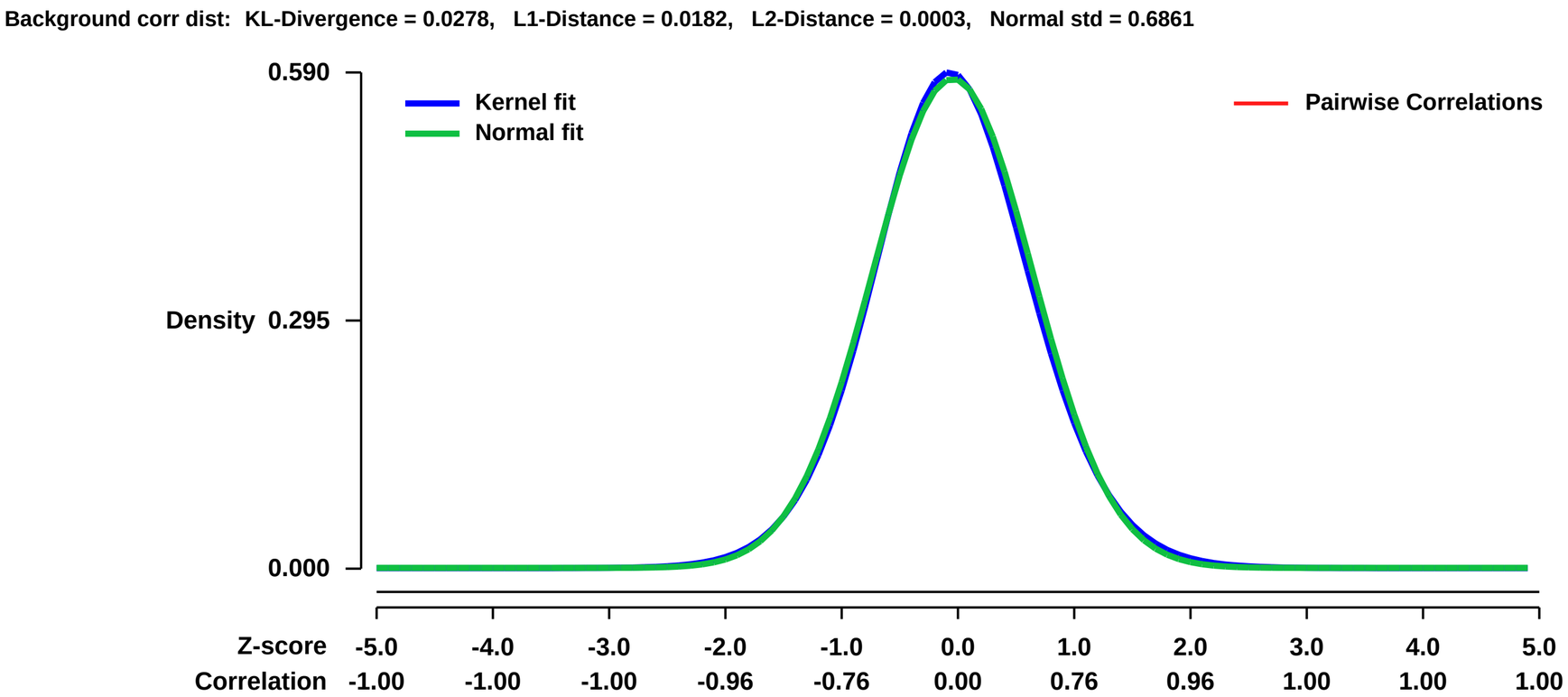

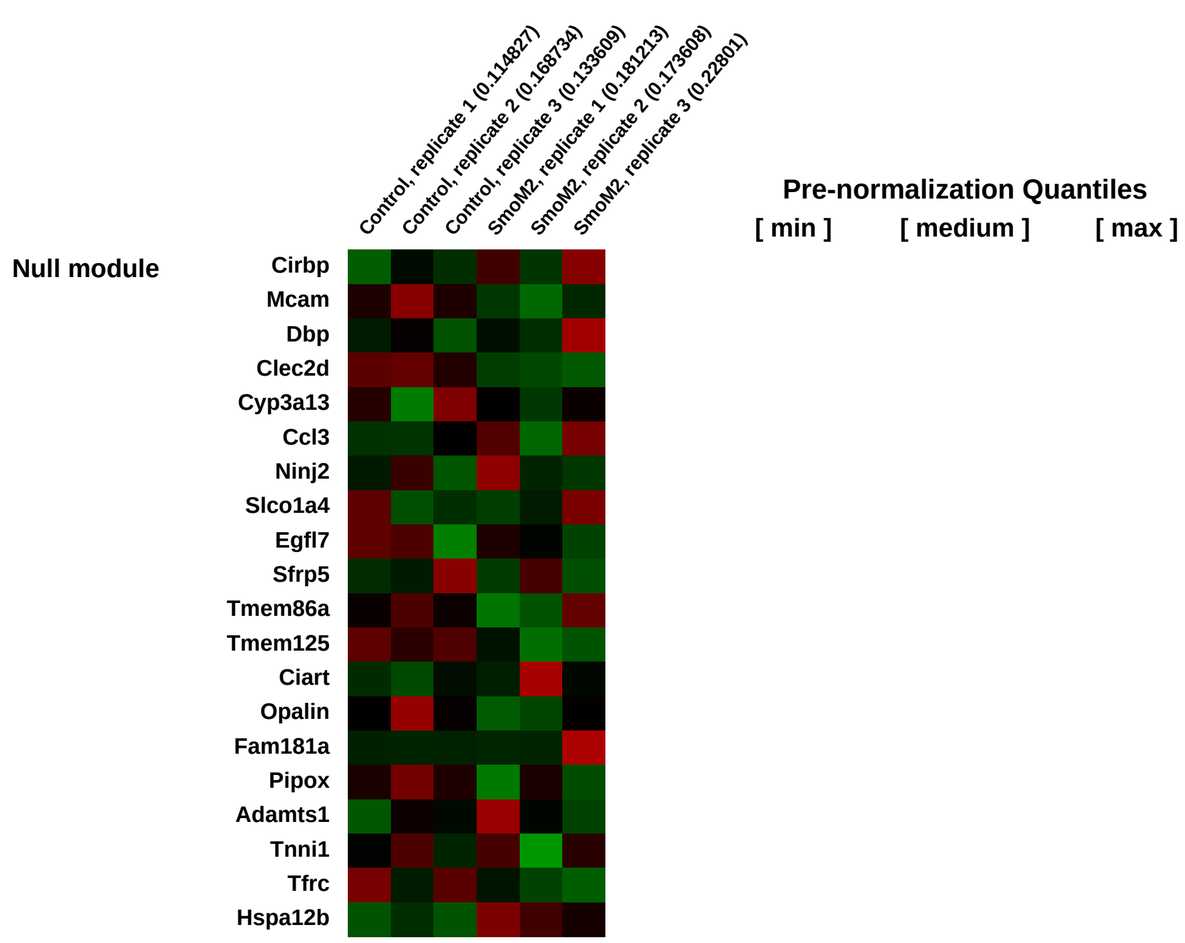

GEO Series "GSE35593" Expression Profiles

Num of samples in this series: 6

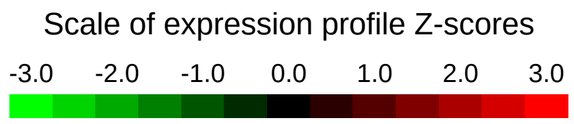

GEO Link:	http://www.ncbi.nlm.nih.gov/geo/query/acc.cgi?acc=GSE35593
Status:	Public on Feb 16 2013
Title:	Foxo1/3 depletion in granulosa cells reveals novel mechanisms controlling follicle growth and death and endocrine regulation of pituitary FSH.
Organism:	Mus musculus
Experiment type:	Expression profiling by array
Platform:	GPL1261
Pubmed ID:	23322722
Summary & Design:	**Summary:** The Foxo transcription factors regulate multiple cellular functions. Foxo1 and Foxo3 are highly expressed in granulosa cells of ovarian follicles. Selective depletion of the Foxo1 and Foxo3 genes in granulosa cells revealed a novel ovarian-pituitary endocrine feedback loop characterized by: 1) undetectable levels of serum FSH but not LH, 2) reduced expression of the pituitary Fshb gene and its transcriptional regulators and 3) ovarian production of a factor(s) that suppresses pituitary cell Fshb. Equally notable and independent of FSH, depletion of Foxo1/3 altered the expression of specific genes associated with follicle growth versus apoptosis by disrupting critical regulatory interactions of Foxo1/3 with the activin and BMP2 pathways, respectively. As a consequence, granulosa cell proliferation and apoptosis were decreased. These data provide the first evidence that Foxo1/3 divergently regulate follicle growth or death by interacting with the activin and BMP pathways in granulosa cells and by modulating pituitary FSH production. **Overall design:** A direct comparison of ovarian granulosa cells from wild type d25, Foxo1/3 dKO d25 and Foxo1/3 dKO 2 month mice.

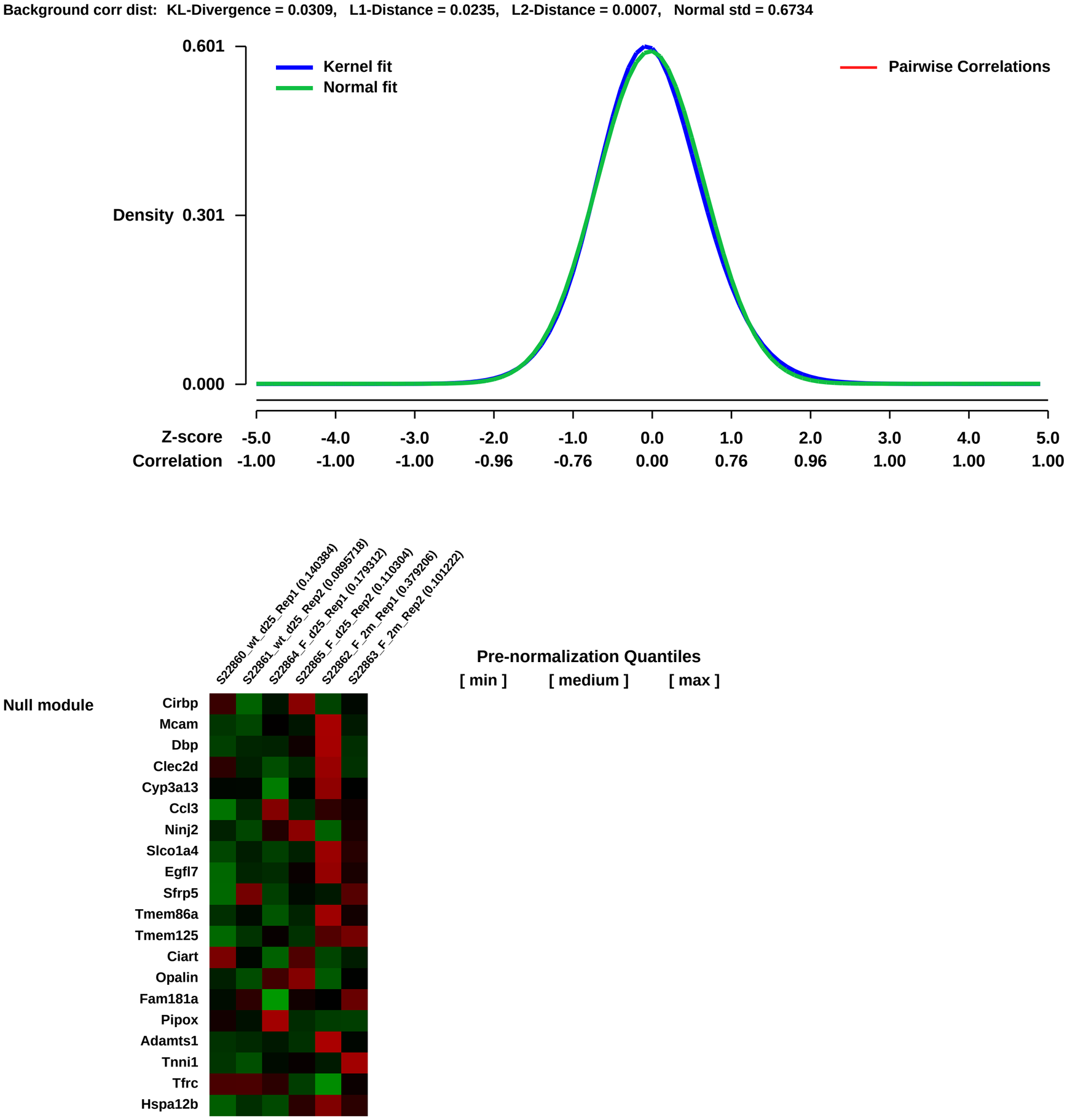

GEO Series "GSE5296" Expression Profiles

Num of samples in this series: 96

Scale of expression profile Z-scores

-3.0 -2.0 -1.0 0.0 1.0 2.0 3.0

GEO Link: http://www.ncbi.nlm.nih.gov/geo/query/acc.cgi?acc=GSE5296
Status: Public on Jul 12 2006
Title: Spinal Cord Injury Murine Model
Organism: Mus musculus
Experiment type: Expression profiling by array
Platform: GPL1261
Pubmed ID:

Summary & Design:

Summary:
Traumatic spinal cord injury (SCI) initiates a complex series of pathophysiological secondary responses that lead to tissue loss and functional deficits.This study represents a comprehensive database of temporal changes in gene expression that underlie the secondary injury response that occurs in a well-defined mouse model of contusion injury.

Keywords: Time-Series

Overall design:
Global changes in gene expression that contribute to secondary injury in a C57BL6 mouse model of contusion injury were evaluated using Affymetrix Mouse Genome 430 2.0 arrays.Mice were subjected to a moderate injury at the T8 spinal segment under isoflurane anesthesia.Sections of cord (0.4 cm in length) were analyzed from the site of impact and from the immediately adjacent rostral and caudal regions at 0.5, 4, 24, 72 h and 7 and 28 days after injury (n=3/per group), sham-injury (n=2 per group), or from na˜flve mice (n=2). Four mice were pooled for each individual n, for a total of 12 mice for each injury time point.

Background corr dist: KL-Divergence = 0.5541, L1-Distance = 0.0744, L2-Distance = 0.0168, Normal std = 0.2171

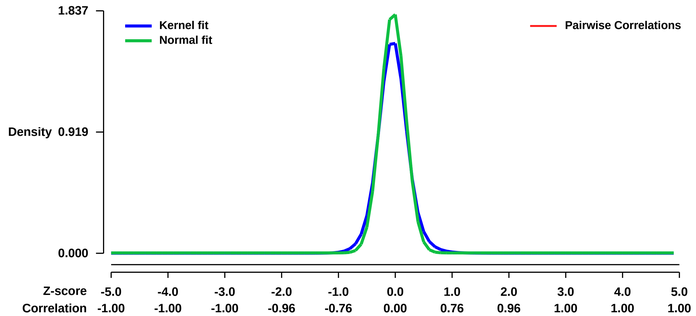

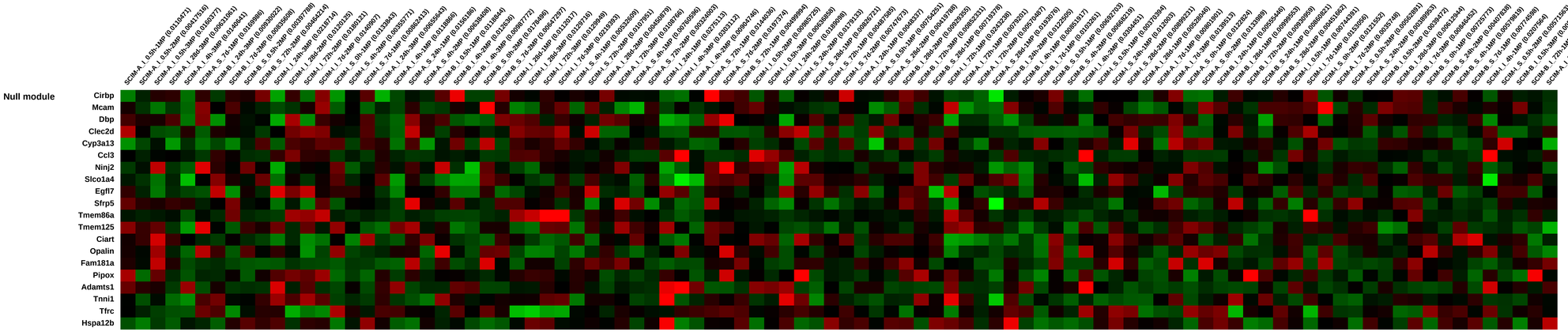

GEO Series "GSE32103" Expression Profiles

Num of samples in this series: 6

Scale of expression profile Z-scores

-3.0 -2.0 -1.0 0.0 1.0 2.0 3.0

GEO Link:	http://www.ncbi.nlm.nih.gov/geo/query/acc.cgi?acc=GSE32103
Status:	Public on Sep 01 2012
Title:	Expression data from mice mammary glands from Elf5 knockout (KO) and wildtype controls
Organism:	Mus musculus
Experiment type:	Expression profiling by array
Platform:	GPL1261
Pubmed ID:	23086238
Summary & Design:	**Summary:** We developed conditional knockout mice where the transcription factor Elf5 (also called ESE-2) is deleted in the mammary glands. Loss of Elf5 results in block in alveologenesis and epithelial differentiation defects. Mammary gland samples from Elf5 knockout and wild type animals were analyzed for global transcriptome changes. **Overall design:** We used microarrays to performing transcriptional profiling of Elf5KO and control mammary glands at Lac1 (Lactation day 1)

Background corr dist: KL-Divergence = 0.0299, L1-Distance = 0.0253, L2-Distance = 0.0009, Normal std = 0.6722

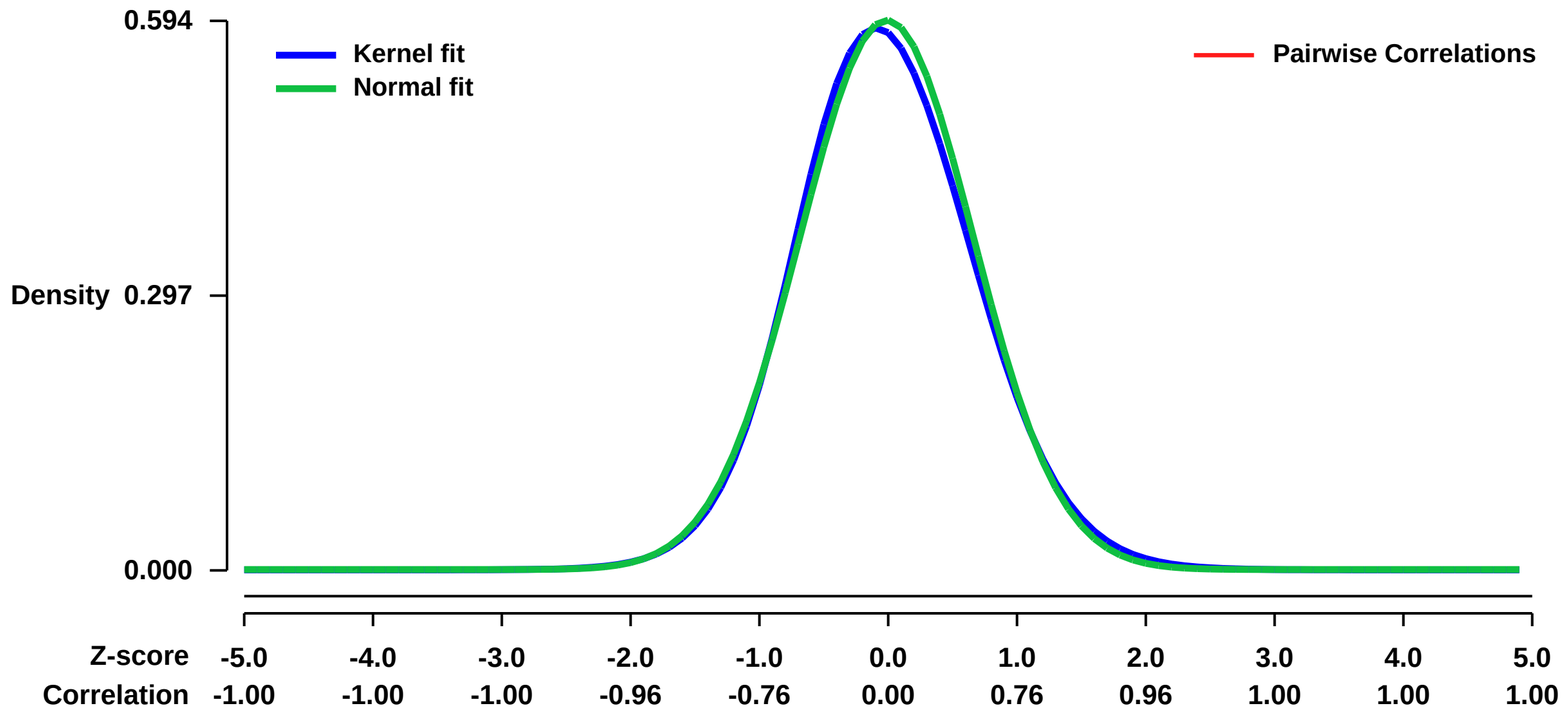

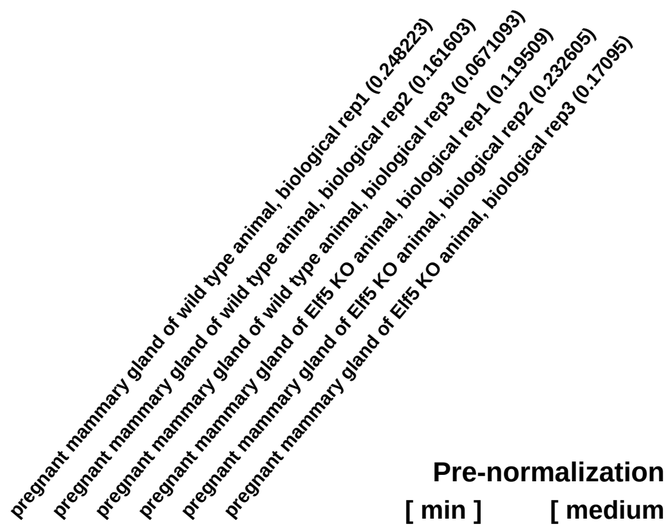

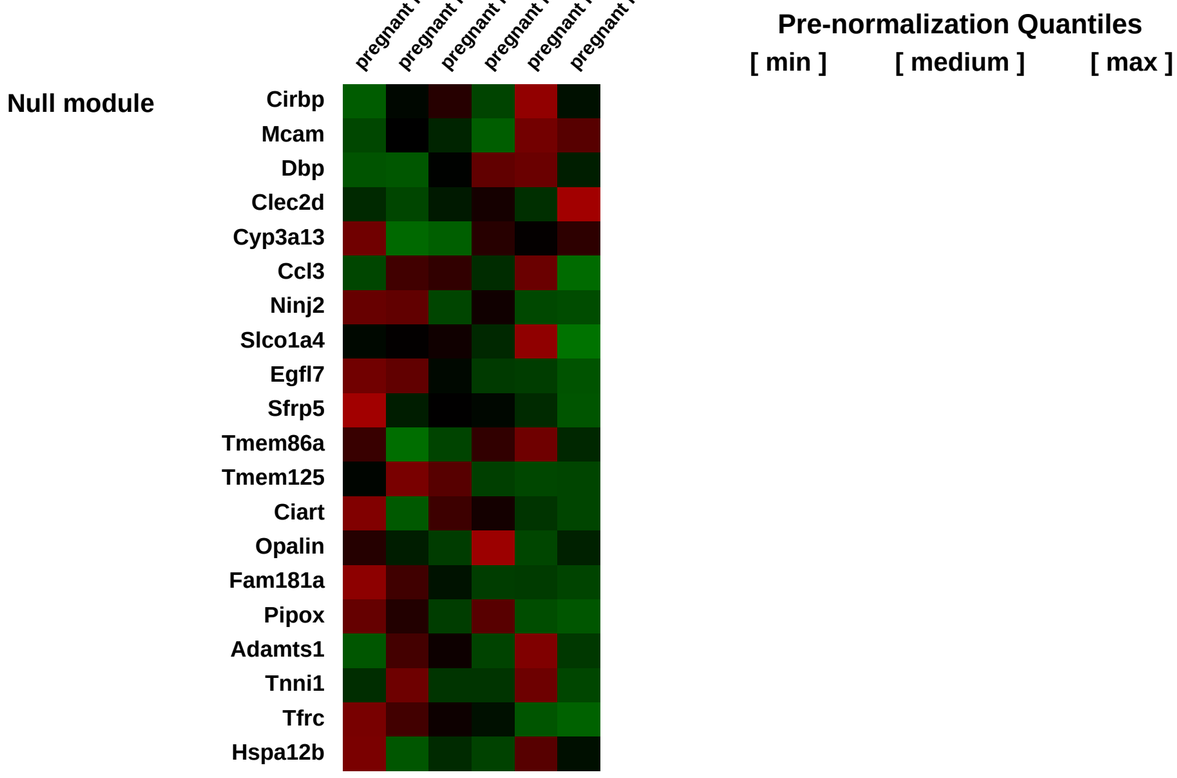

GEO Series "GSE40261" Expression Profiles

Num of samples in this series: 8

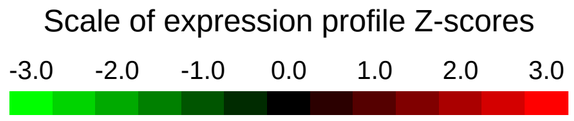

GEO Link:	**http://www.ncbi.nlm.nih.gov/geo/query/acc.cgi?acc=GSE40261**
Status:	**Public on Aug 22 2012**
Title:	**Hepatic gene expression changes following antisense oligonucleotide-based inhibition of miR-29a**
Organism:	**Mus musculus**
Experiment type:	**Expression profiling by array**
Platform:	**GPL1261**
Pubmed ID:	**22167021**
Summary & Design:	**Summary:** **Adult BALB/c female mice were injected intraperitoneally with a single dose at 20 mg per kg of antisense oligonucleotide either against miR-29a (5â -TAACCGATTTCAGATGGTGCTA-3â) or against a scrambled sequence (5â -TCATTGGCATGTACCATGCAGCT-3â Antisense oligonucleotides contained 2â -O-methoxyethyl (2â -MOE), 2â -flouro (2â -F) 2'-alpha-flouro units with a phosphorothioate backbone (Regulus Therapeutics). Six days following the injection, liver was isolated, total RNA was prepared as described above, and the RNA was amplified and biotinylated using the MessageAmp Premier kit (Ambion). Samples (n=4 each experimental and control) were hybridized to Affymetrix GeneChip Mouse Genome 430 2.0 Arrays in the Childrenâ s Hospital of Philadelphia Nucleic Acids Core Facility´ and analyzed with the assistance of the Penn Bioinformatics Core. Probe intensities were normalized using the GCRMA method and the significance of the log2-transformed, GCRMA-normalized signal intensities was determined using SAM** **Overall design:** **Adult mice injected with anti-miR-29a or scrambled control ASO, n=4 per group**

Background corr dist: KL-Divergence = 0.0598, L1-Distance = 0.0534, L2-Distance = 0.0053, Normal std = 0.5600

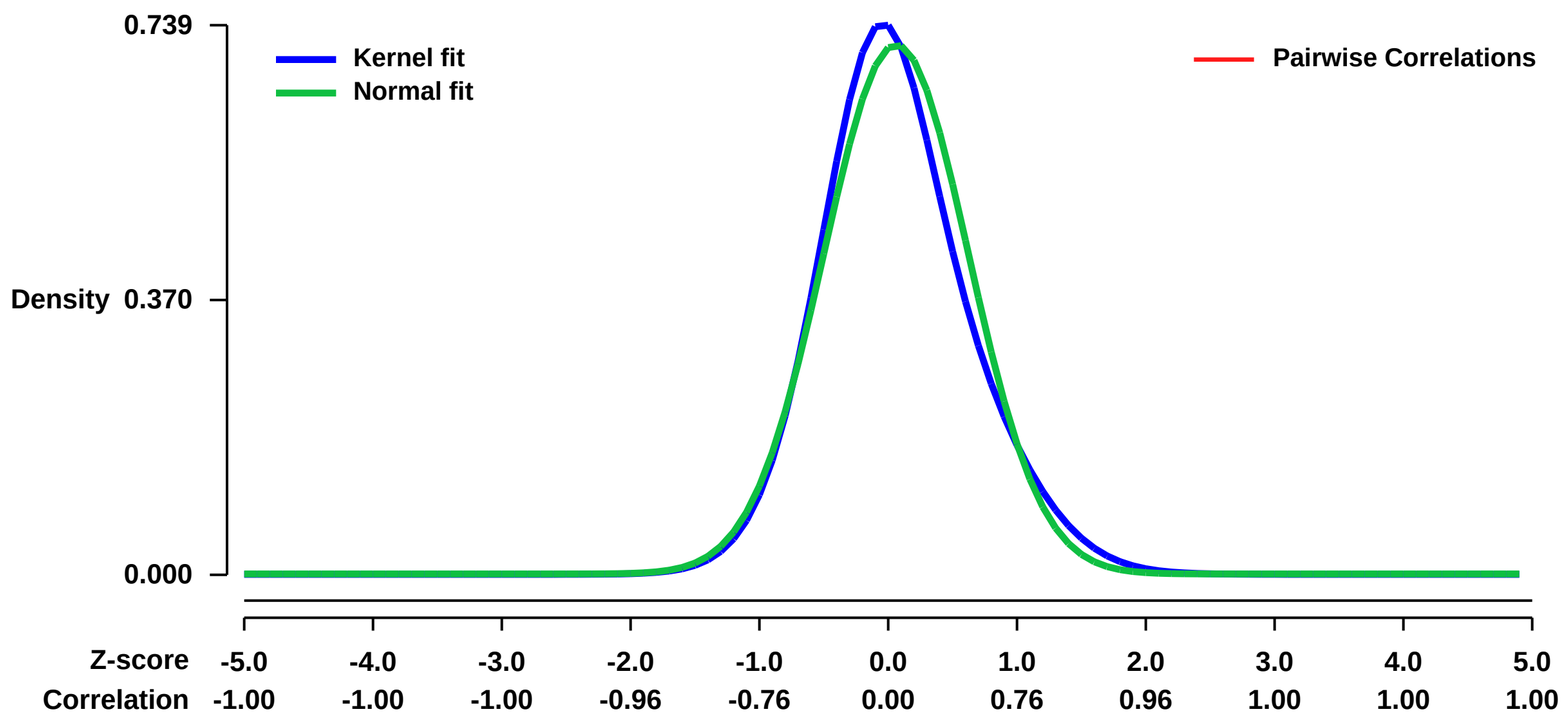

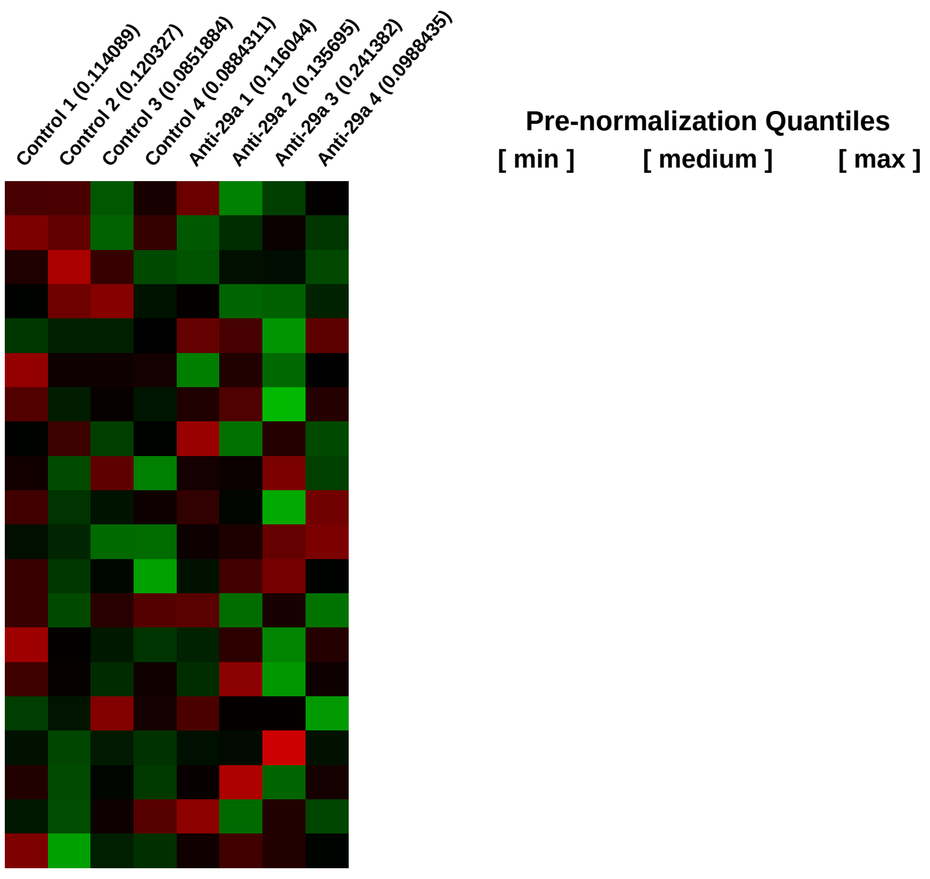

GEO Series "GSE17649" Expression Profiles

Num of samples in this series: 36

Scale of expression profile Z-scores

-3.0 -2.0 -1.0 0.0 1.0 2.0 3.0

GEO Link:	http://www.ncbi.nlm.nih.gov/geo/query/acc.cgi?acc=GSE17649
Status:	Public on Aug 14 2009
Title:	Expression data from mouse liver after Acetaminophen intoxication
Organism:	Mus musculus
Experiment type:	Expression profiling by array
Platform:	GPL1261
Pubmed ID:	19923254
Summary & Design:	**Summary:** Acetaminophen (APAP) is the most widely used analgesic in the United States. Its acute overdose causes liver damage by inducing localized centrilobular cell death. Because of widespread use, APAP toxicity has become the most frequent cause of acute liver failure. Many factors have been associated with the susceptibility of APAP-induced liver injuries, however, few of them have been confirmed and used in the clinical setting. We tried to identify the subset of factors that could affect susceptibility to APAP-induced liver injury by an integrative genetic, transcriptional and 2-D-NMR-based metabolomic analysis across a panel of inbred mouse strains. **Overall design:** After a single administration of high dose (300 mg/kg i.p.) APAP, liver and blood samples were extracted from 3 sensitive (C57B6, DBA/2, and SmJ) and 1 resistant (SJL) mice strains at 0, 3 and 6 hour after APAP exposure. Endogenous metabolites from liver samples were analyzed by 1H-13C 2-dimensional-NMR and gene expression changes occurring within these liver samples were simultaneously analyzed using Affymetrix microarrays. The transcriptional and metabolomic data was jointly analyzed, and functional information within the Gene Ontology database was used to identify the subset of genes that could affect susceptibility to APAP-induced liver injury in the early phase response.

Background corr dist: KL-Divergence = 0.5029, L1-Distance = 0.0901, L2-Distance = 0.0270, Normal std = 0.2244

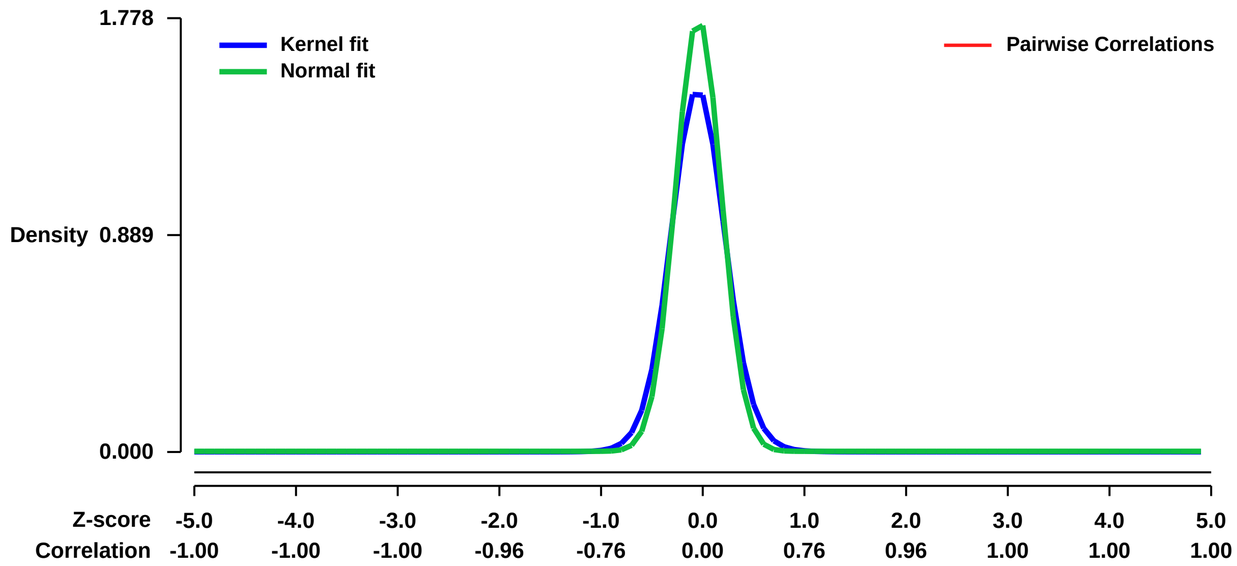

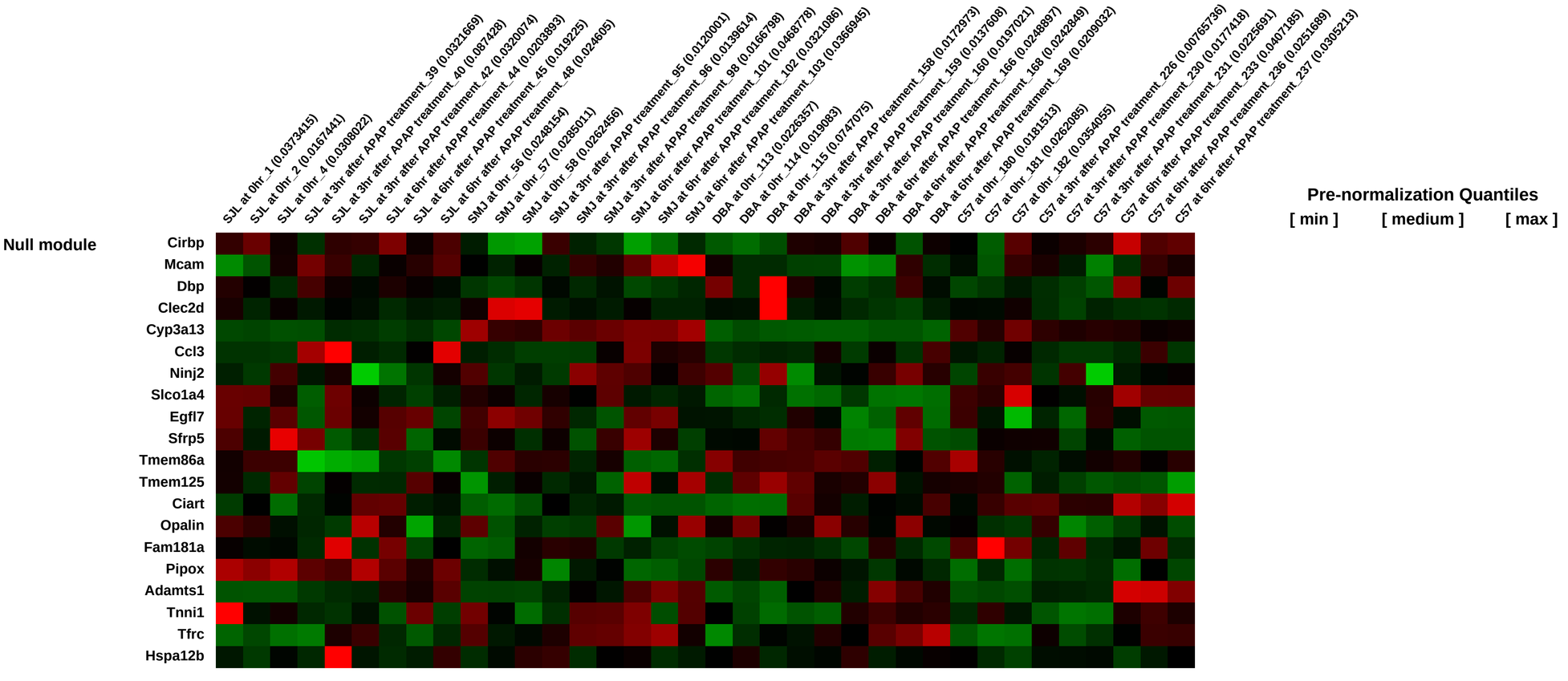

GEO Series "GSE9763" Expression Profiles

Num of samples in this series: 20

Scale of expression profile Z-scores

-3.0 -2.0 -1.0 0.0 1.0 2.0 3.0

GEO Link: http://www.ncbi.nlm.nih.gov/geo/query/acc.cgi?acc=GSE9763
Status: Public on Dec 04 2007
Title: Transformed glial progenitor cells (prosc-affy-mouse-450860)
Organism: Mus musculus
Experiment type: Expression profiling by array
Platform: GPL1261
Pubmed ID:

Summary & Design:

Summary:
The goals of this research are three-fold: (i) One is to identify genetic changes associated with tumorgenesis that interfere with the ability of transformed glial cells to differentiate. This is connected with (ii) our analysis of the regulation of differentiation in normal glial progentor cells, as only by understanding this in normal cells can we understand what is occurring when differentiation fails in transformed versions of the same cells. (iii) The third is to identify the molecular basis for the greater resistance of transformed glial progenitor cells to chemotherapeutic agents as compared with normal glial progenitor cells. Thus, analysis of the populations provided will yield data crucial to two of our central areas of research, as awarded by NINDS in ""Oligodendrocytes & precursors: toxicity of chemotherapy"" (5R01NS044701), and ""Low-level toxicant perturbation of neural cell function"" (1R01ES012708).

Our ability to work with essentially unlimited numbers of primary progenitor cells and transformed derivatives of these cells offers one of the few systems in which side-by-side comparison of normal and transformed cells at both the biochemical and molecular levels is possible. Using defined cell populations, expression profiles will be compared to reveal changes in cell type specific markers and regulatory factors associated with transformation. In addition, retention of markers despite transformation may enable identification of new markers useful in the diagnosis of glial tumors.

Transformation of glial progenitor cells is associated both with loss of the proteins required for normal differentiation and with an inability to normally activate proteins that function in differentiation control. By side-by-side analysis of gene expression in normal and transformed glial progenitor cells, and analysis of the response to inducers of differentiation in each these populations, we will identify candidate regulators critical in the control of normal differentiation. Identification of these regulators will also provide clues as to overcome the blockade of differentiation that occurs in glial cancers (which represent the majority of adult brain tumors).

RNA will be isolated from two separate preparations of glial progenitors. Preparation of purified populations has been described in multiple of our previous publications (Mayer, M. et al. (1994) Development 120, 142-153; Mayer-Prˆ¶schel, M. et al. (1997) Neuron 19, 773-785; Rao, M. and Mayer-Prˆ¶schel, M. (1997) Dev. Biology 188, 48-63). Total RNA from purified cell cultures will be extracted in a two step process. RNA will first be extracted by dounce homogenization in phenol/guanidine isothiocyonate solution (Trizol, Invitrogen, California) followed by isopropanol precipitation. Contaminating traces of DNA and protein will then be removed by silica-based affinity chromatography and Dnase treatment (NucleoSpin RNA Purification system, Clontech, California). Depending on the cell type, 5x105 cells will typically yield 5-15´µg of high quality RNA (OD260/280=2.1 at pH7.5). In order to determine purity and molecular weight distribution, samples will be routinely tested on a Agilent Bioanalyzer. cDNA will be generated from total RNA and then be submitted to one round of amplification and labeling using the messageAmp system (Ambion). Probes are then hybridized to the Affymerix Rat 230 (A/B or 2.0) GeneChip expression array. Array data will be processed using the Micro Array Suite 5.0 (MAS, Affymetrix). .Cel files containing normalized, relative expression data for all genes tested will be used for downstream statistical analysis.

Keywords: other

Overall design:

Background corr dist: KL-Divergence = 0.1052, L1-Distance = 0.0572, L2-Distance = 0.0056, Normal std = 0.4613

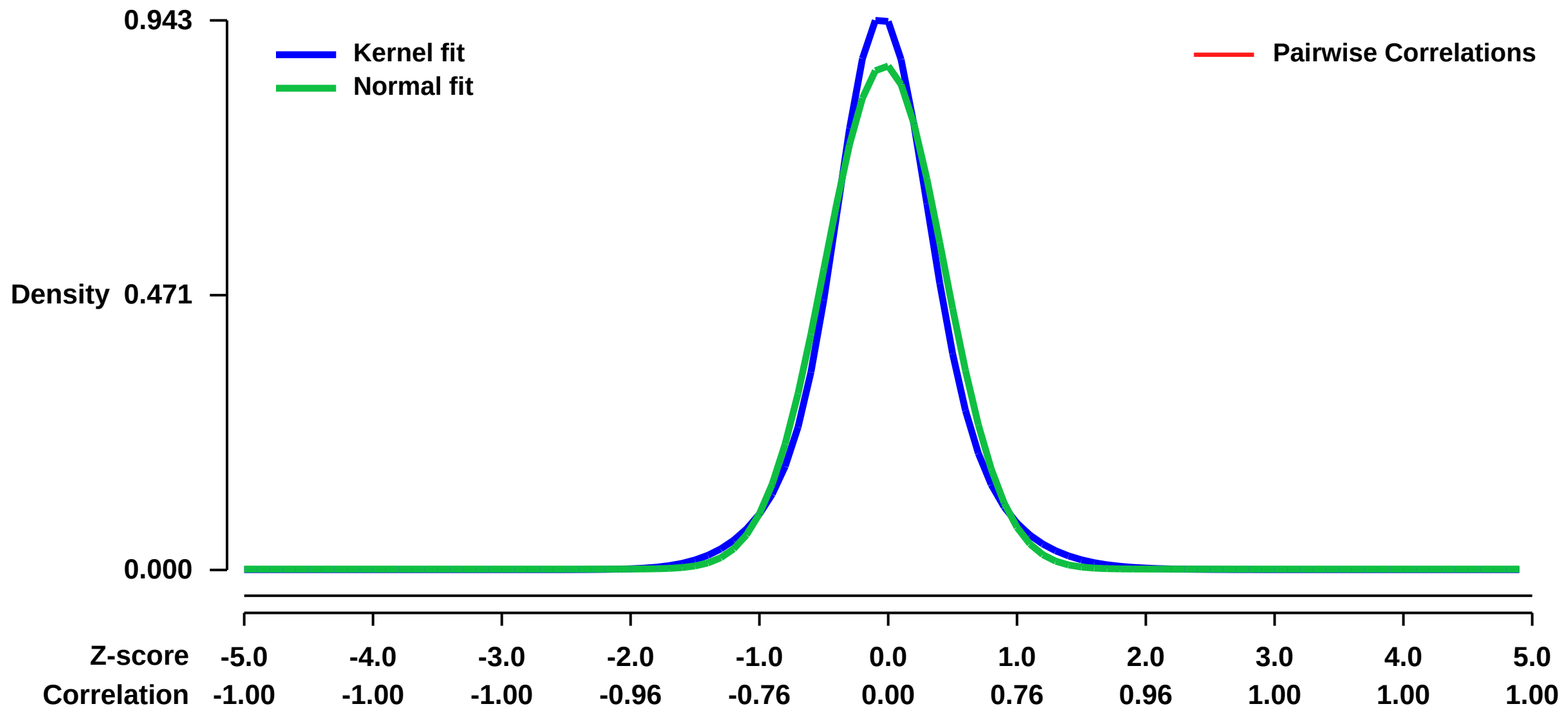

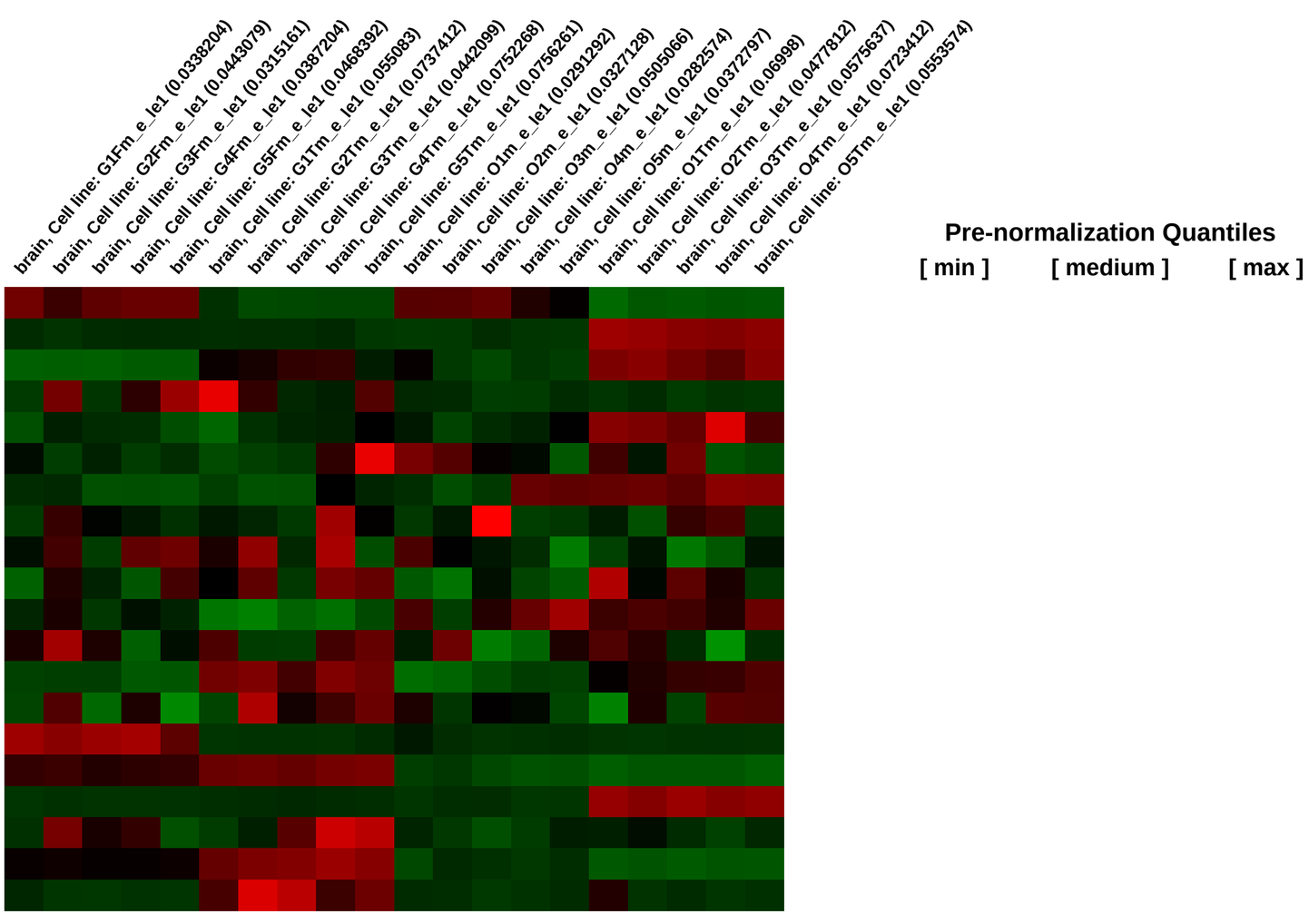

GEO Series "GSE4658" Expression Profiles

Num of samples in this series: 6

Scale of expression profile Z-scores

-3.0 -2.0 -1.0 0.0 1.0 2.0 3.0

GEO Link:	**http://www.ncbi.nlm.nih.gov/geo/query/acc.cgi?acc=GSE4658**
Status:	**Public on Dec 31 2006**
Title:	**static vs simulated microgravity**
Organism:	**Mus musculus**
Experiment type:	**Expression profiling by array**
Platform:	**GPL1261**
Pubmed ID:	**17243119**
Summary & Design:	**Summary:** **The below table includes a smaller list of data that was analyzed by dChip and filtered by pvalue such that a file with about 4600 genes was obtained, which allowed for ease of use from 40,000 genes.** **Keywords: static vs simulated microgravity** **Overall design:** **The total RNA was extracted from 2T3 pre-osteoblast cells exposed to static or simulated microgravity (Rotating Wall Vessel) conditions.** **The RNA was then sent to Affymetrix microarray core facility at Baylor College of Medicine (Houston, TX) for microarray analysis.**

Background corr dist: **KL-Divergence = 0.0342, L1-Distance = 0.0397, L2-Distance = 0.0022, Normal std = 0.6845**

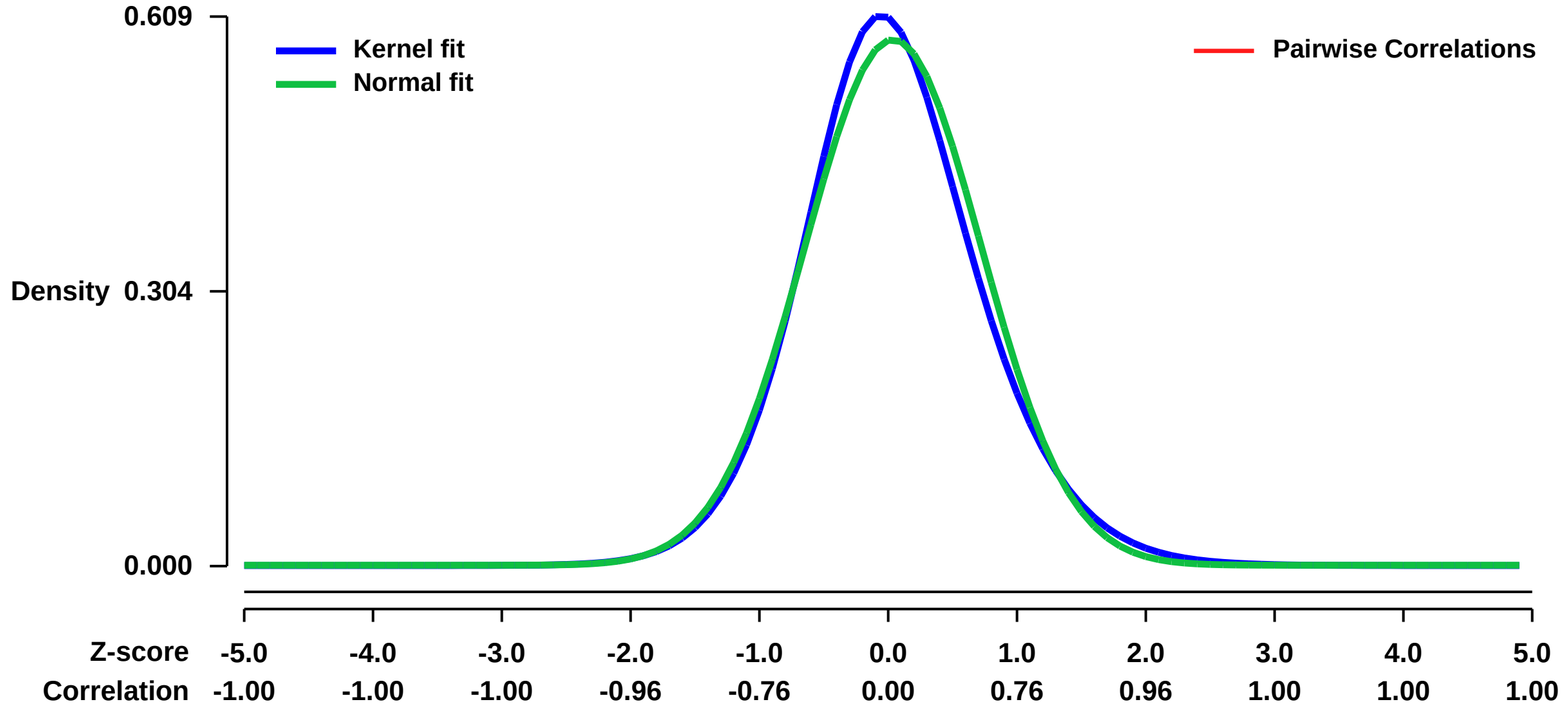

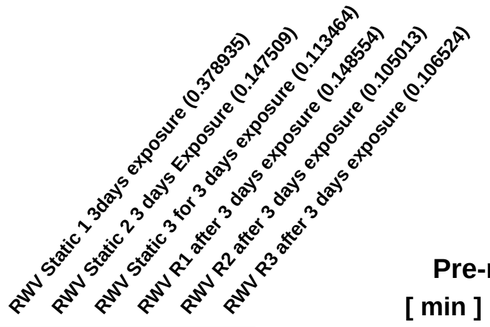

Pre-normalization Quantiles

[min] [medium] [max]

Null module

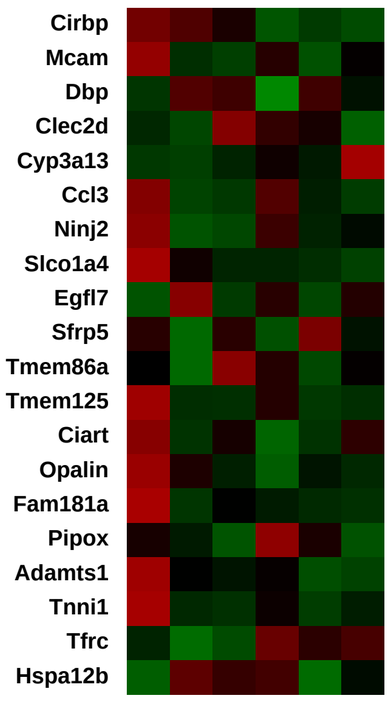

GEO Series "GSE3313" Expression Profiles

Num of samples in this series: 24

Scale of expression profile Z-scores

-3.0 -2.0 -1.0 0.0 1.0 2.0 3.0

GEO Link:	http://www.ncbi.nlm.nih.gov/geo/query/acc.cgi?acc=GSE3313
Status:	Public on Jun 30 2014
Title:	Impaired revascularization in a mouse model of diabetes associated with dysregulation of angiogenic-regulatory network.
Organism:	Mus musculus
Experiment type:	Expression profiling by array
Platform:	GPL1261
Pubmed ID:	15920034
Summary & Design:	**Summary:** Diabetes is a risk factor for the development of cardiovascular diseases that are associated with impaired angiogenesis or increased endothelial cell apoptosis. Here is it shown that angiogenic repair of ischemic hind limbs was impaired in Lepr db/db mice, a leptin receptor deficient model of diabetes, compared to wild-type C57BL/6 (WT) mice as evaluated by laser Doppler flow and capillary density analyses. To identify molecular targets associated with this disease process, hind limb cDNA expression profiles were created from adductor muscle of Lepr db/db and WT mice before and after hind limb ischemia using Affymetrix GeneChip´fi Mouse Expression Set microarrays. The expression patterns of numerous angiogenesis related proteins were altered in Lepr db/db versus WT mice following ischemic injury. These transcripts included neuropilin-1, VEGF-A, placental growth factor, elastin and matrix metalloproteinases that are implicated in blood vessel growth and maintenance of vessel wall integrity. These data illustrate that impaired ischemia-induced neovascularization in type 2 diabetes is associated with the dysregulation of a complex angiogenesis-regulatory network. **Keywords:** Diabetes, ischemia, angiogenesis, microarrays **Overall design:** Gene expression data for adductor muscle in the ischemic limb from wild type mice and Lepr db/db mice of 4 time points (before hind limb ischemia, 1 day, 7 days and 14 days after hind limb ischemia surgery). Three independent experimental replicates of each condition for each time point.

Background corr dist: KL-Divergence = 0.1724, L1-Distance = 0.0358, L2-Distance = 0.0026, Normal std = 0.3616

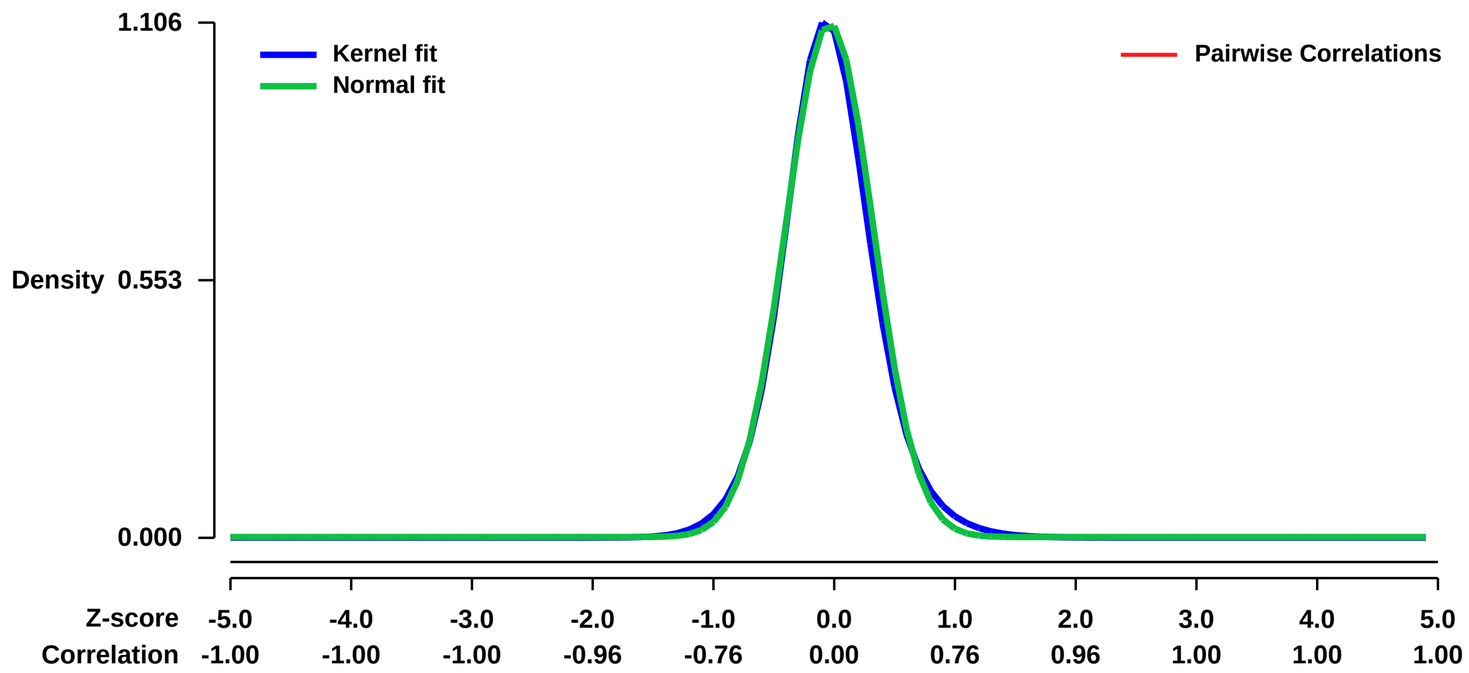

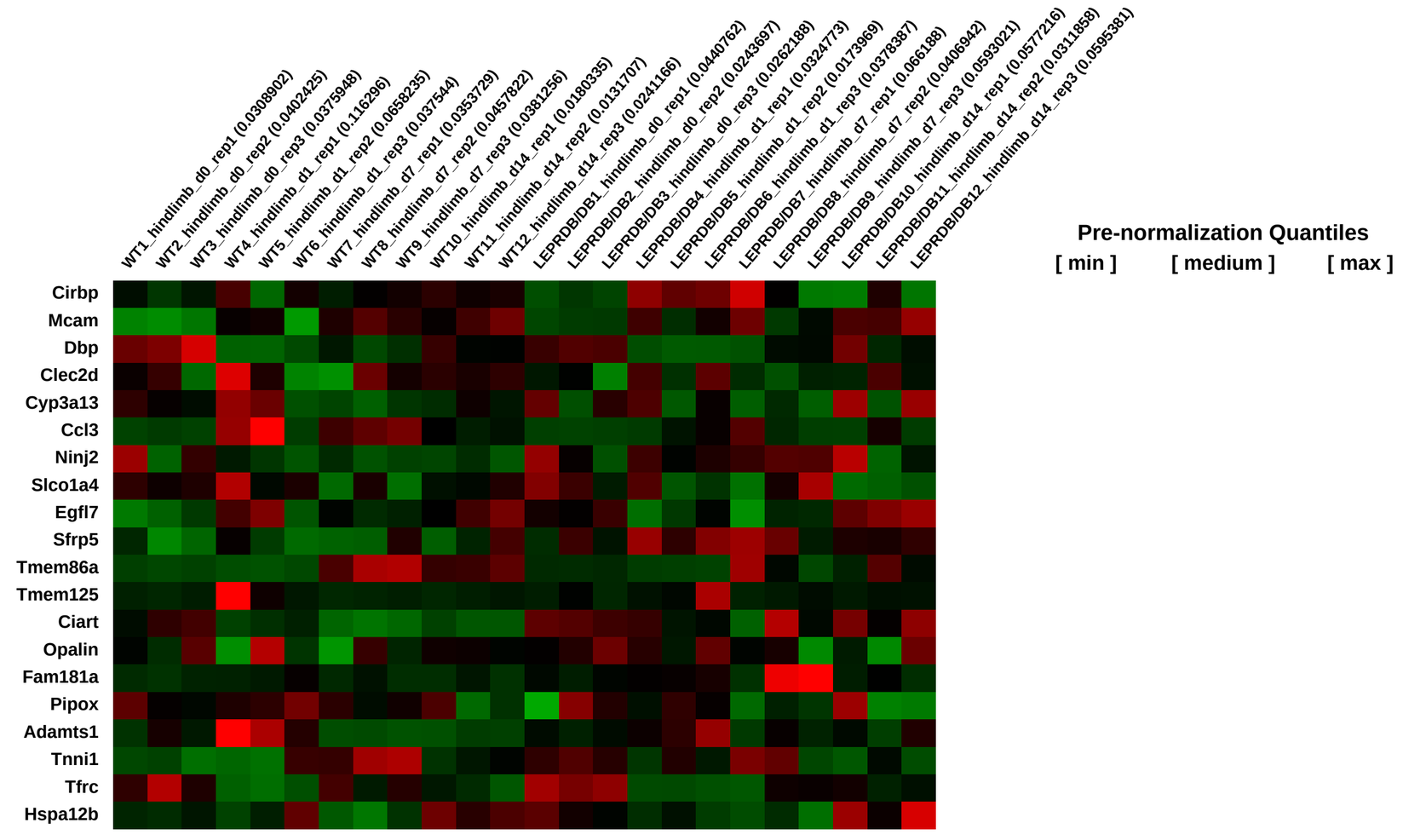

GEO Series "GSE28457" Expression Profiles

Num of samples in this series: 24

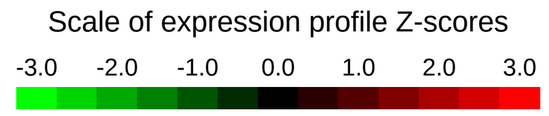

GEO Link:	http://www.ncbi.nlm.nih.gov/geo/query/acc.cgi?acc=GSE28457
Status:	Public on May 31 2012
Title:	Gene expression profile of E1A infected C2C12 myotubes
Organism:	Mus musculus
Experiment type:	Expression profiling by array
Platform:	GPL1261
Pubmed ID:	23027903

Summary & Design:

Summary:
Proliferating C2C12 myoblasts were induced to differentiate into myotubes and then infected with adenovirus expressing E1A (Ad-E1A), which induces cell cycle re-entry and dedifferentiation.

We analyzed the transcriptional profile of E1A infected C2C12-myotubes through the Affymetrix Mouse Genome 430 2.0 Array, searching for genes that were significantly regulated between two independent biological replicates at two different time points (24h and 36h after infection with Ad-E1A). In addition, we took advantage of the E1A mutant known as YH47/dl928 (hereafter referred as YH47), which bears two mutations in the pocket-binding region of E1A (Y48H, C124G) able to disrupt the interaction with Rb and its cognate proteins and to impair cell-cycle re-entry phenotype. YH47 mutant was used to identify the Rb independent transcriptional reprogramming of C2C12.

Overall design:
C2C12 cells were differentiated in vitro to myotubes as previously described. Myotubes were, then, infected with an adenovirus carrying the 12S form of E1A (dl520), with the YH47 E1A mutant (dl928) or with a control adenovirus (CTR) expressing a deletion of essentially the entire E1A gene (dl312). Two different time points after infection were considered (24 hours and 36 hours) to evaluate changes in C2C12 cells expression profile. Technical (A or B) and biological replicates (EXP1 or EXP2) were done for each condition.

Background corr dist: KL-Divergence = 0.1997, L1-Distance = 0.0314, L2-Distance = 0.0016, Normal std = 0.3411

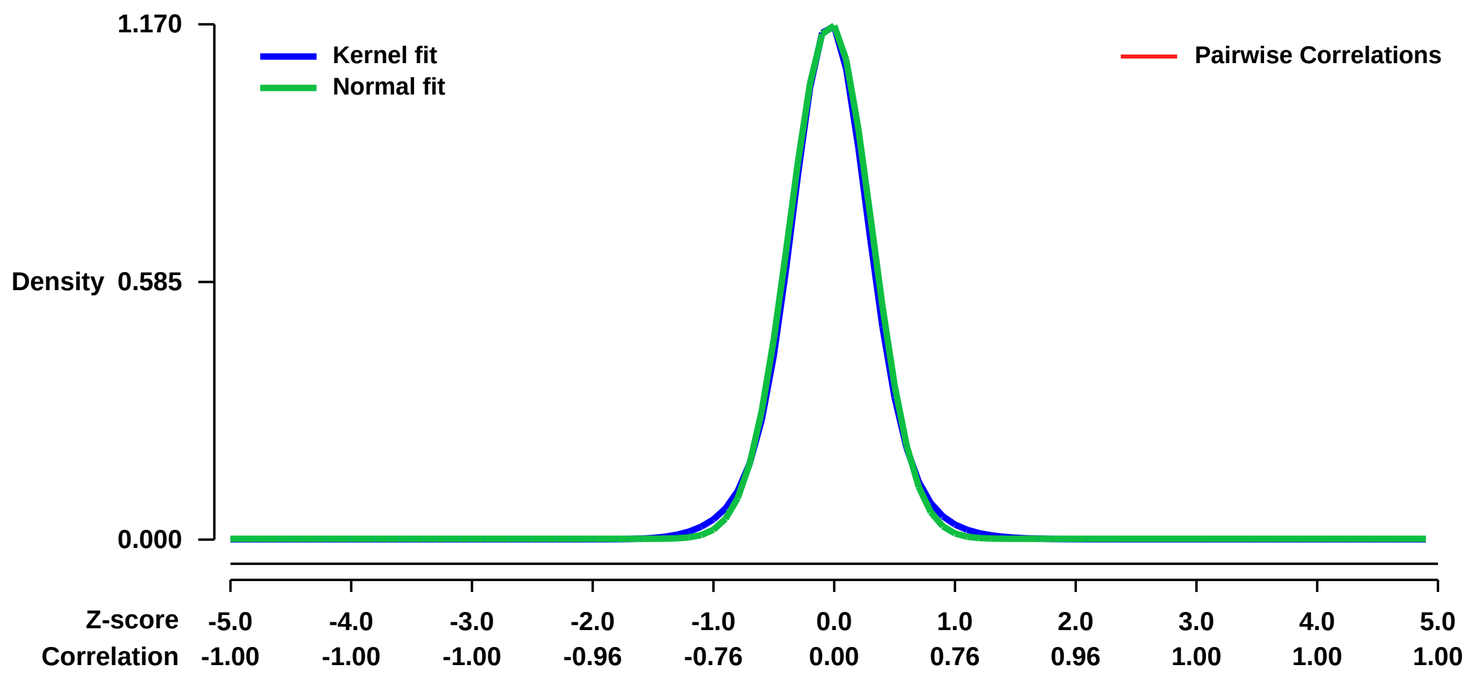

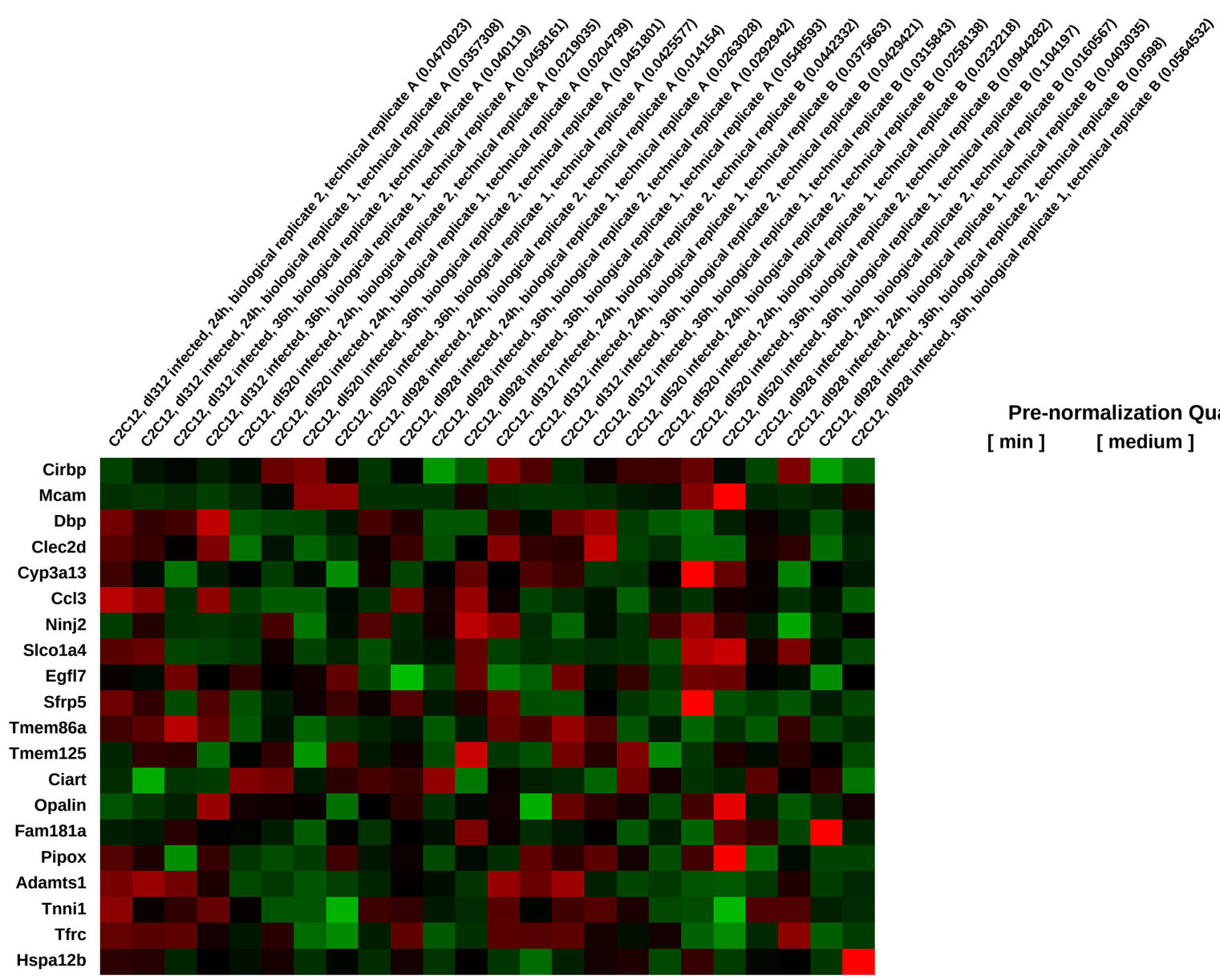

GEO Series "GSE6837" Expression Profiles

Num of samples in this series: 8

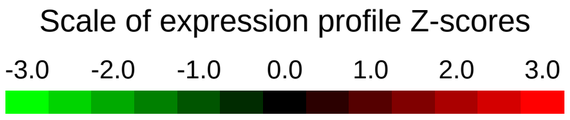

GEO Link:	http://www.ncbi.nlm.nih.gov/geo/query/acc.cgi?acc=GSE6837
Status:	Public on Jan 31 2007
Title:	Expression data from wild type (wt) and Ikbke knockout (Ikke) embryonic fibroblasts (EF)
Organism:	Mus musculus
Experiment type:	Expression profiling by array
Platform:	GPL1261
Pubmed ID:	17332413
Summary & Design:	**Summary:** WT and Ikbke-/- EF cells were stimulated with recombinant interferon beta for 6 hours. Cells lacking IKKe kinase show a defect in a subset of interferon stimulated gene transcription **Keywords: comparative study** **Overall design:** WT and Ikbke cells were either stimulated and left untreated to compare their response to interferon.

Background corr dist: KL-Divergence = 0.0231, L1-Distance = 0.0545, L2-Distance = 0.0038, Normal std = 0.8315

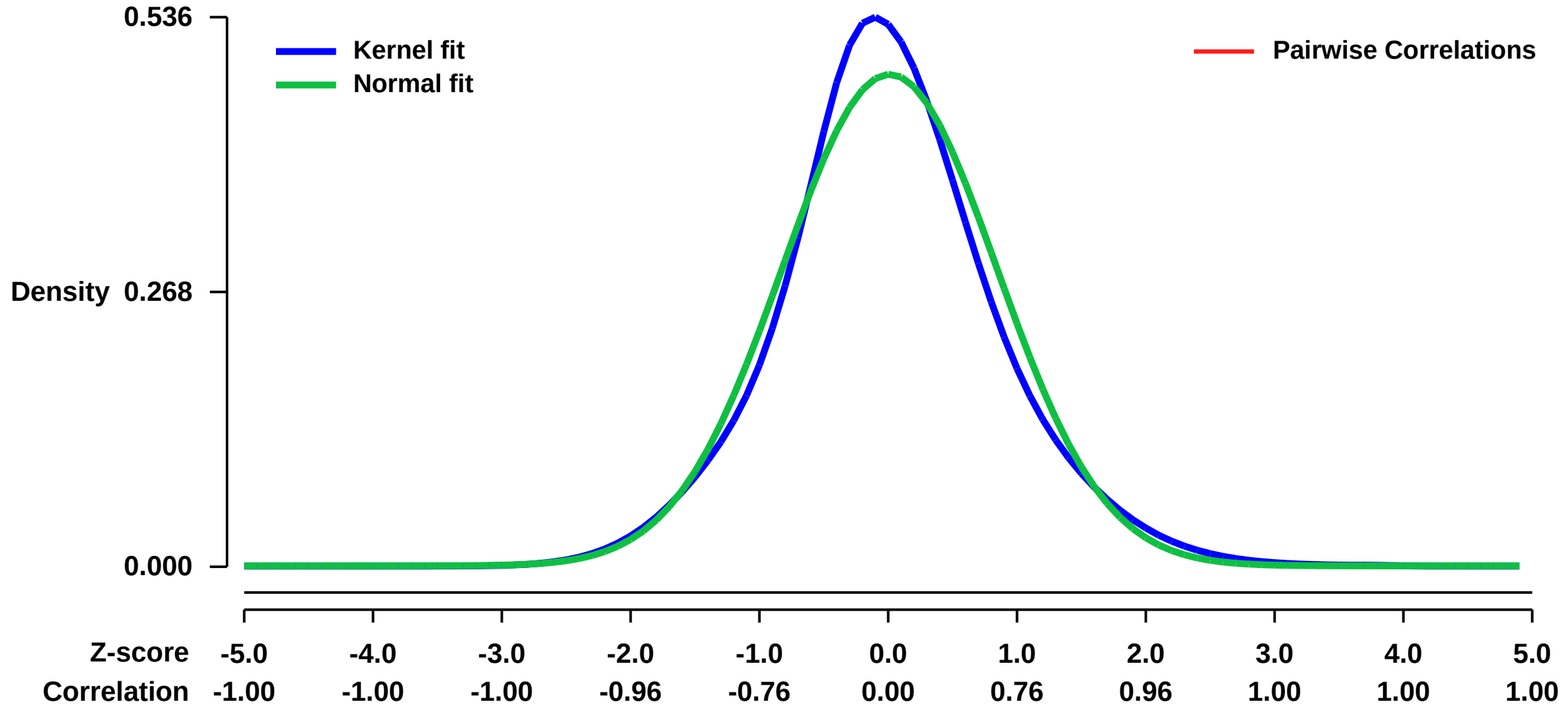

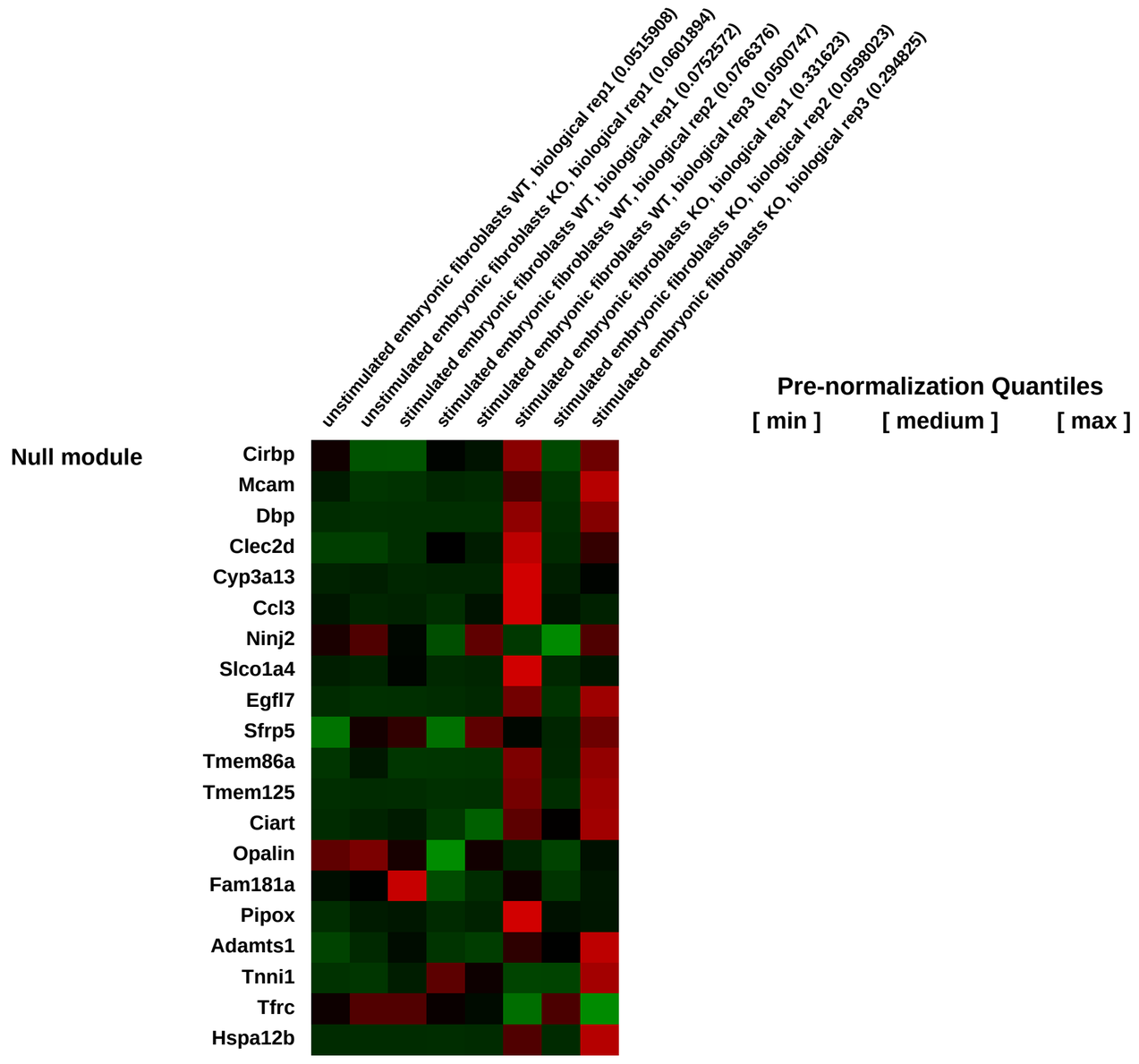

GEO Series "GSE20426" Expression Profiles

Num of samples in this series: 35

Scale of expression profile Z-scores

-3.0 -2.0 -1.0 0.0 1.0 2.0 3.0

GEO Link:	http://www.ncbi.nlm.nih.gov/geo/query/acc.cgi?acc=GSE20426
Status:	Public on Feb 16 2011
Title:	Hepatic gene expression during liver regeneration in response to partial hepatectomy: late time points (24h, 38h, 48h)
Organism:	Mus musculus
Experiment type:	Expression profiling by array
Platform:	GPL1261
Pubmed ID:	21719609
Summary & Design:	**Summary:** The process of liver regeneration can be divided into a series of stages that include initial inductive or priming events through cellular mitosis. Following two-thirds liver resection, the liver undergoes the â primingâ phase, in which cytokines TNF-a and IL-6 activate their respective receptors in hepatocytes. This leads to the activation of several key transcription factors: NF-kB, AP-1, Stat 3, Stat 1, and C/EBP-b and -d . These transcription factors induce the expression of immediate early genes. HGF is also expressed at this time and involved in the transition of quiescent hepatocytes into the G1 phase of the cell cycle. During the G1 phase, delayed early genes are expressed followed by induction of cell cycleâ related genes, both of which require new protein synthesis for their production. Increased expression of FoxM1B and TGF-a occurs at the G1/S transition and is correlated with increased expression of cyclinD1 and decreased expression of cdk inhibitors. During the G2/M phase of the cell cycle, FoxM1B directly elevates cyclinB1, cyclinB2, and cdc25B expression. Additionally, FoxM1B is associated with increased cyclinF and p55cdc, which are involved in completion of the cell cycle following partial hepatectomy. In mice, two-thirds partial hepatectomy promotes proliferation of liver cells and rapid growth of the remaining liver tissue, resulting in complete restoration of organ mass in approximately 7 days (Mackey S. et al. Hepatology 2003 Dec;38(6):1349-52). **Overall design:** Liver tissue was collected 0h, 24h, 38h, and 48h after partial hepatectomy or sham surgery from both young (5-6 months) and old (25-27 months) CB6F1 mice. All control and partial hepatectomy samples were assayed in triplicate. Relative gene expression levels were determined using Affymetrix moe430_2 oligo arrays.

Background corr dist: KL-Divergence = 0.1371, L1-Distance = 0.0498, L2-Distance = 0.0059, Normal std = 0.3856

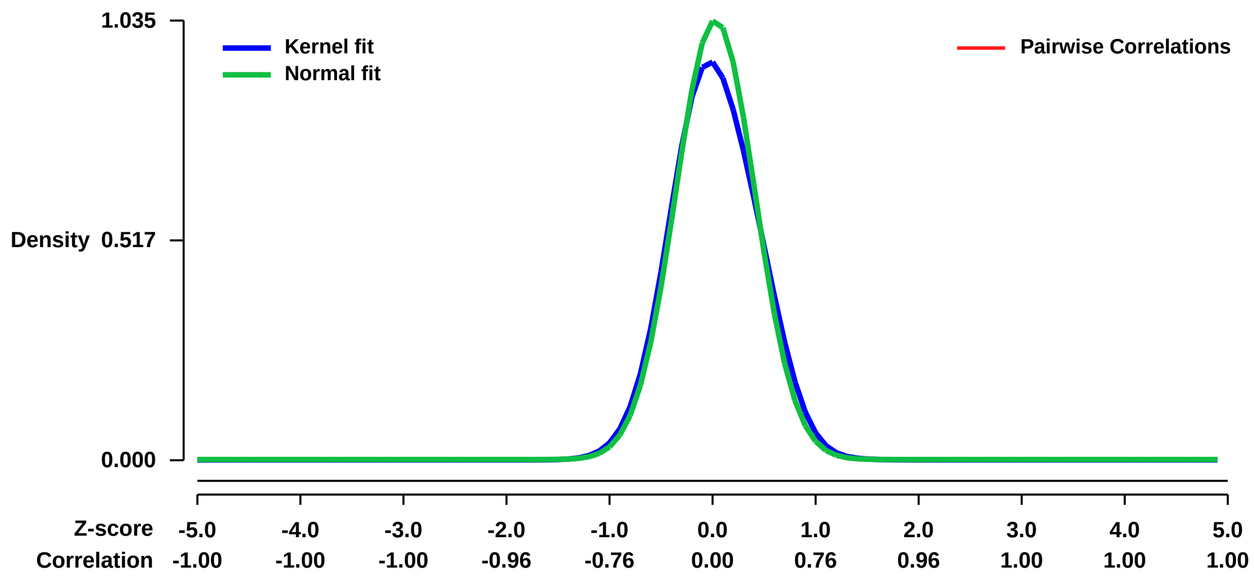

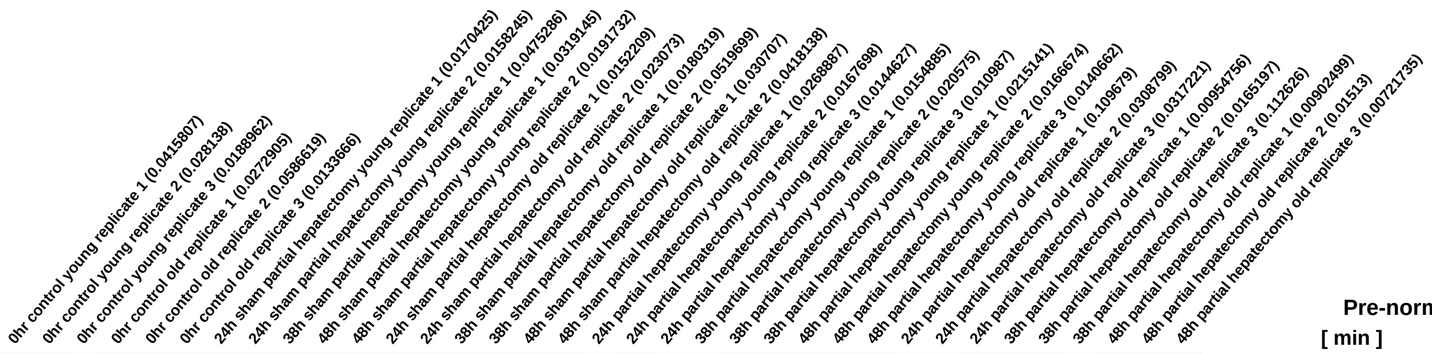

Pre-normalization Quantiles

[min] [medium] [max]

Null module

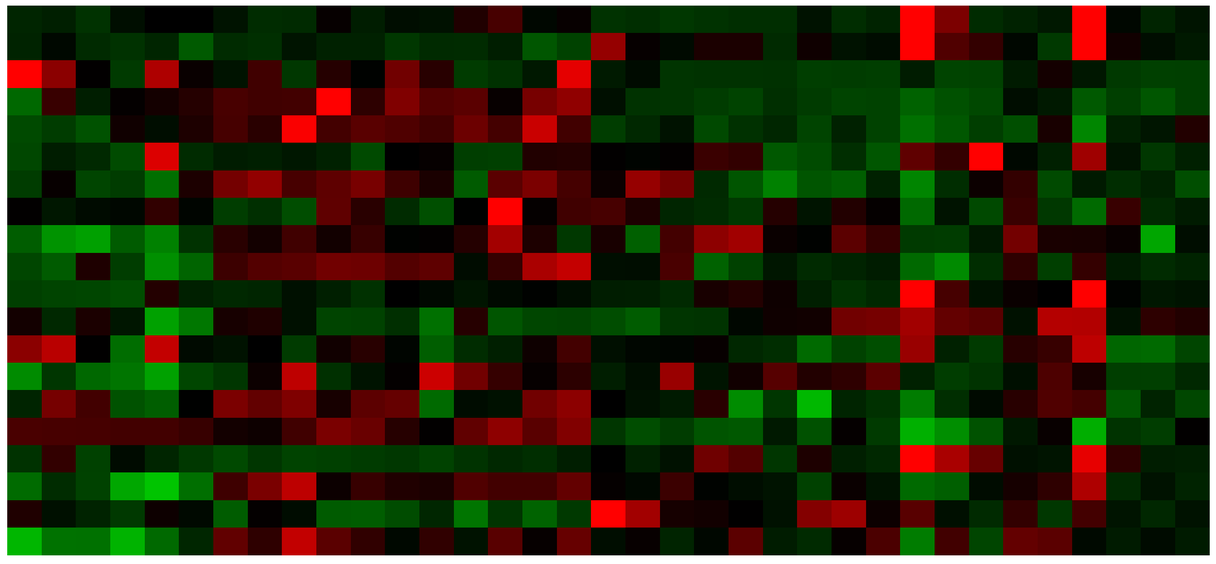

GEO Series "GSE42021" Expression Profiles

Num of samples in this series: 27

Scale of expression profile Z-scores

-3.0 -2.0 -1.0 0.0 1.0 2.0 3.0

GEO Link:	http://www.ncbi.nlm.nih.gov/geo/query/acc.cgi?acc=GSE42021
Status:	Public on Mar 07 2013
Title:	Gene expression profiles of CD4SP Foxp3GFP-CD25+ Treg precursors and Foxp3GFP-CD25- thymocytes
Organism:	Mus musculus
Experiment type:	Expression profiling by array
Platform:	GPL1261
Pubmed ID:	23420886
Summary & Design:	**Summary:** We investigated at which stage of maturation commitment to a stable Foxp3-expressing phenotype takes place. We assessed stability of Foxp3 expression in thymic Foxp3+ Treg subsets of different maturity, defined by CD24 expression. Next we compared gene expression profiles of Foxp3+ Treg subsets (+) of different maturity (24lo, 24int, 24hi) and could identify a set of genes that were specifically up or downregulated in Foxp3+ Tregs, but not in Foxp3- conventional T cells, in a maturation-dependent manner. **Overall design:** Gene expression of Foxp3+ Treg subsets (+) of different maturity (24lo, 24int, 24hi) compared to their Foxp3- conventional Tcell subsets (-) counterpart.

Background corr dist: KL-Divergence = 0.2463, L1-Distance = 0.0487, L2-Distance = 0.0055, Normal std = 0.3050

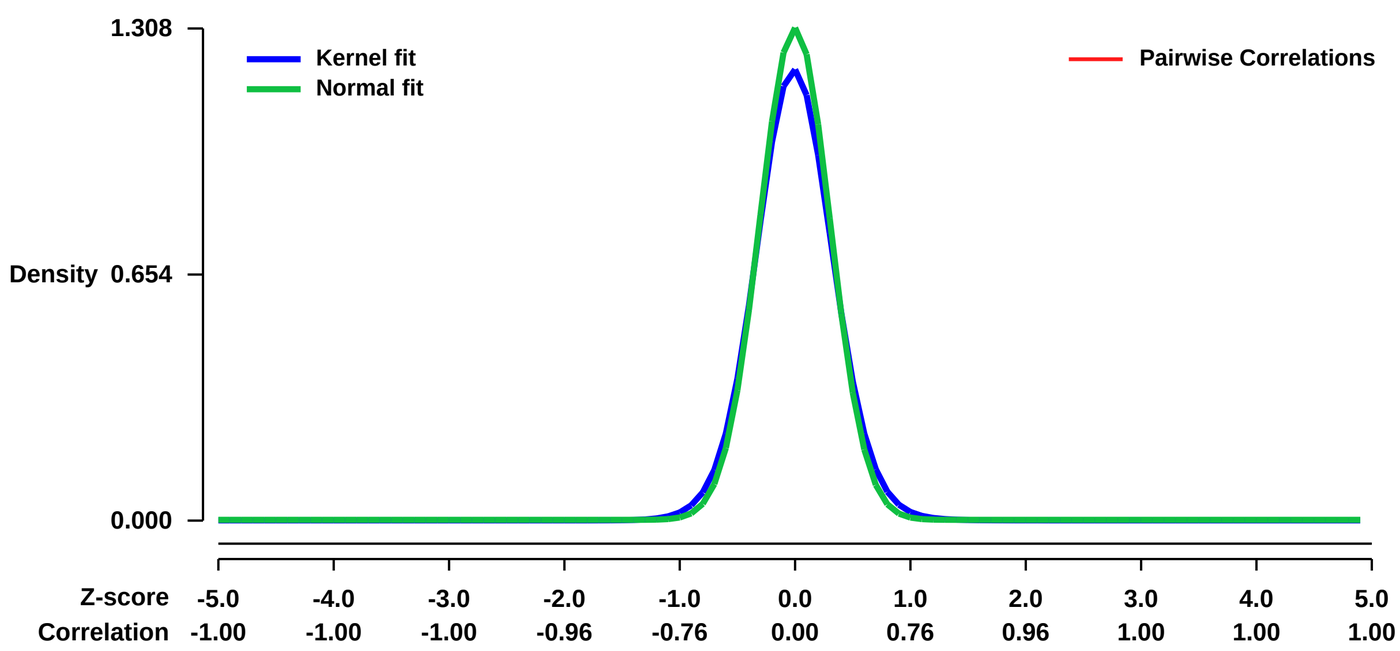

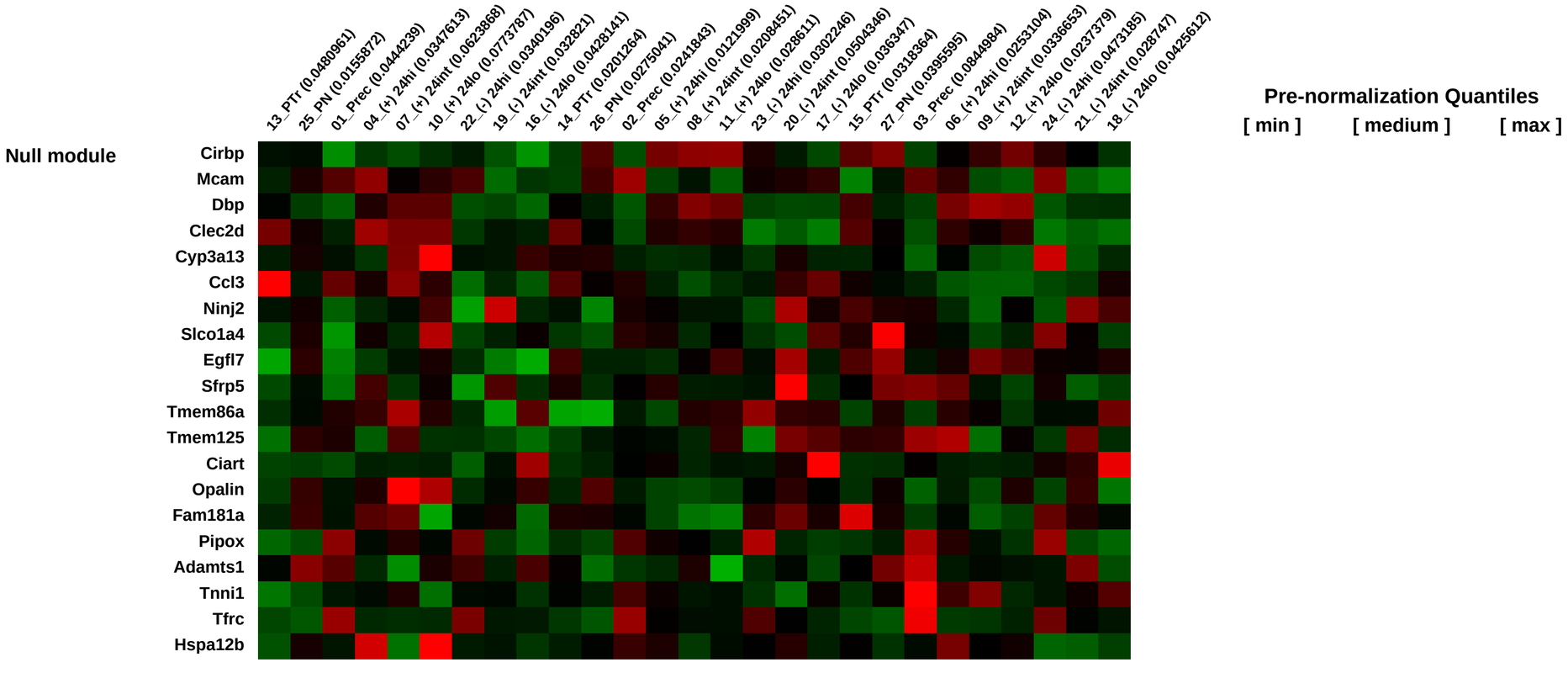

GEO Series "GSE35322" Expression Profiles

Num of samples in this series: 20

Scale of expression profile Z-scores

-3.0 -2.0 -1.0 0.0 1.0 2.0 3.0

GEO Link:	http://www.ncbi.nlm.nih.gov/geo/query/acc.cgi?acc=GSE35322
Status:	Public on Mar 15 2012
Title:	Expression data from tail skin in young (5 months) and old (30 months) CB6F1 mice
Organism:	Mus musculus
Experiment type:	Expression profiling by array
Platform:	GPL1261
Pubmed ID:	22413003
Summary & Design:	**Summary:** **Background: Skin aging is associated with intrinsic processes that compromise structure of the extracellular matrix while promoting loss of functional and regenerative capacity. These processes are accompanied by a large-scale shift in gene expression, but underlying mechanisms are not understood and conservation of these mechanisms between humans and mice is uncertain. Results: We used genome-wide expression profiling to investigate the aging skin transcriptome. In humans, age-related shifts in gene expression were sex-specific. In females, aging increased expression of transcripts associated with T-cells, B-cells and dendritic cells, and decreased expression of genes in regions with elevated Zeb1, AP-2 and YY1 motif density. In males, however, these effects were contrasting or absent. When age-associated gene expression patterns in human skin were compared to those in tail skin from CB6F1 mice, overall human-mouse correspondence was weak. Moreover, inflammatory gene expression patterns were not induced with aging of mouse tail skin, and well-known aging biomarkers were in fact decreased (e.g., Clec7a, Lyz1 and Lyz2). These unexpected patterns and weak human-mouse correspondence may be due to decreased abundance of antigen presenting cells in mouse tail skin with age. Conclusions: Aging is generally associated with a pro-inflammatory state, but we have identified an exception to this pattern with aging of CB6F1 mouse tail skin. Aging therefore does not uniformly heighten inflammatory status across all mouse tissues. Furthermore, we identified both intercellular and intracellular mechanisms of transcriptome aging, including those that are sex- and species-specific.** **We used Affymetrix microarrays to evaluate genome-wide expression in tail skin from young (5 month) and old (30 month) CB6F1 mice (males and females).** **Overall design:** **Genome-wide expression was evaluated in tail skin from young (5 months) and old (30 months) CB6F1 mice of both sexes. Samples were collected simultaneously but RNA samples were processed in two separate batches.**

Background corr dist: KL-Divergence = 0.1813, L1-Distance = 0.0453, L2-Distance = 0.0045, Normal std = 0.3448

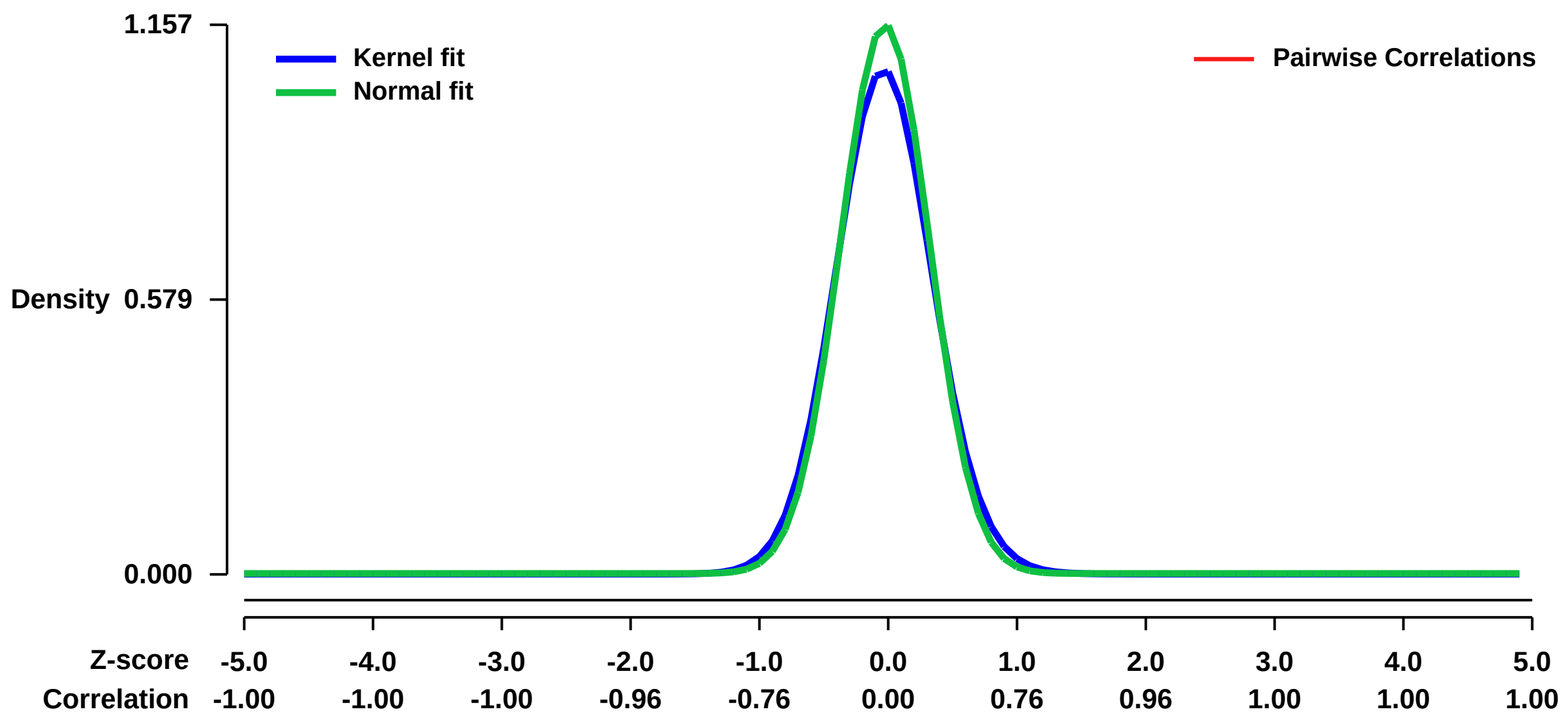

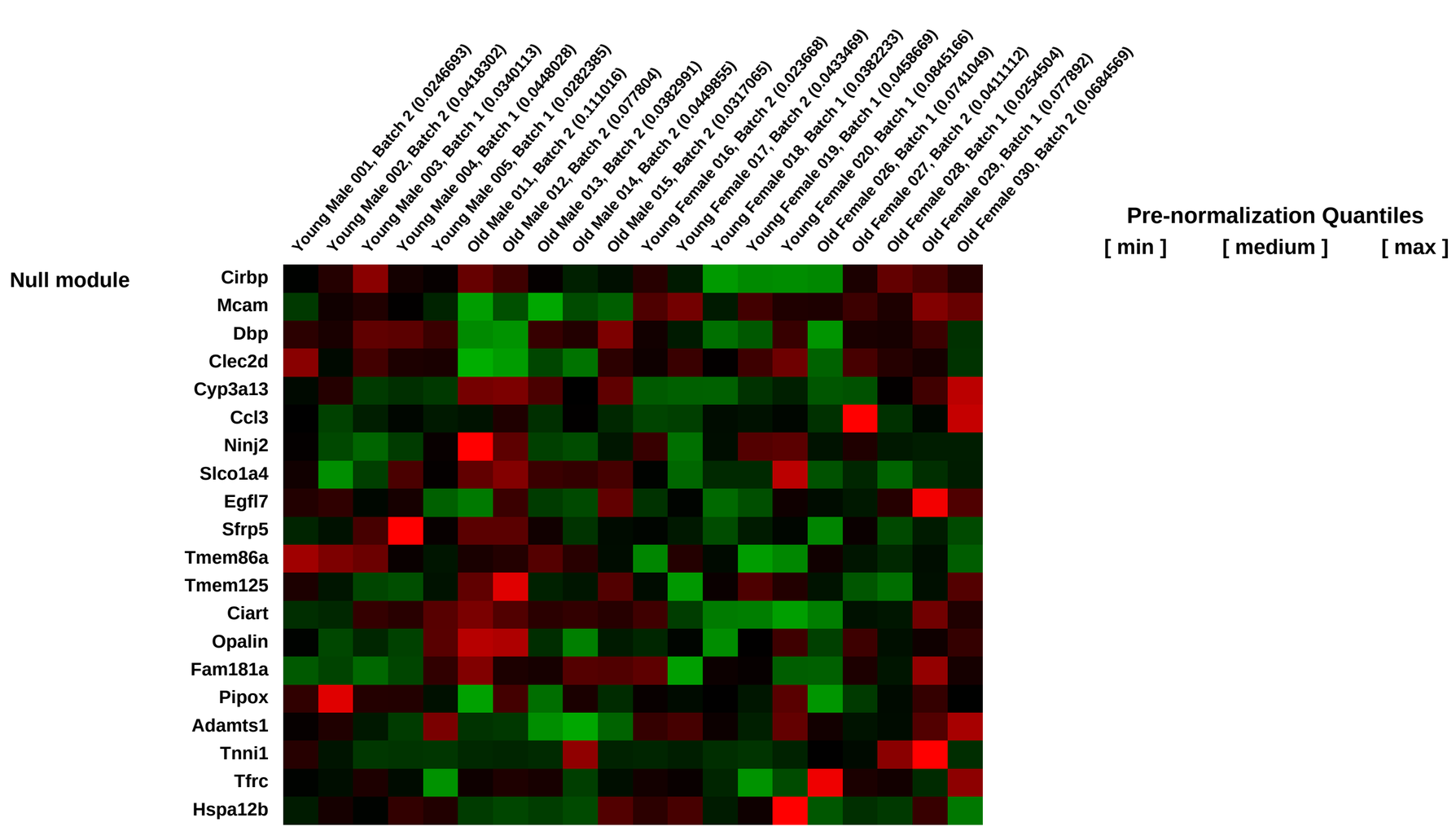

GEO Series "GSE8349" Expression Profiles

Num of samples in this series: 10

Scale of expression profile Z-scores

-3.0 -2.0 -1.0 0.0 1.0 2.0 3.0

GEO Link:	http://www.ncbi.nlm.nih.gov/geo/query/acc.cgi?acc=GSE8349
Status:	Public on Mar 25 2008
Title:	Microarray platform comparison study of hippocampal gene expression in DCLK1 transgenic and wild-type mice
Organism:	Mus musculus
Experiment type:	Expression profiling by array
Platform:	GPL1261
Pubmed ID:	18927111
Summary & Design:	**Summary:** The aim of the present study was to compare, on a statistical basis, the performance of different microarray platforms to detect differences in gene expression in a realistic and challenging biological setting. Gene expression profiles in the hippocampus of five wild-type and five transgenic ¸·C-doublecortin-like kinase mice were evaluated with five microarray platforms: Applied Biosystems, Affymetrix, Agilent, Illumina and home-spotted oligonucleotide arrays. We observed considerable overlap between the different platforms, the overlap being better detectable with significance level-based ranking than with a p-value based cut-off. Confirming the qualitative agreement between platforms, Pathway analysis consistently demonstrated aberrances in GABA-ergic signalling in the transgenic mice, even though pathways were represented by only partially overlapping genes on the different platforms. **Keywords:** microarray platform comparison **Overall design:** Illumina_raw_data.csv contains the raw data for GSM206887 to GSM206896. In these files, the sample identifiers are included in the column headers.

Background corr dist: KL-Divergence = 0.0755, L1-Distance = 0.0346, L2-Distance = 0.0023, Normal std = 0.4822

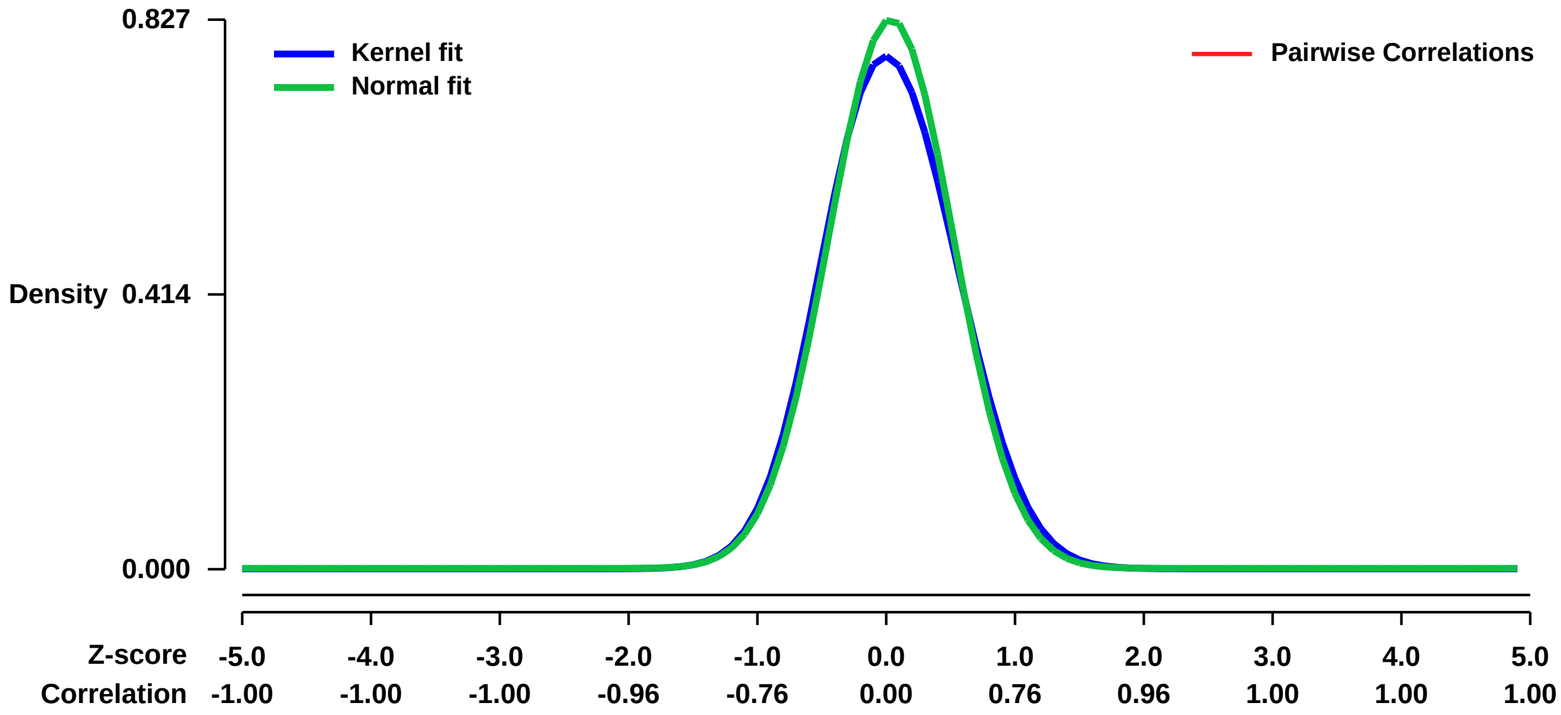

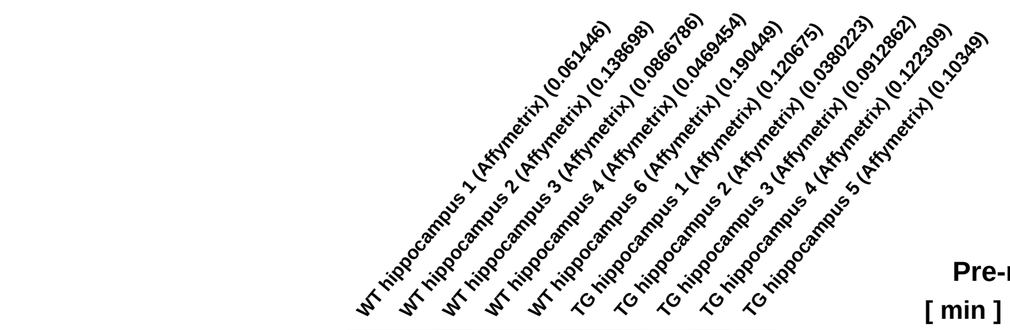

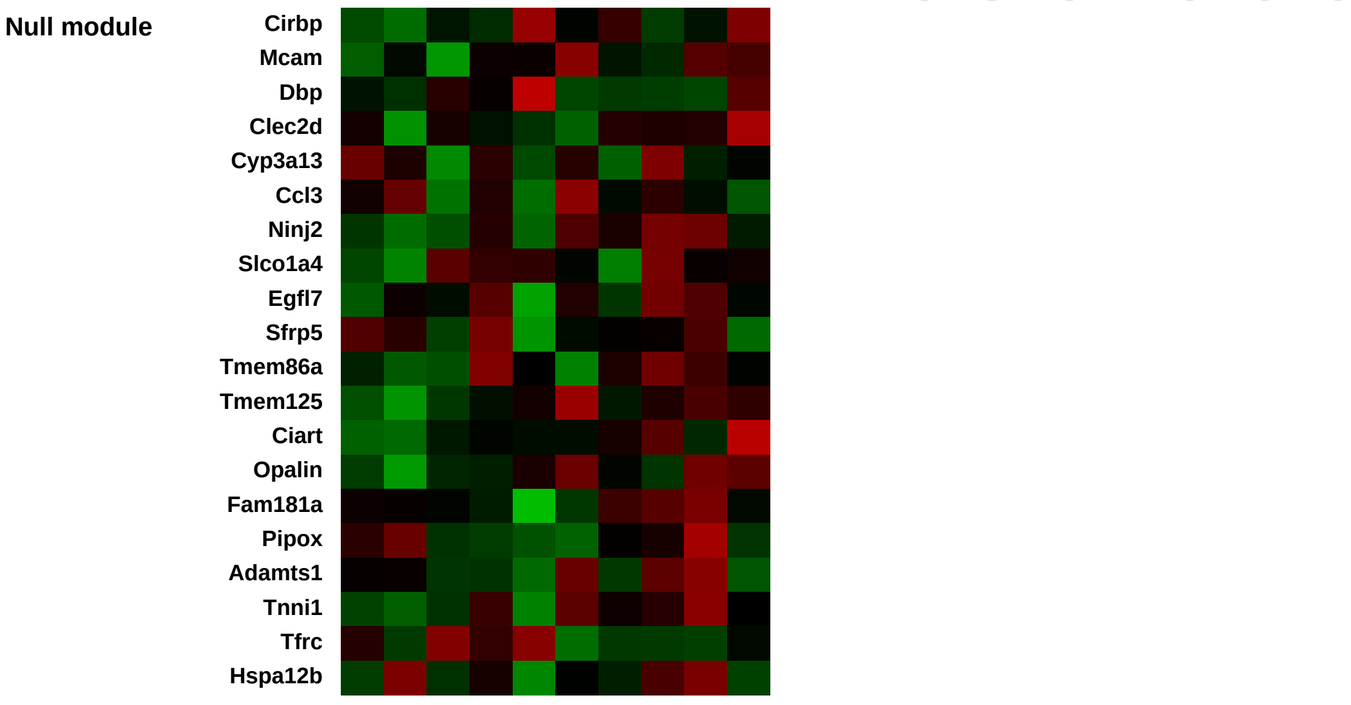

GEO Series "GSE35844" Expression Profiles

Num of samples in this series: 9

Scale of expression profile Z-scores

-3.0 -2.0 -1.0 0.0 1.0 2.0 3.0

GEO Link:	http://www.ncbi.nlm.nih.gov/geo/query/acc.cgi?acc=GSE35844
Status:	Public on Jun 18 2012
Title:	Dicer1 deletion in myeloid-committed progenitors causes neutrophil dysplasia and blocks macrophage/dendritic cell development in mice
Organism:	Mus musculus
Experiment type:	Expression profiling by array
Platform:	GPL1261
Pubmed ID:	22353998
Summary & Design:	**Summary:** MiRNAs have the potential to regulate cellular differentiation programs. However, miRNA-deficiency in primary hematopoietic stem cells (HSCs) results in HSC depletion in mice, leaving the question of whether miRNAs play a role in early-lineage decisions unanswered. To address this issue, we deleted Dicer1, which encodes an essential RNaseIII enzyme for miRNA biogenesis, in murine CCAAT/enhancer-binding protein alpha (C/EBPA)-positive myeloid-committed progenitors in vivo. In contrast to the results in HSCs, we found that miRNA depletion affected neither the number of myeloid progenitors nor the percentage of C/EBPA-positive progenitor cells. Analysis of gene-expression profiles from wild type and Dicer1-deficient granulocyte-macrophage progenitors (GMPs) revealed that 20 miRNA families were active in GMPs. Of the derepressed miRNA targets in Dicer1-null GMPs, 27% are normally exclusively expressed in HSCs or are specific for multi-potent progenitors and erythropoiesis, indicating an altered gene-expression landscape. Dicer1-deficient GMPs were defective in myeloid development in vitro and exhibited an increased replating capacity, indicating a regained self-renewal potential of these cells. In mice, Dicer1 deletion blocked monocytic differentiation, depleted macrophages and caused myeloid dysplasia with morphological features of Pelger-Huˆ«t anomaly. These results provide evidence for a miRNA-controlled switch for a cellular program of self-renewal and expansion towards myeloid differentiation in GMPs. **Overall design:** To generate Cebpa-Cre;R26-LSL-Eyfp;Dicer1wt/fl/Dicer1fl/fl mice, we crossed mice that contain floxed Dicer1 alleles (Dicer1fl) with Cebpa-Cre;R26-LSL-Eyfp reporter mice 2. Fetal livers were obtained on embryonic day (E) 13.5. Routine genotyping of Dicer1; Cebpa-Cre;R26-LSL-Eyfp mice was performed by PCR assays of DNA from tail or toe biopsies. For transplantation, 6 to 8-week-old recipient mice (C57Bl/6, Jackson Laboratories) were irradiated (8.5 Gy) and tail-vein injected with fetal liver single-cell suspensions. Typically, cells from each fetal liver were transplanted into two recipient mice. Hematopoietic tissues were analyzed 6-10 weeks post transplantation. EYFP positive GMPs from the bone marrow of Dicer wt control (n=3), Dicer -/wt (n=3 and Dicer fl/fl (n=3) were sorted and analyzed for gene expression profiles.

Background corr dist: KL-Divergence = 0.1010, L1-Distance = 0.0231, L2-Distance = 0.0009, Normal std = 0.4374

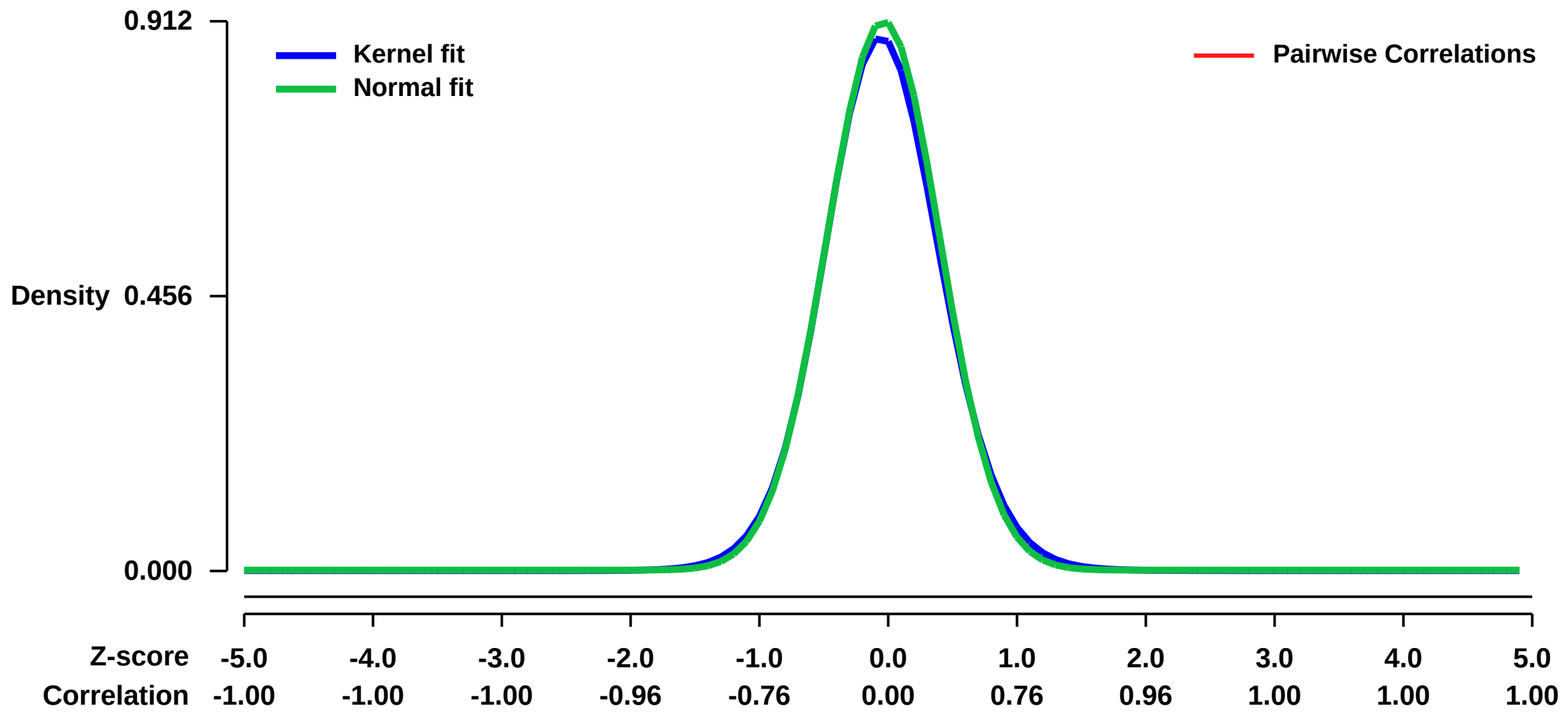

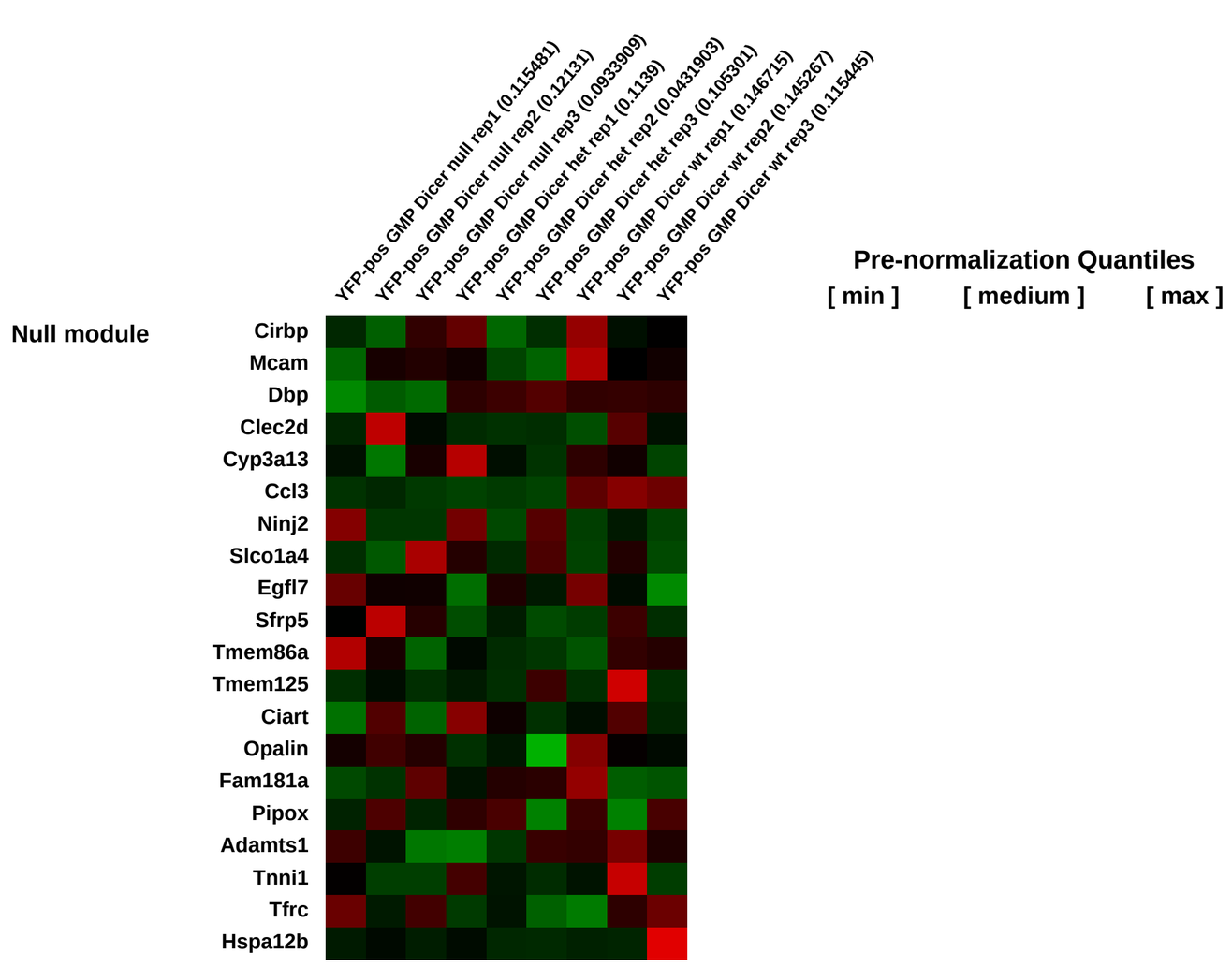

GEO Series "GSE7699" Expression Profiles

Num of samples in this series: 6

Scale of expression profile Z-scores

-3.0 -2.0 -1.0 0.0 1.0 2.0 3.0

GEO Link:	http://www.ncbi.nlm.nih.gov/geo/query/acc.cgi?acc=GSE7699
Status:	Public on May 04 2007
Title:	A high fat, ketogenic diet induces a unique metabolic state in mice.
Organism:	Mus musculus
Experiment type:	Expression profiling by array
Platform:	GPL1261
Pubmed ID:	17299079
Summary & Design:	**Summary:** Analysis of liver gene transcription during feeding of a ketogenic diet. Ketogenic diets may alter physiologic and metabolic profiles in a direction that favors weight loss. C57BL/6J mice were maintained for six weeks on either chow or ketogenic diet. Mice eating KD had lower weights, 90% reduction in insulin levels and increased energy expenditure compared to animals fed chow. Despite consumpiton of a very high fat diet serum lipids remained normal. Here we show that consumption of KD shifted liver metabolism to drastically increased fatty acid oxidation. Concurrently, expression of genes involved in fatty acid synthesis were markedly suppressed. **Keywords: Hepatic profile** **Overall design:** Eight week old C57BL/6 mice were fed either chow (Labdiet 5008, Pharmserv) or KD (F3666, Bio-Serv) for six weeks. Livers were harvested in the morning in ad lib fed animals. Total RNA from 2-3 animals in each group was used for Affymetrix analysis.

Background corr dist: KL-Divergence = 0.0402, L1-Distance = 0.0246, L2-Distance = 0.0007, Normal std = 0.6199

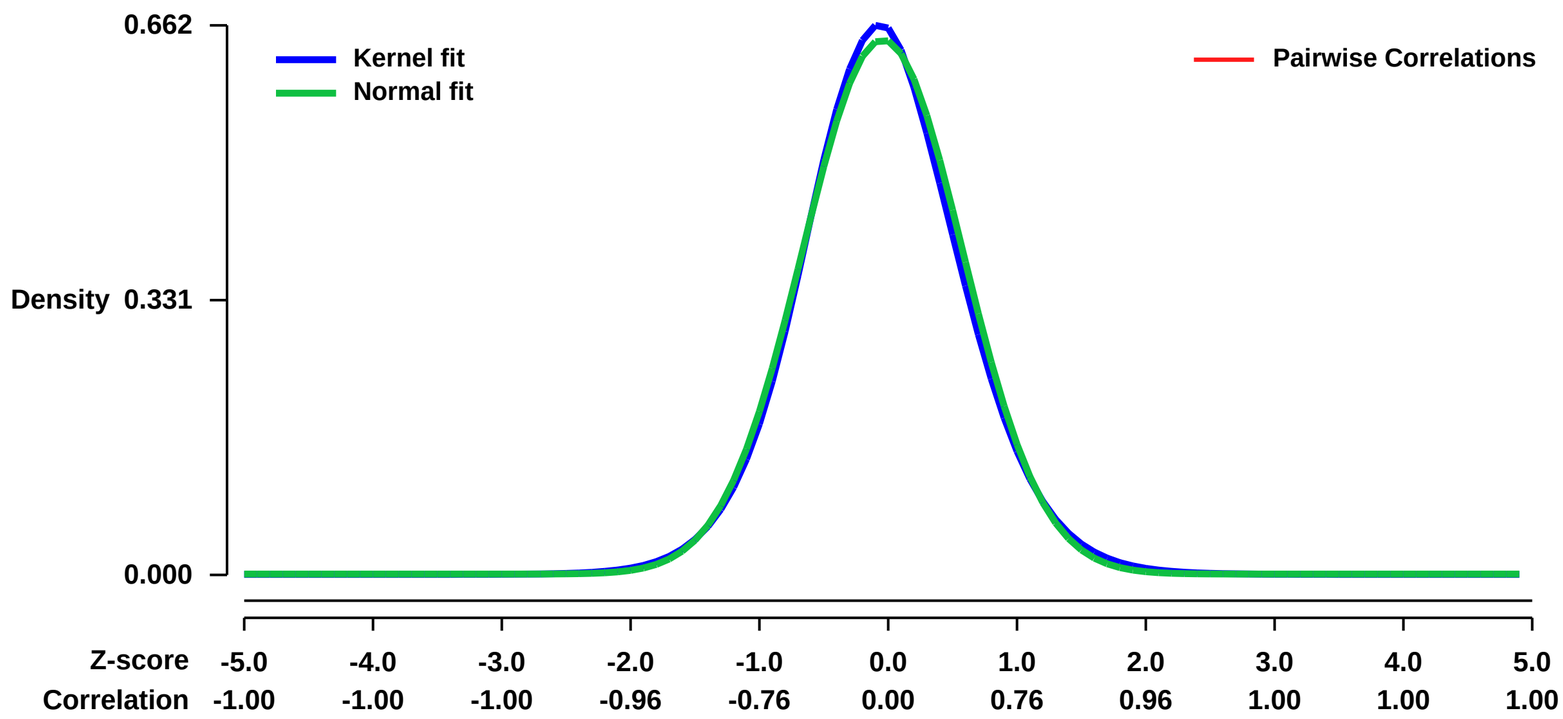

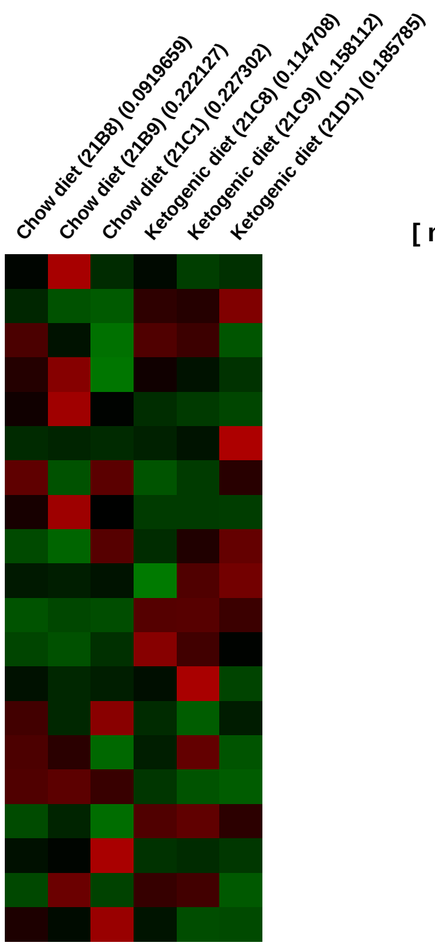

GEO Series "GSE7767" Expression Profiles

Num of samples in this series: 6

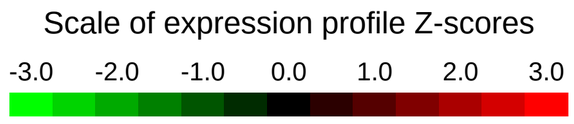

GEO Link:	http://www.ncbi.nlm.nih.gov/geo/query/acc.cgi?acc=GSE7767
Status:	Public on Jul 15 2007
Title:	Differential transcription of ip Chlamydia infected C57BL6J and DBA2J mice
Organism:	Mus musculus
Experiment type:	Expression profiling by array
Platform:	GPL1261
Pubmed ID:	17641048

Summary & Design:

Summary:
C57BL/6J mice were 105-fold more resistant to Chlamydia psittaci infection than DBA/2J mice by LD100 determinations. Linkage analysis using BXD recombinant inbred strains revealed a single effector locus at a 1.5 Mbp region on chromosome 11 encoding a cluster of three p47GTPases (Irgb10, Igtp, and Iigp2). Western blots of infected tissue showed that Irgb10 was elevated in resistant mice and one of the two possible Iigp2 protein isoforms was preferentially expressed in susceptible mice. The BXD39 strain, susceptible at Irgb10 and resistant at Iigp2, had an intermediate phenotype, implicating the non-redundant role of these p47GTPases. C57BL/6J and DBA/2J exhibited a difference in IFNg dependent chlamydial control, which was reversible by Iigp2 siRNA knockdown. Microarrays of infected peritoneal lavage revealed >10 fold up regulation of neutrophil recruiting chemokines in susceptible mice and >100 fold increase in macrophage differentiation genes in resistant mice, indicating that susceptibility pattern involves stimulation of different inflammatory cell recruiting pathways. Massive neutrophil recruitment was seen in susceptible mice by histology and flow cytometry, and neutrophil chemokine receptor (CXCR2) knockout mice on a susceptible background survived lethal challenge confirming that neutrophil recruitment was required for susceptibility. Congenic Igtp knockout mice also susceptible at Irgb10 and Iigp2 on a resistant background recruited neutrophils and succumbed to infection. We conclude that Irgb10 and Iigp2 act together to confer differential susceptibility against murine chlamydial infection. Results indicate that these p47GTPases have cell autonomous effects, which results in vastly different inflammatory stimulation leading to either recovery or death.

Keywords: Comparative disease state analysis

Overall design:
C57BL/6J and DBA2J mice (4 mice each) were infected I.p. with 10E4 IFU of Chlamydia psittaci then peritoneal lavage was collected on day 3 post infection. Cells were centrifuged then treated with Trizol for total RNA extraction.

Background corr dist: KL-Divergence = 0.0126, L1-Distance = 0.0218, L2-Distance = 0.0006, Normal std = 0.8222

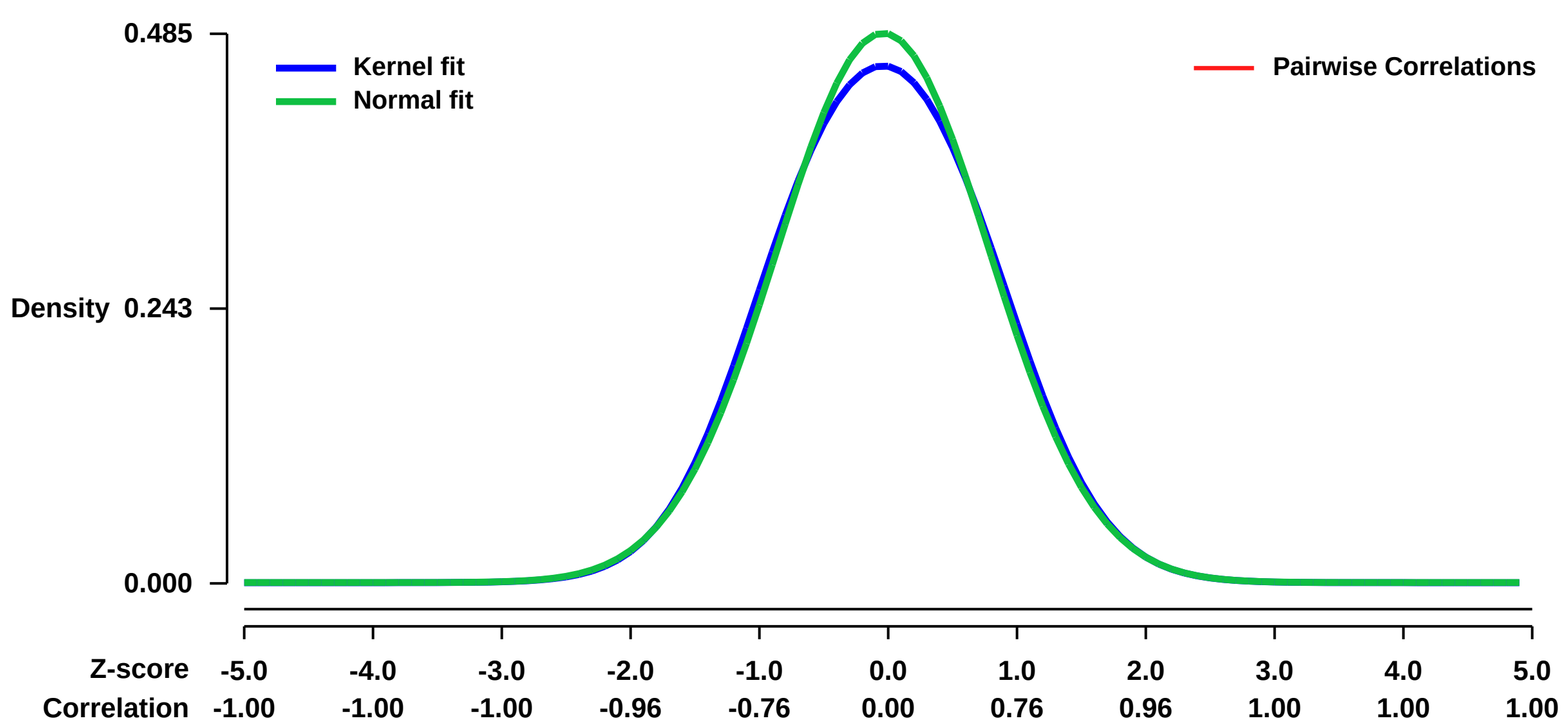

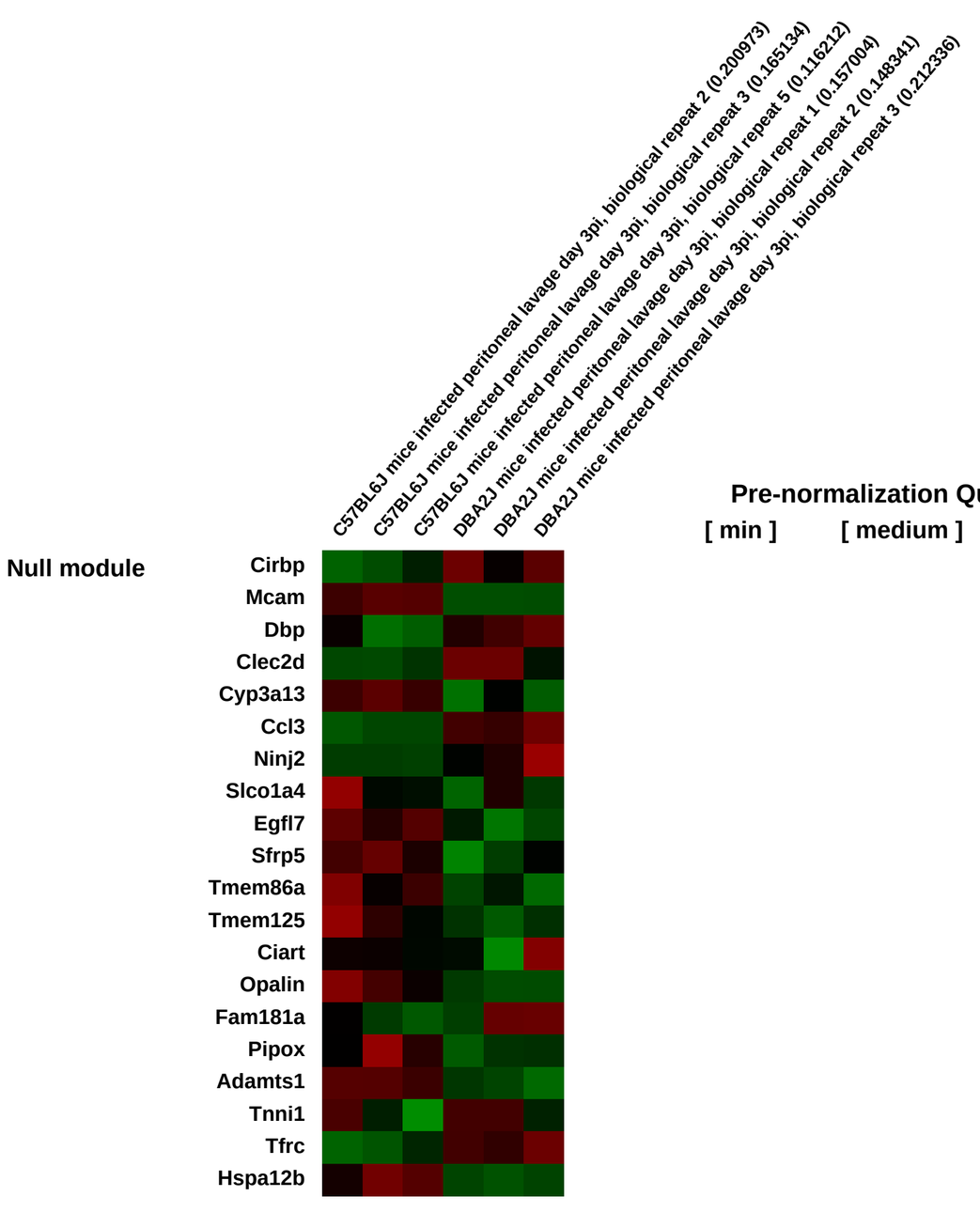

GEO Series "GSE20954" Expression Profiles

Num of samples in this series: 14

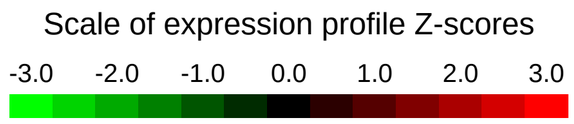

GEO Link:	**http://www.ncbi.nlm.nih.gov/geo/query/acc.cgi?acc=GSE20954**
Status:	**Public on Aug 17 2010**
Title:	**mRNA expression profile in mouse lung development**
Organism:	**Mus musculus**
Experiment type:	**Expression profiling by array**
Platform:	**GPL1261**
Pubmed ID:	**20520778**
Summary & Design:	**Summary:** **We performed miRNA and mRNA profiling over a 7-point time course, encompassing all recognized stages of lung development and explore dynamically regulated miRNAs and potential miRNA-mRNA interaction networks specific to mouse lung development** **Overall design:** **replicated time course of mouse lung development in 7 time points**

Background corr dist: **KL-Divergence = 0.0229, L1-Distance = 0.0372, L2-Distance = 0.0026, Normal std = 0.7245**

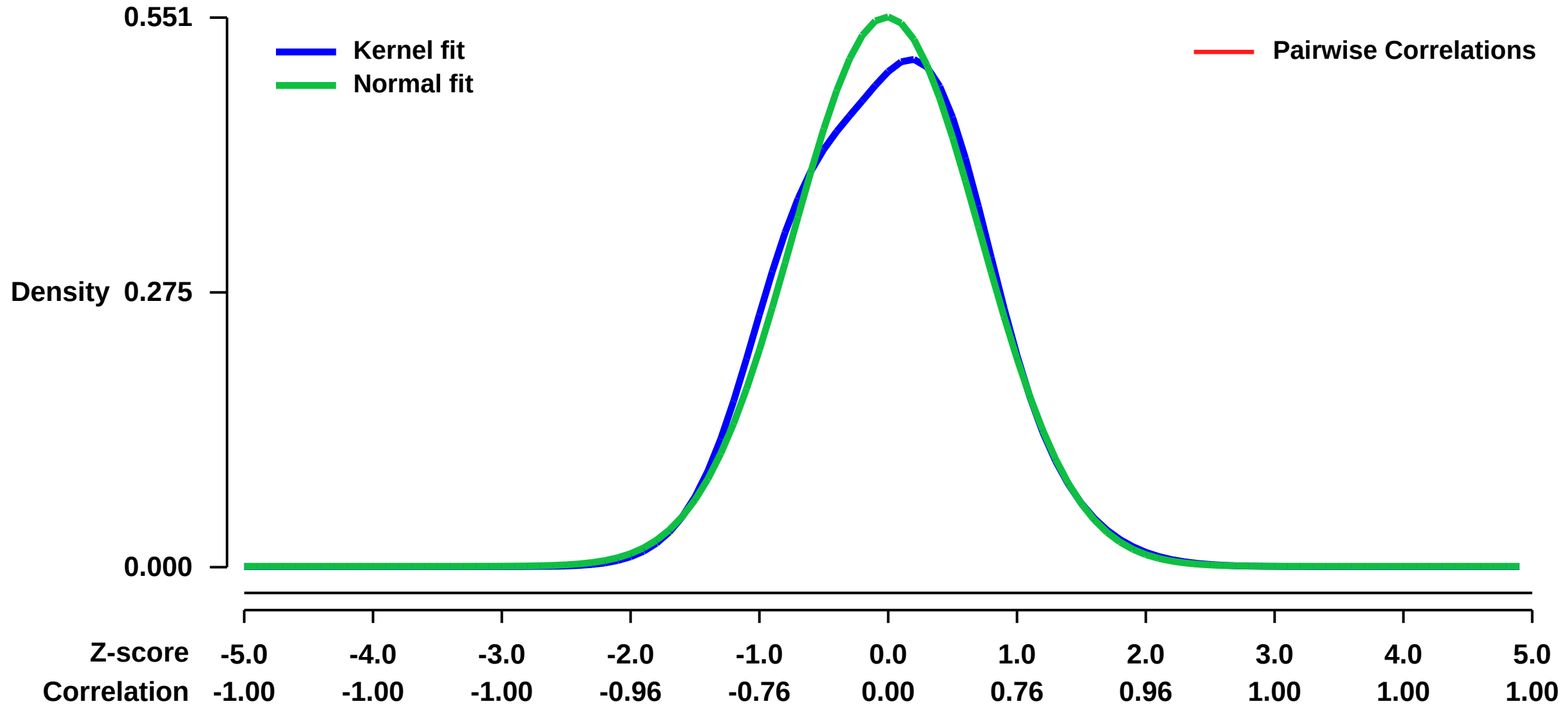

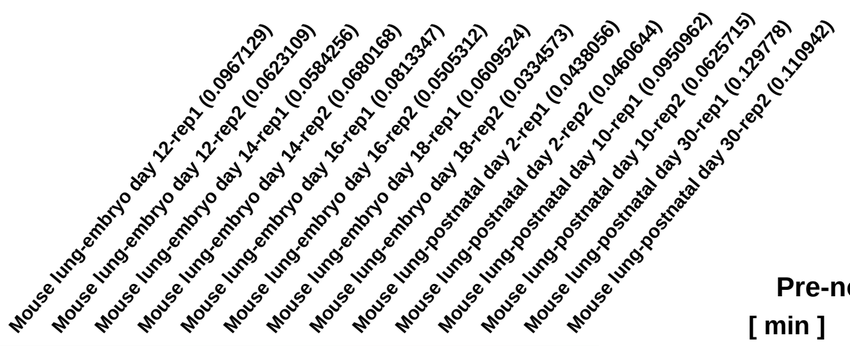

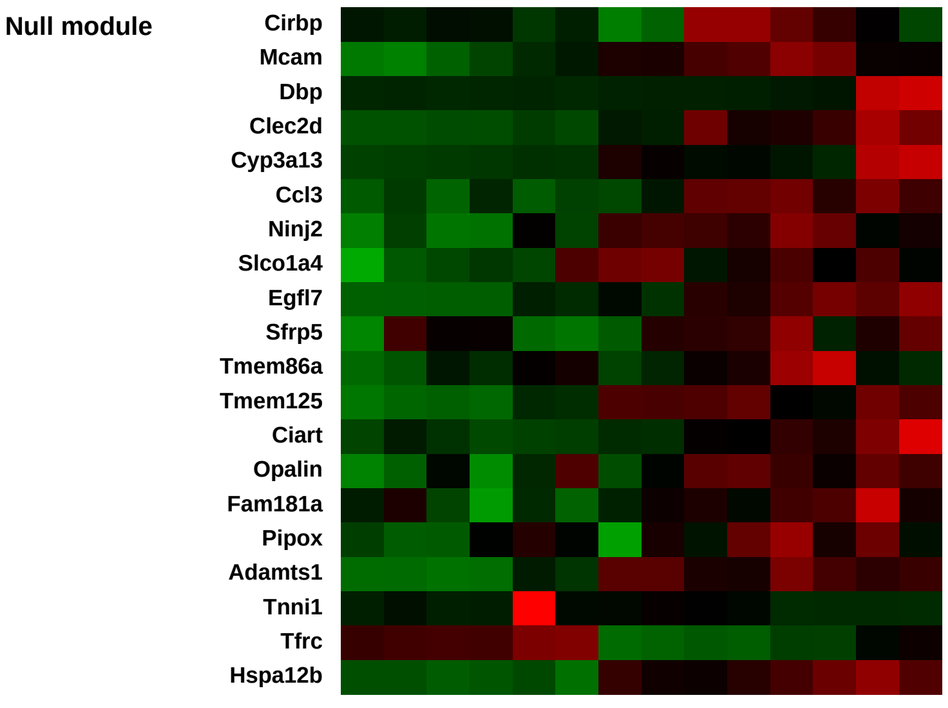

GEO Series "GSE7424" Expression Profiles

Num of samples in this series: 8

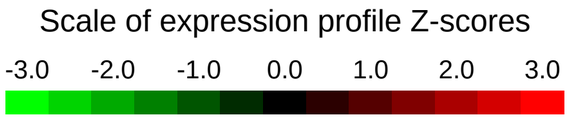

GEO Link:	http://www.ncbi.nlm.nih.gov/geo/query/acc.cgi?acc=GSE7424
Status:	Public on Apr 03 2007
Title:	Intragraft gene expression profile associated with the induction of tolerance
Organism:	Mus musculus
Experiment type:	Expression profiling by array
Platform:	GPL1261
Pubmed ID:	18267024
Summary & Design:	**Summary:** Xenotransplantation holds the promise of providing an unlimited supply of donor organs for terminal patients with organ failure. The gal carbohydrate results in rejection of wild type pig grafts, however, chimerism established by expression of the GalT gene prior to transplantation in GalT knockout mice results in tolerance to Gal+ heart grafts. We used microarrays in order to further understand the early events that occur within grafts that demonstrate tolerance. Keywords: transplntation tolerance **Overall design:** The GalT BMT recipient is a GalT knockout mouse which recieved GalT gene transduced allo-bone marrow cells transplantation after sublethal irradiation. A heart of wild type C57BL/6 was heterotopically transplanted into the recipient after GalT BMT. Syngeneic Control recipient is a wild type C57BL/6 transplanted a heart of wild C57BL/6.

Background corr dist: KL-Divergence = 0.0600, L1-Distance = 0.0214, L2-Distance = 0.0007, Normal std = 0.5344

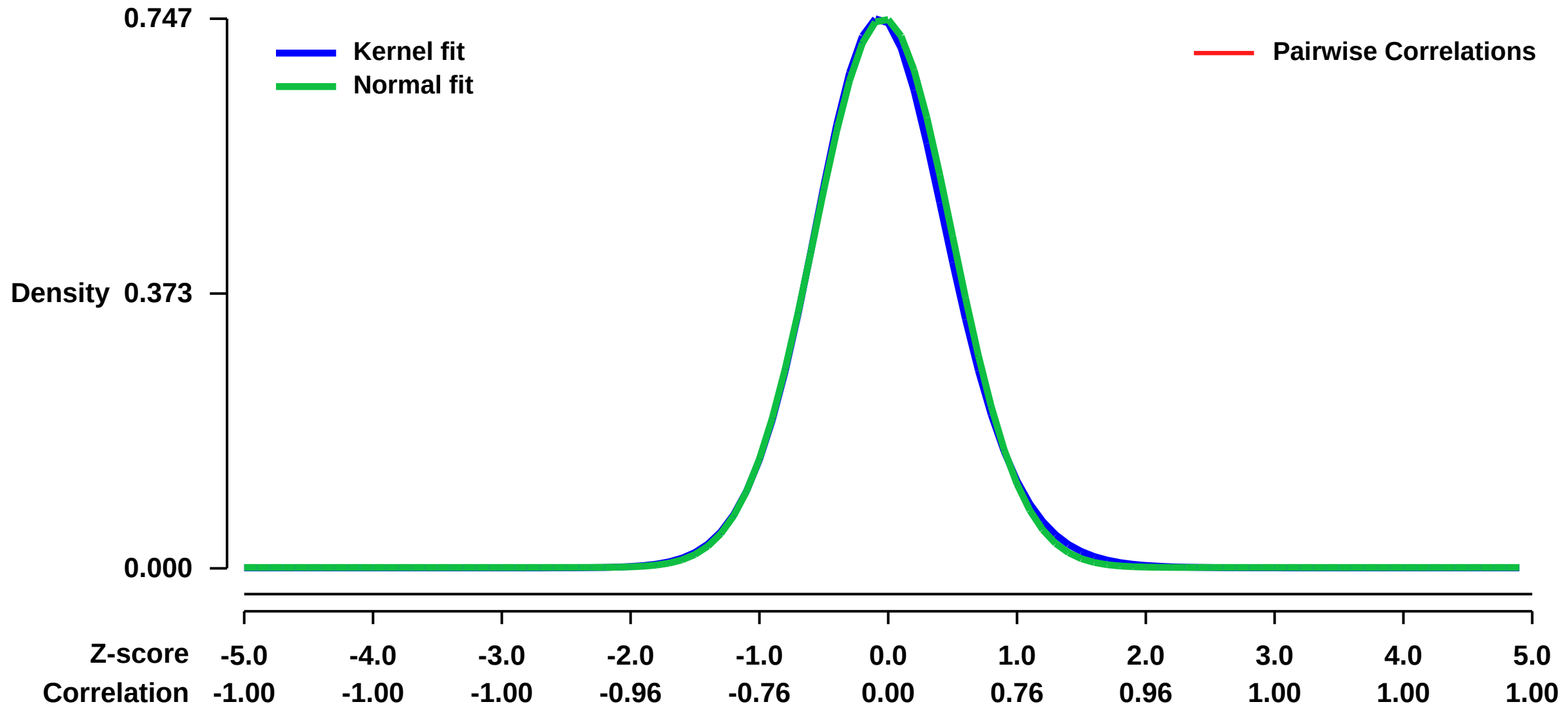

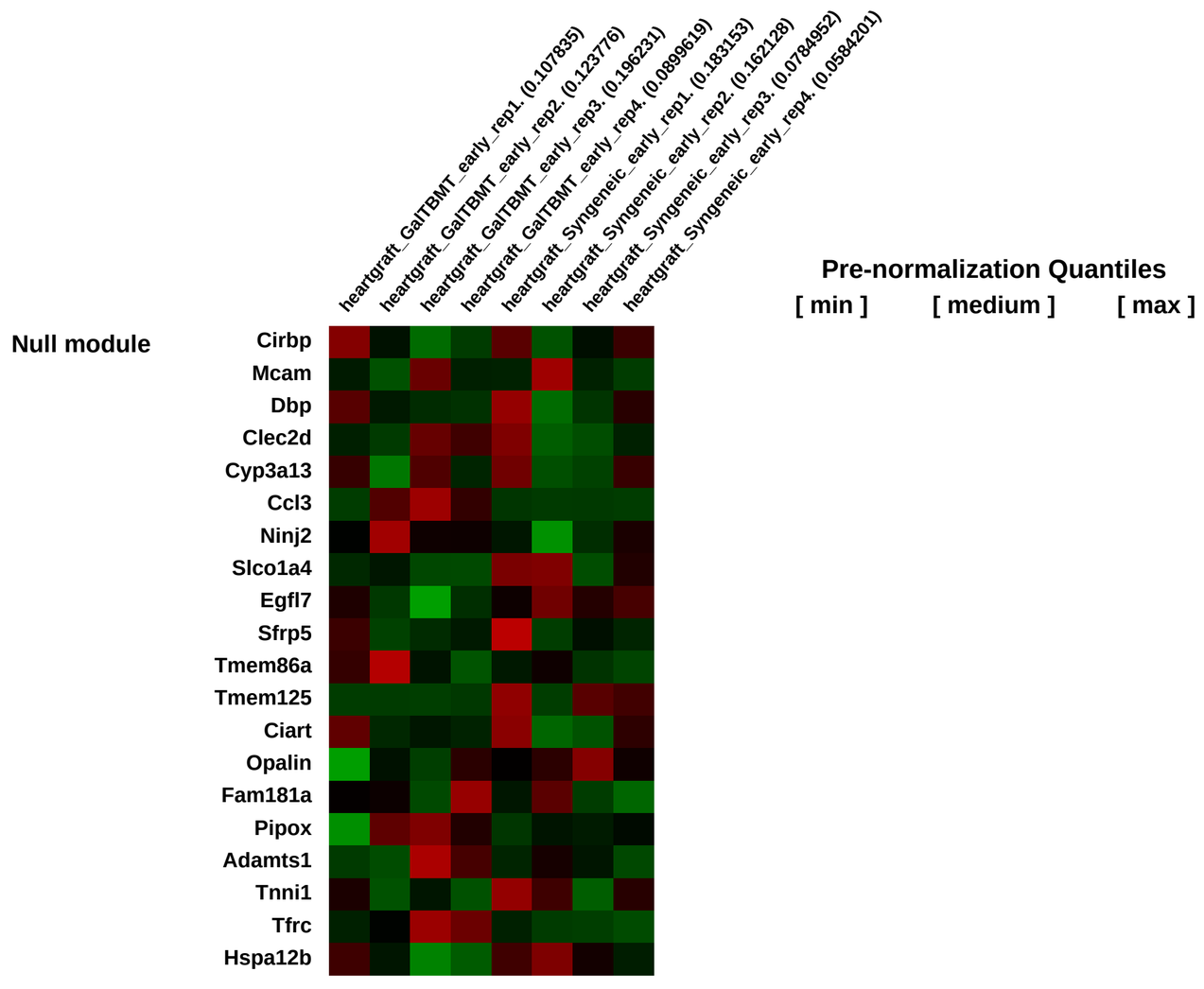

GEO Series "GSE8431" Expression Profiles

Num of samples in this series: 12

Scale of expression profile Z-scores

-3.0 -2.0 -1.0 0.0 1.0 2.0 3.0

GEO Link:	http://www.ncbi.nlm.nih.gov/geo/query/acc.cgi?acc=GSE8431
Status:	Public on Dec 18 2007
Title:	Microarray screening of RARgamma responsive genes in F9 teratocarcinoma cells
Organism:	Mus musculus
Experiment type:	Expression profiling by array
Platform:	GPL1261
Pubmed ID:	18164278
Summary & Design:	**Summary:** We compared the differentially expressed genes between the F9 Wt cells and F9 RAR gamma knock out cells before and after RA treatment. 3 replicates for each conditions. We also identified the RA responsive genes in the F9 Wt cells. **Keywords: mutant type** **Overall design:** F9 wt cells and F9 RAR gamma knock out cells are treated with RA (1 uM) or ethanol for 24 hours. 3 replicates for each condition.

Background corr dist: KL-Divergence = 0.0991, L1-Distance = 0.0302, L2-Distance = 0.0018, Normal std = 0.4467

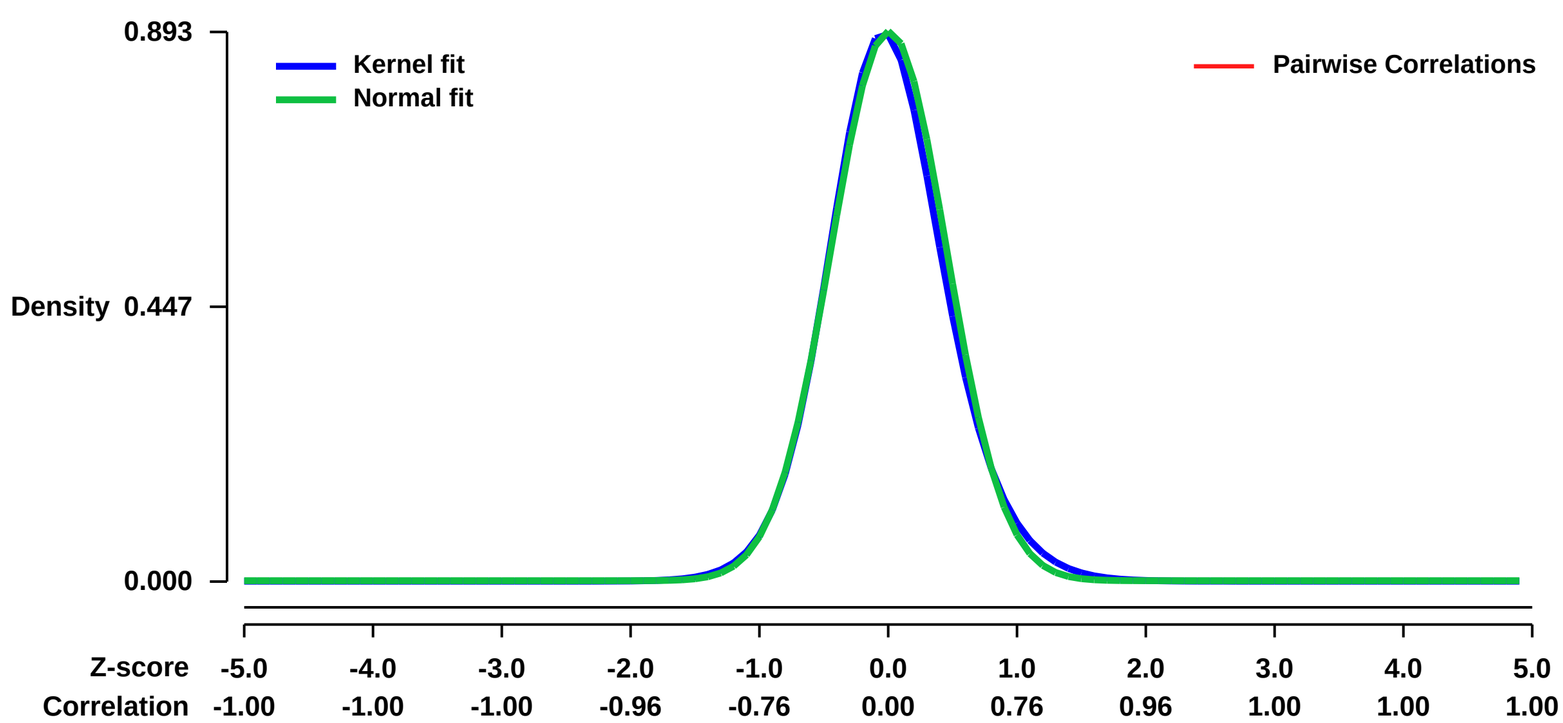

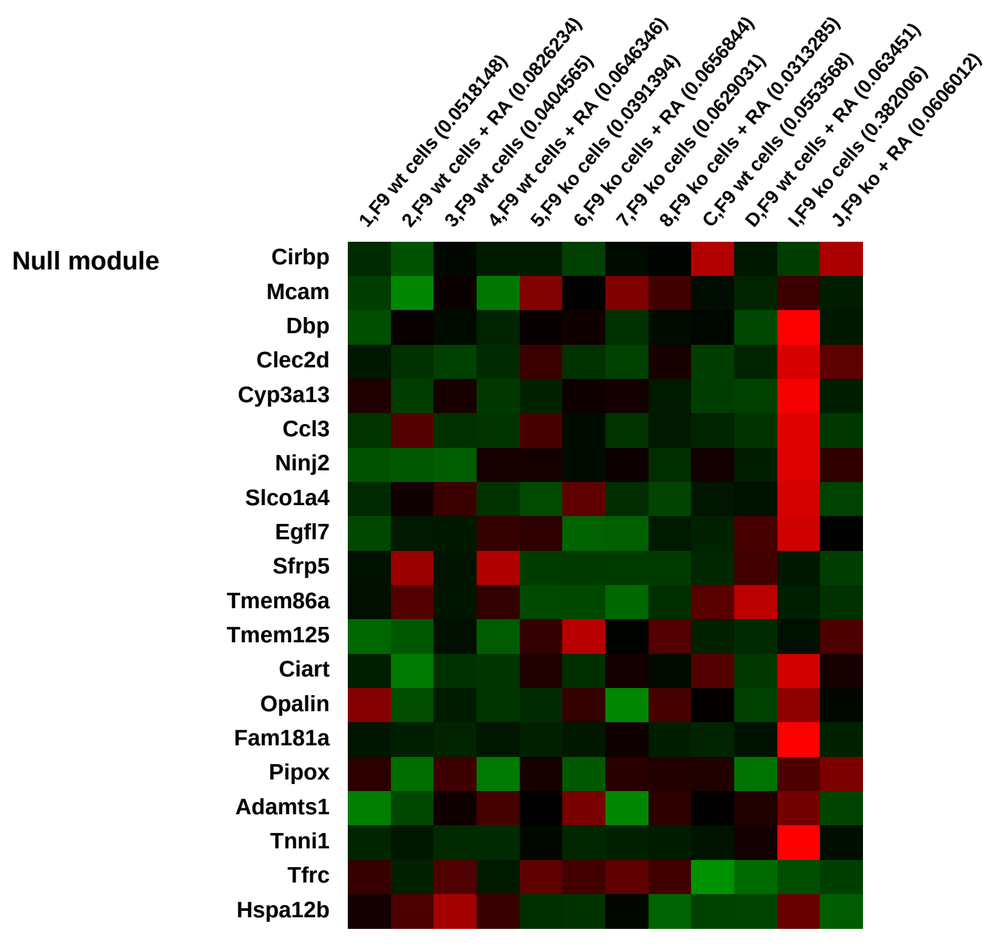

GEO Series "GSE29045" Expression Profiles

Num of samples in this series: 12

Scale of expression profile Z-scores

-3.0 -2.0 -1.0 0.0 1.0 2.0 3.0

GEO Link: http://www.ncbi.nlm.nih.gov/geo/query/acc.cgi?acc=GSE29045

Status: Public on May 01 2012

Title: Genetic modification of STAT5 levels reveals dose-dependent and isoform-specific requirement for cell lineage progression and differentiation.

Organism: Mus musculus

Experiment type: Expression profiling by array

Platform: GPL1261

Pubmed ID:

Summary & Design:

Summary:
Two highly conserved transcription factors STAT5A and STAT5B play an identical role in the intracellular signaling pathway upon cytokine stimulation, while gene deletion experiments have revealed separable and overlapping functions of STAT5. This questions whether the phenotypic differences in the organ development observed in the individual knockout mice result from isoform-specific functions or quantitative differences in the expression levels of each STAT5 isoform among tissues. To elucidate the redundancy and isoform-specificity of STAT5 for development at molecular levels, mice carrying only a single allele of either Stat5a or Stat5b were generated. Both of these mice overcame the lethal anemia observed in Stat5ab-null mice, indicating that development of erythroid cell lineage was totally dependent on the dosage of STAT5. The blocked progression of B cell lineage at the pre-pro B cell stage in Stat5ab-/- mice was rescued in the presence of a single allele of either Stat5a or Stat5b, while the number of total B220+ cells in bone marrow was smaller in Stat5abnull/Stat5b- mice than Stat5abnull/Stat5a- mice. The paucity of alveolar progenitor cells in the Stat5ab-null mammary epithelium was rescued by a single allele of either Stat5a but not Stat5b, suggesting cell-type dependent isoform-specific function. Genome-wide gene expression analyses revealed that different steps of cell lineage progression require different gene sets which expression requires the different isoform of STAT5 in a dose-dependent manner in the mammary epithelium. Taken together, this study demonstrates that dose-dependent isoform specificity of STAT5A and STAT5B controls progression and differentiation of each cell lineage.

Overall design:
Six days after observation of a plug, mammary tissues from three of each Stat5a-/- mice, Stat5ab+/null mice, Stat5abnull/Stat5b- and Stat5abnull/Stat5a- mice were collected, frozen in liquid nitrogen, and stored at -70 ´℃

Background corr dist: KL-Divergence = 0.0195, L1-Distance = 0.0454, L2-Distance = 0.0028, Normal std = 0.7810

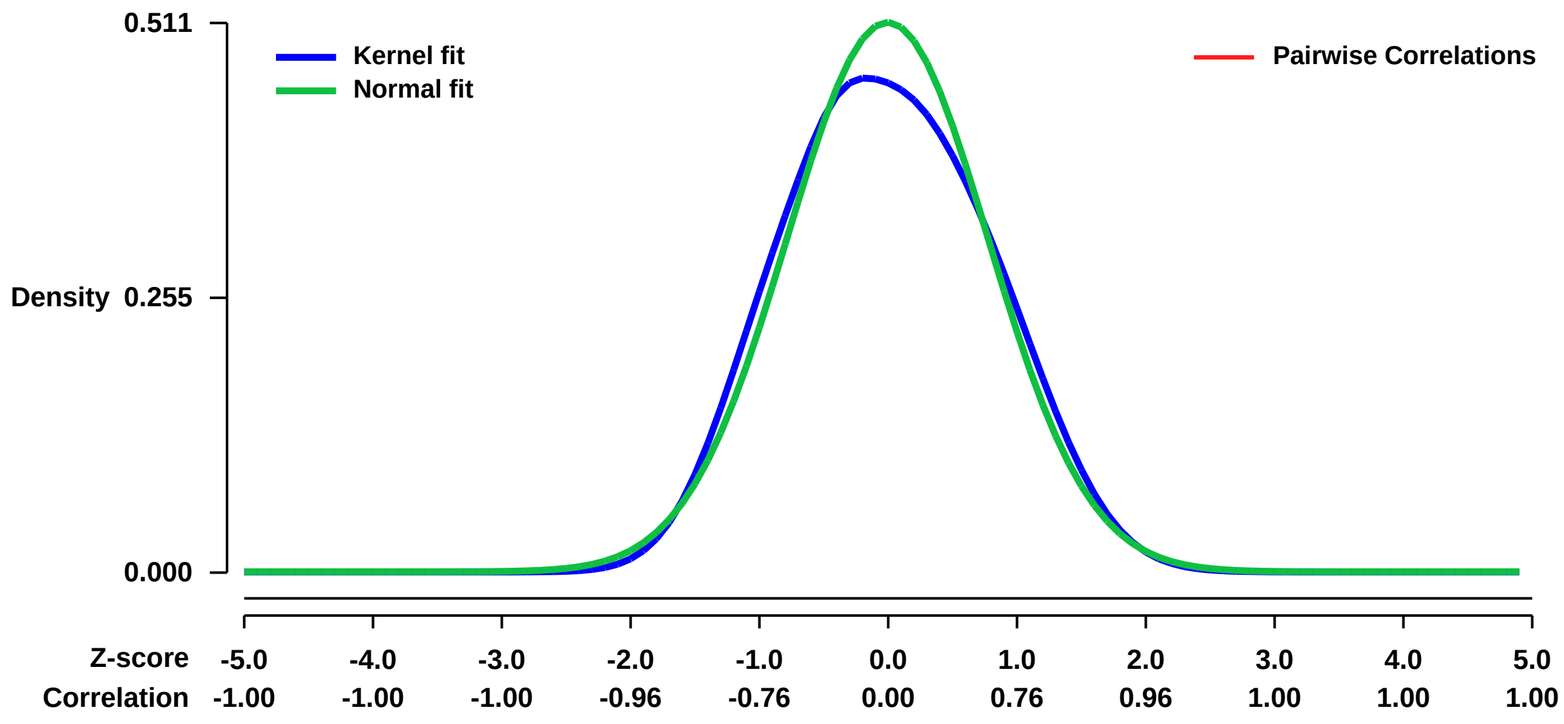

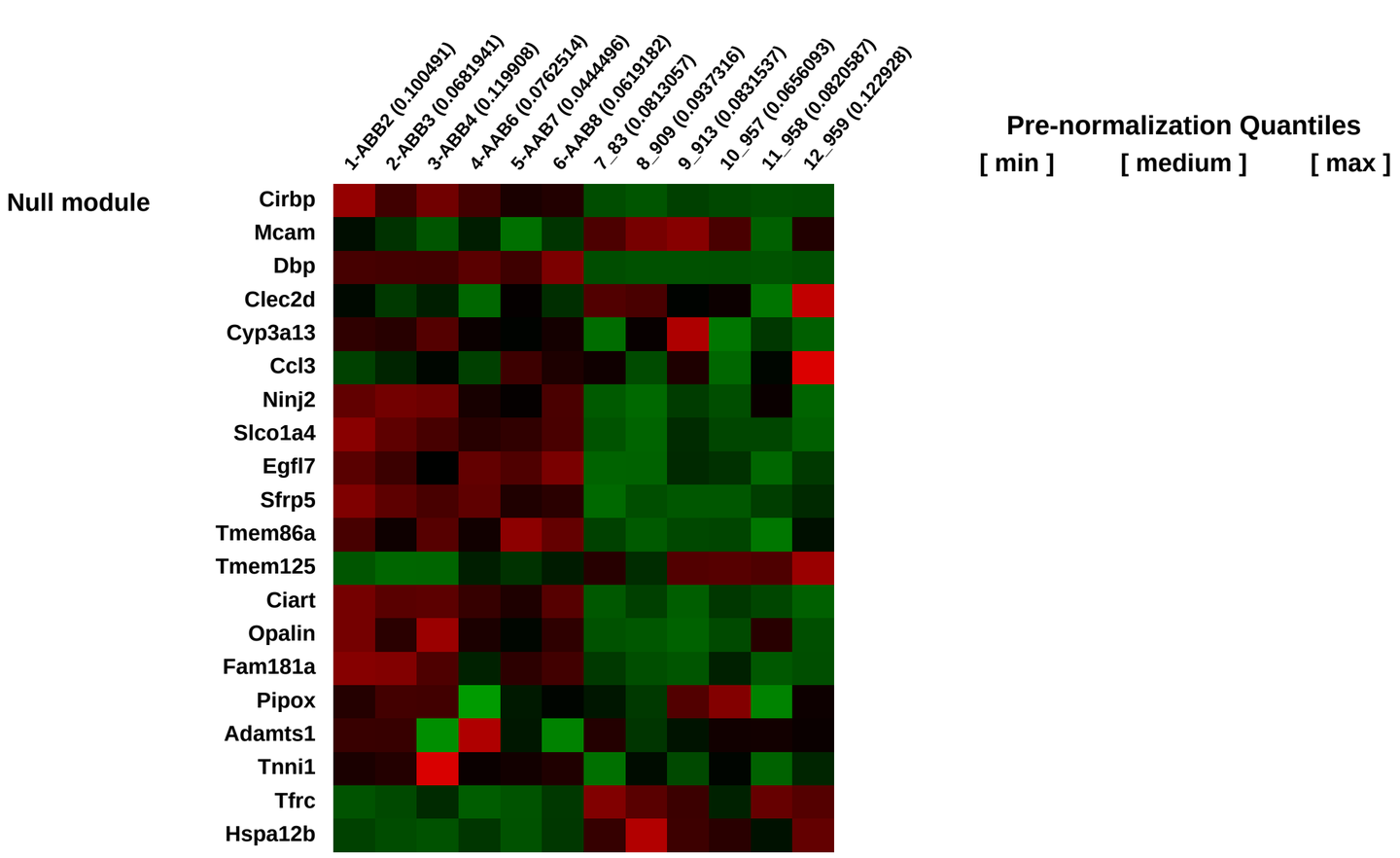

GEO Series "GSE6957" Expression Profiles

Num of samples in this series: 12

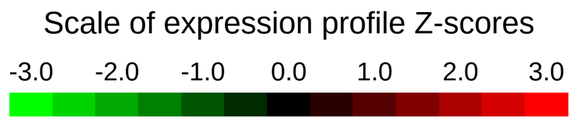

GEO Link:	http://www.ncbi.nlm.nih.gov/geo/query/acc.cgi?acc=GSE6957
Status:	Public on Jul 19 2007
Title:	Transcriptional profiling of bipotential embryonic liver cells to identify liver progenitor cell surface markers (430)
Organism:	Mus musculus
Experiment type:	Expression profiling by array
Platform:	GPL1261
Pubmed ID:	17641245
Summary & Design:	**Summary:** The ability to purify to homogeneity a population of hepatic progenitor cells from adult liver is critical for their characterization prior to any therapeutic application. As a step in this direction, we have utilized gene profiling of a bipotential liver cell line from dpc 14 mouse embryonic liver to catalog genes expressed by liver progenitor cells. These cells, known as Bipotential Mouse Embryonic Liver (BMEL) cells, proliferate in an undifferentiated state and are capable of differentiating into hepatocyte-like and cholangiocyte-like cells in vitro. Upon transplantation, BMEL cells are capable of differentiating into hepatocytes and cholangiocytes in vivo. Microarray analysis of gene expression in the 9A1 and 14B3 BMEL cell lines grown under proliferating and differentiating conditions was used to identify cell surface markers preferentially expressed in the bipotential undifferentiated state. This analysis revealed that proliferating BMEL cells express many genes involved in cell cycle regulation whereas differentiation of BMEL cells by cell aggregation causes a switch in gene expression to functions characteristic of mature hepatocytes. In addition, microarray data and protein analysis indicated that the Notch signaling pathway could be involved in maintaining BMEL cells in an undifferentiated stem cell state. Using GO annotation, a list of cell surface markers preferentially expressed on undifferentiated BMEL cells was generated. One marker, Cd24a, is specifically expressed on progenitor oval cells in livers of DDC treated animals. We therefore consider Cd24a expression a candidate molecule for purification of hepatic progenitor cells. **Keywords:** cell type comparison **Overall design:** RNA was extracted from two independently isolated BMEL cell lines (9A1 and 14B3) after culture under three conditions (basal, aggregate 1 day, and aggregate 5 days). Duplicate biological replicates were collected for each cell line:culture condition combination for a total of 12 samples. Samples were biotin-labeled, hybridized to mouse 430 2.0 chips, and scanned according to established Affymetrix protocols.

Background corr dist: KL-Divergence = 0.0532, L1-Distance = 0.0670, L2-Distance = 0.0087, Normal std = 0.5905

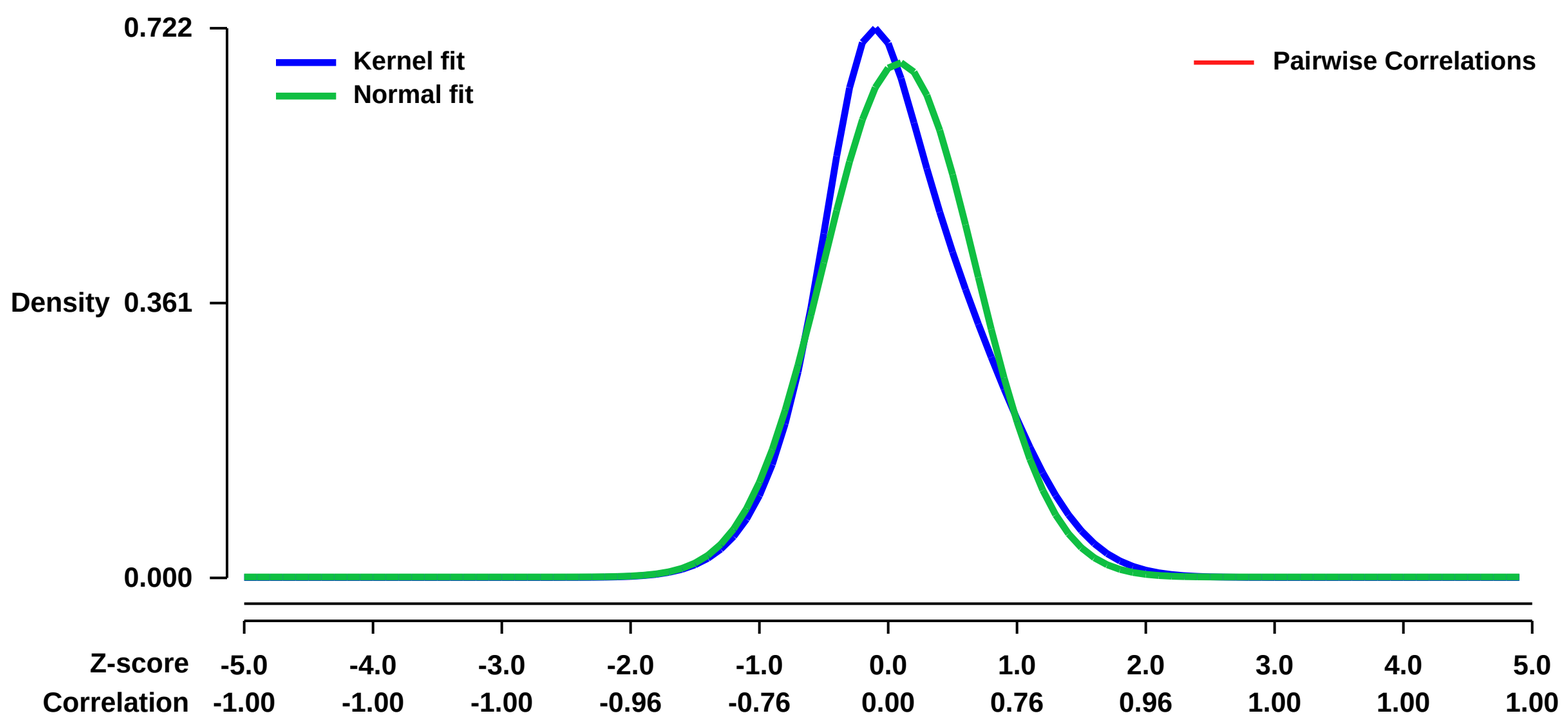

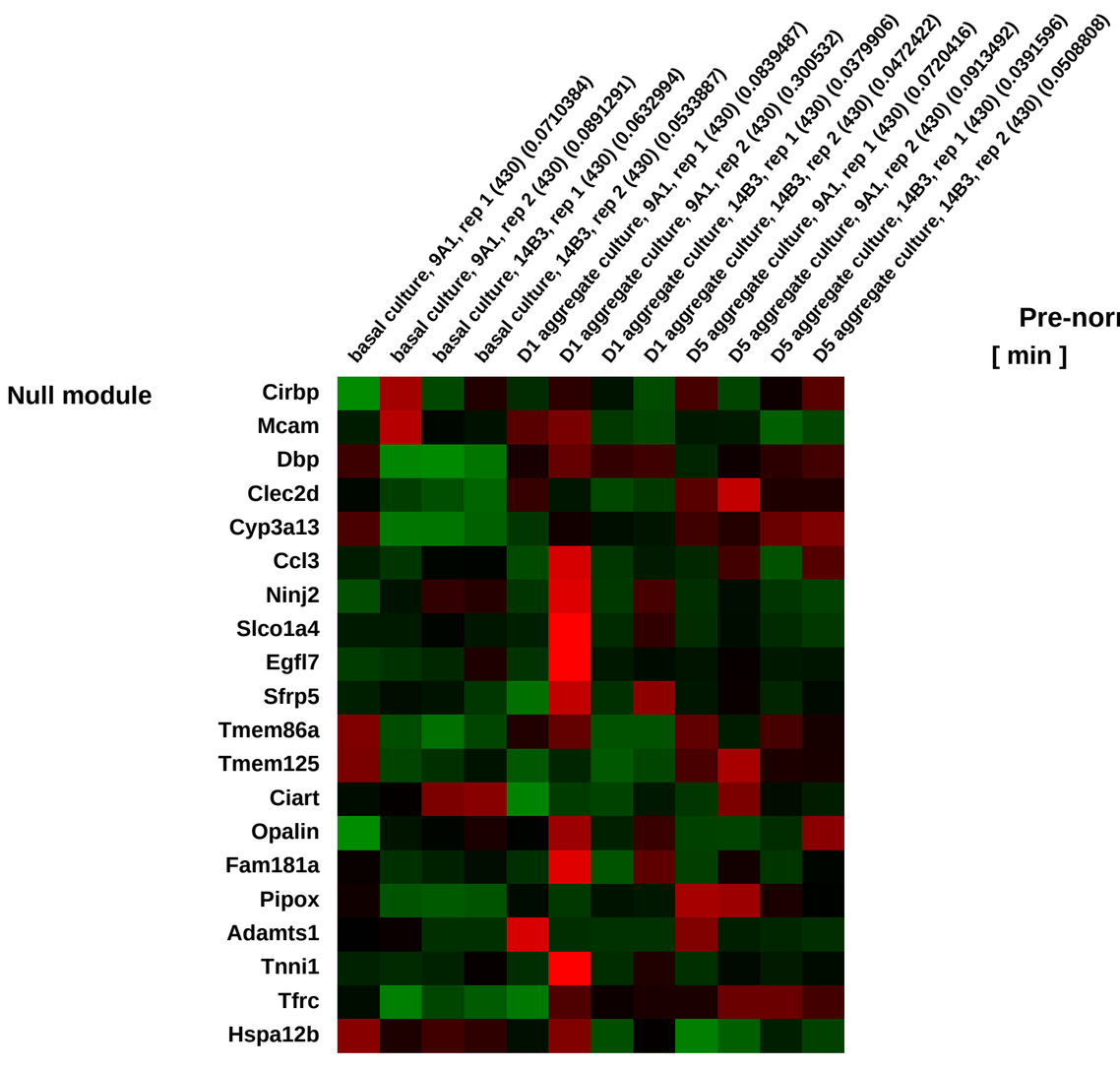

GEO Series "GSE4695" Expression Profiles

Num of samples in this series: 6

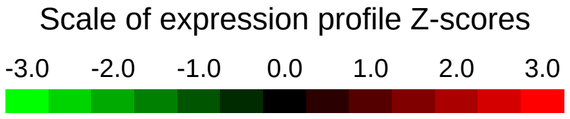

GEO Link:	**http://www.ncbi.nlm.nih.gov/geo/query/acc.cgi?acc=GSE4695**
Status:	**Public on Apr 25 2006**
Title:	**Changes in gene expression in dermal fibroblasts following exposure to Et1 peptide**
Organism:	**Mus musculus**
Experiment type:	**Expression profiling by array**
Platform:	**GPL1261**
Pubmed ID:	**16870175**
Summary & Design:	**Summary:** **To determine if aberrant activation of endothelin-1 (Et1) could lead to the dysregulation of many downstream genes, we exposed fibroblasts to exogenous ET1 peptide and assayed for transcriptional changes by microarray. Mouse dermal fibroblasts were treated with exogenous Et1 peptide for 24 hours. ET1 treatment resulted in significant expression changes â primarily downregulation â of a number of genes. In particular, Tgf‚†2 and Tgf‚†3 were among the downregulated genes, which in turn alter the expression status of their many target genes. These data suggest that the stable silencing of Et1 is important for the phenotypic stability of dermal fibroblasts, and perhaps many other cell types as well.** **Keywords: endothelin-1; Et1; dermal fibroblast** **Overall design:** **Three separate biological replicates were derived for both control and treated samples. The primary dermal fibroblasts were derived by explant procedure from the skin of mouse pups aged 0-3 days. By passage 5, cells were split to two separate cultures-- one with 100nM synthetic Et1 peptide added to the medium (treated) and the other with nothing added (control). Cells were exposed to Et1 for 24 hrs, then treated and control populations were harvested for total RNA.**

Background corr dist: KL-Divergence = 0.0374, L1-Distance = 0.0203, L2-Distance = 0.0004, Normal std = 0.6307

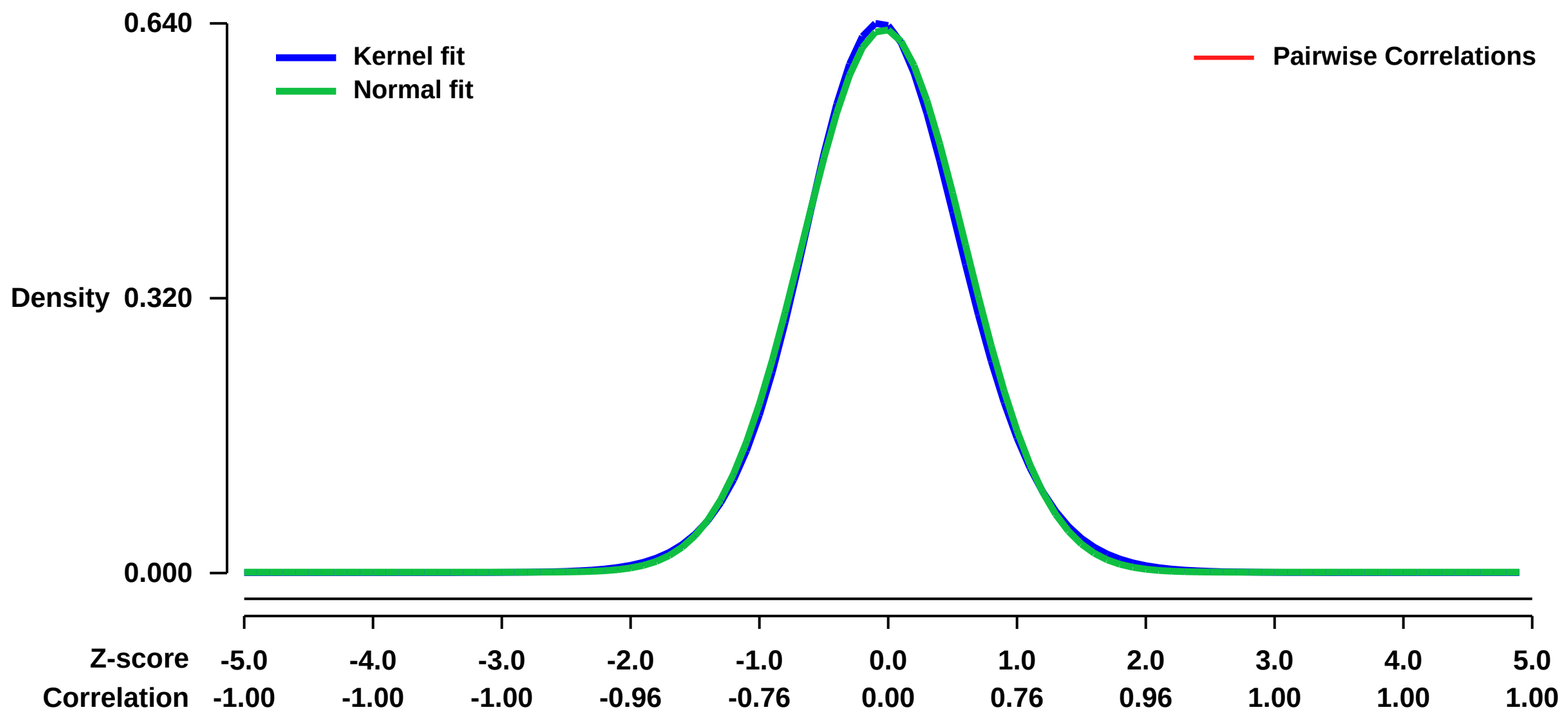

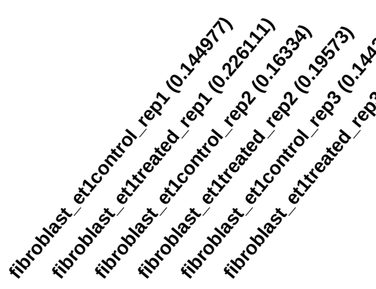

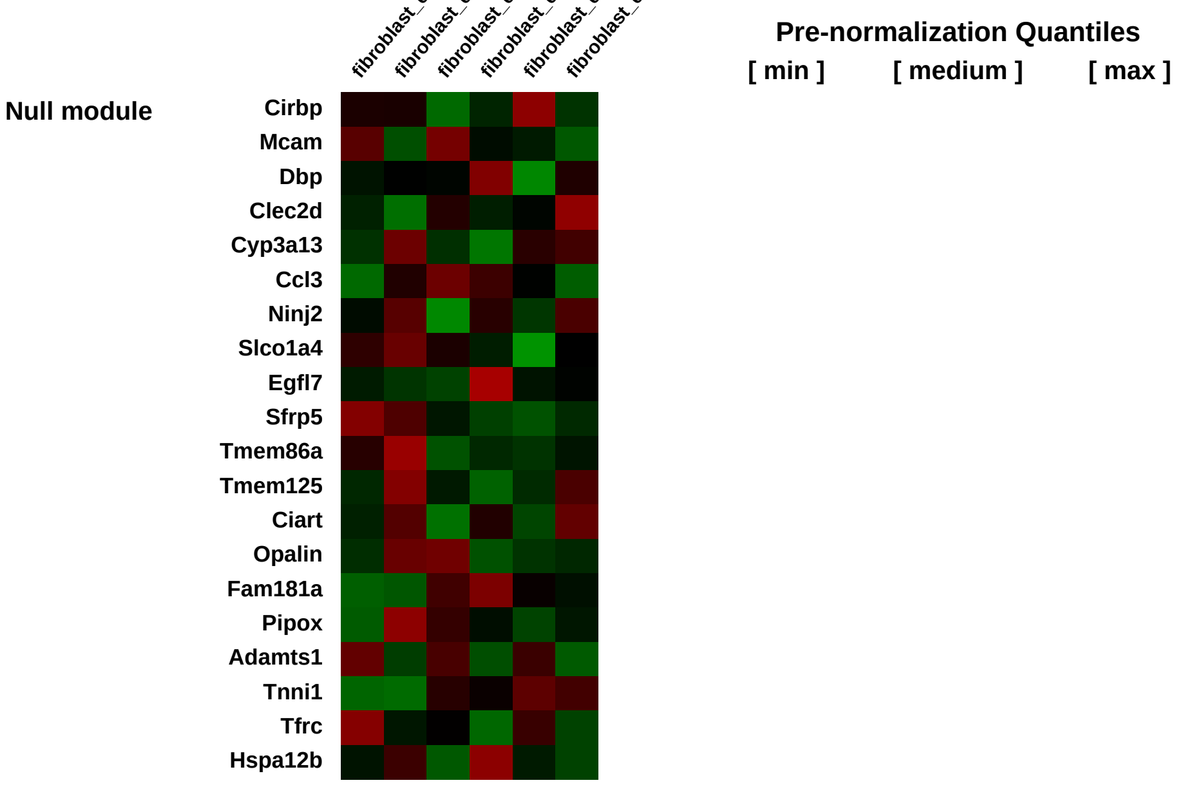

GEO Series "GSE24210" Expression Profiles

Num of samples in this series: 16

Scale of expression profile Z-scores

-3.0 -2.0 -1.0 0.0 1.0 2.0 3.0

GEO Link:	http://www.ncbi.nlm.nih.gov/geo/query/acc.cgi?acc=GSE24210
Status:	Public on Sep 18 2010
Title:	IL-35-mediated induction of a potent regulatory T cell population.
Organism:	Mus musculus
Experiment type:	Expression profiling by array
Platform:	GPL1261
Pubmed ID:	20953201
Summary & Design:	**Summary:** Regulatory T cells (Tregs) play a critical role in the maintenance of immunological self-tolerance. Naˆflve human or murine T cell treatment with the inhibitory cytokine IL35 induces a regulatory population, termed iTR35, that mediates suppression via IL35, but not IL10 or TGF¸†, neither express nor require Foxp3, are strongly suppressive in five in vivo models, and exhibit in vivo stability. Treg-mediated suppression induces iTR35 generation in an IL35- and IL10-dependent manner in vitro, and in inflammatory conditions in vivo in Trichuris-infected intestines and within the tumor microenvironment, where they appear to contribute to the regulatory milieu. iTR35 may constitute a key mediator of infectious tolerance and may contribute to Treg-mediated tumor progression, and ex vivo-generated iTR35 may possess therapeutic utility. **Overall design:** Five IL35-treated samples, in parallel with 5 control-treated samples, were compared to 3 Treg and 3 Tconv cell samples.

Background corr dist: KL-Divergence = 0.1392, L1-Distance = 0.0306, L2-Distance = 0.0015, Normal std = 0.3946

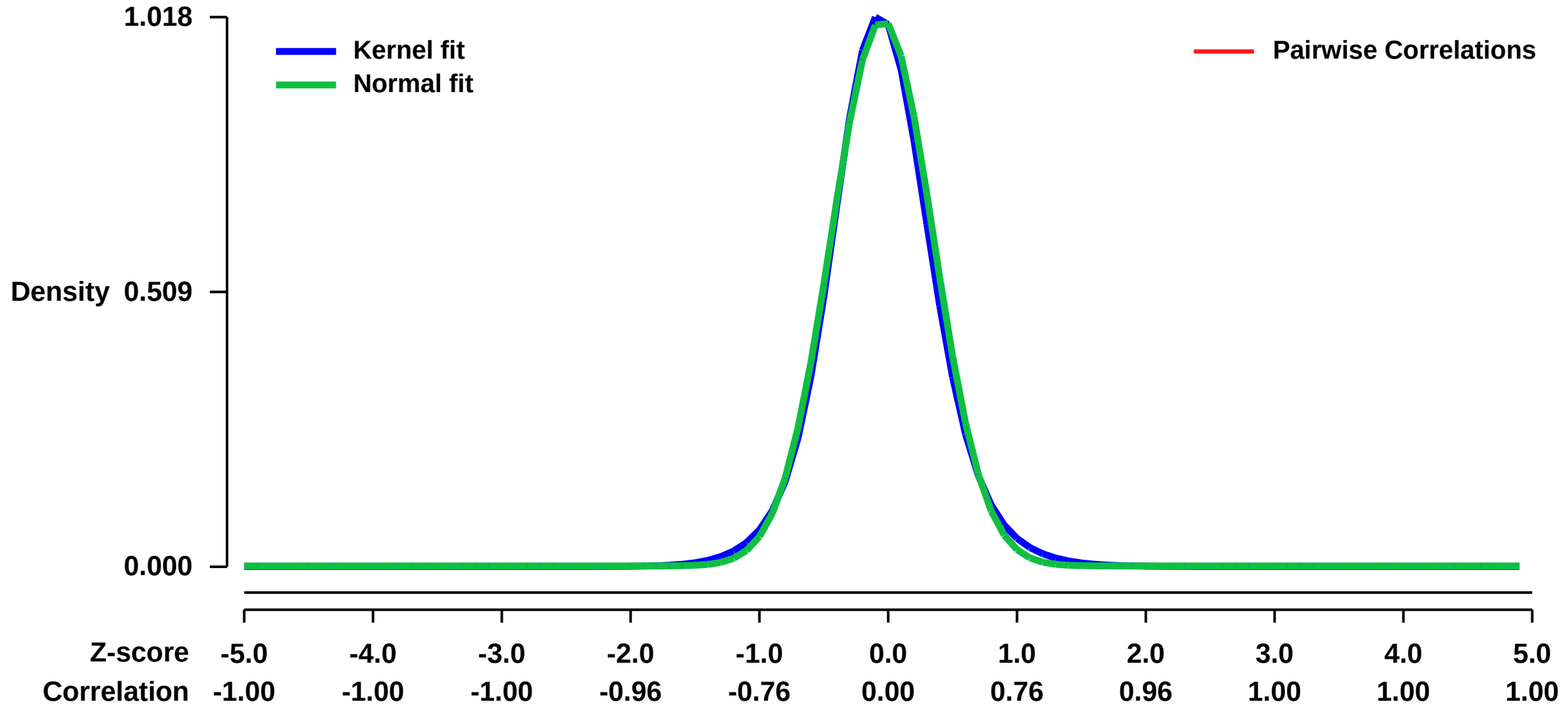

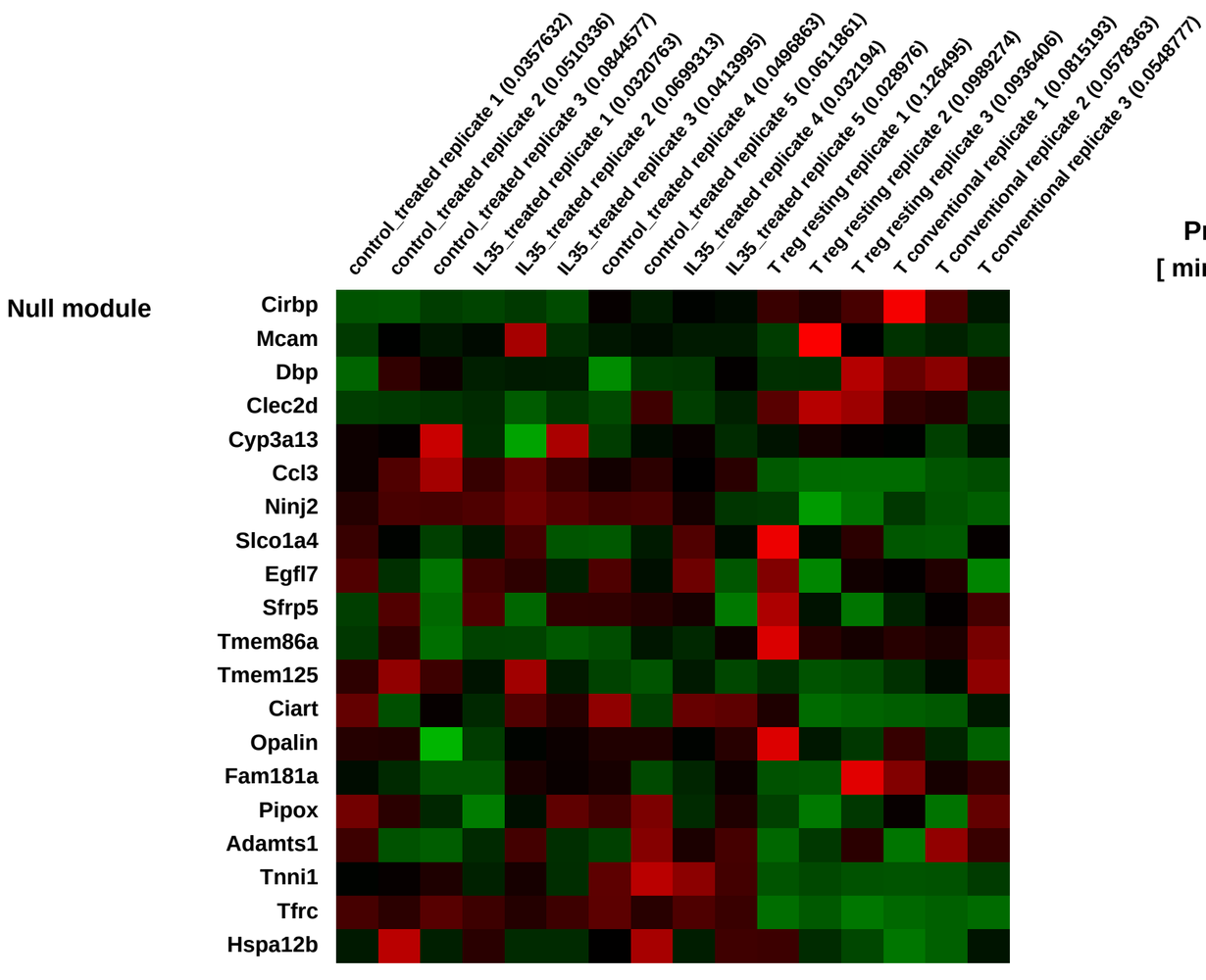

GEO Series "GSE22927" Expression Profiles

Num of samples in this series: 38

Scale of expression profile Z-scores

-3.0 -2.0 -1.0 0.0 1.0 2.0 3.0

GEO Link:	http://www.ncbi.nlm.nih.gov/geo/query/acc.cgi?acc=GSE22927
Status:	Public on Mar 23 2011
Title:	Hierarchical synergy of Pten, p53 and Rb pathways in high-grade astrocytoma induced in adult brain
Organism:	Mus musculus
Experiment type:	Genome variation profiling by genome tiling array
Platform:	GPL1261
Pubmed ID:	21397855
Summary & Design:	**Summary:** Mutations in the PTEN, TP53 and RB1 pathways are obligate events in the pathogenesis of human glioblastomas, the highest grade of astrocytoma. To investigate synergy between these tumor suppressors in mice, we induced various combinations of compound deletions conditionally in astrocytes and neural precursors in the mature brain. The resulting highly penetrant astrocytomas showed a spectrum of histopathological variation reminiscent of human tumors, and ranged from grade III to grade IV (glioblastoma). Secondary somatic mutations varied depending on the combination of initiating deletions and were relevant to human disease. Receptor tyrosine kinase amplifications were frequent in tumors initiated by combined conditional deletion of Pten and Tp53, but not when Rb, Pten and Tp53 were simultaneously deleted. Multiple mutations within PI3K and Rb pathways were acquired, however, Mapk activation was not consistently detected in astrocytomas. Gene expression profiling revealed striking similarities to previously described human astrocytoma subclasses. A subset of astrocytomas initiated outside of proliferative niches in the adult brain. **Overall design:** Gene expression of 8 human brain samples including 2 normal brainstem and 6 brainstem low-grade gliomas were profiled using HG-U133 plus 2 arrays. Gene expression of 38 mouse tumor samples, including 24 Pten;p53 double knockout and 14 Pten;p53;Rb1 triple knockout, were profiled using Affymetrix Mouse Genome 430 v2 arrays. Copy number changes of 51 double knockout tumor samples were analysed using Roswell Park Cancer Institute 6.5k BAC arrays. Copy number changes of 21 triple knockout tumor samples were analysed using Agilent mouse genome CGH mocirarray 244A.

Background corr dist: KL-Divergence = 0.4712, L1-Distance = 0.0871, L2-Distance = 0.0244, Normal std = 0.2319

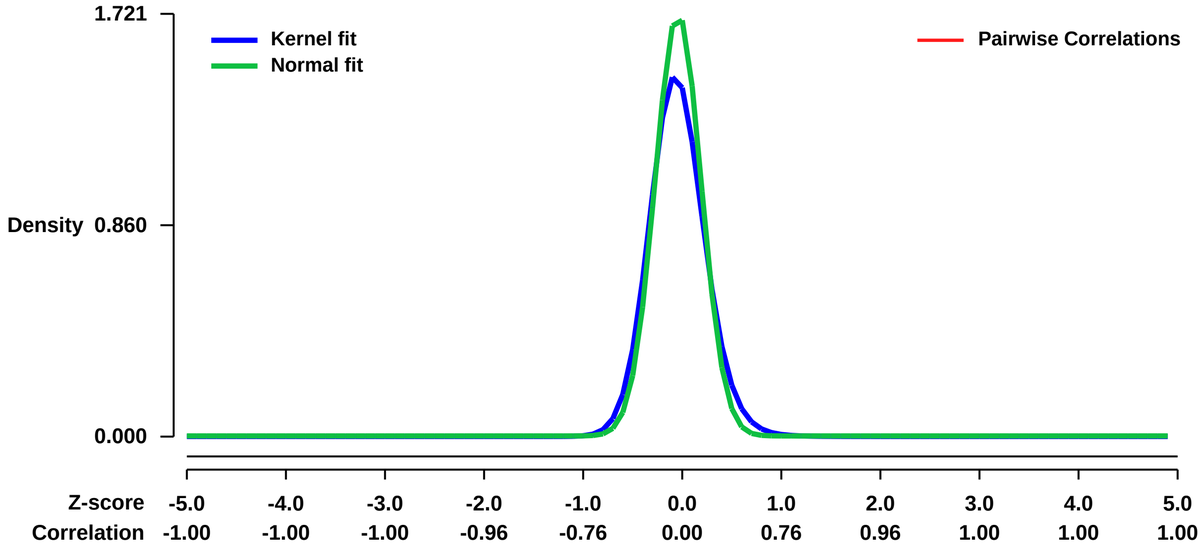

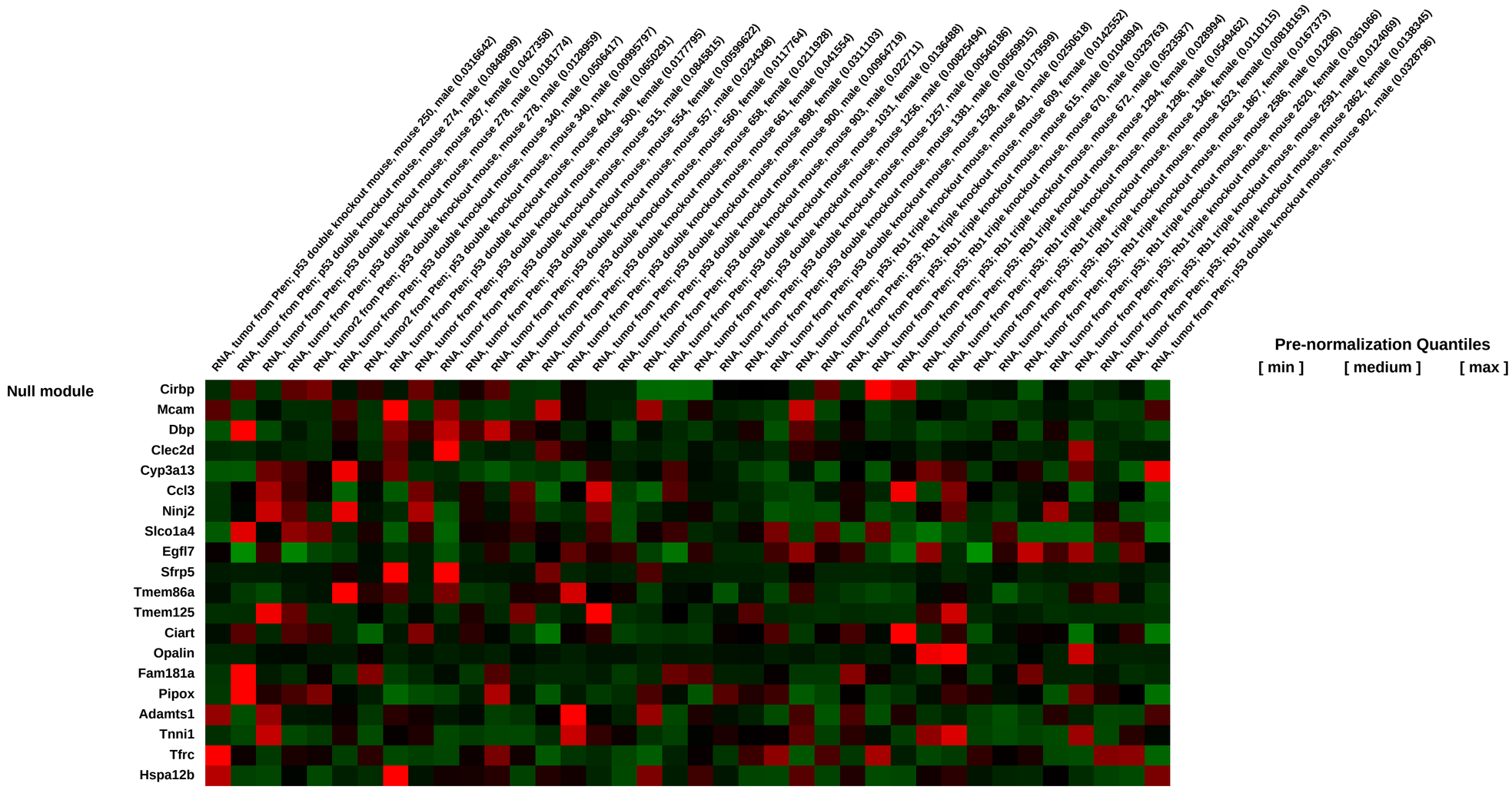

GEO Series "GSE26290" Expression Profiles

Num of samples in this series: 12

Scale of expression profile Z-scores

-3.0 -2.0 -1.0 0.0 1.0 2.0 3.0

GEO Link:	http://www.ncbi.nlm.nih.gov/geo/query/acc.cgi?acc=GSE26290
Status:	Public on Feb 01 2011
Title:	Expression data from control and Phospholipid dependent kinase 1 (PDK1) null cytotoxic T-lymphocytes (CTL) and from control and Akt inhibitor treated CTL
Organism:	Mus musculus
Experiment type:	Expression profiling by array
Platform:	GPL1261
Pubmed ID:	21295499
Summary & Design:	**Summary:** In cytotoxic T cells (CTL), Protein Kinase B /Akt is activated by the T cell antigen receptor (TCR) and the cytokine Interleukin 2 (IL2), in part by phosophorylation of Akt by Phospholipid dependent kinase 1 (PDK1). The role of PDK1 and Akt in CTL has however not been fully defined. In order to explore the relative roles of these kinases in CTL we used microarrays to profile the gene expression of control and PDK1 null CTL. In separate experiments we compared the gene expression profiles of control and Akt inhibitor treated CTL. **Overall design:** The gene expression patterns of the AktI treated and the untreated CTL were then compared by microarray.

Background corr dist: KL-Divergence = 0.0257, L1-Distance = 0.0736, L2-Distance = 0.0070, Normal std = 0.8329

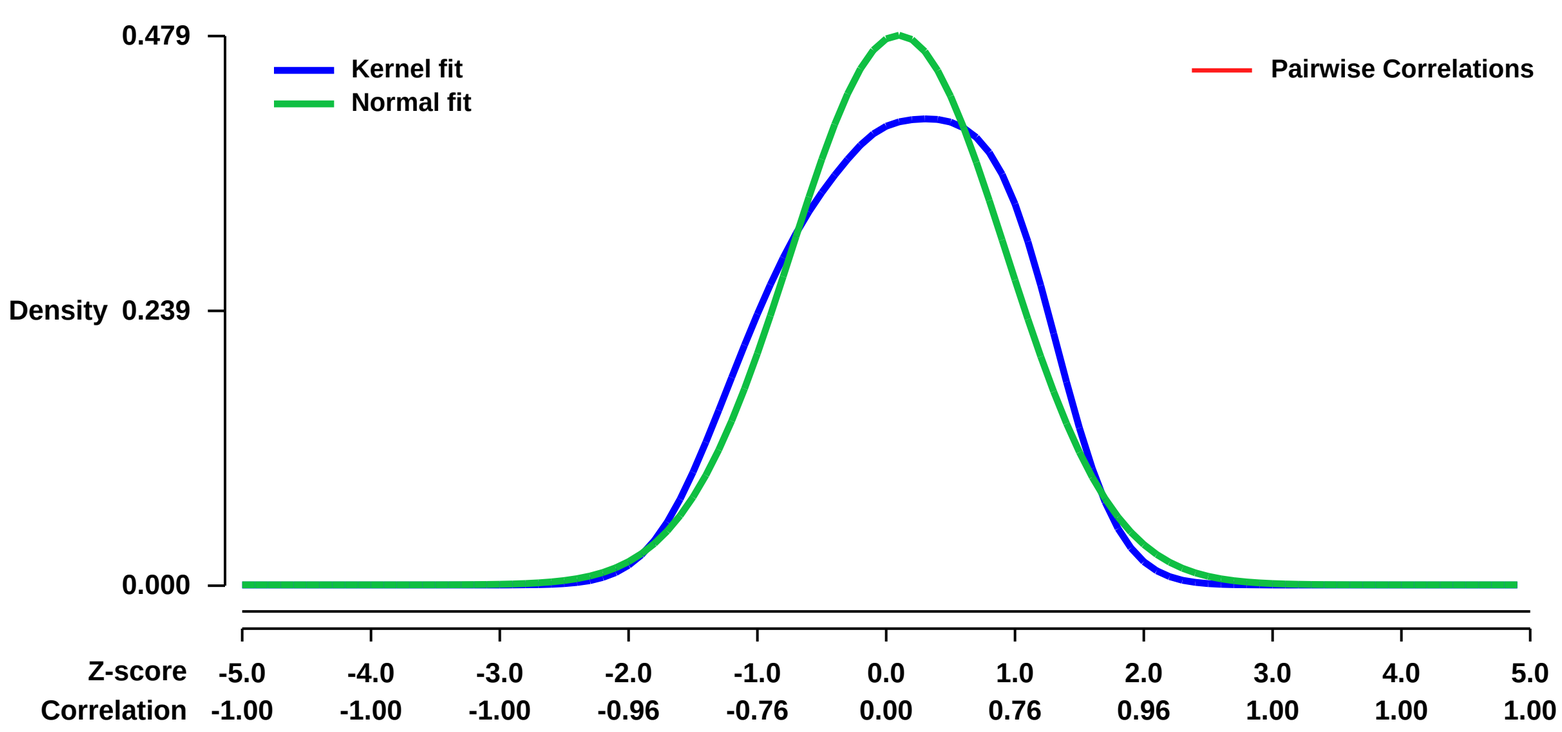

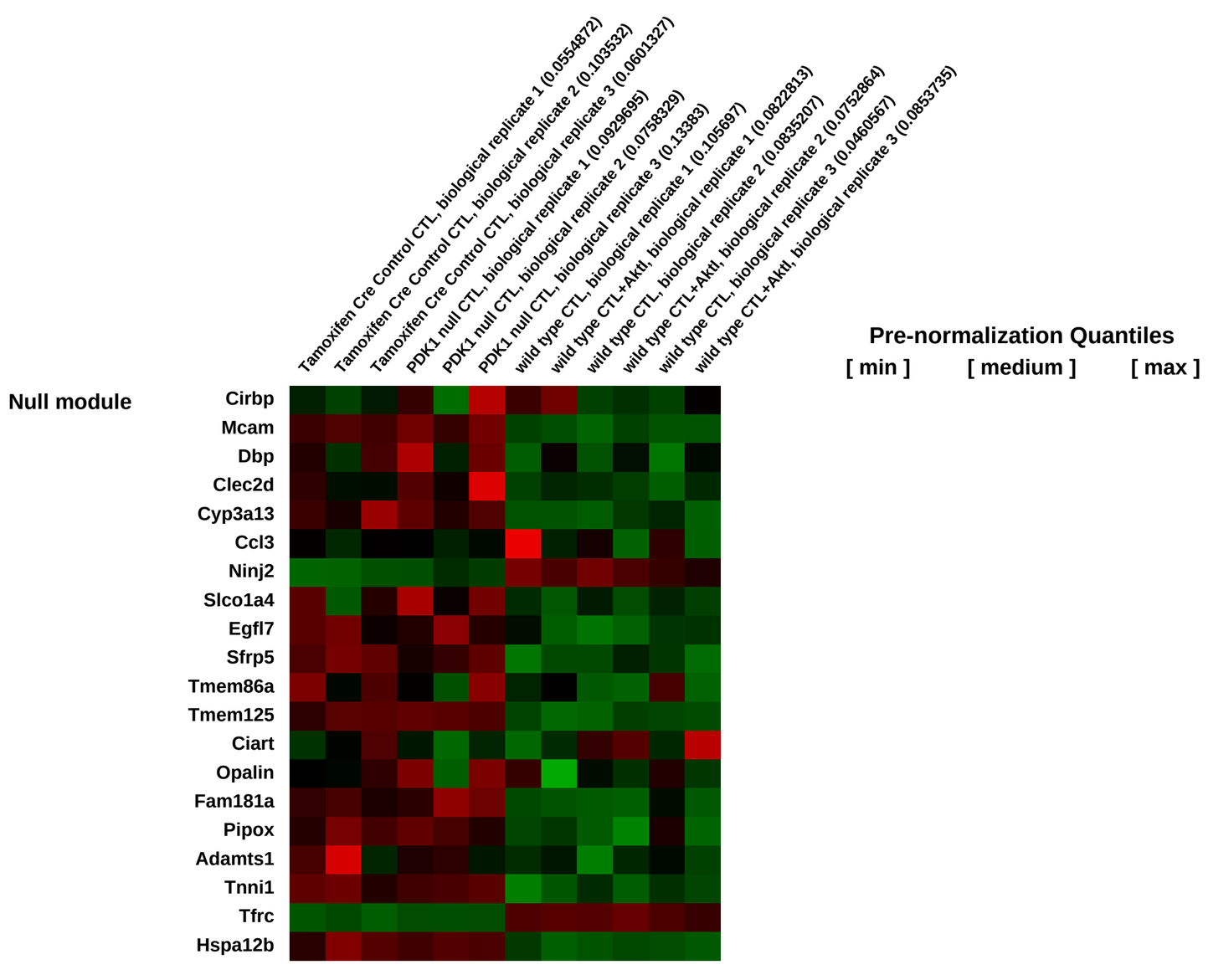

GEO Series "GSE4230" Expression Profiles

Num of samples in this series: 8

Scale of expression profile Z-scores

-3.0 -2.0 -1.0 0.0 1.0 2.0 3.0

GEO Link:	http://www.ncbi.nlm.nih.gov/geo/query/acc.cgi?acc=GSE4230
Status:	Public on Feb 13 2006
Title:	Gene expression profiles in developing nephrons using Lim1 metanephric mesenchyme-specific conditional mutant mice
Organism:	Mus musculus
Experiment type:	Expression profiling by array
Platform:	GPL1261
Pubmed ID:	16464245
Summary & Design:	**Summary:** **BACKGROUND: Lim1 is a homeobox gene that is essential for nephrogenesis. During metanephric kidney development, Lim1 is expressed in the nephric duct, ureteric buds, and the induced metanephric mesenchyme. Conditional ablation of Lim1 in the metanephric mesenchyme blocks the formation of nephrons at the nephric vesicle stage, leading to the production of small, non-functional kidneys that lack nephrons.** **METHODS: In the present study, we used Affymetrix probe arrays to screen for nephron-specific genes by comparing the expression profiles of control and Lim1 conditional mutant kidneys. Kidneys from two developmental stages, embryonic day 14.5 (E14.5) and 18.5 (E18.5), were examined.** **RESULTS: Comparison of E18.5 kidney expression profiles generated a list of 465 nephron-specific gene candidates that showed a more than 2-fold increase in their expression level in control kidney versus the Lim1 conditional mutant kidney. Computational analysis confirmed that this screen enriched for kidney-specific genes. Furthermore, at least twenty-eight of the top fifty (56%) candidates (or their vertebrate orthologs) were previously reported to have a nephron-specific expression pattern. Our analysis of E14.5 expression data yielded 41 candidate genes that are up-regulated in the control kidneys compared to the conditional mutants. Three of them are related to the Notch signaling pathway that is known to be important in cell fate determination and nephron patterning.** **CONCLUSIONS: Therefore, we demonstrate that Lim1 conditional mutant kidneys serve as a novel tissue source for comprehensive expression studies and provide a means to identify nephron-specific genes.** **Keywords: tissue specificity, time course, development, kidney, metanephric mesenchyme, nephron, Lim1, knockout mice, conditional knockout** **Overall design:** **Normalized data were exported in a tab delimited text format. Fold changes of each transcript from different samples were calculated and sorted using Microsoft Excel 5.0 software. Signal obtained from control kidney samples were used as an experiment to compare to the signal obtained from Lim1 conditional mutant kidneys that was designated as a baseline. A 2-fold change in the means of signal obtained from experimental duplicates and those from baseline duplicates was used as the criterion to identify differentially expressed transcripts. To ensure the quality of the data, probe sets that showed a fold change between duplicates greater than between the experimental mean and baseline mean were removed. To study only genes that showed consistent expression on experimental chips, probe sets that did not show consistent present calls in the experimental duplicates were removed. To focus on genes with a significant fold change between the experiment and the baseline, only probe sets that the product of their experimental mean and fold change were more than 100 were retained. To produce a compact differentially expressed gene list, the probe set list was sorted within Microsoft Excel based on Locus Link number and redundant entries were removed. Our experimental design description and the data format provided in the Additional files fulfill the MIAME (minimum information about a microarray experiment) standards.**

Background corr dist: KL-Divergence = 0.0369, L1-Distance = 0.0151, L2-Distance = 0.0003, Normal std = 0.6203

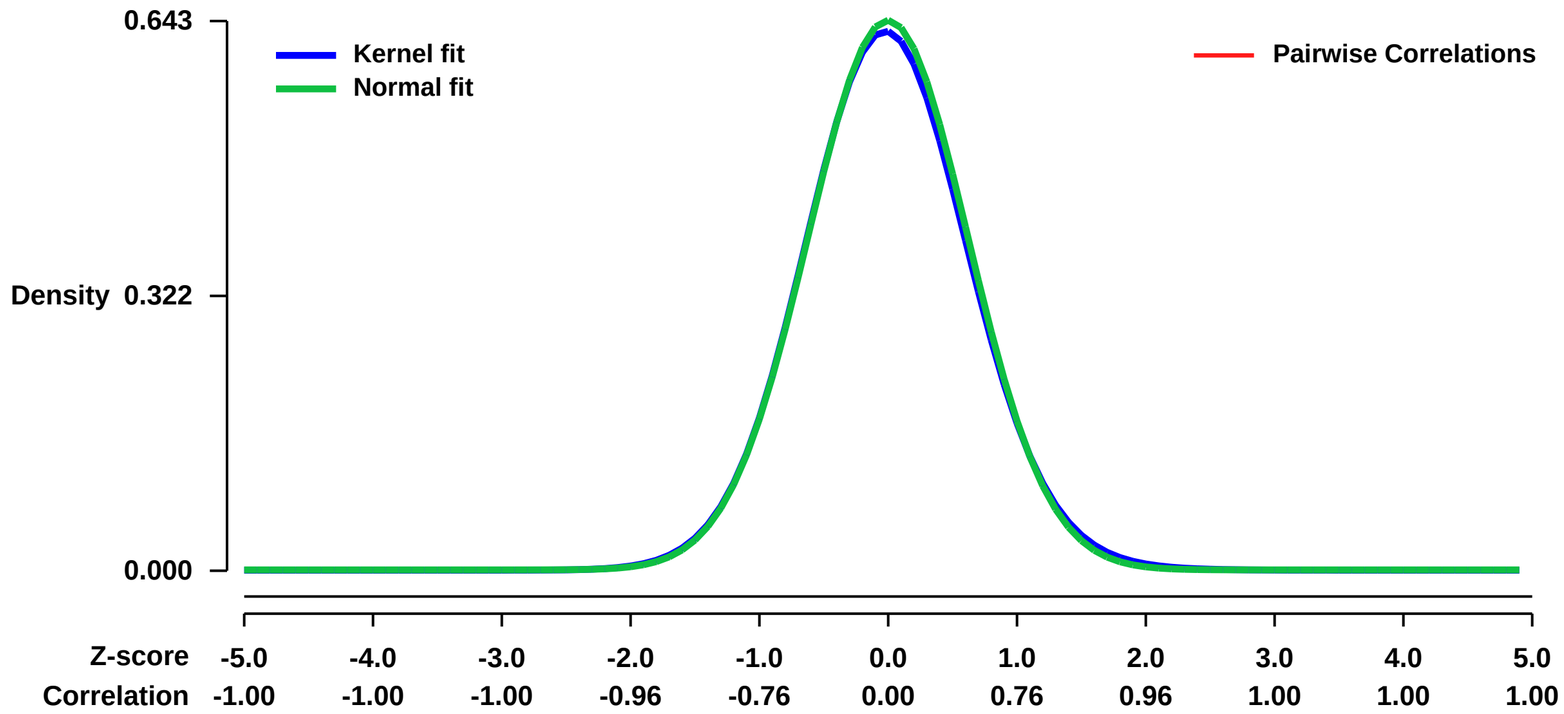

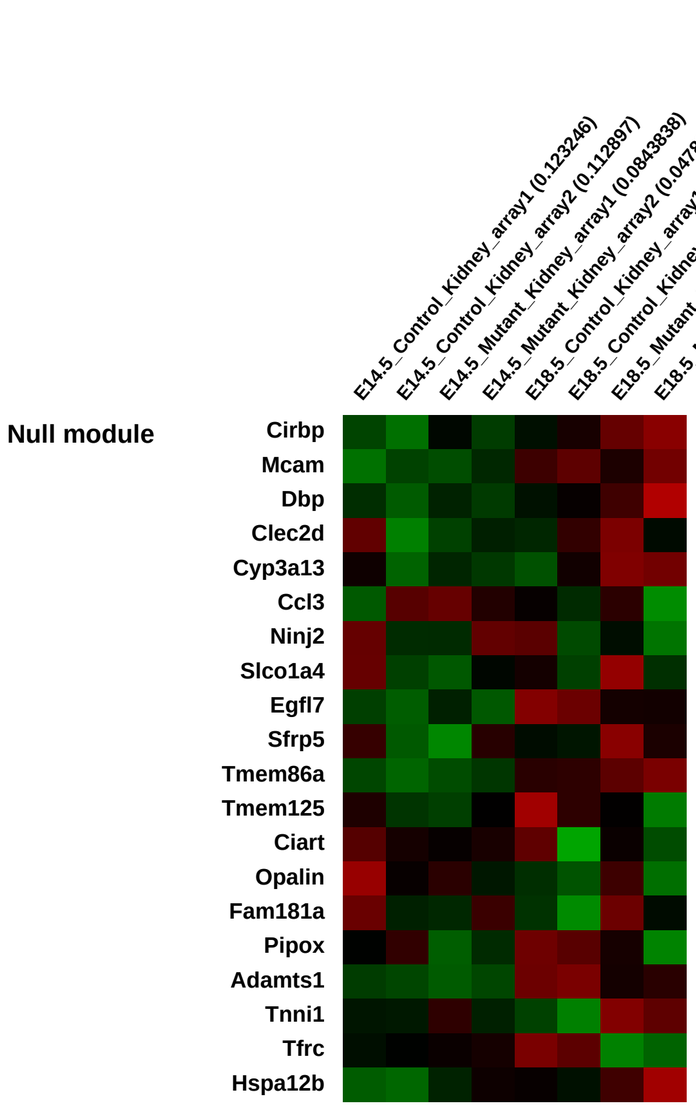

GEO Series "GSE11759" Expression Profiles

Num of samples in this series: 6

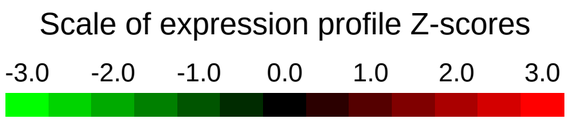

GEO Link:	http://www.ncbi.nlm.nih.gov/geo/query/acc.cgi?acc=GSE11759
Status:	Public on Dec 01 2008
Title:	Role of HNF4alpha in the adult colon
Organism:	Mus musculus
Experiment type:	Expression profiling by array
Platform:	GPL1261
Pubmed ID:	19898610
Summary & Design:	**Summary:** **Background & Aims: HNF4¿– is an important transcriptional regulator of hepatocyte and pancreatic function. Hnf4¿– deletion is embryonically lethal with severe defects in visceral endoderm formation, liver maturation and colon development. However, the precise role of this transcription factor in maintaining homeostasis of the adult intestine remains unclear. Herein, we aimed to elucidate the adult intestinal functions of Hnf4¿–. Methods: A conditional intestinal epithelial Hnf4¿– knockout mouse was generated. Histological abnormality of the colonic mucosa was assessed by immunodetection and Western. Changes in global gene expression and biological network were analyzed. Results: Hnf4¿– intestine null mice developed normally until reaching young adulthood. Crypt distortion became apparent in the Hnf4¿– null colon at 3 months of age followed by focal areas of crypt dropout, increased immune cell infiltrates, crypt hyperplasia and early signs of polyposis later in life. A gene profiling analysis identified cell death and cell cycle related to cancer as the most significant sets of genes altered in the Hnf4¿– colon null mice. Expression levels of the tight junction proteins claudin 4, 8 and 15 were altered early in the colon epithelium of Hnf4¿– mutants and correlated with increased barrier permeability to a molecular tracer that does not normally penetrate normal mucosa. Conclusion: These observations support a functional role for Hnf4¿– in protecting the colonic mucosa against the initiation of the changes resembling inflammatory bowel diseases and polyp formation.** **Overall design:** **HNF4alpha was conditionally knockout in the mouse epithelial colon with the villin CRE. A total of 3 control and 3 mutant littermates individuals were sacrificed at 1 year of age. The colon was harvested and Total RNA was isolated from each individuals. Each RNA sample was independently used to generate probes to screen affymetrix chips.**

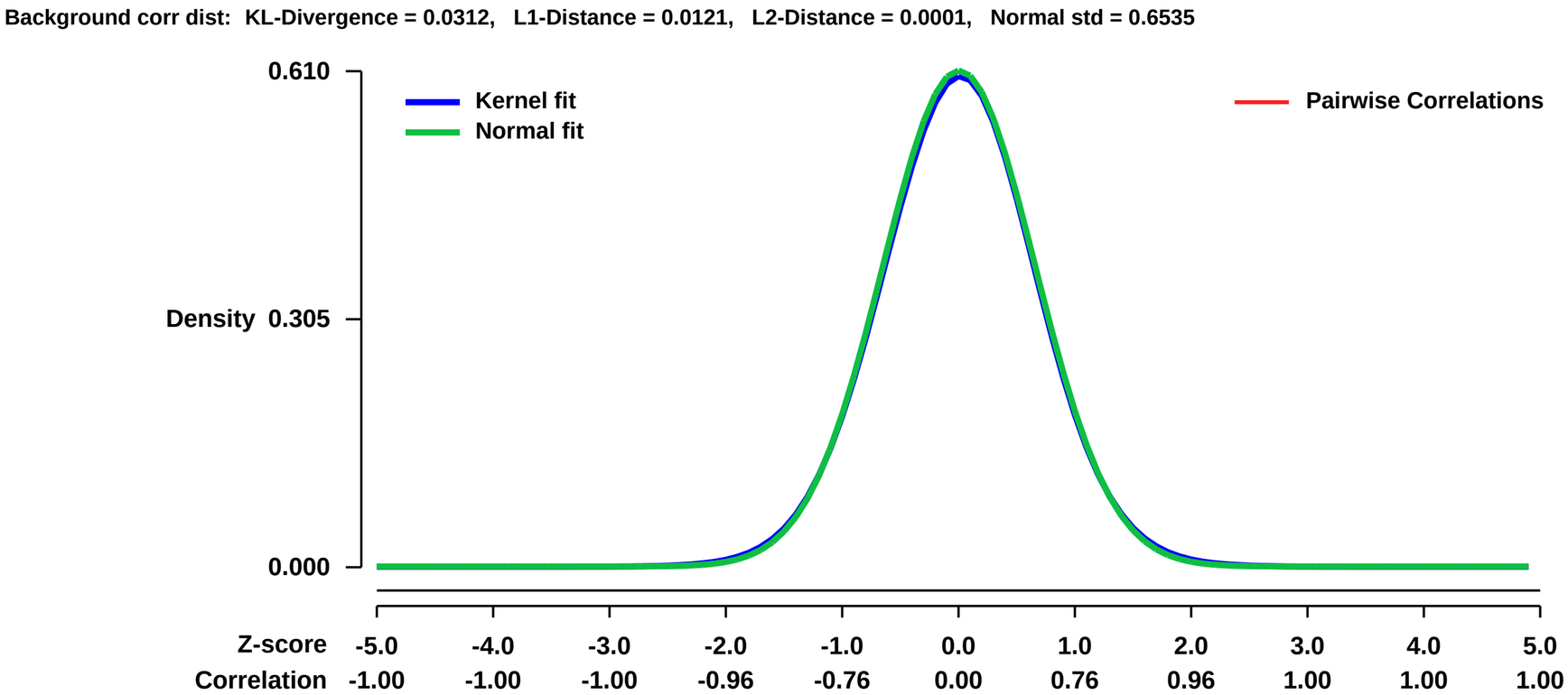

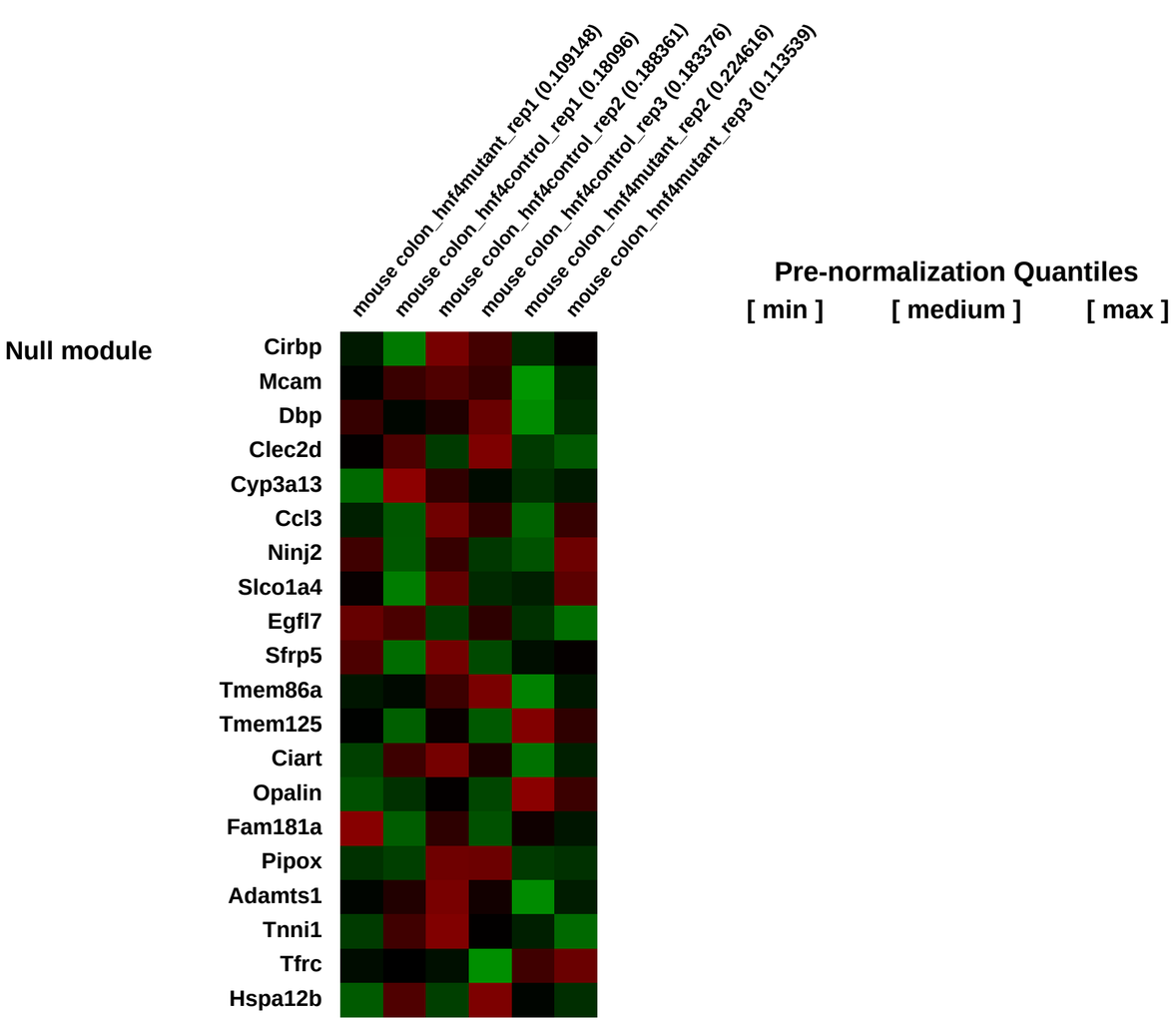

GEO Series "GSE7598" Expression Profiles

Num of samples in this series: 8

Scale of expression profile Z-scores

-3.0 -2.0 -1.0 0.0 1.0 2.0 3.0

GEO Link:	http://www.ncbi.nlm.nih.gov/geo/query/acc.cgi?acc=GSE7598
Status:	Public on Jan 01 2008
Title:	Identification and characterization of genes expressed in the mouse ZPA using a novel microarray approach
Organism:	Mus musculus
Experiment type:	Expression profiling by array
Platform:	GPL1261
Pubmed ID:	17911046
Summary & Design:	**Summary:** Comparing gene expression of cells from the E10.5 limb bud ZPA and the rest of the E10.5 limb bud from Shhgfpcre heterozygotes separated by FACS. **Keywords: comparison, cell-type comparison, experiemental versus control** **Overall design:** 8 samples, 4 ZPA and 4 rest of the limb

Background corr dist: **KL-Divergence = 0.0410, L1-Distance = 0.0441, L2-Distance = 0.0031, Normal std = 0.6311**

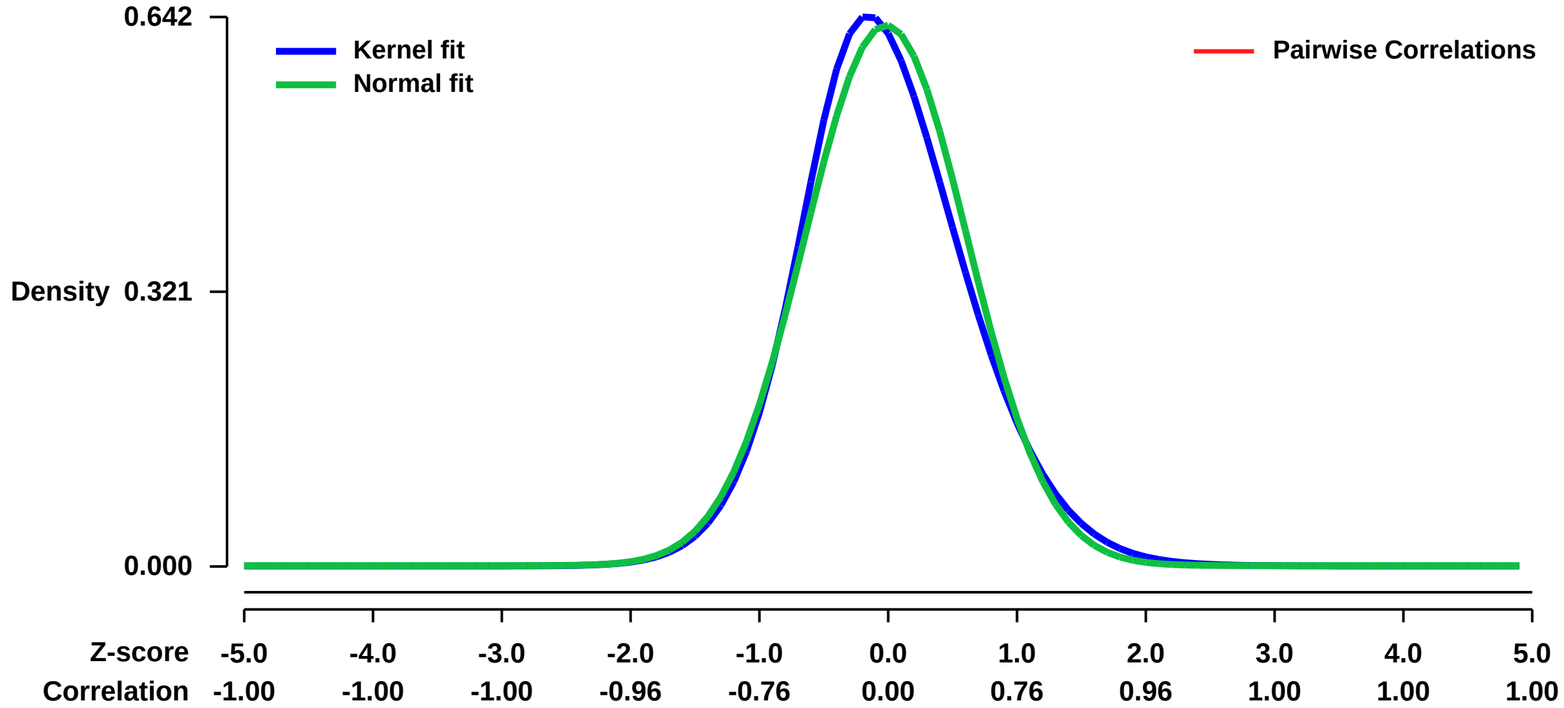

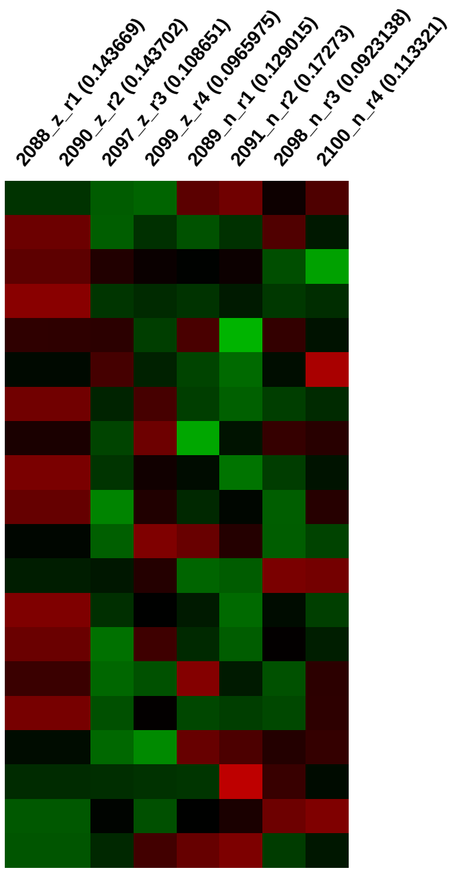

GEO Series "GSE39916" Expression Profiles

Num of samples in this series: 6

Scale of expression profile Z-scores

-3.0 -2.0 -1.0 0.0 1.0 2.0 3.0

GEO Link:	http://www.ncbi.nlm.nih.gov/geo/query/acc.cgi?acc=GSE39916
Status:	Public on Aug 07 2012
Title:	Expression data from murine bone marrow-resident plasma cells and spleen mature follicular B cells
Organism:	Mus musculus
Experiment type:	Expression profiling by array
Platform:	GPL1261
Pubmed ID:	22991471
Summary & Design:	**Summary:** CD138+ B220- plasma cells were sorted from bone marrow and B220+ CD23+ mature follicular B cells were sorted from the spleens. Plasma cells were sorted from C57BL/6 mice 7 days after boosting with antigen, with mice first primed with an i.p. injection of KLH/IFA followed by boost at day 21 with KLH/PBS i.p. Mature B cells were sorted from antigen-naˆflve C57BL/6 mice. We compared expression profiles of plasma cells and mature B cells to identify differentially expressed transcripts. **Overall design:** Seven days after boosting with KLH, plasma cells were enriched by CD138-PE/anti-PE magnetic bead enrichment and then sorted to purity. Affymetrix microarrays were performed on 50,000-70,000 plasma cells and 2,000,000-3,000,000 naˆflve B cells.

Background corr dist: KL-Divergence = 0.0176, L1-Distance = 0.0538, L2-Distance = 0.0034, Normal std = 0.9040

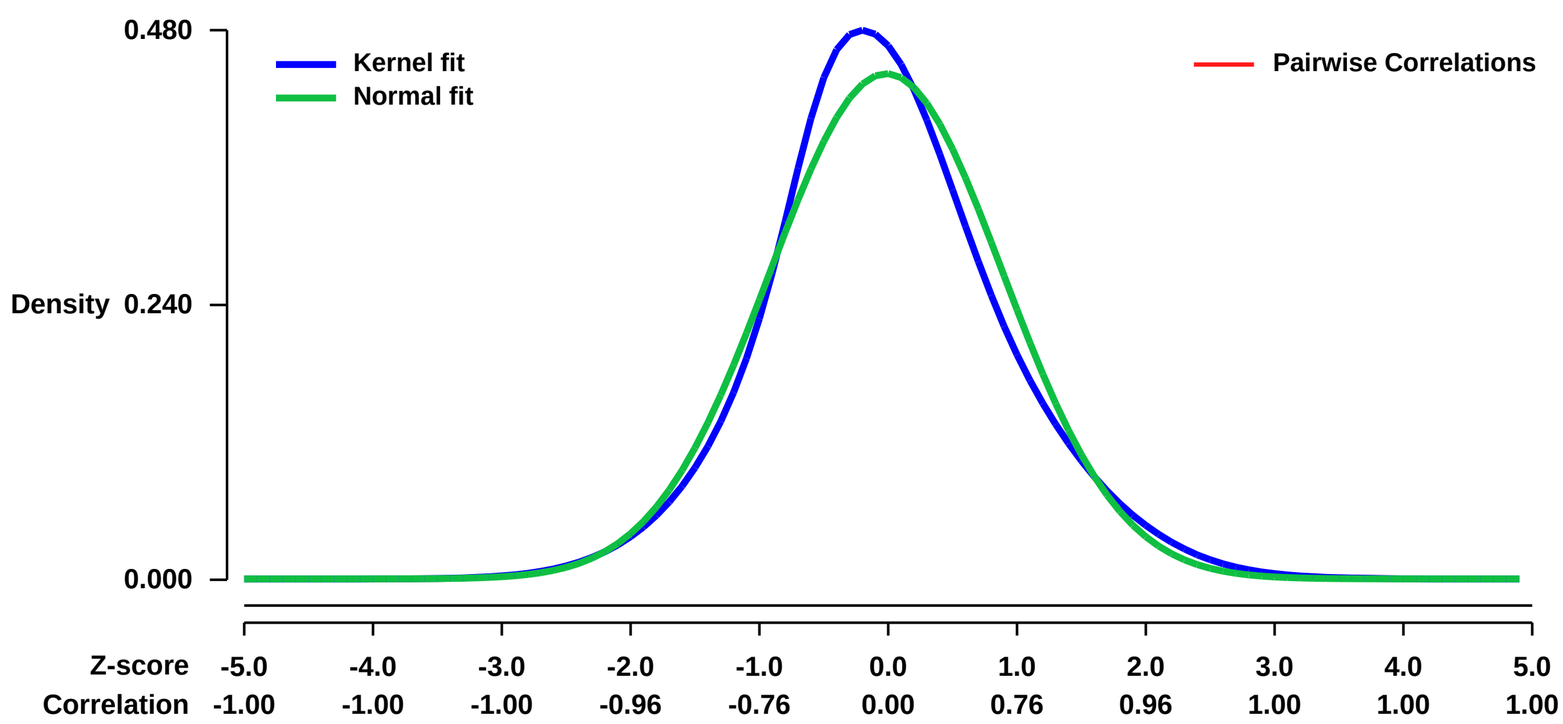

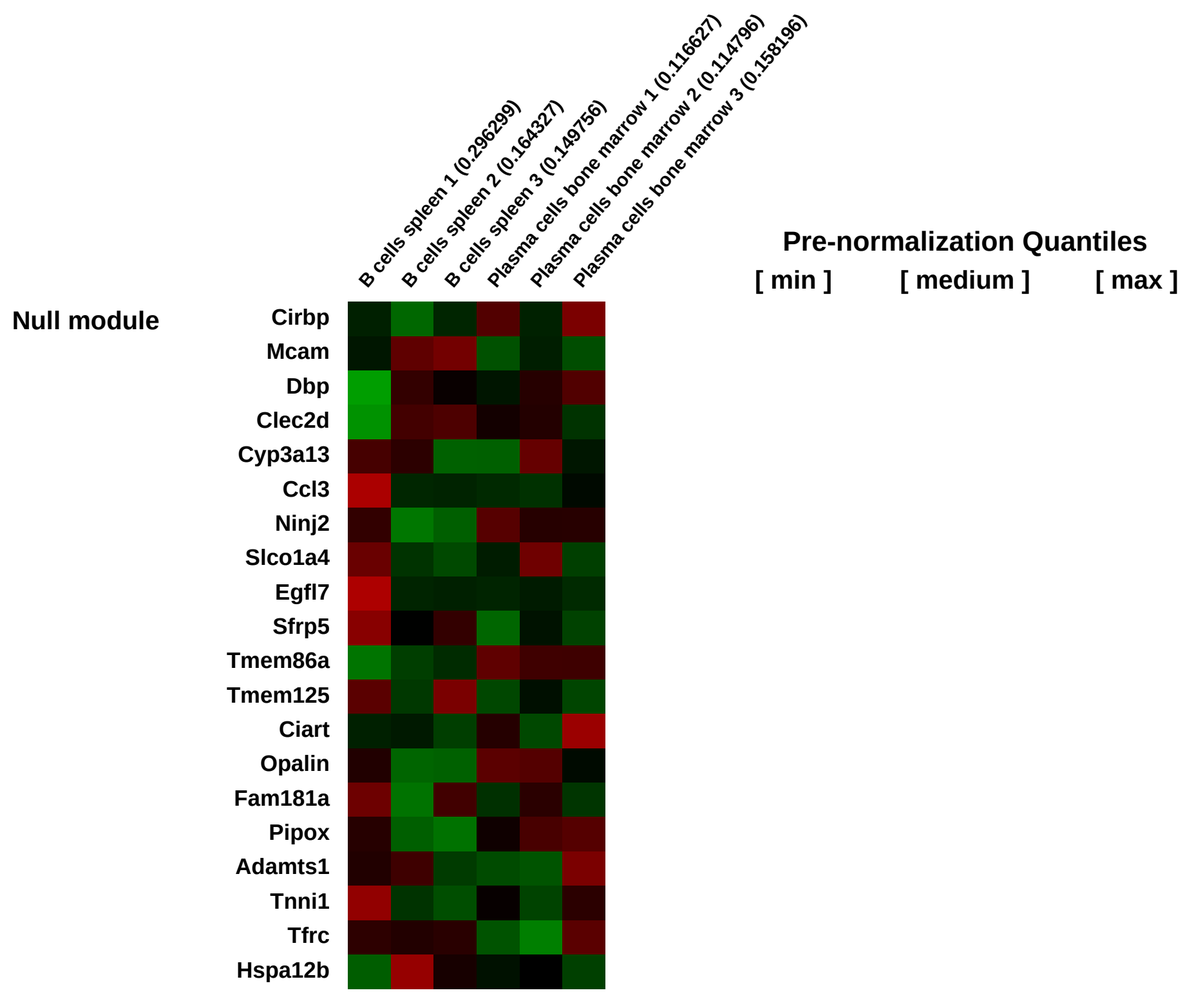

GEO Series "GSE5313" Expression Profiles

Num of samples in this series: 6

Scale of expression profile Z-scores

-3.0 -2.0 -1.0 0.0 1.0 2.0 3.0

GEO Link:	http://www.ncbi.nlm.nih.gov/geo/query/acc.cgi?acc=GSE5313
Status:	Public on Dec 02 2006
Title:	Comparative analysis of gene expression in A/J CB versus DBA/2J
Organism:	Mus musculus
Experiment type:	Expression profiling by array
Platform:	GPL1261
Pubmed ID:	17098806
Summary & Design:	**Summary:** We hypothesize that gene expression in the CBs of these two strains of mice are divergent thus contributing to the disparity in the phenotypes. More specifically, (1) genes related to CB function are expressed less in the A/J mice compared to DBA/2J mice; (2) gene expression levels of morphogenic and trophic factors of the CB maybe significantly lower in the A/J mice than the DBA/2J mice. In order to test these hypotheses, we utilized microarray analysis to examine transcriptional differences between CBs of both strains of mice. **Keywords: comparative expression profiling** **Overall design:** . This study utilizes microarray analysis to test these hypotheses. Three sets of CBs were harvested from both strains. RNA was isolated and used for global gene expression profiling (Affymetrix Mouse 430 2.0 array). Statistically significant gene expression was determined as a minimum 6 counts of 9 pairwise comparisons, minimum 1.5-fold change, and p < 0.05.

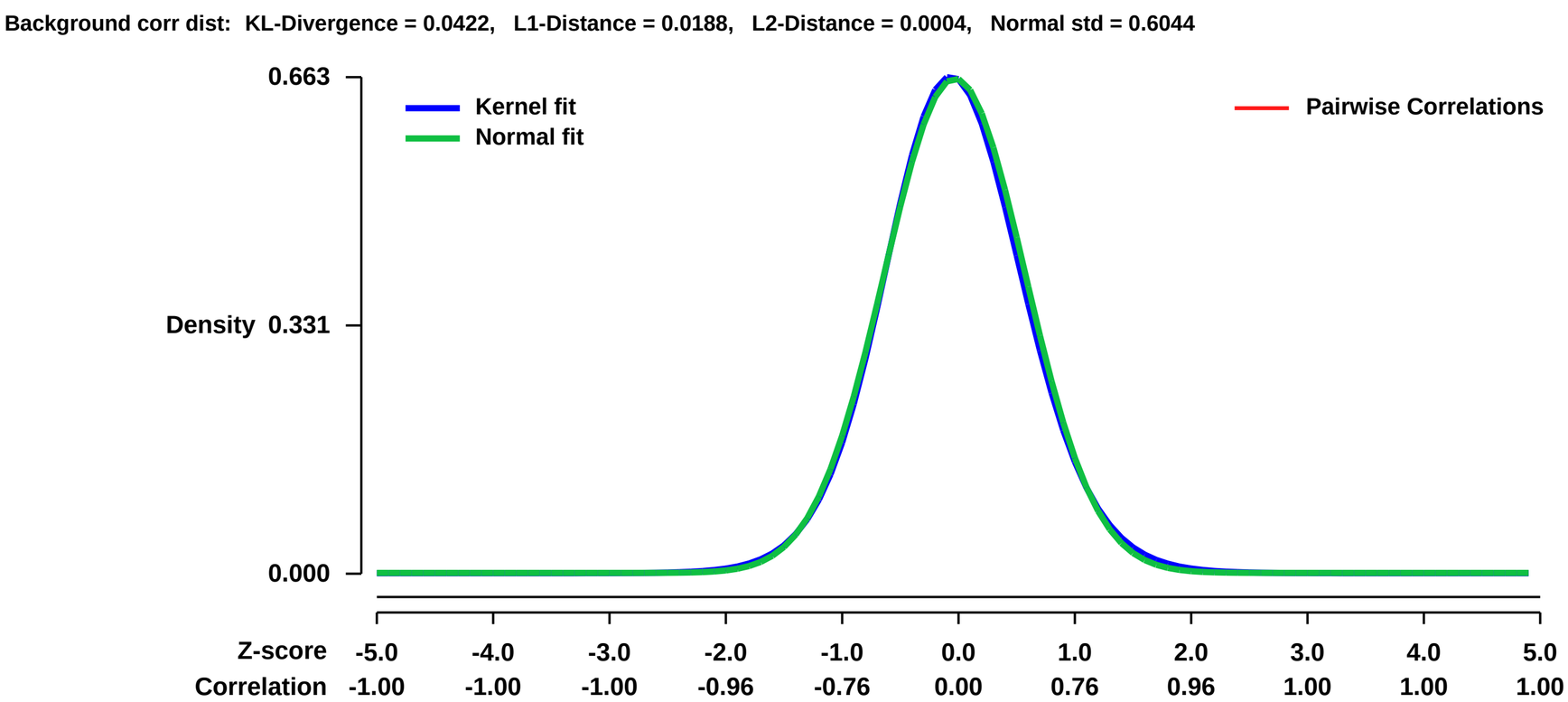

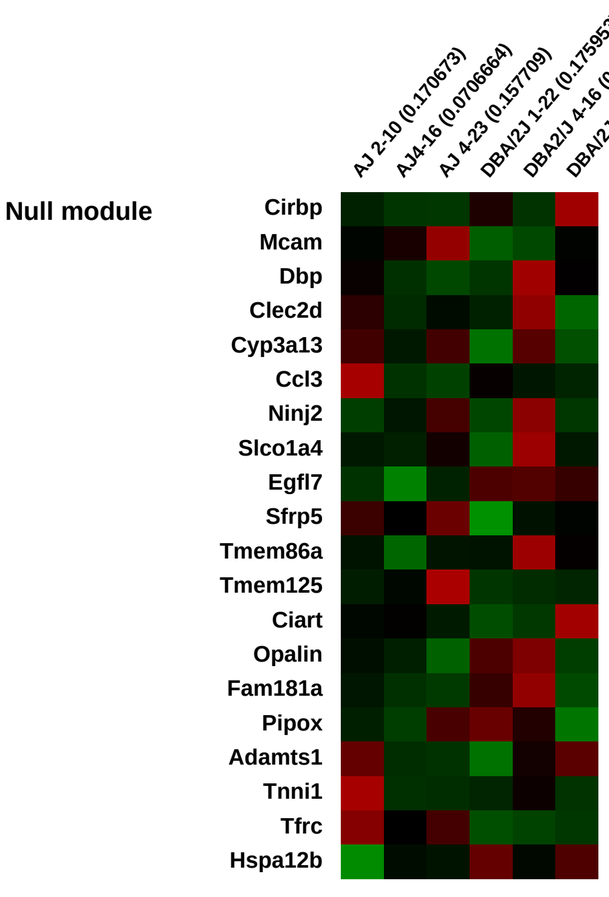

GEO Series "GSE18704" Expression Profiles

Num of samples in this series: 9

Scale of expression profile Z-scores

-3.0 -2.0 -1.0 0.0 1.0 2.0 3.0

GEO Link:	http://www.ncbi.nlm.nih.gov/geo/query/acc.cgi?acc=GSE18704
Status:	Public on Oct 23 2009
Title:	WNT4 is required for ovarian follicle development and female fertility
Organism:	Mus musculus
Experiment type:	Expression profiling by array
Platform:	GPL1261
Pubmed ID:	20371632
Summary & Design:	**Summary:** To study the physiological role of WNT4 in the postnatal ovary, a mouse strain bearing a floxed Wnt4 allele was created and mated to the Amhr2tm3(cre)Bhr strain to target deletion of Wnt4 to granulosa cells. Wnt4flox/-;Amhr2tm3(cre)Bhr/+ mice had significantly reduced ovary weights and produced smaller litters (P<0.05). Serial follicle counting demonstrated that, while Wnt4flox/-;Amhr2tm3(cre)Bhr/+ mice were born with a normal ovarian reserve and maintained normal numbers of small follicles until puberty, they had only 25.2% of the normal number of healthy antral follicles. Some Wnt4flox/-;Amhr2tm3(cre)Bhr/+ mice had no antral follicles or corpora lutea and underwent premature follicle depletion. RTPCR analyses of Wnt4flox/-;Amhr2tm3(cre)Bhr/+ granulosa cells and cultured granulosa cells that overexpress WNT4 demonstrated that WNT4 regulates the expression of Star, Cyp11a1 and Cyp19, steroidogenic genes previously identified as downstream targets of the WNT signaling effector CTNNB1. WNT4- and CTNNB1-overexpressing cultured granulosa cells were analyzed by microarray for alterations in gene expression, which showed that WNT4 also regulates a series of genes involved in late follicle development and the cellular stress response via the WNT/CTNNB1 signaling pathway. Together, these data indicate that WNT4 is required for normal antral follicle development, and may act by regulating granulosa cell functions including steroidogenesis. **Overall design:** Granulosa cells were obtained from 20-26 day-old mice of various genotypes 48h after eCG treatment, using the needle puncture method as previously described. Cells were then infected with adenoviruses to express eGFP or Cre, or overexpress WNT4 in serum-free medium, and subsequently harvested for RNA extraction as described below. Preliminary experiments demonstrated that an infection efficiency of >80% could be obtained at an MOI of ~50 (as determined by analysis of fluorescent signal in Ad-eGFP-infected cells) and that the Ad-Cre and Ad-WNT4 viruses produced efficient recombination of the floxed Ctnnb1 alleles and robust WNT4 overexpression, respectively. Microarray analyses were done using triplicate RNA samples from each adenoviral treatment described above, and using mouse expression set 430 microarrays (Affymetrix, Santa Clara, CA).

Background corr dist: KL-Divergence = 0.0407, L1-Distance = 0.0344, L2-Distance = 0.0022, Normal std = 0.5970

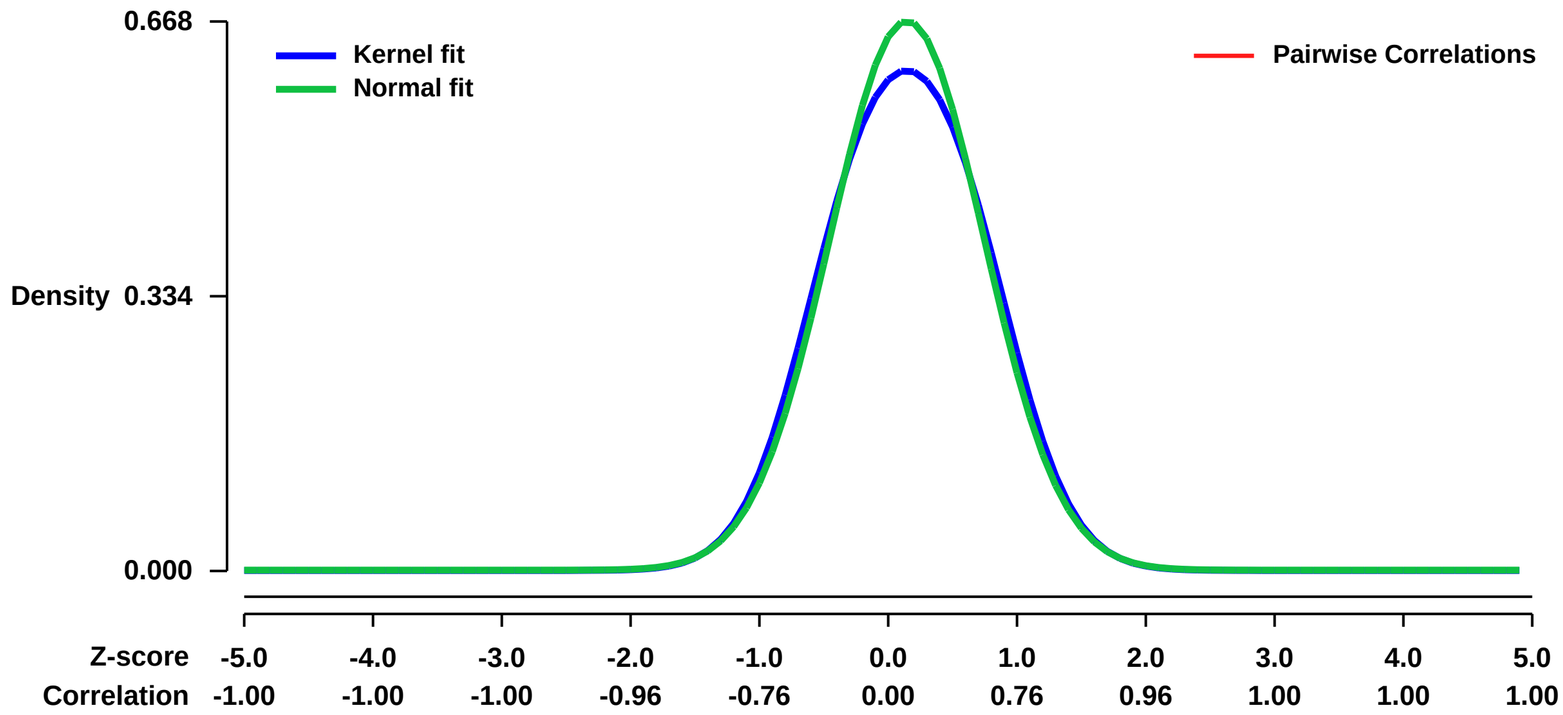

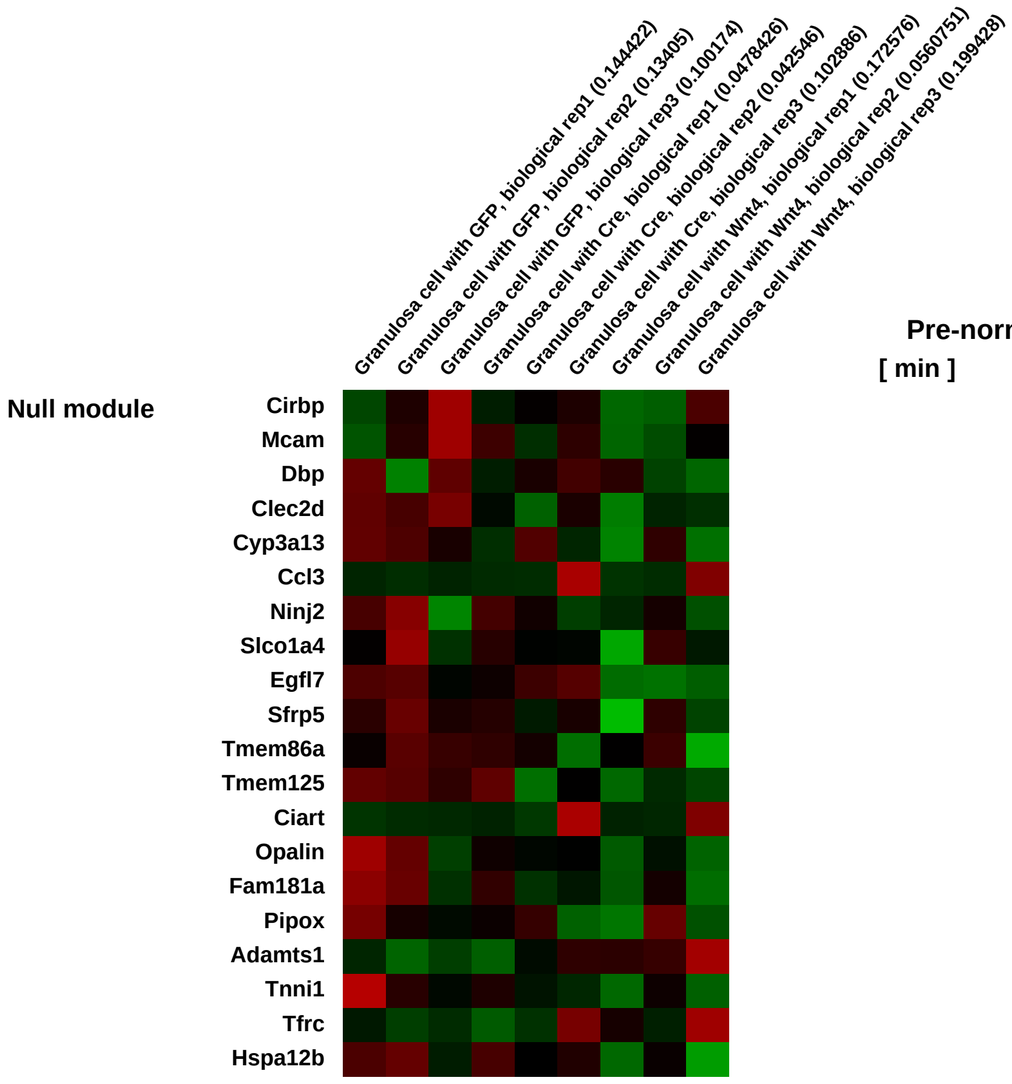

GEO Series "GSE20968" Expression Profiles

Num of samples in this series: 6

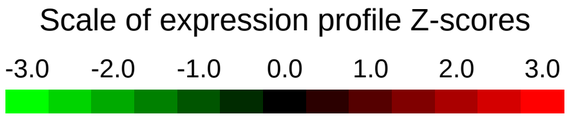

GEO Link:	http://www.ncbi.nlm.nih.gov/geo/query/acc.cgi?acc=GSE20968
Status:	Public on Jan 01 2011
Title:	Hepatocyte-nuclear-factor-4a promotes gut neoplasia in mice and protects against the production of reactive oxygen species
Organism:	Mus musculus
Experiment type:	Expression profiling by array
Platform:	GPL1261
Pubmed ID:	21062980
Summary & Design:	**Summary:** Hepatocyte-nuclear-factor-4¿– (Hnf4¿–) is a transcription factor that controls epithelial cell polarity and maturation during embryogenesis. Hnf4¿– conditional deletion during post-natal development results in minor consequences on intestinal epithelium integrity but promotes activation of the Wnt/¿†-catenin pathway. Here we show that Hnf4¿– does not act as a tumor suppressor gene but is crucial to promote gut tumorigenesis in mice. Polyp multiplicity in ApcMin mice that lacks Hnf4¿– is suppressed in comparison to littermate ApcMin controls. Analysis of microarray gene expression profiles from mice lacking Hnf4¿– in the intestinal epithelium identifies its novel function in regulating the expression of reactive oxygen species (ROS) detoxifying genes. This role is supported with the demonstration that HNF4¿– is functionally involved in the protection against spontaneous and 5-fluorouracil chemotherapy-induced production of intracellular ROS in colorectal cancer cell lines. The analysis of a colorectal cancer patient cohort establishes that HNF4¿– is significantly up-regulated at both gene transcript and protein levels in tumors relative to adjacent benign epithelial resections. Several genes involved in ROS neutralization are also up-regulated in correlation with HNF4¿– expression. All together, the findings point to the nuclear receptor HNF4¿– as a potential therapeutic target to eradicate aberrant epithelial cell resistance to ROS production during intestinal tumorigenesis. **Overall design:** HNF4alpha was conditionally knockout in the mouse epithelial intestine with the 12.4-kb VillinCRE. A total of 3 control and 3 mutant littermates individuals were sacrificed at 7 months of age. The distal jejunum was harvested and Total RNA was isolated from each individuals. Each RNA sample was independently used to generate probes to screen affymetrix chips.

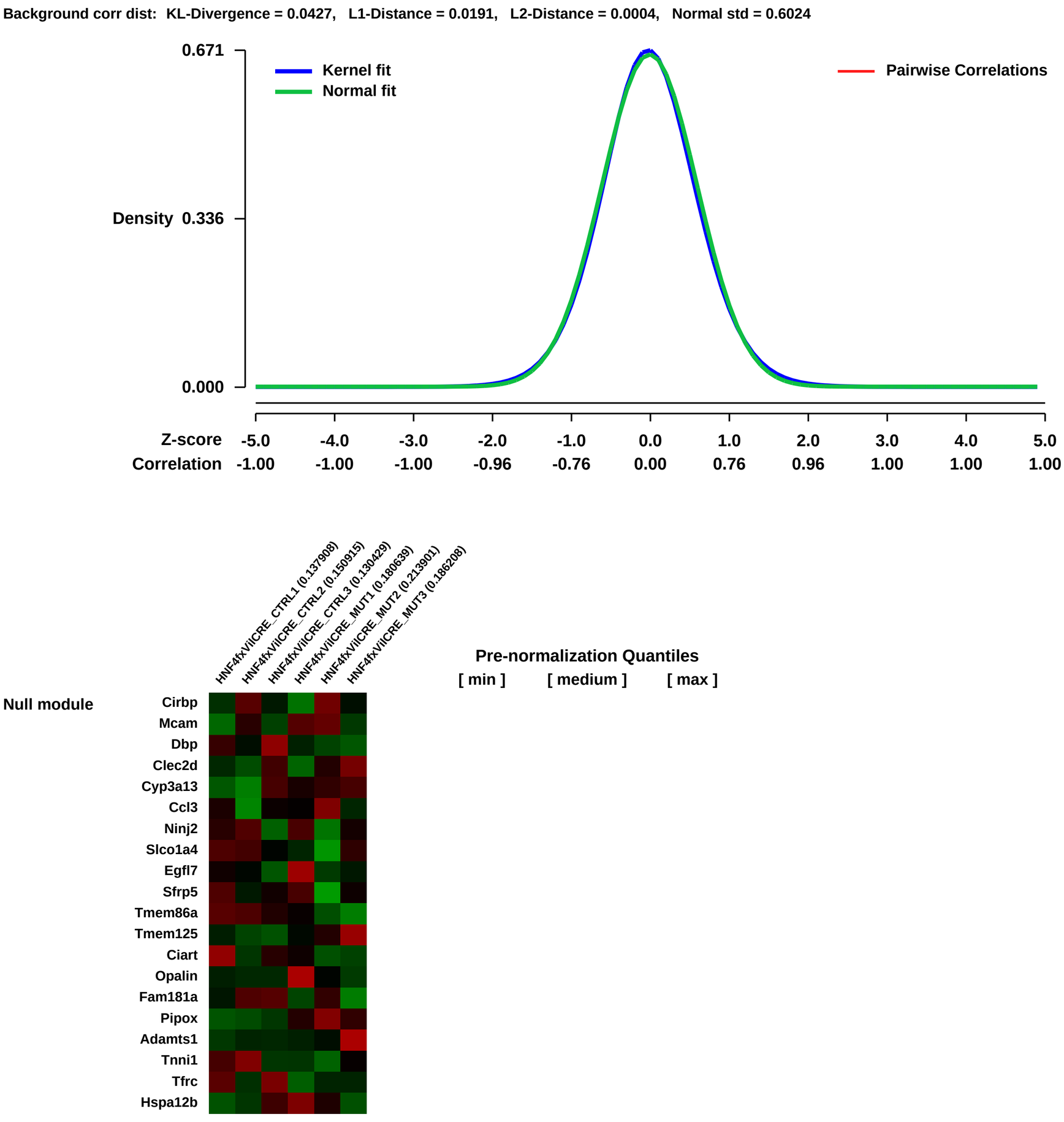

GEO Series "GSE43713" Expression Profiles

Num of samples in this series: 16

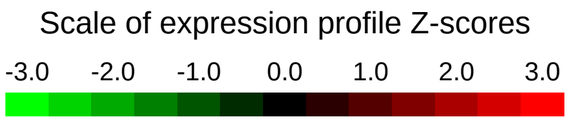

GEO Link:	http://www.ncbi.nlm.nih.gov/geo/query/acc.cgi?acc=GSE43713
Status:	Public on Sep 05 2013
Title:	Microarray to find CHOP dependent genes in response to proteasome inhibition
Organism:	Mus musculus
Experiment type:	Expression profiling by array
Platform:	GPL1261
Pubmed ID:	23761072
Summary & Design:	**Summary:** Environmental stresses that disrupt protein homeostasis induce phosphorylation of eIF2, triggering repression of global protein synthesis coincident with preferential translation of ATF4, a transcriptional activator of the Integrated stress response (ISR). Depending on the extent of protein disruption, ATF4 may not be able to restore proteostatic control and instead switch to a terminal outcome that features elevated expression of the transcription factor CHOP (GADD153/DDIT3). The focus of this study was to define the mechanisms by which CHOP directs gene regulatory networks that determine cell fate. We find that in response to proteasome inhibition, CHOP induces the expression of a collection of genes encoding transcription regulators, including ATF5, which is preferentially translated during eIF2 phosphorylation. Transcriptional expression of ATF5 is directly activated by both CHOP and ATF4. Knock-down of ATF5 increased cell survival in response to proteasome inhibition, supporting the idea that both ATF5 and CHOP have pro-apoptotic functions. Transcriptome analyses of ATF5-dependent genes revealed targets involved in apoptosis, including, NOXA, which is important for inducing cell death during proteasome inhibition. This study suggests that the ISR features a feed-forward loop of stress induced transcriptional regulators, each subject to transcriptional and translational control that can switch cell fate towards apoptosis. **Overall design:** 8 plates (10cm) of WT and and 8 plates (10cm) of CHOP-/- MEF cells were subject to no stress (4 each for a total of 8) or treated for 8 hours with 1uM MG132 (4 each for a total of 8). Unstressed cells were harvested at the same time as the stressed cells

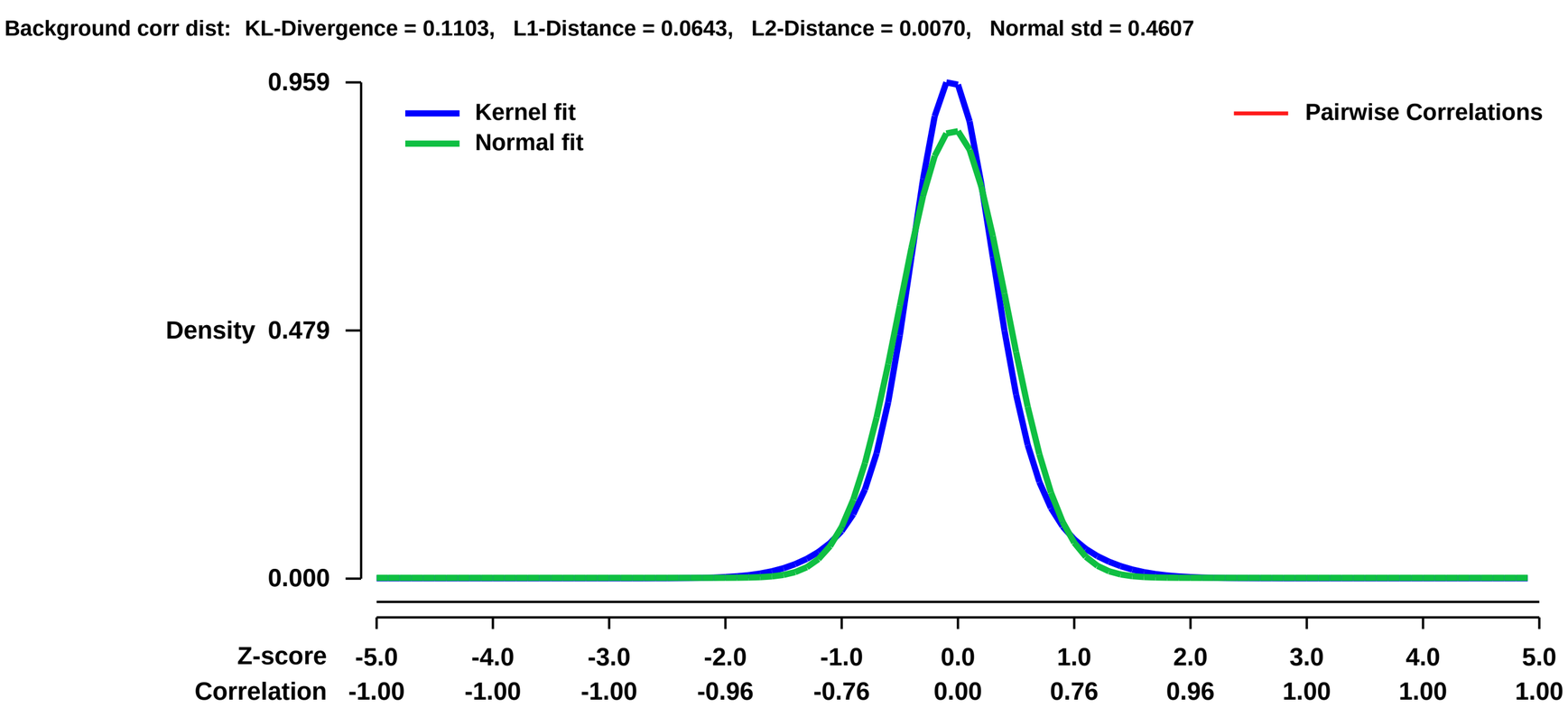

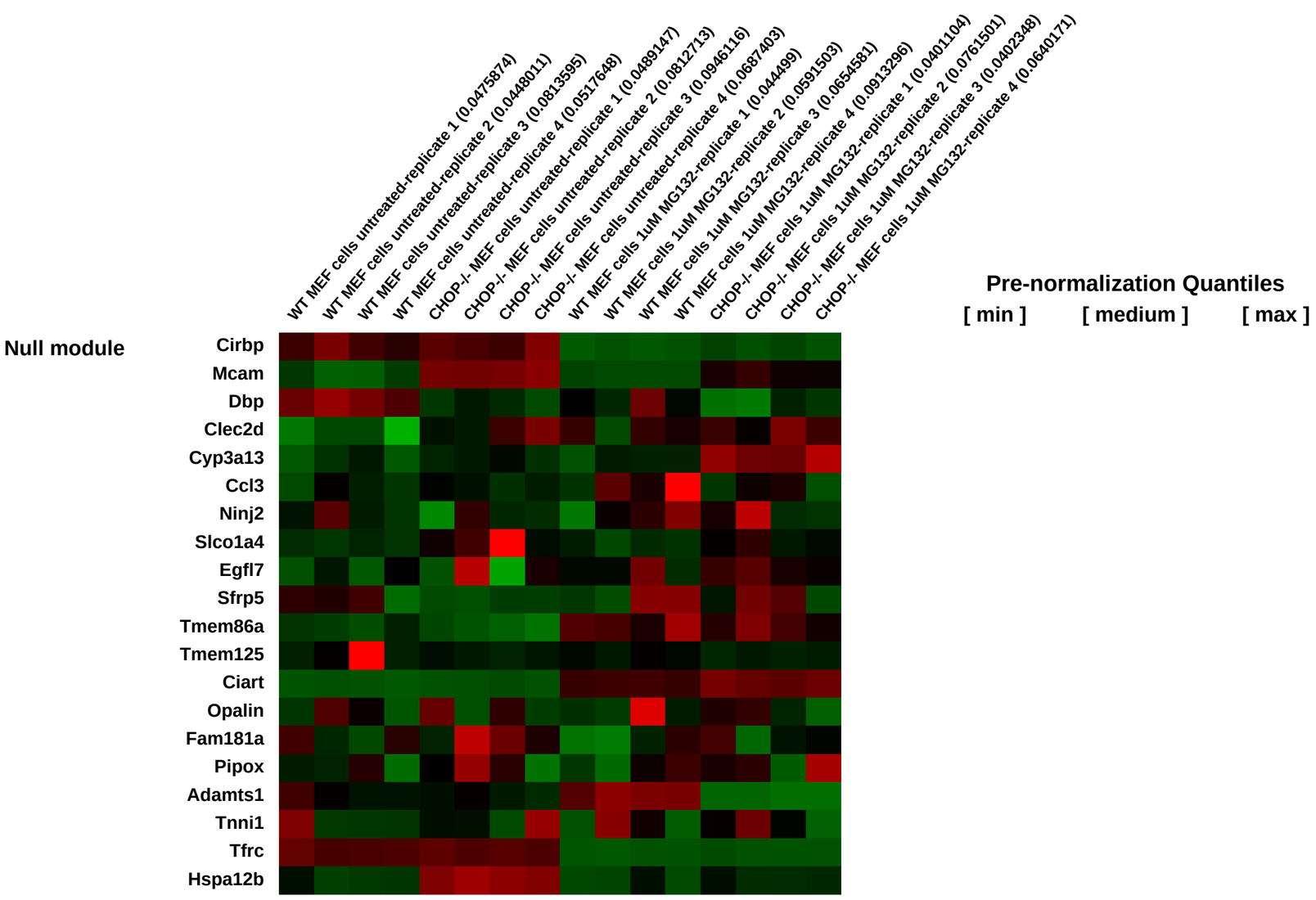

GEO Series "GSE17844" Expression Profiles

Num of samples in this series: 6

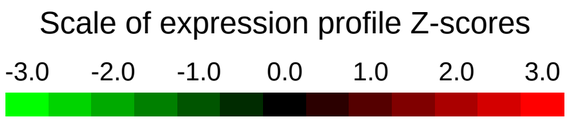

GEO Link:	**http://www.ncbi.nlm.nih.gov/geo/query/acc.cgi?acc=GSE17844**
Status:	**Public on Apr 25 2012**
Title:	**Basal expression in daDREAM transgenic mouse hippocampus**
Organism:	**Mus musculus**
Experiment type:	**Expression profiling by array**
Platform:	**GPL1261**
Pubmed ID:	
Summary & Design:	**Summary:** **Changes in nuclear Ca2+ homeostasis activate specific gene expression programs and are central to the acquisition and the plastic storage of memories. DREAM /KChIP proteins form heterotetramers that bind DNA and repress transcription in a Ca2+-dependent manner. Single ablation of one member of the DREAM/KChIP family may result in a mild or the absence of phenotype due to partial gene compensation. To study the function of DREAM/KChIP proteins in the brain, we used transgenic mice expressing a Ca2+-insensitive/CREB-independent dominant active mutant DREAM (daDREAM). We show that daDREAM controls the expression of several activity-dependent transcription factors including Npas4, Nr4a1, Mef2C, JunB and c-Fos, as well as the chromatin modifying enzyme Mbd4 and proteins related to actin polymerization like Arc and gelsolin. Thus, directly or through these targets, expression of daDREAM in the forebrain resulted in a complex phenotype characterized by i) impaired learning and memory, ii) loss of recurrent inhibition and enhanced LTP in the dentate gyrus without affecting Kv4-mediated potassium currents, and iii) modified spine density in DG granule neurons. Our results propose DREAM as a master-switch transcription factor regulating several activity-dependent gene expression programs to control synaptic plasticity, learning and memory.** **Overall design:** **We used Affymetrix microarrays (GeneChip Mouse Genome 430 2.0) to compare global gene expression in wild type (WT) versus transgenic hippocampi (L26 mice). For ech type of sample three hybridizations were carried-out (independent biological replicates).**

Background corr dist: KL-Divergence = 0.0405, L1-Distance = 0.0155, L2-Distance = 0.0002, Normal std = 0.6101

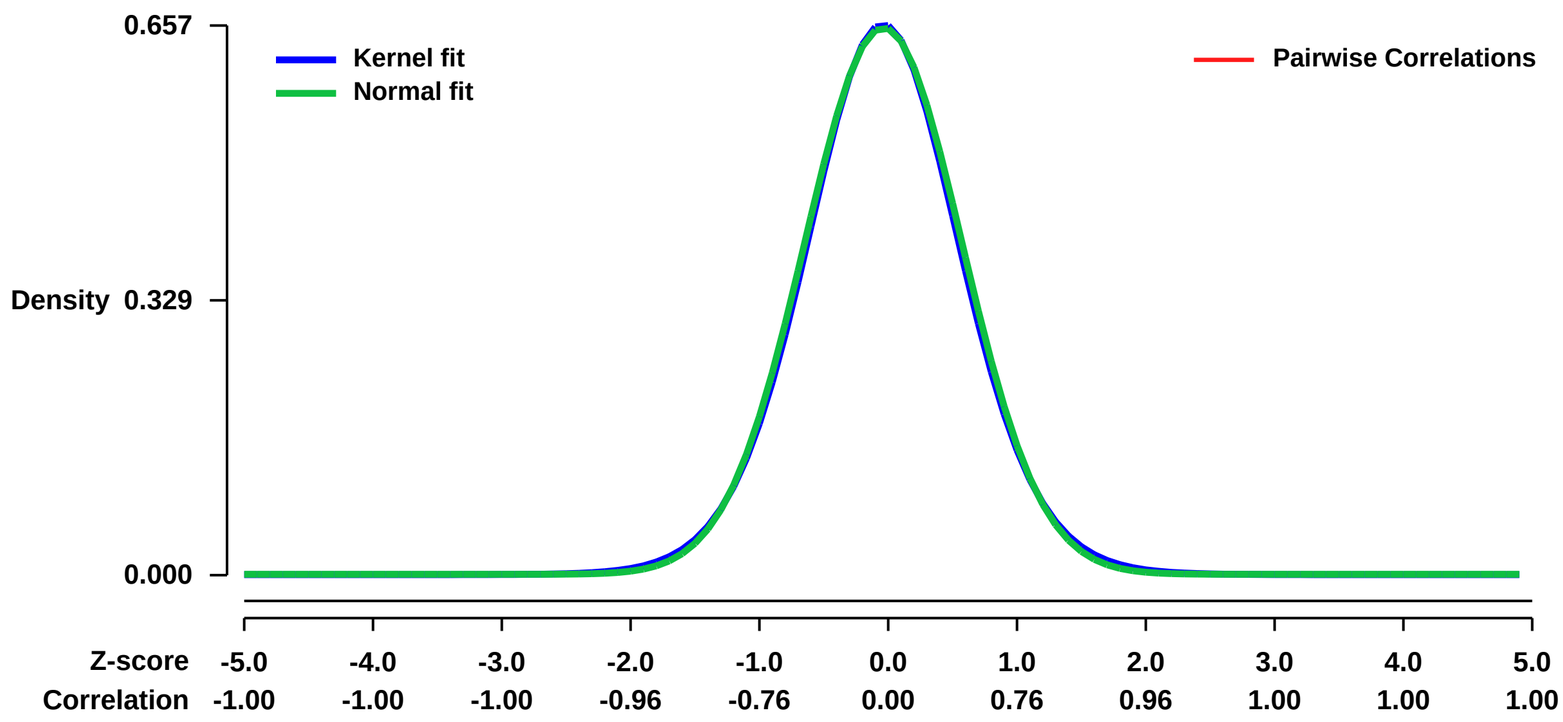

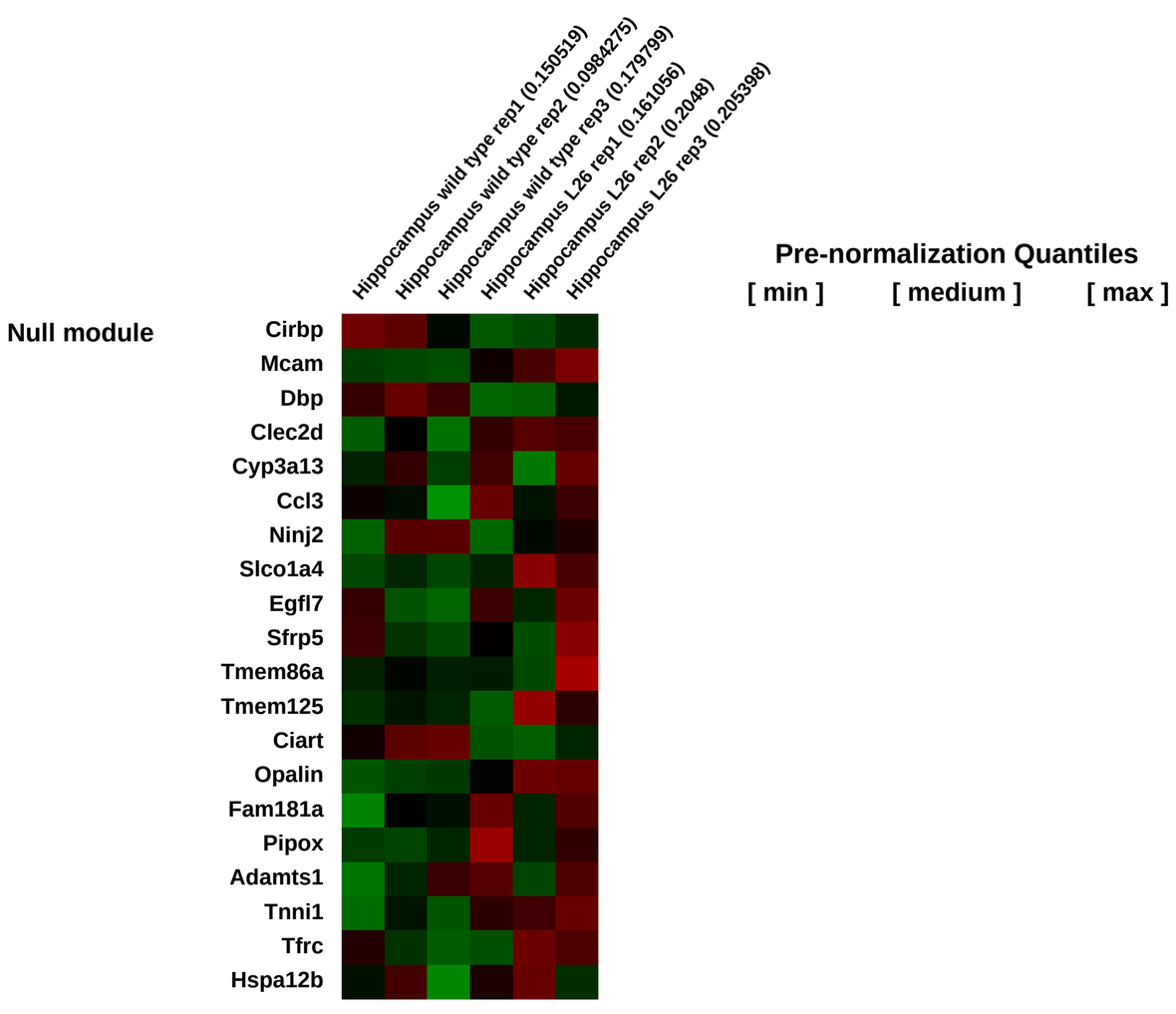

GEO Series "GSE12908" Expression Profiles

Num of samples in this series: 10

Scale of expression profile Z-scores

-3.0 -2.0 -1.0 0.0 1.0 2.0 3.0

GEO Link:	**http://www.ncbi.nlm.nih.gov/geo/query/acc.cgi?acc=GSE12908**
Status:	**Public on Dec 31 2008**
Title:	**Gene expression following miR-30a knockdown in bipotential mouse embryonic liver (BMEL) cells**
Organism:	**Mus musculus**
Experiment type:	**Expression profiling by array**
Platform:	**GPL1261**
Pubmed ID:	**19185580**
Summary & Design:	**Summary:** **The goal was to identify genes targeted by miR-30a.** **Keywords: Transfection of cultured cells with antisense oligonucleotide** **Overall design:** **RNA was isolated from BMELs tranfected with a locked nucleic acid (LNA) antisense oligonucleotide to miR-30a or with a scrambled control oligo.**

Background corr dist: **KL-Divergence = 0.1146, L1-Distance = 0.0300, L2-Distance = 0.0015, Normal std = 0.4135**

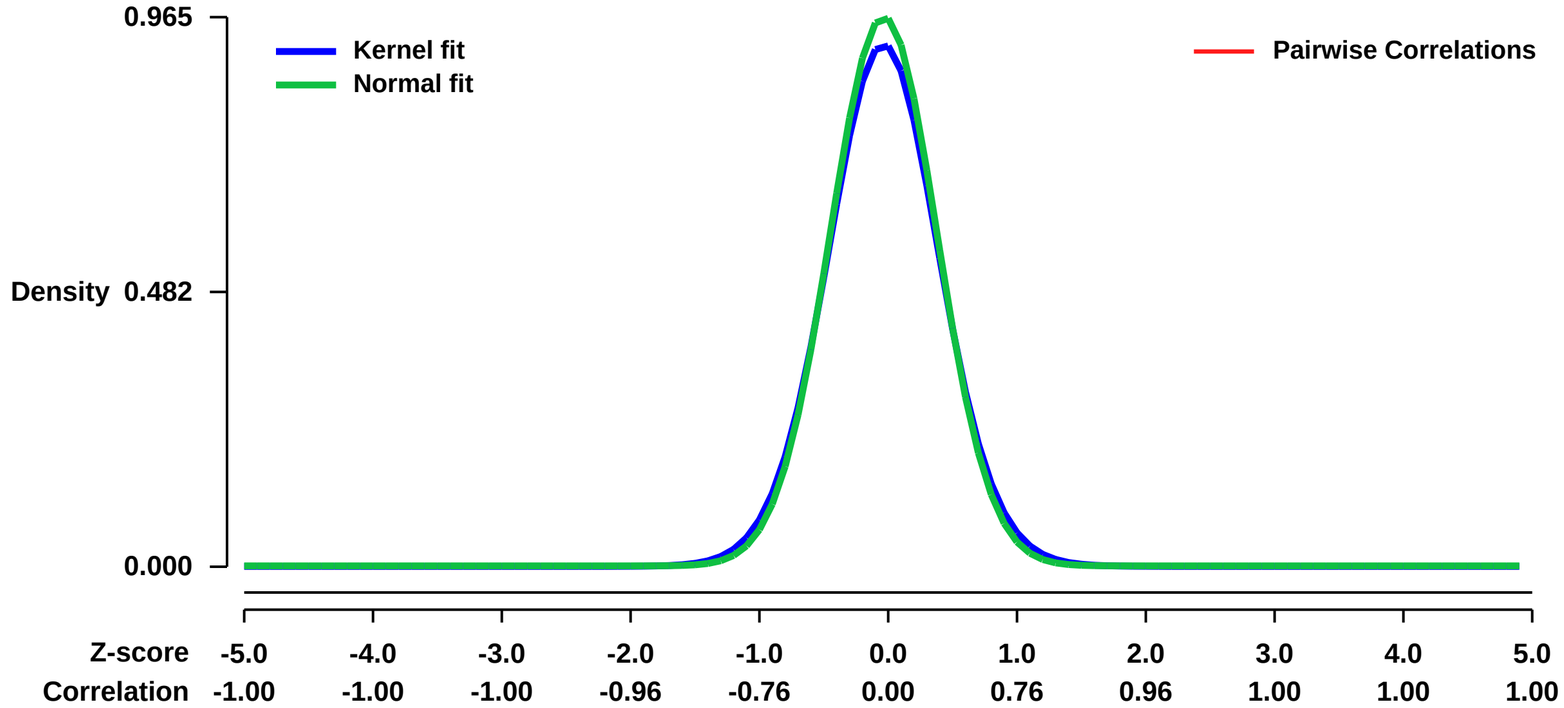

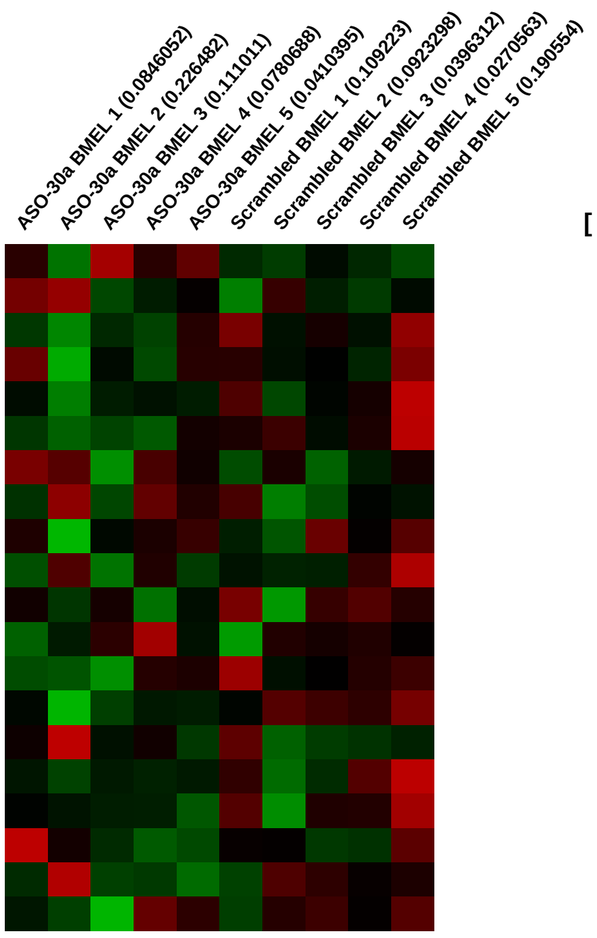

GEO Series "GSE32020" Expression Profiles

Num of samples in this series: 26

Scale of expression profile Z-scores

-3.0 -2.0 -1.0 0.0 1.0 2.0 3.0

GEO Link:	http://www.ncbi.nlm.nih.gov/geo/query/acc.cgi?acc=GSE32020
Status:	Public on Jan 22 2013
Title:	Expression data from mammary gland during pregnancy and lactation of CBA/CaH, QSi5 and Advanced Intercross Line (AIL; CBA/CaH X QSi5, the 14th generation)
Organism:	Mus musculus
Experiment type:	Expression profiling by array
Platform:	GPL1261
Pubmed ID:	23284081
Summary & Design:	**Summary:** Previously we have shown significant differences in lactation performance, mammary gland histology and expression profiles of mammary transcriptome during peak-lactation (lactation day 9; L9) between the ordinary CBA/CaH (CBA) and the superior QSi5 strains of mice. In the present study, we compared mammary gland histology between CBA and QSi5 at mid-pregnancy (pregnancy day 12; P12). We assessed lactation performance during the first 8 days of lactation of the 13th - 14th generation of the Advanced Intercross Line (AIL) (CBA X QSi5) mice. We utilized an integrative approach to analyzing mammary microarray expression profiles of CBA and QSi5 at P12 and CBA, AIL and QSi5 at L9. **Overall design:** The inguinal mammary glands of CBA/CaH and QSi5 during mid-pregnancy (Pregnancy day 12; P12), and the glands of CBA/CaH, AIL and QSi5 during peak lactation (Lactation day 9; L9) were collected and total RNA was extracted for Affymetrix microarray (mouse genome 430 2) assay

Background corr dist: KL-Divergence = 0.0494, L1-Distance = 0.0894, L2-Distance = 0.0125, Normal std = 0.6669

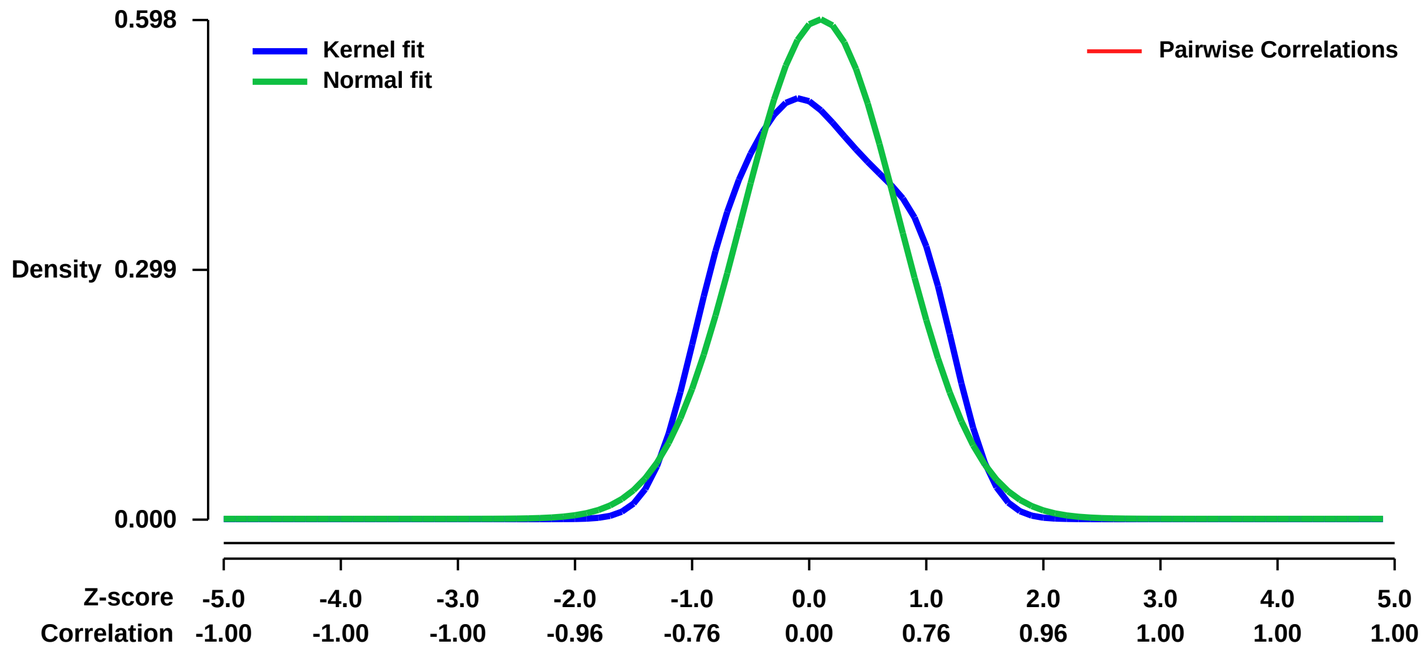

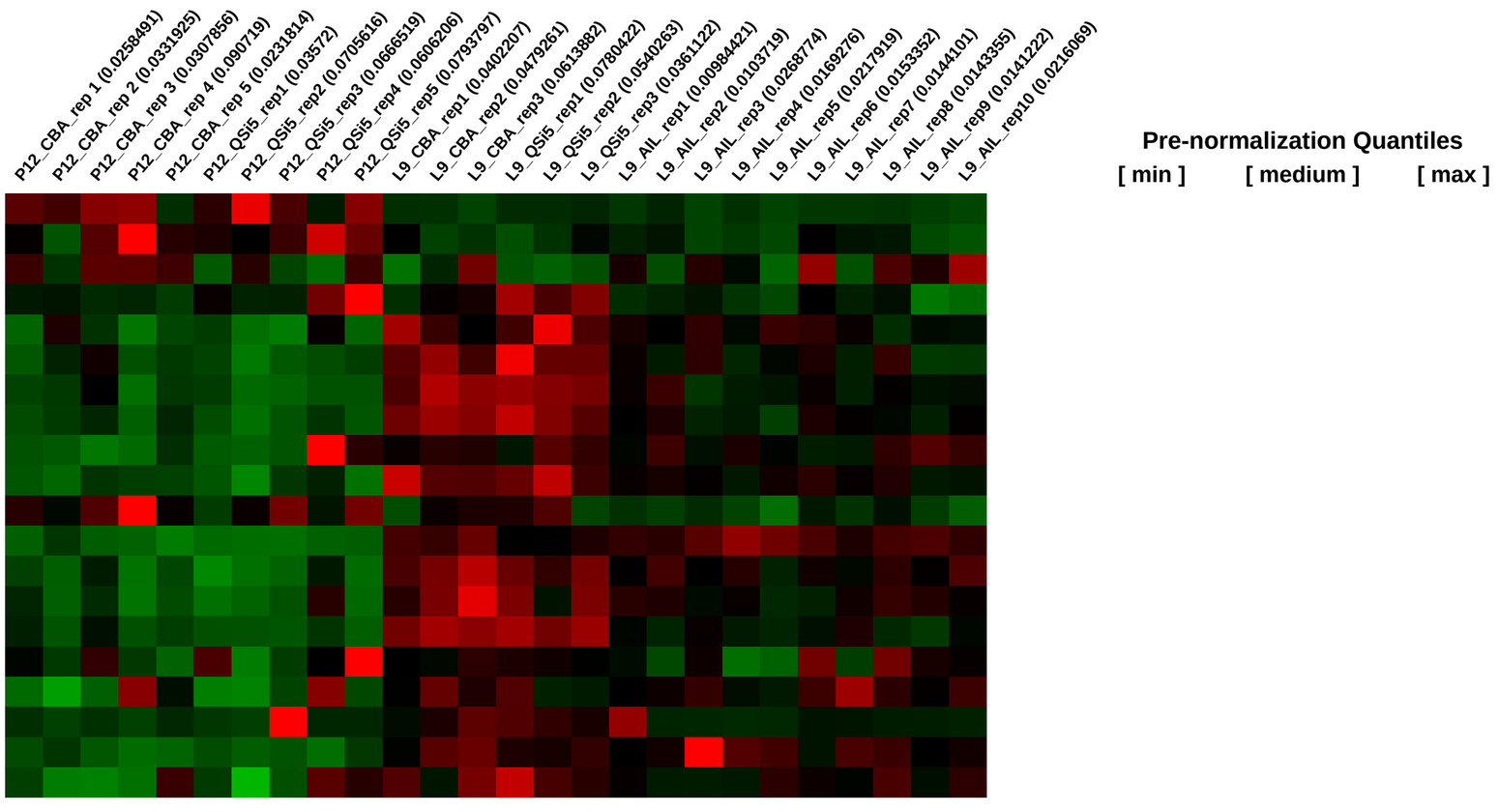

GEO Series "GSE12993" Expression Profiles

Num of samples in this series: 6

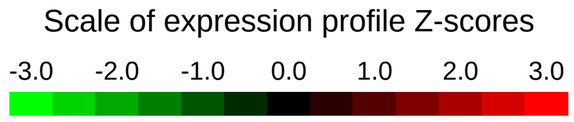

GEO Link:	**http://www.ncbi.nlm.nih.gov/geo/query/acc.cgi?acc=GSE12993**
Status:	**Public on Jul 31 2009**
Title:	**C2C12 culture: myogenesis timecourse and shRp58 treatment**
Organism:	**Mus musculus**
Experiment type:	**Expression profiling by array**
Platform:	**GPL1261**
Pubmed ID:	
Summary & Design:	**Summary:** **To predict Rp58-regulated gene involved in myogenesis, RNA profiling experiments were performed, comparing RNA derived from C2C12 with or without expressing shRNA for Rp58. As a result, 271 genes were upregulated in C2C12 stably expressing shRNA-Rp58 cells compared with control C2C12 cells. As Rp58 is repressor in C2C12, we hypothesized that Rp58 regulates gene cluster which expression is downregulated in accordance with Rp58 expression and myogenesis progression. In this regard, we also characterized dynamic gene expression patterns during myogenesis by microarray at 4 different stage (GM, day 0, 2, 4) of C2C12 myogenesis assays and found that 399 genes expression is characterized as downregulation pattern during myogenesis. Importantly, this down regulation gene set and upregulated genes by shRNA for Rp58 were highly overlapped.** **Keywords: time course, shRNA** **Overall design:** **MAPPFinder (www.genmapp.org) was used to integrate expression data with known pathways.**

Background corr dist: KL-Divergence = 0.0165, L1-Distance = 0.0127, L2-Distance = 0.0002, Normal std = 0.7749

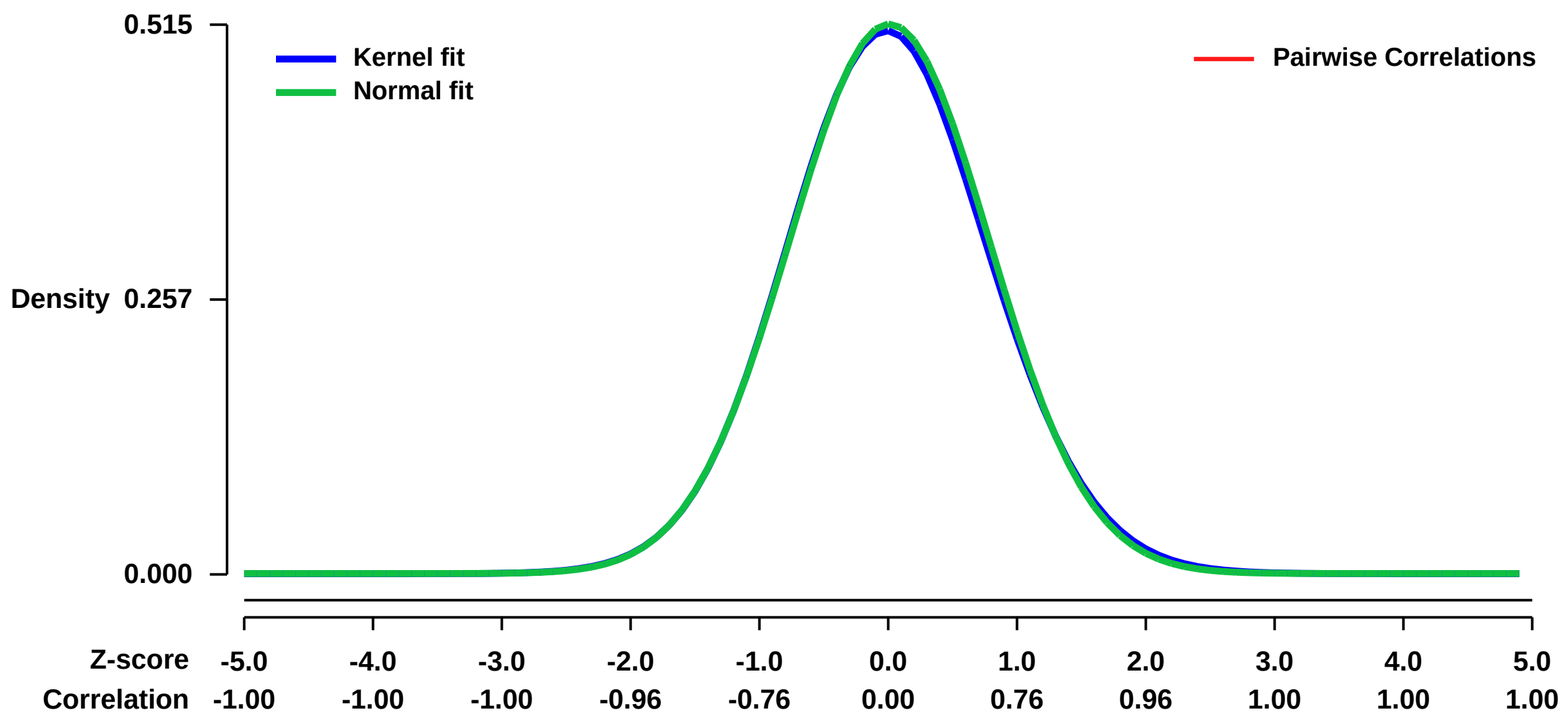

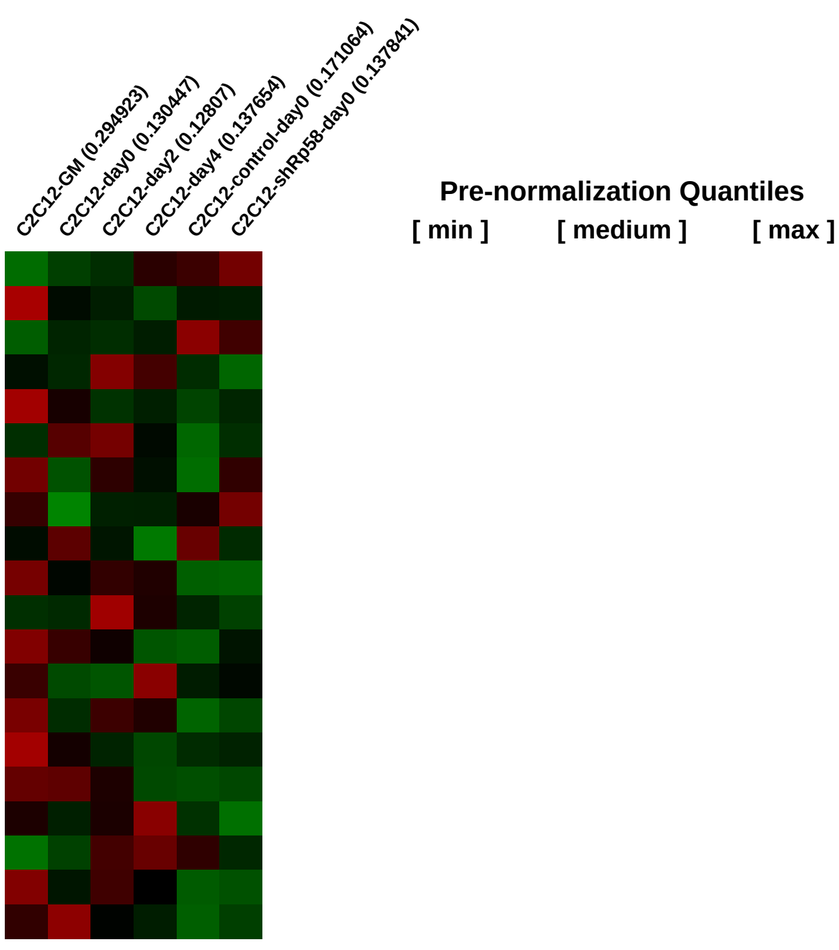

GEO Series "GSE29458" Expression Profiles

Num of samples in this series: 23

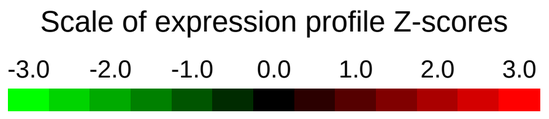

GEO Link:	http://www.ncbi.nlm.nih.gov/geo/query/acc.cgi?acc=GSE29458
Status:	Public on May 23 2011
Title:	Expression data from PDGF driven mouse tumors
Organism:	Mus musculus
Experiment type:	Expression profiling by array
Platform:	GPL1261
Pubmed ID:	21625383
Summary & Design:	**Summary:** **Background** **Tumor heterogeneity is a major obstacle for finding effective treatment of Glioblastoma (GBM). Based on global expression analysis, GBM can be classified into distinct subtypes: Proneural, Neural, Classical and Mesenchymal. The signatures of these different tumor subtypes may reflect the phenotypes of cells giving rise to them.** **However, the experimental evidence connecting any specific subtype of GBM to particular cells of origin is lacking. In addition, it is unclear how different genetic alterations interact with cells of origin in determining tumor heterogeneity. This issue cannot be addressed by studying end-stage human tumors.** **Methodology/Principal Findings** **To address this issue, we used retroviruses to deliver transforming genetic lesions to glial progenitors in adult mouse brain. We compared the resulting tumors to human GBM. We found that different initiating genetic lesions gave rise to tumors with different growth rates.** **However all mouse tumors closely resembled the human Proneural GBM.** **Comparative analysis of these mouse tumors allowed us to identify a set of genes whose expression in humans with Proneural GBM correlates with survival.** **Conclusions/Significance** **This study offers insights into the relationship between adult glial progenitors and Proneural GBM, and allows us to identify molecular alterations that lead to more aggressive tumor growth. In addition, we present a new preclinical model that can be used to test treatments directed at a specific type of GBM in future studies.** **Overall design:** **Gene expression profiling was performed on 20 tumors (12 Ptenf/f and 8 Ptenf/f; p53f/f) and 3 normal brains from mice. End stage tumors were used for expression array analysis. The platform used was Affymetrix GeneChip Mouse Genome 430A 2.0 Array. The microarray labeling, hybridization and quality controls were performed by following Affymetrix protocol.**

Background corr dist: **KL-Divergence = 0.0721, L1-Distance = 0.0373, L2-Distance = 0.0027, Normal std = 0.4903**

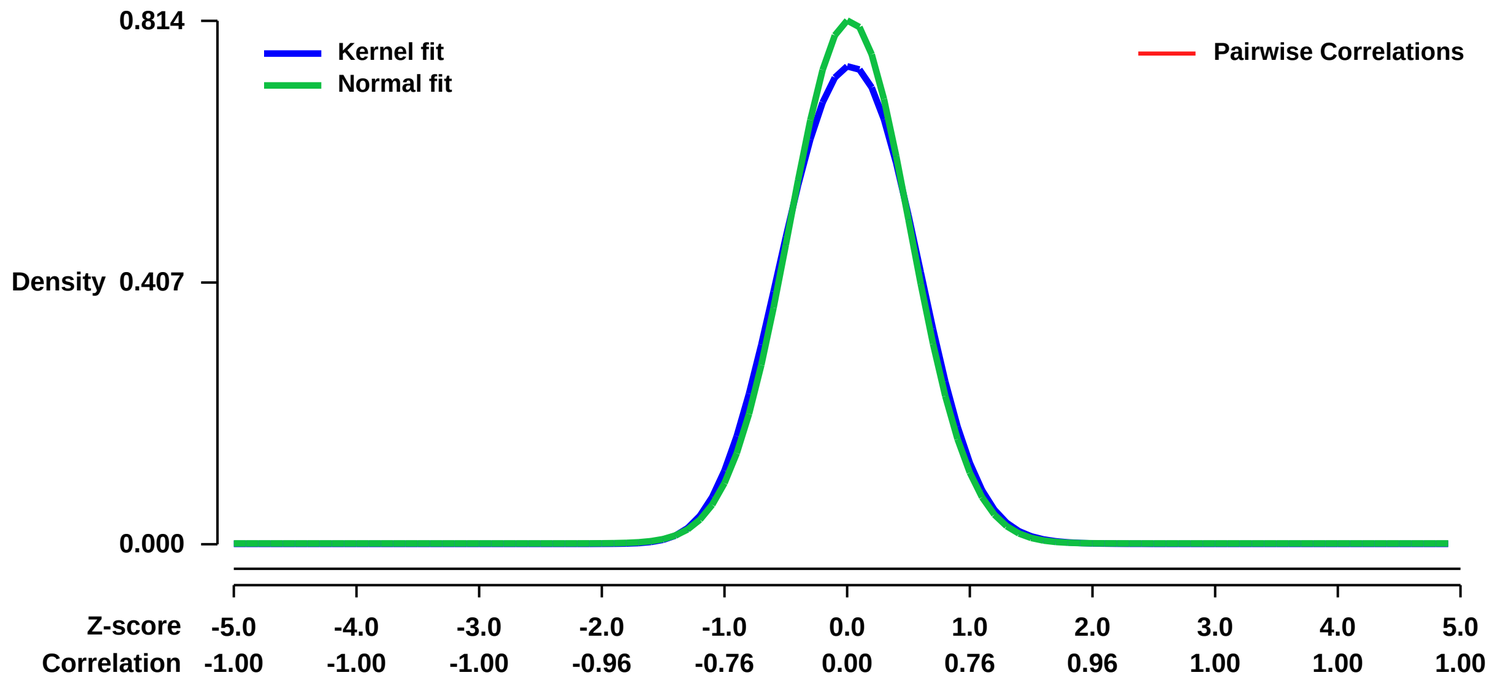

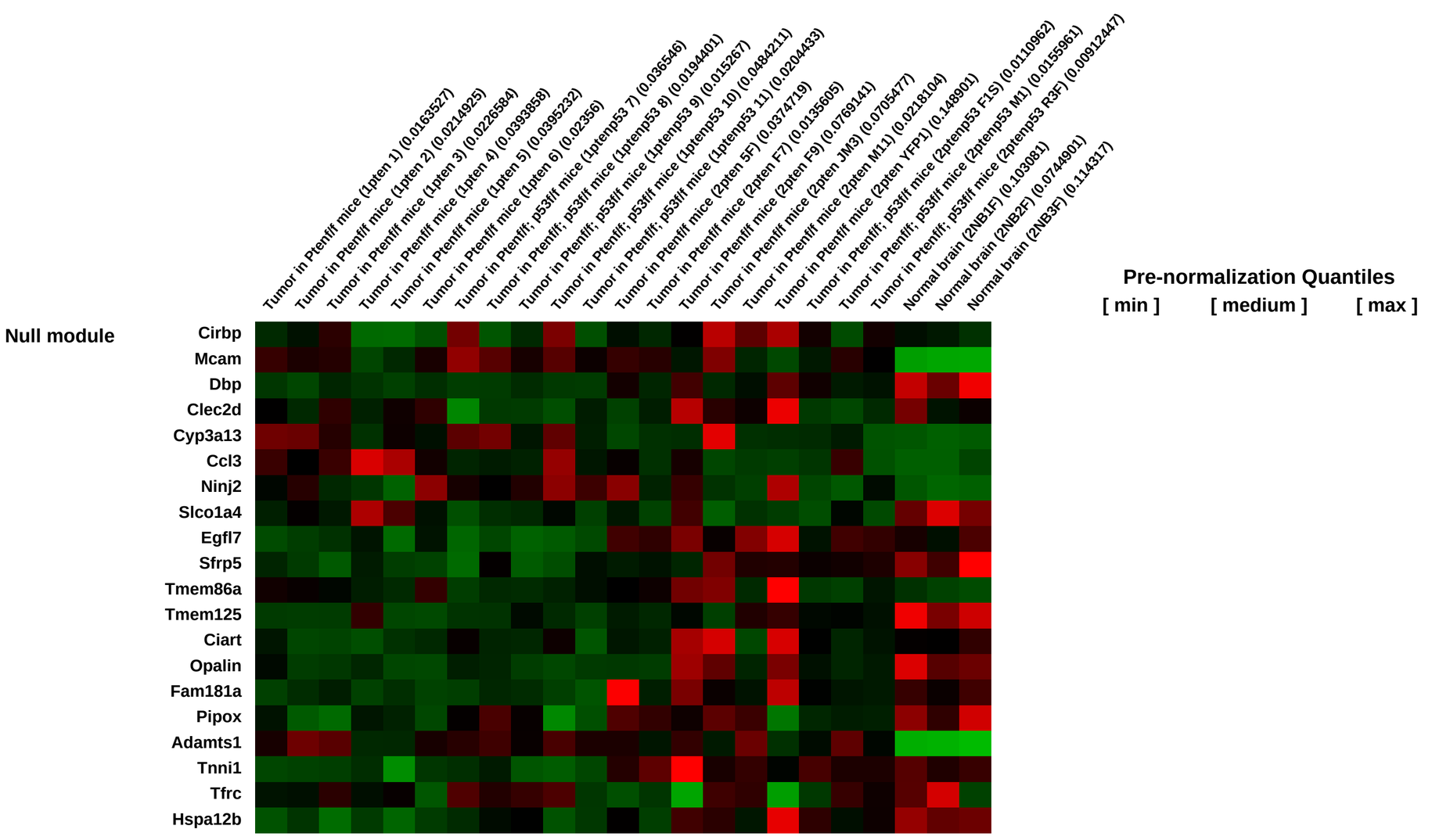

GEO Series "GSE36826" Expression Profiles

Num of samples in this series: 12

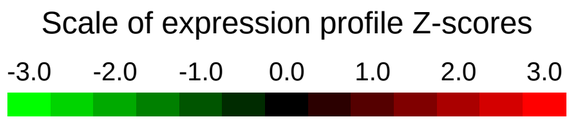

GEO Link:	http://www.ncbi.nlm.nih.gov/geo/query/acc.cgi?acc=GSE36826
Status:	Public on Dec 05 2012
Title:	Neutrophil-derived IL-1¸† is sufficient for abscess formation in immunity against Staphylococcus aureus in mice
Organism:	Mus musculus
Experiment type:	Expression profiling by array
Platform:	GPL1261
Pubmed ID:	23209417
Summary & Design:	**Summary:** Neutrophil abscess formation is critical in innate immunity against many pathogens. Here, the mechanism of neutrophil abscess formation was investigated using a mouse model of Staphylococcus aureus cutaneous infection. Gene expression analysis of S. aureus-infected skin revealed that induction of neutrophil recruitment genes was largely dependent upon IL-1beta/IL-1R activation. Unexpectedly, using IL 1beta reporter mice, neutrophils were identified as the primary source of IL-1beta at the site of infection. Furthermore, IL-1beta-producing neutrophils were necessary and sufficient for abscess formation and bacterial clearance. S. aureus-induced IL 1beta production by neutrophils required TLR2, NOD2, FPRs and the ASC/NLRP3 inflammasome. Taken together, IL-1beta and neutrophil abscess formation during an infection are functionally, spatially and temporally linked as a consequence of direct IL-1beta production by neutrophils. **Overall design:** Lesional skin biopsies obtained from C57BL/6J WT mice or IL-1R-deficient mice at 4 hours post-infection with Staphylococcus aureus. Uninfected skin biopsies were also collected from WT and IL-1R-deficient mice.

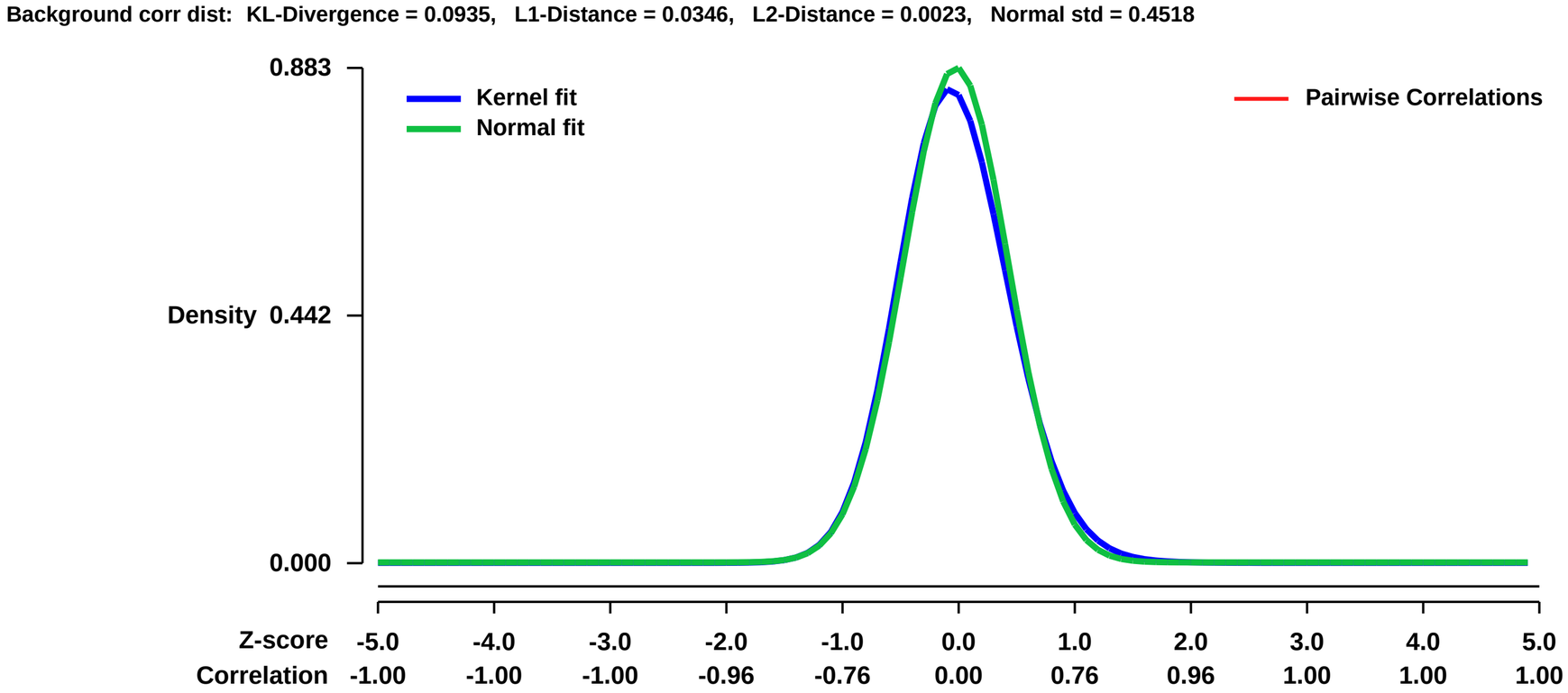

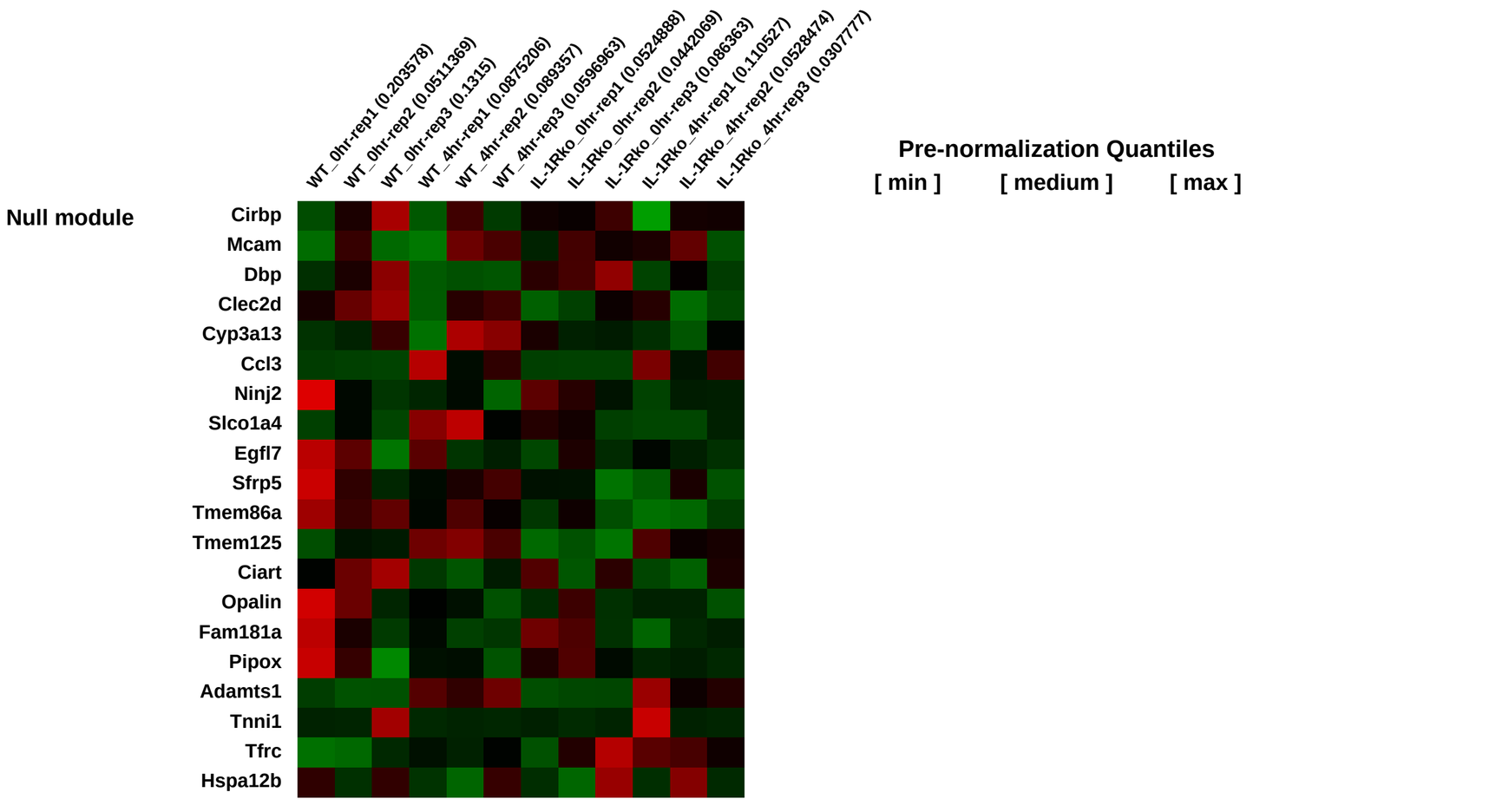

GEO Series "GSE15325" Expression Profiles

Num of samples in this series: 23

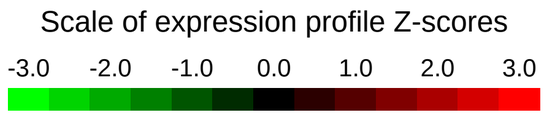

GEO Link:	**http://www.ncbi.nlm.nih.gov/geo/query/acc.cgi?acc=GSE15325**
Status:	**Public on Mar 01 2010**
Title:	**MEF-mKras-WT1**
Organism:	**Mus musculus**
Experiment type:	**Expression profiling by array**
Platform:	**GPL1261**
Pubmed ID:	
Summary & Design:	**Summary:** **K-ras is one of the most frequently mutated human oncogenes. Activation of K-ras can lead to either senescence or proliferation in primary cells. The precise mechanism governing these distinct outcomes remains unclear. Here we utilized a loss-of-function screen to assess the role of specific genes identified as potential key regulators of K-ras driven oncogenesis. Using this approach, we identify the transcription factor Wt1 as an inhibitor of senescence in primary cells expressing oncogenic K-ras. Deletion or suppression of Wt1 expression leads to senescence of primary cells expressing oncogenic K-ras under the control of the native promotor at physiological levels, but has no effect on cells expressing wild-type K-ras. Wt1 contributes to K-ras driven lung tumorigenesis in vivo and loss of Wt1 is specifically deleterious to human lung cancer cell lines that are dependent on oncogenic K-ras. Taken together, these observations reveal a novel role for Wt1 as a key regulator of the complex genetic network required for the oncogenic effect of the small GTPase K-ras.** **We compare the expression profiles of Wild type, K-ras mutant, Wt1-null, and double K-ras mutant/Wt1-null mouse embryonic fibroblasts (MEFs). The study provides insights into the transcriptional role of Wt1 in the context of oncogenic K-ras.** **Overall design:** **MEFs were infected with adenoviral Cre to activate K-ras (6 samples), knockout Wt1 (5 samples), both activate K-ras and knockout Wt1 (7 samples). As a control, MEFs were infected with adenoviral GFP (5 samples). RNA was isolated using Trizol 7 days after infection. RNA was further prepared by passage over an RNeasy column. cDNA synthesis, biotinylation of cRNA and hybridization to mouse Genechip 430A v2 containing 39,000 probes was performed according to the manufacturer's instructions (Affymetrix, Santa Clara). Microarray data was normalized with Expression Console software (Affymetrix, Santa Clara) using RMA algorithms.**

Background corr dist: KL-Divergence = 0.0997, L1-Distance = 0.0402, L2-Distance = 0.0035, Normal std = 0.4350

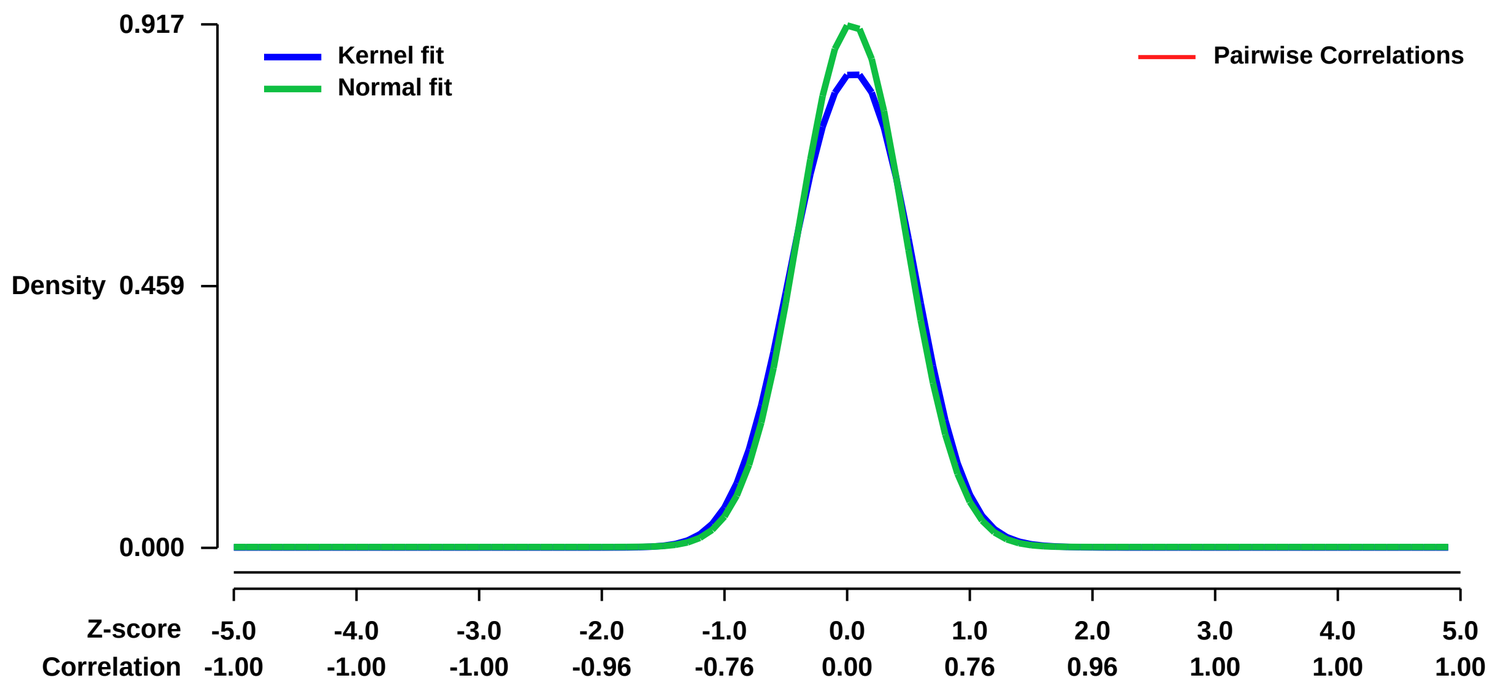

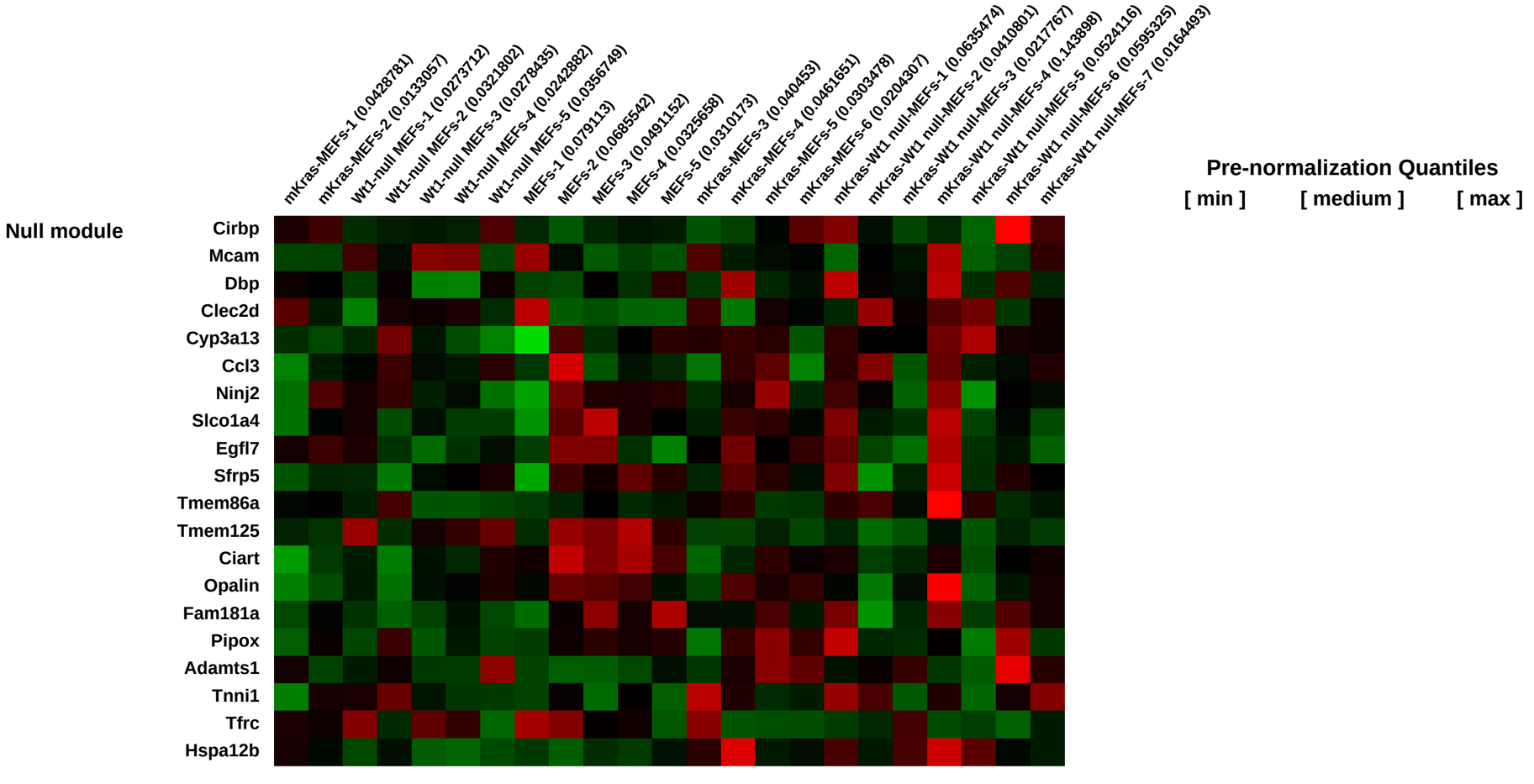

GEO Series "GSE58193" Expression Profiles

Num of samples in this series: 9

Scale of expression profile Z-scores

-3.0 -2.0 -1.0 0.0 1.0 2.0 3.0

GEO Link:	http://www.ncbi.nlm.nih.gov/geo/query/acc.cgi?acc=GSE58193
Status:	Public on Jun 04 2014
Title:	Characterizing the profiles of Ebf1 in mouse fat cells.
Organism:	Mus musculus
Experiment type:	Expression profiling by array
Platform:	GPL1261
Pubmed ID:	24174531
Summary & Design:	**Summary:** gene expression data from mouse adipocyte, with and without Ebf1 knock-down **Overall design:** To ascertain the functional targets of Ebf1 in adipocytes, we depleted Ebf1 from mature 3T3-L1 cells by transducing them with lentivirus harboring one of two different Ebf1-specific hairpins or a scrambled control. We then performed expression profiling using Affymetrix arrays with triplicate samples for each hairpin.

Background corr dist: KL-Divergence = 0.0645, L1-Distance = 0.0174, L2-Distance = 0.0003, Normal std = 0.5180

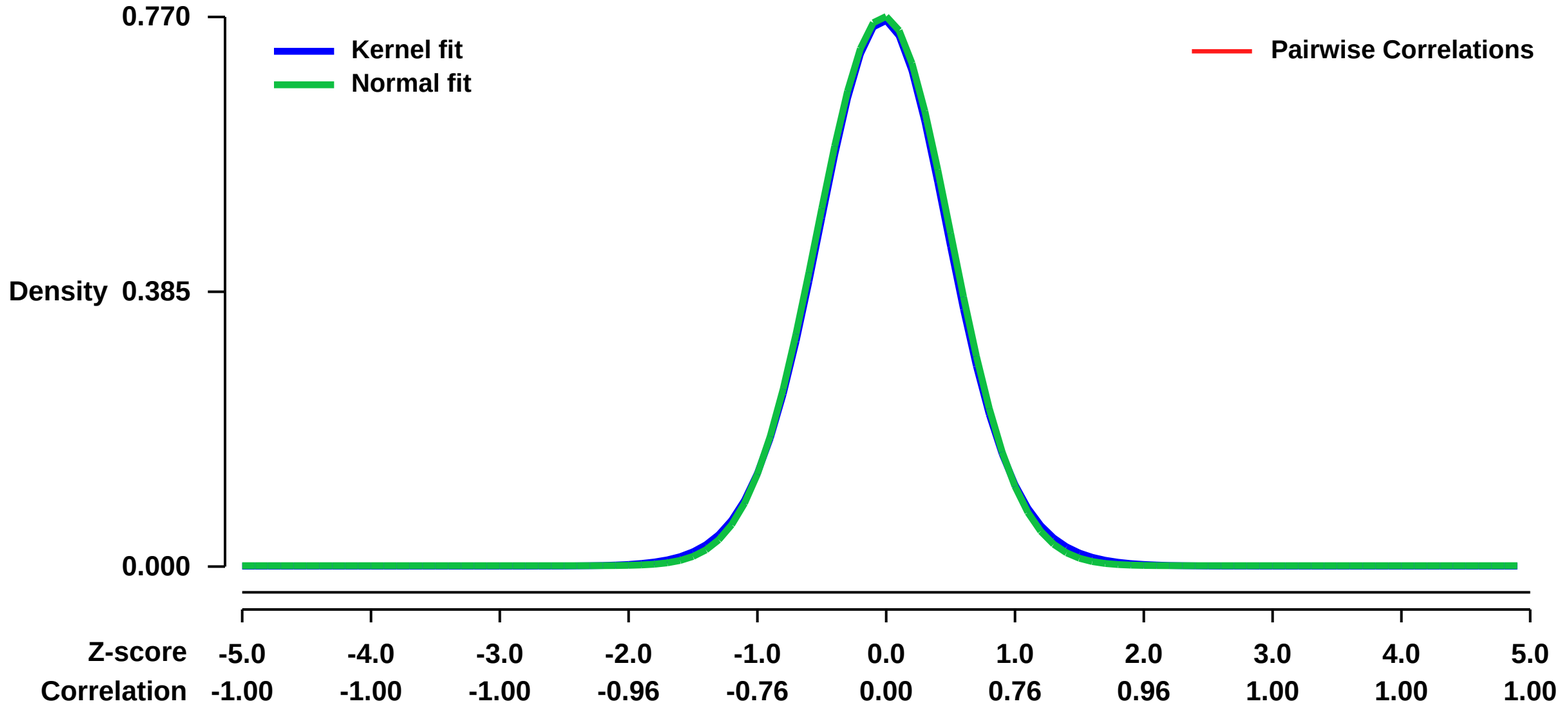

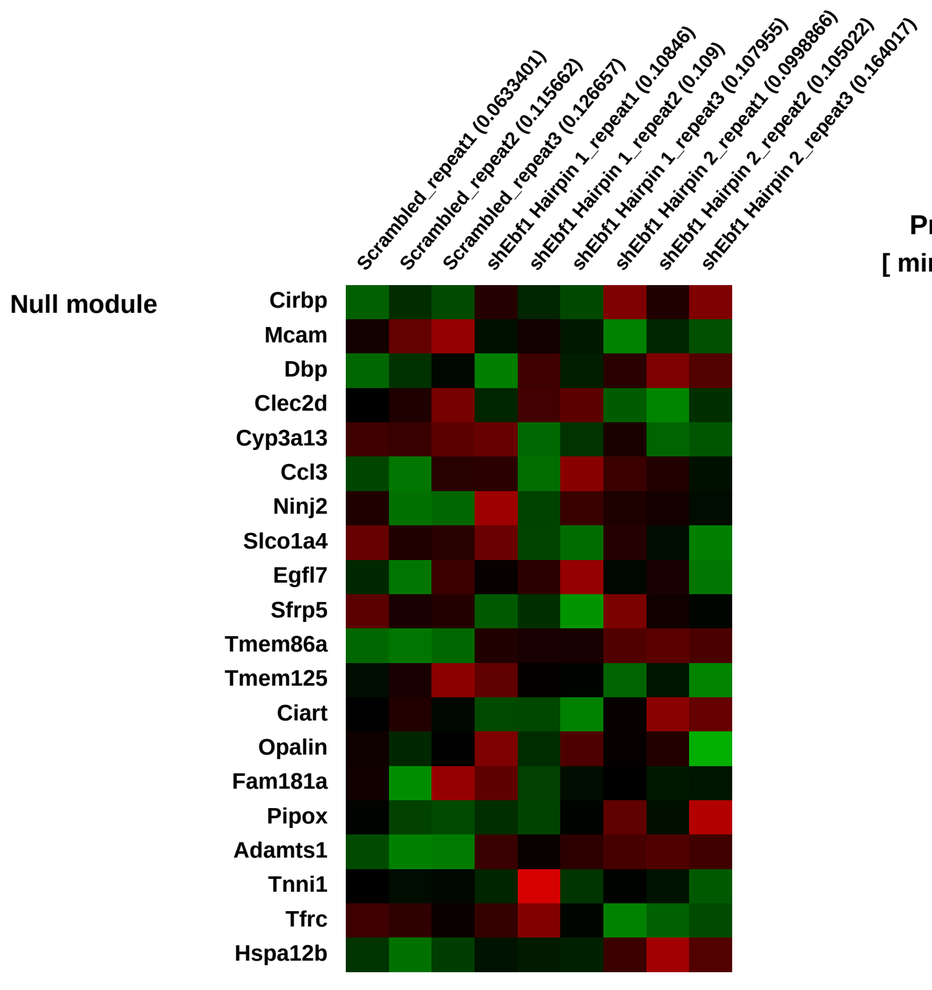

GEO Series "GSE39449" Expression Profiles

Num of samples in this series: 6

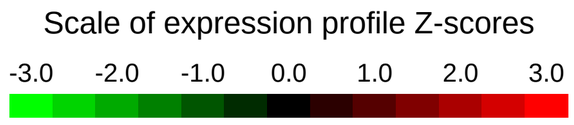

GEO Link:	http://www.ncbi.nlm.nih.gov/geo/query/acc.cgi?acc=GSE39449
Status:	Public on Feb 25 2014
Title:	Differentially activated CD8 T cells in liver and gut
Organism:	Mus musculus
Experiment type:	Expression profiling by array
Platform:	GPL1261
Pubmed ID:	19265543
Summary & Design:	**Summary:** Naˆflve, liver- and gut-activated CD8 OT-I T cells show differential migration behaviour. To analyze which genes could be responsible for different migration patterns, naˆflve, liver-activated and gut-activated CD8 T cells were isolated and compared for their gene expression profile. **Overall design:** After total RNA extraction, reverse transcription, cDNA extraction, the biotinylated cRNA was transcribed, fragmented, and 15 ´µg cRNA hybridized in duplicates for each of the three groups to the GeneChip arrays. Group1: naˆflve, Group2: liver-activated Group3: gut-activated. Lists of differentially regulated genes were created using High Performance Chip Data Analysis (HPCDA) with Bioretis database (http://www.bioretis-analysis.de). Worldwide data sharing is possible via Bioretis, please ask the authors.

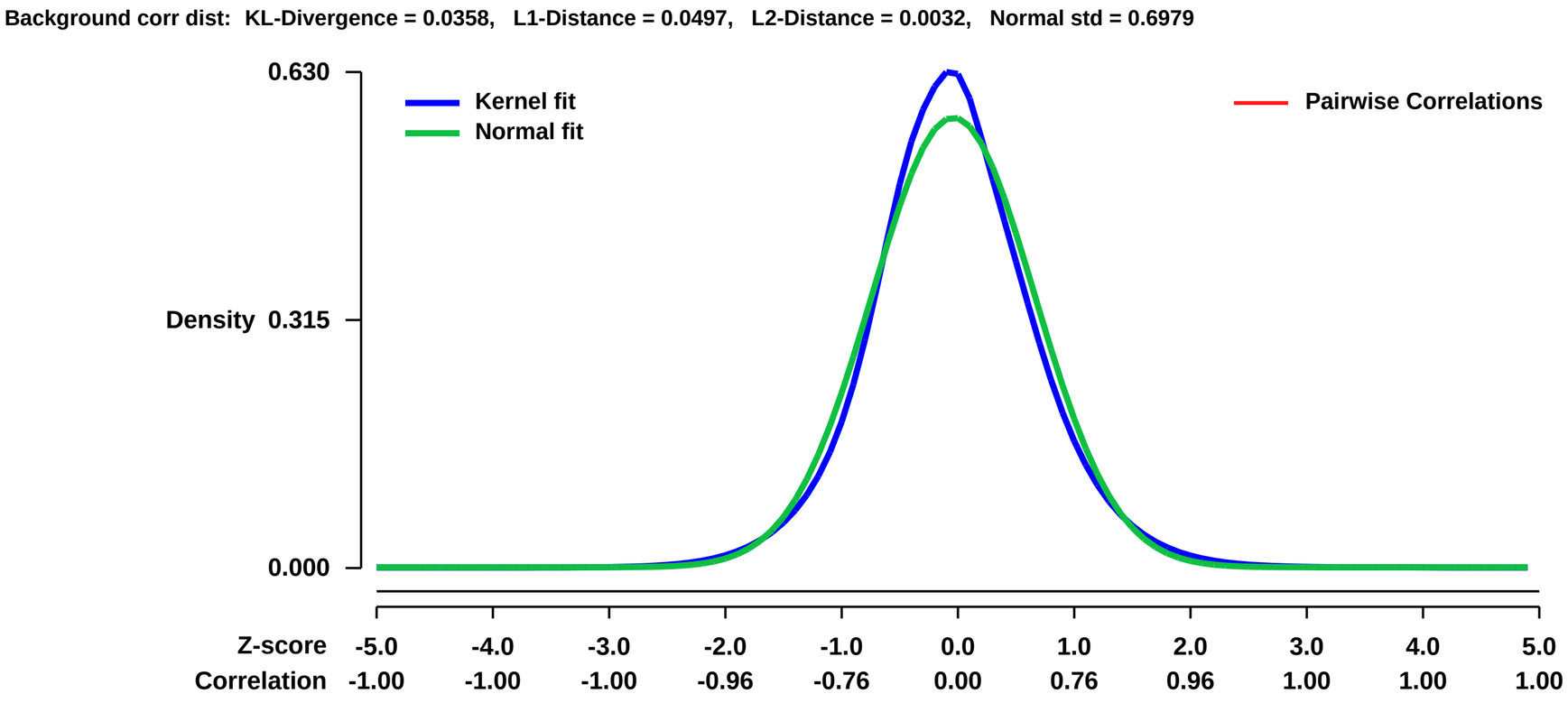

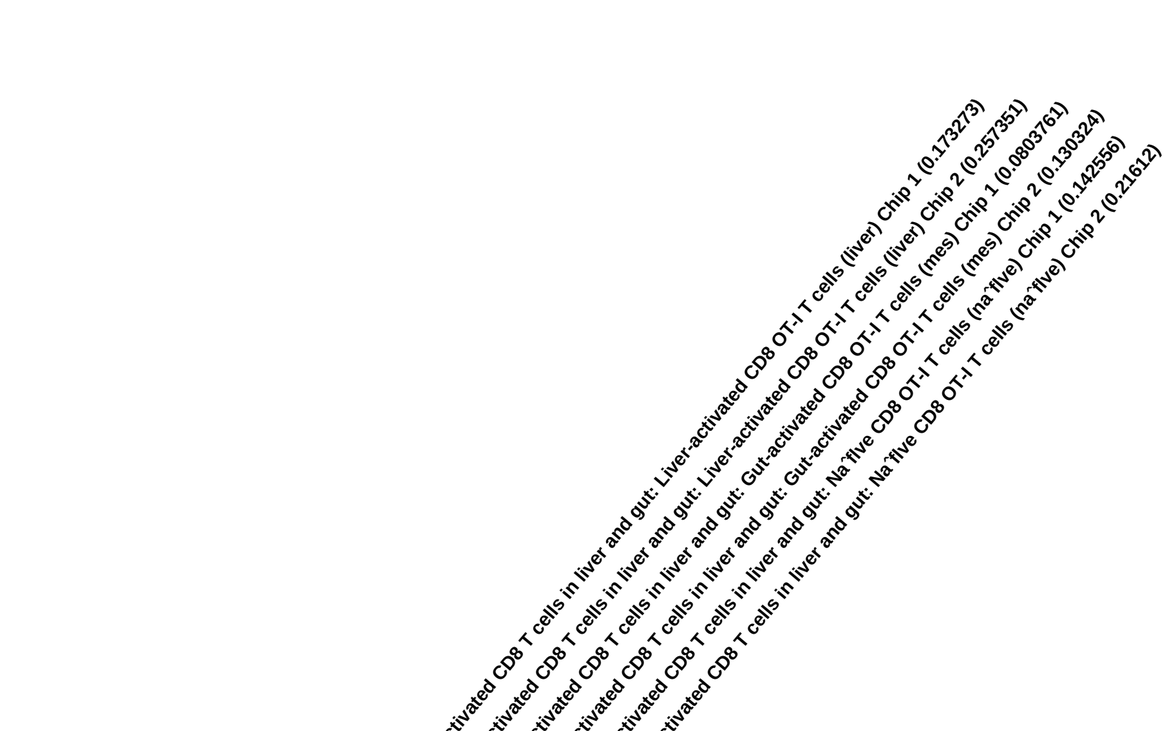

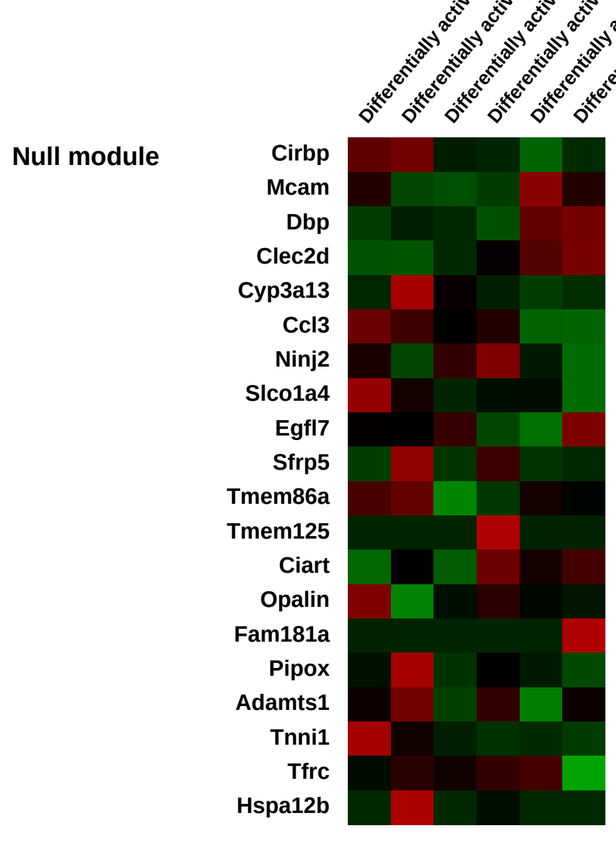

GEO Series "GSE21033" Expression Profiles

Num of samples in this series: 12

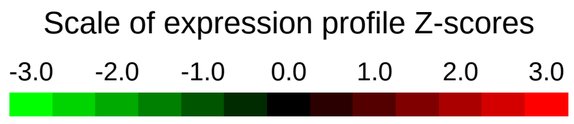

GEO Link:	http://www.ncbi.nlm.nih.gov/geo/query/acc.cgi?acc=GSE21033
Status:	Public on Aug 26 2010
Title:	Timecourse analysis of gene expression by murine bone marrow-generated dendritic cells following treatment with Poly I:C
Organism:	Mus musculus
Experiment type:	Expression profiling by array
Platform:	GPL1261
Pubmed ID:	20682054
Summary & Design:	**Summary:** **BACKGROUND: Dendritic cells (DC) play a central role in primary immune responses and become potent stimulators of the adaptive immune response after undergoing the critical process of maturation. Understanding the dynamics of DC maturation would provide key insights into this important process. Time course microarray experiments can provide unique insights into DC maturation dynamics. Replicate experiments are necessary to address the issues of experimental and biological variability. Statistical methods and averaging are often used to identify significant signals. Here a novel strategy for filtering of replicate time course microarray data, which identifies consistent signals between the replicates, is presented and applied to a DC time course microarray experiment.** **RESULTS: The temporal dynamics of DC maturation were studied by stimulating DC with poly(I:C) and following gene expression at 5 time points from 1 to 24 hours. The novel filtering strategy uses standard statistical and fold change techniques, along with the consistency of replicate temporal profiles, to identify those differentially expressed genes that were consistent in two biological replicate experiments. To address the issue of cluster reproducibility a consensus clustering method, which identifies clusters of genes whose expression varies consistently between replicates, was also developed and applied. Analysis of the resulting clusters revealed many known and novel characteristics of DC maturation, such as the up-regulation of specific immune response pathways. Intriguingly, more genes were down-regulated than up-regulated. Results identify a more comprehensive program of down-regulation, including many genes involved in protein synthesis, metabolism, and housekeeping needed for maintenance of cellular integrity and metabolism.** **CONCLUSIONS: The new filtering strategy emphasizes the importance of consistent and reproducible results when analyzing microarray data and utilizes consistency between replicate experiments as a criterion in both feature selection and clustering, without averaging or otherwise combining replicate data. Observation of a significant down-regulation program during DC maturation indicates that DC are preparing for cell death and provides a path to better understand the process. This new filtering strategy can be adapted for use in analyzing other large-scale time course data sets with replicates. #!#** **Overall design:** **DC were generated from the bone marrow of C57BL/6 mice using GM-CSF, Treated with poly I:C, and RNA was isolated at 0, 1, 3, 6, 12 and 24 hours, and subjected to microarray analysis. Two independent replicate experiments were performed.**

Background corr dist: **KL-Divergence = 0.1114, L1-Distance = 0.0281, L2-Distance = 0.0014, Normal std = 0.4266**

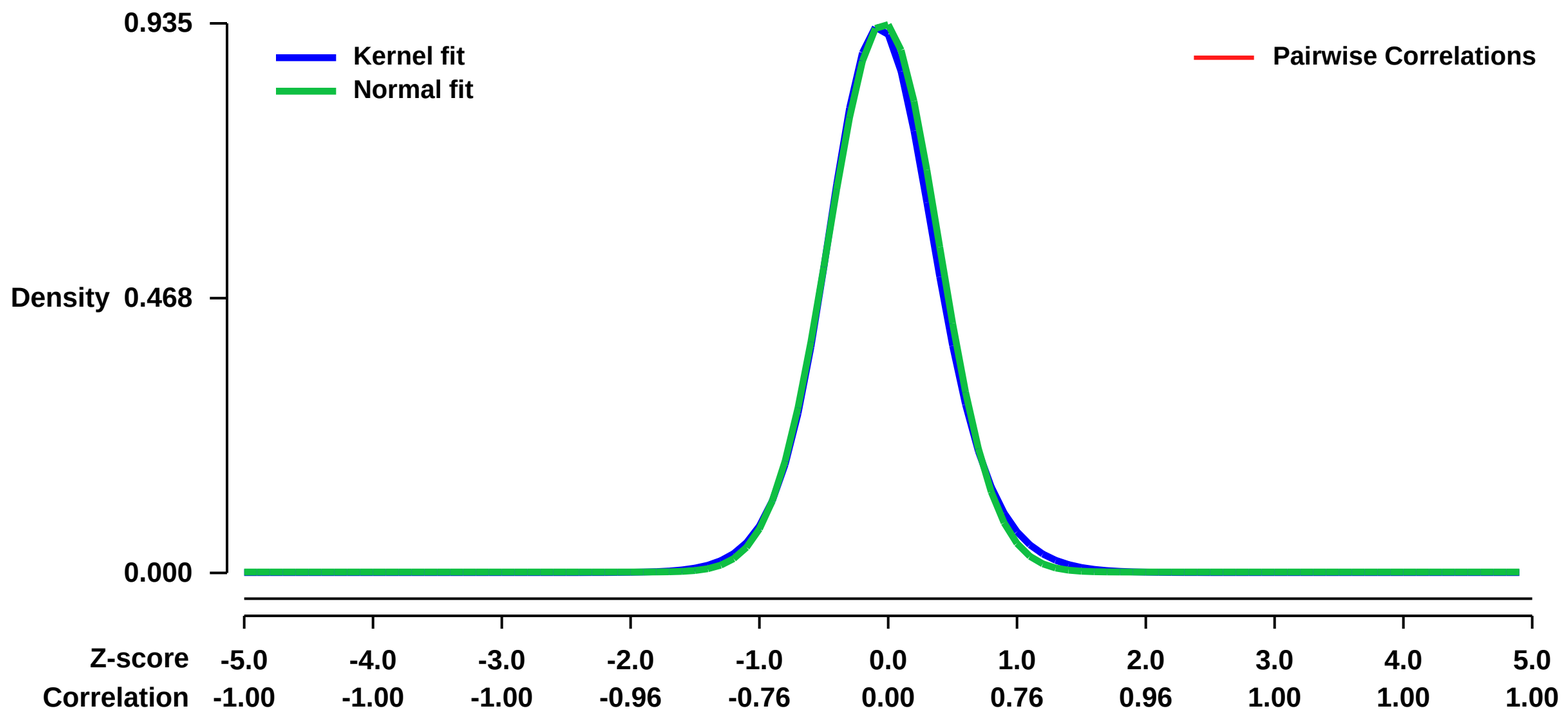

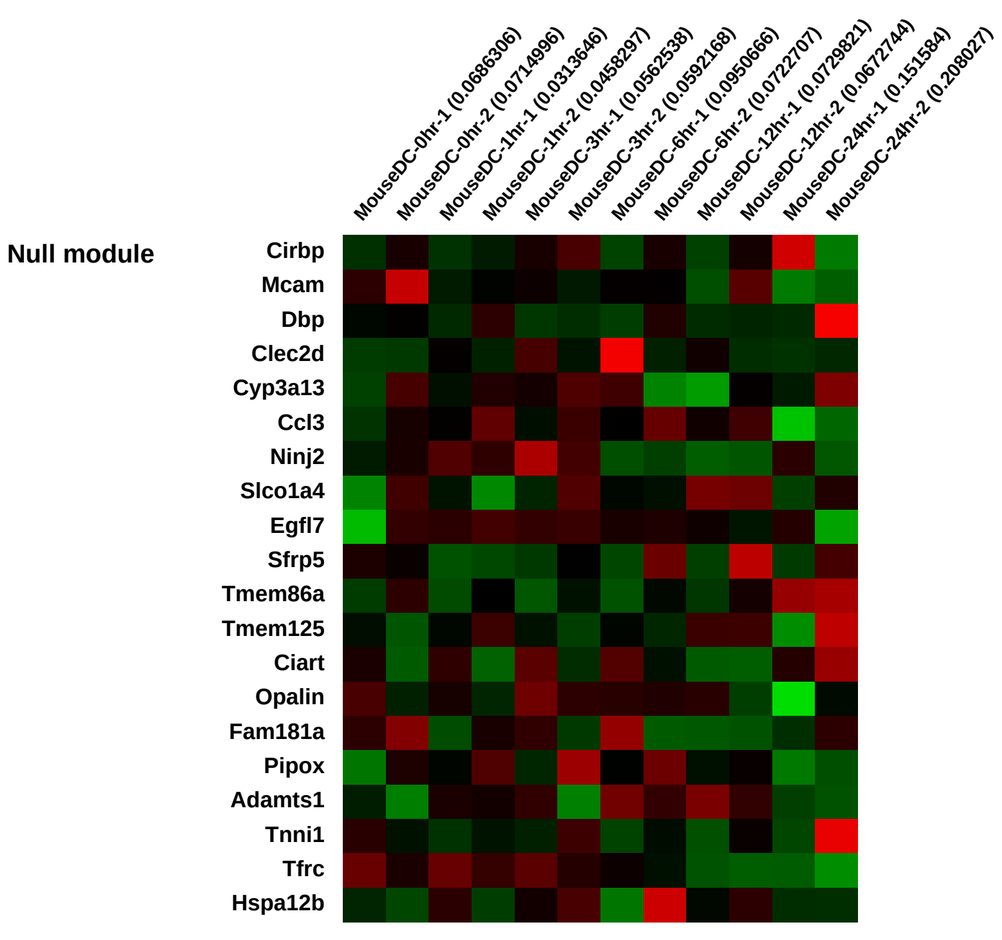

GEO Series "GSE14395" Expression Profiles

Num of samples in this series: 24

Scale of expression profile Z-scores

-3.0 -2.0 -1.0 0.0 1.0 2.0 3.0

GEO Link:	**http://www.ncbi.nlm.nih.gov/geo/query/acc.cgi?acc=GSE14395**
Status:	**Public on Sep 11 2009**
Title:	**Gender-specific gene repression of PPAR-alpha KO mice in liver and heart**
Organism:	**Mus musculus**
Experiment type:	**Expression profiling by array**
Platform:	**GPL1261**
Pubmed ID:	**19729835**
Summary & Design:	**Summary:** **Most metabolic studies are conducted in male animals; thus, the molecular mechanism controlling gender-specific pathways has been neglected, including sex-dependent responses to peroxisome proliferator-activated receptors (PPARs). Here we show that PPARalpha has broad female-dependent repressive actions on hepatic genes involved in steroid metabolism and inflammation. In males, this effect is reproduced by the administration of synthetic PPARalpha ligand. Using the steroid hydroxylase gene Cyp7b1 as a model, we elucidated the molecular mechanism of this PPARalpha-dependent repression. Initial sumoylation of the ligand-binding domain of PPARalpha triggers the interaction of PPARalpha with the GA-binding protein alpha bound to the target promoter. Histone deacetylase is then recruited, and histones and adjacent Sp1-binding site are methylated. These events result in the loss of Sp1-stimulated expression, and thus the down-regulation of Cyp7b1. Physiologically, this repression confers protection against estrogen-induced intrahepatic cholestasis, paving the way for a novel therapy against the most common hepatic disease during pregnancy.** **Keywords: Genetic modification** **Overall design:** **Expression profile difference between male and female PPARalpha wild-type and knock-out mice in liver and heart (3 pools of 4 animals in each group). Wild-type (12 males and 12 females) and knock-out PPARalpha SV129 mice (12 males and 12 females) approximately 10 to 12 weeks of age were killed at ZT14 and their livers and hearts quickly removed and frozen.**

Background corr dist: KL-Divergence = 0.0171, L1-Distance = 0.0604, L2-Distance = 0.0059, Normal std = 0.8714

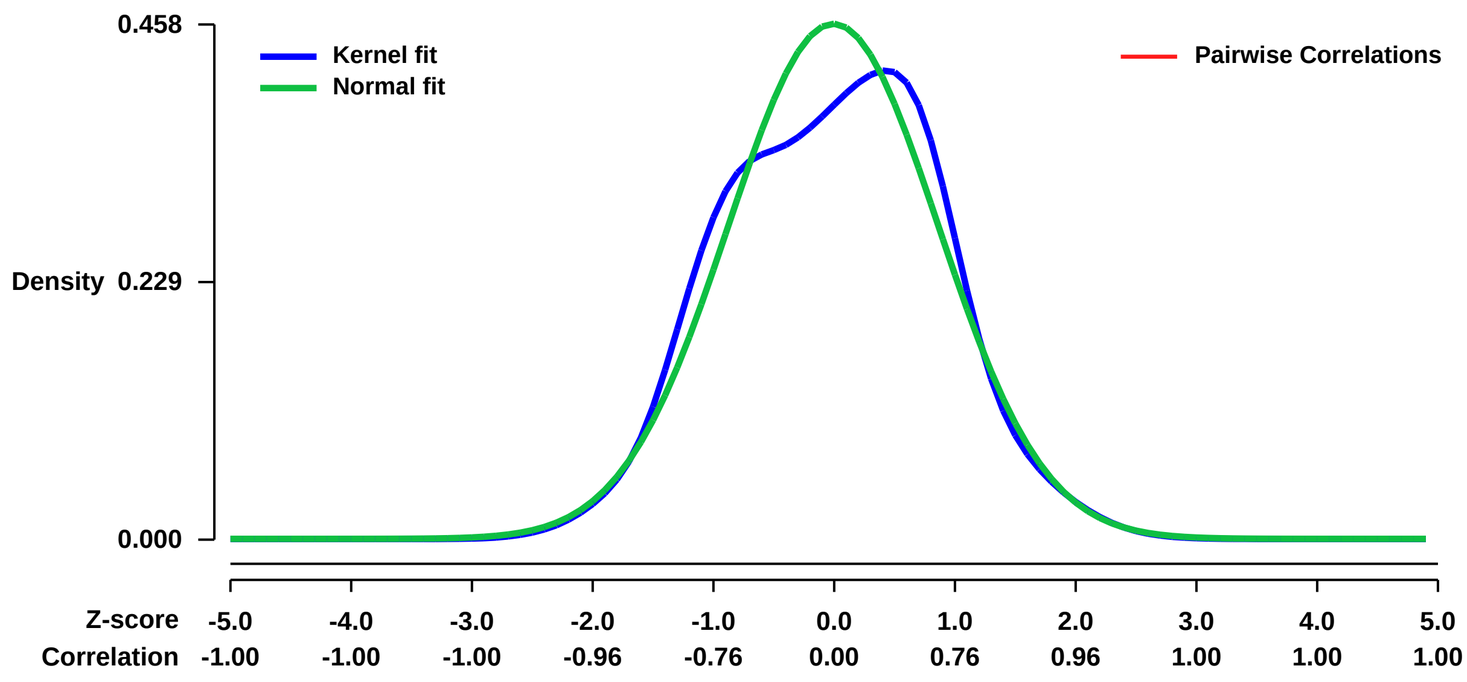

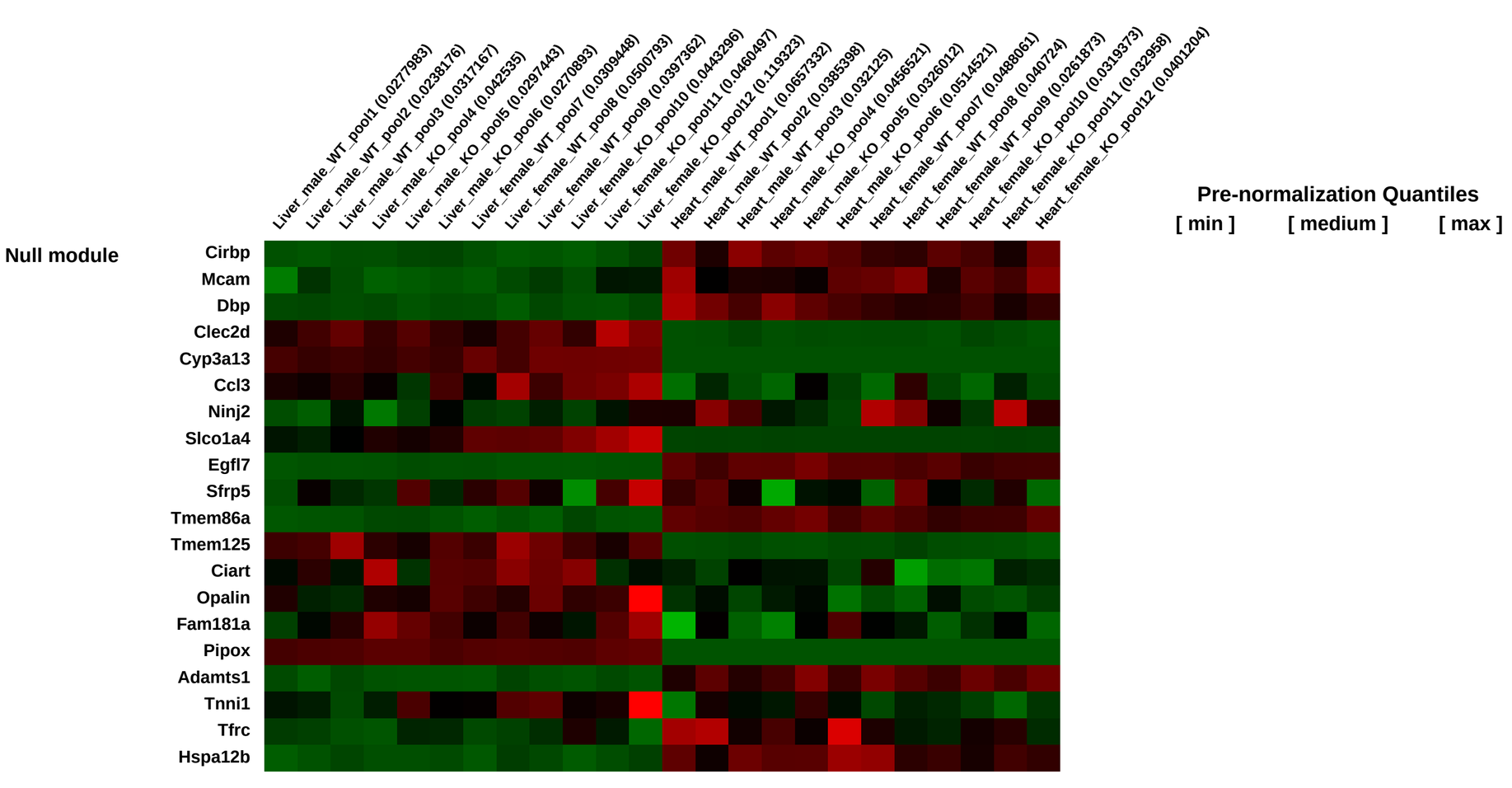

GEO Series "GSE50933" Expression Profiles

Num of samples in this series: 10

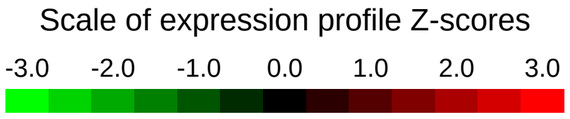

GEO Link:	http://www.ncbi.nlm.nih.gov/geo/query/acc.cgi?acc=GSE50933
Status:	Public on Nov 19 2013
Title:	Essential functions for ID proteins at multiple checkpoints in natural killer T cell development
Organism:	Mus musculus
Experiment type:	Expression profiling by array
Platform:	GPL1261
Pubmed ID:	24244015
Summary & Design:	**Summary:** Thymic iNKT cell development is divided into four stages (stage 0-3) that are characterised, in C57BL/6 mouse strain, by the differential expression of surface markers, such as CD24, CD44 and NK1.1. During transition from immature to mature iNKT cell subsets, gene expression is tightly regulated. Here, we used microarray analysis to detail the influence of the transcriptional regulator ID3 during iNKT cell maturation in the thymus. **Overall design:** Stage 1 (Tet+CD24-CD44-NK1.1-) and Stage 2 (Tet+CD24-CD44+NK1.1-) iNKT cells from WT and Id3KO thymi were FACS sorted for RNA extraction and Affymetrix hybridisation.

Background corr dist: KL-Divergence = 0.1233, L1-Distance = 0.0324, L2-Distance = 0.0018, Normal std = 0.4019

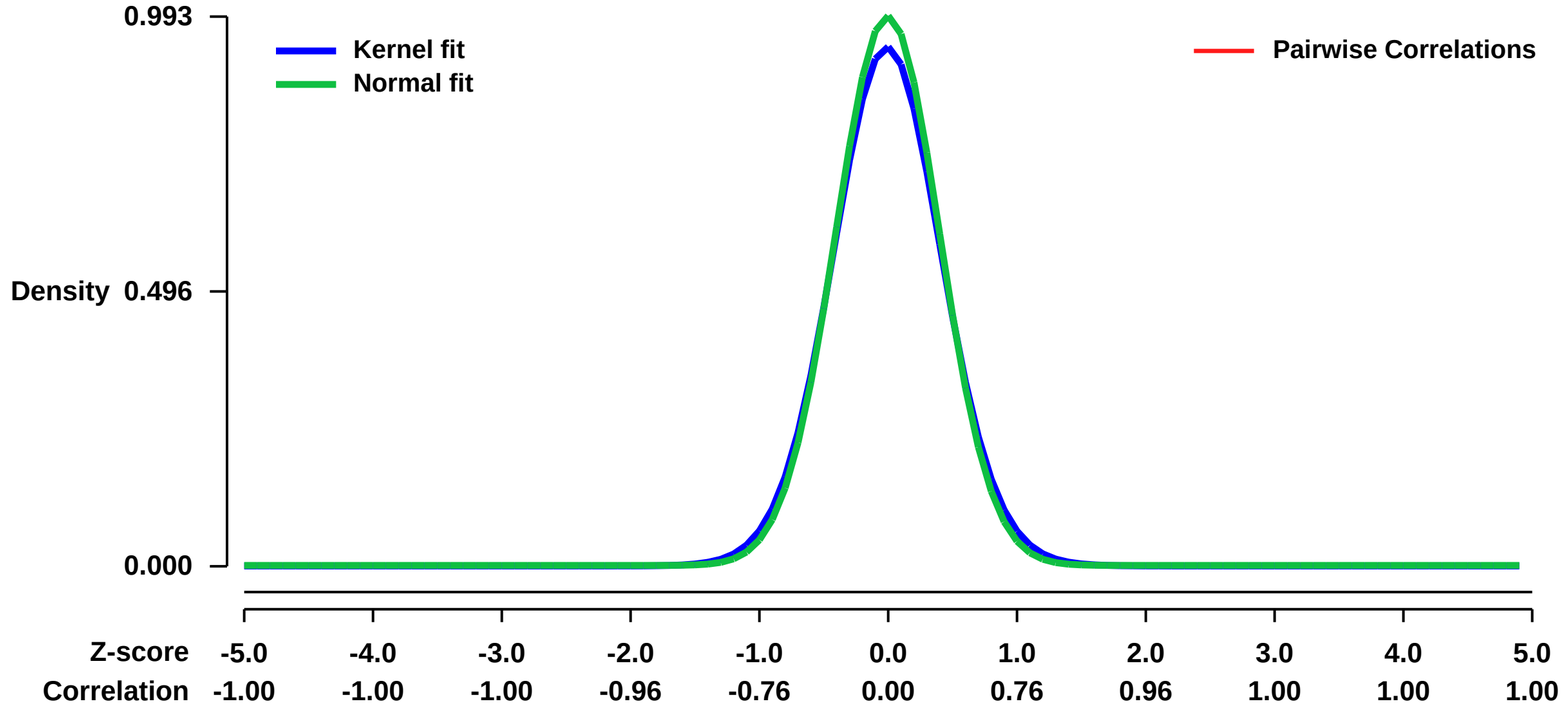

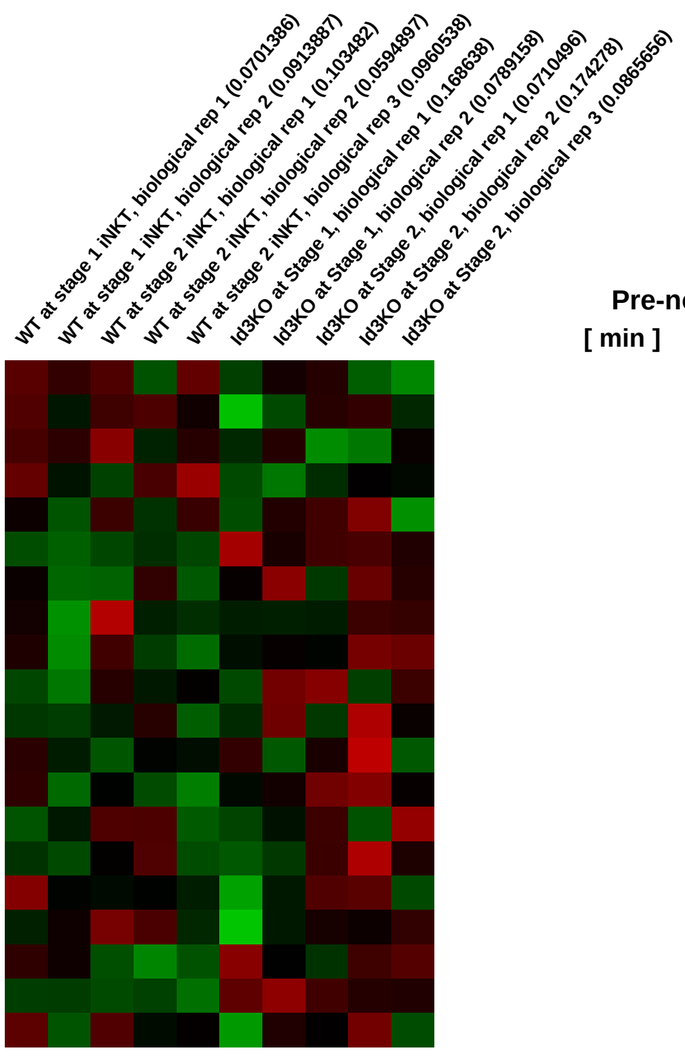

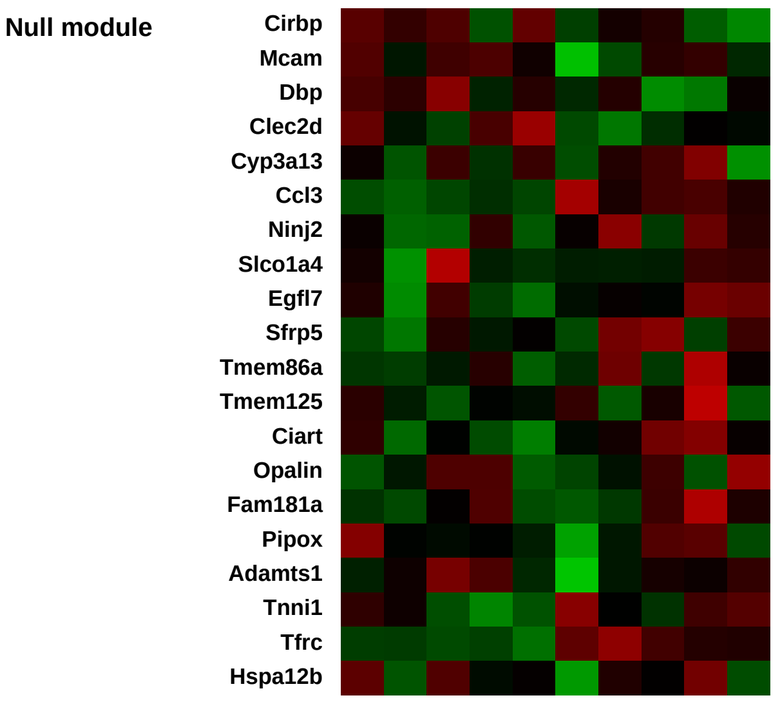

GEO Series "GSE32316" Expression Profiles

Num of samples in this series: 12

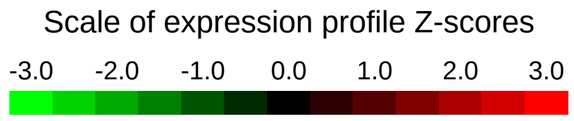

GEO Link:	http://www.ncbi.nlm.nih.gov/geo/query/acc.cgi?acc=GSE32316
Status:	Public on Jan 06 2012
Title:	FGFR1 target genes in brown adipose tissues
Organism:	Mus musculus
Experiment type:	Expression profiling by array
Platform:	GPL1261
Pubmed ID:	22174314
Summary & Design:	**Summary:** We aimed to identify genes that are regulated by FGFR1 in brown adipose tissues of adult male ob/ob mice by injecting 1 mg/kg anti-FGFR1 agonistic antibody. **Overall design:** Brown adipose tissues were isolated from adult male ob/ob mice at day 4 after a single intraperitoneal injection of 1 mg/kg anti-FGFR1 agonistic antibody or pair-fed mice injected with control IgG. N=6 mice per each group.

Background corr dist: KL-Divergence = 0.1245, L1-Distance = 0.0368, L2-Distance = 0.0026, Normal std = 0.3996

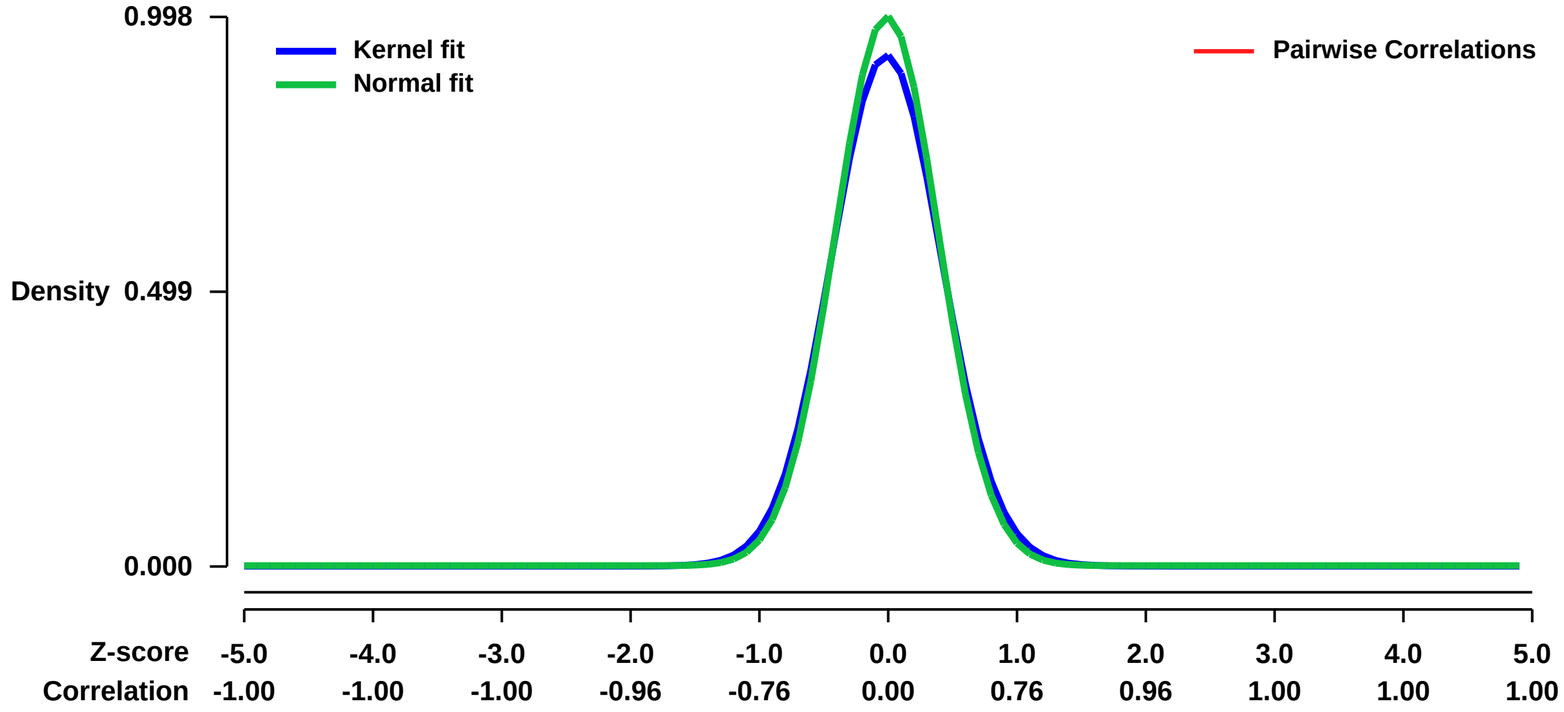

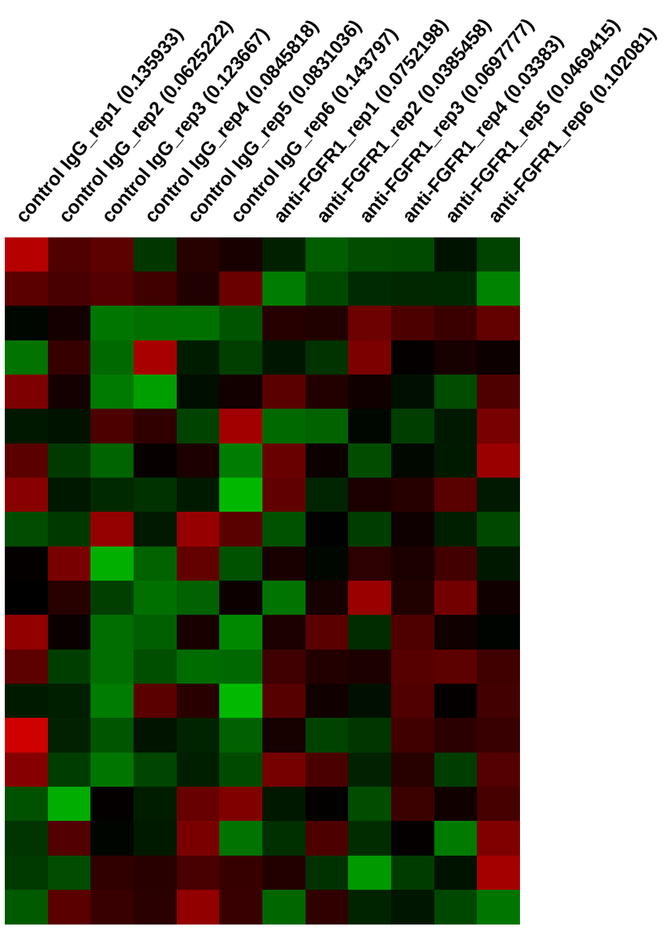

GEO Series "GSE6867" Expression Profiles

Num of samples in this series: 6

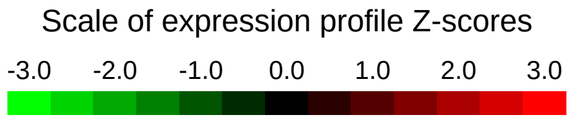

GEO Link:	**http://www.ncbi.nlm.nih.gov/geo/query/acc.cgi?acc=GSE6867**
Status:	**Public on Jan 26 2007**
Title:	**Expression data in the absence of Notch1 in hair follicles**
Organism:	**Mus musculus**
Experiment type:	**Expression profiling by array**
Platform:	**GPL1261**
Pubmed ID:	**17611229**
Summary & Design:	**Summary:** **Notch1 deficient hair matrix keratinocytes have lower mitotic rates, resulting in smaller follicles with fewer cells. In addition, the ratio of melanocytes to keratinocytes is greatly reduced. Microarray was performed to study downstream mechanism of Notch1-deficiency** **Keywords: genetic modification** **Overall design:** **Microarray was first performed using HF_emN1-1 and HF_anN1-1 samples. Later, HF_emN1-2, HF_anN1-2, HF_WT-1, and HF_WT-2 were used to perform another set of microarray. anN1s and WTs were used as wild-type controls.**

Background corr dist: **KL-Divergence = 0.0385, L1-Distance = 0.0217, L2-Distance = 0.0005, Normal std = 0.6256**

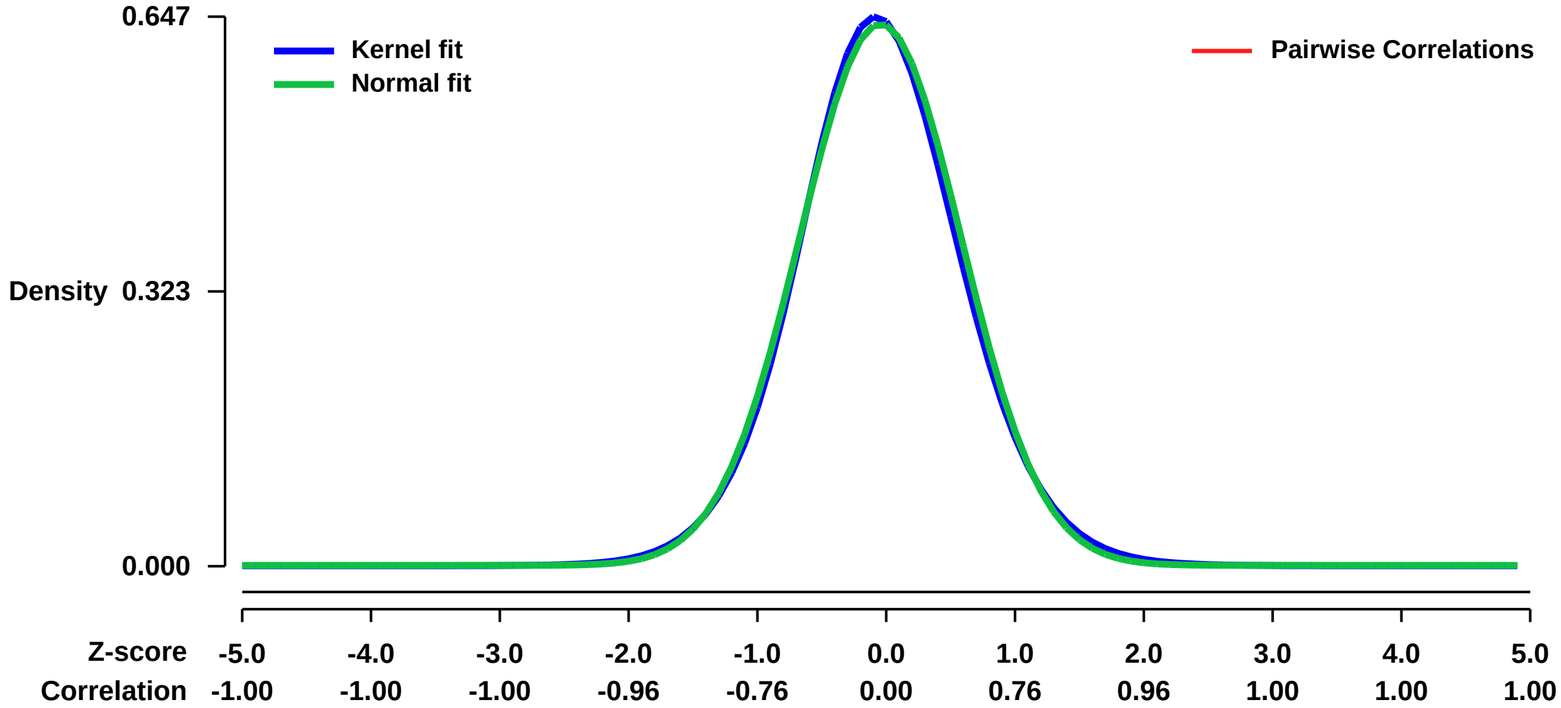

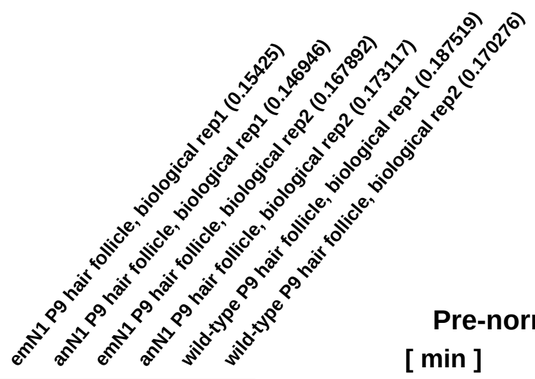

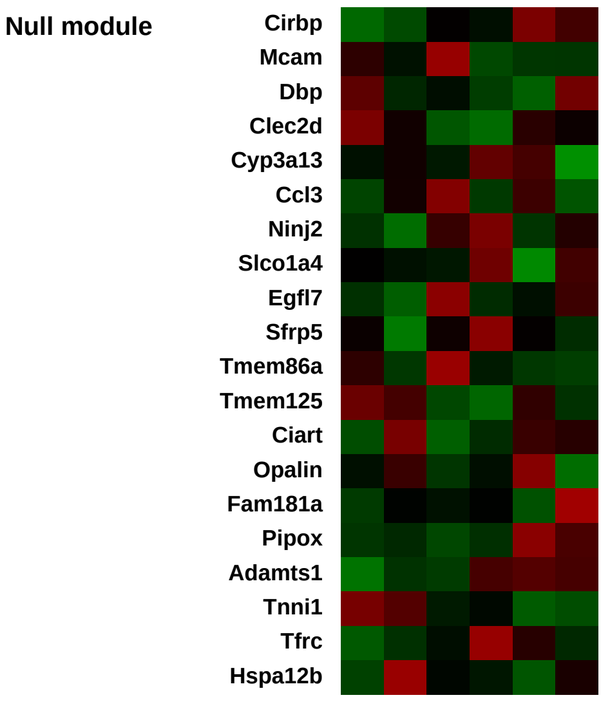

GEO Series "GSE10525" Expression Profiles

Num of samples in this series: 18

Scale of expression profile Z-scores

-3.0 -2.0 -1.0 0.0 1.0 2.0 3.0

GEO Link:	http://www.ncbi.nlm.nih.gov/geo/query/acc.cgi?acc=GSE10525
Status:	Public on Dec 31 2008
Title:	Gene expression profile of Transgenic Adenocarcinoma of the Mouse Prostate (TRAMP)
Organism:	Mus musculus
Experiment type:	Expression profiling by array
Platform:	GPL1261
Pubmed ID:	18668517
Summary & Design:	**Summary:** **Gene expression profile of Transgenic Adenocarcinoma of the Mouse Prostate (TRAMP) reveals murine targets for preclinical development of human prostate cancer therapy** **In this study, we have generated an open source TRAMP microarray dataset to identify differentially expressed genes from human prostate cancer that have concordant expression in TRAMP tumors, and thereby represent lead targets for preclinical therapy development. Affymetrix Mouse 430 2.0 chips were used for microarrays of total RNA from 9 TRAMP tumors and 9 normal prostates (ventral and dorsolateral lobes).** **Keywords: prostate cancer, TRAMP** **Overall design:** **normal prostate vs. TRAMP**

Background corr dist: KL-Divergence = 0.1784, L1-Distance = 0.0411, L2-Distance = 0.0039, Normal std = 0.3571

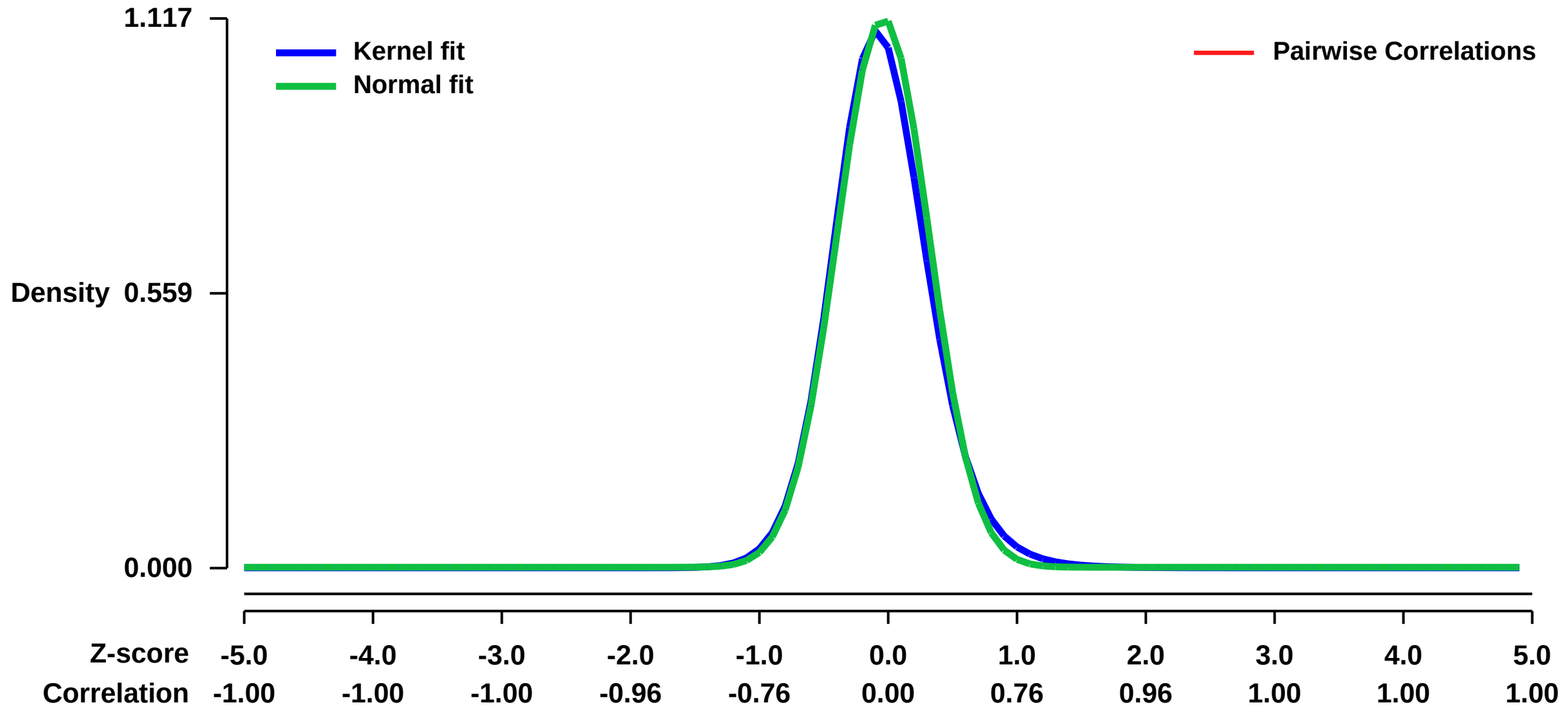

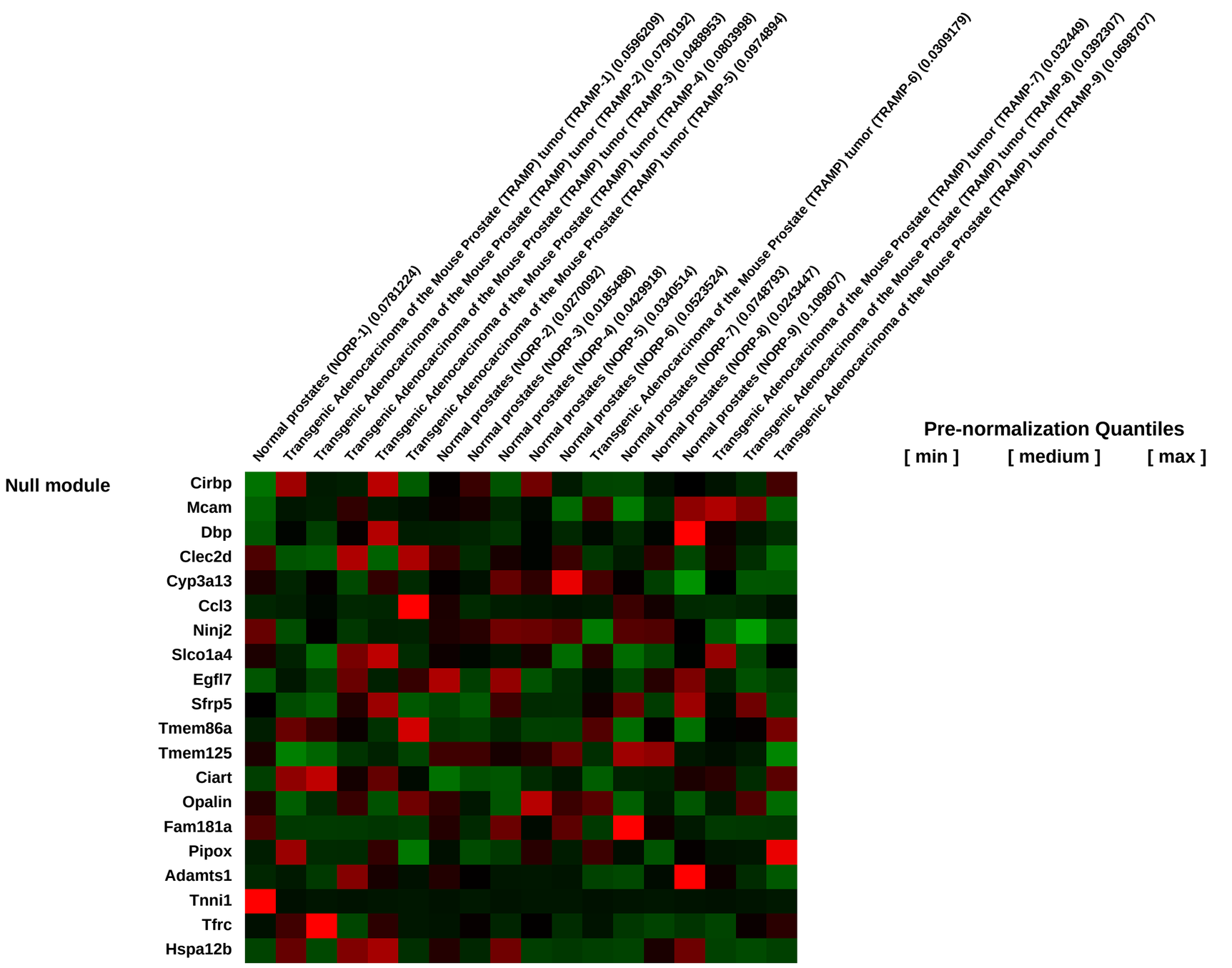

GEO Series "GSE21568" Expression Profiles

Num of samples in this series: 12

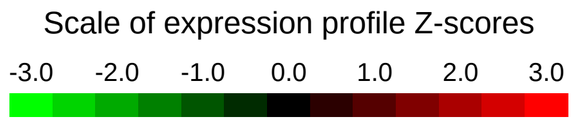

GEO Link:	http://www.ncbi.nlm.nih.gov/geo/query/acc.cgi?acc=GSE21568
Status:	Public on Jan 12 2011
Title:	Mouse bulge (CD34+CD200+CD49+) versus secondary hair germ (CD34-CD200+CD49+) versus interfollicular epidermis (CD34-CD200-CD49+)
Organism:	Mus musculus
Experiment type:	Expression profiling by array
Platform:	GPL1261
Pubmed ID:	21206086
Summary & Design:	**Summary:** Mouse back skin was disassociated to single cells, sorted by cell surface markers and tested by microarrray To compare the gene expression of mouse bulge (CD34+CD200+CD49+) versus secondary hair germ (CD34-CD200+CD49+) versus interfollicular epidermis (CD34-CD200-CD49+) xx Bald scalp retains hair follicle stem cells but lacks CD200-rich and CD34-positive hair follicle progenitor cells Androgenetic alopecia (AGA) or common baldness results from a marked decrease in hair follicle size. This miniaturization may be related to loss of hair follicle stem or progenitor cells. To test this hypothesis, we analyzed bald and non-bald scalp from the same individuals for the presence of hair follicle stem and progenitor cells using flow cytometry to quantitate cells expressing CYTOKERATIN 15 (KRT15), CD200, CD34 and ALPHA-6-INTEGRIN (ITGA6). High levels of KRT15 expression correlated with stem cell properties of small cell size and quiescence. Cells with the highest level of KRT15 expression were maintained in bald scalp; however, distinct populations of CD200high ITGA6high cells and CD34-positive cells were markedly diminished. Consistent with a progenitor cell phenotype, the diminished populations localized closely to the stem-cell rich bulge area but were larger and more proliferative than the bulge stem cells. In functional assays, analogous CD200 high /Itga6 high cells from murine hair follicles were multipotent and generated new hair follicles in skin reconstitution assays. These findings suggest that a defect in stem cell activation plays a role in the pathogenesis of AGA. **Overall design:** 4 independent biologic replicates (each pooled from 3 distinct mice) were sorted for Mouse bulge (CD34+CD200+CD49+) versus secondary hair germ (CD34-CD200+CD49+) versus interfollicular epidermis (CD34-CD200-CD49+)

Background corr dist: KL-Divergence = 0.0683, L1-Distance = 0.0257, L2-Distance = 0.0012, Normal std = 0.5061

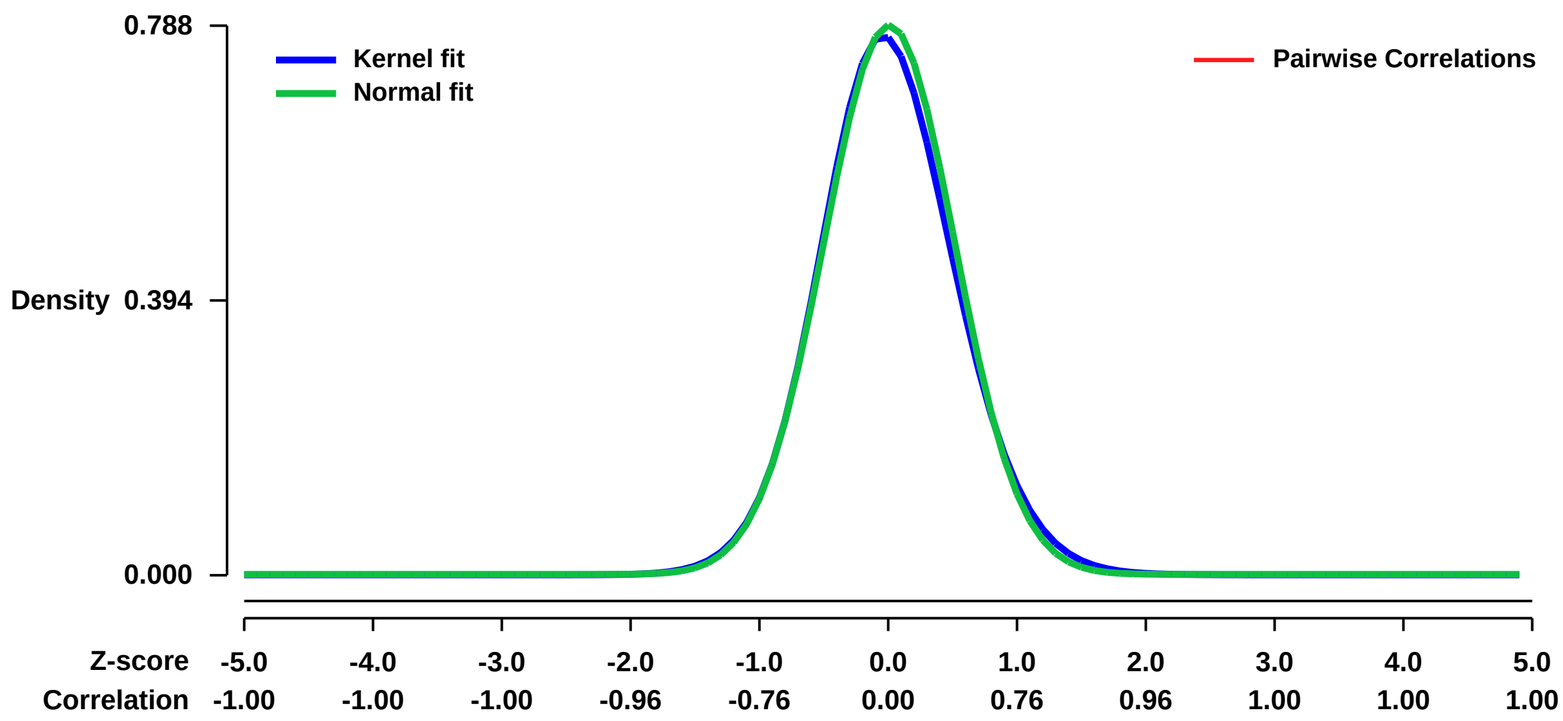

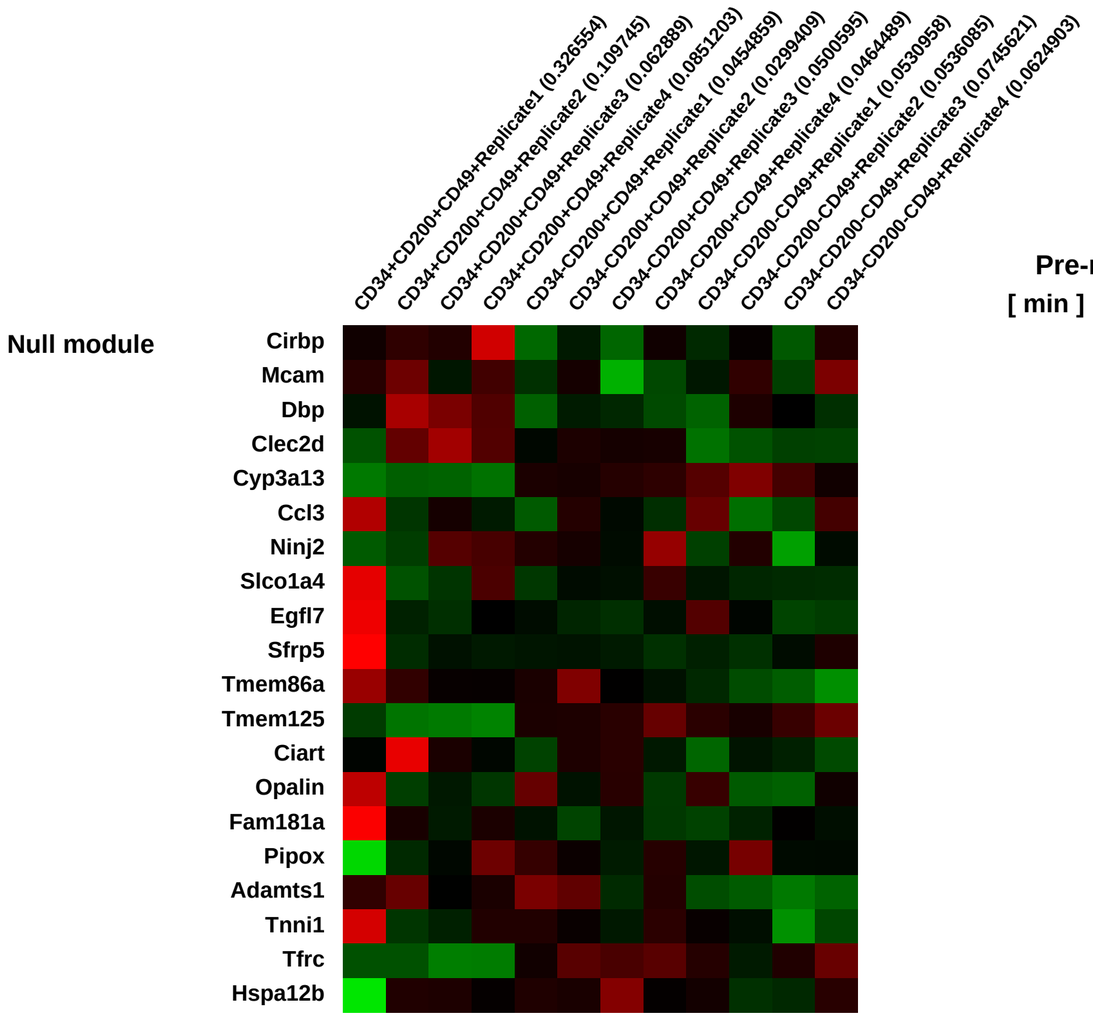

GEO Series "GSE20260" Expression Profiles

Num of samples in this series: 48

Scale of expression profile Z-scores

-3.0 -2.0 -1.0 0.0 1.0 2.0 3.0

GEO Link:	http://www.ncbi.nlm.nih.gov/geo/query/acc.cgi?acc=GSE20260
Status:	Public on Dec 19 2012
Title:	Consequences of exchanging carbohydrates for proteins in the cholesterol metabolism of mice fed a high-fat diet
Organism:	Mus musculus
Experiment type:	Expression profiling by array
Platform:	GPL1261
Pubmed ID:	23139832
Summary & Design:	**Summary:** Dietary proteins have profound effects on lipid metabolism but the mechanism remains to be elucidated. In the present study, we examined the temporal impact of dietary proteins in isoenergetic high fat diets on lipid metabolism of C57BL/6J mice. **Overall design:** Mice were first fed a low protein (P) to carbohydrate (C) ratio high-fat diet (L-P/C-HF) for 10 weeks and then a half of mice were changed to a high protein to carbohydrate ratio high-fat diet (H-P/C-HF) for additional 4 weeks whereas the remaining mice continued eating the L-P/C-HF diet.

Background corr dist: KL-Divergence = 0.1358, L1-Distance = 0.0700, L2-Distance = 0.0128, Normal std = 0.3939

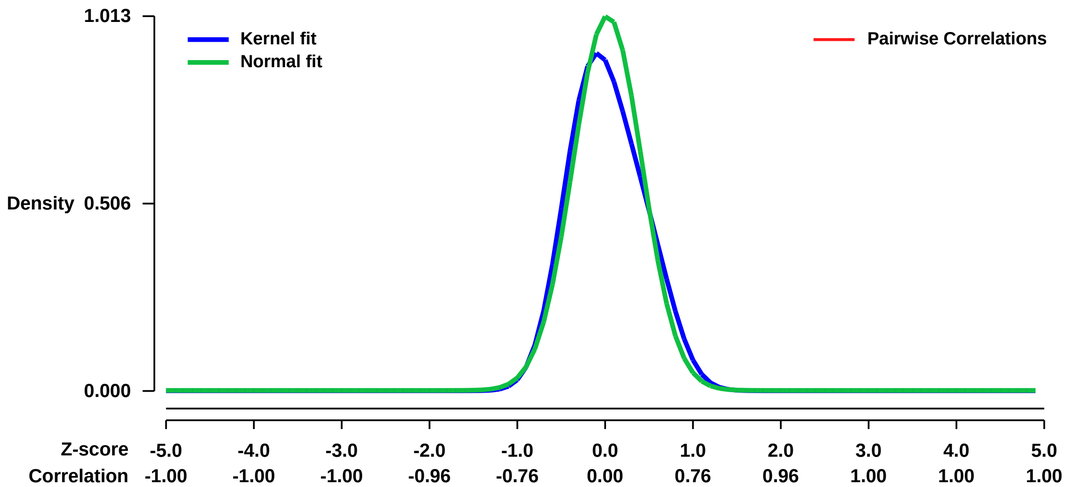

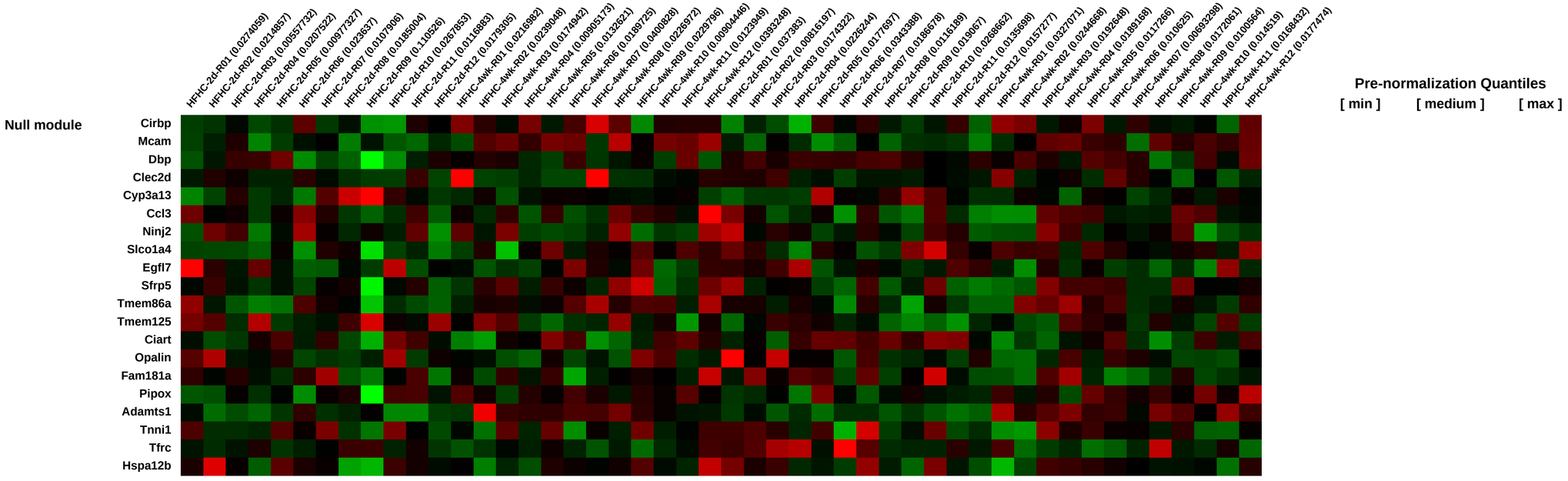

GEO Series "GSE37316" Expression Profiles

Num of samples in this series: 31

Scale of expression profile Z-scores

-3.0 -2.0 -1.0 0.0 1.0 2.0 3.0

GEO Link:	http://www.ncbi.nlm.nih.gov/geo/query/acc.cgi?acc=GSE37316
Status:	Public on Apr 17 2012
Title:	Gene expression data from postnatal day 7 subventricular zone (SVZ), IV ventricle and cerebellar white matter-derived neural stem cells (NSCs) and of cancer stem cells (CSCs) from Ptch het p53 wt and Ptch het p5
Organism:	Mus musculus
Experiment type:	Expression profiling by array
Platform:	GPL1261
Pubmed ID:	22628409
Summary & Design:	**Summary:** We exploited microarrays to detail the global program of gene expression underlying normal stem cells and cancer stem cells in the cerebellum and in medulloblastomas (MBs). **Overall design:** To identify novel molecular mediators involved in medulloblastomagenesis, we compared the distinct postnatal hindbrain-derived NSC populations, which are potentially tumor-initiating, with murine single Ptch and compound Ptch/p53-mutant MB cancer stem cells (CSCs), the latter faithfully phenocopying the different variants of human MB in vivo. Transcriptome analysis of both hindbrain NSCs and MB CSCs resulted in the generation of well-defined gene signatures, each reminiscent of a specific human MB molecular subclass.

Background corr dist: KL-Divergence = 0.1558, L1-Distance = 0.0297, L2-Distance = 0.0016, Normal std = 0.3724

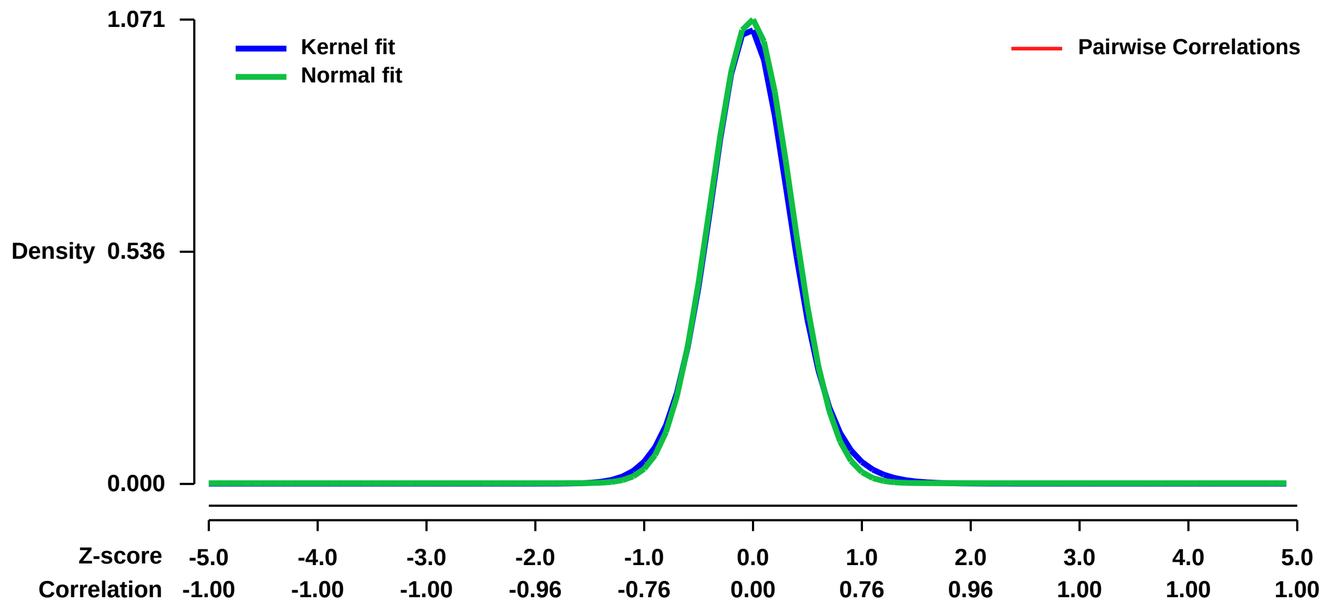

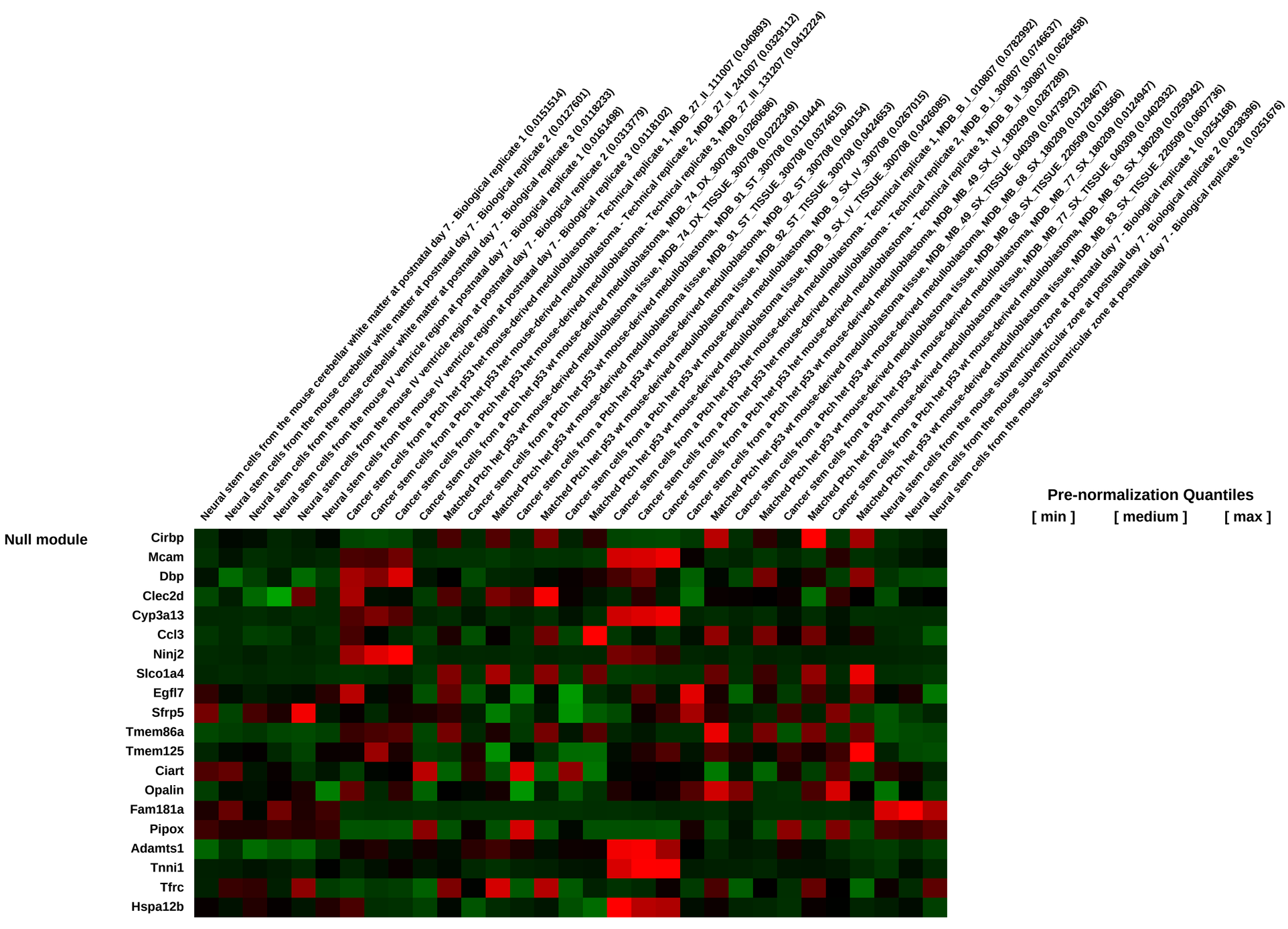

GEO Series "GSE6285" Expression Profiles

Num of samples in this series: 24

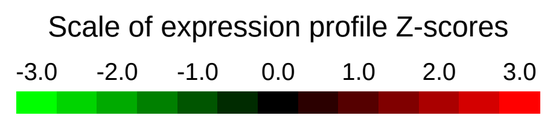

GEO Link:	**http://www.ncbi.nlm.nih.gov/geo/query/acc.cgi?acc=GSE6285**
Status:	**Public on Jan 15 2008**
Title:	**Expression data from brains of mice fed four different diets**
Organism:	**Mus musculus**
Experiment type:	**Expression profiling by array**
Platform:	**GPL1261**
Pubmed ID:	**18231591**
Summary & Design:	**Summary:** **Beyond the DNA sequence difference between humans and closely related apes, there are large differences in the environments that these species experience. One prominent example for this is diet. The human diet diverges from those of other primates in various aspects, such as having a high calorie and protein content, as well as being cooked. Here, we used a laboratory mouse model to identify gene expression differences related to dietary differences.** **Keywords: diet** **Overall design:** **We fed four groups of six genetically identical 8-week-old female NMR1 mice one of four diets ad libidum: (1) a diet consisting of vegetables, fruit and yogurt identical to the diet fed to chimpanzees in our ape facility (’Chimpanzee’); (2) a diet consisting exclusively of McDonalds. fast food (’FastFood’); (3) a diet consisting of cooked food eaten by our staff in the Institute cafeteria (’HumanCafe’); (4) the mouse pellet diet on which they were raised (’Pellet’). At the end of a 2-week period, mice were euthanized by cervical dislocation and both liver and brain (right cerebral hemisphere) tissue were dissected. RNA was extracted from the 24 liver and brain samples as per established lab protocols and processed in two batches (containing equal numbers of individuals from all groups).**

Background corr dist: **KL-Divergence = 0.0423, L1-Distance = 0.0996, L2-Distance = 0.0129, Normal std = 0.8226**

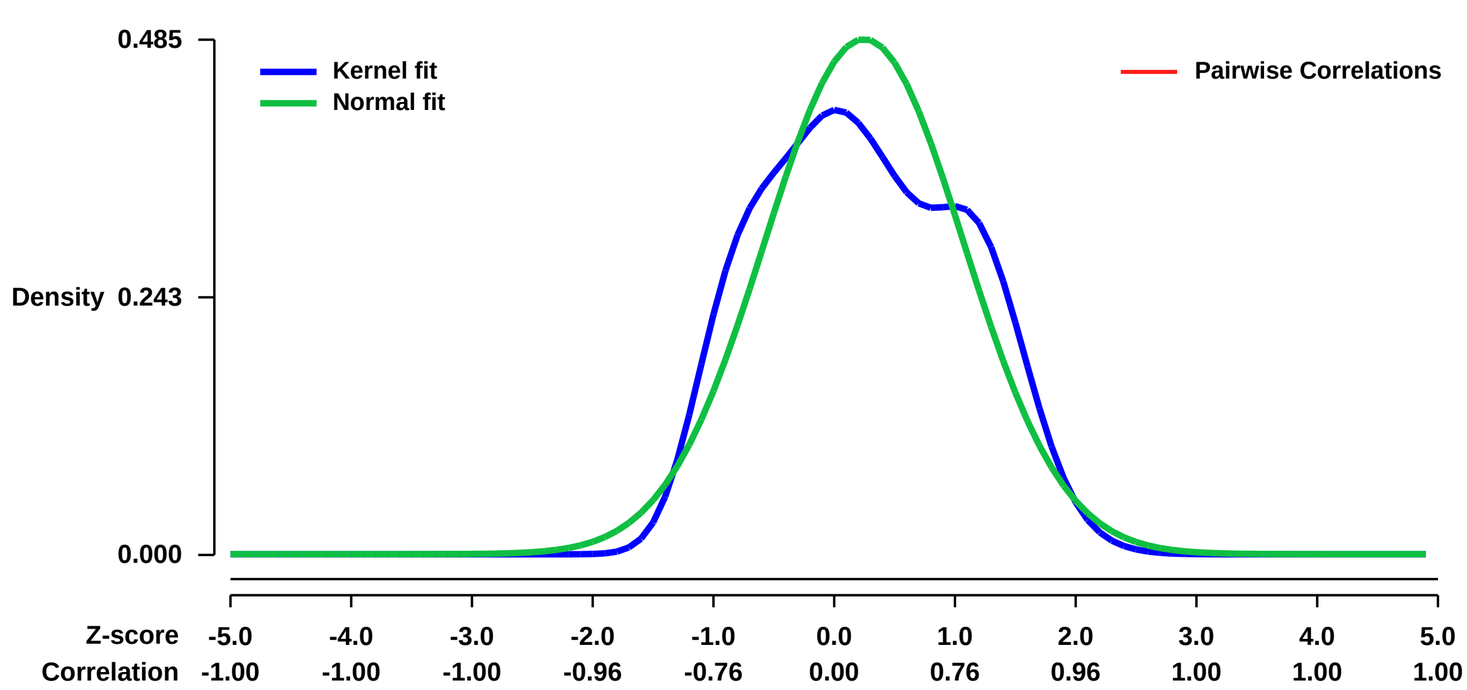

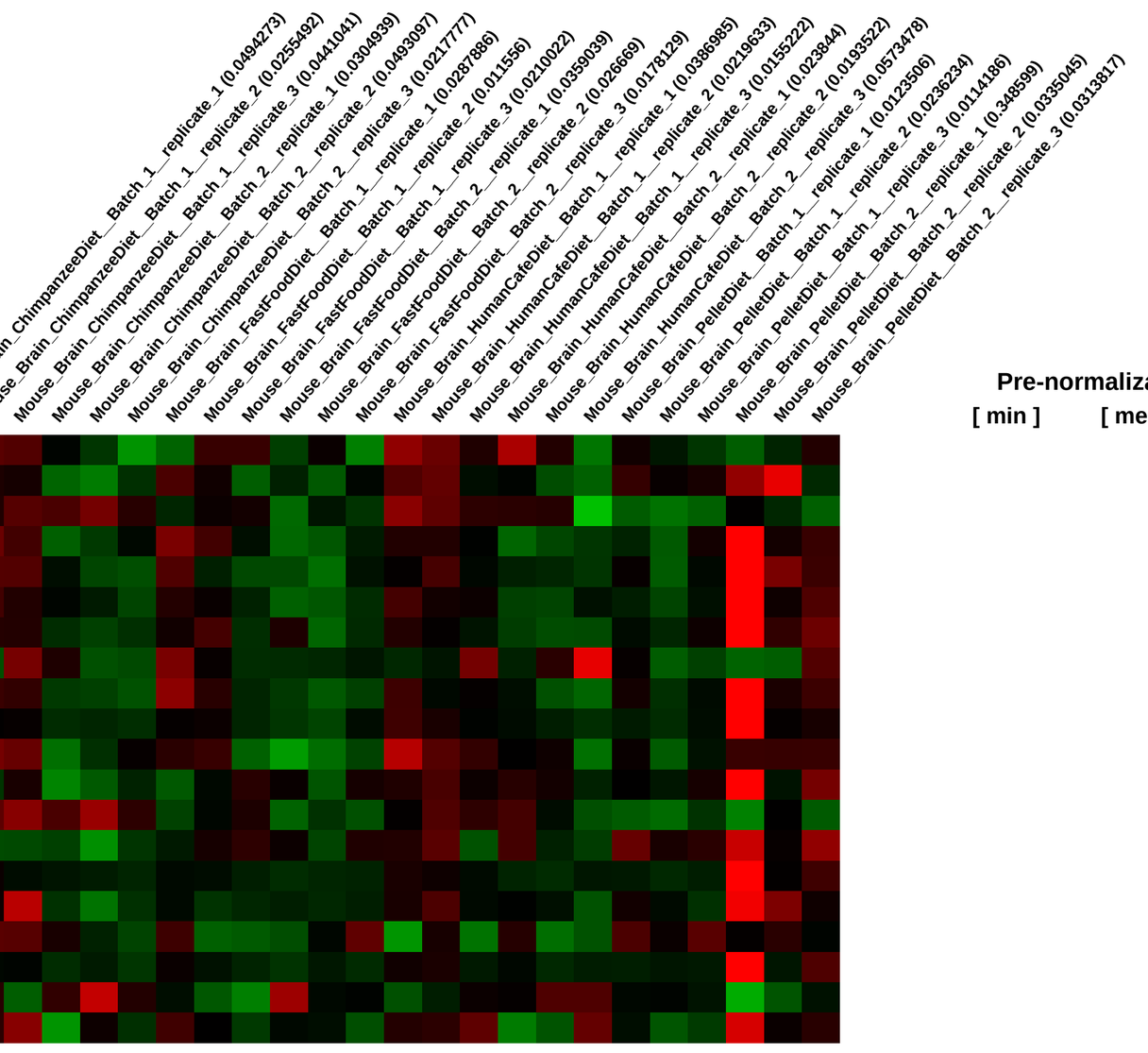

GEO Series "GSE18341" Expression Profiles

Num of samples in this series: 30

Scale of expression profile Z-scores

-3.0 -2.0 -1.0 0.0 1.0 2.0 3.0

GEO Link:	http://www.ncbi.nlm.nih.gov/geo/query/acc.cgi?acc=GSE18341
Status:	Public on Nov 23 2009
Title:	Age Dependent Gene Expression Responses to Inhaled Lipopolysaccharide Combined with Mechanical Ventilation
Organism:	Mus musculus
Experiment type:	Expression profiling by array
Platform:	GPL1261
Pubmed ID:	19901347
Summary & Design:	**Summary:** Children have a lower incidence and mortality from acute lung injury than adults, and infections are the most common event associated with acute lung injury (ALI). To study the effects of age on susceptibility to ALI, we investigated the responses to microbial products combined with mechanical ventilation in juvenile (21 day) and adult (16 week-old) mice. We hypothesized that the increased incidence and severity of lung injury associated with increasing age is due in large part to acquired changes in the way in which inflammatory responses are activated in the lungs in response to microbial products and mechanical ventilation. **Overall design:** Juvenile (21 day) and adult (16 week) C57BL/6 mice were treated with an aerosol of E. coli 0111:B4 lipopolysaccharide (LPS) (20 mL of 0.1 mg/mL) for 30 minutes in a sealed aerosol chamber, immediately followed by mechanical ventilation (LPS+MV) using tidal volume = 15 mL/kg, rate = 80 breaths/min, FiO2 = 30% and positive end expiratory pressure = 2 cm H2O for the duration of the study period time = 2 hours. Comparison groups included mice treated with LPS or mechanical ventilation (MV) alone, and untreated age-matched controls. There were N = 4 animals per group except the juvenile mice treated with MV alone and LPS+MV where there were N = 3. Each sample was an individual animal, therefore there were 30 samples. Mice treated with LPS alone were placed into a sealed aerosol chamber as stated above, and then allowed to breath spontaneously with free access to food and water for the duration of the study period time = 2 hours. Mice treated with MV alone were treated with the mechanical ventilation protocol stated above for the duration of the study period time = 2 hours. At the end of the study period, the mice were euthanized, and the lungs were immediately removed and placed into RNAlater (Ambion, Austin, TX) for at least 24 hr prior to isolation of total lung mRNA.

Background corr dist: KL-Divergence = 0.2657, L1-Distance = 0.0529, L2-Distance = 0.0068, Normal std = 0.2954

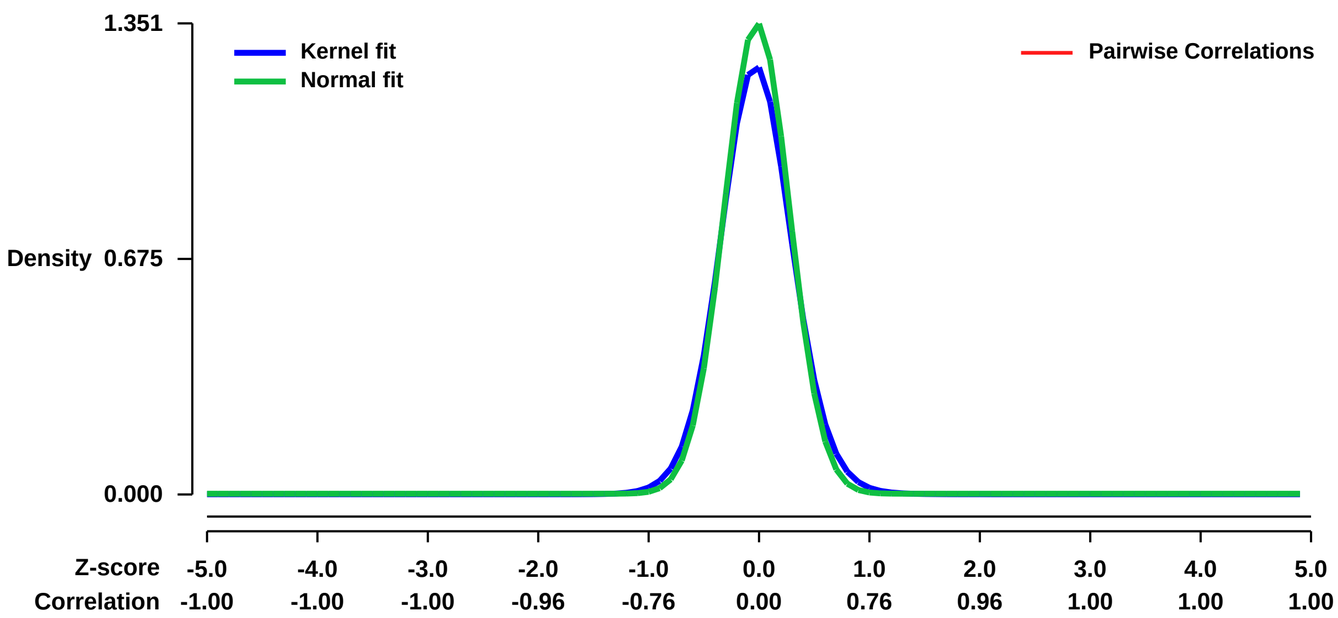

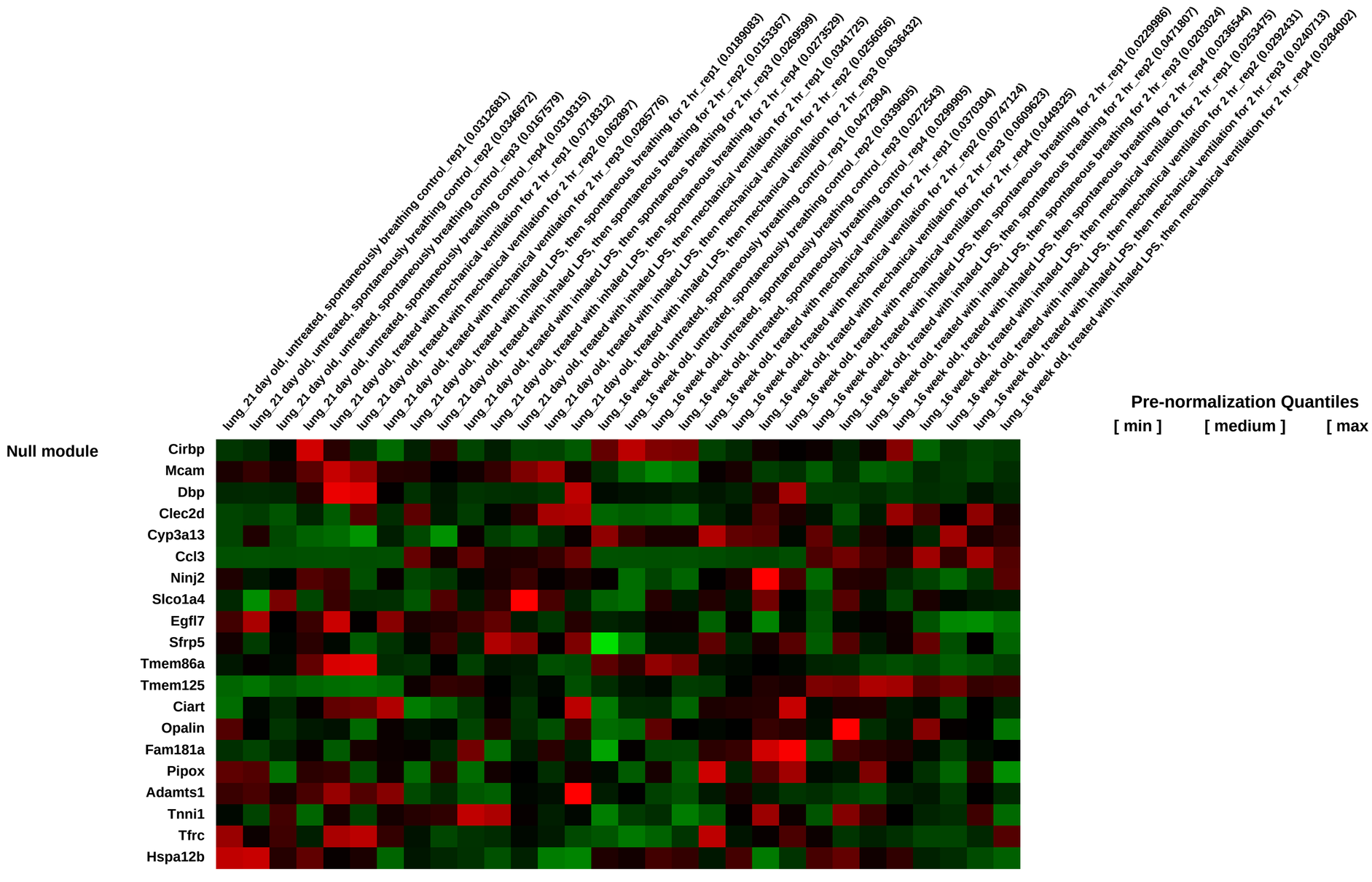

GEO Series "GSE8678" Expression Profiles

Num of samples in this series: 6

Scale of expression profile Z-scores

-3.0 -2.0 -1.0 0.0 1.0 2.0 3.0

GEO Link:	http://www.ncbi.nlm.nih.gov/geo/query/acc.cgi?acc=GSE8678
Status:	Public on Aug 23 2007
Title:	Gene expression data from sorted IL-7Rhi/lo effector CD8 T cells on day 6/7 after LCMV armstrong infection
Organism:	Mus musculus
Experiment type:	Expression profiling by array
Platform:	GPL1261
Pubmed ID:	20921525
Summary & Design:	**Summary:** At the peak of the CD8 T cell response to acture viral and bacterial infections, expression of the Interleukin-7 Receptor (IL-7R) marks Memory Precursor Effector CD8 T Cells (MPECs) from other Short-Lived Effector CD8 T cells (SLECs), which are IL-7Rlo. This study was designed to determine the gene expression differences between these two subsets of effector CD8 T cells. **Keywords: expression comparison** **Overall design:** This study compared IL-7Rhi and IL-7Rlo LCMV-specific P14 Transgenic CD8 T cells, sorted from LCMV armstrong infected recipient mice 6/7 days after infection. Data includes 3 independent replicates for the IL-7Rhi and IL-7Rlo groups.

Background corr dist: KL-Divergence = 0.0428, L1-Distance = 0.0228, L2-Distance = 0.0006, Normal std = 0.6086

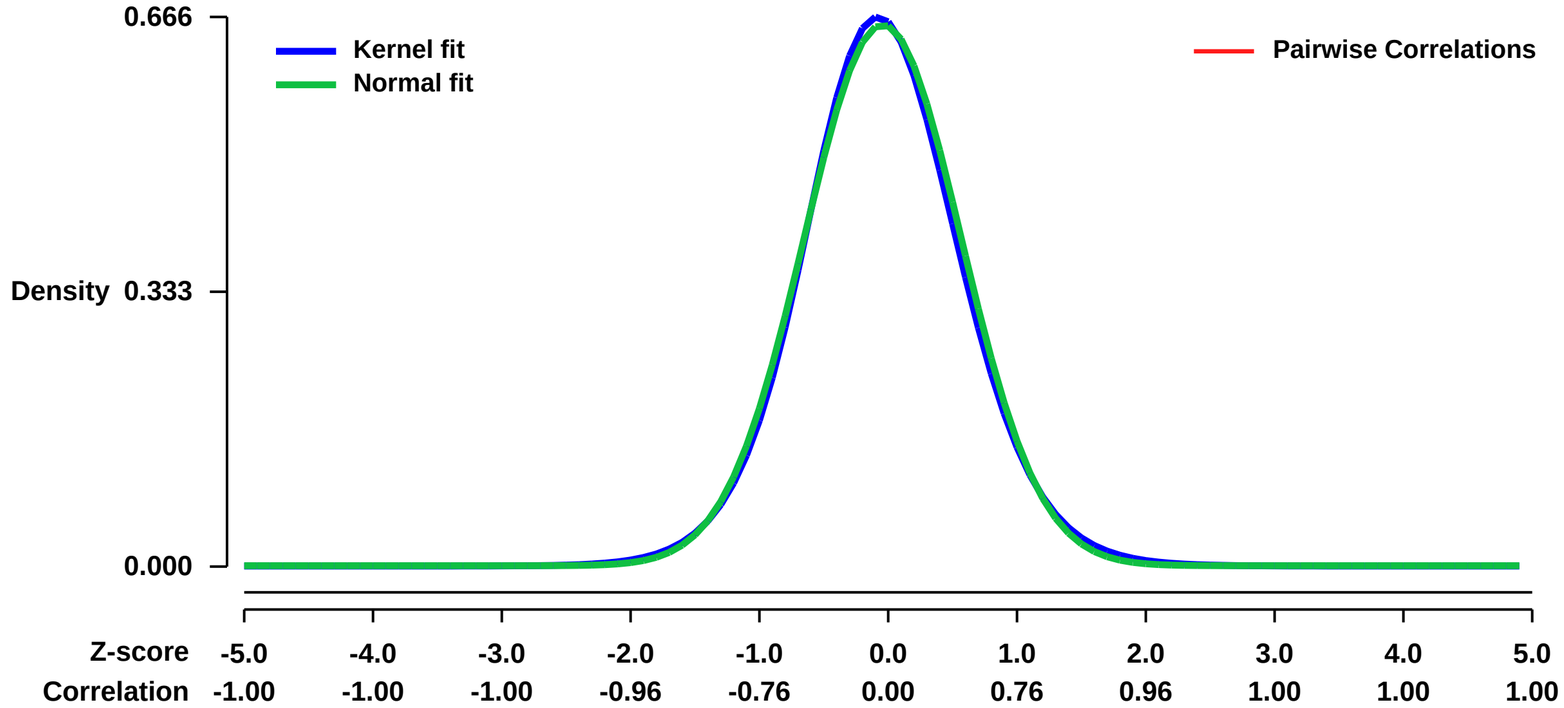

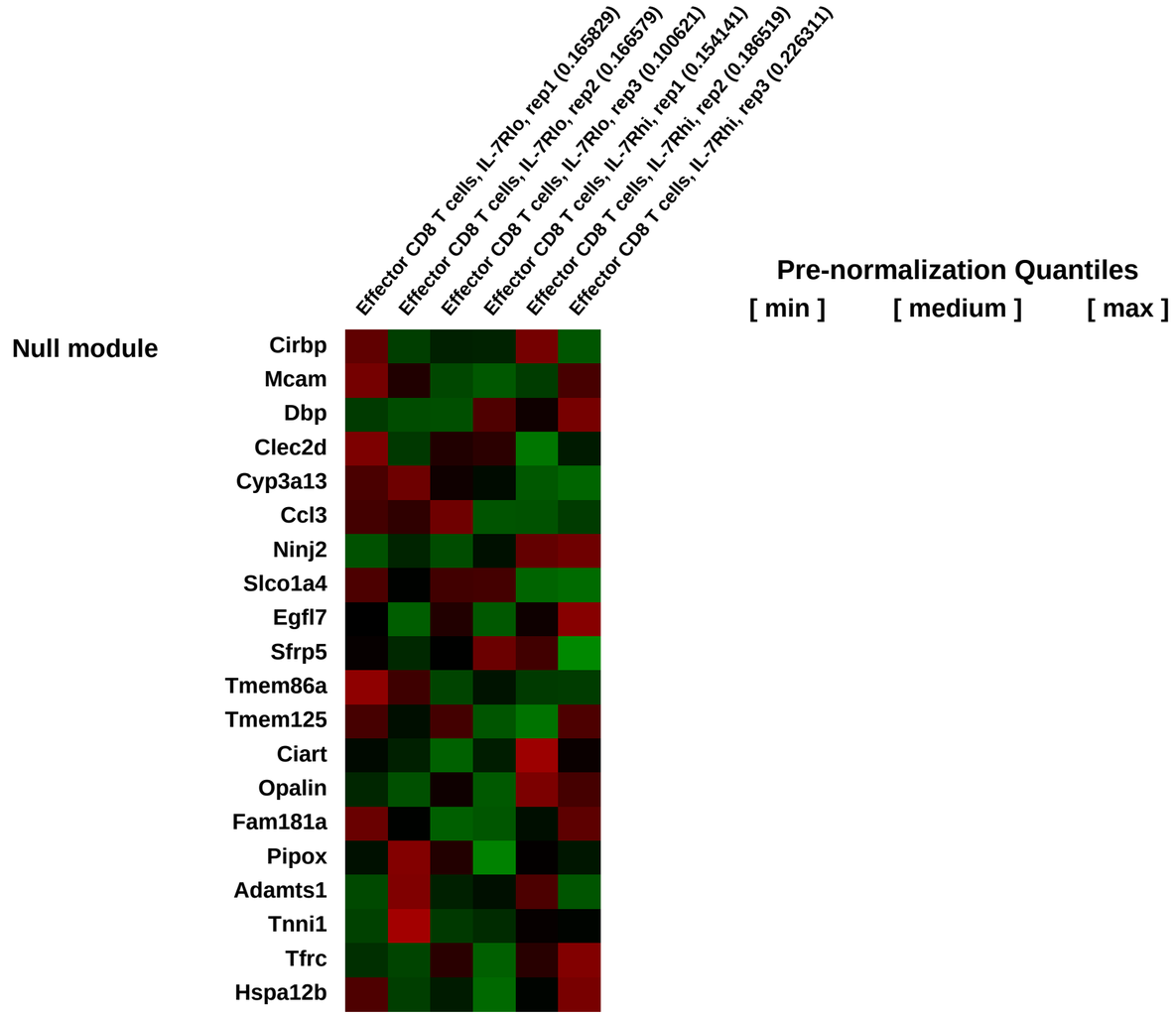

GEO Series "GSE6196" Expression Profiles

Num of samples in this series: 9

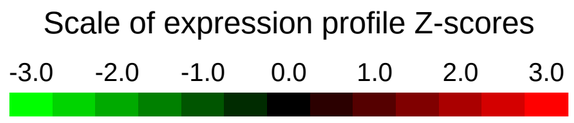

GEO Link:	http://www.ncbi.nlm.nih.gov/geo/query/acc.cgi?acc=GSE6196
Status:	Public on Mar 21 2009
Title:	Mouse Reissner's Membrane Gene Expression studies
Organism:	Mus musculus
Experiment type:	Expression profiling by array
Platform:	GPL1261
Pubmed ID:	19144862
Summary & Design:	**Summary:** The goal was to screen for the expressed genes in Reissner's membrane (RM) that are related to ion transport and its regulation. The objectives were 1) to determine whether short-term incubation altered the transcriptome and 2) to discover which genes changed expression levels in response to glucocorticoids. **Keywords: drug response** **Overall design:** RM was dissected free-hand from mouse cochleae and either immediately subjected to RNA extraction or incubated for 24 as explants. Two series of samples were incubated in the presence or absence of dexamethasone (100 nM) and samples of RM were pooled to obtain sufficient material for gene array analysis. The pooled samples were used to hybridize 3 gene array chips for each biological sample.

Background corr dist: KL-Divergence = 0.0363, L1-Distance = 0.0602, L2-Distance = 0.0046, Normal std = 0.7133

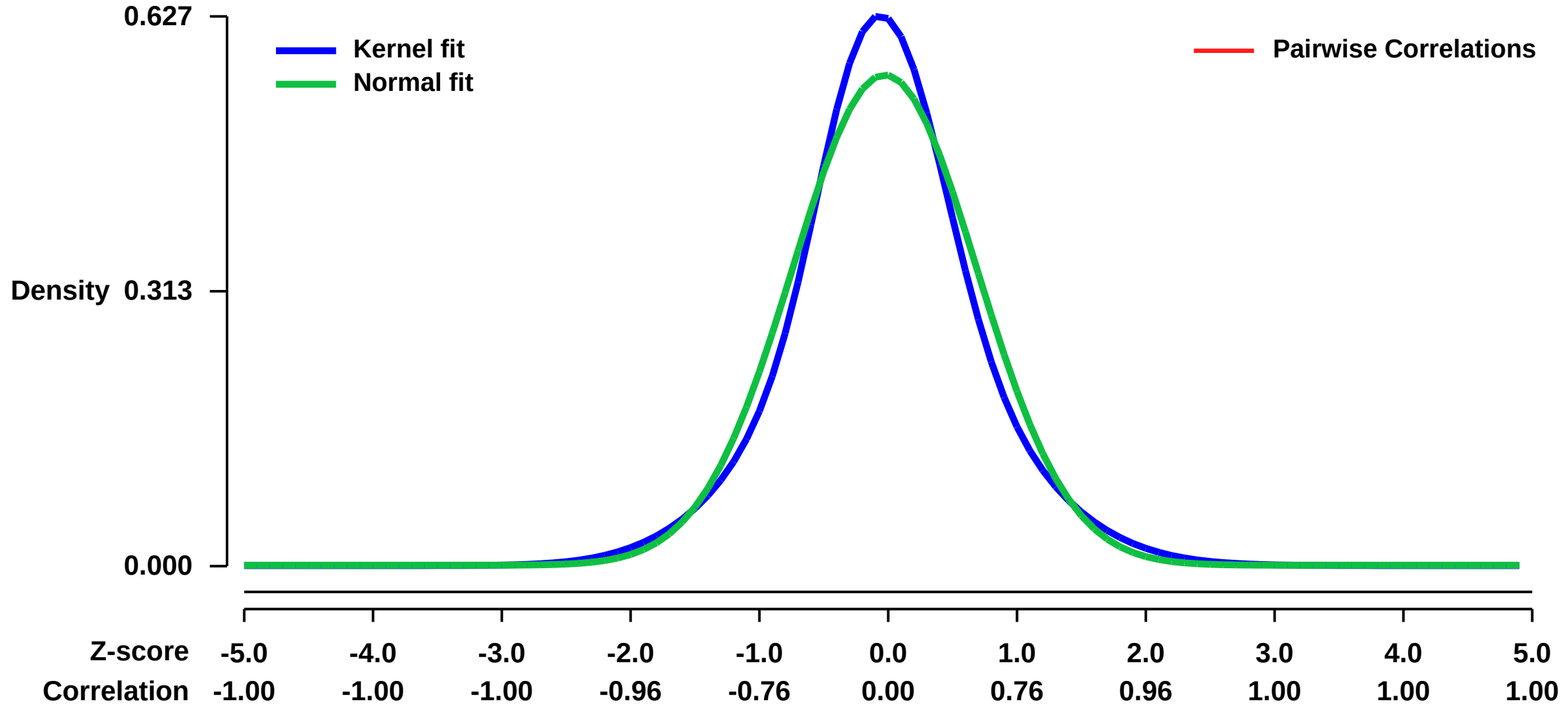

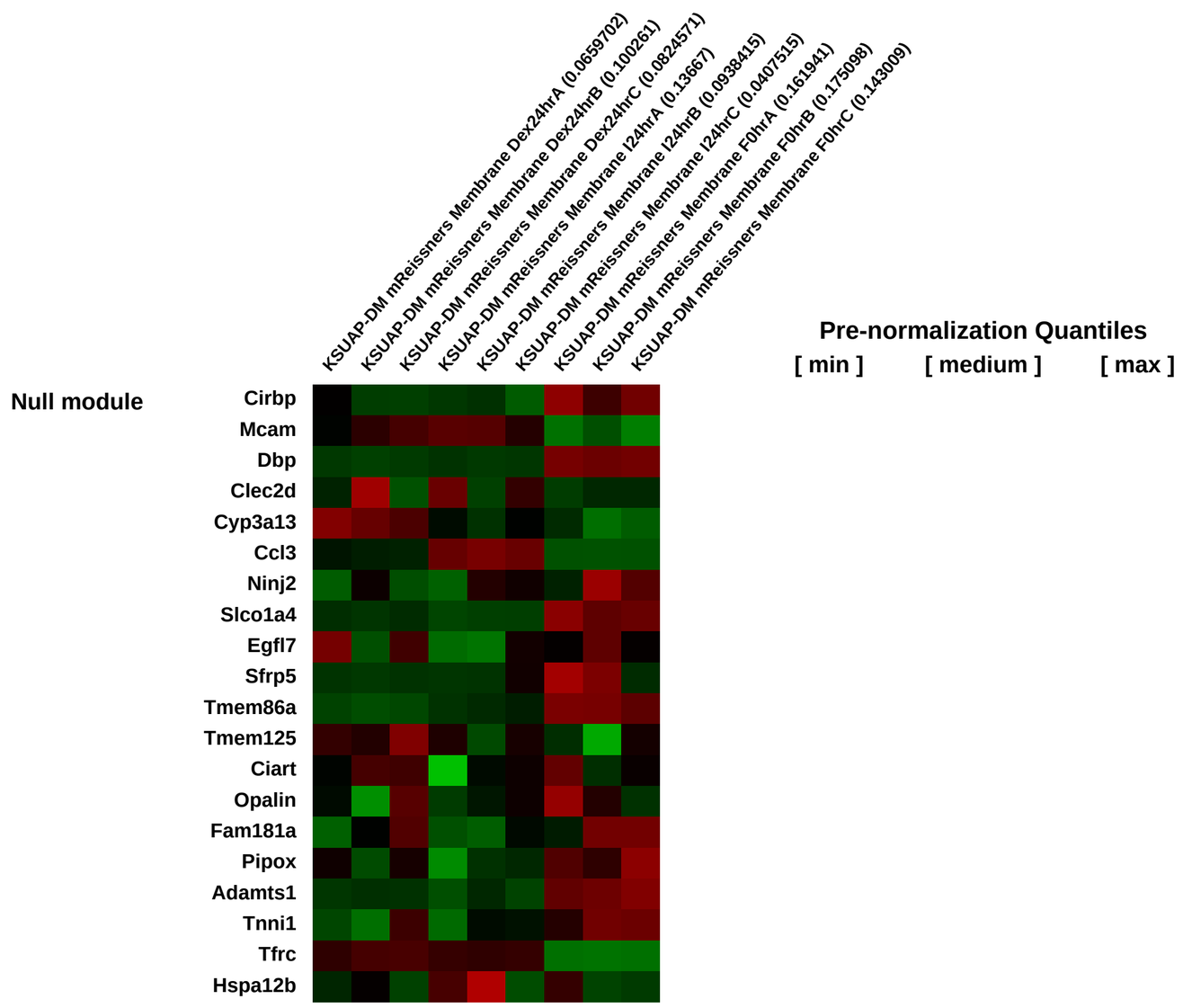

GEO Series "GSE14415" Expression Profiles

Num of samples in this series: 31

Scale of expression profile Z-scores

-3.0 -2.0 -1.0 0.0 1.0 2.0 3.0

GEO Link:	http://www.ncbi.nlm.nih.gov/geo/query/acc.cgi?acc=GSE14415
Status:	Public on Mar 01 2009
Title:	Gene expression profiling of natural and induced regulatory T cells
Organism:	Mus musculus
Experiment type:	Expression profiling by array
Platform:	GPL1261
Pubmed ID:	19265124
Summary & Design:	**Summary:** The gene expression profile of peripheral Foxp3+ natural regulatory T cells isolated from Foxp3/EGFP bicistronic mice was compared to that of in vitro-induced regulatory T cells and to CD4+ conventional (Foxp3-) T cells. The role of the regulatory T cell transcription factor Foxp3 in shaping the transcriptosomes of natural and induced regulatory T cells was analyzed using mice expressing a mutant FOXP3-EGFP fusion protein (Foxp3deltaEGFP). We used gene expression microarrays to examine the transcriptional programs of natural and induced regulatory T cells and the function of Foxp3 in organizing the transcriptosomes of the respective cell type Keywords: Cell population analysis **Overall design:** Conventional T cells and natural and induced regulatory T cells were derived from Foxp3/EGFP bicistronic mice and analyzed for their gene expression profile. Conventional T cells, regulatory T cell precursors (CD4+Foxp3deltaEGFP+) and induced regulatory T cell precursors (CD4+Foxp3deltaEGFP+) cells were deriv ed from Foxp3deltaEGFP mice

Background corr dist: KL-Divergence = 0.1327, L1-Distance = 0.0360, L2-Distance = 0.0024, Normal std = 0.3924

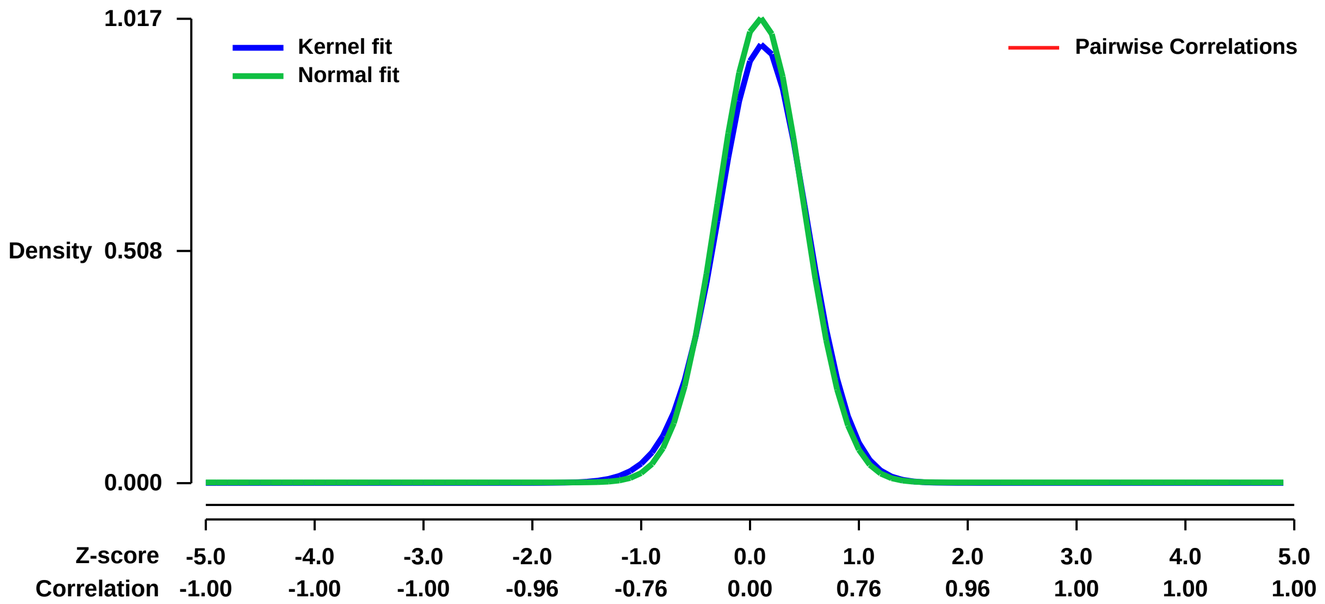

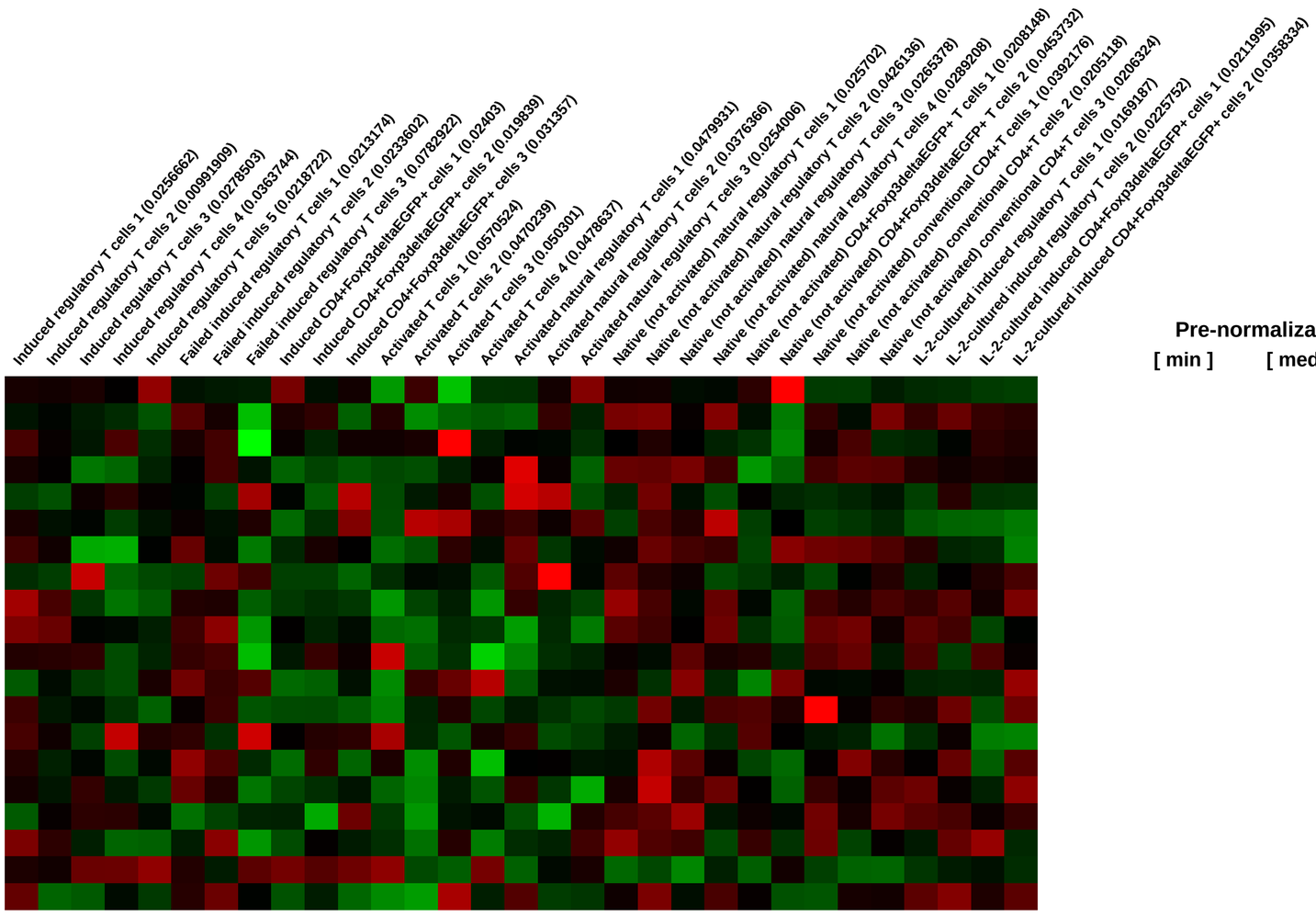

GEO Series "GSE25616" Expression Profiles

Num of samples in this series: 10

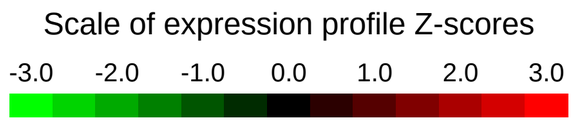

GEO Link:	**http://www.ncbi.nlm.nih.gov/geo/query/acc.cgi?acc=GSE25616**
Status:	**Public on Jun 21 2011**
Title:	**Liver expression data from lactating QSi5 mice**
Organism:	**Mus musculus**
Experiment type:	**Expression profiling by array**
Platform:	**GPL1261**
Pubmed ID:	
Summary & Design:	**Summary:** **The liver plays a crucial role in energy partitioning and is particularly important for the increased demand from the mammary gland during lactation. The present study identifies genes associated with negative energy balance in lactating mice.** **We used microarrays to detail the gene expression underlying negative energy balance and identified distinct classes of up-regulated genes.** **Overall design:** **The pregnant mice was fed a high GI diet during and throughout pregnancy until peak lactation (HGI group; n = 5). The second group was fed a low GI diet over the same period (LGI group; n = 5). The HGI diet included 51.4% (W/W basis) of glucose and a gross energy of 15.6MJ/Kg and the LGI diet contained 51.4% (W/W basis) of high amylase starch (Hi-Maze) and a gross energy of 16.3MJ/Kg. At the end of this period, mice were euthanazed and livers were removed and microarray was performed.**

Background corr dist: KL-Divergence = 0.0978, L1-Distance = 0.0327, L2-Distance = 0.0020, Normal std = 0.4415

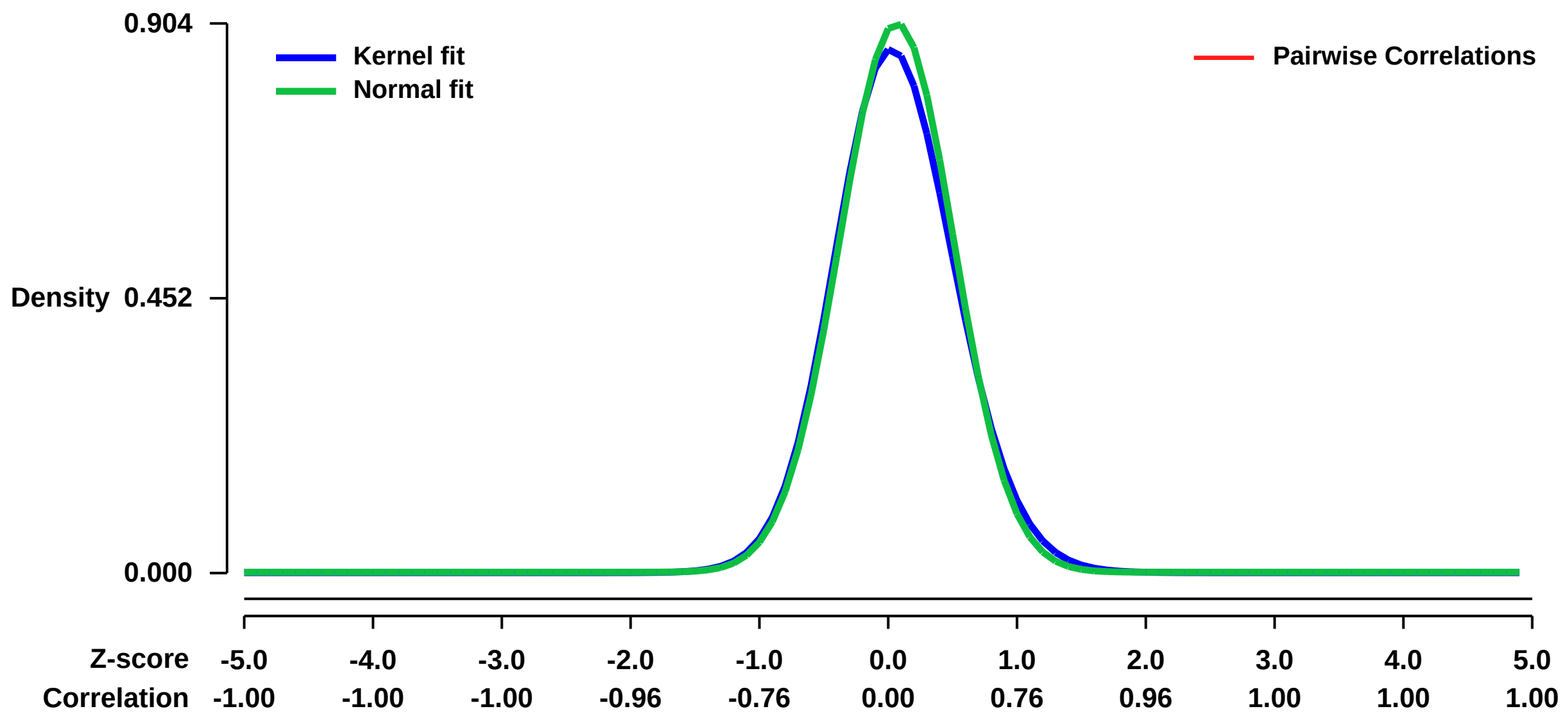

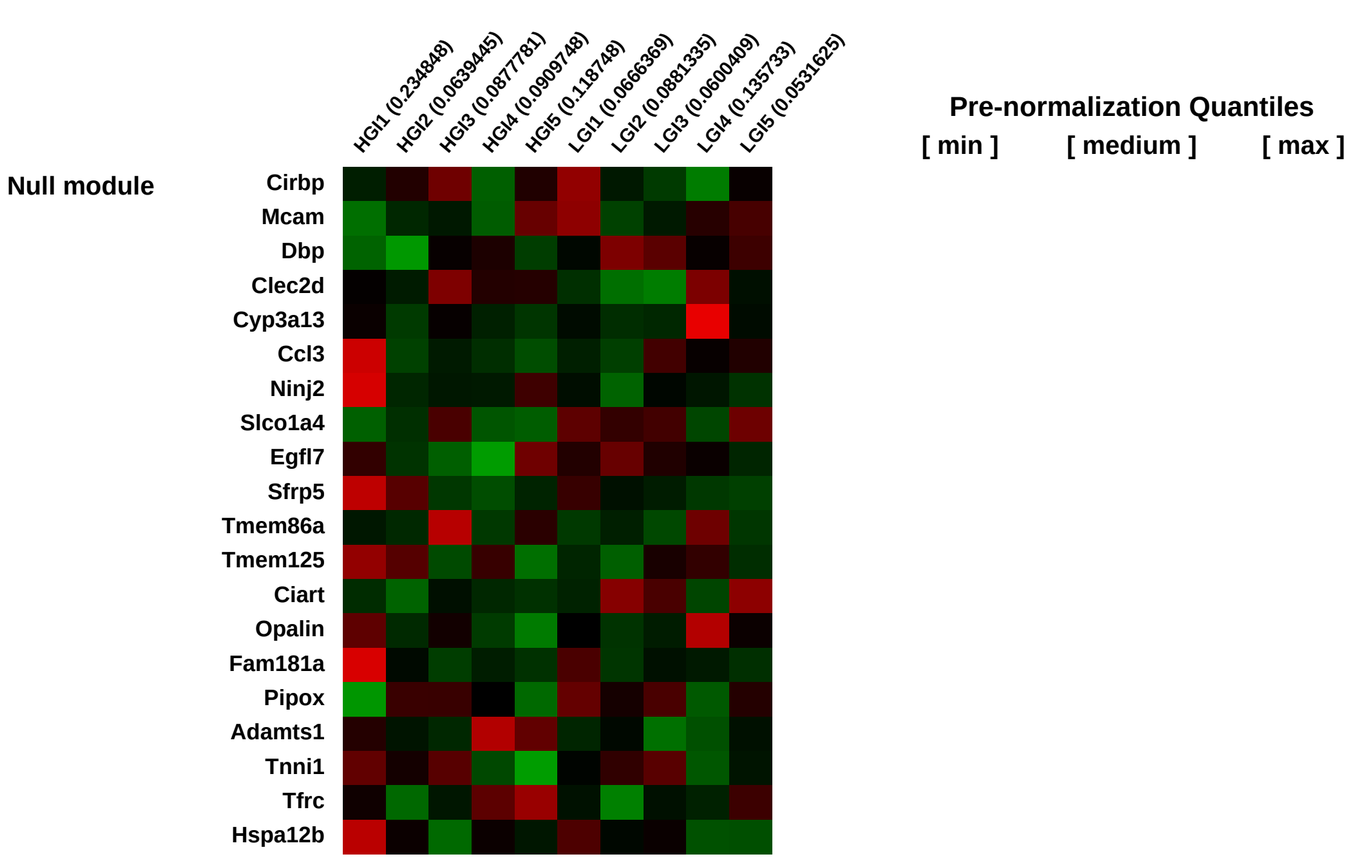

GEO Series "GSE7759" Expression Profiles

Num of samples in this series: 112

Details of this dataset are not shown due to large number of samples and the page size limit.

Find details in http://www.ncbi.nlm.nih.gov/geo/query/acc.cgi?acc=GSE7759

Background corr dist: KL-Divergence = 0.3284, L1-Distance = 0.0565, L2-Distance = 0.0079, Normal std = 0.2710

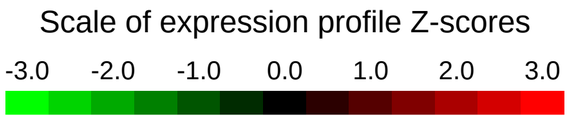

GEO Series "GSE21137" Expression Profiles

Num of samples in this series: 16

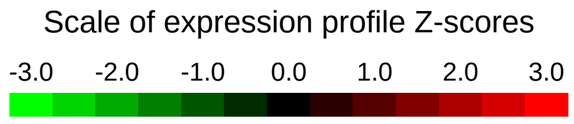

GEO Link:	http://www.ncbi.nlm.nih.gov/geo/query/acc.cgi?acc=GSE21137
Status:	Public on Apr 20 2010
Title:	Ultrastructural and transcriptional profiling of neuropathological misregulation of CREB function
Organism:	Mus musculus
Experiment type:	Expression profiling by array
Platform:	GPL1261
Pubmed ID:	20395962
Summary & Design:	**Summary:** We compare here the neurodegenerative processes observed in the hippocampus of bitransgenic mice with chronically altered levels of cAMP-response element-binding protein (CREB) function. The combination of genome-wide transcriptional profiling of degenerating hippocampal tissue with microscopy analyses reveals that the sustained inhibition of CREB function in A-CREB mice is associated with dark neuron degeneration, whereas its strong chronic activation in VP16-CREB mice primarily causes excitotoxic cell death and inflammation. Furthermore, the meta-analysis with gene expression profiles available in public databases identifies relevant common markers to other neurodegenerative processes and highlights the importance of the immune response in neurodegeneration. Overall, these analyses define the ultrastructural and transcriptional signatures associated with these two forms of hippocampal neurodegeneration, confirm the importance of fine-tuned regulation of CREBdependent gene expression for CA1 neuron survival and function, and provide novel insight into the function of CREB in the etiology of neurodegenerative processes. **Overall design:** For each mouse genome 430 2.0 gene expression array (Affymetrix, Santa Clara, CA, USA), total RNA was extracted from the hippocampi of three to four mice with the same age, sex, and genotype to produce one pooled sample. We analyzed three late A-CREB pooled samples (6-week-old mice) and three late VP16-CREB pooled samples (3-week-off dox) with their corresponding control littermate samples (three pooled samples for each strain). To compare with early changes, we included two pooled A-CREB early samples (3-week-old mice) and two pooled VP16-CREB early samples (1-week-off dox) with their corresponding control littermate samples. In the case of A-CREB mice, we used the dataset GSE14320. We prepared new samples from bitransgenic mice and control littermates 1 week after transgene induction and hybridized them to mouse genome 430 2.0 genechips. The arrays were hybridized, washed, and screened for quality according to the manufacturerâ s protocol.

Background corr dist: KL-Divergence = 0.1496, L1-Distance = 0.0345, L2-Distance = 0.0023, Normal std = 0.3737

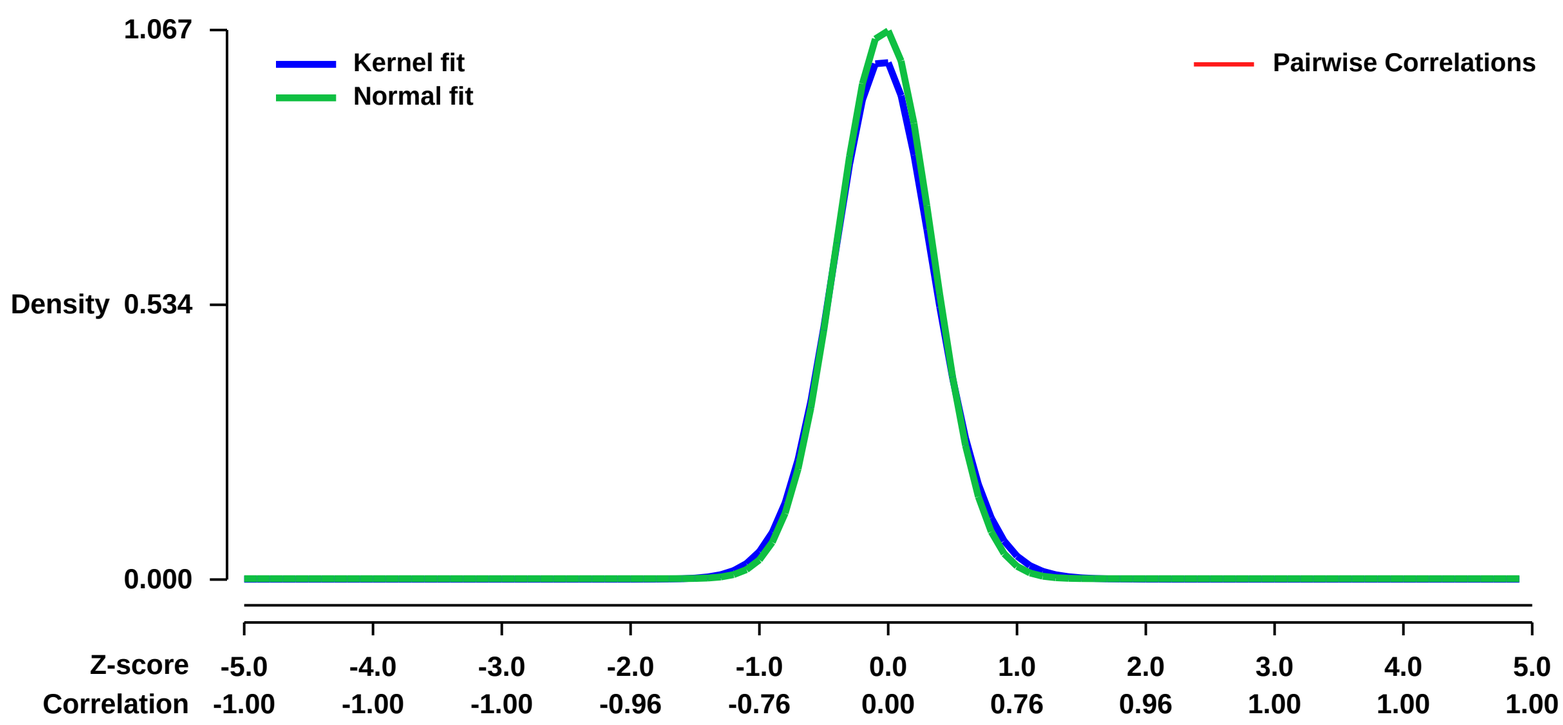

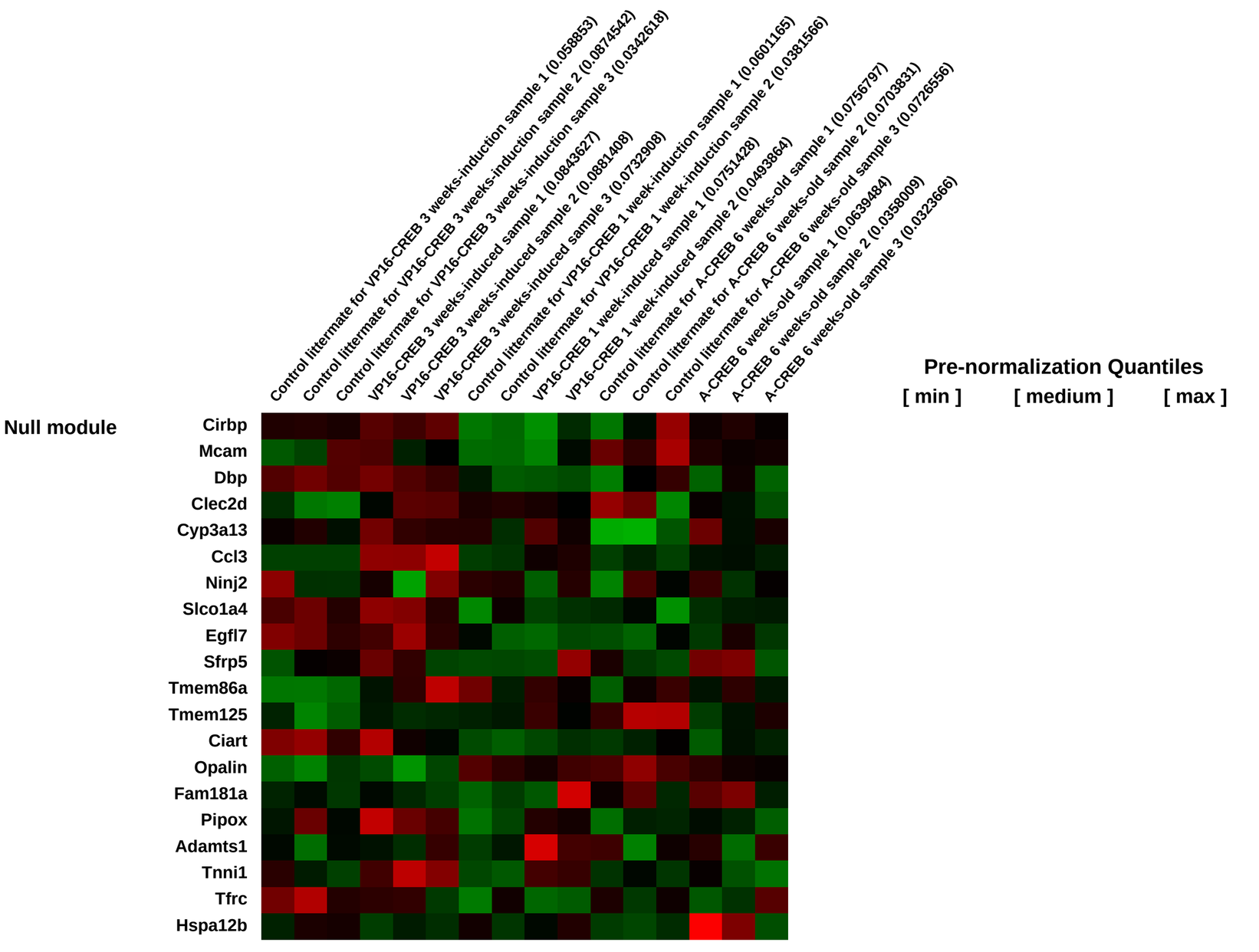

GEO Series "GSE12601" Expression Profiles

Num of samples in this series: 26

Scale of expression profile Z-scores

-3.0 -2.0 -1.0 0.0 1.0 2.0 3.0

GEO Link:	http://www.ncbi.nlm.nih.gov/geo/query/acc.cgi?acc=GSE12601
Status:	Public on Jun 01 2009
Title:	Development and Diversification of Retinal Amacrine Interneurons at Single Cell Resolution
Organism:	Mus musculus
Experiment type:	Expression profiling by array
Platform:	GPL1261
Pubmed ID:	19470466
Summary & Design:	**Summary:** The vertebrate retina uses diverse neuronal cell types arrayed into complex neural circuits to extract, process and relay information from the visual scene to the higher order processing centers of the brain. Amacrine cells, a diverse class of inhibitory interneurons, are thought to mediate the majority of the processing of the visual signal that occurs within the retina. Despite morphological characterization, the number of known molecular markers of amacrine cell types is still much smaller than the 26 morphological types that have been identified. Furthermore, it is not known how this diversity arises during development. Here, we have combined in vivo genetic labeling and single cell genome-wide expression profiling to: 1) Identify specific molecular types of amacrine cells; 2) Demonstrate the molecular diversity of the amacrine cell class. **Overall design:** It is difficult to identify new markers of amacrine cells, due to the fact that they only comprise a small percentage of the total cells in the retina. Additionally, given that there are at least 26 distinct types of amacrine cells, population based approaches fail to achieve the precision necessary to discover markers of each type. To facilitate the identification of new markers for different amacrine cell classes and to more fully characterize the molecular signatures of these classes, we isolated single amacrine cells. To accomplish this goal, we introduced genetic reporters (pNdrg4::GFP or pSynapsin::GFP) into the developing retina (P0) by either in vivo or ex vivo electroporation. These reporters were observed to label morphologically distinct sets of amacrine cells at the different timepoints harvested in this study. Electroporated retinas were then dissociated at different time points and single retinal amacrine cells were isolated by virtue of their GFP expression and placed in tubes containing lysis buffer. Then, their mRNAs were reverse transcribed, and the resulting cDNAs were PCR amplified for 35 cycles. Labeled cDNA samples were hybridized to Affymetrix 430 2.0 microarrays and the data was normalized using MAS5.0 software.

Background corr dist: KL-Divergence = 0.4759, L1-Distance = 0.0934, L2-Distance = 0.0339, Normal std = 0.2404

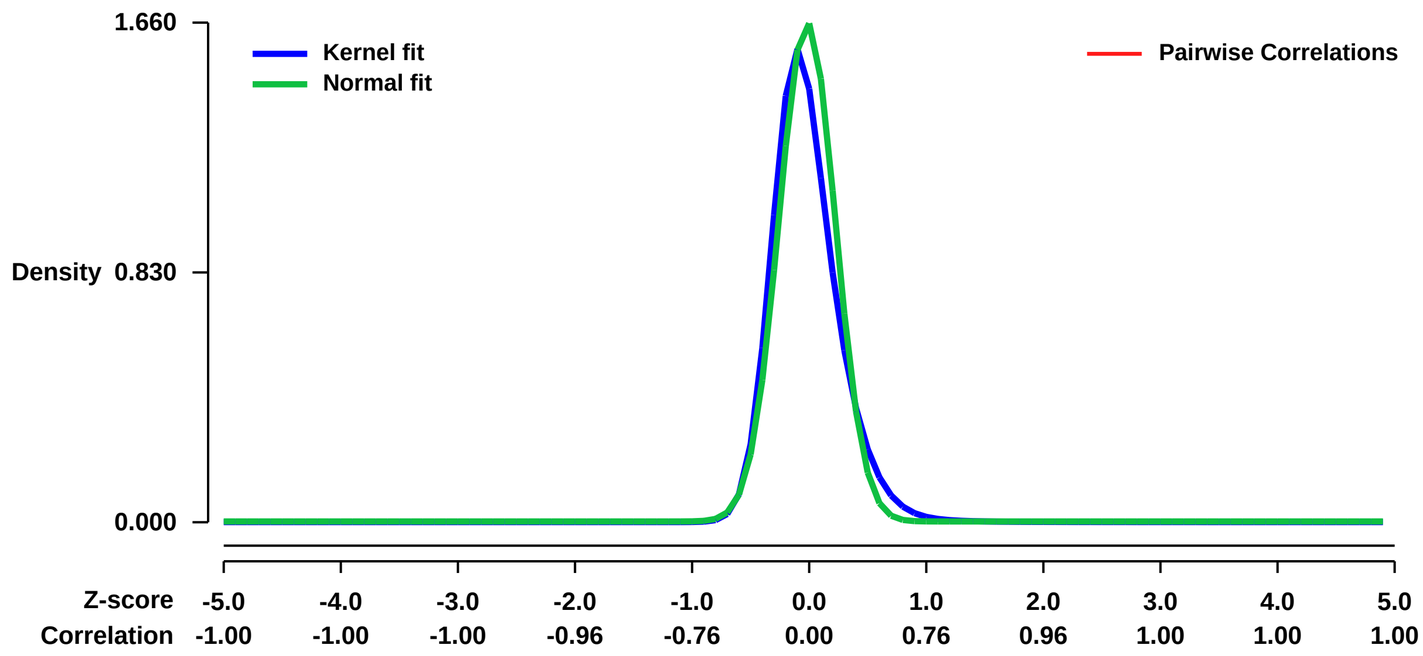

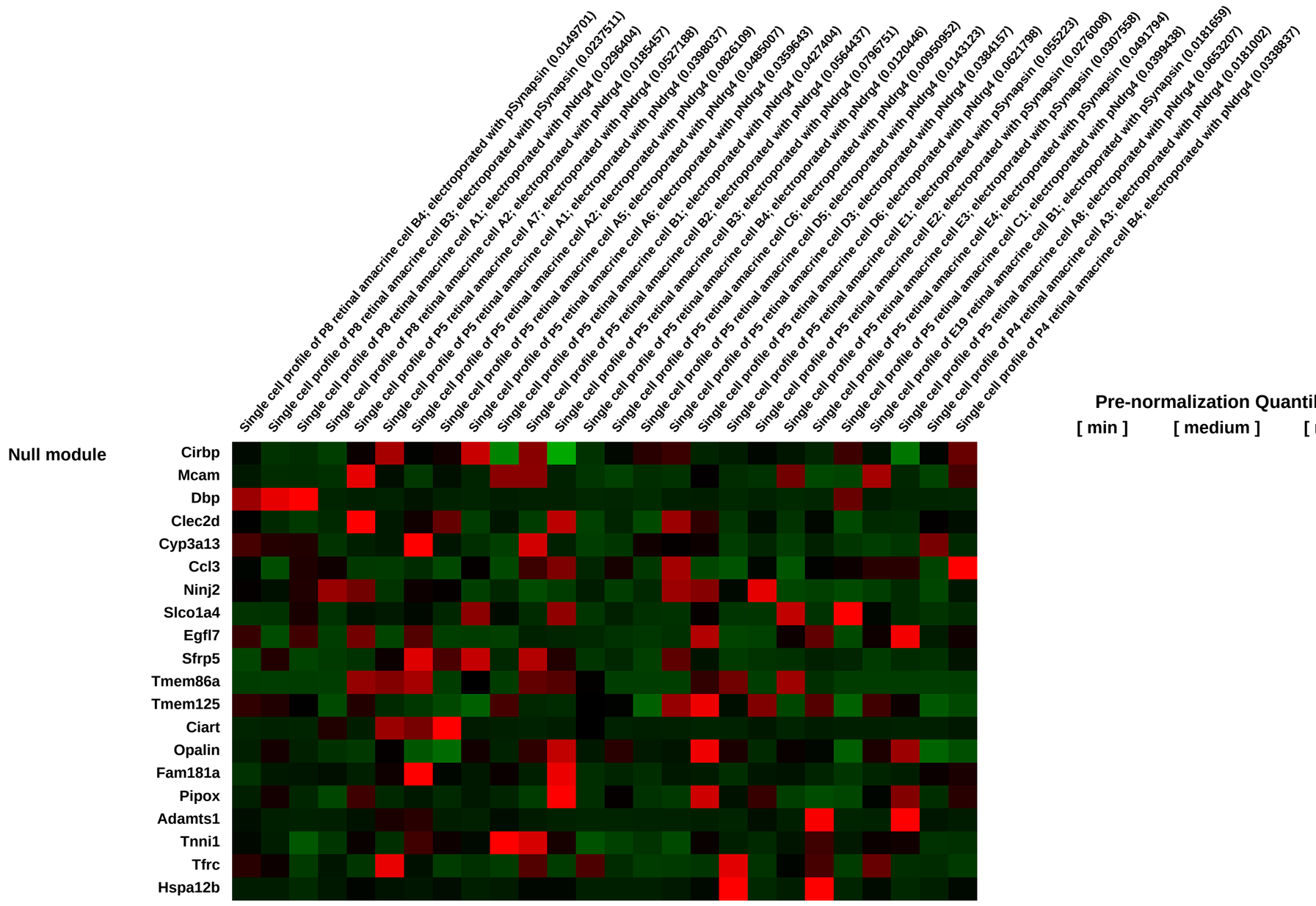

GEO Series "GSE18281" Expression Profiles

Num of samples in this series: 33

Scale of expression profile Z-scores

-3.0 -2.0 -1.0 0.0 1.0 2.0 3.0

GEO Link:	http://www.ncbi.nlm.nih.gov/geo/query/acc.cgi?acc=GSE18281
Status:	Public on Nov 24 2009
Title:	Spatial mapping of thymic stromal microenvironments reveals unique features influencing T lymphoid differentiation
Organism:	Mus musculus
Experiment type:	Expression profiling by array
Platform:	GPL1261
Pubmed ID:	20064453
Summary & Design:	**Summary:** Interaction of hematopoietic progenitors with the thymic stromal microenvironment induces them to proliferate, adopt the T cell fate, and asymmetrically diverge into multiple T lineages. Progenitors at various developmental stages are stratified among different regions of the thymus, implying that the corresponding microenvironments differ from one another, and provide unique sets of signals to progenitors migrating between them. The nature of these differences remains undefined. Here we use novel physical and computational approaches to characterize these stromal subregions, distinguishing gene expression in microdissected tissues from that of their lymphoid constituents. Using this approach, we comprehensively map gene expression in functionally distinct stromal microenvironments, and identify clusters of genes that define each region. Quite unexpectedly, we find that the central cortex lacks distinctive features of its own, and instead appears to function by sequestering unique microenvironments found at the cortical extremities, and modulating the relative proximity of progenitors moving between them. **Overall design:** 4 to 6 weeks old male C57bl6/J were used for microdissection of 3 thymic cortical subregions and thymic medulla or for sorting cortical and medullary thymocytes. These samples were used for subsequent RNA purification, labeling and hybridization to Affymetrix arrays

Background corr dist: KL-Divergence = 0.1533, L1-Distance = 0.0296, L2-Distance = 0.0018, Normal std = 0.3795

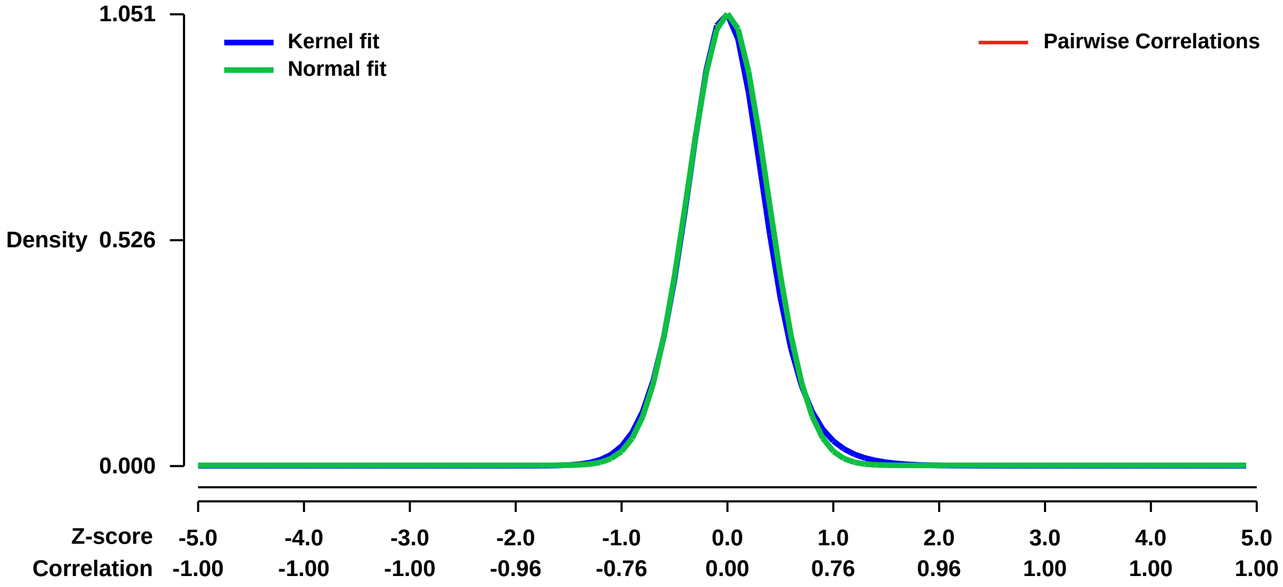

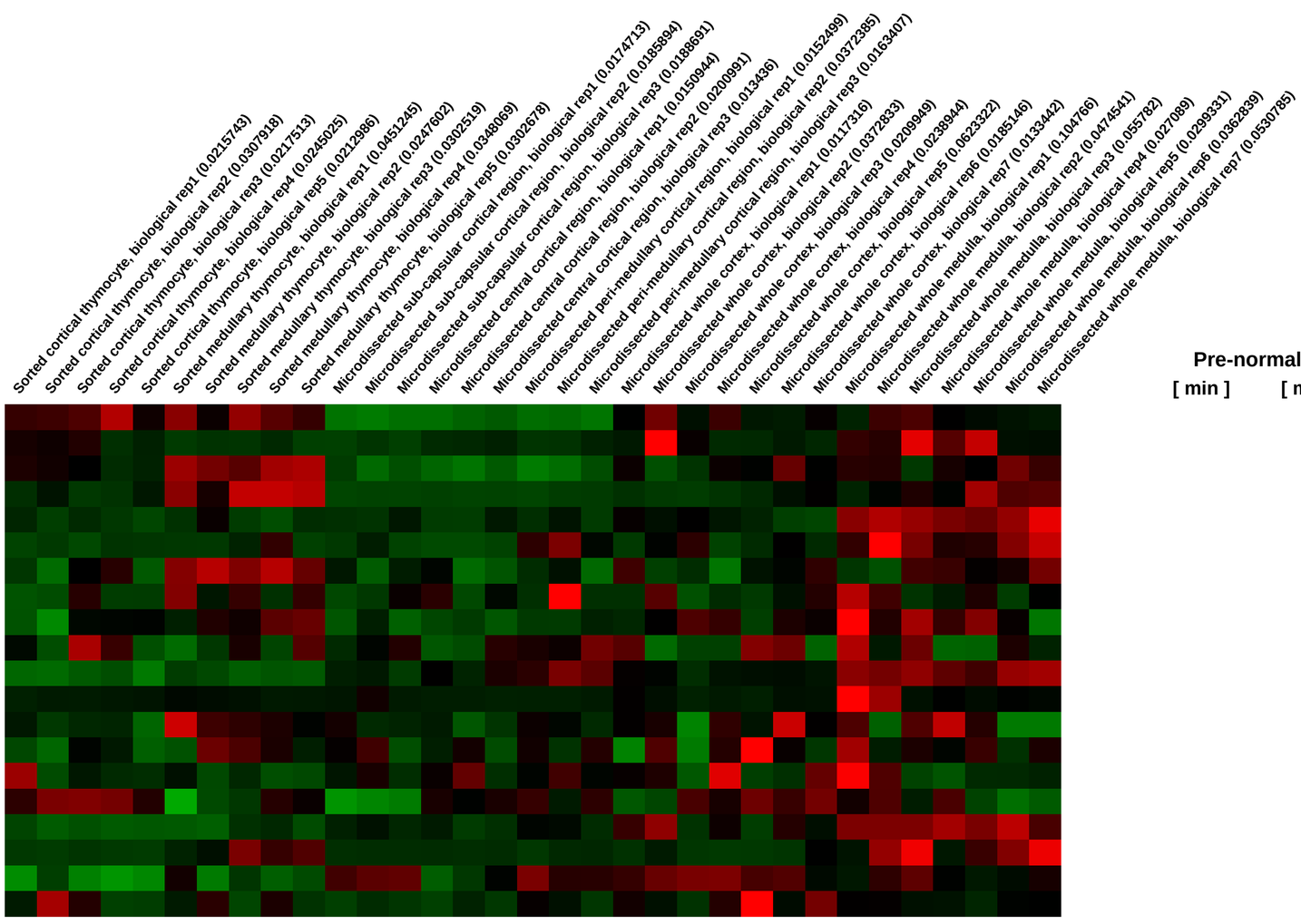

GEO Series "GSE9978" Expression Profiles

Num of samples in this series: 8

Scale of expression profile Z-scores

-3.0 -2.0 -1.0 0.0 1.0 2.0 3.0

GEO Link:	http://www.ncbi.nlm.nih.gov/geo/query/acc.cgi?acc=GSE9978
Status:	Public on Mar 17 2009
Title:	Genes plus and minus LIF
Organism:	Mus musculus
Experiment type:	Expression profiling by array
Platform:	GPL1261
Pubmed ID:	19618472
Summary & Design:	**Summary:** This study was undertaken in order to characterize the functions of Rex-1 and identify potential Rex-1 target genes.Both alleles of the Rex-1 gene were disrupted in J1 mouse embryonic stem cells. Gene expression levels in one of the resulting Rex-1 knockout cell lines was compared to that of J1 wild type cells. **Keywords: cell type comparison** **Overall design:** Gene expression in Rex-1 knockout mouse embryonic stem cells compared to that of J1 wild type cells. Cells were cultured in the presence and absence of LIF. This series utilized eight samples.There are two biological replicates per cell type cultured under this condition. The J1 samples serve as the control.

Background corr dist: KL-Divergence = 0.0670, L1-Distance = 0.0204, L2-Distance = 0.0006, Normal std = 0.5077

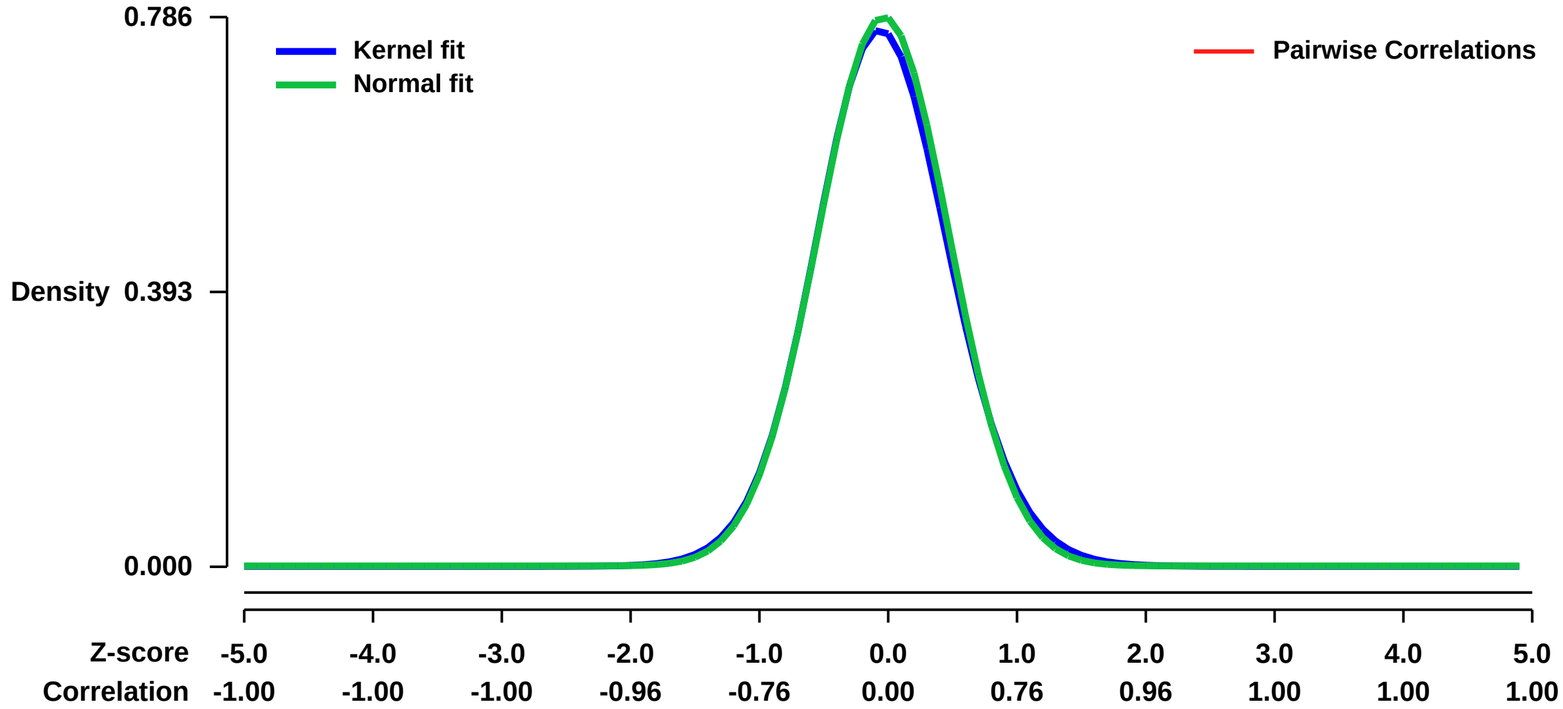

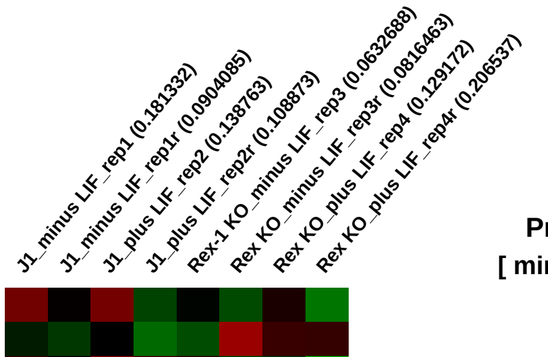

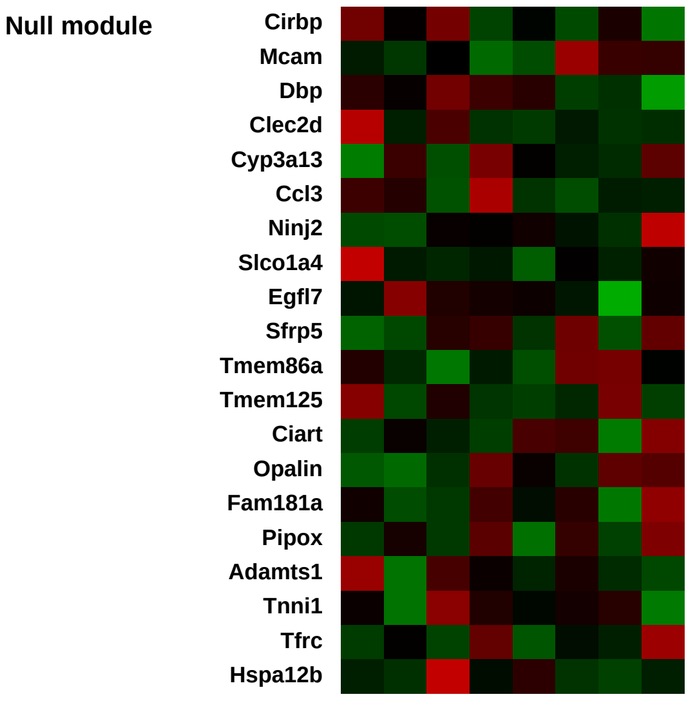

GEO Series "GSE20645" Expression Profiles

Num of samples in this series: 8

Scale of expression profile Z-scores

-3.0 -2.0 -1.0 0.0 1.0 2.0 3.0

GEO Link:	http://www.ncbi.nlm.nih.gov/geo/query/acc.cgi?acc=GSE20645
Status:	Public on Mar 06 2010
Title:	The difference of gene expression in mouse OPCs in normothermic and hypothermic culture
Organism:	Mus musculus
Experiment type:	Expression profiling by array
Platform:	GPL1261
Pubmed ID:	20936704
Summary & Design:	**Summary:** **We have found that the cell yield of oligodendrocyte precursor cells (OPCs) are higher in 31.5 â than in 37 â not by suppression of apoptosis but by enhancement of proliferation.** **Here, we performed transcriptome analysis using Affymetrix GeneChip on the primary cultured oligodendrocyte precursor cells prepared from the brain of ICR mice.** **Overall design:** **Oligodendrocyte precursor cells were prepared from primary mixed cell cultures of embryonic mouse cerebral hemispheres. The cerebral hemispheres from 15-day-old mouse embryos were enzymatically dissociated, seeded and cultured for 5 days in D-MEM containing 10% FBS. The cells were passaged to serum-free basal medium and cultured for further 48 hr at 37 â and 31.5 â .**

Background corr dist: **KL-Divergence = 0.0653, L1-Distance = 0.0185, L2-Distance = 0.0005, Normal std = 0.5114**

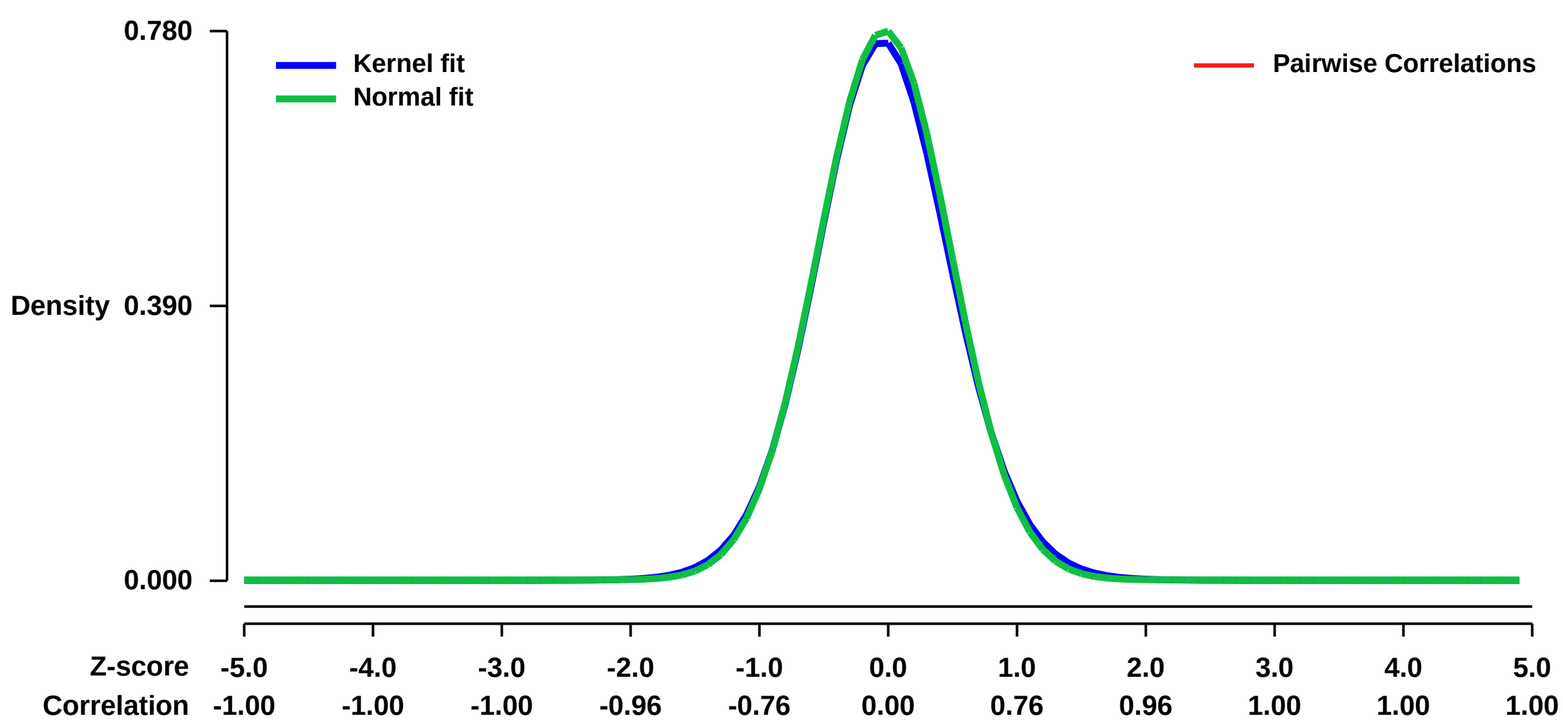

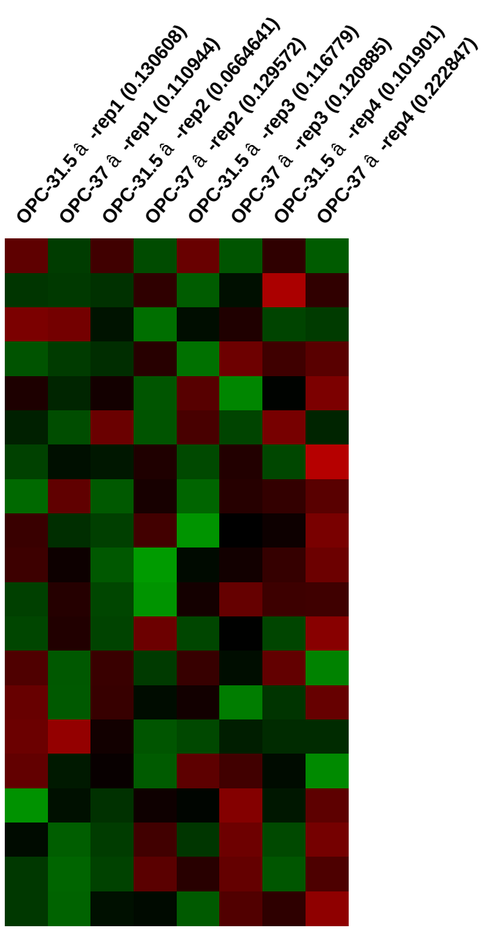

GEO Series "GSE42473" Expression Profiles

Num of samples in this series: 15

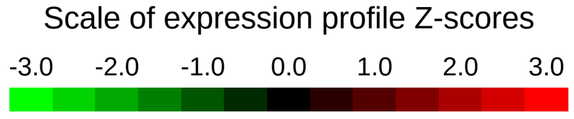

GEO Link:	http://www.ncbi.nlm.nih.gov/geo/query/acc.cgi?acc=GSE42473
Status:	Public on Dec 04 2012
Title:	PGC-1 alpha isoforms and muscle hypertrophy
Organism:	Mus musculus
Experiment type:	Expression profiling by array
Platform:	GPL1261
Pubmed ID:	23217713
Summary & Design:	**Summary:** An alternative promoter of the PGC-1alpha gene gives rise to three new PGC-1alpha isoforms refered to as PGC-1a2 (A2), PGC-1a3 (A3) and PGC-1a4 (A4). The proximal PGC-1 alpha promotor transcribes the canonical PGC-1 alpha which is refered to as PGC-1a1 (A1).G1/G2/G3 samples refer to the Green fluorescent protein (GFP) control samples used in this experiment. Forced expression of the PGC-1a4 isoform results in muslce hypertrophy associated with increased IGF-1 signaling and repression of myostatin signaling. **Overall design:** Mouse primary myoblasts isolated from C57BL/6 mice were differentiated in vitro. Fully differentiated myotubes were transduced with adenoviral vectors expressing GFP (as control) or each of the PGC-1alpha isoforms originating from the proximal or alternative promotor.

Background corr dist: KL-Divergence = 0.1210, L1-Distance = 0.0285, L2-Distance = 0.0011, Normal std = 0.4209

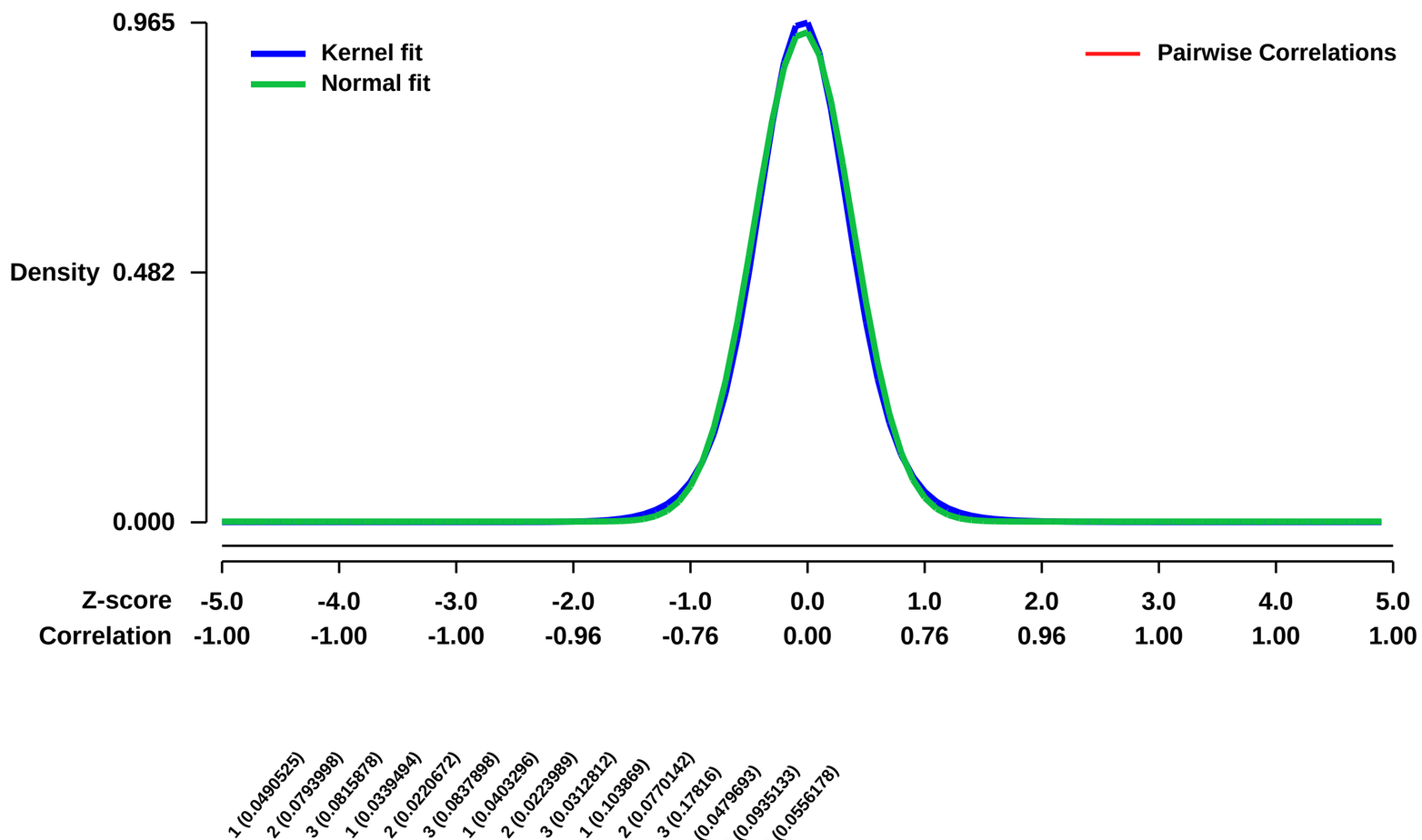

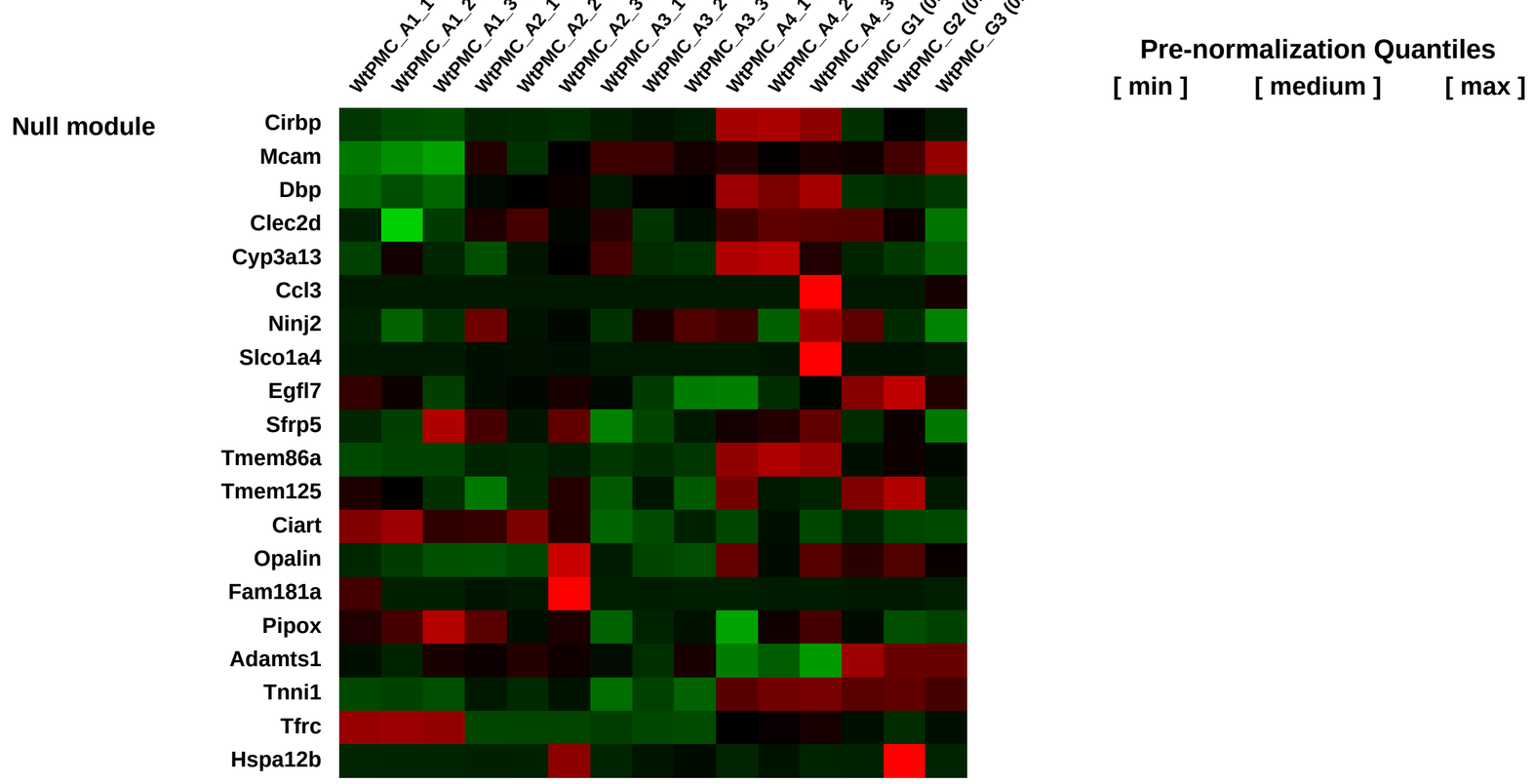

GEO Series "GSE26671" Expression Profiles

Num of samples in this series: 12

Scale of expression profile Z-scores

-3.0 -2.0 -1.0 0.0 1.0 2.0 3.0

GEO Link:	**http://www.ncbi.nlm.nih.gov/geo/query/acc.cgi?acc=GSE26671**
Status:	**Public on Dec 31 2011**
Title:	**Expression data of murine model of cardiac hypertrophy**
Organism:	**Mus musculus**
Experiment type:	**Expression profiling by array**
Platform:	**GPL1261**
Pubmed ID:	
Summary & Design:	**Summary:** **An initial cellular change in the pathogenesis of heart failure is cardiomyocyte hypertrophy, characterized by increased cell size, enhanced protein synthesis and reactivation of fetal genes. In addition to mechanical stresses, several neurohumoral factors have been identified as potent hypertrophic agents, including angiotensin II, endothelin, and catecholamines.** **We used microarrays to study the gene expression during cardiac hypertrophy.** **Overall design:** **Balb/c mice (6-8w) were treated with TAC, ATII infusion, and myocardial infarction. TAC model: The transverse aorta (TAC) was constricted at the upper left sternal border by ligation with a 7-silk surgical thread and 27-gauge needle, which was removed thereafter.** **Sham-operated controls underwent an identical procedure without TAC. At 1 week and 1month after the procedure, LV was harvested. Ang II model.: Ang II was dissolved in 0.9% NaCl at concentrations sufficient to allow an infusion rate of 2.0 mg/kg/day, known to produce hypertension and cardiac hypertrophy. Control mice received a vehicle (saline) via an osmotic minipump. At 1 week after the procedure, LV was harvested. MI model: The proximal portion of the left coronary artery was ligated using an 8-0 nylon thread. Myocardial ischemia was confirmed by the discoloration of the heart and typical ECG changes. After 30 min occlusion, the left coronary artery was reperfused by loosening the ligature. In sham-operated mice (SHAM), the pericardium was opened, but the coronary artery was not ligated. At 1 day, 1week, and 1 month after the procedure, LV was harvested.**

Background corr dist: KL-Divergence = 0.1406, L1-Distance = 0.0310, L2-Distance = 0.0018, Normal std = 0.3847

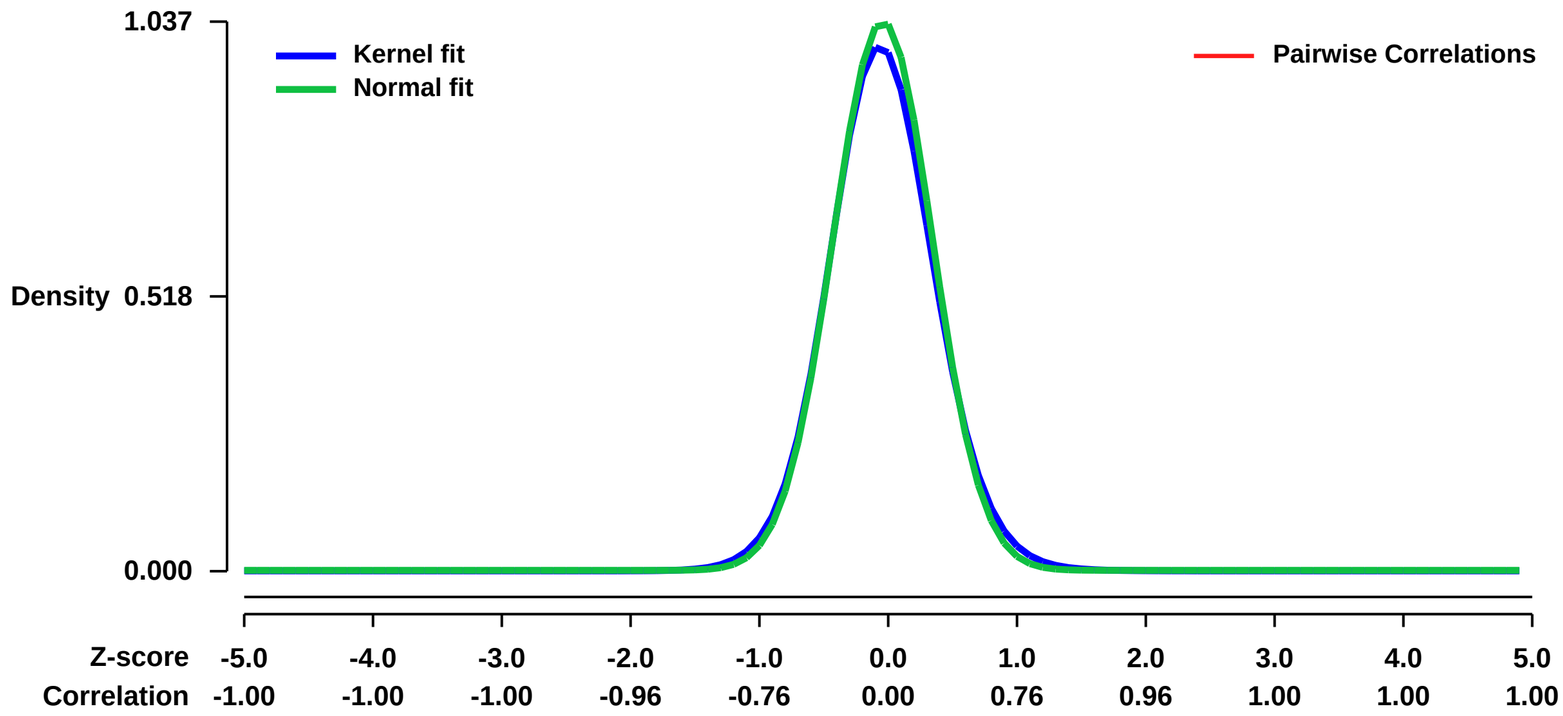

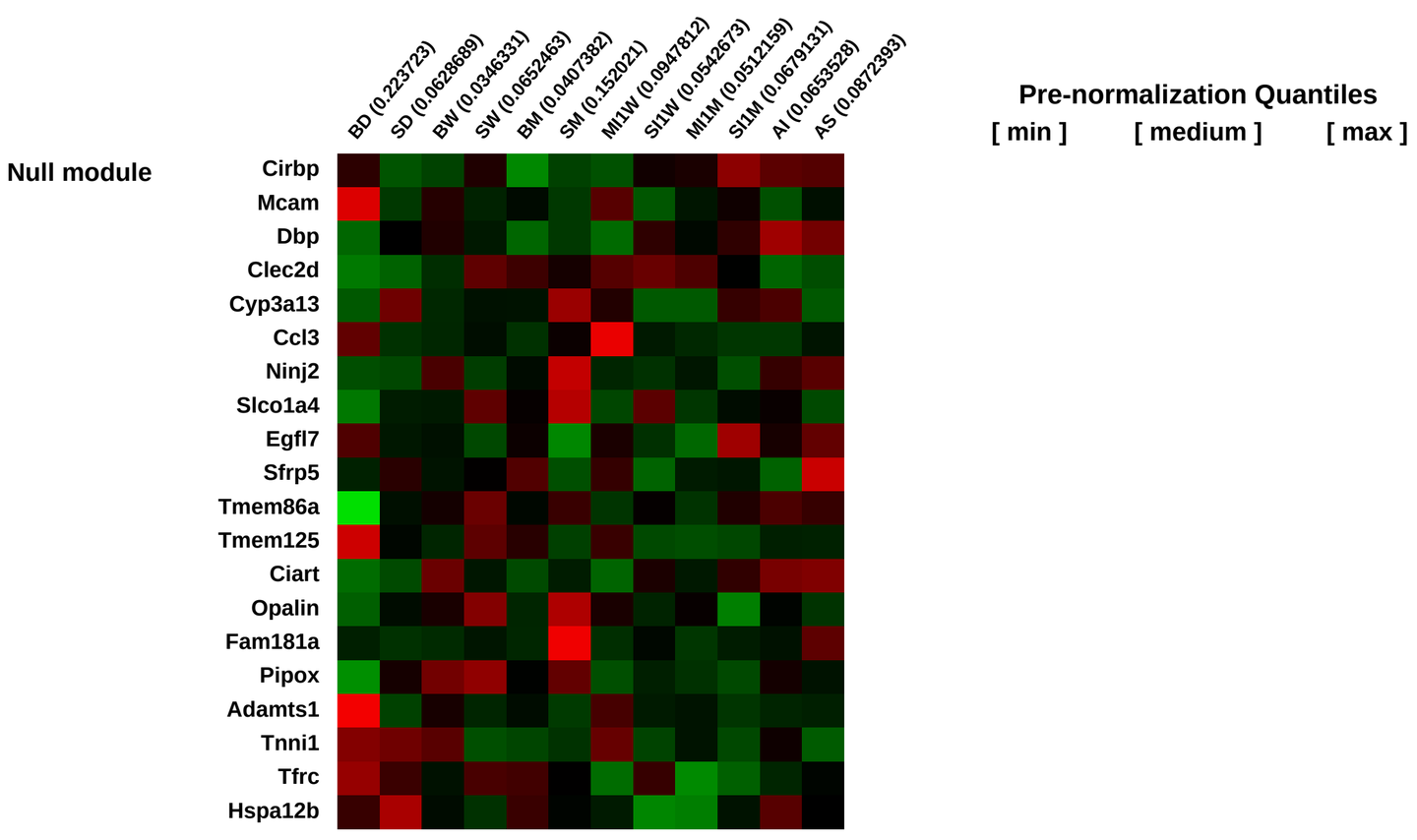

GEO Series "GSE8660" Expression Profiles

Num of samples in this series: 6

Scale of expression profile Z-scores

-3.0 -2.0 -1.0 0.0 1.0 2.0 3.0

GEO Link:	http://www.ncbi.nlm.nih.gov/geo/query/acc.cgi?acc=GSE8660
Status:	Public on Aug 01 2008
Title:	C-terminal diversity within the p53 family accounts for differences in DNA binding and transcriptional activity
Organism:	Mus musculus
Experiment type:	Expression profiling by array
Platform:	GPL1261
Pubmed ID:	18267967
Summary & Design:	**Summary:** The p53 family is known as a family of transcription factors with functions in tumor suppression and development. Whereas the central DNA binding domain is highly conserved among the three family members p53, p63 and p73, the C-terminal domains (CTDs) are diverse and subject to alternative splicing and post-translational modification. Here we demonstrate that the CTDs strongly influence DNA binding and transcriptional activity. While p53 and the p73 isoform p73gamma have basic CTDs and form weak sequence-specific protein-DNA complexes, the major p73 isoforms alpha, beta and delta have neutral CTDs and bind DNA strongly. A basic CTD has been previously shown to enable sliding along the DNA backbone and to facilitate the search for binding sites in the complex genome. Our experiments, however, reveal that a basic CTD also reduces protein-DNA complex stability, intranuclear mobility, promoter occupancy in vivo, transgene activation and induction of cell cycle arrest or apoptosis. A basic CTD in p53 and p73gamma therefore provides both positive and negative regulatory functions presumably to enable rapid switching of protein activity in response to stress. In contrast, most p73 isoforms exhibit constitutive DNA binding activity consistent with a predominant role in developmental control. **Keywords:** Adenoviros, p73 / p53 **Overall design:** Infection of H1299 cell with different p73/p53 constructs by adenoviral system

Background corr dist: KL-Divergence = 0.0374, L1-Distance = 0.0263, L2-Distance = 0.0008, Normal std = 0.6403

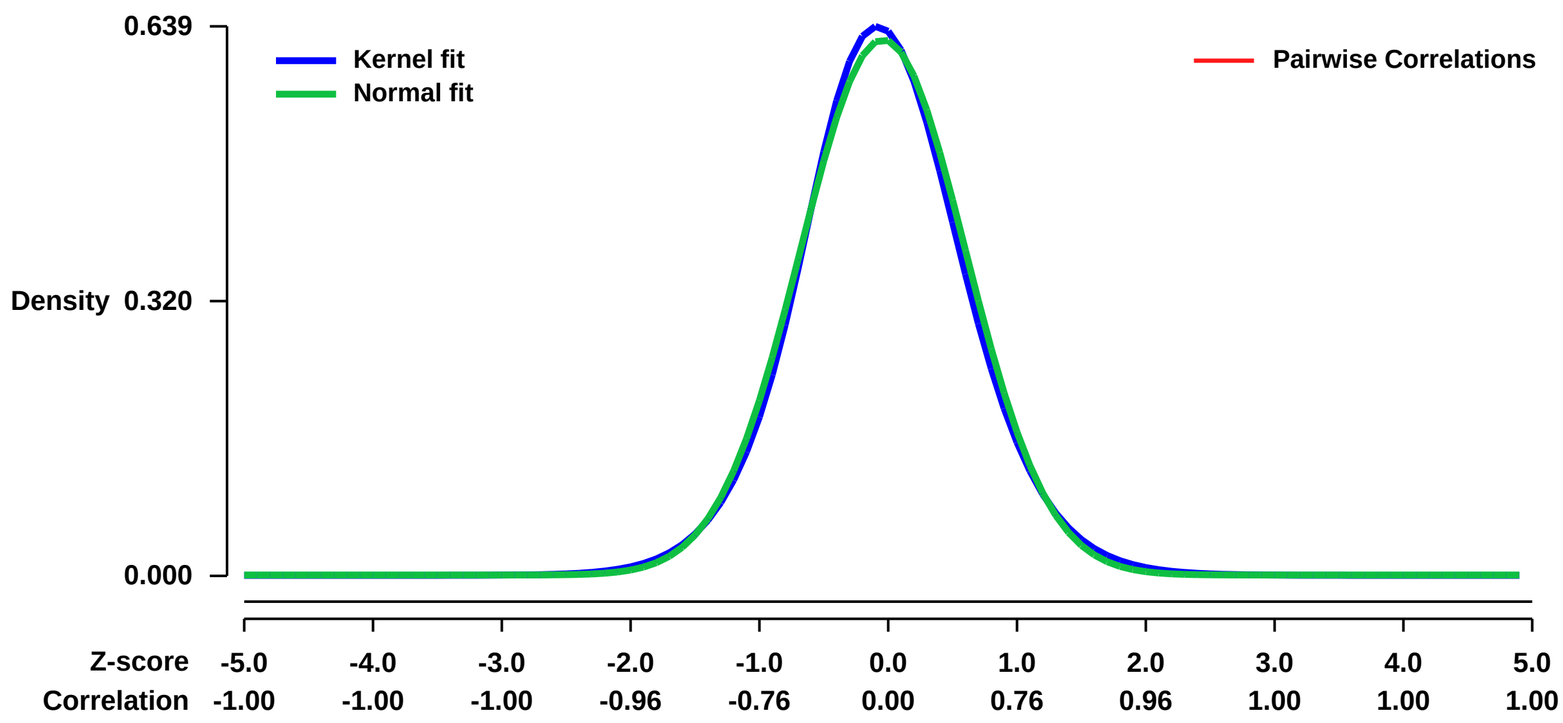

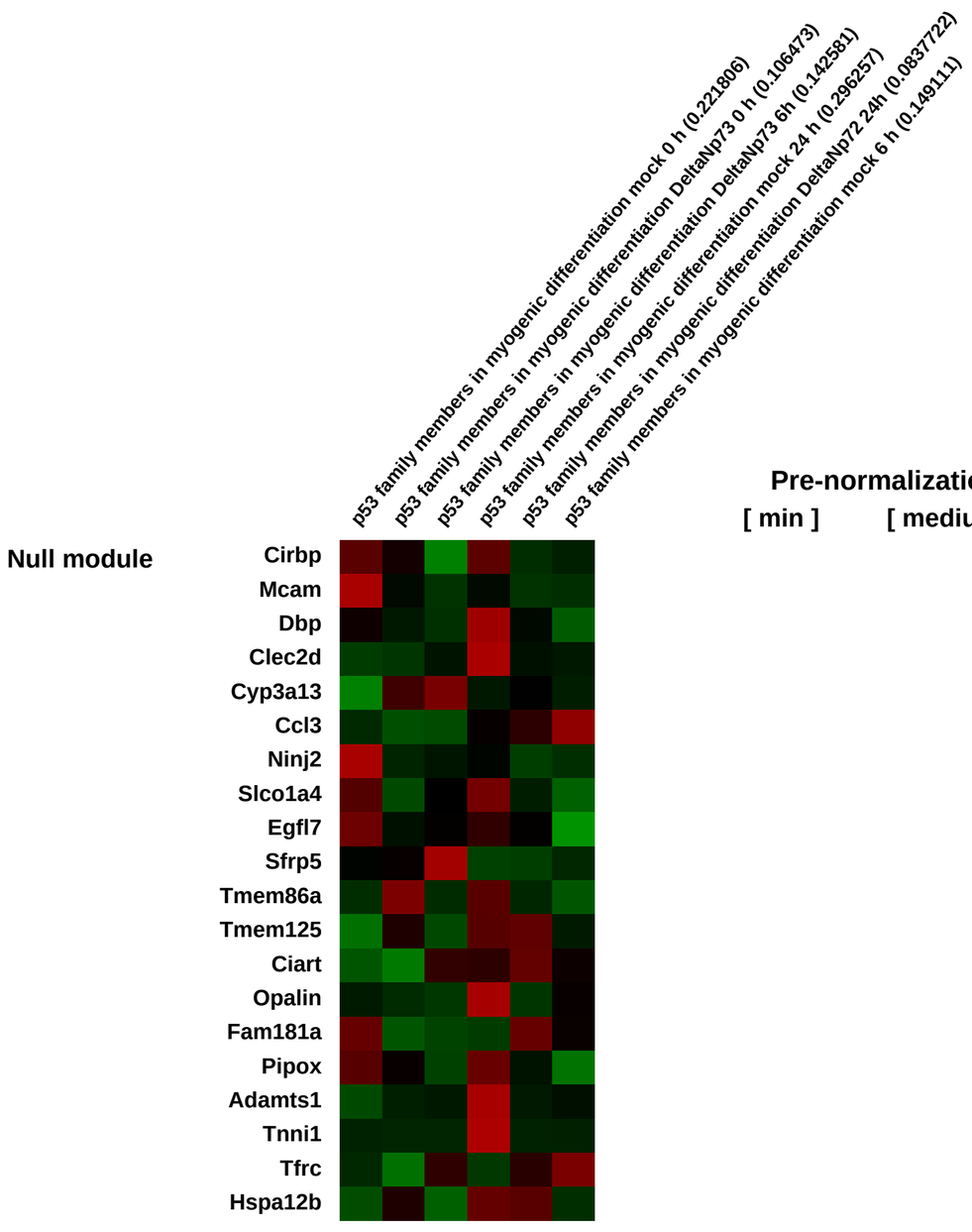

GEO Series "GSE55738" Expression Profiles

Num of samples in this series: 6

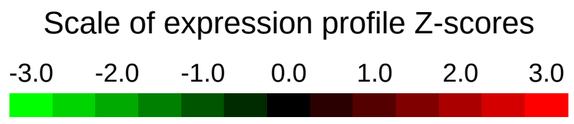

GEO Link:	**http://www.ncbi.nlm.nih.gov/geo/query/acc.cgi?acc=GSE55738**
Status:	**Public on Jun 08 2014**
Title:	**Expression data from chemically-induced skin papillomas (benign tumours)**
Organism:	**Mus musculus**
Experiment type:	**Expression profiling by array**
Platform:	**GPL1261**
Pubmed ID:	

Summary & Design:

Summary:
Cancer stem cells (CSCs) have been reported in various cancers including skin squamous cell carcinoma (SCC). The molecular mechanisms regulating tumour initiation and stemness are still poorly characterized. Here, we found that Sox2, a transcription factor expressed in various types of embryonic and adult stem cells (SCs), was the most upregulated transcription factor in CSCs of squamous skin tumours. Sox2 is absent in normal epidermis and begins to be expressed in the vast majority of mouse and human pre-neoplastic skin tumours and continues to be expressed in a heterogeneous manner in invasive mouse and human SCCs. In contrast to other SCCs, in which Sox2 is frequently genetically amplified, the expression of Sox2 in mouse and human skin SCCs is transcriptionally regulated. Conditional deletion of Sox2 in the mouse epidermis dramatically decreases skin tumour formation following chemical induced carcinogenesis. Using Sox2-GFP knockin mice, we showed that Sox2 expressing cells in invasive SCC are greatly enriched in tumour propagating cells (TPCs) that further increase upon serial transplantations. Lineage ablation of Sox2 expressing cells within primary benign and malignant SCCs leads to tumour regression, consistent with the critical role of Sox2 expressing cells in tumour maintenance. Conditional Sox2 deletion in pre-existing skin papilloma and SCC leads to their regression and decreases their ability to be propagated upon transplantation into immunodeficient mice, supporting the essential role of Sox2 in regulating CSC functions. Transcriptional profiling of Sox2-GFP expressing CSC and upon Sox2 deletion uncovered a gene network regulated by Sox2 in primary tumour cells in vivo. Chromatin immunoprecipitation identified several direct Sox2 target genes controlling tumour stemness, survival, proliferation, adhesion, invasion, and paraneoplastic syndrome. Altogether, our study demonstrates that Sox2, by marking and regulating the functions of skin tumour initiating cells and CSCs, establishes a continuum between tumour initiation and progression in primary skin tumours.

We used microarrays to profile tumour epithelial cells upon Sox2 deletion to uncover a gene network regulated by Sox2 in primary tumour cells in vivo.

Overall design:
Microarray analysis was performed on FACS isolated Epcam+ a6+ TECs from 3 different biological experiments following TAM administration to K14CREER:SOX2fl/fl and control mice. Total RNA was analysed using Mouse whole genome 430 2.0 array from Affymetrix.

Background corr dist: **KL-Divergence = 0.0382, L1-Distance = 0.0141, L2-Distance = 0.0002, Normal std = 0.6180**

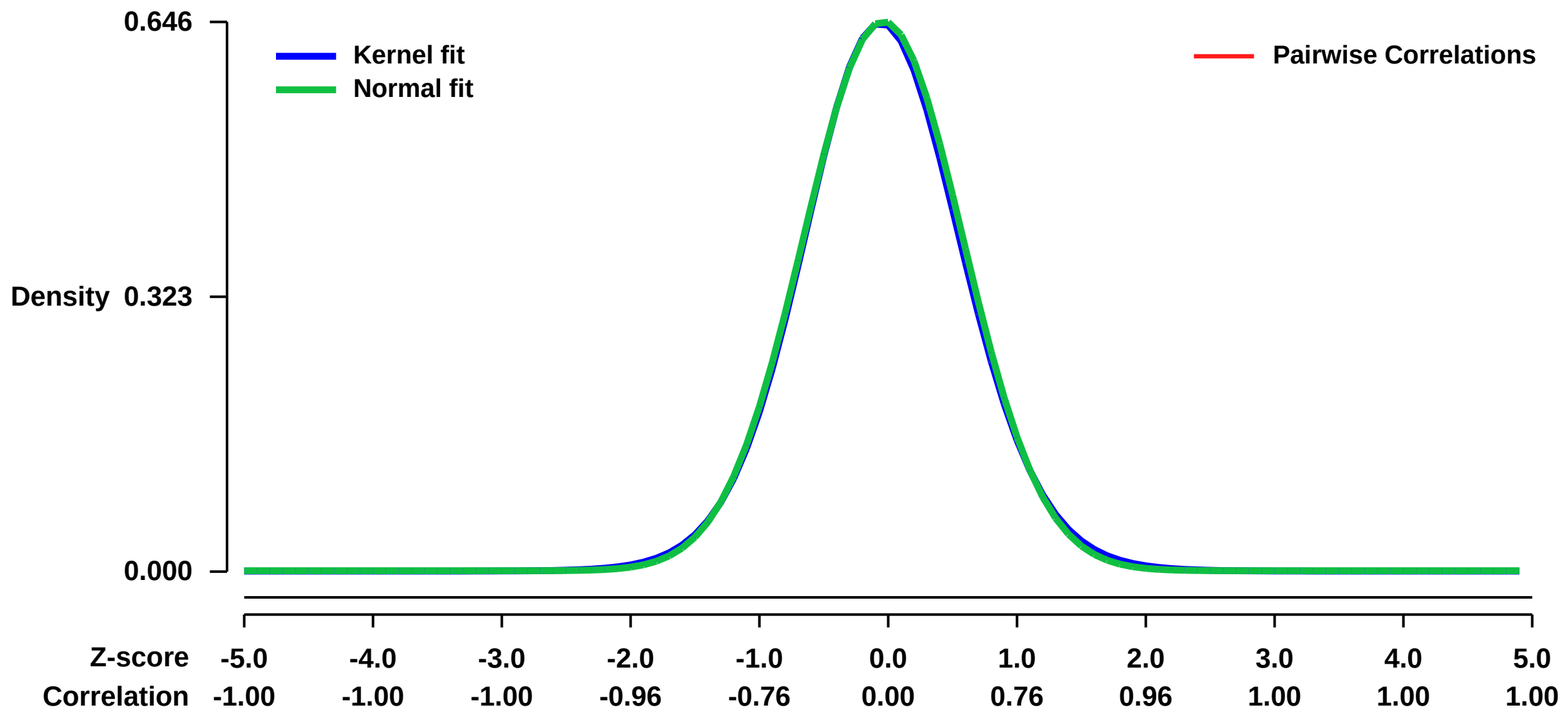

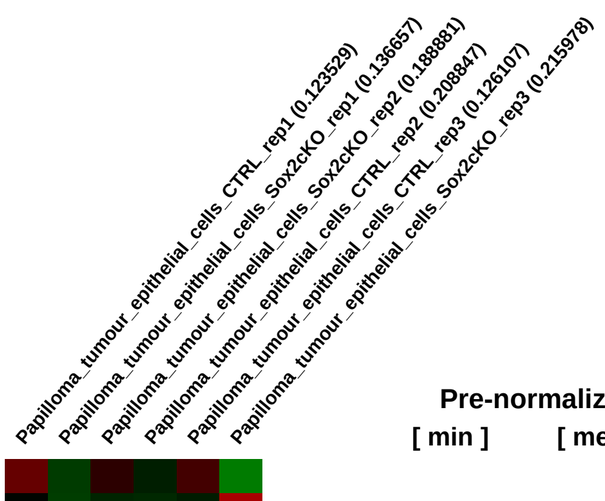

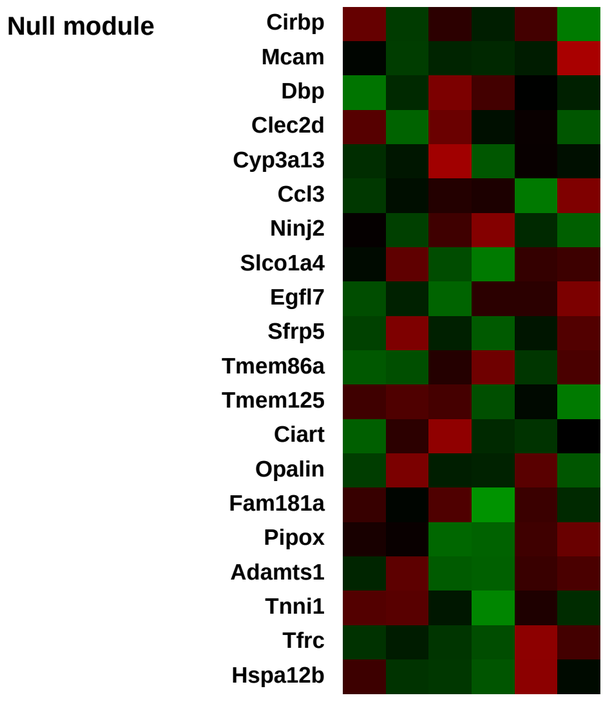

GEO Series "GSE44356" Expression Profiles

Num of samples in this series: 18

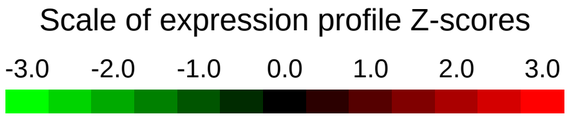

GEO Link:	http://www.ncbi.nlm.nih.gov/geo/query/acc.cgi?acc=GSE44356
Status:	Public on Aug 24 2013
Title:	Expression data from wild-type and HMGN1 knockout mice injected with N-nitrosodiethylamine
Organism:	Mus musculus
Experiment type:	Expression profiling by array
Platform:	GPL1261
Pubmed ID:	24296759
Summary & Design:	**Summary:** HMGN1 contributes to the shortened latency of liver tumorigenesis by changing a chromatin structure and expression of relevant genes To assess the molecular mechanisms underlying accelerated tumor development in Hmgn1-/- mice, we performed the gene expression profiling of liver cells at early stages **Overall design:** Expression profiles has been compared between Hmgn1+/+ and Hmgn1-/- mice livers at 4 weeks after birth and at 12 weeks after DEN or saline (control) injection at 4 weeks

Background corr dist: KL-Divergence = 0.2569, L1-Distance = 0.0562, L2-Distance = 0.0079, Normal std = 0.2990

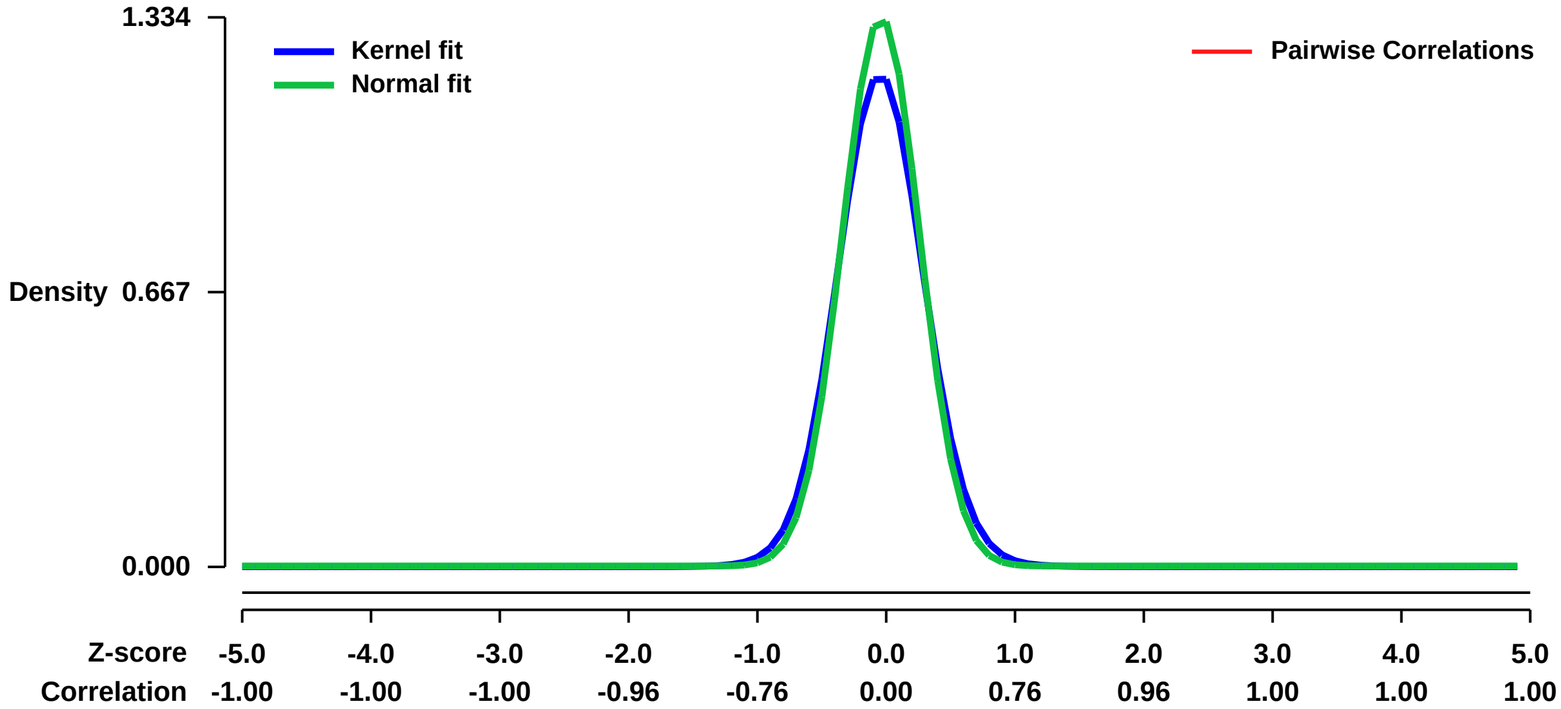

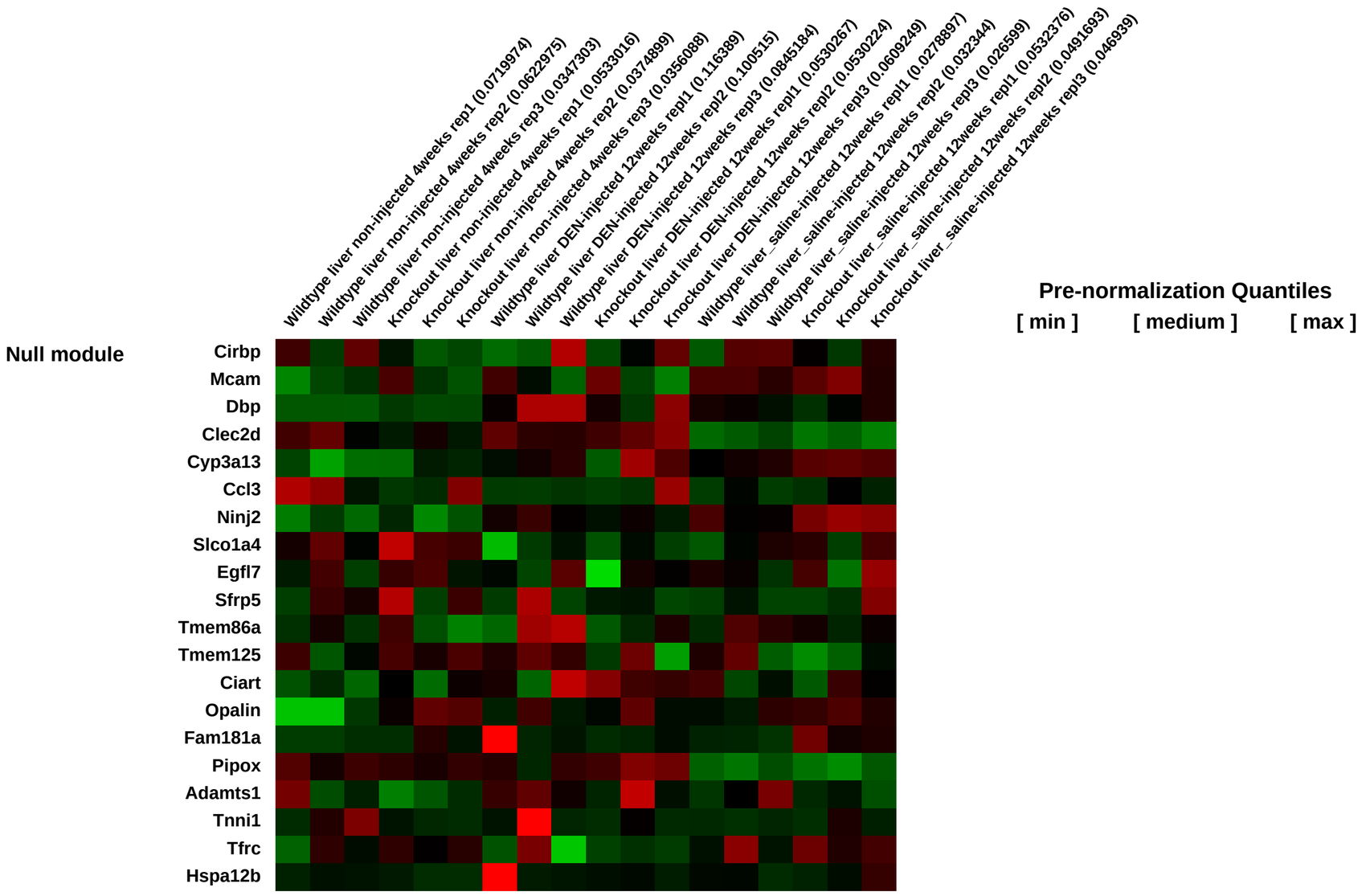

GEO Series "GSE53916" Expression Profiles

Num of samples in this series: 6

Scale of expression profile Z-scores

-3.0 -2.0 -1.0 0.0 1.0 2.0 3.0

GEO Link:	http://www.ncbi.nlm.nih.gov/geo/query/acc.cgi?acc=GSE53916
Status:	Public on Feb 17 2014
Title:	Expression data from mouse bone marrow cells expressing renin driven expression of green fluorescent protein.
Organism:	Mus musculus
Experiment type:	Expression profiling by array
Platform:	GPL1261
Pubmed ID:	24549417
Summary & Design:	**Summary:** Local renin antiotensin systems have been identified for many extra-renal sites. Bone marrow has been proposed as one such site, although the nature of the renin-expressing cell type(s) has not been established. Affymetrix microarrays were used to characterize the expression profile of renin-expressing GFP positive cells. **Overall design:** Green fluorescent protein positive cells were sorted from whole bone marrow collected from adult transgenic mice. Bone marrow from several mice was collected and pooled on the day of a FACS sort. A portion of this was reserved for RNA extraction while the remainder was sorted. RNA was prepared with Trizol. Bone marrow collection and sorting was performed 3 times so that microarrays could be run in triplicate.

Background corr dist: KL-Divergence = 0.0206, L1-Distance = 0.0262, L2-Distance = 0.0007, Normal std = 0.7706

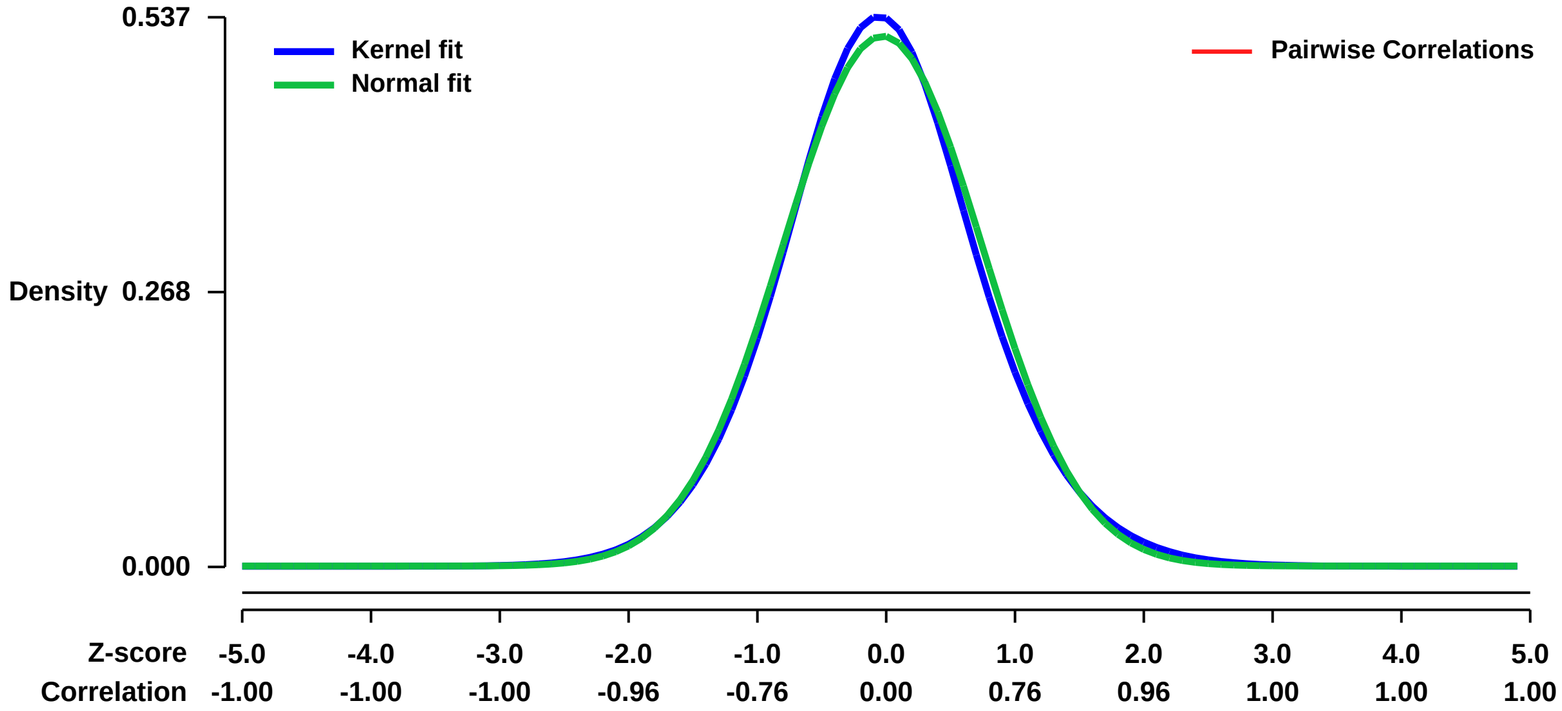

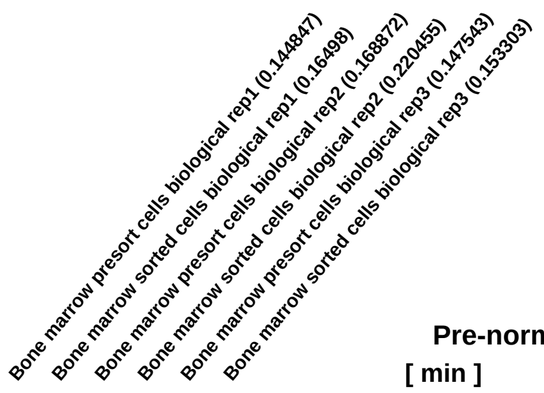

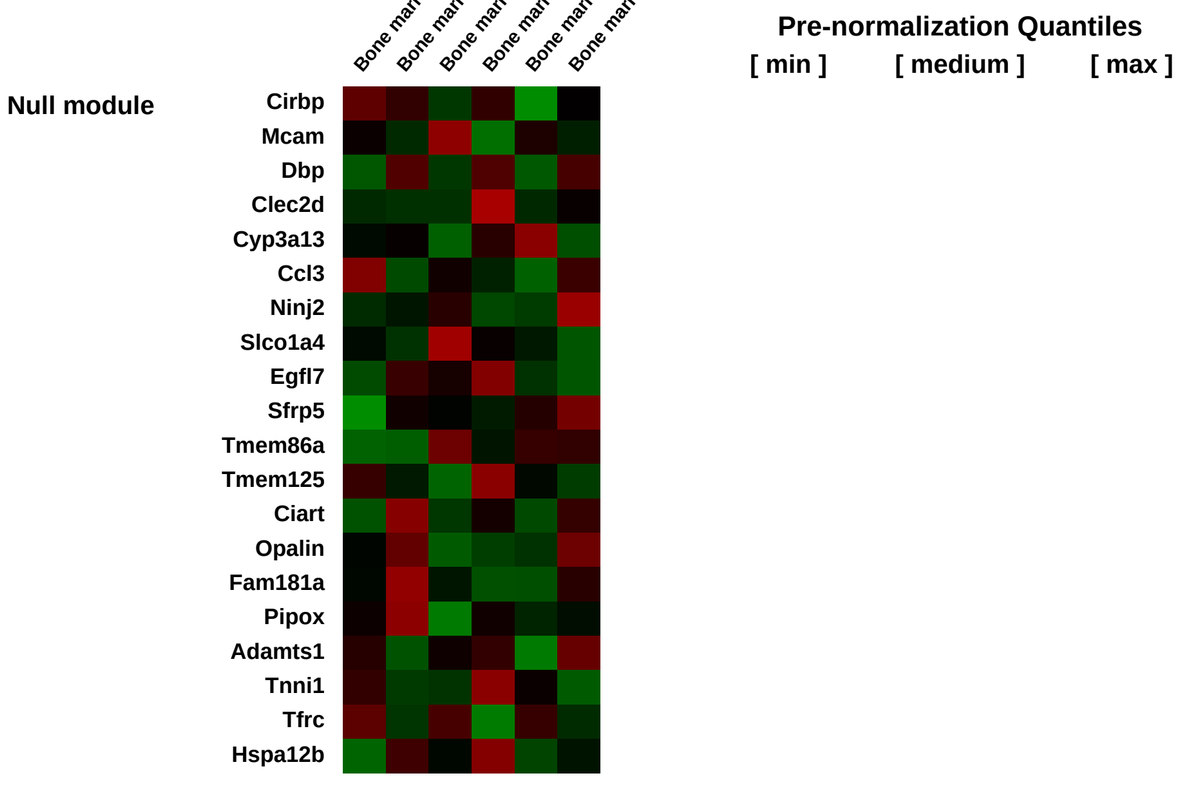

GEO Series "GSE20391" Expression Profiles

Num of samples in this series: 11

Scale of expression profile Z-scores

-3.0 -2.0 -1.0 0.0 1.0 2.0 3.0

GEO Link:	http://www.ncbi.nlm.nih.gov/geo/query/acc.cgi?acc=GSE20391
Status:	Public on Jun 16 2010
Title:	Comprehensive expression profiling across primary fetal liver terminal erythroid differentiation
Organism:	Mus musculus
Experiment type:	Expression profiling by array
Platform:	GPL1261
Pubmed ID:	20231426
Summary & Design:	**Summary:** Primary murine fetal liver cells were freshly isolated from day e14.5 livers and then sorted for successive differentiation stages by Ter119 and CD71 surface expression (ranging from double-negative CFU-Es to Ter-119 positive enucleated erythrocytes) [Zhang, et al. Blood. 2003 Dec 1; 102(12):3938-46]. RNA isolated from each freshly isolated, stage-sorted population was reverse-transcribed, labelled, and then hybridized onto 3' oligo Affymetrix arrays. Important erythroid specific genes as well as the proteins that regulate them were elucidated through this profiling based on coexpression and differential expression patterns as well as by extracting specific GO categories of genes (such as DNA-binding proteins). **Overall design:** Gene-targeting experiments report that the homeodomain-interacting protein kinases 1 and 2, Hipk1 and Hipk2, are essential but redundant in hematopoietic developmentâ because Hipk1/Hipk2 double-deficient animals exhibit severe defects in hematopoiesis and vasculogenesis while the single knockouts do not. These serine-threonine kinases phosphorylate, and consequently modify the functions of, several important hematopoietic transcription factors and cofactors. Here we show that Hipk2 knockdown alone plays a significant role in terminal fetal liver erythroid differentiation. Hipk1 and Hipk2 are highly induced during primary mouse fetal liver erythropoiesis. Specific knockdown of Hipk2 inhibits terminal erythroid cell proliferationâ explained in part by impaired cell cycle progression as well as increased apoptosisâ and terminal enucleation as well as the accumulation of hemoglobin. Hipk2 knockdown also reduces the transcription of many genes involved in proliferation and apoptosis as well as important, erythroid-specific genes involved in hemoglobin biosynthesisâ such as alpha-globin and mitoferrin 1â demonstrating that Hipk2 plays an important role in some but not all aspects of normal terminal erythroid differentiation.

Background corr dist: KL-Divergence = 0.0629, L1-Distance = 0.0458, L2-Distance = 0.0040, Normal std = 0.5380

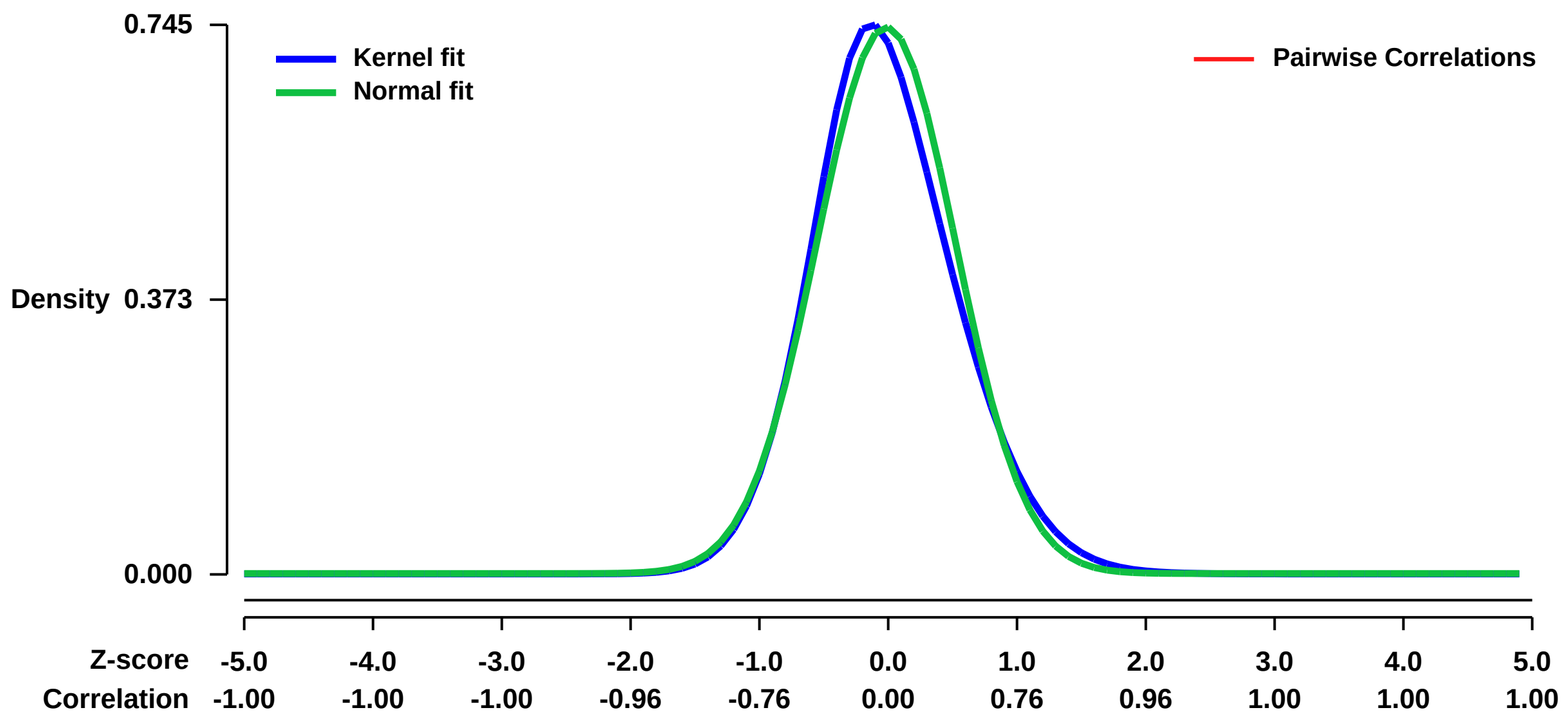

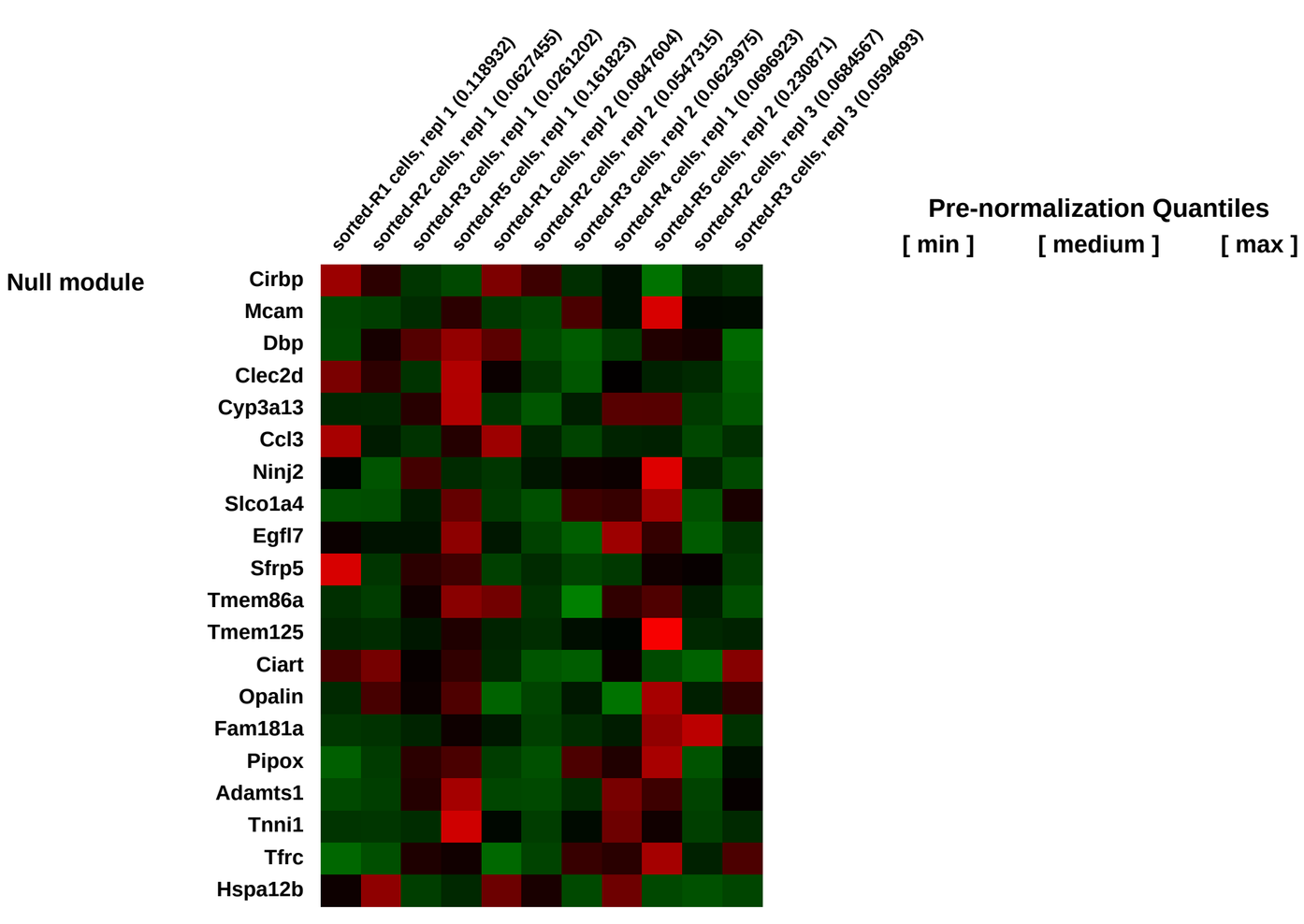

GEO Series "GSE13032" Expression Profiles

Num of samples in this series: 18

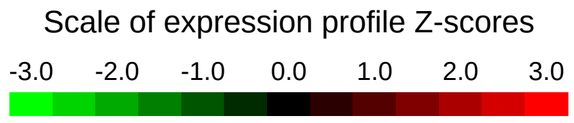

GEO Link:	http://www.ncbi.nlm.nih.gov/geo/query/acc.cgi?acc=GSE13032
Status:	Public on Oct 04 2008
Title:	The Effects of Resiquimod Treatment on the Asthma Transcriptome
Organism:	Mus musculus
Experiment type:	Expression profiling by array
Platform:	GPL1261
Pubmed ID:	19491150
Summary & Design:	**Summary:** Resiquimod is a nucleoside analog belonging to the imidazoquinoline family of compounds which is known to signal through Toll-like receptor 7. Resiquimod treatment has been demonstrated to inhibit the development of allergen induced asthma in experimental models. Despite this demonstrated effectiveness, little is known about the molecular events responsible for this effect. The aim of the present study was to elucidate the molecular processes which were altered following resiquimod treatment and antigen challenge in a mouse model of allergic asthma. Employing microarray analysis, we have characterized the â asthmaticâ transcriptome of the murine lung and determined that it includes genes involved in: the control of cell cycle progression, airway remodelling, the complement and coagulation cascades, and chemokine signalling. We have demonstrated that systemic resiquimod administration resulted in the recruitment of NK cells to the lungs of the mice, although no causal relationship between NK cell recruitment and treatment efficacy was found. Furthermore, results of our studies demonstrated that resiquimod treatment resulted in the normalization of the expression of genes involved with airway remodelling and chemokine signalling, and in the modulation of the expression of genes including cytokines and chemokines, adhesion molecules, and B-cell related genes, involved in several aspects of immune function and antigen presentation. Overall, our findings identified several genes, important in the development of asthma pathology, that were normalized following resiquimod treatment thus improving our understanding of the molecular consequences of resiquimod treatment in the lung milieu. **Keywords:** Disease and treatment state analysis **Overall design:** A total of 18 samples, from 6 sets of biological replicates, were analyzed. 9 A/J and 9 C57BL/6 mice were divided into three equal groups. All animals were sensitized to ovalbumin, one group received PBS aerosol challenges, the other two received 1% ovalbumin aerosol challenges. Of the two ovalbumin challenged groups, one recieved resiquimod 24hours before each challenge.

Background corr dist: KL-Divergence = 0.1972, L1-Distance = 0.0379, L2-Distance = 0.0027, Normal std = 0.3357

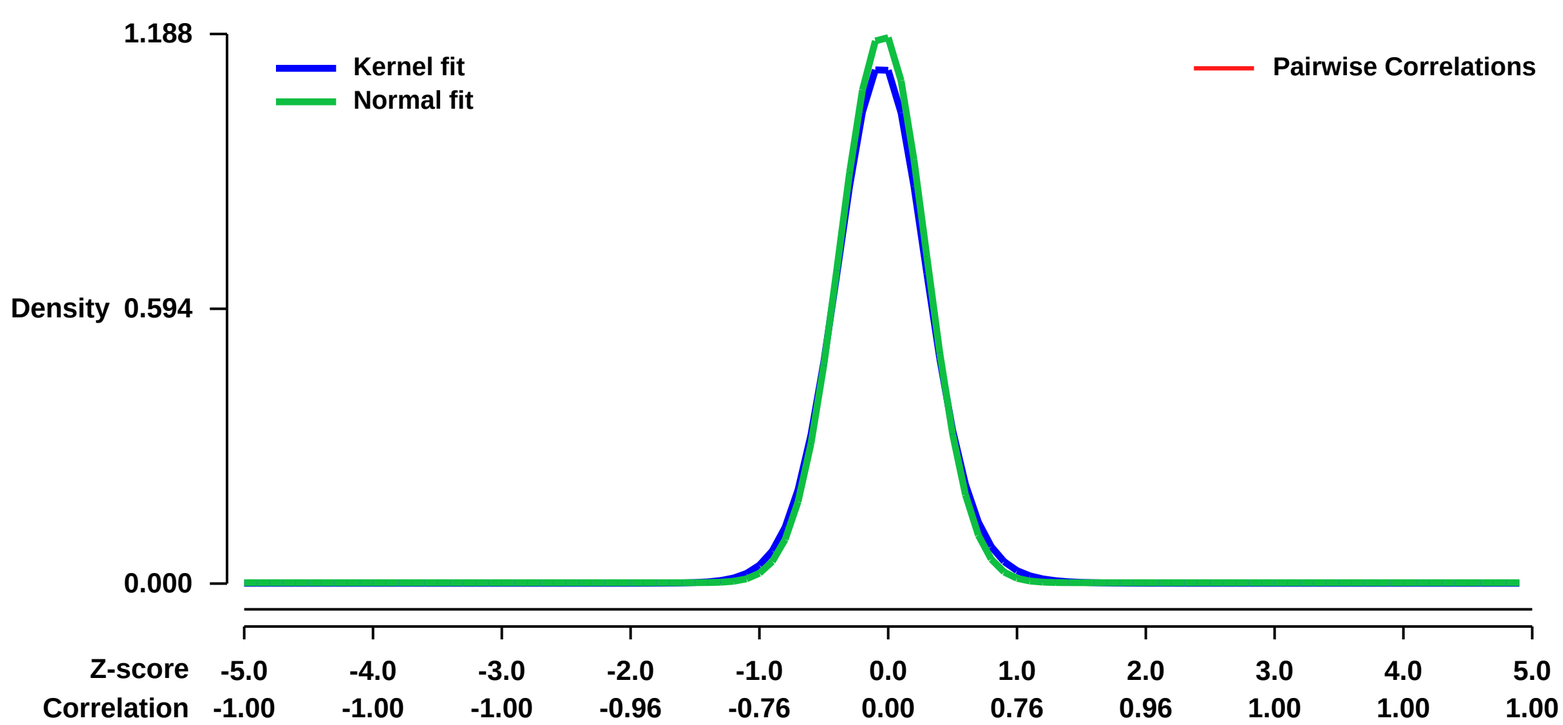

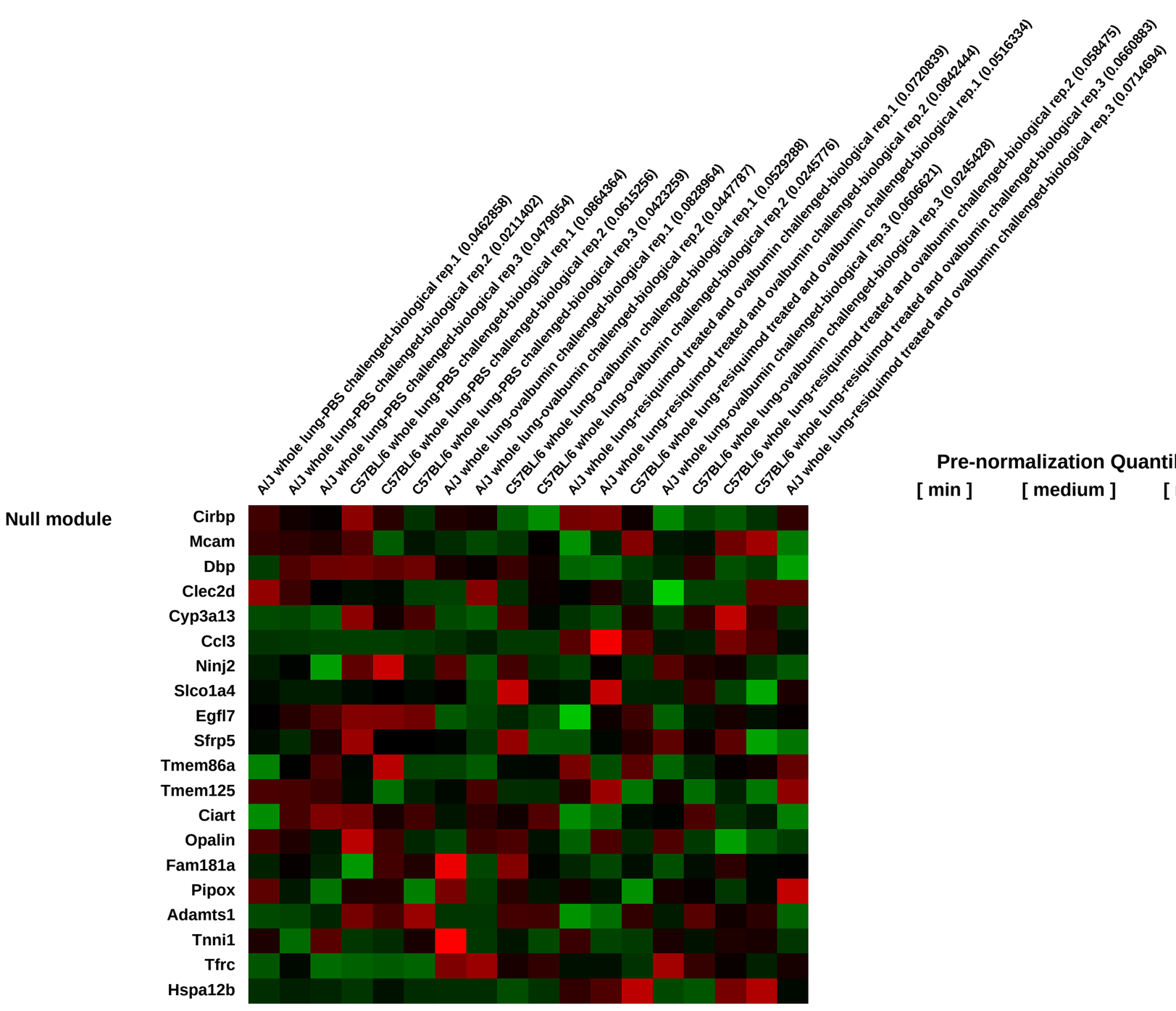

Null module

GEO Series "GSE13432" Expression Profiles

Num of samples in this series: 12

Scale of expression profile Z-scores

-3.0 -2.0 -1.0 0.0 1.0 2.0 3.0

GEO Link:	http://www.ncbi.nlm.nih.gov/geo/query/acc.cgi?acc=GSE13432
Status:	Public on Feb 01 2009
Title:	Adipose tissue exposed to cold
Organism:	Mus musculus
Experiment type:	Expression profiling by array
Platform:	GPL1261
Pubmed ID:	19117550
Summary & Design:	**Summary:** **Cold triggers VEGF dependent but hypoxia independent angiogenesis in adipose tissues and anti-VEGF agents modulate adipose metabolism** **The molecular mechanisms of angiogenesis in relation to adipose tissue metabolism remain poorly understood. Here we show that exposure of mice to cold led to conversion of white adipose tissue (WAT) to brown-like adipose tissue, accompanying the switch of an active angiogenic phenotype. Gene expression profile analysis showed VEGF was upregulated via most likely hypoxia-independent PGC-1 transcriptional activation. Intriguingly, VEGFR2 blockage abolished the cold-induced angiogenesis, significantly impaired nonshivering thermogenesis capacity, and markedly reduced adipose metabolism. Unexpectedly, VEGFR1 blockage resulted in opposite effects by increasing adipose vascularity and metabolism. These findings demonstrate that VEGFR2 and VEGFR1 mediate polarized activities in modulating adipose angiogenesis and metabolism. Taken together, our findings have conceptual implications in applying angiogenesis modulators for the treatment of obesity and metabolic disorders.** **Keywords: Time course** **Overall design:** **Mice were exposed to cold and white addipose tissue was collected at different time points**

Background corr dist: KL-Divergence = 0.0338, L1-Distance = 0.0273, L2-Distance = 0.0009, Normal std = 0.6614

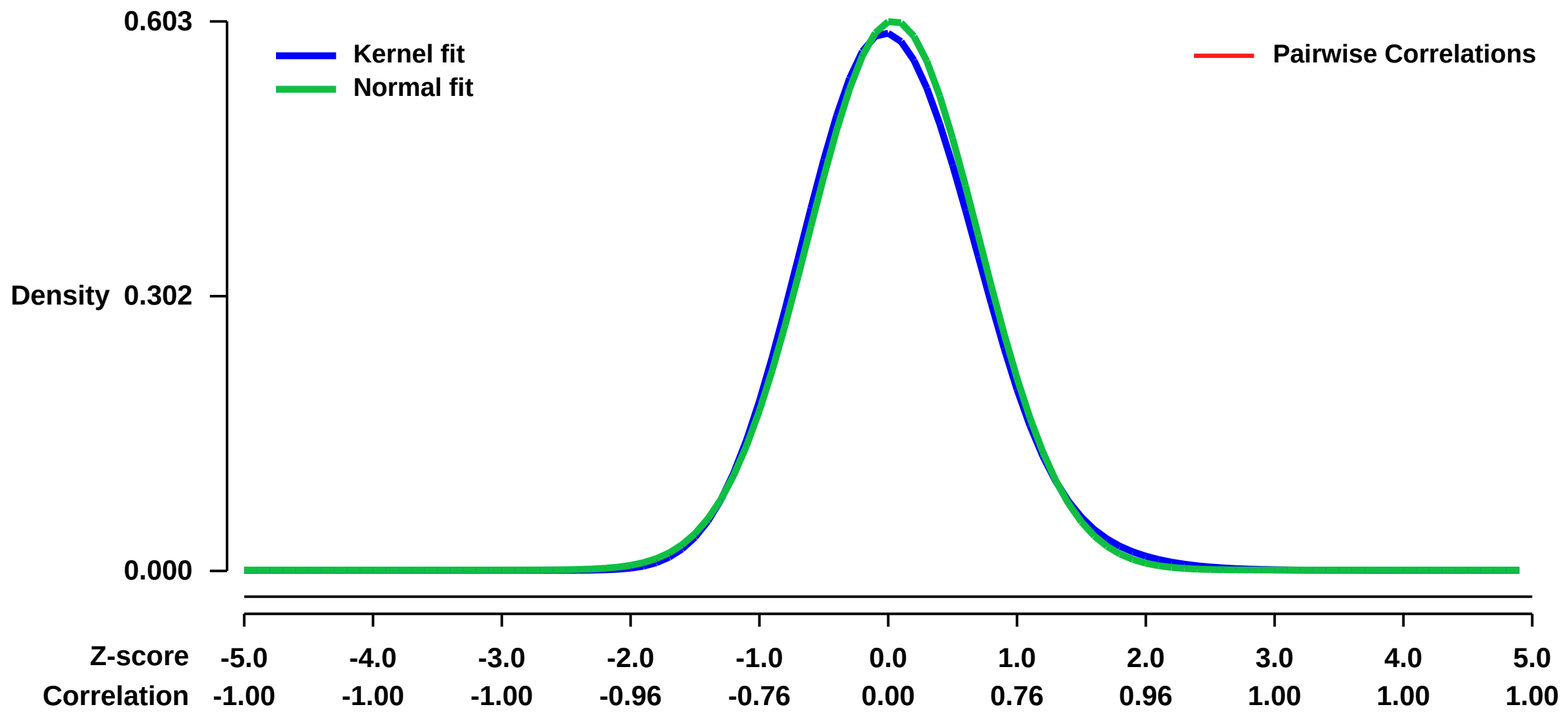

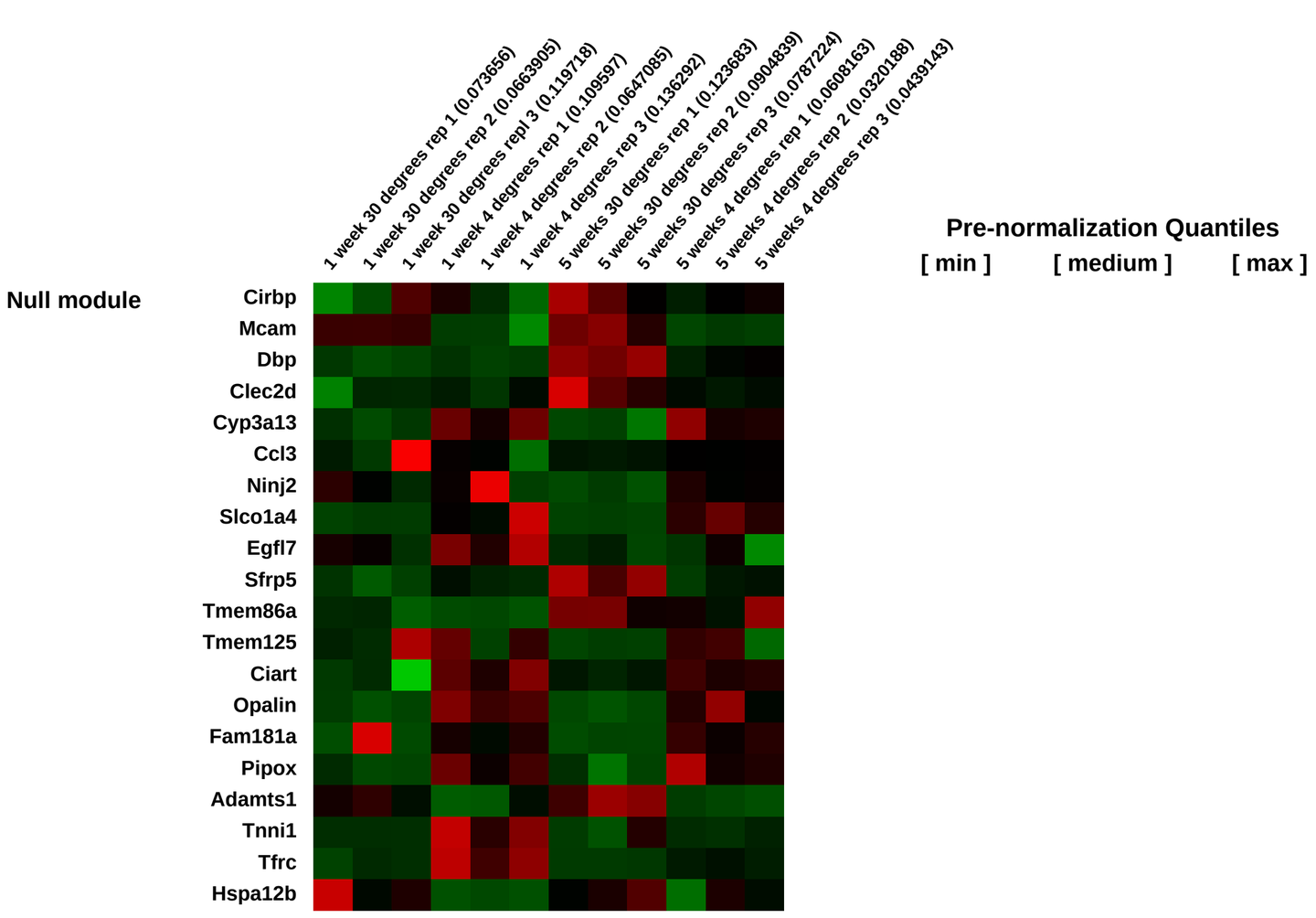

GEO Series "GSE28031" Expression Profiles

Num of samples in this series: 6

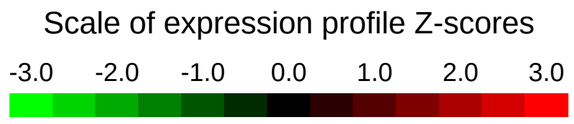

GEO Link:	**http://www.ncbi.nlm.nih.gov/geo/query/acc.cgi?acc=GSE28031**
Status:	**Public on Mar 18 2011**
Title:	**Microarray gene expression profiling of heart failure induced in apolipoprotein E-deficient mice by treatment with rosiglitazone**
Organism:	**Mus musculus**
Experiment type:	**Expression profiling by array**
Platform:	**GPL1261**
Pubmed ID:	
Summary & Design:	**Summary:** **The anti-diabetic drug and agonist of the peroxisome proliferator-activated receptor gamma (Pparg), rosiglitazone, was recently withdrawn in many countries because the drug use was associated with an increased risk of heart failure. To investigate underlying pathomechanisms, we chose 6-month-old apolipoprotein E (apoE)-deficient mice, which are prone to atherosclerosis and insulin resistance, and thereby mimic the risk profile of patients with cardiovascular disease. After 8 weeks of rosiglitazone treatment (30 mg/kg/day), echocardiography and histology analyses demonstrated that rosiglitazone had induced heart failure with cardiac dilation. Concomitantly, cardiac lipid overload and lipid-induced cardiomyocyte death developed. The microarray gene expression study of heart tissue from rosiglitazone-treated apoE-deficient mice relative to untreated apoE-deficient mice and non-transgenic B6 mice identified cardiac Pparg-dependent lipid metabolism genes in rosiglitazone-treated mice, which seem to trigger a major heart failure promoting pathway.** **Overall design:** **Microarray gene expression profiling was performed with heart tissue isolated from three study groups: (i) rosiglitazone-treated 8-month-old apolipoprotein (apoE)-deficient mice with symptoms of heart failure, (ii) untreated 8-month-old apoE-deficient mice, and (iii) age-matched, untreated, non-transgenic B6 control mice.**

Background corr dist: **KL-Divergence = 0.0373, L1-Distance = 0.0241, L2-Distance = 0.0006, Normal std = 0.6413**

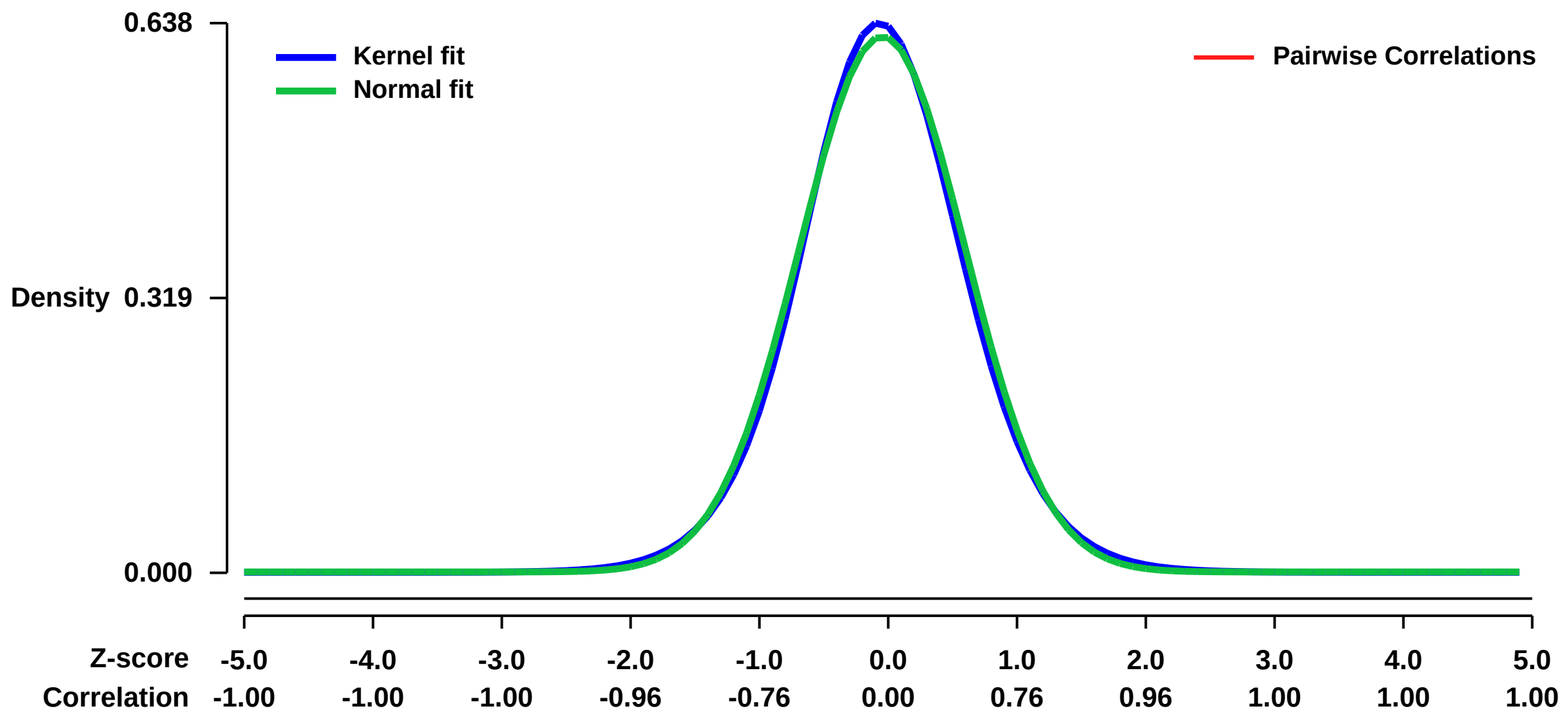

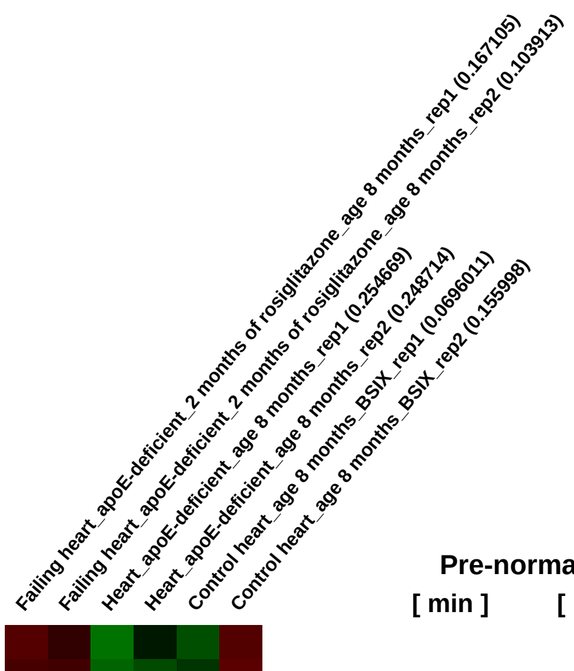

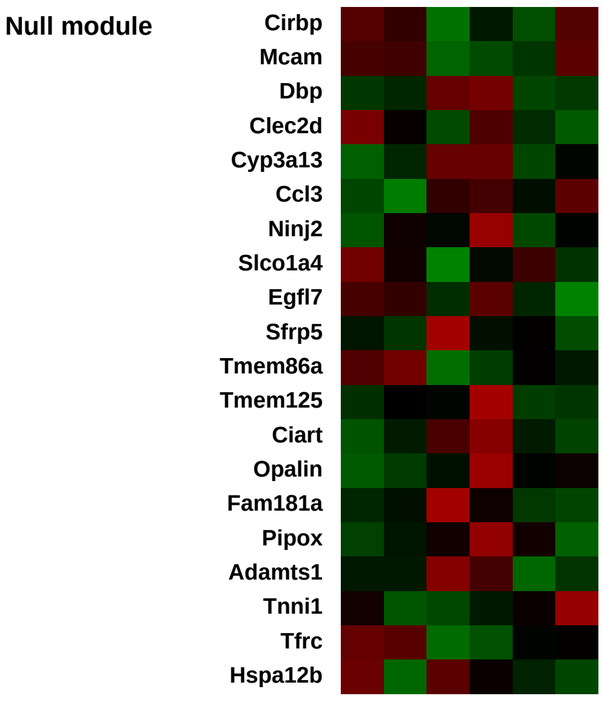

GEO Series "GSE26229" Expression Profiles

Num of samples in this series: 8

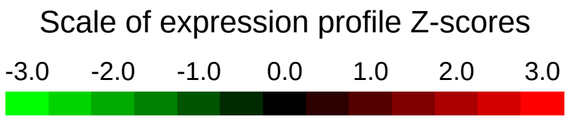

GEO Link:	http://www.ncbi.nlm.nih.gov/geo/query/acc.cgi?acc=GSE26229
Status:	Public on May 20 2011
Title:	Transcriptional profiling of ex vivo isolated inflammed mouse lymphatic endothelial cells
Organism:	Mus musculus
Experiment type:	Expression profiling by array
Platform:	GPL1261
Pubmed ID:	21596851
Summary & Design:	**Summary:** Chemokines and adhesion molecules upregulated in lymphatic endothelial cells (LECs) during tissue inflammation are believed to enhance dendritic cell (DC) migration to draining lymph nodes (dLNs), but the in vivo control of this process is not well understood. By performing transcriptional profiling of LECs isolated from murine skin, we found that inflammation induced by a contact hypersensitivity (CHS) response upregulated the adhesion molecules ICAM-1 and VCAM-1 and inflammatory chemokines in LECs. Furthermore, lymphatic lineage markers like Prox-1, VEGFR3 and LYVE-1 were significantly downregulated during CHS. By contrast, skin inflammation induced by Complete Freundâ s adjuvant (CFA) induced a different pattern of chemokine and lymphatic marker gene expression and almost no ICAM-1 up-regulation in LECs. In FITC painting experiments, DC migration to dLNs was more strongly increased in CFA- as compared to CHS-induced inflammation. Interestingly, DC migration did not correlate with the induction of CCL21 and ICAM-1 in LECs. However, the requirement for CCR7 signaling became further pronounced during inflammation, whereas CCR7-independent signals only had a minor role in enhancing DC migration. Collectively, these findings indicate that inflammation-induced DC migration is stimulus-dependent and only moderately enhanced by LEC-induced genes other than CCL21. **Overall design:** Mouse ear skin single-cell suspensions were prepared by a fast protocol that minimizes the RNA degradation. Fluorescence-activated cell sorting (FACS) was used to sort lymphatic endothelial cells (LEC) from CHS inflammed and control skin. 4 pairs (each with one control and one CHS inflammed sample, sorted and extracted on the same day) of LECs were chosen based on the quality of extracted and amplified material. This gave 8 samples to analyze (4 biological replicates in each condition). Each sample was sorted from 3 mice.

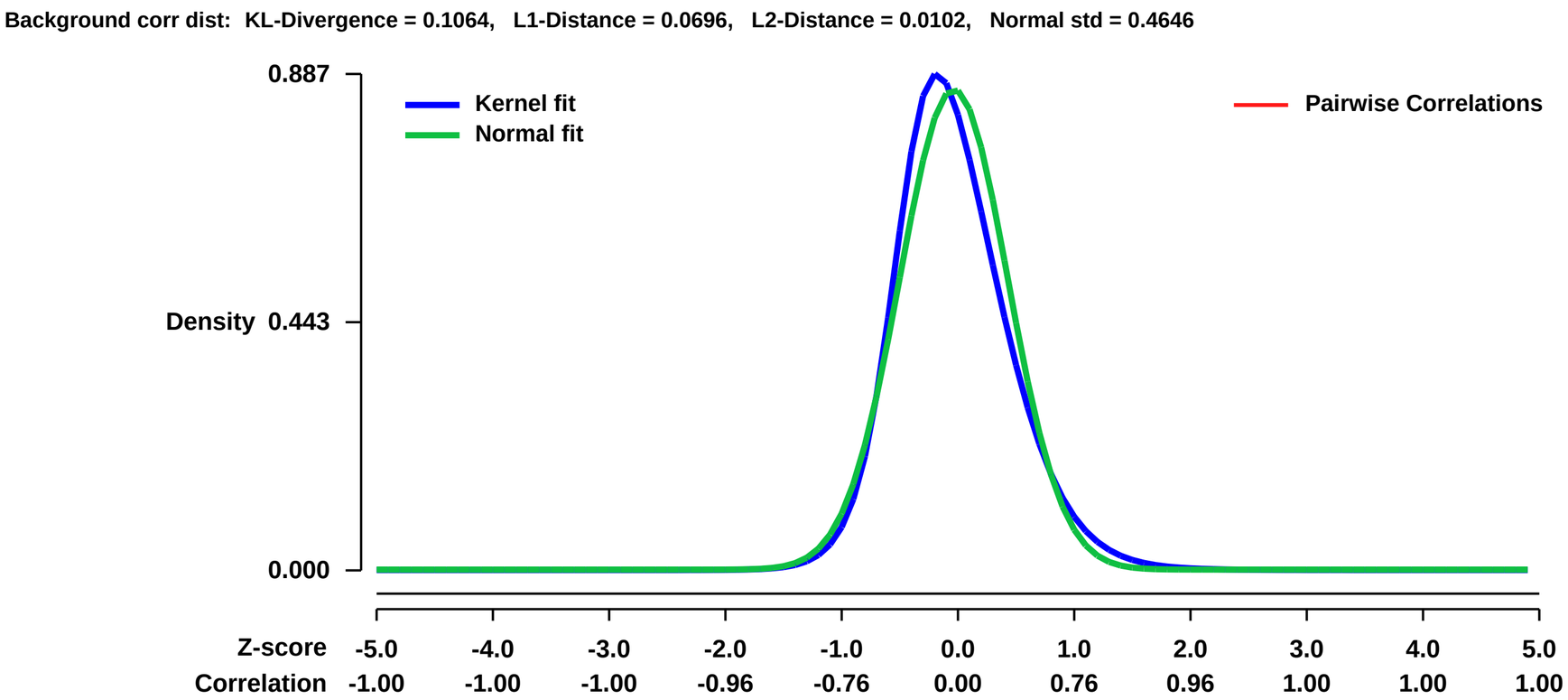

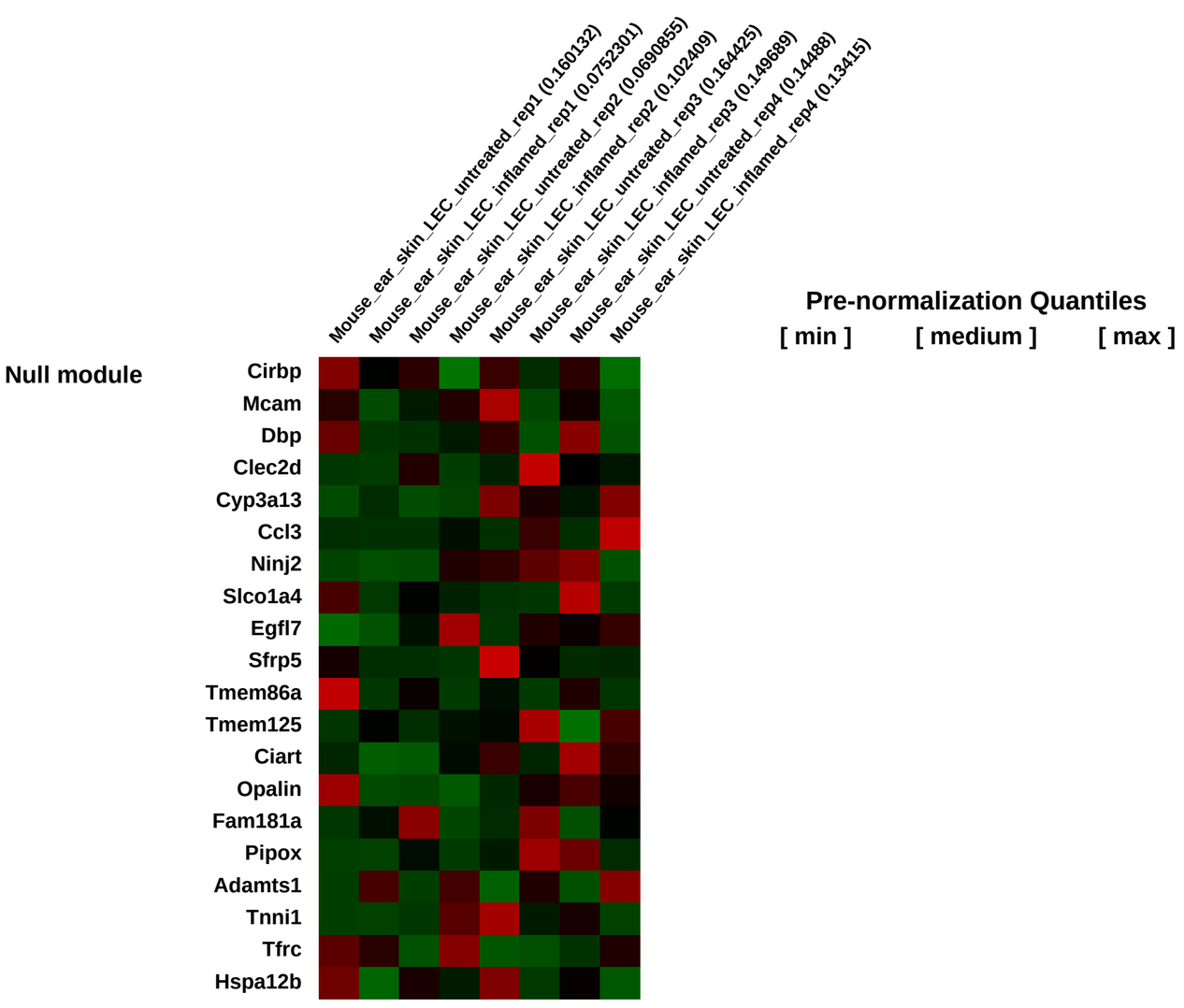

GEO Series "GSE50950" Expression Profiles

Num of samples in this series: 15

Scale of expression profile Z-scores

-3.0 -2.0 -1.0 0.0 1.0 2.0 3.0

GEO Link: http://www.ncbi.nlm.nih.gov/geo/query/acc.cgi?acc=GSE50950

Status: Public on Sep 18 2013

Title: Expression data from adult Shh-responding astroglia cells in mice

Organism: Mus musculus

Experiment type: Expression profiling by array

Platform: GPL1261

Pubmed ID:

Summary & Design:

Summary:
Sonic hedgehog (Shh) signals via Gli transcription factors to promote maintenance and proliferation of neural stem cells in the adult mouse forebrain. We have analyzed the gene expression pattern in neurogenic Shh-responding astroglia (= neural stem cells) in the subventicular zone of the lateral ventricle and dentate gyrus of the hippocampus in comparison to the non-neurogenic Shh-responding glia (=Bergman glia) in the cerebellum to identify the genes specifically involved in neurogenic function downstream of Shh signaling.

In this dataset, we include the expression data obtained from FACS-sorted Gli1+ GFAP+ cells from microdissected SVZ, hippocampus and cerebellum. GFAP expression is based on hGFAP-GFP reporter line and Gli1 expression is lineage marked using Gli1-CreER;ROSA26-tdTomato mice.

Overall design:
15 Total samples were analyzed. We compared expression levels of SVZ vs. Cerebellum, Hippocampus vs. Cerebelllum to identify genes which had more than 4 fold change in expression levels with p < 0.01. From this narrowed list, we compared between SVZ and Hippocampus to identify the common genes up and down regulated. In addition, we also identified commonly expressed genes in hippocampus and SVZ at high level.

Background corr dist: KL-Divergence = 0.1189, L1-Distance = 0.0684, L2-Distance = 0.0115, Normal std = 0.4285

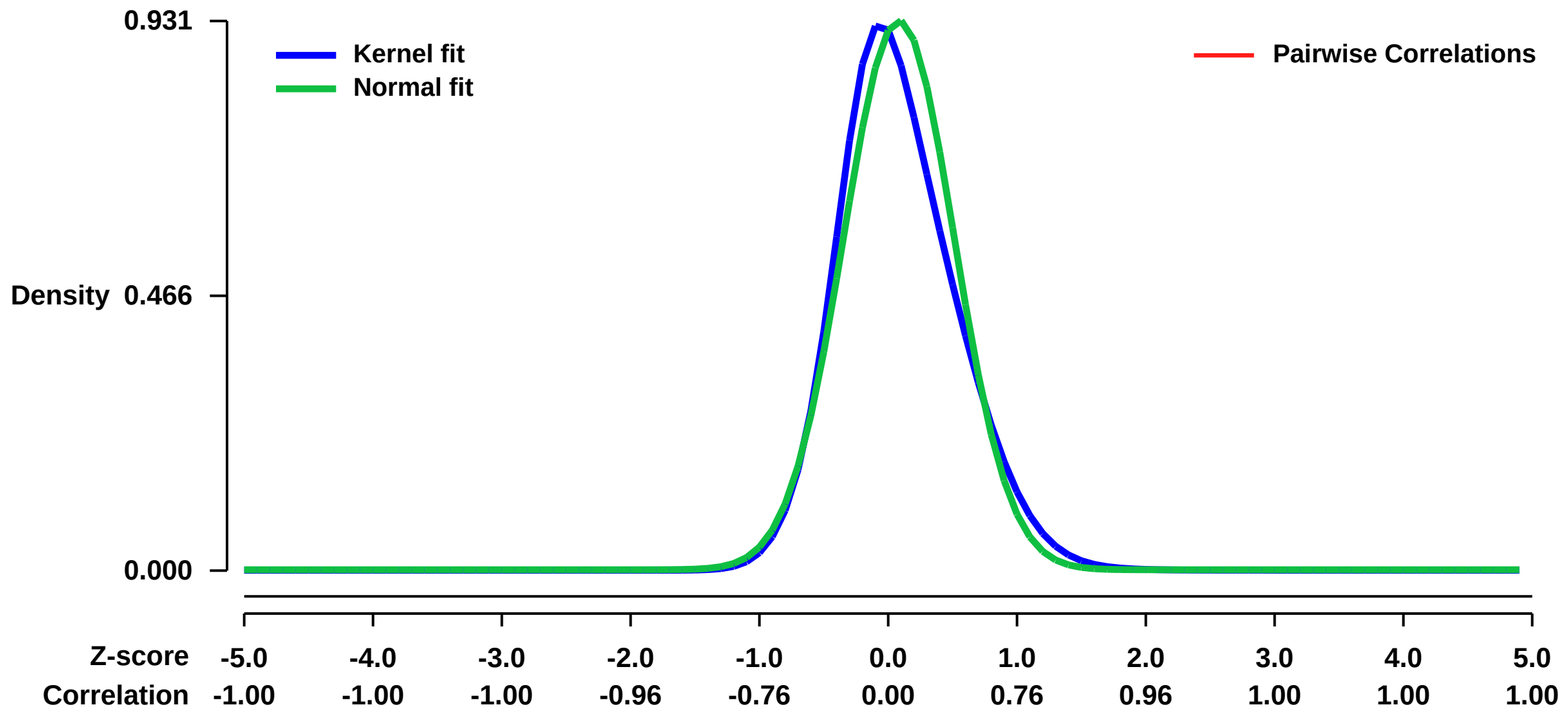

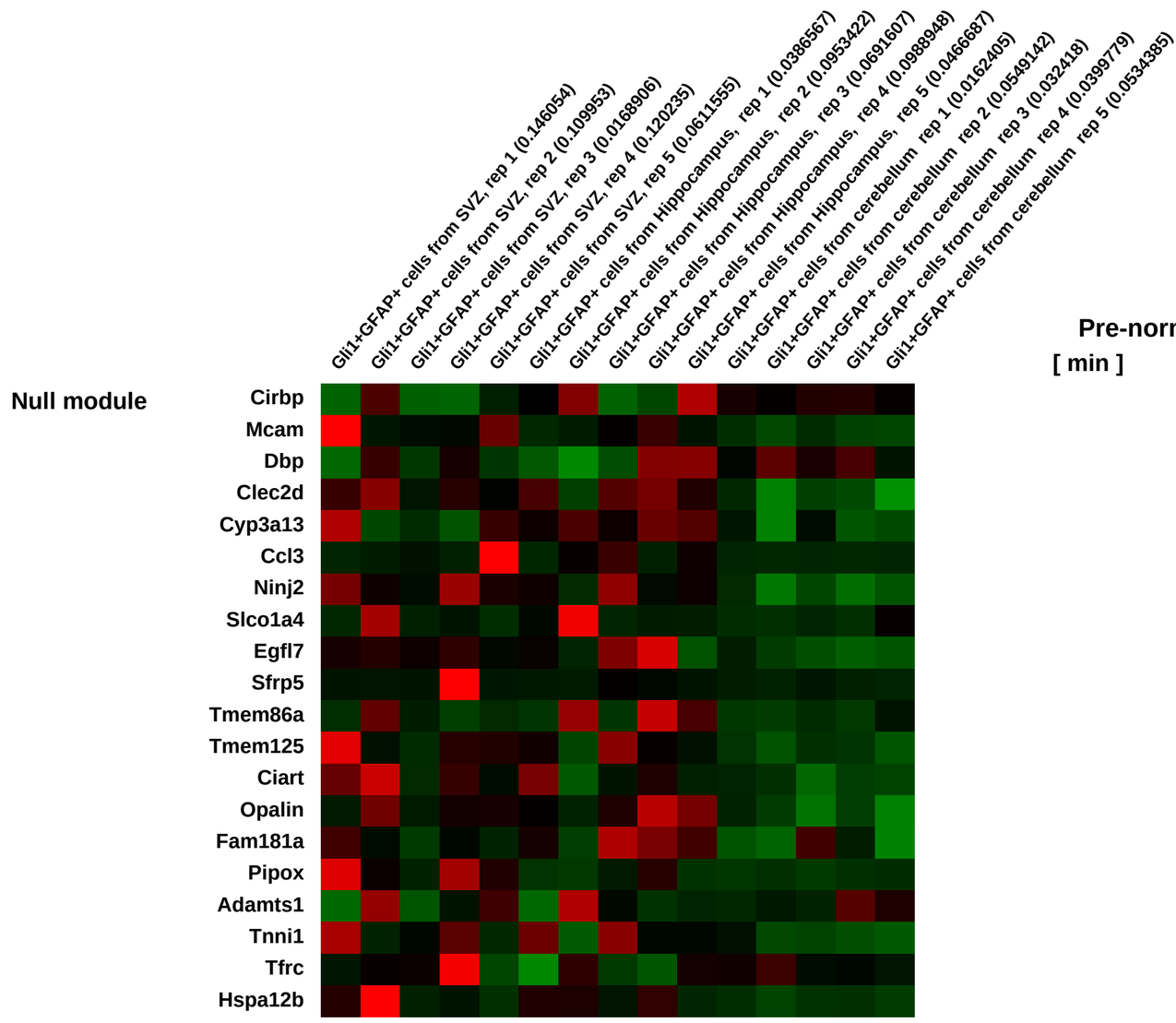

GEO Series "GSE39082" Expression Profiles

Num of samples in this series: 6

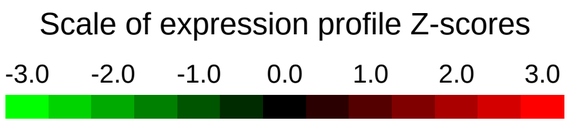

GEO Link:	**http://www.ncbi.nlm.nih.gov/geo/query/acc.cgi?acc=GSE39082**
Status:	**Public on Jul 04 2012**
Title:	**Expression data from cultured c-Kit+Sca-1+Lin- (KSL)cells**
Organism:	**Mus musculus**
Experiment type:	**Expression profiling by array**
Platform:	**GPL1261**
Pubmed ID:	
Summary & Design:	**Summary:** **The Notch signaling pathway plays a critical role in regulating the proliferation and differentiation of stem and progenitor cells including hematopoietic stem and progenitor cells (HSPCs). Notch receptors and ligands are expressed in BM stromal and hematopoietic cells. A large body of evidence has demonstrated that activating Notch signaling enhances HSCs self-renewal and facilitates its expansion ex vivo. We report that an endothelium-targeted soluble Notch ligand, the DSL domain of mouse Delta-like 1 fused with a RGD motif (mD1R), efficiently promotes the expansion ex vivo of mouse bone marrow HSPCs in a Notch signaling and endocytosis dependent manner. HSPCs expanded in the presence of mD1R kept long-term HSPC repopulation capacity.** **We used microarrays to compare the gene expression profiles of HSPCs expanded in the presence of PBS and mD1R.** **Overall design:** **KSL cells were plated on Human umbilical vein endothelial cells (HUVECs) and cultured in a serum-free medium supplemented with a cocktail containing 5 types of mouse cytokines (m5GF) in the presence of PBS or mD1R for 7 days. Then KSL cells were sorted from these cultured hematopoietic cells for RNA extraction and hybridization on Affymetrix microarrays. The experiments were repeated 3 times.**

Background corr dist: KL-Divergence = 0.0342, L1-Distance = 0.0284, L2-Distance = 0.0010, Normal std = 0.6605

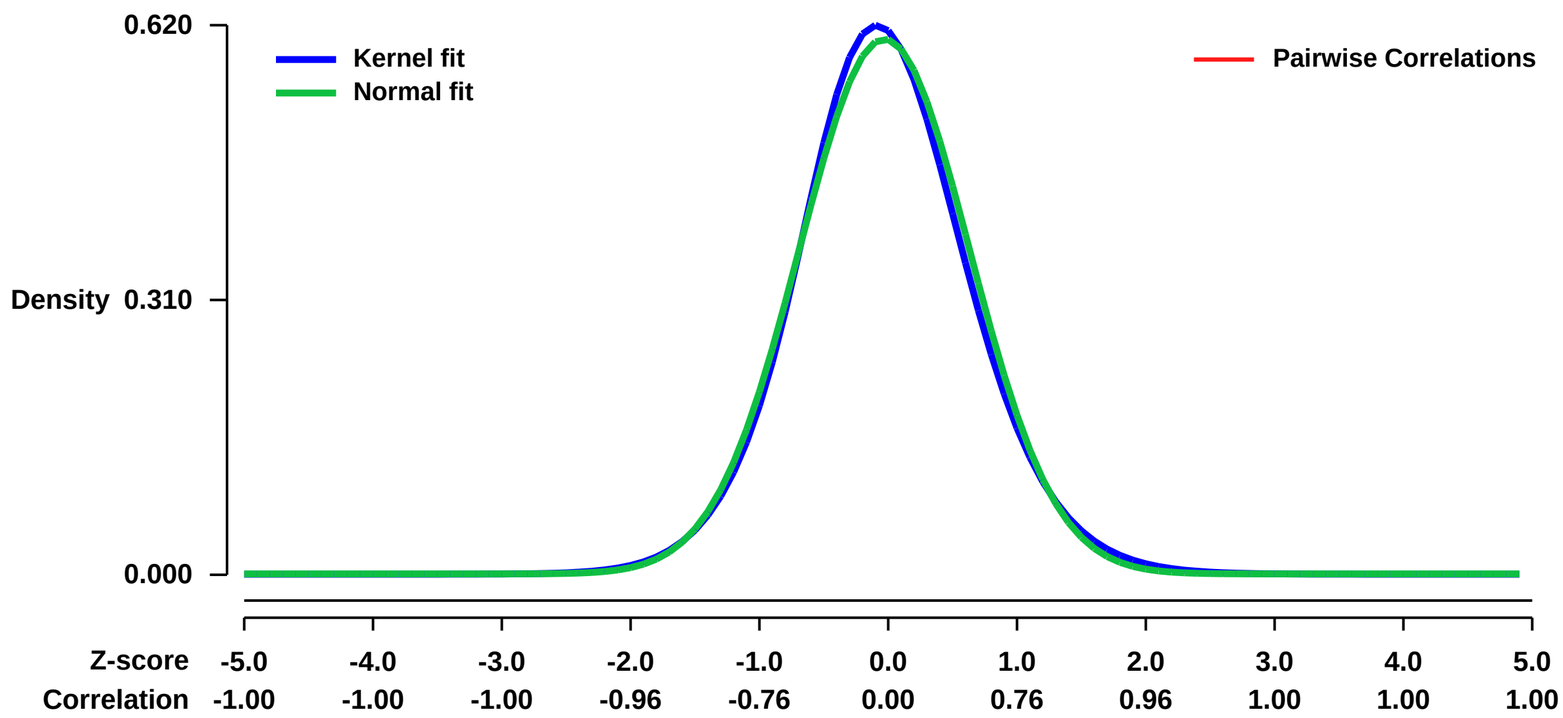

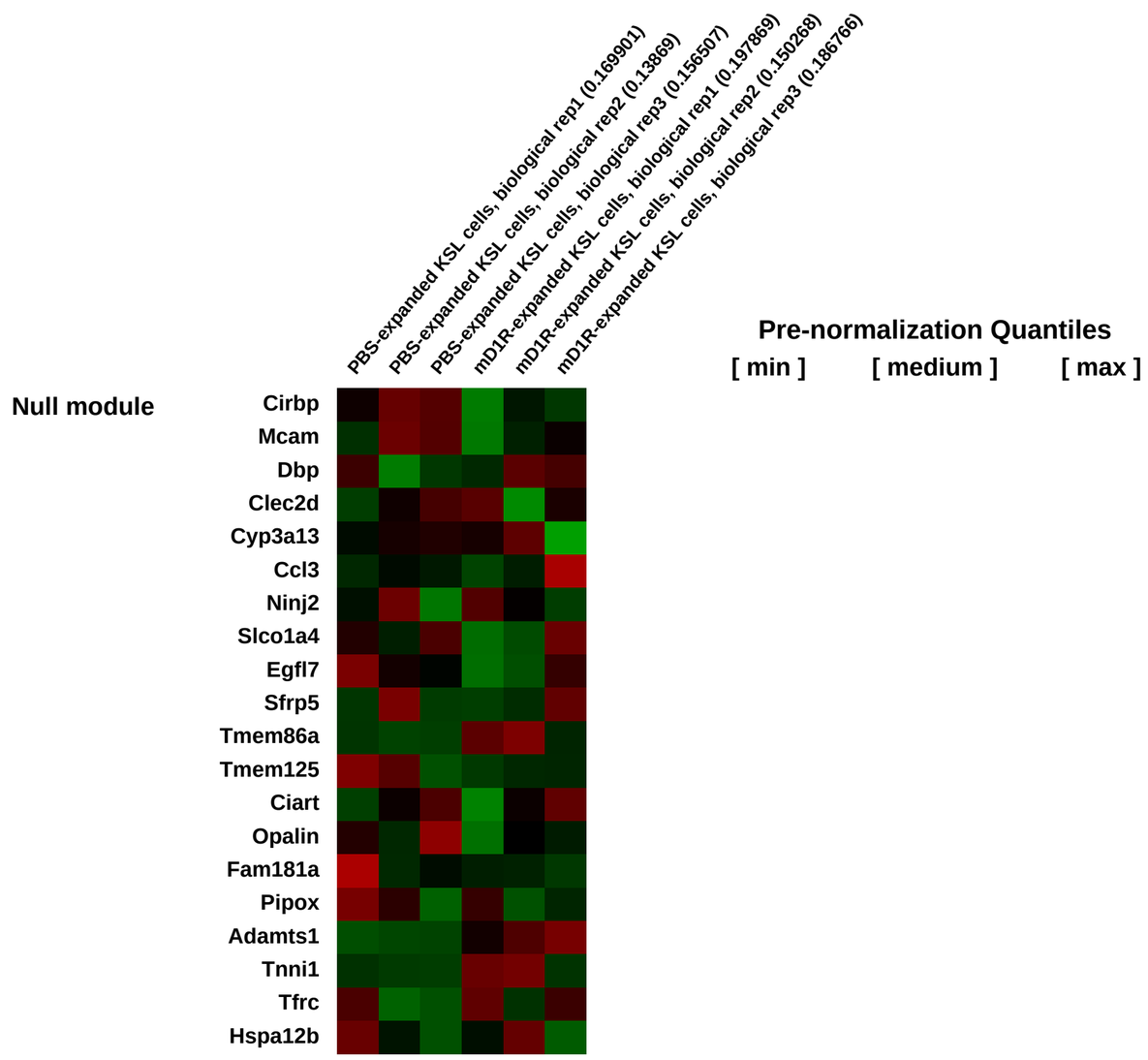

GEO Series "GSE27686" Expression Profiles

Num of samples in this series: 16

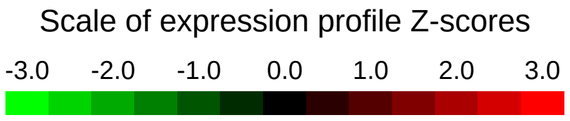

GEO Link:	http://www.ncbi.nlm.nih.gov/geo/query/acc.cgi?acc=GSE27686
Status:	Public on May 06 2011
Title:	Accumulating mitochondrial DNA mutations drive premature hematopoietic aging phenotypes molecularly distinct from physiologic stem cell aging
Organism:	Mus musculus
Experiment type:	Expression profiling by array
Platform:	GPL1261
Pubmed ID:	21549326
Summary & Design:	**Summary:** Somatic stem cells mediate tissue maintenance for the lifetime of an organism. Despite the well-established longevity that is a prerequisite for such function, accumulating data argue for compromised stem cell function with age. Identifying the mechanisms underlying age-dependent stem cell dysfunction is therefore key to understand the aging process. Using a model that carries a proofreading defective mitochondrial DNA polymerase, we demonstrate hematopoietic defects reminiscent of premature HSC aging including anemia, lymphopenia and myeloid lineage skewing. However, in contrast to physiologic stem cell aging, rapidly accumulating mitochondrial DNA mutations displayed little involvement of the hematopoietic stem cell pool but rather with distinct differentiation blocks and/or disappearance of downstream progenitors. **Overall design:** Hematopoietic stem cells (HSC) has been sorted out from midaged wildtype and mutator mice and compared with stem cells sorted from young and and old wt mice

Background corr dist: KL-Divergence = 0.0709, L1-Distance = 0.0577, L2-Distance = 0.0063, Normal std = 0.5126

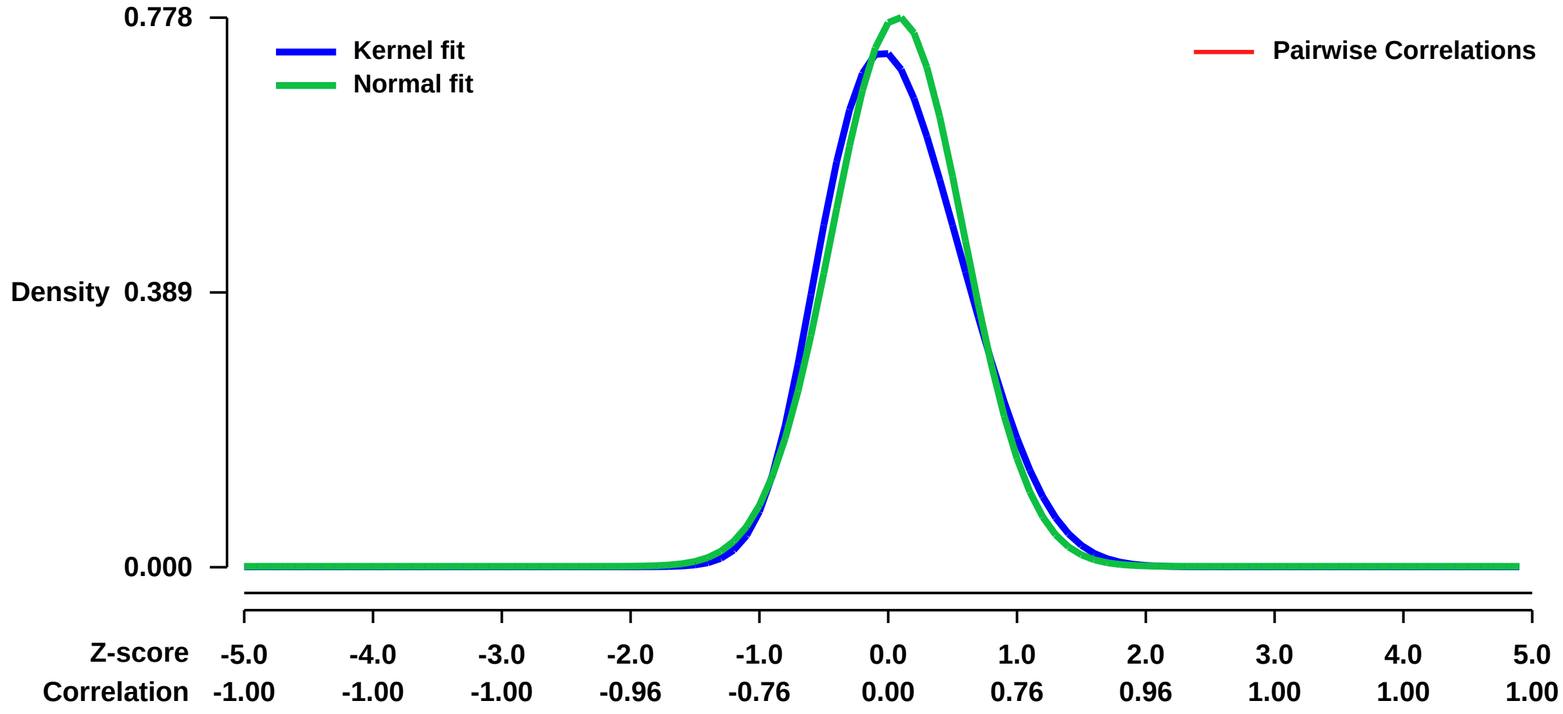

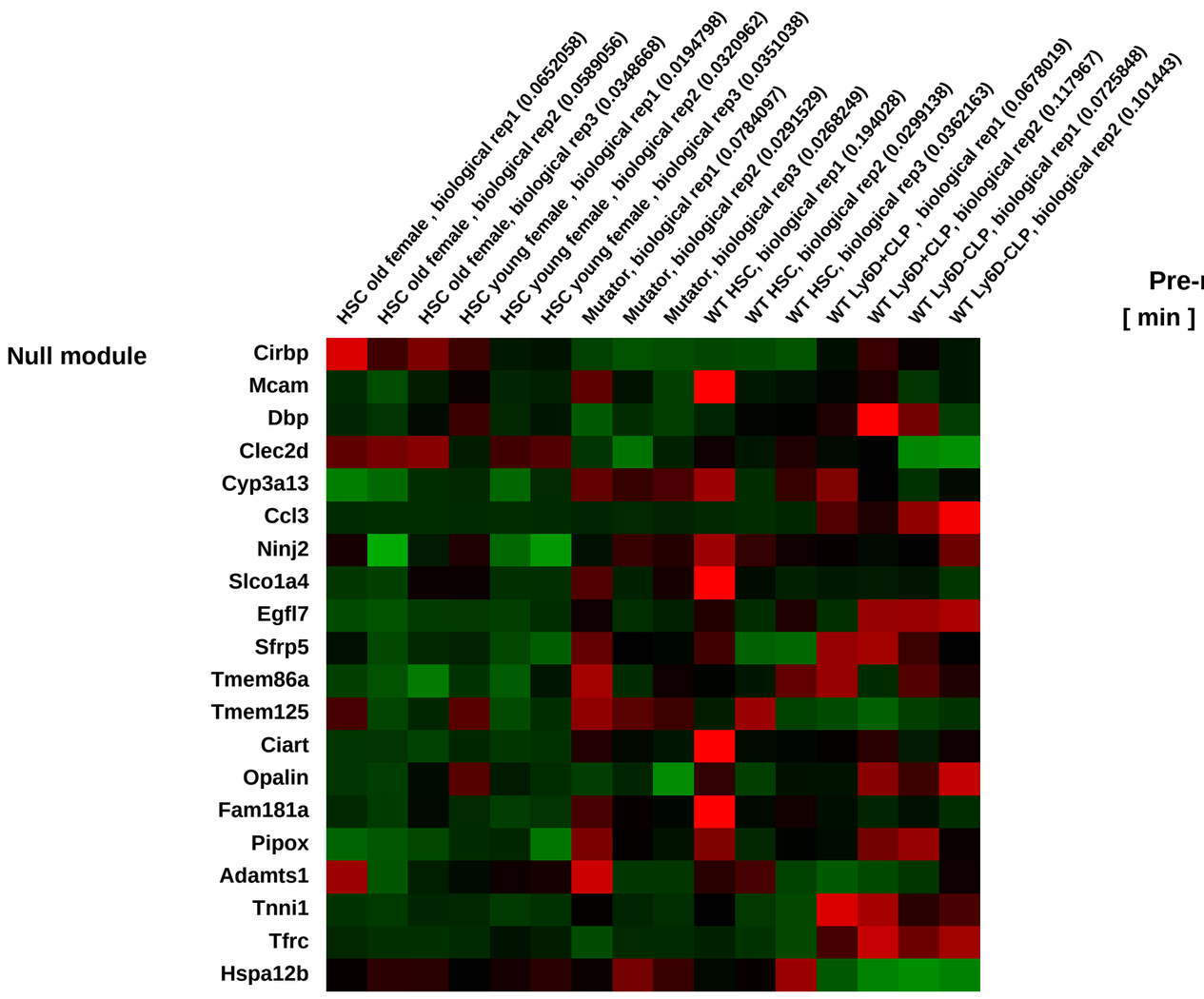

GEO Series "GSE38531" Expression Profiles

Num of samples in this series: 35

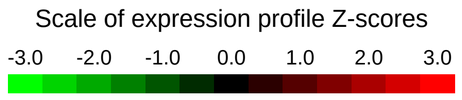

GEO Link:	**http://www.ncbi.nlm.nih.gov/geo/query/acc.cgi?acc=GSE38531**
Status:	**Public on Jun 05 2014**
Title:	**Expression data in Staphylococcus aureus-infected mice with linezolid and vancomycin treatment**
Organism:	**Mus musculus**
Experiment type:	**Expression profiling by array**
Platform:	**GPL1261**
Pubmed ID:	

Summary & Design:

Summary:
The precise mechanism and effects of antibiotics in host gene expression and immunomodulation in MRSA infection is unknown. Using a well characterized Methicillin Resistant Staphylococcus aureus (MRSA) isolate USA300 in a murine model of infection, we determined that linezolid and vancomycin induced differential production of bacterial toxins and host cytokines, differences in host gene expression, and differences in immunomodulators during MRSA bloodstream infection. A total of 35 A/J mice, categorized into seven groups (no infection; no infection with linezolid; no infection with vancomycin; 2 hour post-infection (hpi) S. aureus; 24 hpi S. aureus; 24 hpi S. aureus with linezolid; and 24 hpi S. aureus with vancomycin), were used in this study. Mice were injected with USA300 (6 x 106 CFU/g via i.p. route), then intravenously treated with linezolid (25 mg/kg) or vancomycin (25 mg/kg) at 2 hpi. Control and S. aureus infected mice were euthanized at each time point (2 h or 24h) following injection. Whole blood RNA was used for microarray; three cytokines and two S. aureus toxins [PantonValentine Leukocidin (PVL) and alpha hemolysin] were quantified in mouse serum by ELISA. S. aureus CFUs were significantly reduced in blood and kidney after linezolid or vancomycin treatment in S. aureus-infected mice. In vivo IL-1¸† in mouse serum was significantly reduced in both linezolid (p=0.001) and vancomycin (p=0.006) treated mice compared to untreated ones. IL-6 was significantly reduced only in linezolid treated (p<0.001) but not in vancomycin treated mice. However, another proinflammatory cytokine, TNF-¸–, did not exhibit altered levels in either linezolid or vancomycin treated mice (p=0.3 and p=0.51 respectively). In vivo level of bacterial toxin, Panton-Valentine leukocidin, in mouse serum was significantly reduced only in linezolid treated mice (p=0.02) but not in vancomycin treated mice. There was no significant effect of either treatment in in vivo level of alpha hemolysin production. Unsupervised hierarchical clustering using the gene expression data from 35 microarrays revealed distinct clustering based on infection status and treatment group. Study of the antibiotic-specific difference in gene expression identified the number of genes uniquely expressed in response to S. aureus infection, infection with linezolid treatment, and infection with vancomycin treatment. Pathway associations study for the differentially expressed genes in each comparison group (Control vs. 24 h S. aureus infection, 24 h S. aureus infection vs. 24 h S. aureus linezolid, and 24 h S. aureus infection vs. 24 h S. aureus vancomycin) in mice using Kyoto Encyclopedia of Genes and Genomes (KEGG) identified toll-like receptor signaling pathway to be common to every comparison groups studied. Glycerolipid metabolism pathway was uniquely associated only with linezolid treatment comparison group. The findings of this study provide the evidence that protein synthesis inhibitor like linezolid does a better job in treating MRSA sepsis compared to cell wall acting antibiotics like vancomycin.

Overall design:
To identify differences in host gene expression in a murine sepsis model treated with a) linezolid and b) vancomycin, we used whole blood gene expression (RNA) signatures from A/J inbred mice infected with USA 300 MRSA to evaluate differences in host gene expression among mice treated with linezolid and vancomycin. We used 5 RNA samples from MRSA-infected, linezolid- or vancomycin-treated mice. A total of 7 experimental groups have been employed: 1) Uninfected control group: (negative controls). 2) Uninfected, linezolid-treated group: Uninfected, linezolid-treated mice. 3) Uninfected vancomycin-treated group: Uninfected, vancomycin-treated mice. 4) Infected control group (positive control 2 h) MRSA-infected, untreated mice. 5) Infected control group (positive control 24 h): MRSA-infected, untreated mice. 6) Infected linezolid group: MRSA-infected, linezolid-treated mice. 7) Infected vancomycin group: MRSA-infected, vancomycin-treated mice.

Background corr dist: **KL-Divergence = 0.1180, L1-Distance = 0.0518, L2-Distance = 0.0065, Normal std = 0.4105**

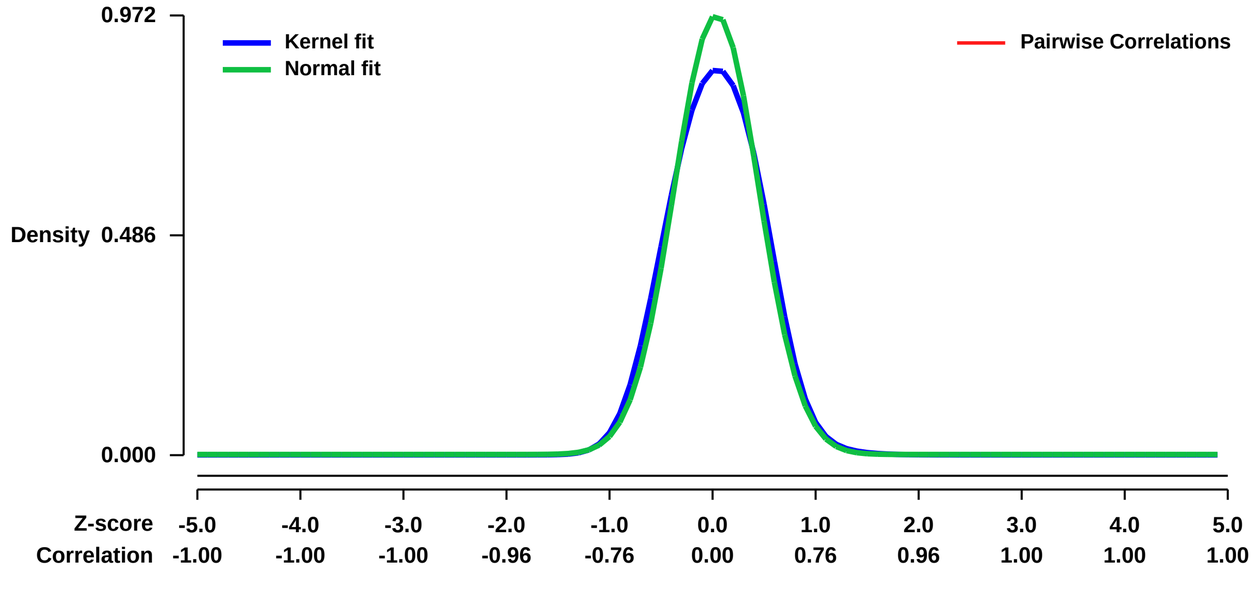

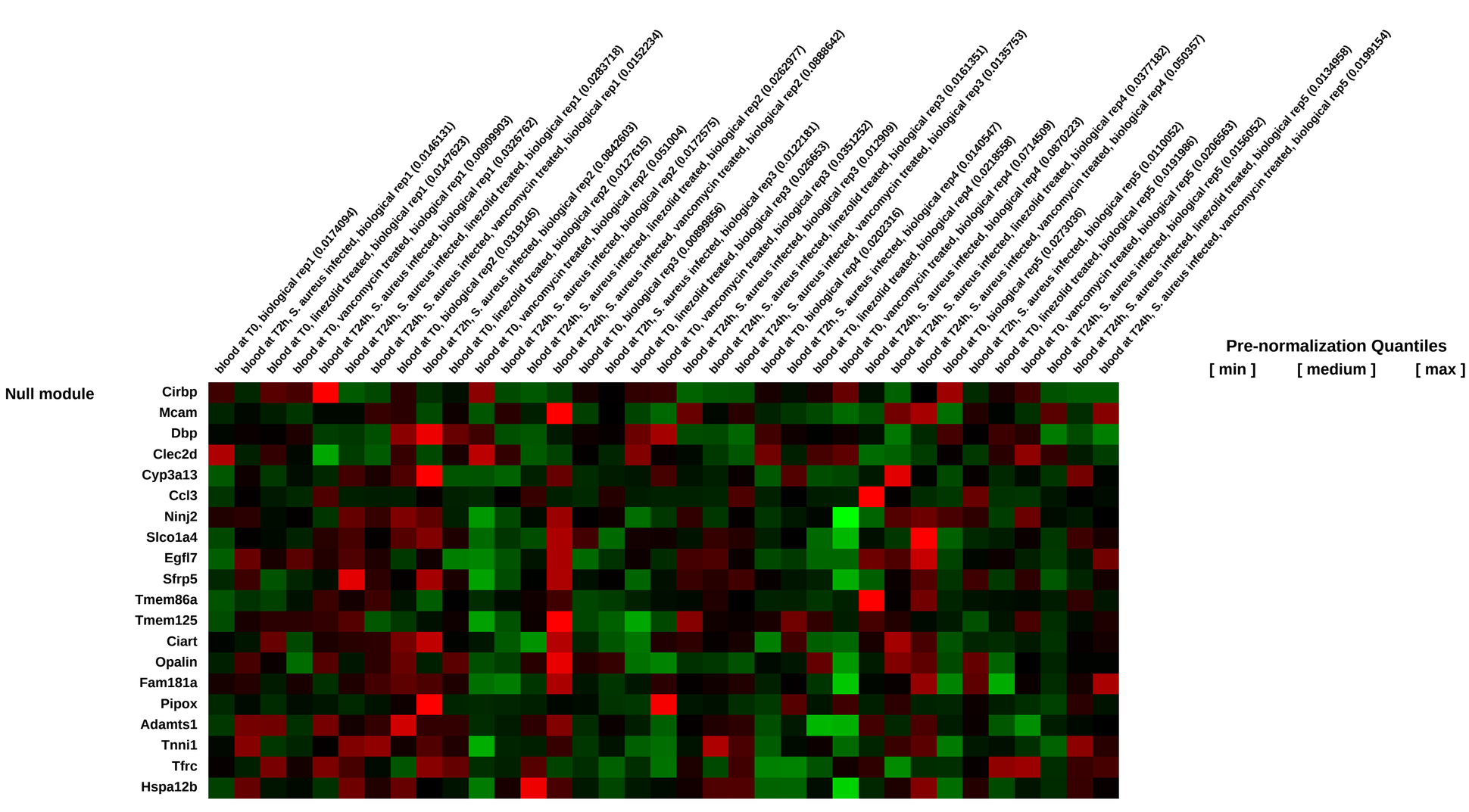

GEO Series "GSE10290" Expression Profiles

Num of samples in this series: 24

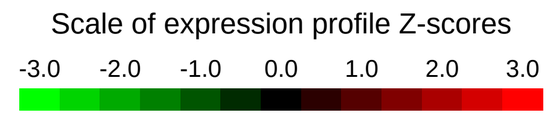

GEO Link:	http://www.ncbi.nlm.nih.gov/geo/query/acc.cgi?acc=GSE10290
Status:	Public on Nov 15 2008
Title:	Gene expression analyses of PR action in the mammary gland of ovariectomized mice
Organism:	Mus musculus
Experiment type:	Expression profiling by array
Platform:	GPL1261
Pubmed ID:	18687774
Summary & Design:	**Summary:** Beyond demonstrating a critical role for progesterone receptor signaling in normal mammary epithelial proliferation, the progesterone receptor knockout mouse disclosed the progesterone receptor along with its effector pathways as key determinants of mammary neoplastic progression. Despite these advances, however, further progress in our mechanistic understanding of progesteroneâ s involvement in mammary morphogenesis and tumorigenesis is contingent upon defining the essential effector pathways responsible for transducing the progesterone signal into a mammary proliferative and/or pro-survival response. Toward this goal, a judiciously chosen acute progesterone treatment regimen together with microarray methods was applied to the mammary gland of the normal mouse to uncover new effectors that operate immediately downstream of the progesterone mammary signal. Examination of the resultant progesterone-responsive transcriptome disclosed â inhibitor of differentiation or DNA binding 4â (Id4) as a molecular target acutely induced by progesterone in the murine mammary epithelium. **Keywords: time course** **Overall design:** Microarray analysis was performed on mammary tissue total RNA obtained from ovariectomized mice previously treated with progesterone for 4, 16, 28, and 76 hours. For each hormone treatment time-point, mammary gland microarray data from sesame oil (vehicle) treated mice was included as controls. Total mammary gland RNA from each time-point and treatment group was interrogated using the Affymetrix GeneChip Mouse Genome 430 2.0 Array. For a given time-point and treatment group, three sets of mice (5 mice in each set) were used for gene expression profiling; mammary RNA pooled from each set was hybridized to one microarray chip. Therefore, a total of 15 mice (or 3 microarray chips) were used per time-point and treatment group.

Background corr dist: KL-Divergence = 0.2584, L1-Distance = 0.0529, L2-Distance = 0.0067, Normal std = 0.2993

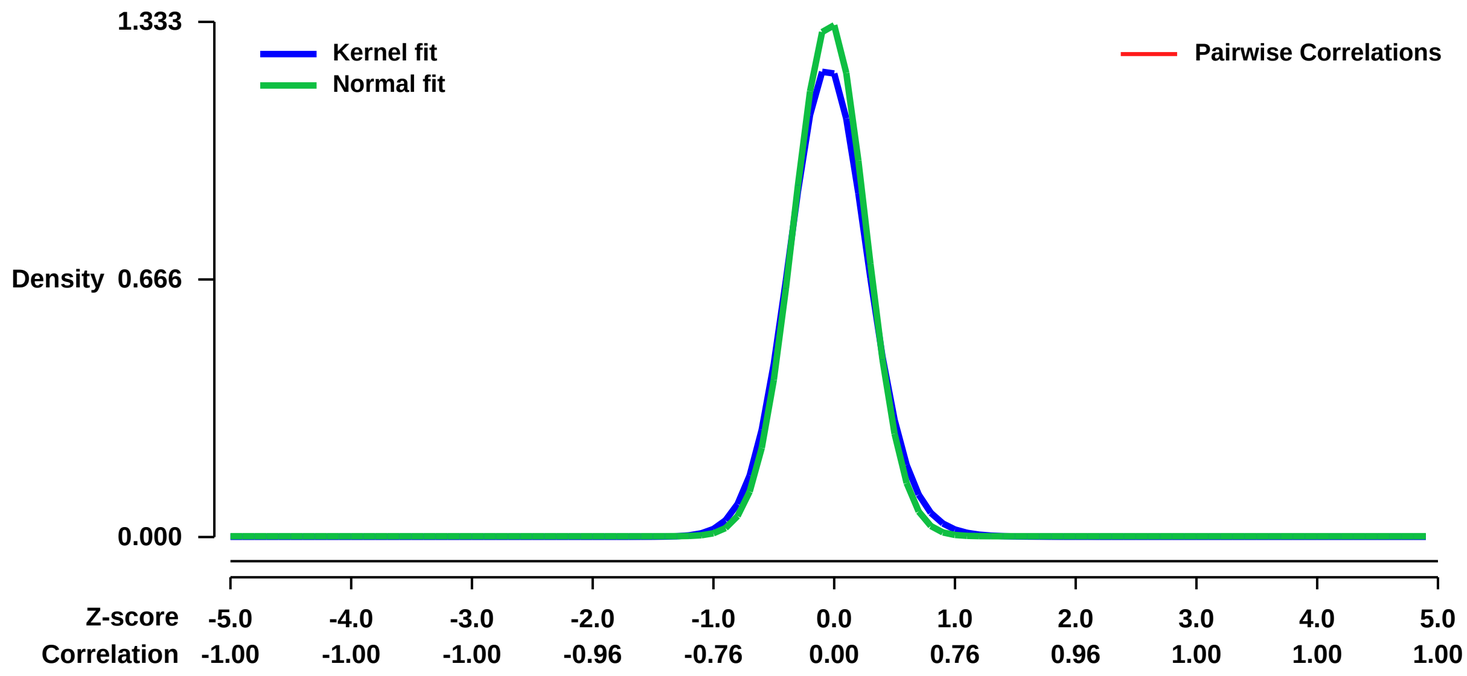

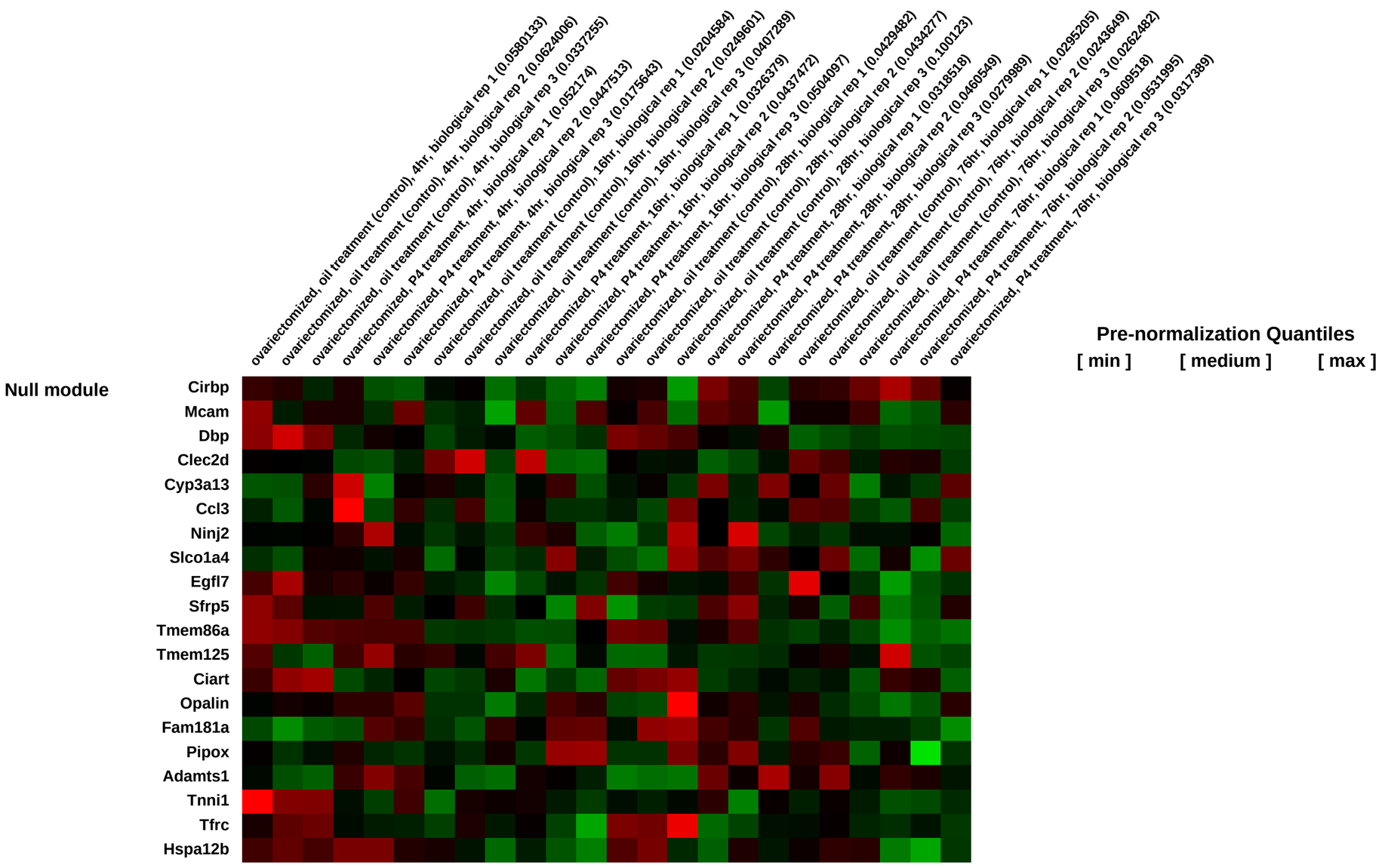

GEO Series "GSE1871" Expression Profiles

Num of samples in this series: 12

Scale of expression profile Z-scores

-3.0 -2.0 -1.0 0.0 1.0 2.0 3.0

GEO Link:	**http://www.ncbi.nlm.nih.gov/geo/query/acc.cgi?acc=GSE1871**
Status:	**Public on Oct 26 2004**
Title:	**SCCOR_MouseLung_Simva_LPS**
Organism:	**Mus musculus**
Experiment type:	**Expression profiling by array**
Platform:	**GPL1261**
Pubmed ID:	**15665042**
Summary & Design:	**Summary:** **This series contain mouse lung samples treated with Simvastatin and LPS and corresponded controls.** **Keywords: other** **Overall design:**

Background corr dist: **KL-Divergence = 0.0617, L1-Distance = 0.0228, L2-Distance = 0.0006, Normal std = 0.5246**

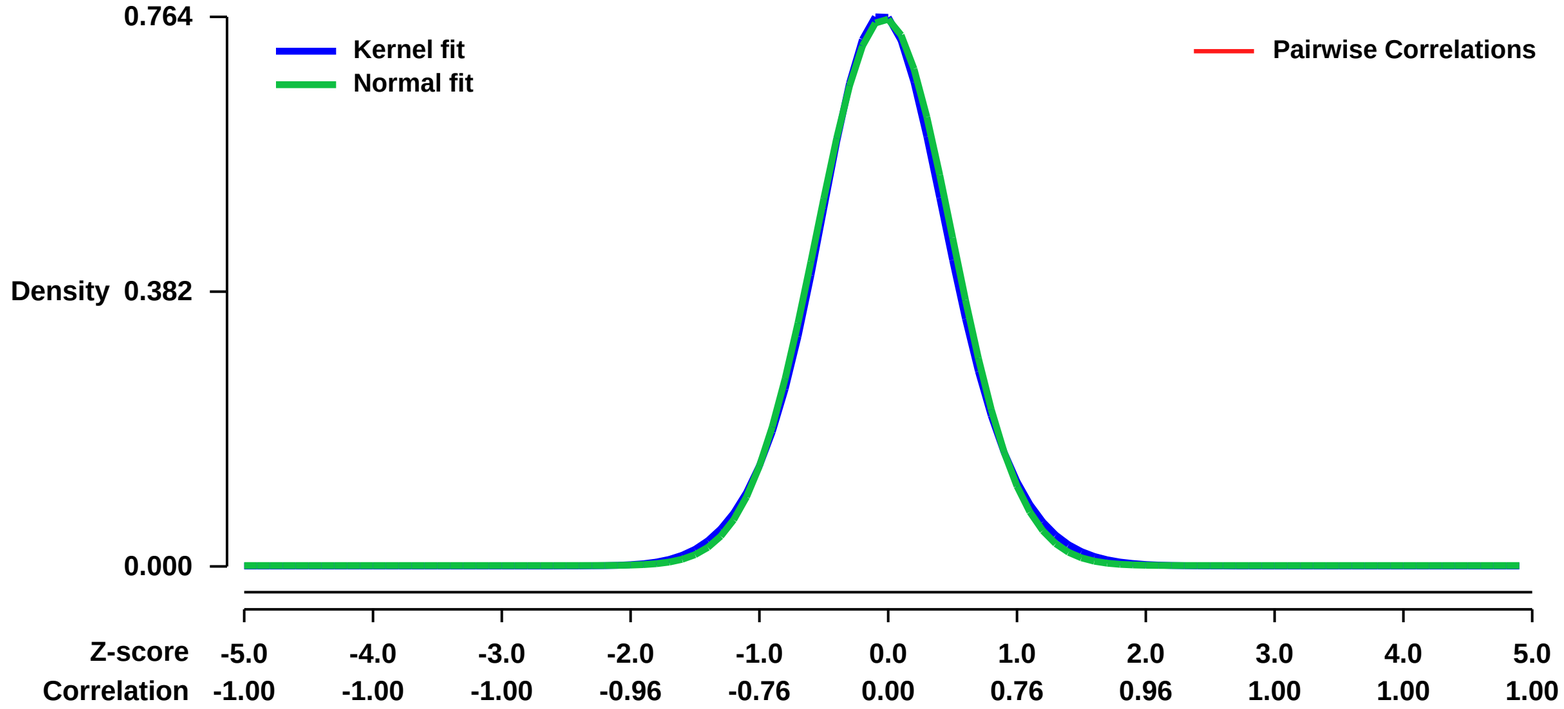

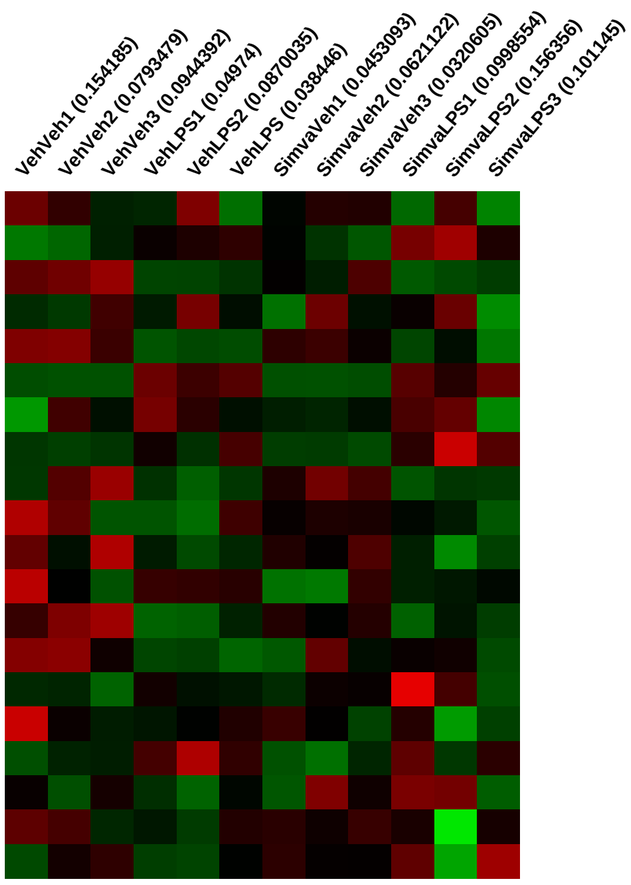

GEO Series "GSE46723" Expression Profiles

Num of samples in this series: 6

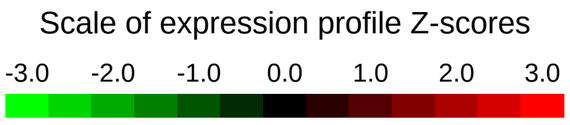

GEO Link:	http://www.ncbi.nlm.nih.gov/geo/query/acc.cgi?acc=GSE46723
Status:	Public on Jul 01 2013
Title:	Expression data from adult Myeloerythroid Progenitors (MP) Hes1-GFP positive and adult Myeloerythroid Progenitors (MP) Hes1-GFP negative
Organism:	Mus musculus
Experiment type:	Expression profiling by array
Platform:	GPL1261
Pubmed ID:	23791481
Summary & Design:	**Summary:** Notch signaling defines a conserved, fundamental pathway, responsible for determination in metazoan development and is widely recognized as an essential component of lineage specific differentiation and stem cell self-renewal in many tissues including the hematopoietic system. Until recently, the majority of studies in the hematopoietic system focused on Notch signaling in lymphocyte differentiation and knowledge of individual Notch receptor roles in early hematopoiesis has been limited due to a paucity of genetic tools available To fate-map Notch receptor expression and pathway activity in the hematopoietic system we used tamoxifen-inducible CreER knock-in mice for individual Notch receptors in combination to a novel Notch reporter strain (Hes1GFP) and a conditional gain of function allele of Notch2 receptor (Rosa-lsl-ICN2). **Overall design:** Bone marrow lineage negative, cKit+, Sca1- cells were sorted from Hes-GFP mice for RNA extraction and hybridization on Affymetrix microarrays

Background corr dist: KL-Divergence = 0.0189, L1-Distance = 0.0122, L2-Distance = 0.0002, Normal std = 0.7520

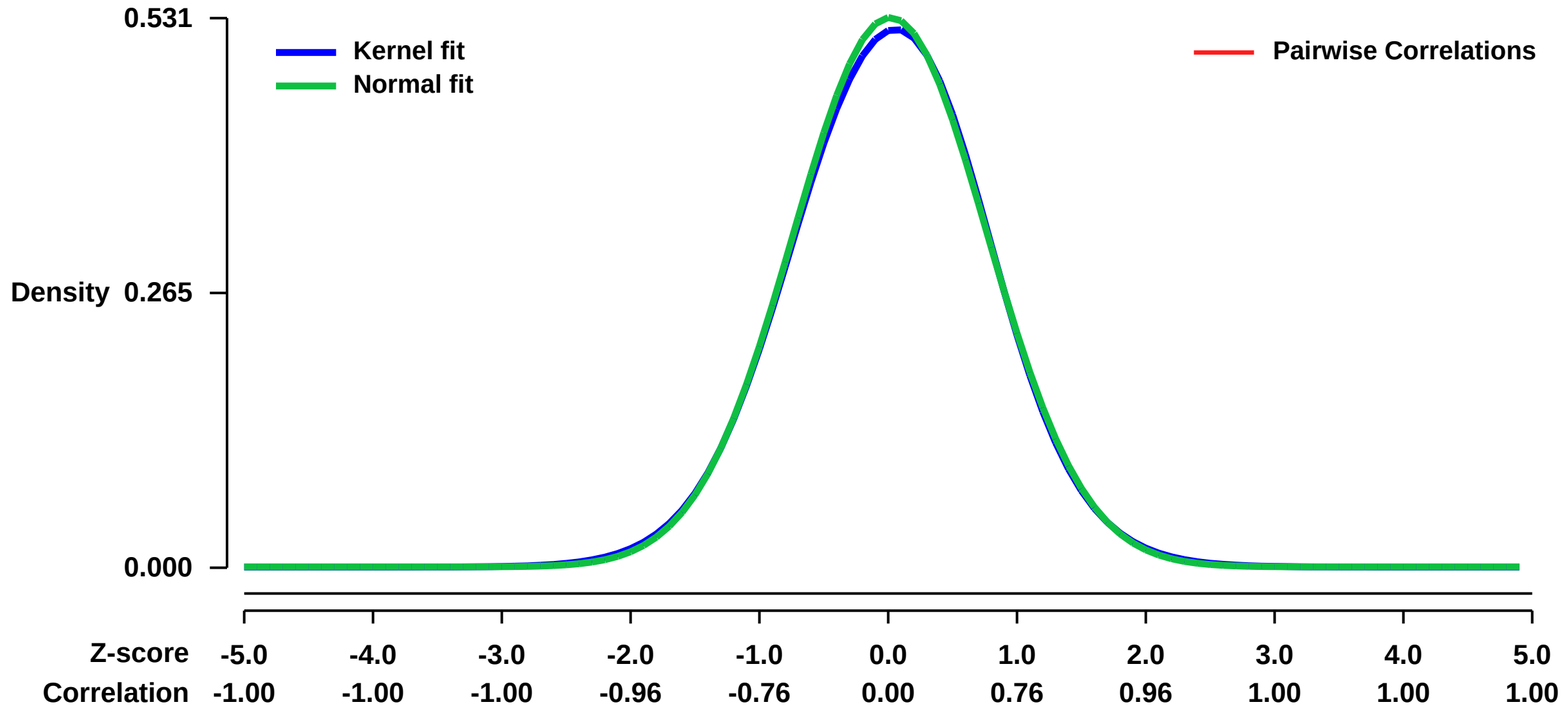

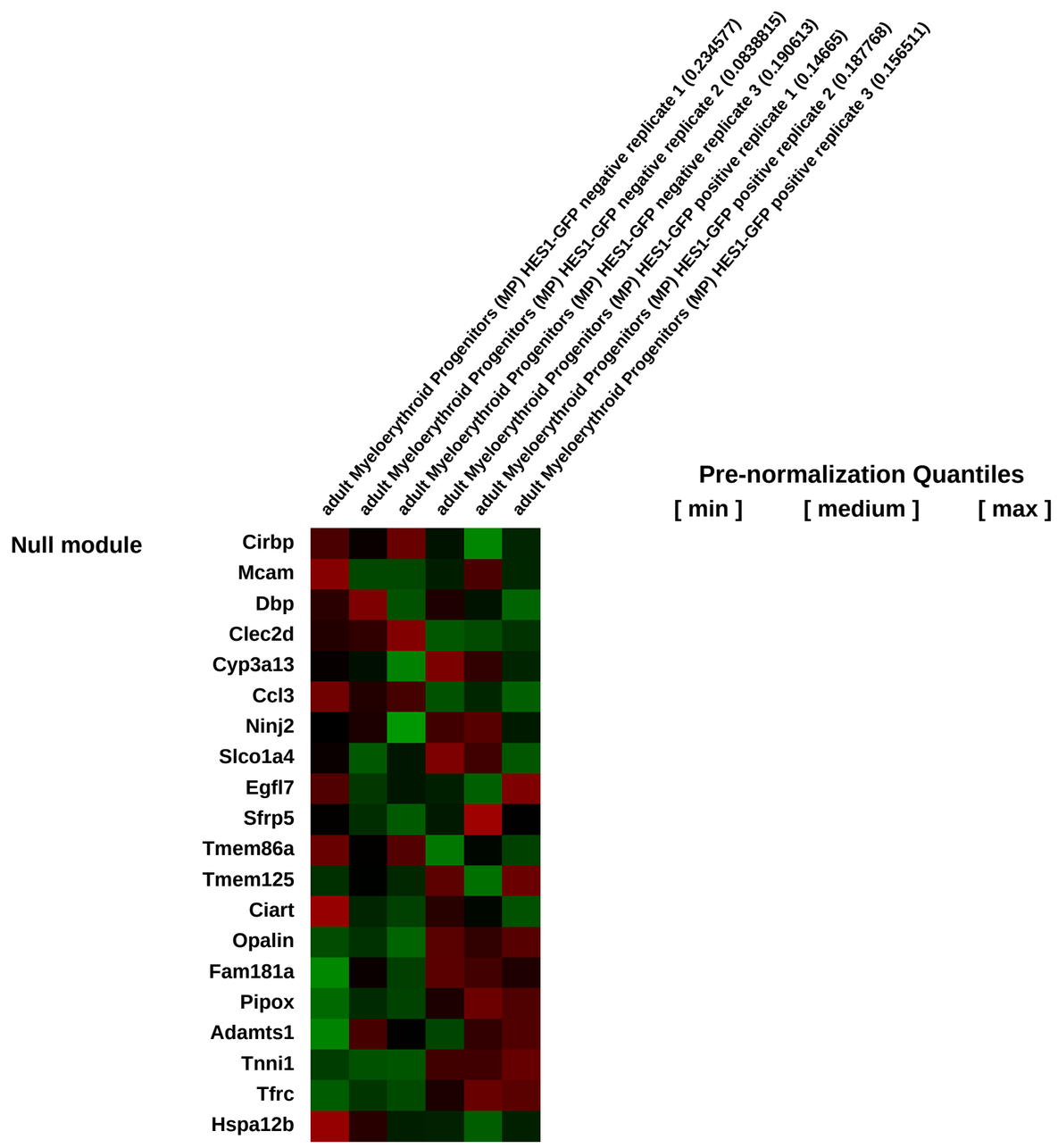

GEO Series "GSE22873" Expression Profiles

Num of samples in this series: 19

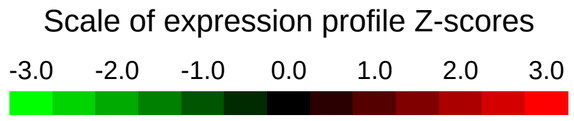

GEO Link:	http://www.ncbi.nlm.nih.gov/geo/query/acc.cgi?acc=GSE22873
Status:	Public on Jun 26 2012
Title:	Ager (Rage) and Myd88 deletion in resected mouse livers
Organism:	Mus musculus
Experiment type:	Expression profiling by array
Platform:	GPL1261
Pubmed ID:	22075646
Summary & Design:	**Summary:** The effect of resection of mouse livers on survival serve as a model for the effect of resection of human livers, which are performed for both the purposes of removing sick tissue and for transplanting healthy tissue. When less than 70% of a mouse liver is resected, the mouse usually lives. However, when more than 70% is resected, there is an increased probability that the mouse will die. We have found that deletion of Ager (Advanced Glycation End products receptor) (Rage) increases the chance of mouse survival relavtive to WT. Conversely, the deletion of Myd88 decreases the chances of survival, as does the simultaneous deletion of both Ager and Myd88. To understand these genotype/phenotype relations, we performed gene expression measurements. **Overall design:** Gene expression of livers of WT C57BL/6 mice, Ager-null C57BL/6 mice, Myd88-null C57BL/6 mice, and Ager-null/Myd88-null C57BL/6 mice, all 10-12 weeks-old and sacrificed 2 hours after 85% liver resection, were compared. 4-6 replicates each group.

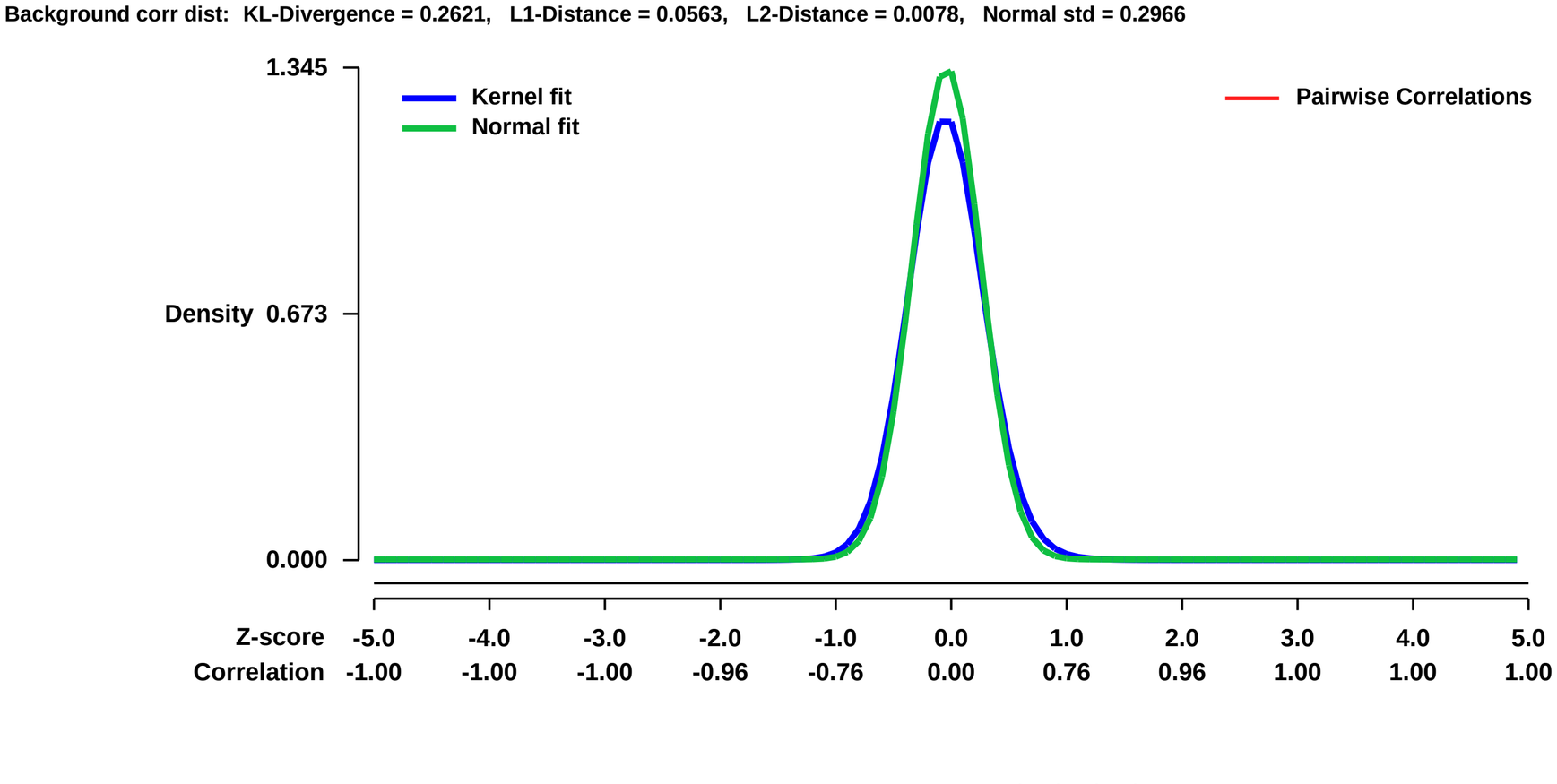

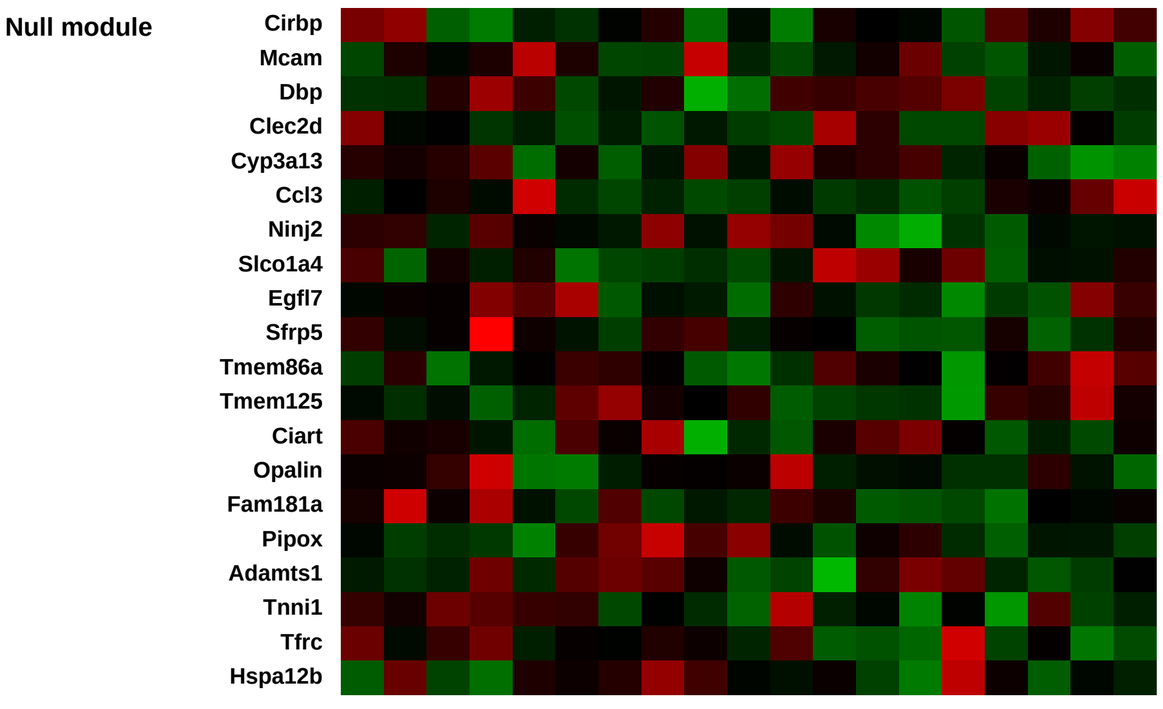

GEO Series "GSE8969" Expression Profiles

Num of samples in this series: 6

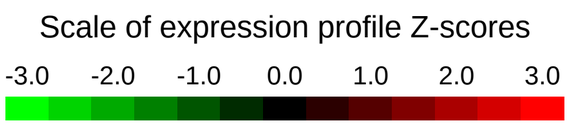

GEO Link:	http://www.ncbi.nlm.nih.gov/geo/query/acc.cgi?acc=GSE8969
Status:	Public on Jan 15 2008
Title:	Impaired liver regeneration in Nrf2 knockout mice caused by ROS-mediated insulin/IGF-1 resistance
Organism:	Mus musculus
Experiment type:	Expression profiling by array
Platform:	GPL1261
Pubmed ID:	18059474
Summary & Design:	**Summary:** The liver is frequently challenged by surgery-induced metabolic overload, viruses, or toxins, which induce the formation of reactive oxygen species. To determine the effect of oxidative stress on liver regeneration and to identify the underlying signalling pathways, we studied liver repair in mice lacking the Nrf2 transcription factor. In these animals, expression of several cytoprotective enzymes was reduced in hepatocytes, resulting in oxidative stress. As a consequence, tissue damage was aggravated, and liver regeneration after partial hepatectomy was delayed. Using in vitro and in vivo studies we identified oxidative stress-induced insulin/insulin-like growth factor resistance as the underlying mechanism. This deficiency impaired the activation of p38 mitogen-activated kinase, Akt kinase, and downstream targets after hepatectomy, resulting in enhanced death and delayed proliferation of hepatocytes. Our results reveal novel roles of Nrf2 in the regulation of growth factor signalling and in tissue repair. In addition, they provide new insight into the mechanisms underlying oxidative stress-induced defects in liver regeneration and thus offer new avenues to improve regeneration in patients with acute or chronic liver damage. **Keywords:** genetic modification, wilde type (wt) vs. knock out (k.o.) liver samples **Overall design:** Livers from Nrf2 k.o. and wt mice; 3 hybridizations per genoype: RNA samples were pooled from 3 individual animals

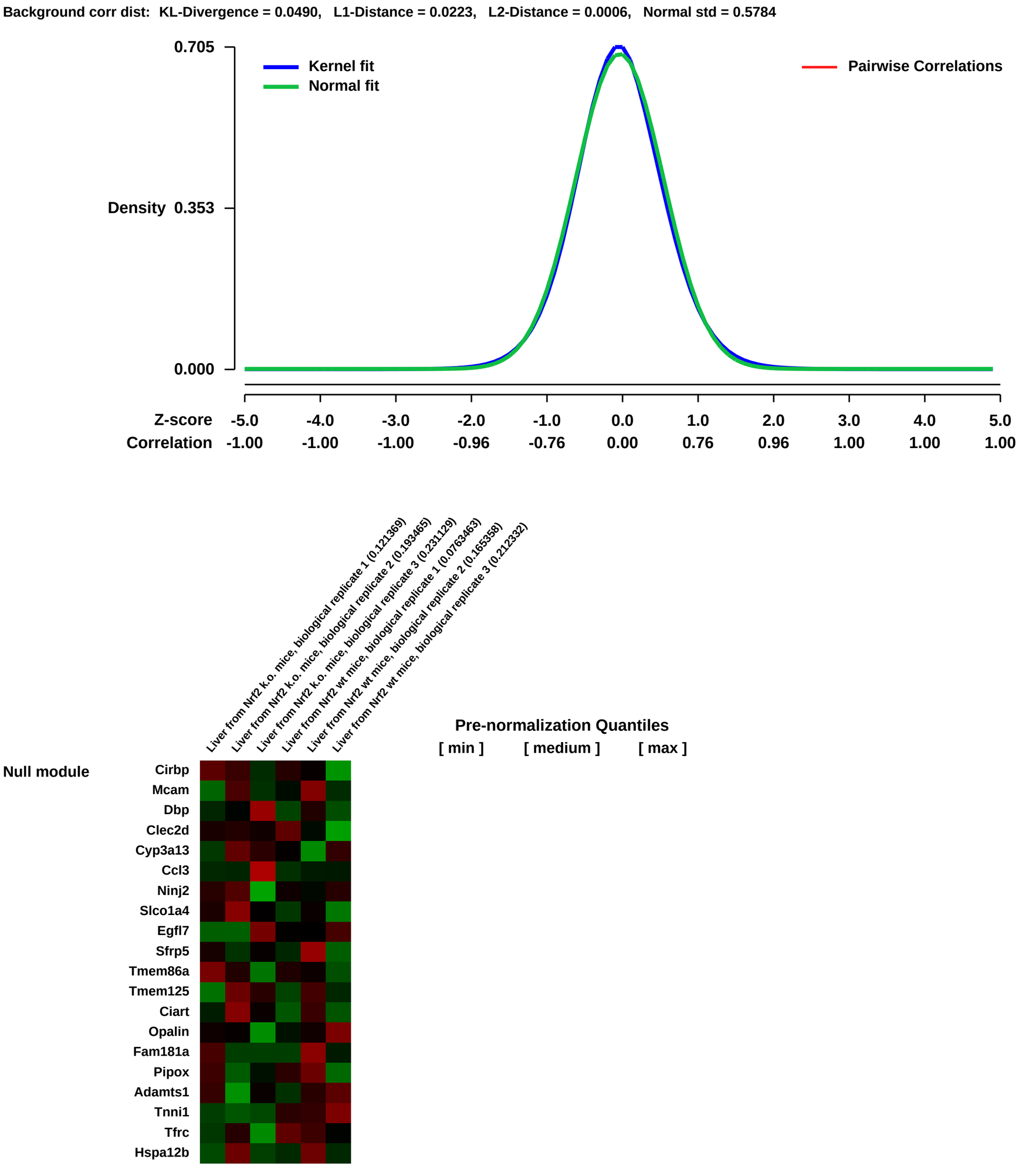

GEO Series "GSE5371" Expression Profiles

Num of samples in this series: 8

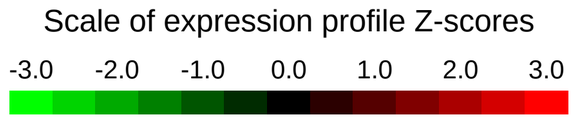

GEO Link:	**http://www.ncbi.nlm.nih.gov/geo/query/acc.cgi?acc=GSE5371**
Status:	**Public on Jul 21 2006**
Title:	**Maternal BRG1 regulates zygotic genome activation in the mouse**
Organism:	**Mus musculus**
Experiment type:	**Expression profiling by array**
Platform:	**GPL1261**
Pubmed ID:	**16818606**
Summary & Design:	**Summary:** **Embryos were collected at 2 cell stage. cRNA from four biological replicates of each were generated and the expression profiles were determined using Affymetrix MOE430 v2.** **Keywords: repeat** **Overall design:** **4 embryo at 2 cell stage biological replicates were analyzed**

Background corr dist: **KL-Divergence = 0.0503, L1-Distance = 0.0327, L2-Distance = 0.0016, Normal std = 0.5980**

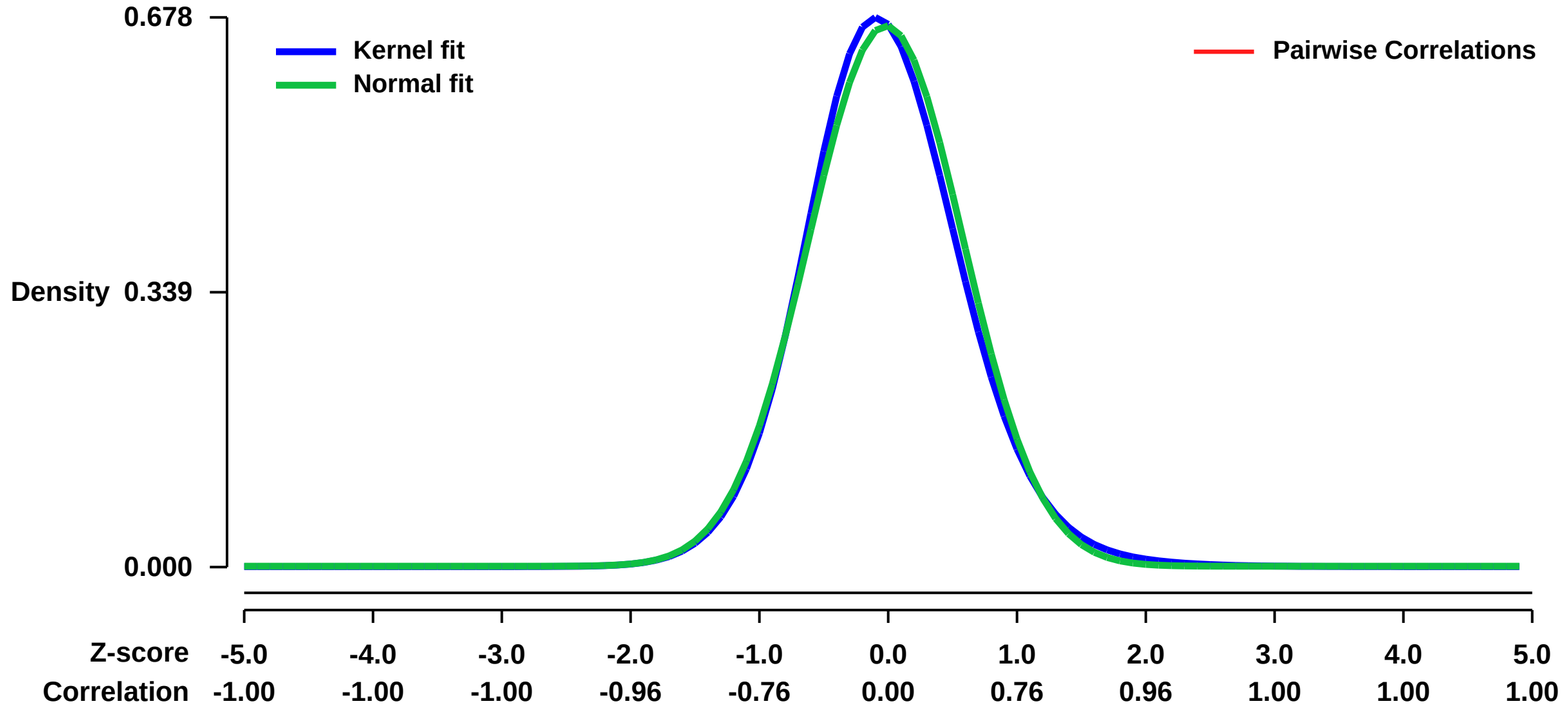

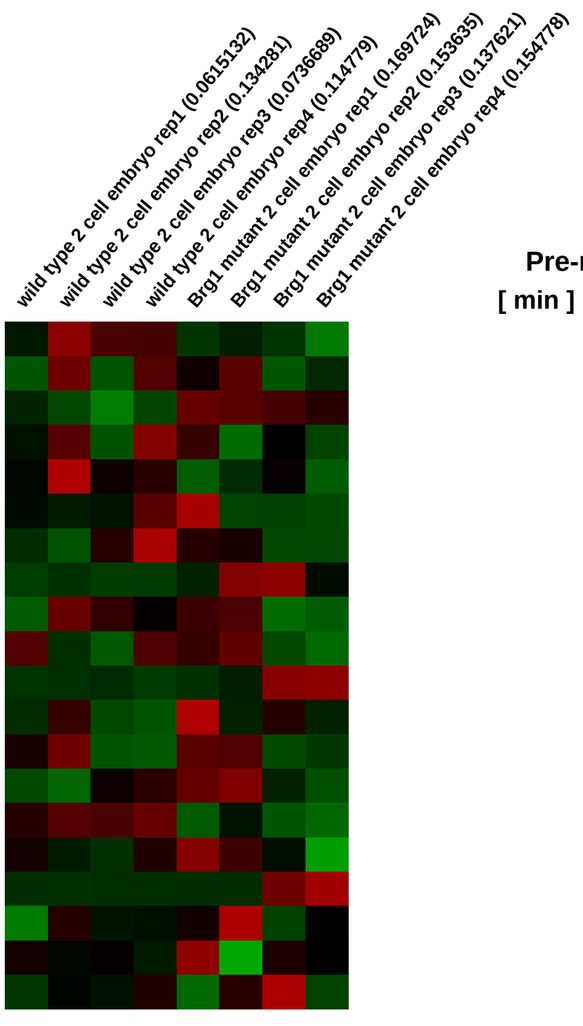

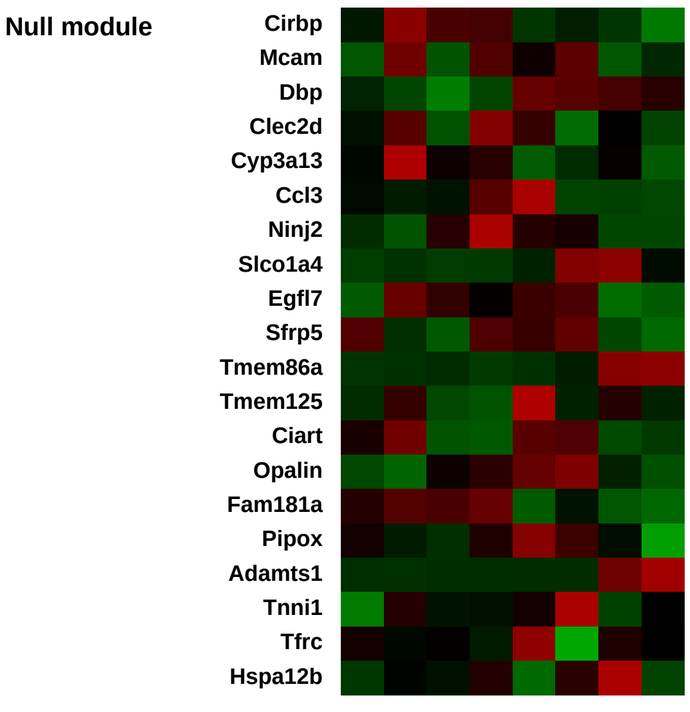

GEO Series "GSE43042" Expression Profiles

Num of samples in this series: 6

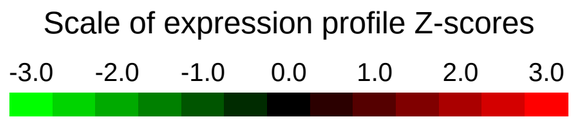

GEO Link:	http://www.ncbi.nlm.nih.gov/geo/query/acc.cgi?acc=GSE43042
Status:	Public on Feb 09 2013
Title:	The role of Ldb1 in hemangioblast development: genome-wide analysis shows that Ldb1 controls essential hematopoietic genes/pathways in mouse early development and
Organism:	Mus musculus
Experiment type:	Expression profiling by array
Platform:	GPL1261
Pubmed ID:	23390196
Summary & Design:	**Summary:** The first site exhibiting hematopoietic activity in mammalian development is the yolk sac blood island, which originates from the hemangioblast. Here we performed differentiation assays, as well as genome-wide molecular and functional studies in BL-CFCs to gain insight into the function of the essential Ldb1 factor in early primitive hematopoietic development. We show that the previously reported lack of yolk sac hematopoiesis and vascular development in Ldb1-/- mouse result from a decreased number of hemangioblasts and a block in their ability to differentiate into erythroid and endothelial progenitor cells. Transcriptome analysis and correlation with the genome wide binding pattern of Ldb1 in hemangioblasts revealed a number of direct target genes and pathways misregulated in the absence of Ldb1. The regulation of essential developmental factors by Ldb1 defines it as an upstream transcriptional regulator of hematopoietic/endothelial development. We show the complex interplay that exists between transcription factors and signaling pathways during the very early stages of hematopoietic/endothelial development and the specific signalling occurring in hemangioblasts in contrast to more advanced hematopoietic developmental stages. Finally, by revealing novel genes and pathways, not previously associated with early development, our study provides novel candidate targets to manipulate the differentiation of hematopoietic and/or endothelial cells. We used microarrays to detail the global programme of gene expression underlying the Ldb1+/+ and Ldb1-/- in Flk1+ cells. **Overall design:** RNA was isolated from Ldb1+/+ and Ldb1-/- Flk1+ cells with the QIAGEN RNeasy Mini Kit and integrity was checked on the Agilent 2100 Bioanalyzer. RNA was converted to biotin-labelled cRNA, hybridised on the Mouse Genome 430 2.0 Array and analyzed with the Affymetrix GeneChip´fi Scanner 3000 according to the manufacturer protocol.

Background corr dist: KL-Divergence = 0.0325, L1-Distance = 0.0414, L2-Distance = 0.0024, Normal std = 0.6850

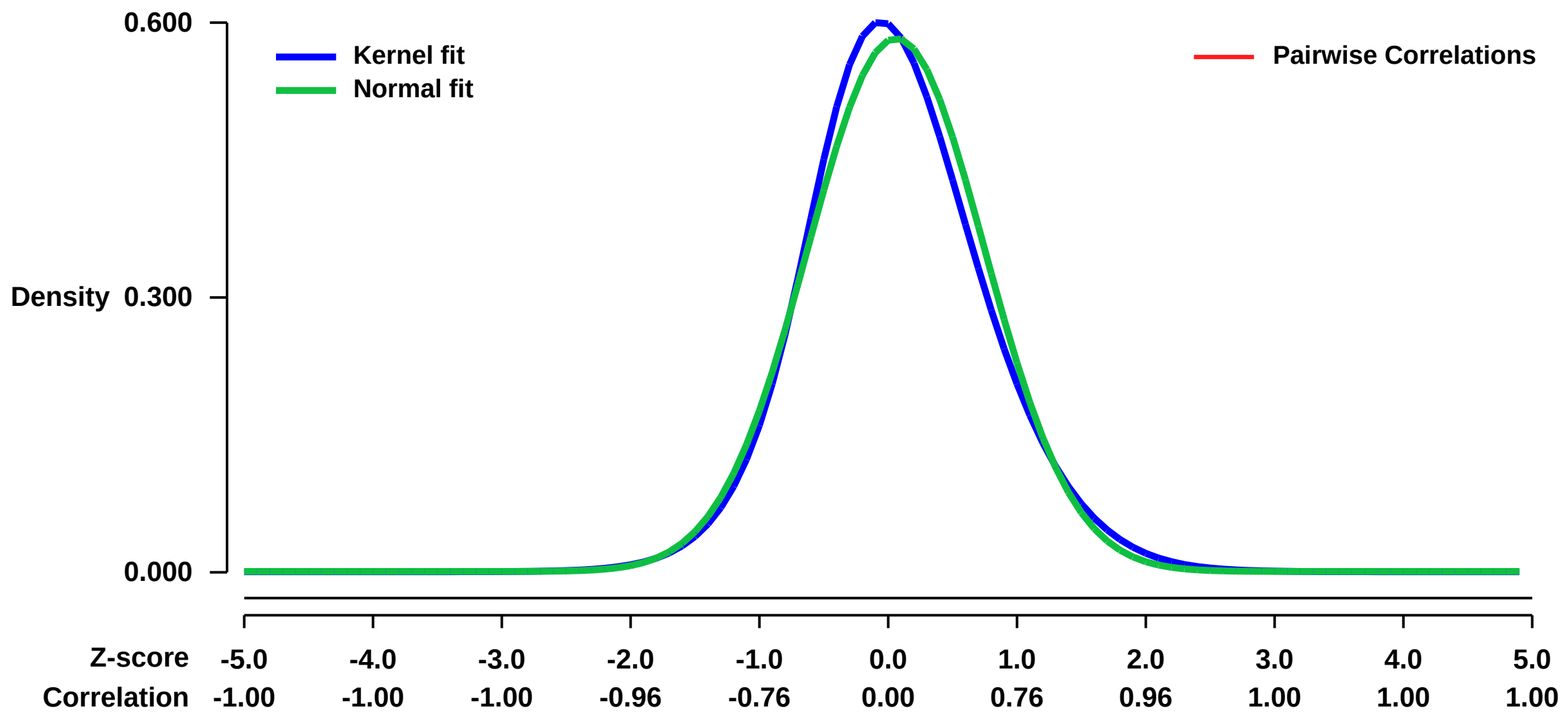

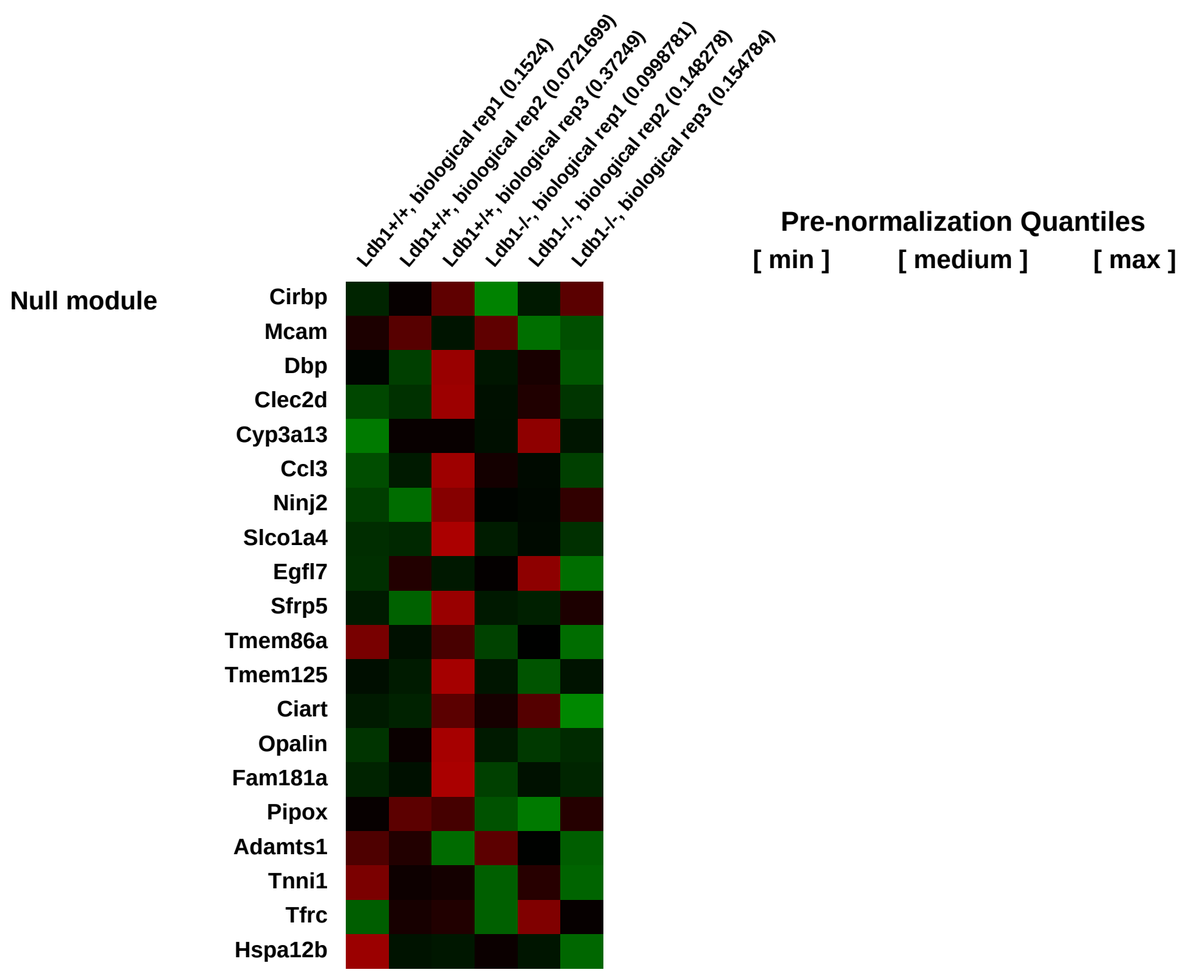

GEO Series "GSE36414" Expression Profiles

Num of samples in this series: 8

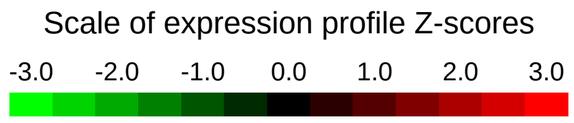

GEO Link:	http://www.ncbi.nlm.nih.gov/geo/query/acc.cgi?acc=GSE36414
Status:	Public on Mar 08 2013
Title:	Gene expression changes induced in the stromal cell line EL08-1D2 by co-culture with leukemic B cells (CLL)
Organism:	Mus musculus
Experiment type:	Expression profiling by array
Platform:	GPL1261
Pubmed ID:	23328482
Summary & Design:	**Summary:** Tumor cell survival critically depends on heterotypic communication with benign cells in the microenvironment. Here we describe a novel survival signaling pathway activated in stromal cells by contact to B-cells from chronic lymphocytic leukemia (CLL) patients. The expression of PKC-¸†II and the subsequent activation of NF-¸”B in bone marrow stromal cells is a prerequisite to support the survival of malignant B-cells. PKC-¸† knockout mice are insusceptible to CLL-transplantations, underscoring the in vivo significance of the PKC-¸†II-NF-¸”B signaling pathway in the tumor microenvironment. Upregulated stromal PKC-¸†II in biopsies from CLL, breast- and pancreatic-cancer patients suggest that this pathway may commonly be activated in a variety of malignancies. We used microarrays to determine gene expression changes induced by co-culturing with leukemic B-cells (CLL) in EL08-1D2 cells. **Overall design:** We compared EL08-1D2 cells co-cultured for 5 days with leukemic B-cells to EL08-1D2 mono-cultured cells by microarray analysis on Affymetrix MG-430_2.0 arrays.

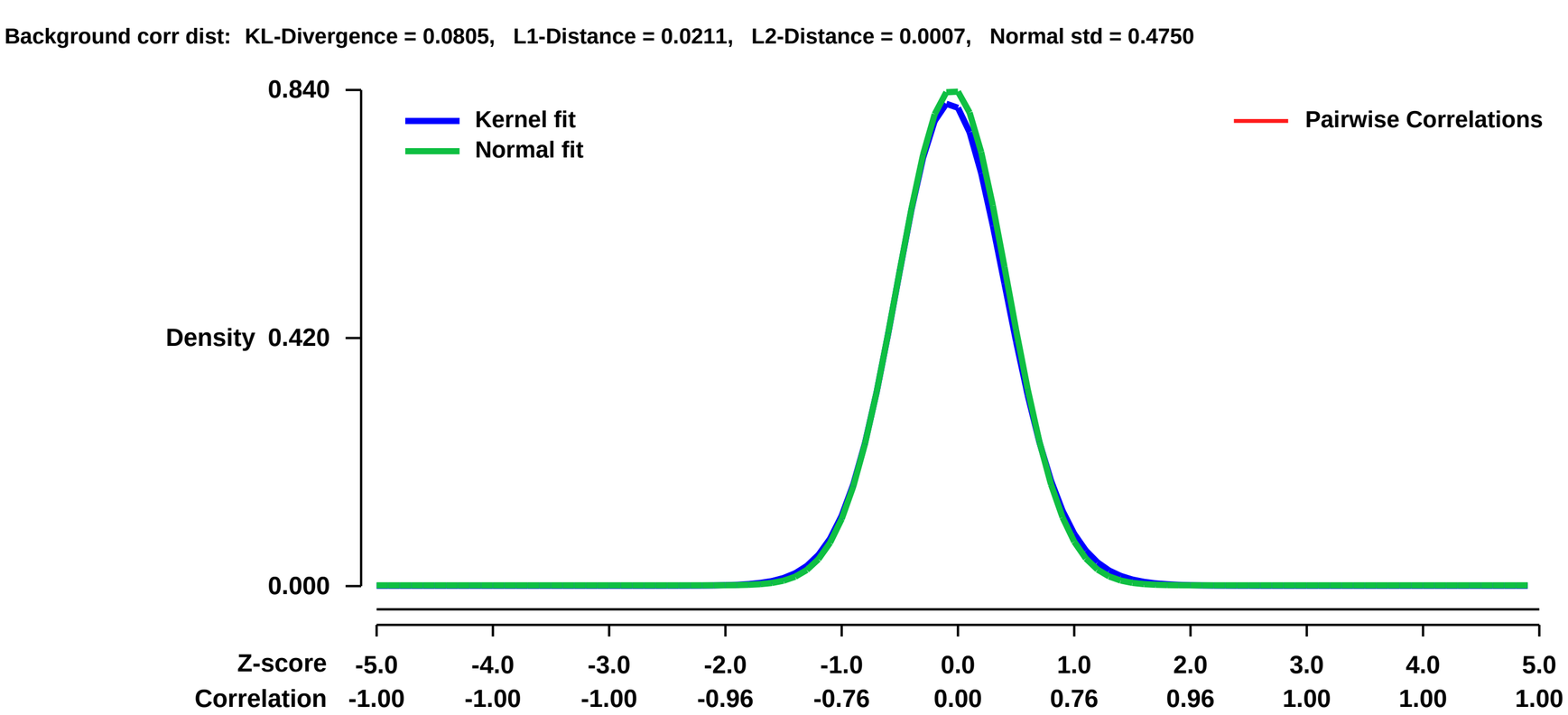

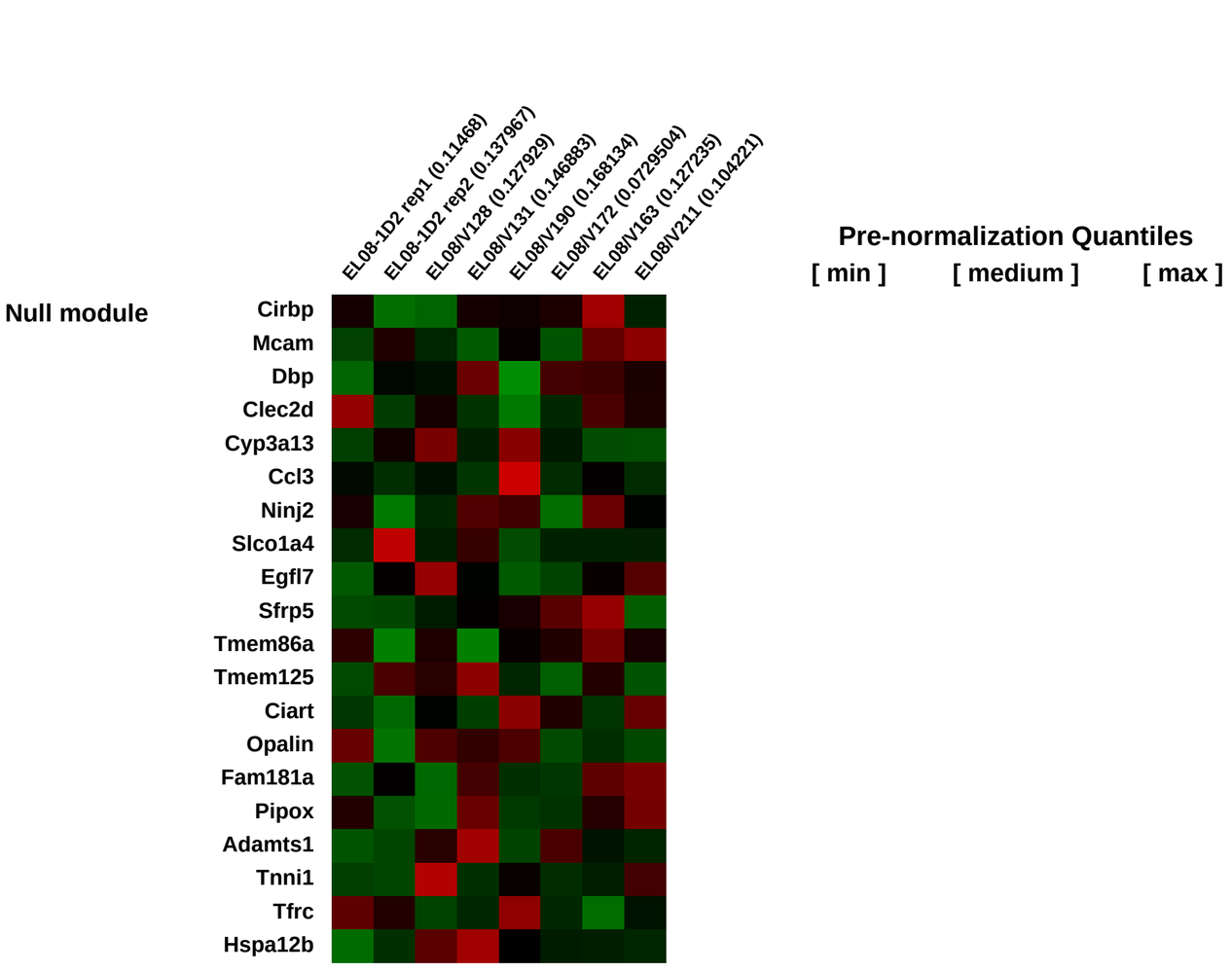

GEO Series "GSE5562" Expression Profiles

Num of samples in this series: 9

Scale of expression profile Z-scores

-3.0 -2.0 -1.0 0.0 1.0 2.0 3.0

GEO Link:	http://www.ncbi.nlm.nih.gov/geo/query/acc.cgi?acc=GSE5562
Status:	Public on Sep 01 2006
Title:	Gene expression profiling in small intestine of mice administered lactoperoxidase
Organism:	Mus musculus
Experiment type:	Expression profiling by array
Platform:	GPL1261
Pubmed ID:	17827675
Summary & Design:	**Summary:** Lactoperoxidase (LPO) is a component of milk and other external secretions. Recently, we found antiinflammatory effect of orally administered LPO in mouse model of influenza virus-induced pneumonia. In order to study influence of bovine LPO on the digestive tract as its possible target organ, we performed comprehensive gene expression analysis of the mouse small intestine using GeneChip microarray to compare the effect of LPO with that of water or bovine serum albumin (BSA). We observed that 3 h after single ingestion of LPO the levels of 78 gene expression are upregulated and those of 9 gene expressions are downregulated. Within most changed genes, 5 upregulated and 1 downregulated genes such as FK506 binding protein 5 (FKBP5) and serum/glucocorticoid regulated kinase (SGK) are known to be transcriptionally modulated by glucocorticoid. This result suggests that ingested LPO modulates gene expressions in the small intestine in a glucocorticoid-like manner and this activity may link to its systemic antiinflammatory effects. **Keywords:** treatment comparison **Overall design:** Mice were orally administered 200 microL of water (n=3), bovine serum albumin (BSA, 2.5 g/kg body weight, n=3), or bovine lactoperoxidase (LPO, 2.5 g/kg body weight, n=3). Three hours after administration, comprehensive gene expressions of jejunum detached payer's patch were analysed for comparison of LPO administration with water or BSA administration.

Background corr dist: KL-Divergence = 0.1144, L1-Distance = 0.0288, L2-Distance = 0.0014, Normal std = 0.4149

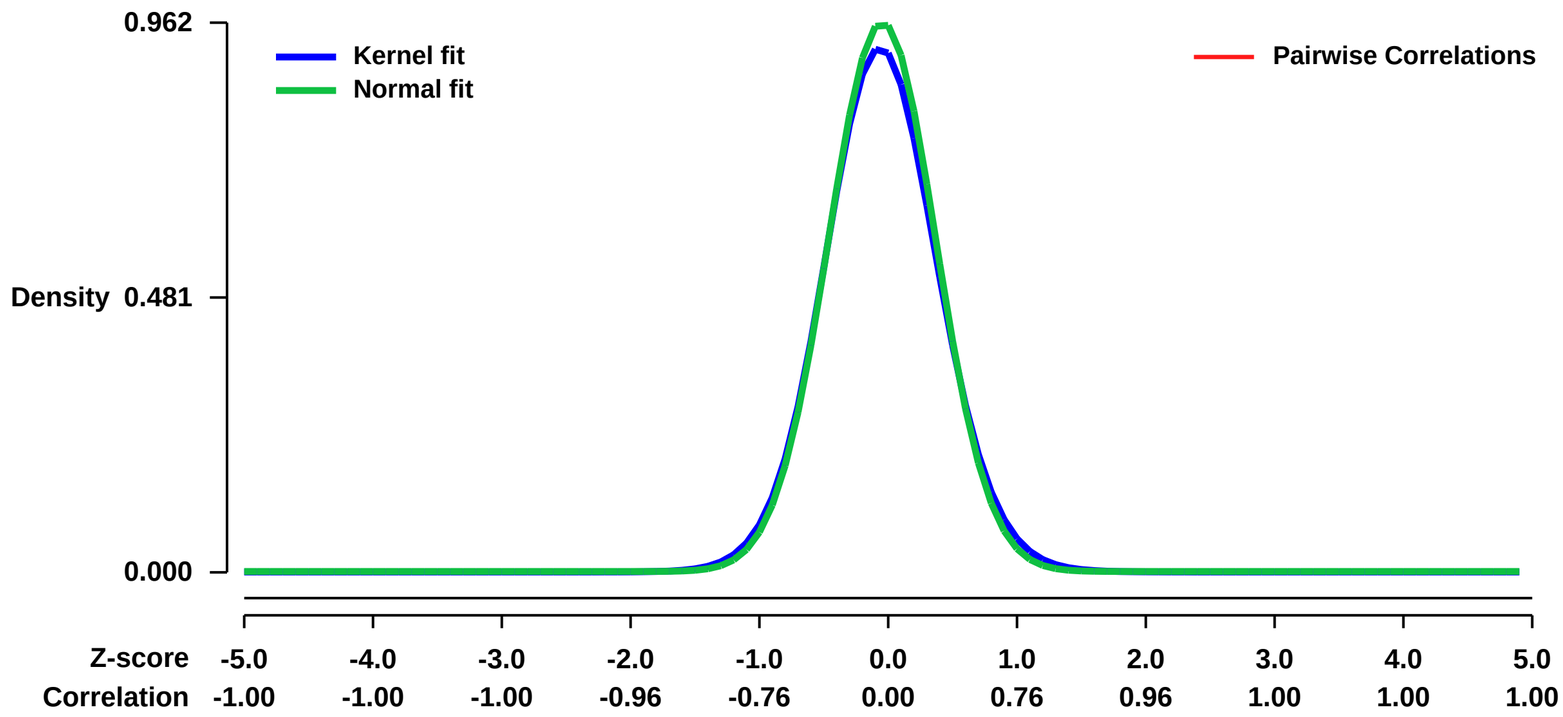

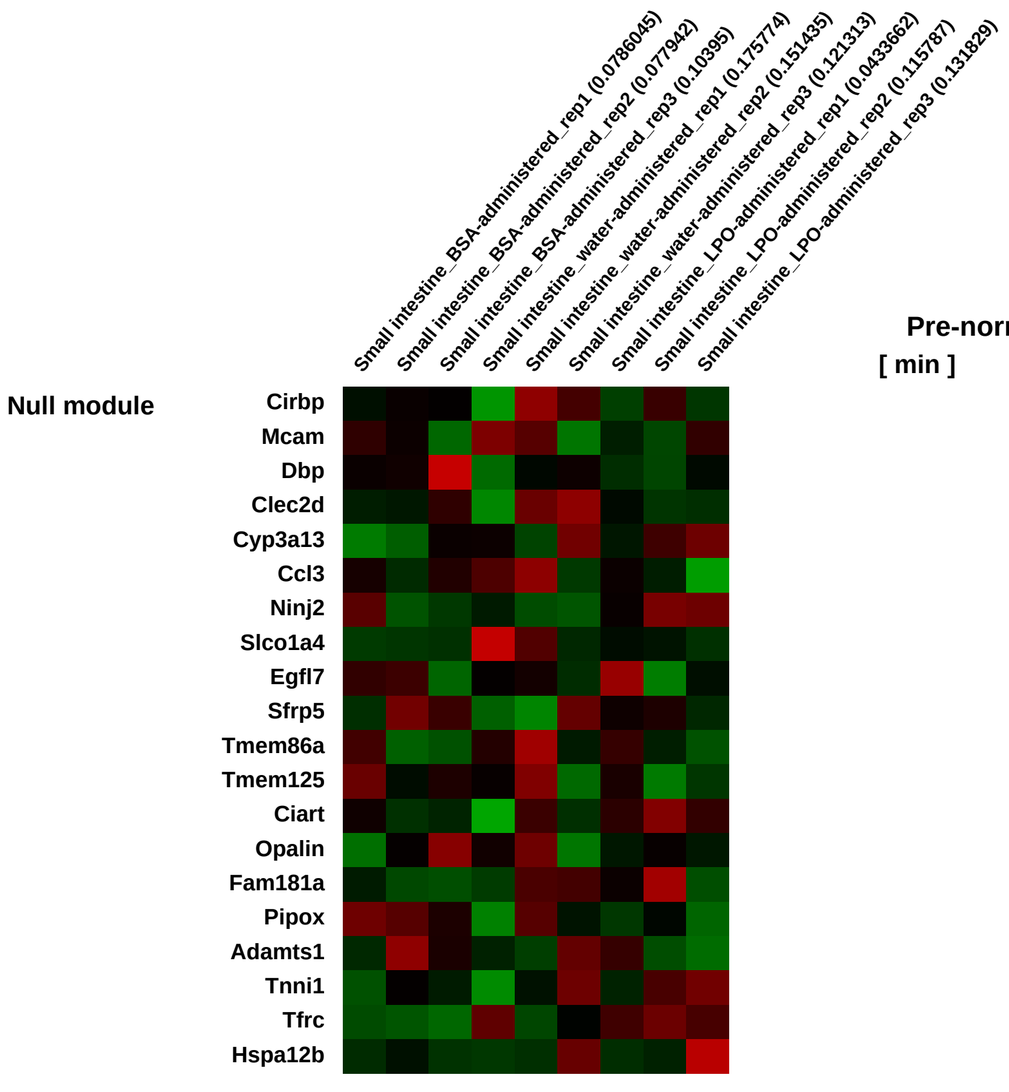

GEO Series "GSE26023" Expression Profiles

Num of samples in this series: 6

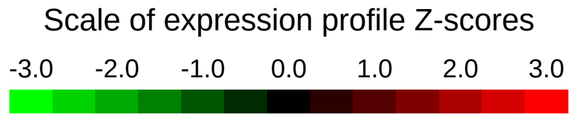

GEO Link:	http://www.ncbi.nlm.nih.gov/geo/query/acc.cgi?acc=GSE26023
Status:	Public on Feb 08 2011
Title:	Prolyl hydroxylase PHD3 is essential for hypoxic regulation of neutrophilic inflammation in humans and mice
Organism:	Mus musculus
Experiment type:	Expression profiling by array
Platform:	GPL1261
Pubmed ID:	21317538
Summary & Design:	**Summary:** Neutrophils were isolated form peripheral blood of wildtype and Phd3 null mice, cultured for 4 hours in hypoxia (3% O2) and micro array analysis performed The aim of the present study is to identify the mechanism by which phd3 is required for the hypoxia mediated survival of neutrophils **Overall design:** Murine peripheral blood neutrophils were isolated from wildtype and phd3 null mice, cultured for 4 hours in hypoxia (3% O2) and micro array analysis performed

Background corr dist: KL-Divergence = 0.0468, L1-Distance = 0.0286, L2-Distance = 0.0011, Normal std = 0.5961

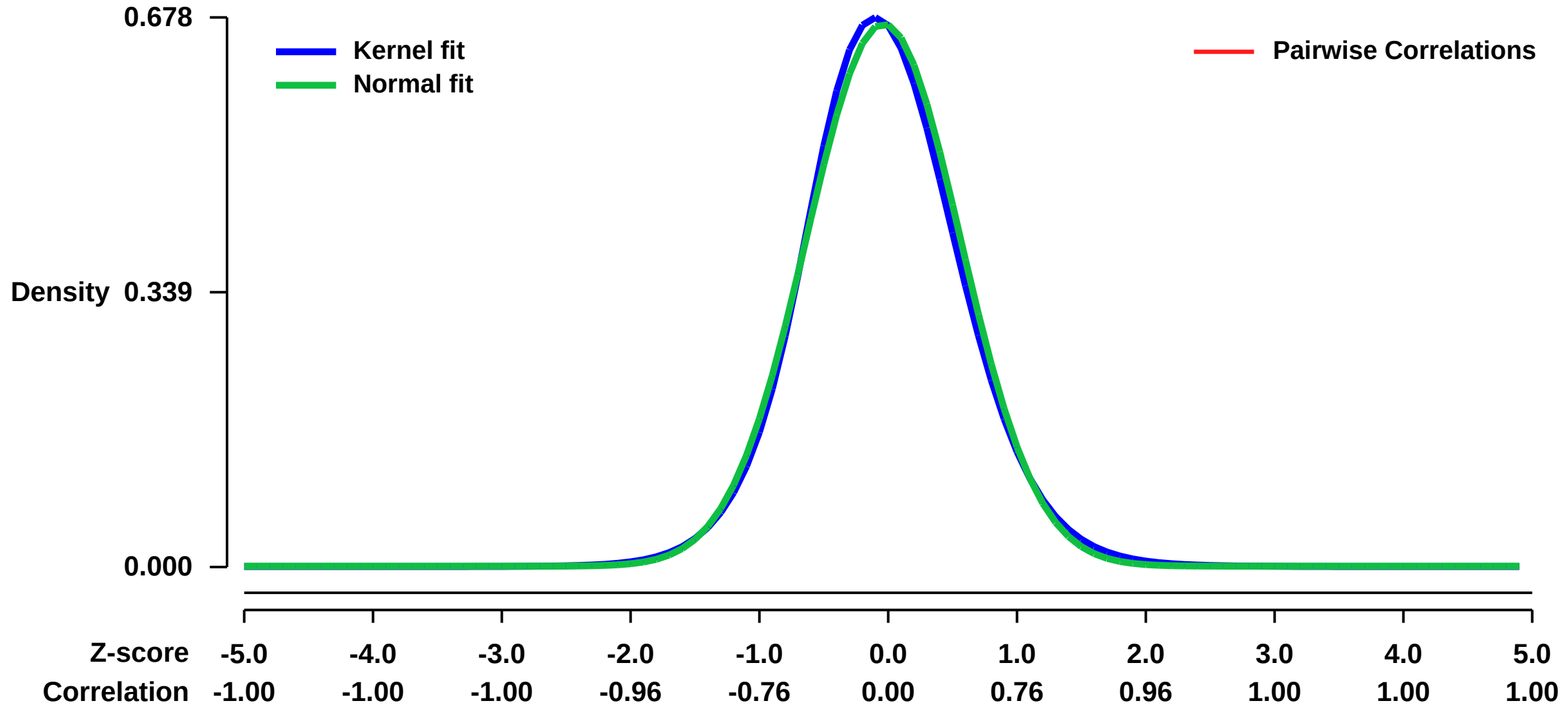

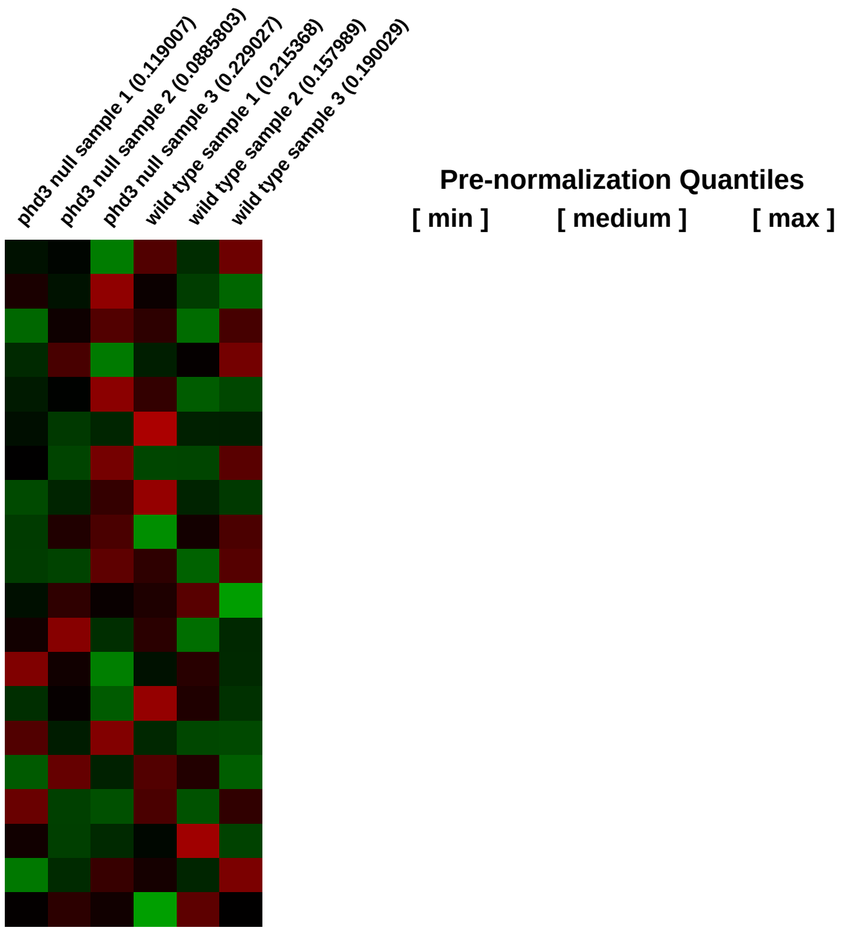

GEO Series "GSE23016" Expression Profiles

Num of samples in this series: 9

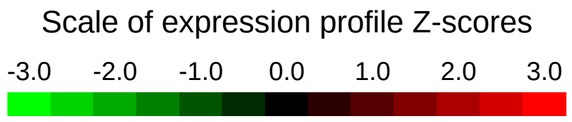

GEO Link:	http://www.ncbi.nlm.nih.gov/geo/query/acc.cgi?acc=GSE23016
Status:	Public on Mar 07 2011
Title:	Alternatively Spliced Variants of Interleukin-4 Promote Inflammation Differentially
Organism:	Mus musculus
Experiment type:	Expression profiling by array
Platform:	GPL1261
Pubmed ID:	21285395
Summary & Design:	**Summary:** IL-4d2 is a natural splice variant of IL-4 which lacks the region encoded by the second exon. Numerous recent reports suggested that the expression levels of IL-4d2 change in various diseases, especially those with pulmonary involvement, but the effects of IL-4d2 on the lungs in vivo have never been studied. Replication-deficient adenovirus-mediated gene delivery of mouse IL-4d2 to mouse lungs in vivo was used, and the effects compared with similar adenoviral delivery of mouse IL-4 or with infection with a NULL viral construct. The objective was to determine whether full-length wild-type Interleukin-4 encoded by exons 1-4 (IL-4) and alternatively spliced variant econded by exons 1,3, and 4 (IL-4d2) differentially affect gene expression in the lungs in vivo. The results show that IL-4d2 and IL-4 affected global gene expression differentially. **Keywords: Comparative analysis of gene delivery of alternative splice variants in vivo** **Overall design:** There were three mice overexpressing mouse IL-4 in their lungs, three mice overexpressing mouse IL-4d2 in their lungs, and three mice similarly infected with control AdV-NULL virus not encoding a cytokine.

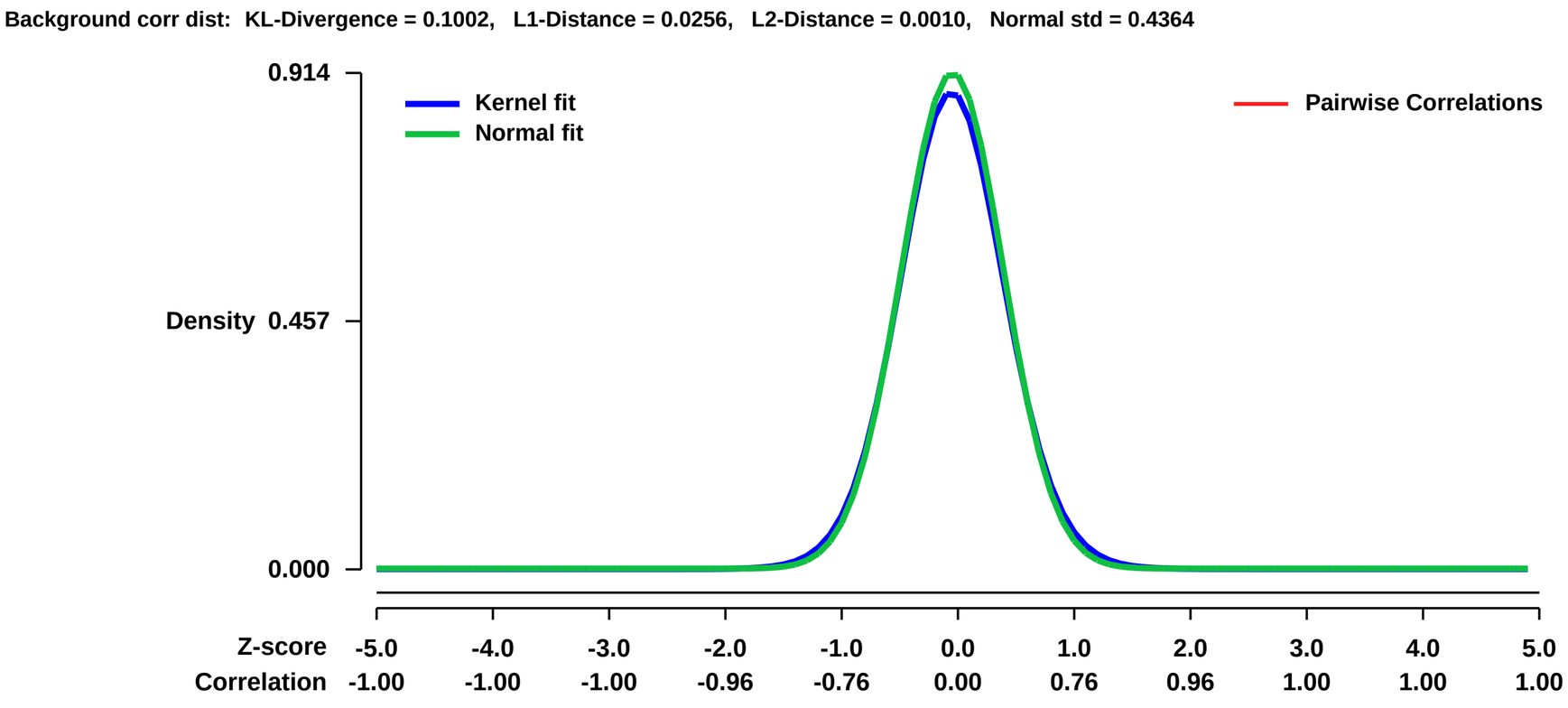

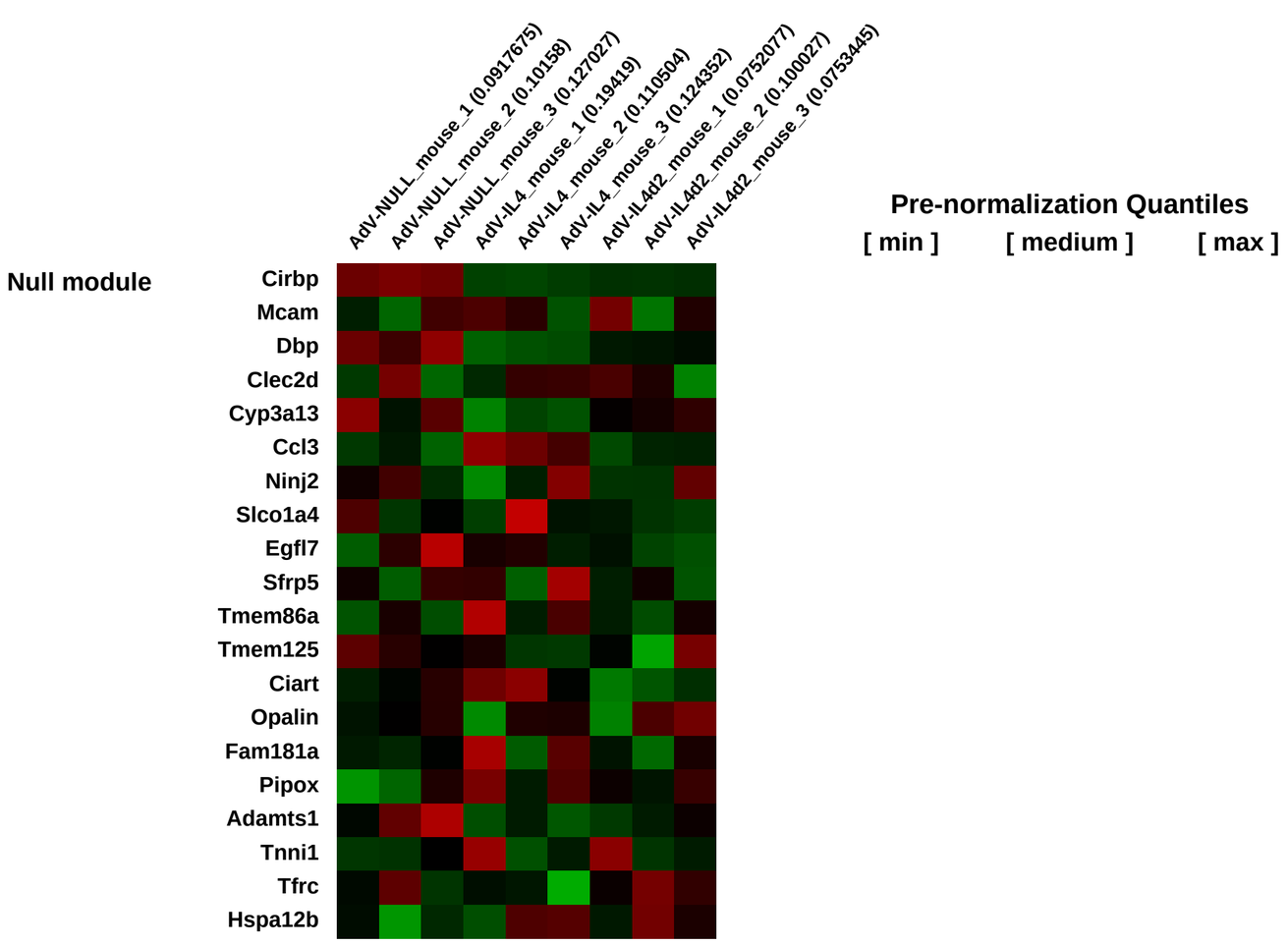

GEO Series "GSE53590" Expression Profiles

Num of samples in this series: 8

Scale of expression profile Z-scores

-3.0 -2.0 -1.0 0.0 1.0 2.0 3.0

GEO Link: http://www.ncbi.nlm.nih.gov/geo/query/acc.cgi?acc=GSE53590

Status: Public on Dec 24 2013

Title: Dietary fat disturbance of of gut microbial diurnal patterns uncouples host metabolic networks.

Organism: Mus musculus

Experiment type: Expression profiling by array

Platform: GPL1261

Pubmed ID:

Summary & Design:

Summary:
Diet-induced obesity (DIO) is rapidly becoming a global health problem, particularly as Westernization of emerging nations continues. Currently, one third of adult Americans are considered obese and, if current trends continue, >90% of US citizens are predicted to be affected by 2050. However, efforts to fight this epidemic have not yet produced sound solutions for prevention or treatment. Our studies reveal a balanced and chronobiological relationship between food consumption, daily variation in gut microbial evenness and function, basomedial hypothalamic circadian clock (CC) gene expression, and key hepatic metabolic regulatory networks , including CC and nuclear receptors (NR), that is are essential for metabolic homeostasis. â Westernâ diets high in saturated fats dramatically alter diurnal variation in microbial composition and function, which in turn lead to uncoupling of the hepatic CC and NR networks from central CC control in ways that offset the timing and types of regulatory factors directing metabolic function. These signals include microbial metabolites such as short chain fatty acids (SCFAs) and hydrogen sulfide (H2S) that can directly regulate or disrupt metabolic networks of the hepatocyte. Our study therefore provides insights into the complex and dynamic relationships between diet, gut microbes, and the host that are critical for maintenance of health. Perturbations of this constellation of processes, in this case by diet-induced dysbiosis and its metabolomic signaling, can potentially promote metabolic imbalances and disease. This knowledge opens up many possibilities for novel therapeutic and interventional strategies to treat and prevent DIO, ranging from the manipulation of gut microbial function to pharmacological targeting of host pathways to restore metabolic balance.

Overall design:
Mice were raised under germ-free or specific pathogen-free condition, or germ-free followed by conventionization. Liver tissues were harvested for total RNA isolation and hybridization on Affymetrix microarrays

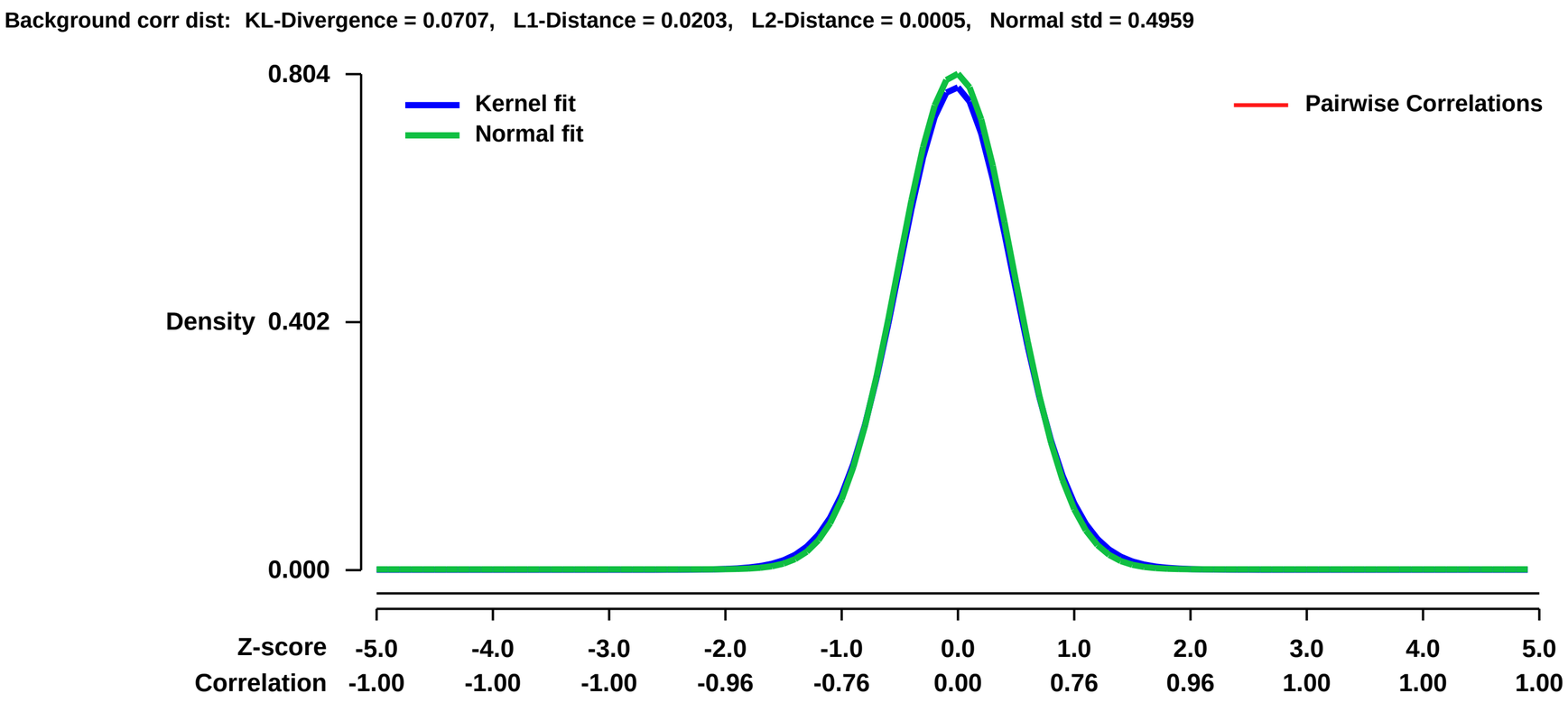

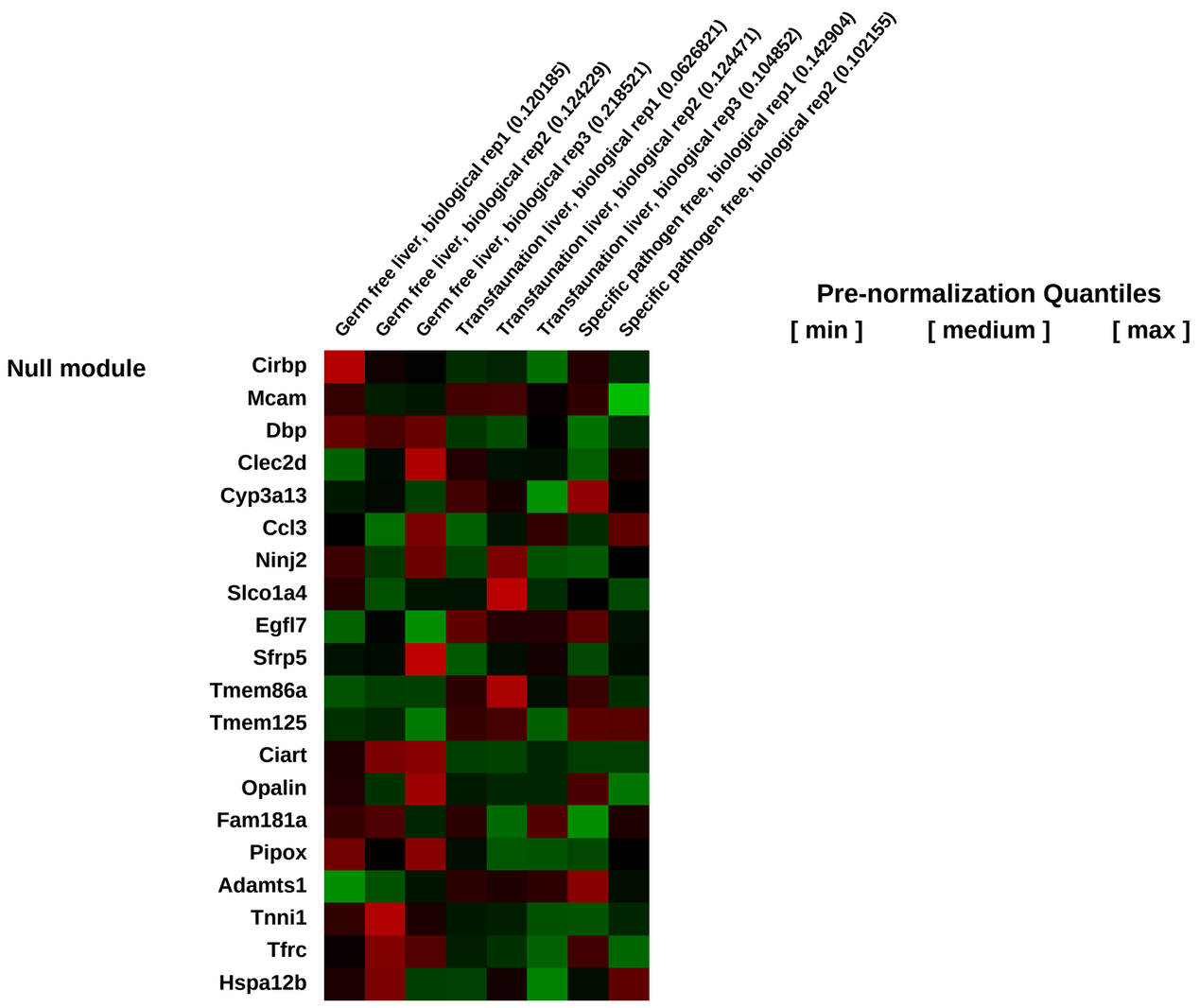

GEO Series "GSE30957" Expression Profiles

Num of samples in this series: 16

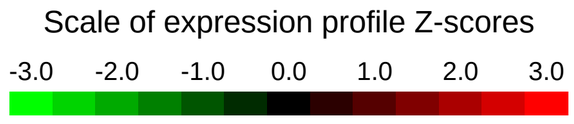

GEO Link:	http://www.ncbi.nlm.nih.gov/geo/query/acc.cgi?acc=GSE30957
Status:	Public on Feb 27 2012
Title:	Expression data from mouse embryo during neural tube closure
Organism:	Mus musculus
Experiment type:	Expression profiling by array
Platform:	GPL1261
Pubmed ID:	22045912

Summary & Design:

Summary:
This data series was used for two separate studies. The initial study was aimed to idenify expression changes brought about by the Cecr2Gt45Bic mutation during neural closure. The study included two different strains, BALB/cCrl in which Cecr2GT45Bic shows a neural tube defect phenotype and FVB/N in which Cecr2Gt45Bic does not manifest neural closure defects. The second was to idenify strain specific expression differences present during neural closure of the mouse embryo between BALB/cCrl and FVB/N in order to identify candidate modifiers of the Cecr2Gt45Bic neural tube defect. Relevant abstracts are included below.

The initial study ;

BACKGROUND: Over 200 mouse genes are associated with neural tube defects (NTDs), including Cecr2, the bromodomain-containing subunit of the CERF chromatin remodeling complex.

METHODS: Gene-trap mutation Cecr2Gt45Bic results in 74% exencephaly (equivalent of human anencephaly) on the BALB/c strain. Gene expression altered during cranial neural tube closure by the Cecr2 mutation was identified through microarray analysis of 11â 14 somites stage Cecr2Gt45Bicembryos.

RESULTS: Analysis of Affymetrix Mouse 430 2.0 chips detected 60 transcripts up-regulated and 54 transcripts down-regulated in the Cecr2Gt45Bic embryos (fold > 1.5, p < 0.05). The Cecr2 transcript was reduced only â…7- to 14-fold from normal levels, suggesting the Cecr2Gt45Bic is a hypomorphic mutation. We therefore generated a novel Cecr2 null allele (Cecr2tm1.1Hemc). Resulting mutants displayed a stronger penetrance of exencephaly than Cecr2Gt45Bic in both BALB/c and FVB/N strains, in addition to midline facial clefts and forebrain encephalocele in the FVB/N strain. The Cecr2 transcript is reduced 260-fold in the Cecr2tm1.1Hemc line. Subsequent qRT-PCR using Cecr2tm1.1Hemc mutant heads confirmed downregulation of transcription factors Alx1/Cart1,Dlx5, Eya1, and Six1.

CONCLUSIONS: As both Alx1/Cart1 and Dlx5 mouse mutations result in exencephaly, we hypothesize that changes in expression of these mesenchymal/ectodermal transcription factors may contribute to NTDs associated with Cecr2. Birth Defects Research (Part A), 2010. 010 Wiley-Liss, Inc.

The second study:

ABSTRACT:Although neural tube defects (NTDs) are common in humans, little is known about their multifactorial genetic causes. While most mouse models involve NTDs caused by a single mutated gene, we have previously described a multigenic system involving susceptibility to NTDs. In mice with a mutation in Cecr2, the cranial NTD exencephaly shows strain specific differences in penetrance, with 74% penetrance in BALB/cCrl and 0% penetrance in FVB/N. Whole genome linkage analysis showed that a region of chromosome 19 was partially responsible for this difference in penetrance. We now reveal by genetic analysis of three subinterval congenic lines that the chromosome 19 region contains more than one modifier gene. Analysis of embryos showed that although a Cecr2 mutation causes wider neural tubes in both strains, FVB/N embryos overcome this abnormality and close. A microarray analysis comparing neurulating female embryos from both strains identified differentially expressed genes within the chromosome 19 region, including Arhgap19, which is expressed at a lower level in BALB/cCrl due to a stop codon specific to that substrain. Modifier genes in this region are of particular interest because it is syntenic to human chromosome 10q25, the site of a human susceptibility locus. (MANUSCRIPT PENDING SUBMISSION)

Overall design:
Thieler STAGE 13-14 (11-14 somite) female embryos where disected away from extraembryonic membranes for RNA extraction and hybridization on Affymetrix microarrays. A single embryo was processed per array, with four biological replicates per genotype BALB/cCrl, Cecr2GT45Bic BALB/cCrl, FVB/N, and Cecr2Gt45Bic FVB/N.

Background corr dist: KL-Divergence = 0.1763, L1-Distance = 0.0411, L2-Distance = 0.0035, Normal std = 0.3492

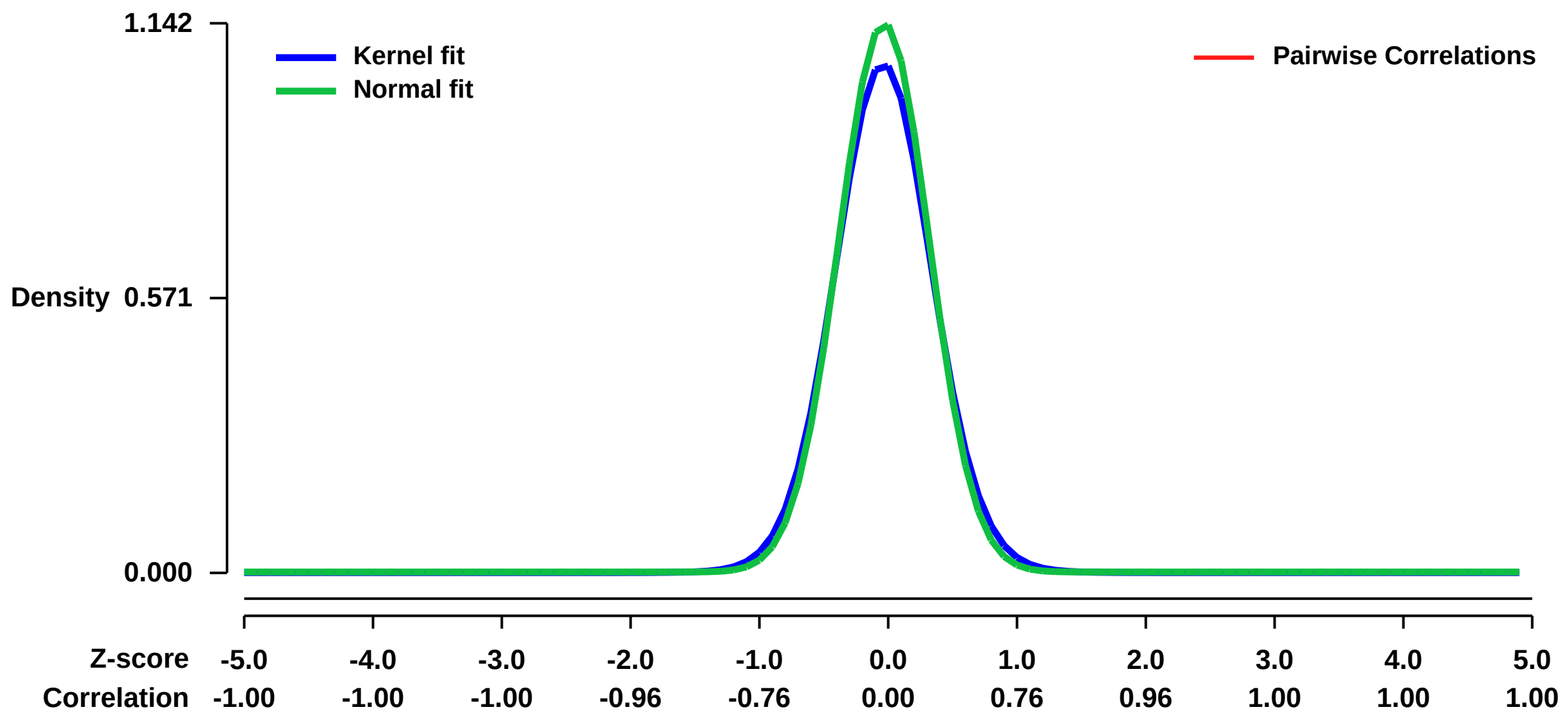

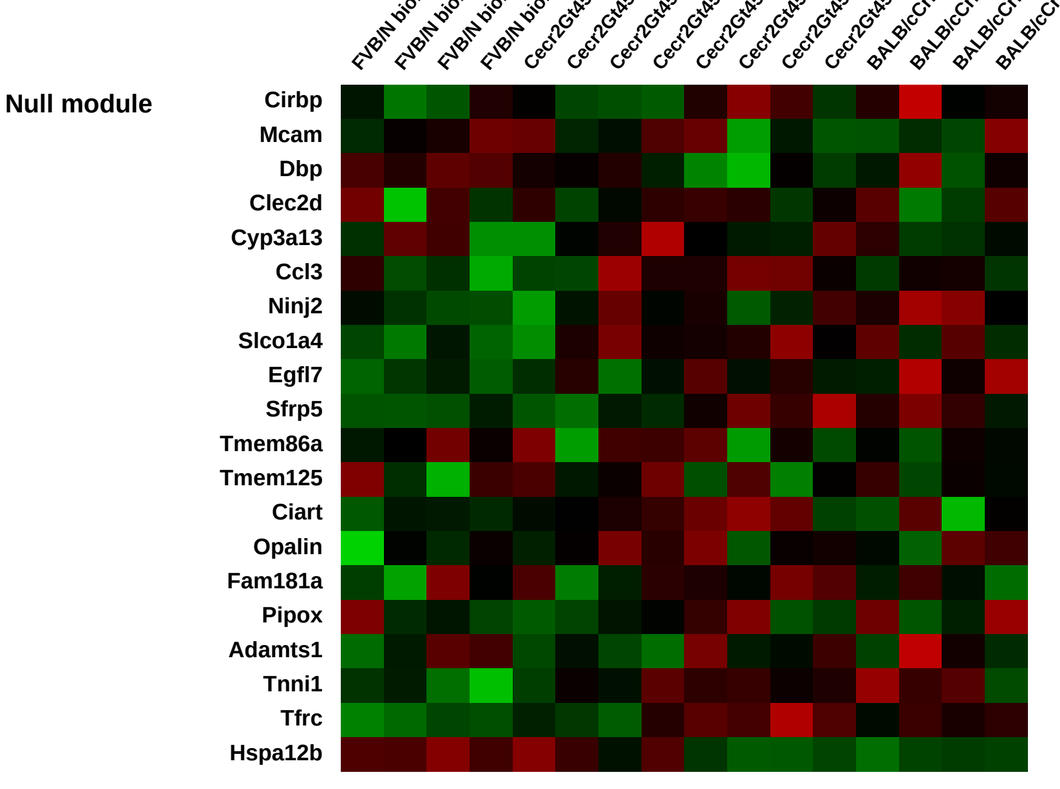

GEO Series "GSE9804" Expression Profiles

Num of samples in this series: 9

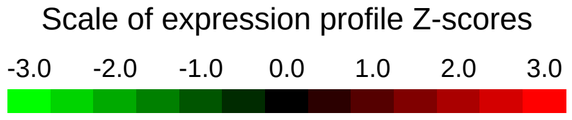

GEO Link:	http://www.ncbi.nlm.nih.gov/geo/query/acc.cgi?acc=GSE9804
Status:	Public on Dec 17 2007
Title:	Striatal gene expression data from 12 weeks-old R6/2 mice and control mice (set 2)
Organism:	Mus musculus
Experiment type:	Expression profiling by array
Platform:	GPL1261
Pubmed ID:	17519223
Summary & Design:	**Summary:** To test the hypotheses that mutant huntingtin protein length and wild-type huntingtin dosage have important effects on disease-related transcriptional dysfunction, we compared the changes in mRNA in seven genetic mouse models of Huntington's disease (HD) and postmortem human HD caudate. Transgenic models expressing short N-terminal fragments of mutant huntingtin (R6/1 and R6/2 mice) exhibited the most rapid effects on gene expression, consistent with previous studies. Although changes in the brains of knock-in and full-length transgenic models of HD took longer to appear, 15- and 22-month CHL2(Q150/Q150), 18-month Hdh(Q92/Q92) and 2-year-old YAC128 animals also exhibited significant HD-like mRNA signatures. Whereas it was expected that the expression of full-length huntingtin transprotein might result in unique gene expression changes compared with those caused by the expression of an N-terminal huntingtin fragment, no discernable differences between full-length and fragment models were detected. In addition, very high correlations between the signatures of mice expressing normal levels of wild-type huntingtin and mice in which the wild-type protein is absent suggest a limited effect of the wild-type protein to change basal gene expression or to influence the qualitative disease-related effect of mutant huntingtin. The combined analysis of mouse and human HD transcriptomes provides important temporal and mechanistic insights into the process by which mutant huntingtin kills striatal neurons. In addition, the discovery that several available lines of HD mice faithfully recapitulate the gene expression signature of the human disorder provides a novel aspect of validation with respect to their use in preclinical therapeutic trials. **Keywords:** genetic modification **Overall design:** Striatal samples from 5 R6/2 mutant mice (12 weeks-old) and 4 age-matched wild-type mice.

Background corr dist: KL-Divergence = 0.0684, L1-Distance = 0.0199, L2-Distance = 0.0005, Normal std = 0.5033

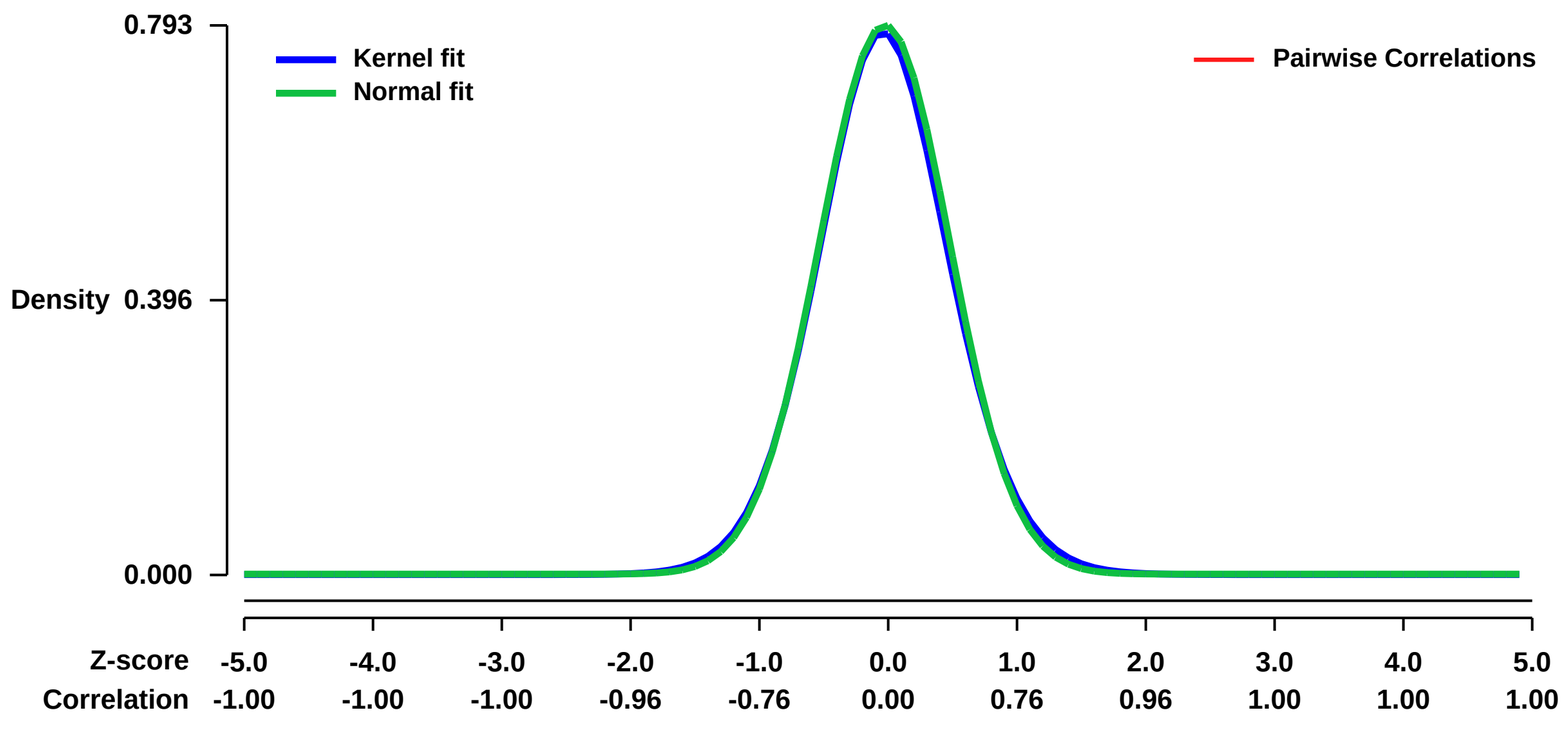

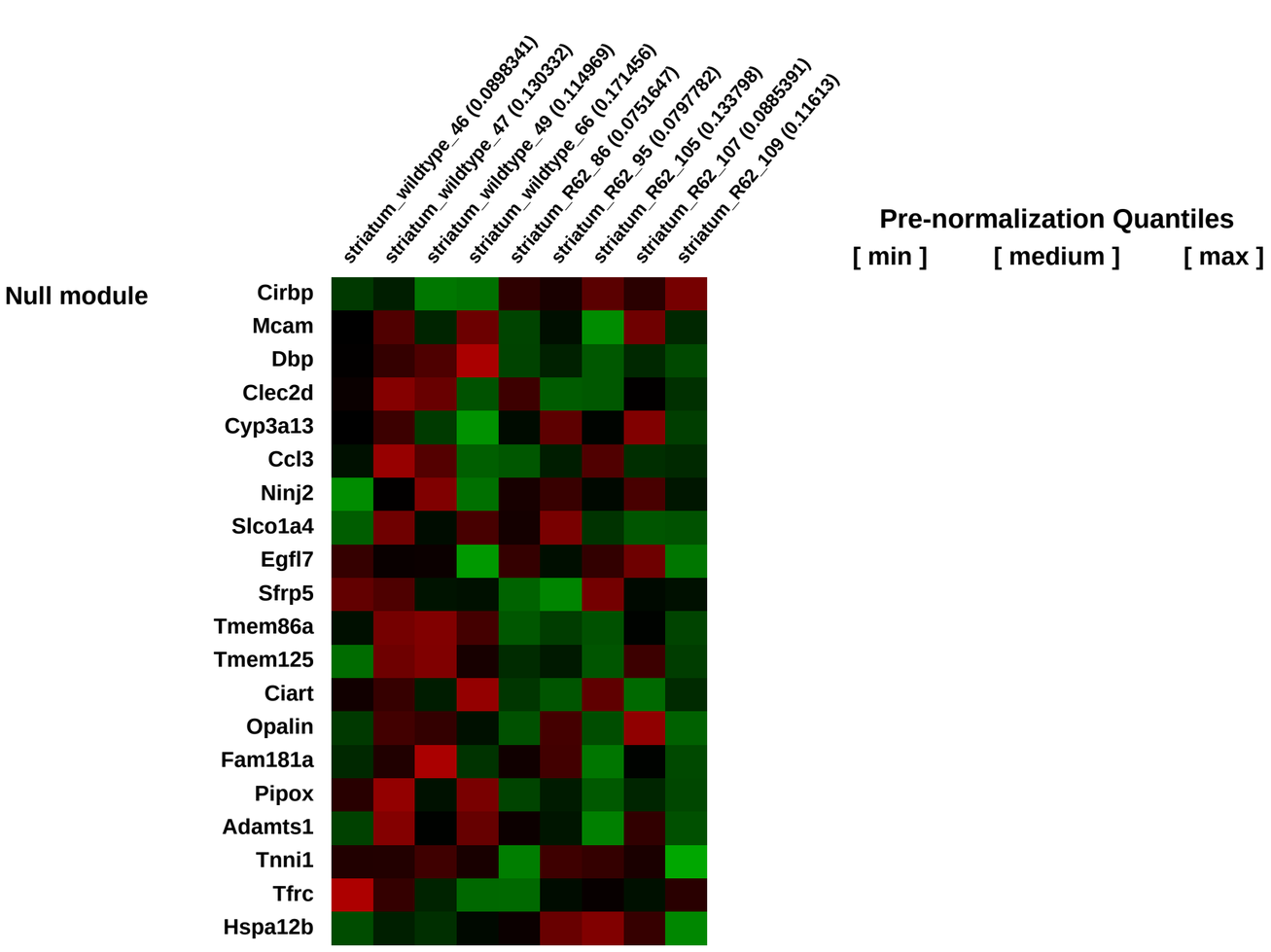

GEO Series "GSE10912" Expression Profiles

Num of samples in this series: 6

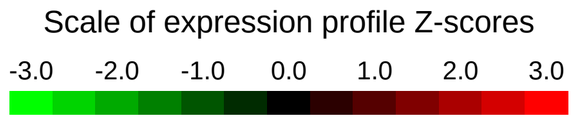

GEO Link:	http://www.ncbi.nlm.nih.gov/geo/query/acc.cgi?acc=GSE10912
Status:	Public on Mar 22 2008
Title:	Gene expression profiling in BCR/ABL expressing HSCs
Organism:	Mus musculus
Experiment type:	Expression profiling by array
Platform:	GPL1261
Pubmed ID:	22431519
Summary & Design:	**Summary:** The BCR-ABL oncogene, generated by Philadelphia chromosome, is present in about 95% human Chronic myeloid leukemia (CML) and 20~30% acute lymphoblastic leukemia (ALL). One of BCR-ABL isoforms, P210, is more often detected in CML and ALL patients. Although BCR-ABL kinase inhibitors are effective in controlling the diseases, they do not provide cure due to the development of drug resistance and the insensitivity of leukemia stem cells to these drugs. Identification of new therapeutic targets is critical. To identify potential target against leukemia stem cells, we studied gene expression in leukemia stem cells, which were identified in mice in our lab (Hu Y, Swerdlow S, Duffy TM, Weinmann R, Lee FY, Li S. 2006. Targeting multiple kinase pathways in leukemic progenitors and stem cells is essential for improved treatment of Ph+ leukemia. Proc Natl Acad Sci USA 103(45):16870-16875.). The sorted leukemia stem cells that expressed BCR-ABL were used for isolation of RNA, followed by the analysis of gene expression using the DNA microarray. The same lineage of non-BCR-ABL-expressing normal hematopoietic stem cells was used as control. We have identified some interesting genes that are up- or down-regulated by BCR-ABL in these leukemia stem cells. We are currently studying the functions of these identified genes. **Keywords:** Genetic modification **Overall design:** Bone marrow cells are isolated from the long bones of CML mice that are untreated or treated with imatinib. BCR-ABL-expressing or non-BCR-ABL-expressing (transduced with the empty GFP vector) hematopoietic stem cells (GFP+Lin-c-Kit+Sca-1+) are stored by FACS directly into RNAlater (Ambion, Austin, TX) and are homogenized in RLT Buffer (RNeasy Micro Kit (Qiagen, Valencia, CA)). Total RNA is isolated by following the protocol for the RNeasy Micro Kit, and quality is assessed using a 2100 Bioanalyzer instrument and RNA 6000 Pico LabChip assay (Agilent Technologies, Palo Alto, CA). Utilizing the GeneChip Whole Transcript Sense Target Labeling Assay kit (Affymetrix, Santa Clara, CA.) between 100-300ng of total RNA undergoes reverse transcription with random hexamers tagged with T7 sequence. The double stranded cDNA that is generated is then amplified by T7 RNA polymerase to produce cRNA. Second cycle first strand cDNA synthesis then takes place incorporating dUTP which is later used as sites where fragmentation occurs by utilizing an uracil DNA glycosylase and apurinic/apyrimidinic endonuclease 1 enzyme mix. The fragmented cDNA is then labeled by terminal transferase attaching a biotin molecule using Affymetrix proprietary DNA labeling Reagent. Approximately 2.0´µg of fragmented and biotin-labeled cDNA is then hybridized onto a Mouse Gene ST 1.0 Array (Affymetrix, Santa Clara, CA.) for 16 hours at 45´ºC. Post-hybridization staining and washing are performed according to manufacturer's protocols using the Fluidics Station 450 instrument (Affymetrix). Finally, the arrays are scanned with a GeneChip? Scanner 3000. Images are acquired and cel files generated which are then used for analysis.

Background corr dist: KL-Divergence = 0.0432, L1-Distance = 0.0407, L2-Distance = 0.0025, Normal std = 0.6321

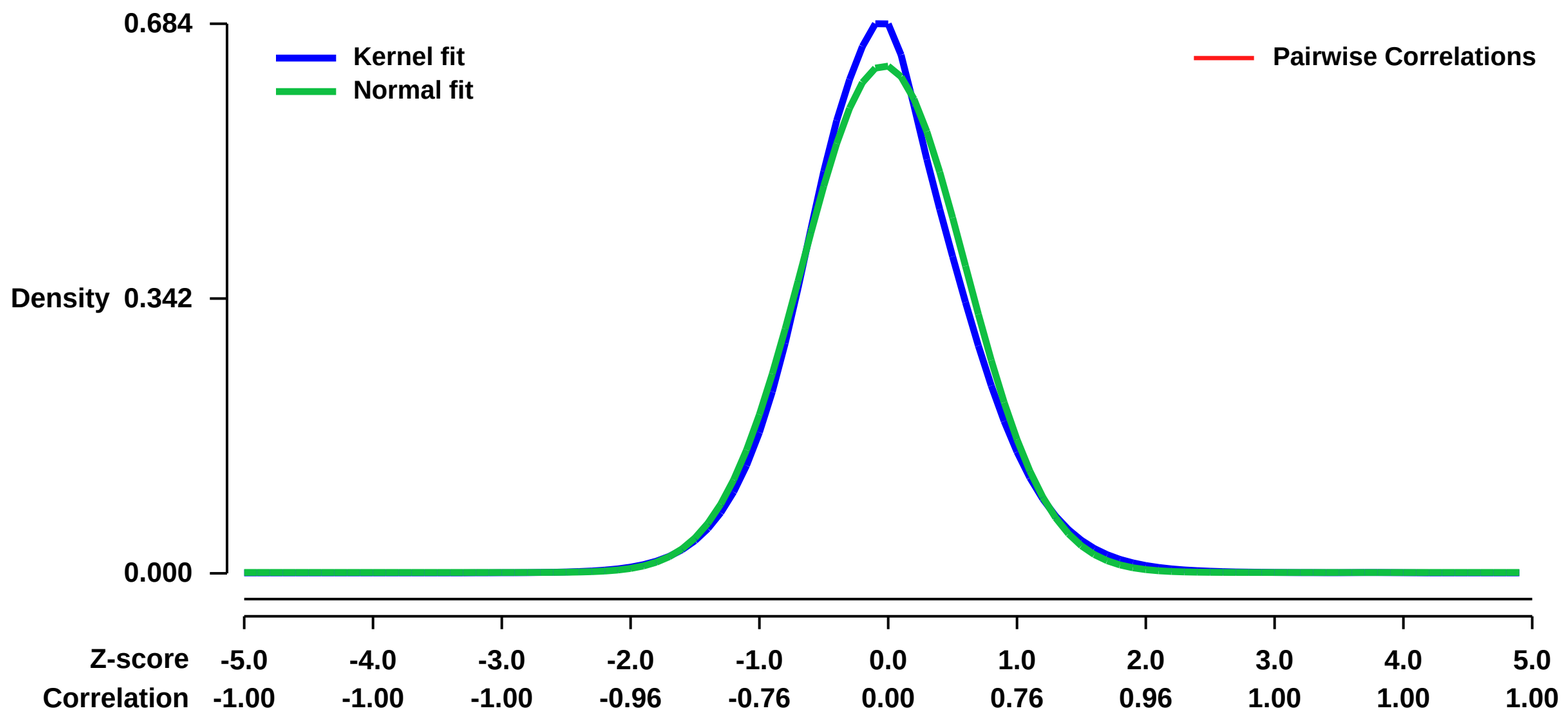

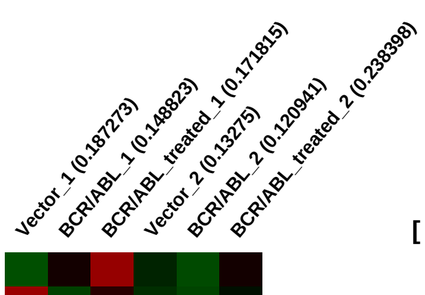

Pre-normalization Quantiles

[min] [medium] [max]

Null module

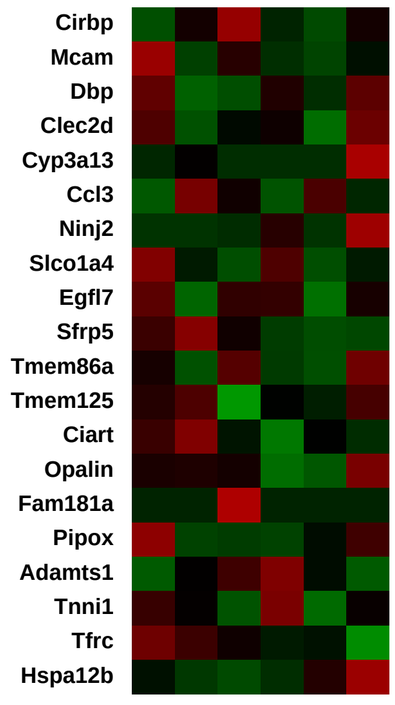

GEO Series "GSE7863" Expression Profiles

Num of samples in this series: 16

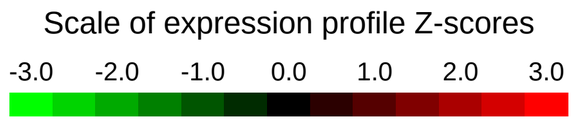

GEO Link:	**http://www.ncbi.nlm.nih.gov/geo/query/acc.cgi?acc=GSE7863**
Status:	**Public on Mar 01 2009**
Title:	**Gene expression profiling of Galgt2 overexpression in mdx skeletal muscle**
Organism:	**Mus musculus**
Experiment type:	**Expression profiling by array**
Platform:	**GPL1261**
Pubmed ID:	

Summary & Design:

Summary:
Transgenic overexpression of Galgt2 in the skeletal muscles of mdx mice inhibits the development of disease pathology associated with muscular dystrophy. This is the case both in transgenic mice, where Galgt2 overexpression occurs from embryonic timepoints onward and in mdx mice where Galgt2 is overexpressed in the early postnatal period using Adeno-associated virus (AAV). Here, we use gene expression profiling to compare transcriptional changes resulting from embryonic and postnatal Galgt2 overexpression in mdx skeletal muscle. A surprising number of changes were in genes known to ameliorate muscular dystrophy when overexpressed (agrin, integrin alpha 7, ADAM12, Bcl2) or to cause muscular dystrophy when mutated (collagen VI (alpha1,alpha2), plectin 1, dystroglycan, selenoprotein N1, integrin alpha7, biglycan, dysferlin). Several genes involved in calcium homeostasis were also changed. In Galgt2 transgenic mice, where embryonic overexpression of Galgt2 in skeletal muscles alters neuromuscular development and muscle growth, the number of gene expression changes was vastly greater, however, 14% of genes altered in postnatal AAV-Galgt2 infected mdx muscles were also changed with embryonic overexpression. These experiments suggest that postnatal overexpression of Galgt2 inhibits muscular dystrophy in mdx mice via induction of a group of genes that, in aggregate, can govern membrane stability, membrane repair, calcium homeostasis, and apoptosis.

Keywords: disease state analysis, gene therapy, comparative gene expression, muscular dystrophy, glycosylation, collagens, integrins, dysferlin, dystroglycan

Overall design:
Microarrays were done in three groups at a time. 1) Transgenic Overexpression of Galgt2 - comprised to Wild Type (WT), Galgt2 Transgenic (CT), Dystrophin-Deficient (mdx), and Galgt2 Transgenic and Dystrophin-Deficient (CTmdx) each in duplicate 2) AAV-Mediated Galgt2 Gene Delivery in to the mdx gastrocnemius muscle in the postnatal period - comprised of AAVGalgt2 and PBS each in duplicate, and 3) Myoblasts and myotubes - comptised of one sample each of C1C12 myoblasts and myotubes, C2C12 myoblasts and myotubes stably transfected with Galgt2

Background corr dist: **KL-Divergence = 0.0693, L1-Distance = 0.0383, L2-Distance = 0.0029, Normal std = 0.5016**

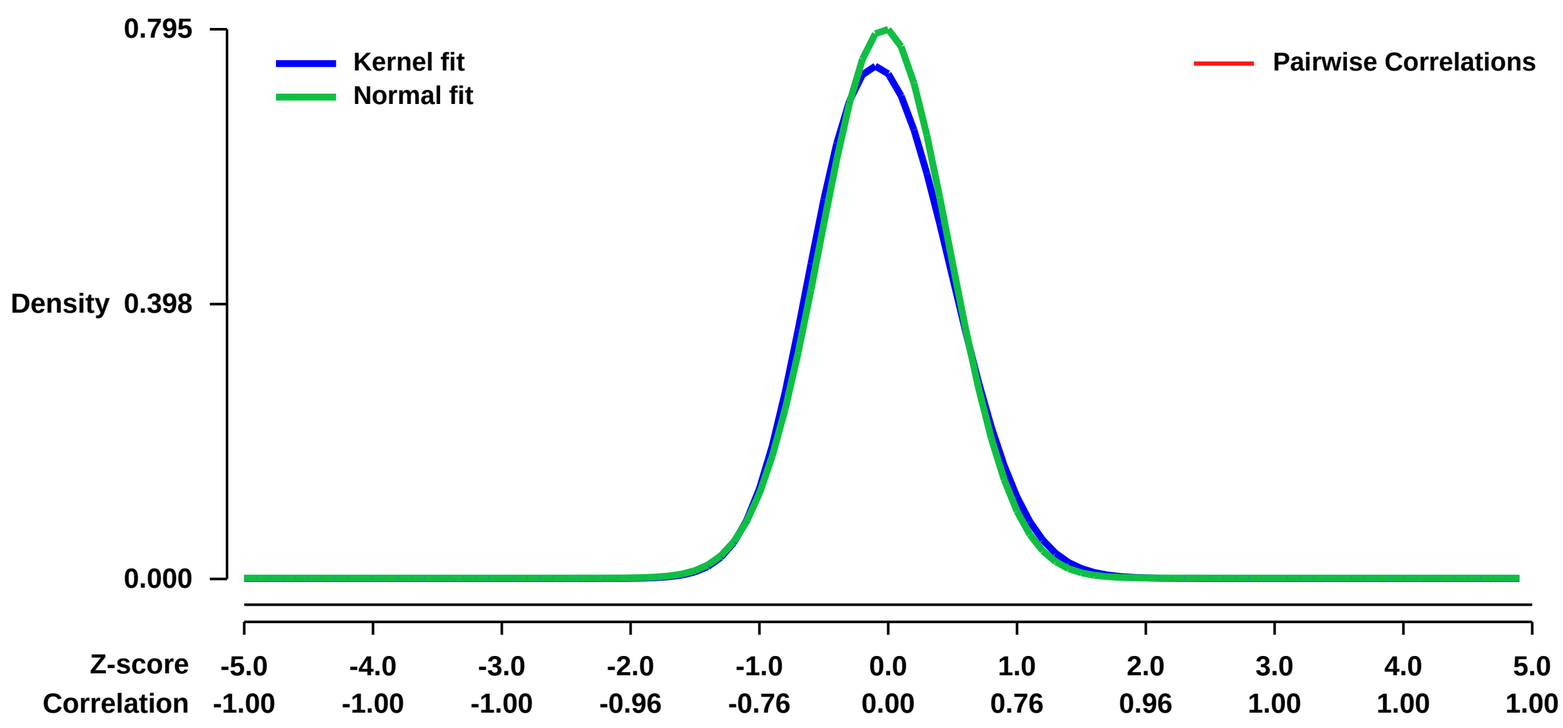

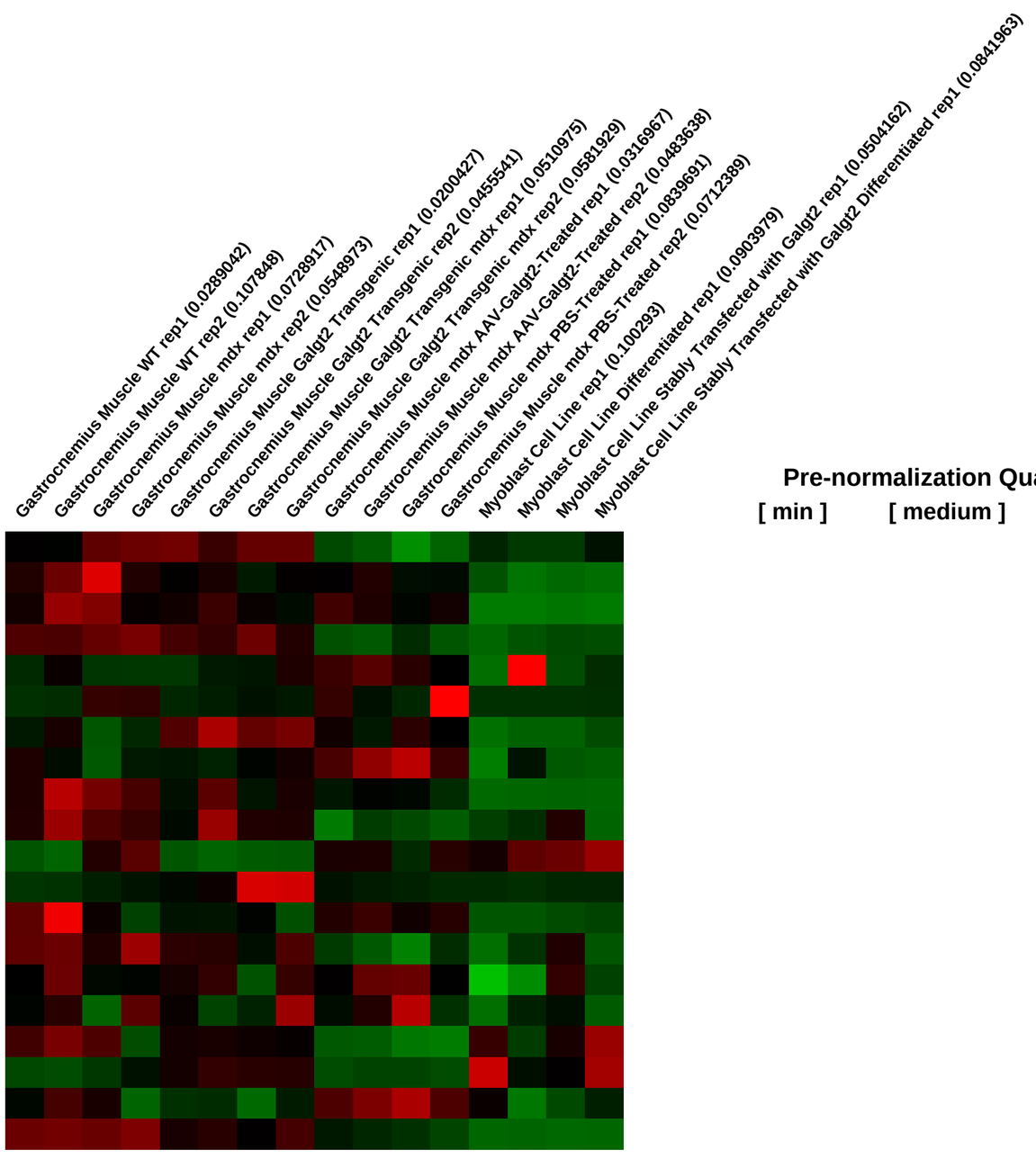

Null module

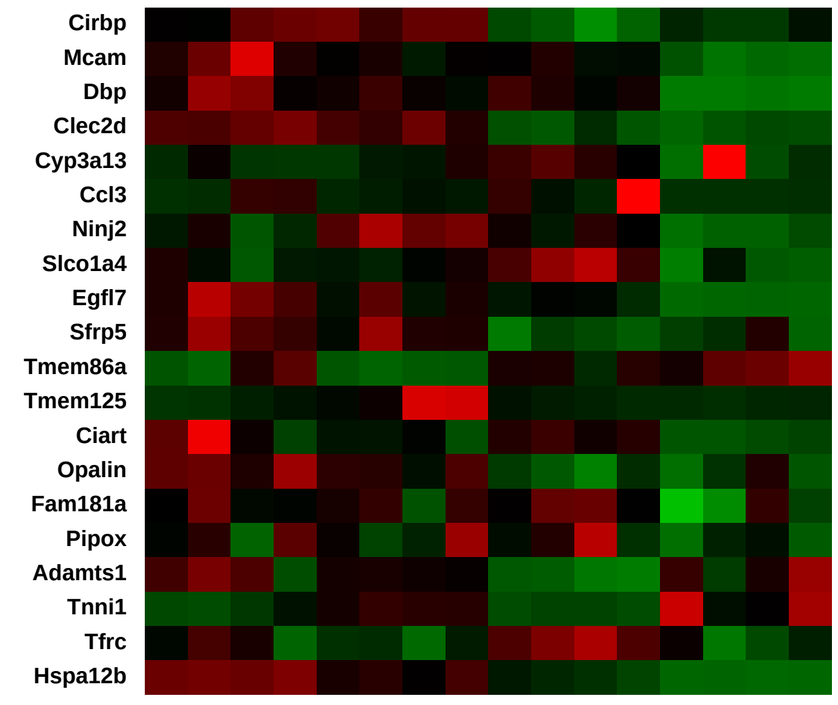

GEO Series "GSE27987" Expression Profiles

Num of samples in this series: 31

Scale of expression profile Z-scores

-3.0 -2.0 -1.0 0.0 1.0 2.0 3.0

GEO Link:	http://www.ncbi.nlm.nih.gov/geo/query/acc.cgi?acc=GSE27987
Status:	Public on Aug 25 2011
Title:	Differential pre-mRNA processing in Crebbp+/- mice
Organism:	Mus musculus
Experiment type:	Expression profiling by array
Platform:	GPL1261
Pubmed ID:	21901164
Summary & Design:	**Summary:** The presence of unspliced transcripts in hematopoietic stem cells (HSCs) and the proposed association of CREBBP with the constitutive production of unspliced RNA and with pre-mRNA processing prompted us to examine more closely an anomaly we had noted in microarray-based gene expression studies but had previously attributed to experimental noise. We noticed that more than half of the probe sets down-regulated in Crebbp+/- fetal liver HSCs (FLHSCs) relative to wild-type (WT) mapped entirely within introns, rather than detecting exonic or spliced sequences. We therefore set out to test whether this might be evidence that reduced CREBBP levels selectively alter the generation of full-length, unspliced pre-mRNA. We also asked whether this process might be associated with differentiation since self-renewal and lineage commitment are the both responses for which HSCs are primed. **Overall design:** cell type comparison

Background corr dist: KL-Divergence = 0.0422, L1-Distance = 0.0924, L2-Distance = 0.0091, Normal std = 0.9341

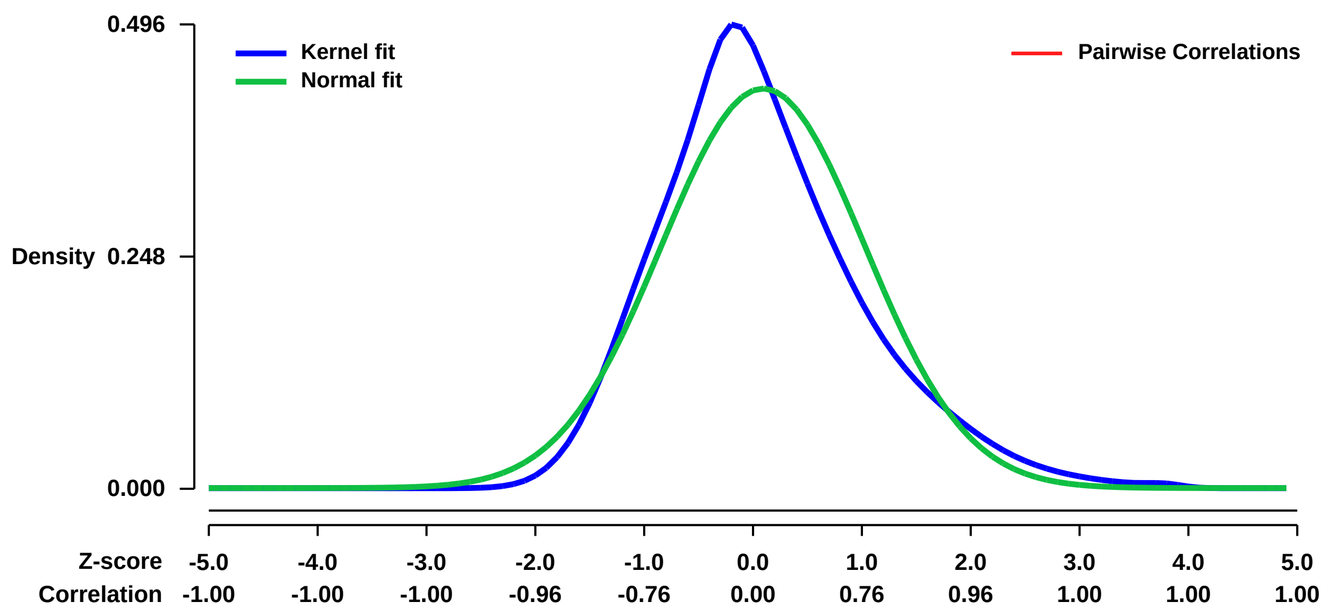

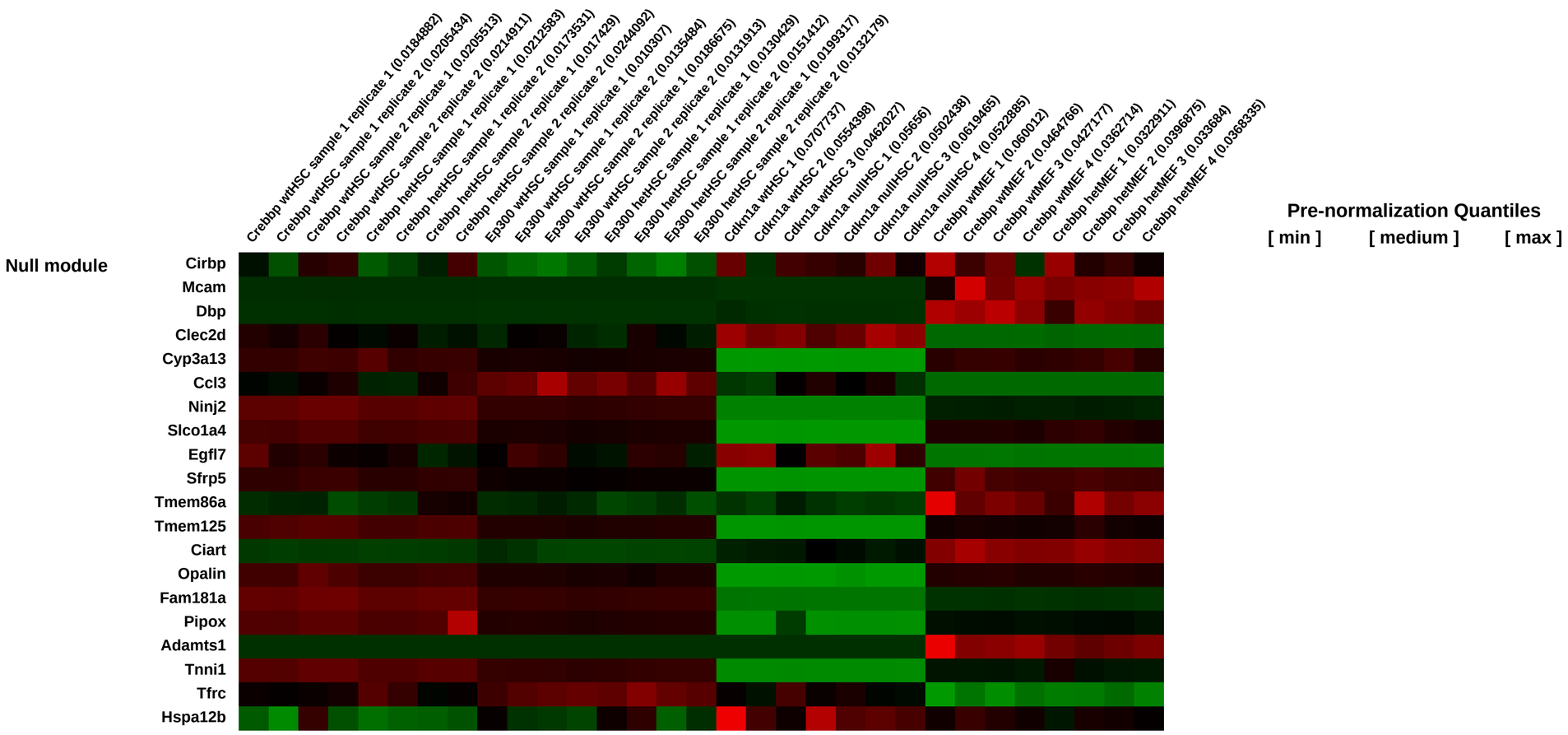

GEO Series "GSE38048" Expression Profiles

Num of samples in this series: 20

Scale of expression profile Z-scores

-3.0 -2.0 -1.0 0.0 1.0 2.0 3.0

GEO Link:	http://www.ncbi.nlm.nih.gov/geo/query/acc.cgi?acc=GSE38048
Status:	Public on Aug 20 2012
Title:	E2F1 loss induces spontaneous tumour development in Rb-deficient epidermis
Organism:	Mus musculus
Experiment type:	Expression profiling by array
Platform:	GPL1261
Pubmed ID:	22890321
Summary & Design:	**Summary:** The specific ablation of Rb1 gene in epidermis (RbF/F;K14cre) promotes proliferation and altered differentiation but does not produce spontaneous tumour development. These phenotypic changes are associated with increased expression of E2F members and E2F-dependent transcriptional activity. Here, we have focused on the possible dependence on E2F1 gene function. We have generated mice that lack Rb1 in epidermis in an inducible manner (RbF/F;K14creERTM). These mice are indistinguishable from those lacking pRb in this tissue in a constitutive manner (RbF/F;K14cre). In an E2F1-null background (RbF/F;K14creERTM; E2F1-/- mice), the phenotype due to acute Rb1 loss is not ameliorated by E2F1 loss, but rather exacerbated, indicating that pRb functions in epidermis do not rely solely on E2F1. On the other hand, RbF/F;K14creERTM;E2F1-/- mice develope spontaneous epidermal tumours of hair follicle origin with high incidence. These tumours, which retain a functional p19arf/p53 axis, also show aberrant activation of ¸†catenin/Wnt pathway. Gene expression studies revealed that these tumours display relevant similarities with specific human tumours. These data demonstrate that the Rb/E2F1 axis exerts essential functions not only in maintaining epidermal homeostasis, but also in suppressing tumour development in epidermis, and that the disruption of this pathway may induce tumour progression through specific alteration of developmental programs. **Overall design:** Gene expression was compared between normal mouse skin, skin from transgenic RbF/F;K14creERTM; E2F1-/- , E2F1-/-, and RbF/F;K14creERTM; E2F1-/- mouse, and carcinomas arising in the skin of RbF/F;K14creERTM; E2F1-/- mouse. All mice were treated with tamoxifen.

Background corr dist: KL-Divergence = 0.1039, L1-Distance = 0.0370, L2-Distance = 0.0028, Normal std = 0.4346

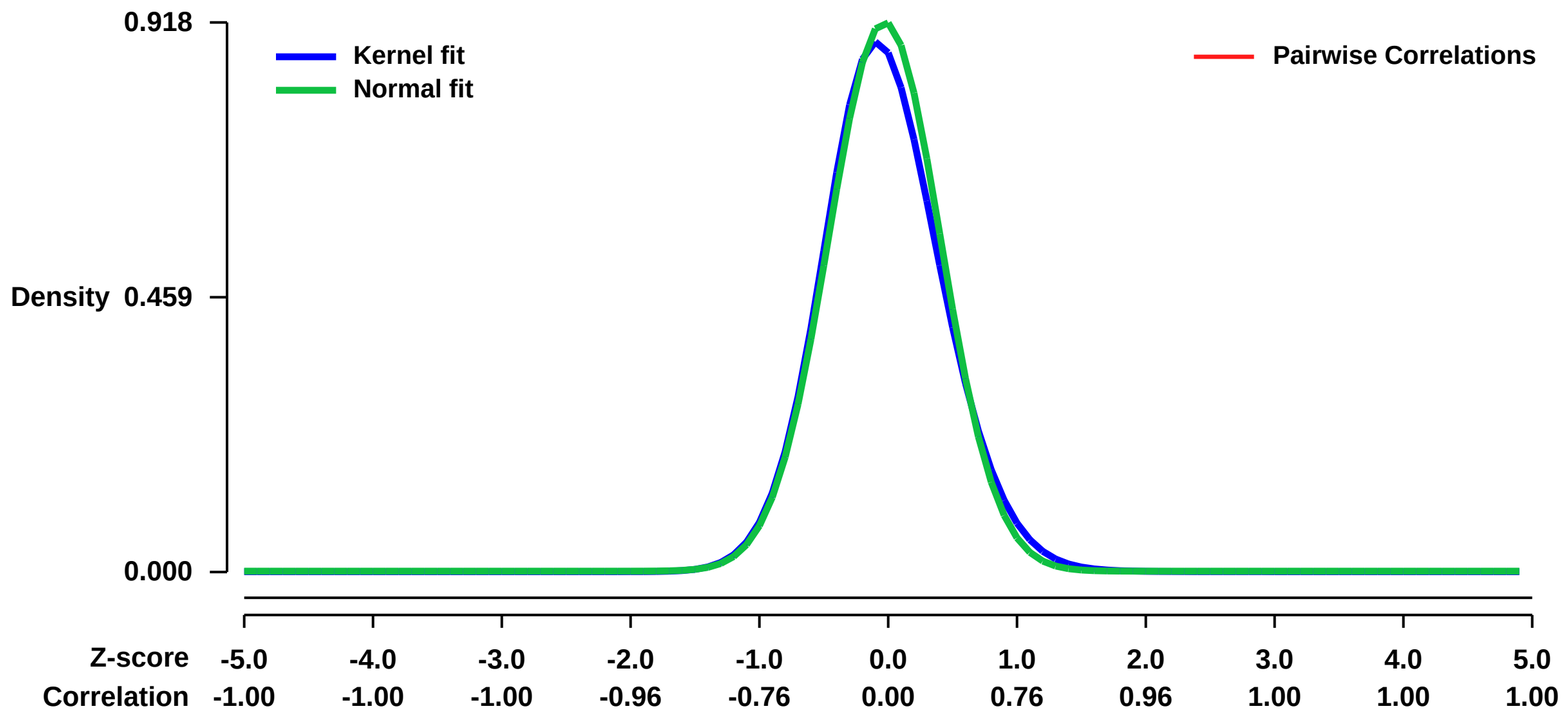

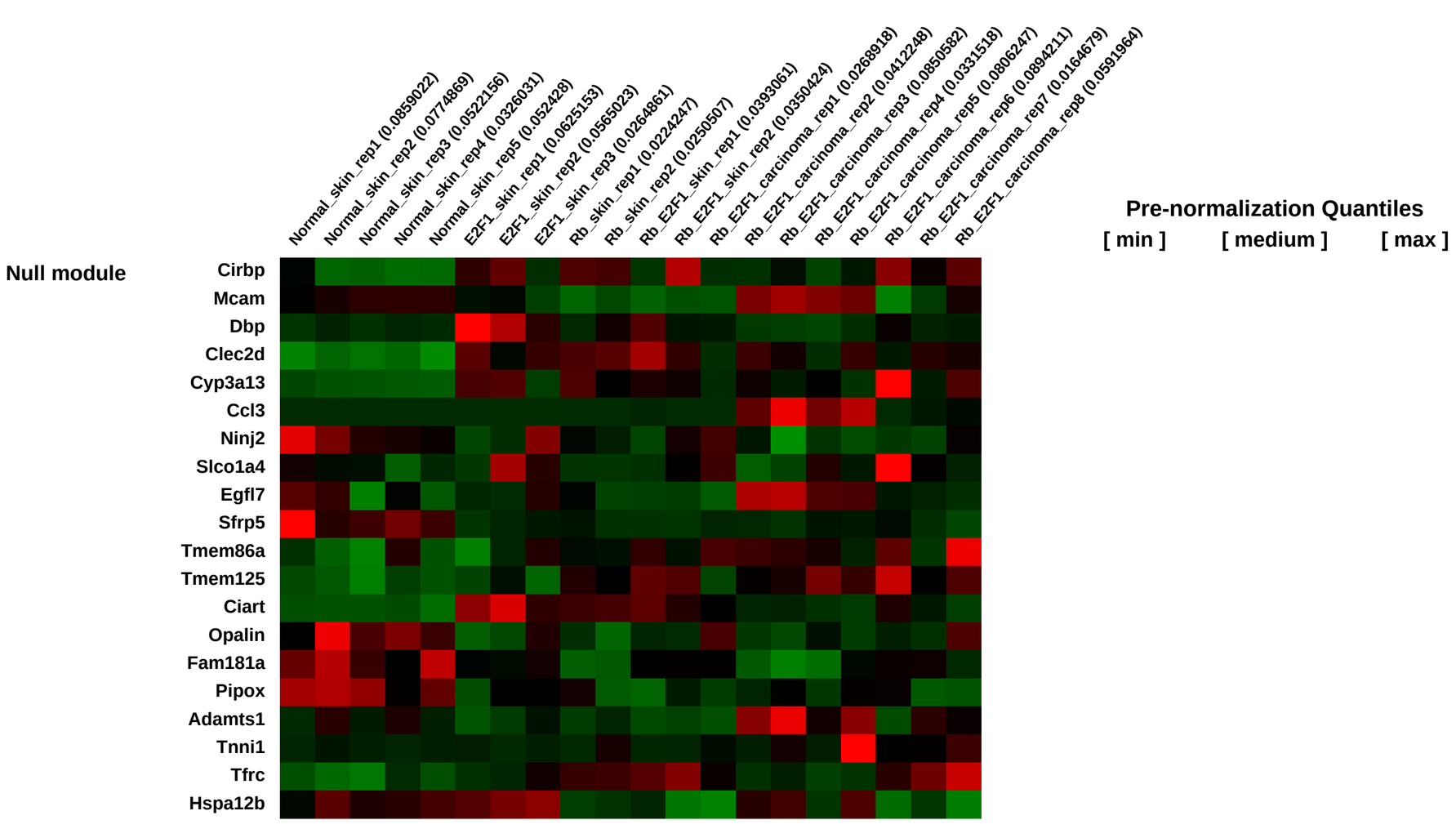

GEO Series "GSE46298" Expression Profiles

Num of samples in this series: 64

Scale of expression profile Z-scores

-3.0 -2.0 -1.0 0.0 1.0 2.0 3.0

GEO Link:	http://www.ncbi.nlm.nih.gov/geo/query/acc.cgi?acc=GSE46298
Status:	Public on Oct 01 2013
Title:	Whole genome transcriptome analysis identifies indices of fast and slow disease progression in two ALS mouse models
Organism:	Mus musculus
Experiment type:	Expression profiling by array
Platform:	GPL1261
Pubmed ID:	24065725
Summary & Design:	**Summary:** Microarray analysis has been applied to the study of ALS in order to investigate gene expression in whole spinal cord homogenates of SOD1 G93A mice and human ALS cases, although the massive presence of glial cells and inflammatory factors has made it difficult to define which gene expression changes were motor neuron specific. Recently, laser capture microdissection (LCM), combined with microarray analysis, has allowed the identification of motor neuron specific changes in gene expression in mouse and human ALS cases. The aim of the present study is to combine LCM and microarray analysis to compare the gene expression profiles of motor neurons from two SOD1G93A mouse strains (129Sv and C57) with different progression of the disease in order to discover the molecular mechanisms that may contribute to the distinct phenotypes and to uncover factors underlying fast and slow disease progression **Overall design:** Motor neurons have been isolated from the spinal cord of 129SvG93A mice, C57G93A mice and non transgenic littermates at different time points and the transcription expression profile of the isolated motor neurons has been analysed

Background corr dist: KL-Divergence = 0.2248, L1-Distance = 0.0369, L2-Distance = 0.0027, Normal std = 0.3165

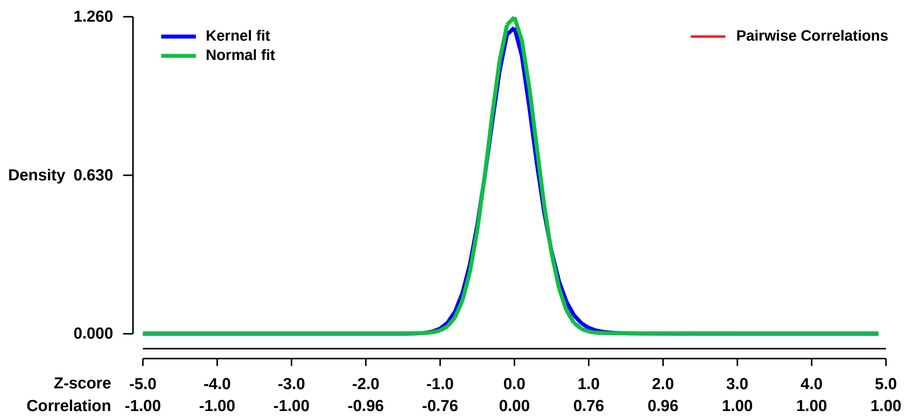

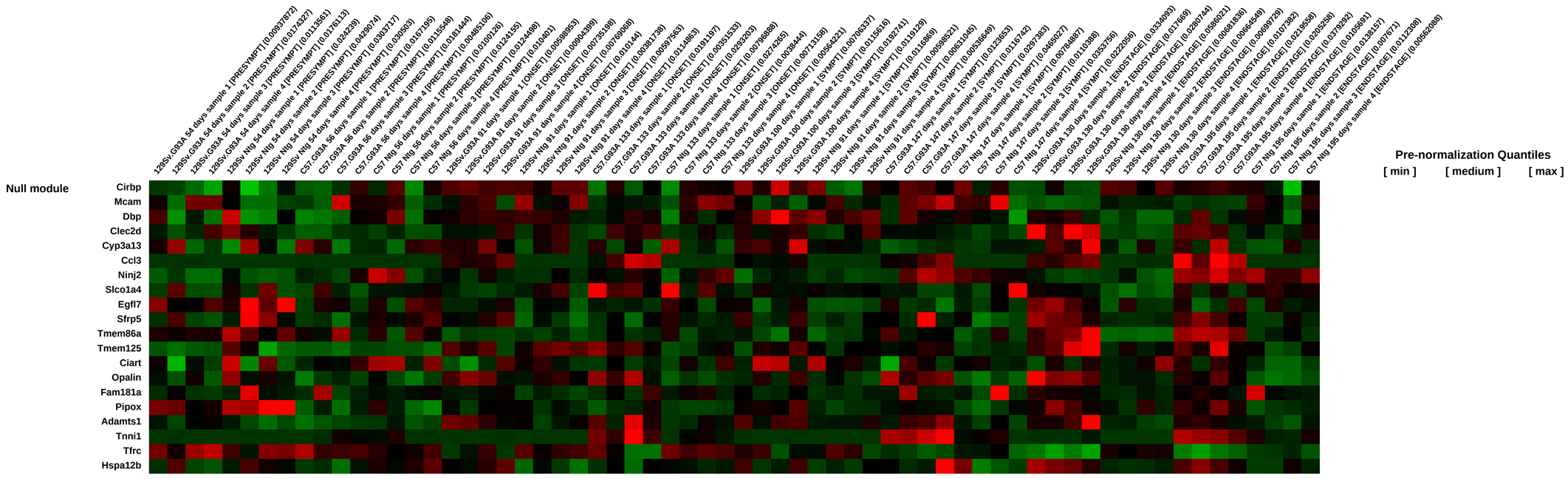

GEO Series "GSE4627" Expression Profiles

Num of samples in this series: 6

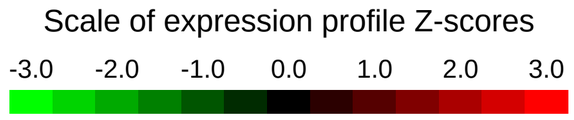

GEO Link:	**http://www.ncbi.nlm.nih.gov/geo/query/acc.cgi?acc=GSE4627**
Status:	**Public on Jul 01 2006**
Title:	**Telomere dysfunction**
Organism:	**Mus musculus**
Experiment type:	**Expression profiling by array**
Platform:	**GPL1261**
Pubmed ID:	
Summary & Design:	**Summary:** **We used microarrays to analyze the prevalence of signalling induced by acute telomere dysfunction (as induced by TRF2DBDM expression = Dataset 1) and in TERC- compared to TERC+ HCC (Dataset 2).** **Keywords: acute telomere dysfunction, hepatocellular cancer** **Overall design:** **Differentially expressed gene clusters were identified using Array Assist 4.0 (Stratagene).**

Background corr dist: **KL-Divergence = 0.0506, L1-Distance = 0.0389, L2-Distance = 0.0023, Normal std = 0.5890**

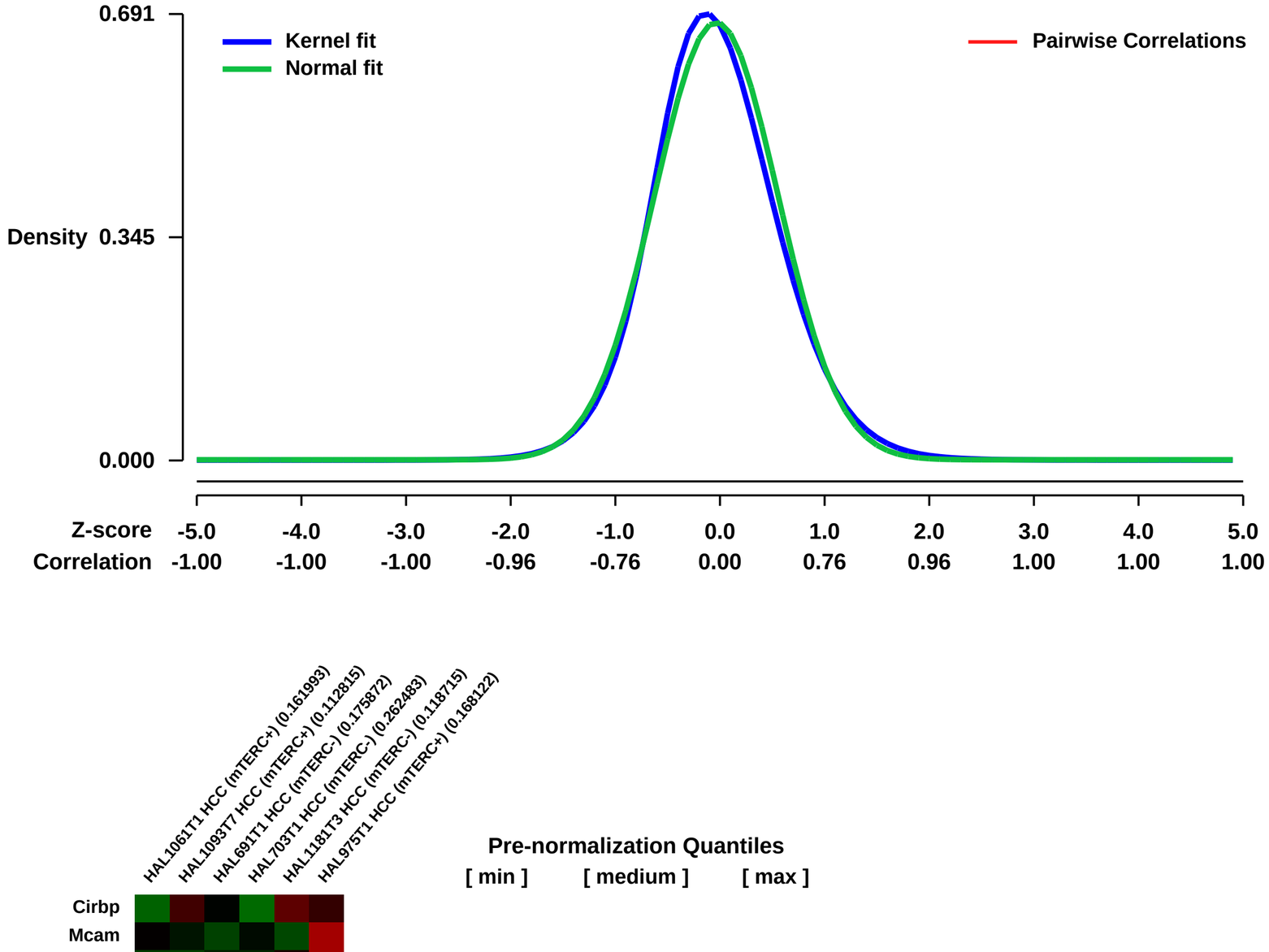

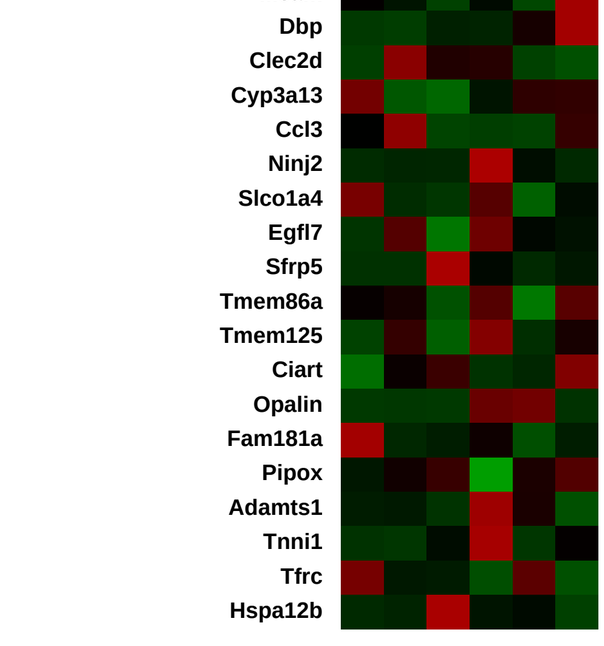

GEO Series "GSE39766" Expression Profiles

Num of samples in this series: 6

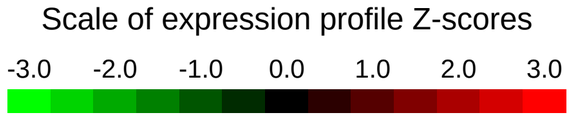

GEO Link:	http://www.ncbi.nlm.nih.gov/geo/query/acc.cgi?acc=GSE39766
Status:	Public on Aug 10 2012
Title:	Blockade of TNF‹– after ischemia reperfusion injury ameliorates renal prognosis
Organism:	Mus musculus
Experiment type:	Expression profiling by array
Platform:	GPL1261
Pubmed ID:	
Summary & Design:	**Summary:** Recently, acute kidney injury (AKI) is thought to develop a predisposition toward chronic kidney disease. But the detailed mechanism of the disease progression after AKI is unknown. We made two ischemia-reperfusion injury (IRI) mice models, repaired kidney model and atrophic kidney model, and studied the mechanism that kidney after IRI became atrophy. We found that the atrophy kidney model had two peaks of apoptosis 3 and 14 days after IRI, whereas the repaired kidney model had only one apoptosis peak 3 days after IRI. We showed that the second apoptosis is responsible for the kidney atrophy. Moreover, apoptotic ligands, TNF‹– and FasL were upregulated at the same time of two apoptosis peaks on the atrophic kidney, and blockade of them before IRI prevented kidney from falling into atrophy. Surprisingly, inhibition of the second apoptosis by anti-TNF‹– antibody protected from renal atrophy. We propose that apoptosis might play a major role in AKI progression and blockade of TNF‹– after IRI will be a new therapeutic approach for AKI. **Overall design:** Mice were subjected for 0, 45, and 60 min of unilateral IRI. Mice kidneys were collected at day 1 and 3 after IRI for RNA extraction and hybridization on Affymetrix microarrays. There are 6 samples, 1day IRI45(1), 1day IRI60(2), 1day IRI0(3), 3day IRI45(4), 3day IRI60(5), 3day IRI0(6).

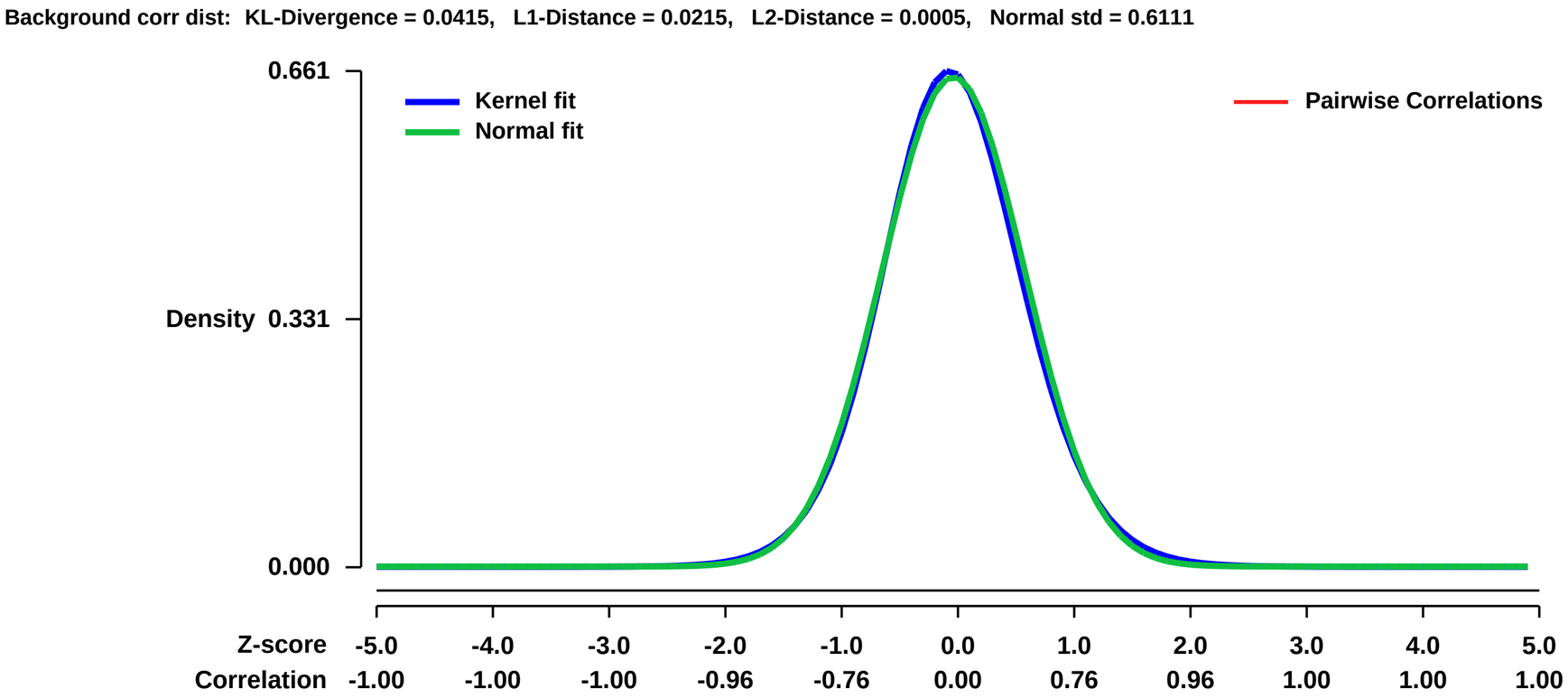

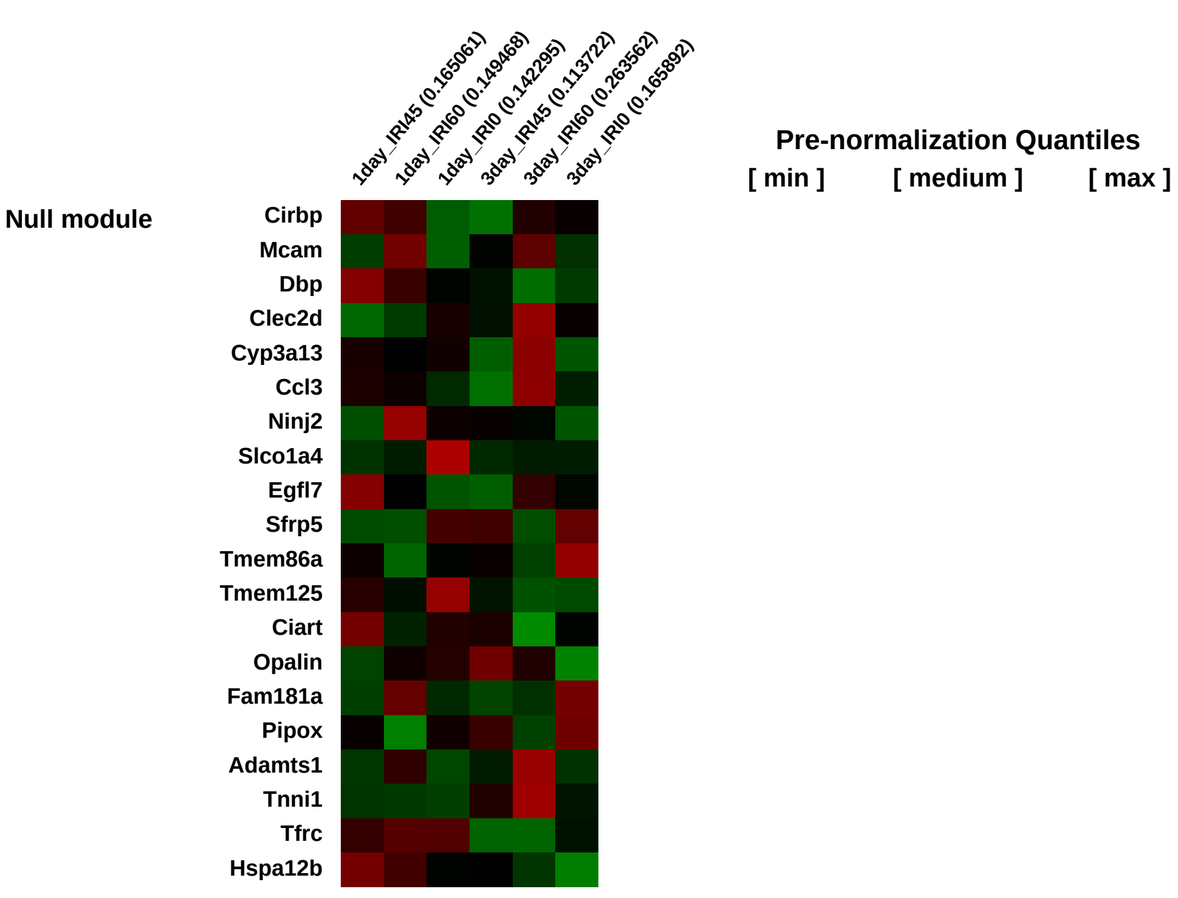

GEO Series "GSE23495" Expression Profiles

Num of samples in this series: 6

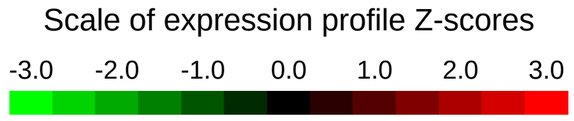

GEO Link:	**http://www.ncbi.nlm.nih.gov/geo/query/acc.cgi?acc=GSE23495**
Status:	**Public on Aug 09 2010**
Title:	**Lmnadelta9 mouse gene expression study**
Organism:	**Mus musculus**
Experiment type:	**Expression profiling by array**
Platform:	**GPL1261**
Pubmed ID:	**20833363**
Summary & Design:	**Summary:** **Lmnadelta9 mice derived in the C57bl6X129S3/J background have been identified as exhibiting a progeric phenotype. Using this mouse model we show that a truncated variant of Lamin A (Lmnaâ 9) causes the proliferative arrest of post-natal fibroblasts. Arrest is due to the cells inability to produce a functional extracellular matrix (ECM).** **We used microarrays to compare gene expression of adult primary fibroblasts from wildtype and Lmnadelta9 mice in order to understand whether the Lmnadelta9 adult MEF defective proliferation is due to alterations of specific signaling associated with ECM functions.** **Overall design:** **Three independent replicate samples of sibling-derived wild-type and Lmnaâ 9 post-natal fibroblast lines at passage 3 were serum-starved for 72 hours and used as the source of mRNA for microarray analysis. RNA was extracted with Trizol, and hybridized to Affymetrix microarrays.**

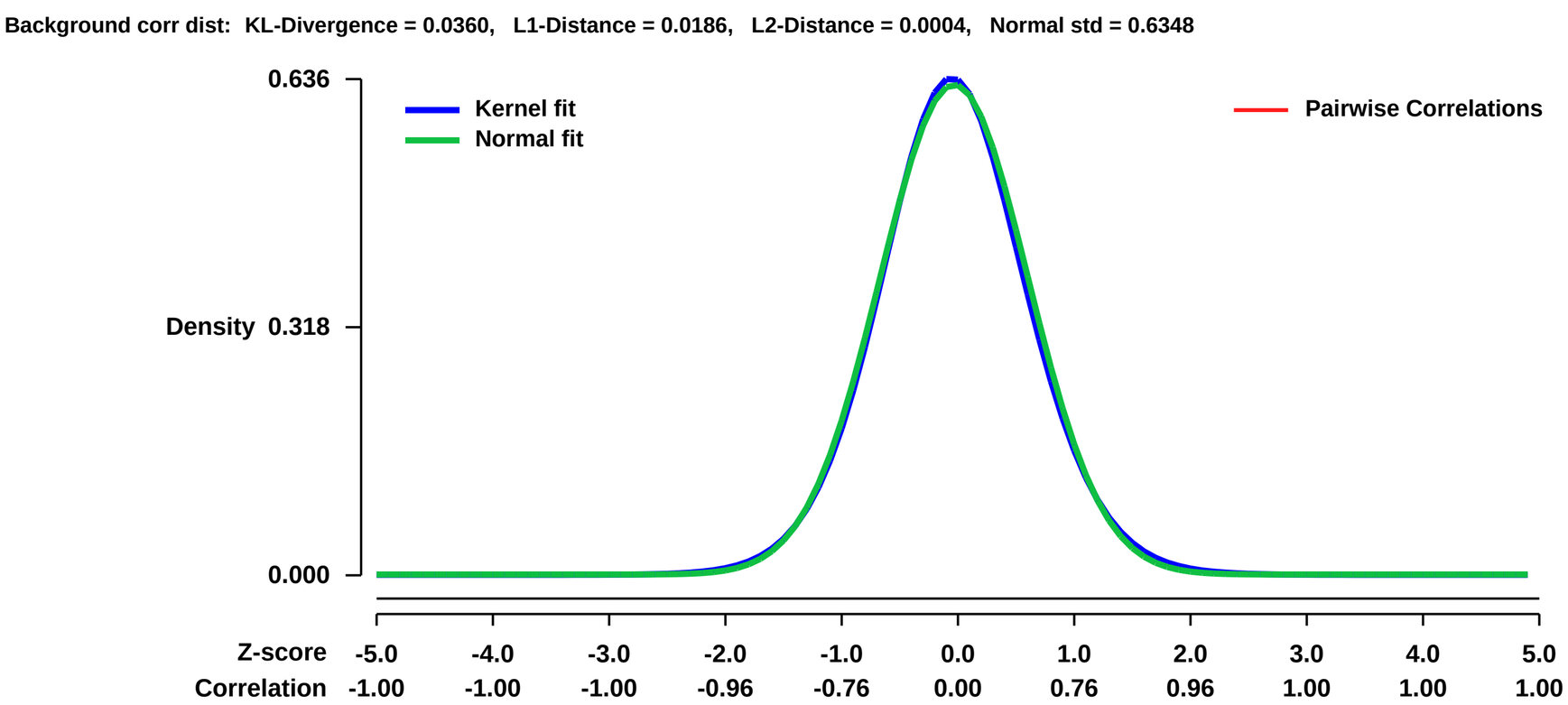

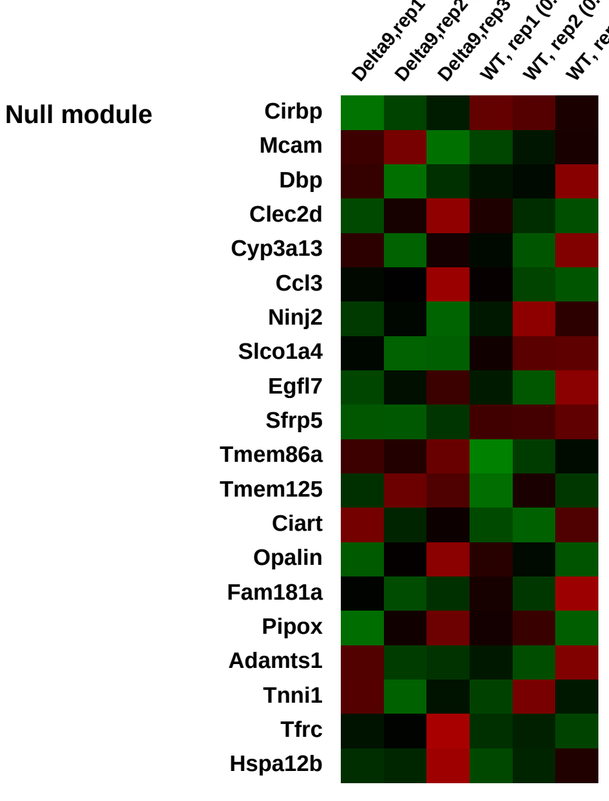

GEO Series "GSE16691" Expression Profiles

Num of samples in this series: 12

Scale of expression profile Z-scores

-3.0 -2.0 -1.0 0.0 1.0 2.0 3.0

GEO Link:	http://www.ncbi.nlm.nih.gov/geo/query/acc.cgi?acc=GSE16691
Status:	Public on Oct 01 2009
Title:	Transcriptional regulation by Norrin-Frizzled4 signaling in the embryonic yolk sac
Organism:	Mus musculus
Experiment type:	Expression profiling by array
Platform:	GPL1261
Pubmed ID:	19837032
Summary & Design:	**Summary:** Transcriptional profiles of the embryonic yolk sac from embryos with ectopic Norrin expression were compared to their wild type littermate controls. The goal is to identify the transcriptional response to Norrin-Frizzled 4 signaling during embryonic angiogenesis. **Overall design:** Ectopic Norrin expression was achieved using a conditional over-expression strategy. Yolk sacs from 3-5 embryos were pooled for each sample and 3 replicates of both control and experimental groups were analyzed.

Background corr dist: KL-Divergence = 0.0423, L1-Distance = 0.0287, L2-Distance = 0.0014, Normal std = 0.5865

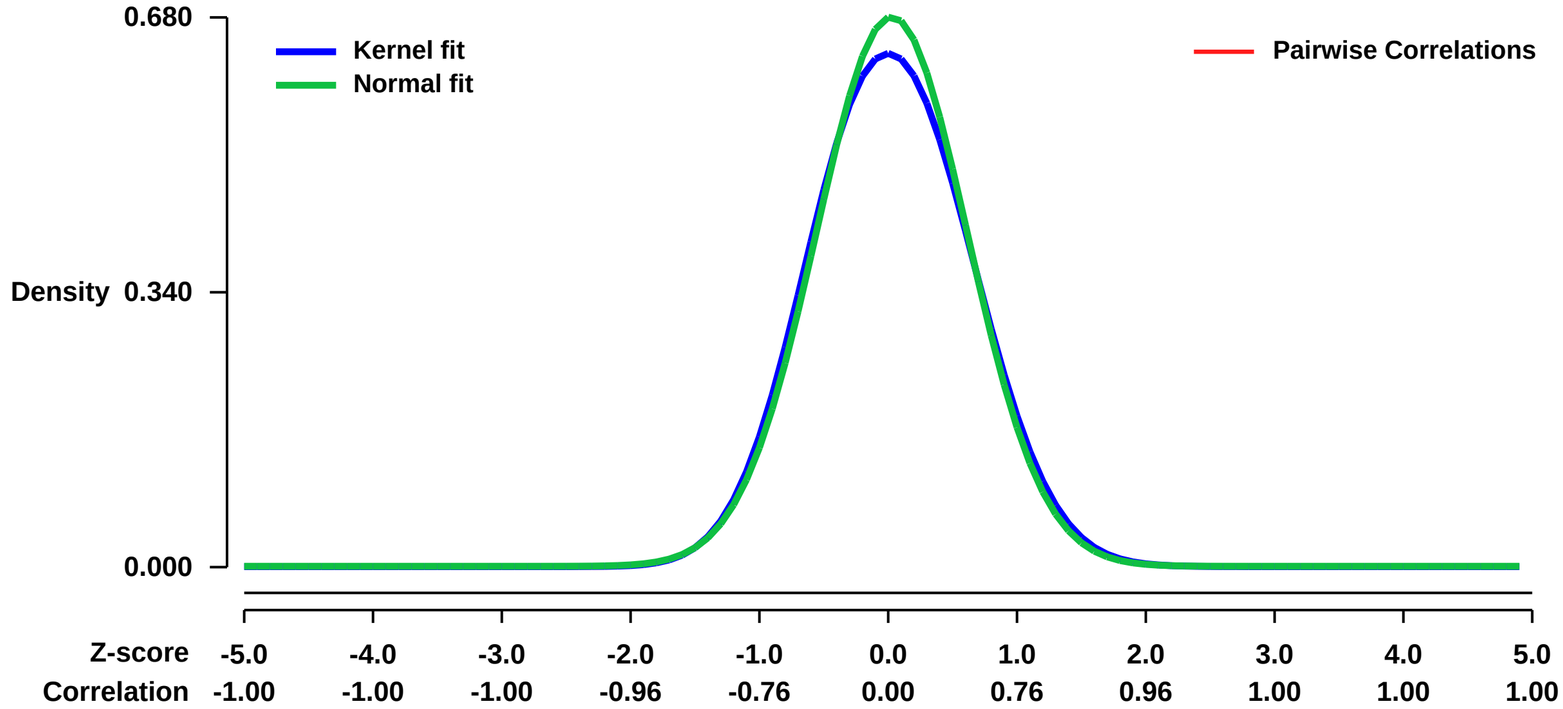

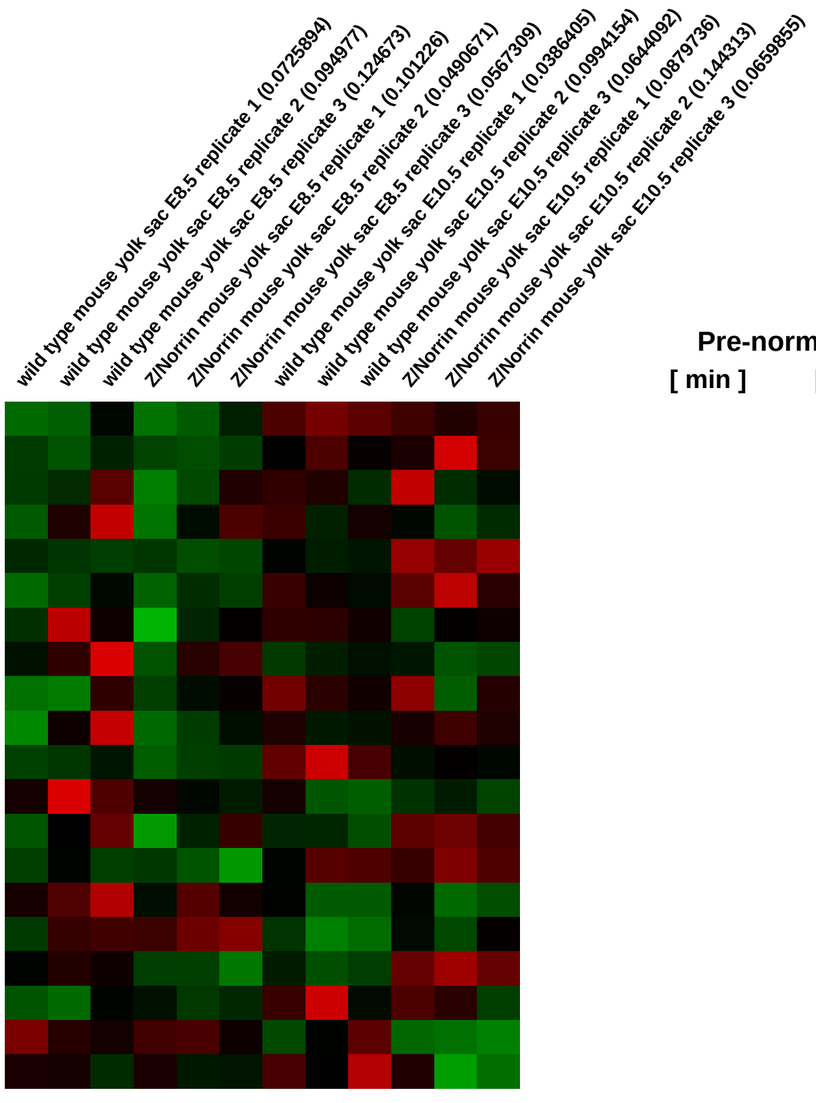

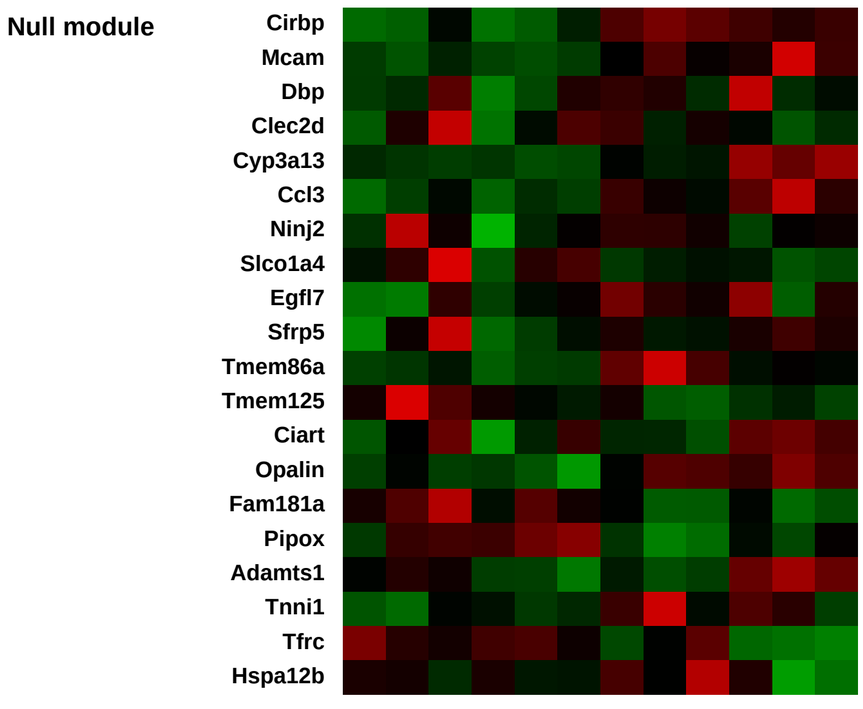

GEO Series "GSE9810" Expression Profiles

Num of samples in this series: 13

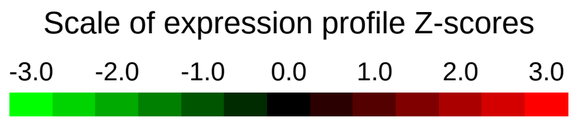

GEO Link:	http://www.ncbi.nlm.nih.gov/geo/query/acc.cgi?acc=GSE9810
Status:	Public on Jan 24 2008
Title:	Comparison of human and mouse dendritic cell subsets by genome-wide expression profiling
Organism:	Mus musculus
Experiment type:	Expression profiling by array
Platform:	GPL1261
Pubmed ID:	18218067
Summary & Design:	**Summary:** Dendritic cells (DCs) are a complex group of cells which play a critical role in vertebrate immunity. Spleen or lymph node resident DCs are subdivided into conventional DC (cDC) subsets (CD11b and CD8alpha in mouse; BDCA1 and BDCA3 in man) and plasmacytoid DCs (pDCs). It is currently unclear if these various DC populations belong to a unique hematopoietic lineage and if the subsets identified in the mouse and human systems are evolutionary homologs. To bring novel insights into these questions, we sought conserved genetic signatures for these DCs through the analysis of a compendium of genome-wide expression profiles of mouse or human leukocytes. We show through clustering analysis that all spleen resident DC subsets form a distinct branch within the leukocyte family tree, and reveal a transcriptomal signature evolutionary conserved in all these DC subsets. Moreover we identify a large gene expression program shared between mouse and human plasmacytoid DCs, and smaller conserved profiles shared between mouse and human cDC subsets. Finally, we use compendium analysis to re-evaluate the classification of interferon-producing killer DCs (IKDCs) and lin-CD16+HLA-DR+ cells, which have both been claimed to be DCs, and show that these cells are more closely linked to NK or myeloid cells, respectively. Our study thus provides a unique resource for future investigation of the evolutionarily conserved molecular pathways governing the ontogeny and functions of leukocyte subsets, especially DCs. **Keywords:** cell type comparison of wild-type spleen leukocyte subsets, including palsmacytoid dendritic cells, CD8alpha conventional dendritic cells, and CD11b conventional dendritic cells **Overall design:** This study includes data from cell sort purified dendritic cells, B cells, NK cells, and CD8 T cells. 2 or 3 independent replicates were made for each cell type. The genearray was performed in an attempt to investigate the relationships between DCs subsets and with other leukocytes, in mouse, in human, and between these 2 species. To this end, public data for mouse CD4 T cells and macrophages, as well as public data for human leukocyte subsets were also used in the analysis. The results have led to the identification of specific transcriptional programs conserved between human and mouse dendritic cell subsets.

Background corr dist: KL-Divergence = 0.1436, L1-Distance = 0.0470, L2-Distance = 0.0054, Normal std = 0.3893

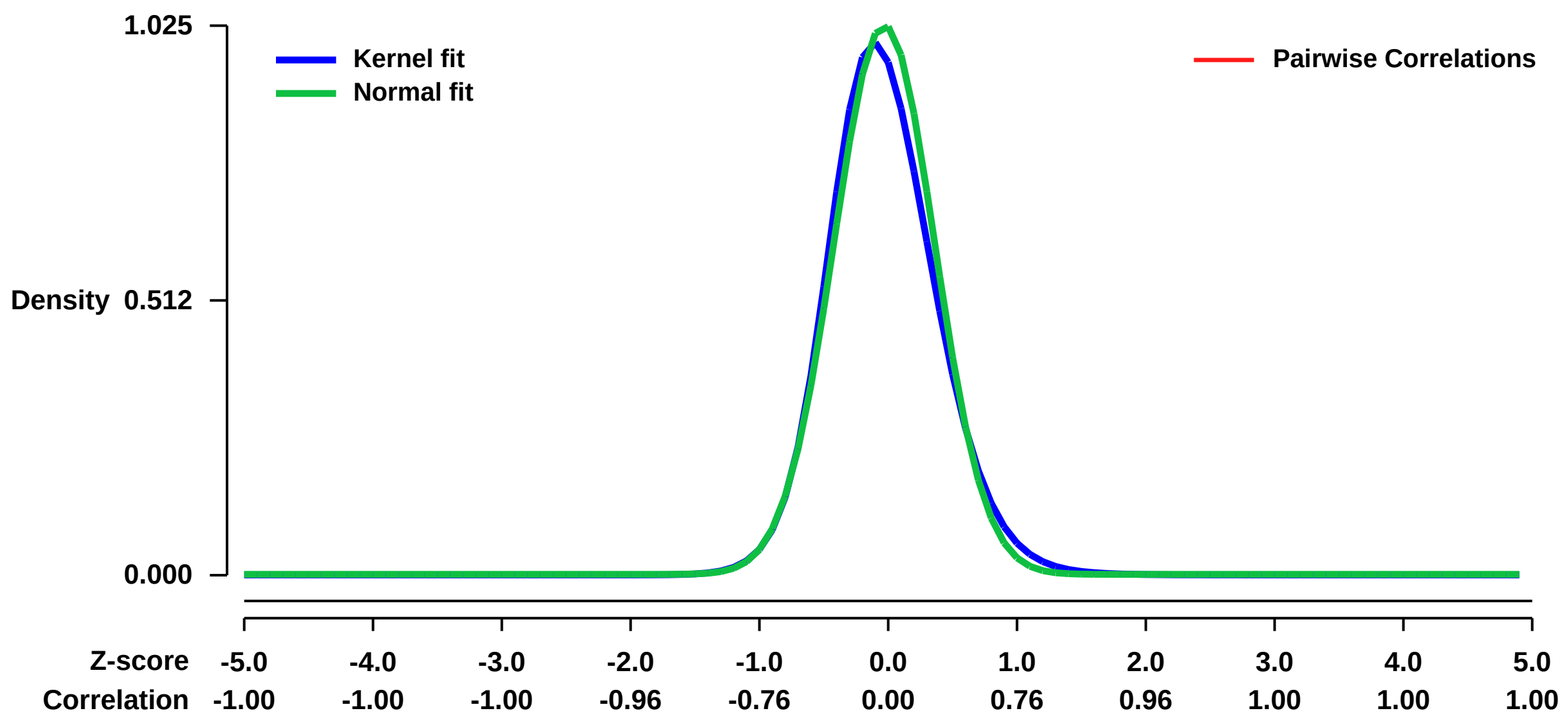

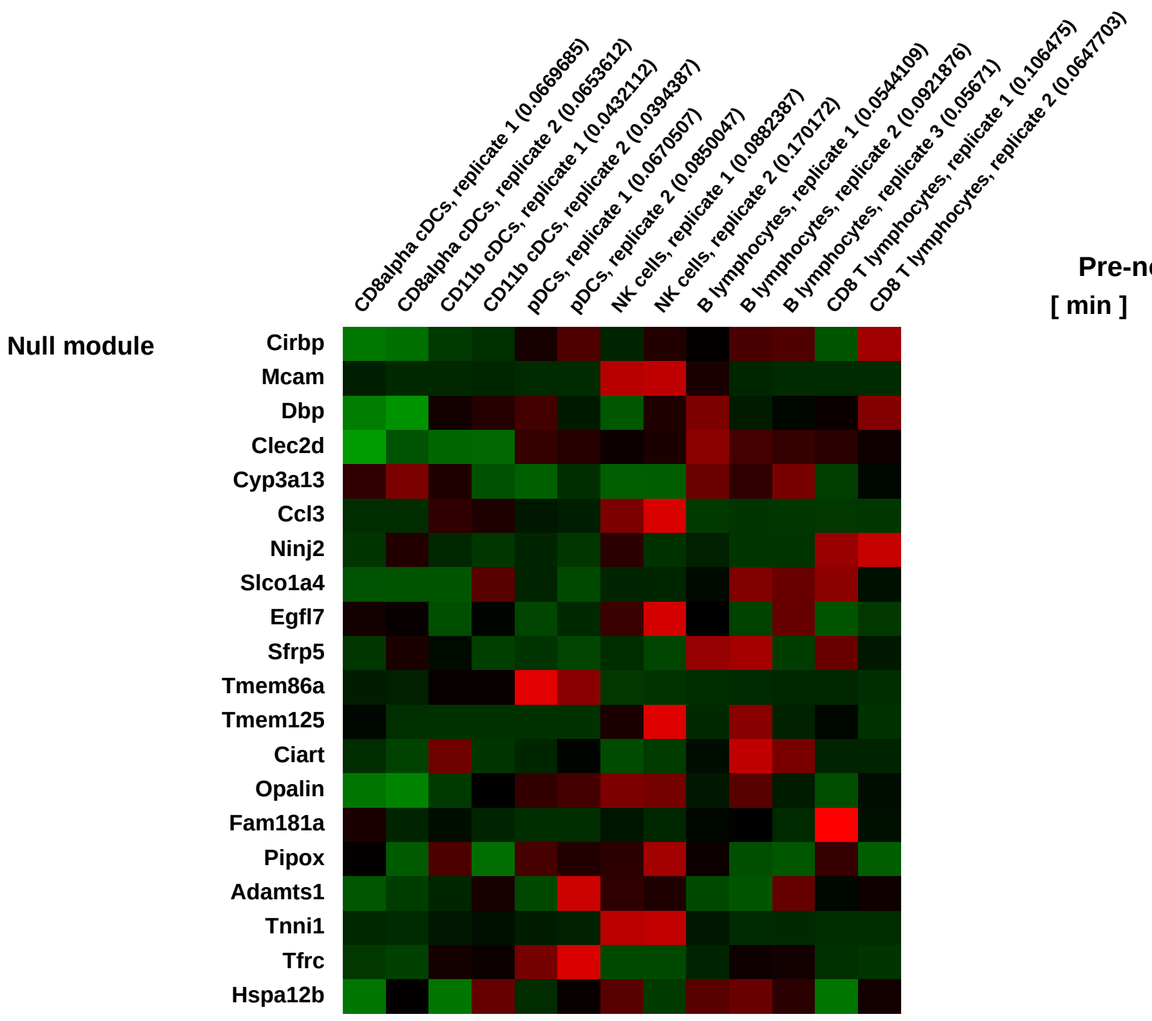

GEO Series "GSE50426" Expression Profiles

Num of samples in this series: 6

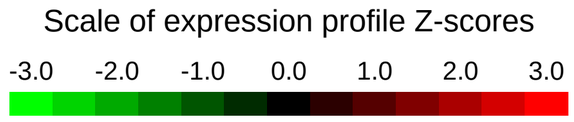

GEO Link:	**http://www.ncbi.nlm.nih.gov/geo/query/acc.cgi?acc=GSE50426**
Status:	**Public on Jan 01 2014**
Title:	**Expression Data from E16.5 hearts from WT and FOG-2R3K5A siblings**
Organism:	**Mus musculus**
Experiment type:	**Expression profiling by array**
Platform:	**GPL1261**
Pubmed ID:	
Summary & Design:	**Summary:** **Heart development is modulated by FOG-2/NuRD interactions. FOG-2R3K5A is unable to recuit the NuRD complex and this results in cardiac defects such as ASD, VSD, and thin ventricular walls** **We used microarrays to detail the changes in gene expression in FOG-2R3K5A hearts to determine misexpression of genes that may be causing the observed phenotypes.** **Overall design:** **Whole hearts from E16.5 Wild-type and FOG-2R3K5A siblings were processed for RNA extraction and hybridization on Affymetrix microarrays. We used three biological replicates of each genotype.**

Background corr dist: **KL-Divergence = 0.0394, L1-Distance = 0.0184, L2-Distance = 0.0003, Normal std = 0.6170**

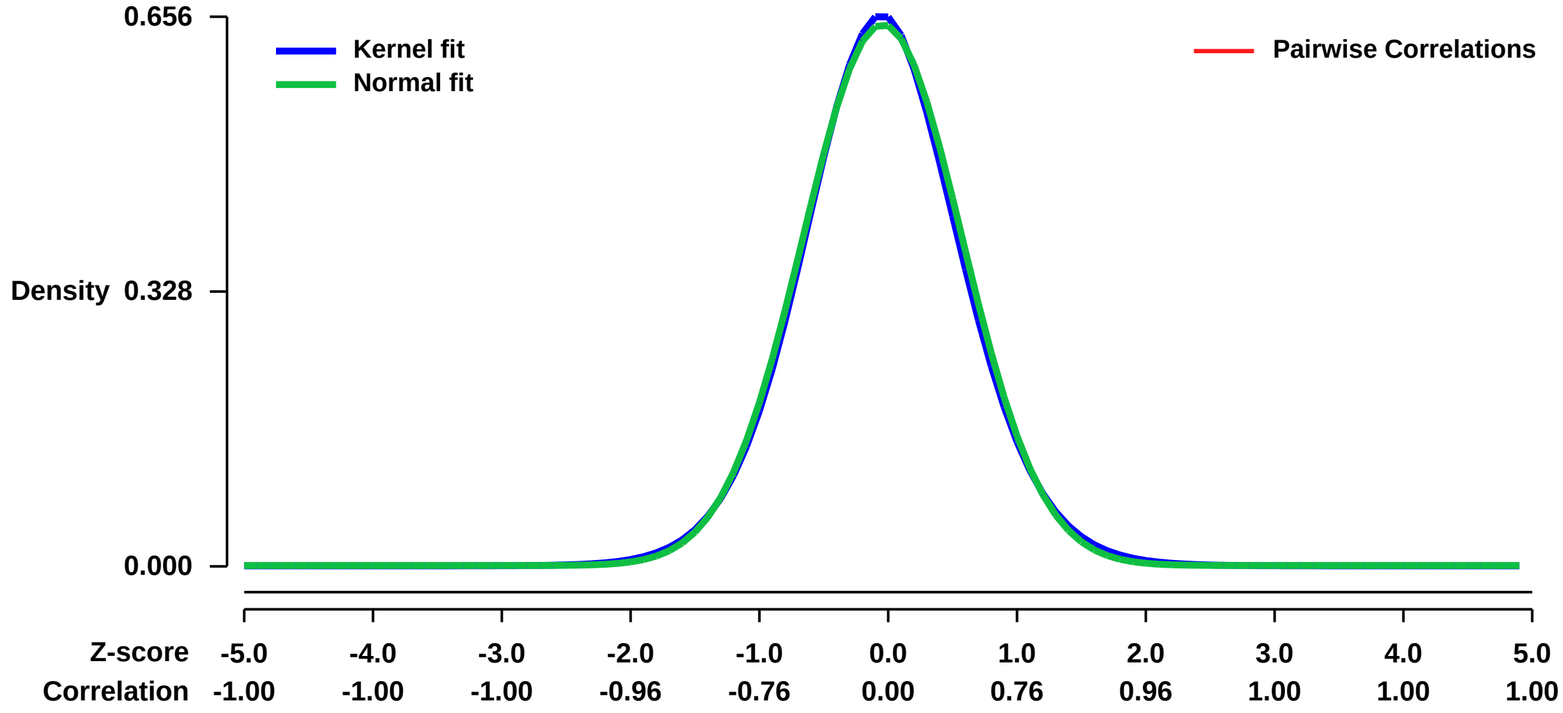

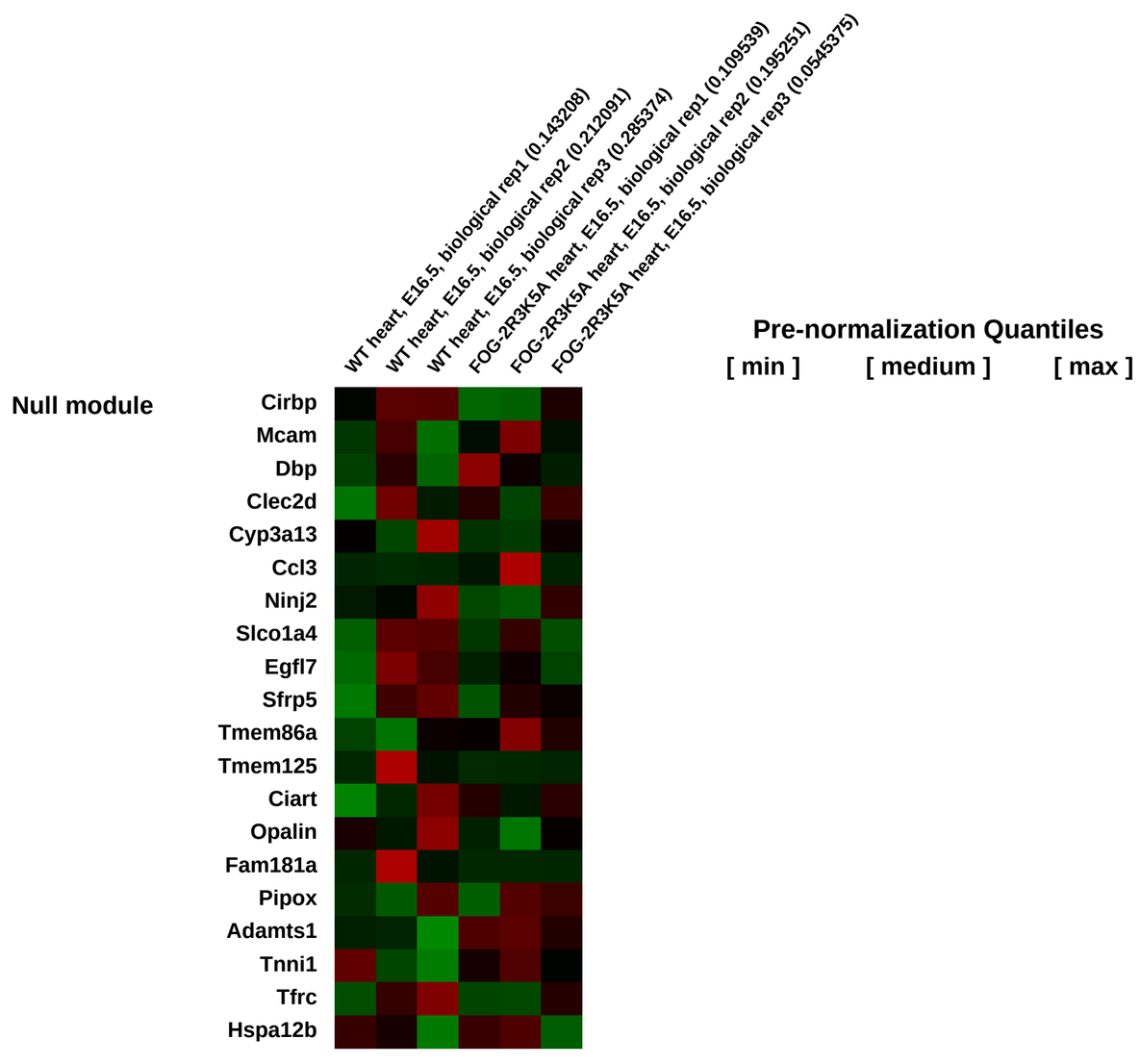

GEO Series "GSE34552" Expression Profiles

Num of samples in this series: 10

Scale of expression profile Z-scores

-3.0 -2.0 -1.0 0.0 1.0 2.0 3.0

GEO Link:	http://www.ncbi.nlm.nih.gov/geo/query/acc.cgi?acc=GSE34552
Status:	Public on Nov 05 2012
Title:	Expression data from mouse kidney tissue
Organism:	Mus musculus
Experiment type:	Expression profiling by array
Platform:	GPL1261
Pubmed ID:	22791343
Summary & Design:	**Summary:** The role of the renin-angiotensin system in chronic kidney disease involves multiple peptides and receptors. Exerting antipodal pathophysiological mechanisms, renin inhibition and AT1 antagonism ameliorate renal damage. This is a comparison between the renin inhibitor aliskiren with the At1 antagonist losartan in mice with chronic kidney disease due to renal ablation. **Overall design:** Renal tissue from ablated mice was used after 6-week treatment with either 500 mg/l losartan or 50 mg/kg aliskiren per day (n = 5)

Background corr dist: KL-Divergence = 0.0759, L1-Distance = 0.0208, L2-Distance = 0.0006, Normal std = 0.4855

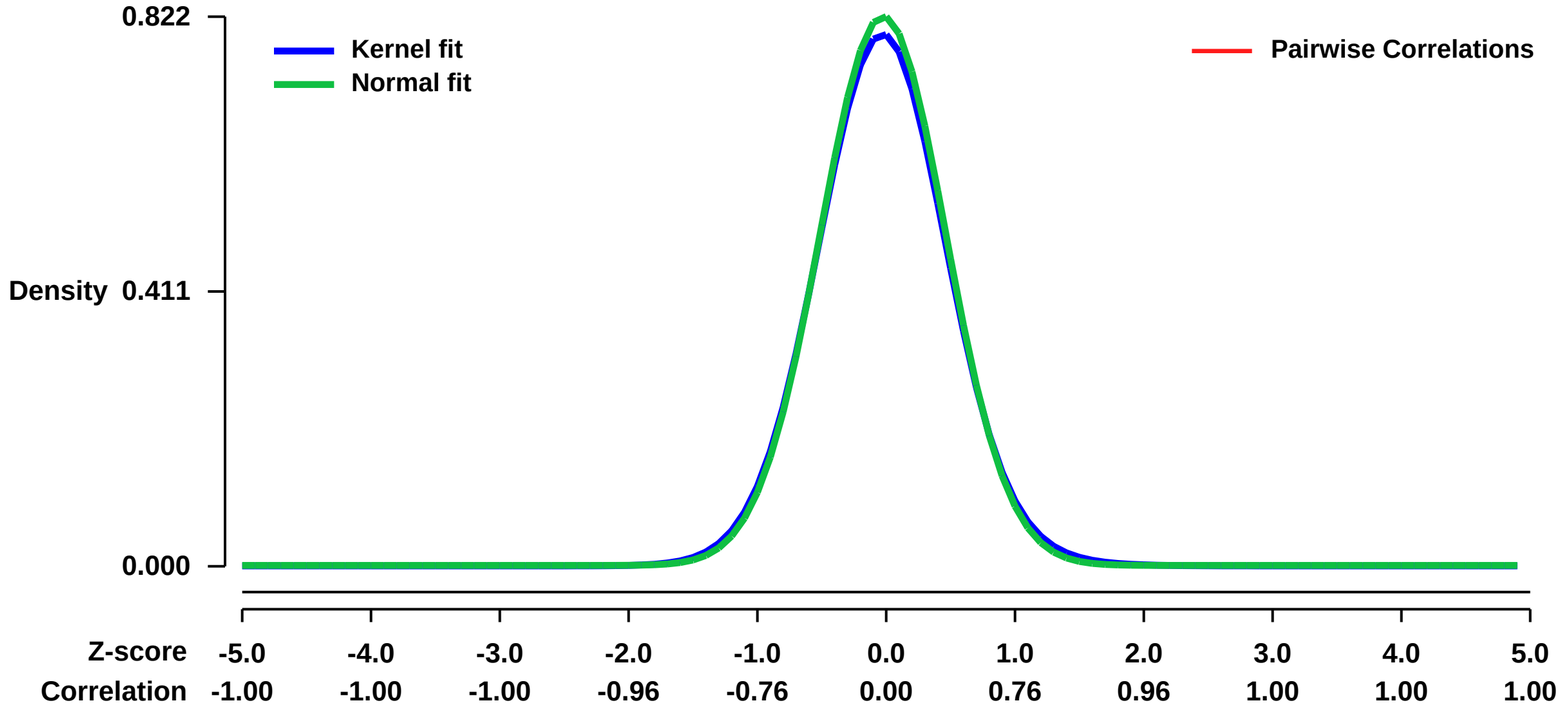

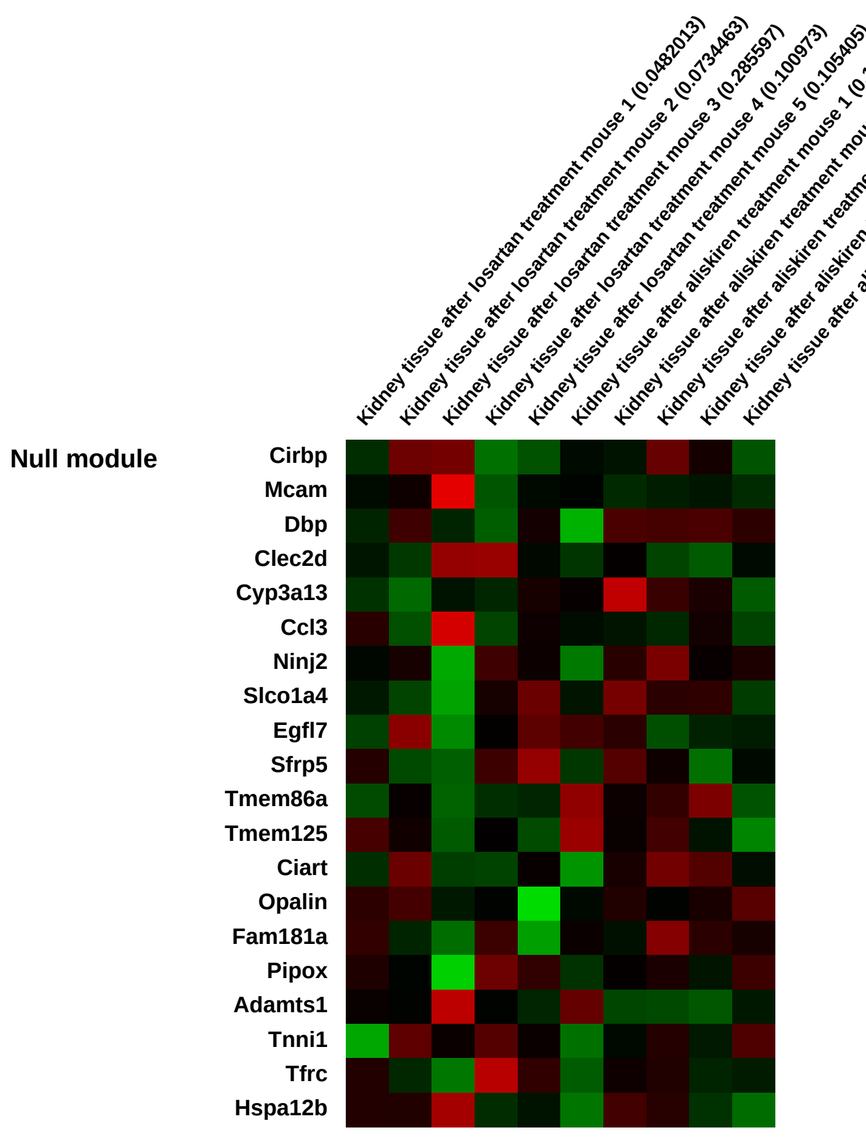

GEO Series "GSE15315" Expression Profiles

Num of samples in this series: 6

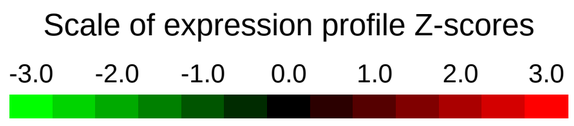

GEO Link:	http://www.ncbi.nlm.nih.gov/geo/query/acc.cgi?acc=GSE15315
Status:	Public on Mar 20 2009
Title:	ERK1/2 in Ovarian Granulosa Cells are Essential for Female Fertility
Organism:	Mus musculus
Experiment type:	Expression profiling by array
Platform:	GPL1261
Pubmed ID:	19443782
Summary & Design:	**Summary:** A surge of luteinizing hormone (LH) from the pituitary gland triggers ovulation, oocyte maturation, and luteinization for successful reproduction in mammals. Since the signaling molecules RAS and ERK1/2 are activated by a LH surge in granulosa cells of preovulatory follicles, we disrupted Erk1/2 in mouse granulosa cells and provide in vivo evidence that these kinases are necessary for LH-induced oocyte resumption of meiosis, ovulation, and luteinization. In addition, biochemical analyses and selected disruption of the Cebpb gene in granulosa cells demonstrate that C/EBP is a critical downstream mediator of ERK1/2 activation. These mouse models provide in vivo systems in which to define the context specific and molecular mechanisms by which granulosa cells respond to LH and these mechanisms are relevant to the regulation of human fertility and infertility. **Overall design:** Immature wild type or ERK1/2 conditonal knock-out mice were injected with 5IU equine chorionic gonadotropin (eCG)-48h followed by 5 IU hCG injection. The ovarian granulosa cells were collected at hCG 0h, 2.5h, or 4h and the gene expression pforiles were compared by microarray method.

Background corr dist: KL-Divergence = 0.0268, L1-Distance = 0.0170, L2-Distance = 0.0004, Normal std = 0.6851

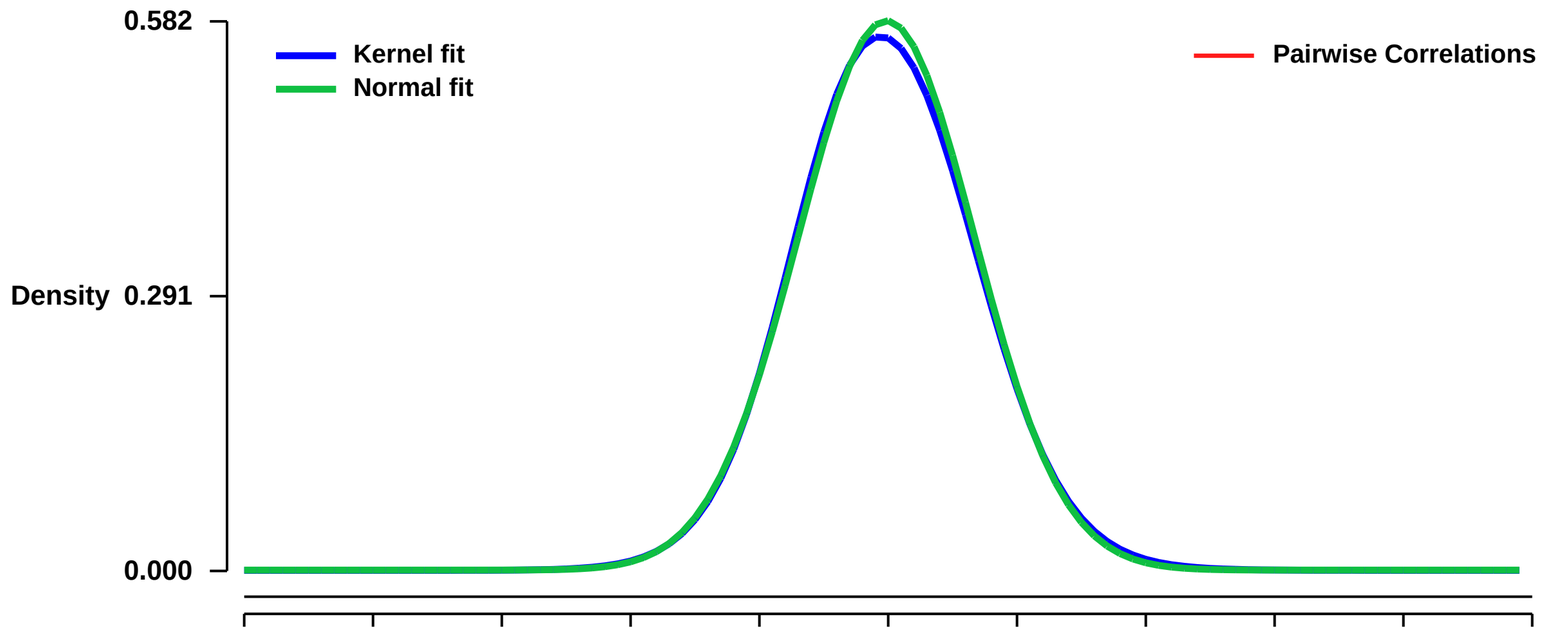

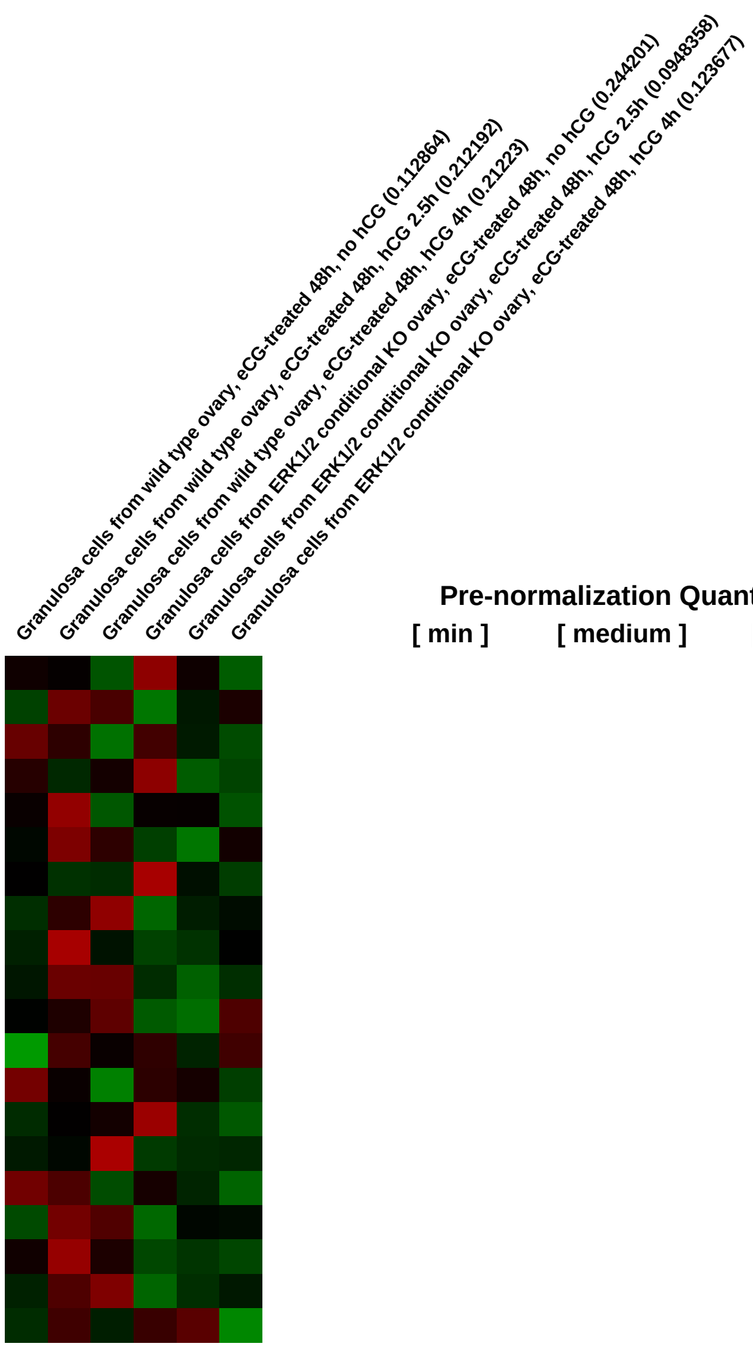

GEO Series "GSE42591" Expression Profiles

Num of samples in this series: 26

Scale of expression profile Z-scores

-3.0 -2.0 -1.0 0.0 1.0 2.0 3.0

GEO Link:	http://www.ncbi.nlm.nih.gov/geo/query/acc.cgi?acc=GSE42591
Status:	Public on Jul 01 2013
Title:	Expression data from fresh and cultured islets at different glucose concentrations
Organism:	Mus musculus
Experiment type:	Expression profiling by array
Platform:	GPL1261
Pubmed ID:	23685457
Summary & Design:	**Summary:** ¸†-cell identity is determined by tightly regulated transcriptional networks that are modulated by extracellular cues, thereby ensuring ¸†-cell adaptation to the organismâ s insulin demands. We have observed in pancreatic islets that stimulatory glucose concentrations induced a gene profile that was similar to that of freshly isolated islets, indicating that glucose-elicited cues are involved in maintaining ¸†-cell identity. Low glucose induces the expression of ubiquitous genes involved in stress responses, nutrient sensing, and organelle biogenesis. By contrast, stimulatory glucose concentrations activate genes with a more restricted expression pattern (¸†- and neuronal-cell identity). Consistently, glucose-induced genes are globally reduced in islets deficient with Hnf1a (MODY3), characterized by a deficient glucose metabolism. Of interest, a cell cycle gene module was the most enriched among the variable genes between intermediate and stimulatory glucose concentrations. Glucose regulation of the islet transcriptome was unexpectedly broadly maintained in islets from aged mice. However, the cell cycle gene module is selectively lost in old islets and the glucose activation of this module is not recovered even in the absence of the cell cycle inhibitor p16. We used microarrays to detail the global programme of gene expression regulated by glucose in young and aged pancreatic islets as well as freshly-isolated islets. **Overall design:** Pancreatic islets from young and old mice were isolated and cultured at different glucose concentrations for RNA extraction and hybridization on Affymetrix microarrays. Islets were cultured at 3mM (G3), 5.5mM (G5), 11mM (G11) and 16mM (G16). Freshly-isolated islets (F) were also processed for RNA extraction . We also assessed the dynamic glucose regulation of gene expression at different time-points after an overnight at 3mM (T0): after 1h at 11mM (T1) and after 4h (T4).

Background corr dist: KL-Divergence = 0.1425, L1-Distance = 0.0297, L2-Distance = 0.0013, Normal std = 0.3825

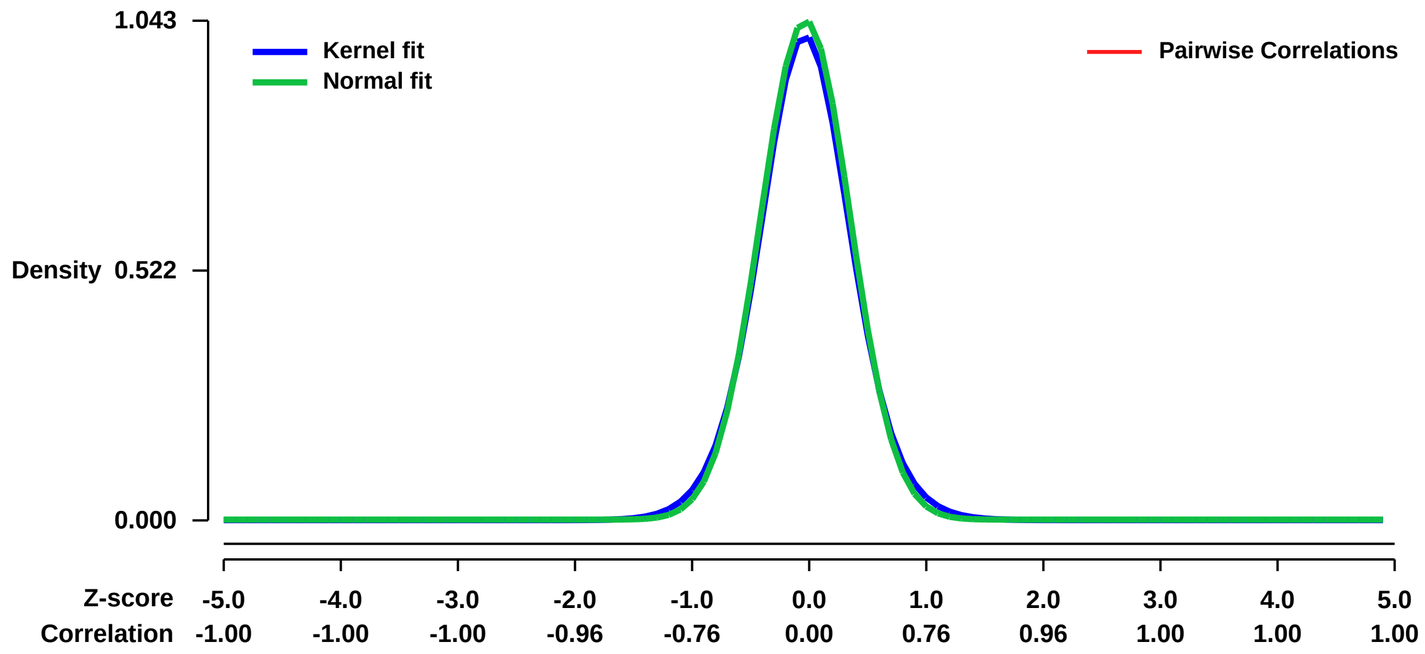

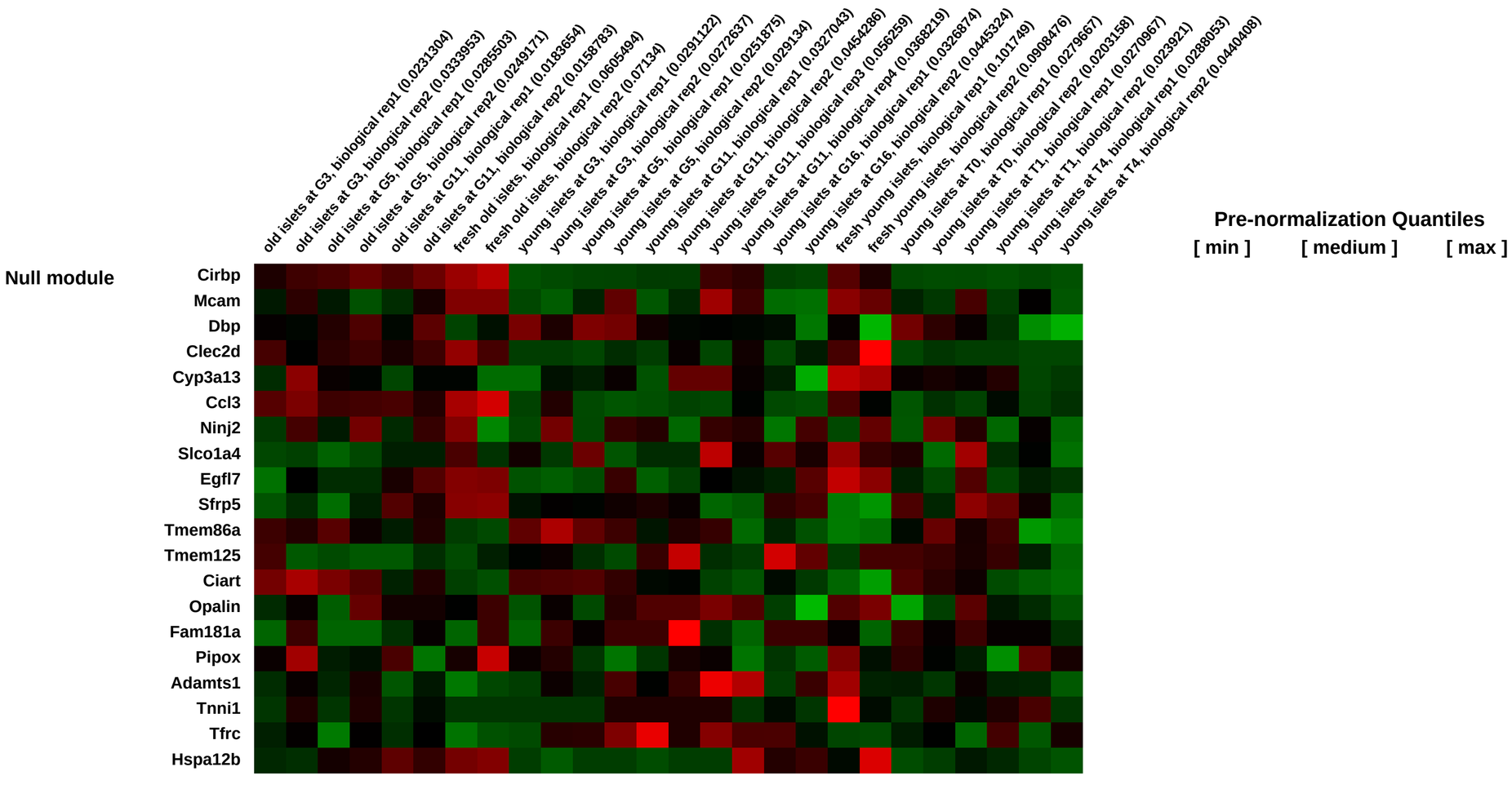

GEO Series "GSE11161" Expression Profiles

Num of samples in this series: 6

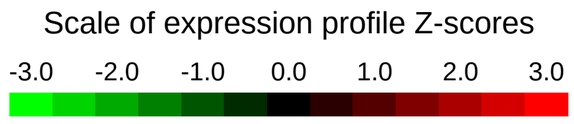

GEO Link:	**http://www.ncbi.nlm.nih.gov/geo/query/acc.cgi?acc=GSE11161**
Status:	**Public on Apr 17 2008**
Title:	**Gene expression profiles of neonatal bladder samples. (GUDMAP Series ID: 19)**
Organism:	**Mus musculus**
Experiment type:	**Expression profiling by array**
Platform:	**GPL1261**
Pubmed ID:	
Summary & Design:	**Summary:** **The long term objective is to create an encyclopedia of the expression levels of all genes in multiple components of the developing bladder. The central thesis is straightforward. The combination of microdissected tissues and FACS sorted cells plus microarray analysis offers a powerful, efficient and effective method for the creation of a global gene expression atlas of the developing urogenital system. Microarrays with essentially complete genome coverage can be used to quantitate expression levels of every gene. The ensuing rapid read-out provides an expression atlas that is more sensitive, more economical and more complete than would be possible by in situ hybridizations alone. The data submitted here represents the gene expression profiles of FACS sorted newborn bladder cells and compares two distinct cell populations of smooth muscle cells since both of these populations contain EGFP from a SMGA (Actg2) promoter shown to be expressed only in smooth muscle cells.** **Gene expression comparison from developing regions of the mouse postnatal day 2 urogenital system.** **Overall design:** **Bladder cells were FACS sorted from newborn double transgenic mice expressing EGFP under the control of a SMGA promoter and EYFP under the control of a SMAA promoter. Total RNA was isolated and underwent 2-round amplification (Epicentre´fi Biotechnologies) for gene expression analysis using the Affymetrix MOE430 microarray chip.**

Background corr dist: **KL-Divergence = 0.0443, L1-Distance = 0.0332, L2-Distance = 0.0016, Normal std = 0.6073**

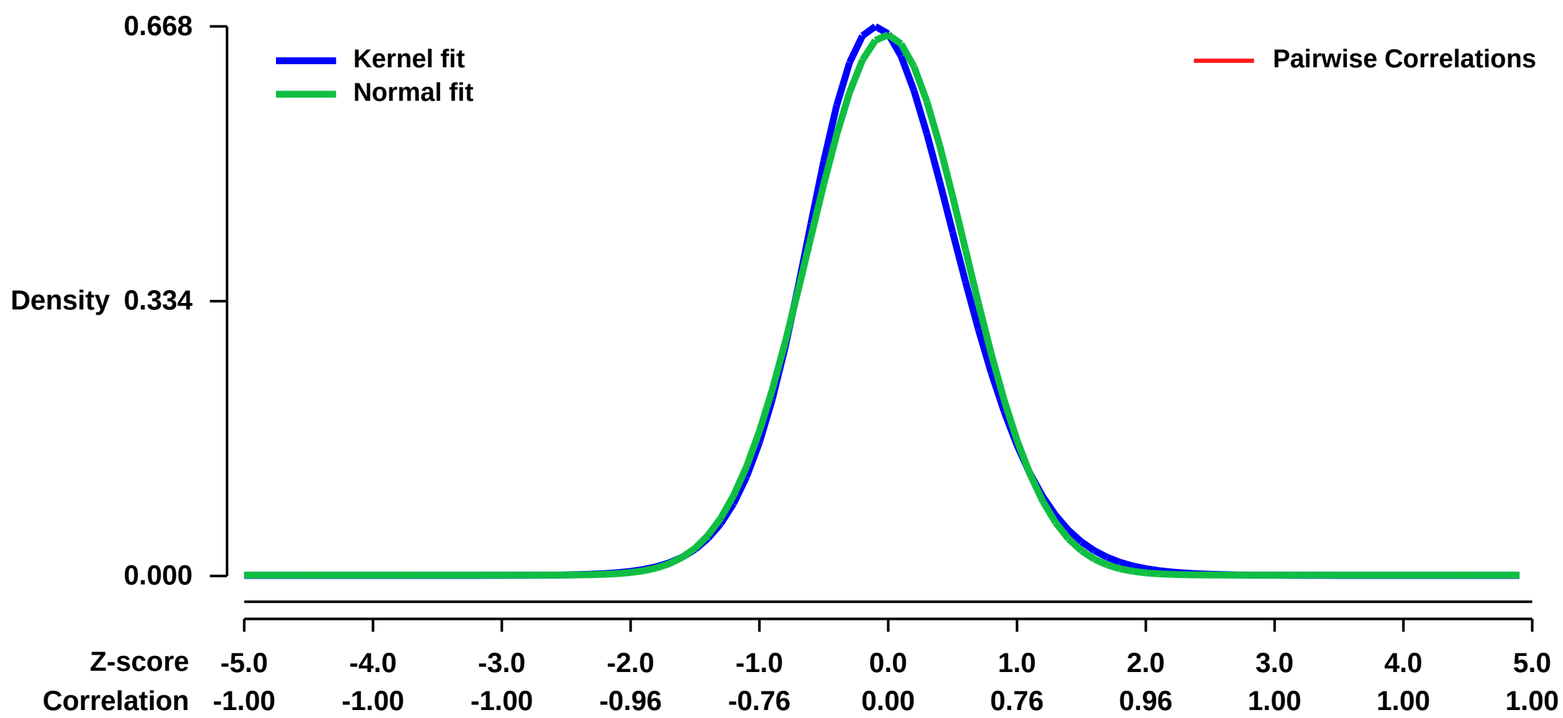

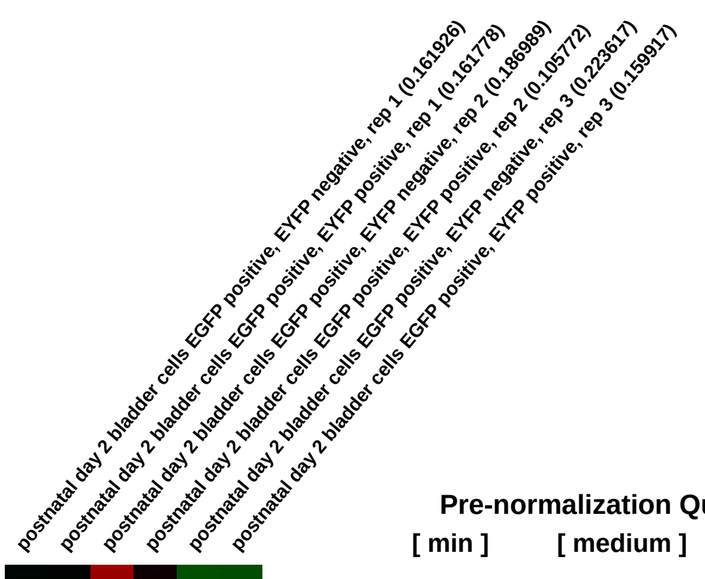

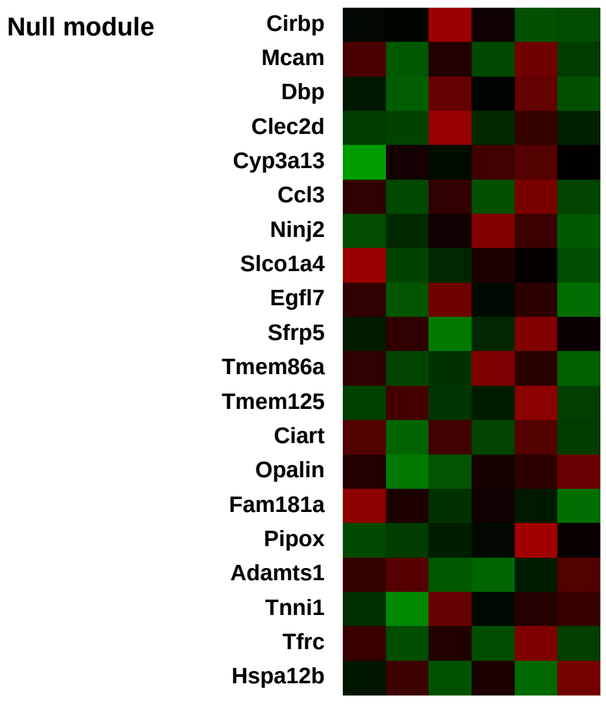

GEO Series "GSE59672" Expression Profiles

Num of samples in this series: 12

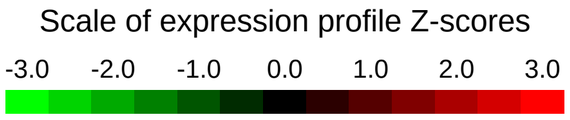

GEO Link:	**http://www.ncbi.nlm.nih.gov/geo/query/acc.cgi?acc=GSE59672**
Status:	**Public on Jul 23 2014**
Title:	**Expression data from DOX(doxorubicin) -treated wild type or CHIP knockout C57BL/6J mice at day 5**
Organism:	**Mus musculus**
Experiment type:	**Expression profiling by array**
Platform:	**GPL1261**
Pubmed ID:	
Summary & Design:	**Summary:** **The clinical application of doxorubicin as a broad-spectrum anti-tumor antibiotic is limited greatly by its cardiotoxicity. Various mechanisms have been studied, but little is known about whether genes or pathways relevant with energy metabolism contributes to doxorubicin-induced cardiomyopathy or not.** **We used microarrays to detail the global expression profiling of acute cardiomyopathy induced by doxorubicin in wild type or CHIP knockout C57BL/6J mice and discovered distinct classes of changed genes during this process.** **Overall design:** **The whole hearts were selected for RNA extraction and hybridization on Affymetrix microarrays at day 5 after a single intraperitoneal injection of doxorubicin at a dose of 15 mg/kg.**

Background corr dist: **KL-Divergence = 0.1136, L1-Distance = 0.0306, L2-Distance = 0.0016, Normal std = 0.4148**

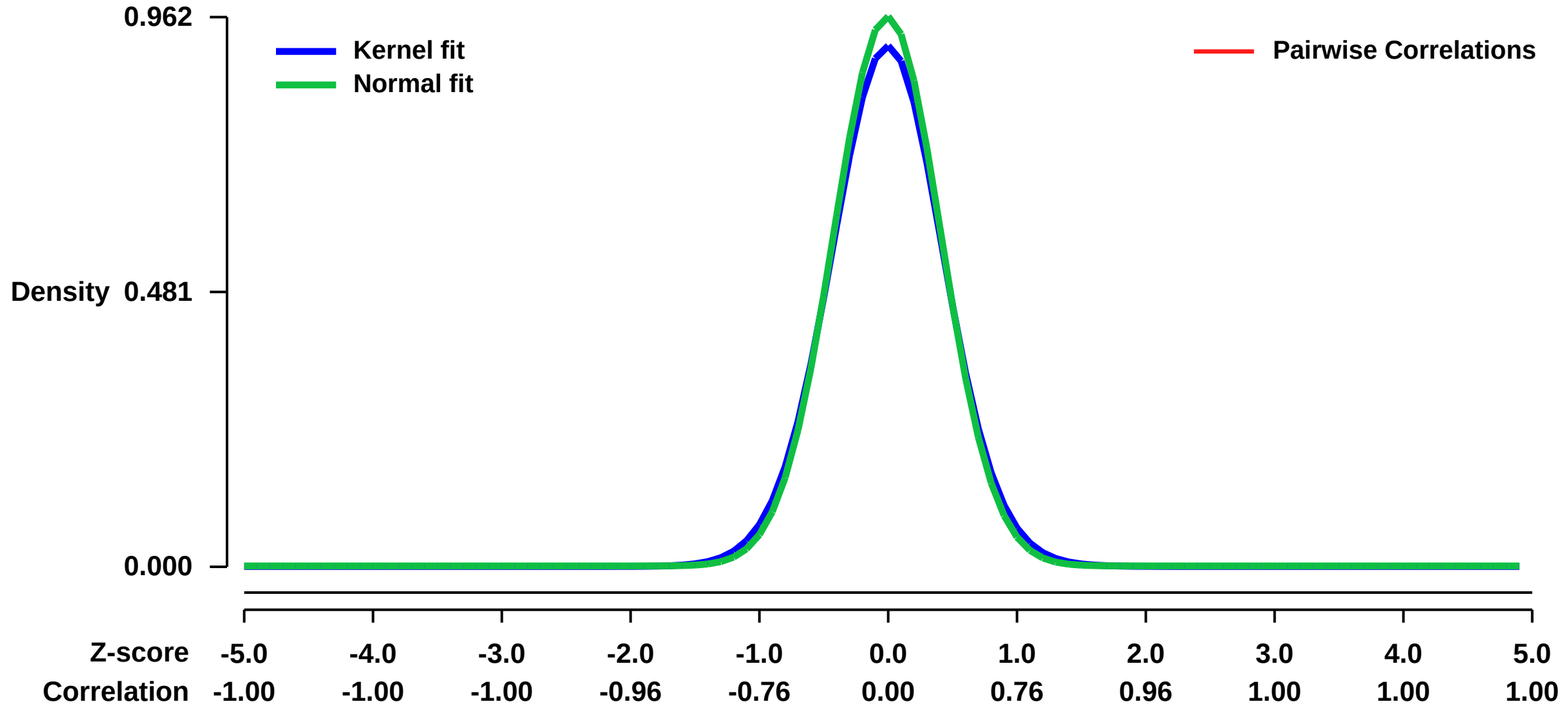

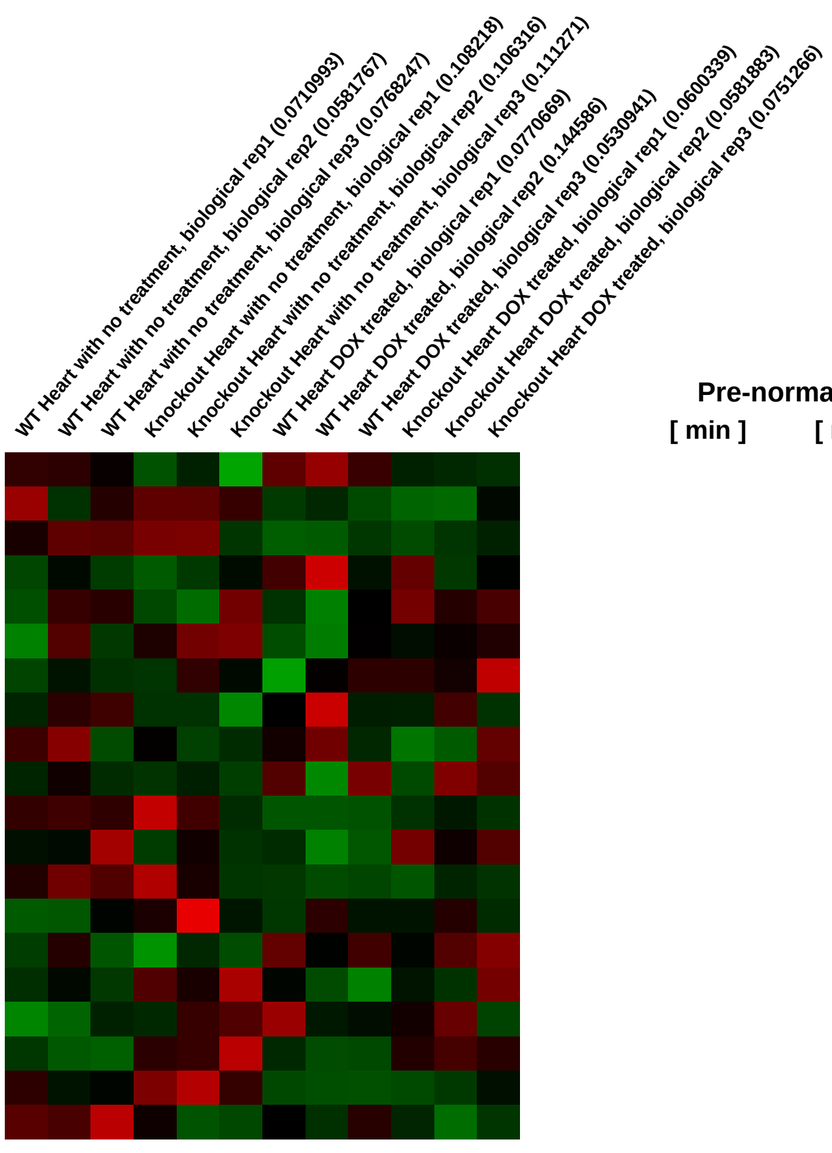

GEO Series "GSE9400" Expression Profiles

Num of samples in this series: 8

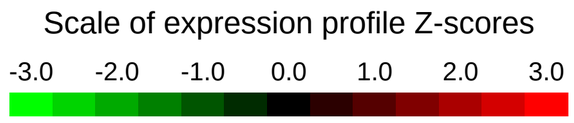

GEO Link:	**http://www.ncbi.nlm.nih.gov/geo/query/acc.cgi?acc=GSE9400**
Status:	**Public on Oct 10 2009**
Title:	**Hypoxic gene regulation on mice Quadriceps muscle**
Organism:	**Mus musculus**
Experiment type:	**Expression profiling by array**
Platform:	**GPL1261**
Pubmed ID:	
Summary & Design:	**Summary:** **To address whether hypoxia contributes to muscle patho-physiology, normal, adult C57 mice were exposed to chronic, normobaric and hypobaric hypoxic environments for 2 weeks in order to simulate levels of hypoxaemia reported in DMD patients with advanced respiratory insufficiency. Control mice were maintained under normoxic conditions. Control and experimental mice were studied.** **Keywords: Hypoxia effect, Comparison type** **Overall design:** **Fifteen micrograms labeled cRNA of hypoxic or normoxic QF muscle was fragmented, and 10¿…g was hybridized to Affymetrix´fi Mouse 430 ver 2.0 GeneChip arrays for 18â 24h (Affymetrix Inc.). Each microarray was washed and stained with streptavidinâ phycoerythrin and scanned at a 6-¿…m resolution with Agilent model G2500A GeneArray scanner A visual quality control measurement was performed to ensure proper hybridization after each chip was scanned.**

Background corr dist: KL-Divergence = 0.0562, L1-Distance = 0.0214, L2-Distance = 0.0005, Normal std = 0.5483

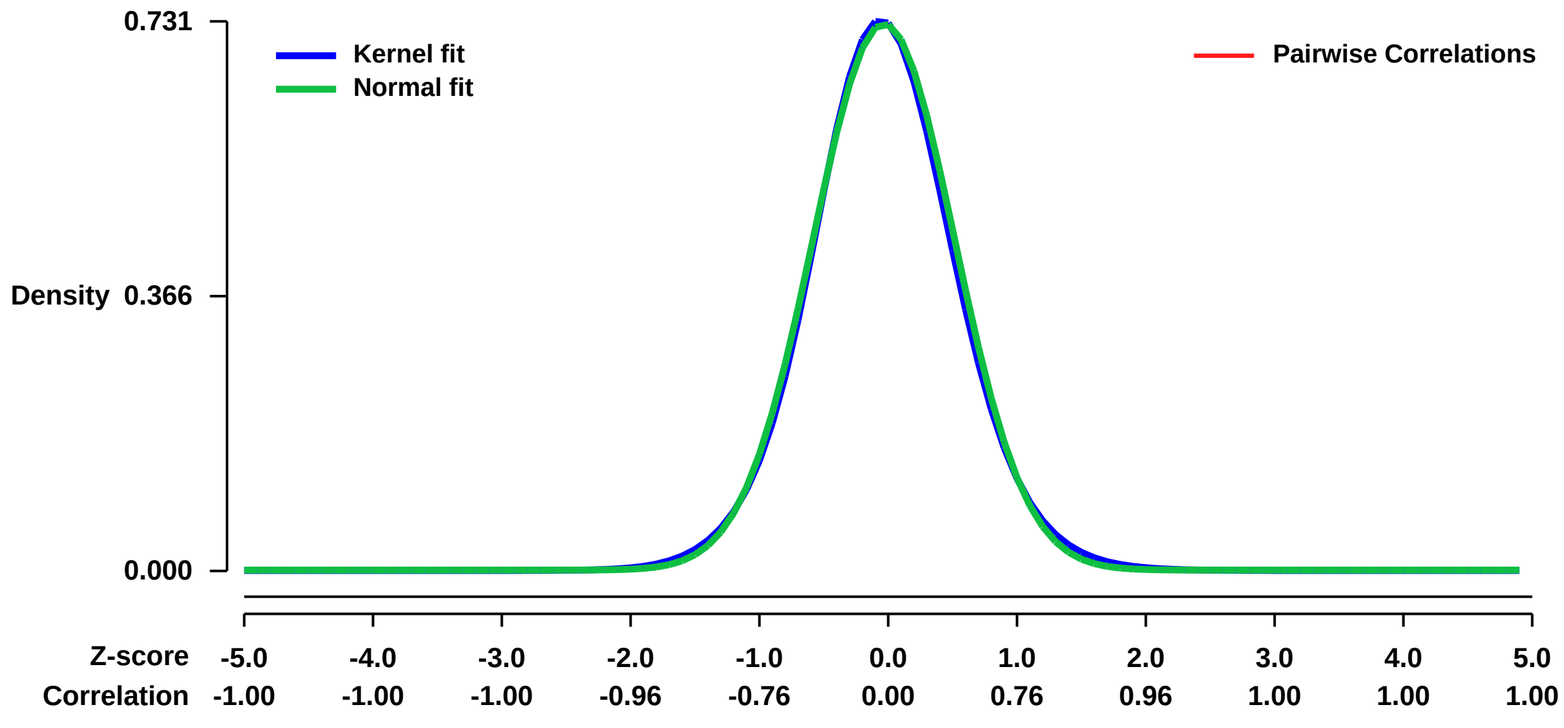

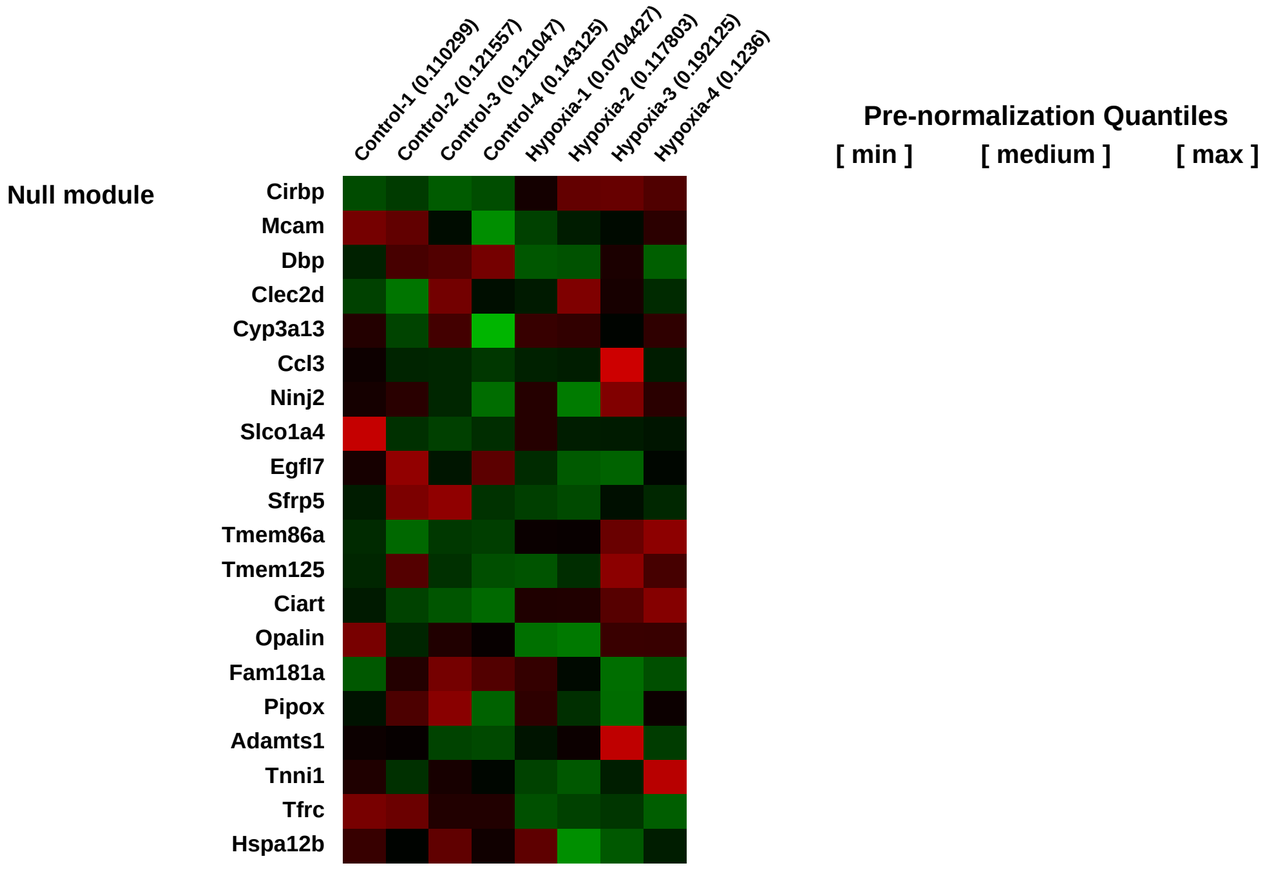

GEO Series "GSE5011" Expression Profiles

Num of samples in this series: 10

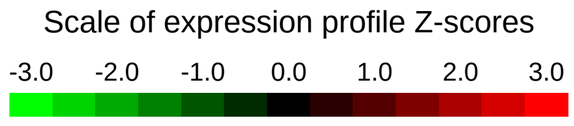

GEO Link:	http://www.ncbi.nlm.nih.gov/geo/query/acc.cgi?acc=GSE5011
Status:	Public on Jun 06 2006
Title:	oksen-affy-mouse-212956
Organism:	Mus musculus
Experiment type:	Expression profiling by array
Platform:	GPL1261
Pubmed ID:	

Summary & Design:

Summary:
Experimental autoimmune encephalomyelitis (EAE) is an autoimmune inflammatory disease of the CNS that is mediated by T cells and macrophages and represents the paradigmatic model for multiple sclerosis (MS). In EAE, therapeutic approaches targeting T cells have been successfully utilized leading to immunosuppression or tolerance. It has been recently shown that mesenchimal stem cells (MSC) isolated from C57BL/6J mice are an effective treatment of EAE induced by the encephalitogenic peptide pMOG 35-55. In this project we aim to track and evaluate the molecular changes the MSC acquire through several in-vitro passages that determine their therapeutic potential. Elucidation of the molecular pathways involved in this process will allow us to formulate better models of disease progression and curative strategies.

Specific aim:The specific aim of this proposal is to dissect the molecular pathways that mesenchimal stem cells undergo during in-vitro treatment and confer them the therapeutic potential to cure EAE. To accomplish this aim, we will purify and grow murine MSC under the same conditions used for therapy as described in Zappia et al (In press. Brain, 2005) and obtain samples at several stages of the culture. RNA will be purified from each sample and profiled using Affymetrix microarrays. Initial bioinformatics analysis will include data transformation, normalization and filtering. A second stage analysis will involve time-series analysis by ANOVA and dynamic events modeling using neural networks.

Stem cells are now viewed as potential source of cells for almost any tissue due to their postulated capacity to give rise to virtually any type of cell. Among them, mesenchymal stem cells (MSC), can extensively proliferate in vitro and differentiate under appropriate conditions in bone, cartilage, and other mesenchymal tissues. It has been also reported that MSC can differentiate into other cells types including neuroectodermal cells. Furthermore, upon tissue injury MSC have been shown to migrate into the damaged brain. These results suggest that MSC could provide an ideal cell source for repair of injured organs including the central nervous system (CNS). In addition to their plasticity, MSC have been recently demonstrated to suppress several T lymphocyte activities thus exerting an immunoregulatory capacity both in vitro and in vivo. The mechanisms mediating such effect are only partially understood. We hypothesize that an analysis of how MSC acquire their therapeutic potential in vitro by expression profiling in a time series fashion will allow us to dissect the involved mechanisms.

Before arriving to our lab in UCSF, samples will be processed as follows: Bone marrow from 6-8 weeks old C57BL/6J mice will be flushed out of tibias and femurs. After two washings by centrifugation at 1500 rpm for 5 min in PBS (Sigma Chemical Co., St. Louis, MO, USA), cells will be plated in 75 cm2 tissue culture flasks at the concentration of 0.3-0.4 x 106 cells/cm2 utilizing Murine Mesencult as medium (Stem Cell Technologies Inc., Vancouver, BC, Canada). Cells will be kept in a humidified 5% CO2 incubator at 37´℃ for about 4-5 weeks, when only adherent cells will be collected following 10 min incubation at 37´℃ with 0.05% trypsin solution containing 0.02% EDTA. After the first cut and for the subsequent 4 or 5 passages, cells will be plated in 25 cm2 flasks at 1.2-2.0 x 104cells/cm2 . For the following passages cells will routinely seeded at 4-10 x 103cells/cm2 reaching confluence only after 4-5 days. Cells will be collected at selected timepoints and immersed in TRizol reagent and shipped to UCSF. For the initial stage of this project cell will be collected at the following 5 time points:

T0: Bone marrow aspirates (uncultured)

T1: pre-mesenchymal stem cells (some cut before the population completely subtracted of Hematopoietic stem cells)

T2: Mesenchymal stem cells (in vitro assessed, functionally and phenotipically)

T3: Mesenchymal stem cells biological active in vivo

T4: Mesenchymal stem cells at the passage in vitro next to the one active in vivo

T5: Mesenchymal stem cells no more active in vitro neither in vivo

Once in our lab, RNA will be extracted using the Trizol reagent (Invitrogen) and further purified by the RNeasy kit (Qiagen). Sample labeling will be performed according to the array manufacturer (Affymetrix) instructions. Subject to initial results, we plan to add intermediate timepoints in subsequent stages.

Keywords: time-course

Overall design:

Background corr dist: KL-Divergence = 0.1086, L1-Distance = 0.0338, L2-Distance = 0.0023, Normal std = 0.4283

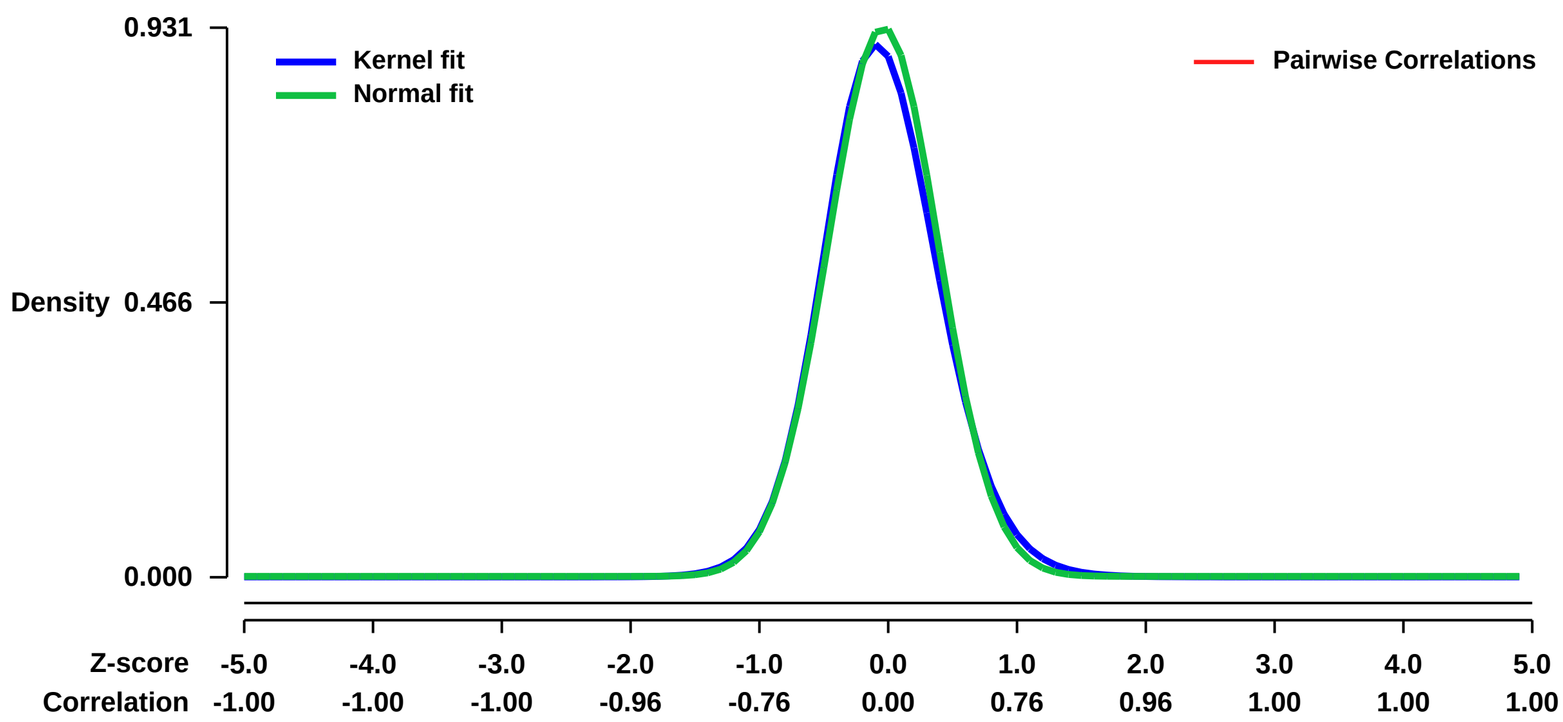

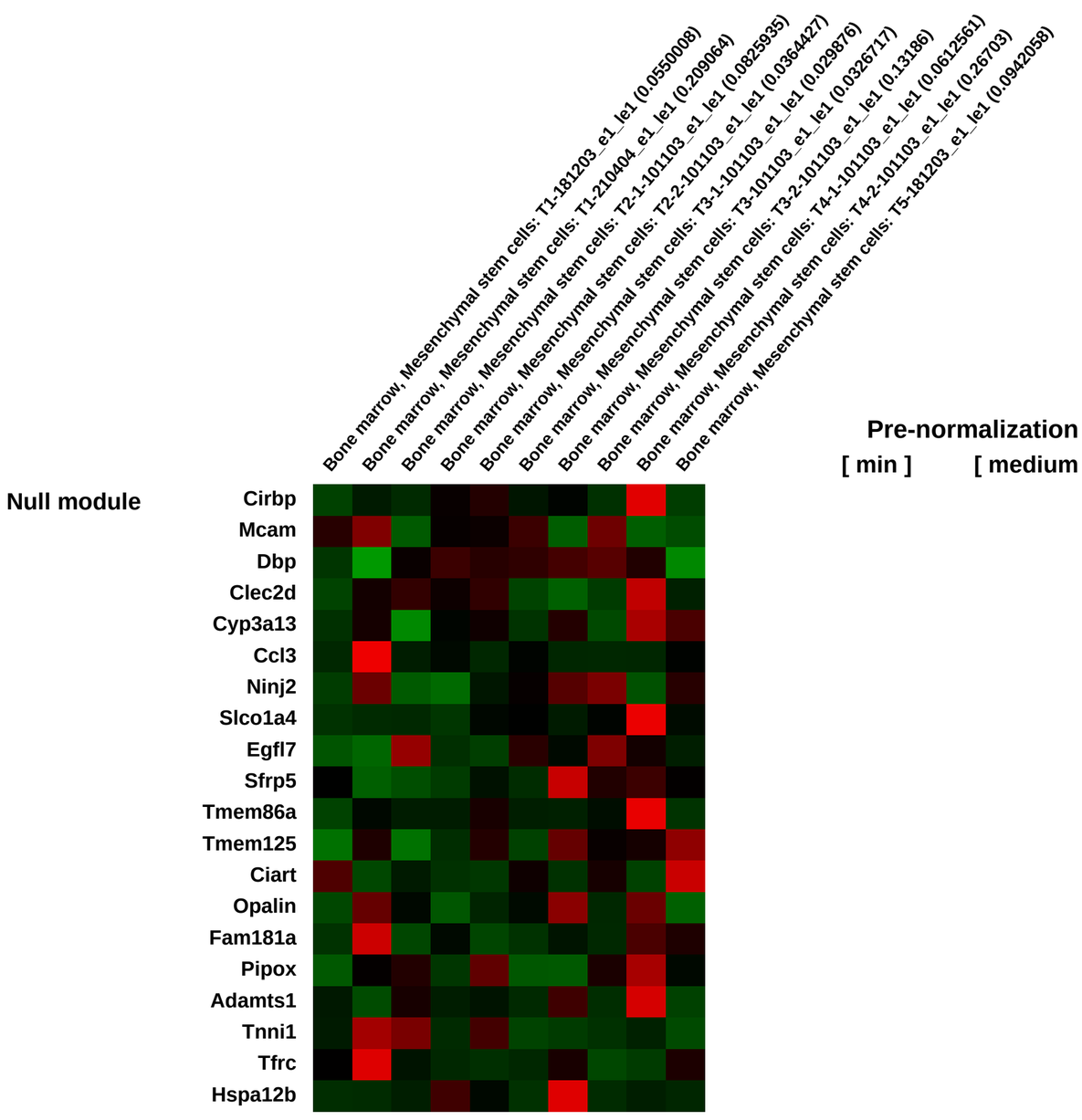

GEO Series "GSE17383" Expression Profiles

Num of samples in this series: 6

Scale of expression profile Z-scores

-3.0 -2.0 -1.0 0.0 1.0 2.0 3.0

GEO Link:	http://www.ncbi.nlm.nih.gov/geo/query/acc.cgi?acc=GSE17383
Status:	Public on Aug 05 2009
Title:	Toward a Better Understanding of Potential Roles of Astrocytes in HIV-1-associated Neurocognitive Disorders
Organism:	Mus musculus
Experiment type:	Expression profiling by array
Platform:	GPL1261
Pubmed ID:	19697136
Summary & Design:	**Summary:** We present a microarray analysis of primary mouse astrocytes exposed to HIV-1 in culture. Results are compared with previous genomic studies of HIV-1 effect in human astrocytes and human and macaque brains. **Overall design:** Day-two neonatal mouse astrocytes were exposed in triplicates to cell-free HIV-1/NL4-3 at m.o.i. of 1 and cultured for 24 hours. As control, cells were treated in triplicates with a mock virus concentrate at the same dilution (vol/vol) as the wild-type virus. As an example of large scale gene expression analysis we shall provide some details of the method; full description is in Kim et al. (S.-Y. Kim et al., 2004). Total RNA was prepared from cell cultures using the RNAeasy total RNA extraction kit (Qiagen, CA). RNA quality was assessed by electrophoresis and spectrophotometric analysis; between 1 and 10 ´µg of total RNA was used to generate a cDNA, and then 1 ´µg of cDNA product was used in an in vitro transcription reaction that contained biotinylated UTP and CTP. Twenty ´µg of full-length cRNA was fragmented and was subjected to gene expression analysis on the Affymetrix Mouse Genome 430 2.0 Array chip. Affymetrix software was used to generate CHP files. Significance analysis was performed using ArrayAssist software (Stratagene).

Background corr dist: KL-Divergence = 0.0419, L1-Distance = 0.0186, L2-Distance = 0.0004, Normal std = 0.6059

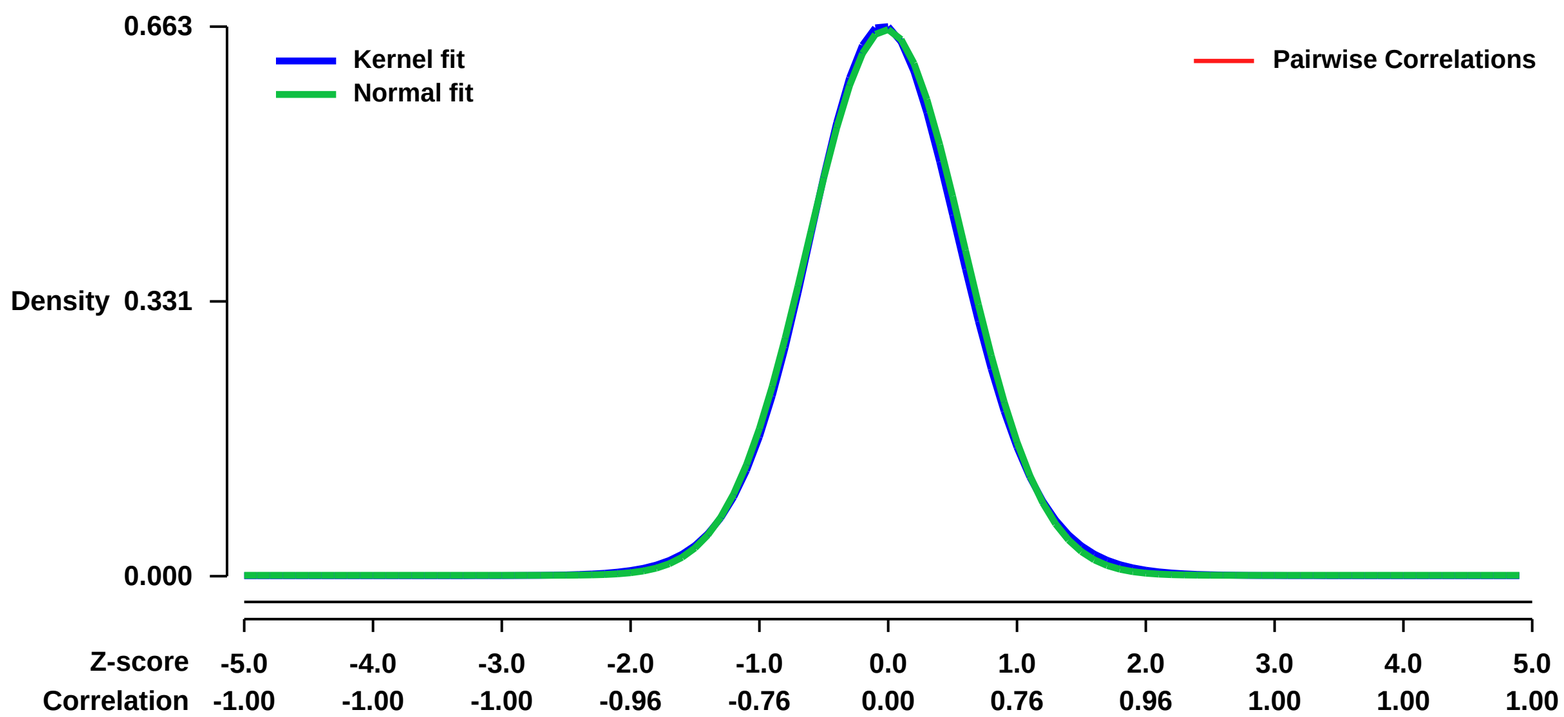

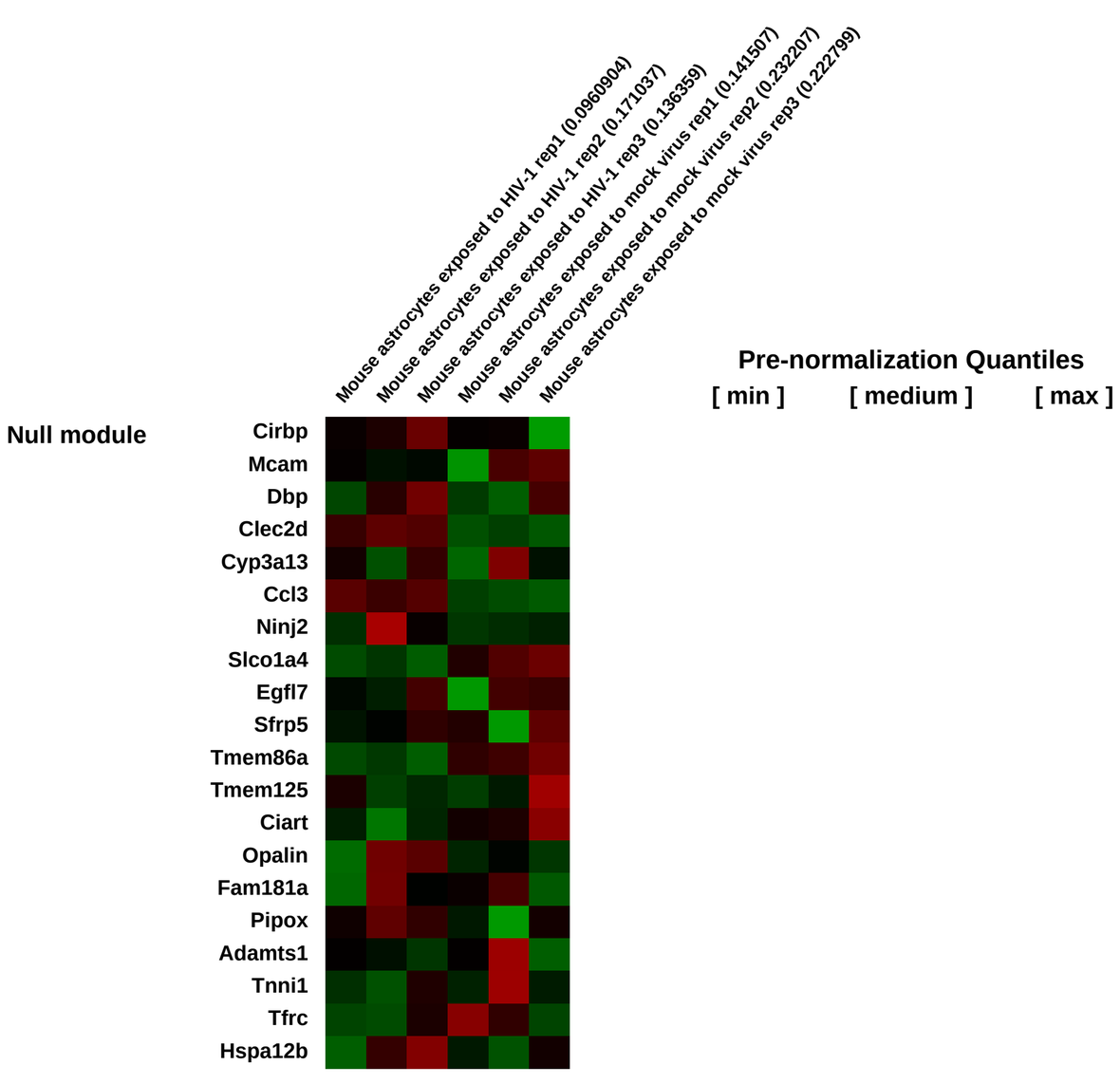

GEO Series "GSE39771" Expression Profiles

Num of samples in this series: 10

Scale of expression profile Z-scores

-3.0 -2.0 -1.0 0.0 1.0 2.0 3.0

GEO Link:	http://www.ncbi.nlm.nih.gov/geo/query/acc.cgi?acc=GSE39771
Status:	Public on Aug 01 2012
Title:	Expression data from embryonic stem cells following siRNA transfection of UPS members [self_renewal]
Organism:	Mus musculus
Experiment type:	Expression profiling by array
Platform:	GPL1261
Pubmed ID:	23103054
Summary & Design:	**Summary:** While transcriptional regulation of stem cell self-renewal and differentiation has been extensively studied, only a small number of studies have addressed the roles for post-translational modifications in these processes. A key mechanism of post-translational modification is ubiquitination by the ubiquitin-proteasome system (UPS). Using UPS-targeted RNAi screens, we identify novel regulators of pluripotency and differentiation. We focus on two of these proteins, the deubiquitinating enzyme, Psmd14, and the E3 ligase, Fbxw7, and characterize their importance in ES cell pluripotency and cellular reprogramming. **Overall design:** Embryonic stem cells were reverse transfected with siRNA, 48 hrs post transfection cells were isloated for RNA extraction and hybridization on Affymetrix microarrays

Background corr dist: KL-Divergence = 0.0991, L1-Distance = 0.0239, L2-Distance = 0.0008, Normal std = 0.4406

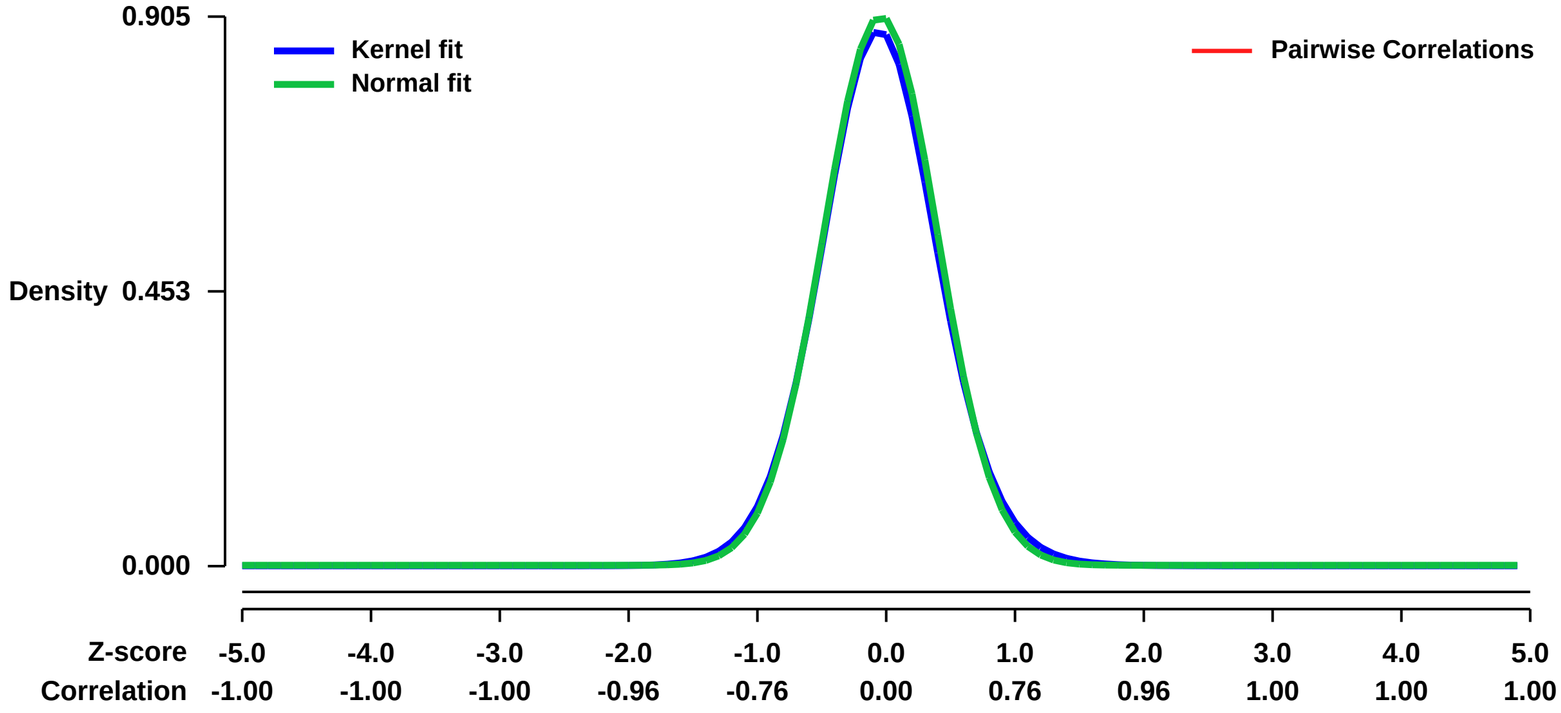

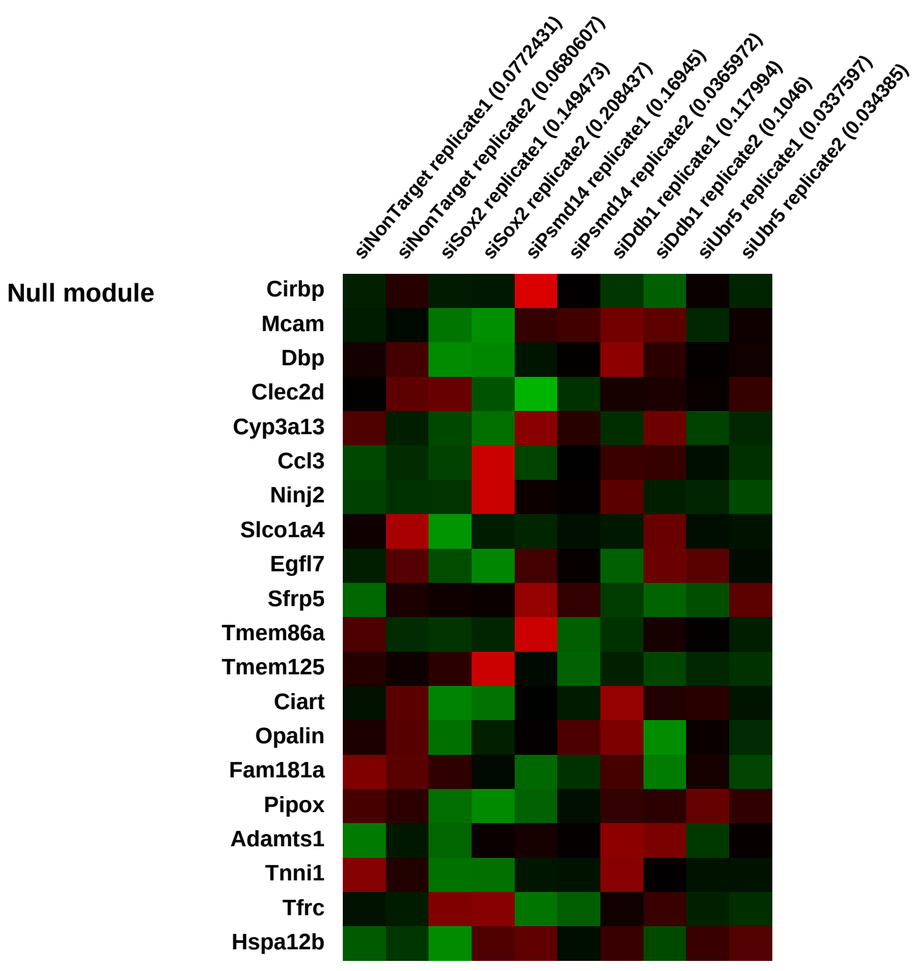

GEO Series "GSE4765" Expression Profiles

Num of samples in this series: 6

Scale of expression profile Z-scores

-3.0 -2.0 -1.0 0.0 1.0 2.0 3.0

GEO Link:	**http://www.ncbi.nlm.nih.gov/geo/query/acc.cgi?acc=GSE4765**
Status:	**Public on Nov 03 2006**
Title:	**SM by NZB Female Liver Gene Expression**
Organism:	**Mus musculus**
Experiment type:	**Expression profiling by array**
Platform:	**GPL1261**
Pubmed ID:	
Summary & Design:	**Summary:** **3 x 3 comparison of the inbred strains SM/J and NZB/BinJ.** **Keywords: Comparitive mRNA** **Overall design:** **Simple comparison of native untreated gene expression profiles of female 8wk old SM mice (x3) by female 8wk old NZB mice (x3)**

Background corr dist: **KL-Divergence = 0.0199, L1-Distance = 0.0258, L2-Distance = 0.0010, Normal std = 0.7416**

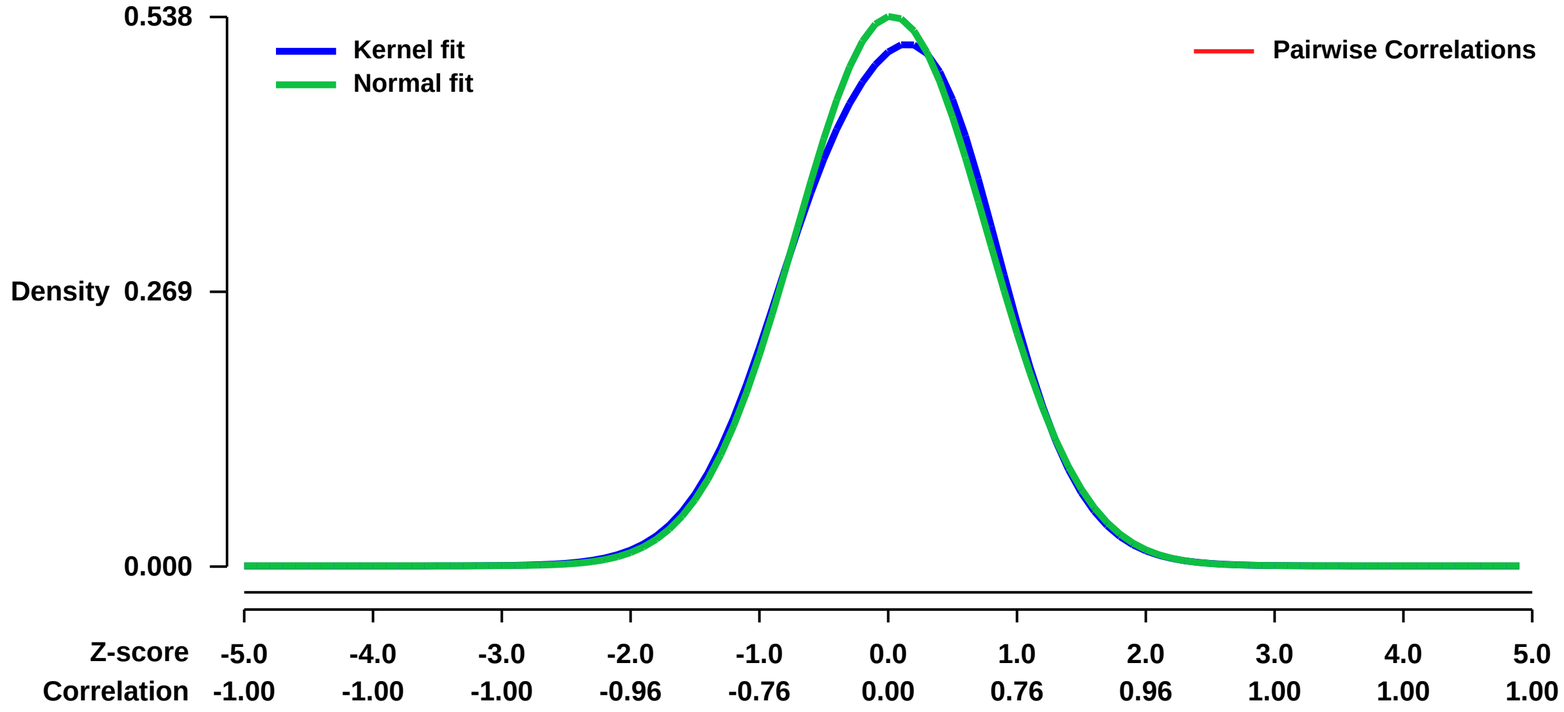

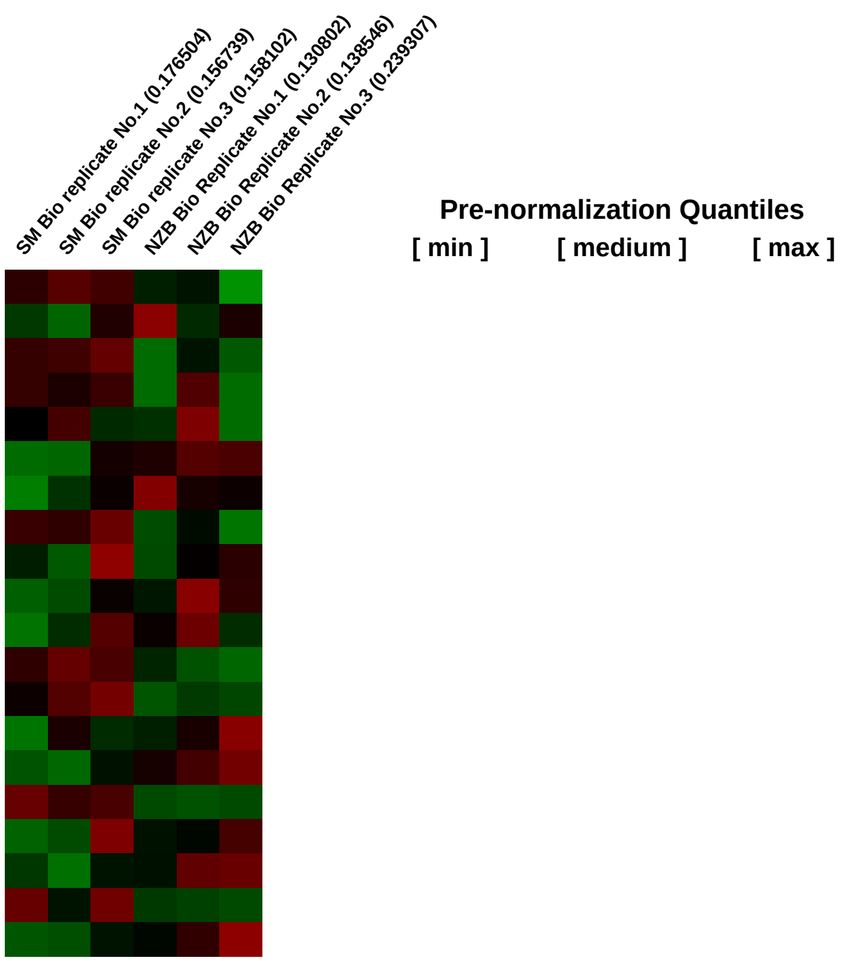

GEO Series "GSE19286" Expression Profiles

Num of samples in this series: 6

Scale of expression profile Z-scores

-3.0 -2.0 -1.0 0.0 1.0 2.0 3.0

GEO Link:	http://www.ncbi.nlm.nih.gov/geo/query/acc.cgi?acc=GSE19286
Status:	Public on Dec 03 2009
Title:	Microarray gene expression profiling of aorta genes of APOE-deficient mice receiving the ACE inhibitor captopril
Organism:	Mus musculus
Experiment type:	Expression profiling by array
Platform:	GPL1261
Pubmed ID:	20504763
Summary & Design:	**Summary:** Microarray gene expression profiling of aorta genes of APOE-deficient mice receiving atherosclerosis treatment with the ACE inhibitor captopril. Hypercholesterolemic APOE-deficient mice were used as a standard model of atherosclerosis to study gene expression changes during atherosclerosis treatment with the ACE inhibitor captopril. Microarray analysis was performed of whole aortas isolated from captopril-treated APOE-deficient mice relative to untreated APOE-deficient mice with overt atherosclerosis, and nontransgenic control mice. Microarray gene expression profiling revealed that captopril-mediated atherosclerosis prevention involved inhibition of aorta-infiltrating immune cells such as pro-atherogenic T lymphocytes and macrophages. **Overall design:** Microarray gene expression profiling was performed of whole aortas isolated from APOE-deficient mice with atherosclerosis relative to captopril-treated APOE-deficient mice, and nontransgenic control mice. Three study groups were analyzed, i.e. 8-months-old untreated APOE-deficient mice with overt atherosclerosis, age-matched APOE-deficient mice treated for 7 months with the angiotensin-converting enzyme (ACE) inhibitor, captopril (20 mg/kg in drinking water), and nontransgenic control C57BL/6J mice. Two biological replicates were made of each group, and total RNA of three aortas was pooled for one gene chip.

Background corr dist: KL-Divergence = 0.0254, L1-Distance = 0.0174, L2-Distance = 0.0003, Normal std = 0.7080

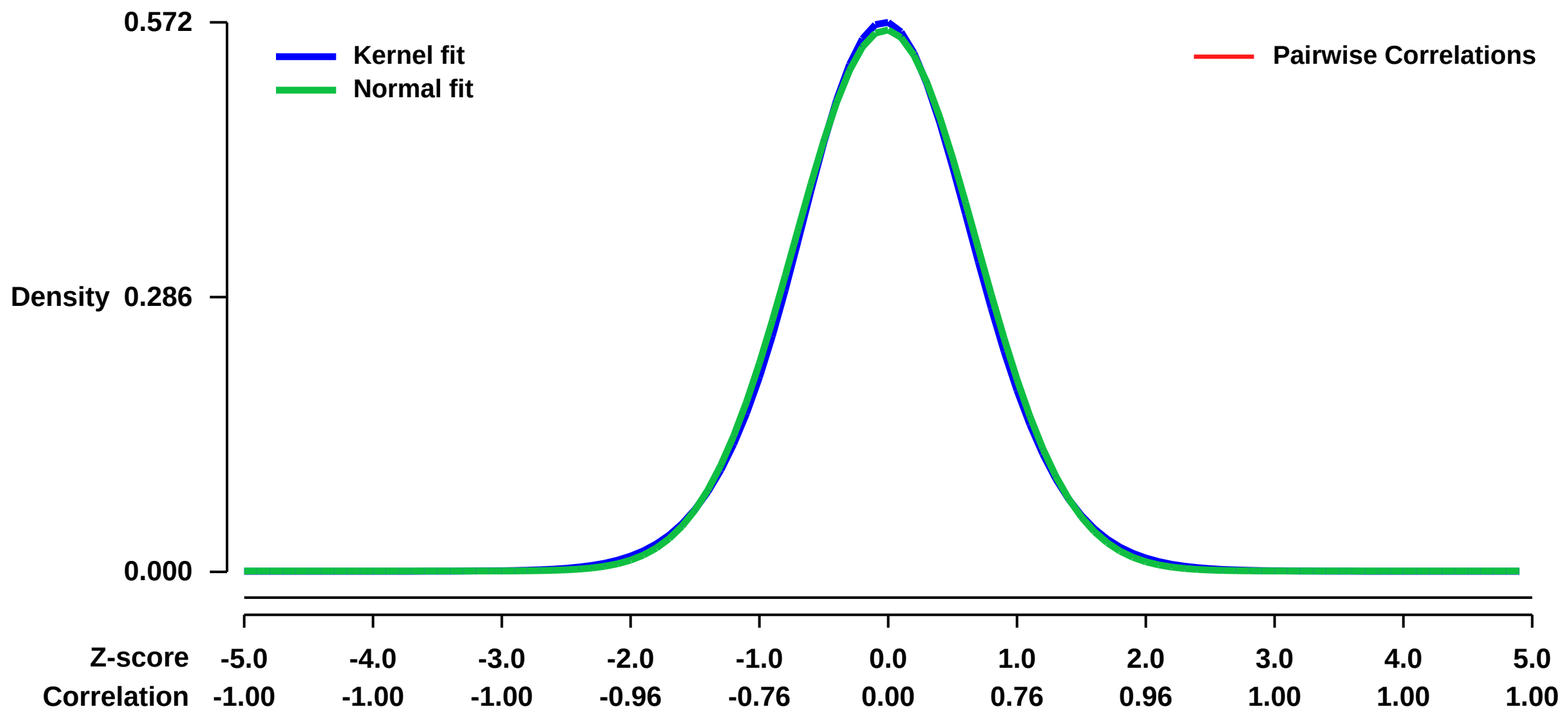

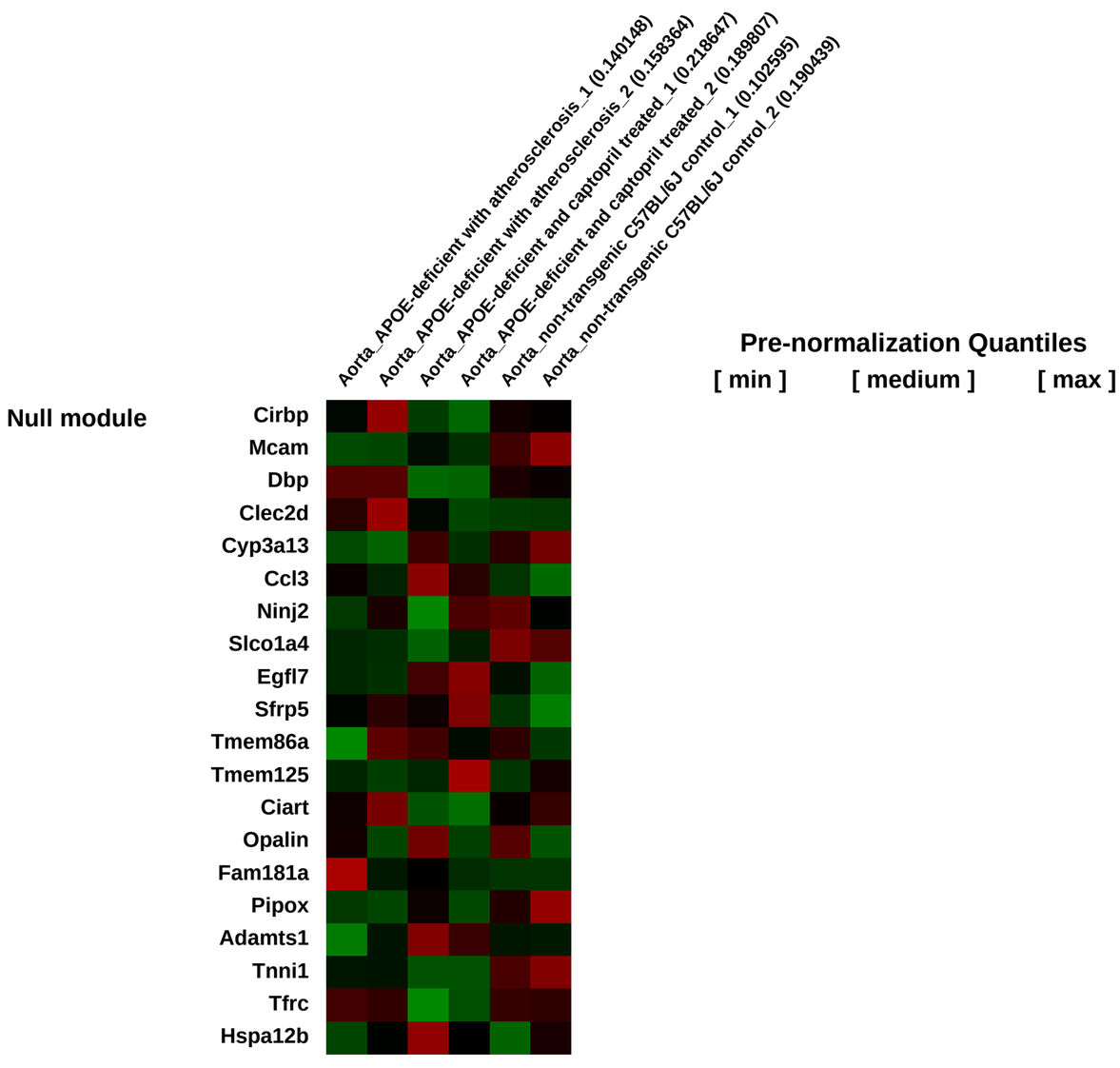

GEO Series "GSE8503" Expression Profiles

Num of samples in this series: 6

Scale of expression profile Z-scores

-3.0 -2.0 -1.0 0.0 1.0 2.0 3.0

GEO Link:	http://www.ncbi.nlm.nih.gov/geo/query/acc.cgi?acc=GSE8503
Status:	Public on Jan 01 2008
Title:	mRNA expression analysis of undifferentiated Dicer -/- (27H10) embryonic stem cells after miRNA transfection
Organism:	Mus musculus
Experiment type:	Expression profiling by array
Platform:	GPL1261
Pubmed ID:	18311153
Summary & Design:	**Summary:** We have analyzed the transcript expression levels in Dicer knock-out embryonic stem (ES) cells 24 hours after transfection with either control siRNA agains Renilla luciferase or miRNA Mimics (Dharmacon) of mmu-miR-290 cluster members in order to identify primary targets of miR-290 cluster miRNAs. **Keywords:** Comparison of effect of two different transfections on transcriptome of Dicer-KO ES cells **Overall design:** Cell were analysed 24h after transfections in an undifferentiated state. Triplicates of both transfections were analyzed.

Background corr dist: KL-Divergence = 0.0399, L1-Distance = 0.0219, L2-Distance = 0.0005, Normal std = 0.6216

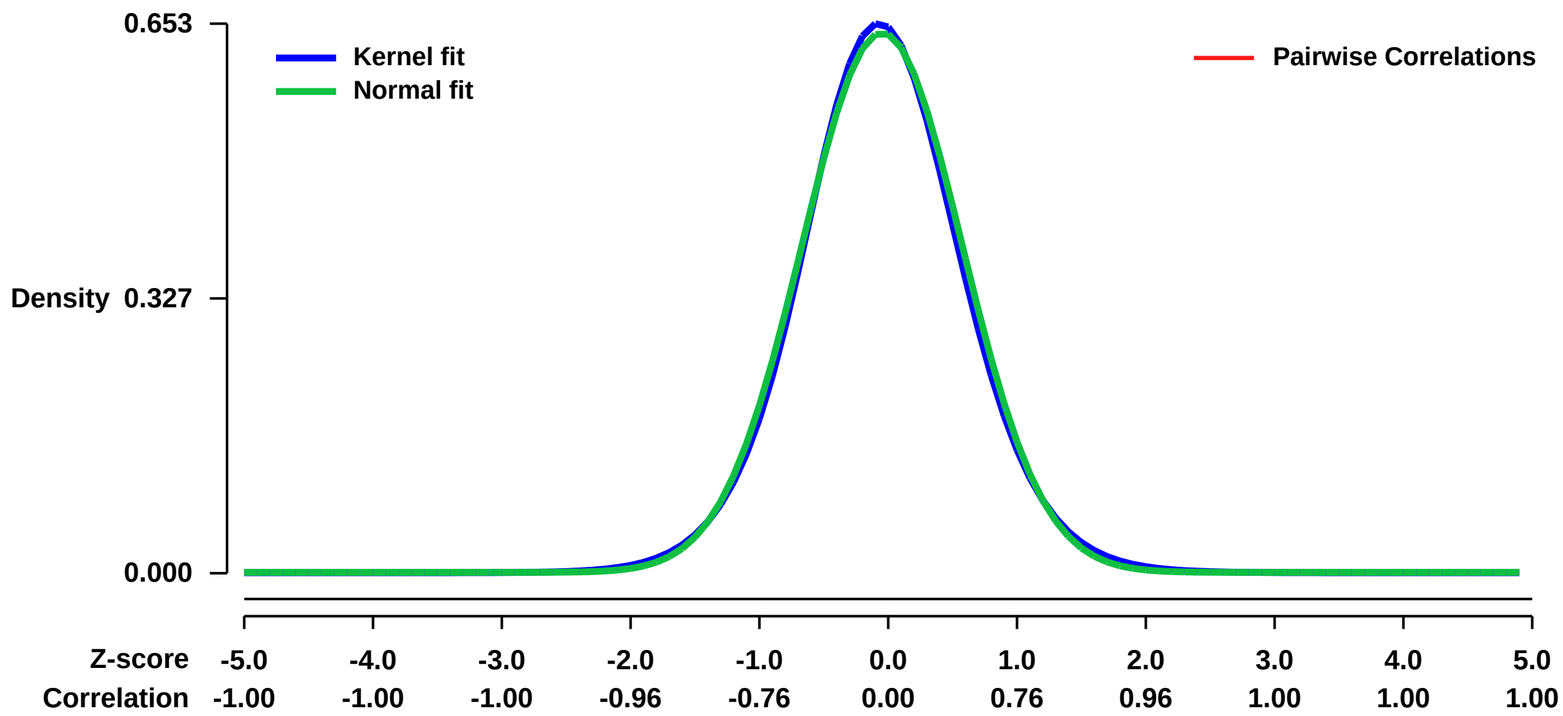

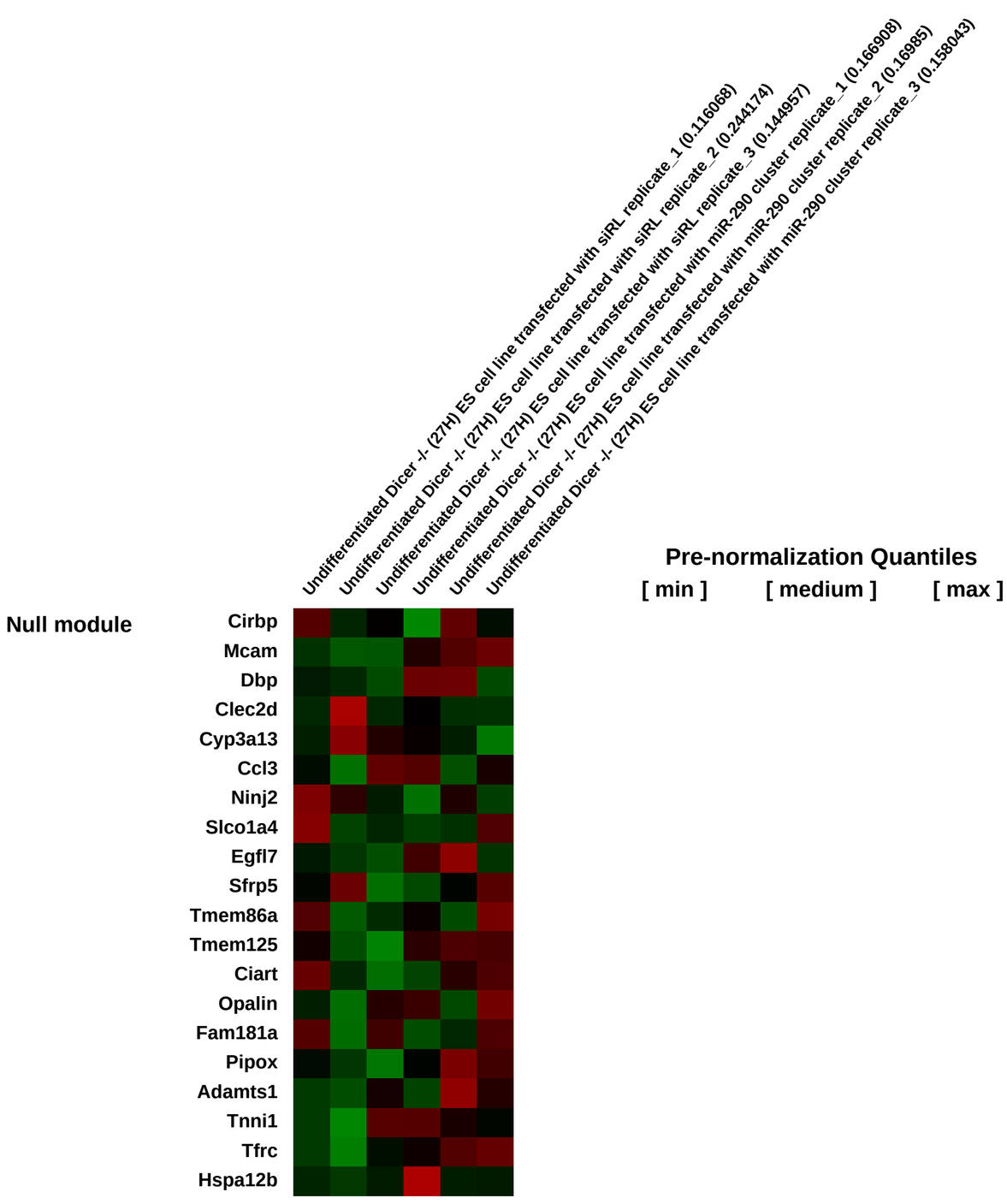

GEO Series "GSE6259" Expression Profiles

Num of samples in this series: 21

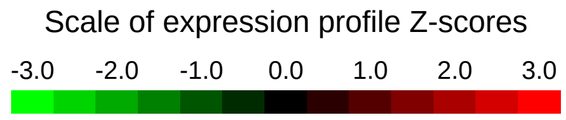

GEO Link:	**http://www.ncbi.nlm.nih.gov/geo/query/acc.cgi?acc=GSE6259**
Status:	**Public on Dec 01 2006**
Title:	**Differential antigen processing by dendritic cell subsets in vivo**
Organism:	**Mus musculus**
Experiment type:	**Expression profiling by array**
Platform:	**GPL1261**
Pubmed ID:	**17204652**
Summary & Design:	**Summary:** **Dendritic cells (DCs) process and present self and foreign antigens to induce tolerance or immunity. In vitro models suggest that induction of immunity is controlled by regulating the presentation of antigen, but little is known about how DCs control antigen presentation in vivo. To examine antigen processing and presentation in vivo we specifically targeted antigens to the two major subsets of DCs using chimeric monoclonal antibodies. Unlike CD8+ DCs that express the cell surface protein CD205, CD8- DCs, which are positive for the 33D1 antigen, are specialized for presentation on MHC class II. This difference in antigen processing is intrinsic to the DC subsets and associated with increased expression of proteins associated with MHC processing.** **Keywords: cell type comparison of wildtype and Flt3L melonom spleen DCs and splenic B cells, CD4 and CD8 T cells** **Overall design:** **This study includes data from cell sort purified dendritic cells, B cells and CD4 and CD8 T cells. The genearray was performed to identify the transmembrane molecule recognized by the antibody 33D1. The antibody 33D1 binds specifically to CD8-CD11cHigh DCs in the spleen. Therfore the data set was reduced in this way that all molecules that are expressed either in CD8=CD11cHigh DCs, B cells and T cells were diminished of the CD8+CD11cHigh DC data set. This Genearray was also used to analyze MHC class I and MHC class II associated moelcules as the DC subsets differ in the antigen presentation. Each Series consists of 3 individuall samples**

Background corr dist: KL-Divergence = 0.1459, L1-Distance = 0.0268, L2-Distance = 0.0013, Normal std = 0.3825

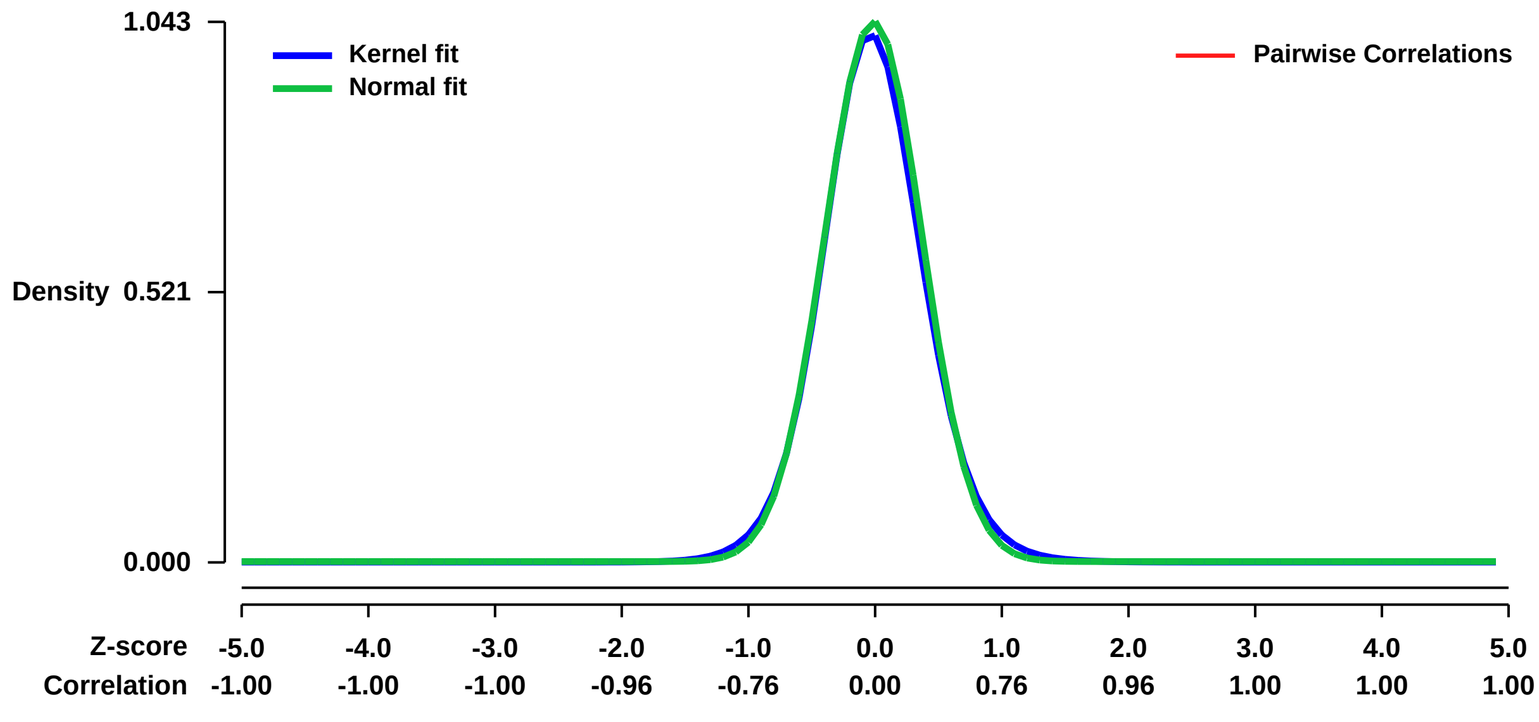

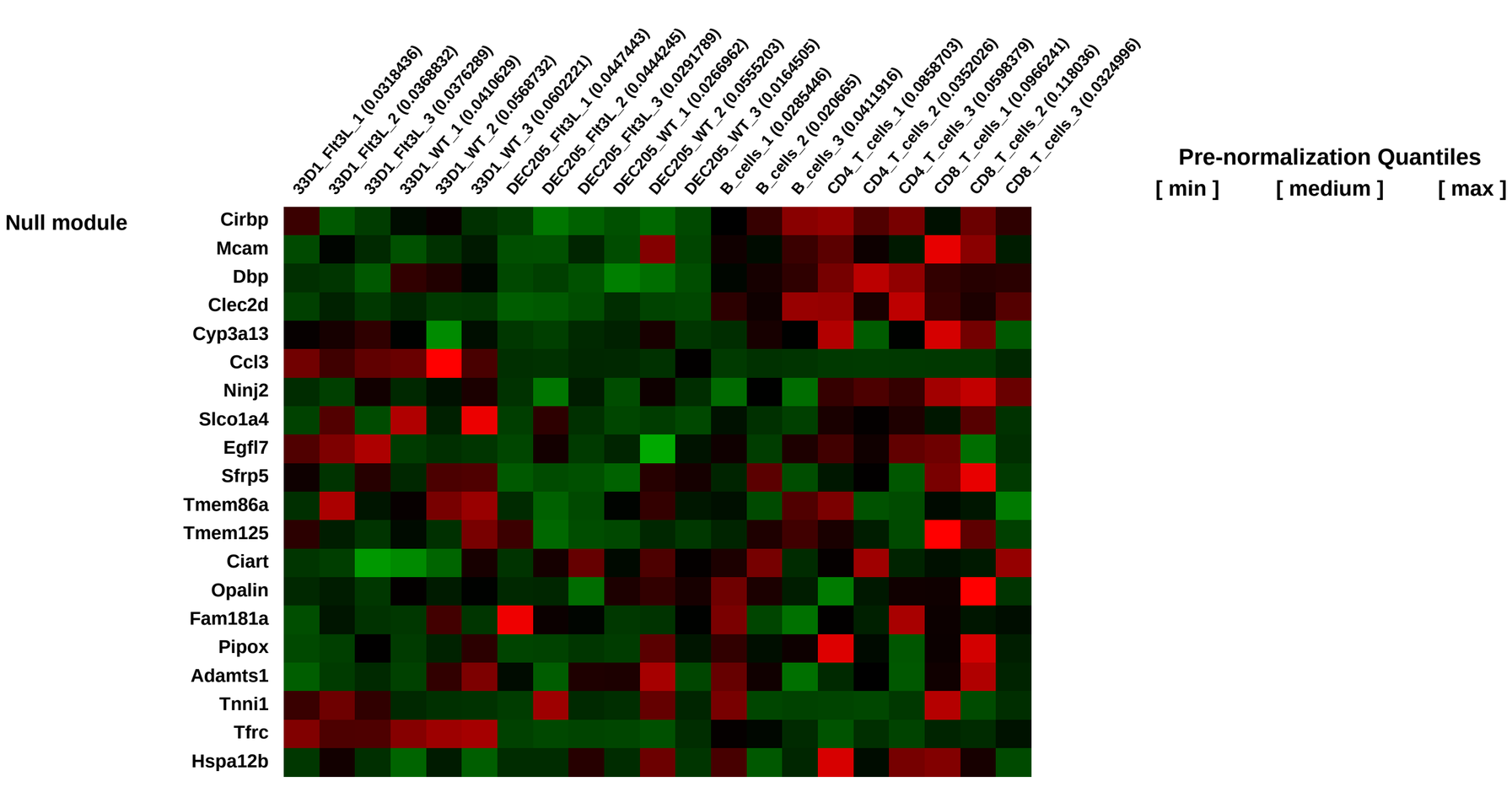

GEO Series "GSE13071" Expression Profiles

Num of samples in this series: 15

Scale of expression profile Z-scores

-3.0 -2.0 -1.0 0.0 1.0 2.0 3.0

GEO Link:	http://www.ncbi.nlm.nih.gov/geo/query/acc.cgi?acc=GSE13071
Status:	Public on Aug 26 2009
Title:	Knee joint synovium from different grades of inflammation in mouse collagen induced arthritis (CIA)
Organism:	Mus musculus
Experiment type:	Expression profiling by array
Platform:	GPL1261
Pubmed ID:	19690516
Summary & Design:	**Summary:** Knee joint synovium was used for gene expression analysis of mouse collagen induced arthritis (CIA). Synovium was prepared at day 30 after initial sensitization from: healthy controls, CIA animals with no, with mild, with moderate, or with severe joint inflammation. Each sample group is represented by three replicates, each consisting of tissue collected from three to four animals. **Keywords: disease severity analysis** **Overall design:** The data set consists of 15 samples: five groups with three replicates each. One sample group is from healthy controls, the other groups are from CIA animals with different degress of joint inflammation.

Background corr dist: KL-Divergence = 0.0611, L1-Distance = 0.0572, L2-Distance = 0.0049, Normal std = 0.5641

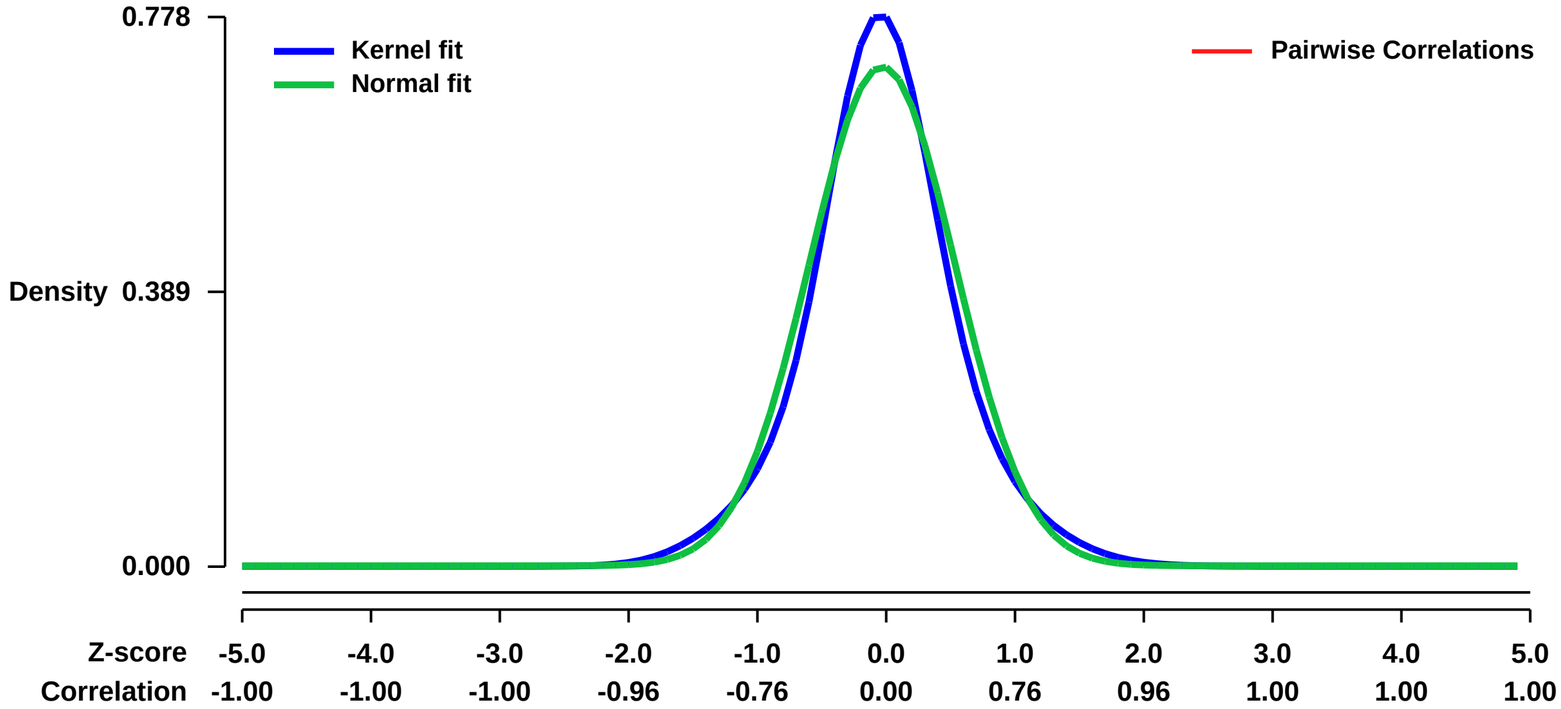

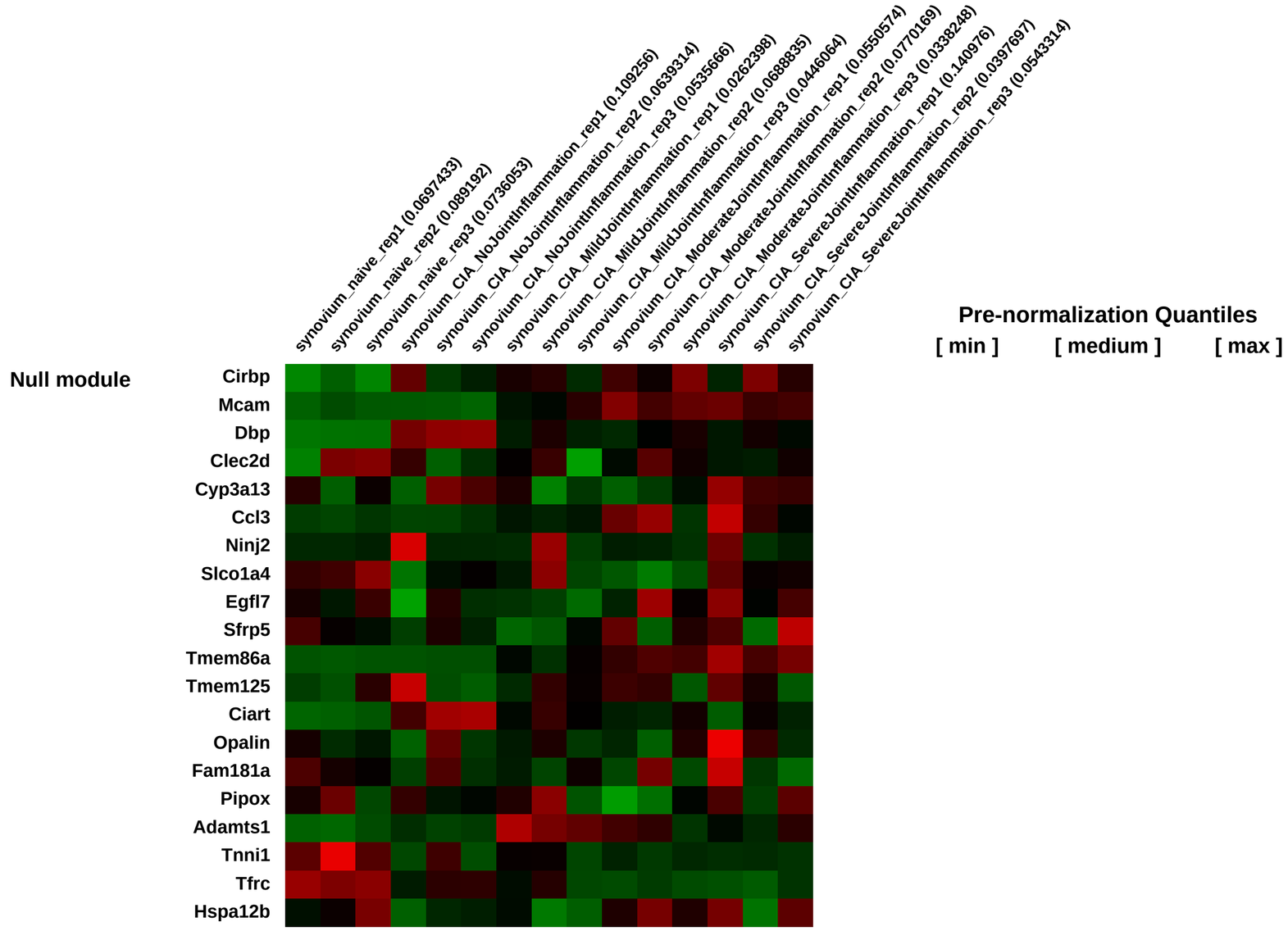

GEO Series "GSE52118" Expression Profiles

Num of samples in this series: 9

Scale of expression profile Z-scores

-3.0 -2.0 -1.0 0.0 1.0 2.0 3.0

GEO Link:	http://www.ncbi.nlm.nih.gov/geo/query/acc.cgi?acc=GSE52118
Status:	Public on Nov 15 2013
Title:	Comparison of gene expression in motor pools with differential vulnerability in ALS
Organism:	Mus musculus
Experiment type:	Expression profiling by array
Platform:	GPL1261
Pubmed ID:	24462097
Summary & Design:	**Summary:** ALS is a uniformly fatal neurodegenerative disease in which motor neurons in the spinal cord and brain stem are selectively lost. Individual motor - groups of motor neurons innervating single muscles - show widely varying degrees of disease resistance: in the final stages of ALS, nearly all voluntary movement is lost but eye movement and eliminative and sexual functions remain relatively unimpaired. These functions are controlled by motor neurons of the oculomotor (III), trochlear (IV) and abducens (VI) nuclei in the midbrain and brainstem, and by Onufâ s nucleus in the lumbosacral spinal cord, respectively. Correspondingly, in ALS autopsies the oculomotor and Onufâ s nuclei are almost completely preserved. We used microarray profiling of isolated wildtype mouse motor neurons to identify genes whose expression was characteristic of both oculomotor and Onufâ s nuclei but not of vulnerable lumbar spinal neurons, or vice versa. **Overall design:** Three wild-type C57BL/6J P7 male animals were perfused with 30% sucrose, lumbosacral spinal cord and midbrain regions were rapidly recovered, embedded in OCT compound, and frozen in liquid nitrogen. 12 ´µm-thick cryosections were mounted on RNAse-free, PEN-foil covered glass slides (Zeiss), fixed for 2 min in 100% EtOH, rinsed in 50% EtOH, stained with 1% cresyl violet for 2 min, rinsed with 50% EtOH, dehydrated in graded solutions of ethanol and air dried prior to LCM using PALM Microbeam system (Zeiss). From each animal, ~200 DL, L5, and oculomotor motor neurons were collected directly in lysis buffer. RNA was purified using Absolutely RNA, NanoPrep kit (Stratagene, La Jolla, CA). RNA integrity was assessed on the Bioanalyzer 2100 (Agilent Technologies, Santa Clara, CA). At least 1.5 ng of purified RNA was the starting material used in the WT-Ovation Pico RNA Amplification System (Nugen, San Carlos,CA) with the FL-Ovation cDNA Biotin Module V2 (Nugen) to generate labeled probe. 10 ´µg of biotinylated cRNA from three independent samples for each motor neuron group isolated by LCM was hybridized to on Affymetrix (Santa Clara, CA) Mouse Genome 430 2.0 Arrays. Gene ontology and pathway analysis was performed using DAVID Bioinformatics Resources 6.7 (National Institute of Allergy and Infectious Diseases, NIH, Bethesda, MD).

Background corr dist: KL-Divergence = 0.1030, L1-Distance = 0.0325, L2-Distance = 0.0021, Normal std = 0.4364

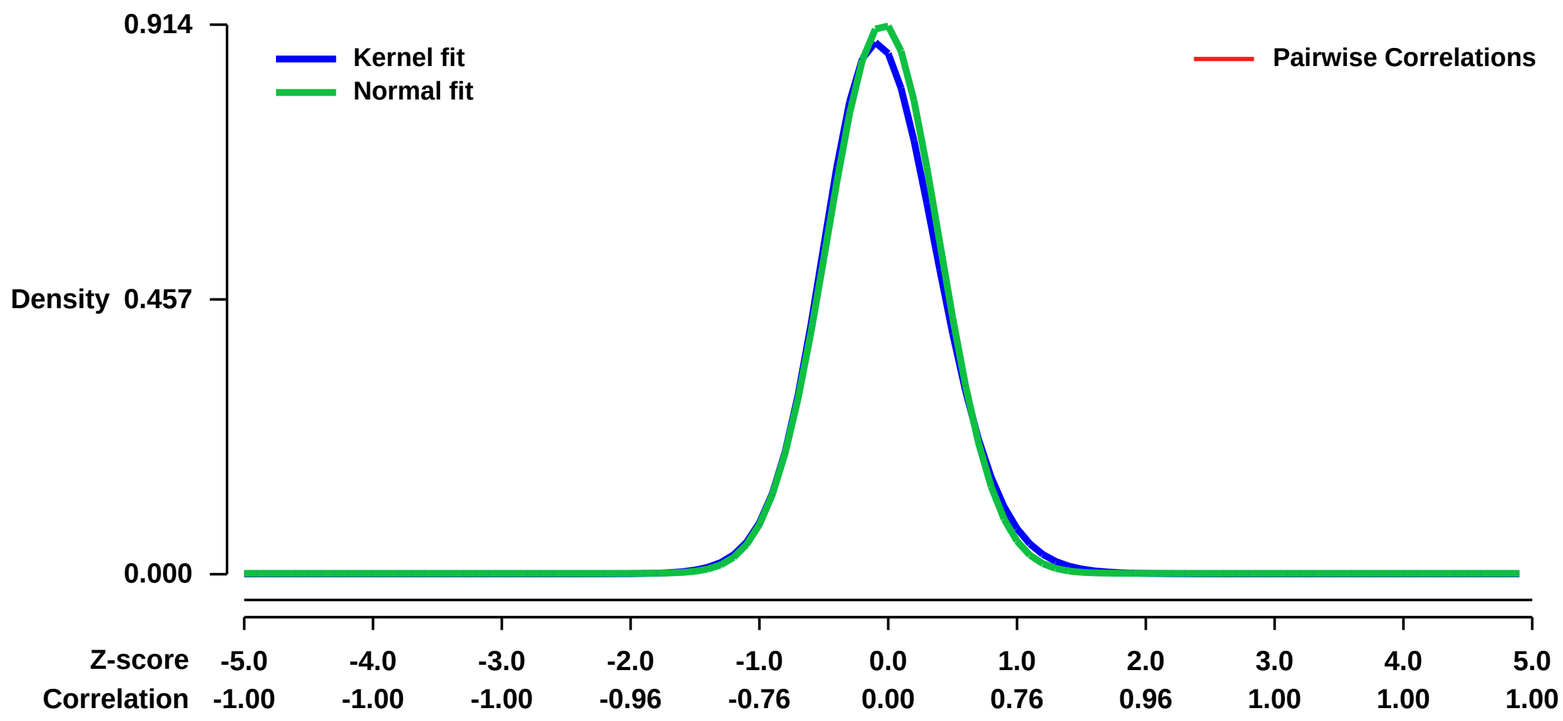

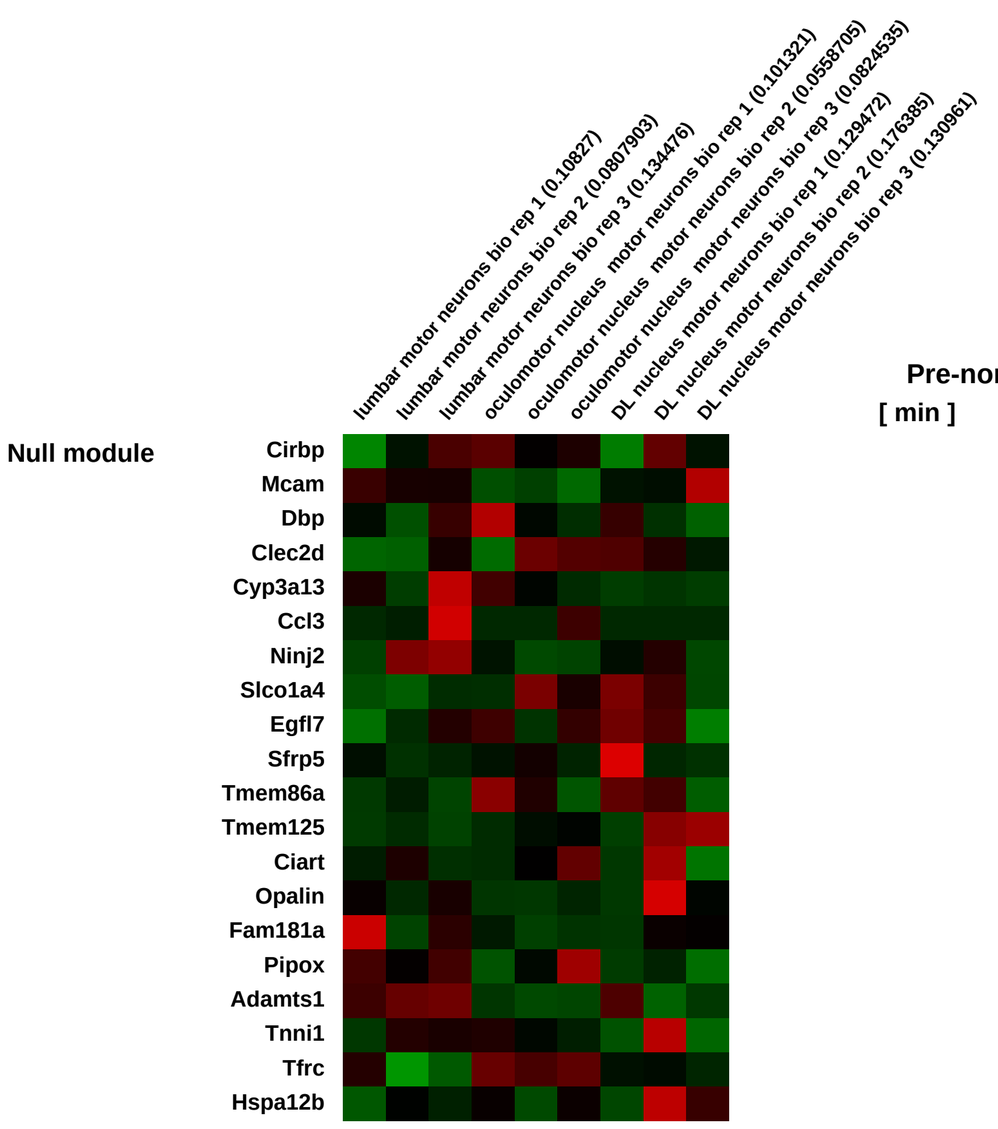

GEO Series "GSE19729" Expression Profiles

Num of samples in this series: 14

Scale of expression profile Z-scores

-3.0 -2.0 -1.0 0.0 1.0 2.0 3.0

GEO Link:	http://www.ncbi.nlm.nih.gov/geo/query/acc.cgi?acc=GSE19729
Status:	Public on Jan 05 2010
Title:	Interactions between developing B-lymphocytes and stromal cells reveal complex interactions and two-way communication
Organism:	Mus musculus
Experiment type:	Expression profiling by array
Platform:	GPL1261
Pubmed ID:	20152025
Summary & Design:	**Summary:** **Full title: Genomics based analysis of interactions between developing B-lymphocytes and stromal cells reveal complex interactions and two-way communication** **In order to identify extra cellular signals that promote B lymphocyte development we created a database with approximately 400 receptor ligand pairs and software matching gene expression data from two cell populations to obtain information about possible communication pathways. Using this database and gene expression data from NIH3T3 cells (unable to support B cell development) and OP-9 cells (strongly supportive of B cell development) and data from pro-B and pre-B cells as well as mature peripheral B-lineage cells, we were able to identify a set of potential stage and stromal cell restricted communication pathways. Functional analysis of some of these potential ways of communication allowed us to identify BMP-4 as a potent stimulator of B-cell development in vitro. Further, the analysis suggested that there existed possibilities for progenitor B cells to send signals to the stroma. The functional consequences of this were investigated by co-culture experiments revealing that the co-incubation of stromal cells with pro-B cells altered both the morphology and the gene expression pattern in the stromal cells.** **Overall design:** **OP9 Stromal cells has been cultured with and without primary PreB cells drived from LSK cells in culture or PreB cell lines 230-238. OP9 cells has been isolated by FACS and microarray performed to study the effect of PreB cells on OP9's at the level of RNA expression. The results have been compared with 3T3 and MC3T3 cells.**

Background corr dist: KL-Divergence = 0.0722, L1-Distance = 0.0433, L2-Distance = 0.0037, Normal std = 0.5033

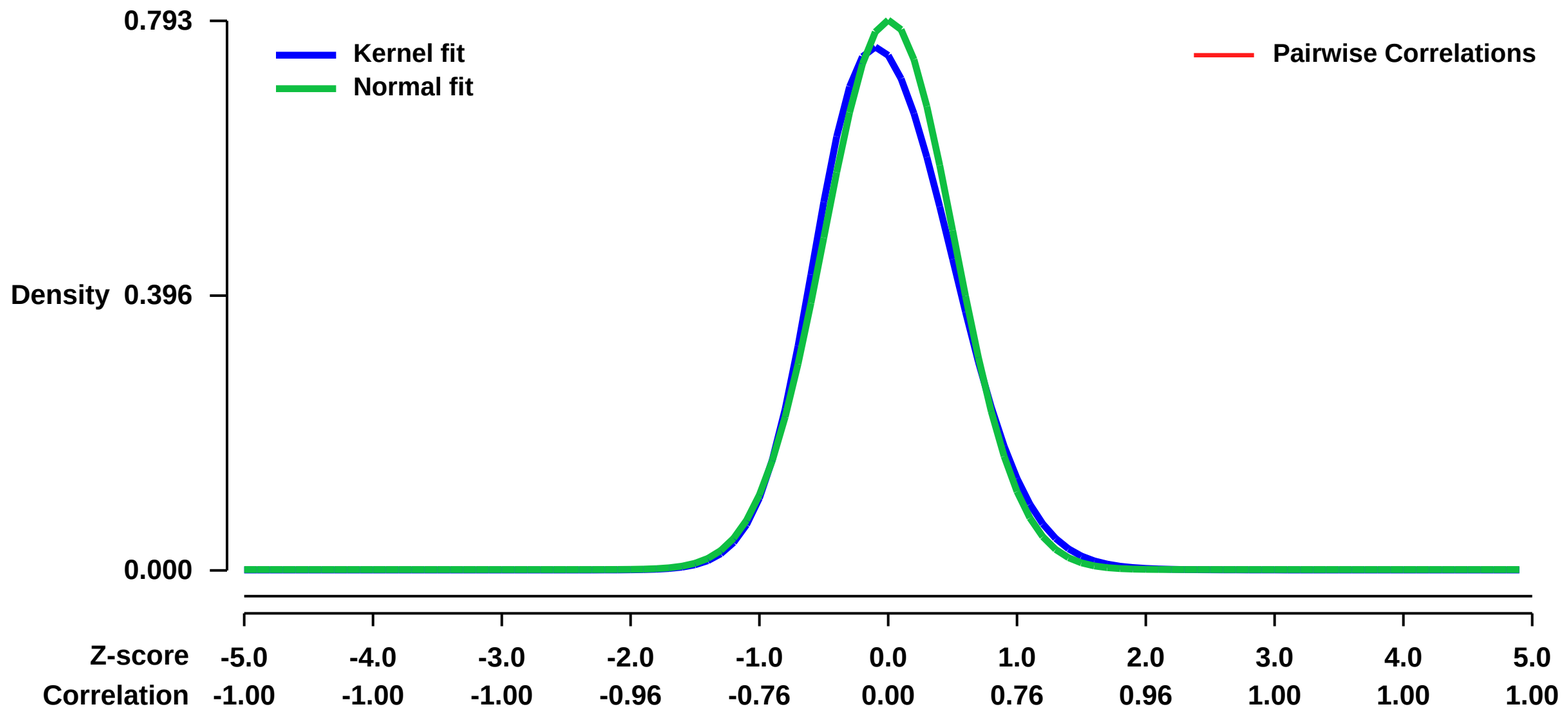

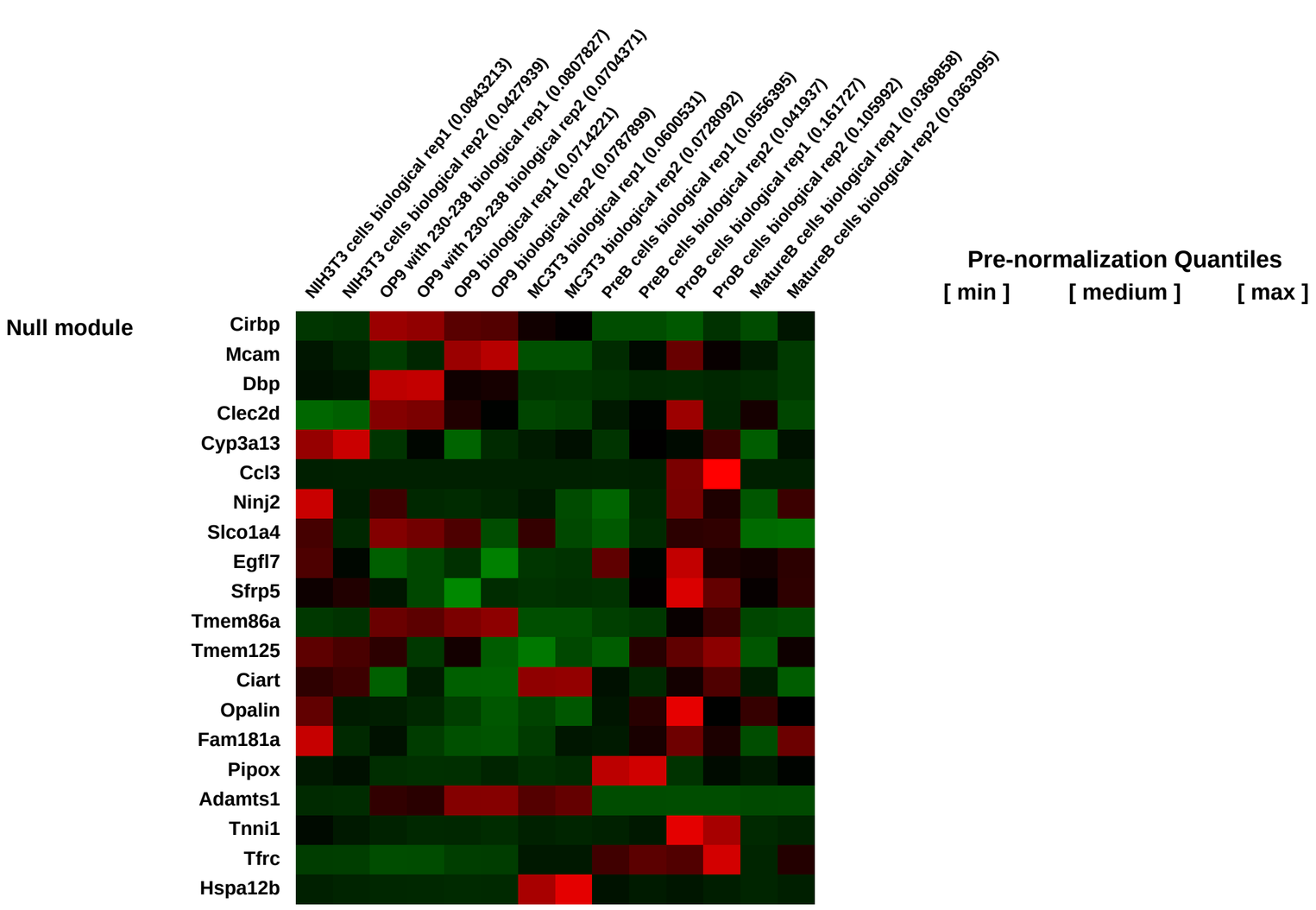

GEO Series "GSE11207" Expression Profiles

Num of samples in this series: 6

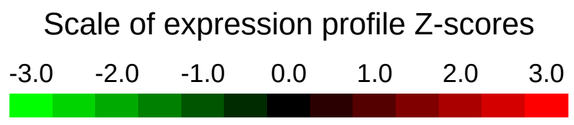

GEO Link:	**http://www.ncbi.nlm.nih.gov/geo/query/acc.cgi?acc=GSE11207**
Status:	**Public on Apr 19 2008**
Title:	**Dorsal root ganglion (katz-affy-mouse-210210)**
Organism:	**Mus musculus**
Experiment type:	**Expression profiling by array**
Platform:	**GPL1261**
Pubmed ID:	
Summary & Design:	**Summary:** **The molecular identity of touch sensation is still largely unknown. We choose an extrem and very specific example, touch sensation of pennis glan, to study this problem. It's known from previous retro-grade labeling result that only one DRG in rat innervate the pennis glan, which makes it idea for microarry analysis.** **To clone the mechanosensory receptor specifically or highly expressed in the primary sensory neurons innervating pennis glan.** **There is a specific mechanosensory receptor in the primary sensory neurons innervating pennis glan.** **1. Retrograde labeling the innervating nerve by DiI** **2. Dissect DRGs, dissociate neurons and pick up the fluorescent cells.** **3. Pool around 20 positive cells and 50 control cells (big diameter neuron and small to medium diameter neuron respectively), purify total RNA.** **4. Two rounds of amplification** **5. Affymetrix analysis** **Keywords: dorsal root ganglion, touch sensatiion** **Overall design:**

Background corr dist: KL-Divergence = 0.0479, L1-Distance = 0.0281, L2-Distance = 0.0010, Normal std = 0.5894

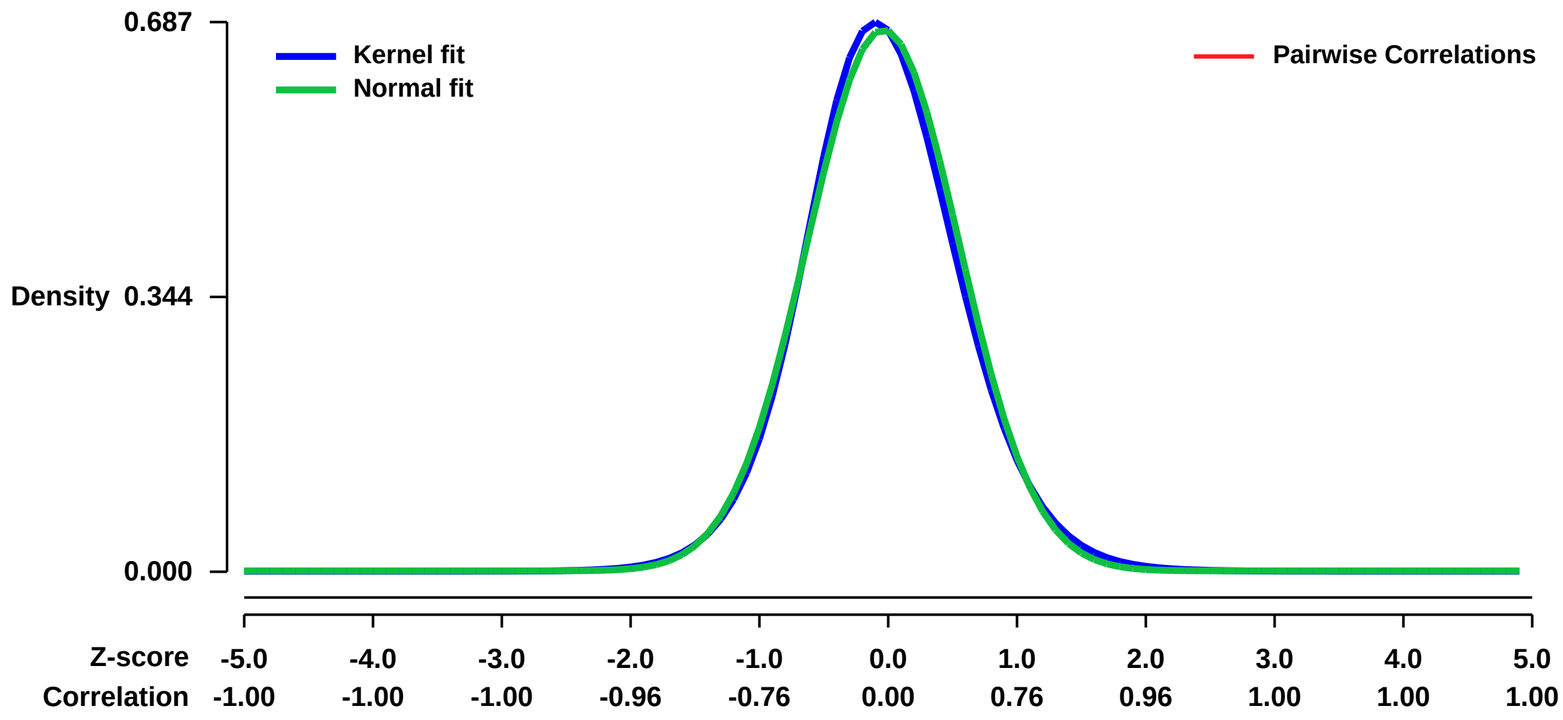

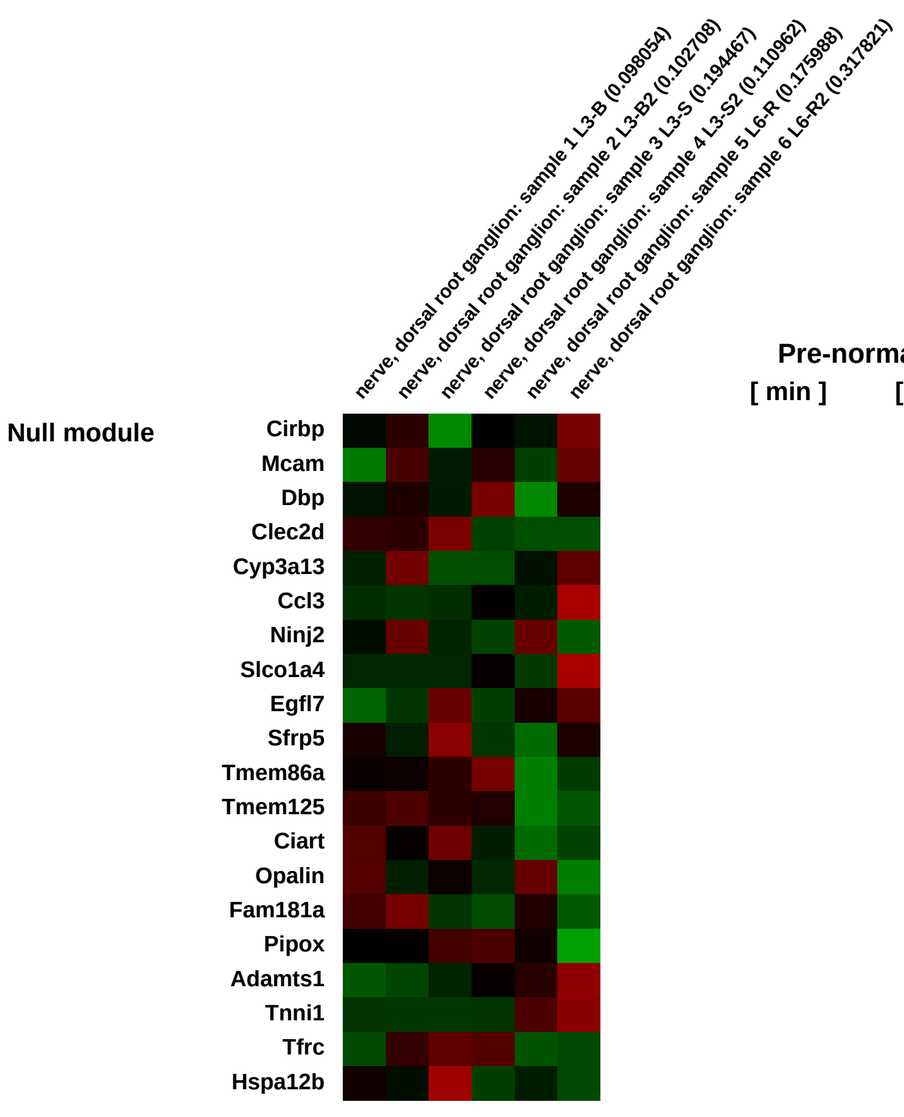

GEO Series "GSE10176" Expression Profiles

Num of samples in this series: 6

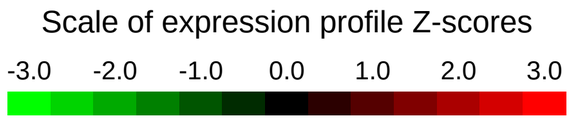

GEO Link:	http://www.ncbi.nlm.nih.gov/geo/query/acc.cgi?acc=GSE10176
Status:	Public on Jan 16 2008
Title:	Inducible repositioning of genes to the inner nuclear membrane
Organism:	Mus musculus
Experiment type:	Expression profiling by array
Platform:	GPL1261
Pubmed ID:	18272965
Summary & Design:	**Summary:** Nuclear compartmentalization appears to play an important role in regulating metazoan genes. While studies on immunoglobulin (Ig) and other loci have correlated positioning at the nuclear lamina with gene repression, the functional consequences of this compartmentalization remain untested. We devised an approach for inducible tethering of genes to the inner nuclear membrane (INM) and demonstrate with 3D DNA-ImmunoFISH, repositioning of chromosomal regions to the nuclear lamina. Relocalization requires mitotic nuclear envelope breakdown and reformation. Tethering leads to the accumulation of lamin and INM proteins but not to association with pericentromeric heterochromatin or nuclear pore complexes. Recruitment of genes to the INM can result in their transcriptional repression. Using DamID we show that as is the case for our model system, inactive Ig loci at the nuclear periphery are contacted by INM and lamina components. We propose that such molecular interactions are used to compartmentalize and limit the accessibility of Ig loci. **Keywords: Inducible** **Overall design:** We used microarray to analyze the transcription status of genomic regions are inducibly tethered to the INM

Background corr dist: KL-Divergence = 0.0247, L1-Distance = 0.0189, L2-Distance = 0.0005, Normal std = 0.7016

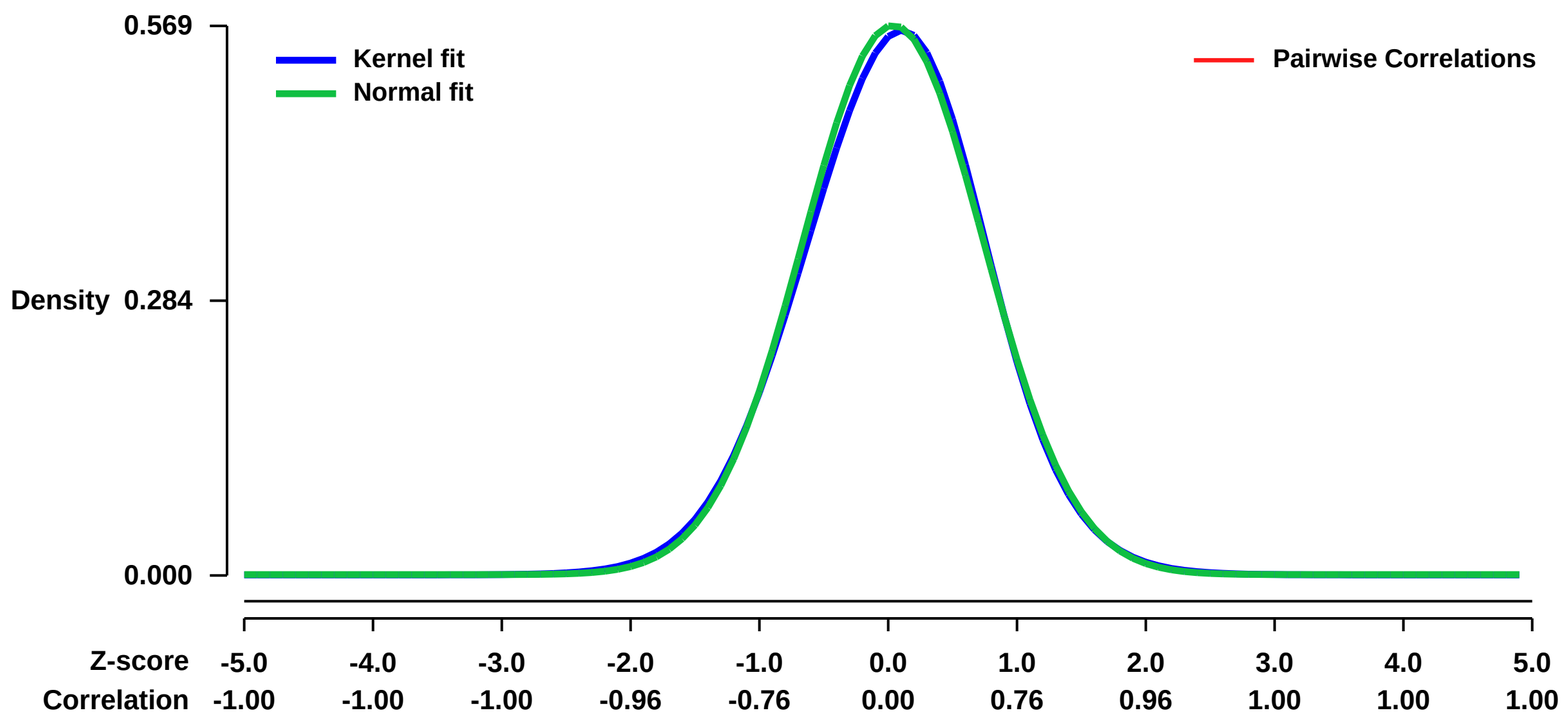

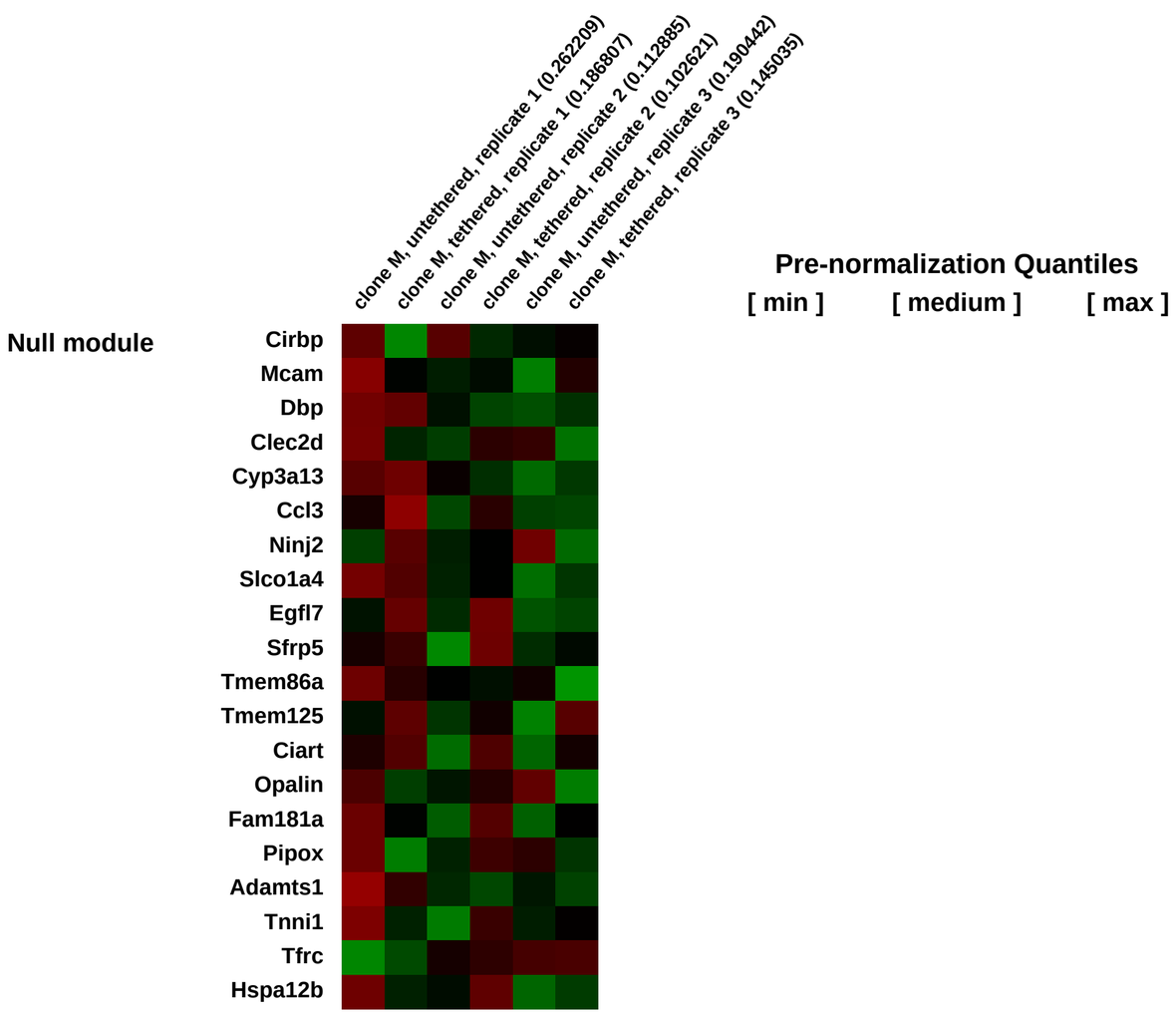

GEO Series "GSE8863" Expression Profiles

Num of samples in this series: 18

Scale of expression profile Z-scores

-3.0 -2.0 -1.0 0.0 1.0 2.0 3.0

GEO Link:	http://www.ncbi.nlm.nih.gov/geo/query/acc.cgi?acc=GSE8863
Status:	Public on Jun 27 2008
Title:	Mouse mammary tumor-initiating cells
Organism:	Mus musculus
Experiment type:	Expression profiling by array
Platform:	GPL1261
Pubmed ID:	18559513
Summary & Design:	**Summary:** Using a syngeneic p53 null mouse mammary gland tumor model that closely mimics human breast cancer, we have identified by limiting dilution transplantation as well as in vitro mammosphere and clonogenic assays a Lin-CD29HighCD24High subpopulation of tumor-initiating cells. Differentially expressed genes in the Lin-CD29HighCD24High mouse mammary gland tumor-initiating cell population include those involved in DNA damage response and repair, as well as genes involved in epigenetic regulation previously shown to be critical for stem cell self-renewal. **Keywords: tumor-initiating cells** **Overall design:** 12 samples (RNA of 4 subpopulations based on expression of CD29 and CD24 for each tumor of 3) were included in the identification of differentially expressed genes of tumor-initiating cells. 5 samples (RNA of subpopulations based on expression of CD29 and CD24 of normal mammary epithelial cells) were included in the normal group analysis. Reference RNA was used to normalize all samples.

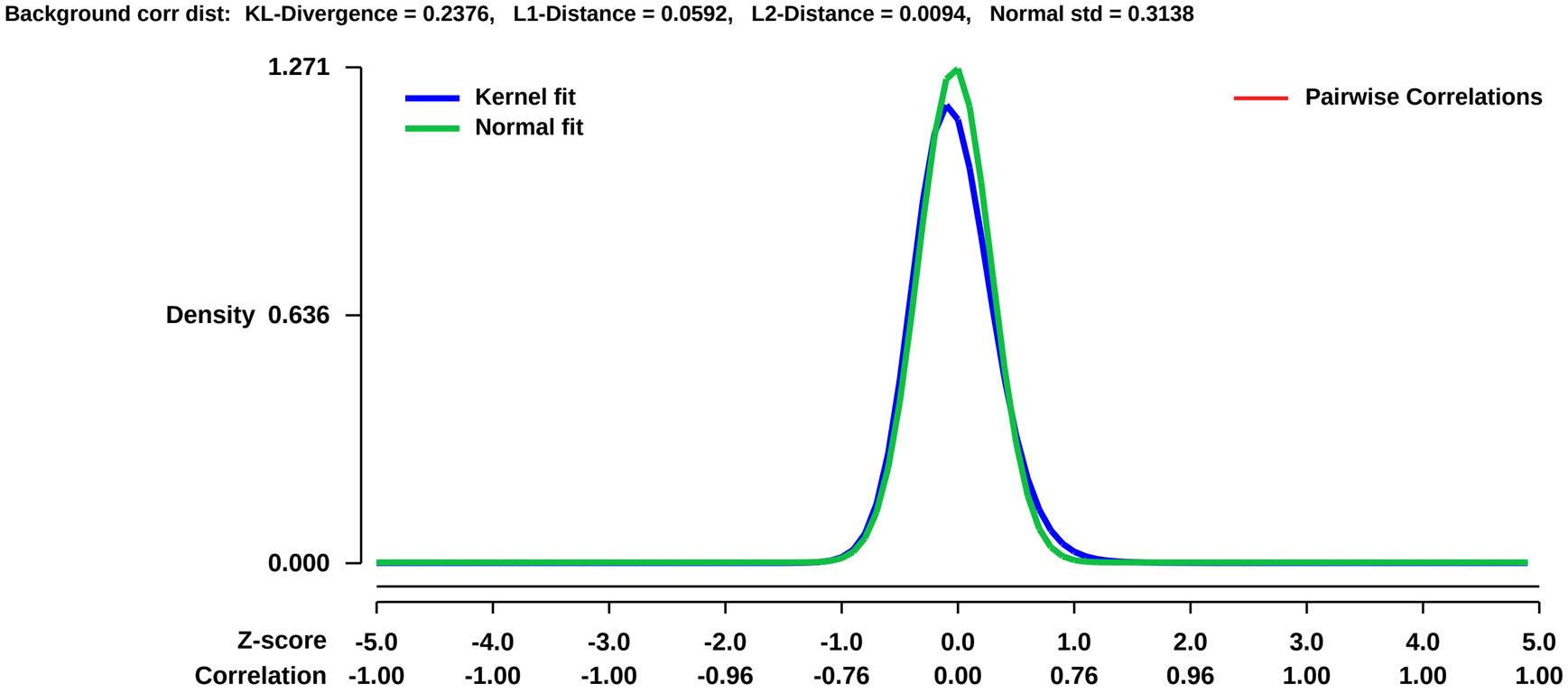

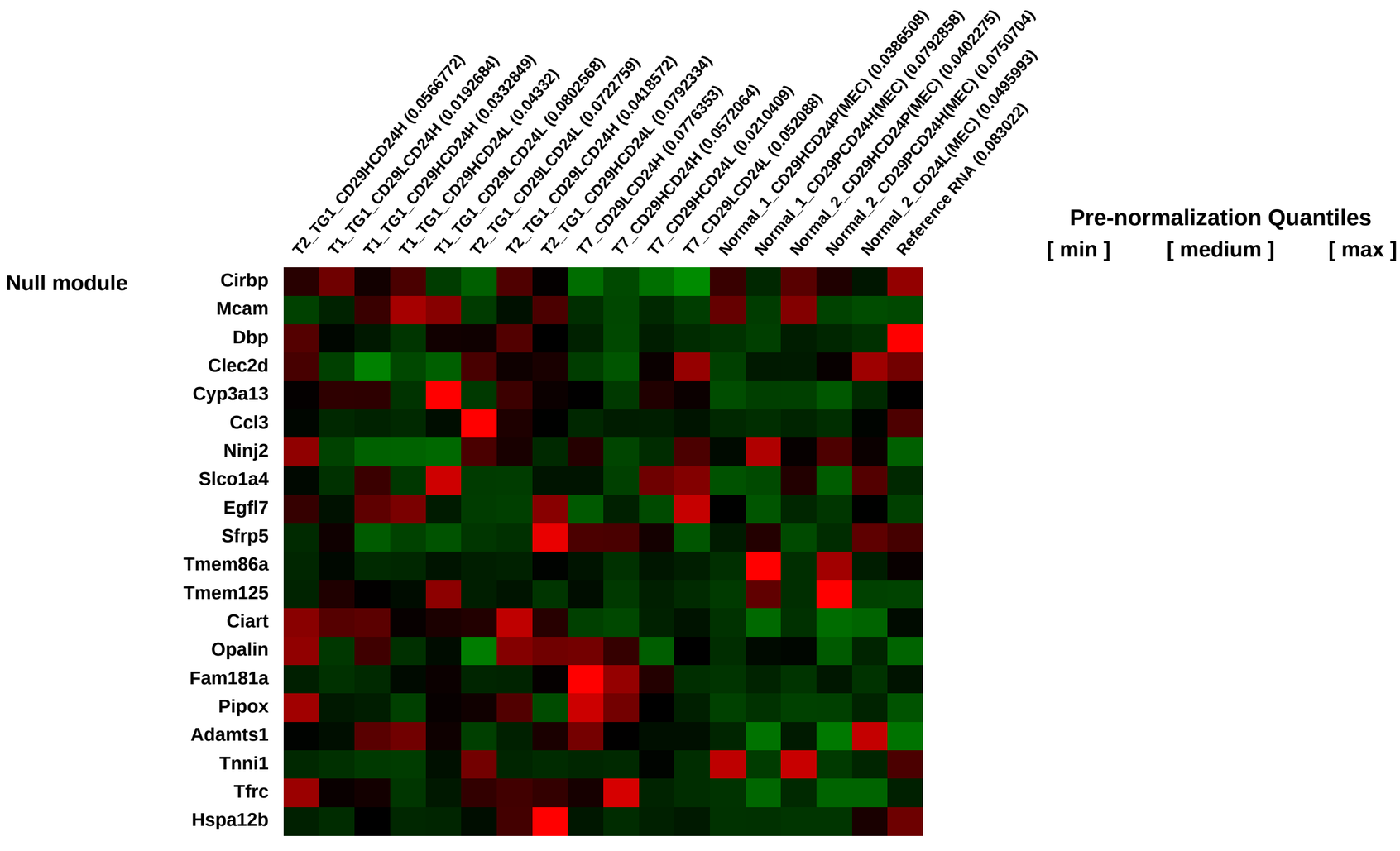

GEO Series "GSE12465" Expression Profiles

Num of samples in this series: 14

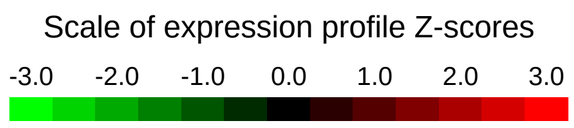

GEO Link:	http://www.ncbi.nlm.nih.gov/geo/query/acc.cgi?acc=GSE12465
Status:	Public on May 20 2009
Title:	Transcriptional signatures of Itk-deficiency using CD3+, CD4+ and CD8+ T-cells
Organism:	Mus musculus
Experiment type:	Expression profiling by array
Platform:	GPL1261
Pubmed ID:	19450280
Summary & Design:	**Summary:** The Tec-family kinase Itk plays an important role during T-cell activation and function, and controls also conventional versus innate-like T-cell development. We have characterized the transcriptome of Itk-deficient CD3+ T-cells, including CD4+ and CD8+ subsets, using Affymetrix microarrays. The largest difference between Itk-/- and Wt CD3+ T-cells was found in unstimulated cells, e.g. for killer cell lectin-like receptors. Compared to anti-CD3-stimulation, anti-CD3/CD28 significantly decreased the number of transcripts suggesting that the CD28 co-stimulatory pathway is mainly independent of Itk. The signatures of CD4+ and CD8+ T-cell subsets identified a greater differential expression than in total CD3+ cells. Cyclosporin (CsA)-treatment had a stronger effect on transcriptional regulation than Itk-deficiency, suggesting that only a fraction of TCR-mediated calcineurin/NFAT-activation is dependent on Itk. Bioinformatic analysis of NFAT-sites of the group of transcripts similarly regulated by Itk-deficiency and CsA-treatment, followed by chromatin-immunoprecipitation, revealed NFATc1-binding to the Bub1, IL7R, Ctla2a, Ctla2b, and Schlafen1 genes. Finally, to identify transcripts that are regulated by Tec-family kinases in general, we compared the expression profile of Itk-deficient T-cells with that of Btk-deficient B-cells and a common set of transcripts was found. Taken together, our study provides a general overview about the global transcriptional changes in the absence of Itk. **Overall design:** CD3+ CD4+ and CD8+ T-cells from pooled suspensions of spleen and lymph nodes of Wt and Itk knockout mice on C57BL/6 background were isolated after negative depletion. Unstimulated as well as stimulated T-cells were studied. Stimulations were done with anti-CD3 (1 mg/ml) for 24 hrs. For the CD4+ T-cells we collected triplicates from the Itk knockout mice and duplicates from the Wt group. For the CD8+ T-cells, we got duplicates from Itk knockout , while we obtained a single sample from Wt owing to the low cell yield for resting Wt CD8+ T-cells. After CD3-stimulation we got a single sample from the CD8+ subset of both Wt and Itk knockout, while for the CD4+ subsets we collected duplicates.

Background corr dist: KL-Divergence = 0.0403, L1-Distance = 0.0459, L2-Distance = 0.0032, Normal std = 0.6284

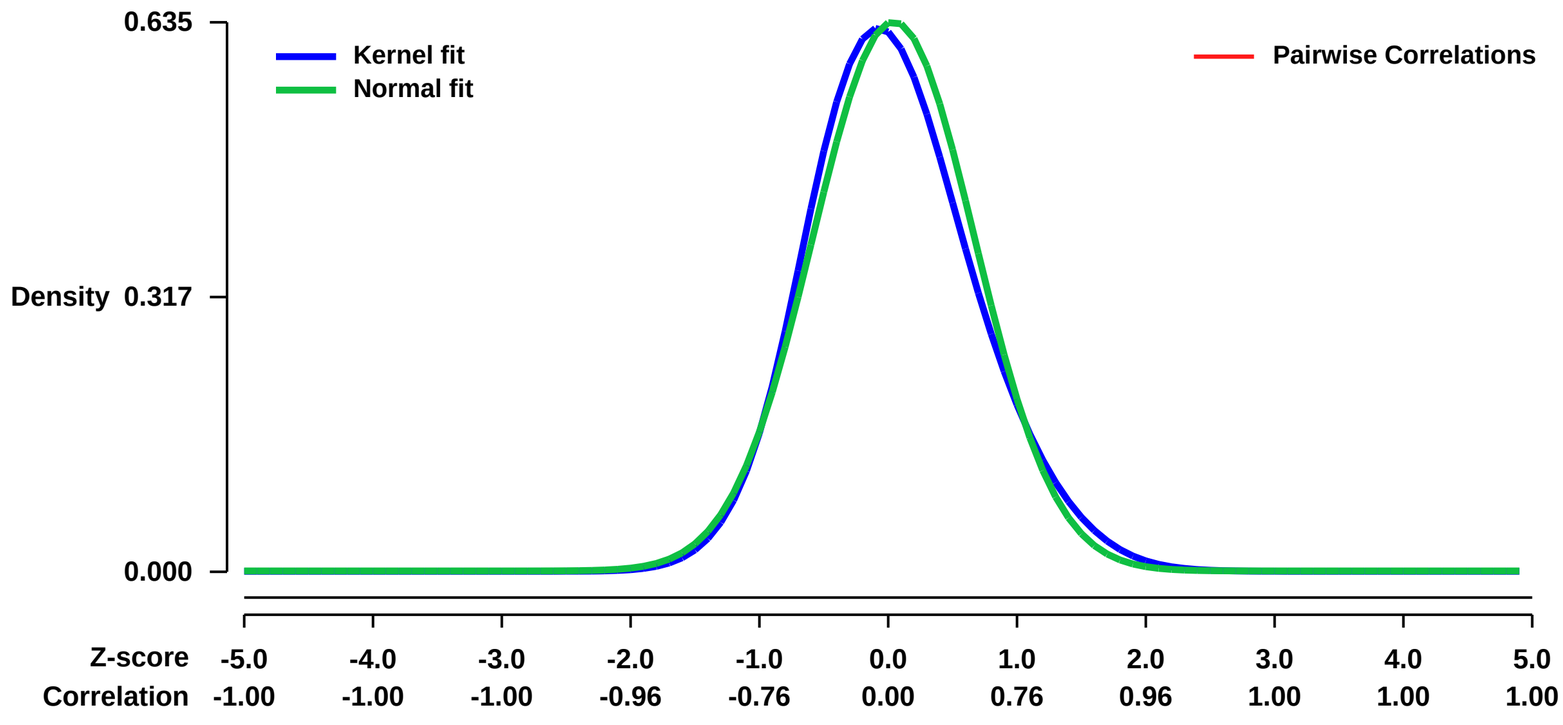

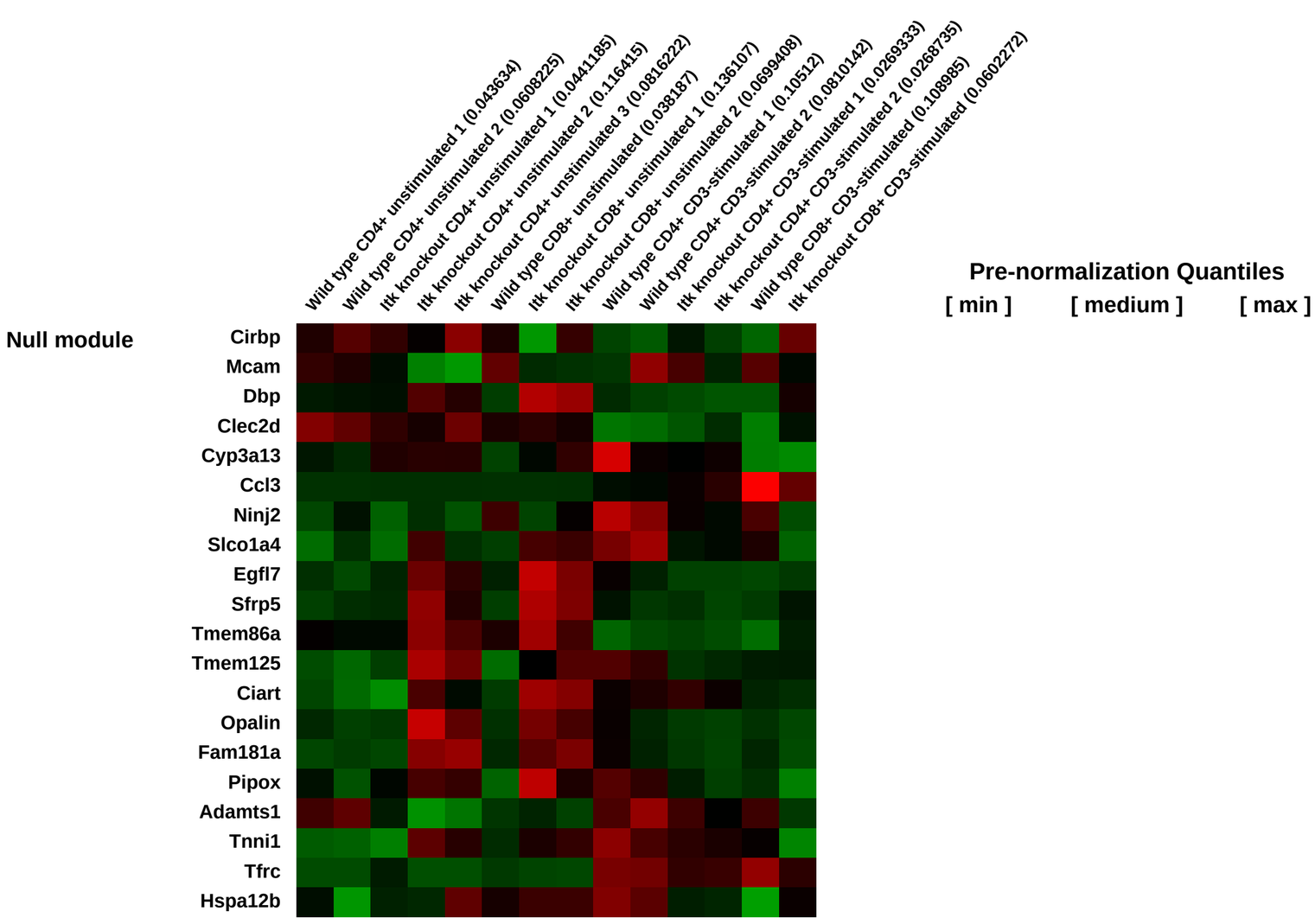

GEO Series "GSE11386" Expression Profiles

Num of samples in this series: 15

Scale of expression profile Z-scores

-3.0 -2.0 -1.0 0.0 1.0 2.0 3.0

GEO Link:	http://www.ncbi.nlm.nih.gov/geo/query/acc.cgi?acc=GSE11386
Status:	Public on Jun 05 2008
Title:	Gene expression in murine memory versus naive B cells (1st generation and 2nd generation screens)
Organism:	Mus musculus
Experiment type:	Expression profiling by array
Platform:	GPL1261
Pubmed ID:	18566367
Summary & Design:	**Summary:** Memory B cells play essential roles in the maintenance of long-term immunity and may be important in the pathogenesis of autoimmune disease, but how these cells are distinguished from their naˆflve precursors is poorly understood. To address this, it would be important to understand how gene expression differs between memory and naive B cells in order to elucidate memory-specific functions. Using model systems that help overcome the lack of murine memory-specific markers and the low frequency of antigen-specific memory and naˆflve cells, we undertook a global comparison of gene expression between memory B cells and their naive precursors. 1st generation screen: These data represent our first generation comparison of gene expression between murine naˆflve and memory splenic B cells. Naˆflve NP-binding splenic B cells were FACS purified from unimmunized mVh186.2 transgenic Balb/c mice. Memory B cells were generated by immunizing mVh186.2 transgenic Balb/c mice with 2 doses of NP-CGG in alum delivered i.p. 6 weeks apart. After a minimum of 12-weeks rest, NP-binding splenic B cells were isolated by FACS. Total RNA was extracted, cRNA synthesized and labeled and hybridized to Affymetrix mouse 430 2.0 chips. 2nd generation screen: These data represent our second generation comparison of gene expression between murine naˆflve and memory splenic B cells. Naˆflve NP-binding AA4.1neg splenic B cells were FACS purified from unimmunized mVh186.2 transgenic Jk KO Balb/c mice. Memory B cells were generated from these naive precursors after adoptive transfer into recipients that mount poor endogenous NP-responses. 12-weeks post i.p. immunization with NP-CGG in alum, NP-specific splenic memory B cells were isolated by FACS. Total RNA was extracted, cRNA synthesized and labeled and hybridized to Affymetrix mouse 430 2.0 chips. Memory/Naˆflve comparison data linked below as Supplementary files. Keywords: Cell type comparison Overall design: 2nd generation screen: 8 samples, 4 biological replicates each of murine splenic naˆflve and memory B cells

Background corr dist: KL-Divergence = 0.0318, L1-Distance = 0.0408, L2-Distance = 0.0027, Normal std = 0.6582

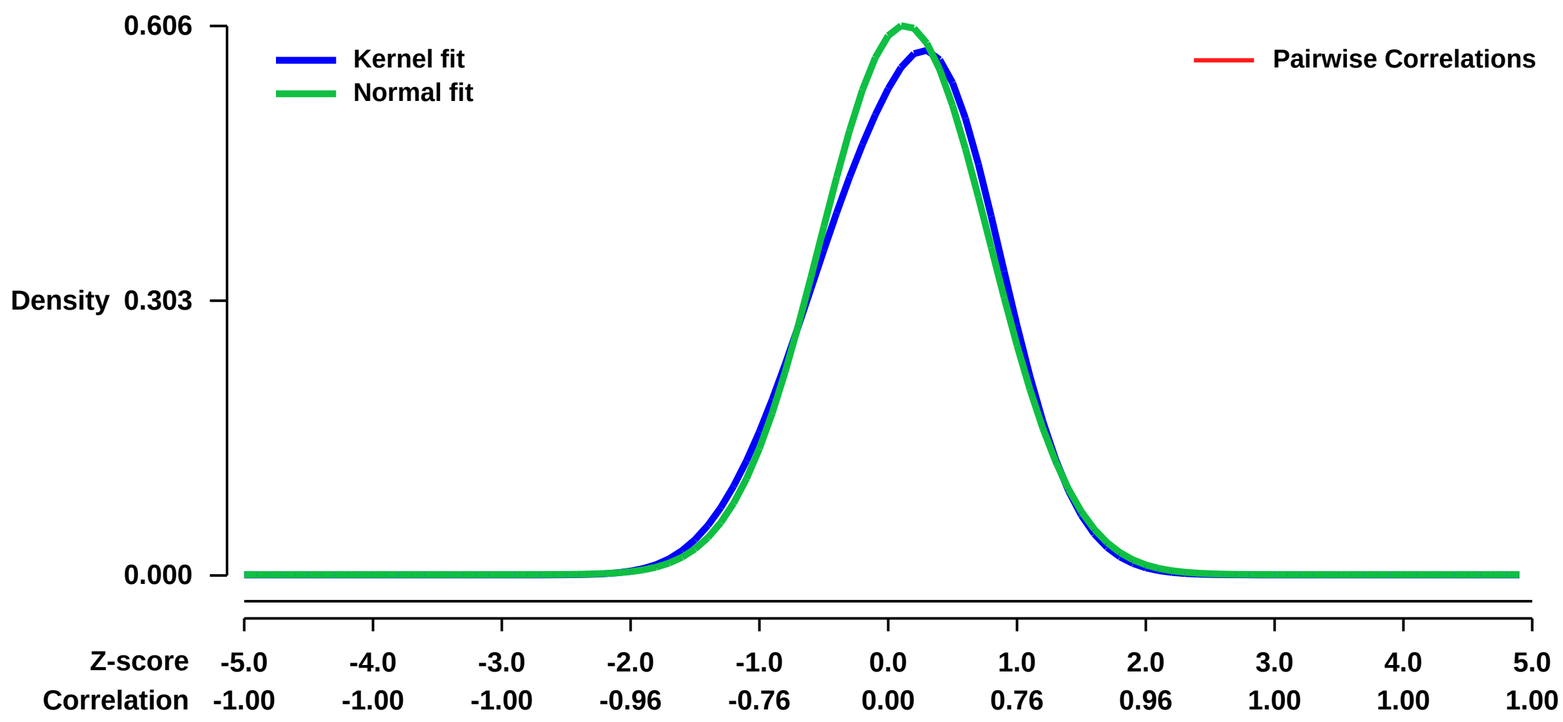

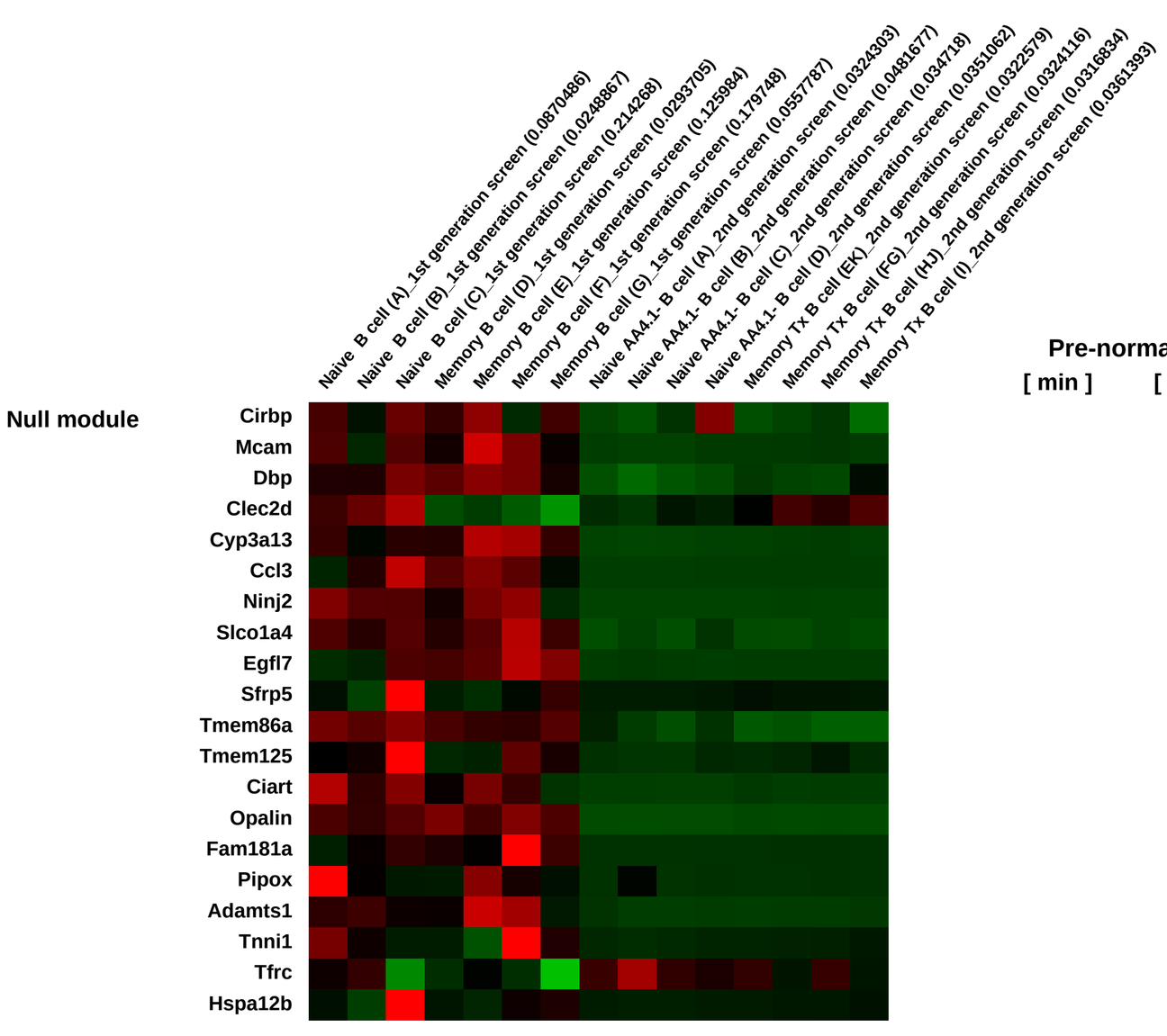

GEO Series "GSE23845" Expression Profiles

Num of samples in this series: 15

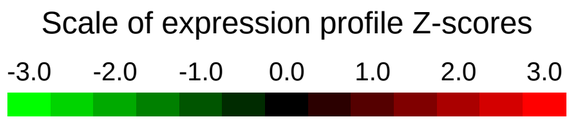

GEO Link:	**http://www.ncbi.nlm.nih.gov/geo/query/acc.cgi?acc=GSE23845**
Status:	**Public on Aug 28 2010**
Title:	**Time course for bladder UCC development in UPII-SV40Tag mice**
Organism:	**Mus musculus**
Experiment type:	**Expression profiling by array**
Platform:	**GPL1261**
Pubmed ID:	**20501863**
Summary & Design:	**Summary:** **We have identified genes that are differentially expressed between the bladders of UPII-SV40Tag mice and their age-matched wild-type littermates at 3, 6, 20, and 30 weeks of age. These are ages that correspond to premalignant, carcinoma in situ, and early-stage and later stage invasive UCC, respectively** **Analysis of the microarray data sets has revealed â…1,900 unique genes differentially expressed (â¥3-fold difference at one or more time points) between wild-type and UPII-SV40Tag urothelium during the time course of tumor development.** **Overall design:** **RNA from the urothelium of duplicate UPII-SV40Tag hemizygous and age-matched wild type littermate mice was isolated at 3, 6, 20, and 30 weeks of age and gene expression profiles were obtained.**

Background corr dist: **KL-Divergence = 0.1356, L1-Distance = 0.0293, L2-Distance = 0.0013, Normal std = 0.3985**

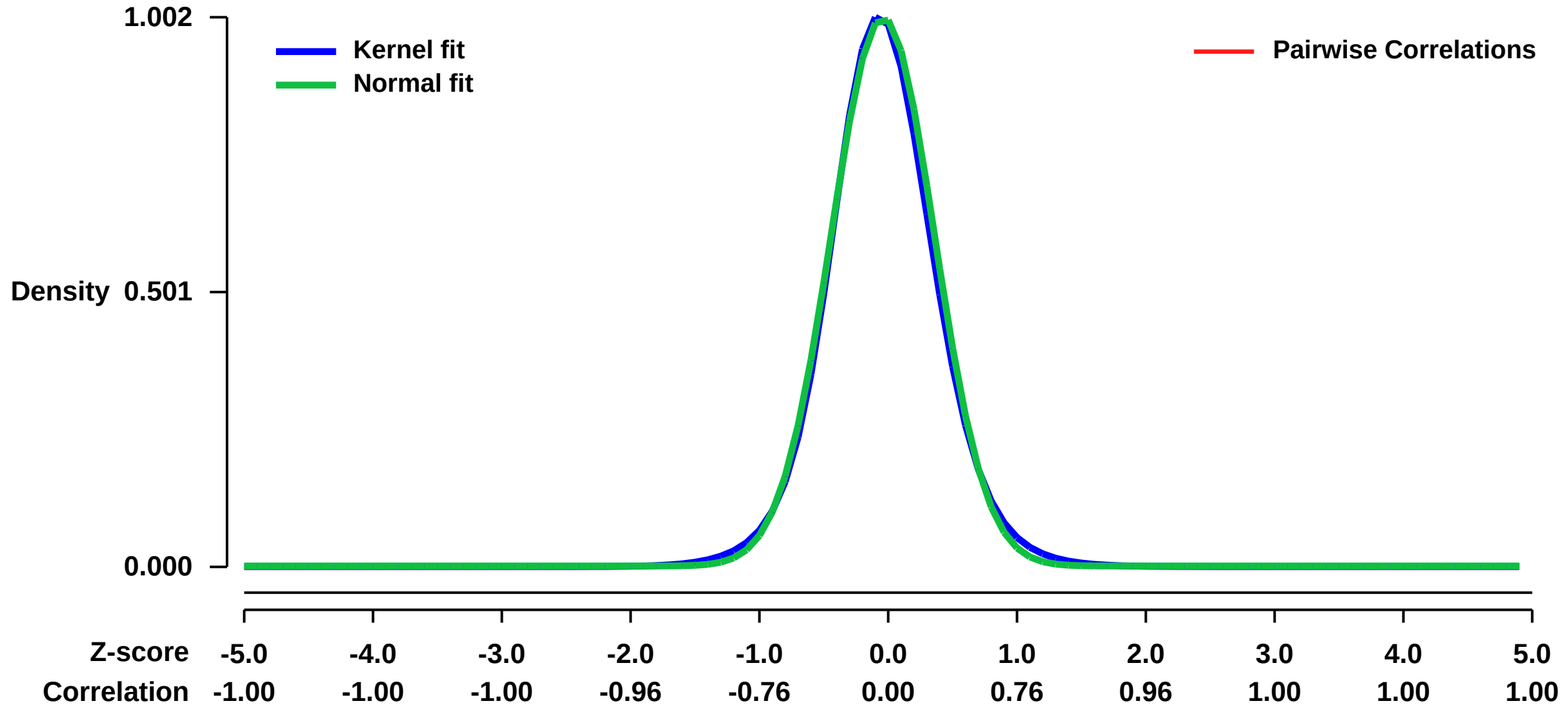

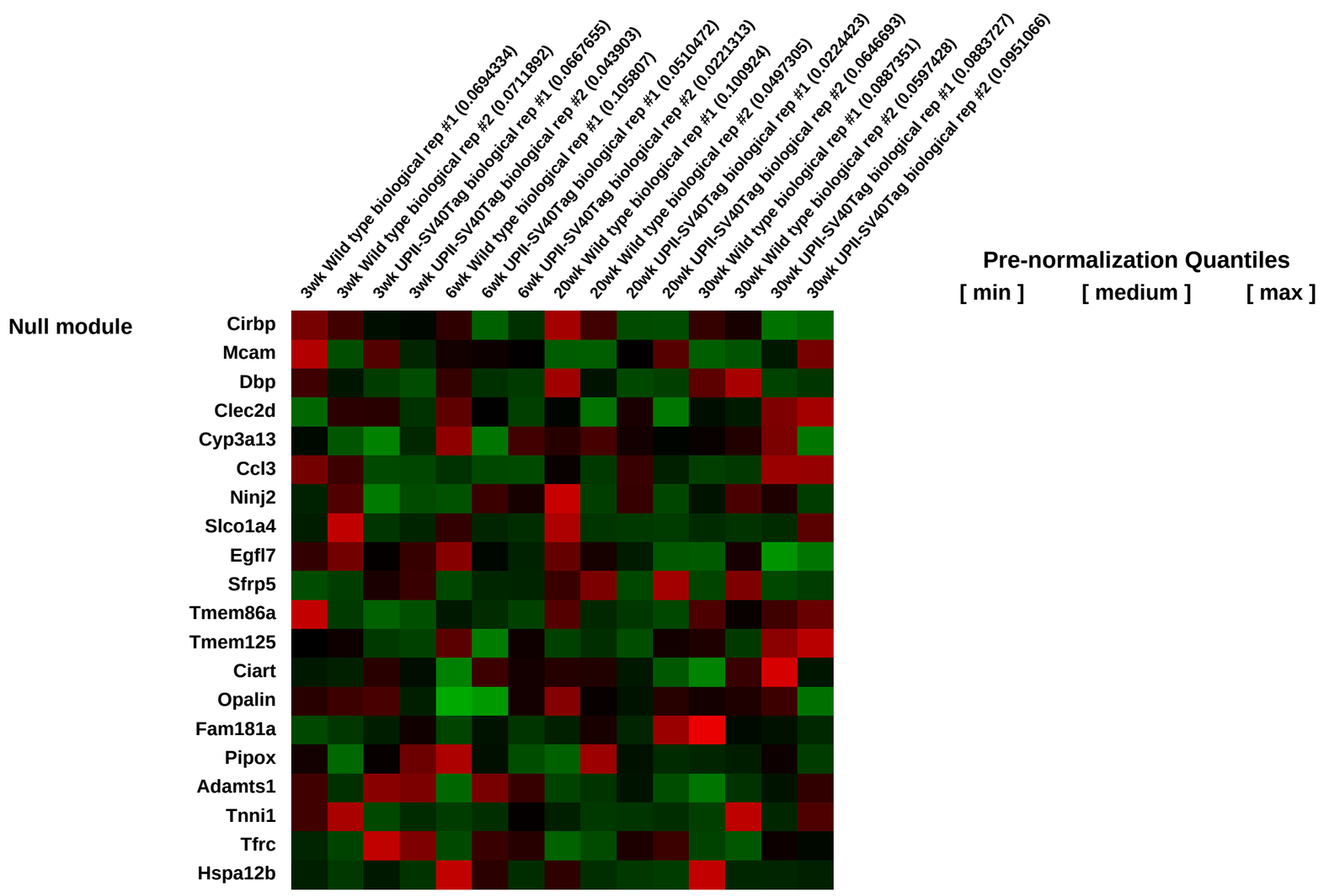

GEO Series "GSE34618" Expression Profiles

Num of samples in this series: 7

Scale of expression profile Z-scores

-3.0 -2.0 -1.0 0.0 1.0 2.0 3.0

GEO Link:	http://www.ncbi.nlm.nih.gov/geo/query/acc.cgi?acc=GSE34618
Status:	Public on May 02 2012
Title:	Expression data from CD8+ Central memory T cells after different time periods of Concanavalin A in vitro activation.
Organism:	Mus musculus
Experiment type:	Expression profiling by array
Platform:	GPL1261
Pubmed ID:	22567129
Summary & Design:	**Summary:** CD8+ tumor infiltrating T cells (TIL) lack effector-phase functions due to defective proximal TCR-mediated signaling shown to result from inactivation of p56lck kinase. We identify a novel interacting partner for p56lck in nonlytic TIL, Protocadherin-18 (â pcdh18â), and show that pcdh18 is transcribed upon in vitro or in vivo activation of CD8+ central memory T cells (CD44+CD62LhiCD127+) coincident with conversion into effector memory cells (CD44+CD62LloCD127+). Expression of pcdh18 in primary CD8+ effector cells induces the phenotype of nonlytic TIL: defective; proximal TCR signaling, cytokine secretion, and cytolysis; and enhanced AICD. pcdh18 contains a motif (centered at Y505) shared with src kinases (QGQYQP) which is required for the inhibitory phenotype. Thus, pcdh18 is a novel marker of CD8+ effector memory T cells expressed upon cell activation that can function as a negative regulator by restricting the effector phase. We used microarrays to detail the global programme of gene expression underlying CD8+ 'Central memory' T cells activation and identified distinct transcriptional pattern clusters. **Overall design:** Ten spleens were pooled from 62 week old C57BL/6 male mice and enriched for CD8+ T cells by negative selection using a cocktail of biotinylated antibodies to deplete CD4, CD11c, CD11b, MHC-II, B220, and NK cells. Cells were then stained for CD8, CD44, CD62L, and CD127 and sorted (using a iCyt Reflection parallel cell sorter). Cells were collected and cultured (0.5 x106 cells/well) in 10% complete RPMI media supplemented with 0.005 ugr Con A and RNA prepared using TRIZOL and the 'RNeasy clean-up kit' (Invitrogen) after activation for different times. We established single transcriptional profiles for 6 time points after T cell activation (4, 6, 8, 16, 20, 24 h) including a control zero h time point (prior to activation). RNA was isolated by standard procedures and its quality was assessed by the NYU Center for Health Informatics and Bioinformatics. cDNAs were hybridized to GeneSpring arrays using the mouse genome MOE430 2.0 array (Affymetrix) which interrogates ~45,000 transcripts.

Background corr dist: KL-Divergence = 0.0627, L1-Distance = 0.0842, L2-Distance = 0.0115, Normal std = 0.6392

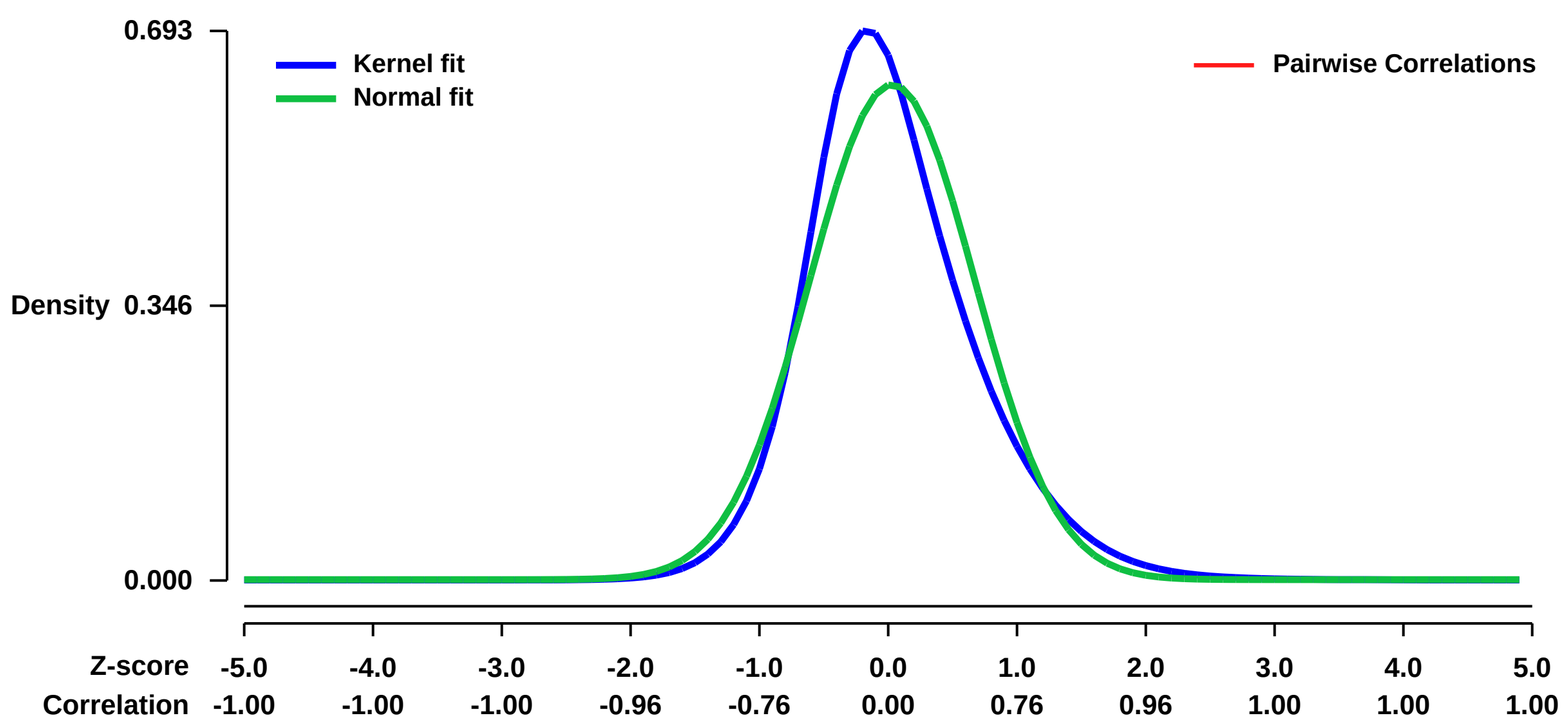

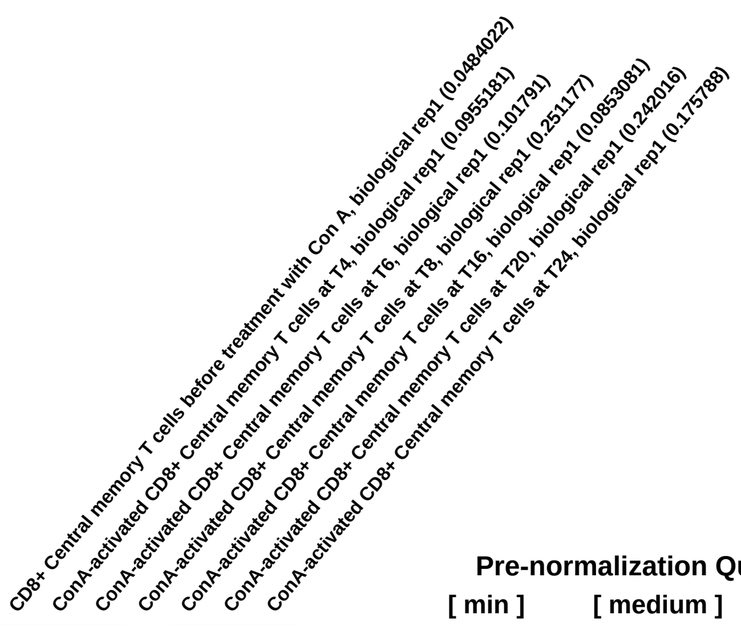

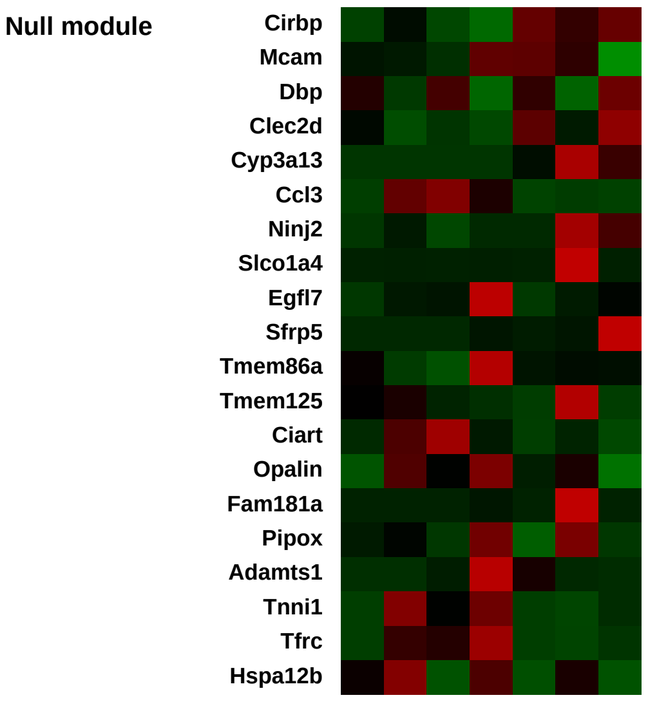

GEO Series "GSE30164" Expression Profiles

Num of samples in this series: 23

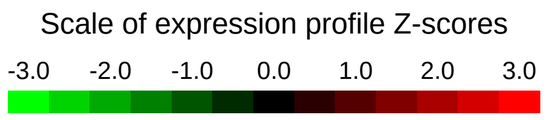

GEO Link:	http://www.ncbi.nlm.nih.gov/geo/query/acc.cgi?acc=GSE30164
Status:	Public on Jun 23 2011
Title:	Transcriptome transfer provides a model for understanding the phenotype of cardiomyocytes
Organism:	Mus musculus
Experiment type:	Expression profiling by array
Platform:	GPL1261
Pubmed ID:	21730152
Summary & Design:	**Summary:** We show that the transfer of the adult ventricular myocyte (AVM) transcriptome into either a fibroblast or an astrocyte converts the host cell into a cardiomyocyte. Transcriptome-effected cardiomyocytes (tCardiomyocytes) display morphologies, immunocytochemical properties, and expression profiles of postnatal cardiomyocytes. Cell morphology analysis shows that tCardiomyoctes are elongated and have a similar length-to-width ratio as AVMs. These global phenotypic changes occur in a time-dependent manner and confer electroexcitability to the tCardiomyocytes. tCardiomyocyte generation does not require continuous overexpression of specific transcription factors; for example, the expression level of transcription factor Mef2c is higher in tCardiomyocytes than in fibroblasts, but similar in tCardiomyocytes and AVMs. These data highlight the dominant role of the gene expression profile in developing and maintaining cellular phenotype. The transcriptomeinduced phenotype remodelingâ generated tCardiomyocyte has significant implications for understanding and modulating cardiac disease development. **Overall design:** Transcriptome transfer can change one cell type to another cell type. We transfect cardiomyocyte transciptome into fibroblast and astrocyte. Transcriptomes from single cells are isolated and amplified and then hybridize on Affymetrix array.

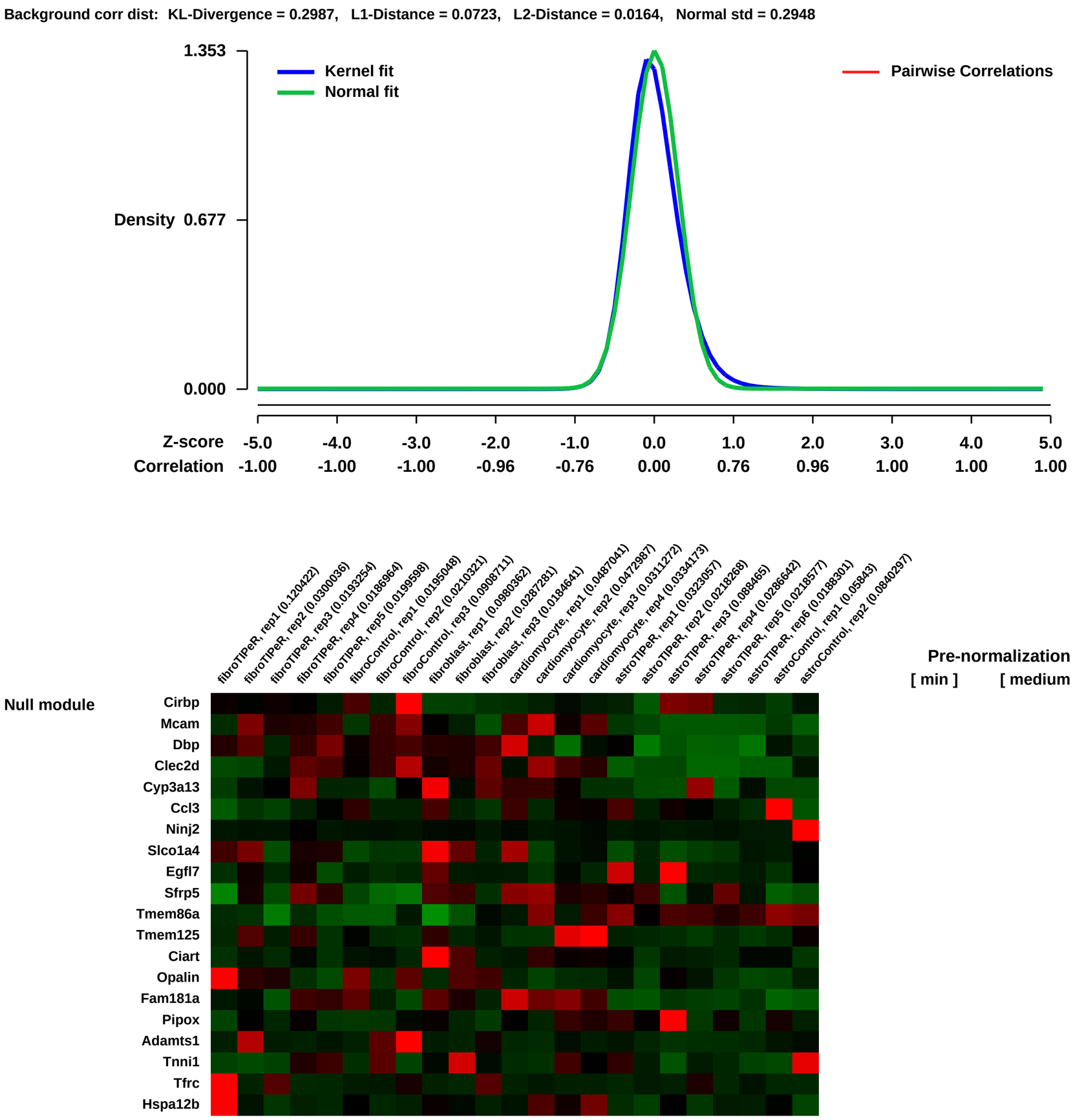

GEO Series "GSE15232" Expression Profiles

Num of samples in this series: 6

Scale of expression profile Z-scores

-3.0 -2.0 -1.0 0.0 1.0 2.0 3.0

GEO Link:	http://www.ncbi.nlm.nih.gov/geo/query/acc.cgi?acc=GSE15232
Status:	Public on May 13 2009
Title:	A Regulatory Pathway Involving Notch1/¸†-Catenin/Isl1 Determines Cardiac Progenitor Cell Fate
Organism:	Mus musculus
Experiment type:	Expression profiling by array
Platform:	GPL1261
Pubmed ID:	19620969
Summary & Design:	**Summary:** The regulation of multipotent cardiac progenitor cell (CPC) expansion and subsequent differentiation into cardiomyocytes, smooth muscle, or endothelial cells is a fundamental aspect of basic cardiovascular biology and cardiac regenerative medicine. However, the mechanisms governing these decisions remain unclear. Here, we show that Wnt/¸†-Catenin signaling, which promotes expansion of CPCs, is negatively regulated by Notch1-mediated control of phosphorylated ¸†-Catenin accumulation within CPCs, and that Notch1 activity in CPCs is required for their differentiation. Notch1 positively, and ¸†-Catenin negatively, regulated expression of the cardiac transcription factors, Isl1, Myocd and Smyd1. Surprisingly, disruption of Isl1, normally expressed transiently in CPCs prior to their differentiation, resulted in expansion of CPCs in vivo and in an embryonic stem (ES) cell system. Furthermore, Isl1 was required for CPC differentiation into cardiomyocyte and smooth muscle cells, but not endothelial cells. These findings reveal a regulatory network controlling CPC expansion and cell fate that involve unanticipated functions of ¸†-Catenin, Notch1 and Isl1 that may be leveraged for regenerative approaches involving CPCs. **Overall design:** YFP+ cells marking precardiac mesoderm (Isl1-cre domain) were FACS-sorted (w/wo stabilized Beta-catenin). Their total RNA was amplified with the WT-Ovation Pico RNA Amplification System, fragmented and labeled with the FL-Ovation cDNA Biotin Module V2 (Nugen). The hybridization, staining and scanning of the Affymetrix GeneChips were performed in the Gladstone Genomics Core Lab. Raw data generated from at least three independent experiments were further analyzed by the group of Dr. Ru-Fang Yeh at the Center for Informatics and Molecular Biostatistics, UCSF.

Background corr dist: KL-Divergence = 0.0450, L1-Distance = 0.0180, L2-Distance = 0.0003, Normal std = 0.5914

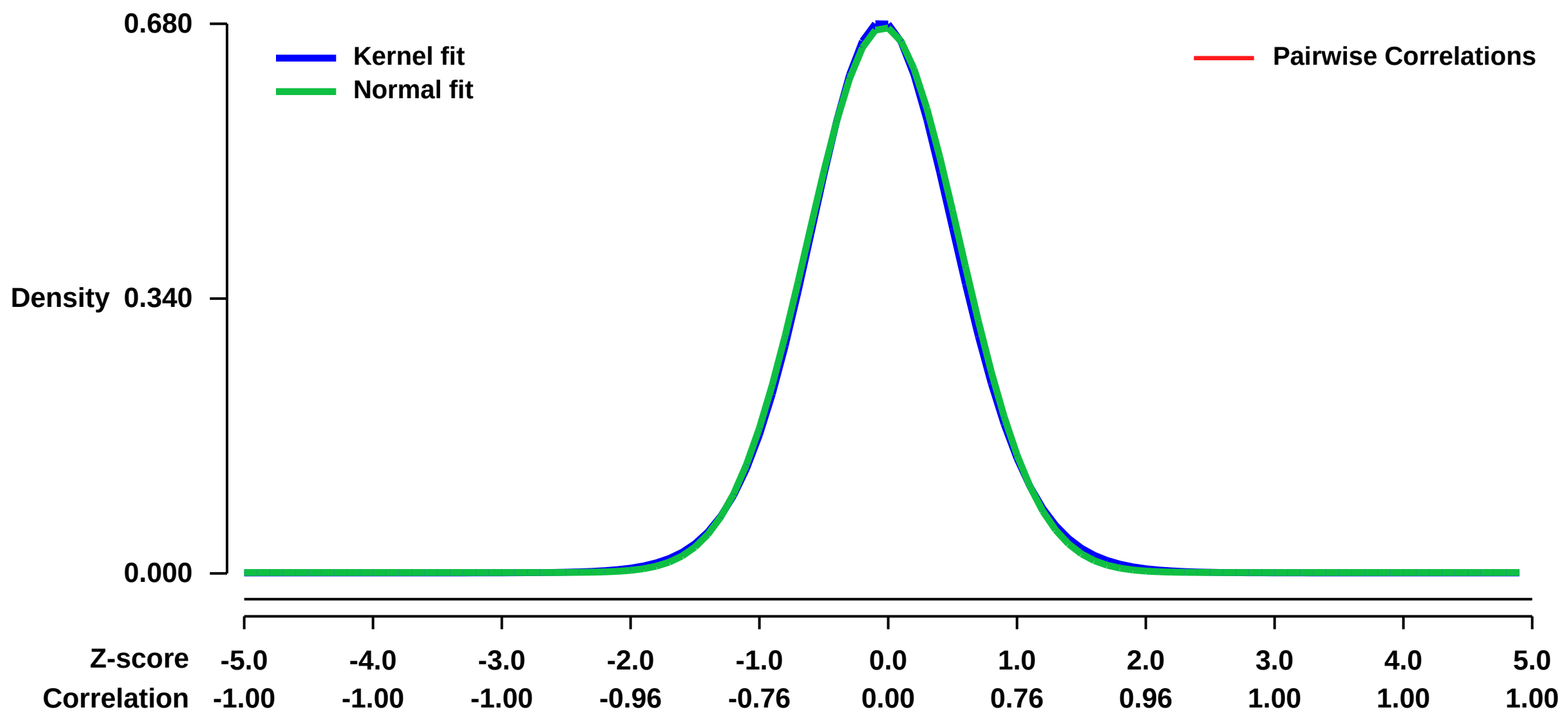

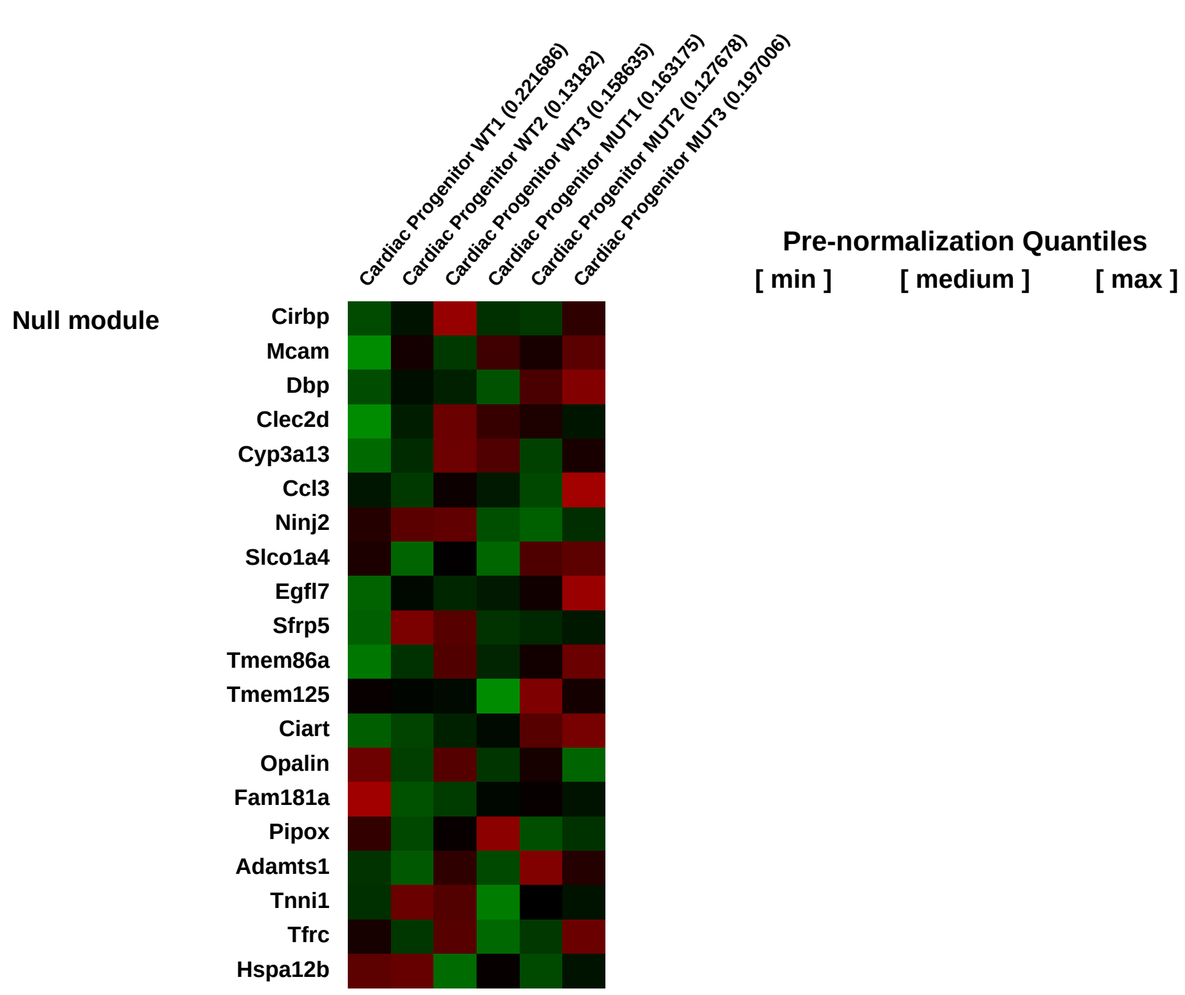

GEO Series "GSE13302" Expression Profiles

Num of samples in this series: 30

Scale of expression profile Z-scores

-3.0 -2.0 -1.0 0.0 1.0 2.0 3.0

GEO Link:	http://www.ncbi.nlm.nih.gov/geo/query/acc.cgi?acc=GSE13302
Status:	Public on May 12 2009
Title:	Gene expression profiling in the lung and liver of Perfluorooctane sulfonate (PFOS) exposed mouse fetuses
Organism:	Mus musculus
Experiment type:	Expression profiling by array
Platform:	GPL1261
Pubmed ID:	19429403
Summary & Design:	**Summary:** Most of the transcriptional changes induced by PFOS in the fetal mouse liver and lung were related to activation of PPARalpha. When compared to the transcript profiles induced by PFOA (Pubmed ID 17681415), few remarkable differences were found other than up-regulation of Cyp3a genes. Because PFOS and PFOA have been shown to differ in their mode of action in the murine neonate, these data suggest that changes related to PFOS-induced neonatal toxicity may not be evident in the fetal transcriptome at term. **Overall design:** Thirty timed-pregnant CD-1 mice were orally dosed from gestation day 1-17 with either 0, 5, or 10 mg/kg/day PFOS in 0.5% Tween 20. At term, fetal lung and liver were collected, total RNA prepared, and samples pooled from three fetuses per litter. Five biological replicates consisting of individual litter samples were then evaluated for each treatment group using Affymetrix mouse 430_2 microarrays.

Background corr dist: KL-Divergence = 0.0214, L1-Distance = 0.0694, L2-Distance = 0.0077, Normal std = 0.8465

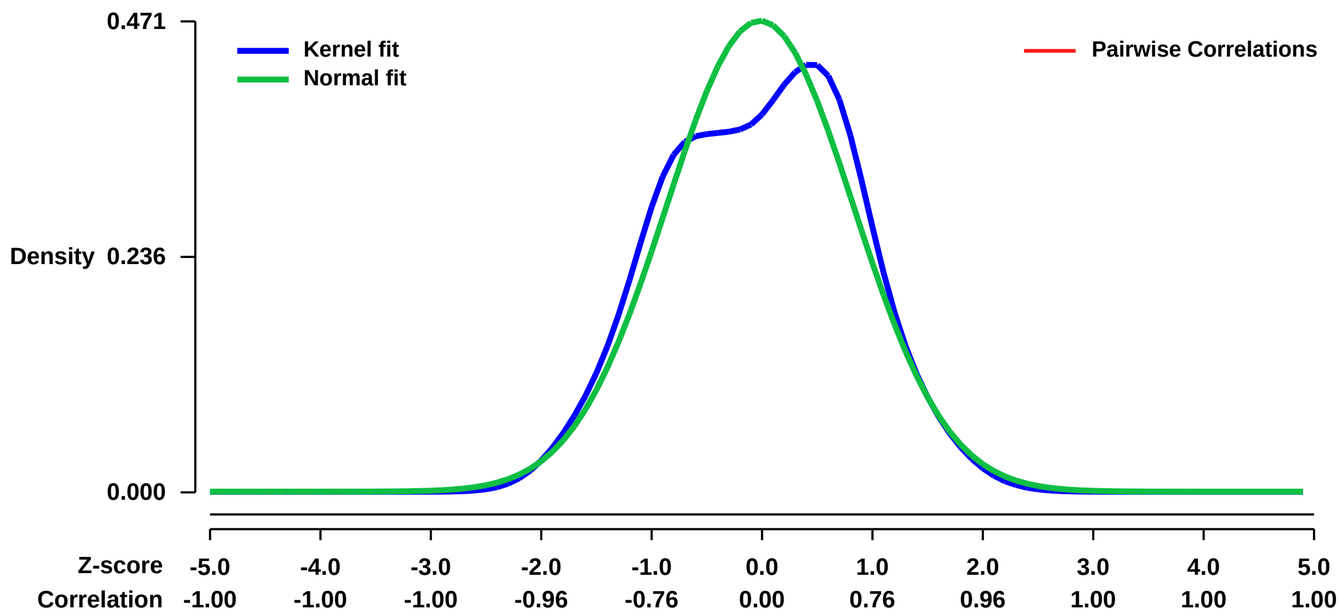

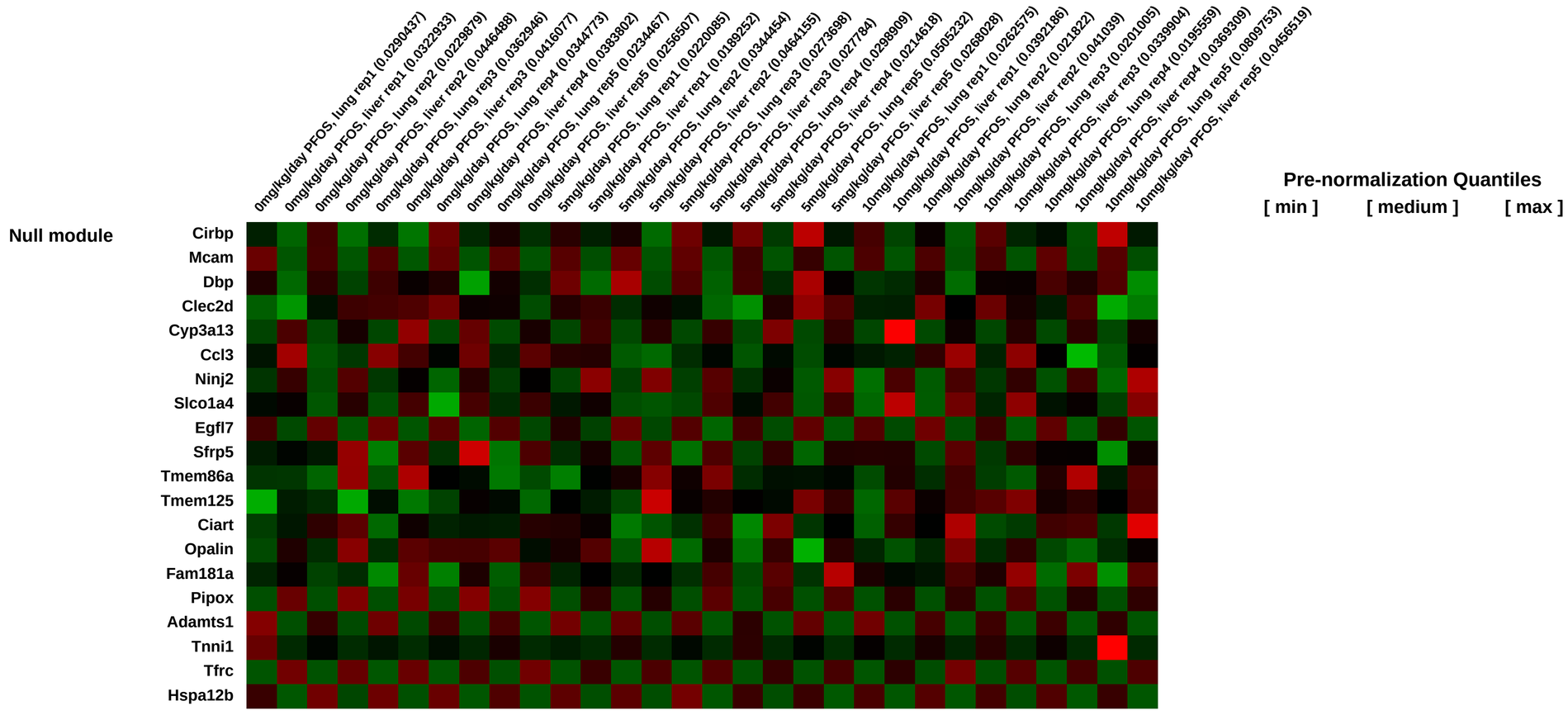

GEO Series "GSE58915" Expression Profiles

Num of samples in this series: 21

Scale of expression profile Z-scores

-3.0 -2.0 -1.0 0.0 1.0 2.0 3.0

GEO Link: http://www.ncbi.nlm.nih.gov/geo/query/acc.cgi?acc=GSE58915
Status: Public on Jul 14 2014
Title: Changes of genes in time-dependent photoaged mouse model
Organism: Mus musculus
Experiment type: Expression profiling by array
Platform: GPL1261
Pubmed ID:

Summary & Design:

Summary:
Photoaging results from the damaging effects of long-term exposure to UV. It is characterized by deep wrinkle, but the mechanism is still lack. To better understand molecular events contributing to photoaging,

We used microarray analysis using an optimized in time-dependent wrinkle model in mice.

Overall design:
We used non UV-irradiated 1 and 8 weeks as a control group and compared expression patterns with UV-irradiated 1, 2, 4, 6 and 8 weeks mouse skin. Three animals were used per each group.

Background corr dist: KL-Divergence = 0.0629, L1-Distance = 0.0739, L2-Distance = 0.0109, Normal std = 0.5481

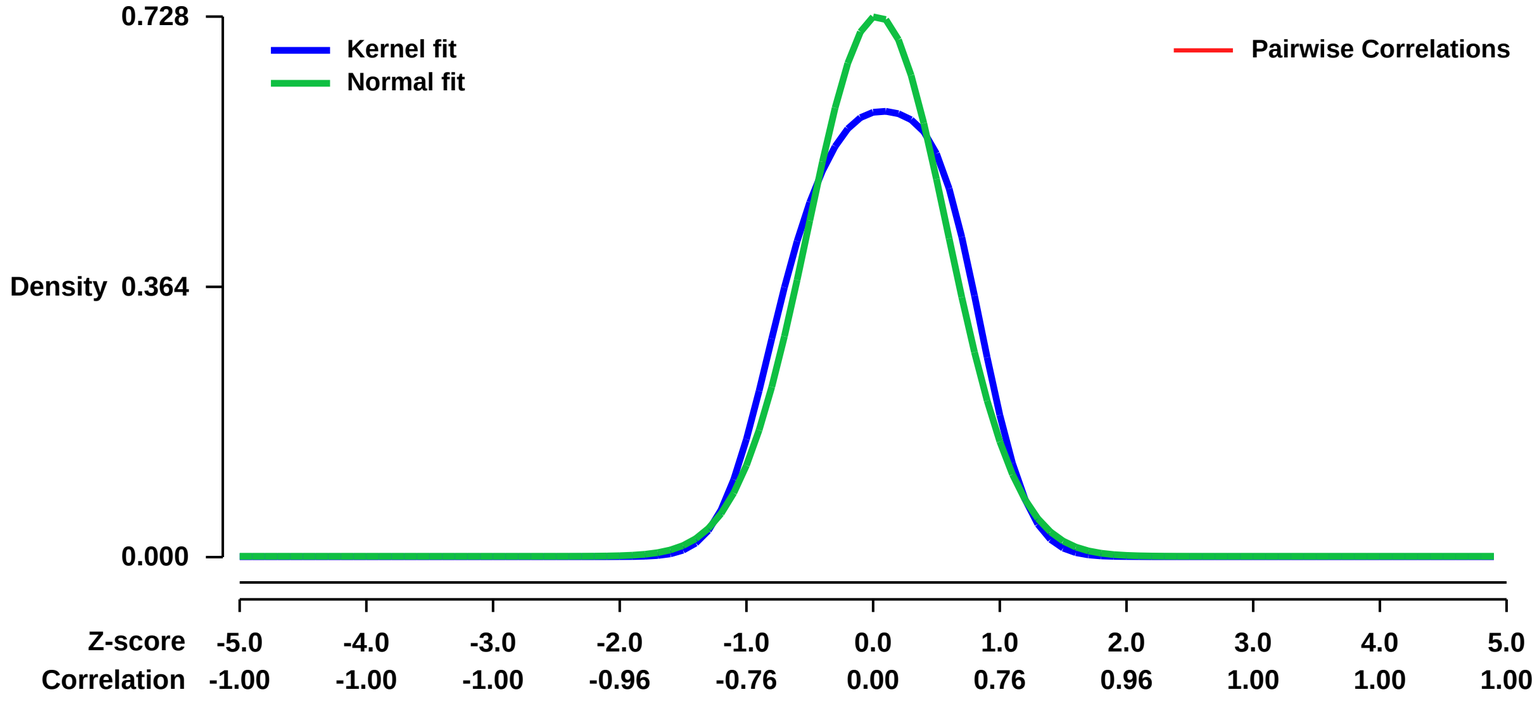

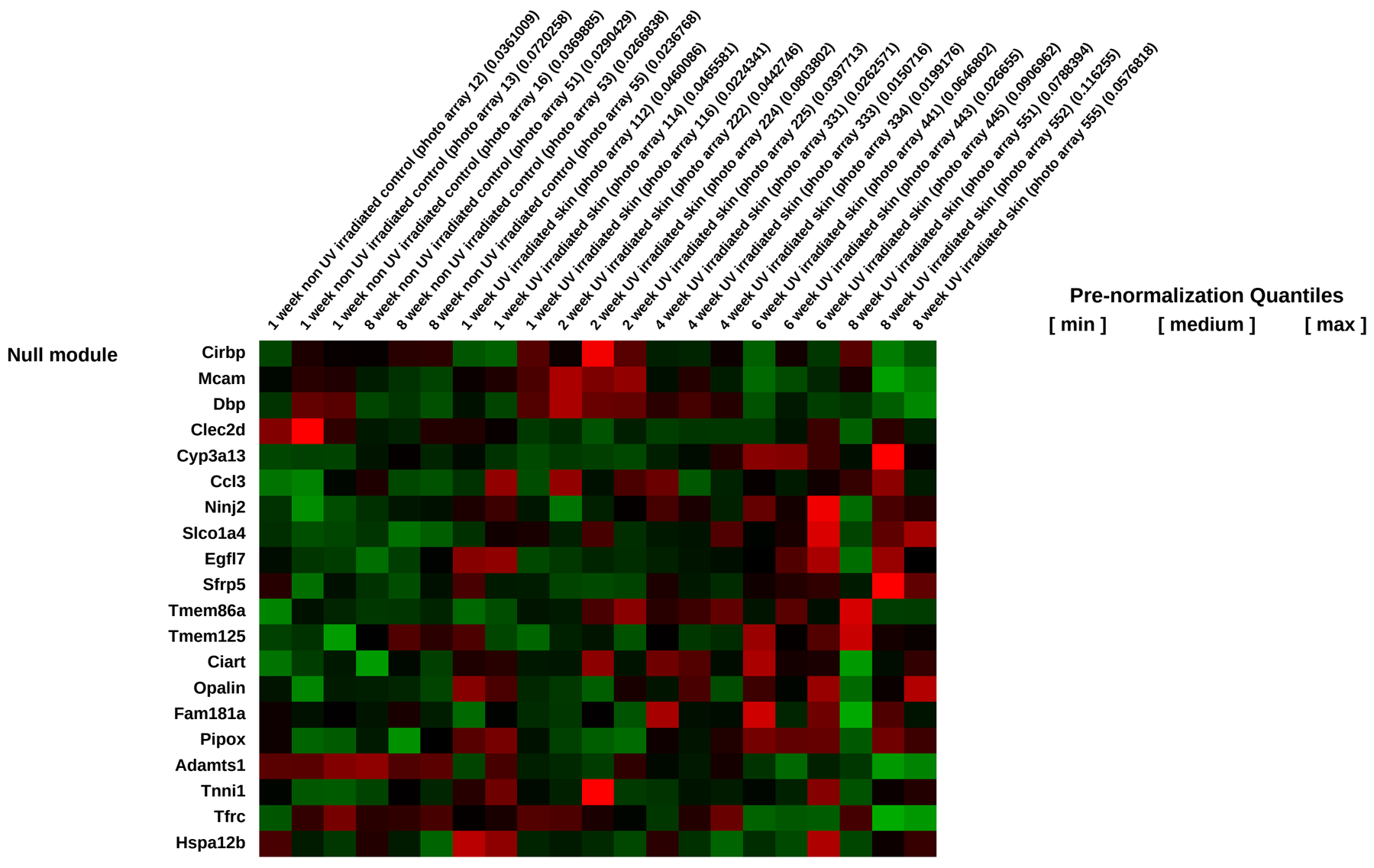

GEO Series "GSE15326" Expression Profiles

Num of samples in this series: 10

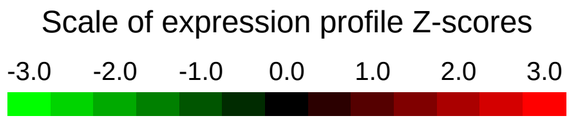

GEO Link:	**http://www.ncbi.nlm.nih.gov/geo/query/acc.cgi?acc=GSE15326**
Status:	**Public on Mar 01 2010**
Title:	**LKR13-Kras-WT1-KO**
Organism:	**Mus musculus**
Experiment type:	**Expression profiling by array**
Platform:	**GPL1261**
Pubmed ID:	
Summary & Design:	**Summary:** **K-ras is one of the most frequently mutated human oncogenes. However, activation of K-ras can lead to either senescence or proliferation in primary cells. The precise mechanism governing these distinct outcomes remains unclear. Here we describe a novel loss-of-function screen to assess the role of specific genes identified as potential key regulators of K-ras driven oncogenesis. Using this approach, we identify the transcription factor Wt1 as an inhibitor of senescence in primary cells expressing oncogenic K-ras. Deletion or suppression of Wt1 expression leads to senescence of primary cells expressing oncogenic K-ras under the control of the native promotor and at physiological levels, but had no effect on cells expressing wild-type K-ras. Furthermore, loss of Wt1 in lung cancer cell lines that harbor mutant K-ras leads to apoptosis. Taken together, these observations reveal a novel role for Wt1 as a key regulator of the complex genetic network required for the oncogenic effect of the small GTPase K-ras.** **We compare the expression profiles of K-ras mutant mouse cell line (LKR13) upon shRNA knockdown of K-ras itself or Wt1. The study provides insights into the transcriptional role of Wt1 in the context of oncogenic K-ras.** **Overall design:** **LKR13 cells were infected with plko.1s vectors carrying one of two shRNAs against K-ras or Wt1. Control cells were infected with an shRNA against GFP. 48 hours after infection, cells were selected with puromycin for 3 days. RNA was isolated using Trizol 7 days after infection. RNA was further prepared by passage over an RNeasy column. cDNA synthesis, biotinylation of cRNA and hybridization to mouse Genechip 430A v2 containing 39,000 probes was performed according to the manufacturerâ s instructions (Affymetrix, Santa Clara). Microarray data was normalized with Expression Console software (Affymetrix, Santa Clara), using RMA algorithms.**

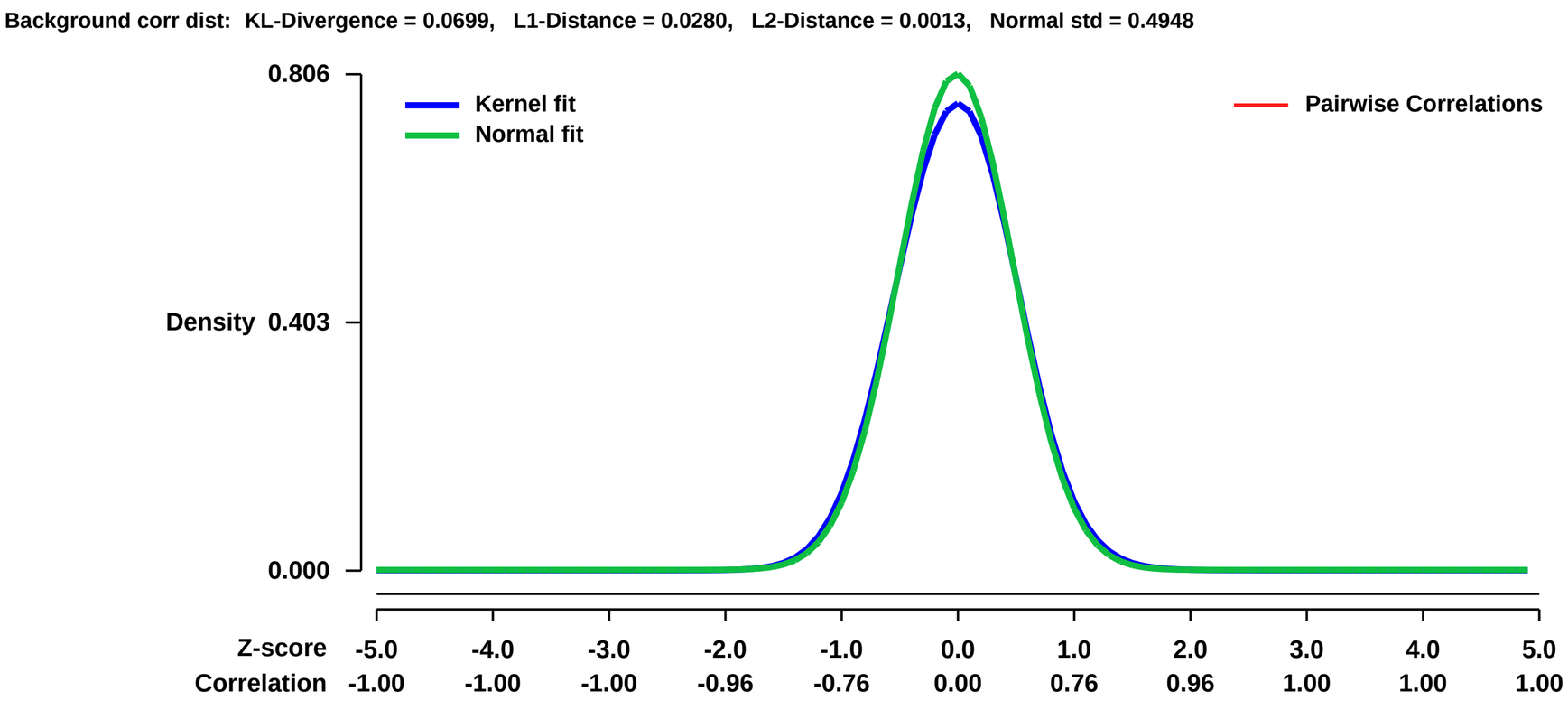

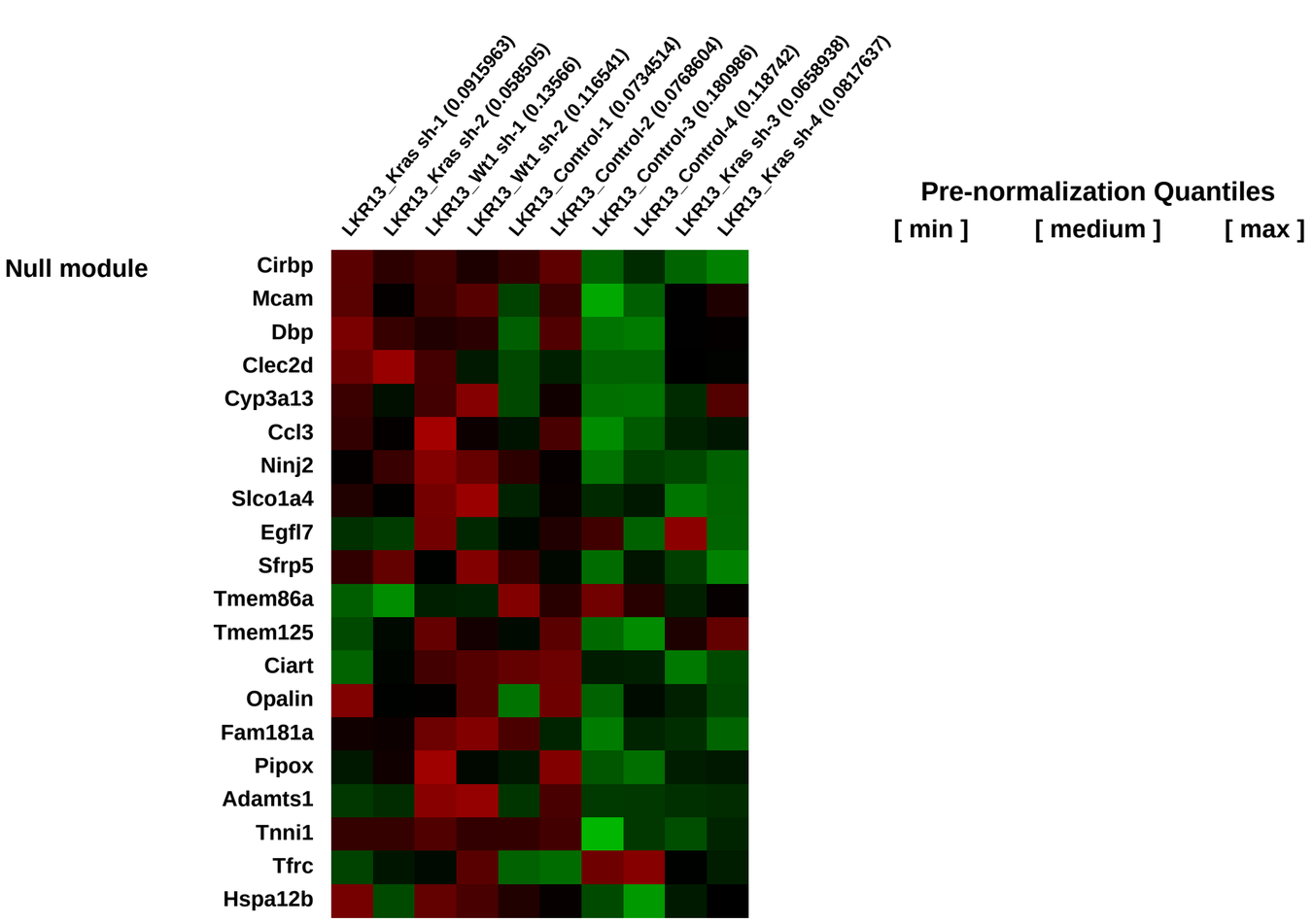

GEO Series "GSE32986" Expression Profiles

Num of samples in this series: 18

Scale of expression profile Z-scores

-3.0 -2.0 -1.0 0.0 1.0 2.0 3.0

GEO Link:	http://www.ncbi.nlm.nih.gov/geo/query/acc.cgi?acc=GSE32986
Status:	Public on Oct 15 2011
Title:	Synergism between curdlan and GM-CSF in mouse dendritic cells
Organism:	Mus musculus
Experiment type:	Expression profiling by array
Platform:	GPL1261
Pubmed ID:	22250091
Summary & Design:	**Summary:** A simultaneous engagement of different pathogen recognition receptors provides a tailor made adaptive immunity for an efficient defence against distinct pathogens. For example, cross talk of TLR and c-type lectin signalling effectively shapes distinct gene expression patterns by integrating the signals at the level of NF-¸”B. Here, we extend this principle to a strong synergism between the Dectin-1 agonist, curdlan, and an inflammatory growth factor, GM-CSF. Both together act in synergy in inducing a strong inflammatory signature which converts immature DCs to potent effector DCs. A variety of cytokines (IL-1¸†, IL-6, TNF-¸–, IL-2 and IL-12p70), costimulatory molecules (CD80, CD86, CD40 and CD70), chemokines (CxCl1, CxCl2, CxCl3, CCl12, CCl17) as well as receptors and molecules involved in fugal recognition and immunity such as Mincle, Dectin-1, Dectin-2 and Pentraxin 3 are strongly up-regulated in DC treated simultaneously with curdlan and GM-CSF. The synergistic effect of both stimuli resulted in strong IKB¸– phosphorylation, in its rapid degradation and in enhanced nuclear translocation of all NF-¸”B subunits. We further identified MAPK ERK, as one possible integration site of both signals, since its phosphorylation was clearly augmented when curdlan was co-applied with GM-CSF. Our data demonstrate that the immunomodulatory activity of curdlan requires an additional signal provided by GM-CSF to successfully initiate a robust ¸†-glucan specific cytokine and chemokine response. The integration of both signals clearly prime and tailor a more effective innate and adaptive response against invading microbes and fungi. **Overall design:** CD11b+ fraction of FLT3L generated BM DCs (3-4 x106) were stimulated for 4 hours with 100 or 1 ¸…g/ml curdlan in presence or absence of 5 ng/ml GM-CSF in triplicates.

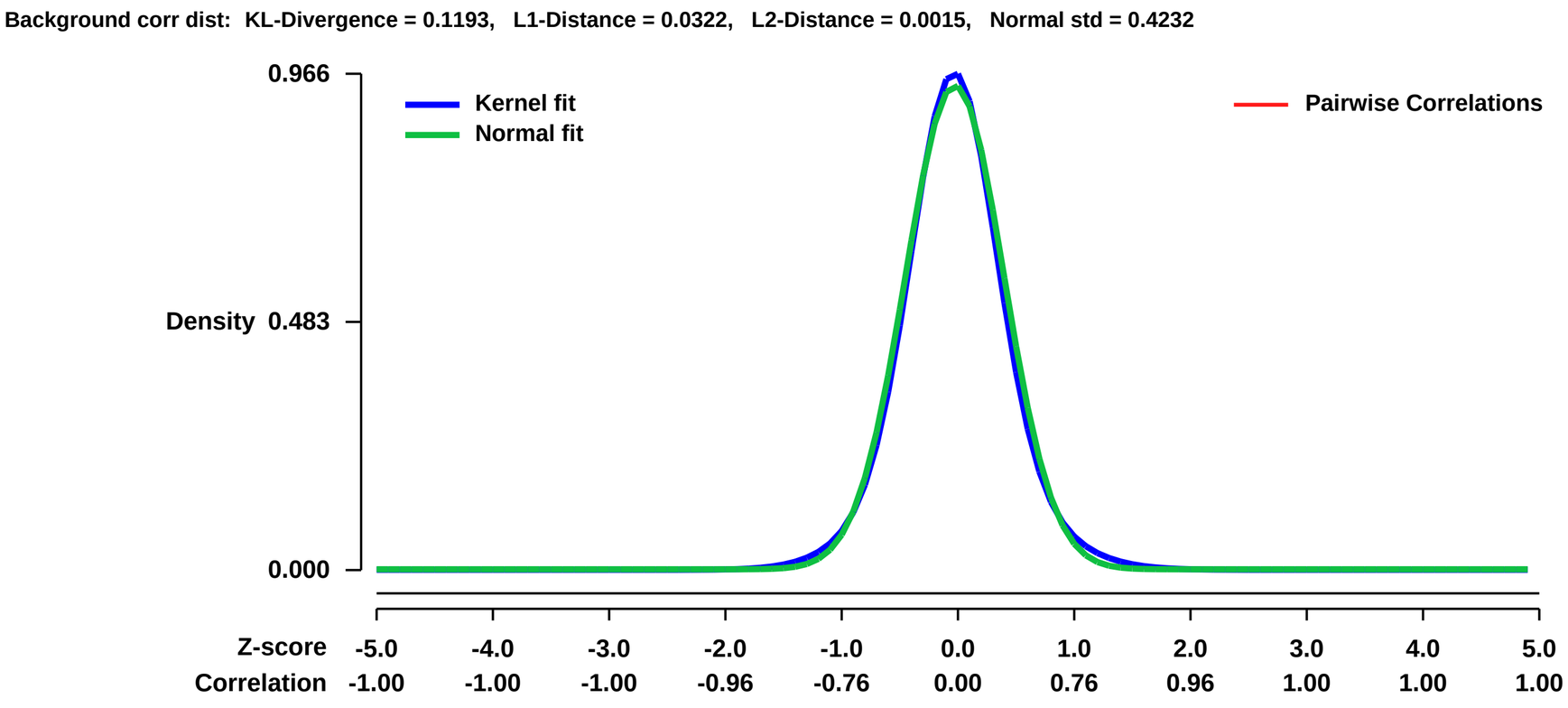

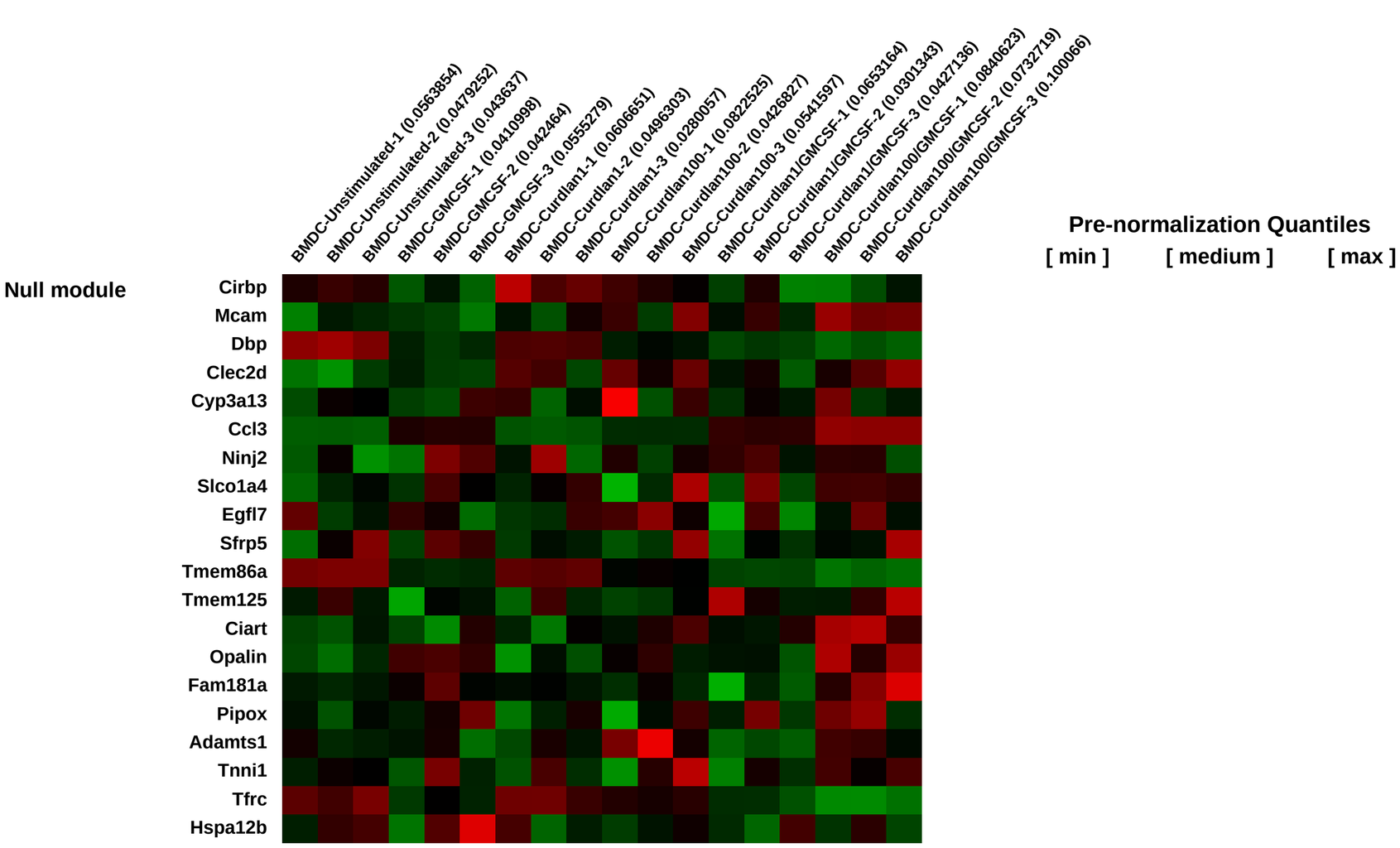

GEO Series "GSE23781" Expression Profiles

Num of samples in this series: 6

Scale of expression profile Z-scores

-3.0 -2.0 -1.0 0.0 1.0 2.0 3.0

GEO Link:	http://www.ncbi.nlm.nih.gov/geo/query/acc.cgi?acc=GSE23781
Status:	Public on Mar 23 2011
Title:	Expression data from E13.5 Fz4-/- and Fz4+/+ kidneys
Organism:	Mus musculus
Experiment type:	Expression profiling by array
Platform:	GPL1261
Pubmed ID:	21343368
Summary & Design:	**Summary:** Fz4 and Fz8 cooperate in regulating the branching morhpogenesis of the developing kidney during mouse embryonic development, hence determines the eventual kidney size. We used microarrays to study the global gene expression profiles regulated by Fz4 and Fz8 signaling during early kidney development, and to understand the collaboration between the signaling events mediated by Fz4 and Fz8 **Overall design:** Kidney rudiments were dissected from E13.5 mouse embryos for RNA extraction and hybridization on Affymetrix MOE430.2 arrays. Three biological replicates of each genotype were analyzed.

Background corr dist: KL-Divergence = 0.0214, L1-Distance = 0.0173, L2-Distance = 0.0004, Normal std = 0.7180

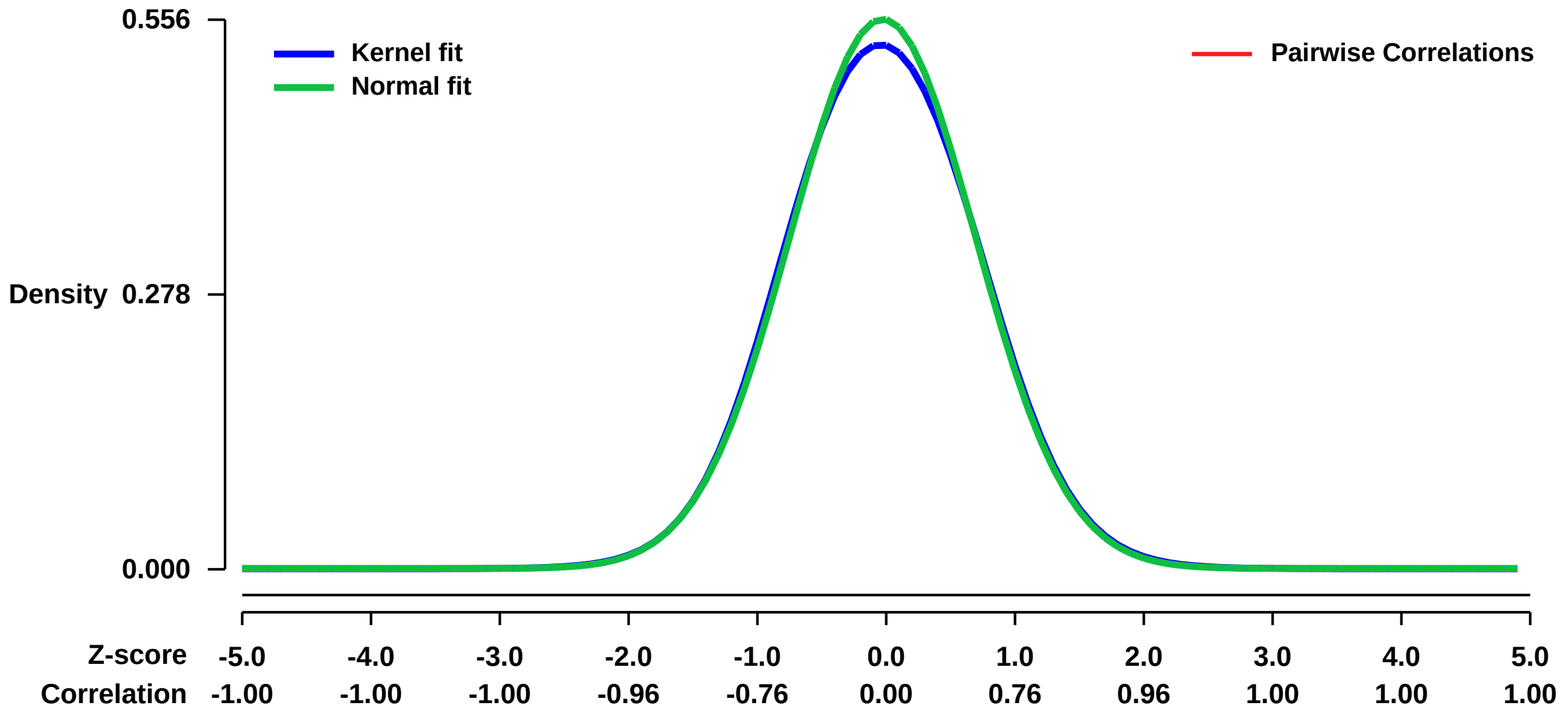

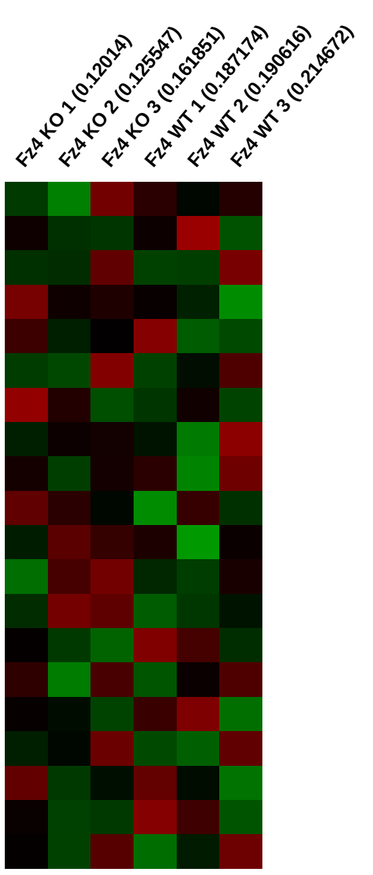

GEO Series "GSE4193" Expression Profiles

Num of samples in this series: 8

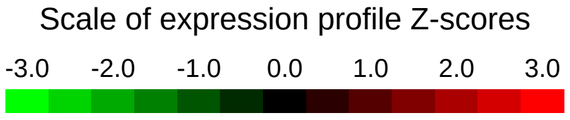

GEO Link:	**http://www.ncbi.nlm.nih.gov/geo/query/acc.cgi?acc=GSE4193**
Status:	**Public on Feb 09 2006**
Title:	**Gene expression in murine germ cells**
Organism:	**Mus musculus**
Experiment type:	**Expression profiling by array**
Platform:	**GPL1261**
Pubmed ID:	**16581510**
Summary & Design:	**Summary:** **In mammals, the X and Y chromosomes are subject to meiotic sex chromosome inactivation (MSCI) during prophase I in the male germline, but their status thereafter is currently unclear. An abundance of X-linked spermatogenesis genes has spawned the view that the X must be active [1-8]. On the other hand, the idea that the imprinted paternal X of the early embryo may be pre-inactivated by MSCI suggests that silencing may persist longer [9-12]. To clarify this issue, we establish a comprehensive X-expression profile during mouse spermatogenesis. Here, we discover that the X and Y occupy a novel compartment in the post-meiotic spermatid and adopt a non-Rabl configuration. We demonstrate that this post-meiotic sex chromatin (PMSC) persists throughout spermiogenesis into mature sperm and exhibits epigenetic similarity to the XY body. In the spermatid, 87% of X-linked genes remain suppressed post-meiotically, while autosomes are largely active. We conclude that chromosome-wide X-silencing continues from meiosis to the end of spermiogenesis and discuss implications for proposed mechanisms of imprinted X-inactivation.** **Keywords: Specific germ cells from murine testis** **Overall design:** **Independent germ cell preps were used for array analysis. Duplicates were provided for each sample.**

Background corr dist: KL-Divergence = 0.0209, L1-Distance = 0.0329, L2-Distance = 0.0015, Normal std = 0.7625

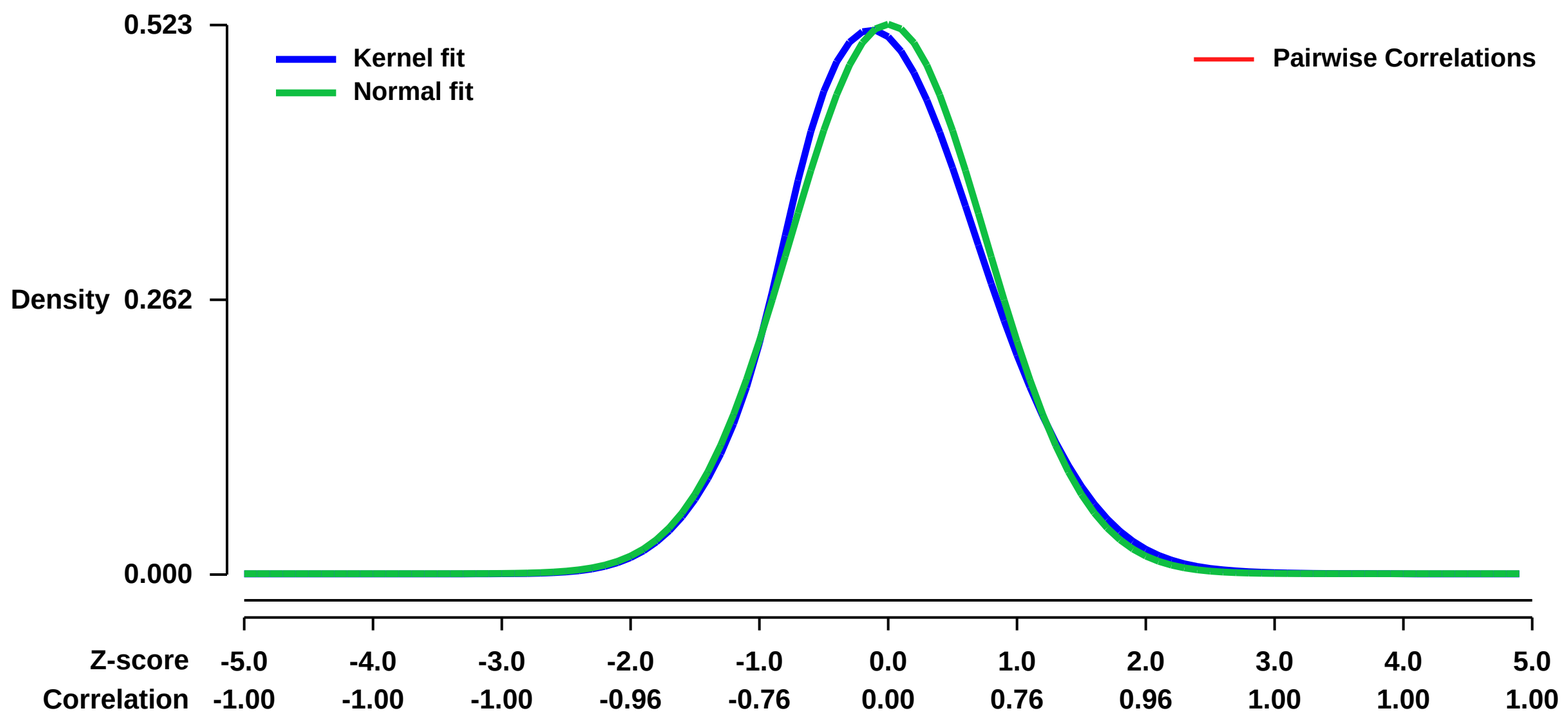

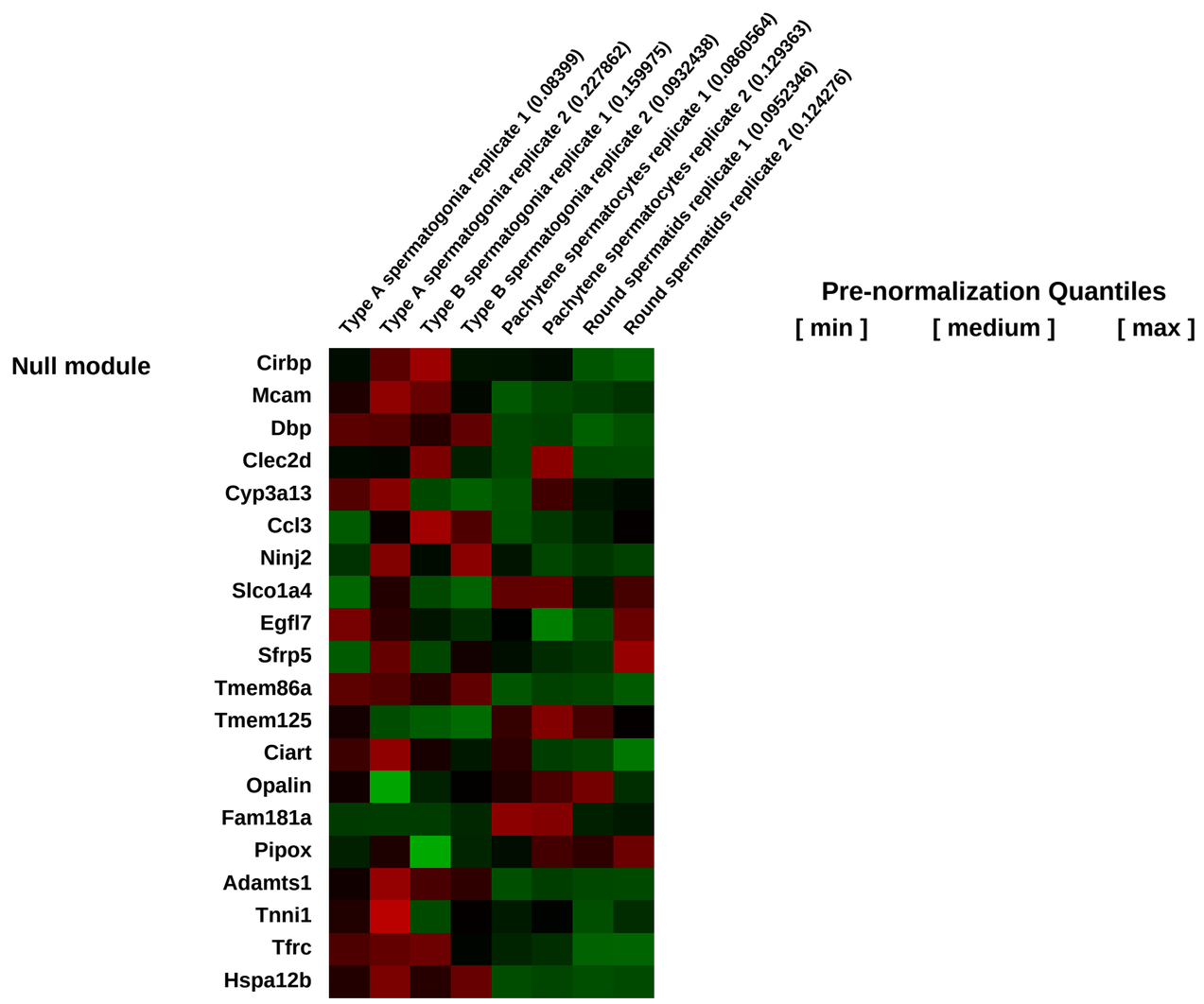

GEO Series "GSE33659" Expression Profiles

Num of samples in this series: 9

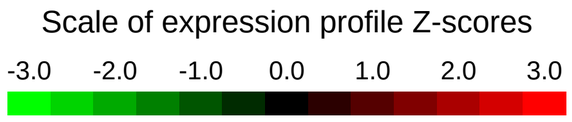

GEO Link:	http://www.ncbi.nlm.nih.gov/geo/query/acc.cgi?acc=GSE33659
Status:	Public on Feb 10 2012
Title:	Direct Recruitment of Polycomb Repressive Complex 1 (PRC1) to Chromatin by Core Binding Transcription Factors (microarray)
Organism:	Mus musculus
Experiment type:	Expression profiling by array
Platform:	GPL1261
Pubmed ID:	22325351
Summary & Design:	**Summary:** Polycomb repressive complexes (PRCs) play key roles in developmental epigenetic regulation. Yet the mechanisms that target PRCs to specific loci in mammalian cells remain incompletely understood. In this study, we show that Bmi1, a core component of Polycomb Repressive Complex 1 (PRC1), binds directly to the Runx1/CBFbeta transcription factor complex. Genome-wide studies in megakaryocytic cells demonstrate considerable chromatin occupancy overlap between the PRC1 core component Ring1b and Runx1/CBFbeta and functional regulation of a significant fraction of commonly bound genes. Bmi1/Ring1b and Runx1/CBFbeta deficiency generate partial phenocopies of one another in vivo. We also show that Ring1b occupies key Runx1 binding sites in primary murine thymocytes and that this occurs via Polycomb Repressive Complex 2 (PRC2) independent mechanisms. Genetic depletion of Runx1 results in reduced Ring1b binding at these sites in vivo. These findings provide evidence for site-specific PRC1 chromatin recruitment by core binding transcription factors in mammalian cells. **Overall design:** shRNA mediated knockdown of CBFb, Ring1b and control in biological triplicate

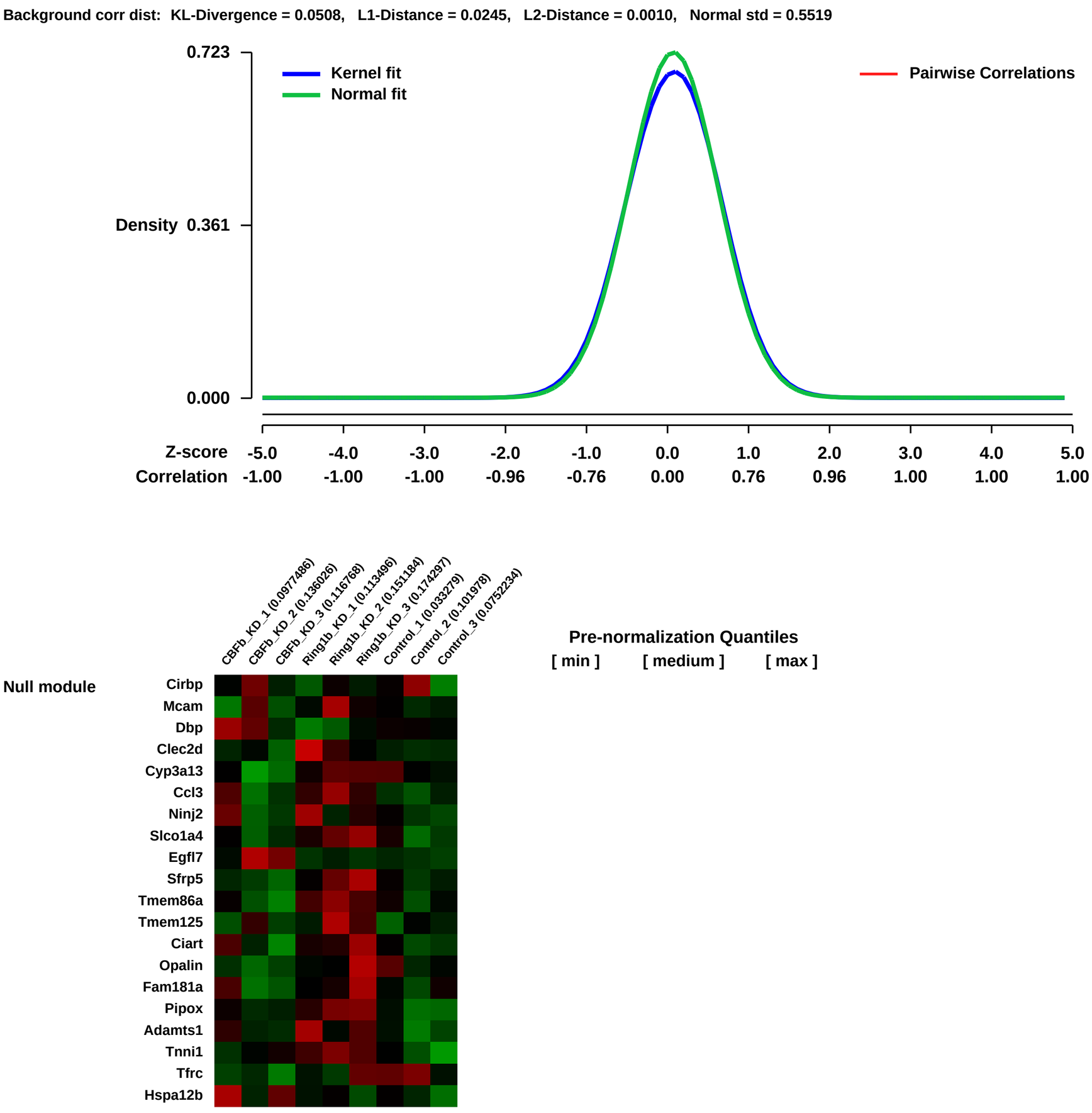

GEO Series "GSE21583" Expression Profiles

Num of samples in this series: 8

Scale of expression profile Z-scores

-3.0 -2.0 -1.0 0.0 1.0 2.0 3.0

GEO Link:	http://www.ncbi.nlm.nih.gov/geo/query/acc.cgi?acc=GSE21583
Status:	Public on Aug 25 2010
Title:	Effects of ACE2 on BMPR2 mutation-mediated defects in gene expression
Organism:	Mus musculus
Experiment type:	Expression profiling by array
Platform:	GPL1261
Pubmed ID:	22180660
Summary & Design:	**Summary:** BMPR2 mutation causes pulmonary arterial hypertension (PAH); ACE2 treatment can resolve established BMPR2-mediated PAH. The purpose of this study was to uncover the molecular mechanism behind this. **Overall design:** Four groups: +/- ACE2 and +/- BMPR2 transgene, two arrays each, each array a pool of three animals.

Background corr dist: KL-Divergence = 0.0925, L1-Distance = 0.0232, L2-Distance = 0.0007, Normal std = 0.4506

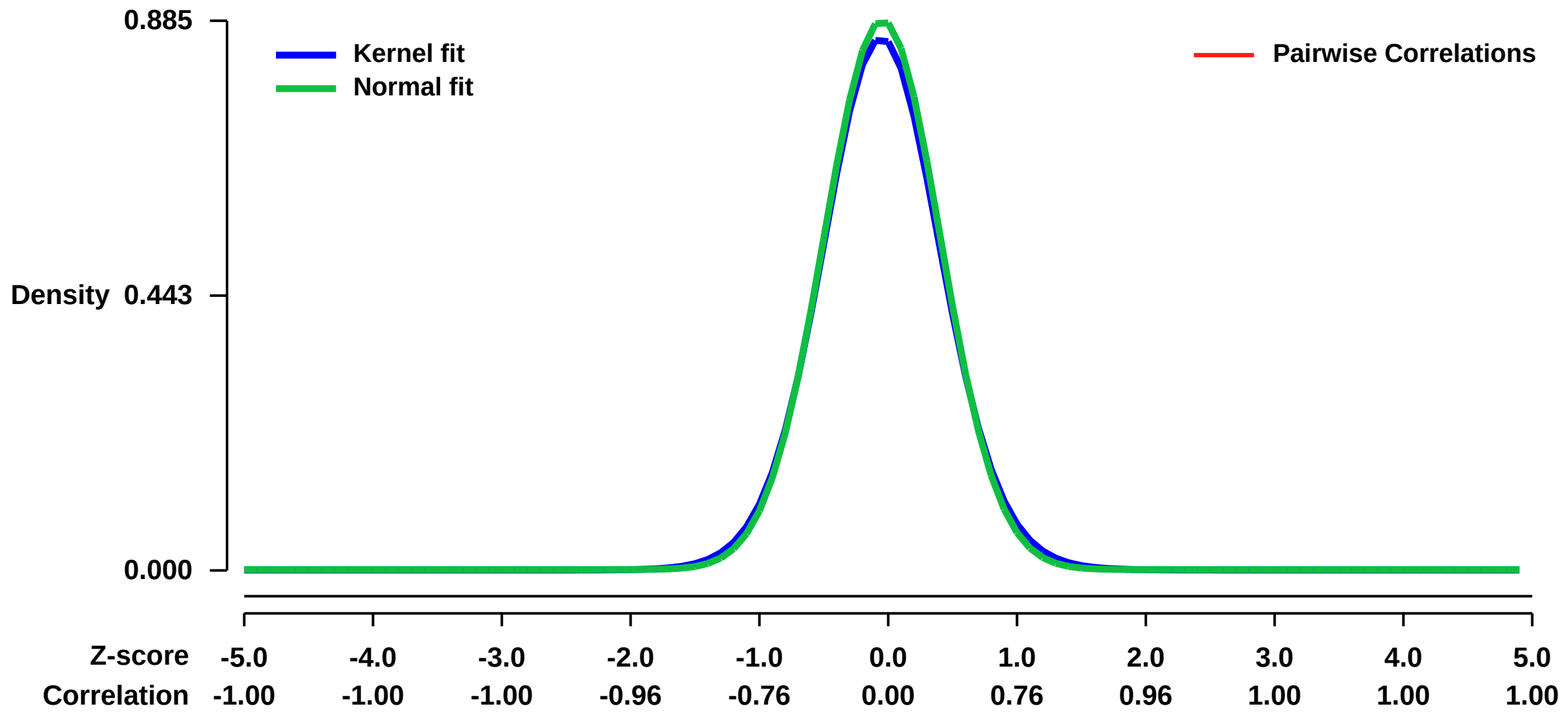

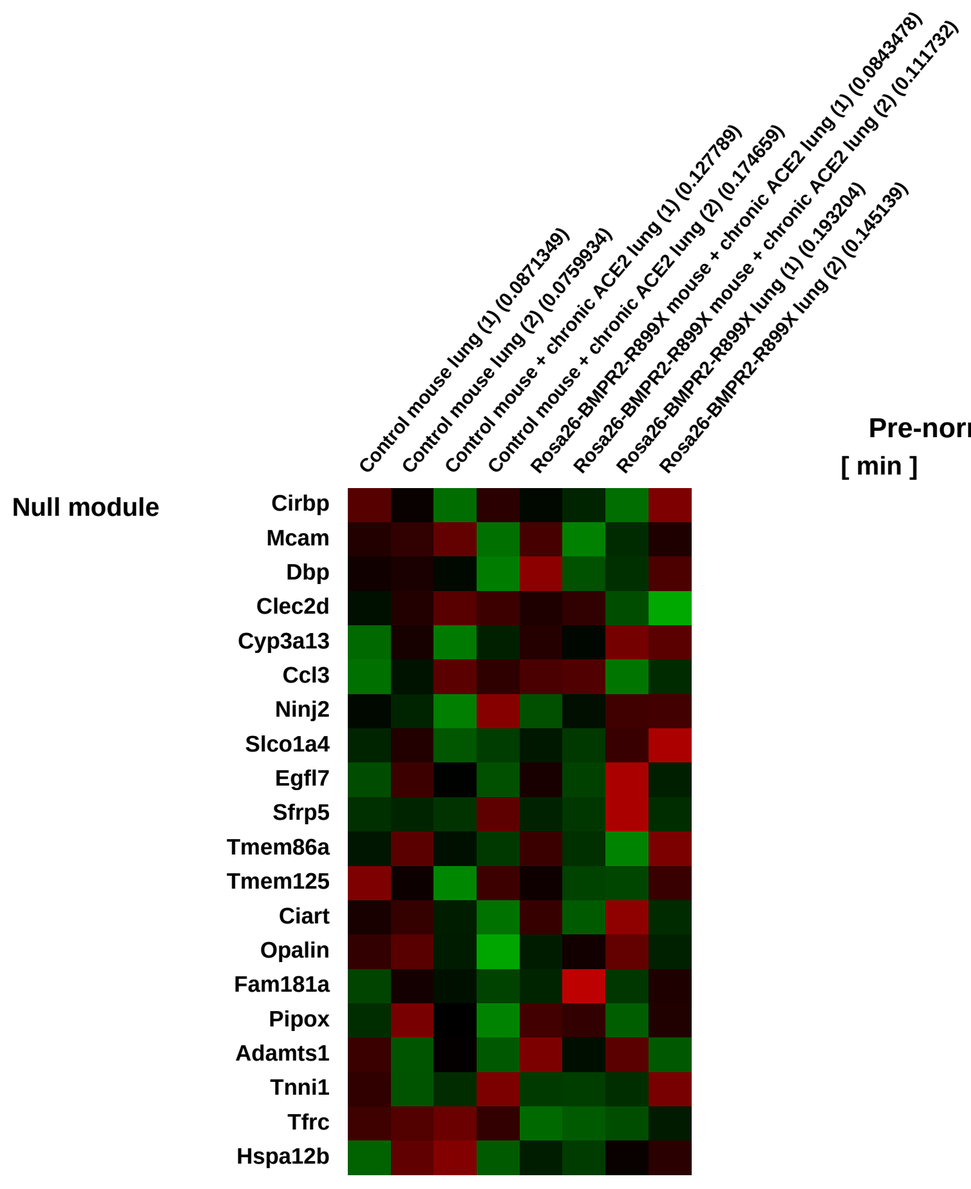

GEO Series "GSE14686" Expression Profiles

Num of samples in this series: 16

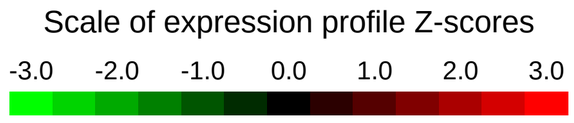

GEO Link:	http://www.ncbi.nlm.nih.gov/geo/query/acc.cgi?acc=GSE14686
Status:	Public on Mar 01 2009
Title:	Colonic transcriptional changes evoked by E. rectale-B. thetaiotaomicron co-colonization
Organism:	Mus musculus
Experiment type:	Expression profiling by array
Platform:	GPL1261
Pubmed ID:	19321416
Summary & Design:	**Summary:** The adult human gut microbial community is typically dominated by two bacterial phyla (divisions), the Firmicutes and the Bacteroidetes. Little is known about the factors that govern the interactions between their members. Here we examine the niches of representatives of both phyla in vivo. Finished genome sequences were generated from E. rectale and E. eligens, which belong to Clostridium Cluster XIVa, one of the most common gut Firmicute clades. Comparison of these and 25 other gut Firmicutes and Bacteroidetes indicated that the former possess smaller genomes and a disproportionately smaller number of glycan-degrading enzymes. Germ-free mice were then colonized with E. rectale and/or a prominent human gut Bacteroidetes, Bacteroides thetaiotaomicron, followed by whole genome transcriptional profiling of both organisms in their distal gut (cecal) habitat as well as host responses, high resolution proteomic analysis of cecal contents, and biochemical assays of carbohydrate metabolism. B. thetaiotaomicron adapts to E. rectale by upregulating expression of a variety of polysaccharide utilization loci (PULs) encoding numerous glycoside hydrolase gene families, and by signaling the host to produce mucosal glycans that it, but not E. rectale, can access. E. rectale adapts to B. thetaiotaomicron by decreasing production of its glycan-degrading enzymes, increasing expression of selected amino acid and sugar transporters, and facilitating glycolysis by reducing levels of NADH, in part via generation of butyrate from acetate, which in turn is utilized by the gut epithelium. This simplified model of the human gut microbiota illustrates niche specialization and functional redundancy within members of major gut bacterial phyla, and the importance of host glycans as a nutrient foundation that ensures ecosystem stability. **Overall design:** four biological replicates per group. NMRI mice, males (12-14 weeks old).

Background corr dist: KL-Divergence = 0.1134, L1-Distance = 0.0264, L2-Distance = 0.0010, Normal std = 0.4187

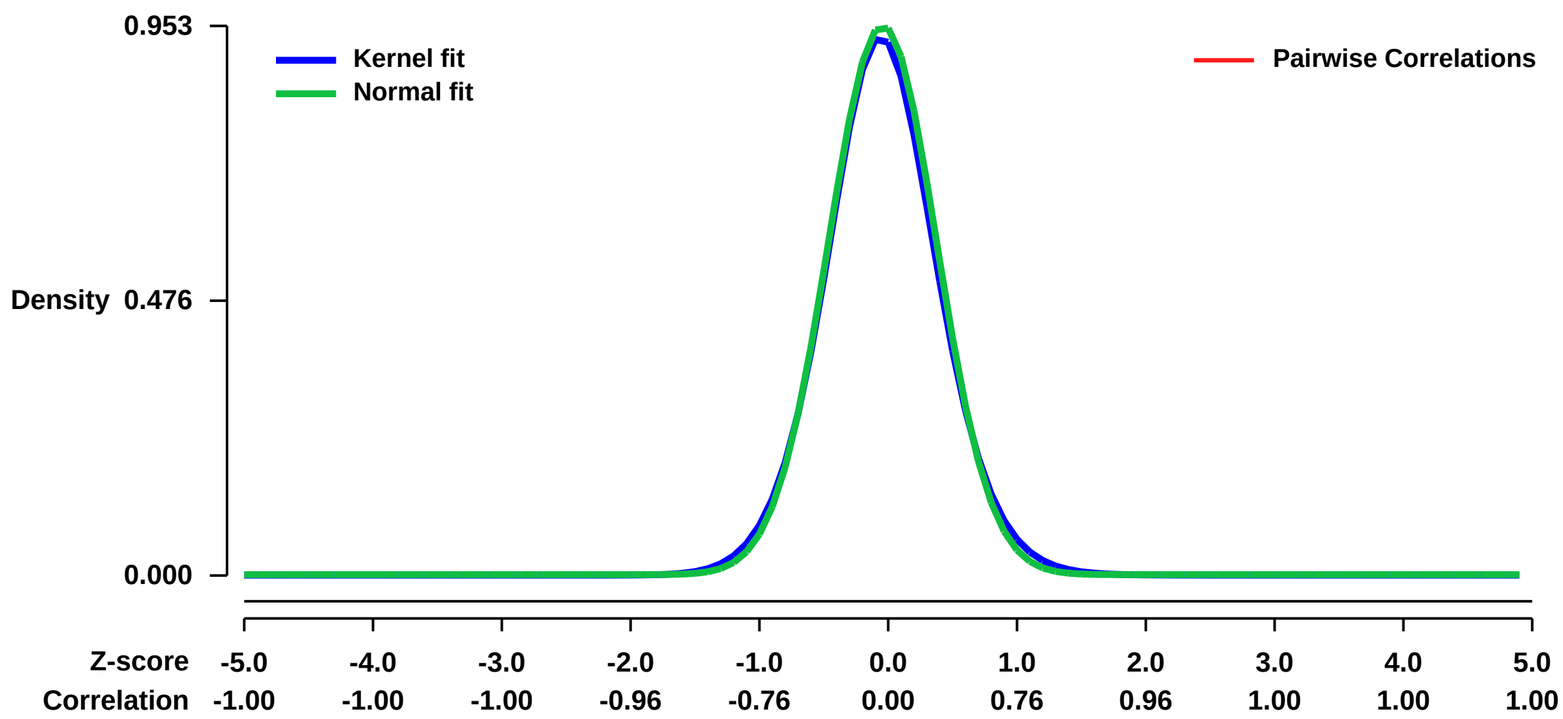

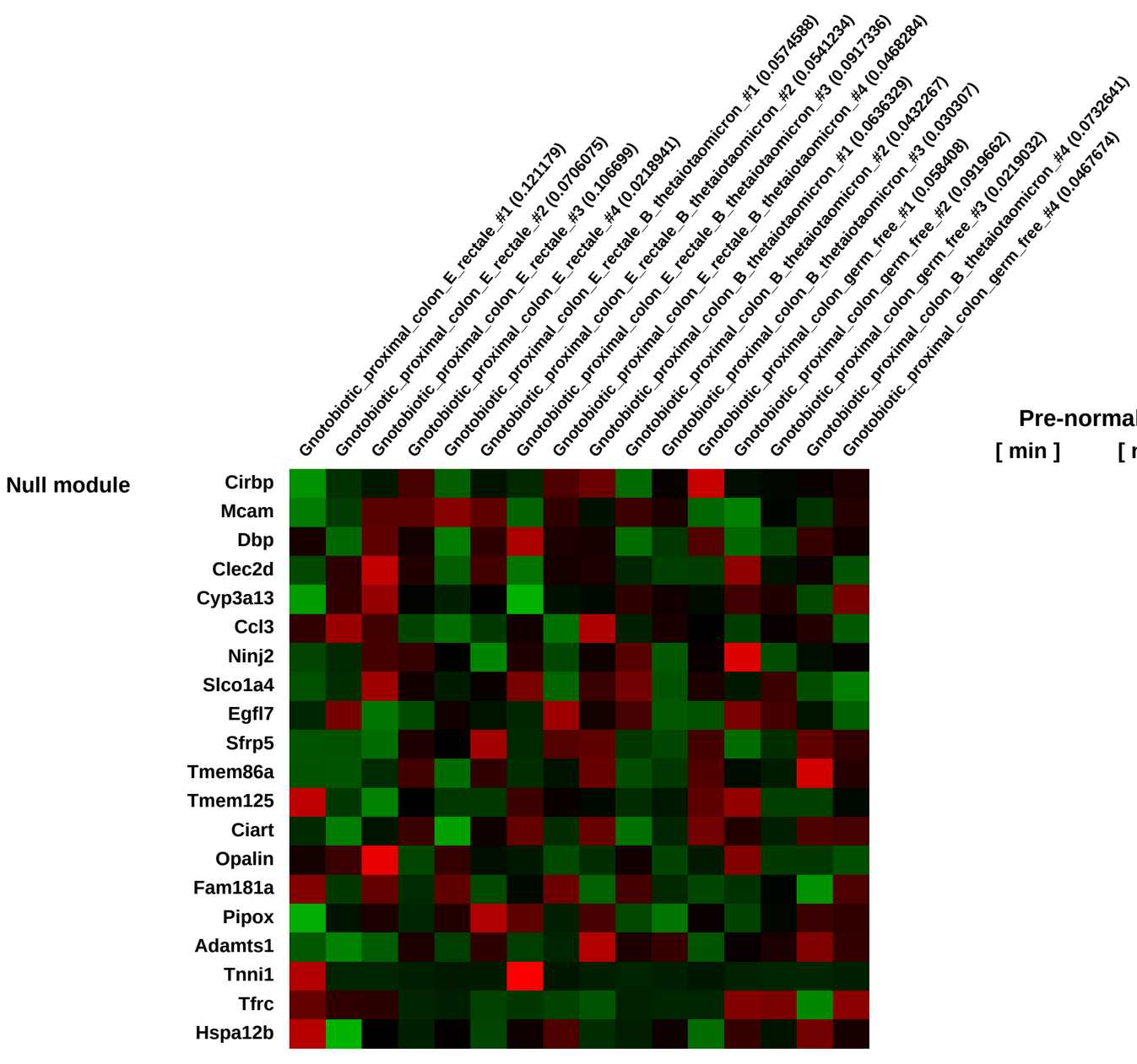

GEO Series "GSE44260" Expression Profiles

Num of samples in this series: 10

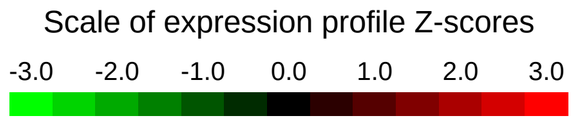

GEO Link:	**http://www.ncbi.nlm.nih.gov/geo/query/acc.cgi?acc=GSE44260**
Status:	**Public on Mar 06 2013**
Title:	**Murine germinal center and naive B cells**
Organism:	**Mus musculus**
Experiment type:	**Expression profiling by array**
Platform:	**GPL1261**
Pubmed ID:	**23514741**
Summary & Design:	**Summary:** **Gene expressions of murine germinal center and naive B cells on Affymetrix platform** **Overall design:** **The experiment include 3 d14 GC B1-8, 3 d14 GC V23 and 4 Naˆflve samples**

Background corr dist: **KL-Divergence = 0.0522, L1-Distance = 0.0558, L2-Distance = 0.0041, Normal std = 0.6145**

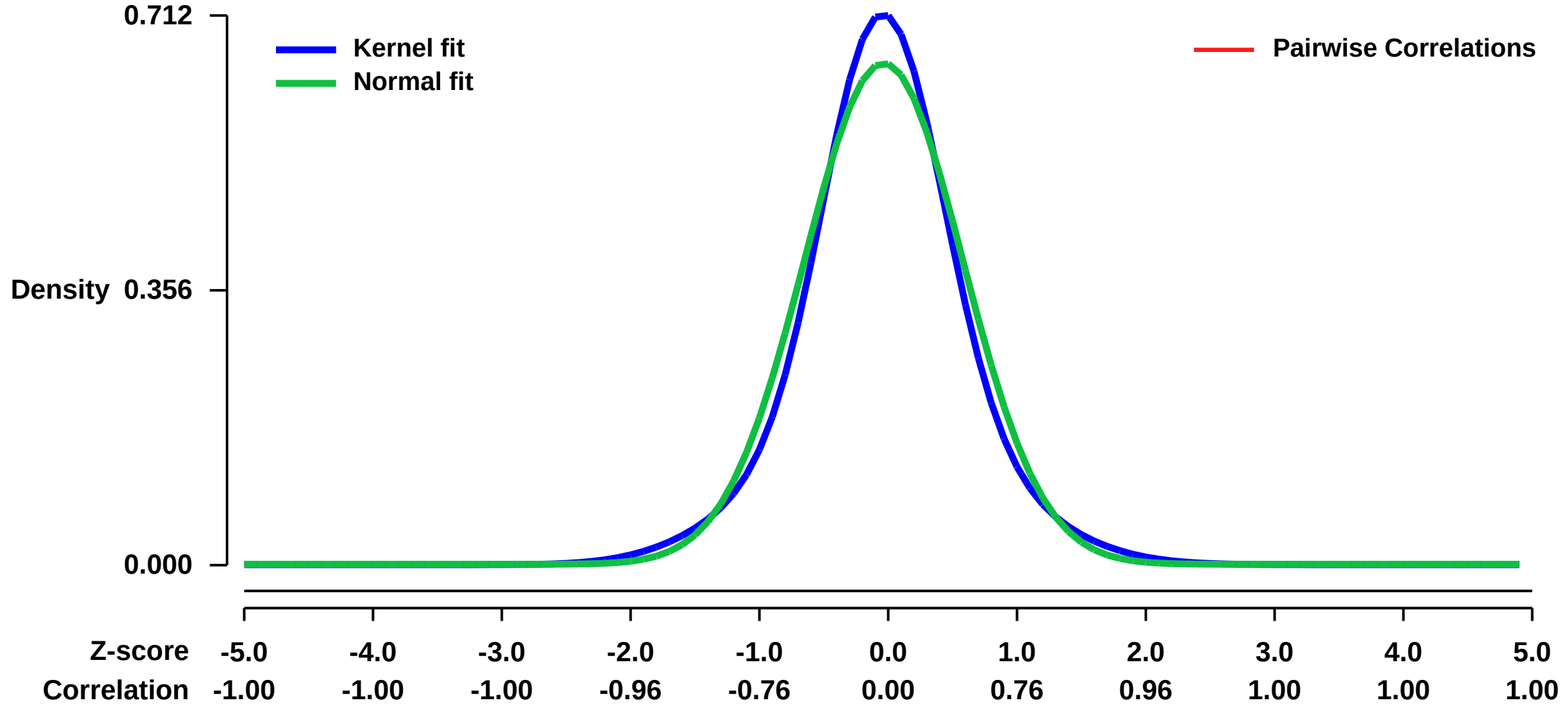

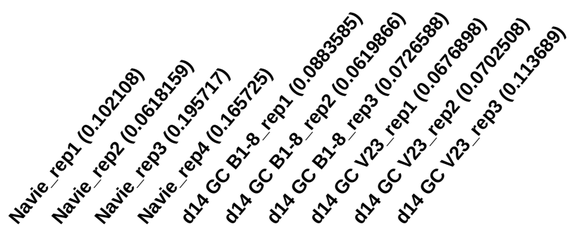

Pre-normalization Quantiles

[min] [medium] [max]

Null module

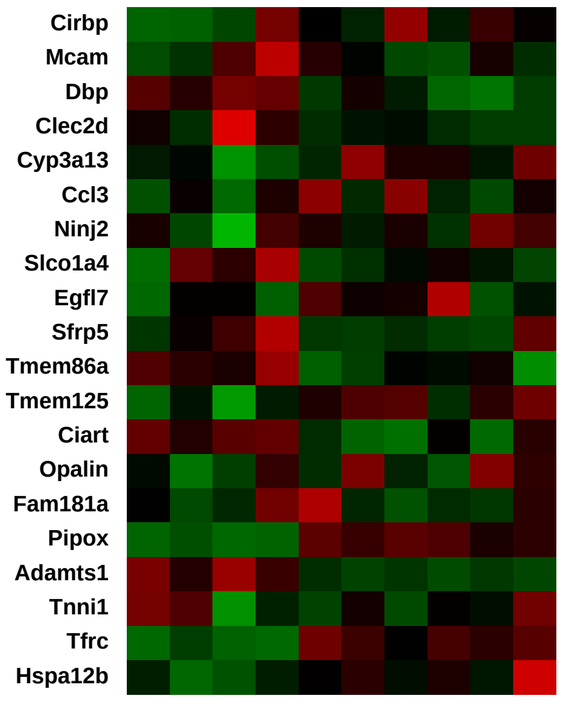

GEO Series "GSE30247" Expression Profiles

Num of samples in this series: 16

Scale of expression profile Z-scores

-3.0 -2.0 -1.0 0.0 1.0 2.0 3.0

GEO Link:	http://www.ncbi.nlm.nih.gov/geo/query/acc.cgi?acc=GSE30247
Status:	Public on Dec 21 2012
Title:	High Fat Diet Triggers SIRT1 Cleavage in Adipose Tissue Providing a Link between Dietary Stress and Metabolic Dysfunction.
Organism:	Mus musculus
Experiment type:	Expression profiling by array
Platform:	GPL1261
Pubmed ID:	22883230
Summary & Design:	**Summary:** Adipose tissue plays an important role in storing excess nutrients and preventing ectopic lipid accumulation in other organs. Obesity leads to excess lipid storage in adipocytes, resulting in the generation of stress signals and the derangement of metabolic functions. SIRT1 is an important regulatory sensor of nutrient availability in many metabolic tissues. Here we report that SIRT1 functions in adipose tissue to protect from the development of inflammation and obesity under normal feeding conditions, and the progression to metabolic dysfunction under dietary stress. Genetic ablation of SIRT1 from adipose tissue leads to gene expression changes that highly overlap with changes induced by high fat diet in wild type mice, suggesting that dietary stress signals inhibit the activity of SIRT1. Indeed, we show that high fat diet induces the cleavage of SIRT1 in adipose tissue by the inflammation-activated caspase-1, providing a link between dietary stress and predisposition to metabolic dysfunction. **Overall design:** Four replicates from four different biological conditions: 1) SIRT1 wild-type fed low fat diet, 2) SIRT1 wild-type fed high fat diet, 3) SIRT1 knock-out fed low fat diet, 4) SIRT1 knock-out fed high fat diet

Background corr dist: KL-Divergence = 0.1238, L1-Distance = 0.0283, L2-Distance = 0.0017, Normal std = 0.4093

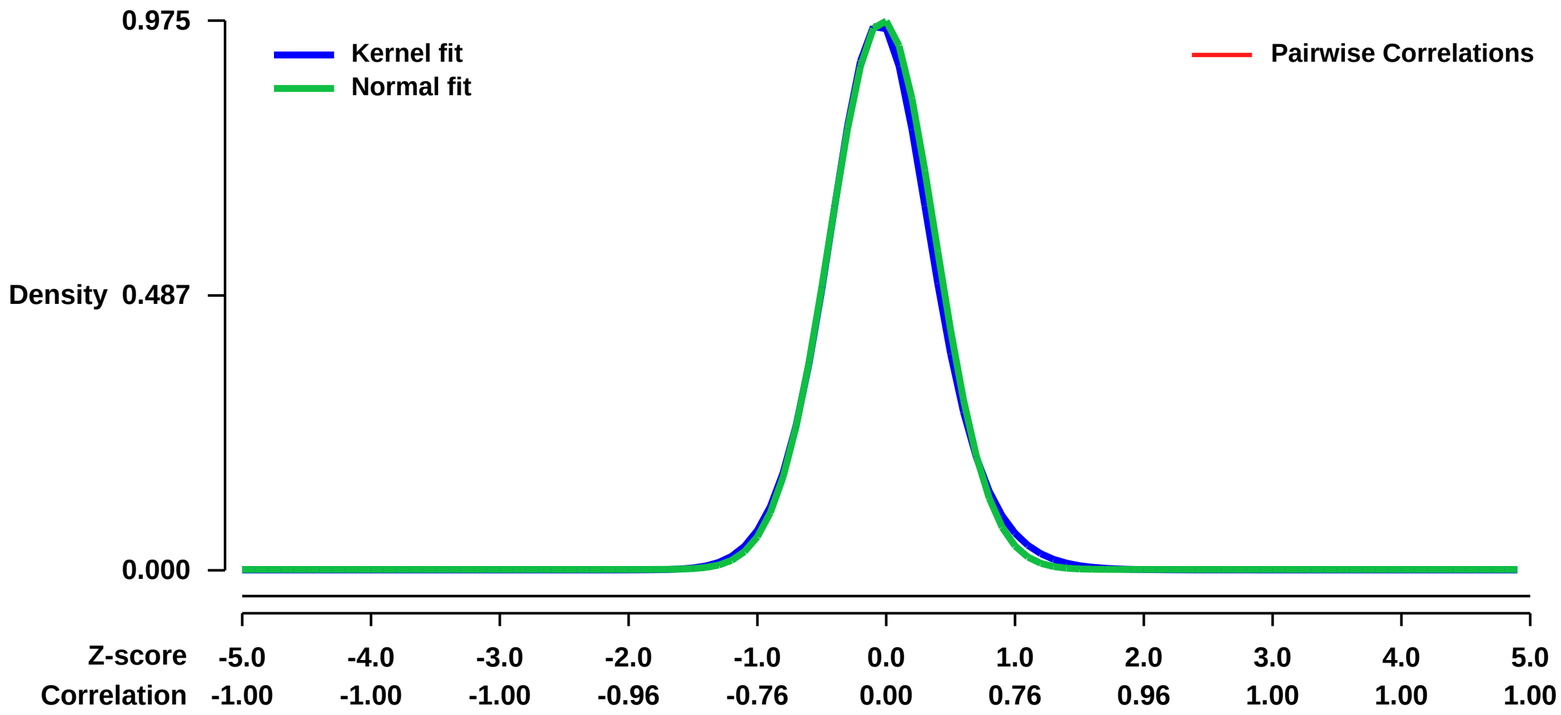

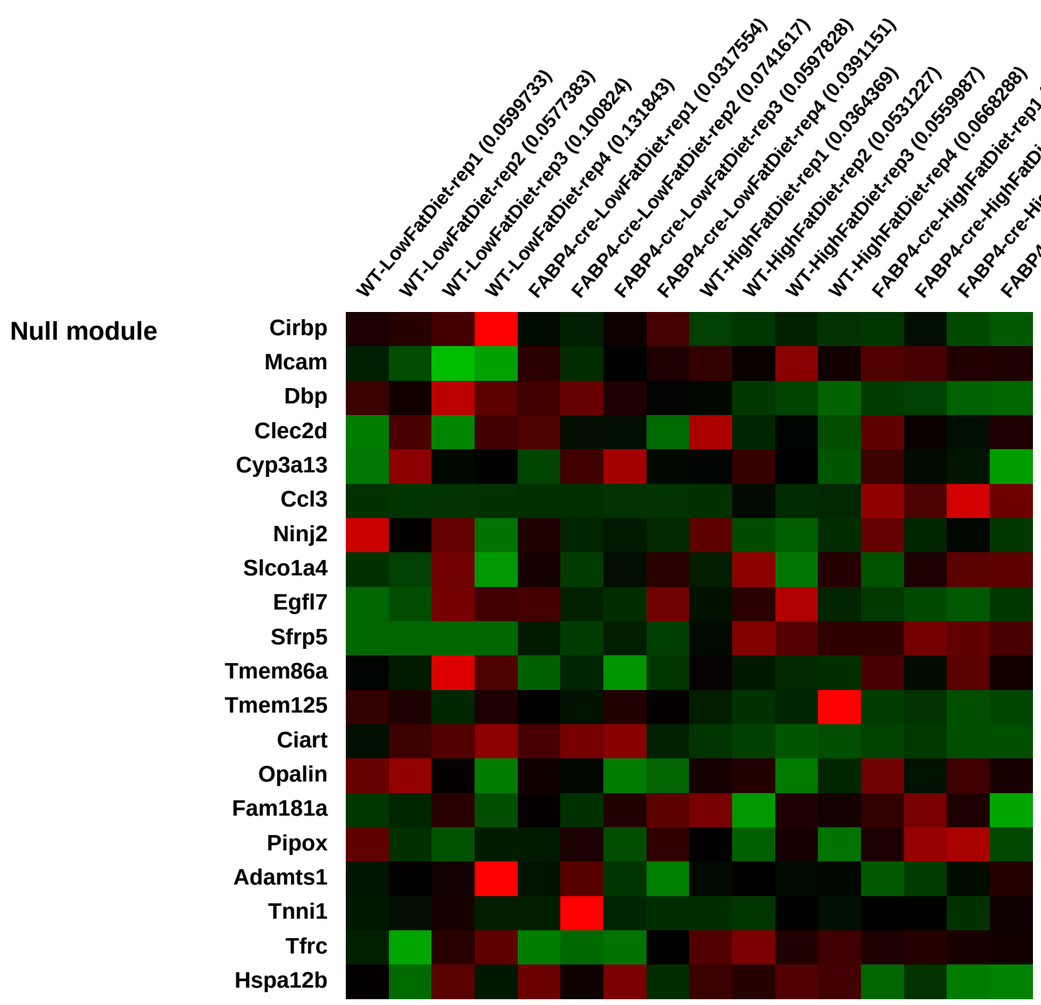

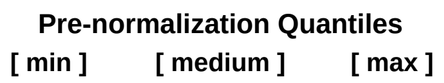

GEO Series "GSE32422" Expression Profiles

Num of samples in this series: 6

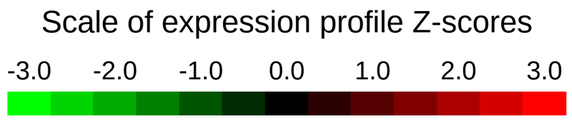

GEO Link:	http://www.ncbi.nlm.nih.gov/geo/query/acc.cgi?acc=GSE32422
Status:	Public on Jan 06 2013
Title:	Expression data from the dorsal and lateral lobes of the prostates of TRAMP mice treated with OSU-CG5
Organism:	Mus musculus
Experiment type:	Expression profiling by array
Platform:	GPL1261
Pubmed ID:	23275006
Summary & Design:	**Summary:** Cells undergoing malignant transformation often shift their cellular metabolism from primarily oxidative phosphorylation to aerobic glycolysis (the Warburg effect). Energy restriction-mimetic agents (ERMAs), such as 2-deoxyglucose and resveratrol, that target this shift in cellular metabolism have been effective in inhibiting cancer cell growth in vitro, and xenograft tumor growth in vivo. We recently developed a novel ERMA, OSU-CG5, that exhibits higher in vivo activity than previously described ERMAs. In this study, we investigated the effect of OSU-CG5 on global gene expression in the dorsal and lateral lobes of the prostate of transgenic adenocarcinoma of the mouse prostate (TRAMP) mice, and on its ability to suppress lesion progression in these mice. **Overall design:** Intact male TRAMP mice were randomized into 2 groups and treated for 4-weeks (from age 6 to 10 weeks) with a vehicle or 100 mg/kg/day OSU-CG5 via oral gavage. At the end of the study, the urogenital tracts were collected and prostates microdissected. RNA was extracted from the dorsal and lateral lobes of the prostates from 3 mice per group, and Affymetrix microarrays were performed.

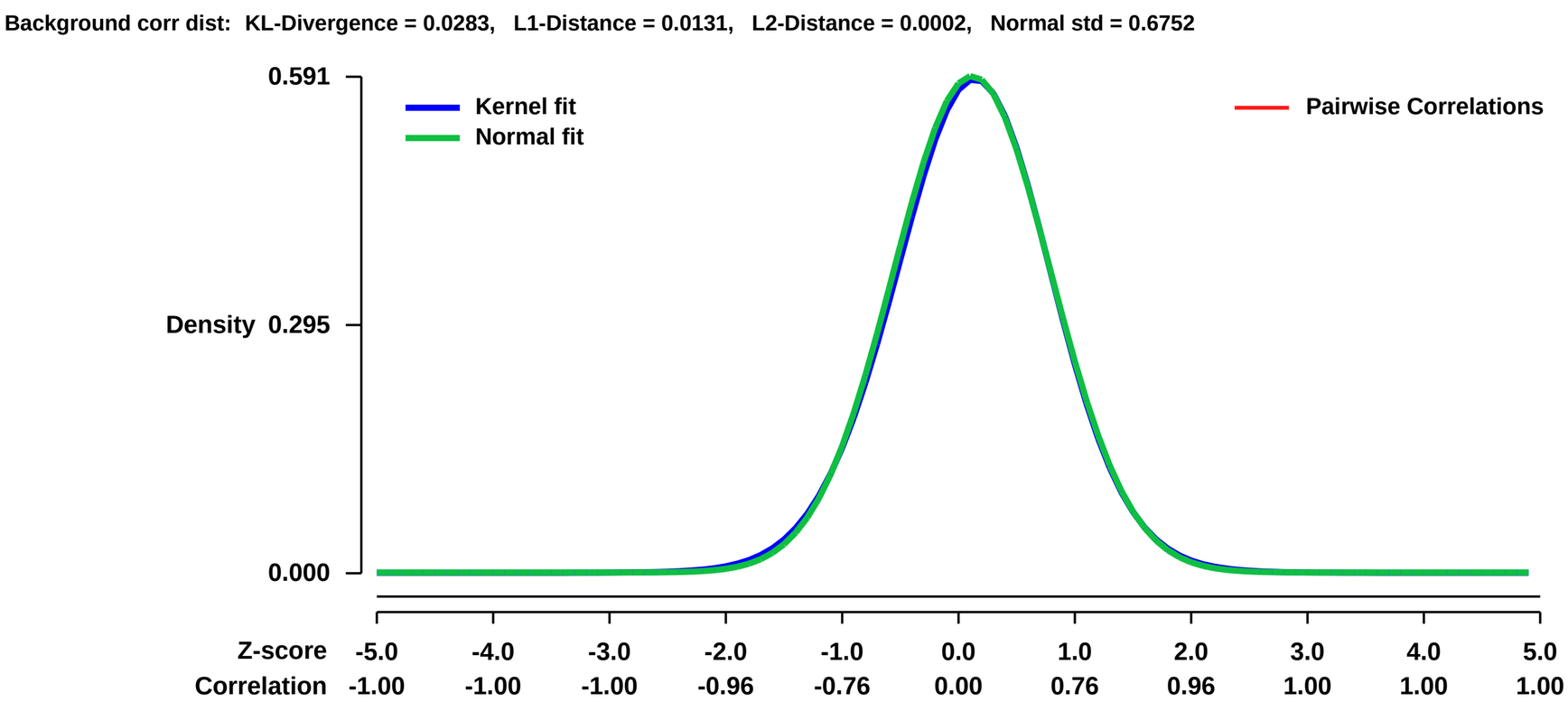

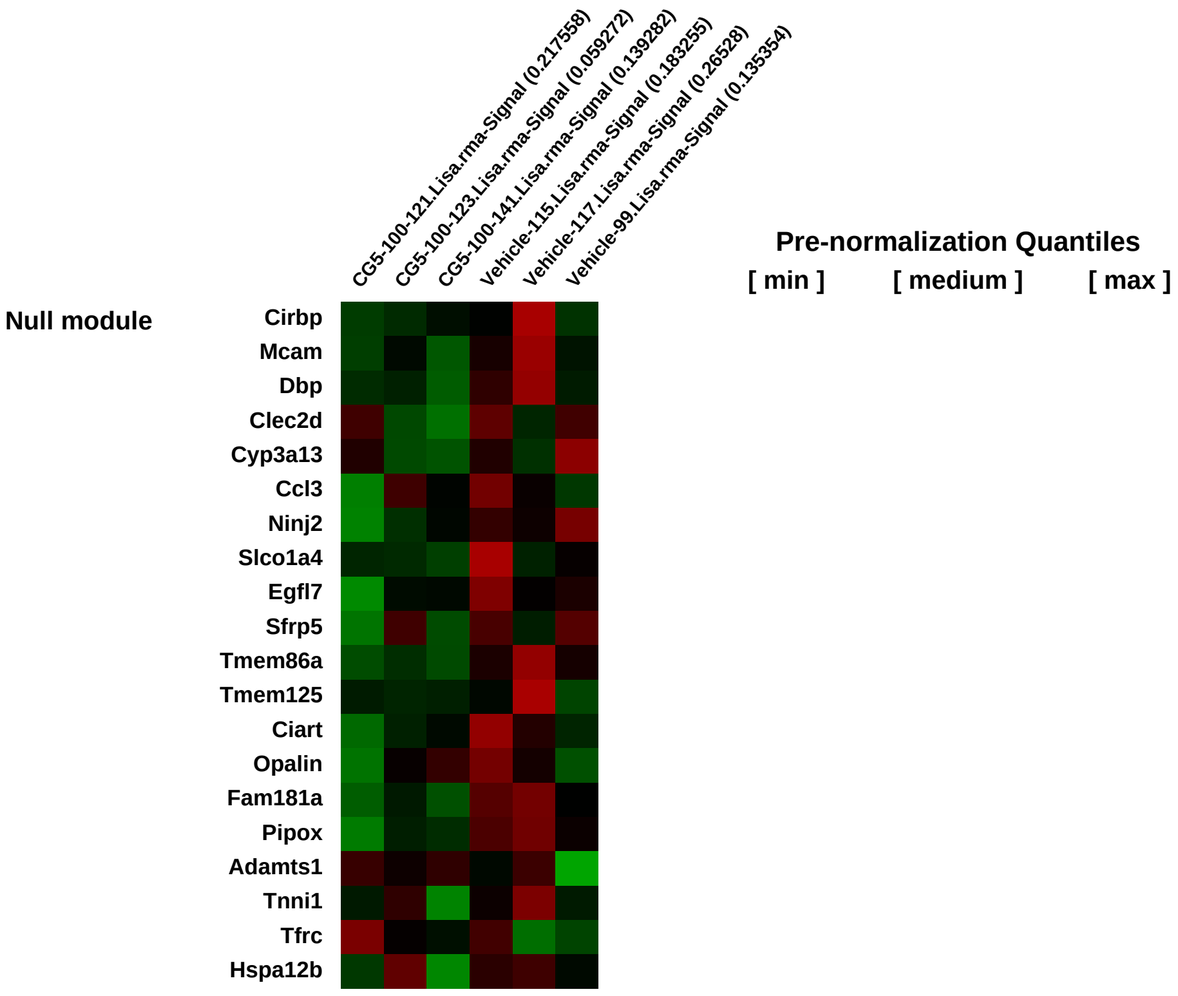

GEO Series "GSE20235" Expression Profiles

Num of samples in this series: 6

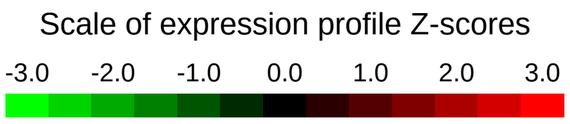

GEO Link:	http://www.ncbi.nlm.nih.gov/geo/query/acc.cgi?acc=GSE20235
Status:	Public on Aug 03 2010
Title:	RNA expression data from glomeruli lacking von Hippel-Lindau protein in podocytes
Organism:	Mus musculus
Experiment type:	Expression profiling by array
Platform:	GPL1261
Pubmed ID:	20522651
Summary & Design:	**Summary:** We and others have previously shown that glomerular endothelial cells and podocytes express hypoxia-inducible transcription factors (HIFs). HIFs bind to hypoxia response elements in target genes, such as vascular endothelial growth factor, which is continually produced by podocytes throughout life. To further assess function of HIFs in podocyte biology, podocin-Cre mice were mated with floxed von Hippel-Lindau (VHL) mice to selectively delete VHL, a component of an E3 ligase complex responsible for degradation of HIFs in normoxia. We reasoned that cells lacking VHL would overexpress stable HIFs and upregulate hypoxia-responsive genes. Progeny from these crosses displayed two phenotypes, non-proteinuric with glomerular basement membrane (GBM) defects and proteinuric with GBM defects and end-stage renal failure at ~6 months of age. Gene changes associated with the mild, non-proteinuric phenotype were studied using isolated glomeruli from wildtype and Pod-Cre fVHL mice. **Overall design:** At 4 weeks of age, urine was collected and urinary albumin was quantified by Albuwell elisa from Pod-Cre fVHL litters. At 6 weeks of age, glomeruli from 3 wildtype littermate controls and 3 non-proteinuric Pod-Cre fVHL mice were collected using the magnetic bead method. RNA was extracted and hybridized to Affymetrix microarrays.

Background corr dist: KL-Divergence = 0.0402, L1-Distance = 0.0228, L2-Distance = 0.0006, Normal std = 0.6194

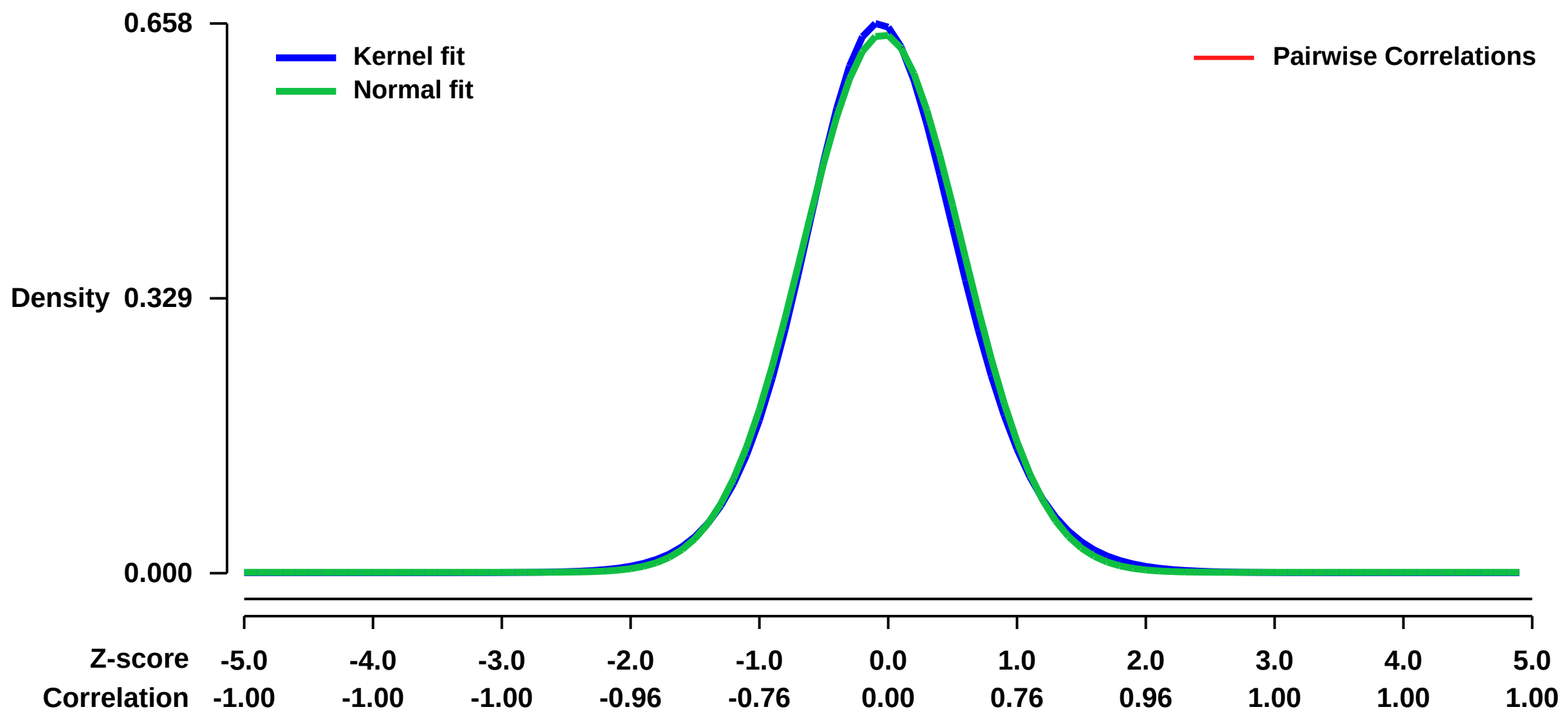

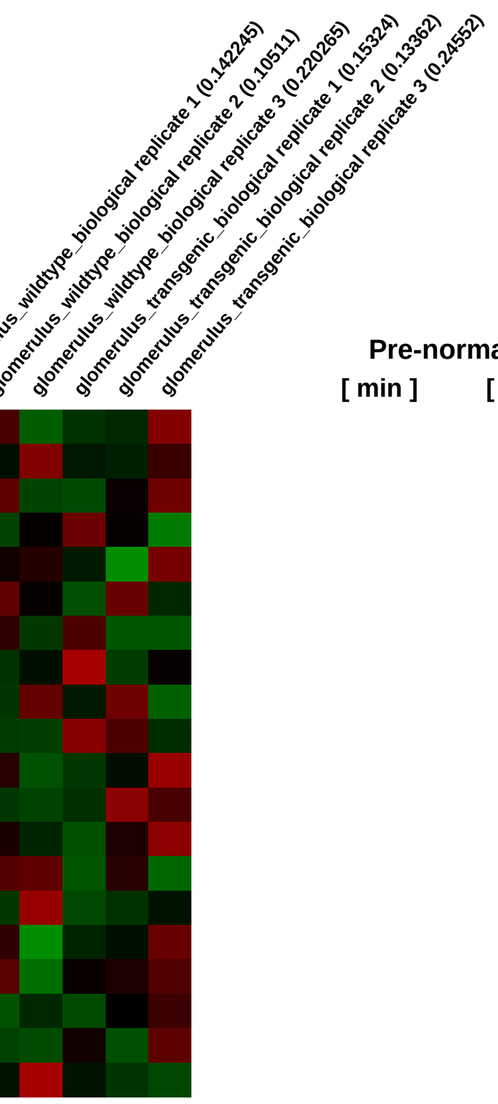

GEO Series "GSE10806" Expression Profiles

Num of samples in this series: 11

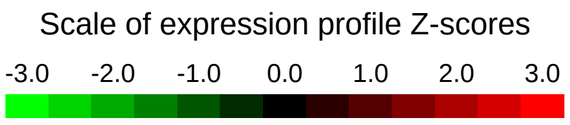

GEO Link:	**http://www.ncbi.nlm.nih.gov/geo/query/acc.cgi?acc=GSE10806**
Status:	**Public on Jun 28 2008**
Title:	**Pluripotent stem cells induced from adult neural stem cells by reprogramming with two factors**
Organism:	**Mus musculus**
Experiment type:	**Expression profiling by array**
Platform:	**GPL1261**
Pubmed ID:	**18594515**
Summary & Design:	**Summary:** **Reprogramming of somatic cells is a valuable tool to understand the mechanisms of regaining pluripotency and further opens up the possibility of generating patient-specific pluripotent stem cells. Reprogramming of mouse and human somatic cells into pluripotent stem cells, designated as induced pluripotent stem (iPS) cells, has been possible with the expression of the transcription factor quartet Oct4 (also known as Pou5f1), Sox2, c-Myc, and Klf4. Considering that ectopic expression of c-Myc causes tumourigenicity in offspring and retroviruses themselves can cause insertional mutagenesis, the generation of iPS cells with a minimal number of factors may hasten the clinical application of this approach. Here, we show that adult mouse neural stem cells express higher endogenous levels of Sox2 and c-Myc than embryonic stem cells, and that exogenous Oct4 together with either Klf4 or c-Myc are sufficient to generate iPS cells from neural stem cells. These two-factor (2F) iPS cells are similar to embryonic stem cells at the molecular level, contribute to development of the germ line, and form chimeras. We propose that, in inducing pluripotency, the number of reprogramming factors can be reduced when using somatic cells that endogenously express appropriate levels of complementing factors.** **Overall design:** **- iPS cell_4F_3**

Background corr dist: **KL-Divergence = 0.0471, L1-Distance = 0.0191, L2-Distance = 0.0004, Normal std = 0.6050**

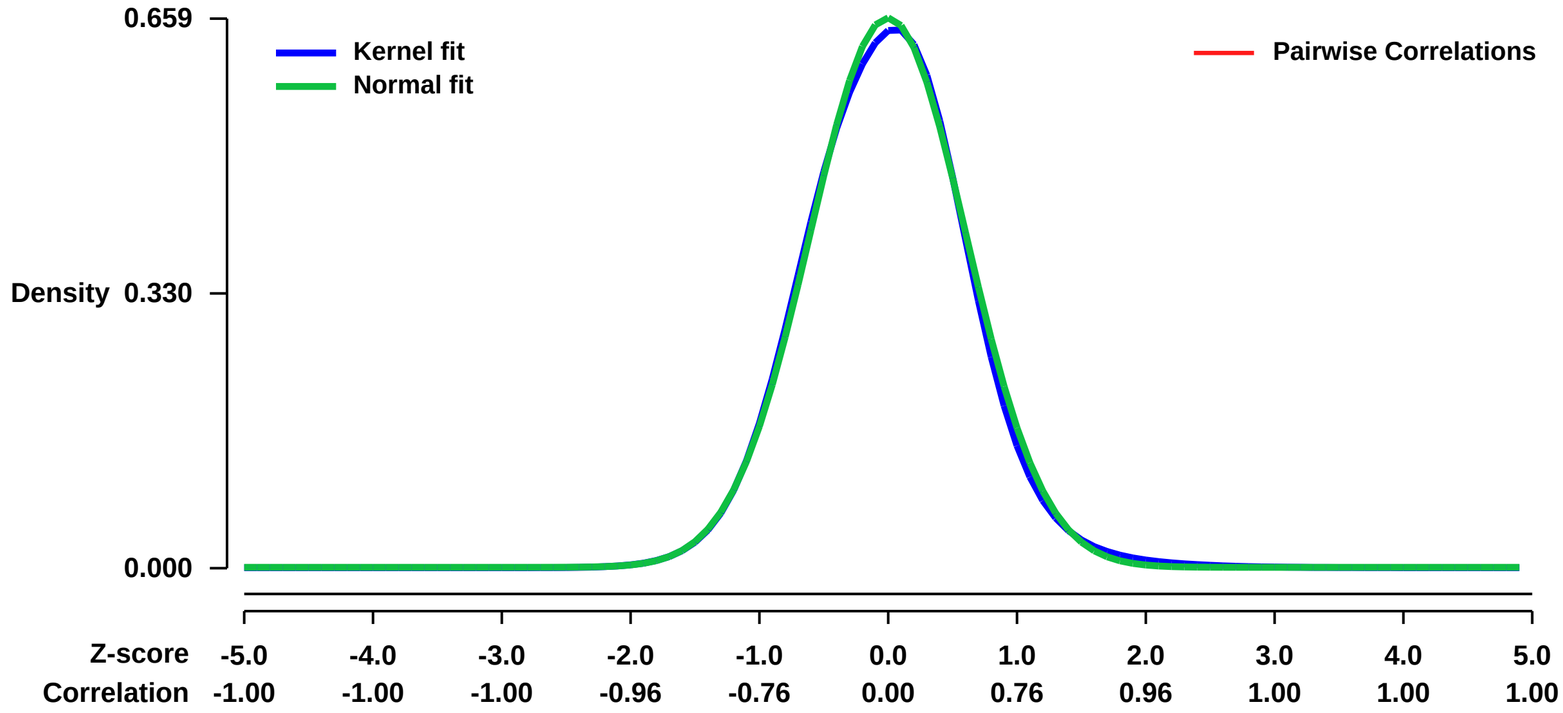

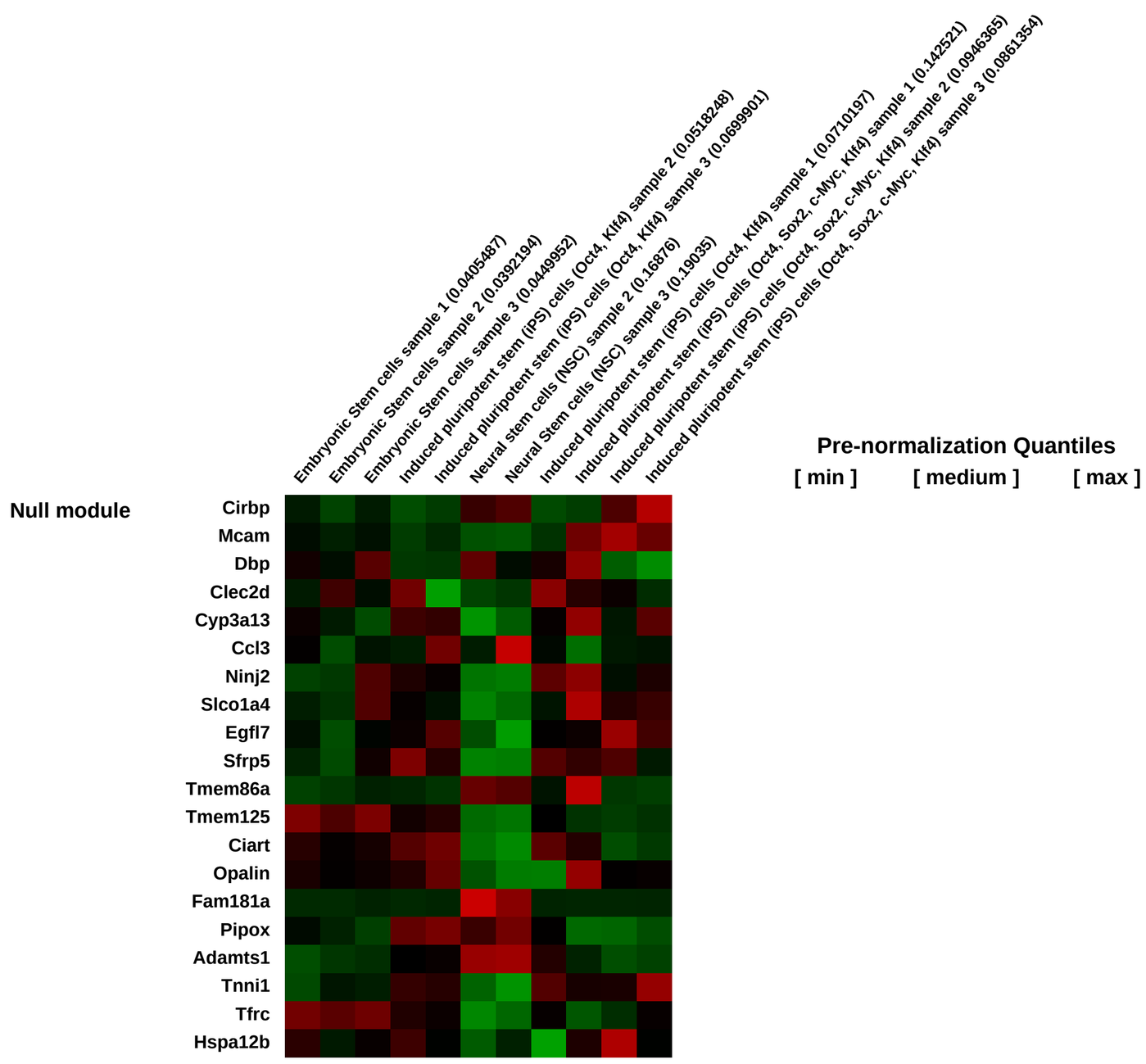

GEO Series "GSE11898" Expression Profiles

Num of samples in this series: 9

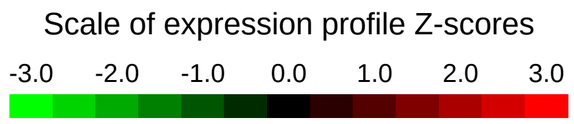

GEO Link:	**http://www.ncbi.nlm.nih.gov/geo/query/acc.cgi?acc=GSE11898**
Status:	**Public on Jun 27 2008**
Title:	**Expression data from primary mesangial cells stimulated with DNA and RNA ligands**
Organism:	**Mus musculus**
Experiment type:	**Expression profiling by array**
Platform:	**GPL1261**
Pubmed ID:	**21949095**
Summary & Design:	**Summary:** **Extrarenal viral infections commonly trigger glomerulonephritis mostly in association with immune complex disease. The immunoglobulin component of immune complexes can activate glomerular cell Fc receptors but whether complexed viral nucleic acids contribute to glomerular inflammation remains unknown. Glomerular mesangial cells express TLR3 but lack TLR7-9, hence, it is unclear whether mesangial cells can recognize and respond to viral ssRNA or DNA. Here we studied the immune responses activated by 3P-RNA (5'Triphosphate RNA) and Non-CpG DNA (Double stranded DNA) in primary mesangial cells (PMC).** **We used microarrays to detail the global programme of gene expression that induced by 3P-RNA and Non-CpG DNA.** **Keywords: diffrent ligands** **Overall design:** **PMC were stimulated with 3P-RNA and Non-CpG DNA for 6 hours and then total RNA was isolated for hybridization to MOE430_2 arrays.**

Background corr dist: KL-Divergence = 0.0613, L1-Distance = 0.0257, L2-Distance = 0.0008, Normal std = 0.5353

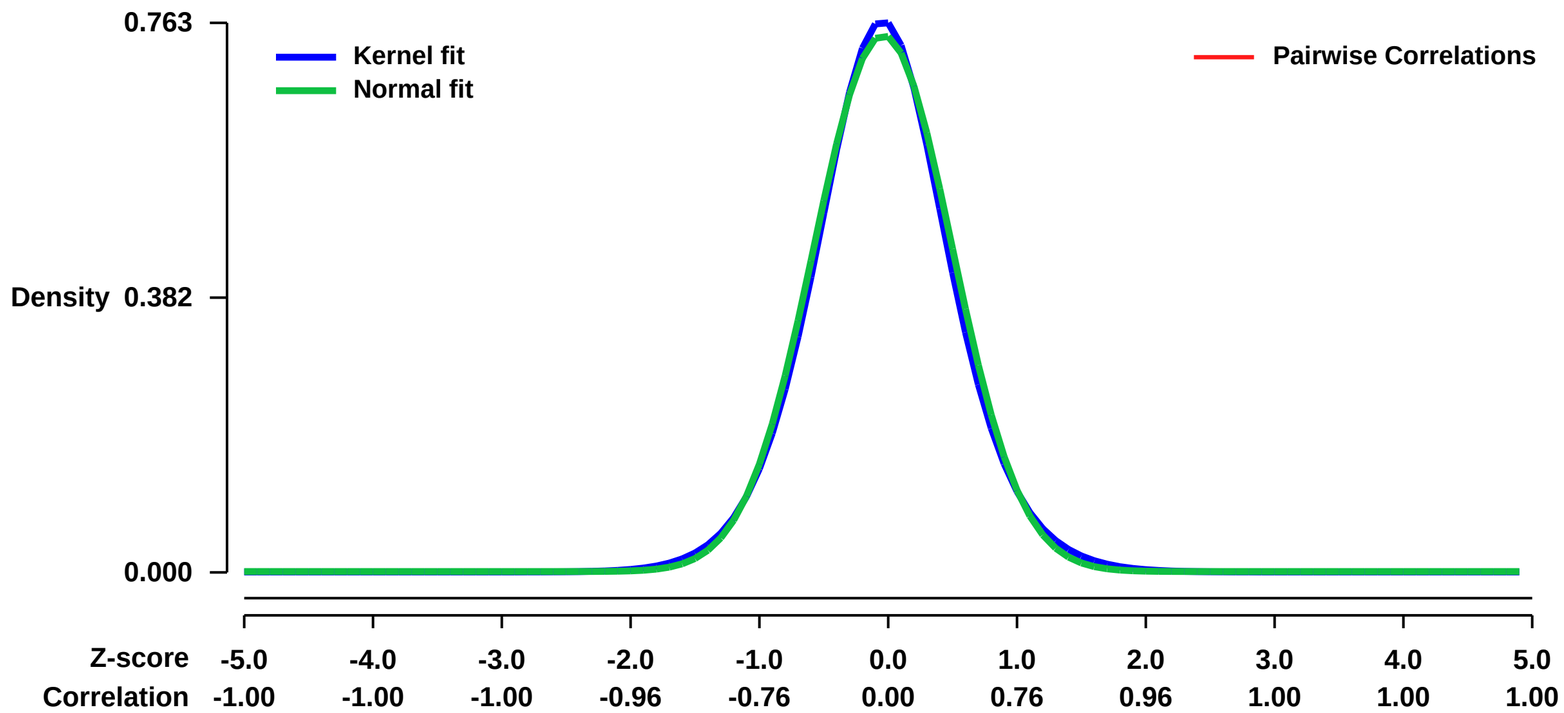

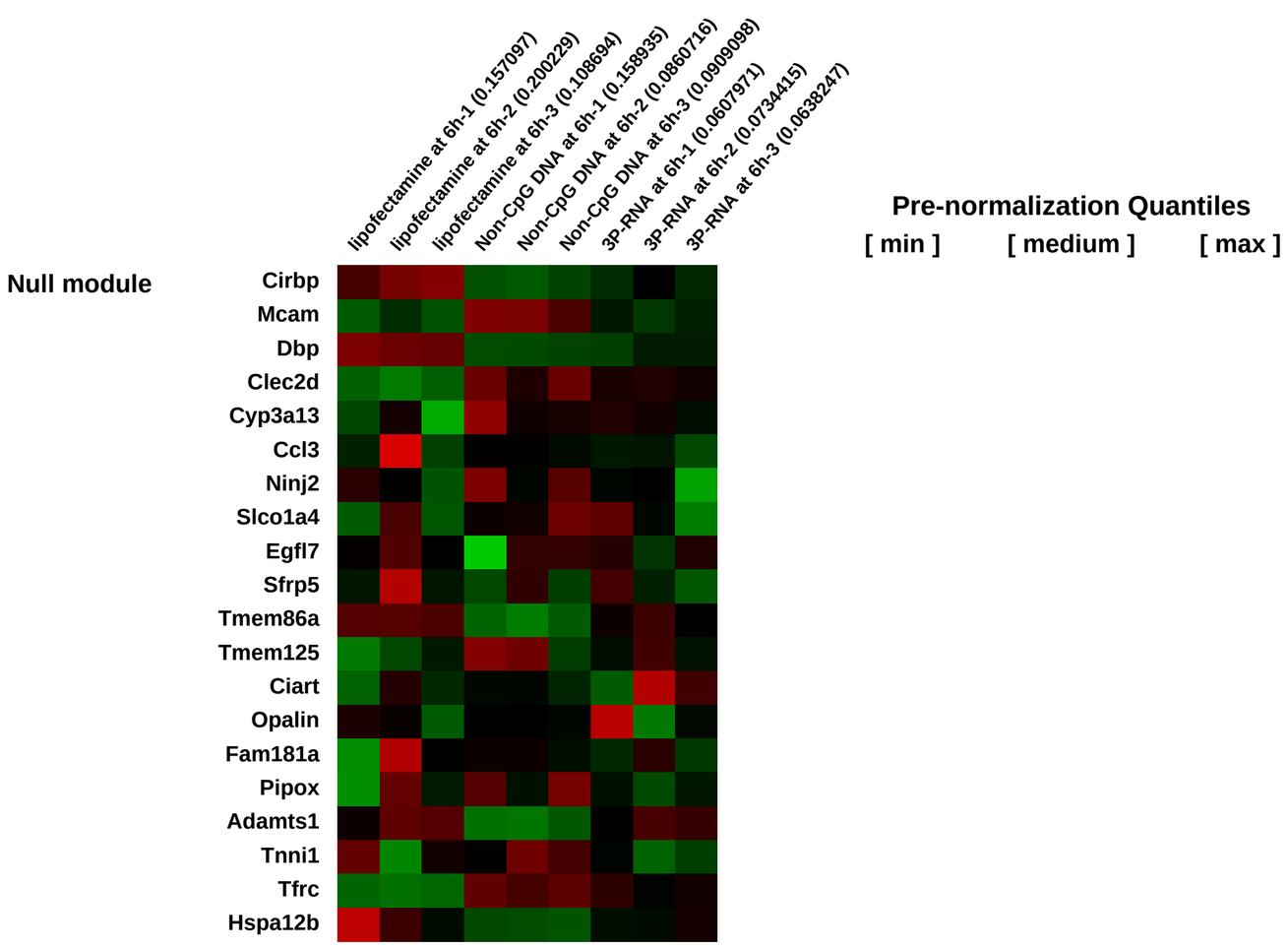

GEO Series "GSE49814" Expression Profiles

Num of samples in this series: 8

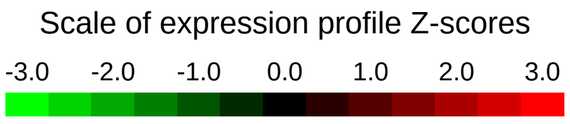

GEO Link:	http://www.ncbi.nlm.nih.gov/geo/query/acc.cgi?acc=GSE49814
Status:	Public on Oct 21 2013
Title:	Genome-wide cheater screen reveals safeguards for cell cooperation during embryogenesis
Organism:	Mus musculus
Experiment type:	Expression profiling by array
Platform:	GPL1261
Pubmed ID:	24030493

Summary & Design:

Summary:
Ensuring cooperation among formerly autonomous cells has been a central challenge in the evolution of multicellular organisms. One solution is monoclonality, but this option does not eliminate genetic and epigenetic variability, leaving room for exploitative behavior. We therefore hypothesized that embryonic development must be protected by robust regulatory mechanisms that prevent aberrant clones from superseding wild-type cells. Using a genome-wide screen in murine induced pluripotent stem cells, we identified a network of genes (centered on p53, topoisomerase 1, and olfactory receptors) whose downregulation caused the cells to replace wild-type cells, both in vitro and in the mouse embryoâ without perturbing normal development. These genes thus appear to fulfill an unexpected role in fostering cell cooperation.

Overall design:
We mixed knockdown (Top1 or p53) and mock embryonic stem cells and collected mRNA on day 4 of coculture, while cells were in the growth phase. These conditions allowed direct comparisons within a single cell type rather than a mixture of different cell types as seen under differentiation conditions. To extract information specific to cell cooperation as opposed to canonical p53 and Top1 functions, we compared results obtained from our mixed (1:4) culture with those obtained after mixing mRNA (also 1:4) from p53- or Top1-knockdown cells and mock cells that were grown homotypically.

Background corr dist: KL-Divergence = 0.0856, L1-Distance = 0.0220, L2-Distance = 0.0007, Normal std = 0.4642

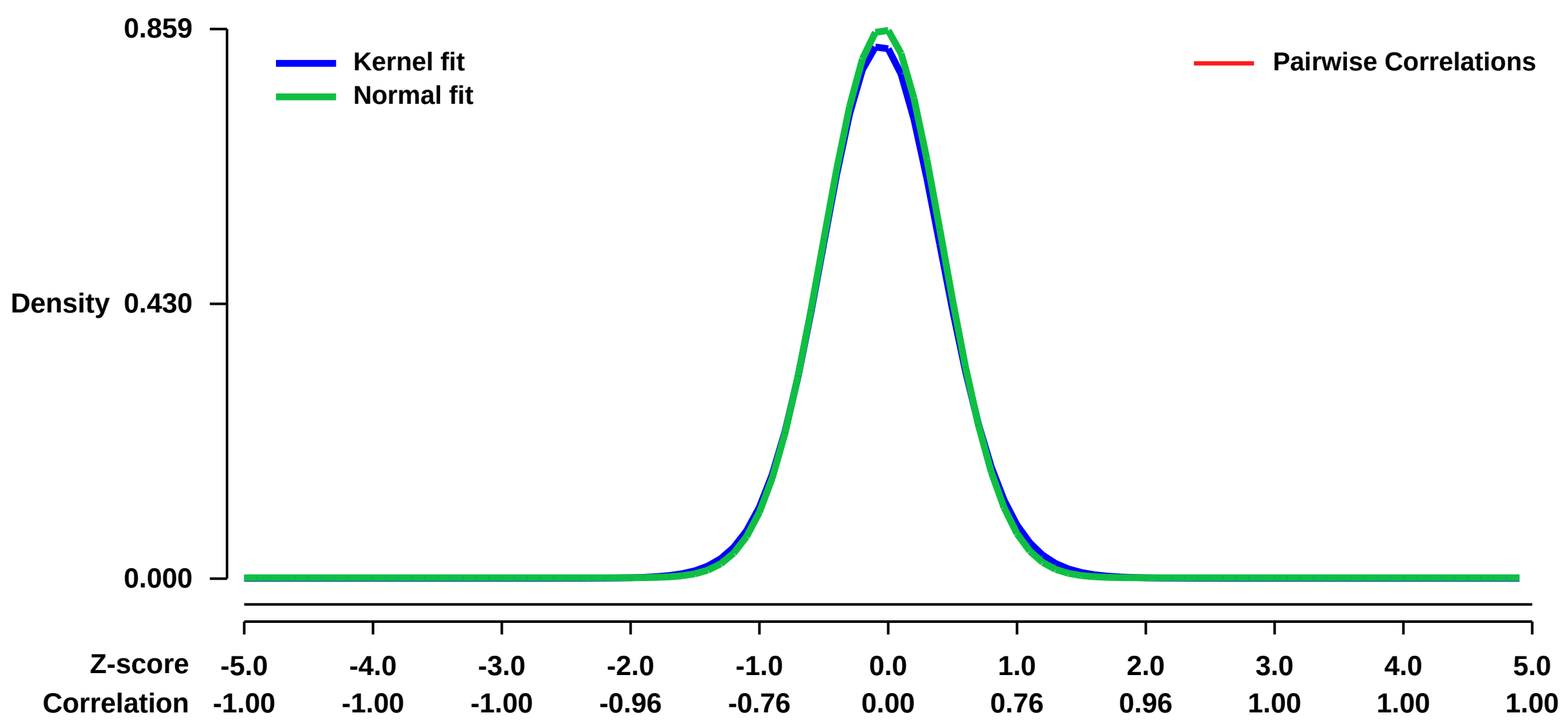

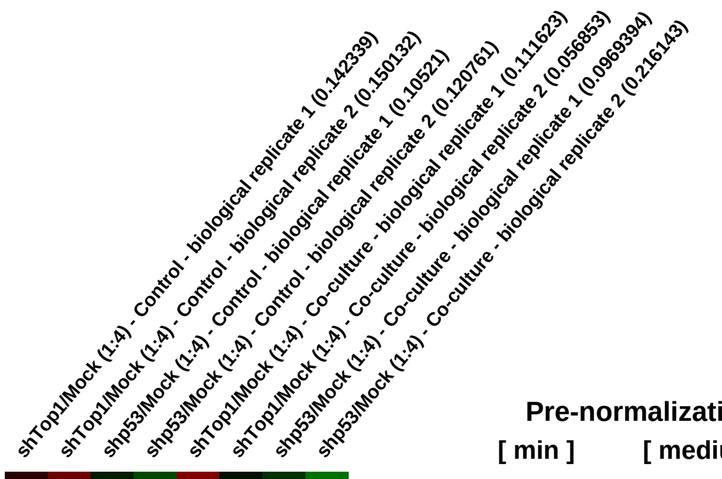

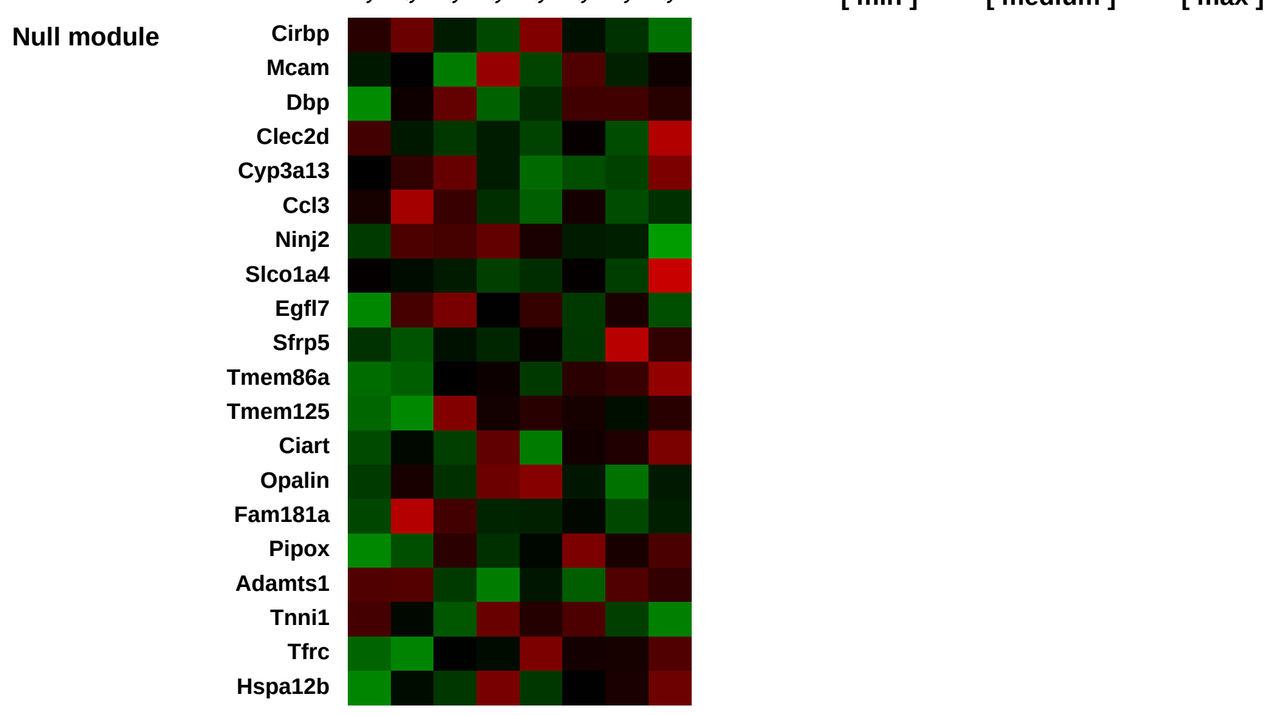

GEO Series "GSE27972" Expression Profiles

Num of samples in this series: 6

Scale of expression profile Z-scores

-3.0 -2.0 -1.0 0.0 1.0 2.0 3.0

GEO Link: http://www.ncbi.nlm.nih.gov/geo/query/acc.cgi?acc=GSE27972
Status: Public on Dec 31 2011
Title: Mouse bone marrow-derived macrophages infected with T. gondii (Type I, RH strain) for 6 hr
Organism: Mus musculus
Experiment type: Expression profiling by array
Platform: GPL1261
Pubmed ID:

Summary & Design:

Summary:
Toxoplasma gondii is a globally distributed parasite pathogen that infects virtually all warm-blooded animals. A hallmark of immunity to acute infection is the production of IFN-¿‡ and IL-12, followed by a protective T cell response that is critical for parasite control. Naˆflve T cell activation requires both TCR stimulation and the engagement of costimulatory receptors. Because of their important function in activating T cells, the expression of co-stimulatory ligands is believed to be under tight control. The molecular mechanisms governing their induction during microbial stimulation, however, are not well understood. We found that all three strains of T. gondii (Types I, II, and III) up-regulated the expression of B7-2, but not B7-1, on the surface of mouse bone marrow-derived macrophages. This induction occurred at the transcriptional level, required active parasite invasion, and was not dependent on MyD88 or TRIF. Genome-wide transcriptional analysis comparing infected and uninfected macrophages revealed the activation of MAPK signaling in infected cells. Using specific inhibitors against MAPKs, we determined that parasite-induced B7-2 is dependent on JNK, but not ERK or p38 signaling. We also observed that T. gondii-induced B7-2 expression on human peripheral blood monocytes is dependent on JNK signaling, indicating that a common mechanism of B7-2 regulation by T. gondii may exist in both humans and mice.

We used microarrays to examine genome-wide changes in host cell gene expression during T. gondii infection at an early time point (6 hpi).

Overall design:
BMdM were mock-treated or infected with T. gondii (Type I, RH strain) at an MOI of 2 and cultured for 6 hours. Biological triplicates were performed. Total RNA was harvested and used for cDNA synthesis, labeling, and hybridization to Affymetrix mouse 430 2.0 expression arrays.

Background corr dist: KL-Divergence = 0.0242, L1-Distance = 0.0274, L2-Distance = 0.0007, Normal std = 0.7449

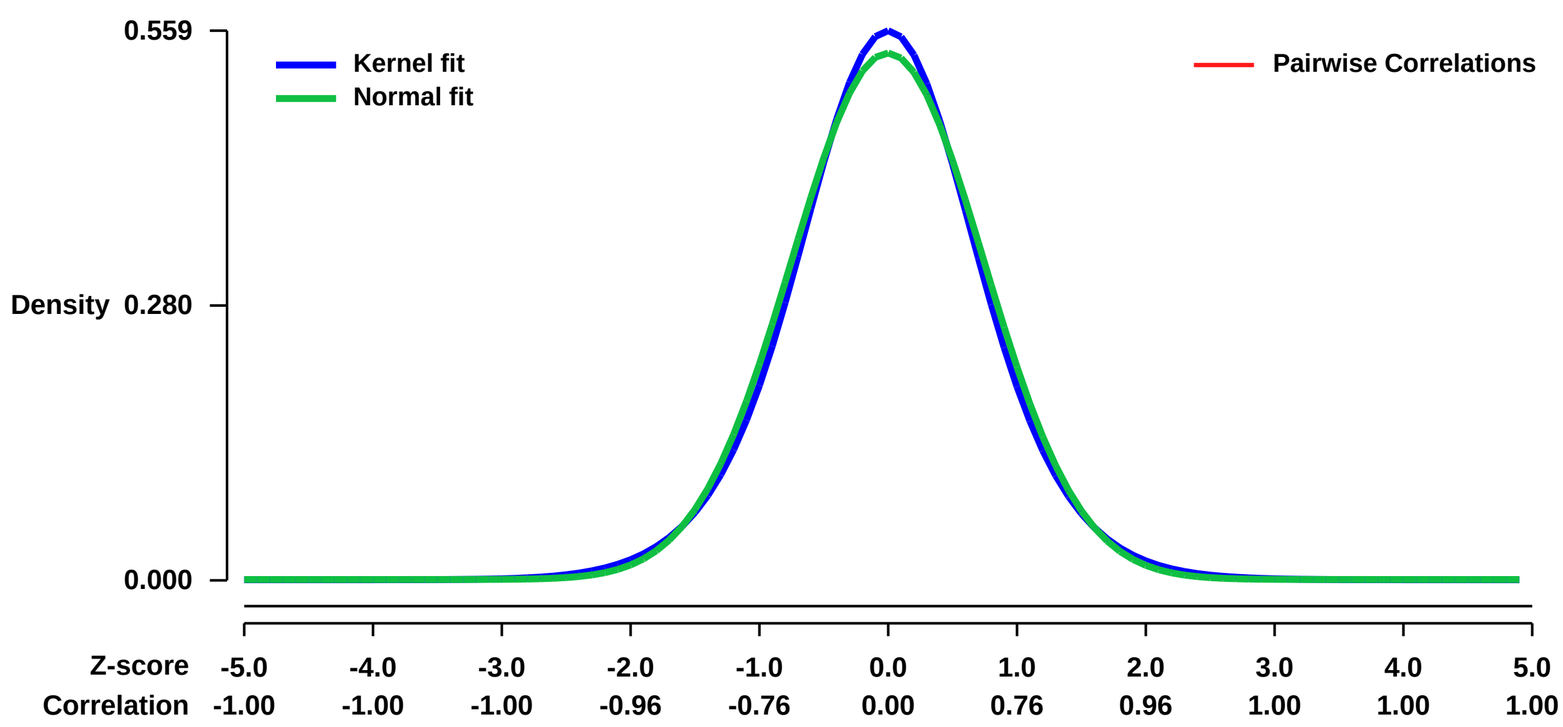

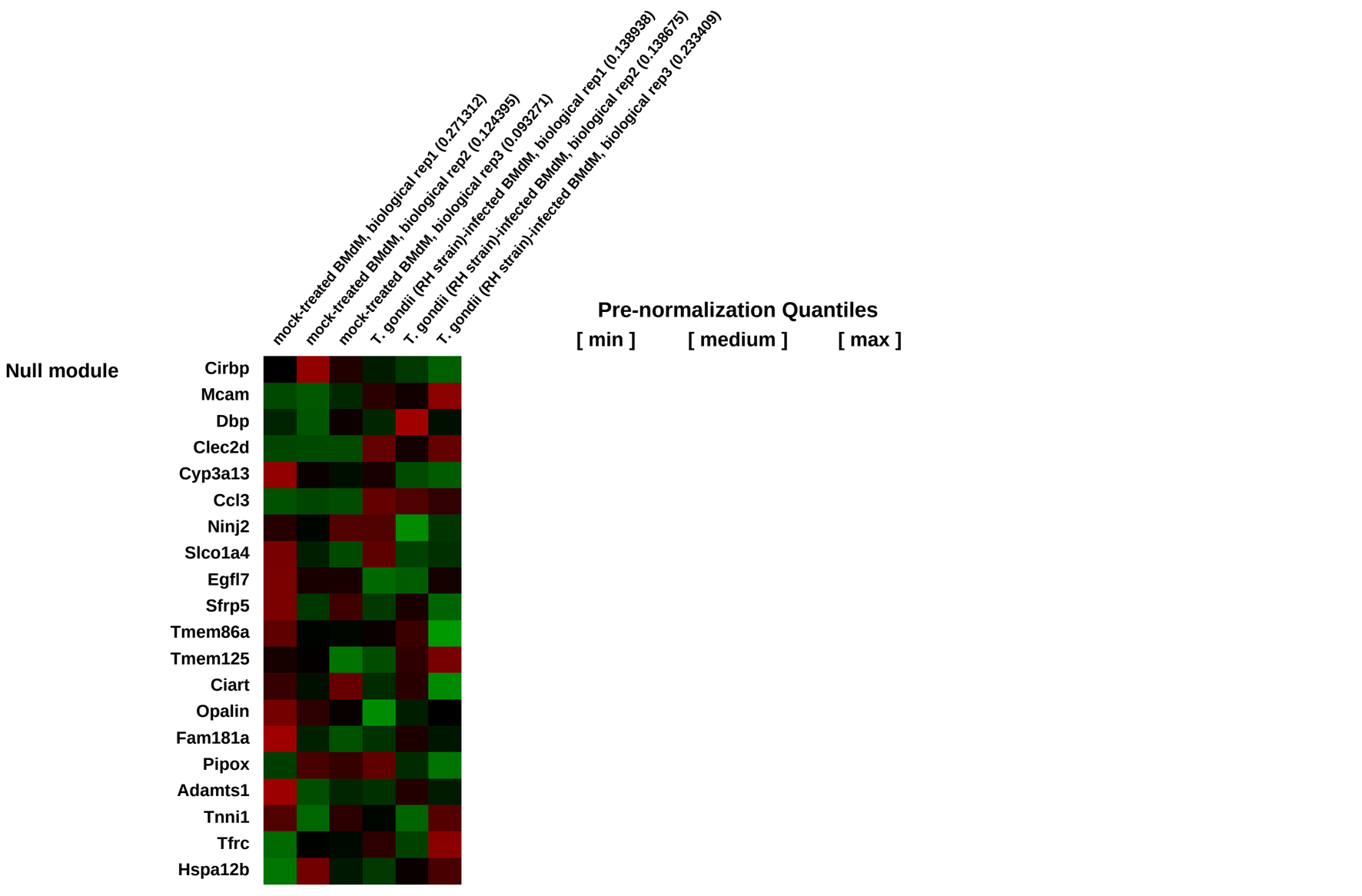

GEO Series "GSE3837" Expression Profiles

Num of samples in this series: 12

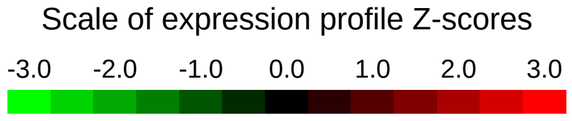

GEO Link:	http://www.ncbi.nlm.nih.gov/geo/query/acc.cgi?acc=GSE3837
Status:	Public on Oct 31 2006
Title:	Methylglyoxal treatment of MH-S cell line induces apoptosis and immune response
Organism:	Mus musculus
Experiment type:	Expression profiling by array
Platform:	GPL1261
Pubmed ID:	17183656
Summary & Design:	**Summary:** Mycobacteria-induced apoptosis of macrophages plays an important role in modulation of the host immune response involving TNF-alpha as major cytokine. The underlying mechanisms are still ill-defined. Here, we show for the first time that methylglyoxal (MG) and AGEs levels were elevated during mycobacterial infection of macrophages and that their increased levels mediated mycobacteria-induced apoptotic and immune response of macrophages. Moreover, we show that high levels of AGEs were formed at the sites of pulmonary tuberculosis. This observation represents the first evidence of the potential involvement of AGEs in tuberculosis and in infectious diseases in general. Global gene expression profiling of MG-treated macrophages reveals diversified potential roles of MG in cellular processes, including apoptosis, immune response, and growth regulation. The results of this study provide new insights into intervention strategies to develop therapeutic tools against infectious diseases in which MG and AGE production plays critical roles. **Keywords:** time course, replicates, immune response, apoptosis **Overall design:** MH-S cells (ATCC Number: CRL-2019), an alveolar macrophage cell line, was treated with 0.8 mM MG. At different time points after treatment (30 min, 4 h, and 8 h) the cells were harvested for total RNA preparation. As negative control the cells without treatment were included. RNA preparation was performed using Trizol method. Totally three independent experiments were performed, so that each time point consists of biological triplicates.

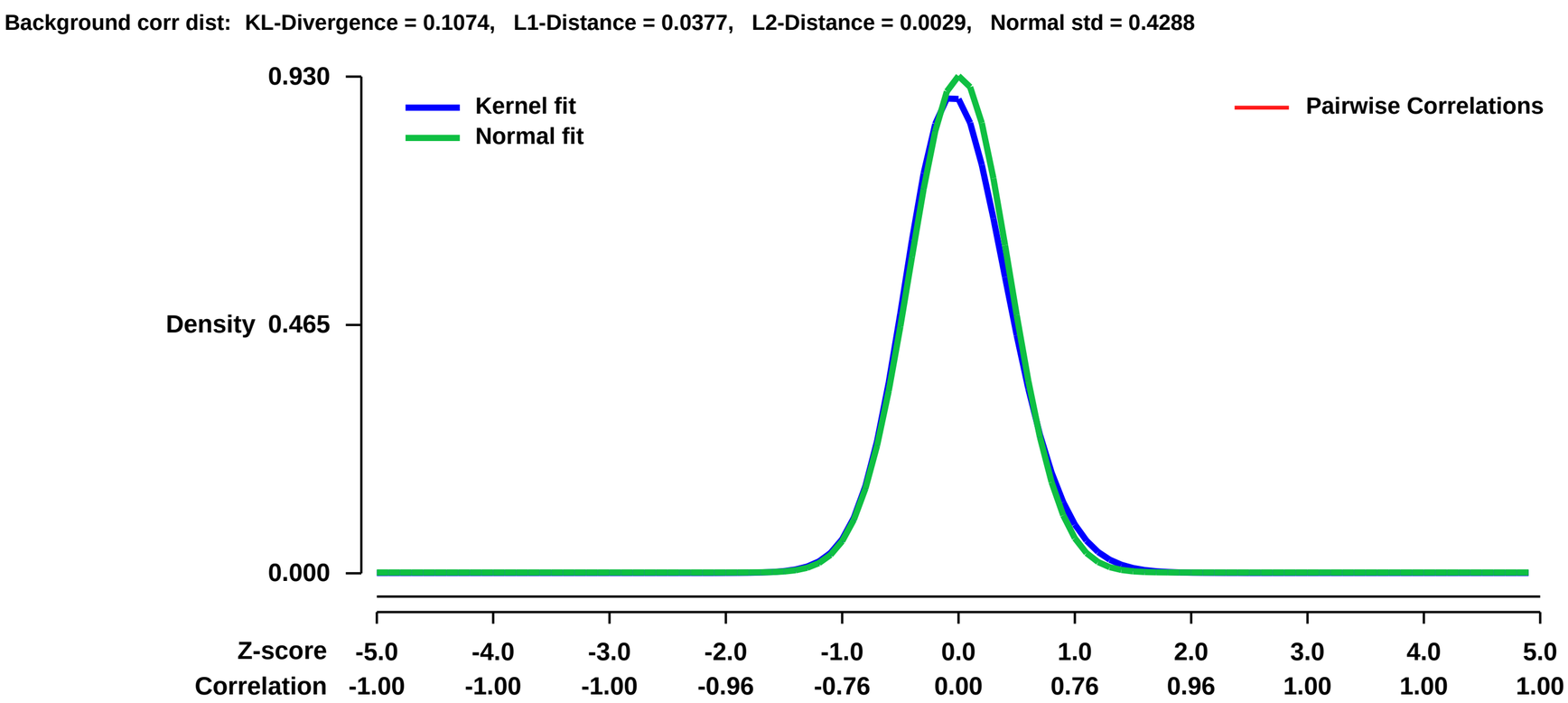

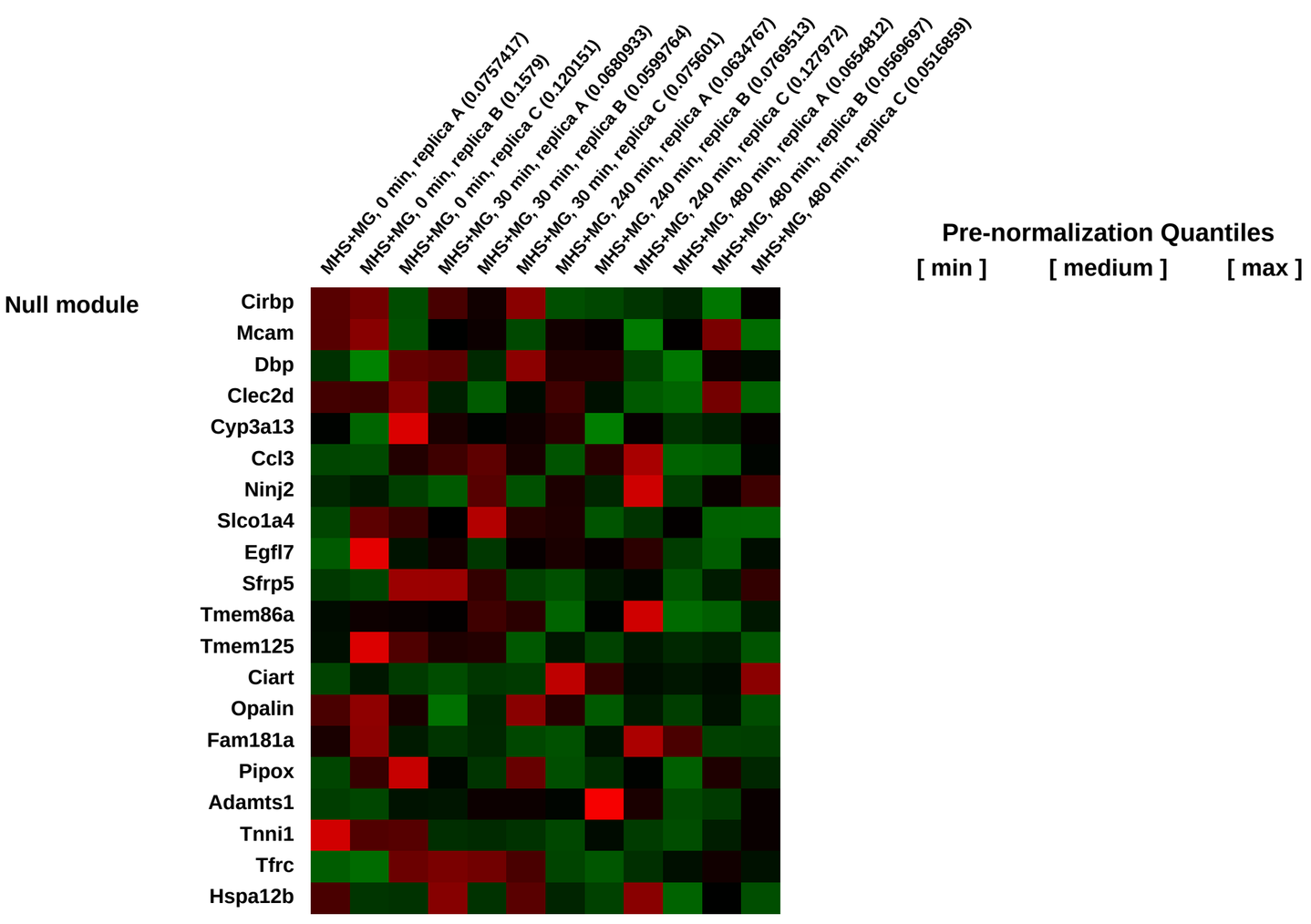

GEO Series "GSE17404" Expression Profiles

Num of samples in this series: 9

Scale of expression profile Z-scores

-3.0 -2.0 -1.0 0.0 1.0 2.0 3.0

GEO Link:	http://www.ncbi.nlm.nih.gov/geo/query/acc.cgi?acc=GSE17404
Status:	Public on Aug 10 2010
Title:	Activated AMPK and prostaglandins are involved in the response to conjugated linoleic acid and are sufficient to cause lipid reductions in adipocytes
Organism:	Mus musculus
Experiment type:	Expression profiling by array
Platform:	GPL1261
Pubmed ID:	20965713
Summary & Design:	**Summary:** Activated AMPK and prostaglandins are involved in the response to conjugated linoleic acid and are sufficient to cause lipid reductions in adipocytes. Trans-10, cis-12 conjugated linoleic acid (t10c12 CLA) reduces triglyceride levels in adipocytes. AMP-activated protein kinase (AMPK) was recently demonstrated to be involved in the emerging pathways regulating this response. This study investigated the role of AMPK and inflammation in lowering triglyceride levels by testing the following hypotheses: 1) A moderate activator of AMPK, such as metformin, and an inflammatory response are sufficient to reduce triglycerides, and 2) Strong activation of AMPK is also sufficient. These experiments were performed by adding compounds that affect these pathways and measuring their effects in 3T3-L1 adipocytes. Tumor necrosis factor ˛– (TNF-˛–), an inflammatory cytokine, increased the ability of metformin to reduce triglycerides, but TNF-˛– was observed to activate AMPK. A comparison of metformin, phenformin, TNF-˛–, and t10c12 CLA found a correlation between AMPK activity level and triglyceride reduction. Inhibitors of the prostaglandin (PG) biosynthetic pathway interfered with t10c12 CLA's ability to reduce triglycerides. Inhibitors of MAPK/ERK kinase or Jun N-terminal kinase interfered with the phosphorylation of phospholipase A2 and triglyceride reductions. Keywords: control/treatment **Overall design:** Limma data are available in the Supplementary files 'GSE17404_limma_CLAvsLA.txt', 'GSE17404_limma_PFMvsLA.txt', and 'GSE17404_limma_PFMvsCLA.txt'.

Background corr dist: KL-Divergence = 0.0361, L1-Distance = 0.0325, L2-Distance = 0.0019, Normal std = 0.6204

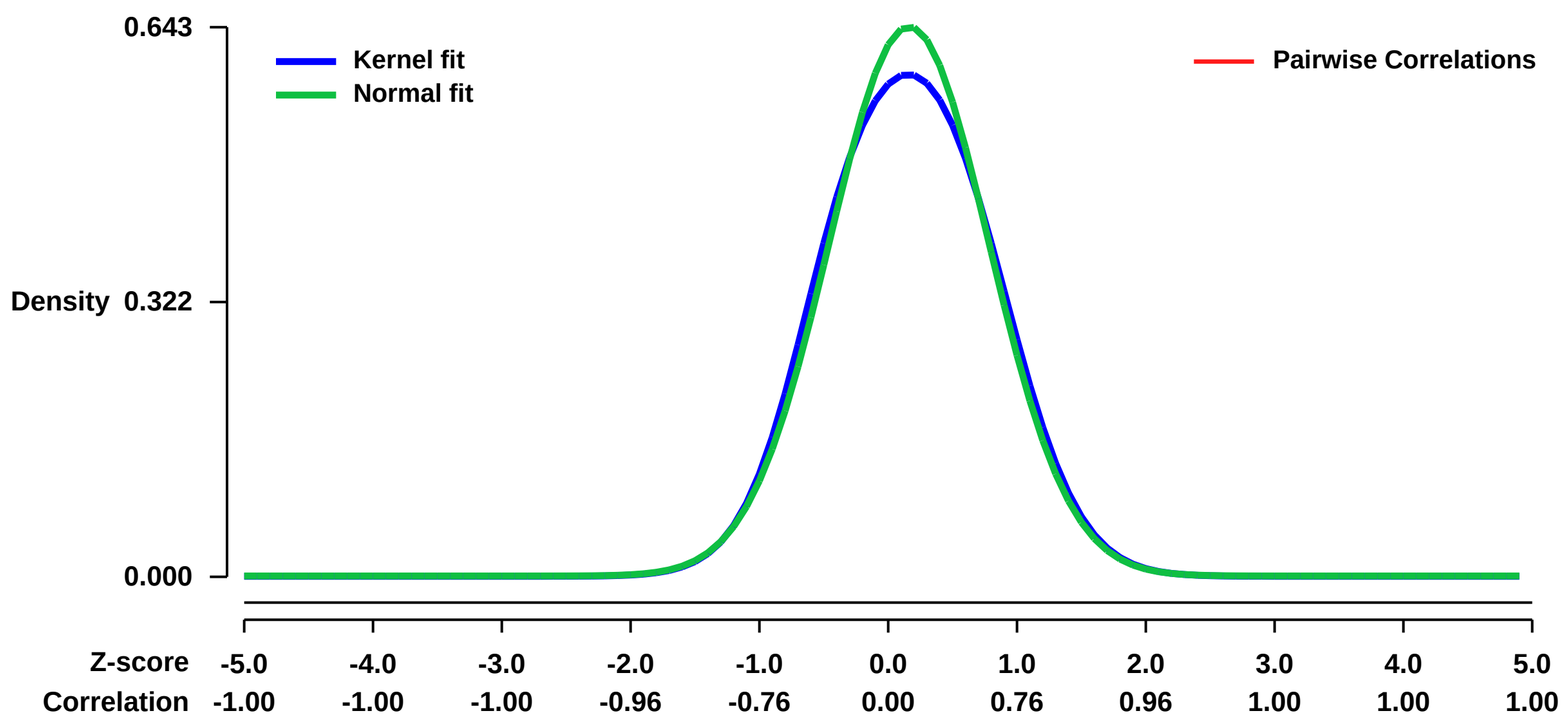

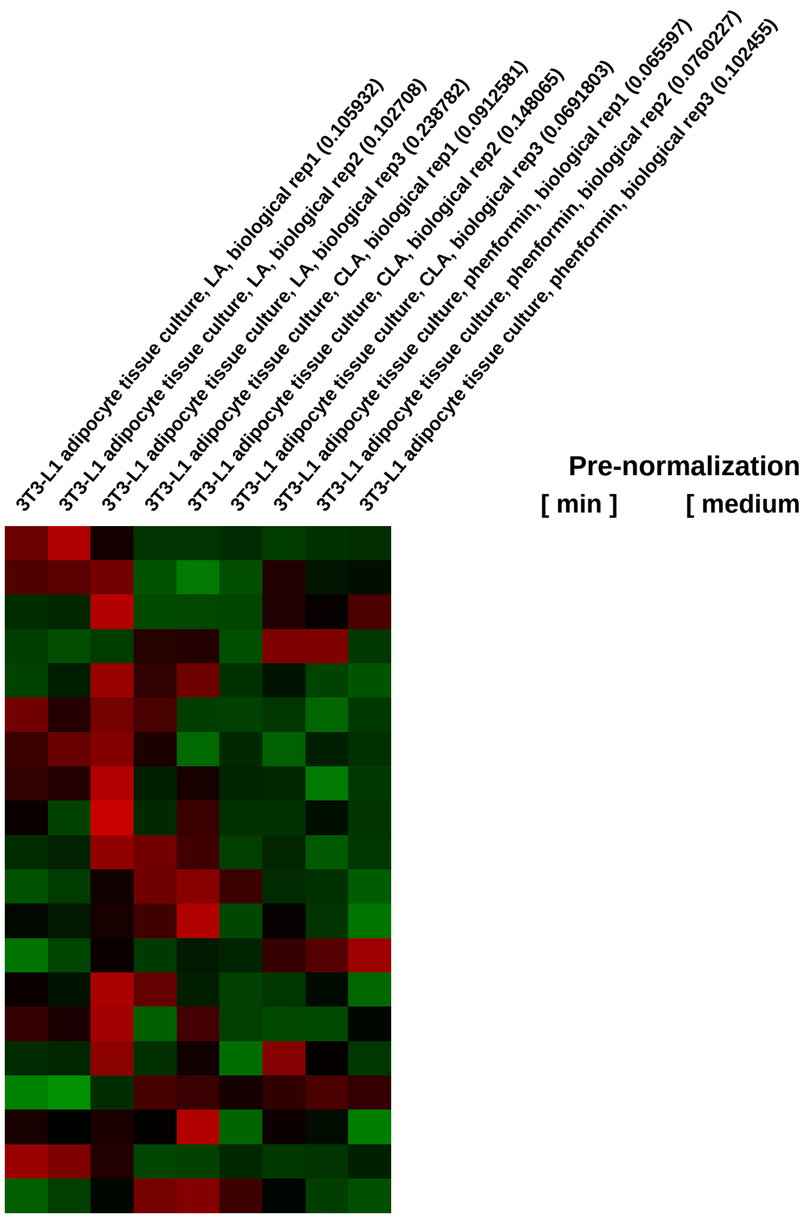

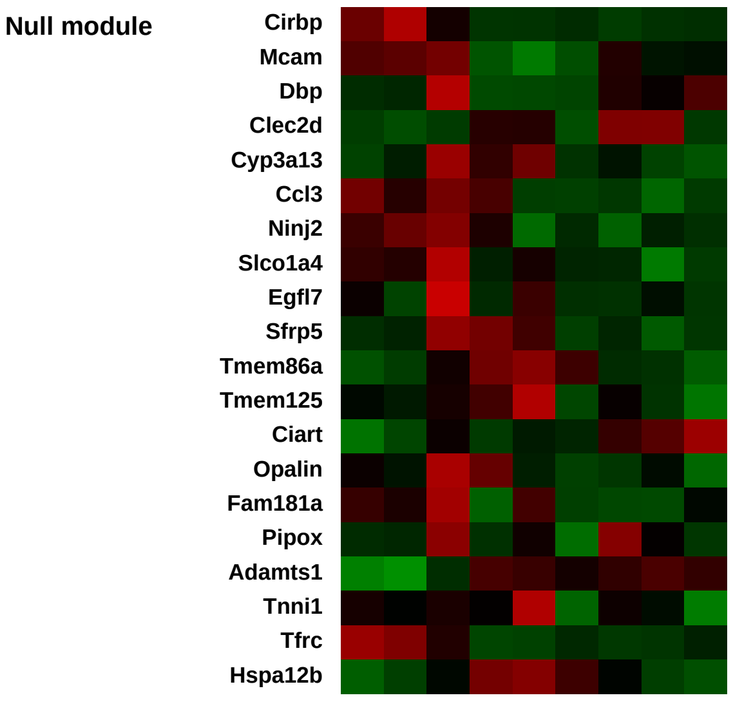

GEO Series "GSE19272" Expression Profiles

Num of samples in this series: 30

Scale of expression profile Z-scores

-3.0 -2.0 -1.0 0.0 1.0 2.0 3.0

GEO Link:	http://www.ncbi.nlm.nih.gov/geo/query/acc.cgi?acc=GSE19272
Status:	Public on Mar 01 2010
Title:	Genome-wide comparison between IL-17 and combined TNF-alpha/ IL-17 induced genes in primary murine hepatocytes
Organism:	Mus musculus
Experiment type:	Expression profiling by array
Platform:	GPL1261
Pubmed ID:	20374638
Summary & Design:	**Summary:** Cytokines such as TNF-alpha and IL-1beta are known for their contribution to inflammatory processes in liver . In contrast, the cytokine IL-17 has not yet been assigned a role in liver diseases. IL-17 can cooperate with TNF-alpha to induce a synergistic response on several target genes in different cell lines, but no data exist for primary hepatocytes. To enhance our knowledge on the impact of IL-17 alone and combined with TNF-alpha in primary murine hepatocytes a comprehensive microarray study was designed. IL-1beta was included as this cytokine is suggested to act in a similar manner as the combination of TNF-alpha and IL-17, especially with respect to its role in mRNA stabilization. Results: The present microarray analysis demonstrates that primary murine hepatocytes responded to IL-17 stimulation by upregulation of chemokines and genes, which are functionally responsible to increase and sustain inflammation. Cxcl2, Nfkbiz and Zc3h12a were strongly induced, whereas the majority of the genes were only very moderately upregulated. Promoter analysis revealed involvement of NF-kappaB in the activation of many genes. Combined stimulation of TNF-alpha/IL-17 resulted in enhanced induction of gene expression, but significantly synergistic effects could be applied only to a few genes, such as Nfkbiz, Cxcl2, Zc3h12 and Steap4. Comparison of the gene expression profile obtained after stimulation of TNF-alpha/IL-17 versus IL-1 proposed a IL-1beta-like effect of the latter cytokine combination. Moreover, evidence was provided that modulation of mRNA stability may be a major mechanism by which IL-17 regulates gene expression in primary hepatocytes. This assumption was exemplarily proven for Nfkbiz mRNA for the first time in hepatocytes. Our studies also suggest that RNA stability can partially be correlated to the existence of AU rich elements, but further mechanisms like the RNase-activity of the upregulated Zc3h12a have to be considered. Conclusions: Our microarray analysis gives new insights in IL-17 induced gene expression in primary hepatocytes highlighting the crosstalk with the NF-kappaB signalling pathway. Gene expression profile suggests IL-17 a role in sustaining liver inflammatory processes most likely by RNA stabilization. Altogether, our results provide evidence that IL-17 alone and in concert with TNF-alpha may play a role in inflammatory liver diseases. **Overall design:** Primary murine hepatocytes of three animals stimulated for 1 or 4h by TNF-alpha, IL-1beta, IL-17 or TNF-alpha followed by IL-17 were used for microarray analysis.

Background corr dist: KL-Divergence = 0.3841, L1-Distance = 0.0661, L2-Distance = 0.0122, Normal std = 0.2530

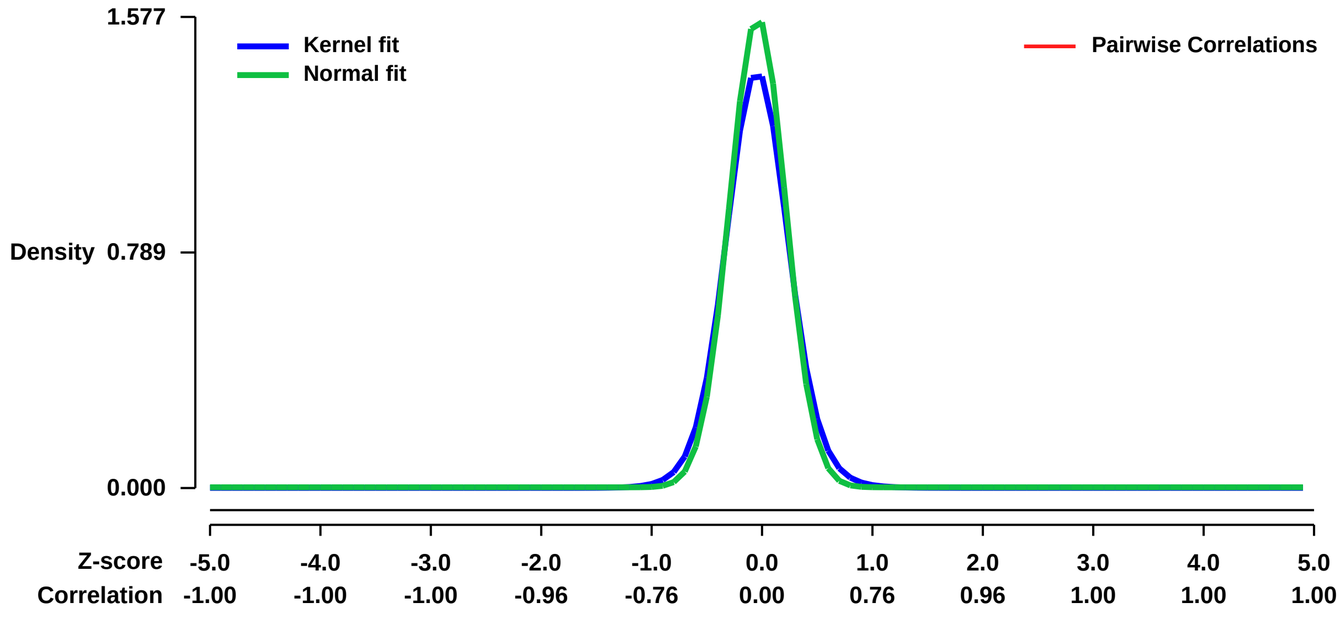

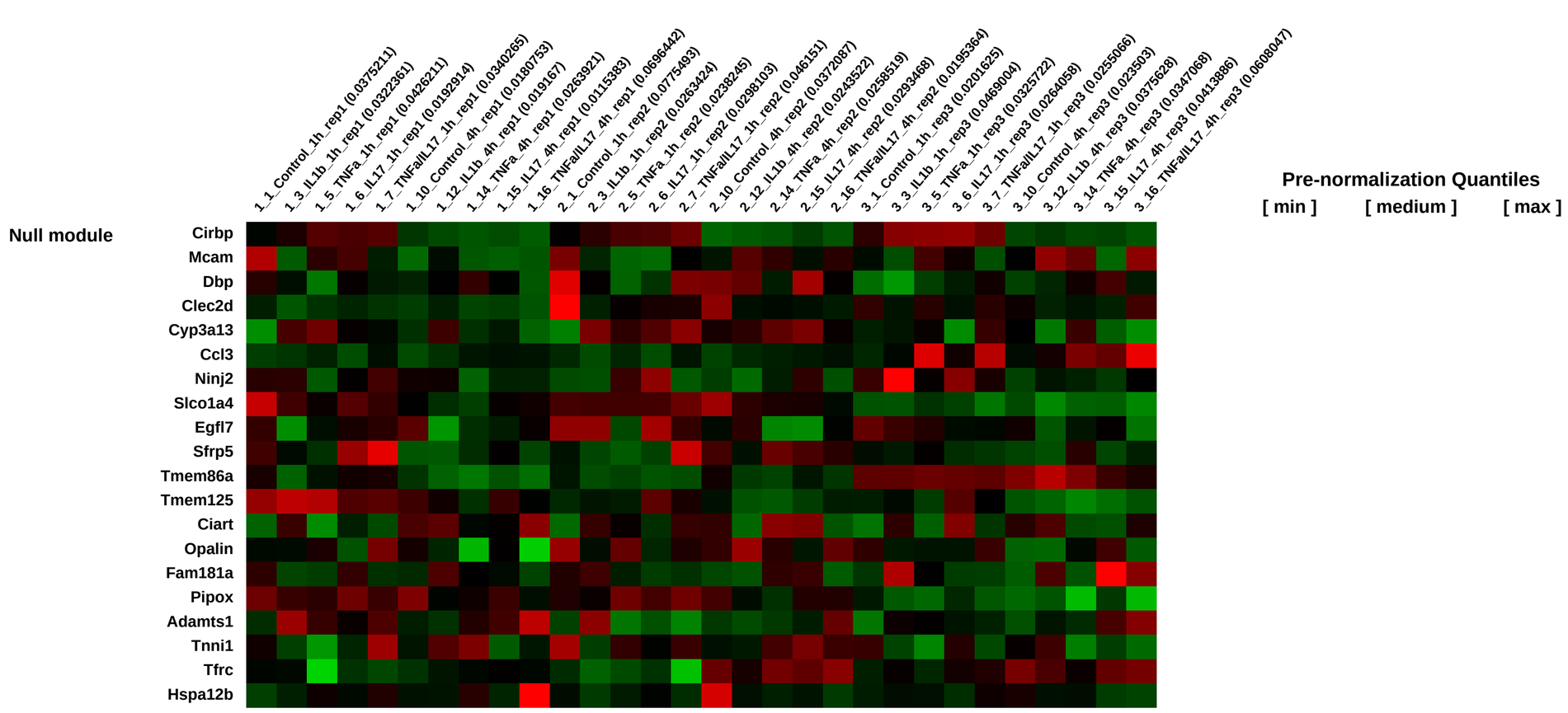

GEO Series "GSE27975" Expression Profiles

Num of samples in this series: 6

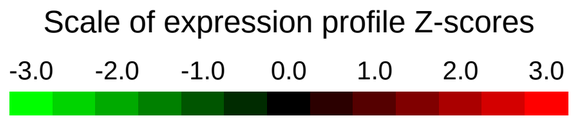

GEO Link:	http://www.ncbi.nlm.nih.gov/geo/query/acc.cgi?acc=GSE27975
Status:	Public on Mar 16 2011
Title:	HL-1 cardiomyocyte response to hypoxia
Organism:	Mus musculus
Experiment type:	Expression profiling by array
Platform:	GPL1261
Pubmed ID:	21670500
Summary & Design:	**Summary:** Expression profiling of cultured HL-1 cardiomyocytes subjected to hypoxia for 8 hours. **Overall design:** Three samples from each condition were analyzed

Background corr dist: KL-Divergence = 0.0443, L1-Distance = 0.0247, L2-Distance = 0.0007, Normal std = 0.6032

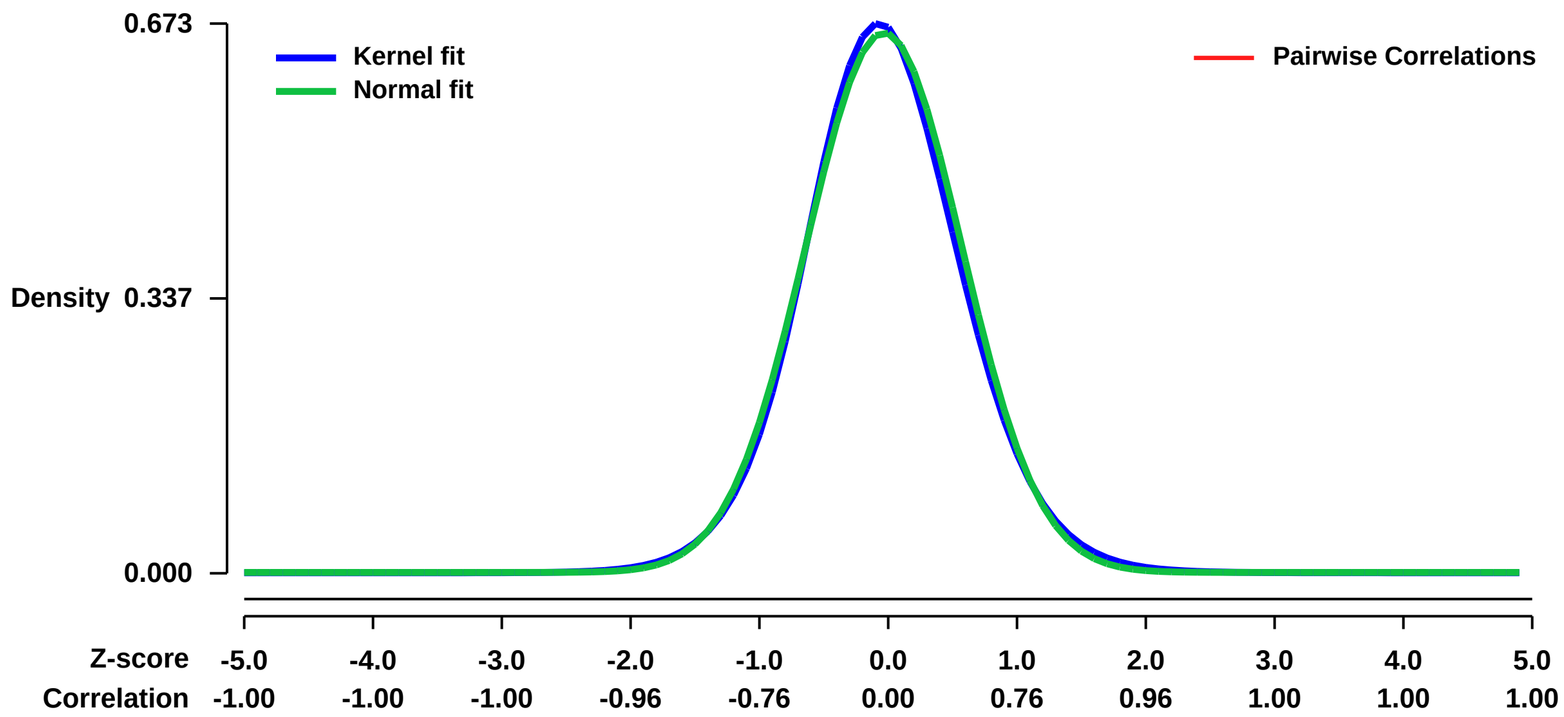

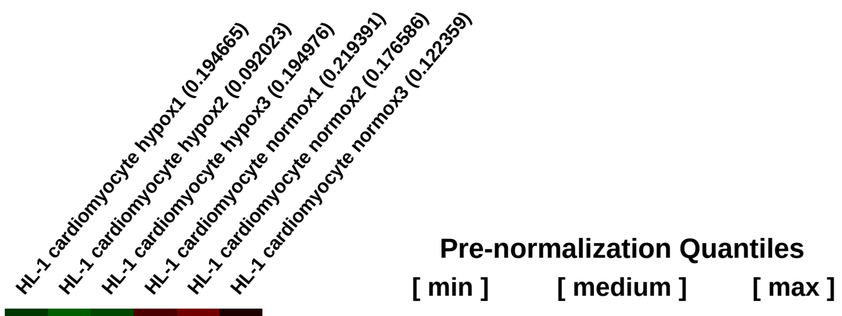

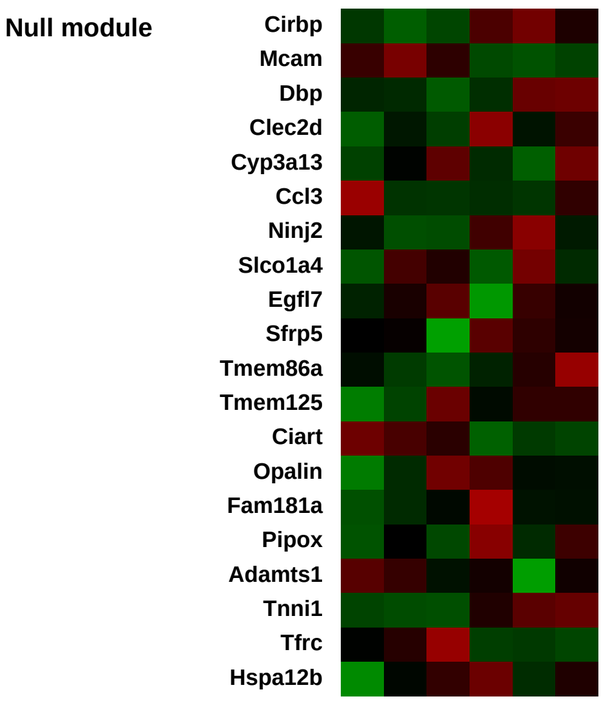

GEO Series "GSE8790" Expression Profiles

Num of samples in this series: 22

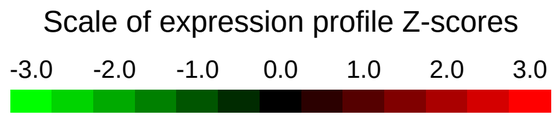

GEO Link:	**http://www.ncbi.nlm.nih.gov/geo/query/acc.cgi?acc=GSE8790**
Status:	**Public on Mar 23 2009**
Title:	**Comparative analysis of gene expression in A/J CS vs Air lungs.**
Organism:	**Mus musculus**
Experiment type:	**Expression profiling by array**
Platform:	**GPL1261**
Pubmed ID:	**19286929**
Summary & Design:	**Summary:** **We hypothesize that gene expression in the CS-exposed lungs of this strain (A/J) of mice would be able to give clues about the molecular mechanism of emphysema development, thus contributing to this phenotype. More specifically, although imbalance in oxidants/antioxidants and proteinase/antiproteinase pathways drives the pathogenesis of COPD, the molecular mechanisms involved in the development of emphysema are poorly understood. In order to test this hypothesis at the gene expression level, we utilized microarray analysis to examine transcriptional differences between CS-exposed and Air-exposed groups of mice.** **Keywords: comparative expression profiling** **Overall design:** **This study utilizes microarray analysis to test these hypotheses. Three sets of lungs were harvested from both groups at each time point (A/J - CS exposed OR Air-exposed: 5 hr, 8 days, 1.5 mos, and 6 mos). RNA was isolated and used for global gene expression profiling (Affymetrix Mouse 430 2.0 array). Statistically significant gene expression was determined as a minimum 6 counts of 9 pairwise comparisons, minimum 1.5-fold change, and p < 0.05.**

Background corr dist: KL-Divergence = 0.1293, L1-Distance = 0.0369, L2-Distance = 0.0027, Normal std = 0.3968

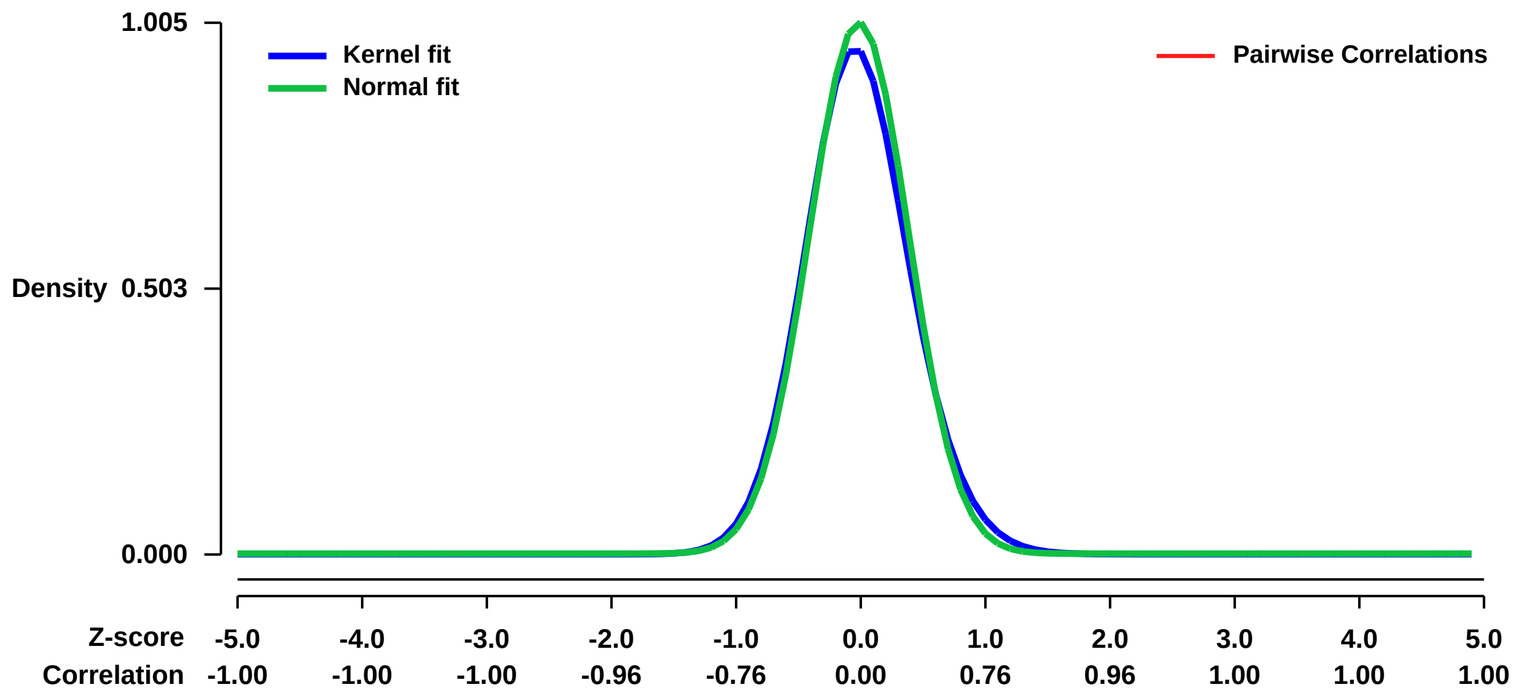

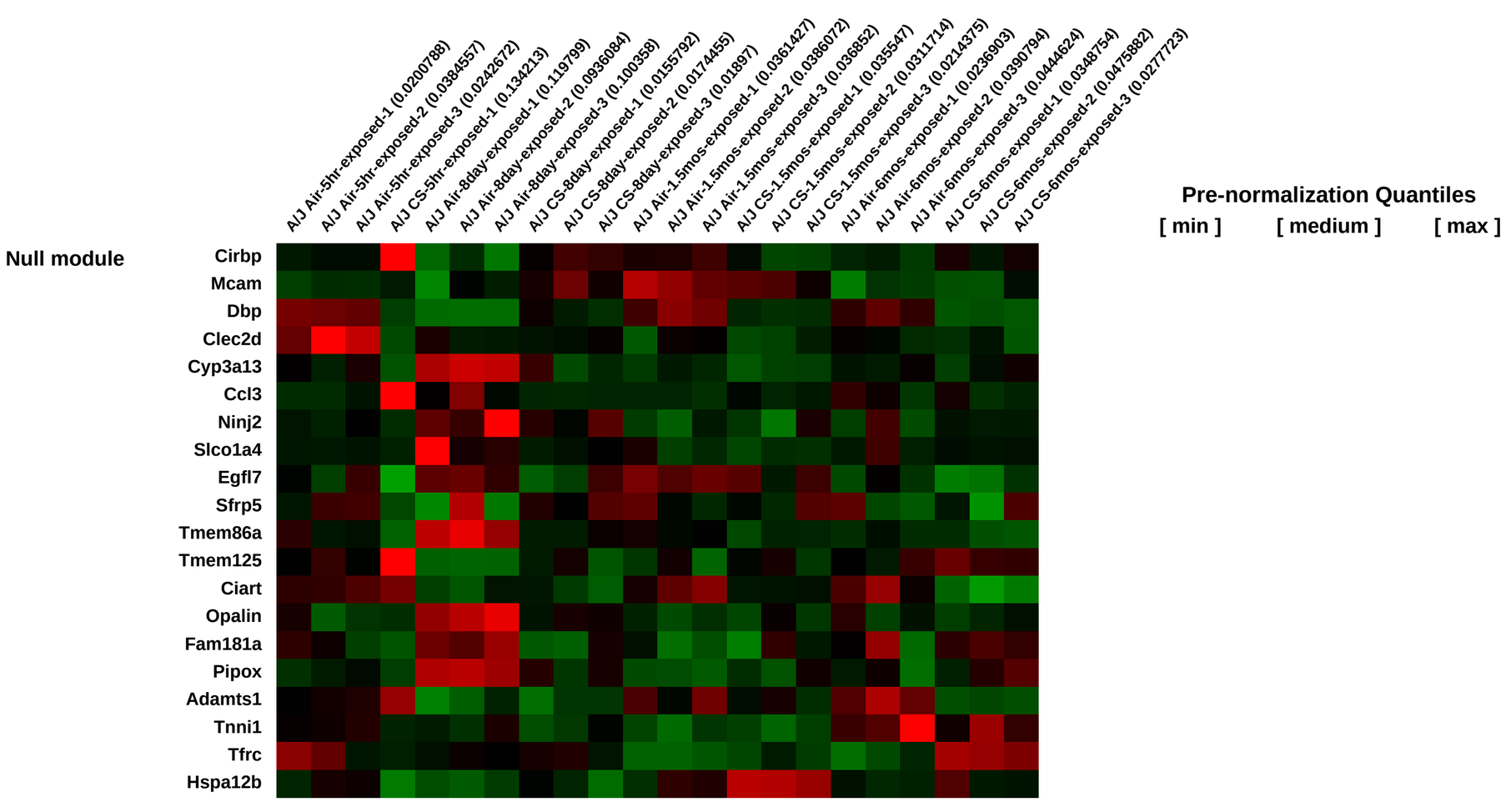

GEO Series "GSE19079" Expression Profiles

Num of samples in this series: 6

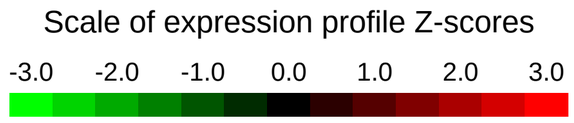

GEO Link:	**http://www.ncbi.nlm.nih.gov/geo/query/acc.cgi?acc=GSE19079**
Status:	**Public on Nov 19 2010**
Title:	**Myocardial expression data from wild-type and akt2-/- mice**
Organism:	**Mus musculus**
Experiment type:	**Expression profiling by array**
Platform:	**GPL1261**
Pubmed ID:	
Summary & Design:	**Summary:** **Wild-type (WT) C57Bl/6 and akt2-/- male mice.** **Keywords: RNA Expression Array** **Overall design:** **Left ventricles (LV) from 12-16 week-old male wild type mice and age-matched akt2-/- mice**

Background corr dist: **KL-Divergence = 0.0153, L1-Distance = 0.0204, L2-Distance = 0.0006, Normal std = 0.7977**

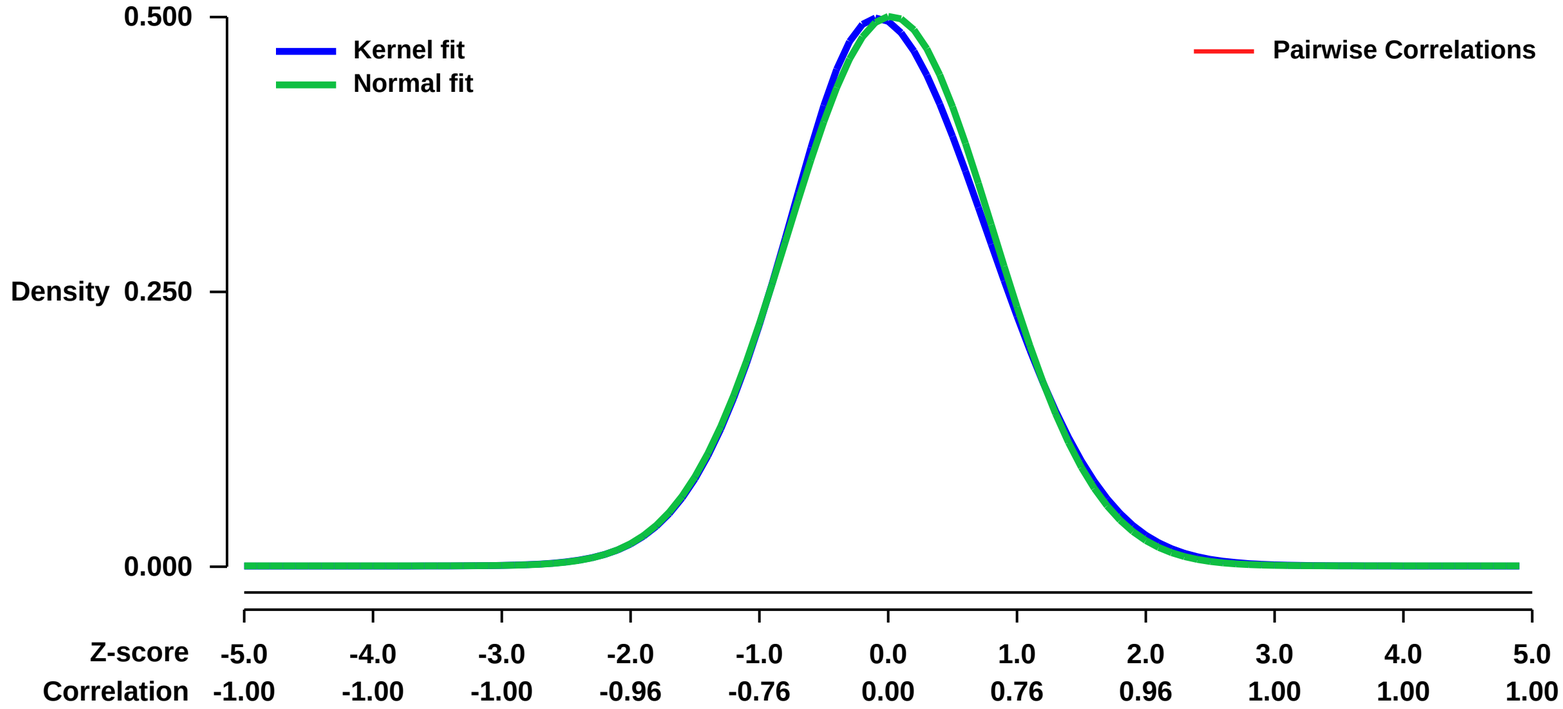

Pre-normalization Quantiles

[min] [medium] [max]

Null module

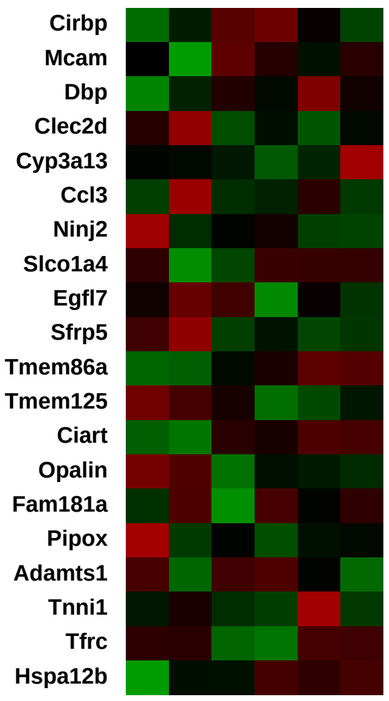

GEO Series "GSE19176" Expression Profiles

Num of samples in this series: 10

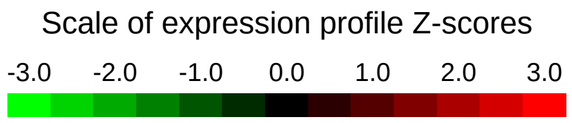

GEO Link:	**http://www.ncbi.nlm.nih.gov/geo/query/acc.cgi?acc=GSE19176**
Status:	**Public on Jan 20 2010**
Title:	**Role of Bmi1 in Shh-mediated shift in gene expression levels**
Organism:	**Mus musculus**
Experiment type:	**Expression profiling by array**
Platform:	**GPL1261**
Pubmed ID:	
Summary & Design:	**Summary:** **We investigated the role of Bmi1 in Shh-mediated shift in gene expression levels** **Overall design:** **Total RNA was isolated using RNeasy Mini Kit (Qiagen) and reverse-transcribed into double-stranded cDNA with One-Cycle cDNA Synthesis Kit (Affymetrix Inc., P/N 900431, Santa Clara, CA) and labelled biotin. Biotin-labeled cRNA samples were fragmented randomly to 35â 200 bp and hybridized to GeneChip´fi Mouse Genome 430 2.0. An Affymetrix GeneChip Scanner 3000 (Affymetrix Inc., Santa Clara, CA) was used to measure the fluorescent intensity emitted by the labeled target.**

Background corr dist: **KL-Divergence = 0.0722, L1-Distance = 0.0262, L2-Distance = 0.0009, Normal std = 0.5022**

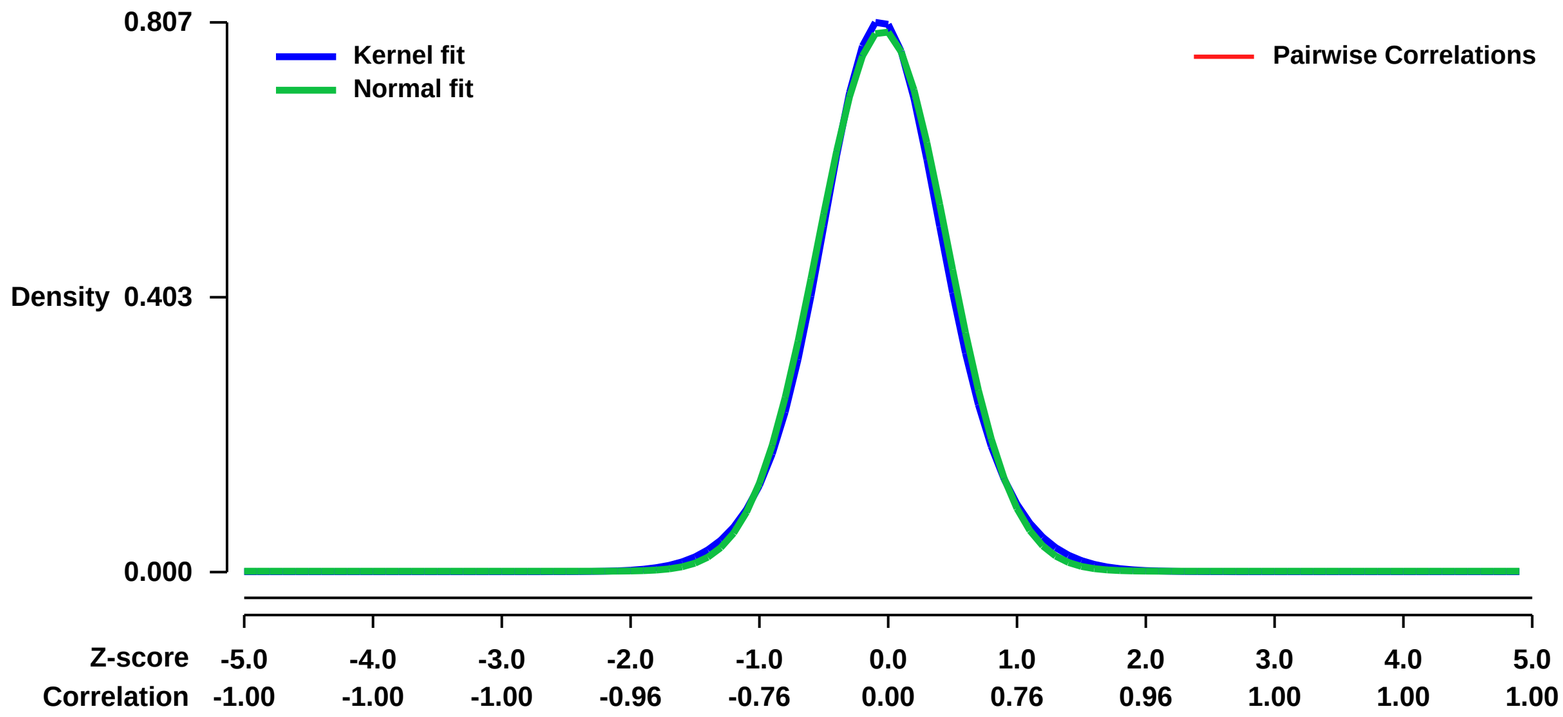

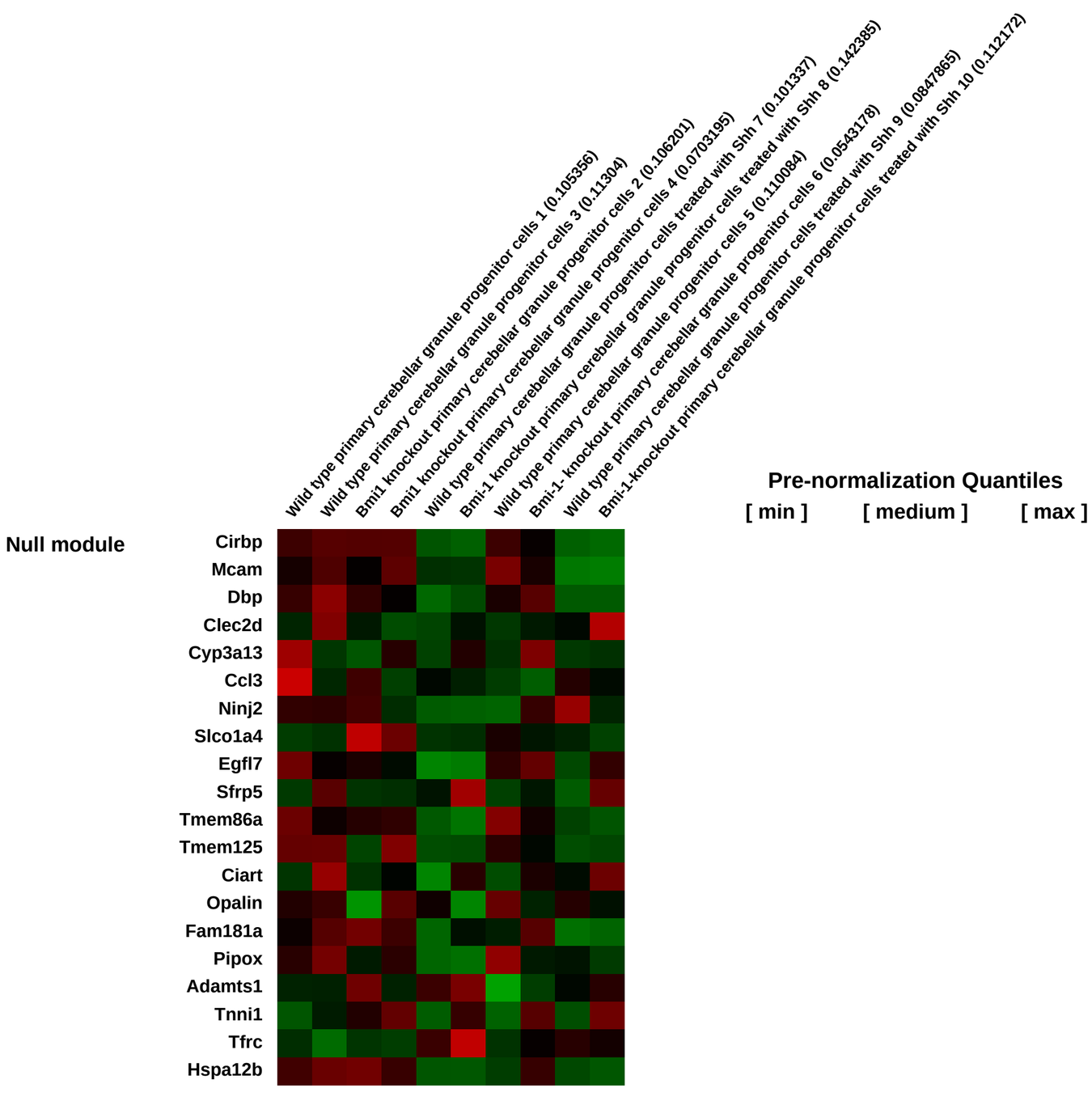

GEO Series "GSE33446" Expression Profiles

Num of samples in this series: 18

Scale of expression profile Z-scores

-3.0 -2.0 -1.0 0.0 1.0 2.0 3.0

GEO Link:	http://www.ncbi.nlm.nih.gov/geo/query/acc.cgi?acc=GSE33446
Status:	Public on Jan 03 2013
Title:	Gene expression accompanying the promotion of hepatocellular carcinoma by intestinal microbiota and Tlr4 in mice.
Organism:	Mus musculus
Experiment type:	Expression profiling by array
Platform:	GPL1261
Pubmed ID:	22516259
Summary & Design:	**Summary:** The effect of Tlr4P712H mutation (rendering TLR4 non-functional), or gut-sterilization by antbiotics, on the induction of tumorgenesis by CCl4 and diethylnitrosamine (DEN) was characterized. Affymetrix Mouse 430 2.0 gene expression measurements were used to characterize the transcriptomic basis of the effects of the above treatments and genotypes on tumorgenesis. **Overall design:** Gene expression of mouse livers of A. Normal liver from WT C3H/HeOuJ mice, B. HCC from WT C3H/HeOuJ mice treated with CCl4 and DEN, C.HCC from TLR4-mutant C3H/HeJ mice (Tlr4P712H) treated with CCl4 and DEN and D.HCC from WT C3H/HeOuJ mice treated with antibiotics (a combination of ampicillin (1 g/l), neomycin [1 g/l], metronidazole[1 g/l] and vancomycin [500 mg/l] in drinking water) and CCl4 and DEN were characterized.

Background corr dist: KL-Divergence = 0.2105, L1-Distance = 0.0448, L2-Distance = 0.0045, Normal std = 0.3261

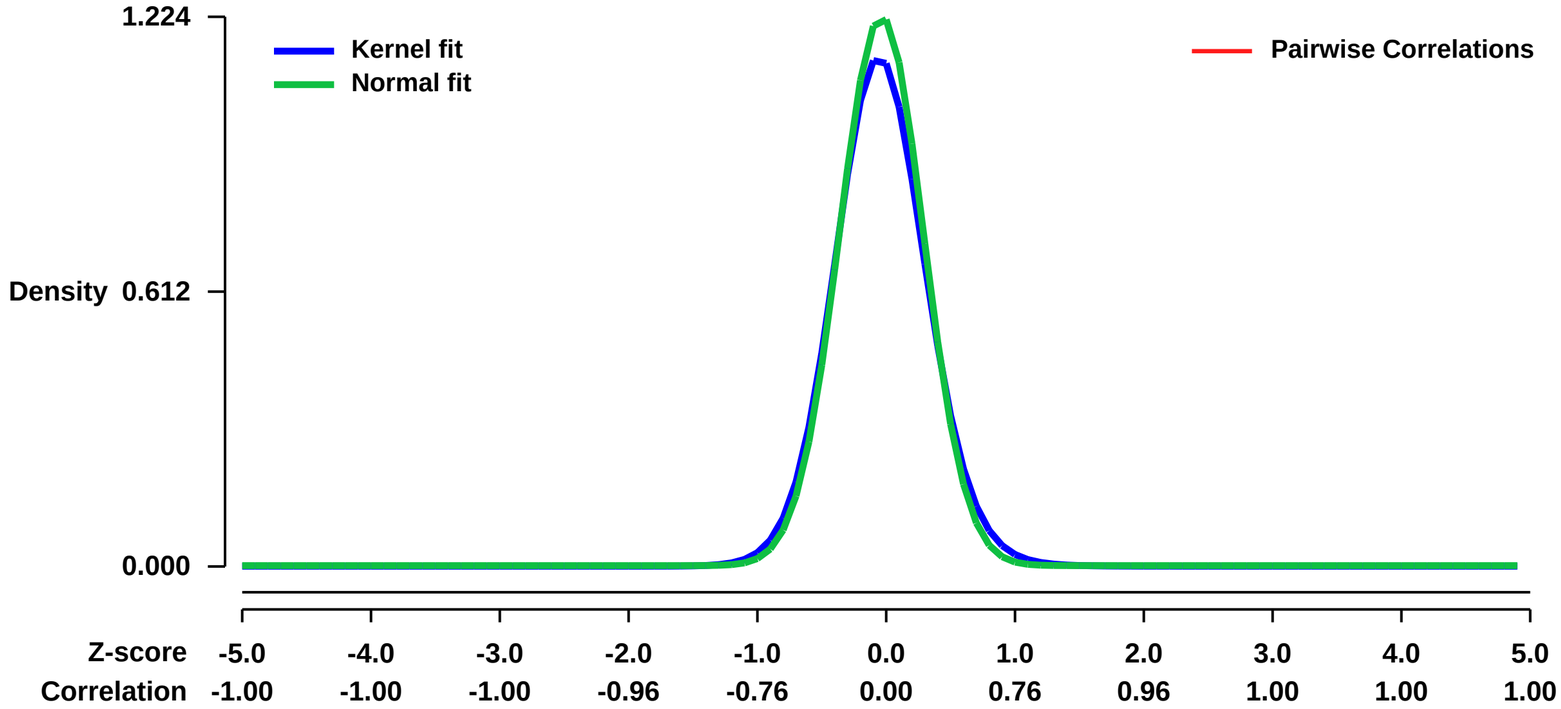

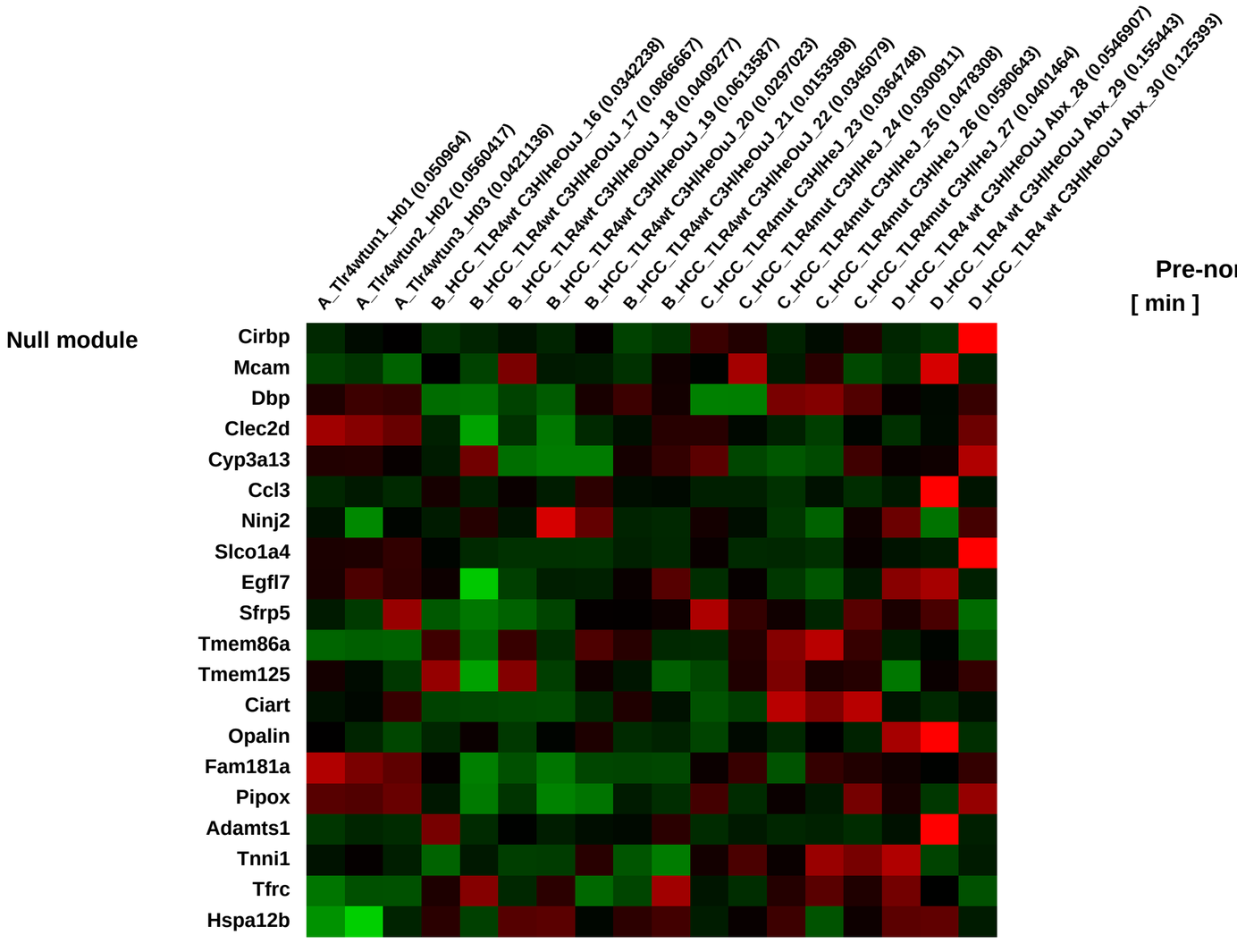

GEO Series "GSE7838" Expression Profiles

Num of samples in this series: 9

Scale of expression profile Z-scores

-3.0 -2.0 -1.0 0.0 1.0 2.0 3.0

GEO Link:	http://www.ncbi.nlm.nih.gov/geo/query/acc.cgi?acc=GSE7838
Status:	Public on Jul 01 2007
Title:	Comprehensive Gene ExpressionProfiling of Peyerâ s Patch M Cells, Villous M-like Cells, and Intestinal Epithelial Cells
Organism:	Mus musculus
Experiment type:	Expression profiling by array
Platform:	GPL1261
Pubmed ID:	
Summary & Design:	**Summary:** Separate populations of M cells have been detected in the follicle-associated epithelium of Peyerâ s patches (PPs) and the villous epithelium of the small intestine, but the traits shared by or distinguishing the two populations have not been characterized. Our separate study has demonstrated that M cells are rare but M-like cells positive for lectin Ulex europaeus agglutinin-1 and our newly developed M cell-specific mAb NKM16-2-4 are induced by oral administration of cholera toxin in the duodenal villous epithelium. Here, we determined the gene expression of PP M cells, villous M-like cells, and intestinal epithelial cells (IECs) isolated by a novel approach using FACS. Specific expression of glycoprotein 2 (GP2) and MARCKS-like protein (MLP) by PP M cells and not villous M-like cells was confirmed by additional mRNA and protein analyses. Comprehensive gene profiling also suggested that villous M-like cells share traits of both PP M cells and IECs, a finding that is supported by their unique expression of specific chemokines. The genome-wide assessment of gene expression facilitates discovery of M cell-specific molecules and enhances the molecular understanding of M cell immunobiology. **Keywords: Cell type comparison** **Overall design:** Epithelial cells in duodenal Peyer's patches or villi of BALB/c mice treated with or without cholera toxin were dissociated and stained with NKM16-2-4 monoclonal antibody (mAb)-FITC, lectin UEA-1-PE, and anti-CD45 mAb-APC-Cy7. Naive PP M cells (NKM16-2-4+, UEA-1+, and CD45- cells), CT-induced villous M-like cells (NKM16-2-4+, UEA-1+, and CD45- cells), and naive intestinal epithelial cells (NKM16-2-4-, UEA-1-, and CD45- cells) were isolated by FACS. Affymetrix GeneChip Mouse Genome 430 2.0 Array was used in triplicate for each cell fraction.

Background corr dist: KL-Divergence = 0.0509, L1-Distance = 0.0296, L2-Distance = 0.0011, Normal std = 0.5720

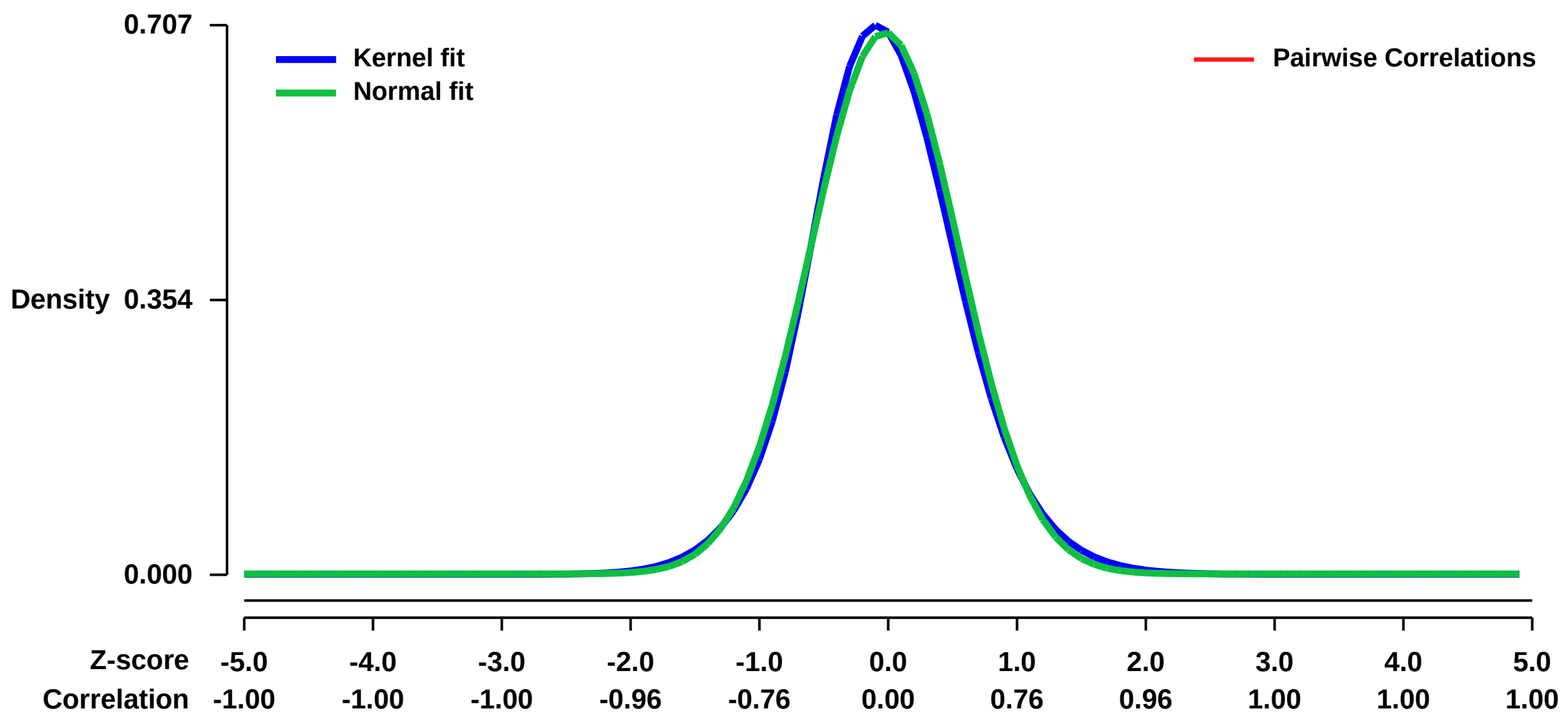

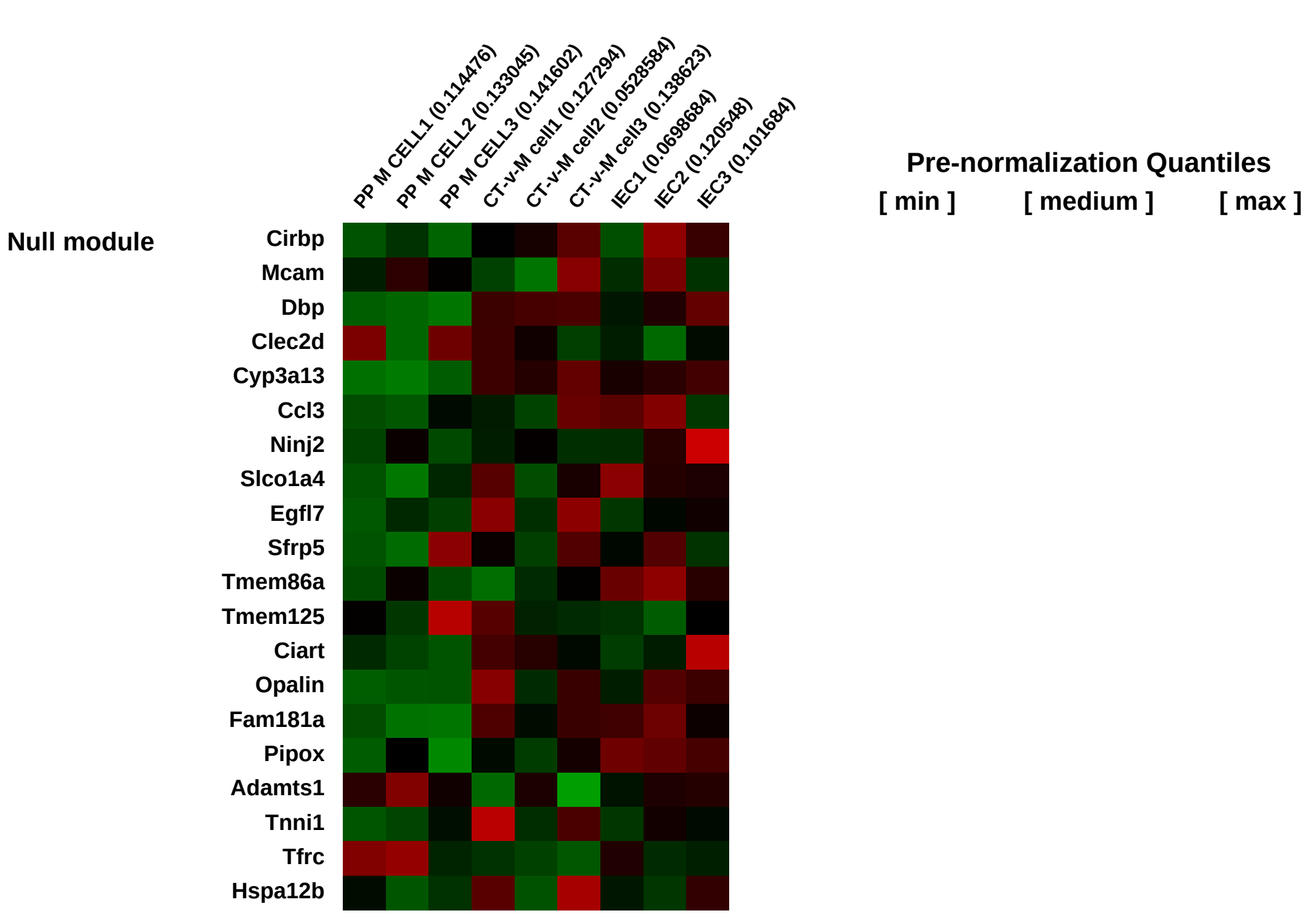

GEO Series "GSE53480" Expression Profiles

Num of samples in this series: 16

Scale of expression profile Z-scores

-3.0 -2.0 -1.0 0.0 1.0 2.0 3.0

GEO Link:	**http://www.ncbi.nlm.nih.gov/geo/query/acc.cgi?acc=GSE53480**
Status:	**Public on Dec 19 2013**
Title:	**Expression data from Tg4510 and Wild-type mice after AAVTFEB injection**
Organism:	**Mus musculus**
Experiment type:	**Expression profiling by array**
Platform:	**GPL1261**
Pubmed ID:	
Summary & Design:	**Summary:** **We used microarrays to detail the global programme of gene expression after 4 months of TFEB overexpression in the brain.** **Overall design:** **Groups of Tg4510 and Wild-type mice were injected at P0 in the brain. Those groups of mice and the respectively controls were sacrificed and analyzed after 4 months from the injection. RNA extraction from the hippocampus and hybridization on Affymetrix microarrays was done.**

Background corr dist: **KL-Divergence = 0.1843, L1-Distance = 0.0396, L2-Distance = 0.0031, Normal std = 0.3439**

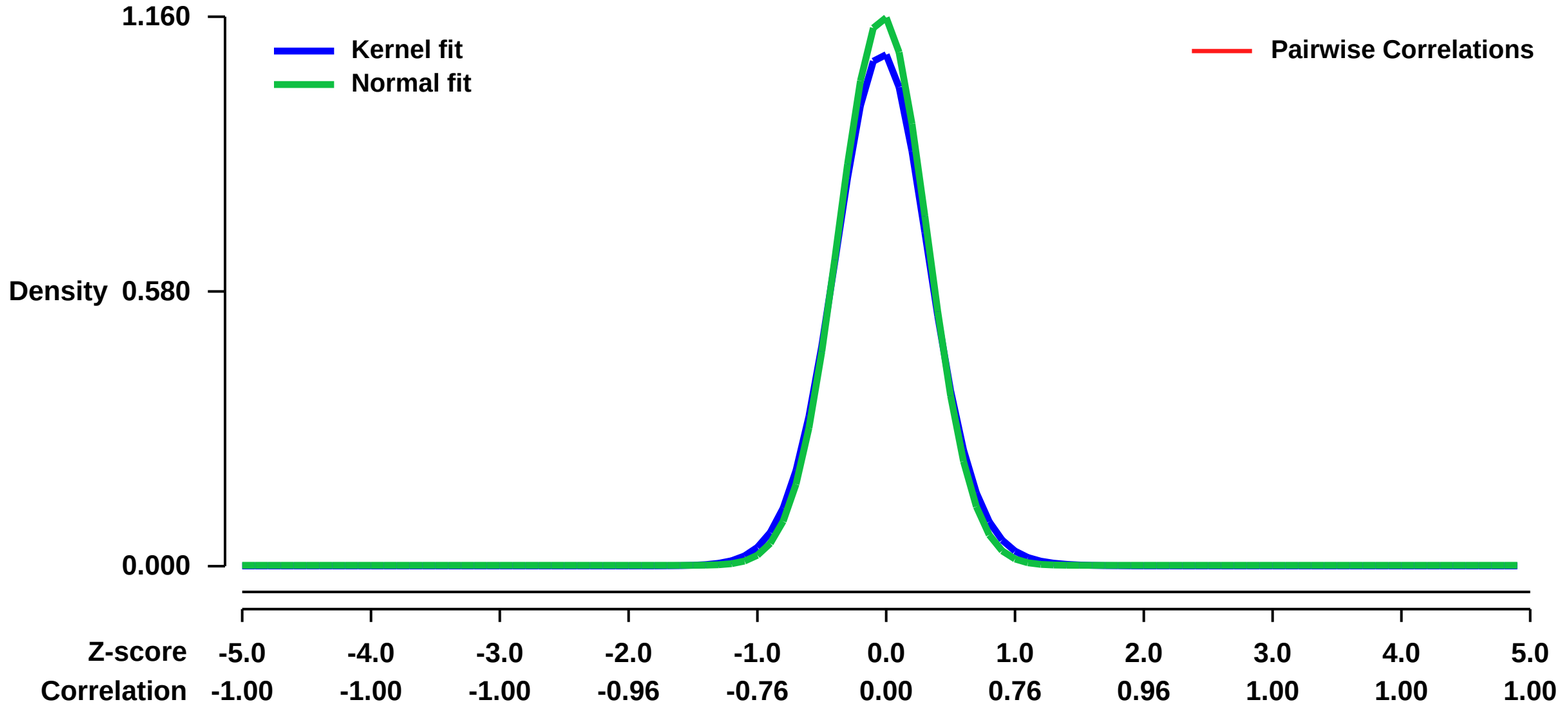

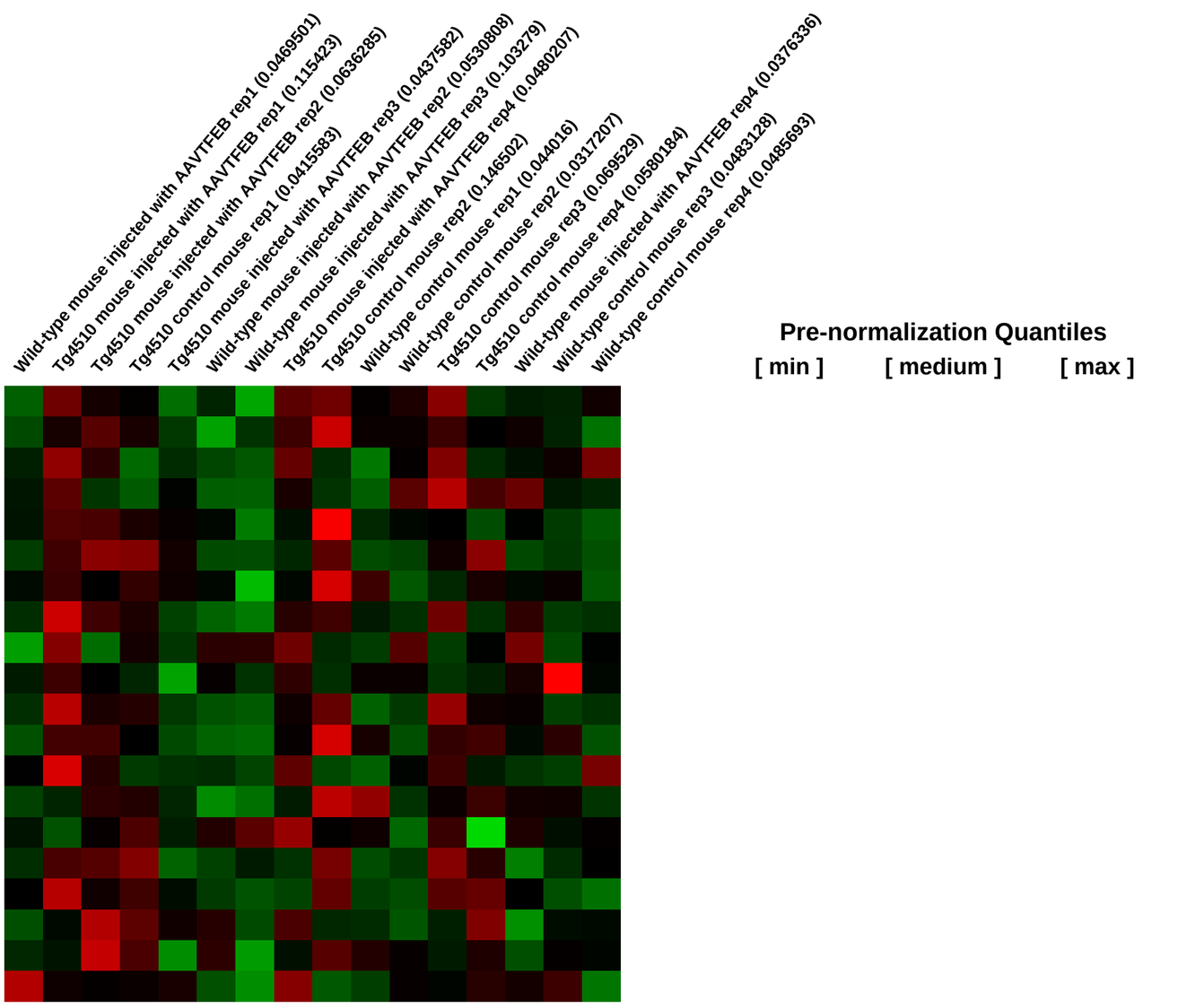

GEO Series "GSE9037" Expression Profiles

Num of samples in this series: 12

Scale of expression profile Z-scores

-3.0 -2.0 -1.0 0.0 1.0 2.0 3.0

GEO Link:	http://www.ncbi.nlm.nih.gov/geo/query/acc.cgi?acc=GSE9037
Status:	Public on Jun 25 2008
Title:	response to LPS of WT and IRAK4 kinase dead mouse bone marrow macrophages
Organism:	Mus musculus
Experiment type:	Expression profiling by array
Platform:	GPL1261
Pubmed ID:	18266302
Summary & Design:	**Summary:** **IRAK-4 is an essential component of the signal transduction complex downstream of the IL-1- and Toll-like receptors. Though regarded as the first kinase in the signaling cascade, the role of IRAK-4 kinase activity versus its scaffold function is still controversial. In order to investigate the role of IRAK-4 kinase function in vivo, â knock-inâ mice were generated by replacing the wild type IRAK-4 gene with a mutant gene encoding kinase deficient IRAK-4 protein (IRAK-4 KD). Analysis of bone marrow macrophages obtained from WT and IRAK-4 KD mice with a number of experimental techniques demonstrated that the IRAK-4 KD cells greatly lack responsiveness to stimulation with the Toll-like receptor 4 (TLR4) agonist LPS. One of the techniques used, microarray analysis, identified IRAK-4 kinase-dependent LPS response genes and revealed that the induction of LPS-responsive mRNAs was largely ablated in IRAK-4 KD cells. In summary, our results suggest that IRAK-4 kinase activity plays a critical role in TLR4-mediated induction of inflammatory responses.** **Keywords: genetic modification, strain comparison, cell stimulation, time course, anti-bacterial response, innate immune response, inflammatory response** **Overall design:** **The response of mouse bone marrow macrophages from WT and IRAK4 kinase dead animals to stimulation with LPS at two time points was determined. There were 12 samples in total, 6 from WT and 6 from IRAK4 kinase dead cells; for each strain there were 3 conditions: growth for 4 hours without stimulation (the strain-specific control), growth for 1 hour with stimulation, and growth for 4 hours with stimulation; for each condition there were two biological replicates.**

Background corr dist: KL-Divergence = 0.1460, L1-Distance = 0.0329, L2-Distance = 0.0021, Normal std = 0.3783

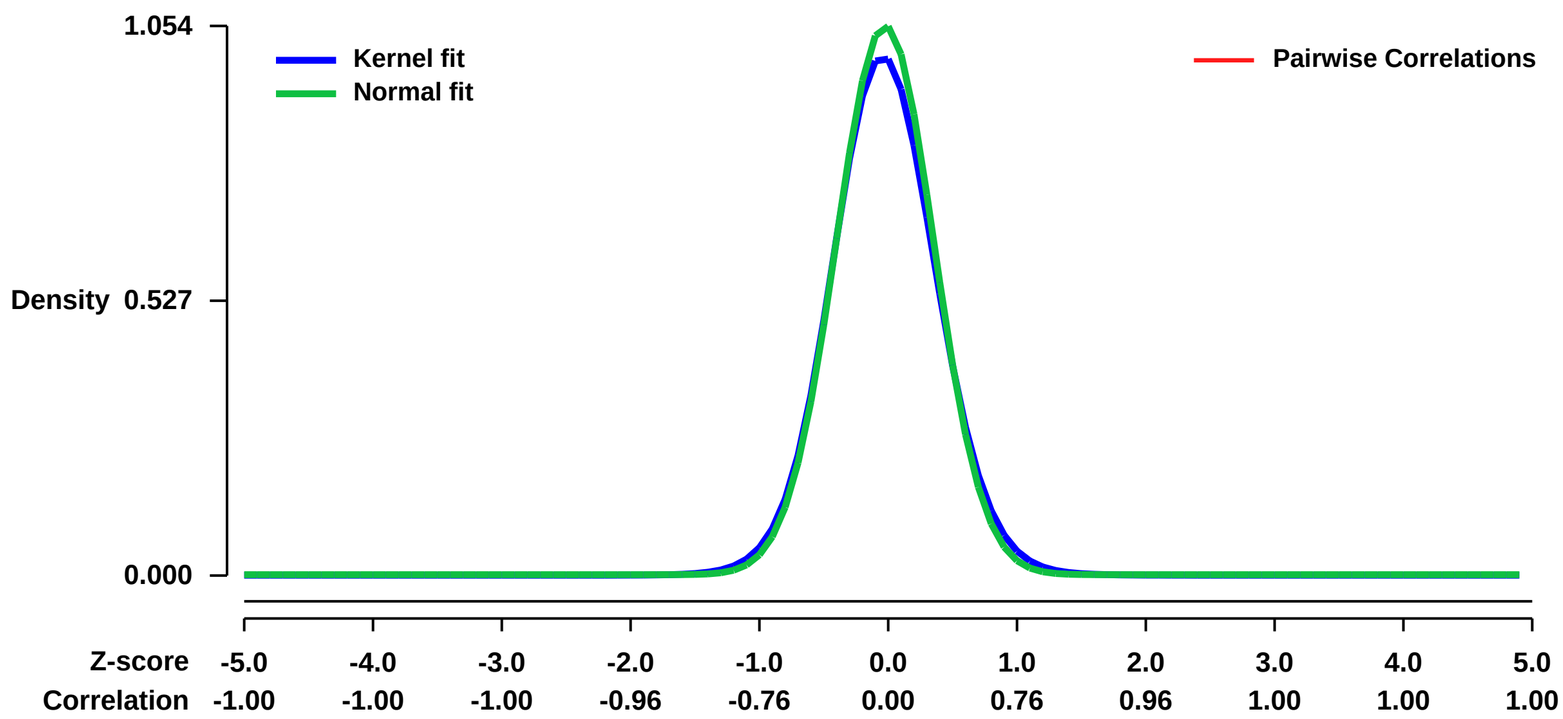

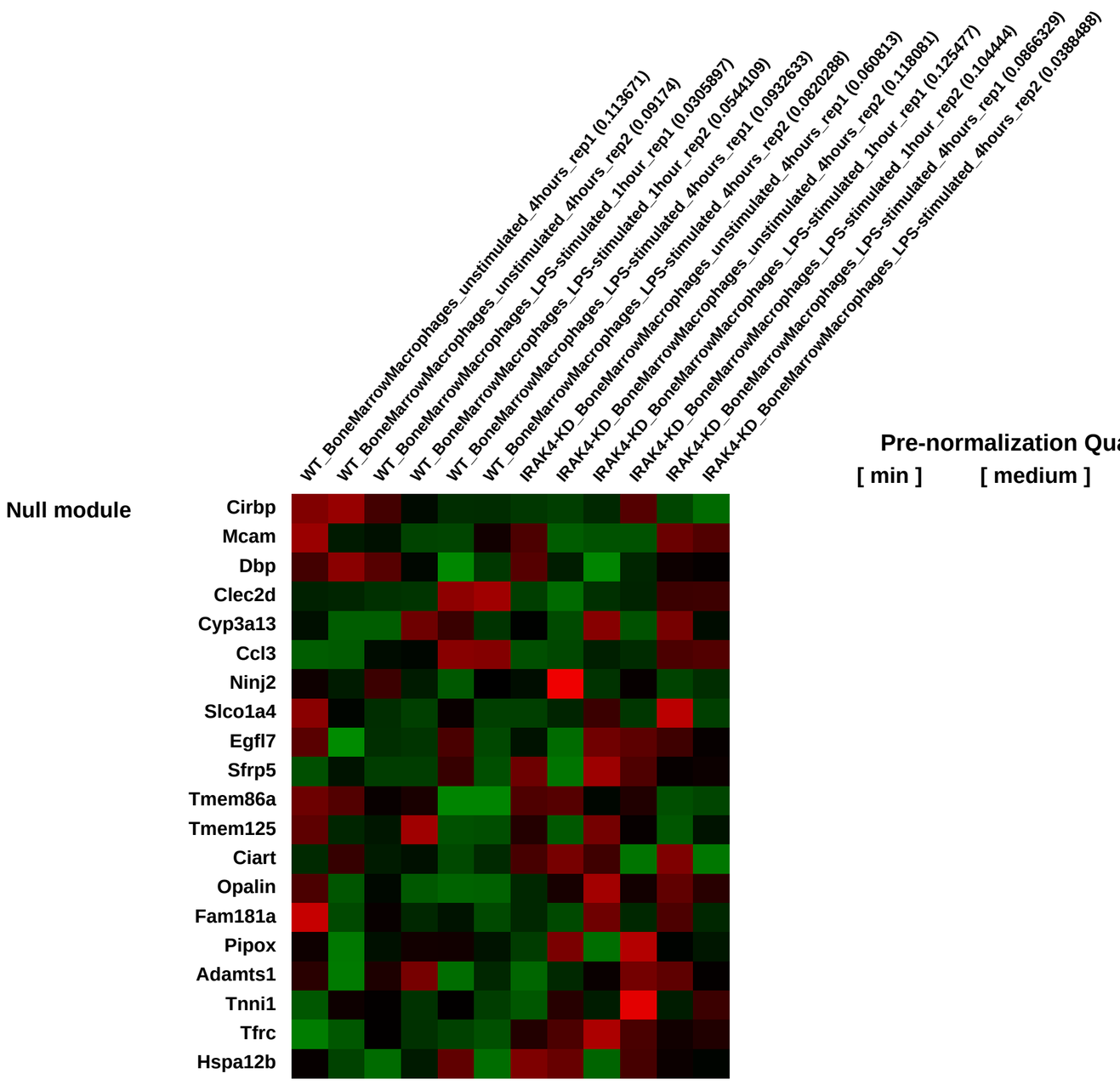

GEO Series "GSE45365" Expression Profiles

Num of samples in this series: 28

Scale of expression profile Z-scores

-3.0 -2.0 -1.0 0.0 1.0 2.0 3.0

GEO Link:	http://www.ncbi.nlm.nih.gov/geo/query/acc.cgi?acc=GSE45365
Status:	Public on Apr 03 2013
Title:	Genome-wide expression study of the early/innate responses of murine B and T cells to MCMV infection
Organism:	Mus musculus
Experiment type:	Expression profiling by array
Platform:	GPL1261
Pubmed ID:	
Summary & Design:	**Summary:** **Murine Cytomegalovirus (MCMV) infection leads to early activation of various immune cells, including B and T lymphocytes, before the actual initiation of antigen-specific adaptive immunity. This activation is partly driven by innate cytokines, including type I interferon (IFN), which are induced early after infection. The objective of this study was to address the role of type I IFN in shaping early/innate B and T cell responses to a primary acute viral infection.** **In order to decipher the specific impact of IFN-I on cell subsets, we performed a genome-wide expression analysis on WT splenic B and CD8 T lymphocytes isolated from C57BL/6 [CD45.1 WT / CD45.2 IFNAR-KO] mixed bone marrow chimera mice. This study complements series GSE39555, which focused on early responses of NK cells and of the two subsets of conventional dendritic cells.** **Overall design:** **This study includes data from B and CD8 T lymphocytes purified by flow cytometry sorting from the spleen of bone marrow chimera (BMC) mice, under steady-state or MCMV conditions. Two independent replicates were made for each cell type, from two independent pools of spleens from uninfected or d1.5 MCMV-infected BMC 5-8 mice, and were hybridized on 3 separate batches of GeneChips.**

Background corr dist: KL-Divergence = 0.2995, L1-Distance = 0.0581, L2-Distance = 0.0091, Normal std = 0.2827

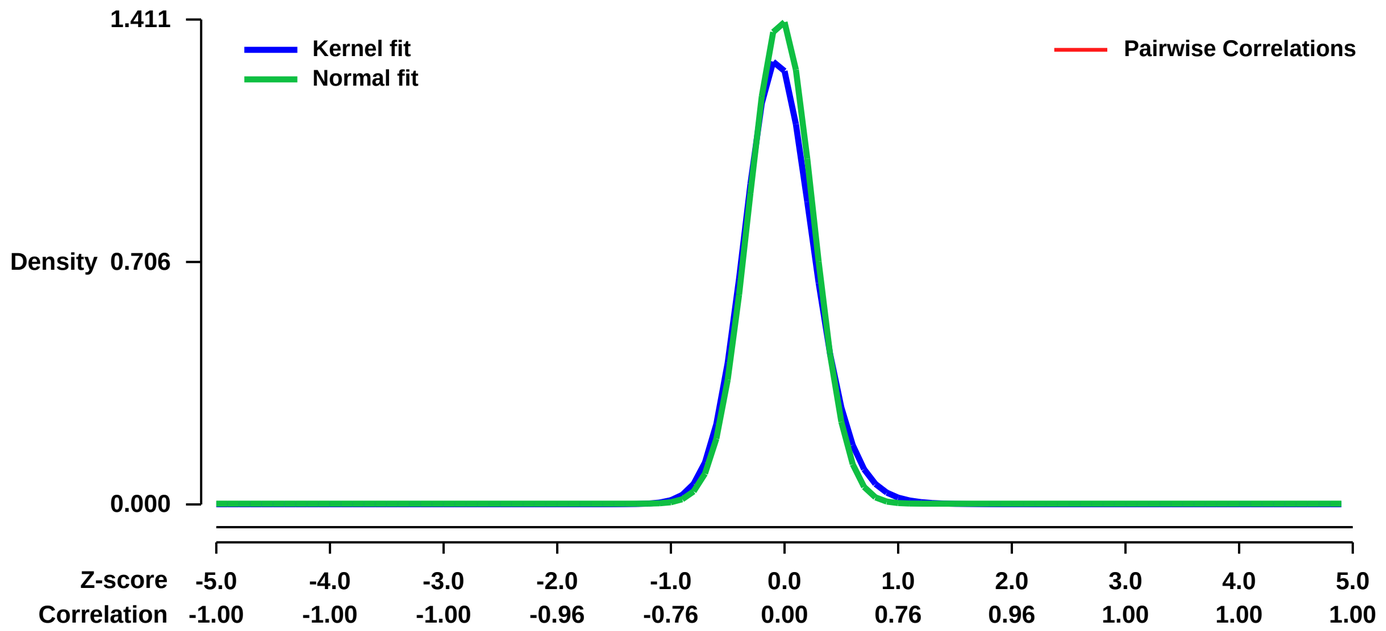

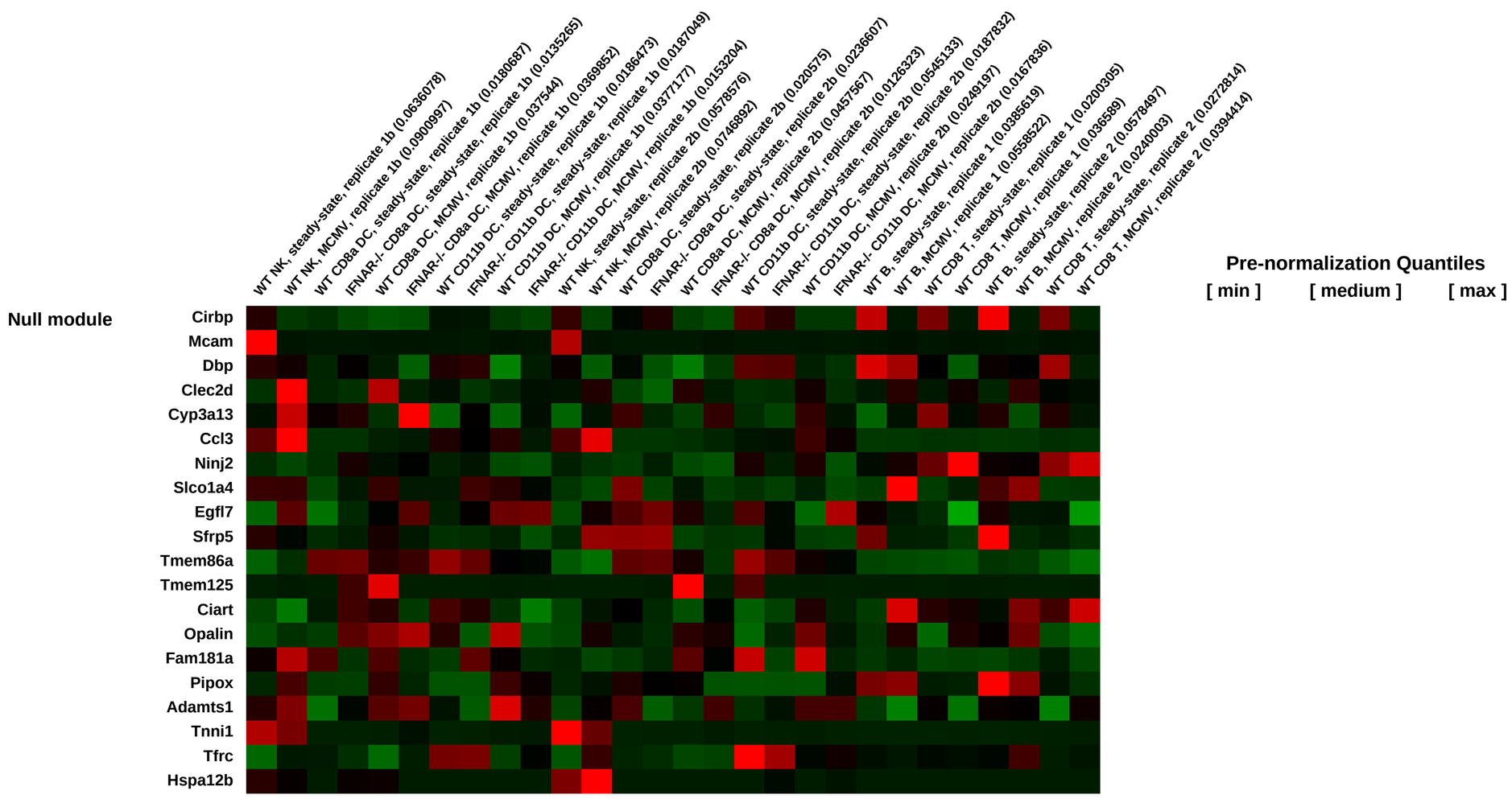

GEO Series "GSE35219" Expression Profiles

Num of samples in this series: 6

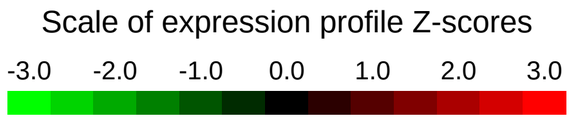

GEO Link:	http://www.ncbi.nlm.nih.gov/geo/query/acc.cgi?acc=GSE35219
Status:	Public on Aug 14 2012
Title:	Synergy between PI3K Signaling and MYC in Burkitt Lymphomagenesis
Organism:	Mus musculus
Experiment type:	Genome variation profiling by SNP array
Platform:	GPL1261
Pubmed ID:	22897848
Summary & Design:	**Summary:** In Burkitt lymphoma (BL), an aggressive germinal-center (GC) derived non-Hodgkin B-cell lymphoma characterized by MYC translocations as early transforming event, the apoptotic properties of MYC must have been overcome by pro-survival signals. Whereas activation of the pro-survival factor NFkappaB is not eminent in BL, PI3K signalling, which mediates B cell receptor associated survival signals in mature B cells, might be the cooperating event. Here we prove this hypothesis by the generation of BL in mice upon concordant expression of MYC and activation of PI3K in GC B cells. Unlike existing murine BL-like models, our tumour model fully phenocopies primary human BL and reflects the complexity of the disease with regard to histological appearance, surface marker expression, and characteristic gene expression profiles. Like in human BL, tumour monoclonality indicated a multistep pathogenesis underlining MYC and PI3K as predisposing events that invariably lead to GC-derived BL formation. In accordance, copy number alteration analysis revealed genomic regions involved in BL pathogenesis. **Overall design:** All samples were obtained from murine lymphomas (Cgamma1-cre; R26StopFLMYC;R26StopFLP110* animals). Cells used for microarray analysis were sorted reporter positive cells. Tumour cells were compared to a matched germline DANN sample to identify acquired aberrations.

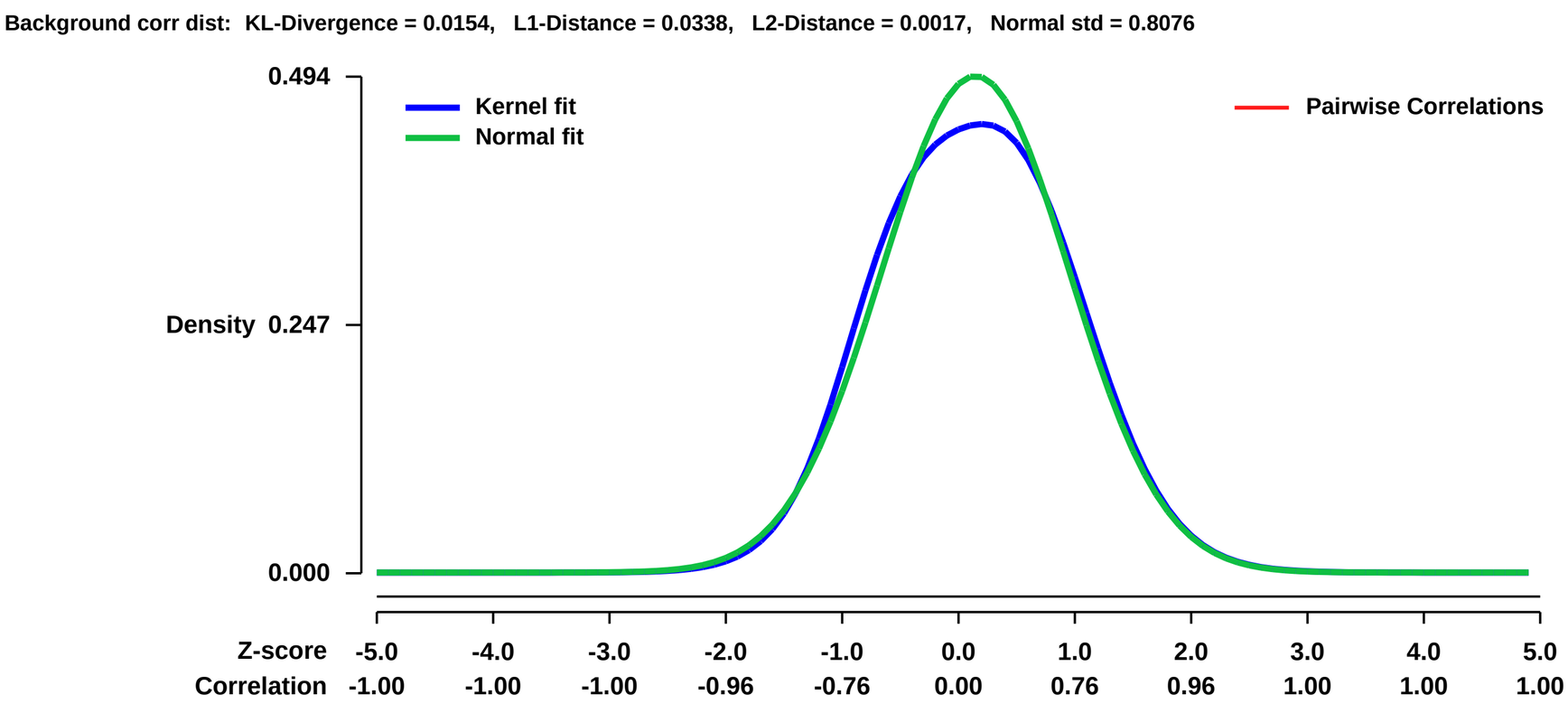

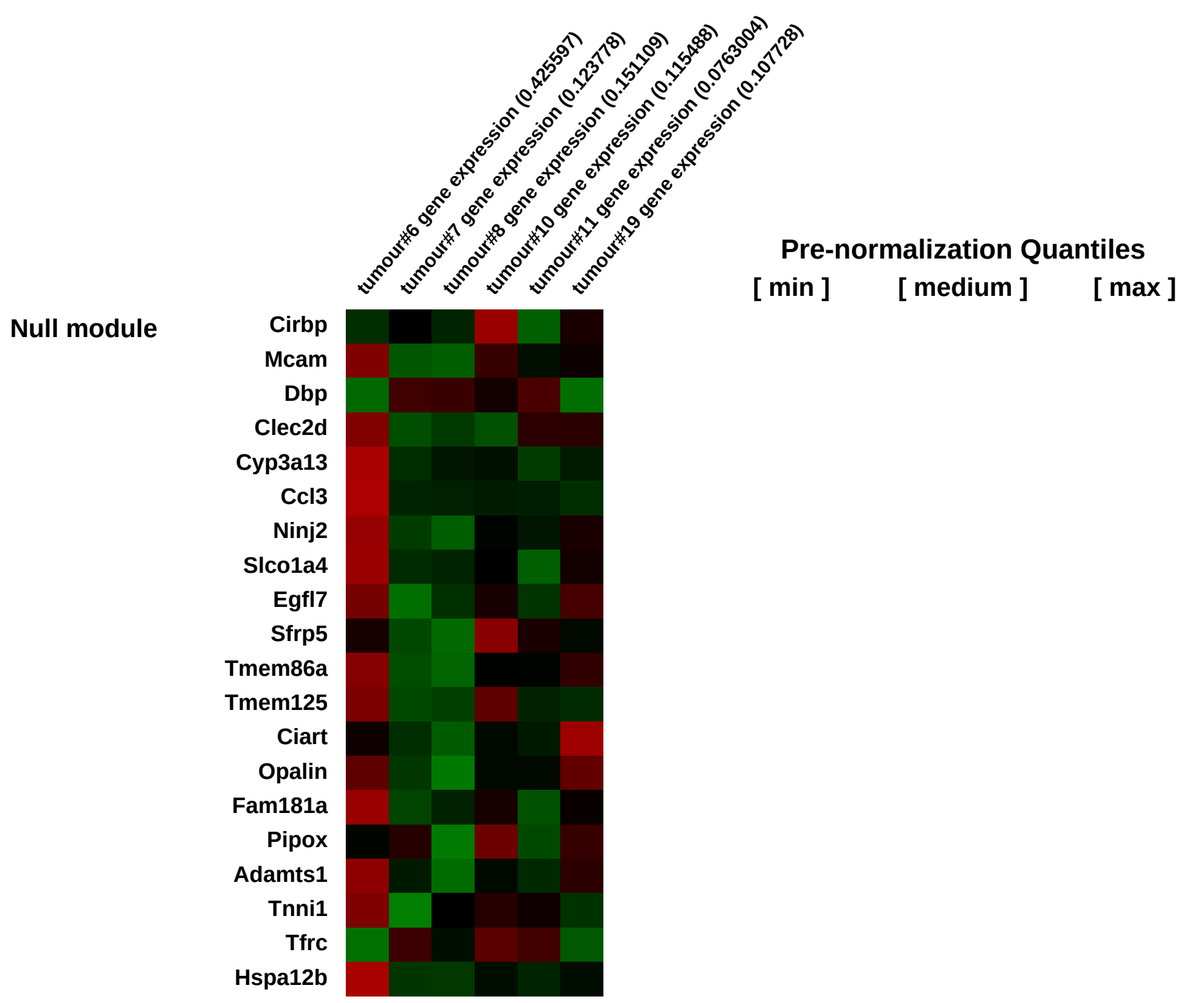

GEO Series "GSE16679" Expression Profiles

Num of samples in this series: 8

Scale of expression profile Z-scores

-3.0 -2.0 -1.0 0.0 1.0 2.0 3.0

GEO Link:	http://www.ncbi.nlm.nih.gov/geo/query/acc.cgi?acc=GSE16679
Status:	Public on Aug 01 2010
Title:	Plag1 overexpression cooperates with Evi1 overexpression and Gata1s mutation in leading to M7 leukemia
Organism:	Mus musculus
Experiment type:	Expression profiling by array
Platform:	GPL1261
Pubmed ID:	20679399
Summary & Design:	**Summary:** **The goal of this study is to develop a Plag1 signature and determine how its overexpression contributes to leukemogenesis.** **To study this, we transduced an immortalized (but not transformed) cell line (derived from Gata1s mutant fetal liver progenitor through insertional mutagenesis) by Plag1-expressing retrovirus. This turned a non-transformed cell line to a leukemogenic cell line. To study whether Plag1 overexpression led to deregulation of signaling pathways that may contribute to leukemic transformation, we generated microarray gene expression profiles of this cell line transduced with either Plag1 or the empty vector.** **Overall design:** **We generated gene expression profiles by microarray from stable cell lines transduced with either the empty vector or the Plag1-expressing vector.**

Background corr dist: **KL-Divergence = 0.0435, L1-Distance = 0.0264, L2-Distance = 0.0008, Normal std = 0.6089**

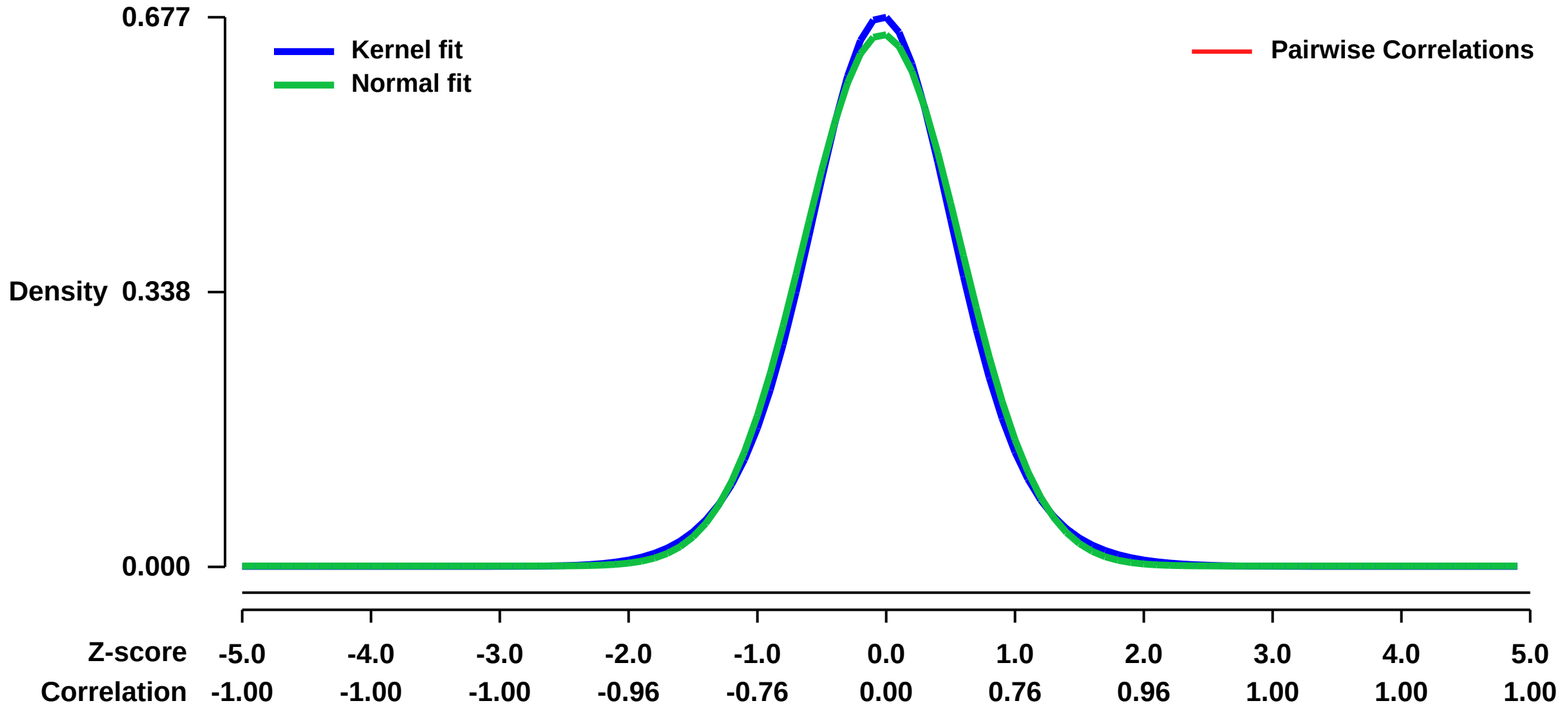

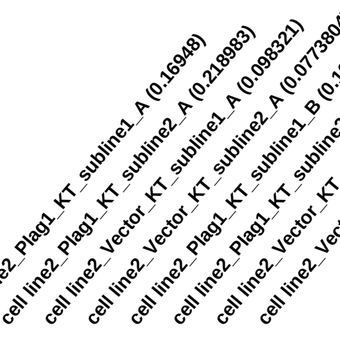

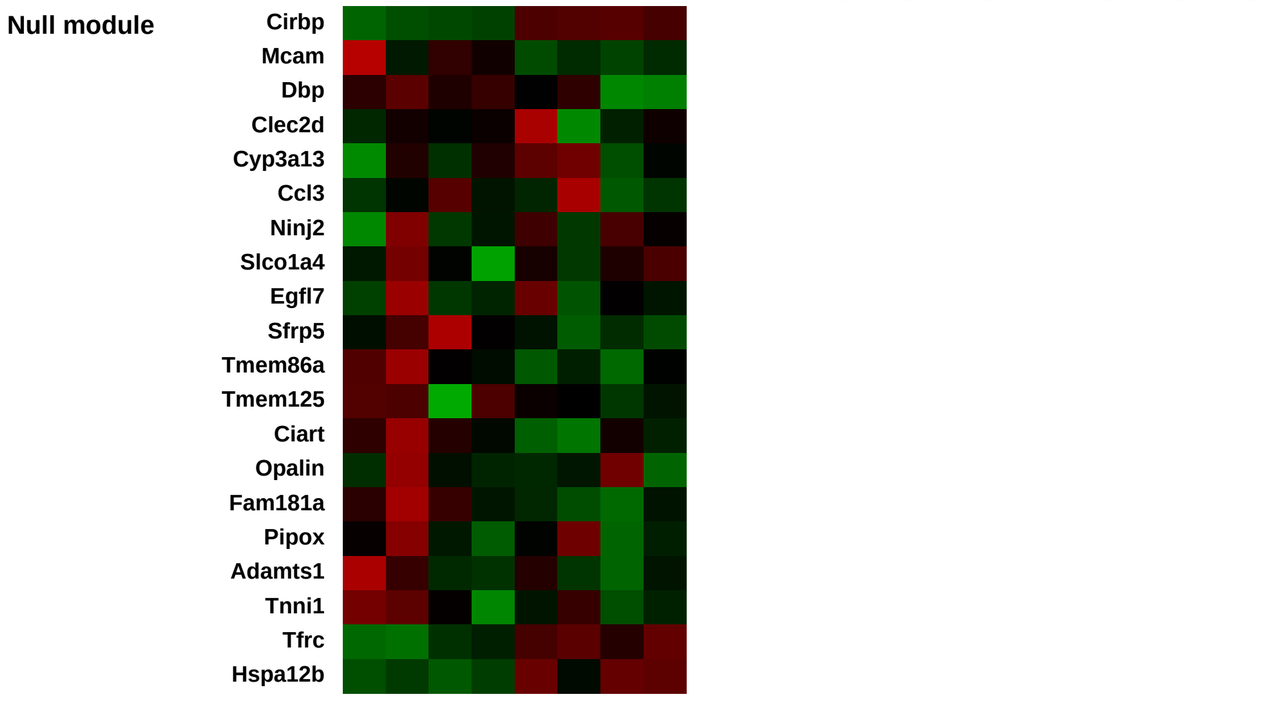

GEO Series "GSE38067" Expression Profiles

Num of samples in this series: 24

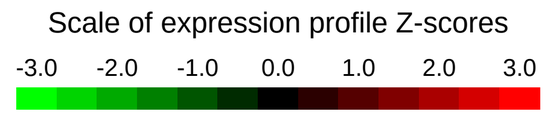

GEO Link:	http://www.ncbi.nlm.nih.gov/geo/query/acc.cgi?acc=GSE38067
Status:	Public on May 23 2012
Title:	Hepatic gene expression in streptozotocin-induced diabetic mice fed a quercetin diet
Organism:	Mus musculus
Experiment type:	Expression profiling by array
Platform:	GPL1261
Pubmed ID:	19496084
Summary & Design:	**Summary:** Quercetin is a food component that may ameliorate the diabetic symptoms. We examined hepatic gene expression of BALB/c mice with streptozotocin (STZ)-induced diabetes to elucidate the mechanism of the protective effect of dietary quercetin on diabetes-associated liver injury. We fed STZ-induced diabetic mice with diets containing 0.1% or 0.5% quercetin for 2 weeks and compared the patterns of hepatic gene expression in these groups of mice using a DNA microarray. Diets containing 0.1% or 0.5% quercetin lowered the STZ-induced increase in blood glucose levels and improved plasma insulin levels. A cluster analysis of the hepatic gene expressions showed that 0.5% quercetin diet suppressed STZ-induced alteration of gene expression. Gene set enrichment analysis (GSEA) and quantitative RT-PCR analysis showed that the quercetin diets had their greatest suppressive effect on the STZ-induced elevation of expression of cyclin dependent kinase inhibitor p21(WAF1/Cip1) (Cdkn1a). **Overall design:** Six-week-old male mice were divided into 4 groups of 6 mice each, housed in groups of 3 per cage. After 1 week mice were intraperitoneally injected with STZ. Mice (n=6) in the untreated control group did not receive any treatment. After 1 week, 18 mice showing non-fasting blood glucose levels of 230-400 mg/dL were divided into 3 groups: one group was fed with AIN93G only (control group), the others with an AIN93G diet containing 0.1% or 0.5% quercetin (Funakoshi, Tokyo, Japan) for 2 weeks.

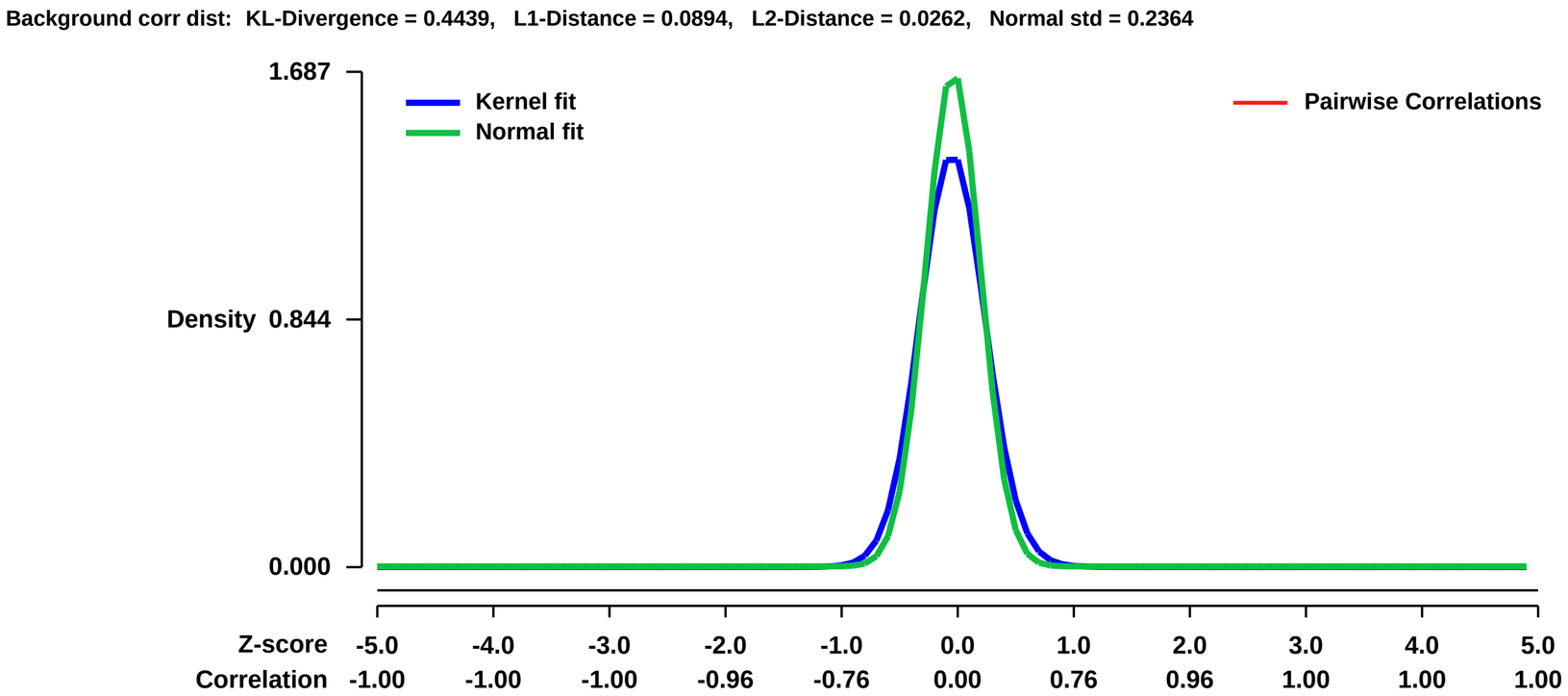

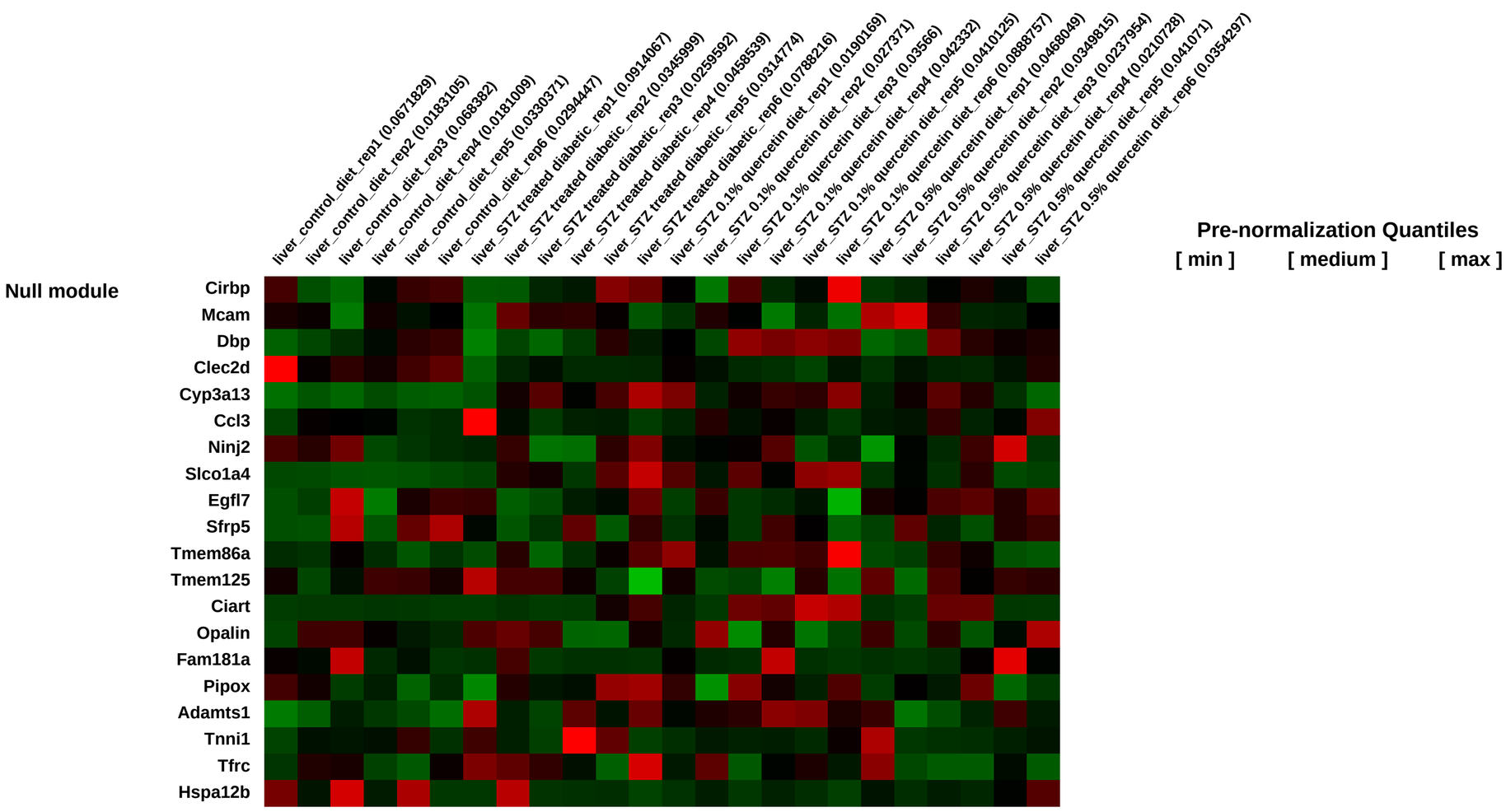

GEO Series "GSE37301" Expression Profiles

Num of samples in this series: 20

Scale of expression profile Z-scores

-3.0 -2.0 -1.0 0.0 1.0 2.0 3.0

GEO Link:	http://www.ncbi.nlm.nih.gov/geo/query/acc.cgi?acc=GSE37301
Status:	Public on Aug 10 2012
Title:	Expression data of Rag2-deficient Ets1++ and Rag2-deficient Ets1-- mature NK cells and WT bone marrow progenitors
Organism:	Mus musculus
Experiment type:	Expression profiling by array
Platform:	GPL1261
Pubmed ID:	22608498
Summary & Design:	**Summary:** Expression profiling of Rag2-deficient Ets1++ and Rag2-deficient Ets1-- mature NK cells and WT bone marrow progenitors, WT T cells, and WT Pro B cells **Overall design:** WT Hematopoietic progenitors, CD4 T cells, Pro B cells, and WT and Ets1-deficient NK cells were FACs sorted. RNA was subsequently extracted, labelled, and hybridized to Affymetrix microarrays. The goal if this experiment was to identify Ets1 dependent genes in NK cells

Background corr dist: KL-Divergence = 0.0889, L1-Distance = 0.0927, L2-Distance = 0.0180, Normal std = 0.4995

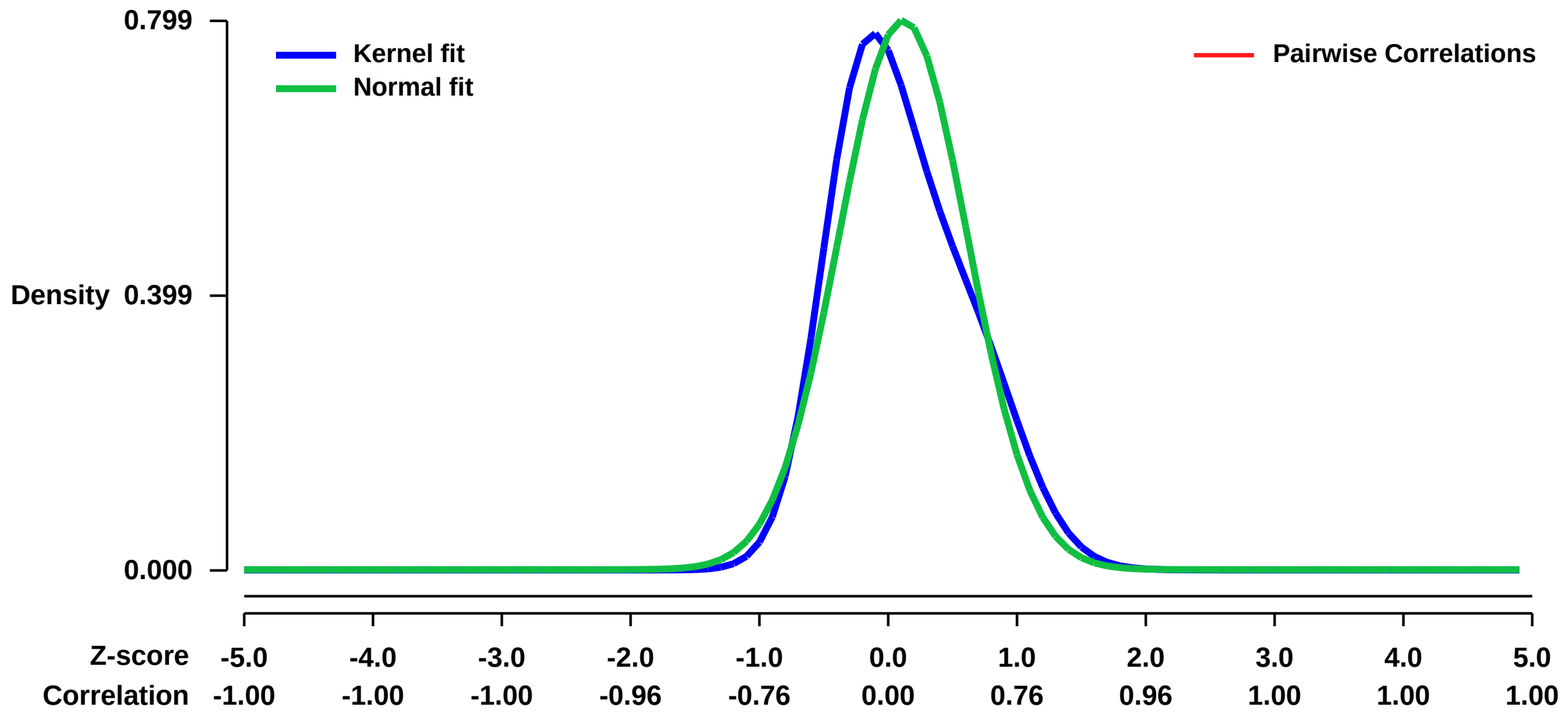

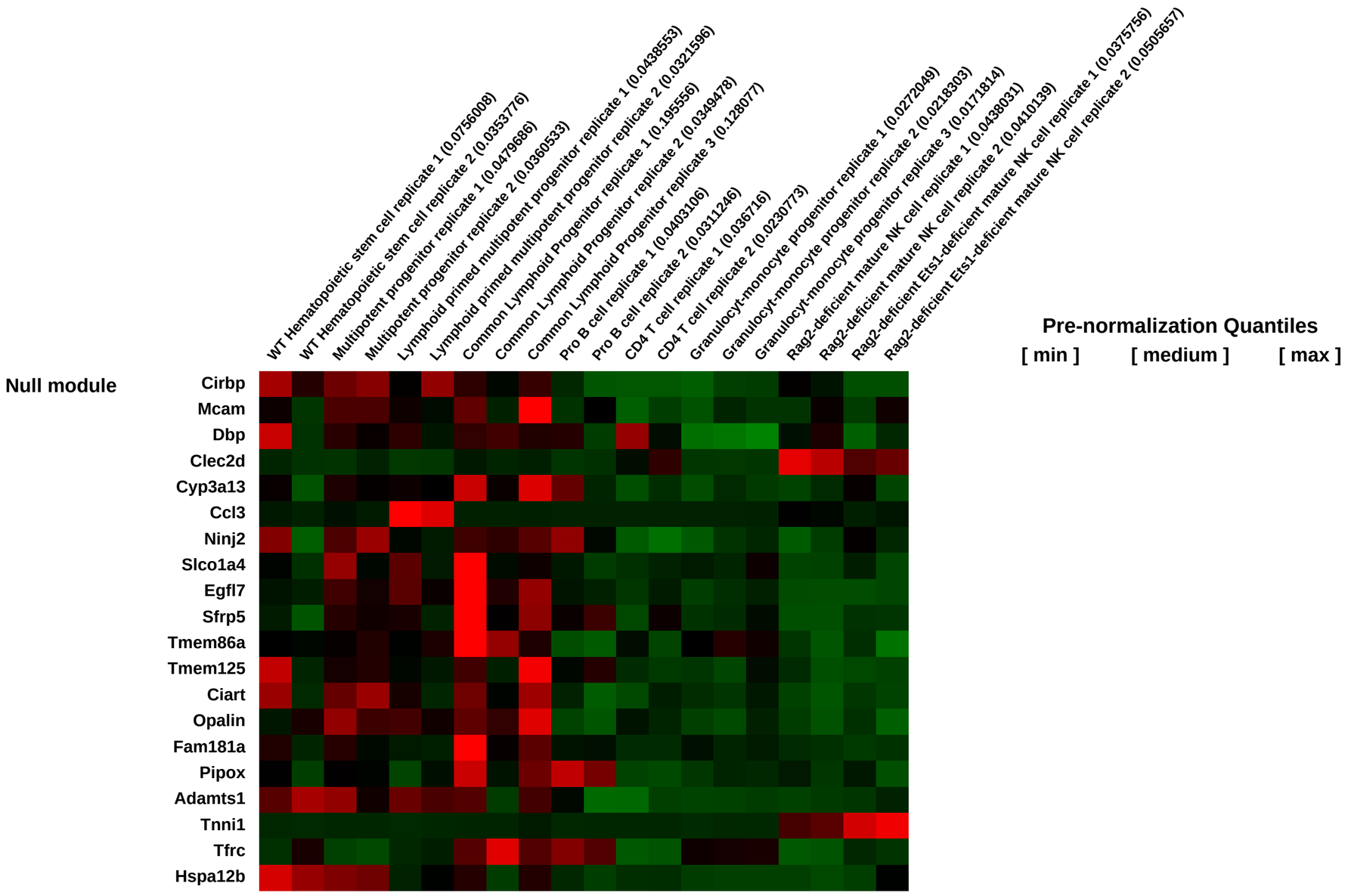

GEO Series "GSE3296" Expression Profiles

Num of samples in this series: 16

Scale of expression profile Z-scores

-3.0 -2.0 -1.0 0.0 1.0 2.0 3.0

GEO Link:	http://www.ncbi.nlm.nih.gov/geo/query/acc.cgi?acc=GSE3296
Status:	Public on Oct 24 2005
Title:	Gene expression in MEFs in response to treatment with dipyridyl and trichostatin A
Organism:	Mus musculus
Experiment type:	Expression profiling by array
Platform:	GPL1261
Pubmed ID:	16237459
Summary & Design:	**Summary:** The CH1 protein interaction domain of the transcriptional coactivators p300 and CBP is thought to interact with HIF-1alpha and this interaction is thought to be critical to the expression of HIF-1alpha target genes in response to hypoxia. Trichostatin A (TSA), an inhibitor of histone deacetylases, has been reported to repress the expression of HIF-1alpha target genes. To test the requirement of the CH1 domain and TSA for gene expression in response to dipyridyl (a hypoxia mimetic), primary mouse embryonic fibroblasts (MEFs) were generated from C57Bl/6x129/Sv F2 e14.5 embryos that contain a deletion in the CH1 domain of three of four alleles of CBP and p300. The remaining allele of p300 or CBP was a conditional knock out allele. Control MEFs with only a single conditional knockout allele of p300 or CBP were also generated. At passage 3 MEFs were infected with Cre Adenovirus and grown until they had expanded at least 100 fold. Subconfluent MEFs were treated with ethanol vehicle or 100ng/ml TSA with 5% carbon dioxide at 37 C in a humid chamber for 30 min., followed by ethanol vehicle or 100 umdipyridyl (DP) for an additional 3hrs. Immediately after treatment, cells were lysed in Trizol for RNA extraction. **Keywords: genetic modification, dose response** **Overall design:** 16 samples; 4 genotypes [CBP+/flox (flox1), p300 +/flox (flox2), CBP CH1/flox;p300 CH1/CH1 (triCH1flox1),CBP CH1/CH1;p300 CH1/flox (triCH1flox2)] , 4 treatments (EtOH, TSA, dipyridyl (DP) and TSA+DP).

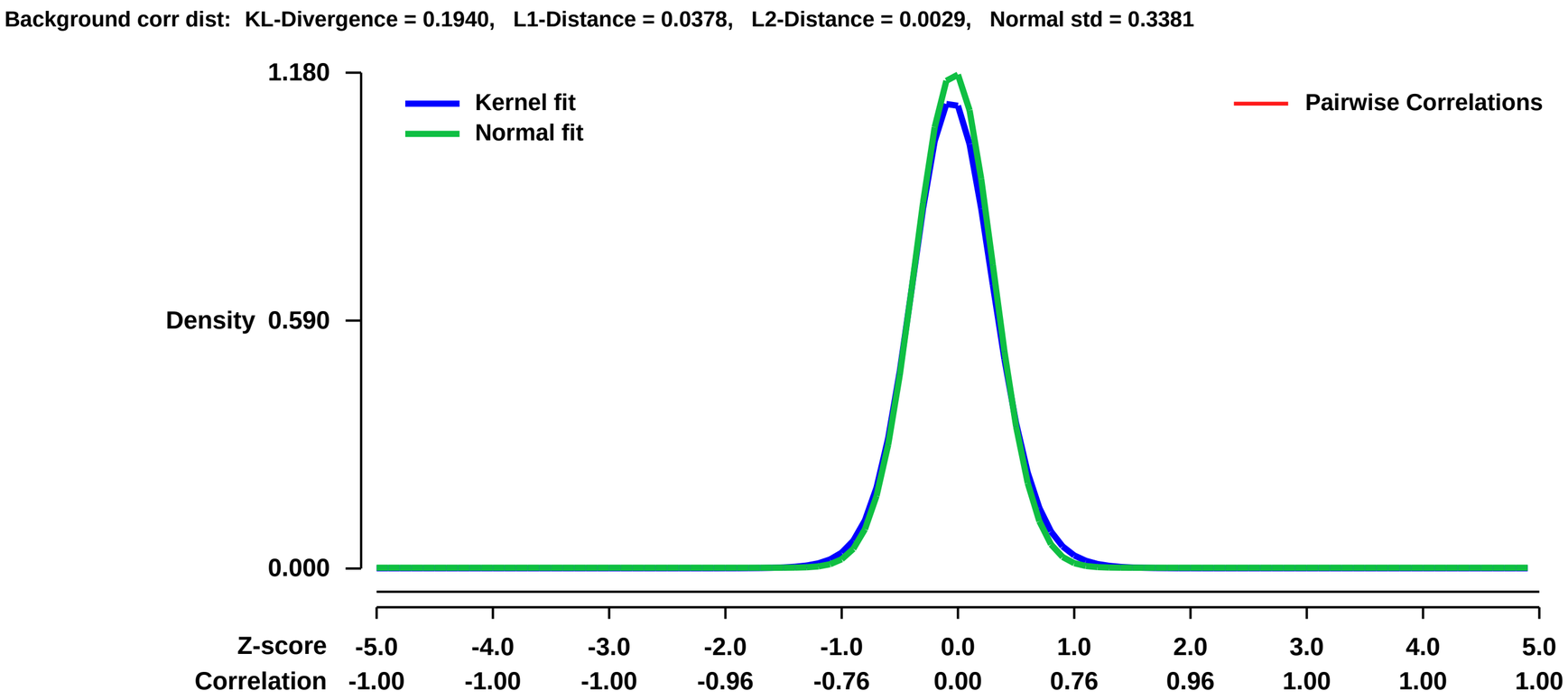

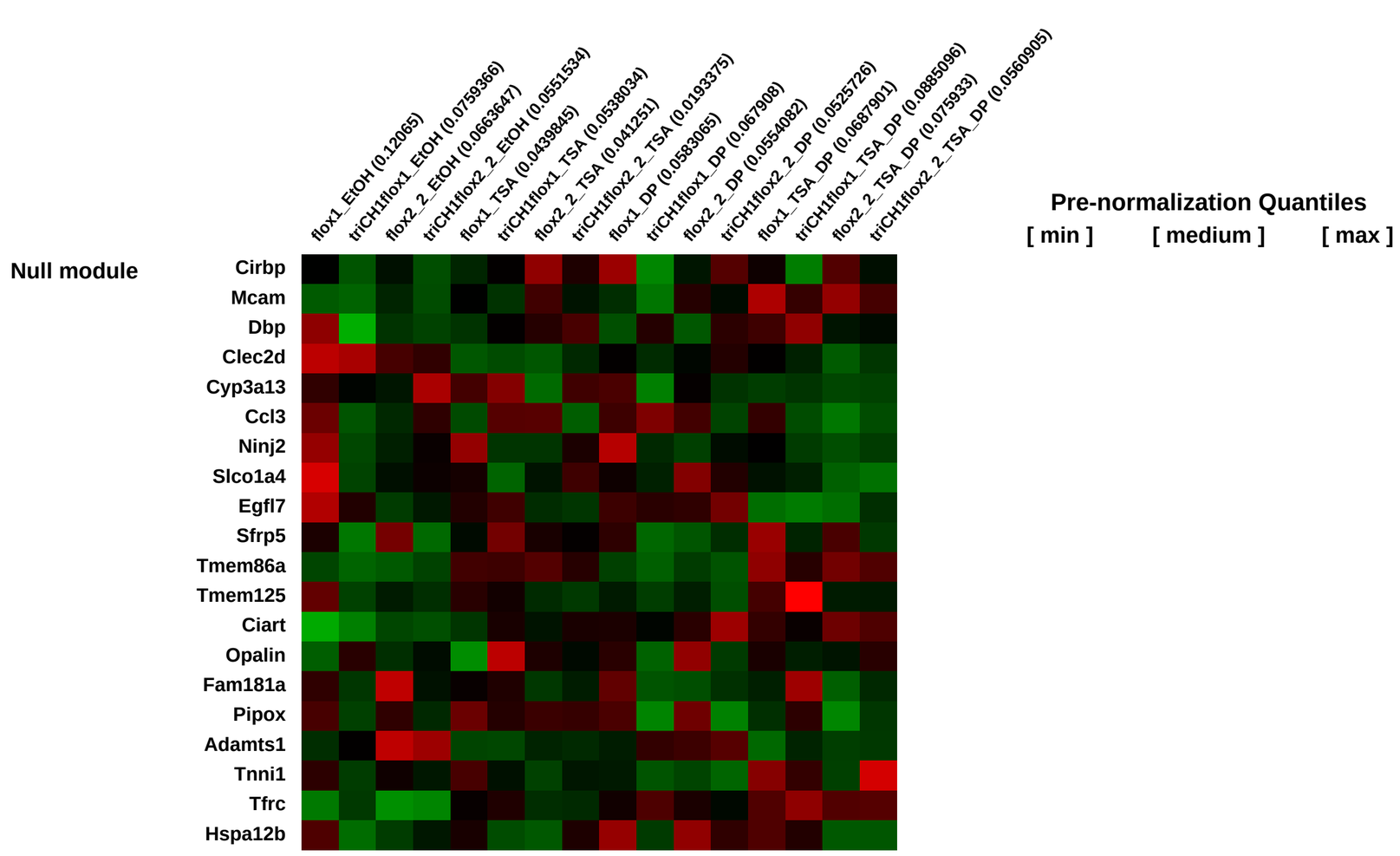

GEO Series "GSE55162" Expression Profiles

Num of samples in this series: 8

Scale of expression profile Z-scores

-3.0 -2.0 -1.0 0.0 1.0 2.0 3.0

GEO Link:	http://www.ncbi.nlm.nih.gov/geo/query/acc.cgi?acc=GSE55162
Status:	Public on Feb 20 2014
Title:	Age-related changes in the cellular composition and epithelial organization of the mouse trachea
Organism:	Mus musculus
Experiment type:	Expression profiling by array
Platform:	GPL1261
Pubmed ID:	24675804
Summary & Design:	**Summary:** We report here senescent changes in the structure and organization of the mucociliary pseudostratified epithelium of the mouse trachea and the main stem bronchi. We confirm previous reports of the graduate appearance of age-related, gland-like structures (ARGLS) in the submucosa, espeically in the intercartilage regions and carina. Immunohistochemistry shows these structures contain ciliated and secretory cells and Krt5+ basal cells, but not the myoepithelial cells or ciliated ducts typical of normal submucosal glands. Data suggests they arise de novo by budding from teh surface epithelium rather than by delayted growth of small or cryptic submucosal glands. In old mice the surface epithelium contains fewer cells per unit length than in young mice and the proportion of Krt5+, p63+ basal cells is reduced in both males and females. However, there appears to be no significant difference in the ability of basal stem cells isolated from individual young and old mice to form clonal tracheospheres in culture or in the ability of the pithelium to repair after damage by inhaled sulfur dioxide. Gene expression analysis by Affymetrix microarray and quantitative PCR, as well as immunohistochemistry and flow sorting studies, are consistent with low-grade chronic inflammation in the tracheas of old versus young mice. The significance of these changes for ARGL formation are not clear since several treatments that induce acute inflammation in young mice did not result in budding of the surface epithelium. **Overall design:** Total RNA from distal tracheas and carinas of four young (2 month) and four older (14 month) C57Bl/6 female mice was extracted using QIAshredder and RNeasy Micro Kits (QIAGEN). The quality was checked with a 2100 Bioanalyzer (Agilent Technologies). Total RNA was processed using Ambion MessageAmpTM Premier by the Duke Microarray Facility. Standard Affymetrix protocols and Affymetrix GeneChip´fi Mouse Genome 430 2.0 Array chips were used to generate .cel files.

Background corr dist: KL-Divergence = 0.0838, L1-Distance = 0.0224, L2-Distance = 0.0006, Normal std = 0.4668

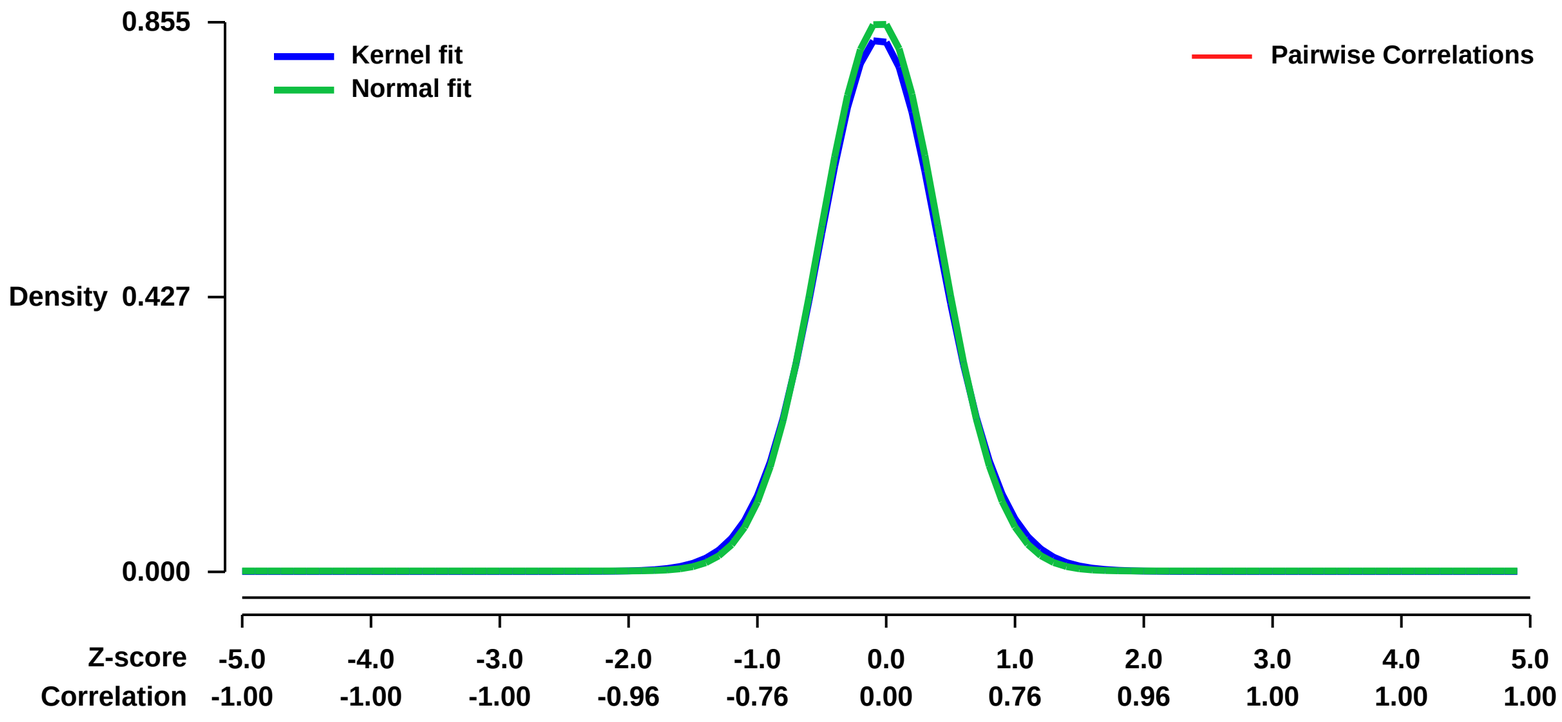

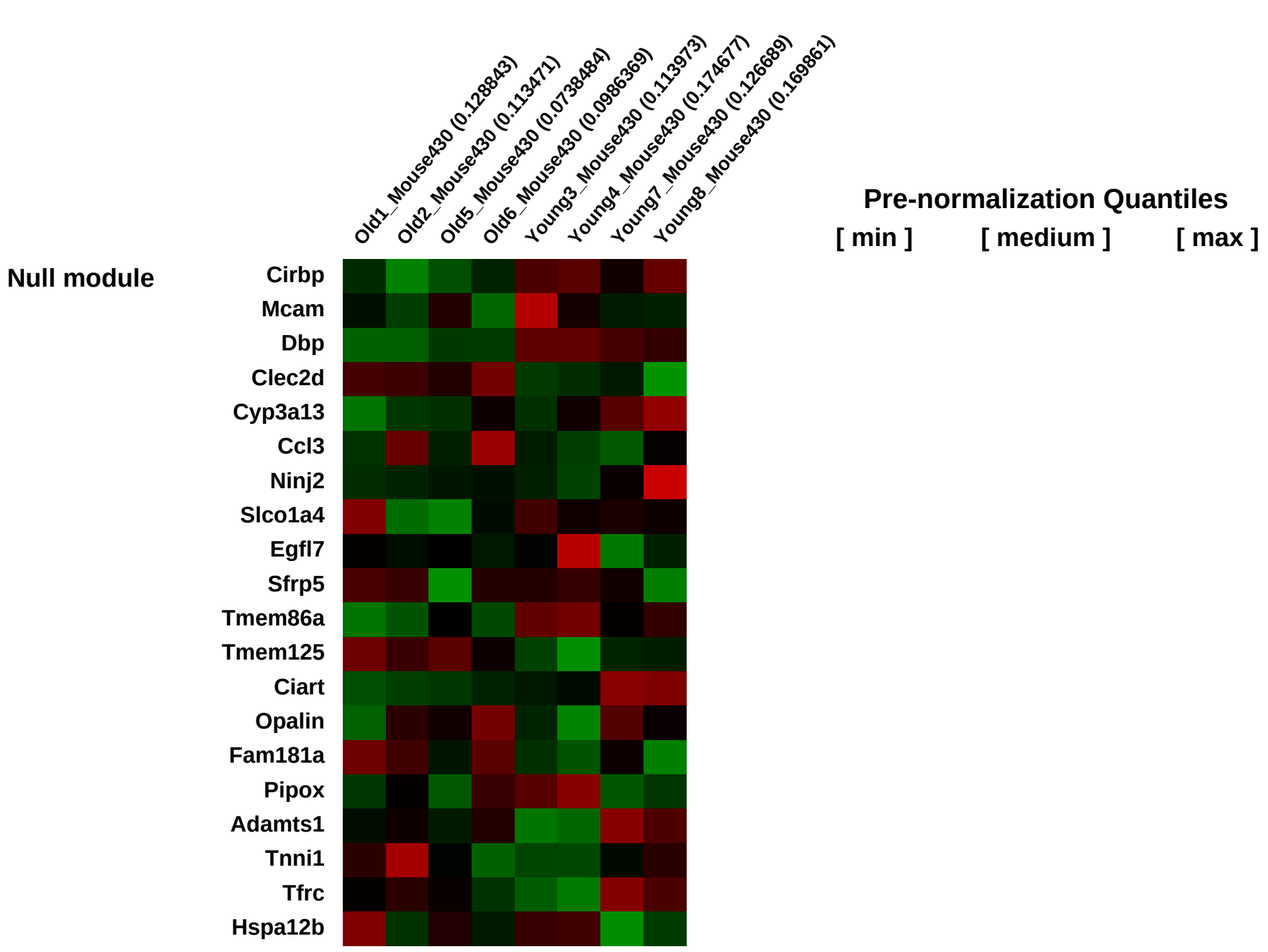

GEO Series "GSE10913" Expression Profiles

Num of samples in this series: 6

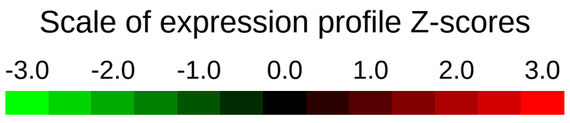

GEO Link:	**http://www.ncbi.nlm.nih.gov/geo/query/acc.cgi?acc=GSE10913**
Status:	**Public on Mar 21 2008**
Title:	**Bmp2 Is Critical for the Murine Decidual Response**
Organism:	**Mus musculus**
Experiment type:	**Expression profiling by array**
Platform:	**GPL1261**
Pubmed ID:	**17515606**
Summary & Design:	**Summary:** **The role of bone morphogenetic protein 2 (Bmp2)in regulating the transformation of the uterine stroma during embryo implantation in the mouse was investigated by the conditional ablation of Bmp2 in the uterus using the (PR-cre) mouse.** **Keywords: Genetic modification** **Overall design:** **Bmp2 gene ablation was confirmed by real-time PCR analysis in the PR-cre; Bmp2fl/fl (termed Bmp2d/d) uterus. While littermate controls average 0.9 litter of 6.2 ´– 0.7 pups per month, Bmp2d/d females are completely infertile. Analysis of the infertility indicates that whereas embryo attachment is normal in the Bmp2d/d as in control mice, the uterine stroma is incapable of undergoing the decidual reaction to support further embryonic development. Recombinant human BMP2 can partially rescue the decidual response, suggesting that the observed phenotypes are not due to a developmental consequence of Bmp2 ablation. Microarray analysis demonstrates that ablation of Bmp2 leads to specific gene changes, including disruption of the Wnt signaling pathway, Progesterone receptor (PR) signaling, and the induction of prostaglandin synthase 2 (Ptgs2). Taken together, these data demonstrate that Bmp2 is a critical regulator of gene expression and function in the murine uterus.**

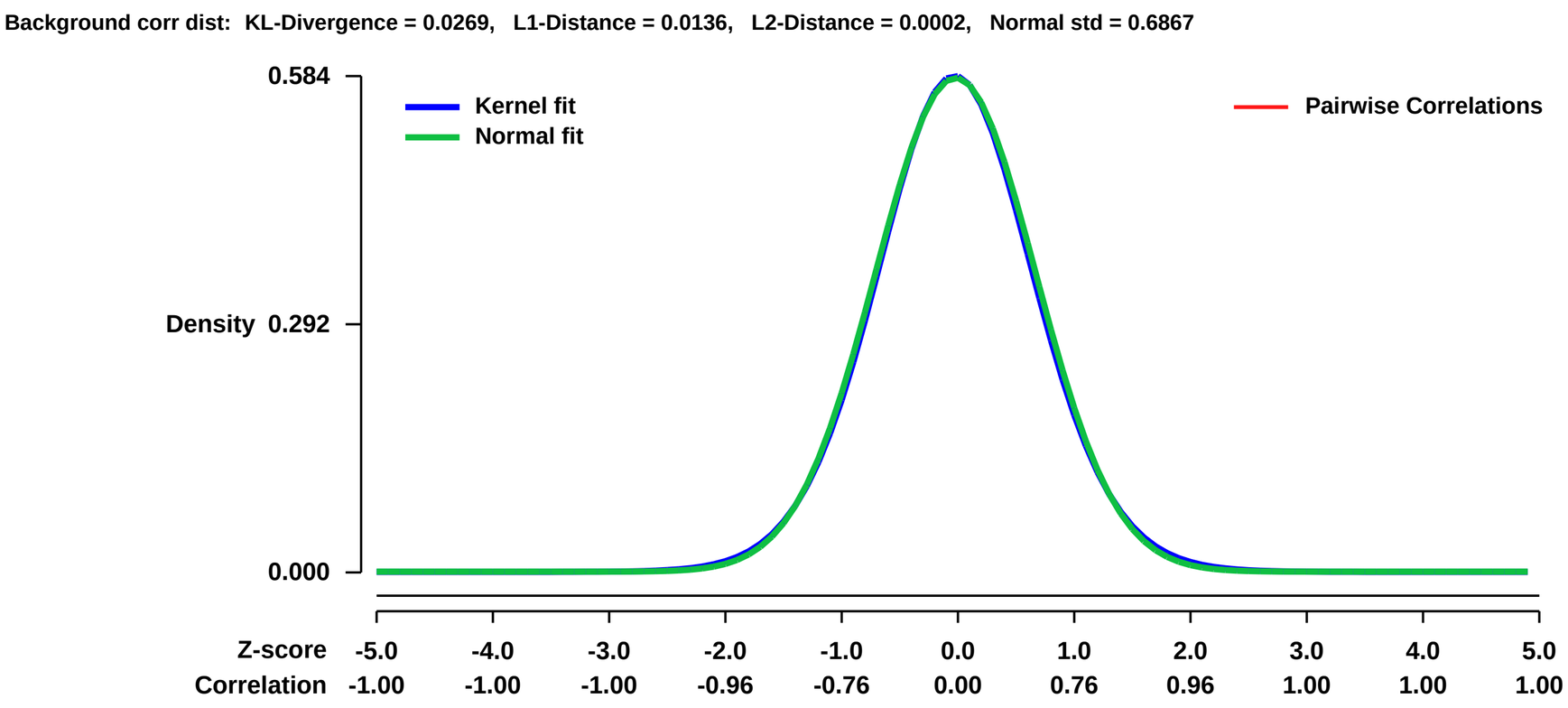

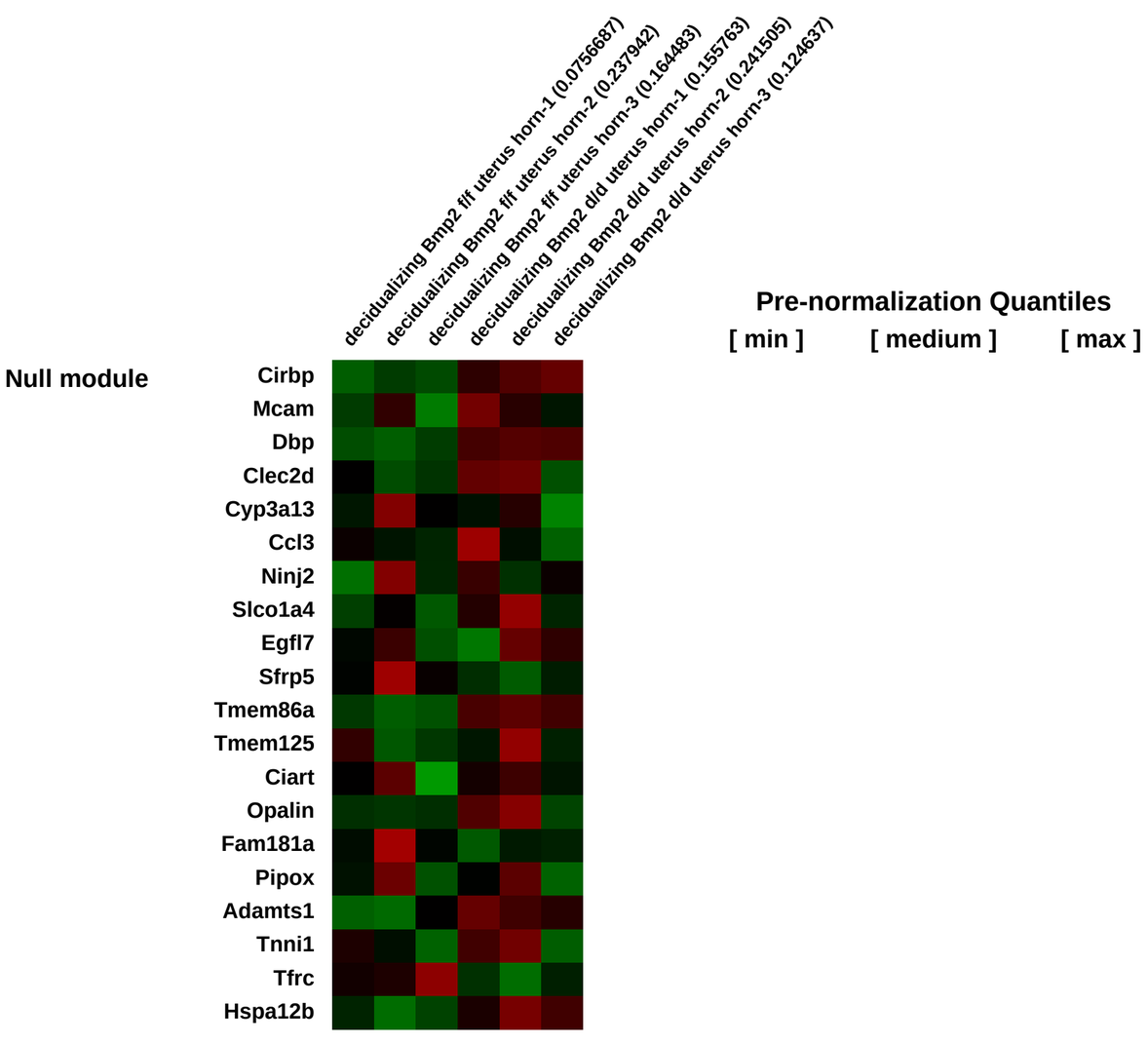

GEO Series "GSE46209" Expression Profiles

Num of samples in this series: 21

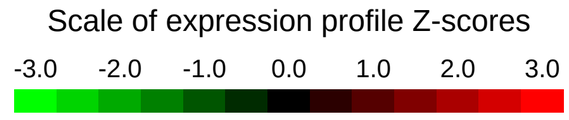

GEO Link:	http://www.ncbi.nlm.nih.gov/geo/query/acc.cgi?acc=GSE46209
Status:	Public on Jun 01 2013
Title:	Non-telomeric role for Rap1 in regulating metabolism and protecting against obesity
Organism:	Mus musculus
Experiment type:	Expression profiling by array
Platform:	GPL1261
Pubmed ID:	23791522
Summary & Design:	**Summary:** The mammalian telomere-binding protein Rap1 was found to have additional non-telomeric functions, acting as a transcriptional cofactor and a regulator of the NF-kB pathway. Here, we assess the effect of disrupting mouse Rap1 in vivo, and report on its unanticipated role in metabolic regulation and body weight homeostasis. Rap1 inhibition causes dysregulation in hepatic as well as adipose function. In addition, using a separation-of-function allele, we show that the metabolic function of Rap1 is independent of its recruitment to TTAGGG binding elements found at telomeres, and at other interstitial loci. We have utilized microarrays to outline gene expression changes resulting from Rap1-deficiency when compared to the wild-type controls. **Overall design:** Total RNA was isolated from the liver and intra-abdominal white adipose tissue of 3 female Rap1 deficient mice and 3 control littermates at 6-8 weeks of age. Rap1 deficient mouse embryonic fibroblasts (MEF) were isolated from 13.5 day embryos, immortalized with SV40LgT, and stably infected with vector, Rap1-wildtype, or Rap1 carrying an isoleucine to arginine mutation at amino acid 312. Total RNA was extracted from MEFs following a similar protocol. The samples were labeled, hybridized, and scanned using standard protocols by the Core Facility at NYU Langone Medical Center on Affymetrix GeneChip Mouse Genome 430 2.0 Arrays.

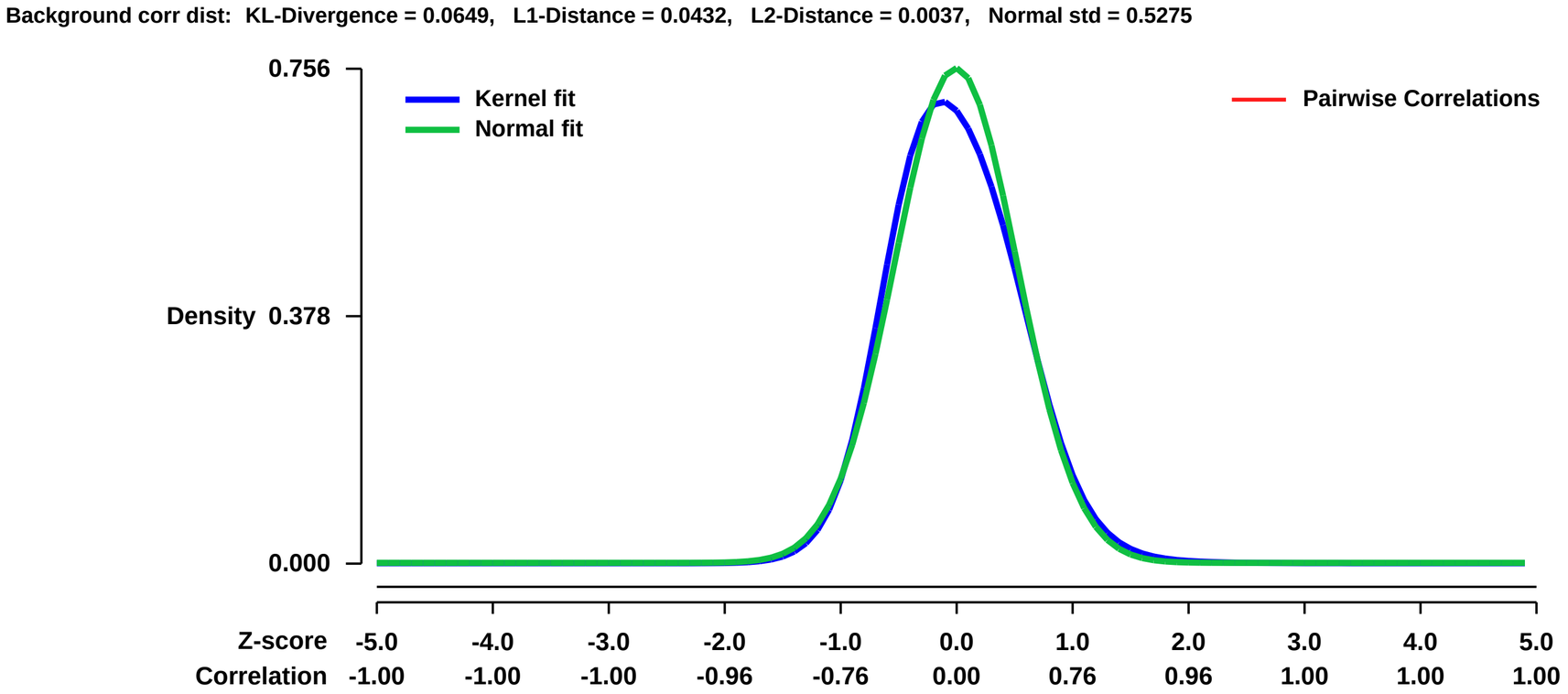

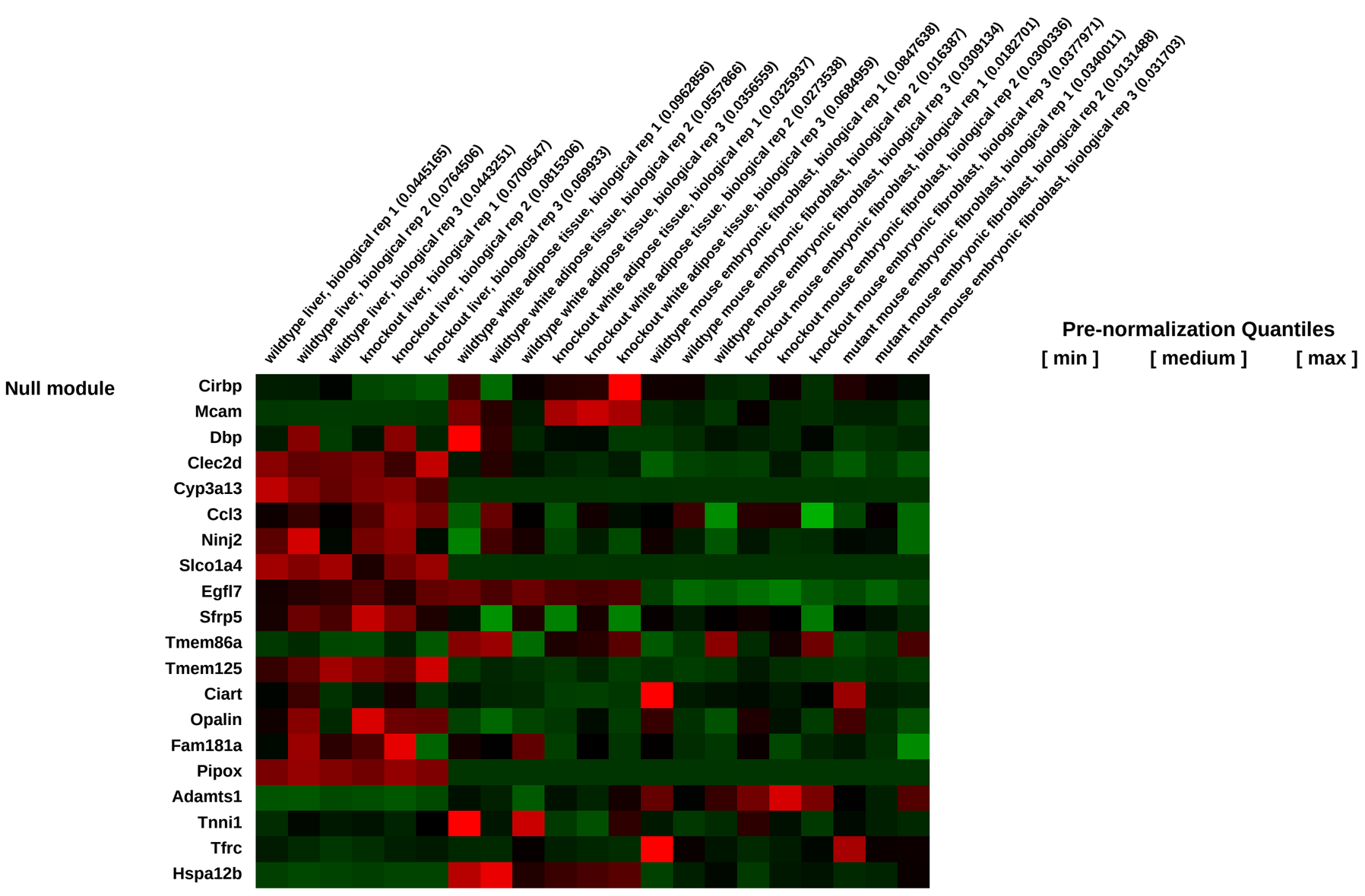

GEO Series "GSE23408" Expression Profiles

Num of samples in this series: 39

Scale of expression profile Z-scores

-3.0 -2.0 -1.0 0.0 1.0 2.0 3.0

GEO Link: http://www.ncbi.nlm.nih.gov/geo/query/acc.cgi?acc=GSE23408
Status: Public on Aug 02 2011
Title: Global gene expression profiles and the progression of pro- and anti-inflammatory pathways in mouse models
Organism: Mus musculus
Experiment type: Expression profiling by array
Platform: GPL1261
Pubmed ID:
Summary & Design:

Summary:
Gaucher Disease (GD) is caused by defective glucocerebrosidase (GCase) activity and the consequent accumulation of its substrate, glucosylceramide (GC). This excess of accumulation of GC leads to broad functional impairments in multiple organs, but the pathogenic pathways leading to lipid laden macrophages (Gaucher cells) in visceral organs and their abnormal function is obscure. To understand the molecular pathogenesis of GD, developmental global gene expression was conducted by microarray analyses of total mRNAs from lung and liver of two distinct GCase point-mutated mice (V394L/V394L and D409V/null) and genetic background matched wild-type controls. INFg regulated pro-inflammatory and IL-4 regulated anti-inflammatory cytokine/mediator network were constructed in the lung and liver of GCase mutant mice. Progressive alterations of the INFg and IL-4 pathways were similar, but to different degrees, in visceral tissues from the two different GCase mutated mice. These analyses implicate IFNg regulated pro-inflammatory and IL-4 regulated anti-inflammatory networks in the differential pathophysiological progression.

Overall design:
In order to understand the molecular pathogenesis of GD, the disease progression in those models were inverstigated in two visceral tissues (lung and liver) at four time points according to the genotypes. 9V/null: 4 weeks (4w), 12 weeks (12w), 18 weeks (18w), 28 weeks (28w); 4L: weeks (4w), 12 weeks (12w), 18 weeks (18w), 28 weeks (28w). The data from those models were analyzed relative to the adult wild type at 28 weeks.

Background corr dist: KL-Divergence = 0.0891, L1-Distance = 0.0753, L2-Distance = 0.0105, Normal std = 0.4948

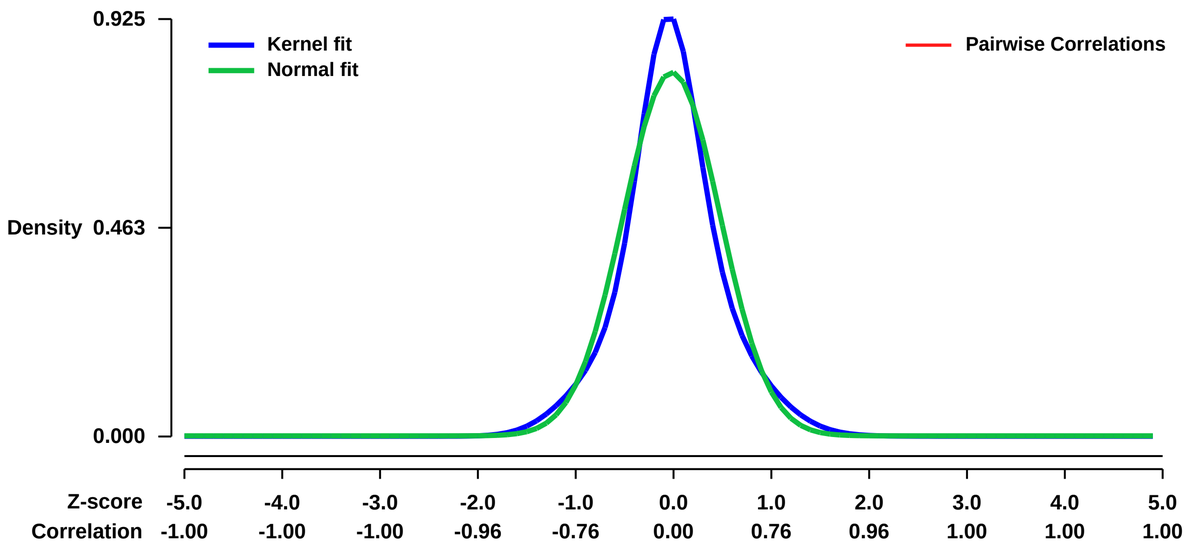

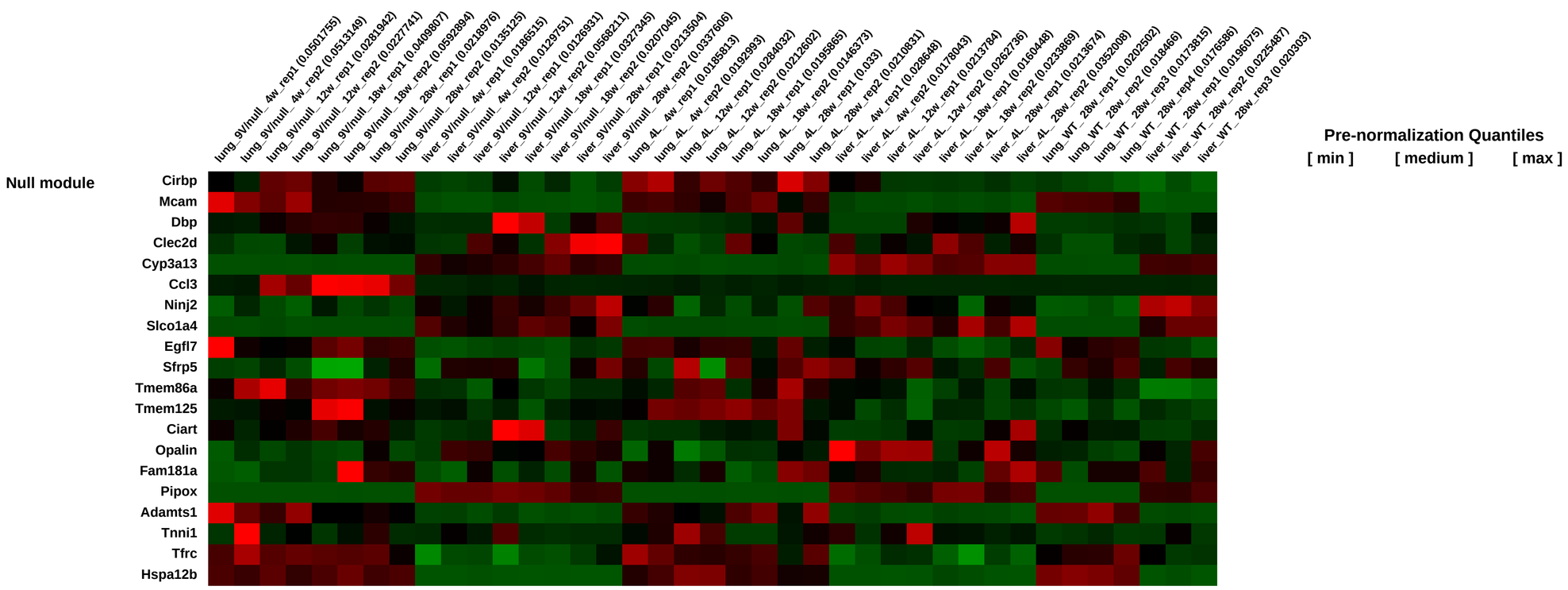

GEO Series "GSE9247" Expression Profiles

Num of samples in this series: 15

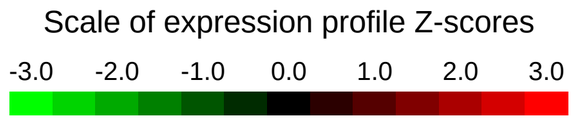

GEO Link:	http://www.ncbi.nlm.nih.gov/geo/query/acc.cgi?acc=GSE9247
Status:	Public on Oct 06 2007
Title:	Effect of histone deacetylase inhibitors on osteoblast gene expression
Organism:	Mus musculus
Experiment type:	Expression profiling by array
Platform:	GPL1261
Pubmed ID:	17925016
Summary & Design:	**Summary:** **Background:** **Osteoblast differentiation requires the coordinated stepwise expression of multiple genes. Histone deacetylase inhibitors (HDIs) accelerate the osteoblast differentiation process by blocking the activity of histone deacetylases (HDACs), which alter gene expression by modifying chromatin structure. We previously demonstrated that HDIs and HDAC3 shRNAs accelerate matrix mineralization and the expression of osteoblast maturation genes (e.g. alkaline phosphatase, osteocalcin). Identifying other genes that are differentially regulated by HDIs might identify new pathways that contribute to osteoblast differentiation.** **Results:** **To identify other osteoblast genes that are altered early by HDIs, we incubated MC3T3-E1 preosteoblasts with HDIs (trichostatin A, MS-275, or valproic acid) for 18 hours in osteogenic conditions. The promotion of osteoblast differentiation by HDIs in this experiment was confirmed by osteogenic assays. Gene expression profiles relative to vehicle-treated cells were assessed by microarray analysis with Affymetrix GeneChip 430 2.0 arrays. The regulation of several genes by HDIs in MC3T3-E1 cells and primary osteoblasts was verified by quantitative real-time PCR. Nine genes were differentially regulated by at least two-fold after exposure to each of the three HDIs and six were verified by PCR in osteoblasts. Four of the verified genes (solute carrier family 9 isoform 3 regulator 1 (Slc9a3r1), sorbitol dehydrogenase 1, a kinase anchor protein, and glutathione S-transferase alpha 4) were induced. Two genes (proteasome subunit, beta type 10 and adaptor-related protein complex AP-4 sigma 1) were suppressed. We also identified eight growth factors and growth factor receptor genes that are significantly altered by each of the HDIs, including Frizzled related proteins 1 and 4, which modulate the Wnt signaling pathway.** **Conclusions: This study identifies osteoblast genes that are regulated early by HDIs and indicates pathways that might promote osteoblast maturation following HDI exposure. One gene whose upregulation following HDI treatment is consistent with this notion is Slc9a3r1. Also known as NHERF1, Slc9a3r1 is required for optimal bone density. Similarly, the regulation of Wnt receptor genes indicates that this crucial pathway in osteoblast development is also affected by HDIs. These data support the hypothesis that HDIs regulate the expression of genes that promote osteoblast differentiation and maturation.** **Keywords: gene expression** **Overall design:** **To identify other osteoblast genes that are altered early by HDIs, we incubated MC3T3-E1 preosteoblasts with HDIs (trichostatin A, MS-275, or valproic acid) or the vehicle control (DMSO) for 18 hours in osteogenic conditions. Gene expression profiles relative to vehicle-treated cells were assessed in triplicate (in some cases quadruplicate) samples by microarray analysis with Affymetrix GeneChip 430 2.0 arrays.**

Background corr dist: **KL-Divergence = 0.1049, L1-Distance = 0.0636, L2-Distance = 0.0067, Normal std = 0.4730**

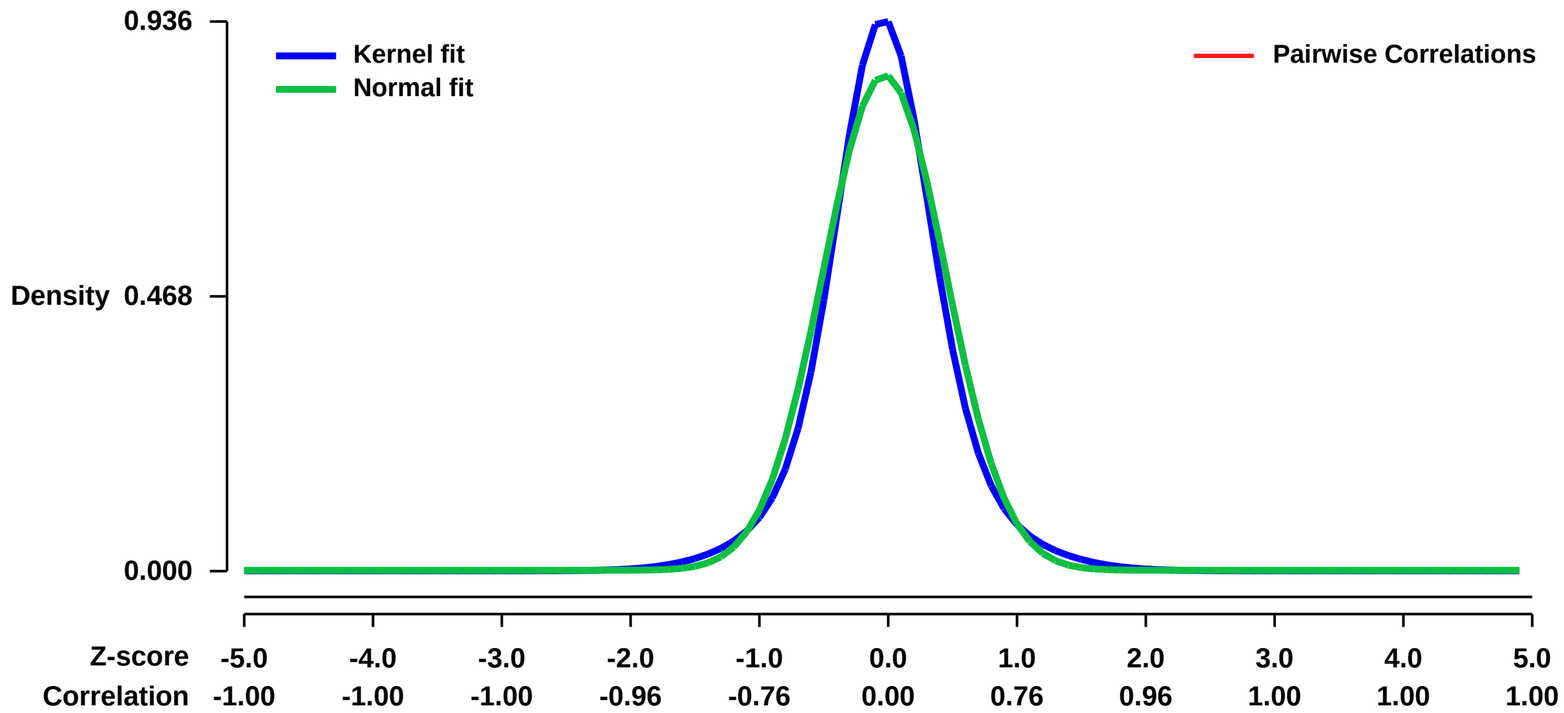

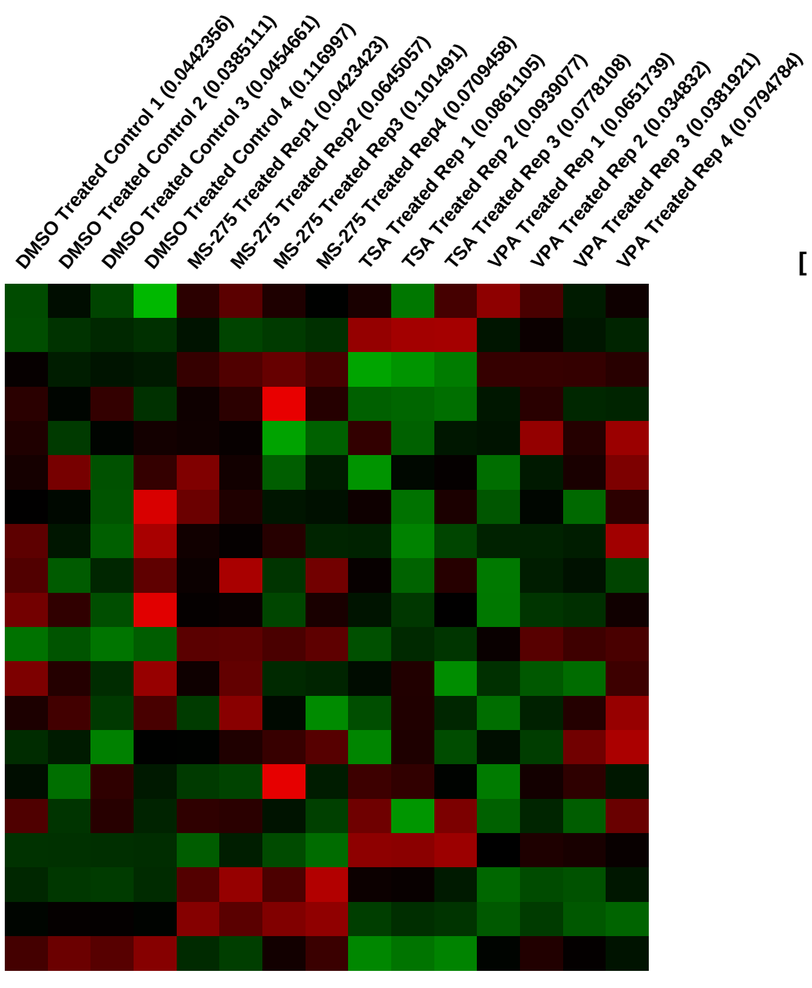

GEO Series "GSE39458" Expression Profiles

Num of samples in this series: 6

Scale of expression profile Z-scores

-3.0 -2.0 -1.0 0.0 1.0 2.0 3.0

GEO Link:	**http://www.ncbi.nlm.nih.gov/geo/query/acc.cgi?acc=GSE39458**
Status:	**Public on Dec 31 2012**
Title:	**Differential gene expression of Kit+Sca1+Lin- (KSL) cells from arthritic versus control mice**
Organism:	**Mus musculus**
Experiment type:	**Expression profiling by array**
Platform:	**GPL1261**
Pubmed ID:	
Summary & Design:	**Summary:** **The involvement of mature hematopoietic cells in disease pathogenesis is well recognized. However it is not clear how if and how primitive progenitors might contribute to inflammatory disease processes.** **This microarray experiment is used together with data from functional assays to determine how primitive progenitors are altered in a mouse model of autoimmune arthritis and how this in turn might contribute to the disease process.** **Overall design:** **All the mice used in this study were C57BL/6 background strain. G7 mice are congenic with C57BL/6 but with MHC II I-Ab replaced with MHC II I-Ag7.**

Background corr dist: **KL-Divergence = 0.0145, L1-Distance = 0.0305, L2-Distance = 0.0010, Normal std = 0.8466**

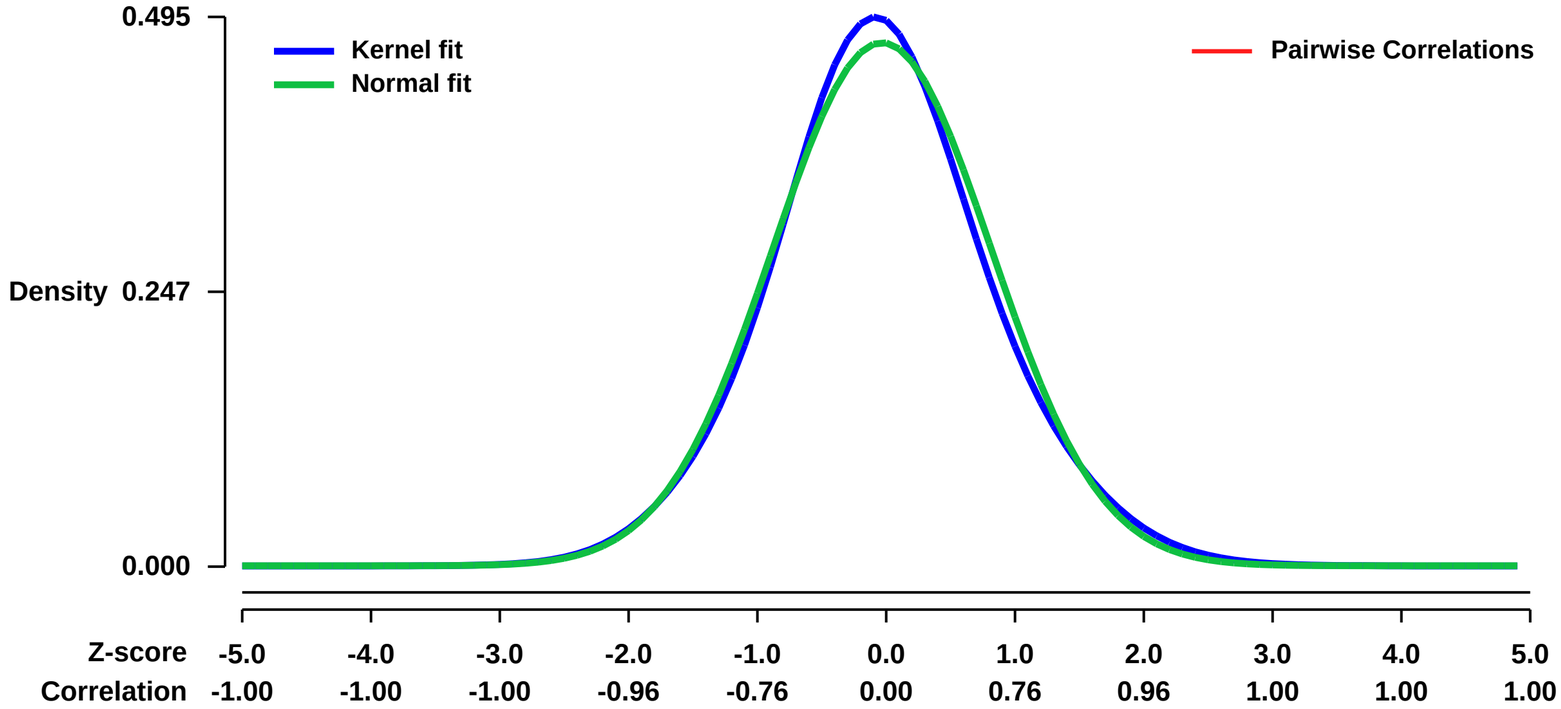

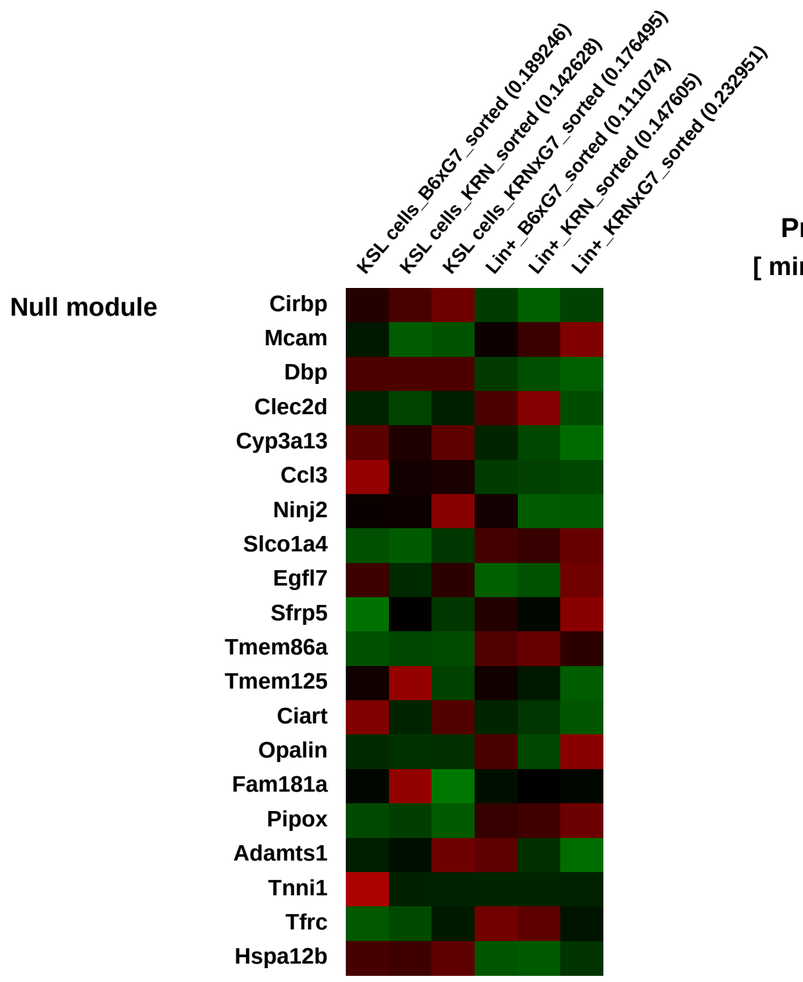

GEO Series "GSE27717" Expression Profiles

Num of samples in this series: 11

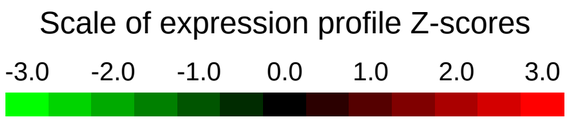

GEO Link:	http://www.ncbi.nlm.nih.gov/geo/query/acc.cgi?acc=GSE27717
Status:	Public on Sep 15 2011
Title:	Expression data from lung tumors of KrasTgfbr2 -/- mouse model
Organism:	Mus musculus
Experiment type:	Expression profiling by array
Platform:	GPL1261
Pubmed ID:	21911454
Summary & Design:	**Summary:** Recent data suggests that repression of the Type II TGF-B Receptor (Tgfr2) repression in human lung adenocarcinoma is important for progression from noninvasive to invasive adenocarcinoma. To test this hypothesis in a animal model of non-invasive lung cancer, we generated an inducible, lung specific Tgfbr2 knockout model in the oncogenic Kras mouse. LSL-KrasG12D positive mice were simultaneously backcrossed to C57/Bl6 mice and to the Tgfbr2 flox/flox mice. To induce tumors, 100 _l of saline containing 3x10e10 particles of an adenovirus containing the Cre recombinase (Ad.Cre) was administered to each LSL-KrasG12D mouse intra-nasally. **Overall design:** Mice were sacrificed at 7 weeks after administration of Adeno-Cre. We used laser capture microdissection to acquire tumor cells from KrasTgfbr2-/- and KrasTgfbr2 wt mouse tumors.

Background corr dist: KL-Divergence = 0.0666, L1-Distance = 0.0266, L2-Distance = 0.0011, Normal std = 0.5027

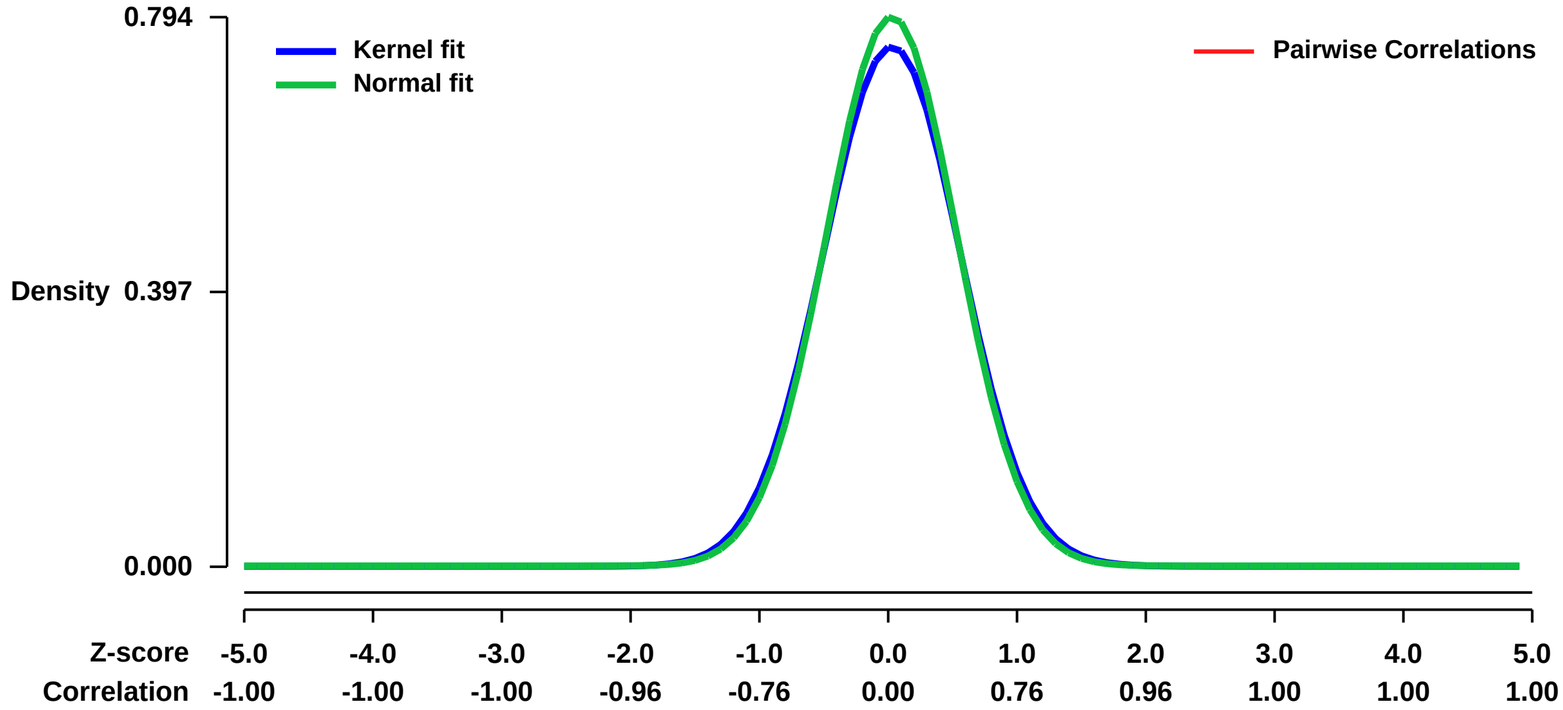

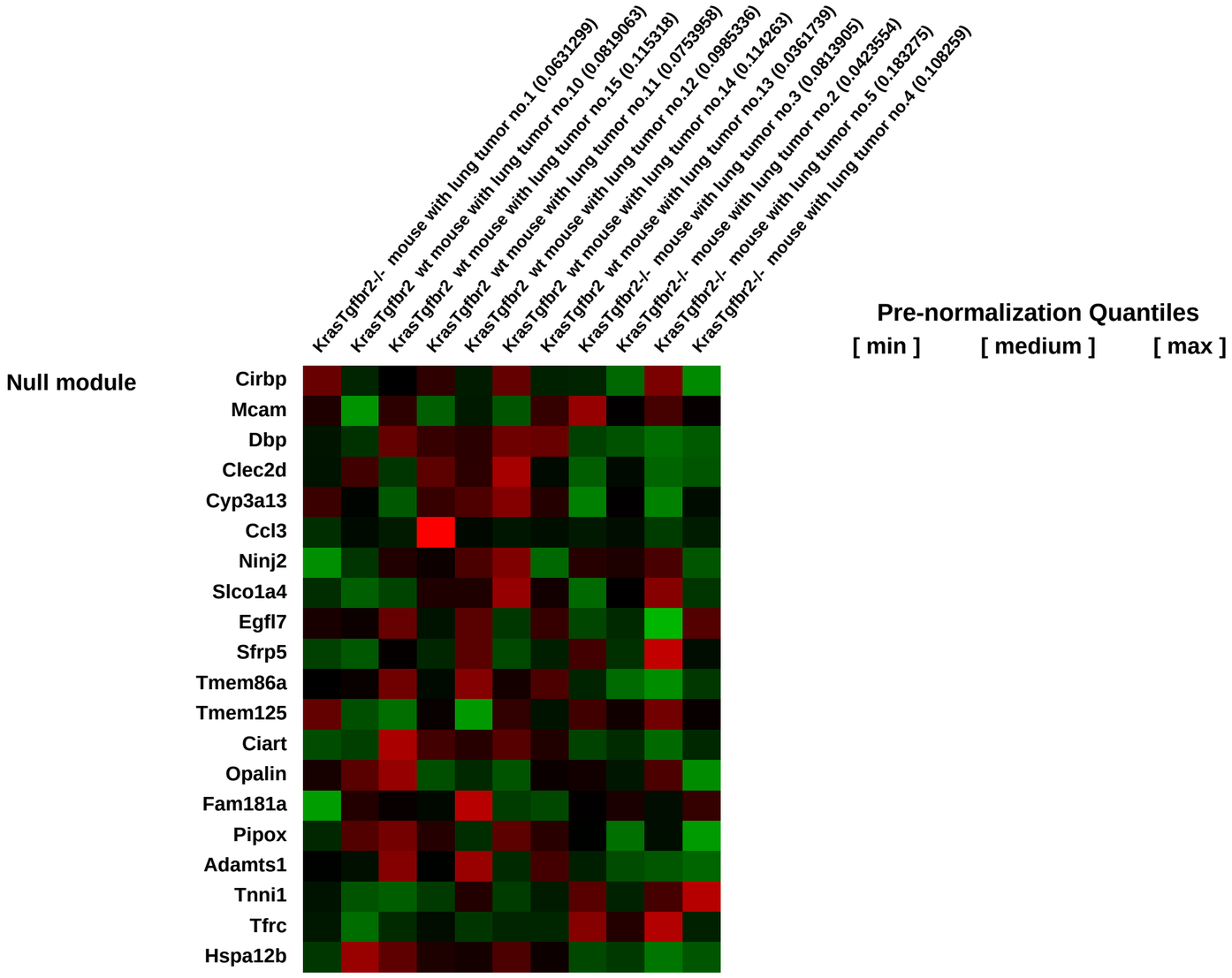

GEO Series "GSE5202" Expression Profiles

Num of samples in this series: 12

Scale of expression profile Z-scores

-3.0 -2.0 -1.0 0.0 1.0 2.0 3.0

GEO Link:	http://www.ncbi.nlm.nih.gov/geo/query/acc.cgi?acc=GSE5202
Status:	Public on Jun 30 2006
Title:	Expression data from B. melitensis infected mouse macrophages
Organism:	Mus musculus
Experiment type:	Expression profiling by array
Platform:	GPL1261
Pubmed ID:	16926395
Summary & Design:	**Summary:** **Facultative intracellular Brucella infect and survive inside macrophages, and the outcome of macrophage-Brucella interaction is a basis for establishment of a chronic Brucella infection. The majority of Brucella are killed at the early infection stage. A subpopulation of virulent Brucella strains is instead trafficked to an intracellular replicative phagosome, and are resistant to further attack and begin to multiply dramatically. Virulent Brucella also inhibit macrophage apoptosis that in turn favors pathogen survival and replication.** **We used the Affymetrix mouse GeneChip 430 2.0 array to analyze mouse macrophage gene expression profiles during the time course of virulent B. melitensis strain 16M infection.** **Keywords: time course** **Overall design:** **Murine J774.A1 macrophage cells were infected with B. melitensis strain 16M at a MOI of 200:1. Brucella cultures derived from different Brucella colonies were used to infect different groups of macrophage cells to reflect independent infections. Following 4 h incubation, the cells were washed with PBS and treated with 50 ug/ml gentamicin to kill extracellular Brucella. At 0 h (no Brucella infection), 4 h, 24 h, and 48 h post-infection, cells were individually collected, and total RNA was isolated. The Affymetrix mouse GeneChip 430 2.0 array was used for microarray hybridization. Microarray intensity data were obtained by using Affymetrix GCOS software and further analyzed by GeneSpring and other software programs.**

Background corr dist: KL-Divergence = 0.1187, L1-Distance = 0.0258, L2-Distance = 0.0010, Normal std = 0.4112

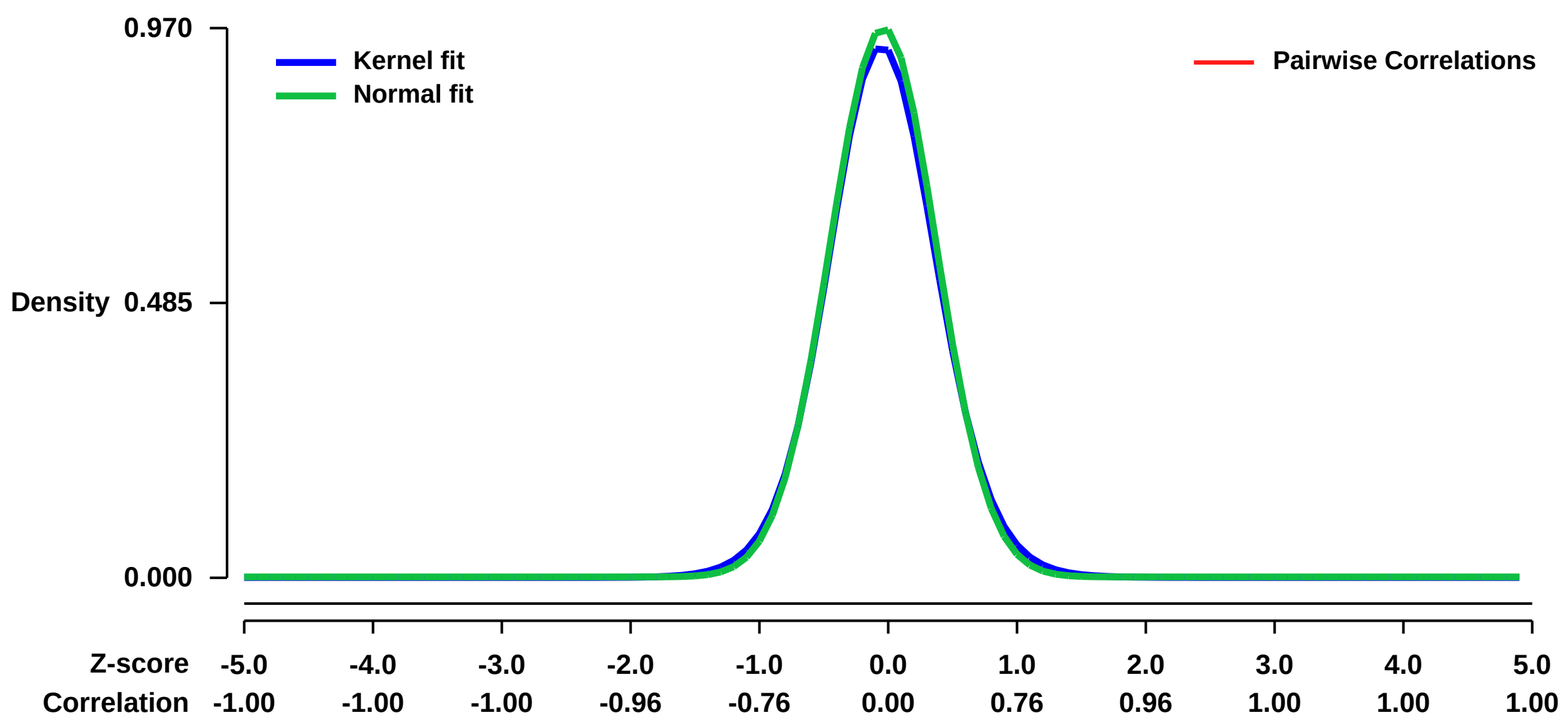

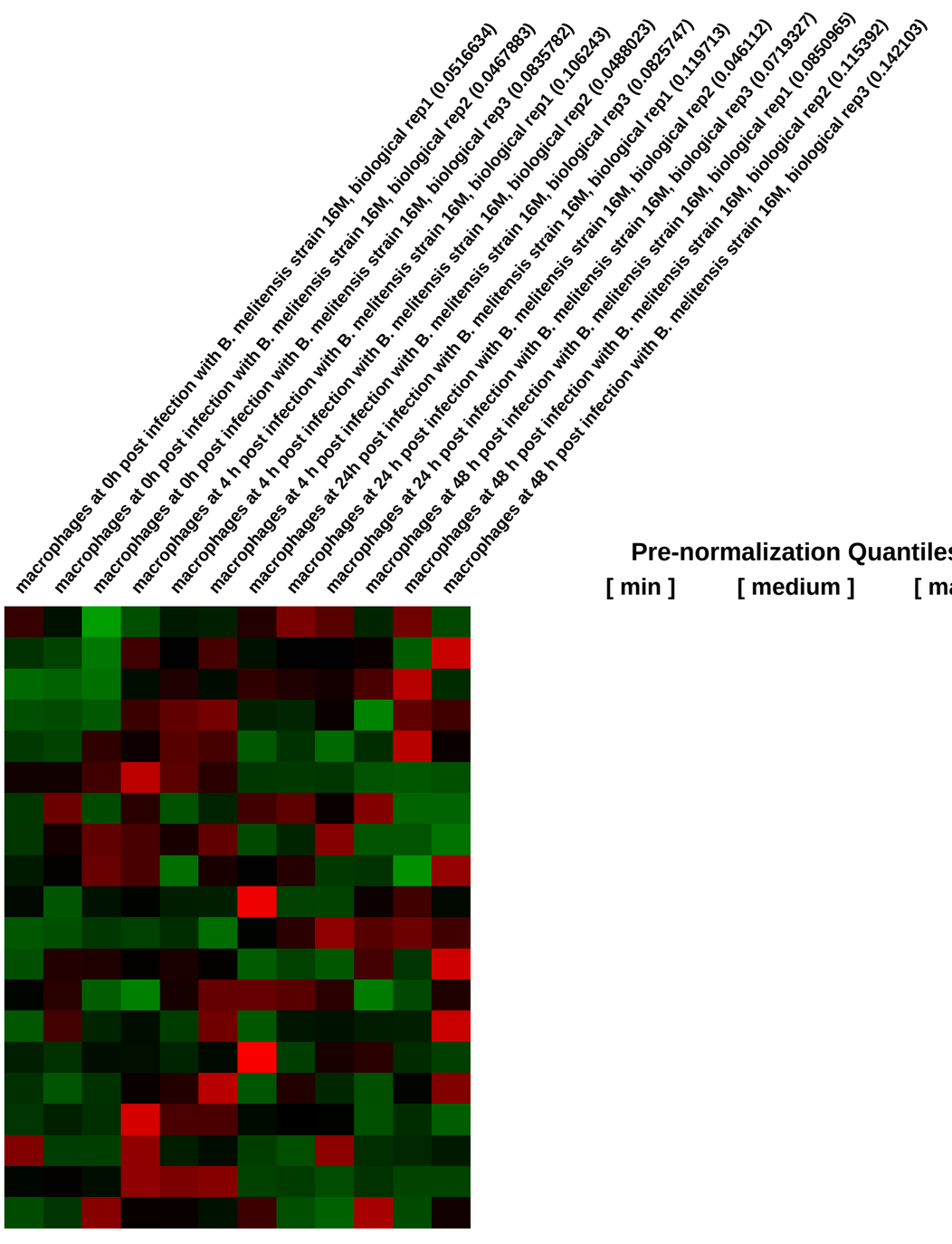

GEO Series "GSE34839" Expression Profiles

Num of samples in this series: 6

Scale of expression profile Z-scores

-3.0 -2.0 -1.0 0.0 1.0 2.0 3.0

GEO Link:	http://www.ncbi.nlm.nih.gov/geo/query/acc.cgi?acc=GSE34839
Status:	Public on Feb 28 2012
Title:	Pten loss and RAS/MAPK activation cooperate to promote EMT and prostate cancer metastasis initiated from stem/progenitor cells
Organism:	Mus musculus
Experiment type:	Expression profiling by array
Platform:	GPL1261
Pubmed ID:	22350410
Summary & Design:	**Summary:** PTEN loss or PI3K/AKT signaling pathway activation correlates with human prostate cancer progression and metastasis. However, in preclinical murine models, deletion of Pten alone fails to mimic the significant metastatic burden that frequently accompanies the end stage of human disease. To identify additional pathway alterations that cooperate with PTEN loss in prostate cancer progression, we surveyed human prostate cancer tissue microarrays and found that the RAS/MAPK pathway is significantly elevated both in primary and metastatic lesions. In an attempt to model this event, we crossed conditional activatable K-rasG12D/WT mice with the prostate conditional Pten deletion model we previously generated. Although RAS activation alone cannot initiate prostate cancer development, it significantly accelerated progression caused by PTEN loss, accompanied by epithelial-to-mesenchymal transition (EMT) and macrometastasis with 100% penitence. A novel stem/progenitor subpopulation with mesenchymal characteristics was isolated from the compound mutant prostates, which was highly metastatic upon orthotopic transplantation. Importantly, inhibition of RAS/MAPK signaling by PD325901, a MEK inhibitor, significantly reduced the metastatic progression initiated from transplanted stem/progenitor cells. Collectively, these data indicate that activation of RAS/MAPK signaling serves as a potentiating second hit to alteration of the PTEN/PI3K/AKT axis and co-targeting both pathways is highly effective in preventing the development of metastatic prostate cancers. **Overall design:** Murine mutants with prostate specific loss of Pten and K-ras activation (K-rasG12D) under regulation of the probasin promoter developed high grade, invasive prostate cancer. RNA was extracted from dissected prostate lobes from individual mutants with pathology thought to closely mimic human disease. Prostate tissue was subject to RNA extraction and hybridization on Affymetrix cDNA microarrays.

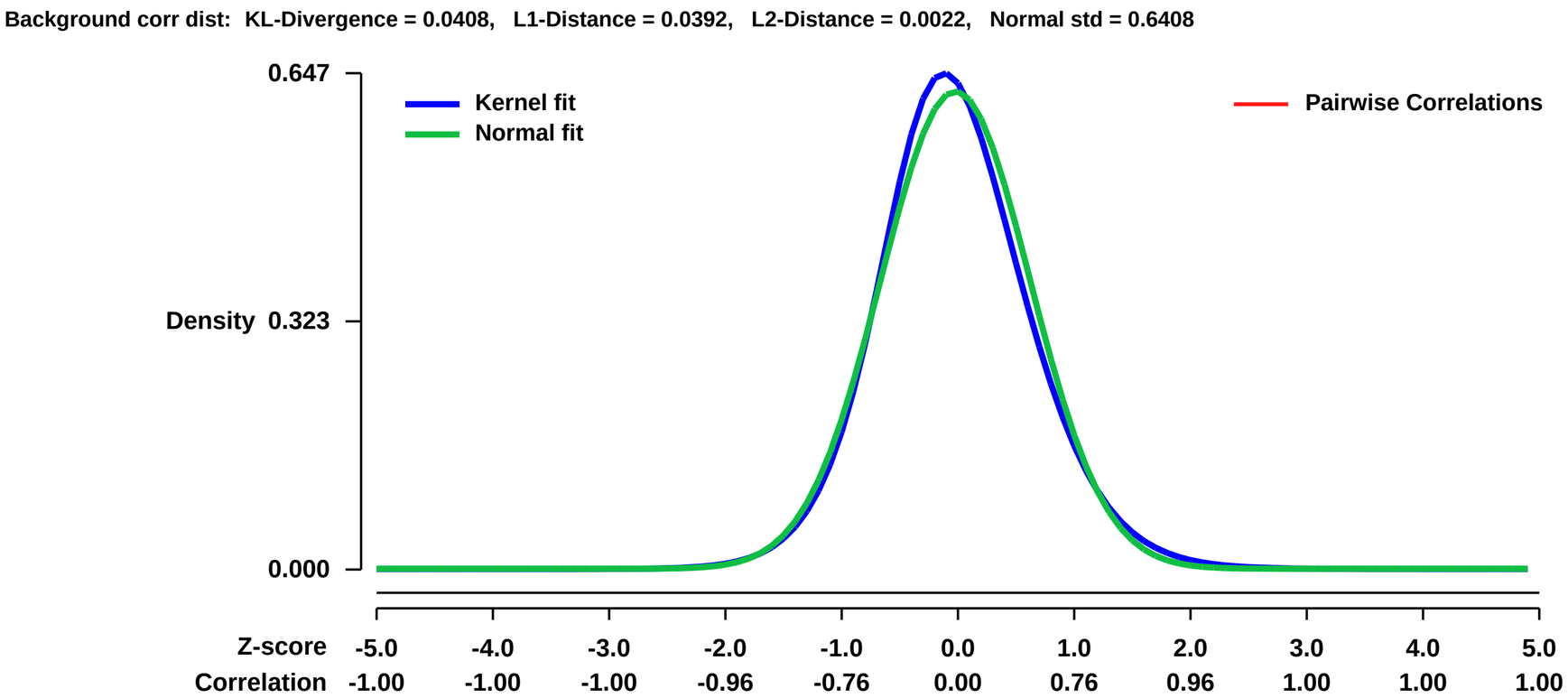

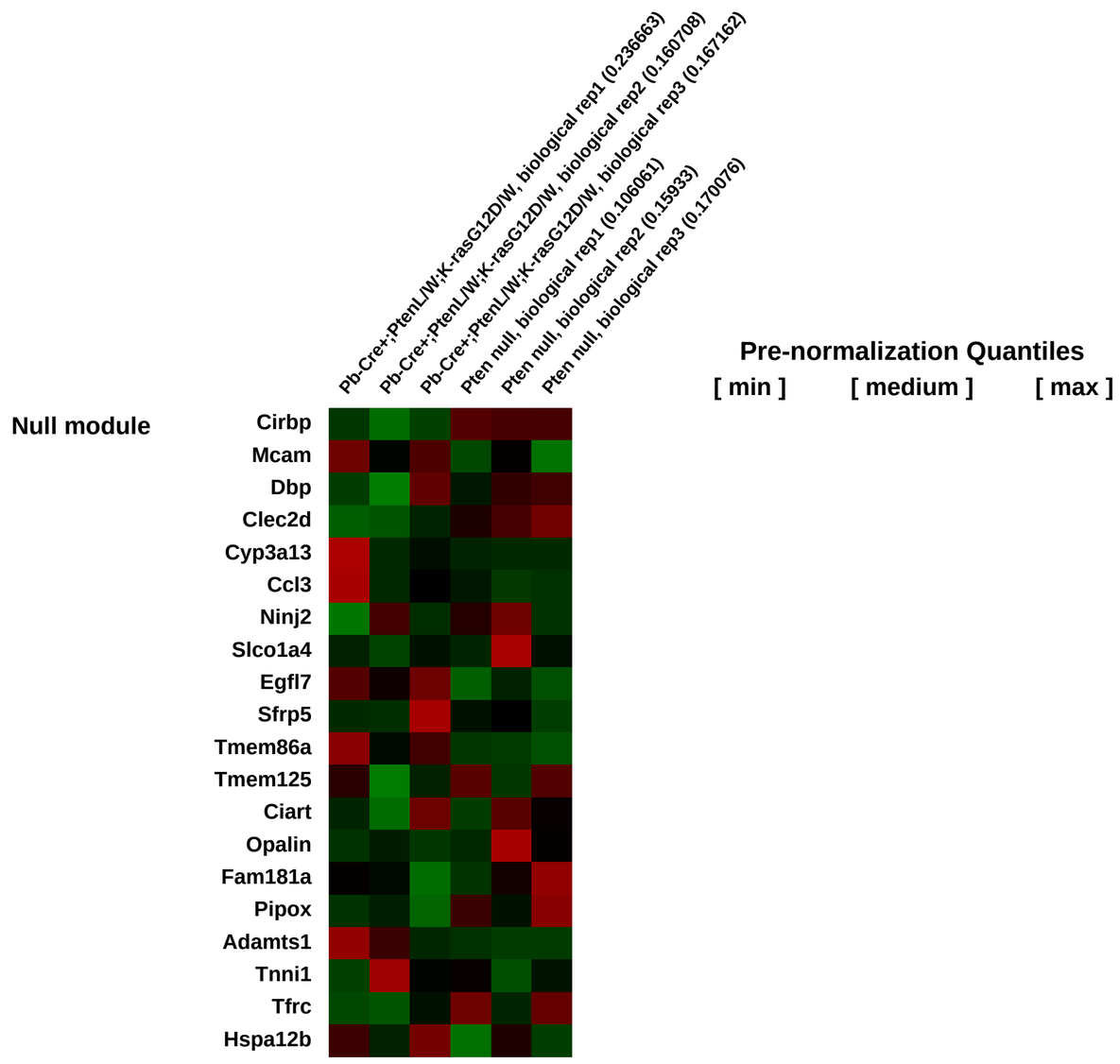

GEO Series "GSE3501" Expression Profiles

Num of samples in this series: 6

Scale of expression profile Z-scores

-3.0 -2.0 -1.0 0.0 1.0 2.0 3.0

GEO Link:	http://www.ncbi.nlm.nih.gov/geo/query/acc.cgi?acc=GSE3501
Status:	Public on Jan 01 2006
Title:	Comparative analysis of 10 week and 5 week Bitransgenic mice (LH mouse crossed with MMTV-neu mouse)
Organism:	Mus musculus
Experiment type:	Expression profiling by array
Platform:	GPL1261
Pubmed ID:	16434967
Summary & Design:	**Summary:** To identify genes that may facilitate early steps of ErbB2/Neu-mediated mammary tumorigenesis, we performed comparative microarray analysis of 5- and 10-week bitransgenic mammary glands (LHxMMTV-neu) in triplicate. **Keywords: transgenic mouse, erbB2, MMTV-neu, HER2, mammary tumor, breast cancer** **Overall design:** We analyzed 3 pooled RNA samples that represented 3 animals for each time point so that a total of 9 bitransgenic mice were analyzed per time point.

Background corr dist: **KL-Divergence = 0.0235, L1-Distance = 0.0195, L2-Distance = 0.0004, Normal std = 0.7222**

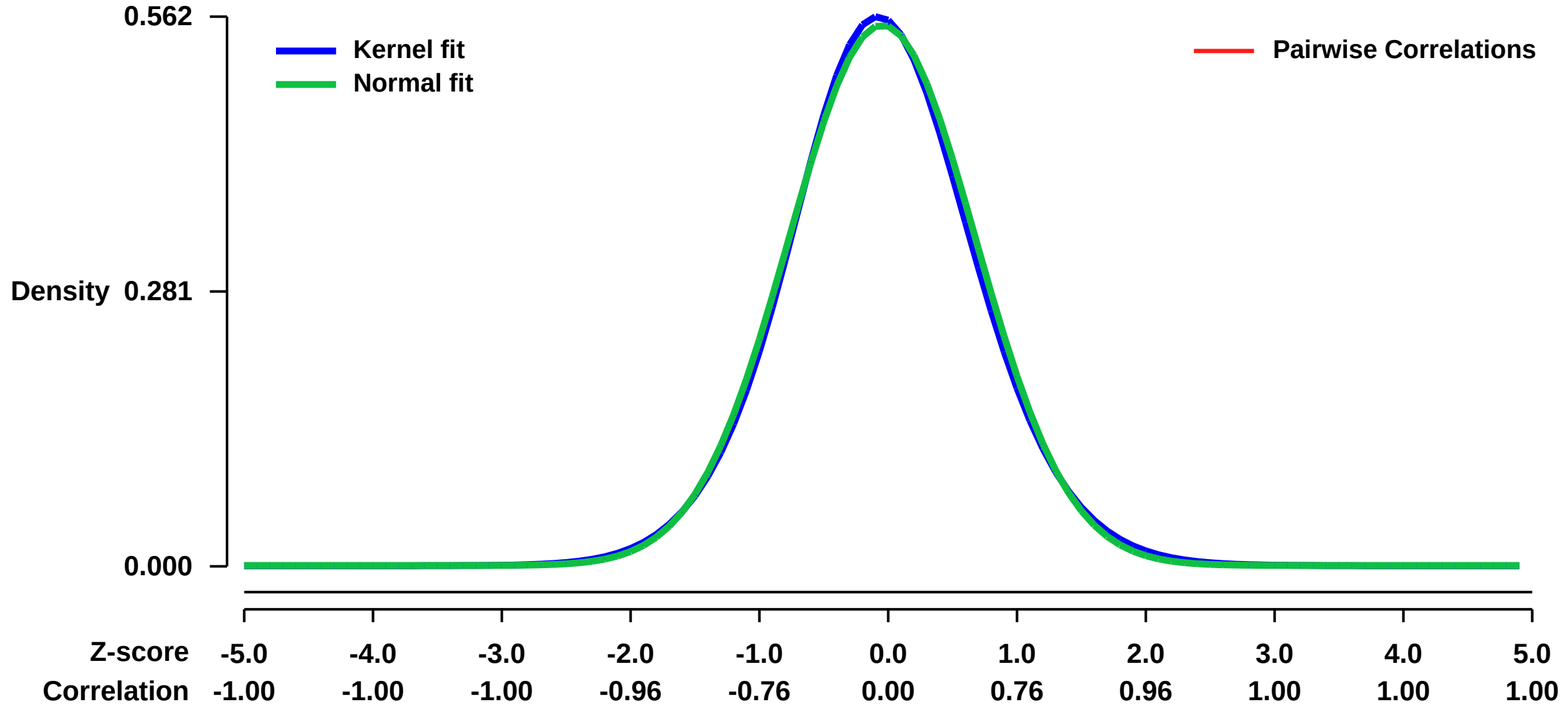

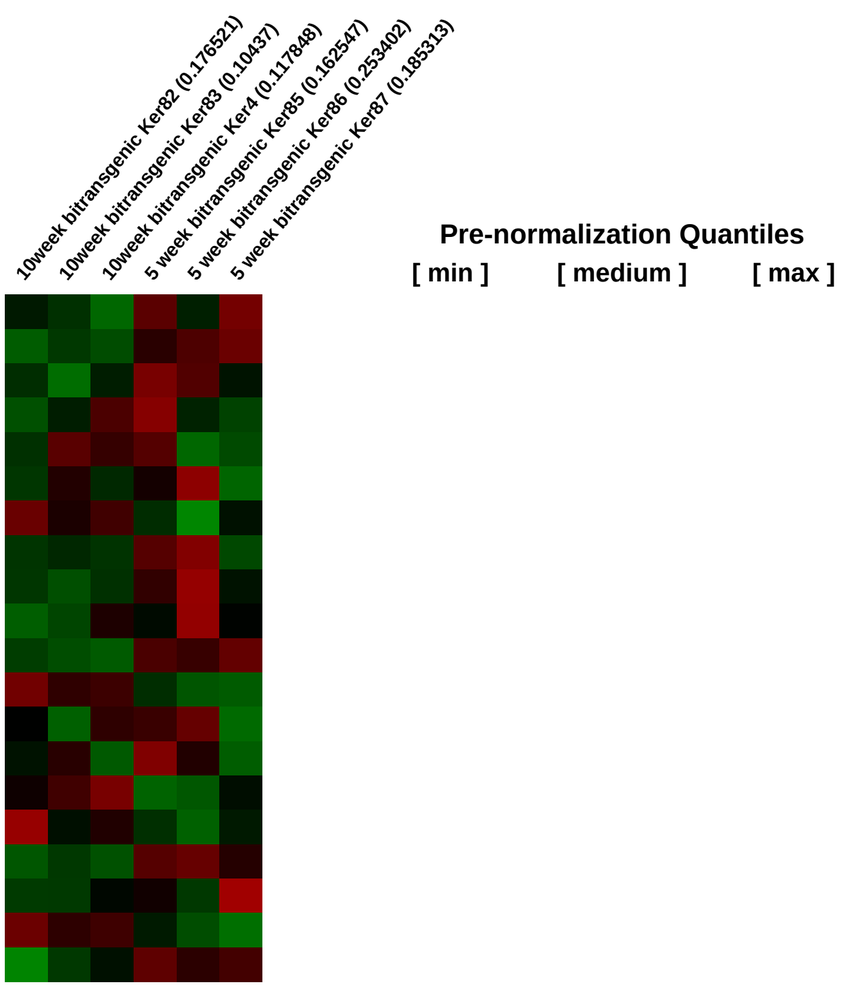

GEO Series "GSE14458" Expression Profiles

Num of samples in this series: 12

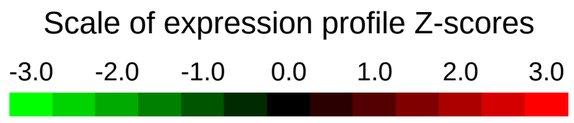

GEO Link:	http://www.ncbi.nlm.nih.gov/geo/query/acc.cgi?acc=GSE14458
Status:	Public on Nov 10 2009
Title:	Gene expression profiles of 344SQ lung adenocarcinoma cells with high metastatic potential (syngeneic mouse model)
Organism:	Mus musculus
Experiment type:	Expression profiling by array
Platform:	GPL1261
Pubmed ID:	19759262
Summary & Design:	**Summary:** The biologic basis for NSCLC metastasis is not well understood. Here we addressed this deficiency by transcriptionally profiling tumors from a genetic mouse model of human lung adenocarcinoma that develops metastatic disease owing to the expression of K-rasG12D and p53R172H. As a tool to investigate the biologic basis for metastasis in this model and to query the roles of specific genes in this signature, we isolated adenocarcinoma cell lines from these mice and used them to develop a syngeneic tumor model in wild-type littermates. Transcriptional profiling of the highly metastatic subcutaneous tumors revealed genes that regulate, among other processes, epithelial-to-mesenchymal transition and intra-tumoral inflammation and angiogenesis, whereas the non-metastatic tumors did not. **Keywords:** two group comparison **Overall design:** Expression profiling performed on 344SQ, 393P, and 393LN

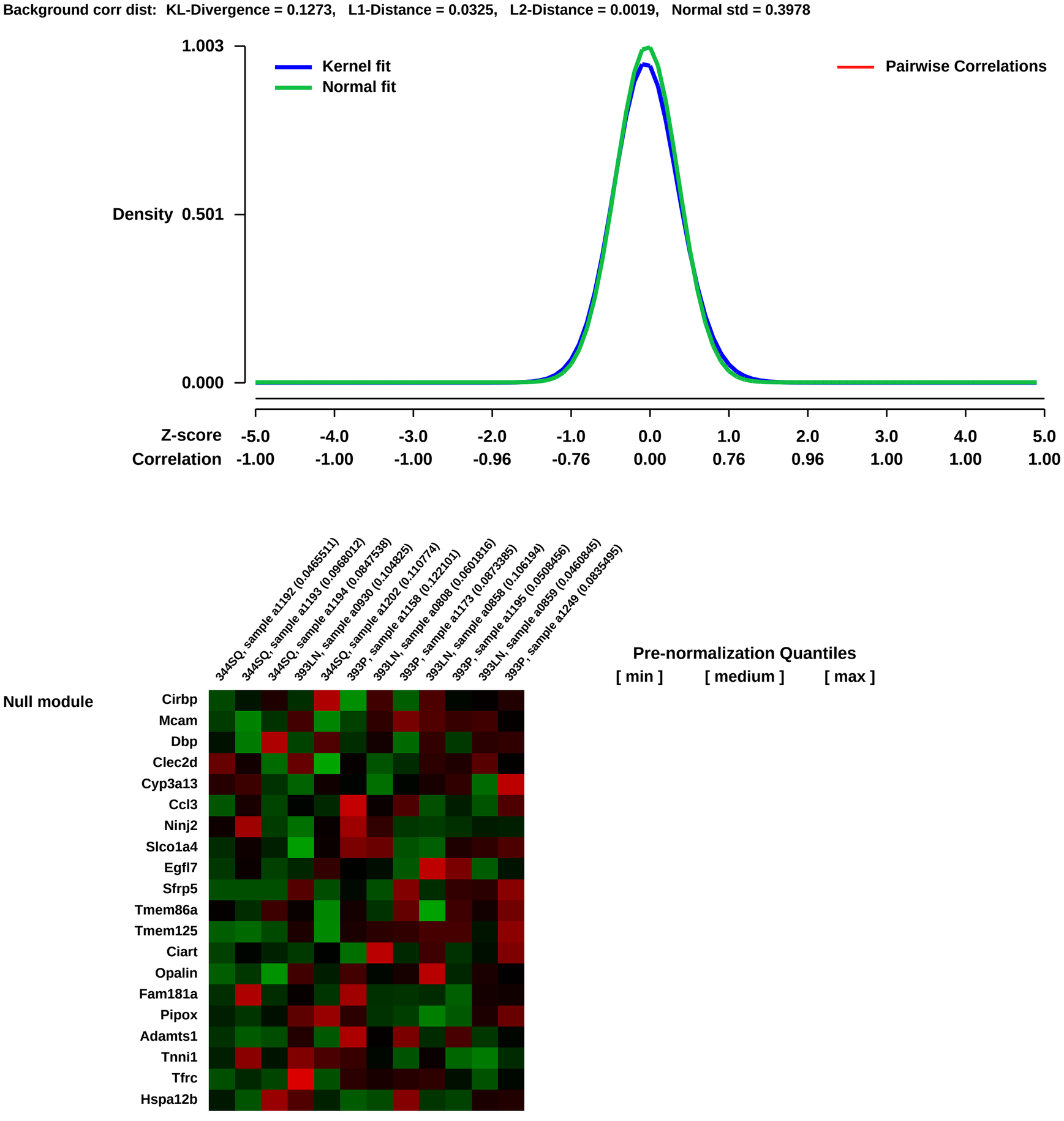

GEO Series "GSE53834" Expression Profiles

Num of samples in this series: 18

Scale of expression profile Z-scores

-3.0 -2.0 -1.0 0.0 1.0 2.0 3.0

GEO Link:	**http://www.ncbi.nlm.nih.gov/geo/query/acc.cgi?acc=GSE53834**
Status:	**Public on Jan 07 2014**
Title:	**Gene expression profiles in the liver of AIM+/+ and AIM-/- mice fed a high-fat diet**
Organism:	**Mus musculus**
Experiment type:	**Expression profiling by array**
Platform:	**GPL1261**
Pubmed ID:	
Summary & Design:	**Summary:** **Expression of genes related to fibrosis was assessed in the liver of AIM+/+ and AM-/- mice fed a high-fat diet (HFD) for various period. Overall, there was no significant difference in the magnitude of expression of fibrosis-related genes during the steatosis progression.** **Overall design:** **AIM+/+ and AIM-/- mice were fed an HFD for 0, 12 or 20 weeks. Liver samples were homogenized with Trizol, and total RNA was extracted according to the manufacturer's instructions. Microarray experiments were performed using Mouse Genome 430 2.0 Arrays (Affymetrix).**

Background corr dist: **KL-Divergence = 0.2329, L1-Distance = 0.0488, L2-Distance = 0.0055, Normal std = 0.3118**

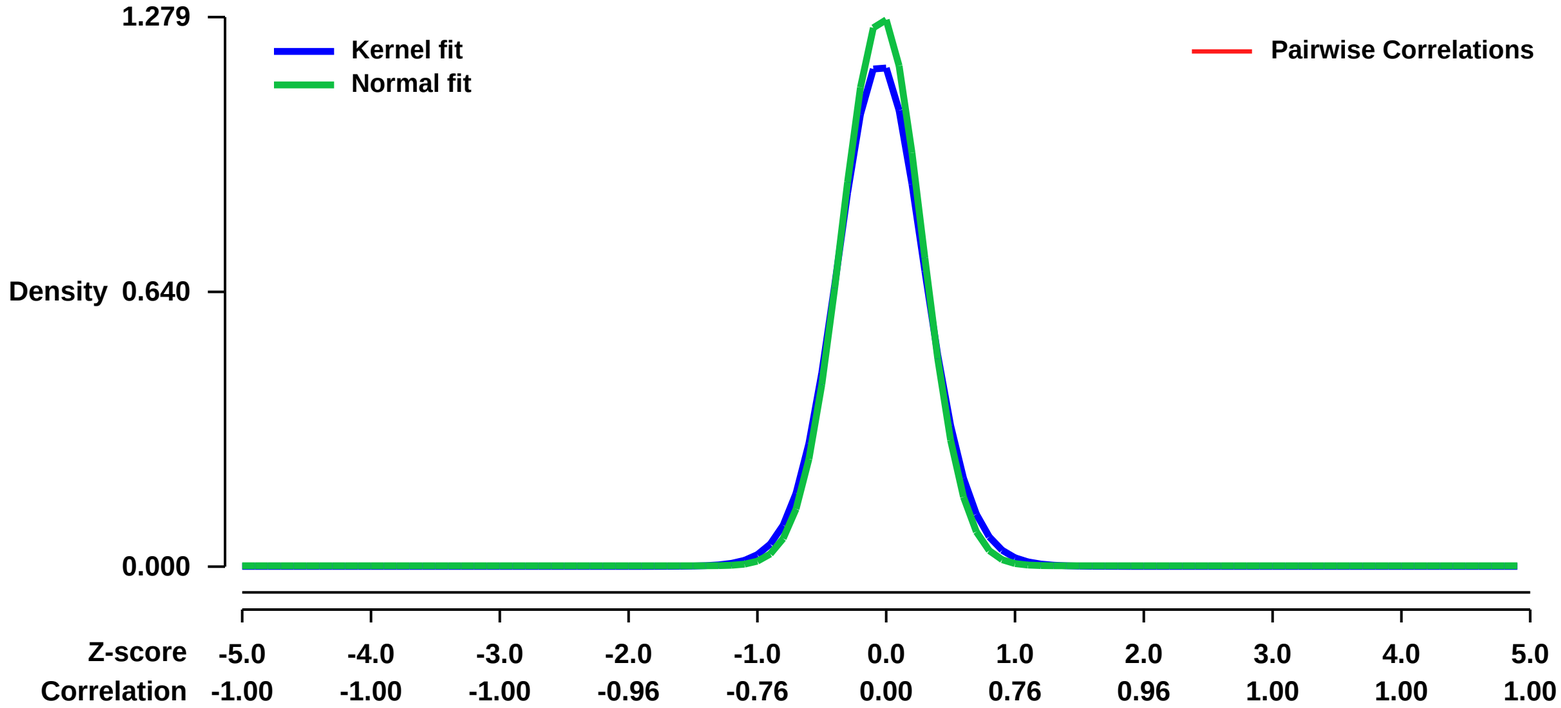

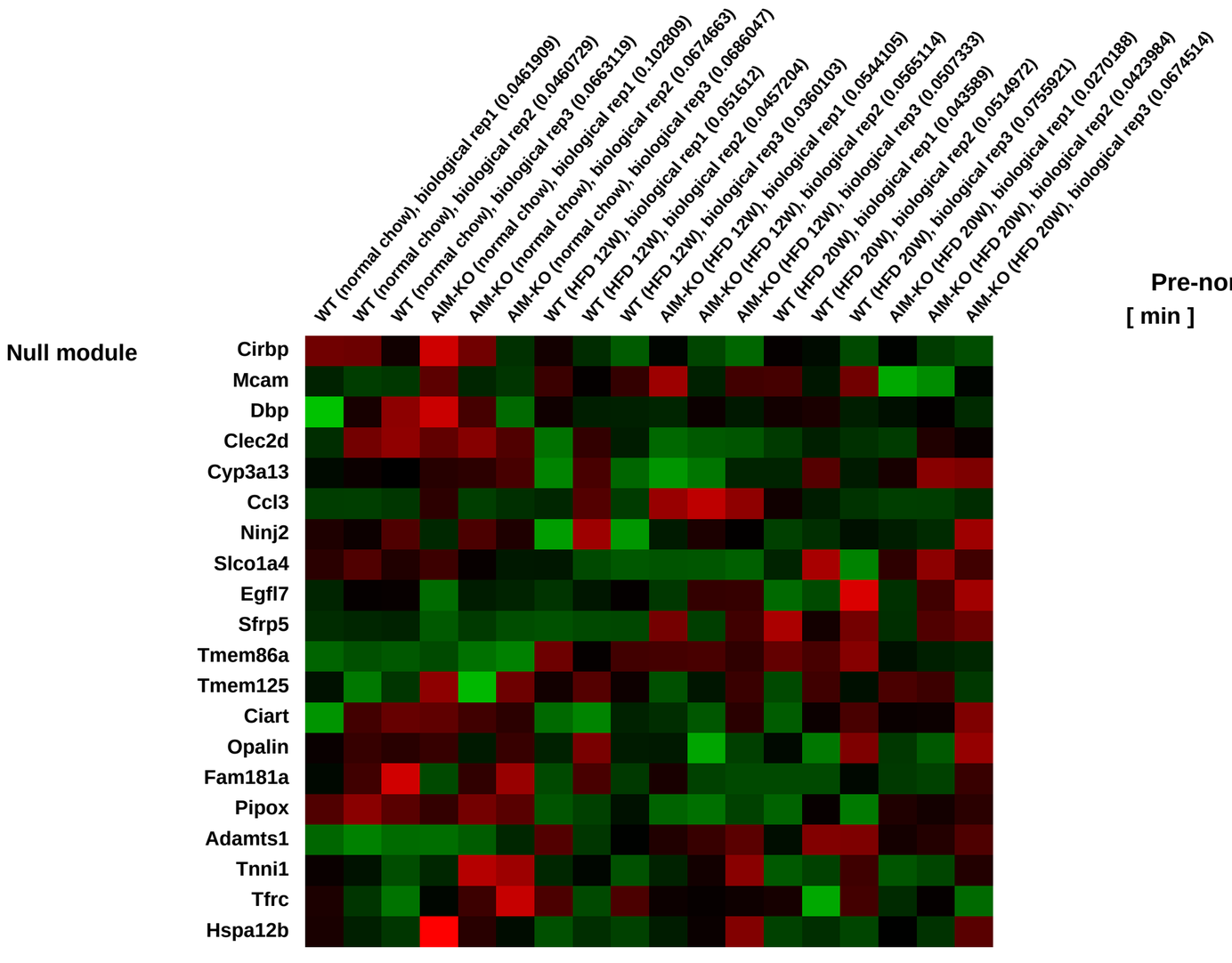

GEO Series "GSE40368" Expression Profiles

Num of samples in this series: 10

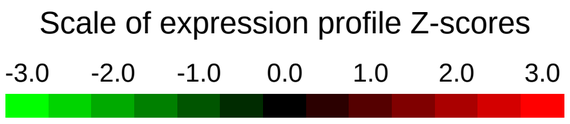

GEO Link:	http://www.ncbi.nlm.nih.gov/geo/query/acc.cgi?acc=GSE40368
Status:	Public on Aug 09 2013
Title:	Sphingosine-1-phosphate phosphatase 1 regulates keratinocyte differentiation and epidermal homeostasis
Organism:	Mus musculus
Experiment type:	Expression profiling by array
Platform:	GPL1261
Pubmed ID:	23637227
Summary & Design:	**Summary:** Sphingosine 1-phosphate (S1P) is a bioactive lipid whose levels are tightly regulated by its synthesis and degradation. Intracellularly, S1P is dephosphoryled by the actions of two S1P-specific phosphatases, sphingosine 1-phosphate phosphatase 1 and 2. To identify the physiologic functions of S1P phosphatase 1, we have studied mice with its gene, Sgpp1, deleted. Sgpp1-/- mice appeared normal at birth but during the first week of life, they exhibited stunted growth, suffered desquamation, and most died before weaning. Interestingly, the epidermal permeability barrier developed normally during embryogenesis. Sgpp1 -/- pups and surviving adults exhibited epidermal hyperplasia and abnormal expression of keratinocyte differentiation markers. Keratinocytes isolated from Sgpp1 -/- skin had increased intracellular S1P levels, and expressed a gene expression profile that indicated enhanced differentiation. The results reveal S1P metabolism as a regulator of keratinocyte differentiation and epidermal homeostasis. **Overall design:** Comparison of KO vs. WT with five replications per treatment sample

Background corr dist: KL-Divergence = 0.0632, L1-Distance = 0.0318, L2-Distance = 0.0018, Normal std = 0.5180

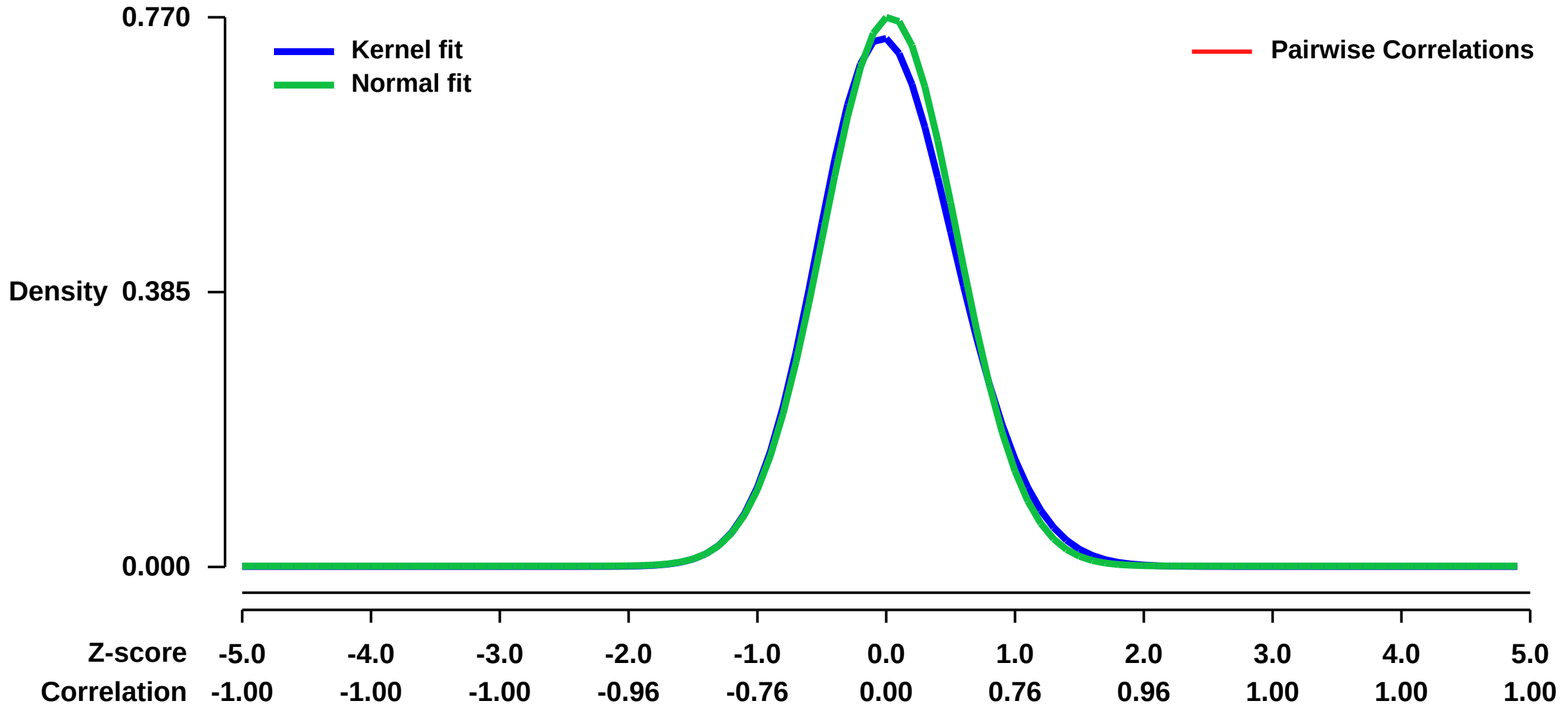

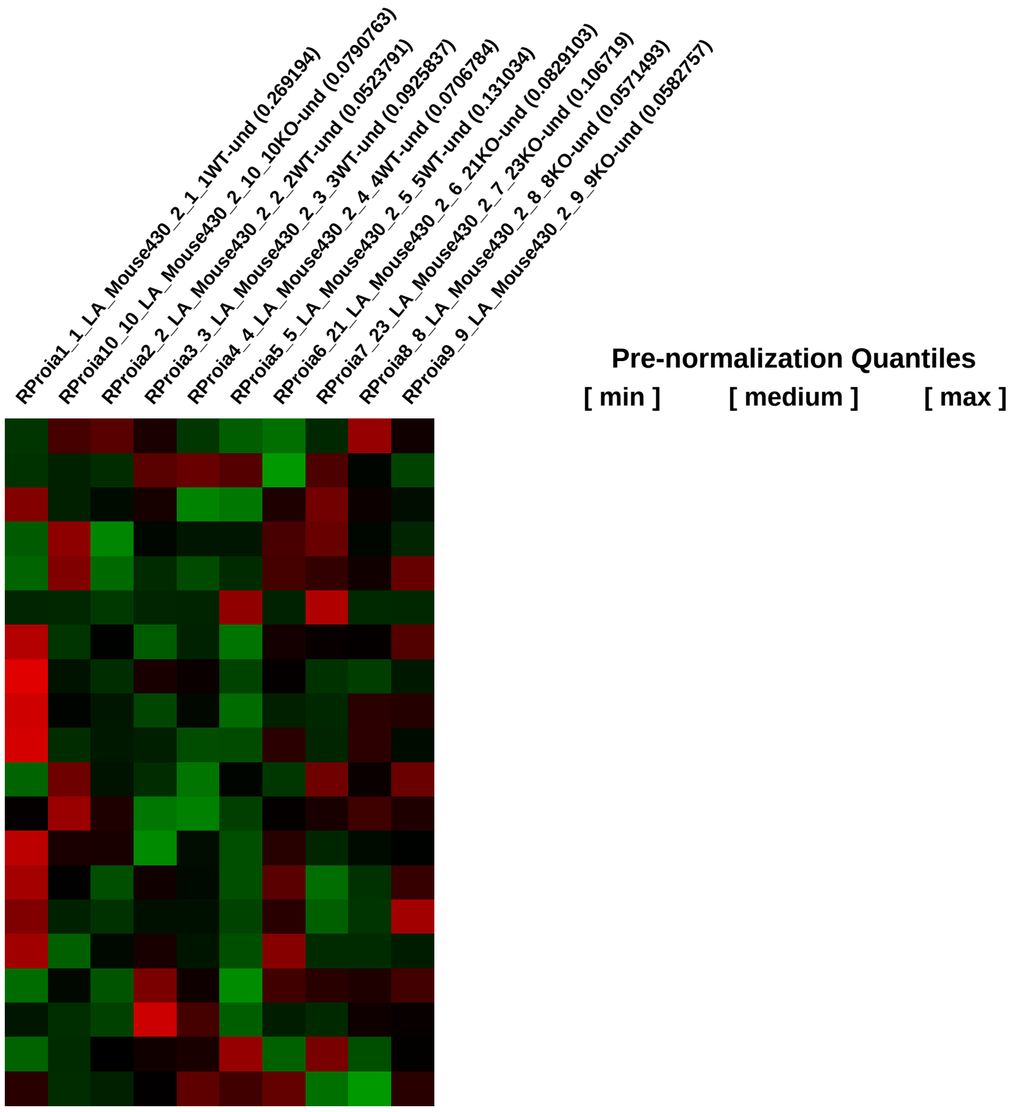

GEO Series "GSE15610" Expression Profiles

Num of samples in this series: 12

Scale of expression profile Z-scores

-3.0 -2.0 -1.0 0.0 1.0 2.0 3.0

GEO Link:	http://www.ncbi.nlm.nih.gov/geo/query/acc.cgi?acc=GSE15610
Status:	Public on Dec 22 2009
Title:	Knockout of the selenocysteine tRNA (Trsp) gene in mouse macrophage
Organism:	Mus musculus
Experiment type:	Expression profiling by array
Platform:	GPL1261
Pubmed ID:	19863805
Summary & Design:	**Summary:** **Comparative analysis of gene expression in bone marrow-derived macrophages (BMDM) from trsp knockout mice (Trspfl/fl-LysM-Cre+/-) and Control (Trspfl/fl-LysM-Cre-/-) mice.** **Selenium, a micronutrient whose deficiency in the diet causes immune dysfunction and inflammatory disorders, exerts its physiological effects partly in the form of selenium-containing proteins (selenoproteins). Incorporation of selenium into the amino acid selenocysteine (Sec), and subsequently into selenoproteins, is mediated by Sec tRNA[Ser]Sec. To identify macrophage-specific selenoprotein function, we generated mice with the Sec tRNA[Ser]Sec gene specifically deleted in myeloid cells. These mutant mice were devoid of the selenoproteome in macrophages, yet exhibited largely normal inflammatory responses. However, selenoprotein deficiency led to aberrant expression of extracellular matrix-related genes, and diminished migration of macrophages in a protein gel matrix. Therefore, selenium status may affect immune defense and tissue homeostasis through its effect on selenoprotein expression and the trafficking of tissue macrophages.** **Overall design:** **We have generated mice in which we have selectively removed the selenocysteine tRNA gene (trsp) in macrophages under the control of LysM-Cre promoter. Microarray analysis was performed on RNA samples taken from bone marrow-derived macrophages in knockout and control mice. 1. Control unstimulated 2. Knockout unstimulated 3. Control lipopolysaccharide (LPS) stimulated (4h) 4. Knockout LPS stimulated (4h). Three replicates for each condition. Thus, a total of 12 samples.**

Background corr dist: KL-Divergence = 0.0769, L1-Distance = 0.0376, L2-Distance = 0.0023, Normal std = 0.4963

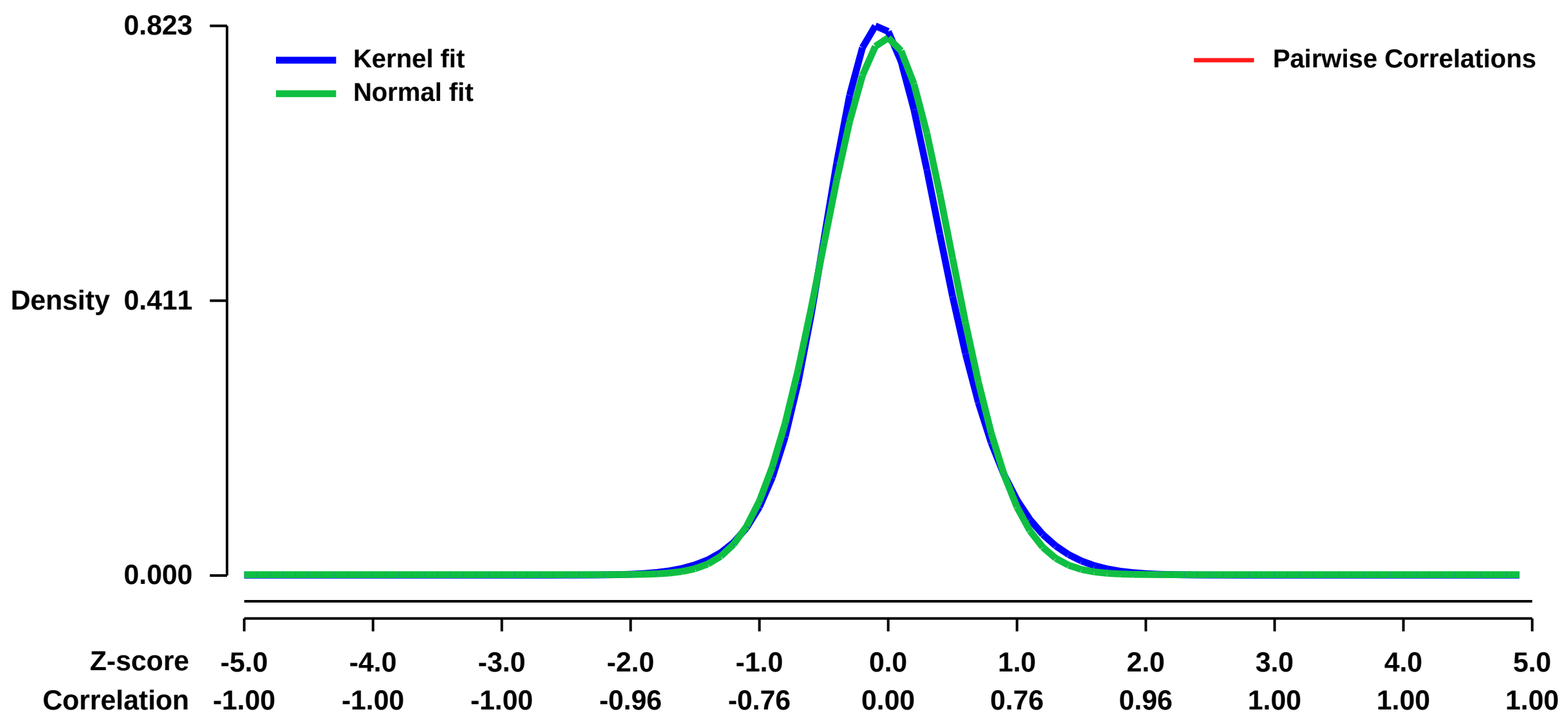

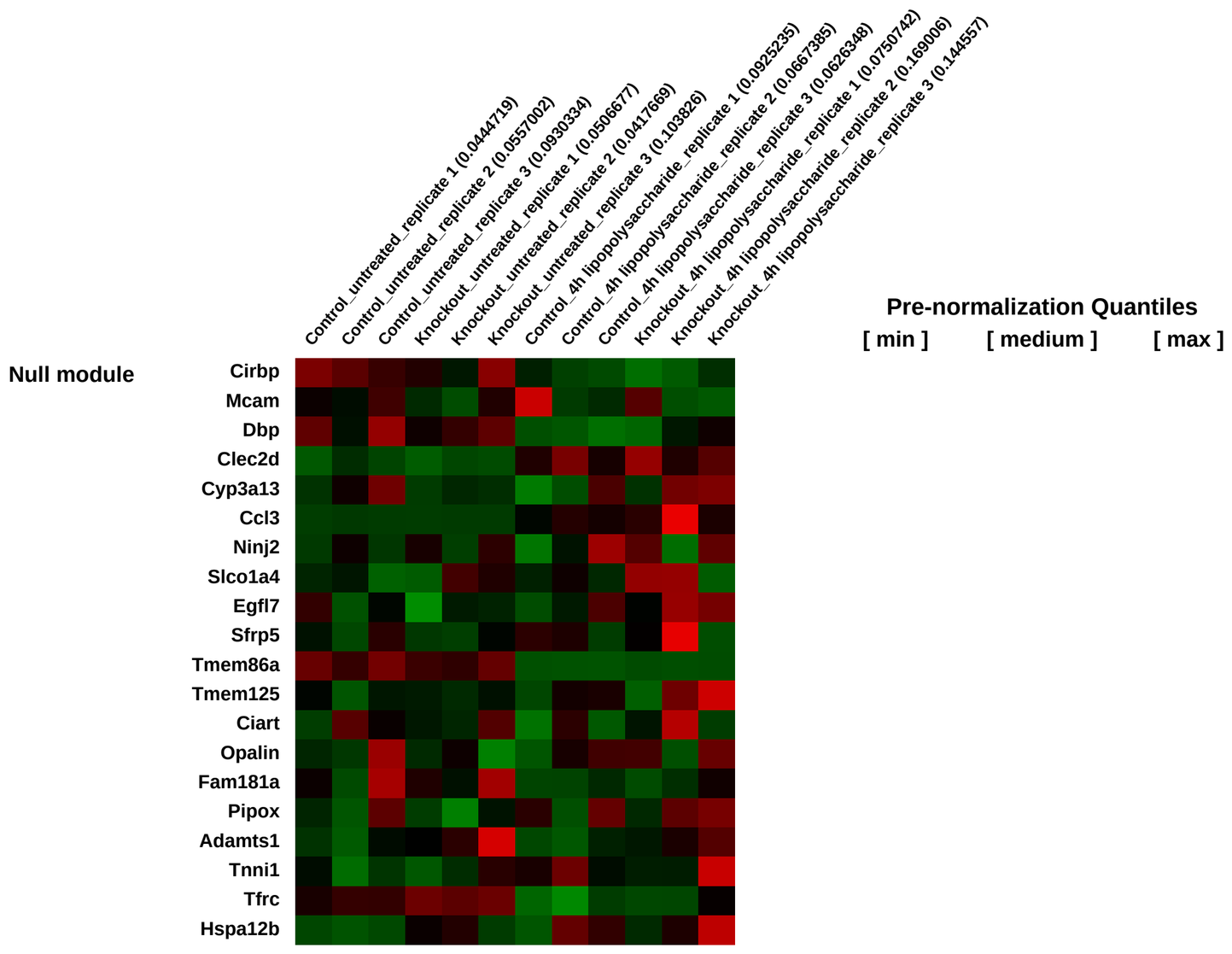

GEO Series "GSE23119" Expression Profiles

Num of samples in this series: 9

Scale of expression profile Z-scores

-3.0 -2.0 -1.0 0.0 1.0 2.0 3.0

GEO Link:	http://www.ncbi.nlm.nih.gov/geo/query/acc.cgi?acc=GSE23119
Status:	Public on Aug 03 2010
Title:	Effect of vitamin A deficiency (VAD) on mouse spermatogonial transcriptome profiles
Organism:	Mus musculus
Experiment type:	Expression profiling by array
Platform:	GPL1261
Pubmed ID:	23253600
Summary & Design:	**Summary:** The objective of this study was to understand the genetic mechanisms of Vitamin-A-Deficiency (VAD)-induced arrest of spermatogonial stem-cell differentiation. Vitamin A and its derivatives (the retinoids) participate in many physiological processes including vision, cellular differentiation and reproduction. VAD affects spermatogenesis, the subject of our present study. Spermatogenesis is a highly regulated process of differentiation and complex morphologic alterations that, in the postnatal testis, leads to the formation of sperm in the seminiferous epithelium. VAD causes early cessation of spermatogenesis, characterized by degeneration of meiotic germ cells, leading to seminiferous tubules containing mostly type A spermatogonia and Sertoli cells. In this study, we investigated the molecular basis of VAD on spermatogenesis in mice. We used adult Balb/C mice fed with a Control or VAD diet for an extended period of time (8-28 weeks) and selected two time points (18 and 25 weeks) for microarray analysis. To understand the effect of VAD on the spermatogonial stem cell transcriptome, we studied isolated pure populations of spermatogonia from control and vitamin-A-deficient mice from two representative time points (18 and 25 weeks) using Affymetrix GeneChip microarrays. We identified target genes involved in the arrest of spermatogonial differentiation and spermatogenesis. Our results establish a better understanding of the chronology and magnitude of the consequences of VAD on mouse testes and add to the current knowledge of the molecular regulatory mechanisms of germ cell development. **Overall design:** Spermatogonia were isolated by the STATPUT procedure with minor modifications. VAD mice were sacrificed at 18 and 25 weeks of VAD treatment for spermatogonia isolation. Decapsulated testes from 2 mice were suspended in RPMI medium containing collagenase (0.6 mg/ml), Hyaluronidase (0.12 mg/ml) and DNAse I (1.25 mg/ml) and incubated at 37´”C for 30 minutes in a shaking water bath. The tissues were then allowed to come down the tube and the supernatant (containing interstitial cells) was removed. The pellet was incubated with 3 ml of 0.25% Trypsin /EDTA (GIBCO, Invitrogen, USA), in the presence of DNAse I (0.2 mg/ml) at 37´”C for 15 minutes in a shaking water bath. The dispersed cells were washed twice with RPMI medium containing 10% heat inactivated FBS to neutralize the protease activity, and filtered through a sterile 0.22 nylon to remove any undigested fragments. Cells of the dissociated seminiferous epithelium were then plated overnight in a 34´”C 3% CO2 incubator. The following day, germ cells, in suspension, were separated by sedimentation with use of a 2-4% BSA gradient. The cells were allowed to sediment for a standard period of 2.5 h, and fractions of 2-ml volume were collected. The cells of each fraction were examined under a phase contrast microscope, and fractions containing cells of similar size and morphology were pooled and spun down by low-speed centrifugation. Purity of spermatogonia was estimated and was routinely higher than 90%. Total RNA was extracted from the isolated germ cells using TRIzol ´fi Reagent, and cleaned with RNeasy minicolumns. RNA content was determined by measurement of optical density at 260 nm. Only the RNA samples showing an OD 260/280 ratio higher than 1.8 were used for microarray hybridization. Raw expression values in Affymetrix CEL file format were generated by GeneChip Operating Software.

Background corr dist: KL-Divergence = 0.0289, L1-Distance = 0.0374, L2-Distance = 0.0019, Normal std = 0.6920

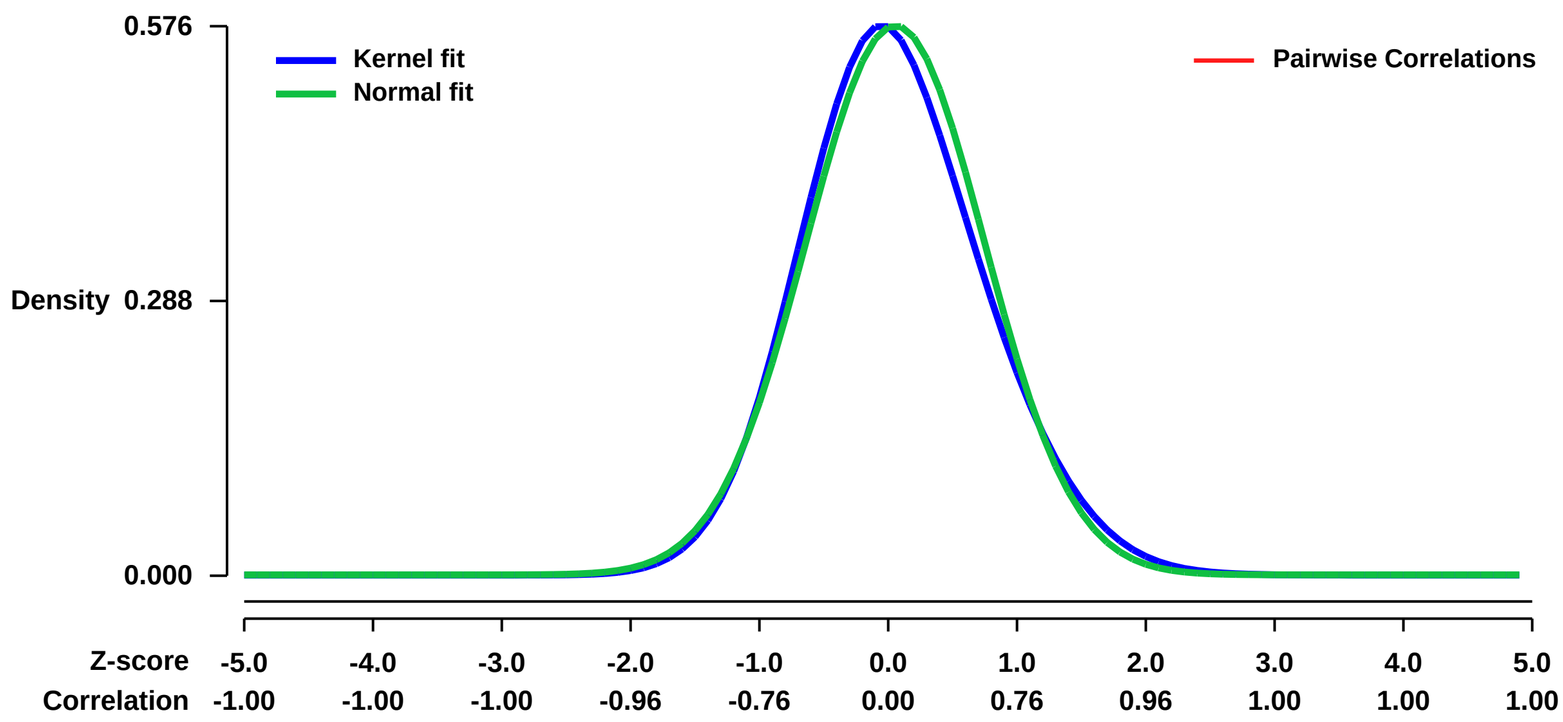

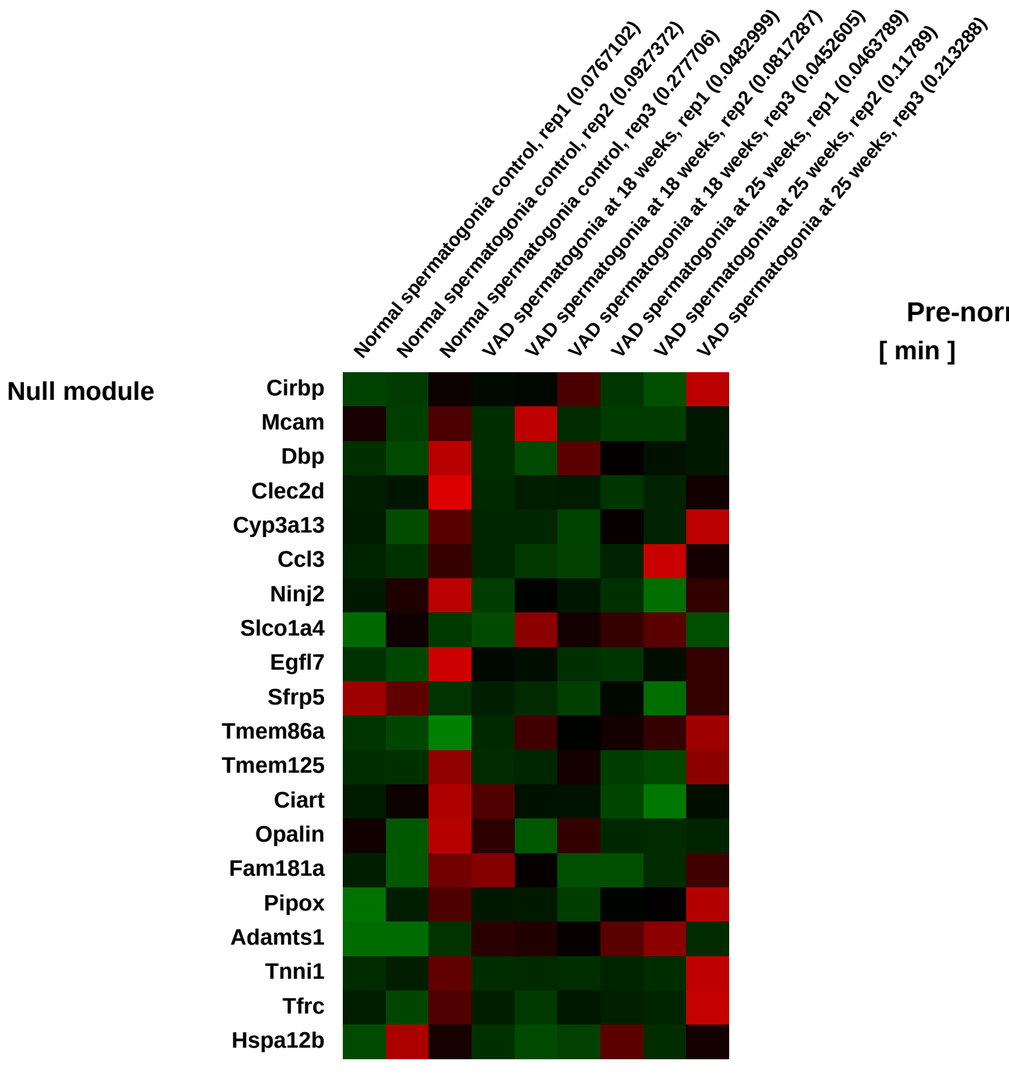

GEO Series "GSE6397" Expression Profiles

Num of samples in this series: 15

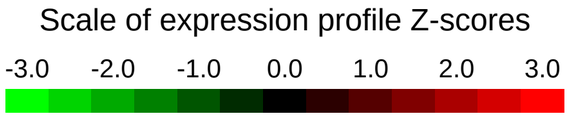

GEO Link:	http://www.ncbi.nlm.nih.gov/geo/query/acc.cgi?acc=GSE6397
Status:	Public on Dec 02 2006
Title:	Comparison between gene expression in heart from Lmna H222P heterozygous and control mice
Organism:	Mus musculus
Experiment type:	Expression profiling by array
Platform:	GPL1261
Pubmed ID:	17446932
Summary & Design:	**Summary:** The present research is devoted to the identification of gene(s) severely affected by LMNA mutations, leading to striated muscle laminopathies and more specifically the cardiomyopathy. For this purpose, we developped a large-scale gene expression approach on heart and skeletal tissues from Lmna H222P heterozygous Knock-In mouse model. **Keywords: disease state modification** **Overall design:** In the project presented here we performed differential expression in heart from a mouse model of EDMD: a LmnaH222P knock-in mouse created via homologous recombination by Gisele Bonne in Paris, France (Arimura et al., 2005). The mutant male LmnaH222P knock-in homozygous mice display reduced locomotion activity with abnormal stiff walking posture and all of them die by 9 months of age. As for cardiac phenotype, they develop chamber dilation and hypokinesia with conduction defects. These results demonstrate that LmnaH222P knock-in homozygous mice represents a good model for studying laminopathies affecting striated muscles as they develop a dystrophic condition of both skeletal and cardiac muscles reminiscent of the human diseases. Genes were identified as differentially expressed if they met a false discovery rate threshold of 0.05 in a two-sample t-test (q-value) and showed at least a two-fold difference in expression independent of absolute signal intensity.

Background corr dist: KL-Divergence = 0.2185, L1-Distance = 0.0538, L2-Distance = 0.0070, Normal std = 0.3196

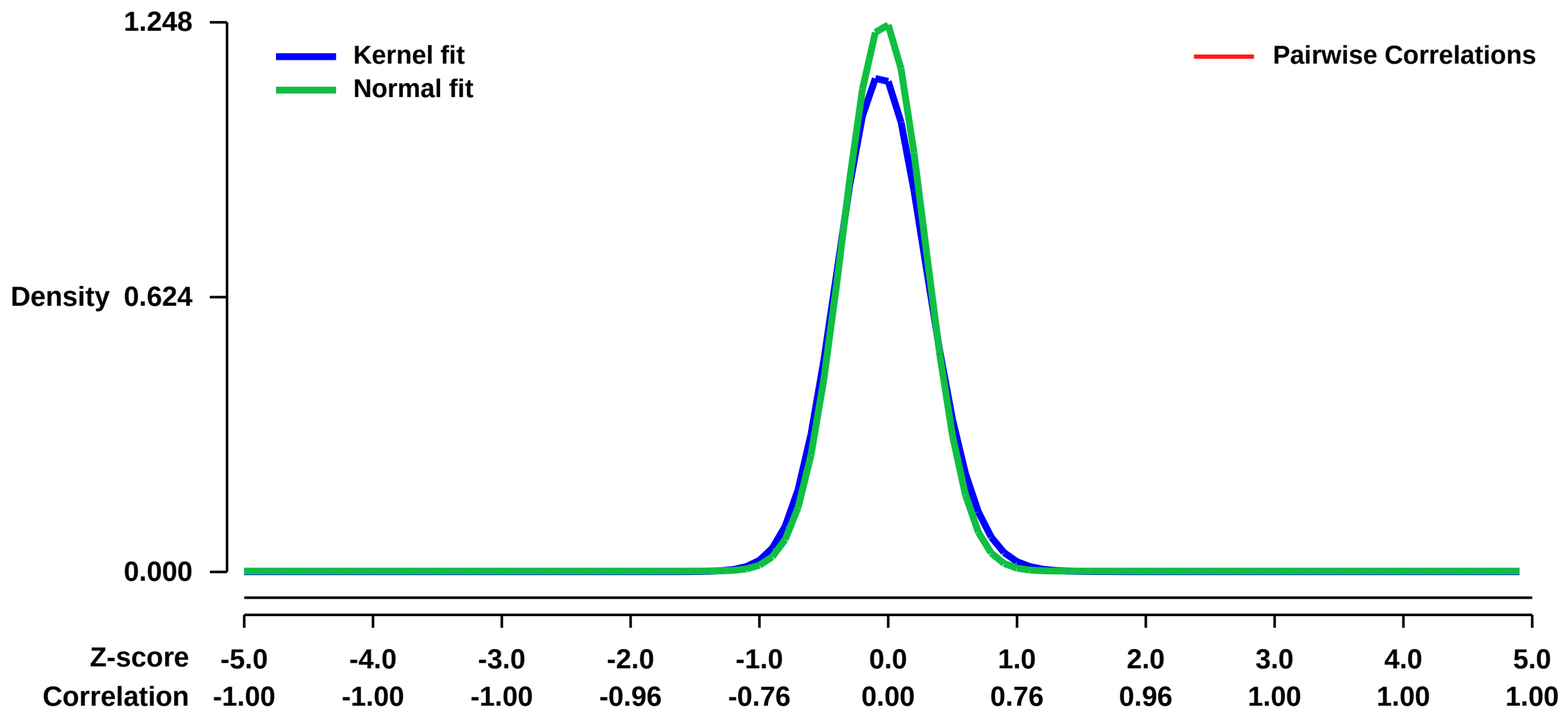

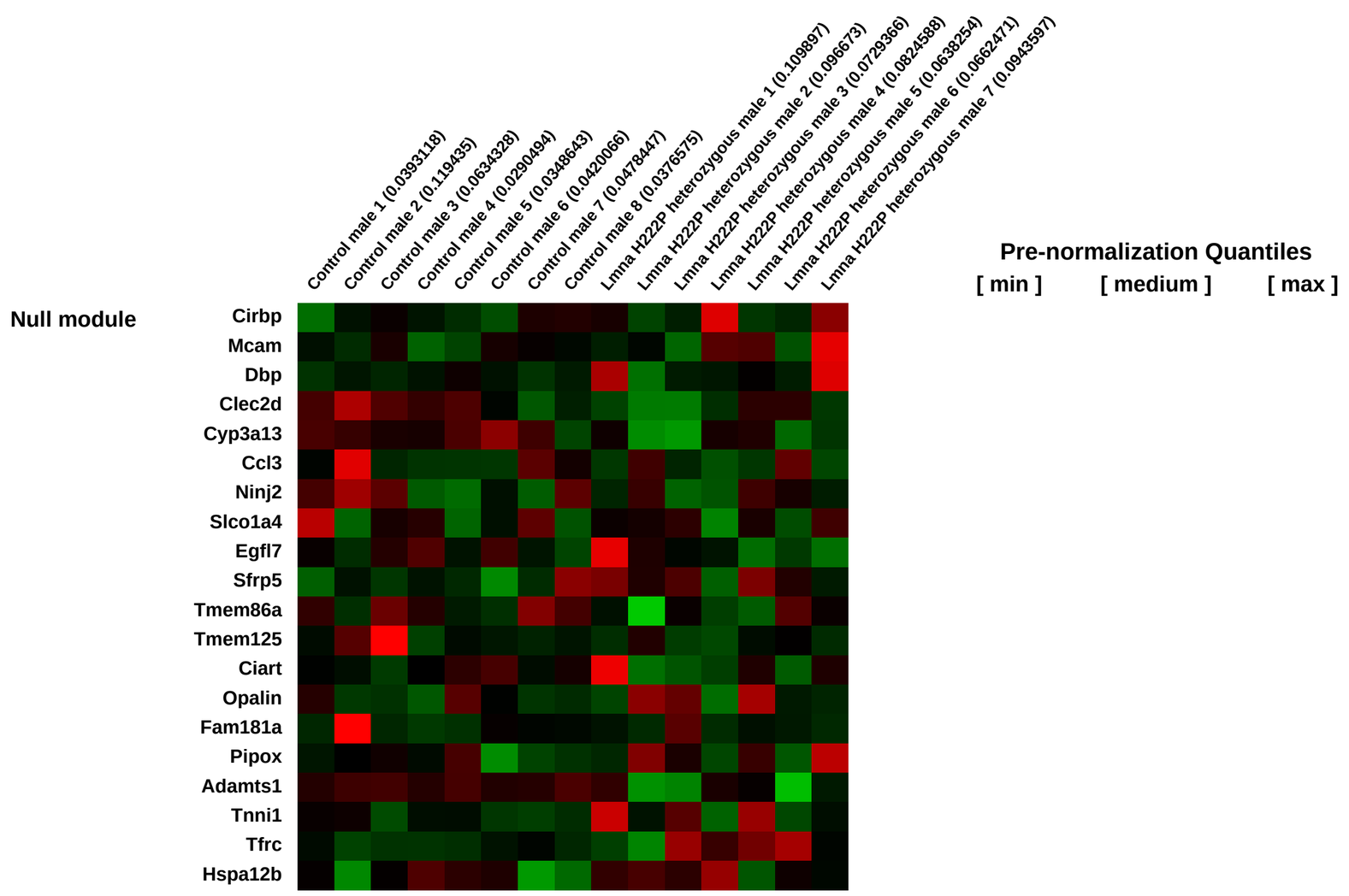

GEO Series "GSE51422" Expression Profiles

Num of samples in this series: 6

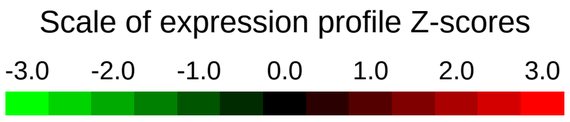

GEO Link:	http://www.ncbi.nlm.nih.gov/geo/query/acc.cgi?acc=GSE51422
Status:	Public on Oct 25 2013
Title:	Gene Expression in wild type and CCR5 knockout mice with lung metastasis
Organism:	Mus musculus
Experiment type:	Expression profiling by array
Platform:	GPL1261
Pubmed ID:	24197118
Summary & Design:	**Summary:** We have shown that C57BL/6J CCR5 knockout mice develop 30.4% ´– 8.6% fewer B16 F10 lung nodules compared to wild type mice after the intravenous injection of 100,000 B16 F10 cells. We sought to understand this phenomenon by comparing gene expression in the lungs of these mice at 6, 24, and 48 hours after tumor injection. **Overall design:** There were 6 groups or conditions (CCR5 - 6 hours, WT - 6 hours, CCR5 - 24 hours, WT - 24 hours, CCR5 - 48 hours, WT - 48 hour); each group had 4 to 5 mice. All of the mice were injected with 100,000 B16 F10 melanoma cells by tail vein. At the designated time, the mice were anesthetized with Avertin and their lungs were perfused with PBS. After this, the lungs were harvested and snap frozen in liquid nitrogen. They were kept at minus 80 degrees C until processing. mRNA was extracted as described below and equivalent amounts of mRNA (by weight) was pooled by group.

Background corr dist: KL-Divergence = 0.0292, L1-Distance = 0.0121, L2-Distance = 0.0001, Normal std = 0.6672

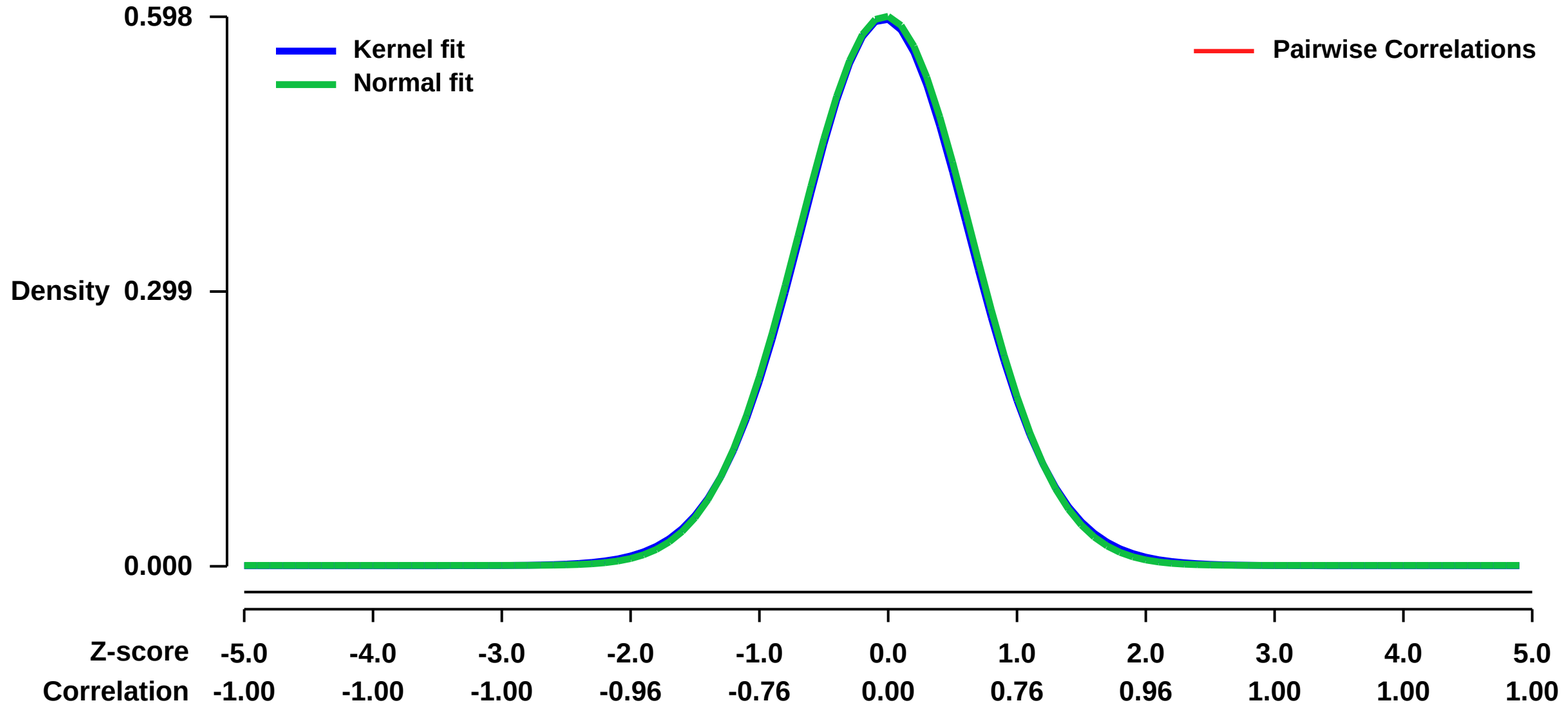

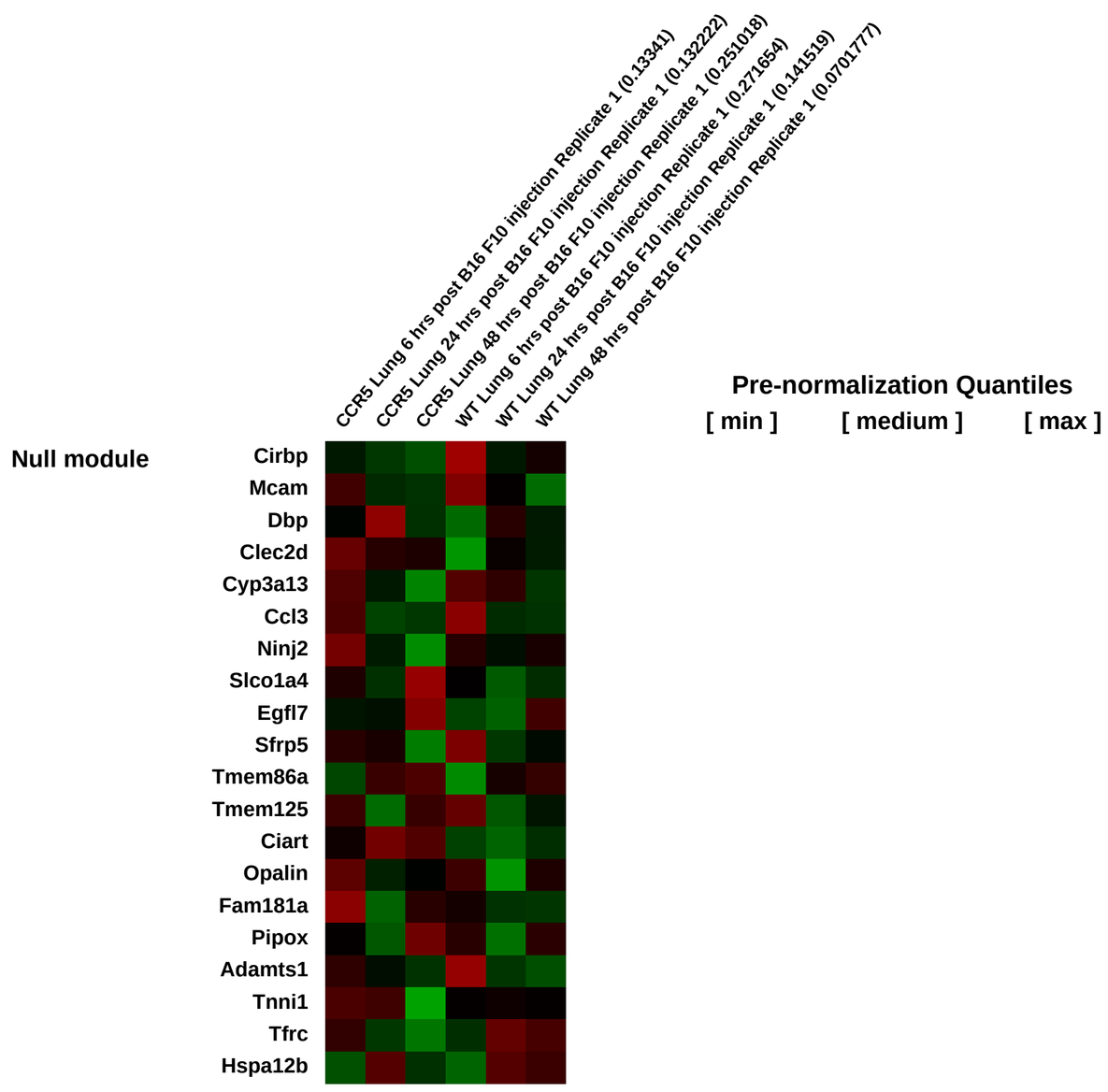

GEO Series "GSE24793" Expression Profiles

Num of samples in this series: 8

Scale of expression profile Z-scores

-3.0 -2.0 -1.0 0.0 1.0 2.0 3.0

GEO Link:	http://www.ncbi.nlm.nih.gov/geo/query/acc.cgi?acc=GSE24793
Status:	Public on Mar 30 2012
Title:	Target genes of thyroid hormone in cerebellum neurons
Organism:	Mus musculus
Experiment type:	Expression profiling by array
Platform:	GPL1261
Pubmed ID:	22586439
Summary & Design:	**Summary:** Cerebellar post-natal development is particularly sensitive to thyroid hormone and low levels of thyroid hormone (hypothyroidism) result in permanent defects in cerebellar architecture and function. All cell types of the cerebellum are affected, but the main sign of hypothyroidism in mice is the persistence of the external granular layer, composed of mitotic neuronal precursors at P21. To make the genetic link between thyroid hormone and cerebellar development, we sought to identify new thyroid hormone target genes, in particular in granule cells which represent the vast majority of cerebellar cells. **Overall design:** Primary cultures of cerebellar neurons were made by dissociation of cerebella from newborn wild-type mice. These cells were plated 48 hours in serum-free medium to avoid invasion of the culture by glial cells. In order to include a kinetic and a maximum number of target genes, several cultures were either treated or left untreated as controls for 6 hours (T1), 16 hours (T2), 24 hours (T3) or 48 hours (T4) and results were pairwise compared for each time point.

Background corr dist: KL-Divergence = 0.0499, L1-Distance = 0.0304, L2-Distance = 0.0014, Normal std = 0.5750

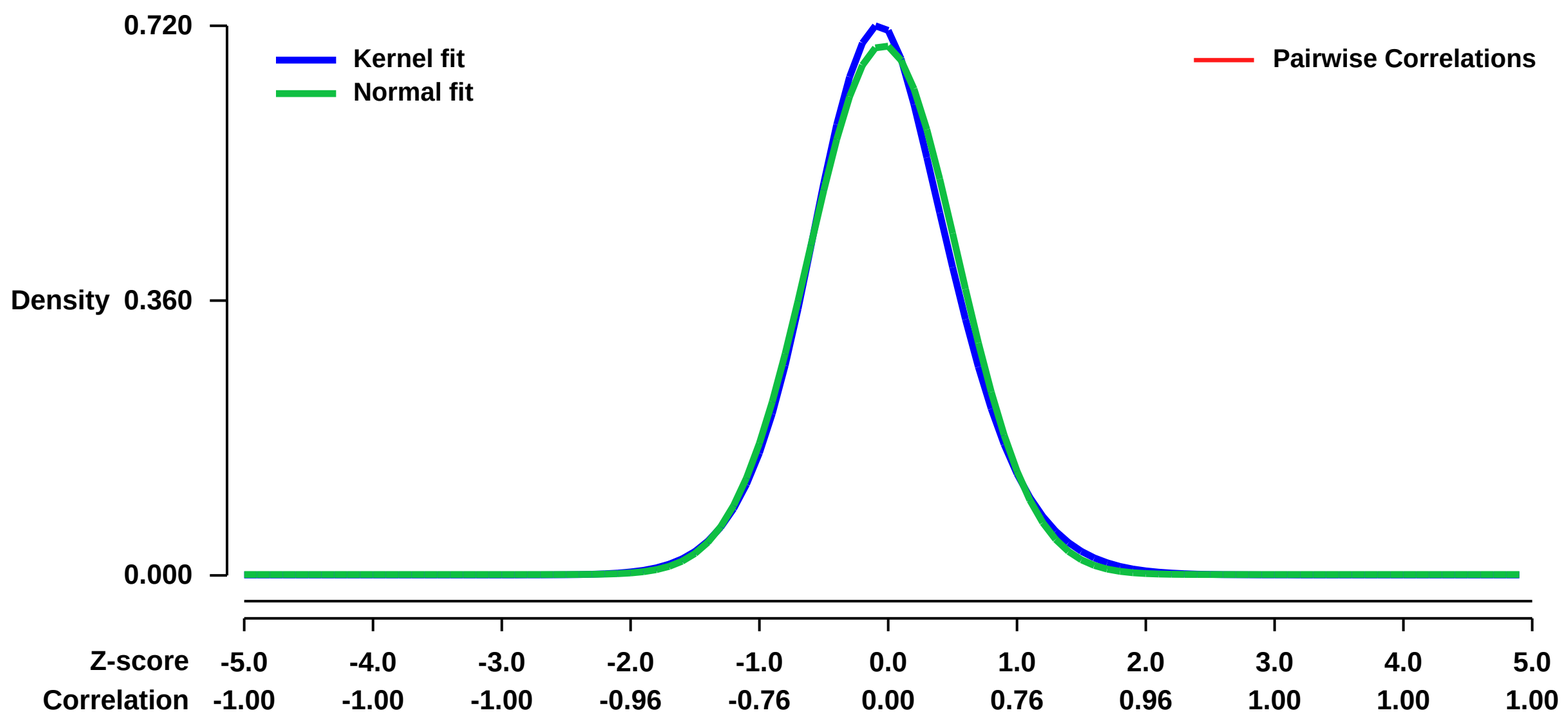

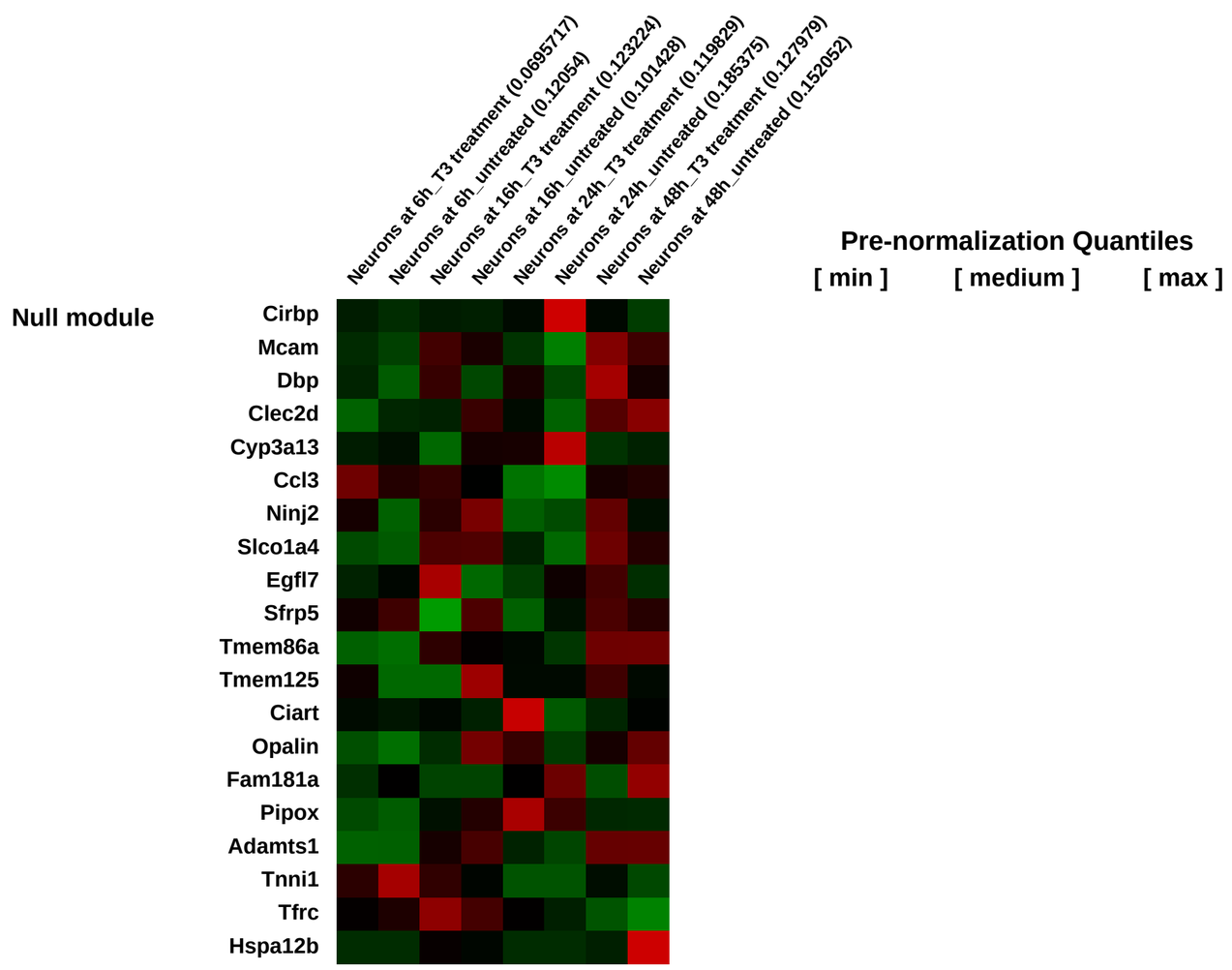

GEO Series "GSE34126" Expression Profiles

Num of samples in this series: 19

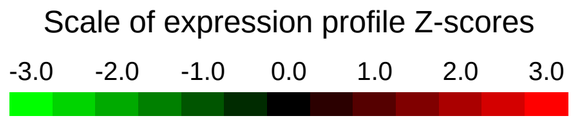

GEO Link:	http://www.ncbi.nlm.nih.gov/geo/query/acc.cgi?acc=GSE34126
Status:	Public on Dec 05 2011
Title:	An Animal Model of Myc-driven medulloblastoma
Organism:	Mus musculus
Experiment type:	Expression profiling by array
Platform:	GPL1261
Pubmed ID:	22340590
Summary & Design:	**Summary:** Medulloblastoma (MB) is the most common malignant brain tumor in children. Patients whose tumors exhibit overexpression or amplification of the MYC oncogene (c-MYC) usually have an extremely poor prognosis, but there are no animal models of this subtype of the disease. Here we show that cerebellar stem cells expressing Myc and mutant Trp53 (p53) generate aggressive tumors following orthotopic transplantation. These tumors consist of large, pleiomorphic cells and resemble human MYC-driven MB at a molecular level. Notably, antagonists of PI3K/mTOR signaling, but not Hedgehog signaling, inhibit growth of tumor cells. These findings suggest that cerebellar stem cells can give rise to MYC-driven MB, and identify a novel model that can be used to test therapies for this devastating disease. To gain insight into the pathways that control growth of MYC-driven MB, we compared gene expression profiles of murine Myc/DNp53 (MP) tumor cells to those of freshly isolated cerebellar stem cells (Prom1+Lin- cells) and of tumors from Ptch1 mutant mice (a model for Sonic Hedgehog-associated MB). RNA was isolated from stem cells and tumor cells using the RNAqueous kit (Ambion). RNA was labeled and hybridized to Affymetrix Mouse Genome 430 2.0 arrays. **Overall design:** 19 mouse cell samples (stem cells and tumor cells) were analyzed. There are four groups of samples, three with five biological replicates and the last with four (one outlier was removed). To gain insight into the mechanisms of transformation into tumors, we compared the gene expression profiles of MP tumor cells derived from stem cells (Myc/DNp53-infected Prom1+Lin- cells, designated MP-pl) or progenitors (Myc/DNp53-infected Prom1+ cells, designated MP-p) to gene expression profiles of uninfected stem cells (designated NSC) and profiles from a distinct model of medulloblastoma, the patched mutant mouse (designated ptch1).

Background corr dist: KL-Divergence = 0.1063, L1-Distance = 0.0311, L2-Distance = 0.0018, Normal std = 0.4292

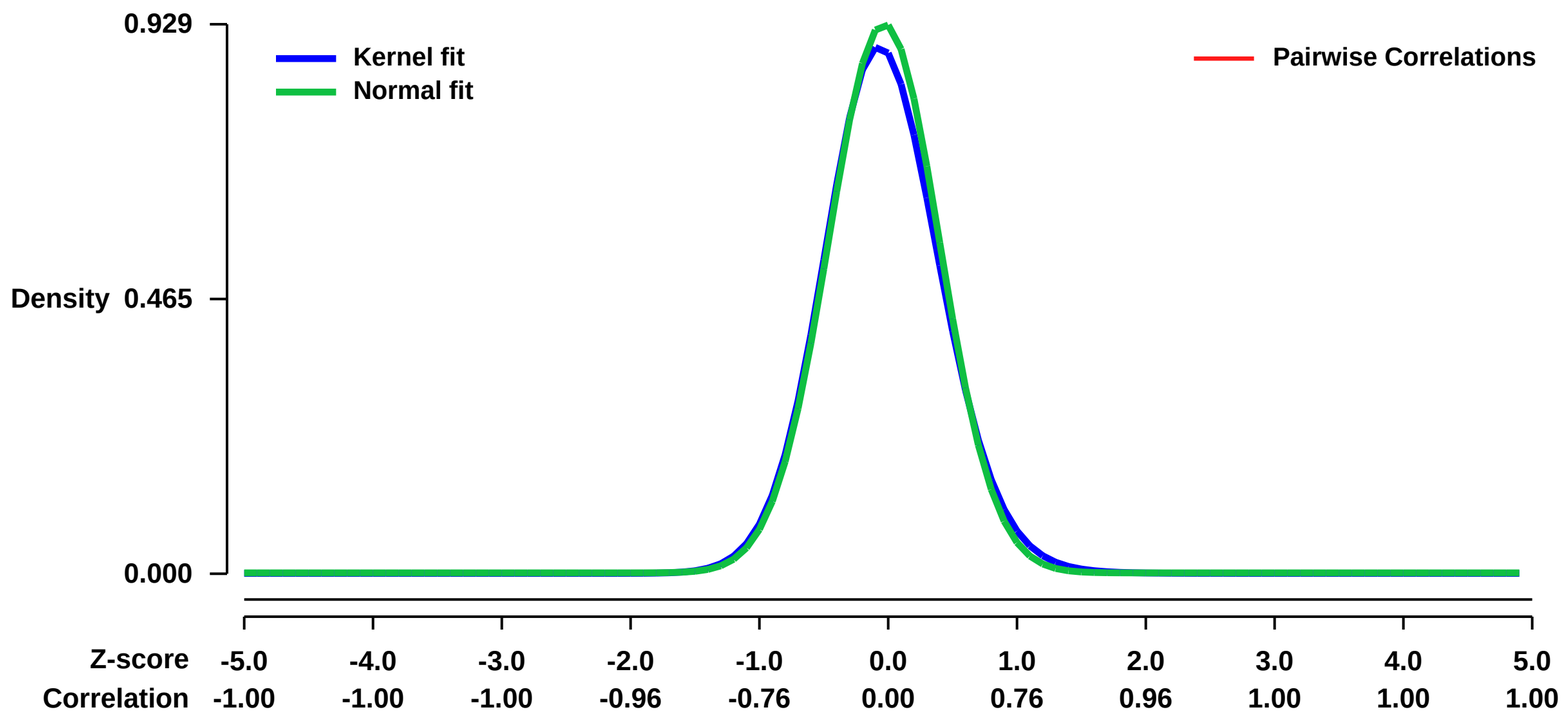

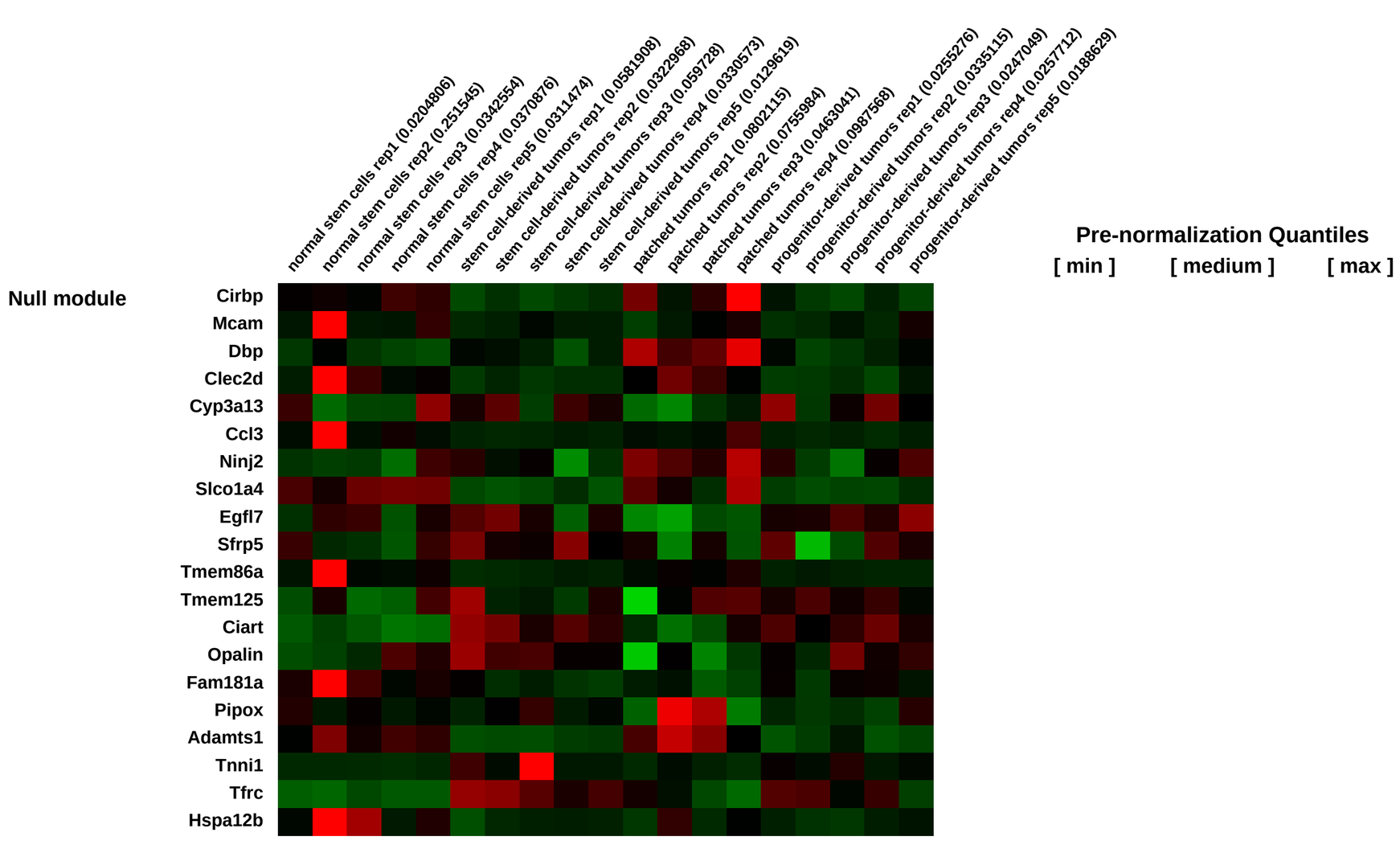

GEO Series "GSE42858" Expression Profiles

Num of samples in this series: 12

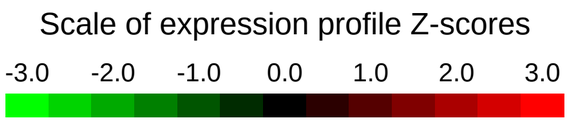

GEO Link:	http://www.ncbi.nlm.nih.gov/geo/query/acc.cgi?acc=GSE42858
Status:	Public on Aug 27 2013
Title:	Progesterone receptor-dependent gene signatures in the mouse mammary gland after acute progesterone treatment
Organism:	Mus musculus
Experiment type:	Expression profiling by array
Platform:	GPL1261
Pubmed ID:	23979845
Summary & Design:	**Summary:** Progesterone (P) acting through its cognate nuclear receptors (PRs) plays an essential role in driving pregnancy-associated branching morphogenesis of the mammary gland. However, the fundamental mechanisms, including global cistromic and acute genomic transcriptional responses that are required to elicit active branching morphogenesis in response to P, have not been elucidated. We used microarray analysis to identify global gene expression signatures that are acutely regulated by PRs in the mouse mammary gland after acute P treatment. **Overall design:** Mammary gland gene expression data from 10-week-old ovariectomized wildtype and progesterone receptor null mice treated subcutaneously with 17¸†-Estradiol for 24 hours and then 17¸†-Estradiol plus Progesterone for 8 or 24 hours. Three replicate pools were tested with three mice per pool.

Background corr dist: KL-Divergence = 0.1073, L1-Distance = 0.0330, L2-Distance = 0.0020, Normal std = 0.4239

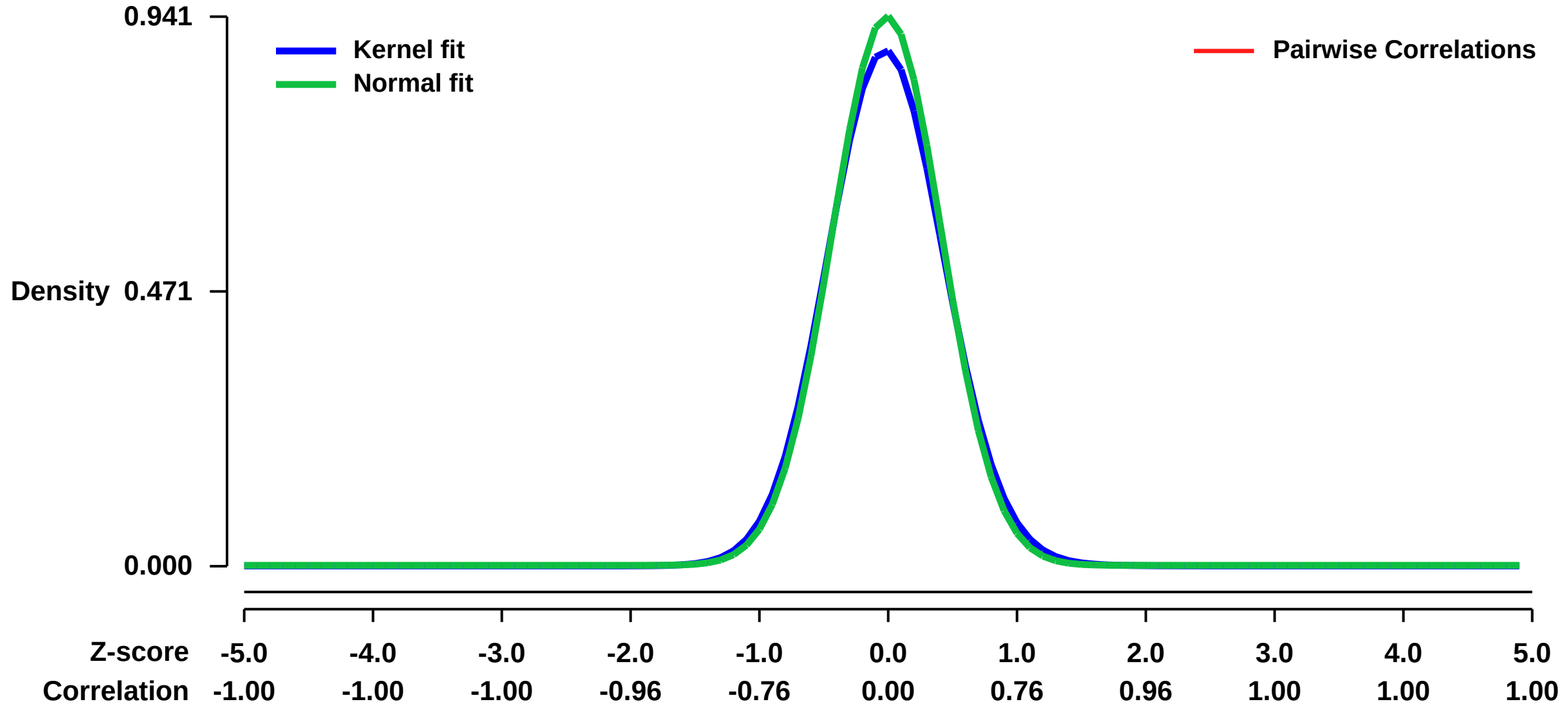

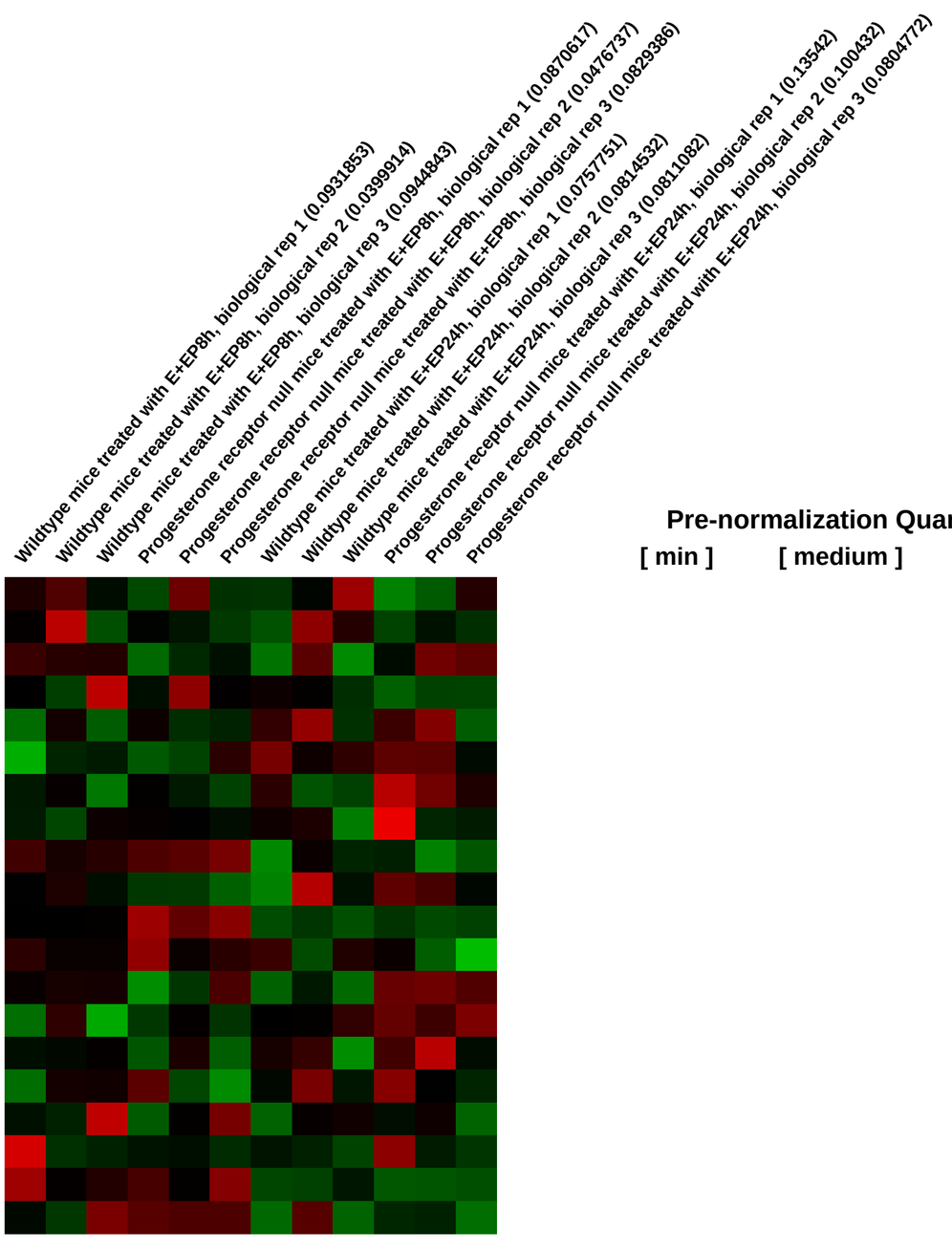

GEO Series "GSE11687" Expression Profiles

Num of samples in this series: 12

Scale of expression profile Z-scores

-3.0 -2.0 -1.0 0.0 1.0 2.0 3.0

GEO Link:	http://www.ncbi.nlm.nih.gov/geo/query/acc.cgi?acc=GSE11687
Status:	Public on Jun 07 2008
Title:	Ca2+ oscillatory pattern in fertilized mouse eggs affects gene expression and development to term.
Organism:	Mus musculus
Experiment type:	Expression profiling by array
Platform:	GPL1261
Pubmed ID:	16996050
Summary & Design:	**Summary:** The Ca2+ oscillations initiated by the fertilizing sperm (but terminating concomitant with pronucleus formation) apparently ensure that the events constituting egg activation occur in the correct temporal order; early events (e.g., cortical granule exocytosis) require fewer oscillations than later events (e.g., recruitment of maternal mRNA). Whether the Ca2+ signaling events impact long-term development, in particular development to term, is unknown. Using fertilized eggs that have undergone the first few Ca2+ oscillations, we developed procedures that result either in inhibiting or stimulating the natural pattern of Ca2+ signaling of inseminated eggs. Although the incidence of development to the blastocyst stage is unaltered by these procedures, fewer offspring are born following embryo transfer, indicating that developmental competence of the blastocysts is reduced. Interestingly, embryo transfer experiments reveal that when the natural regime of Ca2+ oscillations is precociously interrupted, the incidence of implantation is compromised whereas hyper-stimulation of Ca2+ signaling events compromises post-implantation development. Moreover, although there was no major difference in the overall growth rates of the offspring, those obtained following hyper-stimulation exhibited a far greater variability in their weight. Analysis of global patterns of gene expression by microarray analysis revealed that approximately 20% of the transcripts are mis-regulated when too few oscillations are experienced by the embryo and EASE analysis indicates that genes preferentially involved in RNA processing and polymerase II transcription are differentially affected. In addition, a set of genes involved in cell adhesion is also mis-expressed and could thus be mechanistically linked to the observed reduced implantation. Only about 3% of the transcripts were mis-regulated following hyper-stimulation, and EASE analysis indicates that genes preferentially involved in metabolism are differentially affected. In toto, these results indicate that a range Ca2+ signaling events following fertilization (an excess or reduction) has long-term effects on both gene expression and development to term. #!# **Overall design:** We profiled the global gene expression in the blastocysts by treatment of Ca2+ oscillations, and identified the genes differentially expressed.

Background corr dist: KL-Divergence = 0.0856, L1-Distance = 0.0274, L2-Distance = 0.0012, Normal std = 0.4601

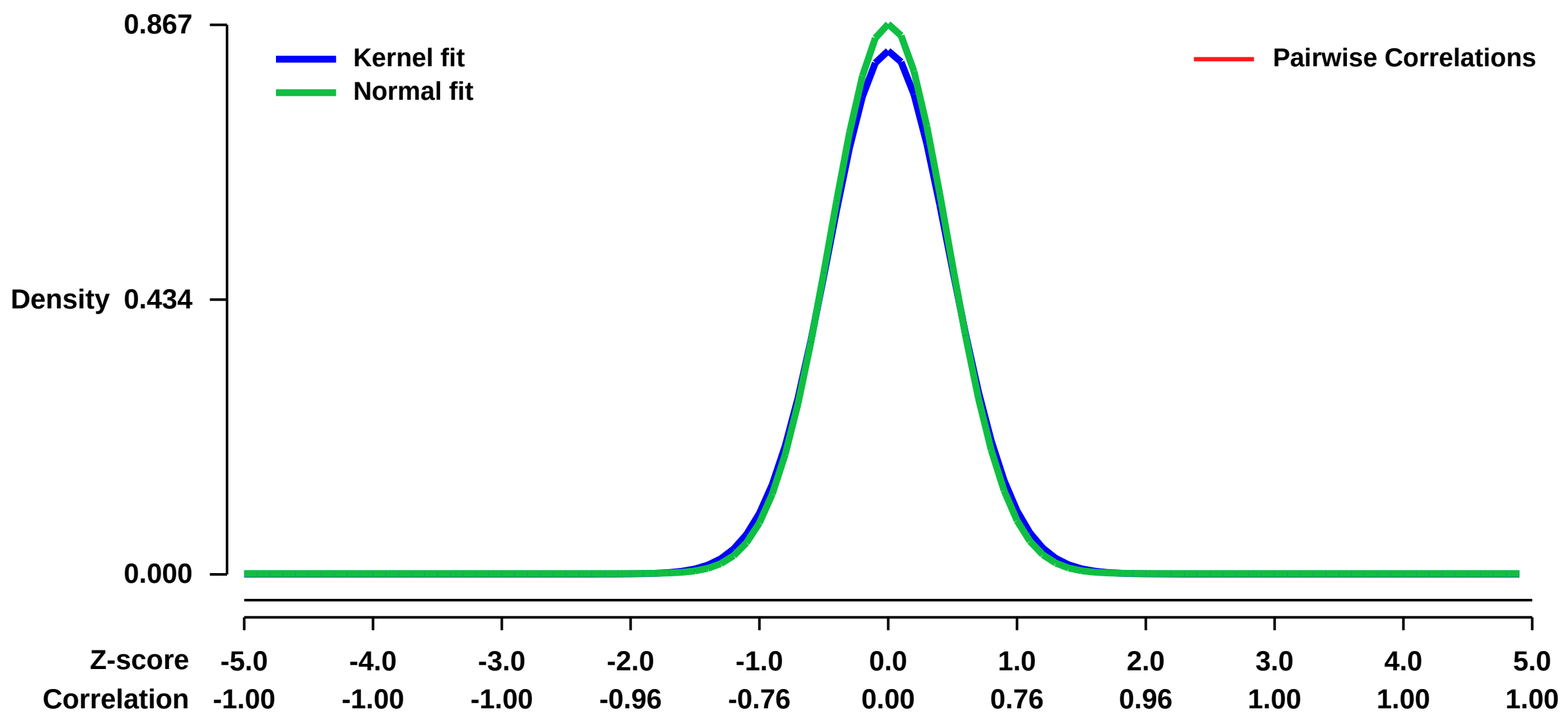

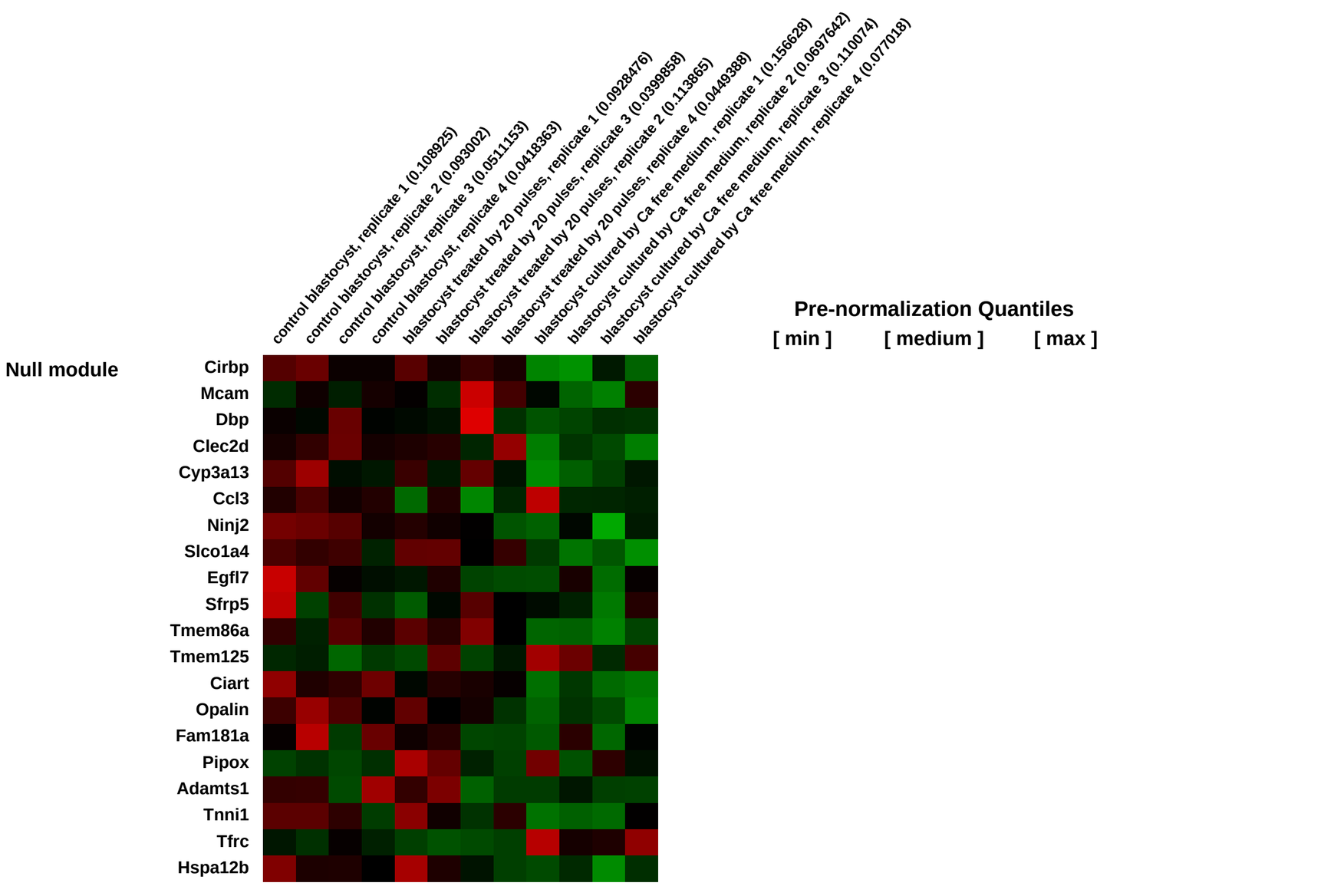

GEO Series "GSE32963" Expression Profiles

Num of samples in this series: 6

Scale of expression profile Z-scores

-3.0 -2.0 -1.0 0.0 1.0 2.0 3.0

GEO Link:	http://www.ncbi.nlm.nih.gov/geo/query/acc.cgi?acc=GSE32963
Status:	Public on Jan 01 2012
Title:	Gene expression profile in the developing and adult mouse cochlear sensory epithelia
Organism:	Mus musculus
Experiment type:	Expression profiling by array
Platform:	GPL1261
Pubmed ID:	22900075
Summary & Design:	**Summary:** To understand the molecular control of development and regeneration in the mammalian cochlear sensory epithelia, we performed a comparative study of gene expression patterns between postnatal day-3 (P3) and adult stages using a microarrays approach. **Overall design:** Two inner ear development stages were used in this study, Post-natal day three and eight-week-old adult. A total number of sixty Swiss mice were exploited for each stage. The cochlear sensory epithelia (CSE) were collected from the inner ears and immediately placed in RNA later solution. A total of six independent dissection experiments were carried out separately in order to obtain three biological replicates for each stage. In each experiment, the CSE from 20 mice were pooled. Total RNA was purified from each biological sample separately using RNAeasy Mini Kit and the RNA integrity was assessed by the Nanodrop 2000

Background corr dist: KL-Divergence = 0.0318, L1-Distance = 0.0515, L2-Distance = 0.0038, Normal std = 0.7289

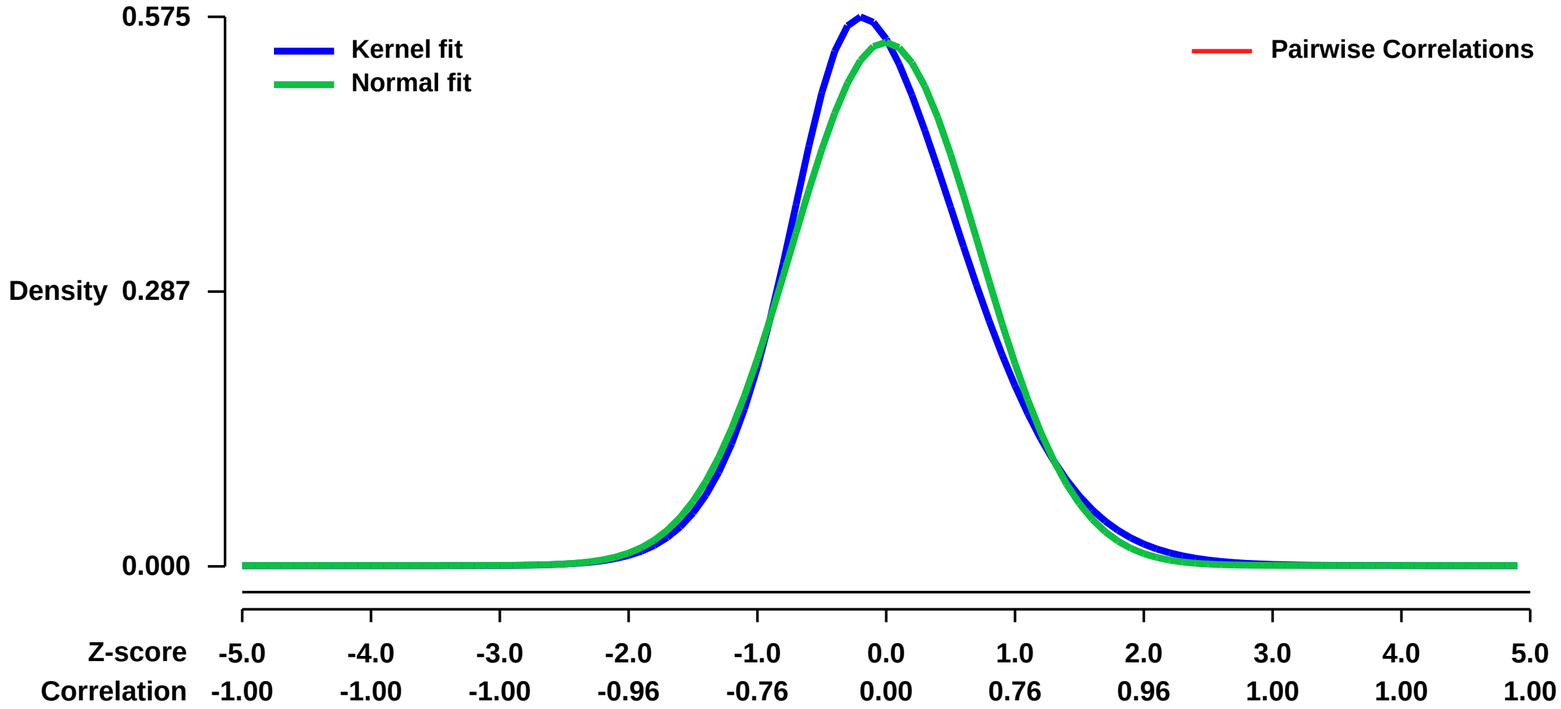

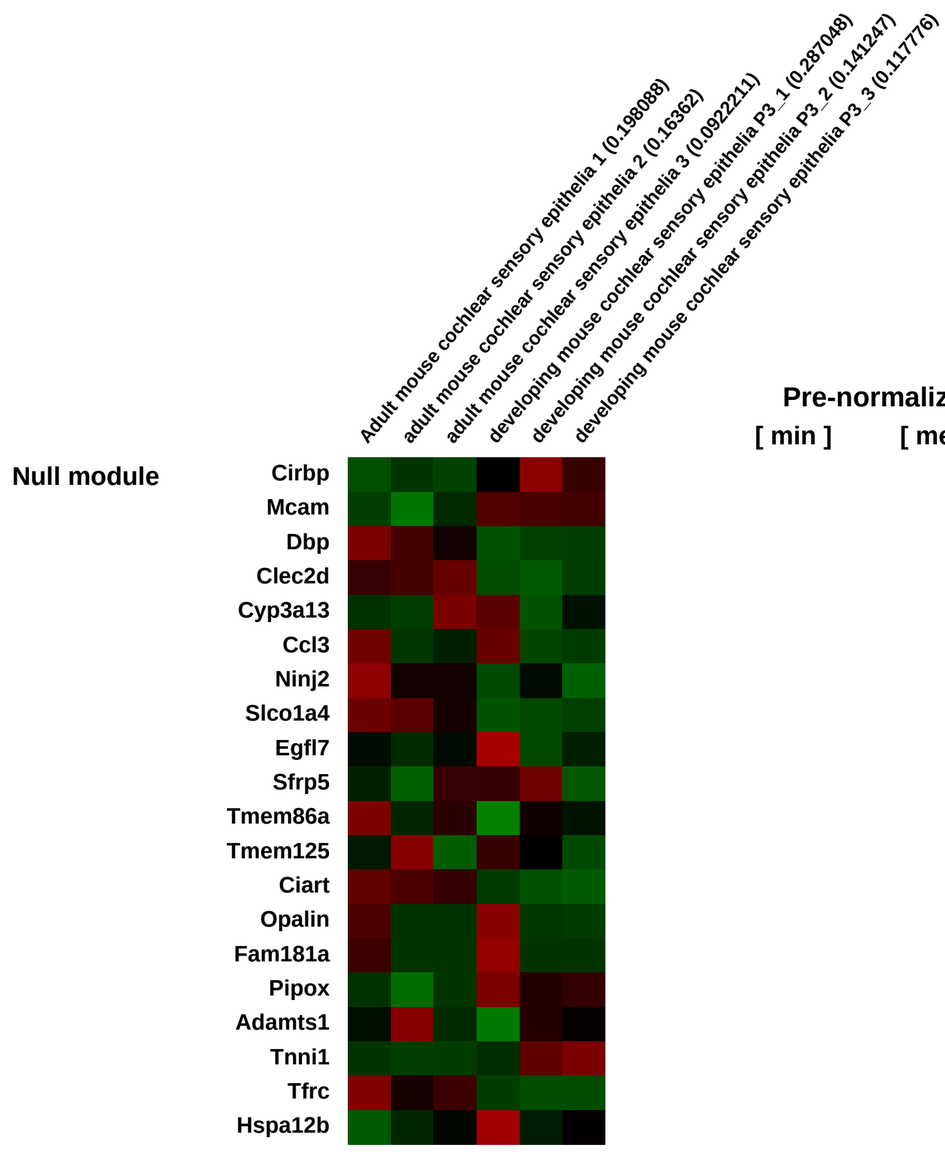

GEO Series "GSE39469" Expression Profiles

Num of samples in this series: 6

Scale of expression profile Z-scores

-3.0 -2.0 -1.0 0.0 1.0 2.0 3.0

GEO Link:	http://www.ncbi.nlm.nih.gov/geo/query/acc.cgi?acc=GSE39469
Status:	Public on Apr 05 2013
Title:	Expression data from proliferating and senescent murine hepatic stellate cells
Organism:	Mus musculus
Experiment type:	Expression profiling by array
Platform:	GPL1261
Pubmed ID:	23562644
Summary & Design:	**Summary:** The p53 protein is a cell-autonomous tumor suppressor that restricts malignant transformation by triggering cell cycle exit or apoptosis. p53 also promotes cellular senescence, a program that triggers a stable cell cycle arrest and can modify the tissue microenvironment through its effect on cell membrane and secretory proteins. Here we show that specific ablation of p53 in hepatic stellate cells, which undergo a process of proliferation and senescence in the fibrogenic response to liver damage, enhances liver cirrhosis, reduces survival and increases the malignant transformation of adjacent epithelial cells into hepatocellular carcinoma. This p53-dependent senescence program involves the release of secreted proteins which skew macrophages into a tumor-inhibiting M1-state that can eliminate senescent stellate cells. In contrast, p53-deficient stellate cells secrete factors that promote M2 polarization, which is pro-tumorigenic. Our study reveals that p53 can exert a non-cell-autonomous tumor suppressor response and suggests that this occurs, in part, by its ability to influence macrophage polarization. We used microarrays to detail the global programme of gene expression underlying p53-dependent senescent and identified distinct classes of up-regulated or down-regulated genes during this process. **Overall design:** Proliferating and senescent stellate cell pellets were collected RNA extraction and hybridization on Affymetrix microarrays.

Background corr dist: KL-Divergence = 0.0299, L1-Distance = 0.0265, L2-Distance = 0.0007, Normal std = 0.6872

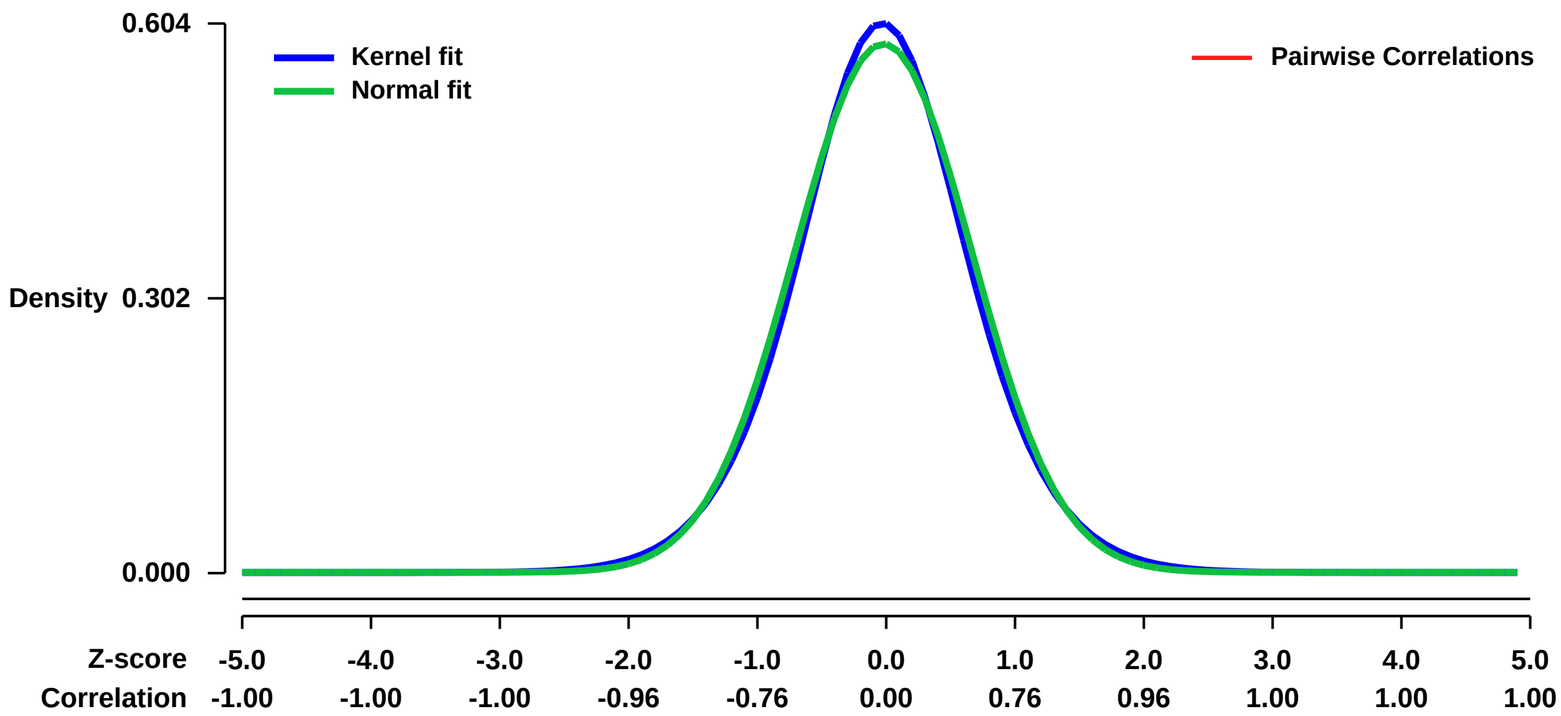

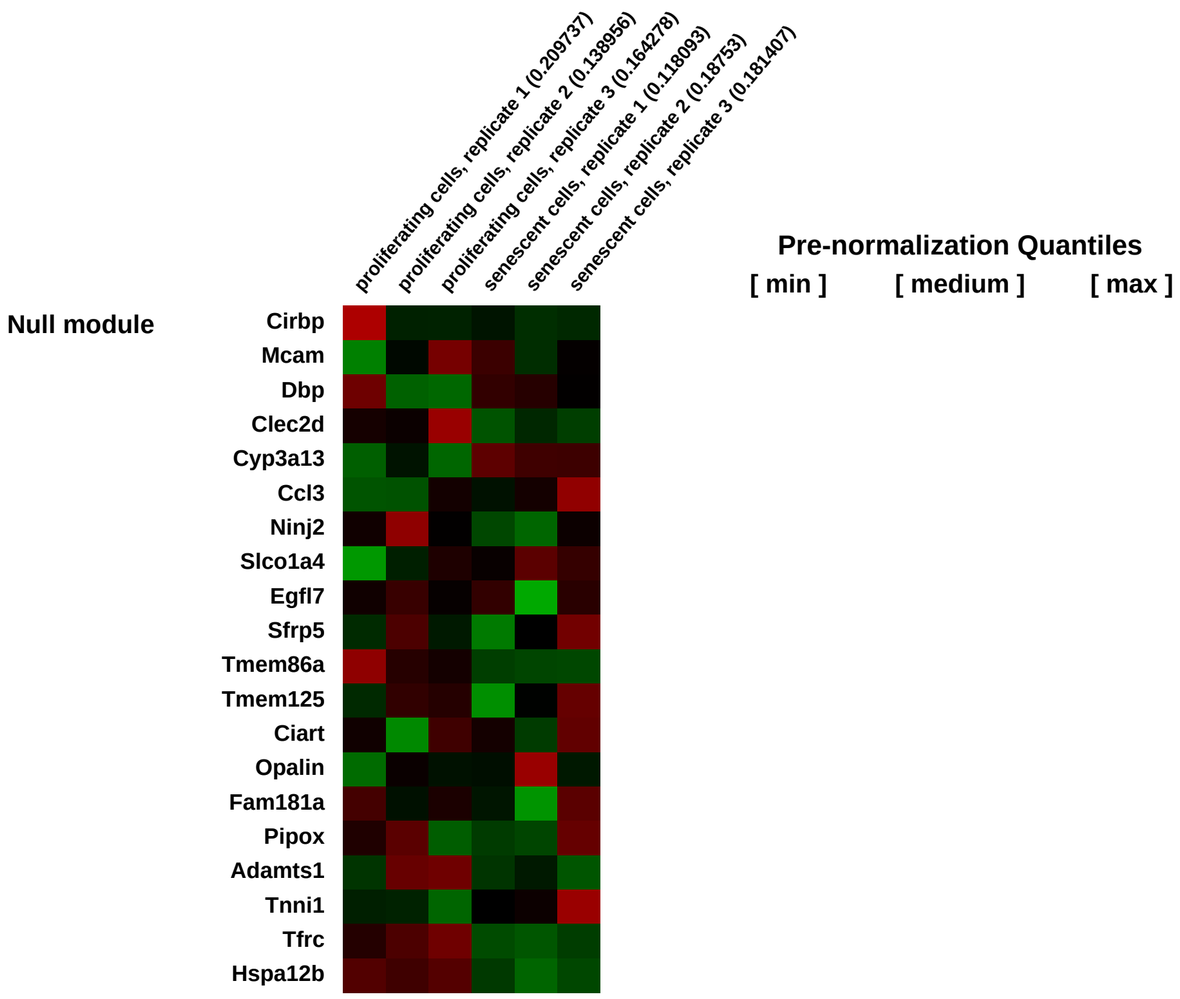

GEO Series "GSE27547" Expression Profiles

Num of samples in this series: 17

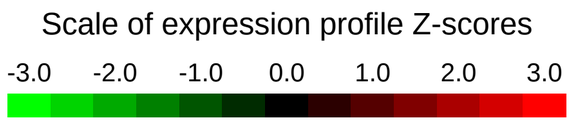

GEO Link:	http://www.ncbi.nlm.nih.gov/geo/query/acc.cgi?acc=GSE27547
Status:	Public on Feb 28 2011
Title:	Gene expression differences in mouse islets after isolation at different time points (0-48hr)
Organism:	Mus musculus
Experiment type:	Expression profiling by array
Platform:	GPL1261
Pubmed ID:	21471441
Summary & Design:	**Summary:** TGFbi (transforming growth factor-beta-induced) is a secreted protein and is capable of binding to both extracellular matrix (ECM) and cells. It thus acts as a bifunctional molecule enhancing ECM and cell interactions, a lack of which results in dysfunction of many cell types. In this study, we investigated the role of TGFbi in the function and survival of islets. Based on DNA microarray analysis followed by qPCR confirmation, the TGFbi gene showed drastic increases in expression in islets after culture. We demonstrated that recombinant TGFbi could preserve the integrity and enhance the function of cultured islets. Such a beneficial effect was mediated via signalling through FAK. Exogenous TGFbi was capable of sustaining high-level FAK phosphorylation in isolated islets, and FAK knockdown by siRNA in islets resulted in compromised islet function. TGFbi Tg islets showed better integrity and insulin release after in vitro culture. In vivo, b-cell proliferation was detectable in Tg but not wild type pancreata. At age above 12 months, Tg pancreata contained giant islets. Tg mice displayed better glucose tolerance than the controls. Tg islets were more potent in lowering blood glucose when transplanted into syngeneic mice with streptozotocin-induced diabetes, and these transplanted islets also underwent regeneration. Our results indicate that TGFbi is a vital trophic factor promoting islet survival, function and regeneration. At least some of its beneficial effect was mediated by signalling through FAK. **Overall design:** Batch 6: YF050524MOT06, YF050524MOT12, YF050524MOT18

Background corr dist: KL-Divergence = 0.1987, L1-Distance = 0.0462, L2-Distance = 0.0047, Normal std = 0.3324

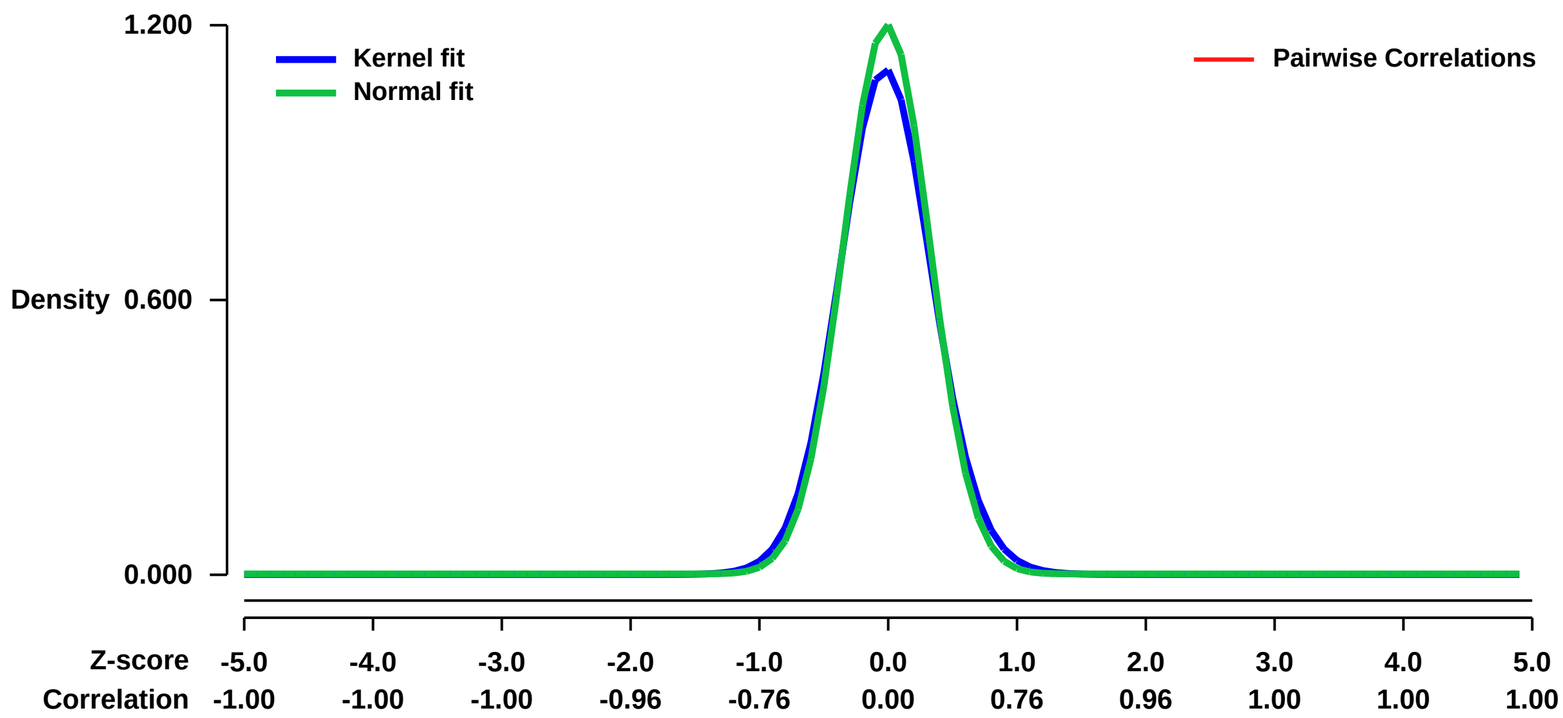

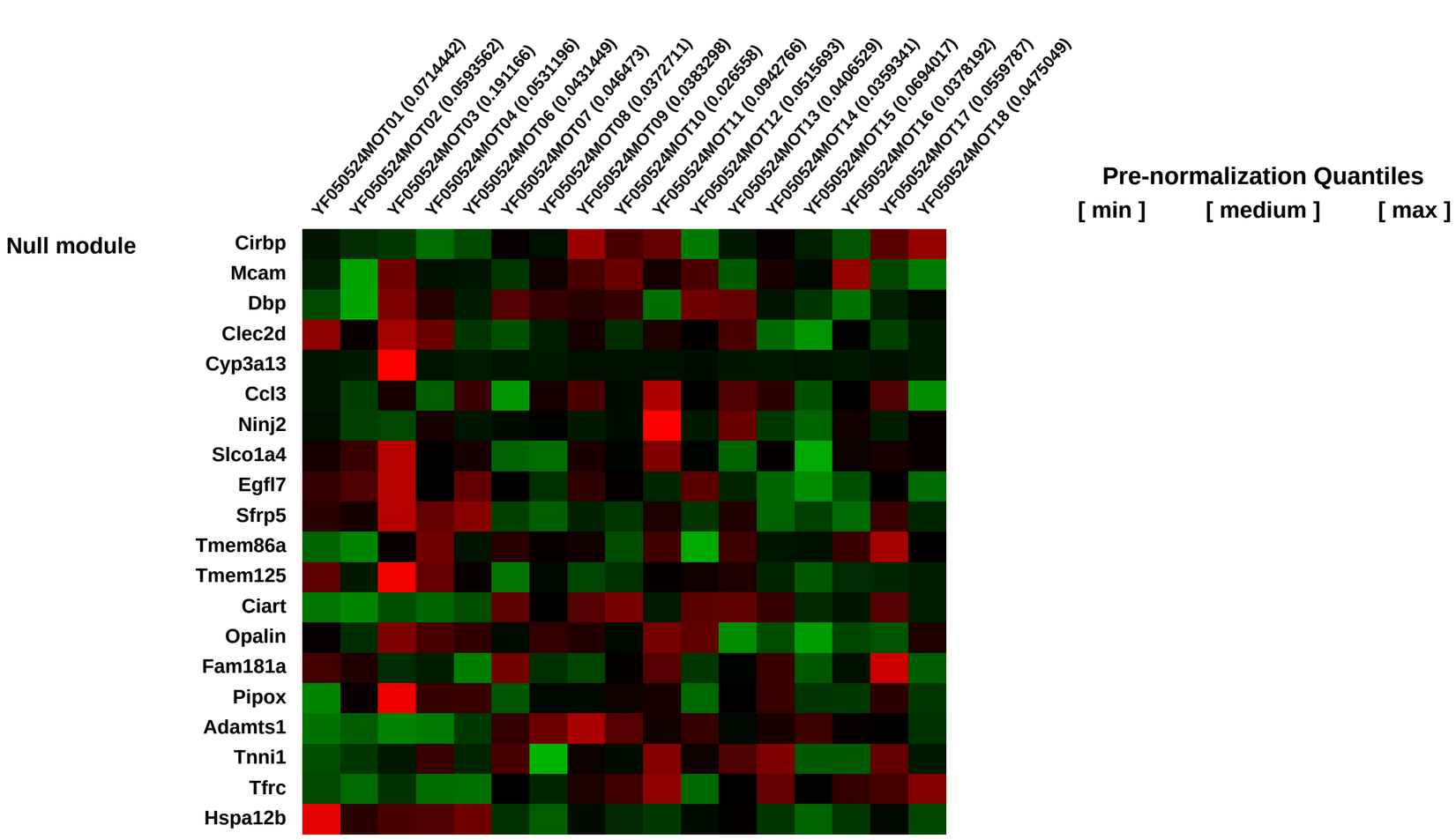

GEO Series "GSE13149" Expression Profiles

Num of samples in this series: 25

Scale of expression profile Z-scores

-3.0 -2.0 -1.0 0.0 1.0 2.0 3.0

GEO Link:	http://www.ncbi.nlm.nih.gov/geo/query/acc.cgi?acc=GSE13149
Status:	Public on Oct 30 2008
Title:	Multi-stage analysis of gene expression in C57/B6 mouse liver development
Organism:	Mus musculus
Experiment type:	Expression profiling by array
Platform:	GPL1261
Pubmed ID:	19015022
Summary & Design:	**Summary:** The liver performs a number of essential functions for life. The development of such a complex organ relies on finely regulated gene expression profiles which change over time in the development and determine the phenotype and function of the liver. We used high-density oligonucleotide microarrays to study the gene expression and transcription regulation at 14 time points across the C57/B6 mouse liver development, which include E11.5 (embryonic day 11.5), E12.5, E13.5, E14.5, E15.5, E16.5, E17.5, E18.5, Day0 (the day of birth), Day3, Day7, Day14, Day21, and normal adult liver. With these data, we made a comprehensive analysis on gene expression patterns, functional preferences and transcriptional regulations during the liver development. **Keywords: time course** **Overall design:** Totally 25 microarrays have been used in this experiment, and 11 of the 14 time points have two technique repeat experiments.

Background corr dist: KL-Divergence = 0.0590, L1-Distance = 0.0653, L2-Distance = 0.0079, Normal std = 0.5560

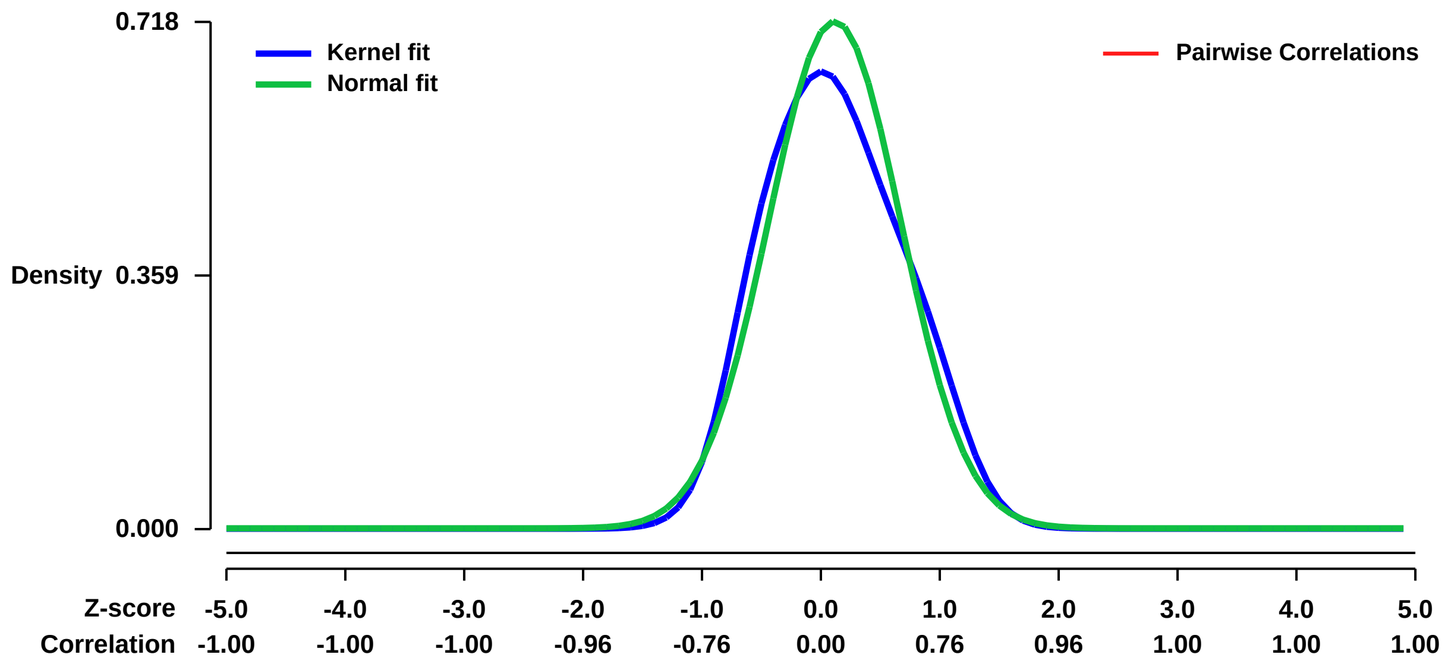

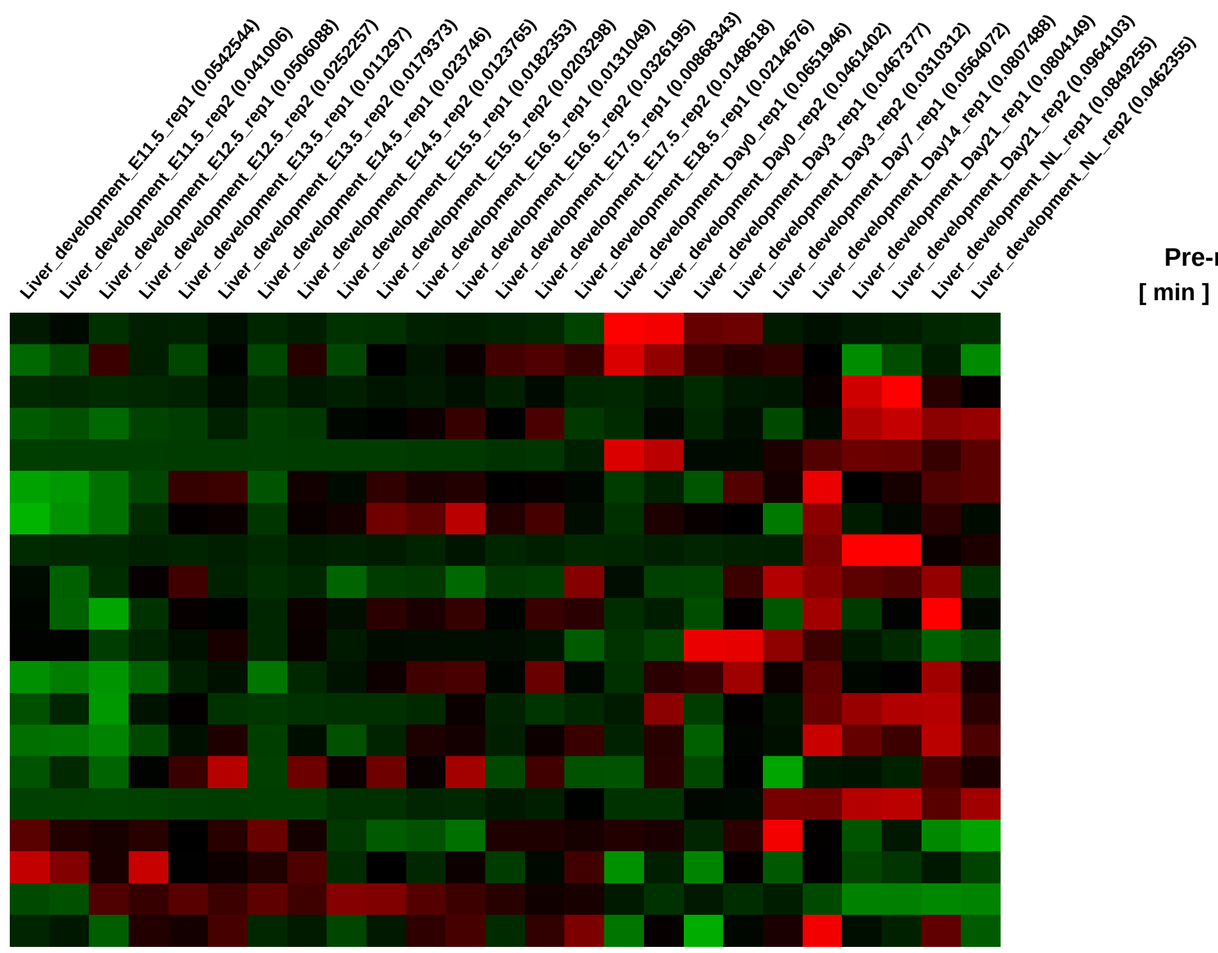

GEO Series "GSE24243" Expression Profiles

Num of samples in this series: 6

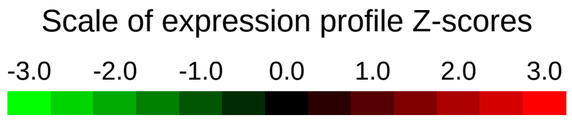

GEO Link:	http://www.ncbi.nlm.nih.gov/geo/query/acc.cgi?acc=GSE24243
Status:	Public on May 09 2011
Title:	Murine skin gene expression analysis of skin-specific Scd1-deficient and control mice
Organism:	Mus musculus
Experiment type:	Expression profiling by array
Platform:	GPL1261
Pubmed ID:	21573029
Summary & Design:	**Summary:** **To help elucidate the metabolic changes in the skin that contribute to the obesity resistance and skin pathology in mice lacking Scd1, we performed microarray analysis of skin gene expression in male skin Scd1 knockout (SKO) and Scd1 flox/flox control (Lox) mice fed a standard rodent diet.** **We identified an extraordinary number of differentially expressed genes that support the previously documented histological observations of sebocyte atrophy, inflammation and epidermal hyperplasia in SKO mice. Additionally, transcript levels were reduced in skin of SKO mice for genes involved in fatty acid synthesis, elongation and desaturation, which may be attributed to decreased abundance of key transcription factors including SREBP1c, ChREBP and LXR$_{\alpha}$–. Conversely, genes involved in cholesterol synthesis were increased, suggesting an imbalance between skin fatty acid and cholesterol synthesis. Unexpectedly, we observed a robust elevation in skin retinol, retinoic acid and retinoic acid-induced genes in SKO mice. These results highlight the importance of monounsaturated fatty acid synthesis for maintaining retinol homeostasis and point to disturbed retinol metabolism as a novel contributor to the Scd1 deficiency-induced skin pathology.** **Overall design:** **We analyzed dorsal skin gene expression in non-fasted 8-9 week old male skin Scd1 knockout (SKO) mice (n=3) and Scd1flox/flox (Lox) control mice (n=3)on a C57BL/6J background using Affymetrix 430 2.0 microarrays.**

Background corr dist: KL-Divergence = 0.0198, L1-Distance = 0.0107, L2-Distance = 0.0001, Normal std = 0.7416

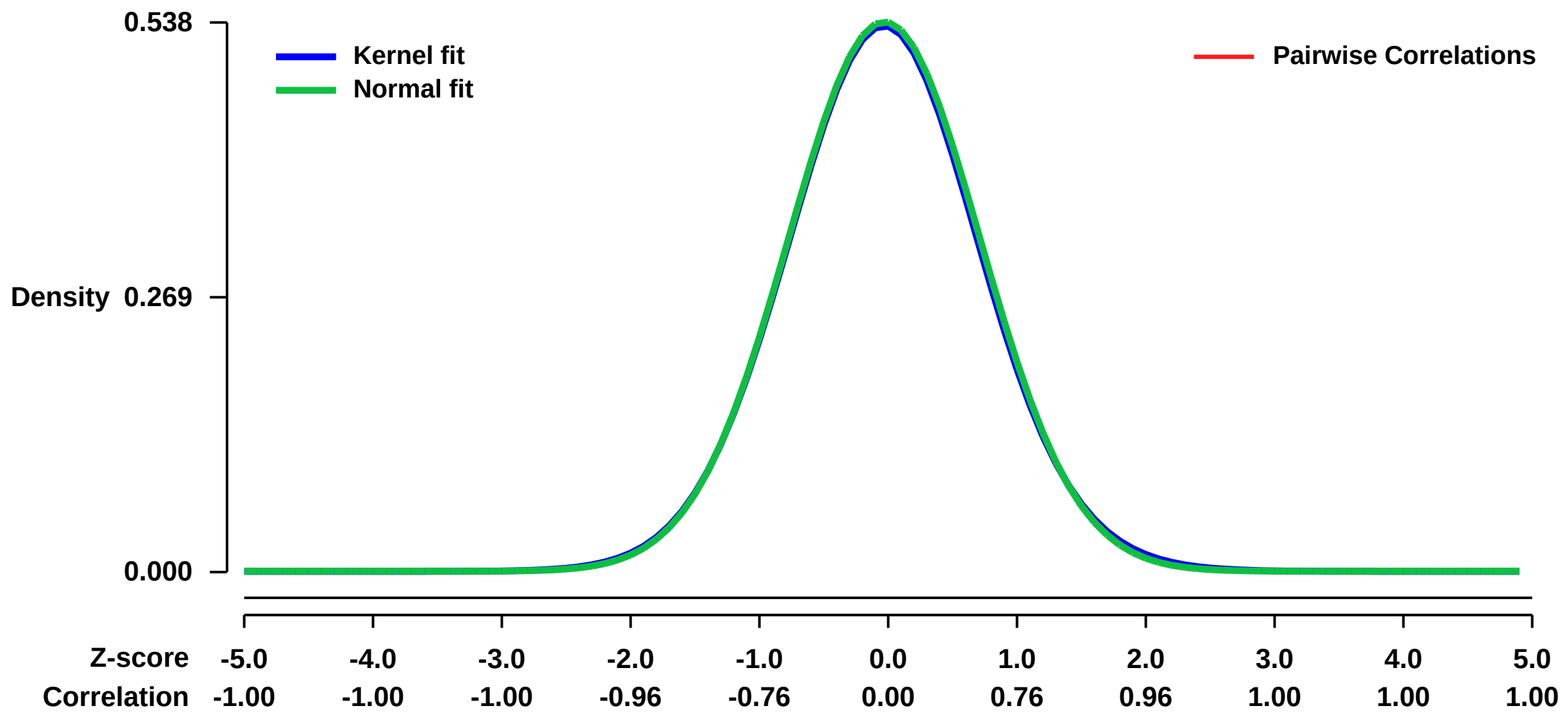

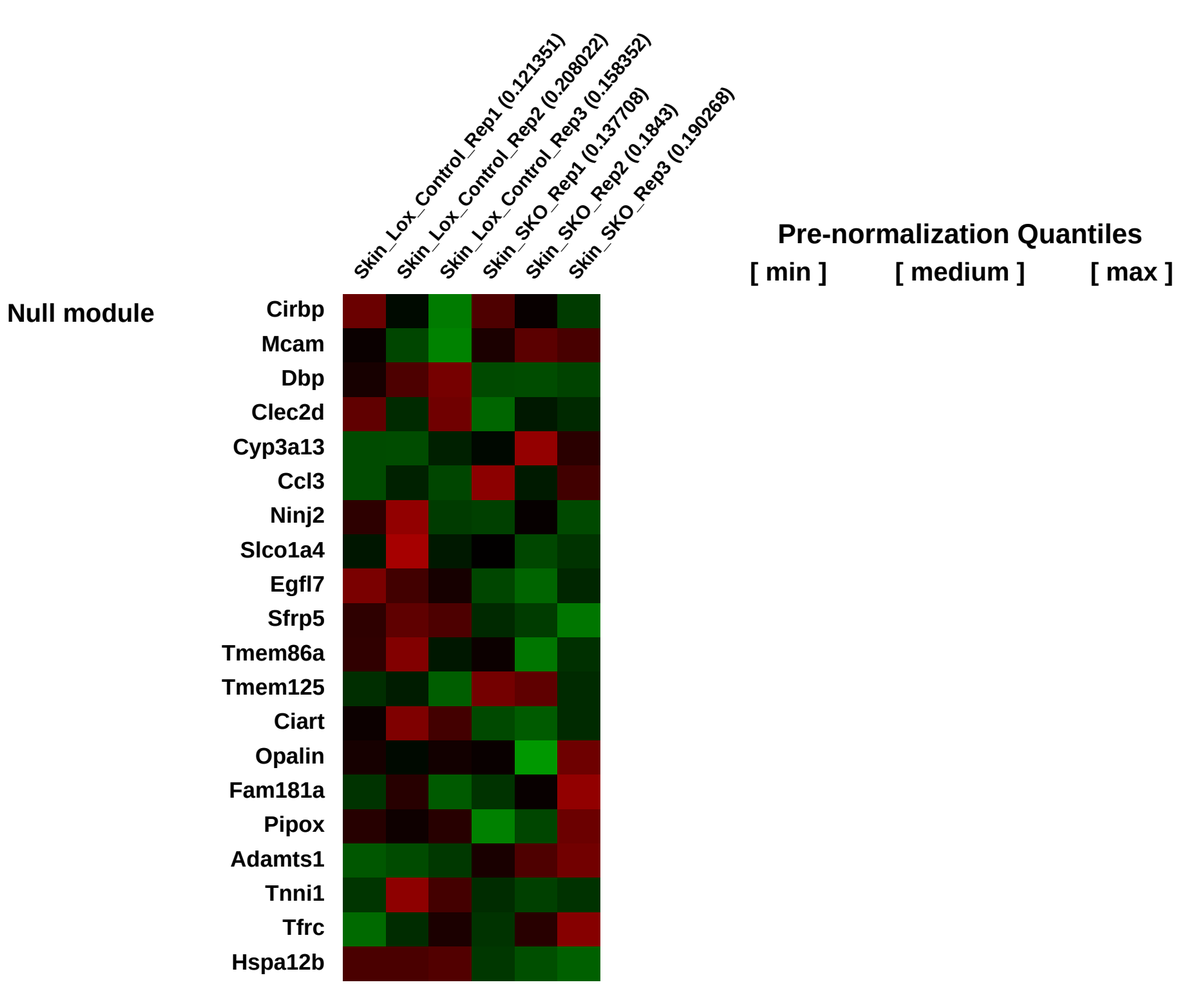

GEO Series "GSE6210" Expression Profiles

Num of samples in this series: 12

Scale of expression profile Z-scores

-3.0 -2.0 -1.0 0.0 1.0 2.0 3.0

GEO Link:	http://www.ncbi.nlm.nih.gov/geo/query/acc.cgi?acc=GSE6210
Status:	Public on Jan 01 2007
Title:	Hypomorphic Mutation in PGC1beta causes mitochondrial dysfunction and liver insulin resistance
Organism:	Mus musculus
Experiment type:	Expression profiling by array
Platform:	GPL1261
Pubmed ID:	17141629
Summary & Design:	**Summary:** PGC1beta is a transcriptional coactivator that potently stimulates mitochondrial biogenesis and respiration of cells. Here, we have generated mice lacking exons 3 to 4 of the Pgc1beta gene (PGC1beta E3,4-/E3,4- mice). These mice express a mutant protein that has reduced coactivation activity on a subset of transcription factors, including ERRalpha, a major target of PGC1beta in the induction of mitochondrial gene expression. The mutant mice have reduced expression of OXPHOS genes and mitochondrial dysfunction in liver and skeletal muscle as well as elevated liver triglycerides. Euglycemic-hyperinsulinemic clamp and insulin signaling studies show that PGC1beta mutant mice have normal skeletal muscle response to insulin, but have hepatic insulin resistance. These results demonstrate that PGC1beta is required for normal expression of OXPHOS genes and mitochondrial function in liver and skeletal muscle. Importantly, these abnormalities do not cause insulin resistance in skeletal muscle but cause substantially reduced insulin action in the liver. **Keywords:** Liver and quadricpes muscle gene expression, WT vs. PGC1beta mutant **Overall design:** Gene expression levels in liver tissue and quadriceps muscle were compared between WT/Control and PGC1beta mutant tissue. Total RNA was extracted from liver and skeletal muscle using RNAeasy kit (Qiagen, Valencia, CA), according to the manufacturerâ s instructions. Synthesis of cRNA, hybridization and scanning of the Affymetrix Murine 430 2.0 chip was performed by Dana Farber Cancer Institute Microarray Core Facility. The microarray data was analyzed by Clustering Analysis using the d-Chip software (Li and Wong, 2001).

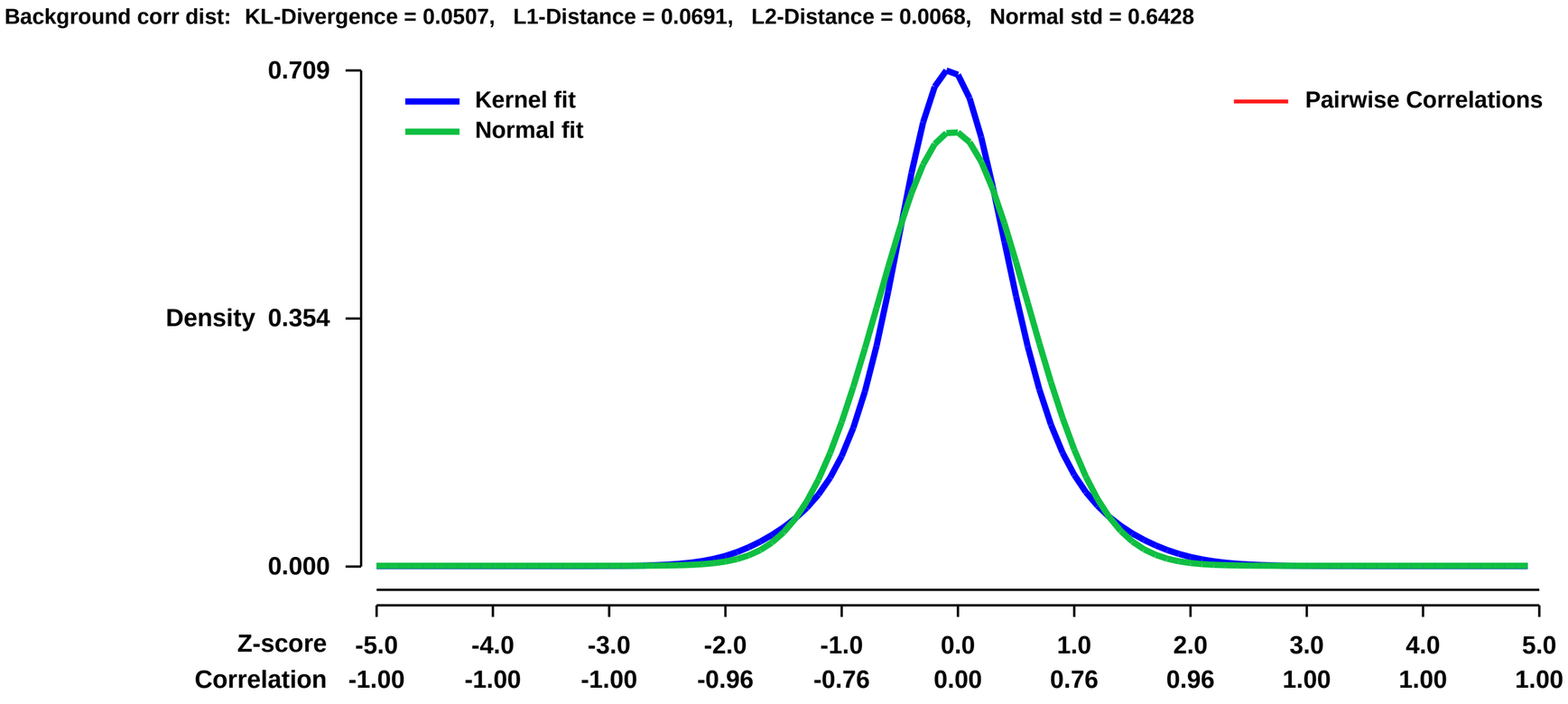

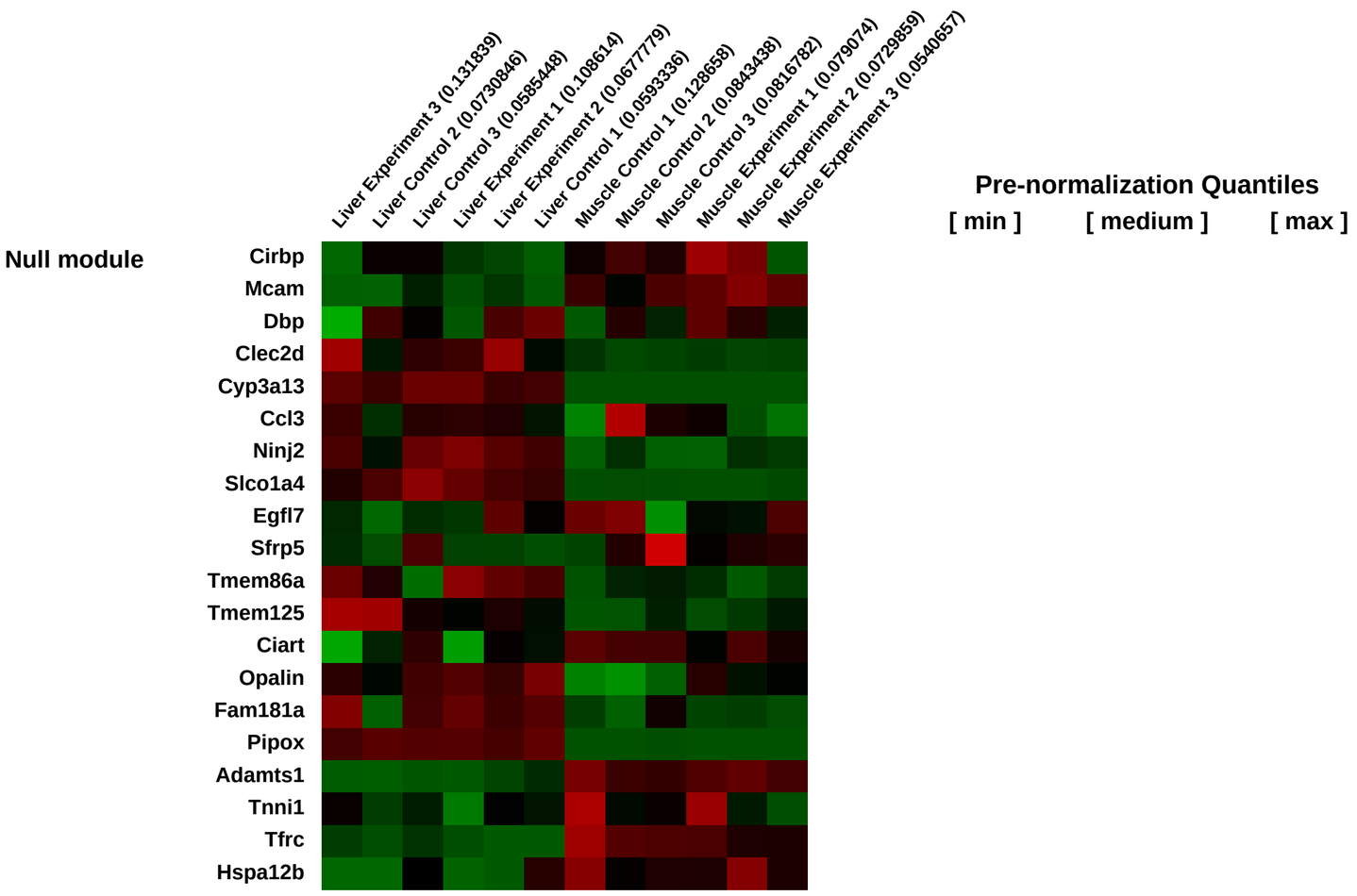

GEO Series "GSE33302" Expression Profiles

Num of samples in this series: 17

Scale of expression profile Z-scores

-3.0 -2.0 -1.0 0.0 1.0 2.0 3.0

GEO Link:	http://www.ncbi.nlm.nih.gov/geo/query/acc.cgi?acc=GSE33302
Status:	Public on Sep 06 2012
Title:	Expression data from sleep deprivation experiment in mouse hippocampus
Organism:	Mus musculus
Experiment type:	Expression profiling by array
Platform:	GPL1261
Pubmed ID:	22930738
Summary & Design:	**Summary:** We used microarrays to detail the global programme of gene expression underlying the effect of sleep deprivation in the mouse hippocampus and identified distinct classes of regulated genes during this process. **Overall design:** Hippocampal tissue was taken from sleep deprived mice and time-matched non-sleep-deprived control animals that were left undisturbed in their home cages during the sleep deprivation period for a total of 8 and 9 replicates per group. RNA was isolated and cDNA was synthesized from hippocampal tissue, and the sample from each animal was hybridized to a separate Affymetrix Mouse 430_2 microarray

Background corr dist: KL-Divergence = 0.1760, L1-Distance = 0.0517, L2-Distance = 0.0063, Normal std = 0.3479

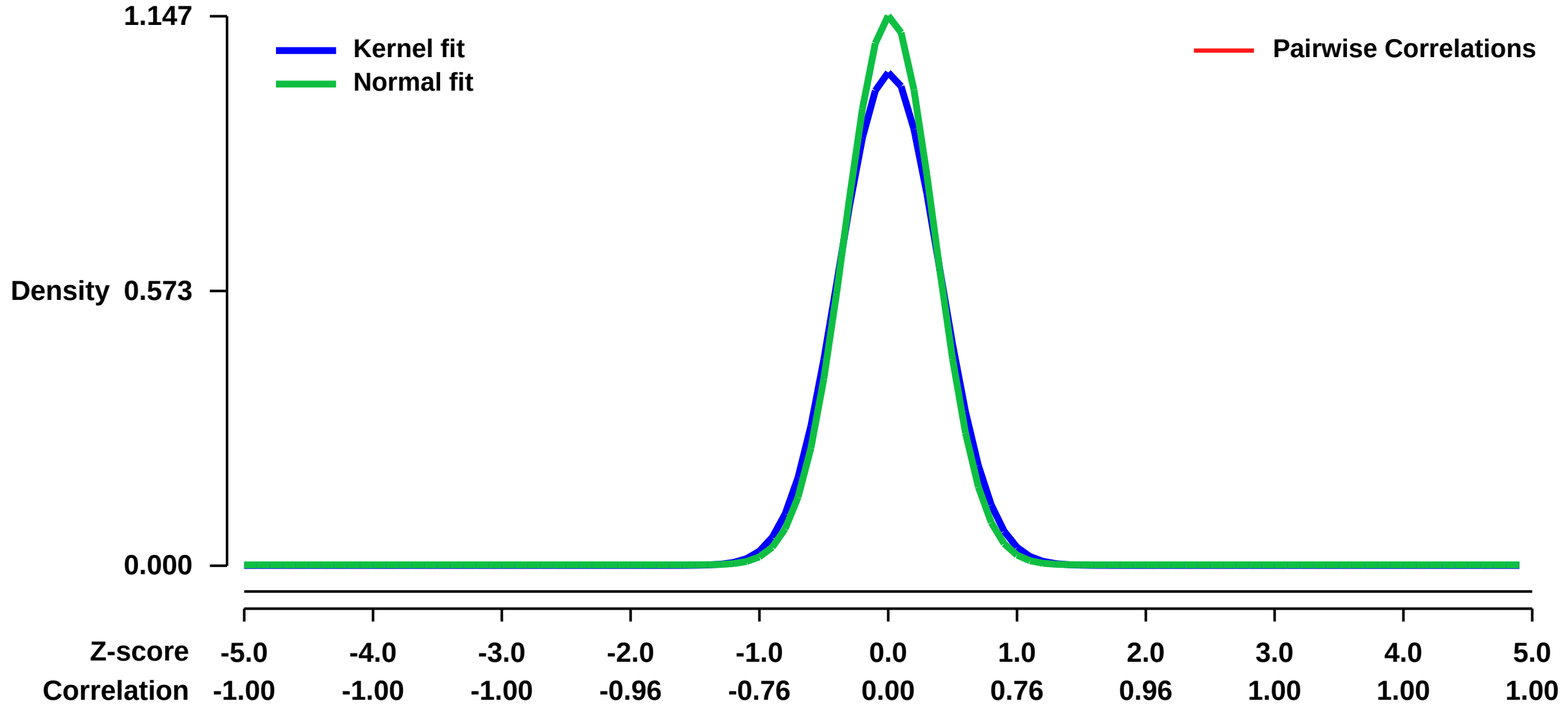

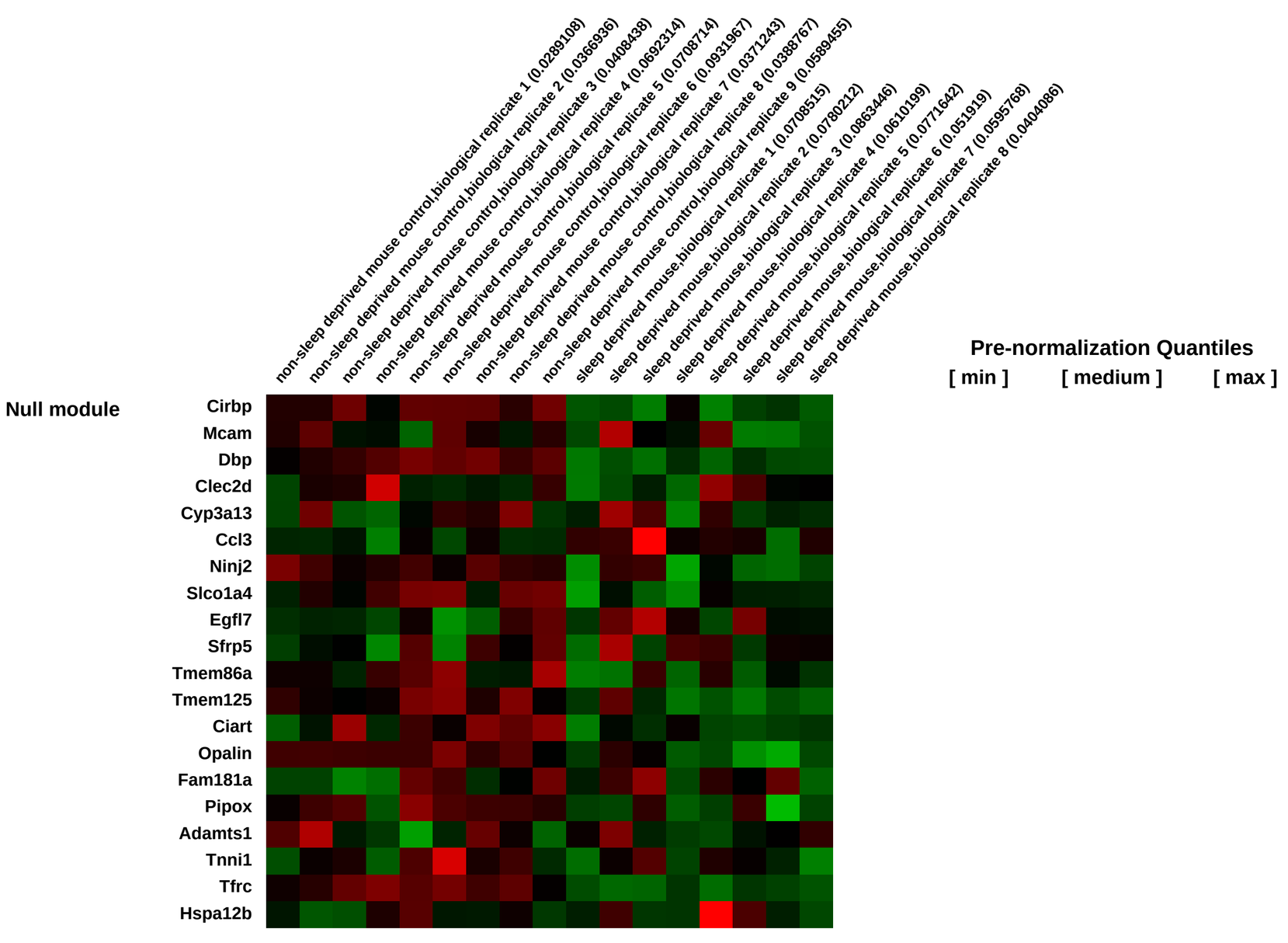

GEO Series "GSE36974" Expression Profiles

Num of samples in this series: 14

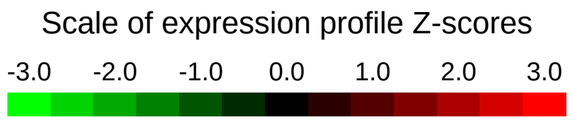

GEO Link:	**http://www.ncbi.nlm.nih.gov/geo/query/acc.cgi?acc=GSE36974**
Status:	**Public on Mar 31 2013**
Title:	**Genotype modulates gene expression profiles in the uterus in response to preconceptual folate supplementation.**
Organism:	**Mus musculus**
Experiment type:	**Expression profiling by array**
Platform:	**GPL1261**
Pubmed ID:	
Summary & Design:	**Summary:** **Periconceptual supplementation of women with folate is considered a great success for public health. Higher folate status, either by supplementation, or via the mandatory fortification of grain products in the United States, has lead to significant reduction in the incidence of neural tube defects. Besides birth defects, folate deficiency has been linked to a variety of morbidities, most notably to increased risk for cancer. However, recent evidence suggests that excess folate may be detrimental - for birth defect incidence or in the progression of cancer. How folate mediates beneficial or detrimental effects is not well understood. It is also unknown what molecular responses are elicited in women taking folate supplements, and thus experience a bolus of folate on top of the status achieved by fortification. To characterize this response, we performed gene expression profiling experiments on uterus tissue of pregnant mice after a preconceptional regimen of supplementation with folinic acid. We suggest that folinic acid supplementation affects expression of genes that contribute to protein synthesis and localization, genes that play a role for mitochondrial biology and oxidative phosphorylation, and genes encoding nucleotide-binding proteins, including protein kinases and GTP-binding intracellular signaling factors. The extent of such a response is strongly modulated by the genetic background. Finally, we suggest that folinic acid supplementation in this paradigm may affect histone methylation status, a potential avenue to mechanisms of gene regulation.** **Overall design:** **Gene expression profiles were generated from uterus tissue. Female mice were either C57BL/6 wildtype, or homozygous for a Folr4 mutation, and received injections of either saline of folininc acid, respectively.**

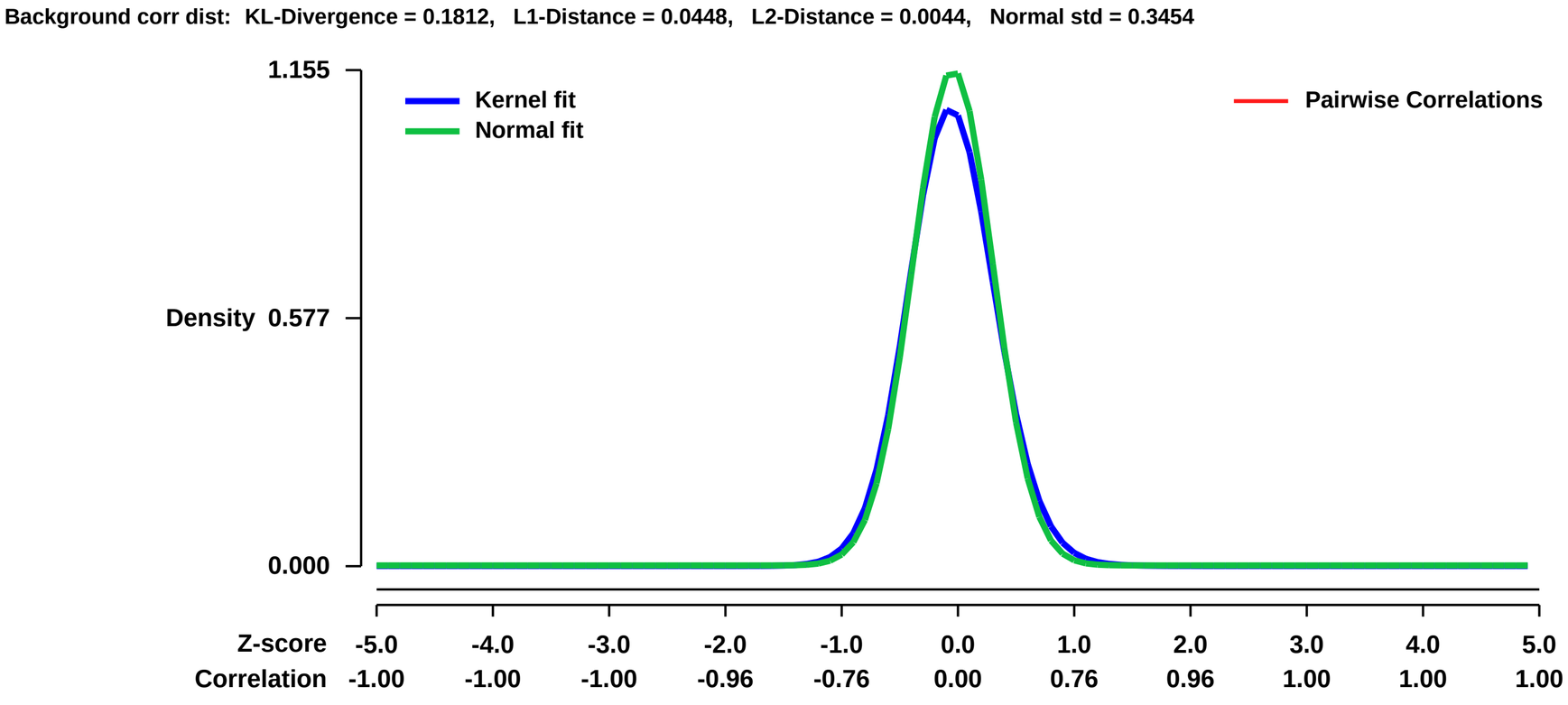

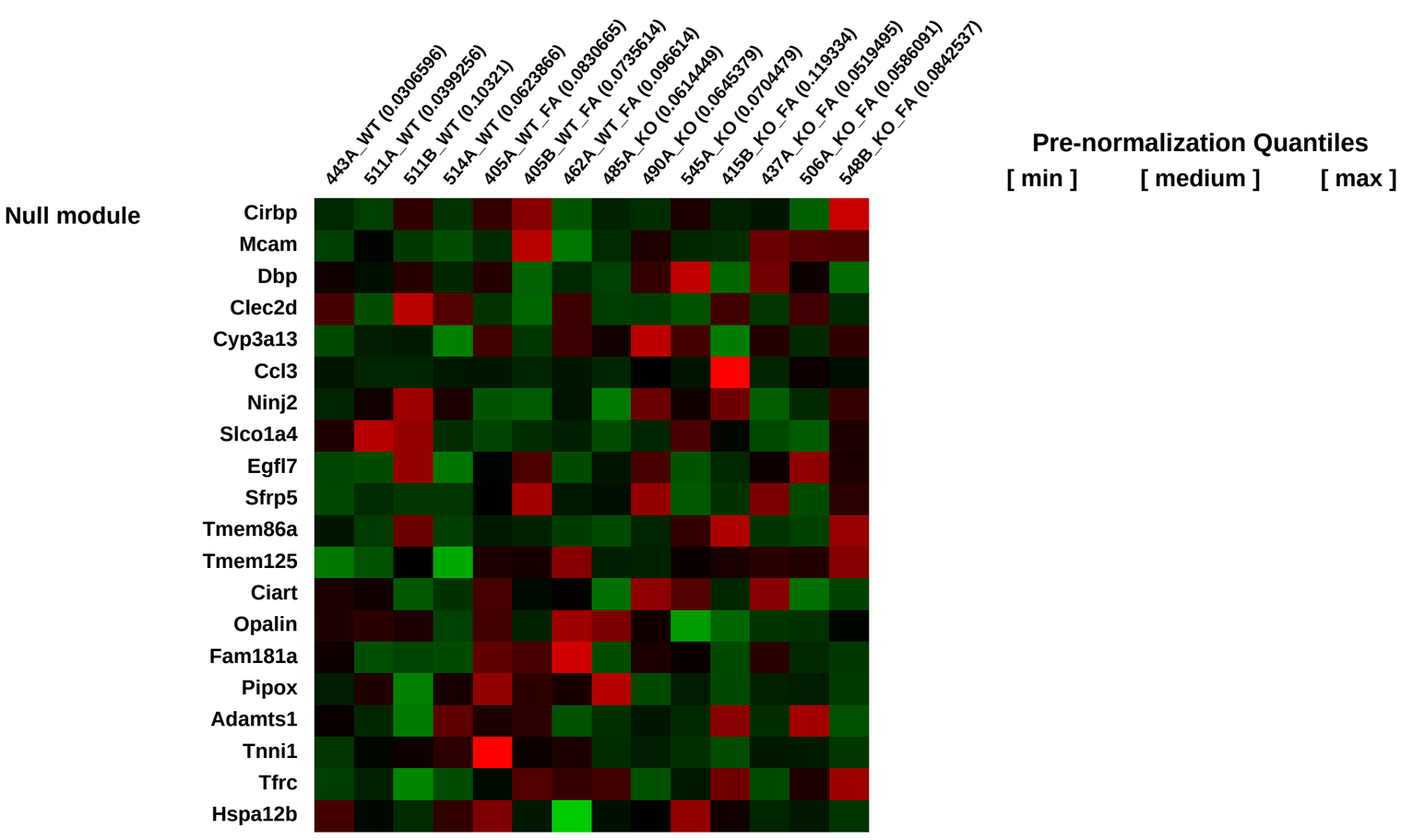

GEO Series "GSE31099" Expression Profiles

Num of samples in this series: 24

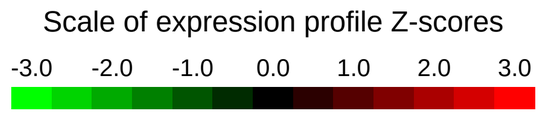

GEO Link:	http://www.ncbi.nlm.nih.gov/geo/query/acc.cgi?acc=GSE31099
Status:	Public on Nov 21 2011
Title:	Expression data from treatment-induced senescence in mouse Emu-myc B-cell lymphoma model
Organism:	Mus musculus
Experiment type:	Expression profiling by array
Platform:	GPL1261
Pubmed ID:	23945590
Summary & Design:	**Summary:** Treatment induced senescence (TIS) is a terminal cell cycle arrest program, increasingly recognized as a tumor suppressor mechanism complementing apoptosis in response to standard chemotherapy regimens. In particular cells with blocked apoptotic pathways rely on senescence as the only remaining failsafe mechanism to keep the neoplastic growth in check. However, little is known about biological properties, long-term fate of senescent tumor cells and their impact on the microenvironment. We used global gene expression profiling by microarrays to gain insight in the molecular programme underlying the treatment-induced senescence in Emu-myc transgenic B-cell lymphomas (apoptosis protected by Bcl2 overexpression), which robustly enter senescence in response to DNA-damaging anticancer agents such as Adriamycin (ADR). **Overall design:** Primary lymphoma cells isolated from lymph nodes of Emu-Myc transgenic mice were used. In this model the the c-Myc oncogene is constitutively expressed in the cells of B-cell lineage, leading to spontaneous development of aggressive B-cell lymphomas, resembling Burkitt lymphoma in humans. In order to bring up the senescence as the main failsafe mechanism, primary lymphoma cells are protected from apoptosis by retroviral over-expression of a strong antiapoptotic protein Bcl2. These cells (Myc;Bcl2) massively undergo senescence upon DNA-damaging treatment. Adriamycin (ADR) is a cytostatic drug, used as a standard part of several lymphoma treatment regimens. In this study, transcriptional profiles of matched pairs of untreated vs. 5 days ADR treated Myc;Bcl2 lymphomas were analysed.

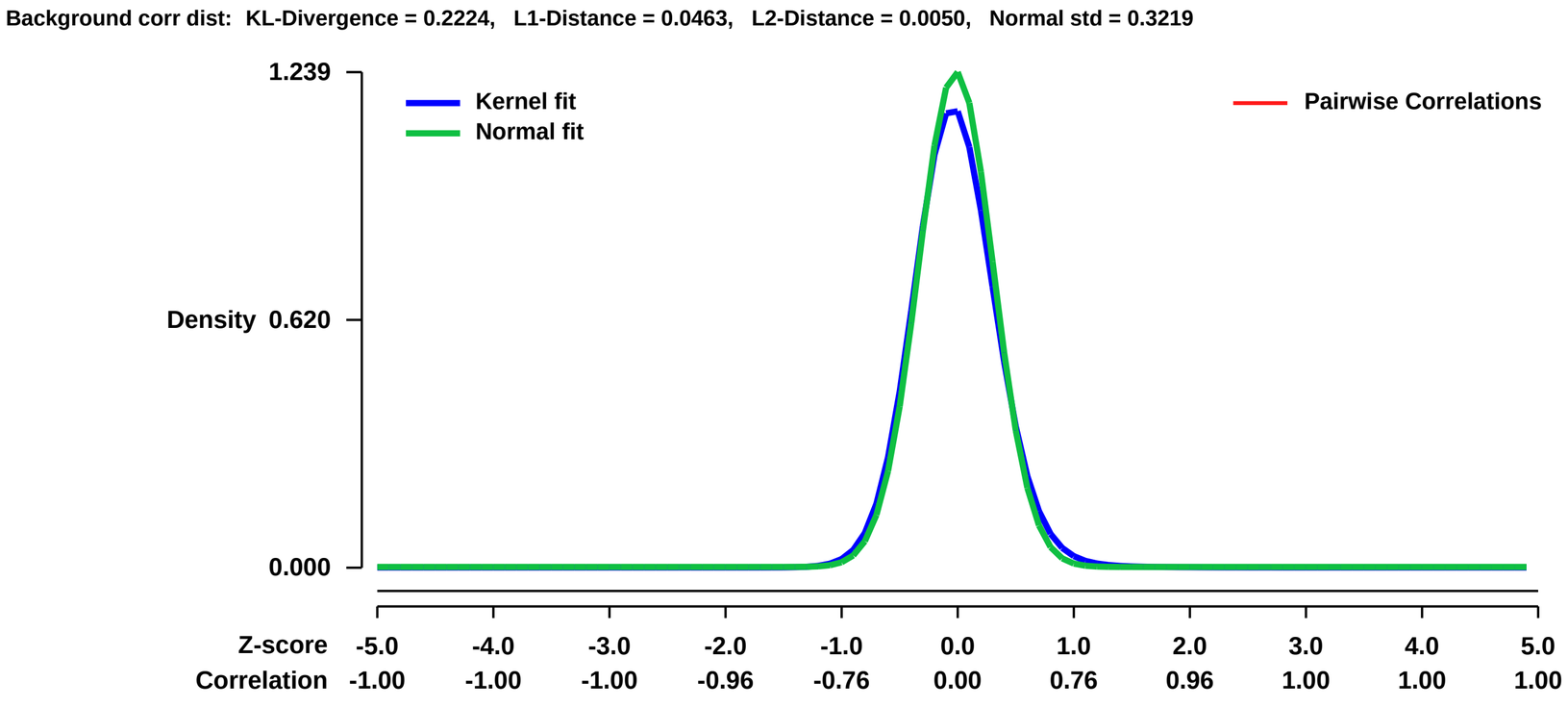

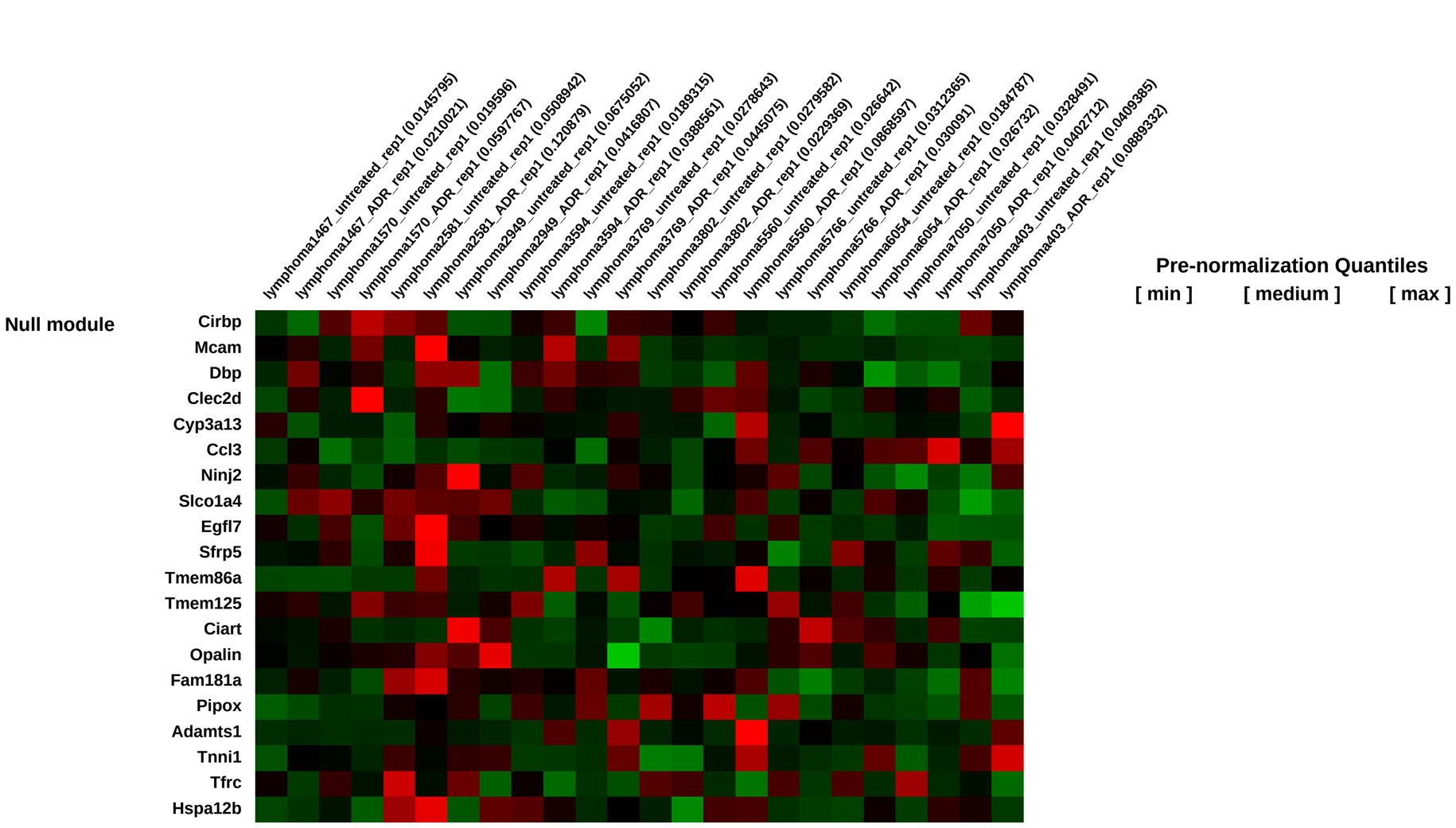

GEO Series "GSE7257" Expression Profiles

Num of samples in this series: 9

Scale of expression profile Z-scores

-3.0 -2.0 -1.0 0.0 1.0 2.0 3.0

GEO Link:	http://www.ncbi.nlm.nih.gov/geo/query/acc.cgi?acc=GSE7257
Status:	Public on Apr 10 2007
Title:	Laser capture-microarray analysis of Lim1 mutant kidney development.
Organism:	Mus musculus
Experiment type:	Expression profiling by array
Platform:	GPL1261
Pubmed ID:	17610272
Summary & Design:	**Summary:** The Lim1 gene has essential functions during several stages of kidney development. In particular, a tissue specific knockout in the early metanephric mesenchyme results in the formation of the earliest nephron precursor, the renal vesicle, but failure of this structure to progress to the next stage, the comma shaped body. To better understand the molecular nature of this developmental arrest we used a laser capture microdissection-microarray strategy to examine the perturbed gene expression pattern of the mutant renal vesicles. Among the genes found differently expressed were Chrdl2, an inhibitor of BMP signaling, the pro-apoptotic factor Bmf, as well as myob5, an atypical myosin which modulates chemokine and transferring signaling, and pdgfr1, which is important in epithelial folding. Of particular interest, the microarray data indicated that the Dkk1 gene, which encodes an inhibitor of Wnt signaling, was downregulated nine fold in mutants. This was confirmed by in situ hybridizations. It is interesting to note that Lim1 and Dkk1 mutant mice have striking similarities in phenotype. These results suggest that the Dkk1 gene might be a key downstream effector of Lim1 function. **Keywords:** Lim1 mutant, kidney development, gene expression profile comparison **Overall design:** We compared gene expression profiles of wild type and mutant Lim1 renal vesicles, which were isolated from E12.5 kidneys by laser capture microdissection. Nine biological independent samples were examined, with four mutant and five wild type. Each sample included approximately 30-50 renal vesicles. Detailed protocols are described at GUDMAP.org

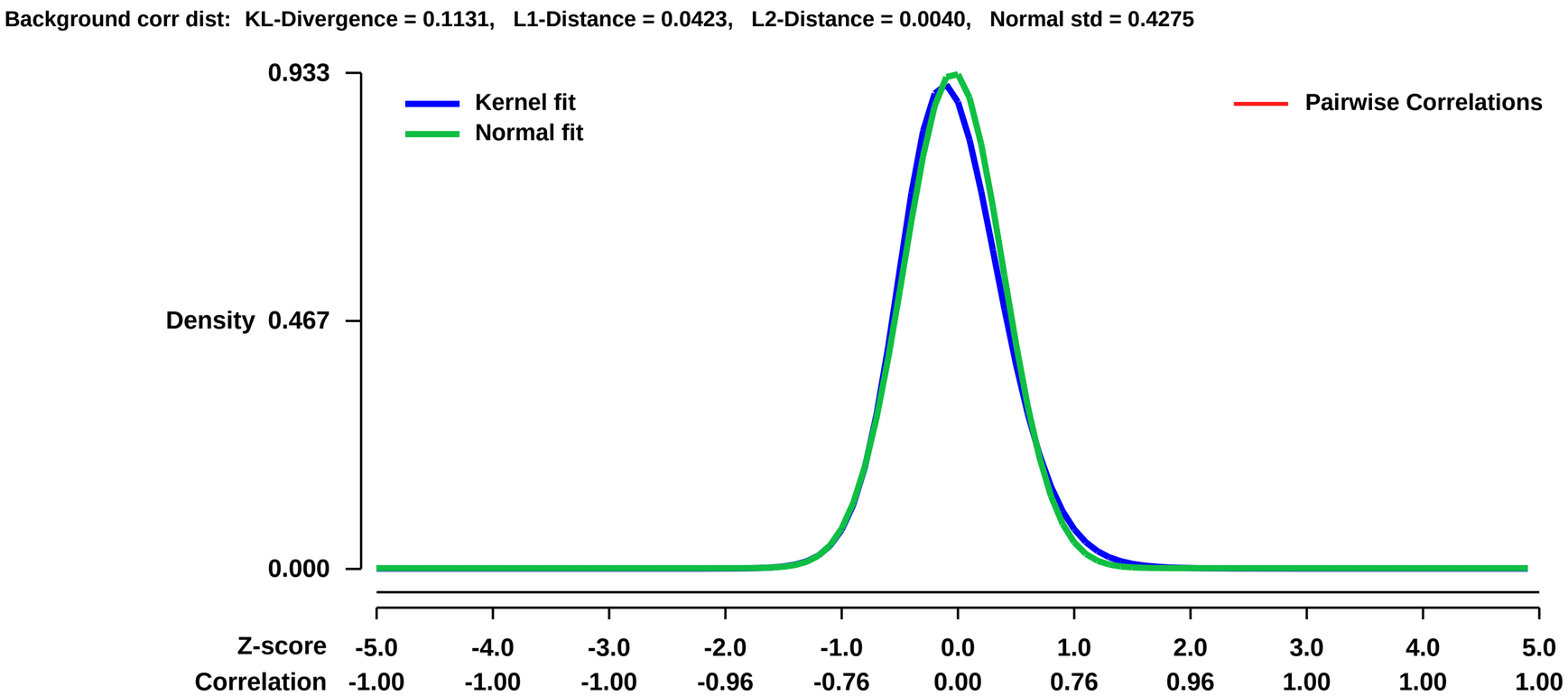

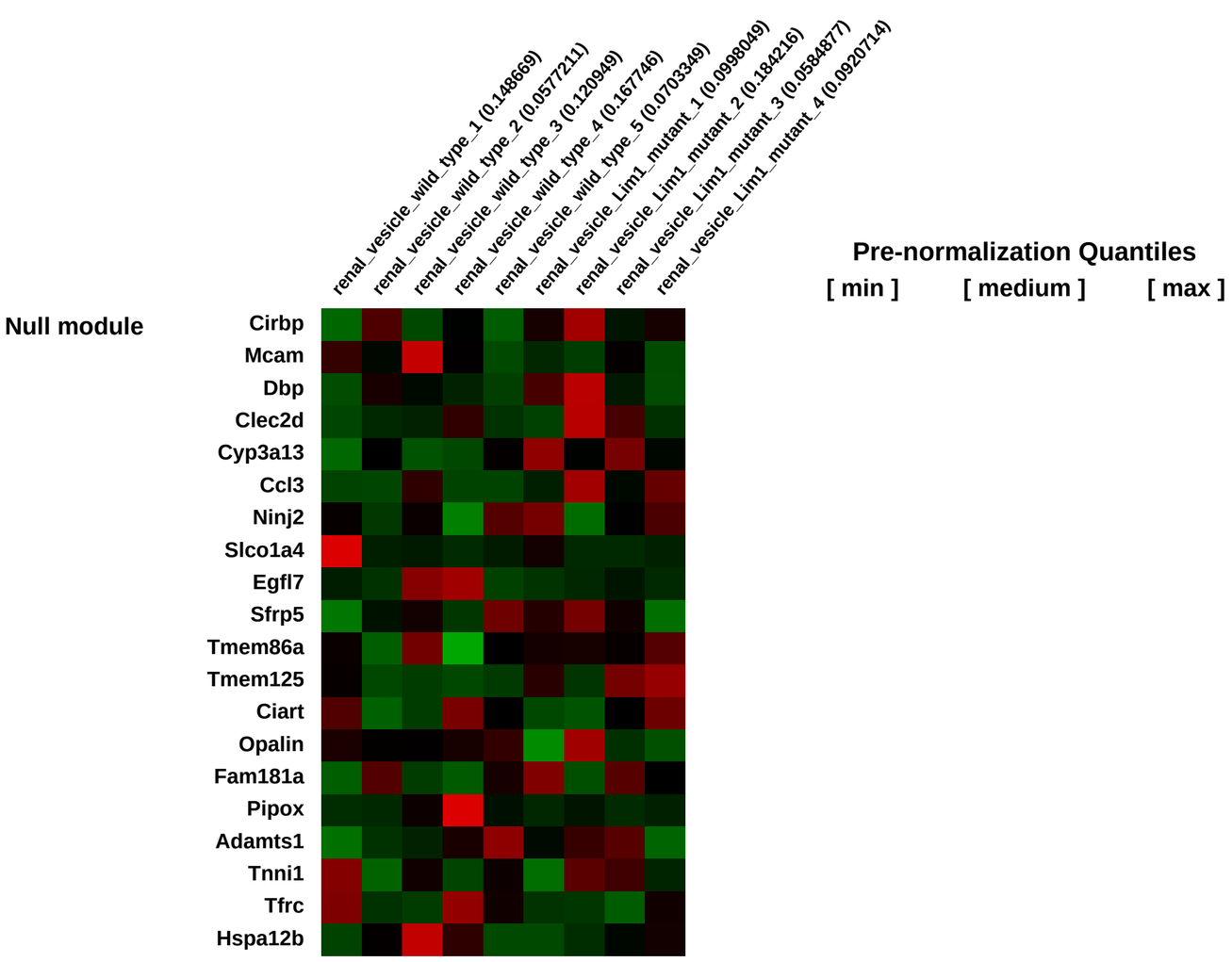

GEO Series "GSE7657" Expression Profiles

Num of samples in this series: 12

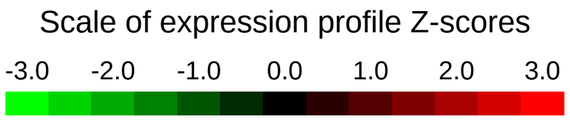

GEO Link:	**http://www.ncbi.nlm.nih.gov/geo/query/acc.cgi?acc=GSE7657**
Status:	**Public on May 01 2008**
Title:	**Identification of phase-specific arthritis-related genes in mice**
Organism:	**Mus musculus**
Experiment type:	**Expression profiling by array**
Platform:	**GPL1261**
Pubmed ID:	
Summary & Design:	**Summary:** **Rheumatoid arthritis (RA), one of the most common polygenic diseases, is characterized by a chronic, progressive inflammation mainly in joints and has an unknown etiology. Numerous studies have revealed the significance of cytokines TNF and IL-1 in the onset and progression of RA. Due to the complexity of interactions among different cytokines and immune cells, little is known about the precise molecular mechanisms underlying RA. In this study, oligonucleotide microarray analysis and a mouse model of RA, IL-1 receptor antagonist deficient mice were used to address this issue. Two hundred and ninety transcripts were found to be dysregulated greater than or equal to 2-fold in the diseased mice. Phase-specific gene expression changes were identified, including early increase and late decrease of heat shock protein coding genes and Cyr61. Moreover, common gene expression changes were also observed, especially the upregulation of paired-Ig-like receptor A (Pira) in both early and late phases of arthritis. We conclude that common and distinct gene expression change patterns that were identified globally may represent novel opportunities for better control of RA through early diagnosis and development of alternative therapeutic strategies.** **Keywords: Time course** **Overall design:** **Six wild-type and 6 Il1rn deficient BALB/c mice at 1 month and 4 month (3 for each time point) were used for microarray analysis of splenic gene expression profiling.**

Background corr dist: KL-Divergence = 0.0960, L1-Distance = 0.0243, L2-Distance = 0.0010, Normal std = 0.4471

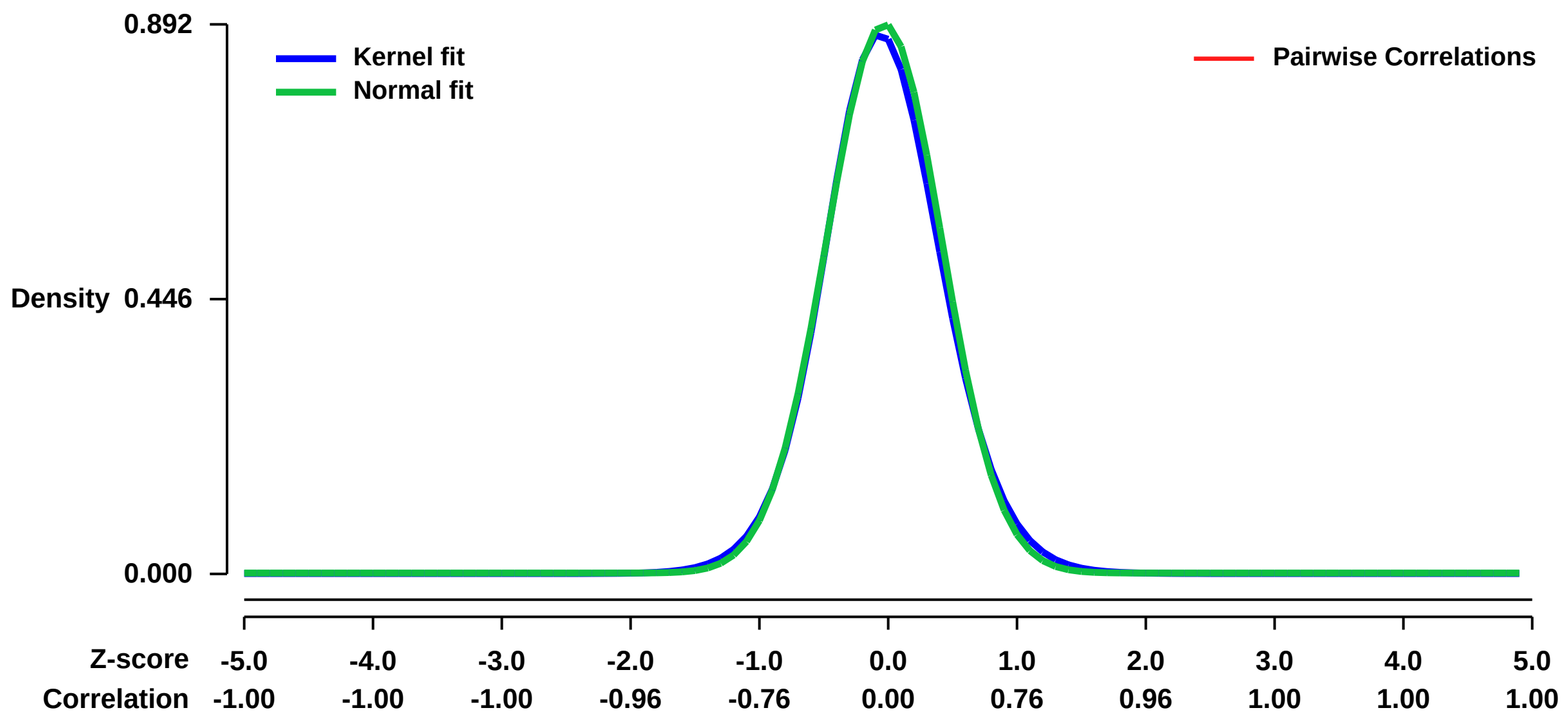

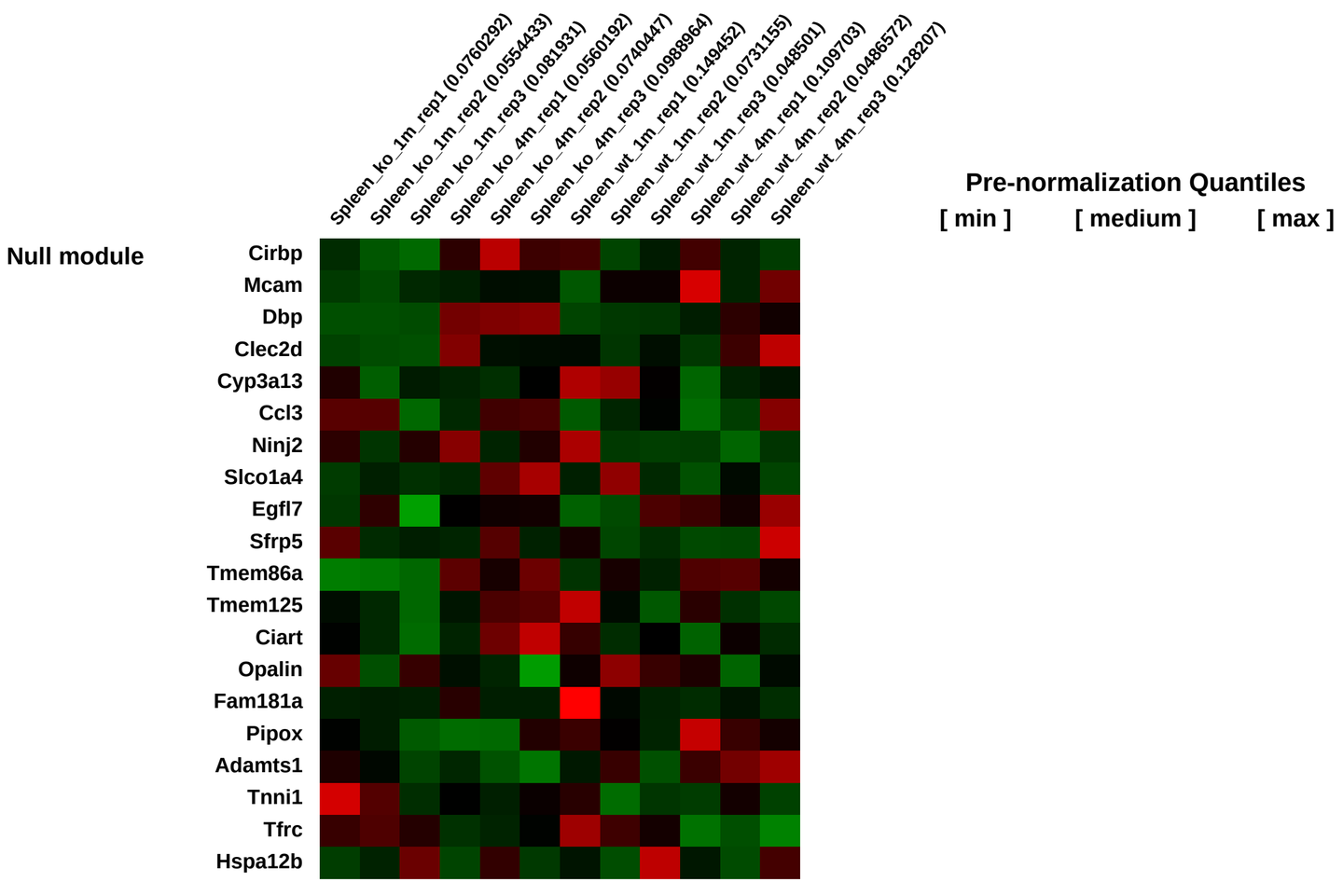

GEO Series "GSE31313" Expression Profiles

Num of samples in this series: 22

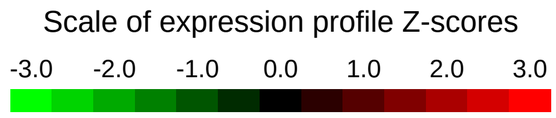

GEO Link:	**http://www.ncbi.nlm.nih.gov/geo/query/acc.cgi?acc=GSE31313**
Status:	**Public on Aug 08 2012**
Title:	**Expression data from anti-EpCAM treated and untreated SP cells compared to lung tissue**
Organism:	**Mus musculus**
Experiment type:	**Expression profiling by array**
Platform:	**GPL1261**
Pubmed ID:	
Summary & Design:	**Summary:** **Targeted therapies against cancer stem cells which are enriched in side populations (SP) involves interruption of Wnt-signalling. Furthermore, EpCAM is a SP marker and modulator of Wnt-signalling. Therefore, the effects of an anti-EpCAM treatment on SP-cells and WNT/¸†-catenin signalling was studied.** **SP of the murine lung adenocarcinoma cell line A2C12 was obtained by fluorescence activated cell sorting and whole genome scans helped to define their molecular phenotype after anti-EpCAM antibody treatment.** **Overall design:** **Anti-EpCAM treated and untreated A2C12 cells were subjected to Hoechst 33342 dye exclusion assay and sorted to SP fractions by FACS. Gene expression of SP cells was compared to non-transgenic lung tissue.**

Background corr dist: **KL-Divergence = 0.0208, L1-Distance = 0.0491, L2-Distance = 0.0029, Normal std = 0.7902**

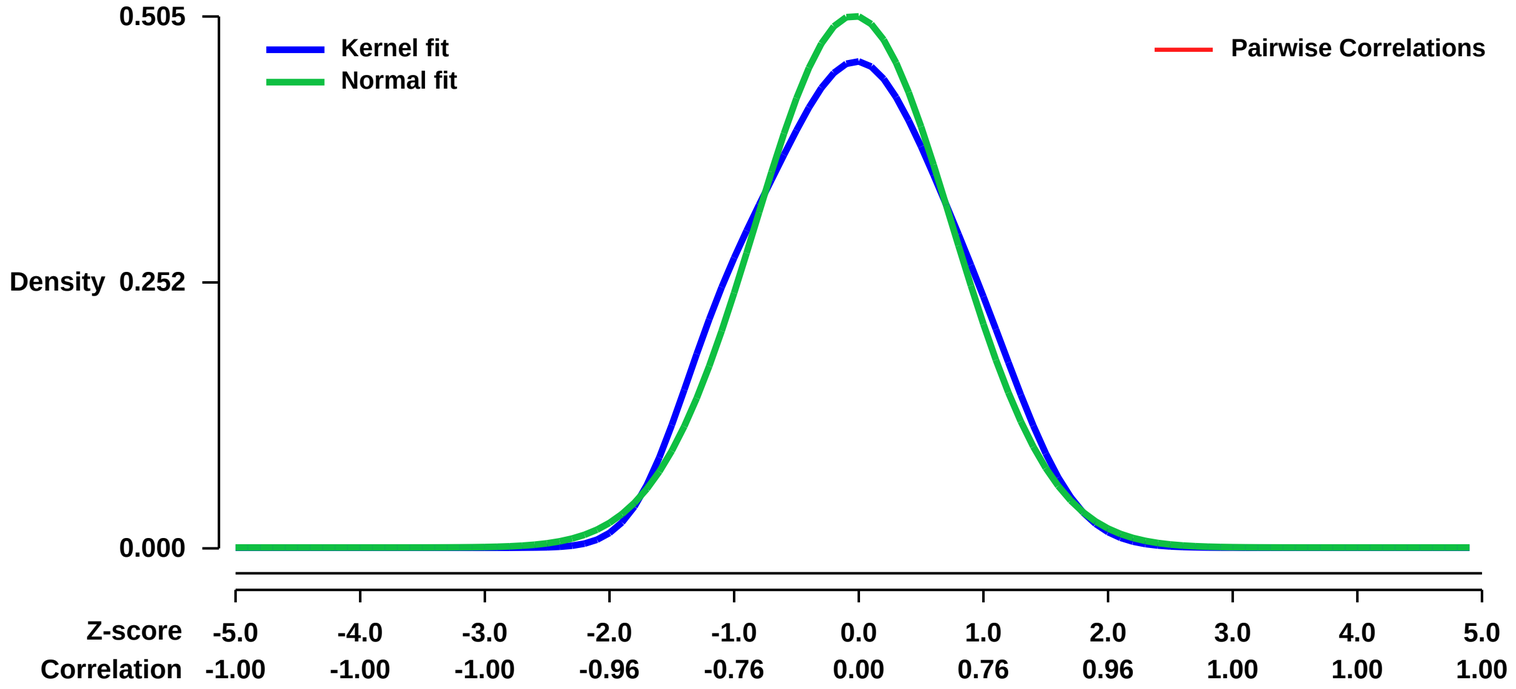

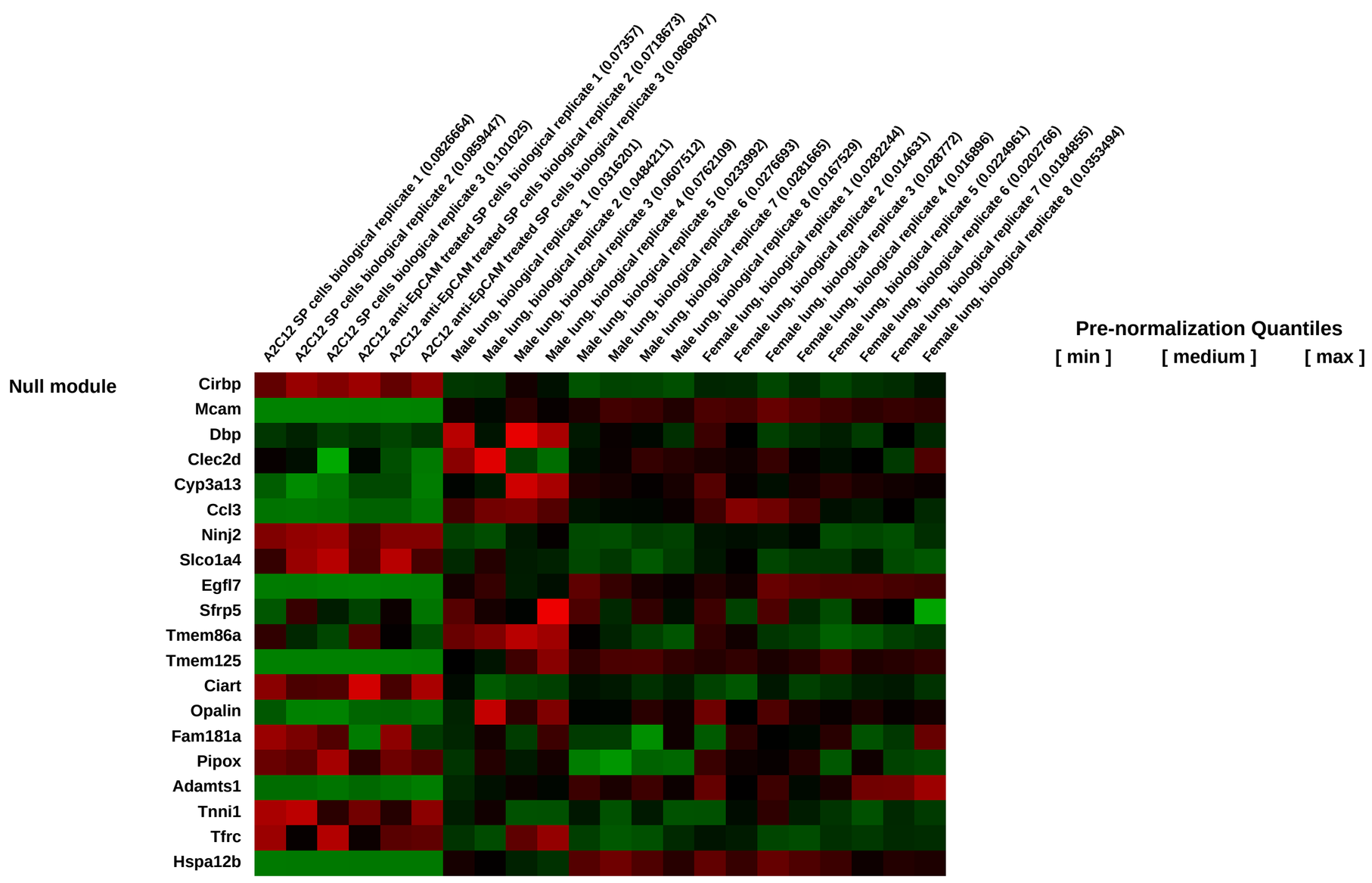

GEO Series "GSE27628" Expression Profiles

Num of samples in this series: 34

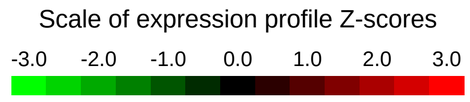

GEO Link:	http://www.ncbi.nlm.nih.gov/geo/query/acc.cgi?acc=GSE27628
Status:	Public on Mar 03 2011
Title:	Expression data from affected skin from psoriasis mouse models and normal skin from control mice
Organism:	Mus musculus
Experiment type:	Expression profiling by array
Platform:	GPL1261
Pubmed ID:	21483750
Summary & Design:	**Summary:** **Development of a suitable mouse model would facilitate the investigation of pathomechanisms underlying human psoriasis and would also assist in development of therapeutic treatments. However, while many psoriasis mouse models have been proposed, no single model recapitulates all features of the human disease, and standardized validation criteria for psoriasis mouse models have not been widely applied. In this study, whole-genome transcriptional profiling is used to compare gene expression patterns manifested by human psoriatic skin lesions with those that occur in five psoriasis mouse models (K5-Tie2, imiquimod, K14-AREG, K5-Stat3C and K5-TGFbeta1). While the cutaneous gene expression profiles associated with each mouse phenotype exhibited statistically significant similarity to the expression profile of psoriasis in humans, each model displayed distinctive sets of similarities and differences in comparison to human psoriasis. For all five models, correspondence to the human disease was strong with respect to genes involved in epidermal development and keratinization. Immune and inflammation-associated gene expression, in contrast, was more variable between models as compared to the human disease. These findings support the value of all five models as research tools, each with identifiable areas of convergence to and divergence from the human disease. Additionally, the approach used in this paper provides an objective and quantitative method for evaluation of proposed mouse models of psoriasis, which can be strategically applied in future studies to score strengths of mouse phenotypes relative to specific aspects of human psoriasis.** **Global transcriptional profiling was utilized to evaluate the similarity between human psoriasis and the psoriasis-like phenotypes that develop in five mouse models (K5-Tie2, IMQ, K14-AREG, K5-Stat3C, K5-TGFbeta1)** **Overall design:** **Expression patterns associated with mouse phenotypes were evaluated by comparing lesional skin from transgenic or IMQ-treated mice (n = 2-3) with normal skin obtained from control mice (n = 2-3).**

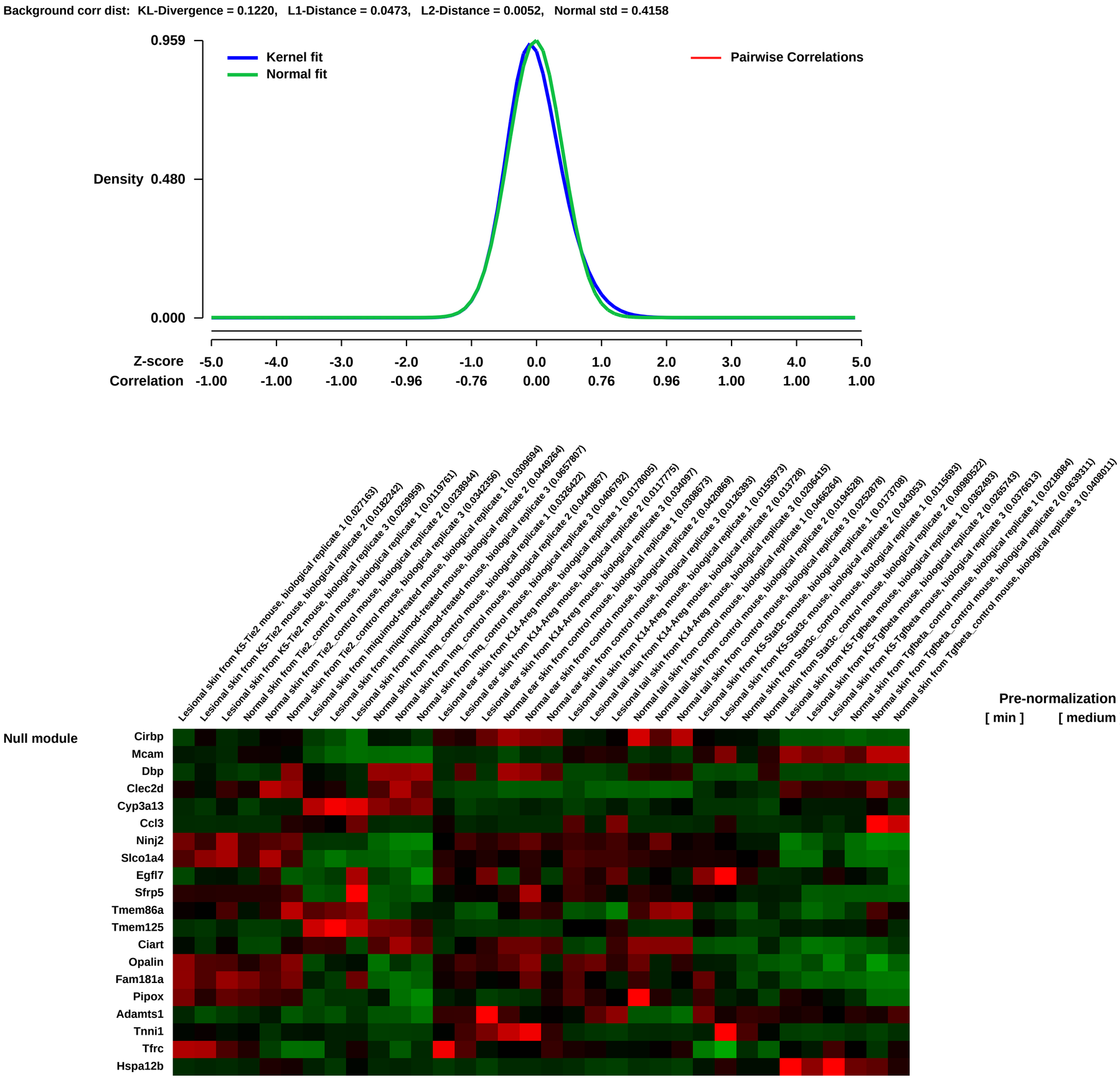

GEO Series "GSE4671" Expression Profiles

Num of samples in this series: 28

Scale of expression profile Z-scores

-3.0 -2.0 -1.0 0.0 1.0 2.0 3.0

GEO Link:	http://www.ncbi.nlm.nih.gov/geo/query/acc.cgi?acc=GSE4671
Status:	Public on Jul 28 2006
Title:	Microarray Analysis of the Delipidation of White Adipose Tissue of Mice Fed Conjugated Linoleic Acid
Organism:	Mus musculus
Experiment type:	Expression profiling by array
Platform:	GPL1261
Pubmed ID:	16868072
Summary & Design:	**Summary:** The white adipose tissue (WAT) rapidly loses mass when mice are fed a diet containing trans-10, cis-12 conjugated linoleic acid (t10c12 CLA). A microarray analysis of WAT due to CLA feeding was performed to better define the processes and genes involved. WAT weight decreased by ca. 80% over 17 days of feeding a 0.5% t10c12 CLA diet. The lipid volume decreased by 90% and the number of adipocytes and total cells were reduced by15% and 47%, respectively. Microarray profiling of replicated pools of control and treated mice (n=140) at seven time points over the 17day feeding indicated between 2798 to 4318 genes showed mRNA changes of 2-fold or more. Transcript levels for genes of glucose and fatty acid import or biosynthesis were significantly reduced. A prolific inflammation response was indicated by the 2 to100-fold induction of many cytokine transcripts, including those for IL-6, IL1?, TNF ligands, and CXC family members We used microarrays to characterize transcriptome changes in mouse adipose tissue due to feeding trans-10 cis-12 linoleic acid . **Keywords:** time course **Overall design:** Mice were fed either diet with 0.5 % CLA or control diet, and the retroperitoneal fat pad mRNA surveyed by high density oligonucleotide array expression profiling. Microarray profiling of replicated pools of control and treated mice (n=140) at seven time points (day 1, 2, 3, 4, 10, 17) over the 17day feeding indicated between 2798 to 4318 genes showed mRNA changes of 2-fold or more.

Background corr dist: KL-Divergence = 0.1498, L1-Distance = 0.0280, L2-Distance = 0.0012, Normal std = 0.3767

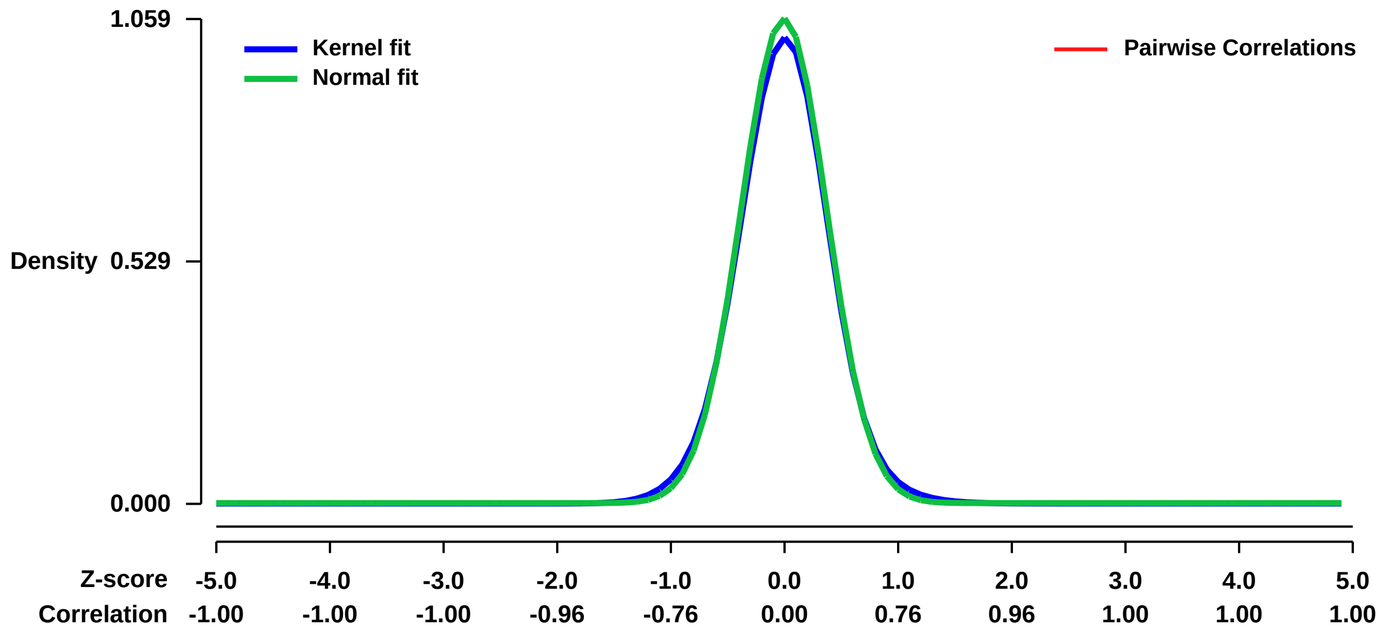

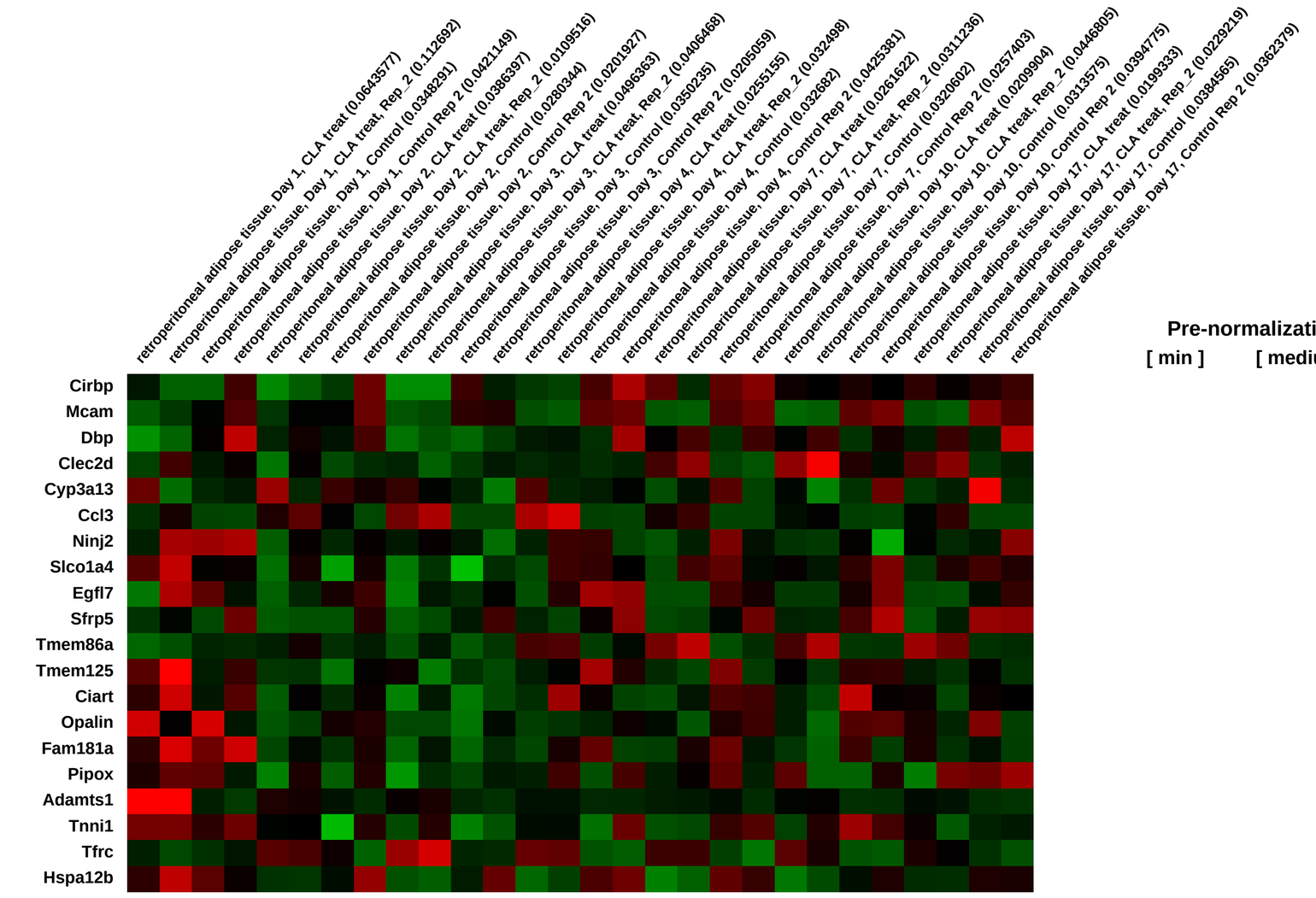

GEO Series "GSE27816" Expression Profiles

Num of samples in this series: 14

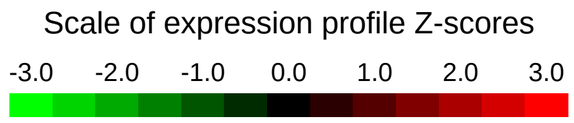

GEO Link:	**http://www.ncbi.nlm.nih.gov/geo/query/acc.cgi?acc=GSE27816**
Status:	**Public on Jul 01 2011**
Title:	**Tet2 loss leads to increased hematopoietic stem cell self-renewal and myeloid transformation**
Organism:	**Mus musculus**
Experiment type:	**Expression profiling by array**
Platform:	**GPL1261**
Pubmed ID:	**21723200**
Summary & Design:	**Summary:** **Recurrent somatic mutations in TET2 and in other genes that regulate the epigenetic state have been identified in patients with myeloid malignancies and in other cancers. However, the in vivo effects of Tet2 loss have not been delineated. We report here that Tet2 loss leads to increased stem-cell self-renewal and to progressive stem cell expansion. Consistent with human mutational data, Tet2 loss leads to myeloproliferation in vivo, notable for splenomegaly and monocytic proliferation. In addition, haploinsufficiency for Tet2 confers increased self-renewal and myeloproliferation, suggesting that the monoallelic TET2 mutations found in most TET2-mutant leukemia patients contribute to myeloid transformation. This work demonstrates that absent or reduced Tet2 function leads to enhanced stem cell function in vivo and to myeloid transformation.** **These studies show that a ubiquitin ligase-substrate pair can orchestrate the molecular program of HSC differentitiation** **Overall design:** **Gene expression profiles from WT and Tet2-/- sorted LSK and myeloid progenitors (CMP and GMP) were compared using genome wide mRNA expression profiling by Affymetrix genechip arrays (Mouse 430 2.0) and key targets were validated by chromatin immunoprecipitation experiments.**

Background corr dist: KL-Divergence = 0.1358, L1-Distance = 0.0335, L2-Distance = 0.0019, Normal std = 0.4092

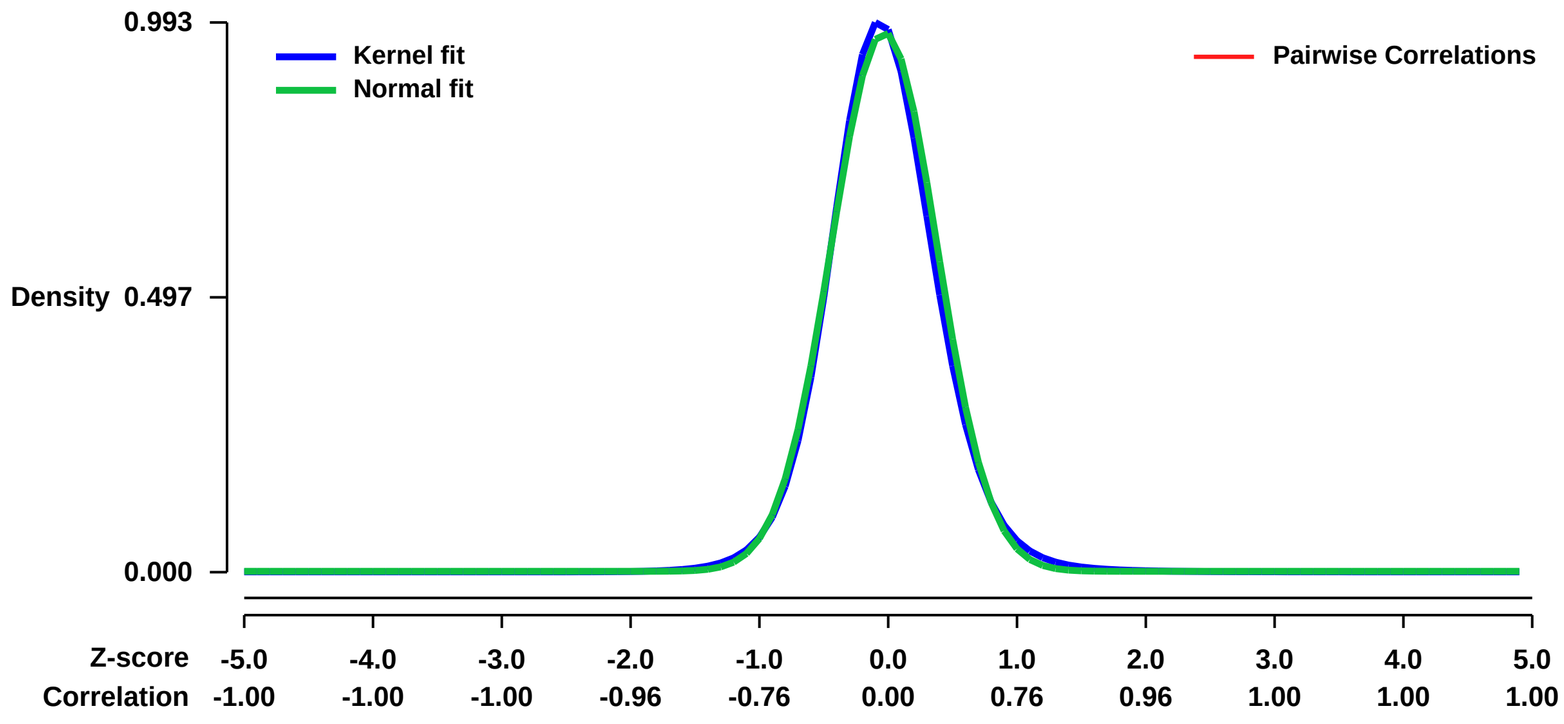

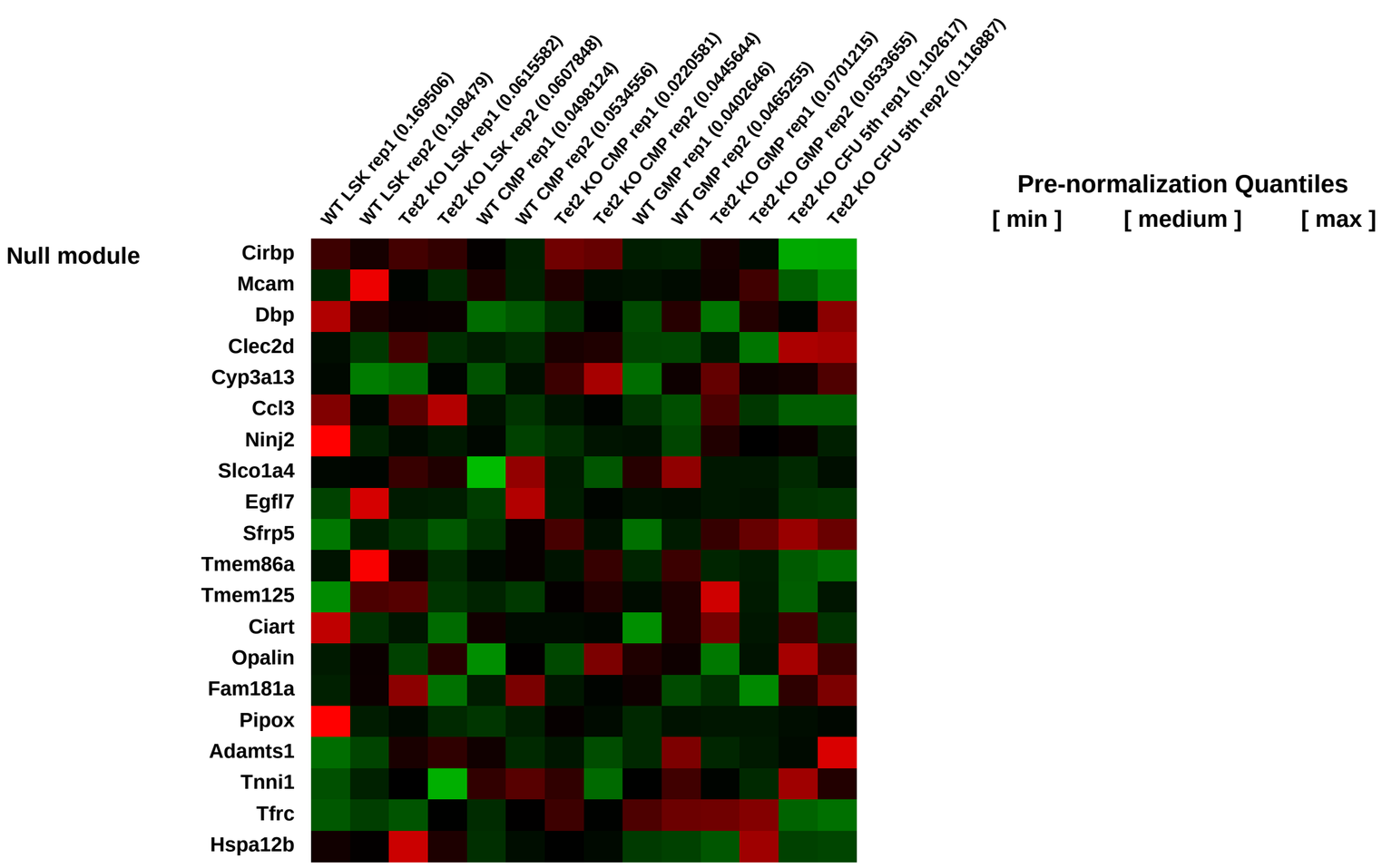

GEO Series "GSE1435" Expression Profiles

Num of samples in this series: 27

Scale of expression profile Z-scores

-3.0 -2.0 -1.0 0.0 1.0 2.0 3.0

GEO Link:	http://www.ncbi.nlm.nih.gov/geo/query/acc.cgi?acc=GSE1435
Status:	Public on May 28 2004
Title:	Microarray Based Comparison of two Amplification Methods For Nanogram Amounts of Total RNA
Organism:	Mus musculus
Experiment type:	Expression profiling by array
Platform:	GPL1261
Pubmed ID:	15613496
Summary & Design:	**Summary:** Two T7 based methods One round of Amplification (Affymetrix) and Two round of Amplification were compared to two Ribo-SPIA based systems, RiboSPIA and pico Ribo SPIA systems. Data for One Round of amplification , Two round of amplification and RiboSPIA are listed here. All Hybridisation were performed using Affymetrix Mouse 430-2 gene chips. Data were all scaled to 500 and scaling factor average was 3.6 +/- 0.9, background intensities 46 +/- 5 , noise 2.9 +/- 0.6, rawQ 1.5 +/- 0.2 Keywords: other Overall design:

Background corr dist: KL-Divergence = 0.0455, L1-Distance = 0.0330, L2-Distance = 0.0017, Normal std = 0.5832

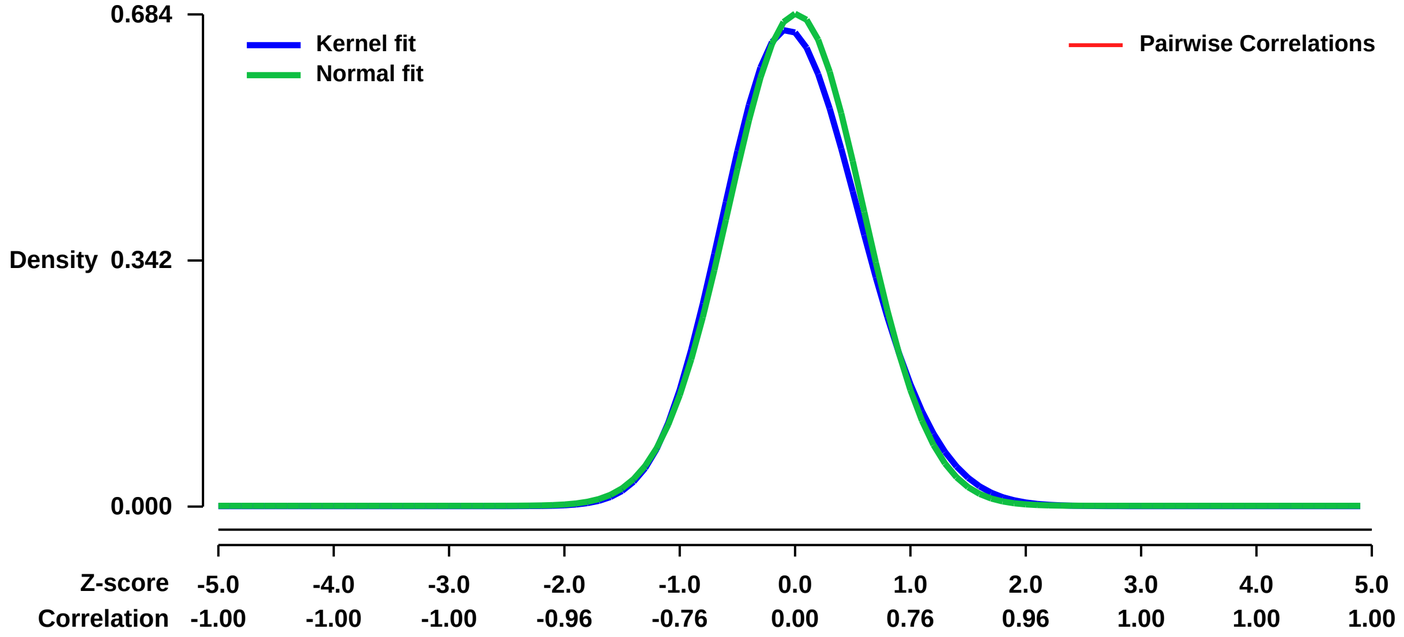

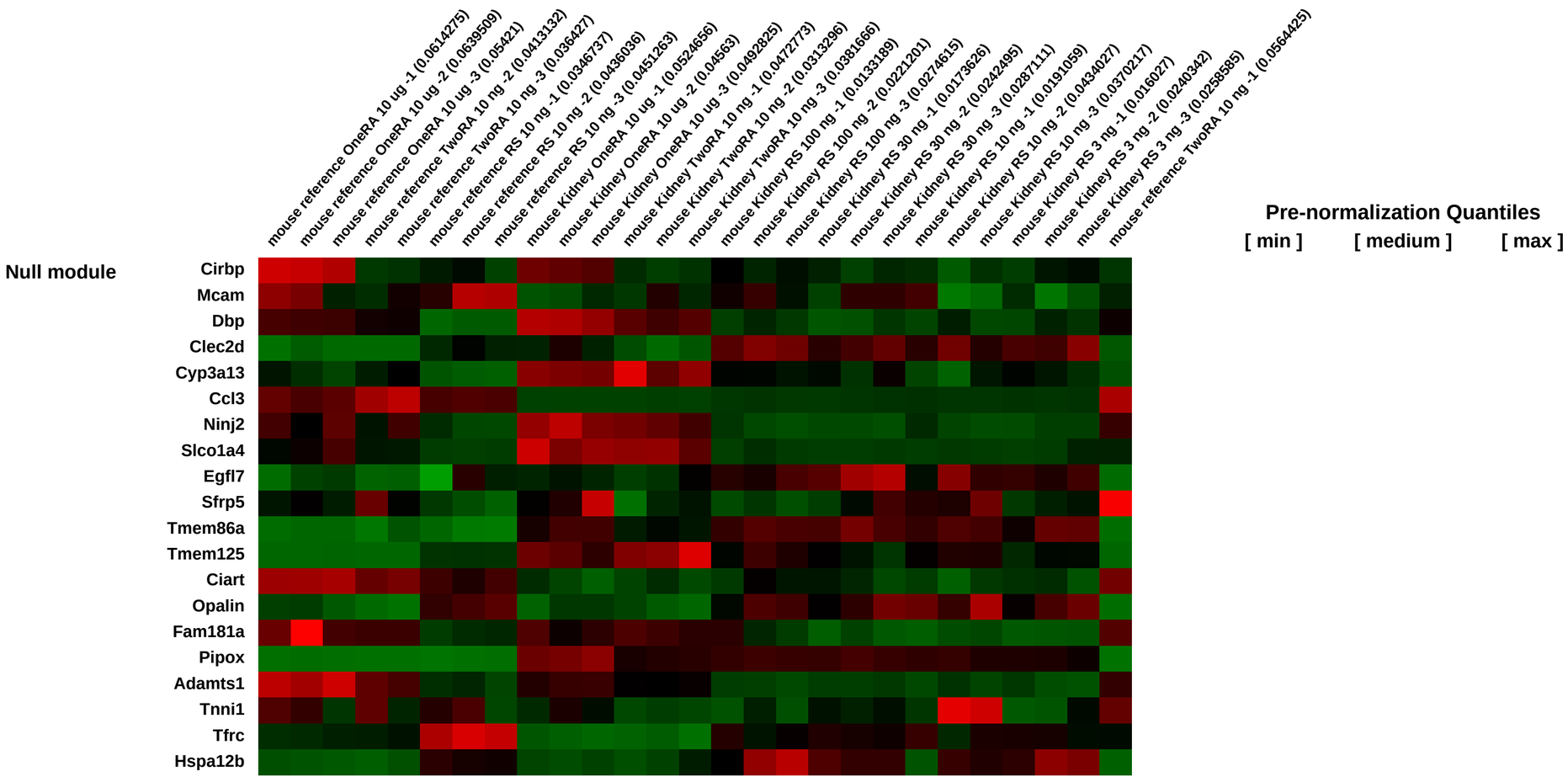

GEO Series "GSE11918" Expression Profiles

Num of samples in this series: 9

Scale of expression profile Z-scores

-3.0 -2.0 -1.0 0.0 1.0 2.0 3.0

GEO Link:	**http://www.ncbi.nlm.nih.gov/geo/query/acc.cgi?acc=GSE11918**
Status:	**Public on Jun 28 2008**
Title:	**Molecular characterization of murine IFN producing killer dendritic cells**
Organism:	**Mus musculus**
Experiment type:	**Expression profiling by array**
Platform:	**GPL1261**
Pubmed ID:	
Summary & Design:	**Summary:** **IKDCs have been newly characterized in mouse and shared functional and phenotypic properties of NK cells and dendritic cells. To formaly distinguish them from NK cells, we have performed a gene expression profile analysis of splenic and LN cell sorted IKDC and compared them with CDC and NK.We are looking for gene or group of genes specifically expressed by IKDCs and which would allow us to specifically isolate and characterize them.** **Keywords: Freshly isolated cells** **Overall design:** **IKDC, NK and CDC were cell-sorted from spleen and lymph node (LN) of naˆflve BALB/c mice (6-8 weeks).**

Background corr dist: **KL-Divergence = 0.0830, L1-Distance = 0.0386, L2-Distance = 0.0029, Normal std = 0.4844**

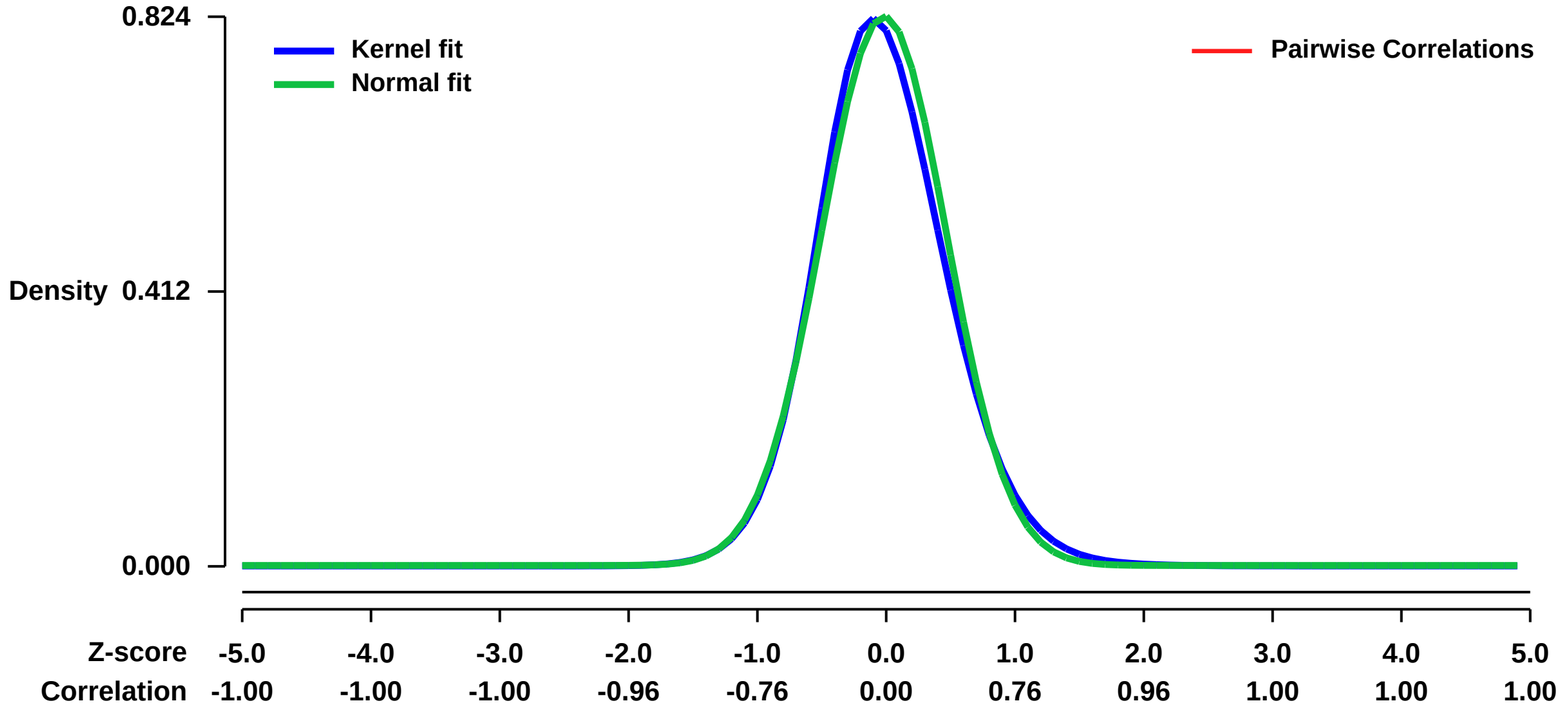

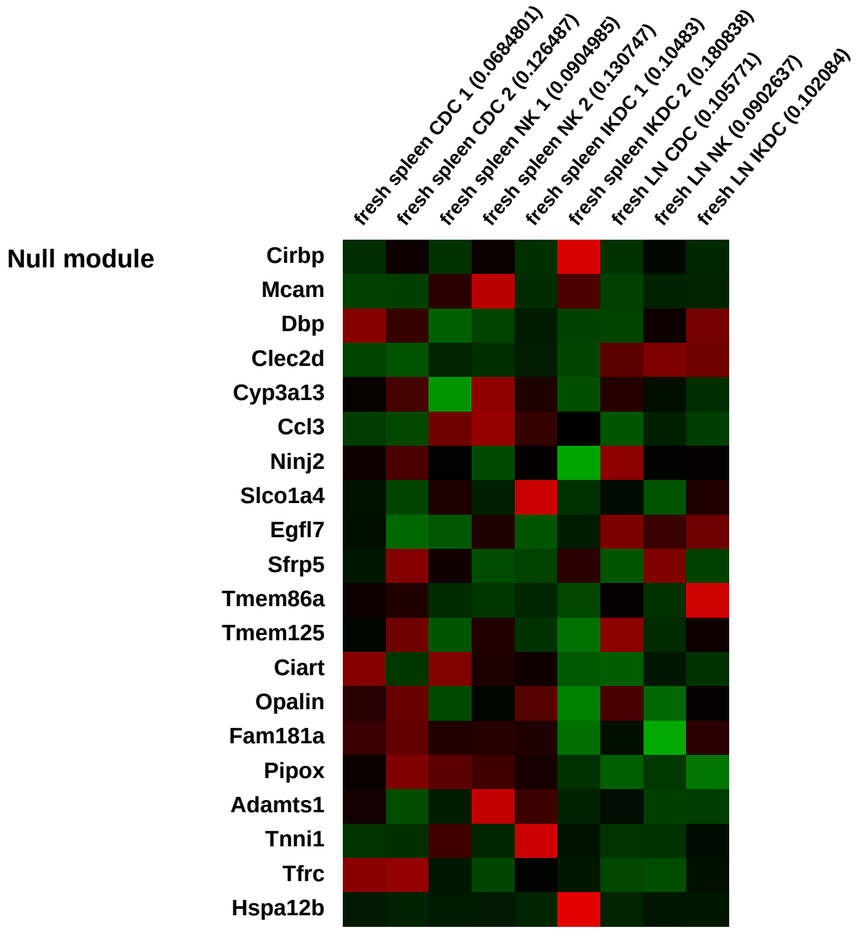

GEO Series "GSE14088" Expression Profiles

Num of samples in this series: 9

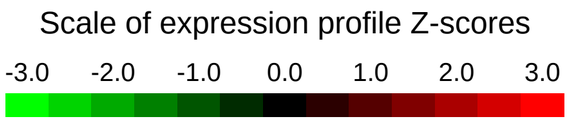

GEO Link:	http://www.ncbi.nlm.nih.gov/geo/query/acc.cgi?acc=GSE14088
Status:	Public on Mar 24 2009
Title:	E2-RING expansion of the NEDD8 cascade confers specificity to cullin modification
Organism:	Mus musculus
Experiment type:	Expression profiling by array
Platform:	GPL1261
Pubmed ID:	19250909
Summary & Design:	**Summary:** Ubiquitin and ubiquitin-like proteins (UBLs) are directed to targets by cascades of E1, E2, and E3 enzymes. The largest ubiquitin E3 subclass consists of cullin-RING ligases (CRLs), which contain one each of several cullins (CUL1, -2, -3, -4, or -5) and RING proteins (RBX1 or -2). CRLs are activated by ligation of the UBL NEDD8 to a conserved cullin lysine. How is cullin NEDD8ylation specificity established? Here we report that, like UBE2M (also known as UBC12), the previously uncharacterized E2 UBE2F is a NEDD8-conjugating enzyme in vitro and in vivo. Biochemical and structural analyses indicate how plasticity of hydrophobic E1-E2 interactions and E1 conformational flexibility allow one E1 to charge multiple E2s. The E2s have distinct functions, with UBE2M/RBX1 and UBE2F/RBX2 displaying different target cullin specificities. Together, these studies reveal the molecular basis for and functional importance of hierarchical expansion of the NEDD8 conjugation system in establishing selective CRL activation. Mol Cell 33:483-495, 2009. Keywords: Comparison of gene expression profiles **Overall design:** NIH 3T3 cells were transduced with retroviral constructs containing shRNA directed against Ube2m or Ube2f. Three replicates of each condition were analyzed.

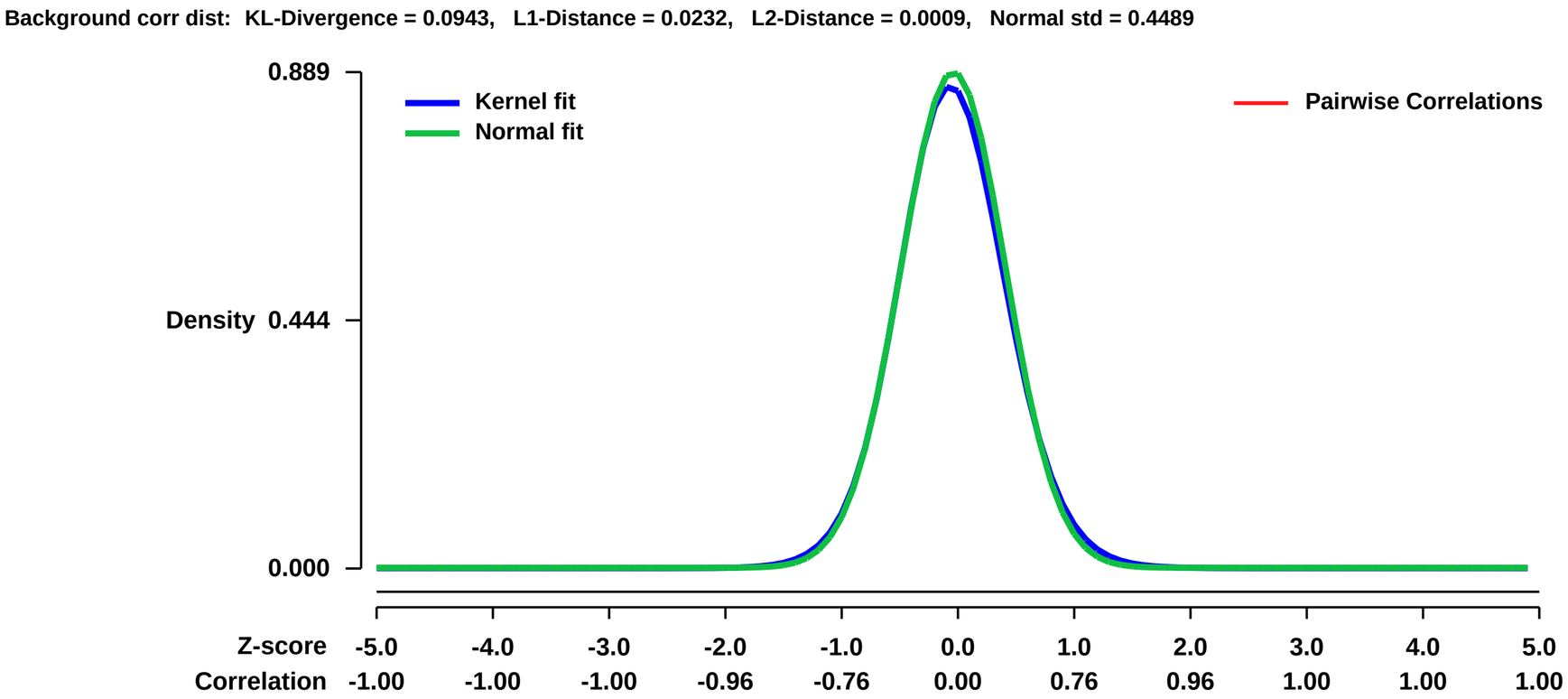

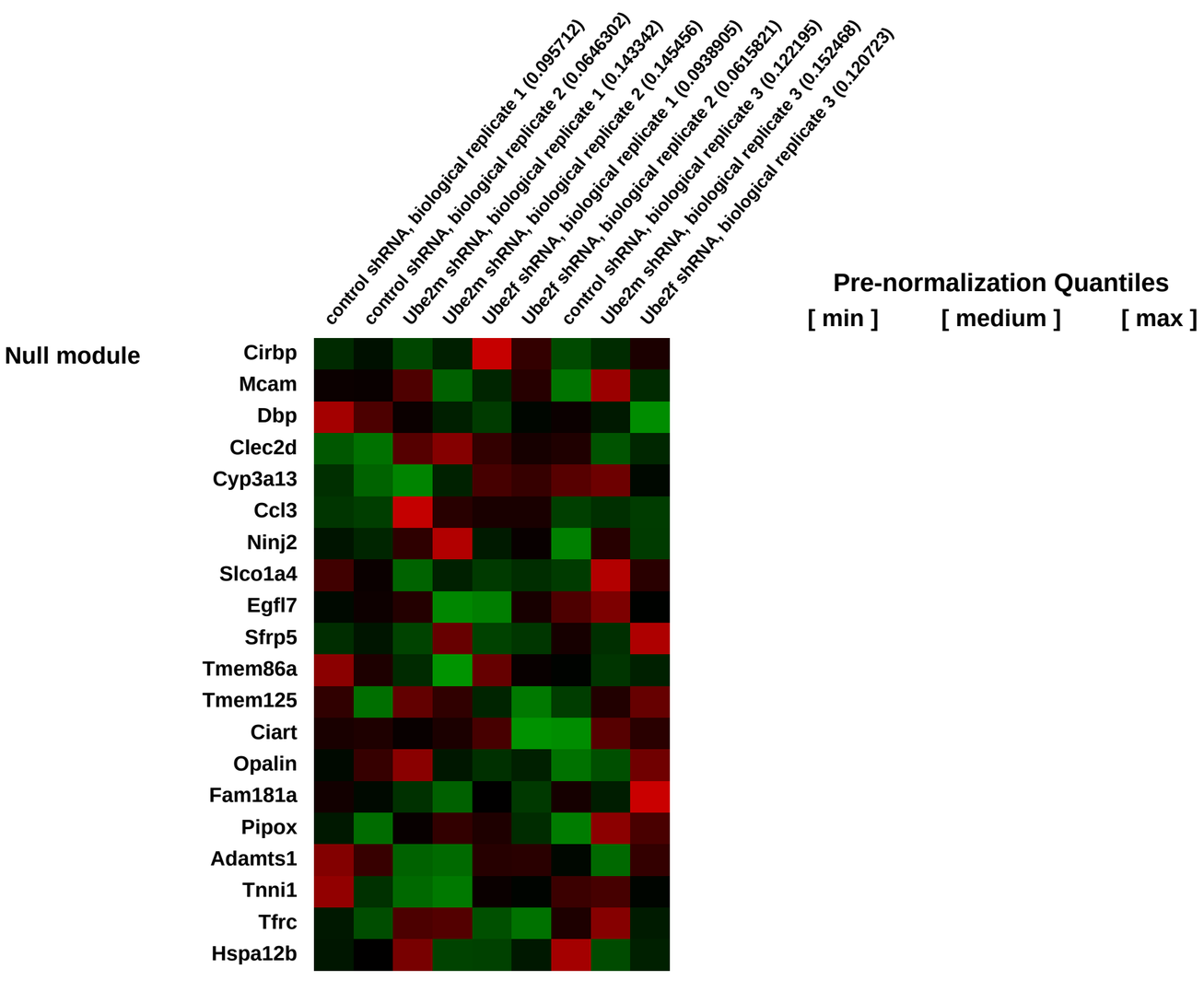

GEO Series "GSE8498" Expression Profiles

Num of samples in this series: 6

Scale of expression profile Z-scores

-3.0 -2.0 -1.0 0.0 1.0 2.0 3.0

GEO Link:	http://www.ncbi.nlm.nih.gov/geo/query/acc.cgi?acc=GSE8498
Status:	Public on Aug 04 2007
Title:	The MicroRNA miR-124 Promotes Neuronal Differentiation by Triggering Brain-Specific Alternative Pre-mRNA Splicing
Organism:	Mus musculus
Experiment type:	Expression profiling by array
Platform:	GPL1261
Pubmed ID:	17679093
Summary & Design:	**Summary:** Both microRNAs and alternative pre-mRNA splicing have been implicated in the development of the nervous system (NS), but functional interactions between these two pathways are poorly understood. We demonstrate that the neuron-specific microRNA miR-124a directly targets PTBP1/PTB/hnRNPI mRNA, which encodes a global repressor of alternative pre-mRNA splicing in non-neuronal cells. Among the targets of PTBP1 is a critical cassette exon in the pre-mRNA of PTBP2/nPTB/brPTB, an NS-enriched PTBP1 homolog. When this exon is skipped, PTBP2 mRNA is subject to nonsense-mediated decay. During neuronal differentiation, miR-124a reduces PTBP1 levels leading to the accumulation of correctly spliced PTBP2 mRNA and a dramatic increase in PTBP2 protein. These events culminate in the transition from non-NS to NS-specific alternative splicing patterns. We also present evidence that miR-124a plays a key role in the differentiation of progenitor cells to mature neurons. Thus, miR-124a promotes NS development at least in part by regulating an intricate network of NS-specific alternative splicing. We used microarrays to detail the global programme of gene expression of CAD cells over-expressing miR-124a-2. Keywords: treatment versus control **Overall design:** Expression data from CAD cells transfected with plasmid expressing miR-124a-2.

Background corr dist: KL-Divergence = 0.0253, L1-Distance = 0.0120, L2-Distance = 0.0002, Normal std = 0.6906

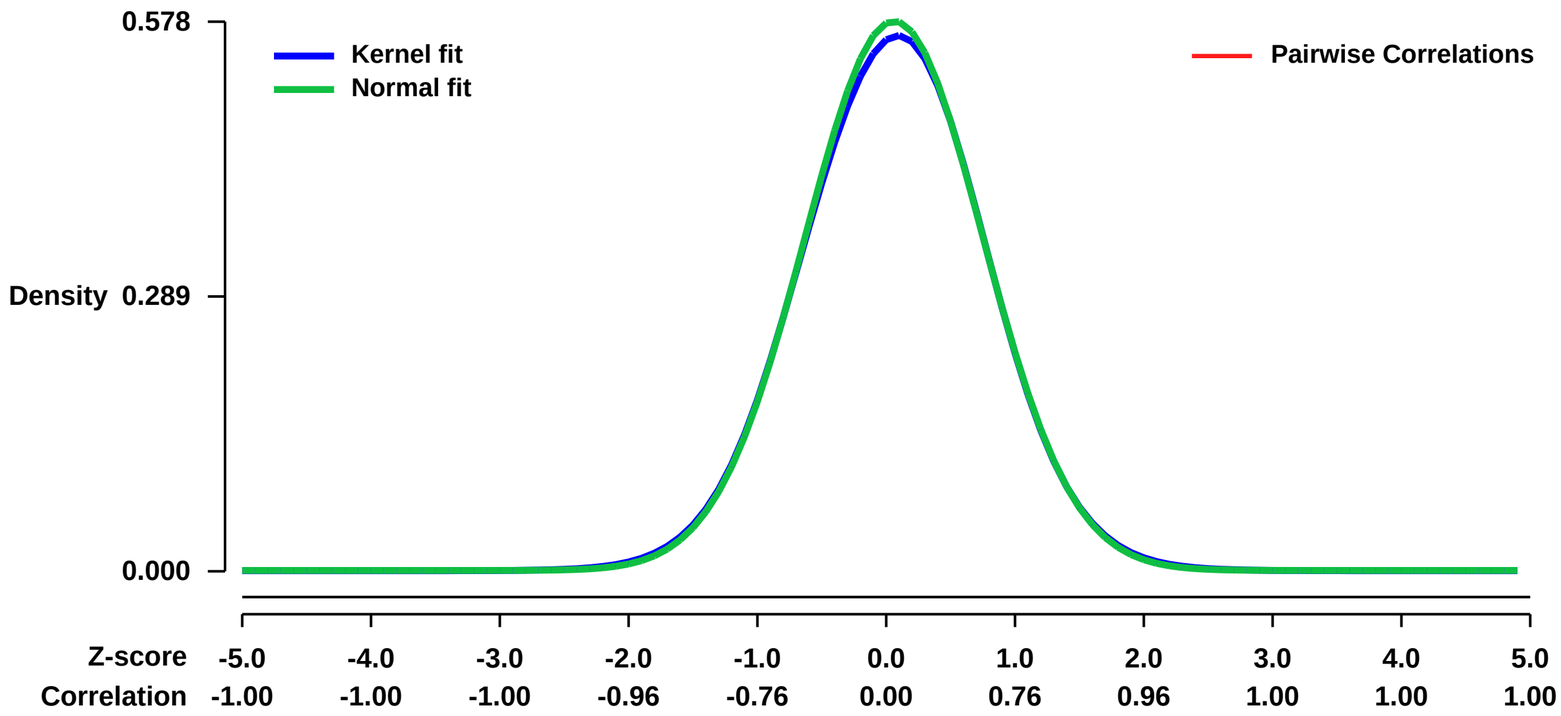

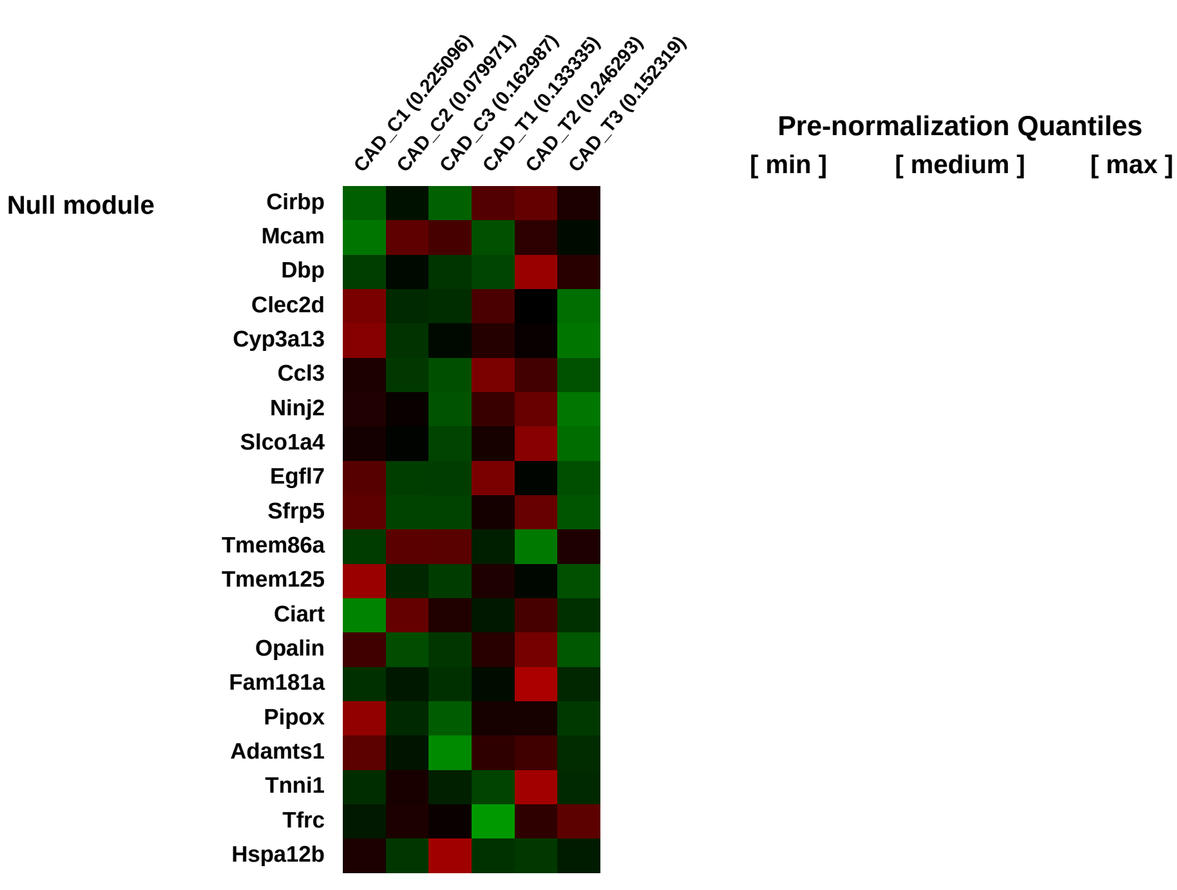

GEO Series "GSE33308" Expression Profiles

Num of samples in this series: 10

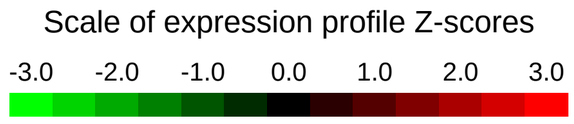

GEO Link:	http://www.ncbi.nlm.nih.gov/geo/query/acc.cgi?acc=GSE33308
Status:	Public on Jan 01 2013
Title:	Keratinocyte Growth Factor and Dexamethasone Plus Elevated cAMP Levels Synergistically Support Pluripotent Stem Cell Differentiation into Alveolar Epithelial Type II Ce
Organism:	Mus musculus
Experiment type:	Expression profiling by array
Platform:	GPL1261
Pubmed ID:	23176317
Summary & Design:	**Summary:** Alveolar epithelial type II (ATII)-like cells can be generated from murine embryonic stem cells (ESCs), although to date, no robust protocols applying specific differentiation factors are established. We hypothesized that the keratinocyte growth factor (KGF), an important mediator of lung organogenesis and primary ATII cell maturation and proliferation, together with dexamethasone, 8-bromoadenosine-cAMP, and isobutylmethylxanthine (DCI), which induce maturation of primary fetal ATII cells, also support the alveolar differentiation of murine ESCs. Here we demonstrate that the above stimuli synergistically potentiate the alveolar differentiation of ESCs as indicated by increased expression of the surfactant proteins (SP-) C and SP-B. This effect is most profound if KGF is supplied not only in the late stage, but at least also during the intermediate stage of differentiation. Our results indicate that KGF most likely does not enhance the generation of (mes)endodermal or NK2 homeobox 1 (Nkx2.1) expressing progenitor cells but rather, supported by DCI, accelerates further differentiation/maturation of respiratory progeny in the intermediate phase and maturation/proliferation of emerging ATII cells in the late stage of differentiation. Ultrastructural analyses confirmed the presence of ATII-like cells with intracellular composite and lamellar bodies. Finally, induced pluripotent stem cells (iPSCs) were generated from transgenic mice with ATII cell-specific lacZ reporter expression. Again, KGF and DCI synergistically increased SP-C and SP-B expression in iPSC cultures, and lacZ expressing ATII-like cells developed. In conclusion, ATII cell-specific reporter expression enabled the first reliable proof for the generation of murine iPSC-derived ATII cells. In addition, we have shown KGF and DCI to synergistically support the generation of ATII-like cells from ESCs and iPSCs. Combined application of these factors will facilitate more efficient generation of stem cell-derived ATII cells for future basic research and potential therapeutic application. **Overall design:** mESCs at d24 of differentiation with KGF and DCI treatment

Background corr dist: KL-Divergence = 0.0344, L1-Distance = 0.0193, L2-Distance = 0.0005, Normal std = 0.6401

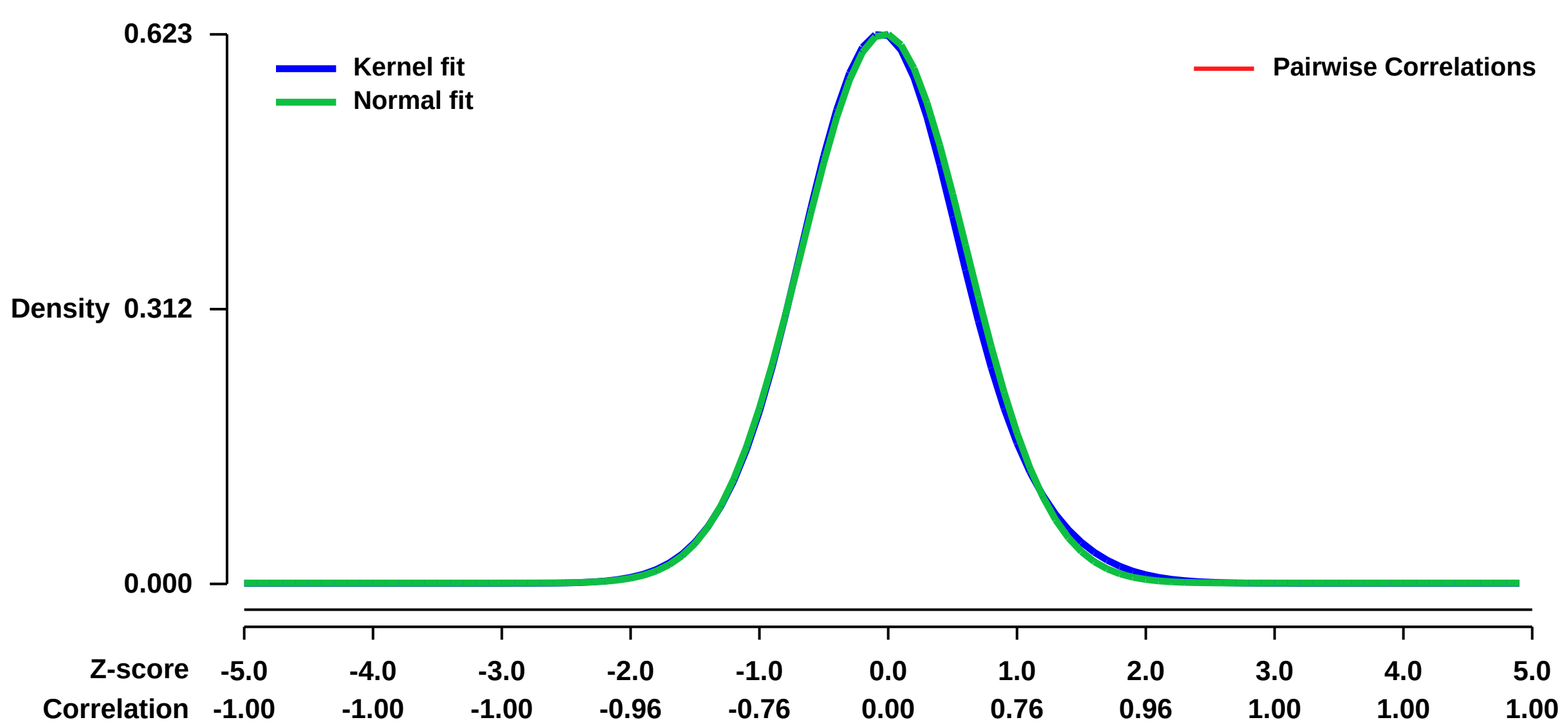

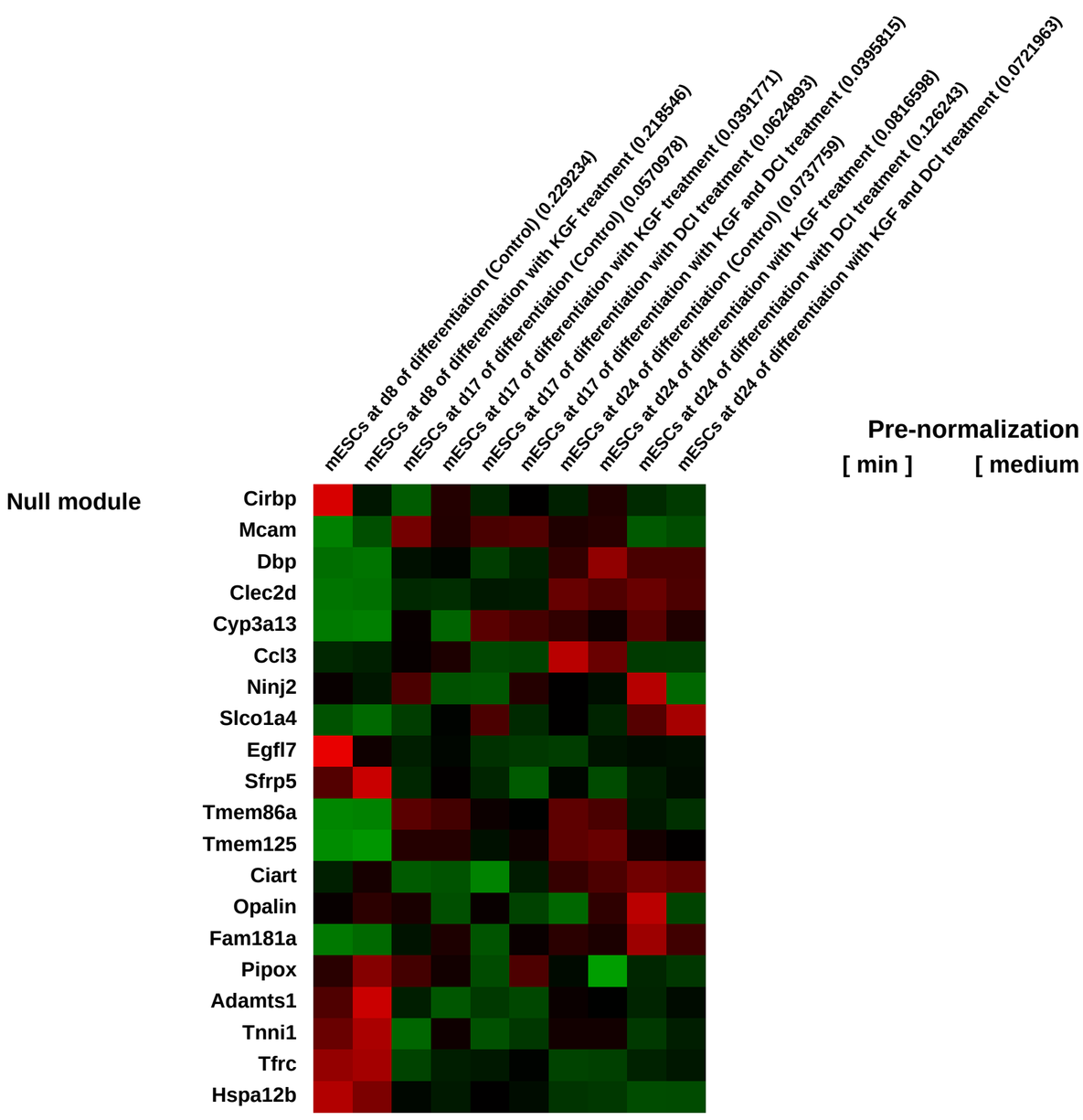

GEO Series "GSE17817" Expression Profiles

Num of samples in this series: 6

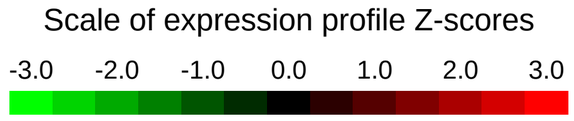

GEO Link:	http://www.ncbi.nlm.nih.gov/geo/query/acc.cgi?acc=GSE17817
Status:	Public on Sep 02 2009
Title:	CAFs are activated in incipient neoplasia to orchestrate tumor promoting inflammation in an NF-¸”B-dependent manner.
Organism:	Mus musculus
Experiment type:	Expression profiling by array
Platform:	GPL1261
Pubmed ID:	20138012
Summary & Design:	**Summary:** **Full title: Cancer Associated Fibroblasts are activated in incipient neoplasia to orchestrate tumor promoting inflammation in an NF-¸”B-dependent manner.** **Cancer Associated Fibroblasts (CAFs) support tumorigenesis by stimulating angiogenesis, cancer cell proliferation, and invasion. We demonstrate that CAFs also mediate tumor-enhancing inflammation. Using a mouse model of squamous skin cancer, we found a pro-inflammatory gene signature in CAFs isolated from dysplastic skin. This signature was also evident in CAFs from skin as well as mammary and pancreatic tumors in mice, and in human cancer. Surprisingly, the inflammatory signature was already activated in CAFs isolated from the incipient hyperplastic stage in multistep tumorigenesis. CAFs from this pathway functioned to promote macrophage recruitment, neovascularization and tumor growth in vivo, activities abolished when NF-¸”B signaling was inhibited. Additionally, we show that normal dermal fibroblasts can be â educatedâ by carcinoma cells to express pro-inflammatory genes.** **Overall design:** **We performed expression profiling analysis of dermal fibroblasts sorted from dysplastic skin tissue of K14-HPV16 mice, and from age matched non transgenic controls. This array analysis was repeated in triplicate. Amplified RNA was hybridized to the 430 2.0 Affymetrix mouse genome arrays.**

Background corr dist: KL-Divergence = 0.0273, L1-Distance = 0.0283, L2-Distance = 0.0010, Normal std = 0.7050

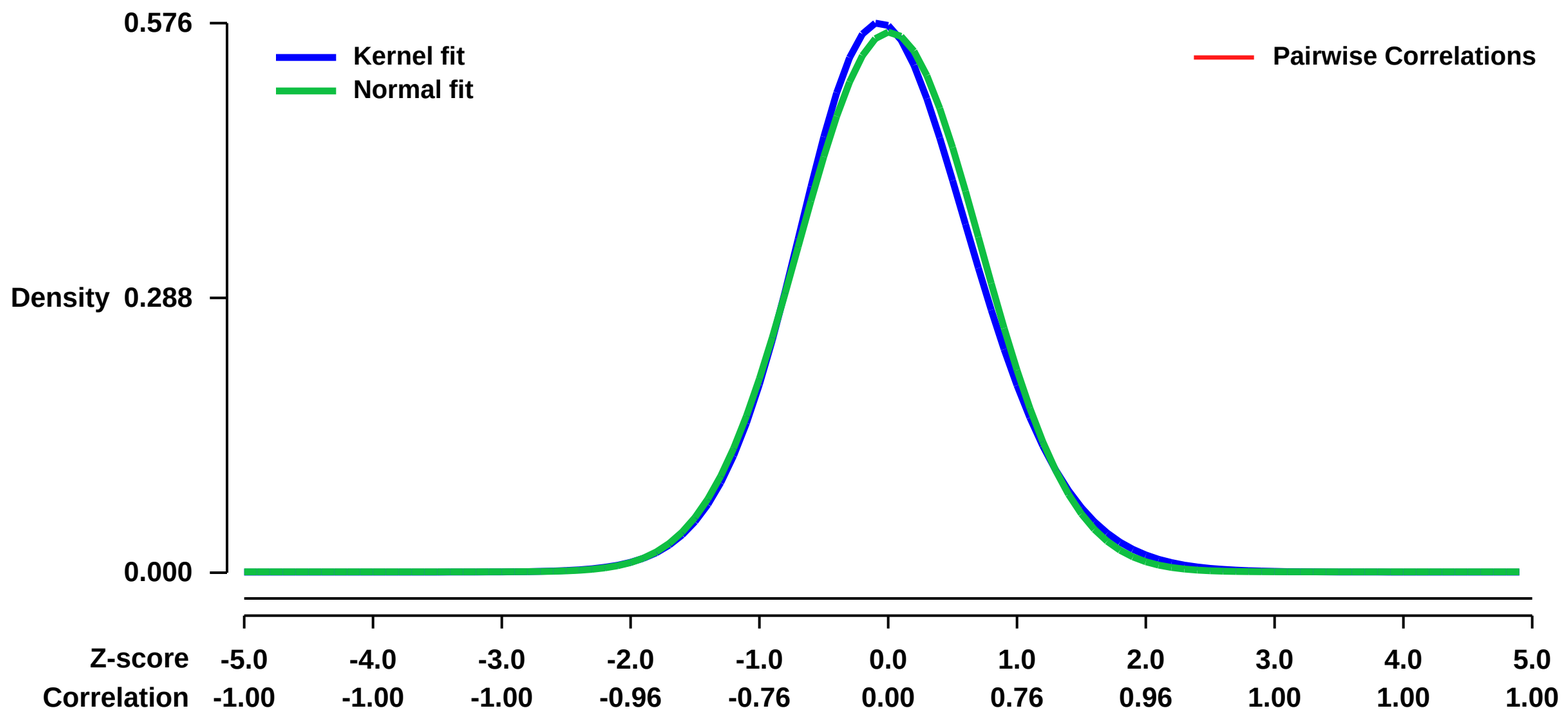

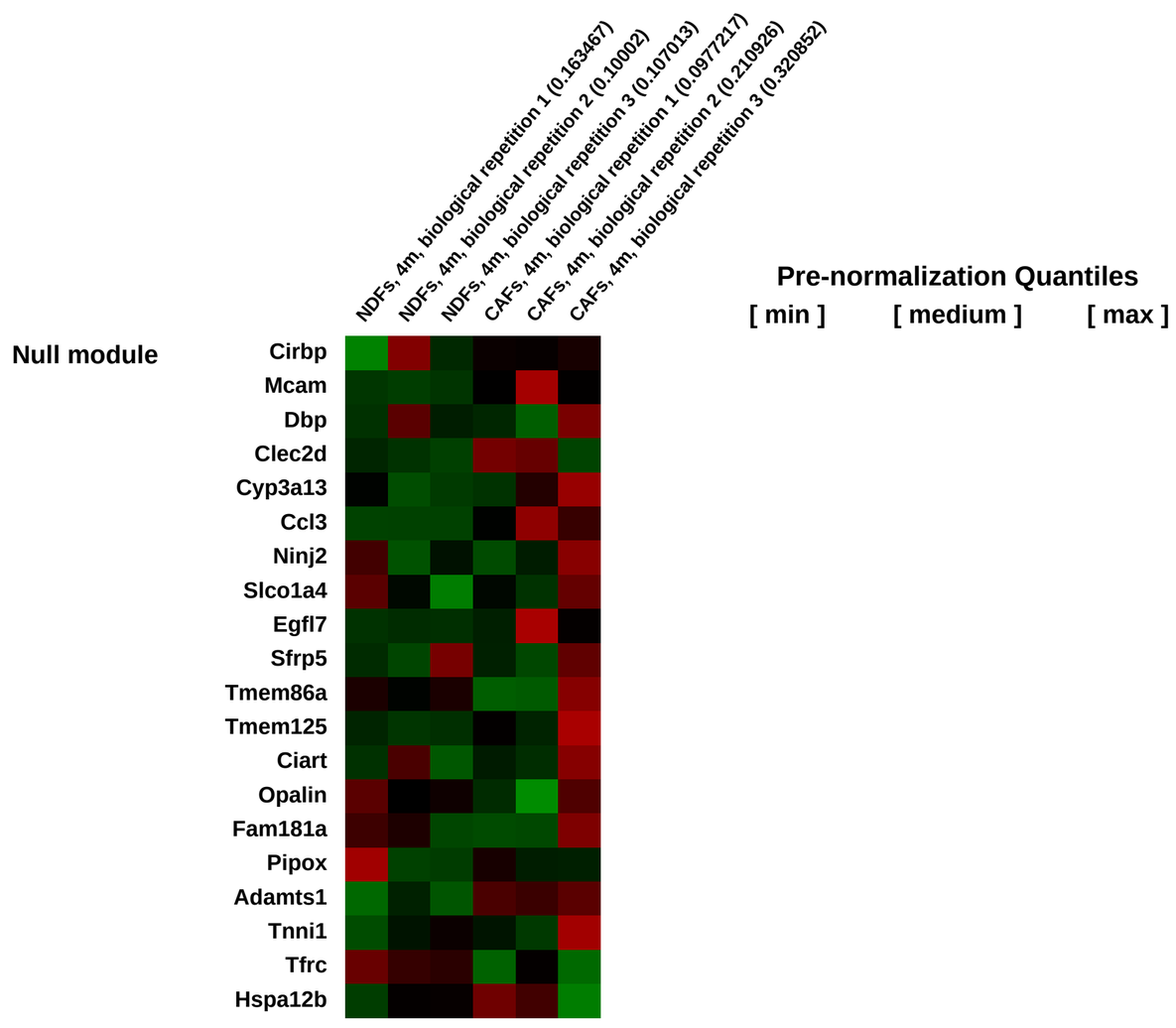

GEO Series "GSE17097" Expression Profiles

Num of samples in this series: 20

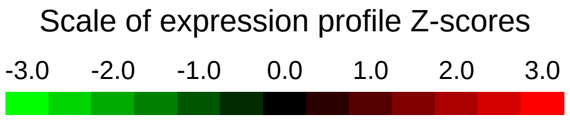

GEO Link:	**http://www.ncbi.nlm.nih.gov/geo/query/acc.cgi?acc=GSE17097**
Status:	**Public on Dec 09 2011**
Title:	**mRNA composition of IRP2 mRNPs in mouse tissues**
Organism:	**Mus musculus**
Experiment type:	**Expression profiling by array**
Platform:	**GPL1261**
Pubmed ID:	**21940823**
Summary & Design:	**Summary:** **Affymetrix microarrays were used to determine the mRNA composition of mRNPs obtained by immunoprecipitation with IRP2 (iron regulatory protein 2).** **Overall design:** **All the microarray procedures were conducted at the EMBL Genomics Core Facility using standard Affymetrix protocols. In brief, approximately 120ng of immunoprecipitated RNA was used as input to a two-step amplification procedure to generate biotin-labeled RNA fragments for hybridization to the Affymetrix GeneChip Mouse Genome 430 2.0 array (Eukaryotic Sample and Array Processing manual 701024 Rev.3). Intensity values for the hybridizations were obtained either using RMA, calculations done in bioconductor (www.bioconductor.org) or MAS5, calculated using Affymetrix GCOS package. MAS5 calculated intensities were further quantile normalized using bioconductor.**

Background corr dist: **KL-Divergence = 0.0612, L1-Distance = 0.0894, L2-Distance = 0.0146, Normal std = 0.5980**

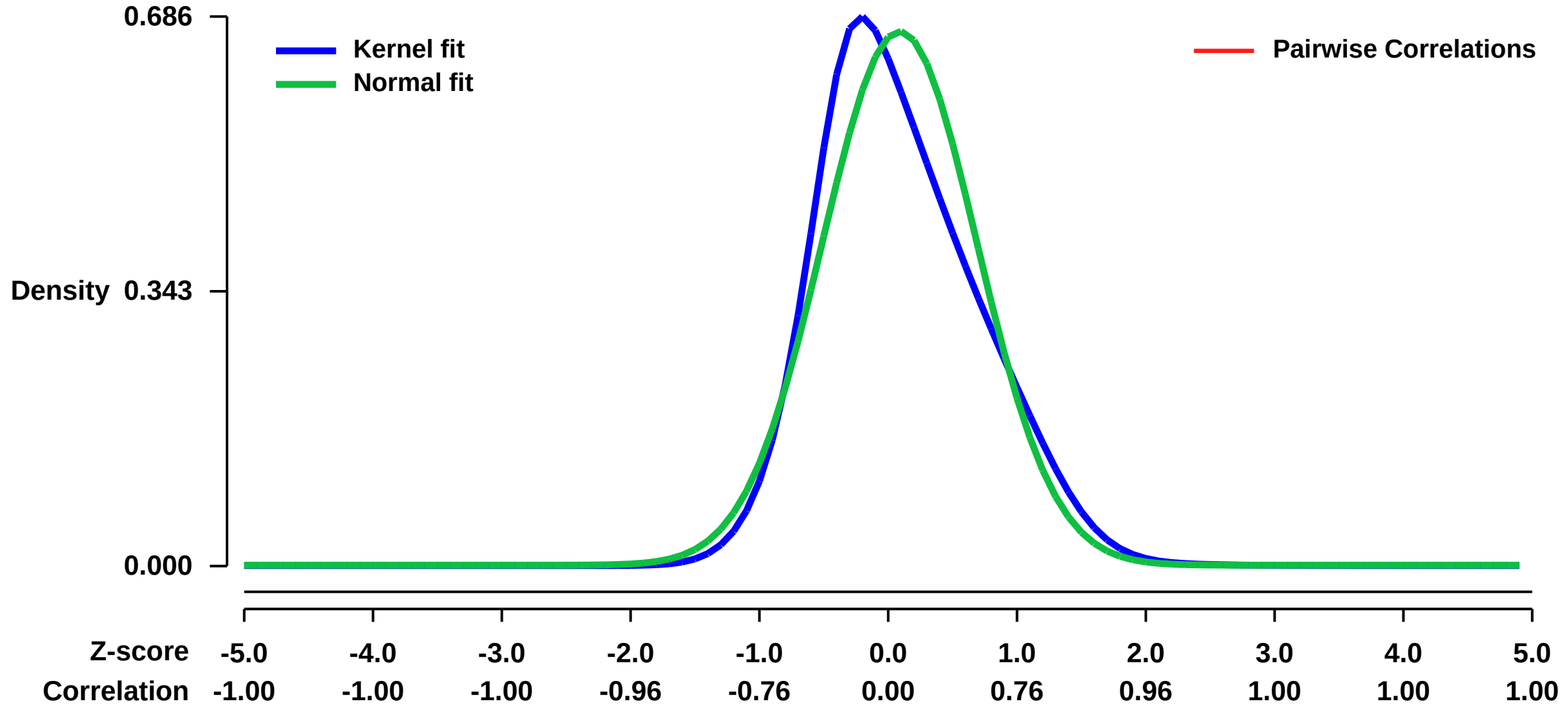

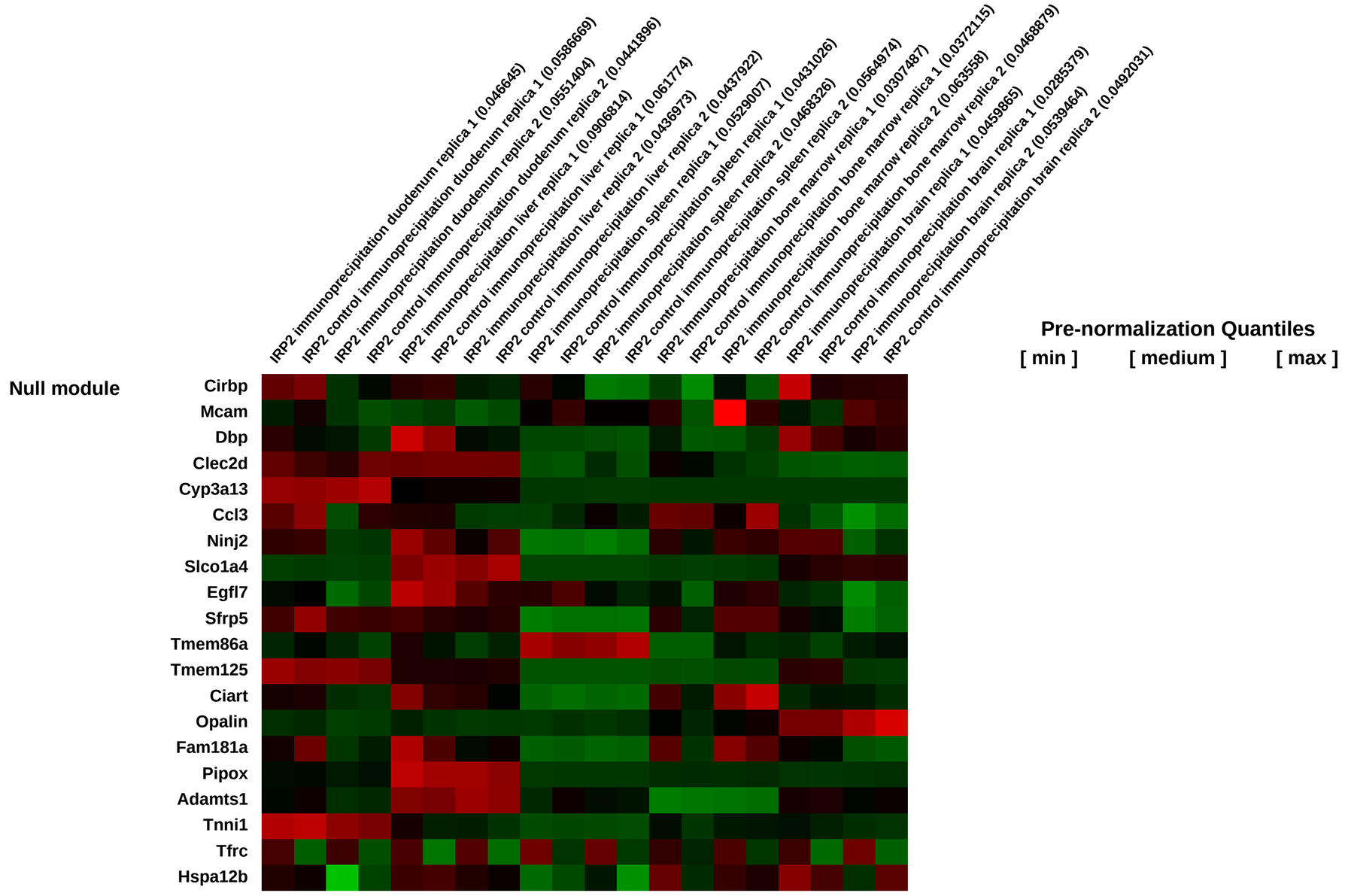

GEO Series "GSE13526" Expression Profiles

Num of samples in this series: 6

Scale of expression profile Z-scores

-3.0 -2.0 -1.0 0.0 1.0 2.0 3.0

GEO Link:	**http://www.ncbi.nlm.nih.gov/geo/query/acc.cgi?acc=GSE13526**
Status:	**Public on Nov 05 2009**
Title:	**Transcript profiling of WT and Nxf2 KO post-natal day 21 testes**
Organism:	**Mus musculus**
Experiment type:	**Expression profiling by array**
Platform:	**GPL1261**
Pubmed ID:	**19345203**
Summary & Design:	**Summary:** **In euakryotes, mRNAs must be exported from the nucleus to the cytsoplasm. NXF2 is highly expressed in the mouse male germ cells. We are interested in its function in spermatogenesis, espically in the nuclear RNA export in the testis. To this end, we made Nxf2 mutant mice by gene targeting. In an attempt to identify the mRNA substrates of NXF2, we perform the microarray experiments on testes.** **We used microarrays to check the expression profiles of the Nxf2 WT and KO 21d testes on C57BL/6 background.** **Overall design:** **To examine the expression difference between WT and Nxf2 KO testes, we collected testes from juvenile mice of three ages (21d, 26d, 28d). Testis weight was similar between WT and KO mice at post-natal day 21. Three pairs of WT and KO 21d testes were chosen for microarray analysis.**

Background corr dist: **KL-Divergence = 0.0259, L1-Distance = 0.0249, L2-Distance = 0.0010, Normal std = 0.6980**

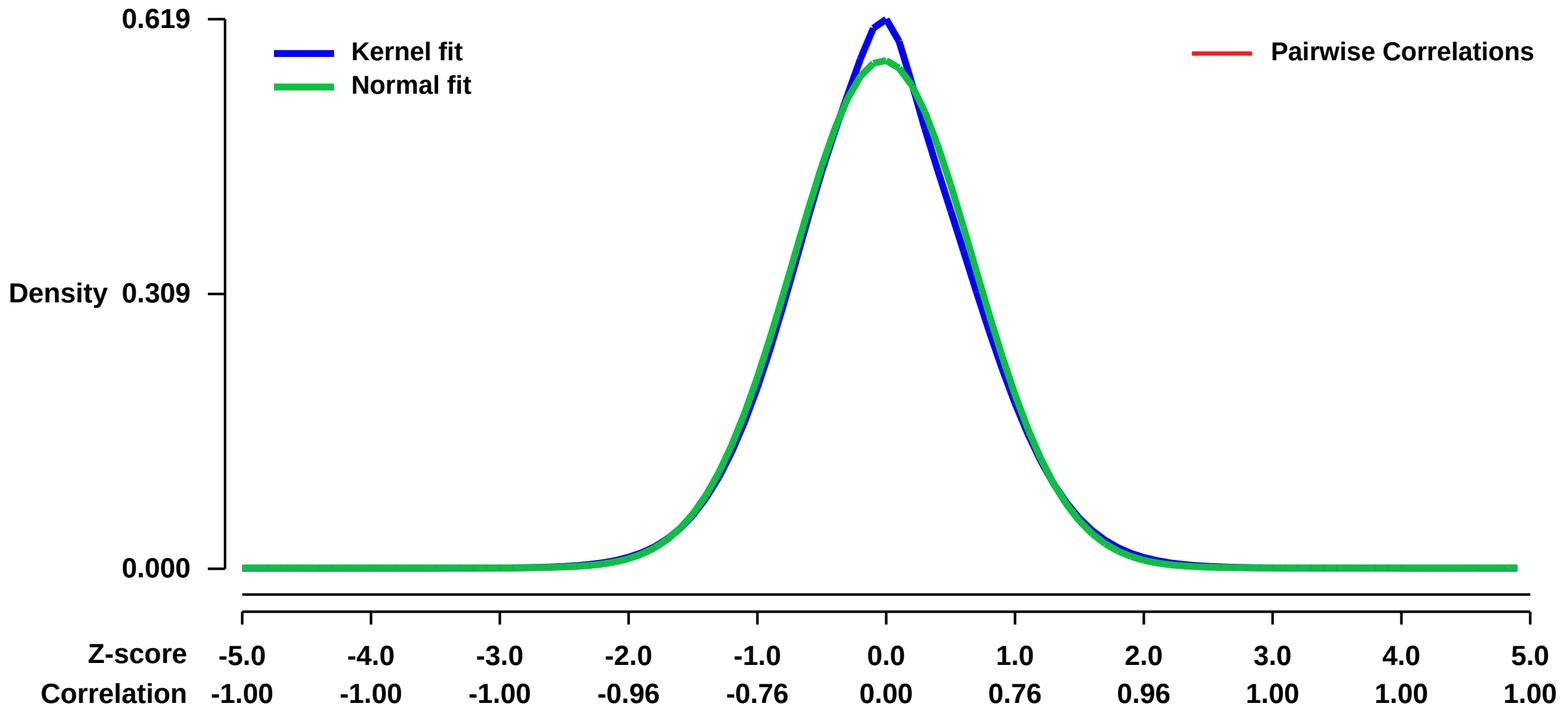

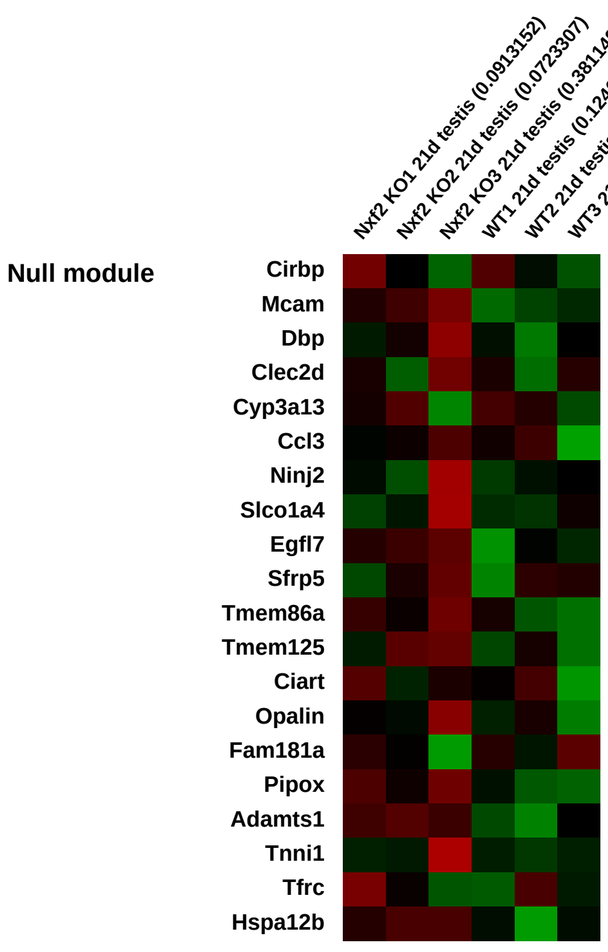

GEO Series "GSE43419" Expression Profiles

Num of samples in this series: 20

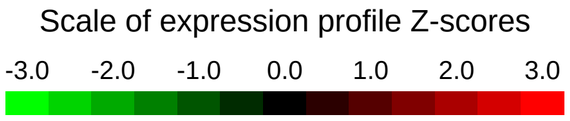

GEO Link:	http://www.ncbi.nlm.nih.gov/geo/query/acc.cgi?acc=GSE43419
Status:	Public on Jan 28 2014
Title:	Expression data from MYCN transgenic mice
Organism:	Mus musculus
Experiment type:	Expression profiling by array
Platform:	GPL1261
Pubmed ID:	24553121
Summary & Design:	**Summary:** **TH-MYCN transgenic (Tg) mice are the model for neuroblastoma. One of the sympathetic ganglia is the origin of neuroblastoma in those mice. The tumor incidences of homozygotes and hemizygotes are 100% and 70-80%, respectively.** **The involvement of midkine (Mdk), a tumor-related growth factor, was also examined by knockout mice.** **Overall design:** **Ganglia and tumor tissues were dissected from several genotypes of mice (MYCN Tg homozygote and hemizygote, knockout (KO) of Mdk gene). In some of cases, we cultured neurosphere and tumorsphere. The mRNA extracted from those samples were subjected to Affymetrix microarrays.**

Background corr dist: **KL-Divergence = 0.1213, L1-Distance = 0.0444, L2-Distance = 0.0046, Normal std = 0.4161**

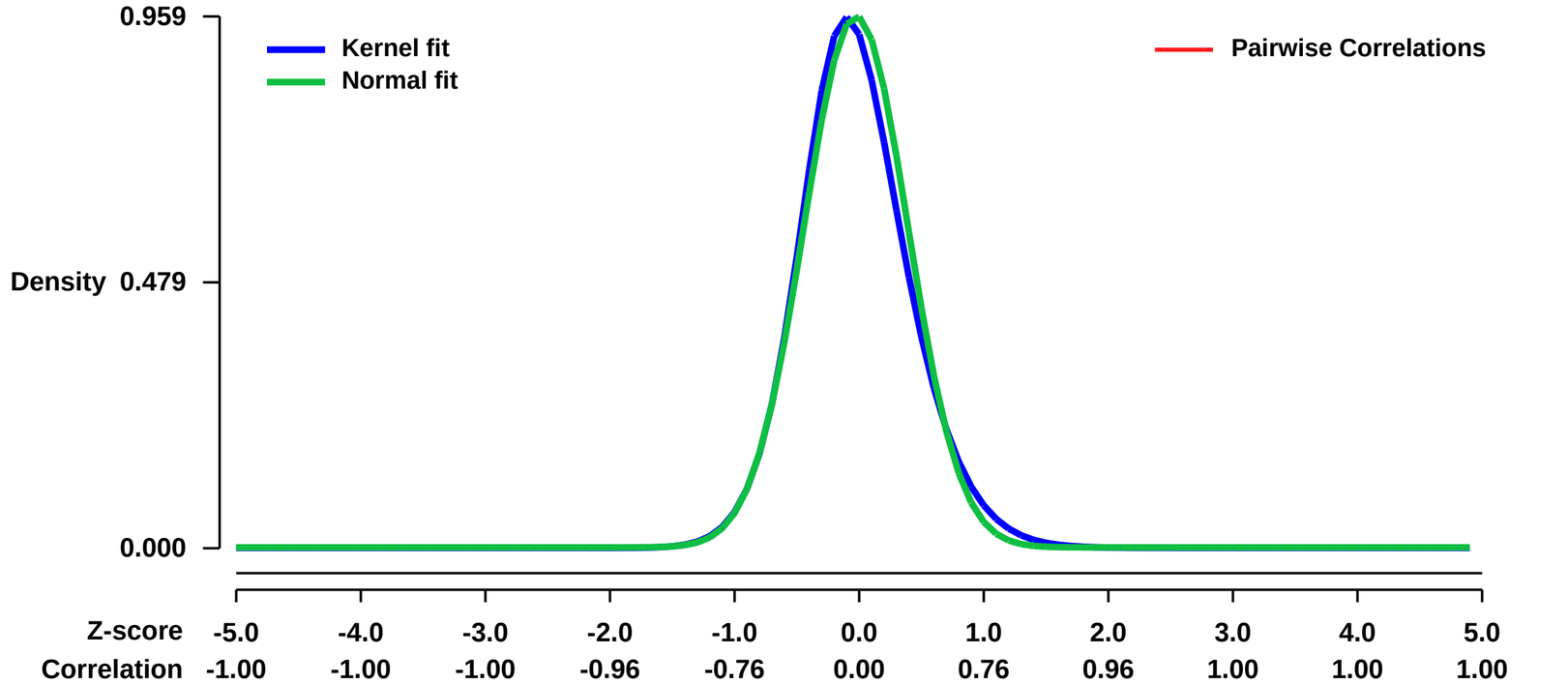

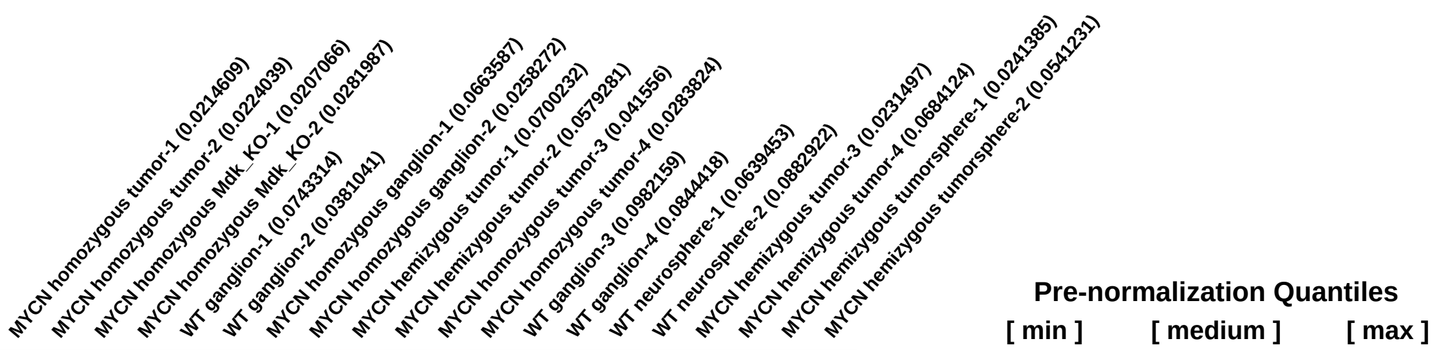

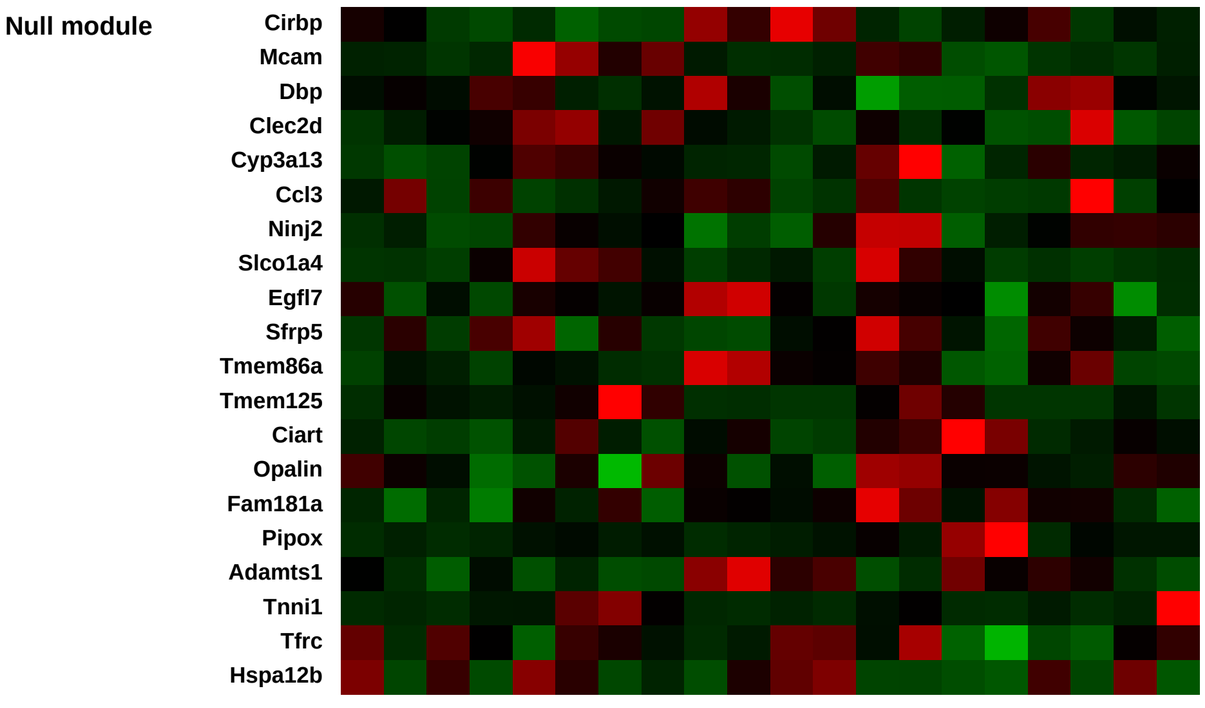

GEO Series "GSE50399" Expression Profiles

Num of samples in this series: 18

Scale of expression profile Z-scores

-3.0 -2.0 -1.0 0.0 1.0 2.0 3.0

GEO Link:	http://www.ncbi.nlm.nih.gov/geo/query/acc.cgi?acc=GSE50399
Status:	Public on Feb 01 2014
Title:	Gene expression data of postnatal Pitx2 deficient heart
Organism:	Mus musculus
Experiment type:	Expression profiling by array
Platform:	GPL1261
Pubmed ID:	24395921
Summary & Design:	**Summary:** Pitx2 is the homeobox gene located in proximity to the human 4q25 familial atrial fibrillation locus. Pitx2 haploinsufficient mice are prone to pacing induced atrial fibrillation indicating that reduced Pitx2 promotes an arrhythmogenic substrate within the atrium. Here, we inactivated Pitx2 in postnatal heart and discovered that unstressed adult Pitx2 mutant mice had sinus node dysfunction with impaired atrial conduction, an arrhythmia closely associated with atrial fibrillation. A genome-wide search for Pitx2 transcriptional targets using ChIP-sequencing and RNA expression profiling shows that Pitx2 represses target genes encoding cell junction proteins, ion channels, and critical transcriptional regulators many of which have been implicated in human atrial fibrillation by genome wide association studies. **Overall design:** Pitx2 control and mutant hearts were collected from 3-, 6- and 12-week-old mice. At each time point, three cotrols and three mutants were collected as biological replicates. cDNA microarray analysis was performed using Affymetrix GeneChip Mouse Genome 430 2.0 Array (Affymetrix, Santa Clara, CA).

Background corr dist: KL-Divergence = 0.1987, L1-Distance = 0.0367, L2-Distance = 0.0025, Normal std = 0.3349

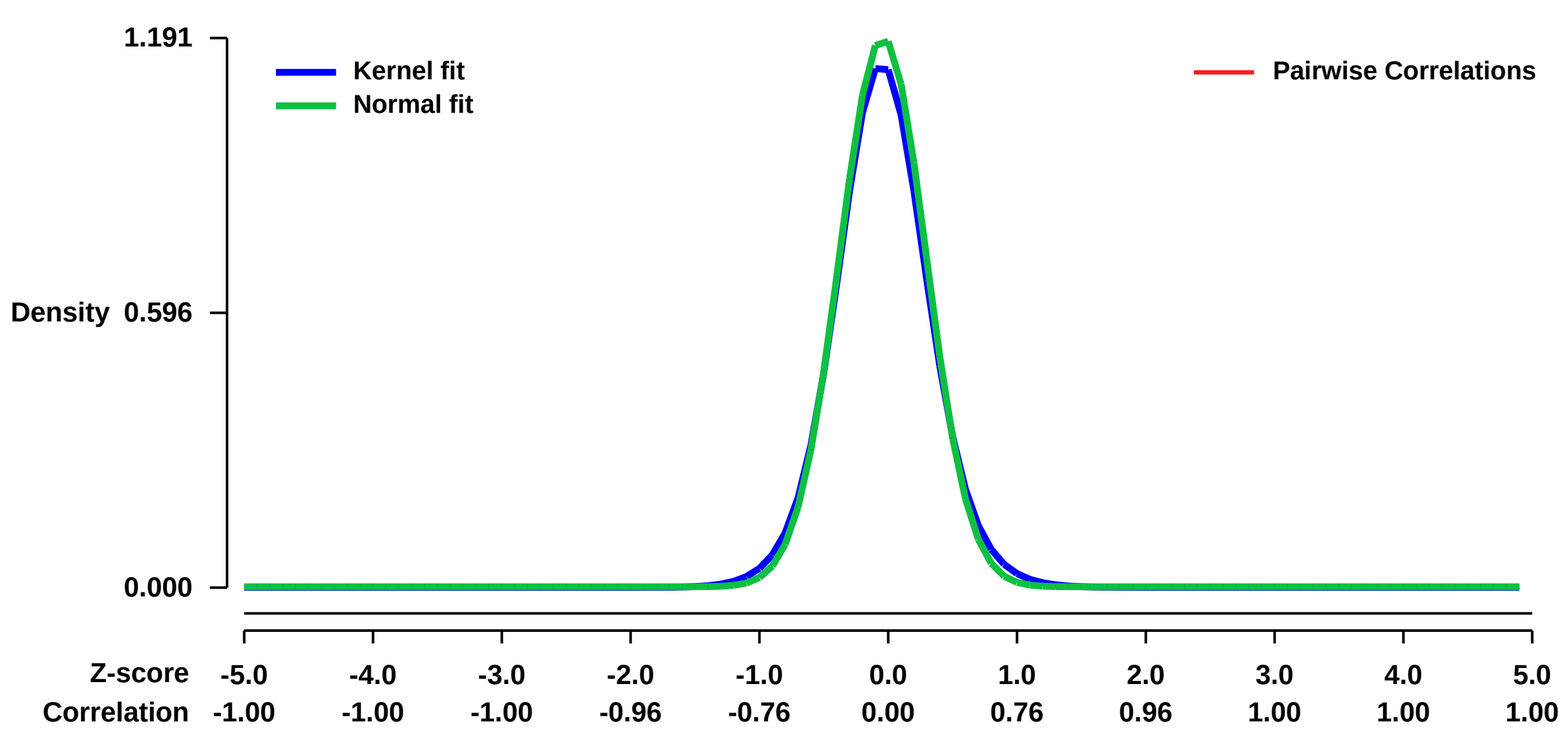

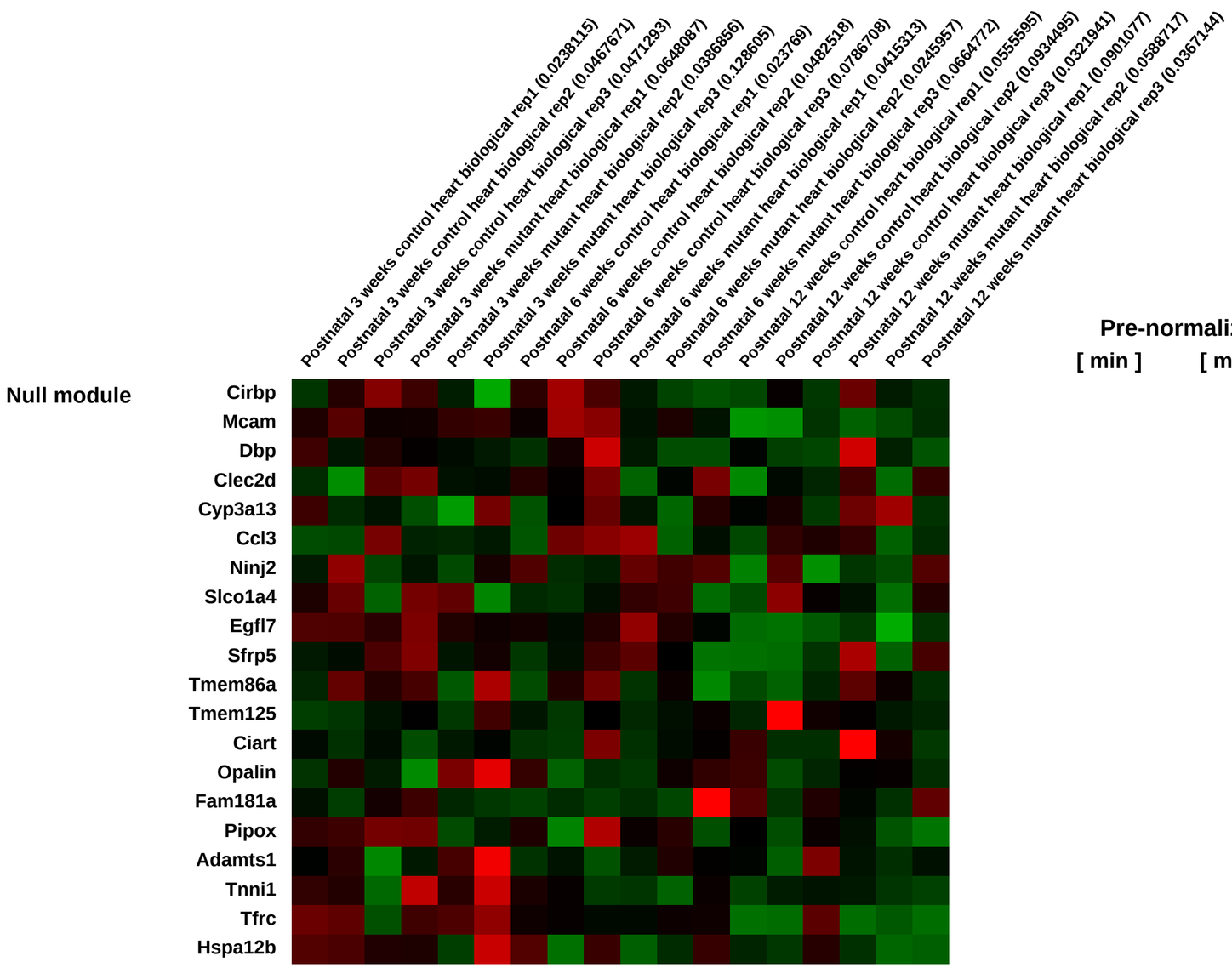

GEO Series "GSE19517" Expression Profiles

Num of samples in this series: 6

Scale of expression profile Z-scores

-3.0 -2.0 -1.0 0.0 1.0 2.0 3.0

GEO Link:	http://www.ncbi.nlm.nih.gov/geo/query/acc.cgi?acc=GSE19517
Status:	Public on Mar 01 2010
Title:	Gene expression profiling of conditional ablation of Indian hedgehog in the mouse uterus
Organism:	Mus musculus
Experiment type:	Expression profiling by array
Platform:	GPL1261
Pubmed ID:	20056671
Summary & Design:	**Summary:** Conditional ablation of Indian hedgehog (Ihh) in the murine uterus results in mice that are sterile due to defects in embryo implantation. We performed microarray analysis on these mice at the time point at which the Ihh target genes are induced by the administration of exogenous hormone to mimic day 3.5 of pregnancy. This analysis identified 863 genes altered by the conditional ablation of Ihh. Of these, genes that regulated the cell cycle were overrepresented. In addition, genes involved in epidermal growth factor (EGF) and estrogen (E2) signaling were found to be deregulated upon Ihh ablation. Furthermore, upon conditional ablation of Ihh, 15 month old mice exhibited hallmarks of estrogenized uteri such as cystically dilated glands and hyalinized stroma. Thus, Ihh regulates embryo implantation by impacting the cell cycle, EGF signaling, and E2 signaling. **Keywords:** two group comparison **Overall design:** We conditionally ablated Indian hedgehog in the mouse uterus using the PRcre mouse model (PRcre/+Ihhf/f; Ihhd/d). High density DNA microarray analysis was performed on Day -1 of the artificial decidual response on Ihhf/f and Ihhd/d uteri.

Background corr dist: KL-Divergence = 0.0158, L1-Distance = 0.0218, L2-Distance = 0.0006, Normal std = 0.7834

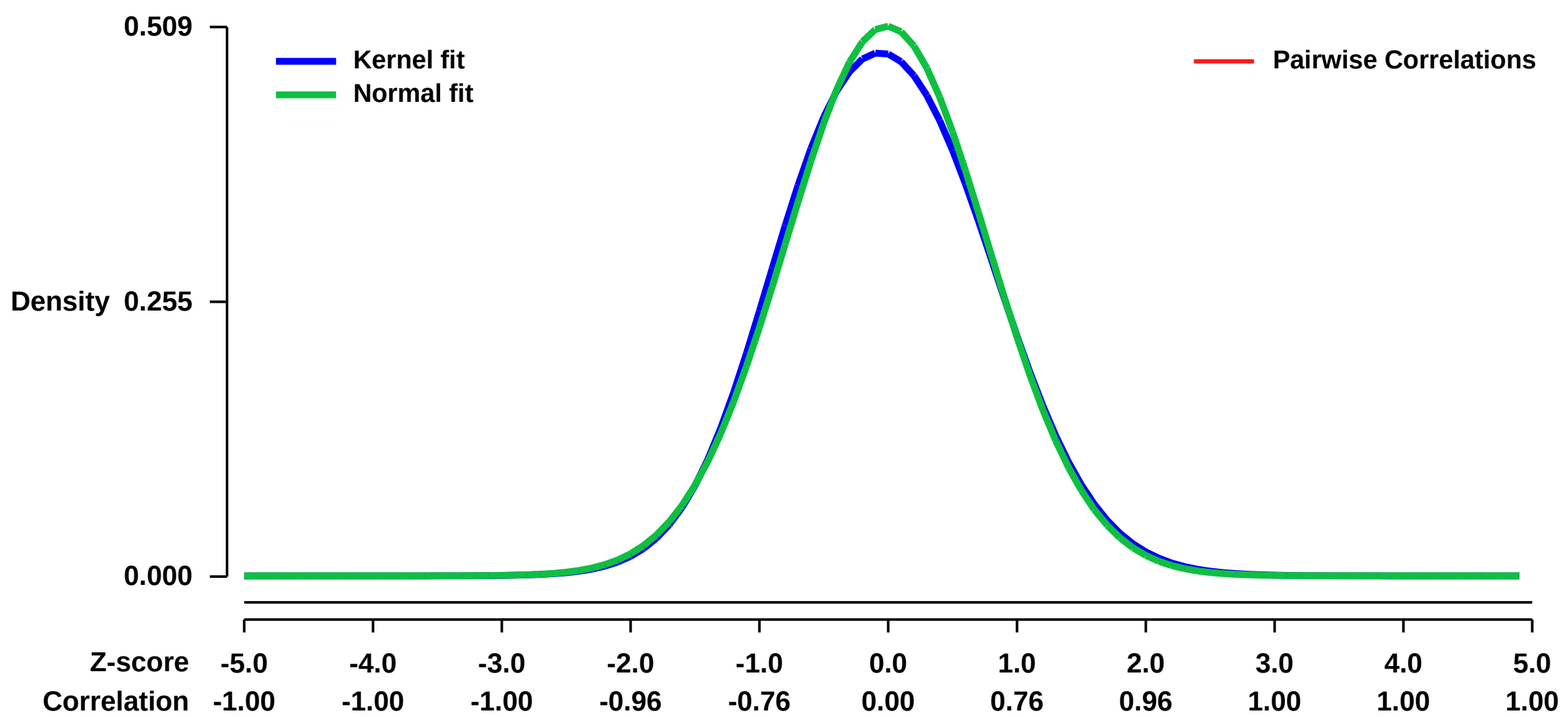

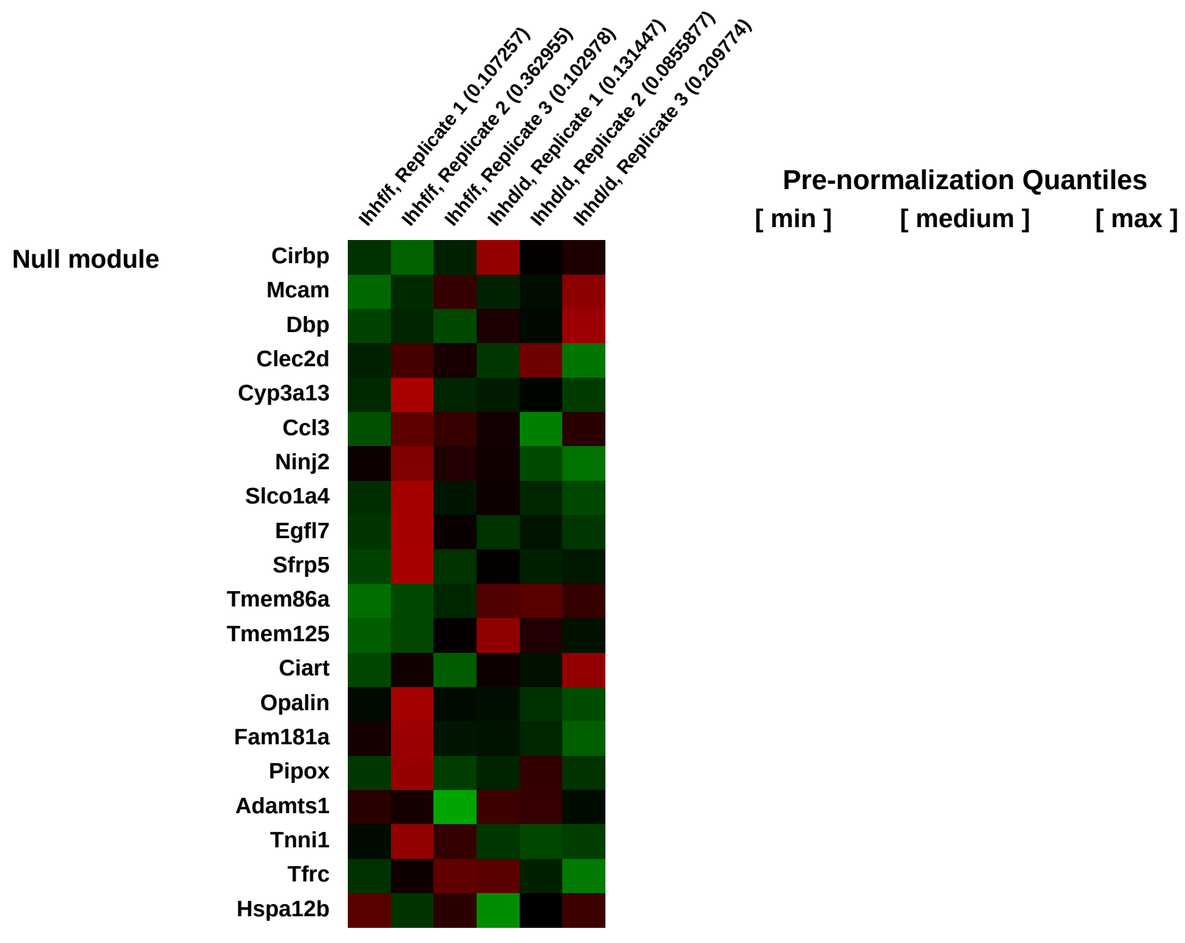

GEO Series "GSE16210" Expression Profiles

Num of samples in this series: 14

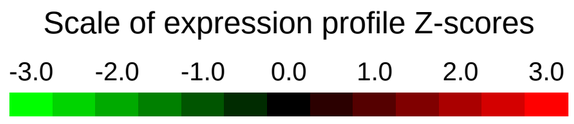

GEO Link:	http://www.ncbi.nlm.nih.gov/geo/query/acc.cgi?acc=GSE16210
Status:	Public on Aug 31 2009
Title:	Expression data of Naive Treg, allogeneic tumor-activated Treg, and GVHD-activated Treg cells
Organism:	Mus musculus
Experiment type:	Expression profiling by array
Platform:	GPL1261
Pubmed ID:	
Summary & Design:	**Summary:** Regulatory T (Treg) cells play an important role in the induction and maintenance of peripheral tolerance. Treg cells also suppress a variety of other immune responses, including anti-tumor and alloimmune responses. We have previously reported that tumor-activated Treg cells express granzyme B and that granzyme B is important for Treg cell-mediated suppression of anti-tumor immune responses (GSE13409). Here, we report that allogeneic mismatch also induces the expression of granzyme B. Granzyme B-deficient mice challenged with fully mismatched allogeneic P815 mastocytoma cells have markedly improved survival compared to WT and other granzyme- or perforin-deficient mice, suggesting an immunoregulatory role for granzyme B in this setting. Treg cells harvested from the tumor environment of P815-challenged mice express granzyme B. Treg cells also express granzyme B in vitro during mixed lymphocyte reactions and in vivo in a mouse model of graft-versus-host disease (GVHD). However, in contrast to findings from our previously published tumor model, granzyme B is not required for the suppression of effector T cell (Teff) proliferation in in vitro Treg suppression assays stimulated by either Concanavalin A or allogeneic antigen presenting cells. Additionally, in an ex vivo assay, sort-purified in vivo-activated CD4+Foxp3+ Treg cells from mice with active GVHD -- under conditions known to induce granzyme B expression in Treg cells -- suppressed Teff cell proliferation in a granzyme B-independent manner. Adoptive transfer of naive granzyme B-deficient CD4+CD25+ Treg cells into a mouse model of GVHD rescued hosts from lethatlity equivalently to naive wild-type Treg cells. Serum analysis of GVHD-associated cytokine production in these recipients also demonstrated that Treg cells suppressed production of IL-2, IL-4, IL-5, GM-CSF, and IFN-gamma in a granzyme B-independent manner. In order to determine whether the context in which Treg cells are activated alters the intrinsic properties of Treg cells, we used Foxp3 reporter mice to obtain gene expression profiles of CD4+Foxp3+ Treg cells purifed from naive resting spleens, spleens from mice with acute GVHD, and from ascites fluid of mice challenged intraperitoneally with allogeneic P815 tumor cells. Unsupervised analyses revealed distinct activation signatures of Treg cells among the 3 experimental groups. Taken together, these findings demonstrate that granzyme B is not required for Treg cell-mediated suppression of GVHD, which is in contrast to what we have previously reported for Treg cell function in the setting of tumor challenge. Cell intrinsic differences could partially account for these differential phenotypes. These data also suggest the therapeutic potential of targeting specific Treg cell suppressive functions in order to segregate GVHD and graft-versus-tumor effector functions. **Keywords:** Normal vs Activated **Overall design:** Naive reps 4-6 are controls for the Allogeneic tumor-activated samples.

Background corr dist: KL-Divergence = 0.1068, L1-Distance = 0.0393, L2-Distance = 0.0033, Normal std = 0.4337

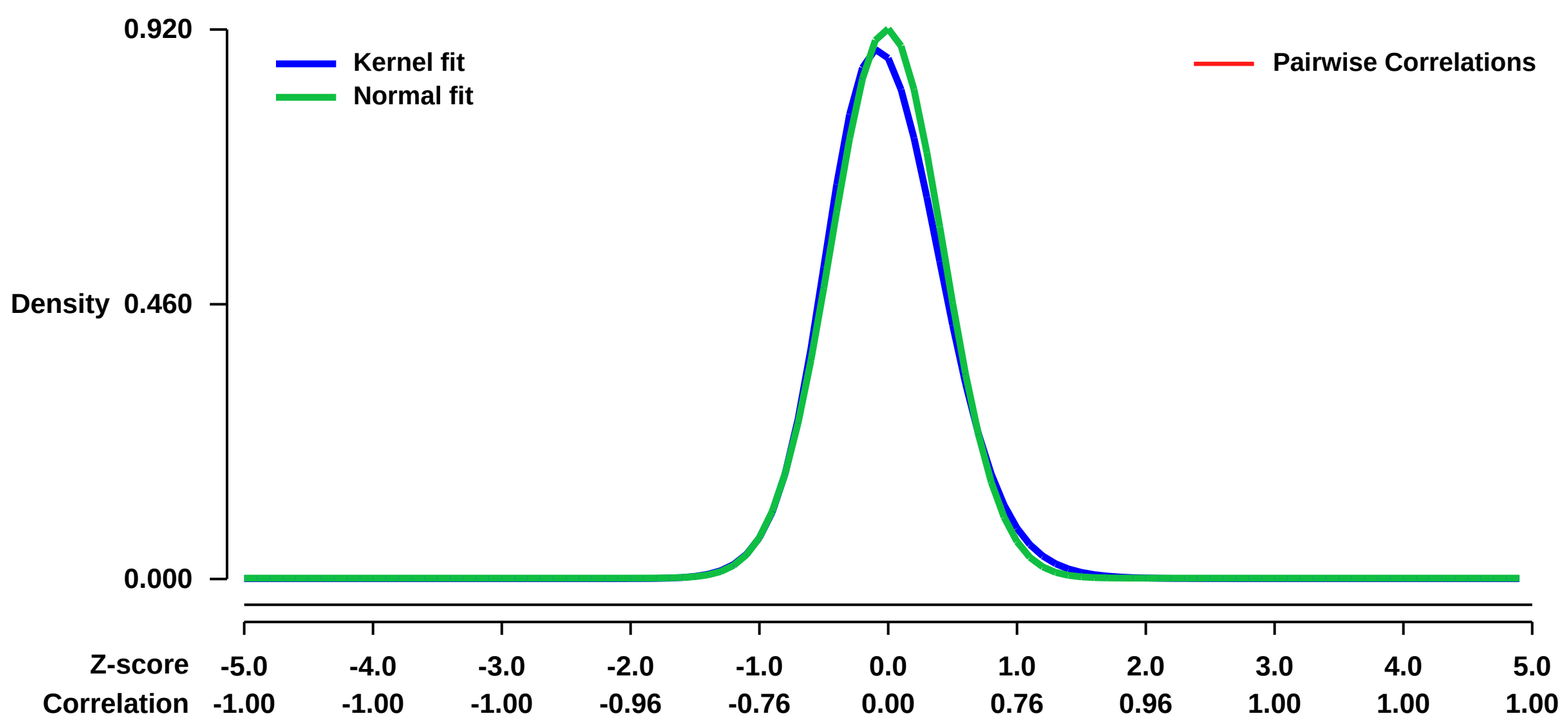

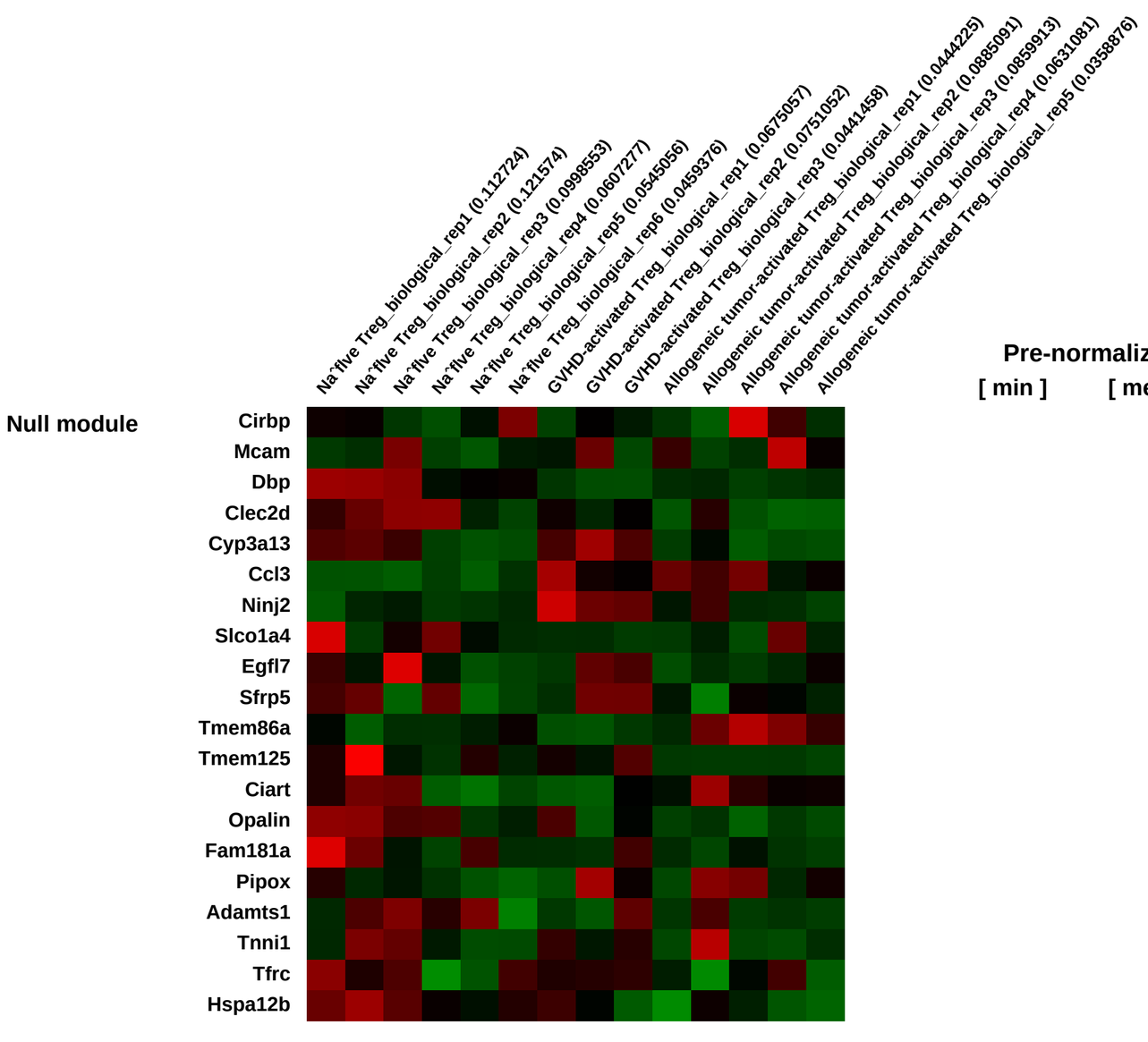

GEO Series "GSE15872" Expression Profiles

Num of samples in this series: 18

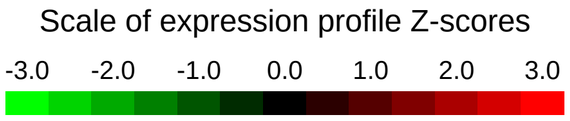

GEO Link:	http://www.ncbi.nlm.nih.gov/geo/query/acc.cgi?acc=GSE15872
Status:	Public on Oct 01 2009
Title:	Dynamic patterning at the pylorus: formation of an epithelial intestine-stomach boundary in late fetal life
Organism:	Mus musculus
Experiment type:	Expression profiling by array
Platform:	GPL1261
Pubmed ID:	19877272
Summary & Design:	**Summary:** In the adult mouse, distinct morphological and transcriptional differences separate stomach from intestinal epithelium. Remarkably, the epithelial boundary between these two organs is literally one cell thick. This discrete junction is established suddenly and precisely at embryonic day (E) 16.5, by sharpening a previously diffuse intermediate zone. In the present study, we define the dynamic transcriptome of stomach, pylorus and intestinal tissues between E14.5 and E16.5. We show that establishment of this boundary is concomitant with the induction of over a thousand genes in intestinal epithelium, and these gene products provide intestinal character. Hence, we call this process intestinalization. We identify specific transcription factors (Hnf4g, Creb3l3 and Tcfec) and examine signaling pathways (Hedgehog and Wnt) that may play a role in this process. Finally, we define a unique expression domain at the pylorus itself and detect novel pylorus-specific patterns for the transcription factor Gata3 and the secreted protein nephrocan. **Overall design:** Stomach, pylorus and duodenum tissue from E14.5 and E16.5 mouse embryos were collected for RNA extraction and hybridization on Affymetrix microarrays. We sought to study the gene expression profiles and identify genes and pathways enriched in these three tissues at two important developmental times.

Background corr dist: KL-Divergence = 0.0387, L1-Distance = 0.0489, L2-Distance = 0.0046, Normal std = 0.6254

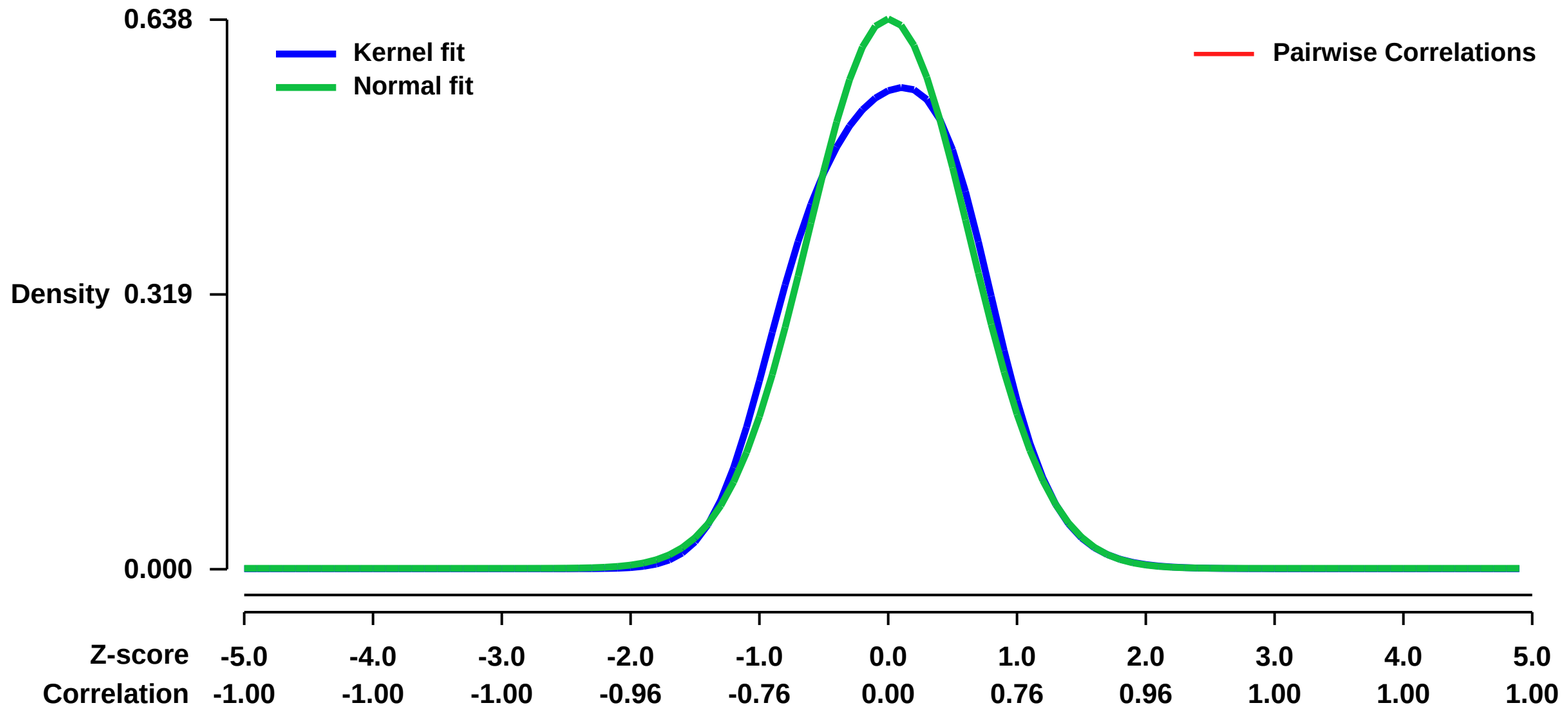

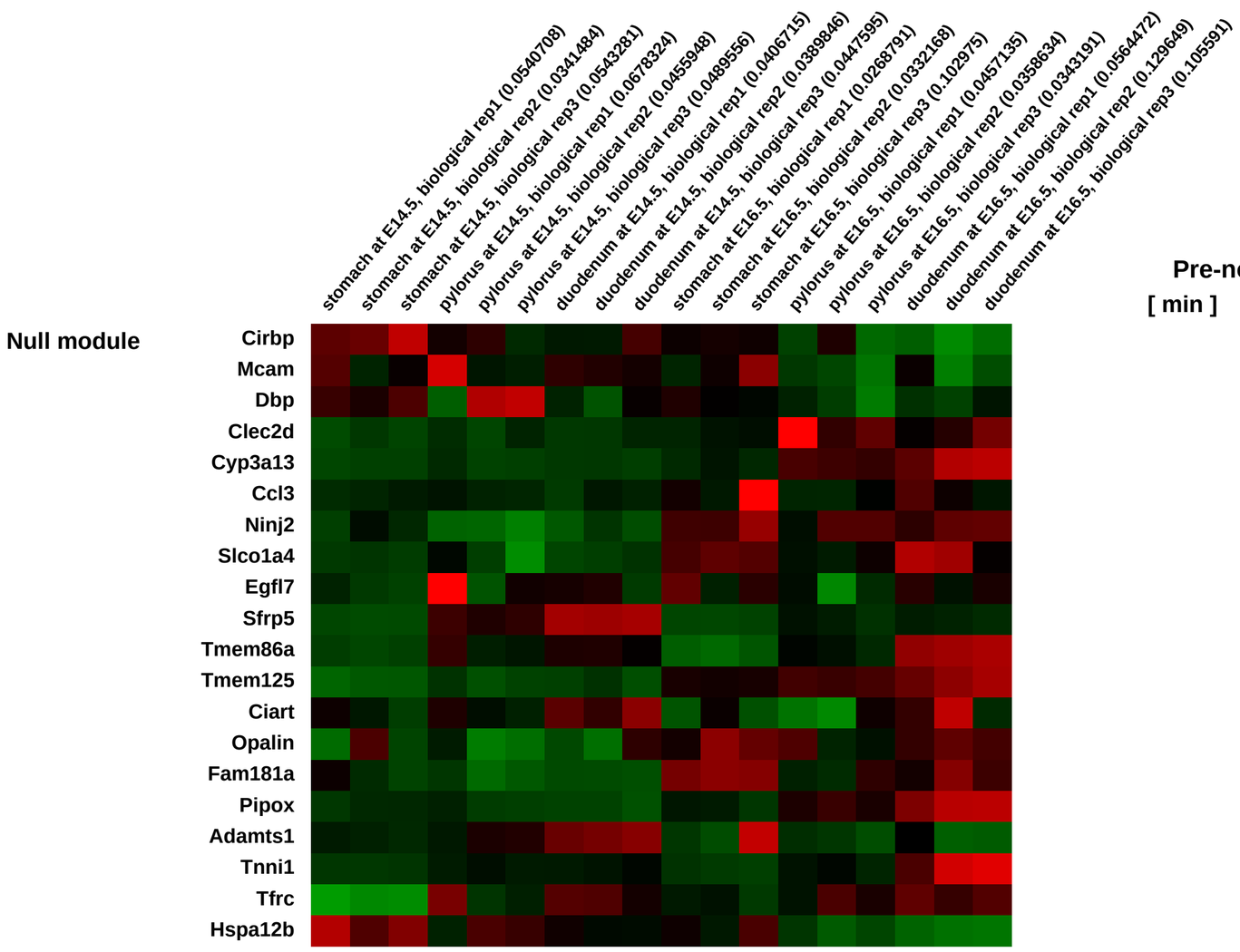

GEO Series "GSE22124" Expression Profiles

Num of samples in this series: 18

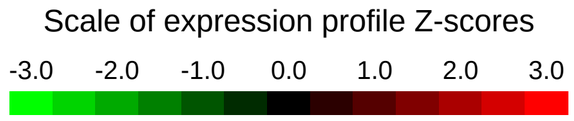

GEO Link:	http://www.ncbi.nlm.nih.gov/geo/query/acc.cgi?acc=GSE22124
Status:	Public on Feb 18 2014
Title:	Microarry datasets for RAW cells stimulated with R848 in the absence or presence of apilimod or API09
Organism:	Mus musculus
Experiment type:	Expression profiling by array
Platform:	GPL1261
Pubmed ID:	24600036
Summary & Design:	**Summary:** Apilimod is a reported TLR pathway antagonist in clinical trial. To understand the mode of action of apilimod, we applied global microarray analysis to explore the effect of apilimod on gene expression of RAW cell in the absence of presence of R848 (TLR7 ligand). **Overall design:** RAW cells were stimulated with R848 in the absence or presence of apilimod (1μ…M). mRNAs were extracted at 0h, 1h,3h, 7h, and 22h for affymetrix analysis. The inactive analog of apilimod (API09) was included as a control.

Background corr dist: KL-Divergence = 0.0783, L1-Distance = 0.0300, L2-Distance = 0.0017, Normal std = 0.4770

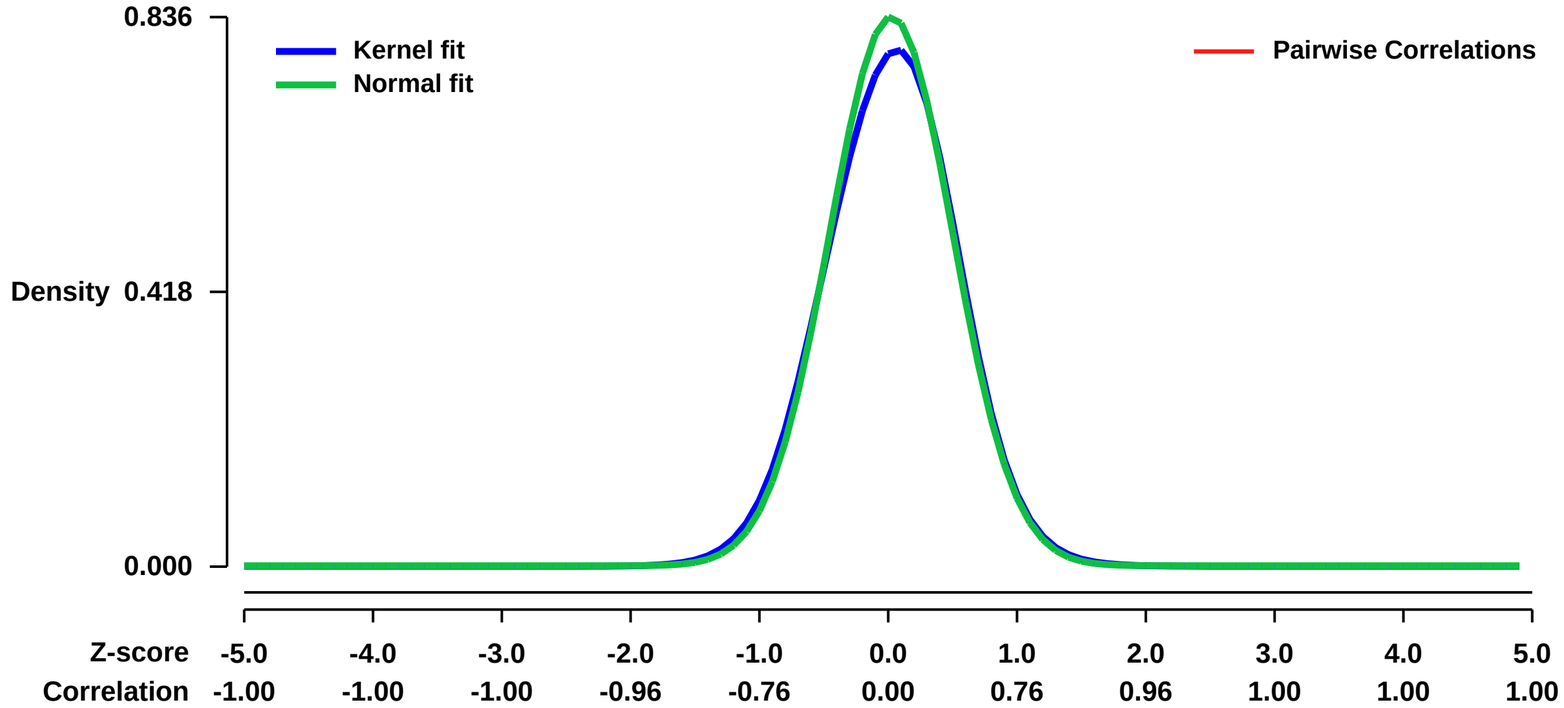

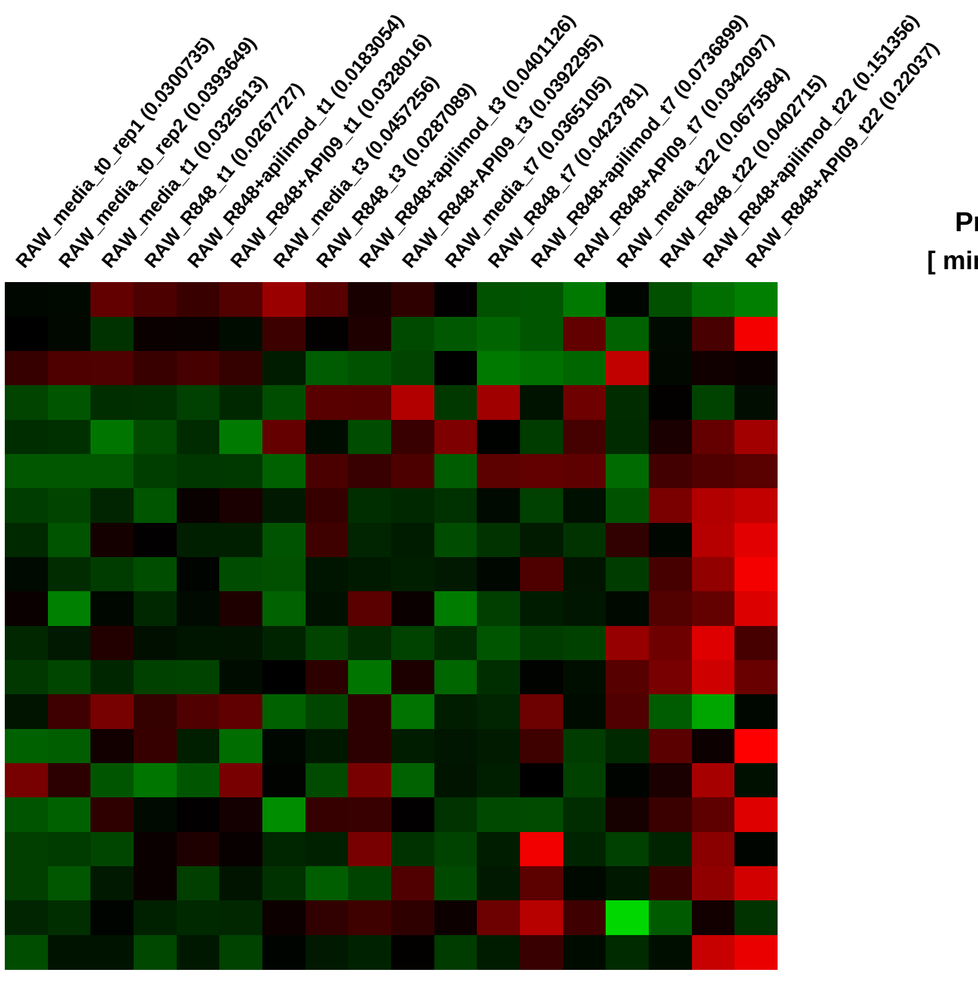

GEO Series "GSE47959" Expression Profiles

Num of samples in this series: 8

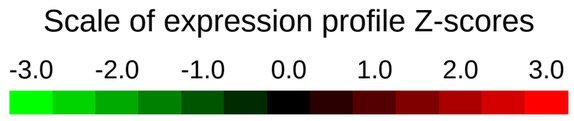

GEO Link:	http://www.ncbi.nlm.nih.gov/geo/query/acc.cgi?acc=GSE47959
Status:	Public on Jul 25 2014
Title:	NKT-10 cells represent a novel invariant NKT cell subset with regulatory characteristics
Organism:	Mus musculus
Experiment type:	Expression profiling by array
Platform:	GPL1261
Pubmed ID:	25061873
Summary & Design:	**Summary:** We compared splenic Va14i NKT cells from C57BL/6 control mice and from mice injected 4 weeks earlier intravenously with 4ug/mouse of the iNKT cell antigen alpha-galactosylceramide (aGalCer). These mice were either left unstimulated or were stimulated with 1ug/mouse aGalCer i.v.. All mice were female and 8 weeks of age at the beginning of the experiment. Va14i NKT cells were enriched via magnetic selection and cell sorted for TCRb+ CD1d/aGalCer-tetramer+. Total RNA were prepared using a Qiagen RNeasy mini kit. IVT probe generation and hybridization to Affymetrix Mouse Genome 430 2.0 arrays was carried out by the Veterans Medical Research Foundation GeneChipTM Microarray located at UCSD. **Overall design:** Group 1 (Ctr_unstim) = iNKT cells from C57BL/6 control mice and left unstimulated / Group 2 (Ctr_stim) = iNKT cells from C57BL/6 control mice and injected 1h before purification with 1ug aGalCer i.v. / Group 3 (Pre_unstim) = iNKT cells from C57BL/6 mice injected 4weeks earlier with 4ug aGalCer i.v. and left unstimulated / Group 4 (Pre_stim) = iNKT cells from C57BL/6 mice injected 4weeks earlier with 4ug aGalCer i.v. and injected 1h before purification with 1ug aGalCer i.v. / Sample were prepared in duplicates in two independent experiments.

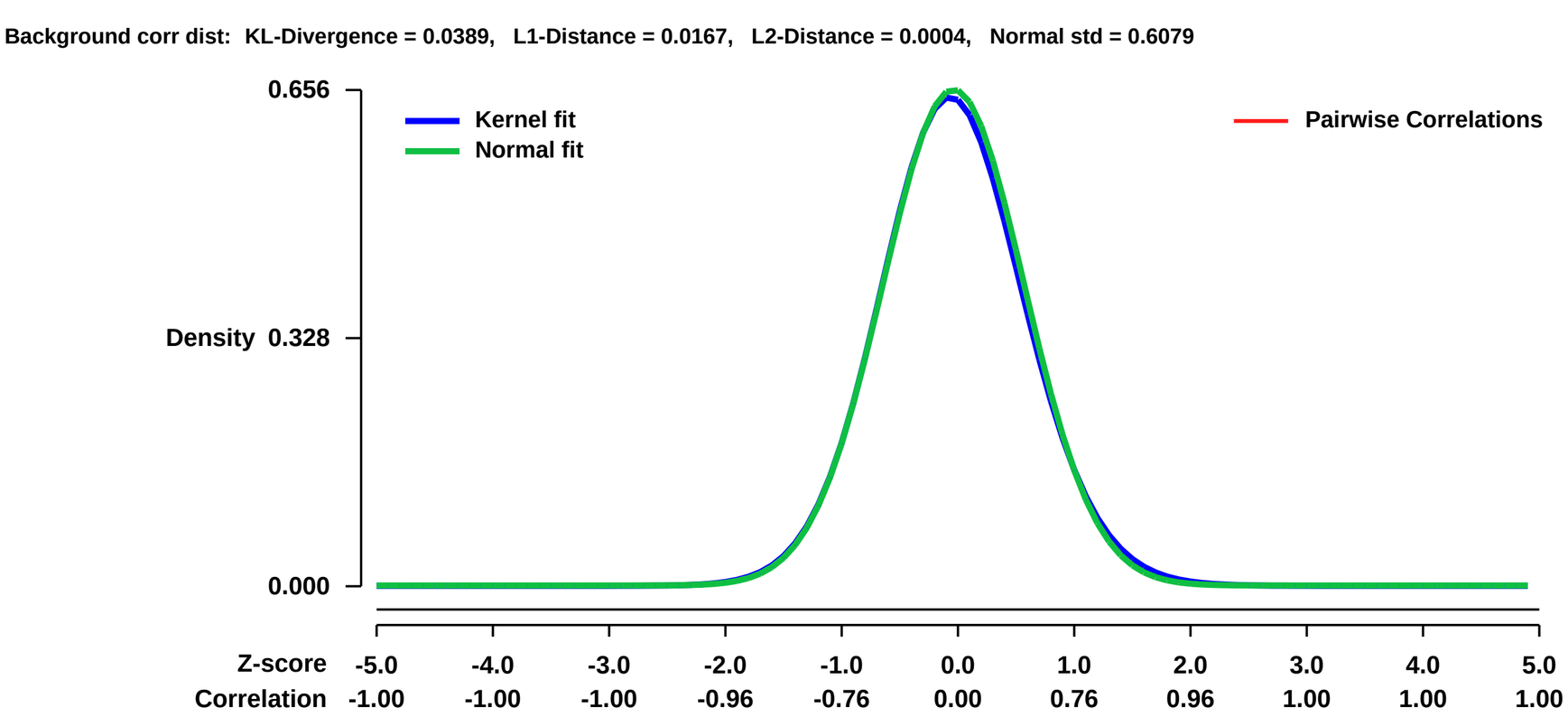

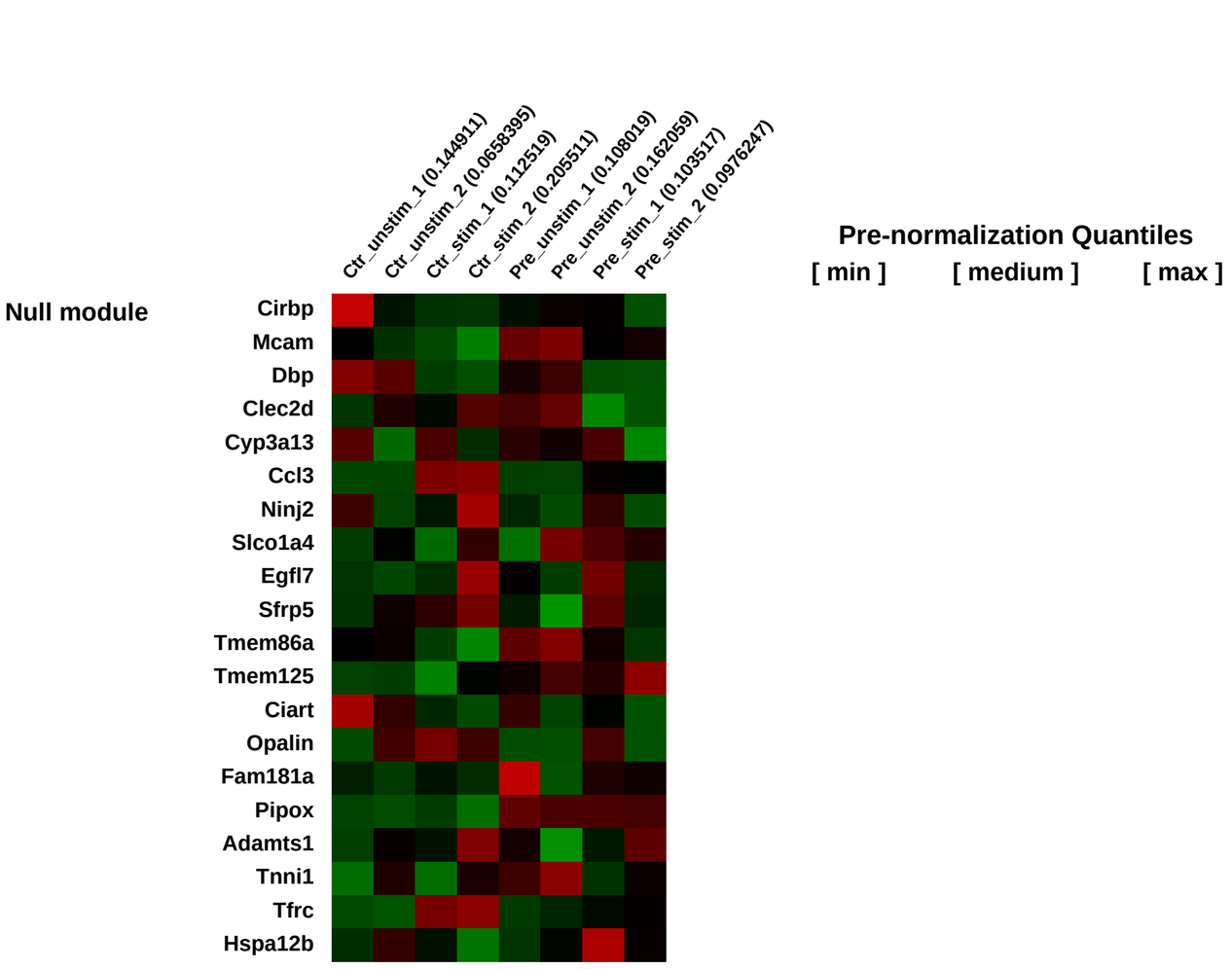

GEO Series "GSE4866" Expression Profiles

Num of samples in this series: 10

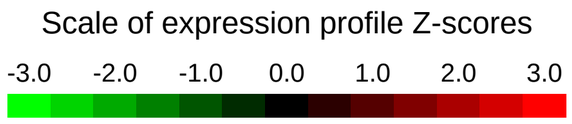

GEO Link:	http://www.ncbi.nlm.nih.gov/geo/query/acc.cgi?acc=GSE4866
Status:	Public on May 18 2007
Title:	The role of mtDNA mutations in age-related hearing loss in mice carrying a mutator DNA polymerase gamma
Organism:	Mus musculus
Experiment type:	Expression profiling by array
Platform:	GPL1261
Pubmed ID:	17363114
Summary & Design:	**Summary:** Mitochondrial DNA (mtDNA) mutations may contribute to aging and age-related disorders. Previously, we created mice expressing a proofreading-deficient version of the mtDNA polymerase gamma (Polg) which accumulate age-related mtDNA mutations and display premature aging. Here we performed microarray gene expression profiling to identify mtDNA mutation-responsive genes in the cochlea of aged mitochondrial mutator mice. Age-related accumulation of mtDNA mutations was associated with transcriptional alternations consistent with reduced inner ear function, mitochondrial dysfunction, neurodegeneration, and reduced cell structural modulation. Hearing assessment and histopathological results confirmed that aged PolgD257A/D257A (D257A) mice exhibited moderate hearing loss and severe cochlear degenerations. Age-related accumulation of mtDNA mutations also resulted in alternations in gene expression consistent with induction of apoptosis, proteolysis, stress response, and reduced DNA repair. TUNEL (Terminal deoxynucleotidyl transferase-mediated dUTP nick-end labeling) assay confirmed that the cochleae from aged D257A mice showed significantly more TUNEL positive cells compared to wild-type (WT) mice. The levels of cleaved caspase-3 were also found to increase in the cochleae of aged D257A mice. These observations provide evidence that age-related accumulation of mtDNA mutations is associated with apoptotic cell death in aged cochlea. Our results provide the first global view of molecular events associated with mtDNA mutations in postmitotic tissue, and suggest that apoptosis is the major mechanism of mtDNA mediated cell death in the development of age-related hearing disorder. **Keywords:** disease state analysis **Overall design:** Affymetrix standard spike controls were used in all experiments (eukaryotic hybridization control kit). Quality control measures were not used. No replicates were done. Dye swap was not used.

Background corr dist: KL-Divergence = 0.0920, L1-Distance = 0.0291, L2-Distance = 0.0015, Normal std = 0.4506

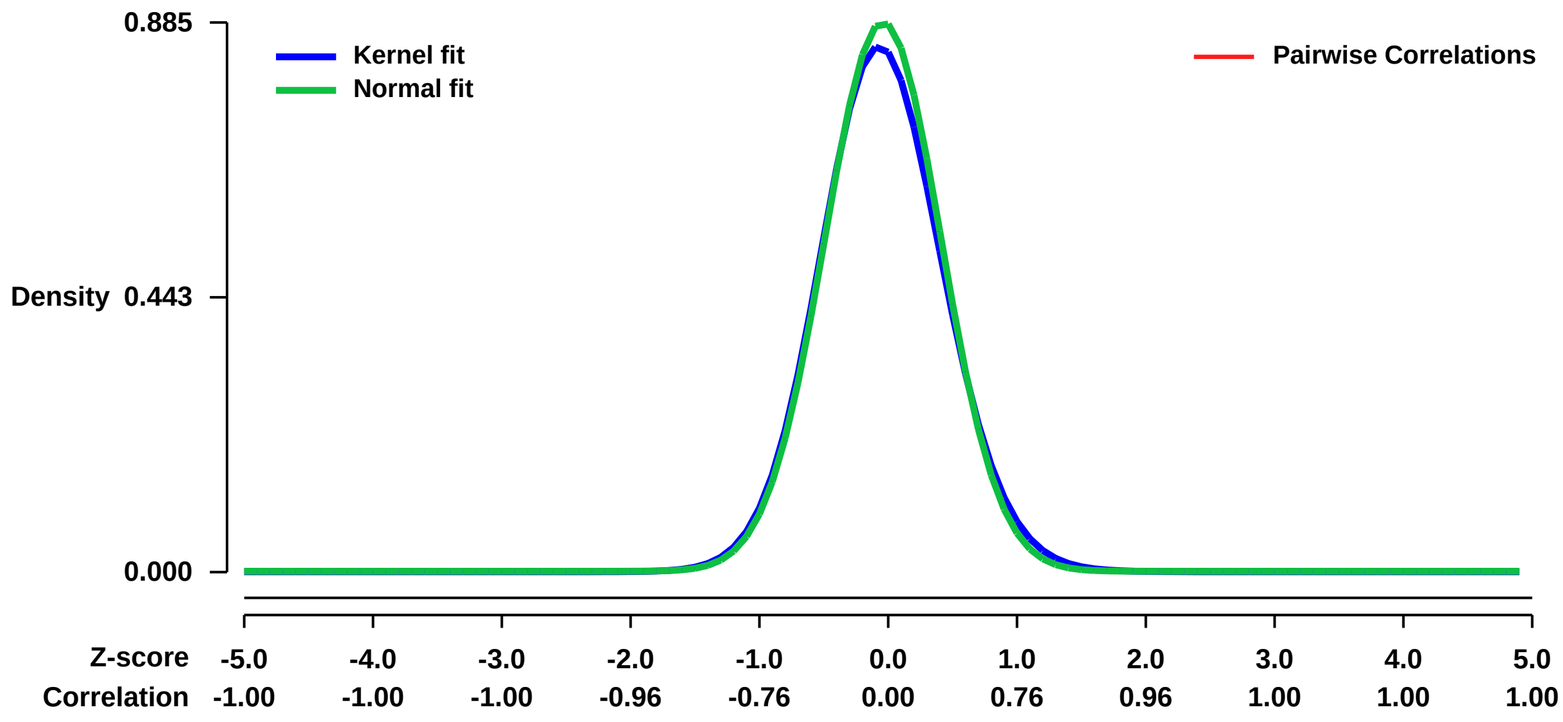

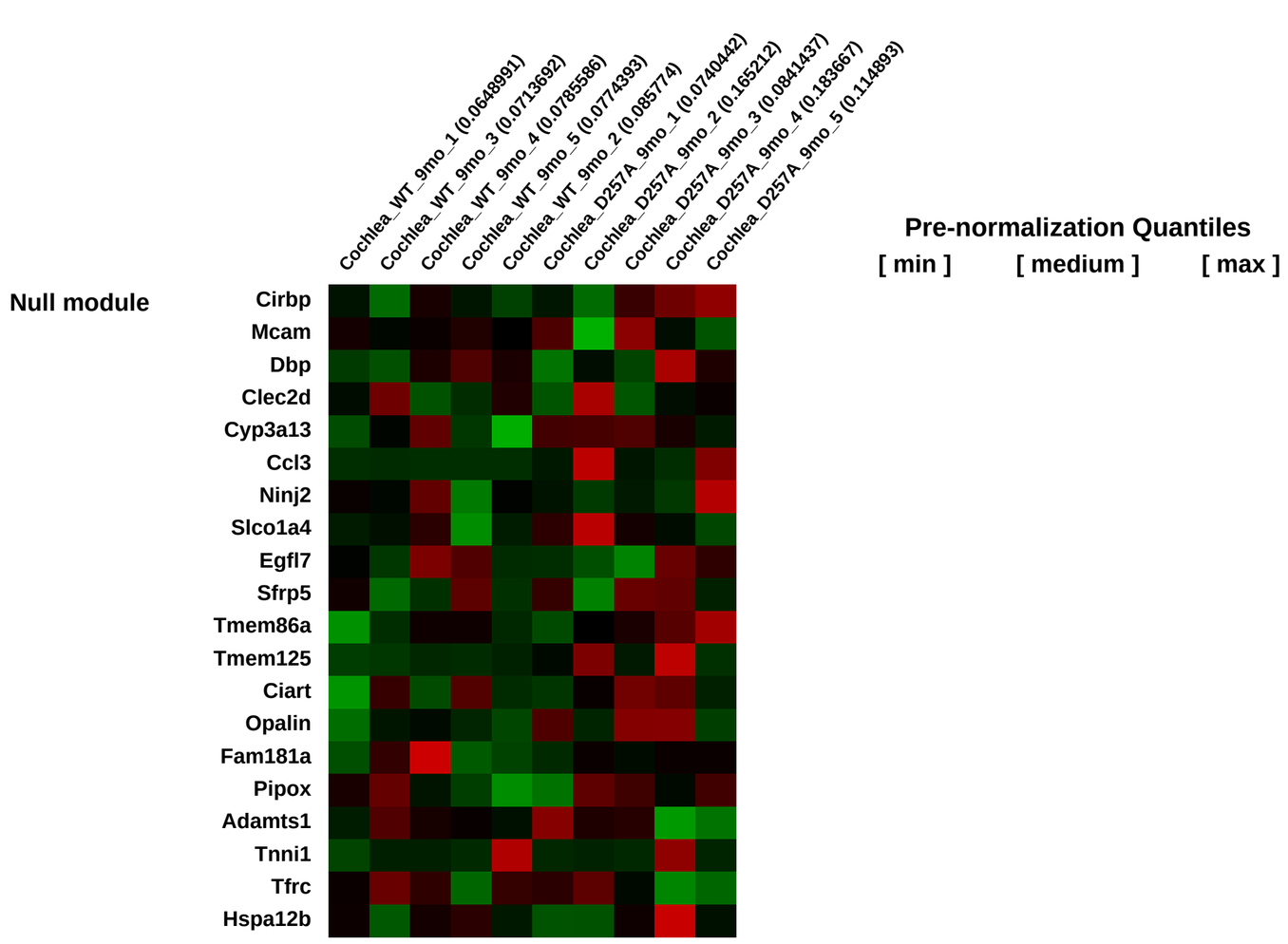

GEO Series "GSE44331" Expression Profiles

Num of samples in this series: 12

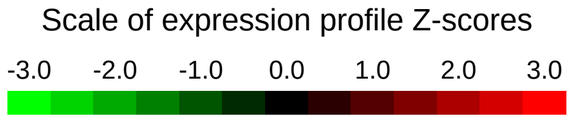

GEO Link:	http://www.ncbi.nlm.nih.gov/geo/query/acc.cgi?acc=GSE44331
Status:	Public on Apr 04 2013
Title:	Expression data from C57BL/6J and C57BL6/J Sarm-deficient mice uninfected or infected with vesicular stomatitis virus (VSV)
Organism:	Mus musculus
Experiment type:	Expression profiling by array
Platform:	GPL1261
Pubmed ID:	23749635
Summary & Design:	**Summary:** Sarm-deficient mice are protected from VSV encephalitis and death. Microarray was done to examine genes contributing to this phenotype **Overall design:** WT and KO mice were infected with VSV and brains were harvested at day 5 post-infection for RNA extraction

Background corr dist: KL-Divergence = 0.1726, L1-Distance = 0.0431, L2-Distance = 0.0039, Normal std = 0.3515

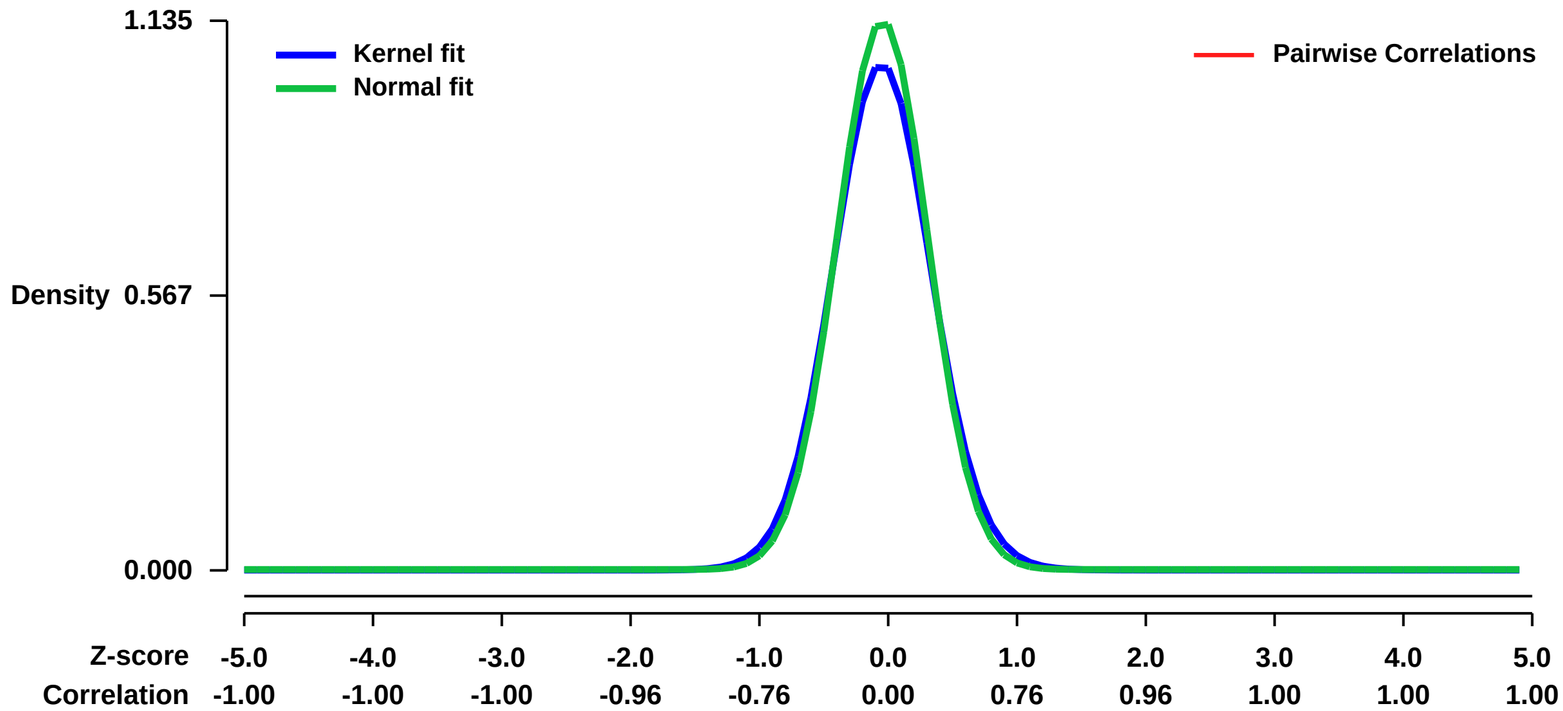

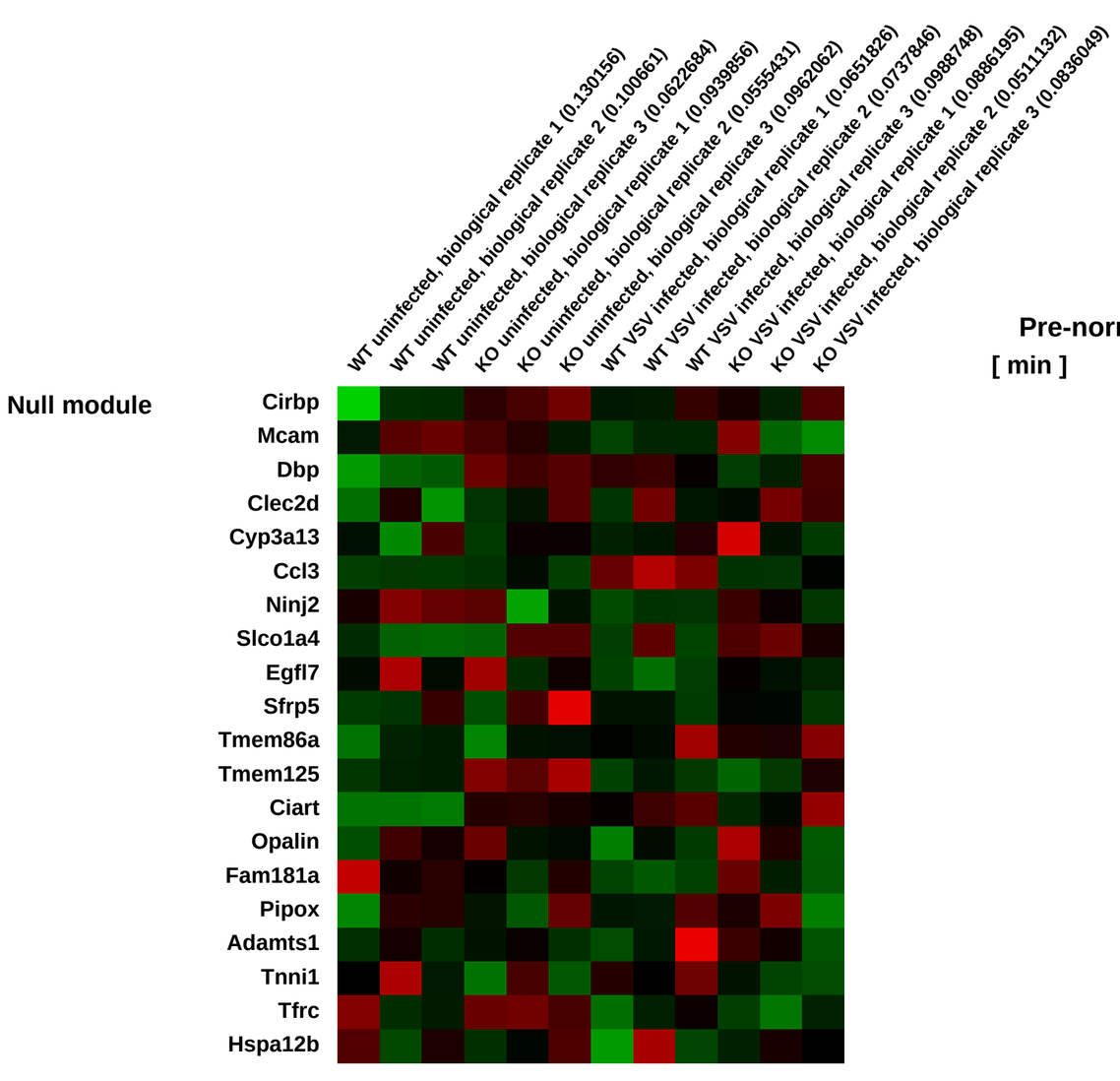

GEO Series "GSE25140" Expression Profiles

Num of samples in this series: 16

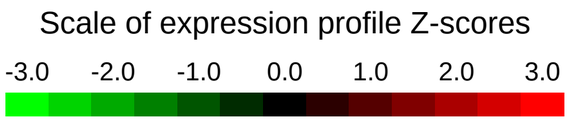

GEO Link:	http://www.ncbi.nlm.nih.gov/geo/query/acc.cgi?acc=GSE25140
Status:	Public on Nov 05 2010
Title:	Prostate specific Pten deletion, Pten-Smad4 deletion, and Pten-p53 deletion
Organism:	Mus musculus
Experiment type:	Expression profiling by array
Platform:	GPL1261
Pubmed ID:	21289624
Summary & Design:	**Summary:** We used microarrays to detail the global gene expression and identified differentially expressed gene list between wild-type anterior prostates and Ptenpc-/- anterior prostates, Ptenpc-/-Smad4pc-/- and Ptenpc-/- anterior prostates, Ptenpc-/-p53pc-/- and Ptenpc-/- anterior prostates at 15 weeks of age. **Overall design:** Prostate-specific Pten deletion (Ptenpc-/-) results in prostate intraepithelial neoplasia (PIN) which, following a long latency, can progress to high-grade adenocarcinoma, albeit with minimally invasive and metastatic features. To understand this feeble progression phenotype, we conducted transcriptome comparison of five Ptenpc-/- PIN relative to three wild-type anterior prostate. Moreover, Ptenpc-/-Smad4pc-/- progress to metastasis, while Ptenpc-/-p53pc-/- not progress to metastasis. To understand this phenotype difference, we conducted transcriptome comparison of five Ptenpc-/-Smad4pc-/-to five Ptenpc-/- prostate tumor, and three Ptenpc-/-p53pc-/- to five Ptenpc-/- tumor.

Background corr dist: KL-Divergence = 0.1614, L1-Distance = 0.0335, L2-Distance = 0.0022, Normal std = 0.3647

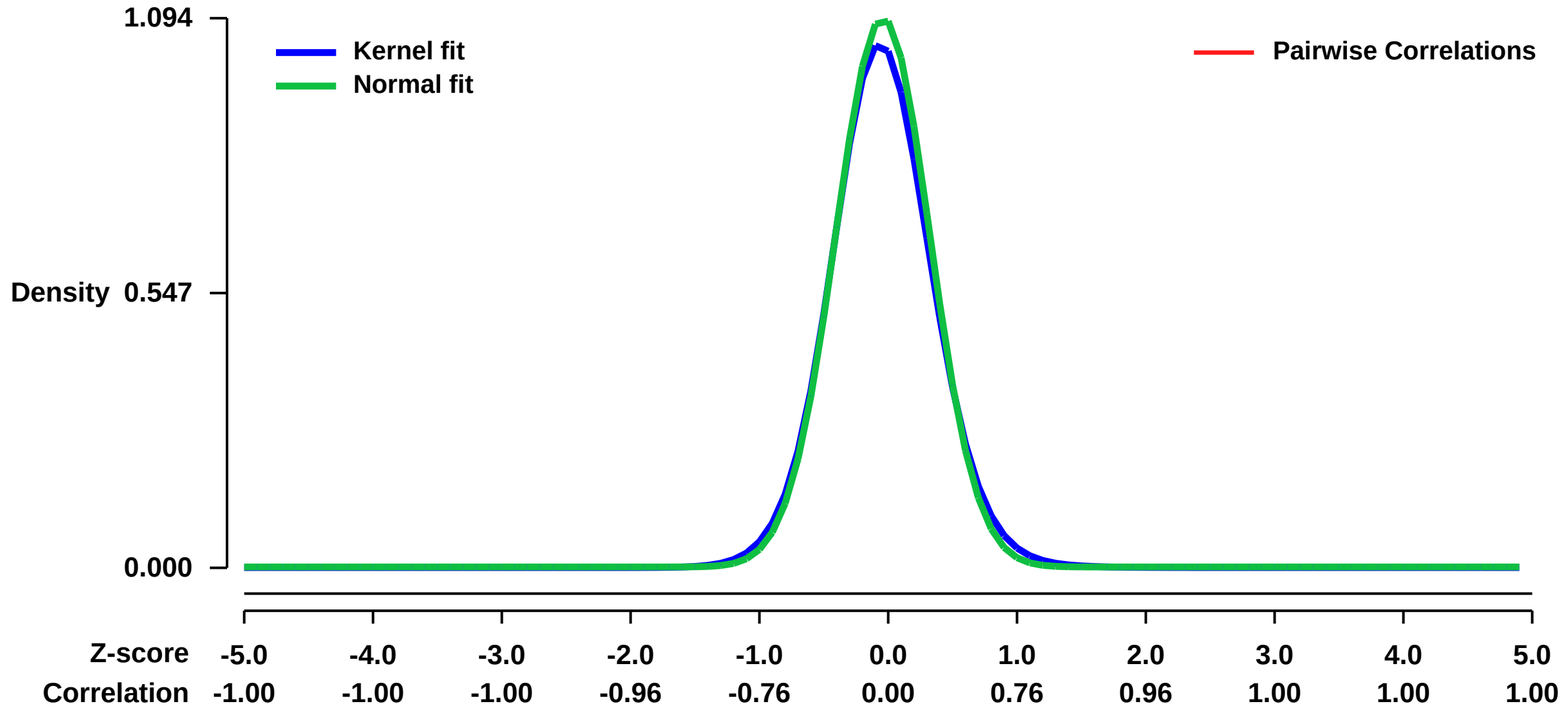

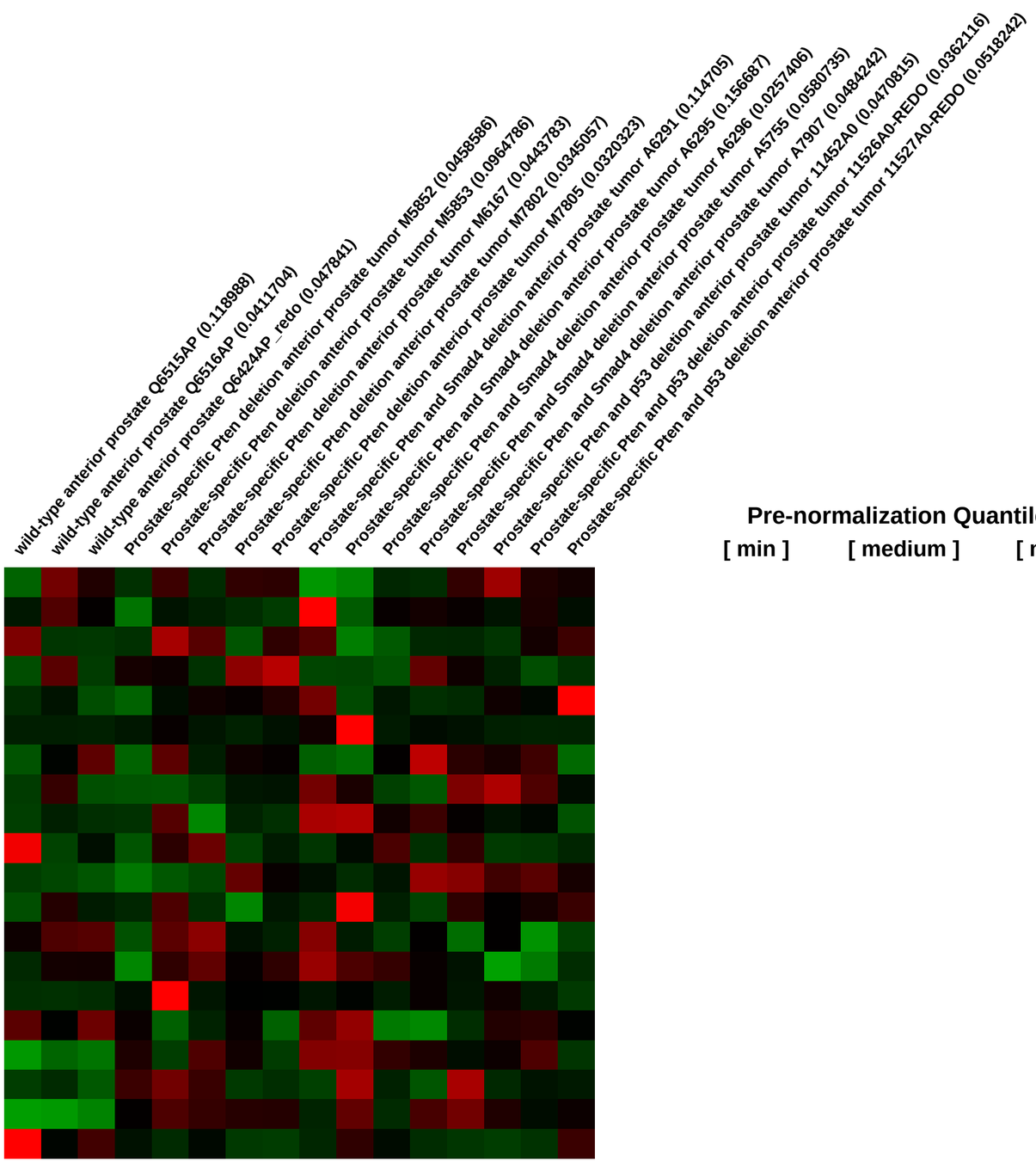

GEO Series "GSE38215" Expression Profiles

Num of samples in this series: 11

Scale of expression profile Z-scores

-3.0 -2.0 -1.0 0.0 1.0 2.0 3.0

GEO Link:	http://www.ncbi.nlm.nih.gov/geo/query/acc.cgi?acc=GSE38215
Status:	Public on Jun 01 2013
Title:	Expression analysis of control and low protein fed mouse offspring subsequently treated with multiple low doses of STZ
Organism:	Mus musculus
Experiment type:	Expression profiling by array
Platform:	GPL1261
Pubmed ID:	23986224
Summary & Design:	**Summary:** Low protein (LP) during gestation leads to low birth weight and poor fetal growth, with altered islet development and glucose intolerance in adulthood. Additionally, LP offspring fail to regenerate their ¸†-cells following depletion with streptozotocin (STZ), in contrast to control-fed offspring that are capable of ¸†-cell regeneration. Our objective was to identify genes and signalling pathways that may be critically altered in LP offspring rendering them susceptible to develop long term glucose intolerance and decreased ¸†-cell plasticity. **Overall design:** Pregnant Balb/C mice were place on a control (20% protein) or isocaloric low protein (8%) diet for the period of gestation, and then all dams were switch to the control diet at birth. Female offspring were injected with streptozotocin (35 mg/kg body weight; sodium citrate buffer 0.1 mol/L, pH 4.5) or vehicle (sham). Total RNA was extracted from pancreas of 30 day old female offspring (n=3) and hybridized to Affymetrix GeneChips.

Background corr dist: KL-Divergence = 0.0800, L1-Distance = 0.0381, L2-Distance = 0.0029, Normal std = 0.4716

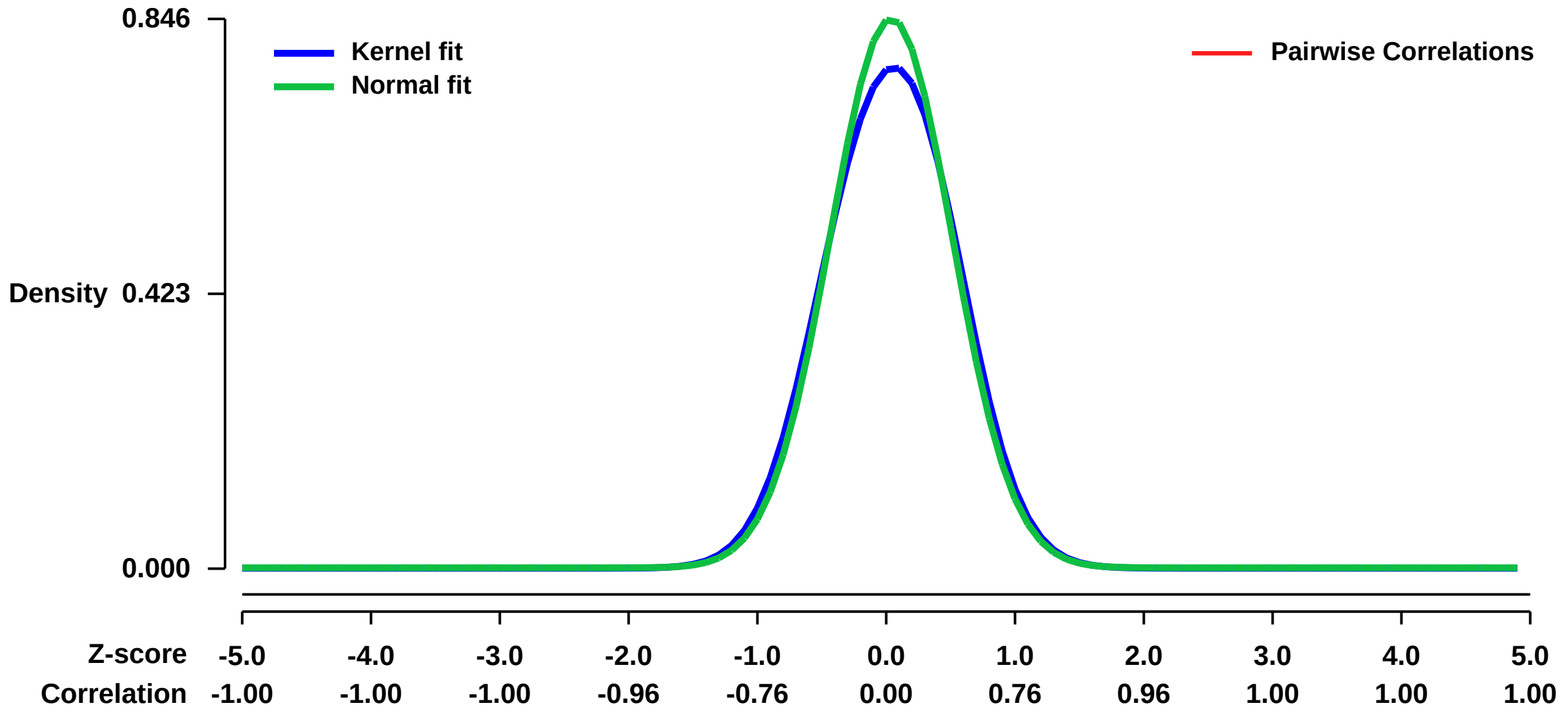

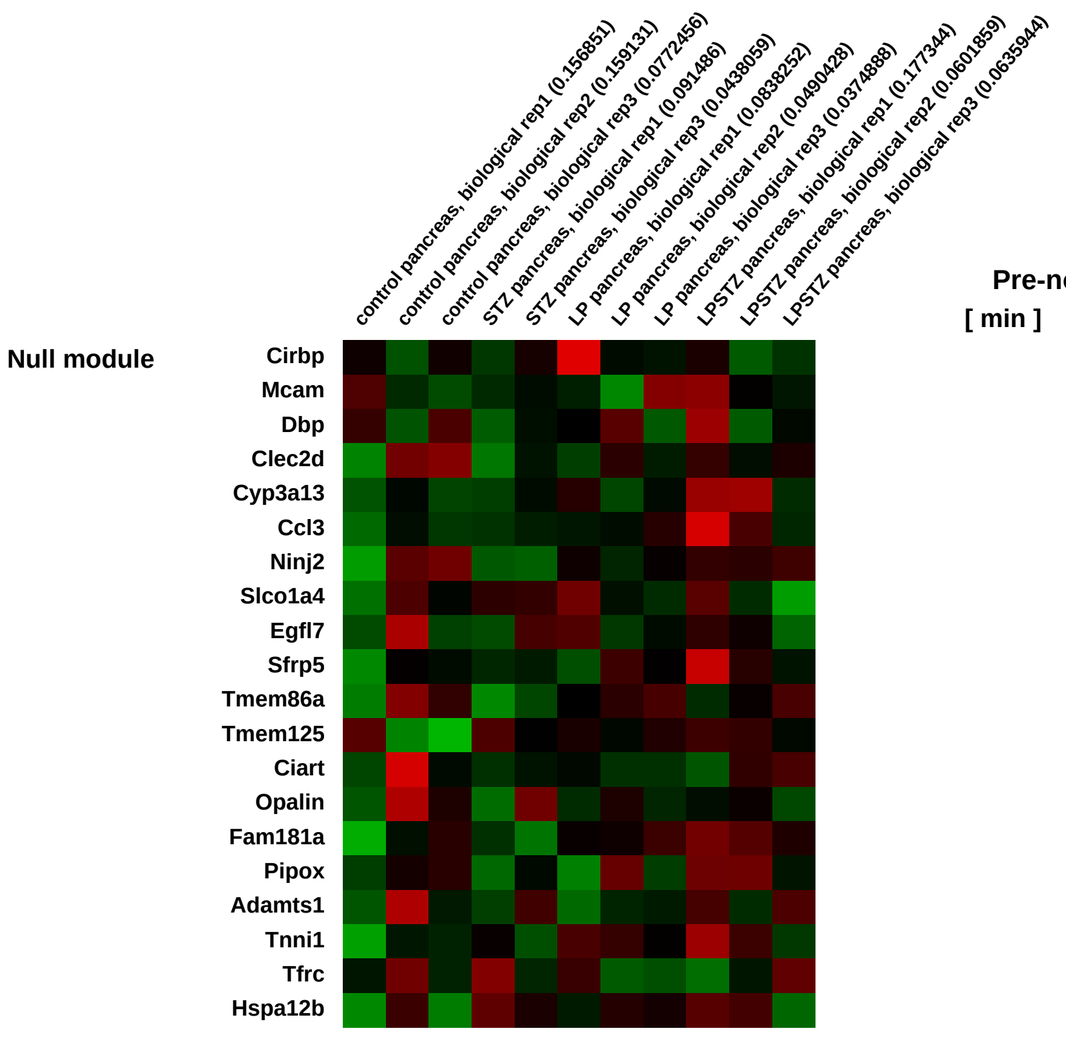

GEO Series "GSE13224" Expression Profiles

Num of samples in this series: 6

Scale of expression profile Z-scores

-3.0 -2.0 -1.0 0.0 1.0 2.0 3.0

GEO Link:	http://www.ncbi.nlm.nih.gov/geo/query/acc.cgi?acc=GSE13224
Status:	Public on Nov 30 2008
Title:	(AKR/J x FVB/NJ)F1 versus (DBA/2J x FVB)F1 lung expression data
Organism:	Mus musculus
Experiment type:	Expression profiling by array
Platform:	GPL1261
Pubmed ID:	19118016
Summary & Design:	**Summary:** F1 hybrids from (AKR/J x FVB/NJ) and (DBA/2J x FVB/NJ) outcrosses display a 20-fold difference in mammary tumor metastatic capacity, due to differences in inherited polymorphisms. Expression studies were performed to determine whether polymorphism-driven gene expression signatures predictive of outcome could be generated from normal tissues **Keywords: Basal transcription profiles** **Overall design:** Lung from adult F1 animals from (AKR/J x FVB/NJ) and (DBA/2J x FVB/NJ) outcrosses was collected and arrayed on Affymetrics chip to identify basal differences in gene expression between the different genotypes

Background corr dist: KL-Divergence = 0.0425, L1-Distance = 0.0175, L2-Distance = 0.0003, Normal std = 0.6020

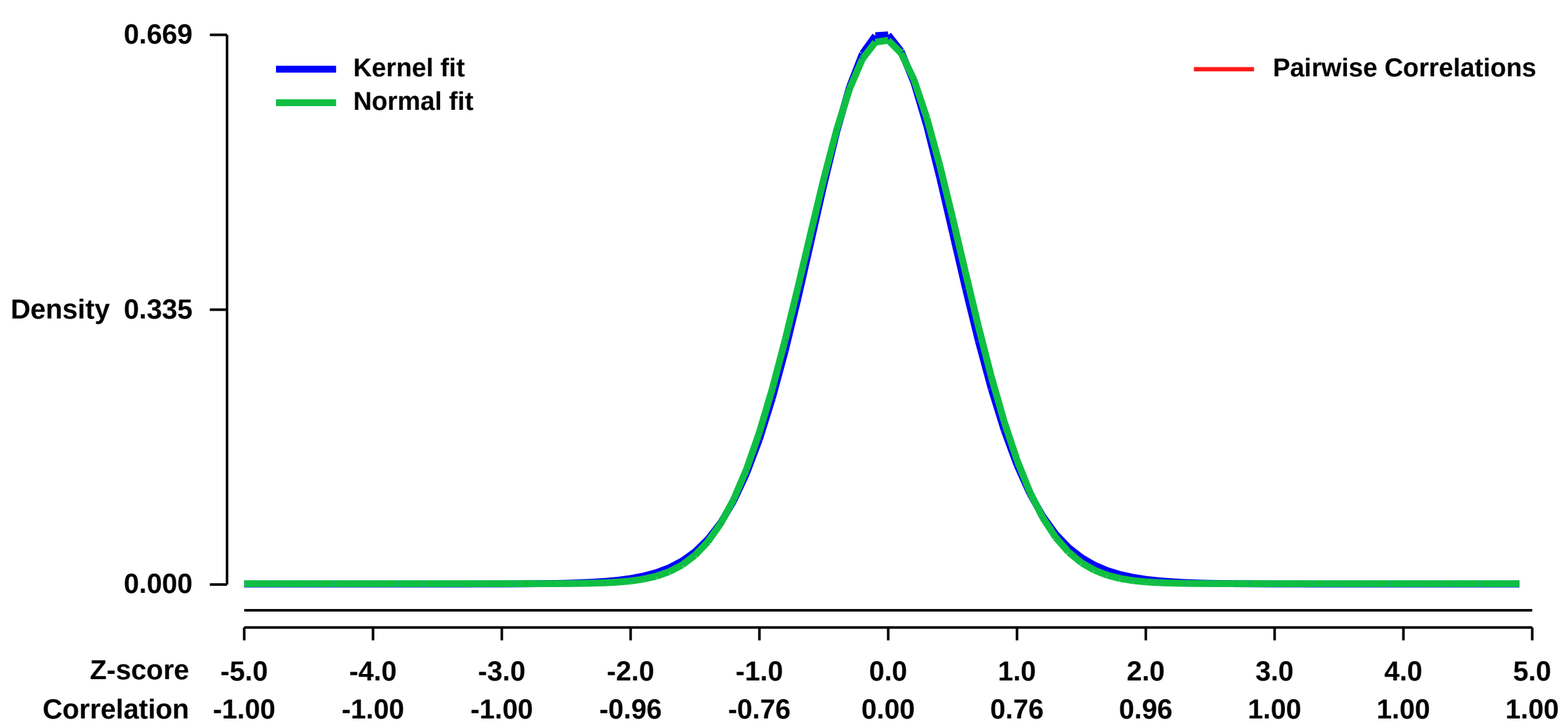

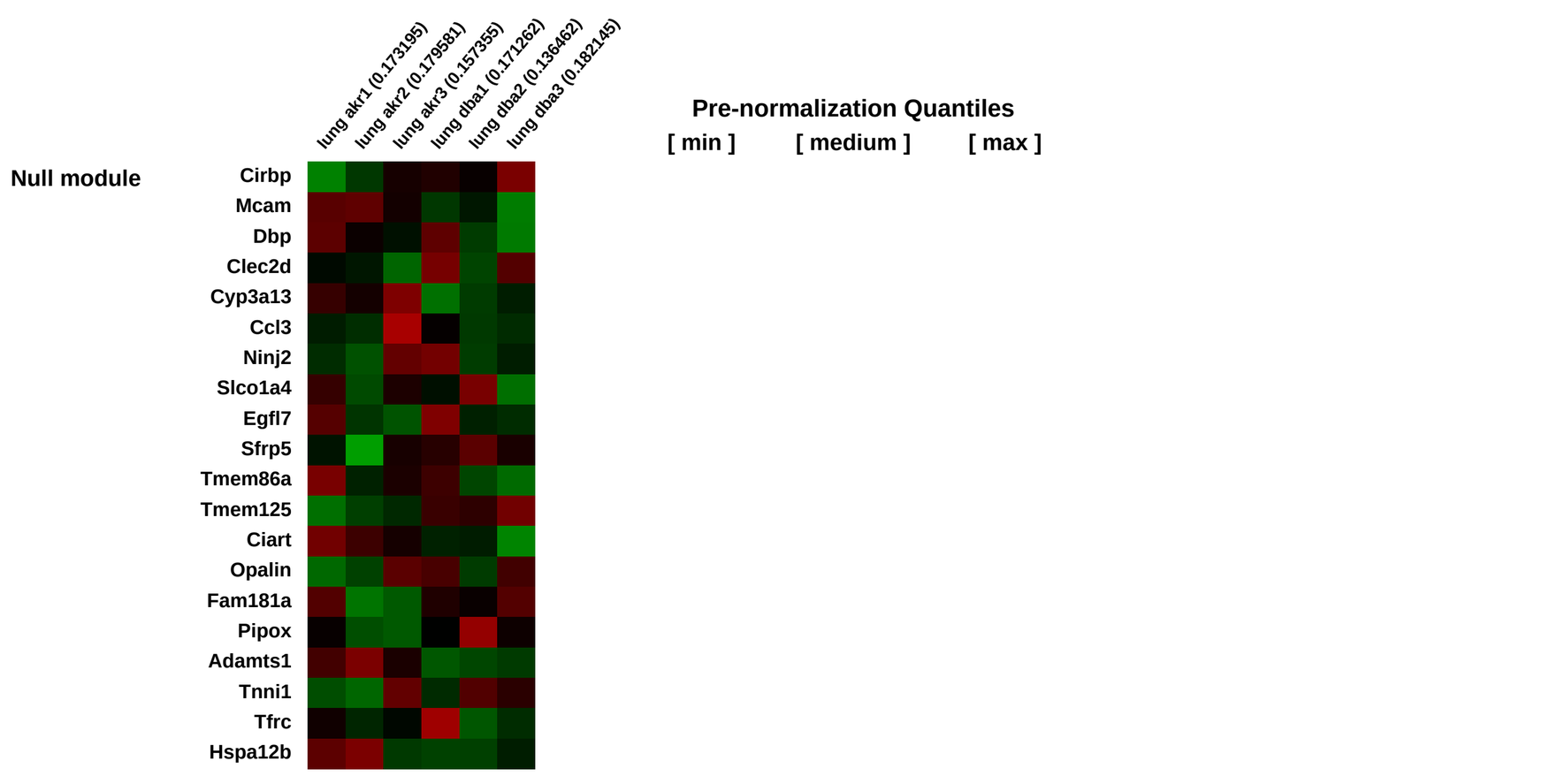

GEO Series "GSE4774" Expression Profiles

Num of samples in this series: 15

Scale of expression profile Z-scores

-3.0 -2.0 -1.0 0.0 1.0 2.0 3.0

GEO Link:	http://www.ncbi.nlm.nih.gov/geo/query/acc.cgi?acc=GSE4774
Status:	Public on Jun 06 2006
Title:	ruben-affy-mouse-187820
Organism:	Mus musculus
Experiment type:	Expression profiling by array
Platform:	GPL1261
Pubmed ID:	18697905
Summary & Design:	**Summary:** The Dlx homeobox genes have central roles in controlling patterning and differentiation of the brain and craniofacial primordia. In the brain, loss of Dlx function results in defects in the production, migration and differentiation of GABAergic neurons, that can lead to epilepsy. In the branchial arches, loss of Dlx function leads to craniofacial malformations that include trigeminal axon pathfinding defects. To determine how these genes function, we wish to identify the transcriptional circuitry that lies downstream of these transcription factors by comparing gene expression in wild type with Dlx mutant CNS and craniofacial tissues. 1) Compare gene expression in the maxillay branch of the first branchial arch (BA) of E10.5 wild type and Dlx2 -/- mutants. 2) Compare gene expression in the maxillary branch of the first BA of E10.5 wild type and Dlx1/2 -/- mutants. 3) Compare gene expression in wild type maxillary and mandibular branchial arches. 4) Compare gene expressionin mandibular branch of Dlx5/6 -/- mutants with wild type mandibular branch. The Dlx transcription factors are essential for controlling patterning of the brain and craniofacial primordia. In the brain, they control differentiation of GABAergic neurons of the basal ganglia. In the branchial arches, they control regional patterning. I hypothesize that there will be some conserved and some divergent mechanisms that the Dlx genes use in controlling brain and craniofacial development. We have already performed array analyses on Dlx function in the developing basal ganglia (with TGEN) by comparing expressed genes in wild type and Dlx1/2 mutants. Here we will compare gene expression in the brachial arches of wild type and Dlx mutant mice. 1) Generate E10.5 mouse embryos that are either wild type, Dlx2-/-, Dlx1/2 -/- or Dlx5/6 -/-. 2) Determine genotype by PCR. 3) Dissect branchial arches from the different genotypes. 4) Separate maxillary and mandibular branch of each branchial arch. 5) Prepare total RNA from the specimens. Obtain sufficient tissue to obtain 10 ug of total RNA - based on previous experience we anticipate that this will require ~ 10 branchial arches. We will pool the tissue from different embryos of the same genotype. 6) Send total RNA to TGEN for probe preparation, hybridization and array result analysis. **Keywords:** other **Overall design:**

Background corr dist: KL-Divergence = 0.2115, L1-Distance = 0.0476, L2-Distance = 0.0052, Normal std = 0.3241

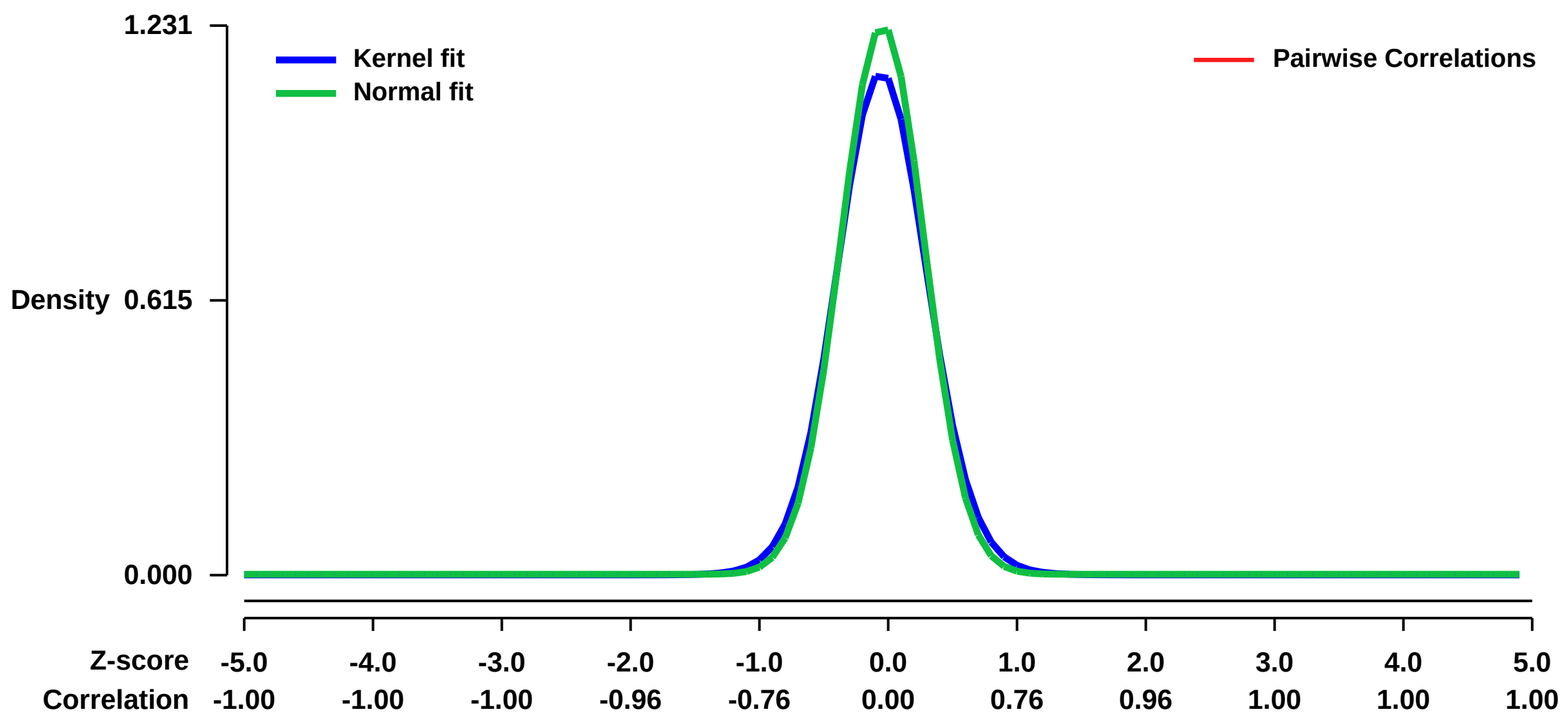

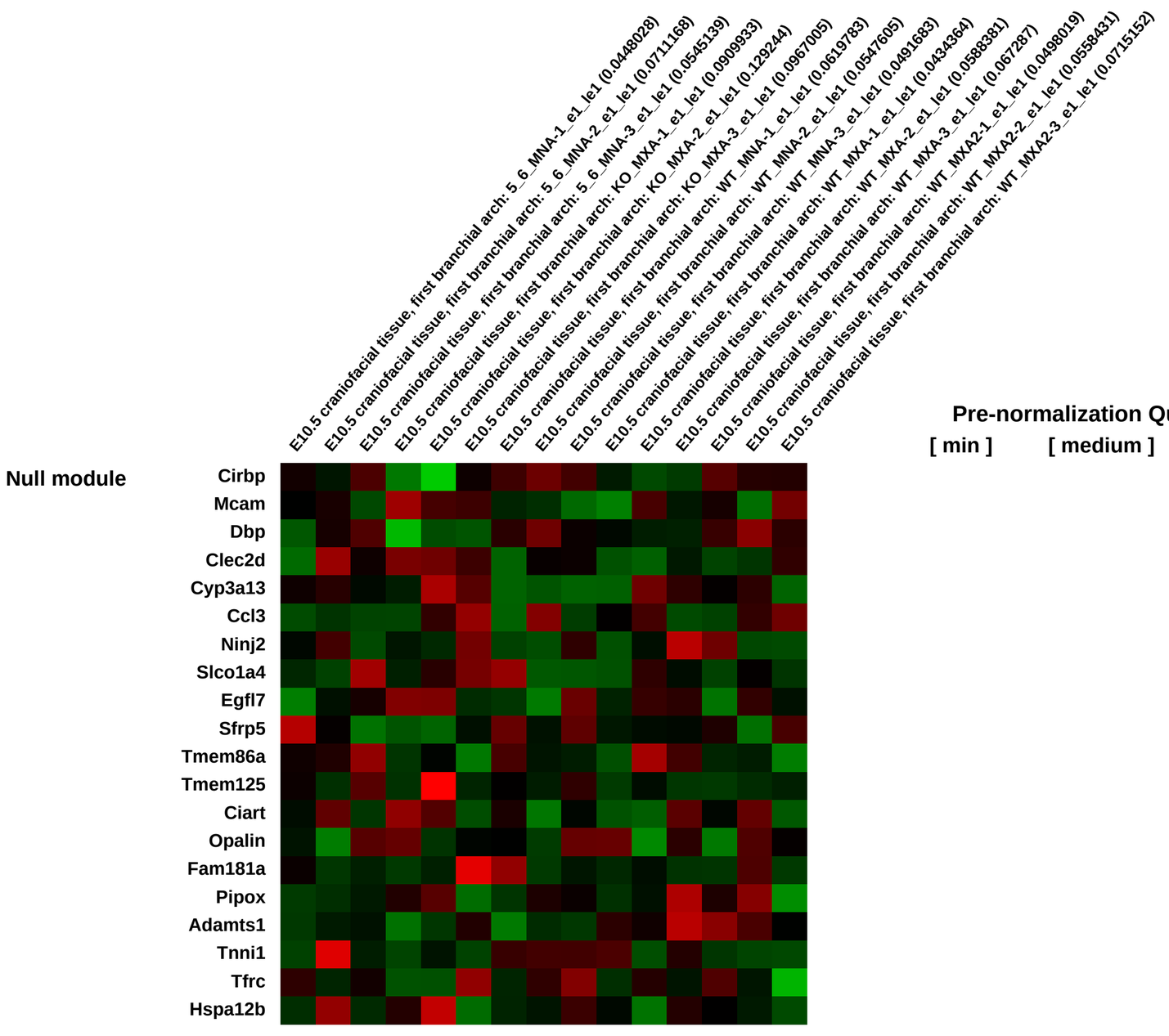

GEO Series "GSE13227" Expression Profiles

Num of samples in this series: 6

Scale of expression profile Z-scores

-3.0 -2.0 -1.0 0.0 1.0 2.0 3.0

GEO Link:	http://www.ncbi.nlm.nih.gov/geo/query/acc.cgi?acc=GSE13227
Status:	Public on Nov 30 2008
Title:	(AKR/J x FVB/NJ)F1 versus (DBA/2J x FVB)F1 Thymus expression data
Organism:	Mus musculus
Experiment type:	Expression profiling by array
Platform:	GPL1261
Pubmed ID:	19118016
Summary & Design:	**Summary:** F1 hybrids from (AKR/J x FVB/NJ) and (DBA/2J x FVB/NJ) outcrosses display a 20-fold difference in mammary tumor metastatic capacity, due to differences in inherited polymorphisms. Expression studies were performed to determine whether polymorphism-driven gene expression signatures predictive of outcome could be generated from normal tissues **Keywords: Basal transcription profiles** **Overall design:** Thymus from adult F1 animals from (AKR/J x FVB/NJ) and (DBA/2J x FVB/NJ) outcrosses was collected and arrayed on Affymetrics chip to identify basal differences in gene expression between the different genotypes

Background corr dist: KL-Divergence = 0.0229, L1-Distance = 0.0141, L2-Distance = 0.0002, Normal std = 0.7131

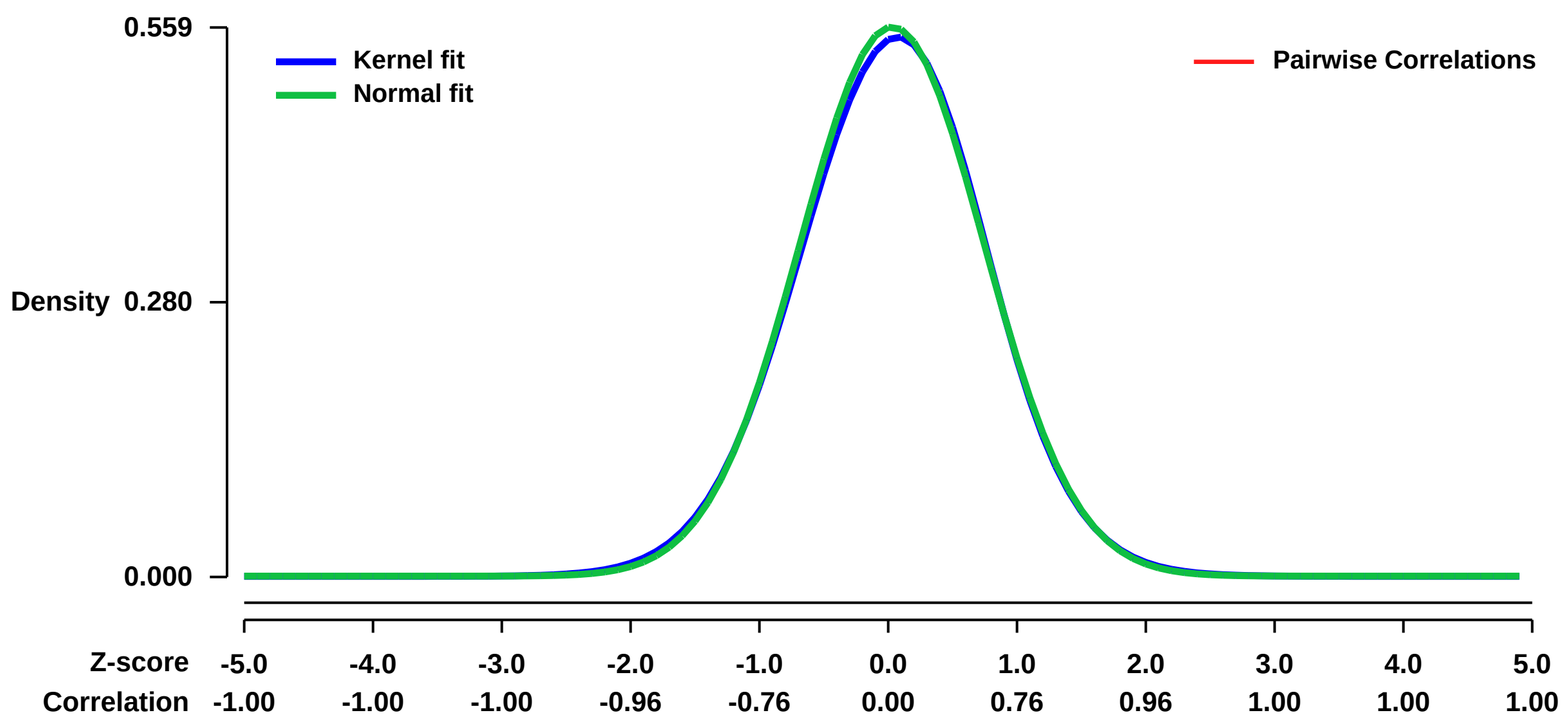

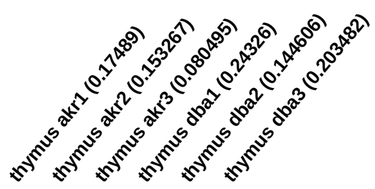

Pre-normalization Quantiles

[min] [medium] [max]

Null module

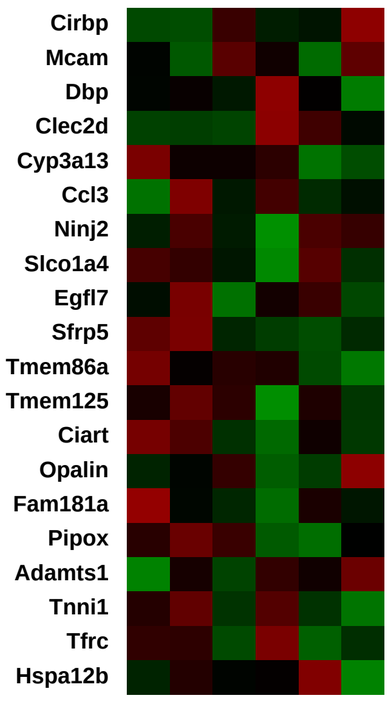

GEO Series "GSE27395" Expression Profiles

Num of samples in this series: 12

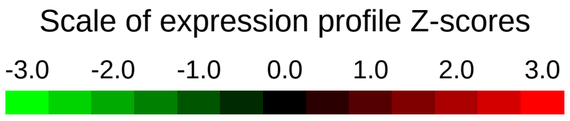

GEO Link:	**http://www.ncbi.nlm.nih.gov/geo/query/acc.cgi?acc=GSE27395**
Status:	**Public on Sep 15 2011**
Title:	**Analysis of Gsk-3-Deficient Embryonic Stem Cells Reveals Large-Scale Alterations in Gene Expression**
Organism:	**Mus musculus**
Experiment type:	**Expression profiling by array**
Platform:	**GPL1261**
Pubmed ID:	
Summary & Design:	**Summary:** **The two vertebrate Gsk-3 isoforms, Gsk-3a and Gsk-3b, are encoded by distinct genetic loci and exhibit mostly redundant function in murine embryonic stem cells (ESCs). Here we report that deletion of both Gsk-3a and Gsk-3b in mouse ESCs results in significant changes in gene expression. In contrast, deletion of either Gsk-3a or Gsk-3b individually had little effect on gene expression. These data support the notion that Gsk-3 isoforms are functionally redundant in embryonic stem cells. In addition, we did not find the expected upregulation of known Wnt target genes. Our data suggests that Gsk-3-meidated regulation of gene expression in embryonic stem cells is complex, and likely involves affects on numerous signaling pathways.** **Overall design:** **The study was designed to examine the changes in gene expression between wild-type, Gsk-3a-/-, Gsk-3b-/-, and Gsk-3a-/-;Gsk-3b-/- mouse embryonic stem cells.**

Background corr dist: **KL-Divergence = 0.1042, L1-Distance = 0.0230, L2-Distance = 0.0009, Normal std = 0.4460**

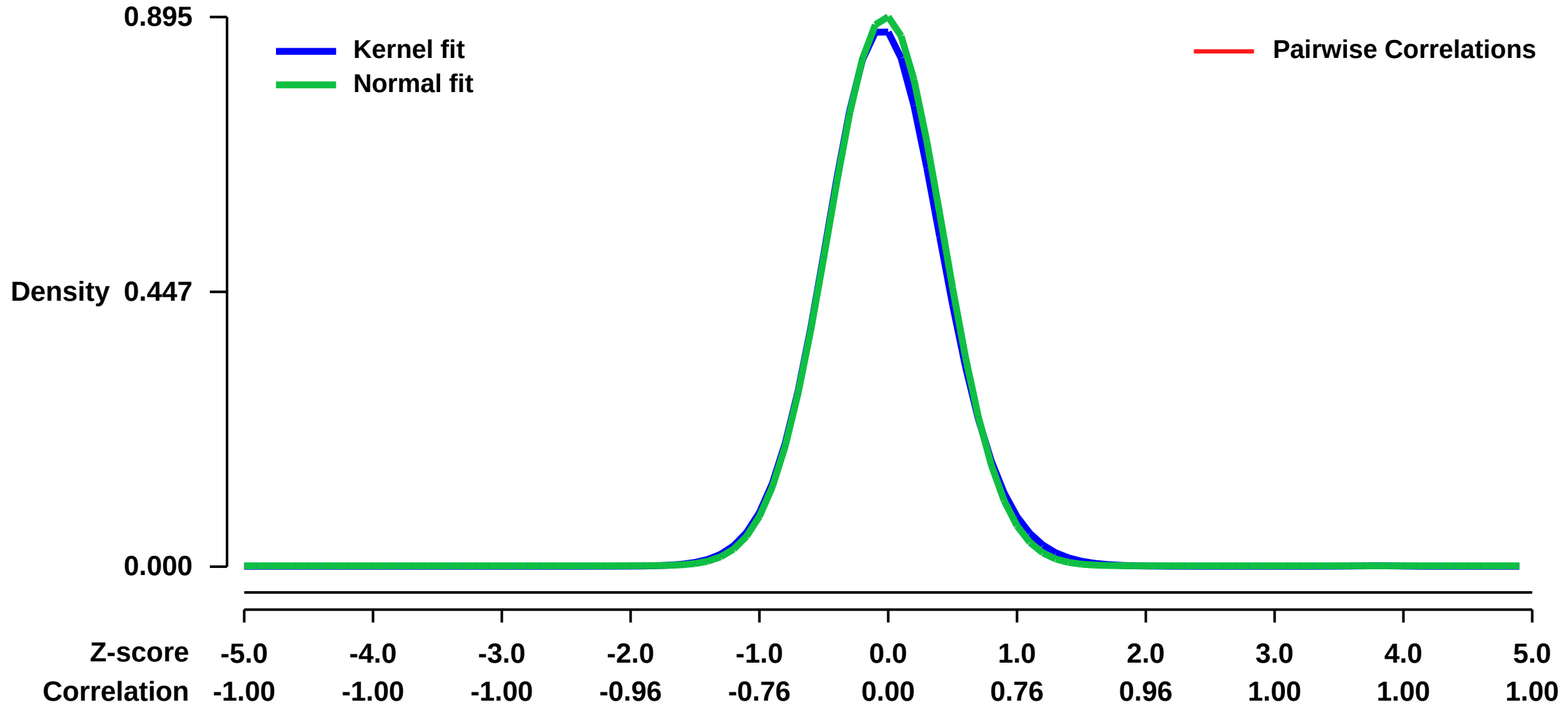

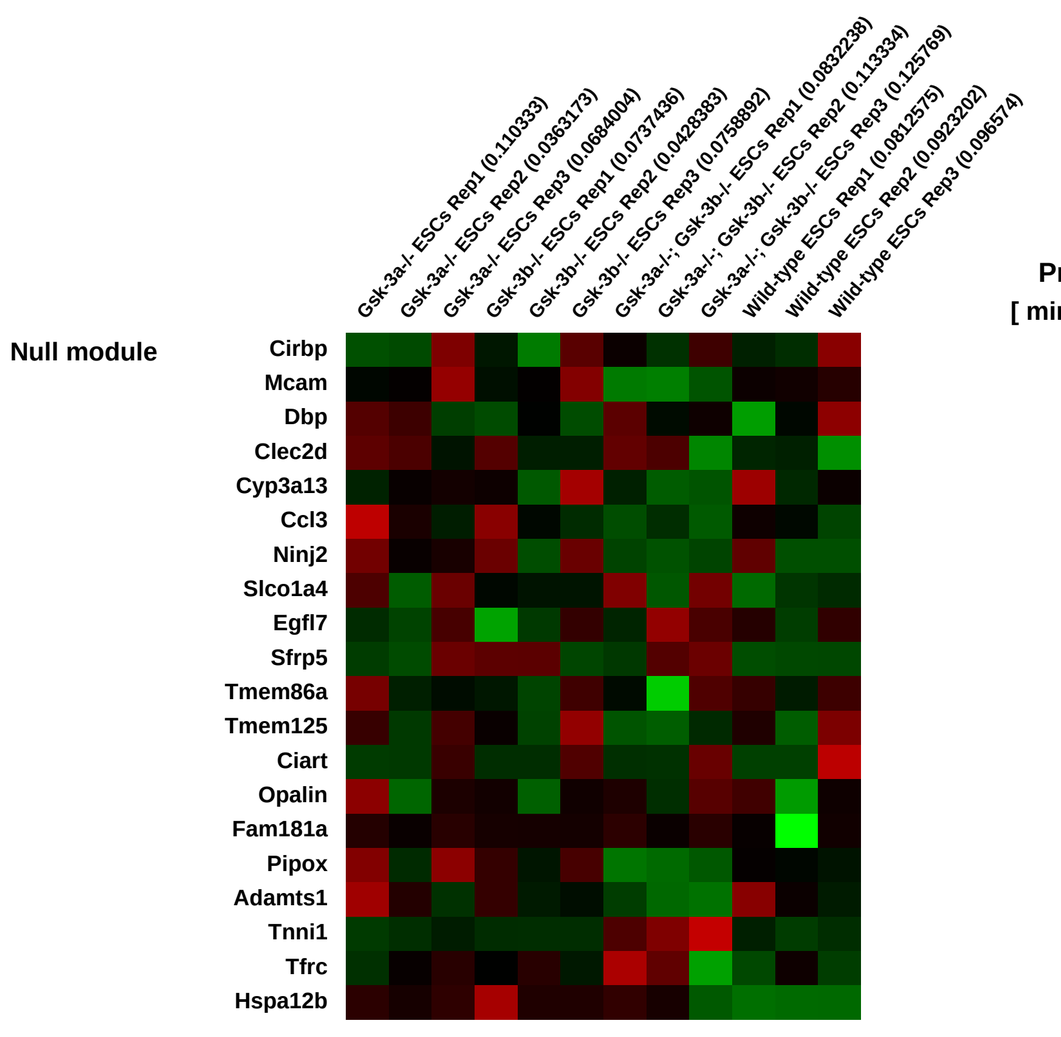

GEO Series "GSE17112" Expression Profiles

Num of samples in this series: 8

Scale of expression profile Z-scores

-3.0 -2.0 -1.0 0.0 1.0 2.0 3.0

GEO Link:	http://www.ncbi.nlm.nih.gov/geo/query/acc.cgi?acc=GSE17112
Status:	Public on Mar 31 2010
Title:	Visualization of cancer initiating cell in the vascular niche utilized with transcriptional activity of PSF1
Organism:	Mus musculus
Experiment type:	Expression profiling by array
Platform:	GPL1261
Pubmed ID:	20103637
Summary & Design:	**Summary:** Identification of cancer stem/initiating cells (CSCs/CICs) by a specific marker is useful for diagnosis and therapy of cancer. We have determined that PSF1 which plays a role in DNA replication in lower species is strongly expressed in wide range of normal stem cell population. Here, utilizing the transcriptional activity of PSF1 promoter in tumor cell xenograft model, we show that PSF1high cancer cells display malignant features including high proliferating activity, serial transplantation potential, and metastatic ability those are used for criteria of CSCs/CICs. PSF1high cancer cells localize in perivascular region and genetically display ES cell like signature. Silencing of PSF1 by RNAi inhibited growth of cancer cells mediated by disruption of DNA synthesis and chromosomal segregation. These suggested that PSF1 is a possible maker and a molecular target of CSCs/CICs. **Overall design:** We have cloned the mouse PSF1 promoter gene and established lung carcinoma (lewis lung carcinoma: LLC) and colon cancer (colon26) cell lines stably expressing enhanced green fluorescent protein (EGFP) under the transcriptional control of PSF1 promoter (LLC- and colon-PSF1P-EGFP, respectively). Mouse xenograft tumor cells were dissociated and sorted into PSF1 low and high expression cells by FACS. We sought whether PSF1 high expression cells possess embryonic stem cells-like signature.

Background corr dist: KL-Divergence = 0.0243, L1-Distance = 0.0419, L2-Distance = 0.0026, Normal std = 0.7181

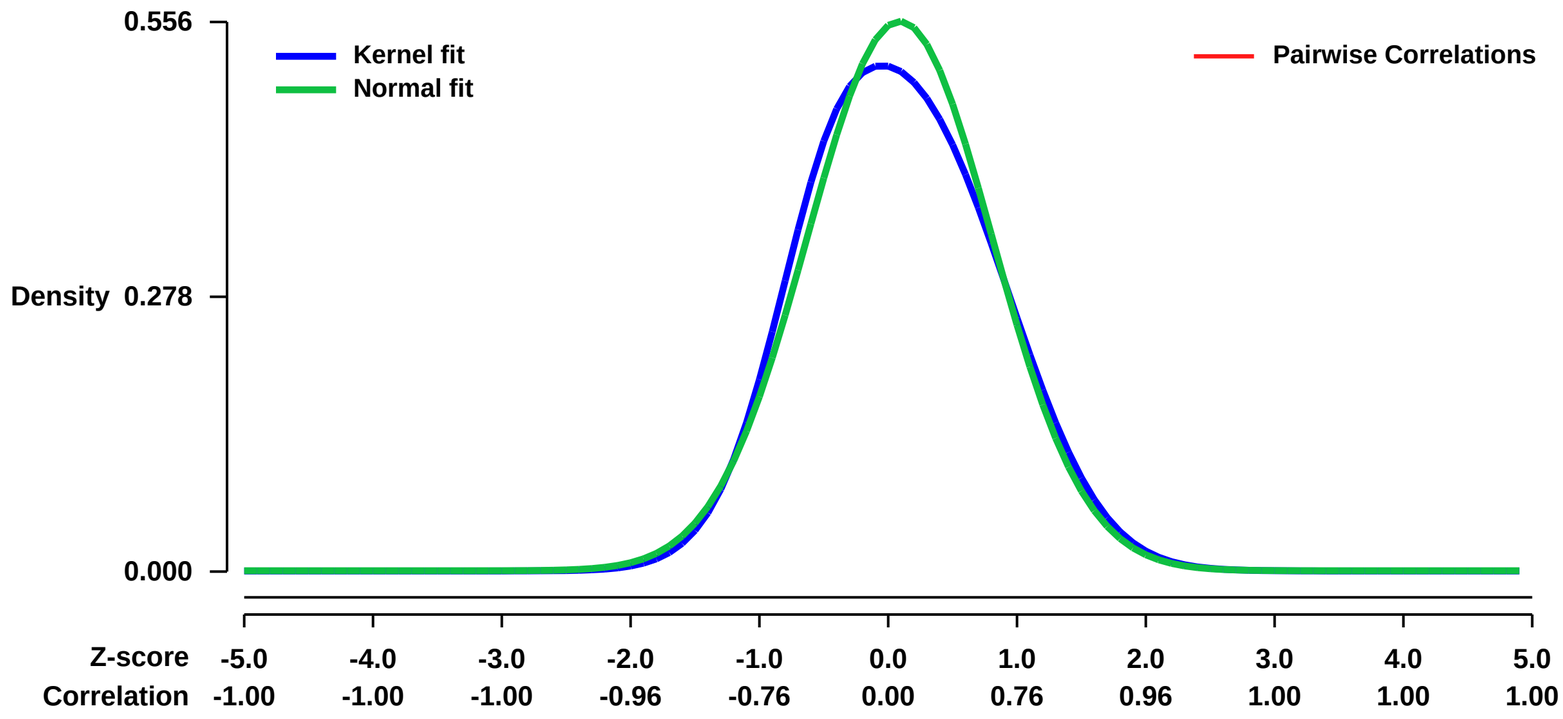

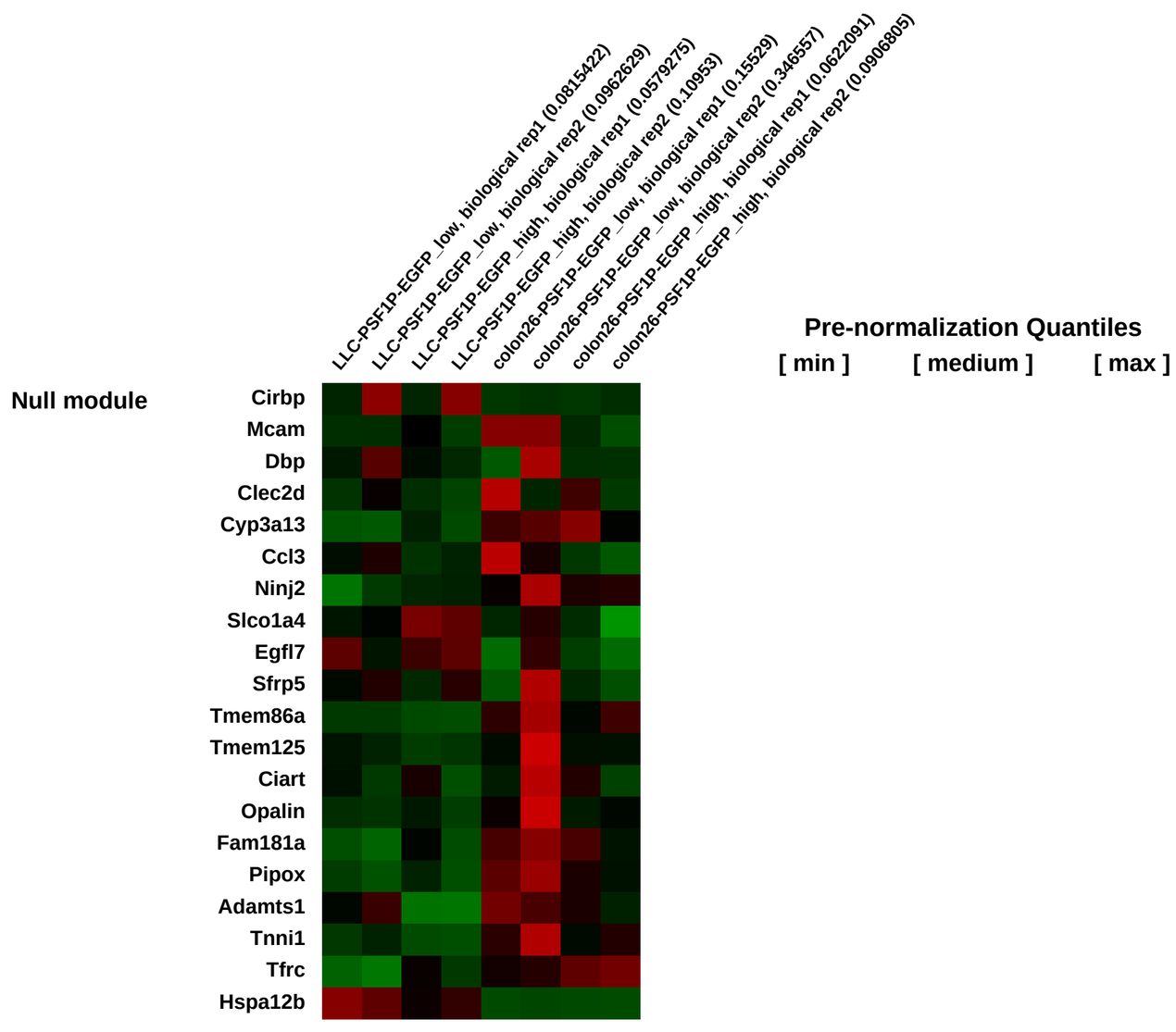

GEO Series "GSE59202" Expression Profiles

Num of samples in this series: 8

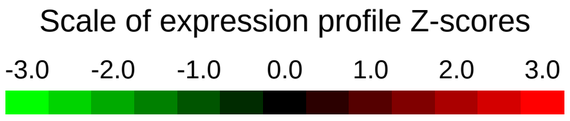

GEO Link:	**http://www.ncbi.nlm.nih.gov/geo/query/acc.cgi?acc=GSE59202**
Status:	**Public on Jul 09 2014**
Title:	**Fluorochrome-based definition of naturally occurring Foxp3+ regulatory T cells of intra- and extrathymic origin**
Organism:	**Mus musculus**
Experiment type:	**Expression profiling by array**
Platform:	**GPL1261**
Pubmed ID:	
Summary & Design:	**Summary:** **Here, we report on experiments in double-transgenic mice, in which RFP is expressed in all Foxp3+ Treg cells, whereas Foxp3-dependent GFP expression is exclusively confined to intrathymically induced Foxp3+ Treg cells. This novel molecular genetic tool enabled us to faithfully track and characterize naturally induced Treg cells of intrathymic (RFP+GFP+) and extrathymic (RFP+GFPâ) origin in otherwise unmanipulated mice.** **These experiments directly demonstrate that extrathymically induced Treg cells substantially contribute to the overall pool of mature Foxp3+ Treg cells residing in peripheral lymphoid tissues of steady-state mice. Furthermore, we provide evidence that intra- and extrathymically induced Foxp3+ Treg cells represent distinct phenotypic and functional sublineages.** **Overall design:** **CD4+CD25+ RFP+GFP- and CD4+CD25+ RFP+GFP+ T cells from pooled lymph nodes and pooled spleens of 20 mice were FACS sorted for RNA extraction and hybridization on Affymetrix microarrays in duplicates.**

Background corr dist: **KL-Divergence = 0.0598, L1-Distance = 0.0245, L2-Distance = 0.0007, Normal std = 0.5412**

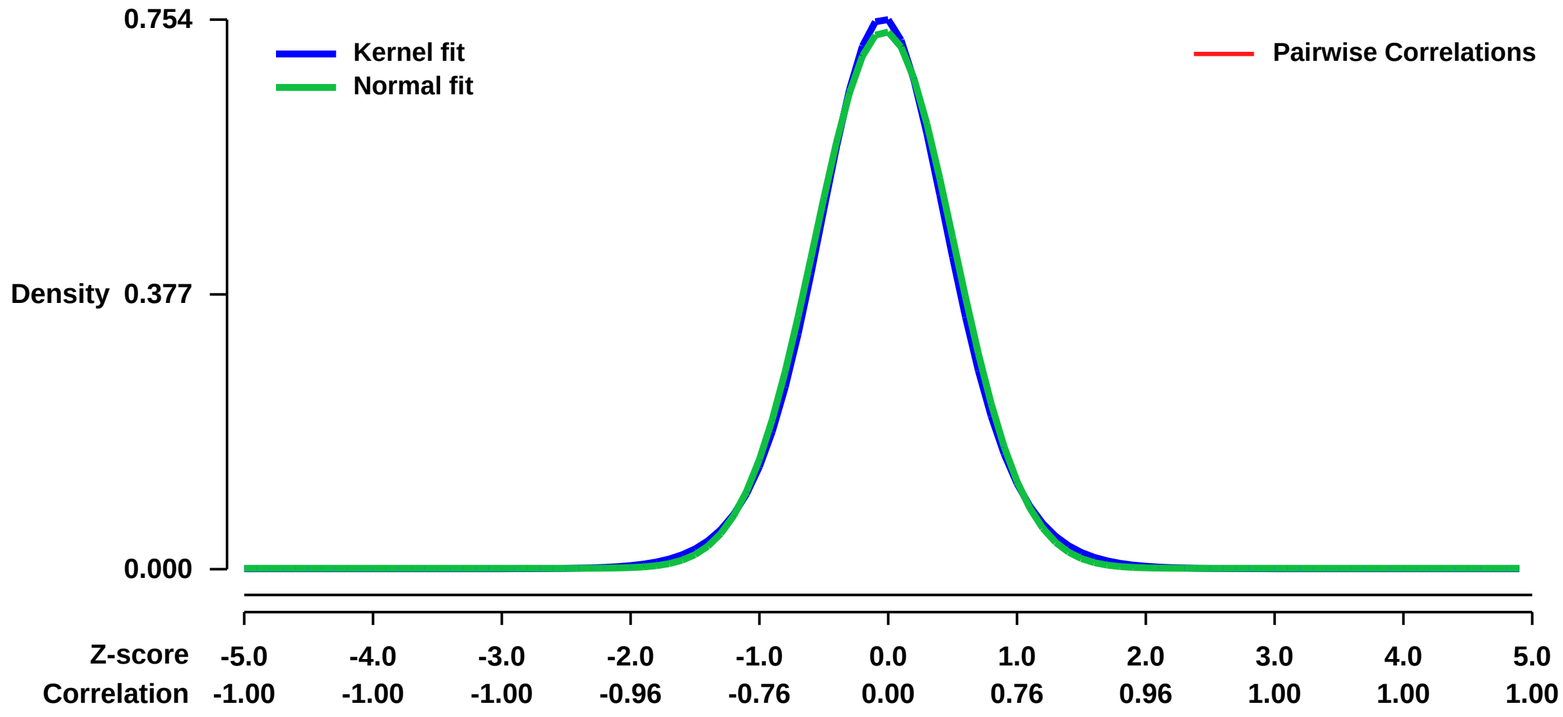

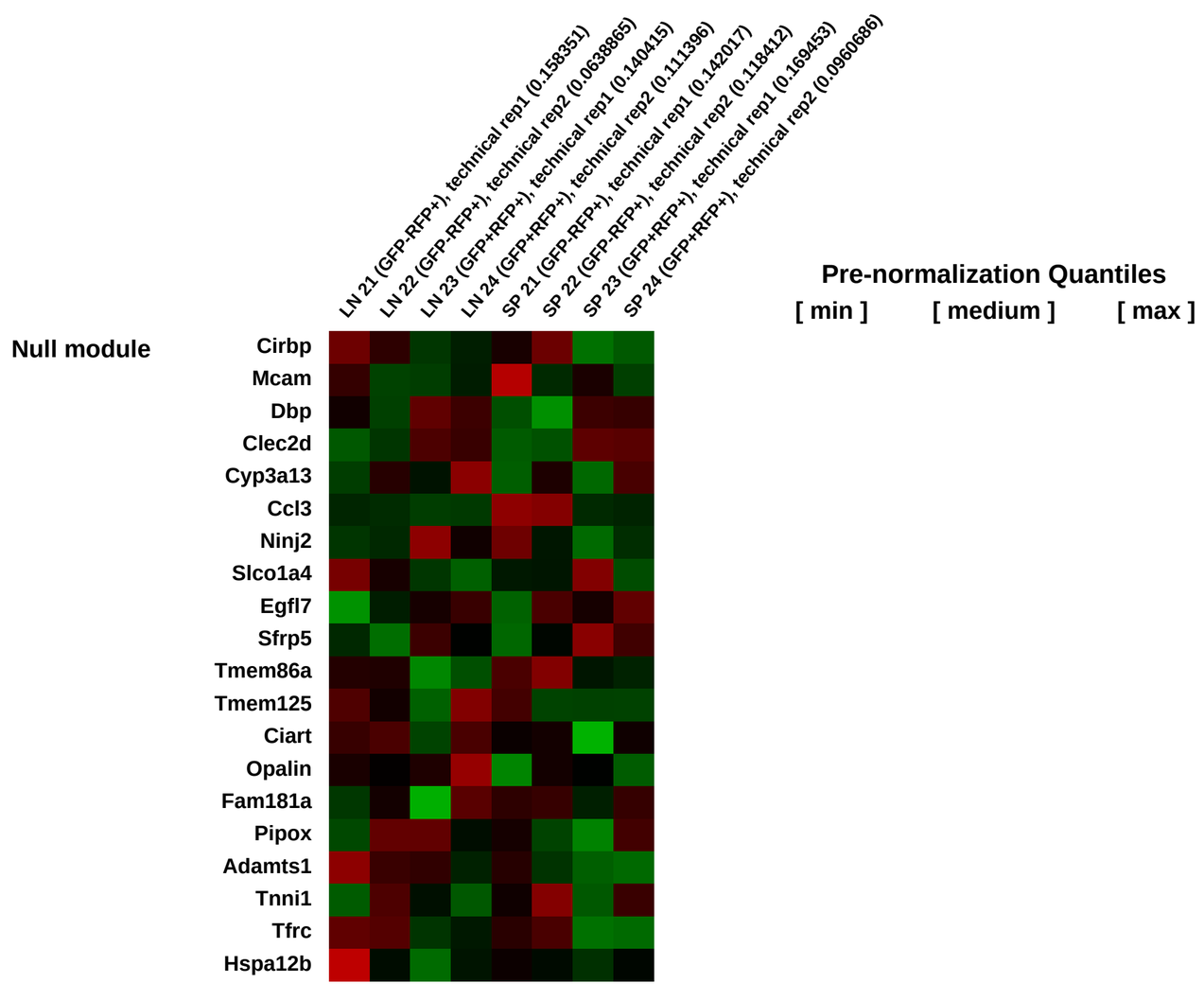

GEO Series "GSE31598" Expression Profiles

Num of samples in this series: 12

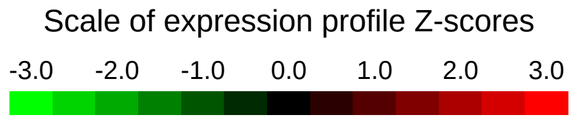

GEO Link:	http://www.ncbi.nlm.nih.gov/geo/query/acc.cgi?acc=GSE31598
Status:	Public on Apr 01 2012
Title:	Expression data from directly induced neural stem cells
Organism:	Mus musculus
Experiment type:	Expression profiling by array
Platform:	GPL1261
Pubmed ID:	22467474
Summary & Design:	**Summary:** Induced pluripotent stem (iPS) cells give rise to neural stem cells, which are applicable for therapeutic transplantation in treatment of neural diseases. However, generation of neural stem cells from iPS cells requires a careful selection of safe iPS clones. We sought to determine whether direct induction of neural stem cells from partially reprogrammed somatic cells is able to generate safer cells rapidly. We have successfully established direct induction system from fibroblast to neural stem cells. To characterize these directly induced neural stem cells, Gene expression profiles were compared with iPS cell or ES cell-derived neurosphere. We used affymetrix microarrays to compare the global gene expression of neurospheres prepared several method. **Overall design:** The mouse strain used in this study except ES/iPS cells was C57BL/6.

Background corr dist: KL-Divergence = 0.1105, L1-Distance = 0.0565, L2-Distance = 0.0068, Normal std = 0.4455

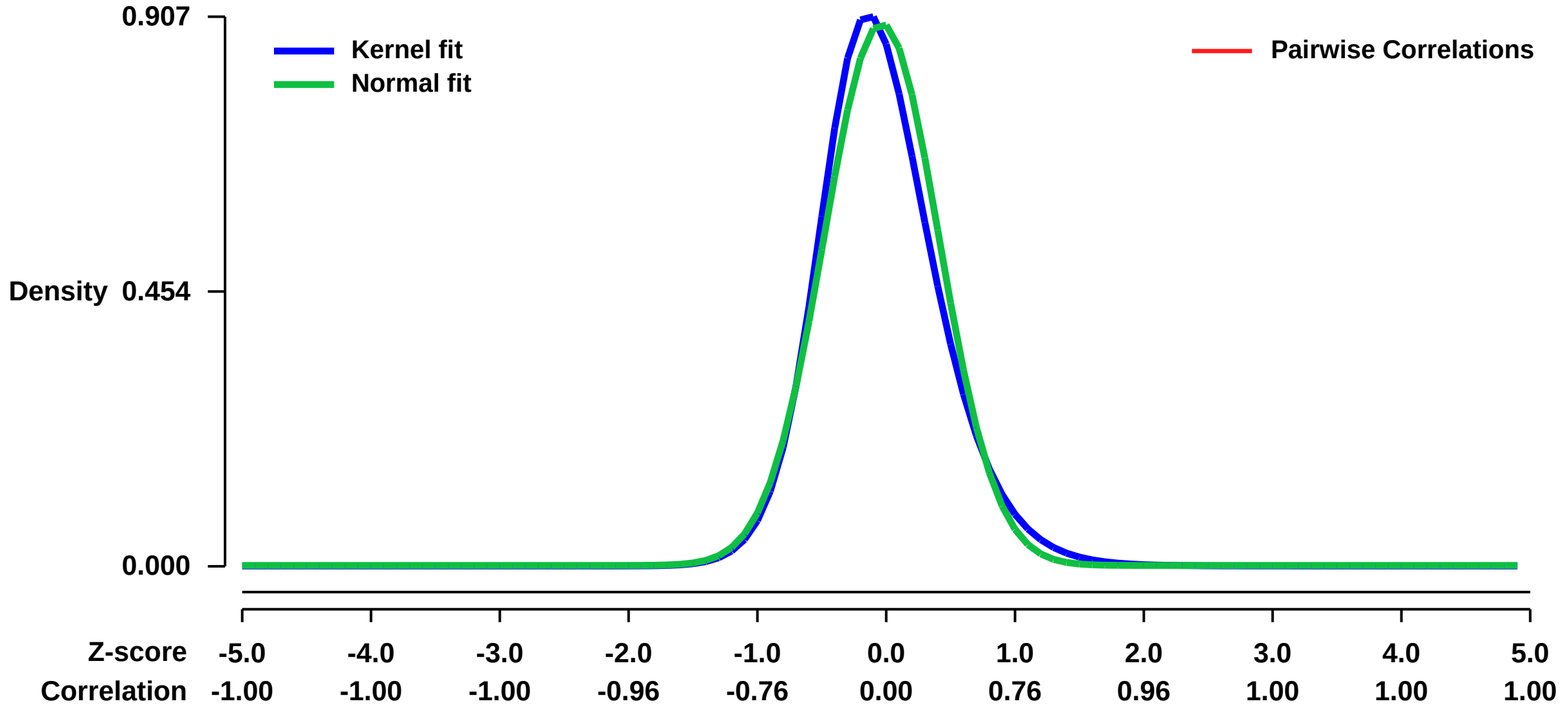

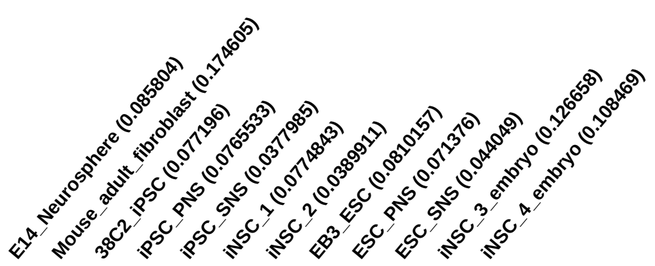

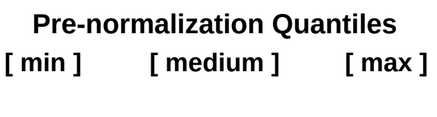

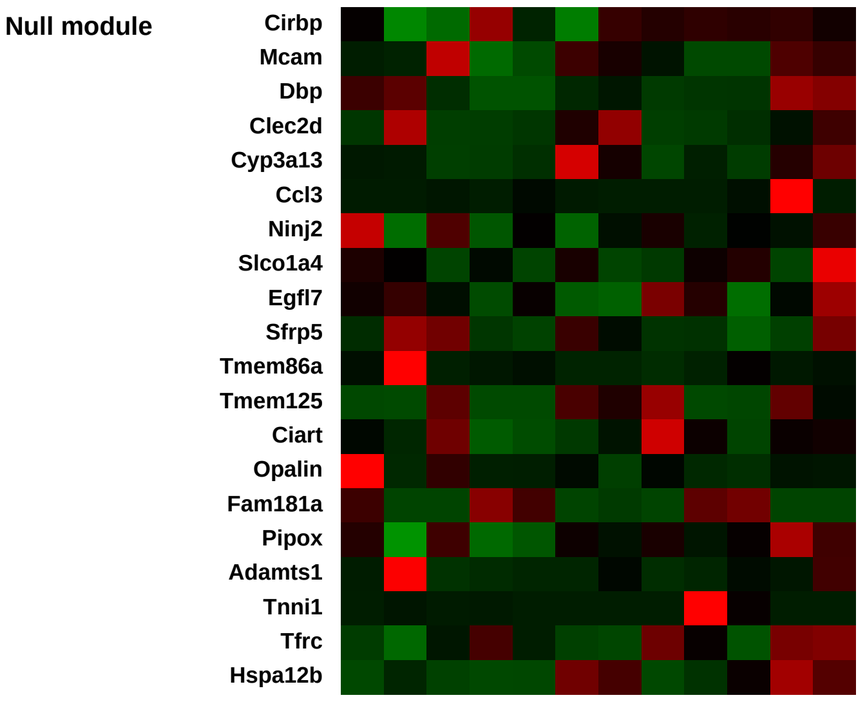

GEO Series "GSE48935" Expression Profiles

Num of samples in this series: 12

Scale of expression profile Z-scores

-3.0 -2.0 -1.0 0.0 1.0 2.0 3.0

GEO Link:	http://www.ncbi.nlm.nih.gov/geo/query/acc.cgi?acc=GSE48935
Status:	Public on Sep 04 2013
Title:	Analysis of gene expression changes induced in wild-type or Atf6a-/- mice by treatment with tunicamycin for 34h
Organism:	Mus musculus
Experiment type:	Expression profiling by array
Platform:	GPL1261
Pubmed ID:	24069029
Summary & Design:	**Summary:** Protein misfolding stress in the endoplasmic reticulum (ER) leads to dysregulation of lipid metabolism in the liver, and ER stress is associated with human diseases that are accompanied by hepatic lipid accumulation, including obesity, alcoholism, and viral hepatitis; yet the pathways leading from ER stress to the regulation of lipid metabolism are poorly understood. Working exclusively in vivo, we used a â bottom-upâ approach to infer pathways in the genetic regulation of lipid metabolism by the UPR. We used a functional genomics to link gene expression patterns taken from microarray data to the severity and persistence of ER stress, using mice lacking the UPR signaling molecule ATF6¸–. This approach revealed that functionally related genes clustered into a small number of distinct expression profiles, and that lipid oxidation and efflux were targets for coordinated transcriptional suppression during ER stress.Our results establish a framework for hepatic gene regulation during ER stress. **Overall design:** Atf6a-/- or +/+ mice of variable age and gender were injected intraperitoneally with 1 mg/kg tunicamycin or vehicle. 3 separate mice were used in each group. 34h after injection, mice were sacrificed and total RNA was prepared from resected livers.

Background corr dist: KL-Divergence = 0.0722, L1-Distance = 0.0377, L2-Distance = 0.0019, Normal std = 0.5191

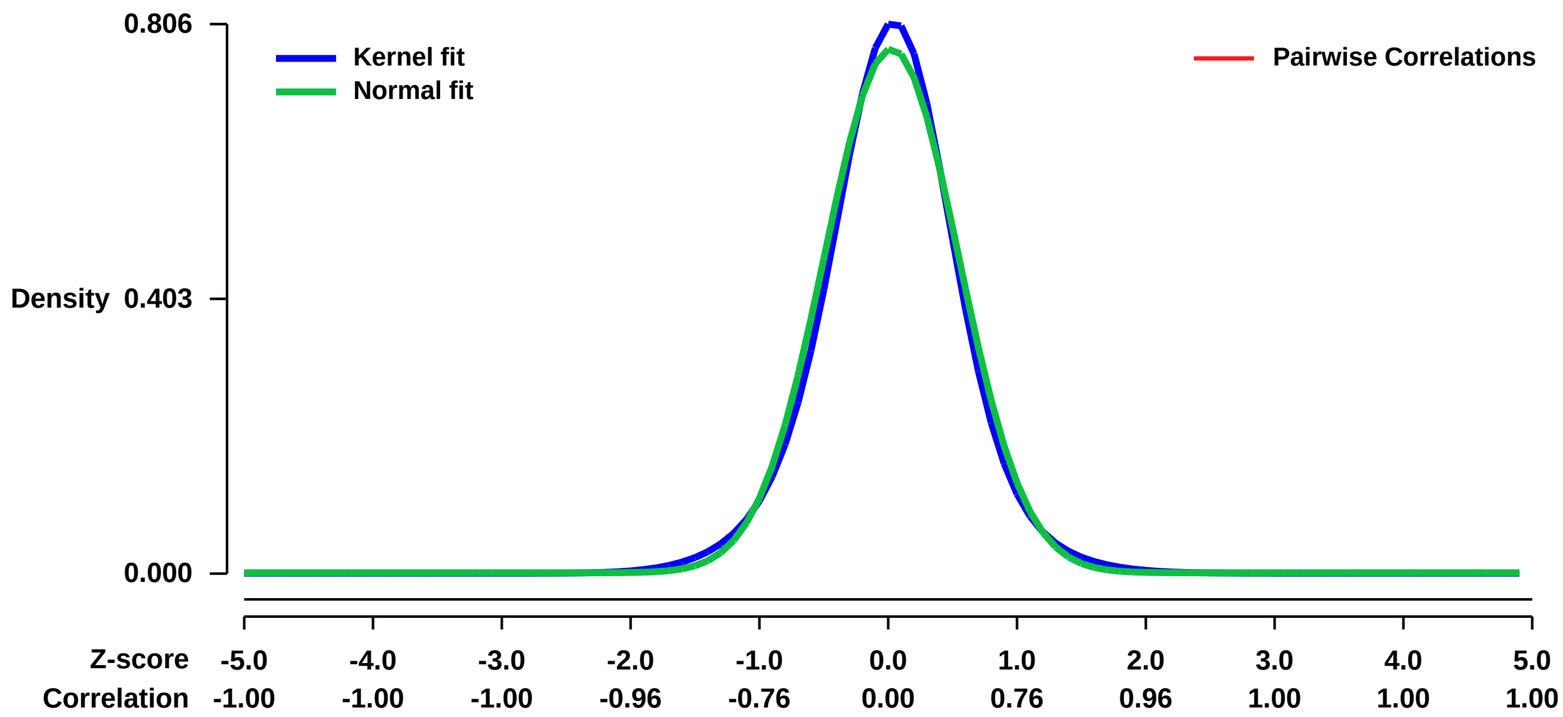

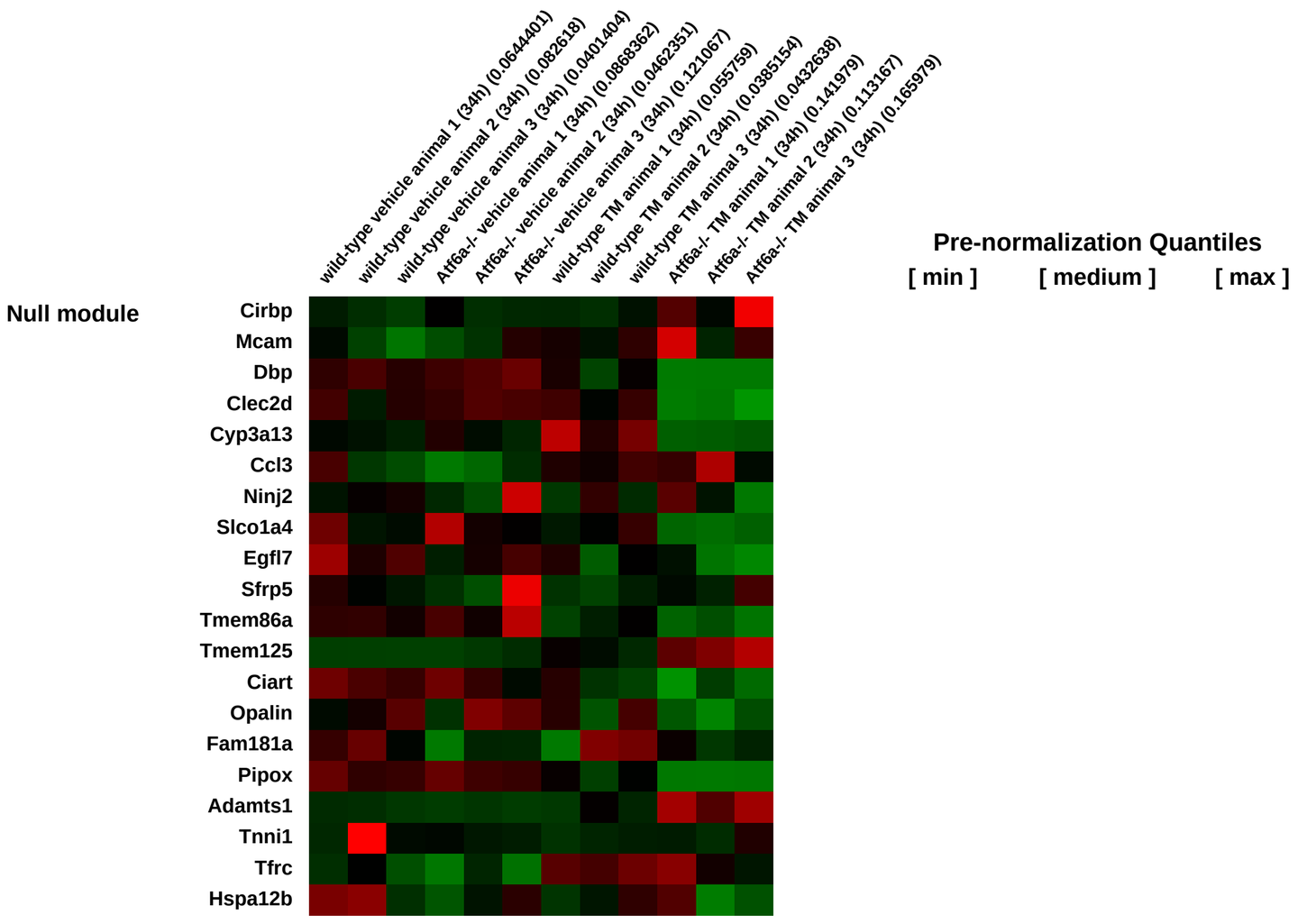

GEO Series "GSE17765" Expression Profiles

Num of samples in this series: 24

Scale of expression profile Z-scores

-3.0 -2.0 -1.0 0.0 1.0 2.0 3.0

GEO Link:	http://www.ncbi.nlm.nih.gov/geo/query/acc.cgi?acc=GSE17765
Status:	Public on Oct 06 2009
Title:	DNA hypomethylation leads to derepression of myeloerythroid genes in hematopoietic stem cells (HSC)
Organism:	Mus musculus
Experiment type:	Expression profiling by array
Platform:	GPL1261
Pubmed ID:	19801979
Summary & Design:	**Summary:** Analysis of hematopoietic stem cells (HSC, LSK Flt3-) and myeloid progenitors (MP, LK CD34+) sorted from wildtype and Dnmt1 hypomorph mice **Overall design:** We FACS sorted HSCs and MPs from bone marrow of 8-12 week old wildtype or Dnmt1 hypomorph (Dnmt1-/chip) mice.

Background corr dist: KL-Divergence = 0.1022, L1-Distance = 0.0336, L2-Distance = 0.0022, Normal std = 0.4334

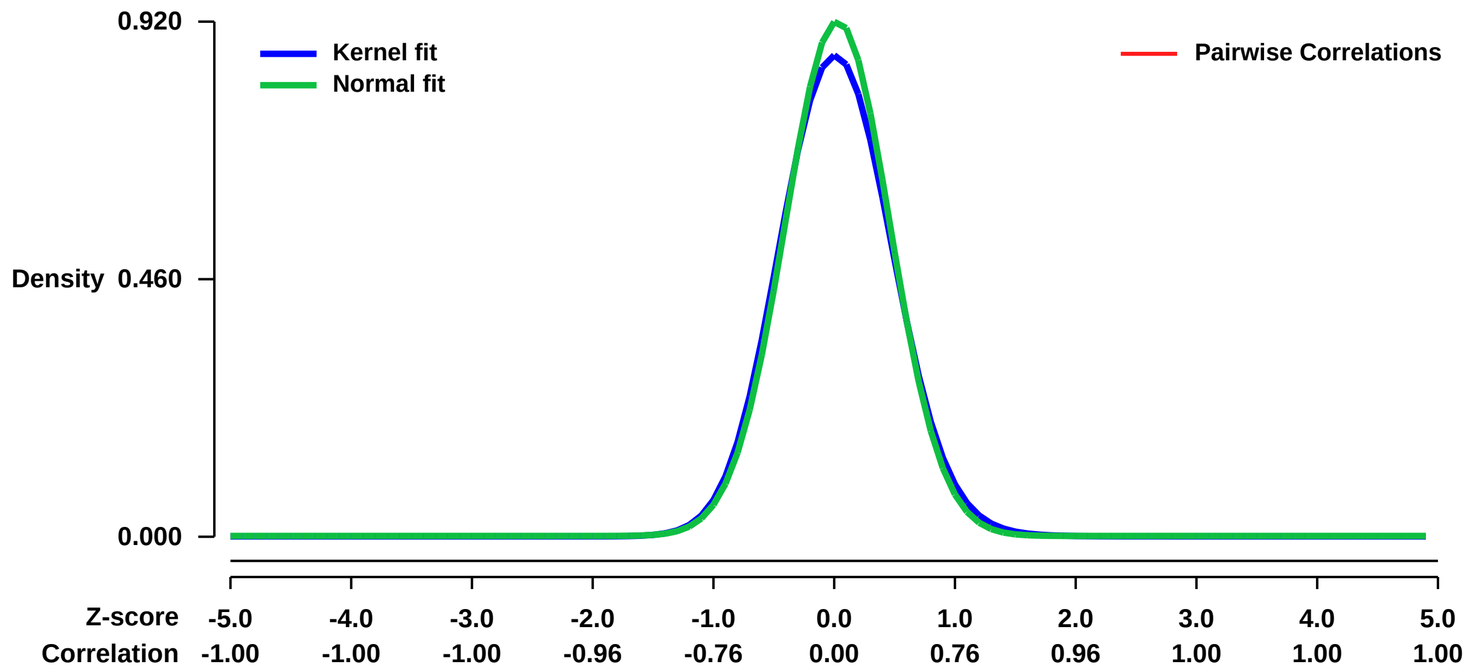

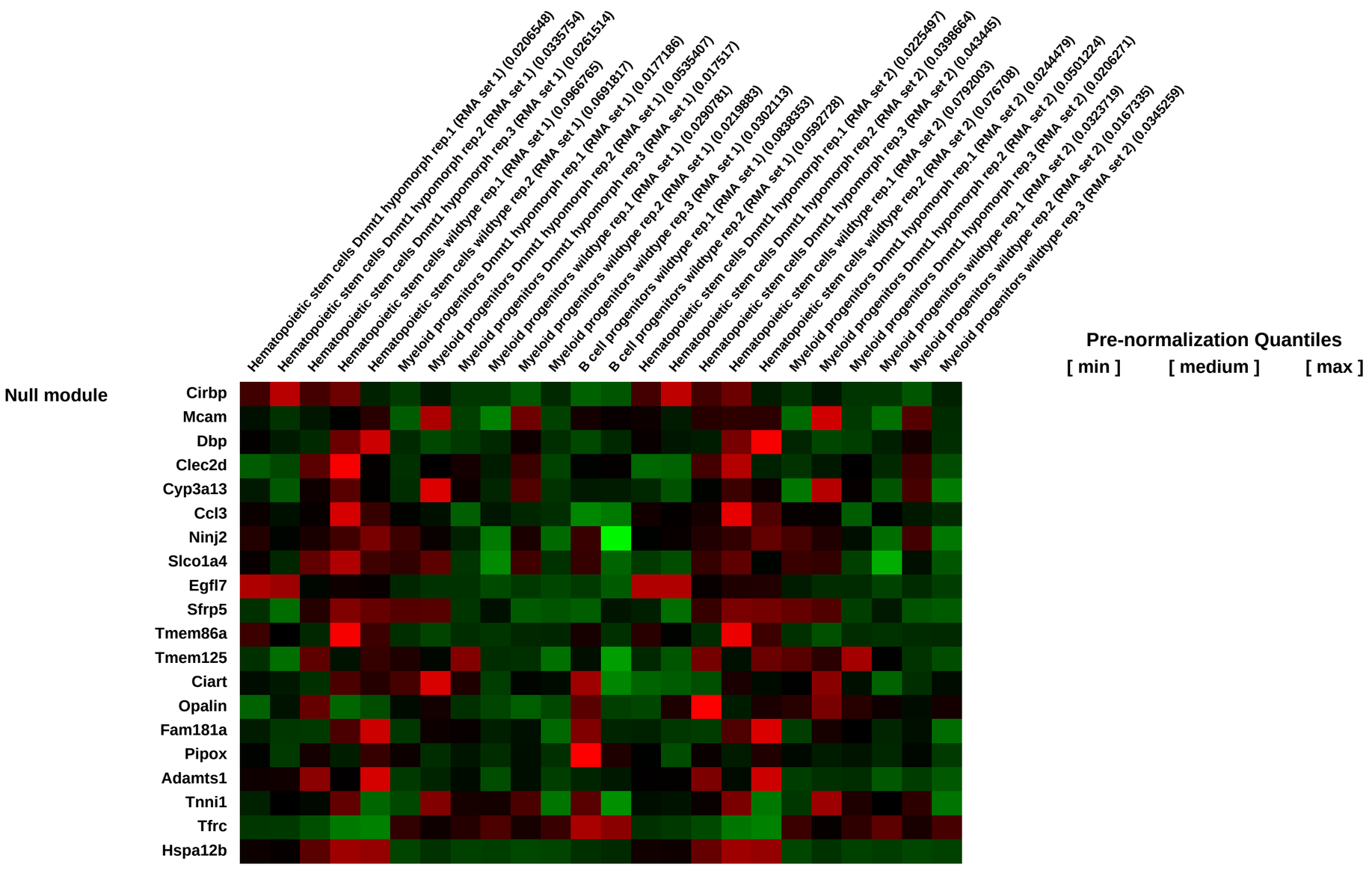

GEO Series "GSE25729" Expression Profiles

Num of samples in this series: 12

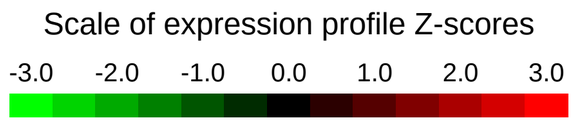

GEO Link:	**http://www.ncbi.nlm.nih.gov/geo/query/acc.cgi?acc=GSE25729**
Status:	**Public on Dec 25 2012**
Title:	**Role of ILK in cardiac regeneration**
Organism:	**Mus musculus**
Experiment type:	**Expression profiling by array**
Platform:	**GPL1261**
Pubmed ID:	
Summary & Design:	**Summary:** **Two different mouse models of cardiac-specific ILK expression (ILKS343D and ILKR211A) were used to investigate the role of ILK in cardiac regeneration** **Overall design:** **4 groups with 3 mice (biological replicates) in each group with the total of 12 heart samples were used in this microarray experiment**

Background corr dist: **KL-Divergence = 0.1828, L1-Distance = 0.0456, L2-Distance = 0.0046, Normal std = 0.3433**

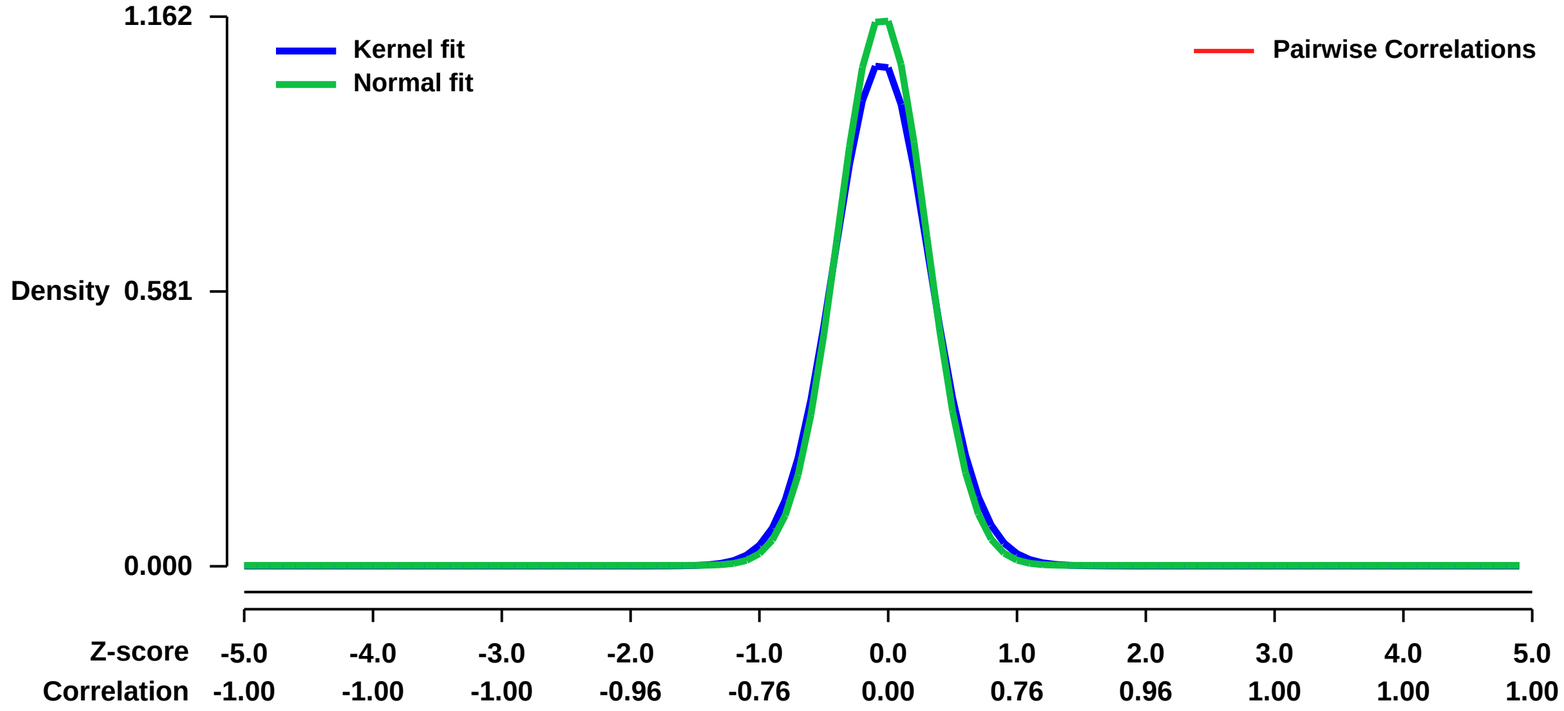

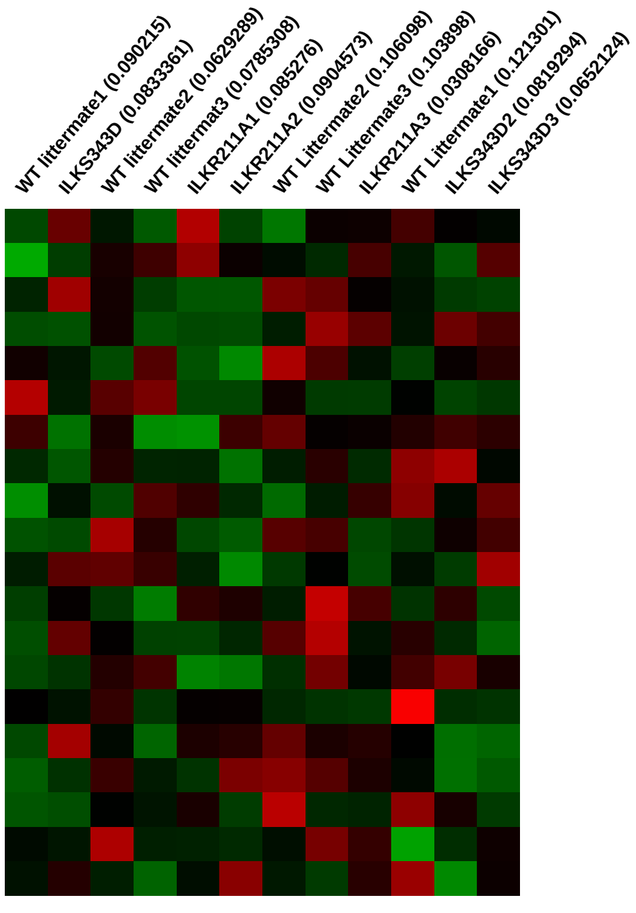

GEO Series "GSE34902" Expression Profiles

Num of samples in this series: 6

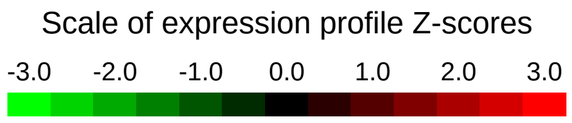

GEO Link:	http://www.ncbi.nlm.nih.gov/geo/query/acc.cgi?acc=GSE34902
Status:	Public on Sep 06 2012
Title:	Genome-wide Profiling of Progesterone Receptor and GATA2 Binding in the Mouse Uterus [Affymetrix]
Organism:	Mus musculus
Experiment type:	Expression profiling by array
Platform:	GPL1261
Pubmed ID:	22638070
Summary & Design:	**Summary:** Progesterone (P4) signaling through its nuclear transcription factor, the progesterone receptor (PR), is essential for normal uterine function. Although deregulation of PR mediated signaling is known to underscore uterine dysfunction and a number of endometrial pathologies, the early molecular mechanisms of this deregulation are unclear. To address this issue, we have defined the genome-wide PR and GATA2 cistrome in the murine uterus using chromatin immunoprecipitation followed by massively parallel sequencing (ChIP-seq). In uteri of ovariectomized mice, we identified 6367 PR binding sites in the absence of P4 ligand; however, this number increased at nearly three fold (18,432) following acute P4 exposure. Sequence analysis revealed that approximately 73% of these binding sites contain a progesterone response element (PRE) or a half-site motif recognized by the PR. Many previously identified P4 target genes known to regulate uterine function were found to contain PR binding sites, confirming the validity of our methodology. In addition we identified 46,183 GATA2 binding sites in P4 treatment conditions with 7,954 binding sites overlapping that of the PR. **Overall design:** Gene expression data from ovariectomized Oil and P4 treated Gata2 f/f uterus horn

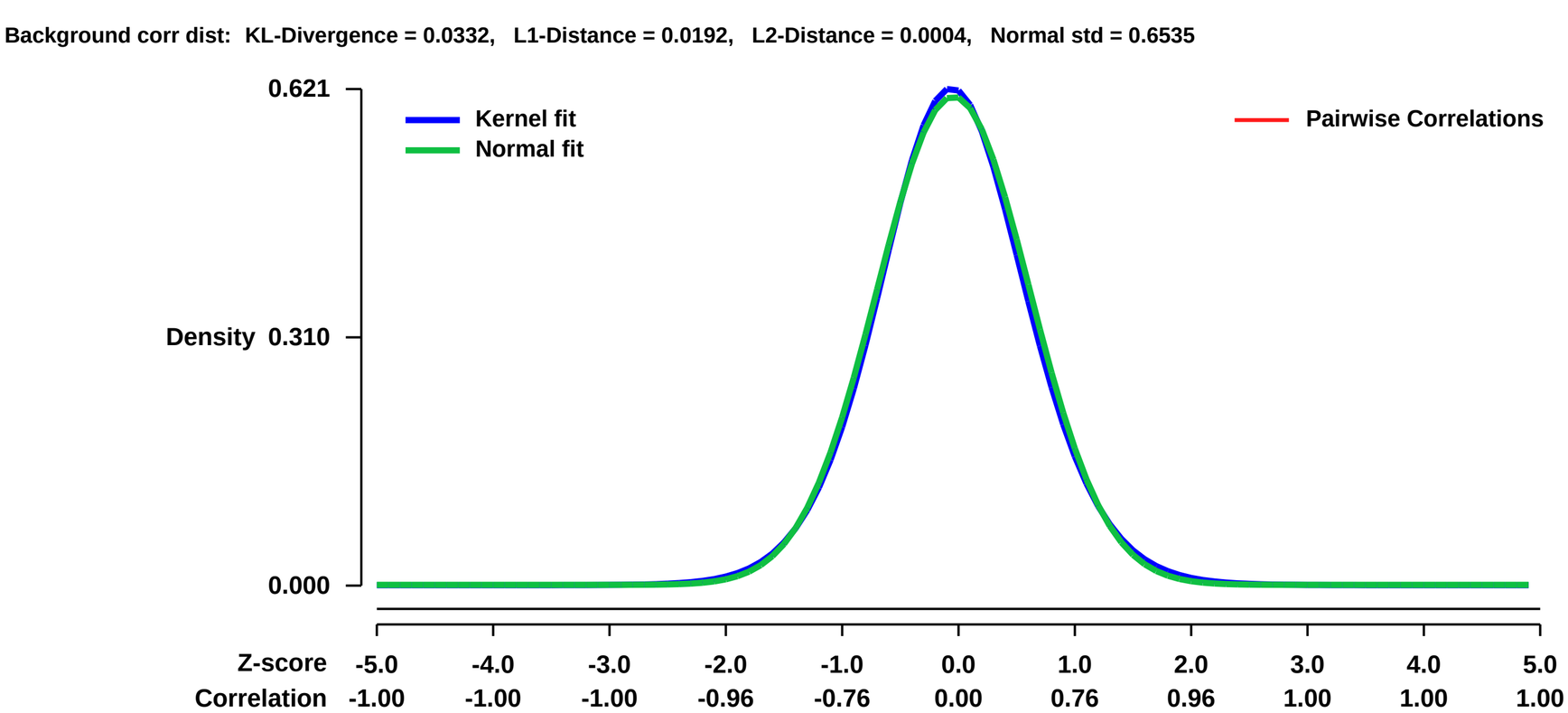

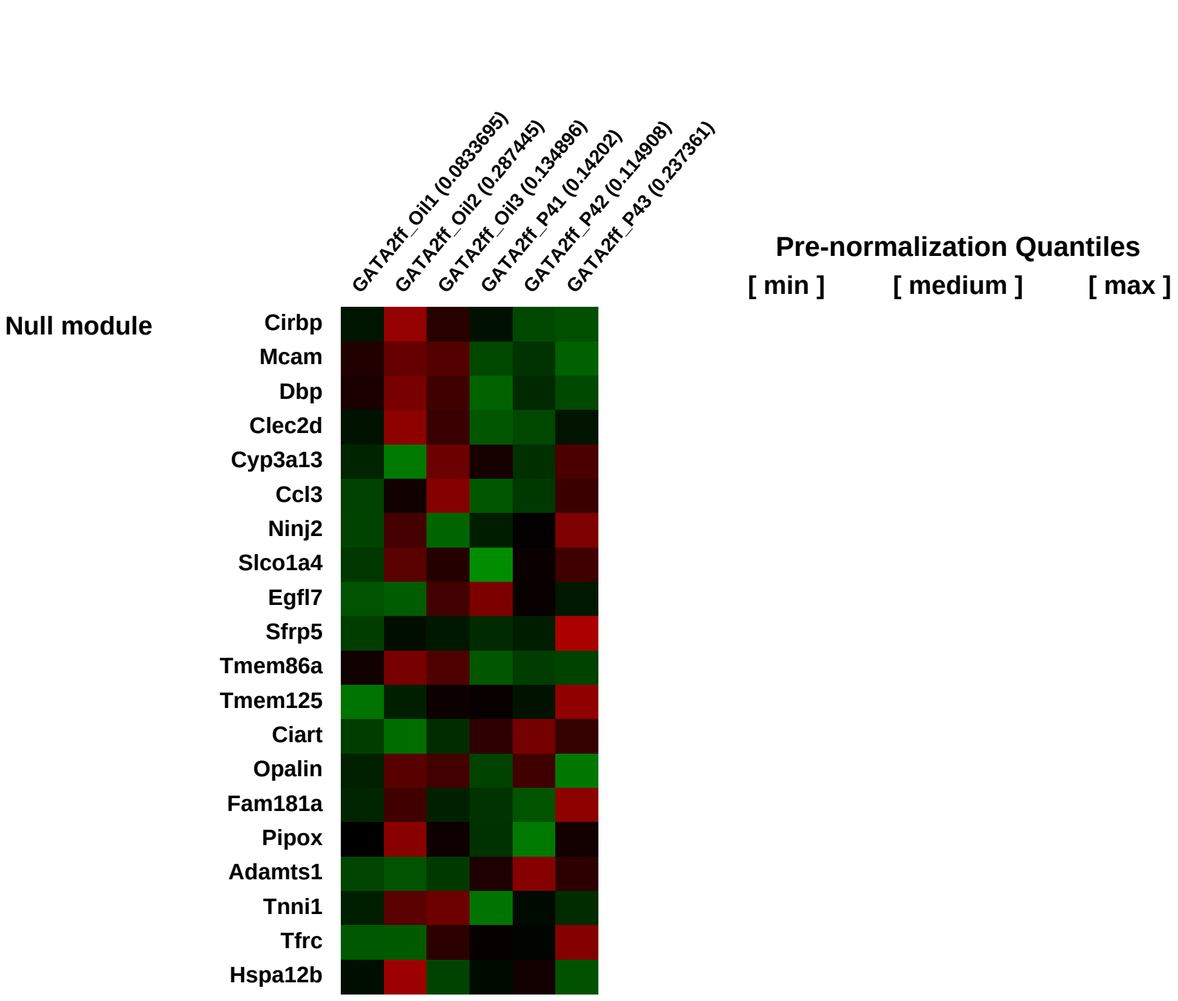

GEO Series "GSE39897" Expression Profiles

Num of samples in this series: 36

Scale of expression profile Z-scores

-3.0 -2.0 -1.0 0.0 1.0 2.0 3.0

GEO Link:	http://www.ncbi.nlm.nih.gov/geo/query/acc.cgi?acc=GSE39897
Status:	Public on Sep 11 2013
Title:	Expression data for mouse embryogenesis from oocyte to newborn
Organism:	Mus musculus
Experiment type:	Expression profiling by array
Platform:	GPL1261
Pubmed ID:	23961710
Summary & Design:	**Summary:** Studies in mouse have led to enormous progress in our understanding of early human development. The identification of genes and the signaling pathways involved in mouse embryogenesis have helped us to better understand fertilization, morulation, gastrulation, organogenesis and embryonic development in mammals. We report a detailed analysis of the global gene expression profiles from oocyte to the end of organogenesis in mouse. Our studies revealed distinct temporal regulation patterns for genes belonging to different functional categories, supporting their roles during organogenesis. **Overall design:** Mouse embryos were selected at successive stage for for RNA extraction and hybridization on Affymetrix microarrays. We sought to obtain homogeneous populations of embryos at each developmental stage in order to increase the temporal resolution of expression profiles. To that end, we hand-selected embryos according to morphological criteria at 12 time-points from embryos to newborn

Background corr dist: KL-Divergence = 0.0939, L1-Distance = 0.0418, L2-Distance = 0.0040, Normal std = 0.4636

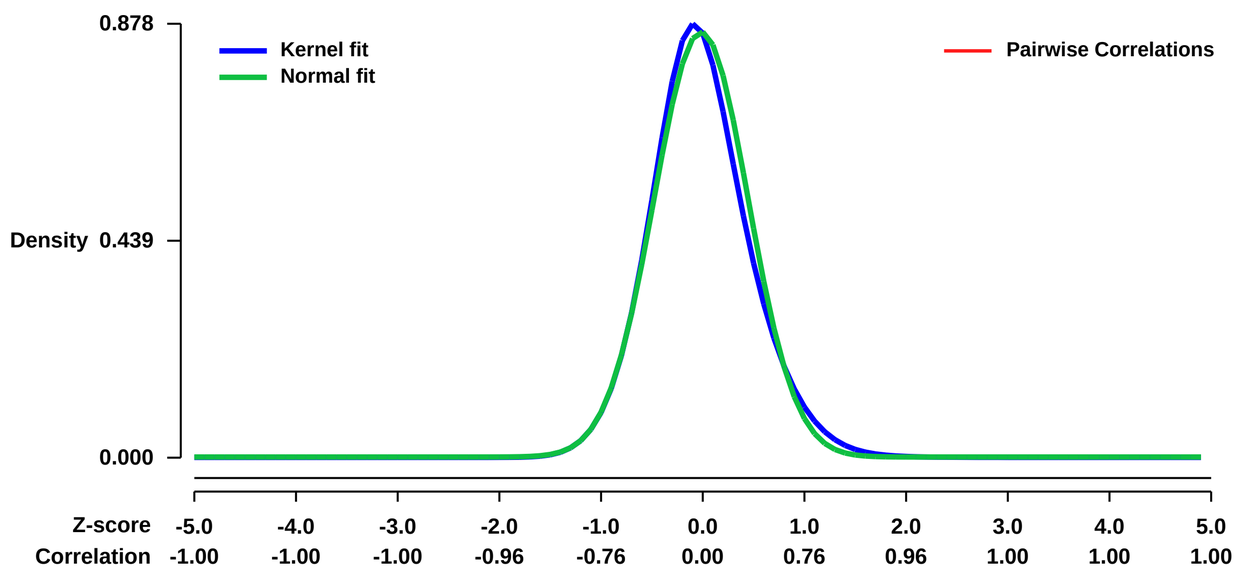

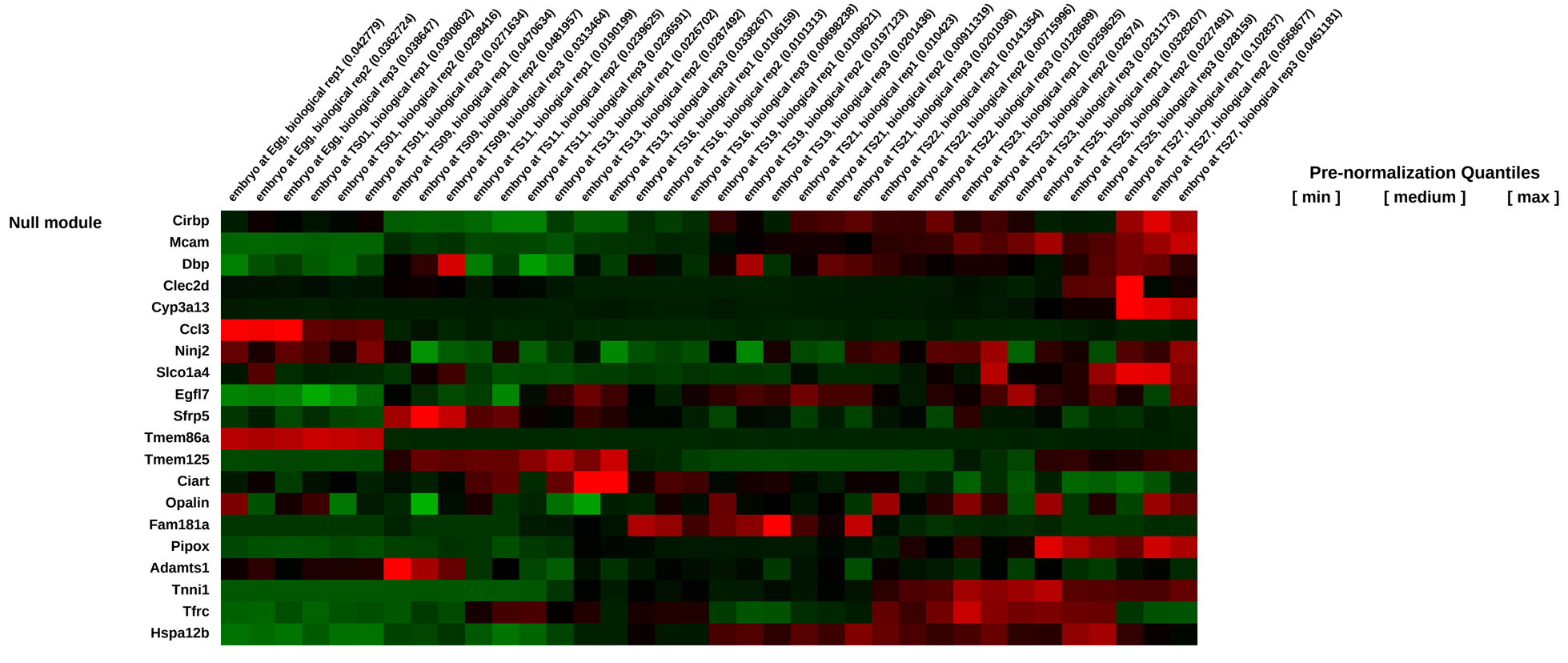

GEO Series "GSE8156" Expression Profiles

Num of samples in this series: 6

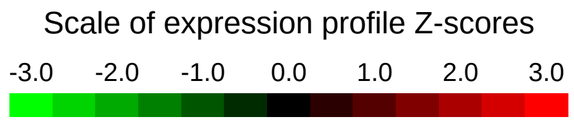

GEO Link:	http://www.ncbi.nlm.nih.gov/geo/query/acc.cgi?acc=GSE8156
Status:	Public on Jun 15 2008
Title:	Smad1/5/8 mutant granulosa cell tumor gene expression
Organism:	Mus musculus
Experiment type:	Expression profiling by array
Platform:	GPL1261
Pubmed ID:	17967875
Summary & Design:	**Summary:** The objective of this study was to understand the gene expression changes during granulosa cell tumor development in Smad1/5/8 mutant ovaries. **Keywords:** Microarray analysis, gene expression **Overall design:** Three independent mouse mutant granulosa cell tumors were compared to three wild type granulosa cells samples.

Background corr dist: KL-Divergence = 0.0332, L1-Distance = 0.0254, L2-Distance = 0.0008, Normal std = 0.6596

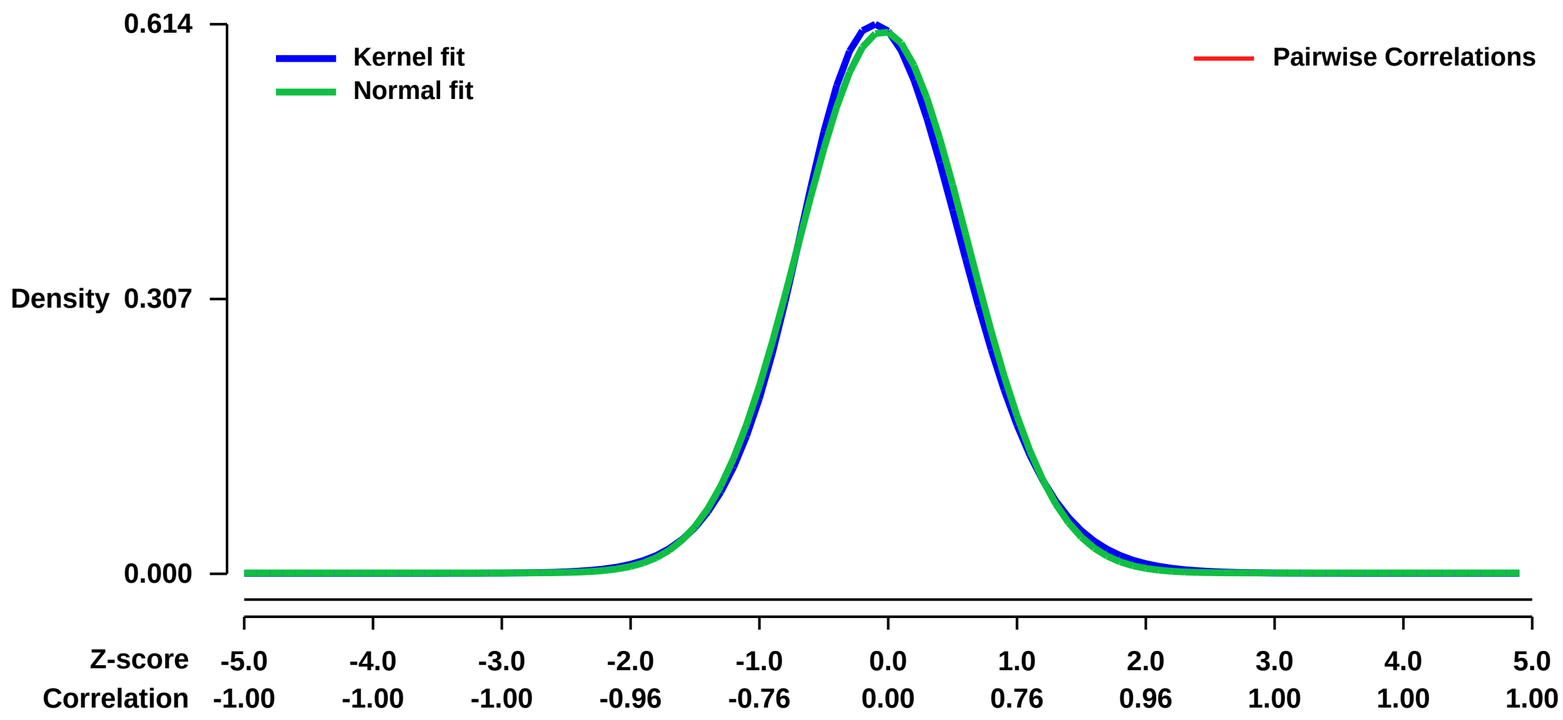

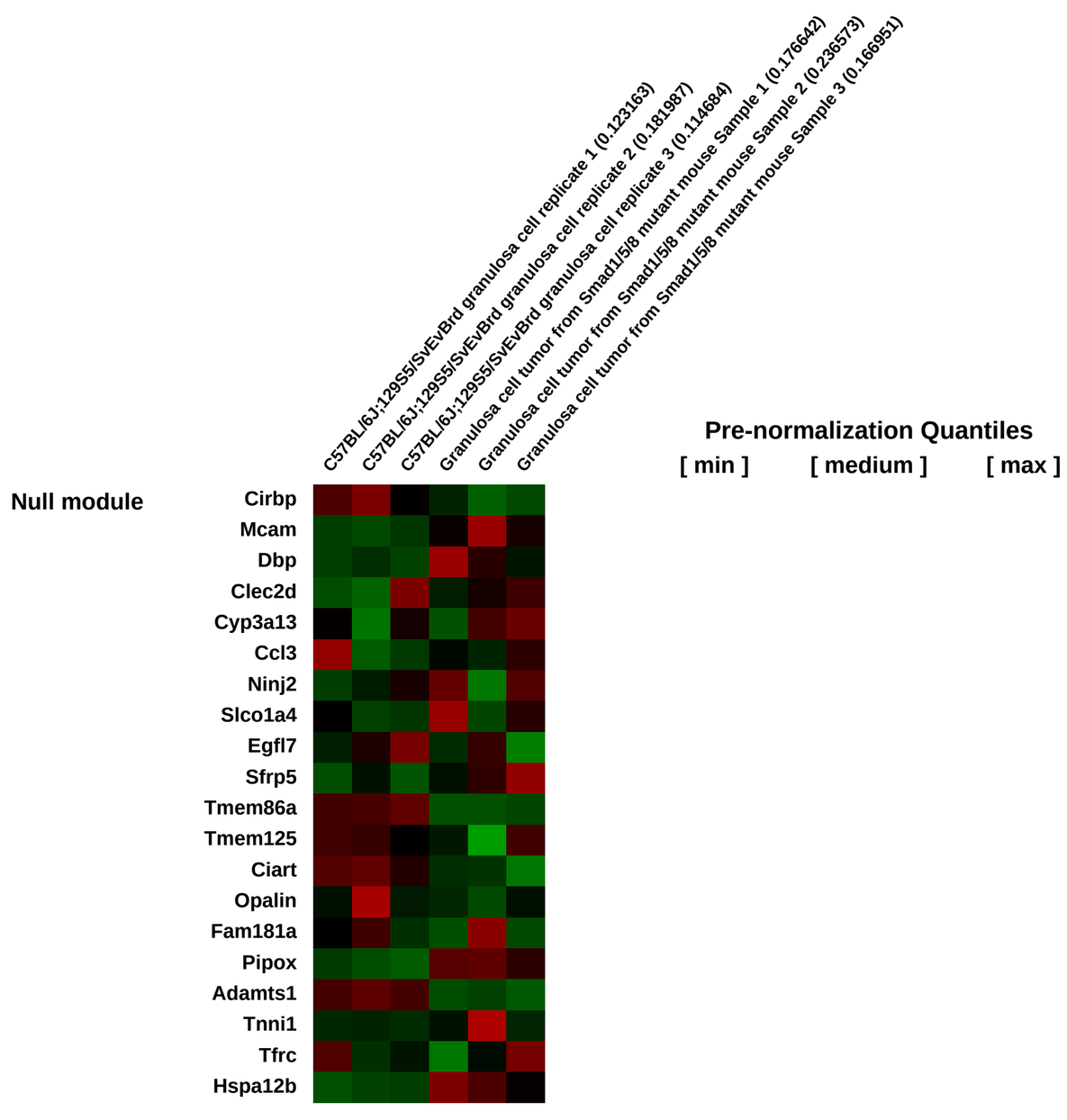

GEO Series "GSE2917" Expression Profiles

Num of samples in this series: 20

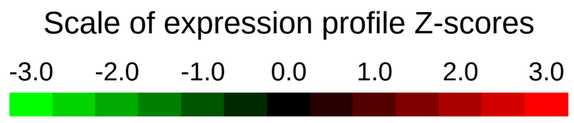

GEO Link:	http://www.ncbi.nlm.nih.gov/geo/query/acc.cgi?acc=GSE2917
Status:	Public on Dec 21 2005
Title:	Profiling of visceral sensory neurons in dorsal root and nodose ganglia in BALB/c mice.
Organism:	Mus musculus
Experiment type:	Expression profiling by array
Platform:	GPL1261
Pubmed ID:	16303873

Summary & Design:

Summary:
Vagal afferent neurons are thought to convey primarily physiological information, whereas spinal afferents transmit noxious signals from the viscera to the central nervous system. In order to elucidate molecular identities for these different properties, we compared gene expression profiles of neurons located in nodose ganglia (NG) and dorsal root ganglia (DRG) in mice. Intraperitoneal administration of Alexa Fluor-488 conjugated Cholera toxin B allowed identification of neurons projecting to the viscera. Fluorescent neurons in DRG (from T10 to T13) and NG were isolated using laser capture microdissection. Gene expression profiles of visceral afferent neurons, obtained by microarray hybridization, were analysed using multivariate spectral map analysis, SAM algorithm (Significance Analysis of Microarray data) and fold-difference filtering. A total of 1996 genes were found to be differentially expressed in DRG versus NG, including 41 G-protein coupled receptors and 60 ion channels. Expression profiles obtained on laser-captured neurons were contrasted to those obtained on whole ganglia demonstrating striking differences and the need for microdissection when studying visceral sensory neurons because of dilution of the signal by somatic sensory neurons. Furthermore, a detailed catalogue of all adrenergic and cholinergic, GABA, glutamate, serotonin and dopamine receptors, voltage-gated potassium, sodium and calcium channels and transient receptor potential cation channels present in visceral afferents is provided. Our genome-wide expression profiling data provide novel insight into molecular signatures that underlie both functional differences and similarities between NG and DRG visceral sensory neurons. Moreover, these findings will offer novel insight into mode of action of pharmacologic agents modulating visceral sensation.

Keywords: Cell type comparison

Overall design:
Three separate experiments were performed. First, 5 whole dorsal root ganglia were compared to 7 whole nodose ganglia. Second, Laser captured visceral neurons derived from 5 dorsal root ganglia and 5 nodose ganglia were compared on MG-U74Av2. Third, Laser captured visceral neurons derived from 9 dorsal root ganglia and 11 nodose ganglia were compared on Mouse430_2.

Background corr dist: KL-Divergence = 0.2526, L1-Distance = 0.0551, L2-Distance = 0.0075, Normal std = 0.3012

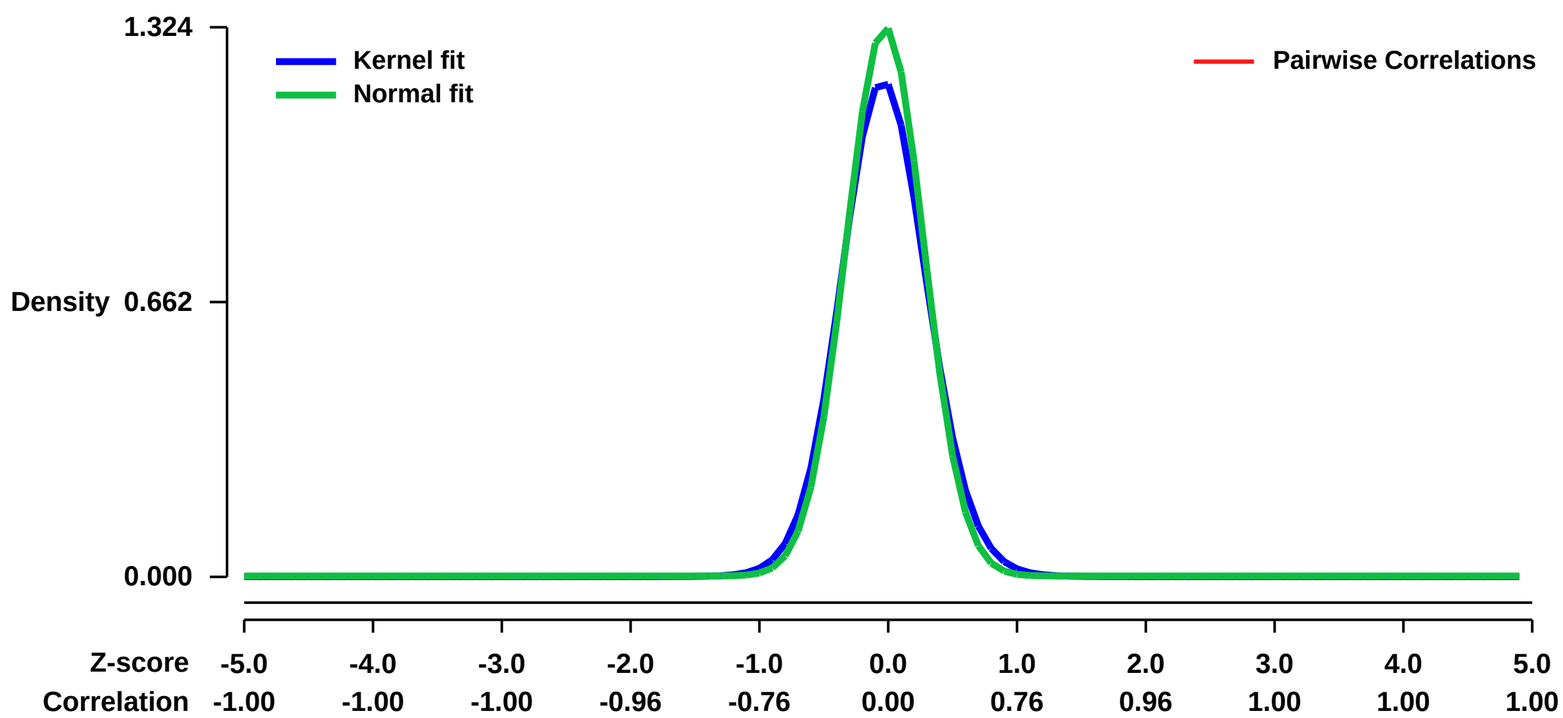

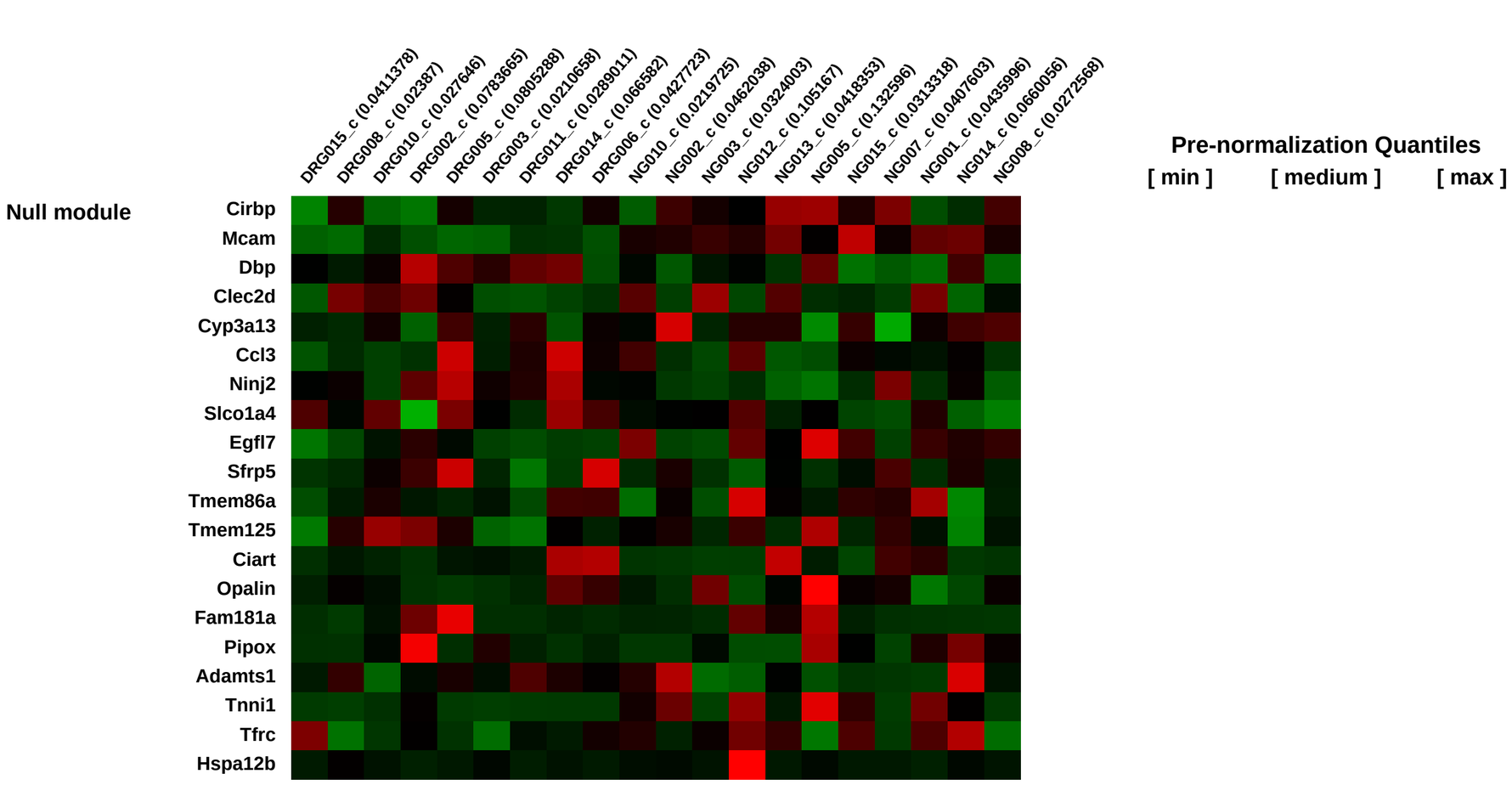

GEO Series "GSE6526" Expression Profiles

Num of samples in this series: 16

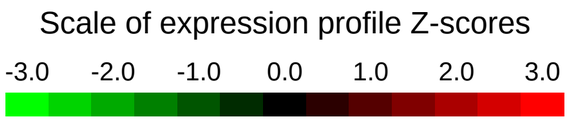

GEO Link:	http://www.ncbi.nlm.nih.gov/geo/query/acc.cgi?acc=GSE6526
Status:	Public on Mar 01 2007
Title:	Expression time course data HEY2 KO and WT MASMC treated with PDGF
Organism:	Mus musculus
Experiment type:	Expression profiling by array
Platform:	GPL1261
Pubmed ID:	17327490
Summary & Design:	**Summary:** **The cardiovascular restricted transcription factor CHF1/Hey2 has been previously shown to regulate the smooth muscle response to growth factors. To determine how CHF1/Hey2 affects the smooth muscle response to growth factors, we performed a genomic screen for transcripts that are differentially expressed in wild type and knockout smooth muscle cells after stimulation with platelet derived growth factor.** **We screened 45101 probes representing more than 39,000 transcripts derived from at least 34,000 genes, at eight different time points. We analyzed the expression data utilizing an algorithm based on Bayesian statistics to derive the best polynomial clustering model to fit the expression data. We found that in a total of 9827 transcripts the normalized ratio of knockout to wild type expression diverged more than 3 fold from baseline in at least one time point, and these transcripts separated into 17 distinct clusters. Further analysis of each cluster revealed distinct alterations in gene expression patterns for immediate early genes, transcription factors, matrix metalloproteinases, signaling molecules and other molecules important in vascular biology.** **Keywords: time course** **Overall design:** **WT and Hey2 knockout mouse aortic smooth muscle cells were treated in parallel with PDGF and harvested at successive time points for RNA extraction and hybridization on Affymetrix microarrays. We sought to identify differentially expressed transcripts through Bayesian statistical methods that would explain the differential response to PDGF observed in vitro.**

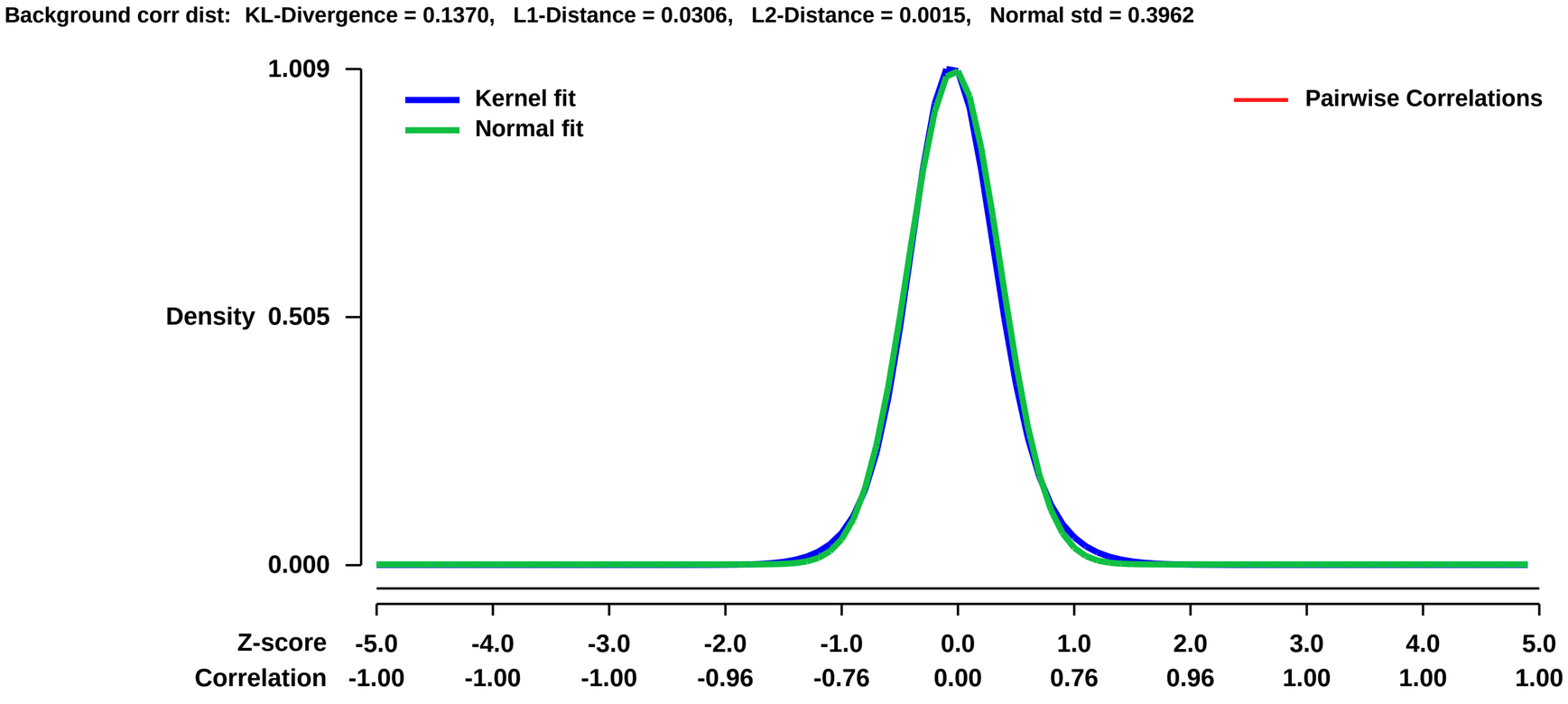

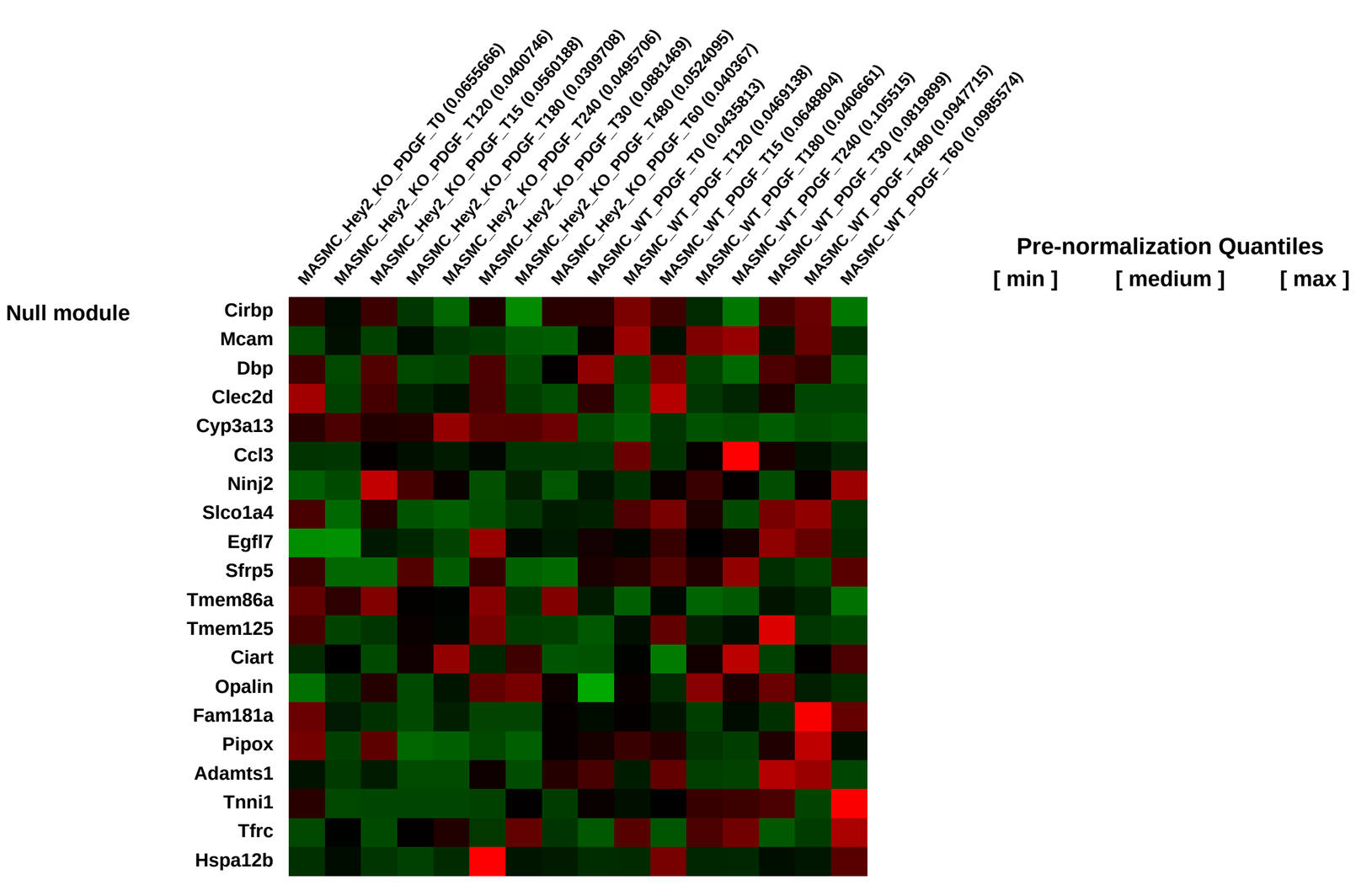

GEO Series "GSE14012" Expression Profiles

Num of samples in this series: 24

Scale of expression profile Z-scores

-3.0 -2.0 -1.0 0.0 1.0 2.0 3.0

GEO Link:	http://www.ncbi.nlm.nih.gov/geo/query/acc.cgi?acc=GSE14012
Status:	Public on Jan 28 2009
Title:	Role of the reprogramming factors in inducing pluripotency
Organism:	Mus musculus
Experiment type:	Genome binding/occupancy profiling by array
Platform:	GPL1261
Pubmed ID:	19167336
Summary & Design:	**Summary:** Induced pluripotent stem (iPS) cells can be obtained from fibroblasts by expression of Oct4, Sox2, Klf4, and c-Myc. To determine how these factors induce this change in cell identity, we carried out genomewide promoter analysis of their binding in iPS and partially reprogrammed cells. Most targets in iPS cells are shared with ES cells and the factors cooperate to activate the ES-like expression program. In partially reprogrammed cells, genes bound by c-Myc have achieved a more ES-like binding and expression pattern. In contrast, genes that are co-bound by Oct4, Sox2, and Klf4 in ES cells and that encode pluripotency regulators show severe lack of both binding and transcriptional activation. Among the factors, c-Myc has a pivotal effect on the initiation of the ES transcription program, including the repression of fibroblast-specific genes. Our analysis begins to unravel how the four factors function together and suggests a temporal and separable order of their effects during reprogramming. **Overall design:** Oct4/Sox2/c-Myc/Klf4 were performed with biological duplicates (2 clonally isolated iPS/partial iPS lines and ES cells were performed with v6.5 and E14 cell lines)

Background corr dist: KL-Divergence = 0.1543, L1-Distance = 0.0420, L2-Distance = 0.0038, Normal std = 0.3796

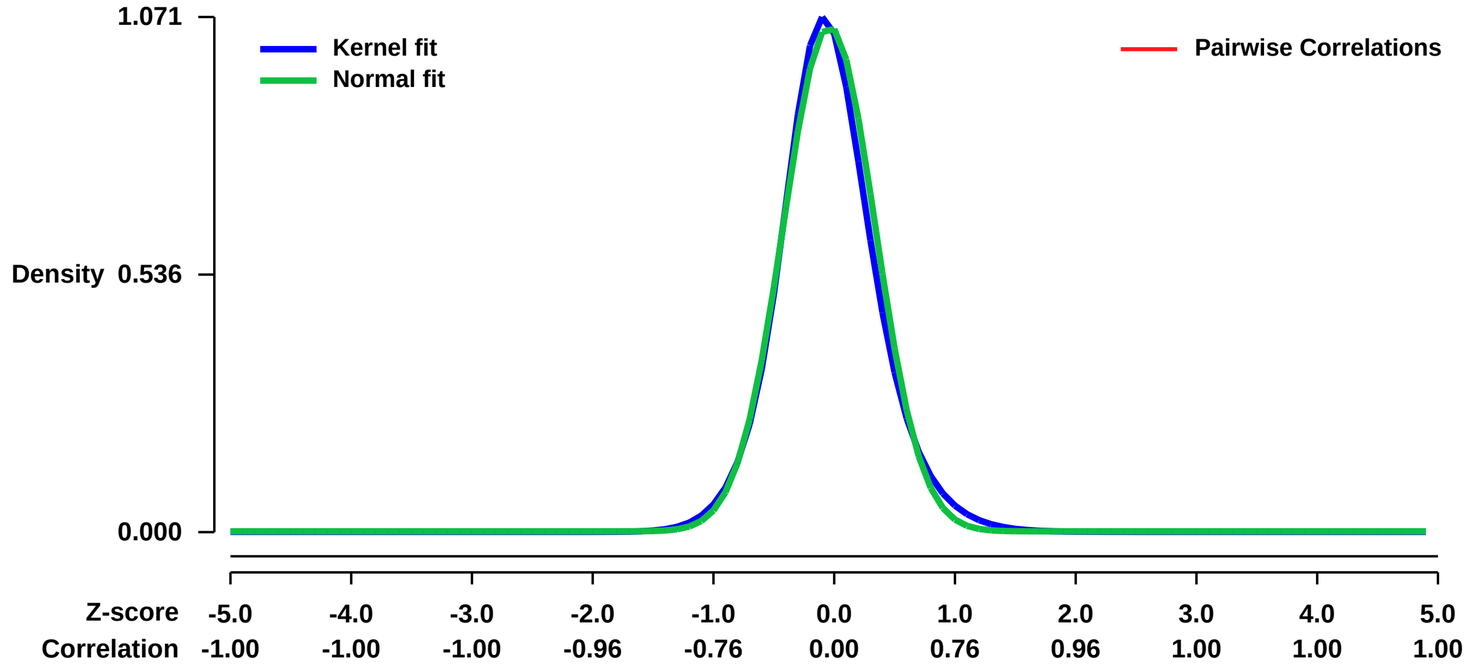

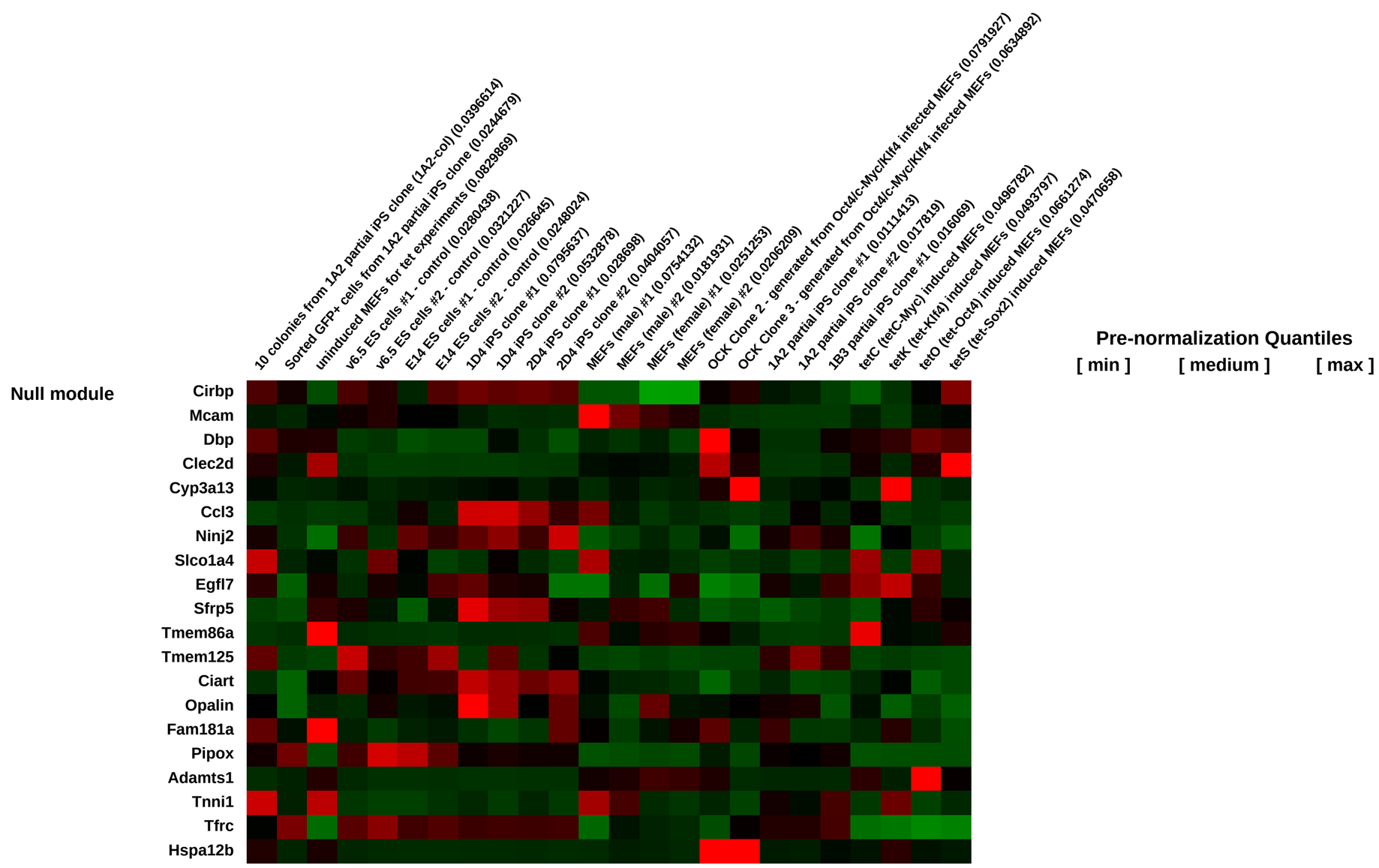

GEO Series "GSE7348" Expression Profiles

Num of samples in this series: 6

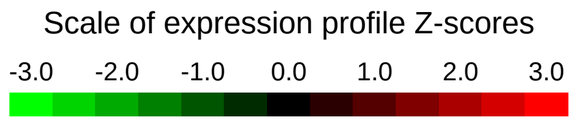

GEO Link:	http://www.ncbi.nlm.nih.gov/geo/query/acc.cgi?acc=GSE7348
Status:	Public on Apr 22 2007
Title:	Gene Expression in Naive and Tolerant Macrophages stimulated with LPS
Organism:	Mus musculus
Experiment type:	Expression profiling by array
Platform:	GPL1261
Pubmed ID:	17538624
Summary & Design:	**Summary:** The inflammatory response initiated by microbial products signaling through Toll-like receptors (TLRs) of the innate immune system is essential for host defense against infection. Because inflammation can be harmful to host tissues, the innate response is highly regulated. Negative regulation of TLR4, the receptor for bacterial lipopolysaccharide (LPS), results in LPS tolerance, defined as hyporesponsiveness to repeated stimulation with LPS. LPS tolerance is thought to protect the host from excessive inflammation by turning off TLR4 signal, which then shuts down TLR-induced genes. However, TLR signaling induces hundreds of genes with very different functions. We reasoned that genes with different functions should have different requirements for regulation. Specifically, genes encoding proinflammatory mediators should be transiently inactivated to limit tissue damage, while genes encoding antimicrobial effectors, which directly target pathogens, should remain inducible in tolerant cells to protect the host from infection. Using an in vitro system of LPS tolerance in macrophages, here we show that TLR-induced genes may indeed be divided into two distinct categories based on their functions and regulatory requirements. Further, we show these distinct groups are regulated by gene-specific, and not signal-specific mechanisms. **Keywords:** Treatment Comparison **Overall design:** We examined gene expression using affymetrix genechips in 3 groups of murine bone-marrow derived macrophages: Naive (untreated), Naive stimulated with LPS, and Tolerant stimulated with LPS. Two biological replicates were performed for each group.

Background corr dist: KL-Divergence = 0.0411, L1-Distance = 0.0357, L2-Distance = 0.0018, Normal std = 0.6261

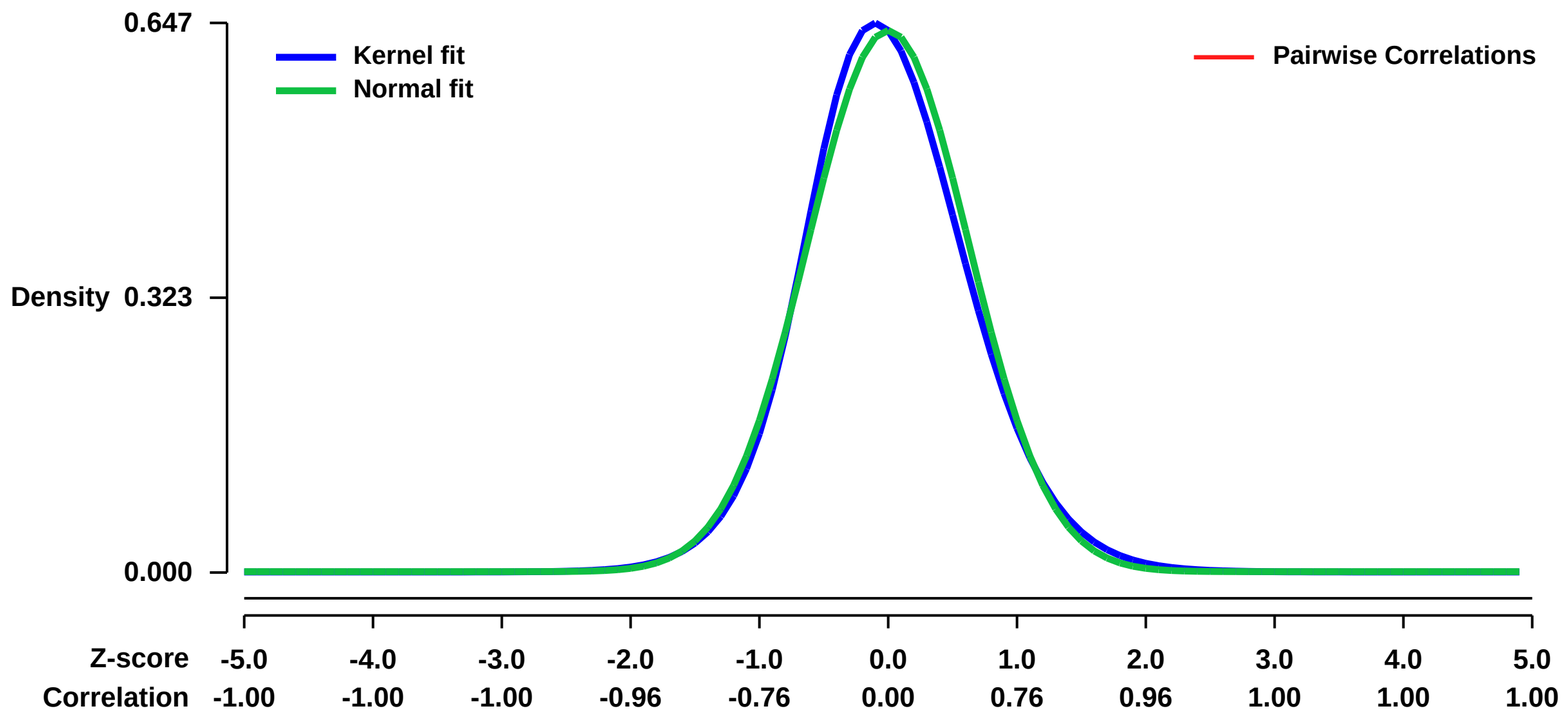

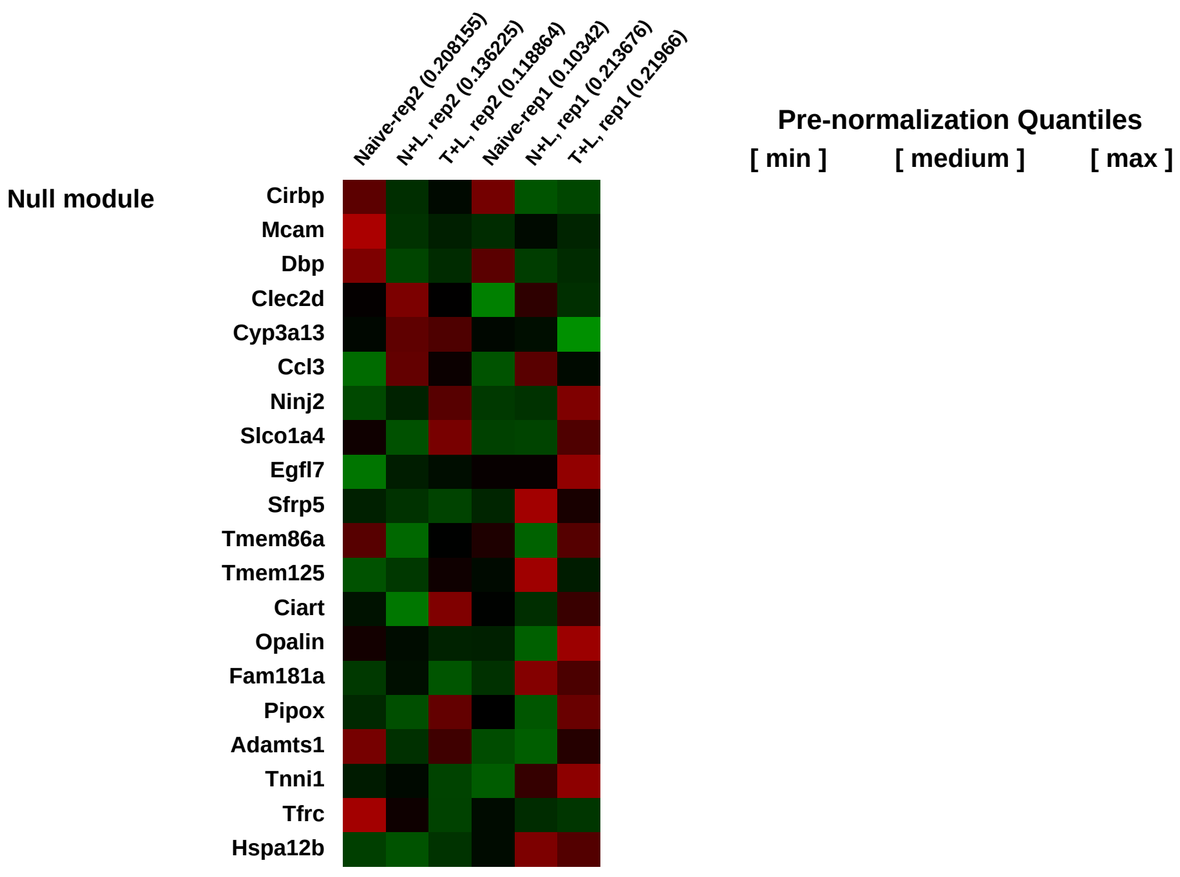

GEO Series "GSE7605" Expression Profiles

Num of samples in this series: 18

Scale of expression profile Z-scores

-3.0 -2.0 -1.0 0.0 1.0 2.0 3.0

GEO Link:	**http://www.ncbi.nlm.nih.gov/geo/query/acc.cgi?acc=GSE7605**
Status:	**Public on Nov 01 2007**
Title:	**Expression in Kir6.1-deficient heart following LPS challenge**
Organism:	**Mus musculus**
Experiment type:	**Expression profiling by array**
Platform:	**GPL1261**
Pubmed ID:	**18026101**
Summary & Design:	**Summary:** **KATP opposes depolarization of cells in the heart, smooth muscle, and other tissues by permitting the efflux of potassium ions and this efflux is evidently required to prevent unopposed vasoconstriction and insufficiency of coronary artery blood flow triggered by one or more cytokines induced in response to LPS. The cytokine(s) involved must elicit a dysfunctional response in the Kir6.1-deficient environment, and to gain further insight into the effects of the mutation, we examined the transcriptional status of whole heart, isolated from normal C57BL/6J mice or KcnJ8Md/Md mice, before and after injection of 1 ¸…g of LPS** **Keywords: Time course, stress response, disease state analysis, genetic modification** **Overall design:** **3 mice per genotype were injected with 0.5 ug LPS in PBS or with PBS alone and hearts were collected after 30 min or 3 h.**

Background corr dist: **KL-Divergence = 0.0549, L1-Distance = 0.0384, L2-Distance = 0.0029, Normal std = 0.5407**

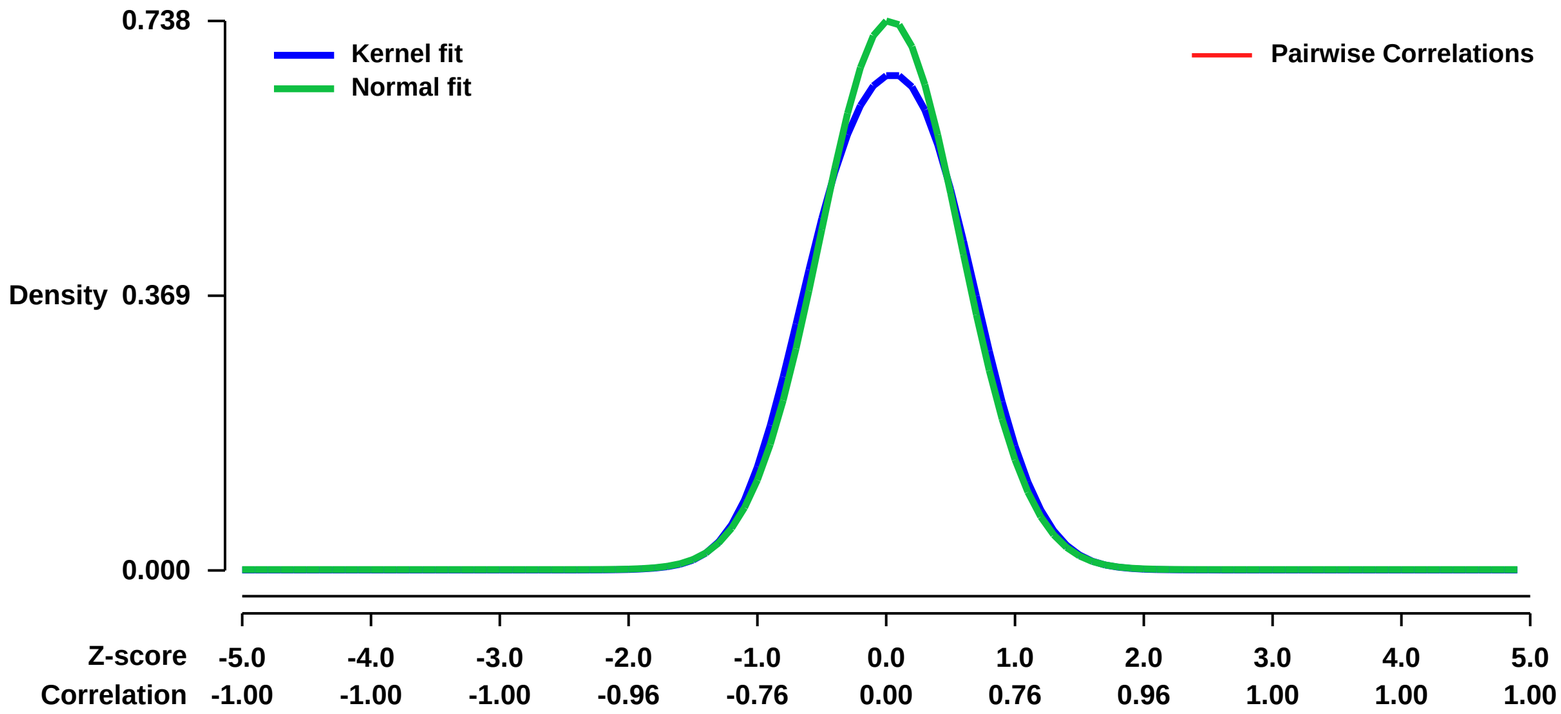

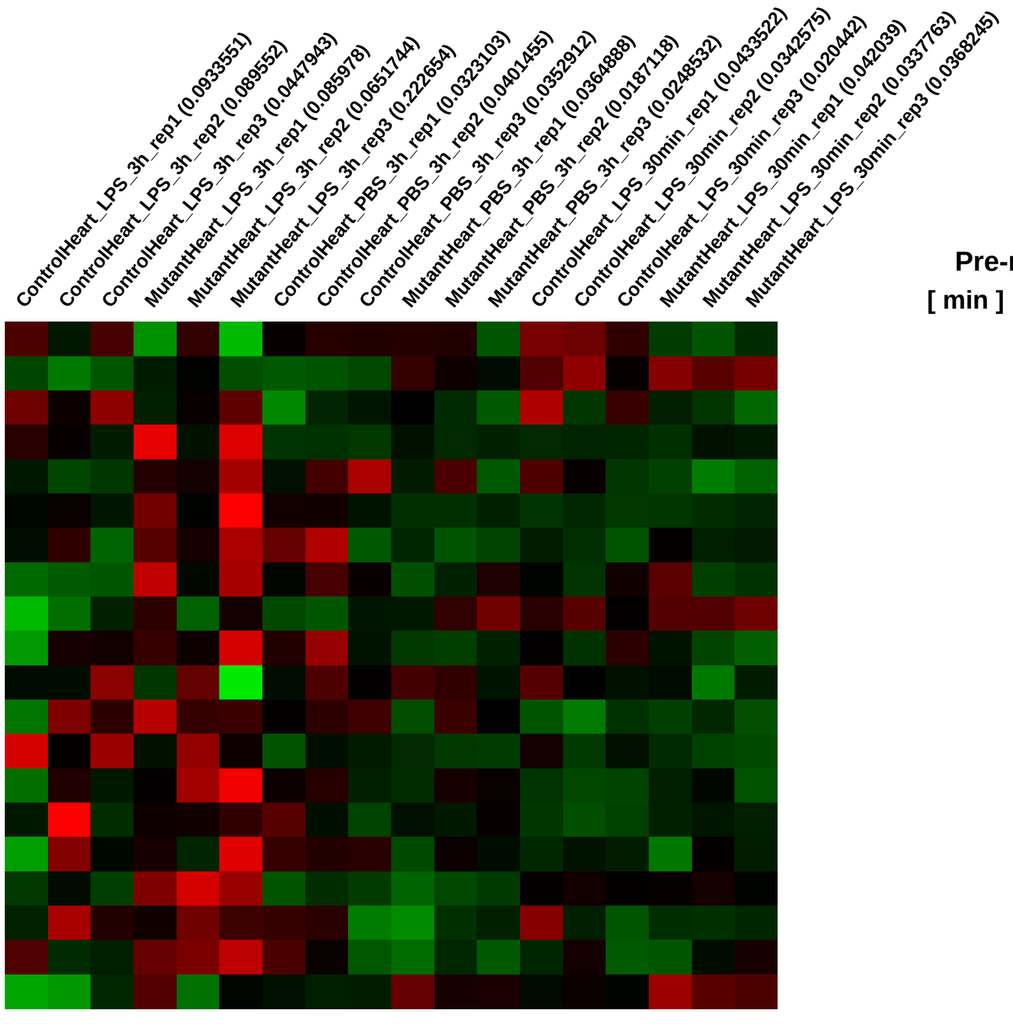

GEO Series "GSE17796" Expression Profiles

Num of samples in this series: 39

Scale of expression profile Z-scores

-3.0 -2.0 -1.0 0.0 1.0 2.0 3.0

GEO Link:	http://www.ncbi.nlm.nih.gov/geo/query/acc.cgi?acc=GSE17796
Status:	Public on Jan 11 2010
Title:	Expression data from B6C3F1 mice treated with reduced oxygen
Organism:	Mus musculus
Experiment type:	Expression profiling by array
Platform:	GPL1261
Pubmed ID:	19812364
Summary & Design:	**Summary:** Mice received decreasing oxygen concentrations from 21% to 6% O2 for ~ 30 minutes. Then, the mice remained an additional 120 minutes at 6% O2, control mice were placed insimilarchambers but recieved normal (21%) oxygen. **Overall design:** Mice were euthanased by cervical dislocation under ketamine / acepromazine (100 mg/kg / 5 mg/kg, I.P) anesthesia. The bone marrow from the right humerus, a portion of the left lateral liver lobe and half a cross-section of the spleen were harvested and the RNA was isolated from these tissues using standard Qiagen reagents. Standard Affymetrix protocols were used for GeneChip probe preparations. 39 arrays.

Background corr dist: KL-Divergence = 0.0270, L1-Distance = 0.0739, L2-Distance = 0.0083, Normal std = 0.7950

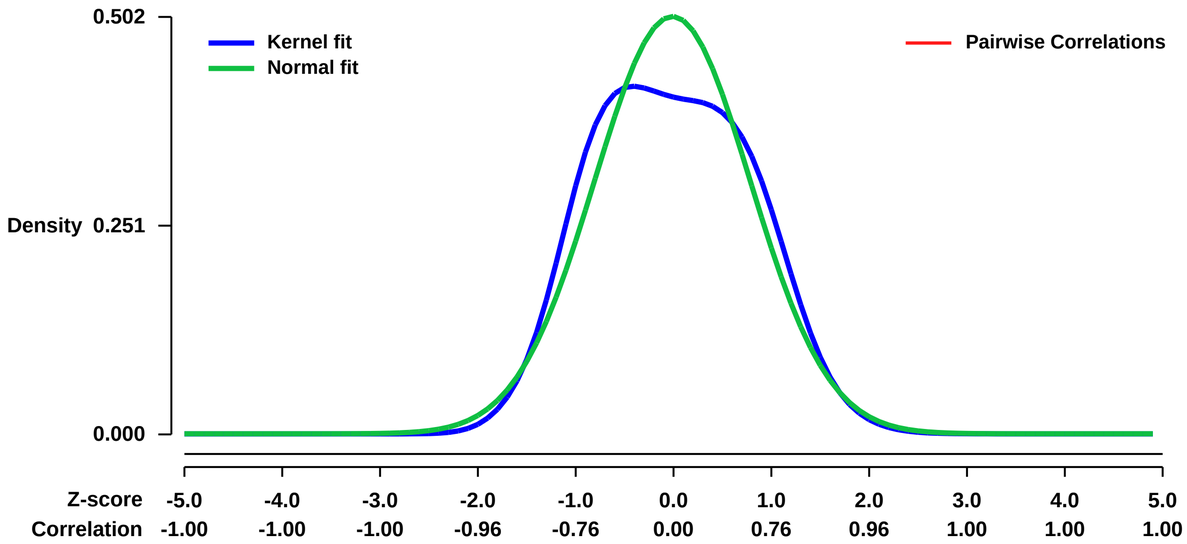

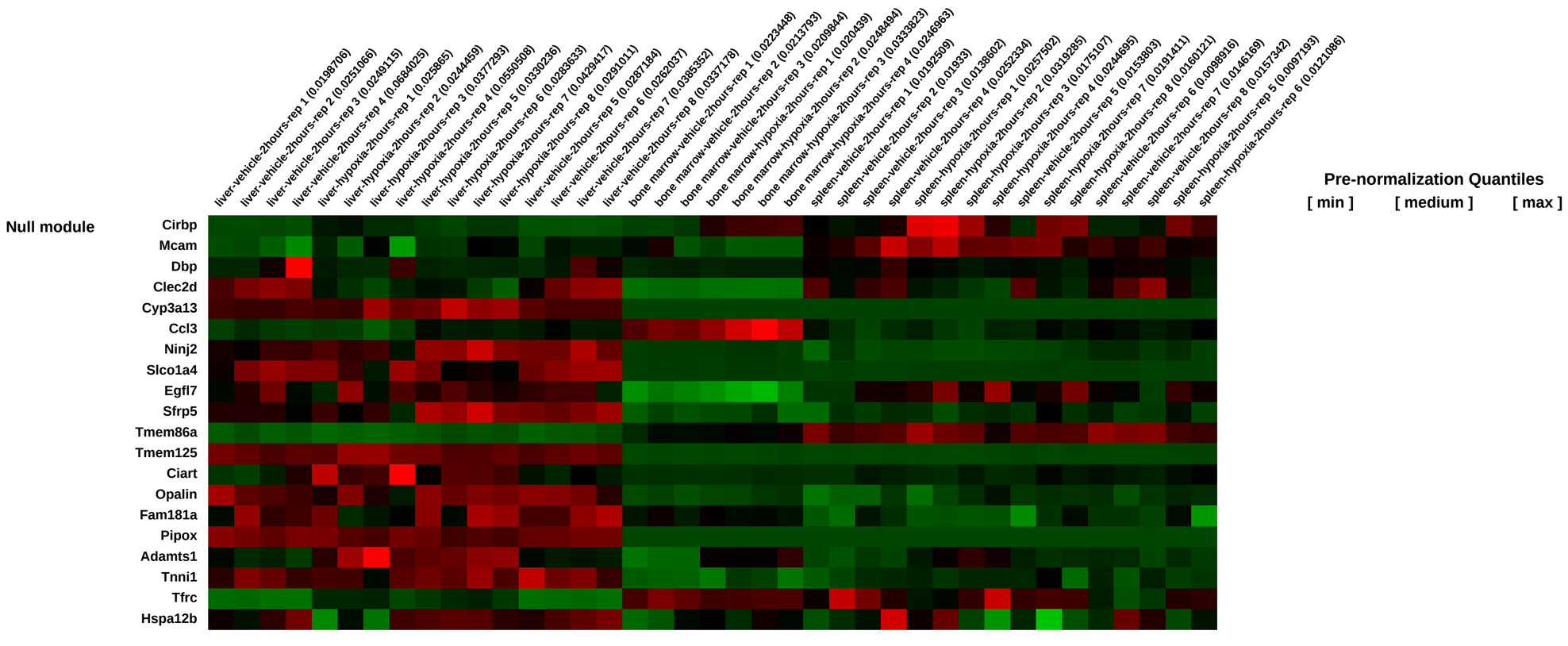

GEO Series "GSE13667" Expression Profiles

Num of samples in this series: 6

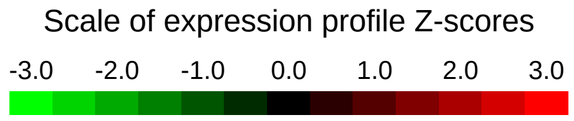

GEO Link:	http://www.ncbi.nlm.nih.gov/geo/query/acc.cgi?acc=GSE13667
Status:	Public on Jan 26 2009
Title:	mpkCCD_Cell_Clones
Organism:	Mus musculus
Experiment type:	Expression profiling by array
Platform:	GPL1261
Pubmed ID:	19190182
Summary & Design:	**Summary:** This series of microarray data contain transcript intensity of mpkCCD cells. **Overall design:** The mpkCCDc14 cells were cloned into colonies with varying aquaporin 2 (AQP2) expression levels in the presence of vasopressin analogy dDAVP. Transcript profiling was done for the original cells and cell clones 2, 3, 9, 10, and 11. By studying transcripts that correlate with AQP2 mRNA levels among cell clones, the objective was to identify transcripts responsible for cell-specific expression of AQP2.

Background corr dist: KL-Divergence = 0.0455, L1-Distance = 0.0247, L2-Distance = 0.0007, Normal std = 0.5960

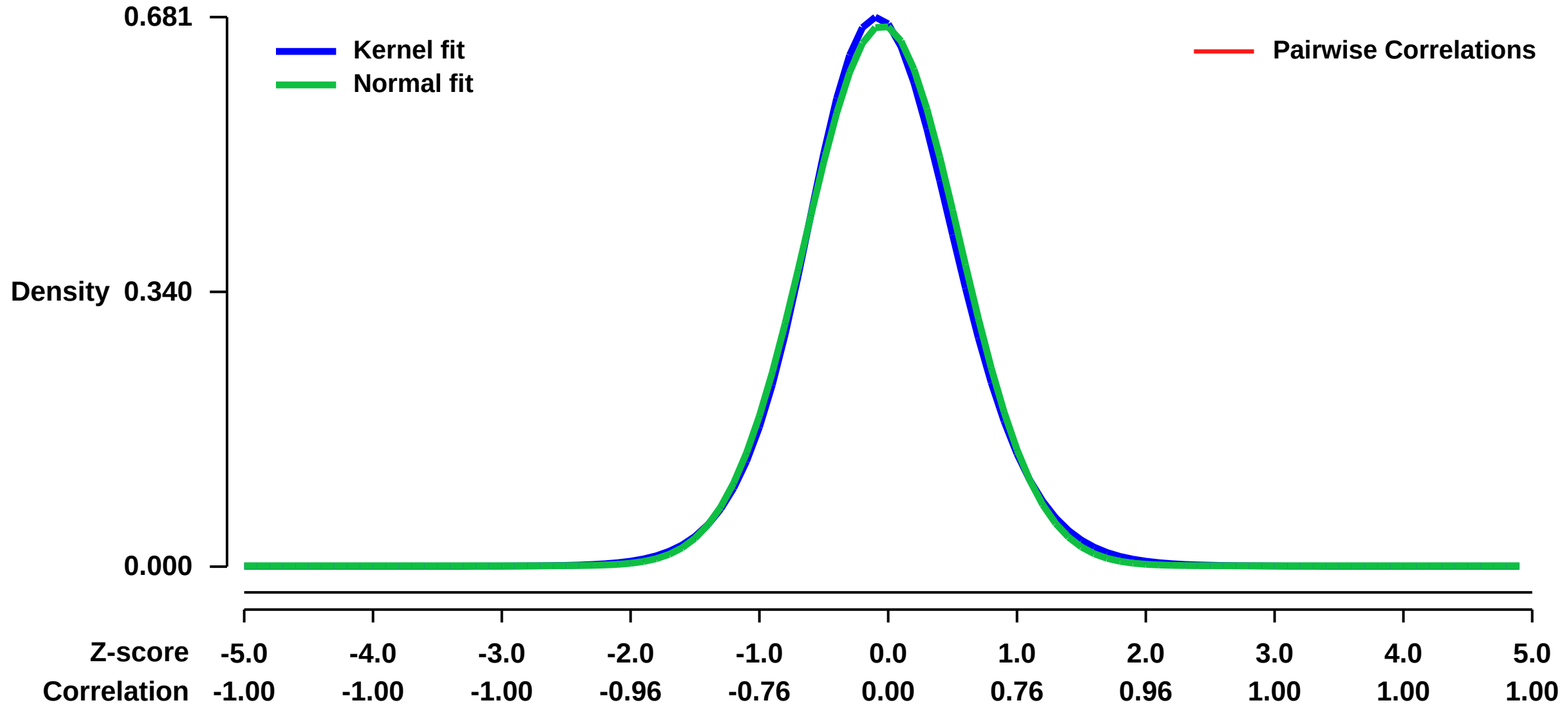

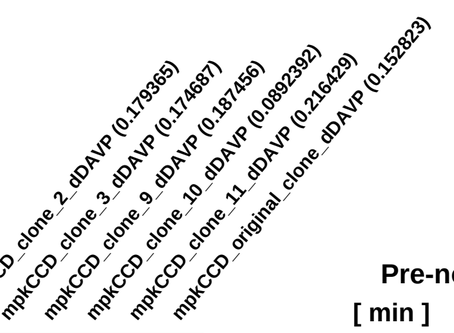

GEO Series "GSE17923" Expression Profiles

Num of samples in this series: 6

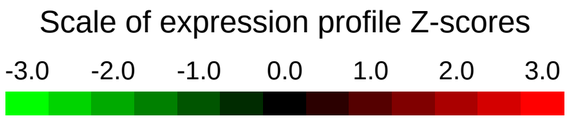

GEO Link:	**http://www.ncbi.nlm.nih.gov/geo/query/acc.cgi?acc=GSE17923**
Status:	**Public on Sep 03 2009**
Title:	**Gene Expression in White Adipose Tissue of KSR2-/- mice compared to wild type mice**
Organism:	**Mus musculus**
Experiment type:	**Expression profiling by array**
Platform:	**GPL1261**
Pubmed ID:	**19883615**
Summary & Design:	**Summary:** **The goal of this study was to define the gene expression changes that take place in the white adipose tissue of KSR2-/- mice at 6 months of age.** **Overall design:** **Three wild type mice and three KSR2-/- mice were used for total RNA extraction from white adipose tissue. The RNA from each mouse was analyzed on one Affymetrix gene chip and the differences were compared using Gene Set Enrichment Analysis.**

Background corr dist: **KL-Divergence = 0.0231, L1-Distance = 0.0257, L2-Distance = 0.0009, Normal std = 0.7211**

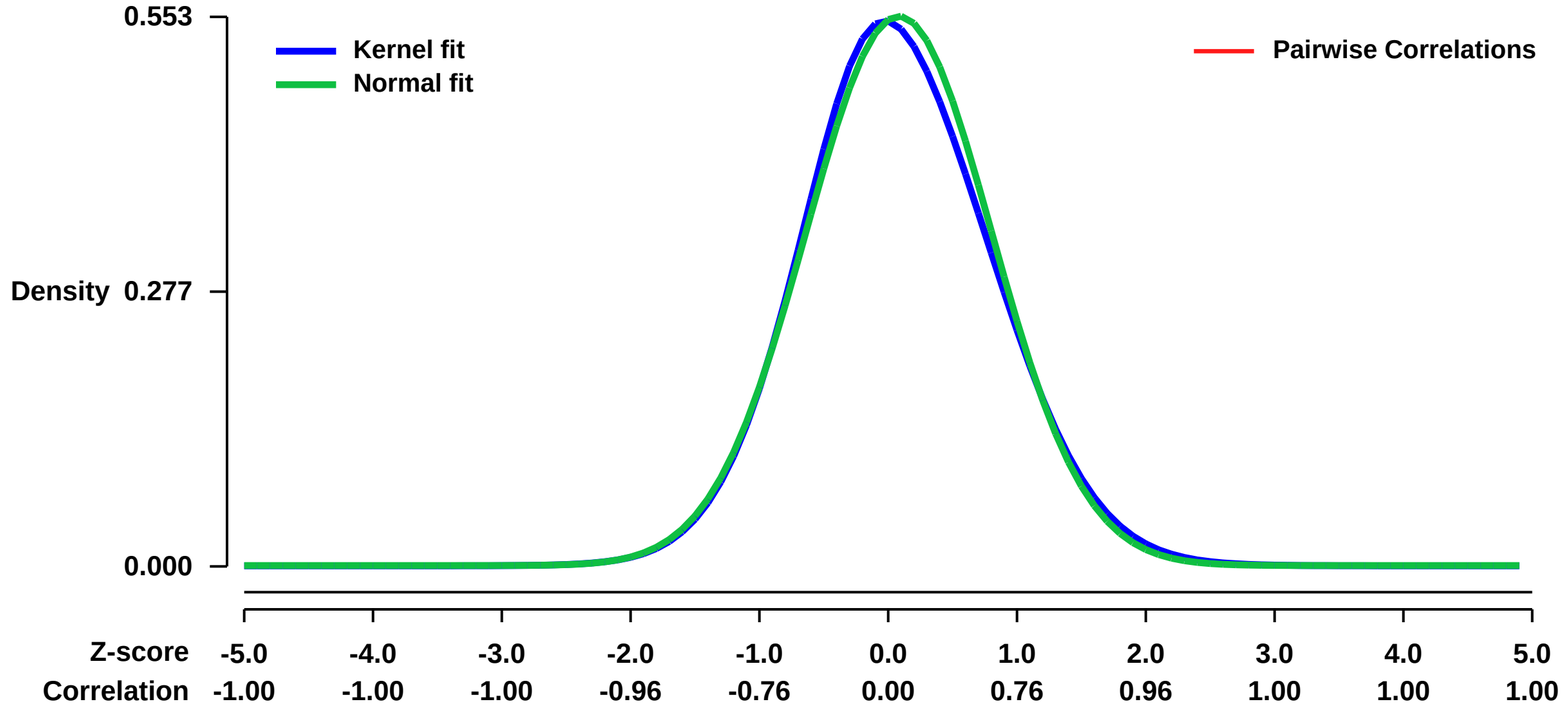

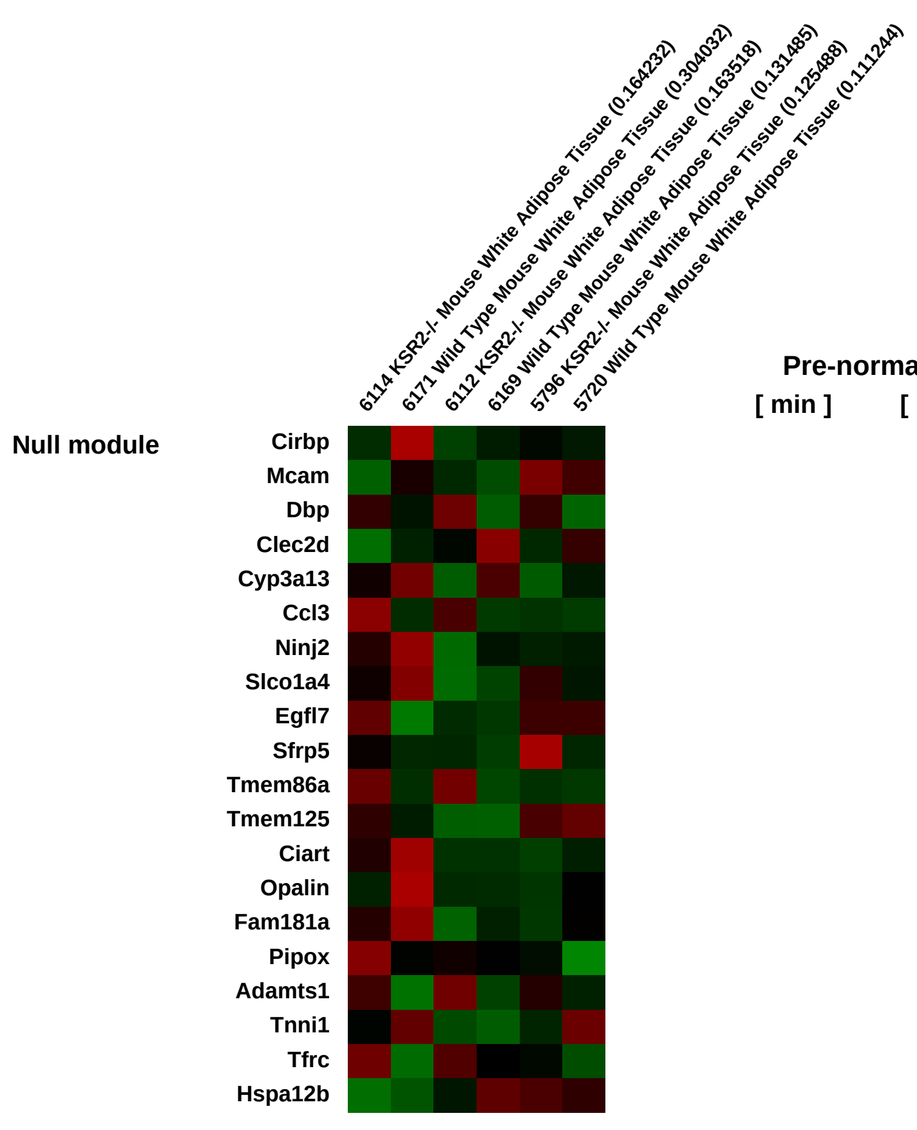

GEO Series "GSE31208" Expression Profiles

Num of samples in this series: 8

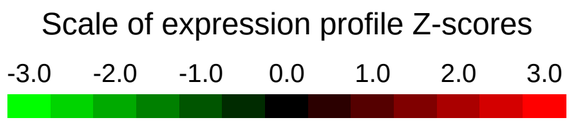

GEO Link:	**http://www.ncbi.nlm.nih.gov/geo/query/acc.cgi?acc=GSE31208**
Status:	**Public on Dec 31 2011**
Title:	**Expression data of MCK conditional frataxin knock-out mice**
Organism:	**Mus musculus**
Experiment type:	**Expression profiling by array**
Platform:	**GPL1261**
Pubmed ID:	
Summary & Design:	**Summary:** **Frataxin deficiency in human is the cause of Friedreich's ataxia (FA), a lethal neuro- and cardio-degenerative disease. Knock-out (KO) mice of this mouse model of FA exhibit classical cardiomyopathy of the patients. The onset of FA phenotypes in the KO mice is approximately 6-7 weeks of age. This genearray analysis was conducted to examine the changes in gene expression in the heart of KO mice relative to their wild-type (WT) littermates at 4- and 10-weeks of age. At 10-weeks of age, the KO mice begin to die from severe cardiomyopathy.** **Overall design:** **RNA from the heart of four female 4-week-old MCK littermates (two WT and two KO) and four female 10-week-old MCK littermates (two WT and two KO) was extracted and hybridised to Affymetrix Mouse Genome 430 2.0 Array.**

Background corr dist: **KL-Divergence = 0.0279, L1-Distance = 0.0409, L2-Distance = 0.0027, Normal std = 0.6823**

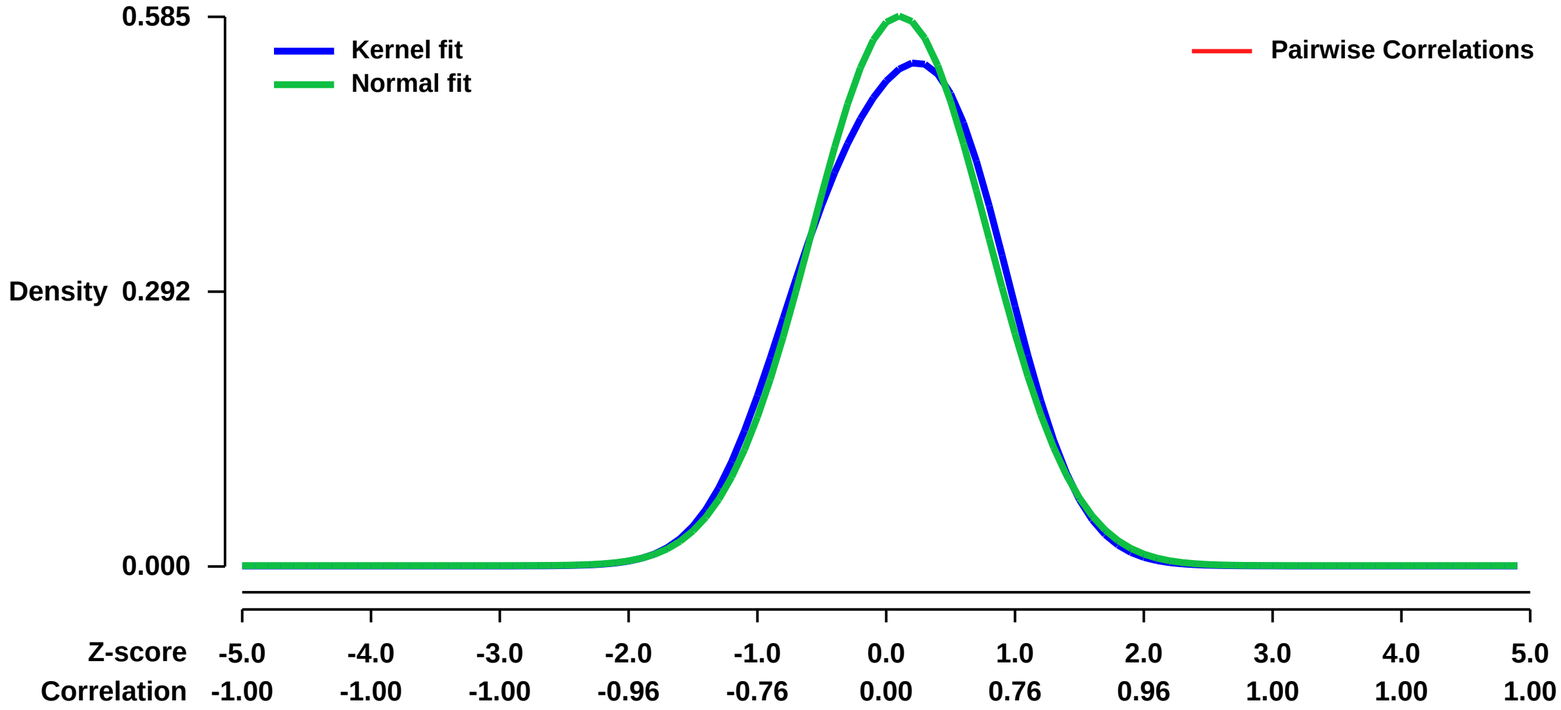

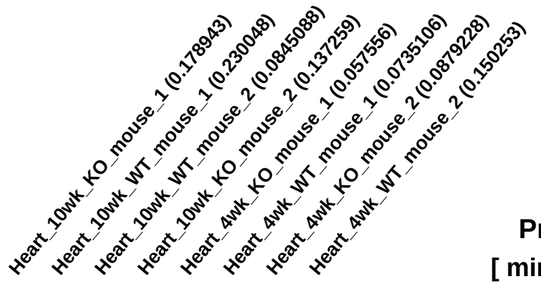

Pre-normalization Quantiles

[min] [medium] [max]

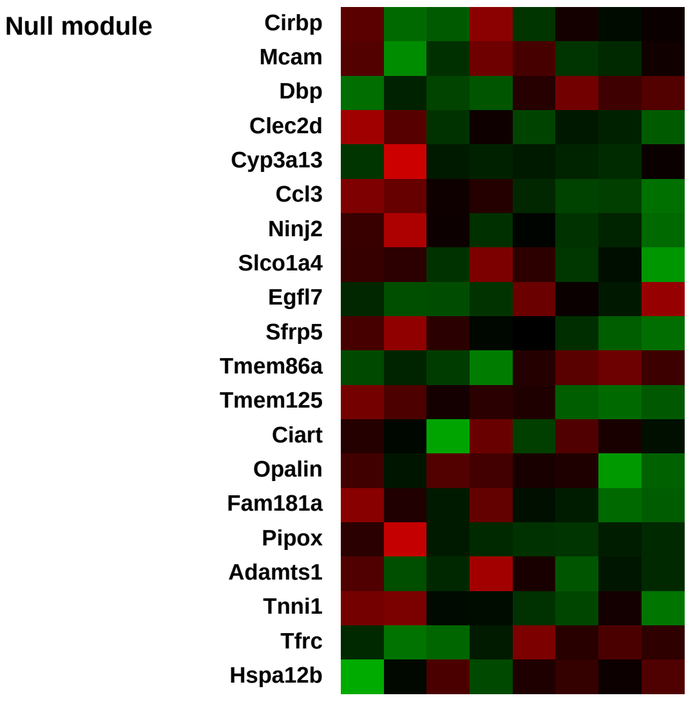

GEO Series "GSE37029" Expression Profiles

Num of samples in this series: 15

Scale of expression profile Z-scores

-3.0 -2.0 -1.0 0.0 1.0 2.0 3.0

GEO Link:	**http://www.ncbi.nlm.nih.gov/geo/query/acc.cgi?acc=GSE37029**
Status:	**Public on May 21 2012**
Title:	**Microarray analysis of WT bone marrow myeloid progenitors, BM cultured with GM-CSF and M-CSF, and monocytes treated with GM-CSF**
Organism:	**Mus musculus**
Experiment type:	**Expression profiling by array**
Platform:	**GPL1261**
Pubmed ID:	
Summary & Design:	**Summary:** **Analysis of genes induced in DC precursors and in BM cells and monocytes treated with GM-CSF** **Overall design:** **For progenitor arrays, bone marrow progenitors (CMP, GMP, CDP, and pre-cDC) were harvested from WT C57Bl/6 mice. For culture arrays, BM was cultured in the presence of GM-CSF or M-CSF and adherent and non-adherent cells sorted. For monocyte cultures, sorted BM monocytes were treated with GM-CSF for 0, 24 or 48 hours.**

Background corr dist: **KL-Divergence = 0.0614, L1-Distance = 0.0519, L2-Distance = 0.0049, Normal std = 0.5449**

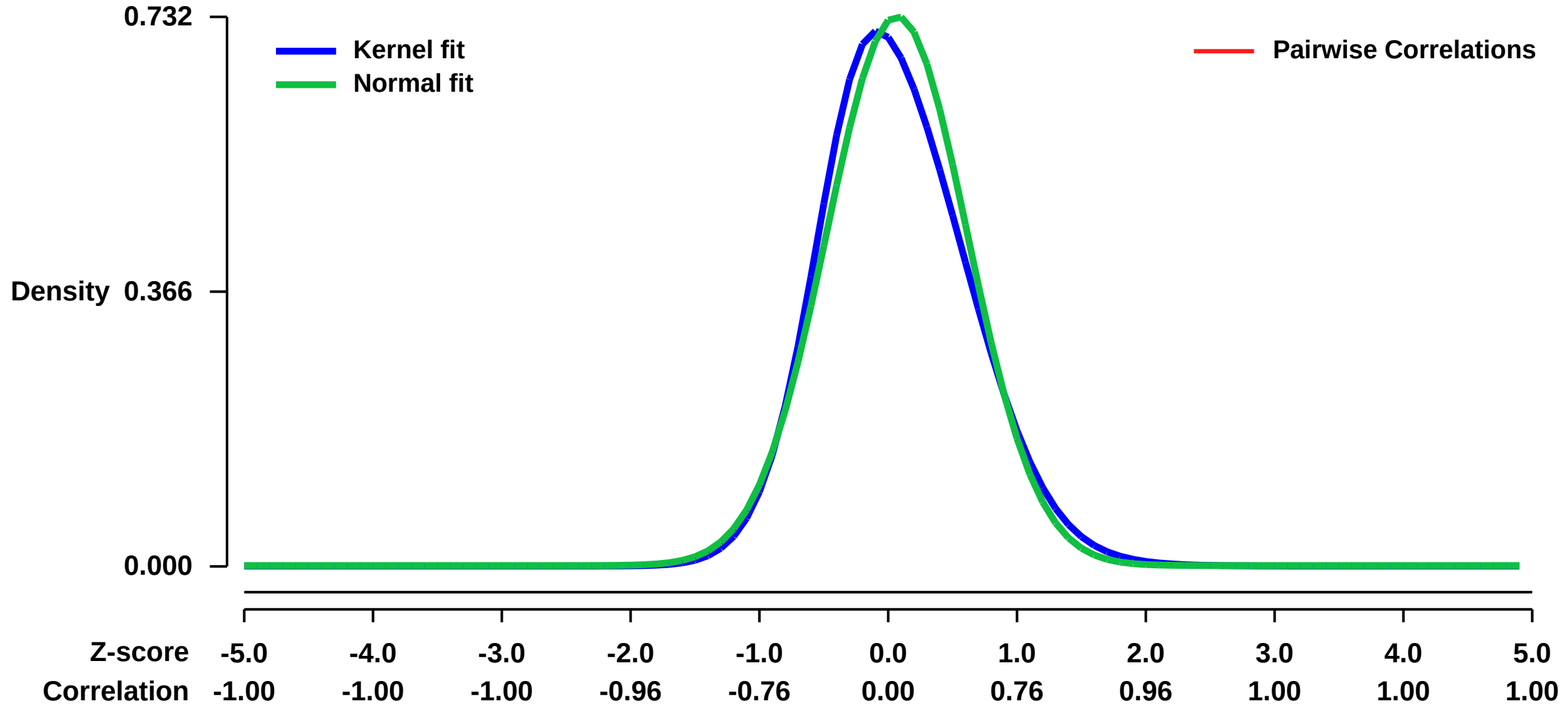

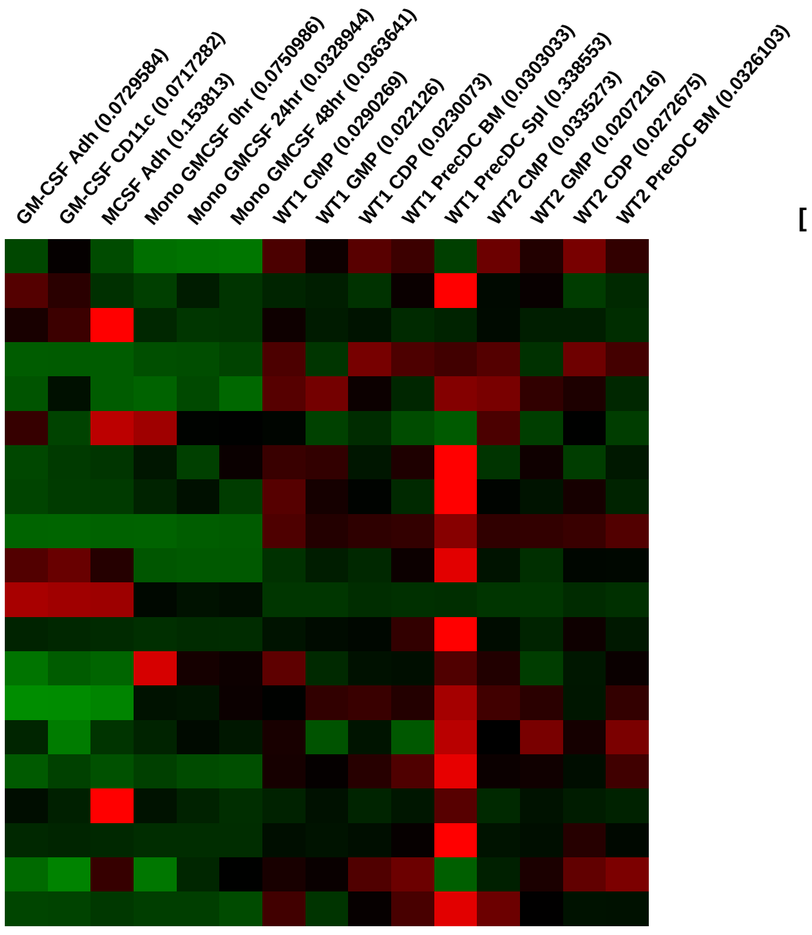

GEO Series "GSE45430" Expression Profiles

Num of samples in this series: 9

Scale of expression profile Z-scores

-3.0 -2.0 -1.0 0.0 1.0 2.0 3.0

GEO Link:	http://www.ncbi.nlm.nih.gov/geo/query/acc.cgi?acc=GSE45430
Status:	Public on Mar 23 2013
Title:	Sox4 is a key oncogenic target in C/EBP‚Äì mutant Acute Myeloid Leukemia
Organism:	Mus musculus
Experiment type:	Expression profiling by array
Platform:	GPL1261
Pubmed ID:	24183681
Summary & Design:	**Summary:** Mutation or epigenetic silencing of the transcription factor C/EBP‚Äì is observed in ~10% of patients with acute myeloid leukemia (AML). In both cases, a common global gene expression profile is observed, but down-stream targets relevant for leukemogenesis are not known. Here we identify Sox4 as a direct target of C/EBP‚Äì whereby its expression is inversely correlated with C/EBP‚Äì activity. Downregulation of Sox4 abrogated increased self-renewal of leukemic cells and restored their differentiation. Gene expression profiles of leukemia initiating cells (LICs) from both Sox4 overexpression and murine mutant C/EBP‚Äì AML models clustered together, but differed from other types of AML. Our data demonstrate that Sox4 overexpression resulting from C/EBP‚Äì inactivation contributes to the development of leukemias with a distinct LIC phenotype. **Overall design:** K/L (bi-allelic Cebpa mutations) leukemic mice and Sox4 overexprssing leukemic mice were used for RNA extraction and hybridization on Affymetrix microarrays. We compared these microarray samples with the C57/BL6 wild type mice.

Background corr dist: KL-Divergence = 0.0498, L1-Distance = 0.0448, L2-Distance = 0.0033, Normal std = 0.5848

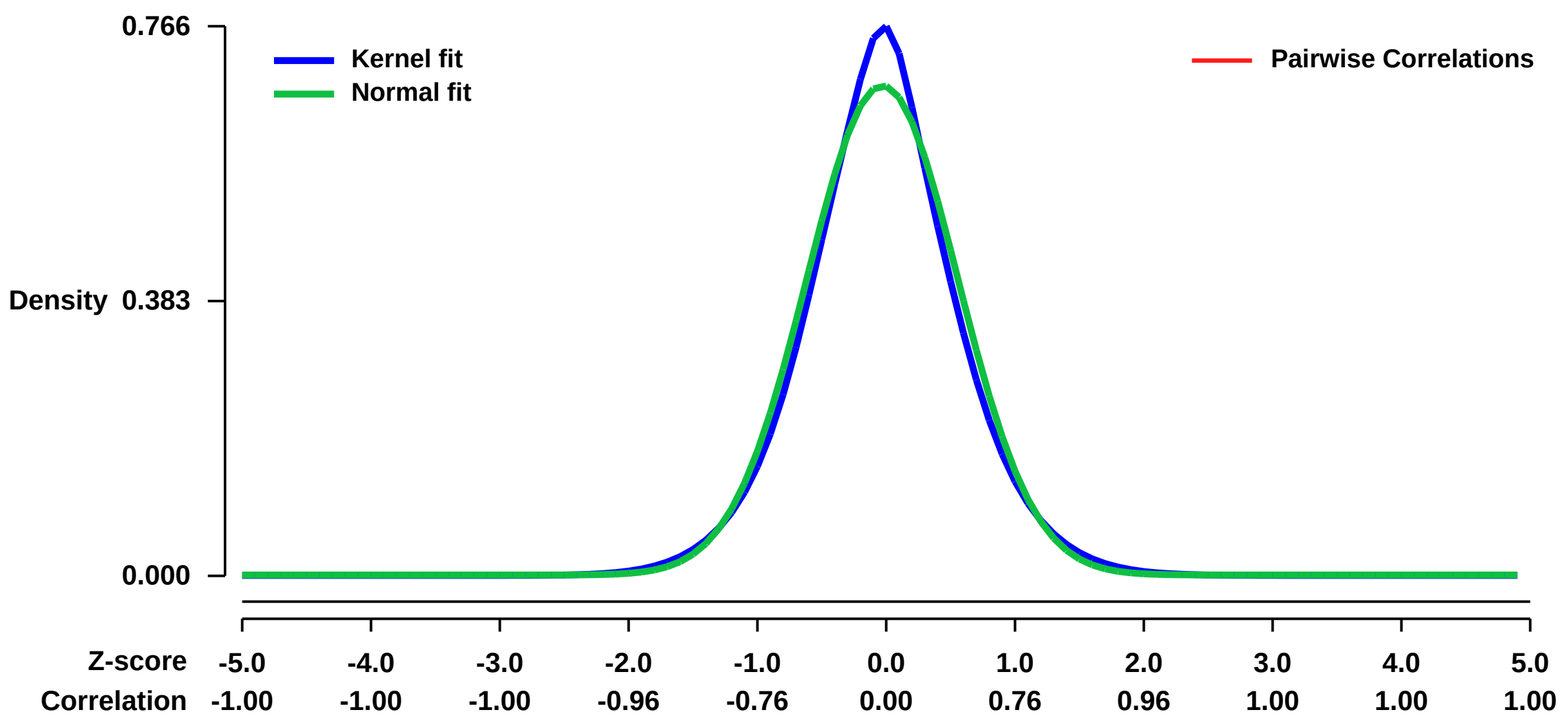

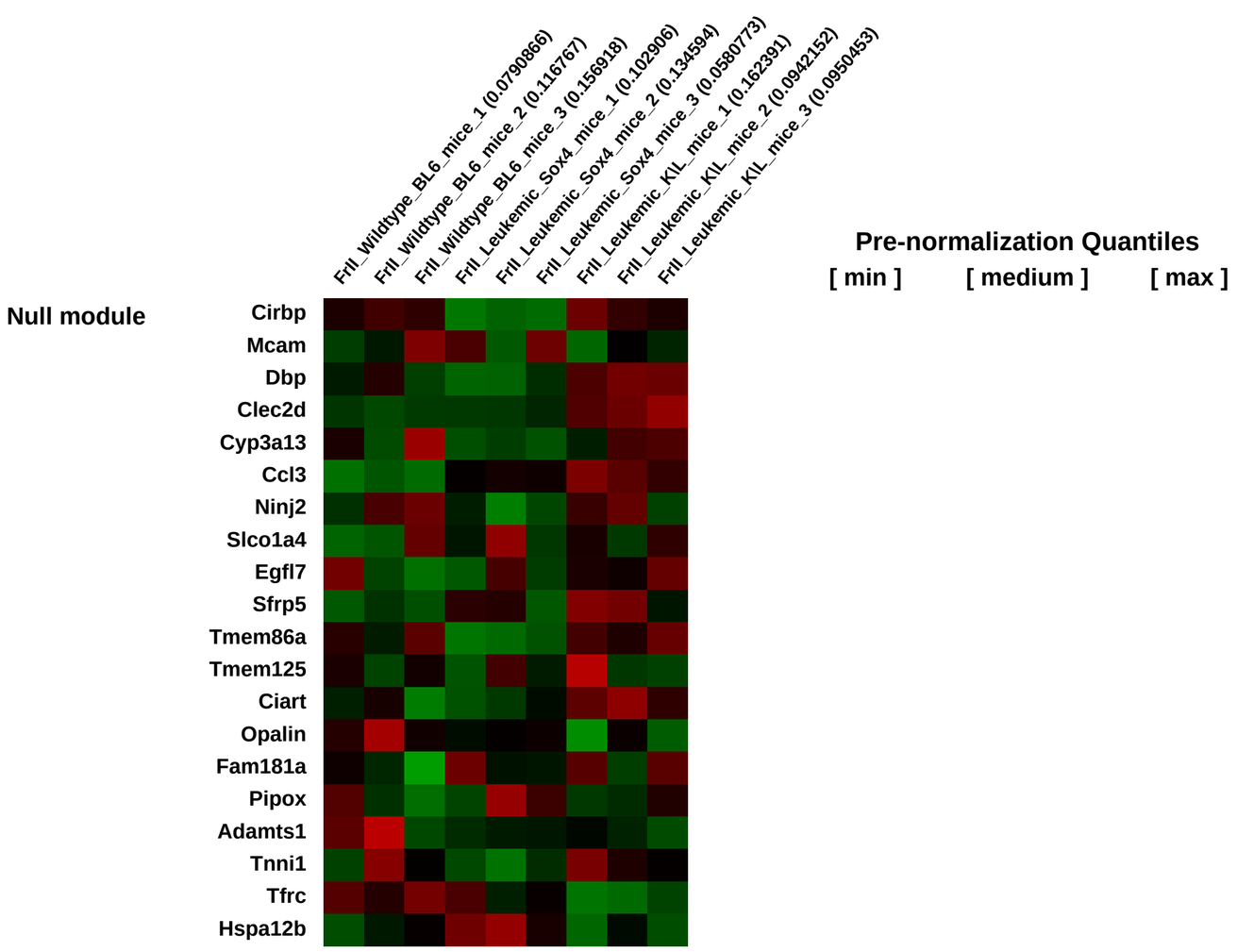

GEO Series "GSE19979" Expression Profiles

Num of samples in this series: 6

Scale of expression profile Z-scores

-3.0 -2.0 -1.0 0.0 1.0 2.0 3.0

GEO Link:	http://www.ncbi.nlm.nih.gov/geo/query/acc.cgi?acc=GSE19979
Status:	Public on Jan 22 2010
Title:	Gene expression profiles of P7 bladder epithelium compartments isolated from Upk1b mice. (GUDMAP Series ID: 34)
Organism:	Mus musculus
Experiment type:	Expression profiling by array
Platform:	GPL1261
Pubmed ID:	
Summary & Design:	**Summary:** The long term objective is to create an encyclopedia of the expression levels of all genes in multiple components of the developing genitourinary tract The central thesis is straightforward. The combination of microdissected tissues and FACS sorted cells plus microarray analysis offers a powerful, efficient and effective method for the creation of a global gene expression atlas of the developing urogenital system. Microarrays with essentially complete genome coverage can be used to quantitate expression levels of every gene. The ensuing rapid read-out provides an expression atlas that is more sensitive, more economical and more complete than would be possible by in situ hybridizations alone. The data submitted here delineates the gene expression profiles of the epithelial compartments of the P7 mouse bladder. **Overall design:** At postnatal day 7 mice were euthanized by CO2 asphyxiation and the bladders were removed and cut at the bladder neck. The bladder was cut into rings and treated with 1 mg/ml trypsin in Tyrode's solution for 30 minutes at 37 ´°C. The layers were separated by gentle microdissection and the epithelial layer was further digested in a mixture of Blendzymes 1 & 4 at 37 ´°C until a single cell suspension was obtained. The samples were placed in RLT and stored at -80 ´°C.RNA was prepared and the Epicentre 2-round amplification scheme described under the Lessard Group Protocols on the GUDMAP pages were performed. The Affymetrix GeneChip Mouse Genome 430 2.0 Array was used to interrogate the amplified RNA.

Background corr dist: KL-Divergence = 0.0264, L1-Distance = 0.0357, L2-Distance = 0.0018, Normal std = 0.7181

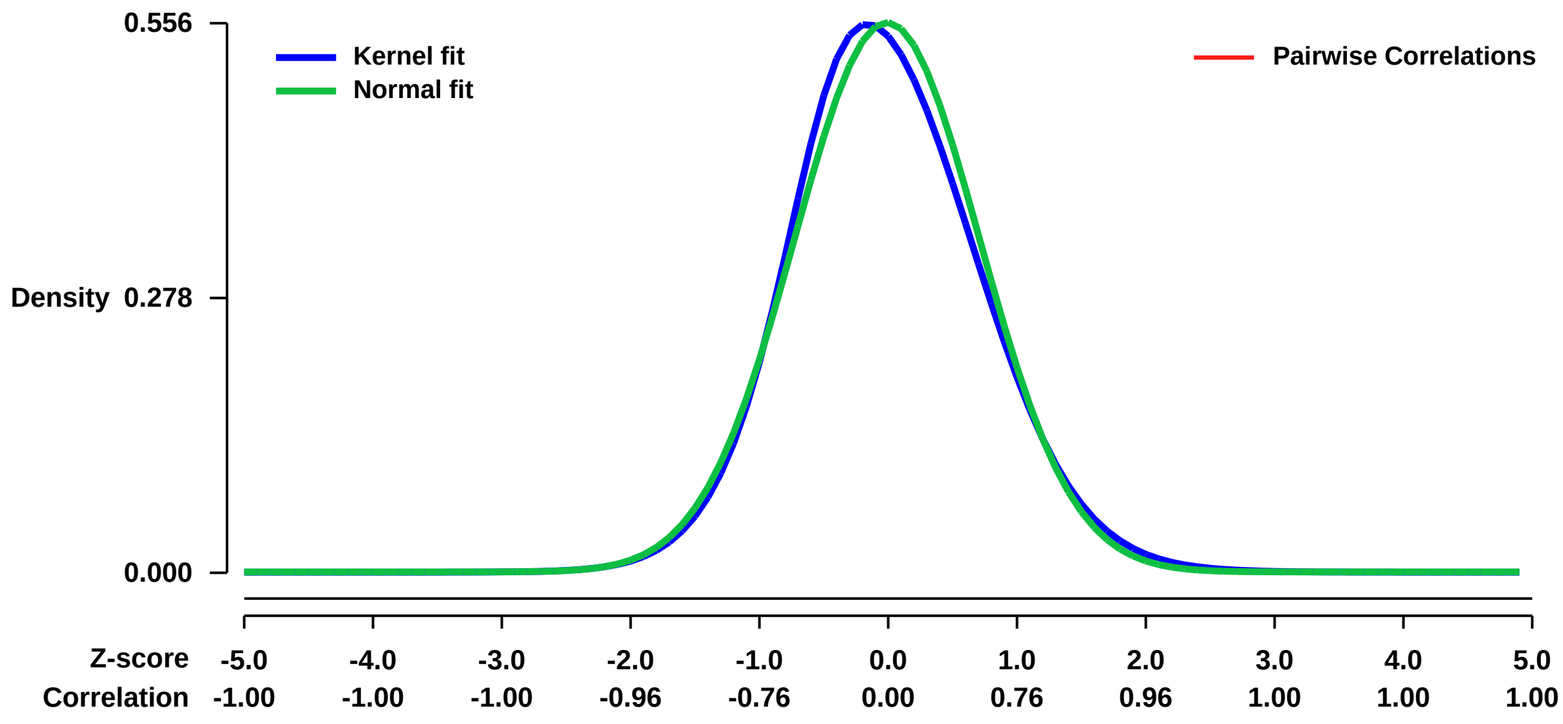

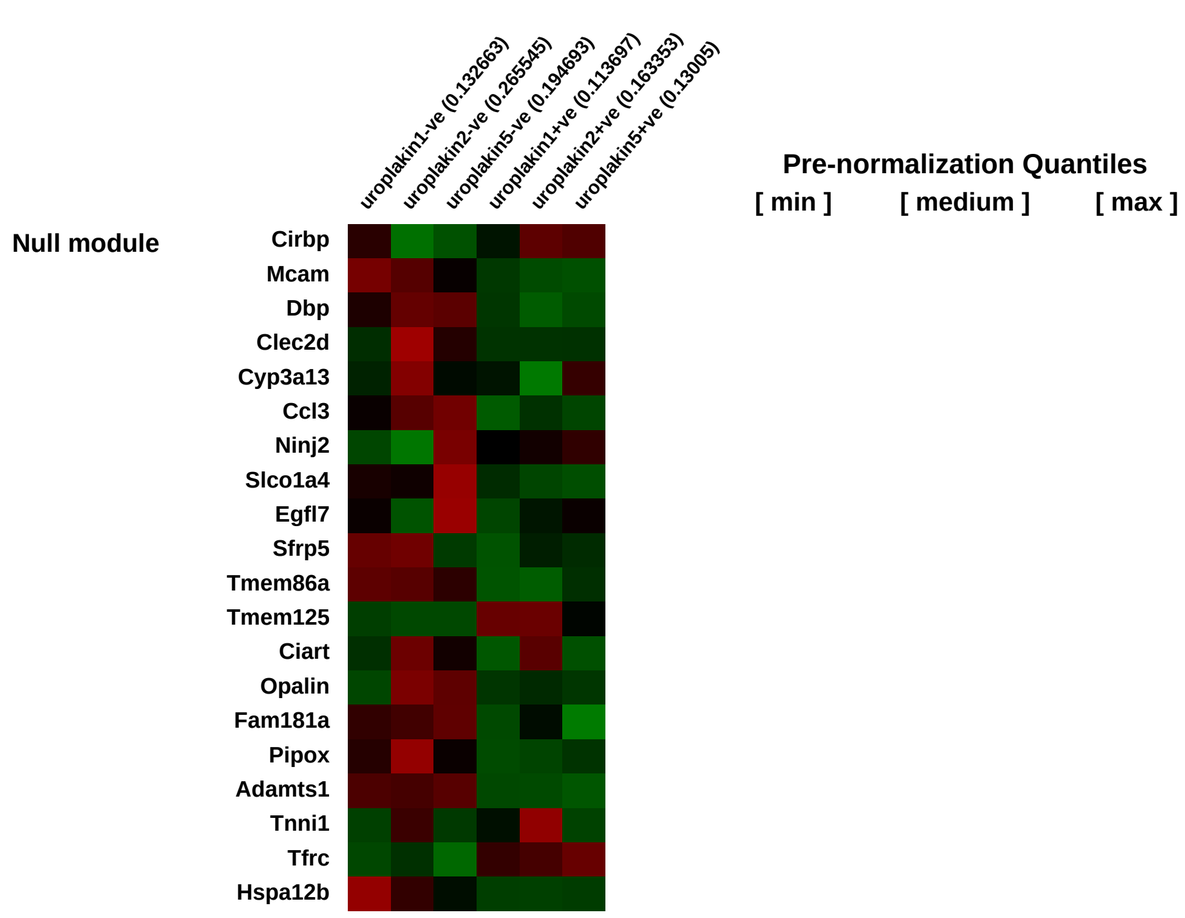

GEO Series "GSE21515" Expression Profiles

Num of samples in this series: 18

Scale of expression profile Z-scores

-3.0 -2.0 -1.0 0.0 1.0 2.0 3.0

GEO Link:	http://www.ncbi.nlm.nih.gov/geo/query/acc.cgi?acc=GSE21515
Status:	Public on May 13 2010
Title:	Expression data from mouse ES and iPS cells
Organism:	Mus musculus
Experiment type:	Expression profiling by array
Platform:	GPL1261
Pubmed ID:	20382743
Summary & Design:	**Summary:** Induced pluripotent stem (iPS) cells were produced from reprogramming of somatic cells, and they are shown to possess pluripotent properties similar to embryonic stem (ES) cells. Here we used microarrays to detail the global expression pattern among the ES cells and iPS cells, as well as the original mouse embryo fibroblast (MEF), to identify important players involved in the reprogramming process. **Overall design:** Mouse ES cell cultures, as well as selected iPS cell lines and the original MEF cells they were derived from, were used for RNA extraction and hybridization on Affymetrix microarrays. Three biological replicates for each sample were processed. GeneChips were processed and data were analyzed using the RMA package of Bioconductor.

Background corr dist: KL-Divergence = 0.0662, L1-Distance = 0.0310, L2-Distance = 0.0018, Normal std = 0.5048

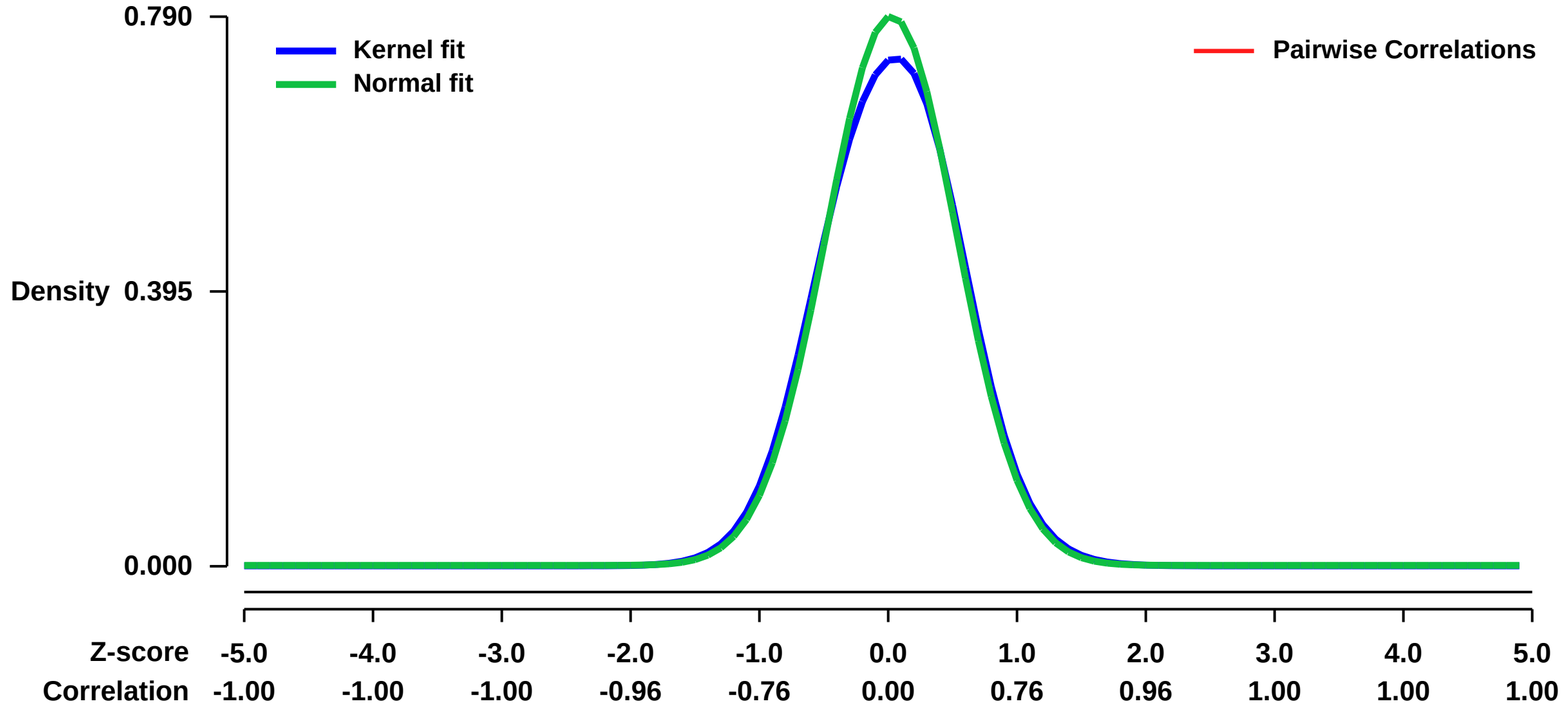

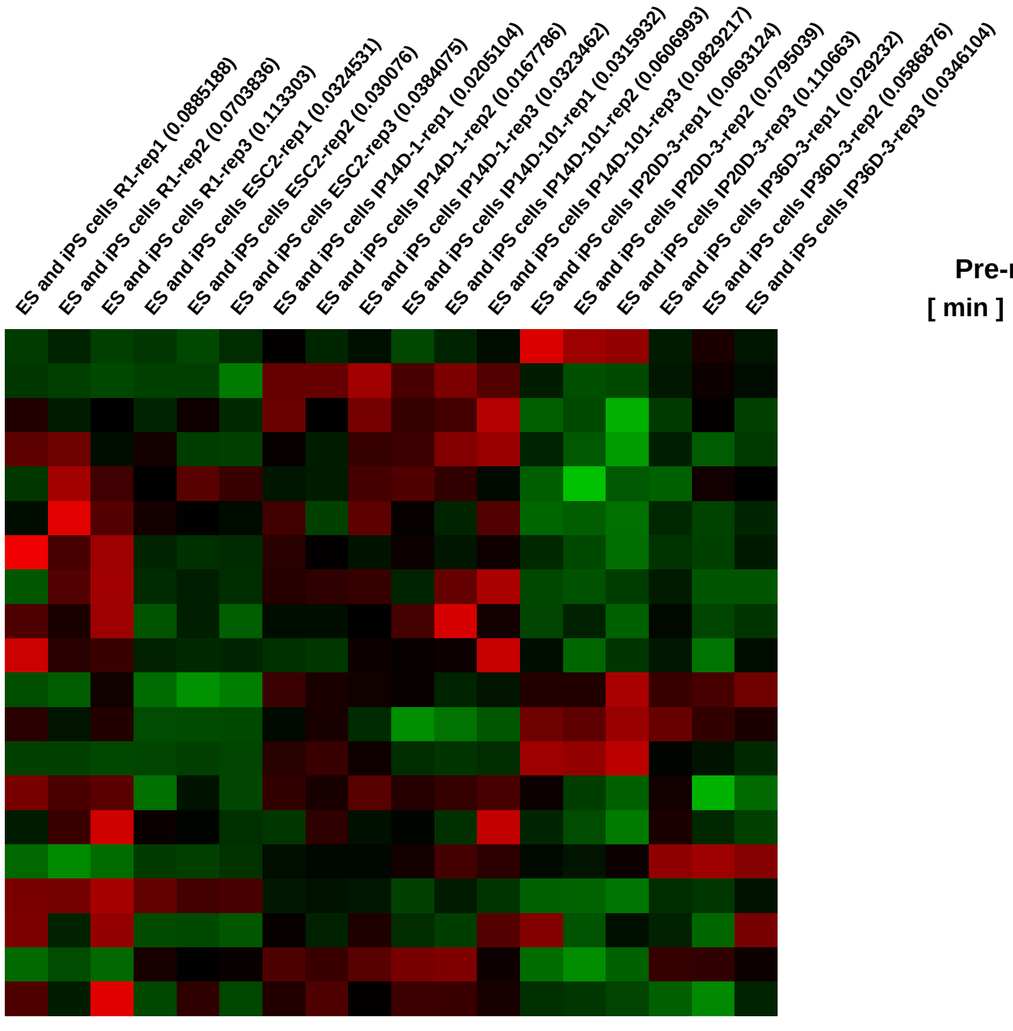

GEO Series "GSE4041" Expression Profiles

Num of samples in this series: 6

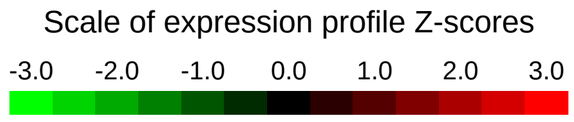

GEO Link:	**http://www.ncbi.nlm.nih.gov/geo/query/acc.cgi?acc=GSE4041**
Status:	**Public on Jan 13 2006**
Title:	**zhang-affy-mouse-200705**
Organism:	**Mus musculus**
Experiment type:	**Expression profiling by array**
Platform:	**GPL1261**
Pubmed ID:	
Summary & Design:	**Summary:** **In our original grant we proposed to use the NR3B-null mouse model to study the role of NR3B subunit in motor neuron function. We have now successfully generated NR3B null mice. Interestingly, NR3B-null mice invariably die at age P4-P8. Our preliminary examination indicates that the motor strength of these mice is severely impaired prior to death. As we continue to explore the cause of death in NR3B null mice, we propose to conduct gene profiling experiments to search for transcription changes in the brain related to ablation of the NR3B gene. We have used the facility provided by the NINDS/NIMH Microarray Consortium to identify genes that show abnormal expression patterns in these mice. We would like to compare these changes with that opccured in SOD1 mice, a mouse model of motor neuron diseases. Analysis of these genes will help to identify changes in networks and pathways that may cause the death of NR3B-null mice. These studies will further help to elucidate the functional role of NR3B in motor neurons.** **We will compare samples from motor neurons of wild type and SOD1 mice to identify genes that show abnormal expression patterns, which may be implicated in the death of SOD1 mice and shared with the same changes in NR3B-null mice.** **We hypothesize that genes with their transcription level changing significantly by ablation of NR3B will be associated with the molecular mechanism underlying the death of motor neurons in NR3B null mice.** **As NR3B is expressed primarily in the motor neurons of hindbrain and spinal cord, we have first collected and analyzed the spinal cord samples from NR3B null mice and wild-type controls in P4, an age of disease onset. We like to compare motor neuron smaples from SOD1 mice at the age around the disease onset. Total RNA from total 6 samples will be purified from ~200 motor neurons obtained by Laser Capture Microdissection. Extracted RNAs will be subjected to two rounds of amplification and the obtained cRNA will be biotinylated. The purified cRNA will be sent to the NINDS/NIMH Microarray Consortium be used to hybridize the GeneChip Mouse Genome 430 2.0 Array. The hybridization, scanning, and initial data analysis of these GeneChips will be conducted by the Consortium staff. We will analyze the collected data further after data collection. We will first identify genes that show significant changes between wild-type and SOD1 mice and then compare that with the result from NR3B null mice.** **Keywords: other** **Overall design:**

Background corr dist: **KL-Divergence = 0.0458, L1-Distance = 0.0243, L2-Distance = 0.0007, Normal std = 0.5932**

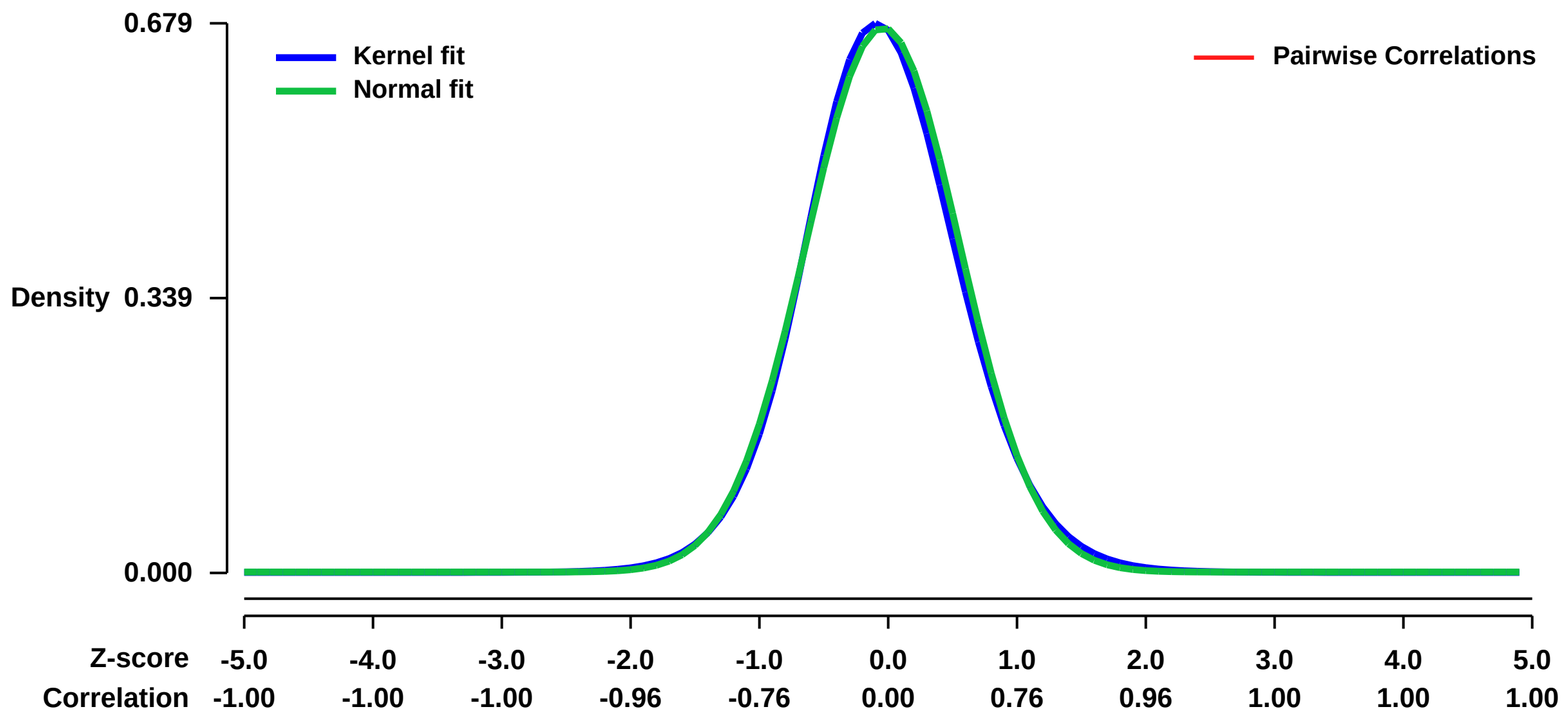

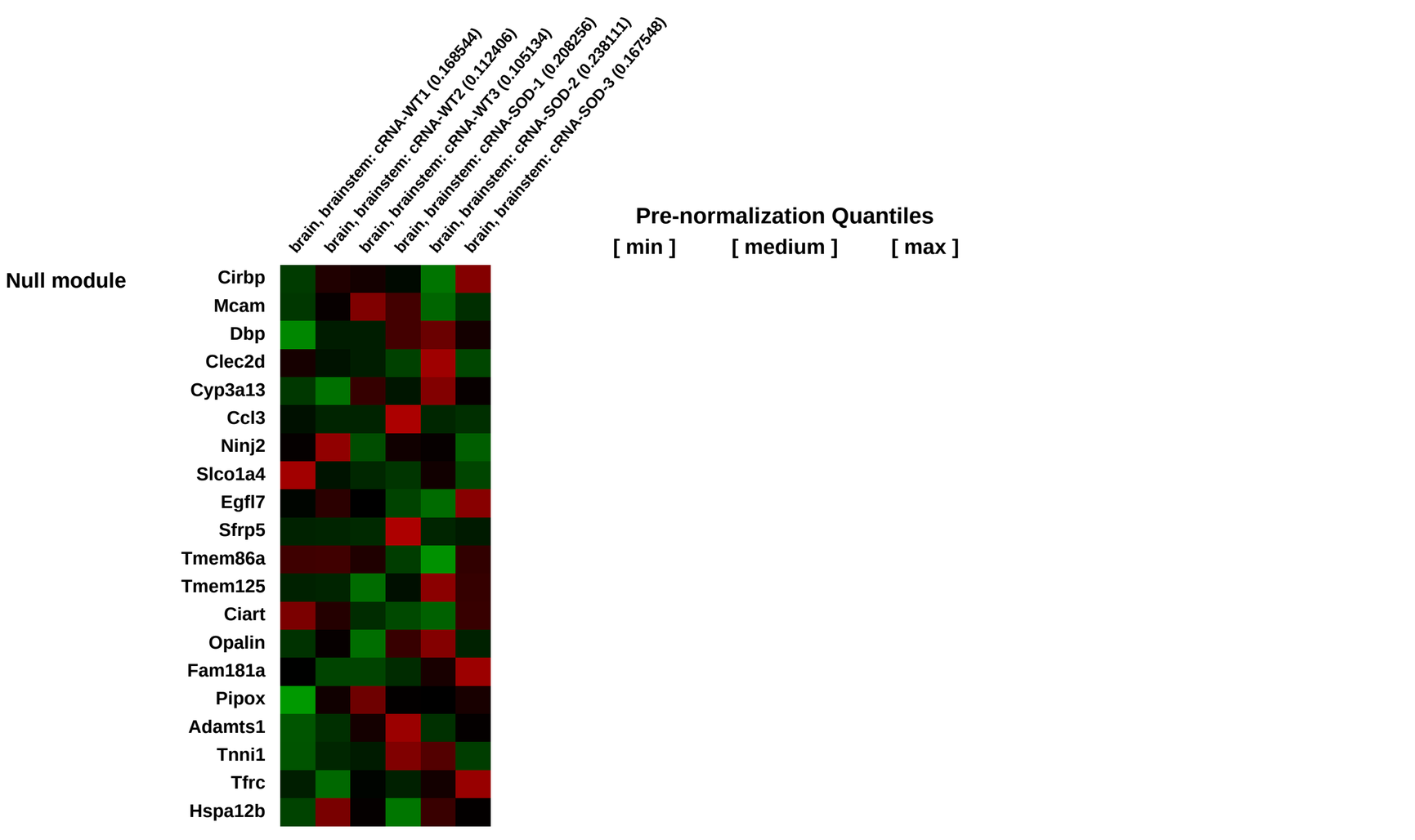

GEO Series "GSE50122" Expression Profiles

Num of samples in this series: 10

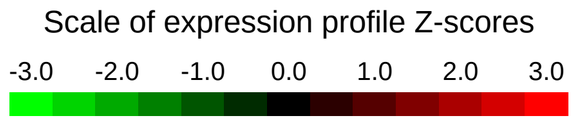

GEO Link:	http://www.ncbi.nlm.nih.gov/geo/query/acc.cgi?acc=GSE50122
Status:	Public on Nov 18 2013
Title:	Runx3 function in splenic NK cells (IL-2 or IL-15)
Organism:	Mus musculus
Experiment type:	Expression profiling by array
Platform:	GPL1261
Pubmed ID:	24236182
Summary & Design:	**Summary:** NK cells are innate immune cells that recognize and kill foreign, virally-infected and tumor cells without the need for prior immunization. NK expansion following viral infection is IL-2 or IL-15-dependent. **Overall design:** To identify Runx3 responsive genes, NK cells were isolated from spleen of WT and Runx3-/- mice . Ten samples (5 WT and 5 Runx3-/-) of freshly isolated NK cells were separately obtained from individual mice. Cells were cultured for 7 days with IL-2 or IL-15.

Background corr dist: KL-Divergence = 0.0244, L1-Distance = 0.0693, L2-Distance = 0.0057, Normal std = 0.8495

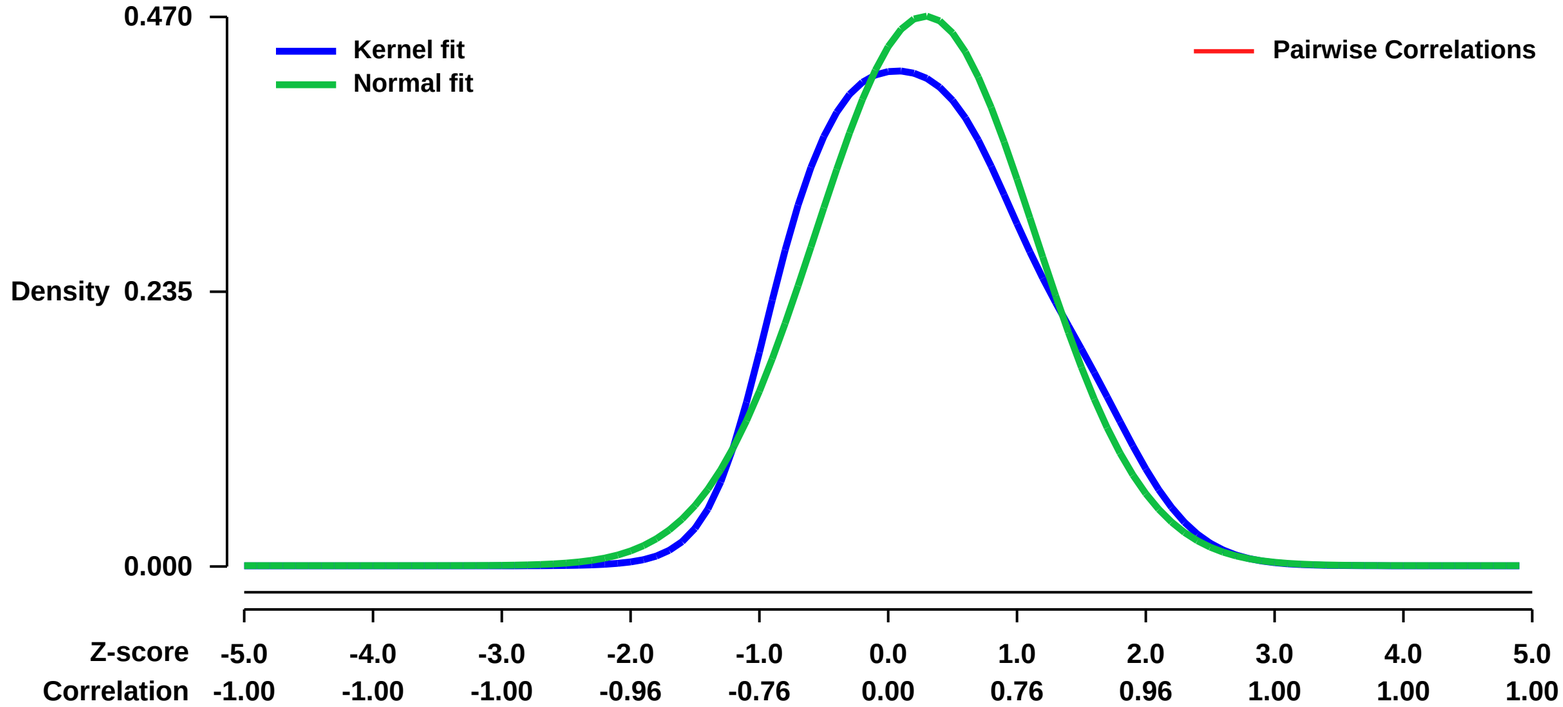

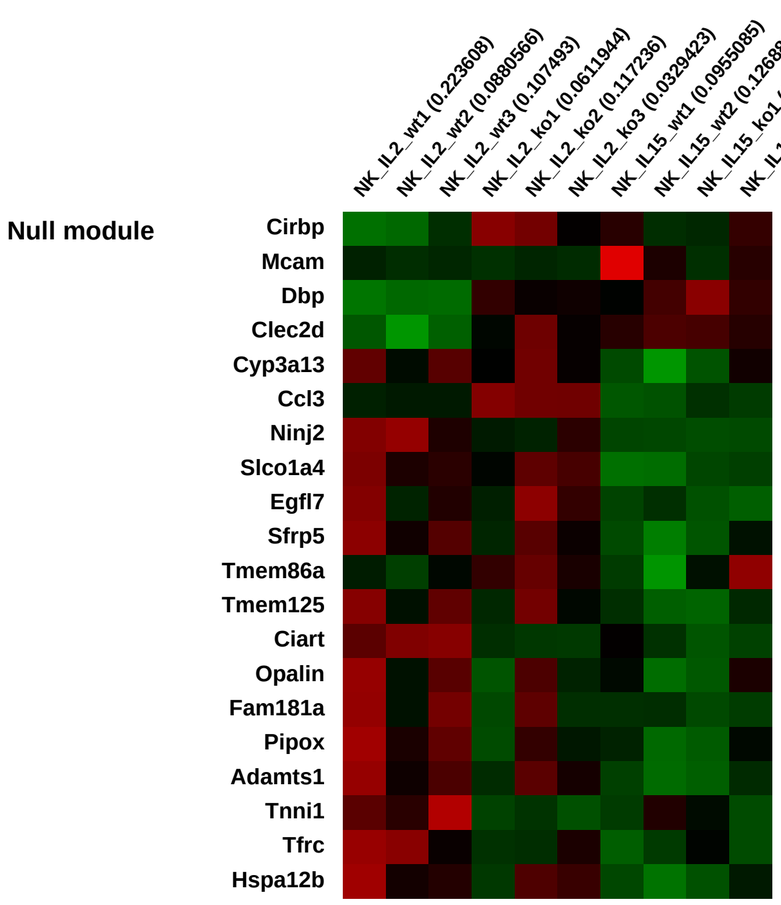

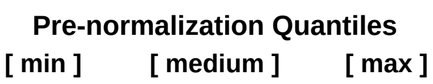

GEO Series "GSE23502" Expression Profiles

Num of samples in this series: 8

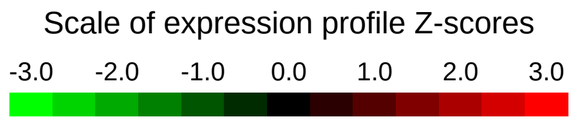

GEO Link:	http://www.ncbi.nlm.nih.gov/geo/query/acc.cgi?acc=GSE23502
Status:	Public on Dec 15 2010
Title:	Differentially expressed genes of CD11b+Gr-1+ myeloid cells
Organism:	Mus musculus
Experiment type:	Expression profiling by array
Platform:	GPL1261
Pubmed ID:	21170045
Summary & Design:	**Summary:** Differentially expressed genes of CD11b+Gr-1+ immature myeloid cells (IMCs) in the bone marrow and colonic tumor setting of histidine decarboxylase (HDC)-KO mice were examined by microarray (Affymetrix Mouse 430.2 array). Myeloid differentiation-related candidate genes were sought to be isolated and functionally studied. **Overall design:** Four sets of comparisons were performed to screen for upregulated or downregulated genes in the HDC-KO CD11b+Gr-1+ IMCs or MDSCs (experiment group) compared to the WT group: (1) HDC-expressing CD11b+Gr-1+ IMCs of bone marrow of HDC KO mice compared to bone marrow IMCs of WT mice; (2) CD11b+Gr-1+ MDSCs in tumors of HDC-KO mice compared to WT mice; (3) CD11b+Gr-1+ MDSCs of WT colon tumors compared to IMCs in the WT bone marrow; and (4) CD11b+Gr-1+ MDSCs of colon tumors of HDC-KO mice compared to IMCs in the bone marrow of HDC-KO mice.

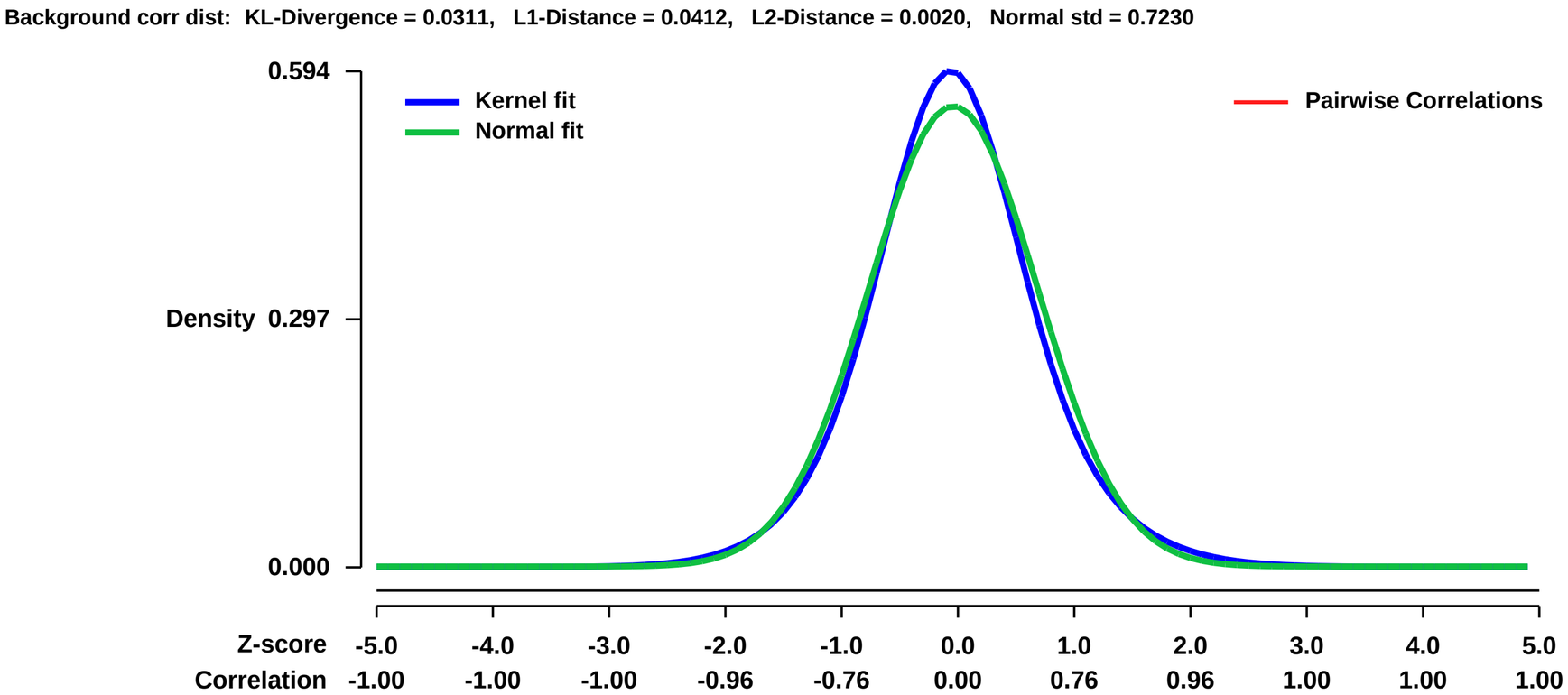

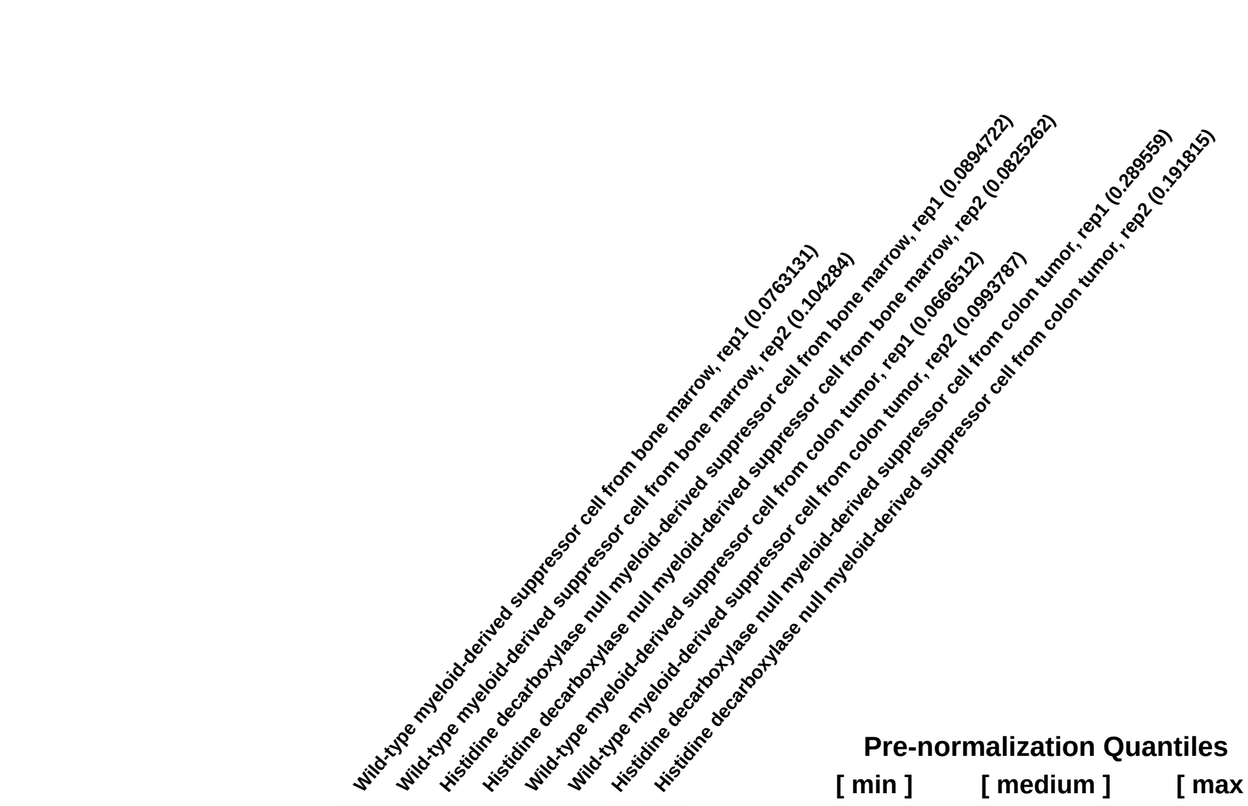

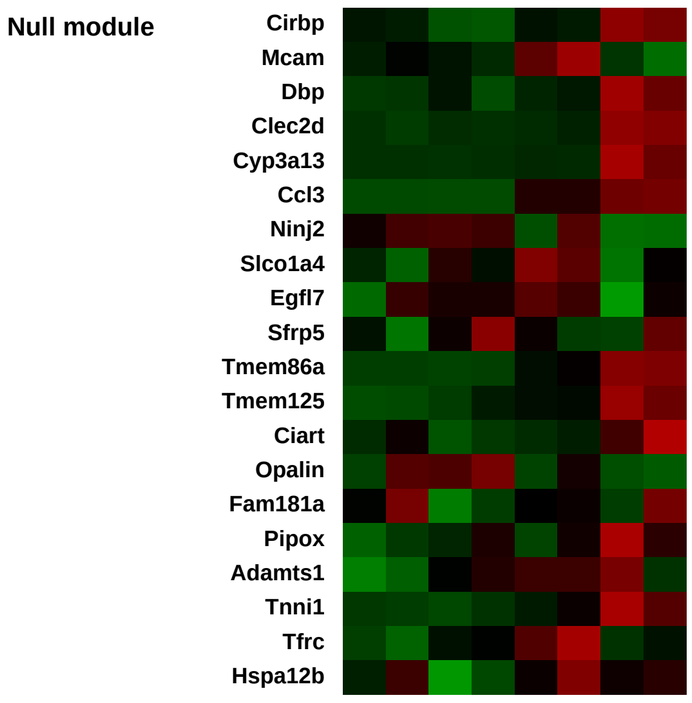

GEO Series "GSE30293" Expression Profiles

Num of samples in this series: 8

Scale of expression profile Z-scores

-3.0 -2.0 -1.0 0.0 1.0 2.0 3.0

GEO Link:	**http://www.ncbi.nlm.nih.gov/geo/query/acc.cgi?acc=GSE30293**
Status:	**Public on Dec 01 2011**
Title:	**Zfp281 Functions as a Transcriptional Repressor for Pluripotency of Mouse Embryonic Stem Cells**
Organism:	**Mus musculus**
Experiment type:	**Expression profiling by array**
Platform:	**GPL1261**
Pubmed ID:	
Summary & Design:	**Summary:** **Zfp281 is a partner protein of Nanog. To identify potential target genes of Zfp281, we generated Zfp281 null ESCs using gene targeting, and compared transcriptomic changes between multiple lines of wildtype, heterozygous and null ESCs.** **Overall design:** **Total 8 ESC lines: 3 wildtype lines, 2 heterozygous lines, and 3 null lines.**

Background corr dist: **KL-Divergence = 0.0694, L1-Distance = 0.0217, L2-Distance = 0.0007, Normal std = 0.5013**

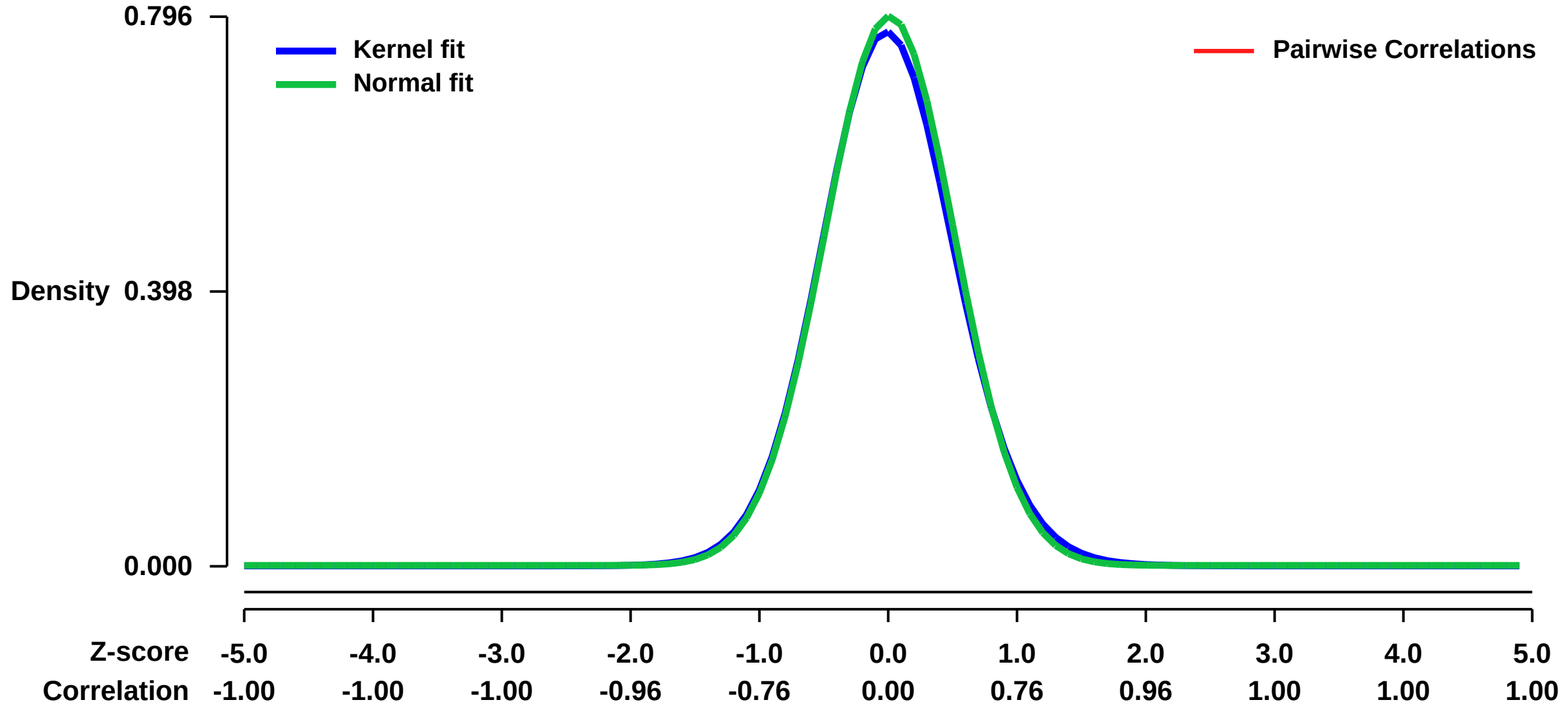

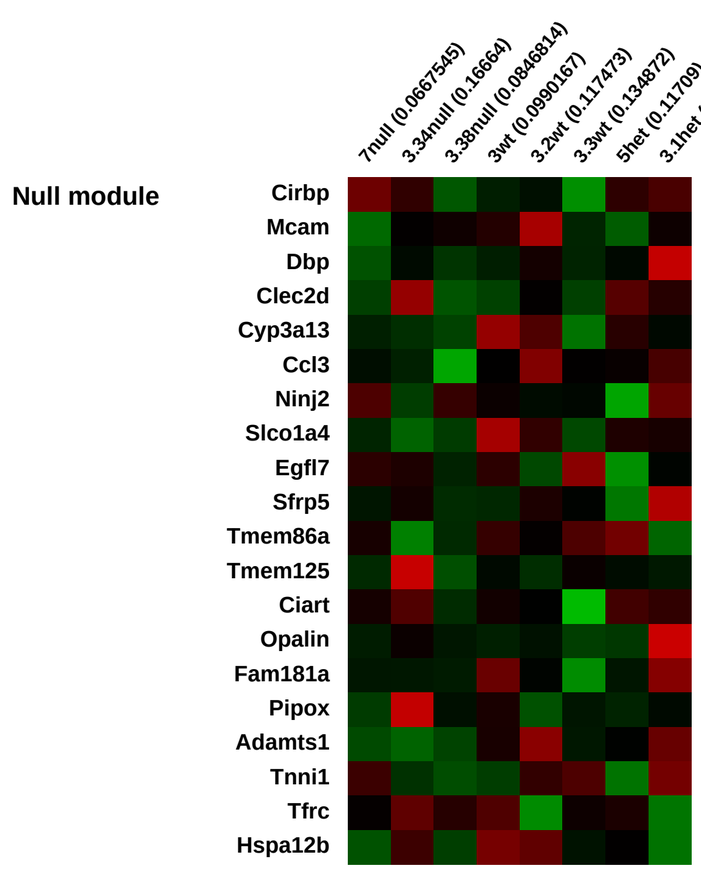

GEO Series "GSE38696" Expression Profiles

Num of samples in this series: 8

Scale of expression profile Z-scores

-3.0 -2.0 -1.0 0.0 1.0 2.0 3.0

GEO Link:	http://www.ncbi.nlm.nih.gov/geo/query/acc.cgi?acc=GSE38696
Status:	Public on Jun 14 2012
Title:	Gene expression in mouse germinal center light zone and dark zone B cells
Organism:	Mus musculus
Experiment type:	Expression profiling by array
Platform:	GPL1261
Pubmed ID:	22740445
Summary & Design:	**Summary:** Microarrays of gene expression in mouse germinal center light zone and dark zone B cells sorted according to the expression of cell surface molecules CD83 and CXCR4 We used microarray data to identify genes differentially expressed by B cells in the light and dark zones of germinal centers from mouse skin-draining lymph nodes 12 days after subcutaneous immunization with NP-OVA in alum. **Overall design:** Germinal center B cells (B220+CD38-CD95+) were sorted from immunized mouse lymph nodes into light zone (CXCR4hi/CD83lo) and dark zone (CXCR4lo/CD83hi) populations, from which RNA was extracted

Background corr dist: KL-Divergence = 0.0538, L1-Distance = 0.0239, L2-Distance = 0.0006, Normal std = 0.5628

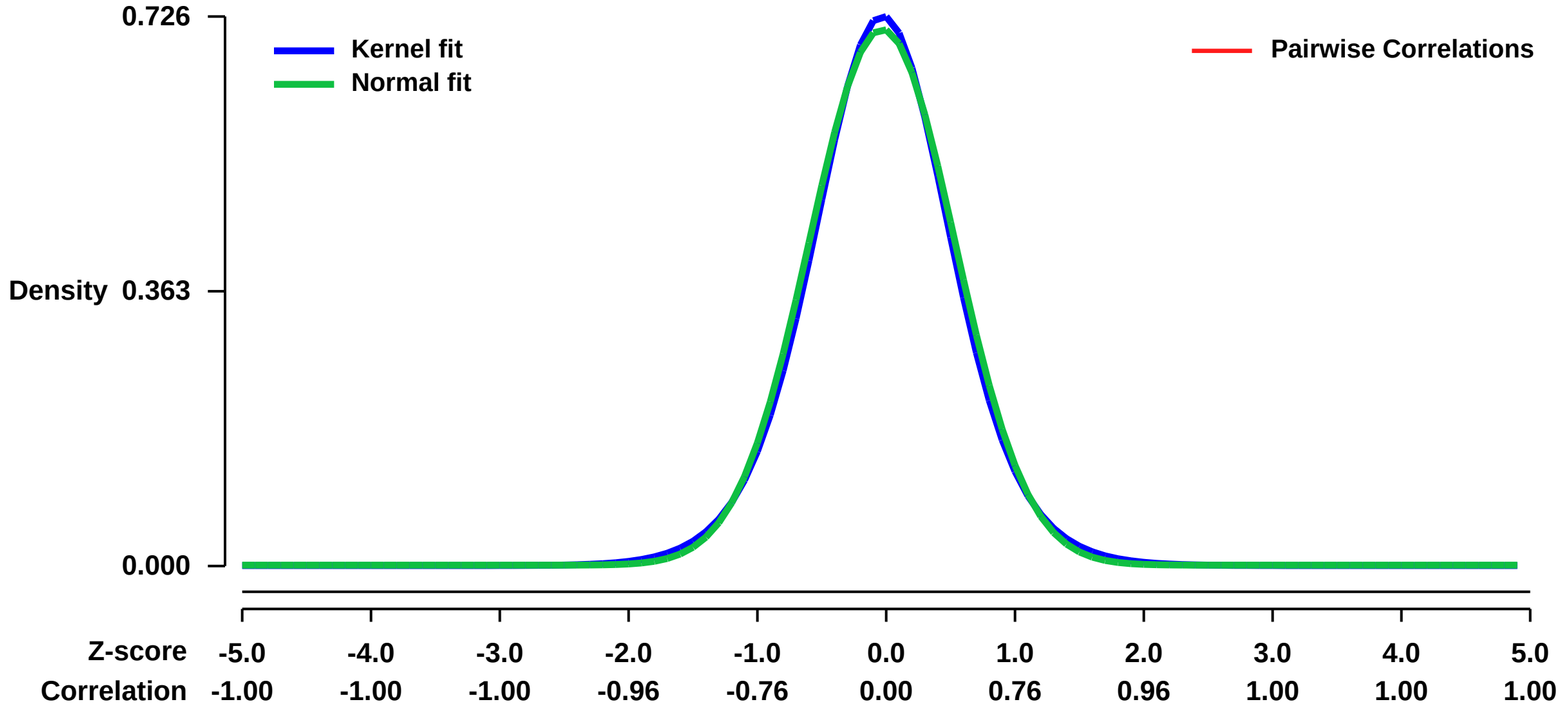

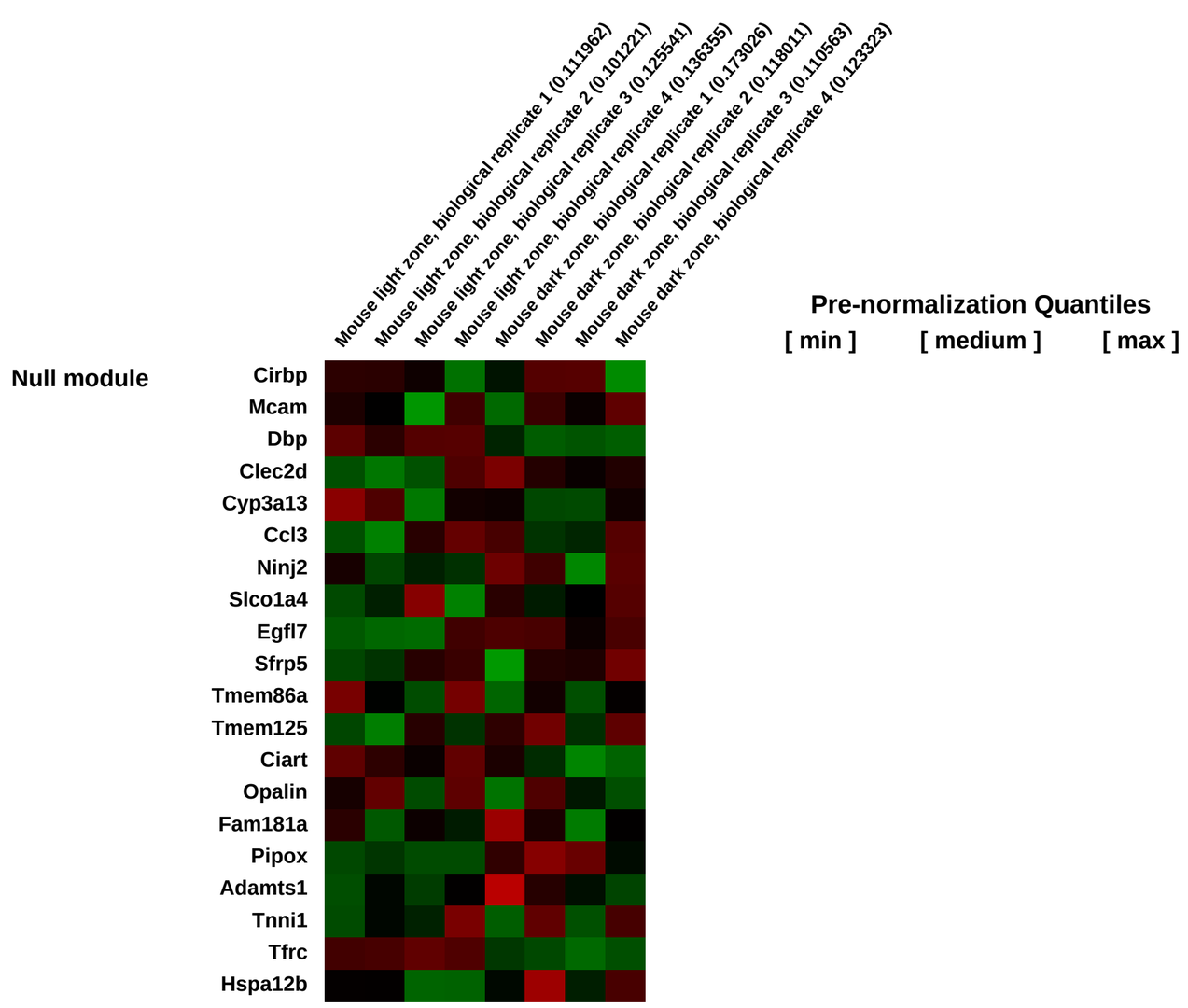

GEO Series "GSE55733" Expression Profiles

Num of samples in this series: 24

Scale of expression profile Z-scores

-3.0 -2.0 -1.0 0.0 1.0 2.0 3.0

GEO Link:	**http://www.ncbi.nlm.nih.gov/geo/query/acc.cgi?acc=GSE55733**
Status:	**Public on Mar 17 2014**
Title:	**Acute Effects Caused by the Rodent Non-Genotoxic Carcinogen Diethylhexylphthalate**
Organism:	**Mus musculus**
Experiment type:	**Expression profiling by array**
Platform:	**GPL1261**
Pubmed ID:	
Summary & Design:	**Summary:** **Acute effects caused by the non-genotoxic carcinogen and peroxisome proliferator (PP) diethylhexylphthalate (DEHP) in the mouse liver** **Overall design:** **Mice (n = 6) were dosed by oral gavage (10 ml/kg body weight) with the non-genotoxic carcinogen diethylhexylphthalate (DEHP), every 24 h for 3 days (1150 mg/kg/day), or with an equivalent volume of vehicle control (corn oil).**

Background corr dist: **KL-Divergence = 0.2626, L1-Distance = 0.0668, L2-Distance = 0.0121, Normal std = 0.2957**

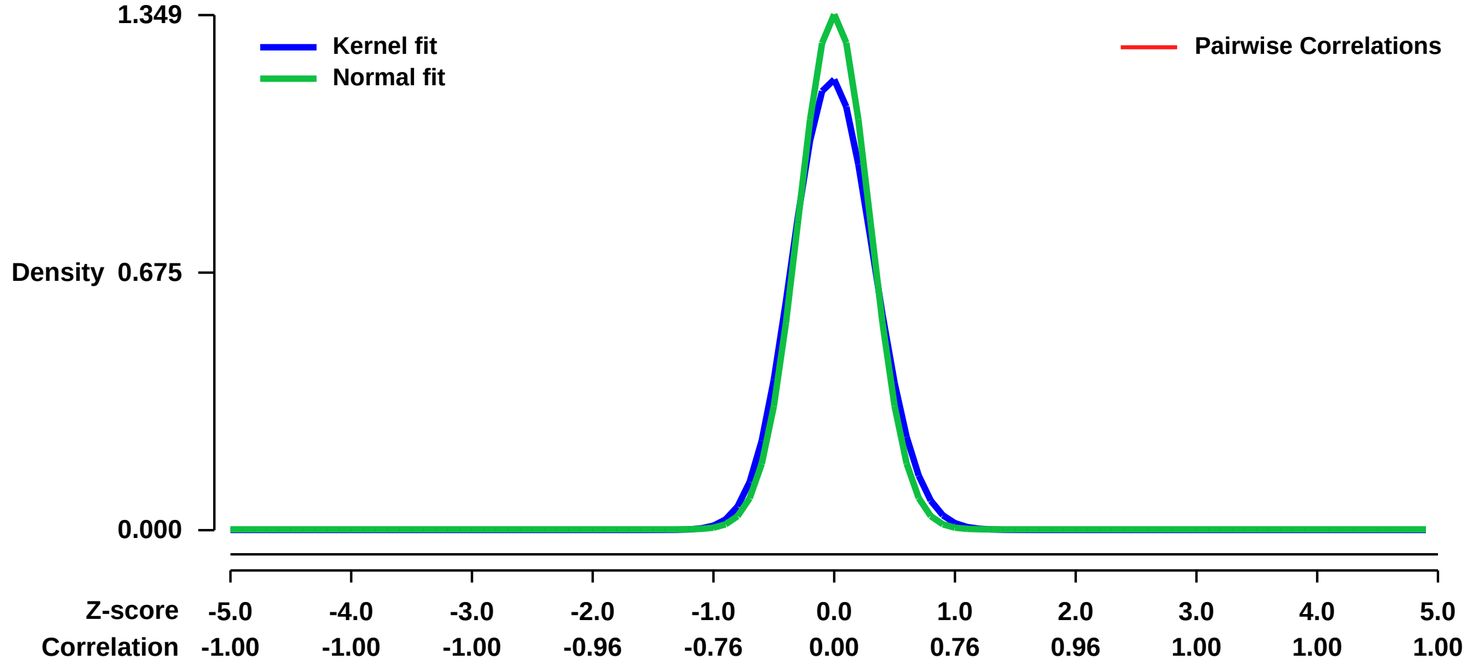

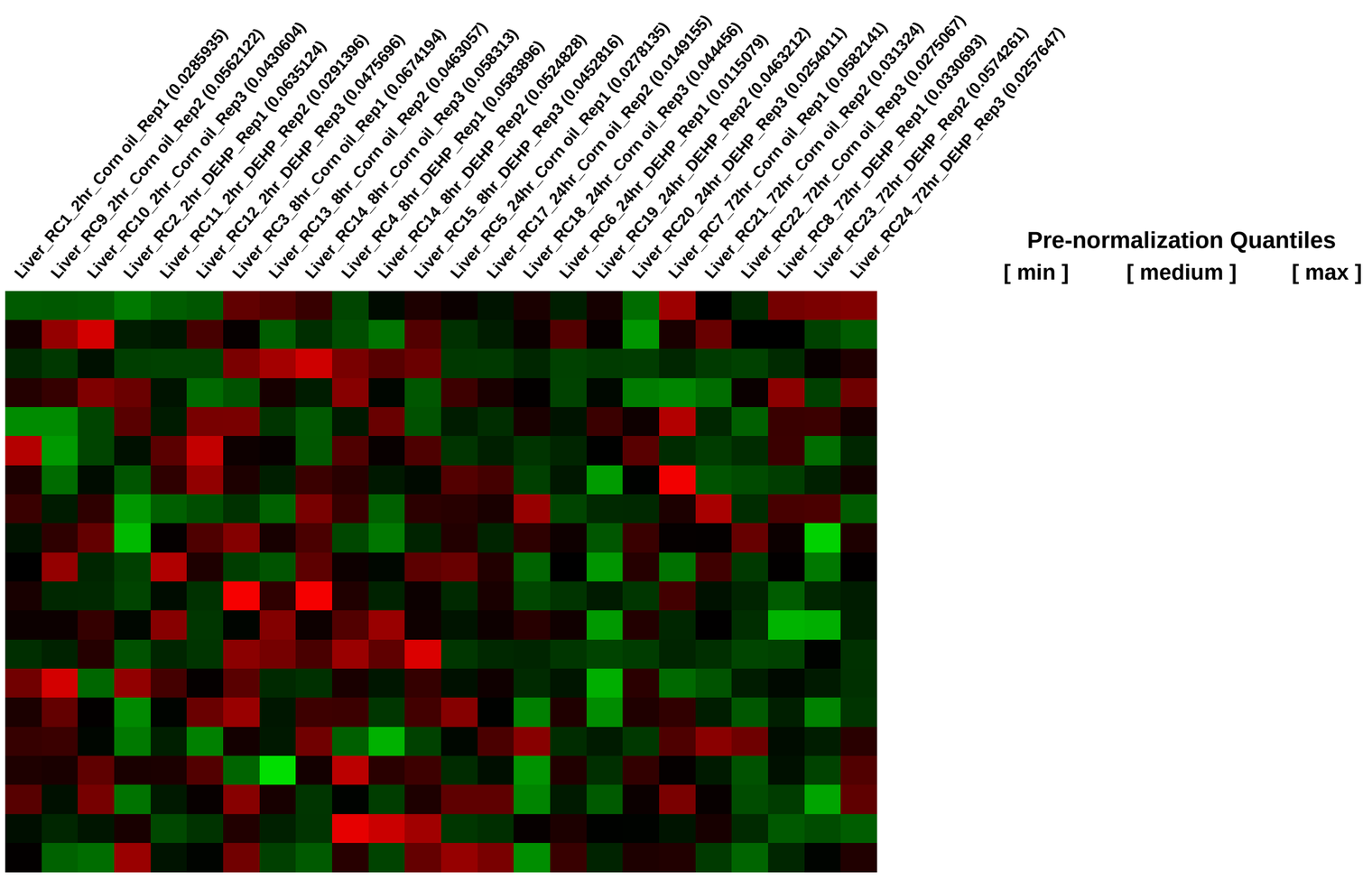

Null module

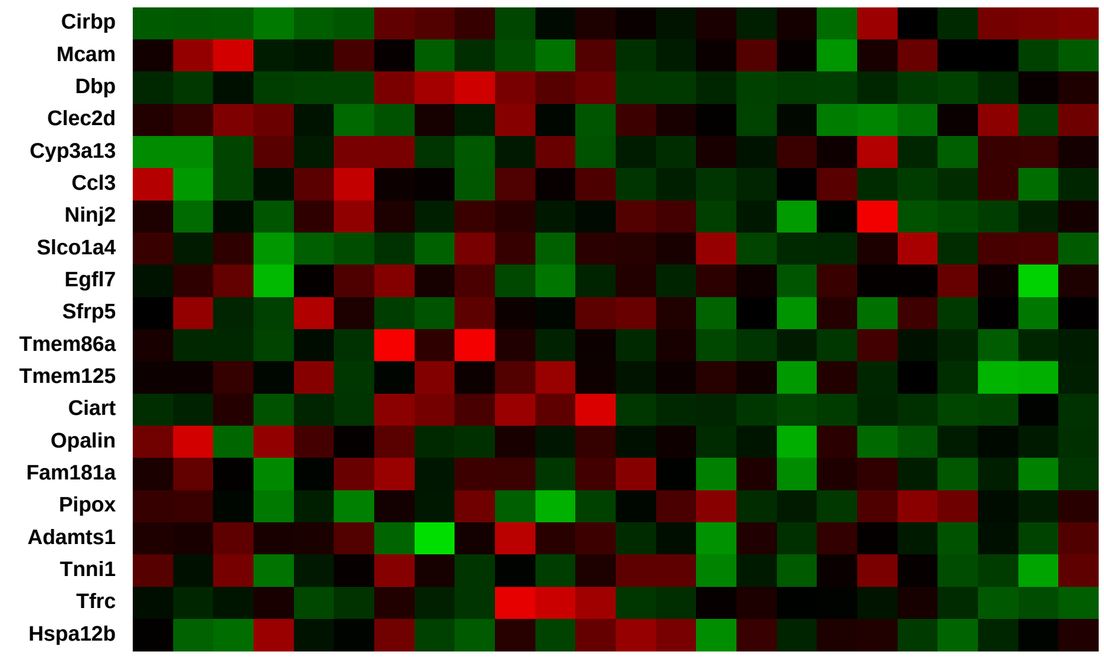

GEO Series "GSE20302" Expression Profiles

Num of samples in this series: 12

Scale of expression profile Z-scores

-3.0 -2.0 -1.0 0.0 1.0 2.0 3.0

GEO Link:	http://www.ncbi.nlm.nih.gov/geo/query/acc.cgi?acc=GSE20302
Status:	Public on Feb 13 2010
Title:	B bifidum actively changes the gene expression profile induced by L acidophilus in murine dendritic cells
Organism:	Mus musculus
Experiment type:	Expression profiling by array
Platform:	GPL1261
Pubmed ID:	20548777
Summary & Design:	**Summary:** Dendritic cells (DC) play a pivotal regulatory role in activation of the innate as well as the adaptive part of the immune system by responding to environmental microorganisms. We have previously shown that some lactobacilli strains induce a strong production of the pro-inflammatory and Th1 polarizing cytokine IL-12 in DC. Contrary, bifidobacteria do not induce IL-12, but are able to inhibit the IL-12 production induced by lactobacilli. In the present study, genome wide microarrays were used to investigate the maturation and gene expression pattern murine bone marrow derived DC stimulated with Lactobacillus acidophilus NCFM and Bifidobacterium bifidum Z9. L. acidophilus NCFM strongly induced expression of interferon (IFN)-¿†, multiple virus defence genes, and cytokine and chemokine genes related to both the adaptive and the innate immune response. Contrary, B. bifidum Z9 mostly up-regulated genes encoding cytokines and chemokines related to the innate immune response. Moreover, B. bifidum Z9 inhibited the expression of the genes initiating the adaptive immune response induced by L. acidophilus NCFM and had an additive effect on genes of the innate immune response and some Th2 skewing genes. The gene encoding Jun dimerization protein 2 (JDP2), a key regulator in cell signalling, was one of the few genes only induced by B. bifidum Z9. Blocking of the JNK1/2 pathway completely inhibited the gene expression of Ifn-¿†. We suggest that B. bifidum Z9 employs an active mechanism to inhibit induction of genes in DC triggering the adaptive immune system and that JPD2 is involved in the regulatory mechanism. **Overall design:** In the experiment saline control, Lactobacillus acidophilus NCFM, Bifidobacterium bifidum Z9 or both bacteria were were added to murine dendritic cells and stimulated for 10 hours. Experiments were run in triplicates and analyzed in a Two-way ANOVA design.

Background corr dist: KL-Divergence = 0.0533, L1-Distance = 0.0180, L2-Distance = 0.0005, Normal std = 0.5475

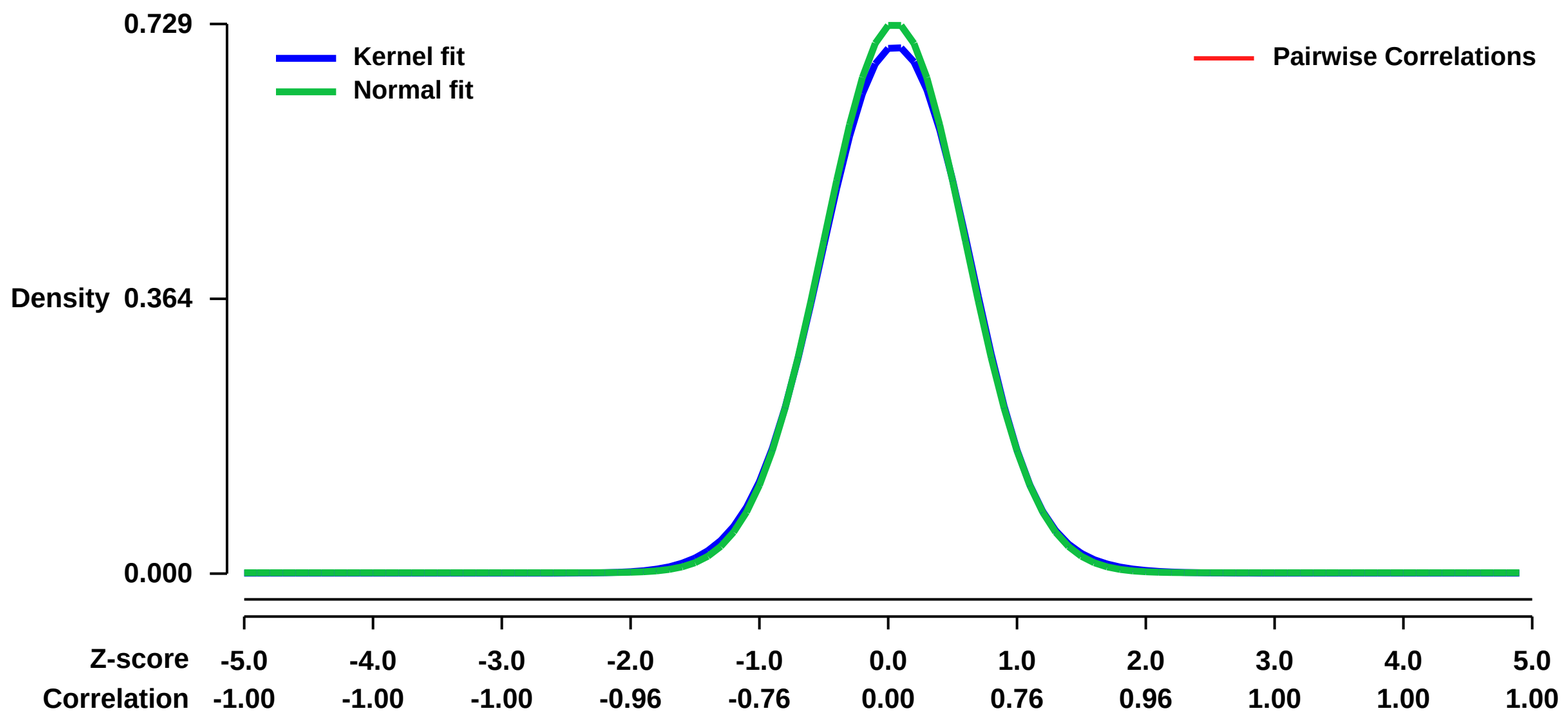

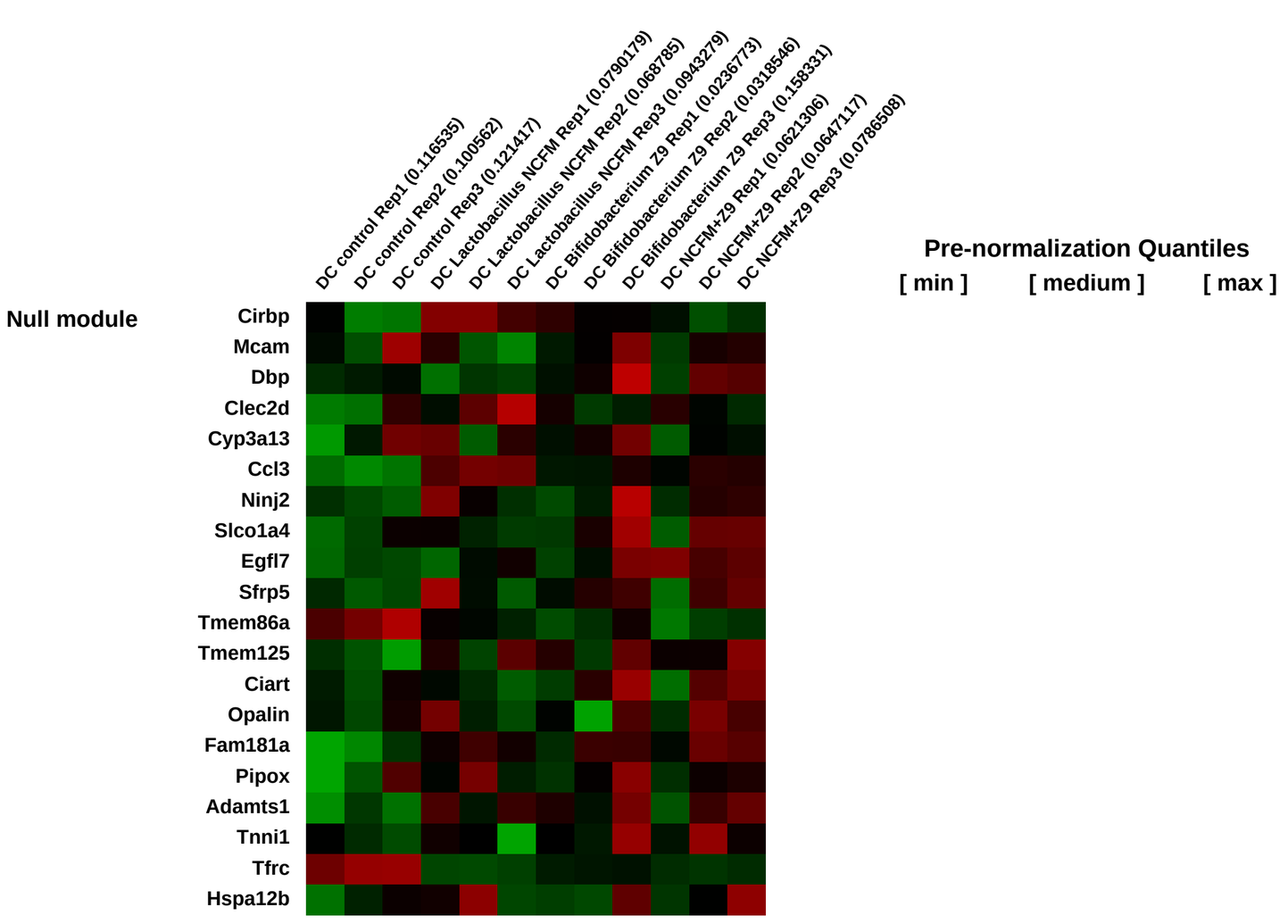

GEO Series "GSE40660" Expression Profiles

Num of samples in this series: 6

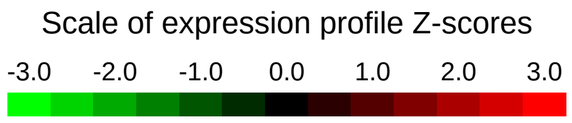

GEO Link:	**http://www.ncbi.nlm.nih.gov/geo/query/acc.cgi?acc=GSE40660**
Status:	**Public on Jan 01 2014**
Title:	**Gata2 is a master regulator of endometrial function and progesterone signaling [Affymetrix]**
Organism:	**Mus musculus**
Experiment type:	**Expression profiling by array**
Platform:	**GPL1261**
Pubmed ID:	
Summary & Design:	**Summary:** **The role of Gata2 in regulating uterine function including fertility, implantation, decidualization and P4 signaling in the mouse was investigated by the conditional ablation of Gata2 in the uterus using the (PR-cre) mouse and ChIP-seq for in vivo GATA2 binding sites in the murine uterus upon acute P4 administration.** **Overall design:** **Gata2 gene ablation was confirmed by real-time PCR analysis in the PR-cre; Gata2fl/fl (termed Gata2d/d) uterus. While littermate controls are fertile, Gata2d/d females are completely infertile. Analysis of the infertility indicates that implantation does not occur, and the uterine stroma is incapable of undergoing the decidual reaction to support further embryonic development. Measure of P4 target genes including PR itself indicate a block in P4 target gene induction and that Gata2 regulates PR expression directly. Microarray analysis demonstrates that ablation of Gata2 leads to specific gene changes, including disruption of the Wnt signaling pathway, Progesterone receptor (PR) signaling, and Ihh signaling pathway. In addition we identified 46,183 GATA2 binding sites in P4 treatment conditions with 7,954 binding sites overlapping that of the PR.Taken together, these data demonstrate that Gata2 is a critical regulator of gene expression and function in the murine uterus.**

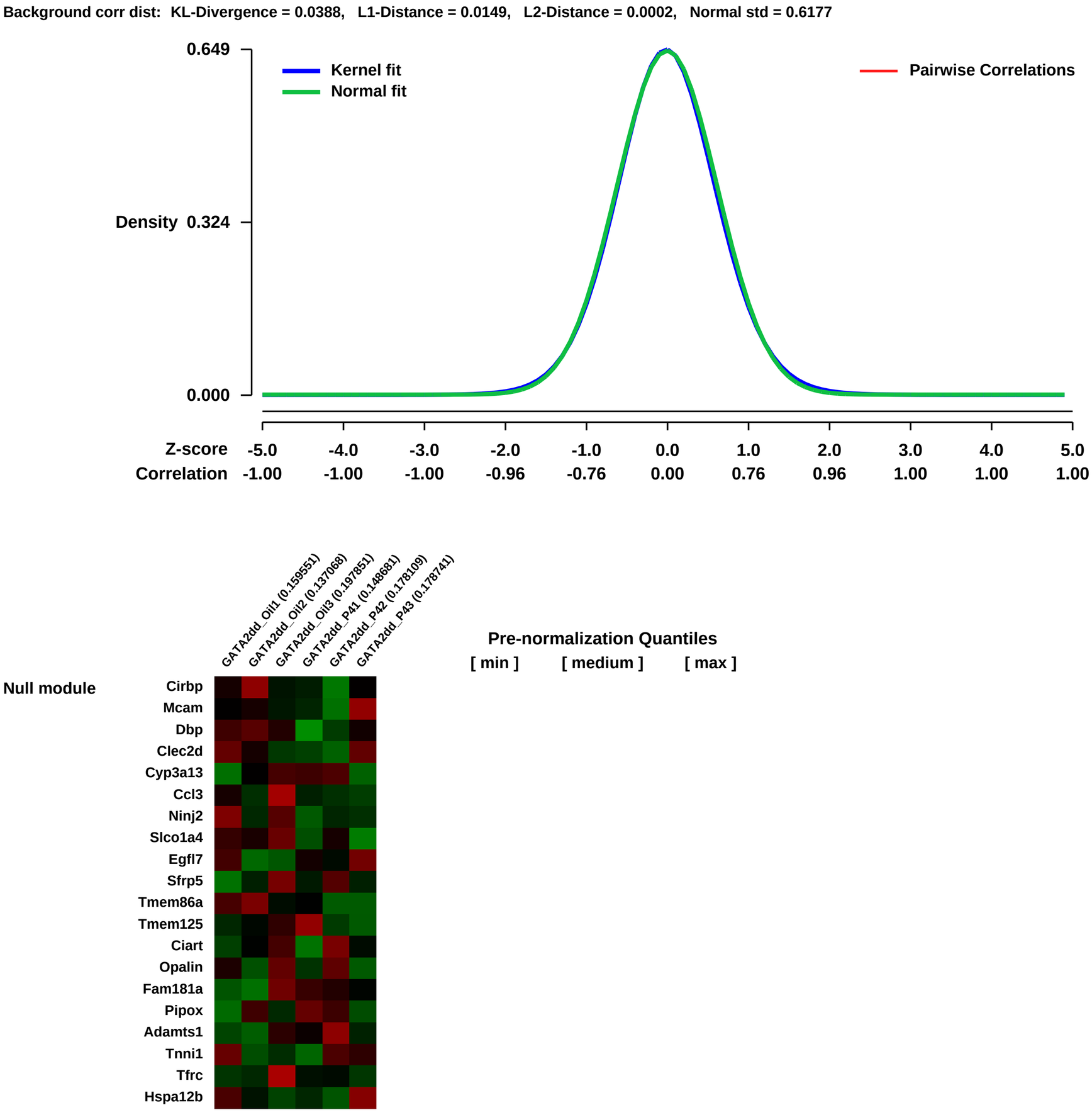

GEO Series "GSE16048" Expression Profiles

Num of samples in this series: 6

Scale of expression profile Z-scores

-3.0 -2.0 -1.0 0.0 1.0 2.0 3.0

GEO Link:	http://www.ncbi.nlm.nih.gov/geo/query/acc.cgi?acc=GSE16048
Status:	Public on Aug 30 2012
Title:	Expression profiling of pancreatic beta-cells harboring a pancreatic-specific deletion of PPAR-beta
Organism:	Mus musculus
Experiment type:	Expression profiling by array
Platform:	GPL1261
Pubmed ID:	23093780
Summary & Design:	**Summary:** Peroxisome proliferator-activated receptor beta/delta protects against obesity by reducing dyslipidemia and insulin resistance via effects in various organs, including muscle, adipose tissue, liver, and heart. However, nothing is known about the function of PPAR-beta in pancreas, a prime organ in the control of glucose metabolism. To gain insight into so far hypothetical functions of this PPAR isotype in insulin production, we specifically ablated Ppar-beta in pancreas. The mutated mice developed a chronic hyperinsulinemia, due to an increase in both beta-cell mass and insulin secretion. Gene expression profiling indicated a broad repressive function of PPAR-beta impacting the vesicular compartment, actin cytoskeleton, and metabolism of glucose and fatty acids. Analyses of insulin release from the islets revealed an increased second-phase glucose-stimulated insulin secretion. Higher levels of PKD, PKC-delta and diacyglycerol in mutated animals lead to an enhanced formation of trans-Golgi network (TGN)-to-plasma-membrane transport carriers in concert with F-actin disassembly, which resulted in increased insulin secretion and its associated systemic effects. Taken together, these results provide evidence for PPAR-beta playing a repressive role on beta-cell growth and insulin exocytosis, which shed new light on its anti-obesity action. **Overall design:** Pancreas-specific knock-out animals were generated by breeding mice harbouring a floxed Ppar-beta (PPARbetafl/fl) to mice expressing the Cre transgene under the control of the Pdx1 promoter (Pdx1Cre). Islets from 3 different animals from the knock-out group Pdx1Cre;PPARbetafl/fl and the control littermates group PPARbetafl/fl were compared.

Background corr dist: KL-Divergence = 0.0416, L1-Distance = 0.0171, L2-Distance = 0.0003, Normal std = 0.6050

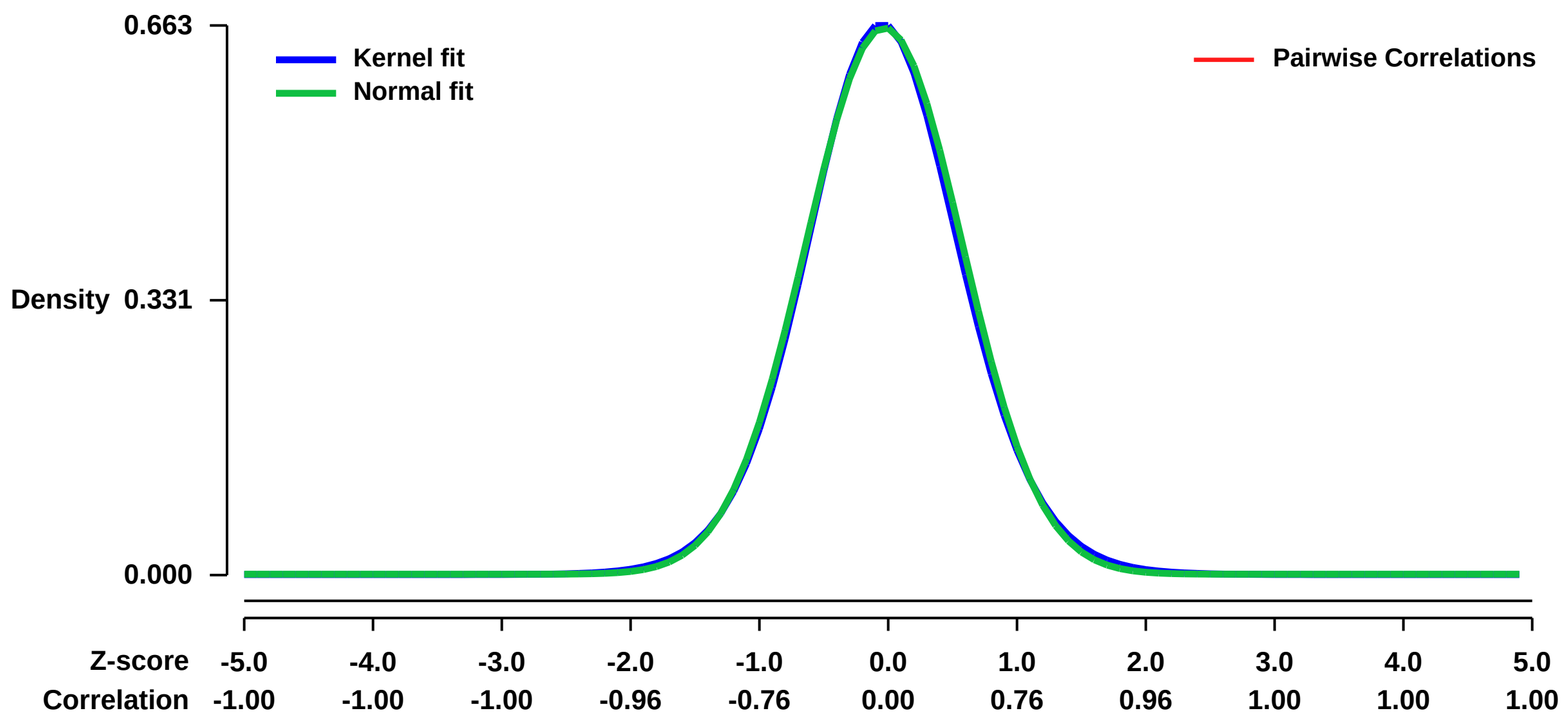

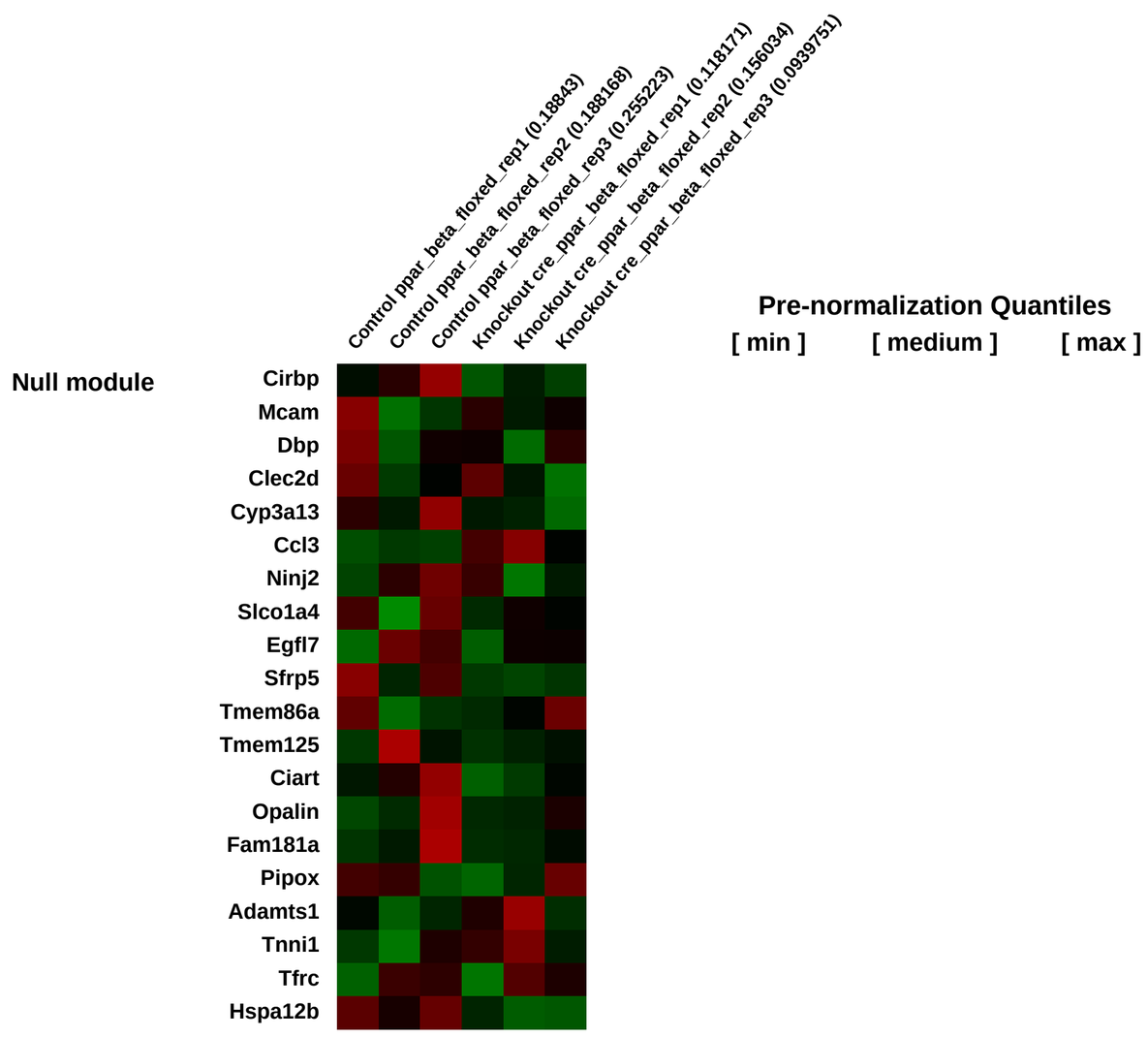

GEO Series "GSE30962" Expression Profiles

Num of samples in this series: 16

Scale of expression profile Z-scores

-3.0 -2.0 -1.0 0.0 1.0 2.0 3.0

GEO Link:	**http://www.ncbi.nlm.nih.gov/geo/query/acc.cgi?acc=GSE30962**
Status:	**Public on Aug 23 2011**
Title:	**Primary and secondary CD8 T cells during acute and chronic LCMV infection**
Organism:	**Mus musculus**
Experiment type:	**Expression profiling by array**
Platform:	**GPL1261**
Pubmed ID:	**21856186**
Summary & Design:	**Summary:** **Understanding the response of memory CD8 T cells to persistent antigen re-stimulation and the role of CD4 T cell help is critical to the design of successful vaccines for chronic diseases. However, studies comparing the protective abilities and qualities of memory and naˆflve cells have been mostly performed in acute infections, and little is known about their roles during chronic infections. Herein, we show that memory cells dominate over naˆflve cells and are protective when present in large enough numbers to quickly reduce infection. In contrast, when infection is not rapidly reduced, memory cells are quickly lost, unlike naˆflve cells. This loss of memory cells is due to (i) an early block in cell proliferation, (ii) selective regulation by the inhibitory receptor 2B4, and (iii) increased reliance on CD4 T cell help. These findings have important implications towards the design of T cell vaccines against chronic infections and tumors.** **Overall design:** **16 samples are analyzed: 3 replicates of secondary effector CD8 P14 T cells at day 8 post-acute lymphocytic choriomeningitis virus (LCMV) infection; 4 replicates of secondary effector CD8 P14 T cells at day 8 post-chronic LCMV infection; 4 replicates of primary effector CD8 P14 T cells at day 8 post-acute LCMV infection; and 5 replicates of primary effector CD8 P14 T cells at day 8 post-chronic LCMV infection.**

Background corr dist: KL-Divergence = 0.1329, L1-Distance = 0.0377, L2-Distance = 0.0028, Normal std = 0.3902

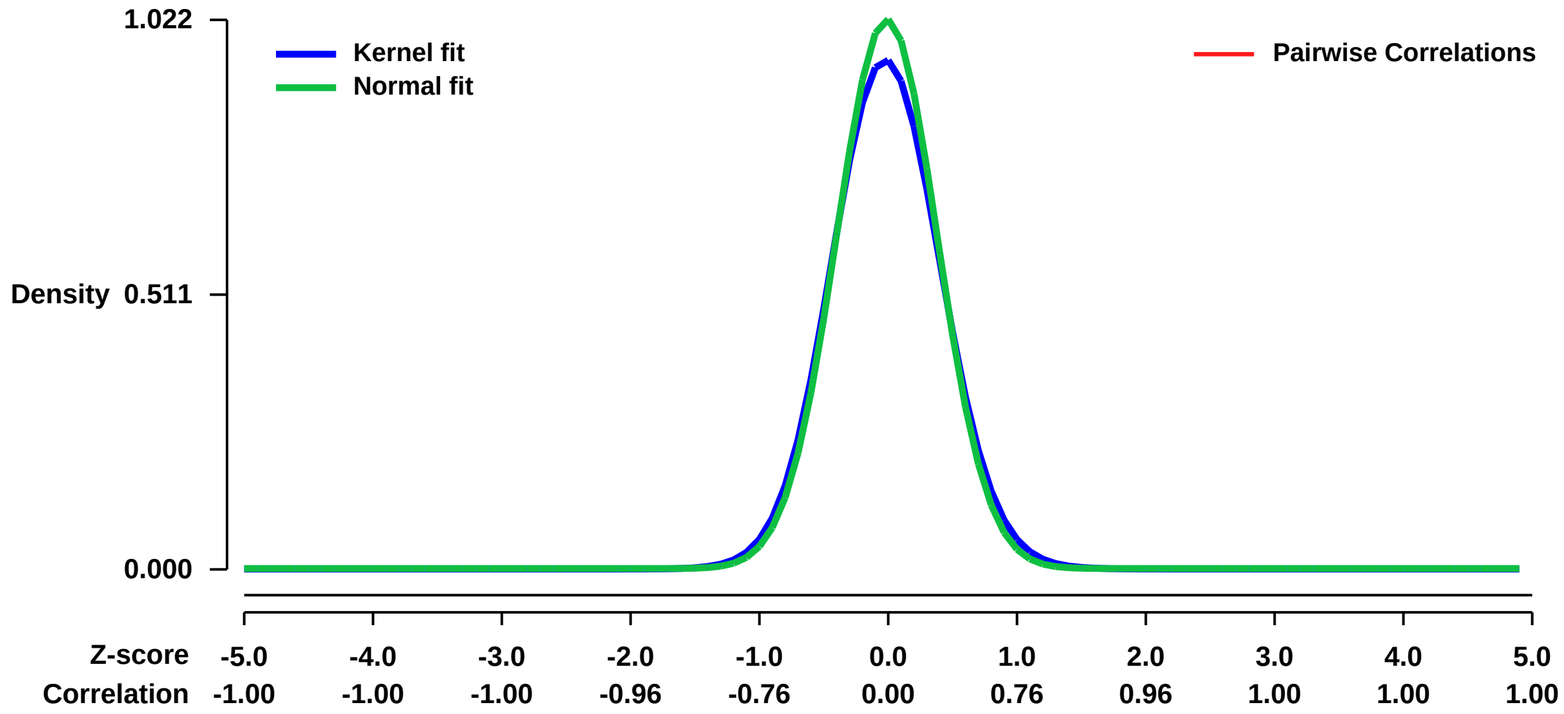

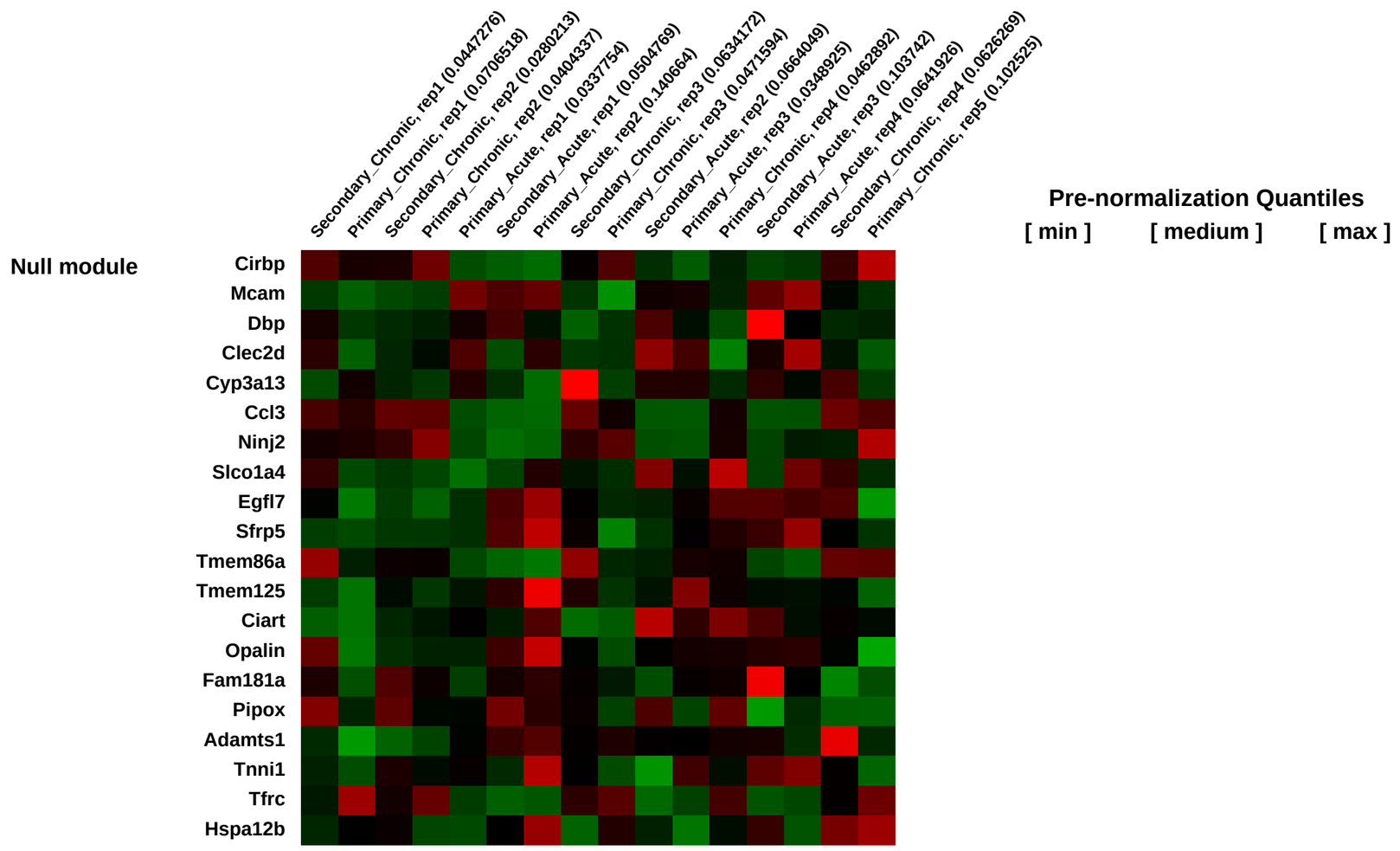

GEO Series "GSE25737" Expression Profiles

Num of samples in this series: 6

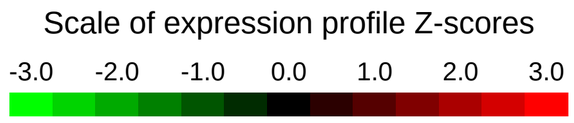

GEO Link:	http://www.ncbi.nlm.nih.gov/geo/query/acc.cgi?acc=GSE25737
Status:	Public on Mar 18 2011
Title:	Geminin-regulated genes during neural fate acquisition of mouse embryonic stem cells
Organism:	Mus musculus
Experiment type:	Expression profiling by array
Platform:	GPL1261
Pubmed ID:	21300881
Summary & Design:	**Summary:** Formation of the complex vertebrate nervous system begins when pluripotent cells of the early embryo are directed to acquire a neural fate. Although cell intrinsic controls play an important role in this process, the molecular nature of this regulation is not well defined. Here we assessed the role for Geminin, a nuclear protein expressed in embryonic cells, in neural fate acquisition from mouse embryonic stem (ES) cells. While Geminin knockdown does not affect the ability of ES cells to maintain or exit pluripotency, we found that it significantly impairs their ability to acquire a neural fate. Conversely, Geminin overexpression promotes neural gene expression, even in the presence of growth factor signaling that antagonizes neural transcriptional responses. These data demonstrate that Gemininâ s activity contributes to mammalian neural cell fate acquisition. We investigated the mechanistic basis of this phenomenon and found that Geminin maintains a hyperacetylated and open chromatin conformation at neural genes. Interestingly, recombinant Geminin protein also rapidly alters chromatin acetylation and accessibility even when Geminin is combined with nuclear extract and chromatin in vitro. These findings define a novel activity for Geminin in regulation of chromatin structure. Together, these data support a role for Geminin as a cell intrinsic regulator of neural fate acquisition that promotes expression of neural genes by regulating chromatin accessibility and histone acetylation. #!# **Overall design:** Mouse embryonic stem cells were differentiated for two days in N2B27 medium, with or without Doxycycline-inducible shRNAmir knockdown of Geminin and compared by microarray. Three independent experiments were conducted, using two different mouse embryonic stem cell lines for Doxycycline-inducible knockdown of Geminin. The two ES lines express unique shRNAmir sequences targeting Geminin (shRNAmir #9 and #11) to control for off-target effects.

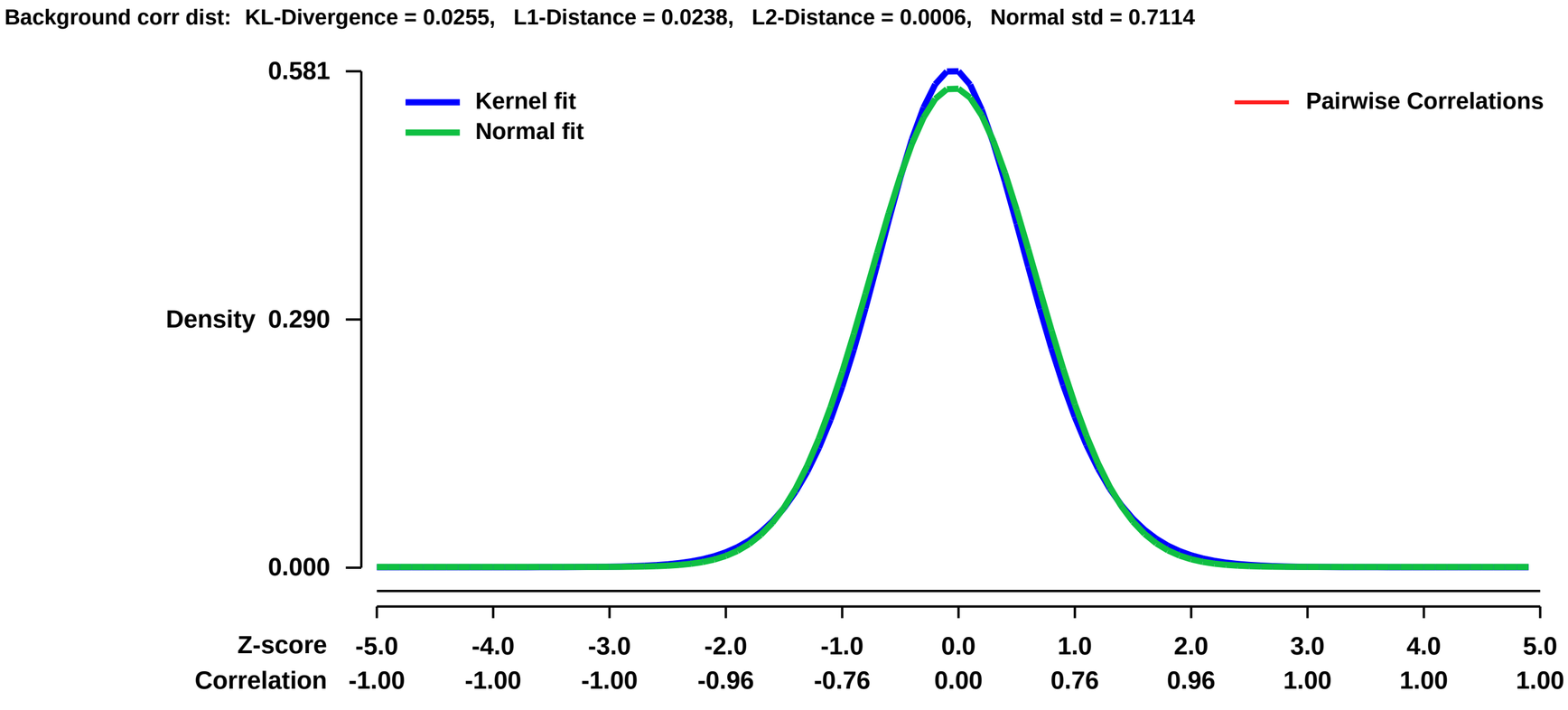

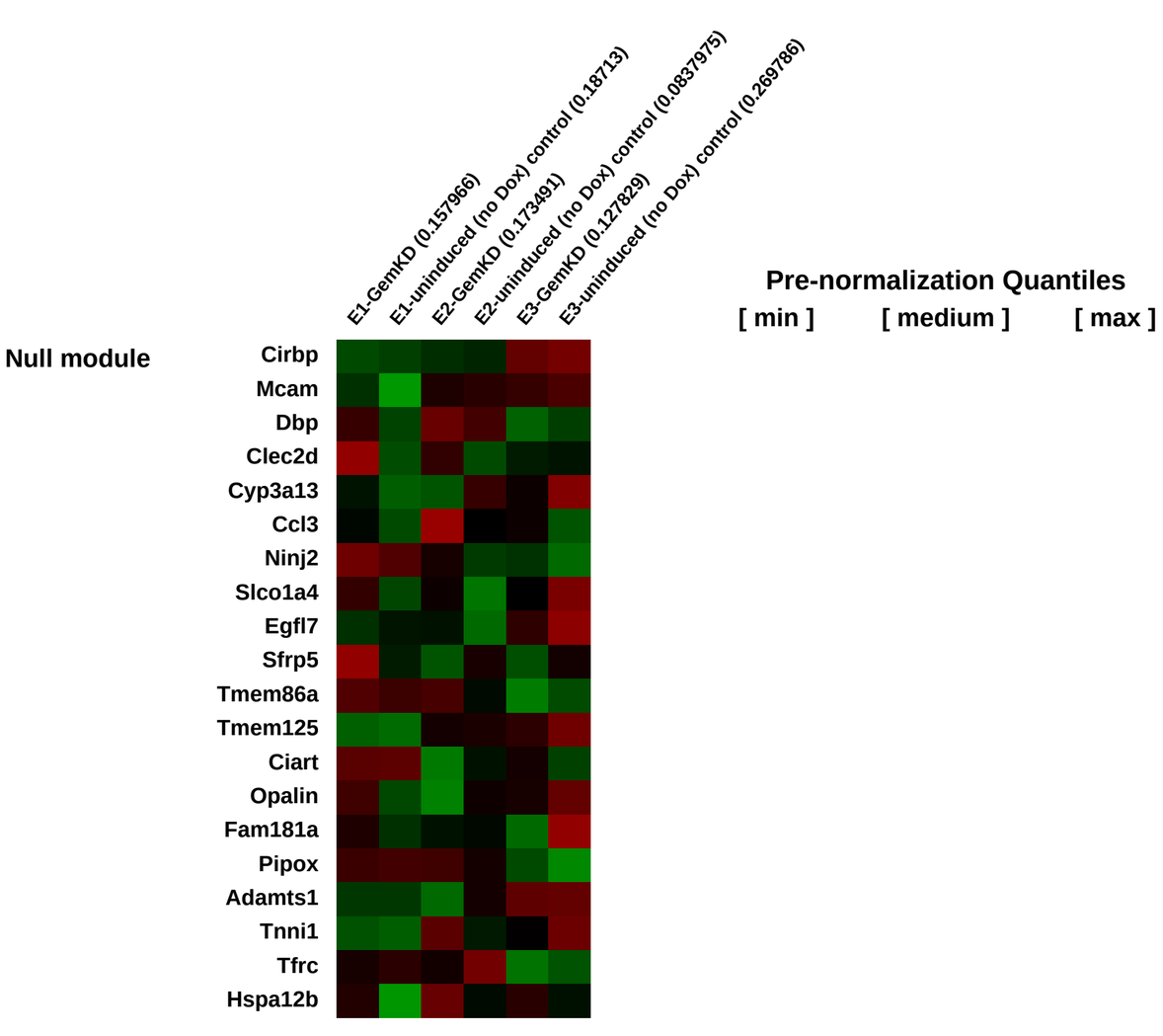

GEO Series "GSE19836" Expression Profiles

Num of samples in this series: 114

Details of this dataset are not shown due to large number of samples and the page size limit.

Find details in http://www.ncbi.nlm.nih.gov/geo/query/acc.cgi?acc=GSE19836

Background corr dist: KL-Divergence = 0.3225, L1-Distance = 0.0725, L2-Distance = 0.0153, Normal std = 0.2720

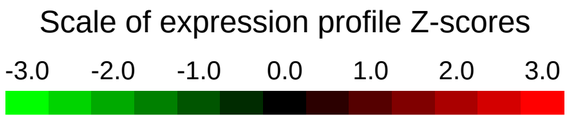

GEO Series "GSE31013" Expression Profiles

Num of samples in this series: 12

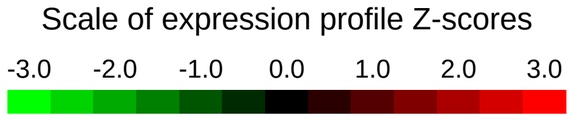

GEO Link:	http://www.ncbi.nlm.nih.gov/geo/query/acc.cgi?acc=GSE31013
Status:	Public on Jun 22 2012
Title:	Global Differential Gene Expression Analysis of Spontaneous Lung Tumors in B6C3F1 Mice: Comparison to Human Non-Small Cell Lung Cancer
Organism:	Mus musculus
Experiment type:	Expression profiling by array
Platform:	GPL1261
Pubmed ID:	22688403
Summary & Design:	**Summary:** **Introduction: Lung cancer is the leading cause of cancer-related death in people. There are several chemically induced and genetically modified mouse models used to study lung cancer. We hypothesized that spontaneous murine (B6C3F1) lung tumors can serve as a model to study human non-small cell lung cancer (NSCLC). Methods: RNA was extracted from untreated 2-year-old B6C3F1 mouse spontaneous lung (SL) tumors and age-matched normal lung tissue from a chronic inhalation NTP study. Global gene expression analysis was performed using Affymetrix Mouse Genome 430 2.0 GeneChip´fi arrays. After data normalization, for each probe set, pairwise comparisons between groups were made using a bootstrap t-test while controlling the mixed directional false discovery rate (mdFDR) to generate a differential gene expression list. IPA, KEGG, and EASE software tools were used to evaluate the overrepresented cancer genes and pathways. Results: MAPK and TGF-beta pathways were overrepresented within the dataset. Almost all of the validated genes by quantitative real time RT-PCR had comparable directional fold changes with the microarray data. The candidate oncogenes included Kras, Braf, Raf1, Id2, Hmga1, Cks1b, and Foxf1. The candidate tumor suppressor genes included Rb1, Cdkn2a, Hnf4a, Tcf21, Ptprd, Hpgd, Hopx, Ogn, Id4, Hoxa5, Smad6, Smad7, Zbtb16, Cyr61, Dusp4, and Ifi16. In addition, several genes important in lung development were also differentially expressed, such as Smad6, Hopx, Sox4, Sox9 and Mycn. Conclusion: In this study, we have demonstrated that several cancer genes and signaling pathways relevant for human NSCLC were similarly altered in spontaneous murine lung tumors.** **Overall design:** **Six spontaneous lung tumors and six normal lungs (as controls) from 2-year-old B6C3F1 mice.**

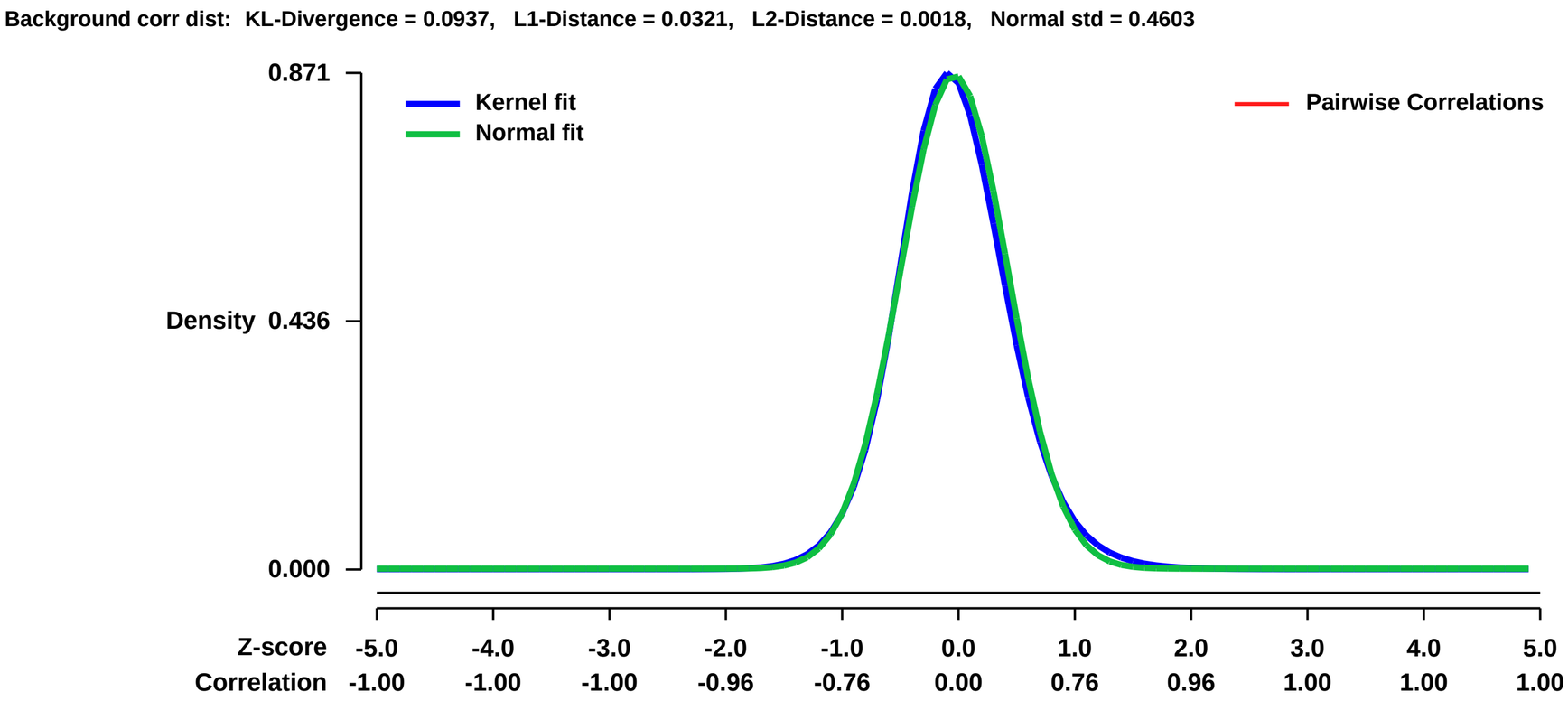

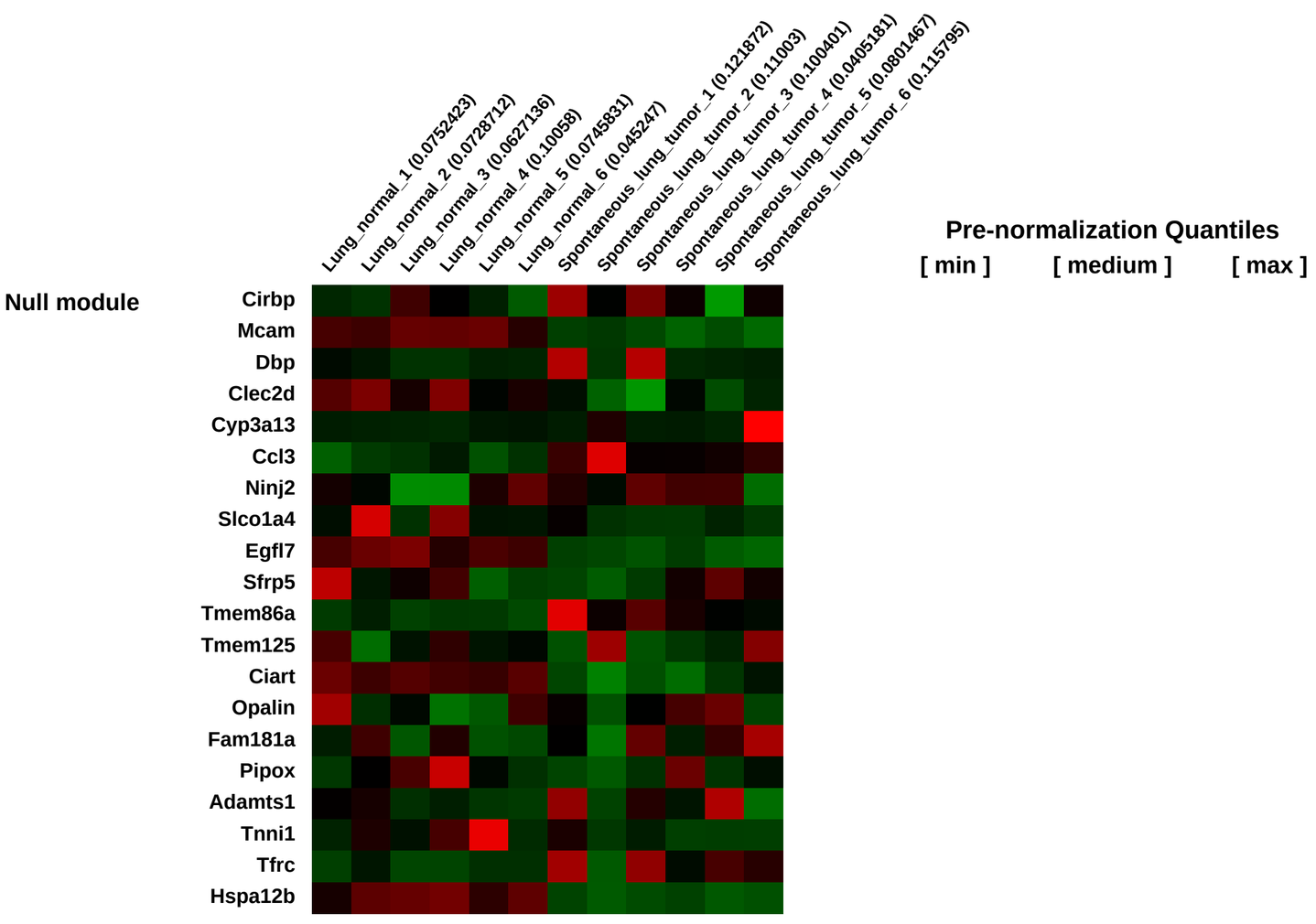

GEO Series "GSE9809" Expression Profiles

Num of samples in this series: 10

Scale of expression profile Z-scores

-3.0 -2.0 -1.0 0.0 1.0 2.0 3.0

GEO Link:	http://www.ncbi.nlm.nih.gov/geo/query/acc.cgi?acc=GSE9809
Status:	Public on Dec 01 2008
Title:	Expression data from GNMT knockout mice
Organism:	Mus musculus
Experiment type:	Expression profiling by array
Platform:	GPL1261
Pubmed ID:	19035462
Summary & Design:	**Summary:** We report that 7 of 7 female Gnmt-/- mice developed hepatocellular carcinoma (HCC), the most common form of liver cancer, at the mean age of 16.1 months. In contrast, only one-third (2/6) of male Gnmt-/- mice had HCC, the remaining had either premature death or liver necrosis. Microarray analysis showed that genes involved in the following pathways were deregulated in different stages of tumorigenesis: S-adenosylmethionine (SAM)-dependent methyltransferases, metabolism, signal transduction, cell proliferation, cell adhesion and immune responses. This study reveals that GNMT plays an important role in the prevention of hapatotumorigenesis through regulating DNA methylaiton and oxidative stress signaling pathways. We postulate that GNMT is a stress-responsive protein and its expression may account for the gender difference of the susceptibility to liver cancer. Keywords: Gnmt knockout **Overall design:** Liver tissues from wild-type or Gnmt knockout mice at young ages, devoloping dysplasia nodules or HCC were used for RNA extraction and hybridization on Affymetrix microarrays. For 11 weeks old mice, total RNA were mixed in equal proportion from 3 mice.

Background corr dist: KL-Divergence = 0.1128, L1-Distance = 0.0327, L2-Distance = 0.0021, Normal std = 0.4199

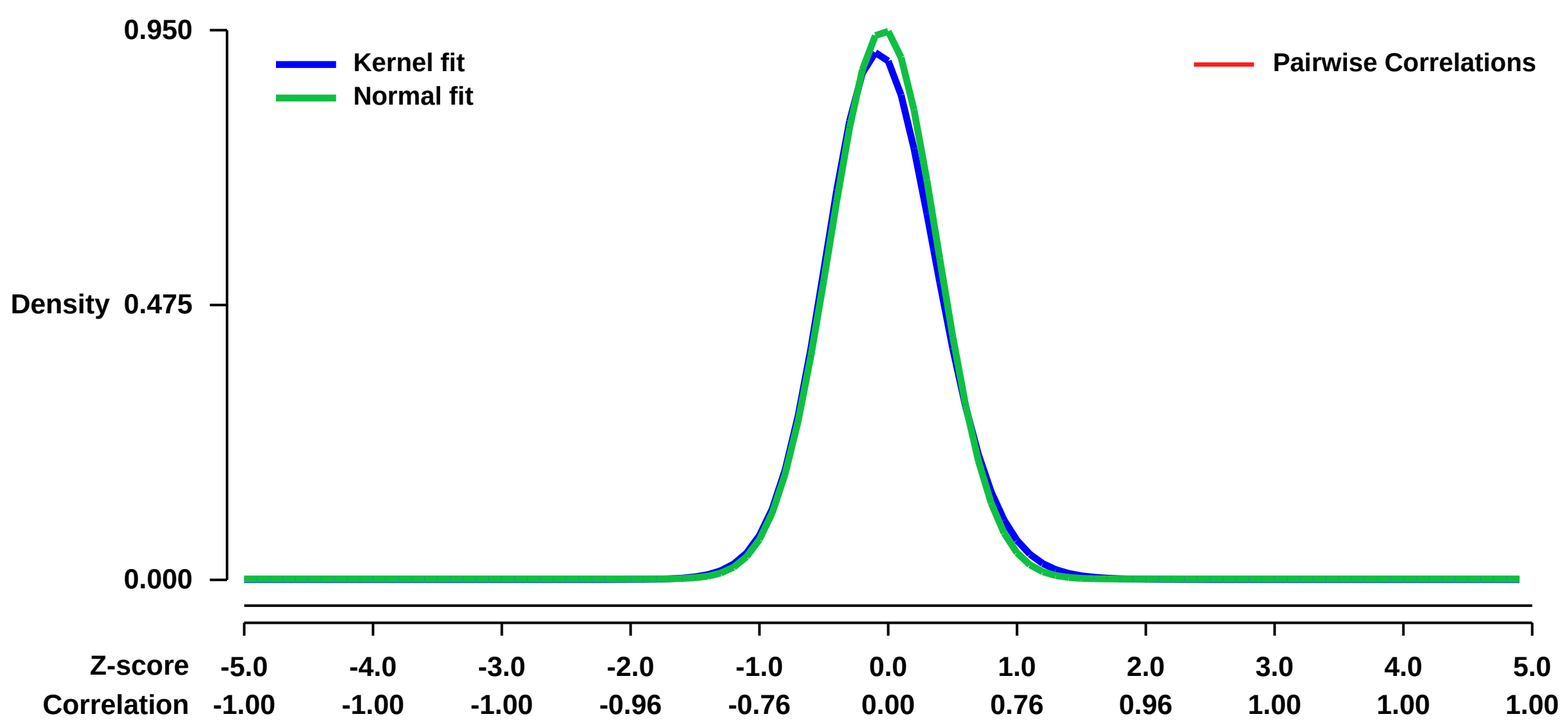

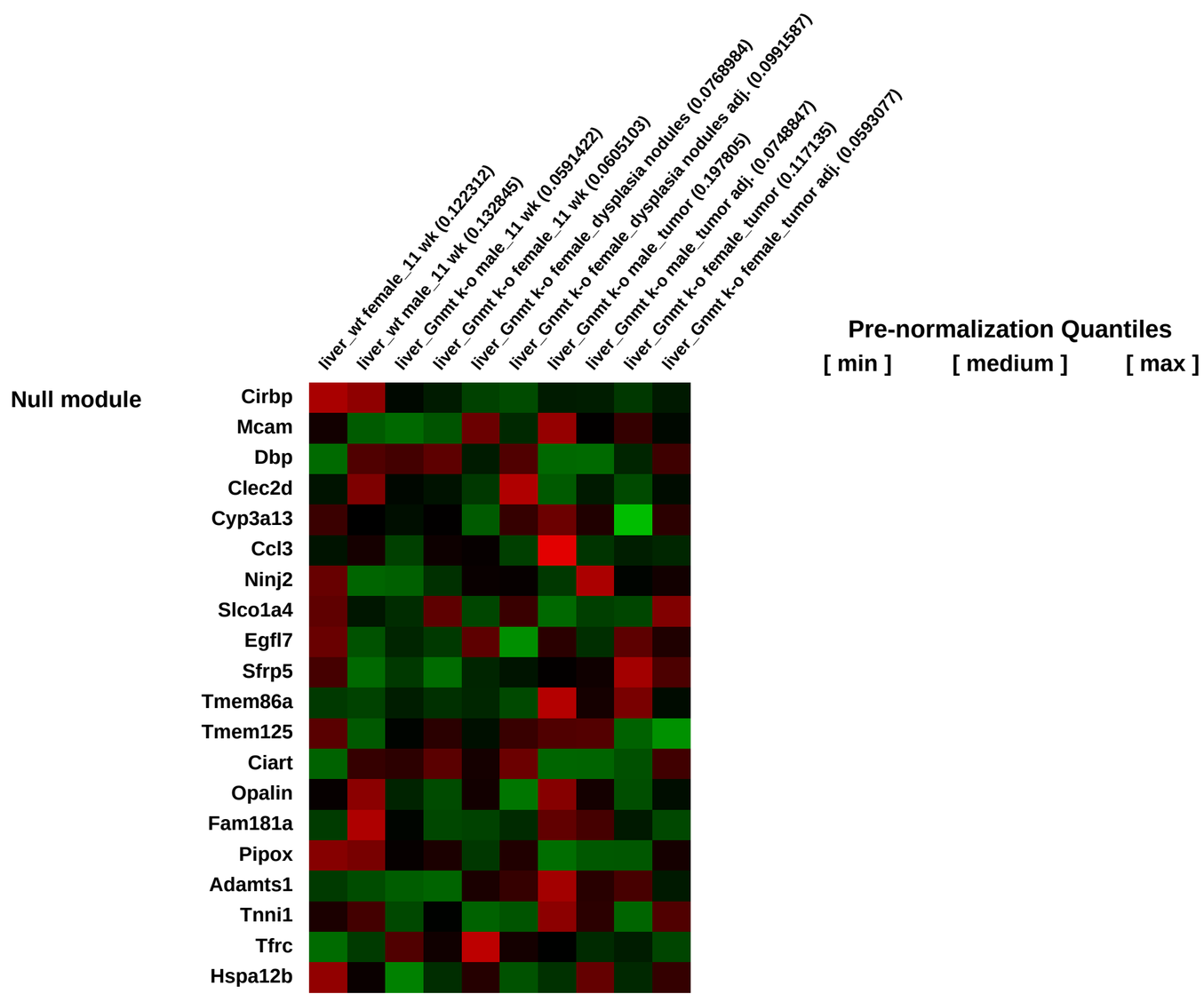

GEO Series "GSE40856" Expression Profiles

Num of samples in this series: 8

Scale of expression profile Z-scores

-3.0 -2.0 -1.0 0.0 1.0 2.0 3.0

GEO Link:	http://www.ncbi.nlm.nih.gov/geo/query/acc.cgi?acc=GSE40856
Status:	Public on Apr 01 2013
Title:	Non-tumor/tumor intestinal tissue of control or intestine-specific HAI-1 deficient Apc(Min/+) mice
Organism:	Mus musculus
Experiment type:	Expression profiling by array
Platform:	GPL1261
Pubmed ID:	23447577
Summary & Design:	**Summary:** To analyse roles of HAI-1/Spint1 in intestinal tumorigenesis, we examined the effect of intestine-specific deletion of Spint1 gene on Apc(Min/+) mice. The loss of Hai-1/Spint1 significantly accelerated tumor formation in ApcMin/+ mice and shortened their survival periods. Mouse small intestine tumor tissue or background mucosa lacking macroscopically visible tumors were proceeded to RNA extraction and hybridization on microarrays (Affymetrix Mouse Genome 430 2.0 Array). **Overall design:** Non-tumor or tumor intestinal mucosa tissues of Apc (Min/+)/Spint1 (flox/flox) mice and non-tumor or tumor intestinal mucosa tissues of Apc (Min/+)/Spint1 (flox/flox)/Vil-Cre mice were analysed. The experiment was repeated respectively.

Background corr dist: KL-Divergence = 0.0508, L1-Distance = 0.0245, L2-Distance = 0.0009, Normal std = 0.5637

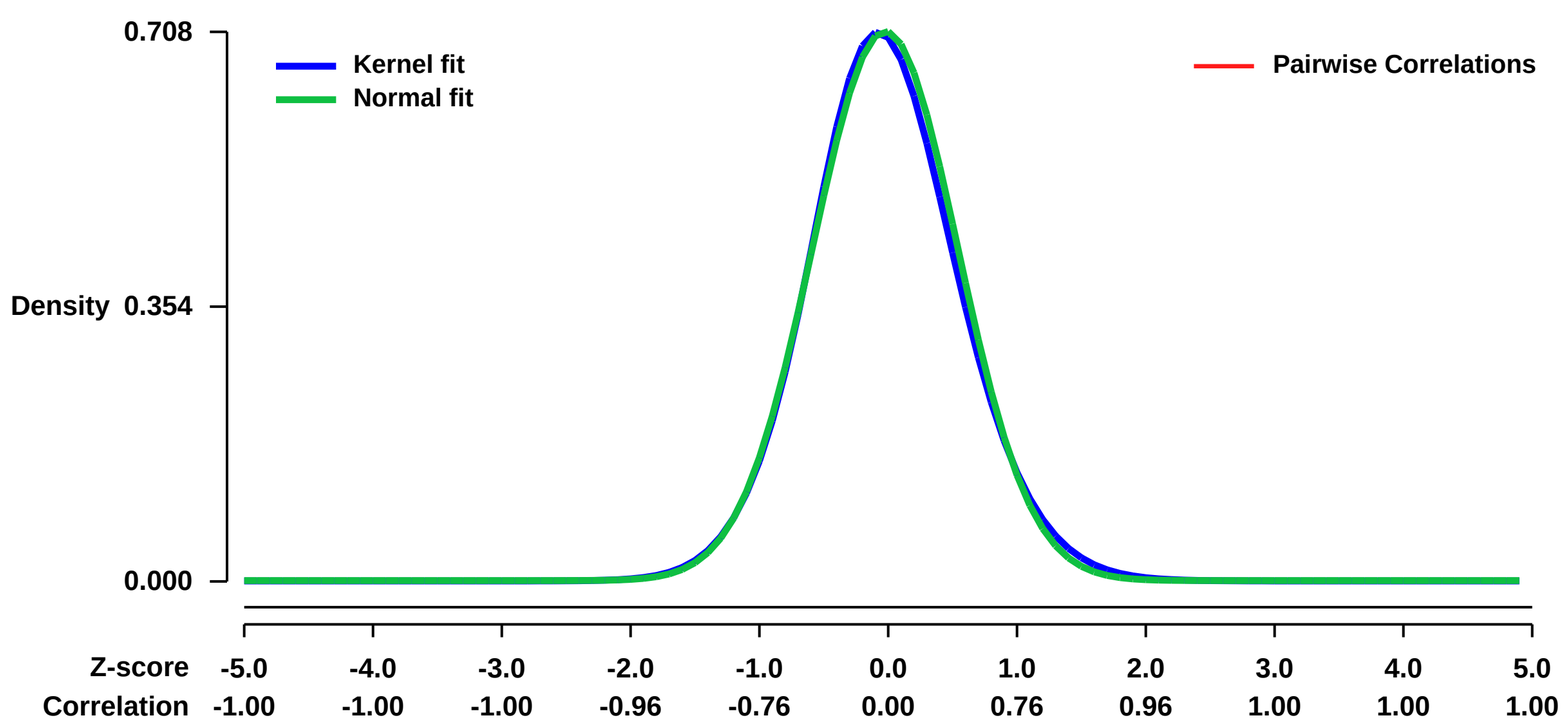

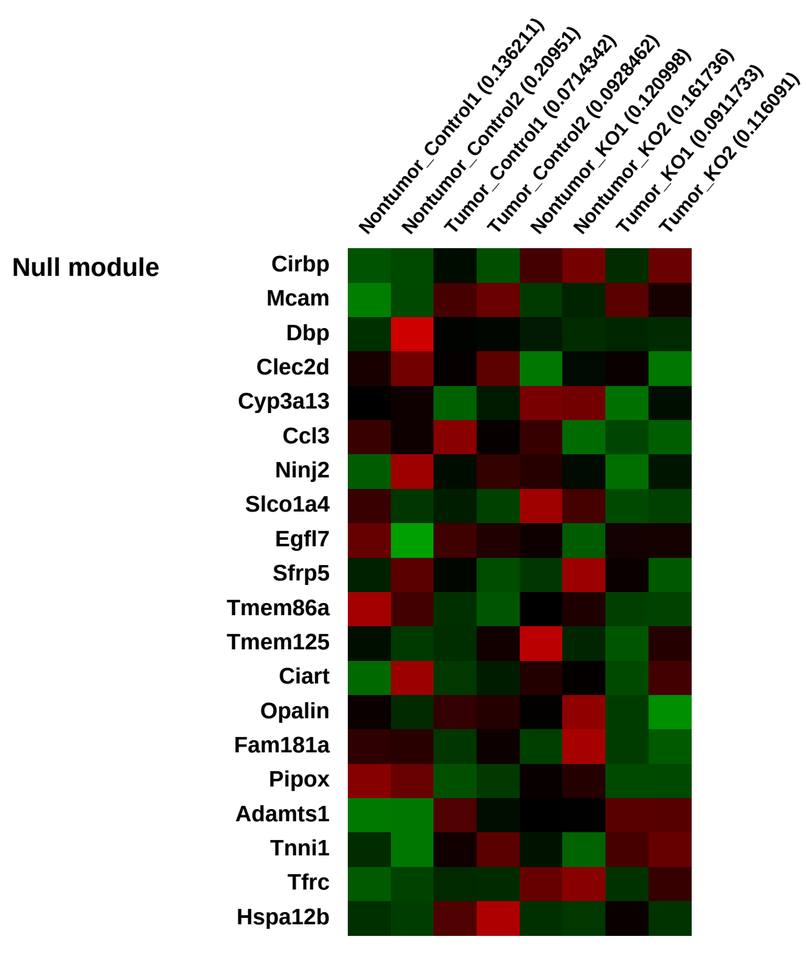

GEO Series "GSE13148" Expression Profiles

Num of samples in this series: 10

Scale of expression profile Z-scores

-3.0 -2.0 -1.0 0.0 1.0 2.0 3.0

GEO Link:	http://www.ncbi.nlm.nih.gov/geo/query/acc.cgi?acc=GSE13148
Status:	Public on Oct 09 2009
Title:	Effect of age on the arthritis susceptibility of BALB/c mice
Organism:	Mus musculus
Experiment type:	Expression profiling by array
Platform:	GPL1261
Pubmed ID:	19519881
Summary & Design:	**Summary:** Rheumatoid arthritis (RA) usually begins in females in their 4th-5th decade, suggesting that the aging of the immune system (immunosenescence) has a major impact on this disease. In the present microarray study, we set out to identify age- and arthritis-related gene expression pattern changes in proteoglycan (aggrecan)-induced arthritis (PGIA) model. Keywords: disease state analysis **Overall design:** We compared the gene expression profile of spleens from PG-immunized but non-arthritic old (older than 4 months) and young (1 month old) mice, and then made a comparison between non-arthritic and age-matched arthritic mice.

Background corr dist: KL-Divergence = 0.0719, L1-Distance = 0.0265, L2-Distance = 0.0011, Normal std = 0.4902

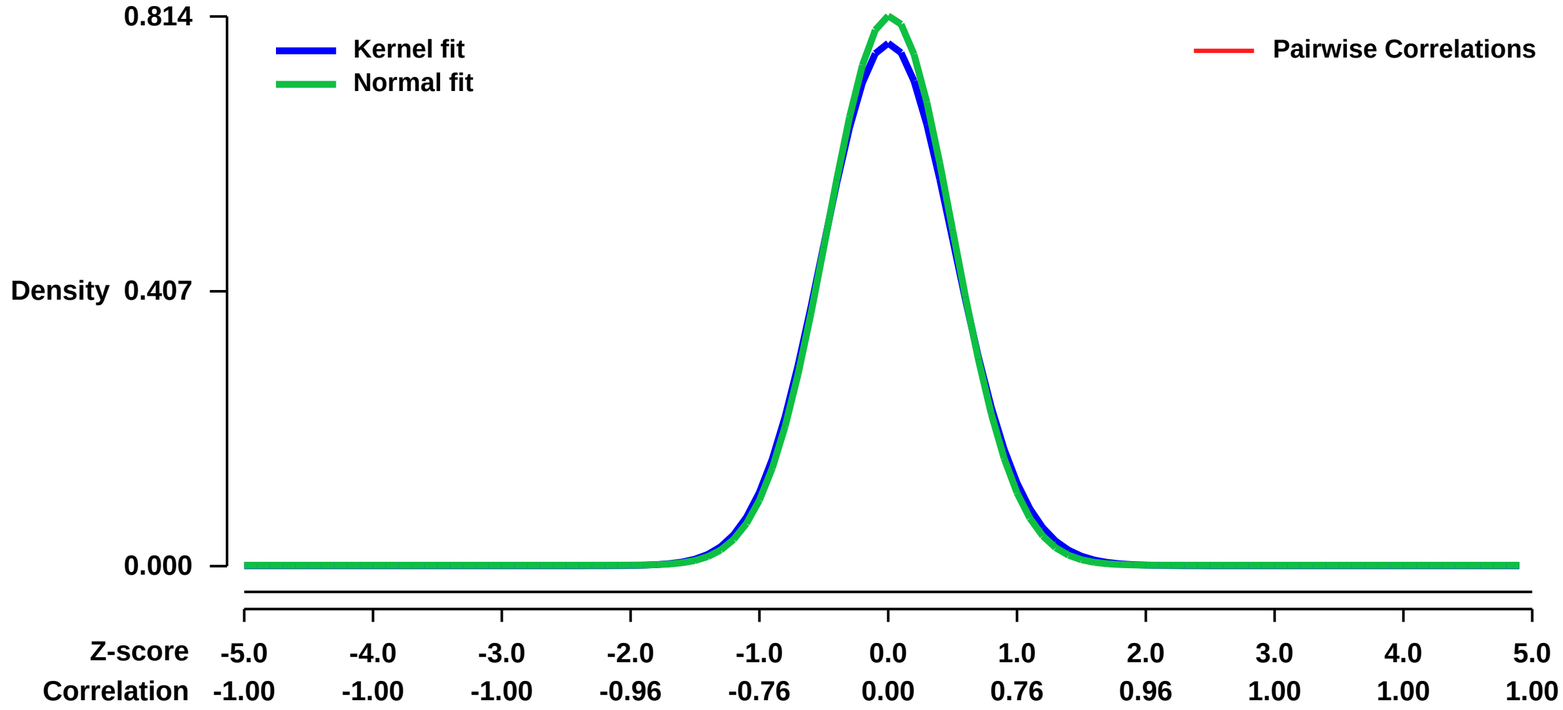

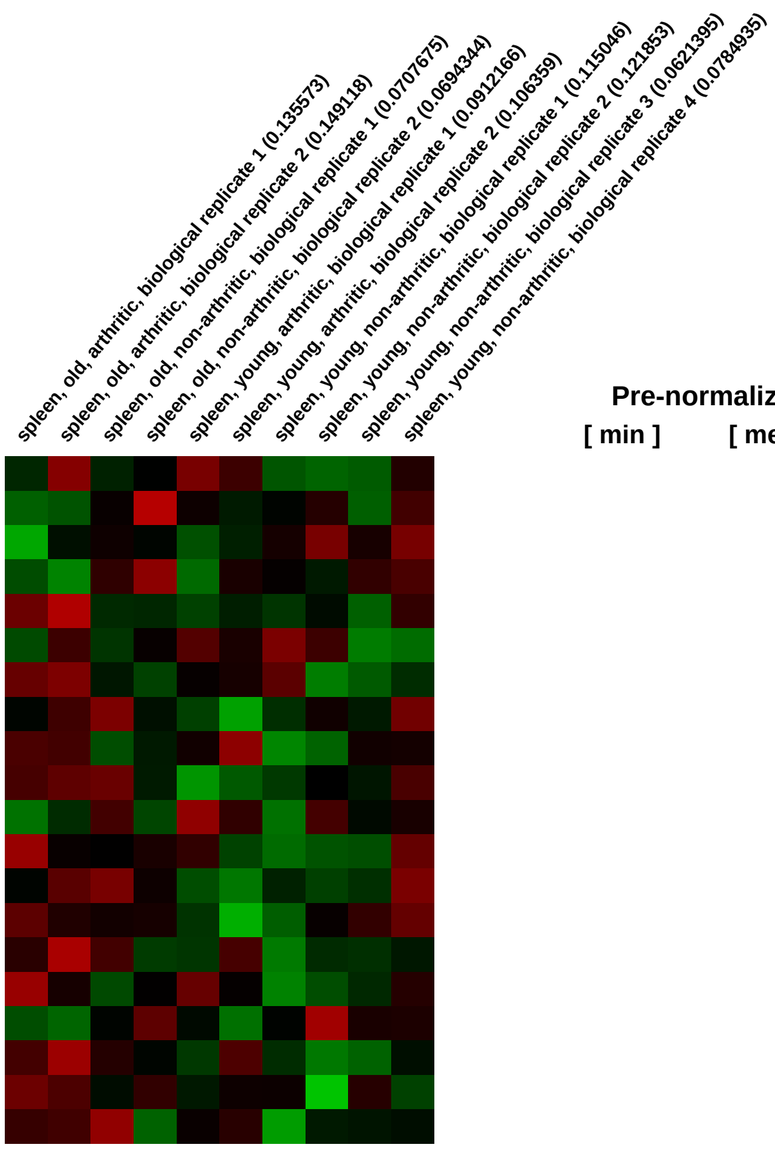

GEO Series "GSE14710" Expression Profiles

Num of samples in this series: 12

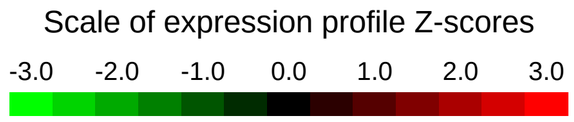

GEO Link:	http://www.ncbi.nlm.nih.gov/geo/query/acc.cgi?acc=GSE14710
Status:	Public on Aug 18 2009
Title:	Skeletal muscle growth and fiber composition in mice are regulated through the transcription factors STAT5a/b
Organism:	Mus musculus
Experiment type:	Expression profiling by array
Platform:	GPL1261
Pubmed ID:	19417088
Summary & Design:	**Summary:** In skeletal muscle, STAT5a/b transcription factors are critical for normal postnatal growth, whole-animal glucose homeostasis, and local IGF-1 production. These observations have led us to hypothesize that STAT5a/b are critical for maintenance of normal muscle mass and function. To investigate this, mice with a skeletal muscle-specific deletion of the Stat5a/b genes (Stat5MKO) were used. Stat5MKO mice displayed reduced muscle mass, altered fiber-type distribution and reduced activity. On a molecular level, gene expression in skeletal muscle of Stat5MKO and control mice was analyzed by microarrays and real-time PCR, both in the presence and absence of growth hormone (GH) stimulation. Several genes involved in muscle growth, fiber-type and metabolism were significantly changed. Specifically in the quadriceps, a muscle almost exclusively composed of type II fibers, the absence of STAT5a/b led to increased expression of several genes associated with type I fibers and the de novo appearance of type I fibers. Additionally, it is shown here that expression of the androgen receptor gene (Ar) is controlled by GH through STAT5a/b. The link between STAT5a/b and Ar gene is likely through direct transcriptional regulation, as chromatin immunoprecipitaion of the Ar promoter region in C2C12 myoblasts was accomplished by antibodies against STAT5a. These experiments demonstrate an important role for STAT5a/b in skeletal muscle physiology and they provide a direct link to androgen signaling. **Keywords:** stat5 KO or WT treated or w/o GH **Overall design:** Total 6 WT controls and 6 stat5a/b KO mice, treated or w/o GH

Background corr dist: KL-Divergence = 0.1214, L1-Distance = 0.0271, L2-Distance = 0.0013, Normal std = 0.4073

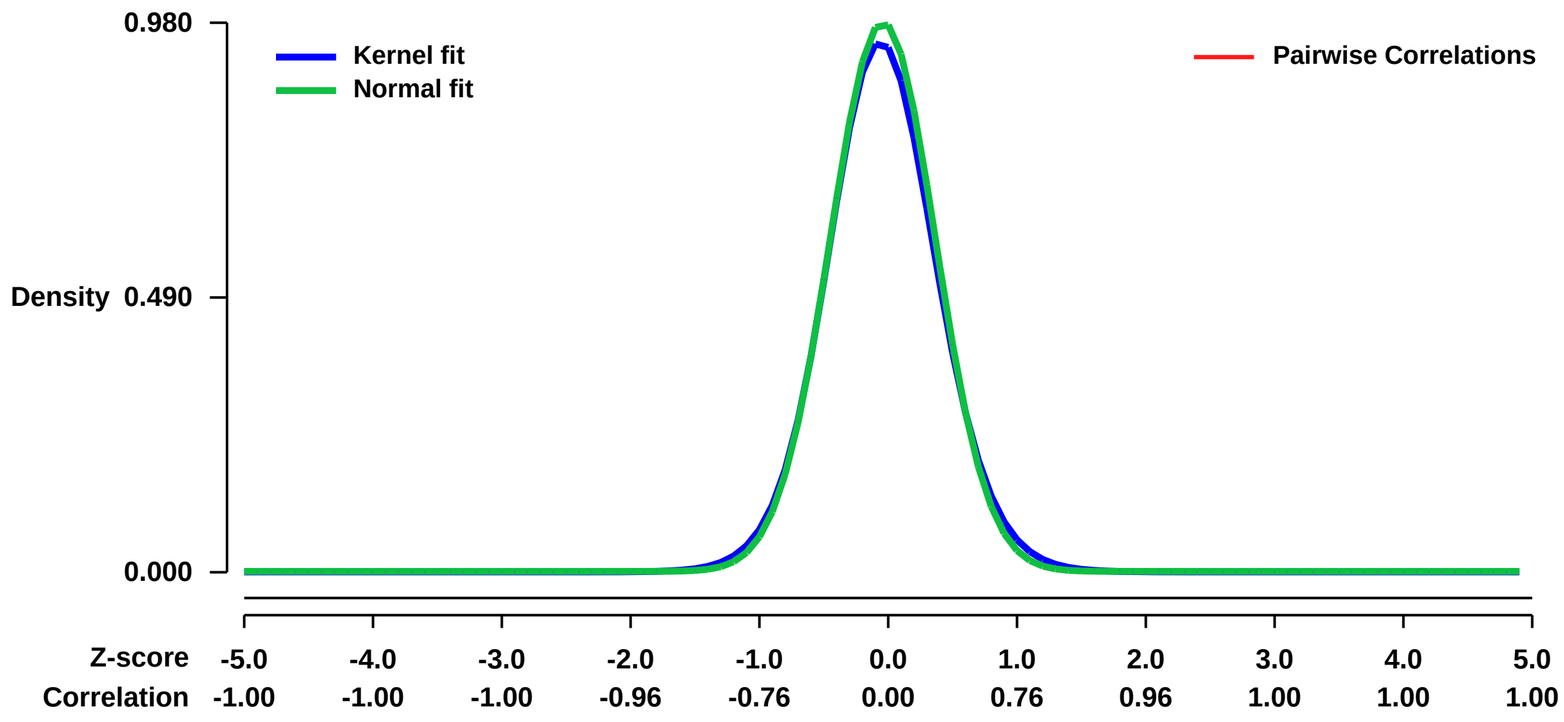

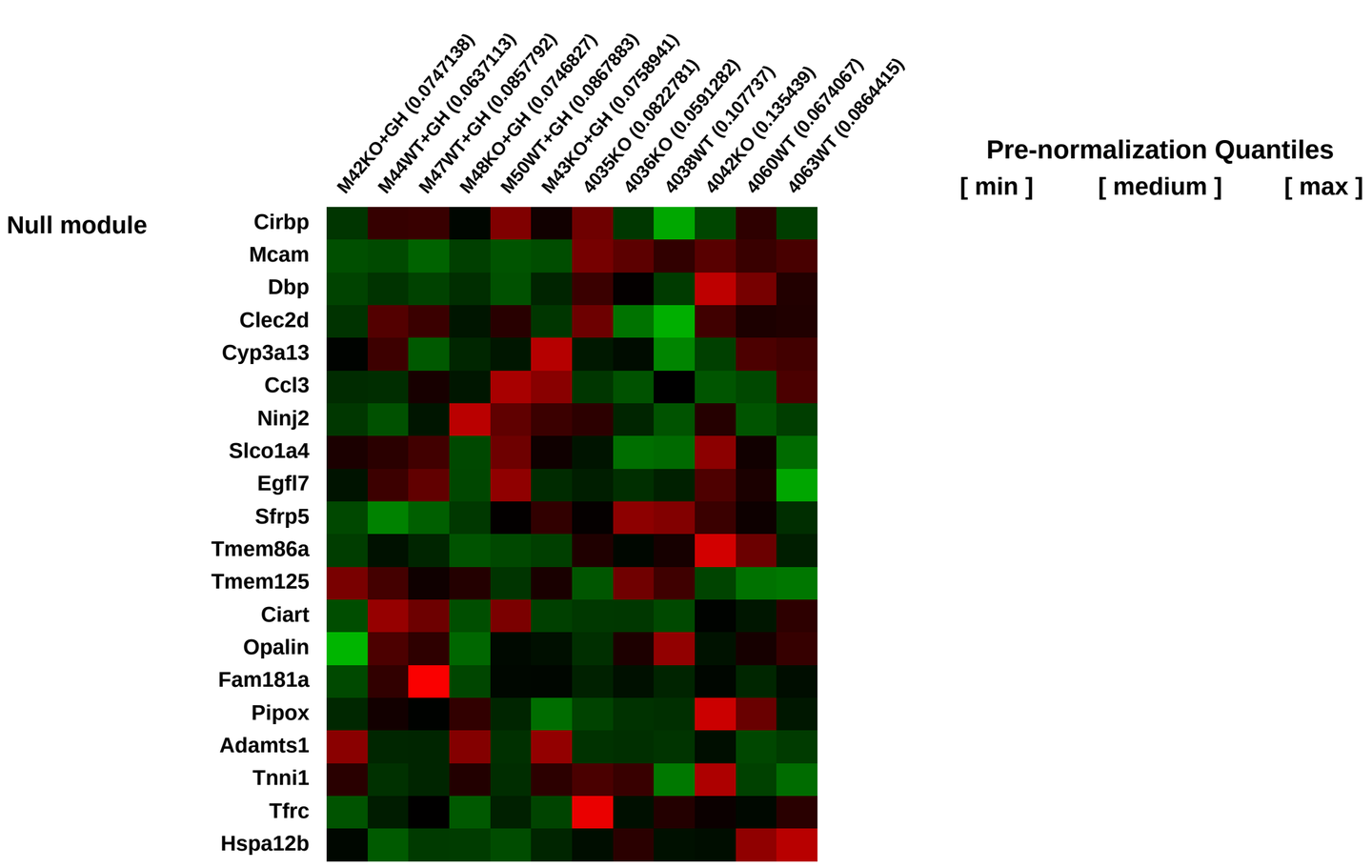

GEO Series "GSE6858" Expression Profiles

Num of samples in this series: 16

Scale of expression profile Z-scores

-3.0 -2.0 -1.0 0.0 1.0 2.0 3.0

GEO Link:	http://www.ncbi.nlm.nih.gov/geo/query/acc.cgi?acc=GSE6858
Status:	Public on Apr 23 2007
Title:	Expression data from experimental murine asthma
Organism:	Mus musculus
Experiment type:	Expression profiling by array
Platform:	GPL1261
Pubmed ID:	17437023
Summary & Design:	**Summary:** Experimental asthma was induced in BALB/c mice by sensitization and challenge with the allergen ovalbumin. Control groups received PBS. To investigate the innate immune component of experimental asthma, we also analyzed recombinase activating gene (RAG) deficient mice following exposure to ovalbumin and control PBS **Keywords: case control** **Overall design:** Each experimental group was exposed to ovalbumin or control PBS. At day 22, 1 day after completion of the allergen exposure, whole lungs were harvested, total mRNA prepared, and gene expression determined by hybridization to Affymetrix microarrays.

Background corr dist: KL-Divergence = 0.1222, L1-Distance = 0.0416, L2-Distance = 0.0036, Normal std = 0.4289

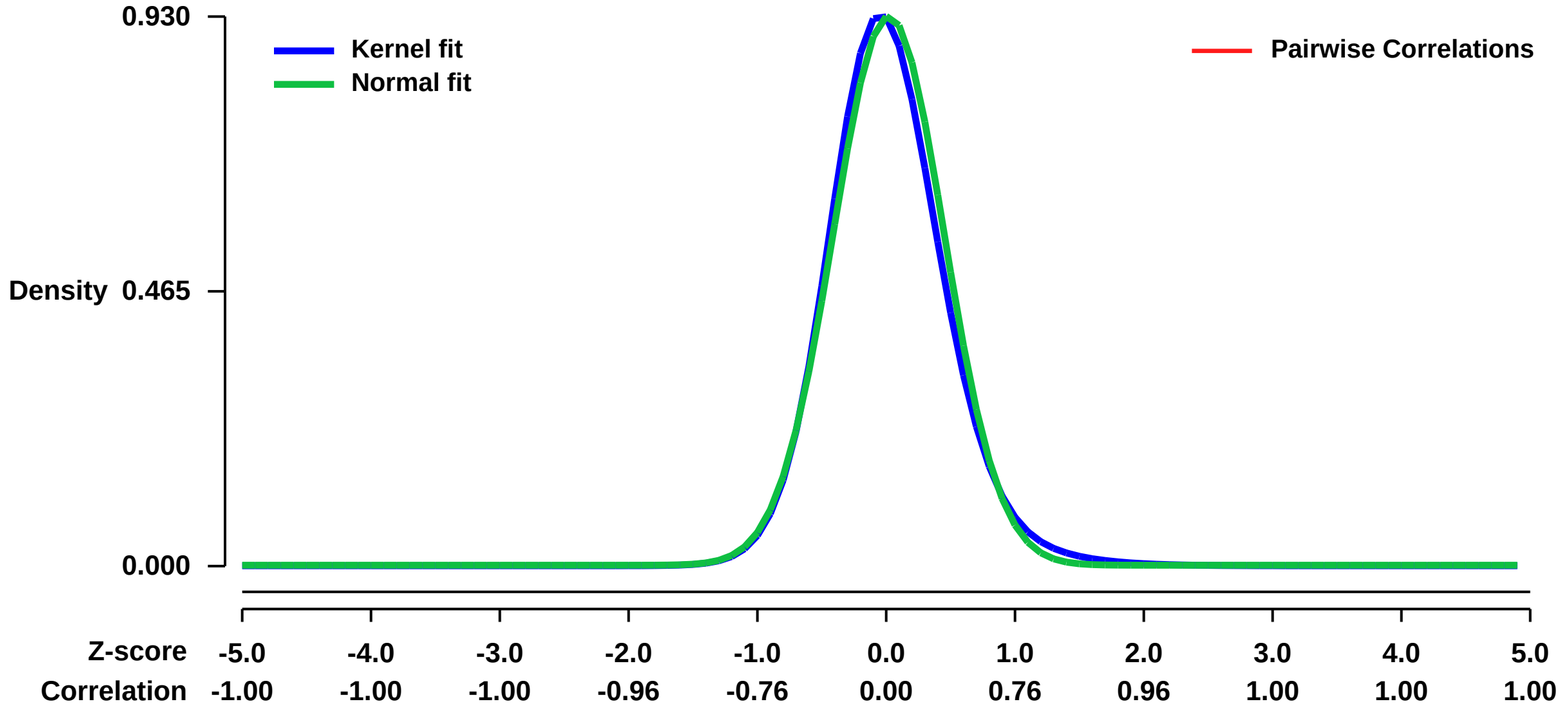

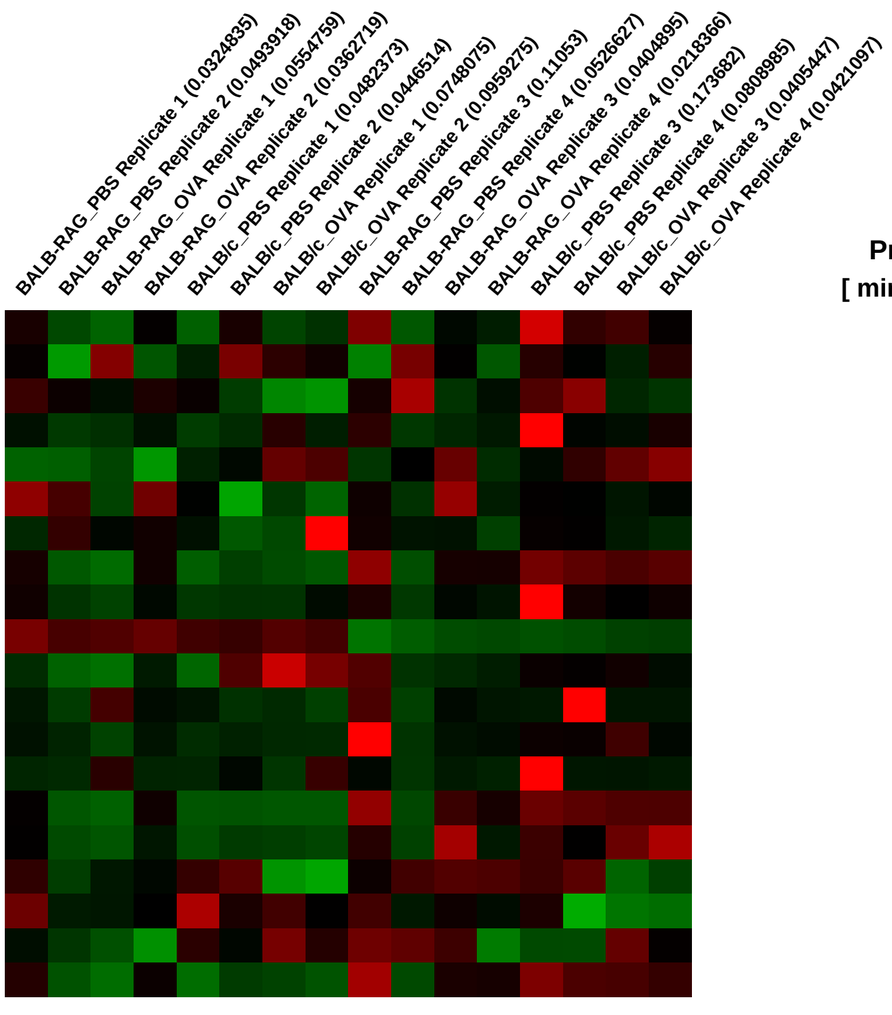

GEO Series "GSE38277" Expression Profiles

Num of samples in this series: 18

Scale of expression profile Z-scores

-3.0 -2.0 -1.0 0.0 1.0 2.0 3.0

GEO Link:	http://www.ncbi.nlm.nih.gov/geo/query/acc.cgi?acc=GSE38277
Status:	Public on Jan 17 2014
Title:	Lsd1 coordinates trophoblast development by retaining stem cells in their niche and directing cell fate
Organism:	Mus musculus
Experiment type:	Expression profiling by array
Platform:	GPL1261
Pubmed ID:	24448552
Summary & Design:	**Summary:** Stem cells reside in specific niches providing stemness-maintaining environments. Thus, the regulated migration from these niches is associated with differentiation onset. However, mechanisms retaining stem cells in their niche remain poorly understood. Here, we show that the epigenetic regulator lysine-specific demethylase 1 (Lsd1) organises the trophoblast niche of the early mouse embryo by coordinating migration and invasion of trophoblast stem cells (TSCs). Lsd1 deficiency leads to the depletion of the stem cell pool resulting from precocious migration of TSCs. Migration is induced by premature expression of the transcription factor Ovol2 that is repressed by Lsd1 in undifferentiated wild-type TSCs. Increasing Ovol2 levels suffices to recapitulate the migration phenotype. Furthermore, Lsd1-deficient TSCs exhibit a developmental bias towards cells of the syncytiotrophoblast and impaired spongiotrophoblast and trophoblast giant cell differentiation. In summary, we describe that the epigenetic modifier Lsd1 coordinates placental development by retaining TSCs in their niche and directing trophoblast differentiation. **Overall design:** Mouse trophoblast stem cells (TSCs) were isoloated from a single conditional Lsd1-deficient mouse (Lsd1tm1Schˆ…le). Deletion of Lsd1 was induced eight days before the collection of RNA by addition of 0.2 ´¡M 4OH-tamoxife. Cells were isolated at successive stages of differentiation for total RNA extraction and hybridization on Affymetrix microarrays. To that end, we harvested cells at three time-points: before induction of differentiation (d0), two days after induction of differentiation (d2), and four days after induction of differentiation (d4). Three replicates (1, 2, 3) for control (-) and Lsd1-deficeint (+) cells were included for each differentiation stage.

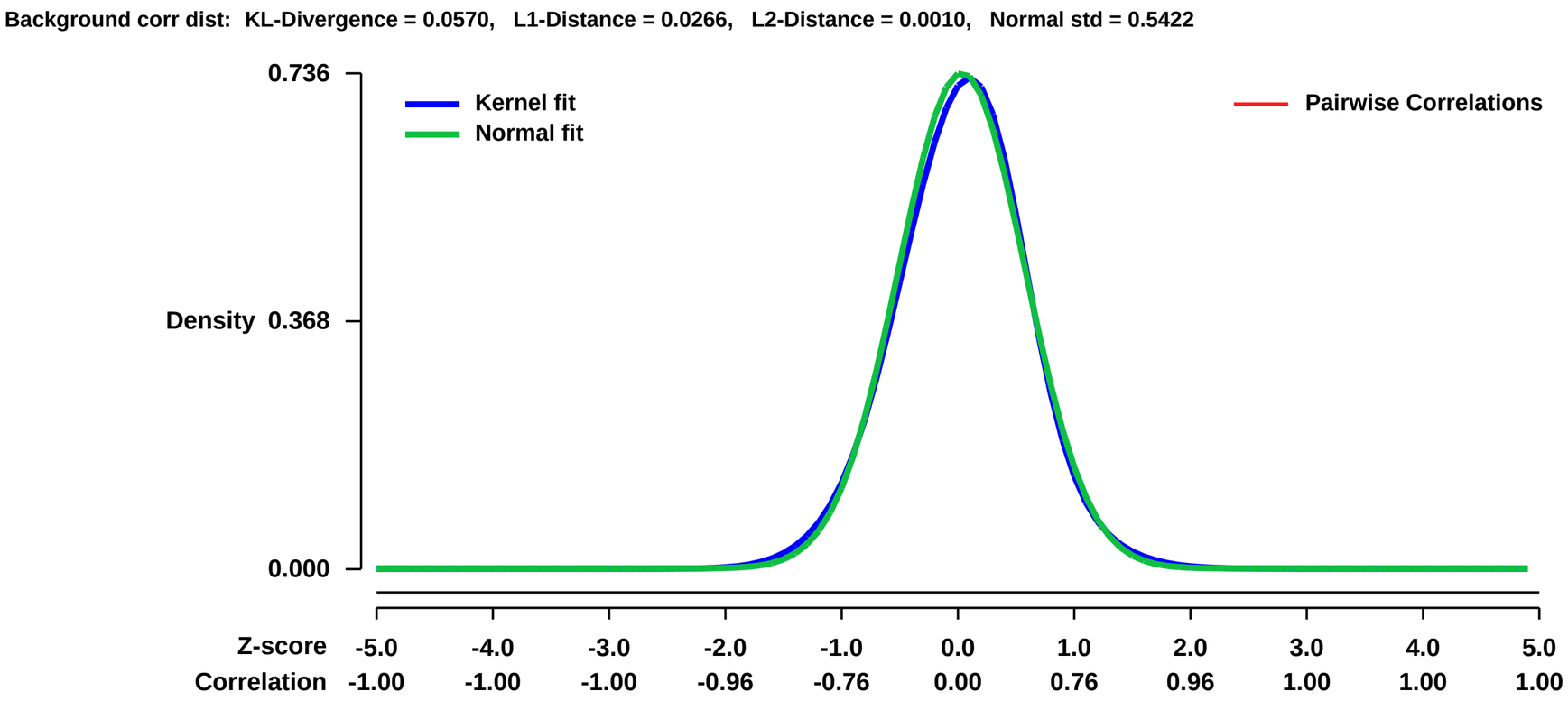

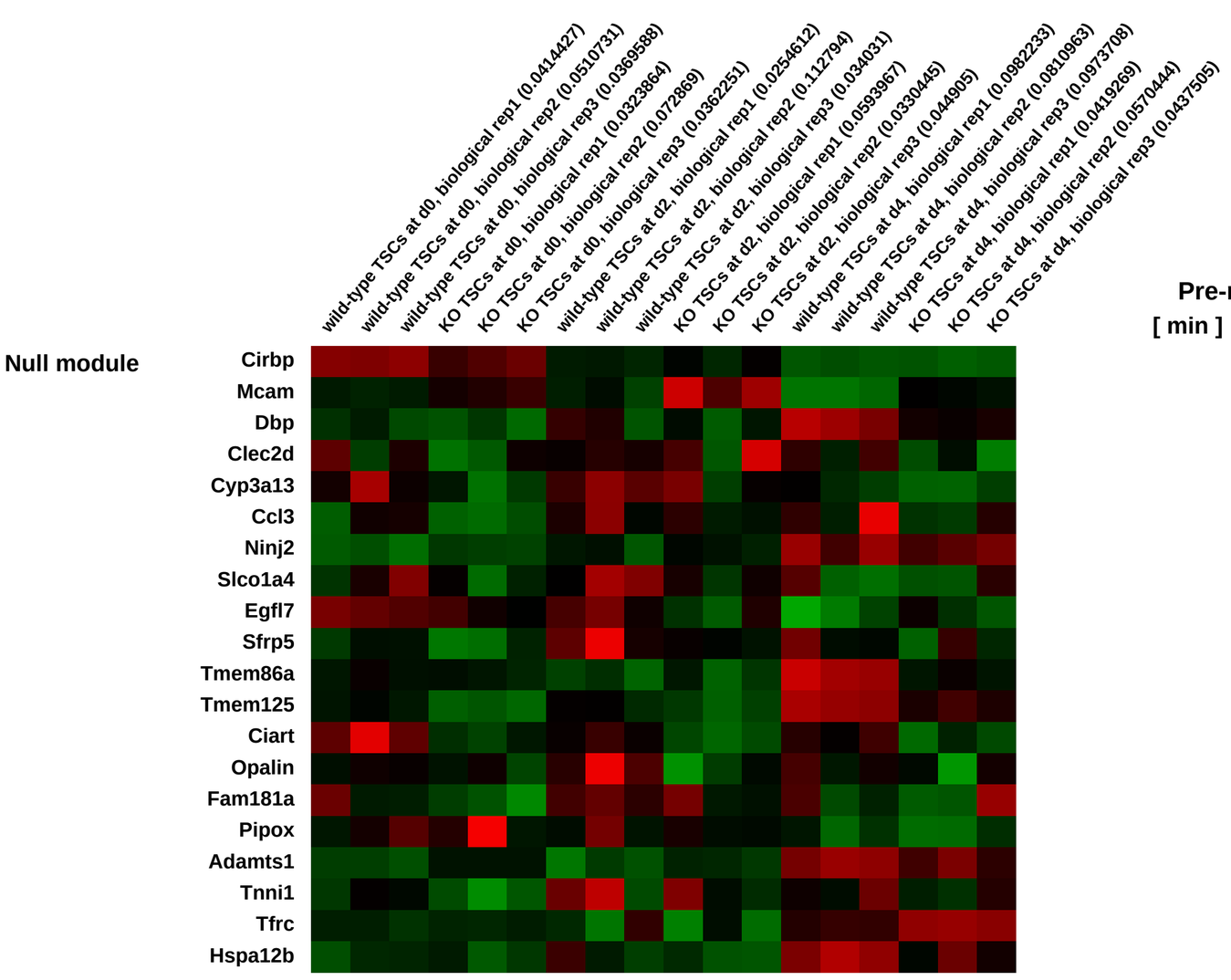

GEO Series "GSE14481" Expression Profiles

Num of samples in this series: 12

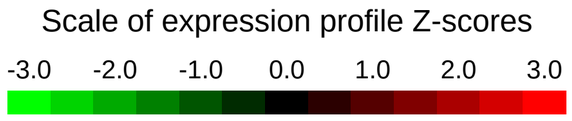

GEO Link:	**http://www.ncbi.nlm.nih.gov/geo/query/acc.cgi?acc=GSE14481**
Status:	**Public on Dec 31 2009**
Title:	**identification of TGCT genes involved in initiation and maintenance of transformed germ cells.**
Organism:	**Mus musculus**
Experiment type:	**Expression profiling by array**
Platform:	**GPL1261**
Pubmed ID:	
Summary & Design:	**Summary:** **Initially, we had compared gene expression differences in the embryonic gonads (E13.5) of the 129 and M19 strains by performing microarray analysis. These studies allowed us to identify downregulation of expression of the D19Bwg1357e, Zfp162 and Cox15 genes in the M19 strain.** **We next decided to examine gene expression profile changes in the embryonic gonads of 129 and M19 at additional stages so as to identify other TGCT genes from M19 that are also involved in initiation and maintenance of transformed germ cells. For this we isolated E13.5, E15.5 and E17.5 genital ridges from male embryos.** **Overall design:** **After data process and quality assessment, 38069 out of 45101 probe sets proceeded for further analysis to identify differentially expressed genes. Hierarchical cluster analysis shows that samples of two strains from the same stage were grouped together and separated from the other stages (Fig.8). The initial analysis indicates a number of trends in gene expression patterns. Moreover, downregulation of expression of D19Bwg1357e, Zfp162 and Cox15 genes in M19 was also verified in this analysis. These data are currently being analyzed with the help of Dr. Y. Ji and L. Xiao from the Department of Bioinformatics and Computational Biology and Department of Biostatistics at M.D. Anderson Cancer Center. The results are unpublished.**

Background corr dist: KL-Divergence = 0.0538, L1-Distance = 0.0246, L2-Distance = 0.0009, Normal std = 0.5415

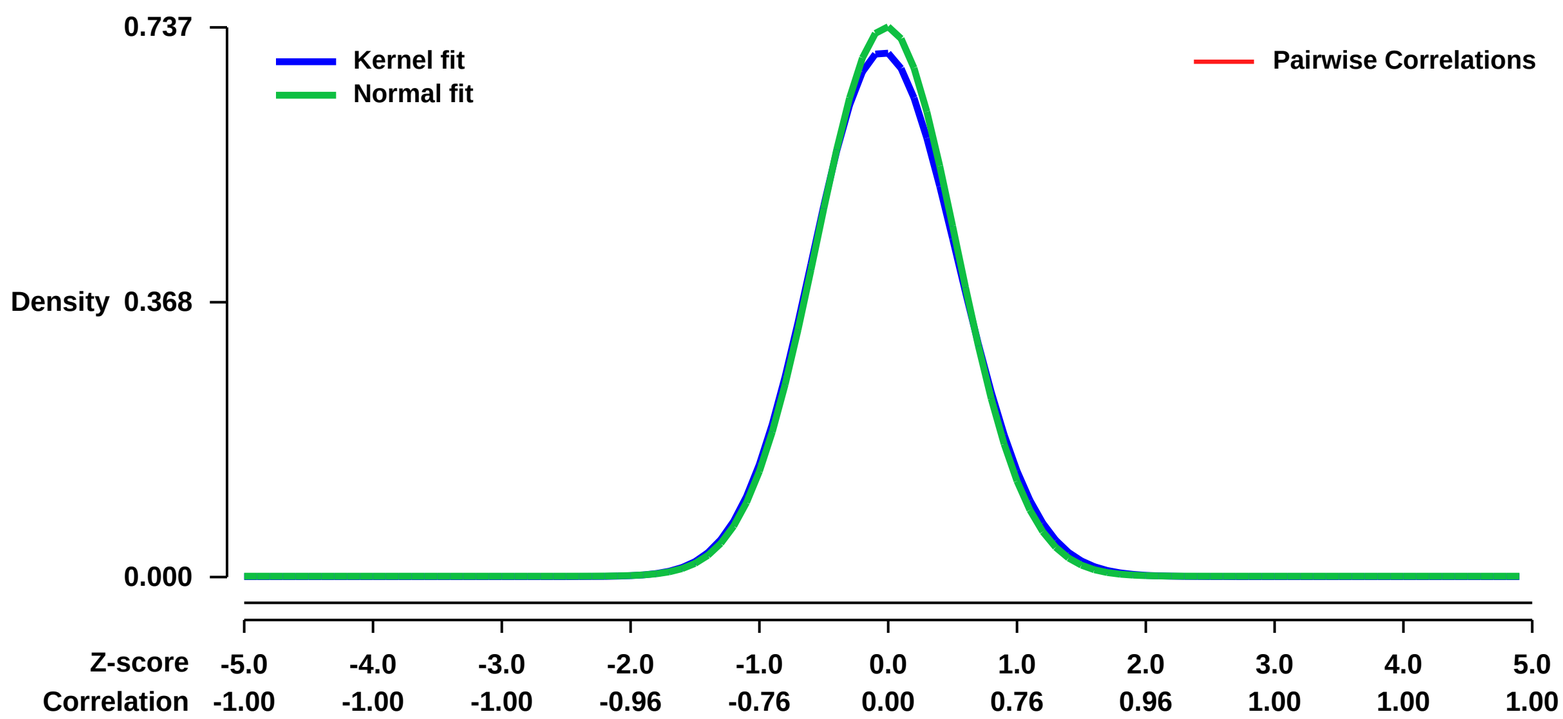

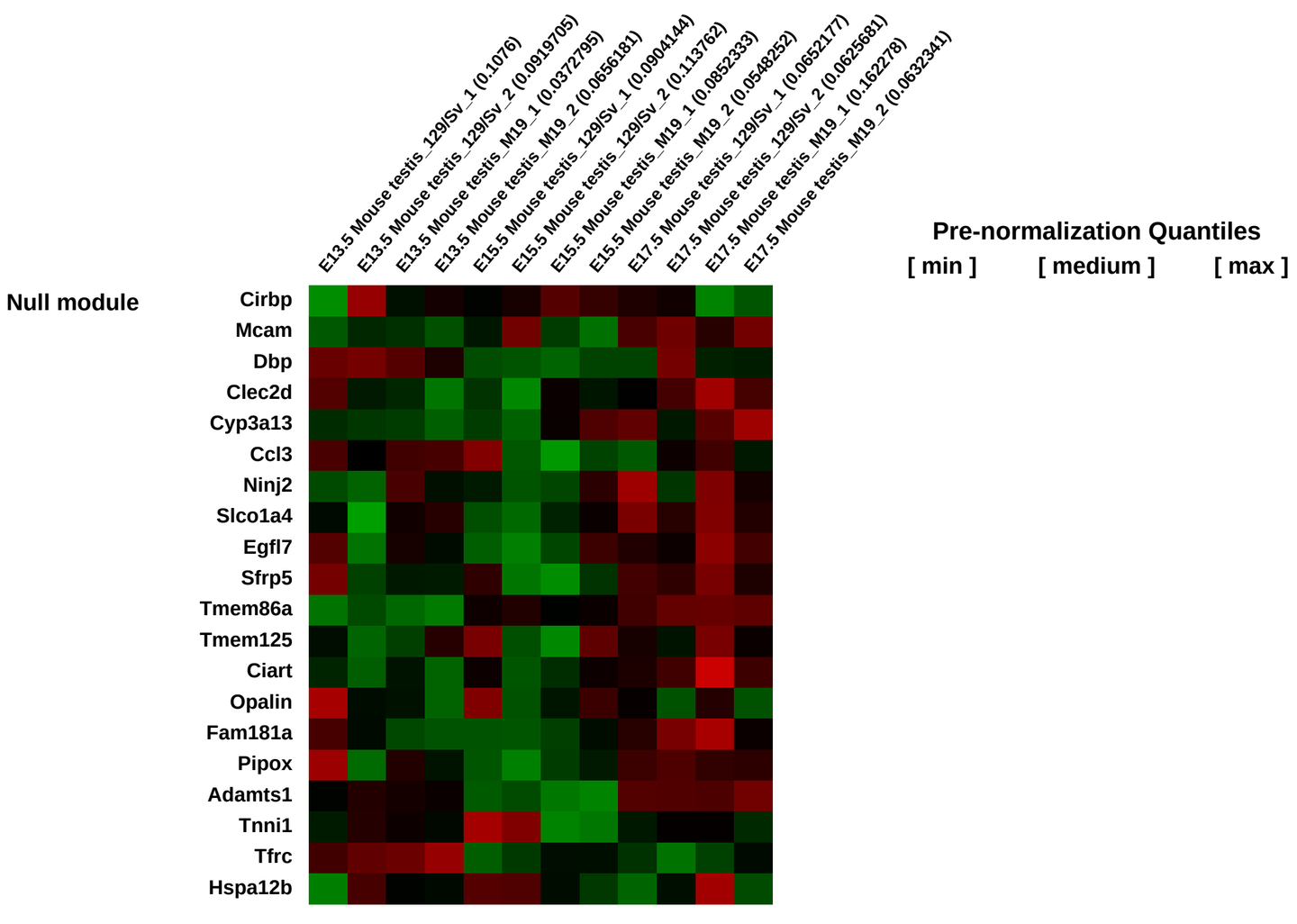

GEO Series "GSE10528" Expression Profiles

Num of samples in this series: 6

Scale of expression profile Z-scores

-3.0 -2.0 -1.0 0.0 1.0 2.0 3.0

GEO Link:	http://www.ncbi.nlm.nih.gov/geo/query/acc.cgi?acc=GSE10528
Status:	Public on Feb 15 2008
Title:	The retinal transcriptional response to light damage
Organism:	Mus musculus
Experiment type:	Expression profiling by array
Platform:	GPL1261
Pubmed ID:	15872101
Summary & Design:	**Summary:** Transcriptional profiles were compared between dark adapted and light damaged BALBc (albino) mouse retinas. **Keywords: stress response** **Overall design:** BALBc mice were dark adapted for one week. To produce light damage a subset of the mice were then exposed to 6,000 lux white fluorescent light for 6 hours. Retinas were collected for RNA extraction 24 hours after light damage.

Background corr dist: KL-Divergence = 0.0225, L1-Distance = 0.0186, L2-Distance = 0.0004, Normal std = 0.7206

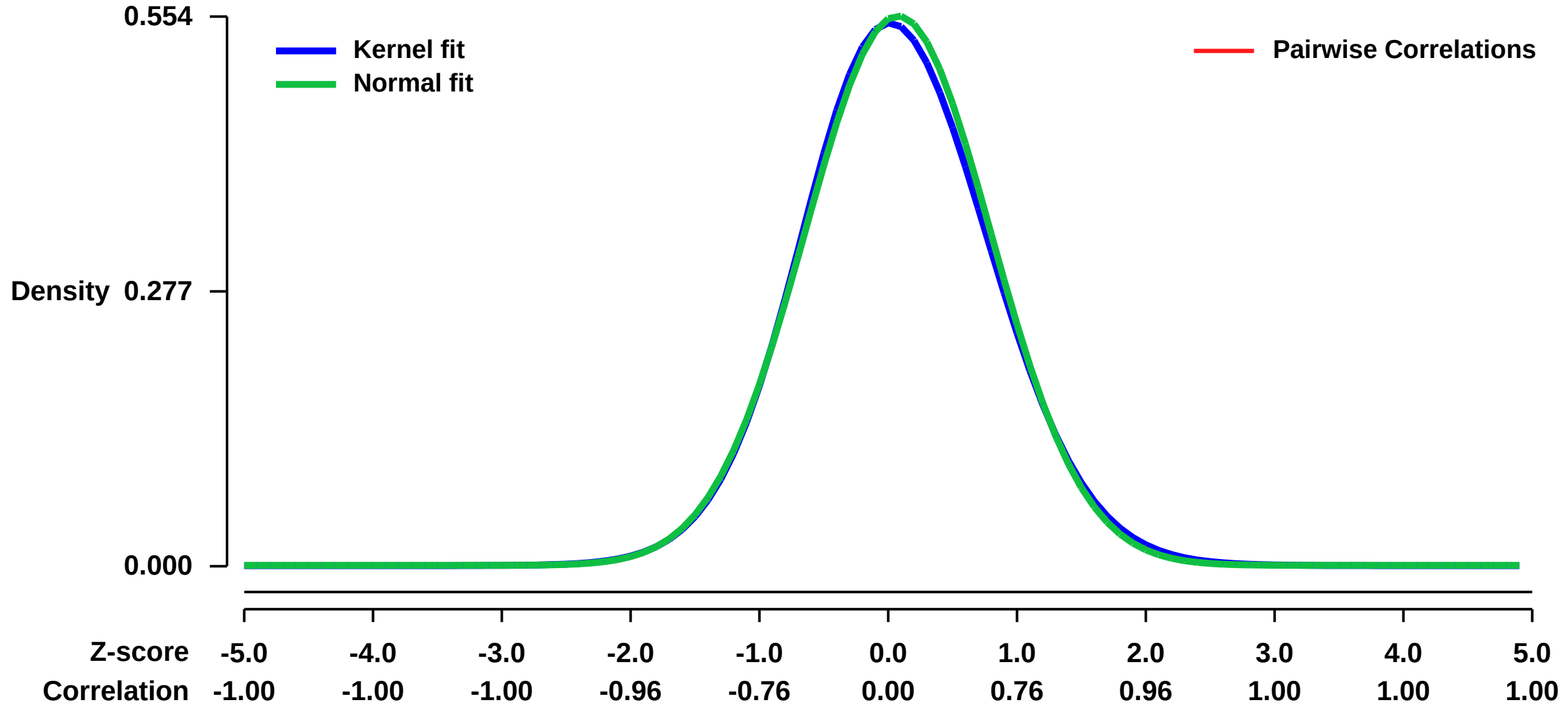

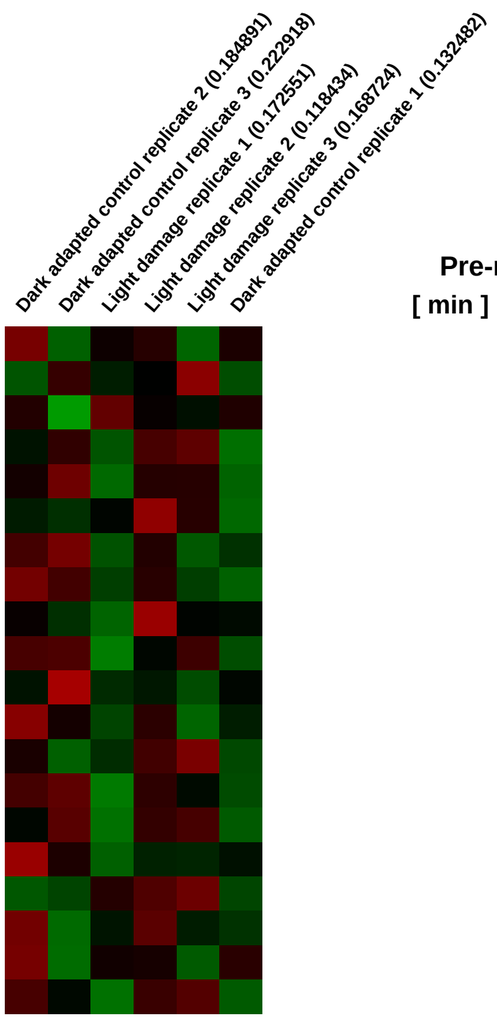

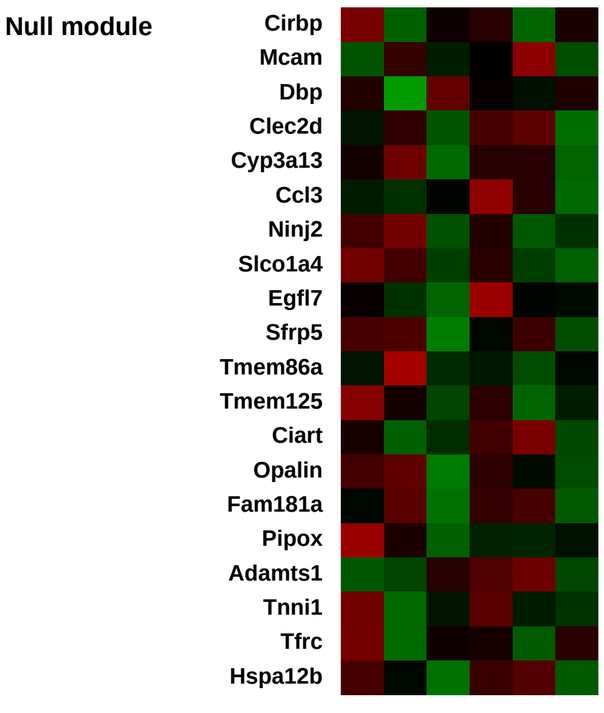

GEO Series "GSE22774" Expression Profiles

Num of samples in this series: 6

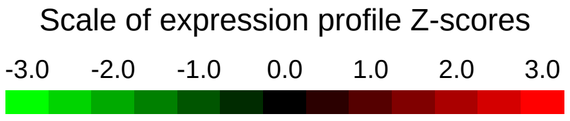

GEO Link:	http://www.ncbi.nlm.nih.gov/geo/query/acc.cgi?acc=GSE22774
Status:	Public on Jul 22 2010
Title:	Musashi 2 regulates normal hematopoiesis and accelerates leukemogenesis (LSK and LK)
Organism:	Mus musculus
Experiment type:	Expression profiling by array
Platform:	GPL1261
Pubmed ID:	20616797
Summary & Design:	**Summary:** We demonstrate that Msi2 is the predominant form expressed in hematopoietic stem cells (HSC), and its knockdown leads to reduced engraftment and depletion of HSCs in vivo. Overexpression of Msi2 in a mouse model increases HSC cell cycle progression and cooperates with BCR-ABL1 to induce an aggressive leukemia. MSI2 is over-expressed in human myeloid leukemia, and expression levels directly correlate with decreased patient survival, thereby defining MSI2 expression as a novel prognostic marker in acute myeloid leukemia (AML). Depletion of MSI2 in human myeloid leukemia cells leads to decreased proliferation and apoptosis. These data implicate the MSI2 RNA binding protein in myeloid leukemogenesis and identify a novel potential target for therapy in AML. **Overall design:** Mouse hematopoietic stem cells (defined as LineageLow, Sca1+, Kit+; LSK; n=3) as well as committed progenitor cells (LineageLow, Sca1-, Kit+; LK; n=3) were sorted and RNA was extracted using Qiagen RNeasy Micro Kit according to manufacturers instruction. cDNA was fragmented and biotinylated before hybridization onto Affymetrix Mouse Expression Array 430 2.0.

Background corr dist: KL-Divergence = 0.0344, L1-Distance = 0.0265, L2-Distance = 0.0009, Normal std = 0.6475

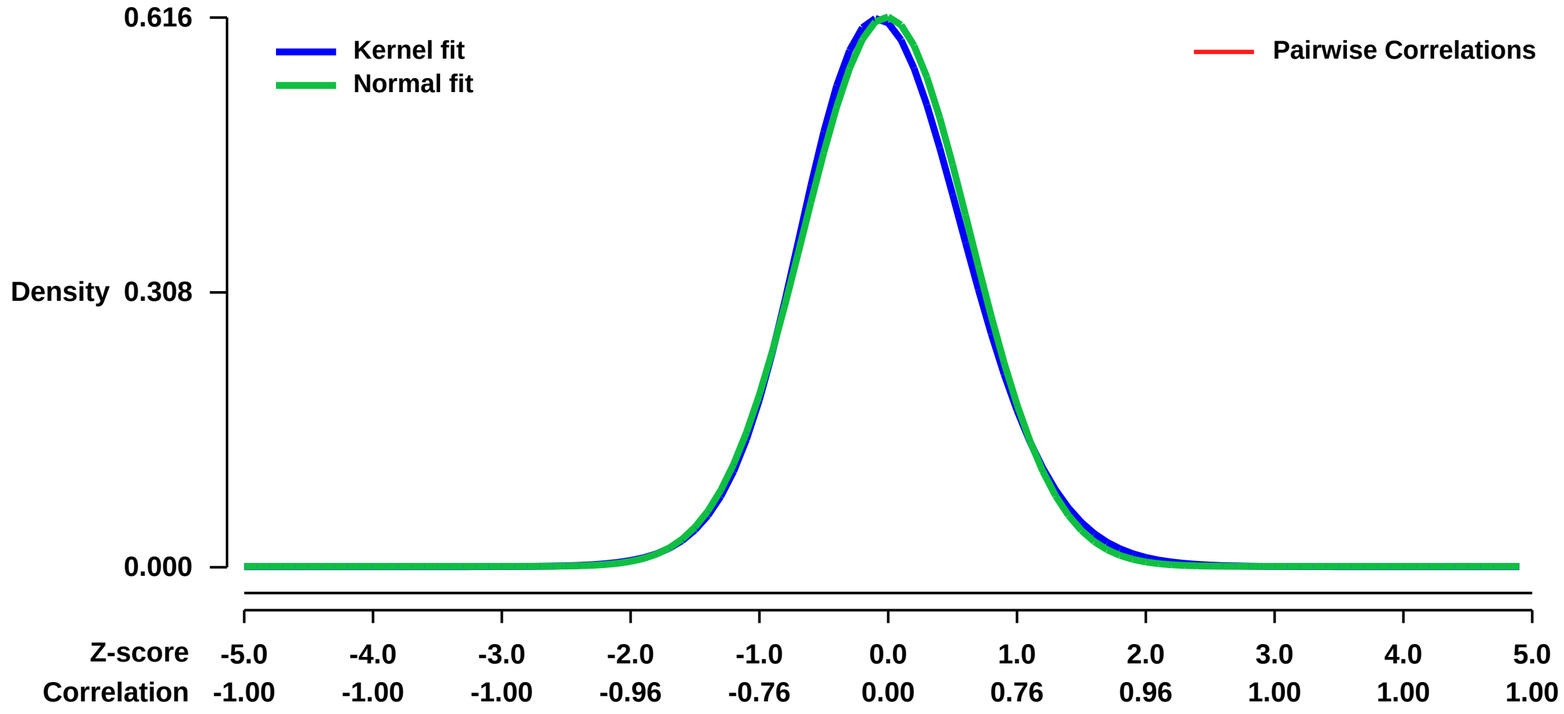

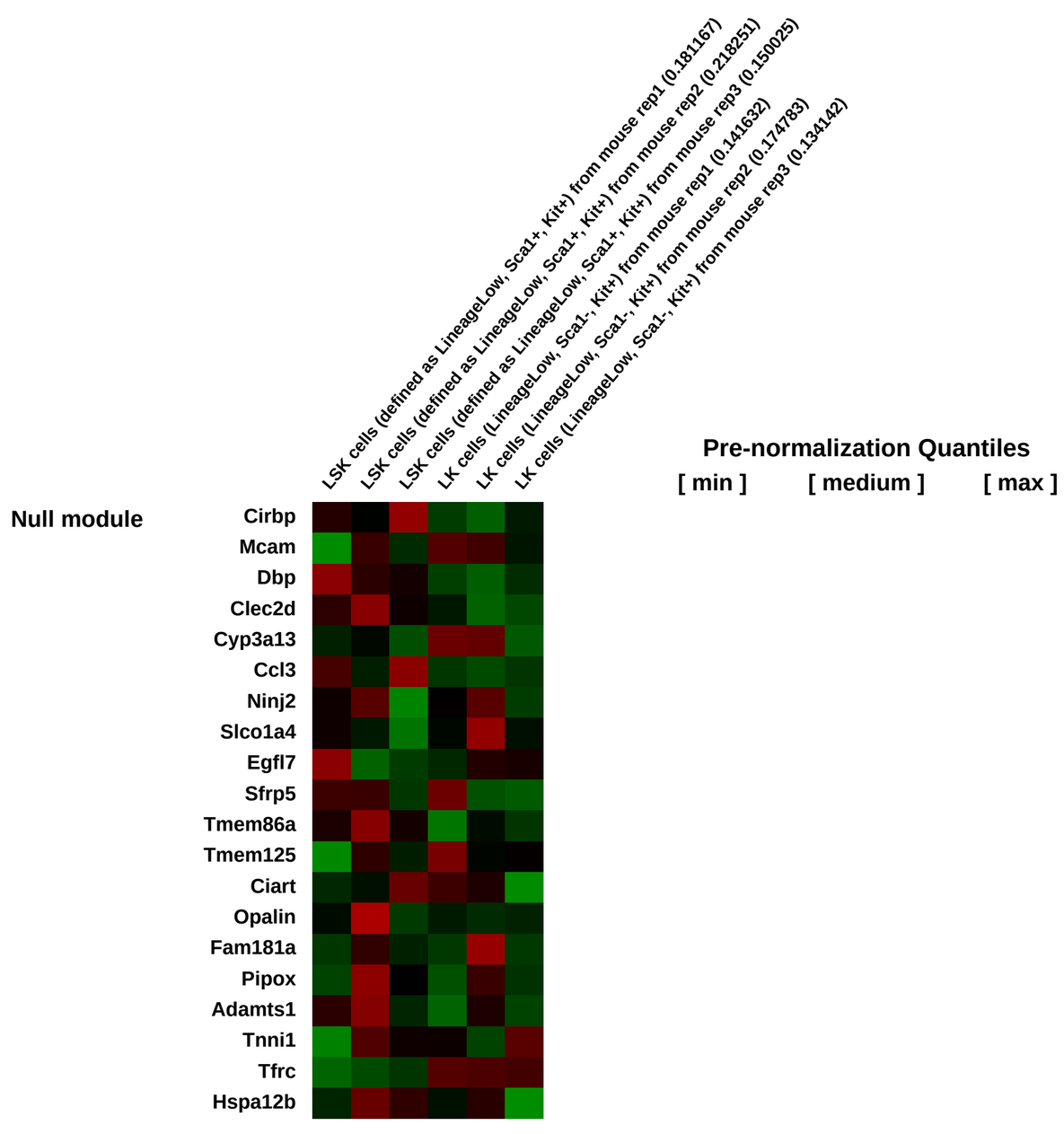

GEO Series "GSE20008" Expression Profiles

Num of samples in this series: 6

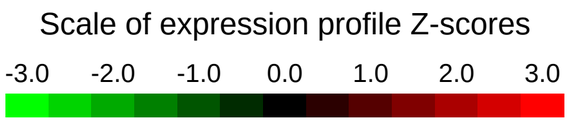

GEO Link:	**http://www.ncbi.nlm.nih.gov/geo/query/acc.cgi?acc=GSE20008**
Status:	**Public on Dec 31 2013**
Title:	**PCAF/GCN5-regulated genes in MEFs**
Organism:	**Mus musculus**
Experiment type:	**Expression profiling by array**
Platform:	**GPL1261**
Pubmed ID:	
Summary & Design:	**Summary:** **Histone acetyltransferases (HATs) GCN5/PCAF and CBP/p300 are transcription coactivators. However, how these HATs regulate ligand-induced nuclear receptor target gene expression remains unclear. Here we show in mouse embryonic fibroblasts (MEFs), deletion of GCN5/PCAF specifically eliminates acetylation on H3K9 (H3K9Ac) while deletion of CBP/p300 selectively reduces acetylation on H3K18 and H3K27 (H3K18/27Ac). Treating MEFs with a specific ligand for nuclear receptor PPARdelta induces sequential increases of H3K18/27Ac and H3K9Ac on the promoter of PPARdelta target gene Angptl4, which correlates with a robust ligand-induced Angptl4 expression. Inhibiting transcription elongation blocks ligand-induced H3K9Ac but not H3K18/27Ac on Angptl4 promoter. Finally, we show CBP/p300 and their HAT activities are required, while GCN5/PCAF and H3K9Ac are dispensable, for ligand-induced PPARdelta target gene expression in MEFs. These results highlight the substrate and site specificities of HATs in cells, and suggest that GCN5/PCAF- and CBP/p300-mediated histone acetylations play distinct roles in regulating ligand-induced nuclear receptor target gene expression.** **Overall design:** **PCAF and GCN5 have some redundant function. To identify PCAF/GCN5-regulated genes, immortalized MEFs with PCAF knockout and GCN5 conditional knockout were infected with retroviruses expressing either Cre recombinase or vector alone. We prepared duplicated RNAs from either vector or Cre infected cells (PCAF-/-;GCN5+/- or PCAF-/-;GCN5+/-) and RNAs from either Vector or Cre infected the other independently immortalized cells for 6 affymetrix microarray.**

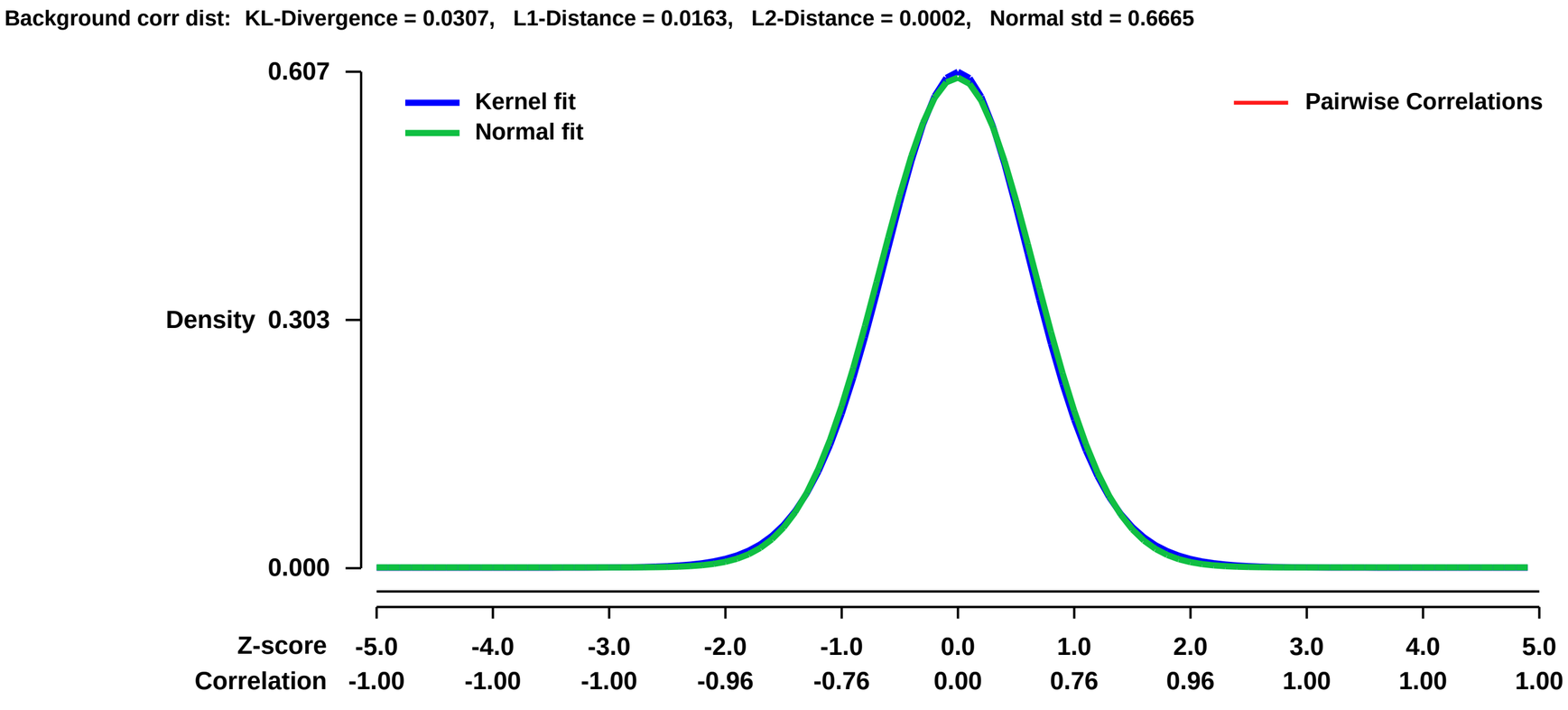

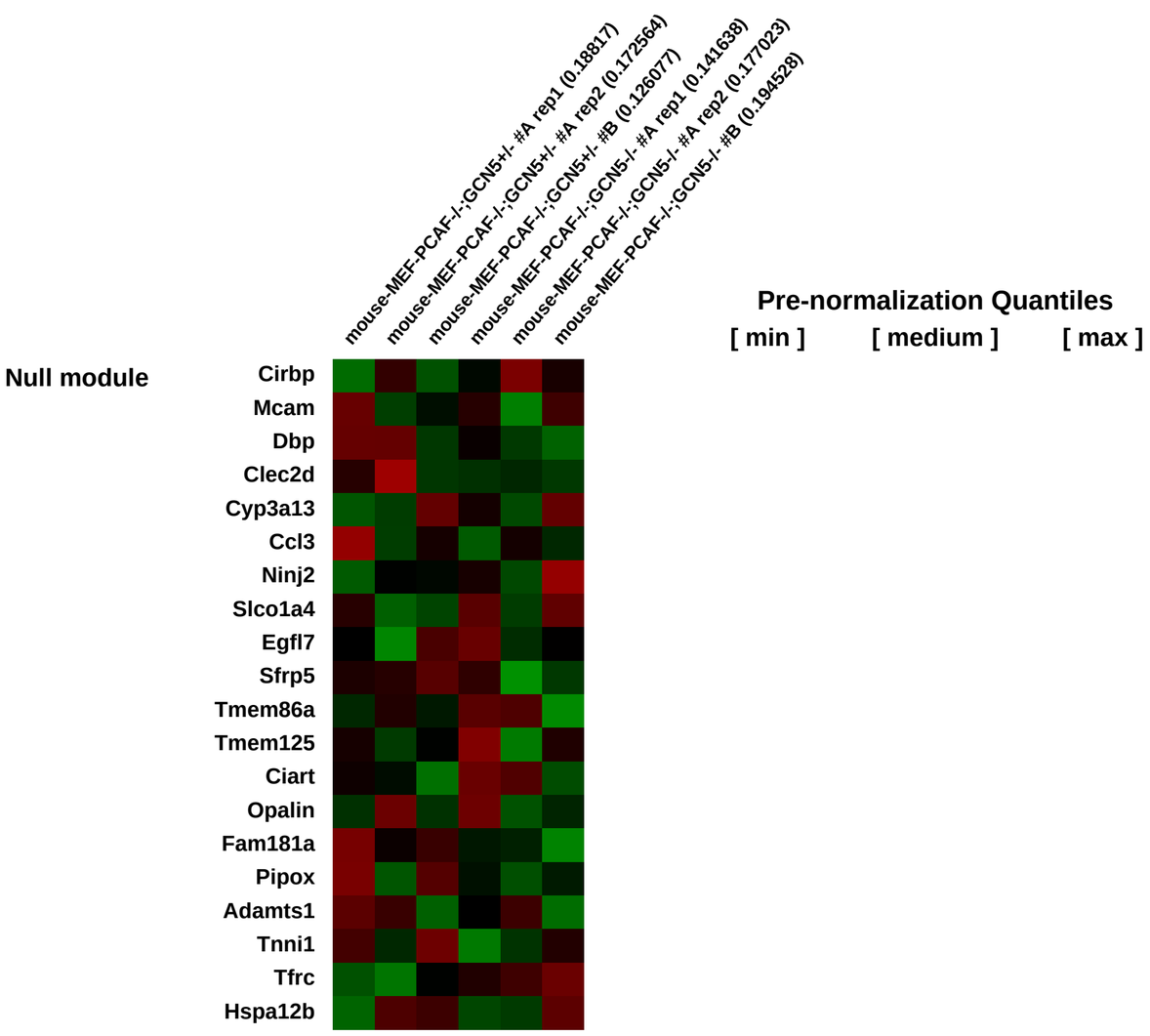

GEO Series "GSE18669" Expression Profiles

Num of samples in this series: 12

Scale of expression profile Z-scores

-3.0 -2.0 -1.0 0.0 1.0 2.0 3.0

GEO Link:	http://www.ncbi.nlm.nih.gov/geo/query/acc.cgi?acc=GSE18669
Status:	Public on Nov 09 2009
Title:	Analysis of murine hematopoieitic stem cells, multipotent progenitors, PreMegE progenitors and mature CD4+ T cells
Organism:	Mus musculus
Experiment type:	Expression profiling by array
Platform:	GPL1261
Pubmed ID:	19887676
Summary & Design:	**Summary:** An investigation of the global gene expression signatures of murine hematopoietic stem cell differentiation during steady state hematopoiesis. This data compliments the miniChIP-chip data obtained from the same cell types as described in Weishaupt et al., 2009 (Blood). **Overall design:** HSCs are phenotypically identified in bone marrow as lineage-, cKit+, Sca1+, CD150+, Flk2/Flt3- (LSKCD150+ cells). MPPs are phenotypically identified in bone marrow as lineage-, cKit+, Sca1+, CD150-, Flk2/Flt3+ (LSKCD150- cells). PreMegEs are phenotypically identified in bone marrow as lineage-, cKit+, Sca1-, CD150+, CD105- and CD41- as described in Pronk et al., 2007. Splenic-derived CD4+ T cells are phentypically identified as CD4+, CD8-, B220-, Nk1.1- cells as described in Rolf et al., 2008.

Background corr dist: KL-Divergence = 0.0714, L1-Distance = 0.0262, L2-Distance = 0.0012, Normal std = 0.4984

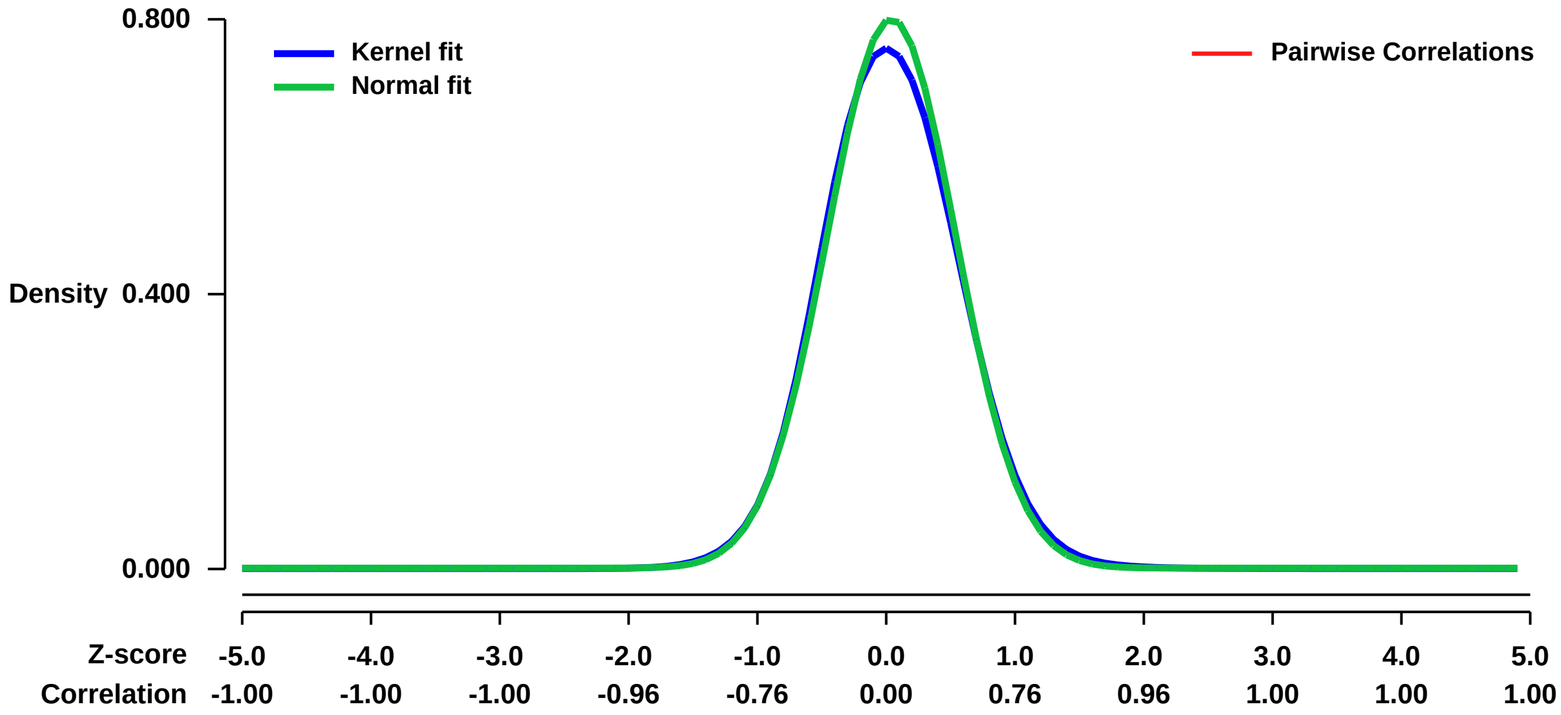

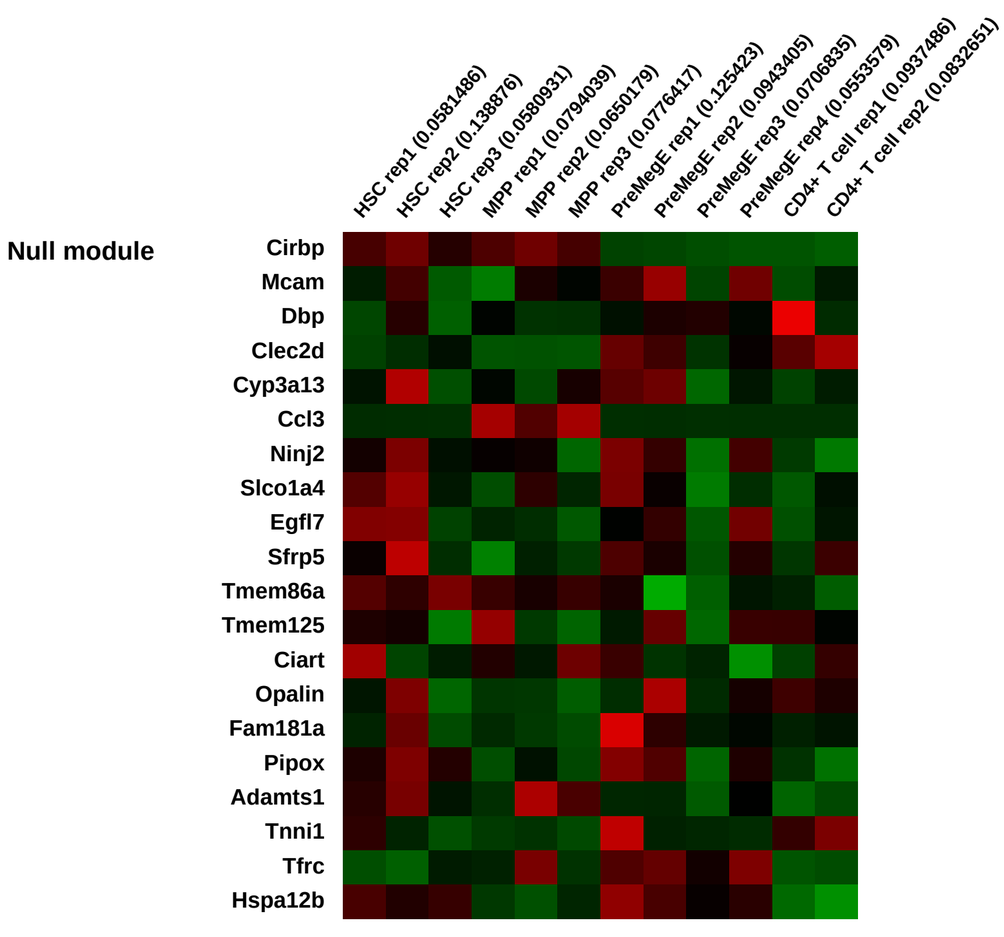

GEO Series "GSE4927" Expression Profiles

Num of samples in this series: 6

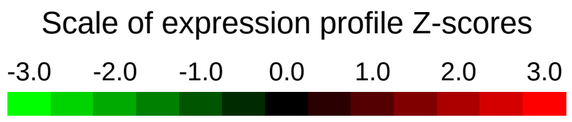

GEO Link:	http://www.ncbi.nlm.nih.gov/geo/query/acc.cgi?acc=GSE4927
Status:	Public on Apr 30 2007
Title:	Effect of OMP on gene expression in the olfactory epithelium
Organism:	Mus musculus
Experiment type:	Expression profiling by array
Platform:	GPL1261
Pubmed ID:	17444493
Summary & Design:	**Summary:** OMP is expressed only in mature olfactory sensory neurons, arguing that its function is specially suited to the needs of OSNs. However none of the properties of OMP suggest any direct role in regulating gene expression in OSNs. Our data confirms that gene expression in the olfactory epithelium of mice lacking OMP is indistinguishable from mice expressing OMP. We used affymerix M430v2.0 gene chips to cover as much of genome as possible and observed no statistically significant differences in mRNA abundance between the two genotypes.These results imply that OMPs ability to regulate signal transduction with in OSNs has little effect on gene expression and that its ability to promote mitosis in neighbouring cells (under culture conditions) is insufficiently active under normal laboratory housing conditions to generate detectable differences in gene expression patterns. **Keywords:** genetic modification **Overall design:** The overall design of the experiment is to undertand the effect of OMP (olfactory marker protein) on gene expression in the olfactory epithelium. We isolated the olfactory epithelium from homozygous and heterozygous OMP-GFP mice, extracted the RNA and hybridized on to the mouse expression set 430 2.0 Chip.

Background corr dist: KL-Divergence = 0.0486, L1-Distance = 0.0184, L2-Distance = 0.0003, Normal std = 0.5777

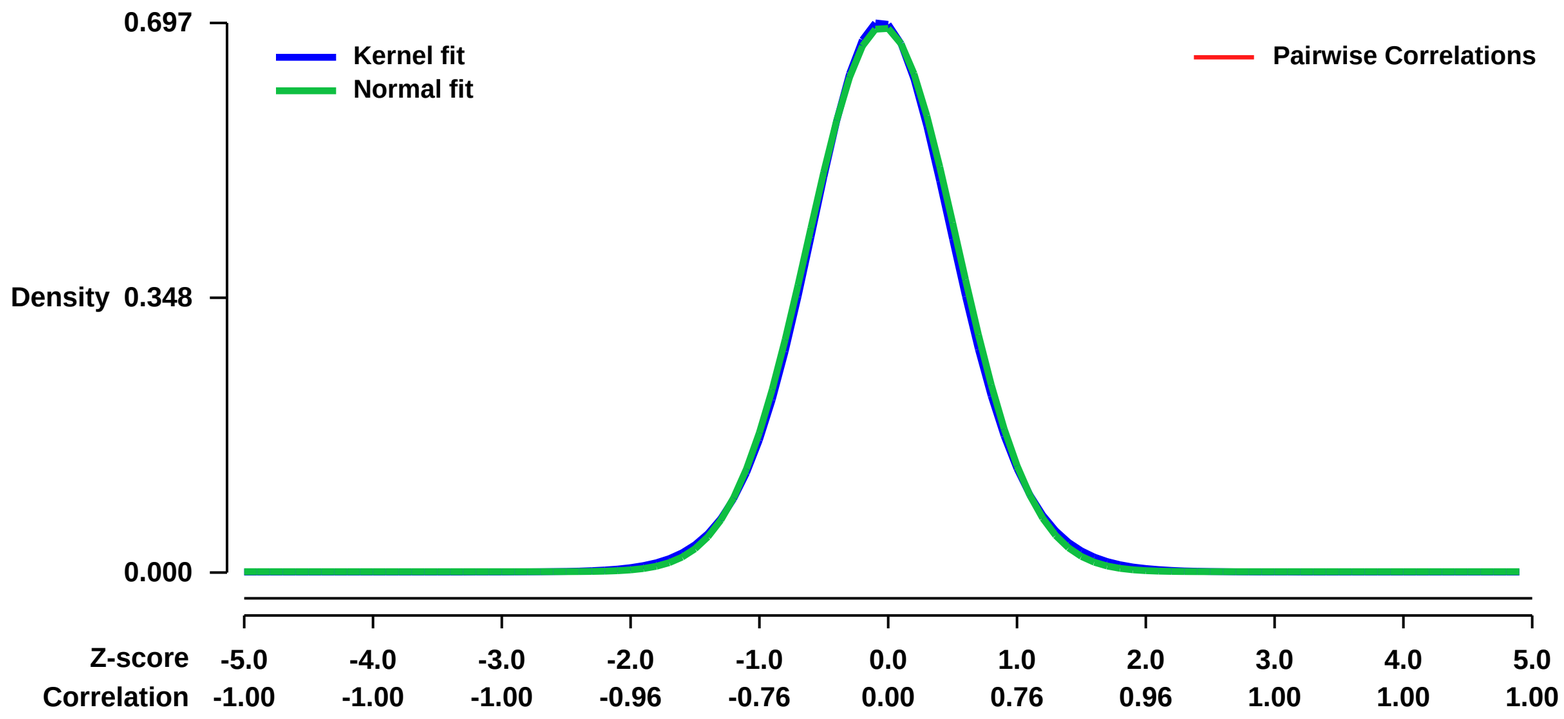

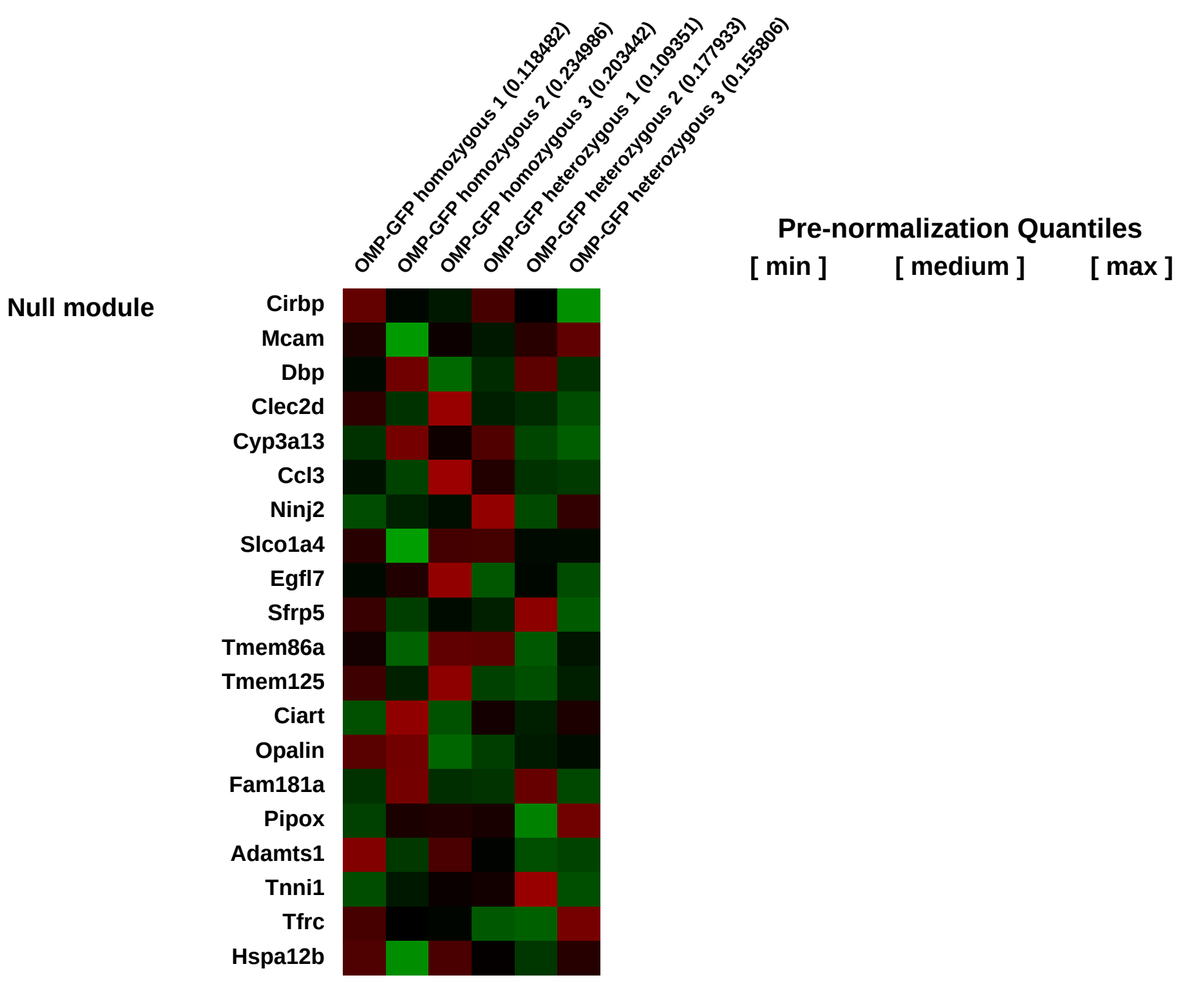

GEO Series "GSE37431" Expression Profiles

Num of samples in this series: 6

Scale of expression profile Z-scores

-3.0 -2.0 -1.0 0.0 1.0 2.0 3.0

GEO Link:	http://www.ncbi.nlm.nih.gov/geo/query/acc.cgi?acc=GSE37431
Status:	Public on Apr 23 2012
Title:	Endothelial cell-enriched genes expression in mouse embryo
Organism:	Mus musculus
Experiment type:	Expression profiling by array
Platform:	GPL1261
Pubmed ID:	22535667
Summary & Design:	**Summary:** The early blood vessels of the embryo and yolk sac in mammals develop by aggregation of de novo forming angioblasts into a primitive vascular plexus, which then undergoes a complex remodeling process. Angiogenesis is also important for disease progression in the adult. However, the precise molecular mechanism of vascular development remains unclear. It is therefore of great interest to determine which genes are specifically expressed in developing endothelial cells.Here, we utilized Flk1-deficient mouse embryos, which lack endothelial cells, to perform a genome-wide survey for genes related to vascular development. **Overall design:** Wild type (WT), Flk1+/GFP and Flk1 KO embryos proper (fetuses) were dissected out at 8.5 dpc. Total RNAs from these embryos were prepared using RNeasy kit. Gene expression analysis was performed by GeneSpring software.

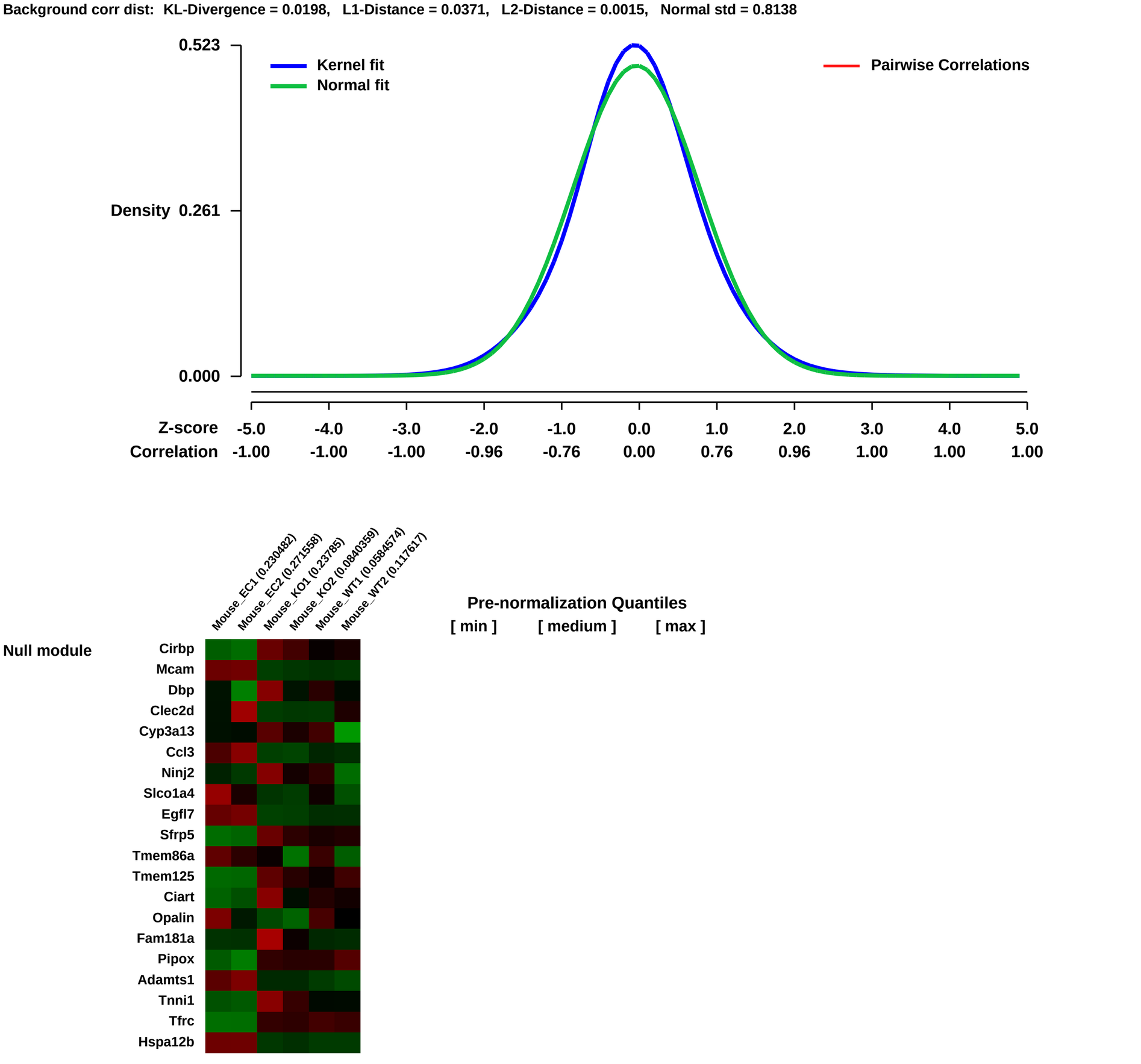

GEO Series "GSE6881" Expression Profiles

Num of samples in this series: 10

Scale of expression profile Z-scores

-3.0 -2.0 -1.0 0.0 1.0 2.0 3.0

GEO Link:	http://www.ncbi.nlm.nih.gov/geo/query/acc.cgi?acc=GSE6881
Status:	Public on Feb 05 2007
Title:	Embryonic Testis Developmental Time Course
Organism:	Mus musculus
Experiment type:	Expression profiling by array
Platform:	GPL1261
Pubmed ID:	15496517
Summary & Design:	**Summary:** Time course of gene expression in the murine embryonic testis from the time of the indifferent gonad (11.5dpc) to birth (18.5dpc) **Keywords: Time Course** **Overall design:** Independent embryonic testis preps were used for array analysis. Duplicates were provided for each sample.

Background corr dist: KL-Divergence = 0.0763, L1-Distance = 0.0229, L2-Distance = 0.0009, Normal std = 0.4853

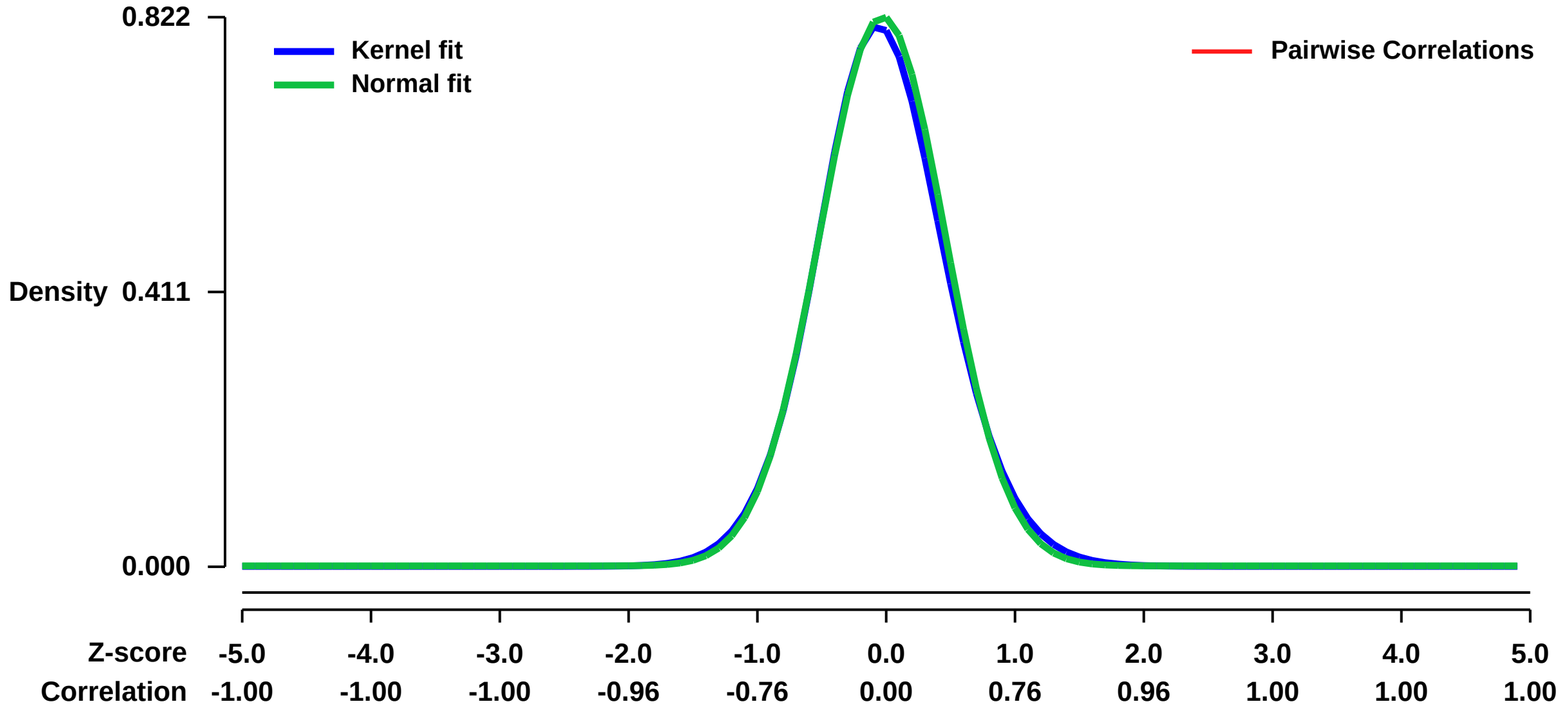

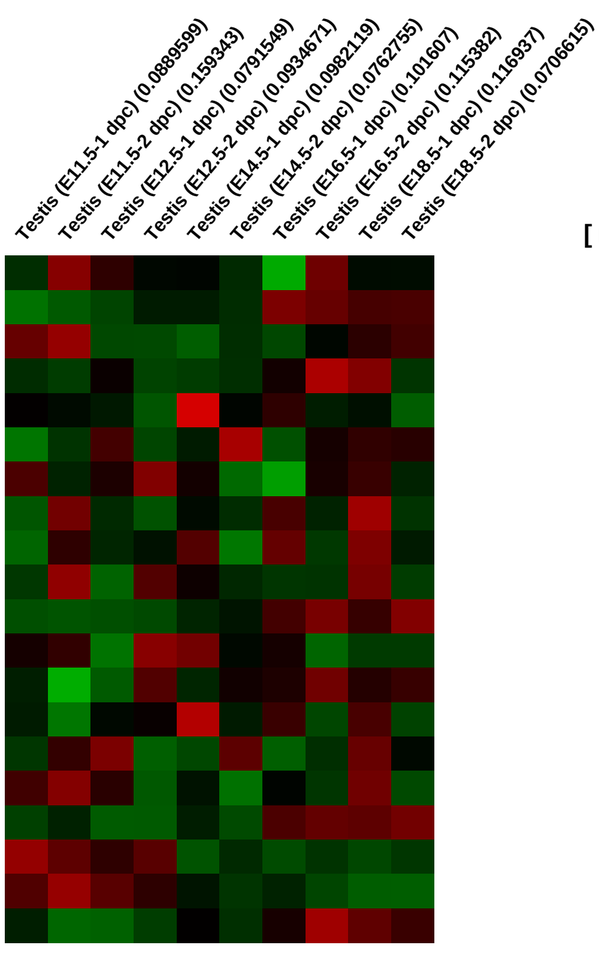

GEO Series "GSE58296" Expression Profiles

Num of samples in this series: 9

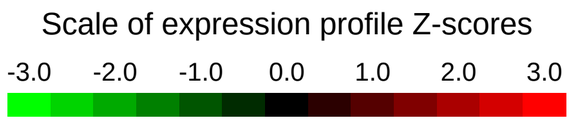

GEO Link:	**http://www.ncbi.nlm.nih.gov/geo/query/acc.cgi?acc=GSE58296**
Status:	**Public on Jun 09 2014**
Title:	**Expression data from intestinal organoids altered for Tgfbeta signaling**
Organism:	**Mus musculus**
Experiment type:	**Expression profiling by array**
Platform:	**GPL1261**
Pubmed ID:	
Summary & Design:	**Summary:** **We treated intestinal organoids continuously for 5 days with or without TgfbR1/2 inhibitor (LY2109761) or Tgfb1 ligand** **Overall design:** **Organoids were continuously treated for 5 days, then RNA was extracted and hybridized to Affymetrix Mouse Genome 430 2.0**

Background corr dist: **KL-Divergence = 0.0550, L1-Distance = 0.0401, L2-Distance = 0.0021, Normal std = 0.5732**

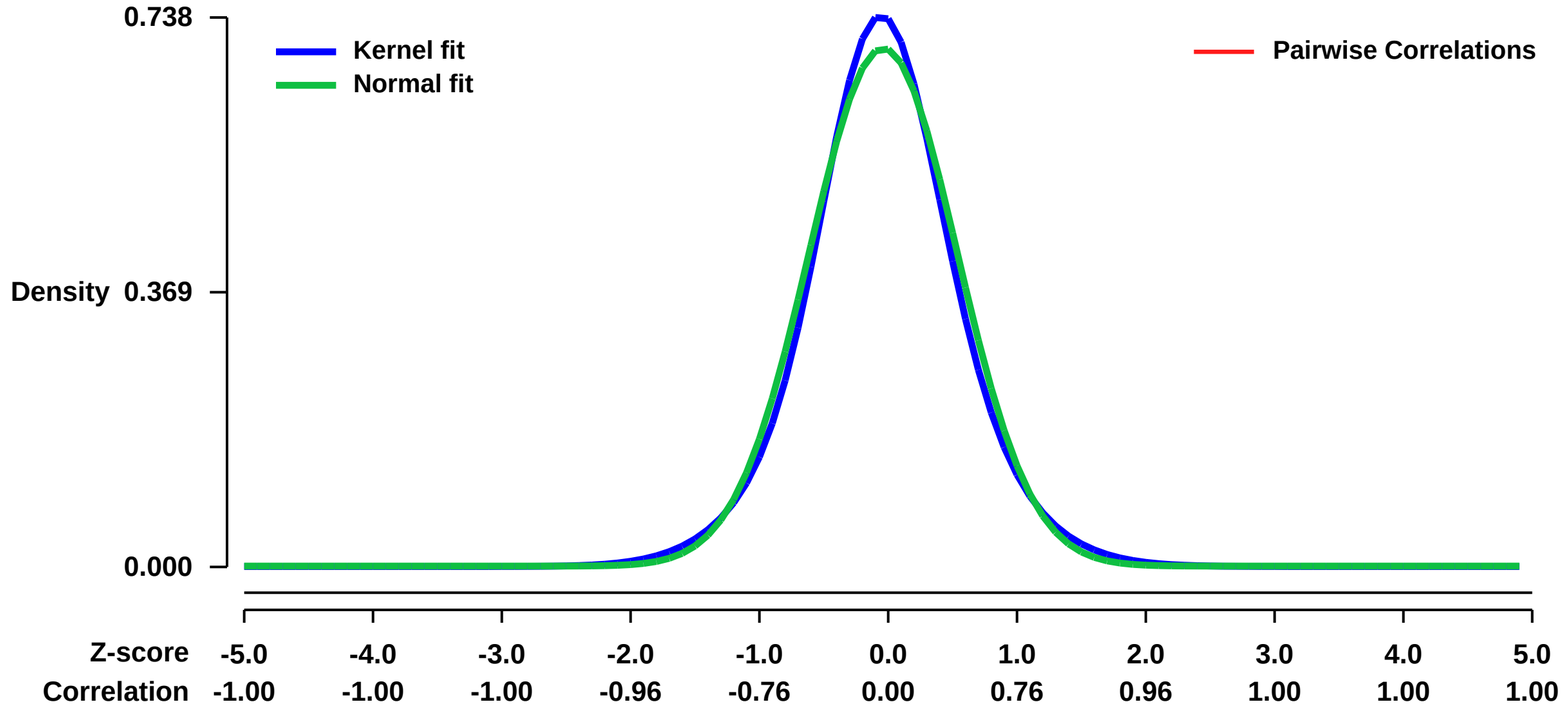

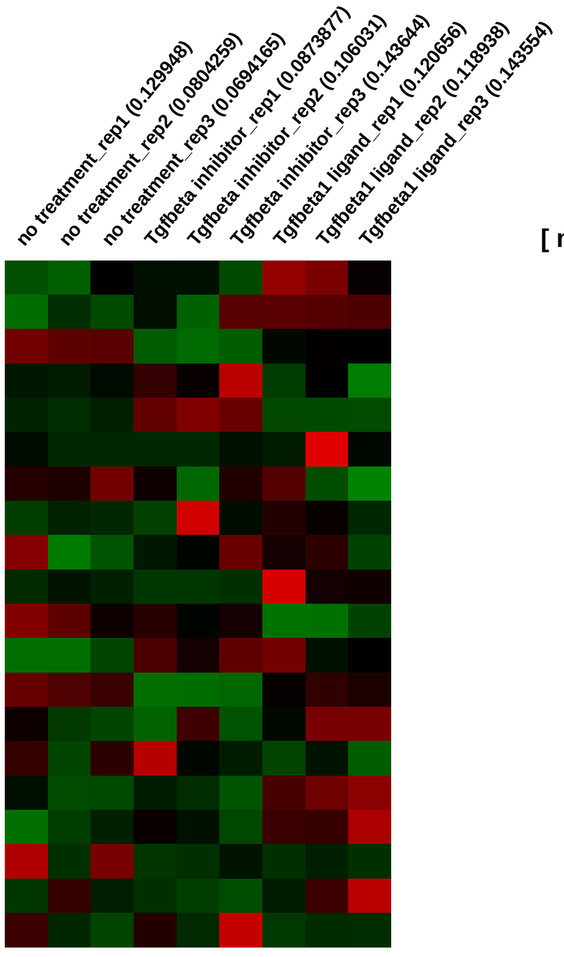

GEO Series "GSE2229" Expression Profiles

Num of samples in this series: 8

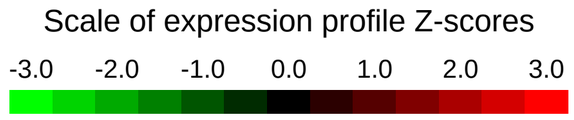

GEO Link:	http://www.ncbi.nlm.nih.gov/geo/query/acc.cgi?acc=GSE2229
Status:	Public on Apr 01 2005
Title:	Mouse preimplantation development
Organism:	Mus musculus
Experiment type:	Expression profiling by array
Platform:	GPL1261
Pubmed ID:	15772134
Summary & Design:	**Summary:** We examined expression profiles of genes that could be regulated by the MAPK pathways during mouse preimplantation development. We used Affymetrix GeneChips for microarray analysis, and three independent experiments were carried out. 8-cell stage embryos were treated or untreated with MAPK inhibitors, and blastocyst stage embryos were recruited for the study. Hybridization was carried out with the GeneChip Mouse Expression Set 430 or GeneChip Mouse Genome 430 2.0 Array following Affymetrix instructions. The array was then washed and stained using the GeneChip fluidics station according to the manufacture's instructions. Hybridized arrays were scanned using an Affymetrix GeneChip Scanner. Expression analysis was performed using GeneChip Operating Software 1.0 (Affymetrix) and scaled to an average probe set intensity of 500. **Keywords:** other **Overall design:**

Background corr dist: KL-Divergence = 0.0853, L1-Distance = 0.0251, L2-Distance = 0.0011, Normal std = 0.4660

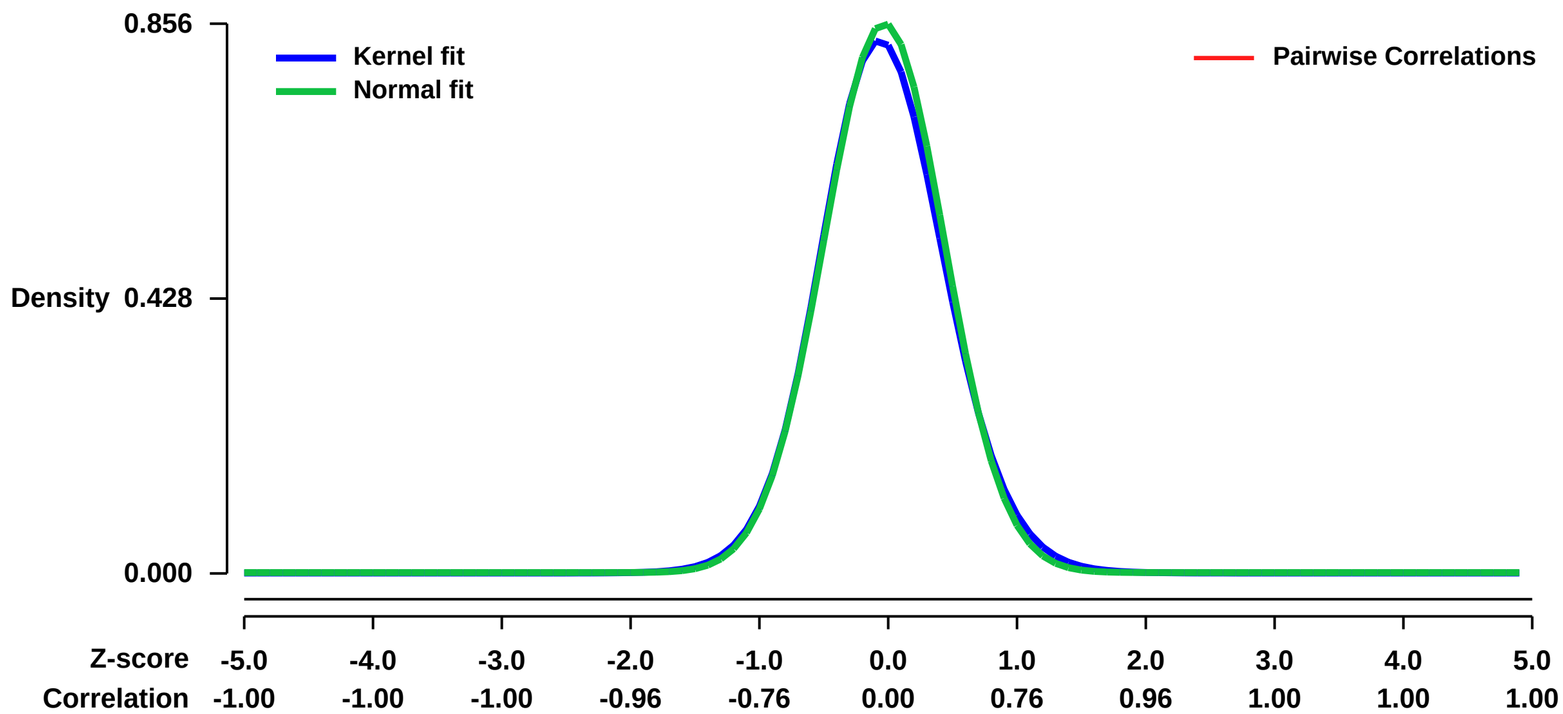

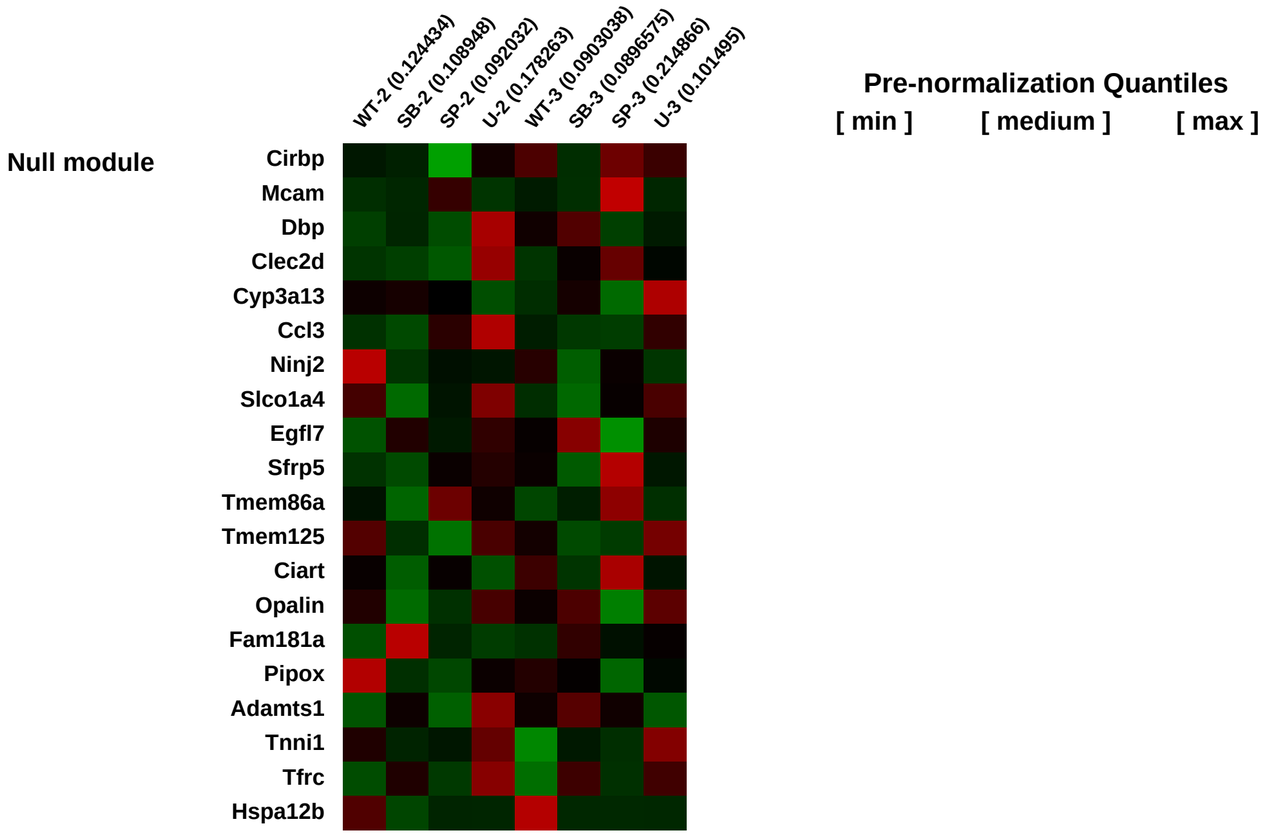

GEO Series "GSE26299" Expression Profiles

Num of samples in this series: 108

Details of this dataset are not shown due to large number of samples and the page size limit.

Find details in http://www.ncbi.nlm.nih.gov/geo/query/acc.cgi?acc=GSE26299

Background corr dist: KL-Divergence = 0.0440, L1-Distance = 0.0244, L2-Distance = 0.0009, Normal std = 0.5775

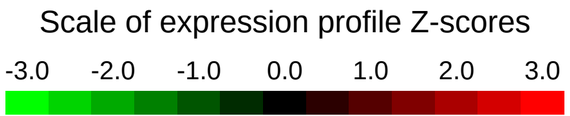

GEO Series "GSE29382" Expression Profiles

Num of samples in this series: 36

Scale of expression profile Z-scores

-3.0 -2.0 -1.0 0.0 1.0 2.0 3.0

GEO Link:	http://www.ncbi.nlm.nih.gov/geo/query/acc.cgi?acc=GSE29382
Status:	Public on Feb 19 2012
Title:	Characterisation of early thymic progenitors and thymus seeding progenitors
Organism:	Mus musculus
Experiment type:	Expression profiling by array
Platform:	GPL1261
Pubmed ID:	22344248
Summary & Design:	**Summary:** Gene expression analysis of early thymic progenitors and thymus seeding progenitors **Overall design:** Eight distinct populations were analysed, each with between 2 and 6 biological replicates.

Background corr dist: KL-Divergence = 0.1002, L1-Distance = 0.0809, L2-Distance = 0.0145, Normal std = 0.4760

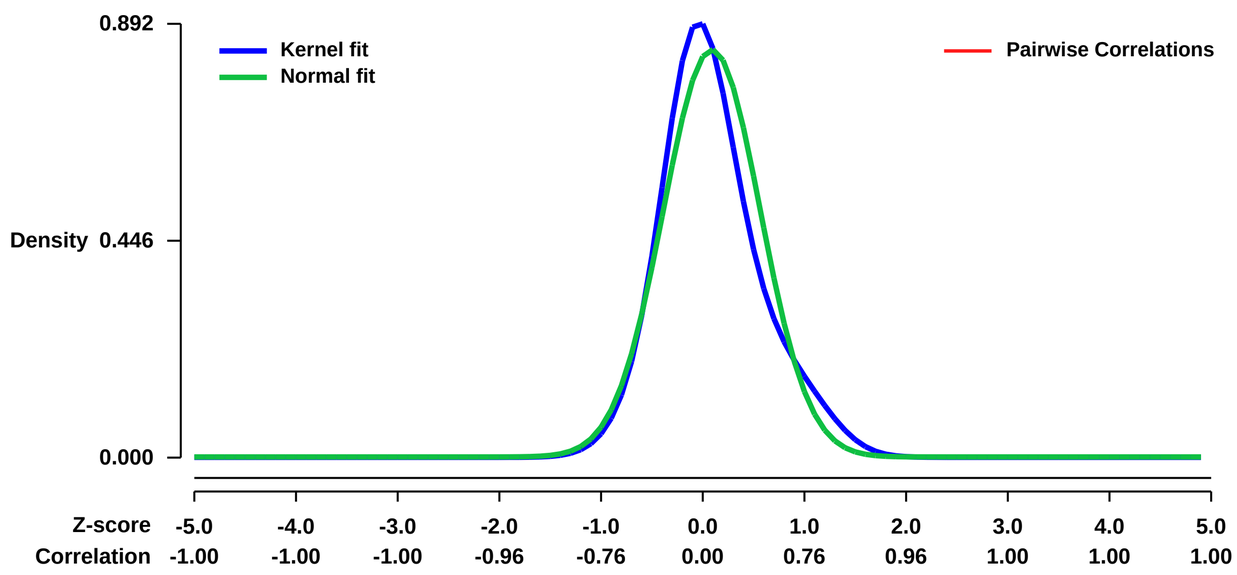

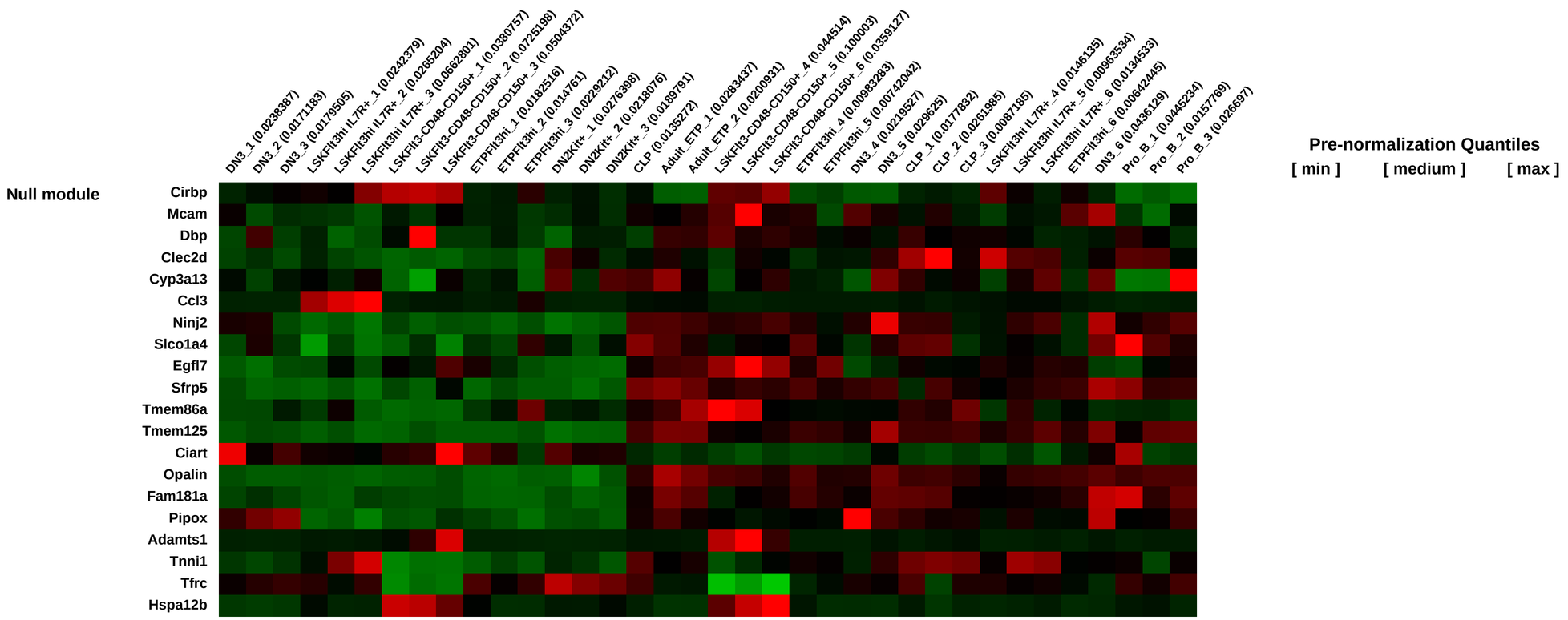

GEO Series "GSE18745" Expression Profiles

Num of samples in this series: 6

Scale of expression profile Z-scores

-3.0 -2.0 -1.0 0.0 1.0 2.0 3.0

GEO Link:	http://www.ncbi.nlm.nih.gov/geo/query/acc.cgi?acc=GSE18745
Status:	Public on Jan 28 2010
Title:	S1P lyase deficiency disrupts lipid homeostasis in liver
Organism:	Mus musculus
Experiment type:	Expression profiling by array
Platform:	GPL1261
Pubmed ID:	21173151
Summary & Design:	**Summary:** The cleavage of sphingoid base phosphates by sphingosine-1-phosphate (S1P) lyase to produce phosphoethanolamine and a fatty aldehyde is the final degradative step in the sphingolipid metabolic pathway. We have studied mice with an inactive S1P lyase gene and have found that, in addition to the expected increase of sphingoid base phosphates, other sphingolipids (including sphingosine, ceramide, and sphingomyelin) were substantially elevated in the serum and /or liver of these mice. This latter increase is consistent with a reutilization of the sphingosine backbone for sphingolipid synthesis due to its inability to exit the sphingolipid metabolic pathway. Furthermore, the S1P lyase deficiency resulted in changes in the levels of serum and liver lipids not directly within the sphingolipid pathway, including phospholipids, triacylglycerol, diacylglycerol, and cholesterol. Even though lipids in serum and lipid storage were elevated in liver, adiposity was reduced in the S1P lyase-deficient mice. Microarray analysis of lipid metabolism genes in liver showed that the S1P lyase deficiency caused widespread changes in their expression pattern. These results demonstrate that S1P lyase is a key regulator of the levels of multiple sphingolipid substrates and reveal functional links between the sphingolipid metabolic pathway and other lipid metabolic pathways that may be mediated by shared lipid substrates and changes in gene expression programs. The disturbance of lipid homeostasis by altered sphingolipid levels may be relevant to metabolic diseases. **Overall design:** RNA samples from liver for three sphingosine-1-phosphate lyase knock-out and three WT mice.

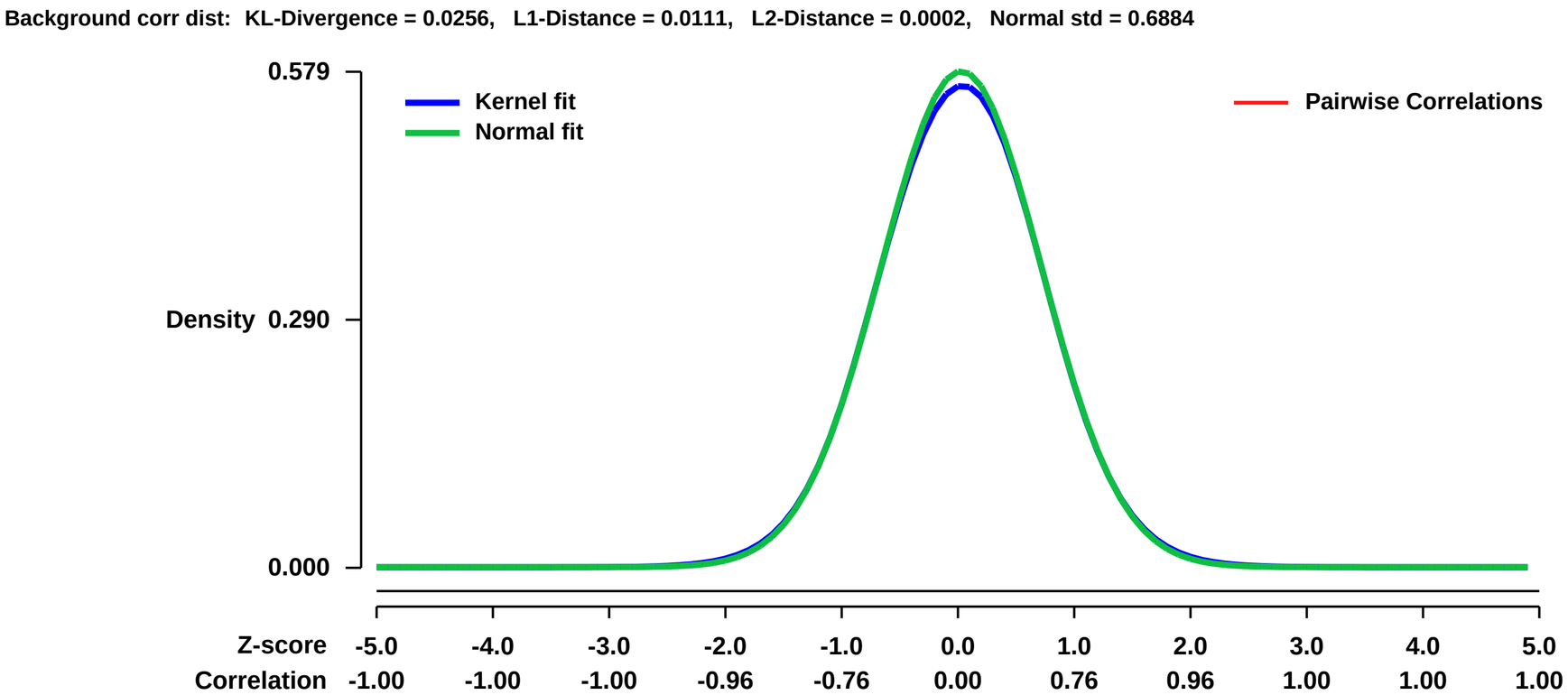

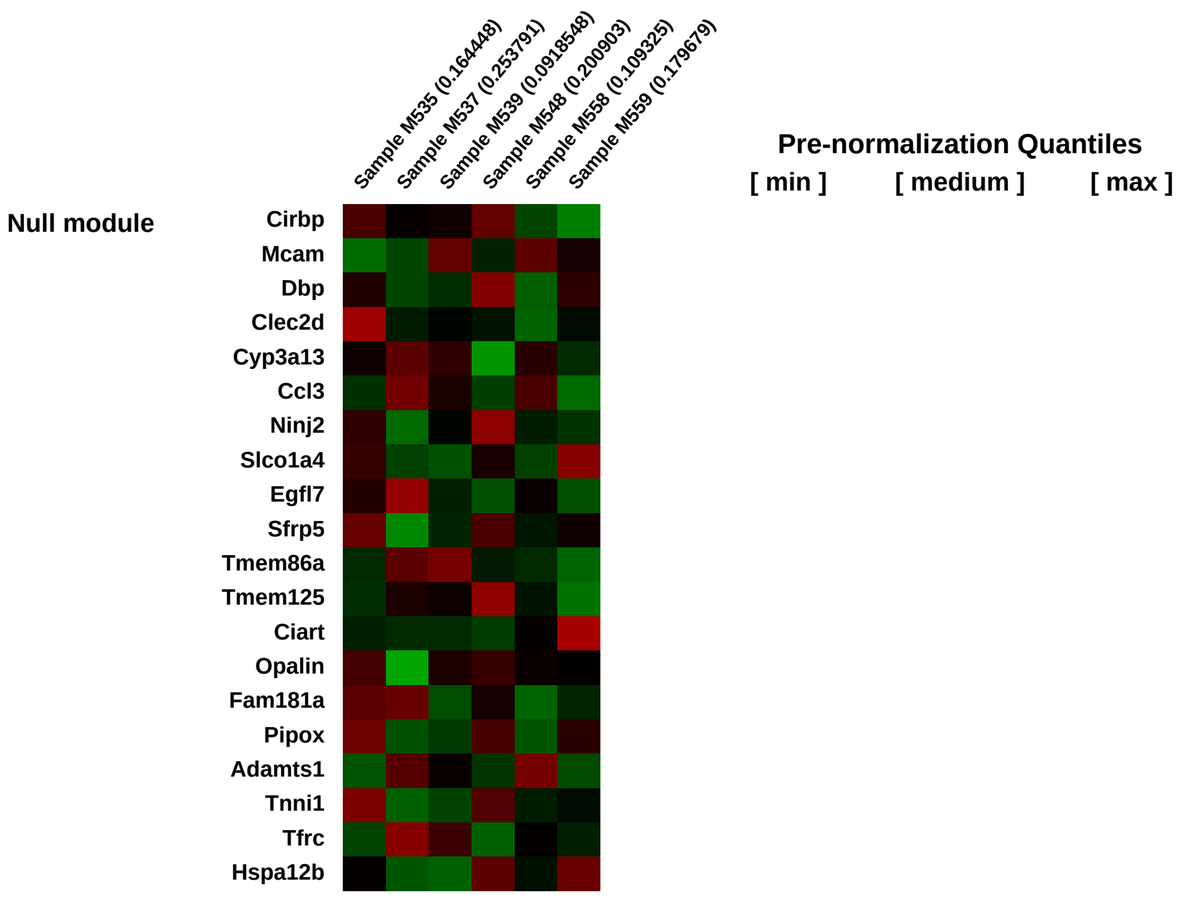

GEO Series "GSE11258" Expression Profiles

Num of samples in this series: 24

Scale of expression profile Z-scores

-3.0 -2.0 -1.0 0.0 1.0 2.0 3.0

GEO Link:	**http://www.ncbi.nlm.nih.gov/geo/query/acc.cgi?acc=GSE11258**
Status:	**Public on Sep 24 2008**
Title:	**Npas4-regulated genes in mouse hippocampal neurons**
Organism:	**Mus musculus**
Experiment type:	**Expression profiling by array**
Platform:	**GPL1261**
Pubmed ID:	**18815592**
Summary & Design:	**Summary:** **we performed a DNA microarray experiment to identify activity-regulated genes that are misregulated in the absence of Npas4.** **Keywords: Primary neuron culture, depolarization, activity-dependent, Npas4** **Overall design:** **We infected mouse hippocampal neurons with lentivirus expressing Npas4-RNAi or control-RNAi @ 3 DIV and depolarized the neurons @ 8 DIV with 50 mM of KCl for 0, 1, 3 or 6 hours. Neurons were lysed, mRNA isolated and hybridized to Affymetrix arrays. Data were collected from 3 independent experiments.**

Background corr dist: **KL-Divergence = 0.2486, L1-Distance = 0.0389, L2-Distance = 0.0028, Normal std = 0.3070**

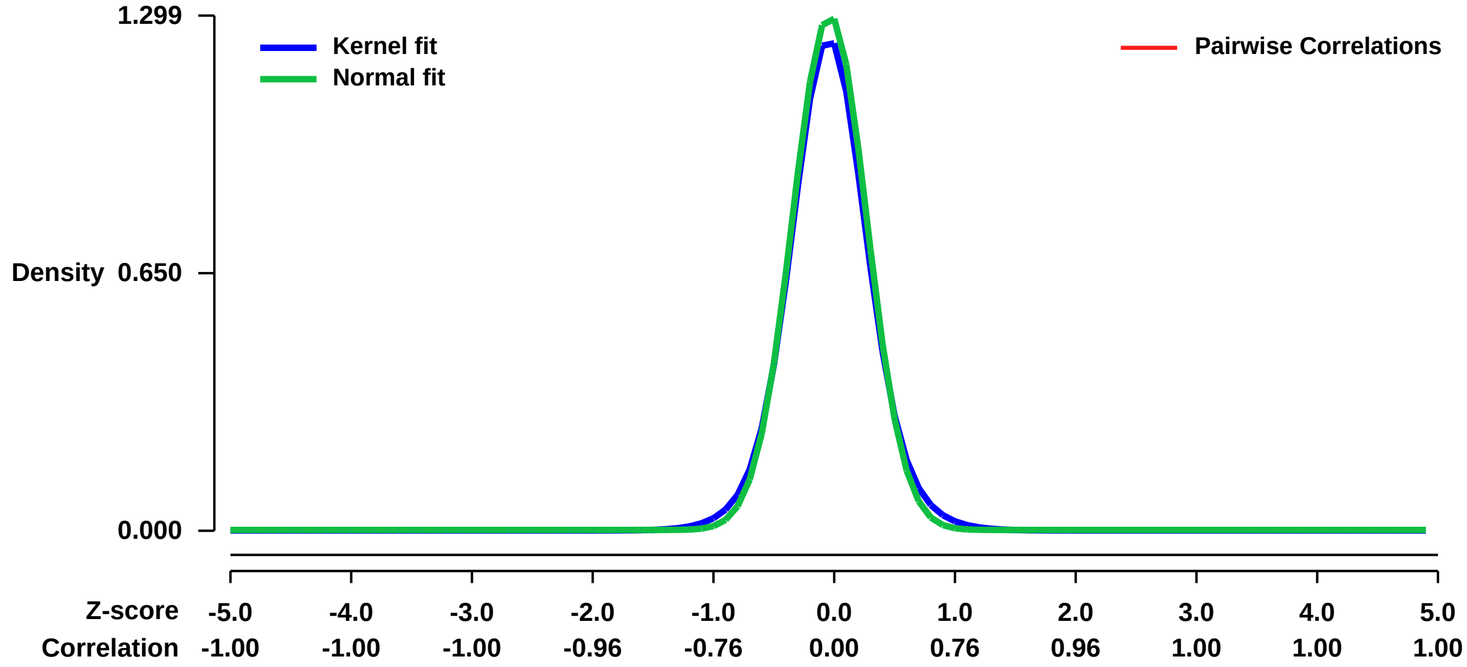

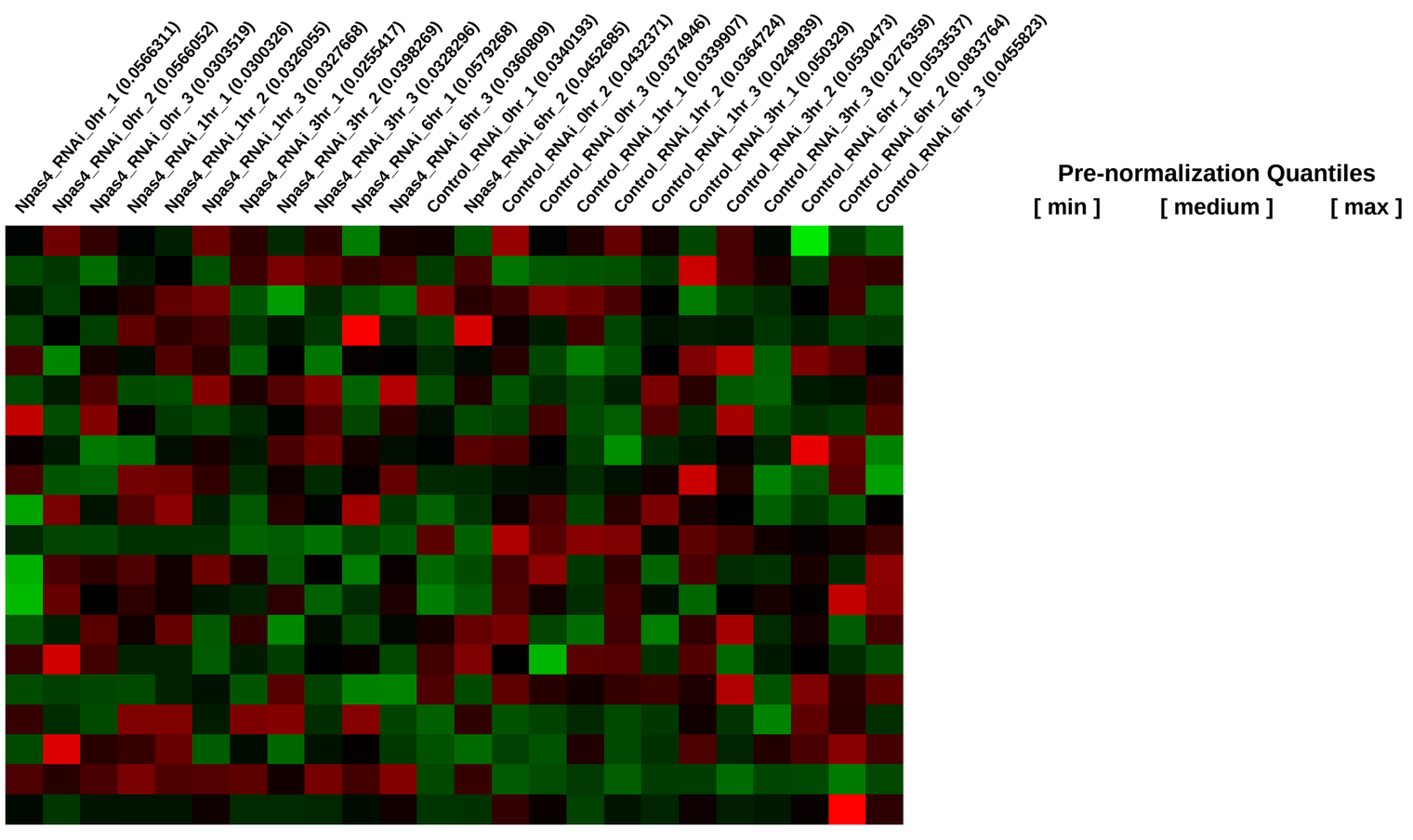

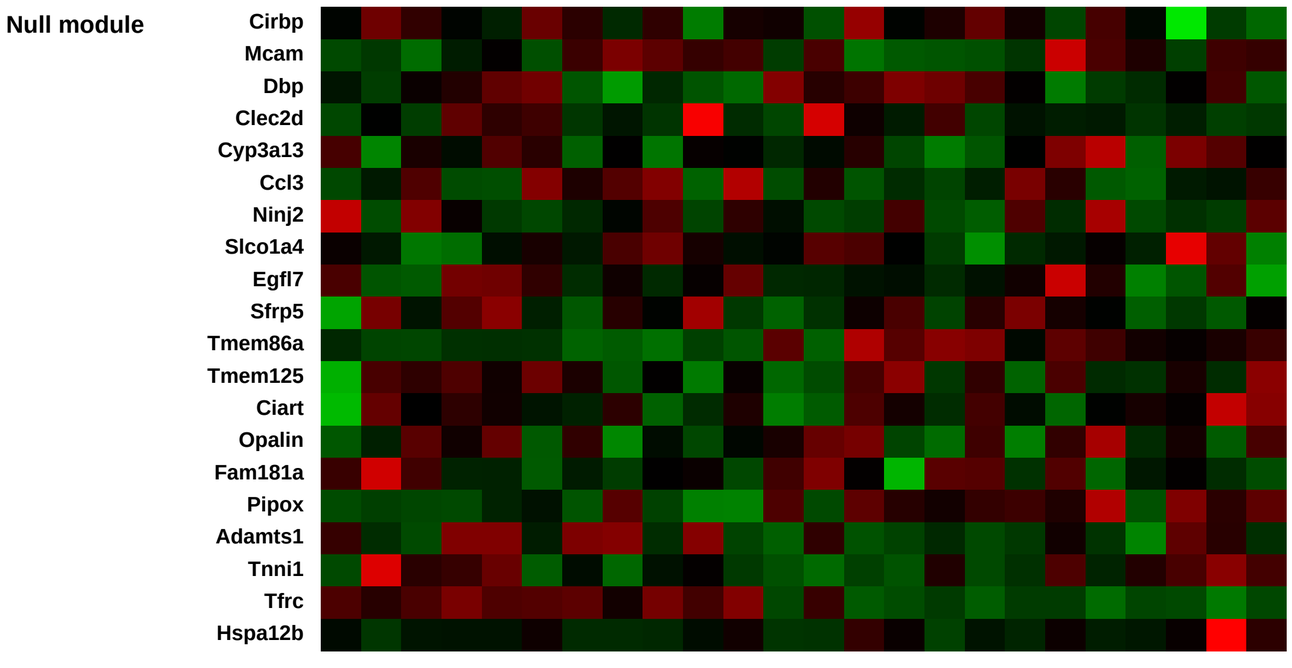

GEO Series "GSE6689" Expression Profiles

Num of samples in this series: 12

Scale of expression profile Z-scores

-3.0 -2.0 -1.0 0.0 1.0 2.0 3.0

GEO Link:	http://www.ncbi.nlm.nih.gov/geo/query/acc.cgi?acc=GSE6689
Status:	Public on Jan 07 2008
Title:	Expression data during stem cell differentiation
Organism:	Mus musculus
Experiment type:	Expression profiling by array
Platform:	GPL1261
Pubmed ID:	18184438
Summary & Design:	**Summary:** Stem cell development requires selection of specific genetic programs to direct cellular fate. Using microarray technology, we profile expression trends at selected timepoints during stem cell differentiation to characterize these changes. **Keyword(s): timecourse** **Overall design:** Total RNA was isolated using the Micro-to-Midi isolation kit (Invitrogen), and subjected to comparative gene expression profiling by labelled cRNA hybridization to the mouse genome 430 2.0 microarray (Affymetrix). Data acquired using the GeneChip Scanner 3000 was analyzed with the Genespring GX 7.3 microarray data software bioinformatics suite (Agilent Technologies) restricting the derived gene list to identify differentially expressed genes defined by a >1.5-fold difference and P<0.05. Data population sets were normalized to the undifferentiated phenotype, and quality filtered to eliminate background noise prior to hierarchical clustering.

Background corr dist: KL-Divergence = 0.0505, L1-Distance = 0.0486, L2-Distance = 0.0033, Normal std = 0.5968

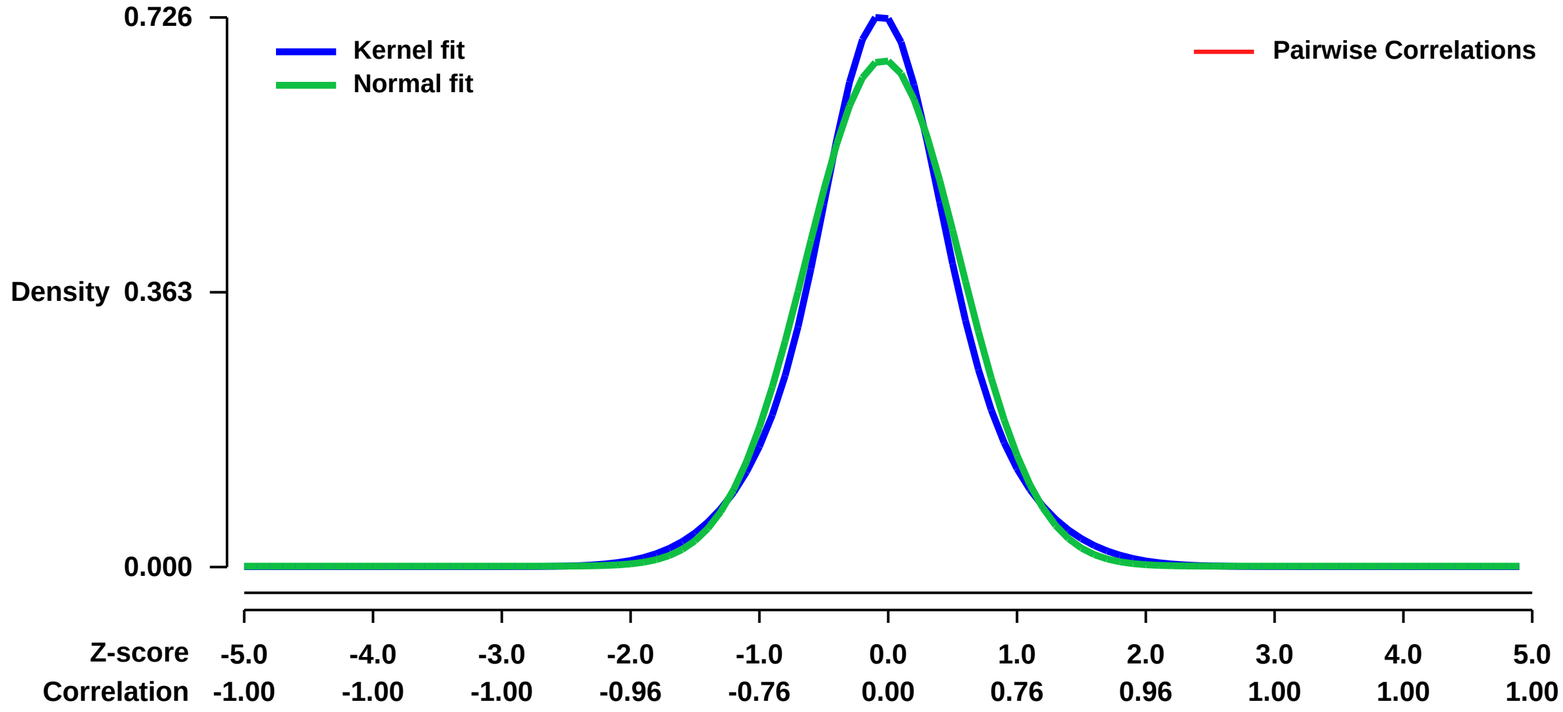

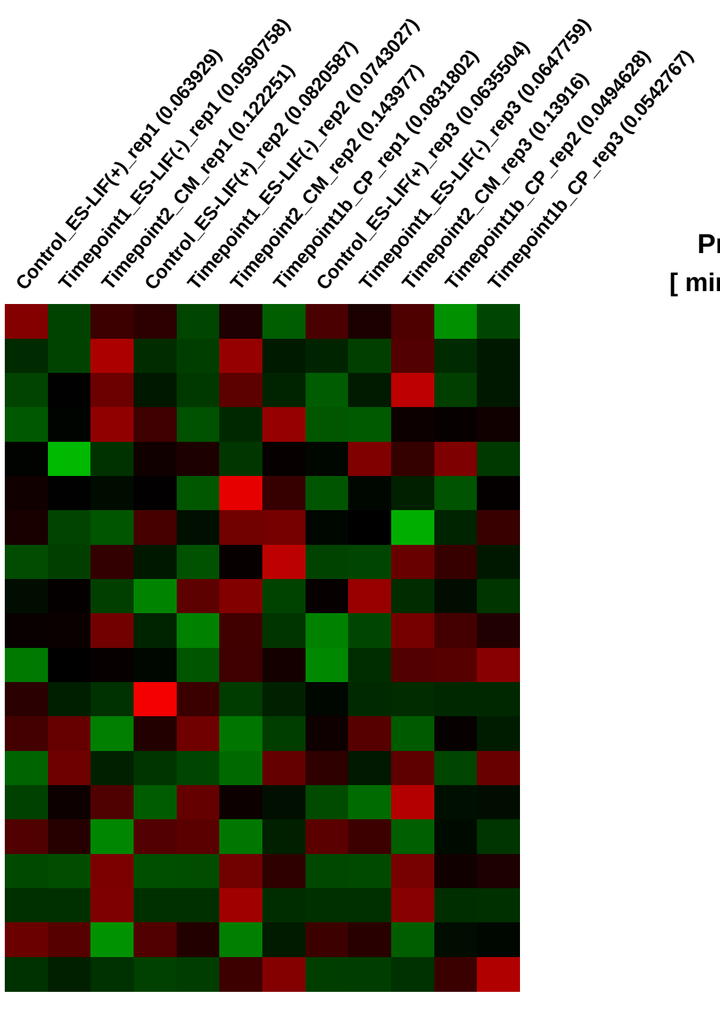

GEO Series "GSE20987" Expression Profiles

Num of samples in this series: 12

Scale of expression profile Z-scores

-3.0 -2.0 -1.0 0.0 1.0 2.0 3.0

GEO Link:	http://www.ncbi.nlm.nih.gov/geo/query/acc.cgi?acc=GSE20987
Status:	Public on May 10 2010
Title:	Gene expression data of BCR-ABL1 transformed B cell precursors from BCL6 wild-type and BCL6 knockout mice
Organism:	Mus musculus
Experiment type:	Expression profiling by array
Platform:	GPL1261
Pubmed ID:	21911423
Summary & Design:	**Summary:** To elucidate the mechanism of BCL6-mediated pre-B cell survival signaling, we investigated the gene expression pattern in BCR-ABL1-transformed BCL6+/+ and BCL6-/- B cell precursors. Pharmacological inhibition of BCR-ABL1 was performed with the BCR-ABL1 kinase inhibitor STI571 (Imatinib). **Overall design:** BCR-ABL1 transformed B cell precursors of BCL6 wildtype and BCL6 knockout mice were either treated with 10´µM STI571 (Imatinib) for 16 hours or cultured in absence of STI571. Three samples for each condition were processed.

Background corr dist: KL-Divergence = 0.0587, L1-Distance = 0.0336, L2-Distance = 0.0015, Normal std = 0.5553

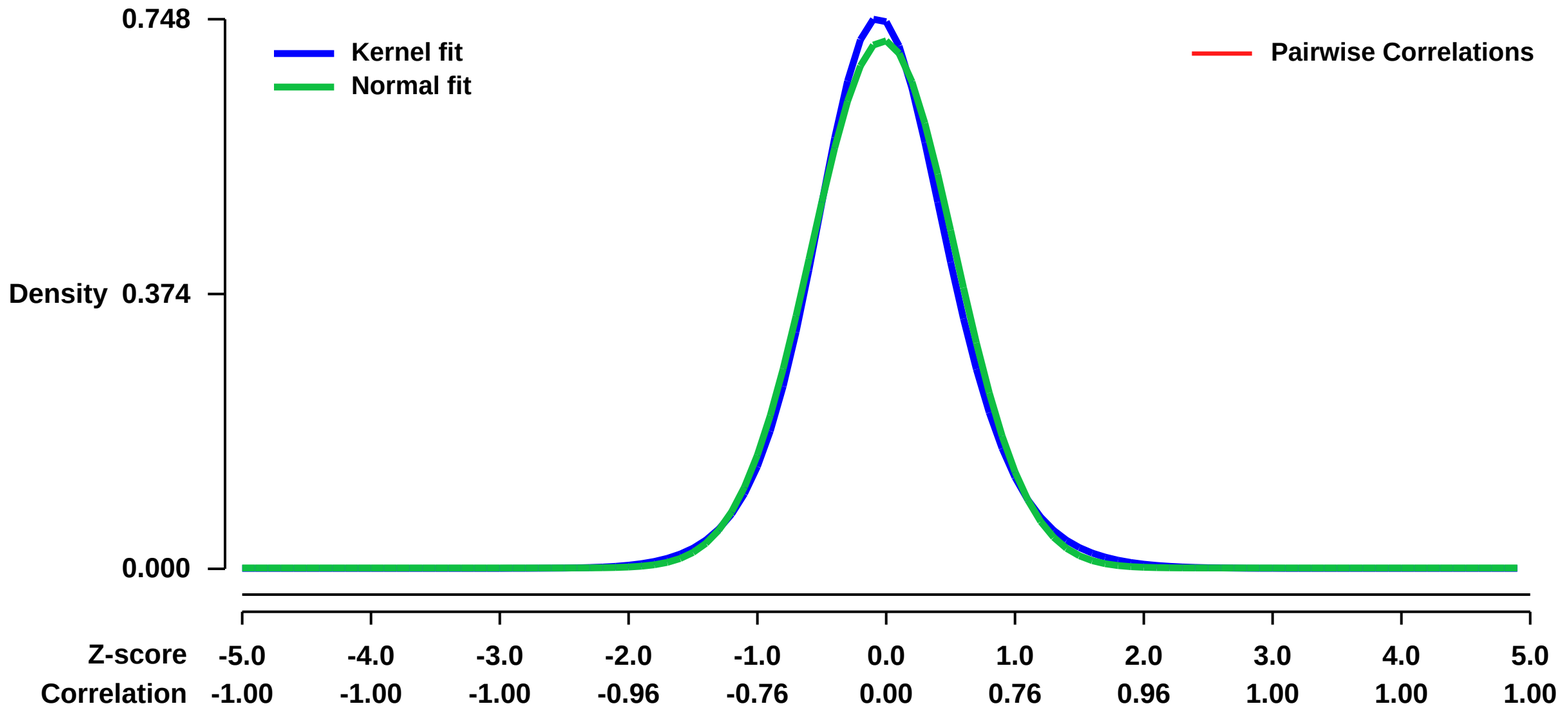

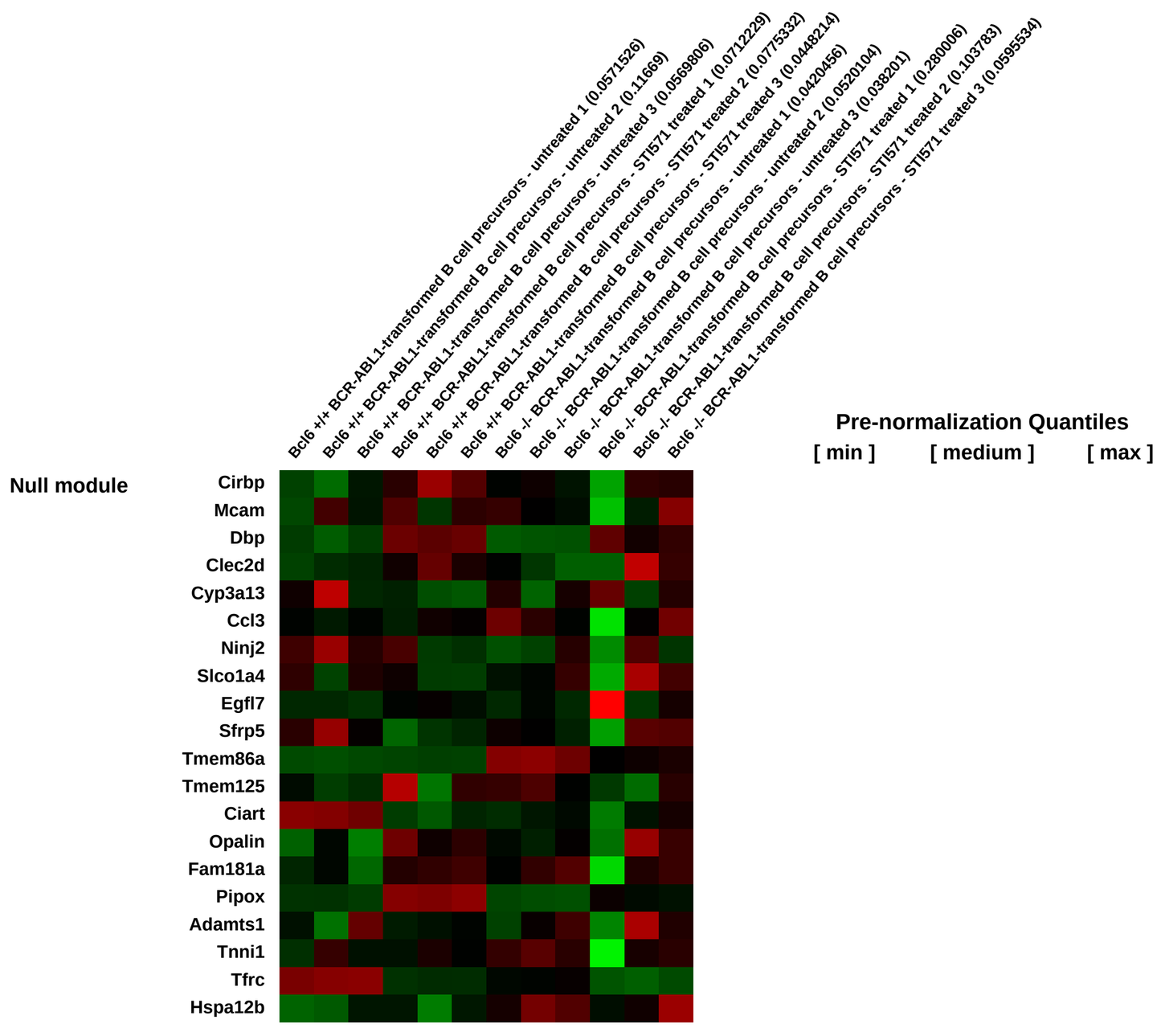

GEO Series "GSE22291" Expression Profiles

Num of samples in this series: 16

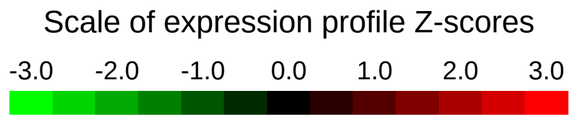

GEO Link:	http://www.ncbi.nlm.nih.gov/geo/query/acc.cgi?acc=GSE22291
Status:	Public on Jun 01 2011
Title:	Timecourse expression data from sciatic nerve distal stump of C57BL/6 and C57BL/6 OlaHsd-Wlds mice.
Organism:	Mus musculus
Experiment type:	Expression profiling by array
Platform:	GPL1261
Pubmed ID:	20688153
Summary & Design:	**Summary:** Wallerian degeneration (WD) involves the fragmentation of axonal segments disconnected from their cell bodies, segmentation of the myelin sheath, and removal of debris by Schwann cells and immune cells. The removal and downregulation of myelin-associated inhibitors of axonal regeneration and synthesis of growth factors by these two cell types are critical responses to successful nerve repair. Here, we analyzed the transcriptome of the sciatic nerve of mice carrying the Wallerian degeneration slow (WldS) mutant gene, a gene that confers axonal protection in the distal stump after injury, therefore causing significant delays in WD, neuroinflammation, and axonal regeneration. **Overall design:** 56 C57BL6 mice and 56 C57BL/6 OlaHsd-Wlds mice were anesthetized with isoflurane and underwent a microcrush lesion of their left sciatic nerve at the mid-thigh level (exept naive mice, t0). At 0, 3, 7 and 14 days post-injury, mice were anesthetized and killed by cervical dislocation. Sciatic nerves were collected and conective tissue removed. A 4-mm long sciatic nerve segment was taken from the nerve distal stump, starting at 1 mm distal from the lesion up to 5 mm distal. Distal nerve stumps were pooled by group and RNA extracted. Samples were hybridized to GeneChip´fi Mouse Genome 430 2.0 Array (Affymetrix). Biological replicate was done.

Background corr dist: KL-Divergence = 0.0729, L1-Distance = 0.0393, L2-Distance = 0.0033, Normal std = 0.4885

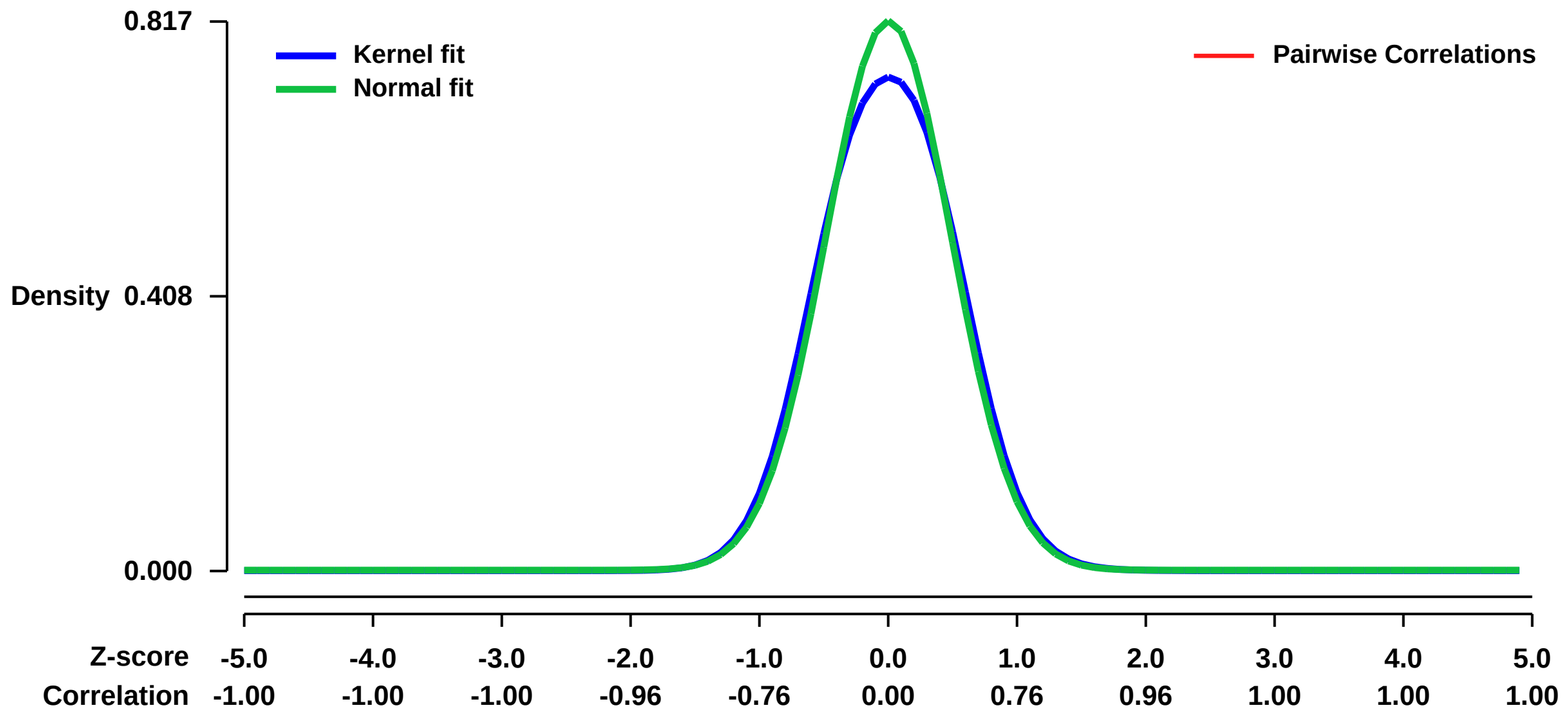

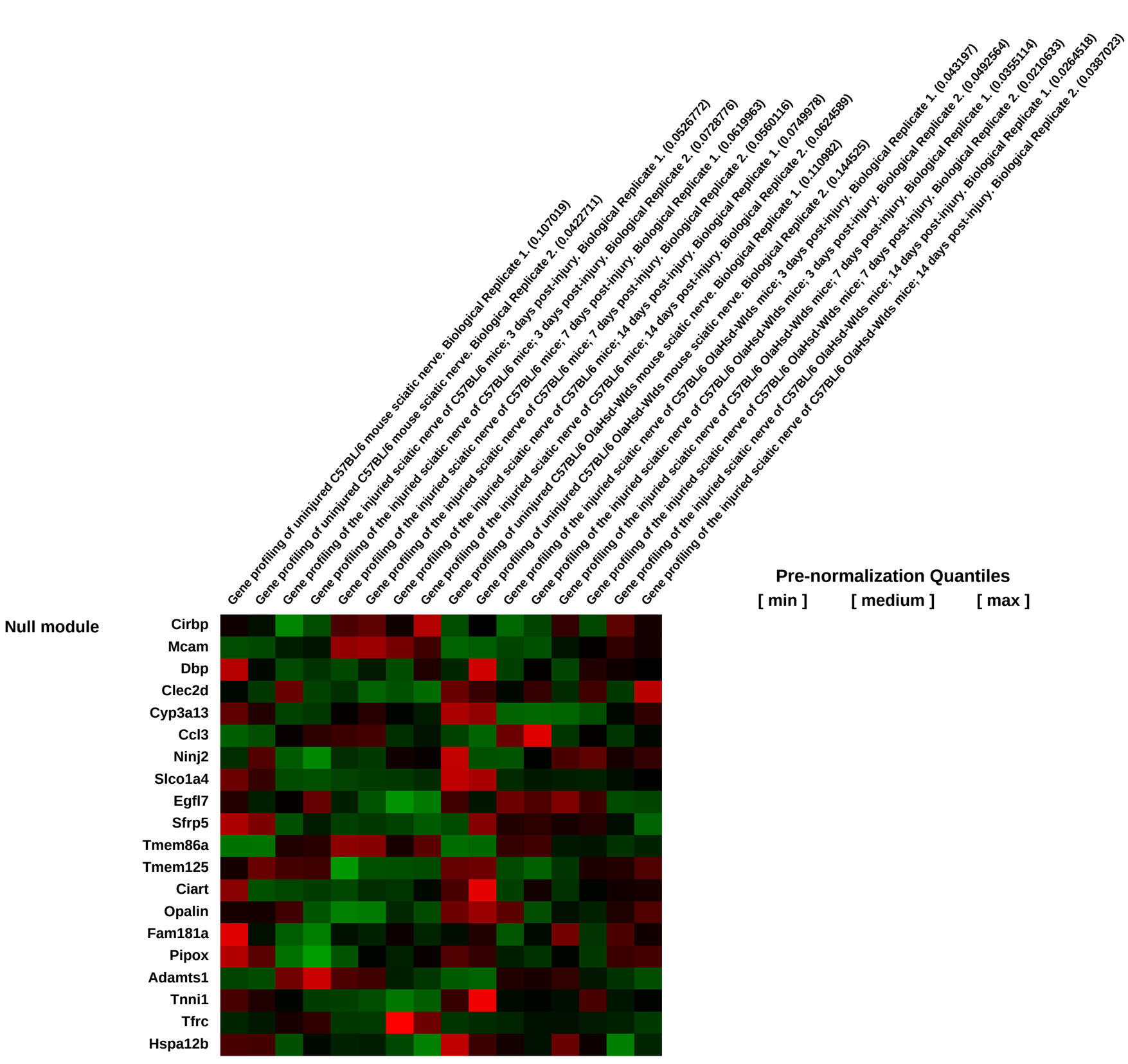

GEO Series "GSE4752" Expression Profiles

Num of samples in this series: 6

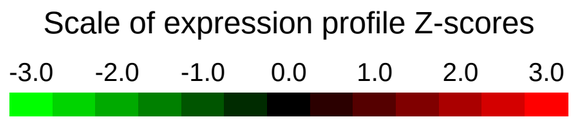

GEO Link:	http://www.ncbi.nlm.nih.gov/geo/query/acc.cgi?acc=GSE4752
Status:	Public on May 02 2006
Title:	tourt-affy-mouse-243760
Organism:	Mus musculus
Experiment type:	Expression profiling by array
Platform:	GPL1261
Pubmed ID:	

Summary & Design:

Summary:
The early growth response (Egr) family of transcriptional regulators consists of four closely related molecules (Egr1-4) that regulate target genes involved in cellular growth and differentiation. In the brain, Egr transcription factors have a critical role in learning and memory processing, presumably by regulating effector target genes that alter synaptic efficacy or mediate structural changes in neurons. Previous work suggests that Egr1 and Egr3 are the most important synaptic activity induced Egr molecules in the brain and they appear to have redundant regulatory function. How Egr transcriptional regulators influence learning and memory processing in the brain is unknown because target genes regulated by them have not been identified. Using Affymetrix microarray analysis and Egr loss-of-function mice, we will begin to characterize the gene regulatory networks modulated by Egr transcription factors in the brain. We anticipate that basic mechanisms related to transcriptional control of learning and memory related plasticity and the identification of plasticity effector molecules that may be involved in synaptic dysfunction associated with degenerative diseases or brain injury will result from these studies.

To identify Egr transcription factor target gene regulation in brain: Target genes regulated by Egr transcription factors have not been identified in the brain, yet the transcription factors are essential for normal learning and memory processes. Using Egr1/3 double knockout and wild type littermate mice, we will compare gene expression profiles from somatosensory cortex to identify genes that are deregulated in Egr1/3 dKO brains.

Egr1 and Egr3 gene expression is coupled to synaptic N-methyl D-aspartate (NMDA) receptor activation, mitogen activated protein kinase (MAPK) signaling engaged by NMDA receptor activation and long term synaptic potentiation (LTP). Previous studies have demonstrated defects in late phase LTP, long-term memory in hippocampal dependent tasks and reconsolidation of memories in Egr1-deficient mice, but the target effector molecules regulated by Egr transcription factors are not known. We hypothesize that it will be possible to identify Egr dependent target genes by using Affymetrix microarray analysis to compare gene expression from wild type cerebral cortex that has high levels of Egr protein expression with gene expression in cortex from Egr1/3 double knockout mice.

Egr1 and Egr3 are highly expressed in mouse cortex and hippocampus twenty one days after birth because of the large amount of maternal stimulation they receive prior to weaning. We will compare the gene expression profile in somatosensory cortex from P21 wild type mice to that of P21 Egr1/3 dKO mice. We will perform microarray analysis using the Mouse 430 2.0 gene array with RNA samples from 3 wild type and 3 1/3 dKO brains (6 arrays total). Differentially regulated genes (up-regulated and down-regulated) will be identified from the list of genes with significantly altered expression greater than or equal to 2-fold by paired T test. Interesting genes will be validated by real-time PCR in wild type and 1/3 dKO brains. Our main goal is to identify genes that are directly regulated by Egr3. Recognizing that both direct and indirect target genes may be identified in the list of differentially expressed genes, real-time PCR validated target genes will be further screened using chromatin immunoprecipitation coupled with PCR (ChIP-PCR) to determine whether Egr1 and/or Egr3 are bound to potential regulatory regions of the putative target genes.

Keywords: other

Overall design:

Background corr dist: KL-Divergence = 0.0459, L1-Distance = 0.0191, L2-Distance = 0.0004, Normal std = 0.5886

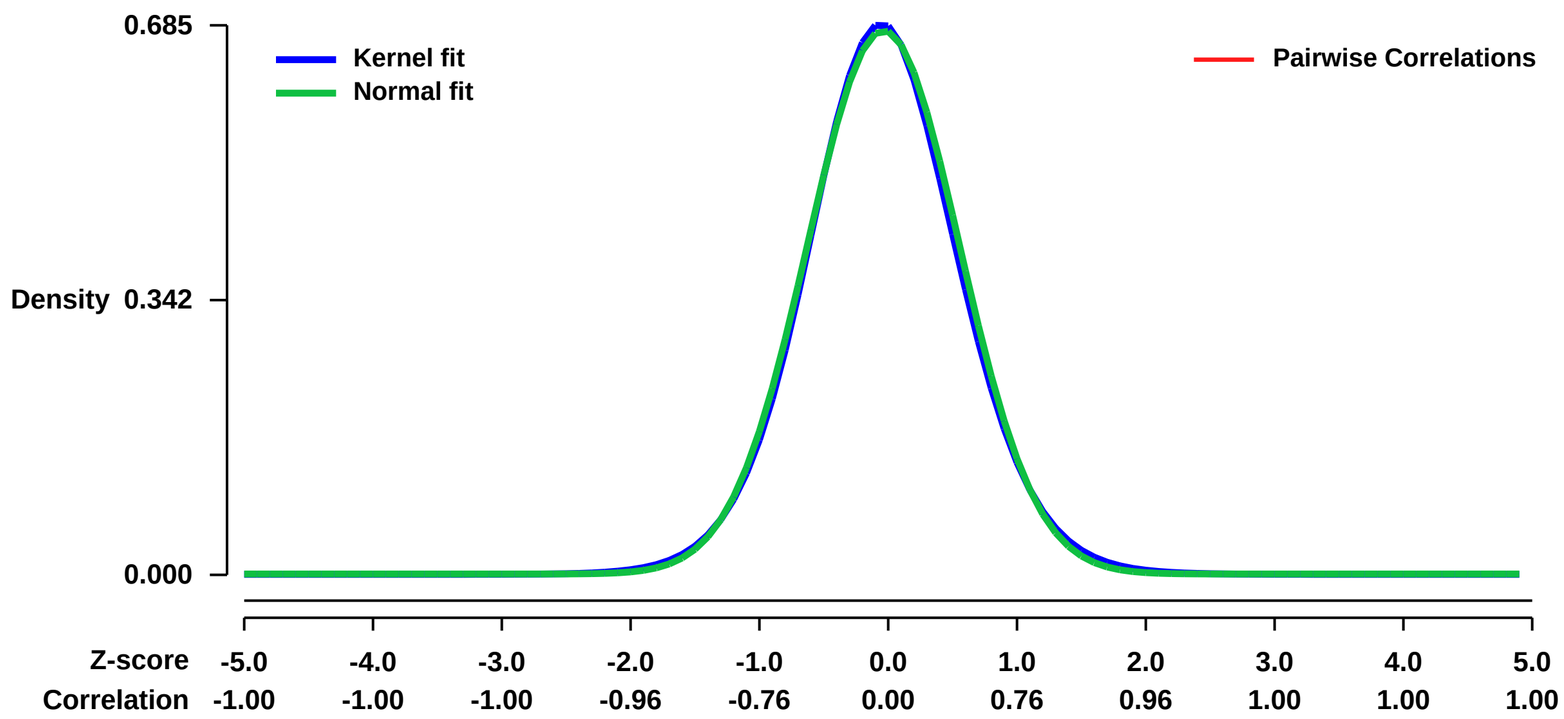

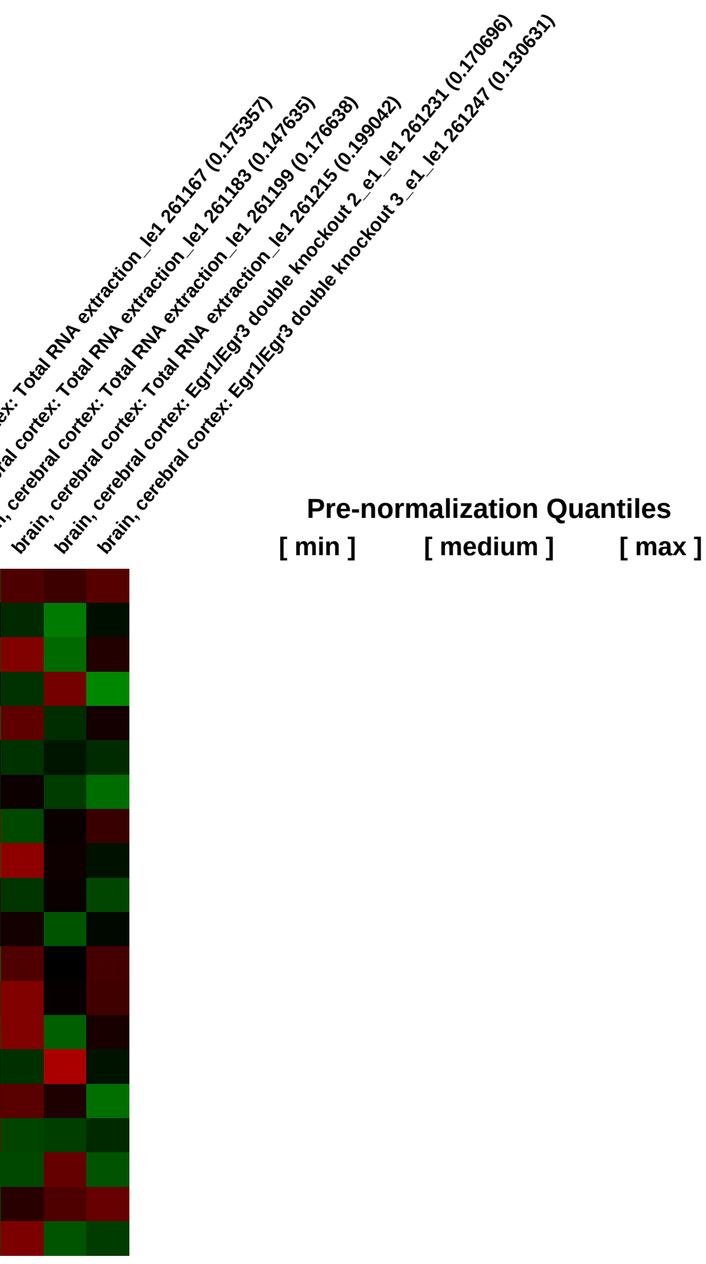

GEO Series "GSE3181" Expression Profiles

Num of samples in this series: 6

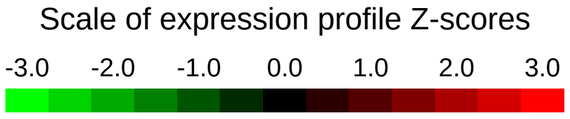

GEO Link:	**http://www.ncbi.nlm.nih.gov/geo/query/acc.cgi?acc=GSE3181**
Status:	**Public on Dec 21 2005**
Title:	**SRF-null neonatal cardiomyocytes**
Organism:	**Mus musculus**
Experiment type:	**Expression profiling by array**
Platform:	**GPL1261**
Pubmed ID:	**16368687**
Summary & Design:	**Summary:** **Serum Response Factor (SRF) is a transcriptional regulator required for mesodermal development. Numerous studies have implicated SRF as a central regulator of muscle gene expression and myogenesis. In this present study we used a loss of function approach to delineate the role of SRF in cardiac myocyte gene expression and function. In SRF null neonatal cardiomyocytes, we observe severe defects in the contractile apparatus, including Z-disc and stress fiber formation, as well as mislocalization and/or attenuation of sarcomeric proteins. Consistent with this, gene array and RT-PCR analyses show downregulation of genes encoding key cardiac transcriptional regulatory factors and proteins required for the maintenance of sarcomeric structure, function, and regulation. Chromatin IP analysis reveals that at least a subset of these proteins are likely regulated directly by SRF. Together the results presented here reveal new cellular and genetic mechanisms through which SRF exacts control over the contractile apparatus in cardiac myocytes.** **Keywords: genetic modification** **Overall design:** **There are three control replicates (cardiomyocytes transduced with Adeno-GFP virus) and three experimental replicates (cardiomyocytes transduced with Adeno-CRE to excise SRF).**

Background corr dist: KL-Divergence = 0.0178, L1-Distance = 0.0149, L2-Distance = 0.0003, Normal std = 0.7593

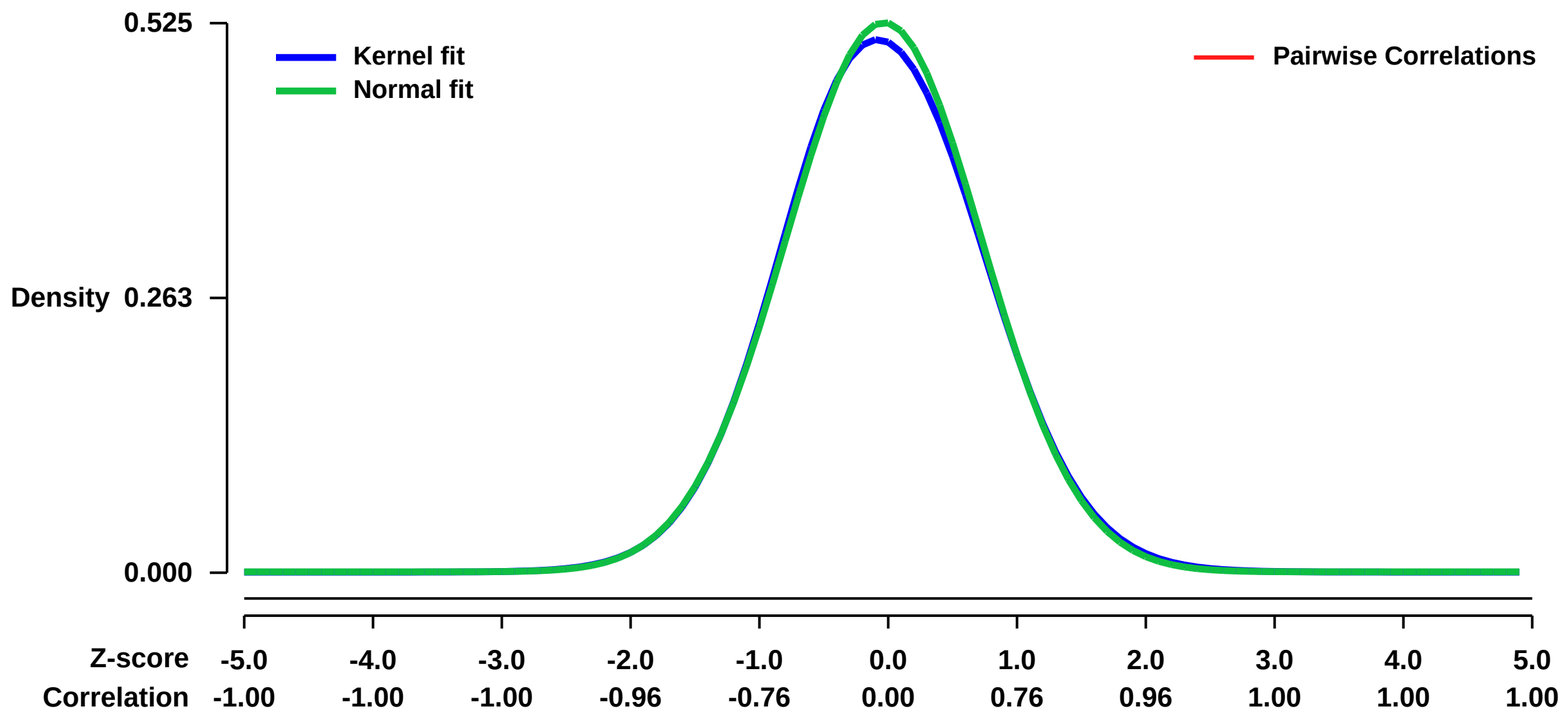

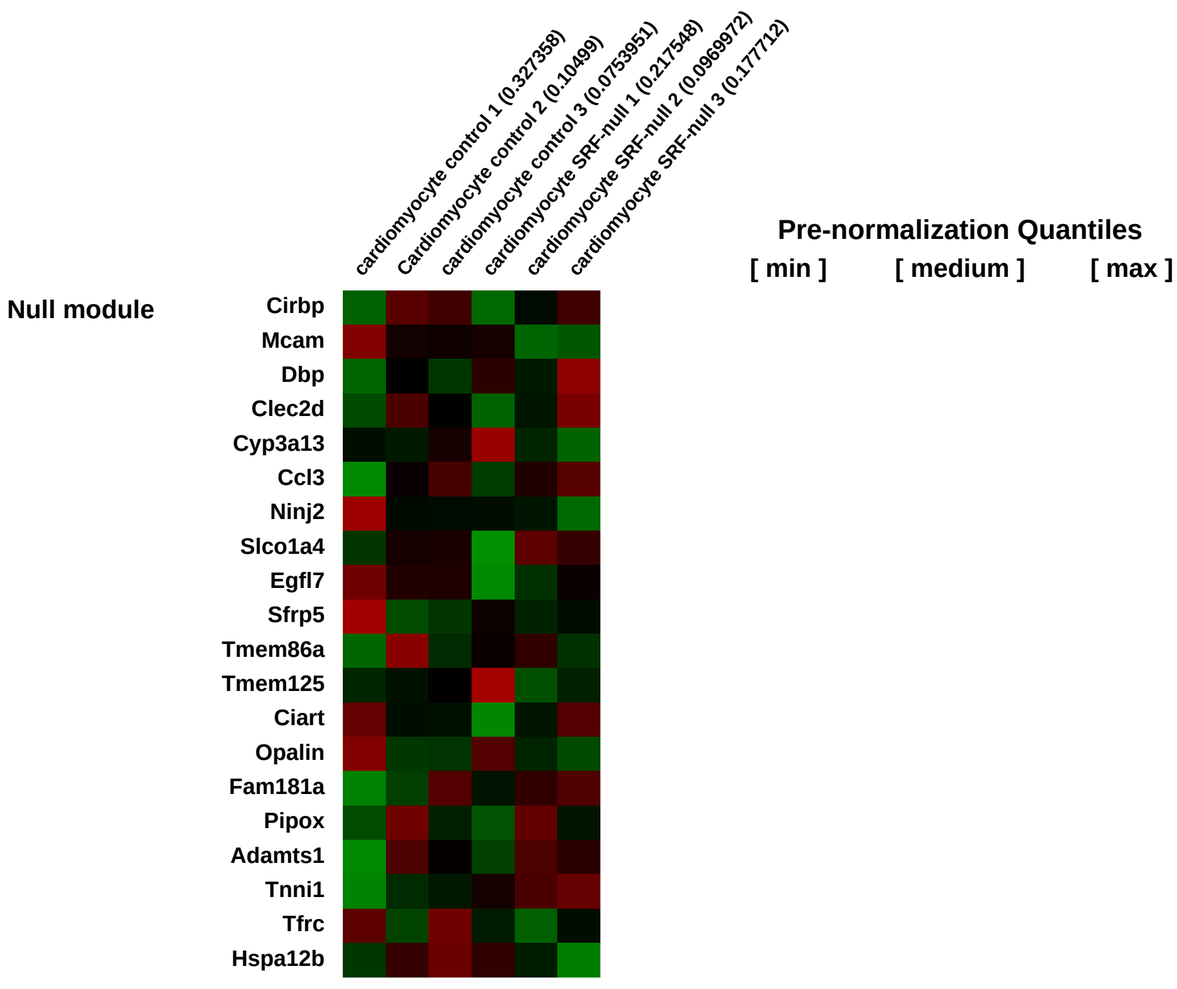

GEO Series "GSE7823" Expression Profiles

Num of samples in this series: 9

Scale of expression profile Z-scores

-3.0 -2.0 -1.0 0.0 1.0 2.0 3.0

GEO Link:	http://www.ncbi.nlm.nih.gov/geo/query/acc.cgi?acc=GSE7823
Status:	Public on May 18 2007
Title:	Murine Pulmonary Response to Chronic Hypoxia is Strain Specific
Organism:	Mus musculus
Experiment type:	Expression profiling by array
Platform:	GPL1261
Pubmed ID:	18600498
Summary & Design:	**Summary:** 6-8 week old BL6, FVB/N and SV129 mouse strains were kept in normoxia or hypobaric hypoxia for 4 weeks and then phenotyped by echocardiogram and right ventricular heart catheterization, followed by tissue collection. In addition, Affymetrix expression analysis was conducted in a paired fashion. **Keywords: Differential response to hypoxia by strain** **Overall design:** This series actually includes another 12 arrays. However, the others had technical difficulties and so aren't really appropriate for general distribution.

Background corr dist: KL-Divergence = 0.0874, L1-Distance = 0.0272, L2-Distance = 0.0013, Normal std = 0.4774

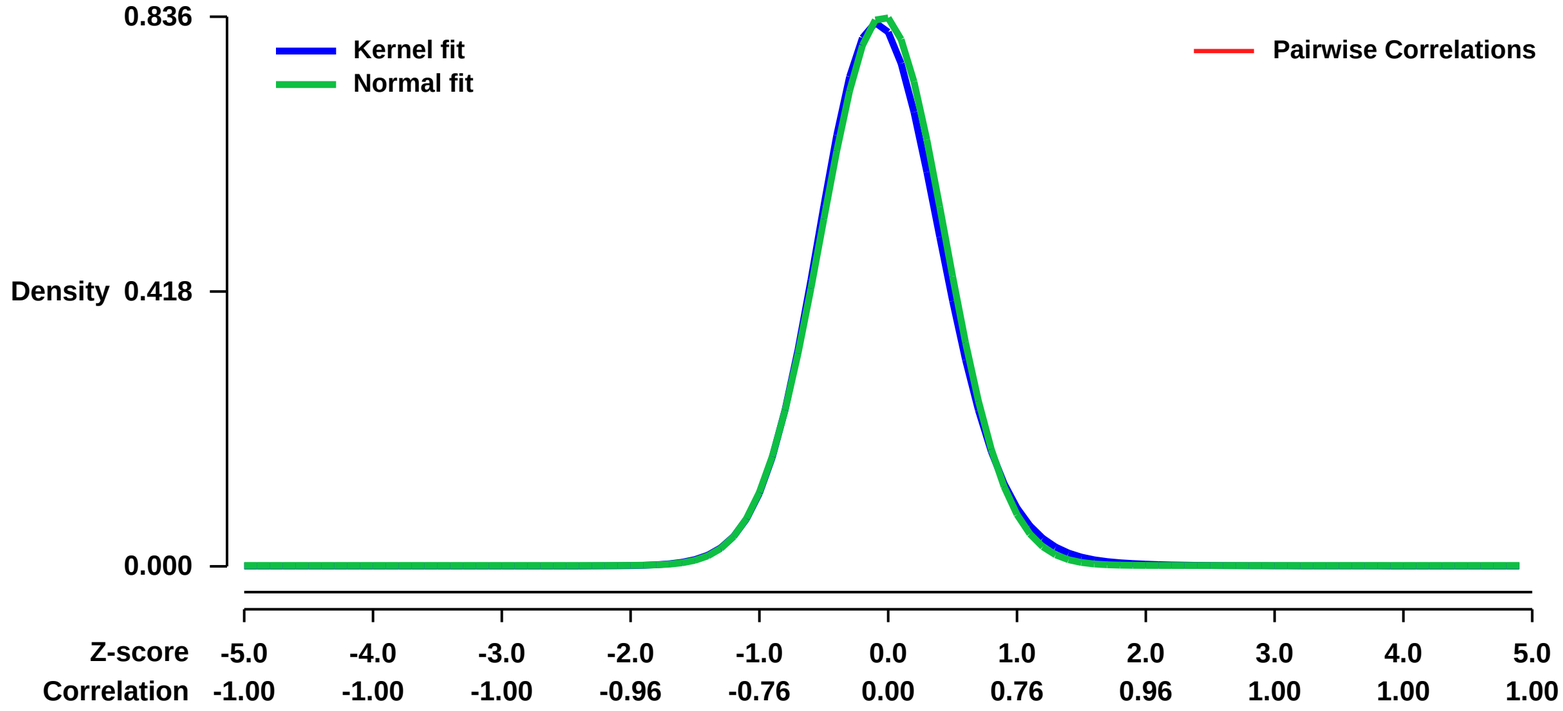

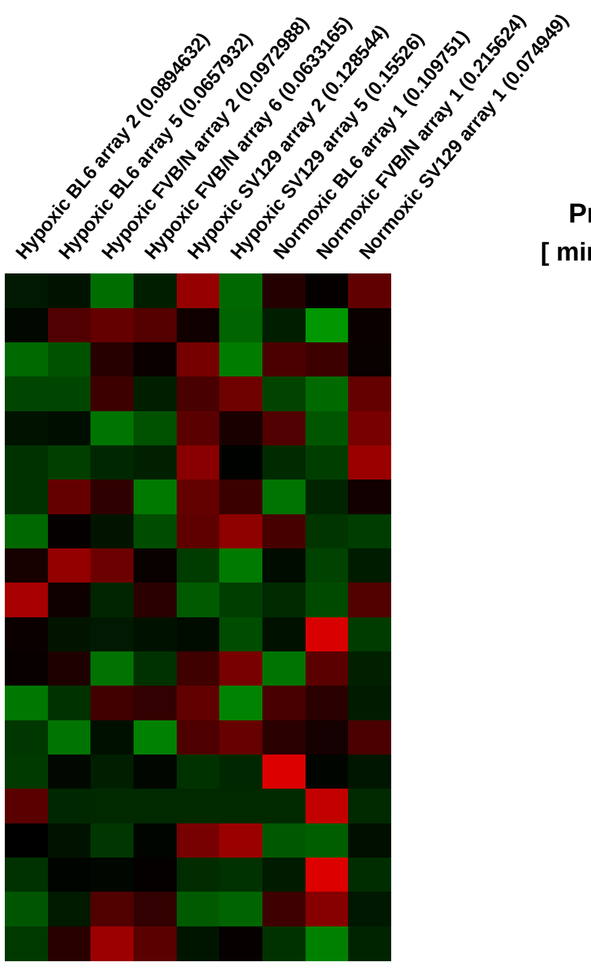

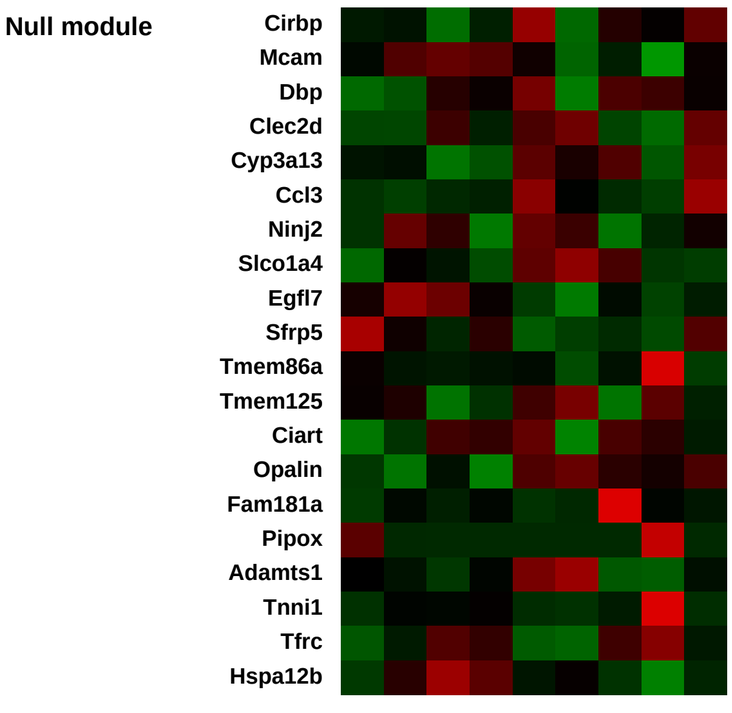

GEO Series "GSE12769" Expression Profiles

Num of samples in this series: 20

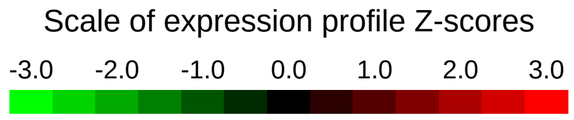

GEO Link:	**http://www.ncbi.nlm.nih.gov/geo/query/acc.cgi?acc=GSE12769**
Status:	**Public on Sep 18 2008**
Title:	**Murine postpartum testis developmental time course (0 to 35 day)**
Organism:	**Mus musculus**
Experiment type:	**Expression profiling by array**
Platform:	**GPL1261**
Pubmed ID:	
Summary & Design:	**Summary:** **Murine testis developmental time course created from tissue samples collected from birth through adulthood and hybridized to M430_2 chips in duplicate.** **Keywords: time-course** **Overall design:** **Time course of gene expression in the murine postpartum testis development (duplicates in day 0, 3, 6, 8, 10, 14, 18, 20, 30, 35). Total 20 samples.**

Background corr dist: **KL-Divergence = 0.0289, L1-Distance = 0.0313, L2-Distance = 0.0017, Normal std = 0.6762**

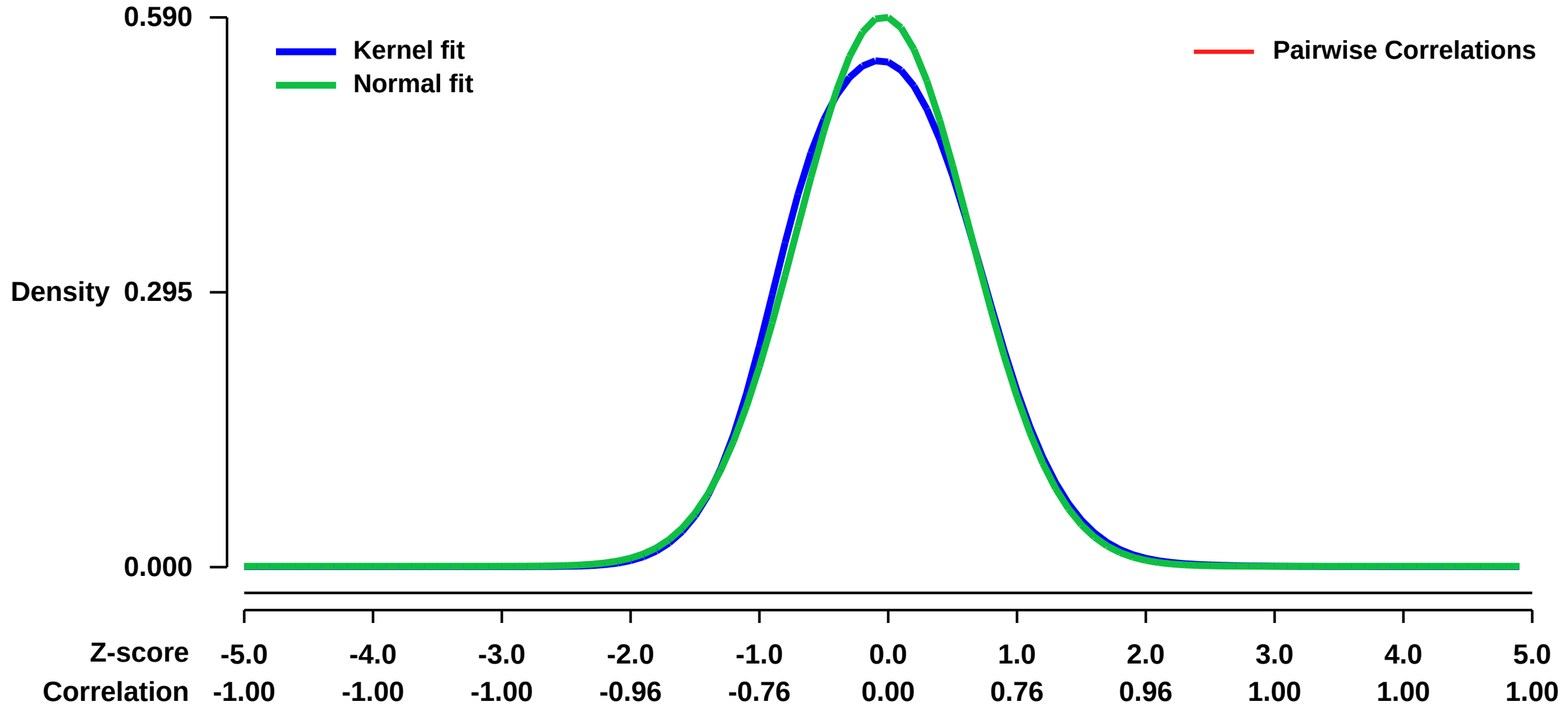

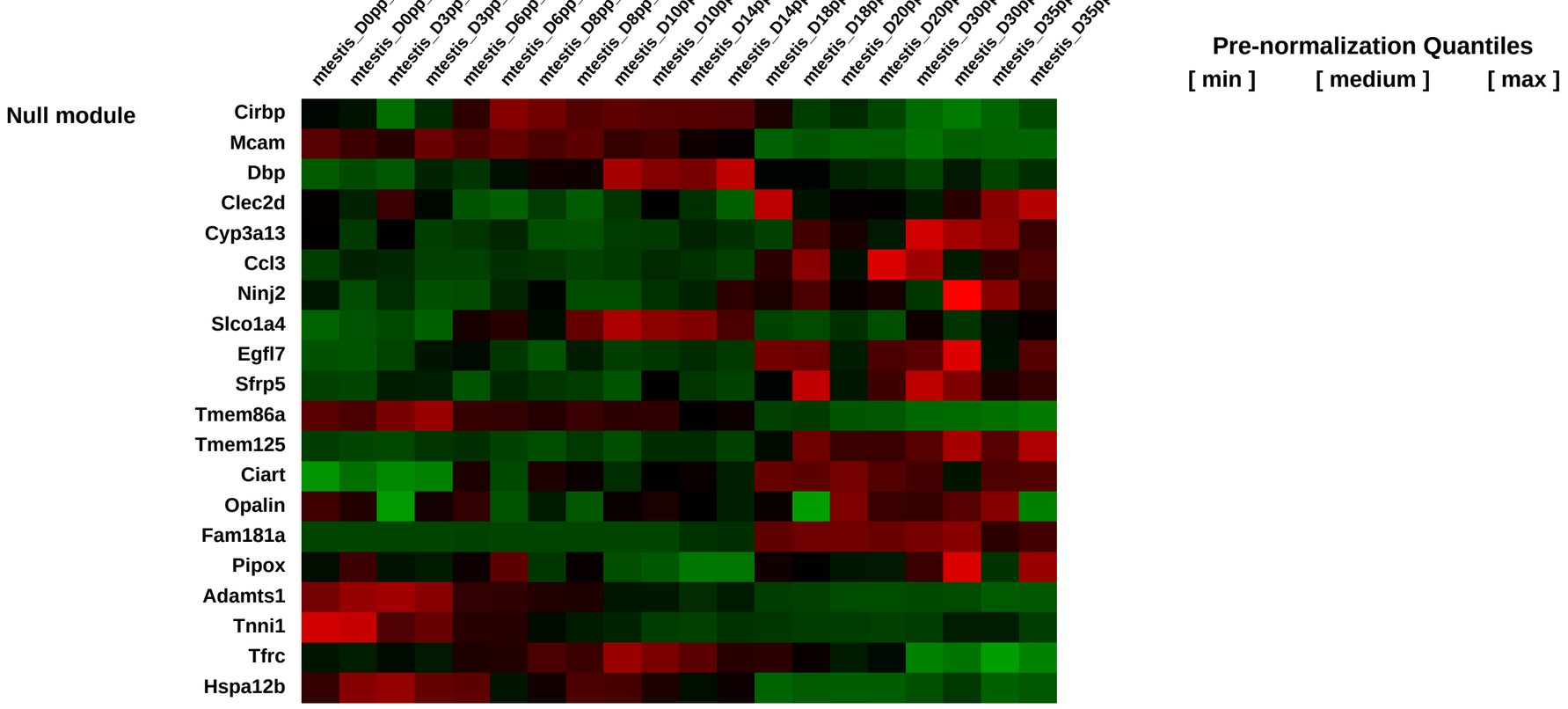

GEO Series "GSE36378" Expression Profiles

Num of samples in this series: 20

Scale of expression profile Z-scores

-3.0 -2.0 -1.0 0.0 1.0 2.0 3.0

GEO Link:	http://www.ncbi.nlm.nih.gov/geo/query/acc.cgi?acc=GSE36378
Status:	Public on Mar 10 2012
Title:	Mapping the Transcriptional Landscape of Autoimmune Targeted Tissues: Transient Alterations in the Extracellular Milieu Precede Innate and Delayed Adaptive Immune Re
Organism:	Mus musculus
Experiment type:	Expression profiling by array
Platform:	GPL1261
Pubmed ID:	
Summary & Design:	**Summary:** The C57BL/6.NOD-Aec1Aec2 mouse is a model for primary Sjˆ¶grenâ s syndrome and was constructed by introducing two genetic intervals derived from the NOD mouse that confers Sjˆ¶grenâ s syndrome (SjS)-like disease in SjS-non-susceptible C57BL/6 mice. To define the chronological interrelationships of biological themes associated with progression from pre- to sub-clinical to overt spontaneous experimental SjS-like disease involving the extracellular milieu (EM) of the salivary glands, we carried out a study utilizing microarray technology in which the parental C57BL/6J mouse was used as the healthy control strain. A bioinformatics-based data analysis methodology designed for comprehensive visualization of global datasets between C57BL/6J and C57BL/6.NOD-Aec1Aec2 mice has permitted a definition of the molecular changes that correlate with onset of stomatitis sicca (xerostomia) in the SjS-susceptible mice. The transcriptome data set of C57BL/6J permitted identification of normal physiological activity. **Overall design:** The study was designed to define the changing gene expression profiles within the salivary glands of C57BL/6.NOD-Aec1Aec2 mice at multiple time points representing a pre-disease stage (4 weeks), the early pre-clinical stage (8 weeks), the initial influx of leukocytes into the salivary glands (12 weeks), and the early clinical phase of autoimmunity (16 weeks) to characterize the influence of the extracellular milieu on early development of disease. Because the C57BL/6.NOD-Aec1Aec2 mouse was derived from the C57BL/6J line, C57BL/6J mice were used as the comparative healthy controls. This comparison permitted the identification of disease-associated gene expressions by subtracting out normal physiological processes. This present study represents the C57BL/6J healthy control mice. Series GSE15640 includes the data for the C57BL/6.NOD-Aec1Aec2 mice.

Background corr dist: KL-Divergence = 0.0794, L1-Distance = 0.0693, L2-Distance = 0.0110, Normal std = 0.4914

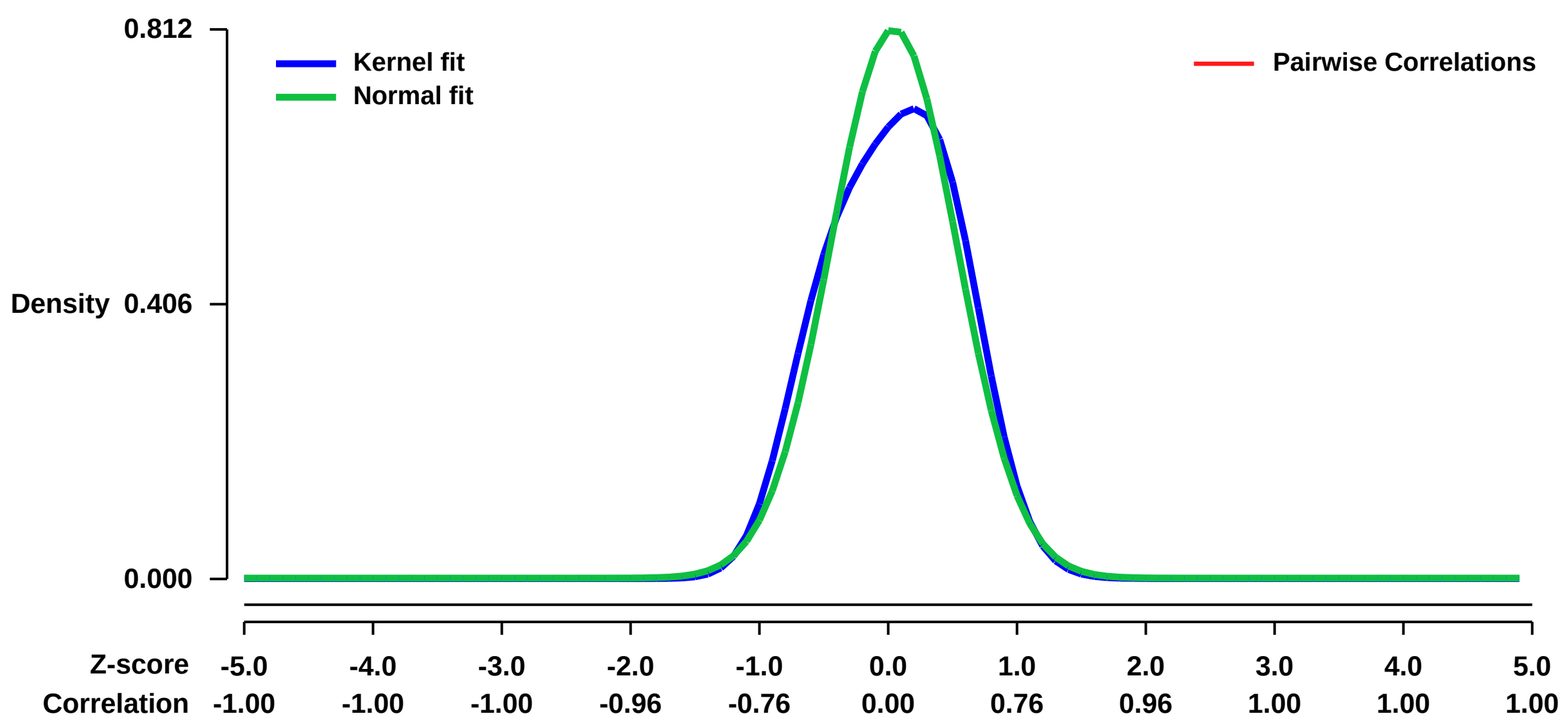

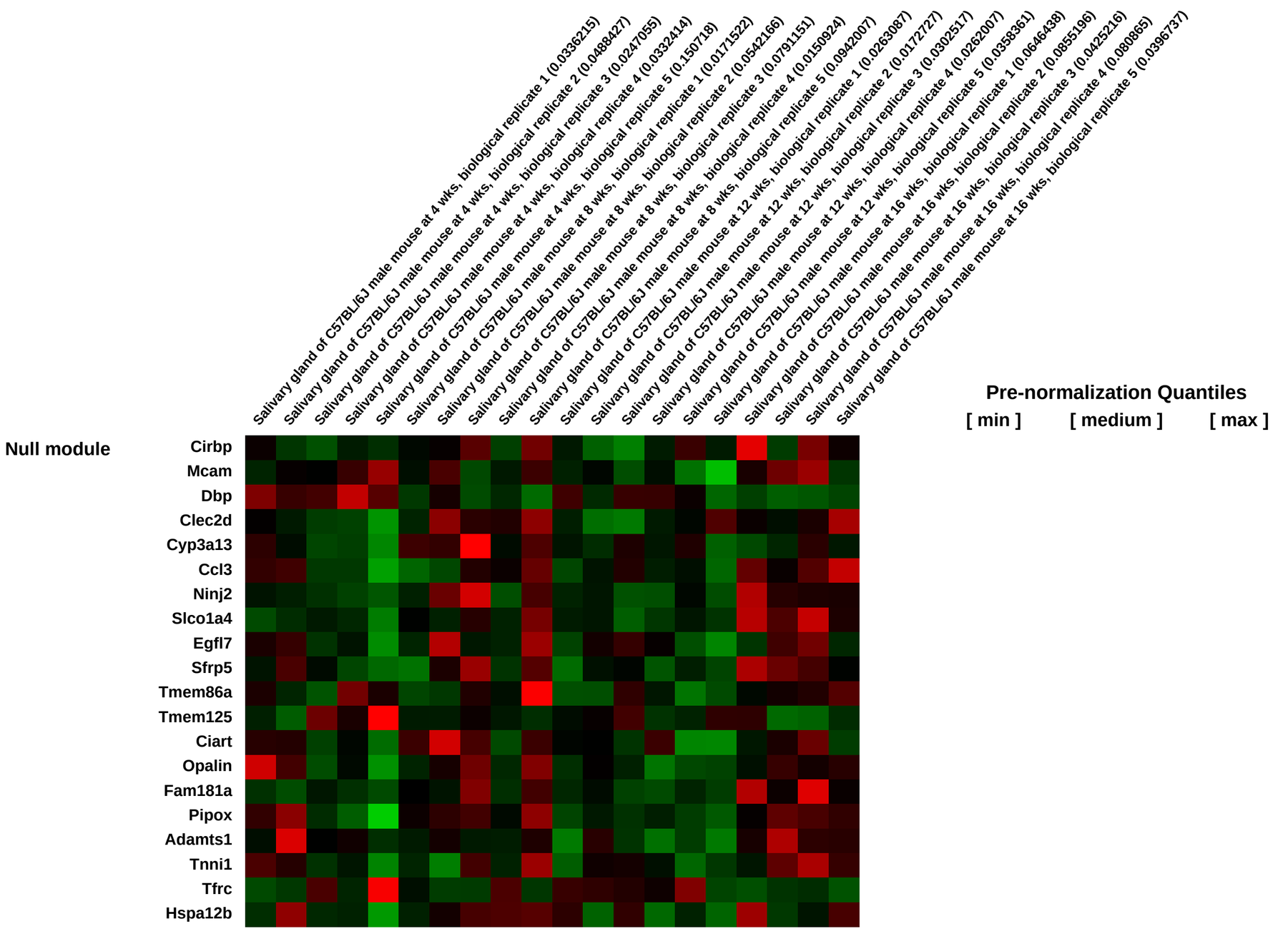

GEO Series "GSE37658" Expression Profiles

Num of samples in this series: 6

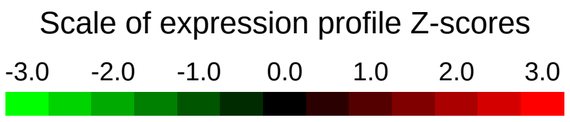

GEO Link:	http://www.ncbi.nlm.nih.gov/geo/query/acc.cgi?acc=GSE37658
Status:	Public on Jul 04 2012
Title:	Gene expression analysis of inducible ES cells overexpressing Etv2 (induced for 12 hours at day 3 of differentiation)
Organism:	Mus musculus
Experiment type:	Expression profiling by array
Platform:	GPL1261
Pubmed ID:	22628281
Summary & Design:	**Summary:** During embryogenesis, the endothelial and the hematopoietic lineages first appear during gastrulation in the blood island of the yolk sac. We have previously reported that an Ets variant gene 2 (Etv2/ER71) mutant embryo lacks hematopoietic and endothelial lineages, however, the precise roles of Etv2 in yolk sac development remains unclear. We carried out a transcriptome analysis using an ES cell line that can inducibly express Etv2. Cells were induced for 12 hours at day 3 of differentiation. **Overall design:** An ES cell line (dervied from mouse of background strain 129P2/Ola) with a doxycycline inducible expression casette of Etv2 (ER71 A2Lox.cre) was differentiated in hanging drops. At 3 days of differentiation, cells were treated with doxycycline for 12 hours, and subsequently Flk1(+) cells were sorted. Experiment was done in triplicate and untreated cells were used for control.

Background corr dist: KL-Divergence = 0.0250, L1-Distance = 0.0262, L2-Distance = 0.0010, Normal std = 0.7073

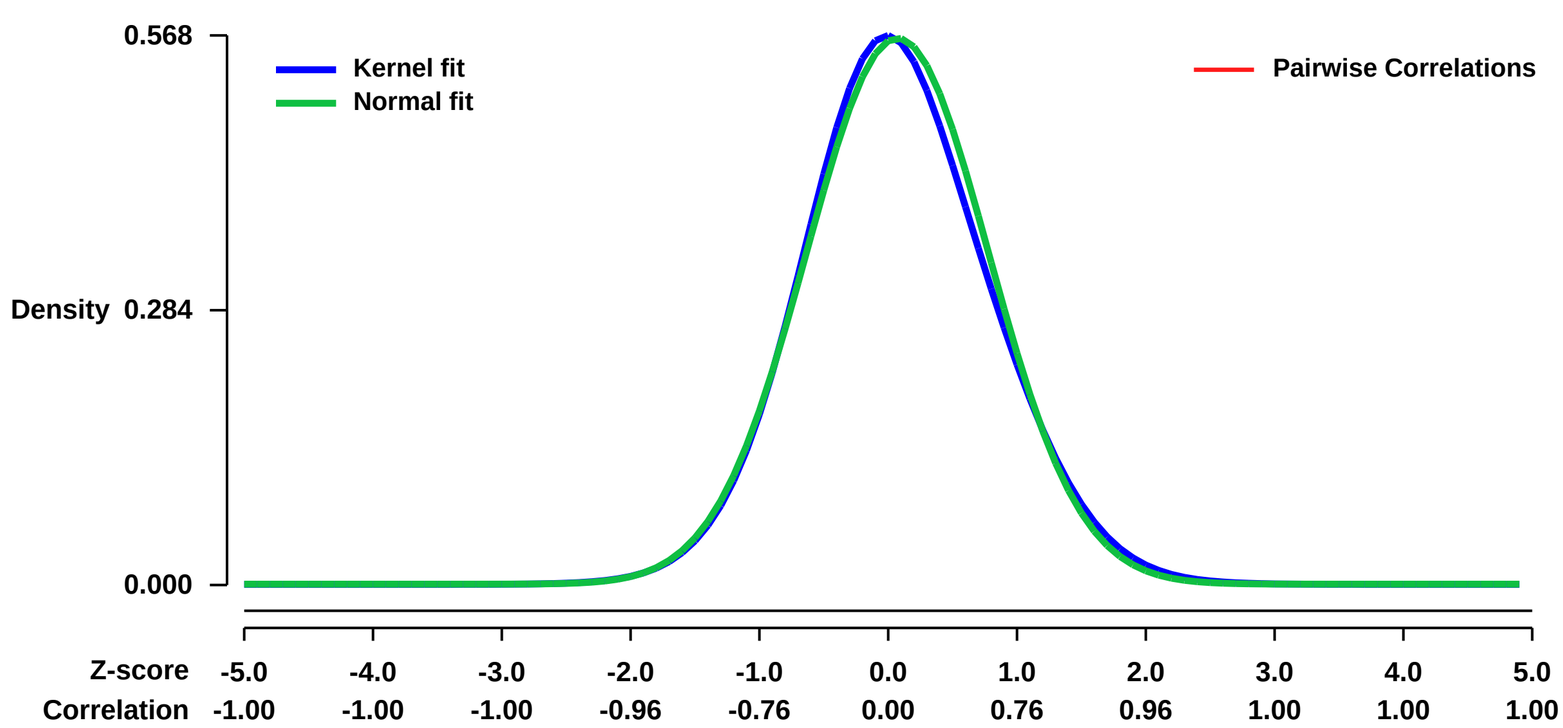

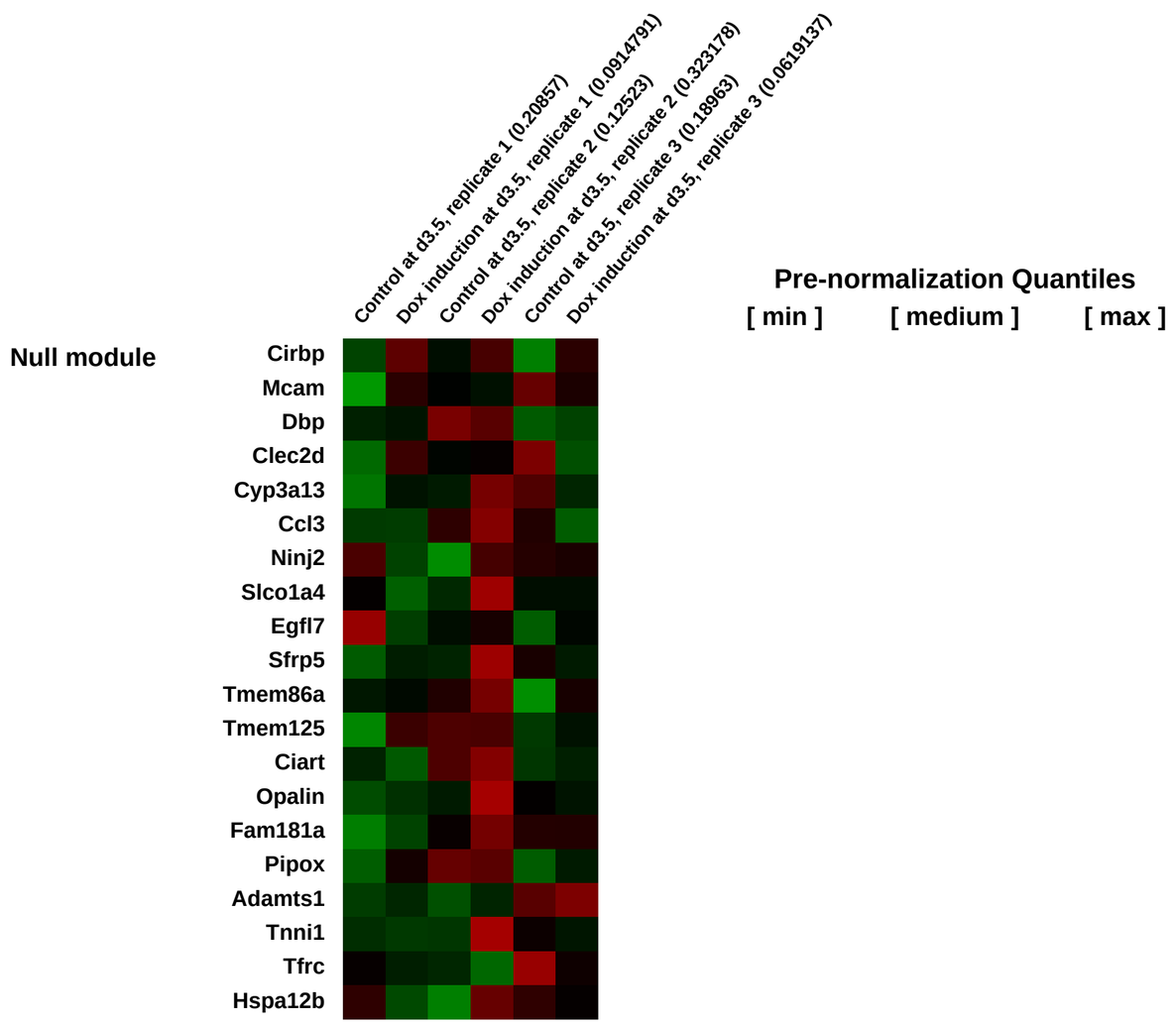

GEO Series "GSE10989" Expression Profiles

Num of samples in this series: 6

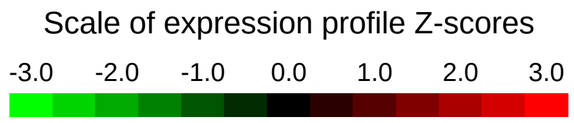

GEO Link:	**http://www.ncbi.nlm.nih.gov/geo/query/acc.cgi?acc=GSE10989**
Status:	**Public on Dec 22 2010**
Title:	**Expression data of cystic renal epithelial tissue from mice deficient for fumarate hydratase.**
Organism:	**Mus musculus**
Experiment type:	**Expression profiling by array**
Platform:	**GPL1261**
Pubmed ID:	
Summary & Design:	**Summary:** **Fumarate hydratase (FH) mutations cause hereditary leiomyomatosis and renal cell cancer (HLRCC). We have conditionally inactivated the murine ortholog (Fh1) in renal tubular epithelial cells in order to generate an in vivo model of HLRCC. Fh1 knockout mice recapitulates important aspects of HLRCC including the development of renal cysts that overexpress hypoxia inducible factor alpha (Hifa) and Hif-target genes.** **We used microarrays to detail the global programme of gene expression underlying cyst development in Fh1 knockout mice and identified distinct classes of up-regulated genes during this process.** **Keywords: gene expression, comparison (wild-type n=3 vs knockout n=3)** **Overall design:** **Renal epithelial tissue was macro-dissected from Fh1 knockout mice and sex-matched litter mate control disease-free animals for RNA extraction and hybridization on Affymetrix microarrays.**

Background corr dist: KL-Divergence = 0.0186, L1-Distance = 0.0758, L2-Distance = 0.0076, Normal std = 0.9701

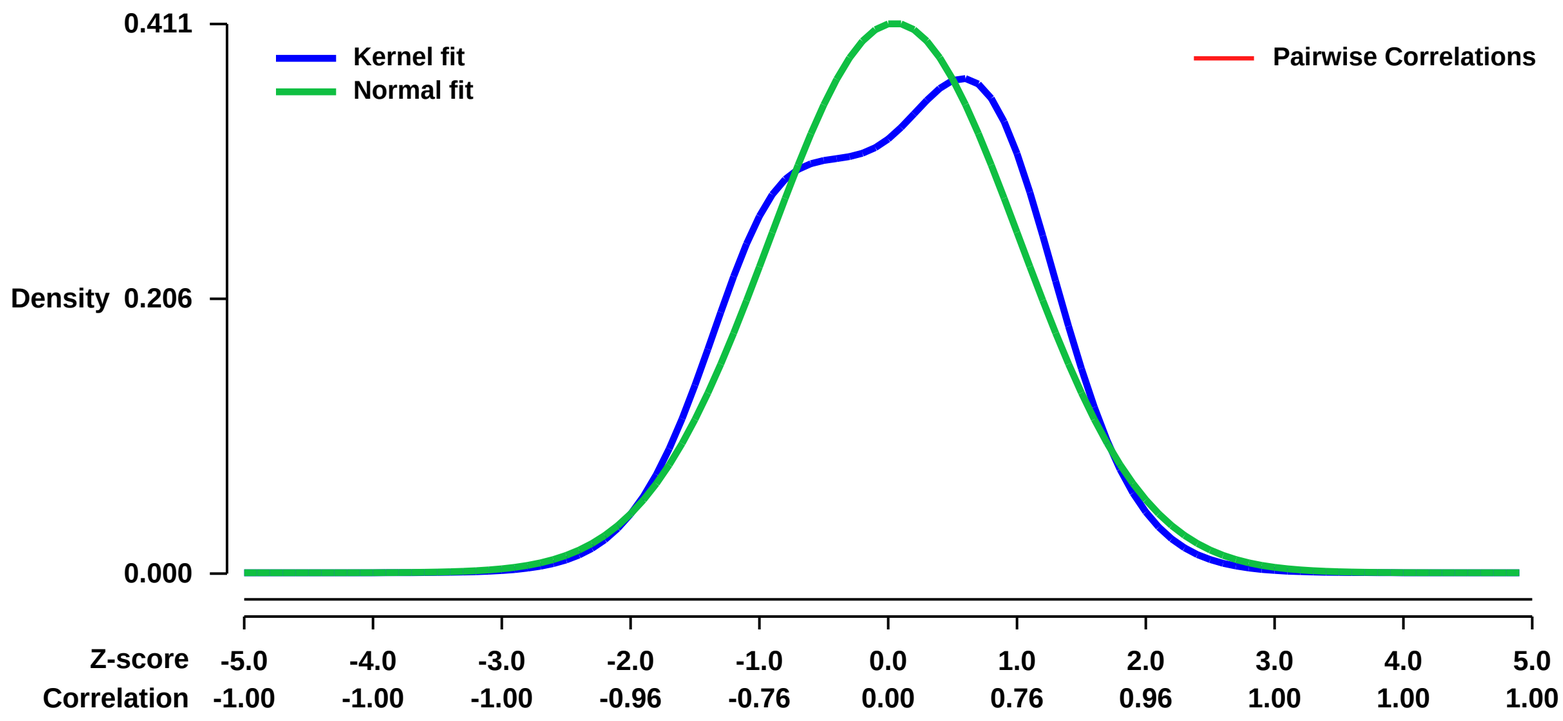

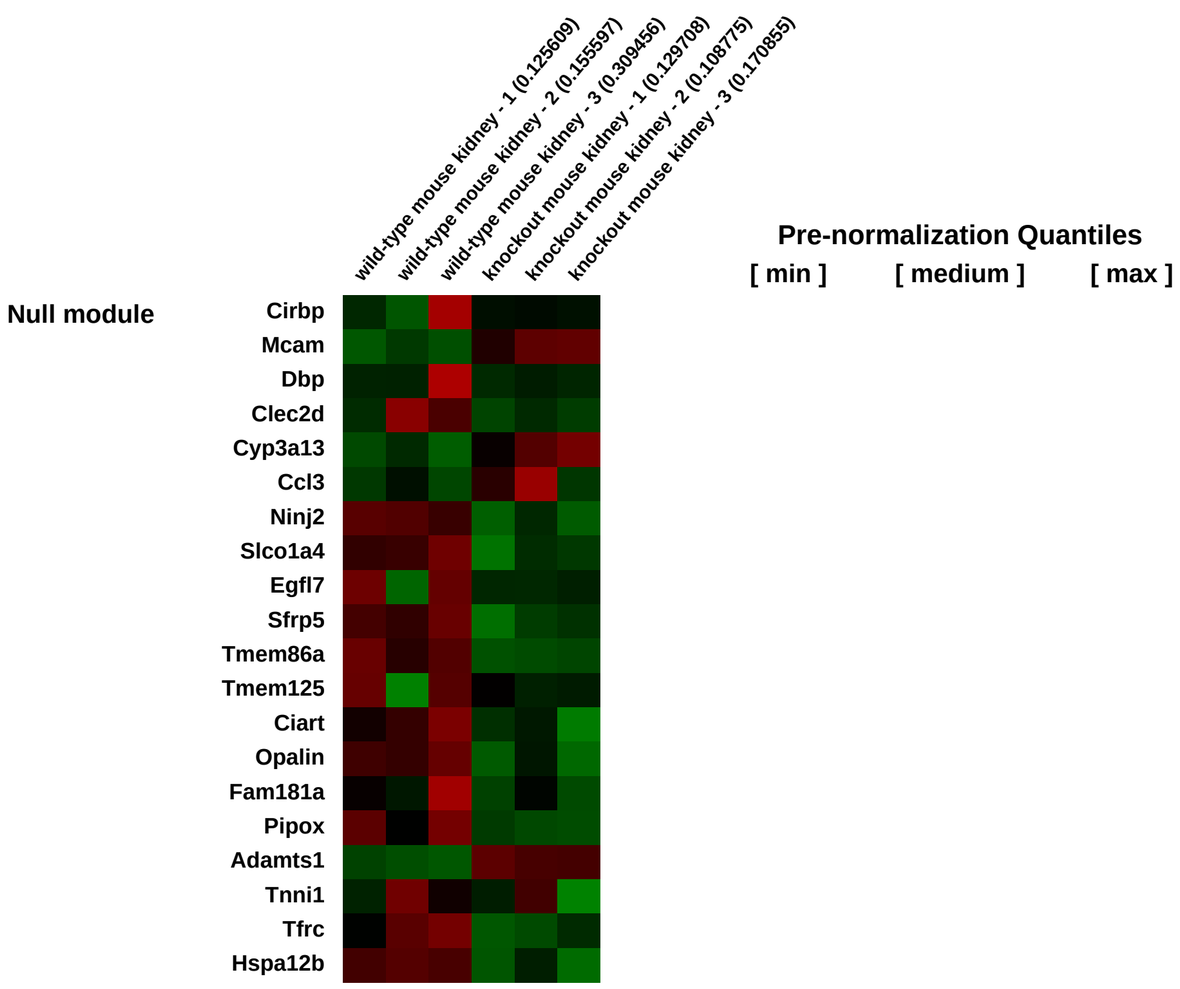

GEO Series "GSE44101" Expression Profiles

Num of samples in this series: 6

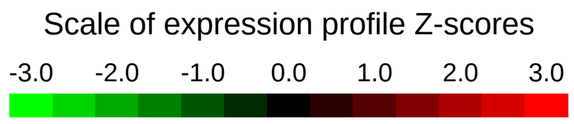

GEO Link:	**http://www.ncbi.nlm.nih.gov/geo/query/acc.cgi?acc=GSE44101**
Status:	**Public on Feb 08 2013**
Title:	**Expression data from Spdef +/+ and Spdef -/- mice**
Organism:	**Mus musculus**
Experiment type:	**Expression profiling by array**
Platform:	**GPL1261**
Pubmed ID:	
Summary & Design:	**Summary:** **Goblet cell numbers decrease within the conjunctival epithelium in drying and cicatrizing ocular surface diseases. Factors regulating goblet cell differentiation in conjunctival epithelium are unknown. Recent data indicate that the transcription factor SAM-pointed domain epithelial-specific transcription factor (Spdef) is essential for goblet cell differentiation in tracheobronchial and gastrointestinal epithelium of mice. Using Spdef -/- mice, we determined that Spdef is required for conjunctival goblet cell differentiation and that Spdef -/- mice, which lack conjunctival goblet cells, have significantly increased corneal surface fluorescein staining and tear volume, a phenotype consistent with dry eye.** **Microarray analysis of conjunctival epithelium in Spdef -/- mice identified 43 signficantly upregulated genes and 110 signficantly downregulated genes in the conjunctival epithelium of Spdef -/- mice compared to that of Spdef +/+ control mice (3 fold change, p<0.01). Downregulated genes of particular interested included goblet cell-specific genes (Muc5ac, Tff1, Gcnt3). Upregulated genes included epithelial cell differentiation/keratinization genes (Sprr2h, Tgm1) and pro-inflammatory genes (Il1-¸–, Il-1¸†, Tnf-¸–), all of which are upregulated in dry eye. Interestingly, four Wnt pathway genes were downregulated.** **Overall design:** **Conjunctival epithelium of Spdef +/+ and Spdef -/- mice was collected by laser capture microdissection for RNA extraction and hybridization on Affymetrix microarrays to determine if gene expression patterns in the conjunctival epithelium of Spdef -/- mice is altered compared to that of Spdef +/+ mice.**

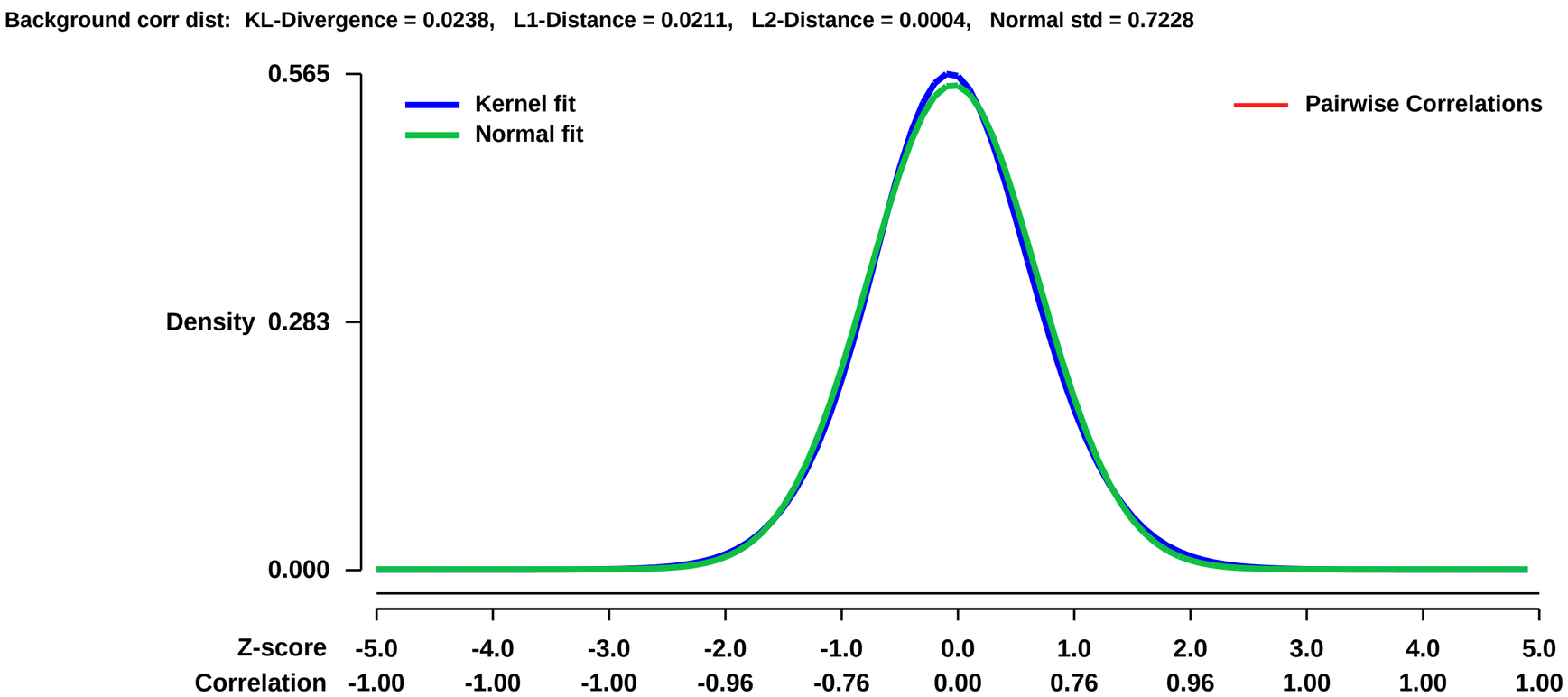

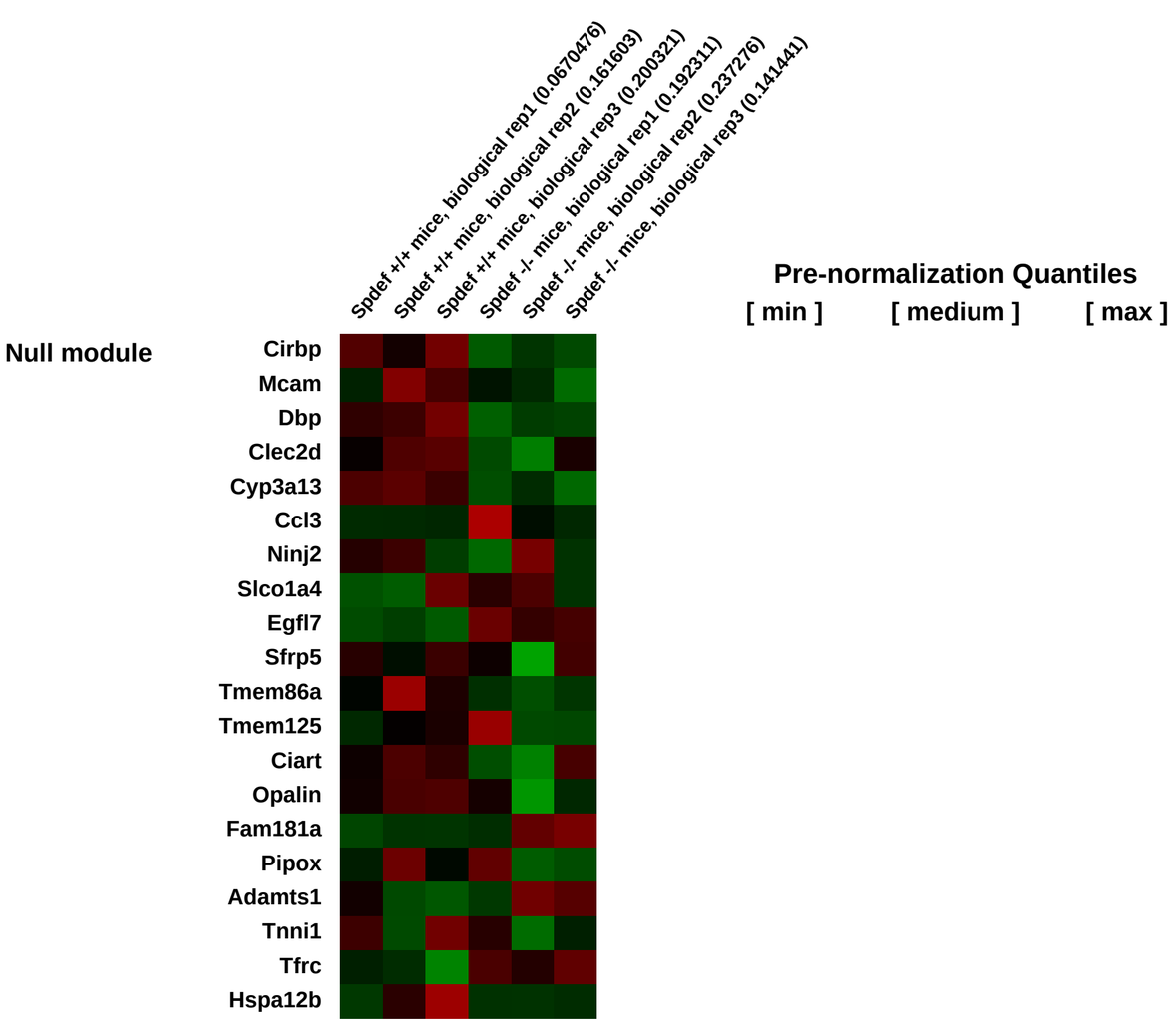

GEO Series "GSE18567" Expression Profiles

Num of samples in this series: 24

Scale of expression profile Z-scores

-3.0 -2.0 -1.0 0.0 1.0 2.0 3.0

GEO Link:	http://www.ncbi.nlm.nih.gov/geo/query/acc.cgi?acc=GSE18567
Status:	Public on Mar 01 2010
Title:	Temporal profiling of gene expression in cochleae of wild type and alpha9 null mice
Organism:	Mus musculus
Experiment type:	Expression profiling by array
Platform:	GPL1261
Pubmed ID:	20140217
Summary & Design:	**Summary:** Efferent inhibition of cochlear outer hair cells is mediated by nicotinic cholinergic receptors containing alpha9 (a9) and alpha10 subunits. Mice lacking a9 nicotinic subunits fail to exhibit classic olivocochlear responses and are characterized by abnormal synaptic morphology at the base of outer hair cells. To detail molecular changes induced upon the loss of a9 subunit, we sampled cochlear RNA from wild type and a9 null mice at postnatal (P) days spanning periods of synapse formation and maturation (P3, P7, P13 and P60). Our findings point to a delay in cochlear maturation starting at the onset of hearing (P13), as well as an up-regulation of various GABA receptor subunits in adult mice lacking the a9 nicotinic subunit. **Overall design:** Cochleae were removed at postnatal ages P3, P7, P13 and P60. Cochlear tissues from 3-5 mice were pooled per replicate; biological triplicates were performed for each age and genotype.

Background corr dist: KL-Divergence = 0.1285, L1-Distance = 0.0372, L2-Distance = 0.0027, Normal std = 0.3964

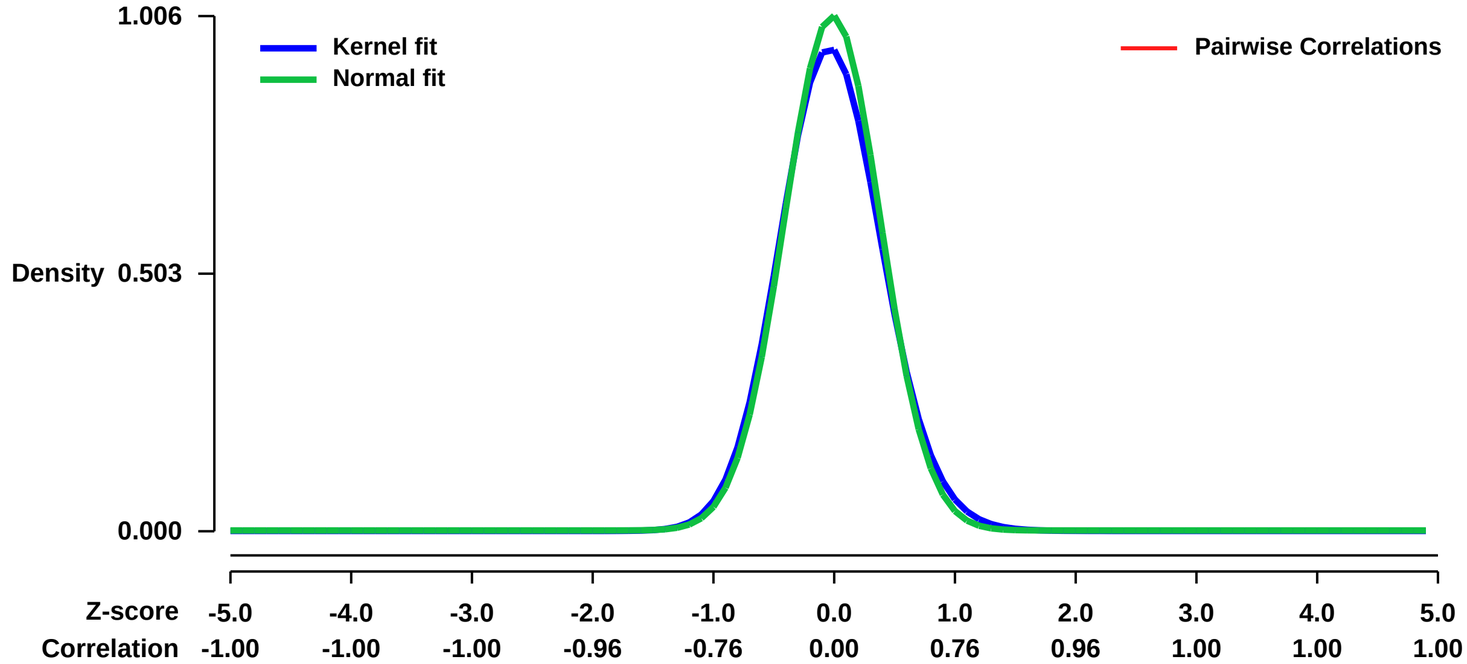

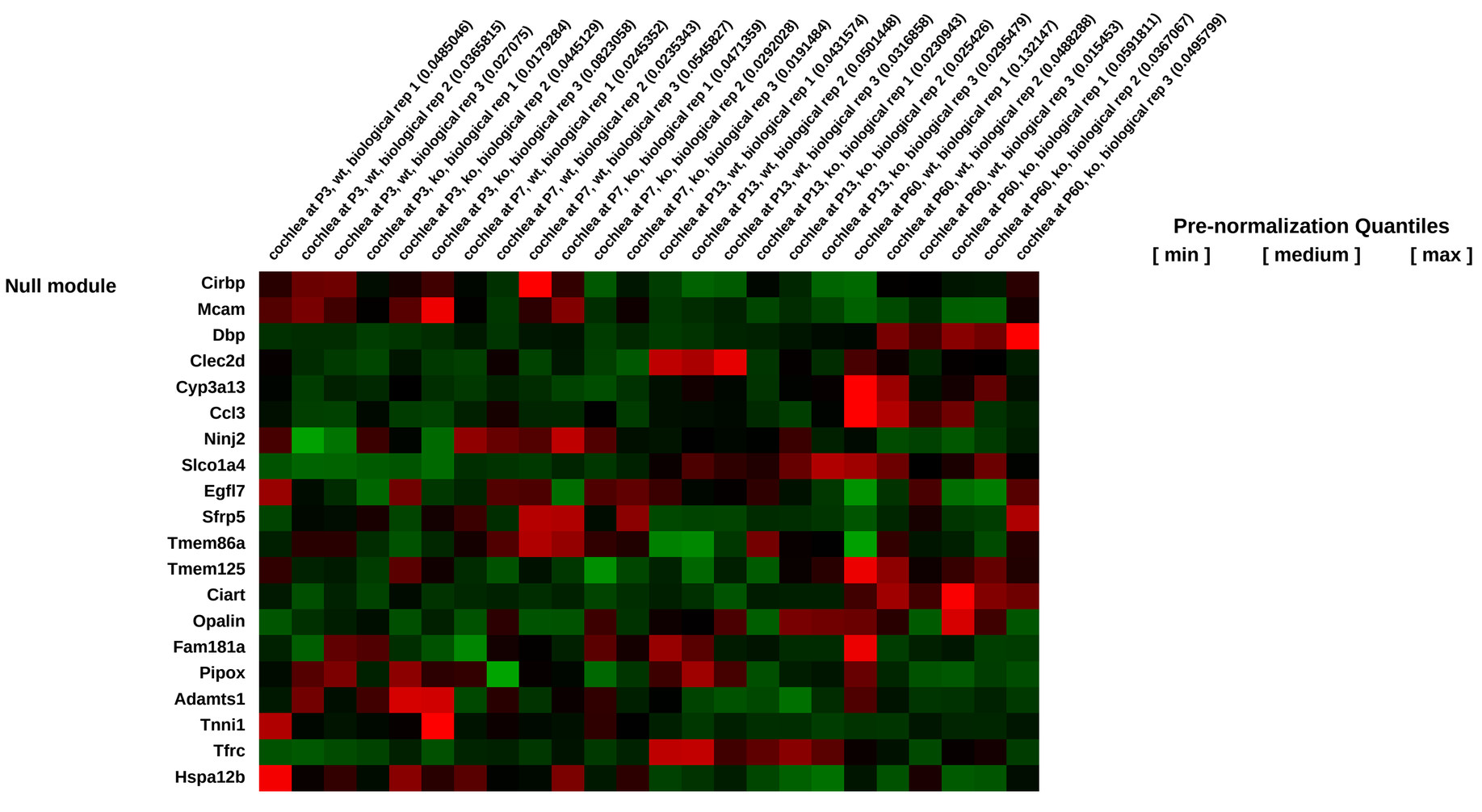

GEO Series "GSE49050" Expression Profiles

Num of samples in this series: 72

Scale of expression profile Z-scores

-3.0 -2.0 -1.0 0.0 1.0 2.0 3.0

GEO Link:	http://www.ncbi.nlm.nih.gov/geo/query/acc.cgi?acc=GSE49050
Status:	Public on Jul 23 2014
Title:	Expression data from postnatal mouse brain regions of Ts1Cje and disomic C57BL/6 mice.
Organism:	Mus musculus
Experiment type:	Expression profiling by array
Platform:	GPL1261
Pubmed ID:	25052193
Summary & Design:	**Summary:** The Ts1Cje mouse model of Down syndrome (DS) has partial triplication of mouse chromosome 16 (MMU16), which is partially homologous to human chromosome 21. The mouse model develops various neuropathological features identified in DS individuals. We analysed the effect of partial triplication of the MMU16 segment on global gene expression in the cerebral cortex, cerebellum and hippocampus of Ts1Cje mice at 4 time-points; postnatal day (P)1, P15, P30 and P84. **Overall design:** RNA was extracted from thre brain regions (Cerebral cortex, hippocampus and cerebellum) for hybridization to arrays from 3 pairs of Ts1Cje and disomic C57BL/6 littermate control for each timepoints at postnatal (P) day 1, P15, P30 and P84.

Background corr dist: KL-Divergence = 0.1628, L1-Distance = 0.0657, L2-Distance = 0.0118, Normal std = 0.3740

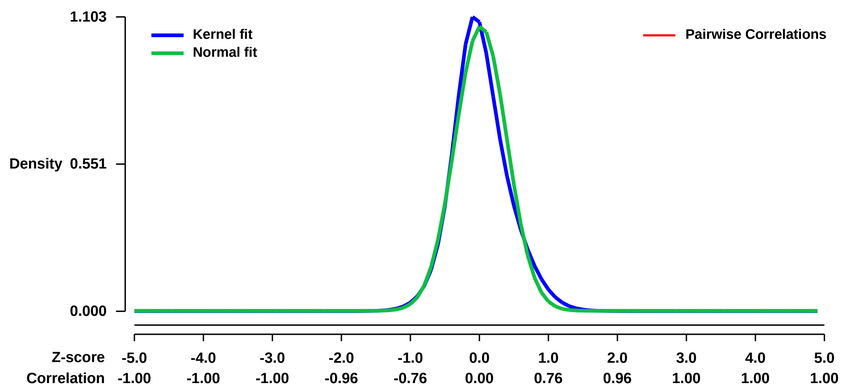

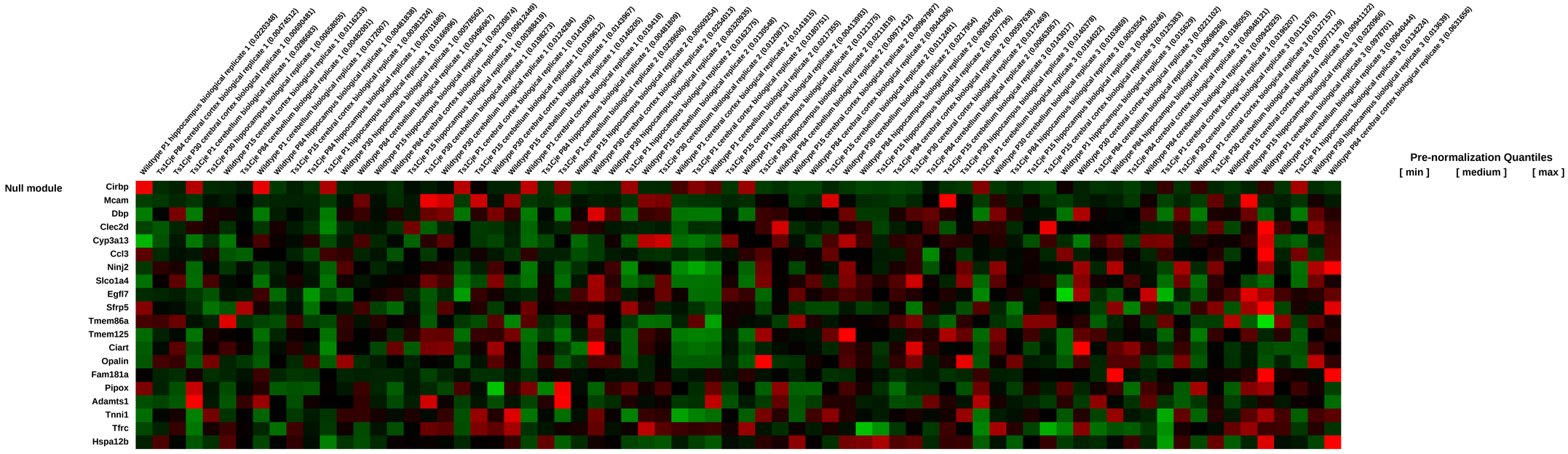

GEO Series "GSE47694" Expression Profiles

Num of samples in this series: 10

Scale of expression profile Z-scores

-3.0 -2.0 -1.0 0.0 1.0 2.0 3.0

GEO Link: http://www.ncbi.nlm.nih.gov/geo/query/acc.cgi?acc=GSE47694
Status: Public on Jul 01 2013
Title: Regulation of Mouse Lens Development and Gene Expression by Krˆ…ppel-Like Factor 4
Organism: Mus musculus
Experiment type: Expression profiling by array
Platform: GPL1261
Pubmed ID:
Summary & Design:

Summary:
Conditional disruption of Klf4 in the ectoderm-derived tissues of the eye results in defective cornea, conjunctiva and the lens.

Expression of Klf4 is first detected in the embryonic day-12 (E12) mouse lens, peaks at E16, and declines thereafter.

Lenses from Mice which were conditional null for Klf4 (Klf4CN) were characterized by morphology and transcriptome.

Overall design:
Wild type and Klf4-conditional null mouse lens gene expression at embryonic day 16.5 (E16.5) and postnatal day 56 (PN56) was surveyed using Affymetrix mouse whole genome 430 2 arrays.

Background corr dist: KL-Divergence = 0.0301, L1-Distance = 0.0216, L2-Distance = 0.0005, Normal std = 0.6597

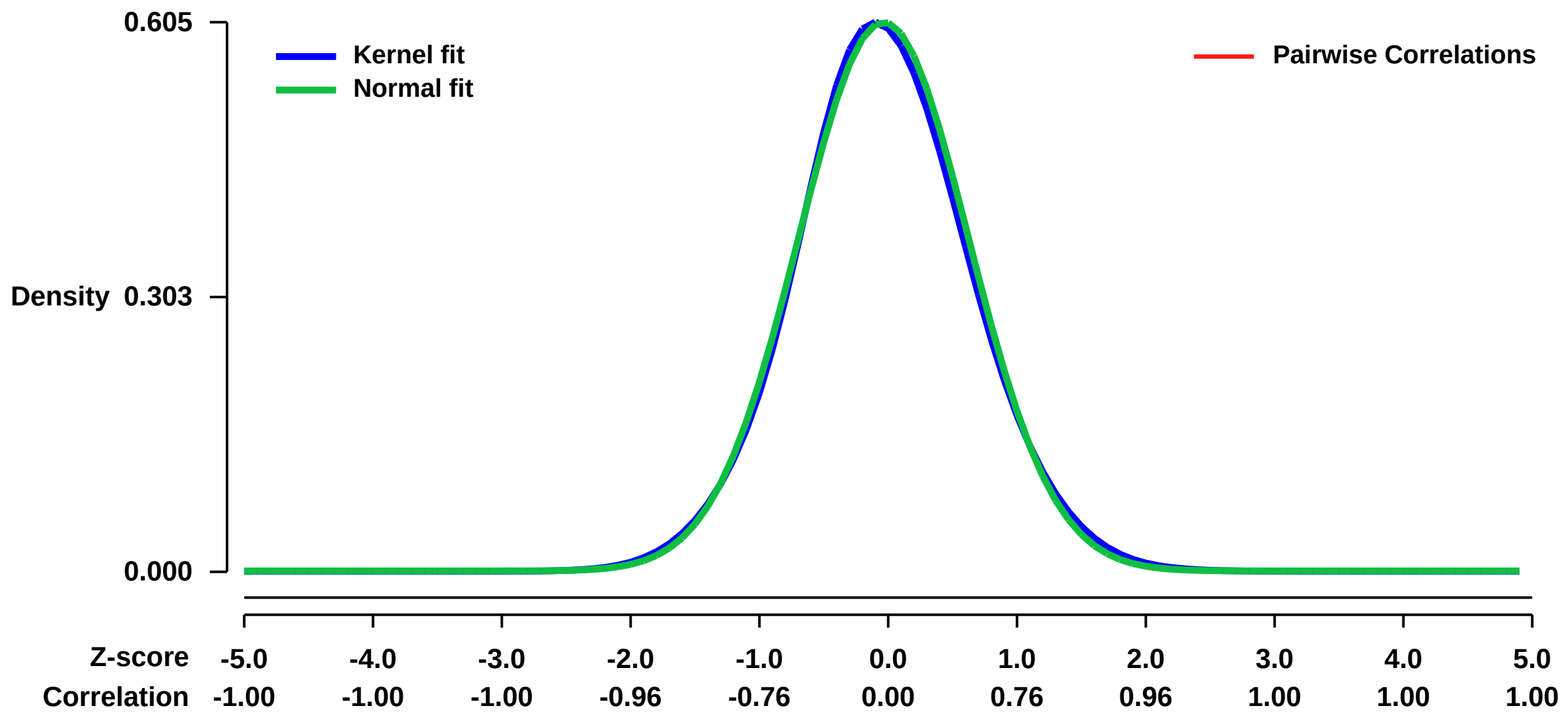

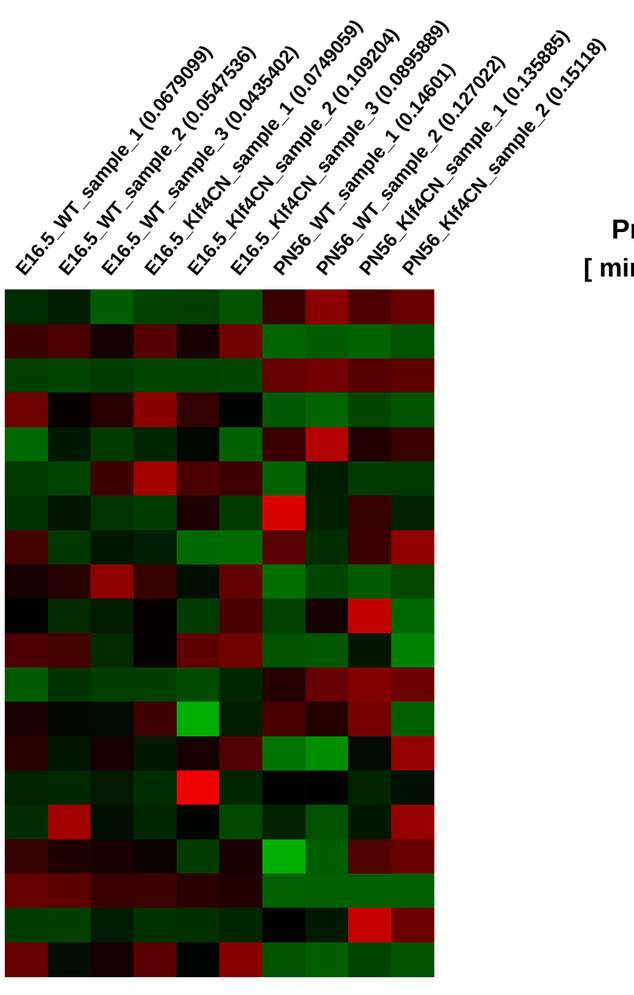

GEO Series "GSE16801" Expression Profiles

Num of samples in this series: 9

Scale of expression profile Z-scores

-3.0 -2.0 -1.0 0.0 1.0 2.0 3.0

GEO Link:	**http://www.ncbi.nlm.nih.gov/geo/query/acc.cgi?acc=GSE16801**
Status:	**Public on Jun 26 2009**
Title:	**Comparative gene expression analysis of 2 subpopulations of dermal papilla cells.**
Organism:	**Mus musculus**
Experiment type:	**Expression profiling by array**
Platform:	**GPL1261**
Pubmed ID:	**19605494**
Summary & Design:	**Summary:** **Different types of hair follicles can be found in the skin of mice. It is believed that the signals that control hair follicle differentiation arise from cells in a structure called the dermal papilla. Understanding the nature of those signals is of interest for the biology of the normal tissue.** **We have developed a technique for isolation of dermal cells by enzymatic digestion of intact skin. We have identified two subpopulations of cells that can be separated by FACS. The Sox2-positive CD133-positive cells are found exclusively in the dermal papillae of guard/awl/auchene hairs, while Sox2-negative, CD133-positive cells are found in the other hair follicle types. We compared these populations with unfractionated dermal cells.** **#!#** **Overall design:** **The yield is approximately 50,000 cells of each population.**

Background corr dist: **KL-Divergence = 0.0780, L1-Distance = 0.0229, L2-Distance = 0.0009, Normal std = 0.4837**

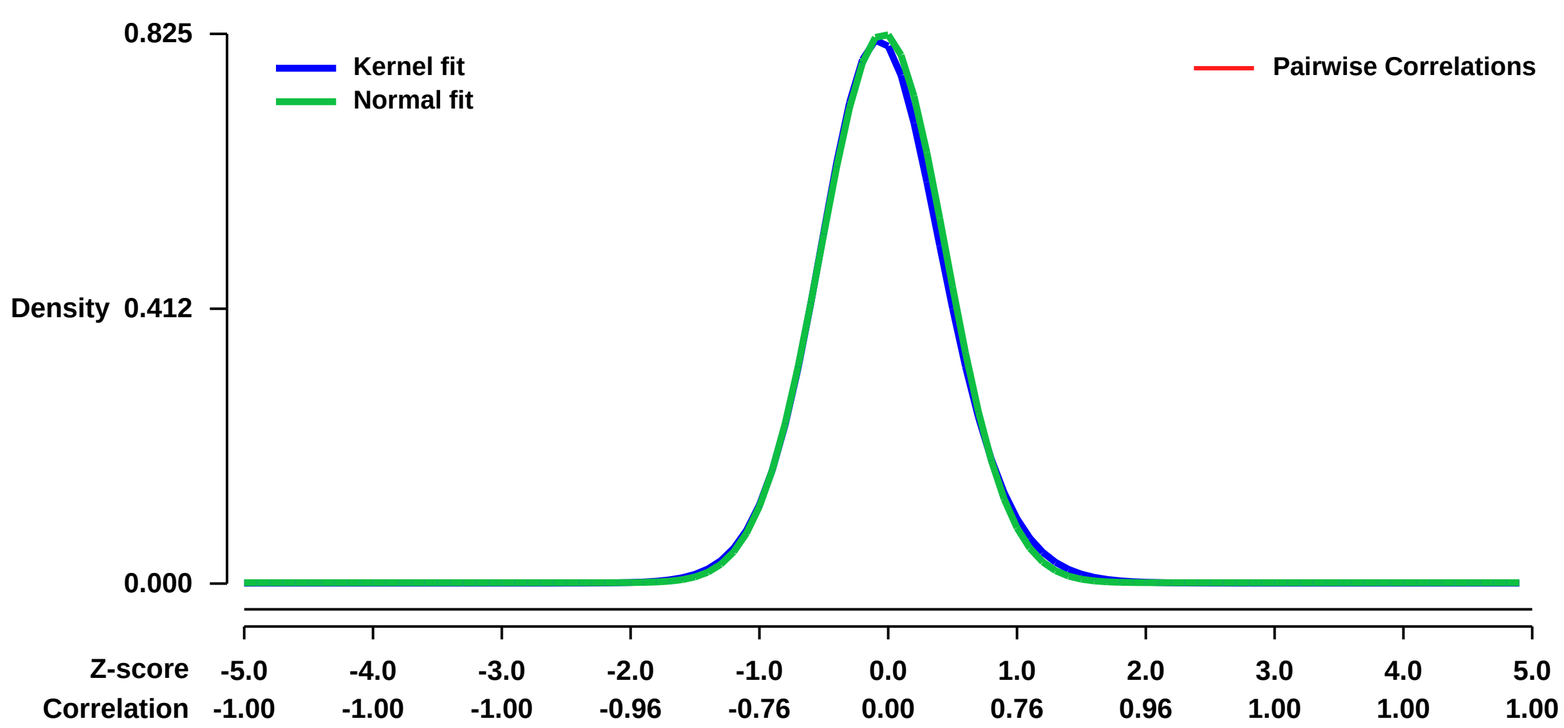

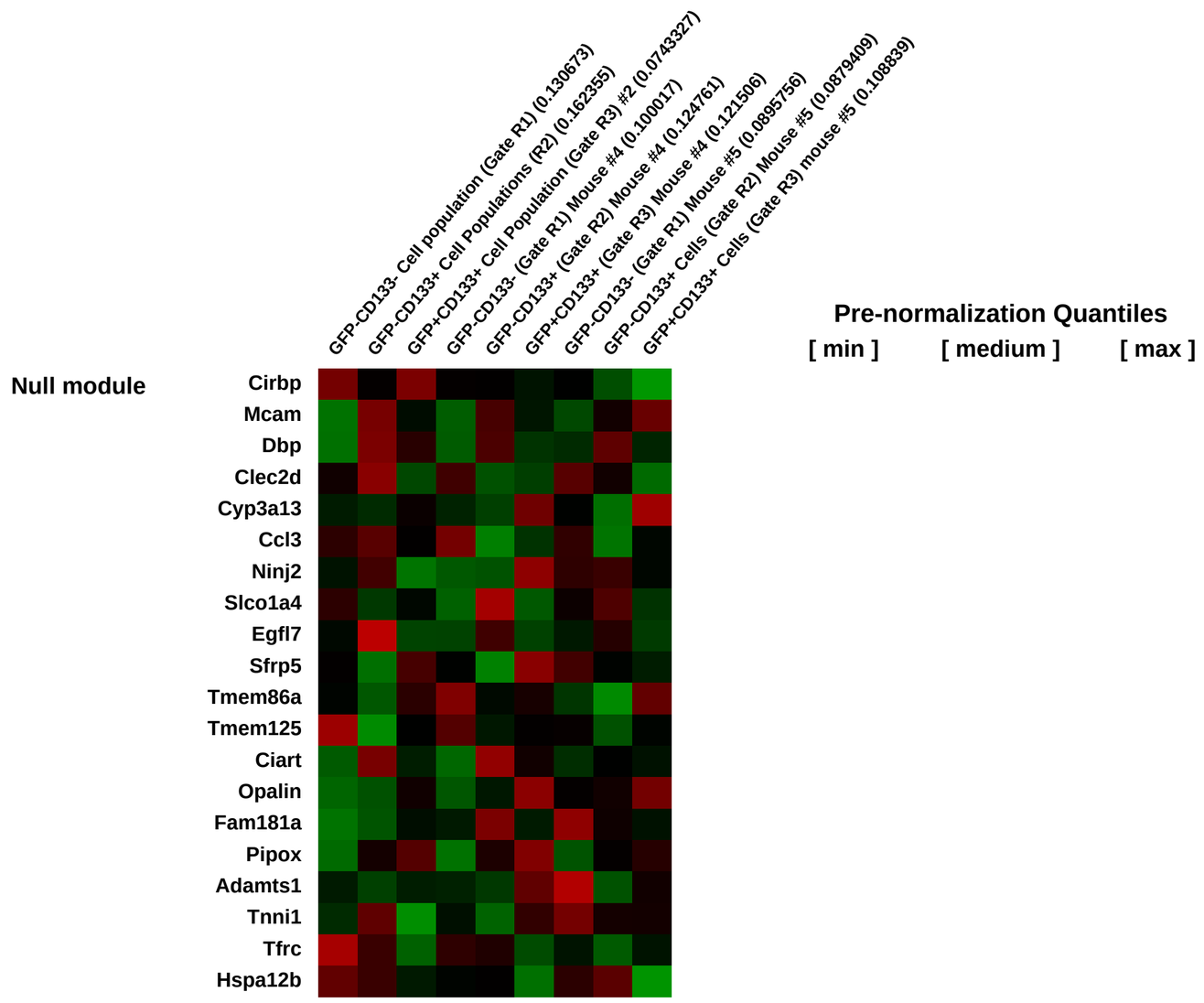

GEO Series "GSE5861" Expression Profiles

Num of samples in this series: 6

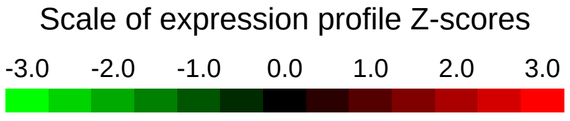

GEO Link:	http://www.ncbi.nlm.nih.gov/geo/query/acc.cgi?acc=GSE5861
Status:	Public on Sep 19 2006
Title:	Searching for Brca1 regulated X-linked genes
Organism:	Mus musculus
Experiment type:	Expression profiling by array
Platform:	GPL1261
Pubmed ID:	17350580
Summary & Design:	**Summary:** We compared the expression levels of X-linked genes in the mammary glands of Brca1 D11/D11;p53+/- mutant and control (p53+/-) mice at three different stages of the mammary cycle: virgin, pregnant day 16.5, and lactation day 1, using a cDNA microarray. In about 690 X-linked genes that are expressed at these three stages of mammary cycle of development, we found 16 X-linked genes showed altered expression levels in Brca1 D11/D11;p53+/- mammary glands in comparison with controls at all three time points. Among them, 9 genes were up-regulated and 7 were down-regulated. This result indicates that mutation of Brca1 could affect expression of a few X-linked genes in mammary tissues. However, this was unlikely caused by failure of X chromosome inactivation, as seven of them were down-regulated, and Xist RNA was expressed in all the Brca1 mutant mammary tissues. **Keywords:** BRCA1 mutation analysis **Overall design:** Mutations in breast cancer associated gene-1 (BRCA1) are associated with hereditary breast and ovarian cancers. BRCA1 encodes a tumor suppressor protein that functions in DNA repair, transcriptional regulation, chromatin remodeling, centrosome duplication and checkpoint control, etc.. We were interested in fishing out the genes regulated by Brca1. Three pairs of mammary glands from Brca1 D11/D11;p53+/- mutant and control (p53+/-) mice at three different stages of the mammary cycle were analyzed by microarray for gene expression levels.

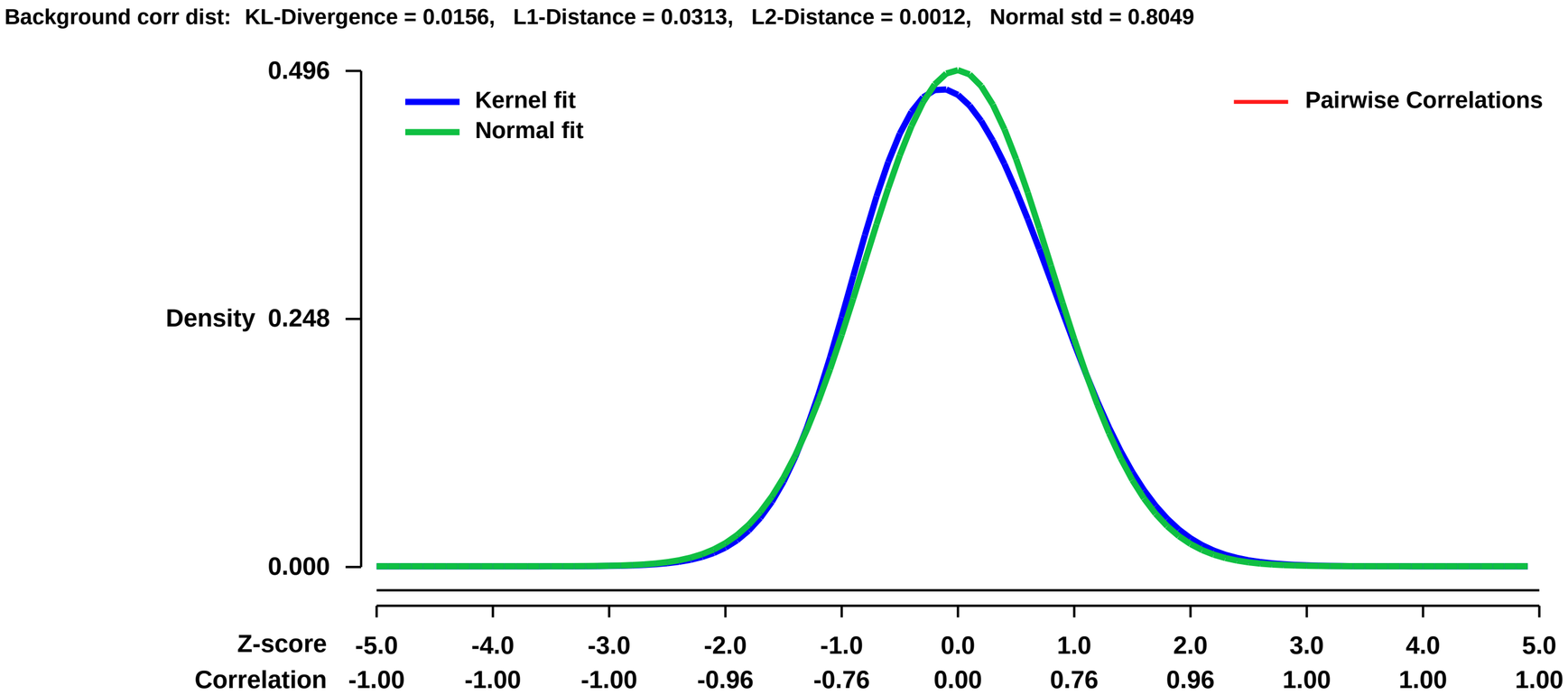

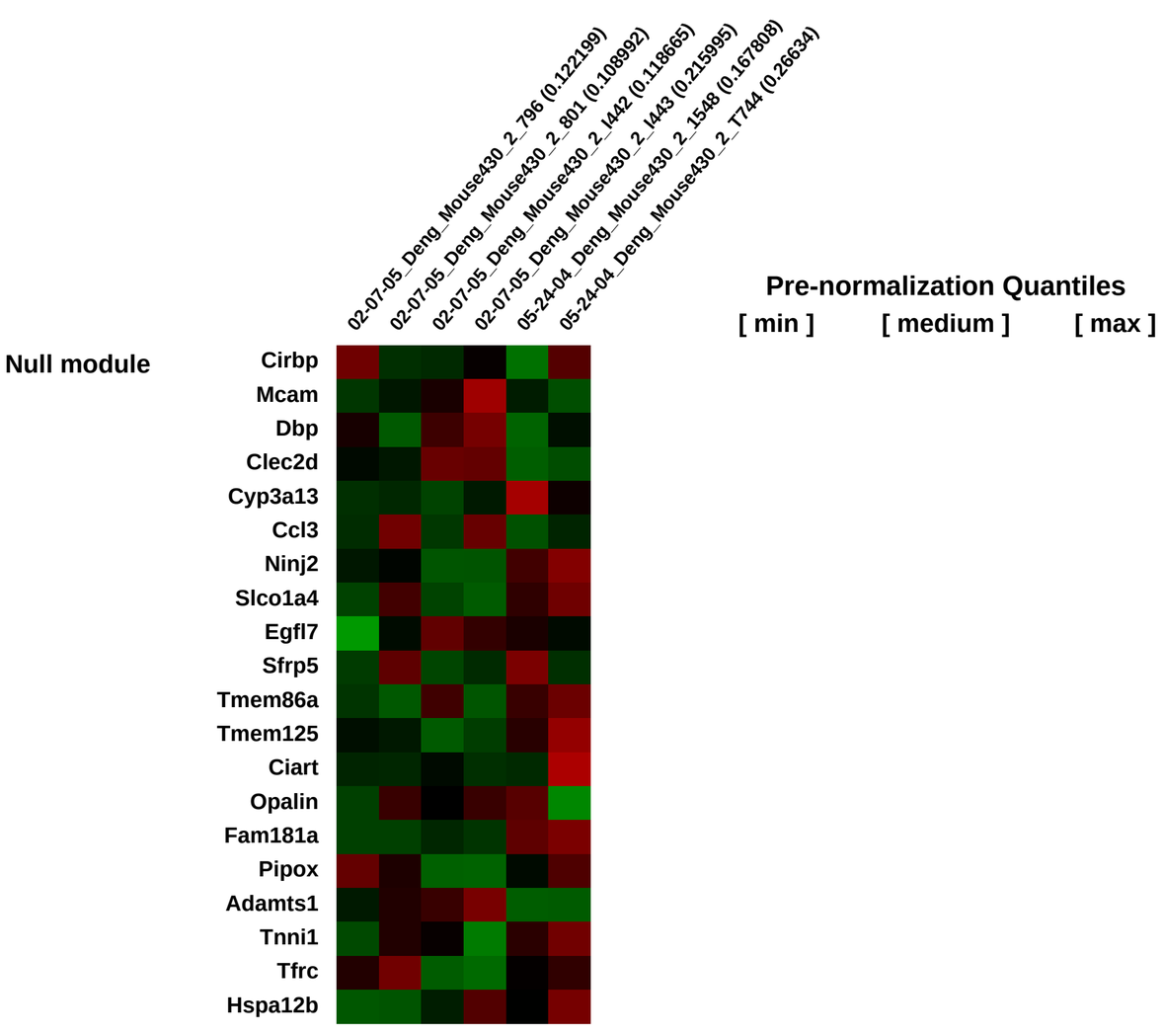

GEO Series "GSE19474" Expression Profiles

Num of samples in this series: 12

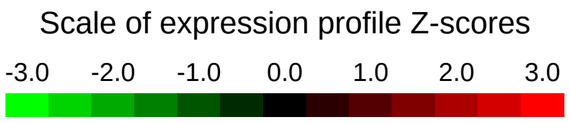

GEO Link:	http://www.ncbi.nlm.nih.gov/geo/query/acc.cgi?acc=GSE19474
Status:	Public on Dec 16 2009
Title:	Expression data from E12.5 ePet-EYFP rostral and caudal serotonin (5HT) neurons purified by flow cytometry
Organism:	Mus musculus
Experiment type:	Expression profiling by array
Platform:	GPL1261
Pubmed ID:	20071532
Summary & Design:	**Summary:** The 5HT system is organized into rostral and caudal populations with discrete anatomical locations and opposite axonal trajectories in the developing hindbrain. 5HT neuron cell bodies in the rostral subdivision migrate to the midbrain and pons and extend ascending projections throughout the forebrain. 5HT cell bodies in the caudal subdivision migrate to the ventral medulla and caudal half of the pons and provide descending projections to the brainstem and spinal cord. **Overall design:** We used microarrays to determine genes expressed by both rostral and caudal 5HT neurons as well as genes that are differentially expressed between rostral and caudal 5HT neurons at E12.5 when axon pathfinding and cell migration are underway. E12.5 neural tubes were isolated from ePet-EYFP embryos and dissected into a rostral domain (mesecephalic flexure to pontine flexure) and a caudal domain (pontine flexure to spinal cord). After cell dissociation (details under growth protocol), cells were subjected to fluorescent activated cell sorting (FACS) to obtain 4 cell populations. R+ = rostral ePetEYFP positive 5HT neurons; R- = YFP negative non-serotonergic cells in the rostral neural tube; C+ = caudal ePetEYFP positive 5HT neurons; C- = YFP negative non-serotonergic cells in the caudal neural tube. 200,000 cells for each of the 4 cell types (R+, R-, C+, C-) were collected for RNA extraction and hybridization to Affymetrix Mouse 430 2.0 arrays.

Background corr dist: KL-Divergence = 0.1218, L1-Distance = 0.0274, L2-Distance = 0.0013, Normal std = 0.4067

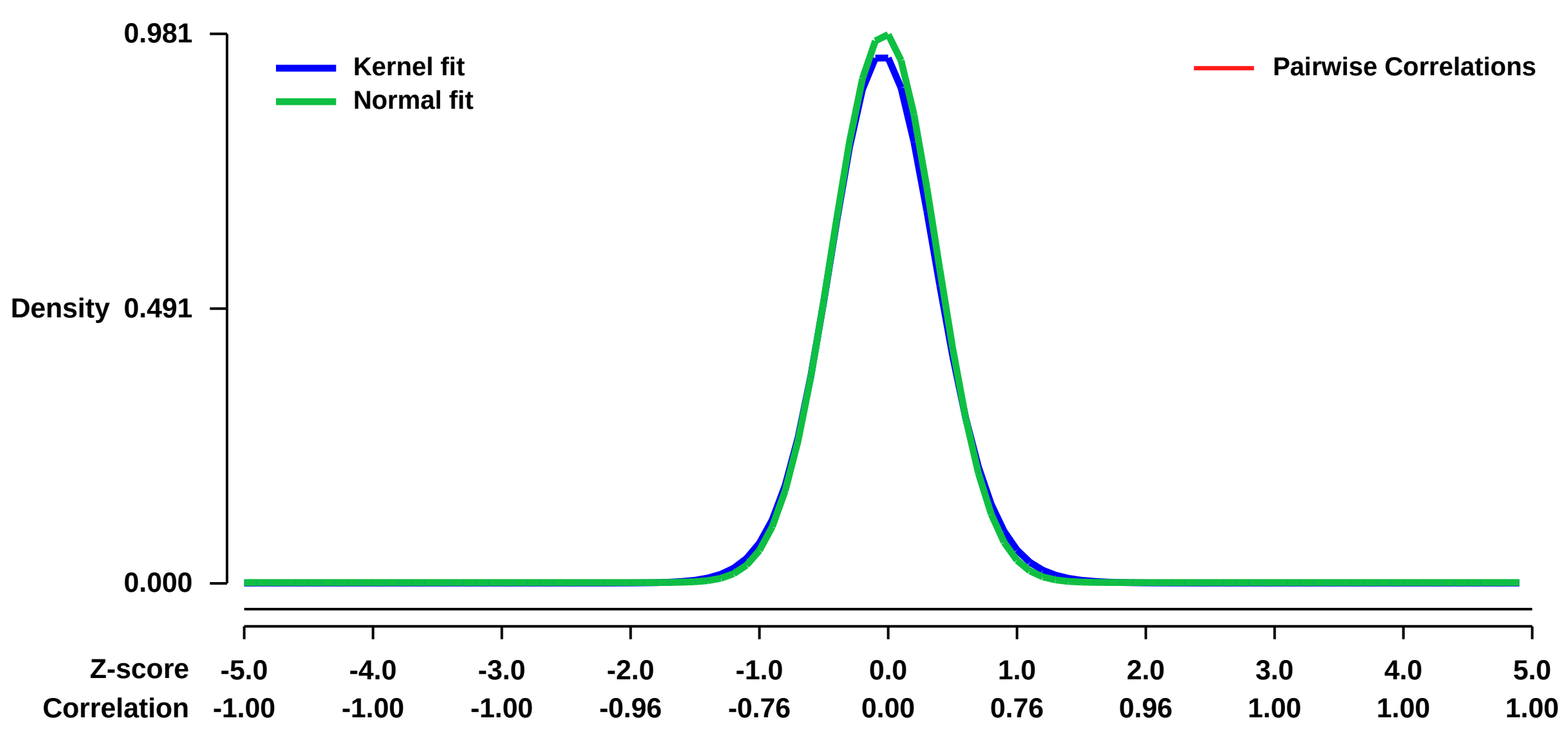

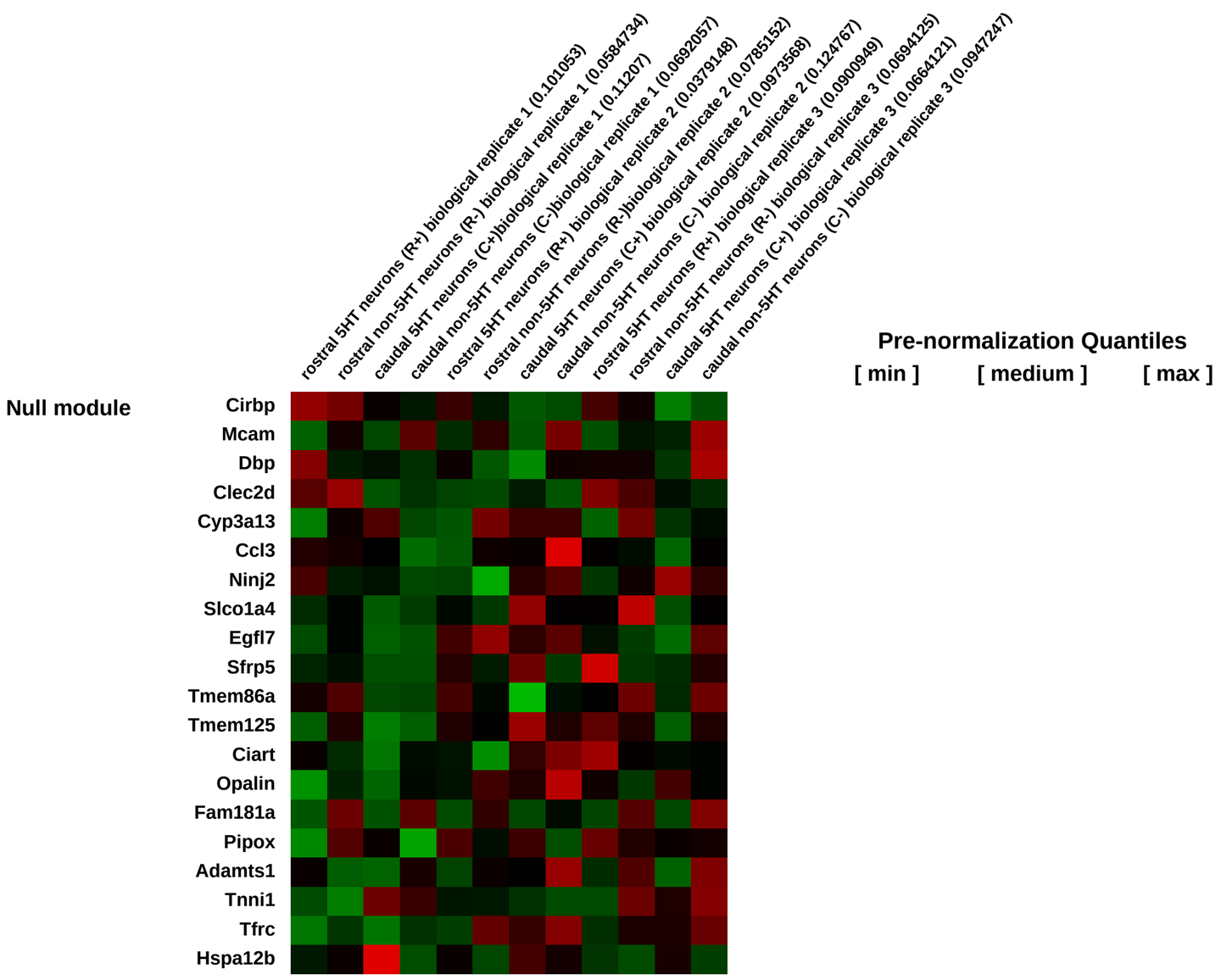

GEO Series "GSE27799" Expression Profiles

Num of samples in this series: 6

Scale of expression profile Z-scores

-3.0 -2.0 -1.0 0.0 1.0 2.0 3.0

GEO Link:	http://www.ncbi.nlm.nih.gov/geo/query/acc.cgi?acc=GSE27799
Status:	Public on May 12 2011
Title:	Expression data from LSK WT and LSK N1-C+
Organism:	Mus musculus
Experiment type:	Expression profiling by array
Platform:	GPL1261
Pubmed ID:	21562564
Summary & Design:	**Summary:** Notch signaling is one of the central regulators of differentiation in a variety of organisms and tissue types. Within the hematopoietic system, Notch is essential for the emergence of definitive HSC during fetal life and controls adult HSC differentiation to the T-cell lineage. Notch activation is controlled by the gamma-secretase complex complex, composed of presenilin, nicastrin (Ncstn), anterior pharynx-1 (Aph1), and presenilin enhancer-2 To determine other role of Notch signaling in HSC we designed a conditional mouse model of Notch activation. WT and N1-IC+ HSC were analysed to determined genes controlled by Notch signaling. **Overall design:** Bone marrow lineage negative, cKit+, Sca1+ cells were sorted from WT and N1-IC+ littermates for RNA extraction and hybridization on Affymetrix microarrays

Background corr dist: KL-Divergence = 0.0326, L1-Distance = 0.0169, L2-Distance = 0.0003, Normal std = 0.6534

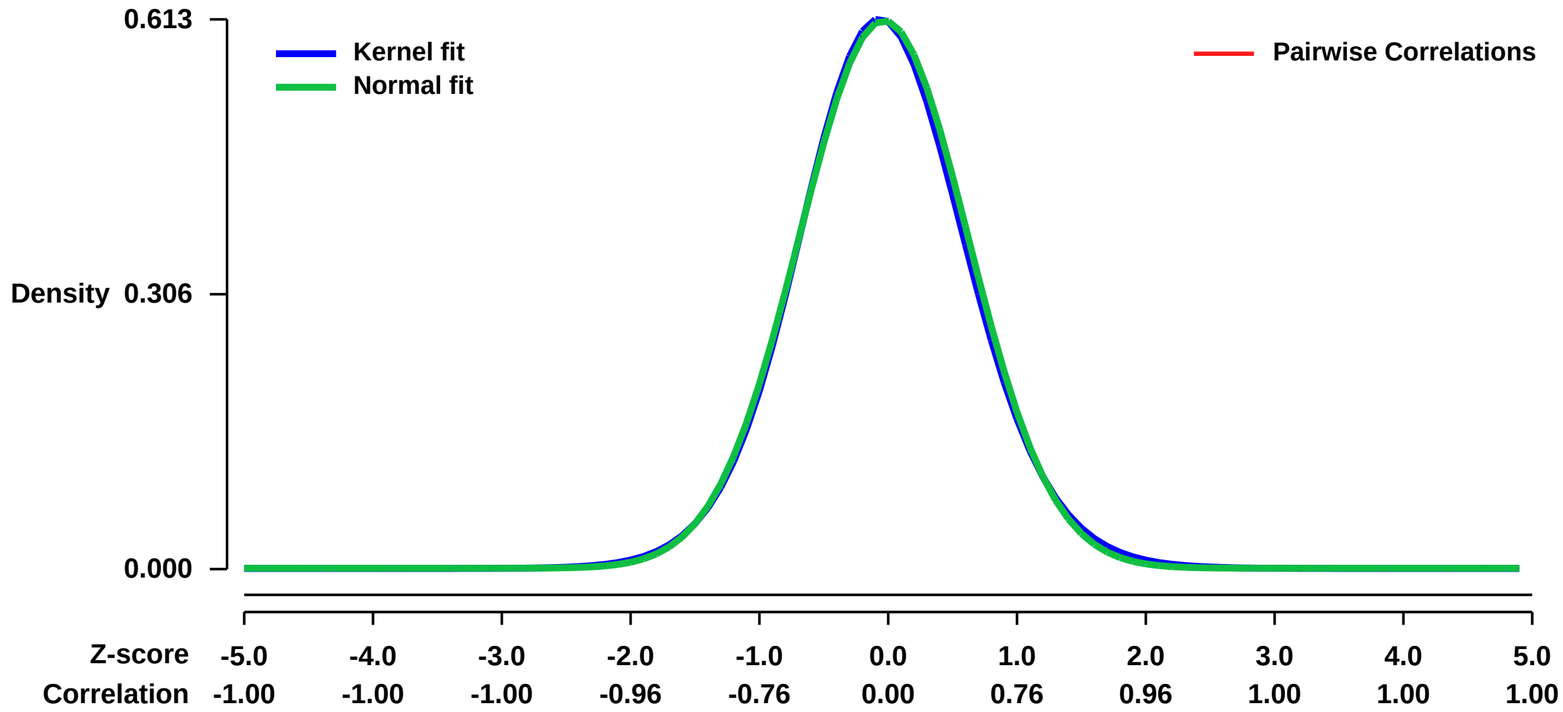

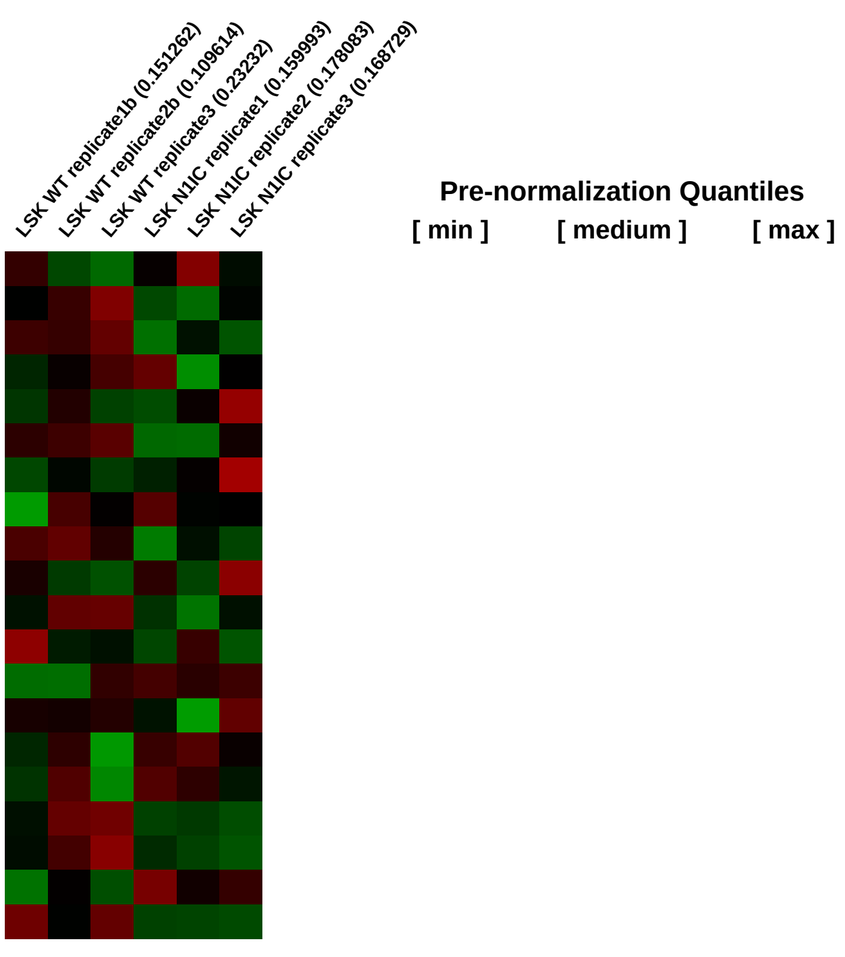

GEO Series "GSE22034" Expression Profiles

Num of samples in this series: 8

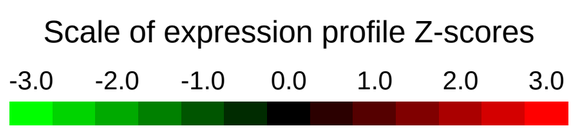

GEO Link:	http://www.ncbi.nlm.nih.gov/geo/query/acc.cgi?acc=GSE22034
Status:	Public on Jun 16 2012
Title:	Transcriptional profiling of ex vivo isolated mouse blood vascular and lymphatic endothelial cells
Organism:	Mus musculus
Experiment type:	Expression profiling by array
Platform:	GPL1261
Pubmed ID:	22723300
Summary & Design:	**Summary:** The lymphatic vascular system plays important roles in the maintenance of interstitial fluid pressure, the afferent immune response and the absorption of dietary lipids. However, the molecular mechanisms that control lymphatic vessel network maturation and function remain largely unknown. To identify novel players in lymphatic vessel function, we isolated pure populations of lymphatic and blood vascular endothelial cells from mouse intestine using fluorescence-activated high-speed cell sorting and performed transcriptional profiling. We found that the axonal guidance molecules semaphorin 3A (Sema3A) and Sema3D were specifically expressed by lymphatic vessels. Quantitative PCR of ex vivo isolated cells and immunohistochemical analysis confirmed these results. Importantly, we found that the semaphorin receptor neuropilin-1 (Nrp-1) is expressed on the valves of collecting lymphatic vessels. Treatment of mice in utero (E12.5-E16.5) with an antibody that blocks Sema3A binding to Nrp-1, but not with an antibody that blocks VEGFA binding to Nrp-1, resulted in abnormal development of collecting lymphatic vessels and valves, and aberrant smooth muscle cell coverage. Conversely, Sema3A-deficient mice displayed branching defects of collecting lymphatic vessels as well as impaired valve development. Together, these results reveal an unanticipated role of Sema3A/Nrp-1 signaling in the maturation of the lymphatic vascular network. **Overall design:** Colon single-cell suspensions were prepared by a fast protocol that minimizes the RNA degradation. Fluorescence-activated cell sorting (FACS) was used to sort blood vascular endothelial cells (BEC) and lymphatic endothelial cells (LEC). 4 animal-matched pairs of LEC and BEC were chosen based on the quality of extracted and amplified material to provide homogenous groups of biological replicates. This gave 8 samples to analyze. Samples present LEC and BEC isolated from 4 healthy normal mice. The 4 mice used present the 4 biological replicates.

Background corr dist: KL-Divergence = 0.1053, L1-Distance = 0.0915, L2-Distance = 0.0169, Normal std = 0.4951

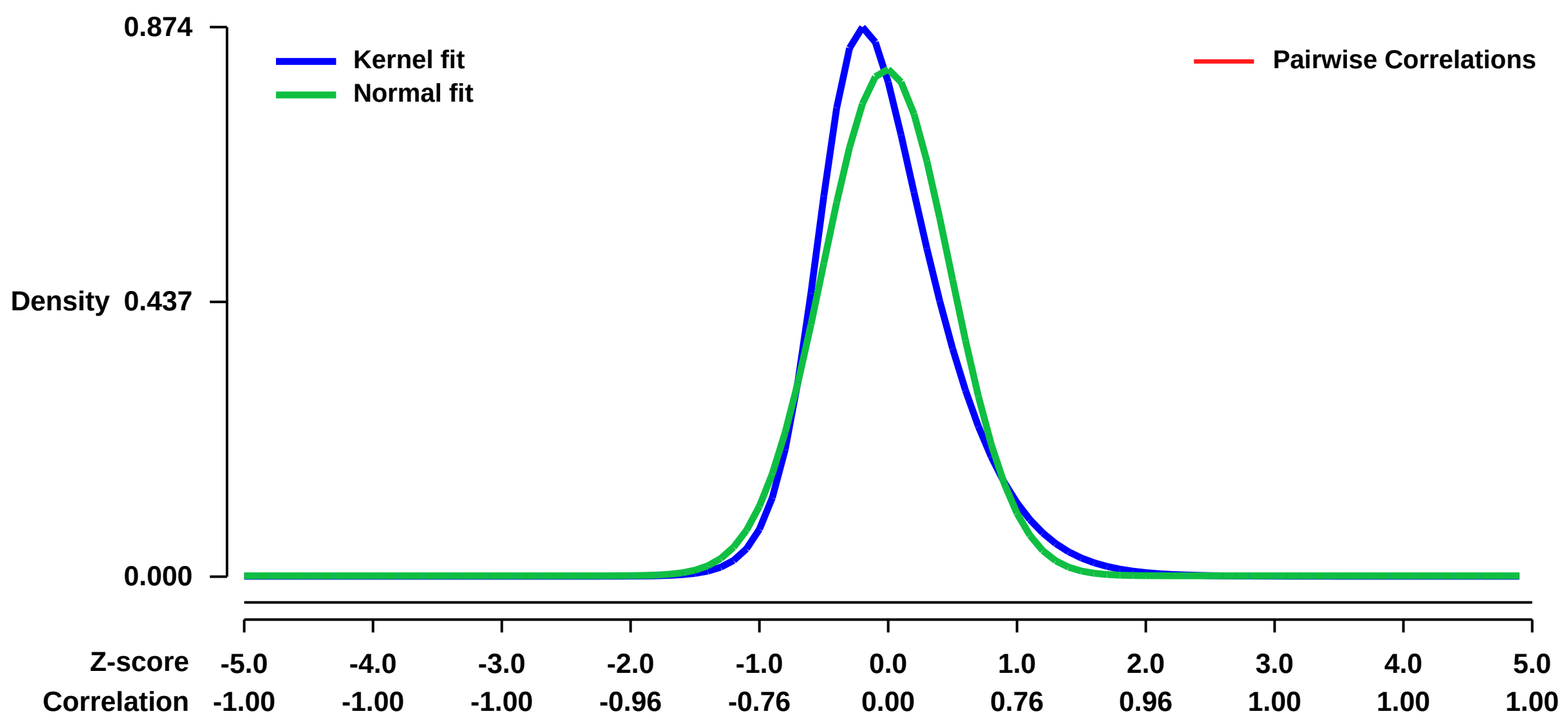

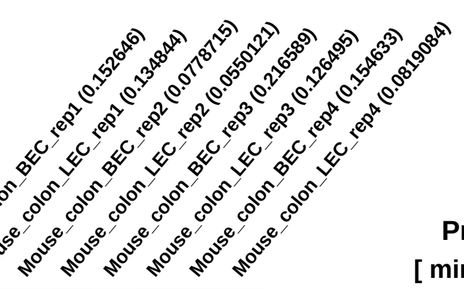

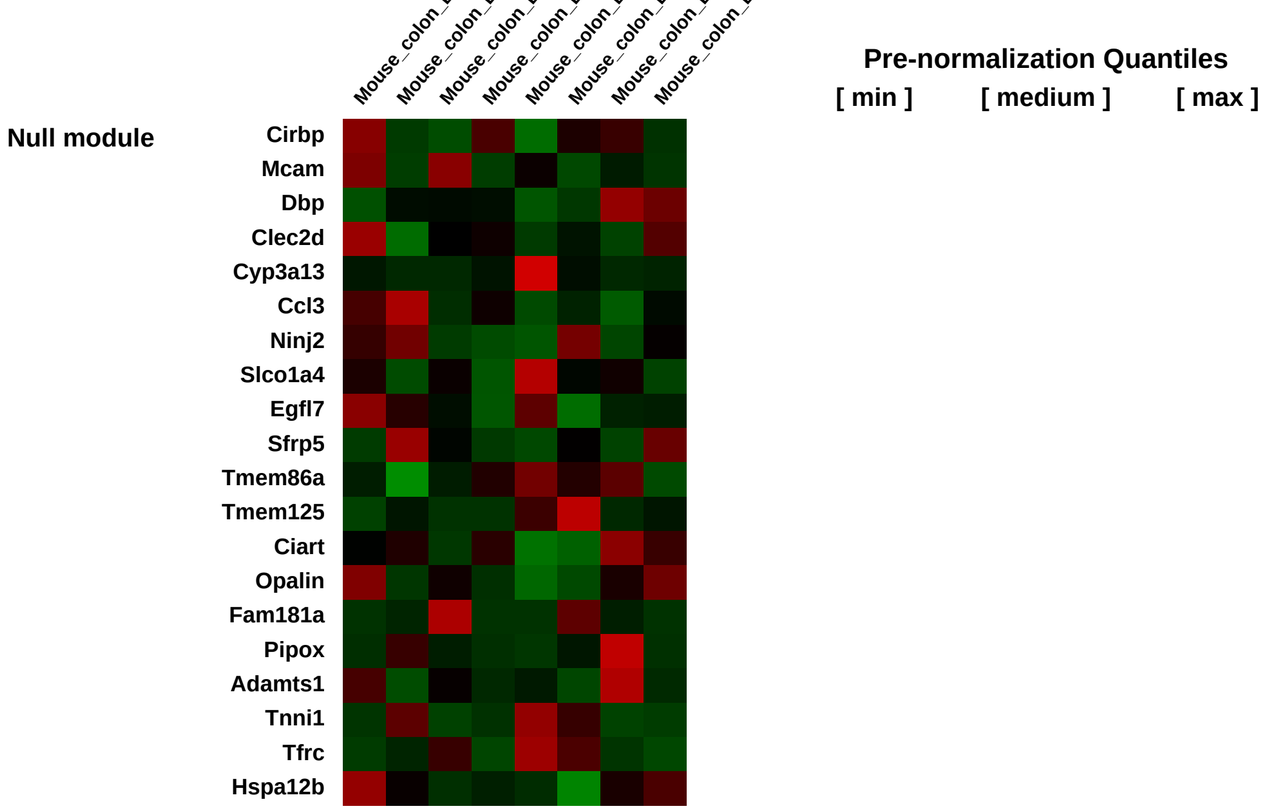

GEO Series "GSE24775" Expression Profiles

Num of samples in this series: 48

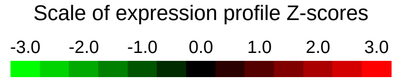

GEO Link:	http://www.ncbi.nlm.nih.gov/geo/query/acc.cgi?acc=GSE24775
Status:	Public on Dec 02 2010
Title:	Genome-wide expression analysis of the mouse pars tuberalis (PT) under chronic short-day and long-day conditions
Organism:	Mus musculus
Experiment type:	Expression profiling by array
Platform:	GPL1261
Pubmed ID:	21129973
Summary & Design:	**Summary:** Living organisms detect seasonal changes in day length (photoperiod), and alter their physiological functions accordingly, to fit seasonal environmental changes. This photoperiodic system is implicated in seasonal affective disorders and the season-associated symptoms observed in bipolar disease and schizophrenia. Thyroid-stimulating hormone beta subunit (Tshb), induced in the pars tuberalis (PT), plays a key role in the pathway that regulates animal photoperiodism. However, the upstream inducers of Tshb expression remain unknown. Here we show that late-night light stimulation acutely triggers the Eya3-Six1 pathway, which directly induces Tshb expression. Using melatonin-proficient CBA/N mice, which preserve the photoperiodic Tshb-expression response, we performed a genome-wide expression analysis of the PT under chronic short-day and long-day conditions. These data comprehensively identified long-day and short-day genes, and indicated that late-night light stimulation induces long-day genes. We verified this by advancing and extending the light period by 8 hours, which acutely induced Tshb expression, within one day. In a genome-wide expression analysis under this condition, we searched for candidate upstream genes by looking for expression that preceded Tshbâ s, and identified Eya3 gene. These results elucidate the comprehensive transcriptional photoperiodic response in the PT, revealing the complex regulation of Tshb expression and unexpectedly rapid response to light changes in the mammalian photoperiodic system. **Overall design:** Mice were separated into 2 groups. One group was maintained under the short-day conditions (light: dark = 8 h:16 h, ZT0 = lights on, ZT8 = lights off, 400 lux) and the other was housed under long-day conditions (light:dark = 16 h:8 h, ZT0 = lights on, ZT16 = lights off, 400 lux) for 2 weeks. The PTs of both groups were retrieved every 4 h for 1 day (6 time points for each group), starting at ZT0. For the experiments performed during the first day of the long-day conditions, we applied two different conditions, following 3 weeks under short-day conditions. In one, the light-onset was advanced by 8 hours (advance condition), and in the other, the dark period was delayed by 8 hours (delay condition). PTs from both groups were obtained every 4 h for 1 day, starting at the lights-on time. (Lights on for the advance condition was ZT16 as defined by the short-day condition. Lights on for the delay condition was ZT0). We sampled 25 mice at each time point. This whole procedure was repeated twice (n = 2) to obtain experimental replicates.

Background corr dist: KL-Divergence = 0.1963, L1-Distance = 0.0481, L2-Distance = 0.0054, Normal std = 0.3344

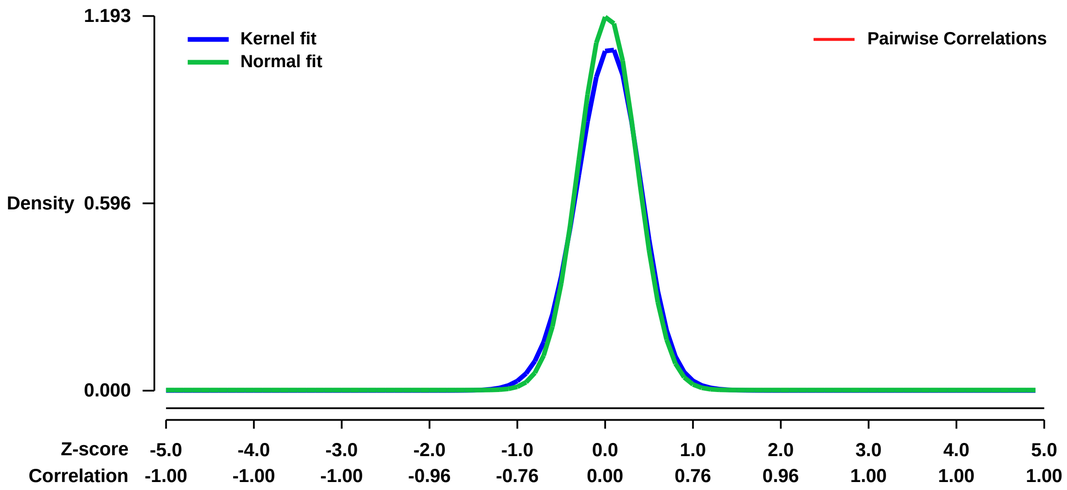

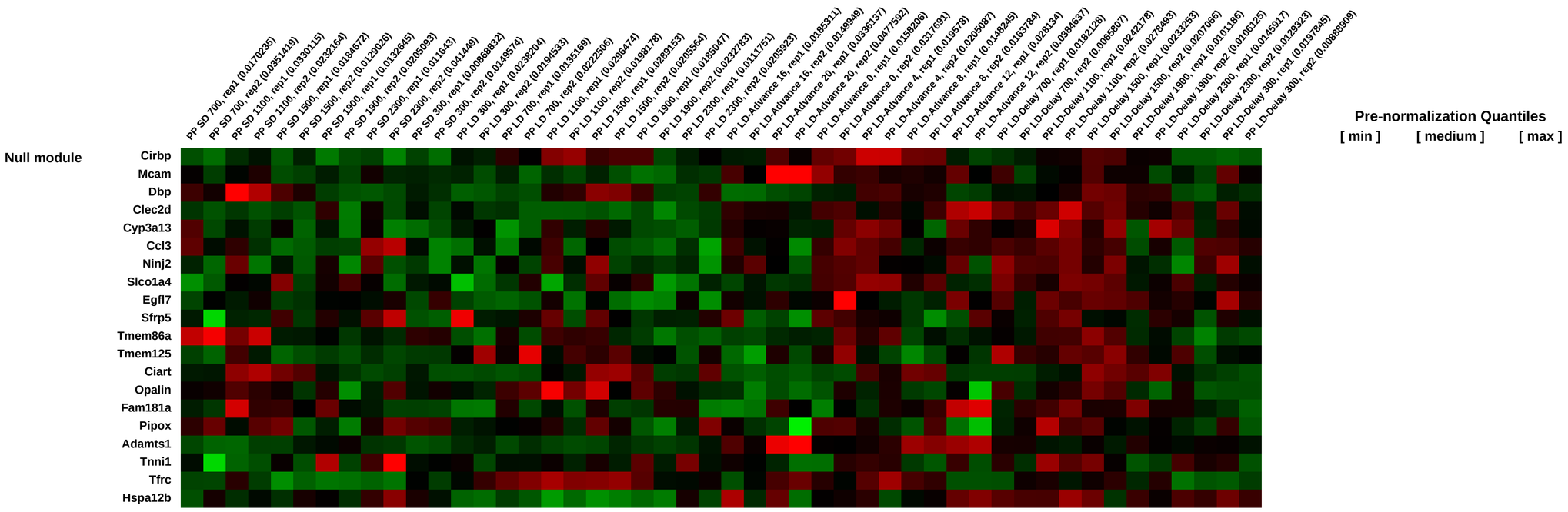

GEO Series "GSE48397" Expression Profiles

Num of samples in this series: 10

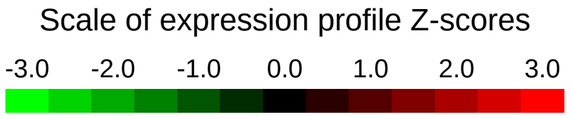

GEO Link:	http://www.ncbi.nlm.nih.gov/geo/query/acc.cgi?acc=GSE48397
Status:	Public on Jul 10 2013
Title:	Expression data from (mouse) normal lung fibroblasts and carcinoma-associated fibroblasts
Organism:	Mus musculus
Experiment type:	Expression profiling by array
Platform:	GPL1261
Pubmed ID:	22962265
Summary & Design:	**Summary:** Cancer-associated fibroblasts (CAFs) have been reported to support tumor progression by a variety of mechanisms. However, their role in the progression of non-small cell lung cancer (NSCLC) remains poorly defined. In addition, the extent to which specific proteins secreted by CAFs contribute directly to tumor growth is unclear. To study the role of CAFs in NSCLC, a cross-species functional characterization of mouse and human lung CAFs was performed, including gene expression analysis comparing normal mouse lung fibroblasts (NFs) and mouse lung CAFs to seek for differentially-expressed secreted proteins. Gene expression microarrays were used to identify transcriptomic changes between NFs and CAFs that may contribute to their different tumor-enhancing capacity. **Overall design:** NFs and CAFs were grown in vitro for RNA extraction and hybridization on mouse 430_2 Affymetrix microarrays

Background corr dist: KL-Divergence = 0.0594, L1-Distance = 0.0233, L2-Distance = 0.0009, Normal std = 0.5290

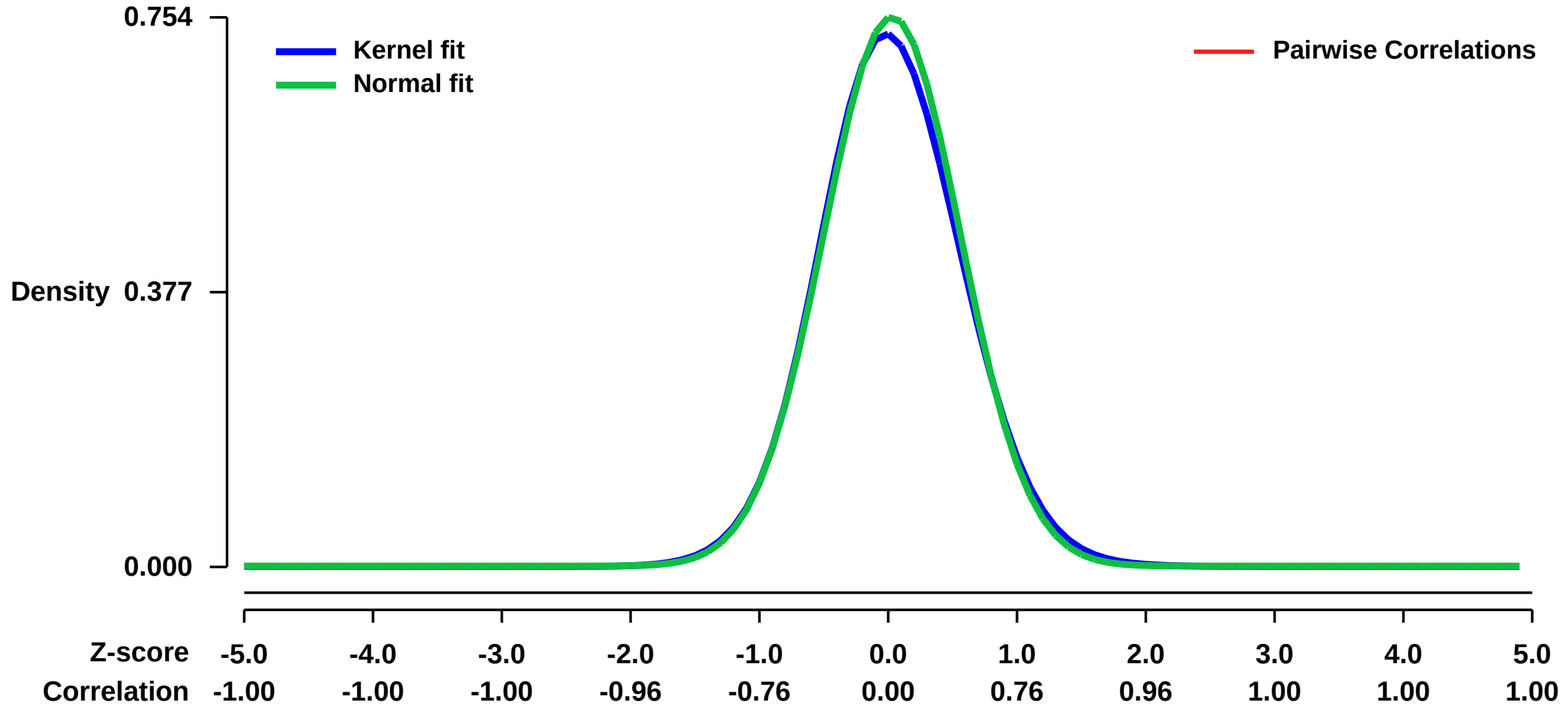

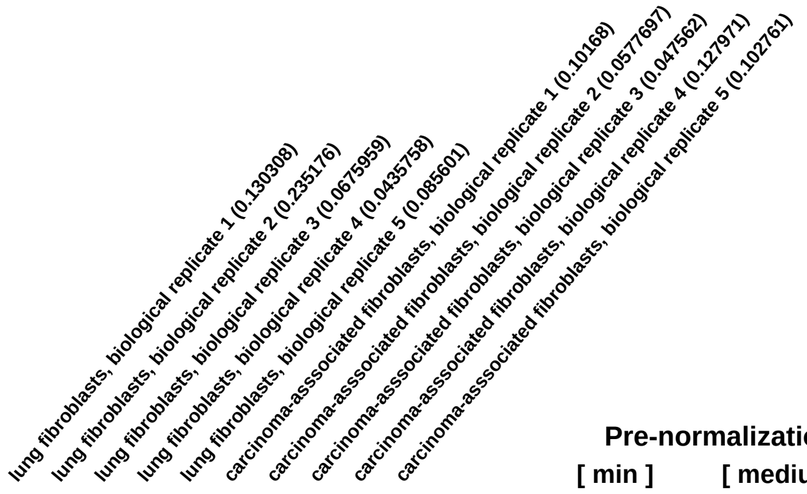

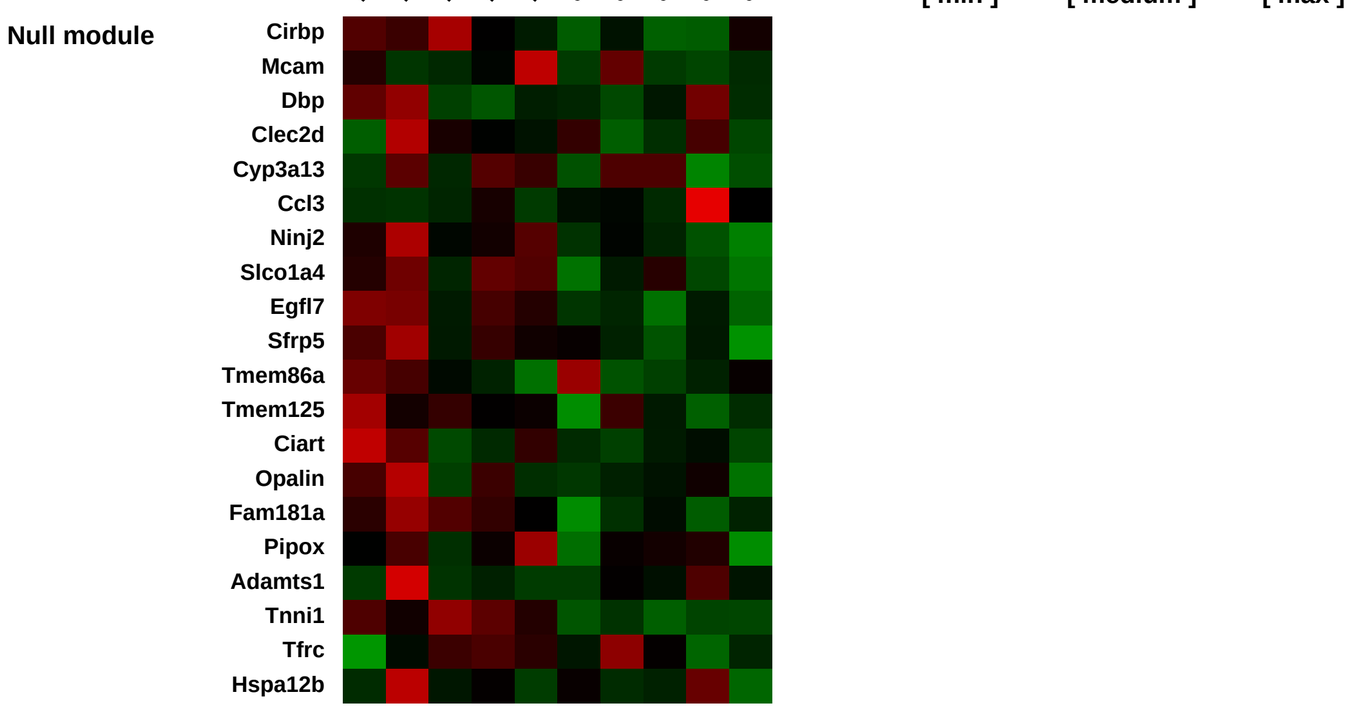

GEO Series "GSE6980" Expression Profiles

Num of samples in this series: 16

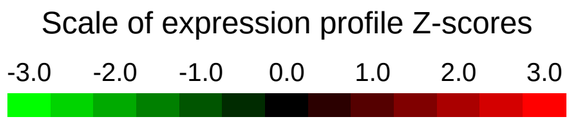

GEO Link:	http://www.ncbi.nlm.nih.gov/geo/query/acc.cgi?acc=GSE6980
Status:	Public on Apr 09 2007
Title:	The Differentiation and Stress Response Factor, XBP-1, Drives Multiple Myeloma Pathogenesis
Organism:	Mus musculus
Experiment type:	Expression profiling by array
Platform:	GPL1261
Pubmed ID:	17418411
Summary & Design:	**Summary:** Multiple myeloma (MM) evolves from highly prevalent premalignant condition termed Monoclonal Gammopathy of Undetermined Significance (MGUS). We report an MGUS-MM phenotype arising in transgenic mice with Emu-directed expression of the unfolded protein/ER stress response and plasma cell development spliced isoform factor XBP-1s. Emu-XBP-1s elicited elevated serum Ig and IL-6 levels, skin alterations and with advancing age, a significant proportion of Emu-xbp-1s transgenic mice develop features diagnostic of human MM including bone lytic lesions. Transcriptional profiles of Emu-xbp-1s B lymphoid and MM cells show aberrant expression of genes known to be dysregulated in human MM including Cyclin D1, MAF, MAFB, and APRIL. This genetic model coupled with documented frequent XBP-1s overexpression in human MM serve to implicate chronic XBP-1s dysregulation in the development of this common and lethal malignancy. **Keywords:** XBP-1, MGUS, multiple myeloma, transgenic mouse **Overall design:** We performed expression analysis of B cells derived from the spleen of 20-week old Emu-xbp-1s mice (n=5) and non-transgenic mice (n=5). Additionally, we analyzed the expression profiles from MM tumor cells arising in Emu-xbp-1s mice (n=6).

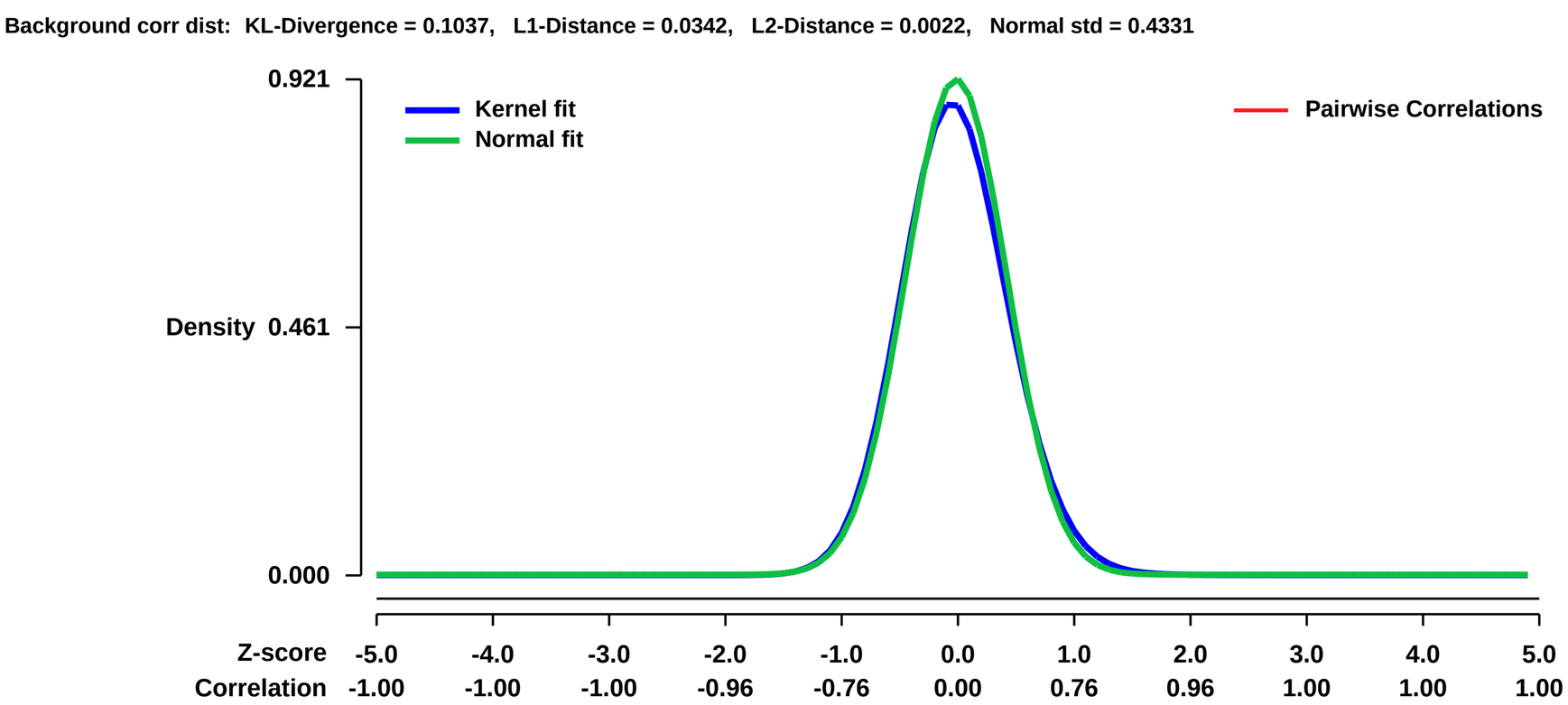

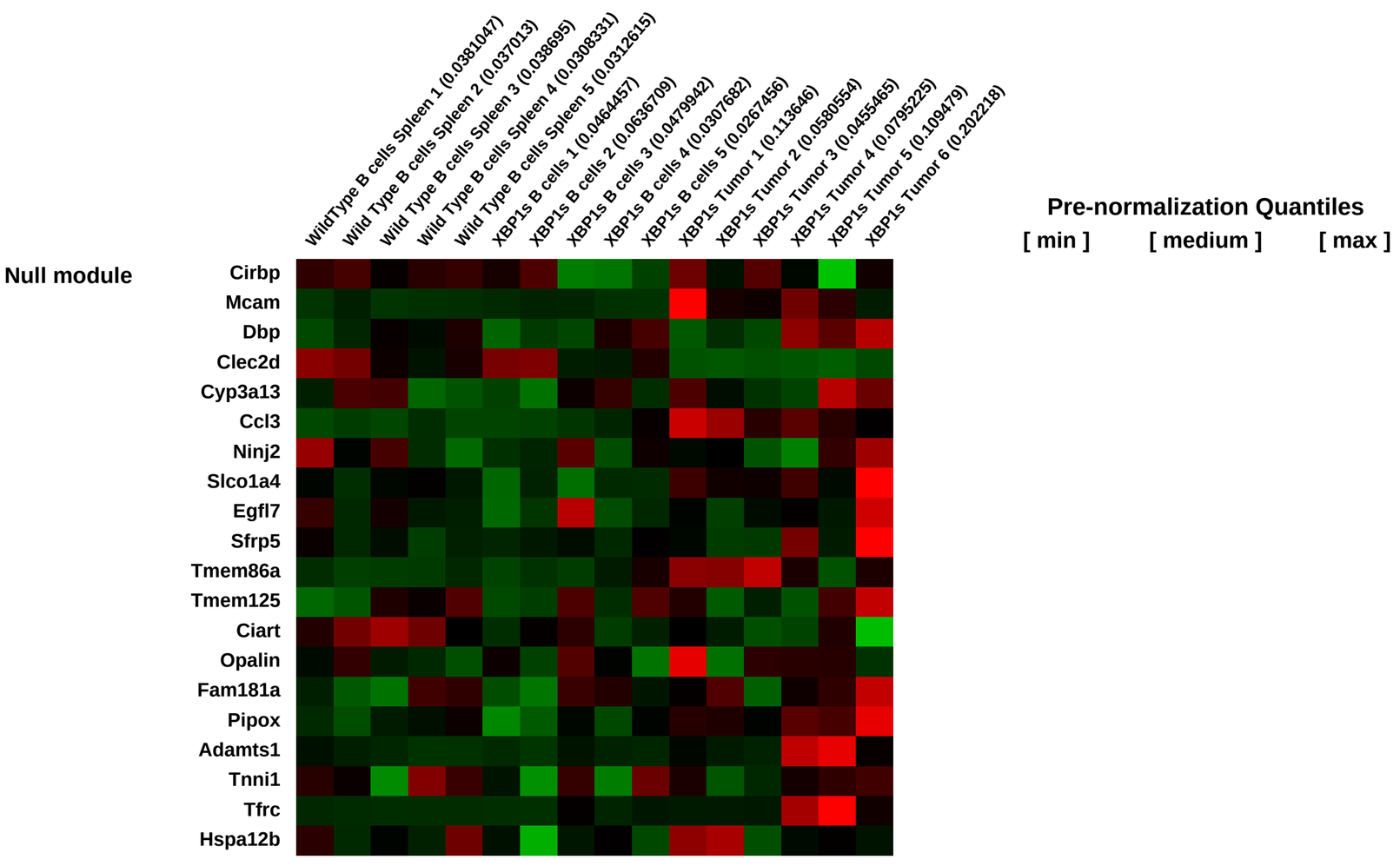

GEO Series "GSE28644" Expression Profiles

Num of samples in this series: 60

Scale of expression profile Z-scores

-3.0 -2.0 -1.0 0.0 1.0 2.0 3.0

GEO Link:	http://www.ncbi.nlm.nih.gov/geo/query/acc.cgi?acc=GSE28644
Status:	Public on Aug 31 2011
Title:	Gene Expression Data Following Chronic Vehicle or Fluoxetine Treatment in Thirty Mouse Inbred Lines
Organism:	Mus musculus
Experiment type:	Expression profiling by array
Platform:	GPL1261
Pubmed ID:	22113448
Summary & Design:	**Summary:** In order to understand how biochemical and genetic differences correlate with treatment response, we measured depressive-like behavior, gene expression and the levels of thirty-six neurobiochemical analytes across a panel of genetically-diverse mouse inbred lines after chronic treatment with vehicle or fluoxetine. Neurobiochemical markers were chosen based on their putative molecular function within pathways proposed to underlie depression, which include neuronal transmission, HPA-axis regulation, and neuroimmune processes. The goal of this study is to establish genetic and biochemical biomarkers that can predict treatment response and to propose a molecular pathway that is critical in mediating anti-depressant response. **Overall design:** Thirty mouse inbred strains (129S1/SvImJ, A/J, AKR/J, BALB/cJ, BTBRT T(+) tf/J, BUB/BnJ, C3H/HeJ, C57BL/6J, C57BLKS/J, C57BR/cdJ, C58/J, CBA/J, CE/J, DBA/2J, FVB/NJ, I/LnJ, LG/J, LP/J, MA/MyJ, MRL/MpJ, NOD/LtJ, NOR/LtJ, NZB/BINJ, NZW/LacJ, P/J, PL/J, RIIIS/J, SJL/J, SM/J, and SWR/J) aged 5-6 weeks old were obtained from The Jackson Laboratory (Bar Harbor, ME). Male mice were kept in polycarbonate cages on a 12-hour light/dark cycle (lights on at 0700h) with access to food and water ad libitum. Following one week of habituation, mice were randomized to either control or treatment group (n=12 male mice per strain per treatment group). Mean water intake for each strain was determined previously by measuring daily water consumption for three weeks (n=12 mice per strain). This information, along with average weight measurements for each strain, was used to determine the amount of fluoxetine required to provide a daily oral dose of 0 or 18 mg/kg per mouse. After chronic administration of 0 or 18 mg/kg of fluoxetine for 21 days, mice aged 9-10 weeks were tested in a tail-suspension and open field apparatus. Upon completion of the study, mice were sacrificed by cervical dislocation and decapitation between 0900h and 1300h. Trunk blood was quickly collected and allowed to clot on ice. Following centrifugation, serum samples were collected and stored at -20C for determination of fluoxetine and norfluoxetine levels using liquid chromatography-mass spectrometry/mass spectrometry (LC-MS/MS). Micro-dissections of individual regions were performed on serial coronal brain sections (approximately 10 ´µm) that were placed on a cold metal block. Cortex was taken from the same section for each animal and immediately snaps frozen on dry ice. Samples were stored at -80C until analysis.

Background corr dist: KL-Divergence = 0.3730, L1-Distance = 0.0800, L2-Distance = 0.0212, Normal std = 0.2917

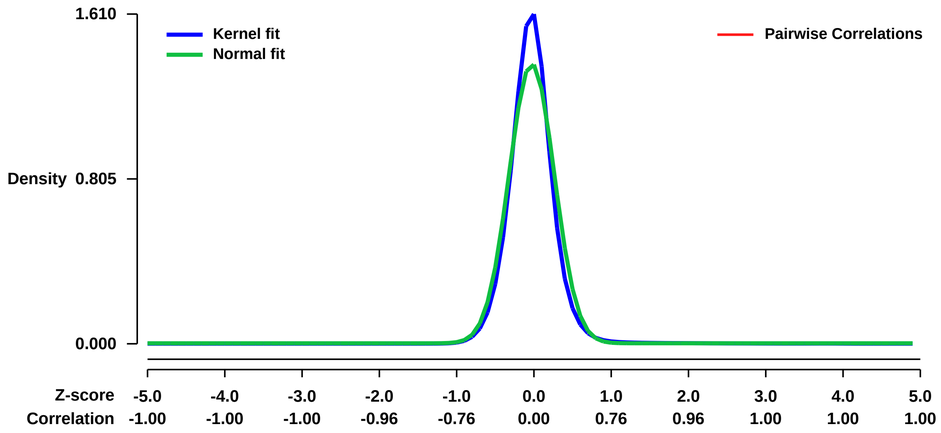

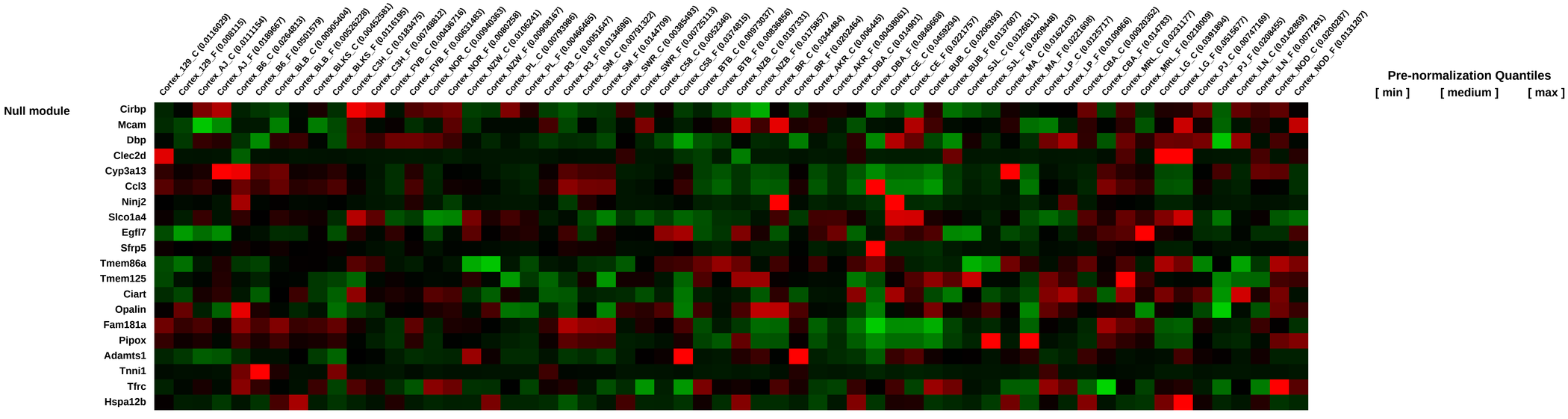

GEO Series "GSE11201" Expression Profiles

Num of samples in this series: 18

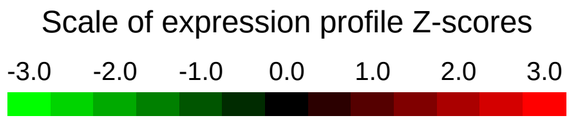

GEO Link:	**http://www.ncbi.nlm.nih.gov/geo/query/acc.cgi?acc=GSE11201**
Status:	**Public on Apr 18 2008**
Title:	**Coordinated Regulation of Signaling Pathways and Biological Processes during Liver Development**
Organism:	**Mus musculus**
Experiment type:	**Expression profiling by array**
Platform:	**GPL1261**
Pubmed ID:	
Summary & Design:	**Summary:** **Understanding congenital liver disease requires elucidation of the signaling pathways and transcriptional events in the developing liver. Comprehensive assessment of gene expression between 10.5 and 16.5 dpc in the developing mouse liver and comparison with adult liver and non-hepatic embryonic tissue was validated with real-time PCR and in situ hybridization. The broad nature of the analysis provides insights into patterns of genetic control of hepatogenesis. Pathways implicated in human disease are highly regulated at the transcriptional level. Rather than activating or inhibiting a pathway or biological process by altering the expression of a single signaling molecule, transcriptional changes in large numbers of genes in a pathway or process are regulated in a coordinated manner. For example, both TGF-beta and Notch signaling is inhibited during hepatogenesis not just by decreasing transcription of multiple pathway members, but also with a complementary increase in the transcription of a pathway inhibitor. Similarly, genes related to specific biological processes exhibit strong temporal synchronization in which multiple members of the pathway have similar transcriptional regulation over time. Global coordination of signaling or functional families at the transcriptional level may be a mechanism to produce robustness of the desired outcomes. In addition, this comprehensive analysis provides a database for the further study of transcriptional events during liver development by identifying liver-specific, highly regulated genes.** **Keywords: time course** **Overall design:** **In order to provide transcriptional profile of the developing liver compared both to normal adult liver and non-hepatic embryonic tissueswe performed high-density microarray analysis using Affymetrix MG 430 2.0 chips for embryonic liver samples at 10.5, 11.5, 12.5, 13.5, 14.5, and 16.5 days post conception (dpc), embryo-minus liver tissues at 10.5, 11.5, 12.5, and 14.5 dpc, and normal 10-week-old adult mouse liver. Each sample consisted of at least five embryos.**

Background corr dist: **KL-Divergence = 0.0374, L1-Distance = 0.0354, L2-Distance = 0.0018, Normal std = 0.6265**

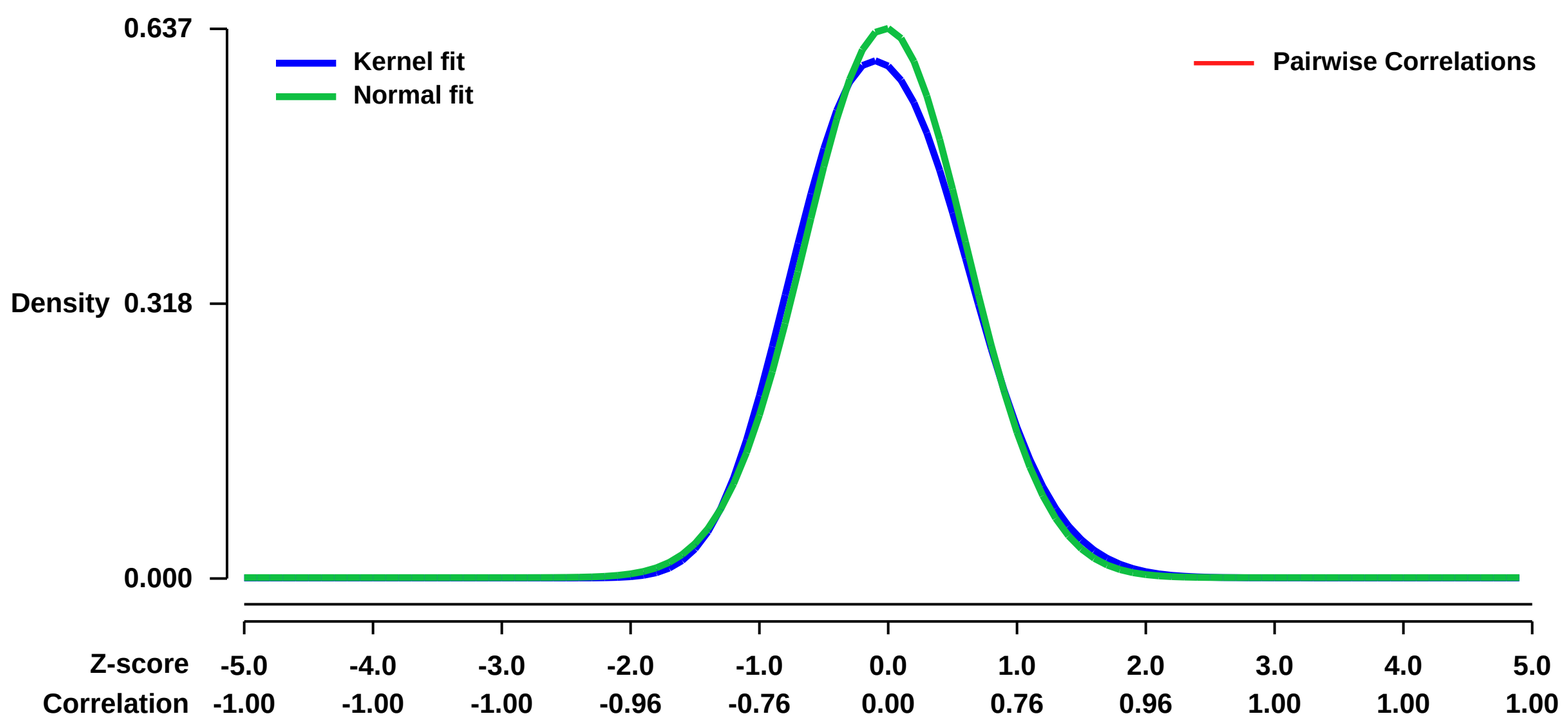

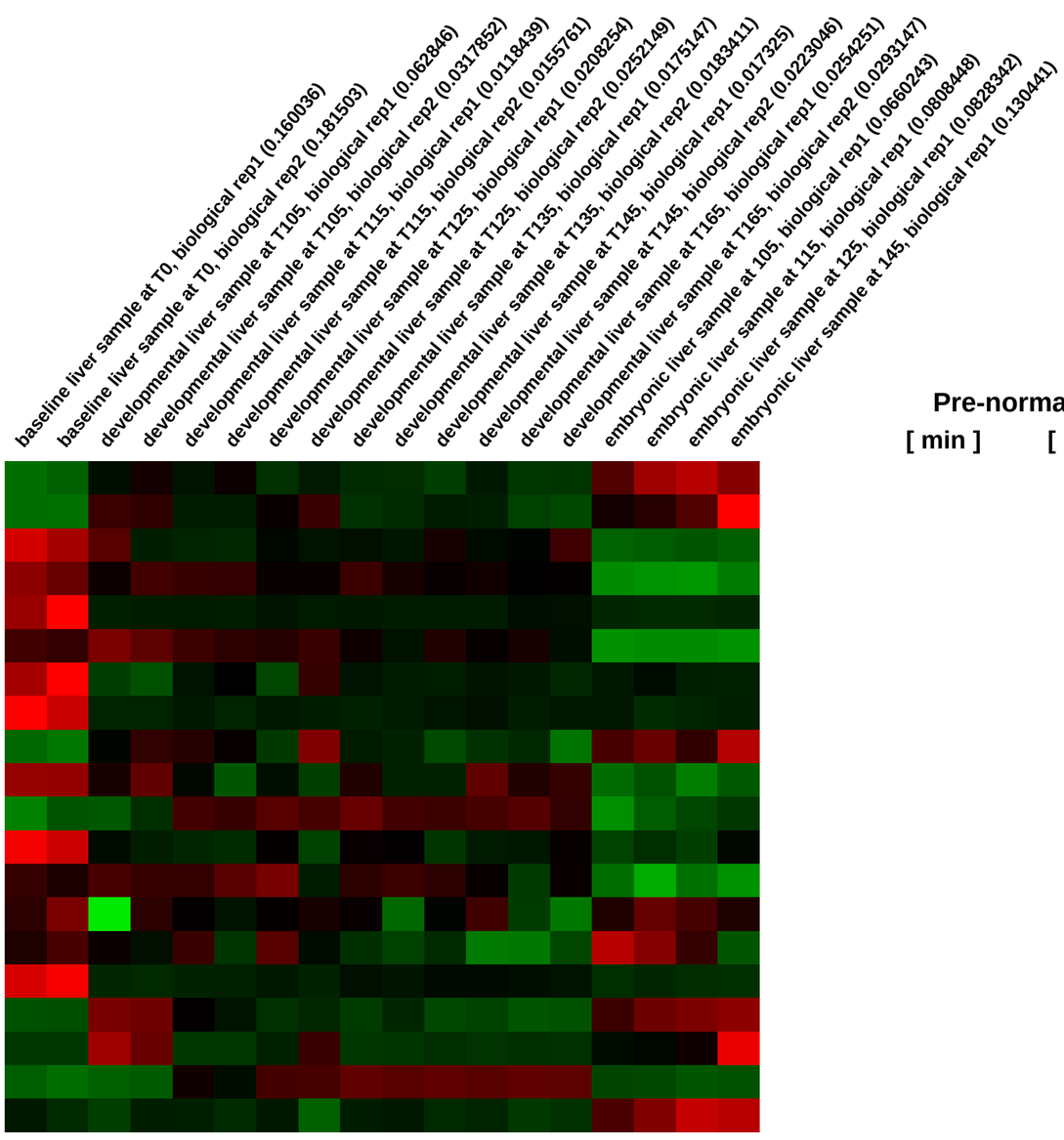

GEO Series "GSE29929" Expression Profiles

Num of samples in this series: 14

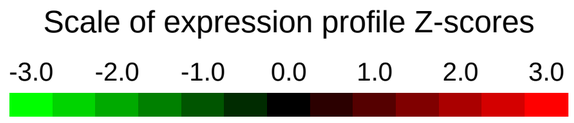

GEO Link:	http://www.ncbi.nlm.nih.gov/geo/query/acc.cgi?acc=GSE29929
Status:	Public on Jan 20 2012
Title:	The eIF2 kinase PERK and the integrated stress response facilitate activation of ATF6 during endoplasmic reticulum stress
Organism:	Mus musculus
Experiment type:	Expression profiling by array
Platform:	GPL1261
Pubmed ID:	21917591
Summary & Design:	**Summary:** Disruptions of the endoplasmic reticulum (ER) that perturb protein folding cause ER stress and elicit an unfolded protein response (UPR) that involves translational and transcriptional changes in gene expression aimed at expanding the ER processing capacity and alleviating cellular injury. Three ER stress sensors PERK, ATF6, and IRE1 implement the UPR. PERK phosphorylation of eIF2 during ER stress represses protein synthesis, which prevents further influx of ER client proteins, along with preferential translation of ATF4, a transcription activator of the integrated stress response. In this study we show that the PERK/eIF2¸–~P/ATF4 pathway is required not only for translational control, but also activation of ATF6 and its target genes. The PERK pathway facilitates both the synthesis of ATF6 and trafficking of ATF6 from the ER to the Golgi for intramembrane proteolysis and activation of ATF6. As a consequence, liver-specific depletion of PERK significantly reduces both the translational and transcriptional phases of the UPR, leading to reduced protein chaperone expression, disruptions of lipid metabolism, and enhanced apoptosis. These findings show that the regulatory networks of the UPR are fully integrated, and helps explain the diverse pathologies associated with loss of PERK. **Overall design:** Comparison of gene expression profiles for treated vs control in wildtype and knock-out.

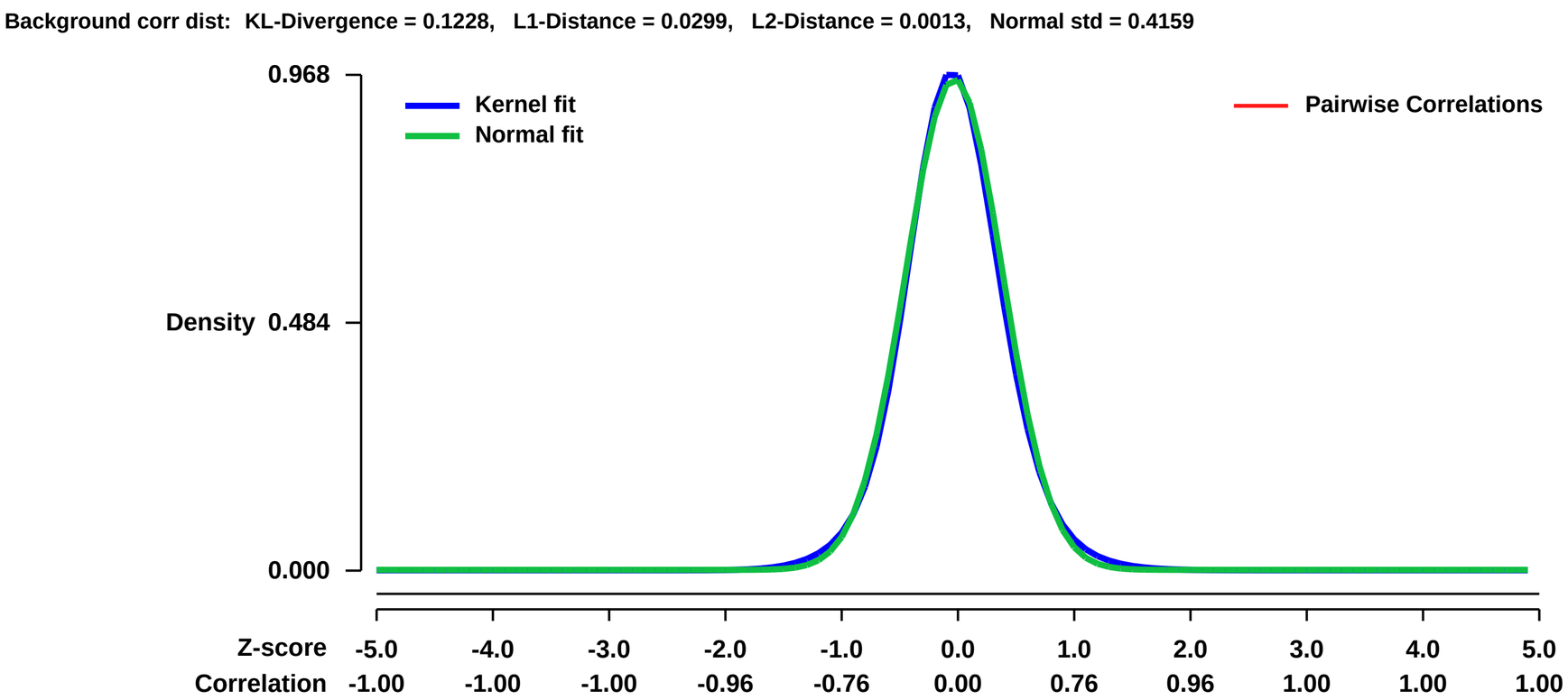

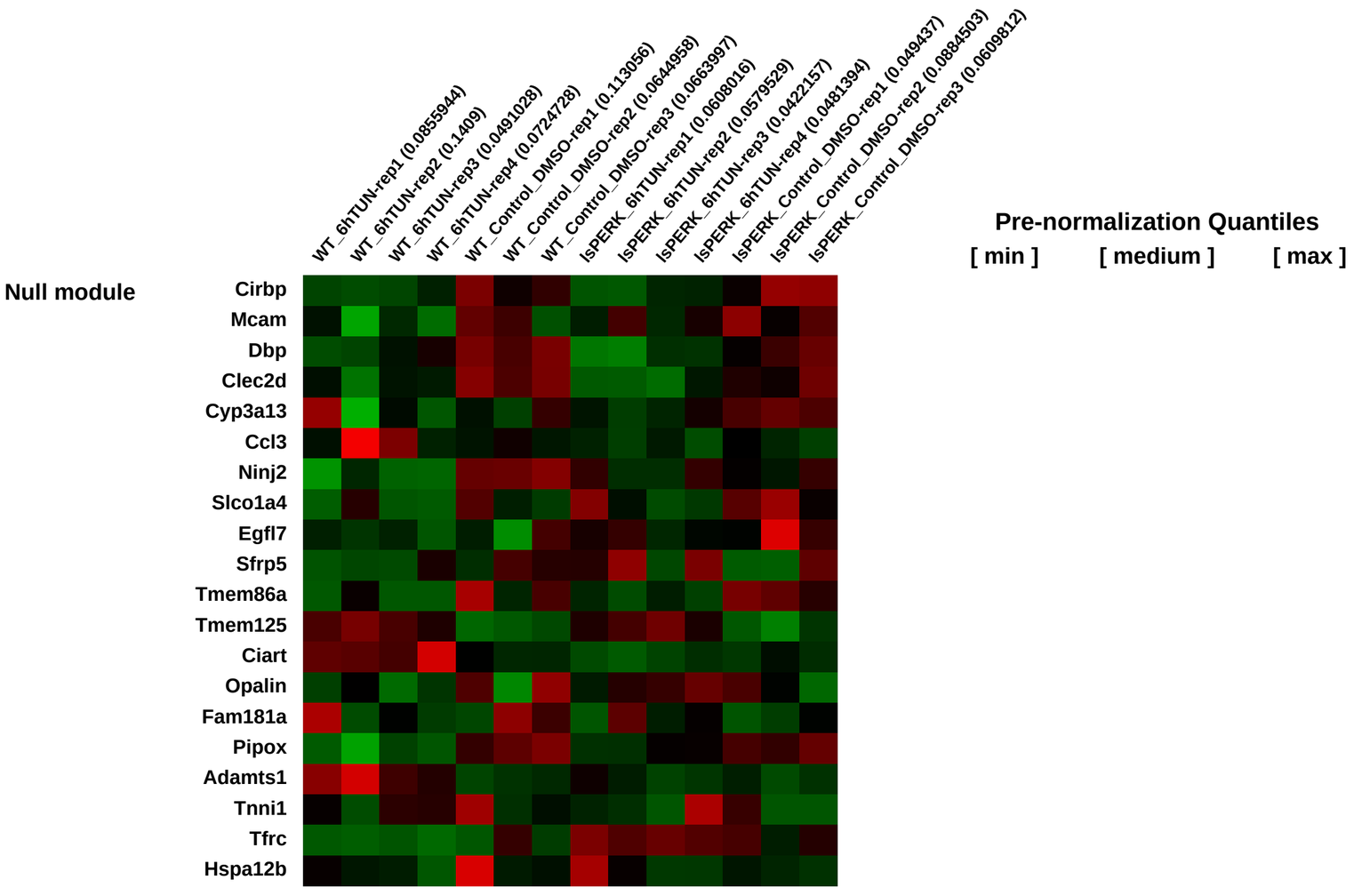

GEO Series "GSE10587" Expression Profiles

Num of samples in this series: 6

Scale of expression profile Z-scores

-3.0 -2.0 -1.0 0.0 1.0 2.0 3.0

GEO Link:	http://www.ncbi.nlm.nih.gov/geo/query/acc.cgi?acc=GSE10587
Status:	Public on Feb 19 2009
Title:	Gene expression in stria vascularis of mice lacking Slc26a4 and heterzygous controls before the onset of hearing.
Organism:	Mus musculus
Experiment type:	Expression profiling by array
Platform:	GPL1261
Pubmed ID:	
Summary & Design:	**Summary:** Determination of differential expression of genes in the stria vascularis of pendrin (Slc26a4) heterozygous and knockout mice before the onset of hearing at postnatal day 10 (P10). **Keywords:** differential expression under disease state **Overall design:** A total of Six samples of stria vascularis RNA obtained from P10 mice were analyzed. Triplicates from pendrin (Slc26a4) heterozygous and knockout mice were run and analyzed.

Background corr dist: KL-Divergence = 0.0370, L1-Distance = 0.0201, L2-Distance = 0.0004, Normal std = 0.6322

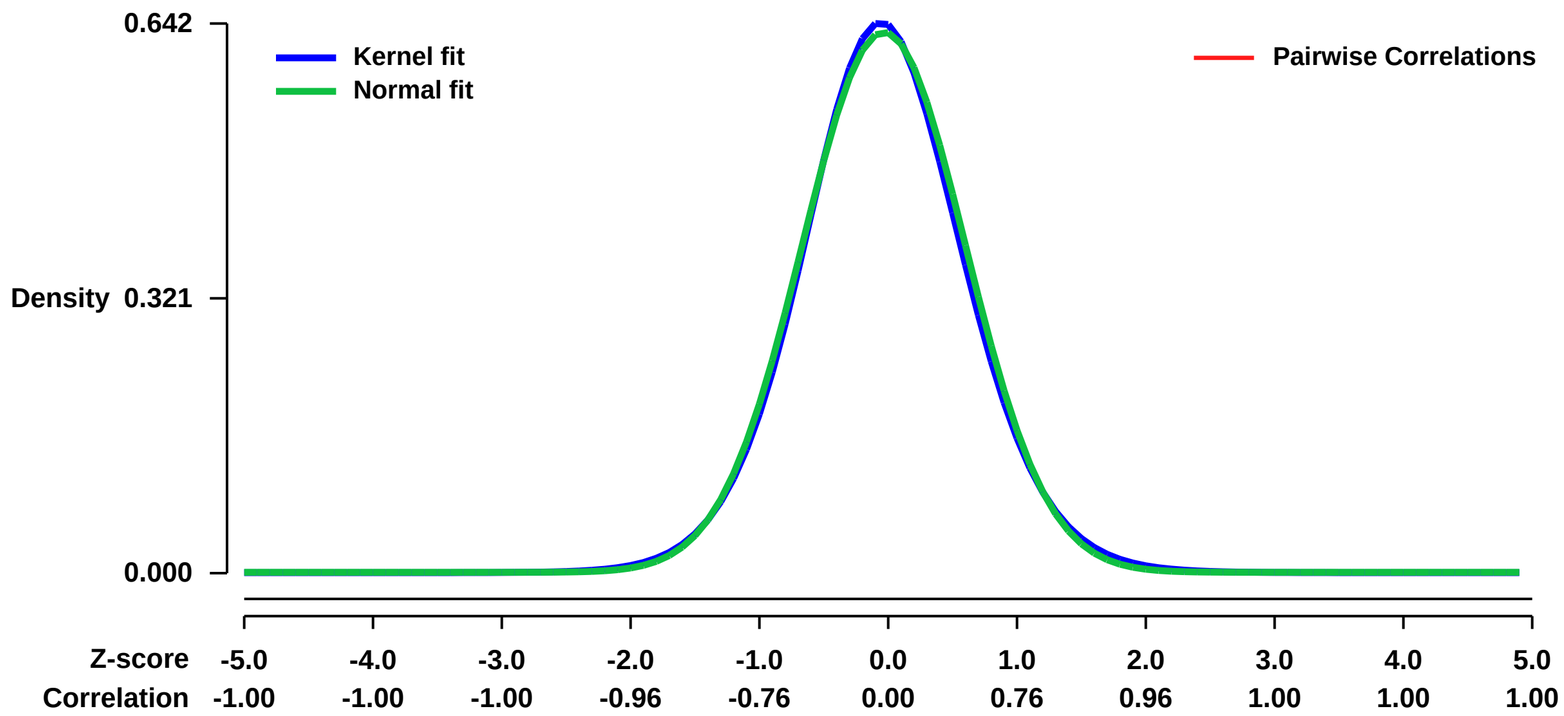

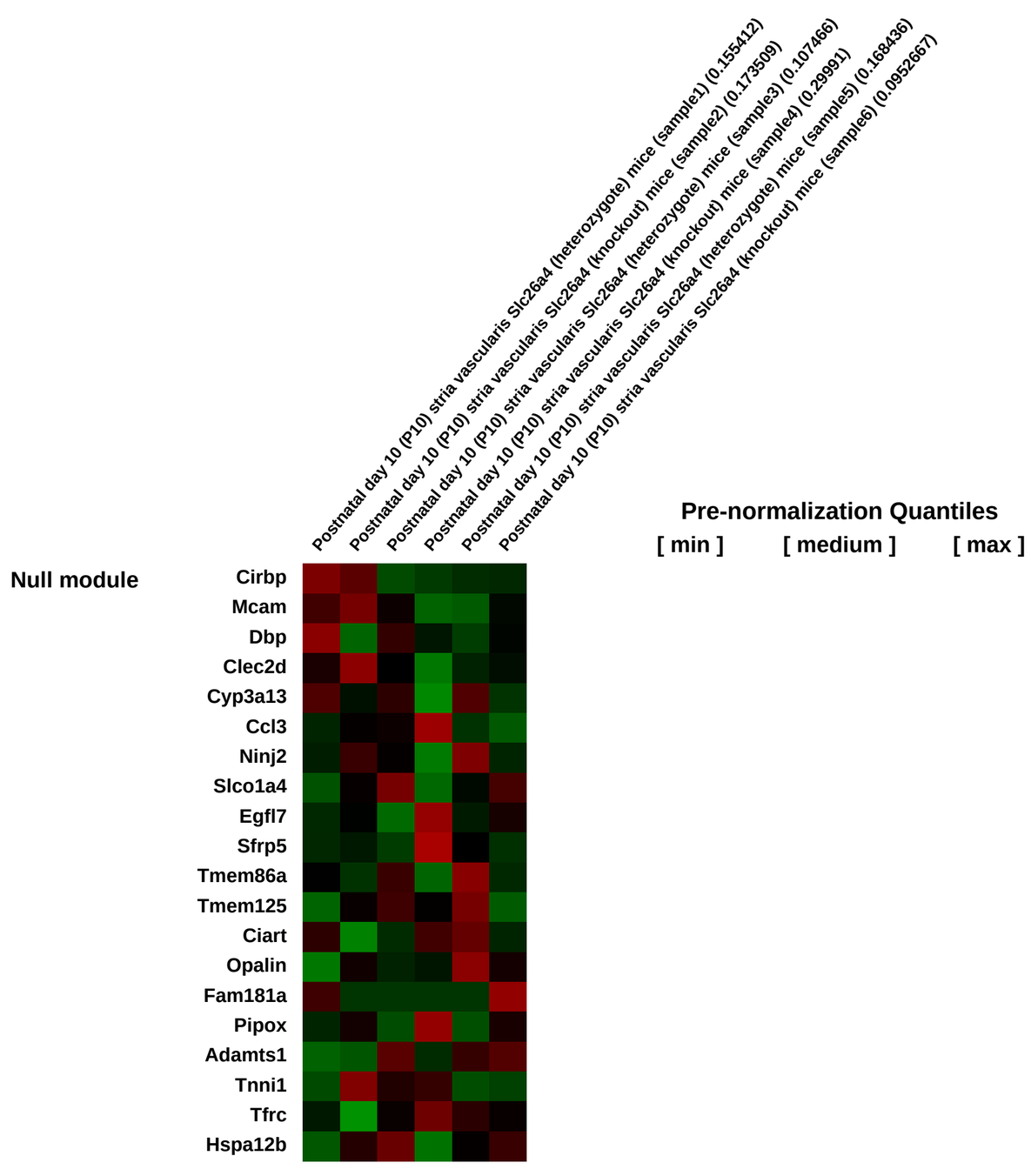

GEO Series "GSE29848" Expression Profiles

Num of samples in this series: 18

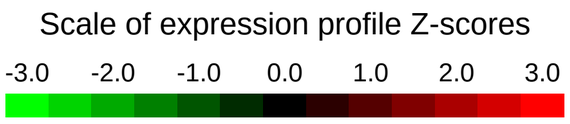

GEO Link:	http://www.ncbi.nlm.nih.gov/geo/query/acc.cgi?acc=GSE29848
Status:	Public on Jul 01 2011
Title:	Microarray data of differentiating embryonic stem cells overexpressing the transcription factor Msgn1
Organism:	Mus musculus
Experiment type:	Expression profiling by array
Platform:	GPL1261
Pubmed ID:	21750544
Summary & Design:	**Summary:** During mammalian gastrulation, pluripotent epiblast stem cells migrate through the primitive streak to form the multipotent progenitors of the mesoderm and endoderm germ layers. Msgn1 is a bHLH transcription factor and is a direct target gene of the Wnt/bcatenin signaling pathway. Msgn1 is expressed in the mesodermal compartment of the primitive streak and is necessary for the proper development of the mesoderm. Msgn1 mutants show defects in somitogenesis leading to a lack of trunk skeletal muscles, vertebra and ribs. To study the molecular and cellular function of Msgn1 in Embryonic Stem Cells (ESC), we have generated doxycycline inducible gain-of-function ESC to overexpress Msgn1 in ESC. In order to identify Msgn1 targets, we performed transcriptional profiling of Msgn1 expressing ES cells and found that upon induction of Msgn1, multiple genes in the Notch pathway were differentially expressed compared to the uninduced cells. Moreover, Whole Mount Insitu Hybridization analysis in Msgn1 null mutants revealed that these Notch pathway genes required Msgn1 for their proper expression in vivo. Our studies demonstrate that Msgn1 is a critical effector of the Wnt pathway during mammalian somitogenesis, mediating crosstalk between the Wnt and Notch pathways. **Overall design:** Inducible A2lox-Flag Msgn1 ES cells were differentiated to form Embryoid bodies (EBs) for 2 days. Flag-Msgn1 was induced on day 2 with doxycycline and samples were collected at three time points, 12h, 24h and 48h after addition of doxycycline. Uninduced cells were used as controls. Experiments were performed in triplicate

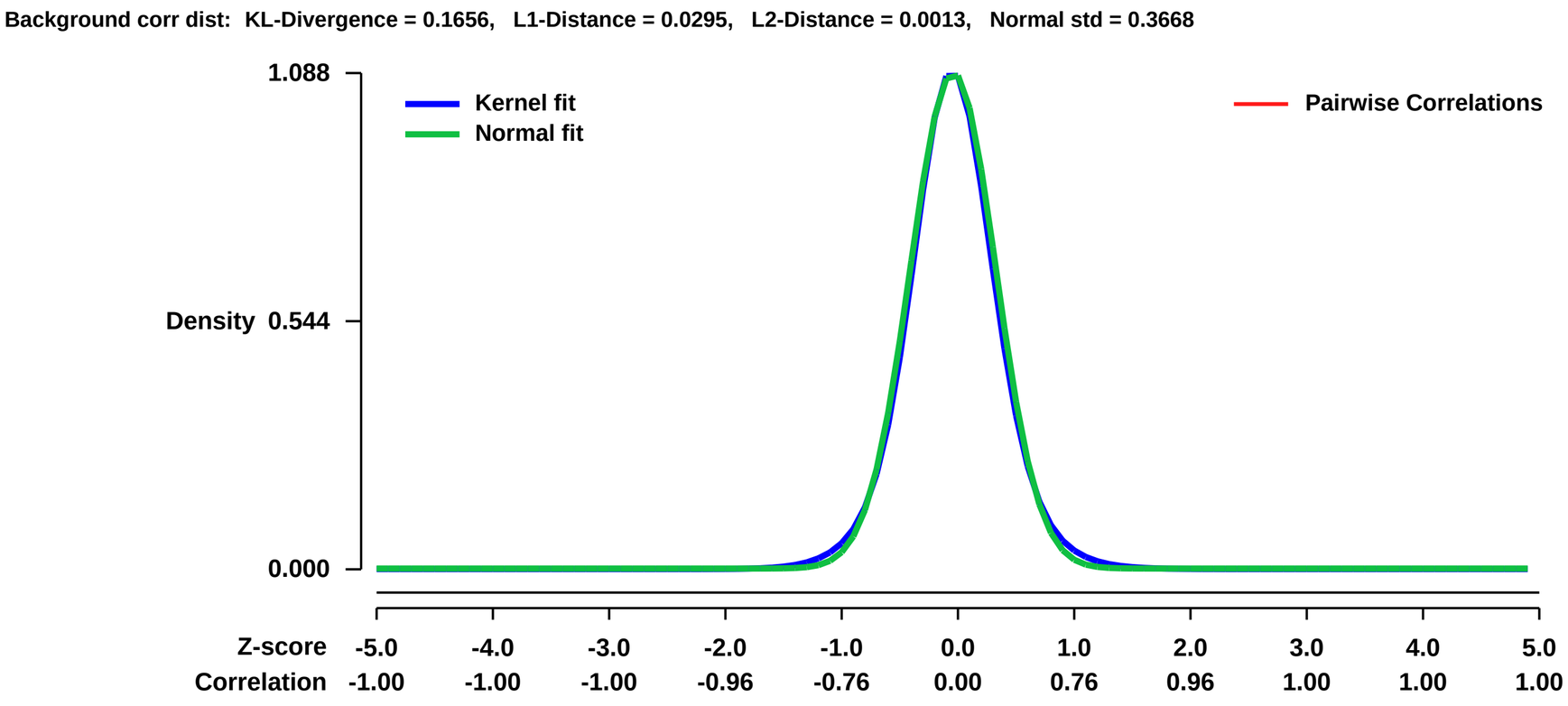

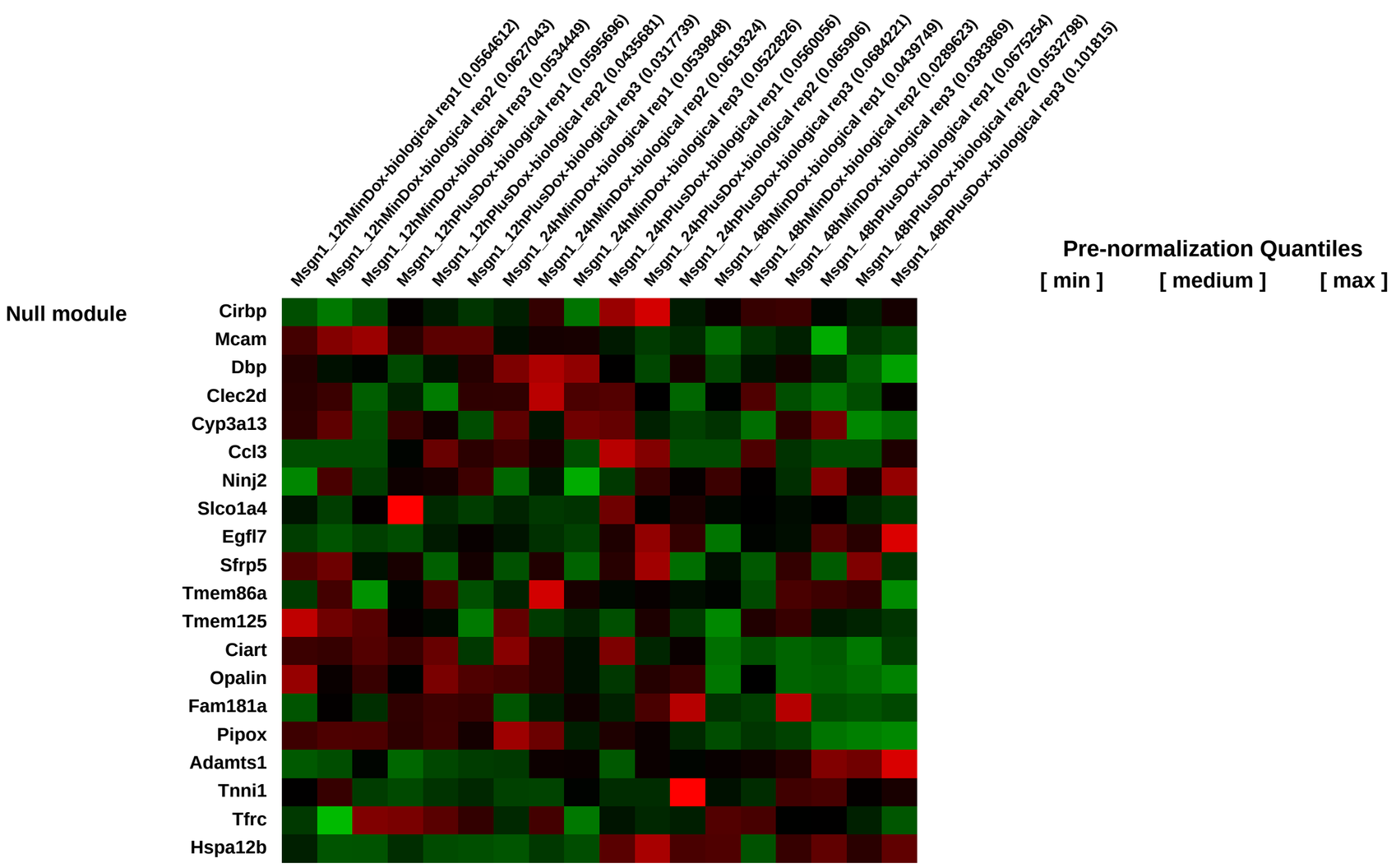

GEO Series "GSE38831" Expression Profiles

Num of samples in this series: 7

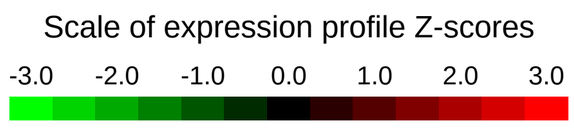

GEO Link:	http://www.ncbi.nlm.nih.gov/geo/query/acc.cgi?acc=GSE38831
Status:	Public on Dec 22 2013
Title:	Deciphering genomic alterations in colorectal cancer through transcriptional subtype-based network analysis
Organism:	Mus musculus
Experiment type:	Expression profiling by array
Platform:	GPL1261
Pubmed ID:	24260186
Summary & Design:	**Summary:** High-throughput genomic studies have identified thousands of genetic alterations in colorectal cancer (CRC). Distinguishing driver from passenger mutations is critical for developing rational therapeutic strategies. Because only a few transcriptional subtypes exist in previously studied tumor types, we hypothesize that highly heterogeneous genomic alterations may converge to a limited number of distinct mechanisms that drive unique gene expression patterns in different transcriptional subtypes. In this study, we defined transcriptional subtypes for CRC and identified driver networks/pathways for each subtype, respectively. Applying consensus clustering to a patient cohort with 1173 samples identified three transcriptional subtypes, which were validated in an independent cohort with 485 samples. The three subtypes were characterized by different transcriptional programs related to normal adult colon, early colon embryonic development, and epithelial mesenchymal transition, respectively. They also showed statistically different clinical outcomes. For each subtype, we mapped somatic mutation and copy number variation data onto an integrated signaling network and identified subtype-specific driver networks using a random walk-based strategy. We found that genomic alterations in the Wnt signaling pathway were common among all three subtypes; however, unique combinations of pathway alterations including Wnt, VEGF, Notch and TGF-beta drove distinct molecular and clinical phenotypes in different CRC subtypes. Our results provide a coherent and integrated picture of human CRC that links genomic alterations to molecular and clinical consequences, and which provides insights for the development of personalized therapeutic strategies for different CRC subtypes. **Overall design:** To characterize the embryonic development of colon, we conducted a time course microarray study using the inbred C57BL/6 (Jackson Laboratories, Bar Harbor, ME) mice. Seven samples corresponding to the mouse colonic development from E13.5 to E18.5 and adult (eight week post-natal) were collected. RNA samples were submitted to the Vanderbilt Functional Genomics Shared Resource (FSGR, http://array.mc.vanderbilt.edu), where RNA was hybridized to the Affymetrix Mouse Genome 430 2.0 GeneChip Expression Arrays (Santa Clara, CA) according to manufacturerâ s instructions. The RMA algorithm was used for data normalization. Mouse gene symbols were mapped to human gene symbols by the Human and Mouse Orthology list available from the Mouse Genome Informatics (http://www.informatics.jax.org/).

Background corr dist: KL-Divergence = 0.0290, L1-Distance = 0.0333, L2-Distance = 0.0015, Normal std = 0.7069

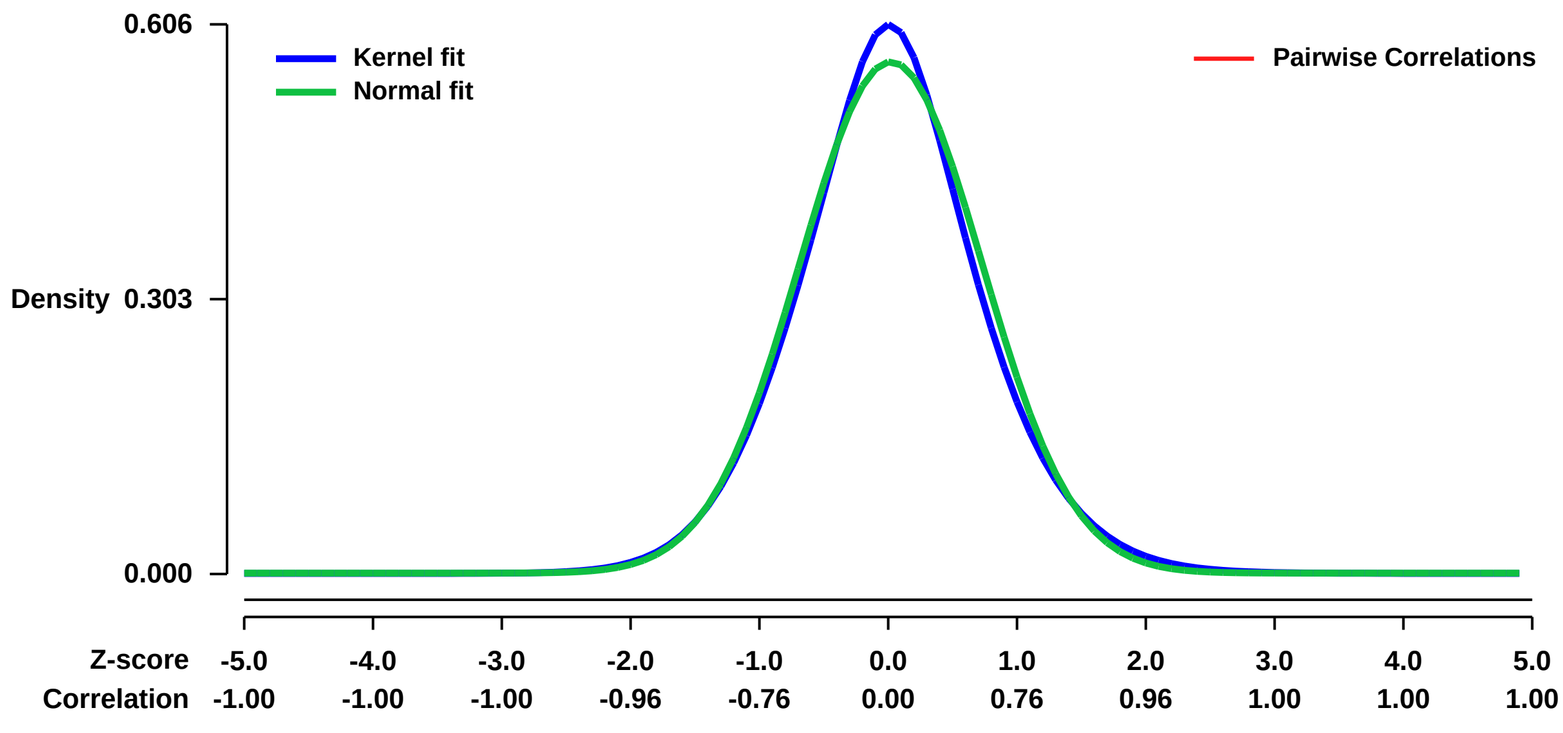

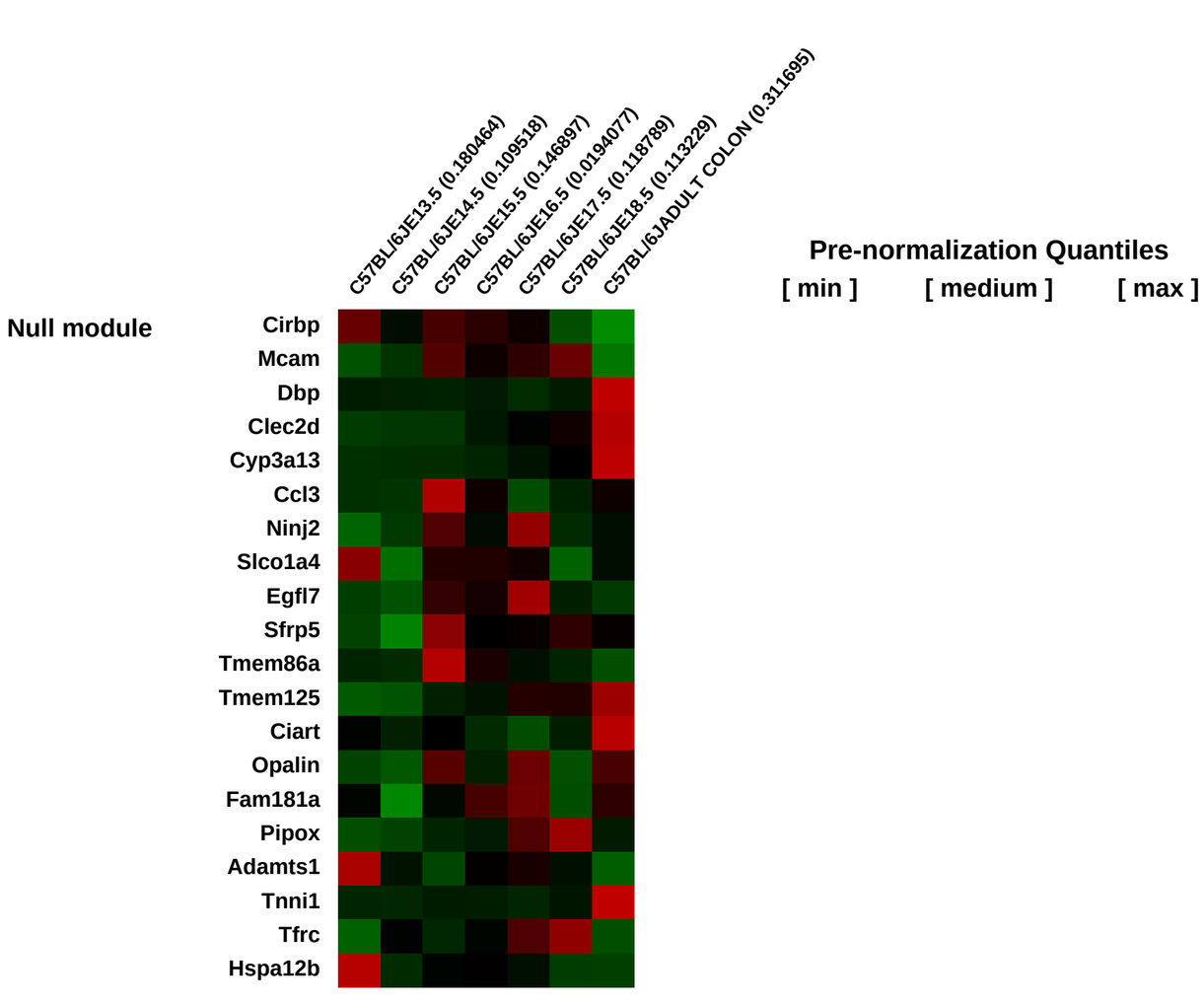

GEO Series "GSE16380" Expression Profiles

Num of samples in this series: 8

Scale of expression profile Z-scores

-3.0 -2.0 -1.0 0.0 1.0 2.0 3.0

GEO Link:	http://www.ncbi.nlm.nih.gov/geo/query/acc.cgi?acc=GSE16380
Status:	Public on Jan 28 2010
Title:	Gene expression analyses of C/EBPb knockout in stem/progenitor cell populations
Organism:	Mus musculus
Experiment type:	Expression profiling by array
Platform:	GPL1261
Pubmed ID:	20054865
Summary & Design:	**Summary:** CCAAT/enhancer binding protein beta (C/EBPb) is a member of a family of highly conserved transcription factors that regulates numerous genes involved in proliferation and differentiation in a variety of tissues. C/EBPb is deregulated in human breast cancer and germline deletion of this gene results in multiple defects in mammary gland development. We hypothesized that C/EBPb regulates mammary stem cell self-renewal, maintenance and/or differentiation through the regulation of multiple target genes that coordinate mammary gland development. Utilizing both a germline knockout mouse model and a conditional knockout strategy, we demonstrated that mammosphere formation was significantly decreased in C/EBPb-deficient mammary epithelial cells (MECs). The ability of C/EBPb-deleted MECs to regenerate the mammary gland in vivo was severely impaired when transplanted at limiting dilution. Furthermore, serial transplantation of C/EBPb-null mammary tissue resulted in decreased outgrowth potential when compared to wildtype, and an early senescence phenotype. Flow cytometric analysis revealed that C/EBPb-null MECs contain a lower frequency of repopulating stem cells accompanied by an increase in committed, differentiated luminal cells as compared to wildtype. Microarray analysis of stem/progenitor cell populations was performed and revealed an alteration in cell fate specification in C/EBPb-null glands, exemplified by the aberrant expression of basal markers in the luminal cell compartment. Collectively, our studies demonstrate that C/EBPb is a critical regulator of mammary stem cell differentiation, and an important determinant of luminal cell fate specification. **Keywords:** multiple group comparison **Overall design:** To identify potential signaling pathways regulated by C/EBPb in stem/progenitor cells, microarray analysis was performed on two stem/progenitor cell subpopulations. For this analysis, subpopulations defined by LIN-CD24+CD29hi and LIN-CD24hiCD29lo were FACS sorted from wildtype and germline C/EBPb-/- glands, and RNA was isolated from each group.

Background corr dist: KL-Divergence = 0.0627, L1-Distance = 0.0241, L2-Distance = 0.0009, Normal std = 0.5244

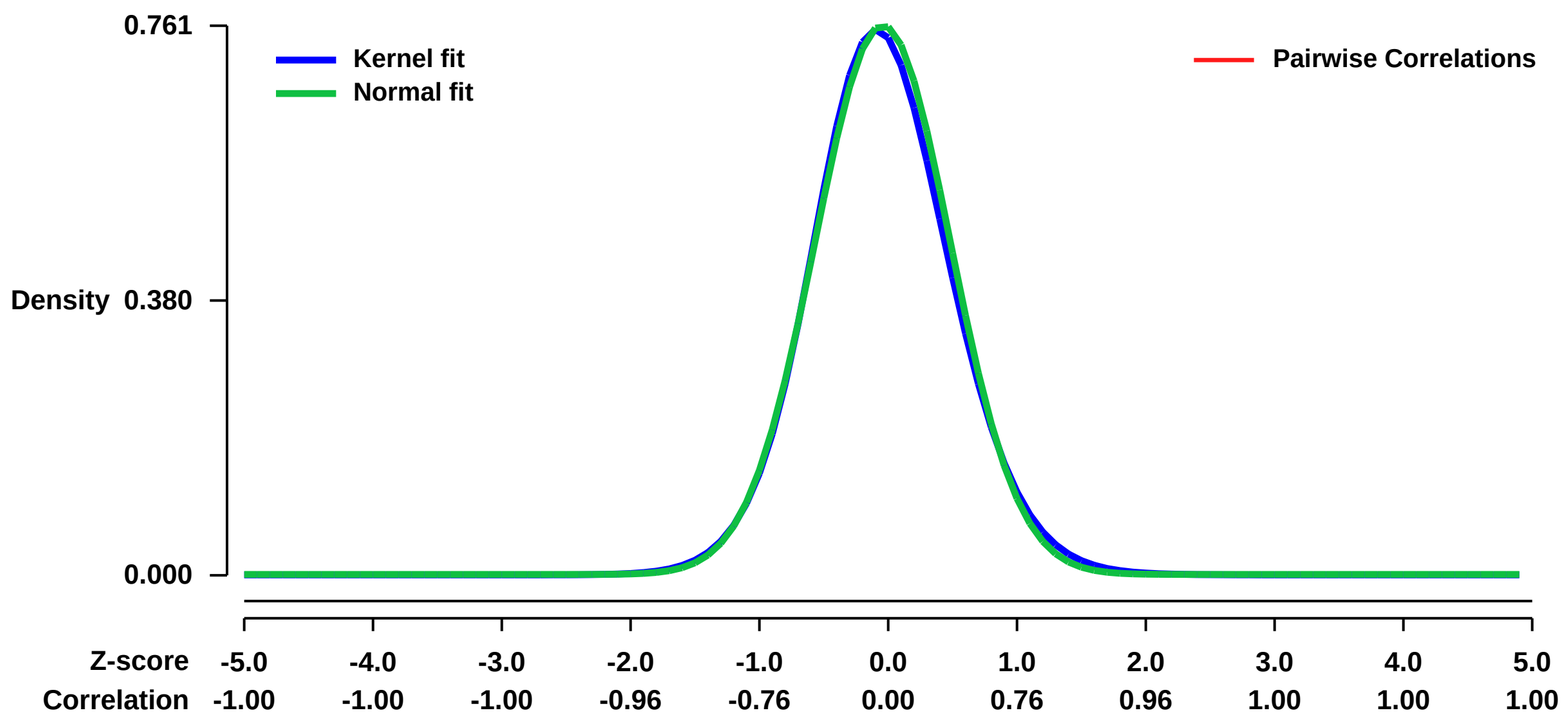

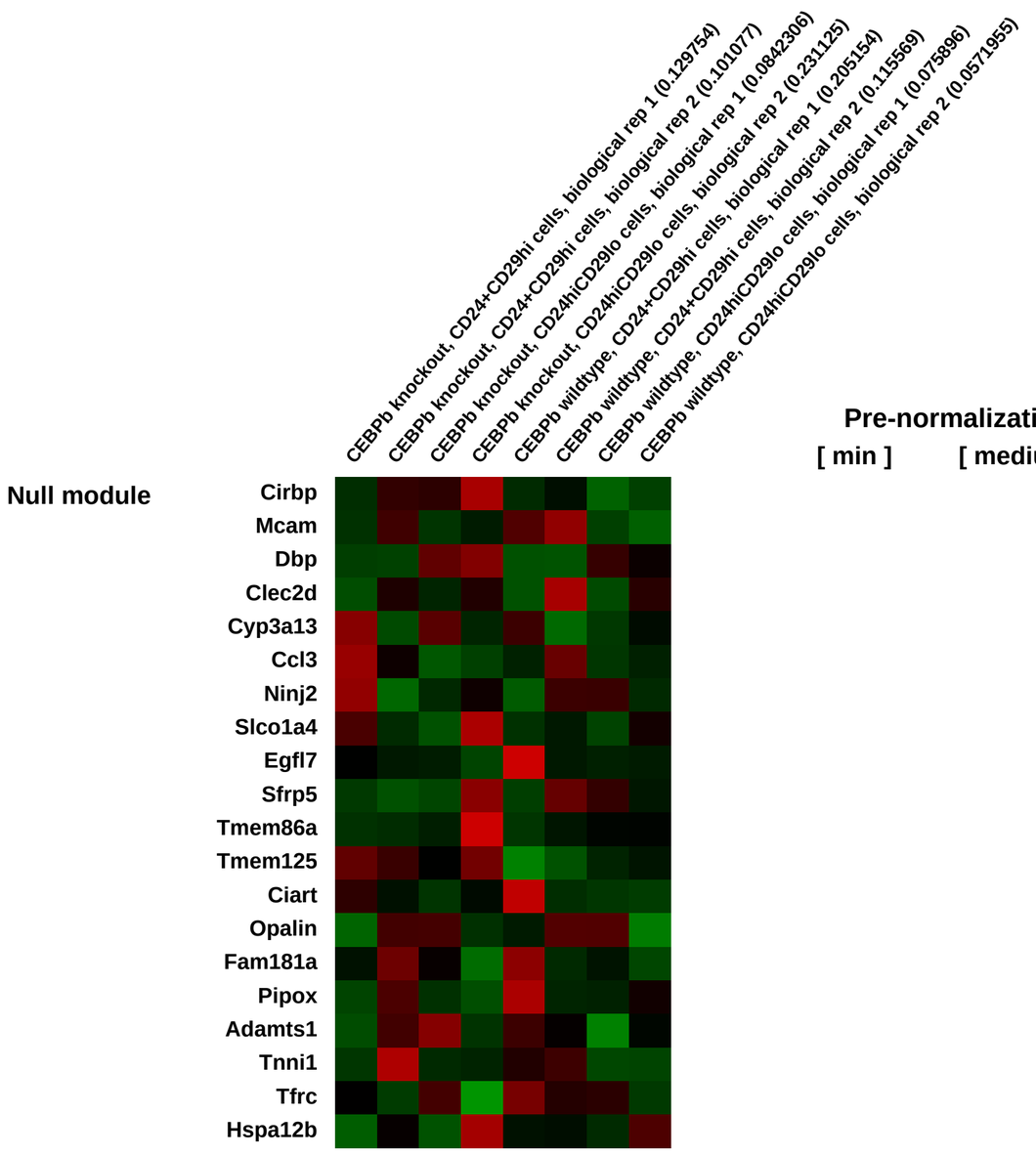

GEO Series "GSE18395" Expression Profiles

Num of samples in this series: 8

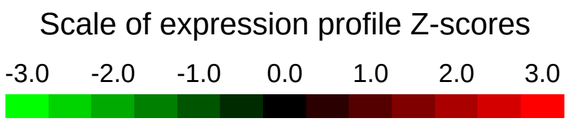

GEO Link:	**http://www.ncbi.nlm.nih.gov/geo/query/acc.cgi?acc=GSE18395**
Status:	**Public on Oct 01 2010**
Title:	**Expression data from mouse adult fibroblasts with Rb deletion and/or p53DD expression exposed to cisplatin (CDDP)**
Organism:	**Mus musculus**
Experiment type:	**Expression profiling by array**
Platform:	**GPL1261**
Pubmed ID:	
Summary & Design:	**Summary:** **The RB and p53 tumor suppressor pathways regulate the transcription of genes involved in cell cycle progression, DNA replication, DNA repair, and apoptosis. These tumor suppressors are critical modulators of the response to genotoxic damage and both pathways are frequently inactivated in human cancers.** **We used microarrays to monitor gene expression patterns upon exposure to cisplatin treatment in fibroblasts harboring loss/inactivation of RB and/or p53.** **Overall design:** **We generated mouse adult fibroblasts harboring loss/inactivation of RB and/or p53 and subjected these cell populations to cisplatin treatment for 24 hours. Treated cell populations were allowed to recover from cisplatin exposure, generating a recurred cell popuation. Untreated and recurred cell populations were then subjected to RNA extraction and hybridization on Affymetrix microarrays.**

Background corr dist: **KL-Divergence = 0.0582, L1-Distance = 0.0193, L2-Distance = 0.0005, Normal std = 0.5297**

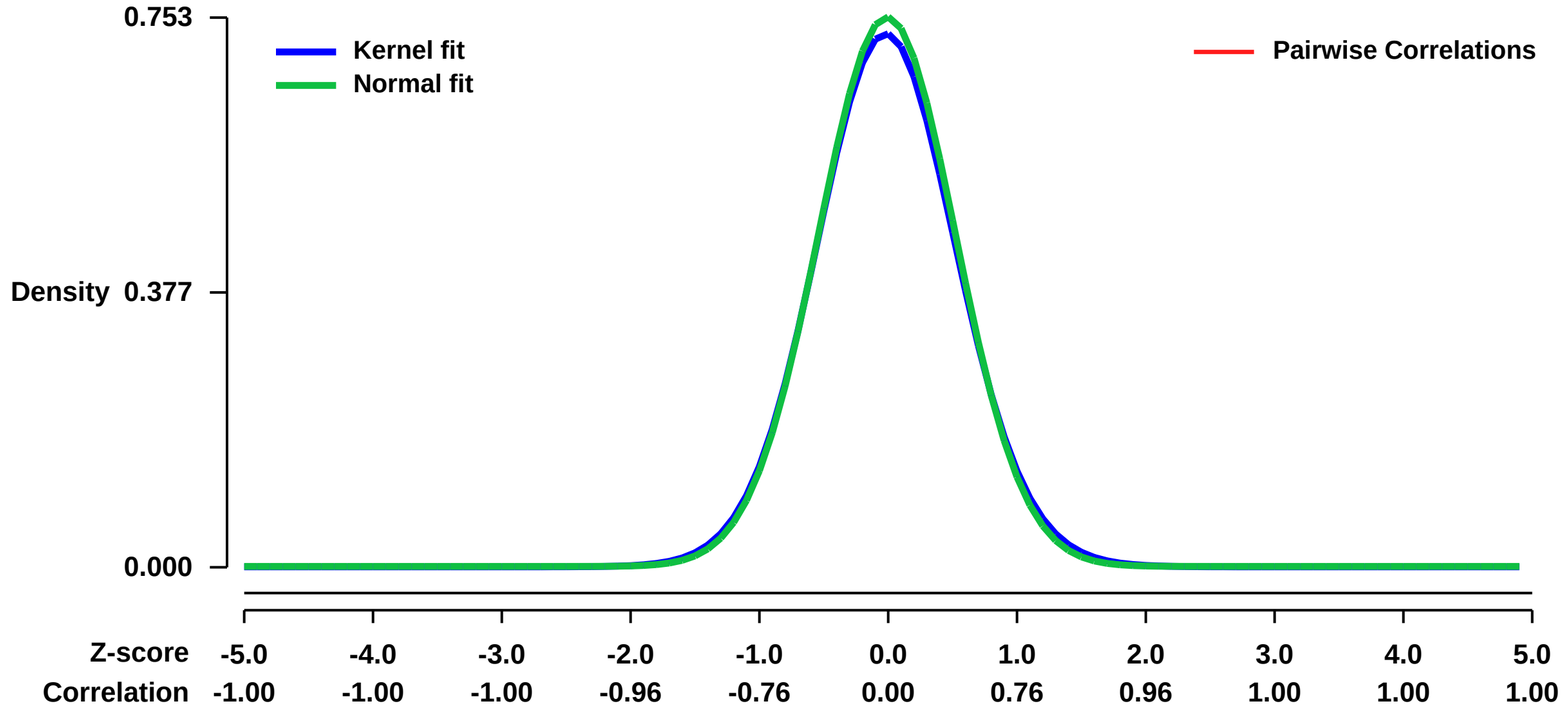

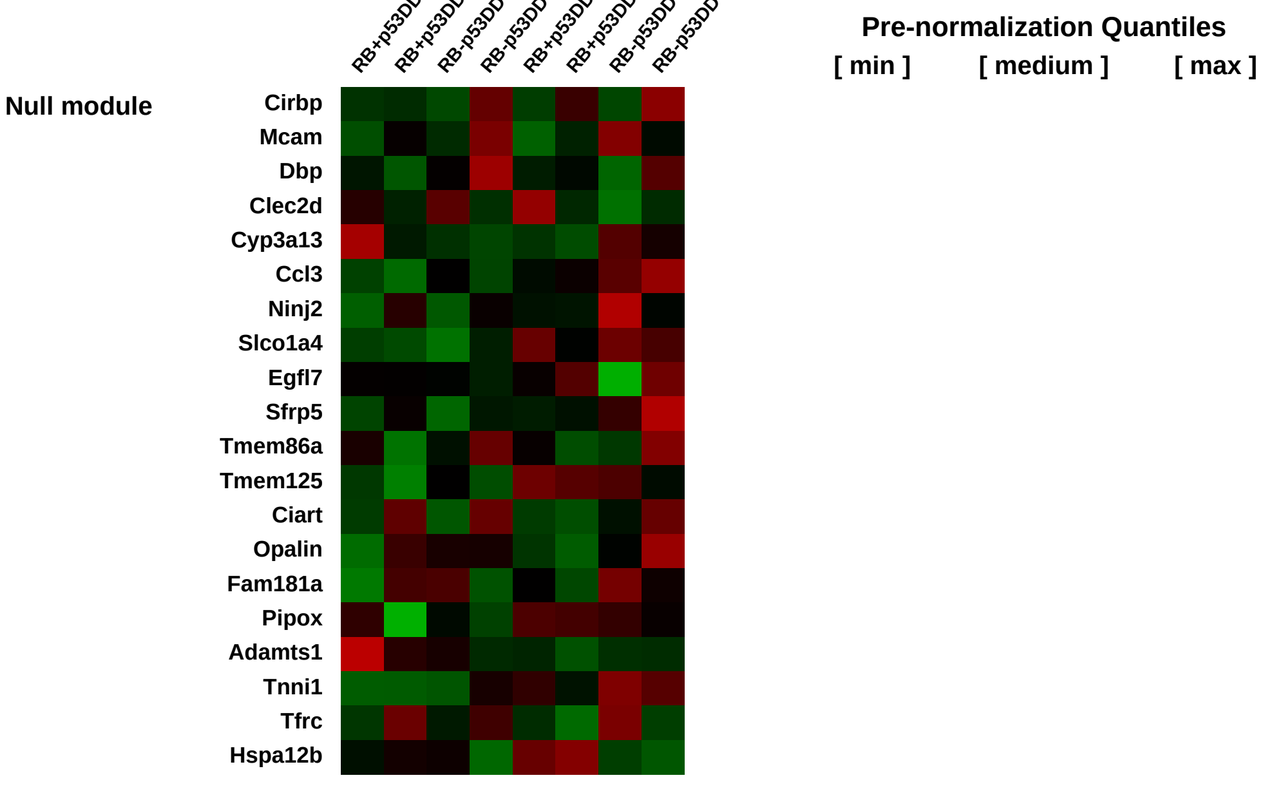

GEO Series "GSE19709" Expression Profiles

Num of samples in this series: 168

Details of this dataset are not shown due to large number of samples and the page size limit.

Find details in http://www.ncbi.nlm.nih.gov/geo/query/acc.cgi?acc=GSE19709

Background corr dist: KL-Divergence = 0.4091, L1-Distance = 0.0481, L2-Distance = 0.0050, Normal std = 0.2525

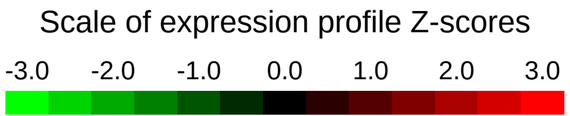

GEO Series "GSE46443" Expression Profiles

Num of samples in this series: 12

Scale of expression profile Z-scores

-3.0 -2.0 -1.0 0.0 1.0 2.0 3.0

GEO Link:	http://www.ncbi.nlm.nih.gov/geo/query/acc.cgi?acc=GSE46443
Status:	Public on Oct 21 2013
Title:	Expression data from mouse cerebral cortex
Organism:	Mus musculus
Experiment type:	Expression profiling by array
Platform:	GPL1261
Pubmed ID:	23800850
Summary & Design:	**Summary:** **Differential gene expression of cerebral cortex might be responsible for distinct neurovascular developments between different mouse strains** **We used Affymetrix microarray to explore the global gene expression patterns of mouse cerebral cortex of different mouse strains at two developmental stages** **Overall design:** **Cerebral cortex from two mouse strains [C57BL/6J(B6) and C3H/J (C3H)] at post-natal day 1 (p1) and post-natal 11 weeks (11 wk) were harvested for microarray experiments**

Background corr dist: **KL-Divergence = 0.0145, L1-Distance = 0.0214, L2-Distance = 0.0004, Normal std = 0.8048**

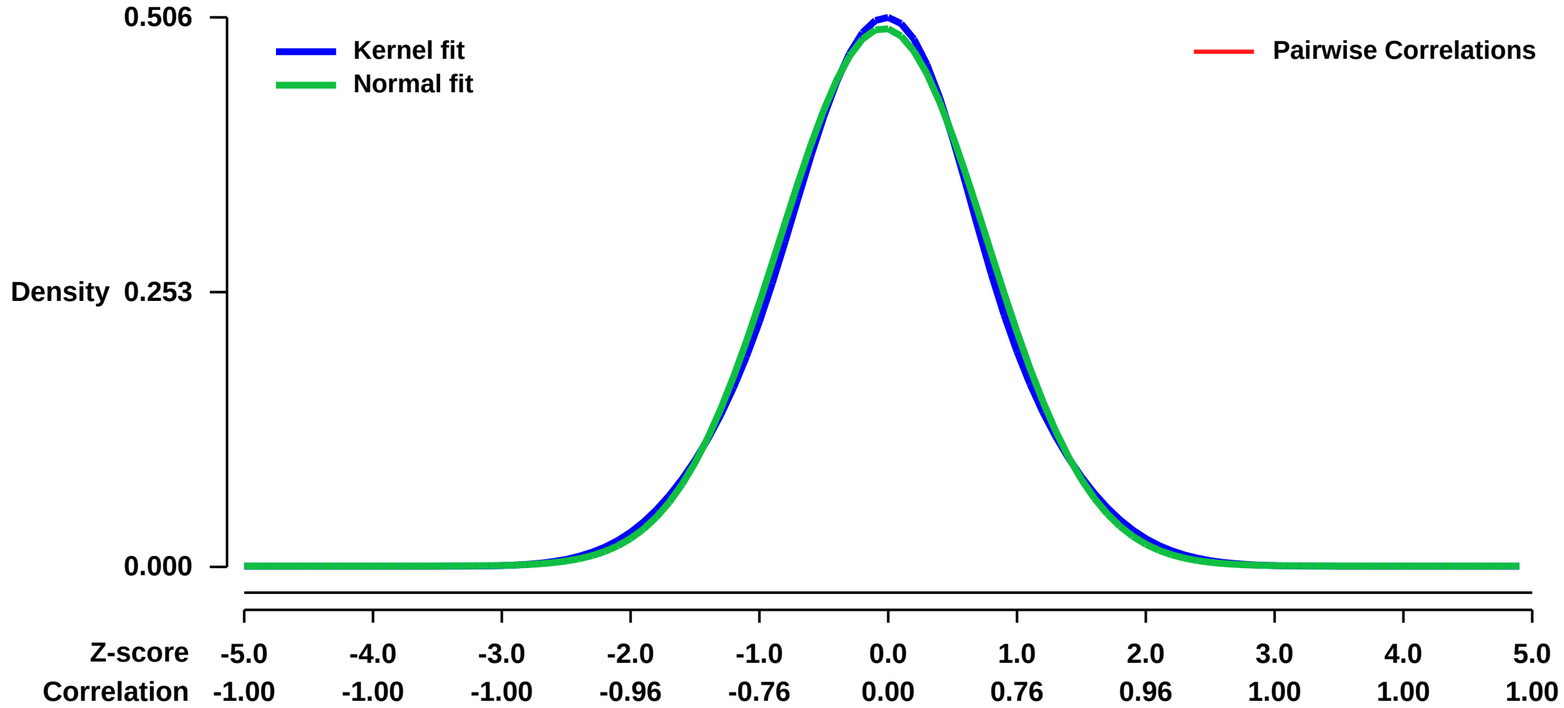

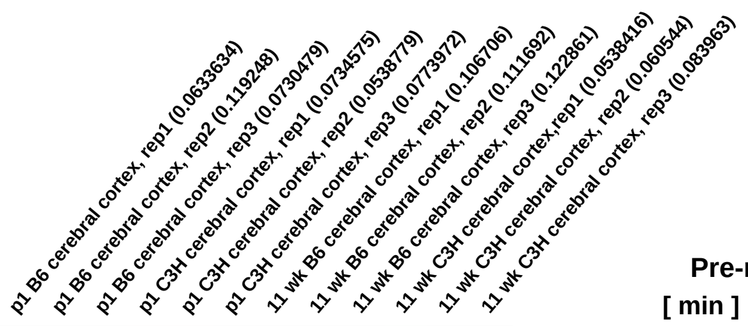

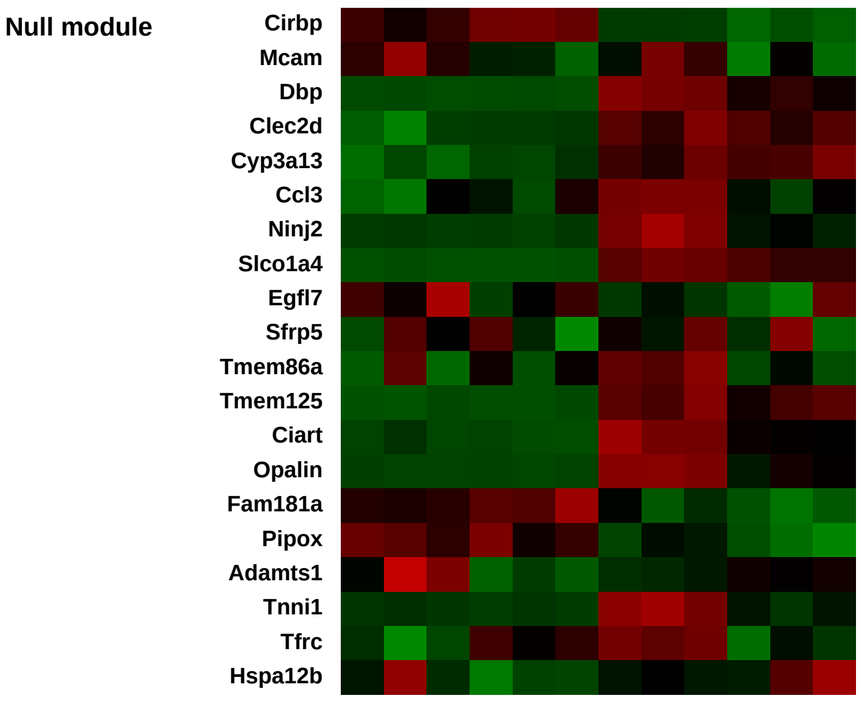

GEO Series "GSE18993" Expression Profiles

Num of samples in this series: 13

Scale of expression profile Z-scores

-3.0 -2.0 -1.0 0.0 1.0 2.0 3.0

GEO Link:	http://www.ncbi.nlm.nih.gov/geo/query/acc.cgi?acc=GSE18993
Status:	Public on Jun 22 2011
Title:	Expression profiles from mouse prostate progenitor/stem cells treated with ethanol or 100nM 1,25 dihydroxyvitamin D3
Organism:	Mus musculus
Experiment type:	Expression profiling by array
Platform:	GPL1261
Pubmed ID:	21653679
Summary & Design:	**Summary:** A major goal in prostate stem cell biology is to identify genes, pathways, or networks that control self-renewal and multilineage differentiation. We hypothesize that 1,25 dihydroxyvitamin D3 can induce differentiation of prostatic progenitor/stem cells, thus serving as an in vitro model with which to study the molecular mechanisms of stem cell differentiation by 1,25 dihydroxyvitamin D3. 1,25 dihydroxyvitamin D3 elicits its effects primarily through transcriptional regulation of genes, so microarray studies were used to gain insight into the cellular response to 1,25 dihydroxyvitamin D3. We used microarrays to detail the global gene expression changes that occur upon 1,25 dihydroxyvitamin D3 treatment of prostatic progenitor/stem cells. **Overall design:** Adult mouse prostate progenitor/stem cells were plated at 1 x 10^5 cells per 10 cm culture dish and grown to 70% confluency before treatment with vehicle (0.1% ethanol) or 100 nM 1,25(OH)2D3 in cell culture media (n = 3 or 4). Cells were treated with control or experimental media for 6 hrs or 48 hrs before RNA isolation. The RNA from 6 hrs and 48 hrs was used to probe Affymetrix 430A oligonucleotide arrays (GPL339).

Background corr dist: KL-Divergence = 0.0617, L1-Distance = 0.0407, L2-Distance = 0.0030, Normal std = 0.5373

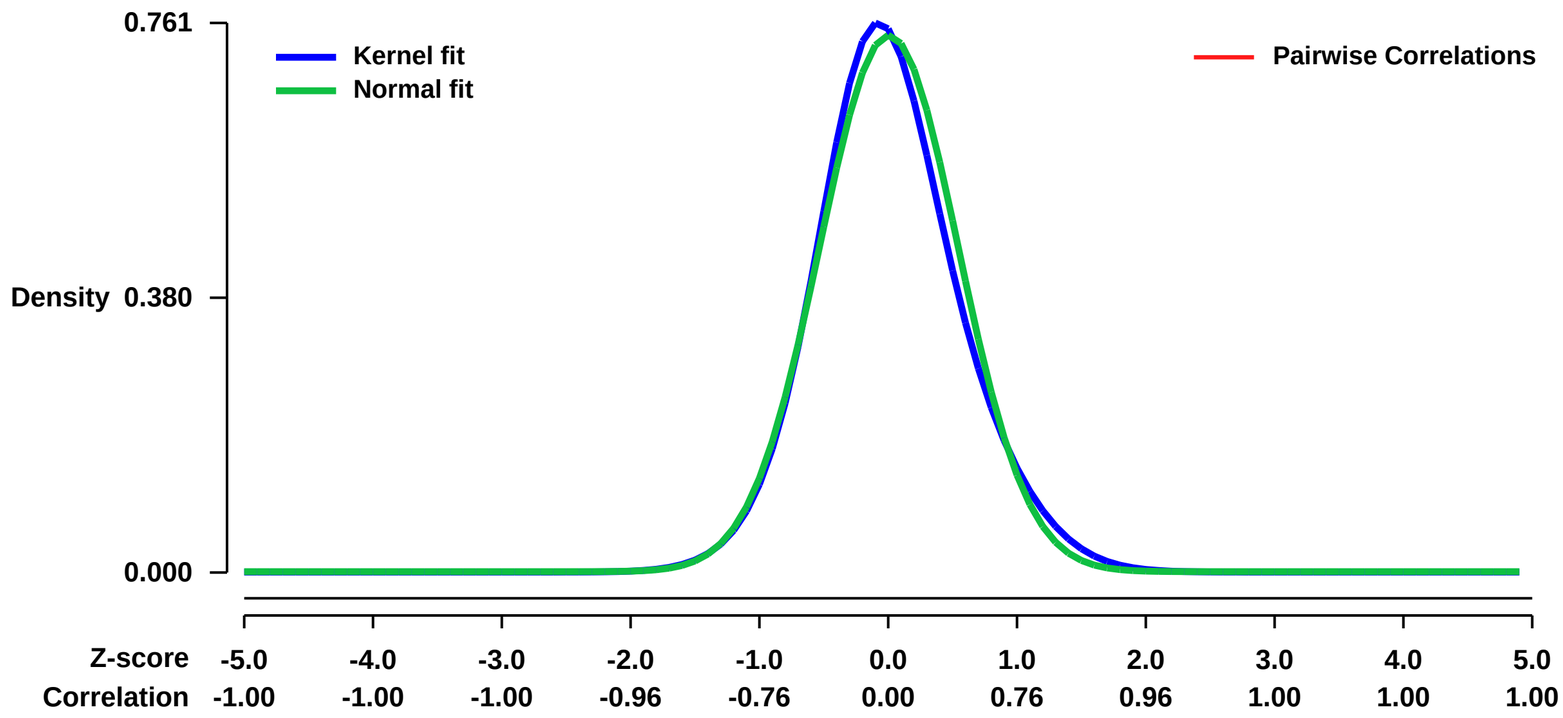

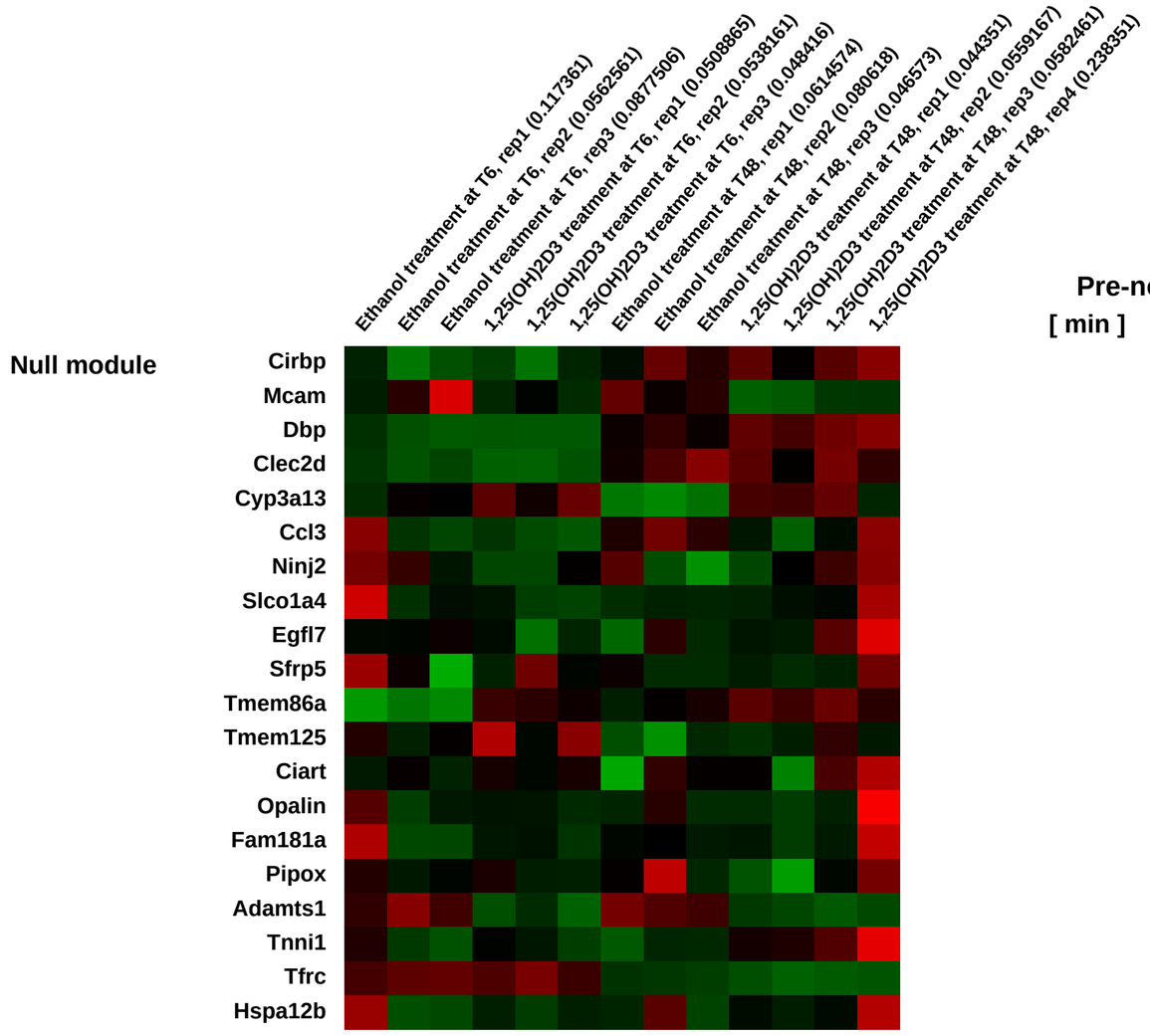

GEO Series "GSE27708" Expression Profiles

Num of samples in this series: 9

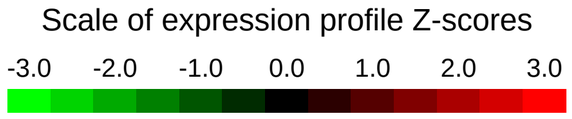

GEO Link:	http://www.ncbi.nlm.nih.gov/geo/query/acc.cgi?acc=GSE27708
Status:	Public on Aug 01 2011
Title:	esBAF facilitates pluripotency by conditioning the genome for LIF/STAT3 signaling and by regulating Polycomb function
Organism:	Mus musculus
Experiment type:	Expression profiling by array
Platform:	GPL1261
Pubmed ID:	21785422
Summary & Design:	**Summary:** Signaling by the cytokine LIF and its downstream transcription factor, STAT3, prevents differentiation of pluripotent embryonic stem cells (ESCs) by opposing MAP kinase signaling. This contrasts with most cell types where STAT3 signaling induces differentiation. We find that STAT3 binding across the pluripotent genome is dependent upon Brg, the ATPase subunit of a specialized chromatin remodeling complex (esBAF) found in ESCs. Brg is required to establish chromatin accessibility at STAT3 binding targets, in essence preparing these sites to respond to LIF signaling. Moreover, Brg deletion leads to rapid Polycomb (PcG) binding and H3K27me3-mediated silencing of many Brg-activated targets genome-wide, including the target genes of the LIF signaling pathway. Hence, one crucial role of Brg in ESCs involves its ability to potentiate LIF signaling by opposing PcG. Contrary to expectations, Brg also facilitates PcG function at classical PcG target including all four Hox loci, reinforcing their repression in ESCs. These findings reveal that esBAF does not simply antagonize PcG, but rather, the two chromatin regulators act both antagonistically and synergistically with the common goal of supporting pluripotency. **Overall design:** ChIP-Seq was used to detect and measure STAT3 occupancy and levels of H3K27me3 in the genome before and after the removal of the SWI/SNF ATPase Brg in mouse ESCs. Total of 4 samples (WT and KO STAT3; WT and KO H3K27me3). Input DNA was sequenced as control.

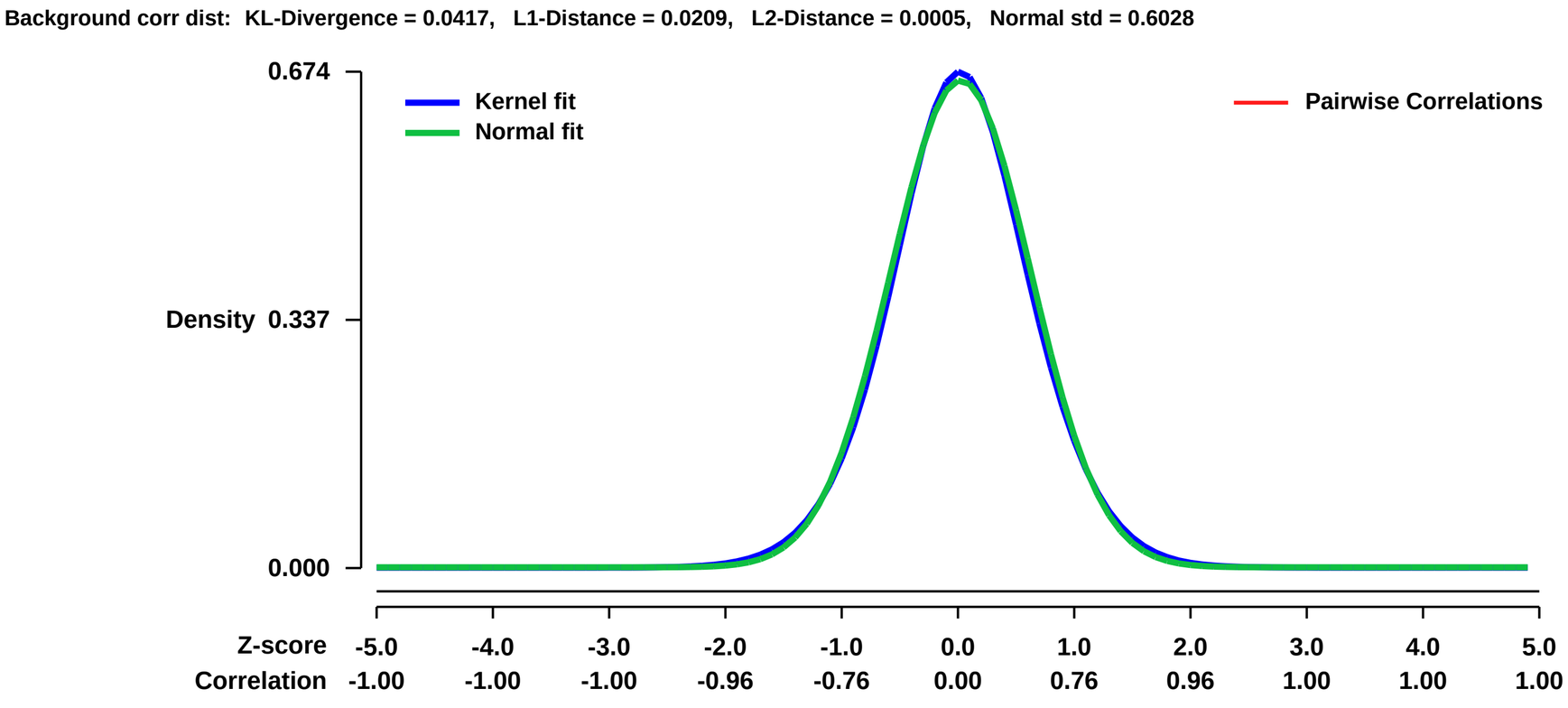

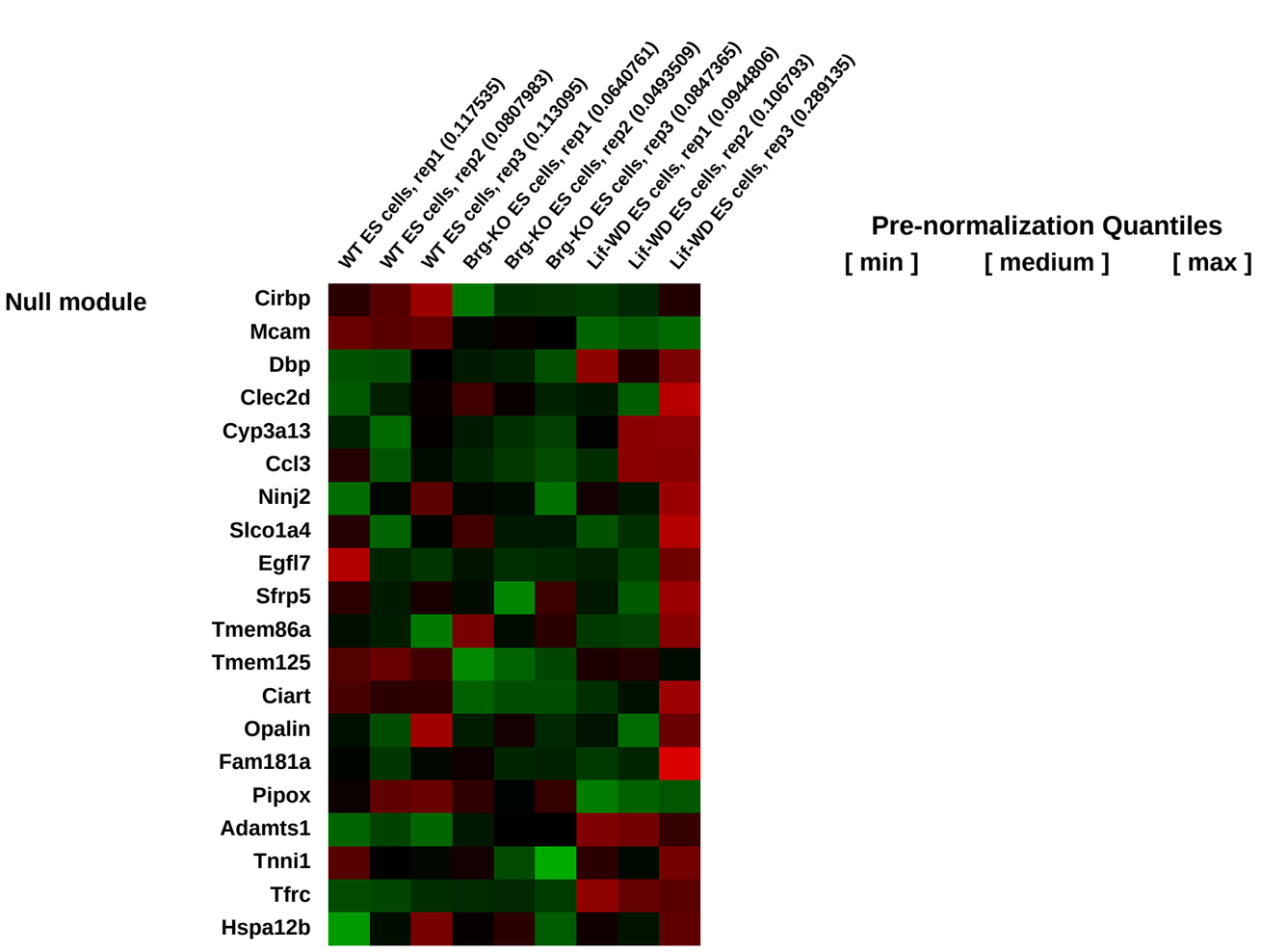

GEO Series "GSE25911" Expression Profiles

Num of samples in this series: 26

Scale of expression profile Z-scores

-3.0 -2.0 -1.0 0.0 1.0 2.0 3.0

GEO Link:	http://www.ncbi.nlm.nih.gov/geo/query/acc.cgi?acc=GSE25911
Status:	Public on Sep 13 2011
Title:	Expression changes after loss of Dot1l in murine MLL-AF9 leukemia cells
Organism:	Mus musculus
Experiment type:	Expression profiling by array
Platform:	GPL1261
Pubmed ID:	21741597
Summary & Design:	**Summary:** MLL-fusions may induce leukemogenic gene expression programs by recruiting the histone H3K79 methyltransferase to MLL-target promoters. We evaluated gene expression changes after cre-mediated loss of Dot1l in leukemia cells obtained from mice injected with MLL-9 transformed lineage negative bone marrow cells. **Overall design:** MLL-AF9 murine leukemia cells carrying two conditional Dot1l alleles were retrovirally transduced with Cre or empty control vector, and gene expression changes were monitored on day 3, 5, and 7 after transduction.

Background corr dist: KL-Divergence = 0.0792, L1-Distance = 0.0746, L2-Distance = 0.0111, Normal std = 0.5107

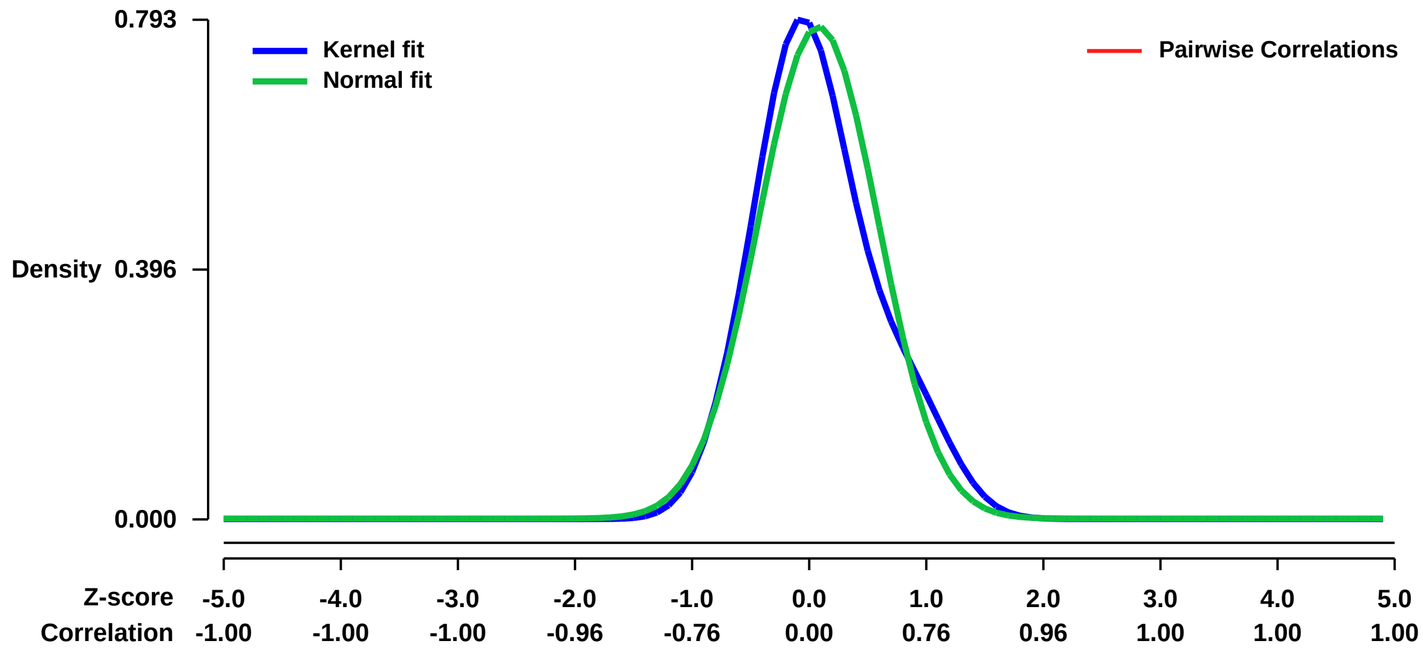

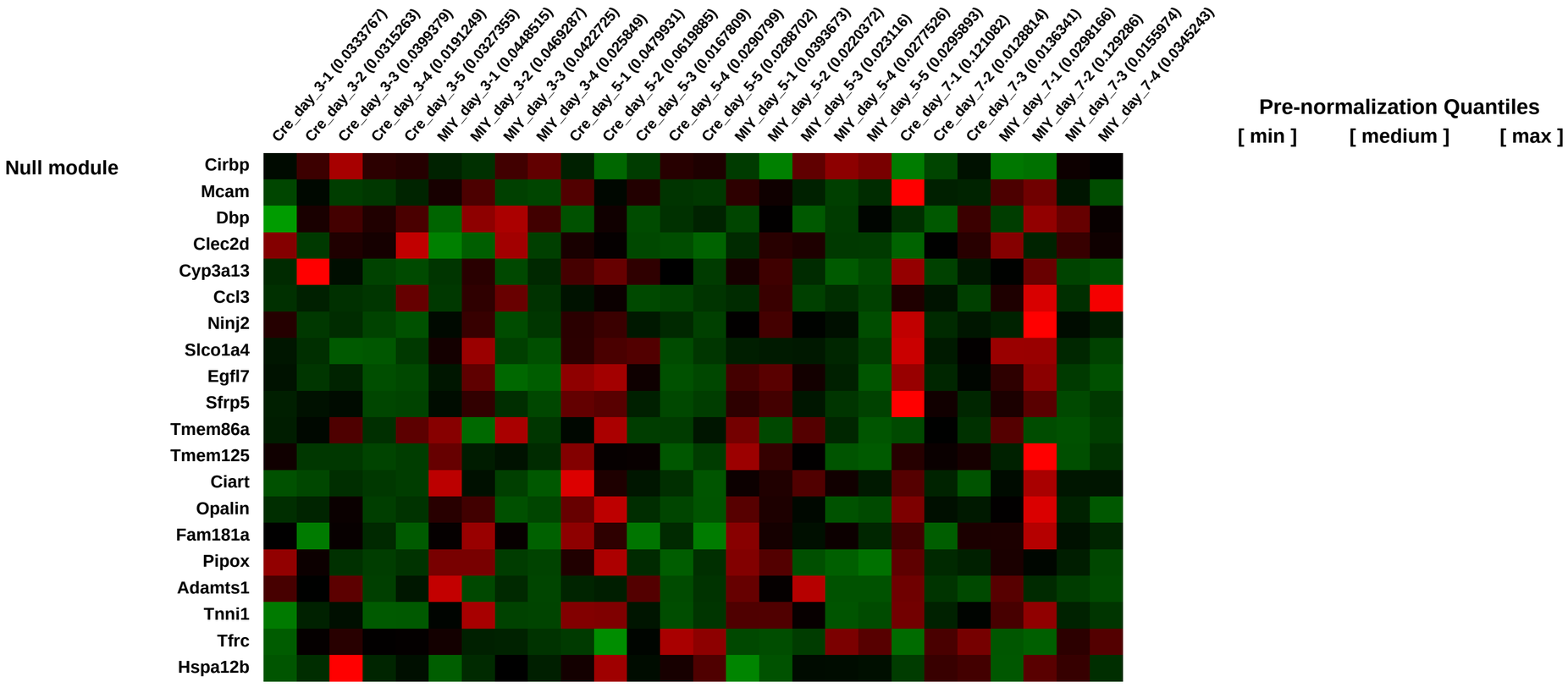

GEO Series "GSE19338" Expression Profiles

Num of samples in this series: 24

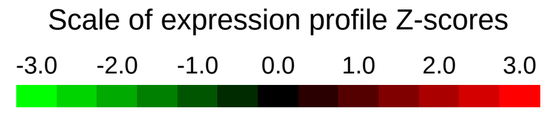

GEO Link:	http://www.ncbi.nlm.nih.gov/geo/query/acc.cgi?acc=GSE19338
Status:	Public on Oct 06 2010
Title:	Expression profiles of villus and crypt layers of large intestine from C57Bl/6, Apc1638N+/-, and p21-/- mice.
Organism:	Mus musculus
Experiment type:	Expression profiling by array
Platform:	GPL1261
Pubmed ID:	20824133
Summary & Design:	**Summary:** Expression profiles obtained from the villus and crypt layers of murine large intestine can elucidate the process of differentiation undergone by epithelial cells as they migrate from the undifferentiated bottom of the crypt to the villus tip before being shed into the intestinal lumen. This series includes profiles from wild type mice, as well as mice harboring mutations in genes (APC and p21) which play key roles in the differentiation process. We used microarrays to characterize gene expression profiles at the base of the crypt and at the villus tip of the lumenal layer of the large intestine in order to better understand the process of differentiation and eventual shedding undergone by cells of the large intestinal epithelium. **Overall design:** Four wild type, four APC1638+/- and four p21-/- mice were sacrified and the large intestines dissected out. Cells from the villus tip and from the bottom of the crypt were isolated from the lumenal face of the each large intestine using the Weiser method of sequential elution. RNA was extracted from each eluted sample and used to hybridize to Affymetrix 3' expression arrays.

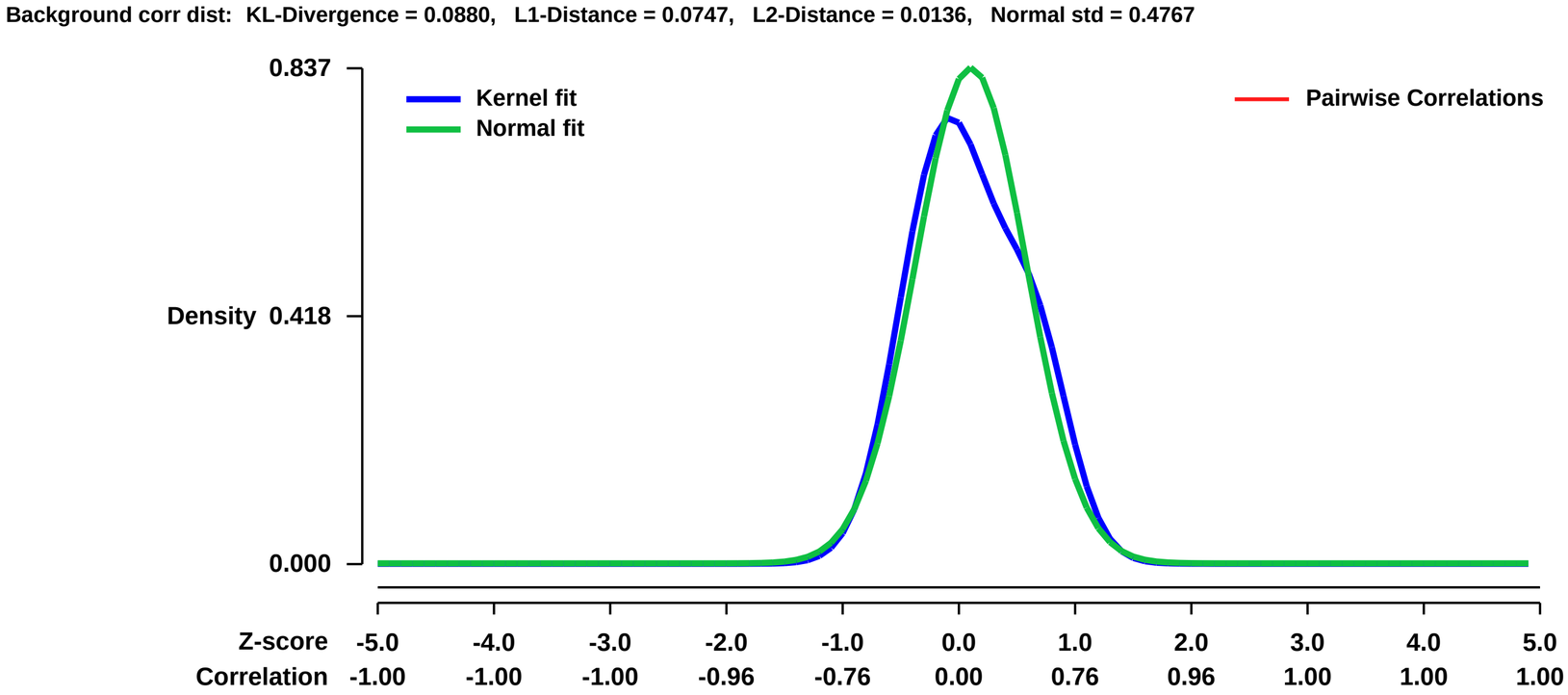

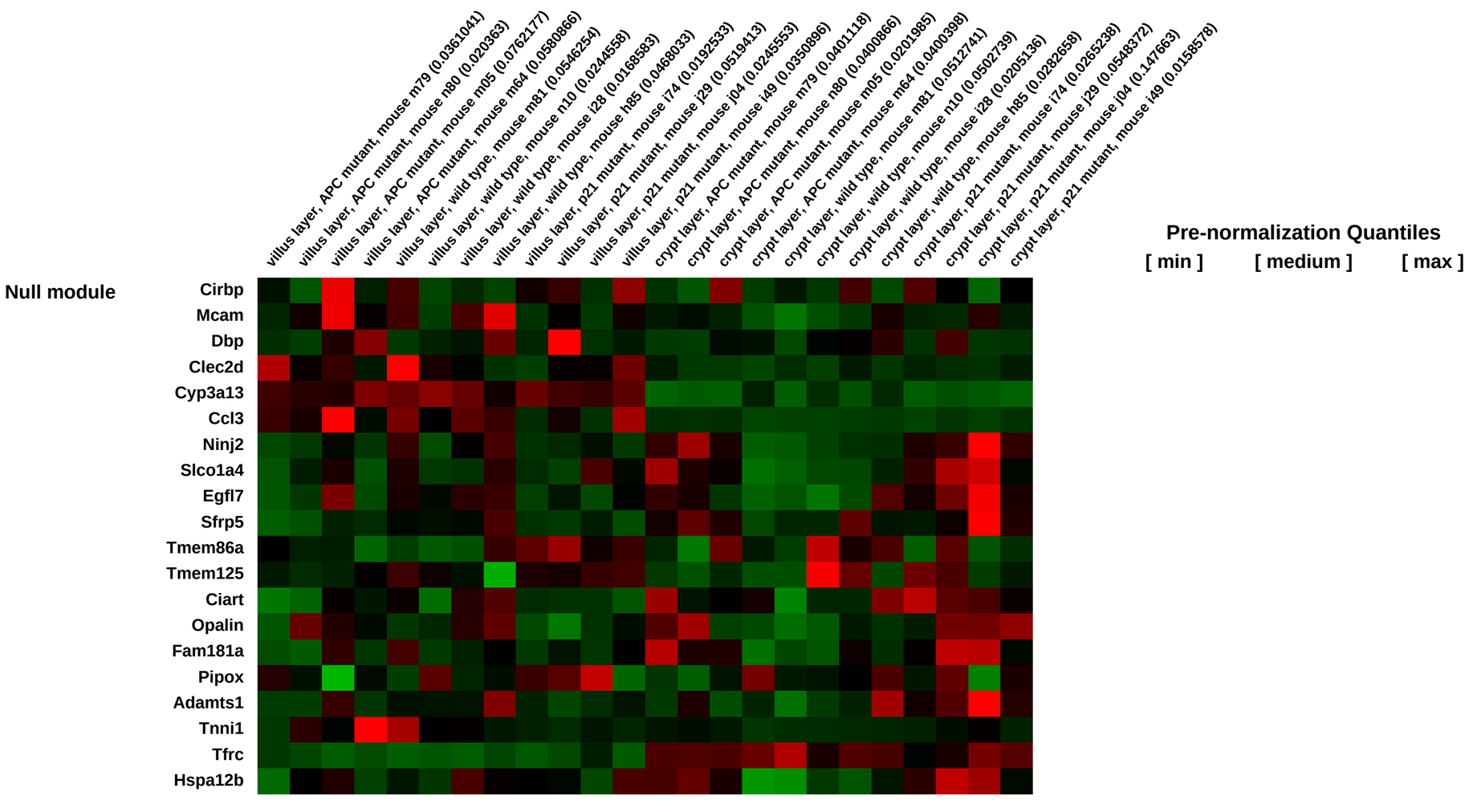

GEO Series "GSE38797" Expression Profiles

Num of samples in this series: 16

Scale of expression profile Z-scores

-3.0 -2.0 -1.0 0.0 1.0 2.0 3.0

GEO Link:	http://www.ncbi.nlm.nih.gov/geo/query/acc.cgi?acc=GSE38797
Status:	Public on Jul 16 2012
Title:	Expression values from wild-type retinas and retinas with a mutant Rhodopsin transgene (Tg(RHO P347S)) with and without Endothelin-2 (EDN2)
Organism:	Mus musculus
Experiment type:	Expression profiling by array
Platform:	GPL1261
Pubmed ID:	
Summary & Design:	**Summary:** Expression of the Endothelin-2 (Edn2) mRNA is greatly increased in the photoreceptors (PRs) of mouse models of inherited PR degeneration. To identify retinasl gene whose expression is directly or indirectly regulated by EDN2 in the presence of the Tg(RHO P347S) mutant allele, we defined mRNAs that were differentially expressed in Edn2+/+, Edn2-/-, Tg(RHO P347S) Edn2+/+, and Tg(RHO P347S) Edn2-/- retinas. **Overall design:** RNA was extracted from Edn2+/+, Edn2-/-, Tg(RHO P347S) Edn2+/+, and Tg(RHO P347S) Edn2-/- retinas at postnatal day 21 (PN21) and hybridized to Affymetrix arrays

Background corr dist: KL-Divergence = 0.1800, L1-Distance = 0.0456, L2-Distance = 0.0046, Normal std = 0.3454

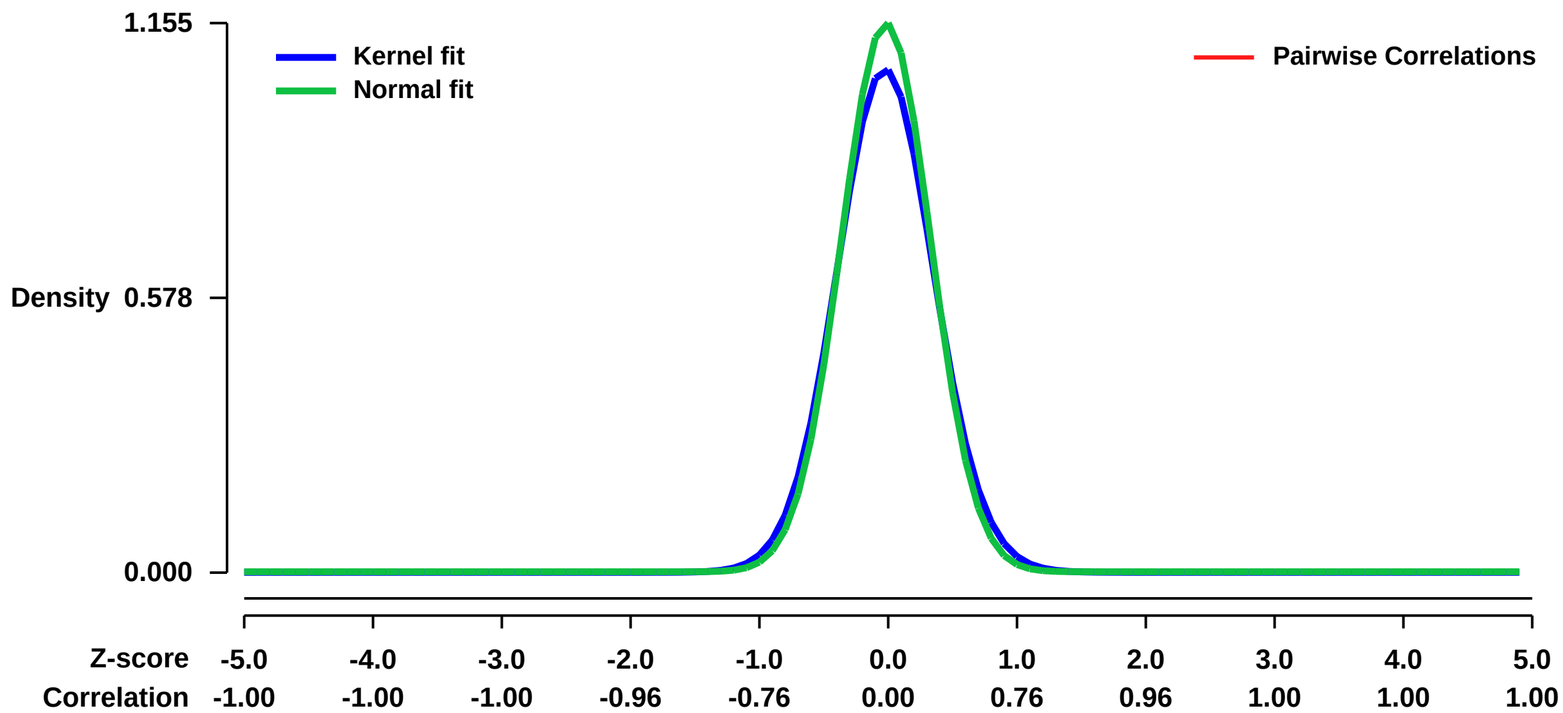

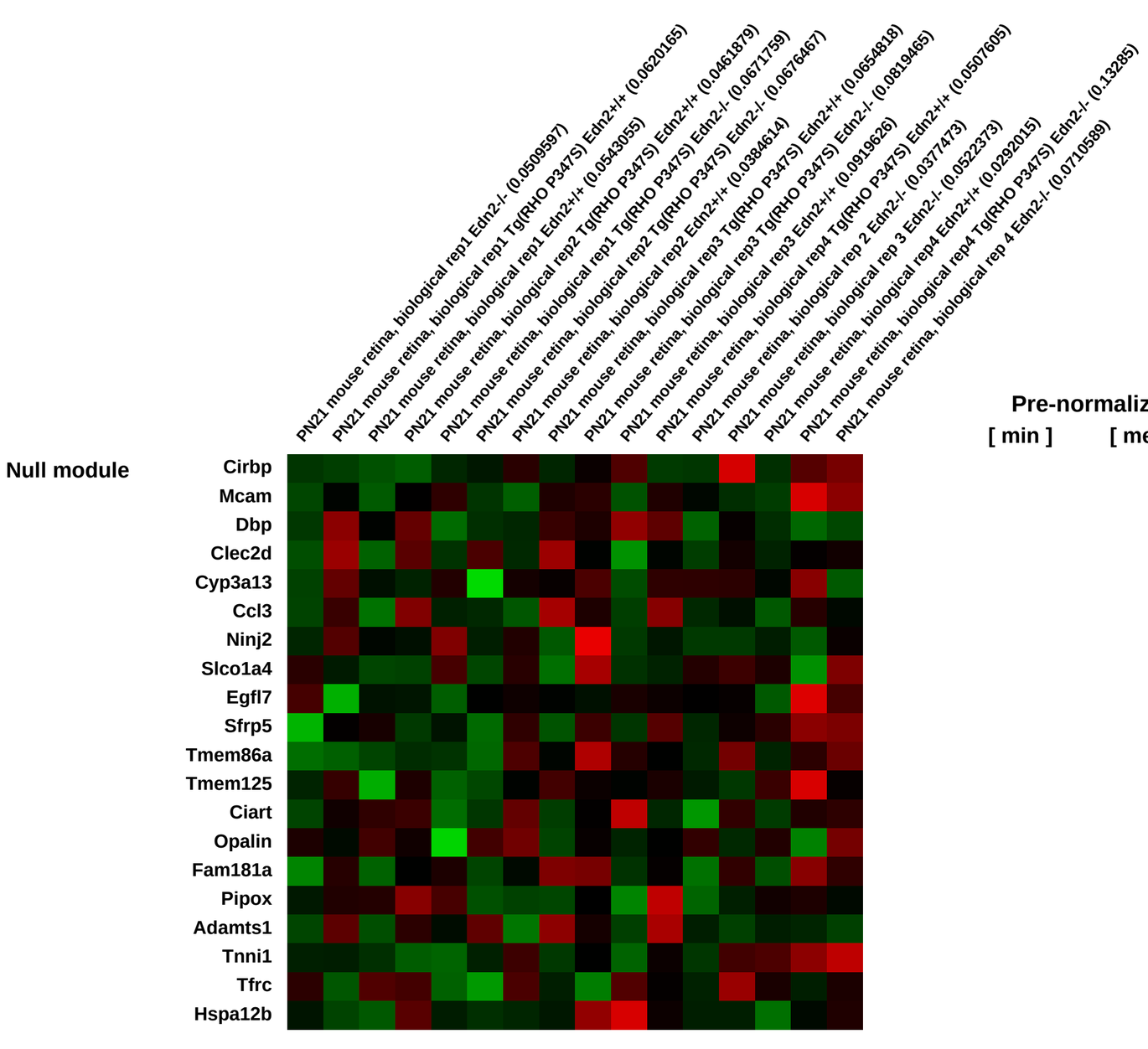

GEO Series "GSE28417" Expression Profiles

Num of samples in this series: 12

Scale of expression profile Z-scores

-3.0 -2.0 -1.0 0.0 1.0 2.0 3.0

GEO Link:	**http://www.ncbi.nlm.nih.gov/geo/query/acc.cgi?acc=GSE28417**
Status:	**Public on Apr 02 2012**
Title:	**Expression data from mouse tissues**
Organism:	**Mus musculus**
Experiment type:	**Expression profiling by array**
Platform:	**GPL1261**
Pubmed ID:	
Summary & Design:	**Summary:** **The role of p53 in assuring longevity through prevention of cancer is well established, but how it specifically regulates aging is still controversial. Our assumption is that distinct p53-pathways regulate tumor suppression and aging and that p66Shc is one of the master regulators of the p53 aging function. p66Shc longevity determinant protein acts as a downstream target of p53 and it is indispensable for the ability of activated p53 to induce elevation of intracellular oxidants and apoptosis.** **We used microarray to gain insight into the mechanism of the physiological activation of p53-p66Shc pathway** **Overall design:** **Total RNA was extracted from freshly isolated thymus, liver, heart and lung of two months old mice (pool of four mice for each genotype)**

Background corr dist: **KL-Divergence = 0.0576, L1-Distance = 0.0878, L2-Distance = 0.0145, Normal std = 0.6092**

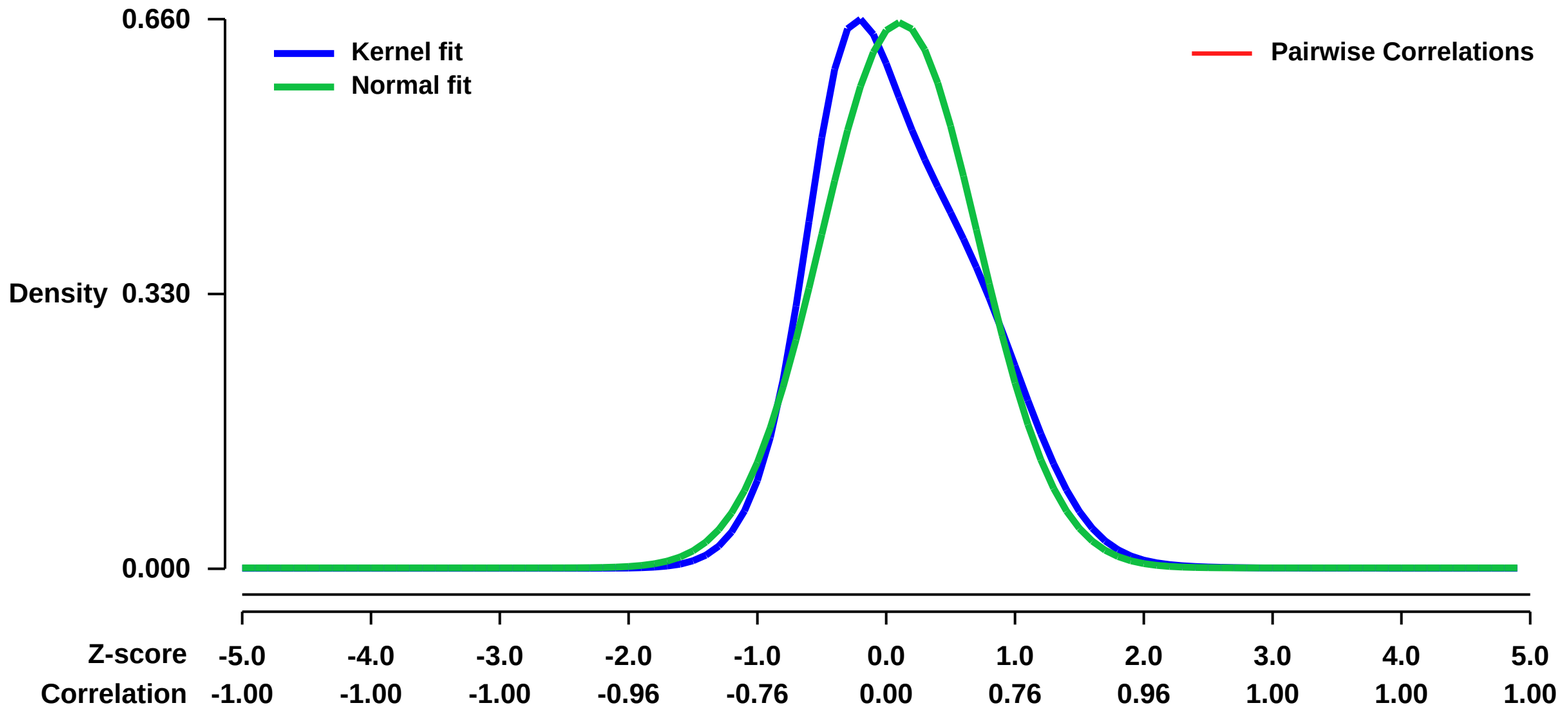

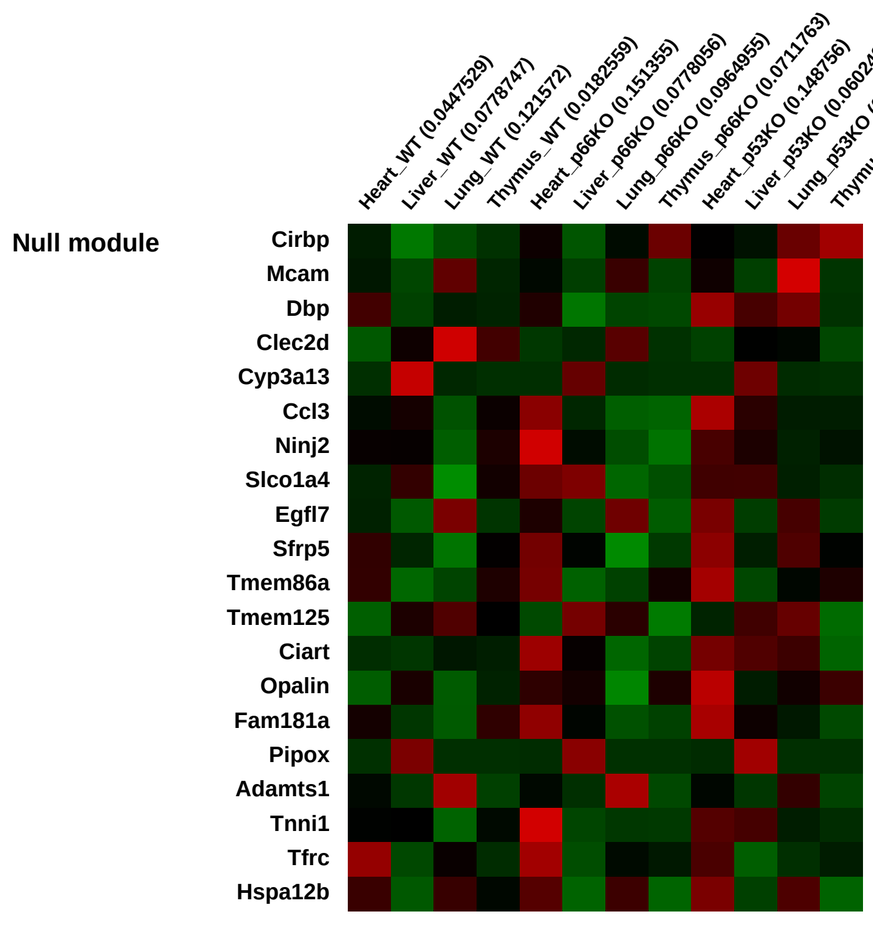

GEO Series "GSE42299" Expression Profiles

Num of samples in this series: 8

Scale of expression profile Z-scores

-3.0 -2.0 -1.0 0.0 1.0 2.0 3.0

GEO Link:	http://www.ncbi.nlm.nih.gov/geo/query/acc.cgi?acc=GSE42299
Status:	Public on Dec 10 2012
Title:	Expression profiles of C2C12 myotubes in response to PGC-1¸– (peroxisome proliferator-activated receptor gamma, coactivator 1 alpha) overexpression and/or iron chelati
Organism:	Mus musculus
Experiment type:	Expression profiling by array
Platform:	GPL1261
Pubmed ID:	23318259
Summary & Design:	**Summary:** Mitochondria are centers of metabolism and signaling whose content and function must adapt to changing cellular environments. The biological signals that initiate mitochondrial restructuring and the cellular processes that drive this adaptive response are largely obscure. To better define these systems, we performed matched quantitative genomic and proteomic analyses of mouse muscle cells as they performed mitochondrial biogenesis. We find that proteins involved in cellular iron homeostasis are highly coordinated with this process, and that depletion of cellular iron results in a rapid, dose-dependent decrease of select mitochondrial protein levels and oxidative capacity. We further show that this process is universal across a broad range of cell types and fully reversed when iron is reintroduced. Collectively, our work reveals that cellular iron is a key regulator of mitochondrial biogenesis, and provides quantitative datasets that can be leveraged to explore post-transcriptional and post-translational processes that are essential for mitochondrial adaptation. **Overall design:** C2C12 mouse myoblasts were differentiated into myotubes for 3 days, at which point they were infected with adenovirus expressing either green fluorescent protein (GFP) or GFP-tagged PGC-1¸– (GFP-PGC-1¸–) ´– treatment with the iron chelator deferoxamine (DFO) (for 4 treatments total). The cells were grown for three more days, then RNA was extracted and applied to Affymetrix Mouse 430 2.0 arrays. Gene expression was measured in biological duplicate (4 treatments ^ 2 replicates = 8 arrays).

Background corr dist: KL-Divergence = 0.0474, L1-Distance = 0.0332, L2-Distance = 0.0013, Normal std = 0.6028

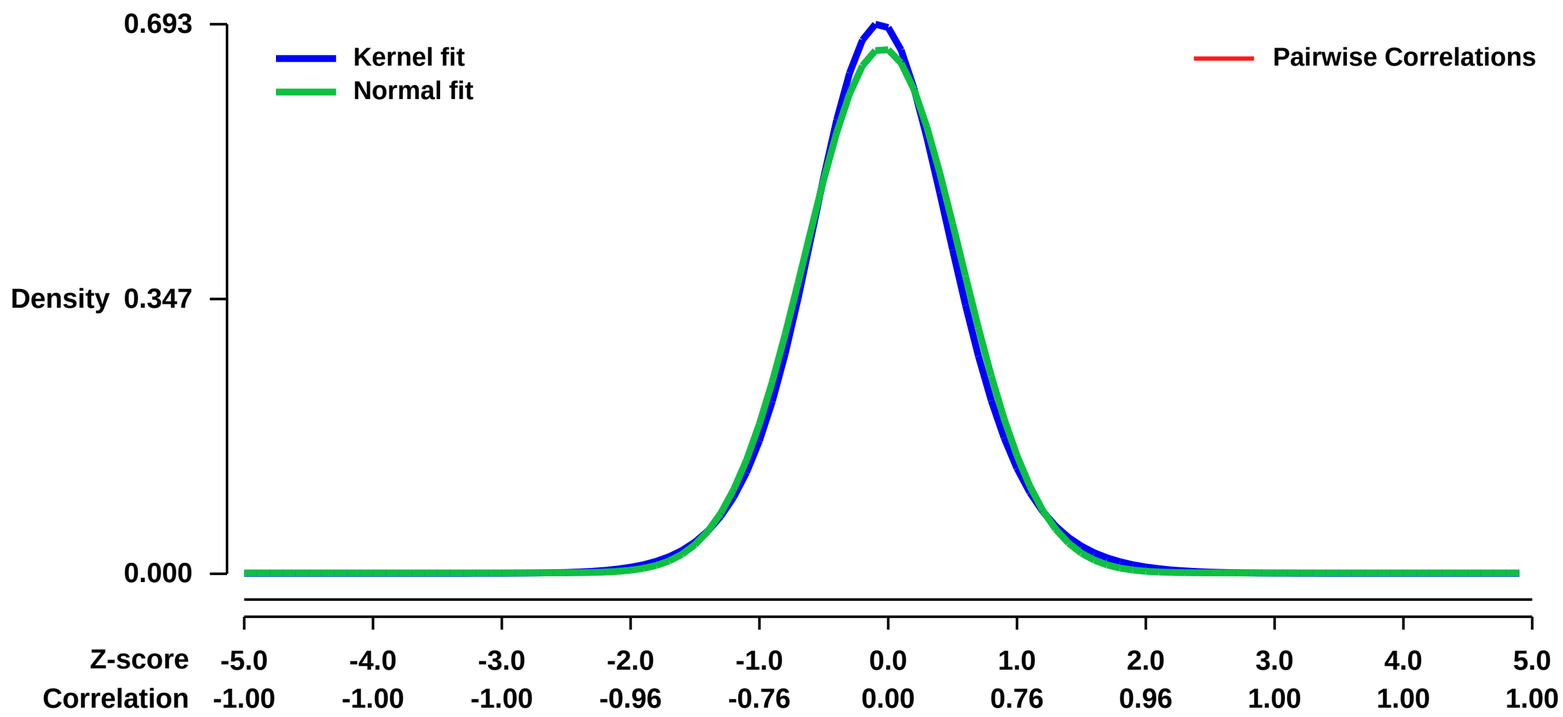

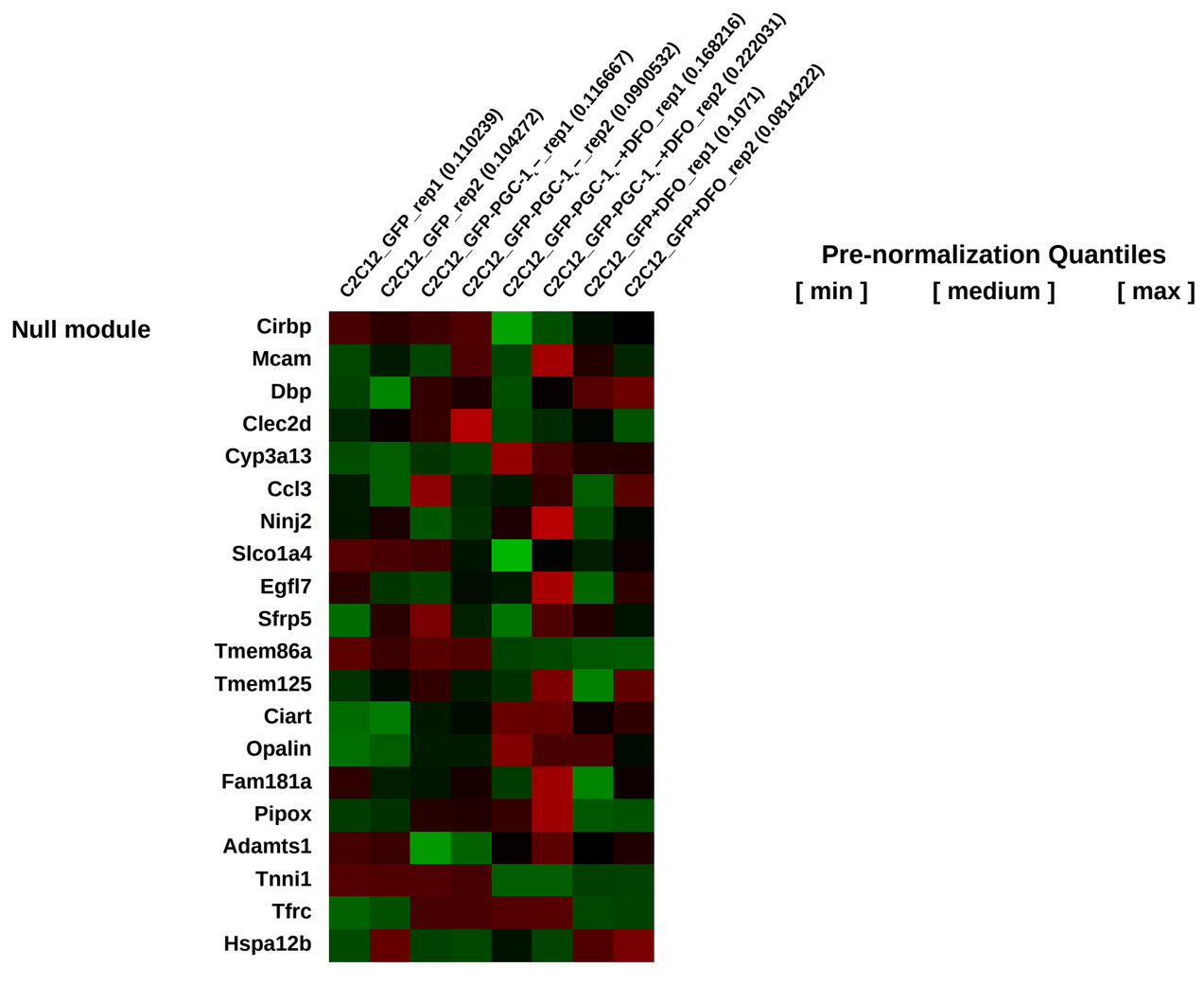

GEO Series "GSE28559" Expression Profiles

Num of samples in this series: 30

Scale of expression profile Z-scores

-3.0 -2.0 -1.0 0.0 1.0 2.0 3.0

GEO Link:	http://www.ncbi.nlm.nih.gov/geo/query/acc.cgi?acc=GSE28559
Status:	Public on Jul 15 2011
Title:	An expression microarray approach for the identification of candidate metastable epialleles in the mouse genome
Organism:	Mus musculus
Experiment type:	Expression profiling by array
Platform:	GPL1261
Pubmed ID:	
Summary & Design:	**Summary:** **Genetic loci displaying environmentally responsive epigenetic marks, termed metastable epialleles, offer a solution to the paradox presented by genetically identical yet phenotypically distinct individuals. The murine viable yellow agouti (Avy) locus is a well-described metastable epiallele that serves as a visual epigenetic biosensor. The Avy locus exhibits a high R-value or ratio of inter-individual (Vi) to inter-tissue (Vt) variance in gene expression, characteristic of what we term the â Agouti Expression Fingerprint.â We propose a novel method for identification of candidate metastable epialleles based on the Agouti Expression Fingerprint, defining candidates as loci with R-values greater than 1.5 on expression microarray.** **Using Expression data from tissues of the three germ layers (liver, kidney, brain), high variance in agouti RNA levels among isogenic animals coupled with low variance among tissue types in individual animals is demonstrated. Here, we provide proof of concept for the â Agouti Expression Fingerprintâ ; the characterization of epigenetically labile loci in humans will be crucial to the development of novel screening and therapeutic targets for human disease prevention.** **Overall design:** **For expression microarray studies, total RNA was isolated from liver, kidney, and brain tissue from 10 male Avy/a mice (2 per each of the 5 coat color classes) at time of weaning and coat color determination (day 22). Using Affymetrix GeneChip Mouse Genome 2.0 arrays (Santa Clara, CA), we queried the entire mouse genome for candidate metastable epialleles that display the Agouti Fingerprint. Approximately 100 of the greater than 40,000 transcripts on the mouse array displayed an expression pattern characterized as high inter-individual variation coupled with low inter-tissue variation (R-value > 1.5).**

Background corr dist: KL-Divergence = 0.0741, L1-Distance = 0.0520, L2-Distance = 0.0050, Normal std = 0.5242

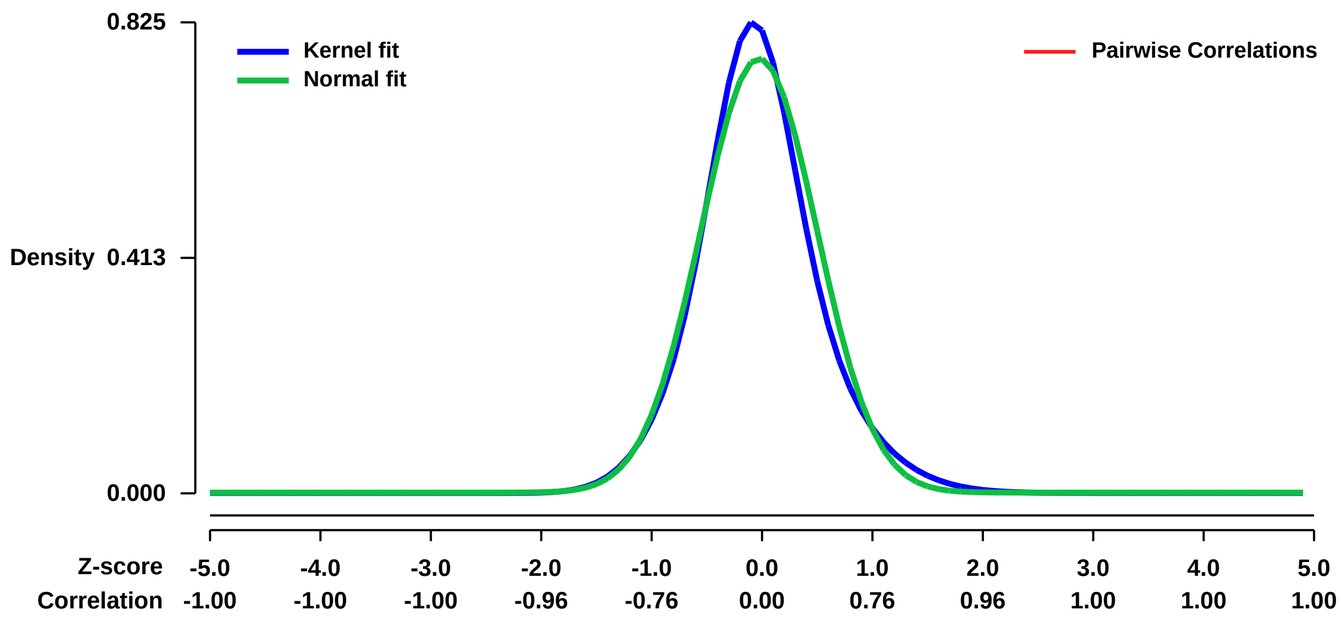

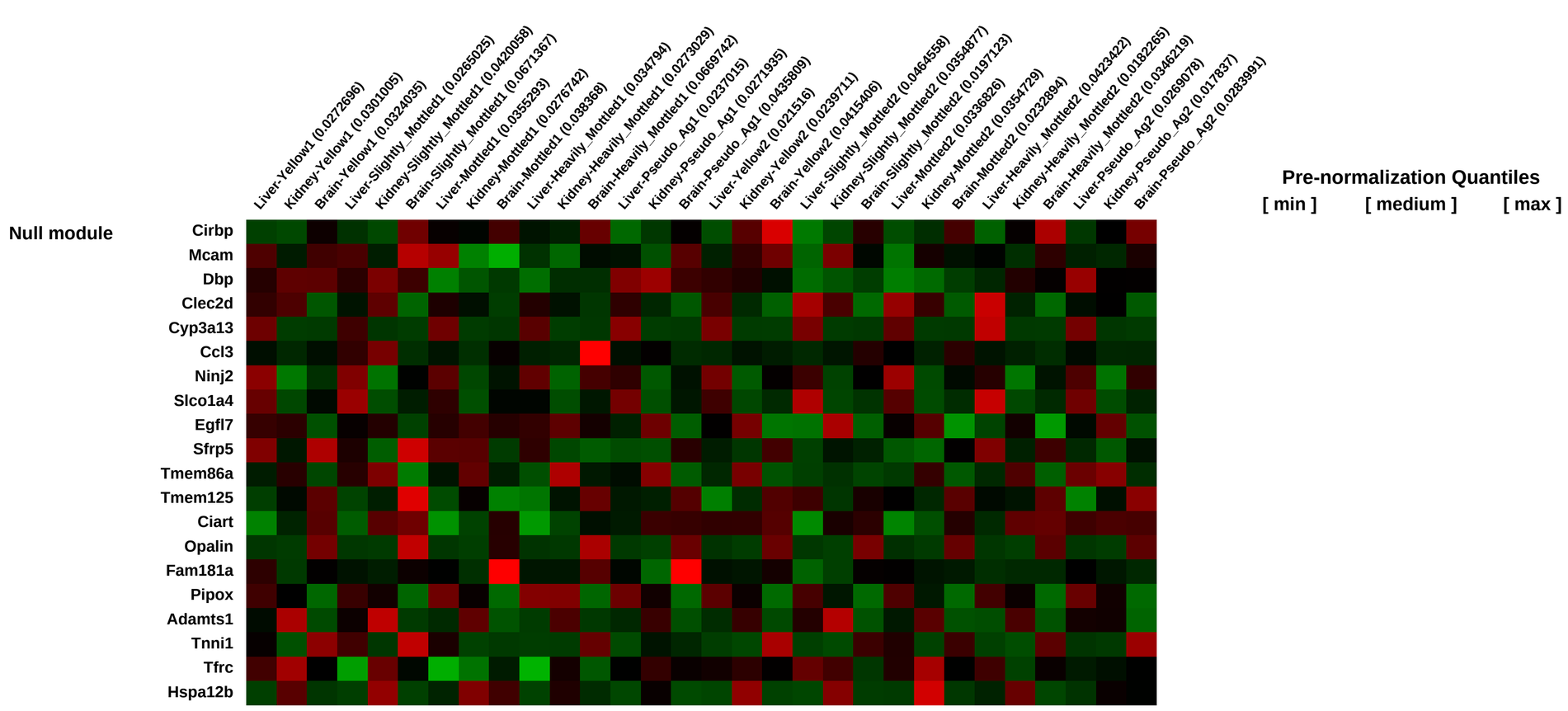

GEO Series "GSE38463" Expression Profiles

Num of samples in this series: 41

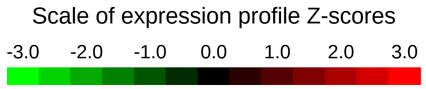

GEO Link:	http://www.ncbi.nlm.nih.gov/geo/query/acc.cgi?acc=GSE38463
Status:	Public on Jan 14 2013
Title:	Gene expression profiling of mouse B cell progenitors
Organism:	Mus musculus
Experiment type:	Expression profiling by array
Platform:	GPL1261
Pubmed ID:	23334668
Summary & Design:	**Summary:** Gene expression profiling was performed of Pax5 wild type bone marrow subsets from common lymphoid progenitors through to Hardy stage F cells. These cells were obtained by flow sorting of bone marrow. **Overall design:** SNP & Sequencing data: dbGaP phs000341.v1.p1

Background corr dist: KL-Divergence = 0.2990, L1-Distance = 0.0620, L2-Distance = 0.0107, Normal std = 0.2837

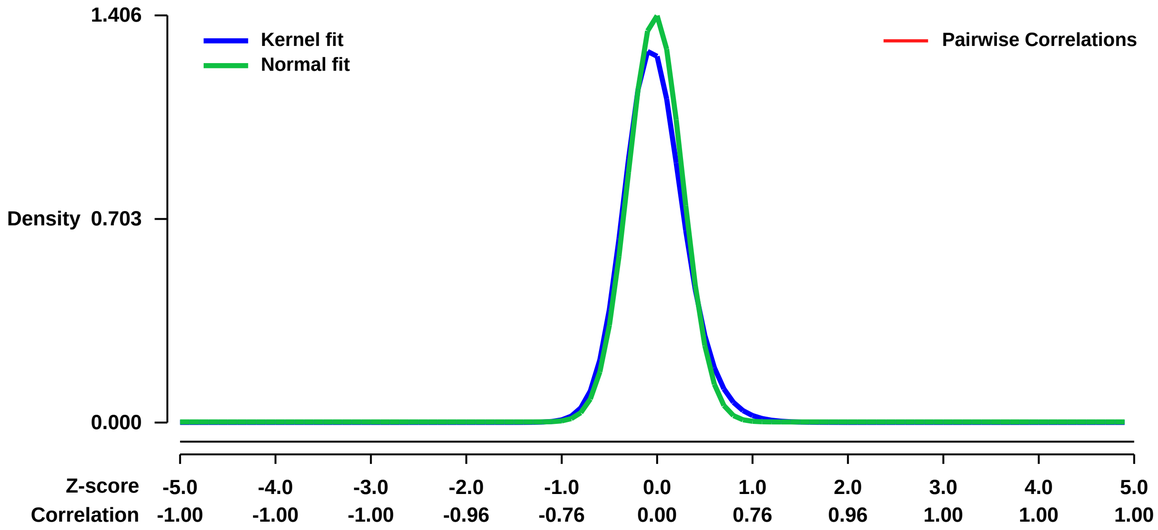

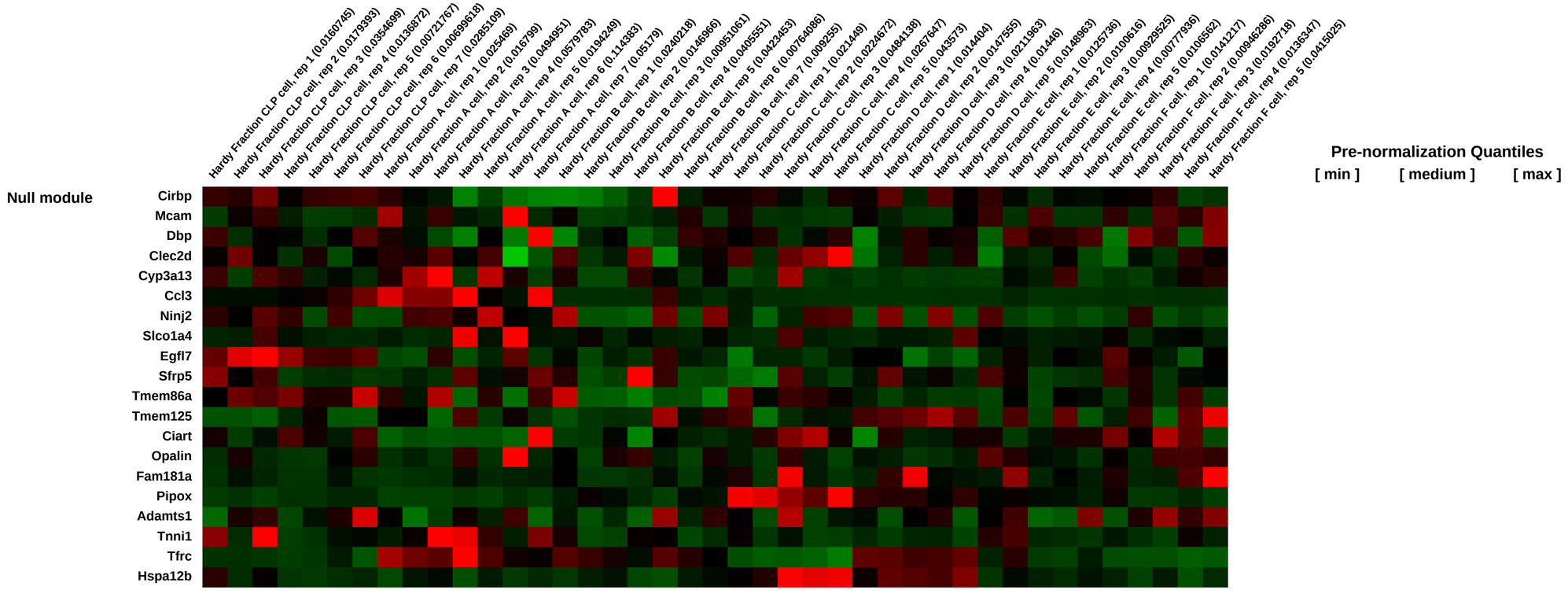

GEO Series "GSE4768" Expression Profiles

Num of samples in this series: 18

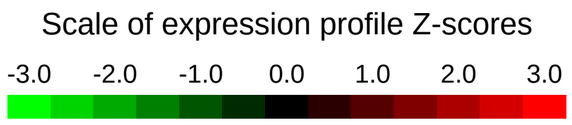

GEO Link:	**http://www.ncbi.nlm.nih.gov/geo/query/acc.cgi?acc=GSE4768**
Status:	**Public on May 06 2006**
Title:	**Global analysis of transcriptional changes following genomic demethylation in chondrocytes, osteoblasts, and fibroblasts**
Organism:	**Mus musculus**
Experiment type:	**Methylation profiling by array**
Platform:	**GPL1261**
Pubmed ID:	
Summary & Design:	**Summary:** **DNA methylation can contribute to the stable transcriptional silencing of mammalian genes. Oftentimes, these genes are important developmental regulators, and their silencing in cell types where they are not supposed to be active is important for the phenotypic stability of the cells. To identify key developmental regulator genes whose expression in terminally differentiated cells may be inhibited by DNA methylation, mouse dermal fibroblasts were demethylated with 5-aza-2â -deoxycytidine, and changes in gene expression monitored by microarray analysis.** **Keywords: 5-aza-2'-deoxycytidine; methylation; dermal fibroblast; chondrocyte; osteoblast** **Overall design:** **Three biological replicates for both control and 5-aza-2'-deoxycytidine treatment were derived. Cells were primary mouse dermal fibroblasts, primary mouse chondrocytes, and primary mouse osteoblasts derived separately for each biological replicate. Treated cells were exposed to 5uM 5-aza-2'-deoxycytidine for 96 hours with recovery in normal medium for 24 hours. Control cells were untreated.**

Background corr dist: KL-Divergence = 0.1372, L1-Distance = 0.0288, L2-Distance = 0.0012, Normal std = 0.3884

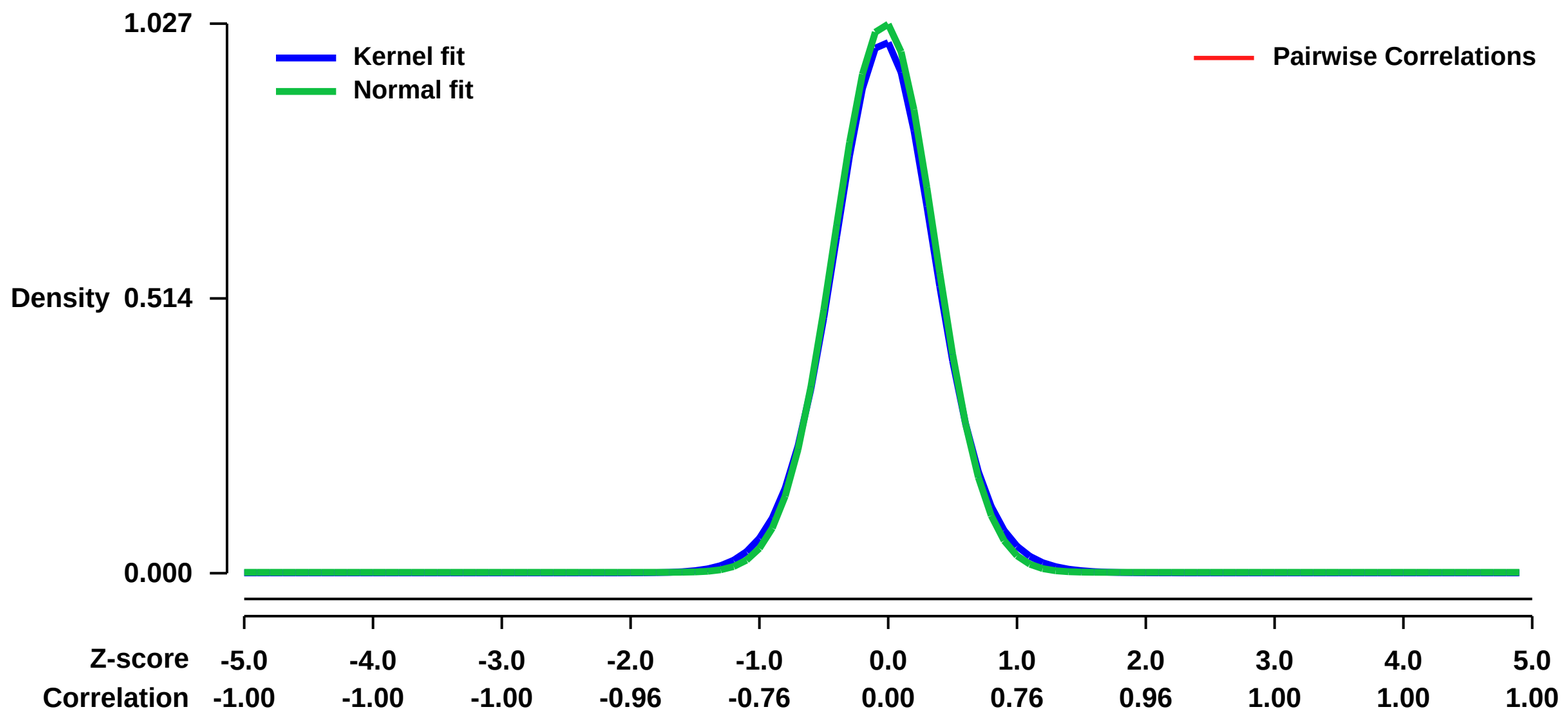

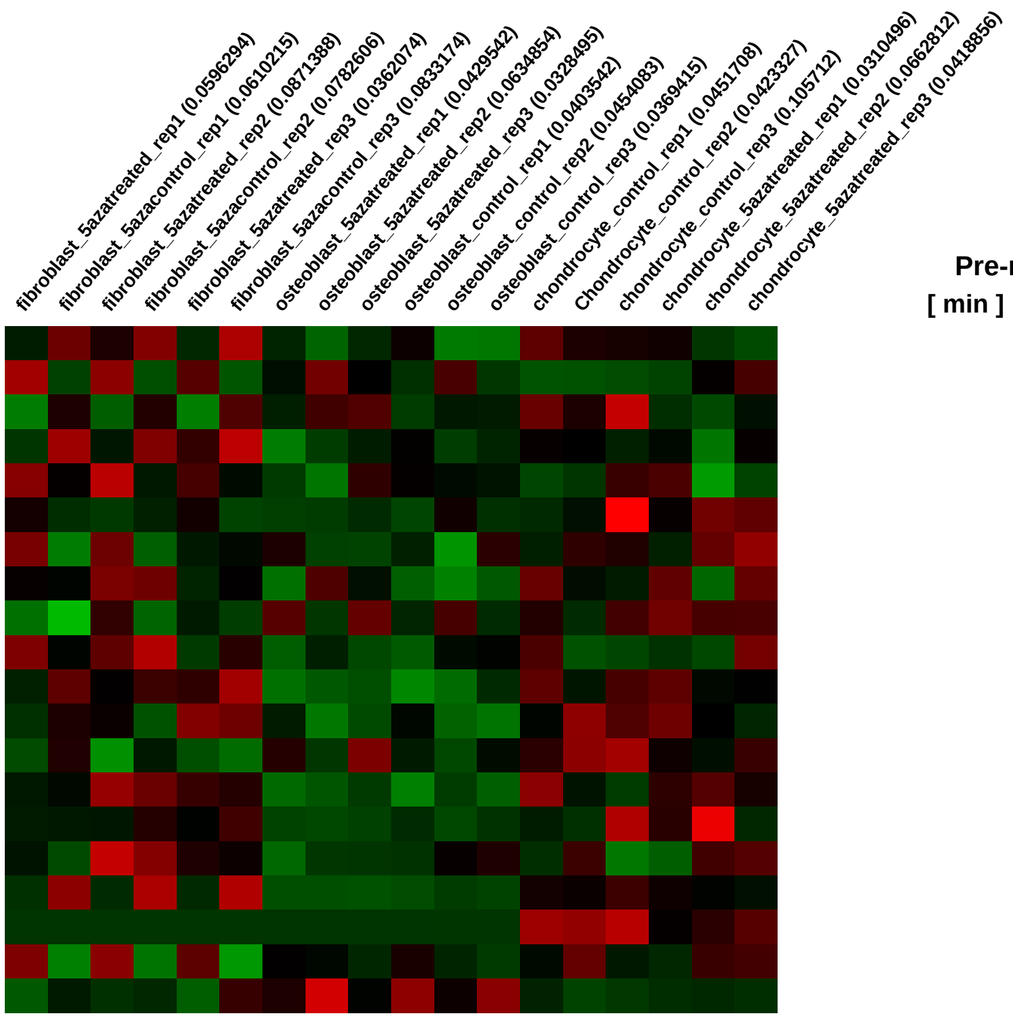

GEO Series "GSE11679" Expression Profiles

Num of samples in this series: 25

Scale of expression profile Z-scores

-3.0 -2.0 -1.0 0.0 1.0 2.0 3.0

GEO Link:	http://www.ncbi.nlm.nih.gov/geo/query/acc.cgi?acc=GSE11679
Status:	Public on Oct 08 2008
Title:	Gene expression changes related to postnatal handling
Organism:	Mus musculus
Experiment type:	Expression profiling by array
Platform:	GPL1261
Pubmed ID:	18836535
Summary & Design:	**Summary:** Postnatal handling in rodents leads to decreased anxiety-like behavior in adulthood. We used microarrays to look at gene expression differences in the CA1 region of the hippocampus in female mice subjected to postnatal handling compared to controls. **Overall design:** Balb c/J offspring were briefly separated from mothers for 15 minutes each morning on postnatal days 1-14 (handled group) or left undisturbed. At 8 weeks of age mice were tested in the open-field and light-dark behavioral paradigms to verify a handling-induced behavioral phenotype. 2 weeks after behavioral testing, animals were sacrificed and the CA1 region was microdissected. CA1 regions were stored at -20C in RNA later. RNA was extracted from 8 samples (4 handled and 4 non-handled) using Trizol. RNA was extracted from second group of animals (7 handled and 10 non-handled) using Qiagen RNA/DNA columns. All total RNA samples were double round amplied and labeled using standard Affymetrix protocols and hybridized to Mouse 430_2.0 arrays in parallel.

Background corr dist: KL-Divergence = 0.1846, L1-Distance = 0.0311, L2-Distance = 0.0015, Normal std = 0.3522

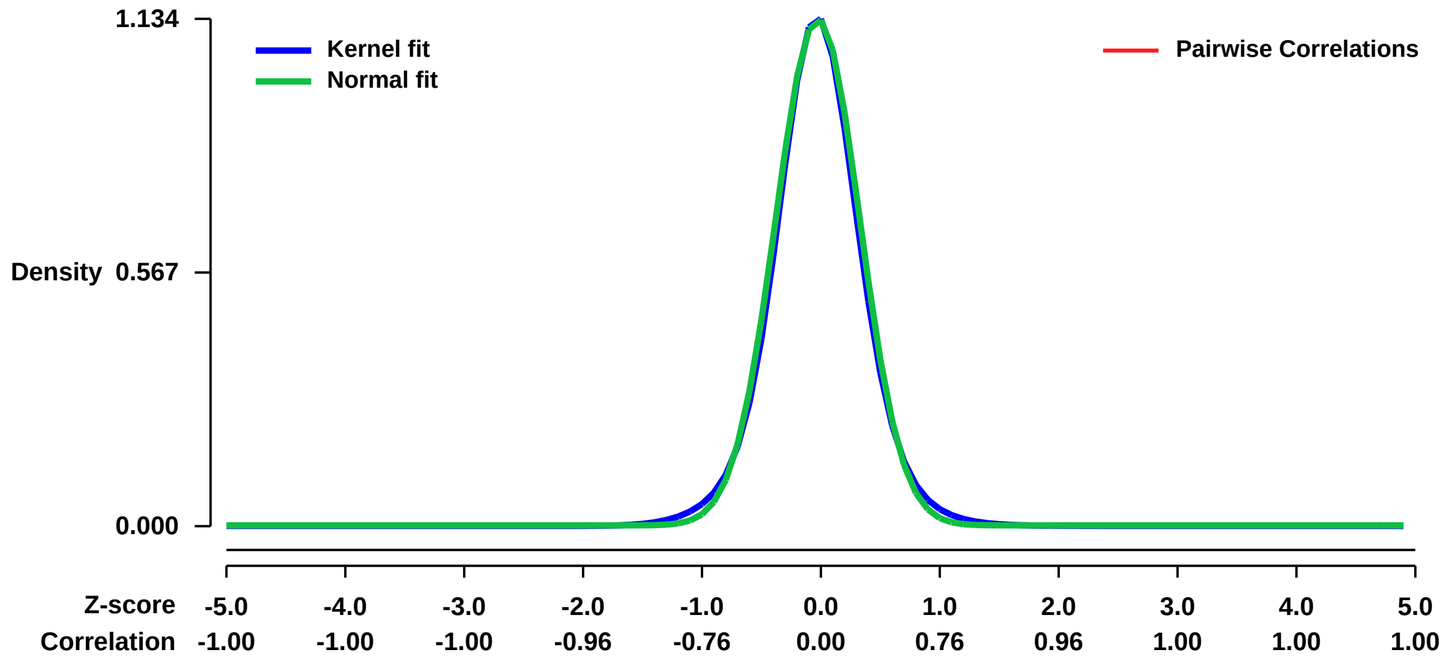

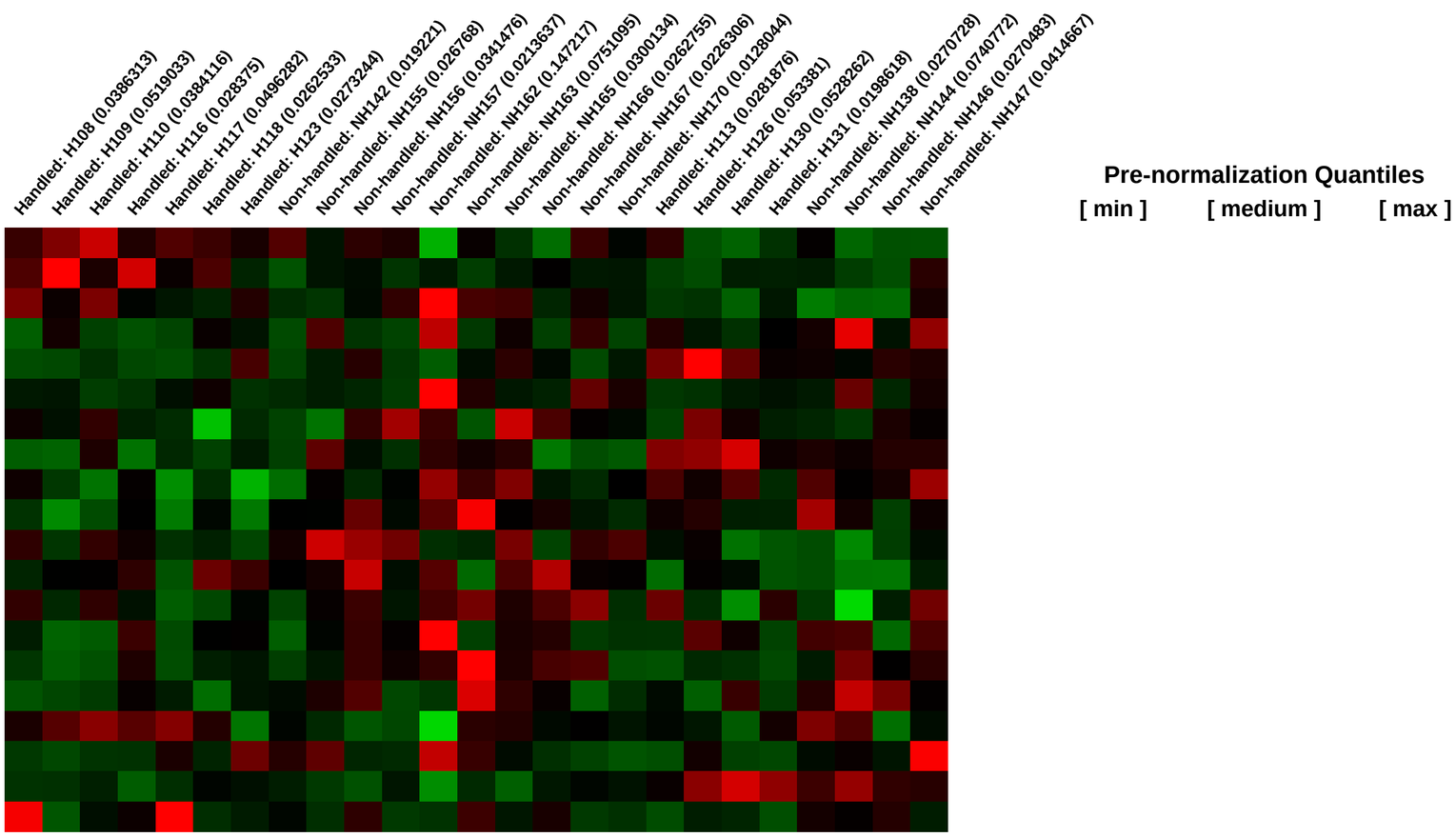

GEO Series "GSE18992" Expression Profiles

Num of samples in this series: 8

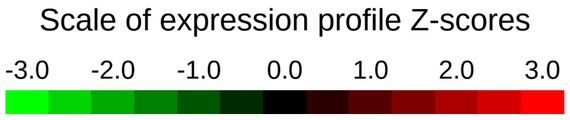

GEO Link:	**http://www.ncbi.nlm.nih.gov/geo/query/acc.cgi?acc=GSE18992**
Status:	**Public on Oct 15 2010**
Title:	**Overexpression of Hoxc8 transcription factor alters transcriptional profiles in mouse chondrocytes at E18.5**
Organism:	**Mus musculus**
Experiment type:	**Expression profiling by array**
Platform:	**GPL1261**
Pubmed ID:	
Summary & Design:	**Summary:** **Homeobox genes of the Hox class are required for proper patterning of skeletal elements and play a role in cartilage differentiation. In transgenic mice with overexpression of Hoxc8 during cartilage development, we observed severe defects, namely physical instability of cartilage, accumulation of immature chondrocytes, and decreased maturation to hypertrophy. To define the molecular basis underlying these defects, we performed gene expression profiling using the Affymetrix microarray platform.** **Overall design:** **Embryos were dissected from four different mouse litters at E18.5. Embryos from each litter were grouped according their genotype: TA=control; TR=transgenic.**

Background corr dist: **KL-Divergence = 0.0799, L1-Distance = 0.0208, L2-Distance = 0.0007, Normal std = 0.4762**

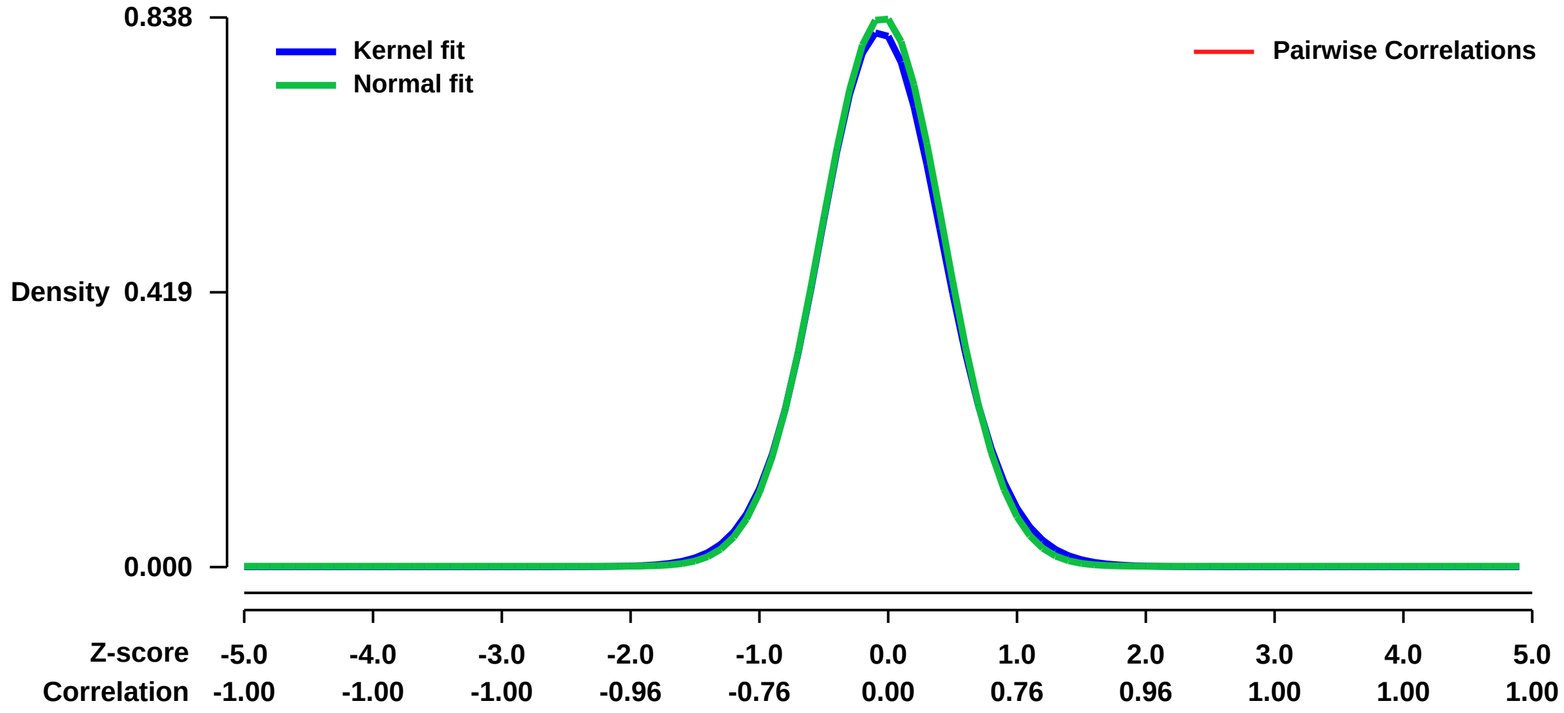

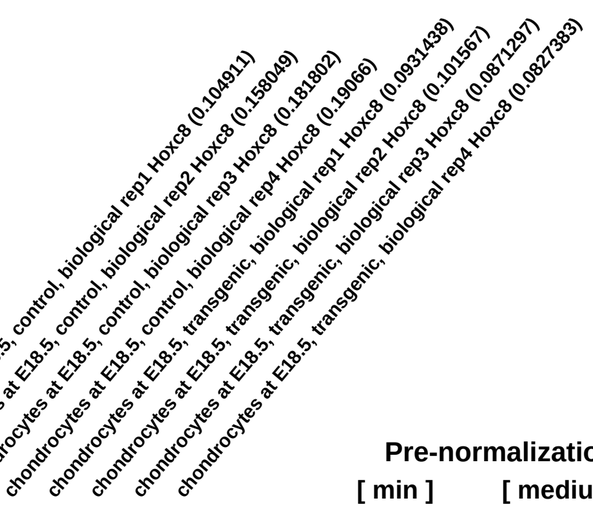

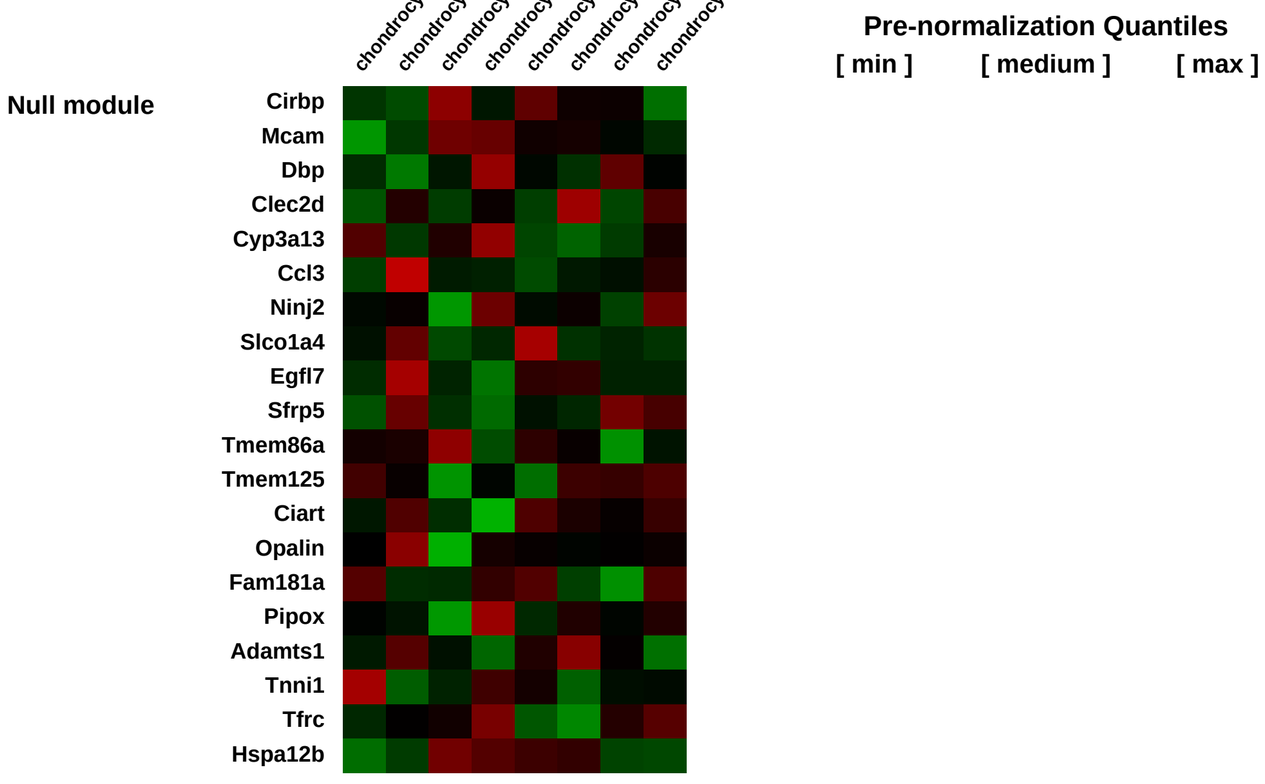

GEO Series "GSE34807" Expression Profiles

Num of samples in this series: 20

Scale of expression profile Z-scores

-3.0 -2.0 -1.0 0.0 1.0 2.0 3.0

GEO Link:	**http://www.ncbi.nlm.nih.gov/geo/query/acc.cgi?acc=GSE34807**
Status:	**Public on Dec 20 2012**
Title:	**The estrogen receptor ¸– is required and sufficient to maintain physiological glucose uptake in the mouse heart**
Organism:	**Mus musculus**
Experiment type:	**Expression profiling by array**
Platform:	**GPL1261**
Pubmed ID:	
Summary & Design:	**Summary:** **Rationale: Estrogens attenuate cardiac hypertrophy and increase cardiac contractility via their cognate receptors ER¸– and ER¸†. Since female sex hormones enhance global glucose utilization and because myocardial function and mass are tightly linked to cardiac glucose metabolism we tested the hypothesis that expression and activation of the estrogen receptor ¸– (ER¸–) might be required and sufficient to maintain physiological cardiac glucose uptake in the murine heart. Methods and Results: Cardiac glucose uptake quantified in vivo by 18F-fluorodeoxyglucose positron emission tomography (FDG-PET) was strongly impaired in ovarectomized compared to gonadal intact female C57BL/6JO mice. The selective ER¸– agonist 16¸–-LE2 and the non-selective ER¸– and ER¸† agonist 17¸†-estradiol completely restored cardiac glucose uptake in ovarectomized mice. Cardiac FDG uptake was strongly decreased in female ER¸– knockout mice (ERKO) compared to wild type littermates. Biochemical assays, affymetrix cDNA array analysis, western blotting and immuno-staining of cardiac glucose transporters revealed a positive correlation of ER¸– dependent cardiac FDG uptake with preserved cardiac glucose transporter-1 expression and micro-vascular localization. Conclusions: Systemic activation of the ER¸– estrogen receptor is sufficient and its expression is required to maintain physiological glucose uptake in the murine heart, which is likely to contribute to known cardio-protective estrogen effects.** **Overall design:** **total samples analysed are 20**

Background corr dist: KL-Divergence = 0.0902, L1-Distance = 0.0670, L2-Distance = 0.0084, Normal std = 0.4873

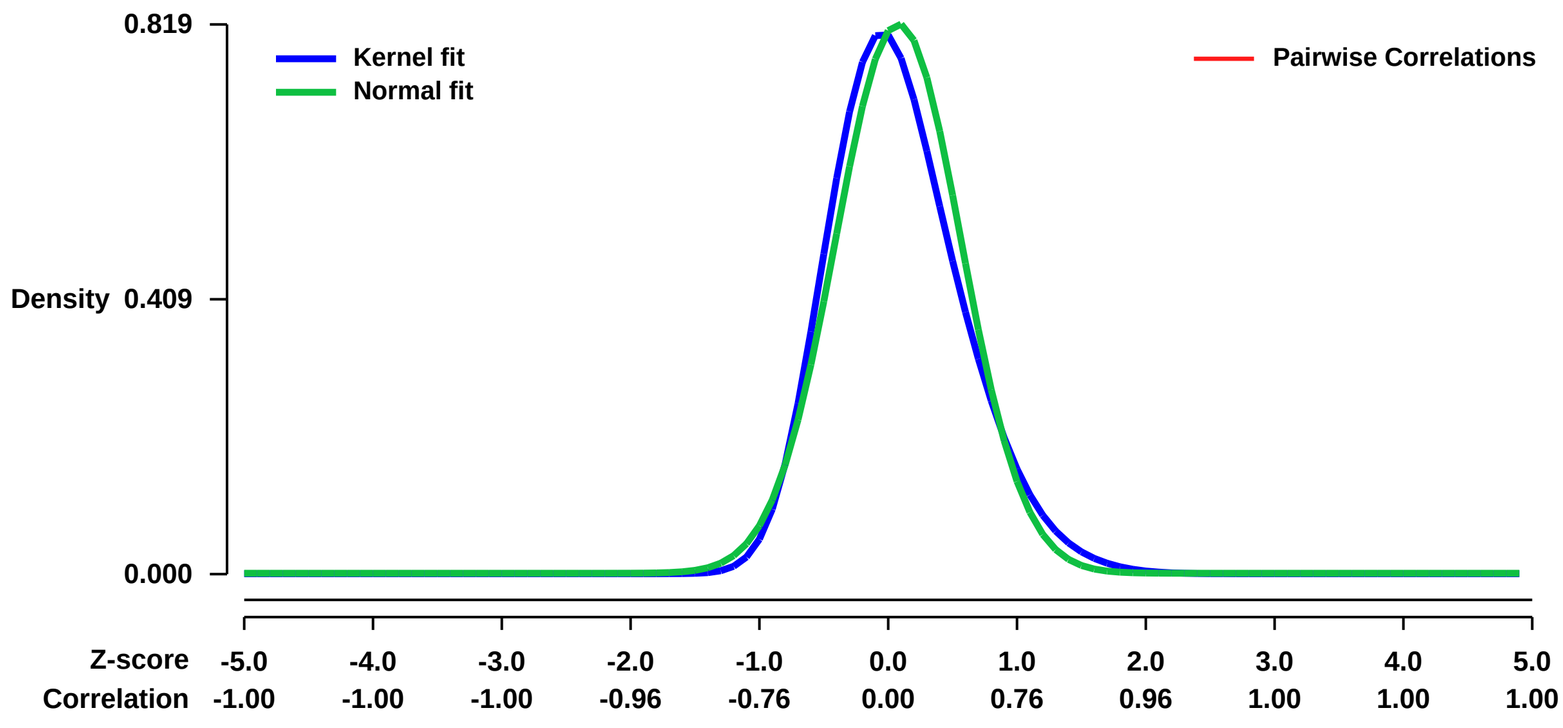

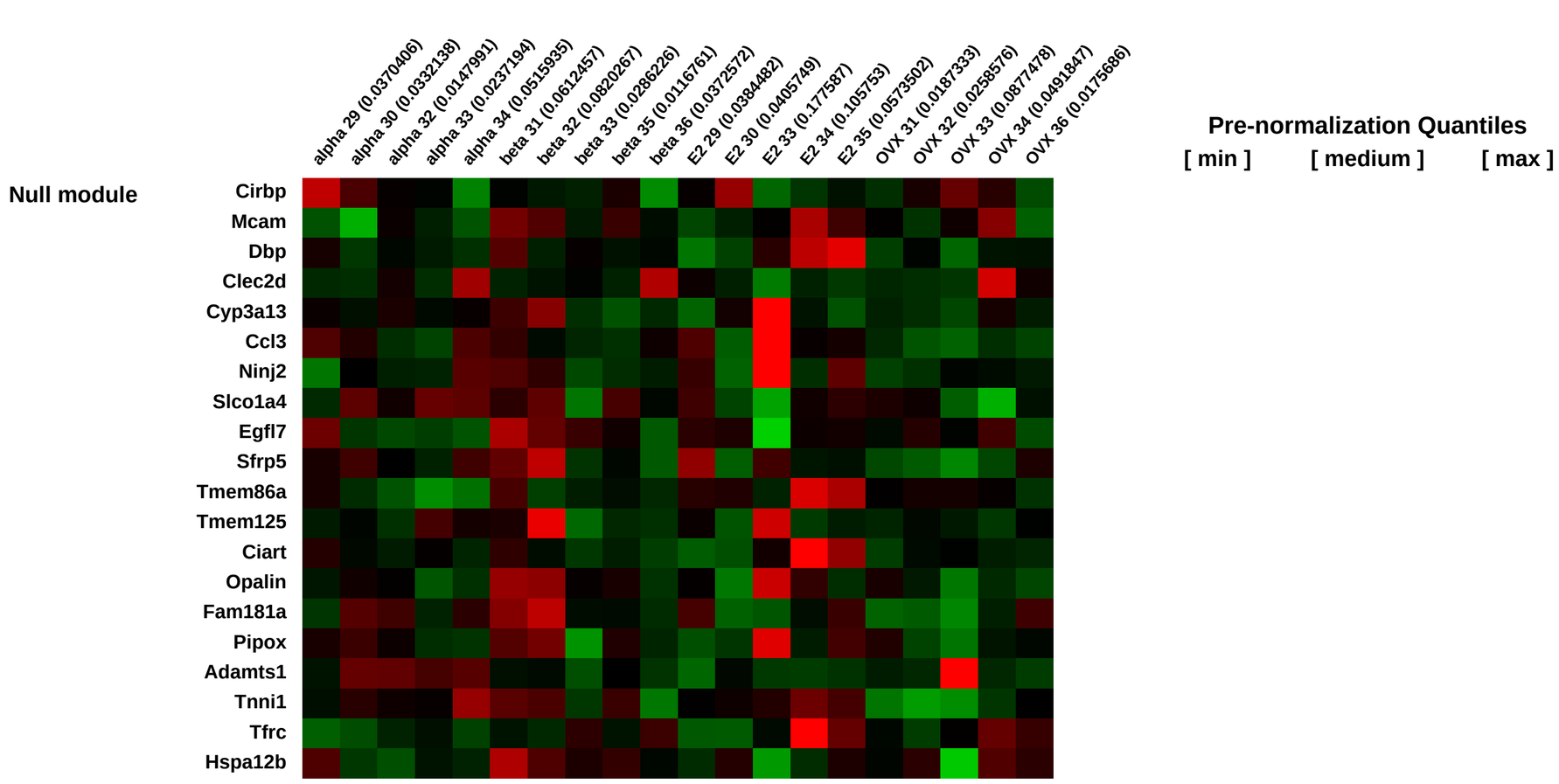

GEO Series "GSE21393" Expression Profiles

Num of samples in this series: 6

Scale of expression profile Z-scores

-3.0 -2.0 -1.0 0.0 1.0 2.0 3.0

GEO Link: http://www.ncbi.nlm.nih.gov/geo/query/acc.cgi?acc=GSE21393
Status: Public on Dec 31 2010
Title: Stroke-brain infiltrating stem cells - mouse
Organism: Mus musculus
Experiment type: Expression profiling by array
Platform: GPL1261
Pubmed ID:

Summary & Design:

Summary:
Genes upregulated in stroke infiltrating stem cells were compared against the parent non-infiltrated mouse stem cell line derived from immortomouseTM.

Abstract

Background and Purpose- Although the therapeutic potential of bone marrow-derived stem cells (SC) has been addressed in different experimental models of ischemic stroke, it is still unclear how SC induce neuroprotection following stroke. In this study, we describe a novel method for recovering SC infiltrating post-stroke brain tissue allowing the determination of genes which become persistently activated / or depressed (compared to their naˆflve counterparts) during SC-mediated neuroprotection.

Methods- Ischemic stroke was induced in C57BL/6 mice by middle cerebral artery occlusion for 1 h, followed by reperfusion. SC were isolated from H-2Kb-tsA58 (immortomouseTM) mice, and were administered (i.v.) 24 h after reperfusion. At the onset of therapeutic improvement (14 days after ischemia), infarcted brain tissue was isolated and infarct-infiltratng SC cultured at 33´℃. Microarray analysis and RT-PCR were performed to compare persistent differential gene expression between naˆflve and infiltrating SC populations.

Results- Z-scoring revealed dramatic changes in extracellular genes of analyzed cells. Pair-wise analysis detected 80 extracellular factor genes that were up-regulated (2 fold, P<0.05, Benjamini-Hochberg correction) between naˆflve and infiltrated SC. Although several conventional neuroregenerative, nerve guidance and angiogenic factors (bFGF, bone morphogenetic protein, angiopoietins, neural growth factors were among the expressed genes detected we identified Cytokine receptor-like factor 1 (Crlf1), Fgf7, family with sequence similarity 19, member A5 (Fam19a5), Glypican 1 (Gpc1), Dickkopf homolog 2 (Dkk2), Endothelial cell-specific molecule 1, Osteopontin (OPN)35, Tissue factor pathway inhibitor 2, Masp3 mRNA for MBL-associated serine protease-3, Glial cell line derived neurotrophic factor (Gdnf), Bone morphogenetic protein 2 (Bmp2), Olfactomedin 1, Sushi-repeat-containing protein, X-linked 2 (Srpx2).

Conclusions- SC infiltrating the post-i schemic brain assume a persistently altered pattern of expressed extracellular genes compared to naˆflve SC that contributes to neuroprotection, regeneration and angiogenesis in infarcts.

Keywords: Gene activation / suppression study

Overall design:
Comparison of persistent stem cell gene expression induced by stroke-infarct infiltration

Background corr dist: KL-Divergence = 0.0364, L1-Distance = 0.0406, L2-Distance = 0.0024, Normal std = 0.6612

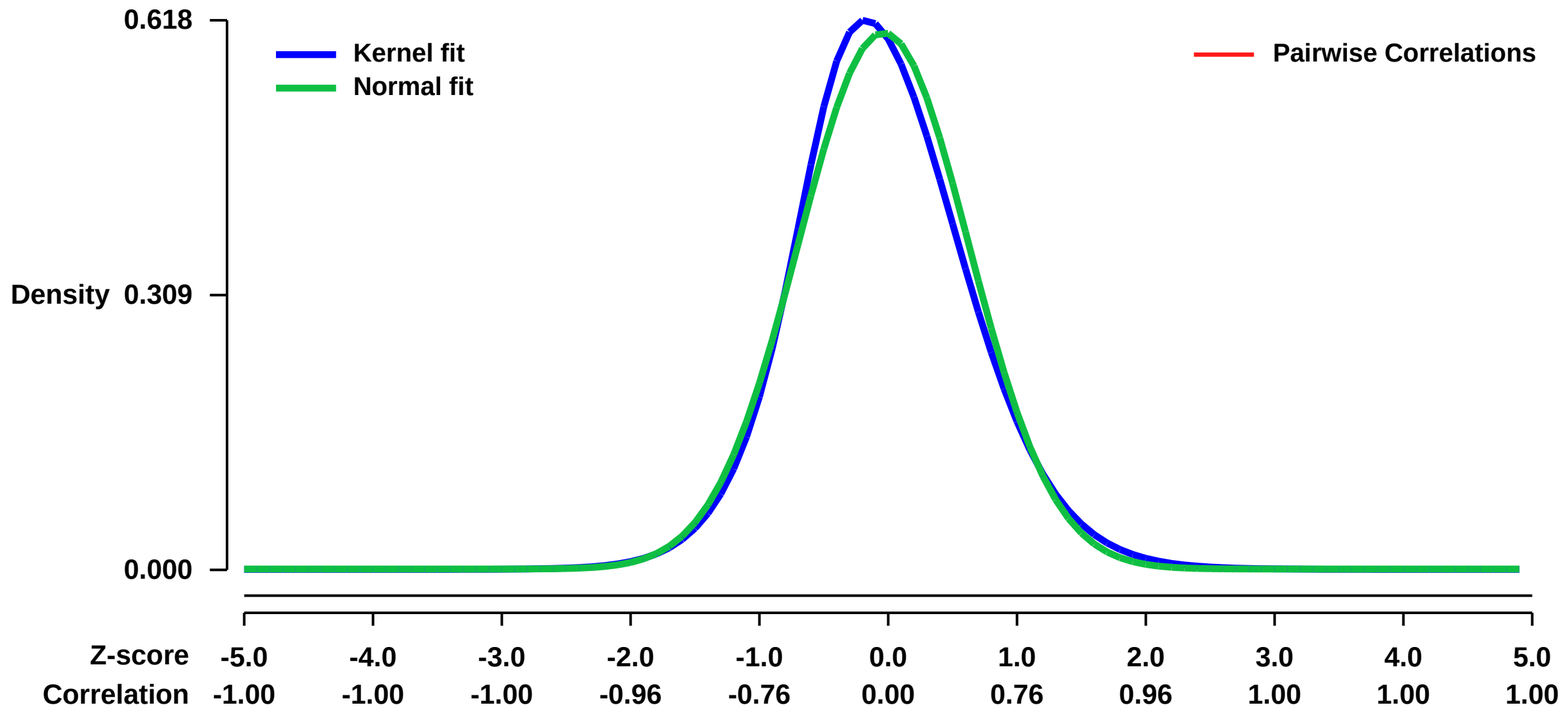

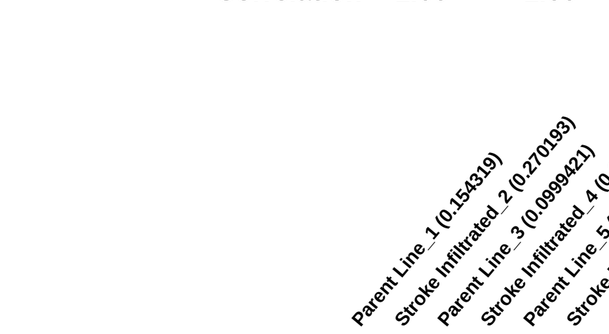

GEO Series "GSE28621" Expression Profiles

Num of samples in this series: 21

Scale of expression profile Z-scores

-3.0 -2.0 -1.0 0.0 1.0 2.0 3.0

GEO Link:	http://www.ncbi.nlm.nih.gov/geo/query/acc.cgi?acc=GSE28621
Status:	Public on May 09 2014
Title:	Transcriptional profiles of macrophages in resolving inflammation
Organism:	Mus musculus
Experiment type:	Expression profiling by array
Platform:	GPL1261
Pubmed ID:	24762537
Summary & Design:	**Summary:** We have performed a comprehensive transcriptional analysis of specific monocyte and macrophage (Mˆ) subsets during an acute self-resolving inflammatory insult. Following initial induction of acute inflammation, tissue resident (Resident) Mˆ are rapidly â clearedâ from the inflammatory foci, only becoming recoverable as inflammation resolves. Monocytes are recruited to the inflammatory lesion where they differentiate into Mˆ. We term these monocyte-derived Mˆ â inflammation-associatedâ to distinguish them from Resident Mˆ which are present throughout the inflammatory response and can renew during the resolution of inflammation by proliferation. Comparative analysis of the Mo and Mˆ populations (both â inflammation-associatedâ and Resident Mˆ) identifies select genes expressed in subsets of â inflammation-associatedâ and Resident Mˆ that play important roles in the resolution of inflammation and/or for immunity, including molecules involved in antigen presentation, cell cycle and others associated with â immaturityâ and Mˆ activation. **Overall design:** We purified monocyte and macrophage populations from the peritoneal cavity of C57BL/6 mice 4, 18, 72 and 168 hours after the induction of inflammation with intraperitoneal administration of zymosan (2x10^7 particles). We also purified tissue resident macrophages and Ly-6B+ bone marrow monocytes from naive mice as reference populations.

Background corr dist: KL-Divergence = 0.1827, L1-Distance = 0.0365, L2-Distance = 0.0024, Normal std = 0.3564

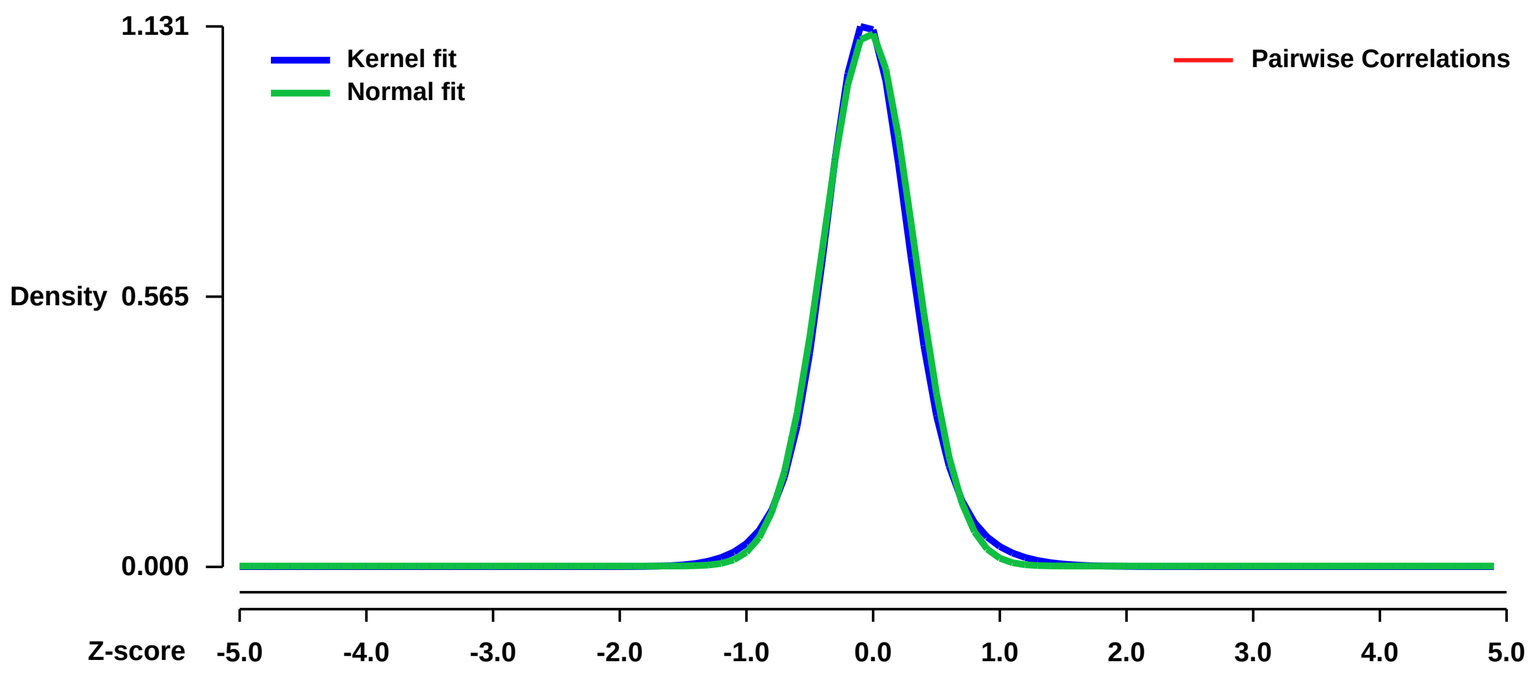

Correlation -1.00 -1.00 -1.00 -0.96 -0.76 0.00 0.76 0.96 1.00 1.00 1.00

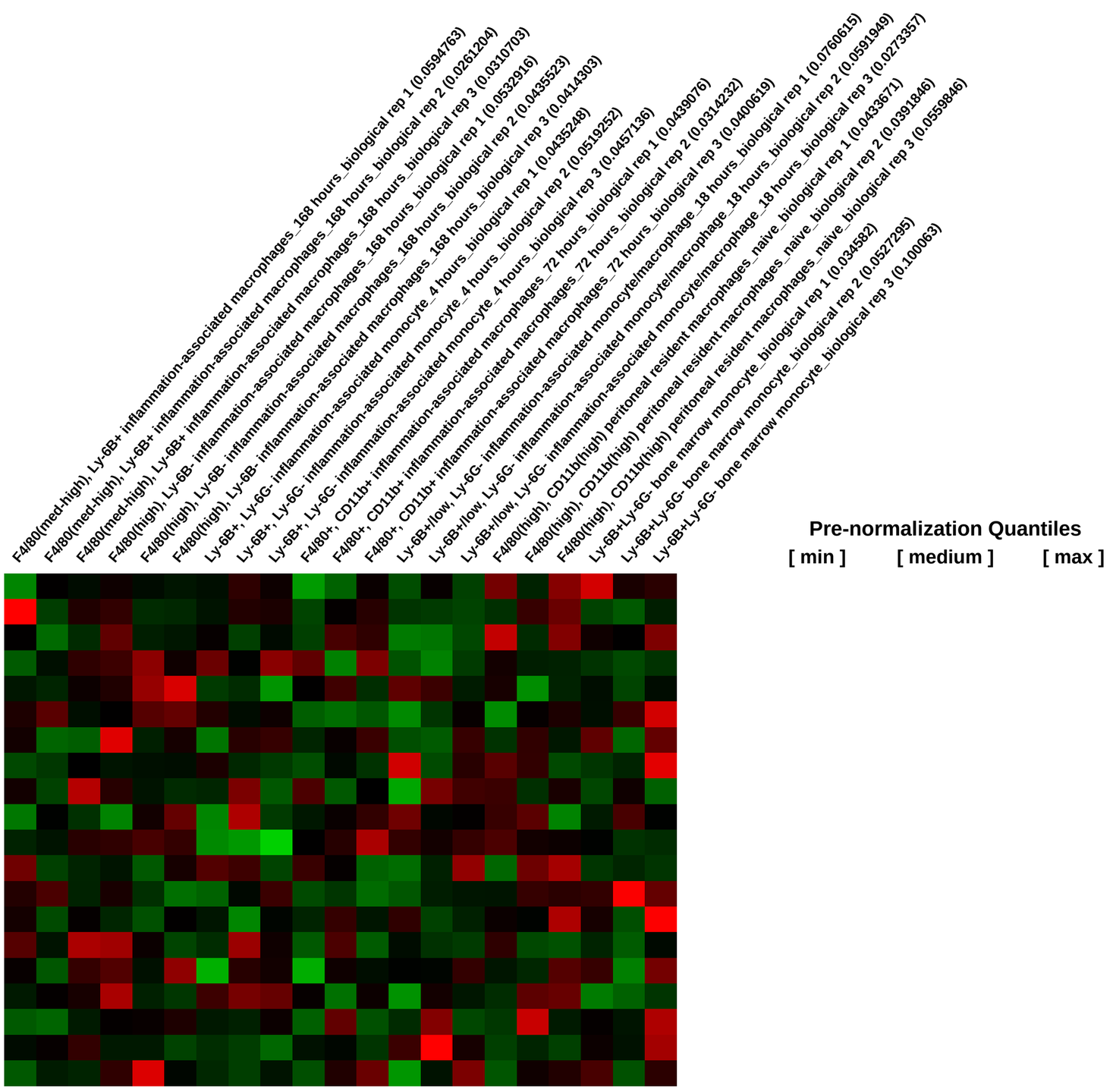

GEO Series "GSE4411" Expression Profiles

Num of samples in this series: 11

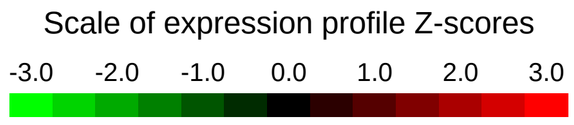

GEO Link:	http://www.ncbi.nlm.nih.gov/geo/query/acc.cgi?acc=GSE4411
Status:	Public on Mar 08 2006
Title:	burde-affy-arabi-64764
Organism:	Mus musculus
Experiment type:	Expression profiling by array
Platform:	GPL1261
Pubmed ID:	16024660

Summary & Design:

Summary:
In skeletal muscle, the pattern of electrical activity regulates the expression of proteins involved in synaptic transmission, contraction and metabolism. Disruptions in electrical activity, resulting from prolonged bed-rest, cast-immobilization or trauma, inevitably lead to muscle atrophy. The mechanisms that regulate muscle atrophy are poorly understood, but it seems likely that changes in gene expression play a key role in initiating and maintaining a muscle atrophy program. Previously, we found that Runx1, a transcription factor previously termed AML1, was substantially induced in muscle following denervation. More recently, we sought to determine whether this increase in Runx1 expression may be causally related to the morphological changes in skeletal muscle that accompany muscle disuse, notably muscle atrophy. We found that Runx1 is indeed required to sustain muscle and to minimize atrophy following denervation. Experiments described here are designed to identify the genes that are regulated by Runx1 in skeletal muscle with the particular goal of identifying genes that regulate muscle atrophy.

We propose to use microarray analysis to identify genes, expressed in skeletal muscle, that are mis-regulated in mice lacking Runx1.

We inactivated runx1 selectively in skeletal muscle and found that denervated myofibers in mutant mice atrophy far more (90% atrophy) than in wild-type mice (30% atrophy). We therefore reason that Runx1 activates and/or represses genes that are required to sustain muscle and to minimize atrophy.

We generated MCK::cre; runx1f/- and runx1f/- control mice. In normal mice, an increase in runx1 expression is detected by two days after denervation and is maximal by five days after denervation. Muscle atrophy is first evident between one and two weeks after denervation. As we wish to avoid detecting global changes in gene expression that are associated with late stages of muscle atrophy, we plan to denervate muscle for three or five days and to compare gene expression in dissected innervated and denervated muscles from mutant and control mice. We will generate thirty samples for comparison-5 replicates per condition: Samples 1-3 from runx1f/- control mice. (1) innervated tibialis anterior muscles (TA); (2) 3-day-denervated TA; (3) 5-day-denervated TA. Samples 4-6 from MCK::cre; runx1f/- mice. (4) innervated TA; (5) 3-day-denervated TA; (6) 5-day-denervated TA. We obtain sufficient total RNA (10 micrograms) from each dissected muscle to avoid pooling samples. We will analyze adult mice of the same age (~six weeks after birth; most will be littermates) and sex-male. It is difficult to anticipate how many genes will be identified in this screen, as few target genes for Runx1 have been identified in any cell type and none in skeletal muscle. Moreover, although we would prefer to focus our attention on genes that are strongly dependent upon Runx1 expression (e.g. more than 5-fold difference in expression in wild-type and mutant mice), we do not know the extent to which target gene expression will depend upon Runx1. For these reasons, in these experiments, we will analyze expression from five â identicalâ samples, so that we can be confident that even small (e.g. three-fold) differences in expression can be reliably determined. Importantly, in order to confirm results obtained from the microarray data, we will use other assays (RNase protection) to measure RNA expression of candidate genes in innervated and denervated muscles of wild-type and mutant mice.

Keywords: other

Overall design:

Background corr dist: KL-Divergence = 0.0801, L1-Distance = 0.0262, L2-Distance = 0.0008, Normal std = 0.4874

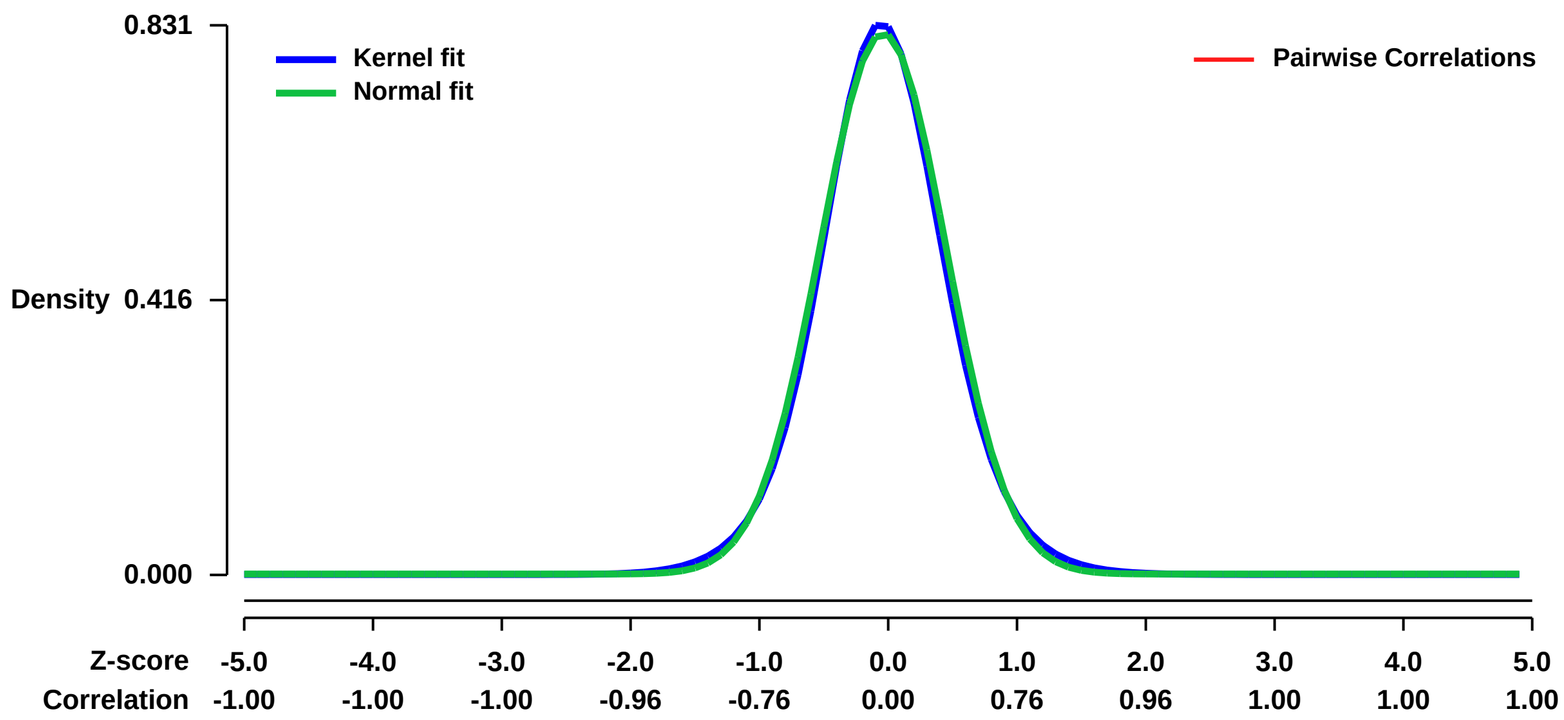

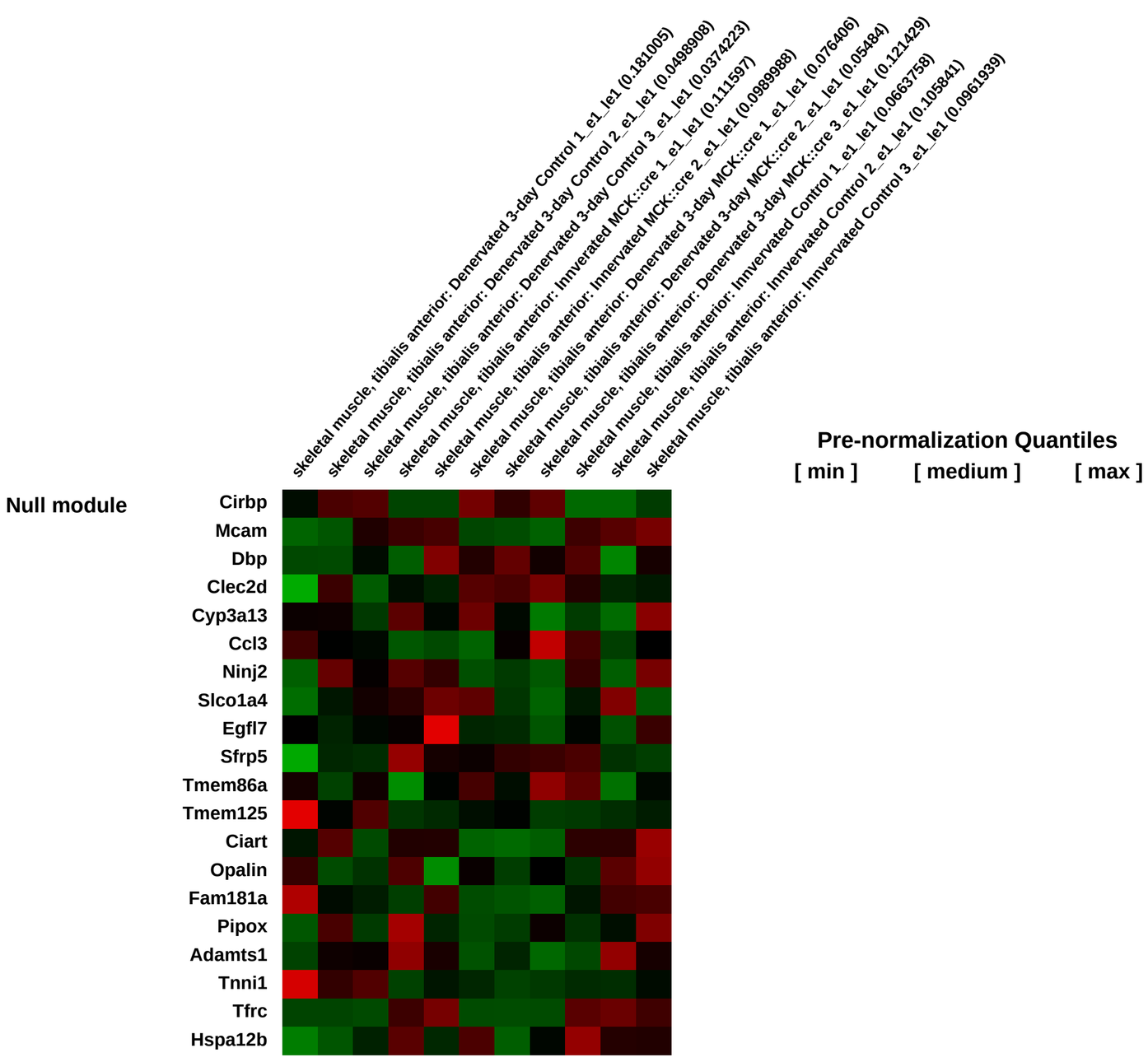

GEO Series "GSE16110" Expression Profiles

Num of samples in this series: 16

Scale of expression profile Z-scores

-3.0 -2.0 -1.0 0.0 1.0 2.0 3.0

GEO Link:	**http://www.ncbi.nlm.nih.gov/geo/query/acc.cgi?acc=GSE16110**
Status:	**Public on Jul 01 2009**
Title:	**Altered mouse mammary gland gene expression and tumor growth following chronic social isolation**
Organism:	**Mus musculus**
Experiment type:	**Expression profiling by array**
Platform:	**GPL1261**
Pubmed ID:	
Summary & Design:	**Summary:** **Clinical studies have revealed that social support improves the outcome of cancer patients while epidemiological studies suggest that social isolation increases the risk of death associated with several chronic diseases. However, the precise biological consequences of an unfavorable social environment have not been defined. To do so, robust, reproducible pre-clinical models are needed to study the mechanisms whereby an adverse environment impacts on gene expression and cancer biology. Because random assignment of inbred laboratory mice to well-defined social environments allows accurate and repeated measurements of behavioral and endocrine parameters, transgenic mice provide a pre-clinical framework with which to begin to determine gene-environment mechanisms. In this study, we found that female C3(1)/SV40 T-antigen mice deprived of social interaction from weaning exhibited increased expression of genes encoding key metabolic pathway enzymes in the pre-malignant mammary gland. Chronic social isolation was associated with upregulated fatty acid synthesis and glycolytic pathway gene expression - both pathways known to contribute to increased breast cancer growth. Consistent with the expression of metabolic genes, isolated mice subsequently developed significantly larger mammary gland tumors compared to group-housed mice. Endocrine evaluation confirmed that isolated mice developed a heightened corticosterone stress response compared to group-housed mice. Together, these transdisciplinary studies show for the first time that an adverse social environment is associated with altered mammary gland gene expression and tumor growth. Moreover, the identification of specific alterations in metabolic pathways favoring tumor growth suggests potential molecular biomarkers and/or targets (e.g. fatty acid synthesis) for preventive intervention in breast cancer.** **Overall design:** **SV40 Tag mice we isolated or grouped at weaning. Mouse mammary glands were rapidly excised at necropsy and immediatley flash frozen to detect difference in gene expression between thoraci MG from isolated versus group-housed female mice.**

Background corr dist: KL-Divergence = 0.0385, L1-Distance = 0.0261, L2-Distance = 0.0009, Normal std = 0.6020

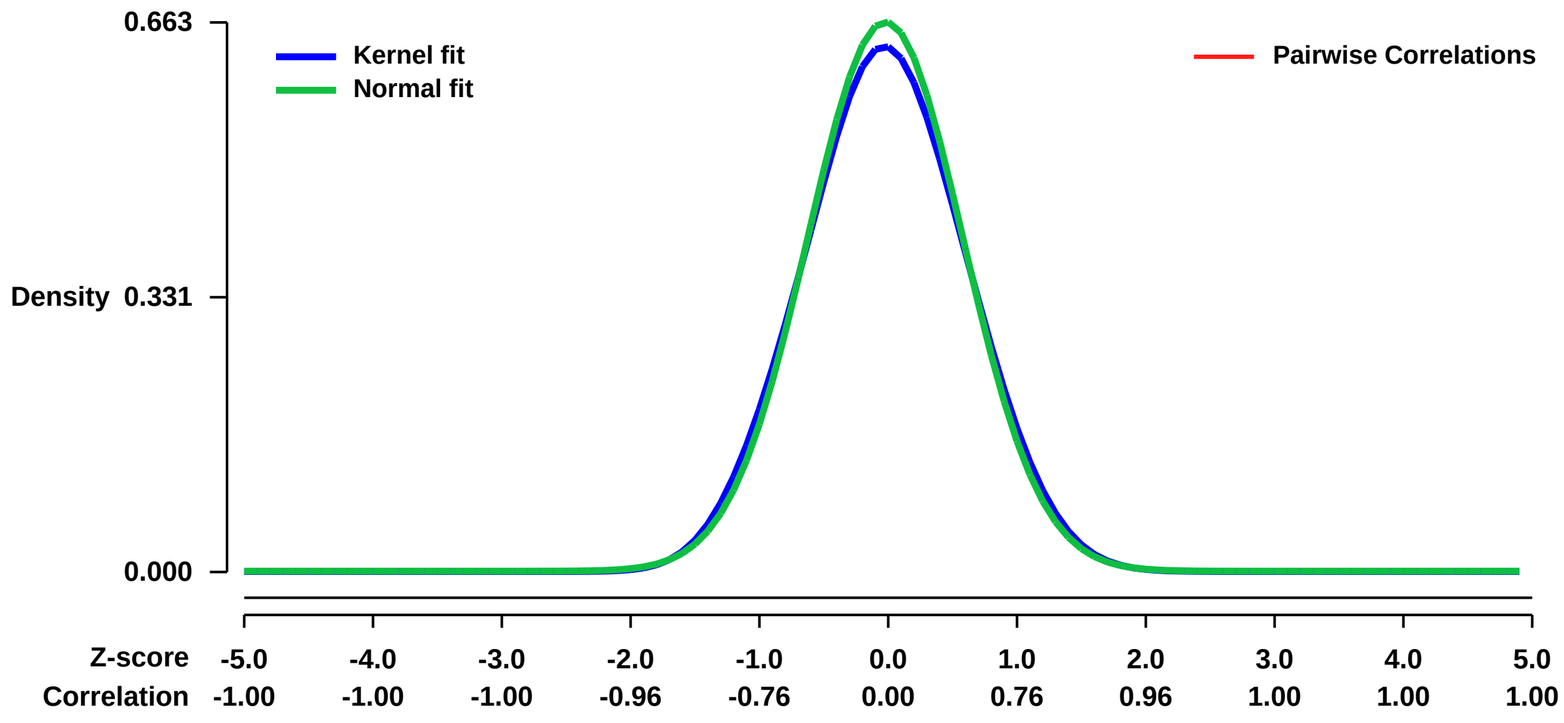

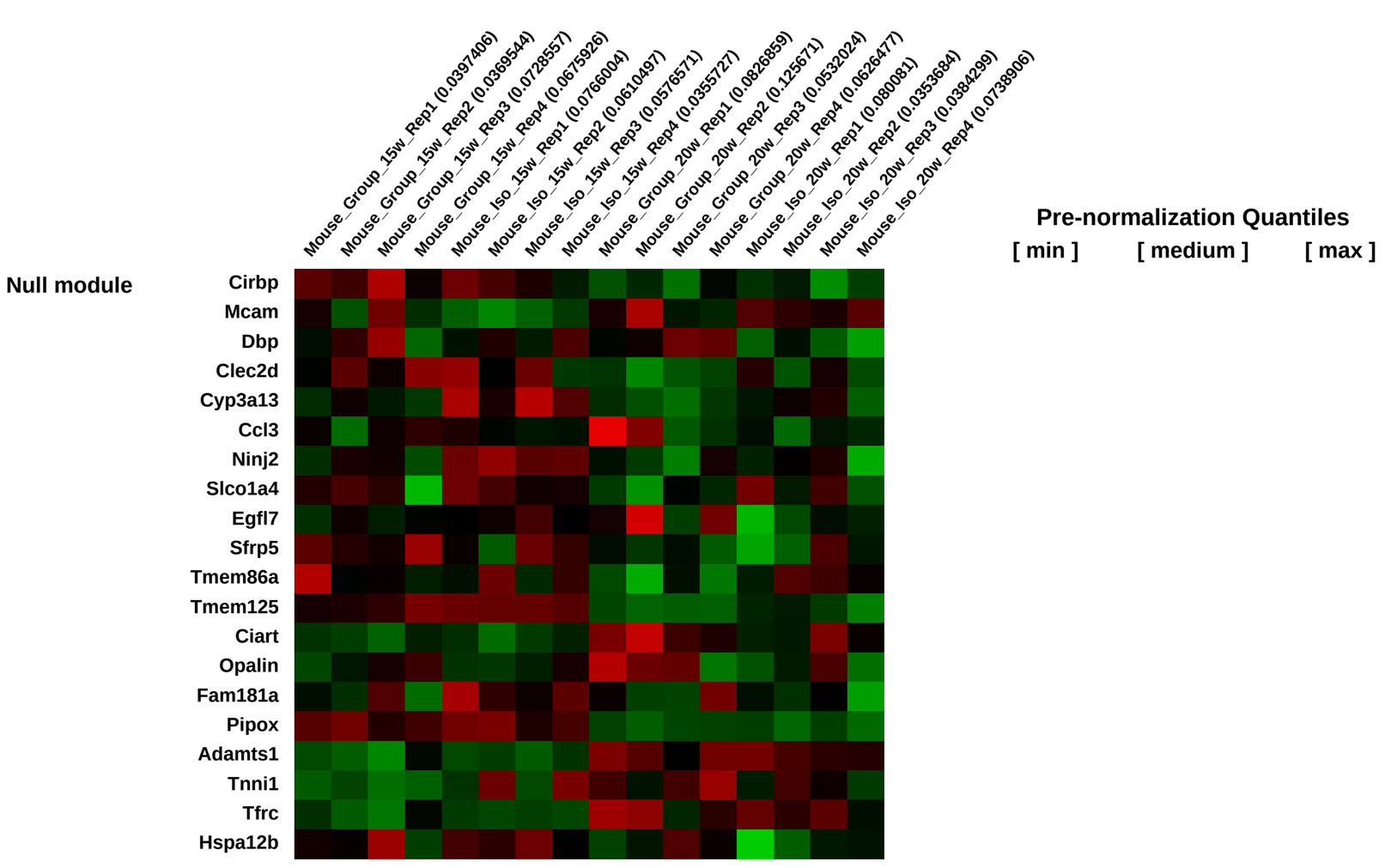

GEO Series "GSE22935" Expression Profiles

Num of samples in this series: 24

Scale of expression profile Z-scores

-3.0 -2.0 -1.0 0.0 1.0 2.0 3.0

GEO Link:	http://www.ncbi.nlm.nih.gov/geo/query/acc.cgi?acc=GSE22935
Status:	Public on Jul 14 2010
Title:	Arginine utilization following mycobacteria infection in macrophages is dependent on autocrine-paracrine signaling
Organism:	Mus musculus
Experiment type:	Expression profiling by array
Platform:	GPL1261
Pubmed ID:	20716764
Summary & Design:	**Summary:** Nitric oxide (NO) produced by macrophages (Mˆ s) is toxic to both host tissues and invading pathogens and its regulation is therefore essential to suppress host cytotoxicity. Mˆ arginase 1 (Arg1) inhibits NO production by competing with NO synthases for arginine, the common substrate of NO synthases and arginases. Two signal transduction pathways control Arg1 expression in Mˆ s. First, a MyD88-dependent pathway induces Arg1 in intracellular infections, while a second Stat6-dependent pathway is required for Arg1 expression in alternativelyactivated Mˆ s. We found that mycobacteria-infected Mˆ s produce soluble factors that induce Arg1 in an autocrine-paracrine manner via Stat3. We identify these factors as IL-6, IL-10 and GCSF. We further establish that Arg1 expression is controlled by the MyD88-dependent production of IL-6, IL-10 and G-CSF rather than cell intrinsic MyD88 signaling to Arg1. Our data reveal the MyD88-dependent pathway of Arg1induction following BCG infection requires Stat3 activation and may result in the development of an immunosuppressive niche in granulomas due to the induced Arg1 production in surrounding uninfected Mˆ s **Overall design:** We used microarrays to perform genome wide expression analysis in mycobacteria-infected macrophages from C57Bl/6 WT and MyD88-knockout mice.

Background corr dist: KL-Divergence = 0.2765, L1-Distance = 0.0406, L2-Distance = 0.0034, Normal std = 0.2944

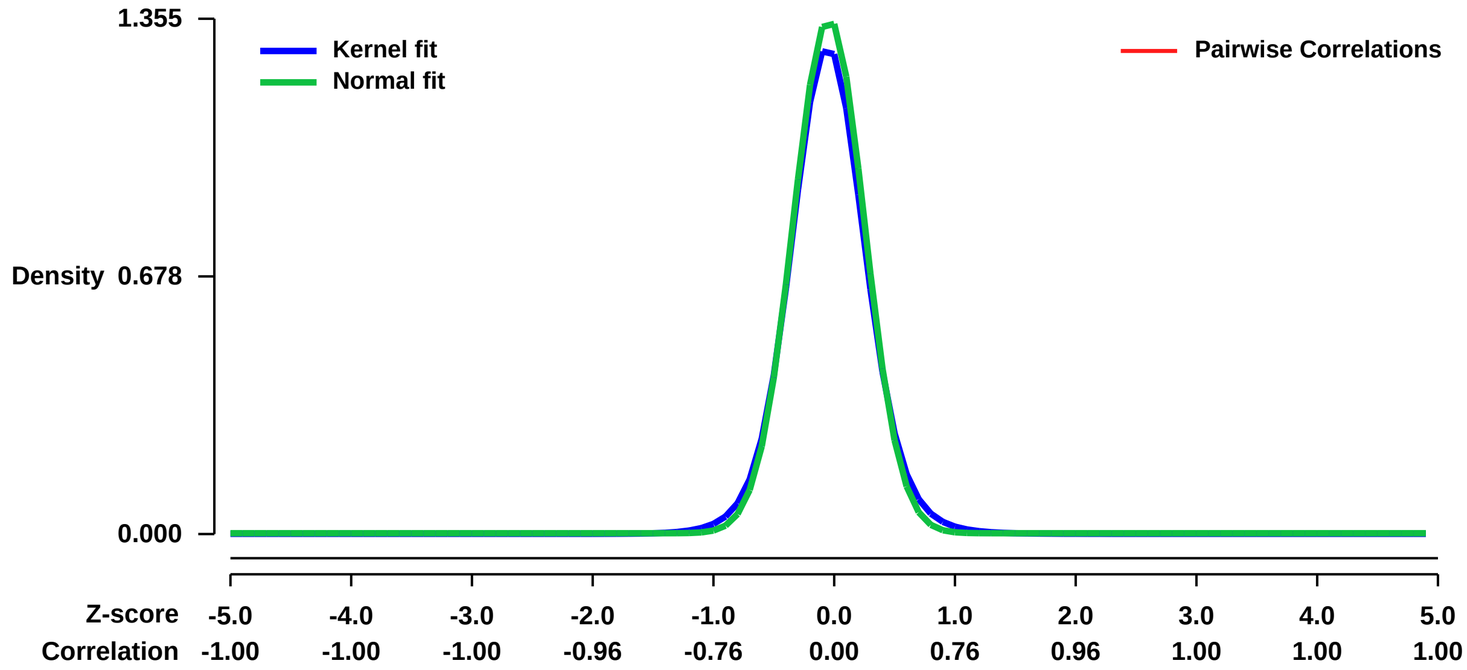

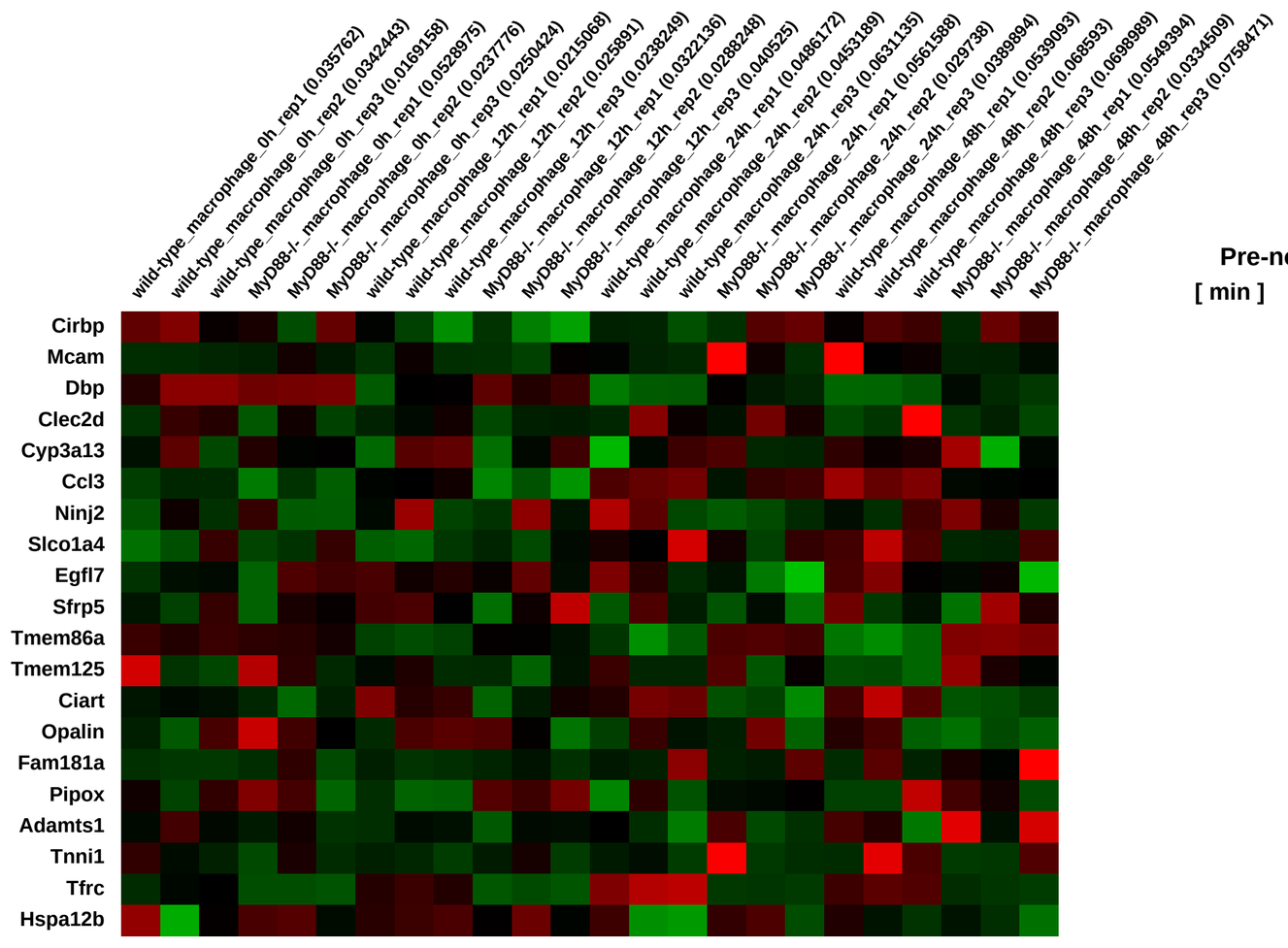

GEO Series "GSE21606" Expression Profiles

Num of samples in this series: 6

Scale of expression profile Z-scores

-3.0 -2.0 -1.0 0.0 1.0 2.0 3.0

GEO Link:	http://www.ncbi.nlm.nih.gov/geo/query/acc.cgi?acc=GSE21606
Status:	Public on Jul 07 2010
Title:	Expression profiling of murine neonatal lung tissue from Carm1 knockouts and wild type controls
Organism:	Mus musculus
Experiment type:	Expression profiling by array
Platform:	GPL1261
Pubmed ID:	20530543
Summary & Design:	**Summary:** Coactivator associated arginine methyltransferase I (CARM1, also known as Protein aRginine MethylTransferase 4, or PRMT4) regulates gene expression by multiple mechanisms including methylation of histones and coactivation of steroid receptor transcription. Mice lacking CARM1 are smaller than their littermates, fail to breath, and die shortly after birth, demonstrating the critical role of CARM1 in development.We performed gene expression analysis to identify genes that are responsible for hyperproliferaion in CARM1 knockout lung. **Overall design:** RNA extracted from murine lung at E18.5 with carm1 knockouts and wild type controls was hybridised to Affymetrix mouse430.2 GeneChips to identify differentially expressed genes in the disease state.

Background corr dist: KL-Divergence = 0.0455, L1-Distance = 0.0209, L2-Distance = 0.0005, Normal std = 0.5932

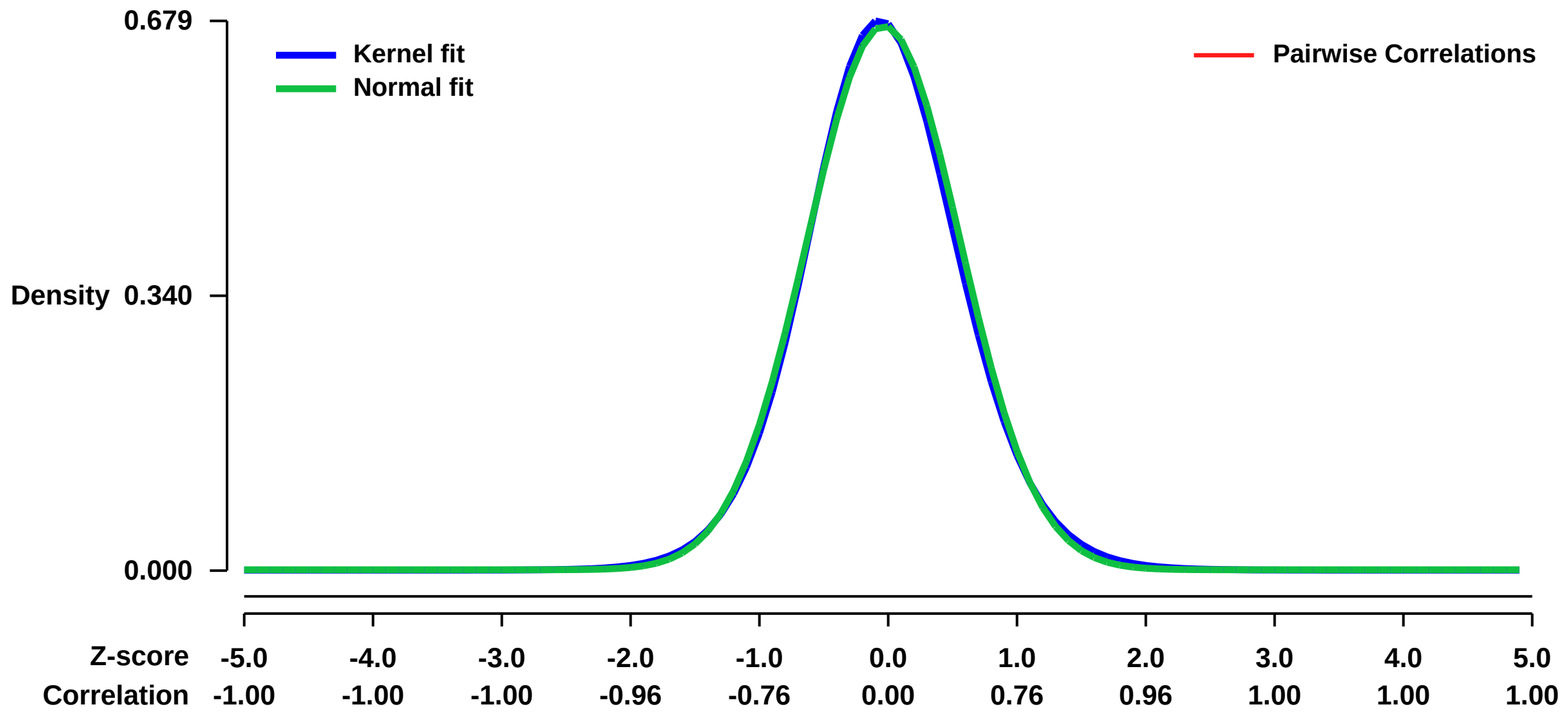

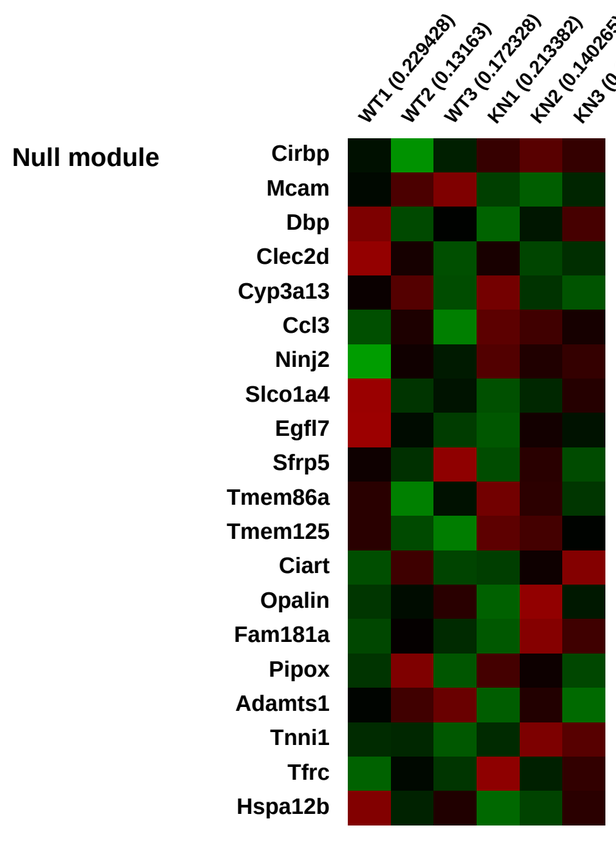

GEO Series "GSE5800" Expression Profiles

Num of samples in this series: 6

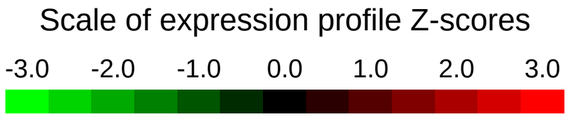

GEO Link:	http://www.ncbi.nlm.nih.gov/geo/query/acc.cgi?acc=GSE5800
Status:	Public on Oct 01 2006
Title:	Expression data from mouse IRF6 null and wt skin
Organism:	Mus musculus
Experiment type:	Expression profiling by array
Platform:	GPL1261
Pubmed ID:	17041601
Summary & Design:	**Summary:** Transcription factor paralogs may share a common role (e.g. Hox) in staged or overlapping expression in specific tissues. In other examples, members have distinct roles in a range of embryologic, differentiation or response pathways (e.g. Tbx, Pax). For the Interferon Regulatory Factor (IRF) family of transcription factors, mice deficient in Irf1, Irf2, Irf3, Irf4, Irf5, Irf7, Irf8 or Irf9, have defects in the immune response but display no embryologic abnormalities. Mice deficient for Irf6 have not been reported, but in humans, mutations in IRF6 cause two Mendelian orofacial clefting syndrome, and genetic variation in IRF6 confers risk for isolated cleft lip and palate. Mice deficient for Irf6 have abnormal skin, limb and craniofacial development. Histological and gene expression analyses indicate that the primary defect is in keratinocyte differentiation and proliferation. This study describes a novel role for an IRF family member in epidermal development. **Keywords:** Comparison of tissue from two genotypes **Overall design:** Skin from E17.5 mice was removed and flash frozen for RNA extraction and hybridization on Affymetrix microarrays.

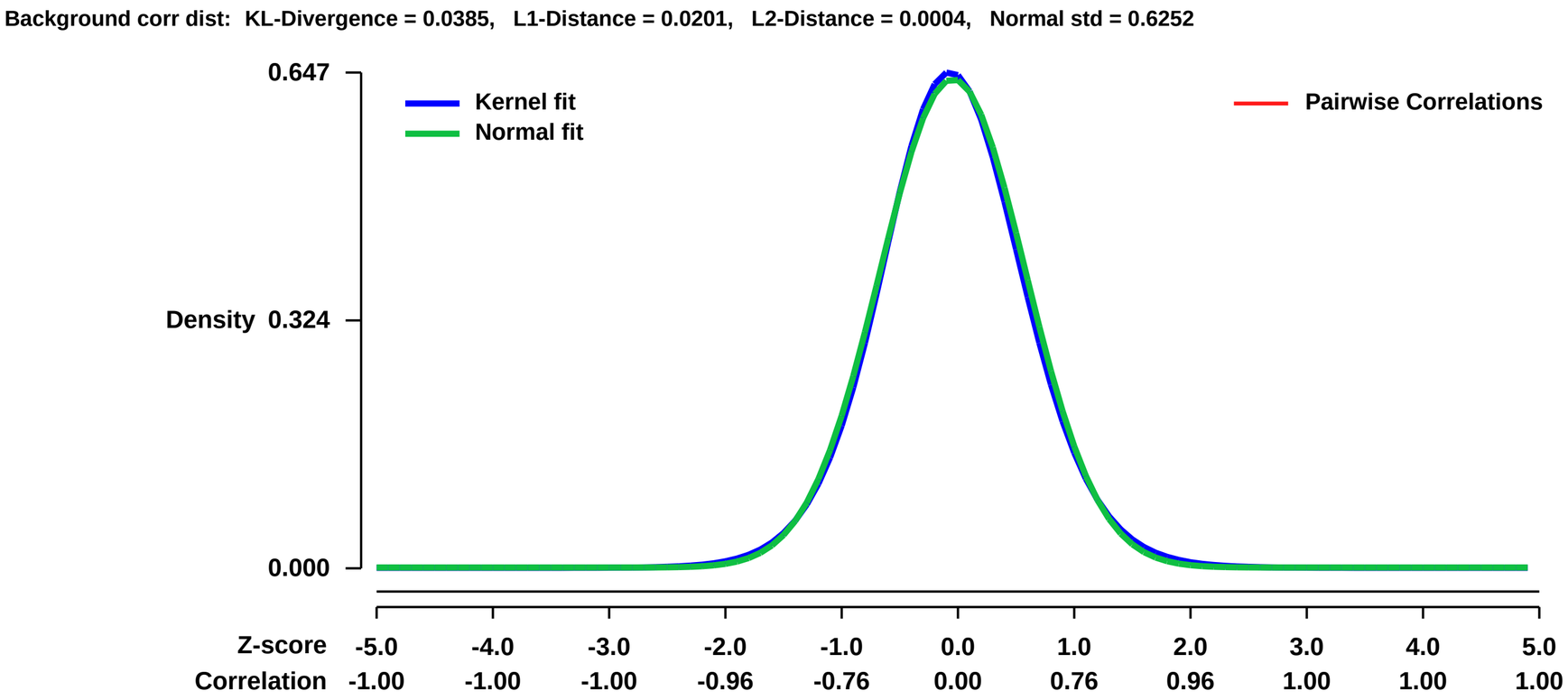

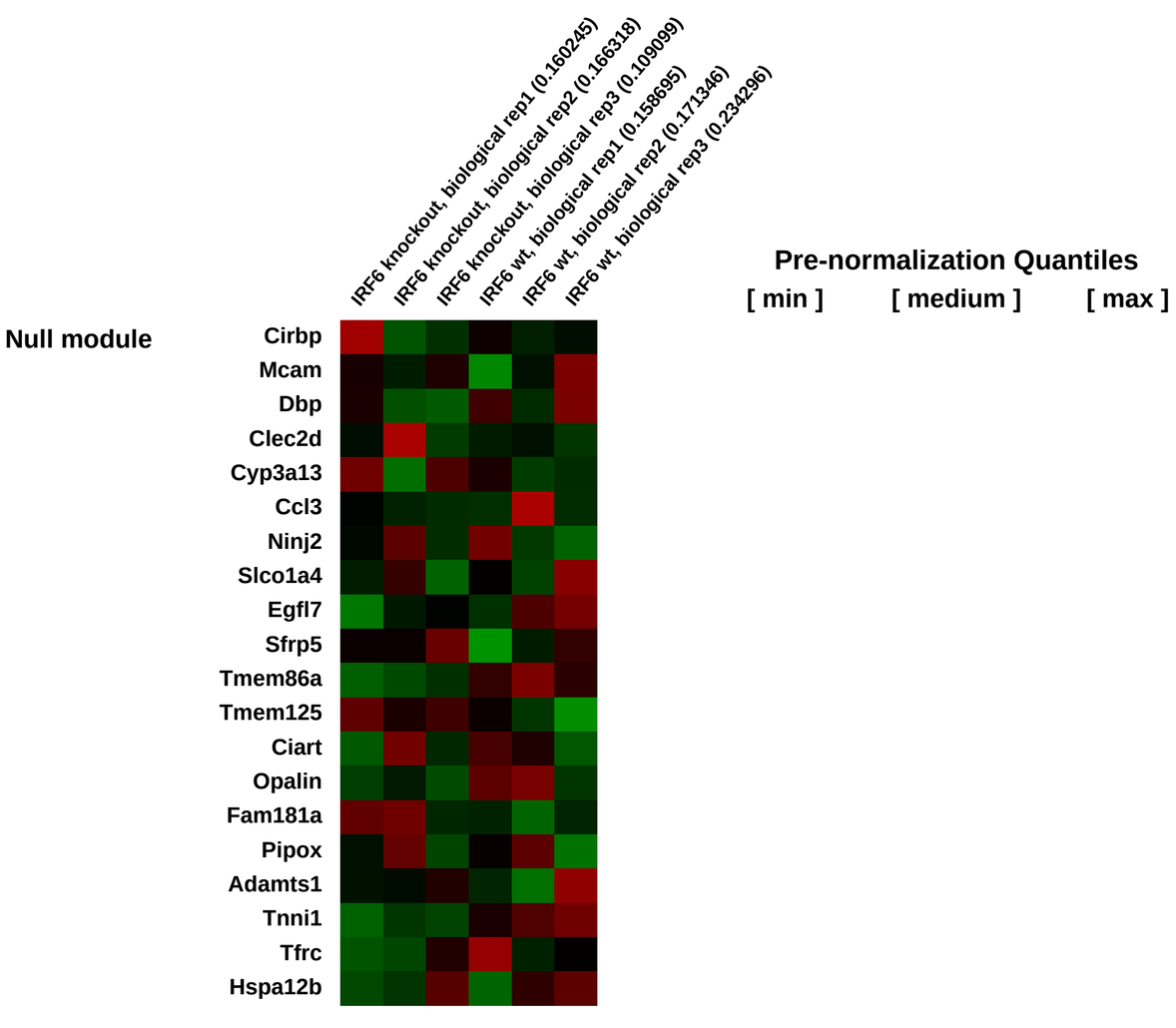

GEO Series "GSE9460" Expression Profiles

Num of samples in this series: 26

Scale of expression profile Z-scores

-3.0 -2.0 -1.0 0.0 1.0 2.0 3.0

GEO Link:	http://www.ncbi.nlm.nih.gov/geo/query/acc.cgi?acc=GSE9460
Status:	Public on Jun 15 2008
Title:	Mouse model of Osteosarcoma
Organism:	Mus musculus
Experiment type:	Expression profiling by array
Platform:	GPL1261
Pubmed ID:	18559481
Summary & Design:	**Summary:** **expression analysis from a genetically engineered mouse model of osteosarcoma** **determine the expression profile of mouse osteosarcoma** **Keywords: disease state analysis** **Overall design:** **3 control in vitro differentiated WT primary osteoblasts; 15 primary osteosarcoma; 4 OS cell lines; 4 secondary tumours**

Background corr dist: **KL-Divergence = 0.2274, L1-Distance = 0.0463, L2-Distance = 0.0048, Normal std = 0.3158**

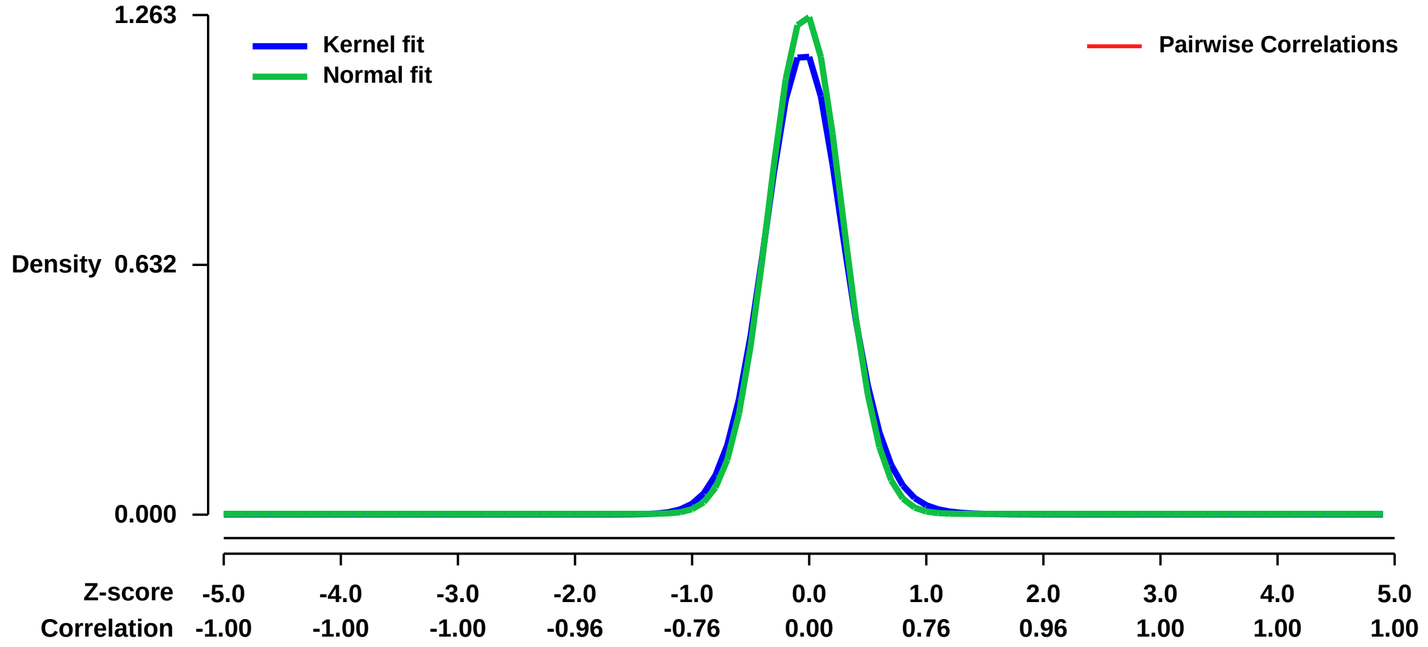

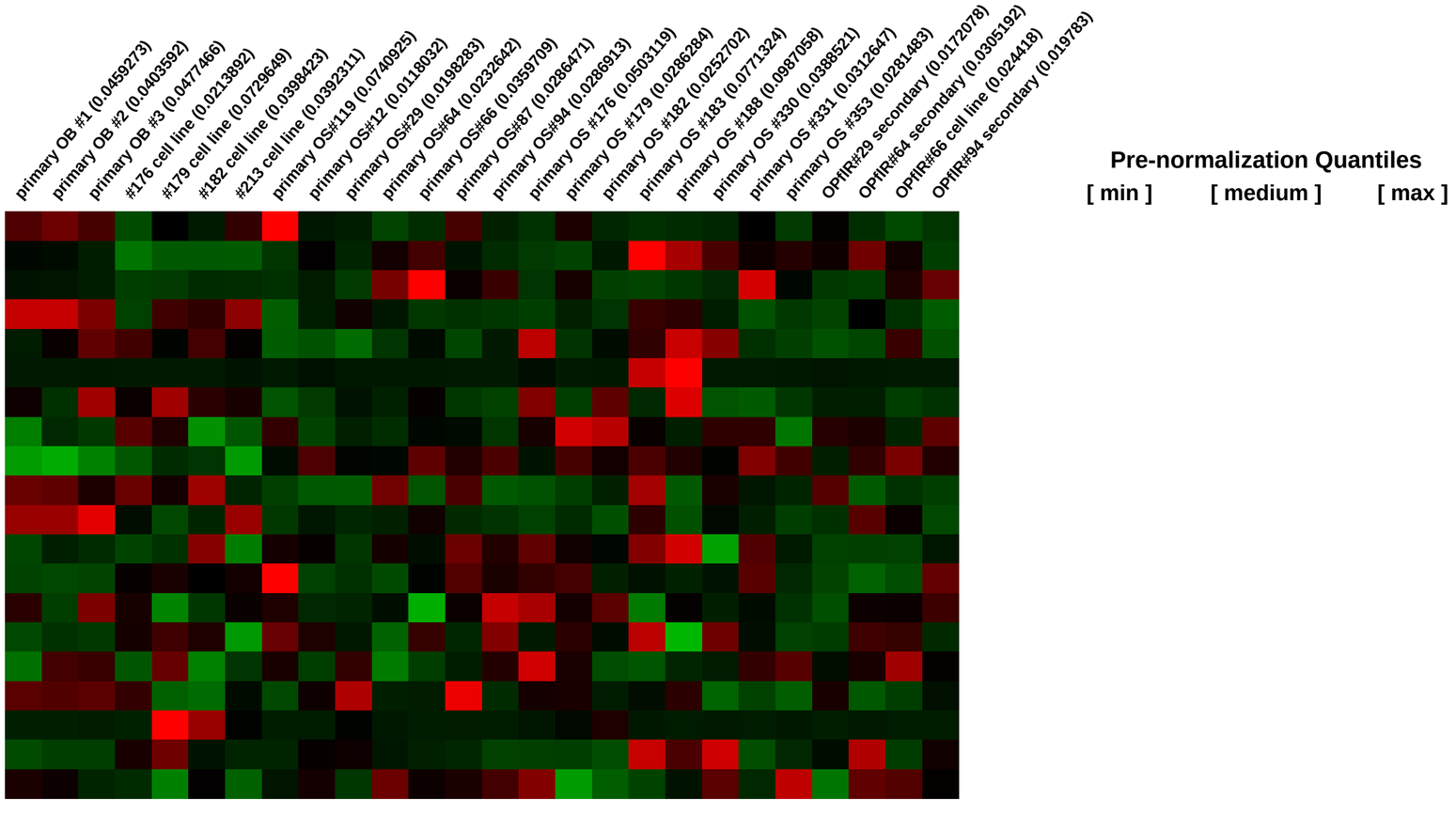

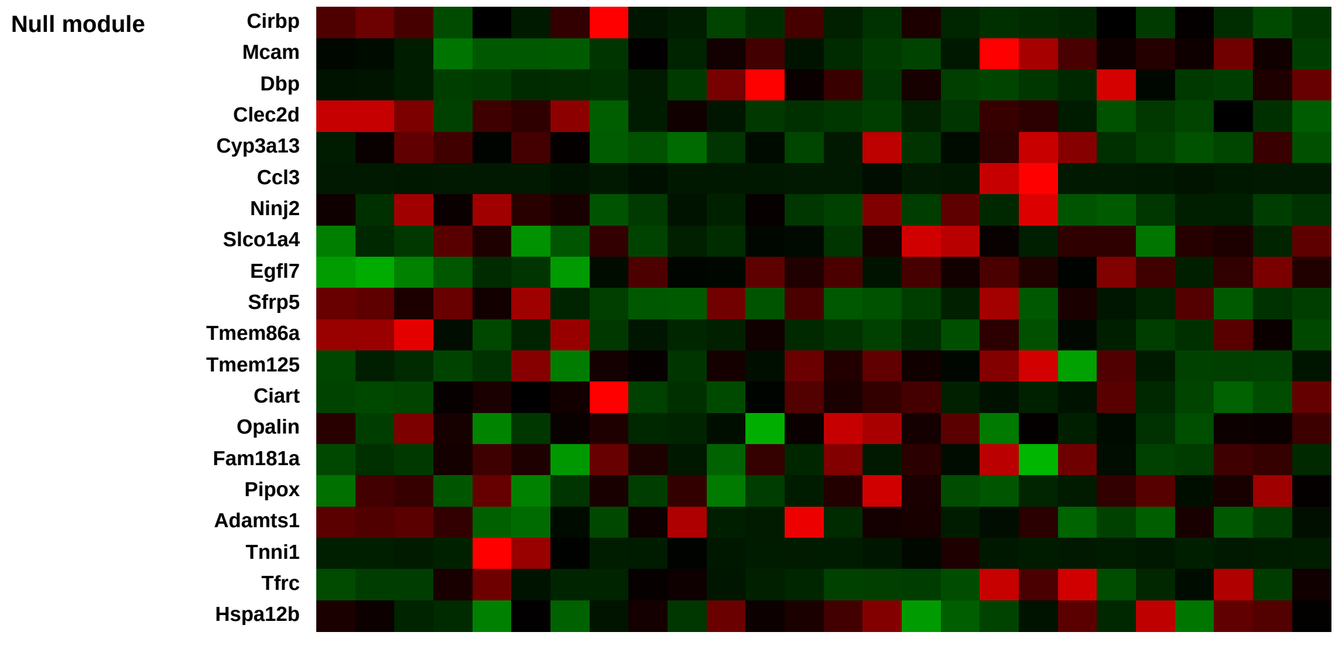

GEO Series "GSE4799" Expression Profiles

Num of samples in this series: 15

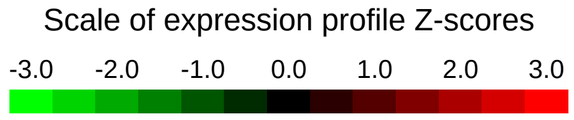

GEO Link:	http://www.ncbi.nlm.nih.gov/geo/query/acc.cgi?acc=GSE4799
Status:	Public on May 11 2006
Title:	GDNF-regulated gene expression in cultured mouse spermatogonial stem cells
Organism:	Mus musculus
Experiment type:	Expression profiling by array
Platform:	GPL1261
Pubmed ID:	16740658
Summary & Design:	**Summary:** GDNF-regulated gene expression was studied in cultures of actively self-renewing spermatogonial stem cells established from 6 day old male mice. GDNF is the essential growth factor regulating mouse spermatogonial stem cell self-renewal. Using a serum-free chemically defined culture system that supports mouse spermatogonial stem cell self-renewal for extended periods of time, GDNF-regulated genes were identified using microarray profiling. **Keywords: GDNF withdrawal and time-course replacement** **Overall design:** Established cultures of highly enriched self-renewing spermatogonial stem cells were subjeted to withrawal of GDNF and GFRalpha1 for 18-hr followed by replacement of the growth factors for 2, 4, and 8-hr. Gene expression was studied using microarray profiling prior to withdrawal, after withdrawal and at each time-point of GDNF/GFRalpha1 replacement.

Background corr dist: KL-Divergence = 0.1956, L1-Distance = 0.0445, L2-Distance = 0.0044, Normal std = 0.3346

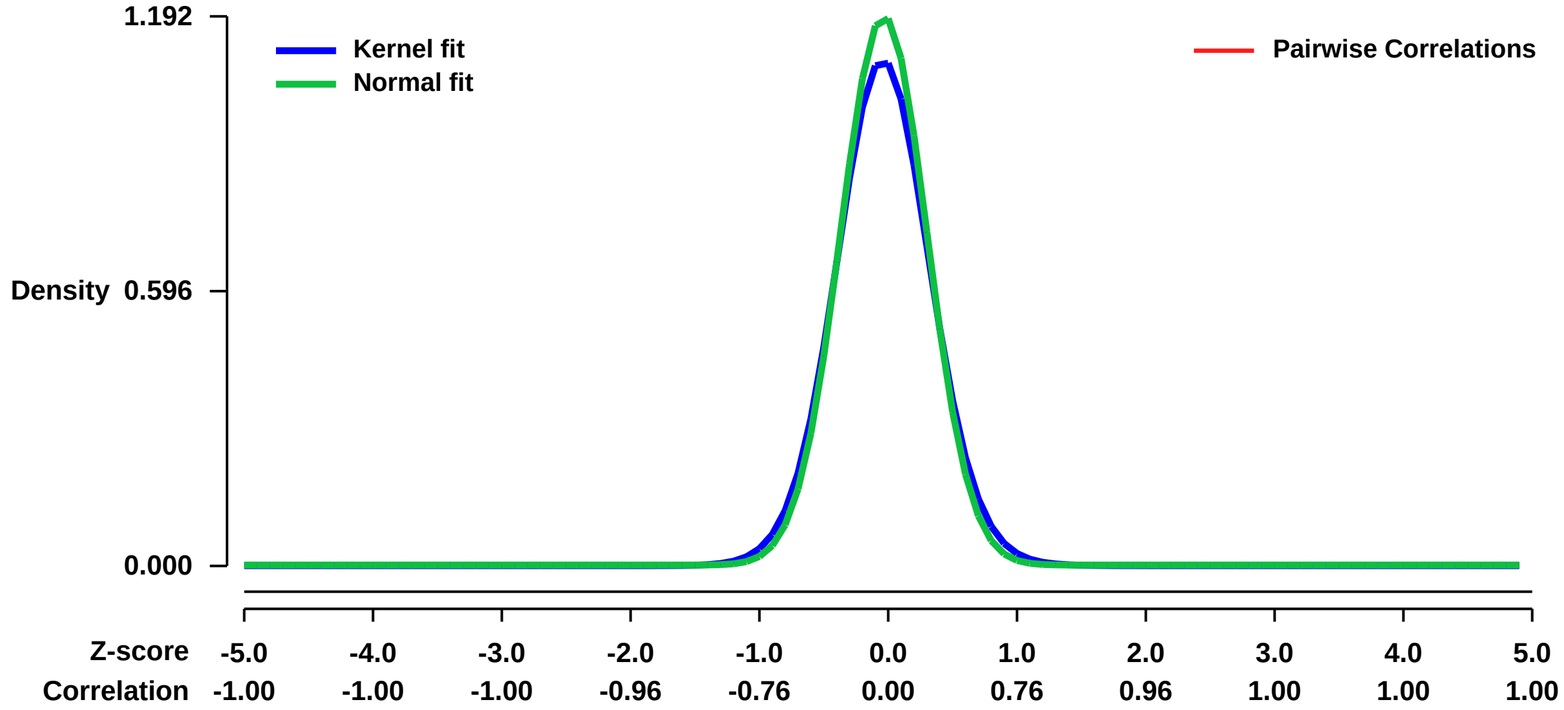

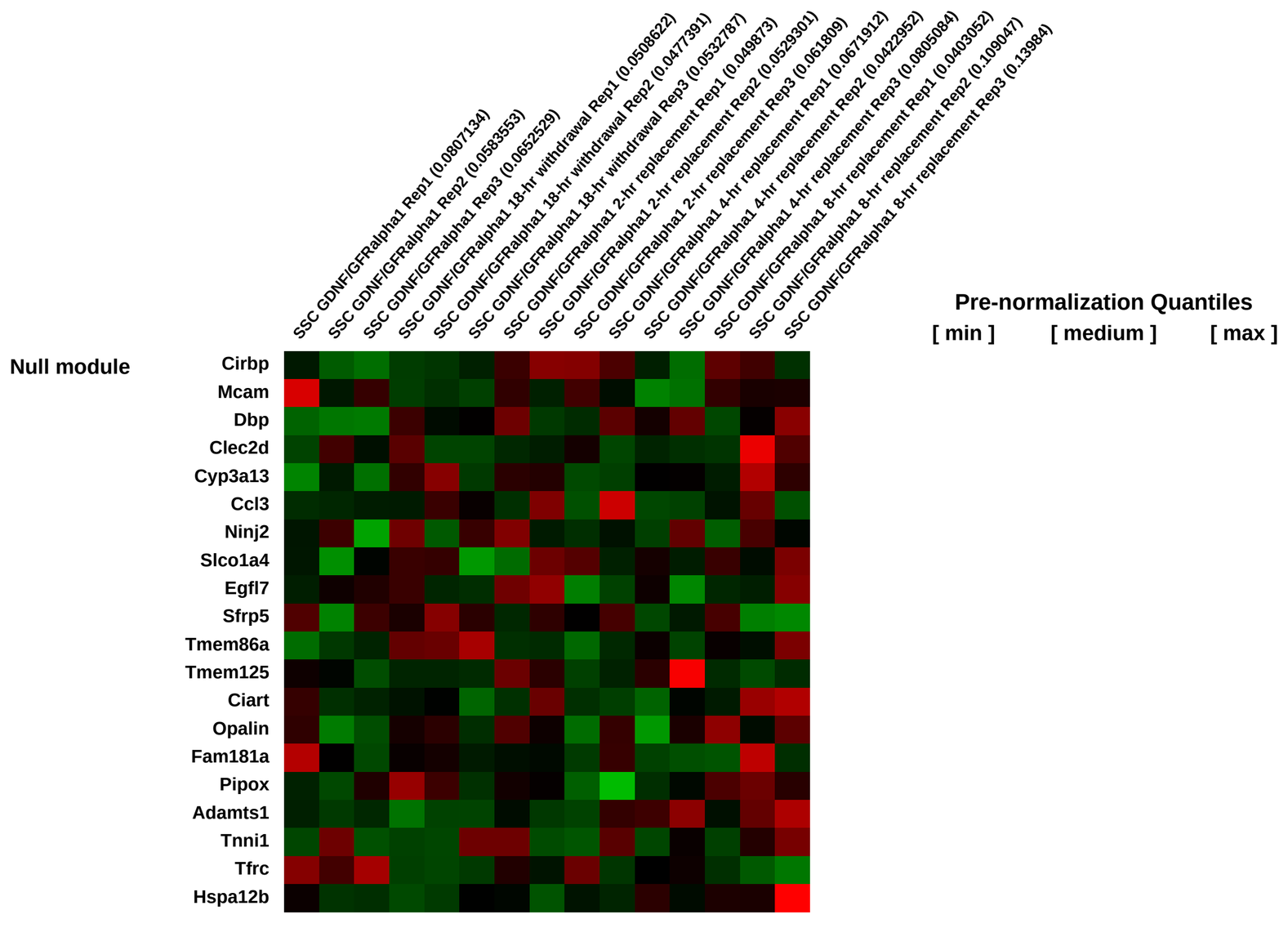

GEO Series "GSE21546" Expression Profiles

Num of samples in this series: 24

Scale of expression profile Z-scores

-3.0 -2.0 -1.0 0.0 1.0 2.0 3.0

GEO Link:	http://www.ncbi.nlm.nih.gov/geo/query/acc.cgi?acc=GSE21546
Status:	Public on Jun 01 2010
Title:	The role of Ternary Complex factors in T-cell Positive Selection
Organism:	Mus musculus
Experiment type:	Expression profiling by array
Platform:	GPL1261
Pubmed ID:	20554967
Summary & Design:	**Summary:** Removal of the transcription factor SAP1a member of the Ternary Complex Factor (TCF) group of transcription factors which in conjunction with Serum Response Factor (SRF) has been shown to have a profound effect on positive selection in the thymus. When another TCF Elk1 is knocked out in mice there is no effect on positive selection unless it is on a Sap1a KO background where the phenotype is very severe. We have stimulated isolated double positive T cells (DPs) with anti-CD3 to mimic positive selection and compared basal and stimulated transcription across the four genotypes to discover the downstream targets of Sap1a involved in positive selection. **Overall design:** The Affymetrix mouse Chip Mouse430_2 arrays were used to define gene expression profiles in purified DPs with and with out CD3 treatment from 3 mice for each genotype (Wt,SapKO, ElkKO and SAP/Elk double KO)

Background corr dist: KL-Divergence = 0.0780, L1-Distance = 0.0515, L2-Distance = 0.0052, Normal std = 0.4892

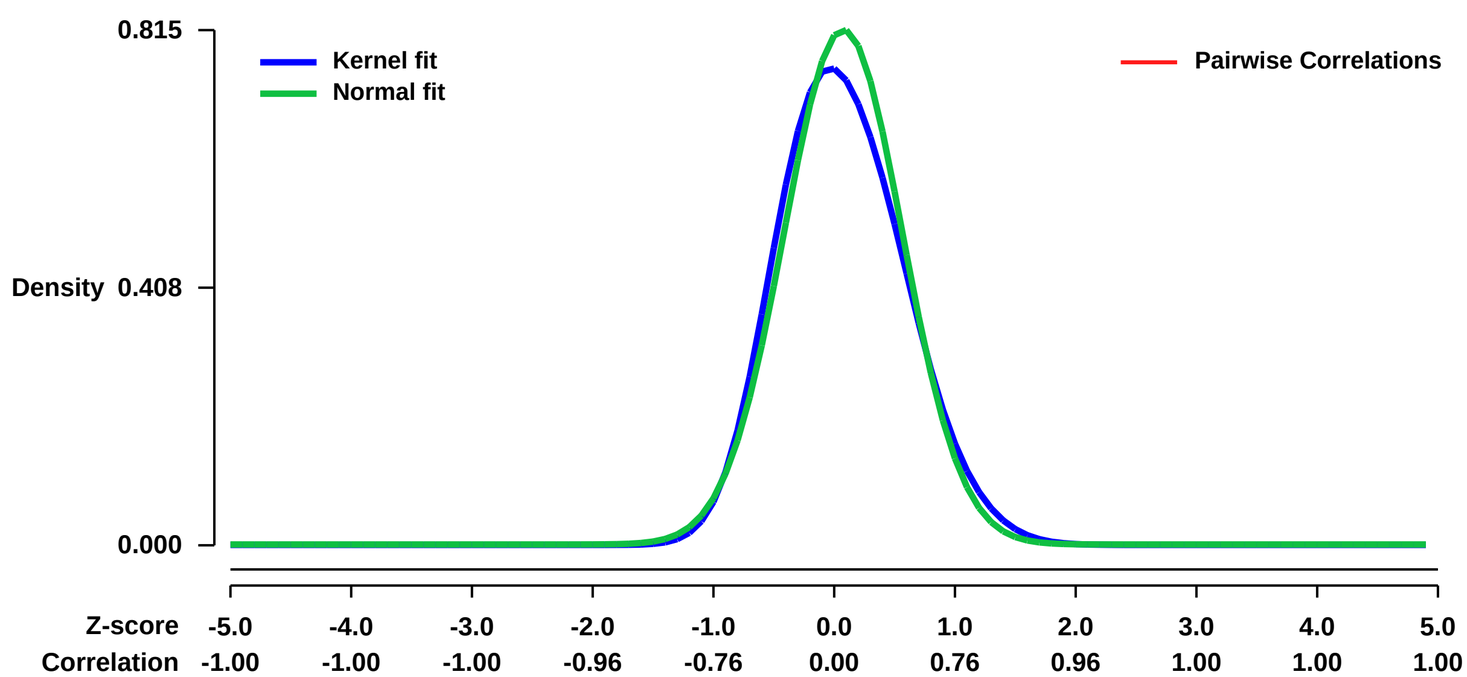

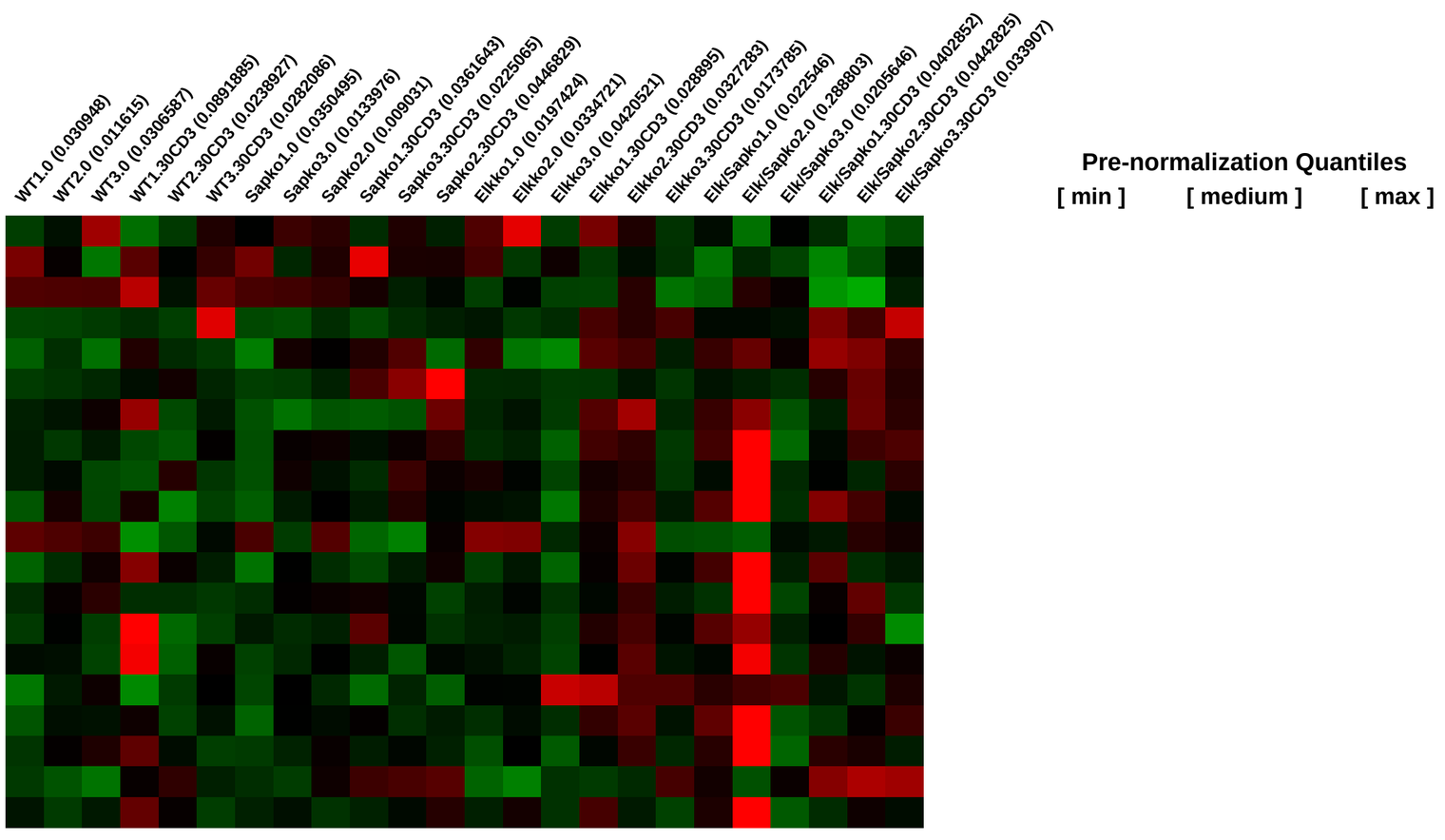

GEO Series "GSE25029" Expression Profiles

Num of samples in this series: 56

Scale of expression profile Z-scores

-3.0 -2.0 -1.0 0.0 1.0 2.0 3.0

GEO Link:	http://www.ncbi.nlm.nih.gov/geo/query/acc.cgi?acc=GSE25029
Status:	Public on Jul 01 2011
Title:	Ionizing radiation in GI tract of Tweak KO mice
Organism:	Mus musculus
Experiment type:	Expression profiling by array
Platform:	GPL1261
Pubmed ID:	21893119
Summary & Design:	**Summary:** TWEAK/Fn14 signaling may regulate the expression of genes involved in epithelial repair and mucosal inflammation. Comparing the gene signatures in WT and TWEAK KO mice will inform the biology of TWEAK/Fn14 pathway in the GI tract. **Overall design:** Mice were treated with 3 Gy of ionizing radiation. After 6h and 24h mice were sacrificed, and whole colon and jejunum were harvested, and RNA was isolated from these tissues. Each CEL file represents a different mouse.

Background corr dist: KL-Divergence = 0.0433, L1-Distance = 0.0713, L2-Distance = 0.0046, Normal std = 0.9679

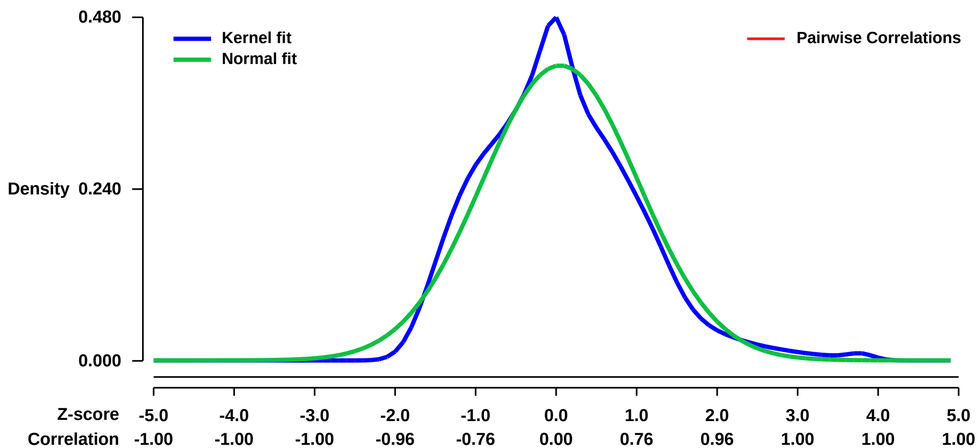

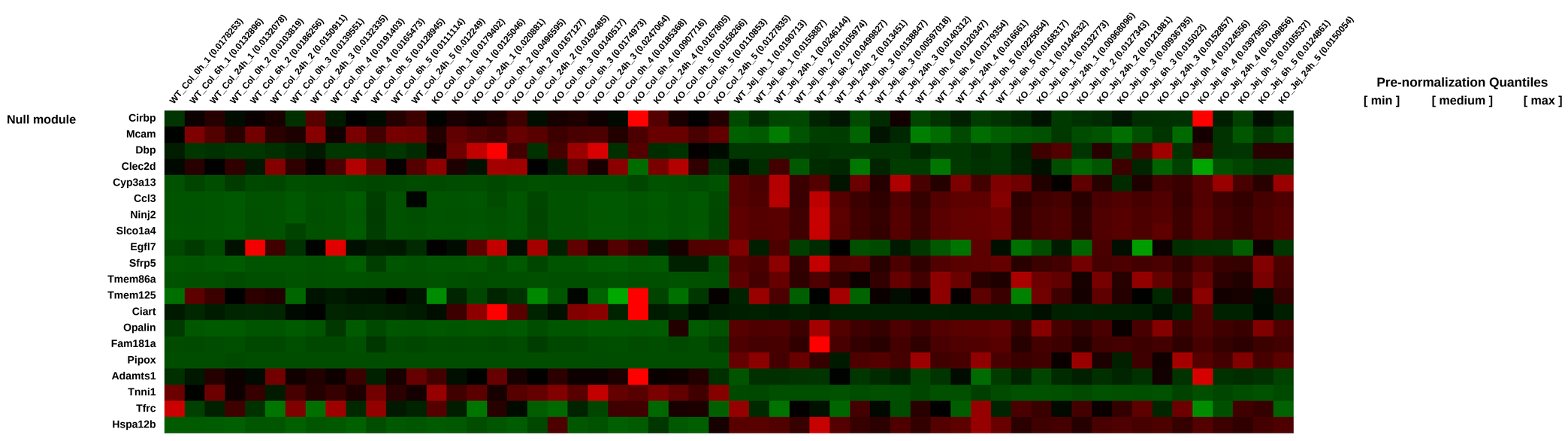

GEO Series "GSE16100" Expression Profiles

Num of samples in this series: 6

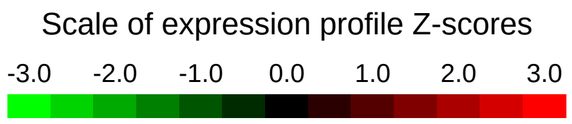

GEO Link:	http://www.ncbi.nlm.nih.gov/geo/query/acc.cgi?acc=GSE16100
Status:	Public on May 15 2009
Title:	Hematopoietic Stem Cells Reversibly Switch from Dormancy to Self-Renewal during Homeostasis and Repair
Organism:	Mus musculus
Experiment type:	Expression profiling by array
Platform:	GPL1261
Pubmed ID:	19062086
Summary & Design:	**Summary:** Bone marrow hematopoietic stem cells (HSCs) are crucial to maintain lifelong production of all blood cells. Although HSCs divide infrequently, it is thought that the entire HSC pool turns over every few weeks, suggesting that HSCs regularly enter and exit cell cycle. Here, we combine flow cytometry with label-retaining assays (BrdU and histone H2B-GFP) to identify a population of dormant mouse HSCs (d-HSCs) within the lin(-)Sca1+cKit+CD150+CD48(-)CD34(-) population. Computational modeling suggests that d-HSCs divide about every 145 days, or five times per lifetime. d-HSCs harbor the vast majority of multilineage long-term self-renewal activity. While they form a silent reservoir of the most potent HSCs during homeostasis, they are efficiently activated to self-renew in response to bone marrow injury or G-CSF stimulation. After re-establishment of homeostasis, activated HSCs return to dormancy, suggesting that HSCs are not stochastically entering the cell cycle but reversibly switch from dormancy to self-renewal under conditions of hematopoietic stress **Overall design:** cDNA microarray analysis was performed on sorted mouse bone marrow after 170 days of doxycycline treatment for CD34 Neg, Lin Neg, Sca1+, cKit+, CD150+, CD48 Neg, HSCs. HSCs were further sorted for GFP+ (LRC) and GFP neg (non-LRC) populations. Per condition, 3 independent biological replicates were analysed.

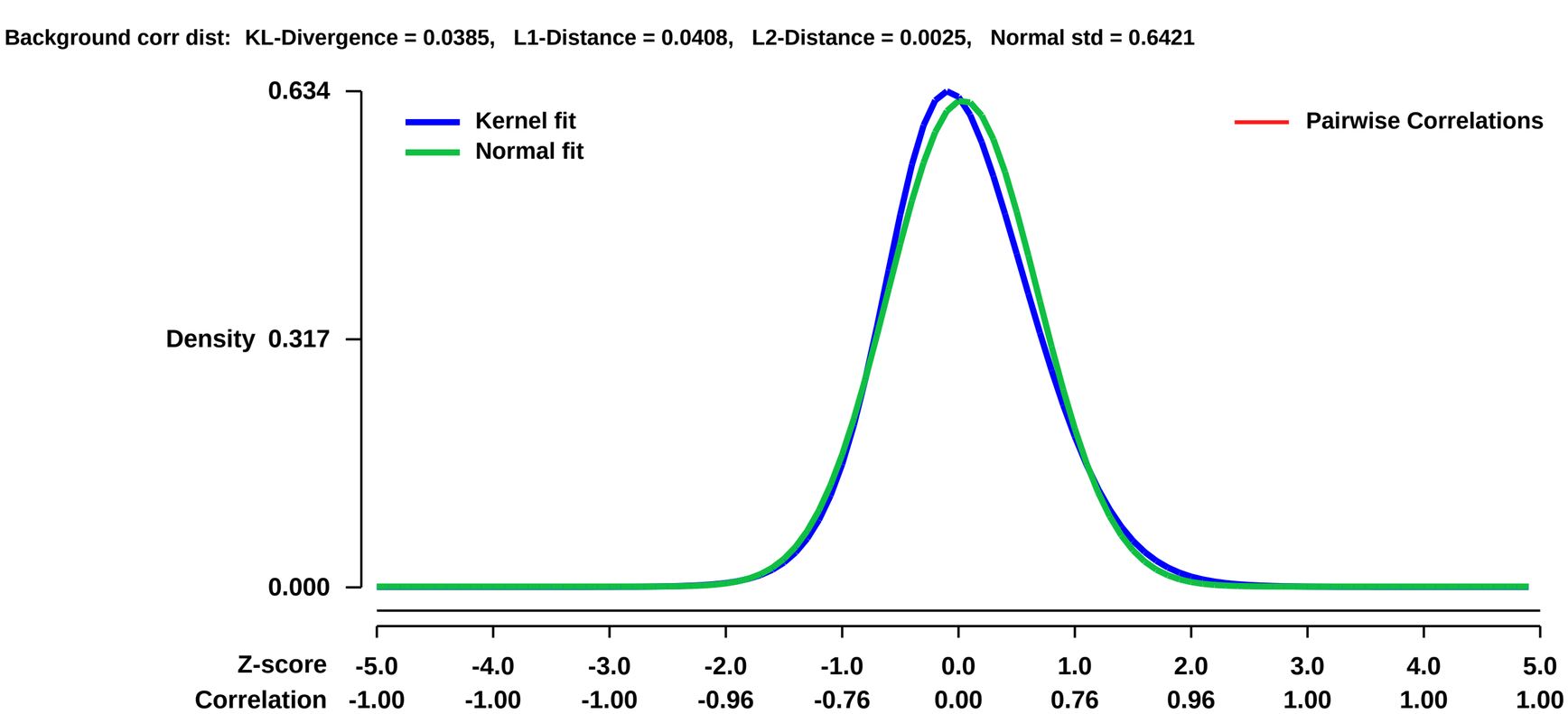

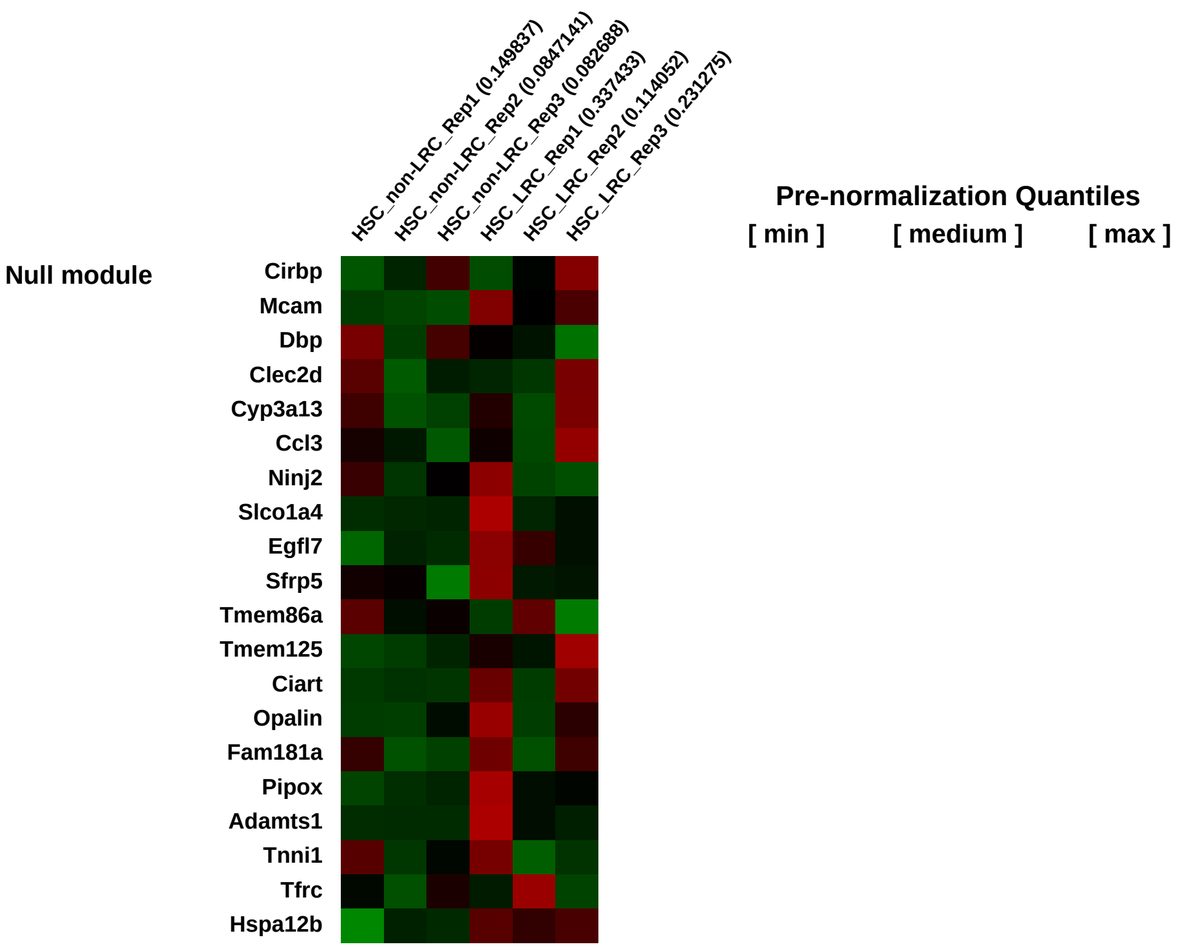

GEO Series "GSE12536" Expression Profiles

Num of samples in this series: 6

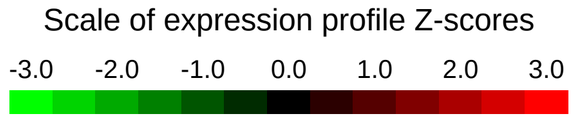

GEO Link:	**http://www.ncbi.nlm.nih.gov/geo/query/acc.cgi?acc=GSE12536**
Status:	**Public on Feb 20 2009**
Title:	**Differentially regulated genes in control and c-myc N-myc deficient progenitors**
Organism:	**Mus musculus**
Experiment type:	**Expression profiling by array**
Platform:	**GPL1261**
Pubmed ID:	**19041778**
Summary & Design:	**Summary:** **Analysis of HSCs from control and c-myc N-myc deficient long-term hematopoietic stem cells. HSCs lacking both c-myc and N-myc display increased apoptosis rates. Data provide insight into the molecular changes occuring upon complete loss of Myc activity, clarifying the resulting apoptotic mechanism and the role of Myc family proteins in HSCs and commited progenitors.** **Overall design:** **Commited progenitors (Lin-Sca1+CD150+CD48+) cells were sorted from the BM of MxCre c-myc flox2 N-myc flox2 (experimental) and c-myc flox2 N-myc flox2 (control) mice 3 days after the last pI-pC injection. Each condition was analysed in triplicates, with each replicate consisting of a pool of 3 dKO mice or 2 control mice.**

Background corr dist: **KL-Divergence = 0.0340, L1-Distance = 0.0285, L2-Distance = 0.0011, Normal std = 0.6522**

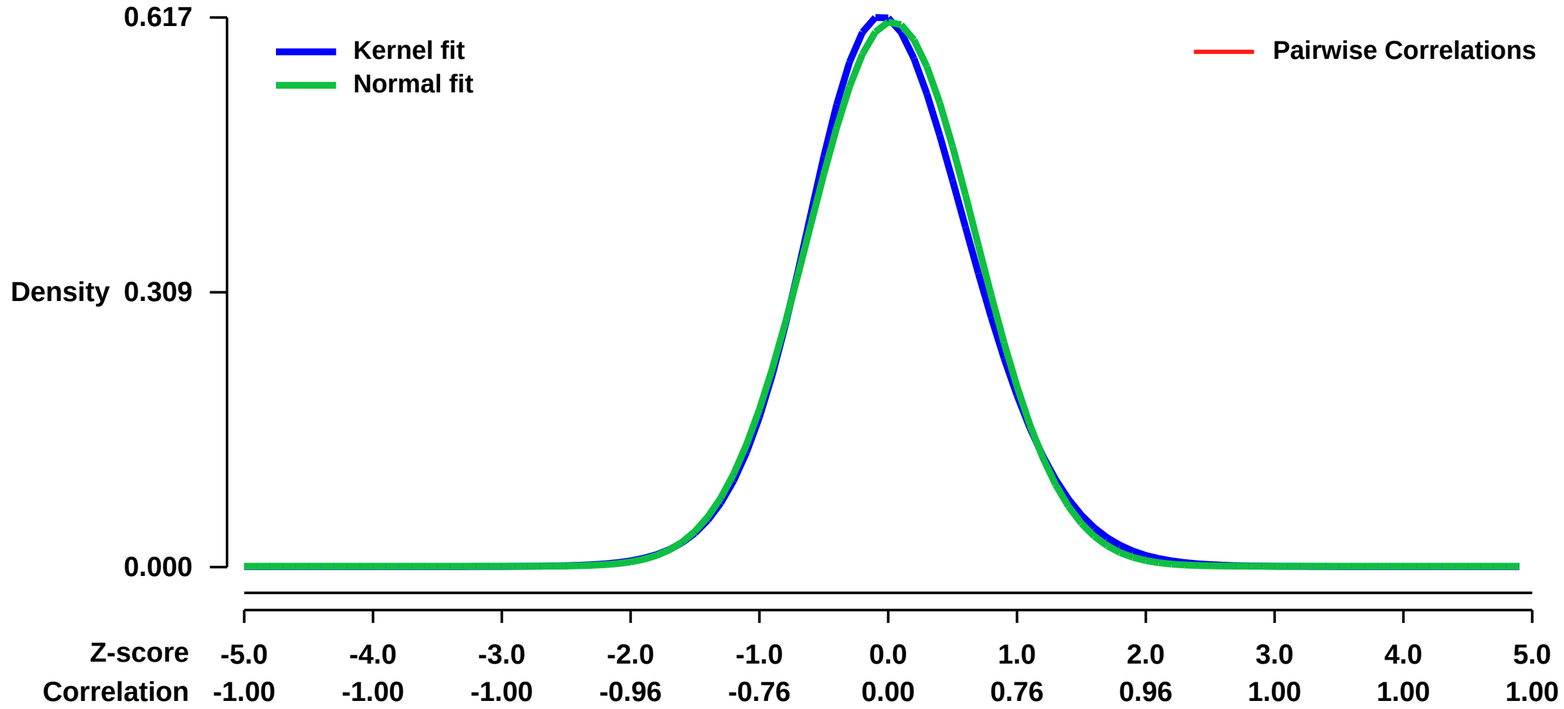

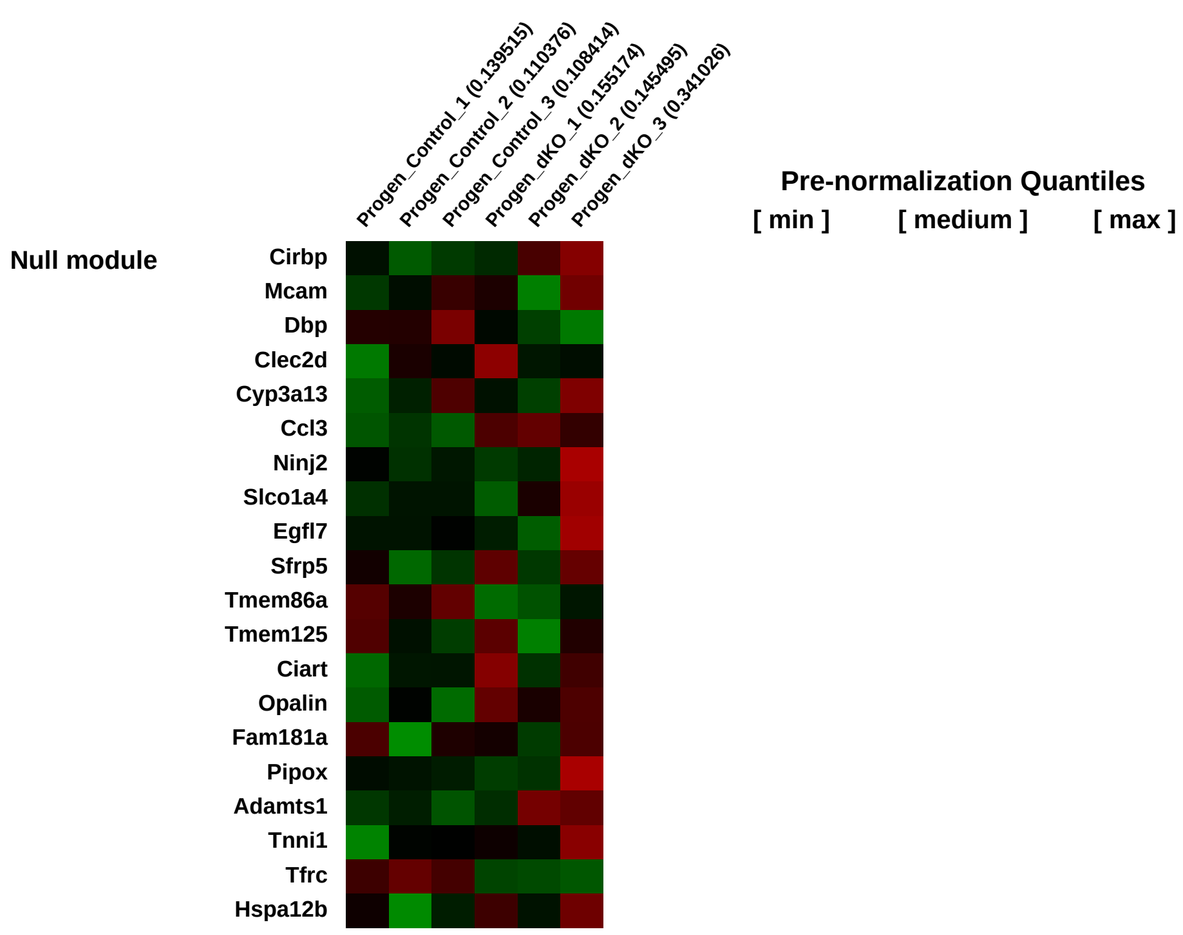

GEO Series "GSE11141" Expression Profiles

Num of samples in this series: 21

Scale of expression profile Z-scores

-3.0 -2.0 -1.0 0.0 1.0 2.0 3.0

GEO Link: http://www.ncbi.nlm.nih.gov/geo/query/acc.cgi?acc=GSE11141

Status: Public on Apr 12 2008

Title: Effects of NgR overexpression on the developing and mature forebrain (backm-affy-mouse-433094)

Organism: Mus musculus

Experiment type: Expression profiling by array

Platform: GPL1261

Pubmed ID:

Summary & Design:

Summary:

The lack of axonal growth after injury in the adult central nervous system (CNS) is partly due to the presence of growth-inhibitory molecules associated with myelin and the intrinsic growth-state of the injured neurons. To date, three inhibitors have been identified in myelin: Myelin- Associated Glycoprotein (MAG), Nogo A, and Oligodendrocyte-Myelin glycoprotein (OMgp). These three proteins all appear to be located in the periaxonal surface of the myelin membrane placing them in an optimal location to mediate axon-glial interaction. In addition, the three proteins have been shown to bind the same neuronal receptor, known as the Nogo-66 receptor (NgR). It has been hypothesized that inhibition of NgR may be a strategy to increase regeneration, plasticity and functional recovery of the lesioned central nervous system. Strong NgR mRNA expression is observed in the hippocampal pyramidal cell layers (CA1-3) and the granular layer of the dentate gyrus. It has been shown that animals exposed to entorhinal lesions show a biphasic regulation of NgR in the hippocampus, suggesting a tightly regulated mechanism mediated by this receptor. We have access to a transgenic model to over-express NgR in forebrain hippocampal neurons. Preliminary results have shown a phenotypic response in behavior and some molecular markers, as result of NgR overexpression. Knowledge of what genes are reacting in this novel transgenic model may provide insights into what pathways are affected by NgR to control synaptic plasticity in normal animals and during injury.

We have access to a bitrasgenic conditional mouse model to everexpress the NgR receptor in forebrain neurons, through the CamKII promoter. This conditional model uses the tetracycline transactivator (tTA), which is expressed through the CamKII promoter. Upon removal of doxycycline, the TetOp target gene becomes active and over-expression of NgR in cells with an active CaMKII promoter is achieved.

We will determine gene expression patterns in the dentate gyrus of transgenic animals engineered to over-express NgR through the CamKII promoter (present in several forebrain areas), and upon removal of doxyxycline.

We hypothesize that over-expression of NgR in the hippocampus inhibits synaptic plasticity, thereby suppressing the formation of new synapses necessary for the formation of memory.

EXPERIMENT 1

- Effects of NgR overexpression in the mature forebrain -

1) Experimental group: Bitrasgenic + water: Overexpresses NgR in forebrain neurons. In this group, doxyxycline was removed from the drinking water in adult animals. All the control groups were aged matched.

2) Control group: Bitransgenic + doxy: Should control for leakage by the TetOp target gene, or for any effects mediated by doxycycline, as compared to other control groups.

3) Control group: Monotransgenic + water: Should control for any leakage mediated by the TetOp target gene, as compared to other control groups.

4) Control group: Monotrangenic + water: Should control for leakage by the TetOp target gene, or for any effects mediated by doxycycline, as compared to other control groups.

EXPERIMENT 2

- Effects of NgR overexpression in the developing forebrain -

We will also analyze the effects of NgR overexpression in bitransgenic animals raised on water. In these animals, the NgR transgene is expressed in the forebrain upon activation of the CamKII promoter. Since neuronal differentiation and neuronal pathways are being formed during development, we anticipate that NgR overexpression (de)effects in these animals will be markedly different to those observed in adult animals.

1) Bitransgenic + water (through entire lifespan): The animals in this group were never treated with doxycycline, and therefore expressed the NgR transgene upon activity of the CamKII promoter.

2) Monotransgenic + water: This control group will control for leakage by the Tet Op gene, or for effects of the tTA expression.

Keywords: NgR, forebrain, development

Overall design:

Background corr dist: KL-Divergence = 0.2830, L1-Distance = 0.0577, L2-Distance = 0.0084, Normal std = 0.2873

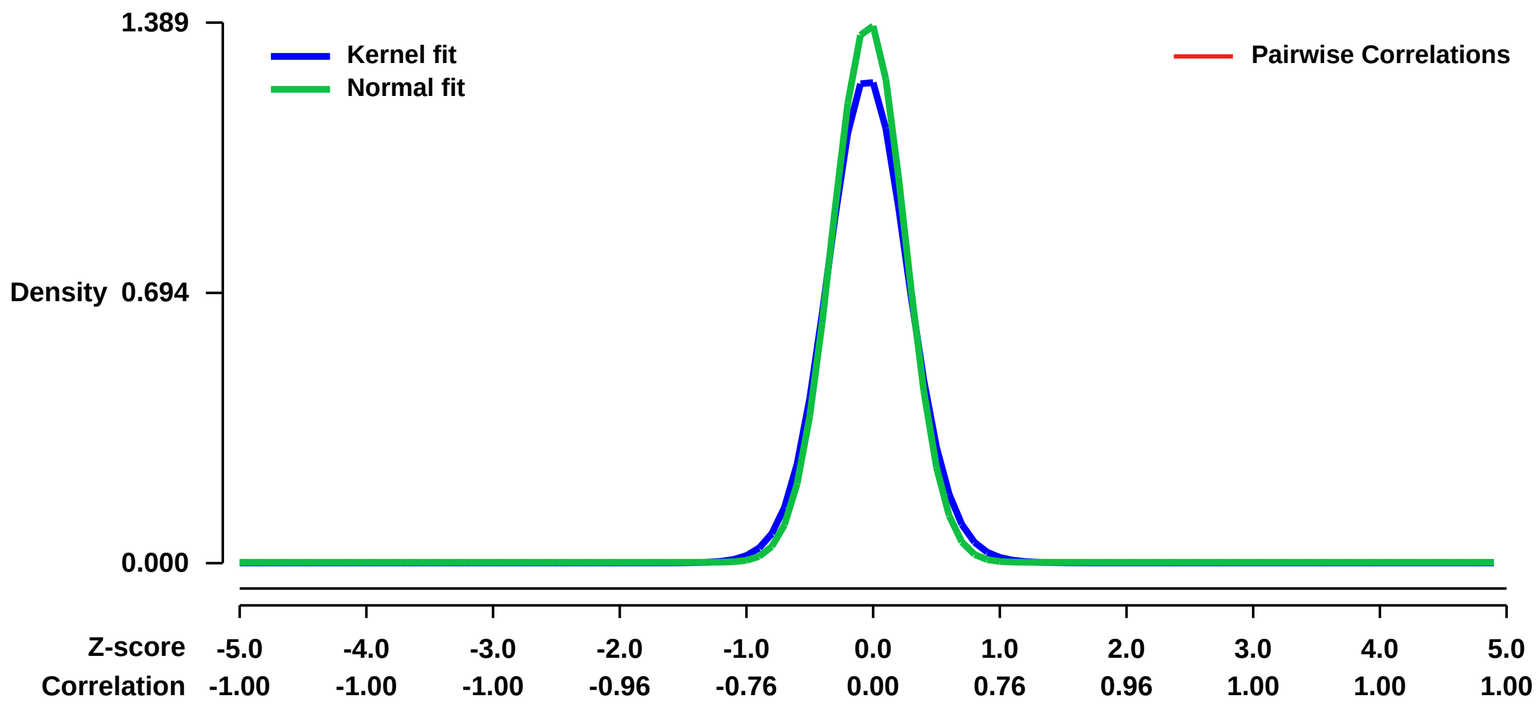

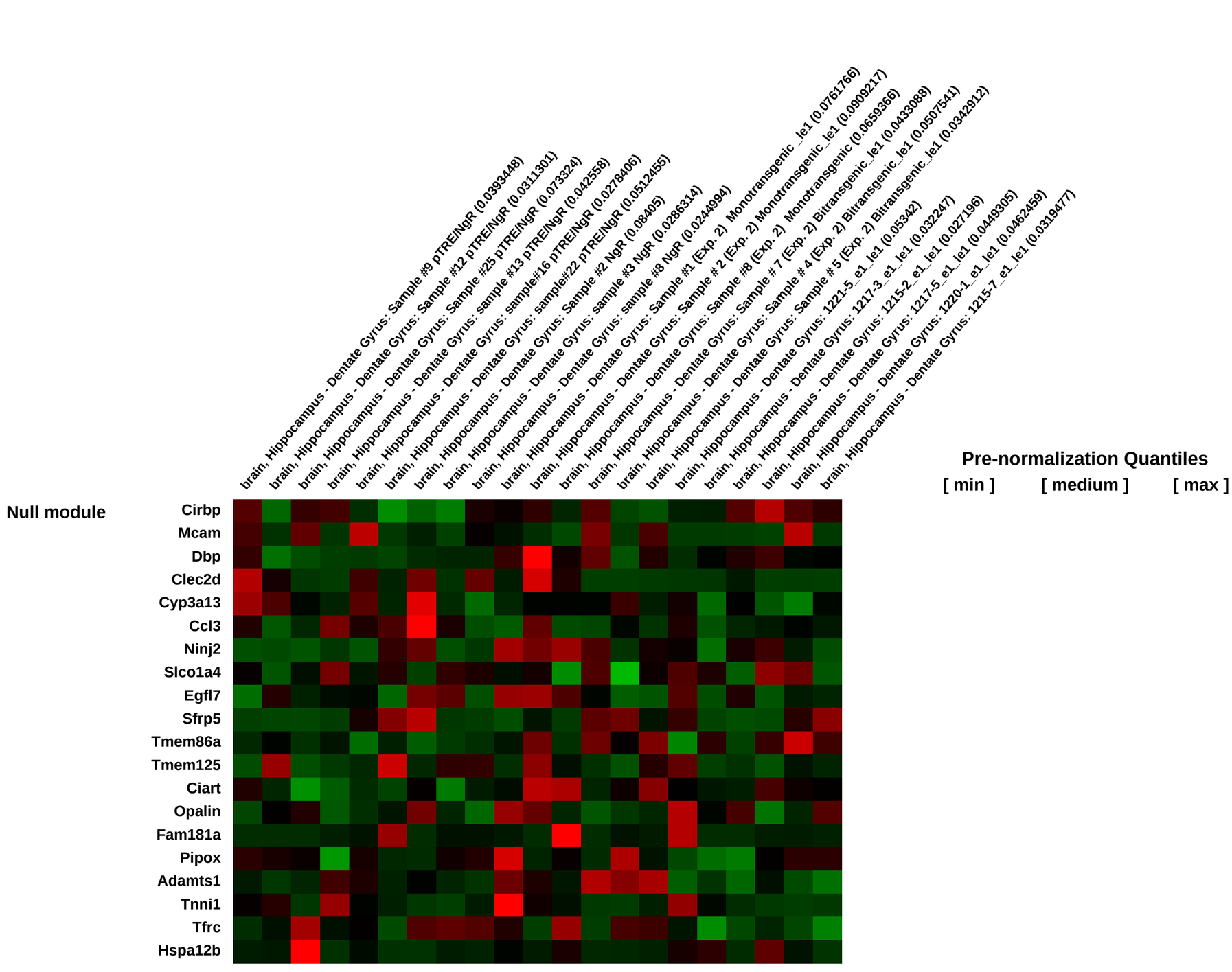

GEO Series "GSE10556" Expression Profiles

Num of samples in this series: 6

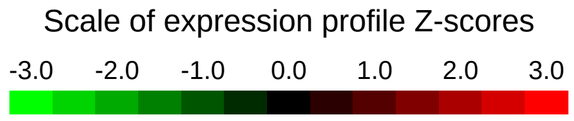

GEO Link:	**http://www.ncbi.nlm.nih.gov/geo/query/acc.cgi?acc=GSE10556**
Status:	**Public on Nov 07 2008**
Title:	**Comparision of expression profile between wild-type and Slc39a13 knockout chondrocytes**
Organism:	**Mus musculus**
Experiment type:	**Expression profiling by array**
Platform:	**GPL1261**
Pubmed ID:	**18985159**
Summary & Design:	**Summary:** **In order to explore molecules whose expression is controlled by Slc39a13, we investigated gene expression profiling of primary chondrocyte isolated from wild-type and Slc39a13 knockout mice.** **Keywords: knockout vs wild-type** **Overall design:** **wild-type vs Slc39a13 knockout**

Background corr dist: **KL-Divergence = 0.0339, L1-Distance = 0.0199, L2-Distance = 0.0004, Normal std = 0.6472**

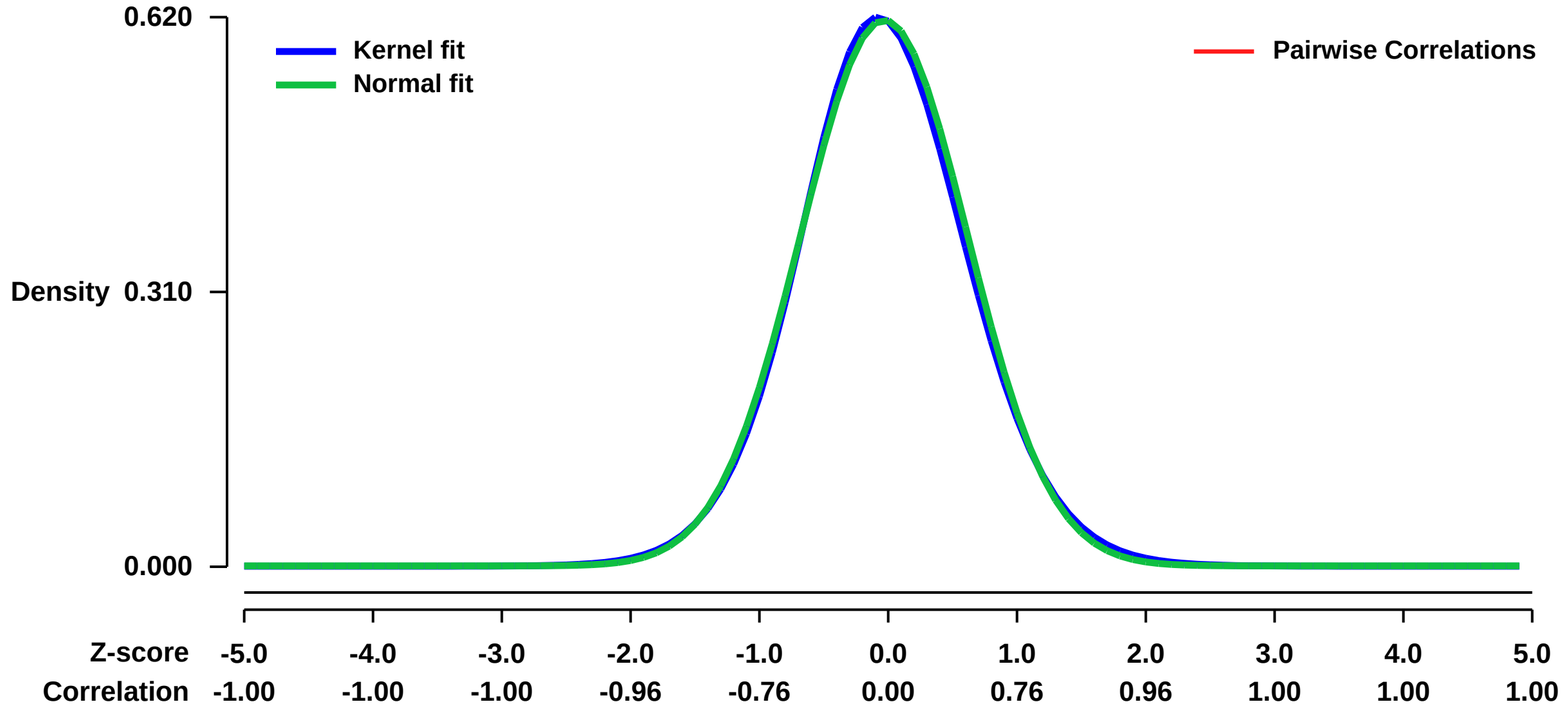

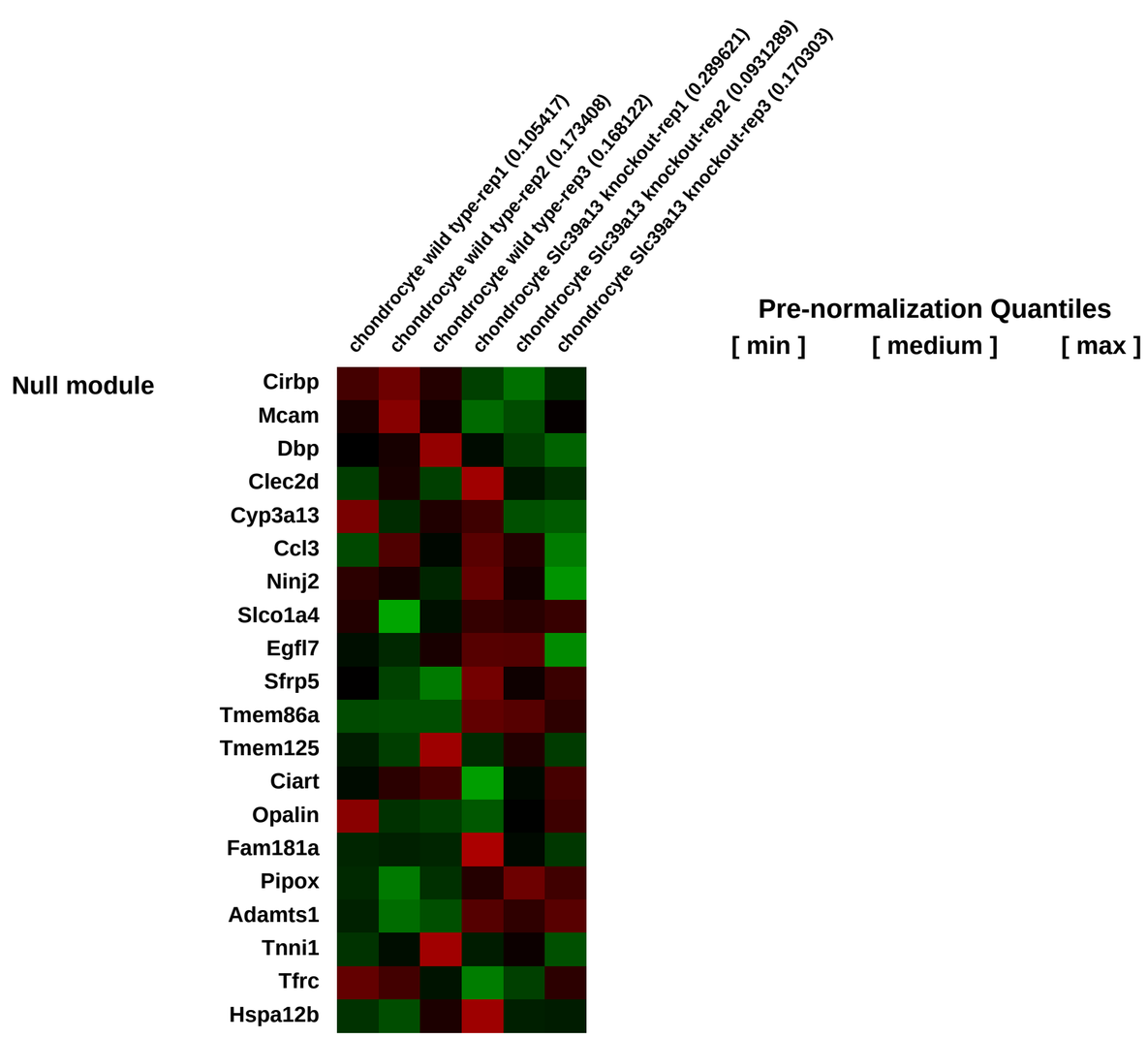

GEO Series "GSE28237" Expression Profiles

Num of samples in this series: 6

Scale of expression profile Z-scores

-3.0 -2.0 -1.0 0.0 1.0 2.0 3.0

GEO Link:	http://www.ncbi.nlm.nih.gov/geo/query/acc.cgi?acc=GSE28237
Status:	Public on Mar 29 2011
Title:	T cell dependent immune responses: B cell activation and differentiation Group1 Fo, Group2 GC1, Group3 GC2
Organism:	Mus musculus
Experiment type:	Expression profiling by array
Platform:	GPL1261
Pubmed ID:	19265543
Summary & Design:	**Summary:** Upon immunization with a T cell dependent antigen naive follicular B cells (Fo) are activated and a germinal center reaction is induced. Within the next 2 weeks large germinal centers develop where the process of affinity maturation takes place. To analyze the gene expression profile of resting and activated B cells, follicular B cells (Fo), B cells from early (GC1) and late germinal centers (GC2) were isolated and their gene expression profile compared. **Overall design:** After total RNA extraction, reverse transcription, cDNA extraction, the biotinylated cRNA was transcribed, fragmented, and 15 ´µg cRNA hybridized in duplicates for each of the three groups to the GeneChip arrays. Group1: Fo, Group2: GC1, Group3: GC2. Lists of differentially regulated genes were created using High Performance Chip Data Analysis (HPCDA) with Bioretis database (http://www.bioretis-analysis.de). Worldwide data sharing is possible via Bioretis, please ask the authors.

Background corr dist: KL-Divergence = 0.0482, L1-Distance = 0.0328, L2-Distance = 0.0015, Normal std = 0.5930

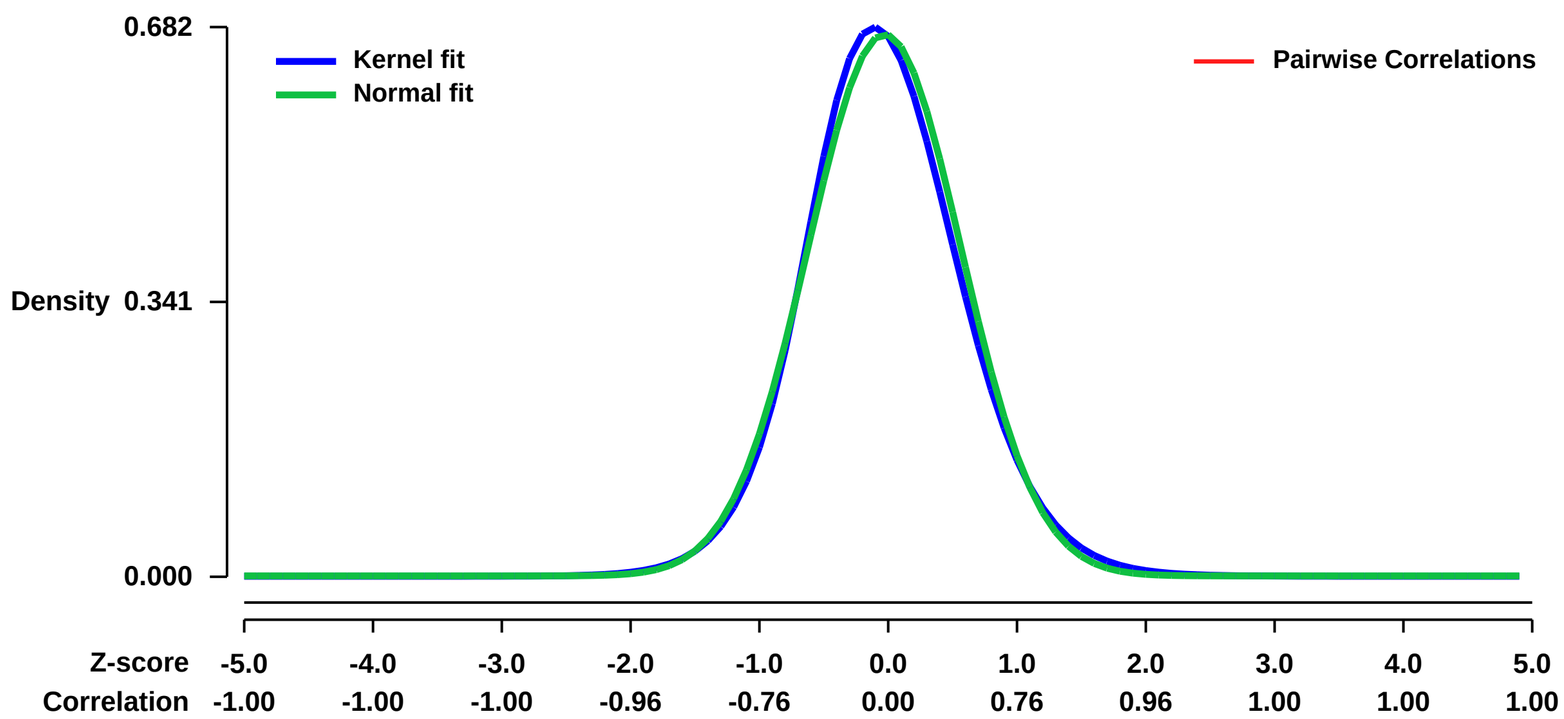

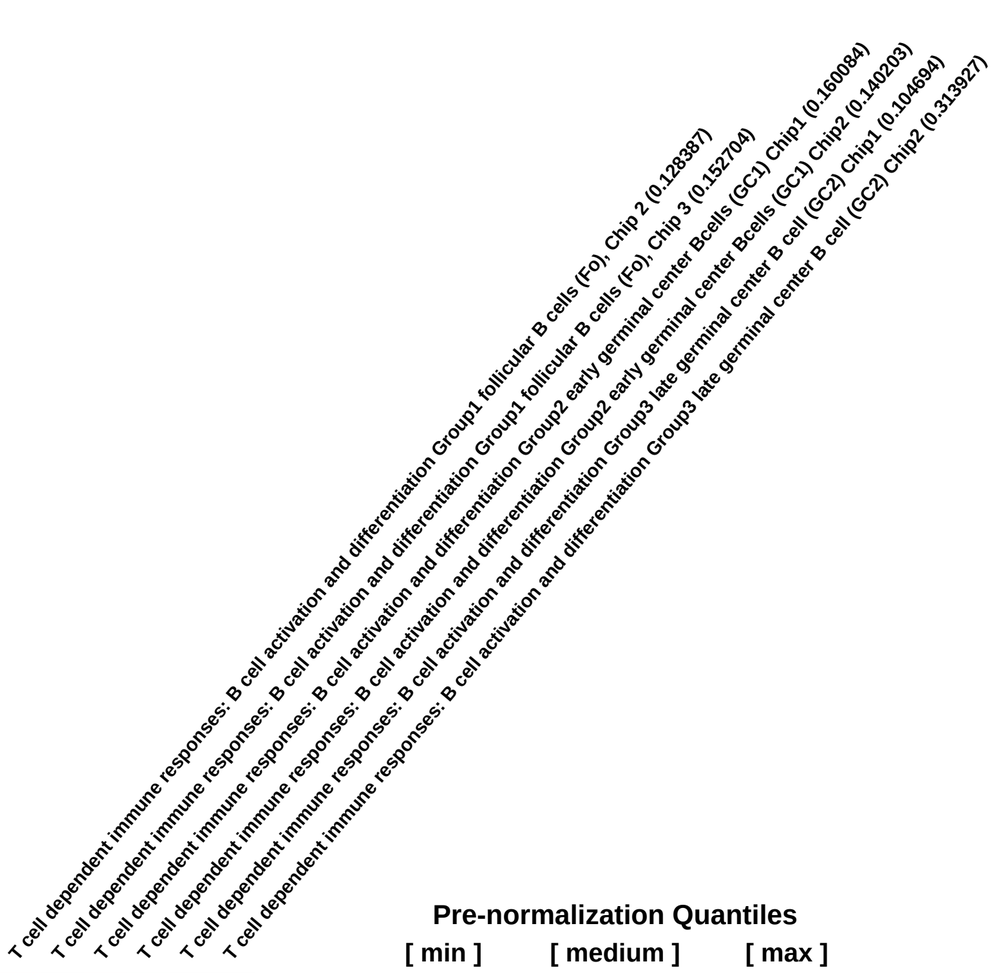

Pre-normalization Quantiles

[min] [medium] [max]

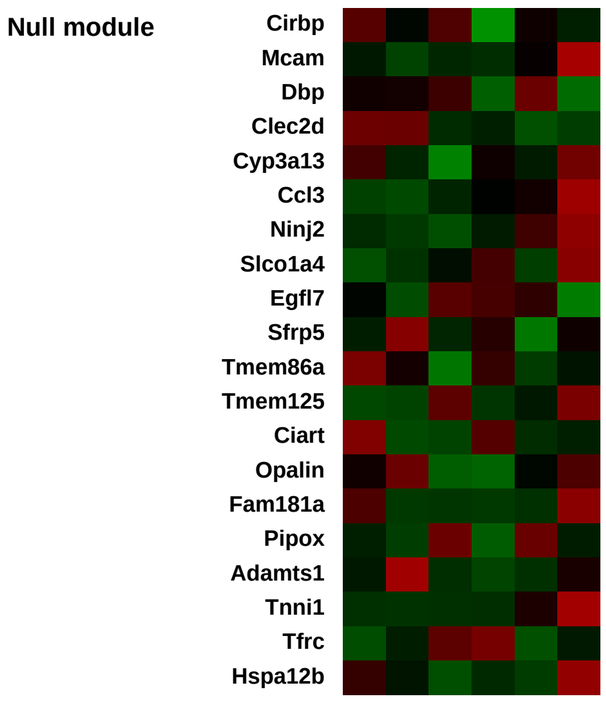

GEO Series "GSE11723" Expression Profiles

Num of samples in this series: 9

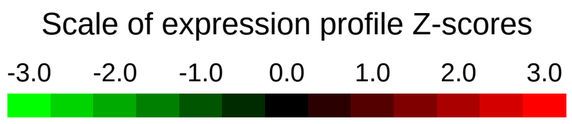

GEO Link:	http://www.ncbi.nlm.nih.gov/geo/query/acc.cgi?acc=GSE11723
Status:	Public on Jun 02 2009
Title:	Role of Notch signaling on hematopoietic stem cell differentiation
Organism:	Mus musculus
Experiment type:	Expression profiling by array
Platform:	GPL1261
Pubmed ID:	18786418
Summary & Design:	**Summary:** **Although Notch signaling has been clearly implicated in lymphoid differentiation, its role in myeloid lineages differentiation is unclear.** **Expression data from hematopoietic stem cells plated on OP9 stroma expressing or not the Notch ligand Delta-like1. Results provide insight into the role of Notch signalling in megakaryocyte fate specification.** **Keywords: Gene expression array-based (RNA / in situ oligonucleotide)** **Overall design:** **LSK cells were co-cultured for 3 days on OP9, OP9-DL1 and OP9-DL1+CompoundE (gamma-secretase inhibitor) and expression analysis was performed.**

Background corr dist: **KL-Divergence = 0.0364, L1-Distance = 0.0225, L2-Distance = 0.0005, Normal std = 0.6430**

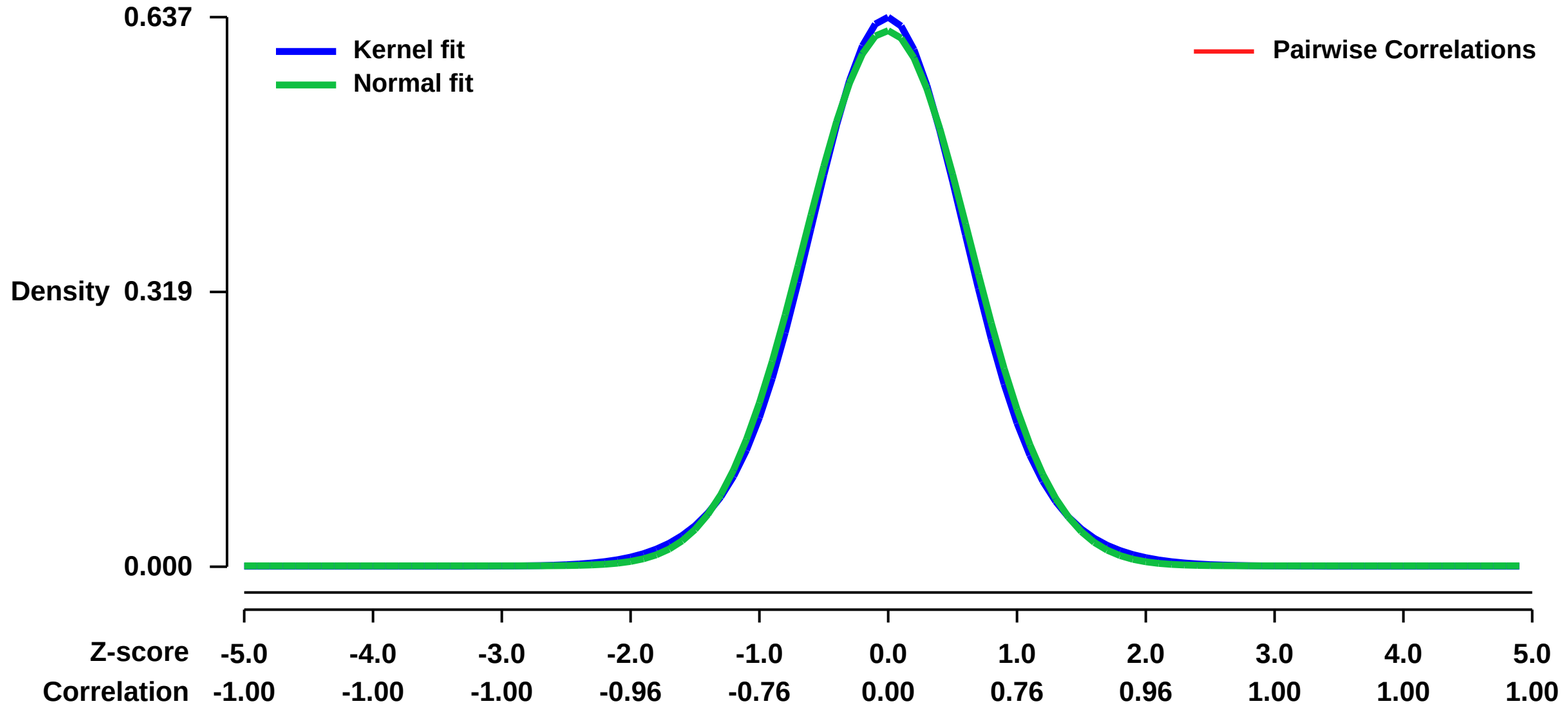

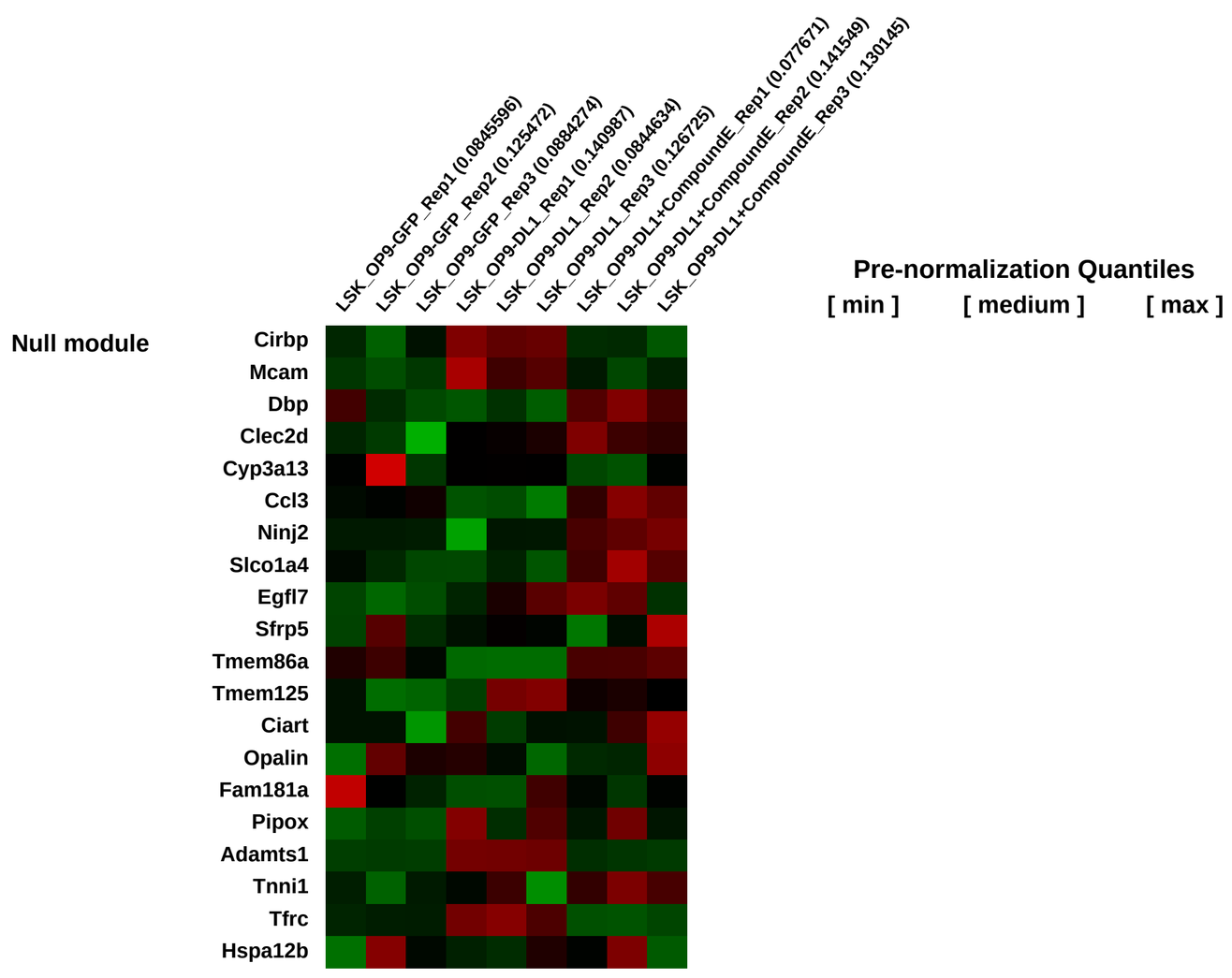

GEO Series "GSE55622" Expression Profiles

Num of samples in this series: 22

Scale of expression profile Z-scores

-3.0 -2.0 -1.0 0.0 1.0 2.0 3.0

GEO Link:	http://www.ncbi.nlm.nih.gov/geo/query/acc.cgi?acc=GSE55622
Status:	Public on Jun 26 2014
Title:	Cytoplasmic YAP and TAZ are intrinsic components of the b-catenin destruction complex
Organism:	Mus musculus
Experiment type:	Expression profiling by array
Platform:	GPL1261
Pubmed ID:	
Summary & Design:	**Summary:** To investigate the role of YAP/TAZ as b-catenin inhibitors, we compared the expression profiles of Rex1GFPd2 ES cells transfected with siControl#1, siControl#2, siYAP/TAZ#1, siYAP/TAZ#2 and cultured in 2i medium or PD-only medium **Overall design:** We collected RNA from Rex1GFPd2 embryonic stem (ES) cells transfected with siControl#1, siControl#2, siYAP/TAZ#1, siYAP/TAZ#2. Cells were maintained in 2i medium (2i=PD0325901+CHIR99021) or switched to PD (PD0325901)-only medium after 24 hours from siRNA transfection. Cells were harvested 72 hours post-siRNA transfection. Samples were then processed for total RNA extraction and hybridization on Affymetrix microarrays.

Background corr dist: KL-Divergence = 0.0811, L1-Distance = 0.0749, L2-Distance = 0.0091, Normal std = 0.5416

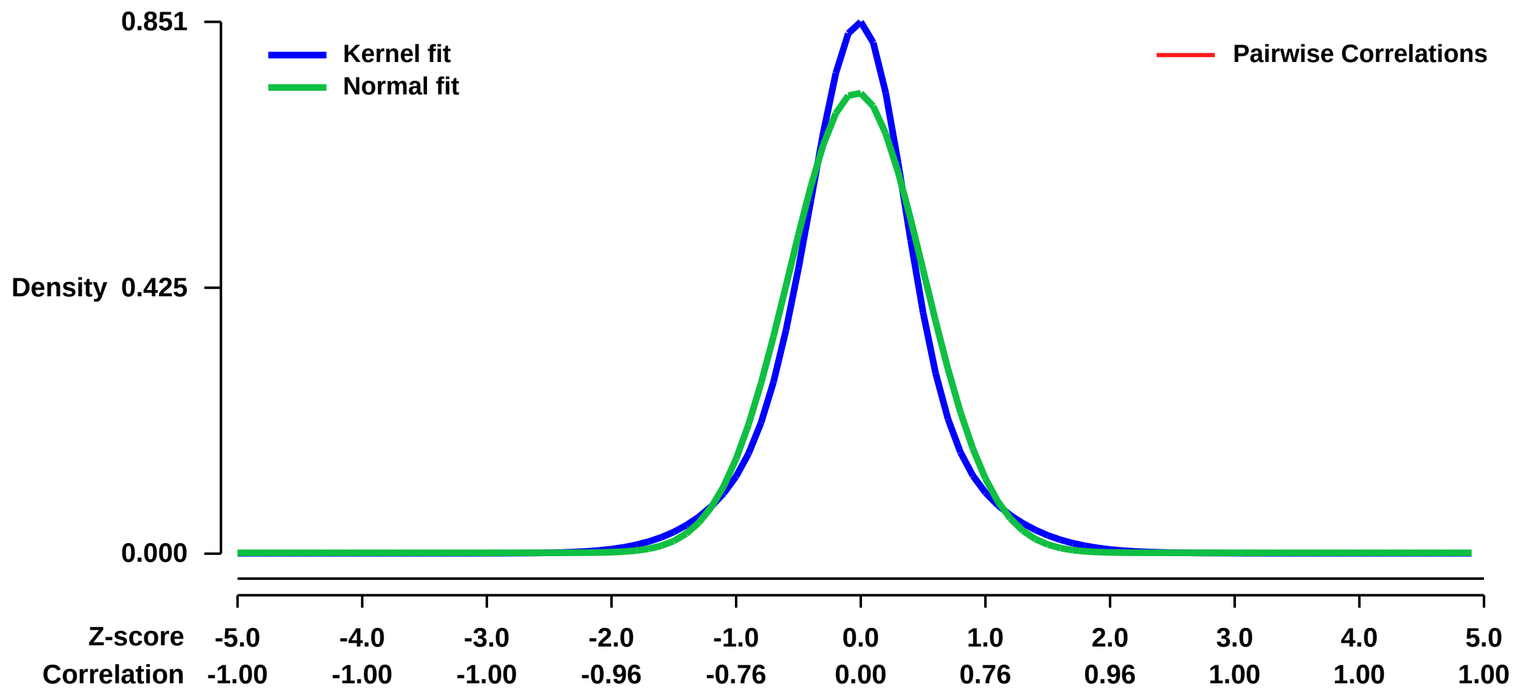

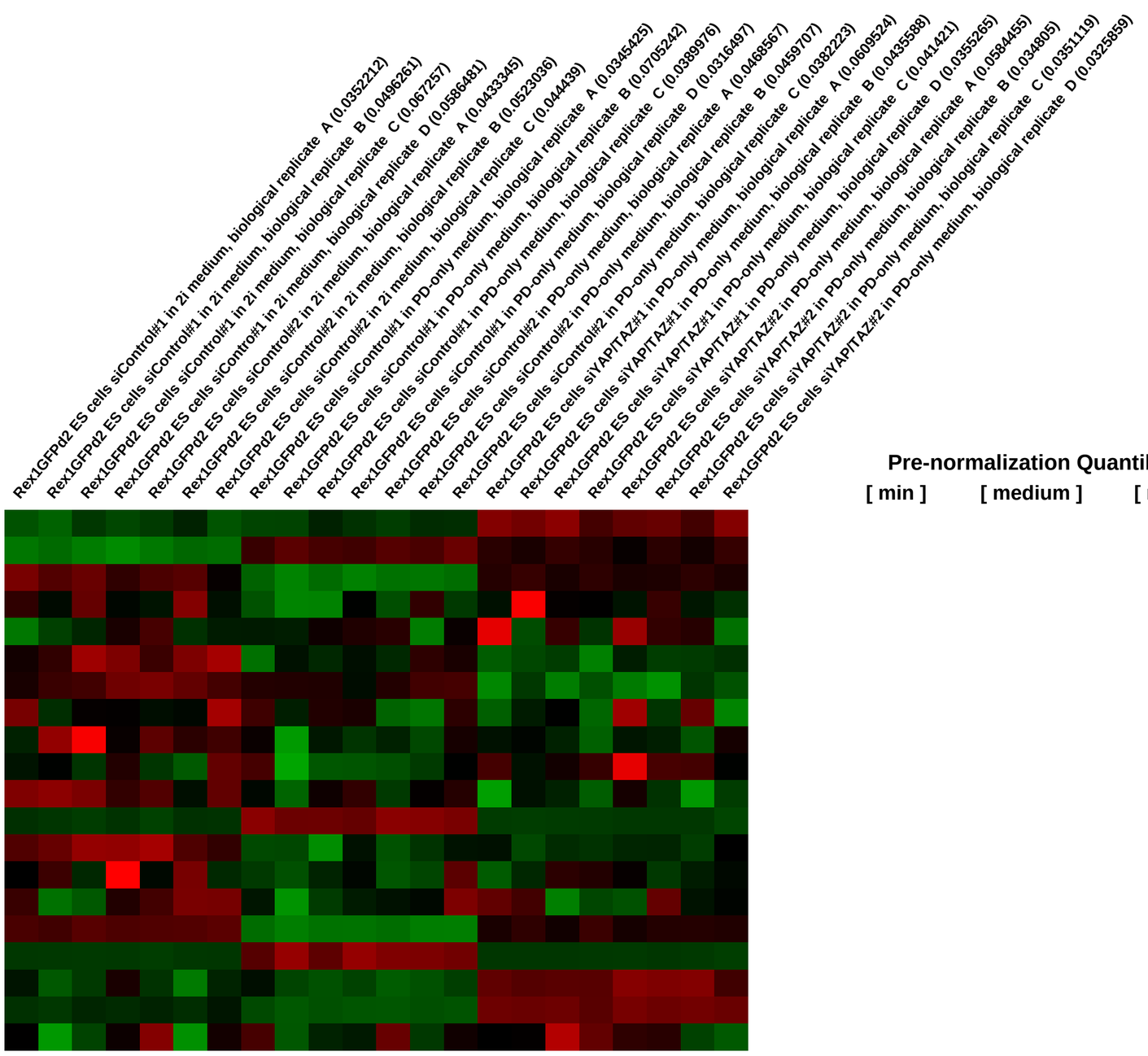

Pre-normalization Quantiles

[min] [medium] [max]

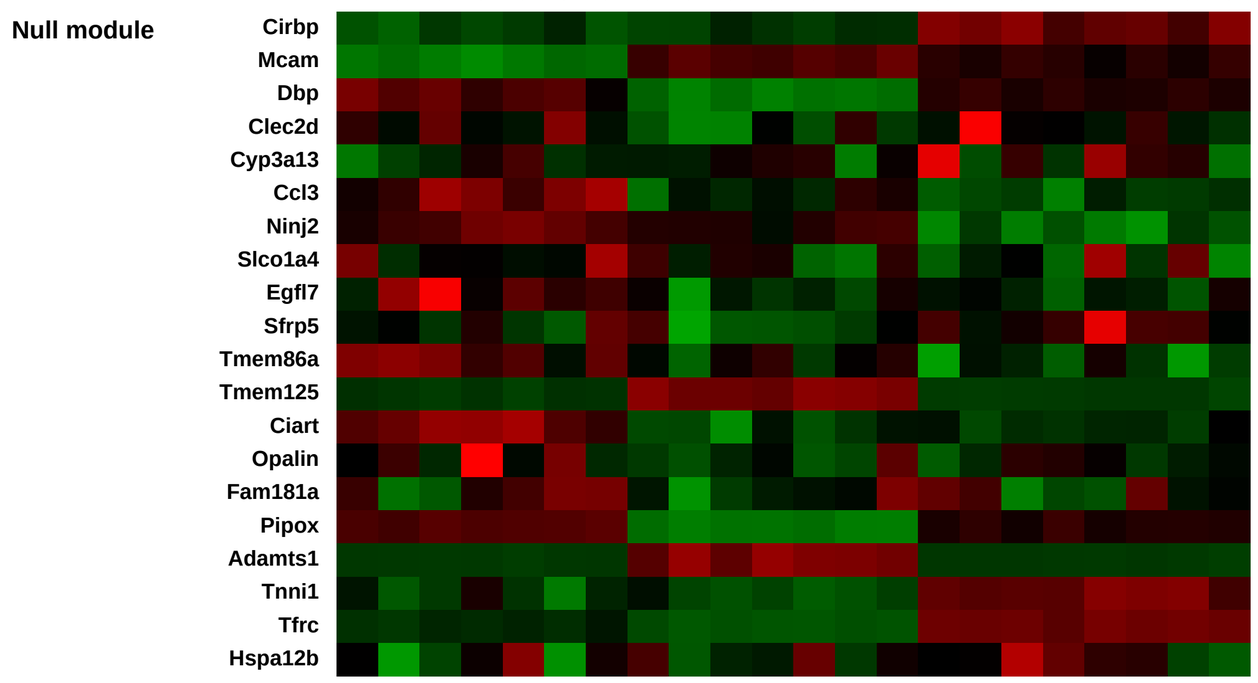

GEO Series "GSE44339" Expression Profiles

Num of samples in this series: 14

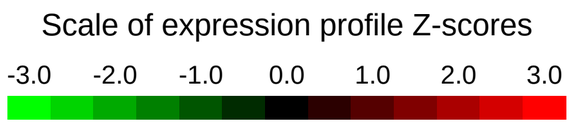

GEO Link:	http://www.ncbi.nlm.nih.gov/geo/query/acc.cgi?acc=GSE44339
Status:	Public on Jan 07 2014
Title:	Identification of Ccr4-Not complex as a regulator of transition from partial to genuine iPS cells
Organism:	Mus musculus
Experiment type:	Expression profiling by array
Platform:	GPL1261
Pubmed ID:	24200330
Summary & Design:	**Summary:** Partial induced pluripotent cells (iPSCs) are cell lines strayed from normal route from somatic cells to iPSCs and are immortalized. Mouse partial iPSCs are able to convert to real iPSCs by the exposure to 2i condition using MAPK and GSK3? inhibitors. However, the molecular mechanisms of this conversion are totally not known. Our piggyback vector mediated genome-wide screen revealed that Cnot2, one of core components of Ccr4-Not complex participates in this conversion. Subsequent analyses revealed other core components, i.e., Cnot1 and Cnot3 and Trim28 which is known to extensively share genomic binding sites with Cnot3 contribute to this conversion as well. Our bioinformatics analyses indicate that the major role of these factors in the conversion is the down-regulation of developmental genes in partial iPSCs. **Overall design:** Two partial iPSC clones (2B1 and 5C5) cultured under conventional culture condition with leukemia inhibitory factor (LIF) and serum and those converted to iPSCs by the exposure to 2i condition were used for RNA source. Partial iPSCs (2B1) cultured under conventional condition in which either one of Cnot1, Cnot2, Cnot3 and Trim28 cDNA or these factors were combinatorially incorporated after retrovirus infection and those in which empty vector or Nanog were stably integrated were also used for RNA source. In addition, embryonic fibroblasts and embryonic stem cells (ESCs) from 13.5 dpc embryos and blastocysts, respectively, from Nanog-GFP transgenic mice and wild-type ESC line (EBRTcH3) were used for RNA source.

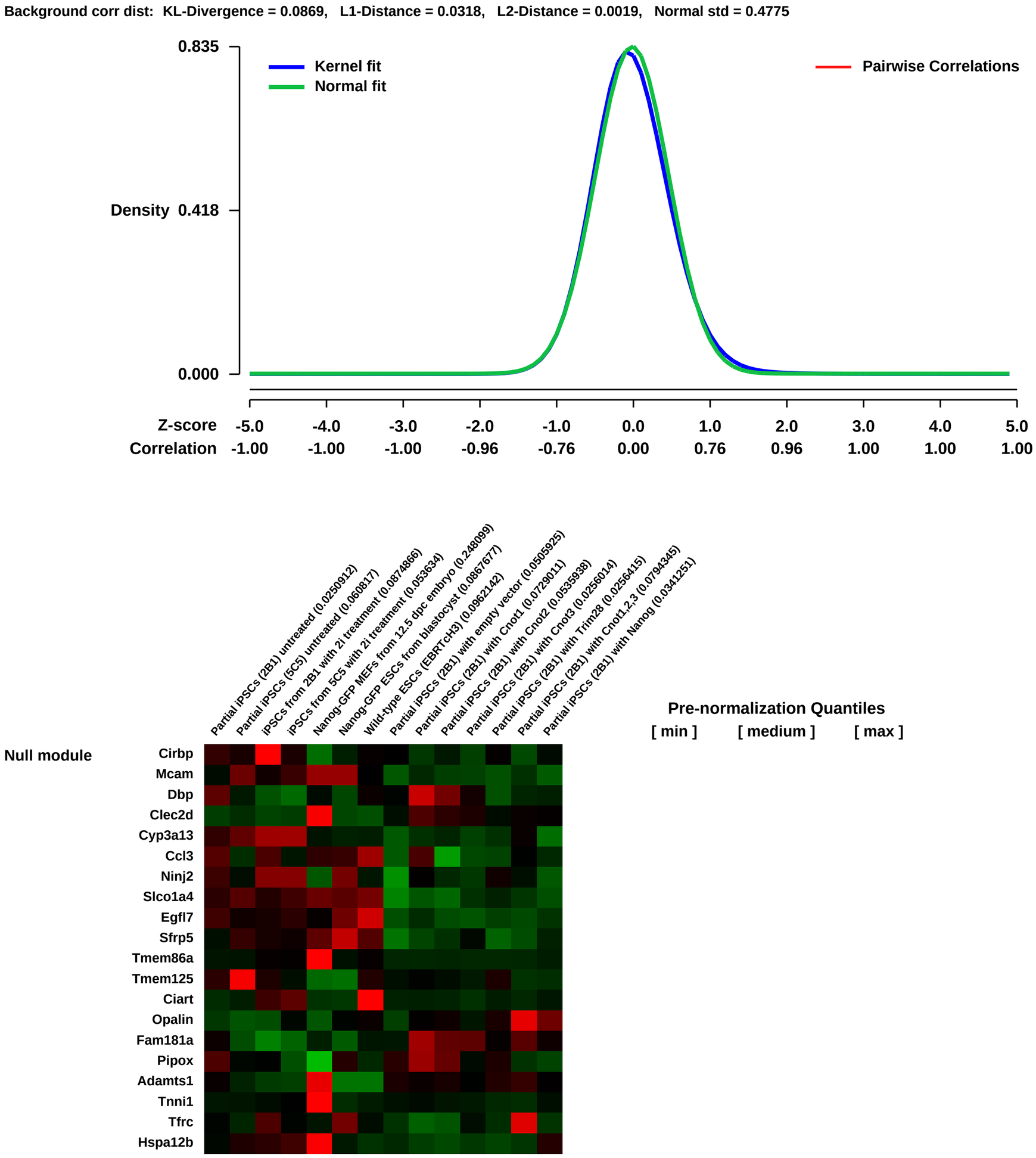

GEO Series "GSE18224" Expression Profiles

Num of samples in this series: 32

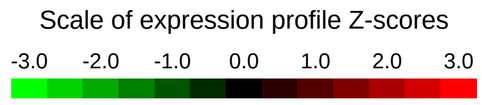

GEO Link:	http://www.ncbi.nlm.nih.gov/geo/query/acc.cgi?acc=GSE18224
Status:	Public on Jan 20 2010
Title:	Female sex and oestrogen receptor ¸† attenuate cardiac remodelling and apoptosis in pressure overload
Organism:	Mus musculus
Experiment type:	Expression profiling by array
Platform:	GPL1261
Pubmed ID:	21325064
Summary & Design:	**Summary:** Aims: We investigate sex differences and the role of oestrogen receptor beta (ERbeta) in a mouse model of pressure overload-induced myocardial hypertrophy. Methods and results: We performed transverse aortic constriction (TAC) or sham surgery in male and female wild-type (WT) and ERbeta knockout (ERbeta-/-) C57Bl6 mice. All mice were characterised by echocardiography and haemodynamic measurements and were sacrificed nine weeks after surgery. Left ventricular (LV) samples were analysed by microarray profiling, real-time RT-PCR and histology. After nine weeks, WT males showed more hypertrophy and heart failure signs than WT females. Notably, WT females developed a concentric form of hypertrophy, while males developed eccentric hypertrophy. These sex differences were abolished in ERbeta-/- mice. ERbeta deletion augmented the TAC-induced increase in cardiomyocyte diameter in both sexes. Gene expression profiling revealed that male WT hearts had a stronger induction of matrix-related genes and a stronger repression of mitochondrial genes than female hearts. ERbeta-/- mice exhibited a different transcriptome. Induction of pro-apoptotic genes after TAC occurred in ERbeta-/- mice of both sexes with a stronger expression in ERbeta-/- males. Histological analysis revealed, that cardiac fibrosis was more pronounced in male WT TAC than in female mice. This was abolished in ERbeta-/- mice. Apoptosis was significantly induced in both sexes of ERbeta-/- TAC mice, but it was most prominent in males. Conclusion: Female sex offers protection against ventricular chamber dilation in the TAC model. Both the female sex and ERbeta attenuate the development of fibrosis and apoptosis; thus slowing the progression to heart failure. **Overall design:** The influence of sex (male/female) and estrogen receptor beta expression (ERbeta knockout/wildtype) on cardiac hypertrophy (transverse aortic constriction/sham operated) was investigated. The left ventricular transcriptome of four individual mice for each combination of the three factors (sex, genotype, surgery) was detected with Affymetrix RAE 430 2.0 GeneChip arrays.

Background corr dist: KL-Divergence = 0.2814, L1-Distance = 0.0423, L2-Distance = 0.0033, Normal std = 0.2916

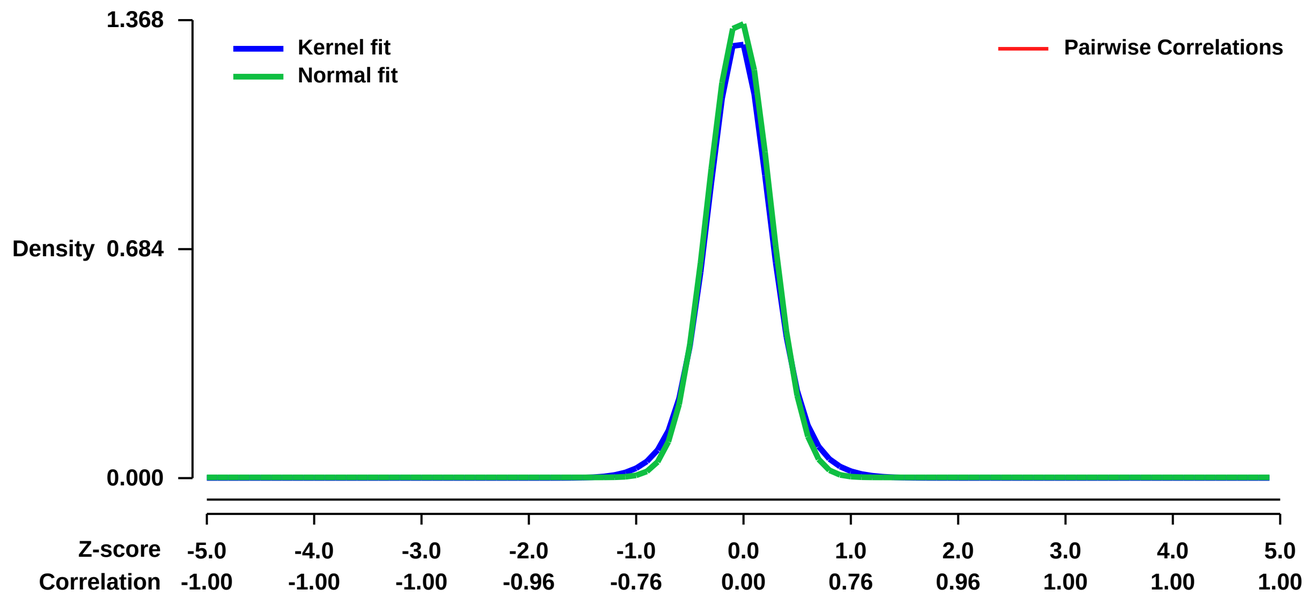

GEO Series "GSE7528" Expression Profiles

Num of samples in this series: 18

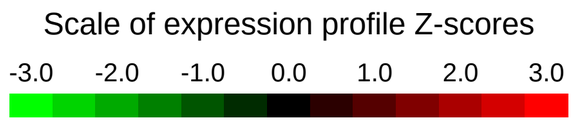

GEO Link:	http://www.ncbi.nlm.nih.gov/geo/query/acc.cgi?acc=GSE7528
Status:	Public on Jan 02 2008
Title:	Gene expression of Wt vs CYP26A1-/- murine ES cells treated with control or 100 nM RA for 8 or 72 hr.
Organism:	Mus musculus
Experiment type:	Expression profiling by array
Platform:	GPL1261
Pubmed ID:	18241852
Summary & Design:	**Summary:** The goal of this study was to identify genes that are differentially expressed after genetic deletion of both alleles of the Cyp26a1 gene in murine embryonic stem cells. Cyp26a1 codes for the CYP26A1 enzyme which metabolizes RA to polar RA metabolites, such as 4-oxo-RA and 4-OH-RA. CYP26A1-/- ES cells do not metabolize RA within 48 hours of RA treatment while in Wt ES cells, polar RA metabolites are already detectable by 8 hr. In addition, the absence of CYP26A1 enzyme increases intracellular RA levels. By gene microarray analysis, we wanted to identify genes that would be affected by the lack of the Cyp26a1 gene. **Keywords:** cell type comparison, time course **Overall design:** Wt and CYP26A1-/- ES cells were treated with control+LIF for 8 hours, and this was repeated 3 times. Wt and CYP26A1-/- ES cells were treated with 100 nM RA +LIF for 8 hours, and this was repeated 3 times. Wt and CYP26A1-/- ES cells were treated with 100 nM RA +LIF for 72 hours, and this was repeated 2 times.

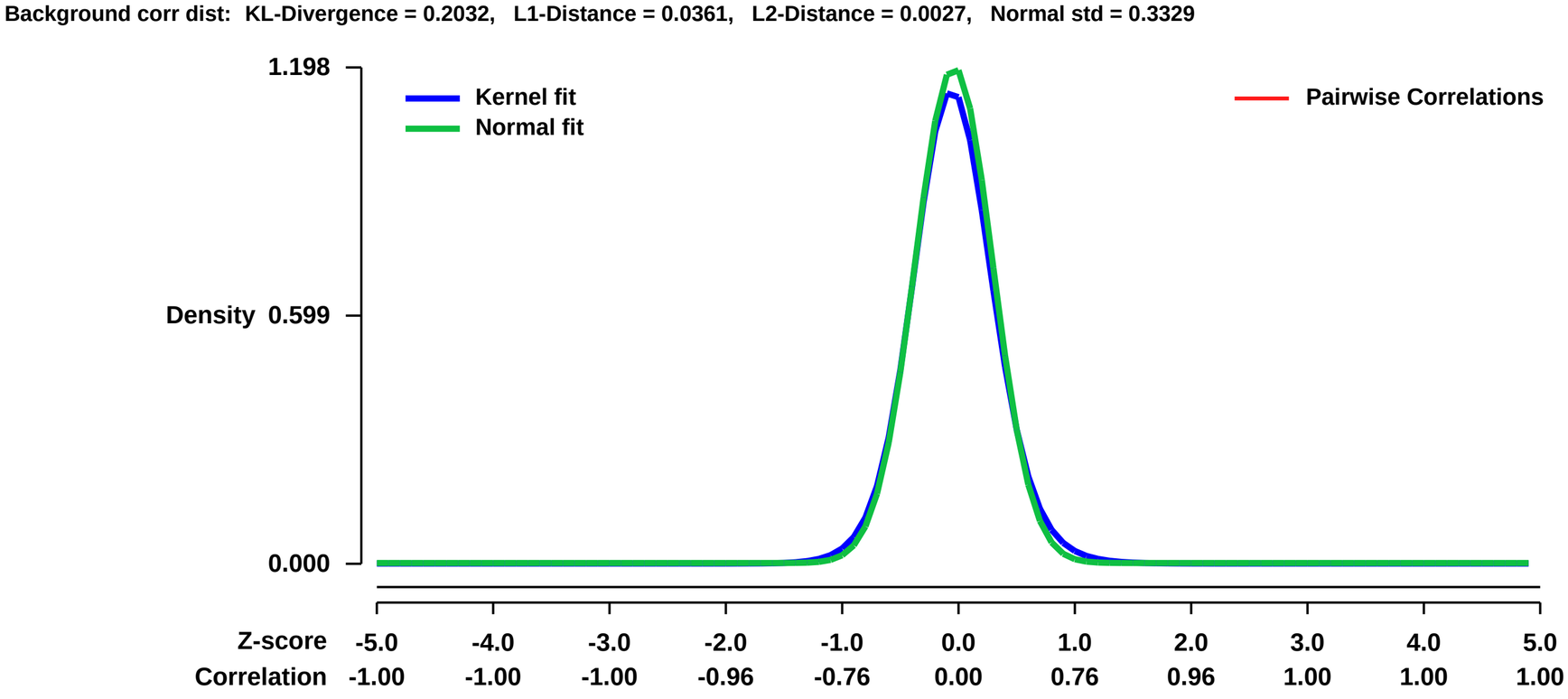

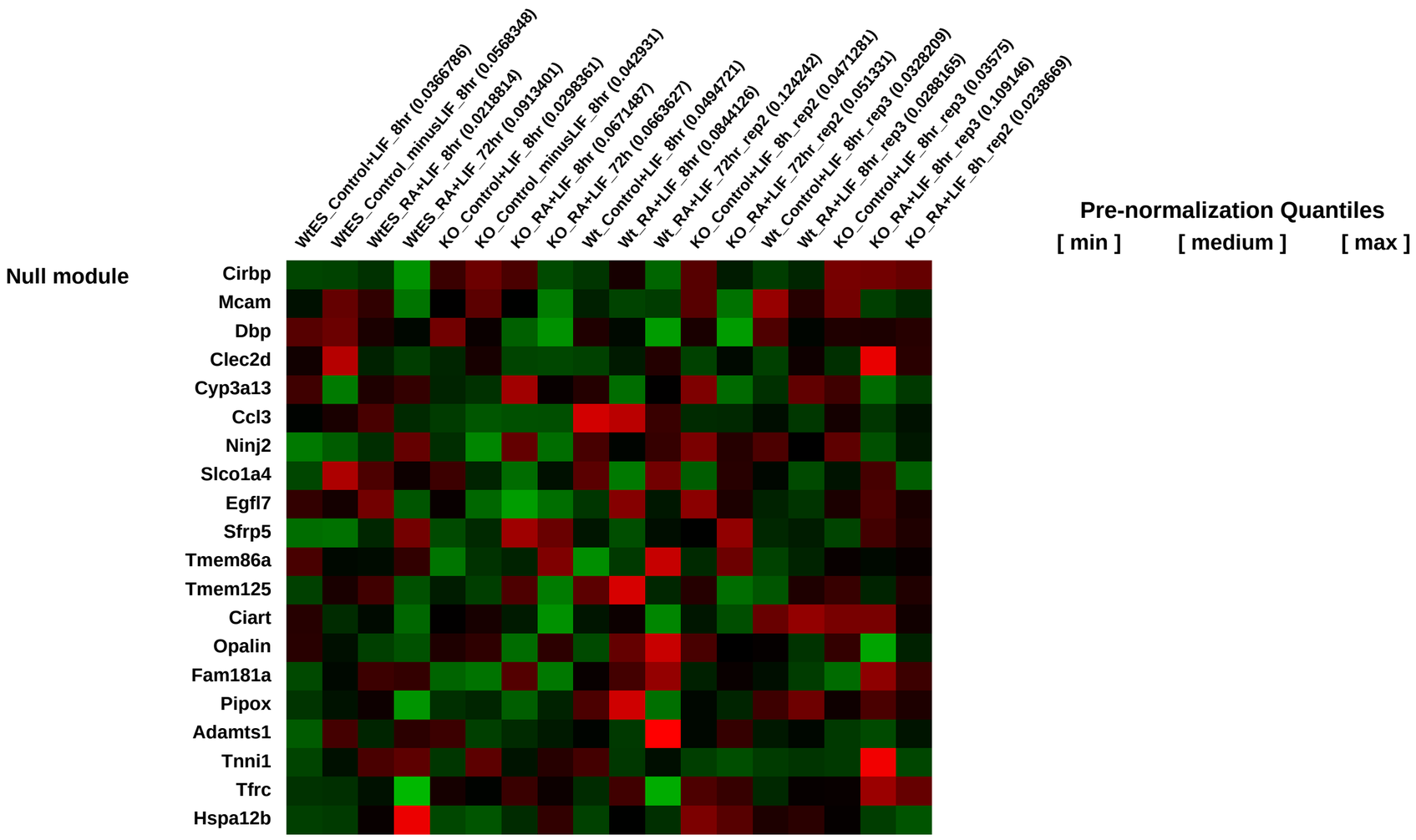

GEO Series "GSE41260" Expression Profiles

Num of samples in this series: 6

Scale of expression profile Z-scores

-3.0 -2.0 -1.0 0.0 1.0 2.0 3.0

GEO Link:	http://www.ncbi.nlm.nih.gov/geo/query/acc.cgi?acc=GSE41260
Status:	Public on Oct 02 2012
Title:	Expression Profiles of E11.5 Mouse Optic Fissure
Organism:	Mus musculus
Experiment type:	Expression profiling by array
Platform:	GPL1261
Pubmed ID:	23147794
Summary & Design:	**Summary:** Mice that are mutant for both Fgfr1 and Fgfr2 specifically in the developing retina develop coloboma. To analyze the transcripts that are affected by defective FGF signaling, we micro-dissected the optic fissure region from the control and FGFR condtional mutant mice and did microarray analysis. **Overall design:** E11.5 control and Six3Cre+; Fgfr1fx/fx;Fgfr2 fx/fx optic fissures are dissected using laser-assisted micro-dissection microscope, RNAs are extracted and labelled and hybridyzed to chips

Background corr dist: KL-Divergence = 0.0386, L1-Distance = 0.0255, L2-Distance = 0.0007, Normal std = 0.6295

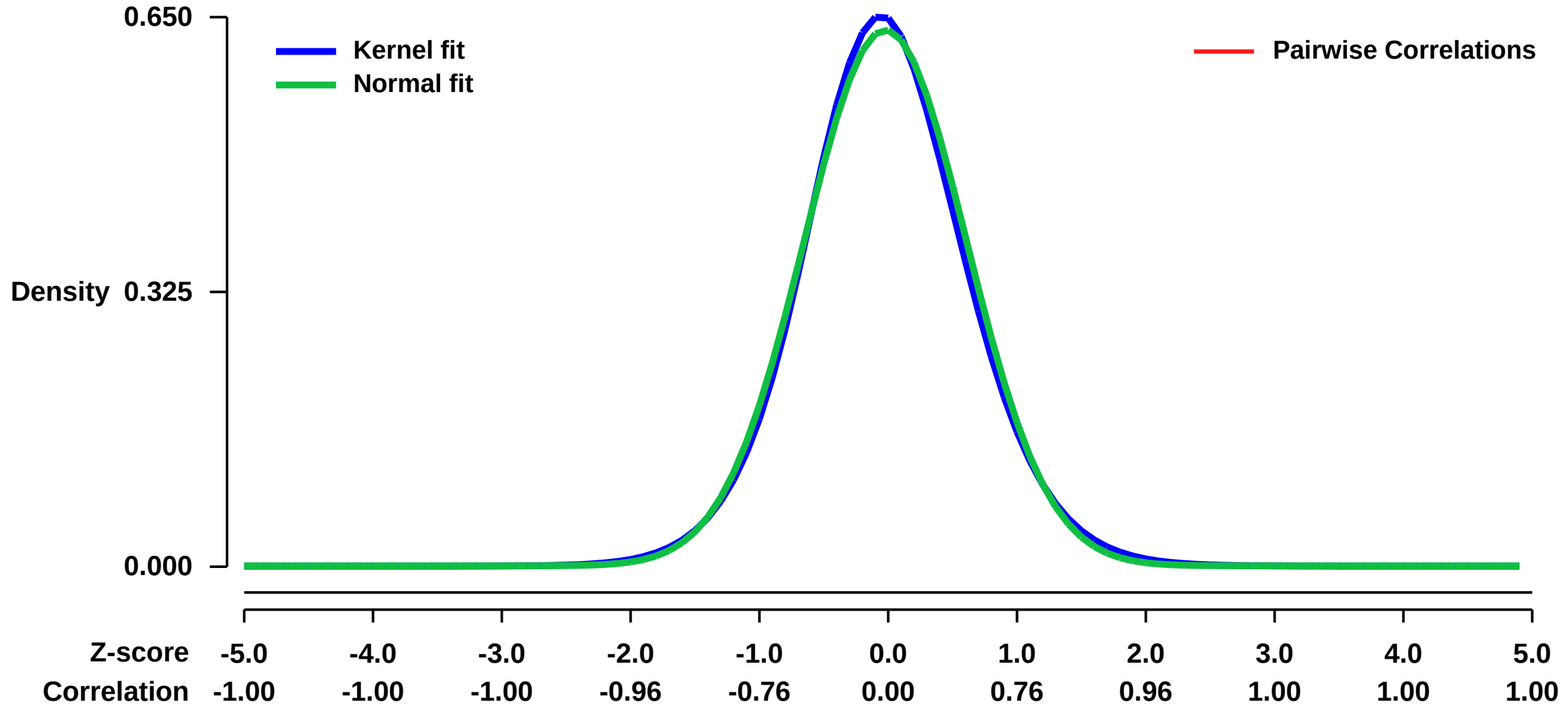

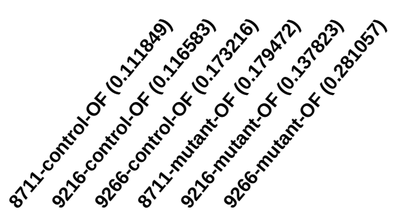

Pre-normalization Quantiles

[min] [medium] [max]

Null module

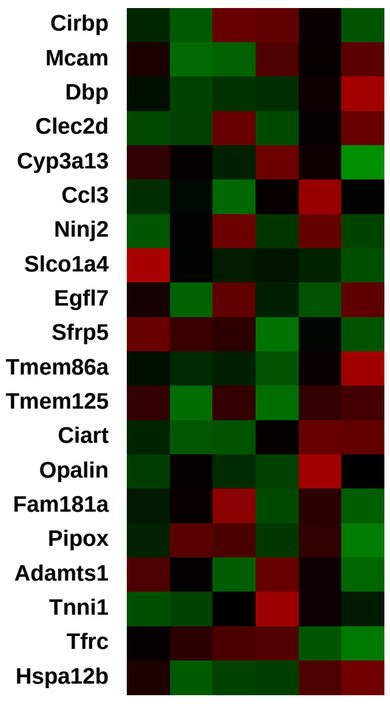

GEO Series "GSE9566" Expression Profiles

Num of samples in this series: 38

Scale of expression profile Z-scores

-3.0 -2.0 -1.0 0.0 1.0 2.0 3.0

GEO Link:	http://www.ncbi.nlm.nih.gov/geo/query/acc.cgi?acc=GSE9566
Status:	Public on Dec 31 2007
Title:	A Transcriptome Database for Astrocytes, Neurons, and Oligodendrocytes
Organism:	Mus musculus
Experiment type:	Expression profiling by array
Platform:	GPL1261
Pubmed ID:	18171944
Summary & Design:	**Summary:** **A Transcriptome Database for Astrocytes, Neurons, and Oligodendrocytes: A New Resource for Understanding Brain Development and Function** **Understanding the cell-cell interactions that control CNS development and function has long been limited by the lack of methods to cleanly separate astrocytes, neurons, and oligodendrocytes. Here we describe the first method for the isolation and purification of developing and mature astrocytes from mouse forebrain. This method takes advantage of the expression of S100‚† by astrocytes. We used fluorescent activated cell sorting (FACS) to isolate EGFP positive cells from transgenic mice that express EGFP under the control of an S100‚† promoter. By depletion of astrocytes and oligodendrocytes we obtained purified populations of neurons, while by panning with oligodendrocyte-specific antibodies we obtained purified populations of oligodendrocytes. Using GeneChip Arrays we then created a transcriptome database of the expression levels of over 20,000 genes by gene profiling these three main CNS neural cell types at postnatal ages day 1 to 30. This database provides the first global characterization of the genes expressed by mammalian astrocytes in vivo and is the first direct comparison between the astrocyte, neuron, and oligodendrocyte transcriptomes. We demonstrate that Aldh1L1, a highly expressed astrocyte gene, is a highly specific antigenic marker for astrocytes with a substantially broader, and therefore potentially more useful, pattern of astrocyte expression than the traditional astrocyte marker GFAP. This transcriptome database of acutely isolated and highly pure populations of astrocytes, neurons and oligodendrocytes provides a resource to the neuroscience community by providing improved cell type specific markers and for better understanding of neural development, function, and disease.** **We acutely purified mouse astrocytes from early postnatal ages (P1) to later postnatal ages (P30), when astrocyte differentiation is morphologically complete (Bushong et al., 2004), and acutely purified mouse OL-lineage cells from stages ranging from OPCs to newly differentiated OLs to myelinating OLs. We extracted RNA from each of these highly purified, acutely isolated cell types and used GeneChip Arrays to determine the expression levels of over 20,000 genes and construct a comprehensive database of cell type specific gene expression in the mouse forebrain. Analysis of this database confirms cell type specific expression of many well characterized and functionally important genes. In addition, we have identified thousands of new cell type enriched genes, thereby providing important new information about astrocyte, OL, and neuron interactions, metabolism, development, and function. This database provides a comparison of the genome-wide transcriptional profiles of the main CNS cell types and is a resource to the neuroscience community for better understanding the development, physiology, and pathology of the CNS.** **Keywords: Developmental CNS Cell type comparision** **Overall design:** **FACS purification of astrocytes: Dissociated forebrains from S100‚†-EGFP mice were resuspended in panning buffer (DBPS containing 0.02% BSA and 12.5 U/ml DNase) and sequentially incubated on the following panning plates: secondary antibody only plate to deplete microglia, O4 plate to deplete OLs, PDGFR‚– plate to deplete OPCs, and a second O4 plate to deplete any remaining OLs. This procedure was sufficient to deplete all OL-lineage cells from animals P8 and younger, however, in older animals that had begun to myelinate, additional depletion of OLs and myelin debris was accomplished as follows. The nonadherent cells from the last O4 dish were harvested by centrifugation, and the cells were resuspended in panning buffer containing GalC, MOG, and O1 supernatant and incubated for 15 minutes at room temperature. The cell suspension was washed and then resuspended in panning buffer containing 20 ‚…g donkey anti-mouse APC for 15 minutes. The cells were washed and resuspended in panning buffer containing propidium iodide (PI). EGFP+ astrocytes were then purified by fluorescence activated cell sorting (FACS). Dead cells were gated out using high PI staining and forward light scatter. Astrocytes were identified based on high EGFP fluorescence and negative APC fluorescence from indirect immunostaining for OL markers GalC, MOG, and O1. Cells were sorted twice and routinely yielded >99.5% purity based on reanalysis of double sorted cells.; FACS purification of neurons: EGFP- cells were the remaining forebrain cells after microglia, OLs, and astrocytes had been removed, and were primarily composed of neurons, and to a lesser extent, endothelial cells (we estimate < 4% endothelial cells at P7 and < 20% endothelial cells at P17). EGFP- cells from S100‚†-EGFP dissociated forebrain were FACS purified in parallel with astrocyte purification and were sorted based on their negative EGFP fluorescence immunofluorescence. Cells were sorted twice and routinely yielded >99.9% purity. In independent preparations, the EGFP- cell population was additionally depleted of endothelial cells and pericytes by sequentially labeling with biotin-BSL1 lectin and streptavidin-APC while also labeling for OL markers as described above. Cells were sorted twice and routinely yielded >99.9% purity.; Panning purification of oligodendrocyte lineage cells: Dissociated mouse forebrains were resuspended in panning buffer. In order to deplete microglia, the single-cell suspension was sequentially panned on four BSL1 panning plates. The cell suspension was then sequentially incubated on two PDGFR‚– plates (to purify and deplete OPCs), one A2B5 plate (to deplete any remaining OPCs), two MOG plates (to purify and deplete myelinating OLs), and one GalC plate (to purify the remaining PDGFR‚–-, MOG-, OLs). The adherent cells on the first PDGFR‚–, MOG, and GalC plates were washed to remove all antigen-negative nonadherent cells. The cells were then lysed while still attached to the panning plate with Qiagen RLT lysis buffer, and total RNA was purified. Purified OPCs were >95% NG2 positive and 0% MOG positive. Purified Myelin OLs were 100% MOG positive, >95% MBP positive, and 0% NG2 positive. Purified GalC OLs depleted of OPCs and Myelin OLs were <10% MOG positive and ~50% weakly NG2 positive, a reflection of their recent development as early OLs.; Data normalization and analysis: Raw image files were processed using Affymetrix GCOS and the MAS 5.0 algorithm. Intensity data was normalized per chip to a target intensity TGT value of 500, and expression data and absent/present calls for individual probe sets were determined. Gene expression values were normalized and modeled across arrays using the dChip software package with invariant-set normalization and a PM model. (www.dchip.org, Li and Wong, 2001). The 29 samples were grouped into 9 sample types: Astros P7-P8, Astros P17, Astros P17-gray matter (P17g), Neurons P7, Neurons P17, Neurons-endothelial cell depleted (P7n, P17n), OPCs, GalC-OLs, and MOG-OLs. Gene filtering was performed to select probe sets that were consistently expressed in at least one cell type, where consistently expressed was defined as being called present and having a MAS 5.0 intensity level greater than 200 in at least two-thirds of the samples in the cell type. We identified 20,932 of the 45,037 probe sets that were consistently expressed in at least one of the nine cell types. The Significance Analysis of Microarrays (SAM) method (Tusher et al., 2001) was used to determine genes that were significantly differentially expressed between different cell types (see Supplemental Table S2 for SAM cell type groupings). Clustering was performed using the hclust method with complete linkage in R. Expression values were transformed for clustering by computing a mean expression value for the gene using those samples in the corresponding SAM statistical analysis, and then subtracting the mean from expression intensities. In order to preserve the log2 scale of the data, unless otherwise indicated, no normalization by variance was performed. Plots were created using the gplots package in R. The Bioconductor software package (Gentleman et al., 2004) was used throughout the expression analyses. Functional analyses were performed through the use of Ingenuity Pathways Analysis (Ingenuity´fi Systems, www.ingenuity.com).**

Background corr dist: KL-Divergence = 0.1819, L1-Distance = 0.0468, L2-Distance = 0.0051, Normal std = 0.3520

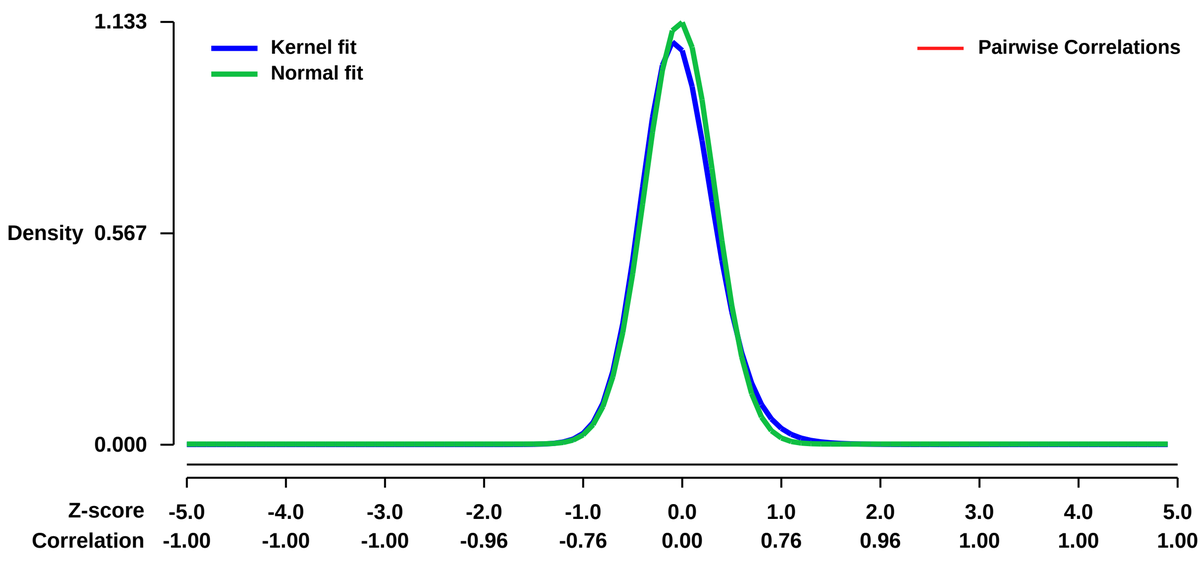

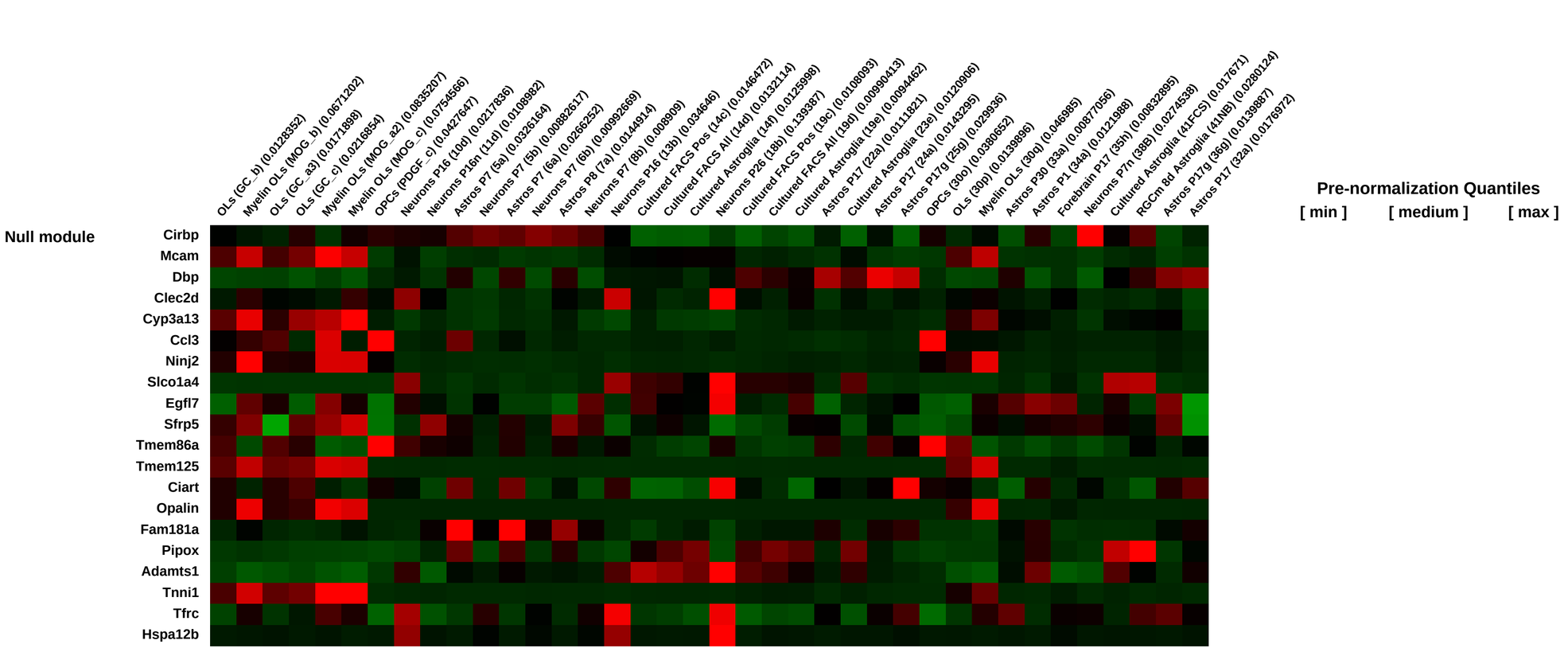

GEO Series "GSE45194" Expression Profiles

Num of samples in this series: 12

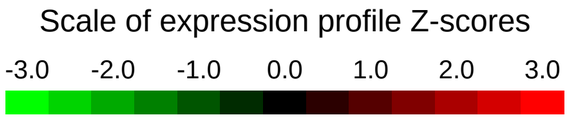

GEO Link:	**http://www.ncbi.nlm.nih.gov/geo/query/acc.cgi?acc=GSE45194**
Status:	**Public on Mar 14 2014**
Title:	**Oncogenic Nras has a bimodal effect on hematopoietic stem cells promoting proliferation and self-renewal**
Organism:	**Mus musculus**
Experiment type:	**Expression profiling by array**
Platform:	**GPL1261**
Pubmed ID:	**24284627**
Summary & Design:	**Summary:** **Pre-leukemic mutations are thought to promote clonal expansion of hematopoietic stem cells (HSCs) by increasing self-renewal and competitiveness. However, mutations that increase HSC proliferation tend to reduce competitiveness and self-renewal potential, raising the question of how a mutant HSC can sustainably outcompete wild-type HSCs. Activating mutations in NRAS are prevalent in human myeloproliferative disease and leukemia. Here we show that a single allele of oncogenic NrasG12D increases HSC proliferation but also increases reconstituting and self-renewal potential upon serial transplantation in irradiated mice, all without immortalizing HSCs or causing leukemia in our experiments. NrasG12D also confers long-term self-renewal potential upon multipotent progenitors. To explore the mechanism by which NrasG12D promotes HSC proliferation and self-renewal we assessed HSC cell cycle kinetics using H2B-GFP label retention. We found that NrasG12D had a bimodal effect on HSCs, increasing the proliferation of some HSCs while increasing the quiescence and competitiveness of other HSCs. One signal can therefore increase HSC proliferation, competitiveness, and self-renewal through a bimodal effect that promotes proliferation in some HSCs and quiescence in others.** **Overall design:** **12 RNA samples from mouse bone marrows were analyzed. There are three biological replicates for each subtype.**

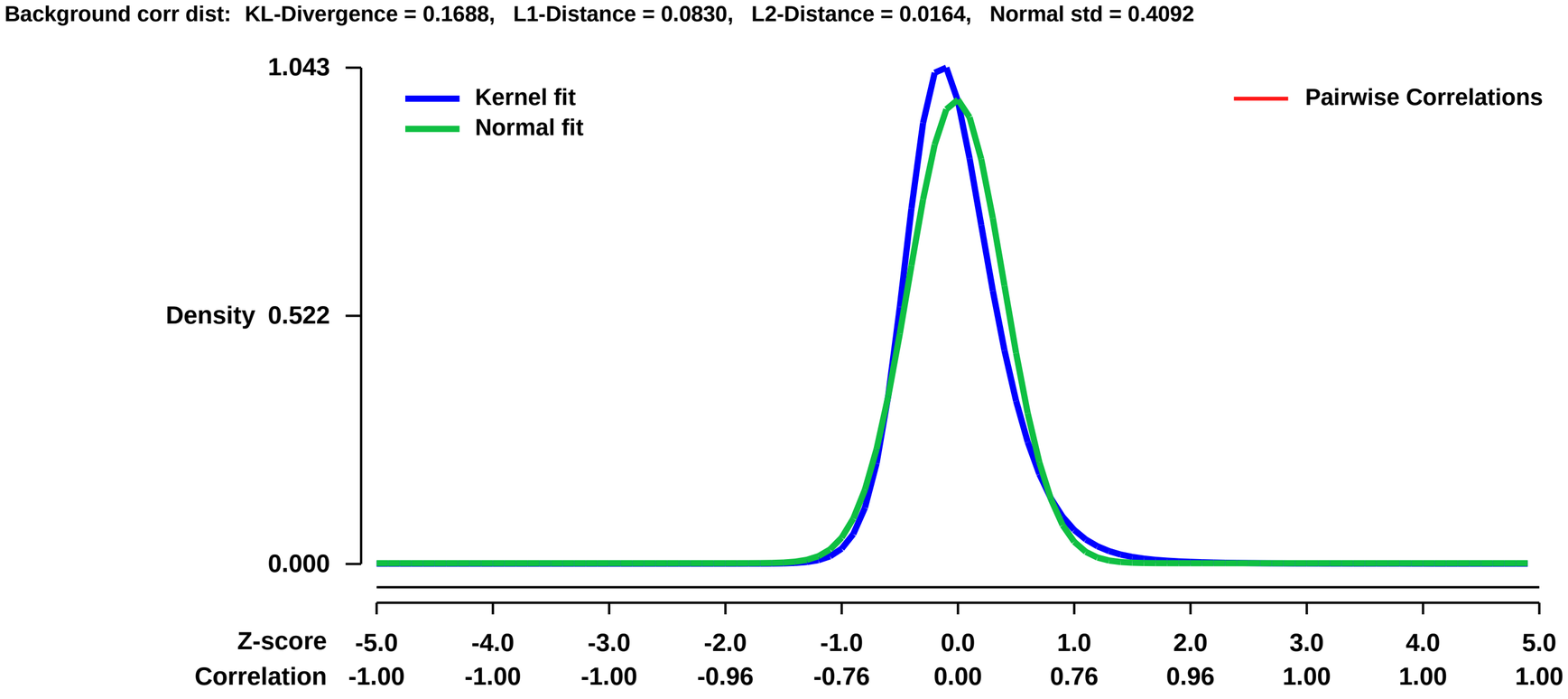

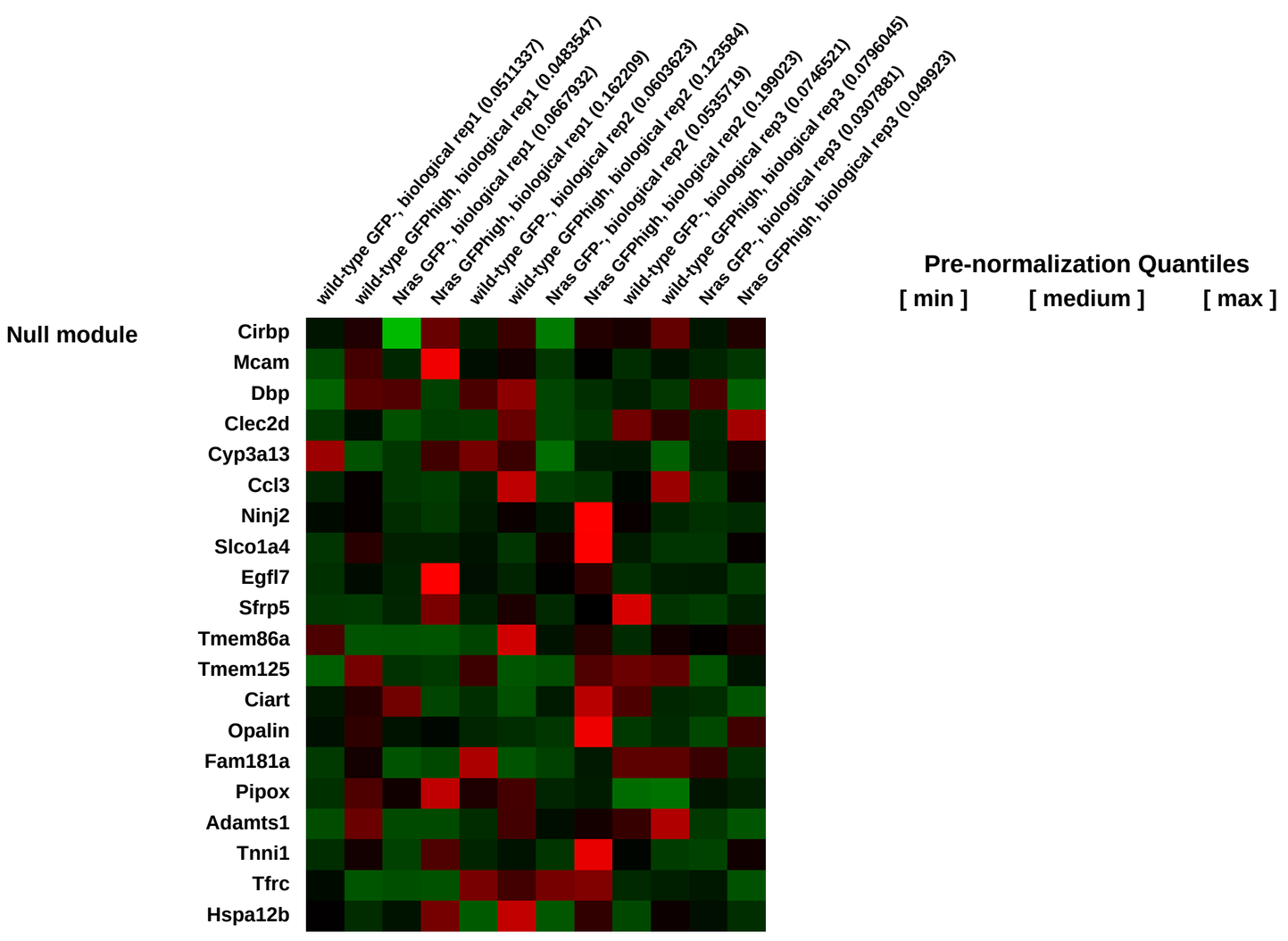

GEO Series "GSE32288" Expression Profiles

Num of samples in this series: 6

Scale of expression profile Z-scores

-3.0 -2.0 -1.0 0.0 1.0 2.0 3.0

GEO Link:	**http://www.ncbi.nlm.nih.gov/geo/query/acc.cgi?acc=GSE32288**
Status:	**Public on Apr 04 2012**
Title:	**Gene expression profile in Yaf2 KD and/or RYBP KO ES cells.**
Organism:	**Mus musculus**
Experiment type:	**Expression profiling by array**
Platform:	**GPL1261**
Pubmed ID:	**22269950**
Summary & Design:	**Summary:** **Gene expression change by Yaf2 KD in wild type or RYBP KO ES cells.** **Overall design:** **Total RNAs were extracted from the respective ES cells, and were subjected to microarray analysis using Affymetrix GeneChip Mouse Genome 430A 2.0 arrays**
Background corr dist:	**KL-Divergence = 0.0452, L1-Distance = 0.0174, L2-Distance = 0.0003, Normal std = 0.5903**

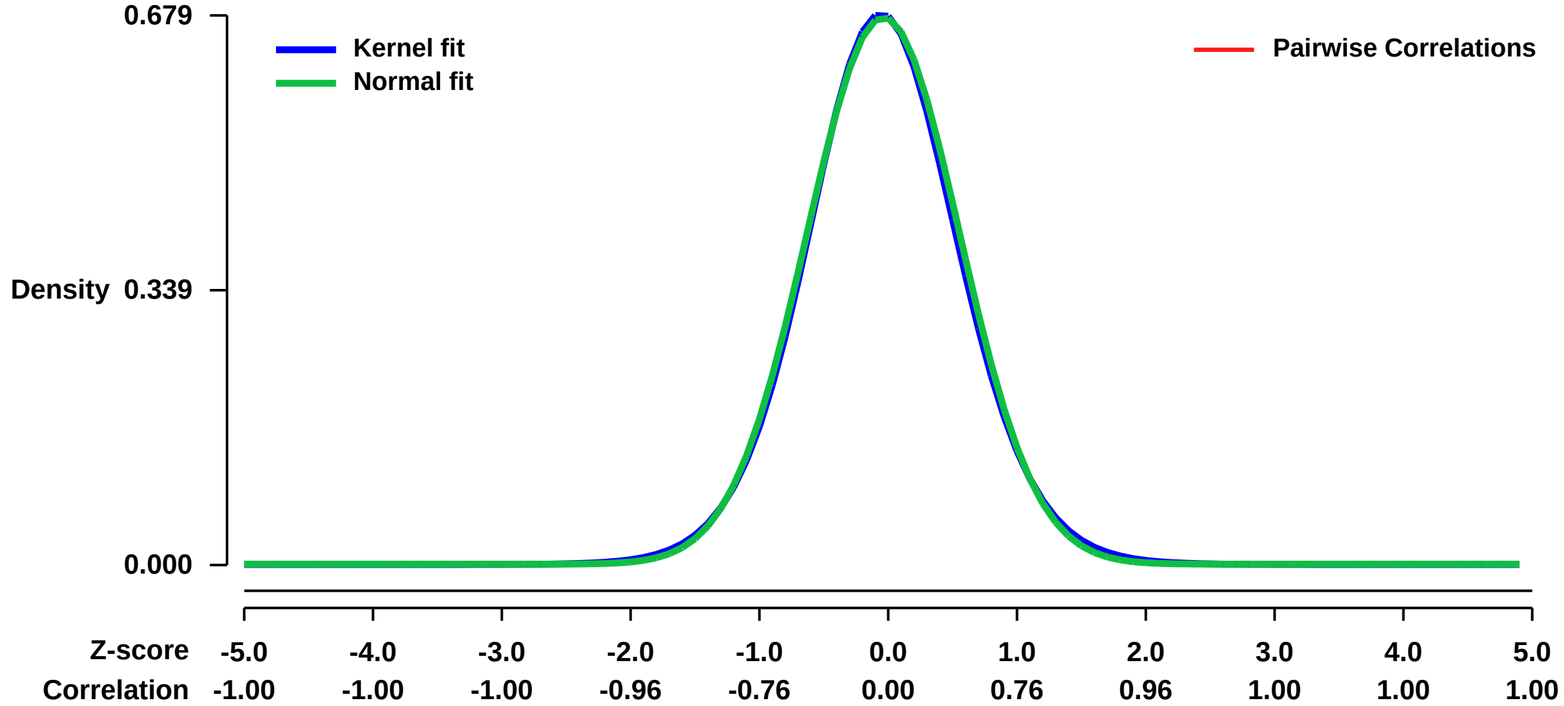

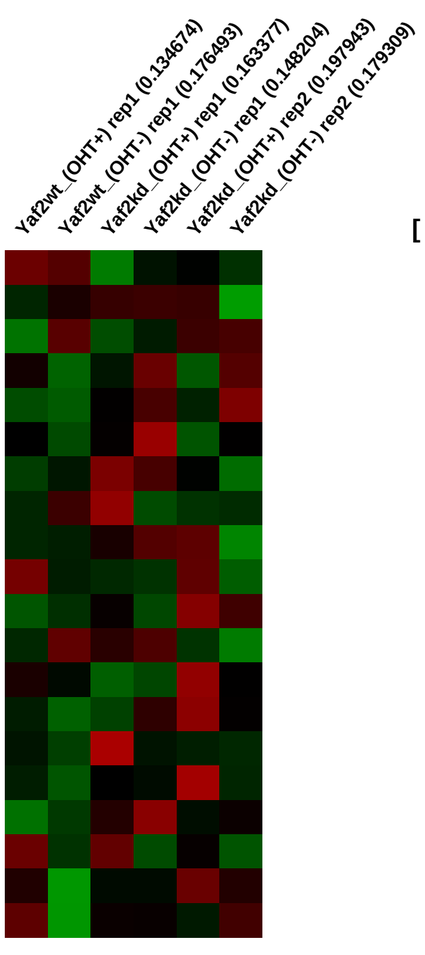

GEO Series "GSE7784" Expression Profiles

Num of samples in this series: 12

Scale of expression profile Z-scores

-3.0 -2.0 -1.0 0.0 1.0 2.0 3.0

GEO Link:	http://www.ncbi.nlm.nih.gov/geo/query/acc.cgi?acc=GSE7784
Status:	Public on May 17 2007
Title:	Expression profiling of double negative thymocytes
Organism:	Mus musculus
Experiment type:	Expression profiling by array
Platform:	GPL1261
Pubmed ID:	17911620
Summary & Design:	**Summary:** In order to understand the molecular mechanisms of DN thymocyte development, it may be also of use to clarify how these developmental processes are regulated in terms of their entire gene expression, to which cell differentiation is ultimately ascribed. In the current study, we approached this issue by investigating gene expression profiles in discrete subsets of DN thymocytes under development, in which DN2, DN3, and DN4 thymocytes were sorted and subjected to expression profiling analysis with high-density oligonucleotide microarrays. Keywords: developmental stages **Overall design:** The DN2, DN3, and DN4 populations were FACS-sorted from DN thymocytes harvested from four C57BL/6 mice and analyzed by Affymetrix´fi Mouse Genome 430 2.0 Array´fi for gene expression. Four independent experiments were performed using 16 mice.

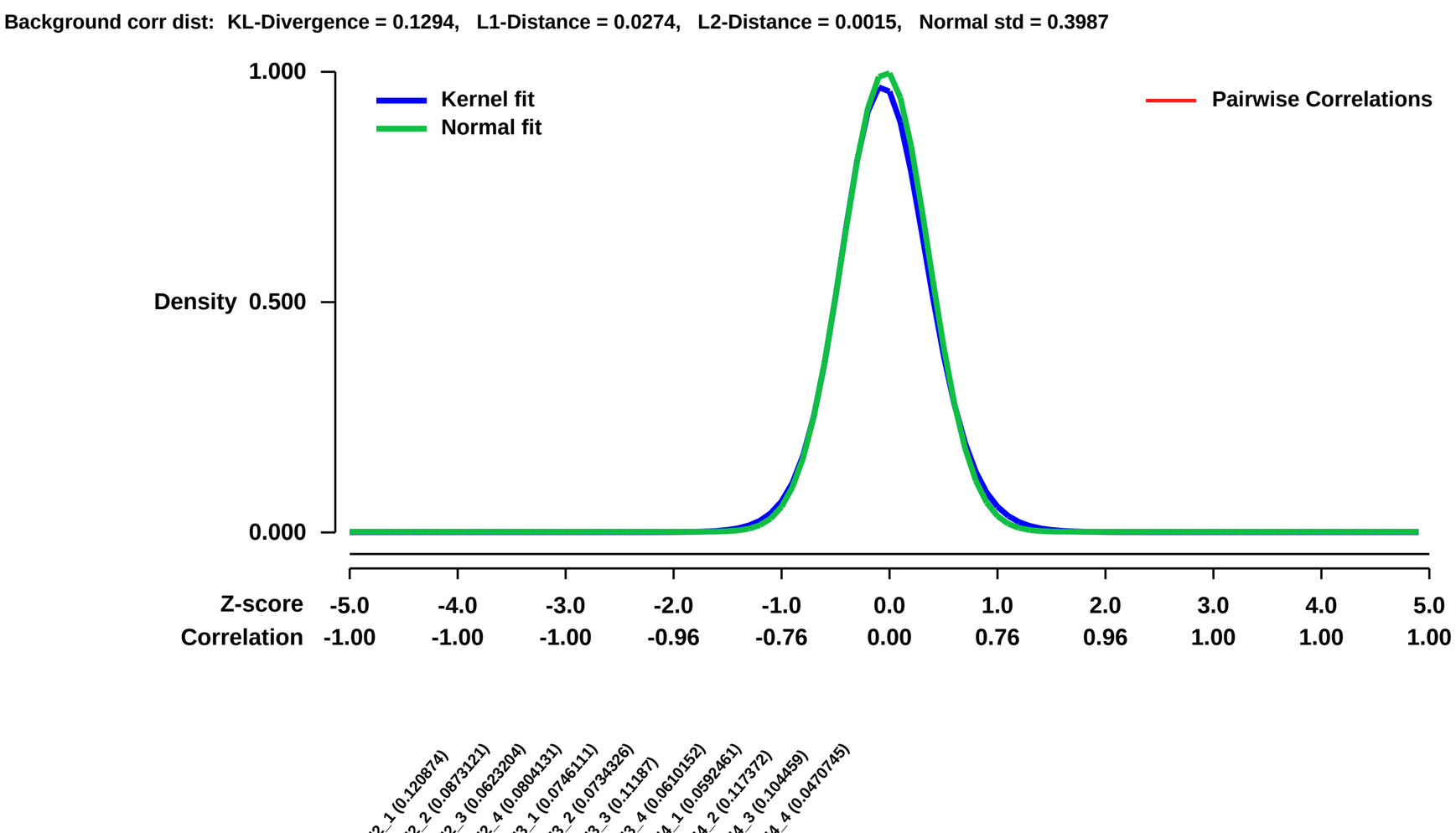

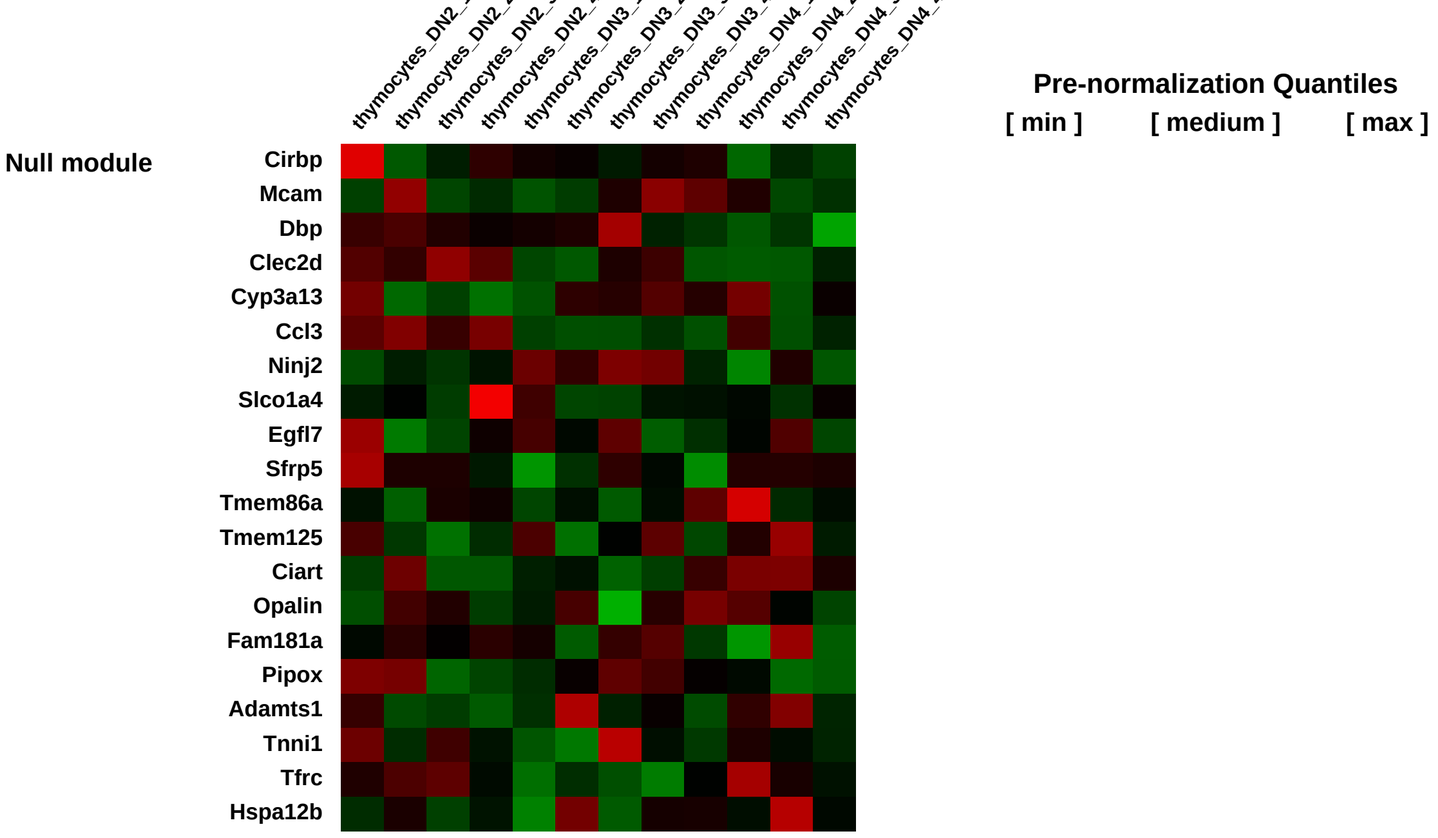

Pre-normalization Quantiles

[min] [medium] [max]

GEO Series "GSE30176" Expression Profiles

Num of samples in this series: 12

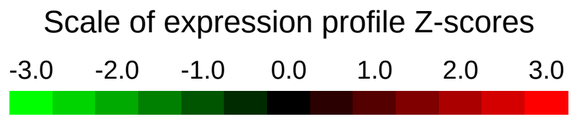

GEO Link:	**http://www.ncbi.nlm.nih.gov/geo/query/acc.cgi?acc=GSE30176**
Status:	**Public on Jul 19 2011**
Title:	**Retinoic acid (RA) induction time-course to profile gene expression during mES cell differentiation.**
Organism:	**Mus musculus**
Experiment type:	**Expression profiling by array**
Platform:	**GPL1261**
Pubmed ID:	**21764852**
Summary & Design:	**Summary:** **Murine ES cell gene expression before RA induction are used to compare gene expression for time-points of 2, 4, 6hrs post-induction.** **Overall design:** **KH2 ES Cell RA Differentiation Time-course**

Background corr dist: **KL-Divergence = 0.0719, L1-Distance = 0.0287, L2-Distance = 0.0010, Normal std = 0.5040**

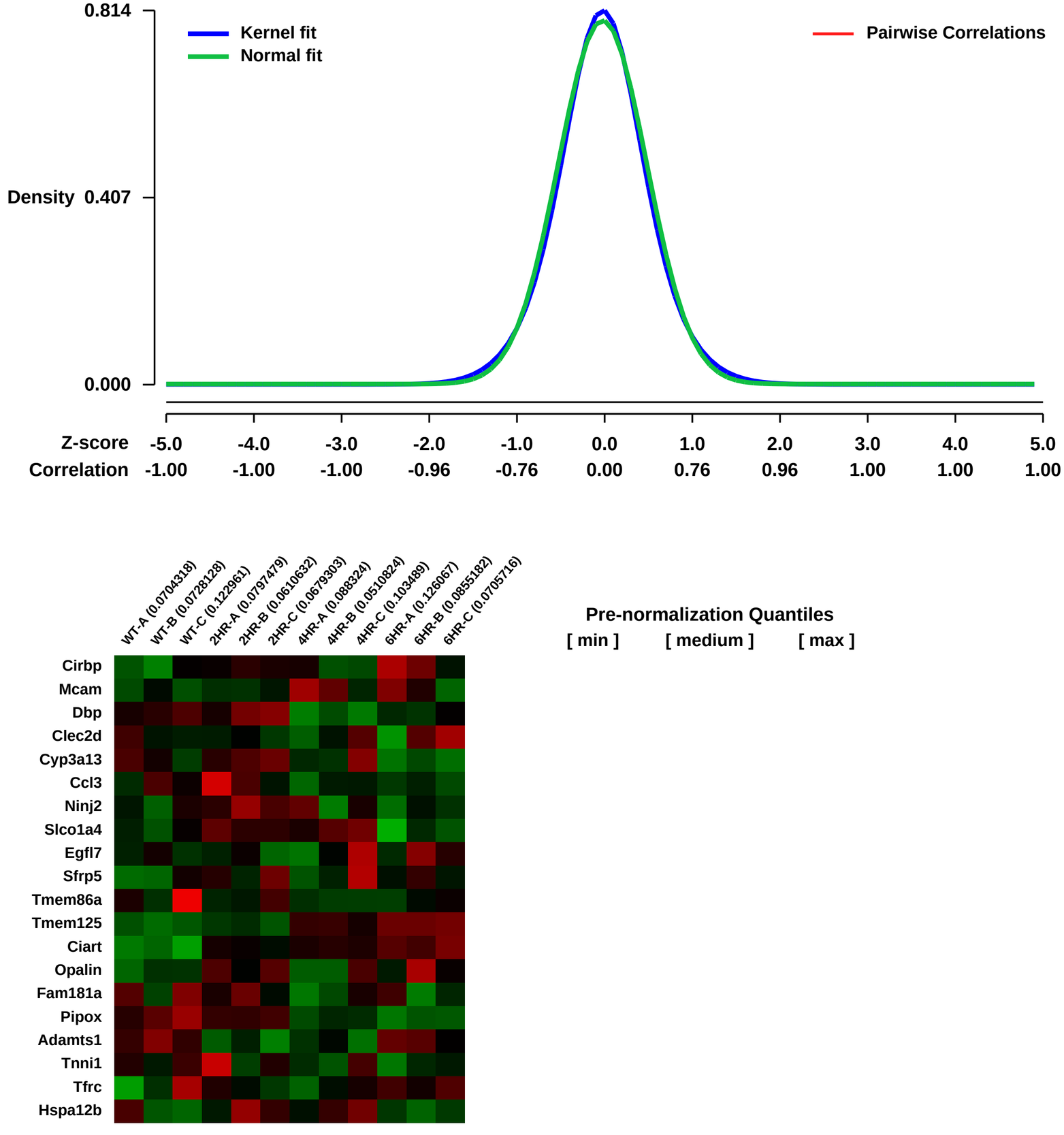

GEO Series "GSE9043" Expression Profiles

Num of samples in this series: 6

Scale of expression profile Z-scores

-3.0 -2.0 -1.0 0.0 1.0 2.0 3.0

GEO Link: http://www.ncbi.nlm.nih.gov/geo/query/acc.cgi?acc=GSE9043
Status: Public on Aug 24 2011
Title: Dap12 microglia
Organism: Mus musculus
Experiment type: Expression profiling by array
Platform: GPL1261
Pubmed ID:

Summary & Design:

Summary:
Polycystic lipomembranous osteodysplasia with sclerosing leukoencephalopathy (PLOSL) is an inherited brain and bone disease. It manifests as dementia and bone fractures. The PLOSL phenotype is caused by loss-of-function mutations in one of the two genes encoding the components of the DAP12/TREM2 receptor complex. The DAP12/TREM2 complex is expressed in cells of the myeloid lineage, including microglia in the central nervous system (CNS). The molecular mechanisms producing the CNS phenotype of PLOSL remain largely unknown. To gain insight into dysfunctional CNS pathways behind PLOSL, we performed genome-wide expression analysis of Dap12 (Tyrobp)-deficient mouse microglial cells.

Keywords: knock-out response

Overall design:
Transcript profiles of three wild type and three Dap12-deficient primary microglial cultures were analyzed.

Background corr dist: KL-Divergence = 0.0465, L1-Distance = 0.0288, L2-Distance = 0.0011, Normal std = 0.5993

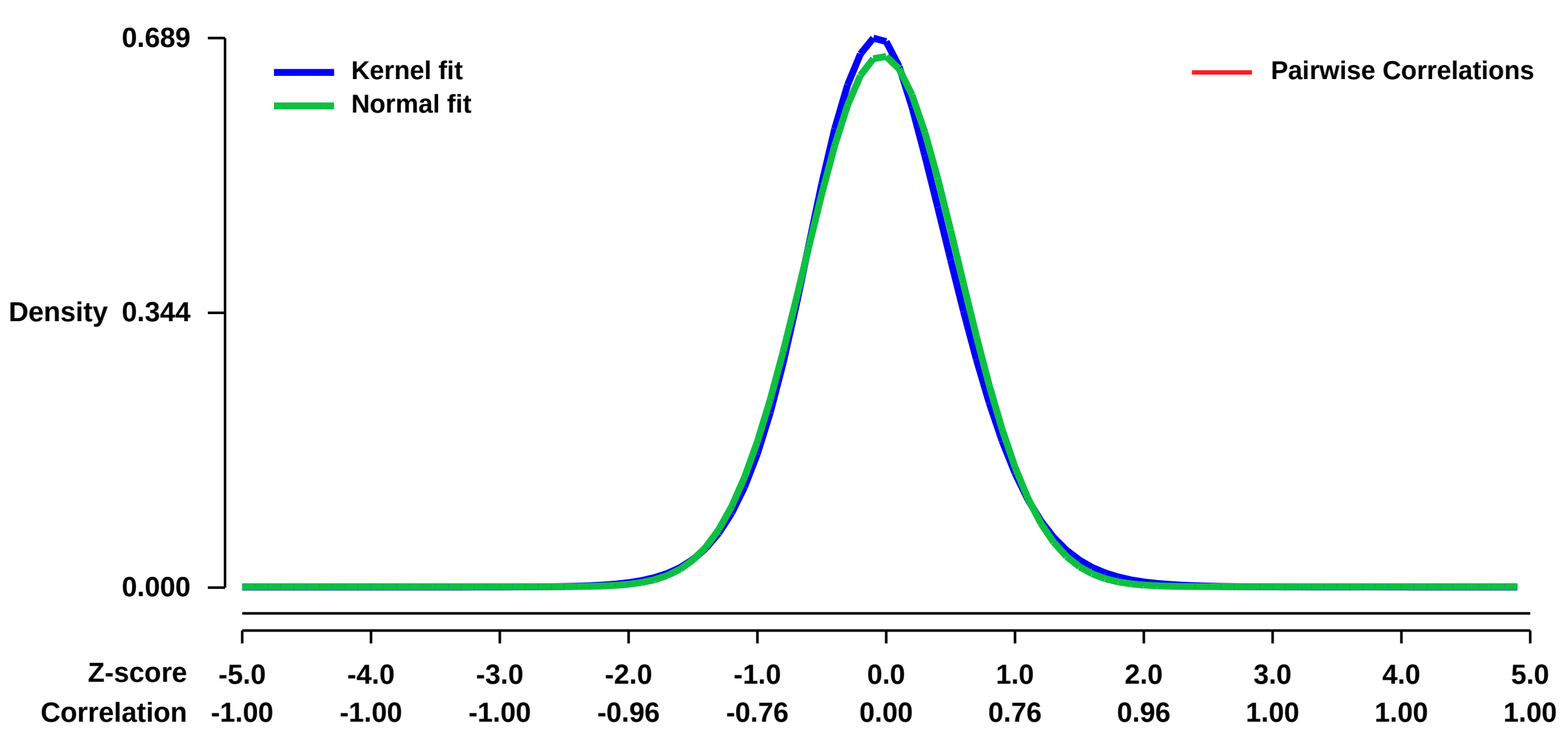

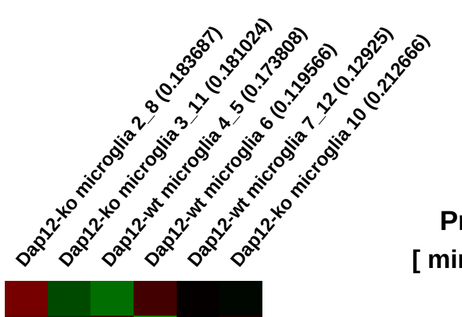

Pre-normalization Quantiles
[min] [medium] [max]

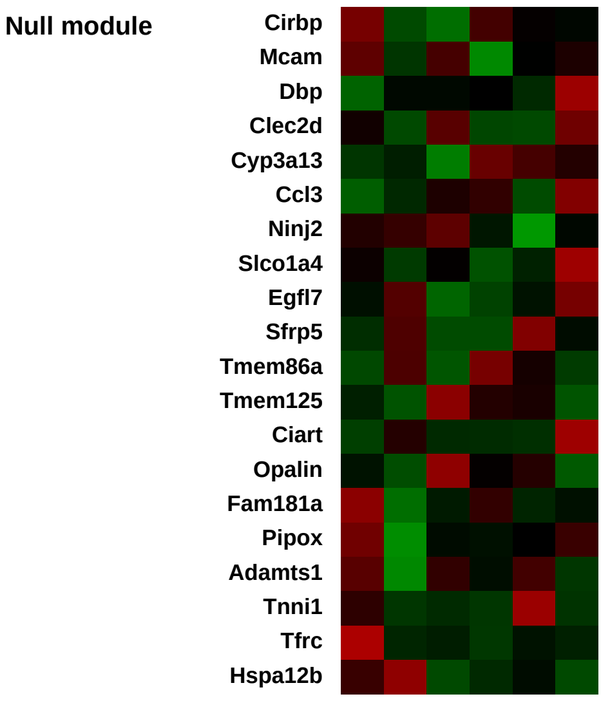

GEO Series "GSE8025" Expression Profiles

Num of samples in this series: 21

Scale of expression profile Z-scores

-3.0 -2.0 -1.0 0.0 1.0 2.0 3.0

GEO Link:	**http://www.ncbi.nlm.nih.gov/geo/query/acc.cgi?acc=GSE8025**
Status:	**Public on Dec 01 2007**
Title:	**Diarrhea as a Cause of Mortality in a Mouse Model of Infectious Colitis**
Organism:	**Mus musculus**
Experiment type:	**Expression profiling by array**
Platform:	**GPL1261**
Pubmed ID:	
Summary & Design:	**Summary:** **Examination of host genome-wide changes upon encounters with pathogens provides insight into the pathogenesis of infection and disease. When performed comparatively, it may shed light on the mechanisms underlying host susceptibility. In this study, gene expression in the mouse colon was investigated in two cognate lines of mice that differ in their response to Citrobacter rodentium infection; susceptible inbred FVB/N (FVB) and resistant outbred Swiss Webster (SW) mice. Gene expression in the distal colon was investigated prior to infection and at 4 and 9 days post-inoculation using a whole mouse genome Affymetrix array. Computational analysis identified 462 (1%) probe sets differentially expressed by more than 2-fold between uninoculated SW and FVB mice. In response to C. rodentium infection, 5,123 probe sets (11.4%) were significantly modulated in one or both lines of mice. Microarray data were validated by quantitative real time RT-PCR on 35 selected genes (r = 0.87, p < 0.001) and were found to have a 94% concordance. Transcripts represented by 1,547 probe sets (3.4%), were differentially expressed between FVB and SW mice regardless of infection status (host effect). Genes associated with transport were over-represented to a greater extent than immune response-related genes (25% vs. 11% of enrichment, respectively). Electrolyte analysis revealed hypochloremia and hyponatremia in susceptible animals. The results support the hypothesis that mortality in C. rodentium-infected FVB mice is associated with impaired ion transport and development of fatal hypovolemia. These studies contribute to our understanding of the pathogenesis of C. rodentium and suggest novel strategies for the prevention and treatment of diarrhea associated with bacterial infections of the intestinal tract.** **Keywords: temporal change (post infection)** **Overall design:** **Global gene expression analysis was performed on the distal colon with 2-3 mice per group. Because no difference for any parameters was observed in uninfected mice at 4 or 9 dpi, the animals were pooled into an uninoculated control groups for each line of mouse. The selection of representative samples for microarray analysis was based on known infection status and colonic lesions. The final number of biological replicates for each condition was n = 5 for uninoculated FVB mice (â Fpâ group), n = 4 for uninoculated SW mice (â Spâ group), and n = 3 for infected animals from each line at each time point (â Fi4â , â Si4â , â Fi9â , and â Si9â respectively).**

Background corr dist: KL-Divergence = 0.1088, L1-Distance = 0.0280, L2-Distance = 0.0012, Normal std = 0.4228

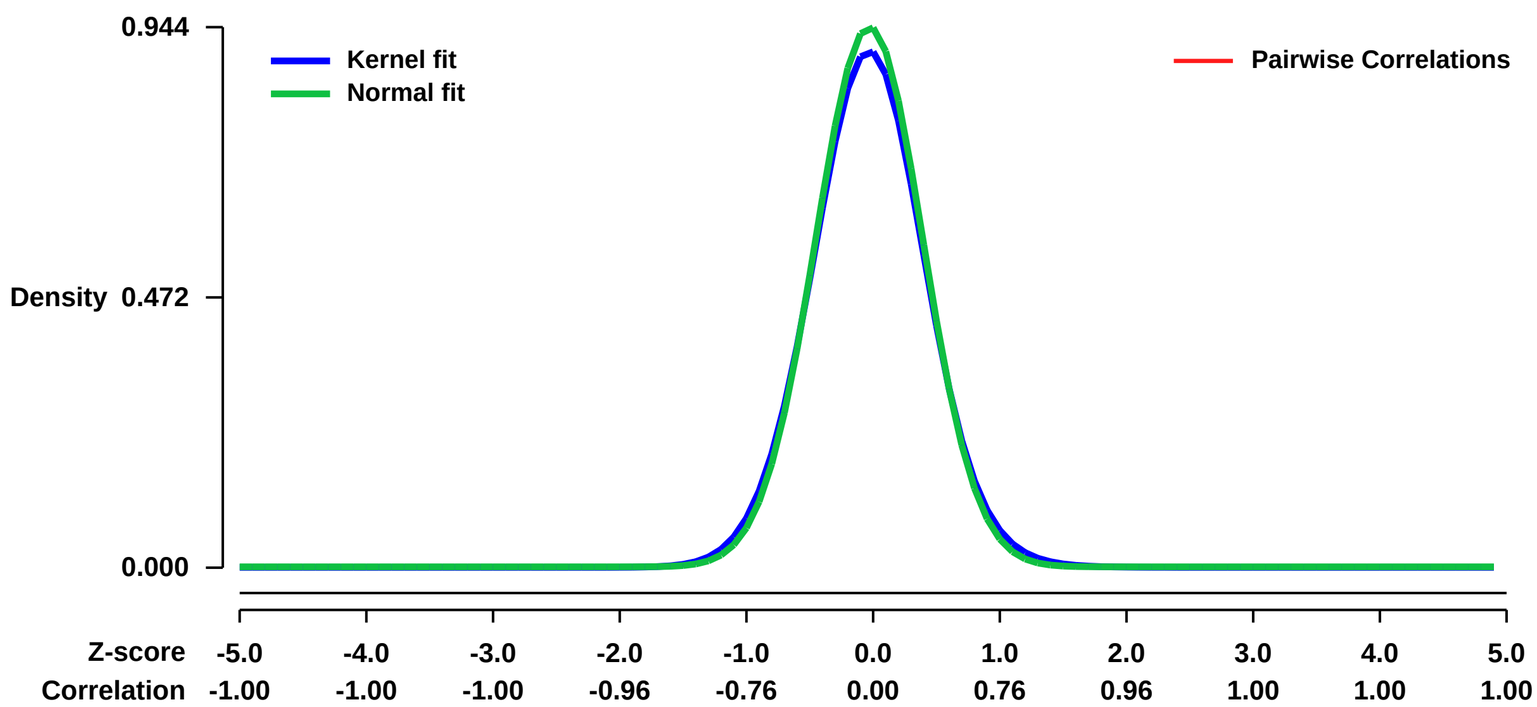

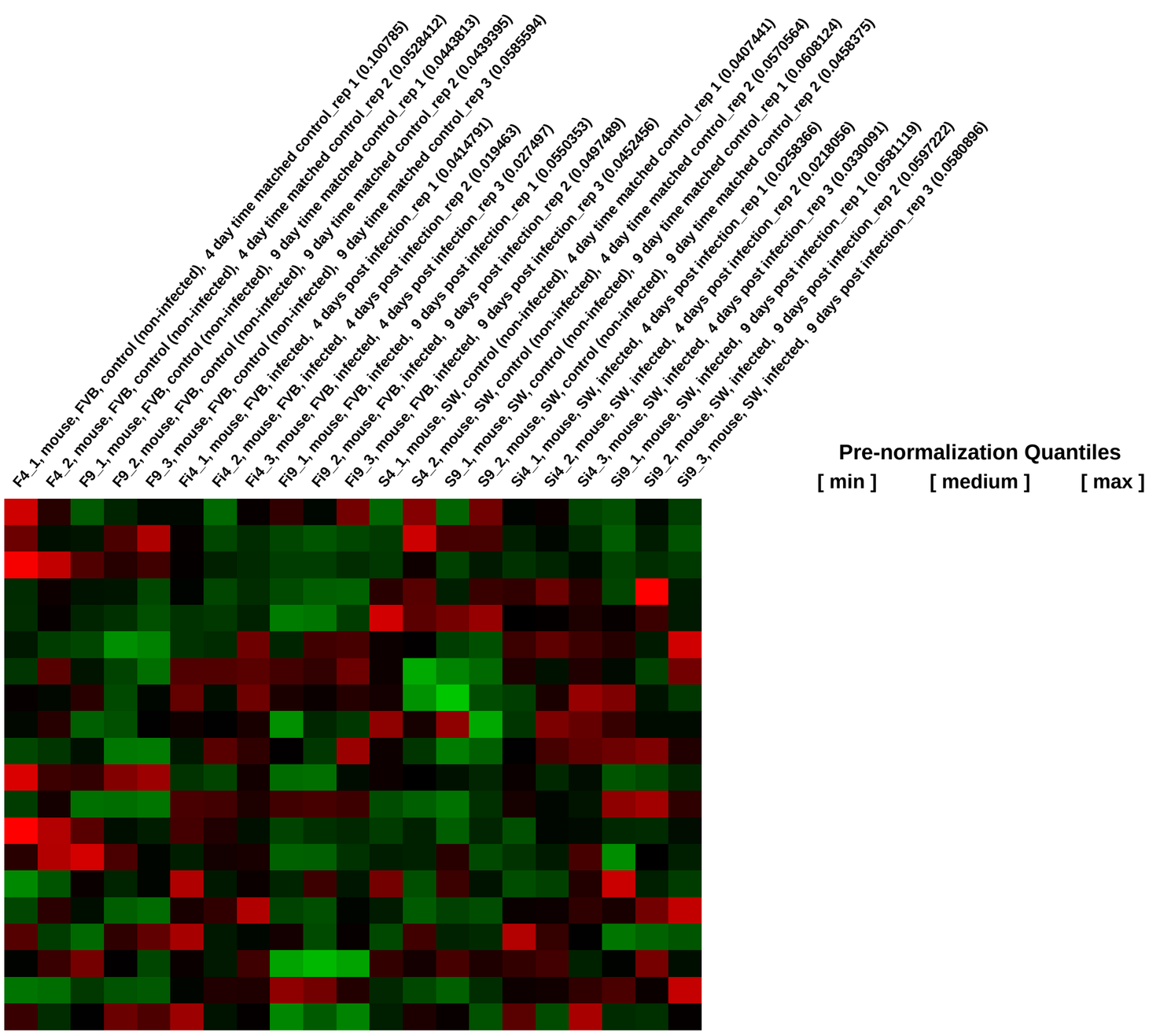

GEO Series "GSE32287" Expression Profiles

Num of samples in this series: 16

Scale of expression profile Z-scores

-3.0 -2.0 -1.0 0.0 1.0 2.0 3.0

GEO Link:	http://www.ncbi.nlm.nih.gov/geo/query/acc.cgi?acc=GSE32287
Status:	Public on Apr 04 2012
Title:	Expression data from wild-type and Rybp-deficient ES cells
Organism:	Mus musculus
Experiment type:	Expression profiling by array
Platform:	GPL1261
Pubmed ID:	22269950
Summary & Design:	**Summary:** We used microarrays to investigate a global change in gene expression by conditional depletion of Rybp in mouse ES cells. **Overall design:** Total RNAs were extracted from wild-type and Rybp-deficient ES cells, and were subjected to microarray analysis using Affymetrix GeneChip Mouse Genome 430A 2.0 arrays

Background corr dist: KL-Divergence = 0.1704, L1-Distance = 0.0323, L2-Distance = 0.0018, Normal std = 0.3569

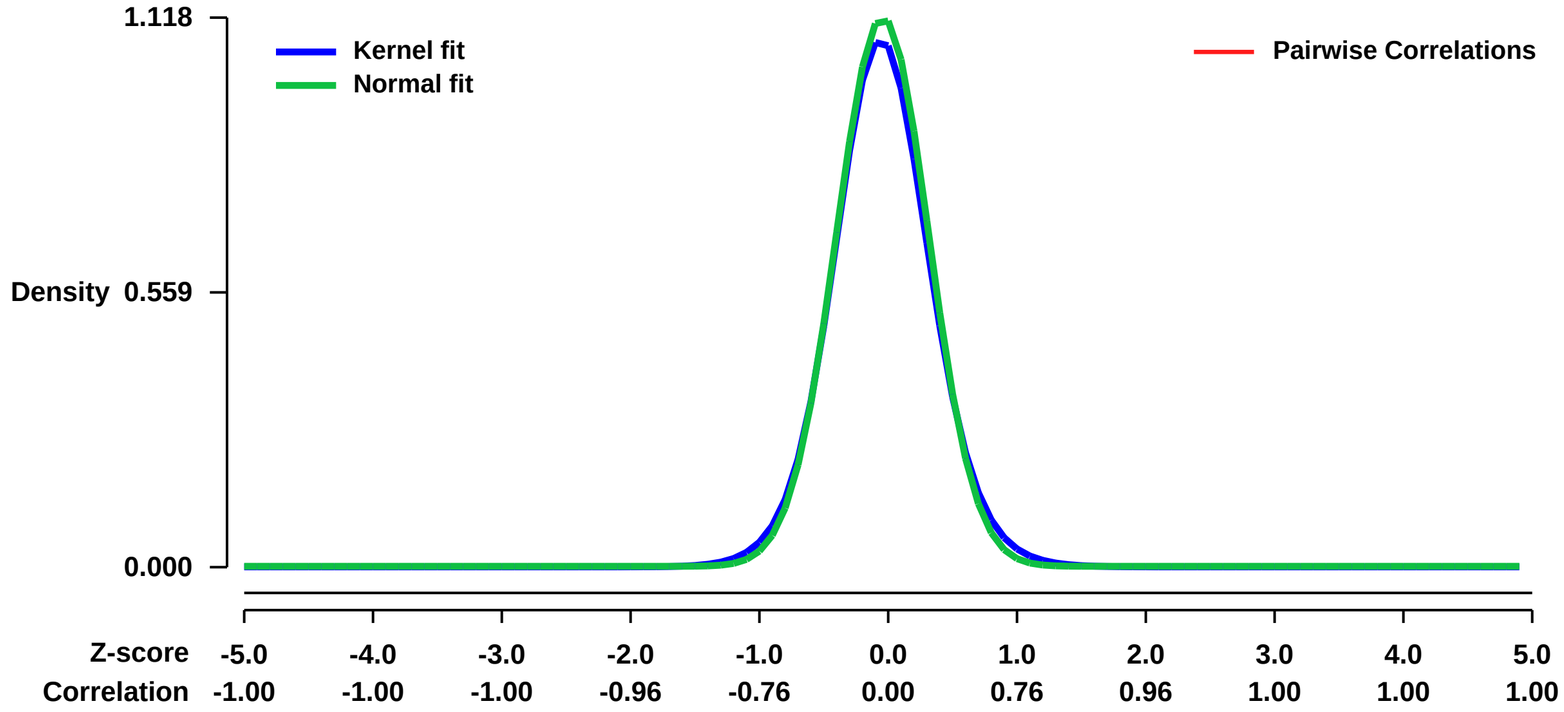

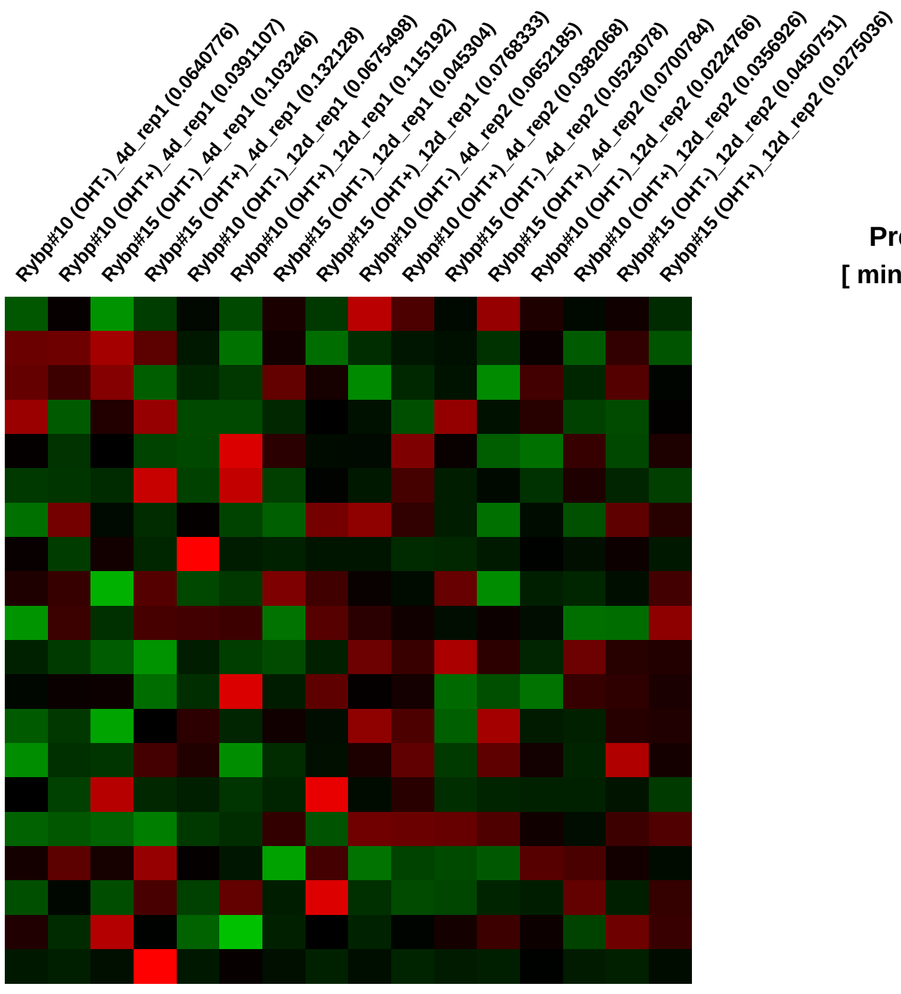

GEO Series "GSE38001" Expression Profiles

Num of samples in this series: 12

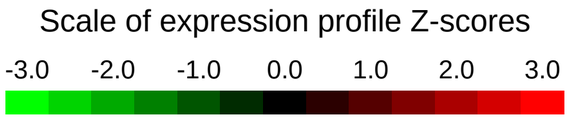

GEO Link:	**http://www.ncbi.nlm.nih.gov/geo/query/acc.cgi?acc=GSE38001**
Status:	**Public on Jun 19 2012**
Title:	**Polyglutamine expanded huntingtin dramatically alters the genome-wide binding of HSF1 (mRNA)**
Organism:	**Mus musculus**
Experiment type:	**Expression profiling by array**
Platform:	**GPL1261**
Pubmed ID:	
Summary & Design:	**Summary:** **In Huntingtonâ s disease (HD), polyglutamine expansions in the huntingtin (Htt) protein cause subtle changes in cellular functions that, over-time, lead to neurodegeneration and death. Studies have indicated that activation of the heat shock response can reduce many of the effects of mutant Htt in disease models, suggesting that the heat shock response is impaired in the disease. To understand the basis for this impairment, we have used genome-wide chromatin immunoprecipitation followed by massively parallel sequencing (ChIP-Seq) to examine the effects of mutant Htt on the master regulator of the heat shock response, HSF1. We find that, under normal conditions, HSF1 function is highly similar in cells carrying either wild-type or mutant Htt. However, polyQ-expanded Htt severely blunts the HSF1-mediated stress response. Surprisingly, we find that the HSF1 targets most affected upon stress are not directly associated with proteostasis, but with cytoskeletal binding, focal adhesion and GTPase activity. Our data raise the intriguing hypothesis that the accumulated damage from life-long impairment in these stress responses may contribute significantly to the etiology of Huntington's disease.** **Overall design:** **Affymetrix MG430 2.0 expression levels of wild-type (STHdhQ7/Q7) and mutant (STHdhQ111/Q111) striatal cells under growth condition (33˚C) and upon heat shock (42˚C for six hours)**

Background corr dist: KL-Divergence = 0.0496, L1-Distance = 0.0405, L2-Distance = 0.0027, Normal std = 0.5782

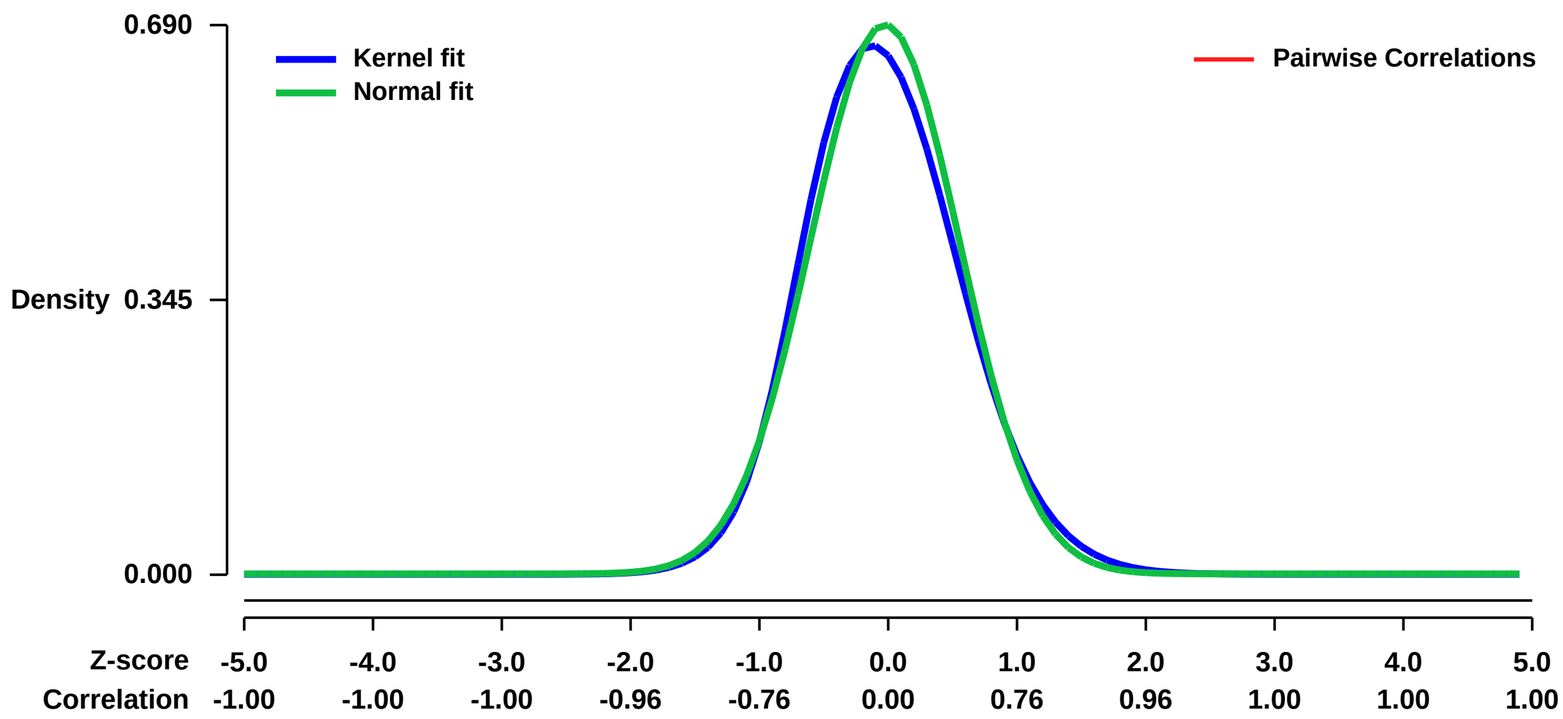

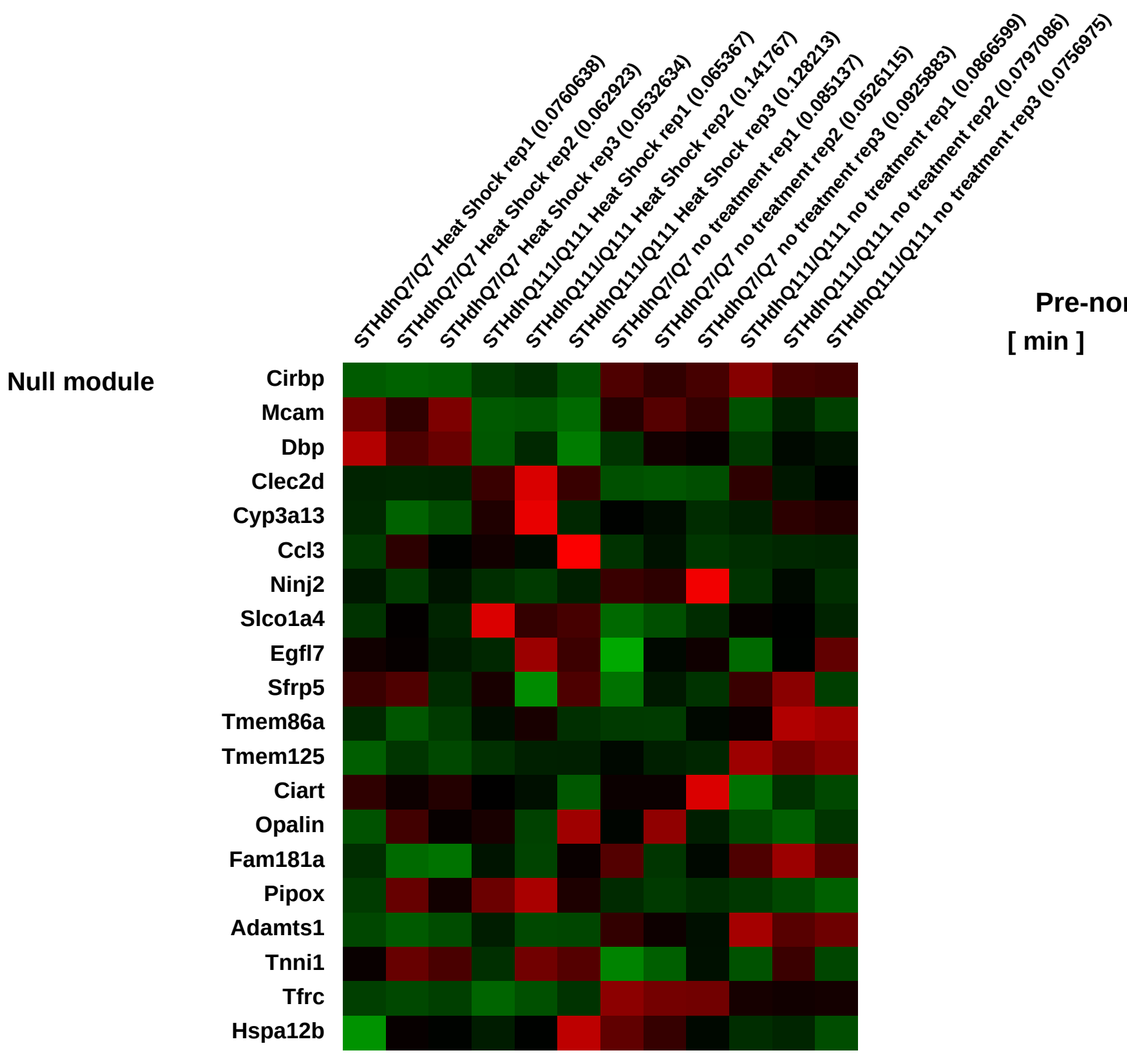

GEO Series "GSE22371" Expression Profiles

Num of samples in this series: 6

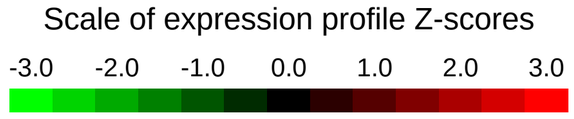

GEO Link:	http://www.ncbi.nlm.nih.gov/geo/query/acc.cgi?acc=GSE22371
Status:	Public on Jul 27 2010
Title:	Tbr1 regulates regional and laminar identity of postmitotic neurons in developing neocortex
Organism:	Mus musculus
Experiment type:	Expression profiling by array
Platform:	GPL1261
Pubmed ID:	20615956
Summary & Design:	**Summary:** Areas and layers of the cerebral cortex are specified by genetic programs that are initiated in progenitor cells and then, implemented in postmitotic neurons. Here, we report that Tbr1, a transcription factor expressed in postmitotic projection neurons, exerts positive and negative control over both regional (areal) and laminar identity. Tbr1 null mice exhibited profound defects of frontal cortex and layer 6 differentiation, as indicated by down-regulation of gene-expression markers such as Bcl6 and Cdh9. Conversely, genes that implement caudal cortex and layer 5 identity, such as Bhlhb5 and Fezf2, were up-regulated in Tbr1 mutants. Tbr1 implements frontal identity in part by direct promoter binding and activation of Auts2, a frontal cortex gene implicated in autism. Tbr1 regulates laminar identity in part by downstream activation or maintenance of Sox5, an important transcription factor controlling neuronal migration and corticofugal axon projections. Similar to Sox5 mutants, Tbr1 mutants exhibit ectopic axon projections to the hypothalamus and cerebral peduncle. Together, our findings show that Tbr1 coordinately regulates regional and laminar identity of postmitotic cortical neurons. **Overall design:** Mouse E14.5 neocortices and Postnatal day (P) 0.5 brains: E14.5 neocortices KO, 3; E14.5 neocortices WT, 3; Postnatal day (P) 0.5 brains frontal WT, 4; Postnatal day (P) 0.5 brains frontal KO, 4; Postnatal day (P) 0.5 brains parietal WT, 4; Postnatal day (P) 0.5 brains parietal KO, 4; Postnatal day (P) 0.5 brains occipital WT, 4; Postnatal day (P) 0.5 brains occipital KO, 4.

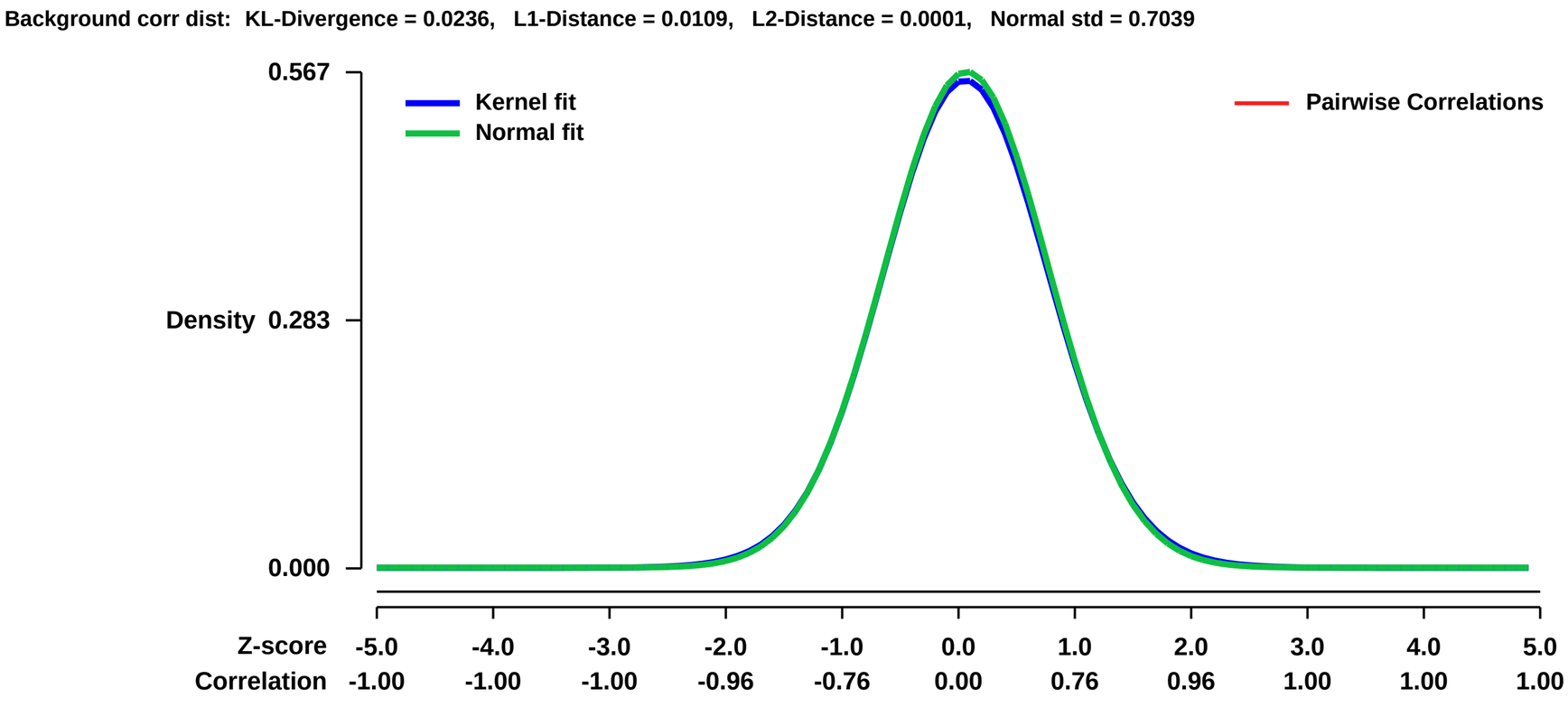

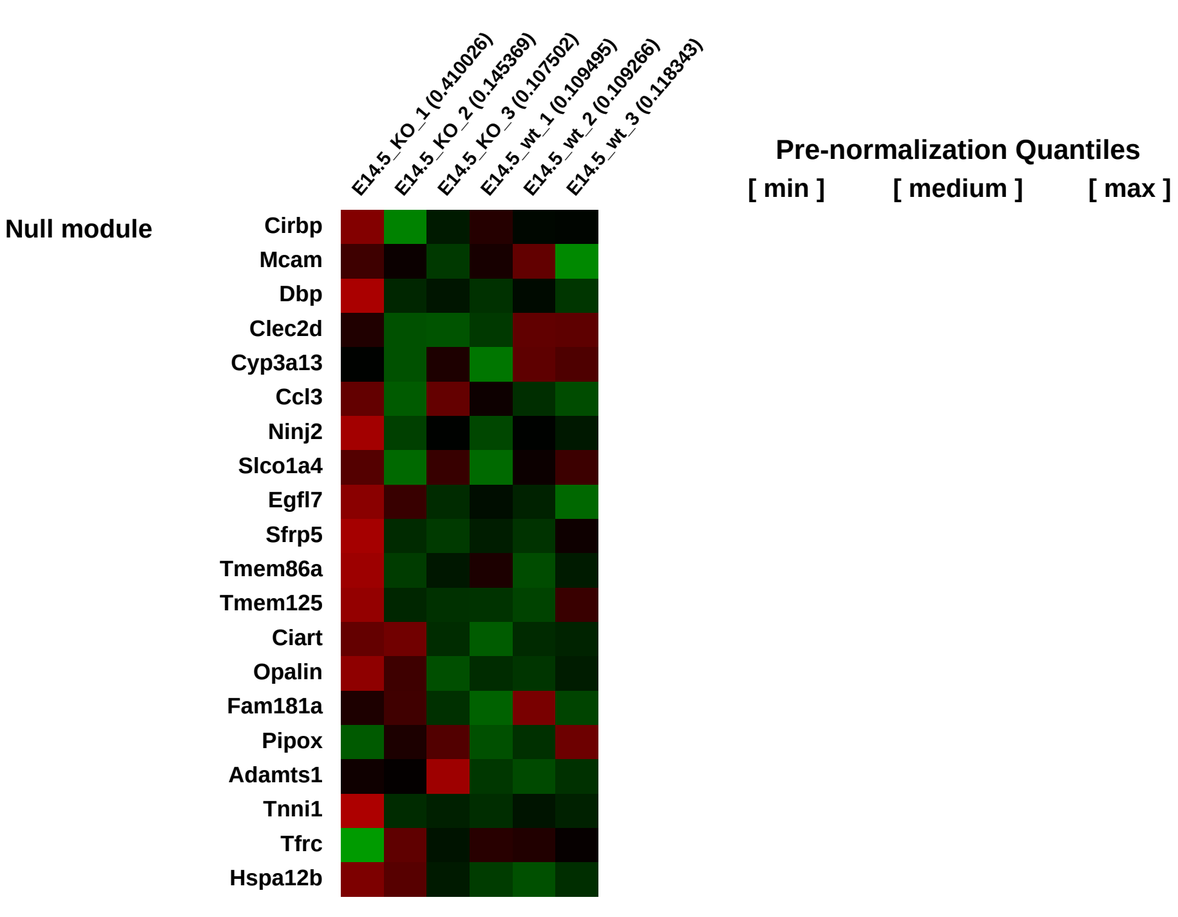

GEO Series "GSE8684" Expression Profiles

Num of samples in this series: 10

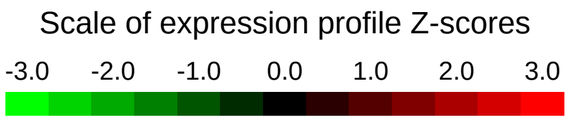

GEO Link:	http://www.ncbi.nlm.nih.gov/geo/query/acc.cgi?acc=GSE8684
Status:	Public on Jan 11 2008
Title:	Gene expression in mouse 3T3-L1 adipocyte tissue culture treated with cis-9,trans-11 conjugated linoleic acid(c9t11 CLA)
Organism:	Mus musculus
Experiment type:	Expression profiling by array
Platform:	GPL1261
Pubmed ID:	17878318
Summary & Design:	**Summary:** Trans-10, Cis-12 conjugated linoleic acid (t10c12 CLA) causes fat loss in mouse 3T3-L1 adipocyte tissue culture; however cis-9, trans-11 CLA does not (this series). The early transcriptome changes were analyzed using high-density microarrays to better characterize the signaling pathways responding to c9t11 CLA. Their gene expression responses between 8 to 12 hr after treatment showed no gene expression changes indicative of an integrated stress response (ISR). **Keywords: control/treatment time course** **Overall design:** Mouse 3T3-L1 RNA for each time point was isolated from control and treatment samples for analysis on microarrays; there are four biological reps for the controls for each timepoint, and only one rep for the treatment.

Background corr dist: KL-Divergence = 0.0618, L1-Distance = 0.0610, L2-Distance = 0.0079, Normal std = 0.5509

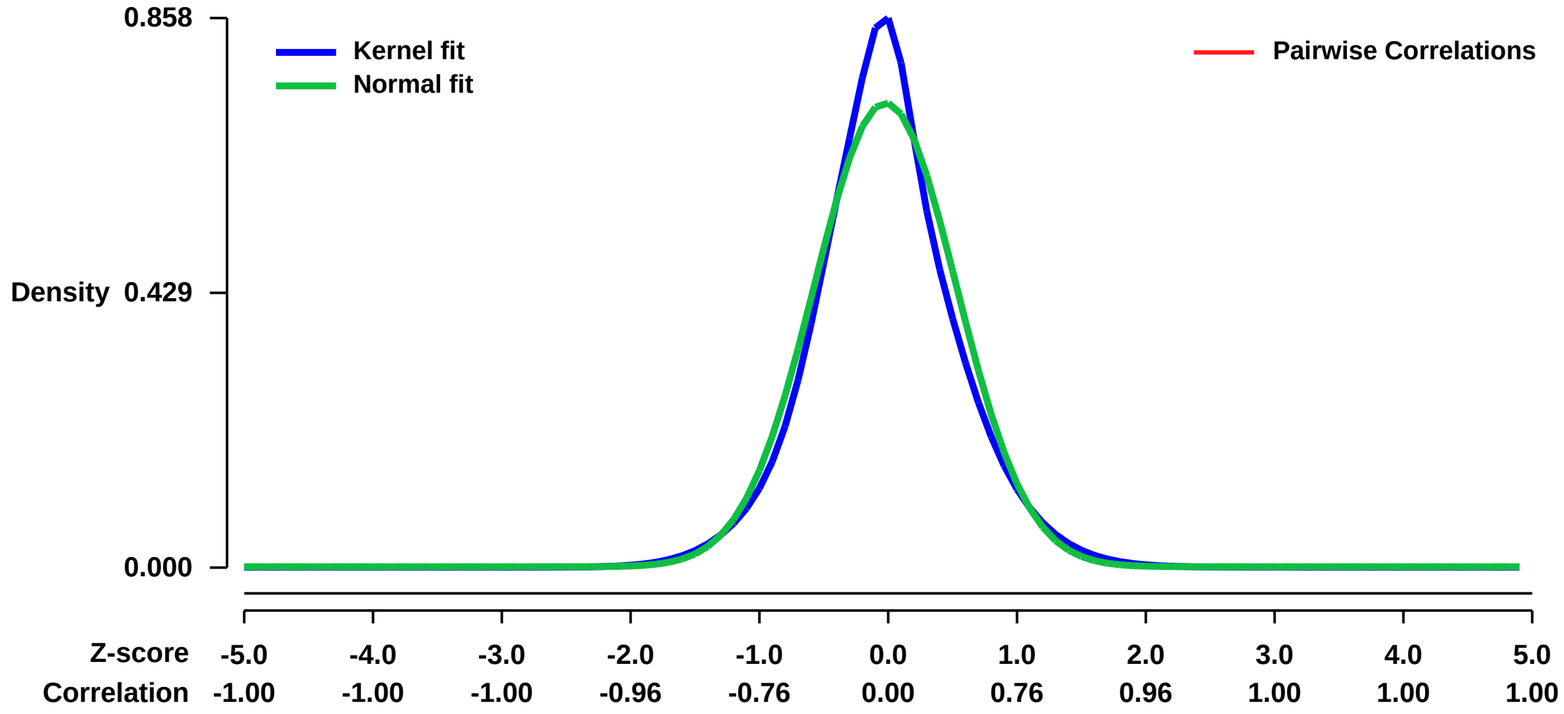

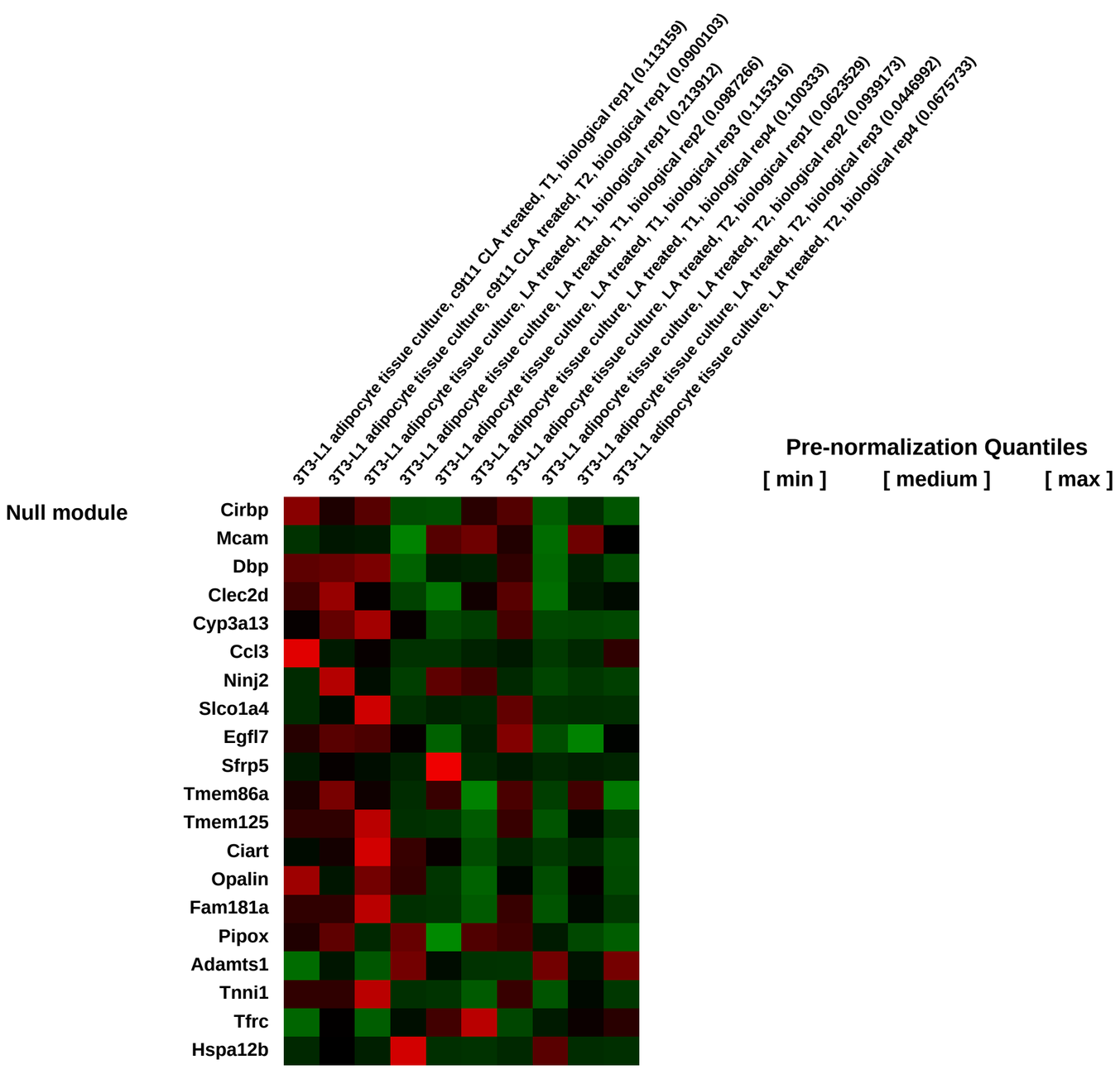

GEO Series "GSE53299" Expression Profiles

Num of samples in this series: 6

Scale of expression profile Z-scores

-3.0 -2.0 -1.0 0.0 1.0 2.0 3.0

GEO Link:	**http://www.ncbi.nlm.nih.gov/geo/query/acc.cgi?acc=GSE53299**
Status:	**Public on Mar 08 2014**
Title:	**Expression data from mouse protein iPS cells compared to mouse embryonic stem cells and mouse hepatocyte.**
Organism:	**Mus musculus**
Experiment type:	**Expression profiling by array**
Platform:	**GPL1261**
Pubmed ID:	
Summary & Design:	**Summary:** **Increased genomic integrity an improved protein-based iPS cell method compared to current viral induced strategies** **We used microarrays to detail the global gene expression of protein-based iPS cells** **Overall design:** **Total RNAs were prepared from mH, mES, miPS cells usingTRIzol reagent (Invitrogen, Carlsbad, CA) and their cDNAs were allowed to hybridize to Affymetrix Mouse Expression Array 430 containing over 43,000 mouse transcripts at the Harvard Partners Center for Genomics and Genetics.**

Background corr dist: **KL-Divergence = 0.0349, L1-Distance = 0.0396, L2-Distance = 0.0020, Normal std = 0.7013**

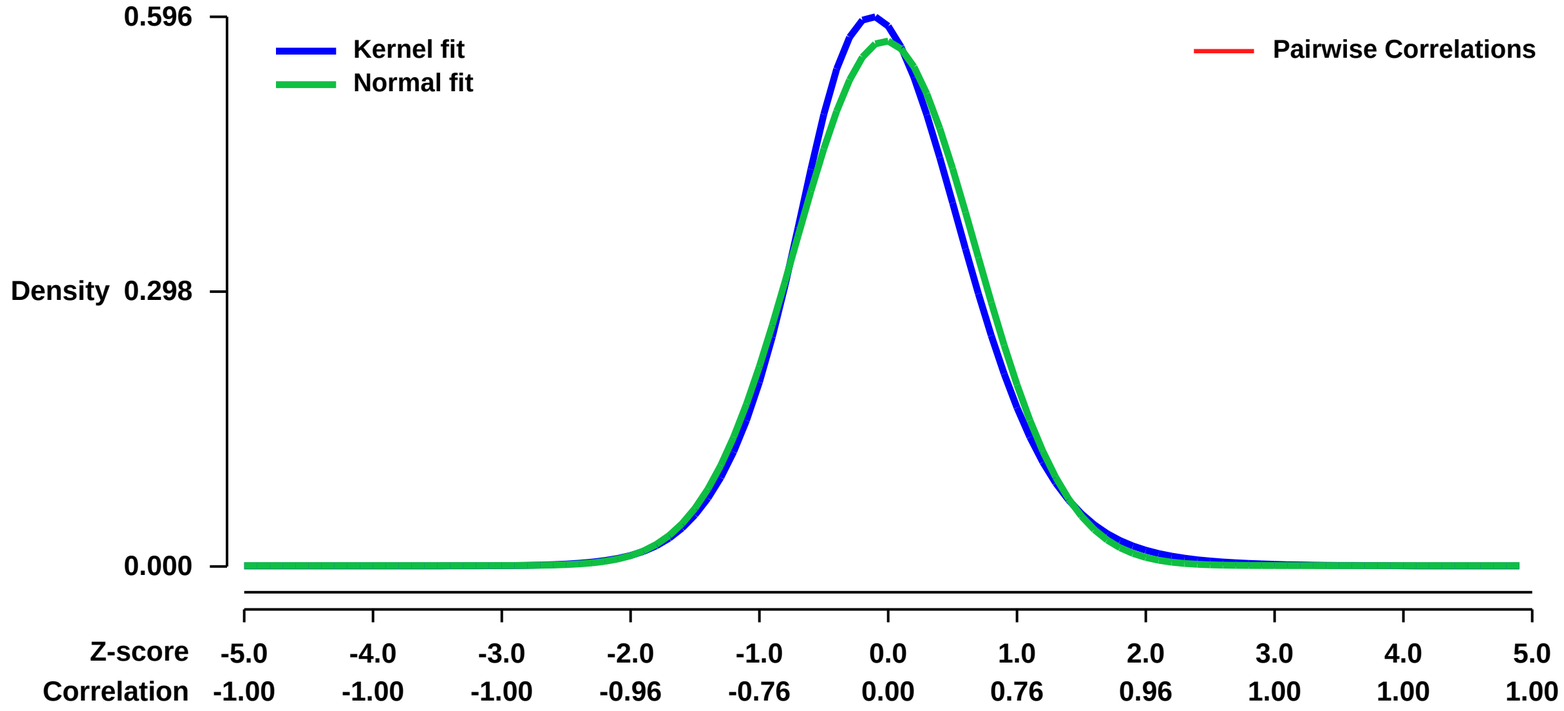

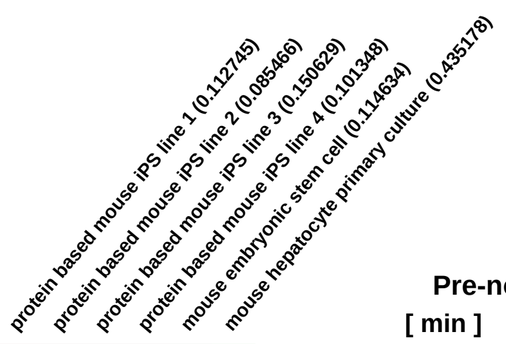

Pre-normalization Quantiles

[min] [medium] [max]

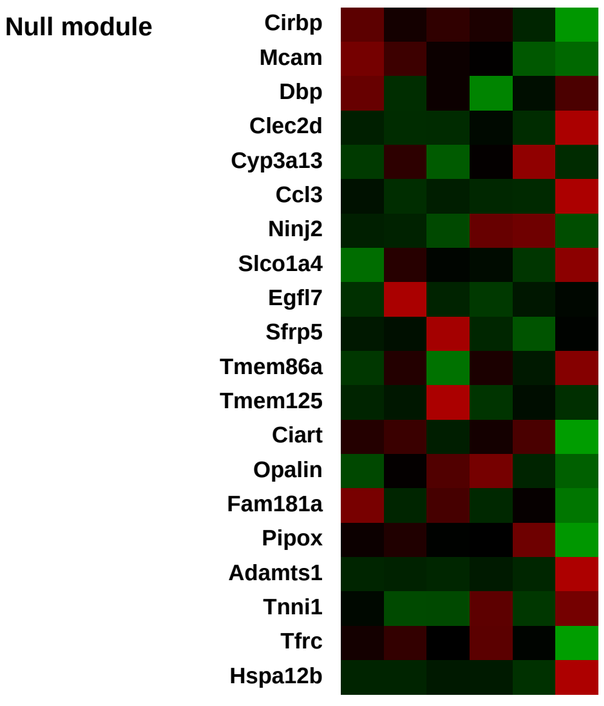

GEO Series "GSE9010" Expression Profiles

Num of samples in this series: 10

Scale of expression profile Z-scores

-3.0 -2.0 -1.0 0.0 1.0 2.0 3.0

GEO Link:	http://www.ncbi.nlm.nih.gov/geo/query/acc.cgi?acc=GSE9010
Status:	Public on Sep 11 2007
Title:	HOXB4 target genes in adult hematopoietic stem and progenitor cells (HSC/HPCs)
Organism:	Mus musculus
Experiment type:	Expression profiling by array
Platform:	GPL1261
Pubmed ID:	17940039
Summary & Design:	**Summary:** HOXB4 mediates expansion of adult and embryo-derived hematopoietic stem cells (HSCs) when expressed ectopically. To define the underlying molecular mechanisms, we performed gene expression profiling in combination with subsequent functional analysis using enriched adult HSCs expressing inducible HOXB4. A substantial number of the identified HOXB4 target genes are involved in signaling pathways important for controlling self-renewal, maintenance and differentiation of stem cells. Functional assays performed on selected pathways confirmed the biological coherence of the array results. HOXB4 activity protected adult HSCs from the detrimental effects mediated by the proinflammatory cytokine TNF-alpha. Furthermore, we demonstrate that HOXB4 activity and FGF-signaling are intertwined. HOXB4-mediated expansion of adult HSCs was enhanced by specific and complete inhibition of FGF-receptors. Based on our results we propose that HOXB4 governs pivotal cell-intrinsic pathways involved in the regulation of cell cycle, differentiation and apoptosis. Our results strongly suggest that HOXB4 modulates the response of HSCs to multiple extrinsic signals in a concerted manner, thereby shifting the balance towards stem cell self-renewal. **Keywords:** plus/minus induction of HOXB4 activity by treatment with 4-hydroxytamoxifen (TMX) **Overall design:** To understand the mechanisms of HOXB4 activity, we wished to identify target genes of HOXB4 in adult hematopoietic stem and progenitor cells (HSC/HPCs). We thus transduced murine HSC/HPCs with a retroviral vector that co-expresses EGFP and a tamoxifen-inducible form of HOXB4 (HOXB4-ER). Upon addition of 4-hydroxytamoxifen (TMX), the HOXB4-ER fusion protein translocates from the cytoplasm to the nucleus, consequently being capable of modulating gene expression. Transduced cell populations were expanded for 14 days in the presence of TMX. Thereafter, HOXB4-ER+LSK (GFP+ , lineage negative, Sca1+, ckit+) cells were flow cytometrically isolated and cultivated either with or without TMX for 1 or 4 hours. Inactivation of HOXB4 activity by TMX withdrawal was intended to mimic the naturally occurring down-regulation of HOXB4 in differentiating stem cells. RNA was prepared after the aforementioned times and the transcriptional profiles of HOXB4-ER+LSK +/- TMX analyzed using the Affymetrixâ¢ platform. As a control, profiling was also performed with LSK cells expressing unmodified constitutively active HOXB4 (HOXB4const) ´– TMX, to exclude changes in gene expression due to unknown effects of tamoxifen itself. RNAs from adult LSK cells were processed for use on Affymetrix GeneChips Mouse Genome 430 2.0. All quality parameters for the arrays were confirmed to be in the recommended range.

Background corr dist: KL-Divergence = 0.0863, L1-Distance = 0.0379, L2-Distance = 0.0029, Normal std = 0.4736

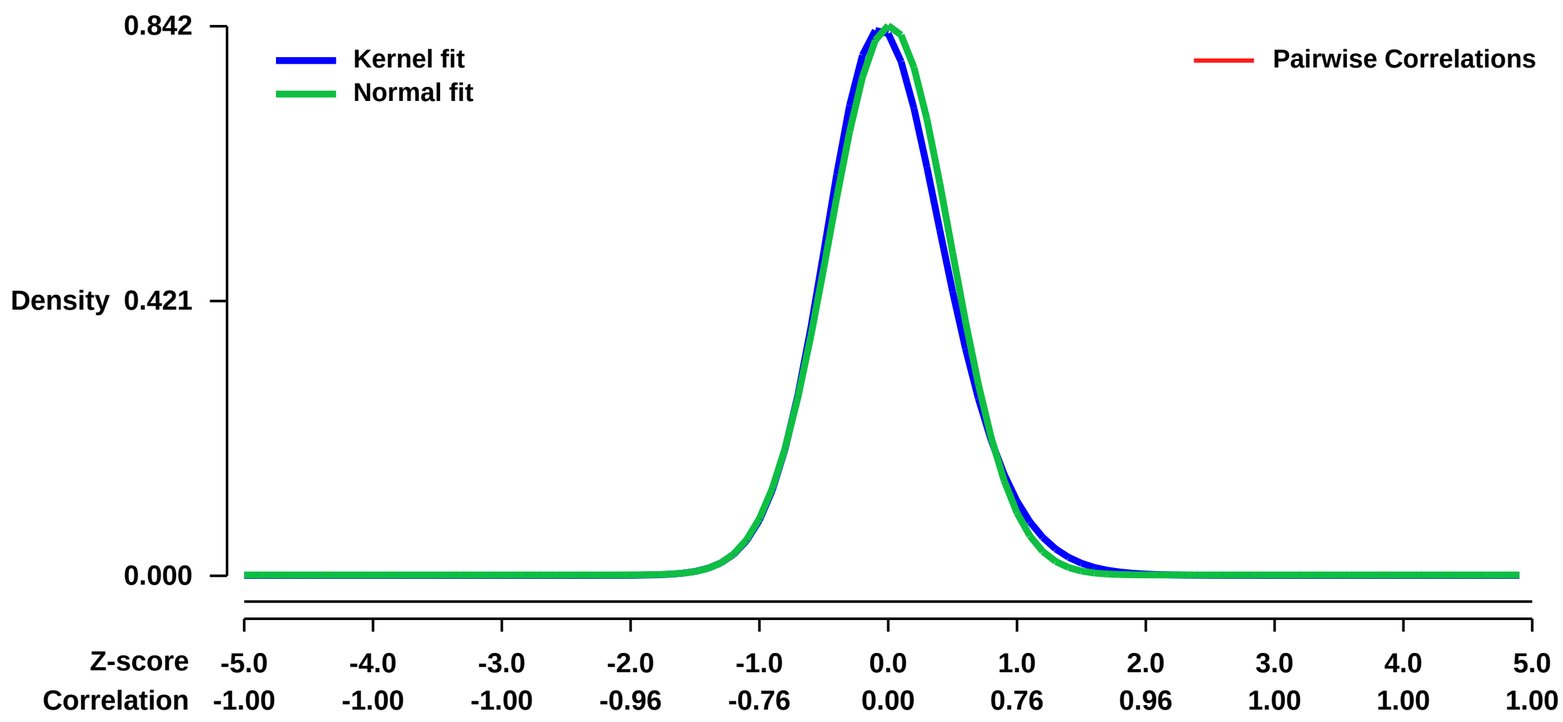

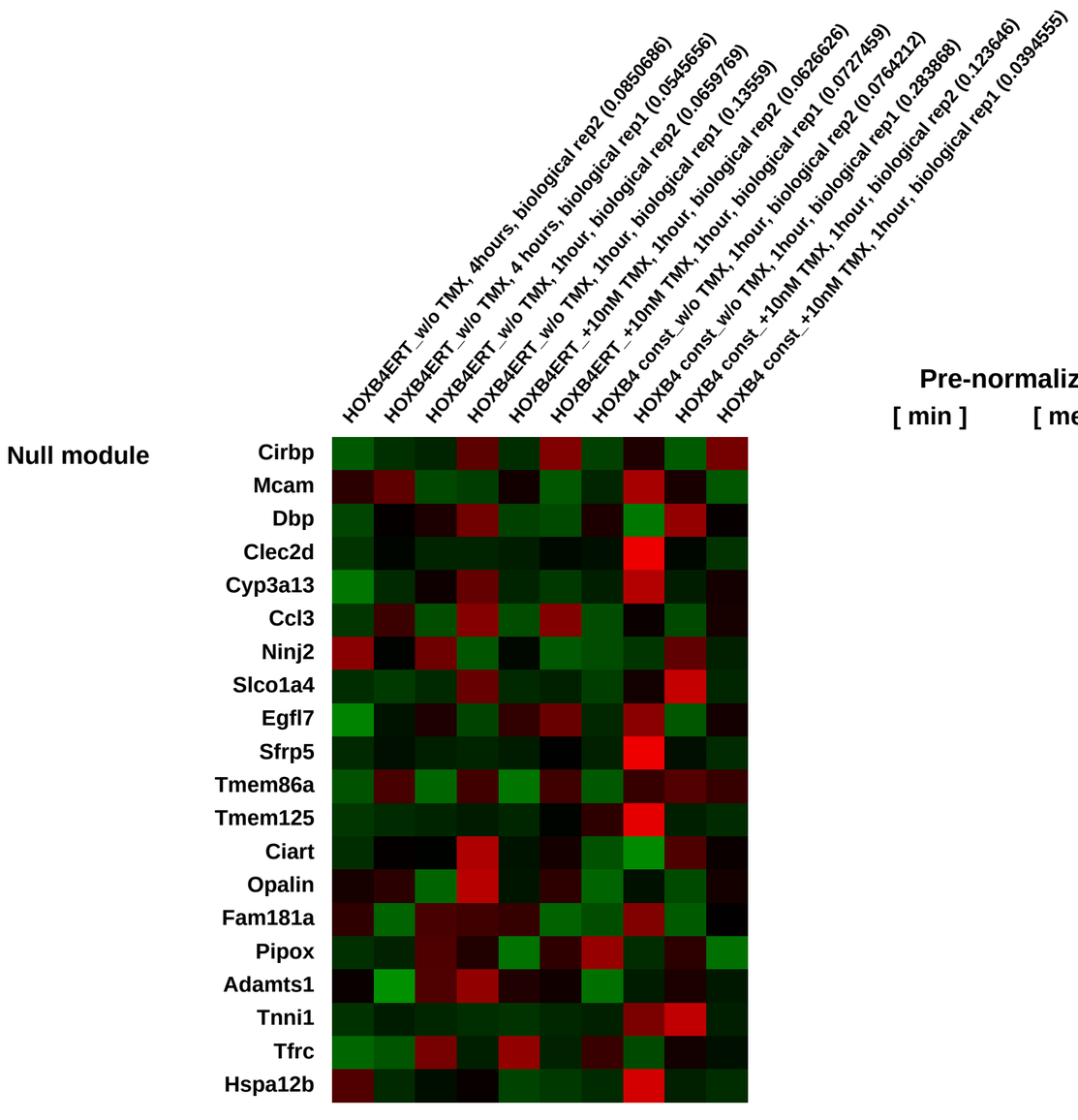

GEO Series "GSE53403" Expression Profiles

Num of samples in this series: 16

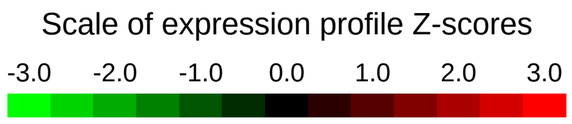

GEO Link:	http://www.ncbi.nlm.nih.gov/geo/query/acc.cgi?acc=GSE53403
Status:	Public on Dec 18 2013
Title:	Expression data from mouse adipose tissue macrophage
Organism:	Mus musculus
Experiment type:	Expression profiling by array
Platform:	GPL1261
Pubmed ID:	24315368
Summary & Design:	**Summary:** In mammals, expansion of adipose tissue mass induces accumulation of adipose tissue macrophages (ATMs). We isolated CD11c- (FB) and CD11c+ (FBC) perigonadal ATMs from SVCs of lean (C57BL/6J Lep +/+) and obese leptin-deficient (C57BL/6J Lep ob/ob) mice. We used expression microarrays to generate transcription profiles of perigonadal ATMs from lean (C57BL/6J Lep +/+) and obese (C57BL/6J Lep ob/ob) mice. Profiling purified FBs and FBCs, we identified 521 transcripts whose expression was differentially (nominal p-value < 0.01) expressed between FBs from lean and obese mice and 1509 genes whose expression was differentially (nominal p-value <0.01) expressed between FBC from lean and obese mice **Overall design:** RNA was isolated from sorted FBC (F4/80+, CD11b+, CD11c+) cells and FB (F4/80+, CD11b+, CD11c-) cells and using RNeasy micro-kits (Qiagen), using a PicoPure RNA isolation kit then amplified two-rounds. Labeled cRNA Mouse Genome 430 2.0 arrays (purified FB and FBC adipose tissue macrophages. There was a total of sixteen samples. FB and FBC populations were isolated from 4 lean and 4 obese mice.

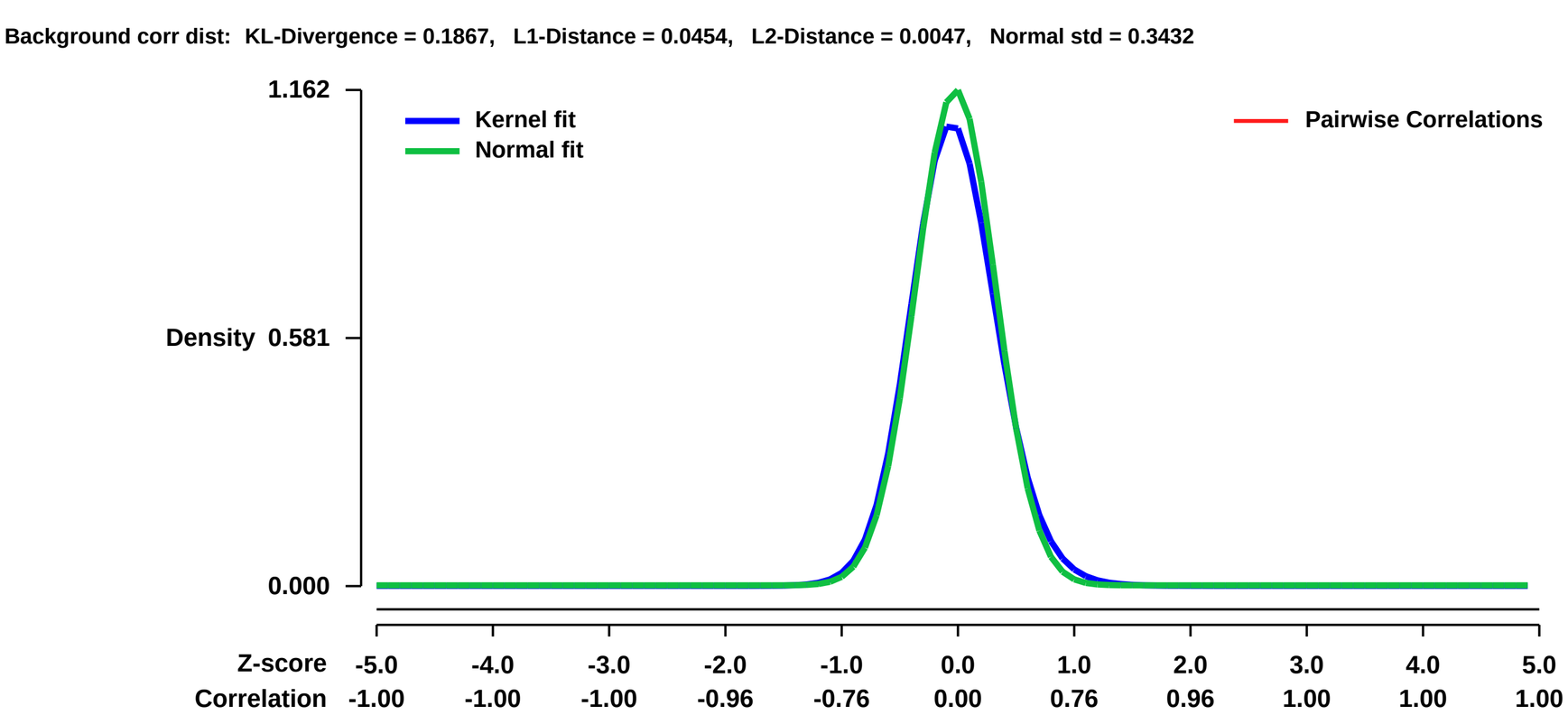

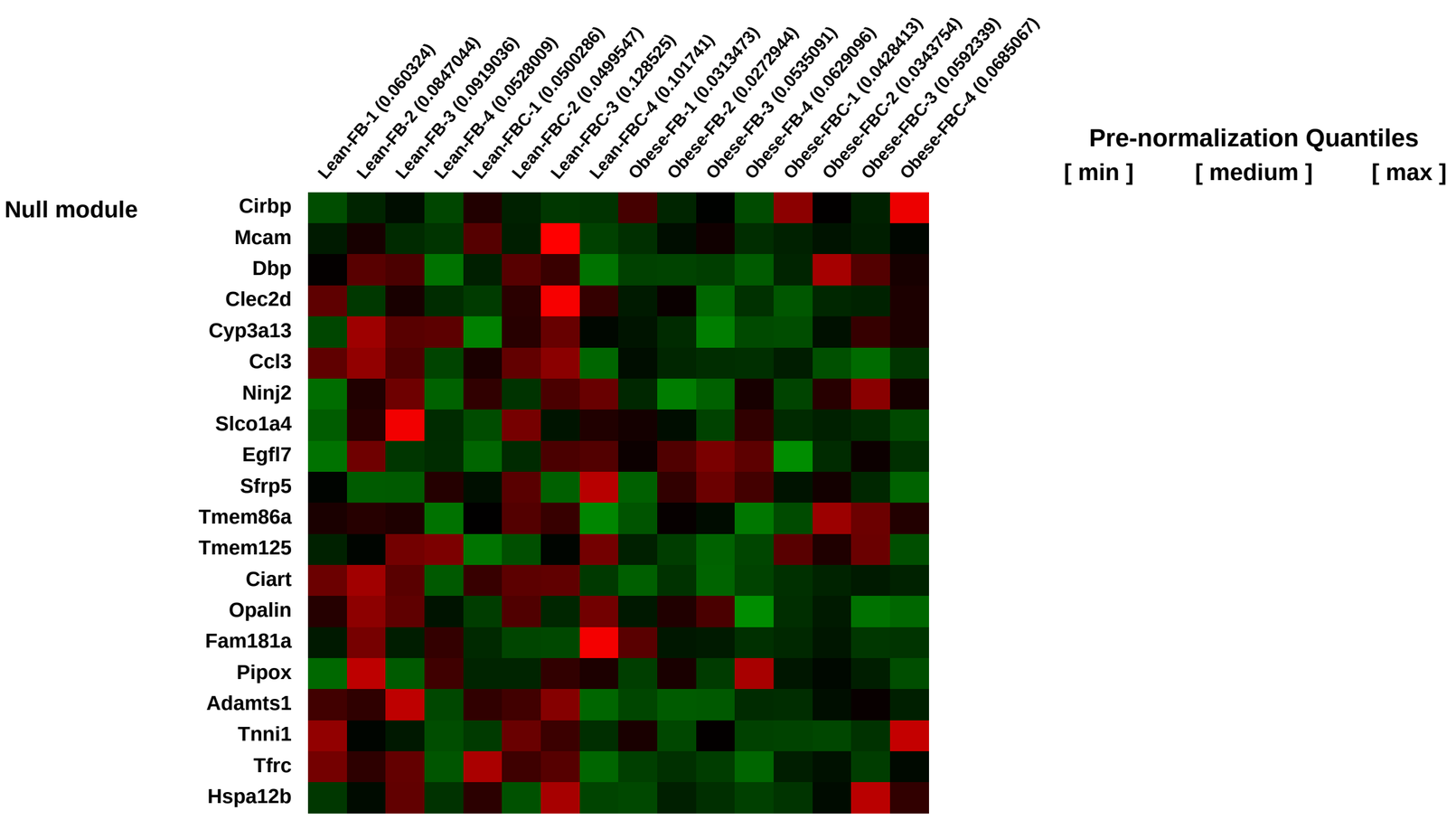

GEO Series "GSE34732" Expression Profiles

Num of samples in this series: 12

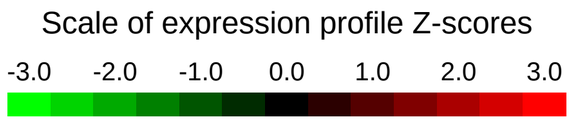

GEO Link:	**http://www.ncbi.nlm.nih.gov/geo/query/acc.cgi?acc=GSE34732**
Status:	**Public on May 22 2012**
Title:	**Differenetial Gene Expression in Limbs of Wild Type and Lmx1b KO mice during limb dorsalization (e11.5, e12.5 & e13.5)**
Organism:	**Mus musculus**
Experiment type:	**Expression profiling by array**
Platform:	**GPL1261**
Pubmed ID:	
Summary & Design:	**Summary:** **Lmx1b regulates dorsalization of limb fates, but the mechanism of this regulation has not been characterized. To identify candidate genes regulated by Lmx1b we compared the limbs from Lmx1b KO mice to wild type mice during limb dorsalization (e11.5-13.5). Differentially expressed genes that we common to all three stages examined were considered to be likely candidates for Lmx1b regulation and further evaluated.** **Overall design:** **At 11.5 and 12.5 dpc, embryos were harvested and the limb buds with the limb girdles were isolated. Embryos at 13.5dpc were also harvested and their distal limb buds (zeugopods and autopods) were isolated. Embryos were genotyped to confirm Lmx1b homozygosity (-/- or +/+). RNA from embryonic forelimbs and hindlimbs of wild type (WT) and Lmx1b KO mice was harvested using the Rneasy Kit (Qiagen). RNA was pooled to decrease genetic variability, i.e., six limbs at 11.5 dpc, three limbs at 12.5 dpc and six limbs at 13.5 dpc. Duplicate samples were generated using different embryos for each stage and then hybridized to the Affymetrix GeneChip´fi Mouse Genome 430 2.0 Array (UCI, Irvine, CA).**

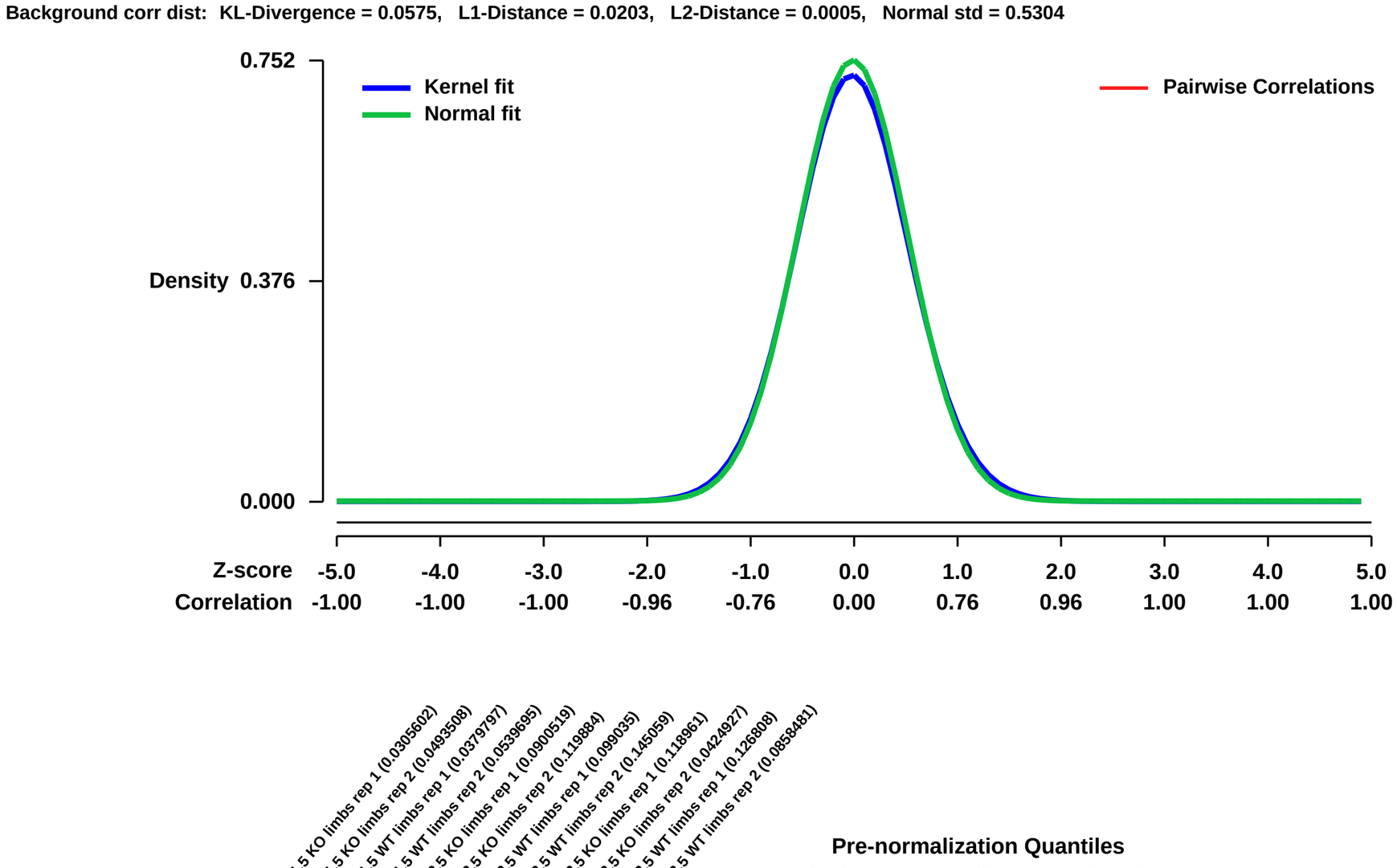

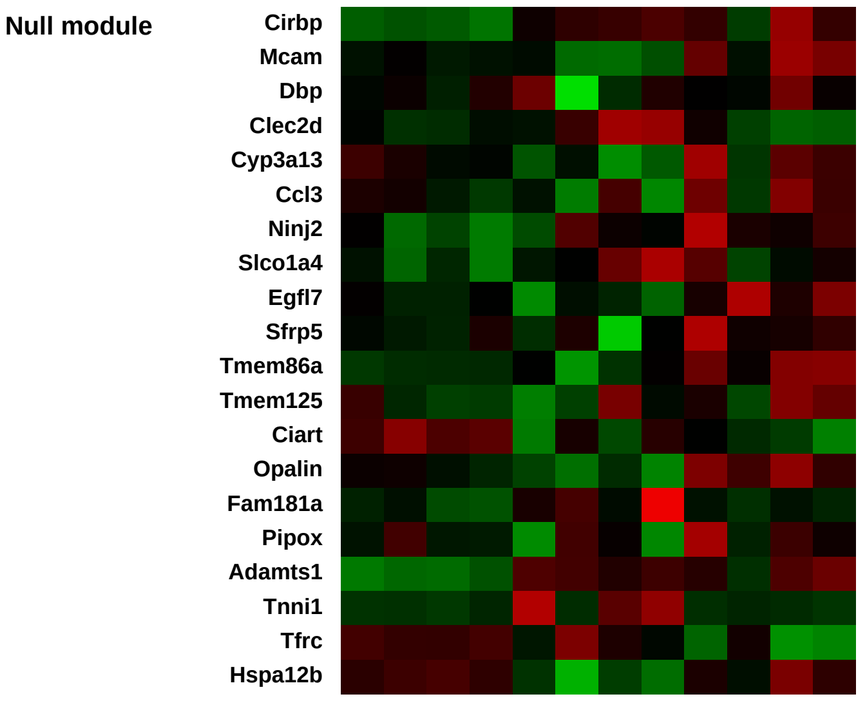

GEO Series "GSE29072" Expression Profiles

Num of samples in this series: 18

Scale of expression profile Z-scores

-3.0 -2.0 -1.0 0.0 1.0 2.0 3.0

GEO Link:	**http://www.ncbi.nlm.nih.gov/geo/query/acc.cgi?acc=GSE29072**
Status:	**Public on May 05 2011**
Title:	**Zebularine effect on mouse embryonic stem cells manifested as cardiod-myogenic potential: testable hypothesis generation using microarray data**
Organism:	**Mus musculus**
Experiment type:	**Expression profiling by array**
Platform:	**GPL1261**
Pubmed ID:	
Summary & Design:	**Summary:** **Lineage commitment during Embryonic Stem Cells (ESCs) differentiation is controlled not only by a gamut of transcription factors but also by epigenetic events, mainly histone deacetylation and promoter DNA methylation. Moreover, the DNA demethylation agent 5â†-Aza-2â†-deoxycytidine (AzadC) has been widely described in the literature as an effective chemical stimulus used to promote cardiomyogenic differentiation in various stem cell types; however, its toxicity and instability complicate its use. Thus, the purpose of this study was to examine the effects of zebularine, a stable and non-toxic DNA cytosine methylation inhibitor, on ESCs differentiation. Herein are the Affymetrix Expression data obtained from RNA of murine ESCs treated with zebularine.** **Overall design:** **9 control samples (replicates) and 9 zebularine samples (replicates).**

Background corr dist: **KL-Divergence = 0.1776, L1-Distance = 0.0403, L2-Distance = 0.0032, Normal std = 0.3481**

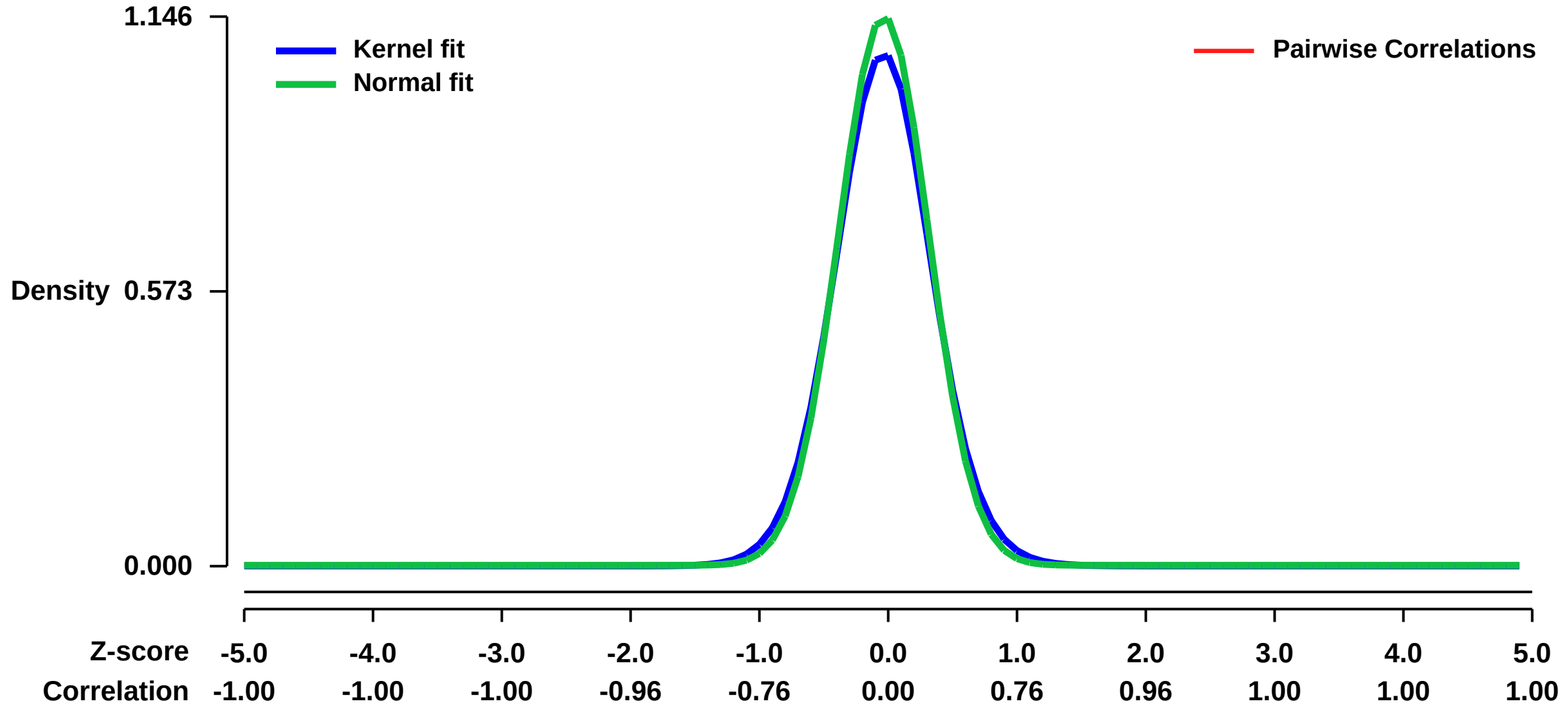

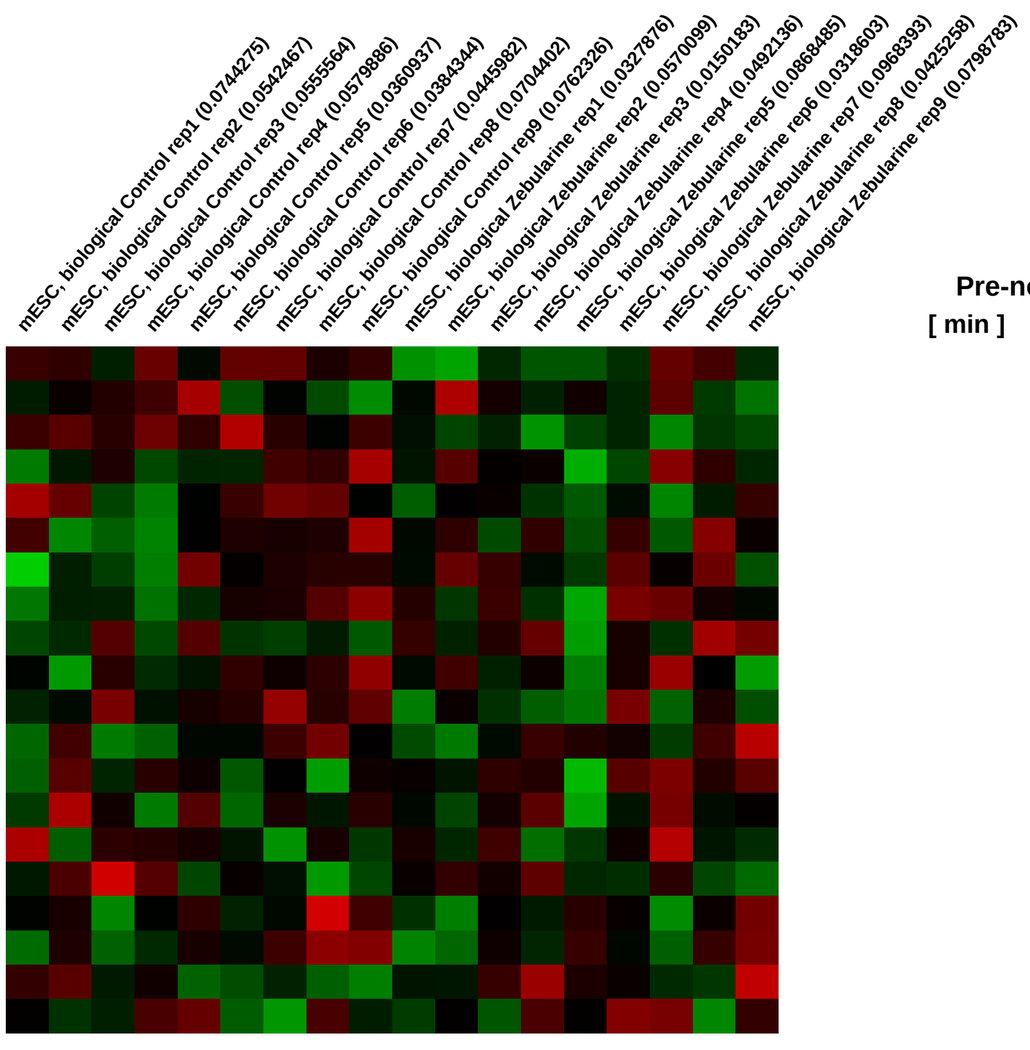

GEO Series "GSE10965" Expression Profiles

Num of samples in this series: 8

Scale of expression profile Z-scores

-3.0 -2.0 -1.0 0.0 1.0 2.0 3.0

GEO Link:	http://www.ncbi.nlm.nih.gov/geo/query/acc.cgi?acc=GSE10965
Status:	Public on Mar 29 2008
Title:	Comparison of the transcriptional profiles of the retinal pigmental epithelium/choroid from young and old mice
Organism:	Mus musculus
Experiment type:	Expression profiling by array
Platform:	GPL1261
Pubmed ID:	18523633
Summary & Design:	**Summary:** To characterize underlying changes in the retinal pigment epithelium (RPE)/choroid with age, we produced gene expression profiles for the RPE/choroid and compared the transcriptional profiles of the RPE/choroid from young and old mice. The changes in the aged RPE/choroid suggest that the tissue has become immunologically active. Such phenotypic changes in the normal aged RPE/choroid may provide a background for the development of age-related macular degeneration. **Keywords:** age-related change **Overall design:** We compared the gene expression of retinal pigmental epithelium/choroid from young and old animals. There were 4 samples from young mice and 4 samples from old mice. Each sample contained 4 retinal pigmental epithelium/choroid from 2 animals

Background corr dist: KL-Divergence = 0.0376, L1-Distance = 0.0149, L2-Distance = 0.0002, Normal std = 0.6113

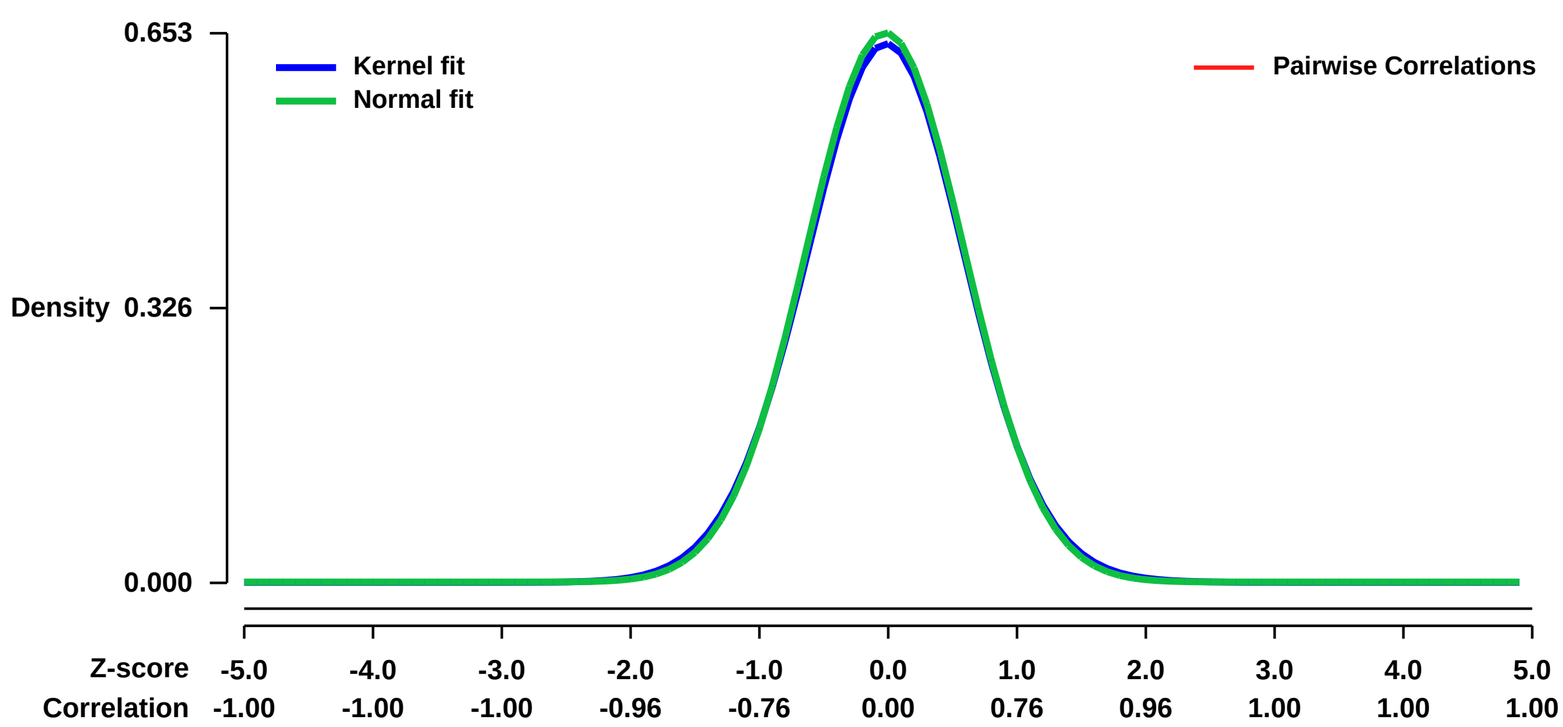

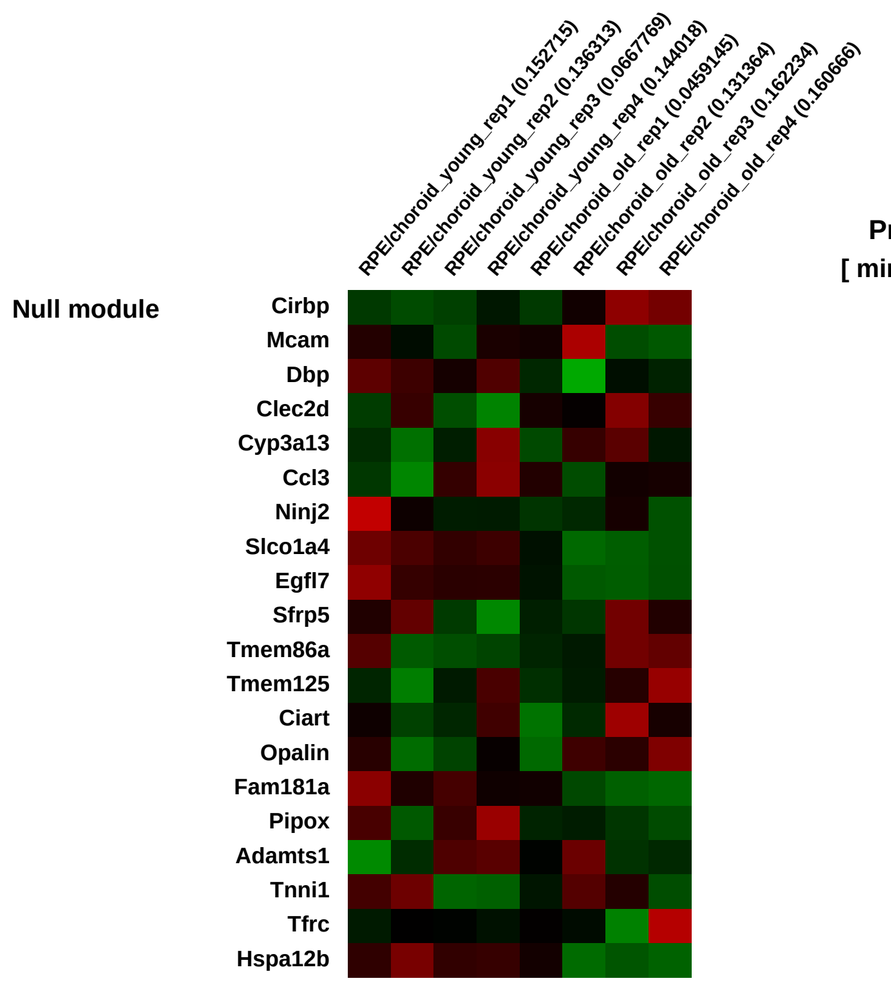

GEO Series "GSE21902" Expression Profiles

Num of samples in this series: 31

Scale of expression profile Z-scores

-3.0 -2.0 -1.0 0.0 1.0 2.0 3.0

GEO Link:	http://www.ncbi.nlm.nih.gov/geo/query/acc.cgi?acc=GSE21902
Status:	Public on Jun 16 2010
Title:	Expression Data from chemical induced tumors obtained from NDR1+/+, NDR1+/- and NDR1-/- mice
Organism:	Mus musculus
Experiment type:	Expression profiling by array
Platform:	GPL1261
Pubmed ID:	20551432
Summary & Design:	**Summary:** Loss and heterozygosity for NDR1 predisposes mice to T-cell lymphoma development. To analyze mechanisms of tumor development in these mice chemically (ENU)-induced tumors were collected and RNA was extracted. **Overall design:** Tumors were collected from mice upon tumor development or 9 months after ENU treatment. Tumors were flash frozen and parts of the tumors were analyzed for RNA, proteins and histology.

Background corr dist: KL-Divergence = 0.2115, L1-Distance = 0.0483, L2-Distance = 0.0061, Normal std = 0.3362

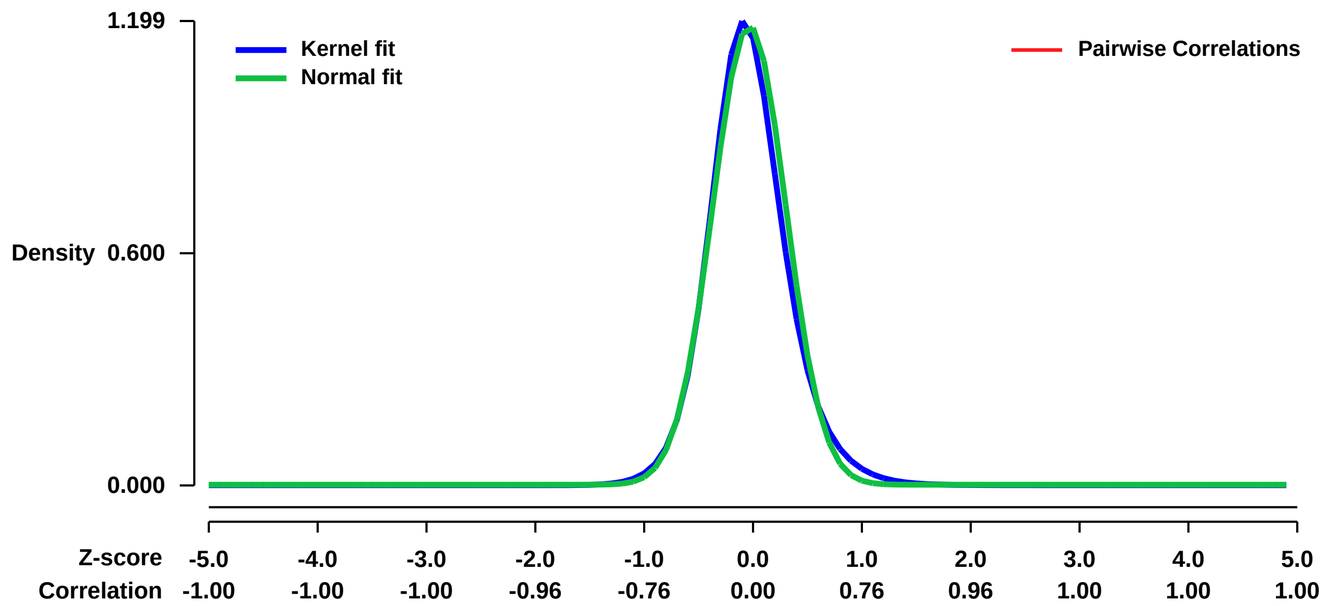

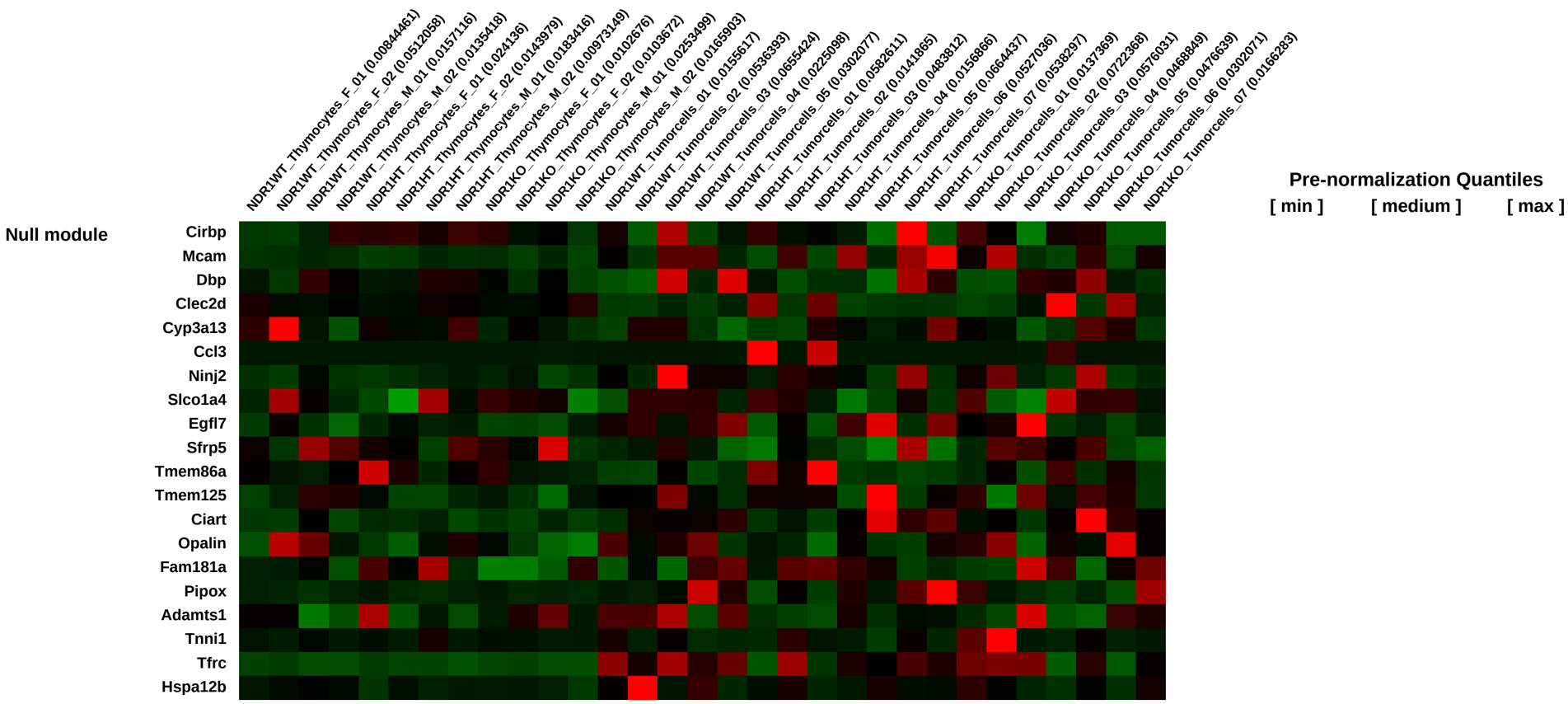

GEO Series "GSE9803" Expression Profiles

Num of samples in this series: 9

Scale of expression profile Z-scores

-3.0 -2.0 -1.0 0.0 1.0 2.0 3.0

GEO Link:	http://www.ncbi.nlm.nih.gov/geo/query/acc.cgi?acc=GSE9803
Status:	Public on Dec 17 2007
Title:	Striatal gene expression data from 12 weeks-old R6/2 mice and control mice (set 1)
Organism:	Mus musculus
Experiment type:	Expression profiling by array
Platform:	GPL1261
Pubmed ID:	17519223
Summary & Design:	**Summary:** To test the hypotheses that mutant huntingtin protein length and wild-type huntingtin dosage have important effects on disease-related transcriptional dysfunction, we compared the changes in mRNA in seven genetic mouse models of Huntington's disease (HD) and postmortem human HD caudate. Transgenic models expressing short N-terminal fragments of mutant huntingtin (R6/1 and R6/2 mice) exhibited the most rapid effects on gene expression, consistent with previous studies. Although changes in the brains of knock-in and full-length transgenic models of HD took longer to appear, 15- and 22-month CHL2(Q150/Q150), 18-month Hdh(Q92/Q92) and 2-year-old YAC128 animals also exhibited significant HD-like mRNA signatures. Whereas it was expected that the expression of full-length huntingtin transprotein might result in unique gene expression changes compared with those caused by the expression of an N-terminal huntingtin fragment, no discernable differences between full-length and fragment models were detected. In addition, very high correlations between the signatures of mice expressing normal levels of wild-type huntingtin and mice in which the wild-type protein is absent suggest a limited effect of the wild-type protein to change basal gene expression or to influence the qualitative disease-related effect of mutant huntingtin. The combined analysis of mouse and human HD transcriptomes provides important temporal and mechanistic insights into the process by which mutant huntingtin kills striatal neurons. In addition, the discovery that several available lines of HD mice faithfully recapitulate the gene expression signature of the human disorder provides a novel aspect of validation with respect to their use in preclinical therapeutic trials. **Keywords:** genetic modification **Overall design:** Striatal samples from 4 R6/2 mutant mice (12 weeks-old) and 5 age-matched wild-type mice.

Background corr dist: KL-Divergence = 0.0775, L1-Distance = 0.0213, L2-Distance = 0.0006, Normal std = 0.4814

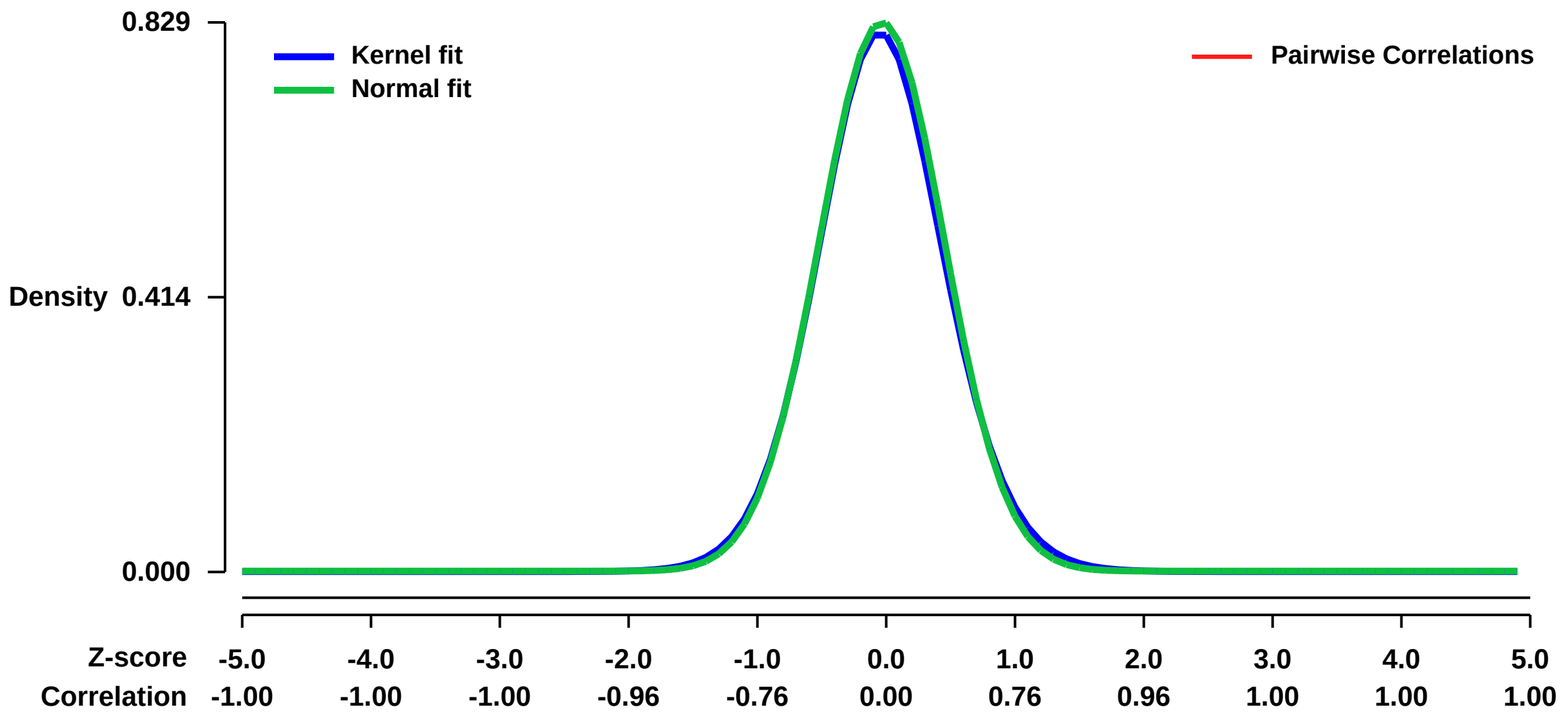

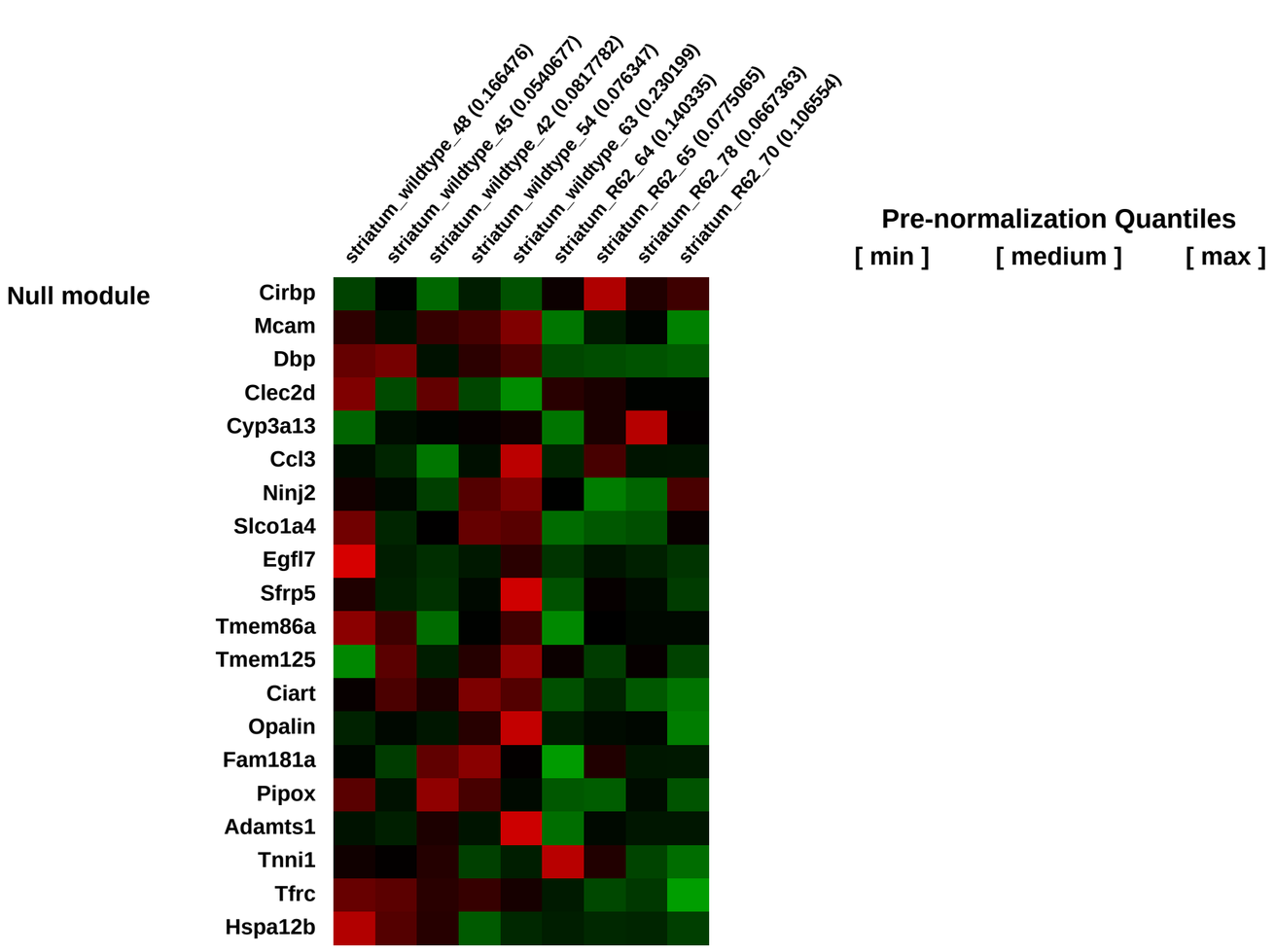

GEO Series "GSE39820" Expression Profiles

Num of samples in this series: 22

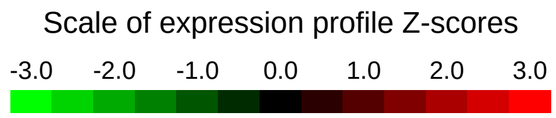

GEO Link:	**http://www.ncbi.nlm.nih.gov/geo/query/acc.cgi?acc=GSE39820**
Status:	**Public on Sep 01 2012**
Title:	**Induction and molecular signature of pathogenic Th17 cells**
Organism:	**Mus musculus**
Experiment type:	**Expression profiling by array**
Platform:	**GPL1261**
Pubmed ID:	**22961052**
Summary & Design:	**Summary:** **TGF-beta3 produced by developing Th17 cells induces highly pathogenic T cells that are functionally and molecularly distinct from TGF-beta1-induced Th17 cells. The microarray data represent a distinct molecular signature for pathogenic versus non-pathogenic Th17 cells.** **Overall design:** **NOCYTO: no cytokines**

Background corr dist: **KL-Divergence = 0.0991, L1-Distance = 0.0309, L2-Distance = 0.0017, Normal std = 0.4374**

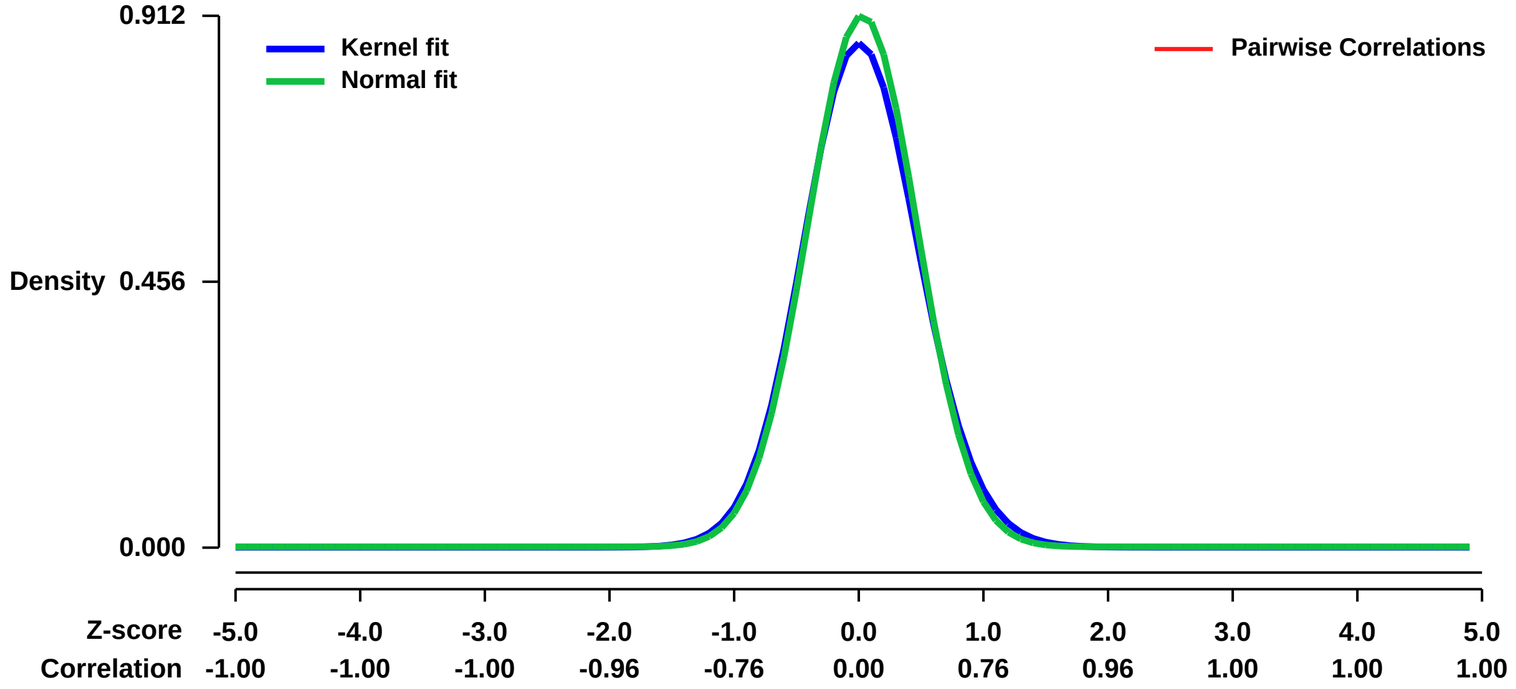

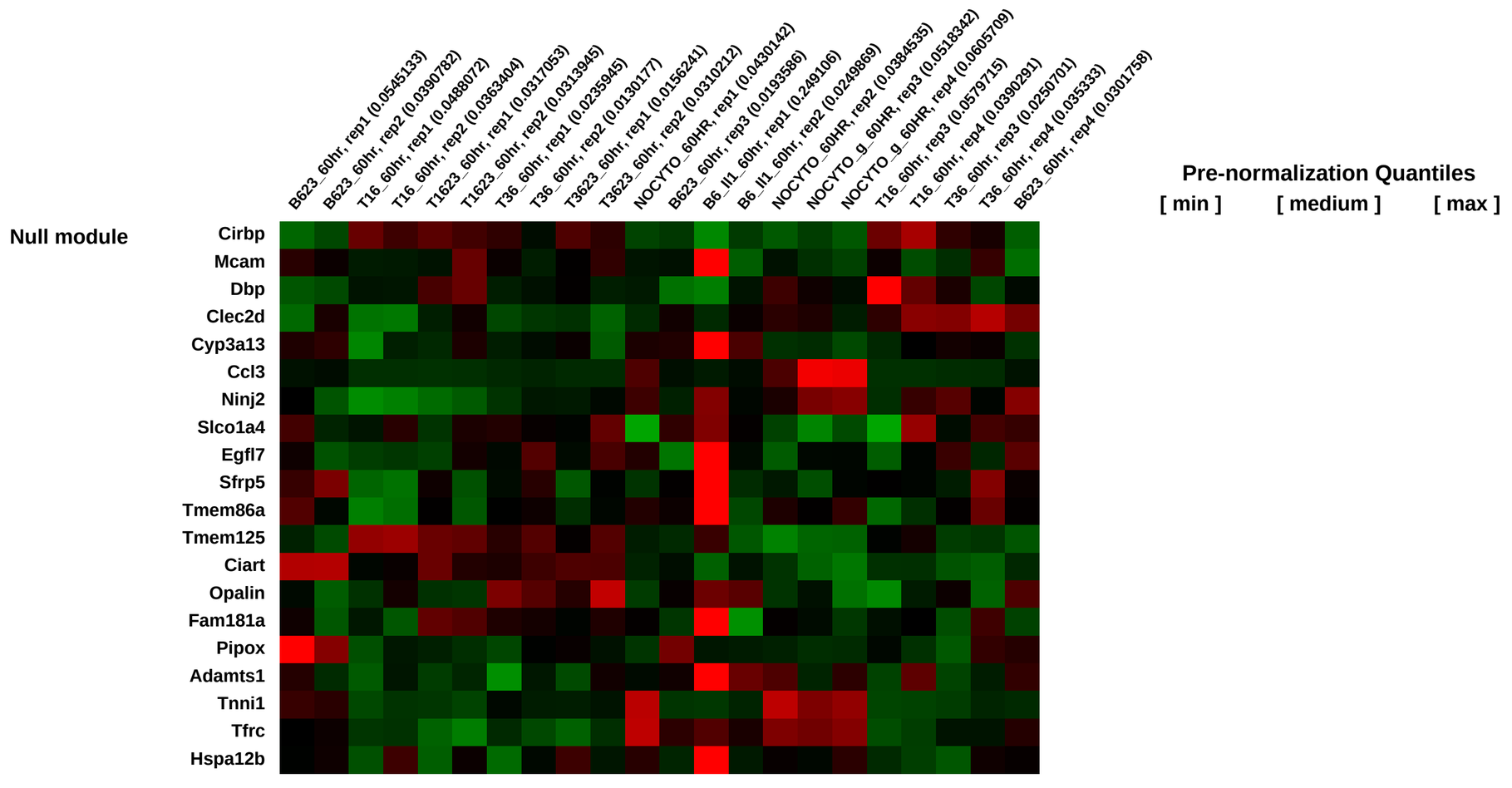

GEO Series "GSE4479" Expression Profiles

Num of samples in this series: 10

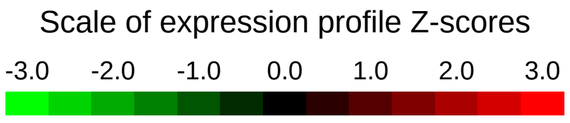

GEO Link:	http://www.ncbi.nlm.nih.gov/geo/query/acc.cgi?acc=GSE4479
Status:	Public on Jun 01 2006
Title:	Expression data from CD4+ splenocytes 6h post-sepsis
Organism:	Mus musculus
Experiment type:	Expression profiling by array
Platform:	GPL1261
Pubmed ID:	16931309
Summary & Design:	**Summary:** Lymphocytes are adversely affected during sepsis. Some CD4+ splenocytes undergo apoptosis while others become Th2 polarized. The molecular determinants of these phenotypic changes are not known. Here we compare the transcriptional response of septic CD4 splenocytes to CD4 splenocytes from sham-manipulated animals 6h after sepsis and identify an early transcriptional component to the septic CD4+ splenocyte phenotype. We used microarrays to detail the global program of gene expression underlying the sepsis-induced changes in CD4+ splenocyte phenotype. Keywords: disease state analysis **Overall design:** CD4+ splenocytes were isolated 6h after the surgical induction of sepsis for RNA extraction and hybridization on Affymetrix microarrays. We sought to obtain a homogeneous cell population in order to reduce any effects of cellular heterogeneity on expression profiles. To that end, immunomagnetic negative selection was used to enrich CD4+ splenocyte populations to ~91%. (n=5 biological replicates each CLP and sham)

Background corr dist: KL-Divergence = 0.0880, L1-Distance = 0.0271, L2-Distance = 0.0012, Normal std = 0.4568

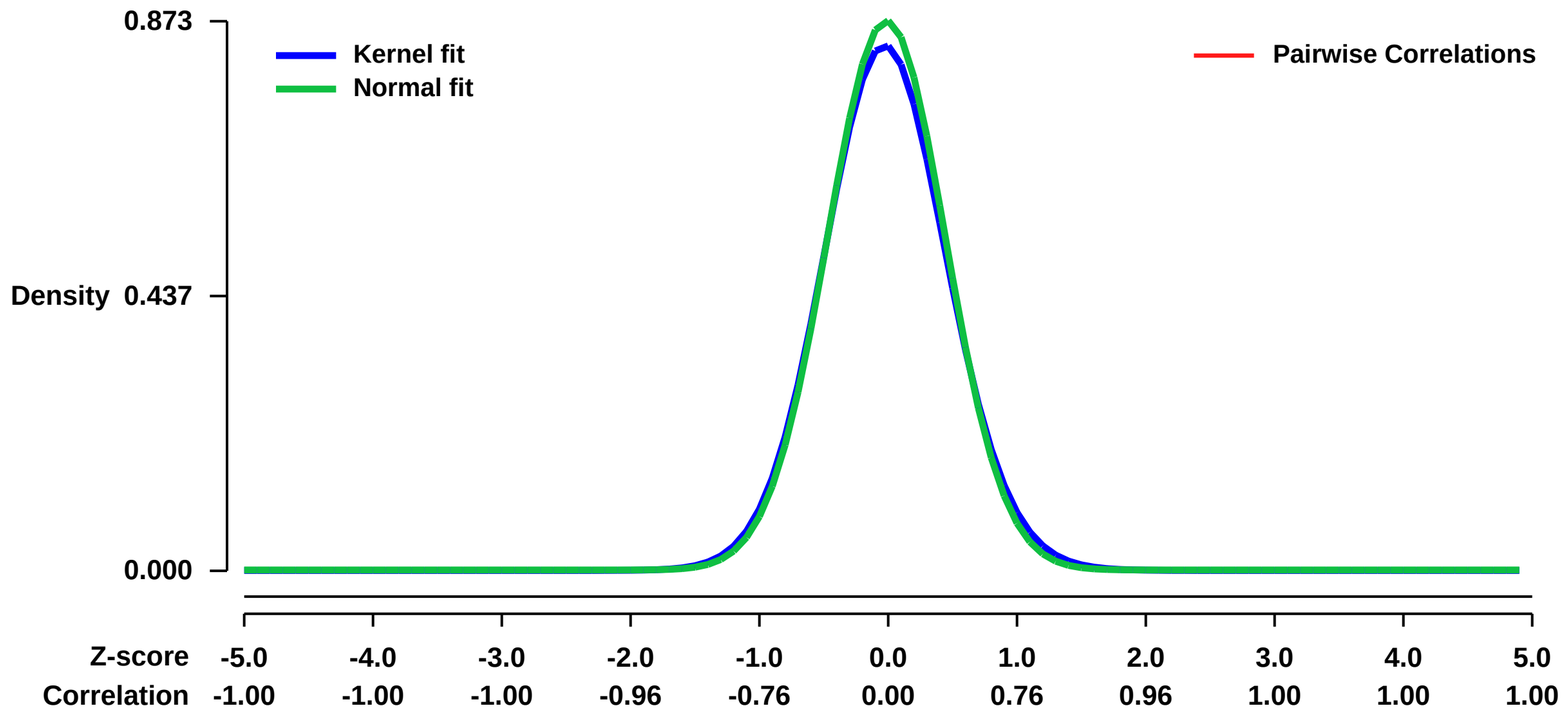

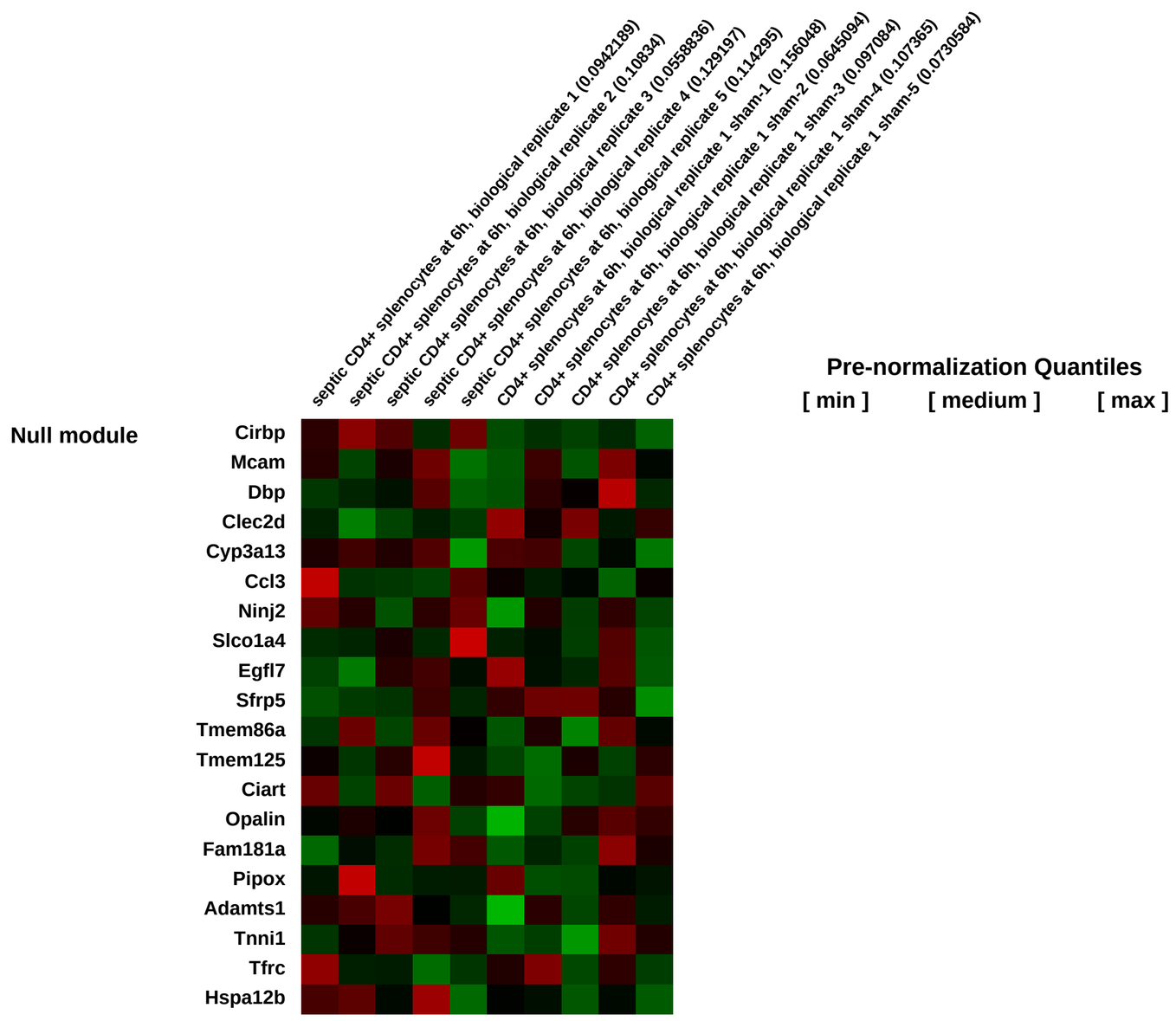

GEO Series "GSE12881" Expression Profiles

Num of samples in this series: 6

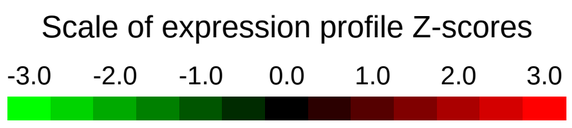

GEO Link:	http://www.ncbi.nlm.nih.gov/geo/query/acc.cgi?acc=GSE12881
Status:	Public on Jan 26 2009
Title:	Loss of Caveolin-3 Induces the Development of a Lactogenic Microenvironment
Organism:	Mus musculus
Experiment type:	Expression profiling by array
Platform:	GPL1261
Pubmed ID:	19164602
Summary & Design:	**Summary:** Here, we show that functional loss of a single gene is sufficient to confer constitutive milk protein production and protection against mammary tumor formation. Caveolin-3 (Cav-3), a muscle-specific caveolin-related gene, is highly expressed in striated and smooth muscle cells. We demonstrate that Cav-3 is also expressed in myoepithelial cells within the mammary gland. To determine if genetic ablation of Cav-3 expression affects adult mammary gland development, we next studied the phenotype(s) of Cav-3 (-/-) null mice. Interestingly, detailed analysis of Cav-3 (-/-) virgin mammary glands shows dramatic increases in ductal thickness, side-branching, and the development of extensive lobulo-alveolar hyperplasia, akin to the changes normally observed during pregnancy and lactation. Analysis by genome-wide expression profiling reveals the upregulation of gene transcripts associated with pregnancy/lactation, mammary stem cells, and human breast cancers, consistent with a constitutive lactogenic phenotype. The expression levels of three key transcriptional regulators of lactation, namely Elf5, Stat5a, and c-Myc are also significantly elevated. Experiments with pregnant mice directly show that Cav-3 (-/-) mice undergo precocious lactation. Finally, using orthotopic implantation of a transformed mammary cell line (known as Met-1), we demonstrate that virgin Cav-3 (-/-) mice are dramatically protected against mammary tumor formation. Interestingly, Cav-3 (+/-) mice also show similar protection, indicating that even reductions in Cav-3 levels are sufficient to render these mice resistant to tumorigenesis. Thus, Cav-3 (-/-) mice are a novel preclinical model to study the protective effects of a constitutive lactogenic microenviroment on mammary tumor onset and progression. Our current studies have broad implications for using the lactogenic micro-environment as a paradigm to discover new therapies for the prevention and/or treatment of human breast cancers. Most importantly, a lactation-based therapeutic strategy would provide a more natural and nontoxic approach to the development of novel anti-cancer therapies. **Overall design:** All WT and Cav-3 knockout (KO) mice used in this study were in the FVB/N genetic background. 4-month old virgin female mice were utilized in a micro array study between 3 wildtype and 3 Caveolin-3 knock-out mammary glands.

Background corr dist: KL-Divergence = 0.0260, L1-Distance = 0.0141, L2-Distance = 0.0002, Normal std = 0.6931

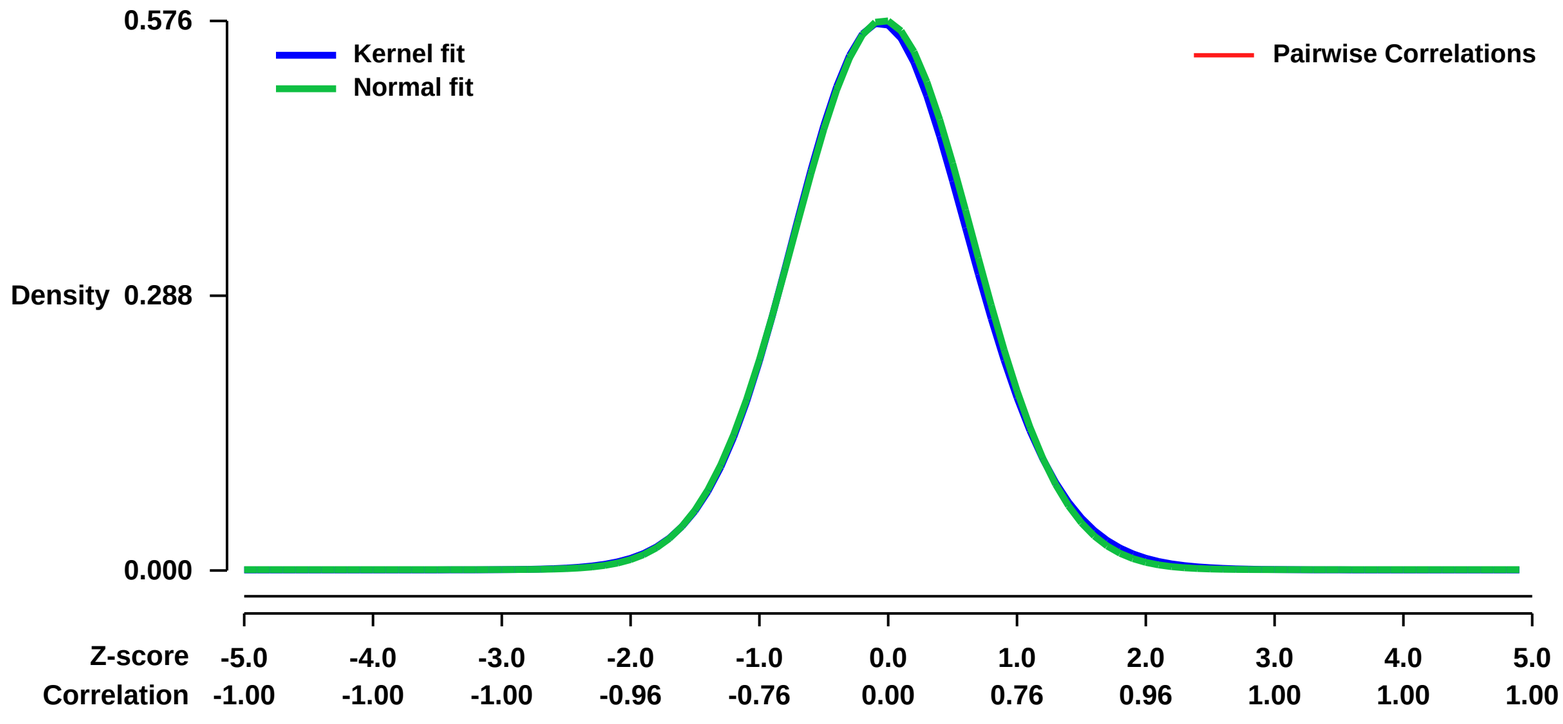

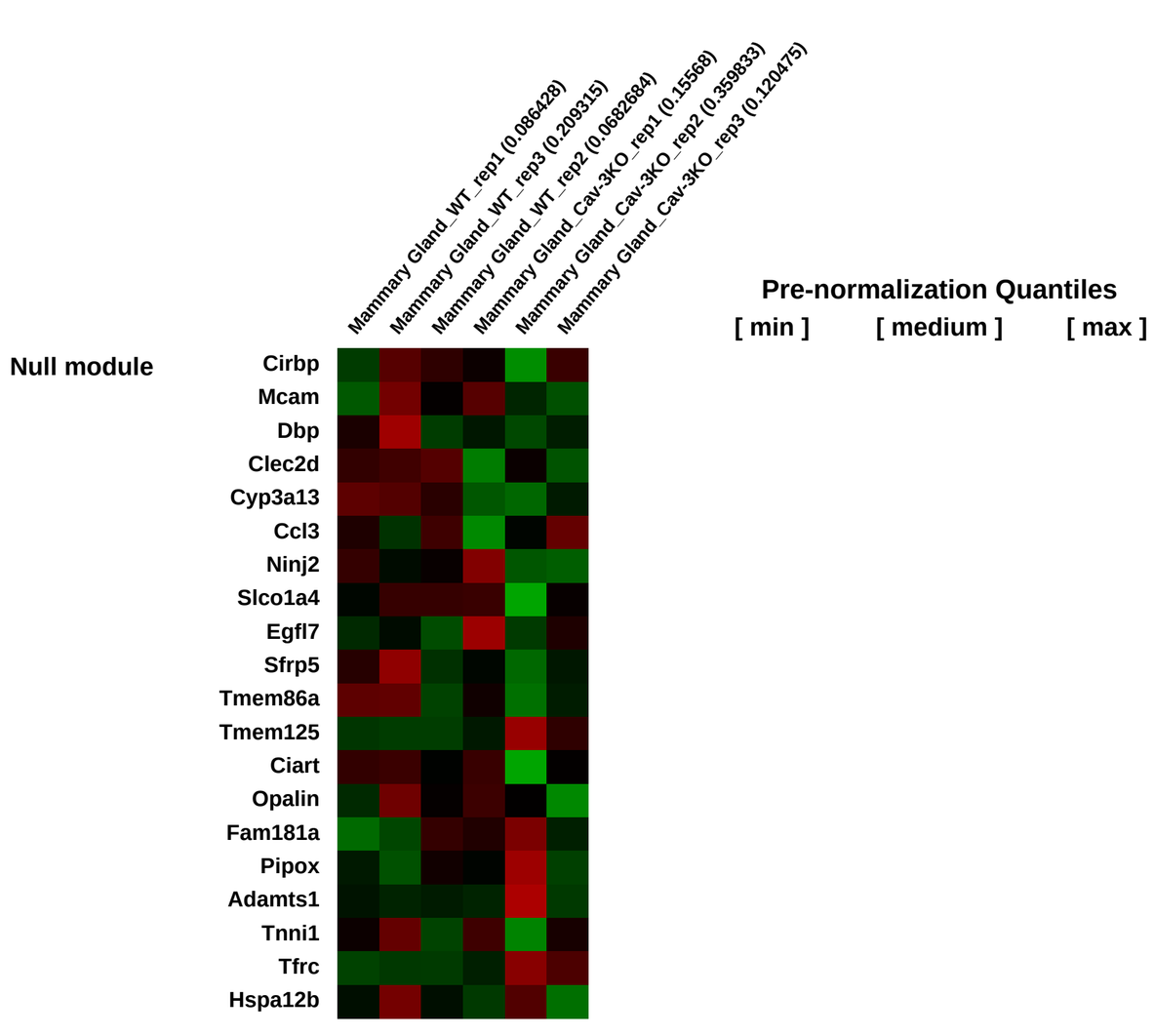

GEO Series "GSE46094" Expression Profiles

Num of samples in this series: 10

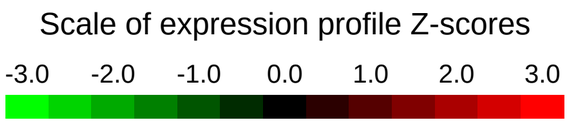

GEO Link:	**http://www.ncbi.nlm.nih.gov/geo/query/acc.cgi?acc=GSE46094**
Status:	**Public on May 01 2014**
Title:	**Expression data from PML-RAR$_{\alpha}$– transgenic mouse APL(acute promyelocyte leukemia) cells**
Organism:	**Mus musculus**
Experiment type:	**Expression profiling by array**
Platform:	**GPL1261**
Pubmed ID:	
Summary & Design:	**Summary:** **The differentiation of leukemia stem cells (LSCs) is generally regarded as a one-way alterative process to self-renewal. However, how differentiation impacts LSC stemness has largely been unexplored. Here we show that before reaching terminal differentiation (TD), apical LSCs of mouse acute promyelocytic leukemia passed through a partial differentiation (PD) stage, wherein the leukemia cells re-initiated leukemia via de-differentiation albeit at a reduced rate. Notably, while retinoic acid (RA) preferentially drove the transition of LSC to PD, monocytic Irf8 skewed PD cells to terminal maturation over de-differentiation and/or expansion. Remarkably, the combined use of RA and Irf8 induction depleted the total leukemogenic potential, which indicates that discrete stage- or lineage-specific mechanisms elaborate a step-wise LSC differentiation.** **We used microarrays to detail the global programme of gene expression indicating the molecular mechanisms unerlying the the process of LSC step-wise differentiation.** **Overall design:** **Retroviral GFP-labled mouse APL cells (bone marrow sample) were repopulated in vivo through transplantation into syngenic recipients. At the proper time points, the GFP positive APL bone marrow cells were collected and sorted for UNSC, UNPD and UNTD samples through FACS. RA-PD and RA-TD cells were sorted from bone marrow tissue treated with ATRA (all trans retinoic acid) for 5 days. The freshly isolated samples were then lysed for RNA extration. Each sample had two biological replicates.**

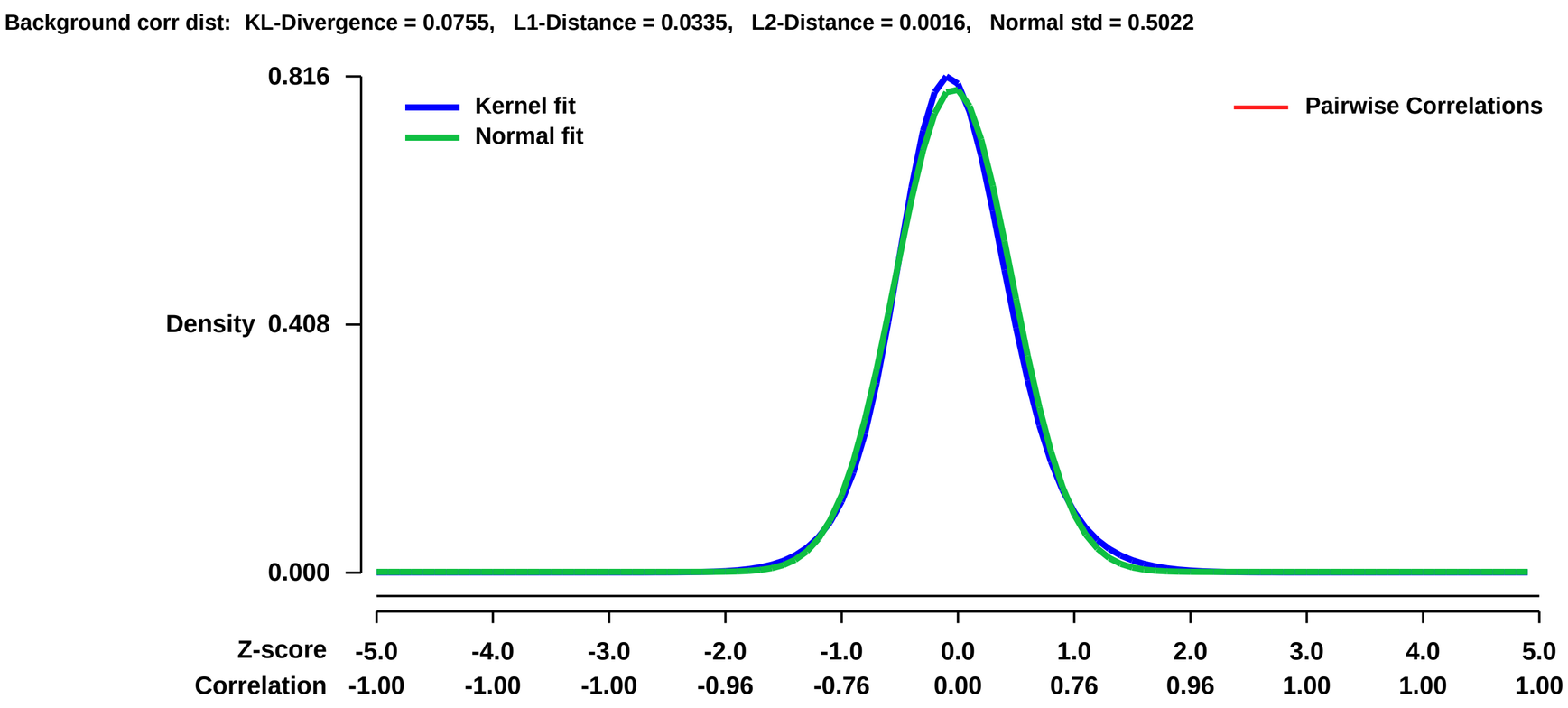

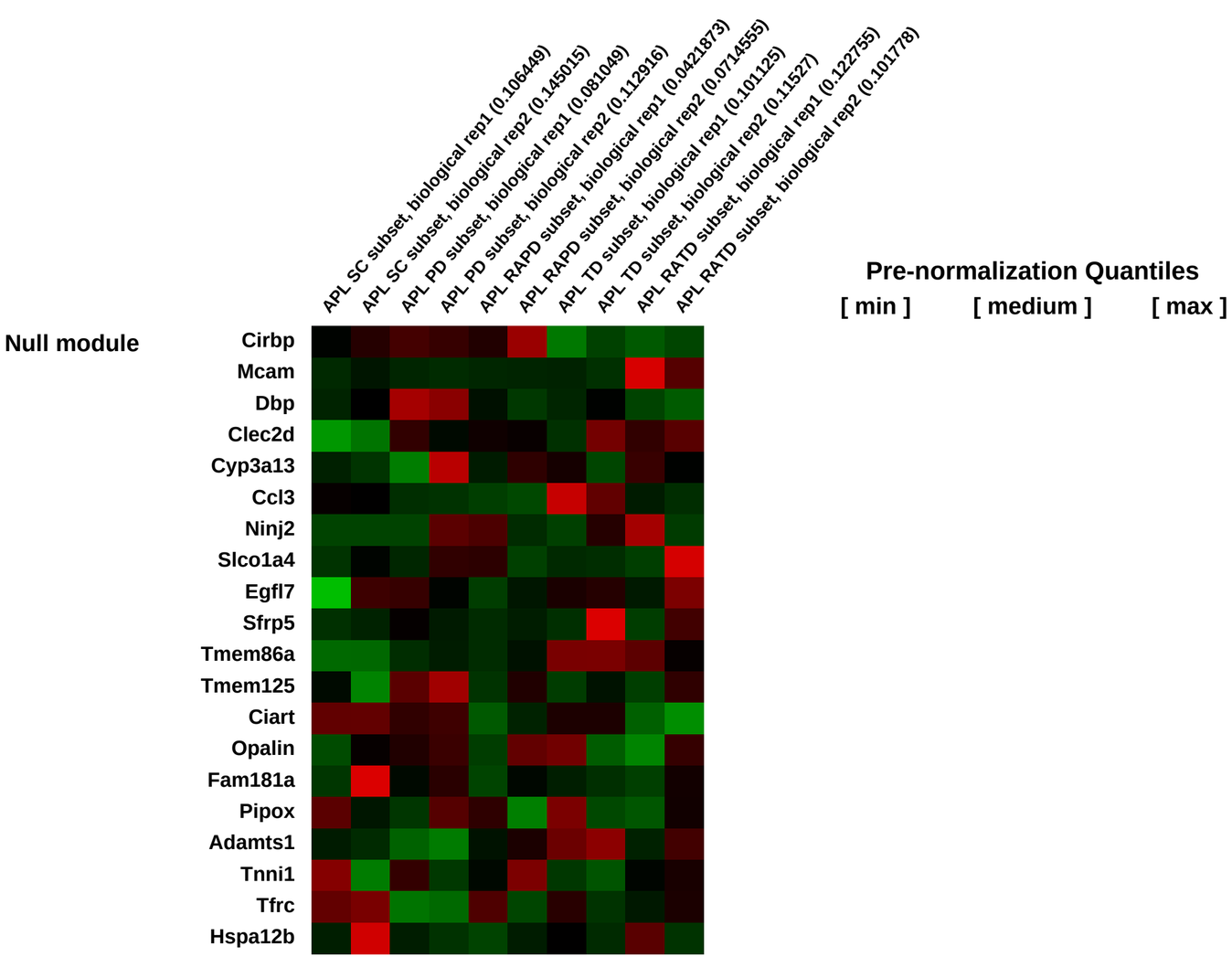

GEO Series "GSE26476" Expression Profiles

Num of samples in this series: 6

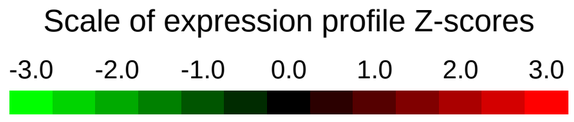

GEO Link:	http://www.ncbi.nlm.nih.gov/geo/query/acc.cgi?acc=GSE26476
Status:	Public on Jan 07 2011
Title:	Smooth muscle IL-4 receptor activation induces airway hyper-responsiveness
Organism:	Mus musculus
Experiment type:	Expression profiling by array
Platform:	GPL1261
Pubmed ID:	21464224
Summary & Design:	**Summary:** **Selective stimulation of IL-4 receptor on smooth muscle induces airway hyper-responsiveness in mice.** **Abstract: Production of the cytokines IL-4 and IL-13 is increased in both human asthma and mouse asthma models and Stat6 activation by the common IL-4/IL-13R drives most mouse model pathophysiology, including airway hyperresponsiveness (AHR). However, the precise cellular mechanisms through which IL-4R$_{\alpha}$– induces AHR remain unclear. Overzealous bronchial smooth muscle constriction is thought to underlie AHR in human asthma, but the smooth muscle contribution to AHR has never been directly assessed. Furthermore, differences in mouse vs. human airway anatomy and observations that selective IL-13 stimulation of Stat6 in airway epithelium induces murine AHR raise questions about the importance of direct IL-4R effects on smooth muscle in murine asthma models and relevance of these models to human asthma. Using transgenic mice in which smooth muscle is the only cell type that expresses or fails to express IL-4R$_{\alpha}$–, we demonstrate that direct smooth muscle activation by IL-4, IL-13, or allergen is sufficient, but not necessary, to induce AHR and show that 5 genes known to promote smooth muscle migration, proliferation and contractility are activated by IL-13 in smooth muscle in vivo. These observations demonstrate that IL-4R$_{\alpha}$– promotes AHR through multiple mechanisms and provide a model for testing smooth muscle-directed asthma therapeutics.** **Overall design:** **Gene transcripts were identified that differed in their relative expression as a function of IL4R expression on the smooth muscle cells.**

Background corr dist: KL-Divergence = 0.0370, L1-Distance = 0.0163, L2-Distance = 0.0003, Normal std = 0.6281

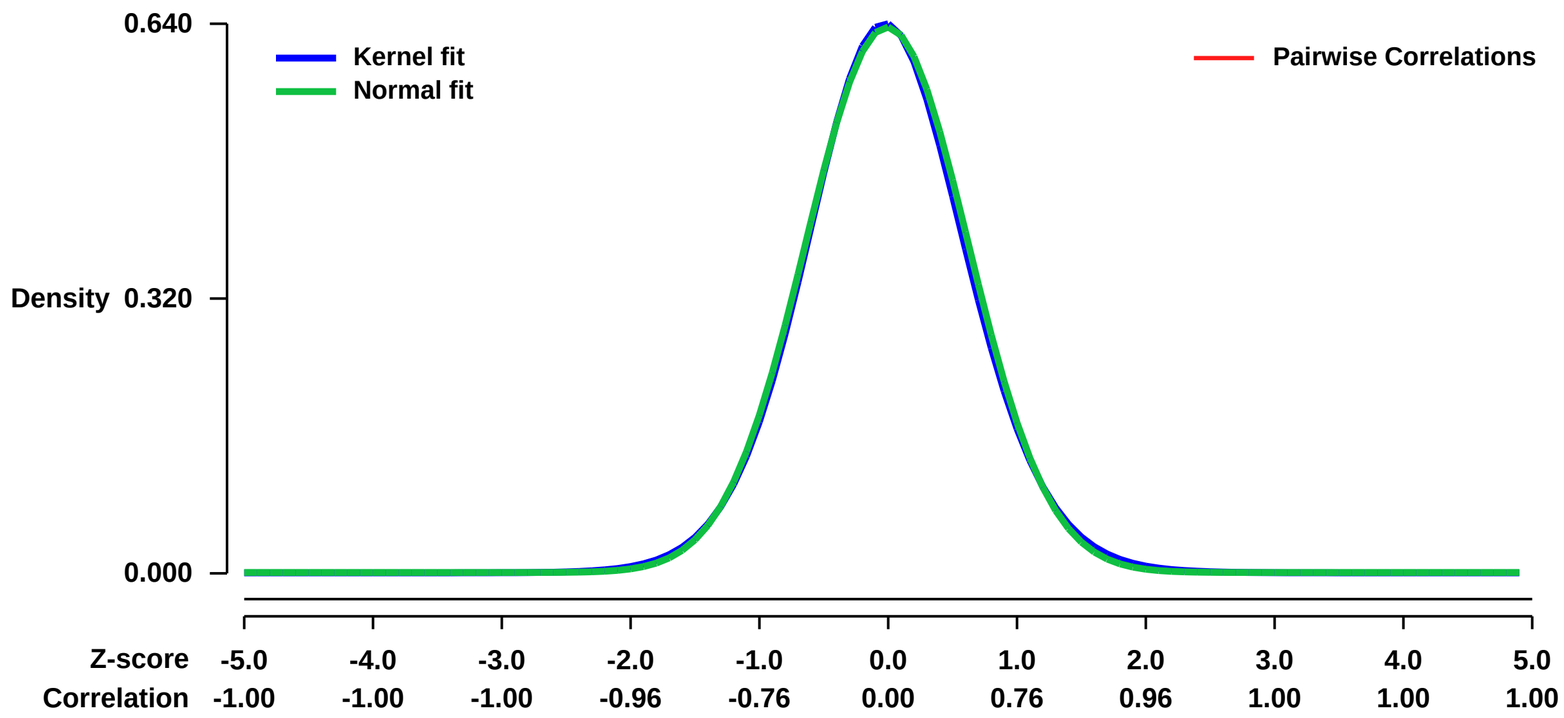

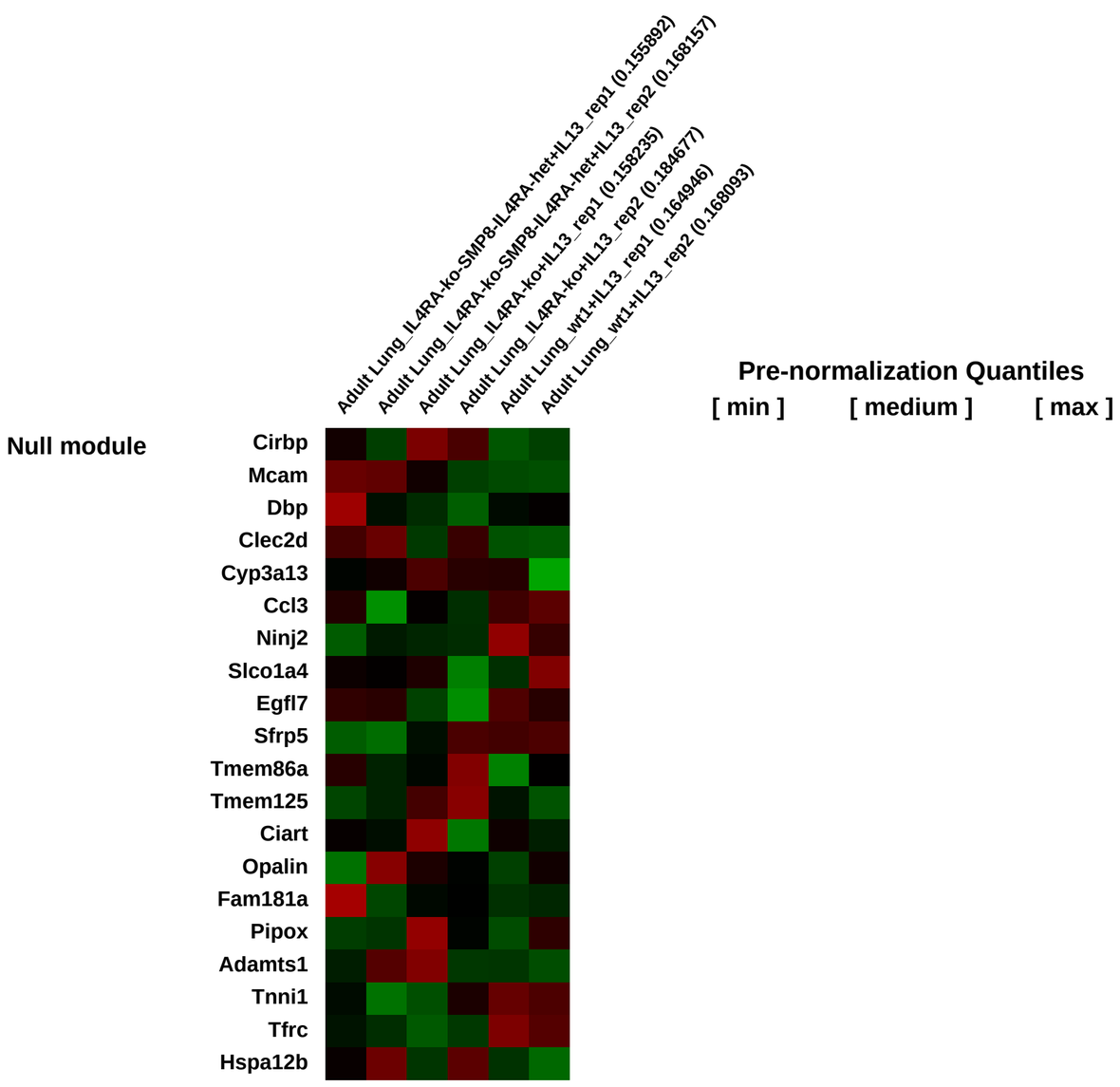

GEO Series "GSE14843" Expression Profiles

Num of samples in this series: 6

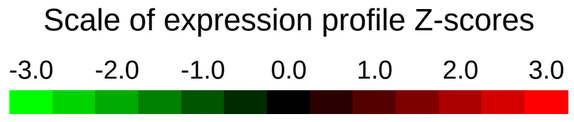

GEO Link:	http://www.ncbi.nlm.nih.gov/geo/query/acc.cgi?acc=GSE14843
Status:	Public on Nov 12 2009
Title:	Altered Hepatic Gene Expression Profiles Associated with Myocardial Ischemia
Organism:	Mus musculus
Experiment type:	Expression profiling by array
Platform:	GPL1261
Pubmed ID:	20160198

Summary & Design:

Summary:
Backgroundâ Acute coronary syndrome (ACS) is sometimes accompanied by accelerated coagulability, lipid metabolism, and inflammatory responses, which are not attributable to the cardiac events alone. We hypothesized that the liver plays a pivotal role in the pathophysiology of ACS. We simultaneously analyzed the gene expression profiles of the liver and heart during acute myocardial ischemia in mice.

Methods and Resultsâ Mice were divided into three treatment groups: sham-operation, ischemia-reperfusion (I/R), and myocardial infarction. Mice with liver I/R were included as additional controls. Marked changes in hepatic gene expression were observed after 24 hours, despite the lack of histological changes in the liver. Genes related to tissue remodeling, adhesion molecules, and morphogenesis were significantly upregulated in the livers of mice with myocardial I/R or infarction, but not in those with liver I/R. Myocardial ischemia, but not changes in the hemodynamic state, was postulated to significantly alter hepatic gene expression. Moreover, detailed analysis of the signaling pathway suggested the presence of humoral factors that intervened between the heart and liver. To address these points, we utilized isolated primary hepatocytes and showed that osteopontin released from the heart actually altered the signaling pathways of primary hepatocytes to those observed in the livers of mice under myocardial ischemia. Moreover, osteopontin stimulated primary hepatocytes to secrete vascular endothelial growth factor-A, which is important for tissue remodeling.

Conclusionsâ Hepatic gene expression is potentially regulated by cardiac humoral factors under myocardial ischemia. These results provide new insights into the pathophysiology of ACS.

Overall design:
C57BL/6J mice (n=46, BW 24.1´–1.42 g, 8â 10 weeks of age; Charles River Laboratories) were divided into the following treatment groups: sham-operated (n=11), I/R (n=10), myocardial infarction (n=10), liver I/R (n=10), and sham-operated plus hydralazine (n=5). In this study, we examined the response of hepatic gene expression to myocardial ischemia. Given the systemic inflammation that characterizes acute coronary syndromes, we postulated that regulation of hepatic genes occurs via inflammatory mediators and not via alterations in hemodynamics or hepatic perfusion. We therefore used whole genome transcriptional profiling to identify hepatic genes selectively regulated in the setting of myocardial ischemia. Moreover, detailed analysis of the signaling pathway suggested the presence of humoral factors that intervened between the heart and liver under myocardial ischemia. As a candidate humoral factors, osteopontin was further investigated. To evaluate whether the cardiac secreted protein affects hepatic gene expressions, we investigated primary hepatocytes treated with osteopontin by using microarray analysis. Affymetrix GeneChip Mouse Genome 430 2.0 Array was used to measure gene expression levels in primary hepatocytes at 8 hours after osteopontin stimulation (mock: n=3 and osteopontin: n=3).

Background corr dist: KL-Divergence = 0.0156, L1-Distance = 0.0483, L2-Distance = 0.0024, Normal std = 0.9256

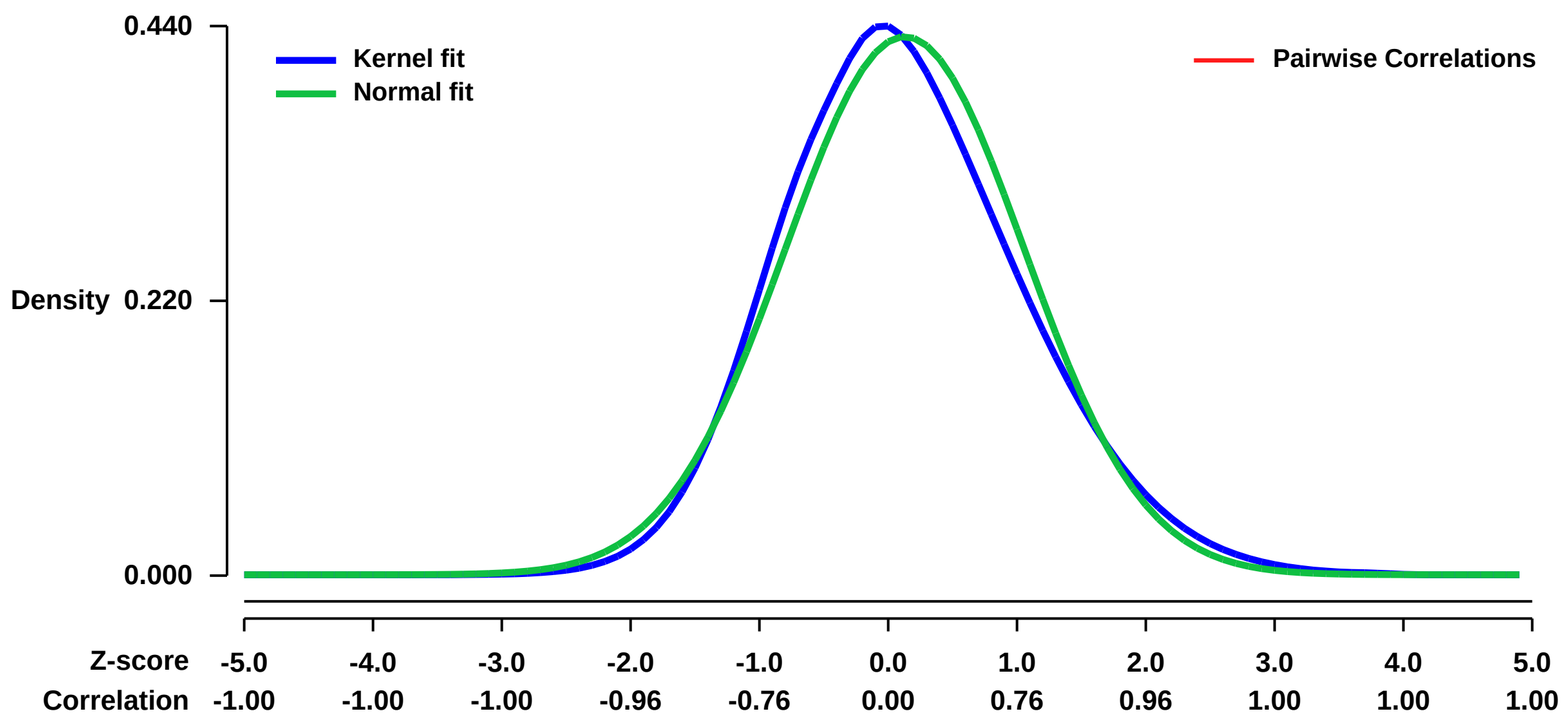

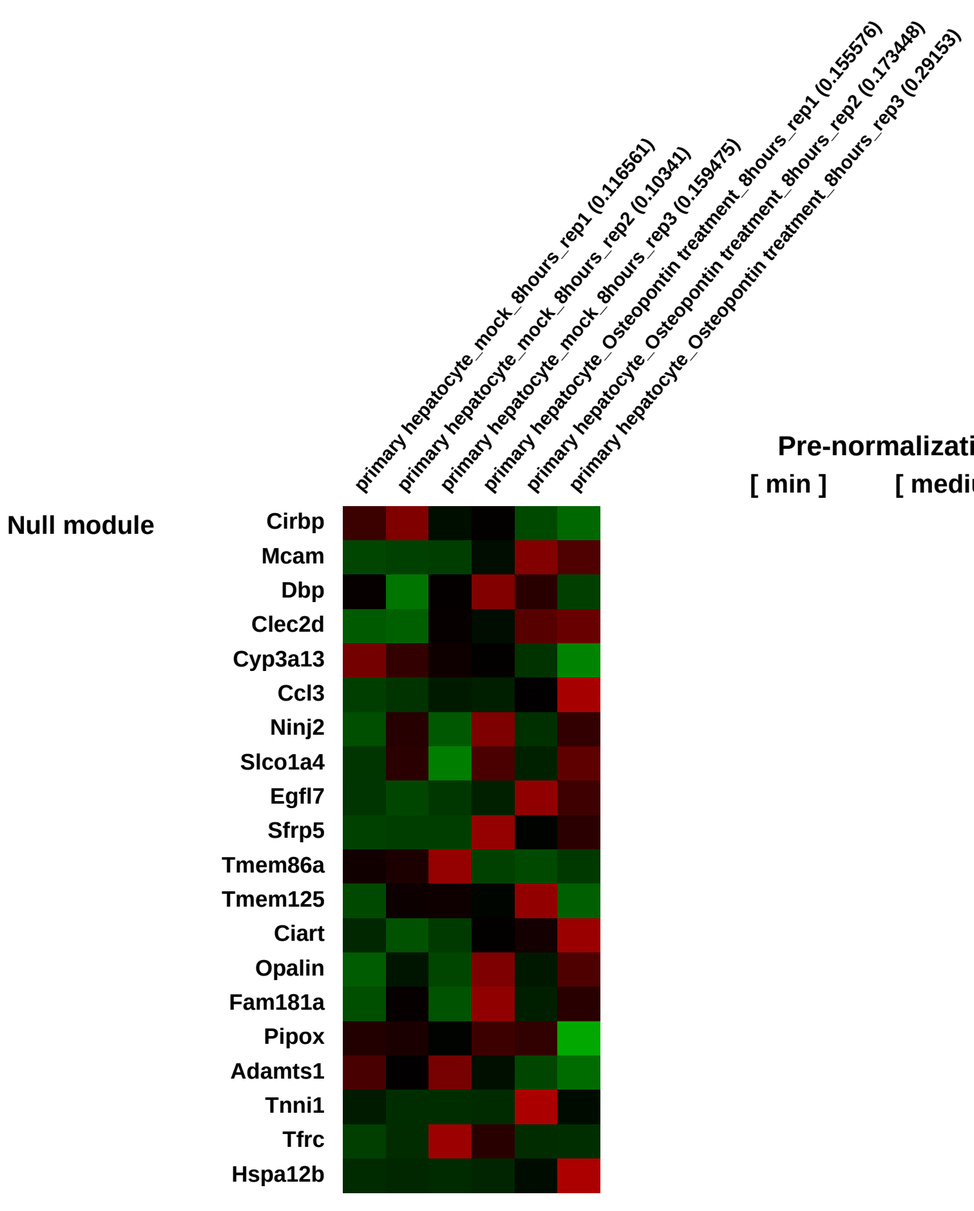

GEO Series "GSE47772" Expression Profiles

Num of samples in this series: 24

Scale of expression profile Z-scores

-3.0 -2.0 -1.0 0.0 1.0 2.0 3.0

GEO Link:	http://www.ncbi.nlm.nih.gov/geo/query/acc.cgi?acc=GSE47772
Status:	Public on Oct 01 2013
Title:	Expression data from subpopulations of Apc1638N/+ intestinal adeno tumors versus Apc1638N/+ / KRAS v12G intestinal adenocarcinomas tumors
Organism:	Mus musculus
Experiment type:	Expression profiling by array
Platform:	GPL1261
Pubmed ID:	24069241
Summary & Design:	**Summary:** Constitutive activation of the Wnt pathway leads to adenoma formation, an obligatory step towards intestinal cancer. In view of the established role of Wnt in regulating stemness, we attempted the isolation of cancer stem cells (CSCs) from Apc- and Apc/KRAS-mutant intestinal tumours. Whereas CSCs are present in malignant Apc/KRASâ mutant carcinomas, they appear to be very rare (<10-6) in the benign Apcâ mutant adenomas. In contrast, the Lin-CD24hiCD29+ subpopulation of adenocarcinoma cells appear to be enriched in CSCs with increased levels of active ï ¢-catenin. Expression profiling analysis of the CSC-enriched subpopulation confirmed their enhanced Wnt activity and revealed additional differential expression of other signalling pathways, growth factor binding proteins, and extracellular matrix components. As expected, genes characteristic of the Paneth cell lineage (e.g. defensins) are co-expressed together with stem cell genes (e.g. Lgr5) within the CSC-enriched subpopulation. This is of interest as it may indicate a cancer stem cell niche role for tumor-derived Paneth-like cells, similar to their role in supporting Lgr5+ stem cells in the normal intestinal crypt. Overall, our results indicate that oncogenic KRAS activation in Apc-driven tumours results in the expansion of the CSCs compartment by increasing b-catenin intracellular stabilization. **Overall design:** To identify molecular differences between stem-like and more differentiated (bulk) tumour cells from Apc1638N/+ and Apc1638N/+/KRASV12G intestinal adenomas and adenocarcinomas, we isolated total RNA from 104 Lin-CD24hiCD29+, Lin-CD24medCD29+/Lin-CD24loCD29+ and Lin- (bulk) tumour cells from 5 individual mice of each genotype (Apc1638N/+ and Apc1638N/+/KRASV12G). Total RNA samples were then employed to hybridize oligonucleotide microarrays (Affymetrix Mouse Genome 430A 2.0 Array) according to conventional protocols.

Background corr dist: KL-Divergence = 0.2441, L1-Distance = 0.0549, L2-Distance = 0.0075, Normal std = 0.3060

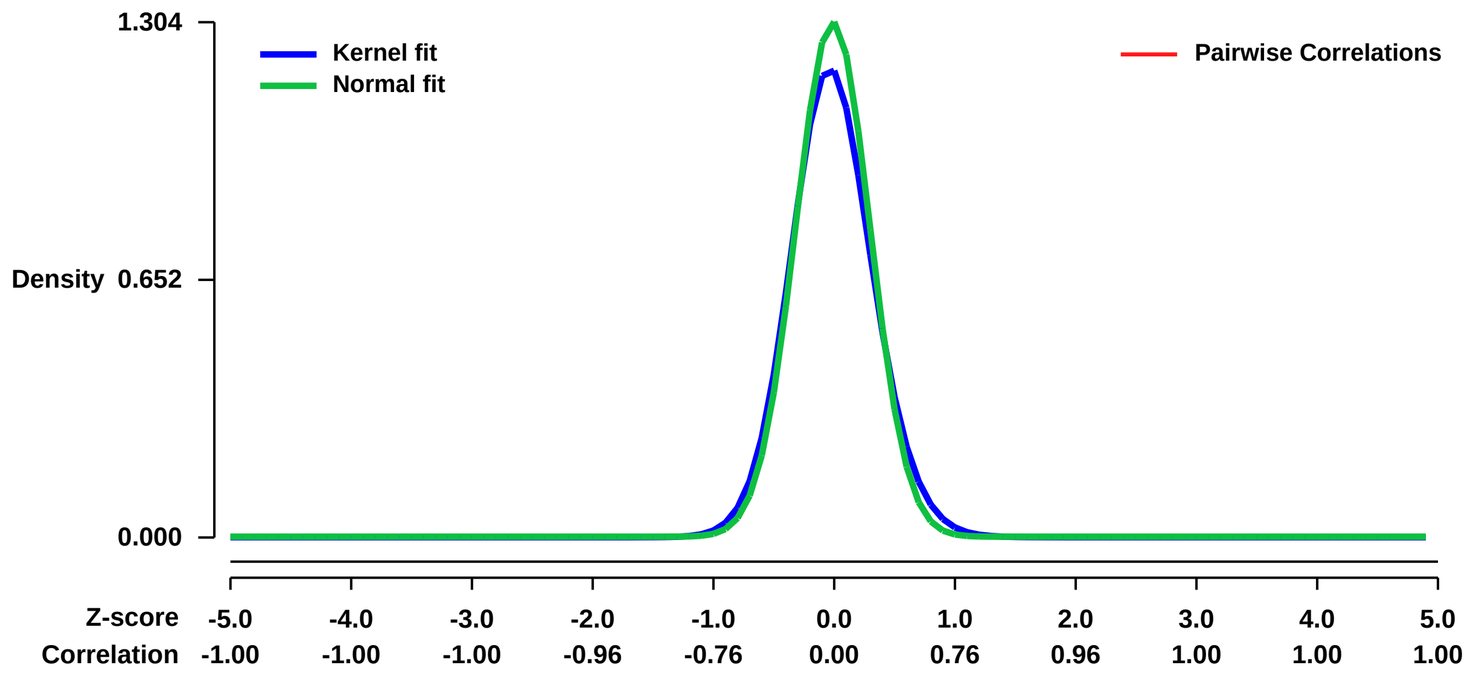

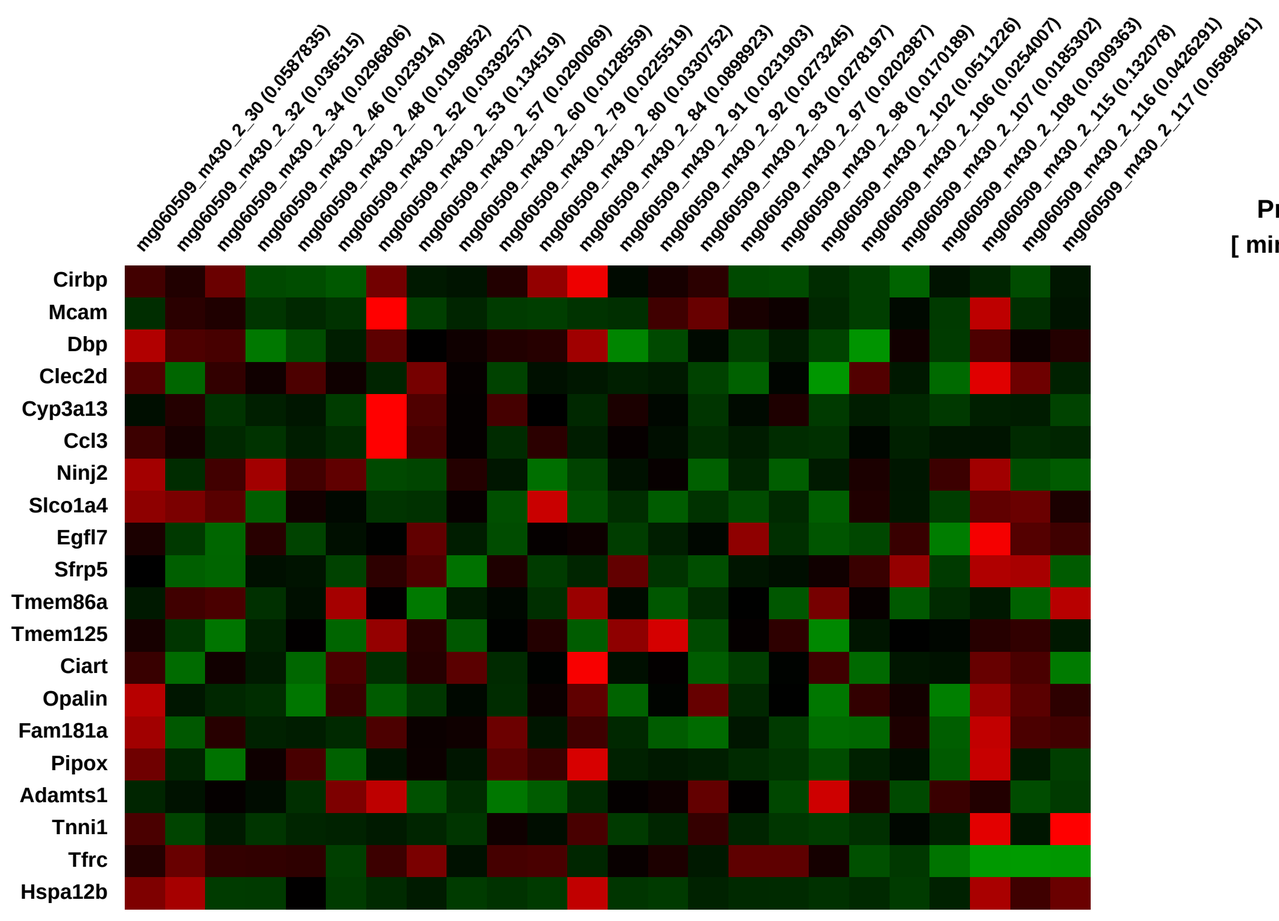

GEO Series "GSE25637" Expression Profiles

Num of samples in this series: 9

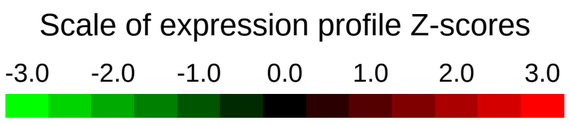

GEO Link:	http://www.ncbi.nlm.nih.gov/geo/query/acc.cgi?acc=GSE25637
Status:	Public on Jul 10 2012
Title:	A mouse model of deregulation of the malt1 oncogene recapitulates the pathogenesis of human malt lymphoma [Spleen dataset]
Organism:	Mus musculus
Experiment type:	Expression profiling by array
Platform:	GPL1261
Pubmed ID:	22689981
Summary & Design:	**Summary:** Attempts at modeling chromosomal translocations involving MALT1 gene, hallmarks of human mucosa-associated lymphoid tissue (MALT) lymphoma, have failed to reproduce the disease in mice. Here we describe a transgenic model in which MALT1 expression was targeted to mouse hematopoietic stem/progenitor cells. In Sca1-MALT1 mice, MALT1 deregulation activated the NF-kappaB pathway in Sca1+ cells, promoting selective B-cell differentiation and mature lymphocyte accumulation in extranodal tissues, progressively leading to the development of clonal B-cell lymphomas. These tumors recapitulated the histopathological features of human MALT lymphomas, presenting typical lymphoepithelial lesions and plasmacytic differentiation. Transcriptional profiling of Sca1-MALT1 murine lymphomas revealed overlapping molecular signatures with human MALT lymphomas, including MALT1-mediated NFkappaB activation, pro-inflammatory signaling and XBP1-induced plasmacytic differentiation. Moreover, murine Malt1 showed proteolytic activity by cleaving Bcl10 in Sca1-MALT1 lymphomas. Our novel technological approach has allowed modeling human MALT lymphoma in mice, which represent unique tools study MALT lymphoma biology and evaluate anti-MALT1 therapies. **Keywords:** Genetic modification, wt vs. transgenic, disease analysis, MALT lymphoma **Overall design:** 9 samples were analized of which 5 were splenic lymphomas from Sca1-MALT1 transgenic mice and 4 were spleens from WT mice.

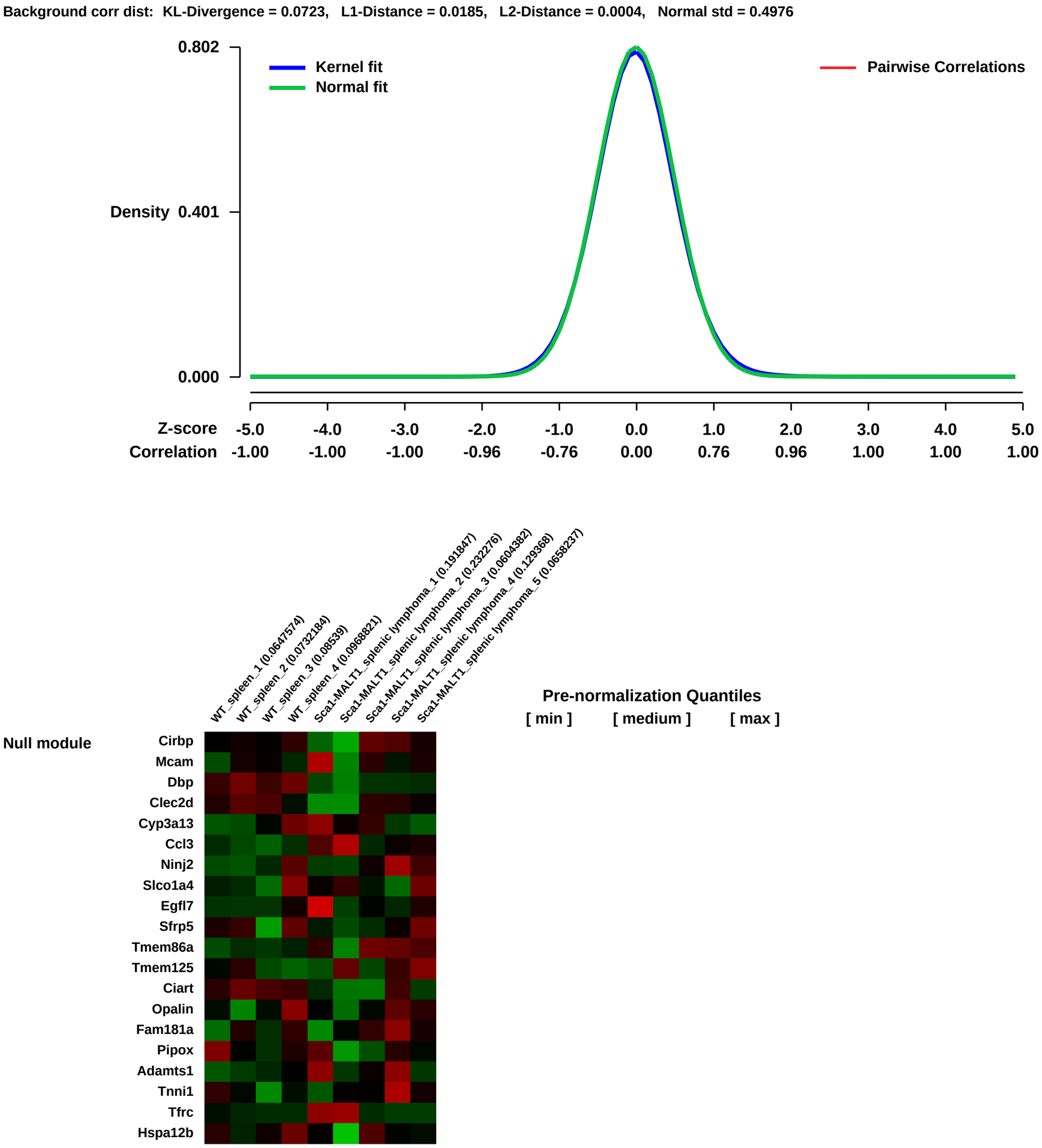

GEO Series "GSE42238" Expression Profiles

Num of samples in this series: 9

Scale of expression profile Z-scores

-3.0 -2.0 -1.0 0.0 1.0 2.0 3.0

GEO Link:	http://www.ncbi.nlm.nih.gov/geo/query/acc.cgi?acc=GSE42238
Status:	Public on Feb 19 2013
Title:	The C-terminus of CBFˆ -SMMHC is required to induce embryonic hematopoietic defects and leukemogenesis.
Organism:	Mus musculus
Experiment type:	Expression profiling by array
Platform:	GPL1261
Pubmed ID:	23152542
Summary & Design:	**Summary:** The C-terminus of CBFˆ -SMMHC, the fusion protein produced by a chromosome 16 inversion in acute myeloid leukemia subtype M4Eo, contains domains for self-mulimerization and transcriptional repression, both of which have been proposed to be important for leukemogenesis by CBFˆ -SMMHC. To test the role of the fusion protein's C-terminus in vivo, we generated knock-in mice expressing a C-terminally truncated CBFˆ -SMMHC (CBFˆ -SMMHC¸ C95). Embryos with a single copy of CBFˆ -SMMHCDC95 were viable and showed no defects in hematopoiesis, while embryos homozygous for the CBFˆ -SMMHC¸ C95 allele had hematopoietic defects and died in mid-gestation, similar to embryos with a single-copy of the full-length CBFˆ -SMMHC¸ C95. To identify gene expression changes induced by CBFˆ -SMMHCDC95, we compared the gene expression profile in the blood cells of Cbfb+/+, Cbfb+/¸ C95, and Cbfb¸ C95/¸ C95 embryonic day 12.5 (E12.5) mice. **Overall design:** Cbfb+/¸ C95 were mated together to generate Cbfb+/+, Cbfb+/¸ C95, and Cbfb¸ C95/¸ C95 embryos. Blood from 8-10 E12.5 embryos of the same genotype was pooled, and RNA was isolated, labeled, and hybridized to Affymetrix Genechip mouse microarray (430 2.0) chips. 3 chips were used for each genotype.

Background corr dist: KL-Divergence = 0.0484, L1-Distance = 0.0351, L2-Distance = 0.0021, Normal std = 0.5825

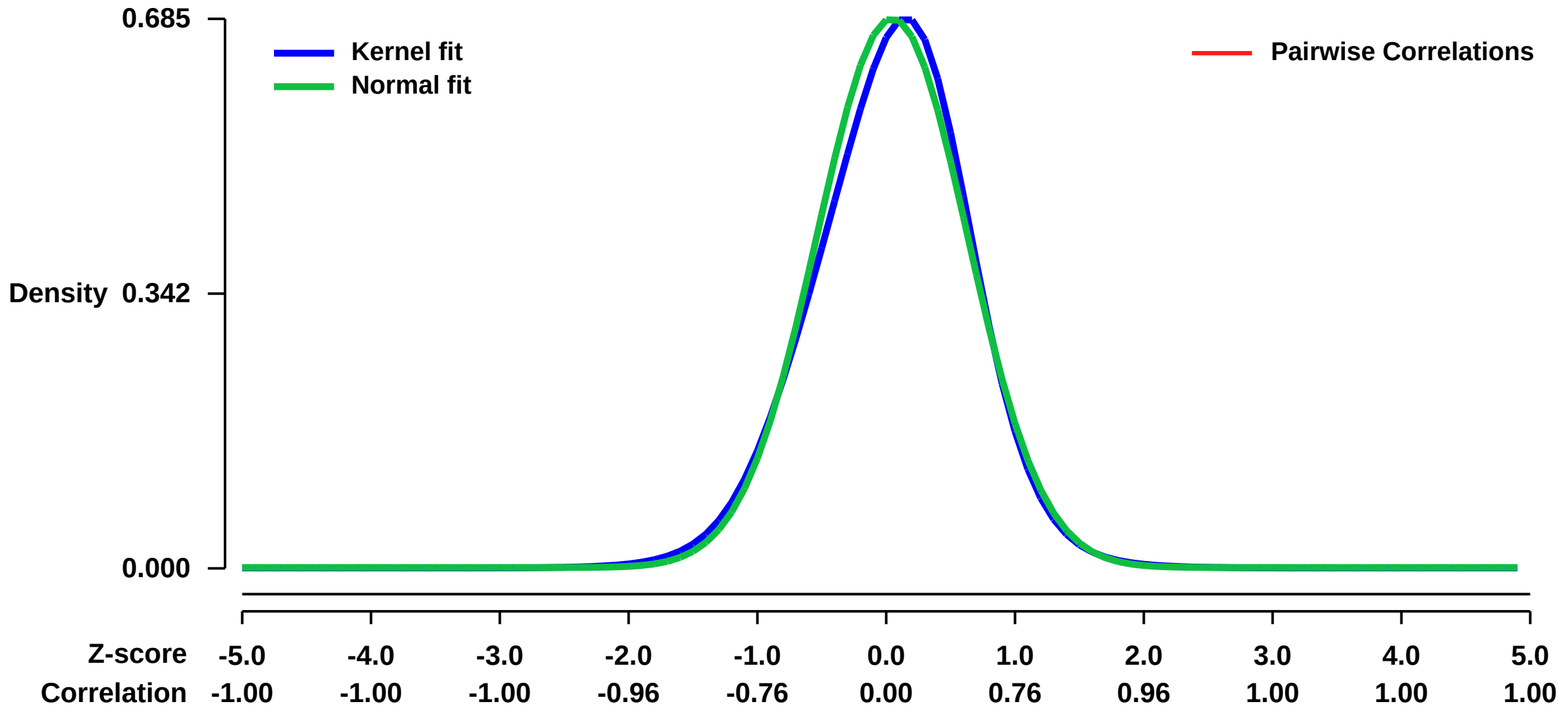

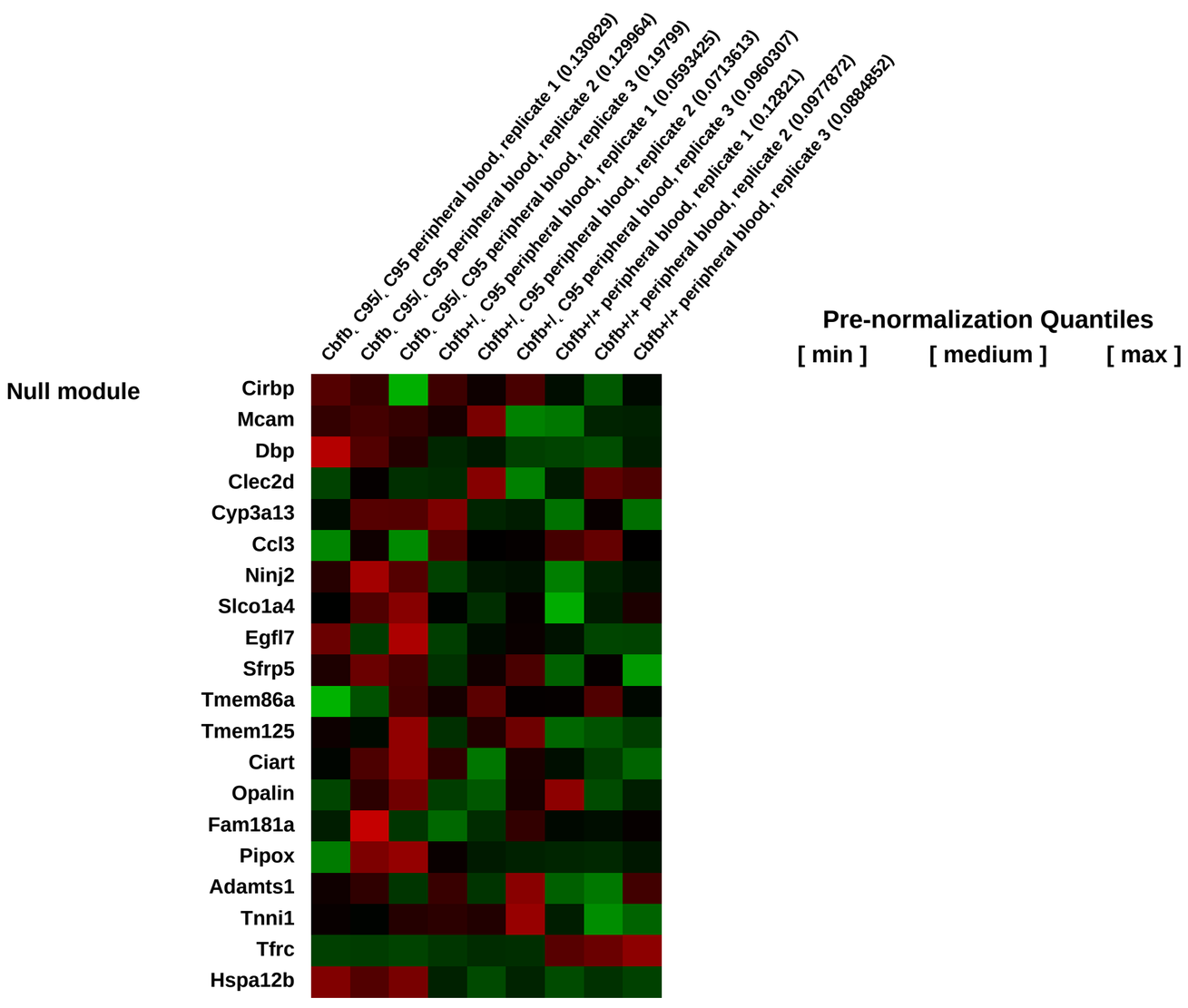

GEO Series "GSE33134" Expression Profiles

Num of samples in this series: 31

Scale of expression profile Z-scores

-3.0 -2.0 -1.0 0.0 1.0 2.0 3.0

GEO Link: http://www.ncbi.nlm.nih.gov/geo/query/acc.cgi?acc=GSE33134

Status: Public on Dec 31 2011

Title: Protective gene expression changes elicited by an inherited defect in photoreceptor structure.

Organism: Mus musculus

Experiment type: Expression profiling by array

Platform: GPL1261

Pubmed ID:

Summary & Design:

Summary:
To investigate pathogenic mechanisms in such instances, we have characterized rod photoreceptor and retinal gene expression changes in response to a defined insult to photoreceptor structure, using the retinal degeneration slow (rds) mouse model. Global gene expression profiling was performed on flow-sorted rds and wild-type rod photoreceptors immediately prior and subsequent to times at which OSs are normally elaborated. Dysregulated genes were identified via microarray hybridization, and selected candidates were validated using quantitative PCR analyses. We identified a single key gene, Egr1, that was dysregulated in a sustained fashion in rds rod photoreceptors and in the retina. Egr1 upregulation was associated with microglial activation and migration, into the outer retina at times subsequent to the major peak of photoreceptor cell death. Interestingly, this response was accompanied by neurotrophic factor upregulation. We hypothesize that activation of Egr1 and neurotrophic factors represents a protective immune mechanism, contributing to the characteristically slow retinal degeneration of the rds mouse model.

Overall design:
We had two conditions WT and Rds-KO at 4 different time points: postnatal (P) 6, P9, P14 and P21.

Background corr dist: KL-Divergence = 0.0735, L1-Distance = 0.0832, L2-Distance = 0.0128, Normal std = 0.6445

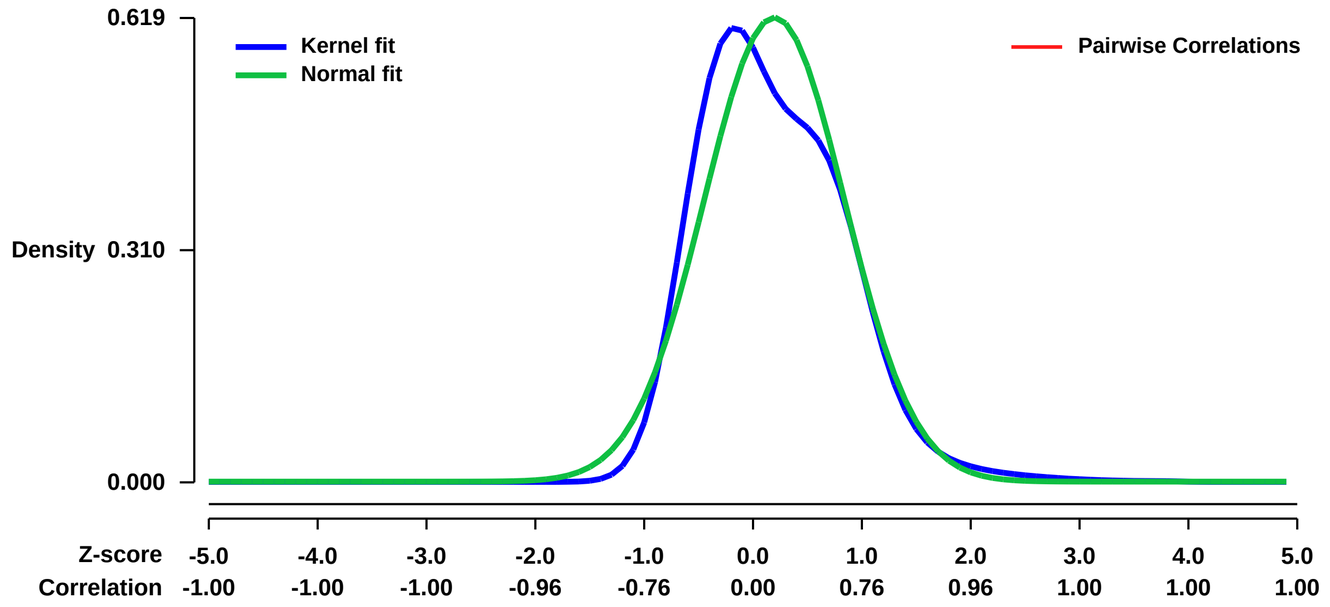

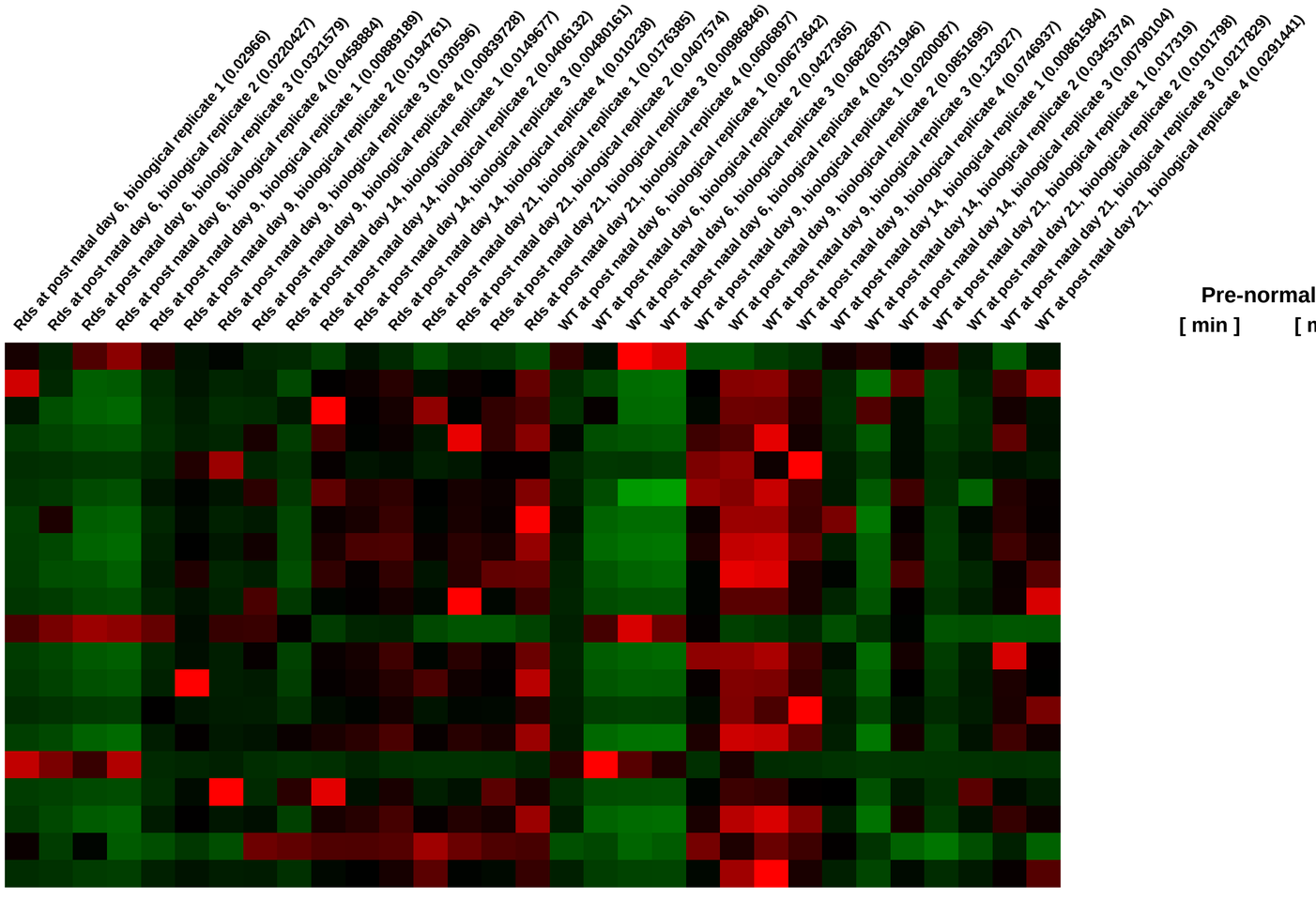

GEO Series "GSE32598" Expression Profiles

Num of samples in this series: 11

Scale of expression profile Z-scores

-3.0 -2.0 -1.0 0.0 1.0 2.0 3.0

GEO Link:	http://www.ncbi.nlm.nih.gov/geo/query/acc.cgi?acc=GSE32598
Status:	Public on Oct 05 2011
Title:	Highly efficient derivation of ventricular cardiomyocytes from induced pluripotent stem cells with a distinct epigenetic signature
Organism:	Mus musculus
Experiment type:	Expression profiling by array
Platform:	GPL1261
Pubmed ID:	22064699
Summary & Design:	**Summary:** The generation of sufficient numbers of mature ventricular myocytes for effective cell-based therapy is a central barrier for cardiac regenerative medicine. Here we demonstrate that induced pluripotent stem cells (iPSCs) can be derived from murine ventricular myocytes, and consistent with other reports of iPSCs derived from various somatic cell types, ventricular myocyte derived iPSCs (ViPSCs) exhibit a markedly higher propensity to differentiate into beating cardiomyocytes as compared to genetically-matched embryonic stem cells (ESCs) or iPSCs derived from tail-tip fibroblasts. Strikingly, ViPSC-derived cardiomyocytes form up to 99% ventricular myocytes suggesting that ventricular myocyte-derived iPSCs may be a viable strategy to generate specific cardiomyocyte subtypes for cell-based therapies. The enhanced ventricular myogenesis in ViPSCs is mediated via increased numbers of cardiovascular progenitors at early stages of differentiation. In order to investigate the mechanism of enhanced ventricular myogenesis from ViPSCs, we performed global gene expression and DNA methylation analysis, which revealed a distinct epigenetic signature that may be involved in specifying the ventricular myocyte fate in pluripotent stem cells. **Overall design:** Total RNA was extracted from mouse ES cells, tail tip fibroblasts (TTFs), ventricular myocytes (VMs), TTF-derived induced pluripotent stem cells (TiPSCs) and VM-derived induced pluripotent stem cells (ViPSCs). Global gene expression profiling was performed using affymetrix mouse 430 2.0 gene arrays.

Background corr dist: KL-Divergence = 0.0622, L1-Distance = 0.0594, L2-Distance = 0.0055, Normal std = 0.6305

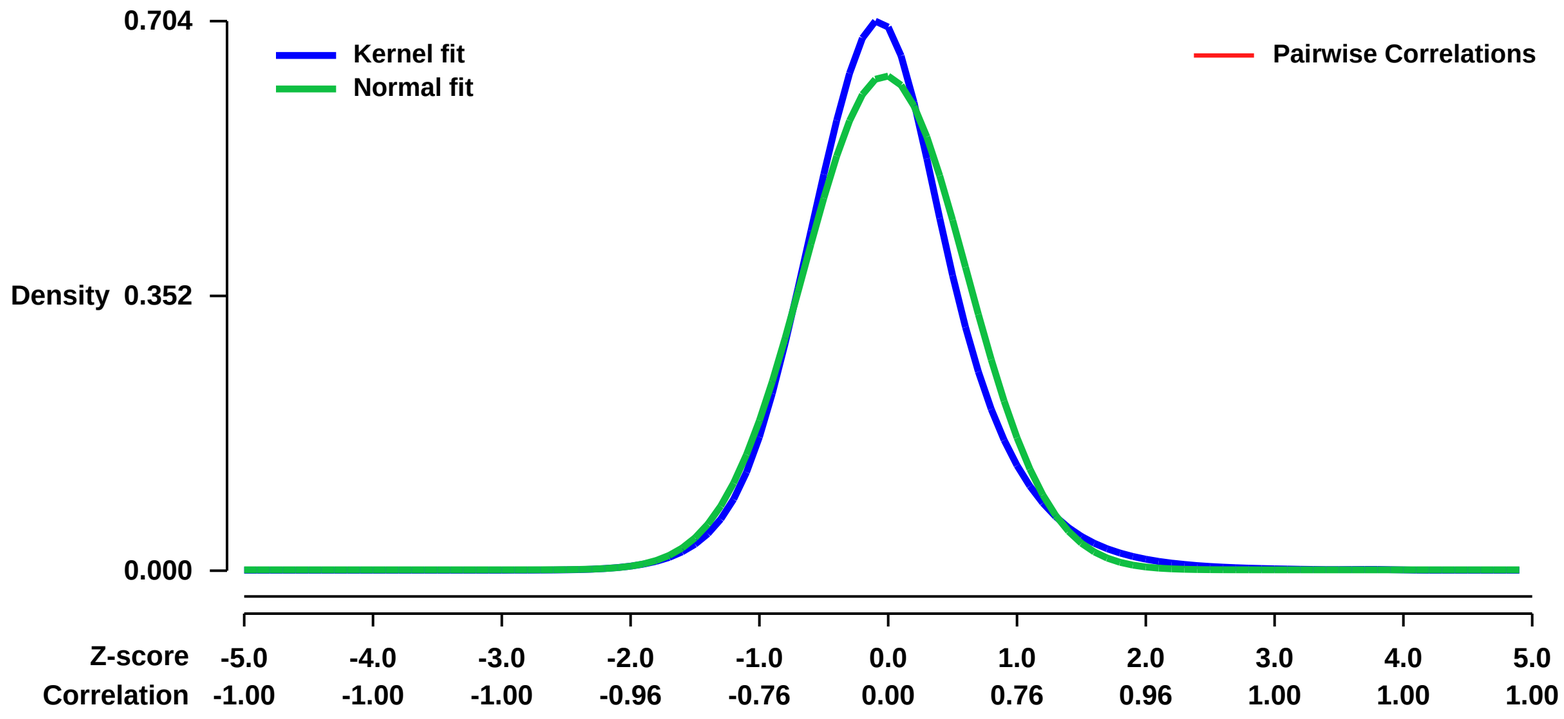

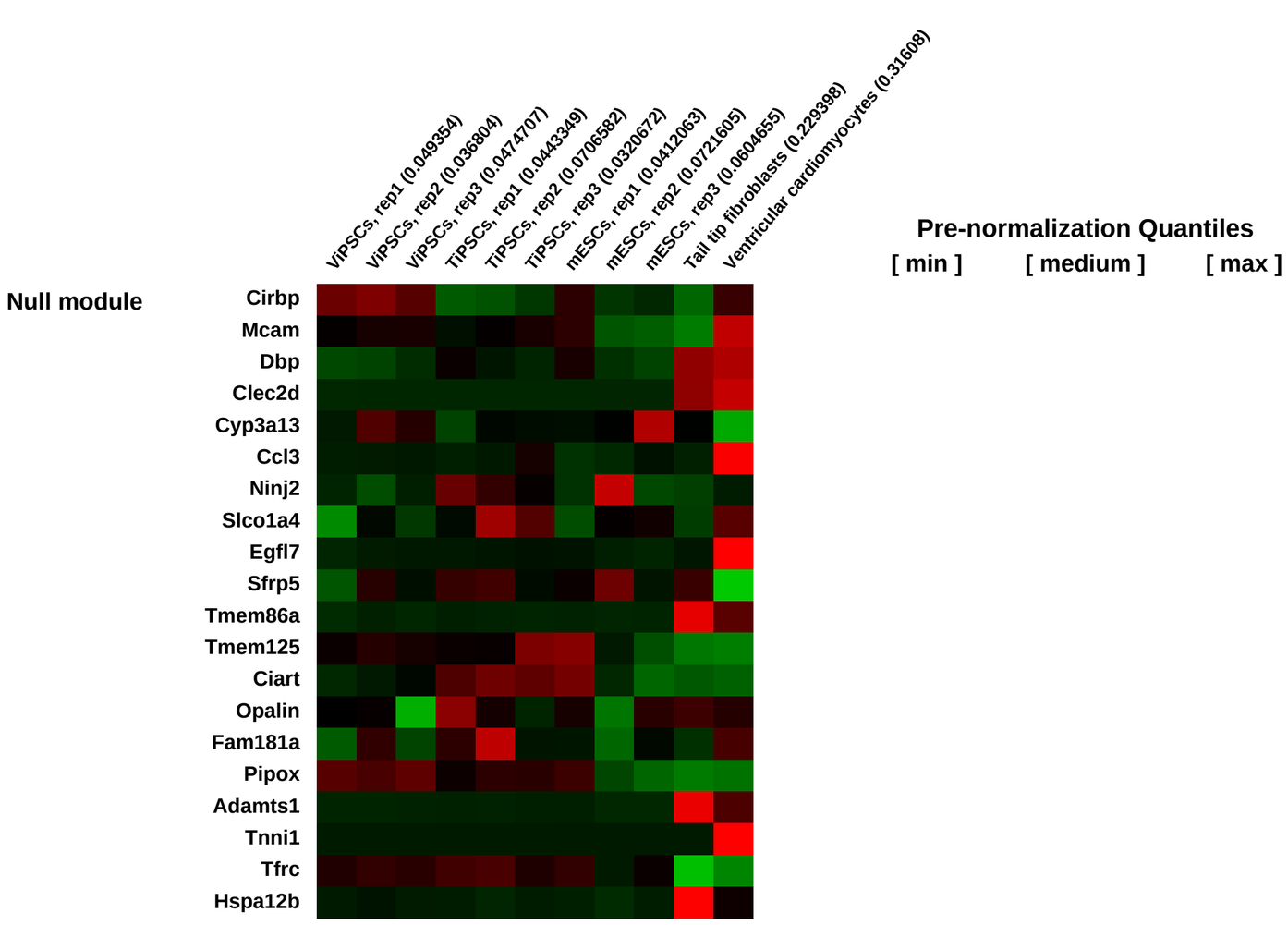

GEO Series "GSE21247" Expression Profiles

Num of samples in this series: 60

Scale of expression profile Z-scores

-3.0 -2.0 -1.0 0.0 1.0 2.0 3.0

GEO Link:	http://www.ncbi.nlm.nih.gov/geo/query/acc.cgi?acc=GSE21247
Status:	Public on Dec 22 2010
Title:	Network Analysis of Skin Tumor Progression Identifies a Rewired Genetic Architecture Affecting Inflammation and Tumor Susceptibility (carcinomas)
Organism:	Mus musculus
Experiment type:	Expression profiling by array
Platform:	GPL1261
Pubmed ID:	21244661
Summary & Design:	**Summary:** Germline polymorphisms influence gene expression networks in normal mammalian tissues. Analysis of this genetic architecture can identify single genes and whole pathways that influence to complex traits including inflammation and cancer susceptibility. Changes in the genetic architecture during the development of benign and malignant tumours have not been investigated. Here, we document major changes in germline control of gene expression during skin tumour development as a consequence of cell selection, somatic genetic events, and changes in tumour microenvironment. Immune response genes such as Interleukin 18 and Granzyme E are under germline control in tumours but not in normal skin. Gene expression networks linked to tumour susceptibility and hair follicle stem cell markers in normal skin undergo significant reorganization during tumour progression. Our data highlight opposing roles of Interleukin-1 signaling networks in tumour susceptibility and tumour progression and have implications for the development of chemopreventive strategies to reduce cancer incidence. **Overall design:** Skin tumors were induced on dorsal back skin from a Mus spretus / Mus musculus backcross ([SPRET/Ei X FVB/N] X FVB/N) mice by treatment of dorsal back skin with dimethyl benzanthracene (DMBA) and tetradecanoyl-phorbol acetate (TPA). This treatment induced multiple benign papillomas as well as malignant squamous cell carcinomas (SCC) and spindle cell carcinomas. 60 carcinomas were harvested from 55 mice; five mice provided two carcinomas each.

Background corr dist: KL-Divergence = 0.5541, L1-Distance = 0.0998, L2-Distance = 0.0338, Normal std = 0.2152

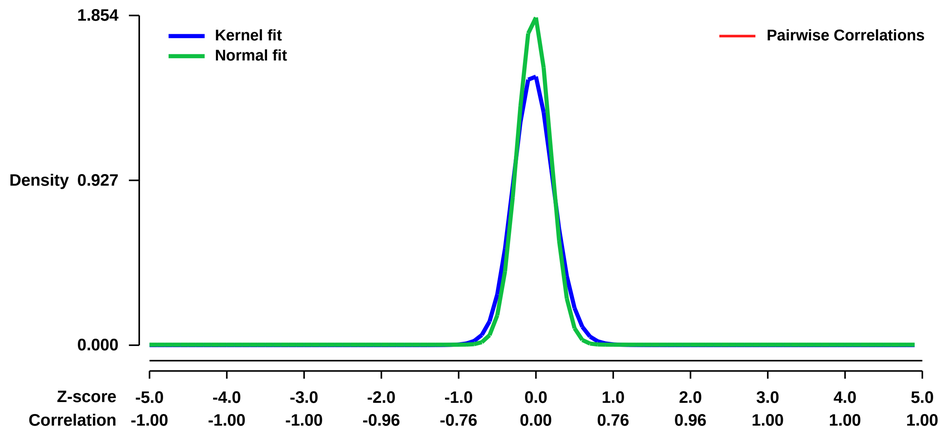

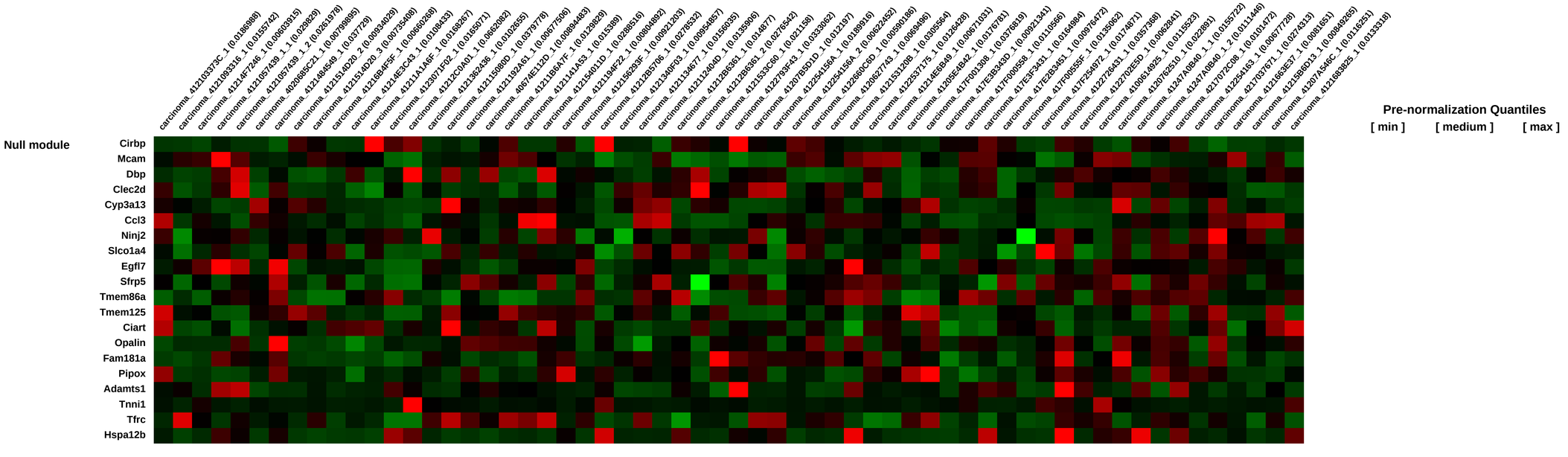

GEO Series "GSE6116" Expression Profiles

Num of samples in this series: 70

Scale of expression profile Z-scores

-3.0 -2.0 -1.0 0.0 1.0 2.0 3.0

GEO Link:	http://www.ncbi.nlm.nih.gov/geo/query/acc.cgi?acc=GSE6116
Status:	Public on Feb 14 2007
Title:	Transcriptional Biomarkers to Predict Female Mouse Lung Tumors in Rodent Cancer Bioassays - A 13 Chemical Training Set
Organism:	Mus musculus
Experiment type:	Expression profiling by array
Platform:	GPL1261
Pubmed ID:	17311802
Summary & Design:	**Summary:** The primary goal of toxicology and safety testing is to identify agents that have the potential to cause adverse effects in humans. Unfortunately, many of these tests have not changed significantly in the past 30 years and most are inefficient, costly, and rely heavily on the use of animals. The rodent cancer bioassay is one of these safety tests and was originally established as a screen to identify potential carcinogens that would be further analyzed in human epidemiological studies. Today, the rodent cancer bioassay has evolved into the primary means to determine the carcinogenic potential of a chemical and generate quantitative information on dose-response behavior in chemical risk assessments. Due to the resource-intensive nature of these studies, each bioassay costs $2 to $4 million and takes over three years to complete. Over the past 30 years, only 1,468 chemicals have been tested in a rodent cancer bioassay. By comparison, approximately 9,000 chemicals are used by industry in quantities greater than 10,000 lbs and nearly 90,000 chemicals have been inventoried by the U.S. Environmental Protection Agency as part of the Toxic Substances Control Act. Given the disparity between the number of chemicals tested in a rodent cancer bioassay and the number of chemicals used by industry, a more efficient and economical system of identifying chemical carcinogens needs to be developed. **Keywords: toxicology, chemical carcinogenesis, lung** **Overall design:** Five-week old female B6C3F1 mice were exposed for 13 weeks in the following dose groups: 1) 1,5-Naphthalenediamine, CAS No. 2243-62-1, feed, 2000 ppm, positive lung carcinogen; 2) 2,3-Benzofuran, CAS No. 271-89-6, gavage, 240 mg/kg, positive lung carcinogen; 3) 2,2-Bis(bromomethyl)-1,3-propanediol, CAS No. 3296-90-0, feed, 1250 ppm, positive lung carcinogen; 4) N-Methylolacrylamide, CAS No. 924-42-5, gavage (water), 50 mg/kg, positive lung carcinogen; 5) 1,2-Dibromoethane, CAS No. 106-93-4, gavage (corn oil), 62 mg/kg, positive lung carcinogen; 6) Coumarin, CAS No. 91-64-5, gavage (corn oil), 200 mg/kg, positive lung carcinogen; 7) Benzene, CAS No. 71-43-2, gavage (corn oil), 100 mg/kg, positive lung carcinogen; 8) N-(1-naphthyl)ethylenediamine dihydrochloride, CAS No. 1465-25-4, feed, 2000 ppm, negative lung carcinogen; 9) Pentachloronitrobenzene, CAS No. 82-68-8, feed, 8187 ppm, negative lung carcinogen; 10) 4-Nitroanthranilic acid, CAS No. 619-17-0, feed, 10000 ppm, negative lung carcinogen; 11) 2-Chloromethylpyridine hydrochloride, CAS No. 6959-47-3, gavage (water), 250 mg/kg, negative lung carcinogen; 12) Diazinon, CAS No. 333-41-5, feed, 200 ppm, negative lung carcinogen; 13) Malathion, CAS No. 121-75-5, feed, 16000 ppm, negative lung carcinogen; 14) Corn oil control, gavage; 15) Water control, gavage; 16) Rodent diet control, feed. Feed animals were exposed 7 days/week and gavage animals were exposed 5 days/week (5 ml/kg). After 13 weeks, animals were euthanized and lungs were collected. The right lobe was used for microarray analysis. Microarray analysis was performed on the lungs of three to four mice per treatment group.

Background corr dist: KL-Divergence = 0.0952, L1-Distance = 0.0327, L2-Distance = 0.0020, Normal std = 0.4508

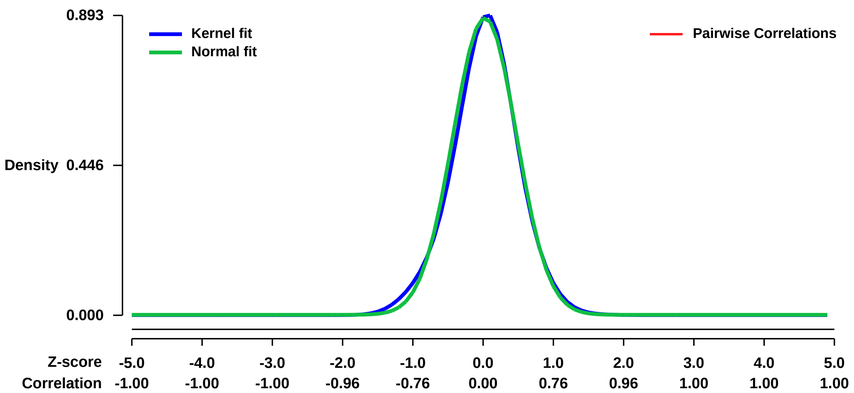

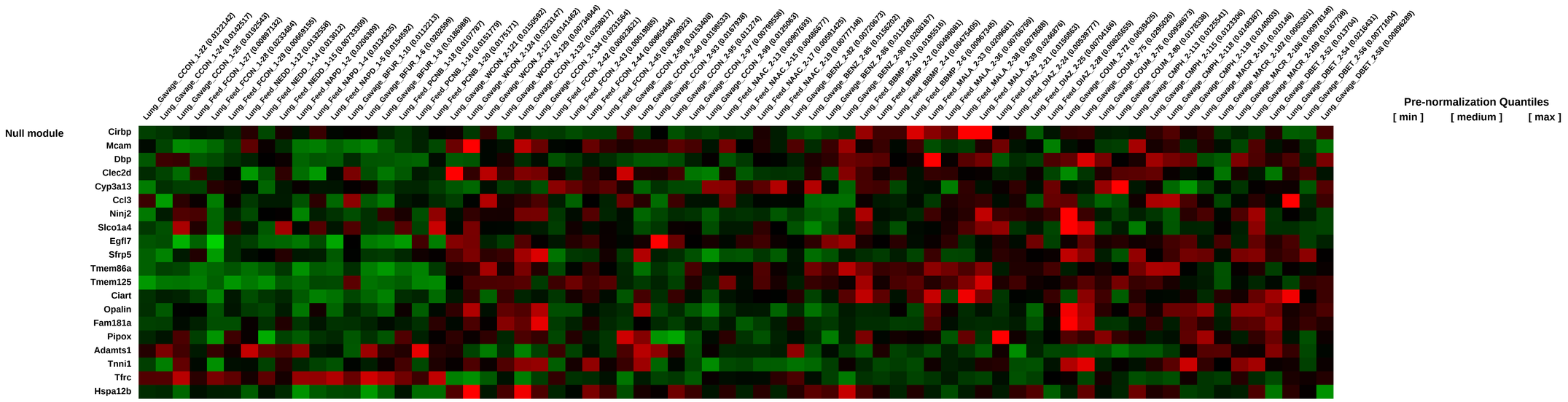

GEO Series "GSE3621" Expression Profiles

Num of samples in this series: 18

Scale of expression profile Z-scores

-3.0 -2.0 -1.0 0.0 1.0 2.0 3.0

GEO Link:	http://www.ncbi.nlm.nih.gov/geo/query/acc.cgi?acc=GSE3621
Status:	Public on Jul 31 2007
Title:	R6/1 brain hemisphere time series gene expression
Organism:	Mus musculus
Experiment type:	Expression profiling by array
Platform:	GPL1261
Pubmed ID:	17696994
Summary & Design:	**Summary:** HD R6/1 transgenic mouse line brain hemispheres dissected. RNA targets were created for transgenics and wildtypes at time points 18, 22 and 27 weeks. Profiles and data analysis performed using the Bioconductor software and linear model contrasts using LIMMA on RMA probeset summarys. **Keywords: timecourse** **Overall design:** 18 samples extracted, 3 transgenic plus 3 littermate controls analysed at each timepoint.

Background corr dist: KL-Divergence = 0.2701, L1-Distance = 0.0575, L2-Distance = 0.0085, Normal std = 0.2927

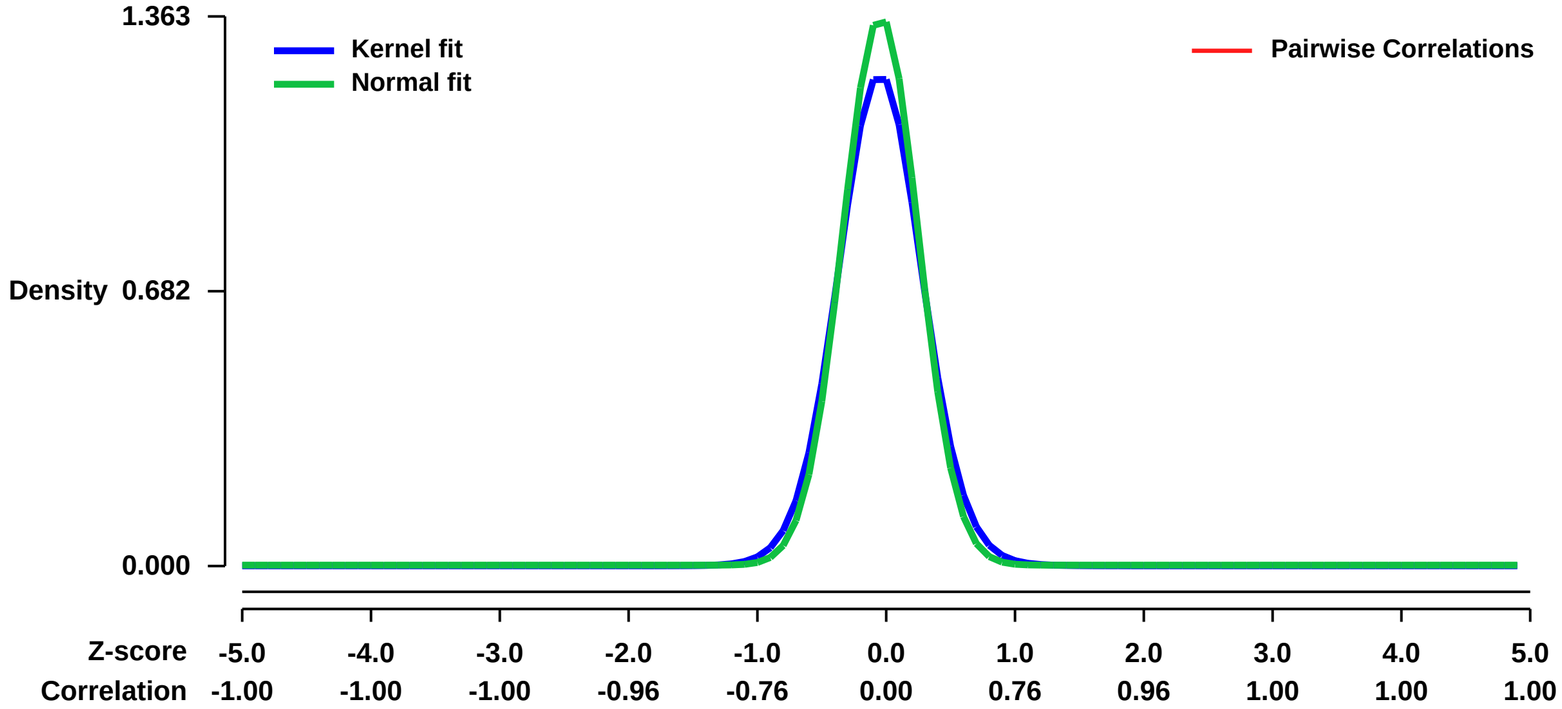

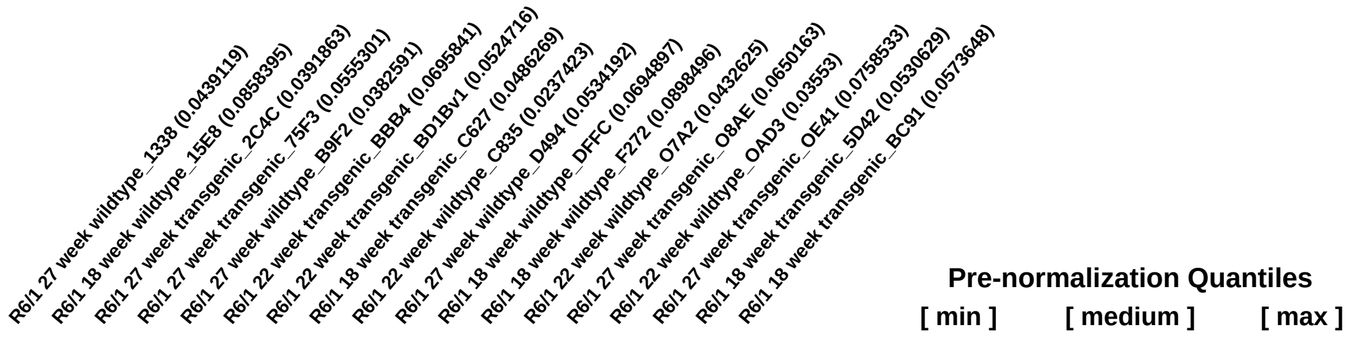

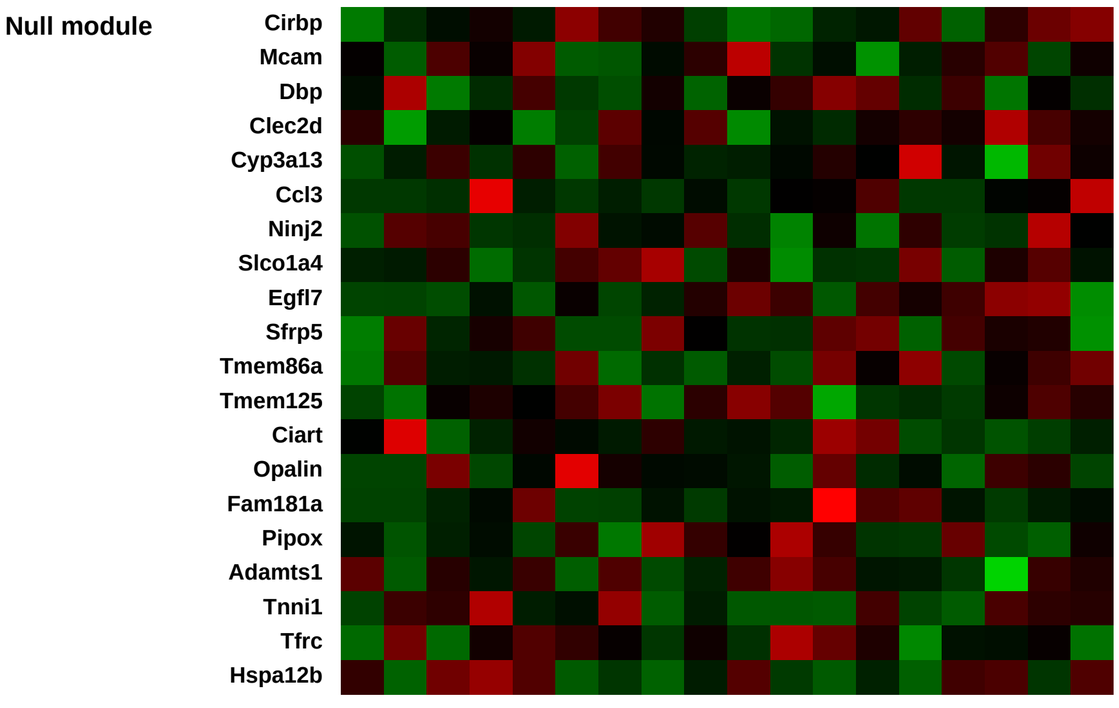

GEO Series "GSE5245" Expression Profiles

Num of samples in this series: 16

Scale of expression profile Z-scores

-3.0 -2.0 -1.0 0.0 1.0 2.0 3.0

GEO Link:	http://www.ncbi.nlm.nih.gov/geo/query/acc.cgi?acc=GSE5245
Status:	Public on Apr 03 2008
Title:	Profiling of CD4+ T cells responding to transient or persistent antigen presented by dendritic cells in vivo
Organism:	Mus musculus
Experiment type:	Expression profiling by array
Platform:	GPL1261
Pubmed ID:	17881563
Summary & Design:	**Summary:** These experiments were done to compare the gene expression profiles in CD4+ T cells responding to antigen presented by dendritic cells transiently or persistently. Some treatments include the activation of the dendritic cells by CD40 engagement. **Keywords: immune response** **Overall design:** 2-4x106 lymph node cells from AND TCR-transgenic animals that expressed the congenic marker CD90.1 were transferred into double-transgenic (Ii-rTA/TIM) recipient animals that expressed the corresponding peptide from moth cytochrome c under a doxycycline-controllable promoter and were FACS-sorted 60 hours later. Recipients expressed the antigen not at all (â ctrlâ), transiently (â shortâ) or throughout the experiment (â longâ) due to different doxycycline treatment protocols. A second variable tested was the activation status of the dendritic cells: recipients were either injected by the stimulatory antibody FGK45.5 targeting CD40 (â FGKâ) or PBS (â PBSâ).

Background corr dist: KL-Divergence = 0.0477, L1-Distance = 0.0650, L2-Distance = 0.0079, Normal std = 0.5996

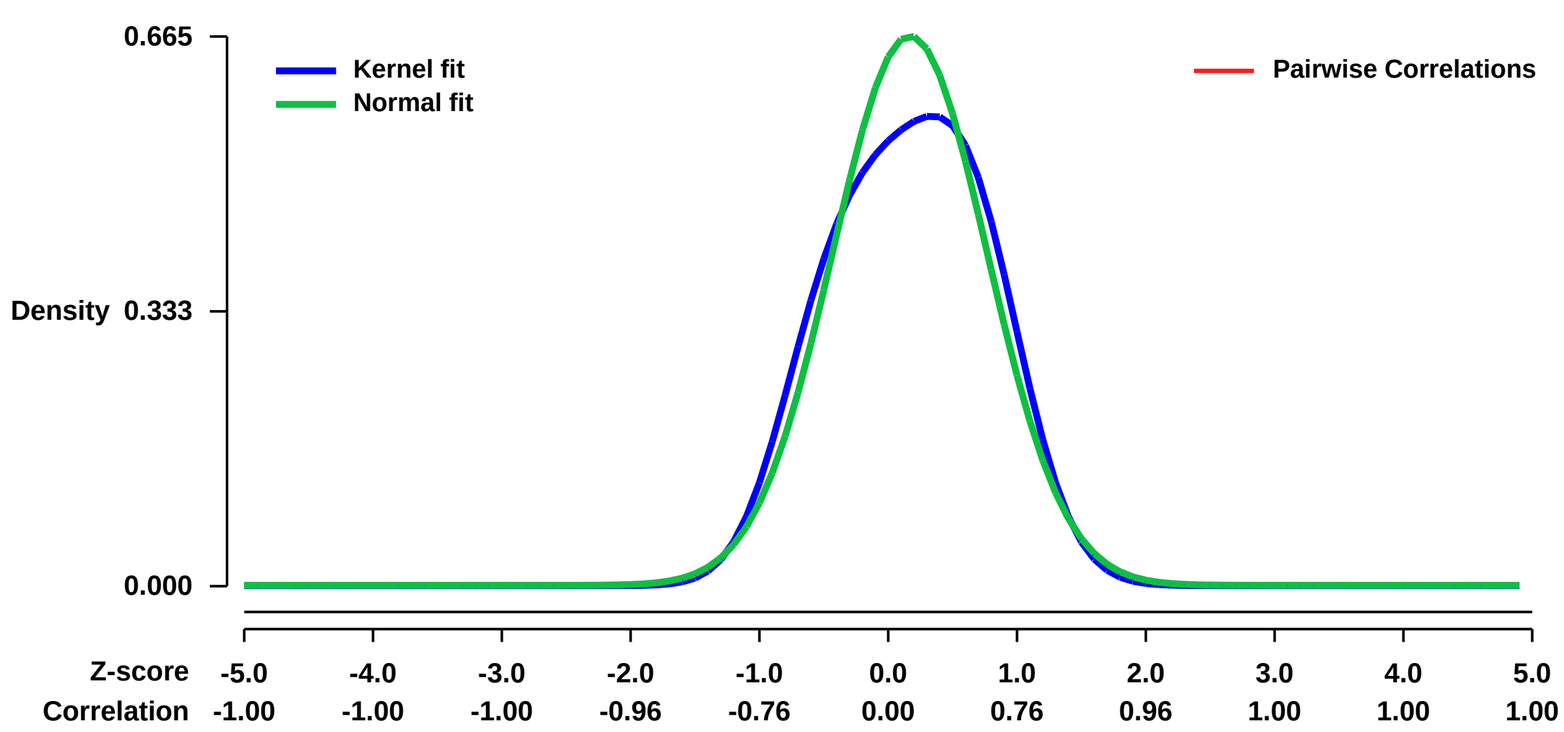

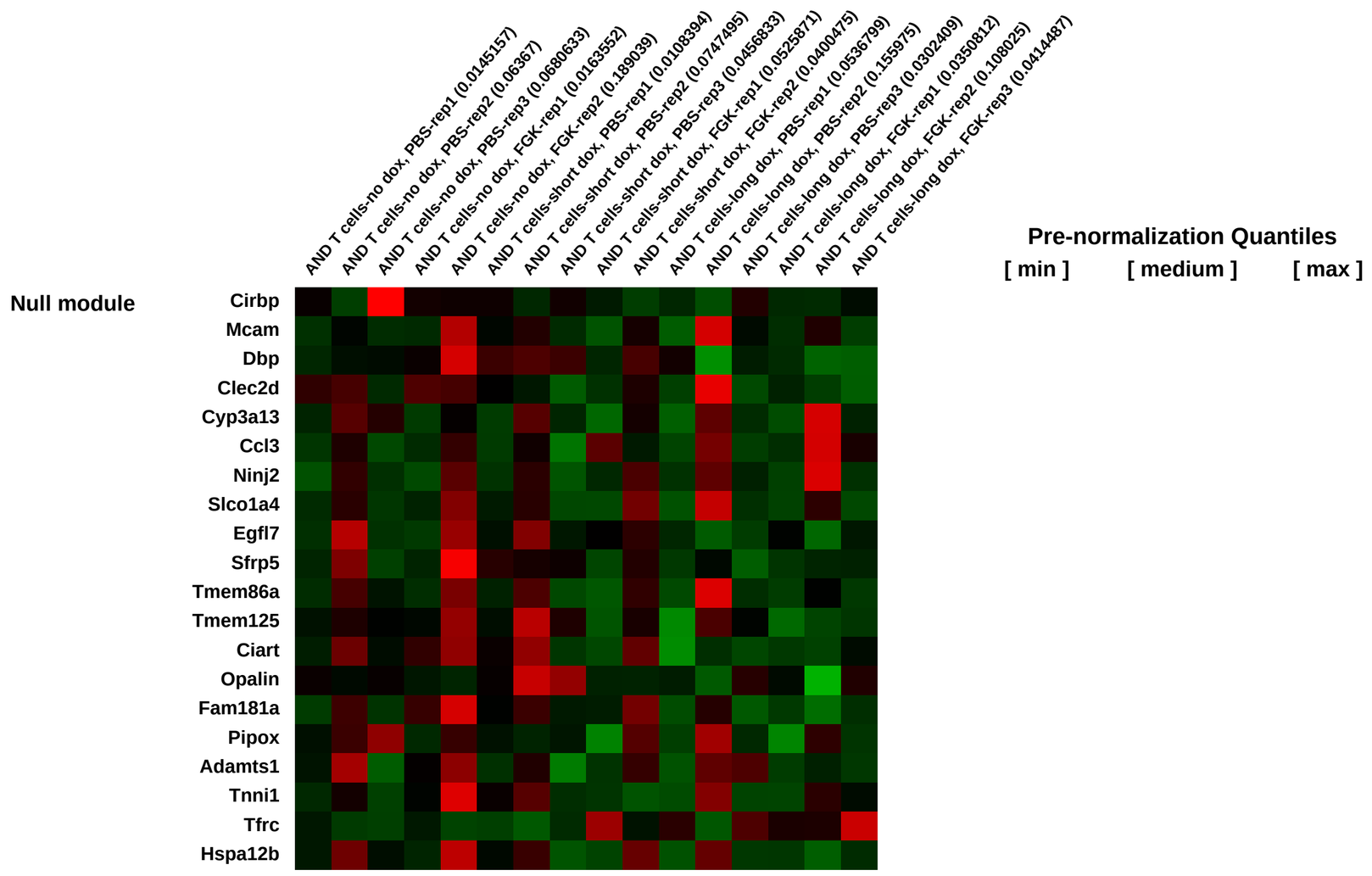

GEO Series "GSE49689" Expression Profiles

Num of samples in this series: 23

Scale of expression profile Z-scores

-3.0 -2.0 -1.0 0.0 1.0 2.0 3.0

GEO Link:	http://www.ncbi.nlm.nih.gov/geo/query/acc.cgi?acc=GSE49689
Status:	Public on Dec 11 2013
Title:	A Mesodermal Factor, T (BRACHYURY), specifies mouse germ cell fate by directly activating germline determinants.
Organism:	Mus musculus
Experiment type:	Expression profiling by array
Platform:	GPL1261
Pubmed ID:	24331926
Summary & Design:	**Summary:** The germ cell lineage ensures reproduction and heredity in metazoans. Primordial germ cells (PGCs) in mice are induced in pluripotent epiblast cells by BMP4 and WNT3, yet their mechanism of action remains elusive. Here, using in vitro PGC specification system, we show that WNT3, but not BMP4, induces many transcription factors associated with mesoderm in epiblast-like cells (EpiLCs) through beta-CATENIN. Among these, T (BRACHYURY), a classical and conserved mesodermal factor, was essential for robust activation of Blimp1 and Prdm14, two of the germline determinants. T, but not SMAD1 or beta-CATENIN/TCF1, binds distinct regulatory elements of both Blimp1 and Prdm14, and directly up-regulates these genes without BMP4 and WNT3. Without BMP4, a program induced by WNT3 prevents T from activating Blimp1 and Prdm14, demonstrating that BMP4 is permissive for PGC specification. These findings establish a fundamental role of a mesodermal gene in PGC specification, a potentially evolutionarily conserved mechanism across metazoans. **Overall design:** Wnt3 (+/+) and Wnt3 (-/-) mouse embryonic stem cells (mESCs) bearing the BV transgenes expressing membrane-targeted Venus under the control of Blimp1 regulatory elements (Blimp1-mVenus: BV; PMID 18583473) were established and maintained. Epiblast-like cells (EpiLCs) were then induced from the established ES lines, followed by the cytokine stimulation (No cytokines [negative control], BMP4, Wnt3a, BMP4+Wnt3a) for different periods (0h, 12h, 24h, 36h).

Background corr dist: KL-Divergence = 0.2220, L1-Distance = 0.0407, L2-Distance = 0.0033, Normal std = 0.3199

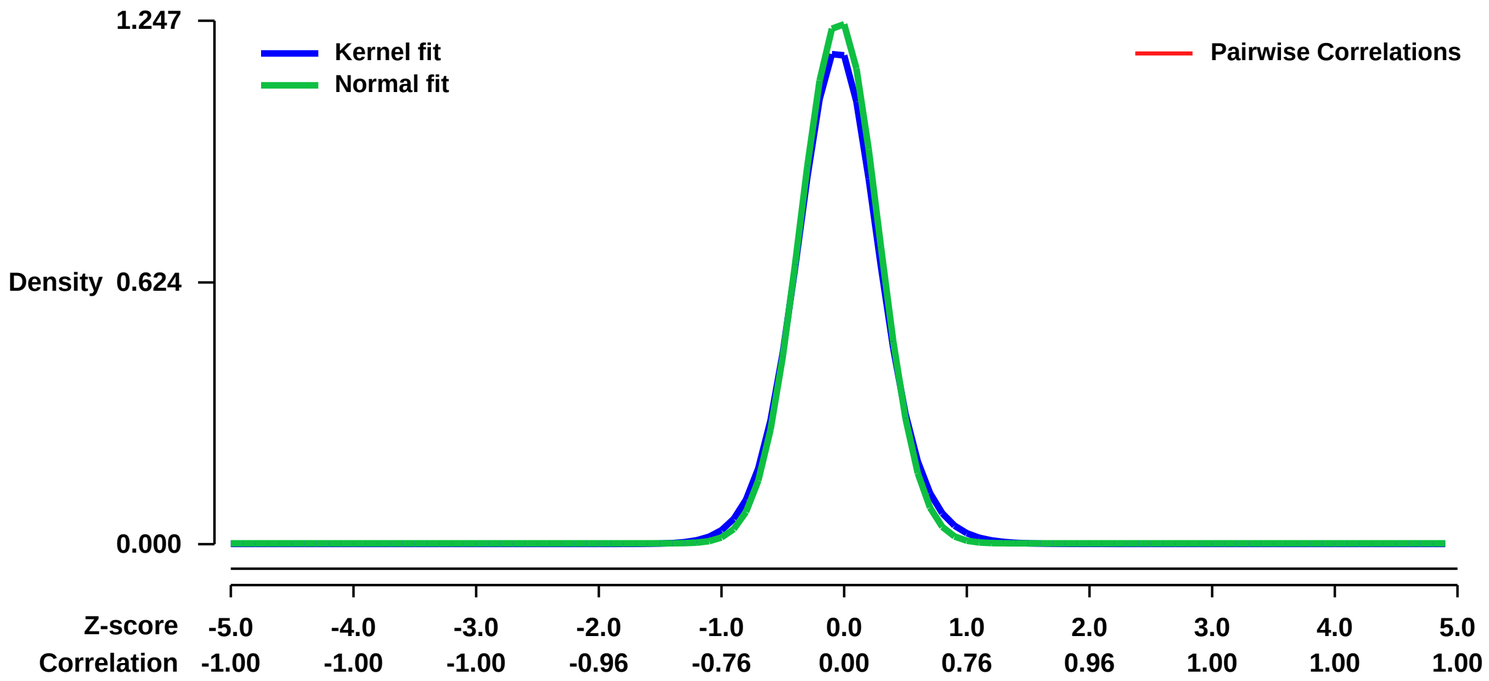

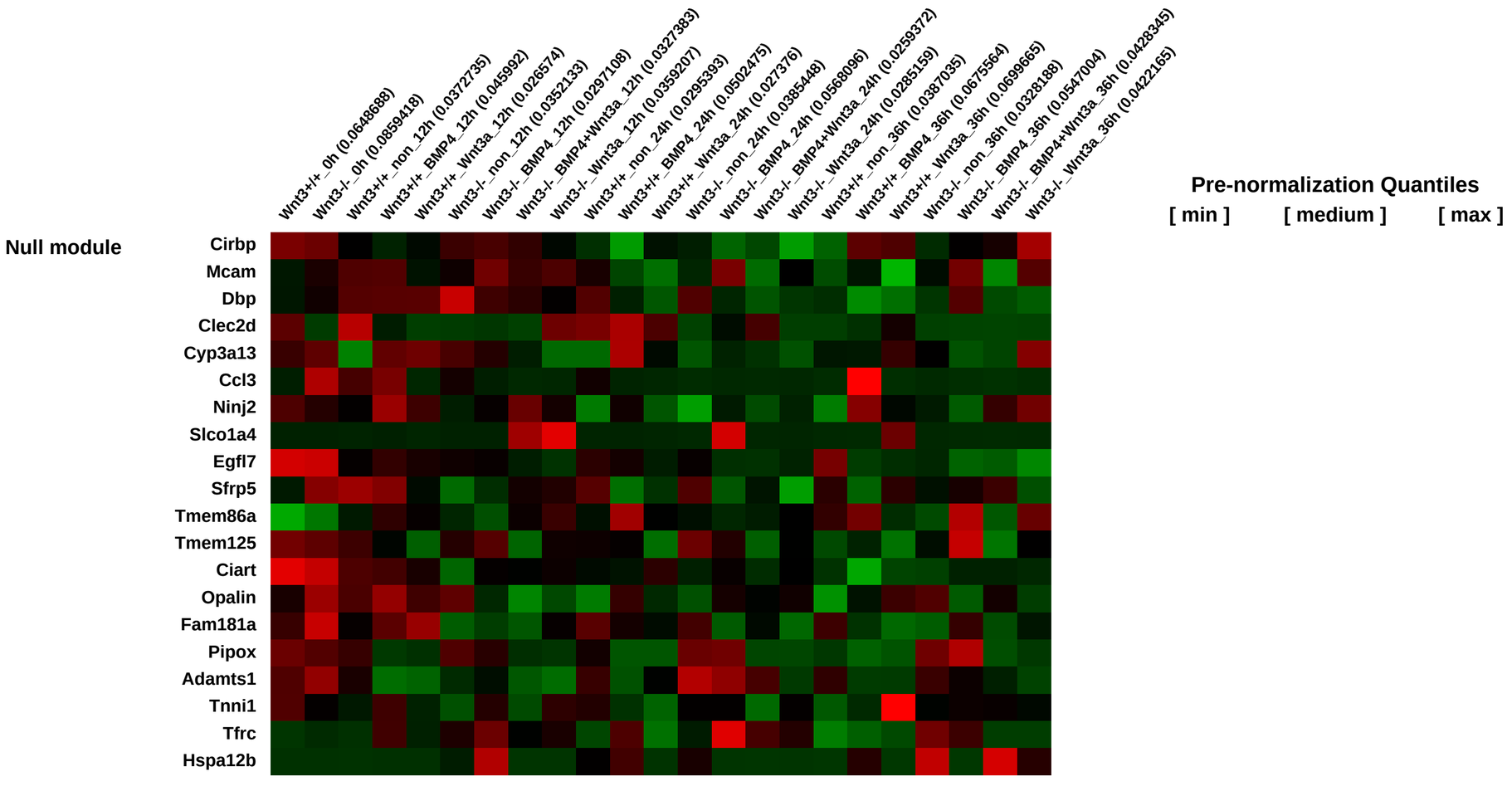

GEO Series "GSE12388" Expression Profiles

Num of samples in this series: 8

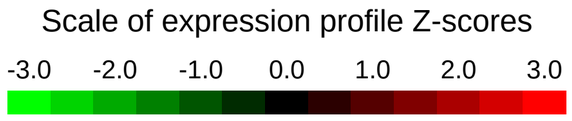

GEO Link:	**http://www.ncbi.nlm.nih.gov/geo/query/acc.cgi?acc=GSE12388**
Status:	**Public on Aug 08 2008**
Title:	**Deletional Tolerance Mediated by Extrathymic Aire-Expressing Cells**
Organism:	**Mus musculus**
Experiment type:	**Expression profiling by array**
Platform:	**GPL1261**
Pubmed ID:	**18687966**
Summary & Design:	**Summary:** **The prevention of autoimmunity requires elimination of self-reactive T cells during their development and maturation. Expression of diverse self-antigens by stromal cells in the thymus is essential to this process, and depends, in part, on the activity of the Autoimmune Regulator (Aire) gene. Here we report the identification of extrathymic Aire-expressing cells (eTACs) resident within the secondary lymphoid organs. These stromally-derived eTACs express a diverse array of unique self-antigens and are capable of interacting with and deleting naive autoreactive T cells. Using two-photon microscopy we observe stable, antigen-specific interactions between eTACs and autoreactive T cells. We propose that such a secondary network of self-antigen-expressing stromal cells may help reinforce immune tolerance by preventing the maturation of autoreactive T cells that escape thymic negative selection.** **A genetic modification design type is where an organism(s) has had genetic material removed, rearranged, mutagenized or added, such as knock out.** **Keywords: genetic_modification_design** **Overall design:** **8 samples**

Background corr dist: KL-Divergence = 0.0859, L1-Distance = 0.0309, L2-Distance = 0.0018, Normal std = 0.4689

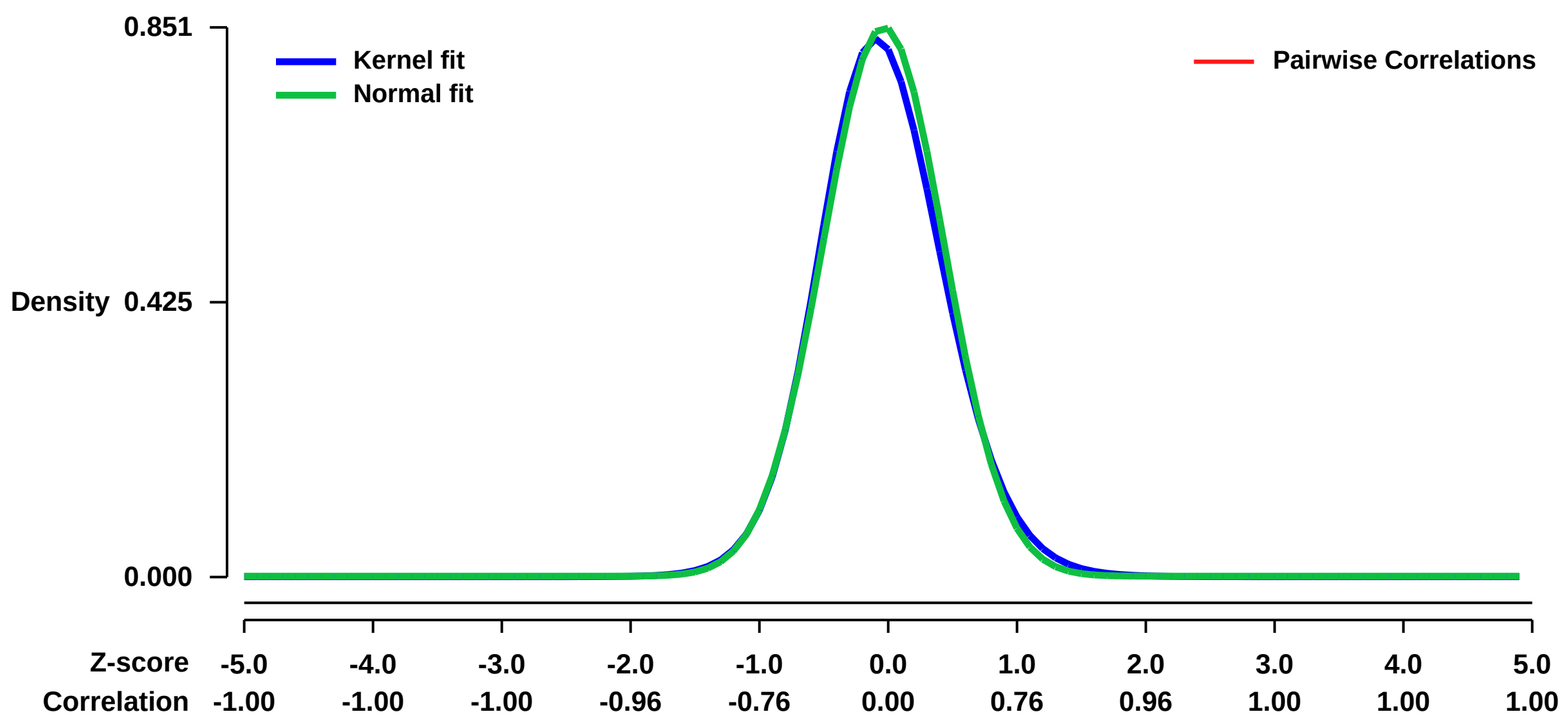

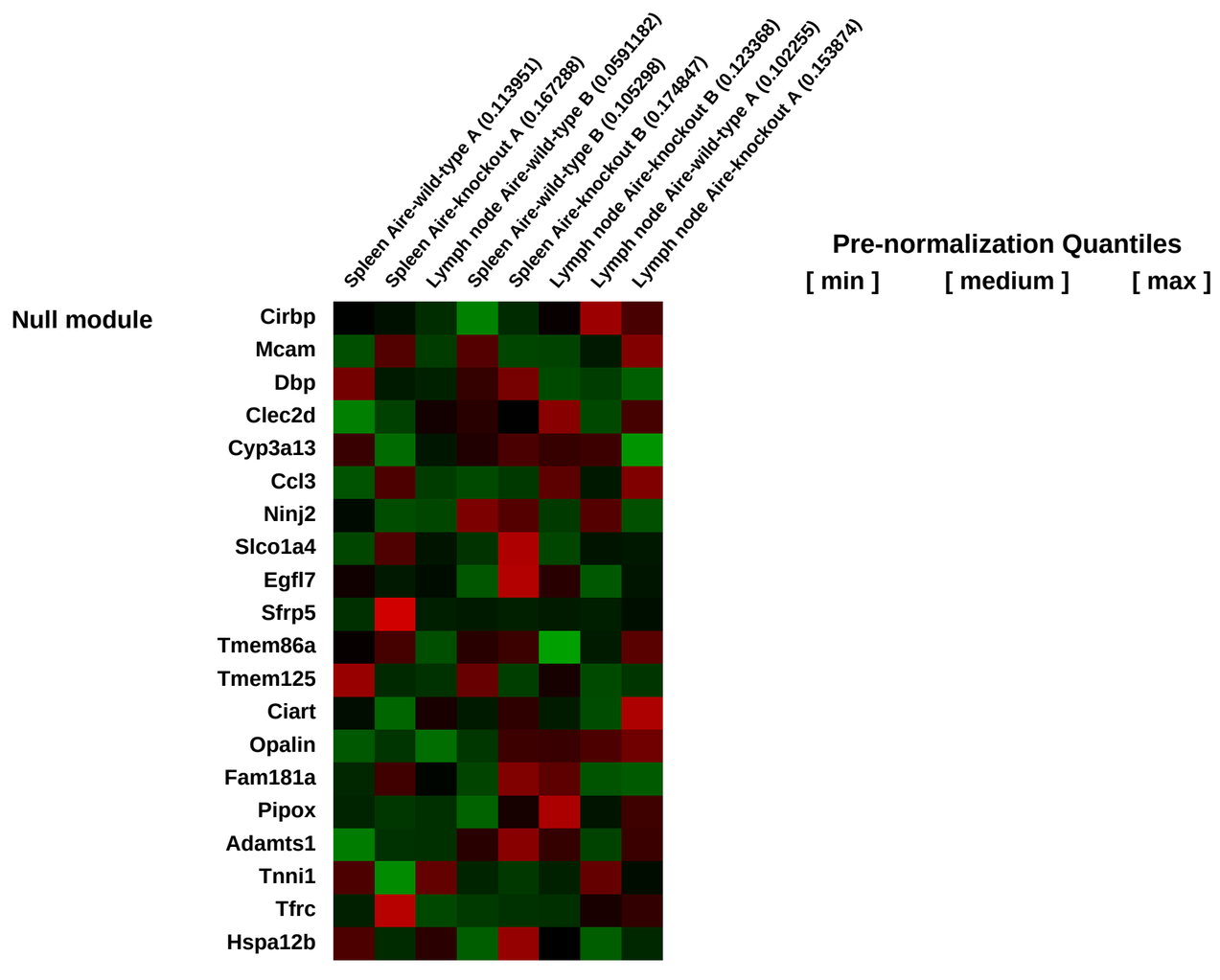

GEO Series "GSE25295" Expression Profiles

Num of samples in this series: 25

Scale of expression profile Z-scores

-3.0 -2.0 -1.0 0.0 1.0 2.0 3.0

GEO Link: http://www.ncbi.nlm.nih.gov/geo/query/acc.cgi?acc=GSE25295

Status: Public on Nov 17 2010

Title: Critical Role of Sphingolipid Pathway Components in Murine Radiation-Induced Lung Injury: Protection by Sphingosine-1-Phosphate Analogues

Organism: Mus musculus

Experiment type: Expression profiling by array

Platform: GPL1261

Pubmed ID: 21712494

Summary & Design:

Summary:
Clinically significant radiation-induced lung injury (RILI) is associated with significant morbidity and mortality and a common toxicity in patients administered thoracic radiotherapy. While the molecular etiology of RILI is poorly understood, we previously characterized a murine model of RILI in which alterations in lung endothelial barrier integrity surfaced as a potentially important pathobiologic event. In these studies, inhibition of HMG-CoA reductase activity (simvastatin) reduced murine RILI-associated lung inflammation and vascular leak and attenuated radiation-induced dysregulation of sphingolipid metabolic pathway genes identified by genome-wide lung gene expression profiling. In the present study, we test the hypothesis that sphingolipid signaling components serve as important modulators of RILI pathobiology and novel therapeutic targets. Sphingolipid involvement in murine RILI was confirmed by radiation-induced increases in lung expression of sphingosine kinase (SphK) isoforms 1 and 2 and increases in the ratio of ceramide to cumulative sphingosine-1-phosphate (S1P) and dihydro-S1P (DHS1P) levels in plasma, bronchoalveolar lavage (BAL) fluid and lung tissue following 25 Gy exposure (6 weeks). Moreover, genetically-engineered mice with either targeted deletion of SphK1 (SphK1-/-), or with reduced expression of selective members of the S1P receptor family (S1PR1+/-, S1PR2-/-, S1PR3-/-,), exhibited marked susceptibility to RILI-mediated lung inflammation. Finally, we assessed the efficacy of three potent vascular barrier-protective S1P analogues FTY720 (FTY), fTysiponate (fTyS) and SEW-2871 (SEW) in attenuating indices of RILI. The phosphonate analogue, fTyS, and to a lesser degree SEW, exhibited significant attenuation of RILI and RILI-induced gene dysregulation compared to control RILI-challenged mice (6 weeks). In contrast, FTY failed to significantly alter physiologic or genomic changes compared to RILI-challenged controls. Together, these results support the targeting of sphingolipid components as a novel and effective therapeutic strategy in RILI.

Overall design:
Four mice were treated with PBS as a control. Three mice were treated with (S)-FTY-phosphonate (0.1mg/kg) as a drug control. Three mice were treated with SEW-2871 (0.1mg/kg) as a drug control. Three mice were treated with FTY720 (0.1mg/kg) as a drug control. Three mice were treated with administered radiation (25 Gy) alone. Three mice were treated with both administered radiation (25 Gy) and (S)-FTY-phosphonate (0.1mg/kg). Three mice were treated with both administered radiation (25 Gy) and SEW-2871 (0.1mg/kg). Three mice were treated with both administered radiation (25 Gy) and FTY720 (0.1mg/kg).

Background corr dist: KL-Divergence = 0.2603, L1-Distance = 0.0508, L2-Distance = 0.0060, Normal std = 0.2985

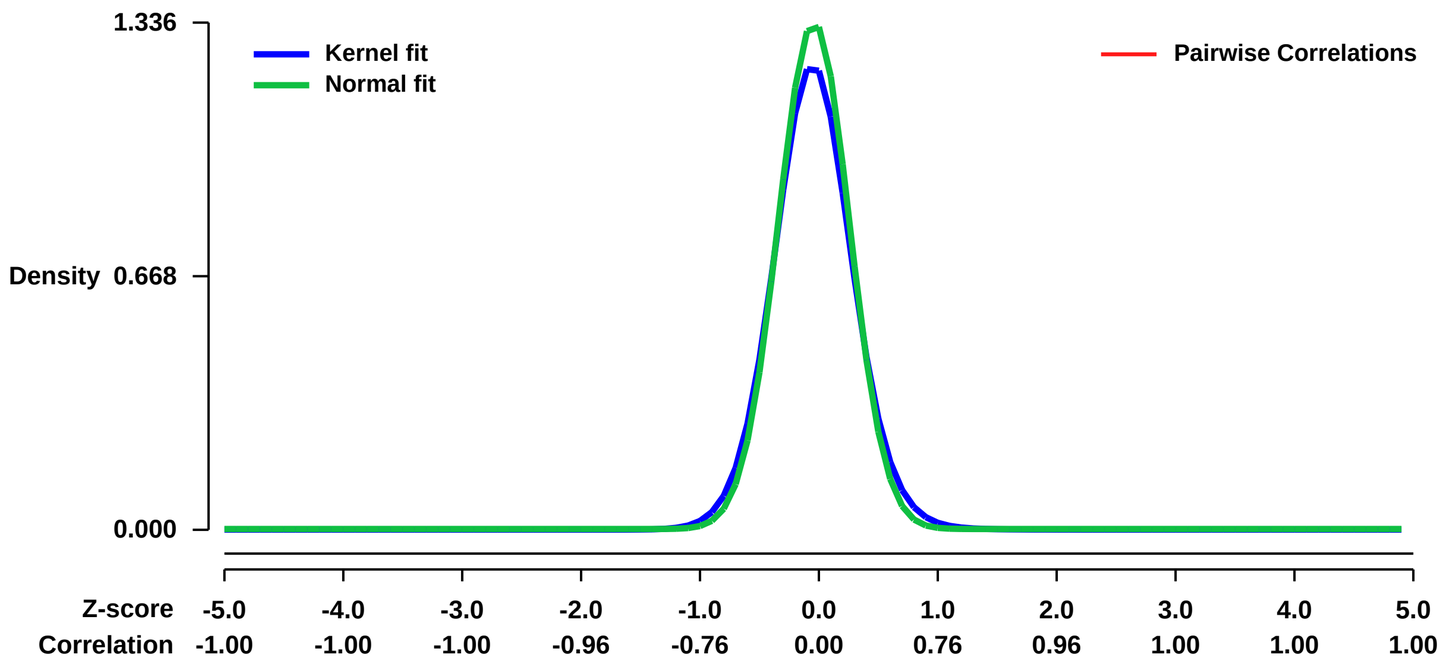

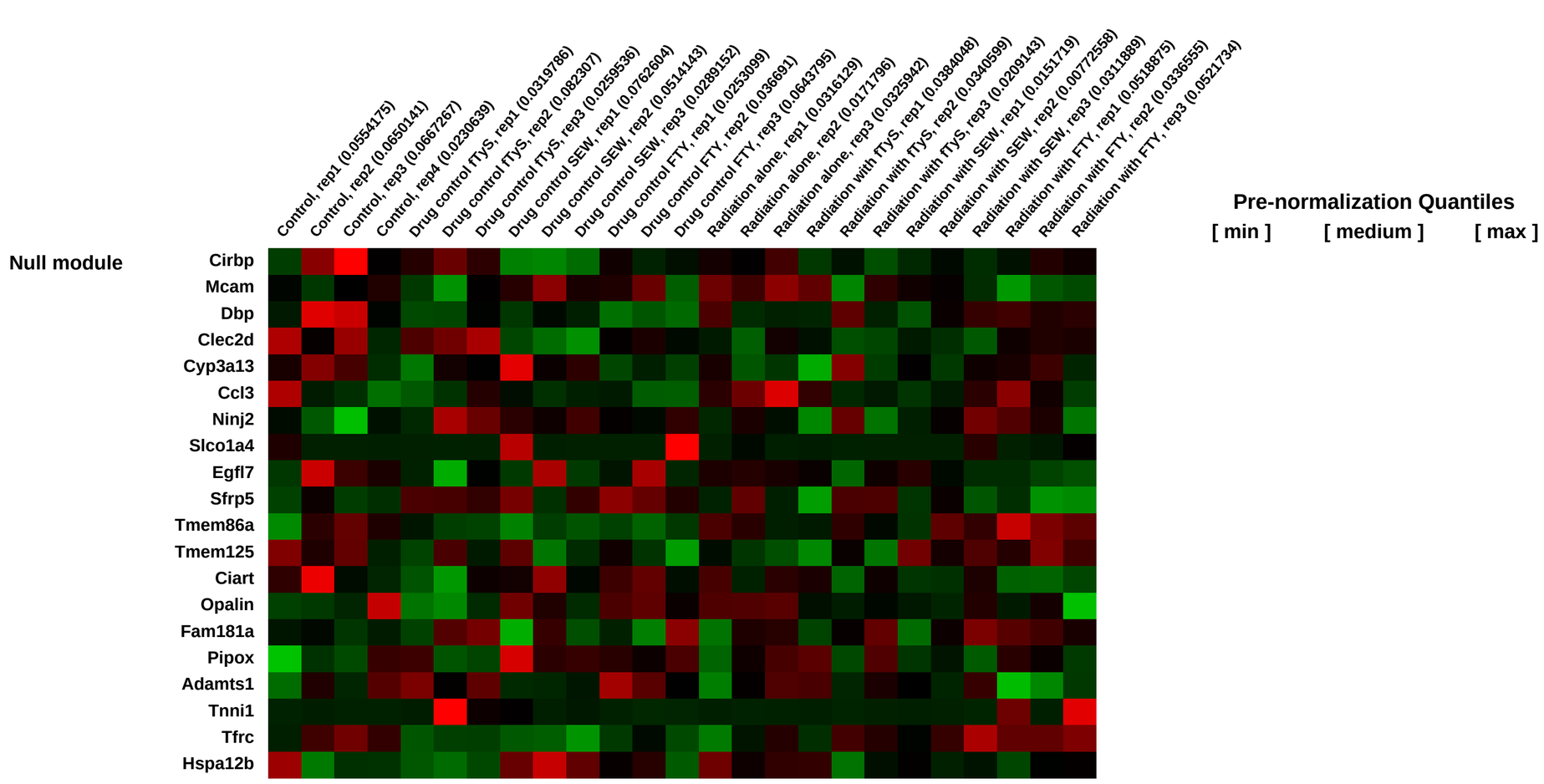

GEO Series "GSE19091" Expression Profiles

Num of samples in this series: 6

Scale of expression profile Z-scores

-3.0 -2.0 -1.0 0.0 1.0 2.0 3.0

GEO Link:	http://www.ncbi.nlm.nih.gov/geo/query/acc.cgi?acc=GSE19091
Status:	Public on Oct 01 2011
Title:	Transcriptional profiling of MKK4-depleted cells
Organism:	Mus musculus
Experiment type:	Expression profiling by array
Platform:	GPL1261
Pubmed ID:	21896780
Summary & Design:	**Summary:** Mitogen-activated protein kinase kinase 4 (MKK4) is a dual-specificity kinase activated by environmental stress, cytokines, and peptide growth factors that reportedly can promote or inhibit tumor cell growth and metastasis. Somatic mutations in the gene encoding MKK4 (MAP2K4) have been identified in various human cancers, but the consequences of these mutations on MKK4 function and the biology of tumor cells that have them have not been elucidated. Here we report that, of the eleven mutations within the MAP2K kinase domain described thus far, one had gain-of-function (Q142L) and six had loss-of-function. Three of the loss-of-function mutations are nonsense mutations that produced C-terminally-truncated proteins (I295fs*23, R304*, and W310*) that were highly ubiqitinated and rapidly degraded when introduced into cells, and three are missense mutations in the ATP-binding pocket (N234I), activation loop (S251N), or C-lobe (P326L). We modeled the consequences of MAP2K4 loss-of-function mutations on cells by introducing MKK4 short-hairpin RNA constructs and found that MKK4 depletion enhanced the ability of a weakly tumorigenic murine cancer cell to metastasize when injected into syngeneic mice but had no effect on primary tumor formation. MKK4-depleted cells exhibited an increased capacity to migrate across PET filters and to invade through matrigel but no change in anchorage-dependent or -independent proliferation. Transcriptional profiling of these cells revealed gene expression changes that promote epithelial-to-mesenchymal transition and angiogenesis. We conclude that MKK4 inactivation promoted metastasis but not primary tumor formation. Collectively, these findings implicate loss-of-function MAP2K4 somatic mutations in tumor metastasis and provide one of the few examples of a somatic mutation in cancer cells that exerts a metastasis-specific effect. **Keywords:** Two-group comparison. **Overall design:** 393P cells were infected with retroviruses expressing a MKK4-specific shRNA construct (shZ) or scrambled control (scr). 393P-shZ and 393P-scr were transcriptionally profiled in triplicate cultures.

Background corr dist: KL-Divergence = 0.0393, L1-Distance = 0.0240, L2-Distance = 0.0006, Normal std = 0.6276

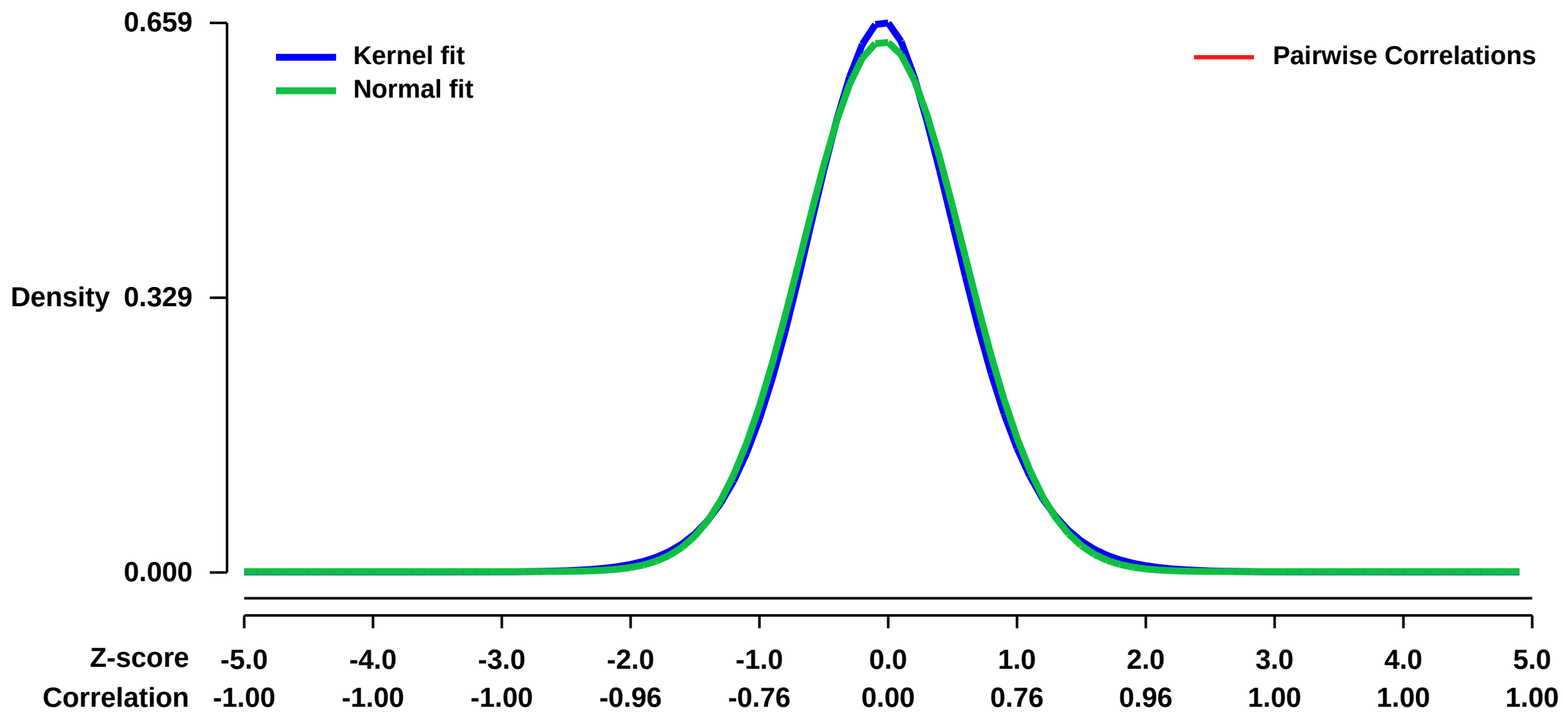

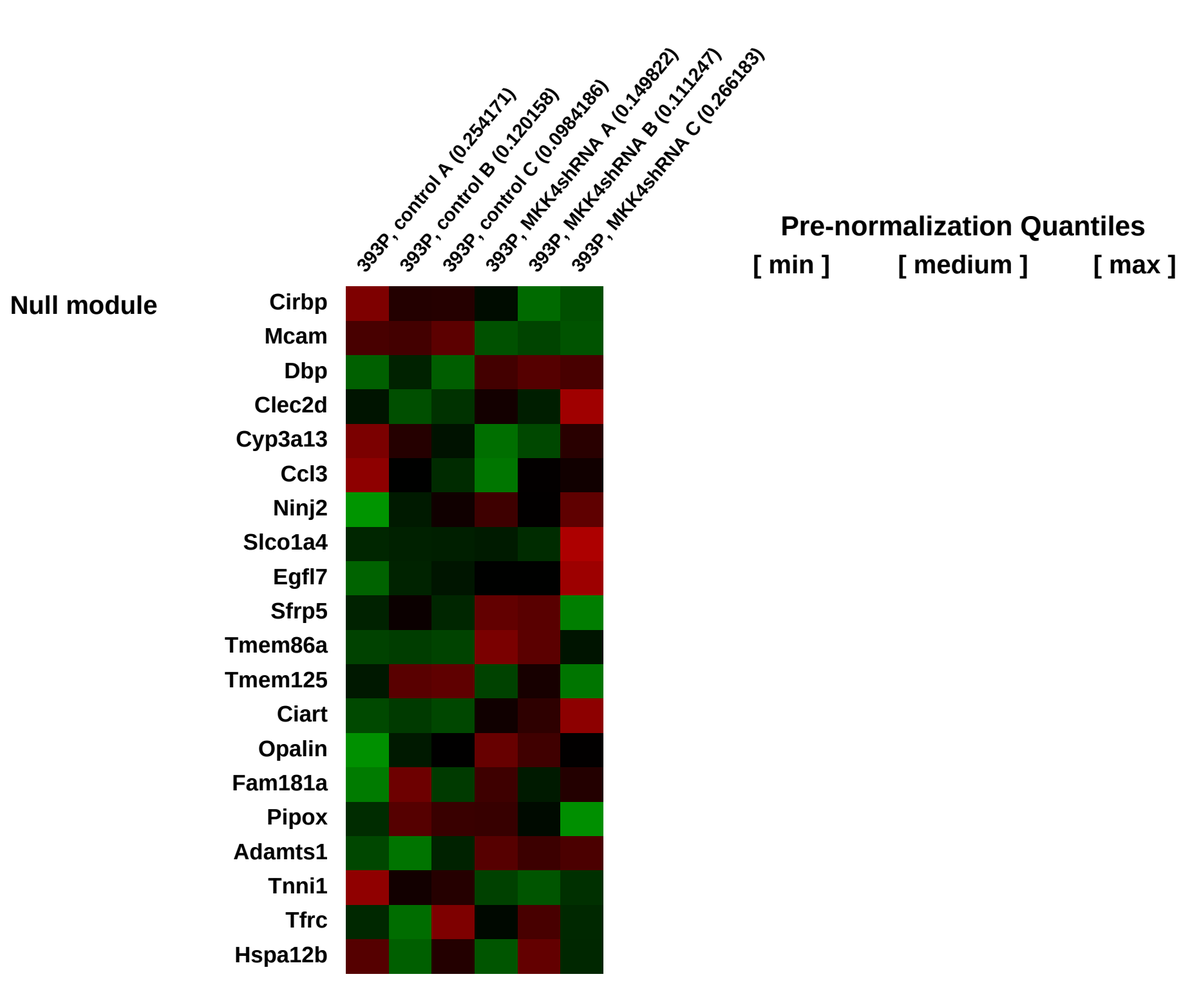

GEO Series "GSE36477" Expression Profiles

Num of samples in this series: 8

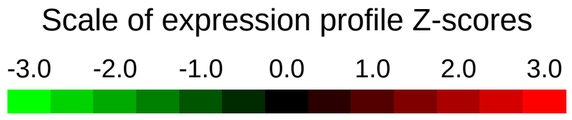

GEO Link:	**http://www.ncbi.nlm.nih.gov/geo/query/acc.cgi?acc=GSE36477**
Status:	**Public on Jun 01 2012**
Title:	**Expression data from mammary macrophages isolated from MMTV-iFGFR1 transgenic mice**
Organism:	**Mus musculus**
Experiment type:	**Expression profiling by array**
Platform:	**GPL1261**
Pubmed ID:	
Summary & Design:	**Summary:** **The goal of this experiment was to profile macrophages from mammary glands isolated from transgenic mice that express inducible FGFR1 in mammary epithelial cells (MMTV-iFGFR1 transgenic mice). The mice were treated with with dimerizer to activates iFGFR1 for 48 hours and 4 weeks to induce mammary hyperplasias. Control mice included non-transgenic littermates treated with dimerizer for the same amount of time.** **Overall design:** **Macrophages were sorted from mammary glands of MMTV-iFGFR1 transgenic mice and non-transgenic mice following dimerizer treatment using Cd11b-PE. Macrophages from 3 mice were pooled for each sample. RNA was extracted and analyzed using the Affymetrix Mouse 2.0 chip.**

Background corr dist: **KL-Divergence = 0.0876, L1-Distance = 0.0270, L2-Distance = 0.0013, Normal std = 0.4631**

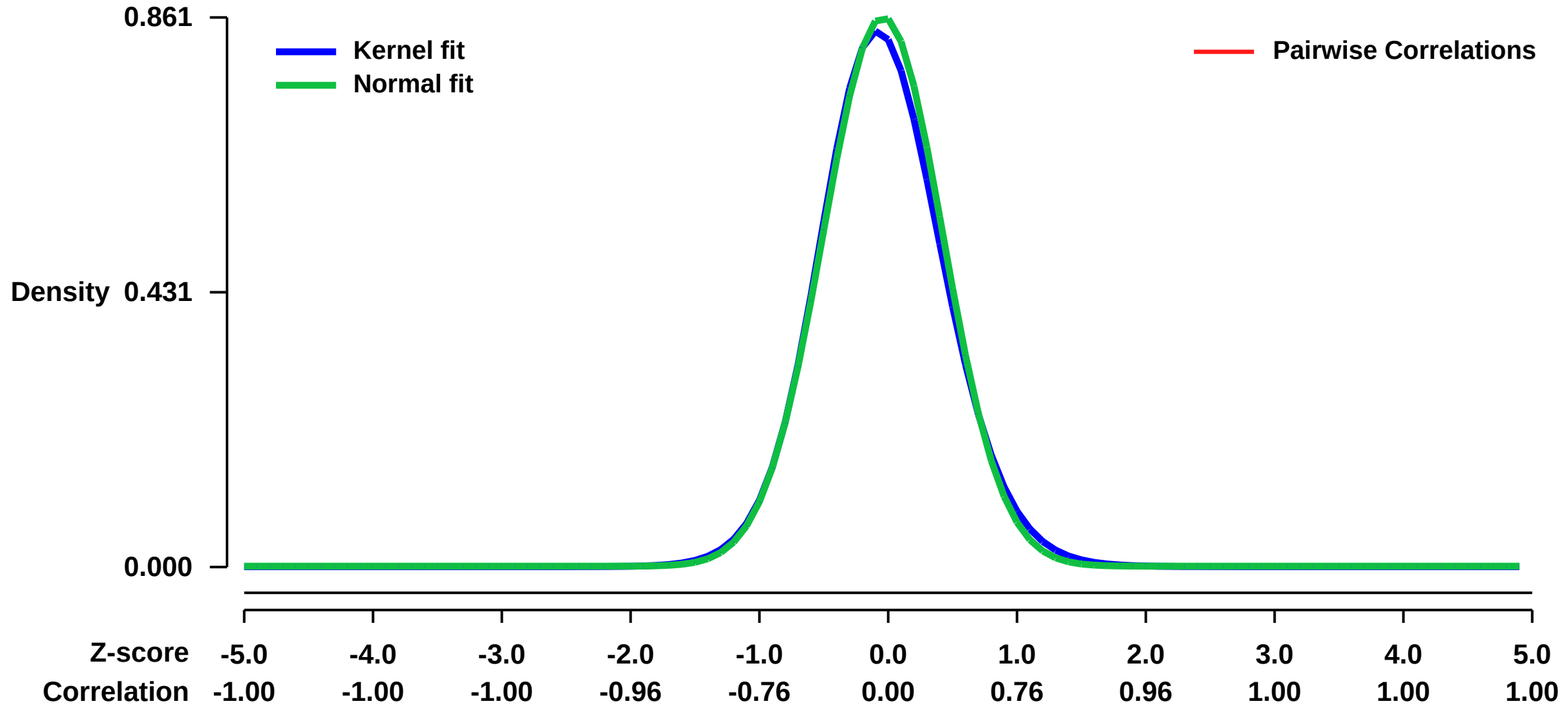

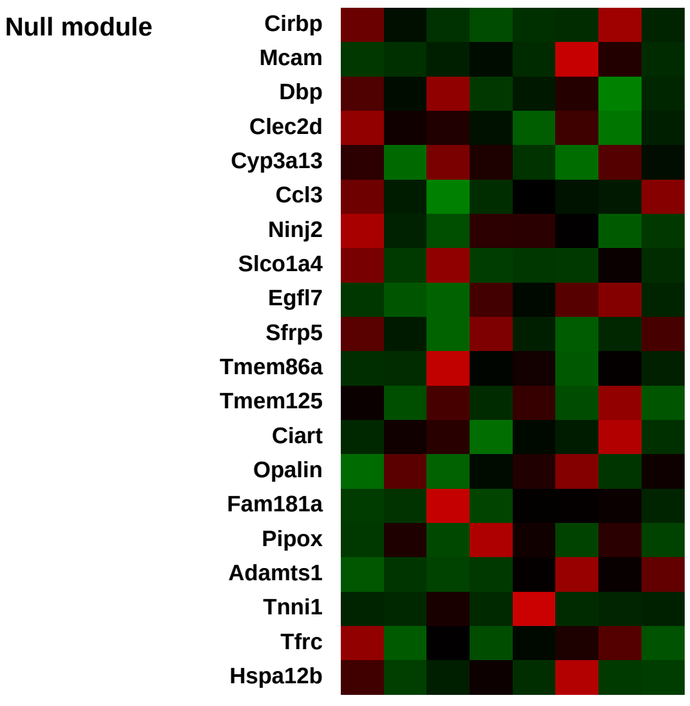

GEO Series "GSE25244" Expression Profiles

Num of samples in this series: 9

Scale of expression profile Z-scores

-3.0 -2.0 -1.0 0.0 1.0 2.0 3.0

GEO Link:	http://www.ncbi.nlm.nih.gov/geo/query/acc.cgi?acc=GSE25244
Status:	Public on Aug 03 2011
Title:	Patterns of gene expression associated with temporal phases of S. aureus infection
Organism:	Mus musculus
Experiment type:	Expression profiling by array
Platform:	GPL1261
Pubmed ID:	21887823
Summary & Design:	**Summary:** To acquire more information regarding the local immune events during the different phases of S. aureus infection, gene profiling using microarray technology was used to identify host genes whose expression is substantively altered in the kidneys during the acute (T2) and persistent phase of infection (T28). Genes associated with the distinct transcript profiles were identified by comparing the relative abundance of transcripts at 2 days (acute) and 28 days (persistent) of infection to their abundance in the kidneys of uninfected control animals (CTL). **Keywords: gene expression** **Overall design:** identification of host genes whose expression is substantively altered in the kidneys during the acute (T2) and persistent phase of infection (T28) compared to uninfected control (CTL).

Background corr dist: KL-Divergence = 0.0707, L1-Distance = 0.0248, L2-Distance = 0.0011, Normal std = 0.5021

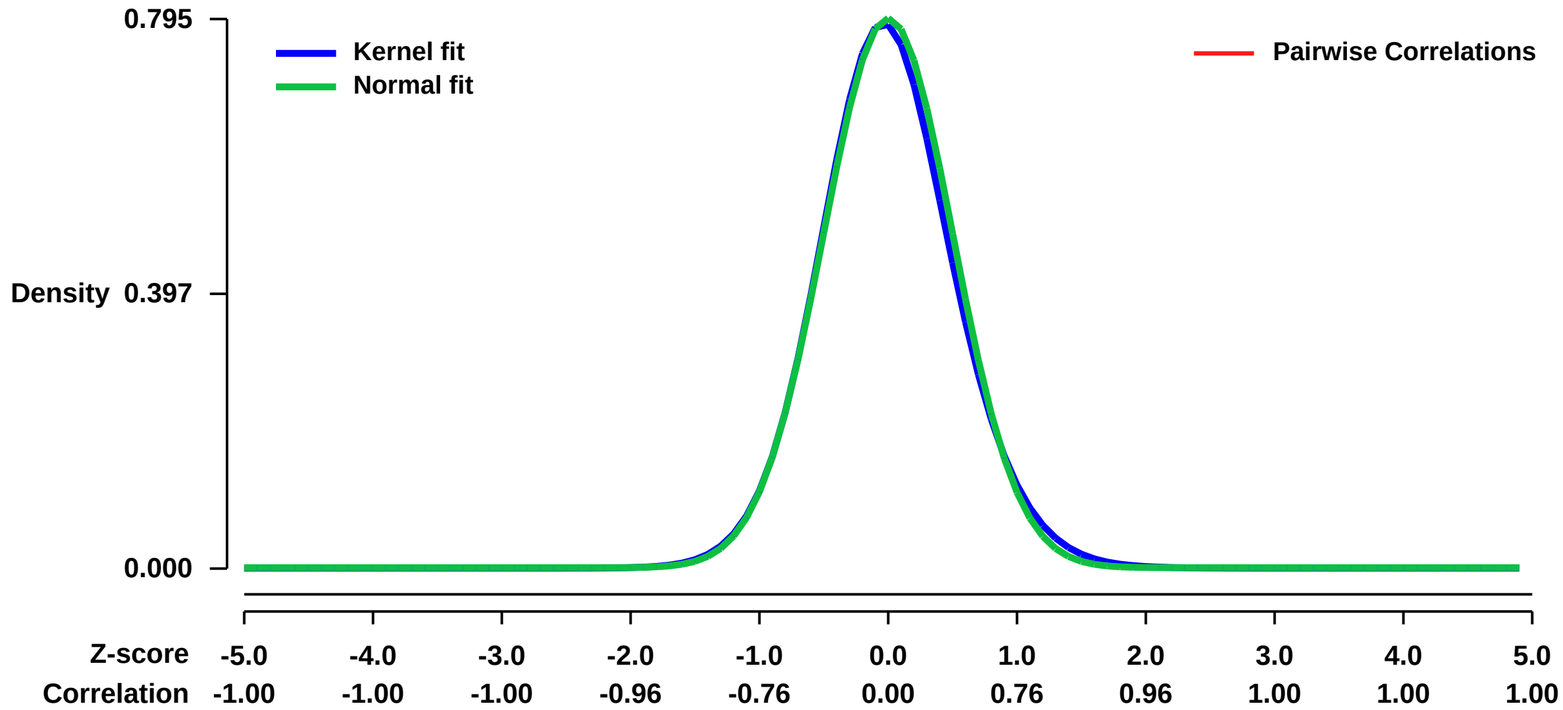

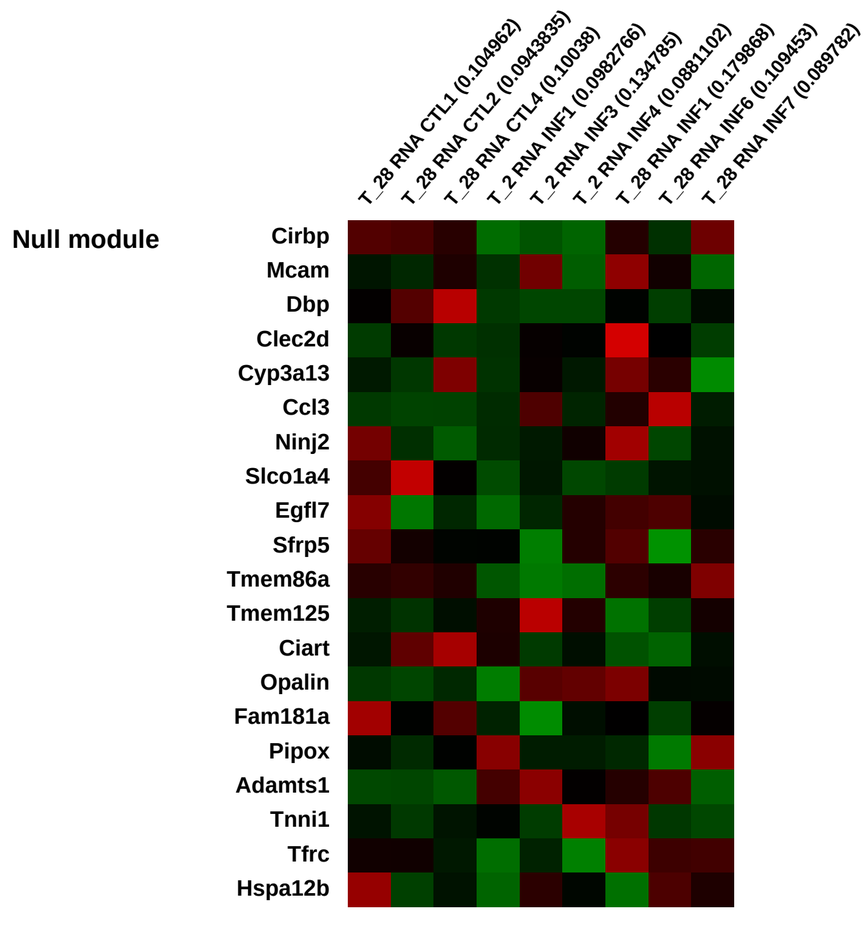

GEO Series "GSE54056" Expression Profiles

Num of samples in this series: 12

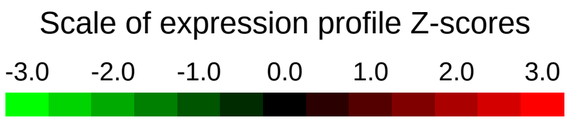

GEO Link:	http://www.ncbi.nlm.nih.gov/geo/query/acc.cgi?acc=GSE54056
Status:	Public on Mar 06 2014
Title:	Expression data from adult mouse normal and damaged retina from B6 and 129 mouse strains
Organism:	Mus musculus
Experiment type:	Expression profiling by array
Platform:	GPL1261
Pubmed ID:	24747725
Summary & Design:	**Summary:** Retinal damage causes proliferation of Muller glia, but the degree of proliferation depends on mouse strains. Muller glial proliferation was significantly promoted by the addition of GSK3 inhibitor in 129, but not in B6. We used retinal explant culture as a model for retinal damage which caused preferential photoreceptor death in a few days. We used microarrays to detail the global programme of gene expression regulating the proliferative potential of Muller glia after retinal damage. **Overall design:** Total RNA from intact whole retina, retinal tissue cultured for three days, and retinal tissue cultured with chir99021 for three days was used. Retinal tissues from 10 weeks old mice were used.

Background corr dist: KL-Divergence = 0.0576, L1-Distance = 0.0272, L2-Distance = 0.0009, Normal std = 0.5454

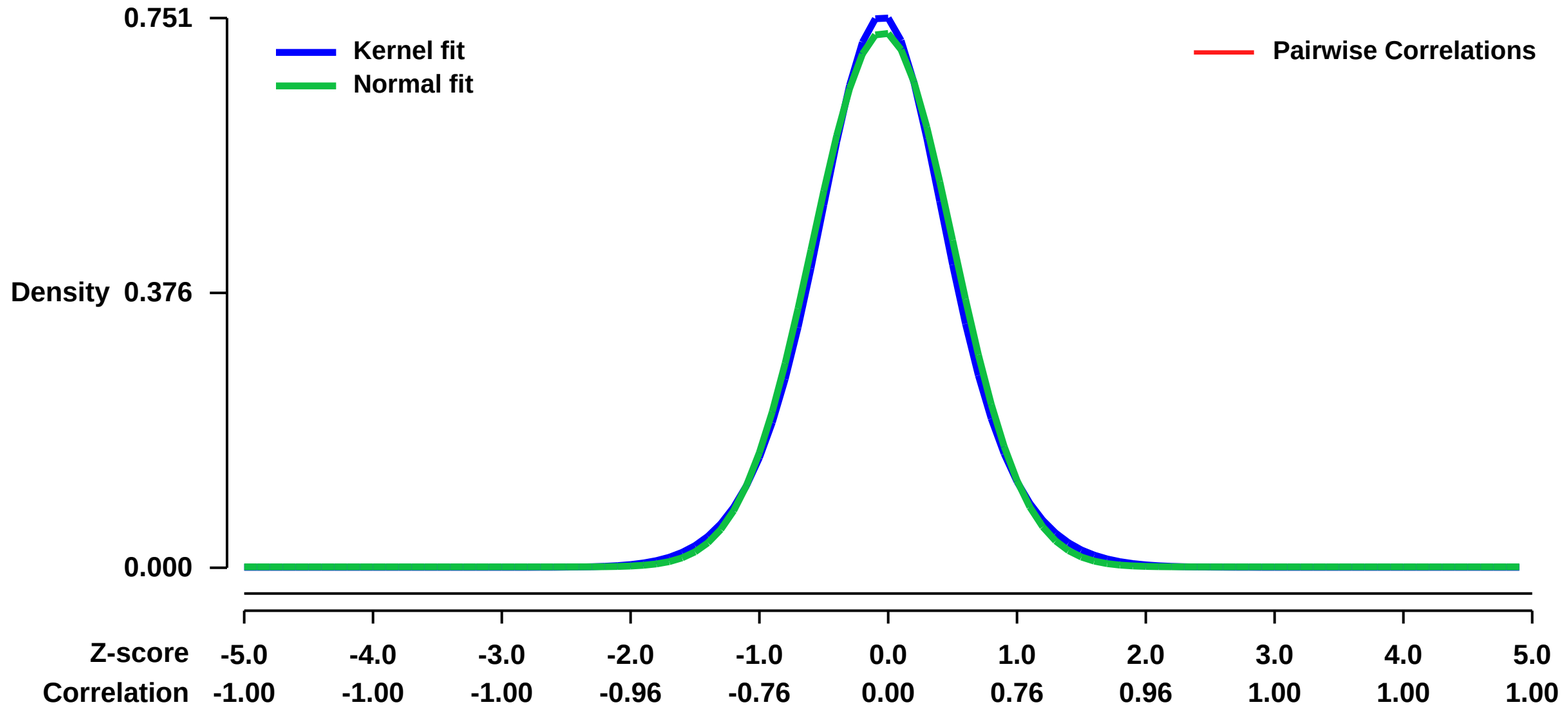

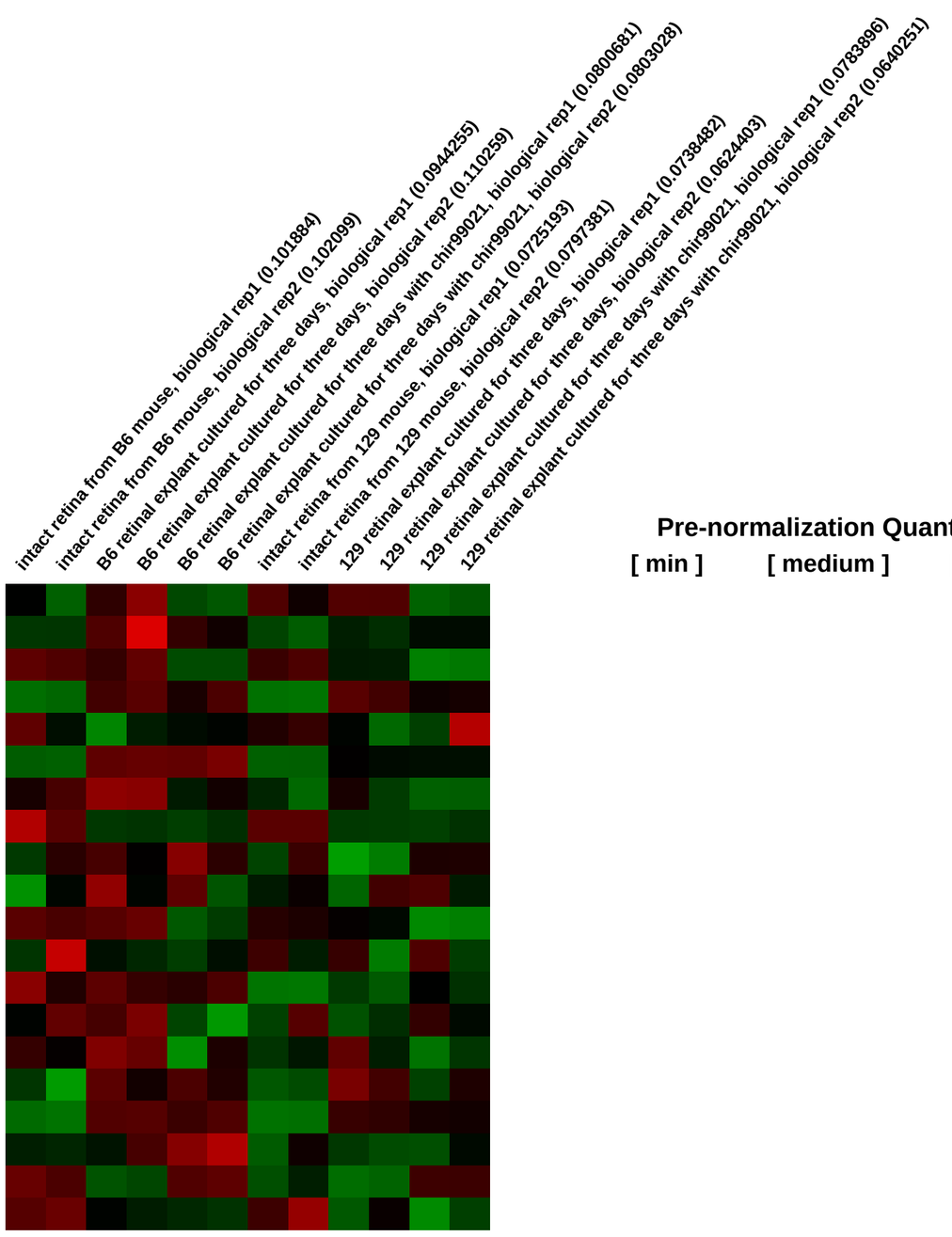

GEO Series "GSE46797" Expression Profiles

Num of samples in this series: 6

Scale of expression profile Z-scores

-3.0 -2.0 -1.0 0.0 1.0 2.0 3.0

GEO Link:	http://www.ncbi.nlm.nih.gov/geo/query/acc.cgi?acc=GSE46797
Status:	Public on May 10 2013
Title:	Expression data from c-Myc+ Notch1 T-ALL initiating cells
Organism:	Mus musculus
Experiment type:	Expression profiling by array
Platform:	GPL1261
Pubmed ID:	23791182
Summary & Design:	**Summary:** Missense FBXW7 mutations are prevalent in various tumors, including T-cell acute lymphoblastic leukemia (T-ALL). To study the effects of such lesions, we generated animals carrying regulatable Fbxw7 mutant alleles. We show here that these mutations specifically bolster cancer-initiating cell activity in collaboration with Notch1 oncogenes, but spare normal hematopoietic stem cell function. We were also able to show that FBXW7 mutations specifically affect the ubiquitylation and half-life of c-Myc protein, a key T-ALL oncogene. Using animals carrying c-Myc fusion alleles, we connected Fbxw7 function to c-Myc abundance and correlated c-Myc expression to leukemia-initiating activity. **Overall design:** Three independent Notch1 T-ALL were derived on c-Myc-GFP background and sorted from the spleen of leukemic mice on the basis of GFP expression for RNA extraction and hybridization on Affymetrix microarrays

Background corr dist: KL-Divergence = 0.0376, L1-Distance = 0.0289, L2-Distance = 0.0011, Normal std = 0.6371

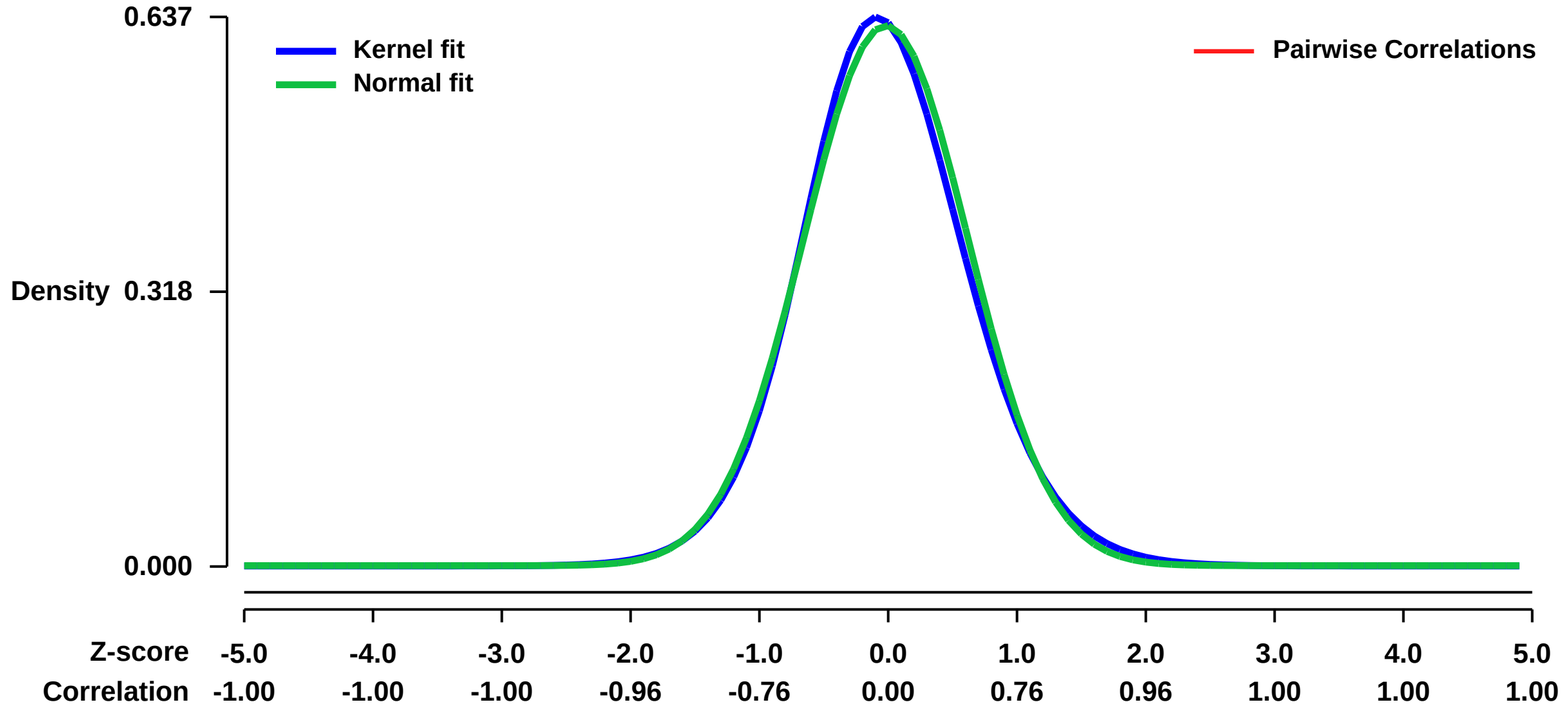

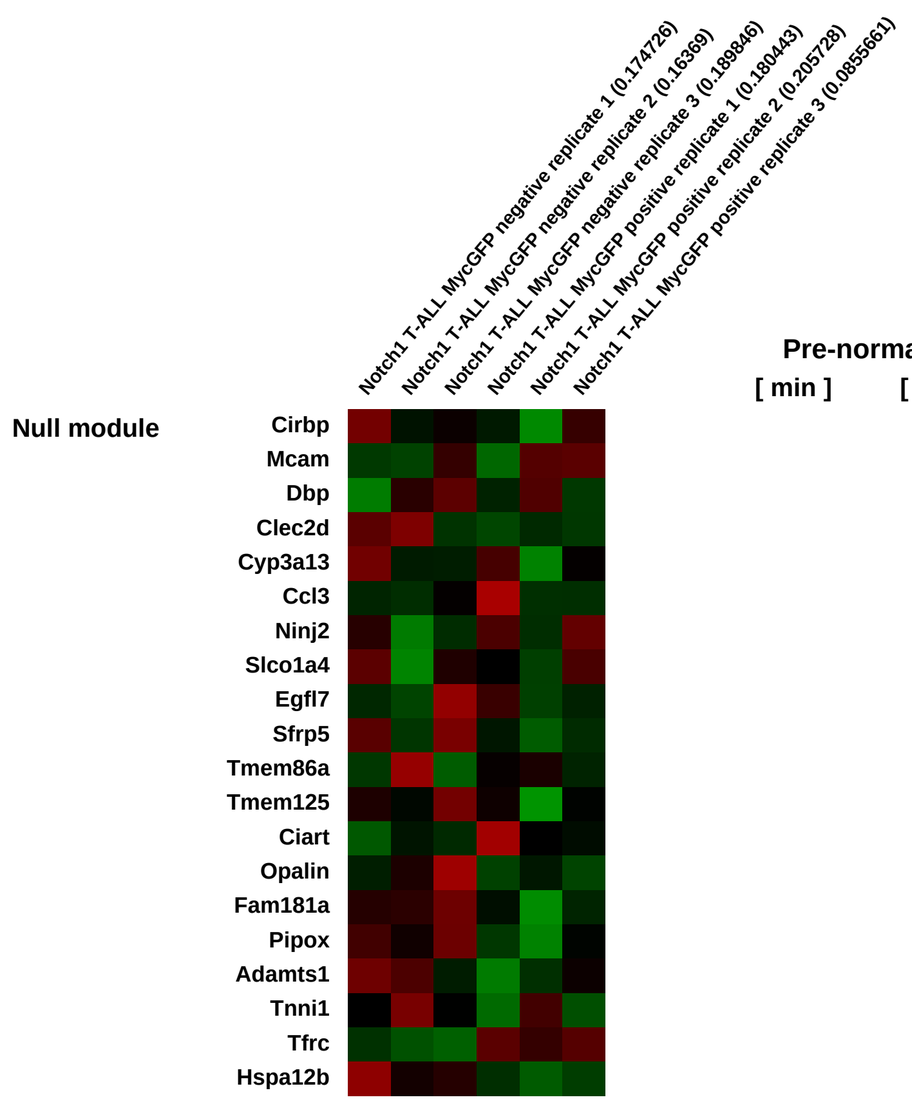

GEO Series "GSE20335" Expression Profiles

Num of samples in this series: 8

Scale of expression profile Z-scores

-3.0 -2.0 -1.0 0.0 1.0 2.0 3.0

GEO Link:	http://www.ncbi.nlm.nih.gov/geo/query/acc.cgi?acc=GSE20335
Status:	Public on Apr 17 2010
Title:	Expression analysis data from large T antigen-immortalized murine embryonic fibroblasts (MEFs)
Organism:	Mus musculus
Experiment type:	Expression profiling by array
Platform:	GPL1261
Pubmed ID:	20399150
Summary & Design:	**Summary:** Microarrays were used to examine the genome-wide expression in FIH null, VHL null and VHL/FIH double null MEFs. We used these data to analyze how deletion of FIH or VHL alone affects gene expression and if VHL and FIH have synergistic effects and differential selectivity on regulating gene expression. **Overall design:** To assess how deletion of FIH, VHL or both VHL and FIH affect gene expression genome-wide, we generated FIH null, VHL null and VHL/FIH double null MEFs after adeno-cre virus infection on large T-immortalized FIHdf, VHLdf, and VHLdf/FIHdf MEFs. These MEFs were cultured under normoxia (21% O2) with complete culture medium before RNA extraction. Total RNA were isolated by using the Qiagen RNeasy kit and treated with on-column DNase digestion. Affymetrix GeneChip Mouse Genome 430 2.0 Array was used.

Background corr dist: KL-Divergence = 0.0547, L1-Distance = 0.0269, L2-Distance = 0.0009, Normal std = 0.5587

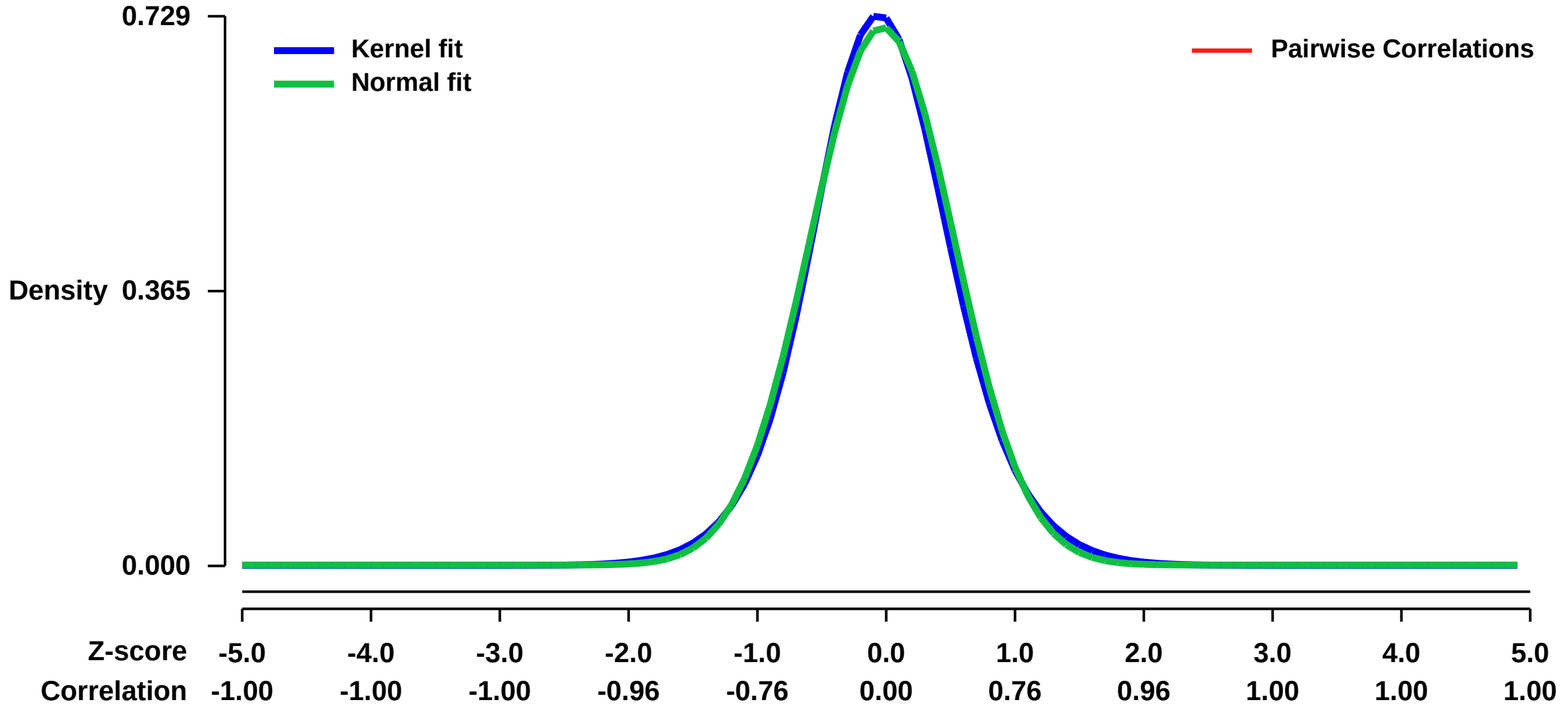

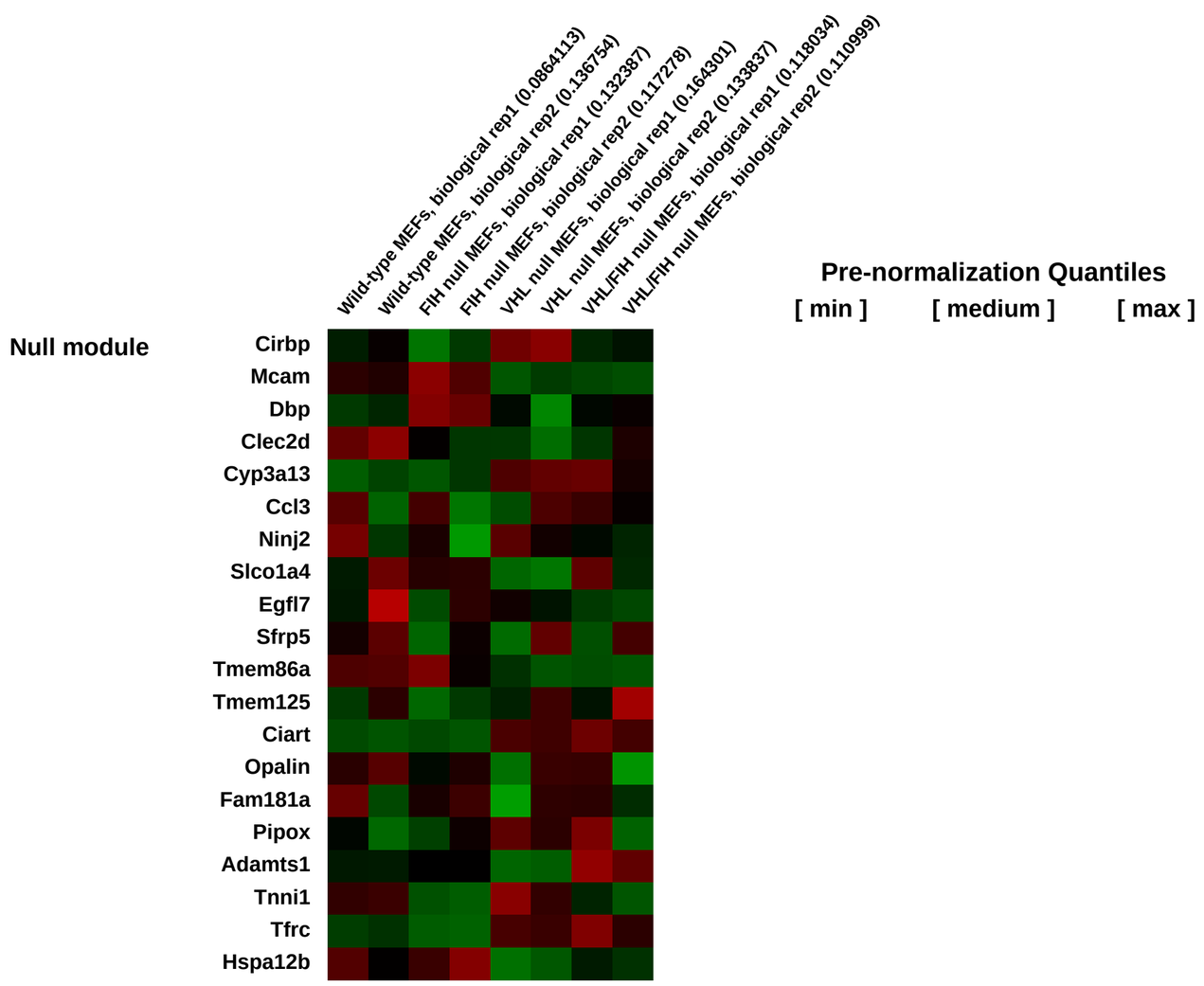

GEO Series "GSE24061" Expression Profiles

Num of samples in this series: 88

Scale of expression profile Z-scores

-3.0 -2.0 -1.0 0.0 1.0 2.0 3.0

GEO Link:	http://www.ncbi.nlm.nih.gov/geo/query/acc.cgi?acc=GSE24061
Status:	Public on Sep 10 2010
Title:	MAQC-II Project: Hamner data set
Organism:	Mus musculus
Experiment type:	Expression profiling by array
Platform:	GPL1261
Pubmed ID:	20676074
Summary & Design:	**Summary:** The Hamner data set (endpoint A) was provided by The Hamner Institutes for Health Sciences (Research Triangle Park, NC, USA). The study objective was to apply microarray gene expression data from the lung of female B6C3F1 mice exposed to a 13-week treatment of chemicals to predict increased lung tumor incidence in the 2-year rodent cancer bioassays of the National Toxicology Program. If successful, the results may form the basis of a more efficient and economical approach for evaluating the carcinogenic activity of chemicals. Microarray analysis was performed using Affymetrix Mouse Genome 430 2.0 arrays on three to four mice per treatment group, and a total of 70 mice were analyzed and used as the MAQC-II's training set (GEO Series GSE6116). Additional data from another set of 88 mice were collected later and provided as the MAQC-II's external validation set (this Series). The training dataset had already been deposited in GEO by its provider and its accession number is GSE6116. **Overall design:** 88 Samples

Background corr dist: KL-Divergence = 0.2466, L1-Distance = 0.0659, L2-Distance = 0.0092, Normal std = 0.3191

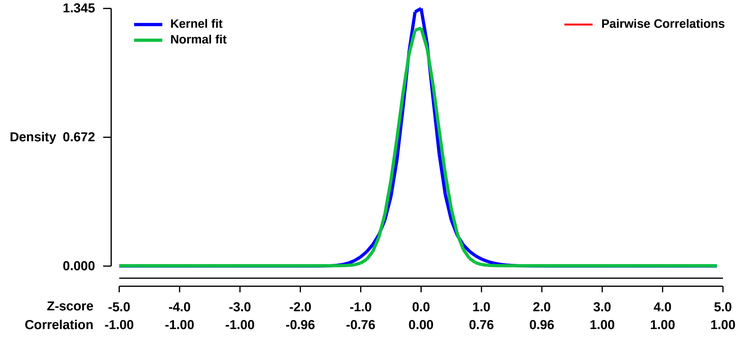

Z-score	-5.0	-4.0	-3.0	-2.0	-1.0	0.0	1.0	2.0	3.0	4.0	5.0
Correlation	-1.00	-1.00	-1.00	-0.96	-0.76	0.00	0.76	0.96	1.00	1.00	1.00

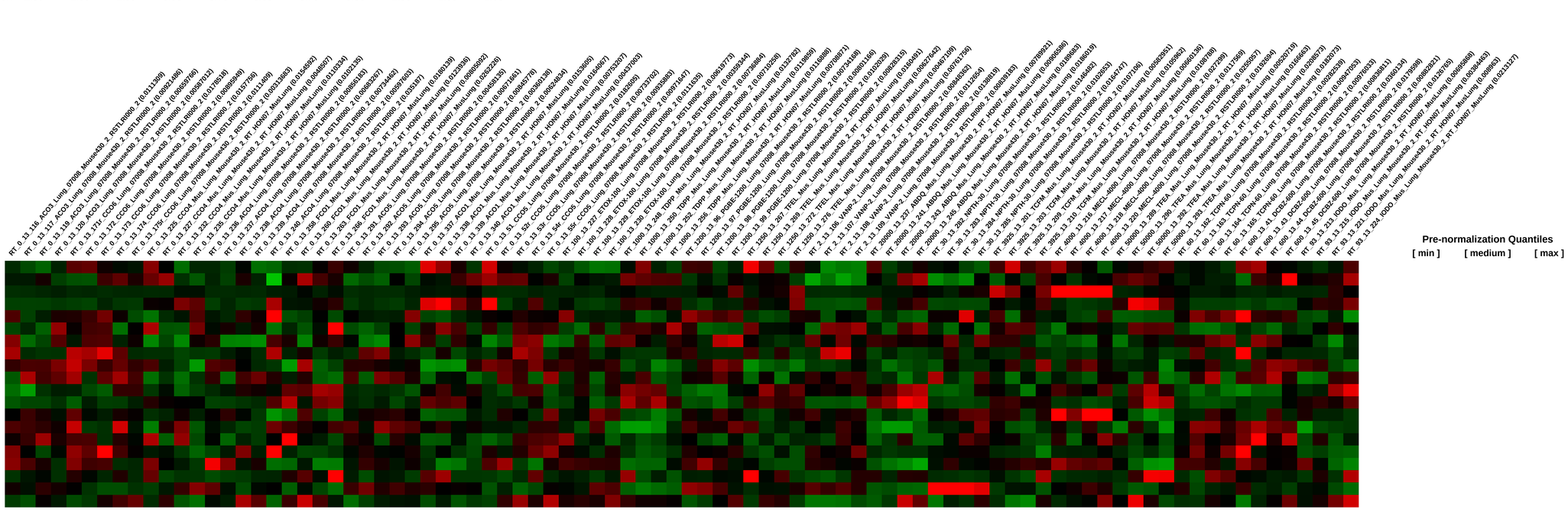

GEO Series "GSE41746" Expression Profiles

Num of samples in this series: 18

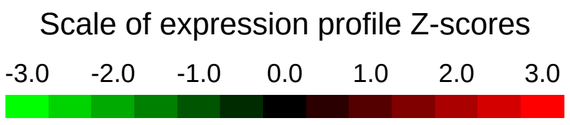

GEO Link:	**http://www.ncbi.nlm.nih.gov/geo/query/acc.cgi?acc=GSE41746**
Status:	**Public on Oct 23 2012**
Title:	**Comparative expression data of PD21 Pik3cd+/- and Pik3cd-/- female mice ovaries responsed to exogenous gonadotropins.**
Organism:	**Mus musculus**
Experiment type:	**Expression profiling by array**
Platform:	**GPL1261**
Pubmed ID:	
Summary & Design:	**Summary:** **The Pik3cd null females are subfertile and have less growing follicles than their heterozygous littermates in the ovary. These mice poorly respond to the exogenous gonadotropins and ovulate much less oocytes than controls. In addition, the estrodial stimulated GC proliferation in preantral follicles is also impaired in Pik3cd null ovaries. FSH and E2 dramatically activates PI3K/AKT pathway in GCs of wild type mice, but not in the Pik3cd null mice.** **we used microarray to identify those genes regulated by Pik3cd in response to PMSG (Pregnant Mare Serum Gonadotropin) and E2 treatment in ovary.** **Overall design:** **We set 3 treatment groups of both Pik3cd+/- and Pik3cd-/- female mice, including PD21 untreatment, PD21 after PMSG administration for 44 hours, PD21 after E2 administration for 72 hours, each group contained three biological repeats. The genes up/down-regulated significantly (not less than 2 fold change) in Pik3cd+/- mice after PMSG and E2 treatment were listed out as PMSG or E2 target genes, in which, those had not the same change trends in Pik3cd-/- were considered as Pik3cd-dependent genes.**

Background corr dist: **KL-Divergence = 0.1591, L1-Distance = 0.0396, L2-Distance = 0.0032, Normal std = 0.3654**

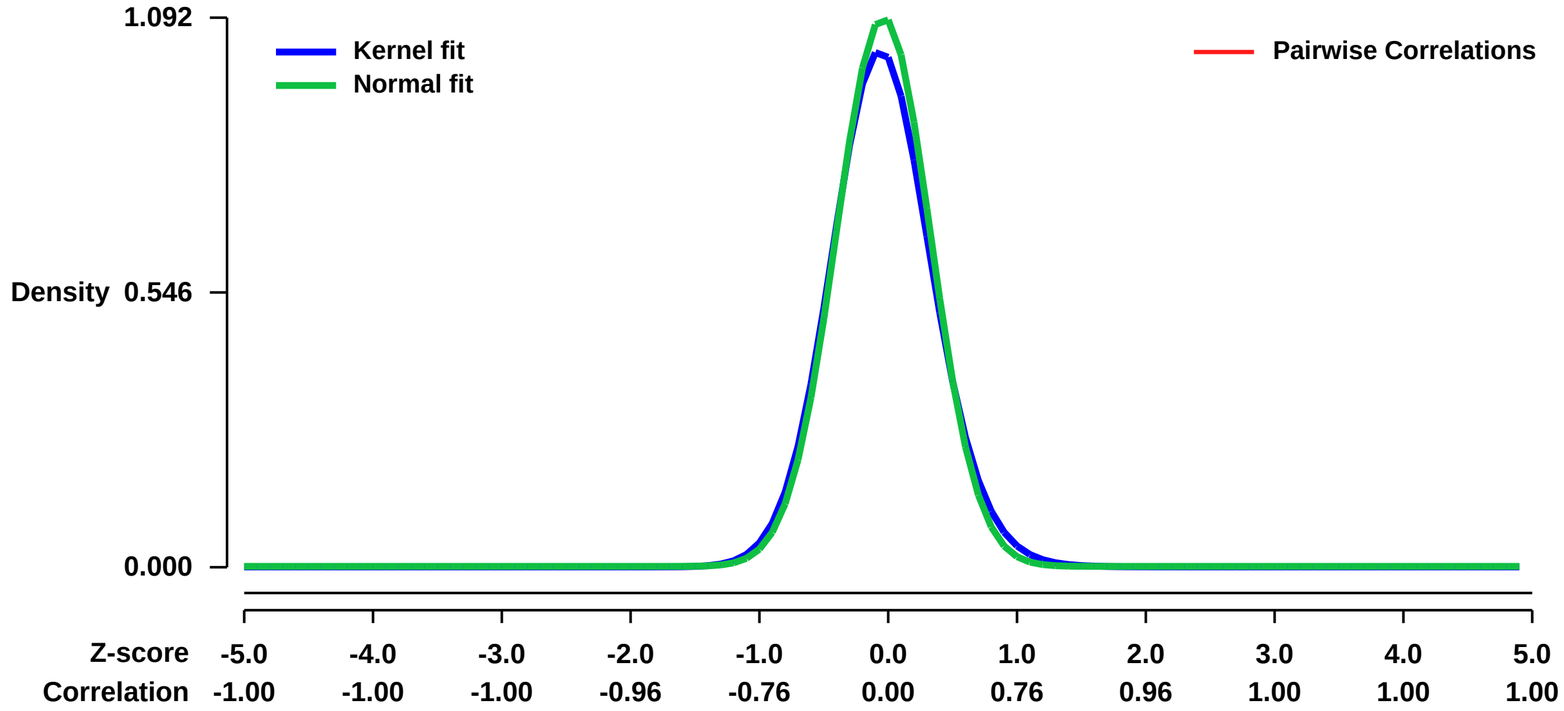

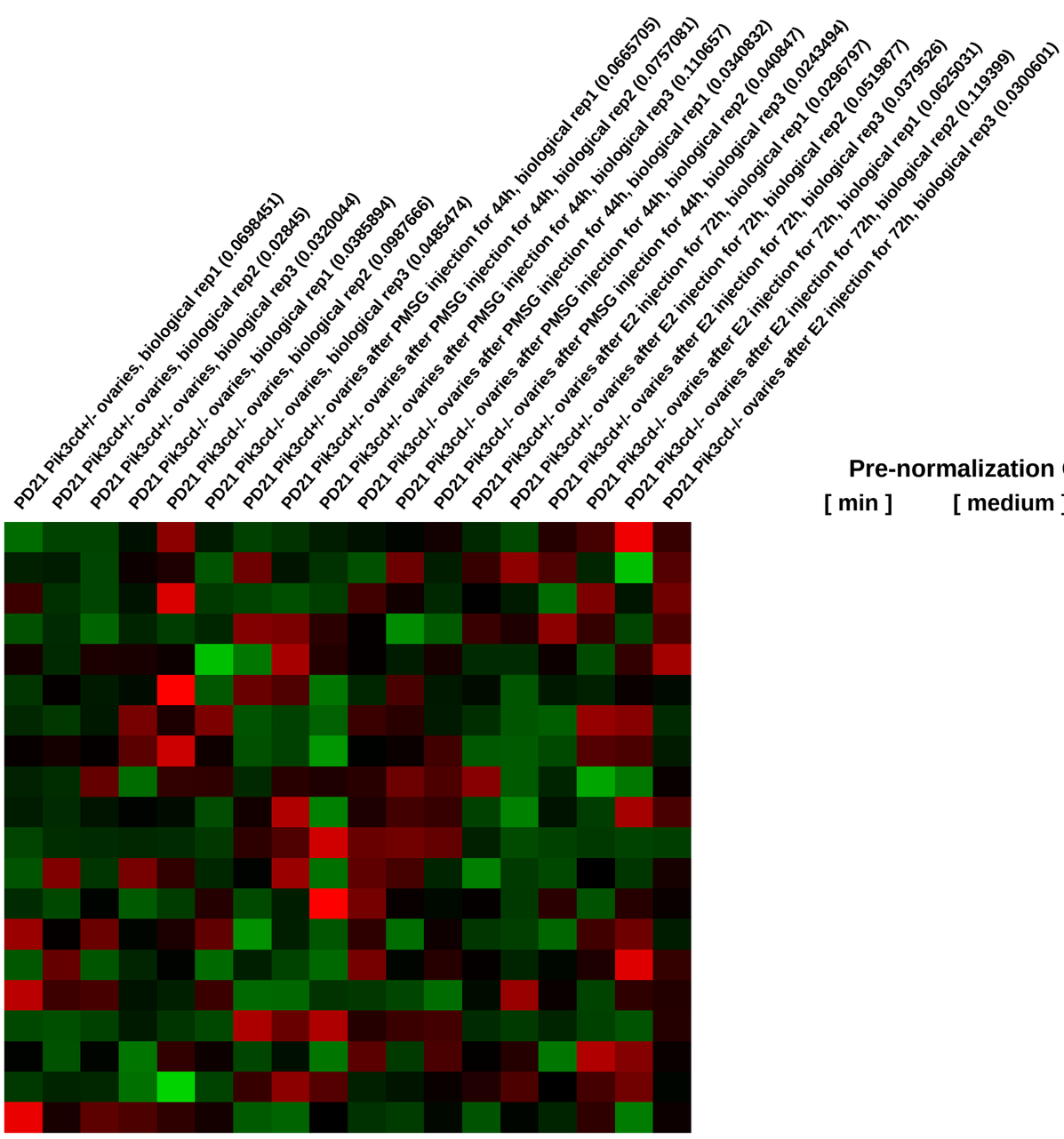

GEO Series "GSE9545" Expression Profiles

Num of samples in this series: 11

Scale of expression profile Z-scores

-3.0 -2.0 -1.0 0.0 1.0 2.0 3.0

GEO Link:	http://www.ncbi.nlm.nih.gov/geo/query/acc.cgi?acc=GSE9545
Status:	Public on Aug 24 2009
Title:	Gene Expression Profiles Associated with Ethanol-Induced Teratogenic Effects in a C57BL/6 Mouse Embryo Culture Model
Organism:	Mus musculus
Experiment type:	Expression profiling by array
Platform:	GPL1261
Pubmed ID:	18366608
Summary & Design:	**Summary:** **Mouse model for Fetal Alcohol Syndrome. Embryos exposed to alcohol in controlled environment to assess teratogenic effects.** **Fetal Alcohol Syndrome (FAS) is a leading developmental disorder. To date, a holistic view of molecular gene changes is largely unexplored. Using microarray analysis of whole embryo mouse culture with strict-control over alcohol-level, we found, directly related alcohol-metabolism, a reduction of retinol binding protein 1(Rbp1), and a, de novo expression of aldehyde dehydrogenase 1B1 (ALDH1B1). Remarkably, four key hemopoiesis genes (glycophorin A, adducin 2, beta-2 microglobulin, and ceruloplasmin) became absent, and many histone variants genes were reduced. Hypothesis-driven informatics analysis and intersection analysis of two independent experiments indicated that the altered genes are involved in cell growth, hemopoiesis, histone modification, eye and heart development, and a collective reduction in expression of growth factor genes (Igf1, Efemp1, Tieg, and Edil3) and neural specification genes (neurogenin, Sox 5, bHLHb5). Down-regulated neural specification phenotypes further supported the above findings. Further more, the gene expression profile indicated distinct subgroups which overlapped with the teratogenesis of the open- and the closed-neural tubes known in FAS. In summary, our data reveal genes alteration with causal potential for dysmorpology (e.g. retinoic acid, neuronal specification, and neurotrophic factors, and epigenetics related histone genes) and those downstream responsive genes related to alcohol metabolism, and developmental teratogenesis.** **Keywords: comparison of gene expression profiles for treated vs. control** **Overall design:** **Comparison of whole embryo gene expression after exposure to ethanol for 46 hours. Note 2 independent experiments completed.**

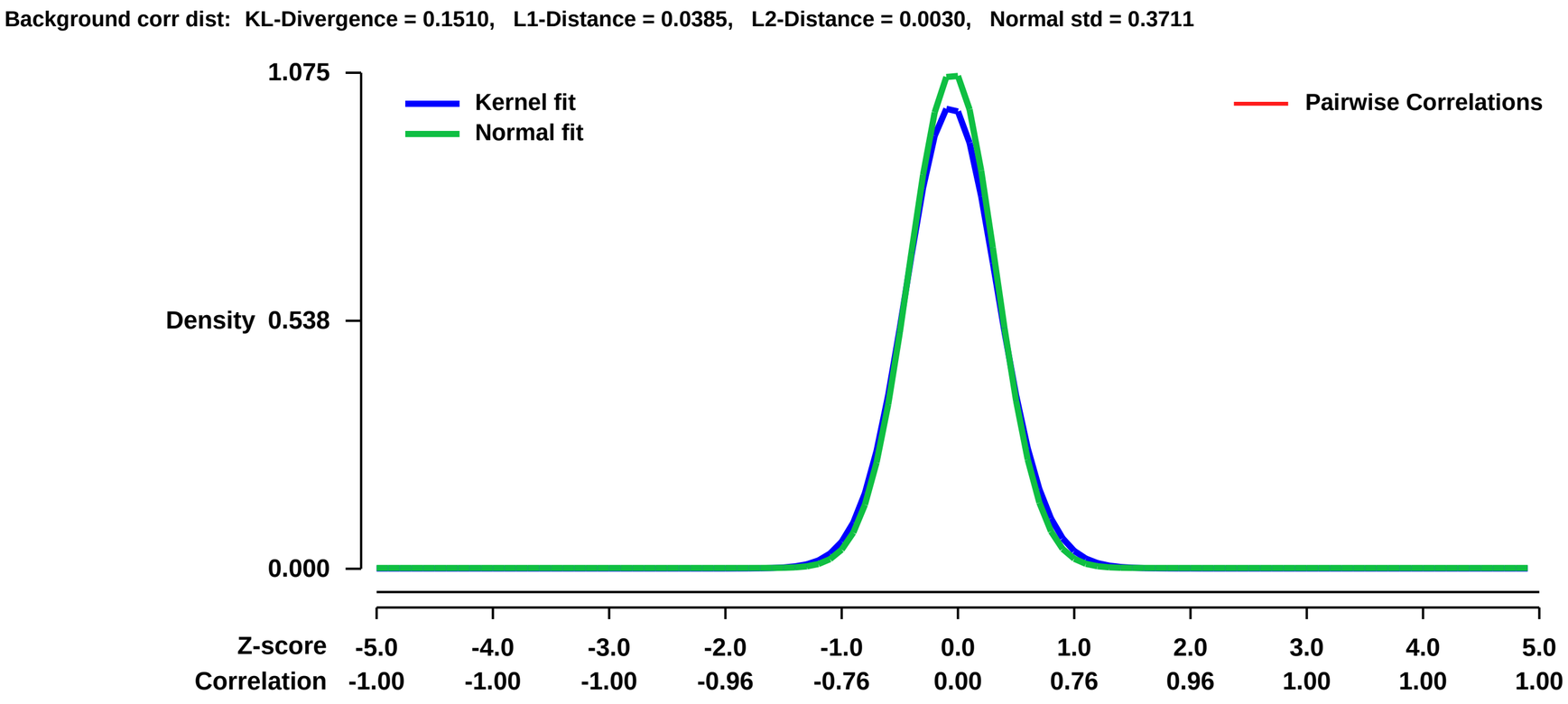

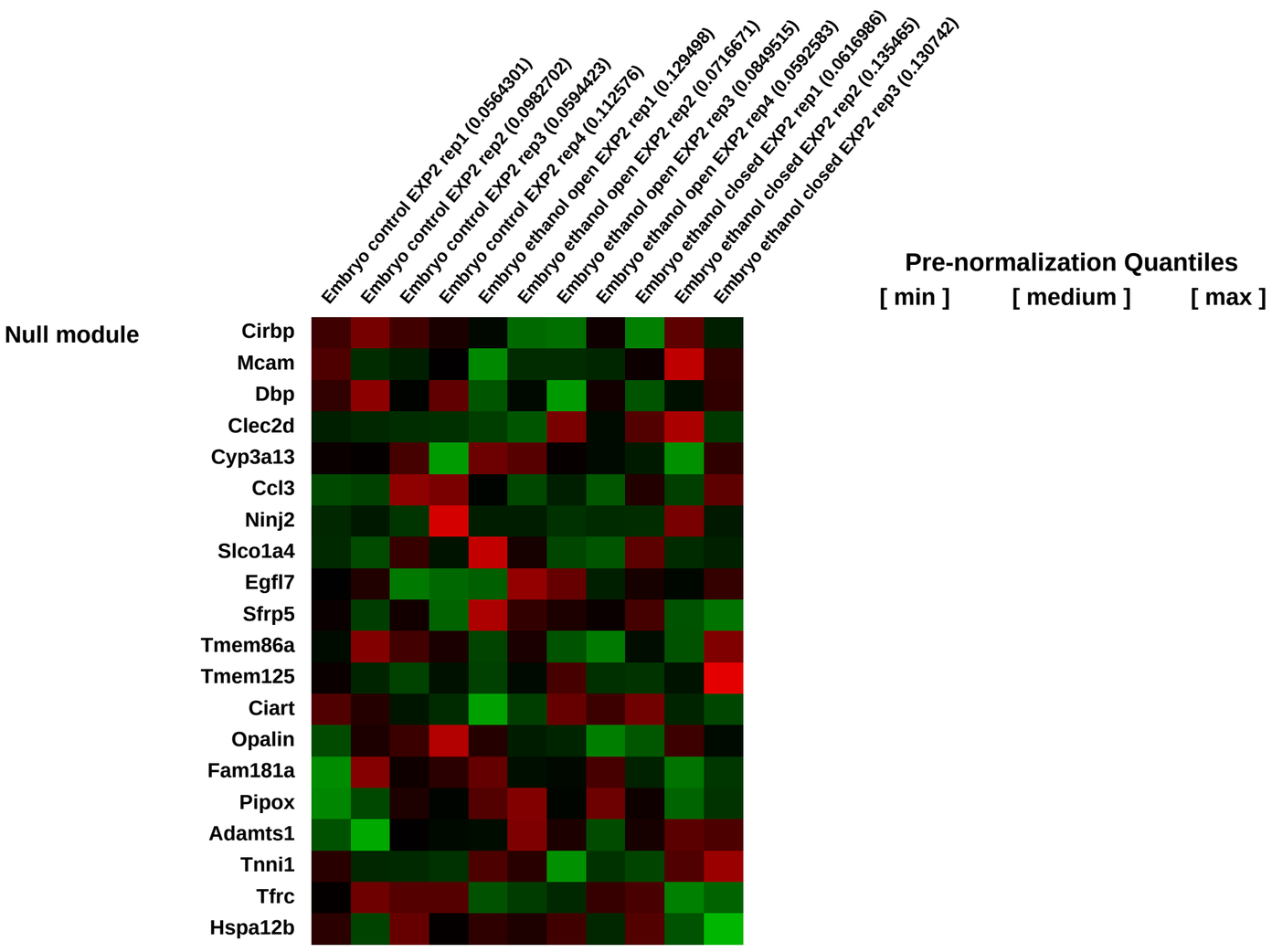

GEO Series "GSE18042" Expression Profiles

Num of samples in this series: 18

Scale of expression profile Z-scores

-3.0 -2.0 -1.0 0.0 1.0 2.0 3.0

GEO Link:	http://www.ncbi.nlm.nih.gov/geo/query/acc.cgi?acc=GSE18042
Status:	Public on Sep 10 2009
Title:	Erythroid differentiation: G1E model
Organism:	Mus musculus
Experiment type:	Expression profiling by array
Platform:	GPL1261
Pubmed ID:	19887574
Summary & Design:	**Summary:** Analysis of erythroid differentiation using Gata1 gene-disrupted G1E ER4 clone cells. Estradiol addition activates an ectopically expressed Gata-1-estrogen receptor fusion protein, triggering synchronous differentiation. 30 hour time course corresponds roughly to late burst-forming unit-erythroid stage (t=0 hrs) through orthochromatic erythroblast stage (t=30 hrs). **Overall design:** G1E ER4 cells cultured in G1E medium were treated at 6 time points with estradiol to initiate erythroid differentiation by activating Gata1 transcription factor and total RNAs from treated cells were extracted for microarray experiment. The erythroid differentiation status was confirmed by cell pellet color and expression of microRNA miR451. The design was similar to an earlier studies (Welch, J. J., Watts, J. A., Vakoc, C. R., Yao, Y., Wang, H., Hardison, R. C., Blobel, G. A., Chodosh, L. A., and Weiss, M. J. (2004)). Global regulation of erythroid gene expression by transcription factor GATA-1. Blood 104, 3136-3147), except that a more recent version of Affymetric chip was used to acheive greater transcriptome coverage.

Background corr dist: KL-Divergence = 0.0901, L1-Distance = 0.0663, L2-Distance = 0.0070, Normal std = 0.5071

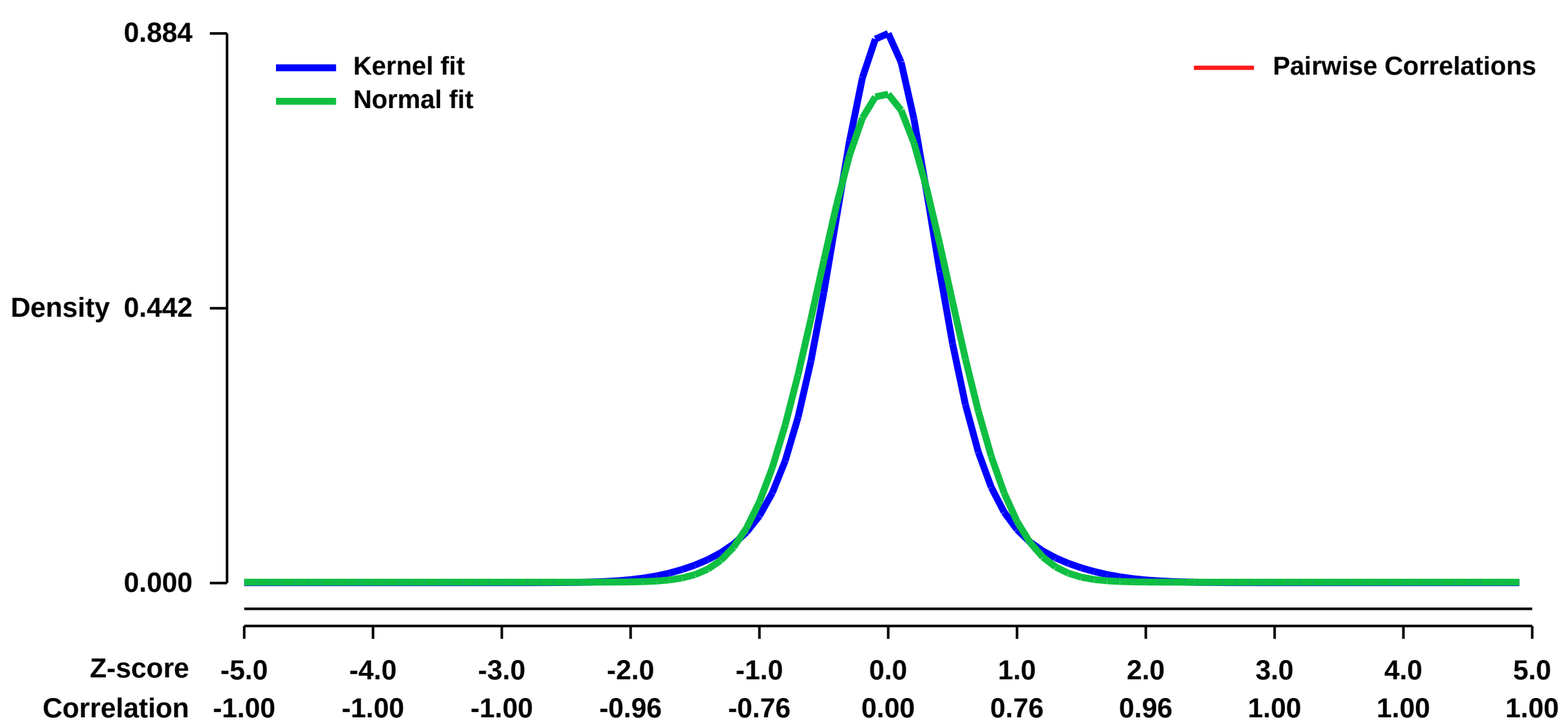

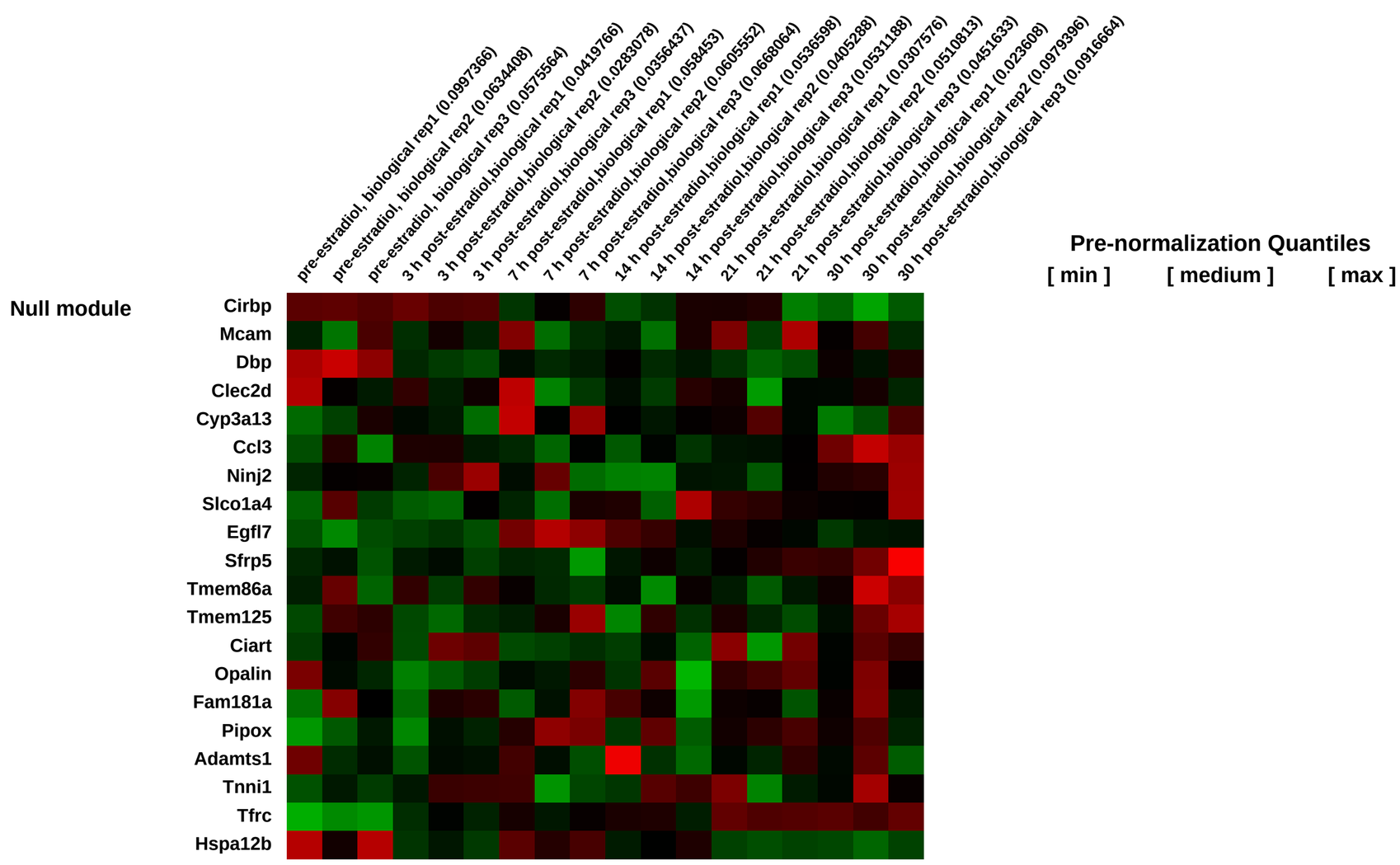

GEO Series "GSE24614" Expression Profiles

Num of samples in this series: 6

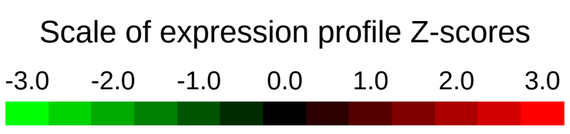

GEO Link:	**http://www.ncbi.nlm.nih.gov/geo/query/acc.cgi?acc=GSE24614**
Status:	**Public on Jun 15 2011**
Title:	**Variegated gene expression caused by cell-specific long-range DNA interactions**
Organism:	**Mus musculus**
Experiment type:	**Other**
Platform:	**GPL1261**
Pubmed ID:	**21706023**
Summary & Design:	**Summary:** **Mammalian genomes contain numerous DNA elements with potential transcription regulatory function but unknown target genes. We used transgenic, gain-of-function mice with an ectopic copy of the beta-globin locus control region (LCR) to better understand how regulatory elements dynamically search the genome for target genes. We find that the LCR samples a restricted nuclear sub-volume in which it forms preferential contacts with genes controlled by shared transcription factors. One contacted gene, betah1, located on another chromosome, is upregulated, providing genetic demonstration that mammalian enhancers can function between chromosomes. Upregulation is not pan-cellular but confined to selected â jackpotâ cells significantly enriched for inter-chromosomal LCR-betah1 interactions. This implies that long-range DNA contacts are relatively stable and cell-specific and, when functional, cause variegated expression. We refer to this as spatial effect variegation (SEV). The data provide a dynamic and mechanistic framework for enhancer action, important for assigning function to the one- and three-dimensional structure of DNA.** **Overall design:** **At the RNA level these mice were characterized with Affymetrix expression arrays. We analyzed three biological replicates for the WT and the knock-in.**

Background corr dist: **KL-Divergence = 0.0272, L1-Distance = 0.0584, L2-Distance = 0.0041, Normal std = 0.8832**

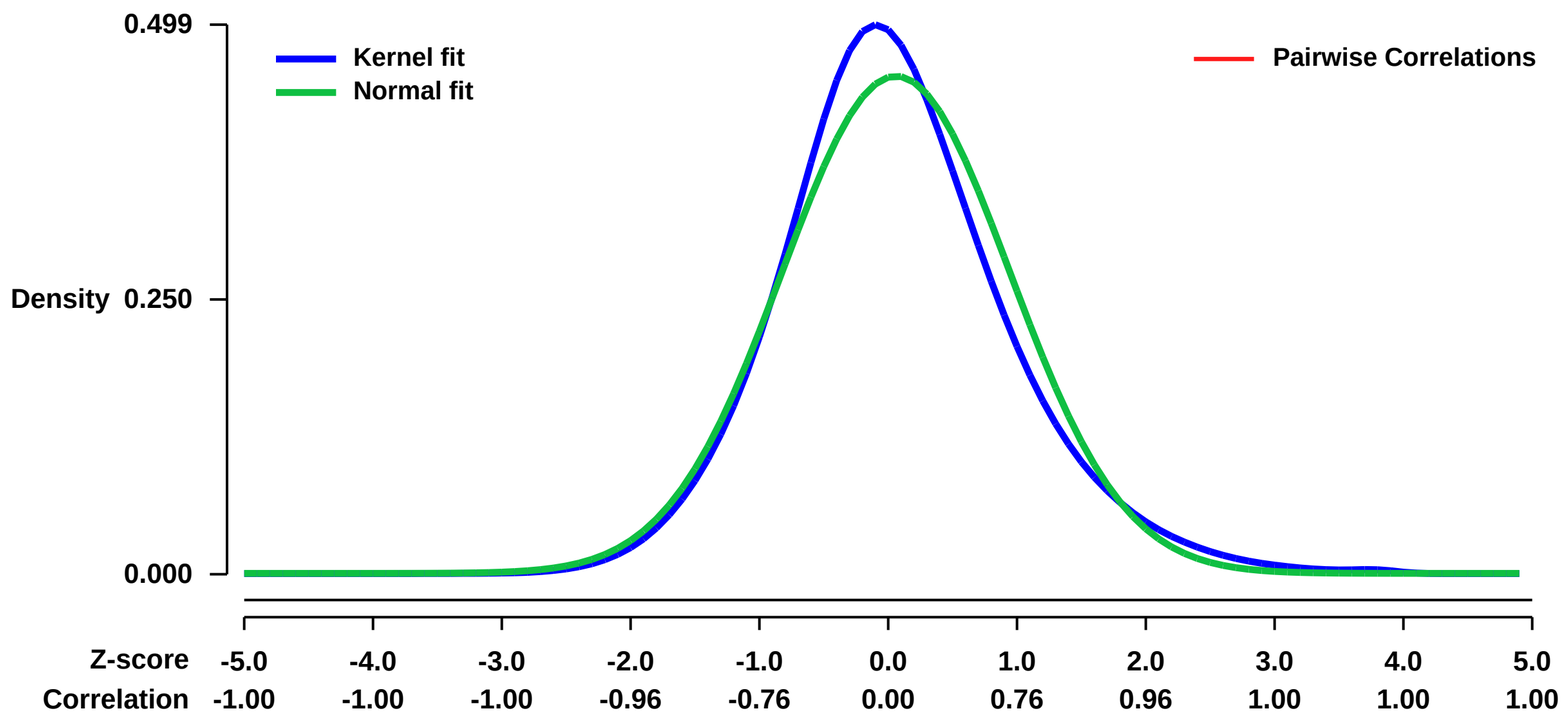

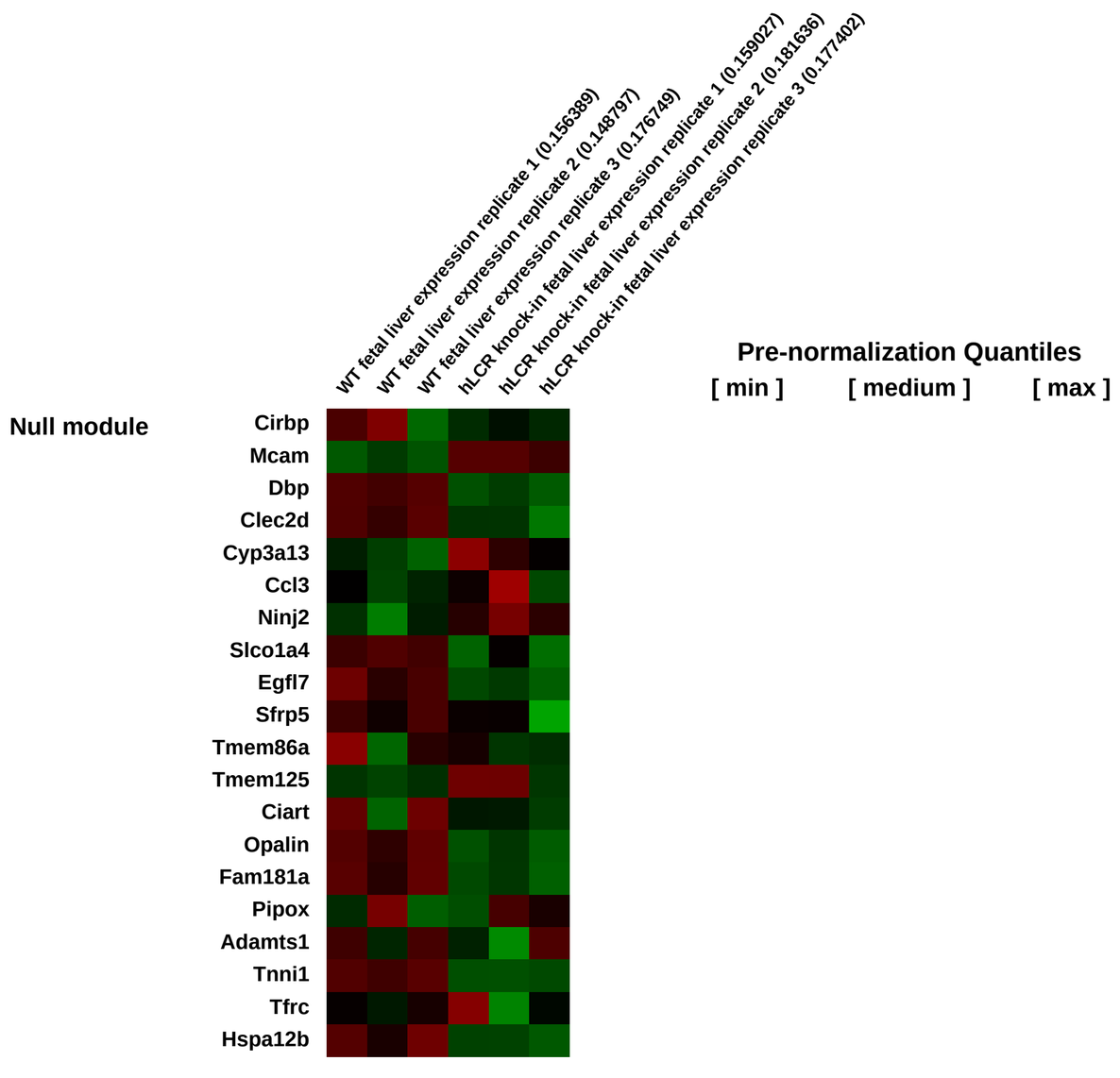

GEO Series "GSE54976" Expression Profiles

Num of samples in this series: 17

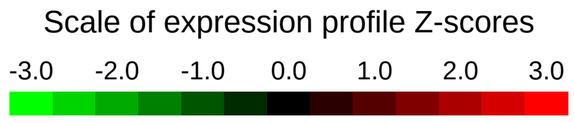

GEO Link:	**http://www.ncbi.nlm.nih.gov/geo/query/acc.cgi?acc=GSE54976**
Status:	**Public on Feb 14 2014**
Title:	**Gene expression in thymi of Tcf1 -/-, Tcf +/- or Tcf1 -/- mice with tumor.**
Organism:	**Mus musculus**
Experiment type:	**Expression profiling by array**
Platform:	**GPL1261**
Pubmed ID:	**23185135**

Summary & Design:

Summary:
The HMG-box factor Tcf1 is required during T-cell development in the thymus and mediates the nuclear response to Wnt signals. Tcf1â /â mice have previously been characterized and show developmental blocks at the CD4â CD8â double negative (DN) to CD4+CD8+ double positive transition. Due to the blocks in T-cell development, Tcf1â /â mice normally have a very small thymus. Unexpectedly, a large proportion of Tcf1â /â mice spontaneously develop thymic lymphomas with 50% of mice developing a thymic lymphoma/leukemia at the age of 16 wk. These lymphomas are clonal, highly metastatic, and paradoxically show high Wnt signaling when crossed with Wnt reporter mice and have high expression of Wnt target genes Lef1 and Axin2. In wild-type thymocytes, Tcf1 is higher expressed than Lef1, with a predominance of Wnt inhibitory isoforms. Loss of Tcf1 as repressor of Lef1 leads to high Wnt activity and is the initiating event in lymphoma development, which is exacerbated by activating Notch1 mutations. Thus, Notch1 and loss of Tcf1 functionally act as collaborating oncogenic events. Tcf1 deficiency predisposes to the development of thymic lymphomas by ectopic up-regulation of Lef1 due to lack of Tcf1 repressive isoforms and frequently by cooperating activating mutations in Notch1. Tcf1 therefore functions as a T-cellâ specific tumor suppressor gene, besides its established role as a Wnt responsive transcription factor. Thus, Tcf1 acts as a molecular switch between proliferative and repressive signals during T-lymphocyte development in the thymus.

Using the Tcf1â /â ¸ VII/¸ VII knockout mouse (Verbeek et al. Nature 1995), thymocytes of 17 mice (5 control Tcf+/-, 4 Tcf-/- and 8 Tcf-/- with thymic lymphoma) were homogenized for RNA isolation using Qiagen RNeasy minicolumns. The quantity and quality of total RNA was determined using spectrophotometry (Nanodrop) and an Agilent Bioanalyzer. One ´µg of RNA was used to generate cRNA using Affymetrix One cycle cDNA synthesis kit (Affymetrix, Santa Clara, CA, USA), after which the samples were biotinylated using an Affymetrix IVT labeling kit (Affymetrix). The samples were hybridized overnight at 42´℃ to GeneChip mouse genome 430 2.0 Arrays (Affymetrix). Washing and staining steps were performed on a Fluidics station 450, and the Genechips were scanned using a GeneChip scanner 3000 (Affymetrix) at the Department of Immunology, Erasmus Medical Center. Raw data were normalized and summarized using Robust Multichip Average (RMA) method.

Overall design:
The experiment consists of 5 control Tcf+/- thymi, 4 Tcf-/- thymi and 8 Tcf-/- thymus samples with thymic lymphoma.

Background corr dist: KL-Divergence = 0.0678, L1-Distance = 0.0800, L2-Distance = 0.0128, Normal std = 0.5432

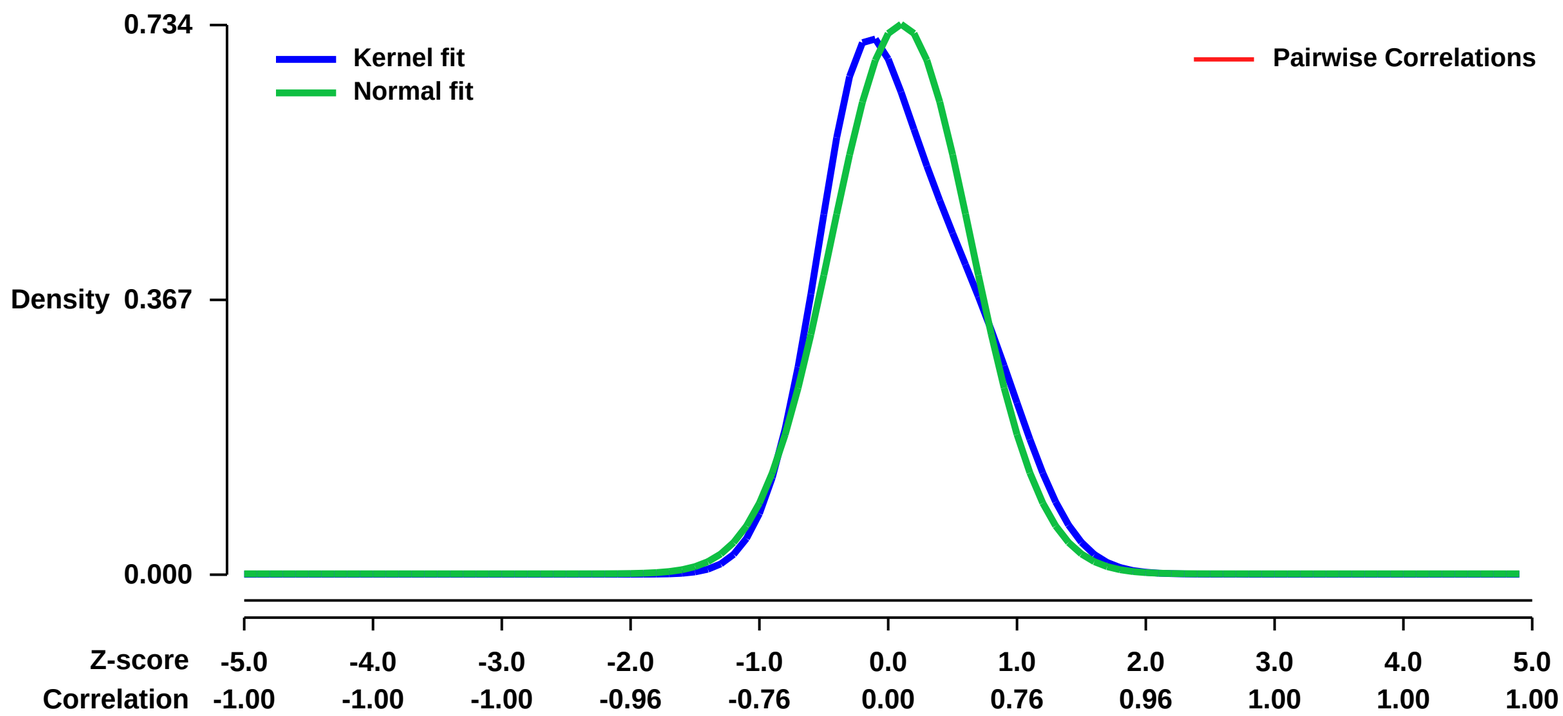

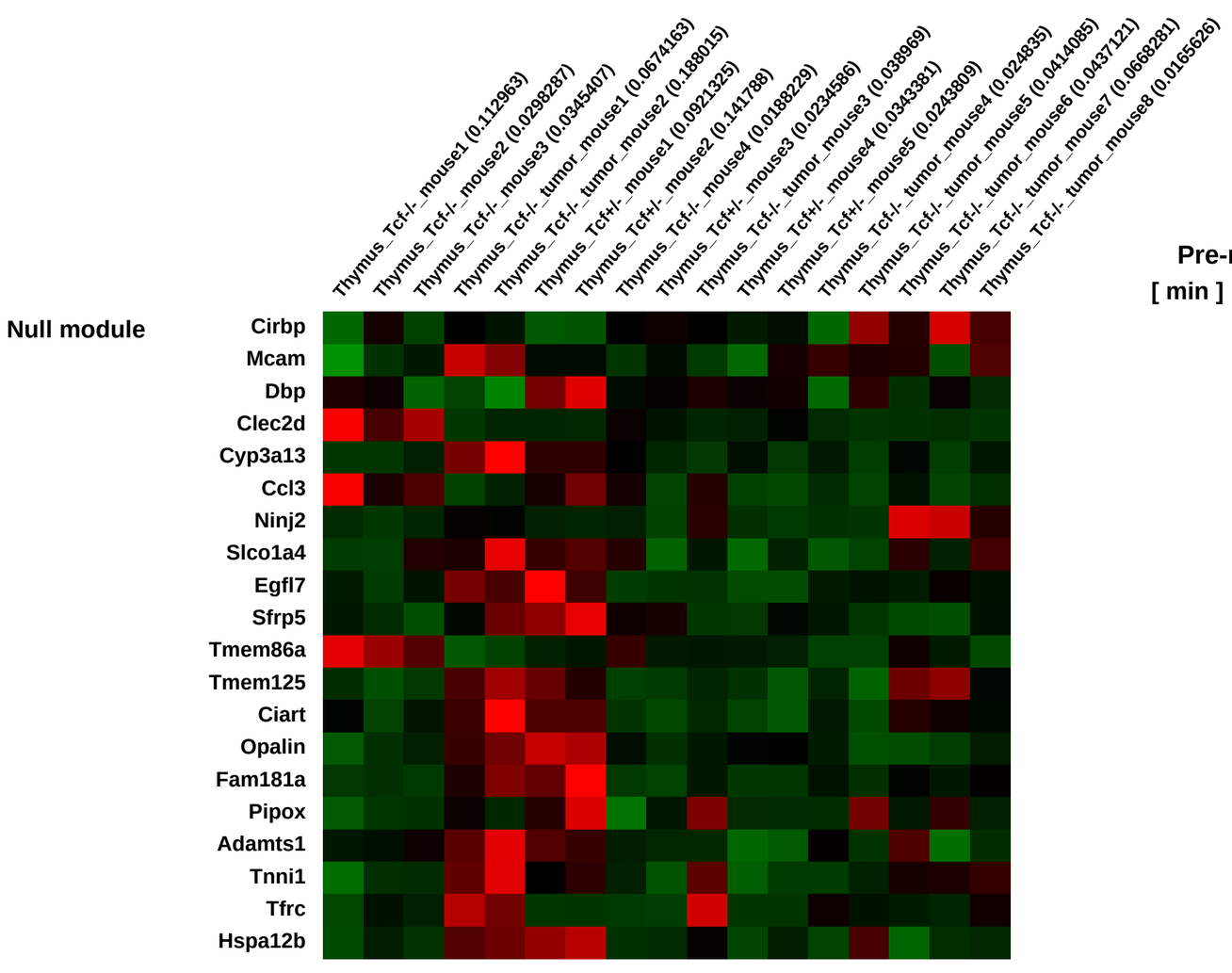

GEO Series "GSE30485" Expression Profiles

Num of samples in this series: 15

Scale of expression profile Z-scores

-3.0 -2.0 -1.0 0.0 1.0 2.0 3.0

GEO Link:	http://www.ncbi.nlm.nih.gov/geo/query/acc.cgi?acc=GSE30485
Status:	Public on Jul 04 2014
Title:	Gene expression accompanying the promotion of hepatocellular carcinoma by intestinal microbiota and Tlr4 in mice.
Organism:	Mus musculus
Experiment type:	Expression profiling by array
Platform:	GPL1261
Pubmed ID:	
Summary & Design:	**Summary:** The effect of Tlr4P712H mutation (rendering TLR4 non-functional), or gut-sterilization by antibiotics, on the induction of tumorgenesis by CCl4 and diethylnitrosamine (DEN) was characterized. Affymetrix Mouse 430 2.0 gene expression measurements were used to characterize the transcriptomic basis of the effects of the above treatments and genotypes on tumorgenesis. **Overall design:** Gene expression of mouse livers of A. WT C3H/HeOuJ mice, B. WT C3H/HeOuJ mice treated with CCl4 and DEN, C. TLR4-mutant C3H/HeJ mice (Tlr4P712H) treated with CCl4 and DEN and D. WT C3H/HeOuJ mice treated with antibiotics (a combination of ampicillin (1 g/l), neomycin [1 g/l], metronidazole[1 g/l] and vancomycin [500 mg/l] in drinking water) and CCl4 and DEN were characterized.

Background corr dist: KL-Divergence = 0.1032, L1-Distance = 0.0263, L2-Distance = 0.0011, Normal std = 0.4349

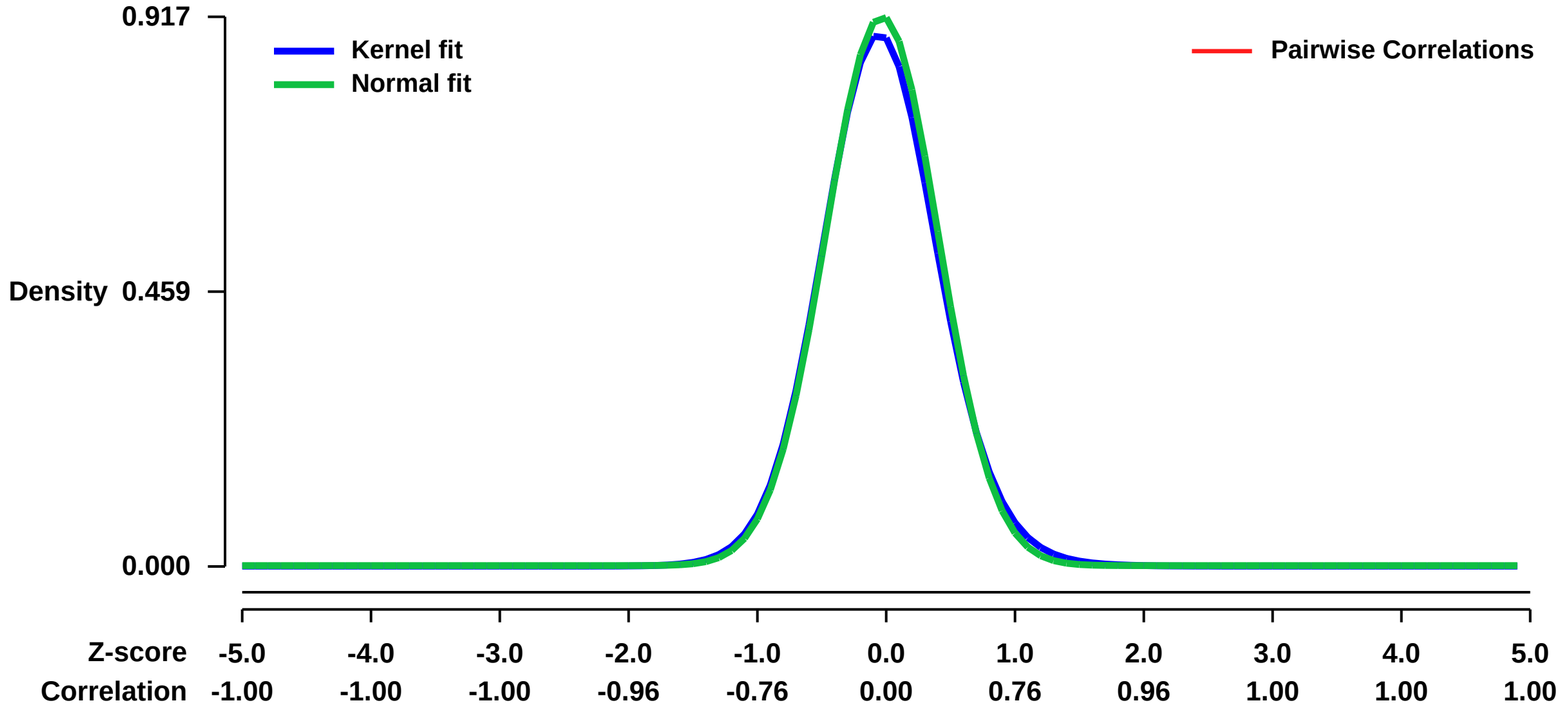

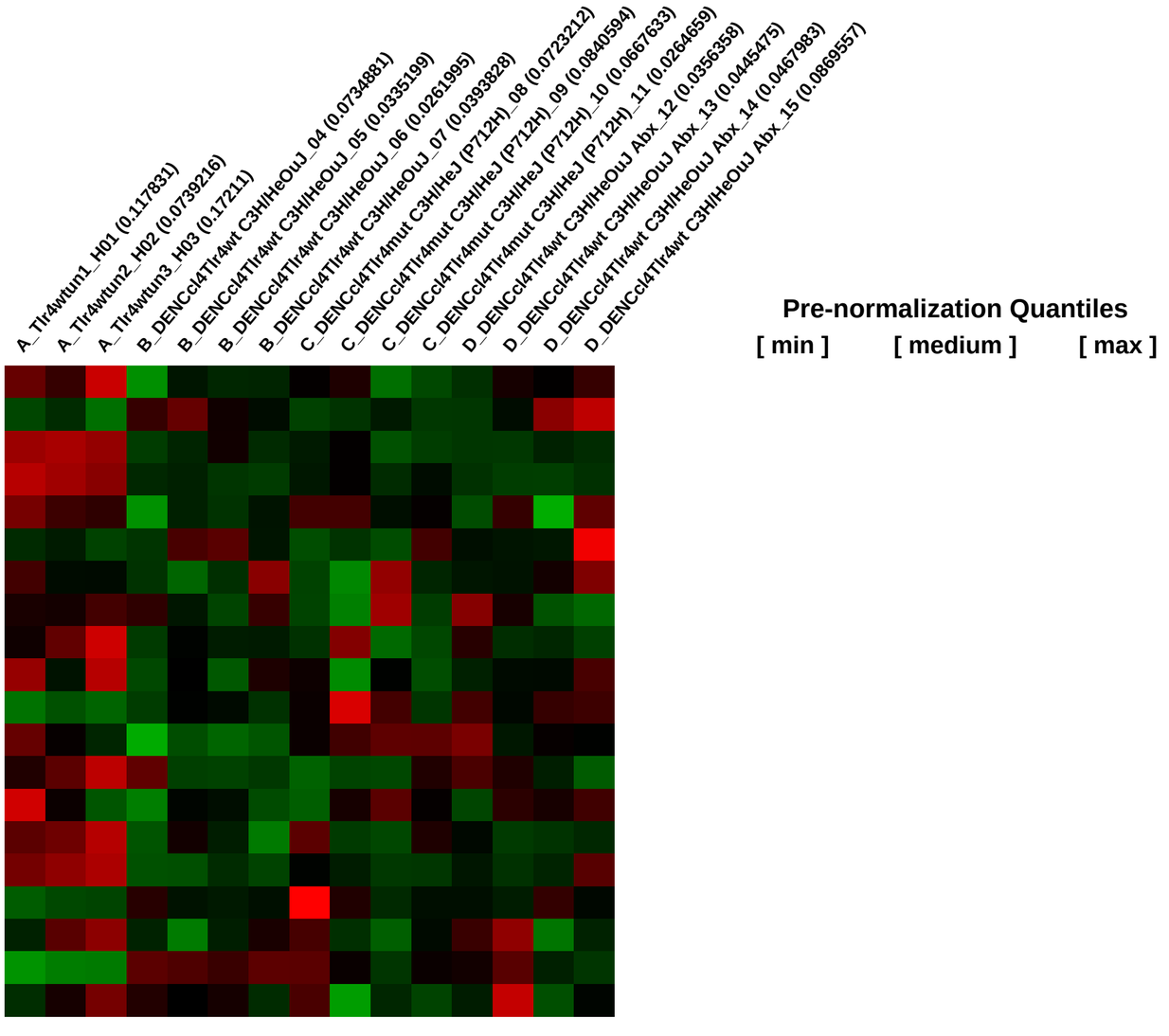

GEO Series "GSE18136" Expression Profiles

Num of samples in this series: 12

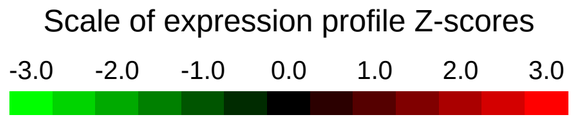

GEO Link:	**http://www.ncbi.nlm.nih.gov/geo/query/acc.cgi?acc=GSE18136**
Status:	**Public on Oct 15 2009**
Title:	**Punctual ablation of Foxp3+ T cells unleashes an autoimmune lesion**
Organism:	**Mus musculus**
Experiment type:	**Expression profiling by array**
Platform:	**GPL1261**
Pubmed ID:	
Summary & Design:	**Summary:** **How do Treg cells control an autoimmune lesion? We depleted Foxp3+ Treg cells in autoimmune prone TCR transgenic BDC2.5 mice on the NOD background** **Kinetic of gene-expression changes in CD4 T cells isolated for pancreas and pancreas draining lymph node (PLN) of Foxp3-DTR.BDC2.5/NOD mice after Treg cell ablation** **Keywords: T cell activation/ differentiation after Treg depletion timecourse** **Overall design:** **CD4 T cells were isolated from pancreas and PLN at 0, 15 and 24 hours after diphtheria toxin application into 4-6 week old female Foxp3-DTR.BDC2.5/NOD transgenic mice**

Background corr dist: KL-Divergence = 0.1270, L1-Distance = 0.0313, L2-Distance = 0.0017, Normal std = 0.3983

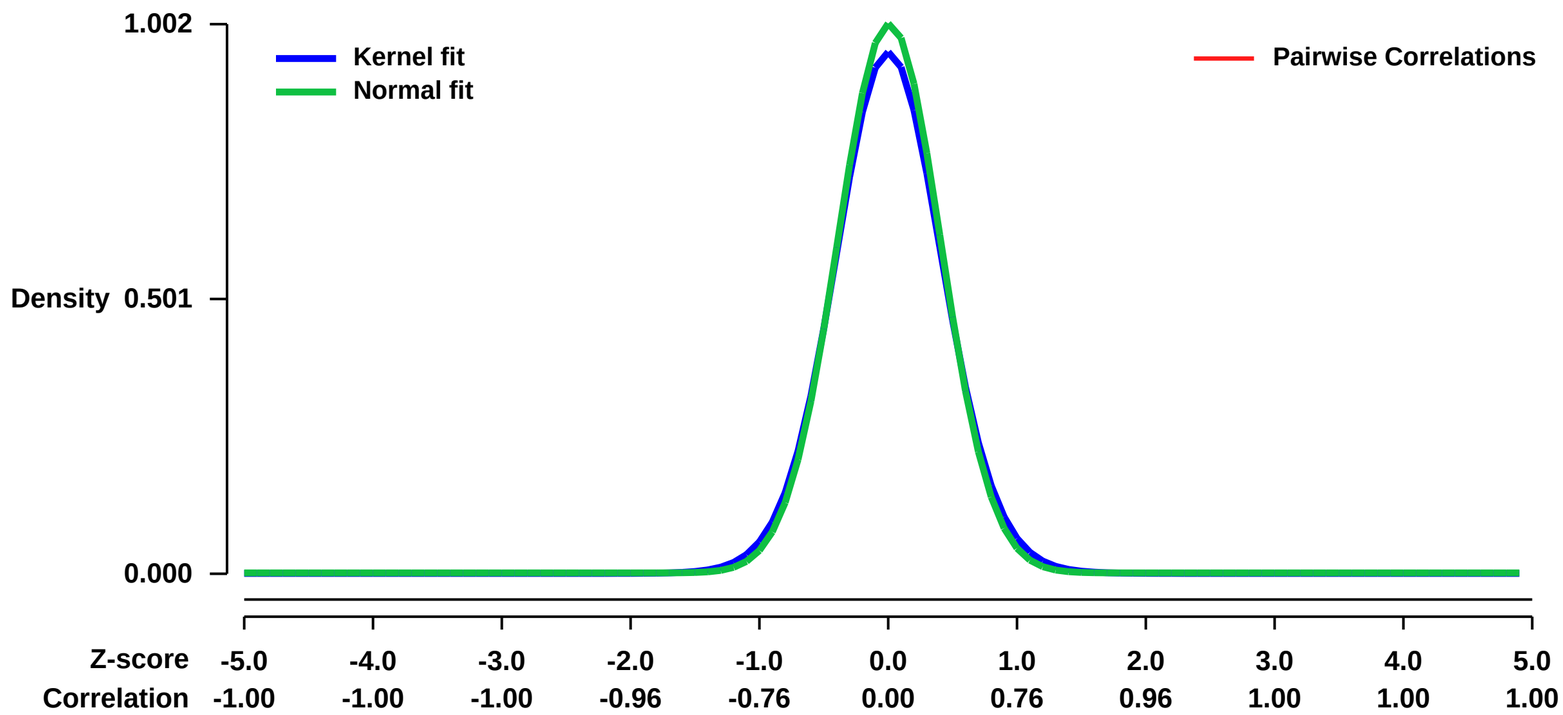

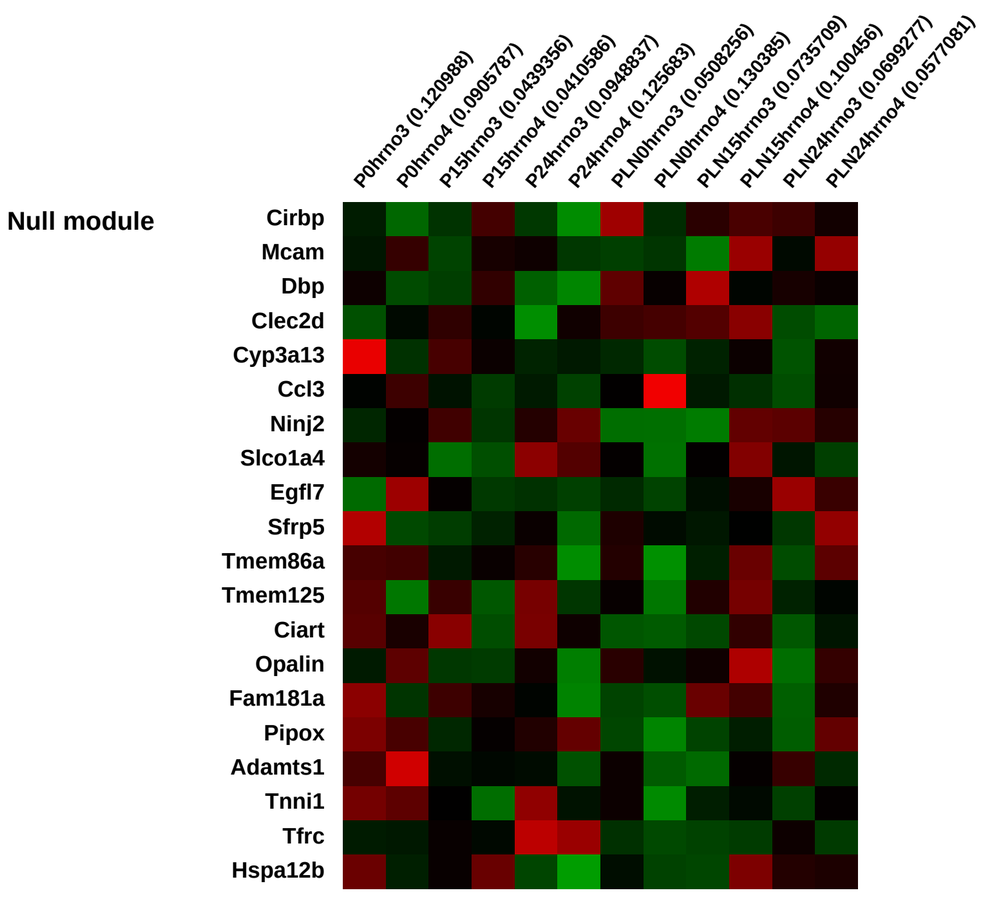

GEO Series "GSE45028" Expression Profiles

Num of samples in this series: 22

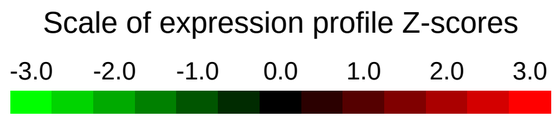

GEO Link:	**http://www.ncbi.nlm.nih.gov/geo/query/acc.cgi?acc=GSE45028**
Status:	**Public on Jul 01 2014**
Title:	**Expression data from NOD and C57BL/6 mouse pancreas CD8ˌ–- Dendritic Cells (DCs) under steady-state and after in-vitro LPS stimulation**
Organism:	**Mus musculus**
Experiment type:	**Expression profiling by array**
Platform:	**GPL1261**
Pubmed ID:	
Summary & Design:	**Summary:** **Abstract Two major dendritic cell (DC) subsets have been described in the islets of mice: The immunogenic CD8ˌ–-CD11b+ DCs and the tolerogenic CD8ˌ–+CD103+ DCs. We have recently reported on reduced numbers of the minor population of tolerogenic CD8ˌ–+CD103+ DCs in the pancreas of 5 week old pre-diabetic non-obese diabetic (NOD) mice. Aim: To analyze also the larger subset of CD11c+CD8ˌ–- DCs isolated from the pancreas of pre-diabetic NOD mice 1) for maturation and tolerance inducing molecules found abnormally expressed on CD8ˌ–+CD103+ DCs, and 2) for genome-wide gene expression to further elucidate abnormalities in underlying gene expression networks. Methods: CD11c+CD8ˌ–- DCs were isolated from 5 week old C57BL/6 and NOD pancreas. Expression of cell surface markers including CD86, CCR5, CD11b, CD103, Clec9a, CD24 and CD200R3 were measured by FACS. Genome-wide gene expression by microarray was assessed during the steady state and after in vitro LPS stimulation. Results: The steady state pancreatic CD11c+ CD8ˌ–- DCs during the pre-diabetic stage showed: 1) A reduced expression of several gene networks important for the prime functions of the cell, such as for cell renewal, immune stimulation and immune tolerance induction, for migration and for the provision of growth factors for beta cell regeneration. This general deficiency state was corroborated by a reduced in vivo proliferation (BrdU incorporation) of the cells and the reduced expression in FACS analysis of CD86, CCR5, CD103, Clec9a, CD24 and CD200R3 on the cells. 2) A hyper reactivity of these cells to LPS correlated with an enhanced pro-inflammatory state characterized by altered expression of a number of classical pro-inflammatory factors and cytokines. Conclusion: The NOD CD11c+CD8ˌ–- DCs seem to be Janus-faced depending on the conditions: Deficient in steady state with reduced immune stimulation capabilities also for tolerance induction; over-inflammatory with a molecular profile suggesting a preferential stimulatory capacity for Th1 cells when encountering a Pathogen-Associated Molecular Pattern (PAMP) in the form of LPS.** **We used microarray gene expression analysis to explain the abnormal expression of several cell surface markers involved in tolerace, migration and maturation in the steady-state and to measure the effect of a PAMP such as LPS** **Overall design:** **We isolated RNA from FACS sorted CD11c+CD8ˌ–- DCs in 10 pooled pancreases from pre-diabetic NOD and non-diabetic C57BL/6 mice at 5 weeks. In addition, we treated in another experiment the isolated pancreas DCs with LPS (and PBS), incubated for 18h and measured gene expression. We compared gene expression between strains NOD vs C57BL/6 under steady-state and after in-vitro LPS/PBS stimulation.**

Background corr dist: KL-Divergence = 0.0365, L1-Distance = 0.0850, L2-Distance = 0.0118, Normal std = 0.7351

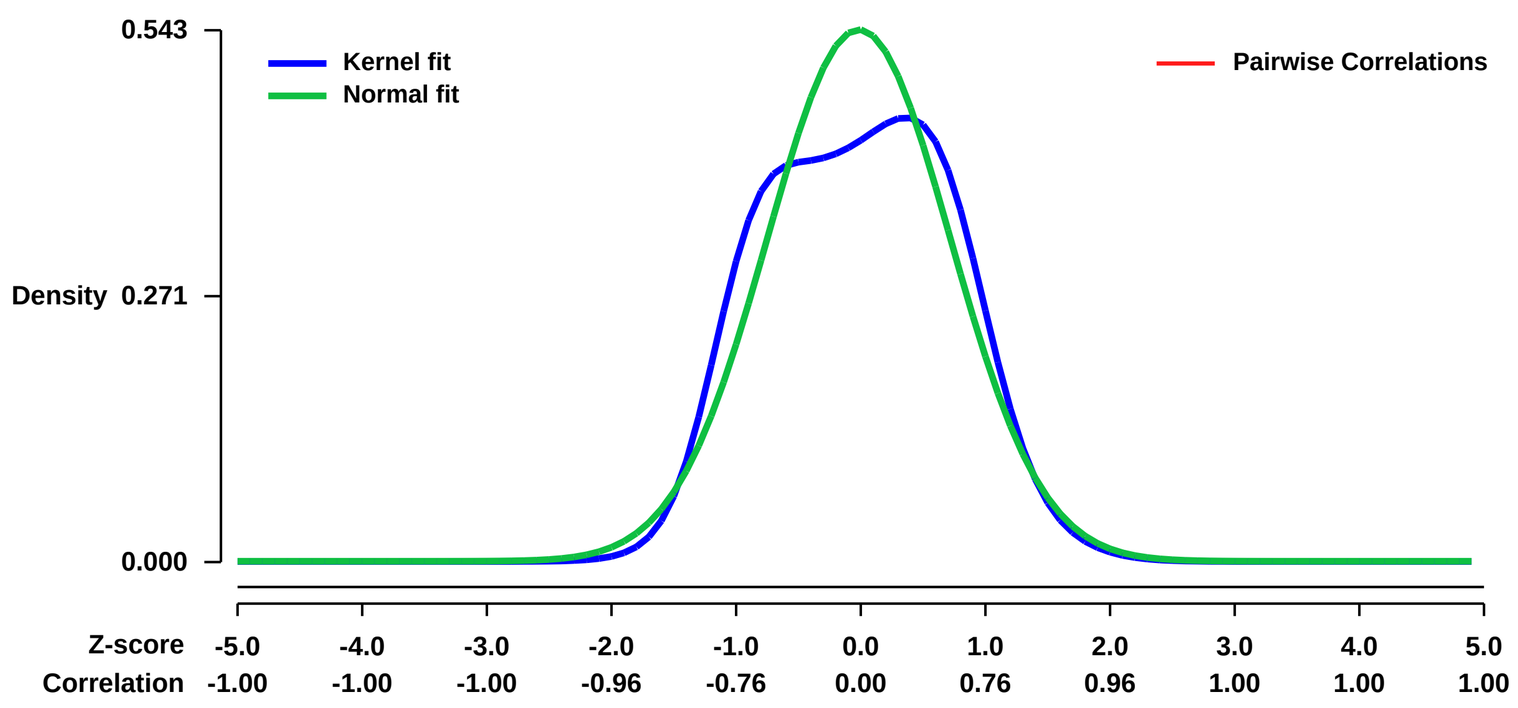

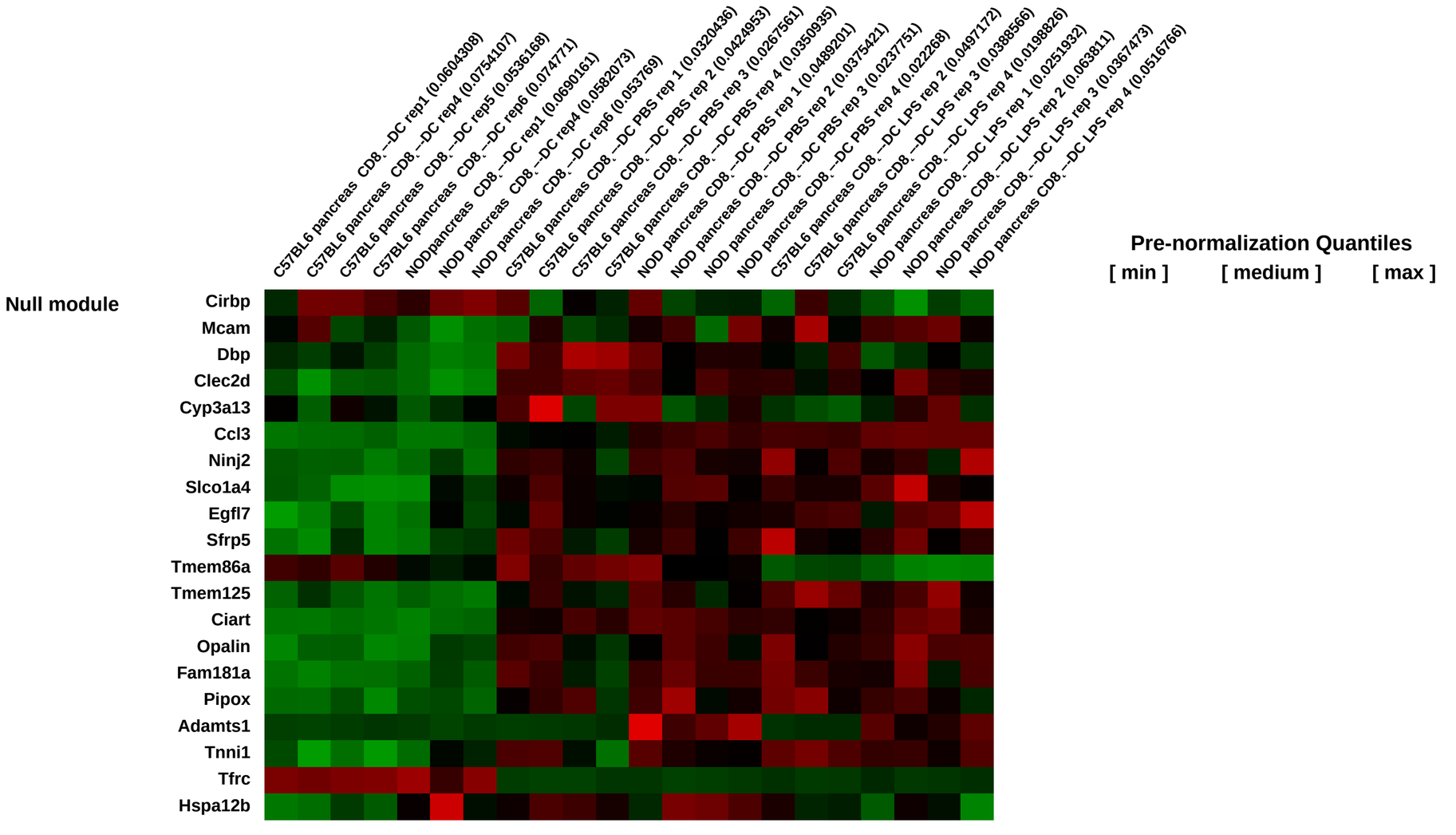

GEO Series "GSE5715" Expression Profiles

Num of samples in this series: 10

Scale of expression profile Z-scores

-3.0 -2.0 -1.0 0.0 1.0 2.0 3.0

GEO Link:	http://www.ncbi.nlm.nih.gov/geo/query/acc.cgi?acc=GSE5715
Status:	Public on May 21 2007
Title:	Intestinal Phenotype of Variable Weight Cystic Fibrosis Knockout Mice
Organism:	Mus musculus
Experiment type:	Expression profiling by array
Platform:	GPL1261
Pubmed ID:	17615178
Summary & Design:	**Summary:** Cystic fibrosis transmembrane conductance regulator (Cftr) knockout mice present the clinical features of low body weight and intestinal disease permitting an assessment of the interrelatedness of these phenotypes in a controlled environment. To identify intestinal alterations which affect body weight in CF mice the histological phenotypes of crypt-villus axis height, goblet cell hyperplasia, and mast cell infiltrate were measured, cardiac blood samples assessed, and gene expression profiling of the ileum was completed for 12 week old (C57BL/6xBALB) F2 Cftrtm1UNC and non-CF mice presenting a range of body weight. Crypt-villus axis height decreased with increasing weight in CF, but not control, mice. Goblet cell hyperplasia and mast cell infiltration in the submucosa and muscularis externa layers of the CF intestine, were identified to be independent of bodyweight. Blood triglyceride levels were found to be significantly lower in CF mice than control mice (p = 3.02 x 10-5) but were not dependent on CF mouse body weight. By expression profiling, genes of DNA replication and lipid metabolism were among those altered in CF mice relative to non-CF controls; and no differences in gene expression were measured between samples from CF mice in the 25th and 75th percentile for weight. This study indicates that the absence of Cftr leads to altered morphology in the CF intestine the extent of which is correlated with body weight in CF mice while CF related changes in blood triglyceride levels and in the intestinal gene expression profile were not dependent on body weight in this model. **Keywords:** disease state analysis **Overall design:** B6xBALB F2 mice gene expression was collected for nine CF-/- mice and 6 controls. Differential expression was analyzed between the groups

Background corr dist: KL-Divergence = 0.0959, L1-Distance = 0.0285, L2-Distance = 0.0013, Normal std = 0.4421

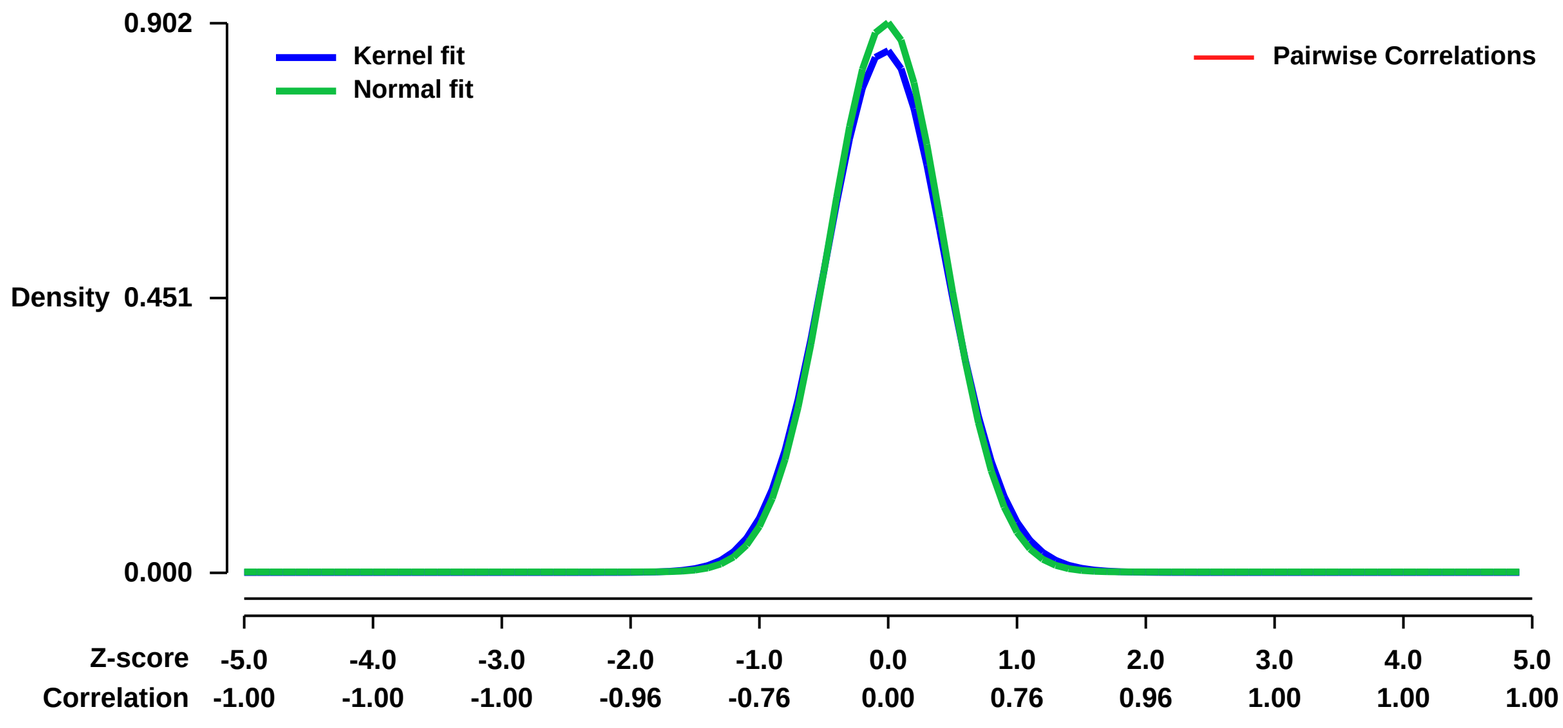

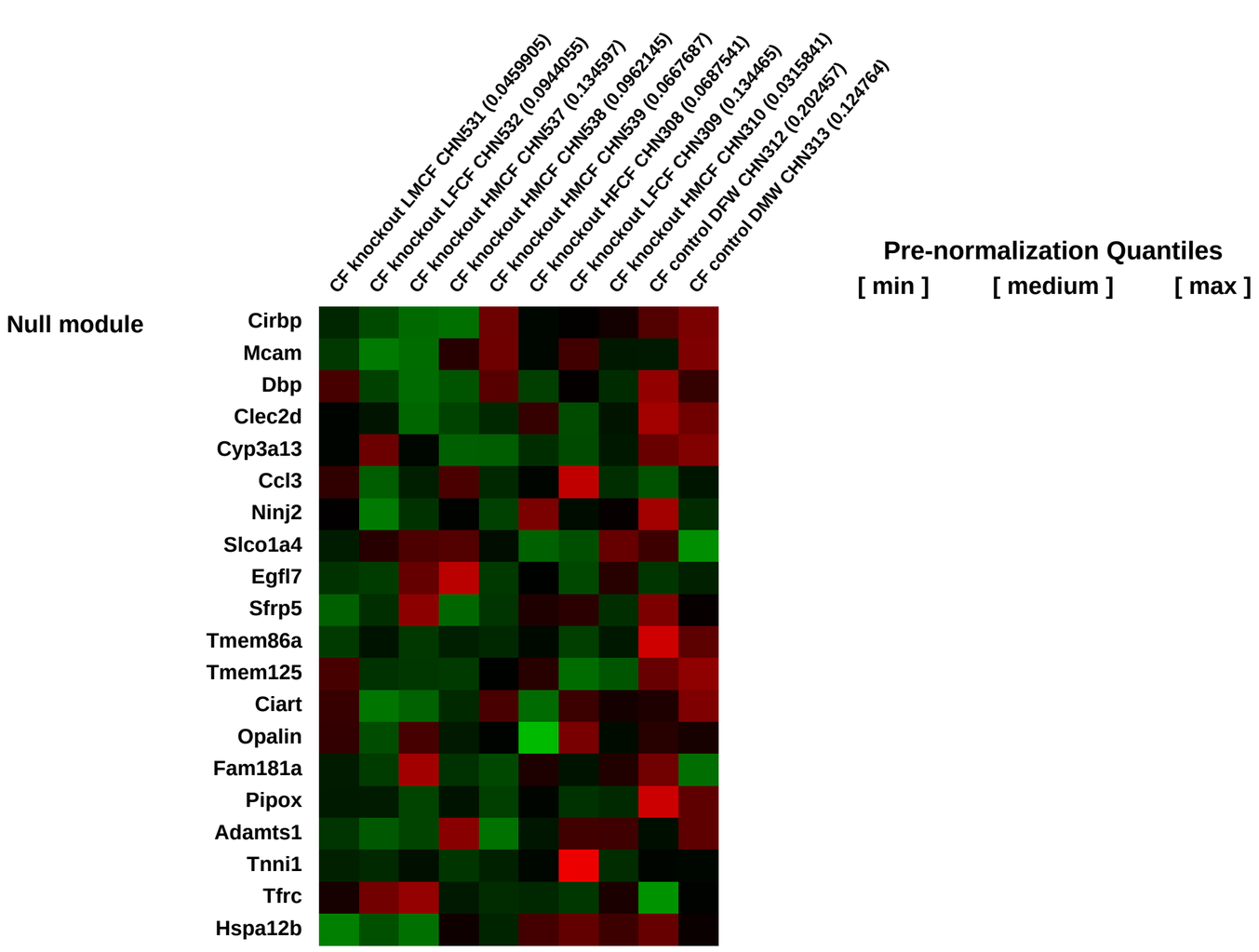

GEO Series "GSE24121" Expression Profiles

Num of samples in this series: 9

Scale of expression profile Z-scores

-3.0 -2.0 -1.0 0.0 1.0 2.0 3.0

GEO Link:	**http://www.ncbi.nlm.nih.gov/geo/query/acc.cgi?acc=GSE24121**
Status:	**Public on Oct 20 2010**
Title:	**Oligoarray analysis of mRNA species from DCs treated with C. parvum for 24 h.**
Organism:	**Mus musculus**
Experiment type:	**Expression profiling by array**
Platform:	**GPL1261**
Pubmed ID:	
Summary & Design:	**Summary:** **To investigate whether C. parvum treatment of DCs regulates other inflammatory genes, mouse BMDCs (CD11c and CD11b positive) were treated with C. parvum for 24 hr. Control groups included untreated BMDCs and DCs treated with E. cuniculi. We noticed that a significant upregulation of the expression of interferon-related genes, which may correlation the critical role of interferon in host defense against C. parvum infection.** **Overall design:** **DCs were treated with C. parvum for 24 hr. Control groups included untreated BMDCs and DCs treated with E. cuniculi. Group comparison was performed using the data of 3 replicate arrays from each time point.**

Background corr dist: **KL-Divergence = 0.0664, L1-Distance = 0.0336, L2-Distance = 0.0016, Normal std = 0.5257**

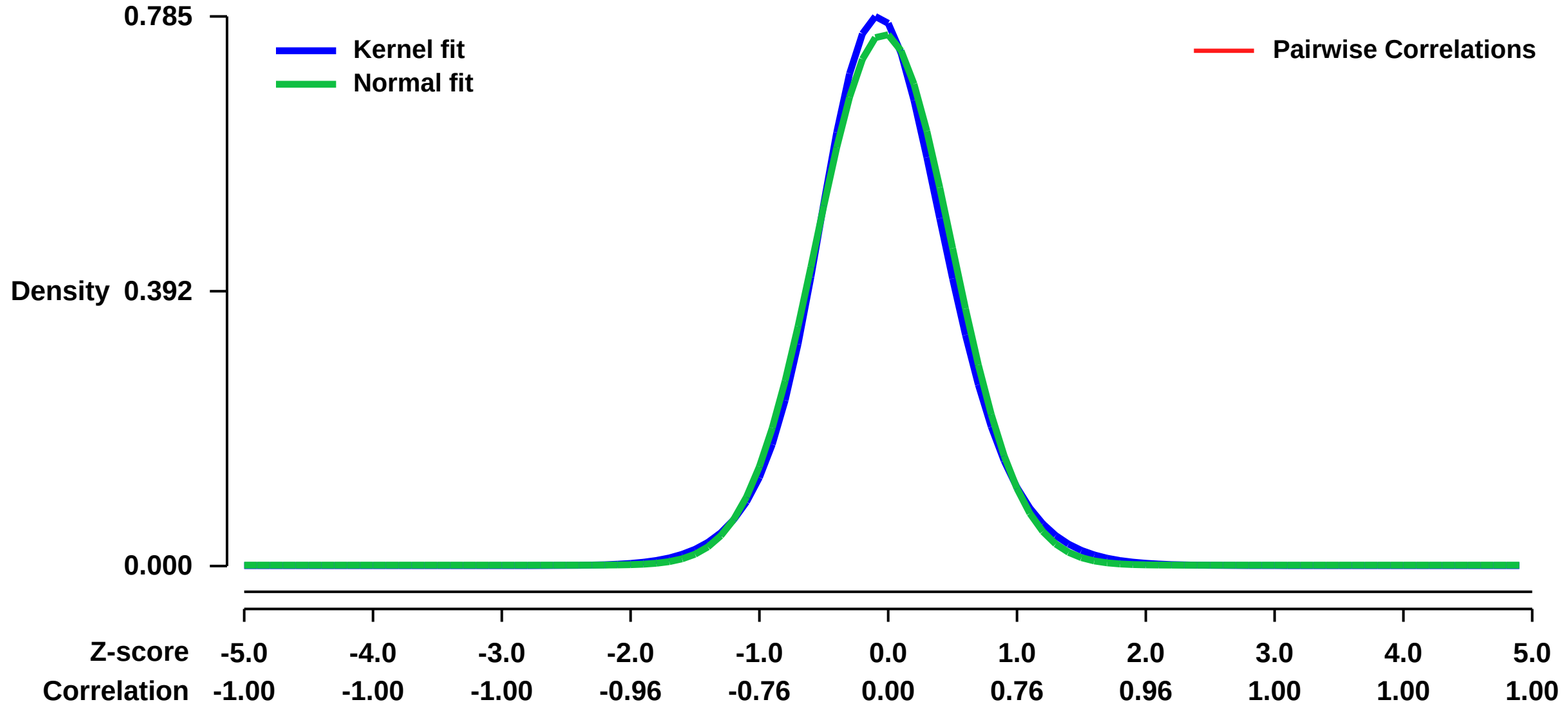

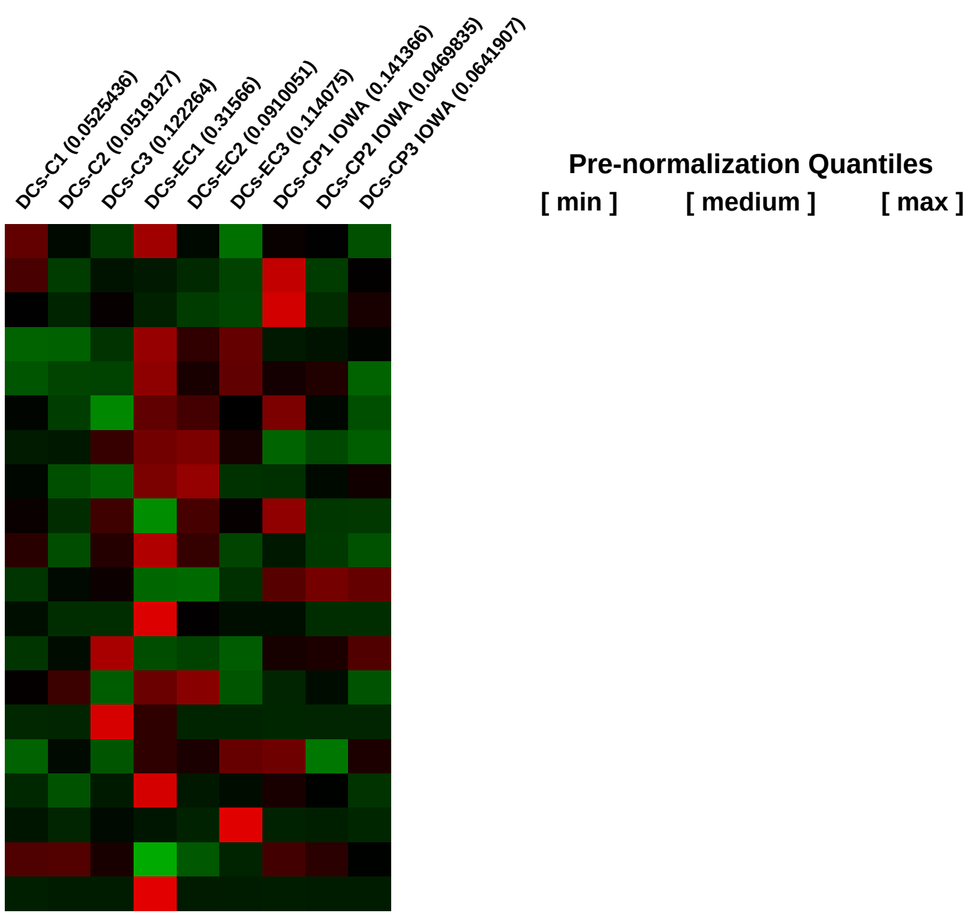

GEO Series "GSE3253" Expression Profiles

Num of samples in this series: 12

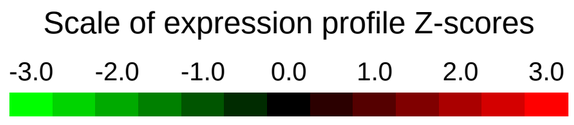

GEO Link:	http://www.ncbi.nlm.nih.gov/geo/query/acc.cgi?acc=GSE3253
Status:	Public on Sep 12 2005
Title:	Exaggerated neuroinflammation and sickness behavior in aged mice after activation of the peripheral innate immune system
Organism:	Mus musculus
Experiment type:	Expression profiling by array
Platform:	GPL1261
Pubmed ID:	15919760
Summary & Design:	**Summary:** Acute cognitive impairment (i.e., delirium) is common in elderly emergency department patients and frequently results from infections that are unrelated to the central nervous system. Since activation of the peripheral innate immune system induces brain microglia to produce inflammatory cytokines that are responsible for behavioral deficits, we investigated if aging exacerbated neuroinflammation and sickness behavior after peripheral injection of lipopolysaccharide (LPS). Microarray analysis revealed a transcriptional profile indicating the presence of primed or activated microglia and increased inflammation in the aged brain. Furthermore, aged mice had a unique gene expression profile in the brain after an intraperitoneal injection of LPS, and the LPS-induced elevation in the brain inflammatory cytokines and oxidative stress was both exaggerated and prolonged compared with adults. Aged mice were anorectic longer and lost more weight than adults after peripheral LPS administration. Moreover, reductions in both locomotor and social behavior remained 24 h later in aged mice, when adults had fully recovered, and the exaggerated neuroinflammatory response in aged mice was not reliably paralleled by increased circulating cytokines in the periphery. Taken together, these data establish that activation of the peripheral innate immune system leads to exacerbated neuroinflammation in the aged as compared with adult mice. This dysregulated link between the peripheral and central innate immune system is likely to be involved in the severe behavioral deficits that frequently occur in older adults with systemic infections. Keywords: Aging, cytokines, brain, inflammation, behavior **Overall design:** In this study, adult and aged mice were injected intraperitoneal with sterile saline or Escherichia coli LPS (0.33 mg/kg, ~10 ´¦g/mouse; serotype 0127:B8, Sigma). This dosage of LPS was used because it induces a mild transient sickness behavior in young adults. Mice were killed 4 h after saline or LPS injection by CO2 asphyxiation. Blood samples were collected and brains were removed, separated in half at the longitudinal fissure, frozen in liquid nitrogen, and stored (-80´℃) until assaying. Total RNA was later isolated from some brain samples for microarray analysis (n=3).

Background corr dist: KL-Divergence = 0.1805, L1-Distance = 0.0447, L2-Distance = 0.0044, Normal std = 0.3453

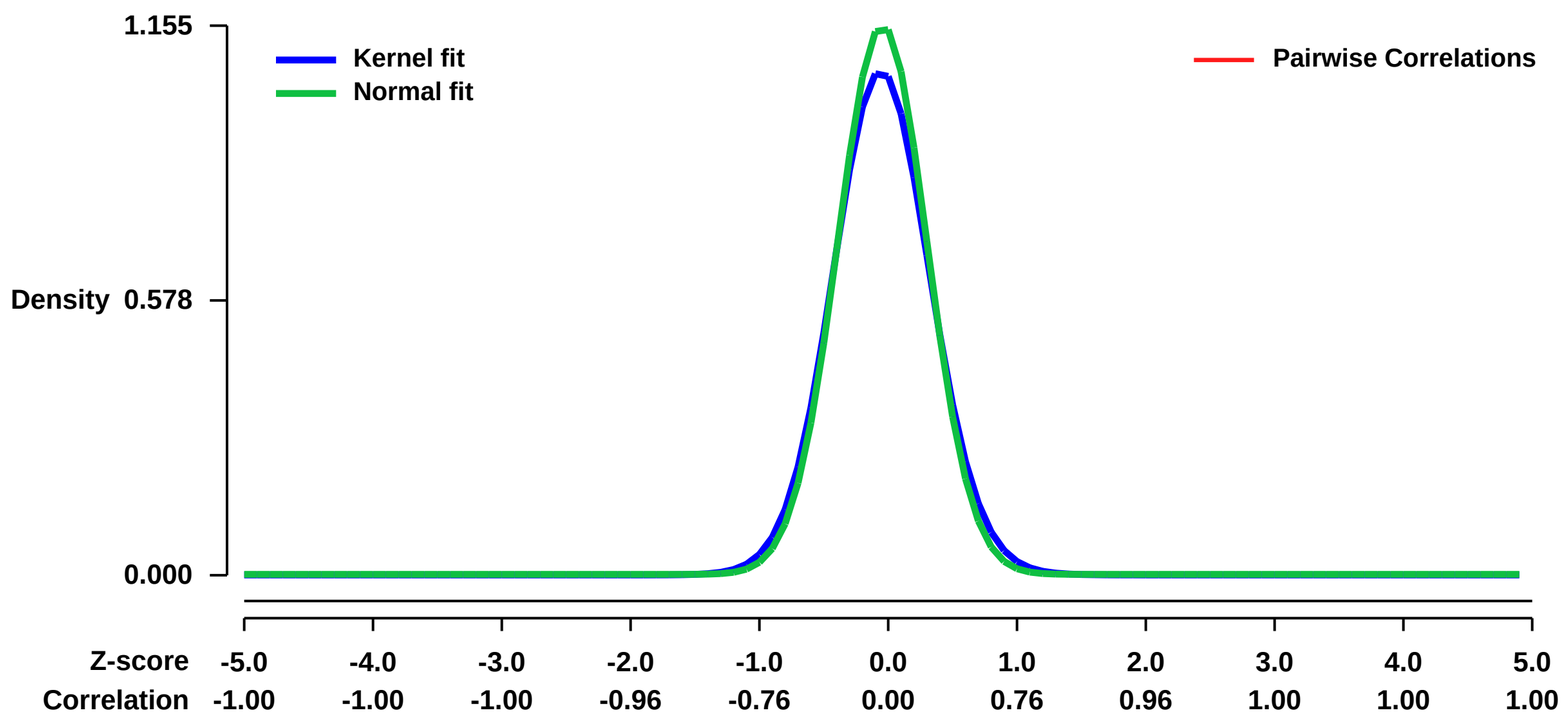

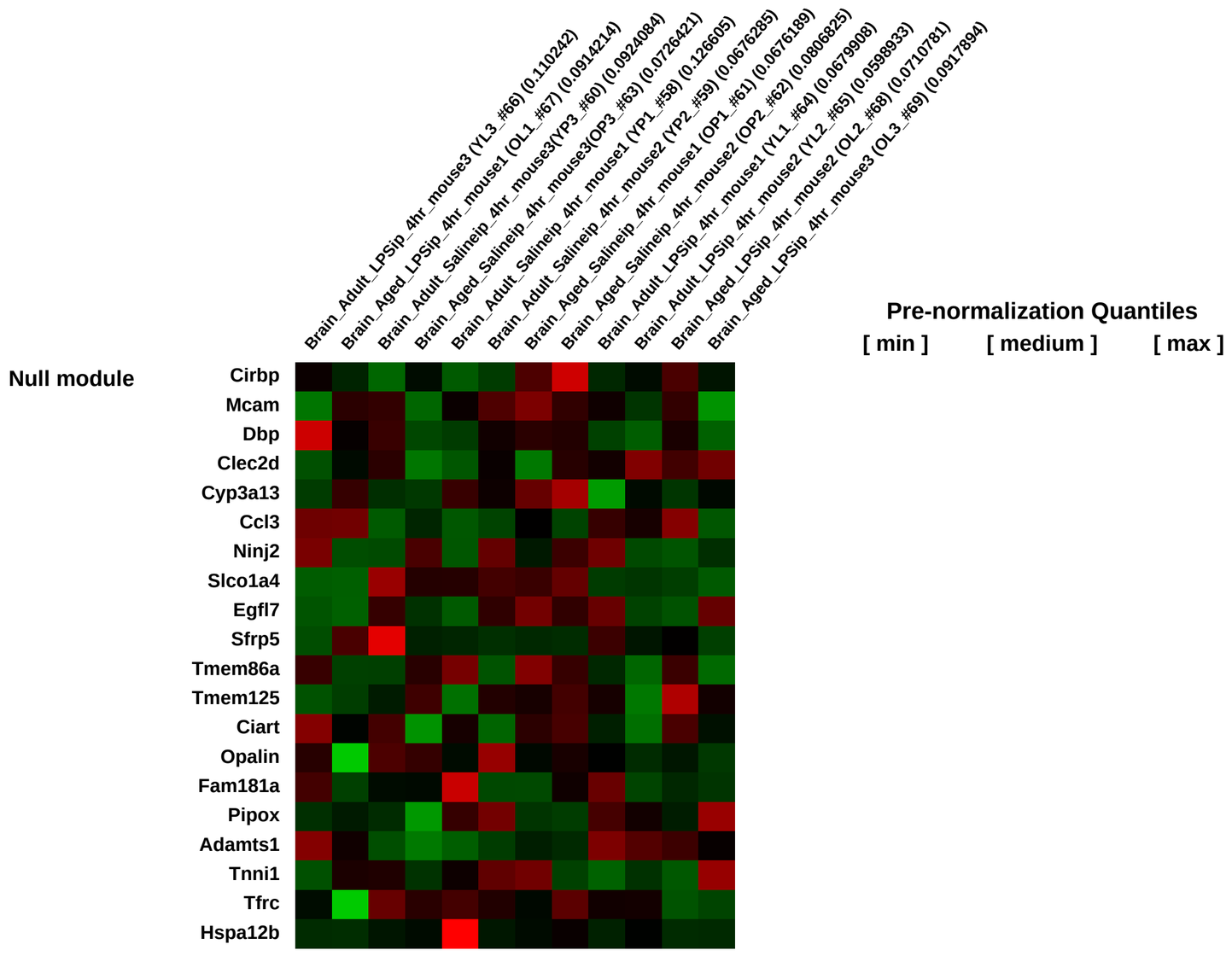

GEO Series "GSE9717" Expression Profiles

Num of samples in this series: 6

Scale of expression profile Z-scores

-3.0 -2.0 -1.0 0.0 1.0 2.0 3.0

GEO Link:	http://www.ncbi.nlm.nih.gov/geo/query/acc.cgi?acc=GSE9717
Status:	Public on Feb 14 2008
Title:	Rb Intrinsically Promotes Erythropoiesis by Coupling Cell Cycle Exit with Mitochondrial Biogenesis
Organism:	Mus musculus
Experiment type:	Expression profiling by array
Platform:	GPL1261
Pubmed ID:	18258751
Summary & Design:	**Summary:** Regulation of the cell cycle is intimately linked to erythroid differentiation, yet how these processes are coupled is not well understood. To gain insight into this coordinate regulation, we examined the role that the retinoblastoma protein (Rb), a central regulator of the cell cycle, plays in erythropoiesis. We found that Rb serves a cell-intrinsic role and its absence causes ineffective erythropoiesis, with a differentiation block at the transition from early to late erythroblasts. Unexpectedly, in addition to a failure to properly exit the cell cycle, mitochondrial biogenesis fails to be upregulated concomitantly, contributing to this differentiation block. The link between erythropoiesis and mitochondrial function was validated by inhibition of mitochondrial biogenesis. Erythropoiesis in the absence of Rb resembles the human myelodysplastic syndromes, where defects in cell cycle regulation and mitochondrial function frequently occur. Our work demonstrates how these seemingly disparate pathways play a role in coordinately regulating cellular differentiation. **Keywords:** disease state analysis **Overall design:** Microarray expression analysis from sorted CD71+/Ter-119+ bone marrow erythroid progenitors of Rb-null animals and controls. The Rb-null genotype was EpoR-GFPcre/+; Rb fl/fl and the control genotype was EpoR-GFPcre/+; Rb fl/+. We have analyzed 3 Rb-null datasets and 3 control datasets.

Background corr dist: KL-Divergence = 0.0253, L1-Distance = 0.0283, L2-Distance = 0.0011, Normal std = 0.7113

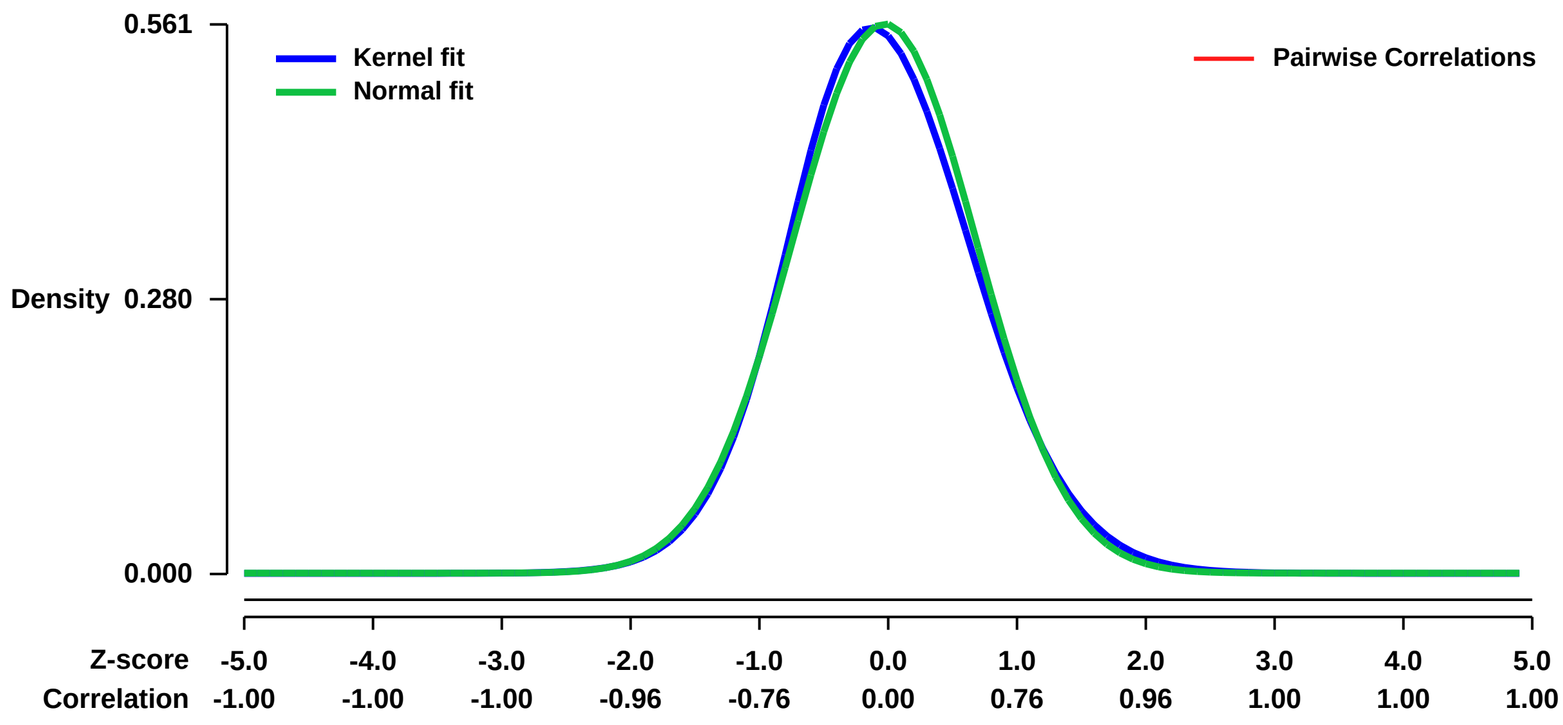

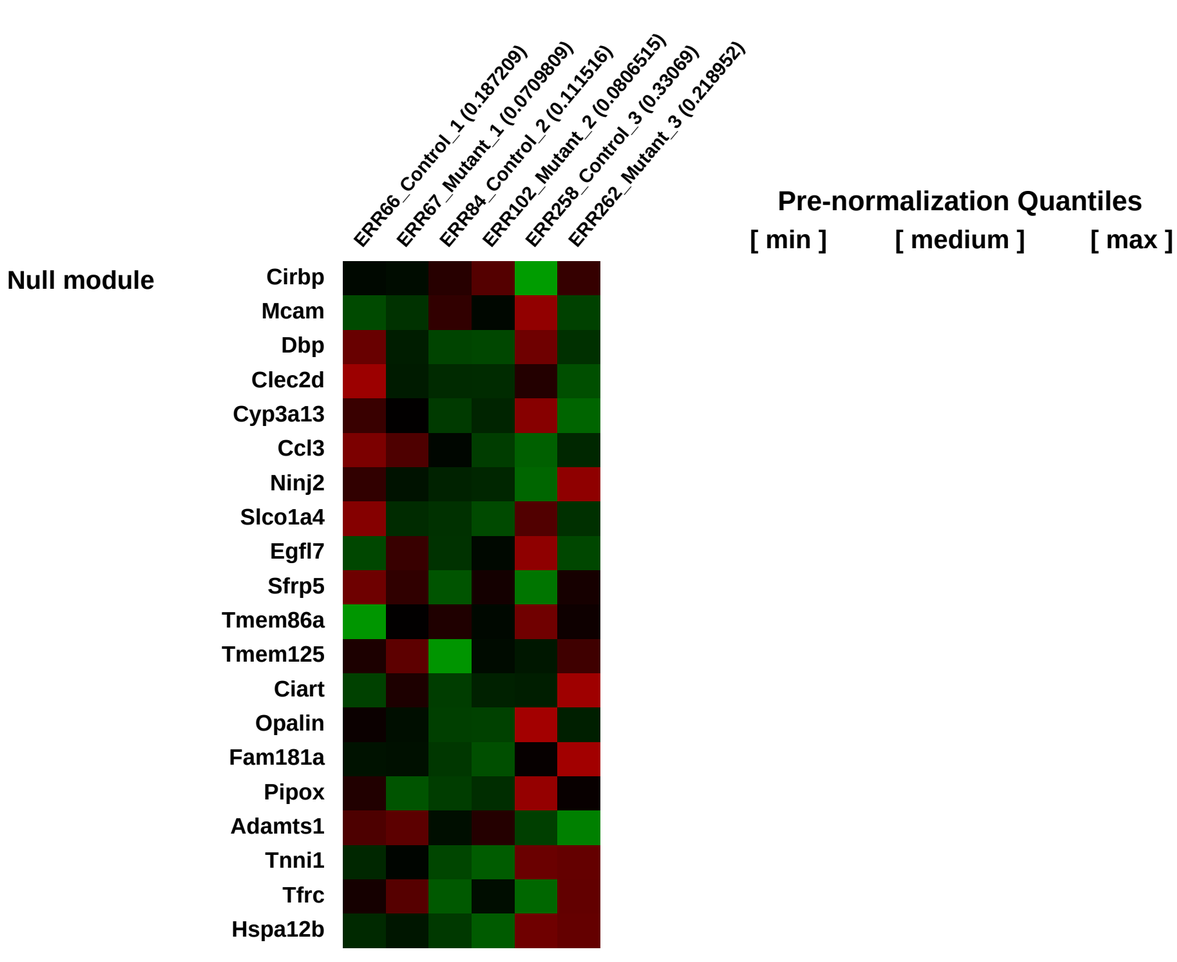

GEO Series "GSE16994" Expression Profiles

Num of samples in this series: 12

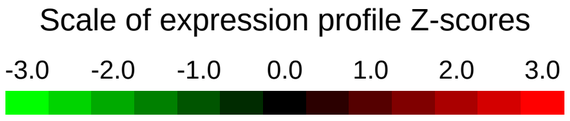

GEO Link:	http://www.ncbi.nlm.nih.gov/geo/query/acc.cgi?acc=GSE16994
Status:	Public on Jul 01 2010
Title:	Microarray analysis of iris gene expression in mice with mutations influencing pigmentation
Organism:	Mus musculus
Experiment type:	Expression profiling by array
Platform:	GPL1261
Pubmed ID:	20739468
Summary & Design:	**Summary:** Several ocular diseases involve the iris, notably including oculocutaneous albinism, pigment dispersion syndrome, and exfoliation syndrome. To screen for candidate genes that may be active in these diseases, genome-wide iris gene expression patterns were comparatively analyzed from mouse models of these conditions. **Overall design:** Irides were obtained from healthy C57Bl/6J, B6-Lystbg-J/J which carry a mutation in the Lyst gene, B6(Cg)-TyrC-2J/J which carry a mutation in the tyr gene, and B6.D2-Tryp1bGpnmbR150X/Sj with mutations in both Tryp1 and Gpnmb. Four eyes from two mice were pooled for one sample. Three samples were prepared for each strain.

Background corr dist: KL-Divergence = 0.0783, L1-Distance = 0.0357, L2-Distance = 0.0025, Normal std = 0.4764

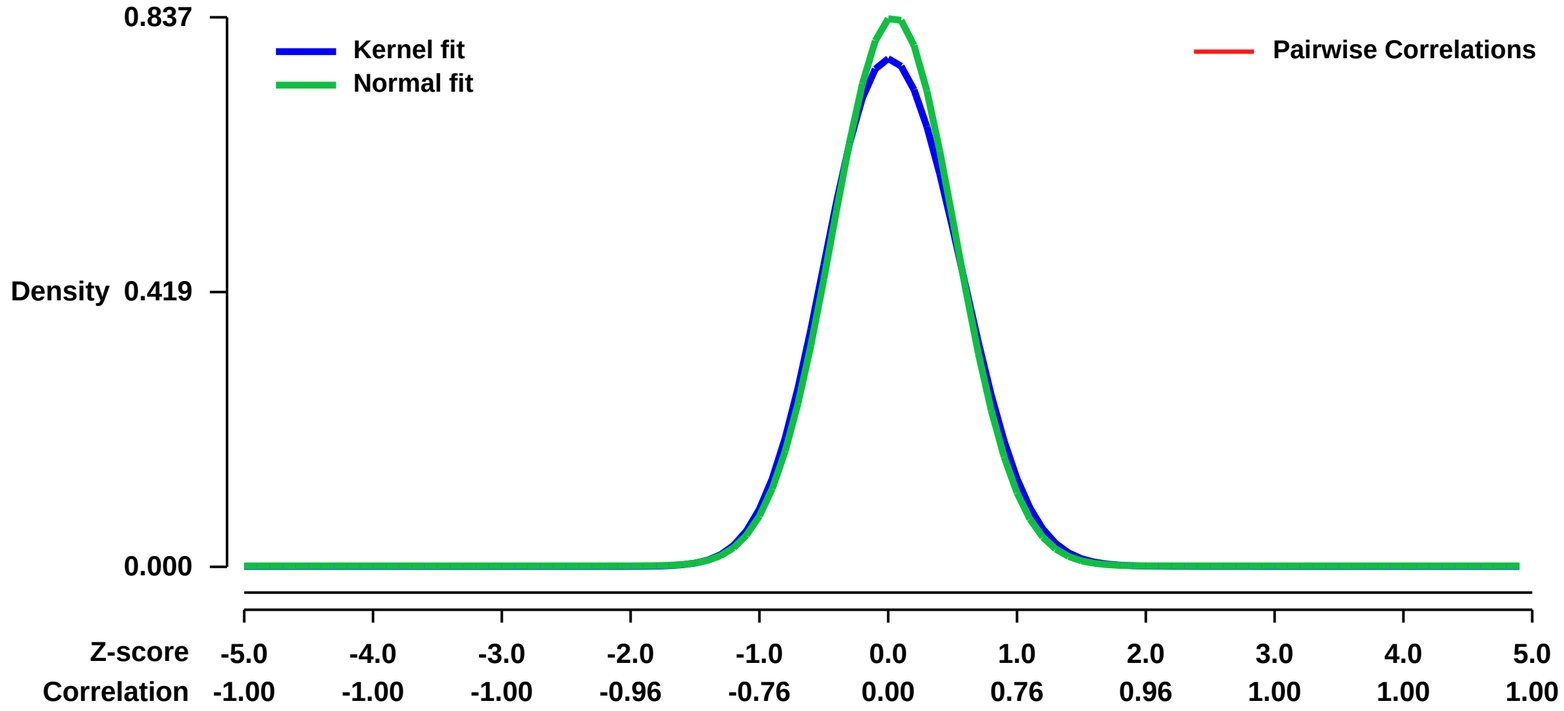

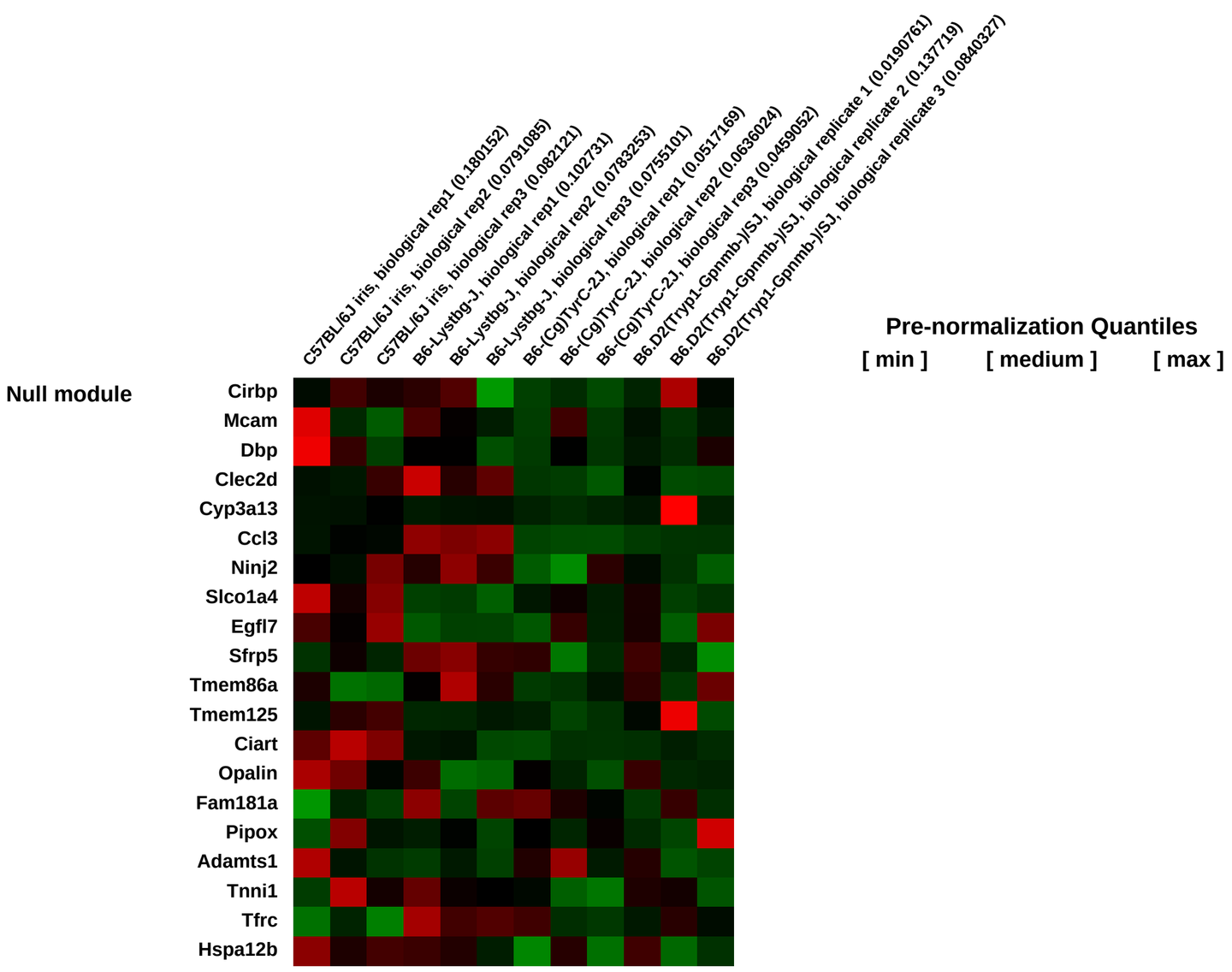

GEO Series "GSE2250" Expression Profiles

Num of samples in this series: 18

Scale of expression profile Z-scores

-3.0 -2.0 -1.0 0.0 1.0 2.0 3.0

GEO Link: http://www.ncbi.nlm.nih.gov/geo/query/acc.cgi?acc=GSE2250
Status: Public on Sep 11 2009
Title: Effects of irradiation on mouse lung
Organism: Mus musculus
Experiment type: Expression profiling by array
Platform: GPL1261
Pubmed ID:
Summary & Design:

Summary:
Total lung RNA from 3 mouse strains after 18Gy thoracic irradiation.

Thoracic cavity radiotherapy is limited by the development of alveolitis and fibrosis in susceptible patients. To define the response to 18 Gy pulmonary irradiation in mice, at the expression level, and to identify pathways which may influence the alveolitis and fibrosis phenotypes expression profiling was completed. Male mice of three strains, A/J (late alveolitis response), C3H/HeJ (C3H, early alveolitis response) and C57BL/6J (B6, fibrosis response) were exposed to thoracic radiation, euthanised when moribund and lung tissue gene expression was assessed with microarrays.

Overall design:
treated vs. control in 3 strains

Background corr dist: KL-Divergence = 0.2095, L1-Distance = 0.0449, L2-Distance = 0.0045, Normal std = 0.3259

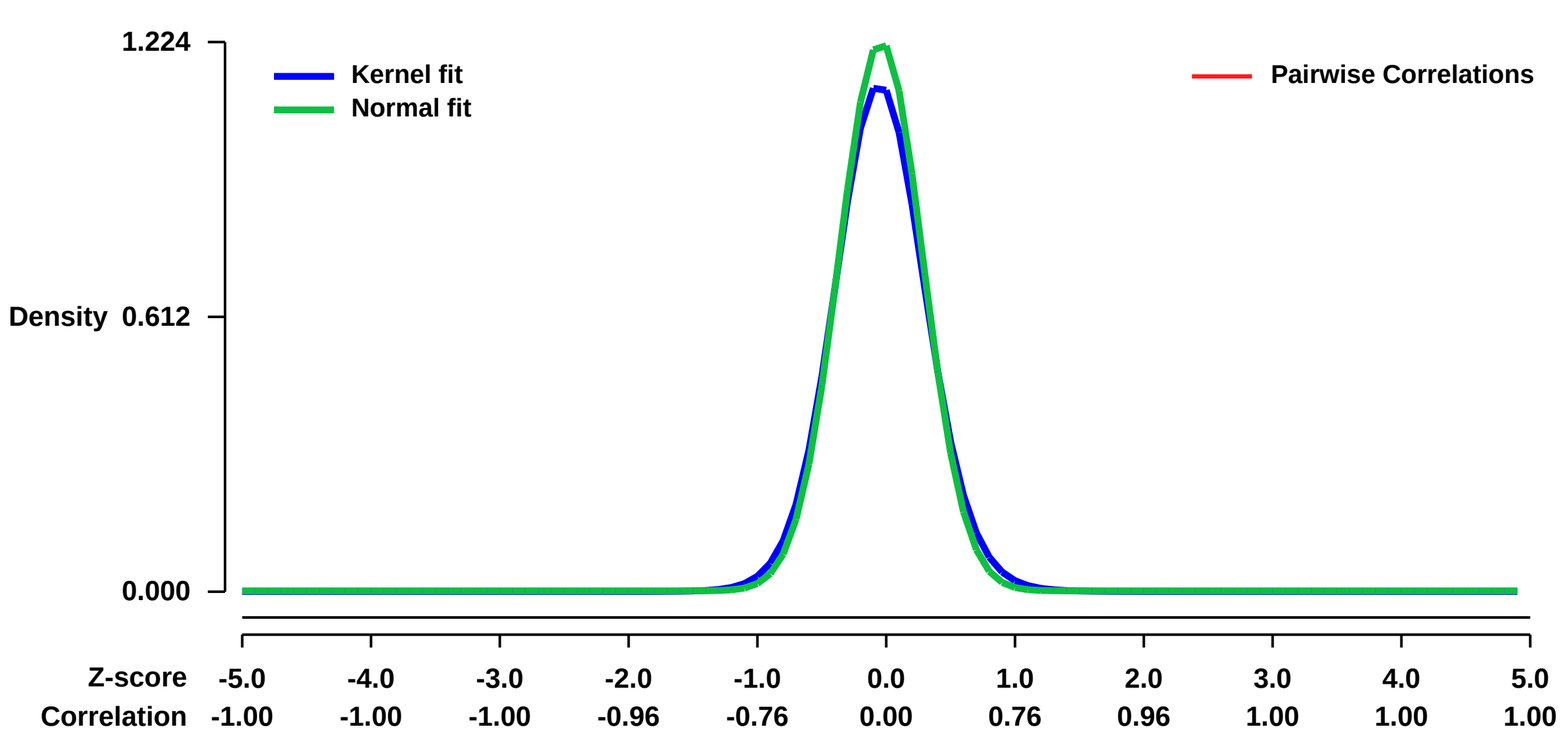

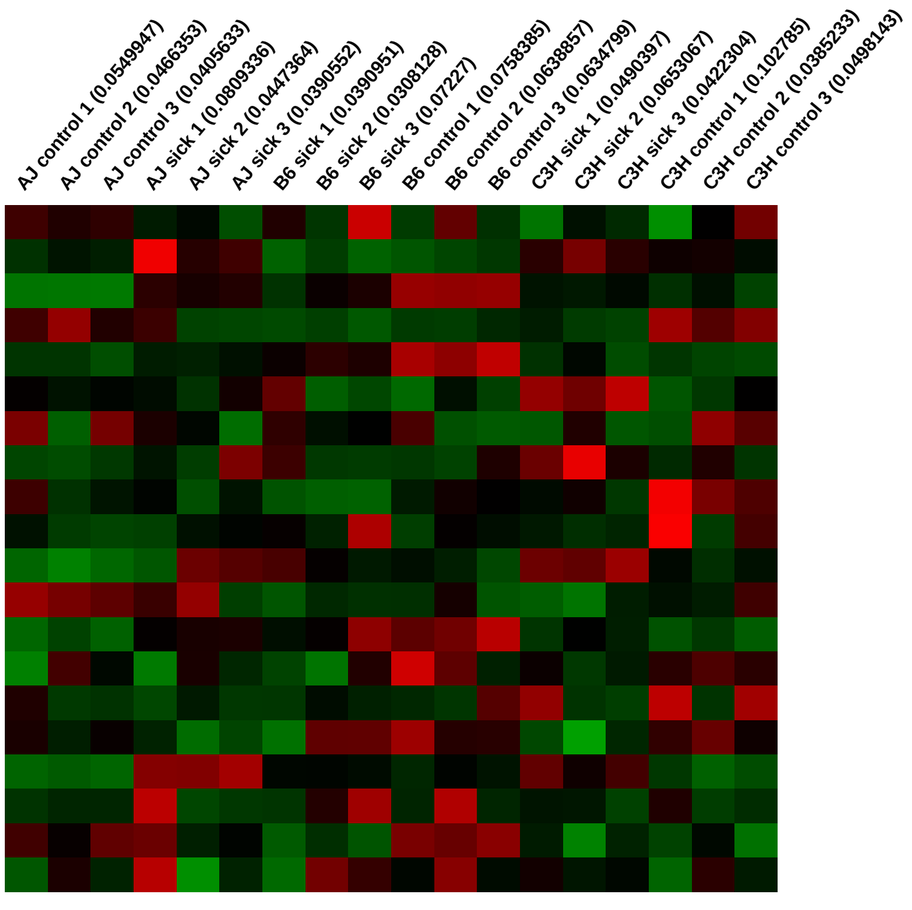

GEO Series "GSE33064" Expression Profiles

Num of samples in this series: 18

Scale of expression profile Z-scores

-3.0 -2.0 -1.0 0.0 1.0 2.0 3.0

GEO Link:	http://www.ncbi.nlm.nih.gov/geo/query/acc.cgi?acc=GSE33064
Status:	Public on Apr 04 2012
Title:	Expression data from a Tbx1 gene allelic series
Organism:	Mus musculus
Experiment type:	Expression profiling by array
Platform:	GPL1261
Pubmed ID:	22367967
Summary & Design:	**Summary:** This study was aimed at identifying Tbx1 dosage-dependent genes in vivo, so we performed a transcriptome analysis of Tbx1 mutants with nine different genotypes corresponding to different Tbx1 mRNA dosages. **Overall design:** Tbx1 gene dosage

Background corr dist: KL-Divergence = 0.1151, L1-Distance = 0.0368, L2-Distance = 0.0028, Normal std = 0.4198

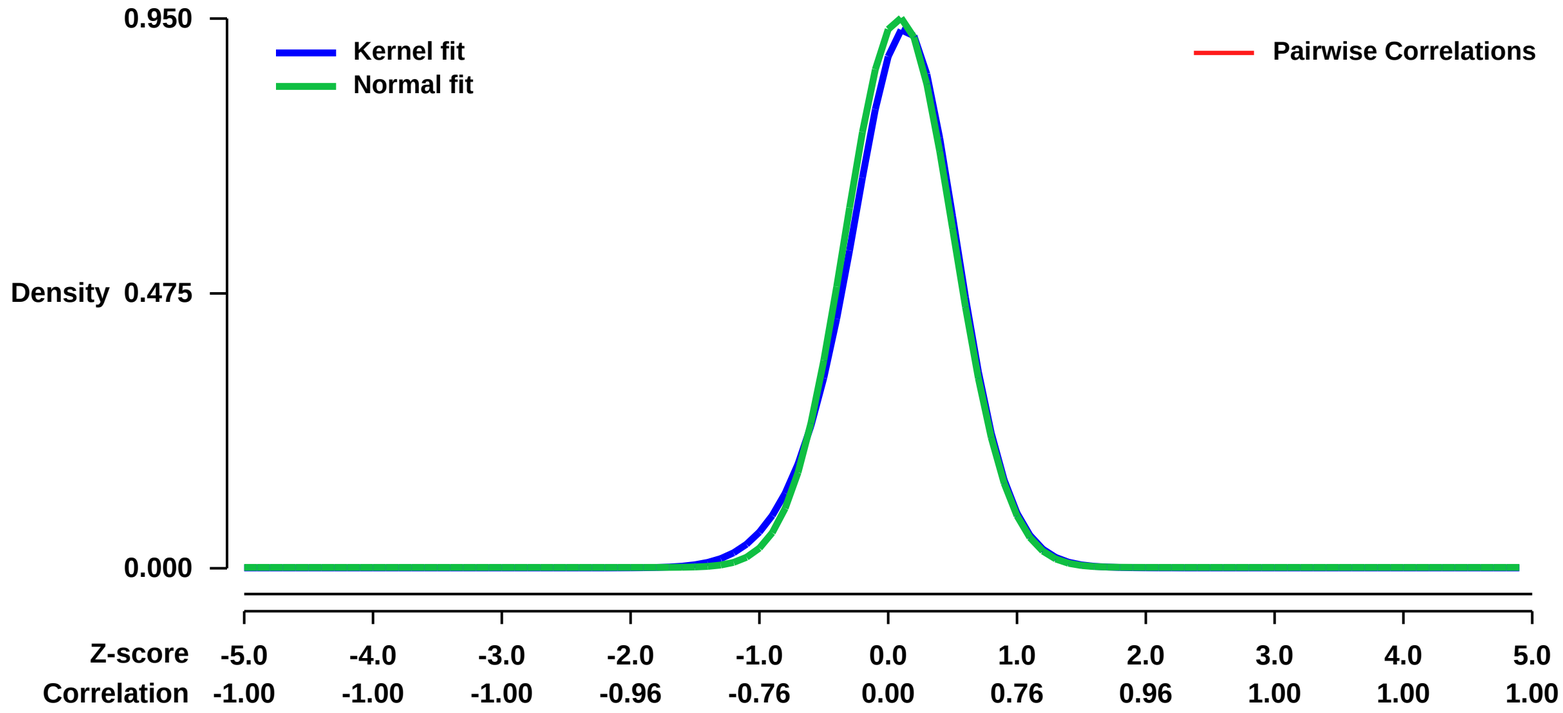

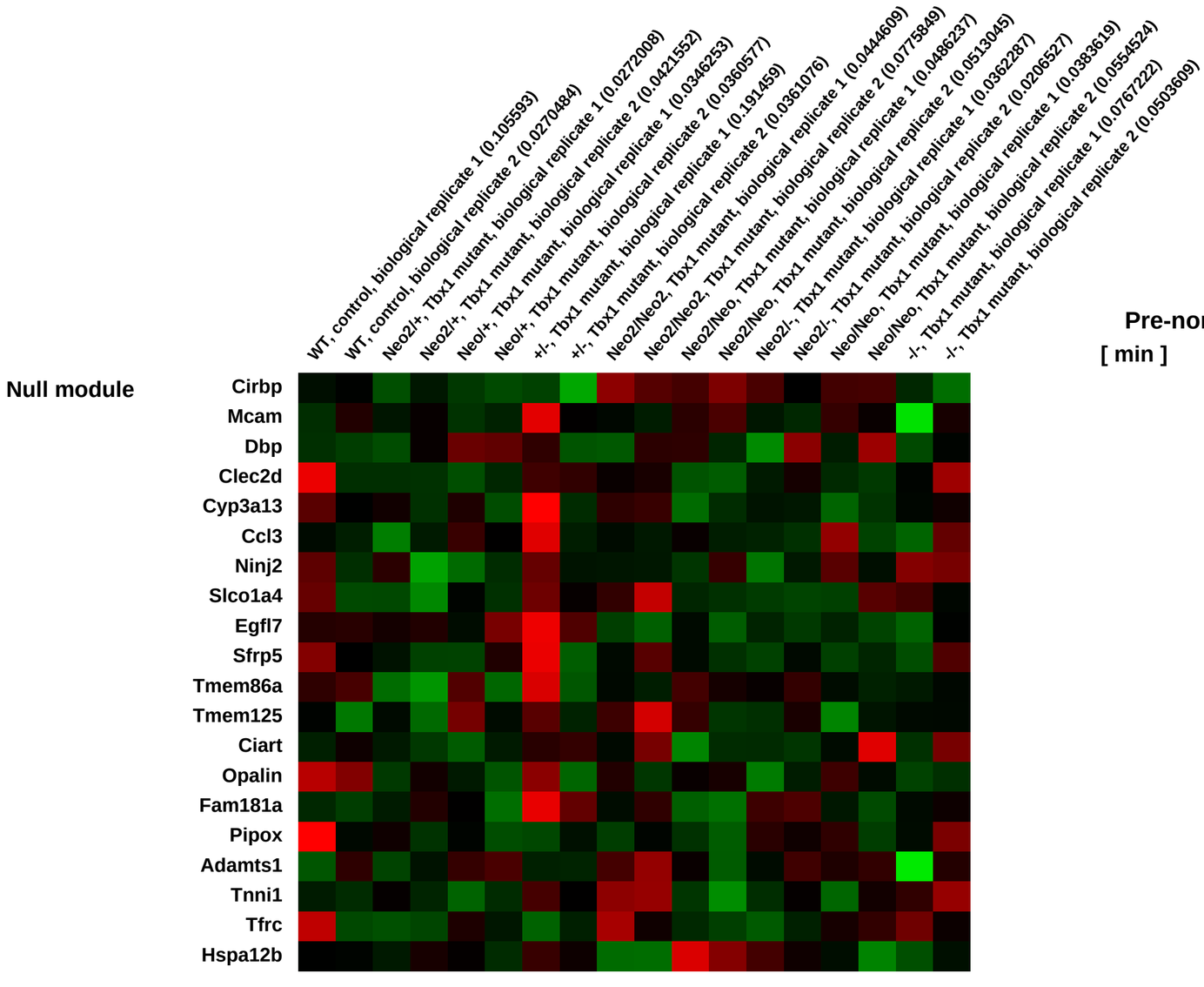

GEO Series "GSE31431" Expression Profiles

Num of samples in this series: 34

Scale of expression profile Z-scores

-3.0 -2.0 -1.0 0.0 1.0 2.0 3.0

GEO Link:	http://www.ncbi.nlm.nih.gov/geo/query/acc.cgi?acc=GSE31431
Status:	Public on Oct 03 2012
Title:	Serial gene expression profiling in the liver of Pdgf-c Tg mice that developed hepatic fibrosis and tumors
Organism:	Mus musculus
Experiment type:	Expression profiling by array
Platform:	GPL1261
Pubmed ID:	22651928
Summary & Design:	**Summary:** Over expression of PDGF-C in mouse liver resulted in the progression of hepatic fibrosis, steatosis and the development of HCC; this mouse model closely resembles the human HCC that is frequently associated with hepatic fibrosis. Peretinoin (generic name; code, NIK-333), developed by the Kowa Company, (Tokyo, Japan), is an oral acyclic retinoid (ACR) with a vitamin A-like structure that targets the retinoid nuclear receptor. Peretinoin effectively inhibits the progression of hepatic fibrosis and tumors in Pdgf-c Tg mice. Gene expression profiling was evaluated during the progression of hepatic fibrosis and tumors. **Overall design:** After weaning at week 4, Pdgf-c Tg or non-transgenic WT mice were fed a basal diet or a diet containing+0.06% peretinoin respectively. At week 20, mice were sacrificed for the analysis of progression of hepatic fibrosis. At week 48, mice were sacrificed for the analysis of the development of hepatic tumors.

Background corr dist: KL-Divergence = 0.3939, L1-Distance = 0.0727, L2-Distance = 0.0157, Normal std = 0.2498

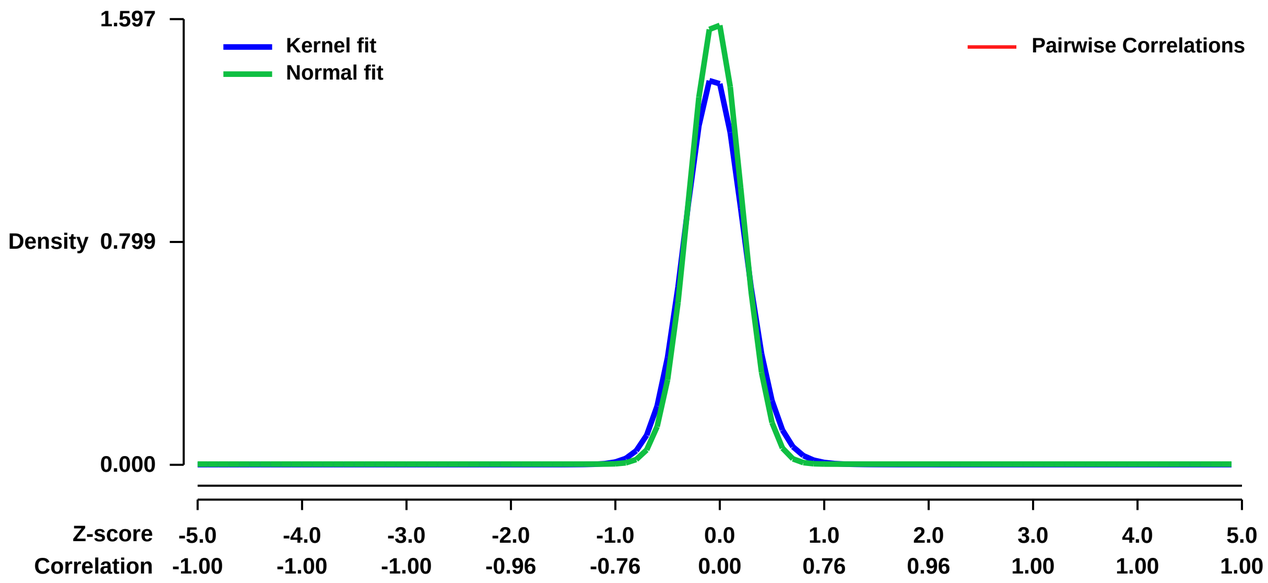

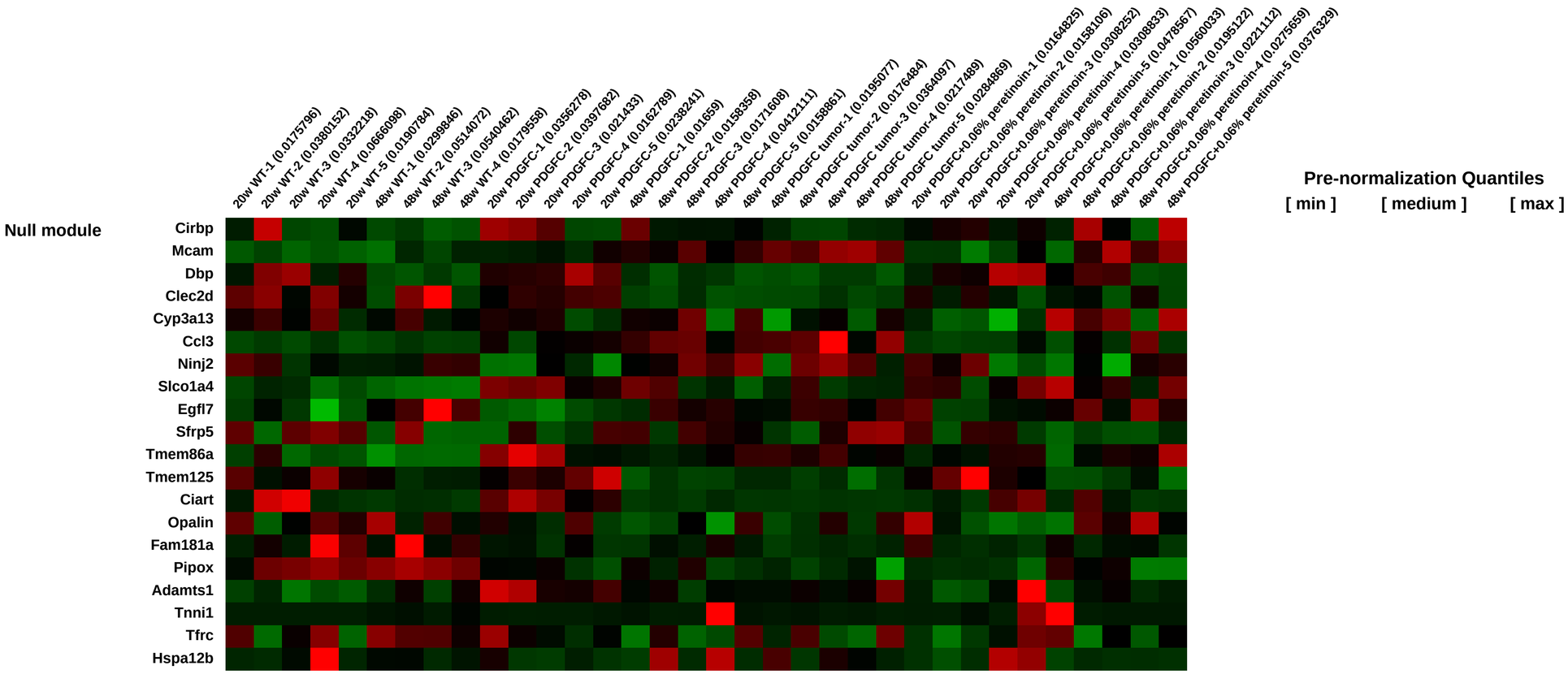

GEO Series "GSE35357" Expression Profiles

Num of samples in this series: 12

Scale of expression profile Z-scores

-3.0 -2.0 -1.0 0.0 1.0 2.0 3.0

GEO Link:	http://www.ncbi.nlm.nih.gov/geo/query/acc.cgi?acc=GSE35357
Status:	Public on Feb 03 2012
Title:	Gene expression profiling of Myf5-Cre;Smad4flox/flox mouse models of tongue development
Organism:	Mus musculus
Experiment type:	Expression profiling by array
Platform:	GPL1261
Pubmed ID:	22438570
Summary & Design:	**Summary:** We investigated Smad4-mediated TGF-beta signaling in the development of occipital somite-derived myogenic progenitors during tongue morphogenesis by comparing the transcriptomes of tongue derived from Myf5-Cre;Smad4flox/flox mutant and Myf5-Cre;Smad4flox/+ control mice at day E13.5. Based on gene expression profiles and functional studies, we elucidated the influences Smad4 activity and TGF-beta signaling have on the gene expression profiles underlying tongue development. The data are consistent with the hypothesis that TGF-beta-Smad4-FGF6 signaling cascade plays a crucial role in myogenic cell fate determination and lineage progression during tongue myogenesis. **Overall design:** We obtained RNA samples from tongue tissues of mutant and control mouse embryos (C57BL/6J) at day E13.5 RNA and subjected them to analysis on Affymetrix GeneChip Mouse Genome 430 2.0 Arrays.

Background corr dist: KL-Divergence = 0.1151, L1-Distance = 0.0296, L2-Distance = 0.0014, Normal std = 0.4133

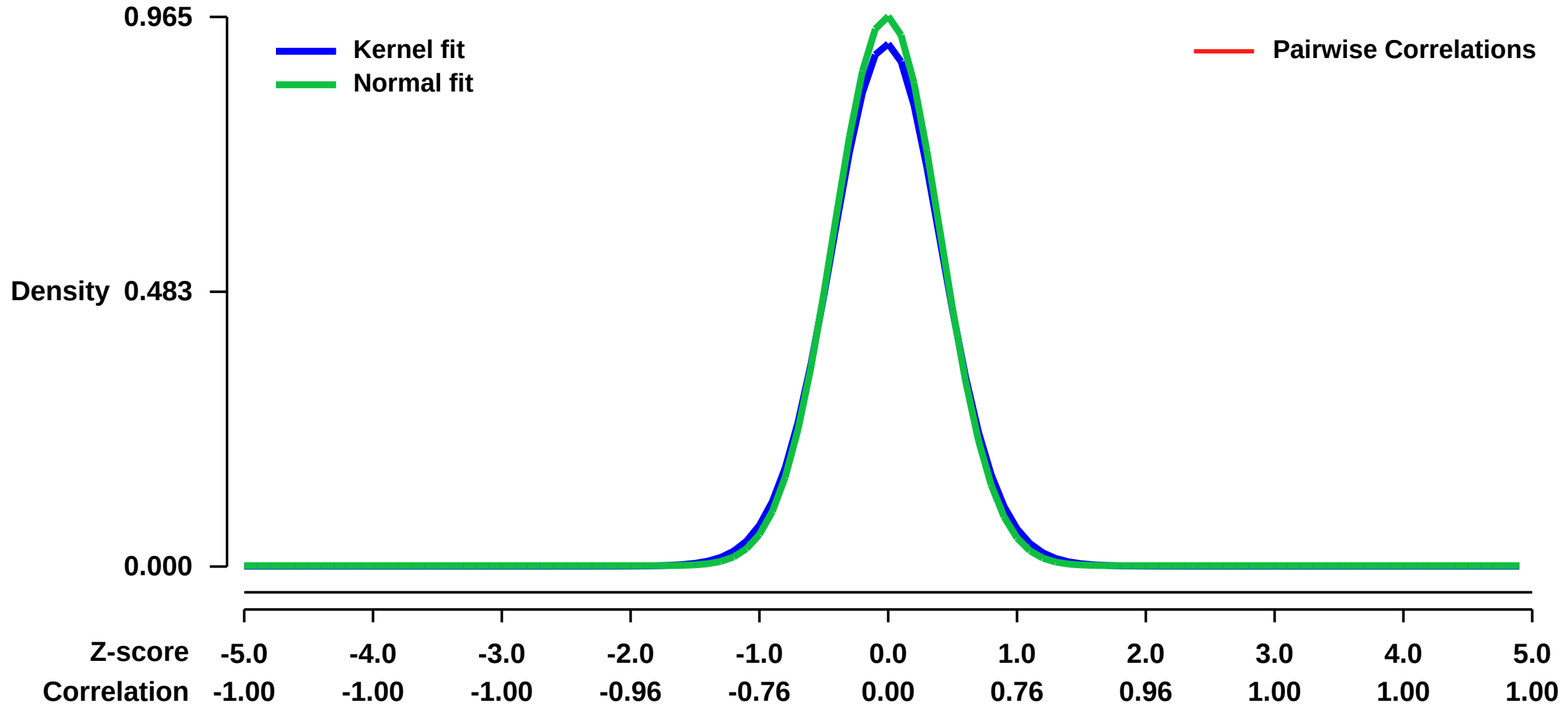

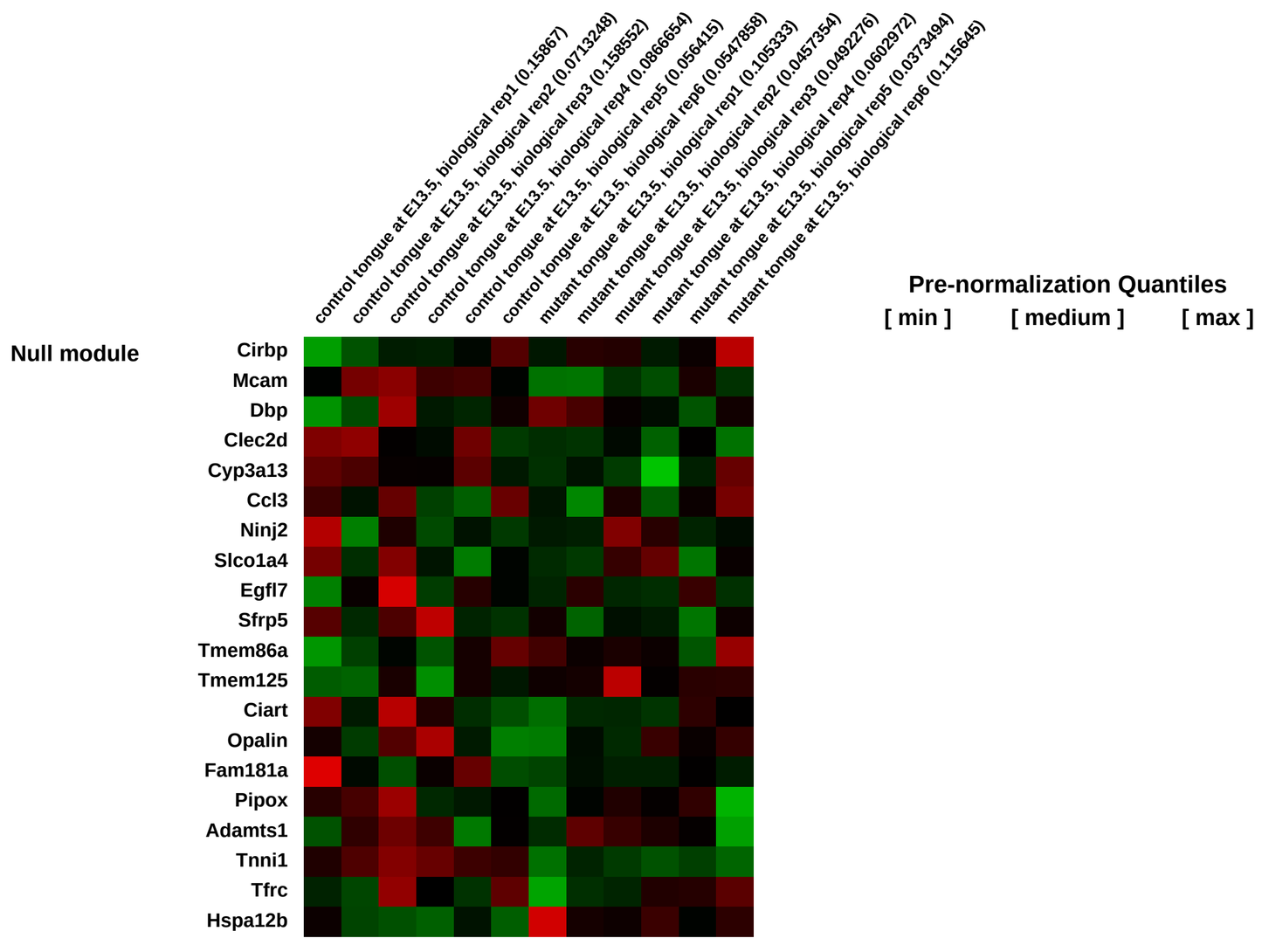

GEO Series "GSE9878" Expression Profiles

Num of samples in this series: 6

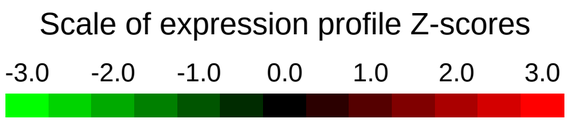

GEO Link:	http://www.ncbi.nlm.nih.gov/geo/query/acc.cgi?acc=GSE9878
Status:	Public on Dec 15 2007
Title:	Gene expression analysis of Pax5-/- proB cells transduced with control or EBF retrovirus.
Organism:	Mus musculus
Experiment type:	Expression profiling by array
Platform:	GPL1261
Pubmed ID:	18176567
Summary & Design:	**Summary:** We have determined that sustained expression of EBF suppresses alternate lineage genes independently of Pax5. Keywords: Transcription factor EBF restricts alternate lineage options and promotes B cell fate commitment independently of Pax5. **Overall design:** Pax5-/- pro-B cells transduced with control or EBF retrovirus. Transduced cells were FACS sorted based on GFP expression and total RNA was isolated. RNA isolated from control or EBF transduced cells was analyzed using the Affymetrix Rat 230A microarrays.

Background corr dist: KL-Divergence = 0.0260, L1-Distance = 0.0124, L2-Distance = 0.0002, Normal std = 0.6863

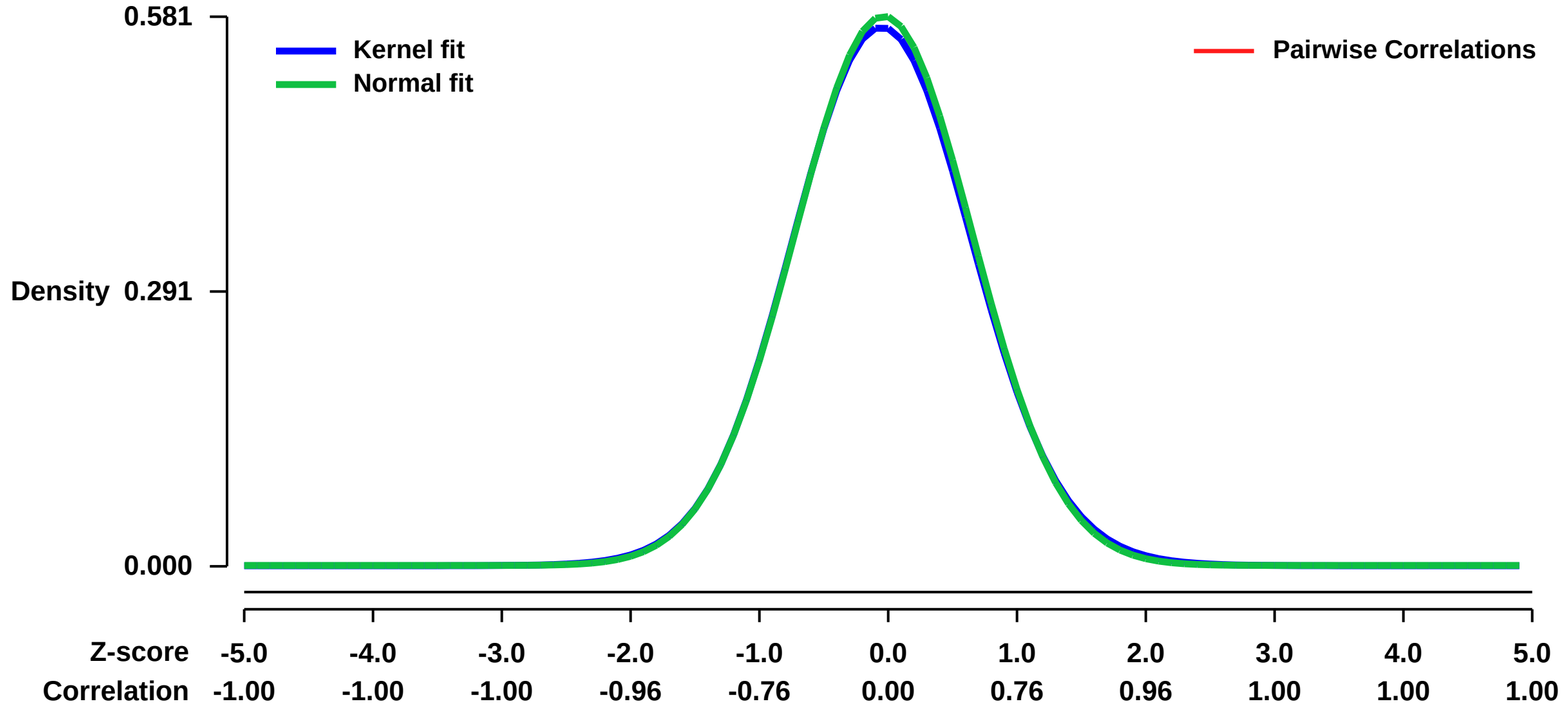

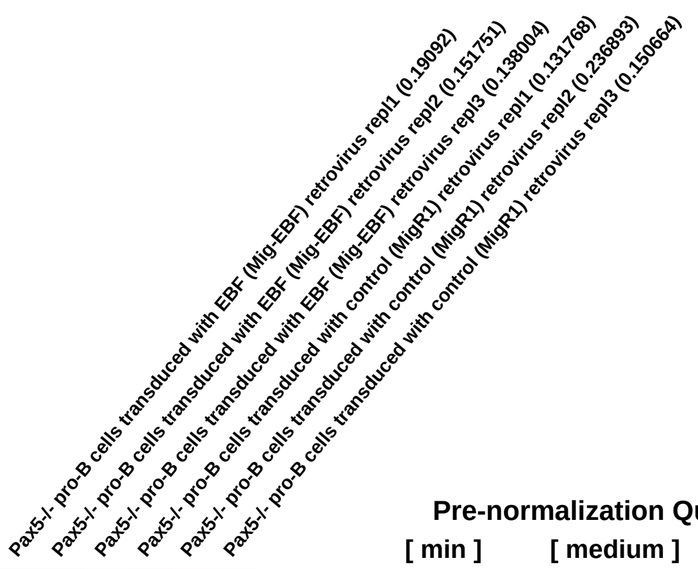

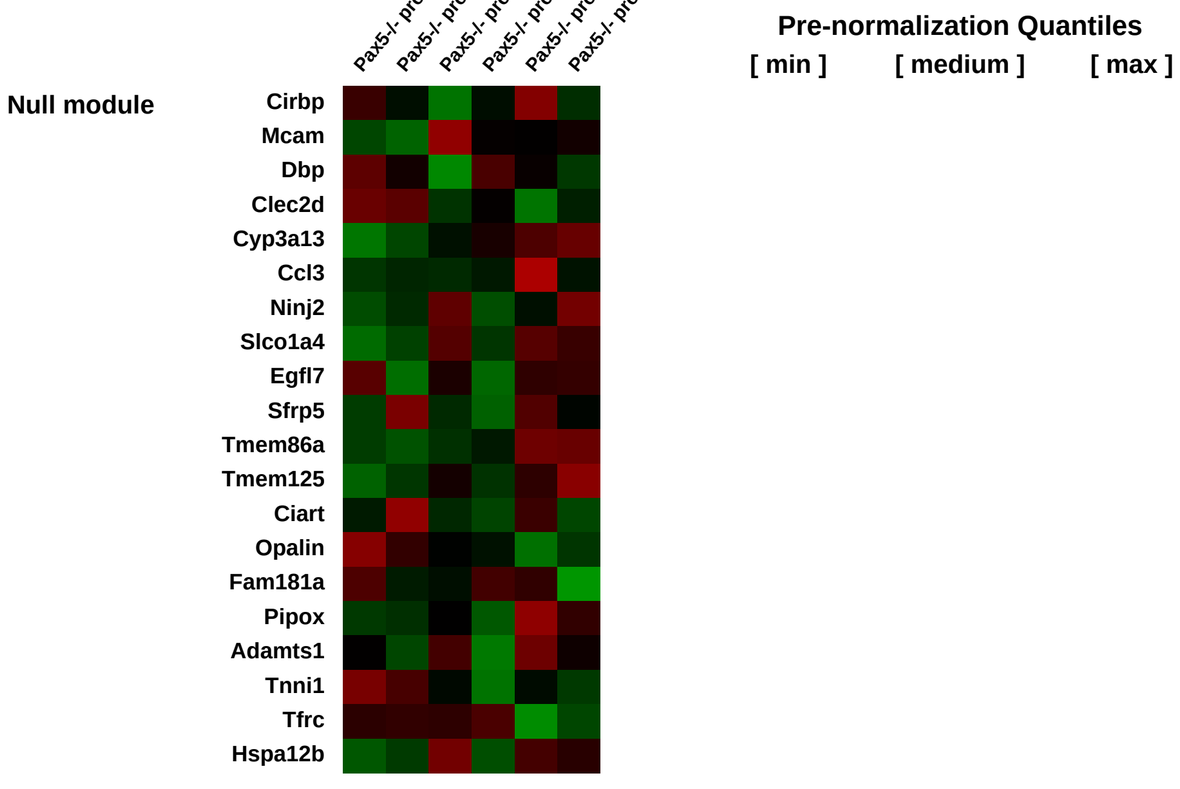

GEO Series "GSE11276" Expression Profiles

Num of samples in this series: 6

Scale of expression profile Z-scores

-3.0 -2.0 -1.0 0.0 1.0 2.0 3.0

GEO Link:	**http://www.ncbi.nlm.nih.gov/geo/query/acc.cgi?acc=GSE11276**
Status:	**Public on Nov 01 2010**
Title:	**Comparison of adult intact naive C57Bl/6 Nogo-A KO versus WT spinal cord**
Organism:	**Mus musculus**
Experiment type:	**Expression profiling by array**
Platform:	**GPL1261**
Pubmed ID:	
Summary & Design:	**Summary:** **Nogo-A localized on myelin adaxonal membrane in the adult CNS is well known for its role as neurite outgrowth inhibitor following a lesion. Nogo-A KO mice show enhanced regenerative/compensatory fiber growth following CNS lesion. However, changes undergoing in their intact CNS have not been studied. Moreover, Nogo-A in the intact adult CNS in also expressed in some neuronal subpopulations, e.g. in the hippocampus, olfactory bulbs and dorsal root ganglia.** **We compared the intact adult CNS (spinal cord) of Nogo-A KO mice in order to identify: potential compensating molecules which could be interesting new inhibitory neurite outgrowth candidates, possible molecules involved in the up to now not yet clarified downstream signalling pathway of Nogo-A, additional new functions for myelin or neuronal Nogo-A in the intact adult CNS.**
	Keywords: gene expression, Nogo-A KO, spinal cord, adult, naive, unlesioned
	Overall design: **Spinal cords from 3 adult C57Bl/6 wild type and Nogo-A KO mice have been explanted. Total RNA has been extracted and processed for hybridization on Mouse 430 2.0 Affymetrix GeneChips. Following scanning and first analysis with MAS 5.0, further analysis was performed by GeneSpring 7.2 (Silicon Genetics, Redwood City, CA). A present call filter (2 out of 3 present calls in at least one out of the different studied conditions) was applied. Normalization was run per chip as well as per gene to the median of the control replicates. Data were statistical restricted through a 1-way Anova (p=0.05). A final threshold of =1.2 folds of increase or decrease in the expression level of each single transcript was applied. Regulated transcripts have been assigned to functional categories according to GeneOntology as well as literature and database mining (Pubmed and Bioinformatics Harvester EMBL Heidelberg).**

Background corr dist: **KL-Divergence = 0.0322, L1-Distance = 0.0218, L2-Distance = 0.0006, Normal std = 0.6601**

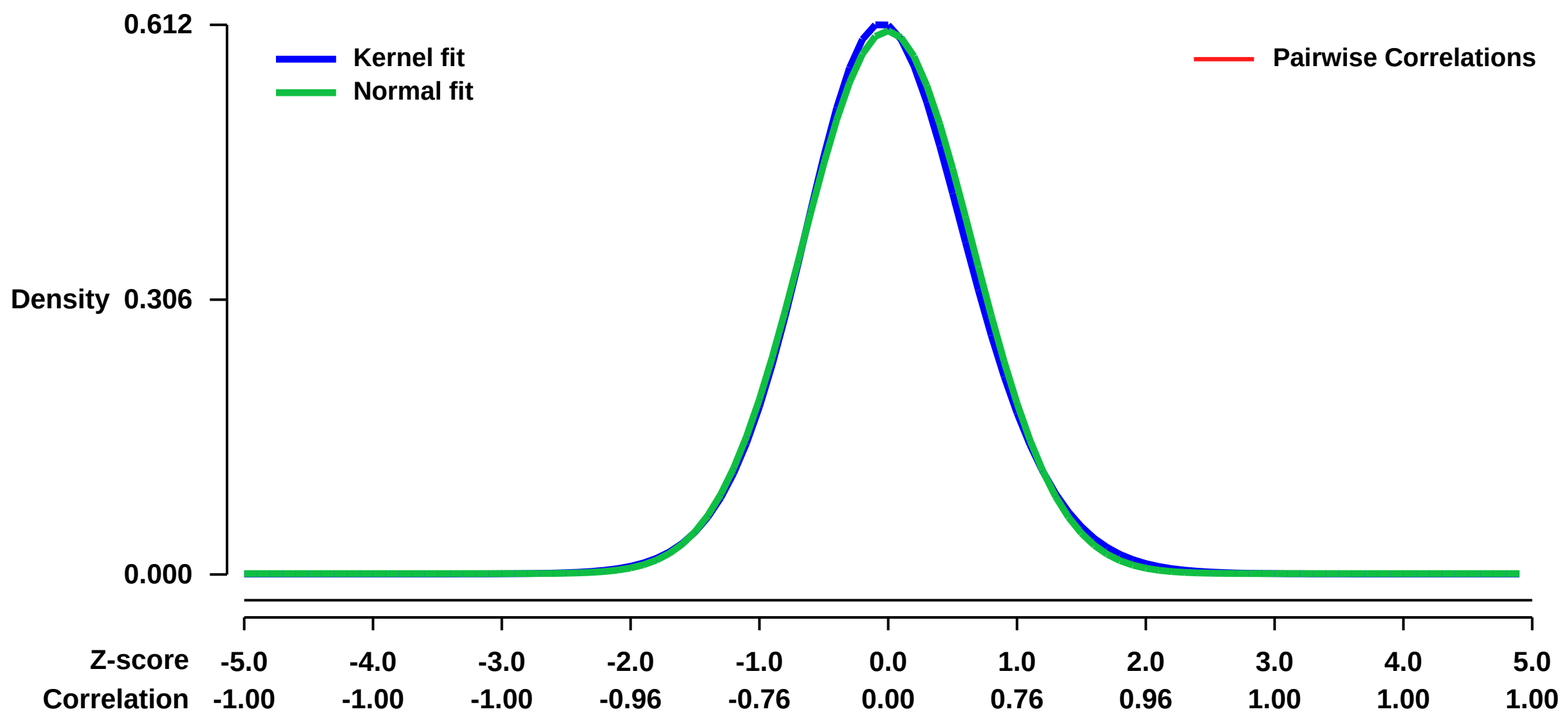

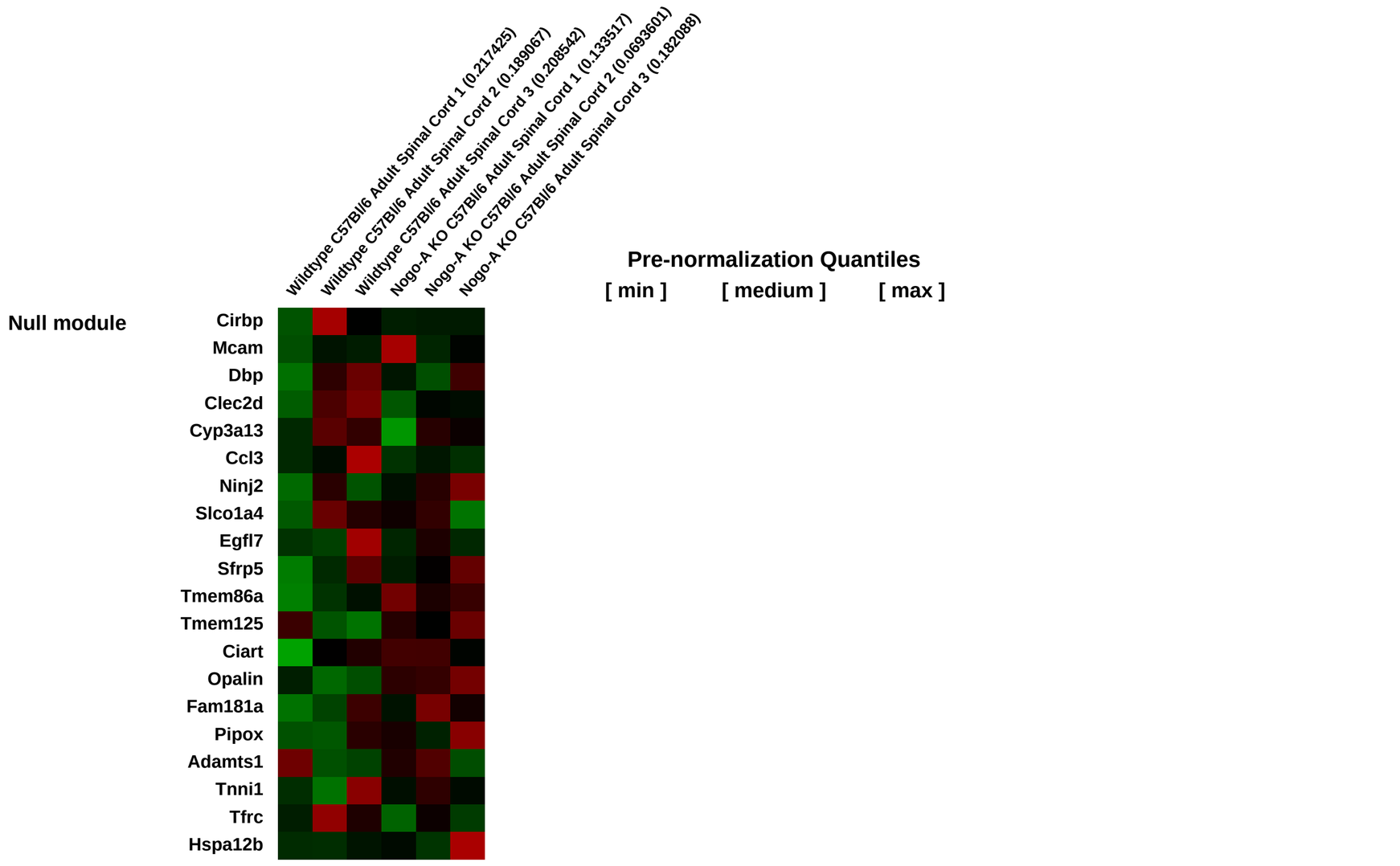

GEO Series "GSE41942" Expression Profiles

Num of samples in this series: 6

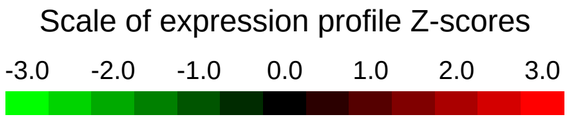

GEO Link:	**http://www.ncbi.nlm.nih.gov/geo/query/acc.cgi?acc=GSE41942**
Status:	**Public on Nov 01 2012**
Title:	**Overexpression of miR-9 and miR-9* in 32D cells**
Organism:	**Mus musculus**
Experiment type:	**Expression profiling by array**
Platform:	**GPL1261**
Pubmed ID:	
Summary & Design:	**Summary:** **Overexpression of miR-9 and miR-9* in 32D cells, cells grown under IL-3 conditions and miR-9 and miR-9* were introduced with retroviral vectors containing about ~150 bp up and downstream of mmu-mir-9-2.** **Expression was determined to find out the effect of miR-9/9*overexpression on the transcriptome level compared to introduction of empty vector control.** **Overall design:** **Transcriptome levels were determined for 32D cells expressing miR-9 and miR-9* and empty vector control. Experiment performed in three independent replicates.**

Background corr dist: **KL-Divergence = 0.0444, L1-Distance = 0.0310, L2-Distance = 0.0014, Normal std = 0.6092**

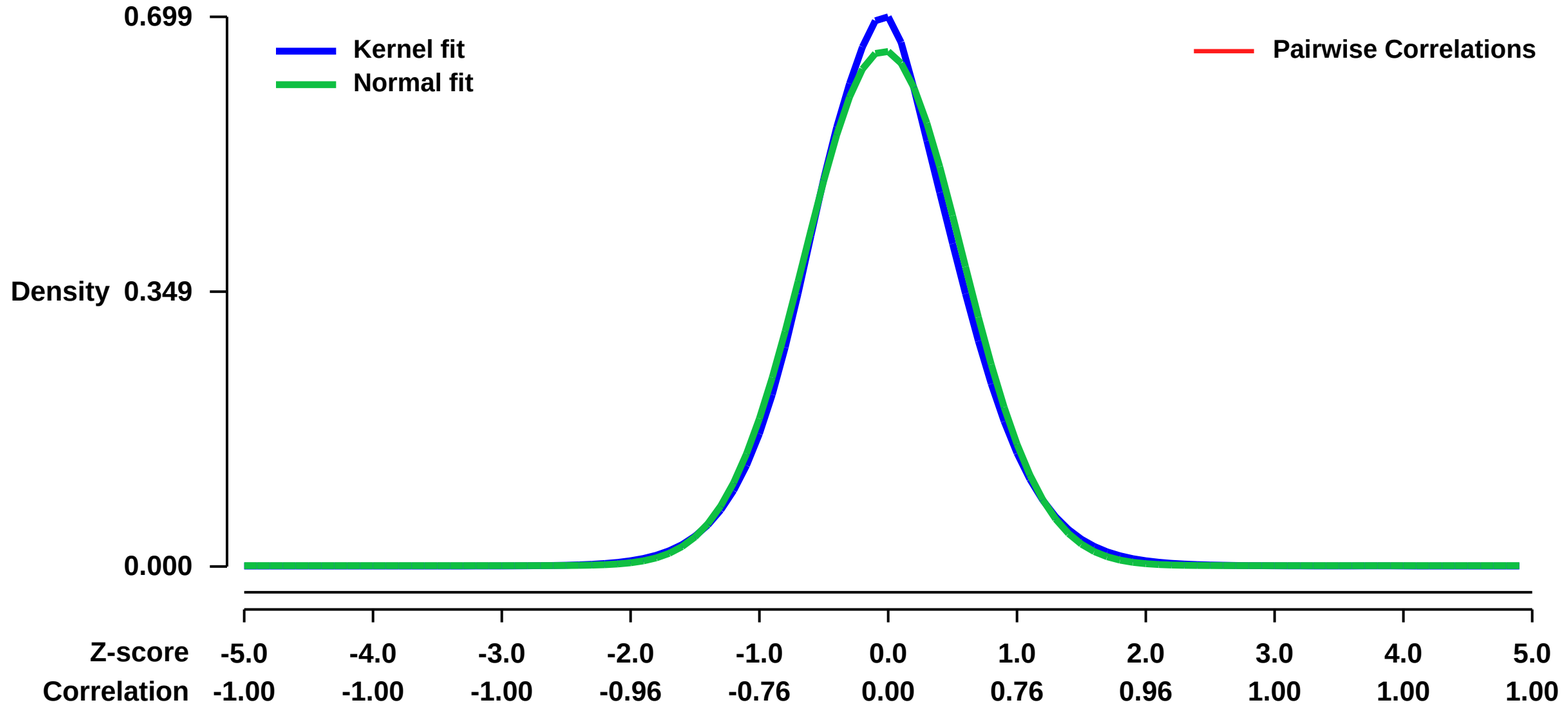

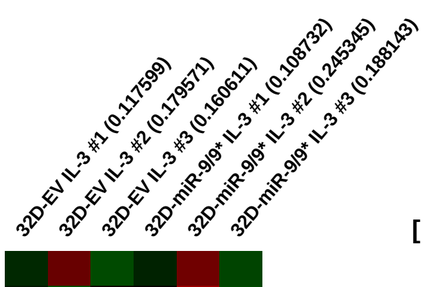

Pre-normalization Quantiles

[min] [medium] [max]

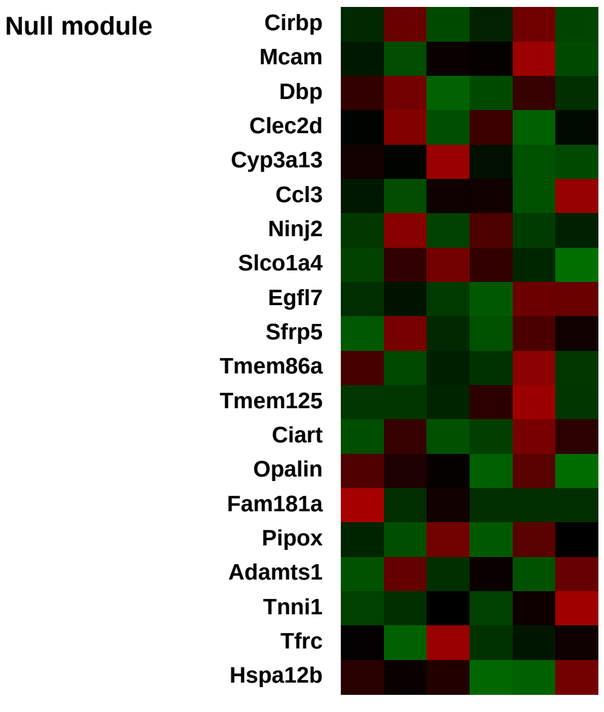

GEO Series "GSE40795" Expression Profiles

Num of samples in this series: 50

Scale of expression profile Z-scores

-3.0 -2.0 -1.0 0.0 1.0 2.0 3.0

GEO Link:	http://www.ncbi.nlm.nih.gov/geo/query/acc.cgi?acc=GSE40795
Status:	Public on Oct 12 2012
Title:	Transcriptomic Dose Response Changes in Female Mouse and Rat Lungs following Chloroprene Exposure
Organism:	Mus musculus
Experiment type:	Expression profiling by array
Platform:	GPL1261
Pubmed ID:	23125180
Summary & Design:	**Summary:** ˆ-chloroprene (2-chloro-1,3-butadiene), a monomer used in the production of neoprene elastomers, is of regulatory interest due to the production of multi-organ tumors in mouse and rat cancer bioassays. A significant increase in female mouse lung tumors was observed at the lowest exposure concentration of 12.8 ppm while a small, but not statistically significant, increase was observed in female rats only at the highest exposure concentration of 80 ppm. The metabolism of chloroprene results in the generation of reactive epoxides and the rate of overall chloroprene metabolism is highly species dependent. To identify potential key events in the mode-of-action of chloroprene lung tumorigenesis, dose response and time course gene expression microarray measurements were made in the lungs of female mice and female rats. The gene expression changes were analyzed using both a traditional analysis of variance approach followed by pathway enrichment analysis and a pathway-based benchmark dose (BMD) analysis approach. Pathways related to glutathione biosynthesis and metabolism were the primary pathways consistent with cross-species differences in tumor incidence and transcriptional BMD values for the pathway were more similar to differences in tumor response than were estimated target tissue dose surrogates based on the total amount of chloroprene metabolized per unit mass of lung tissue per day. The closer correspondence of the transcriptional changes with the tumor response are likely due to their reflection of the overall balance between metabolic activation and detoxication reactions whereas the current tissue dose surrogate reflects only oxidative metabolism. **Overall design:** Female mice (B6C3F1/Crl) were exposed to chloroprene (CAS 126-99-8) by whole-body inhalation exposure at 0, 0.3, 2, 13, or 90 ppm. Exposures were performed for 6 hr/day, 5 days per week. The animals were sacrified at 5 days or 19 days (15 exposure days) post initiation of exposure. The right lung was excised and gene expression microarray analysis was performed using Affymetrix Mouse 430_2 arrays. Female rats (F344/NCrl) were exposed to chloroprene (CAS 126-99-8) by whole-body inhalation exposure at 0, 5, 30, 90, or 200 ppm. Exposures were performed for 6 hr/day, 5 days per week. The animals were sacrified at 5 days or 19 days (15 exposure days) post initiation of exposure. The right lung was excised and gene expression microarray analysis was performed using Affymetrix Rat 230_2 arrays.

Background corr dist: KL-Divergence = 0.1693, L1-Distance = 0.0369, L2-Distance = 0.0026, Normal std = 0.3558

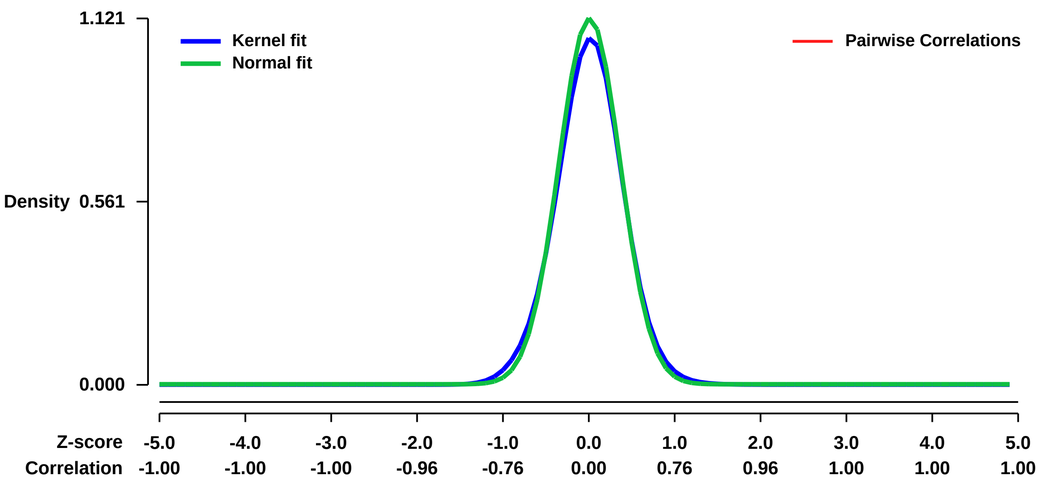

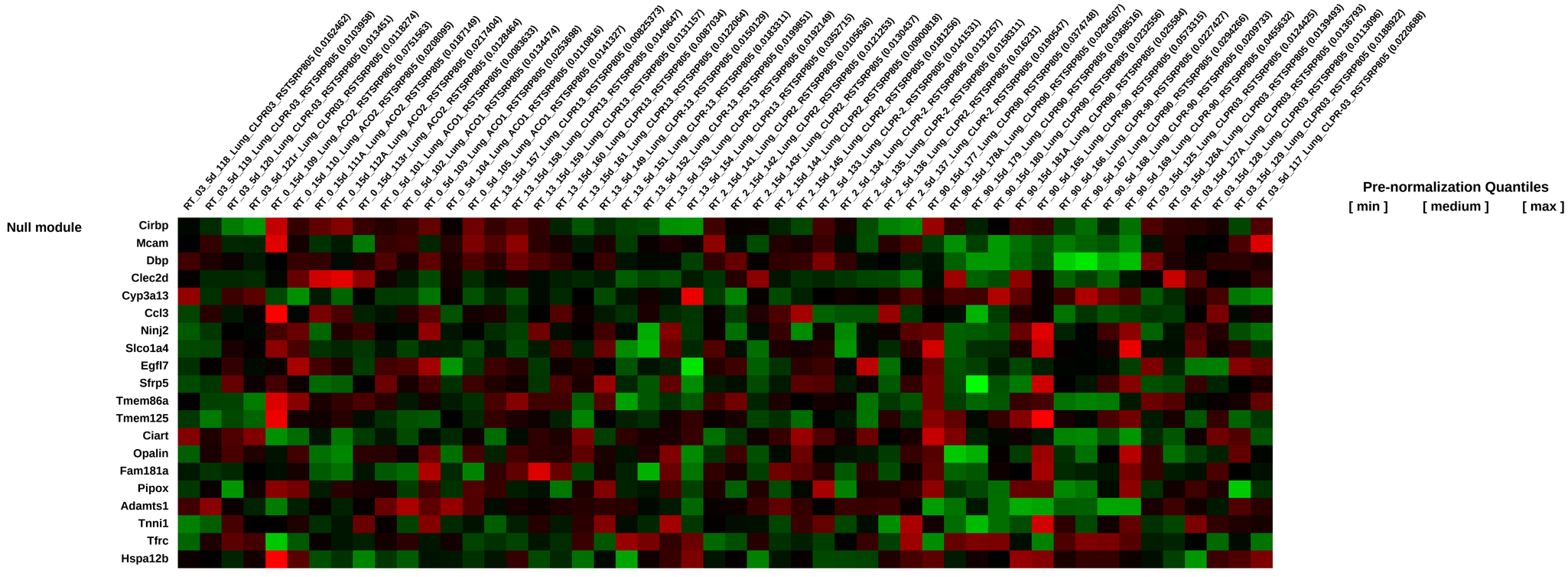

GEO Series "GSE24489" Expression Profiles

Num of samples in this series: 14

Scale of expression profile Z-scores

-3.0 -2.0 -1.0 0.0 1.0 2.0 3.0

GEO Link:	http://www.ncbi.nlm.nih.gov/geo/query/acc.cgi?acc=GSE24489
Status:	Public on Dec 31 2010
Title:	Effect of H11 Kinase/Hsp22 deletion in response to cardiac stress
Organism:	Mus musculus
Experiment type:	Expression profiling by array
Platform:	GPL1261
Pubmed ID:	21747053
Summary & Design:	**Summary:** The expression of the small molecular weight heat shock protein (Hsp) H11 kinase/Hsp22 (Hsp22) is restricted to a limited number of tissues, including the heart and skeletal muscle, both in rodents and in humans. We generated a mouse knockout (KO) model, and investigated the role of Hsp22 in regulating cardiac hypertrophy in response to pressure overload. We compared gene expression profiles between WT and KO mice in basal condition and three days pressure overload after transverse aortic constriction (TAC). These data illustrated a novel mechanism of Hsp22-related gene expression in response to cardiac stress. **Overall design:** We used microarray to examine differential gene expression by Hsp22 deletion at baseline and 3-day pressure overload. Left ventricles from wild type and Hsp22 knockout mice were selected from basal condition (each, n=3) and TAC surgery (each, n=4).

Background corr dist: KL-Divergence = 0.0453, L1-Distance = 0.0832, L2-Distance = 0.0130, Normal std = 0.6502

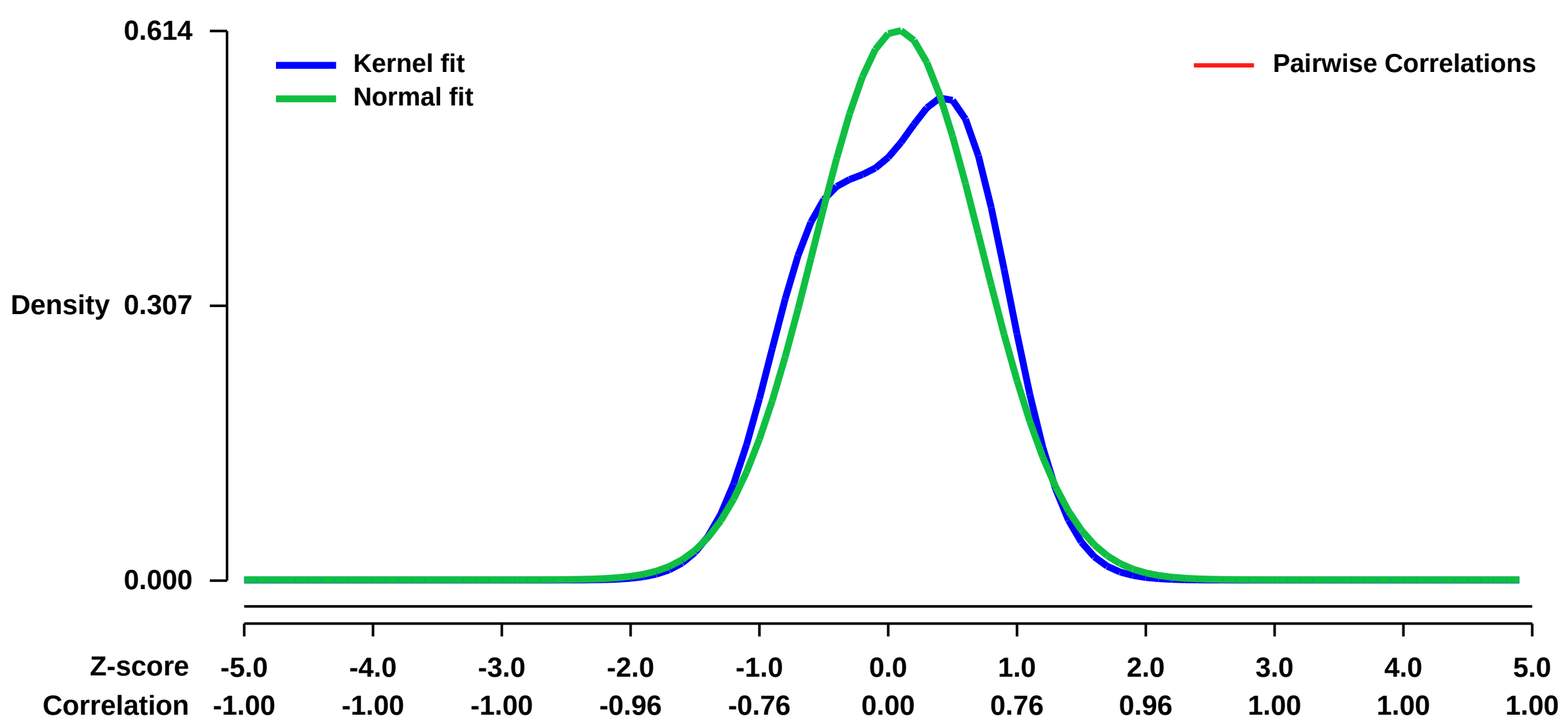

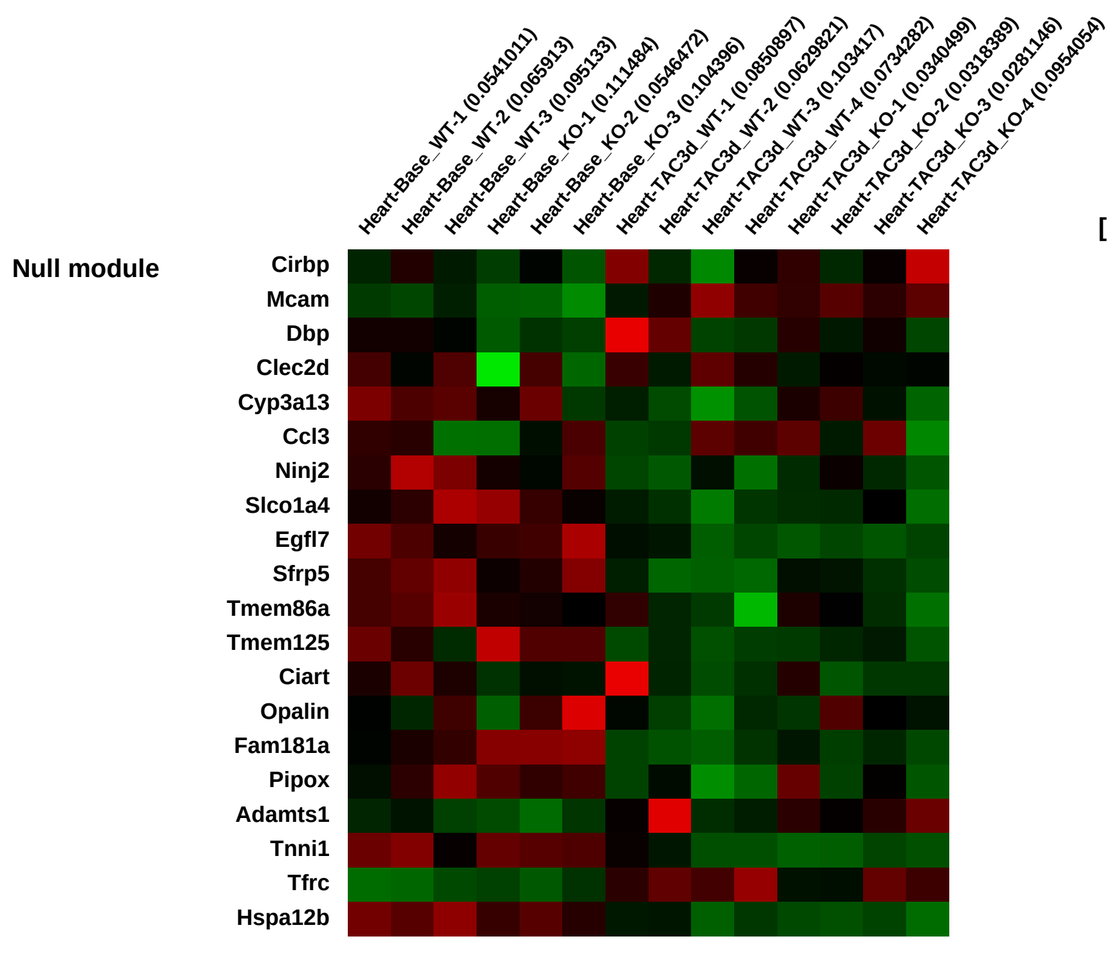

GEO Series "GSE13443" Expression Profiles

Num of samples in this series: 27

Scale of expression profile Z-scores

-3.0 -2.0 -1.0 0.0 1.0 2.0 3.0

GEO Link:	http://www.ncbi.nlm.nih.gov/geo/query/acc.cgi?acc=GSE13443
Status:	Public on Nov 11 2008
Title:	Induction of systemic disease-specific salivary biomarker profiles in mouse cancer models
Organism:	Mus musculus
Experiment type:	Expression profiling by array
Platform:	GPL1261
Pubmed ID:	19517020
Summary & Design:	**Summary:** Saliva (oral fluids) is an emerging biofluid poised for clinical diseases detection. Although the rationale for oral diseases applications (e.g. oral cancer) is clear, the rationale and relationship between systemic diseases and saliva biomarkers are unknown. In this study, we used mouse models of melanoma and non-small cell lung cancer and compared the transcriptome biomarker profiles of tumor-bearing mice to those of control mice. Microarray analysis showed that salivary transcriptomes were significantly altered in tumor-bearing mice vs. controls. Analysis of the transcriptomes in the mouse tumors, serum, salivary glands and saliva revealed that salivary biomarkers have multiple origins. Furthermore, we identified that the expression of two groups of significantly altered transcription factors Runx1, Mlxipl, Trim30 and Egr1, Tbx1, Nr1d1 in melanoma-bearing mice that can potentially be responsible for 82.6% of the up-regulated genes expression and 62.5% of the down-regulated gene expression in the mice saliva, respectively. We also confirmed that the ectopic production of nerve growth factor (NGF) in the melanoma tumor tissue as a tumor-released mediator that can induce expression of the transcription factor Egr-1 in the salivary gland. Taken together, our data support the conclusion that upon systemic disease development, a disease-specific change occurs in the salivary biomarker profile. Although the origins of the disease-specific salivary biomarkers are both systemic and local, stimulation of salivary gland by mediators released from remote tumors play an important role in regulating the salivary surrogate biomarker profiles. **Overall design:** Salivary,salivary gland, serum or tumor RNA was isolated using the RNeasy Mini Kit (Qiagen) as described previously. There are 15 mice in the control group or tumor group (totally 30 C57BL/6 mice for melanoma mouse model, another 30 DBA/2 mice for lung cancer mouse model). Samples derived from 5 mice in each group were pooled and RNA extracted. The pooling is necessary to ensure sufficient salivary mRNA can be obtained for microarray analyses. Isolated total RNA was treated with recombinant DNase (Ambion, Austin, TX). For microarray analysis, mRNA from mouse saliva, gland or tumor was linearly amplified using the RiboAmp RNA Amplification kit (Molecular Devices, Sunnyvale, CA). After purification, cDNA were in vitro transcribed and biotinylated using GeneChip Expression 3â -Amplification Reagents for in vitro transcription labeling (Affymetrix, Santa Clara, CA). The labeled RNAs was subsequently fragmented, hybridization and scanning.

Background corr dist: KL-Divergence = 0.1726, L1-Distance = 0.0919, L2-Distance = 0.0202, Normal std = 0.3872

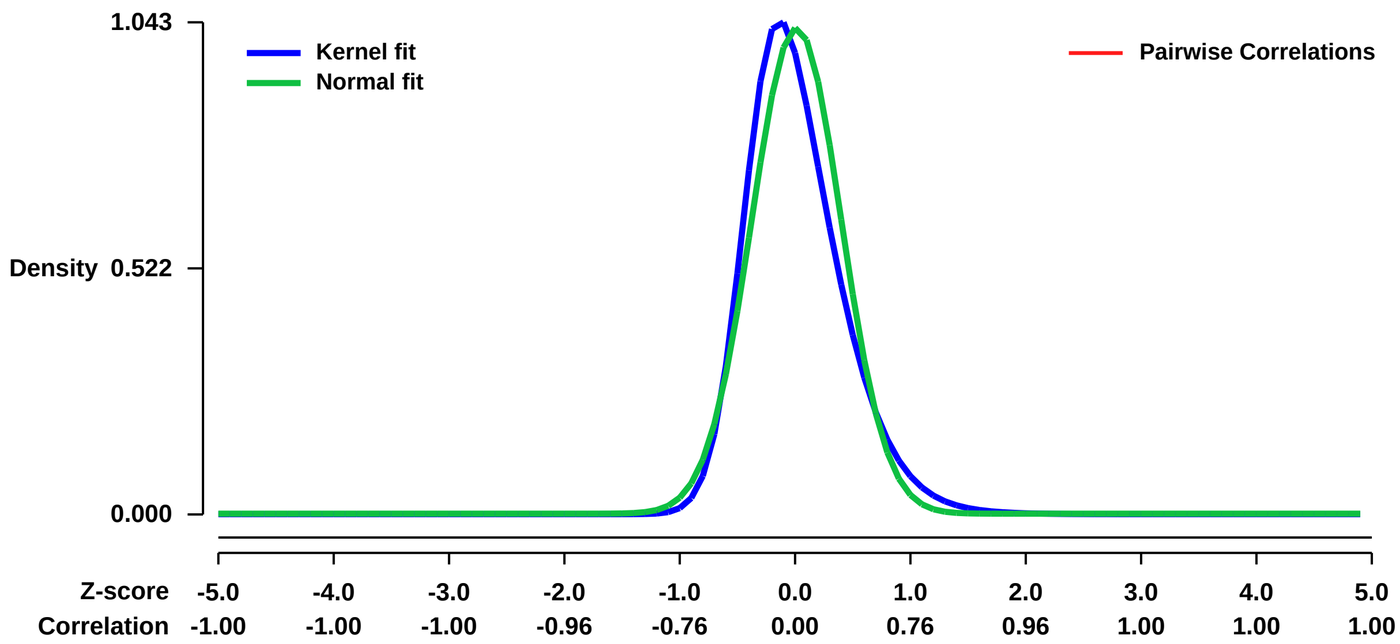

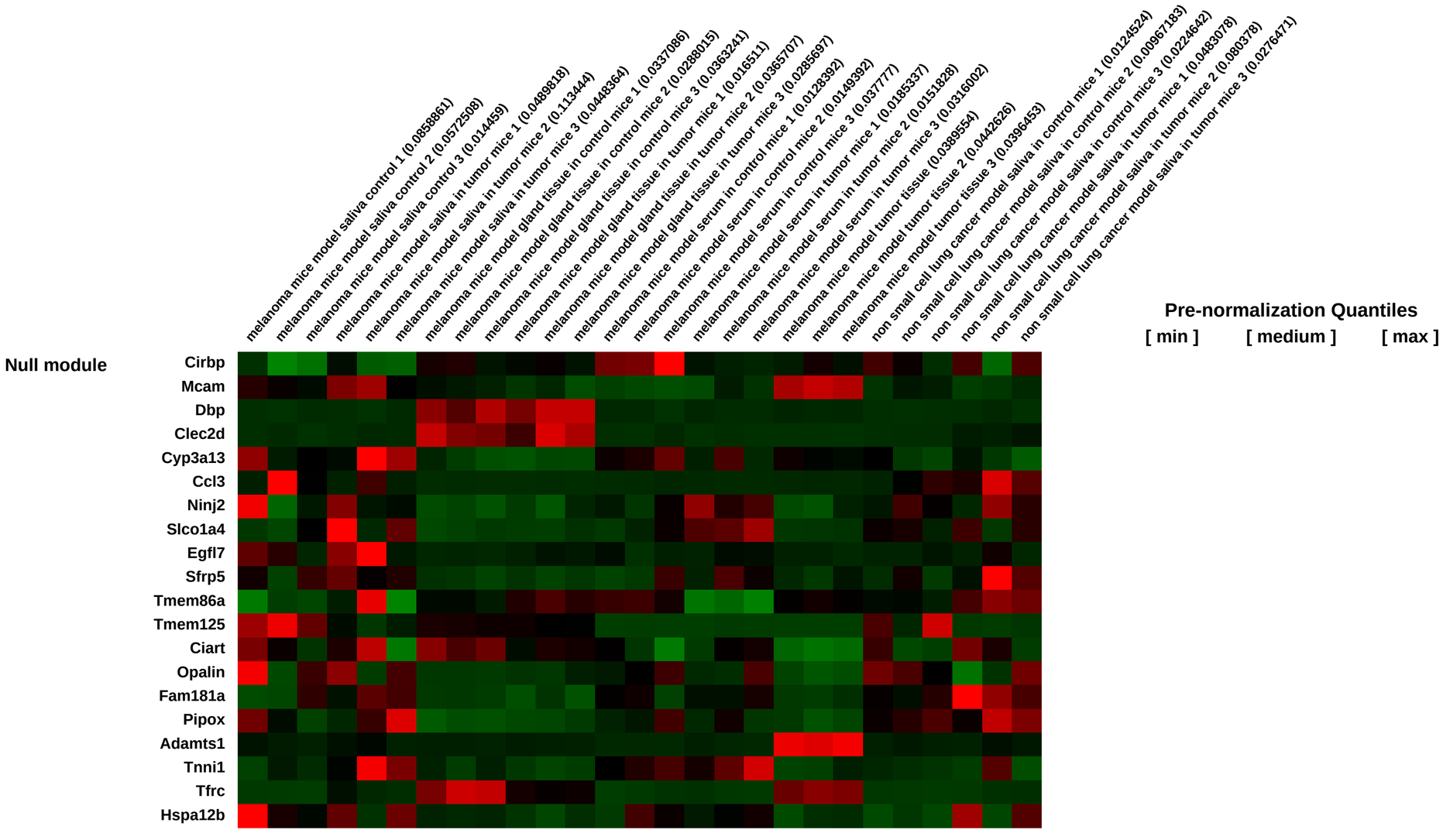

GEO Series "GSE3067" Expression Profiles

Num of samples in this series: 28

Scale of expression profile Z-scores

-3.0 -2.0 -1.0 0.0 1.0 2.0 3.0

GEO Link:	http://www.ncbi.nlm.nih.gov/geo/query/acc.cgi?acc=GSE3067
Status:	Public on Sep 26 2005
Title:	Resistance to thyroid hormone (RTH) and PPARa activation
Organism:	Mus musculus
Experiment type:	Expression profiling by array
Platform:	GPL1261
Pubmed ID:	16985257
Summary & Design:	**Summary:** In this study we used the d337T TRb transgenic mouse that has been created to reproduce the human genetic disease known as resistance to thyroid hormone (RTH) as a model to determine if the d337T TRb mutation would have an effect on PPARa activation. A single amino acid deletion (d337T) abrogates thyroid hormone (T3) binding and transforms the thyroid hormone receptor (TRb) into a constitutive repressor. The principle goal was to determine if T3 regulates myocardial energy metabolism through its nuclear receptors. We introduced a known PPARa activator (WY14, 643) into control and d337T TRb transgenic mice then examined cardiac gene expression using Affymetrix 430_2 expression arrays and RT-PCR. We compared the gene expression of PPARa, RXRb and TRa,b and three PPARa target genes among four studies groups [control, control with WY14, 643, d337T TRb, and d337T TRb with WY14, 643] consisting of seven mice per group. Microarray analysis revealed that these genes responded to the WY14, 643 treatments of control and d337T TRb mice. Analysis of the array and RT-PCR data indicates that mRNA expression levels of PPARa and mRXRb decrease after a six hour drug treatment in both control and d337T TRb mice (P<0.01) as did the array mRNA expression levels for TRa & b (P<0.025). Three target genes (AMPD3, PDK4 and UCP3) of PPARa were up regulated in control and down regulated in the d337T TRb transgenic mouse, indicating a direct action on these metabolic genes when the TRb becomes a repressor. In conclusion, PPARa activation by WY14, 643 has a positive effect on control mice and a negative effect on the TRb transgenic mice which supports our hypothesis that T3 regulates myocardial energy metabolism through its nuclear receptors. **Keywords:** treatment and deletion effects **Overall design:** 7 control, 7 deletion strain individuals, 7 controls with a PPARalpha activator, 7 deletion strain individuals with a PPARalpha activator

Background corr dist: KL-Divergence = 0.4896, L1-Distance = 0.0956, L2-Distance = 0.0315, Normal std = 0.2267

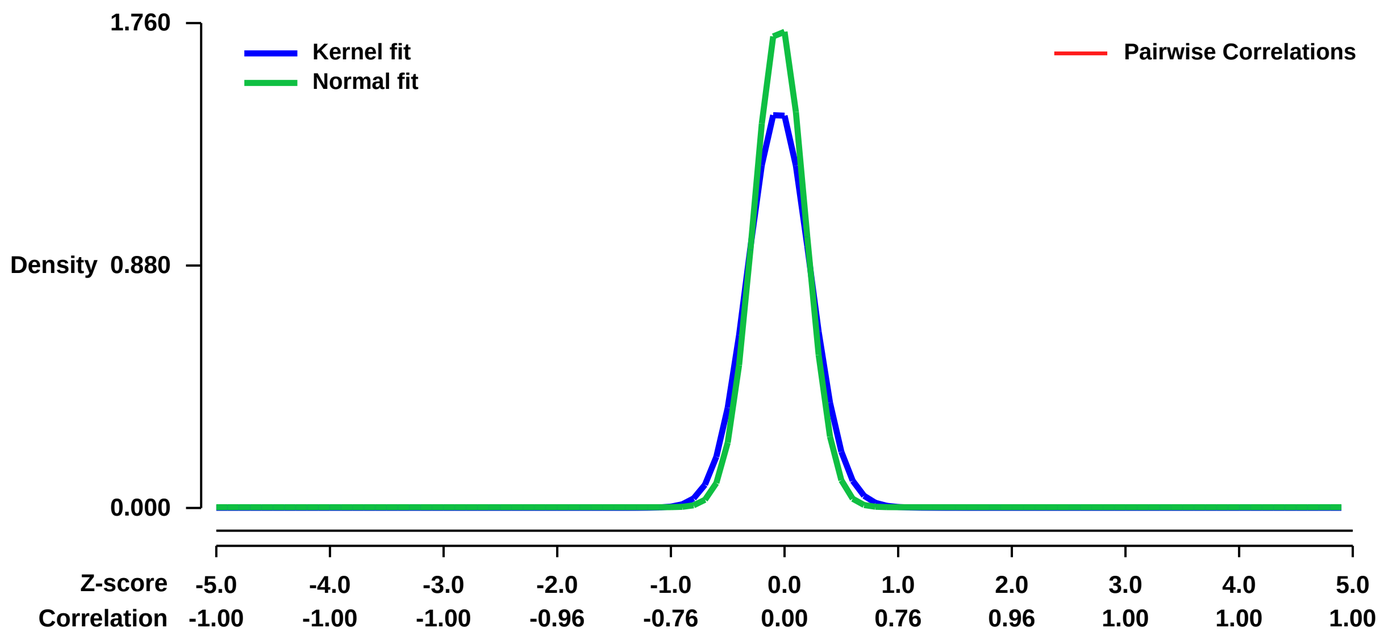

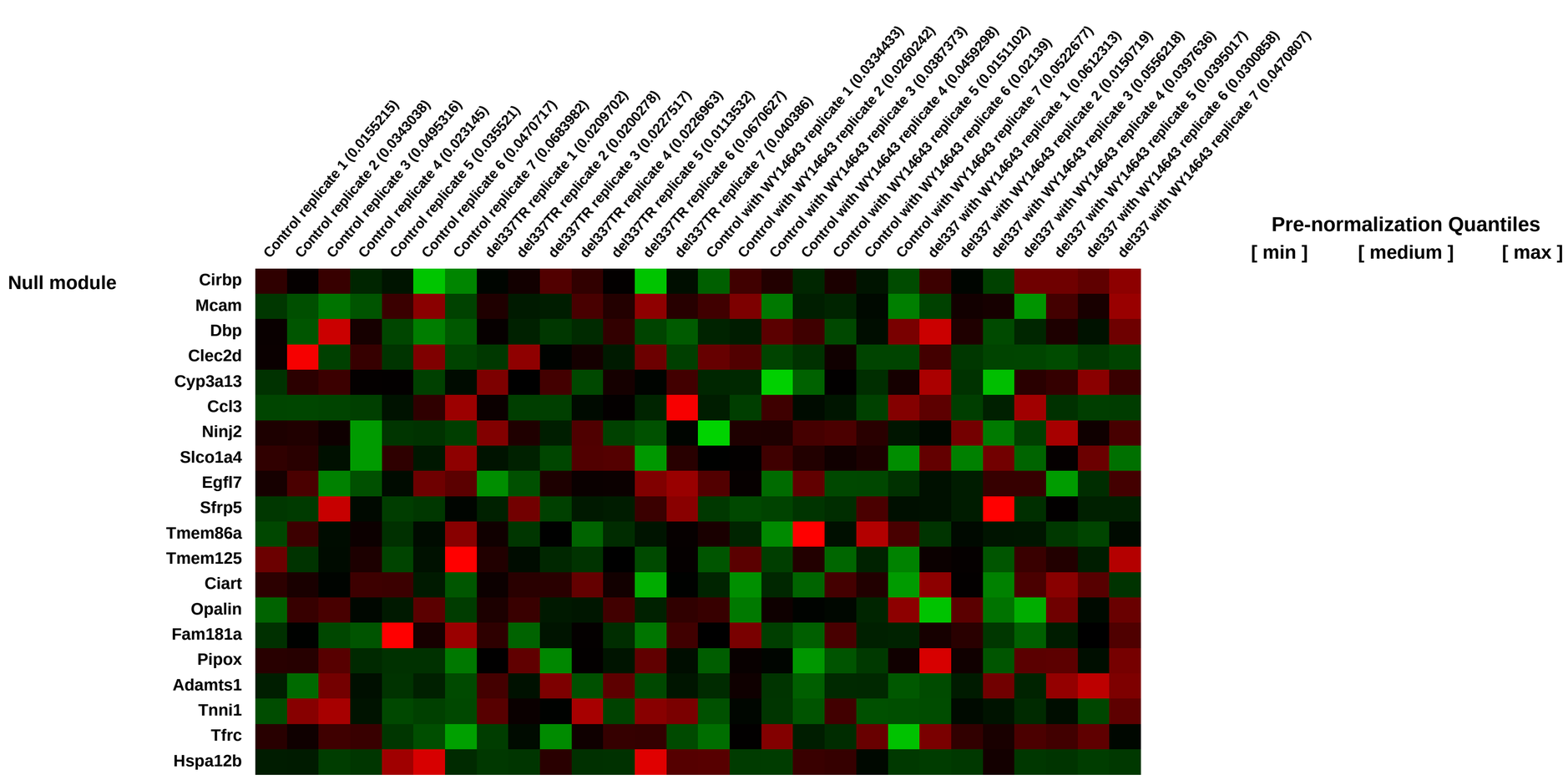

GEO Series "GSE4420" Expression Profiles

Num of samples in this series: 8

Scale of expression profile Z-scores

-3.0 -2.0 -1.0 0.0 1.0 2.0 3.0

GEO Link:	http://www.ncbi.nlm.nih.gov/geo/query/acc.cgi?acc=GSE4420
Status:	Public on Mar 05 2007
Title:	Diabetic mice fat- niacin bound chromium
Organism:	Mus musculus
Experiment type:	Expression profiling by array
Platform:	GPL1261
Pubmed ID:	16940432
Summary & Design:	**Summary:** To study effect of niacin bound chromium in changing genetic profile of subcutaneous fat from diabetic mice **Keywords: nutritional supplemetation, obesity** **Overall design:** Two groups (n=4 each group) of mice were supplemented (oral gavage) with: i) niacin bound chromium (10 mg/kg body wt) in water for 10 wks (5d/wk) or ii) matching volume of water. After 10 wks of supplementation the subcutaneous fat was harvested and gene expression profile was studied using Affymetrix mouse genome 430 v 2.0 chips.

Background corr dist: KL-Divergence = 0.0863, L1-Distance = 0.0220, L2-Distance = 0.0007, Normal std = 0.4630

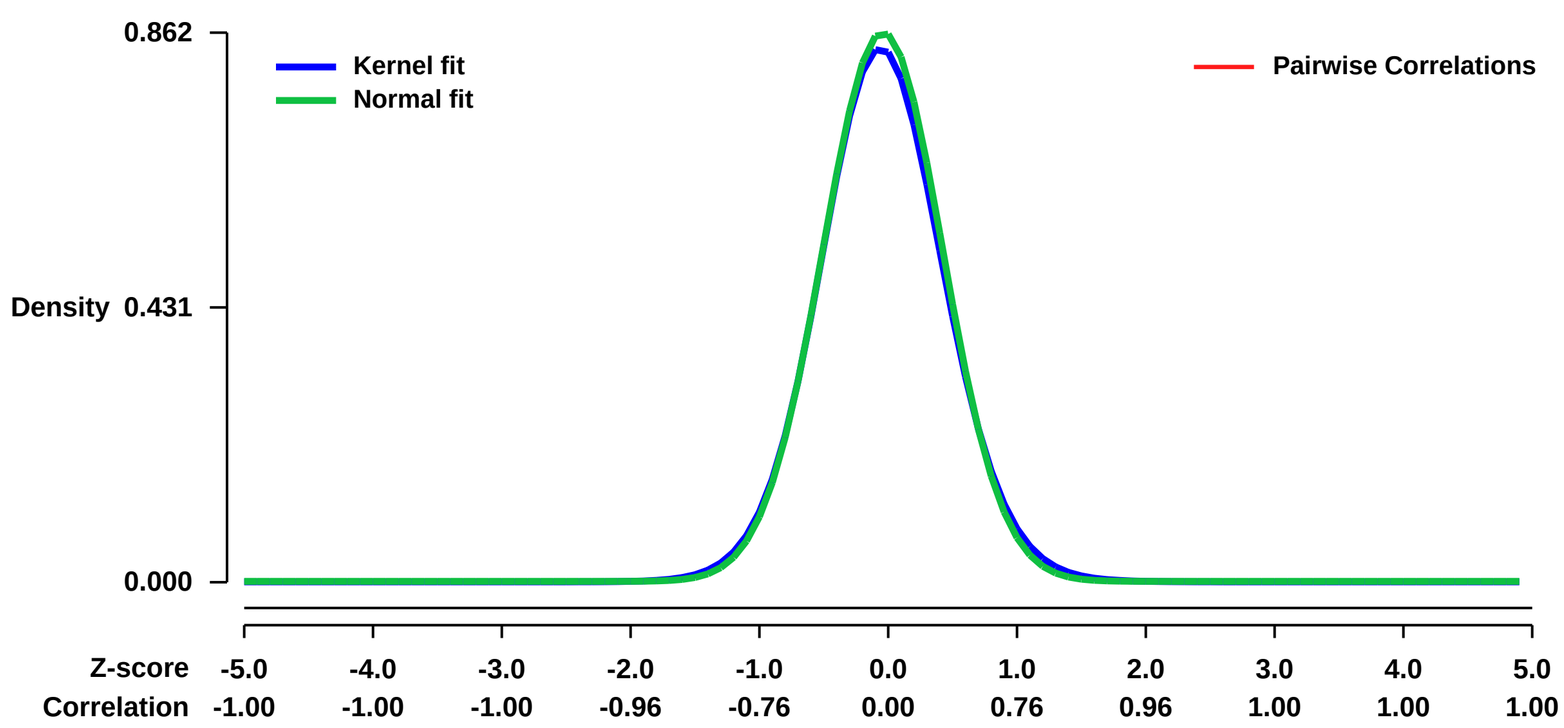

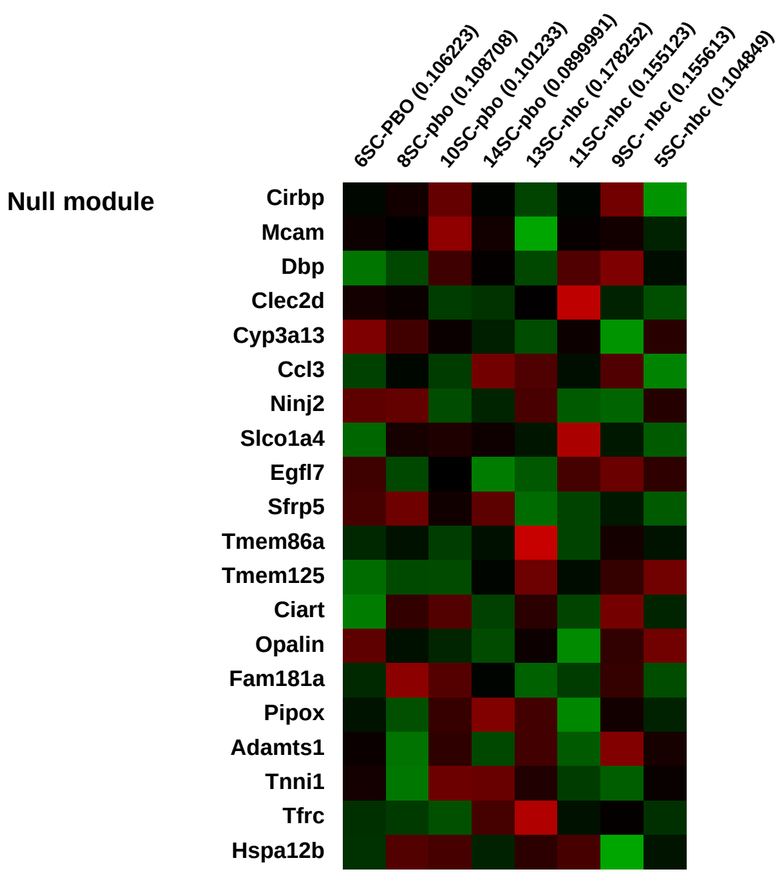

GEO Series "GSE39233" Expression Profiles

Num of samples in this series: 40

Scale of expression profile Z-scores

-3.0 -2.0 -1.0 0.0 1.0 2.0 3.0

GEO Link:	http://www.ncbi.nlm.nih.gov/geo/query/acc.cgi?acc=GSE39233
Status:	Public on Jul 10 2012
Title:	Placental PPARg-Regulated Genes
Organism:	Mus musculus
Experiment type:	Expression profiling by array
Platform:	GPL1261
Pubmed ID:	
Summary & Design:	**Summary:** **Robust identification of placental PPARg target genes via mutliple PPARg-dependence criteria.** **Integration of differential expression data from Pparg-null, Rxra-null, Med1-nul and Ncoa6-null placentas and from WT and Pparg-null Trophoblast stem cells (TSC) differentiated for 2 or 4 days in the presence or absence of the PPARg agonist Rosiglitazone (Rosi).** **Overall design:** **Three independent WT TSC lines differentiated for two and four days in the presence or absence of Rosi vs two independent Pparg-null TSC lines differntiated for the same durations in the presence of Rosi**

Background corr dist: **KL-Divergence = 0.1354, L1-Distance = 0.0395, L2-Distance = 0.0024, Normal std = 0.3994**

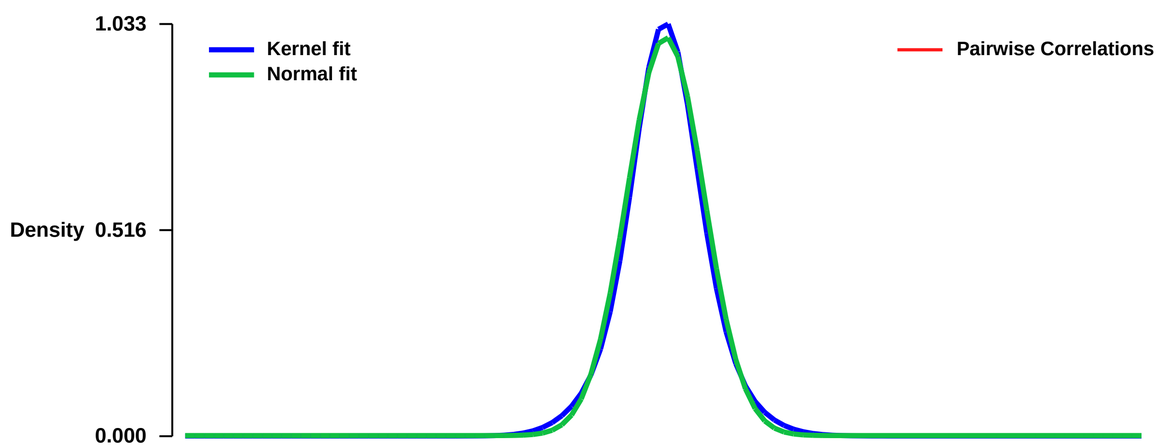

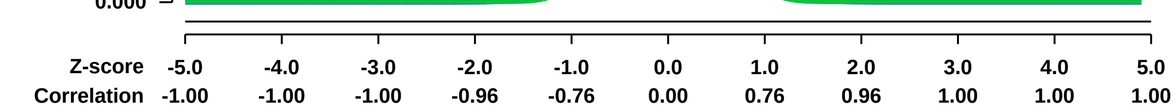

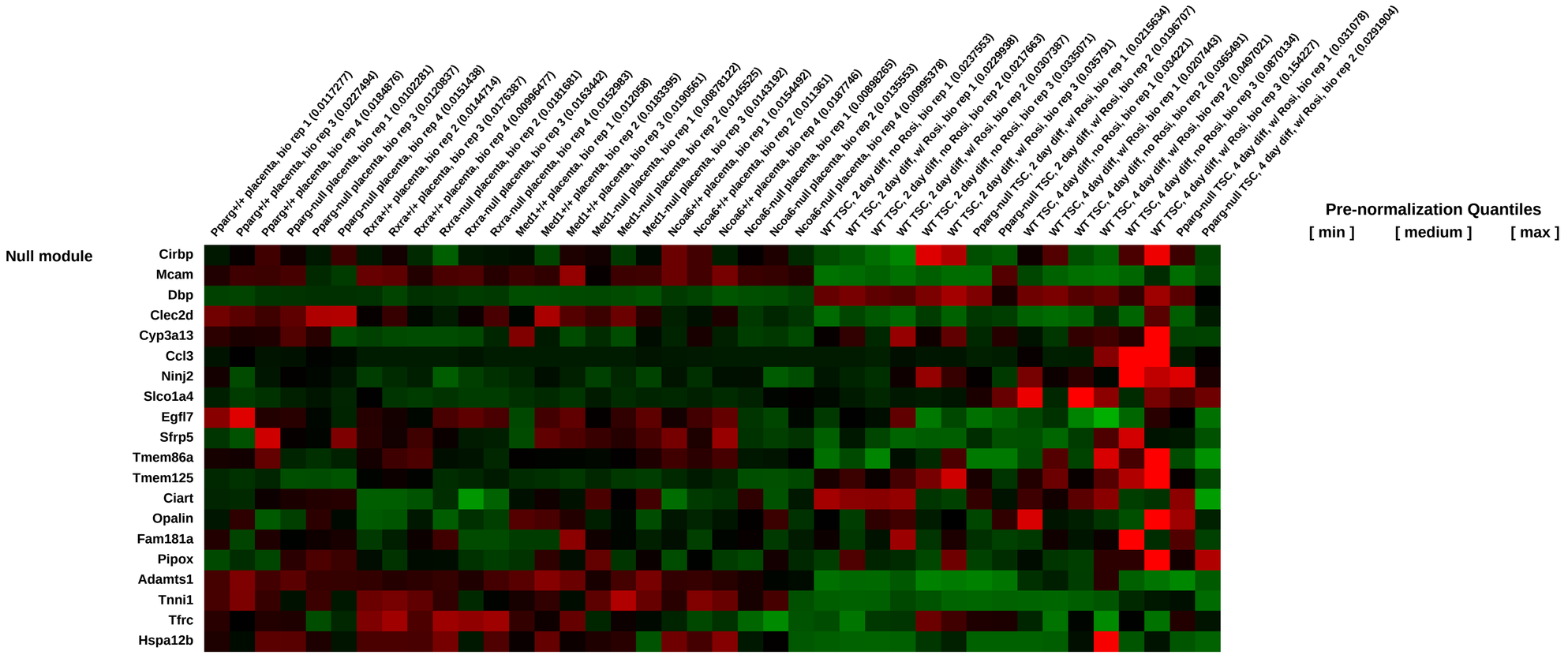

GEO Series "GSE19875" Expression Profiles

Num of samples in this series: 12

Scale of expression profile Z-scores

-3.0 -2.0 -1.0 0.0 1.0 2.0 3.0

GEO Link:	http://www.ncbi.nlm.nih.gov/geo/query/acc.cgi?acc=GSE19875
Status:	Public on Jan 14 2010
Title:	Expression data from murine hearts exposed to ischemic preconditioning comparing A2BAR null and wildtype BL6/C57 mice
Organism:	Mus musculus
Experiment type:	Expression profiling by array
Platform:	GPL1261
Pubmed ID:	22504483
Summary & Design:	**Summary:** Genetically targeted mice with deficiency for the A2BAR show increased susceptibility to acute myocardial ischemia and are not protected by IP, a powerful strategy for cardioprotection, where short and repeated episodes of ischemia and reperfusion prior to myocardial infarction result in attenuation of infarct size. The purpose of this study was to identify genes that are potentially under the control of the cardiac A2B adenosine receptor **Overall design:** Untreated wildtype and A2BAR-/- mice were compared to wildtype and A2BAR-/- mice with IP treatment following a 2 hours reperfusion period

Background corr dist: KL-Divergence = 0.1380, L1-Distance = 0.0290, L2-Distance = 0.0015, Normal std = 0.3889

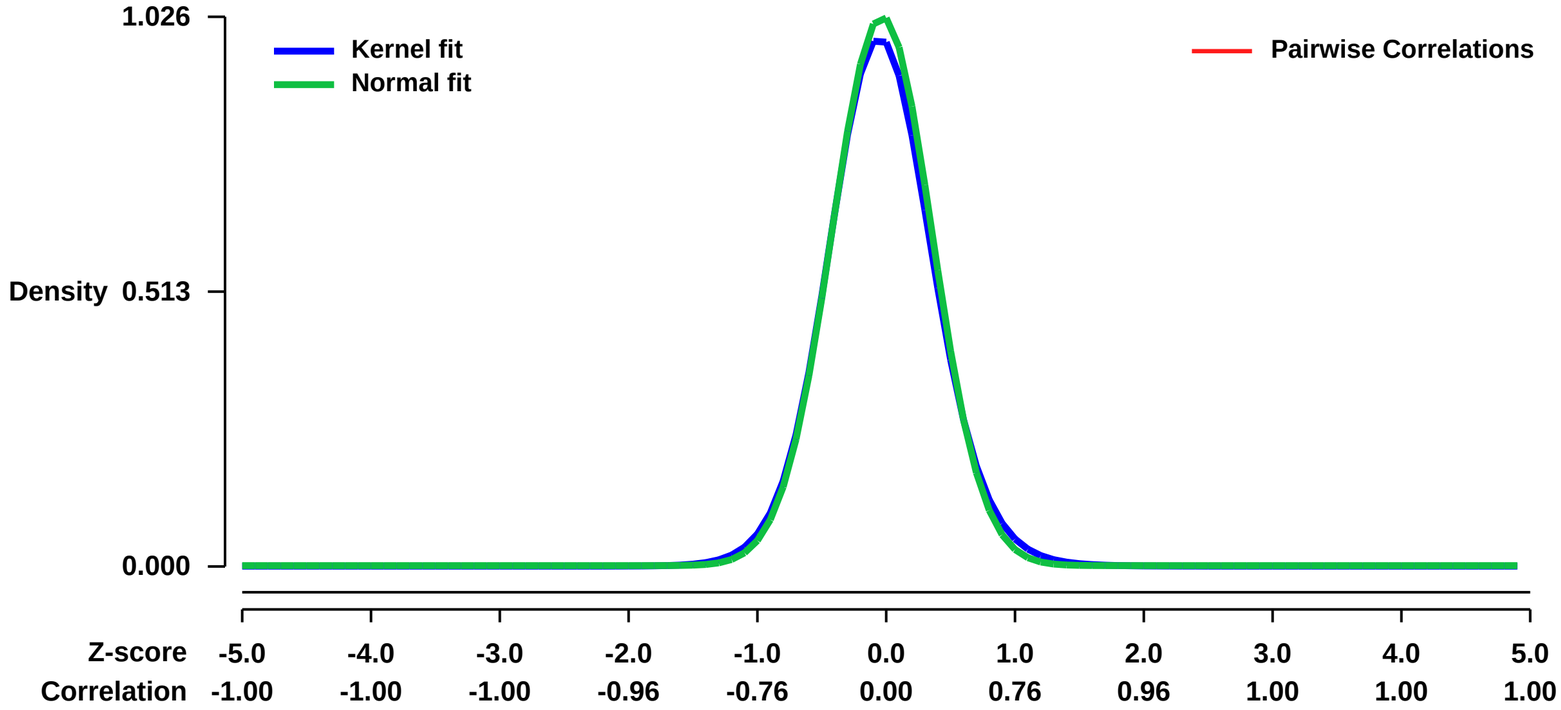

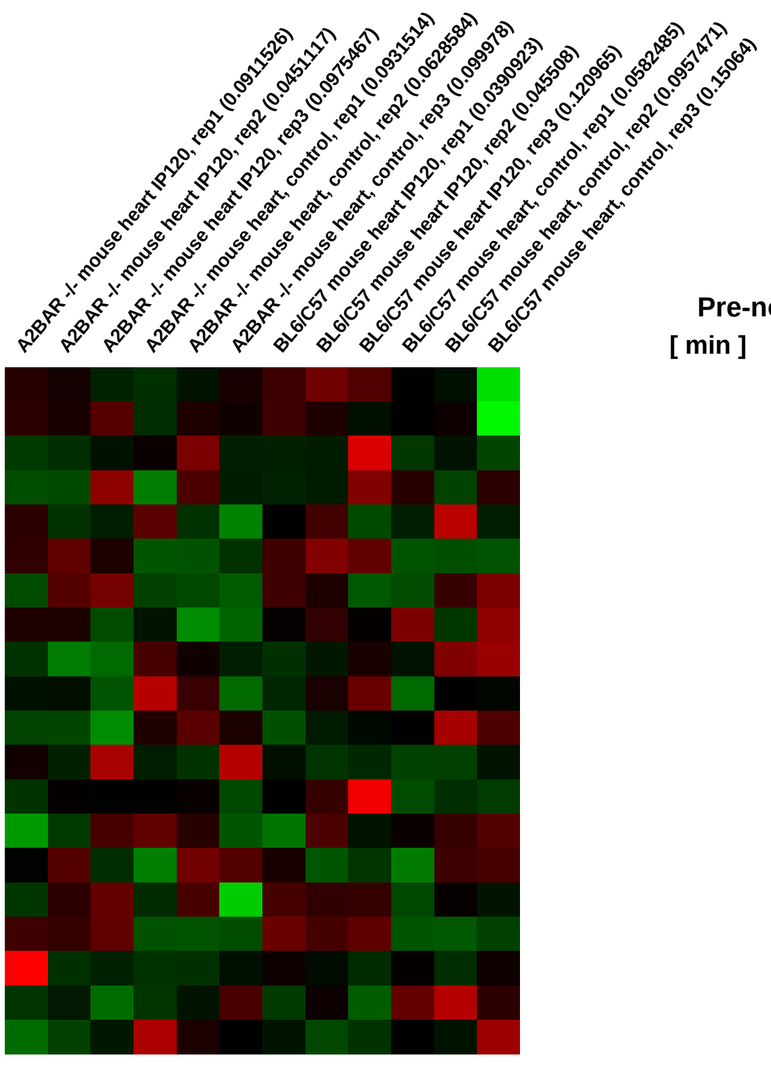

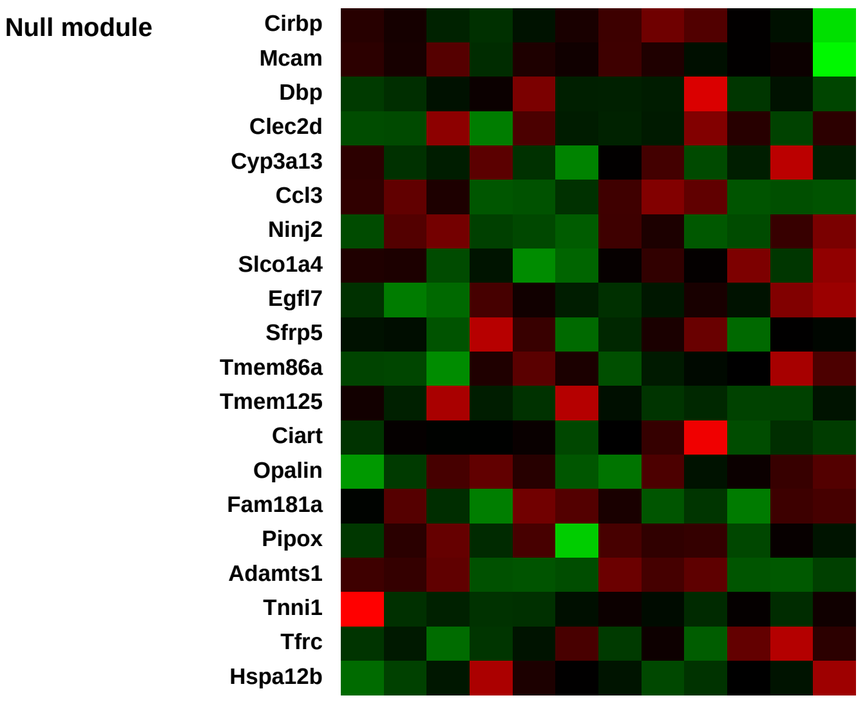

GEO Series "GSE11981" Expression Profiles

Num of samples in this series: 8

Scale of expression profile Z-scores

-3.0 -2.0 -1.0 0.0 1.0 2.0 3.0

GEO Link:	**http://www.ncbi.nlm.nih.gov/geo/query/acc.cgi?acc=GSE11981**
Status:	**Public on Sep 12 2008**
Title:	**Gene expression profiling of HhAntag-treated pancreatic xenografts**
Organism:	**Mus musculus**
Experiment type:	**Expression profiling by array**
Platform:	**GPL1261**
Pubmed ID:	**18754008**
Summary & Design:	**Summary:** **Four vehicle-treated and four HhAntag-treated pancreatic xenograft tumors were profiled for gene expression changes using Affymetrix U133 Plus 2.0 and Affymetrix Mouse Genome 430 2.0 arrays.** **Keywords: comparative gene expression, hedgehog, hh** **Overall design:** **A primary human pancreatic tumor xenograft (1051178-A) was established by direct implantation of surgical material into female CD1 nu/nu mice of 6-8 weeks of age. Tumors were serially passaged into larger cohorts of mice for efficacy testing and subsequently distributed into tumor volume-matched cohorts upon tumors reaching between 200 to 350 mm3. HhAntag was resuspended in 0.5% methyl-cellulose, 0.2% Tween-80 (MCT) and administered orally twice daily at 75 mg/kg from a 10 mg/ml suspension. MCT alone served as vehicle control. Tumor xenografts (4/group) were excised following 21 days of dosing and RNA was extracted. Preparation of complementary RNA, Human Genome U133 Plus 2.0 array and Mouse Genome 430 2.0 array hybridizations, and subsequent data analysis were carried out using Affymetrix protocols, with signal intensities being determined by the MAS5.0 algorithm.**

Background corr dist: KL-Divergence = 0.0855, L1-Distance = 0.0227, L2-Distance = 0.0007, Normal std = 0.4633

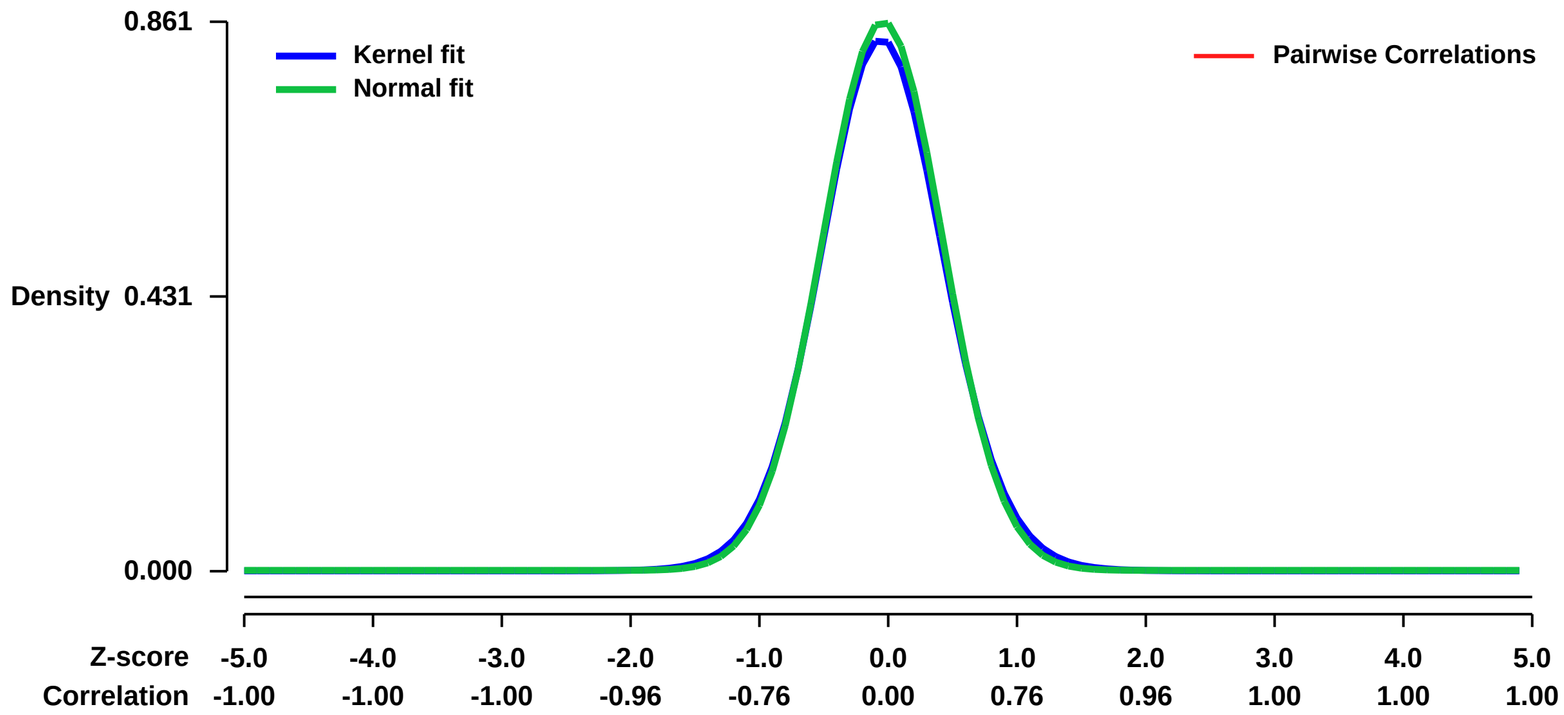

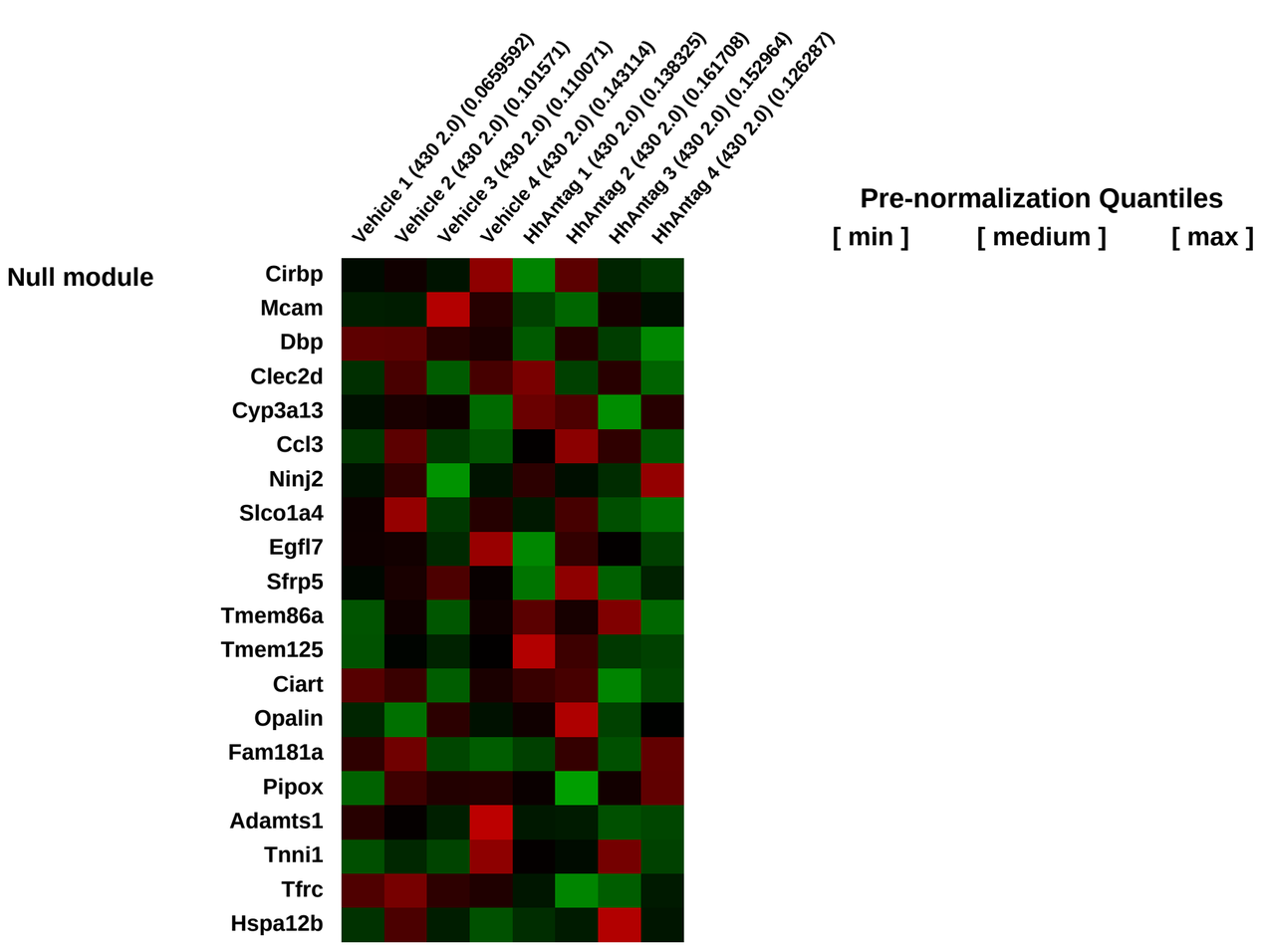

GEO Series "GSE51804" Expression Profiles

Num of samples in this series: 10

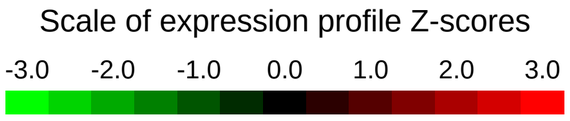

GEO Link:	**http://www.ncbi.nlm.nih.gov/geo/query/acc.cgi?acc=GSE51804**
Status:	**Public on Nov 09 2013**
Title:	**Effect of W805EC nanoemulsion (NE) on global gene transcription in JawsII dendritic cells in vitro**
Organism:	**Mus musculus**
Experiment type:	**Expression profiling by array**
Platform:	**GPL1261**
Pubmed ID:	**24532579**
Summary & Design:	**Summary:** **Nanoemulsion adjuvant affects immune gene expression in dendritic cells.** **Microarray was used to asses global changes in gene expression in JAWS II dendritic cells upon treatment with nanoemulsion (NE) adjuvant W805EC** **Overall design:** **JawsII cell were incubated with NE formulation for 6 and 24 hours, and RNA was extracted for Affymetrix hybridization**

Background corr dist: **KL-Divergence = 0.0882, L1-Distance = 0.0213, L2-Distance = 0.0006, Normal std = 0.4633**

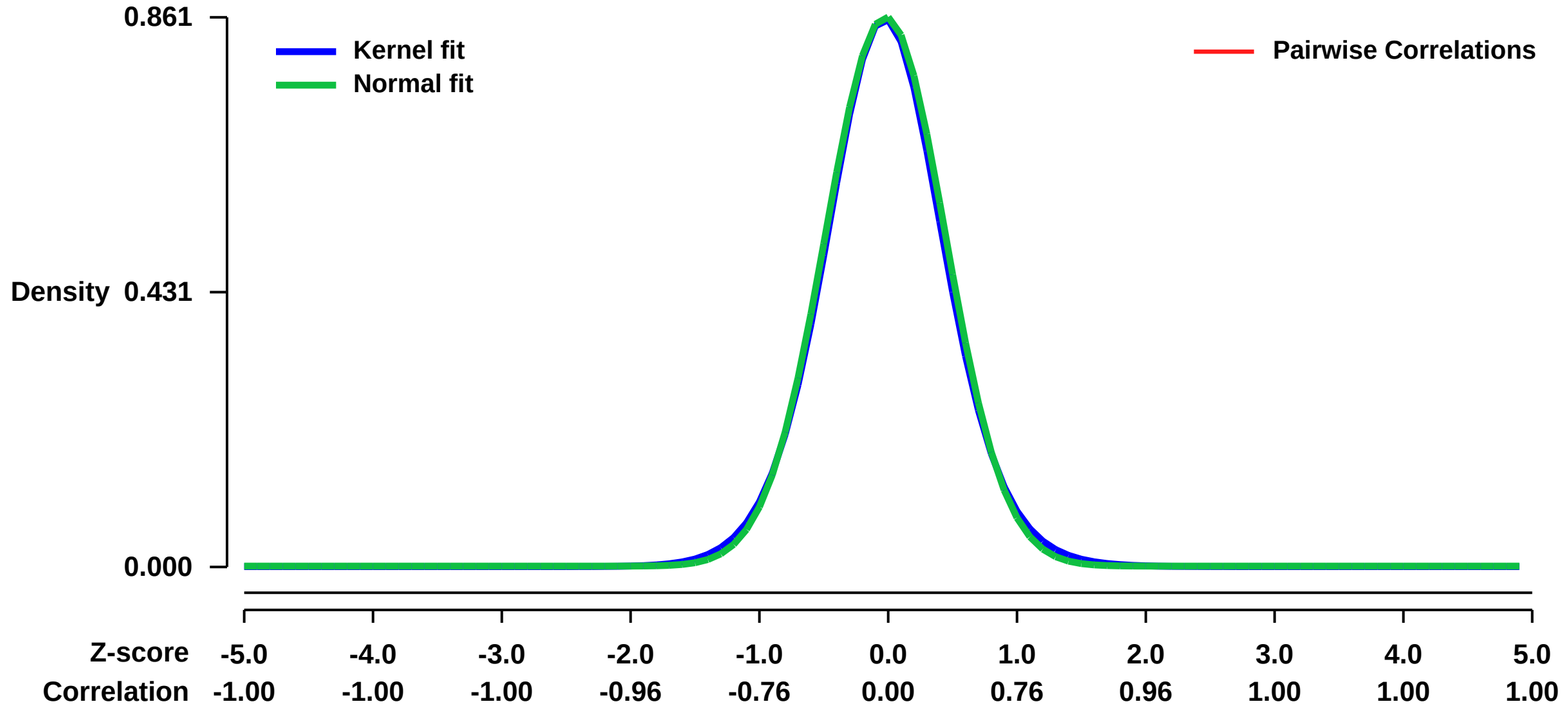

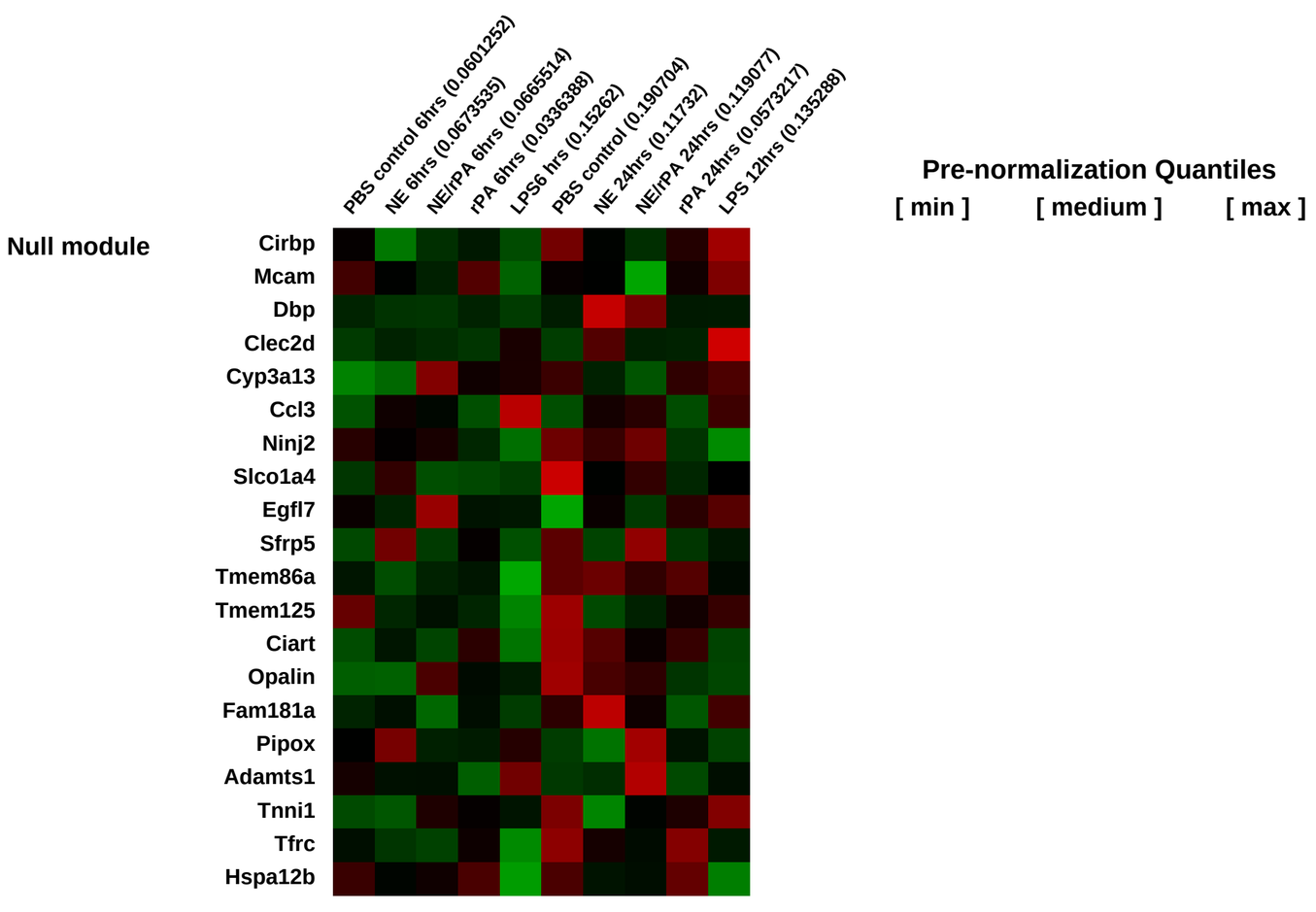

GEO Series "GSE31244" Expression Profiles

Num of samples in this series: 6

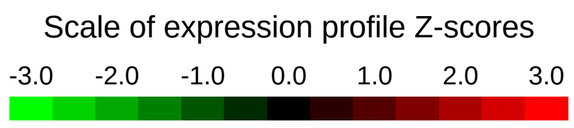

GEO Link:	http://www.ncbi.nlm.nih.gov/geo/query/acc.cgi?acc=GSE31244
Status:	Public on Aug 09 2011
Title:	Notch1 mediates cell fate decisions in the mouse uterus and is critical for complete decidualization
Organism:	Mus musculus
Experiment type:	Expression profiling by array
Platform:	GPL1261
Pubmed ID:	21990372
Summary & Design:	**Summary:** Uterine receptivity implies a dialogue between the hormonally primed maternal endometrium and the free-floating blastocyst. Endometrial stromal cells proliferate, avert apoptosis, and undergo decidualization in preparation for implantation; however, the molecular mechanisms that underlie differentiation into the decidual phenotype remain largely undefined. The Notch family of transmembrane receptors transduce extracellular signals responsible for cell survival, cell-to-cell communication, and trans-differentiation, all fundamental processes for decidualization and pregnancy. Using a murine artificial decidualization model, pharmacological inhibition of Notch signaling by gamma-secretase inhibition resulted in significantly decreased deciduoma. Furthermore, a progesterone receptor (PR)-Cre Notch1 bigenic (Notch1d/d) confirmed a Notch1-dependant hypomorphic decidual phenotype. Microarray and pathway analysis, following Notch1 ablation, demonstrated significantly altered signaling repertoire. Concomitantly, hierarchical clustering demonstrated Notch1-dependent differences in gene expression. Uteri deprived of Notch1 signaling demonstrated decreased cellular proliferation; namely, reduced proliferation-specific antigen, Ki67, altered p21, cdk6, and cyclinD activity, and increased apoptotic-profile, augmented cleaved caspase-3, Bad, and attenuated Bcl2. Demonstrated here, the pre-implantation uterus relies on Notch signaling to inhibit apoptosis of stromal fibroblasts and regulate cell cycle progression, which together promotes successful decidualization. In summary, Notch1 signaling modulates multiple signaling mechanisms crucial for decidualization and we provide greater perspective to the coordination of multiple signaling modalities required during decidualization **Overall design:** RNA samples from 3-5 separate mice were extracted. All mRNA quantities were normalized against 18S gene expression. Gene expression levels were measured by real-time RT-PCR SYBR Green analysis using the ABI Prism 7700 Sequence Detector System according to manufacturerâ s instructions (Applied Biosystems).

Background corr dist: KL-Divergence = 0.0271, L1-Distance = 0.0121, L2-Distance = 0.0002, Normal std = 0.6810

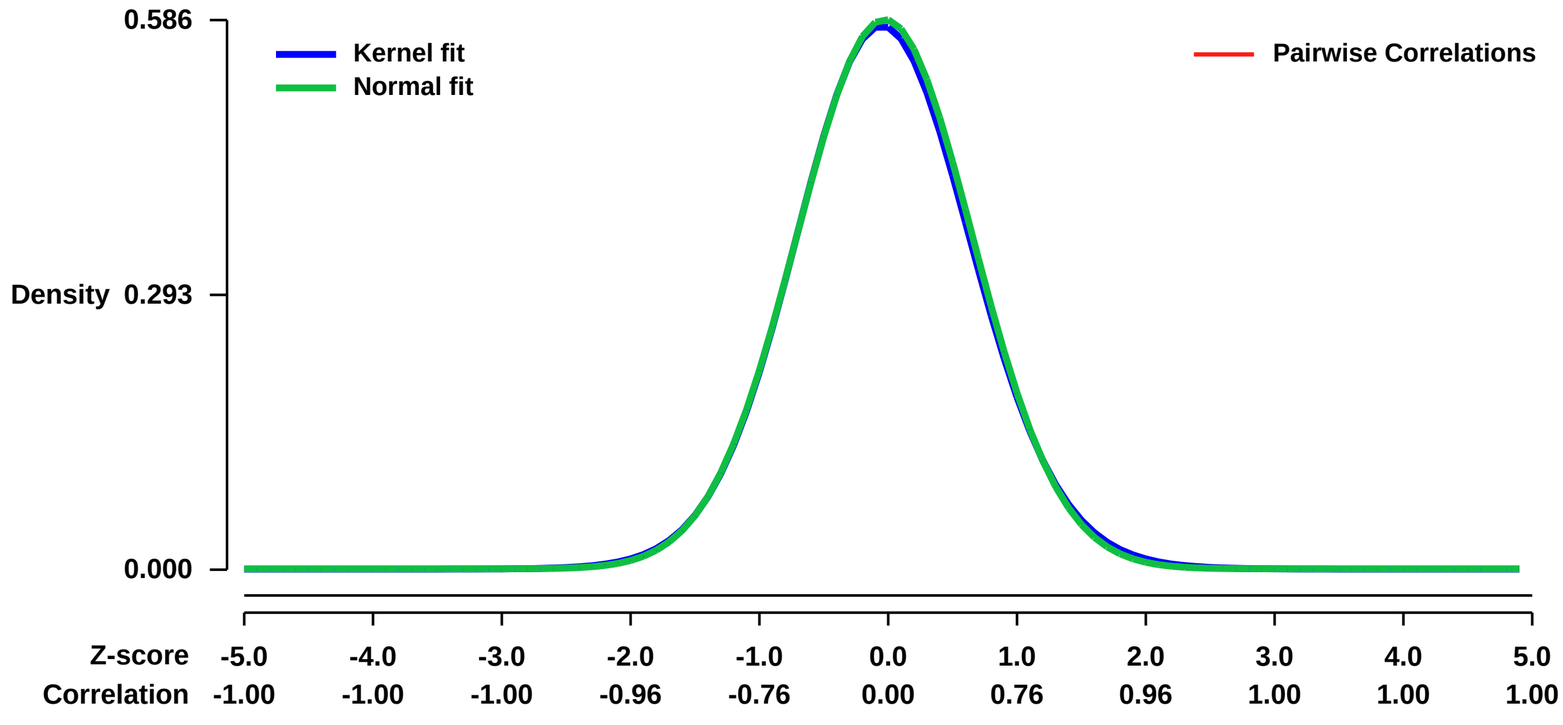

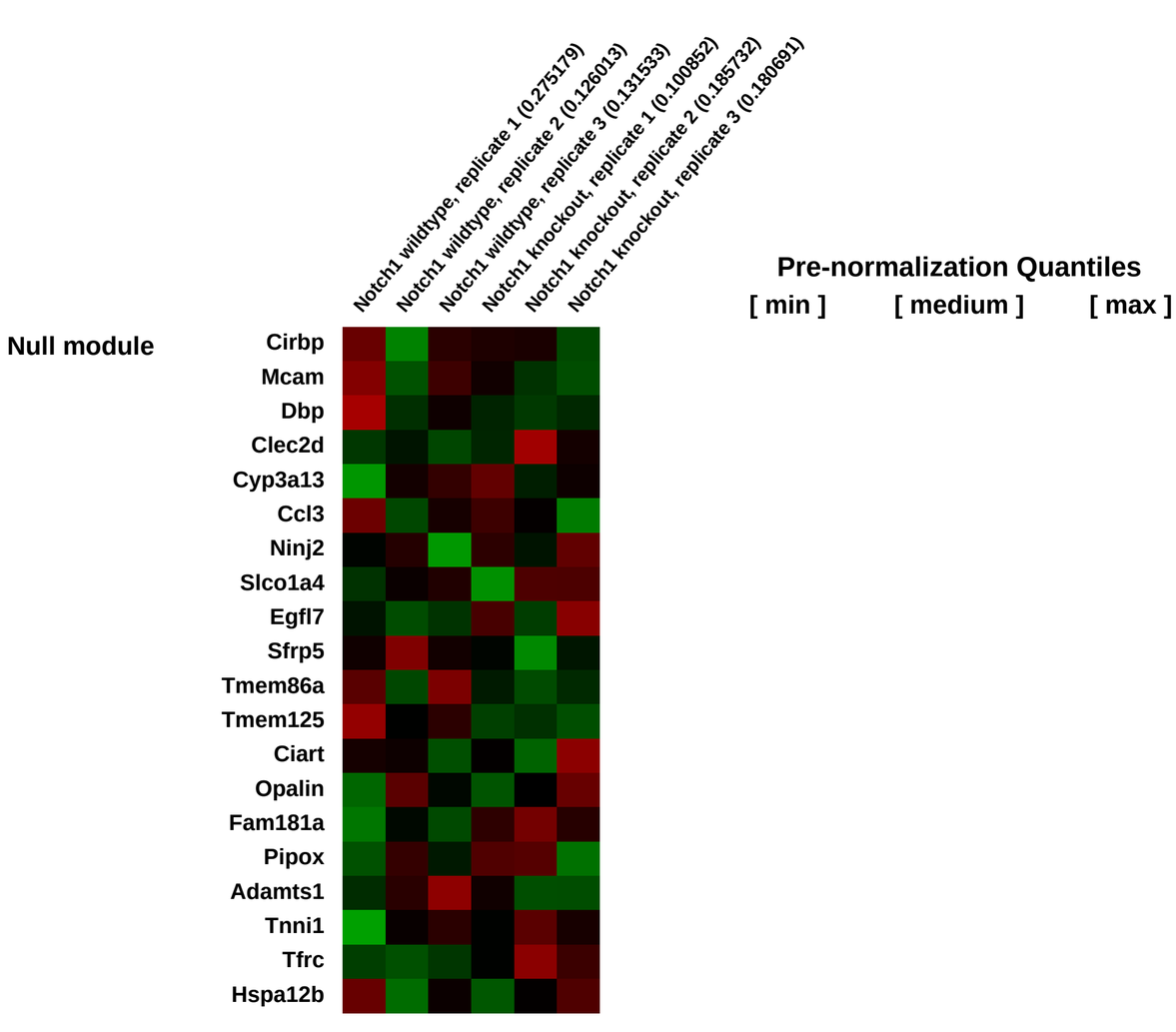

GEO Series "GSE21594" Expression Profiles

Num of samples in this series: 12

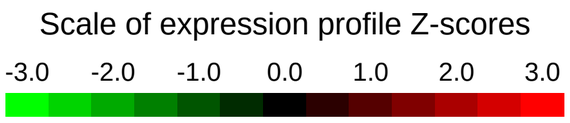

GEO Link:	http://www.ncbi.nlm.nih.gov/geo/query/acc.cgi?acc=GSE21594
Status:	Public on May 07 2013
Title:	Multiple Roles for Steroid Receptor RNA Activator (SRA) in Regulation of Adipogenesis and Insulin Sensitivity
Organism:	Mus musculus
Experiment type:	Expression profiling by array
Platform:	GPL1261
Pubmed ID:	21152033
Summary & Design:	**Summary:** PPARγ‡ is a master transcriptional regulator of adipogenesis. Hence, the identification of PPARγ‡ coactivators should help reveal mechanisms controlling gene expression in adipose tissue development and physiology. We show that the non-coding RNA Steroid receptor RNA Activator, SRA, associates with PPARγ‡ and coactivates PPARγ‡-dependent reporter gene expression. Overexpression of SRA in ST2 adipocyte precursor cells promotes their differentiation into adipocytes. Conversely, knockdown of endogenous SRA inhibits 3T3-L1 preadipocyte differentiation. Microarray analysis reveals hundreds of SRA-responsive genes in adipocytes, including genes in cell cycle, insulin and TNFγ– signaling pathways. Some functions of SRA may involve mechanisms other than coactivation of PPARγ‡. SRA increases insulin-stimulated glucose uptake in adipocytes. SRA promotes S-phase entry during mitotic clonal expansion, decreases expression of cyclin-dependent kinase inhibiters p21Cip1 and p27Kip1, and increases phosphorylation of Cdk1/Cdc2. SRA also inhibits the TNFγ–-induced phosphorylation of c-Jun NH2-terminal kinase. In conclusion, SRA enhances adipogenesis and adipocyte function through multiple pathways. **Overall design:** Total RNA was isolated from fully differentiated (MDIT day 4) SRA overexpressing (pMSCV-SRA) and control (pMSCV empty vector) ST2 adipocytes, or fully differentiated (MDIT day 8) shSRA knockdown (pSuperior-shSRA) or shControl (pSuperior-shcontrol) 3T3-L1 adipocytes. Genome wide gene expression analysis was performed using Affymetrix mouse genome 430 2.0 arrays. Triplicate samples were analyzed.

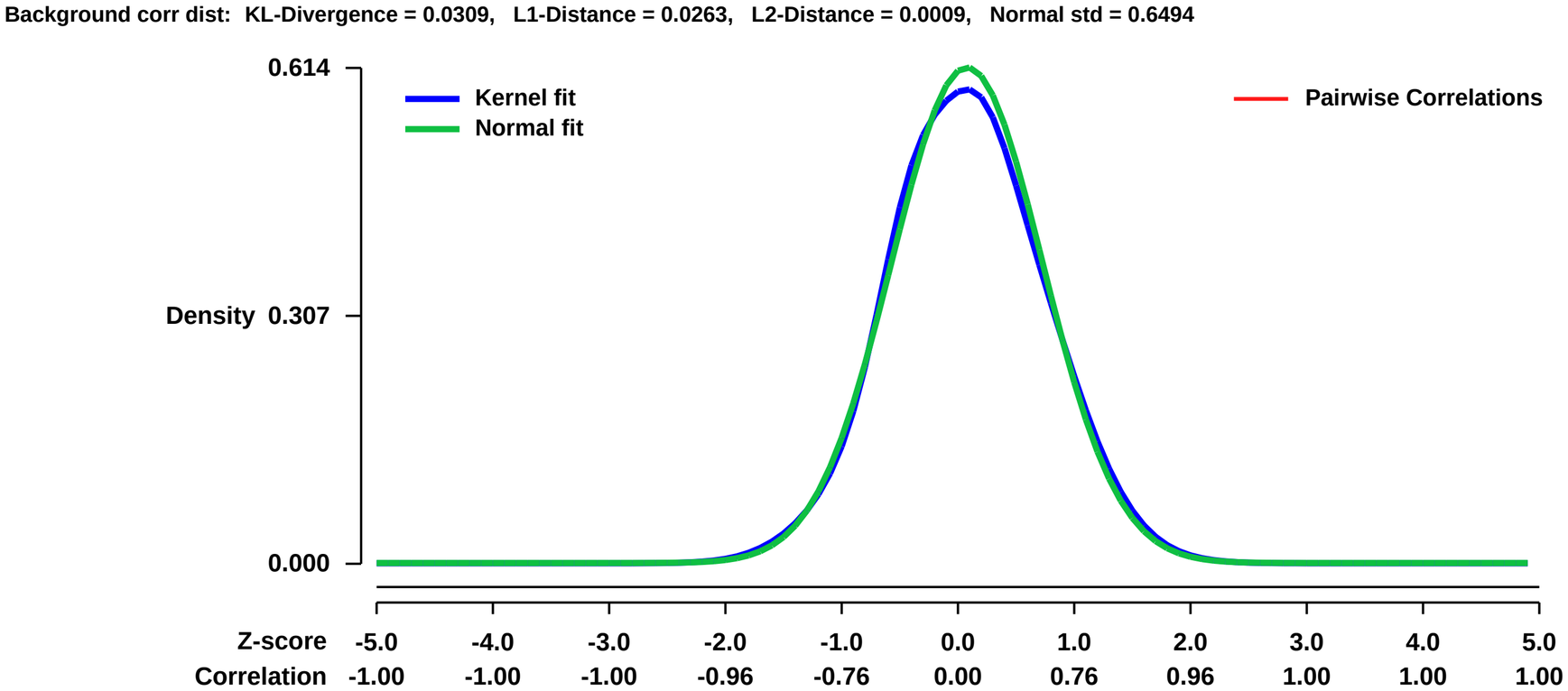

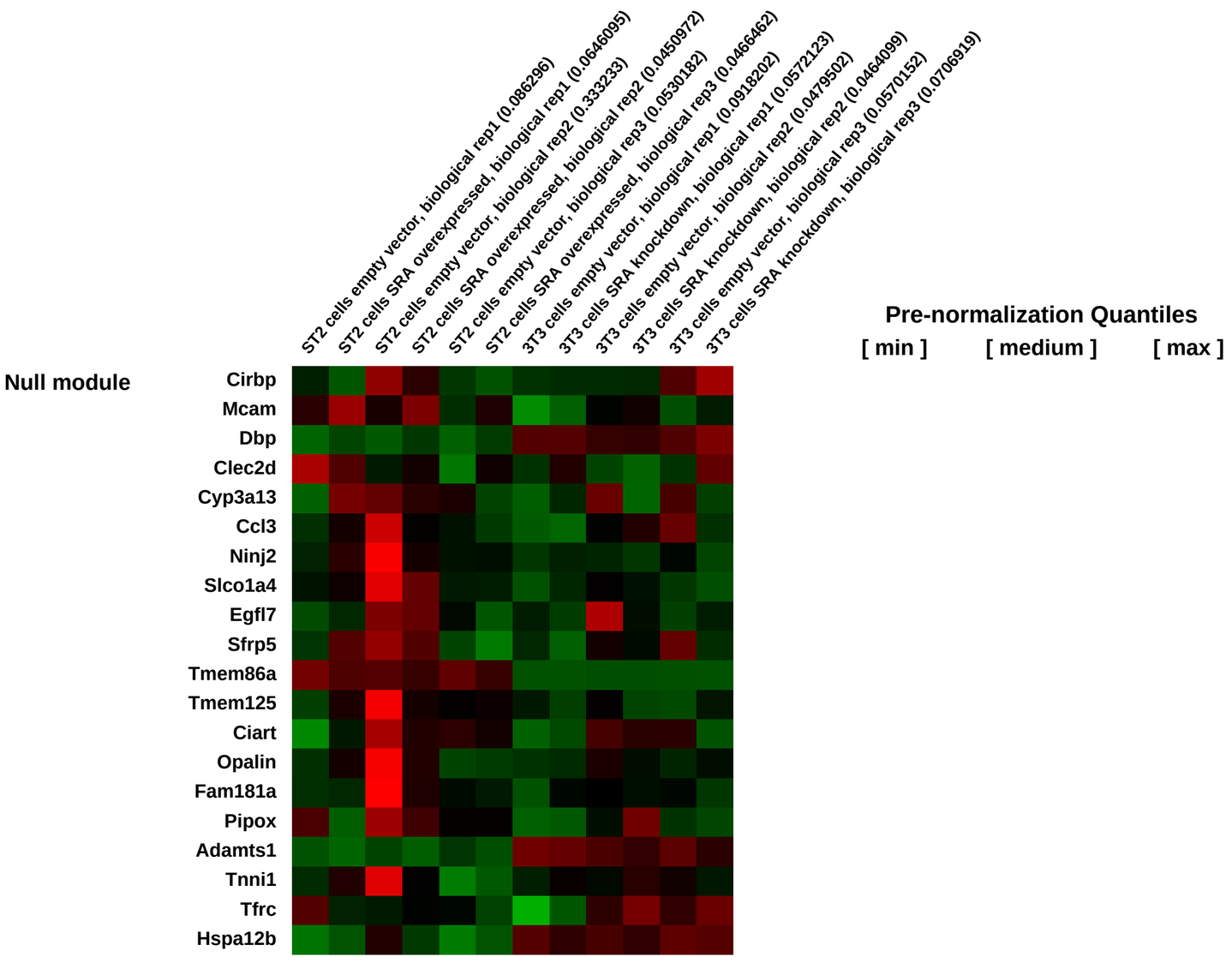

GEO Series "GSE20177" Expression Profiles

Num of samples in this series: 14

Scale of expression profile Z-scores

-3.0 -2.0 -1.0 0.0 1.0 2.0 3.0

GEO Link:	http://www.ncbi.nlm.nih.gov/geo/query/acc.cgi?acc=GSE20177
Status:	Public on Sep 03 2010
Title:	Expression data from mouse wild-type and Dnmt1-/-Dnmt3a-/-Dnmt3b-/- embryonic stem(ES) cells and nuclear transfer-trophoblastic stem(ntTS) cells, and wild-type tropho
Organism:	Mus musculus
Experiment type:	Expression profiling by array
Platform:	GPL1261
Pubmed ID:	20637626
Summary & Design:	**Summary:** To investigate the role of DNA methylation in early embryogenesis, we created Dnmt1-/-Dnmt3a-/-Dnmt3b-/- triple knockout (TKO) embryos by the nuclear transfer (NT) technique using TKO ES cells as the nucleus donor, and found that the TKO NT embryos could develop into blastocysts. From the TKO NT blastocysts, we successfully established trophoblastic stem cells (ntTS cells), and these TKO ntTS cells could self-renew and contribute to the placenta in vivo. Expression profile analysis using microarray revealed that, although many genes were aberrantly expressed, the fundamental gene expression patterns of stem cells were retained in these TKO ntTS cells. **Overall design:** To investigate the properties of the TKO ntTS cells from their expression profiles, we compared the microarray data from the TKO ntTS cells with data from wild-type (WT) ntTS cells and other cell types that represent the three blastocyst-derived lineages: the epiblast (EPI), trophectoderm (TE), and primitive endoderm (PE). WT and TKO ES cells were used as EPI, TS cells derived from wild-type blastocysts were used as TE, and extra-embryonic endoderm (XEN) cells derived from wild-type blastocysts were used as PE. We also treated WT ES cells with Gata4 to induce parietal endoderm cells as PE. The total RNA was extracted from these cell lines, and microarray data were obtained using mouse expression microarrays.

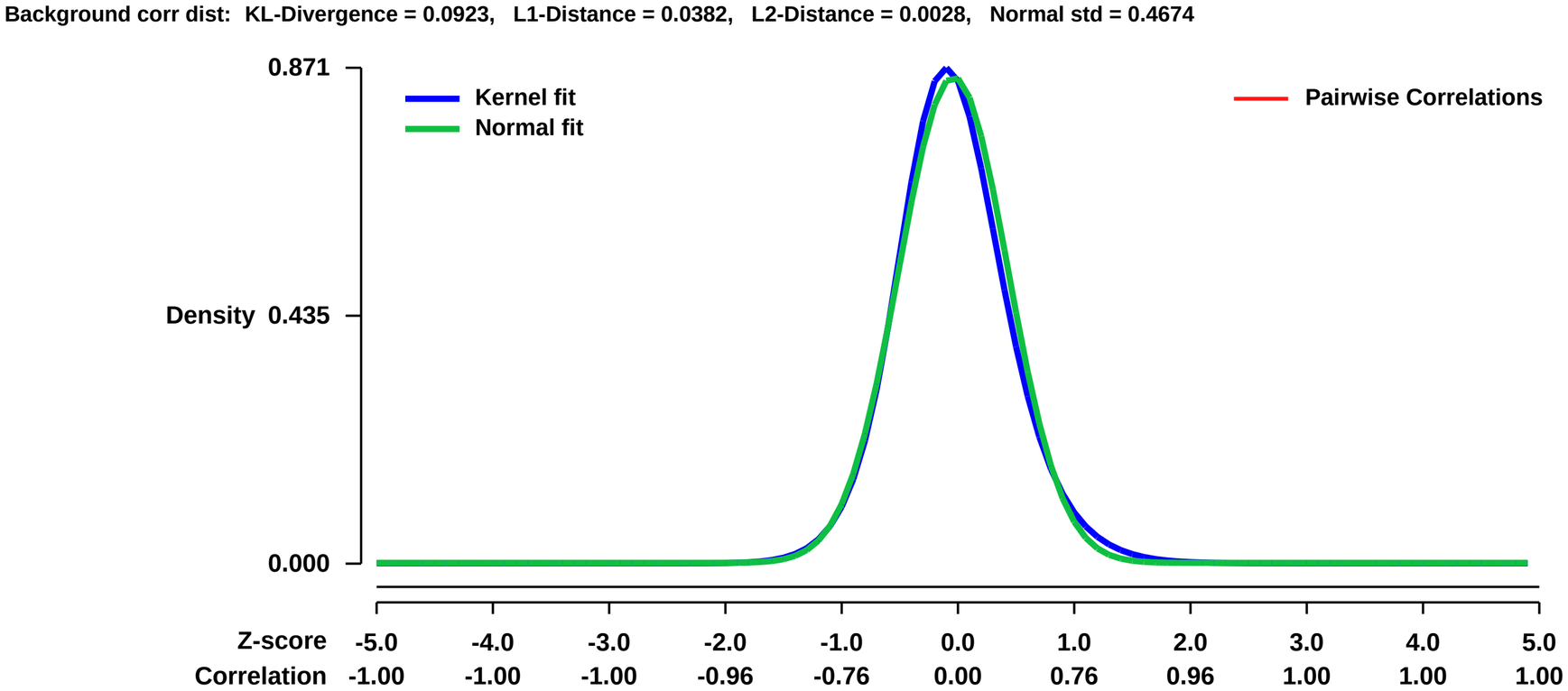

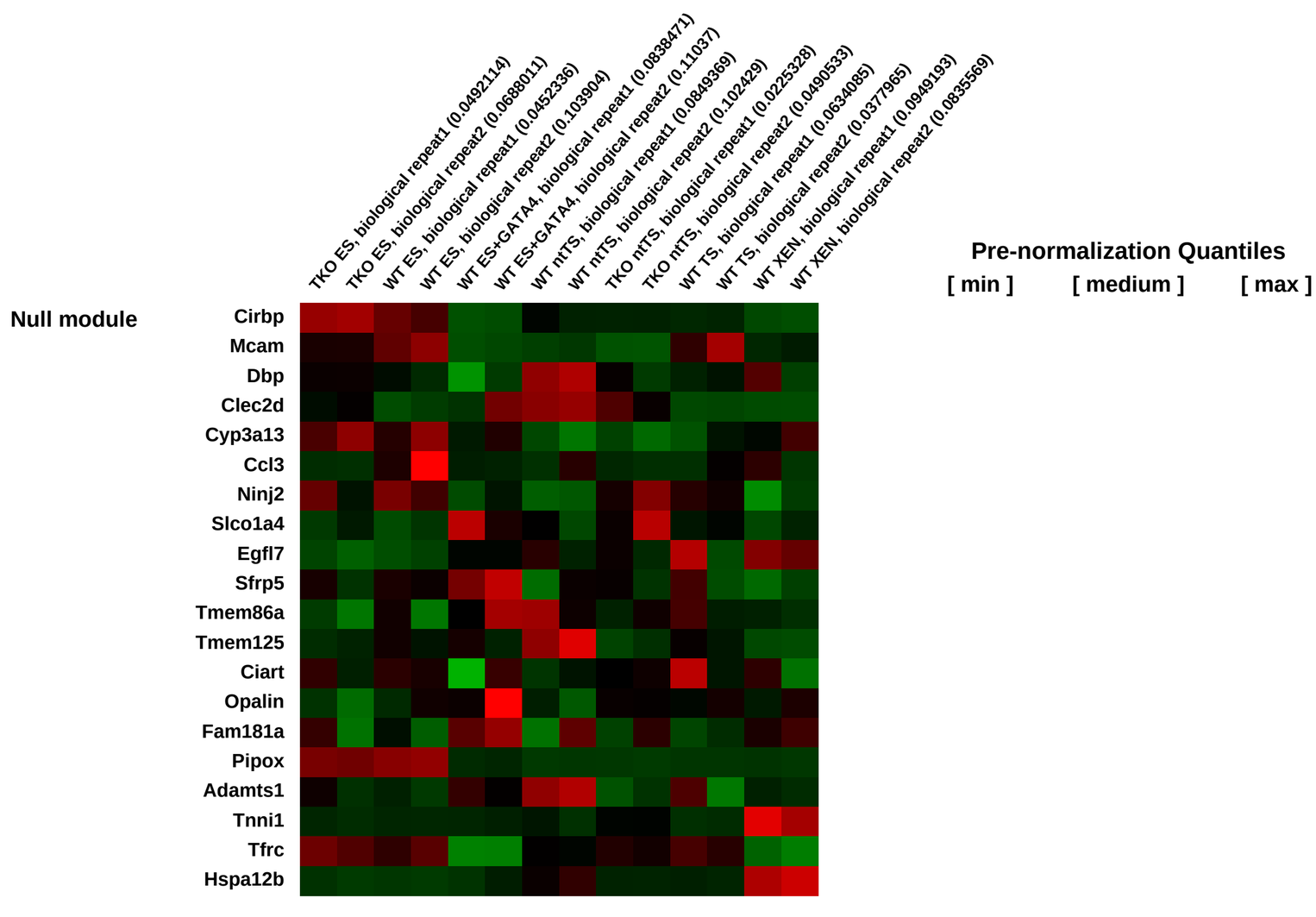

GEO Series "GSE34773" Expression Profiles

Num of samples in this series: 26

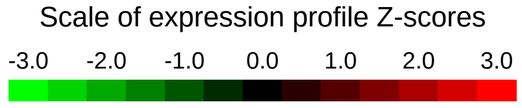

GEO Link:	http://www.ncbi.nlm.nih.gov/geo/query/acc.cgi?acc=GSE34773
Status:	Public on Feb 04 2012
Title:	Skeletal muscle PGC-1a mediates mitochondrial, but not metabolic, changes during calorie restriction.
Organism:	Mus musculus
Experiment type:	Expression profiling by array
Platform:	GPL1261
Pubmed ID:	22308395
Summary & Design:	**Summary:** Calorie restriction (CR) is a dietary intervention that extends lifespan and healthspan in a variety of organisms. CR improves mitochondrial energy production, fuel oxidation and reactive oxygen species scavenging in skeletal muscle and other tissues, and these processes are thought to be critical to the benefits of CR. PGC-1a is a transcriptional coactivator that regulates mitochondrial function and is induced by CR. Consequently, many of the mitochondrial and metabolic benefits of CR are attributed to increased PGC-1a activity. To test this model for the first time, we examined the metabolic and mitochondrial response to CR in mice lacking skeletal muscle PGC-1a (MKO). Surprisingly, MKO mice demonstrated a normal improvement in glucose homeostasis in response to CR, indicating that skeletal muscle PGC-1a is dispensable for the whole-body benefits of CR. In contrast, gene expression profiling and electron microscopy demonstrated that PGC-1a is required for the full CR-induced increases in mitochondrial gene expression and mitochondrial density in skeletal muscle. These results demonstrate that PGC-1a is a major regulator of the mitochondrial response to CR in skeletal muscle, but surprisingly show that neither PGC-1a nor mitochondrial biogenesis in skeletal muscle are required for the metabolic benefits of CR. **Overall design:** Control (FLOX) and PGC-1a skeletal muscle specific knock out (MKO) mice were placed on a control diet [C] or a calorie restriction diet [CR] for 12 weeks. RNA was isolated from TA/EDL muscles for microarray analysis. The following numbers of mice were analyzed from each group: C FLOX: n = 6; C MKO: n = 7; CR FLOX: n = 6; CR MKO: n = 7. Mice were mixed C57/BL6 and 129 background.

Background corr dist: KL-Divergence = 0.2204, L1-Distance = 0.0535, L2-Distance = 0.0068, Normal std = 0.3180

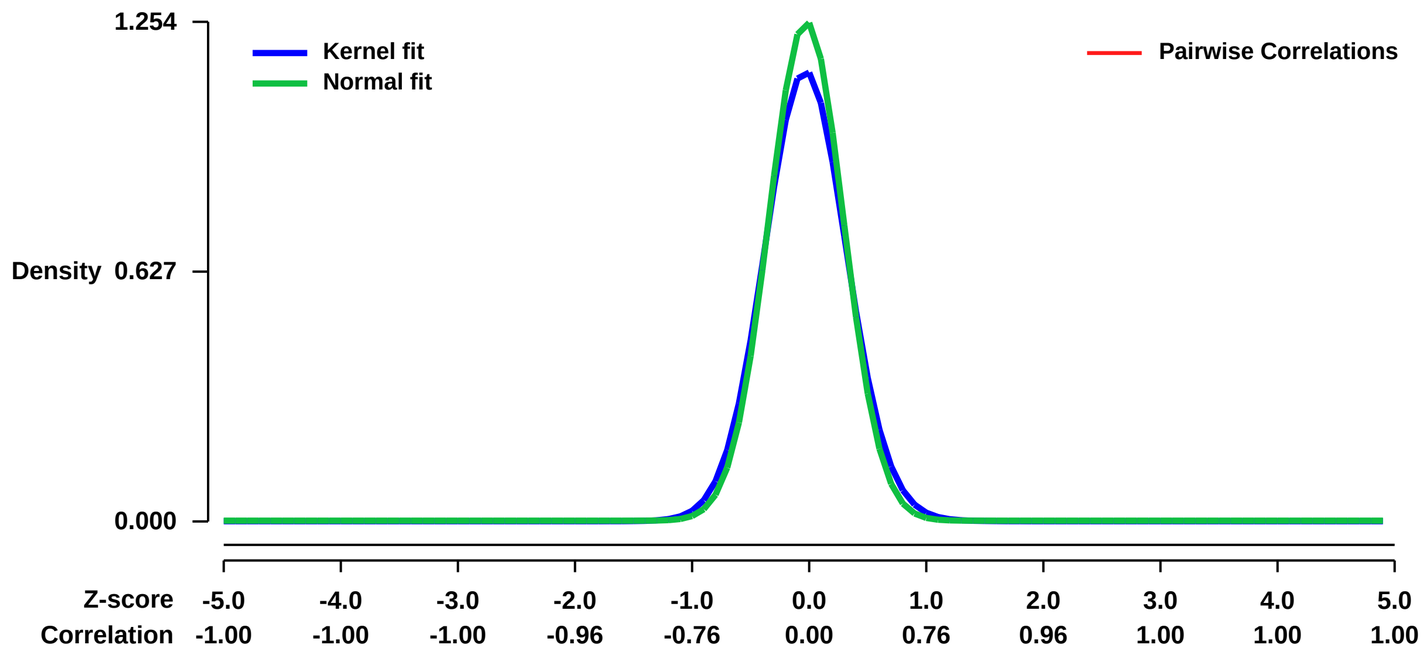

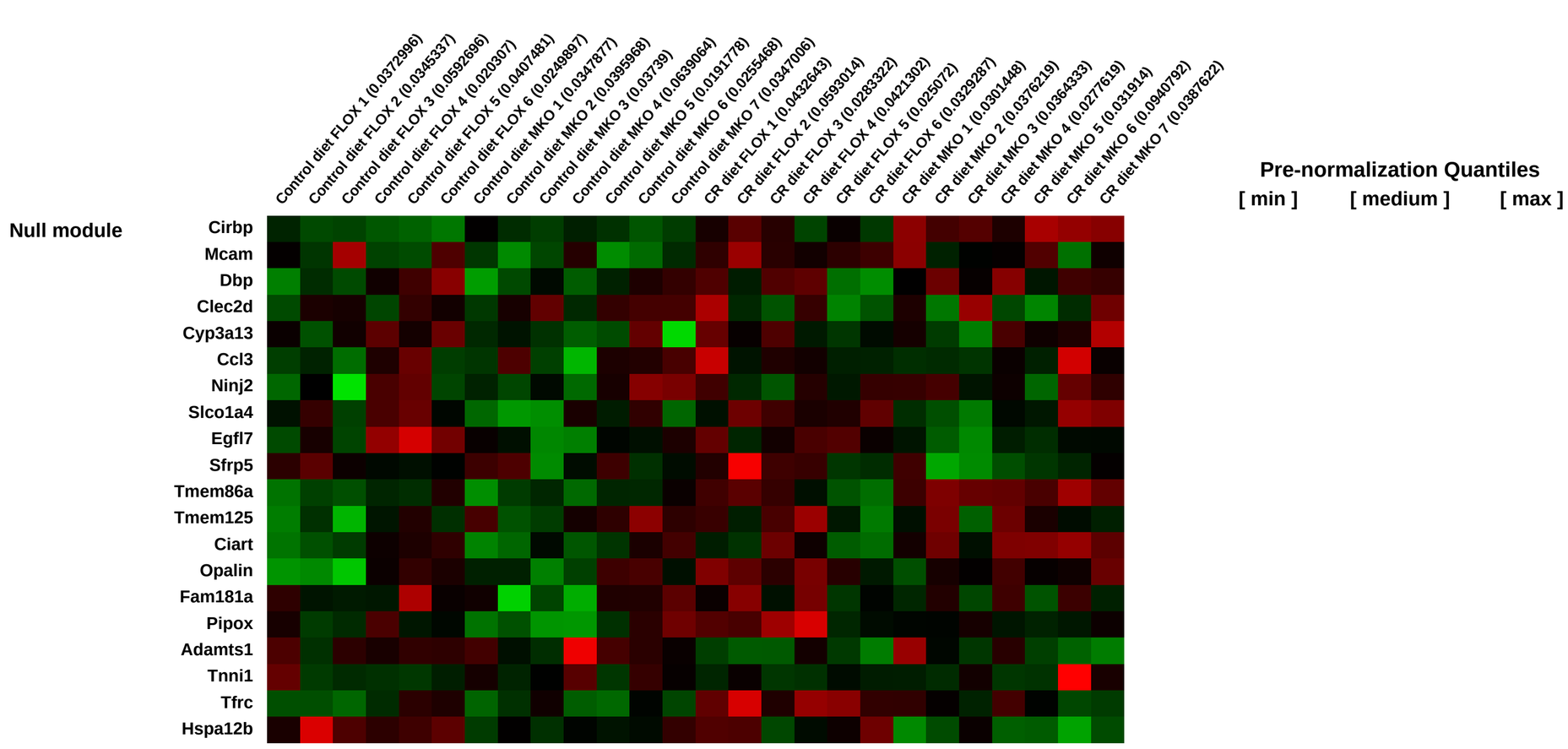

GEO Series "GSE10765" Expression Profiles

Num of samples in this series: 12

Scale of expression profile Z-scores

-3.0 -2.0 -1.0 0.0 1.0 2.0 3.0

GEO Link:	http://www.ncbi.nlm.nih.gov/geo/query/acc.cgi?acc=GSE10765
Status:	Public on Mar 08 2008
Title:	Expression data from MALP-2-stimulated macrophages from wild-type, IRAK-2-/- and IRAK-1-/IRAK-2-/- mice
Organism:	Mus musculus
Experiment type:	Expression profiling by array
Platform:	GPL1261
Pubmed ID:	18438411
Summary & Design:	**Summary:** **IL-1R-associated kinases (IRAKs) participate in Toll-like receptor (TLR) signal transduction. MALP-2 is a TLR2 ligand, and stimulation of macrophages with MALP-2 activates expression of various genes including proinflammatory cytokines.** **We used microarrays to examine influence of IRAK-2 or IRAK-1/IRAK-2 deficiency in MALP-2-inducible gene expression.** **Keywords: Time course after MALP-2 stimulation** **Overall design:** **Peritoneal macrophages from wild-type, IRAK-2-/- and IRAK-1/IRAK-2 mice were stimulated with MALP-2 for 0, 2, 4, and 8 hours, followed by RNA extraction. Then hybridization on affymetrix microarrays was performed.**

Background corr dist: **KL-Divergence = 0.0314, L1-Distance = 0.0844, L2-Distance = 0.0107, Normal std = 0.7991**

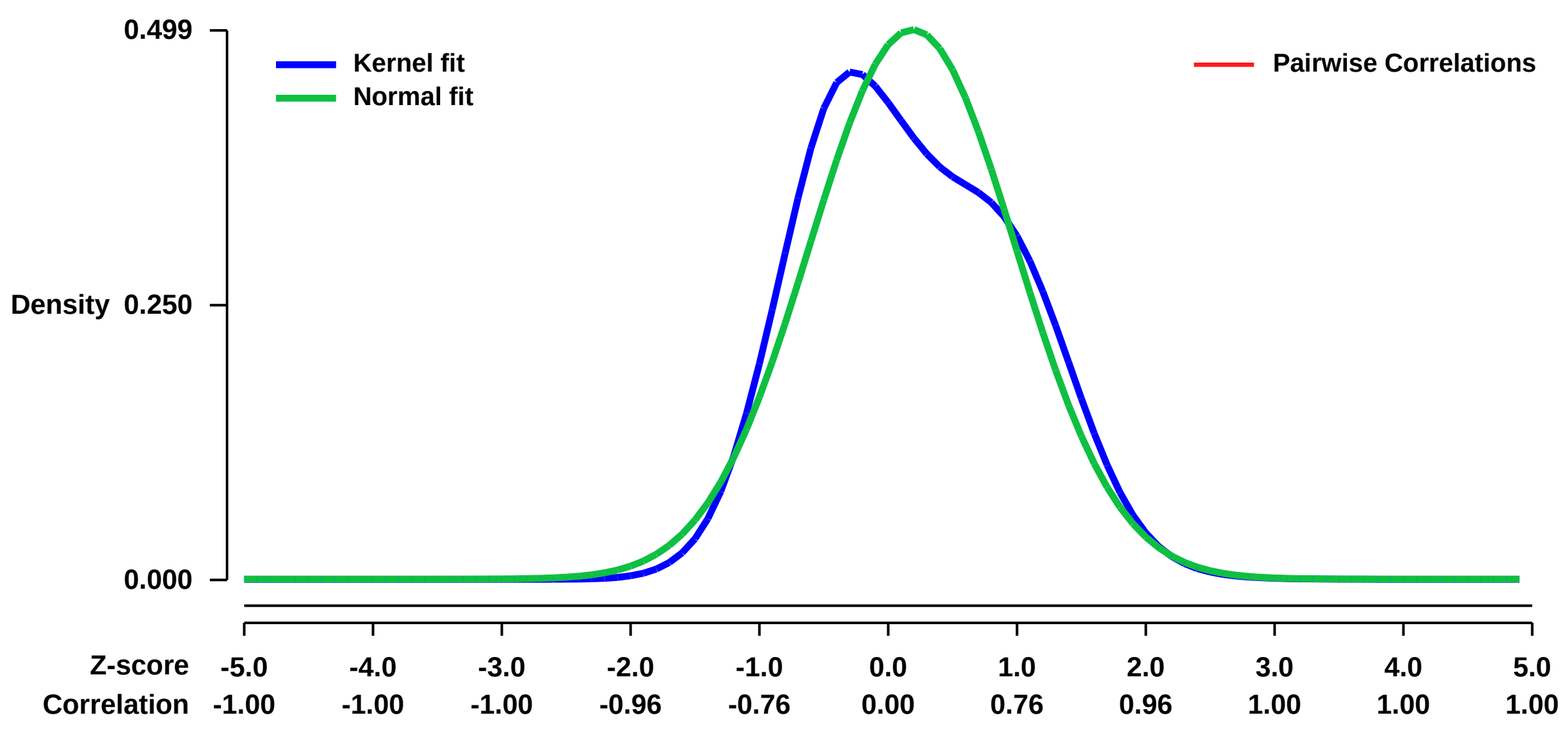

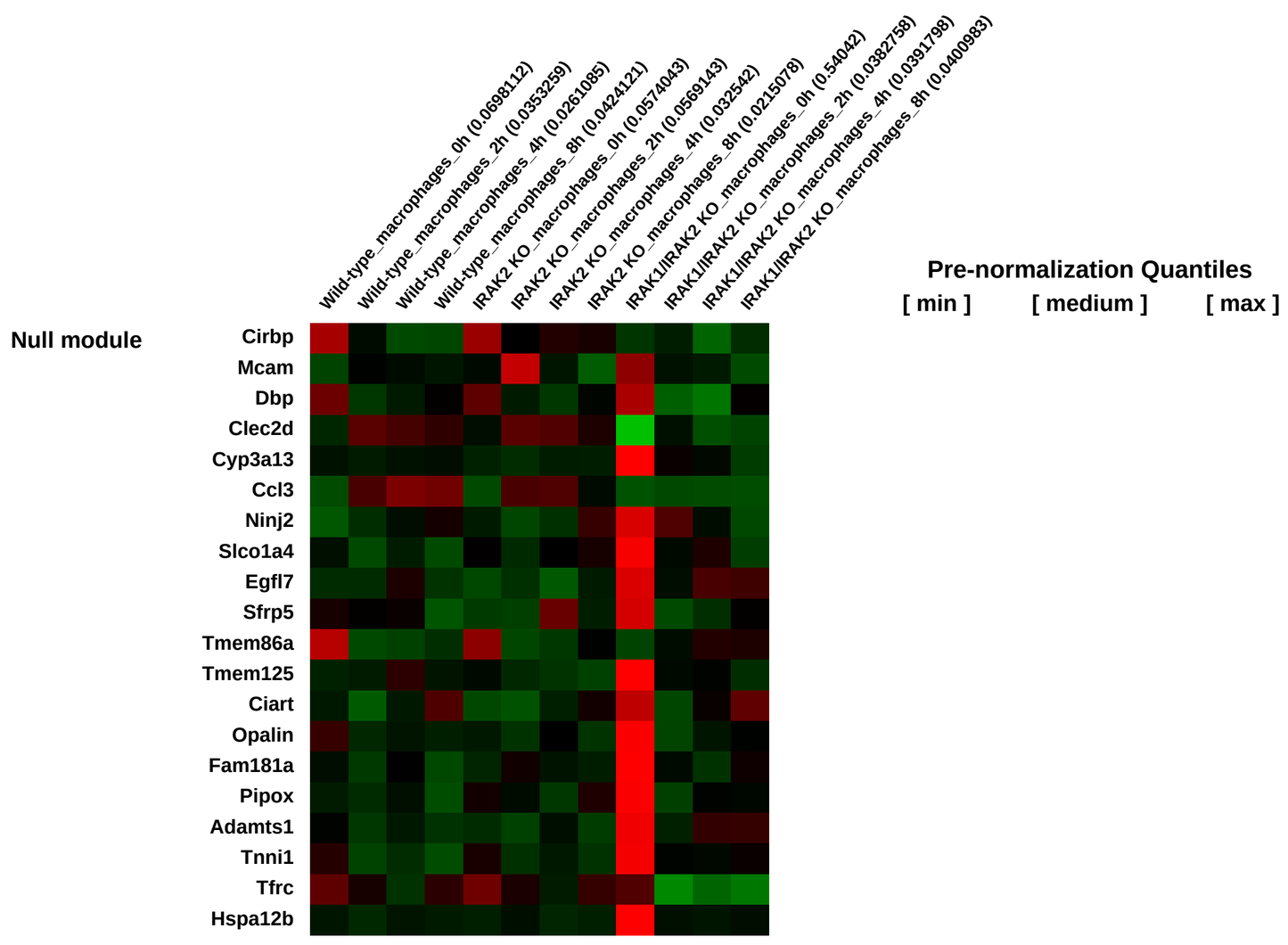

GEO Series "GSE27546" Expression Profiles

Num of samples in this series: 51

Scale of expression profile Z-scores

-3.0 -2.0 -1.0 0.0 1.0 2.0 3.0

GEO Link:	http://www.ncbi.nlm.nih.gov/geo/query/acc.cgi?acc=GSE27546
Status:	Public on Feb 28 2011
Title:	Effects of HMGN variants on cellular transcription profile
Organism:	Mus musculus
Experiment type:	Expression profiling by array
Platform:	GPL1261
Pubmed ID:	21278158
Summary & Design:	**Summary:** HMGN (high mobility group N) is a family of intrinsically disordered nuclear proteins that binds to nucleosomes, alters the structure of chromatin and affects transcription. A major unresolved question is the extent of functional specificity, or redundancy, between the various members of the HMGN protein family. Here we analyze the transcriptional profile of cells in which the expression of various HMGN proteins has been either deleted or doubled. The results reveal an HMGN-variant specific effect on the fidelity of the cellular transcription profile, indicating that functionally, the various HMGN subtypes are not fully redundant. **Overall design:** RNA was collected from either primary knock-out MEFs or SV40-transformed MEFs and MIN6 cells over expressing various HMGN proteins and mutants and hybridized to Affymetrix arrays. We obtained a double ammount of HMGN proteins in MEFs and MIN6 cells by retroviral infection and subsequent selection procedure. We collected all infected cells (pools, not clones) in order to eliminate the effect of viral integration in the genome.

Background corr dist: KL-Divergence = 0.0270, L1-Distance = 0.0406, L2-Distance = 0.0025, Normal std = 0.6975

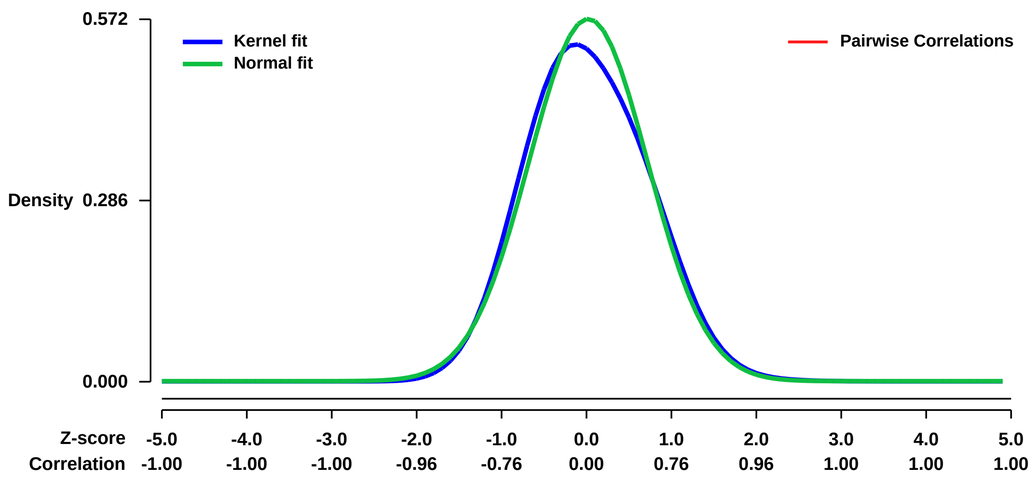

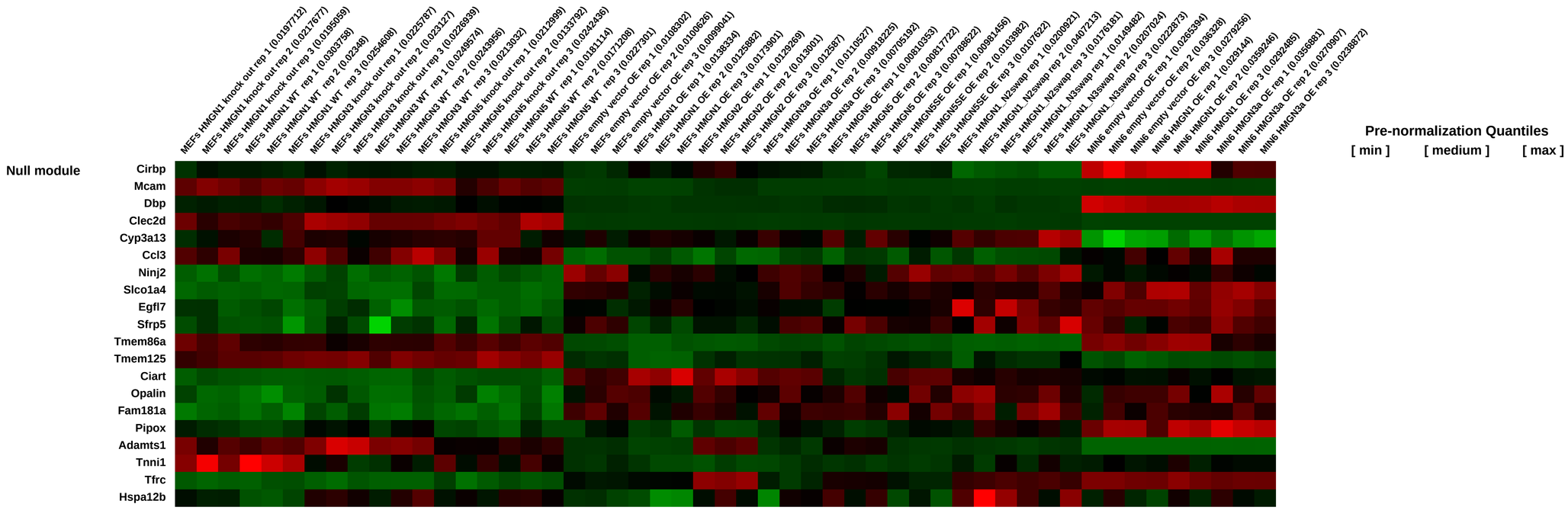

GEO Series "GSE20604" Expression Profiles

Num of samples in this series: 6

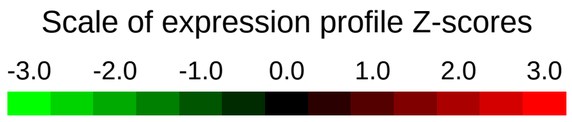

GEO Link:	http://www.ncbi.nlm.nih.gov/geo/query/acc.cgi?acc=GSE20604
Status:	Public on Apr 20 2010
Title:	Downstream Targets of HOXB4 in the primitive hematopoietic progenitor EML Cell line
Organism:	Mus musculus
Experiment type:	Genome binding/occupancy profiling by genome tiling array
Platform:	GPL1261
Pubmed ID:	20404135
Summary & Design:	**Summary:** Enforced expression of the homeobox transcription factor HOXB4 has been shown to enhance hematopoietic stem cell (HSC) self-renewal and expansion ex vivo and in vivo. In order to investigate the largely unknown downstream targets of HOXB4 in hematopoietic progenitor cells, HOXB4 was constitutively overexpressed in the primitive hematopoietic progenitor cell line, EML. Gene expression differences were compared between KLS (c-Kit+, Lin-, Sca-1+)-EML cells that overexpressed HOXB4 (KLS-EML-HOXB4) to control KLS-EML cells that were transduced with vector alone. ChIP-chip was used to identify promoter regions bound by HOXB4. **Overall design:** We overexpressed HOXB4 in EML cells. We isolated 3 separate single cell clones as assessed by Southern Blot Analysis (3 clones for EML-HOXB4 and 3 clones for control EML-GFP cells). RNA was isolated from the KLS (c-Kit+, Lin-, Sca-1+) fraction of each single cell clone population and processed for hybridization to array chips using established lab protocols. Chip-Chip analysis of the three HOXB4 overexpressing clones was performed to identify HOXB4 bound promoters.

Background corr dist: KL-Divergence = 0.0195, L1-Distance = 0.0316, L2-Distance = 0.0018, Normal std = 0.7515

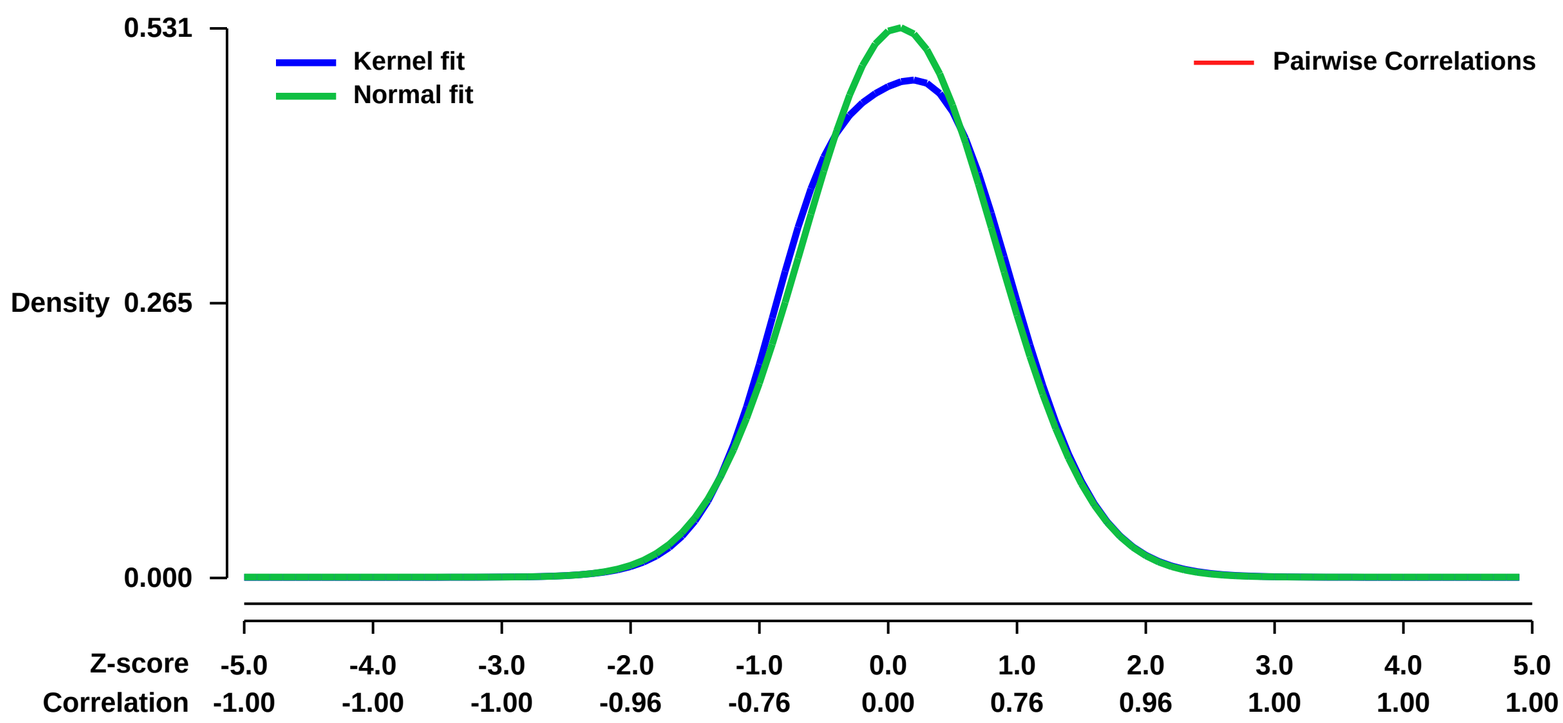

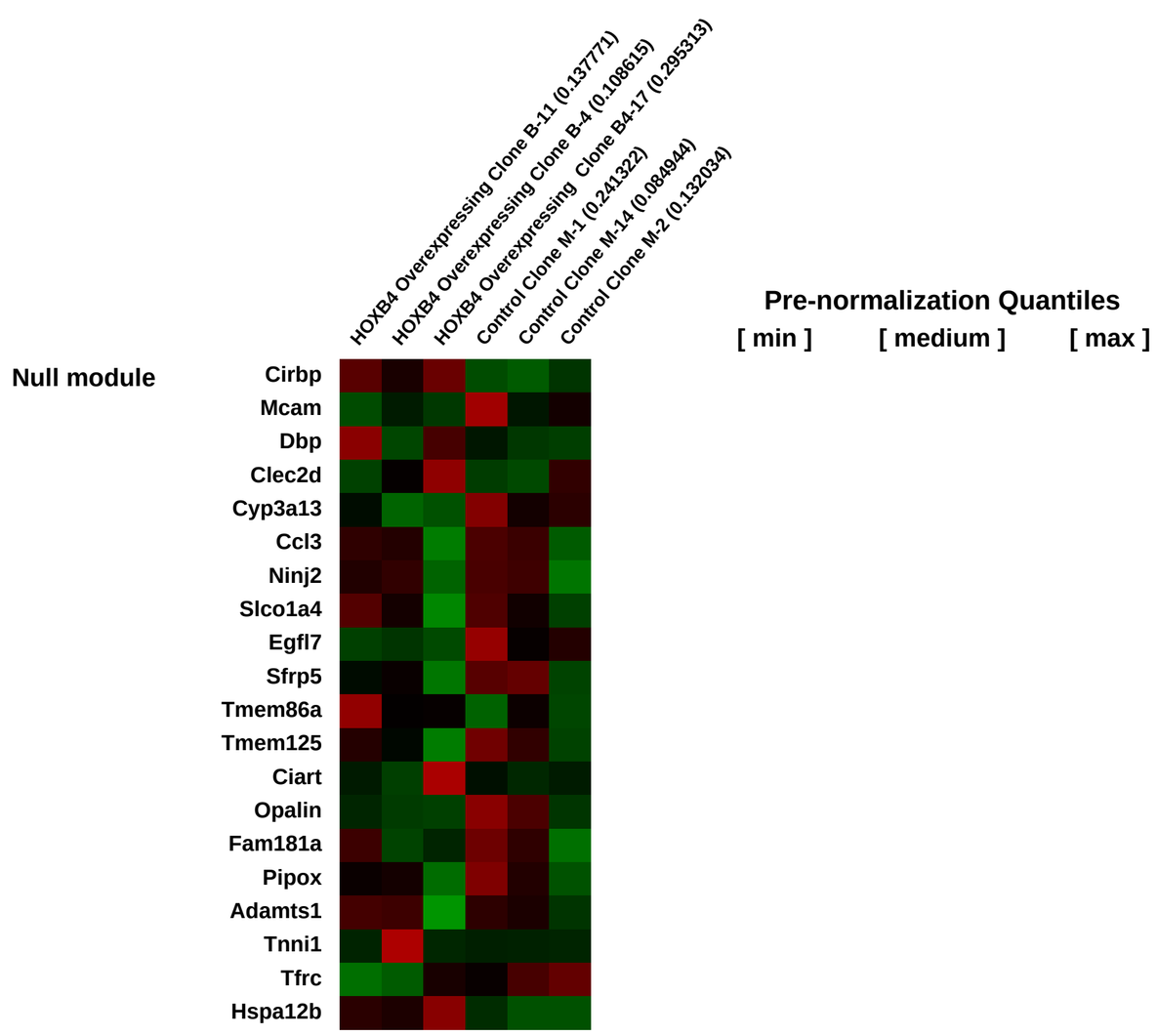

GEO Series "GSE8513" Expression Profiles

Num of samples in this series: 10

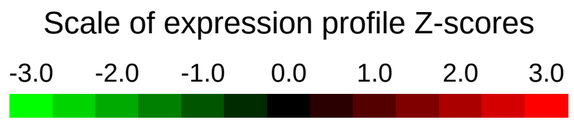

GEO Link:	http://www.ncbi.nlm.nih.gov/geo/query/acc.cgi?acc=GSE8513
Status:	Public on Dec 26 2007
Title:	Eradication of Solid Human Tumors in Nude Mice with an Intravenously Injected Light-Emitting Oncolytic Vaccinia Virus
Organism:	Mus musculus
Experiment type:	Expression profiling by array
Platform:	GPL1261
Pubmed ID:	17942938

Summary & Design:

Summary:
Previously we reported that a recombinant vaccinia virus (VACV) carrying a light-emitting fusion gene enters, replicates in, and reveals the locations of tumors in mice. A new recombinant VACV, GLV-1h68, as a simultaneous diagnostic and therapeutic agent, was constructed by inserting three expression cassettes (encoding Renilla luciferase-green fluorescent protein (RUC-GFP) fusion, b-galactosidase, and b-glucuronidase) into the F14.5L, J2R (encoding thymidine kinase, TK), and A56R (encoding hemagglutinin, HA) loci of the viral genome, respectively. Intravenous (i.v.) injections of GLV-1h68 (1 ^ 107 pfu/mouse) into nude mice with established (500 mm3) subcutaneous (s.c.) GI-101A human breast tumors were used to evaluate its toxicity, tumor targeting specificity and oncolytic efficacy. GLV-1h68 demonstrated an enhanced tumor targeting specificity and much reduced toxicity compared to its parental LIVP strains. The tumors colonized by GLV-1h68 exhibited growth, inhibition, and regression phases followed by tumor eradication within 130 days in 95% of the mice tested. Tumor regression in live animals was monitored in real time based on decreasing light emission, hence demonstrating the concept of a combined oncolytic virus-mediated tumor diagnosis and therapy system. Transcriptional profiling of regressing tumors based on a mouse-specific platform revealed gene expression signatures consistent with immune defense activation, inclusive of interferon stimulated genes (STAT-1 and IRF-7), cytokines, chemokines and innate immune effector function. These findings suggest that immune activation may combine with viral oncolysis to induce tumor eradication in this model, providing a novel perspective for the design of oncolytic viral therapies for human cancers.

Objective: To determine the gene expression changes induced by GLV-1h68 vaccinia virus injection in mouse carrying human breast cancer implant and leading to tumor eradication.

Methods: Gene expression was analyzed using oligonucleotide microarrays. Responsiveness to vaccina virus injection was assessed by toxicity and survival study, gene expression anaysis and tumor volume change.

Result: The tumors colonized by GLV-1h68 exhibited growth, inhibition, and regression phases followed by tumor eradication within 130 days in 95% of the mice tested. Tumor regression in live animals was monitored in real time based on decreasing light emission, hence demonstrating the concept of a combined oncolytic virus-mediated tumor diagnosis and therapy system. Transcriptional profiling of regressing tumors based on a mouse-specific platform revealed gene expression signatures consistent with immune defense activation, inclusive of interferon stimulated genes (STAT-1 and IRF-7), cytokines, chemokines and innate immune effector function.

Conclusion: Our findings suggest that immune activation may combine with viral oncolysis to induce tumor eradication in this model, providing a novel perspective for the design of oncolytic viral therapies for human cancers.

Keywords: Responsiveness to vaccina virus injection

Overall design:
tumor tissues 3 and 6 weeks post virus injection

Background corr dist: KL-Divergence = 0.0674, L1-Distance = 0.0268, L2-Distance = 0.0012, Normal std = 0.5037

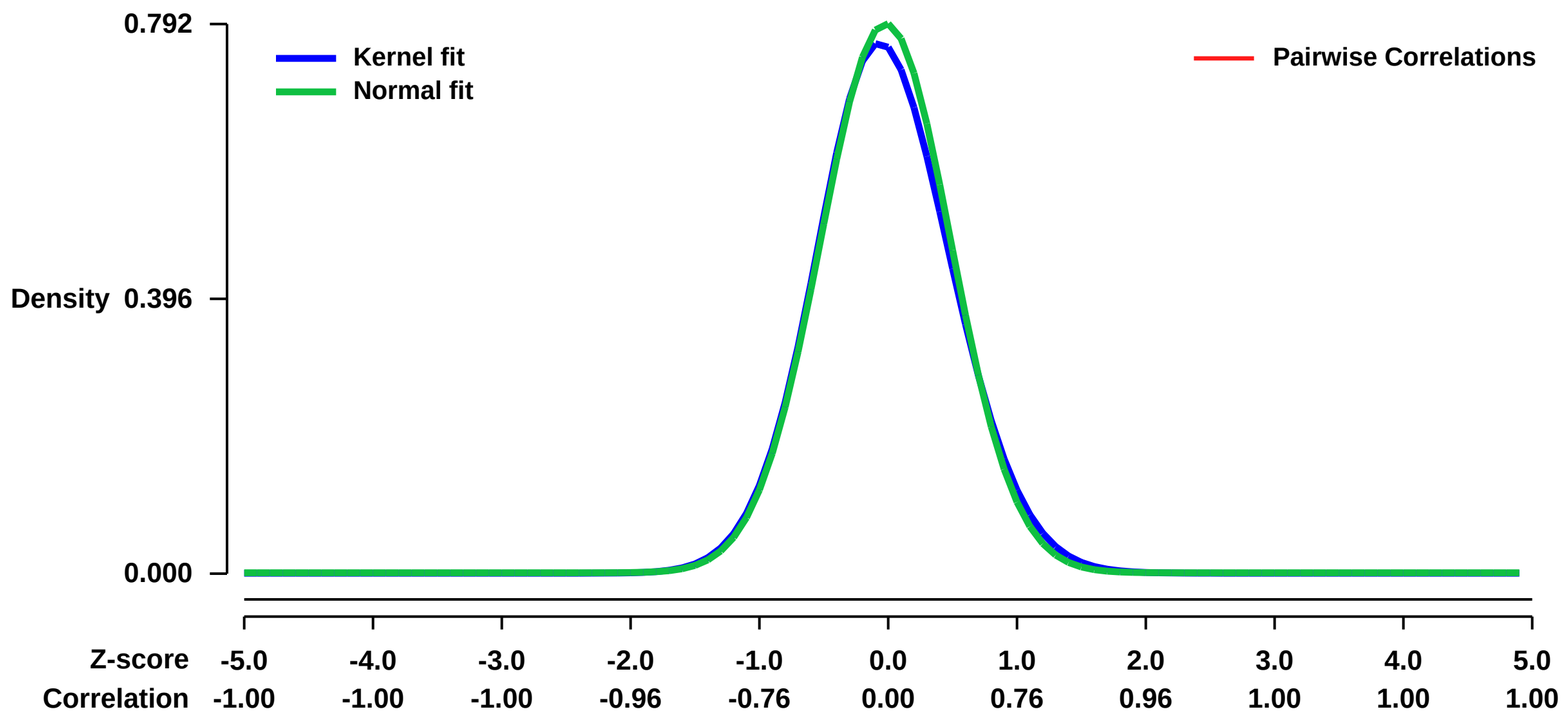

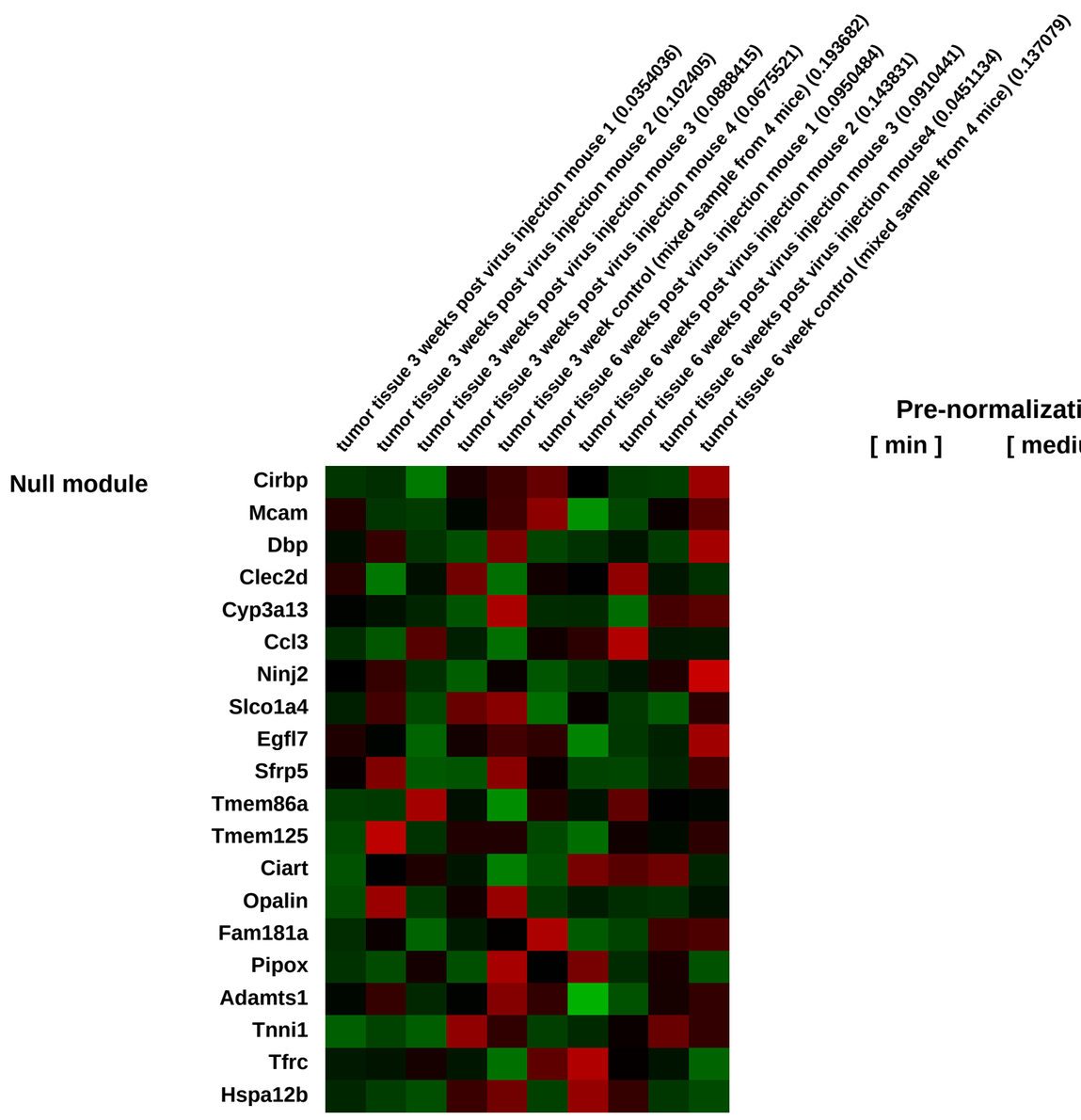

GEO Series "GSE37676" Expression Profiles

Num of samples in this series: 6

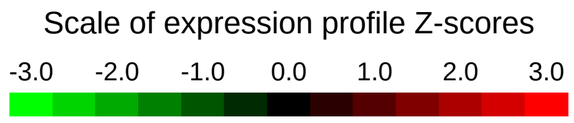

GEO Link:	http://www.ncbi.nlm.nih.gov/geo/query/acc.cgi?acc=GSE37676
Status:	Public on May 02 2012
Title:	Expression data from control and Ascorbic Acid (AA) stimulated Mc-3T3-E1 osteoblasts
Organism:	Mus musculus
Experiment type:	Expression profiling by array
Platform:	GPL1261
Pubmed ID:	23740245
Summary & Design:	**Summary:** Despite advances in investigating functional aspects of osteoblast (OB) differentiation, especially studies on how bone proteins are deposited and mineralized, there has been little research on the intracellular trafficking of bone proteins during OB differentiation. Collagen synthesis and secretion is markedly upregulated upon Ascorbic Acid (AA) stimulation. Understanding the mechanism by which collagen is mobilized in specialized OB cells is important for both basic cell biology and diseases involving defects in bone secretion and deposition. RabGTPases are major regulators on protein trafficking throughout the cell. In this study, we identified the Rab GTPases that are upregulated during 5-day AA differentiation of OBs using microarray analysis, namely Rab1, Rab3d and Rab27b. We used microarrays to detail the global programme of gene expression underlying procollagen production and trafficking and identified up-regulated genes during this process. **Overall design:** Control Mc3T3-E1 cells and 5 day Ascorbic Acid stimulated cells were processed for RNA extraction and hybridization on Affymetrix microarrays.

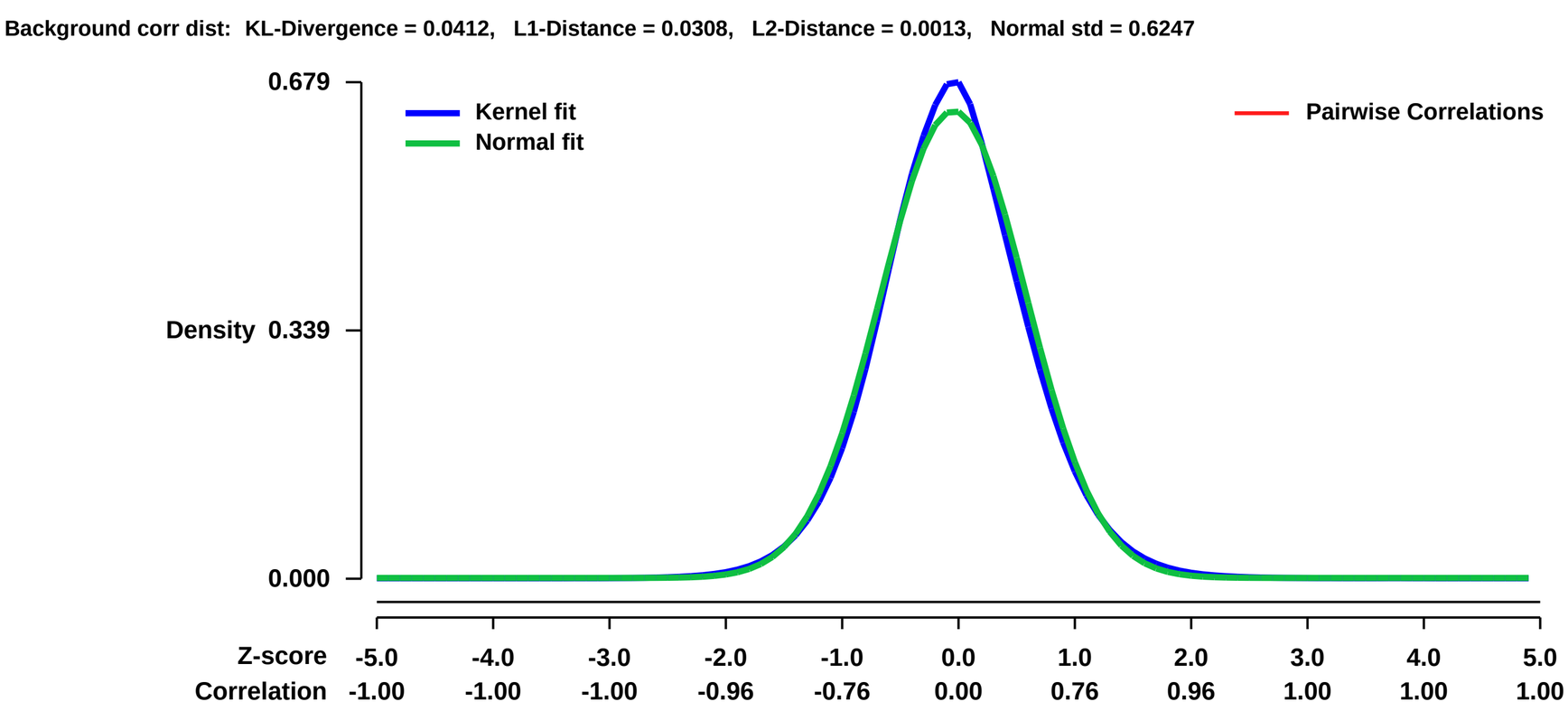

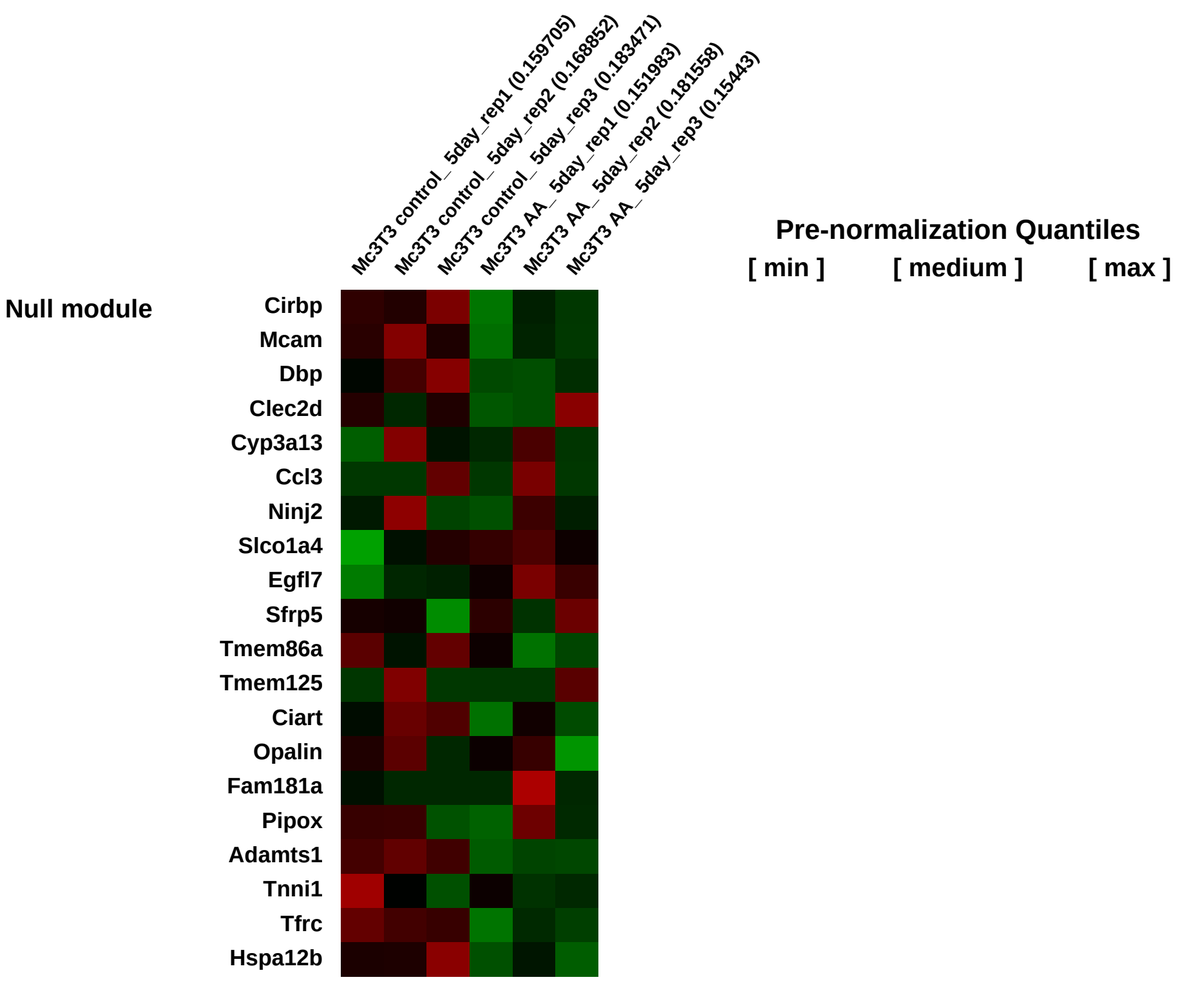

GEO Series "GSE19885" Expression Profiles

Num of samples in this series: 9

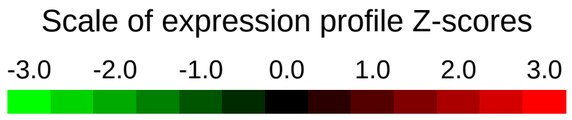

GEO Link:	http://www.ncbi.nlm.nih.gov/geo/query/acc.cgi?acc=GSE19885
Status:	Public on Feb 08 2013
Title:	Gene expression data from rapamycin resistant and sensitive cell lines
Organism:	Mus musculus
Experiment type:	Expression profiling by array
Platform:	GPL1261
Pubmed ID:	23300087
Summary & Design:	**Summary:** The mammalian target of rapamycin (mTOR) is a central regulator of cell proliferation. Inhibitors of mTOR are being evaluated as anti-tumor agents. Given the emerging role of microRNAs (miRNAs) in tumorgenesis we hypothesized that miRNAs could play important roles in the response of tumors to mTOR inhibitors. Rapamycin resistant myogenic cells developed by long-term rapamycin treatment showed extensive reprogramming of miRNAs expression, characterized by up-regulation of the mir-17~92 and related clusters and down-regulation of tumor-suppressor miRNAs. Antagonists of oncogenic miRNA families and mimics of tumor suppressor miRNAs (let-7) restored rapamycin sensitivity in resistant tumor cells. This study identified miRNAs as new downstream components of the mTOR-signaling pathway, which may determine the response of tumors to mTOR inhibitors. **Overall design:** Total RNA extraction and hybridization on Affymetrix microarrays of rapamycin sensitive (RS) cells (BC3H1, mouse brain tumor cell line with myogenic properties, ATCC) cultured in Dulbeccoâ s modified essential medium (DMEM) media supplemented with 20% fetal bovine serum (FBS), penicillin (100 U/ml) and streptomycin (100 mg/ml). Rapamycin resistant cells (RR1) were developed by culturing BC3H1 cells in the presence of 1 uM rapamycin for 6 months. Three samples in triplicates: 1) Rapamycin sensitive cells treated with DMSO for 24 h(BC3H1, reference), 2) Rapamycin sensitive cells treated for 24 h with 100 nM rapamycin (BC3H1+R), 3) Rapamycin resistant cells constantly treated with 1uM Rapamycion (RR1+R).

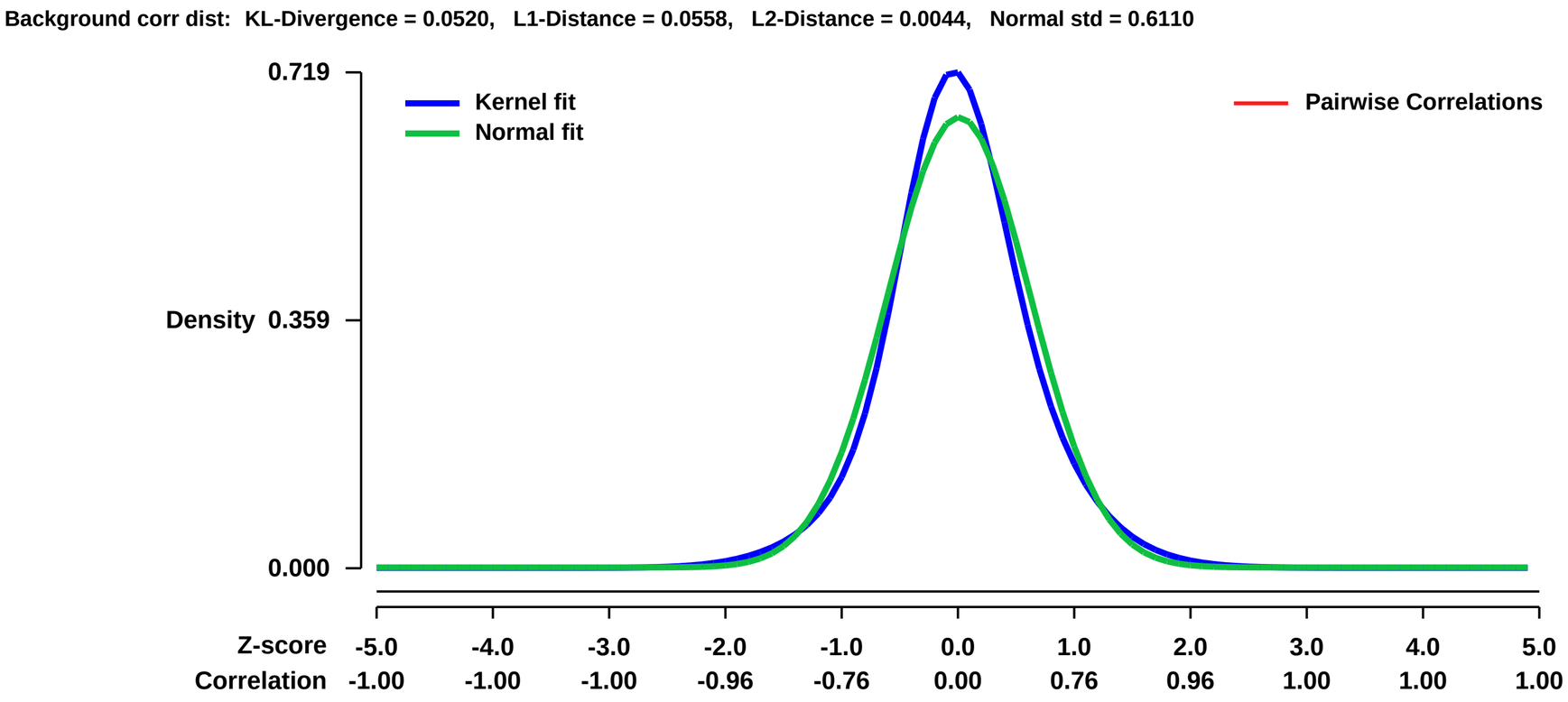

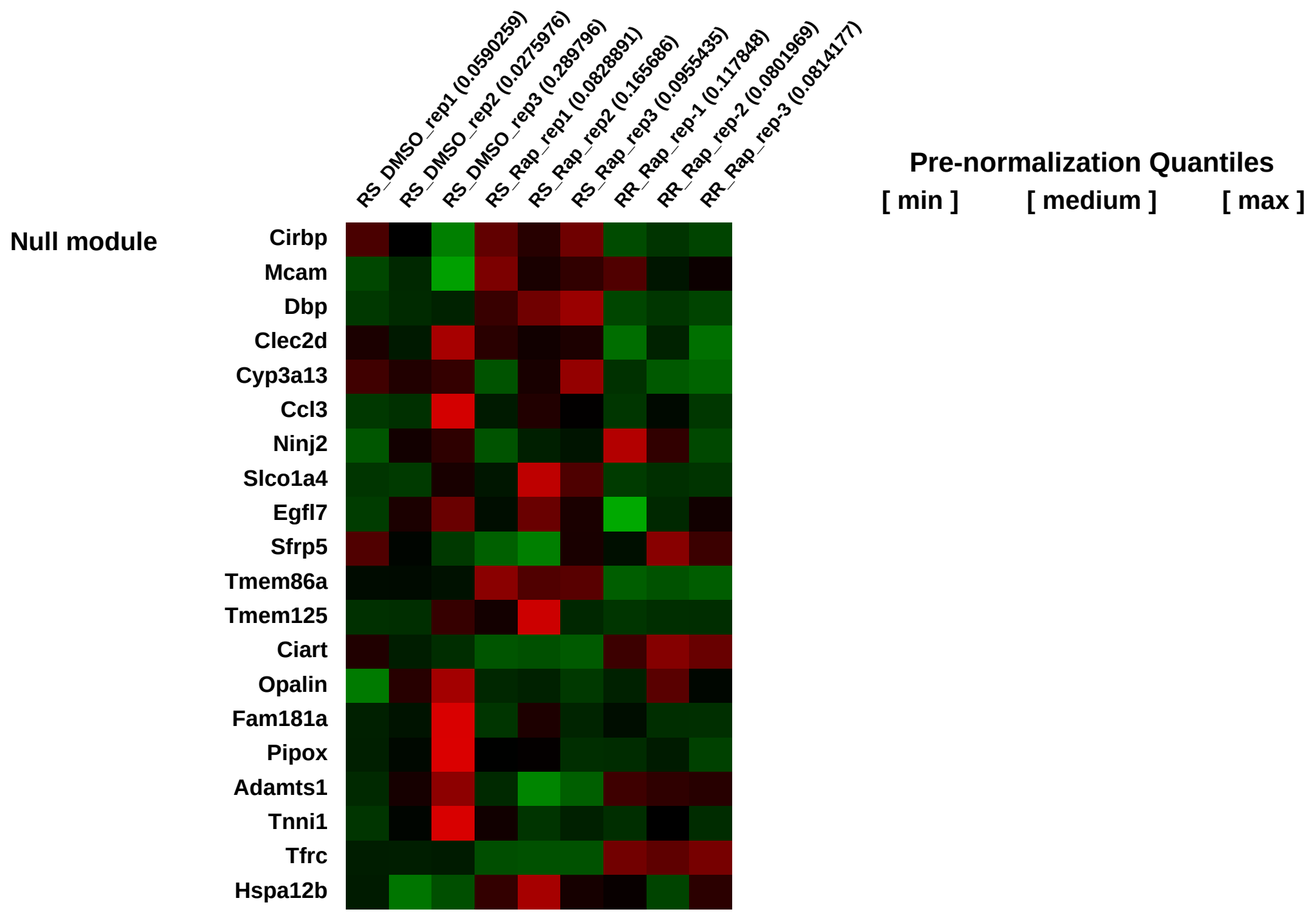

GEO Series "GSE33931" Expression Profiles

Num of samples in this series: 42

Scale of expression profile Z-scores

-3.0 -2.0 -1.0 0.0 1.0 2.0 3.0

GEO Link:	http://www.ncbi.nlm.nih.gov/geo/query/acc.cgi?acc=GSE33931
Status:	Public on Jul 05 2012
Title:	Expression data from mouse muscle
Organism:	Mus musculus
Experiment type:	Expression profiling by array
Platform:	GPL1261
Pubmed ID:	22820870
Summary & Design:	**Summary:** The knock-out of calpain 3 (C3KO) is a murine model for calpainopathies wich shows a mild dystrophic phenotype with signs of muscle degeneration. Adult (A) mice show a more severe phenotype than young (Y) mice which only present inflammatory infiltrates in most severely affected muscles, such as the soleus. Other muscles (e.g. quadriceps) are much less affected. We used microarray technology to compare gene expression profiles of young and adult muscles in wild-type (wt) and C3KO mice, in two types of muscle: soleus (affected) and quadriceps (much less affected). **Overall design:** 11 wt (7 adult and 4 young) and 11 C3KO (7 adult and 4 young) mice were used in this study for RNA extraction and hybridization on Affymetrix microarrays. The soleus and the quadriceps muscles were obtained from each mouse. All mice were males.

Background corr dist: KL-Divergence = 0.2490, L1-Distance = 0.0280, L2-Distance = 0.0013, Normal std = 0.3185

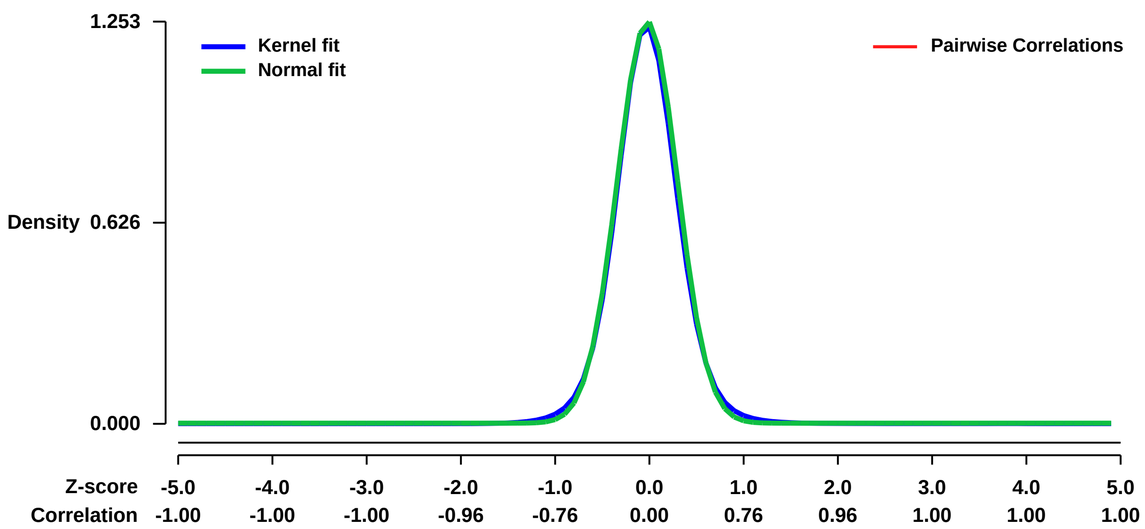

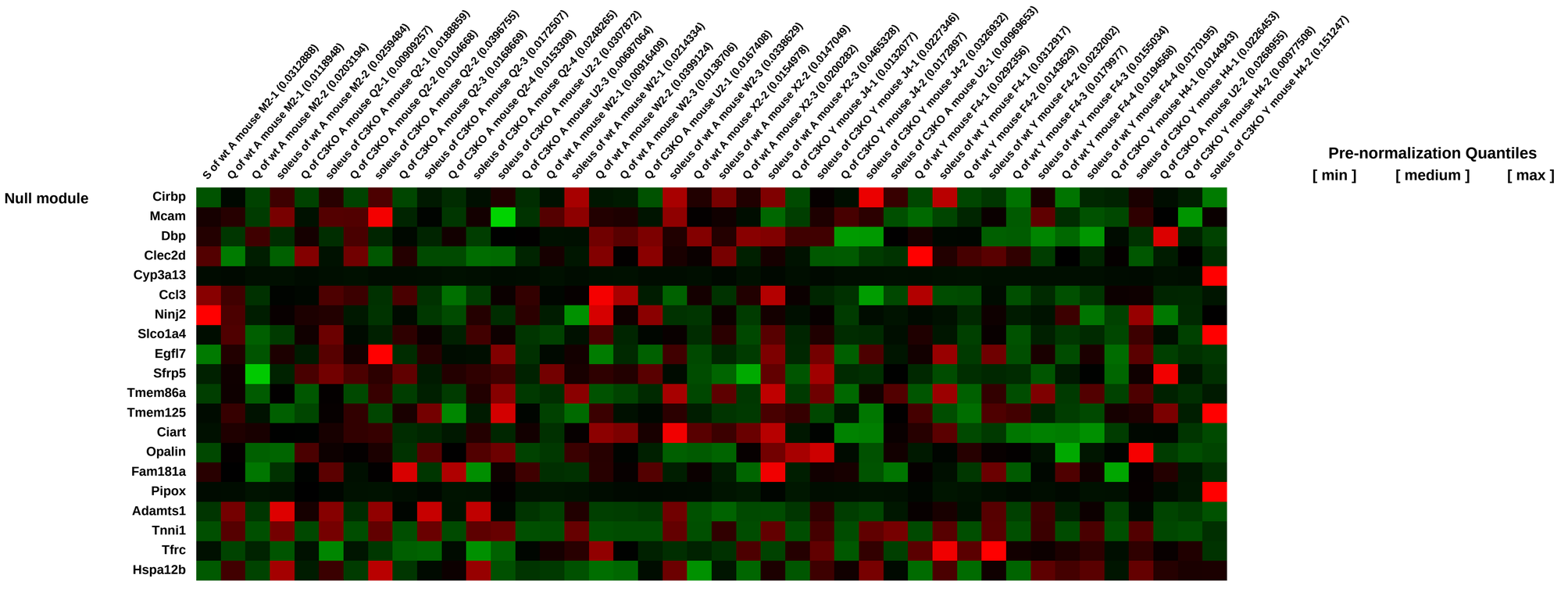

GEO Series "GSE29685" Expression Profiles

Num of samples in this series: 132

Details of this dataset are not shown due to large number of samples and the page size limit.

Find details in http://www.ncbi.nlm.nih.gov/geo/query/acc.cgi?acc=GSE29685

Background corr dist: KL-Divergence = 0.3964, L1-Distance = 0.0812, L2-Distance = 0.0207, Normal std = 0.2500

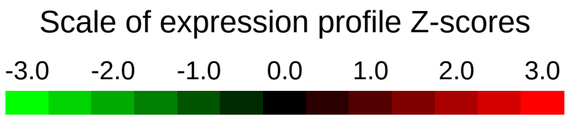

GEO Series "GSE26025" Expression Profiles

Num of samples in this series: 12

Scale of expression profile Z-scores

-3.0 -2.0 -1.0 0.0 1.0 2.0 3.0

GEO Link:	http://www.ncbi.nlm.nih.gov/geo/query/acc.cgi?acc=GSE26025
Status:	Public on Dec 12 2011
Title:	Sex-specific effects of prenatal stress in 5-Htt deficient mice: towards molecular mechanisms of gene x environment interactions
Organism:	Mus musculus
Experiment type:	Expression profiling by array
Platform:	GPL1261
Pubmed ID:	21857948
Summary & Design:	**Summary:** **prenatal stress response, genetic modification** **Background: Prenatal stress (PS) exposure has been shown to increase the risk for emotional disorders in later life. Furthermore, the serotonin transporter (5-HTT) genotype is suggested to exert a modulating effect on the association between early life stress and the risk for depression. In the present study, we use a 5-HTT x PS paradigm to investigate whether the effects of PS are dependent upon the 5-HTT genotype. Methods: The effects of PS on cognition, anxiety- and depression-related behaviour were examined using a maternal restraint stress paradigm of PS in C57BL6 wild-type (WT) and heterozygous (+/-) 5-HTT knockout mice. Additionally, in the female offspring, a genome-wide hippocampal gene expression screening was performed. Results: 5-HTT +/- offspring showed enhanced memory performance and signs of reduced anxiety as compared to WT offspring. Conversely, exposure of 5-HTT +/- mice to PS was associated with altered stress-responsivity and increased depressive-like behaviour, particularly in female offspring. Further, 5-HTT genotype, PS and their interaction differentially affected the expression of numerous genes and related pathways within the female hippocampus. Specifically, MAPK and neurotrophin signalling were regulated by both the 5-HTT +/- genotype and PS exposure, whereas cytokine and Wnt signalling were affected in a 5-HTT genotype x PS manner, indicating a gene x environment interaction at the molecular level. Conclusions: The long-term behavioural effects of PS in C57BL6 mice are partly dependent on the 5-HTT genotype. Further, hippocampal gene expression profiles suggest that distinct molecular mechanisms mediate the behavioural effects of the 5-HTT genotype, PS exposure, and their interaction.** **Overall design:** **total samples analysed are 12**

Background corr dist: KL-Divergence = 0.1377, L1-Distance = 0.0366, L2-Distance = 0.0025, Normal std = 0.3848

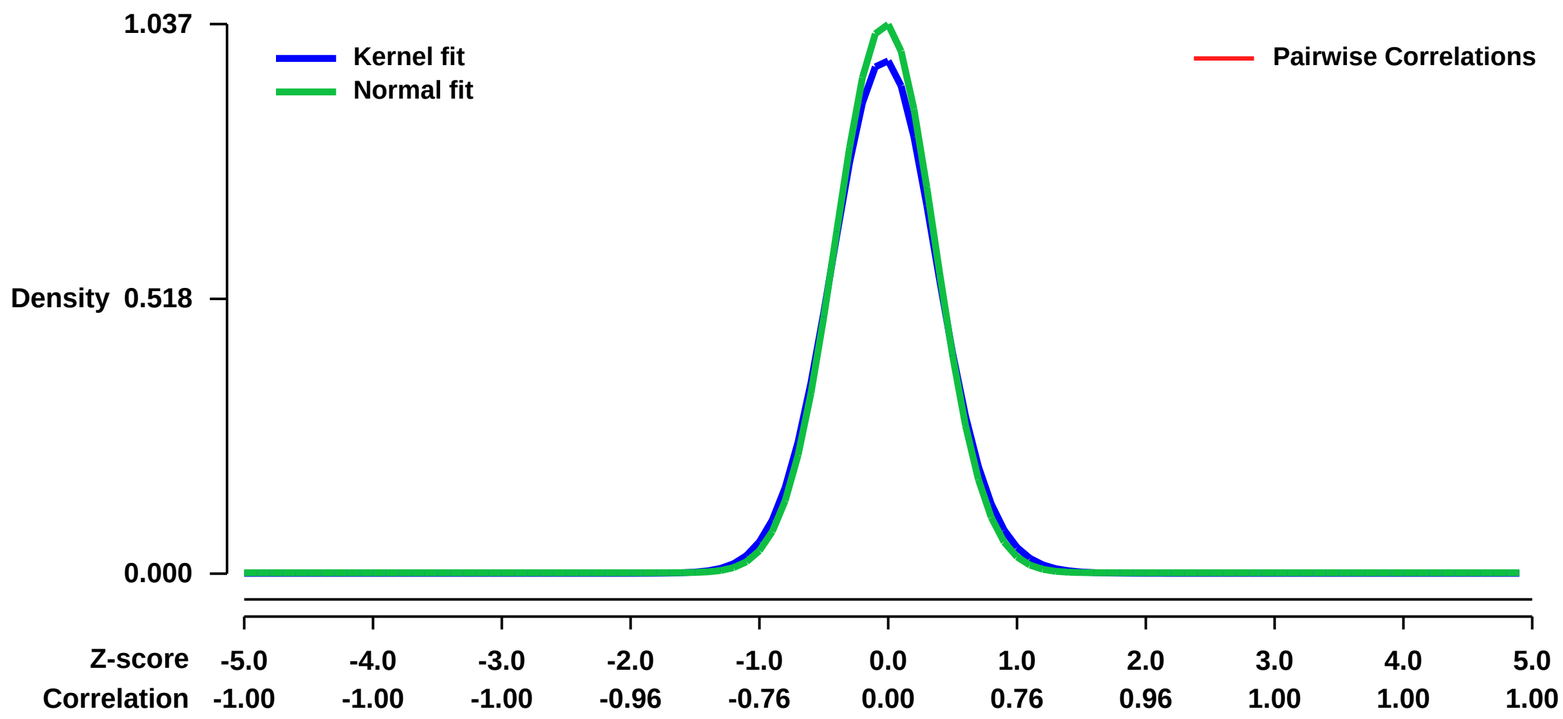

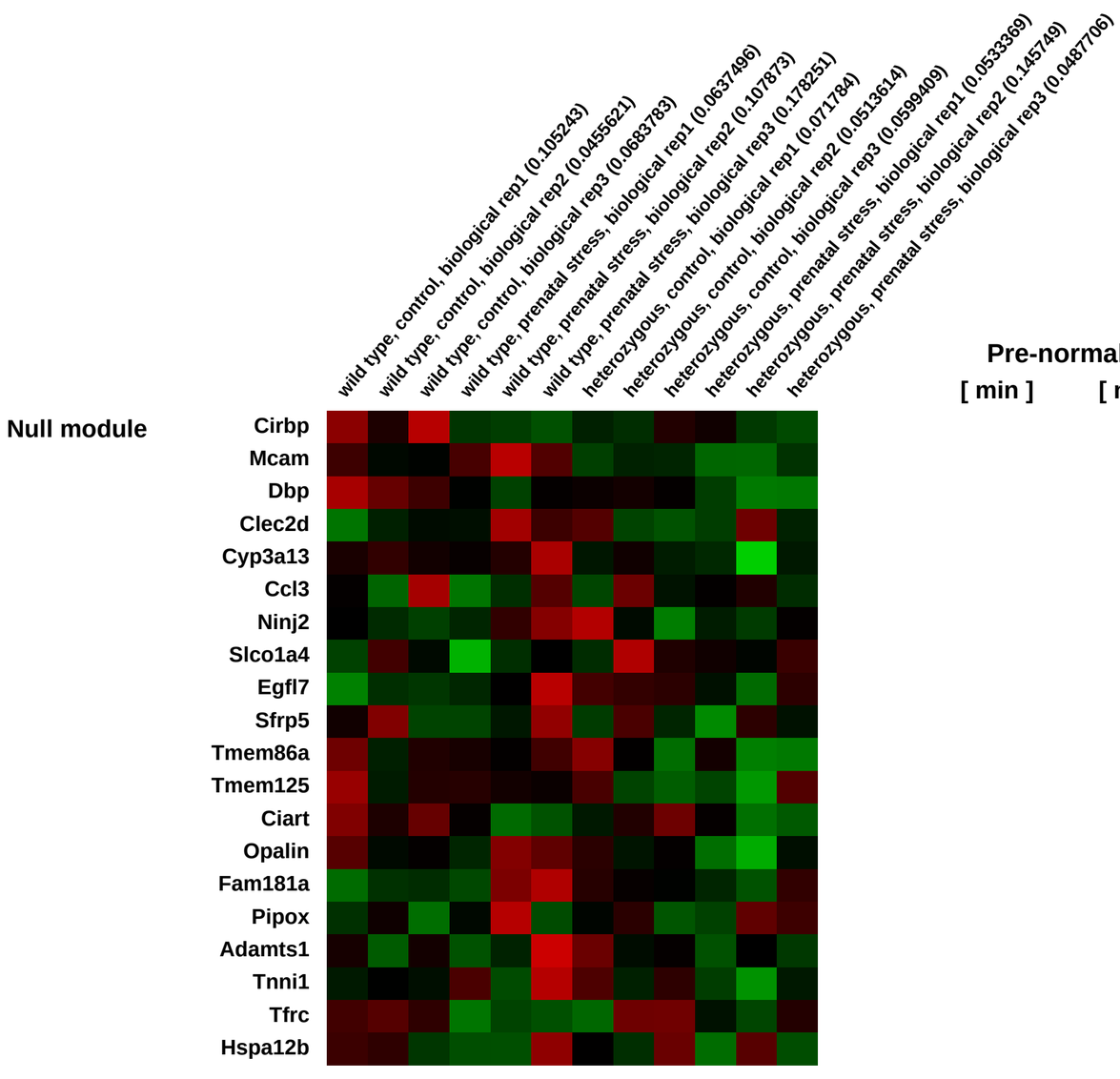

GEO Series "GSE34959" Expression Profiles

Num of samples in this series: 10

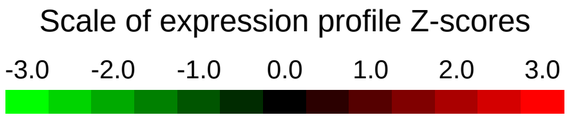

GEO Link:	http://www.ncbi.nlm.nih.gov/geo/query/acc.cgi?acc=GSE34959
Status:	Public on Feb 22 2012
Title:	Expression profiling of primary wild type (WT), Ezh2-null and Eed-null murine MLL-AF9 AML
Organism:	Mus musculus
Experiment type:	Expression profiling by array
Platform:	GPL1261
Pubmed ID:	22396593
Summary & Design:	**Summary:** We evaluated gene expression changes in murine leukemia caused by retroviral overexpression of MLL-AF9. We compared wild-type (WT) leukemia cells with mutant leukemia cells after cre-mediated inactivation of homozygous conditional alleles for Ezh2 or Eed, both of which are components of the Polycomb Repressive Complex2. **Overall design:** For WT cells, 3 biological replicates were hybridized. For Ezh2-null cells, 4 biological replicates were hybridized. For Eed-cells, 3 biological replicates were hybridized.

Background corr dist: KL-Divergence = 0.0919, L1-Distance = 0.0330, L2-Distance = 0.0021, Normal std = 0.4512

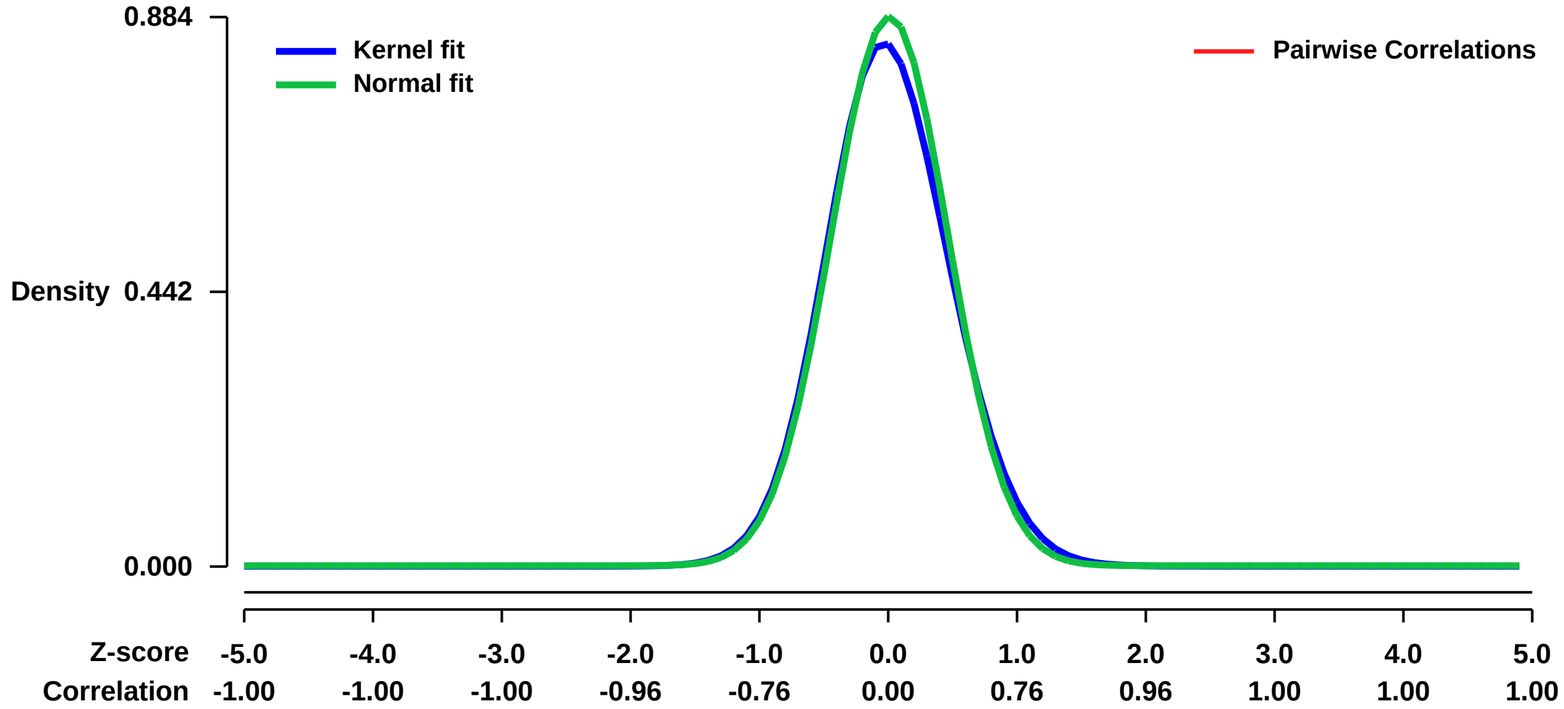

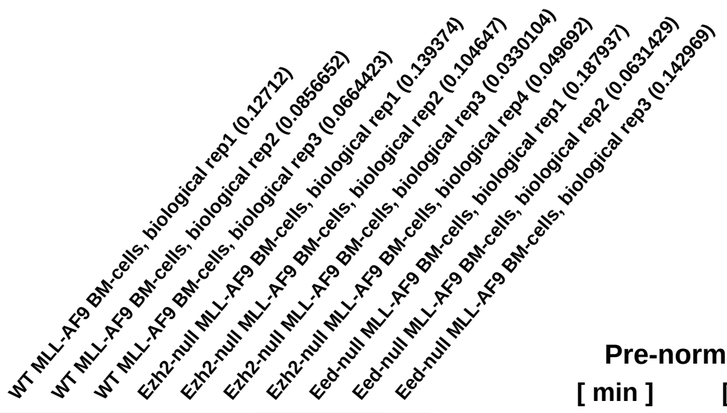

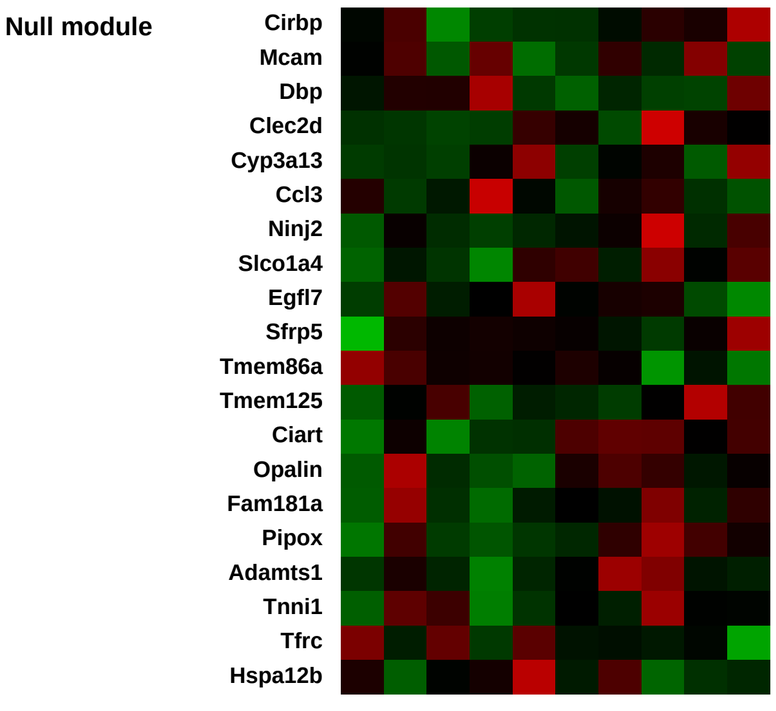

GEO Series "GSE22125" Expression Profiles

Num of samples in this series: 6

Scale of expression profile Z-scores

-3.0 -2.0 -1.0 0.0 1.0 2.0 3.0

GEO Link:	http://www.ncbi.nlm.nih.gov/geo/query/acc.cgi?acc=GSE22125
Status:	Public on Jun 04 2010
Title:	Mouse pancreatic islets during pregnancy
Organism:	Mus musculus
Experiment type:	Expression profiling by array
Platform:	GPL1261
Pubmed ID:	20581837
Summary & Design:	**Summary:** During pregnancy, pancreatic islets undergo structural and functional changes that lead to enhance insulin release in response to increased insulin demand, which is rapidly reversed at parturition. One of the most important changes is expansion of pancreatic ¸†-cell mass mainly by increased proliferation of ¸† cells. We used microarrays to detail the global programme of gene expression and identified distinct up- or down-regulated genes during pregnancy. **Overall design:** Maternal islet were isolated from mice at dpc 0 and 12.5 dpc of pregnancy for RNA extraction and hybridization on Affymetrix microarrays. We sought to identify the responsible factors for the proliferation of islets during pregnancy.

Background corr dist: KL-Divergence = 0.0435, L1-Distance = 0.0196, L2-Distance = 0.0004, Normal std = 0.6024

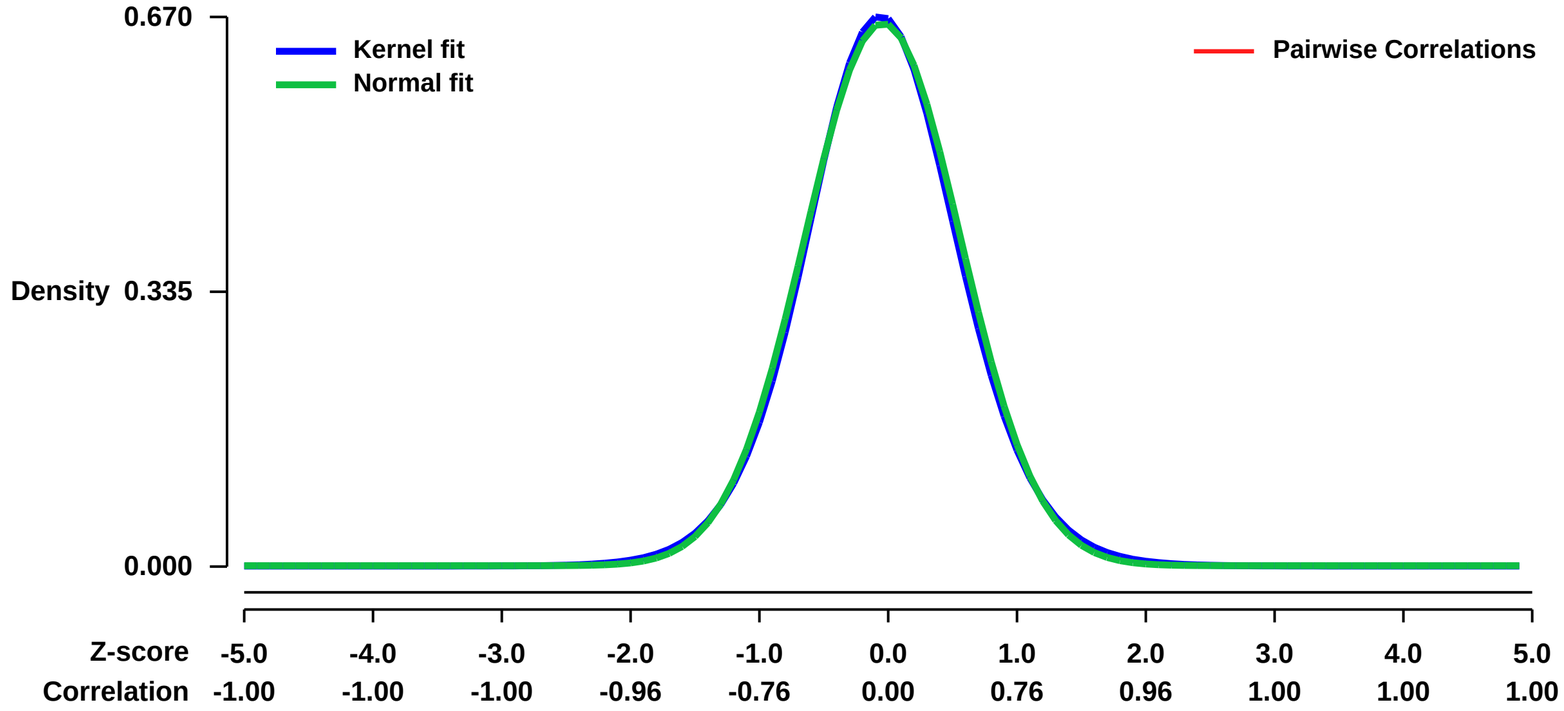

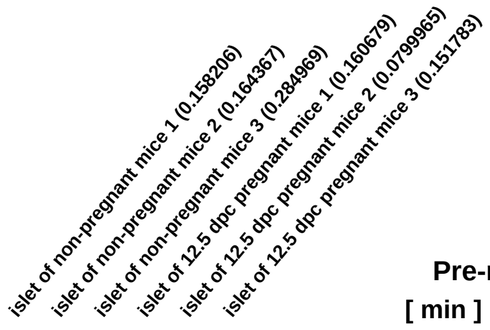

Pre-normalization Quantiles

[min] [medium] [max]

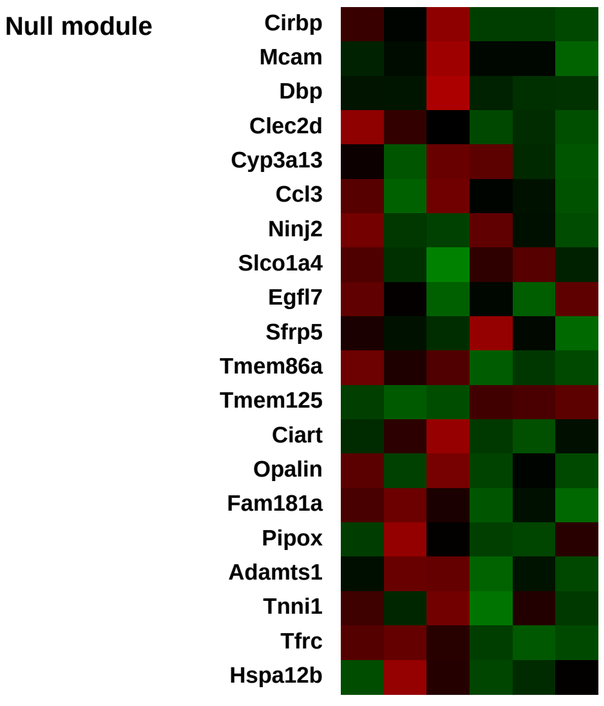

GEO Series "GSE8679" Expression Profiles

Num of samples in this series: 12

Scale of expression profile Z-scores

-3.0 -2.0 -1.0 0.0 1.0 2.0 3.0

GEO Link:	http://www.ncbi.nlm.nih.gov/geo/query/acc.cgi?acc=GSE8679
Status:	Public on Jan 11 2008
Title:	Gene expression in mouse white adipose tissue
Organism:	Mus musculus
Experiment type:	Expression profiling by array
Platform:	GPL1261
Pubmed ID:	17878318
Summary & Design:	**Summary:** Trans-10, Cis-12 conjugated linoleic acid (t10c12 CLA) causes fat loss in mouse white adipose tissue (WAT). The early transcriptome changes in WAT were analyzed using high-density microarrays to better characterize the signaling pathways responding to t10c12 CLA. Their gene expression responses between 4 to 24 hr after treatment showed a common set of early gene expression changes indicative of an integrated stress response (ISR). **Keywords: control/treatment time course** **Overall design:** Mouse WAT RNA for each time point was isolated from two control and two treatment samples for analysis on four microarrays. The two control and two treatment samples consisted of RP tissues from 5 pooled mice for each sample, requiring a total of twenty mice for the four samples taken at each time point.

Background corr dist: KL-Divergence = 0.1214, L1-Distance = 0.0366, L2-Distance = 0.0027, Normal std = 0.4127

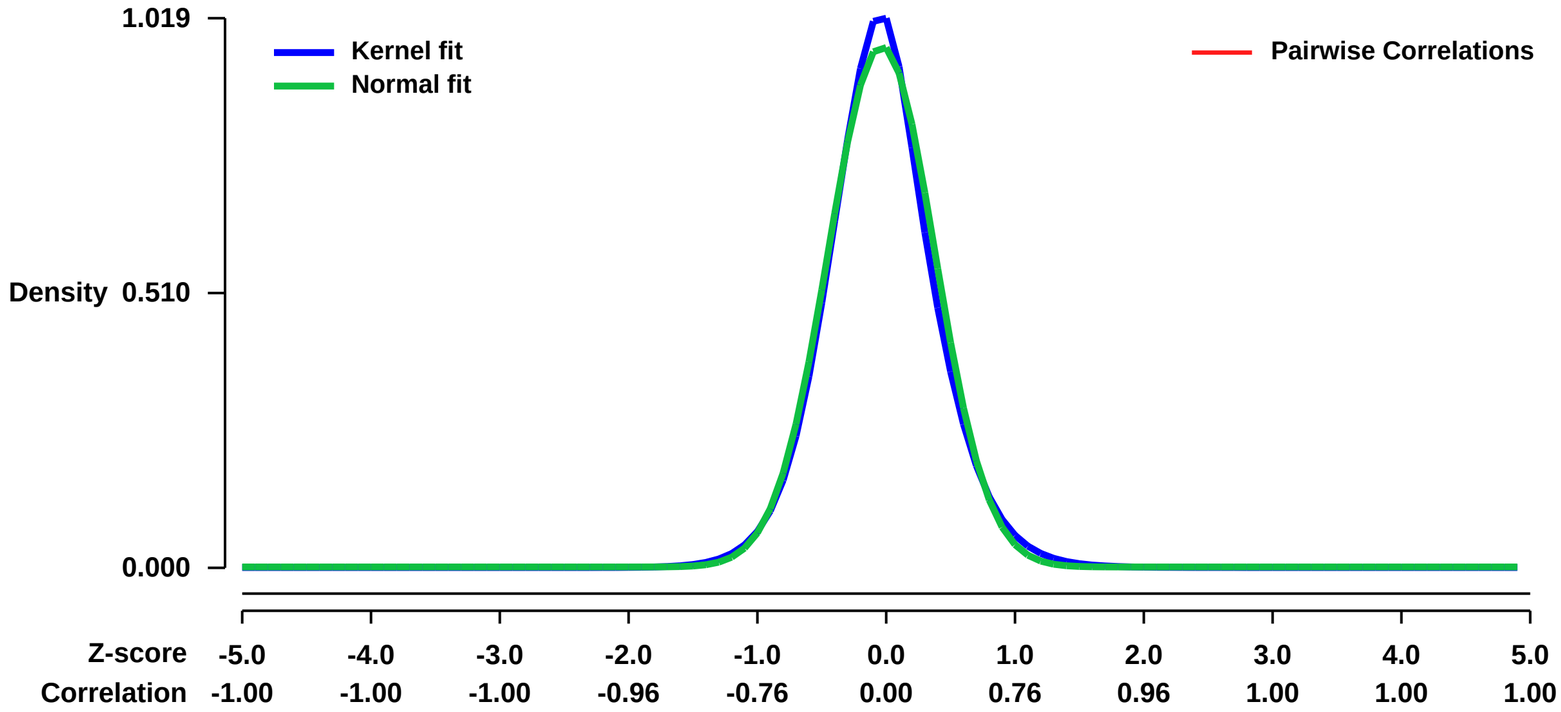

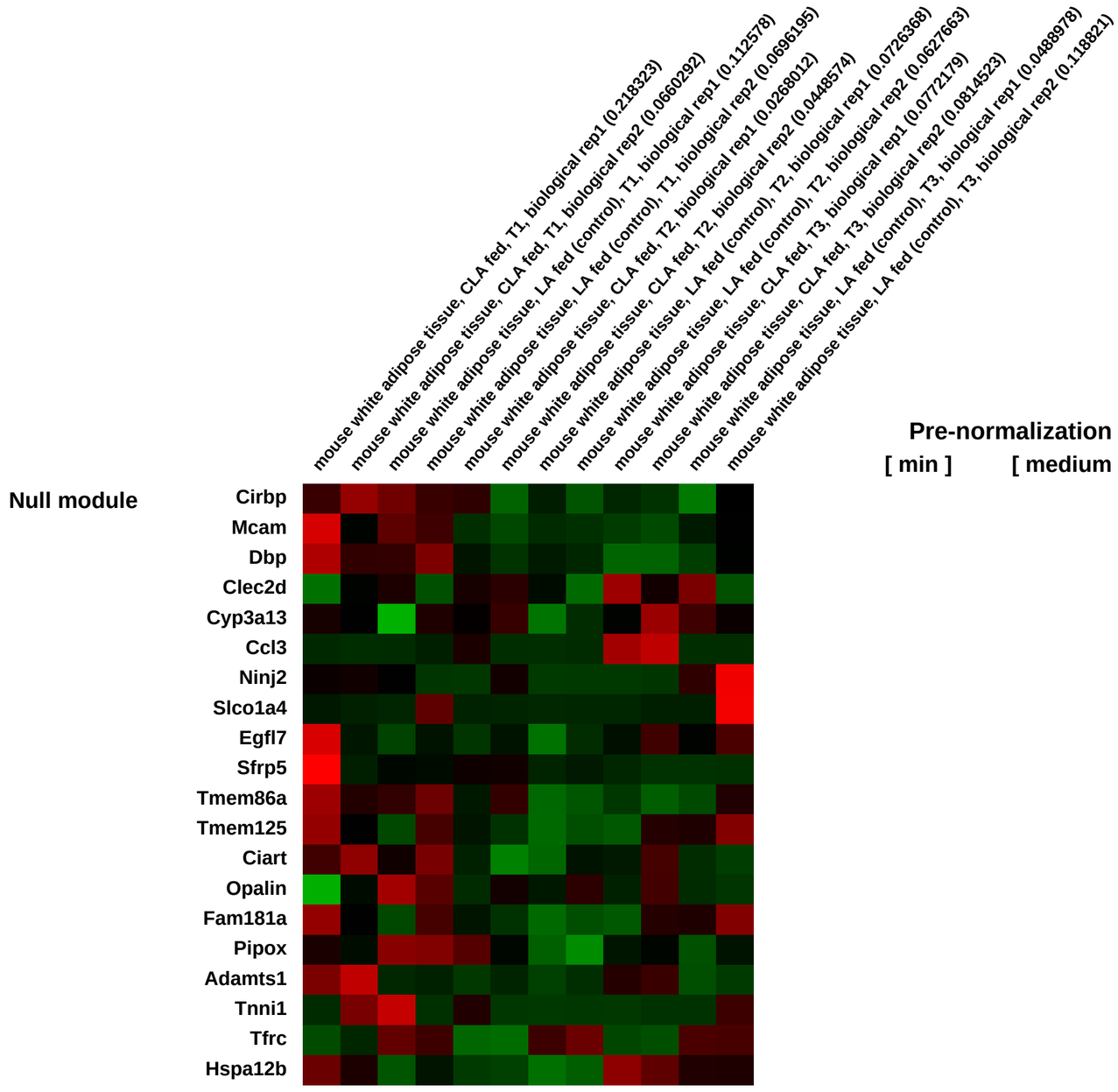

GEO Series "GSE16585" Expression Profiles

Num of samples in this series: 31

Scale of expression profile Z-scores

-3.0 -2.0 -1.0 0.0 1.0 2.0 3.0

GEO Link:	http://www.ncbi.nlm.nih.gov/geo/query/acc.cgi?acc=GSE16585
Status:	Public on Oct 19 2009
Title:	Expression profiling of P14 and P28 mouse retina from 4 genotypes: +/+, Rorb-/- , +/+;CrxpNrl and Rorb-/-;CrxpNrl
Organism:	Mus musculus
Experiment type:	Expression profiling by array
Platform:	GPL1261
Pubmed ID:	19805139
Summary & Design:	**Summary:** Rorb is essential for rod photoreceptor development in the mouse retina. Using Affymetrix mouse GeneChips, we have generated expression profiles of the +/+, Rorb-/- , +/+;CrxpNrl and Rorb-/-;CrxpNrl retina at P14 and P28. In this dataset, we include the expression data obtained from retina of wt and mutants. These data are used to obtain 1189 genes that are differentially expressed in Rorb-/- vs wt. **Overall design:** 31 total samples were analyzed

Background corr dist: KL-Divergence = 0.1975, L1-Distance = 0.0336, L2-Distance = 0.0018, Normal std = 0.3390

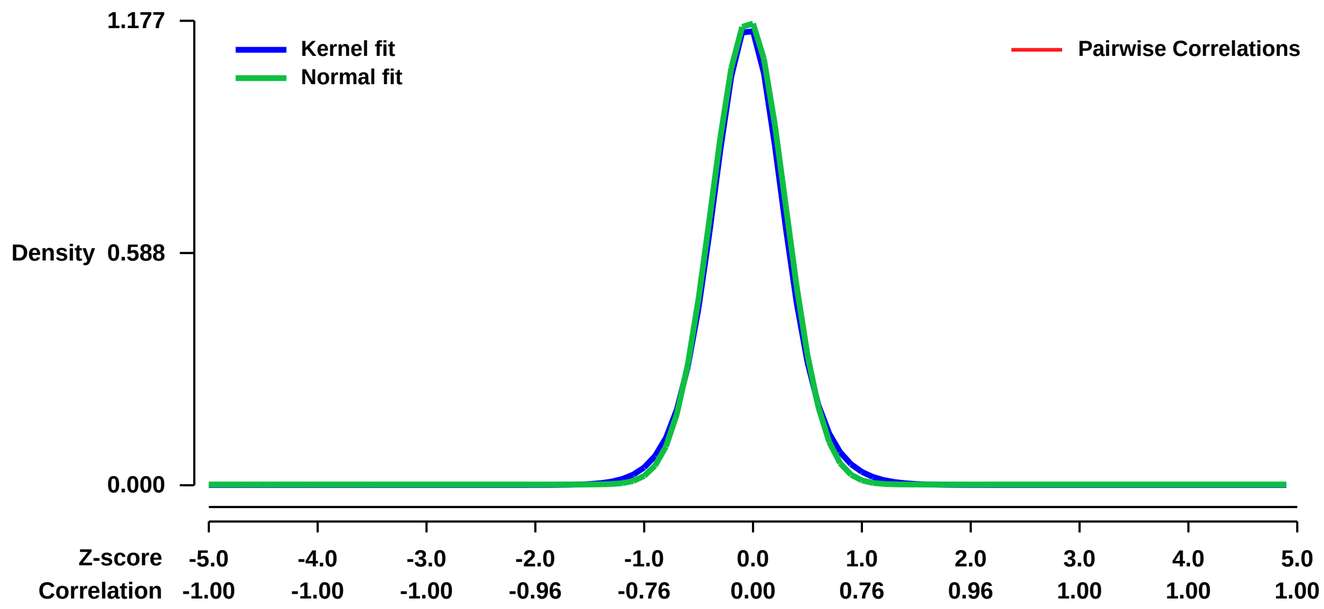

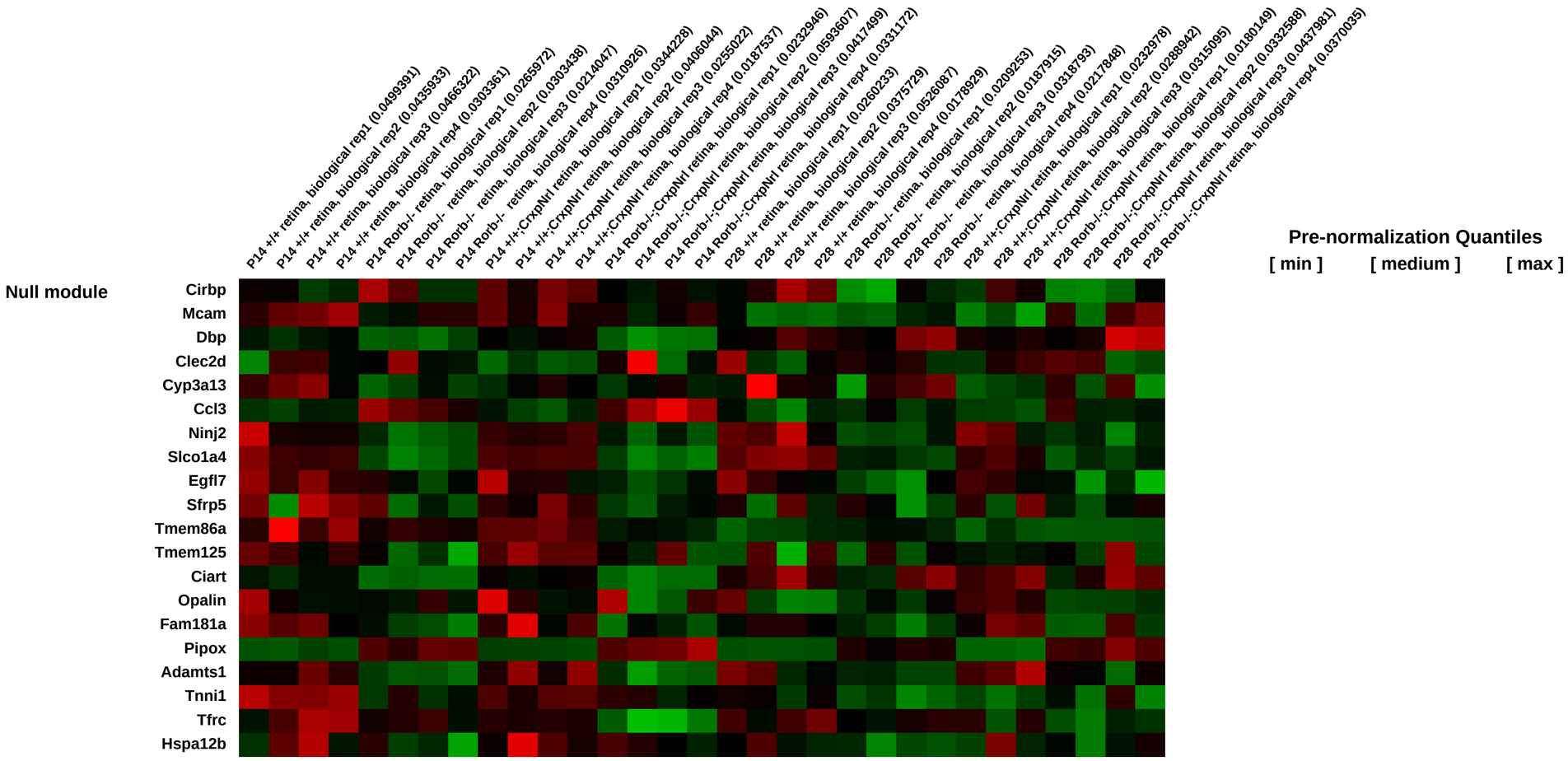

GEO Series "GSE13690" Expression Profiles

Num of samples in this series: 38

Scale of expression profile Z-scores

-3.0 -2.0 -1.0 0.0 1.0 2.0 3.0

GEO Link:	http://www.ncbi.nlm.nih.gov/geo/query/acc.cgi?acc=GSE13690
Status:	Public on Feb 06 2009
Title:	Gene expression profiling of murine MLL leukemias (whole BM)
Organism:	Mus musculus
Experiment type:	Expression profiling by array
Platform:	GPL1261
Pubmed ID:	19200802
Summary & Design:	**Summary:** The genetic programs that promote retention of self-renewing leukemia stem cells (LSCs) at the apex of cellular hierarchies in acute myeloid leukemia (AML) are not known. In a mouse model of human AML, LSCs exhibit variable frequencies that correlate with the initiating MLL oncogene and are maintained in a self-renewing state by a transcriptional sub-program more akin to that of embryonic stem cells (ESCs) than adult stem cells. The transcription/chromatin regulatory factors Myb, Hmgb3 and Cbx5 are critical components of the program and suffice for Hoxa/Meis-independent immortalization of myeloid progenitors when co-expressed, establishing the cooperative and essential role of an ESC-like LSC maintenance program ancillary to the leukemia initiating MLL/Hox/Meis program. Enriched expression of LSC maintenance and ESC-like program genes in normal myeloid progenitors and poor prognosis human malignancies links the frequency of aberrantly self-renewing progenitor-like cancer stem cells to prognosis in human cancer. **Overall design:** Samples are from five separate cohorts of mice where leukemia was initiated using distinct MLL fusion oncogenes: MLL-AF1p (n=9), MLL-AF10 (n=8), MLL-GAS7 (n=5), MLL-AF9 (n=5) and MLL-ENL (n=7). Four normal BM samples were also used as controls.

Background corr dist: KL-Divergence = 0.4095, L1-Distance = 0.0716, L2-Distance = 0.0154, Normal std = 0.2466

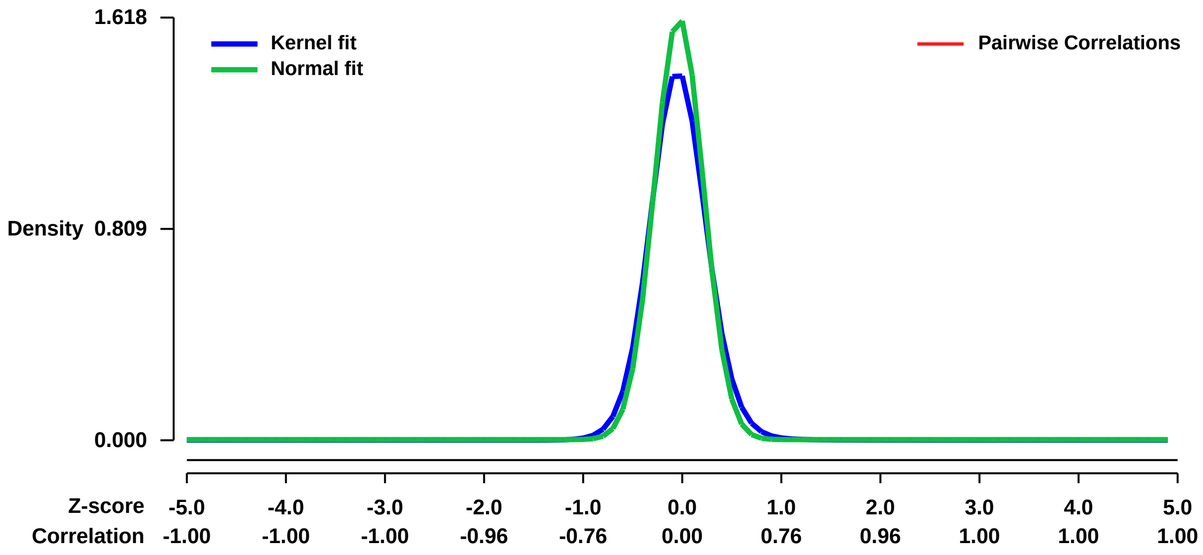

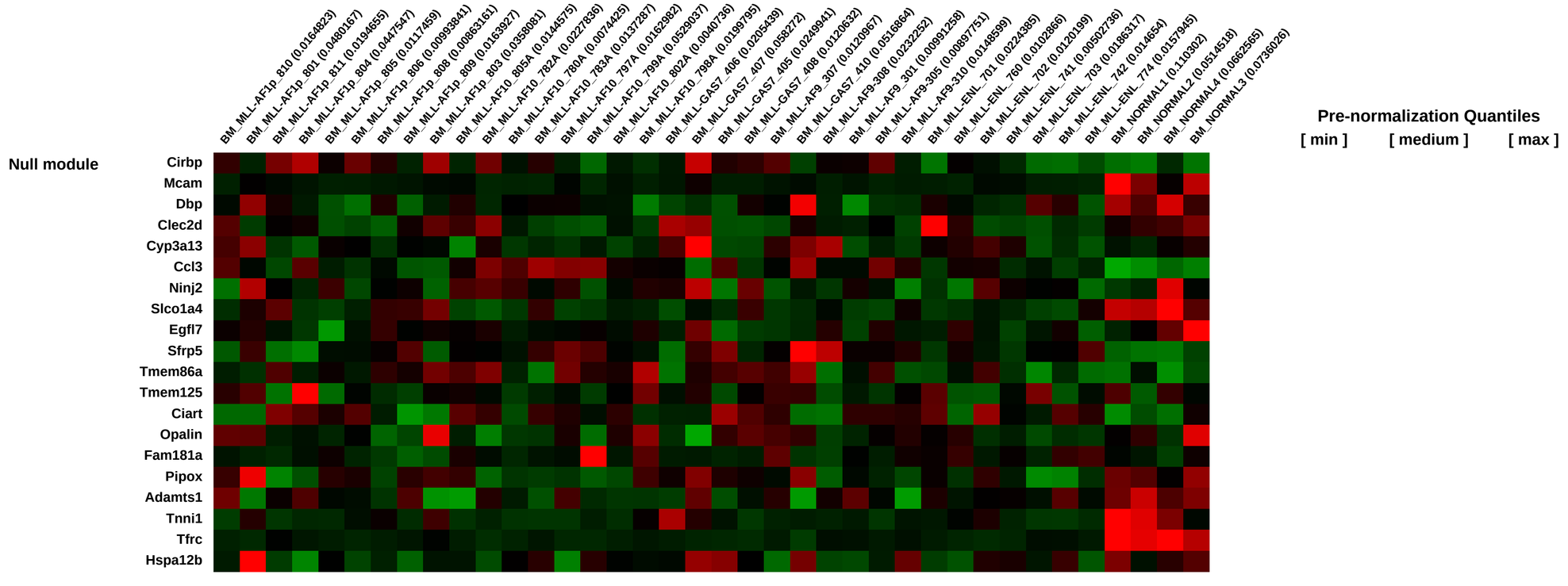

GEO Series "GSE15303" Expression Profiles

Num of samples in this series: 11

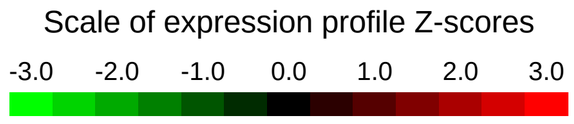

GEO Link:	http://www.ncbi.nlm.nih.gov/geo/query/acc.cgi?acc=GSE15303
Status:	Public on May 31 2009
Title:	Identification of Myelin-gene Regulatory Factor as a Critical Transcriptional Regulator Required for CNS Myelination
Organism:	Mus musculus
Experiment type:	Expression profiling by array
Platform:	GPL1261
Pubmed ID:	19596243

Summary & Design:

Summary:
The transcriptional control of CNS myelin gene expression is poorly understood. Here we identify gene model 98, which we have named Myelin-gene Regulatory Factor (MRF), as a transcriptional regulator required for CNS myelination. Within the CNS, MRF is specifically expressed by postmitotic oligodendrocytes. MRF is a nuclear protein containing an evolutionarily conserved DNA binding domain homologous to a yeast transcription factor. Knockdown of MRF in oligodendrocytes by RNA interference prevents expression of most CNS myelin genes; conversely, overexpression of MRF within cultured oligodendrocyte progenitors or the chick spinal cord promotes expression of myelin genes. In mice lacking MRF within the oligodendrocyte lineage, pre-myelinating oligodendrocytes are generated but display severe deficits in myelin gene expression and fail to myelinate. These mice display severe neurological abnormalities, and die due to seizures during the third postnatal week. These findings establish MRF as a critical transcriptional regulator essential for oligodendrocyte maturation and CNS myelination.

We used microarrays to compare cultured oligodendrocytes (differentiated in vitro for 4 days) from MRF conditional knockouts and control litteramates to look at the effects of MRF deficiency on myelin gene expression. Mouse OPCs grown in vitro in the presence of PDGF serve as a baseline for gene expression prior to differentiation.

Overall design:
Mouse OPCs from MRF conditional knockout (MRF fl/fl, Olig2 wt/cre) mice and control littermates (MRF wt/fl; Olig2 wt/cre) were isolated from enzymatically dissociated P7 mouse brains as previously described (Cahoy et al., 2008), positively immunopanning for PDGFR-alpha following a depletion of microglia with BSL1. Cells were grown in defined serum-free media as previously described (Dugas et al., 2006), but with the addition of 2% B-27 (Invitrogen). Cells were proliferated for several days in the presence of PDGF-AA (10 ng/ml, PeproTech) and then differentiation induced by withdrawal of PDGF-AA and addition of triiodothyronine (T3) (40 ng/ml; Sigma). RNA was isolated from cells 4 days after induction of differentiation; OPCs maintained in PDGF-AA serve as a baseline of OPC gene expression. Total RNA was isolated from cells with the RNeasy micro kit (Qiagen, Valencia, CA) using Qiagen on-column DNase treatment to remove any contaminating genomic DNA. The integrity of RNA was assessed using an Agilent 2100 Bioanalyzer (Agilent Technologies) and RNA concentration was determined using a NanoDrop ND-1000 spectrophotometer (NanoDrop, Rockland, DE). Biotinylated cRNAs for hybridization to Affymetrix 3'-arrays were prepared from 1ug total RNA using the Affymetrix two-cycle target labeling assay with spike in controls (Affymetrix Inc., Santa Clara, CA, 900494). Labeled-cRNA was fragmented and hybridized to Mouse Genome 430 2.0 Arrays (3'-arrays, Affymetrix, 900495) following the manufacturer's protocols. Raw image files were processed using Affymetrix GCOS 1.3 software to calculate individual probe cell intensity data and generate CEL data files. Using GCOS and the MAS 5.0 algorithm, intensity data was normalized per chip to a target intensity TGT value of 500 and expression data and present/absent calls for individual probe sets calculated. Gene symbols and names for data analyzed with the MAS 5.0 algorithm were from the Affymetrix Netaffx Mouse430_2 annotations file (http://www.affymetrix.com/support/technical/byproduct.affx?product=moe430-20). Quality control was performed by examining raw DAT image files for anomalies, confirming each GeneChip array had a background value less than 100, monitoring that the percencelle present calls was appropriate for the cell type, and inspecting the poly(A) spike in controls, housekeeping genes, and hybridization controls to confirm labeling and hybridization consistency.

Background corr dist: KL-Divergence = 0.0695, L1-Distance = 0.0313, L2-Distance = 0.0016, Normal std = 0.5115

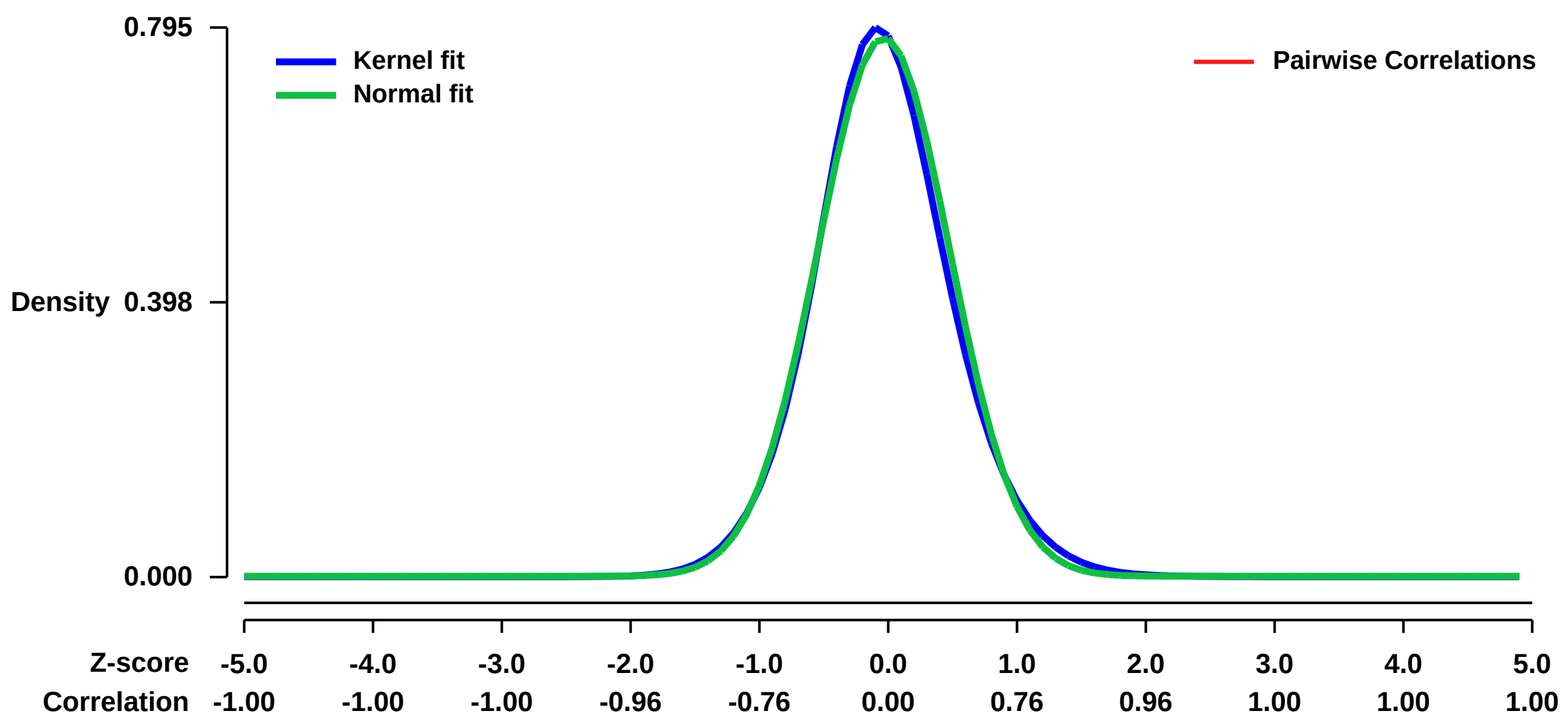

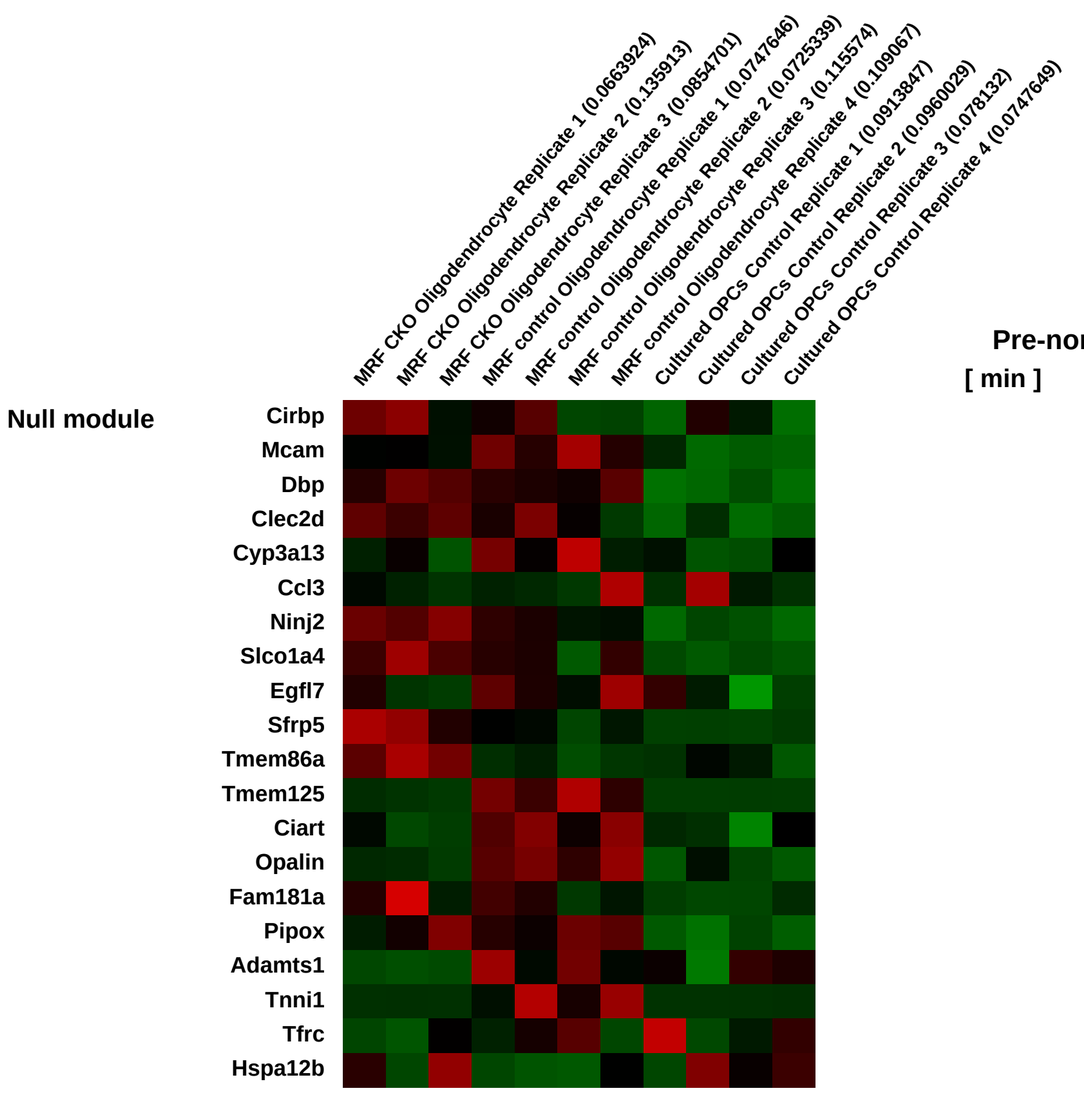

GEO Series "GSE25767" Expression Profiles

Num of samples in this series: 6

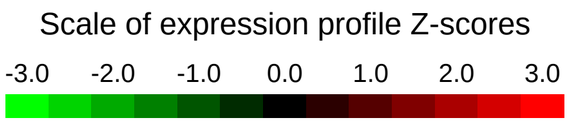

GEO Link:	http://www.ncbi.nlm.nih.gov/geo/query/acc.cgi?acc=GSE25767
Status:	Public on Dec 03 2010
Title:	Cardiac gene expression profiling of apoE-deficient mice receiving heart failure treatment with the anti-ischemic drug ranolazine
Organism:	Mus musculus
Experiment type:	Expression profiling by array
Platform:	GPL1261
Pubmed ID:	21711241
Summary & Design:	**Summary:** Heart failure is a leading cause of cardiovascular mortality with limited options for treatment. We used 18 month-old apolipoprotein E (apoE)- deficient mice as a model of atherosclerosis-induced heart failure to analyze whether the anti-ischemic drug ranolazine could retard the progression of heart failure. The study showed that 2 months of ranolazine treatment improved cardiac function of 18 month-old apoE-deficient mice with symptoms of heart failure as assessed by echocardiography. To identify changes in cardiac gene expression induced by treatment with ranolazine a microarray study was performed with heart tissue from failing hearts relative to ranolazine-treated and healthy control hearts. The microarray approach identified heart failure-specific genes that were normalized during treatment with the anti-ischemic drug ranolazine. **Overall design:** Microarray gene expression profiling was performed with heart tissue isolated from (i) untreated 18 month-old apoE-deficient mice with heart failure relative to (ii) 18 month-old apoE-deficient mice treated for two months with the anti-ischemic drug ranolazine (200 mg/kg), and (iii) age-matched non-transgenic C57BL/6J (B6) control mice.

Background corr dist: KL-Divergence = 0.0357, L1-Distance = 0.0287, L2-Distance = 0.0009, Normal std = 0.6630

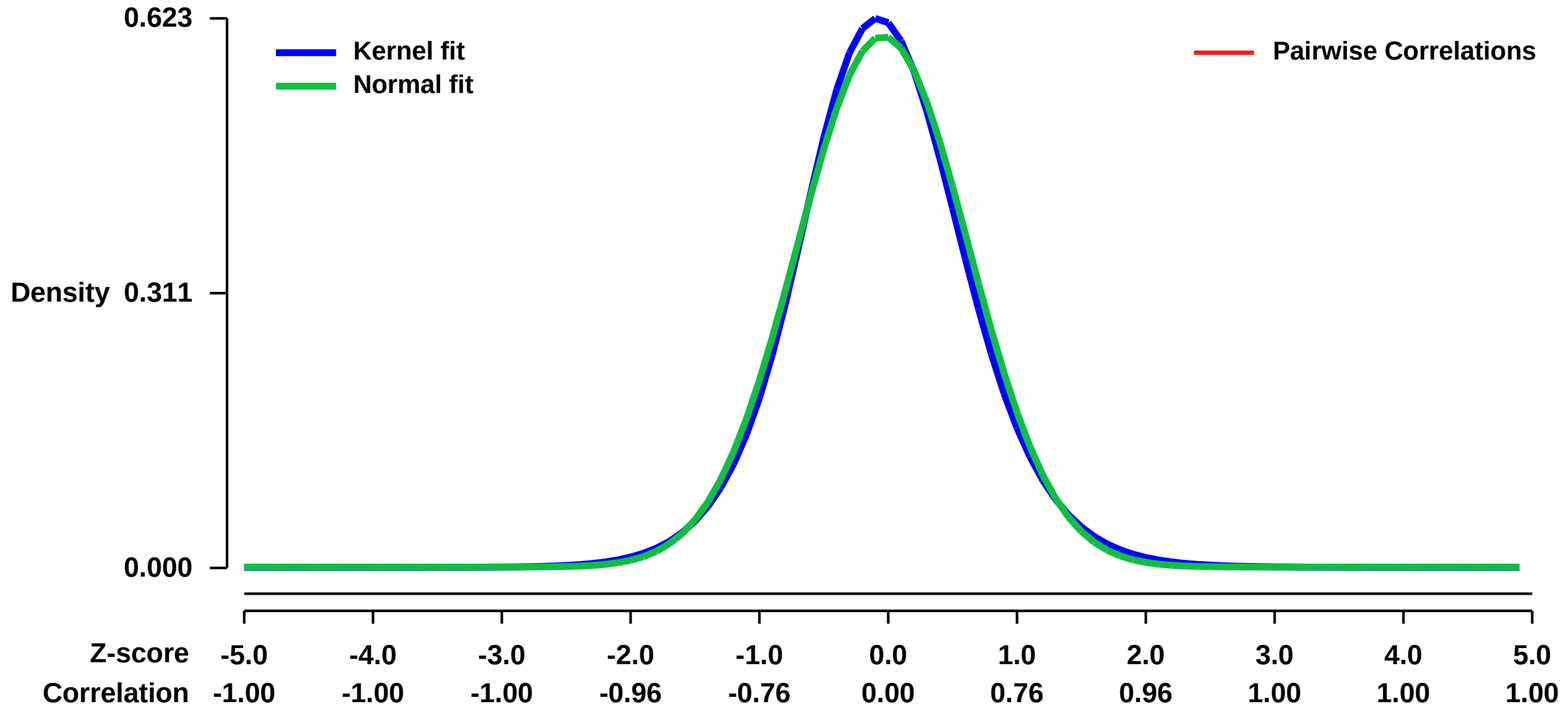

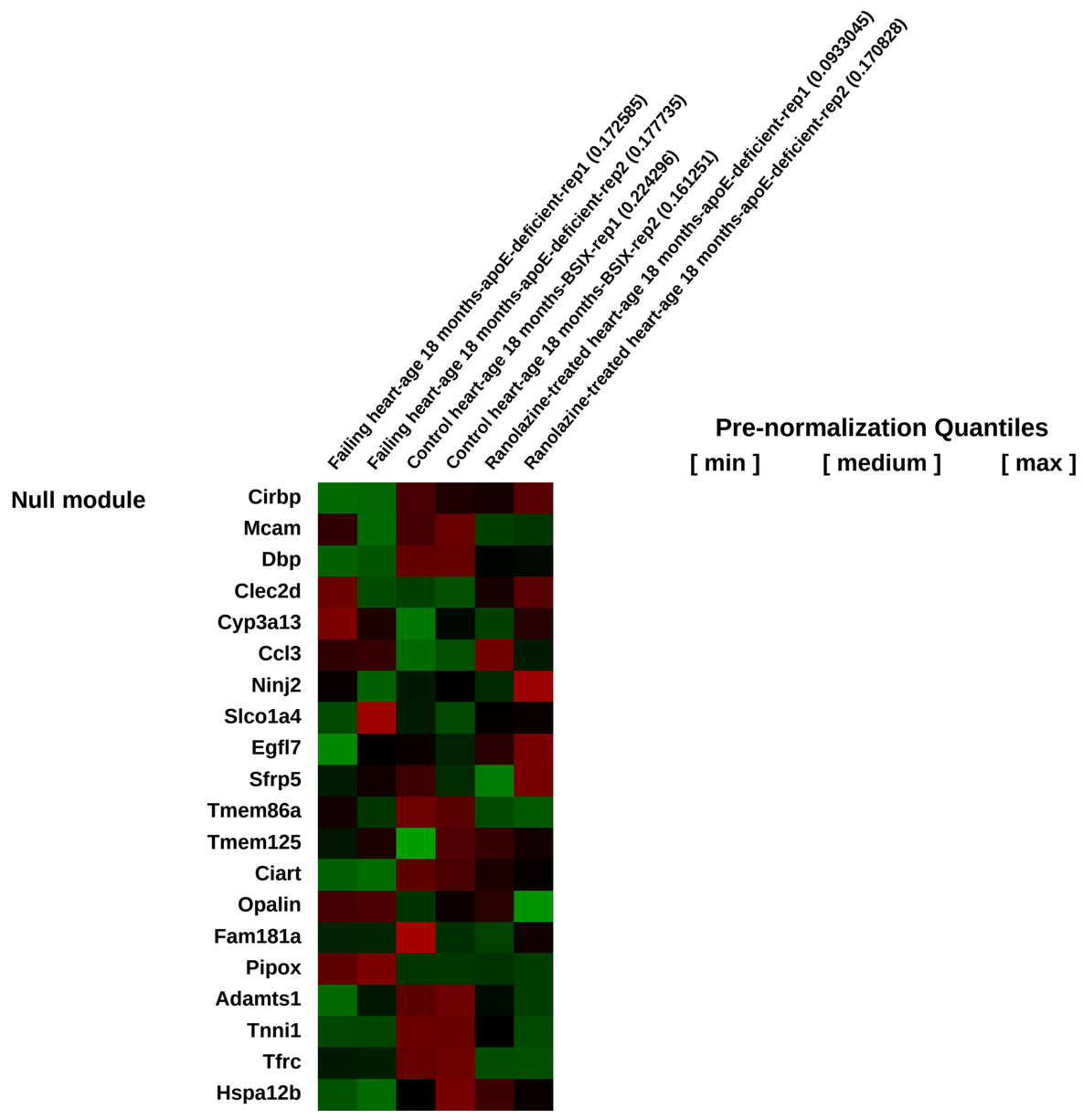

GEO Series "GSE21687" Expression Profiles

Num of samples in this series: 192

Details of this dataset are not shown due to large number of samples and the page size limit.

Find details in http://www.ncbi.nlm.nih.gov/geo/query/acc.cgi?acc=GSE21687

Background corr dist: KL-Divergence = 0.4486, L1-Distance = 0.0571, L2-Distance = 0.0084, Normal std = 0.2410

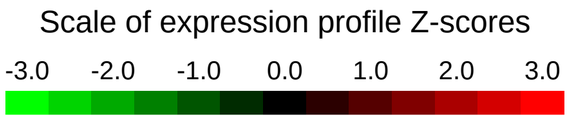

GEO Series "GSE33132" Expression Profiles

Num of samples in this series: 8

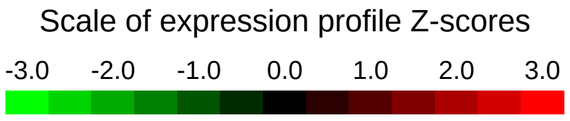

GEO Link:	http://www.ncbi.nlm.nih.gov/geo/query/acc.cgi?acc=GSE33132
Status:	Public on Oct 21 2011
Title:	Expression data from purified control and Brdt˛ BD1 round spermatids.
Organism:	Mus musculus
Experiment type:	Expression profiling by array
Platform:	GPL1261
Pubmed ID:	22570411
Summary & Design:	**Summary:** Brdt is a testis specific member of a family of chromatin interacting proteins. All of the family members have been shown to regulate transcription. Brdt is highly expressed in round spermatids, and may play a role in transcriptional regulation in these cells. We investigated transcriptional changes in mutant round spermatids that were homozygous for a mutation in which the first bromodomain of Brdt was removed. **Overall design:** Round spermatids were purified from seven adult animals of each genotype for each Affymetrix microarray. Purity of round spermatids was assessed by propidium iodide staining.

Background corr dist: KL-Divergence = 0.0577, L1-Distance = 0.0221, L2-Distance = 0.0007, Normal std = 0.5318

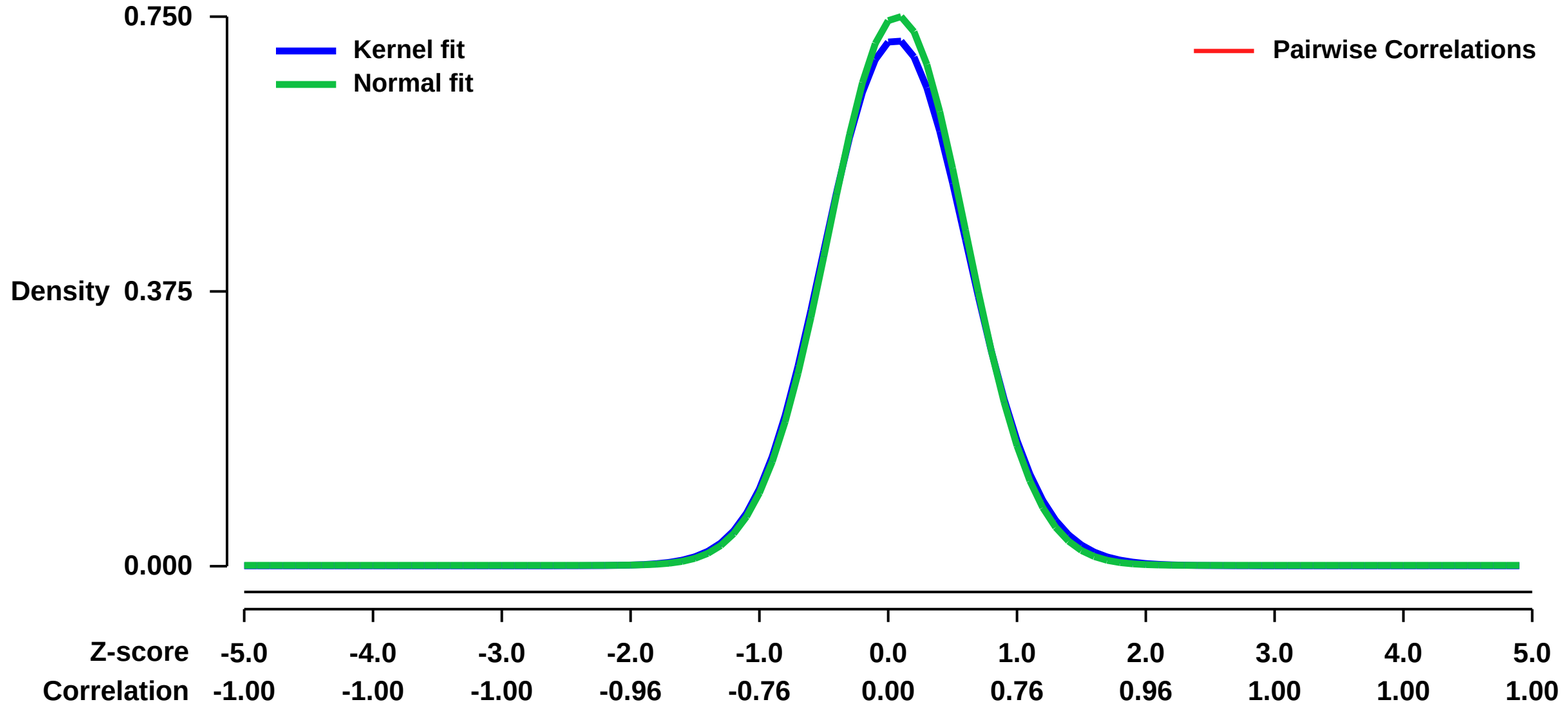

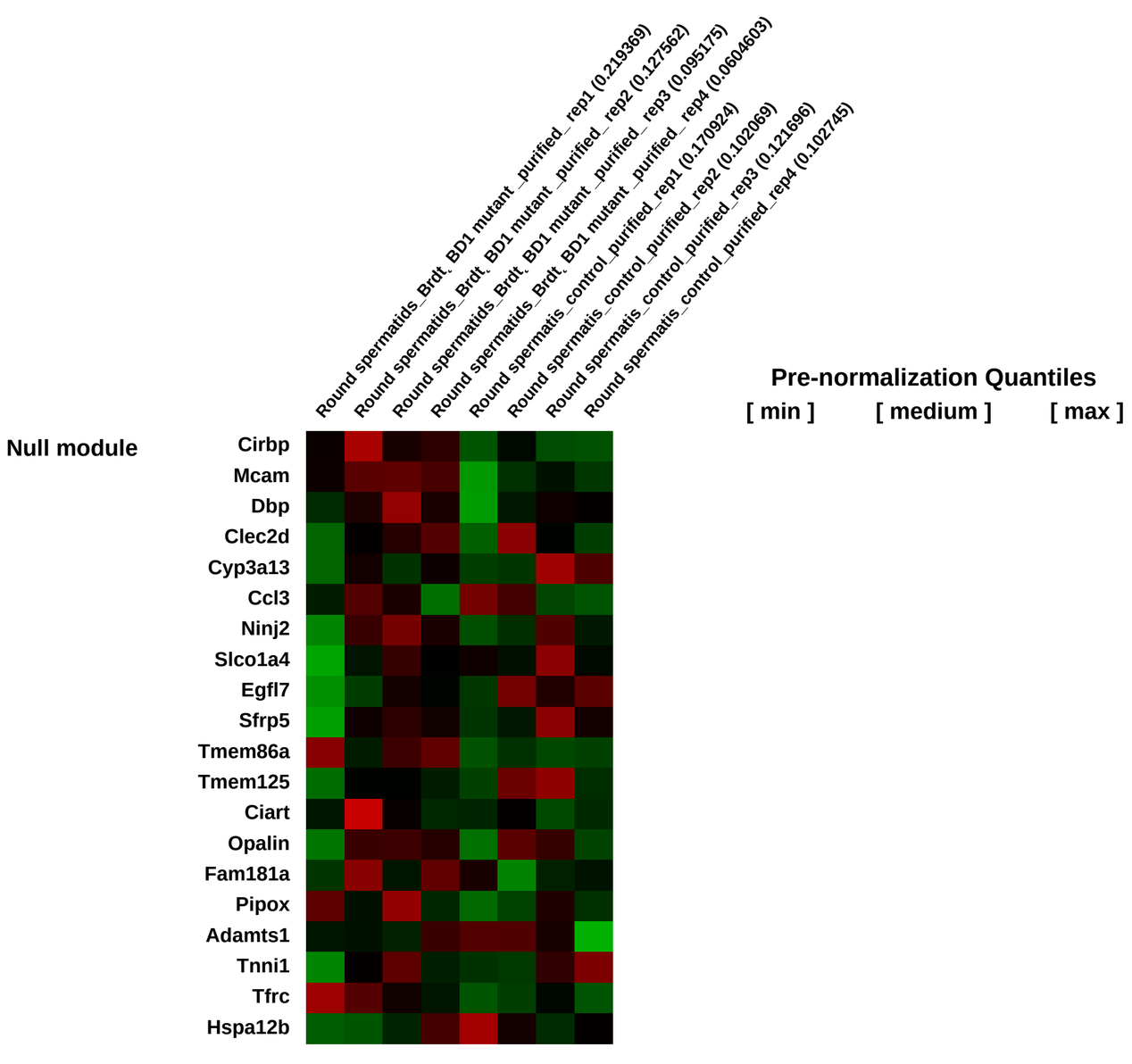

GEO Series "GSE10552" Expression Profiles

Num of samples in this series: 6

Scale of expression profile Z-scores

-3.0 -2.0 -1.0 0.0 1.0 2.0 3.0

GEO Link:	http://www.ncbi.nlm.nih.gov/geo/query/acc.cgi?acc=GSE10552
Status:	Public on Dec 31 2008
Title:	Genome wide expression analysis in AtT-20 cells following Dnmt1 knockdown
Organism:	Mus musculus
Experiment type:	Expression profiling by array
Platform:	GPL1261
Pubmed ID:	18922972
Summary & Design:	**Summary:** Efficient and sustained knockdown of DNMT1 transcript and protein was achieved using a consecutive transfection protocol in the mouse pituitary adenoma cell line, AtT-20. Genome wide microarray analysis identified 91 transcripts that were significantly differentially expressed relative to cells treated with a non-targeting control. **Keywords: Differential expression** **Overall design:** AtT-20 cells were repeatedly treated with 20 nM siRNA (siDNMT1 or siNT) over an eight day period. After eight days total RNA was extracted and prepared for microarray analysis. The procedure was repeated three times independently.

Background corr dist: KL-Divergence = 0.0482, L1-Distance = 0.0201, L2-Distance = 0.0004, Normal std = 0.5806

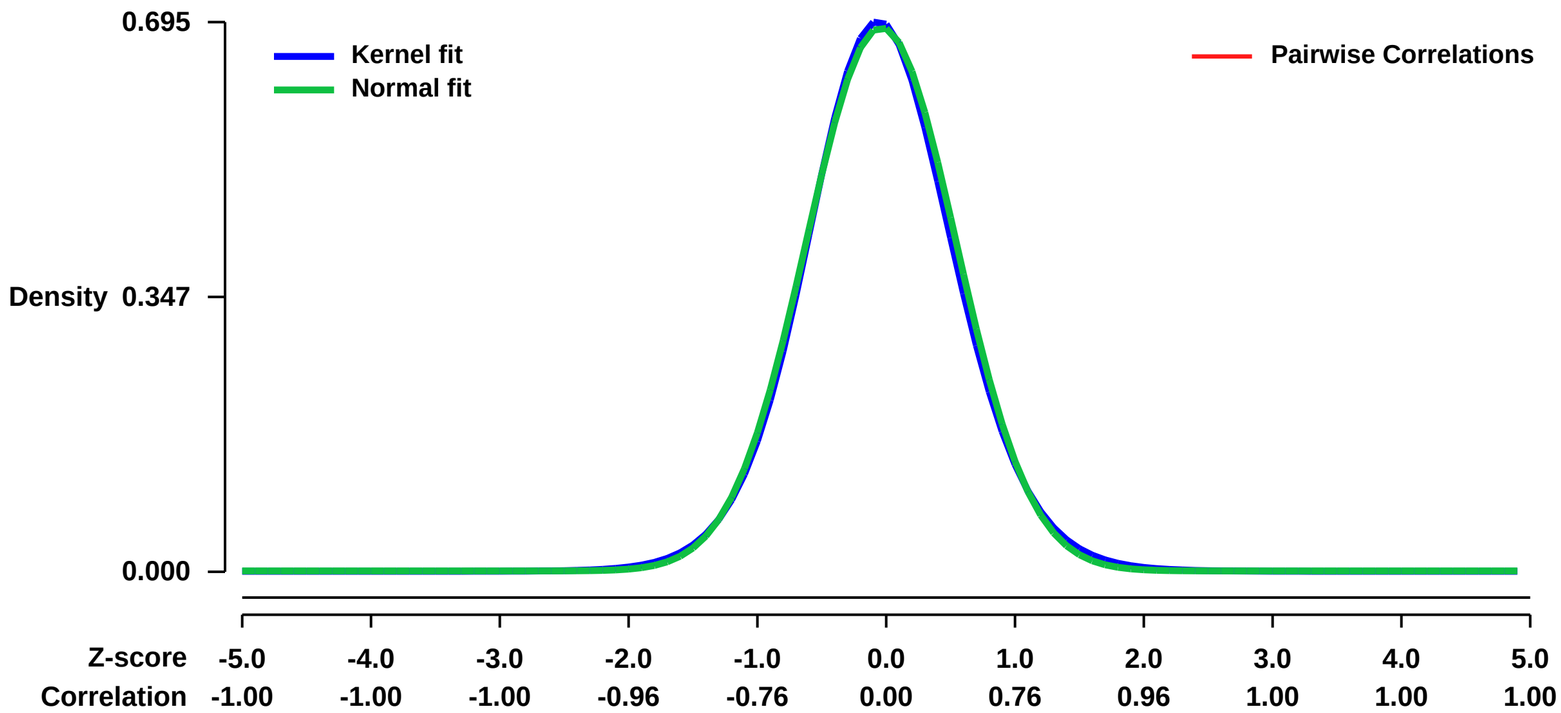

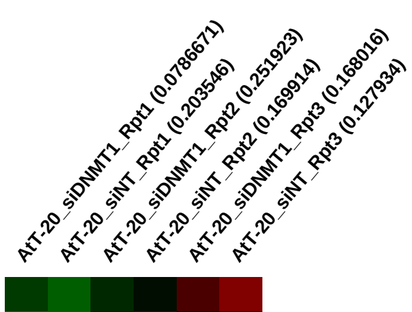

Pre-normalization Quantiles

[min] [medium] [max]

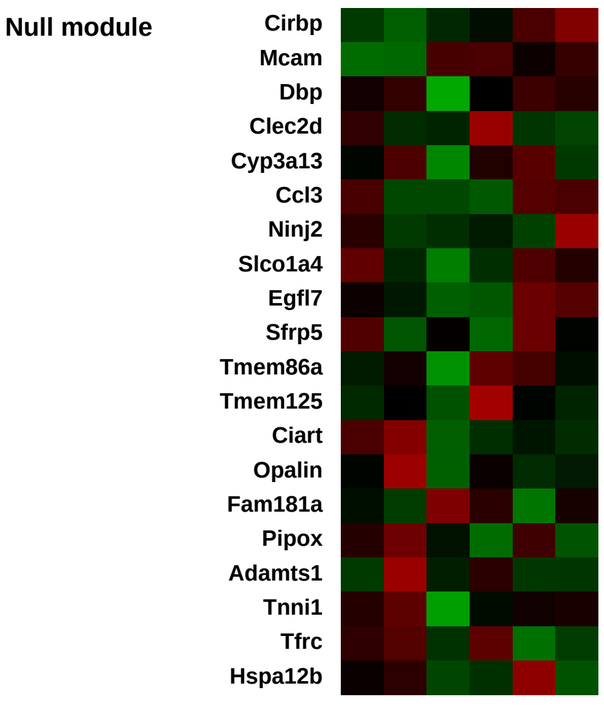

GEO Series "GSE7503" Expression Profiles

Num of samples in this series: 6

Scale of expression profile Z-scores

-3.0 -2.0 -1.0 0.0 1.0 2.0 3.0

GEO Link: http://www.ncbi.nlm.nih.gov/geo/query/acc.cgi?acc=GSE7503

Status: Public on Aug 01 2007

Title: Effects of JNK on TGF-beta responses of mouse B lymphoma derived A20 cells

Organism: Mus musculus

Experiment type: Expression profiling by array

Platform: GPL1261

Pubmed ID:

Summary & Design:

Summary:
TGF-beta plays multiple functions in a board range of cellular responses such as proliferation, differentiation, motility and survival by activating several cellular signaling pathways, including Smads and MAP kinases (Erk, JNK and p38). In particular, TGF-beta can activate pro- or anti-apoptotic signals depending on the target cells. We found that blockage of JNK activation sensitized mouse B lymphoma derived A20 cells to TGF-beta-induced apoptosis. These results suggest that TGF-beta activate JNK to inhibit the activation of death signal that is simultaneously activated by TGF-beta.

We used microarrays to gain insight into the effects of JNK inhibition on gene expression in TGF-b-stimulated A20 cells and identified JNK-dependent TGF-beta inducible genes.

Keywords: time course

Overall design:
The following six samples were prepared: untreated A20 cells (non-stimulated, DMSO): A20 cells cultured with SP600125 for 24 h (non-stimulated, SP600125): A20 cells stimulated with TGF-beta for 12 h (TGF-beta 12 h, DMSO) and 24 h (TGF-beta 24 h, DMSO): and A20 cells stimulated with TGF-beta in the presence of SP600125 for 12 h (TGF-beta 12 h, SP600125) and 24 h (TGF-beta 24 h, SP600125), respectively. Total RNA was prepared and hybridized to the Affymetrix Mouse Genome 430 2.0 array. Genes whose expression was increased by more than 2-fold at either 12 or 24 h after TGF-beta stimulation were identified as TGF-beta inducible genes. Amongst them, we identified genes whose induction levels were reduced by more than 75% by co-treatment with the JNK inhibitor SP600125.

Background corr dist: KL-Divergence = 0.0429, L1-Distance = 0.0241, L2-Distance = 0.0007, Normal std = 0.6069

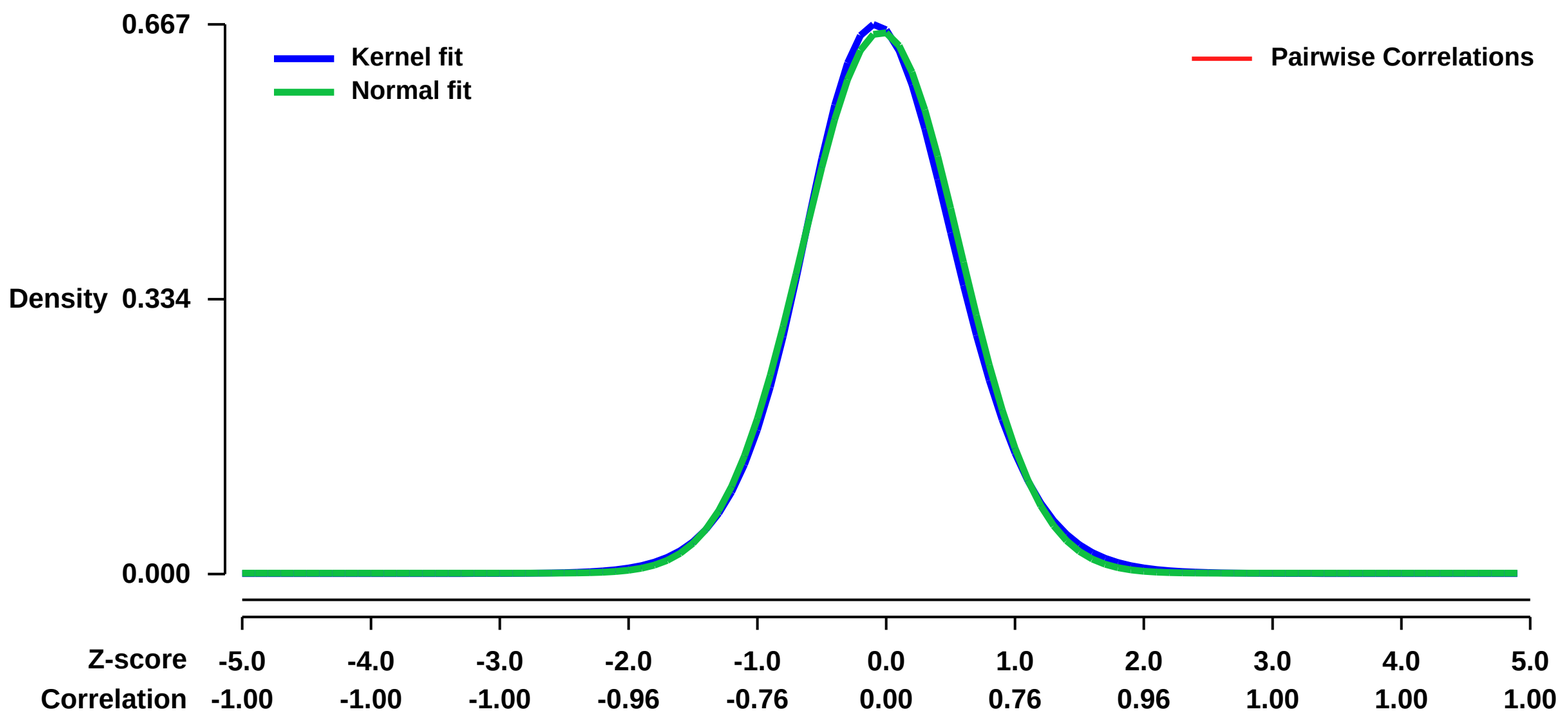

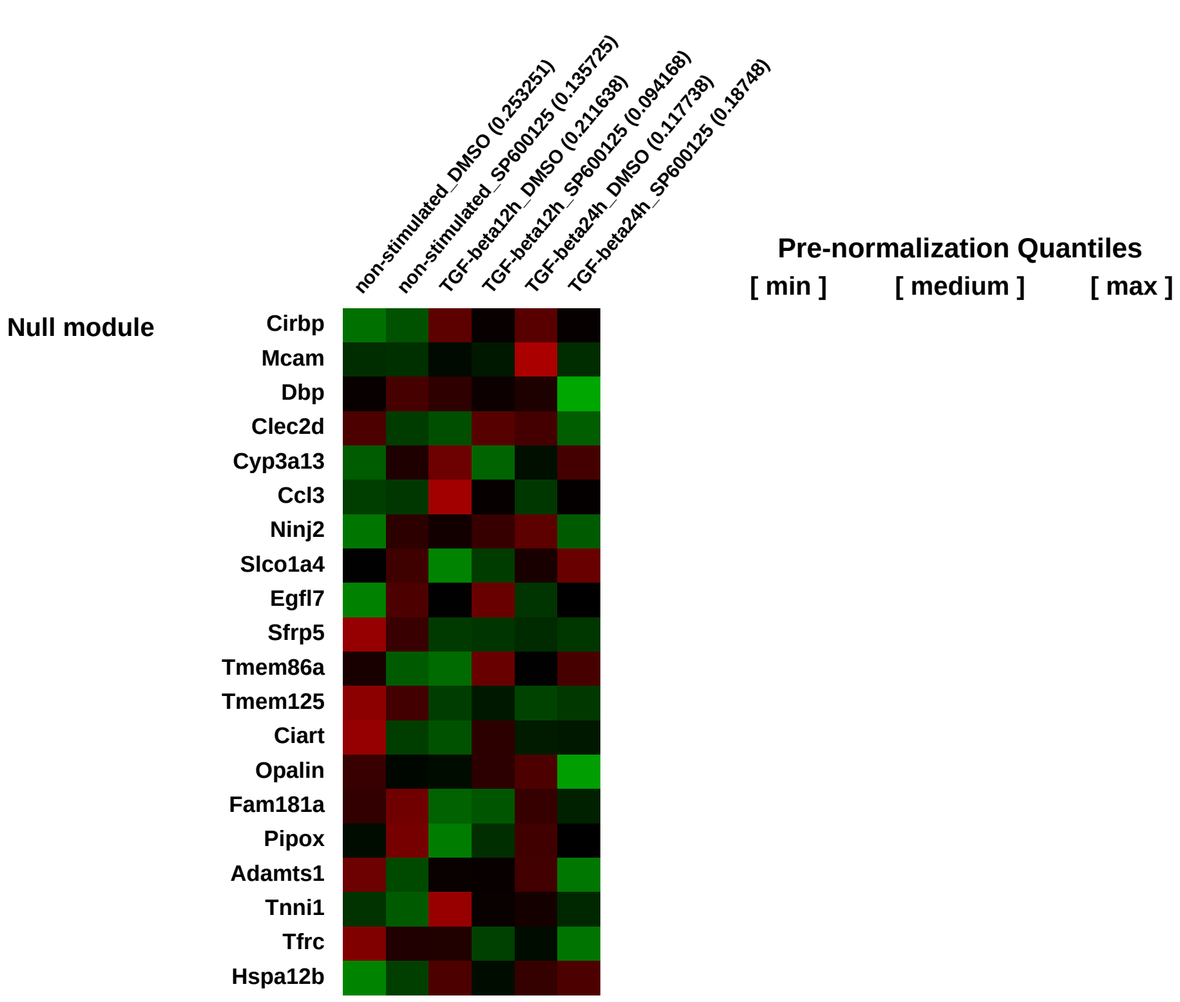

GEO Series "GSE40716" Expression Profiles

Num of samples in this series: 12

Scale of expression profile Z-scores

-3.0 -2.0 -1.0 0.0 1.0 2.0 3.0

GEO Link:	http://www.ncbi.nlm.nih.gov/geo/query/acc.cgi?acc=GSE40716
Status:	Public on Nov 05 2012
Title:	Offspring from oocytes derived from in vitro primordial germ cell-like cells in mice
Organism:	Mus musculus
Experiment type:	Expression profiling by array
Platform:	GPL1261
Pubmed ID:	23042295
Summary & Design:	**Summary:** Reconstitution of female germ-cell development in vitro is a key challenge in reproductive biology and medicine. We show here that female (XX) embryonic stem cells (ESCs) and induced pluripotent stem cells (iPSCs) in mice are induced into primordial germ cell-like cells (PGCLCs), which, when aggregated with female gonadal somatic cells as reconstituted ovaries, develop pre-meiotic germ cell characteristics, including X-reactivation, imprint erasure, and cyst formation. Upon transplantation under ovarian bursa, PGCLCs in the reconstituted ovaries mature into germinal vesicle-stage oocytes, which, through in vitro maturation and fertilization, contribute to fertile offspring. Our culture system serves as a robust foundation for the investigation of key properties of female germ cells, including the acquisition of totipotency, and for the reconstitution of whole female germ-cell development in vitro. **Overall design:** We performed expression analysis of female PGC-like cells [PGCLCs; day 3 (d3), day 6 (d6), and day 3 followed by day 6 in aggregation with female embryonic day (E) 12.5 gonadal somatic cells (d3ag6)] in comparison to in vivo embryonic PGCs (E12.5 female PGCs and E9.5 PGCs) and male d6 PGCLCs. PGCLCs were marked with fluorescence of Blimp1-mVenus, stella-ECFP transgenic reporters (BVSC). PGCs were marked with fluorescence of the stella-EGFP transgenic reporter.

Background corr dist: KL-Divergence = 0.1231, L1-Distance = 0.0294, L2-Distance = 0.0015, Normal std = 0.4047

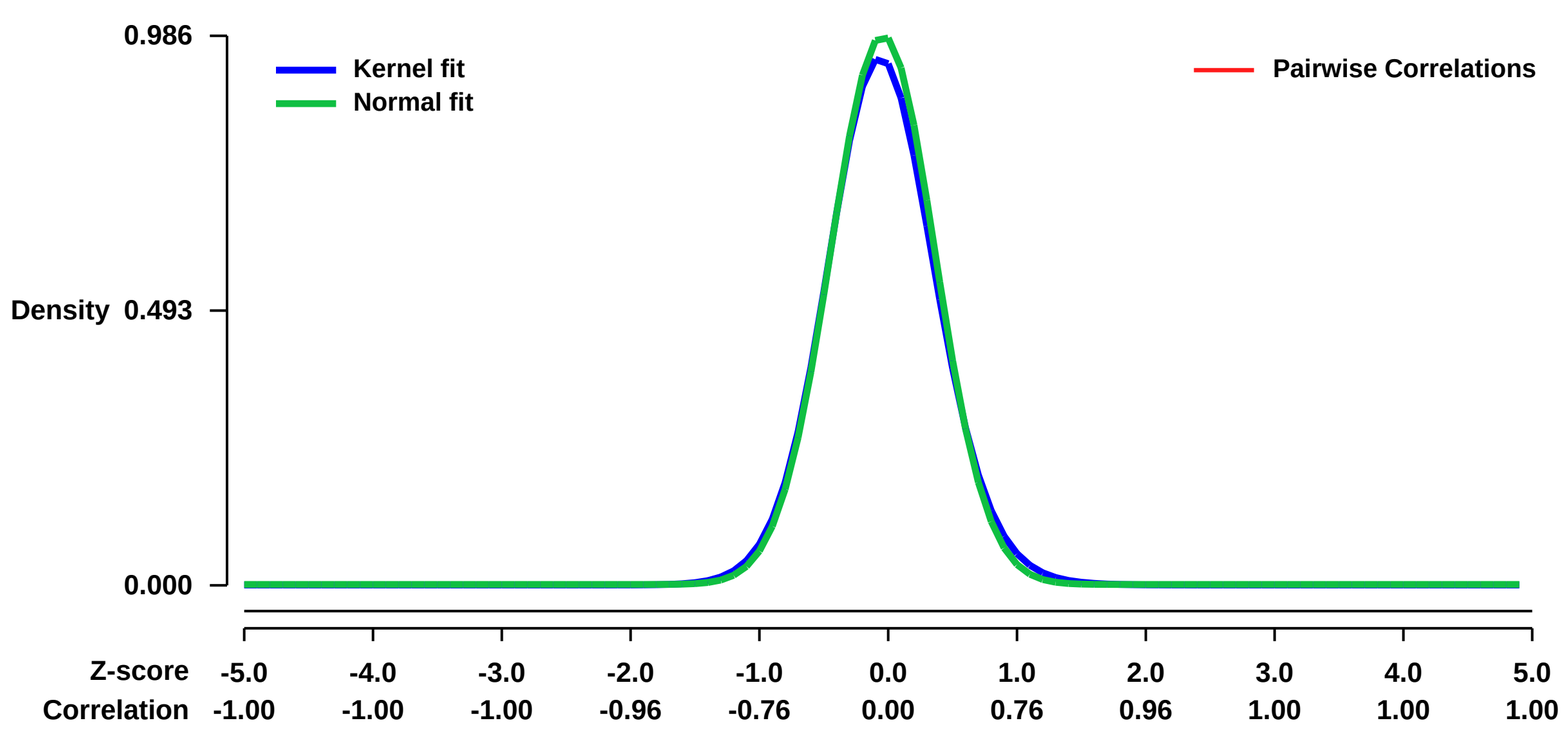

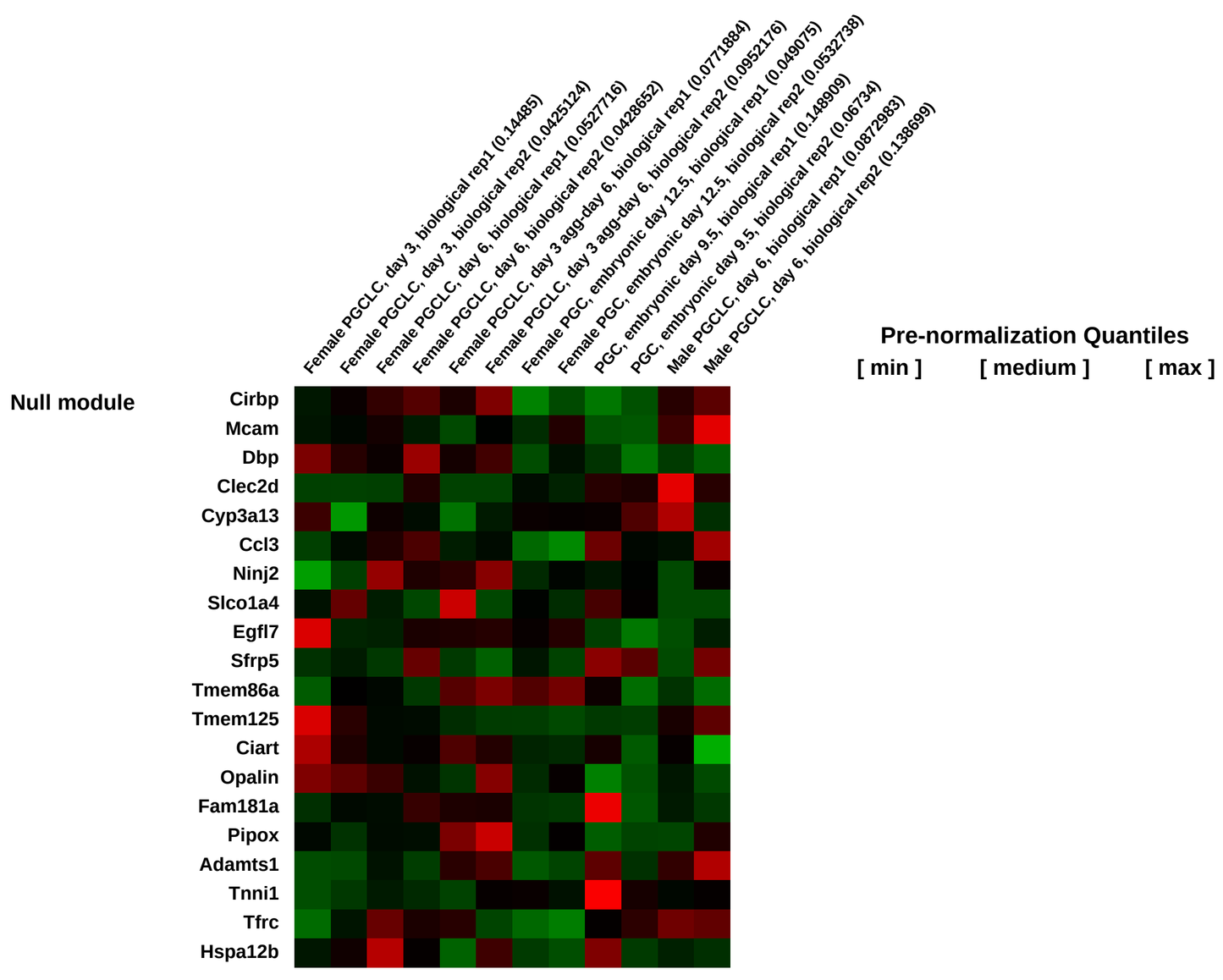

GEO Series "GSE9563" Expression Profiles

Num of samples in this series: 30

Scale of expression profile Z-scores

-3.0 -2.0 -1.0 0.0 1.0 2.0 3.0

GEO Link:	http://www.ncbi.nlm.nih.gov/geo/query/acc.cgi?acc=GSE9563
Status:	Public on May 14 2008
Title:	Translation state array analysis of Mouse embryonic stem cells and embryoid bodies
Organism:	Mus musculus
Experiment type:	Expression profiling by array
Platform:	GPL1261
Pubmed ID:	18462695
Summary & Design:	**Summary:** Stem cell differentiation is known to involve changes in RNA expression, but little is known about translational control during differentiation. We comprehensively profiled gene expression during differentiation of embryonic stem cells (ESCs) into embyroid bodies (EBs) by integrating conventional transcriptome analysis with global assessment of ribosome loading. Differentiation was accompanied by an anabolic switch, characterized by global increases in transcript abundance, polysome content, protein synthesis rates and protein content. Furthermore, 78% of expressed transcripts showed increased ribosome loading, thereby enhancing translational efficiency. Elevated protein synthesis was accompanied by enhanced phosphorylation of eIF-4E binding protein, suggesting regulation by the mTOR pathway. Some transcripts were under exclusive translational control, including Activated Transcription Factor 5 (ATF5) a b-zip transcription factor, Deleted in Colon Cancer (DCC) the tumor suppressor and Wnt1, the beta-catenin agonist. Parsimonious translation in ESCs may provide a layer of quality control to prevent inappropriate gene expression in the pluripotent state. Keywords: Translation state array analysis during embryonic stem cell differentiation **Overall design:** Embryonic stem cells (ESC) maintained in an undifferentiated state and day-5 Embryoid bodies (EB) were selected for RNA was extraction and hybridization on Affymetrix 430_2 mouse expression arrays. For polysome fractionation, twelve fractions collected from the gradients were combined to form four pools. One ml of each pool (Pools: 1-4) was used for RNA isolation, labeling and hybridization for undifferentiated ESCs (UD1, UD2, UD3 and UD4) and EBs (EB1, EB2, EB3 and EB4). In parallel, total RNA was also isolated from unfractionated lysates for transcript abundance analysis. Three biological replicates of ESCs and EB cultures were used for polysome fractionation and total RNA analysis.

Background corr dist: KL-Divergence = 0.1431, L1-Distance = 0.0539, L2-Distance = 0.0065, Normal std = 0.3901

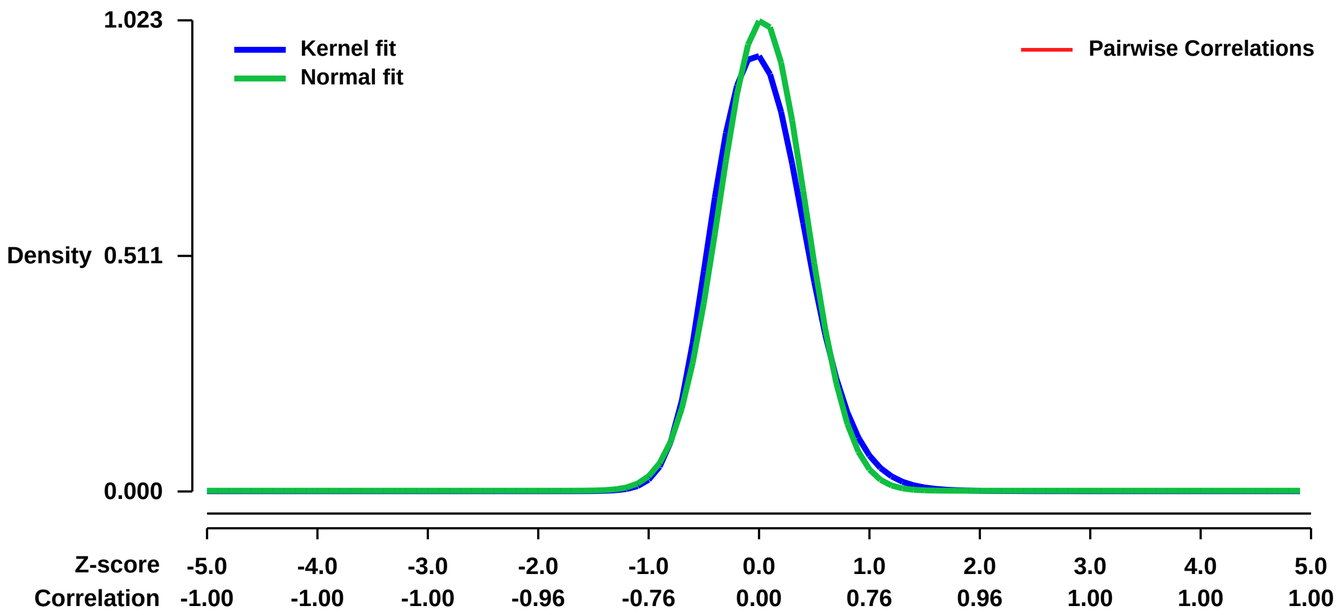

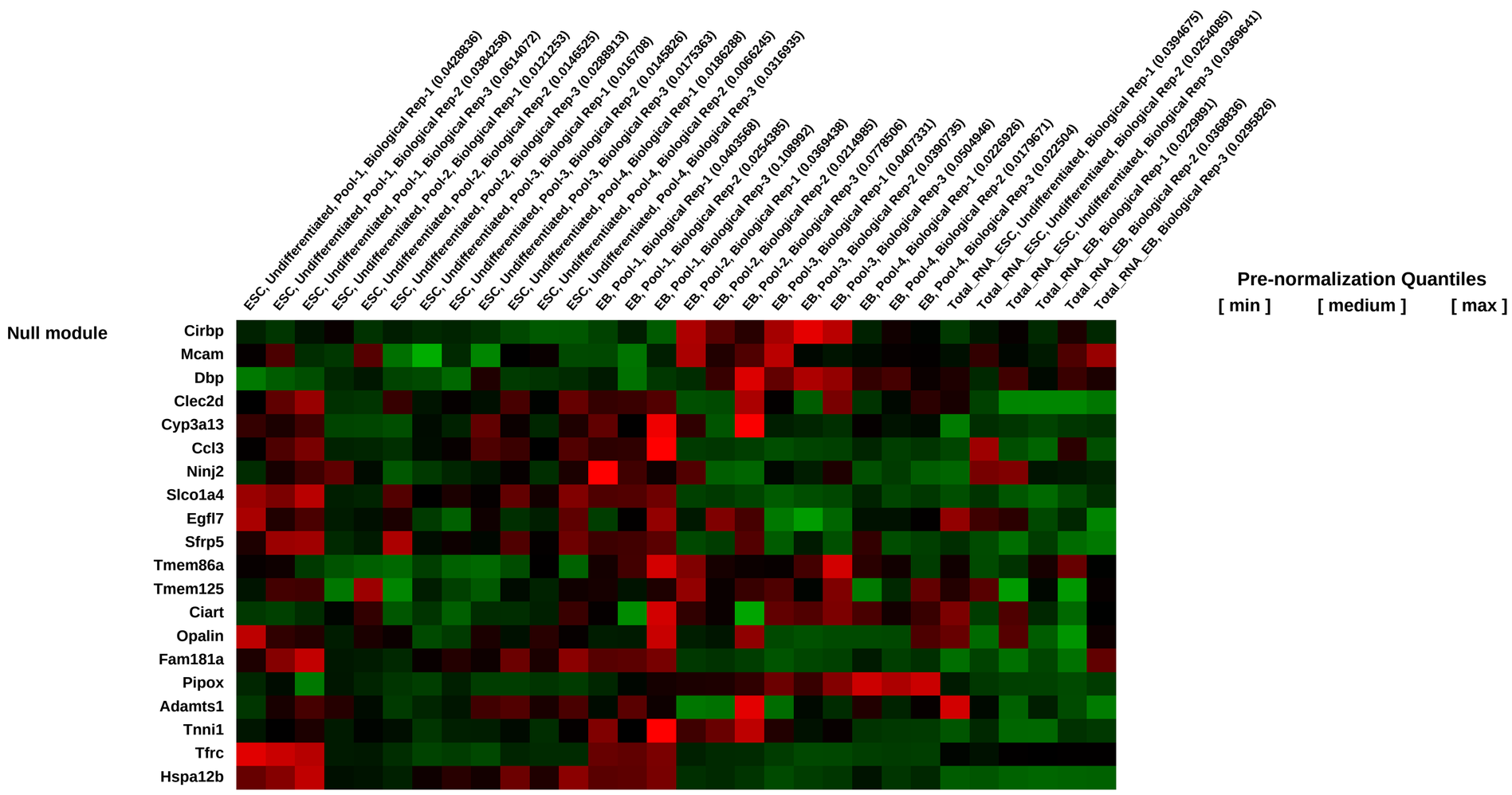

GEO Series "GSE54656" Expression Profiles

Num of samples in this series: 27

Scale of expression profile Z-scores

-3.0 -2.0 -1.0 0.0 1.0 2.0 3.0

GEO Link:	http://www.ncbi.nlm.nih.gov/geo/query/acc.cgi?acc=GSE54656
Status:	Public on Feb 05 2014
Title:	G9a influences neuronal subtype specification in striatum
Organism:	Mus musculus
Experiment type:	Expression profiling by array
Platform:	GPL1261
Pubmed ID:	24584053
Summary & Design:	**Summary:** Cocaine-mediated repression of the histone methyltransferase (HMT) G9a has recently been implicated in transcriptional, morphological, and behavioral responses to chronic cocaine administration. Here, using a ribosomal affinity purification approach, we find that G9a repression by cocaine occurs in both Drd1 (striatonigral)- and Drd2 (striatopallidal)-expressing medium spiny neurons (MSNs). Conditional knockout and overexpression of G9a within these distinct cell types, however, reveals divergent behavioral phenotypes in response to repeated cocaine treatment. Our studies further indicate that such developmental deletion of G9a selectively in Drd2 neurons results in the unsilencing of transcriptional programs normally specific to striatonigral neurons, and the acquisition of Drd1-associated projection and electrophysiological properties. This partial striatopallidal to striatonigral â switchingâ phenotype in mice indicates a novel role for G9a in contributing to neuronal subtype identity, and suggests a critical function for cell-type specific histone methylation patterns in the regulation of behavioral responses to environmental stimuli. **Overall design:** Polyribosome associated mRNAs from 2-5 month old, age and sex matched Drd1-Cre; Drd1-TRAP; G9afl/fl and Drd1-TRAP; G9afl/fl, Drd2-Cre; Drd2-TRAP; G9afl/fl and Drd2-TRAP; G9afl/fl mice (n = 2-4 mice/genotype/drug treatment, 2 hours after the last of eight repeated cocaine injections of 20 mg/kg/day) were obtained as previously described. EGFP labeled ribosomes and associated mRNAs were immunoprecipitated using a mix of two monoclonal anti-GFP antibodies (50 ¸…g of clones #19C8 and #19F7 for each IP, available at Sloan-Kettering Monoclonal Antibody Facility). Purified mRNA was amplified and processed for microarray and qPCR analysis using the Affymetrix two-cycle cDNA Synthesis kit (Affymetrix) as previously described. Affymetrix Mouse Genome 430 2.0 arrays were used in all experiments. Information regarding the array design and features can be found at www.affymetrix.com. Mouse Genome 430 2.0 arrays were scanned using the GeneChip Scanner 3000 (Affymetrix) and globally scaled to 150 using the Affymetrix GeneChip Operating Software (GCOS v1.4).

Background corr dist: KL-Divergence = 0.1756, L1-Distance = 0.0521, L2-Distance = 0.0065, Normal std = 0.3487

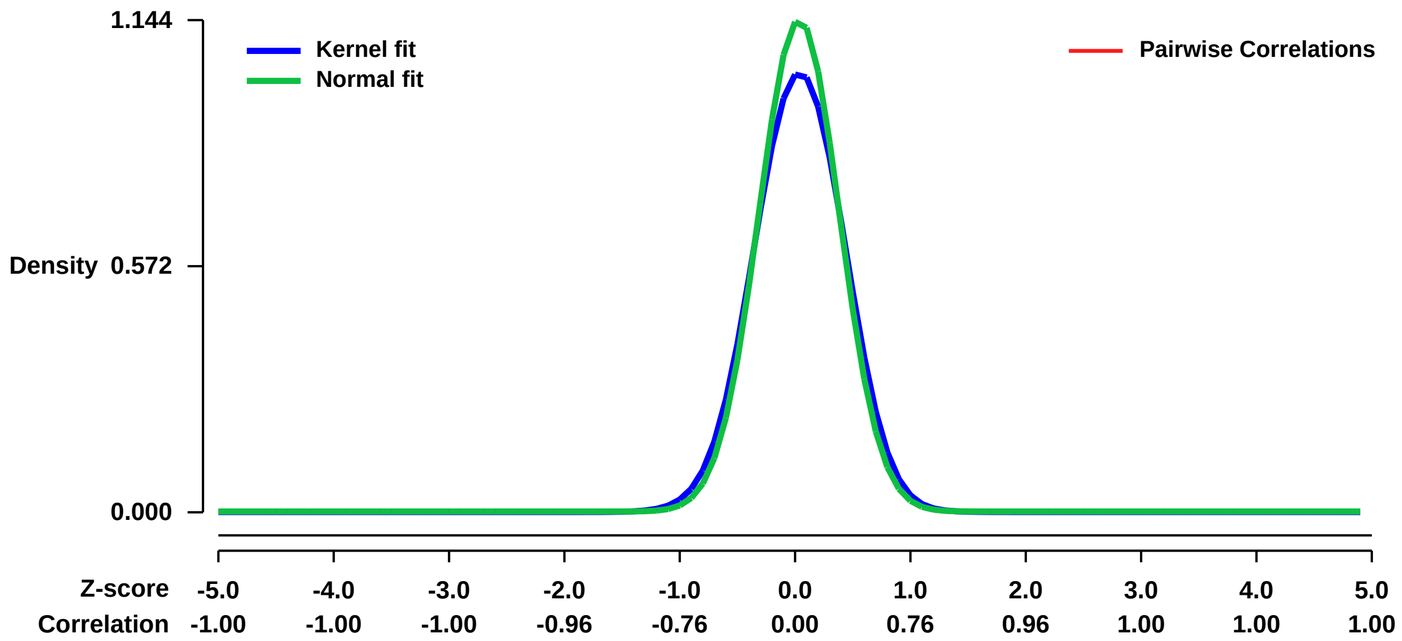

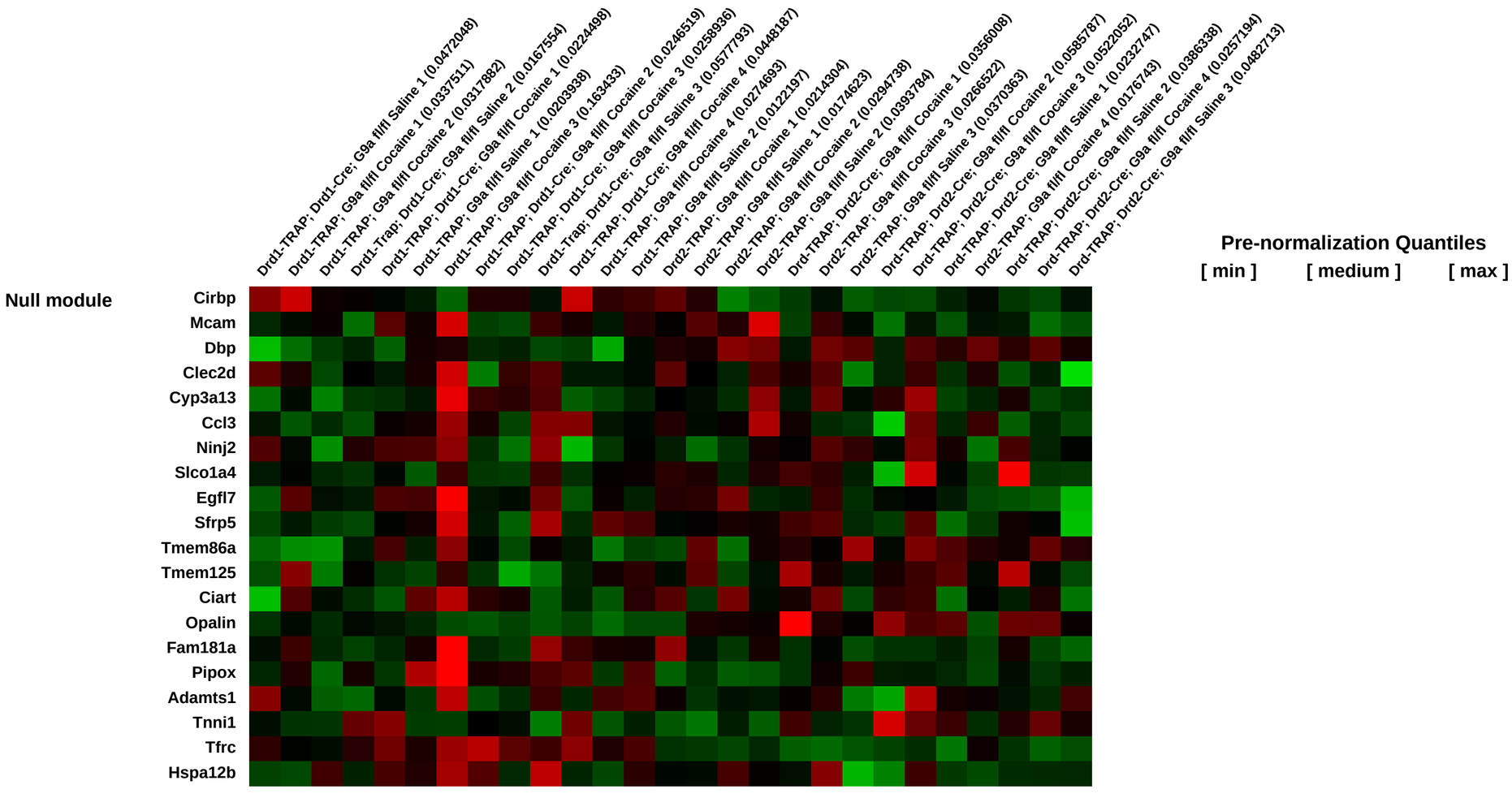

GEO Series "GSE55028" Expression Profiles

Num of samples in this series: 6

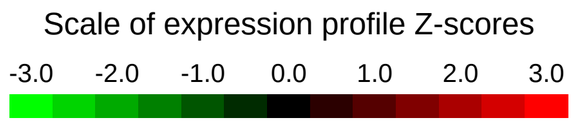

GEO Link:	**http://www.ncbi.nlm.nih.gov/geo/query/acc.cgi?acc=GSE55028**
Status:	**Public on Apr 01 2014**
Title:	**CMPF alters expression of genes related to metabolism in isolated mouse islets**
Organism:	**Mus musculus**
Experiment type:	**Expression profiling by array**
Platform:	**GPL1261**
Pubmed ID:	
Summary & Design:	**Summary:** **CMPF is elevated in diabetes and is associated with impaired insulin secretion. We used microarrays to determine the effect of CMPF on gene expression in isolated islets.** **Overall design:** **Isolated islets from male CD1 mice were treated for 24h with vehicle control or 200uM CMPF.**

Background corr dist: **KL-Divergence = 0.0294, L1-Distance = 0.0116, L2-Distance = 0.0001, Normal std = 0.6652**

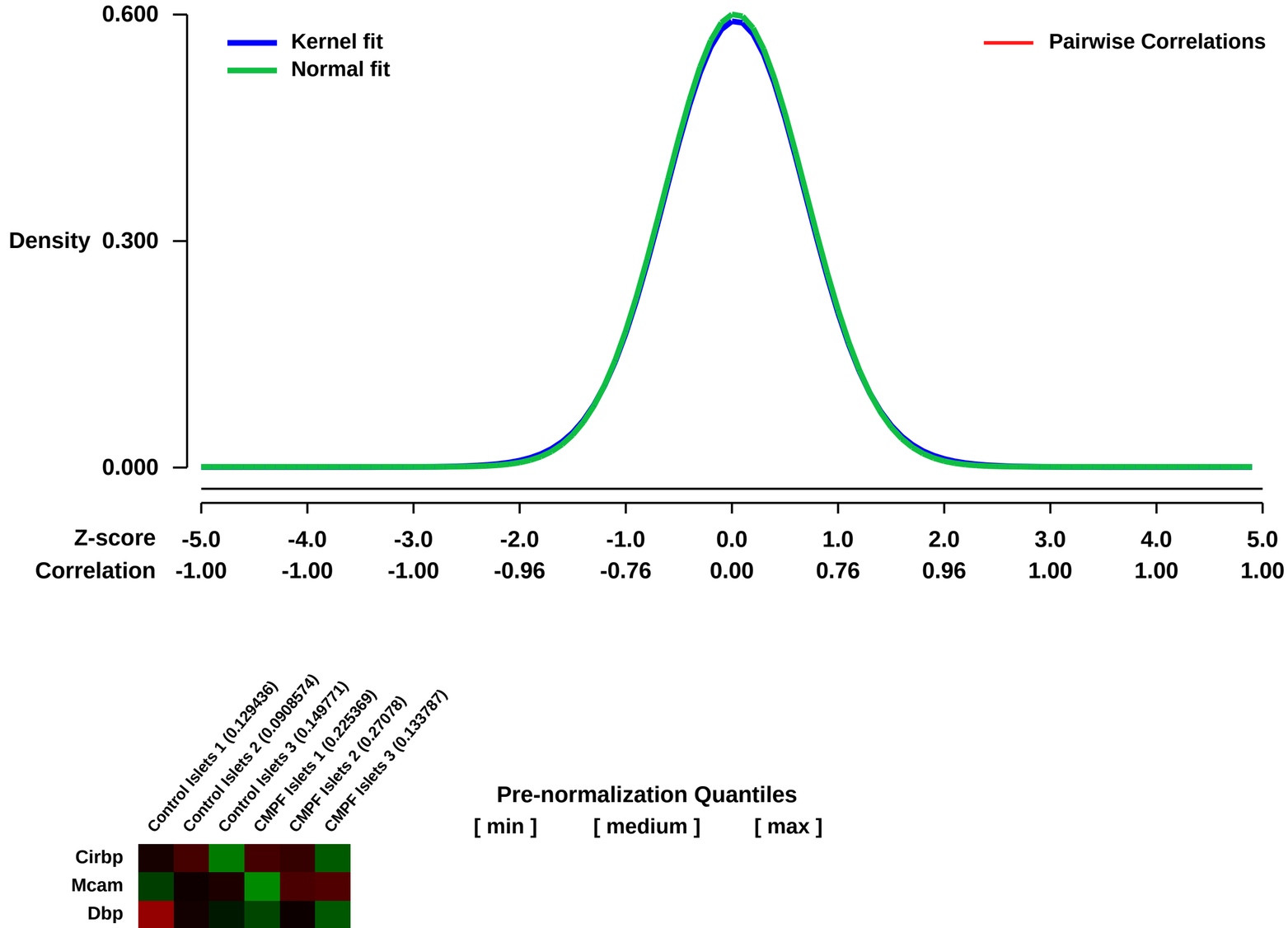

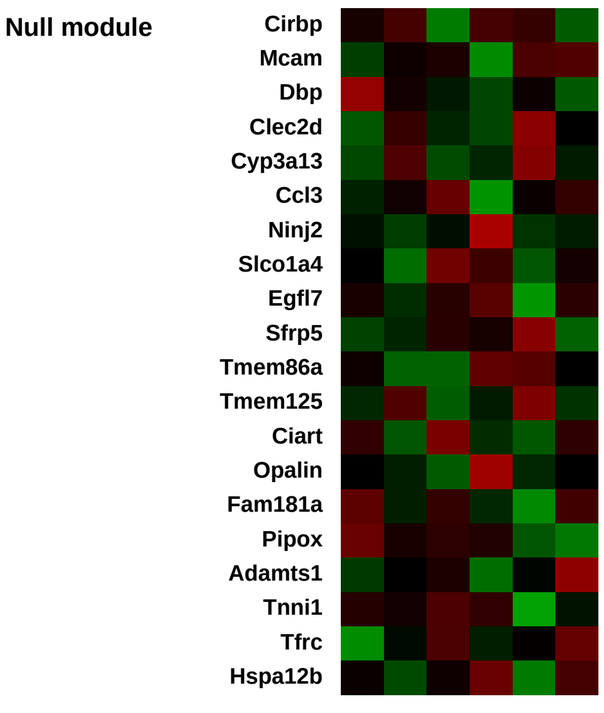

GEO Series "GSE46942" Expression Profiles

Num of samples in this series: 7

Scale of expression profile Z-scores

-3.0 -2.0 -1.0 0.0 1.0 2.0 3.0

GEO Link:	http://www.ncbi.nlm.nih.gov/geo/query/acc.cgi?acc=GSE46942
Status:	Public on May 16 2013
Title:	Transcription Factor Foxo1 Controls Memory CD8+ T Cell Responses To Infection [Affymetrix]
Organism:	Mus musculus
Experiment type:	Expression profiling by array
Platform:	GPL1261
Pubmed ID:	23932570
Summary & Design:	**Summary:** Memory T cells provide immunity against pathogen reinvasion, but mechanisms of their long-term maintenance is unclear. Here we show that mice with the deletion of the transcription factor Foxo1 in activated CD8+ T cells had defective secondary but not primary responses to Listeria monocytogenes infection. Compared to short-lived effector T cells, memory precursor effector T cells expressed higher amounts of Foxo1 that promoted their generation and maintenance. Gene expression profiling and chromatin immunoprecipitation sequencing experiments revealed the chemokine receptor CCR7 and the transcription factor TCF1 as novel Foxo1-bound target genes with critical functions in memory T cell trafficking and transcriptional regulation. These findings demonstrate that Foxo1 is selectively incorporated into the genetic program that regulates memory but not effector CD8+ T cell responses to infection. **Overall design:** Wild-type and GzmB-cre Foxo1fl/fl CD27hiKLRG1lo OT-I T cells were isolated by FACS sorting at 7 days post LM-OVA infection. RNA was prepared with the miRNeasy kit according to the manufacturerâ s instructions (Qiagen). RNA amplification, labeling and hybridization to Mouse 430 2.0 Array chips (Affymetrix) were carried out at the Genomics Core Facility of Memorial Sloan-Kettering Cancer Center.

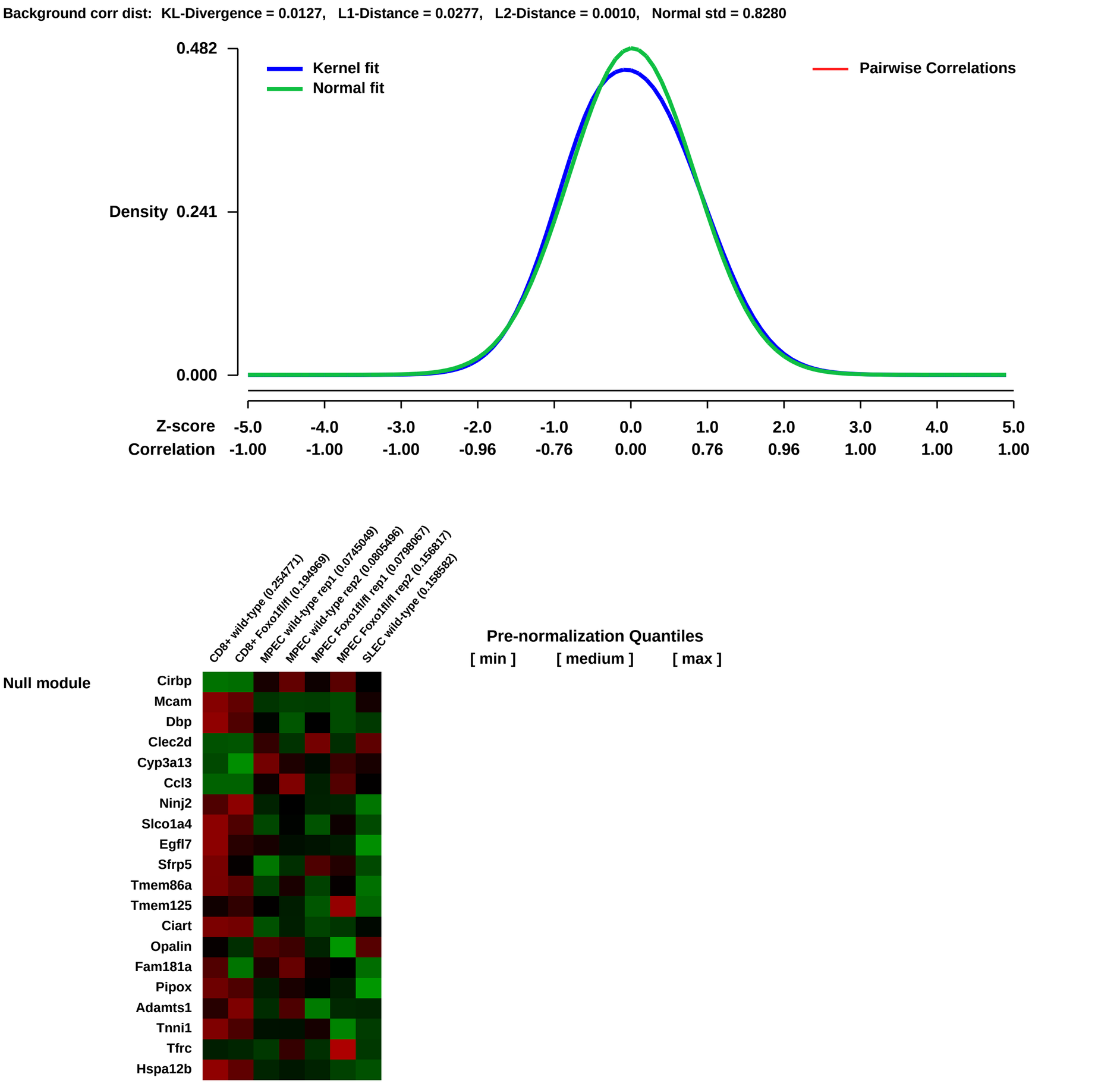

GEO Series "GSE35763" Expression Profiles

Num of samples in this series: 6

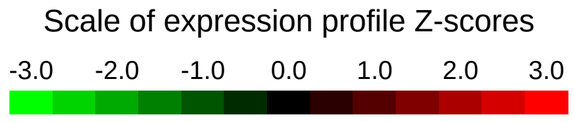

GEO Link:	http://www.ncbi.nlm.nih.gov/geo/query/acc.cgi?acc=GSE35763
Status:	Public on Jun 01 2012
Title:	Effect of fluoxetine treatment on translational profiles of Glt25d2 cortical pyramidal cells
Organism:	Mus musculus
Experiment type:	Expression profiling by array
Platform:	GPL1261
Pubmed ID:	22632977
Summary & Design:	**Summary:** Molecular phenotyping of cell types and neural circuits underlying pathological neuropsychiatric conditions and their responses to therapy provides one avenue for the development of more specific and effective treatments. In this study, we identify a cell population in the cerebral cortex that shows robust and specific molecular adaptations following long-term SSRI treatment. We employed the bacTRAP strategy, which uses BAC transgenic mice expressing EGFP-tagged ribosomal protein L10a in specific cell populations, to affinity purify polysome-bound mRNAs from S100a10-expressing corticostriatal projection neurons. We show that the S100a10 cells are a unique population of cortical cells that are strongly and specifically responsive to chronic SSRI administration and that this response requires p11 (the protein product of S100a10). Our data demonstrate that the beneficial actions of antidepressant therapy can be mediated by a single cell type that is positioned to normalize activity between cortical and subcortical sites, and suggest that development of drugs that specifically target the activity of these cells may result in improved therapies to treat depression. **Overall design:** Glt25d2 bacTRAP mice were administered either fluoxetine (FLX) or vehicle (VEH) in their drinking water for 15-18 days. Three independent TRAP replicates from cortex of each group were then collected. Total RNA from the immunoprecipitates was amplified and hybridized. Data were normalized with the GCRMA algorithm and replicates were averaged across conditions. We recommend filtering data to remove probe sets with normalized expression values less than 50 in at least one condition. Because the S100a10 BAC labels some non-neuronal cells, we recommend only probe sets listed in Table S1 of the accompanying paper be included in the analysis.

Background corr dist: KL-Divergence = 0.0307, L1-Distance = 0.0183, L2-Distance = 0.0004, Normal std = 0.6655

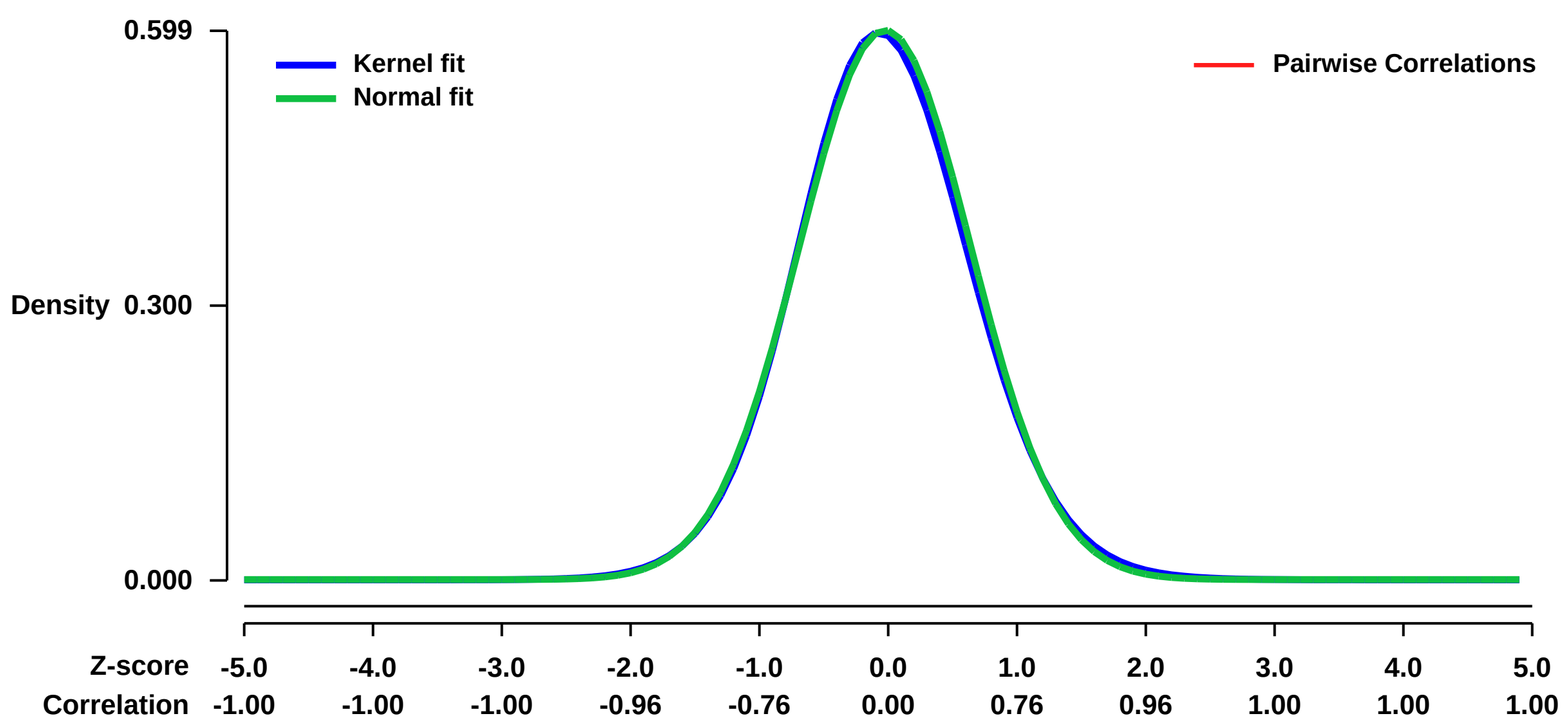

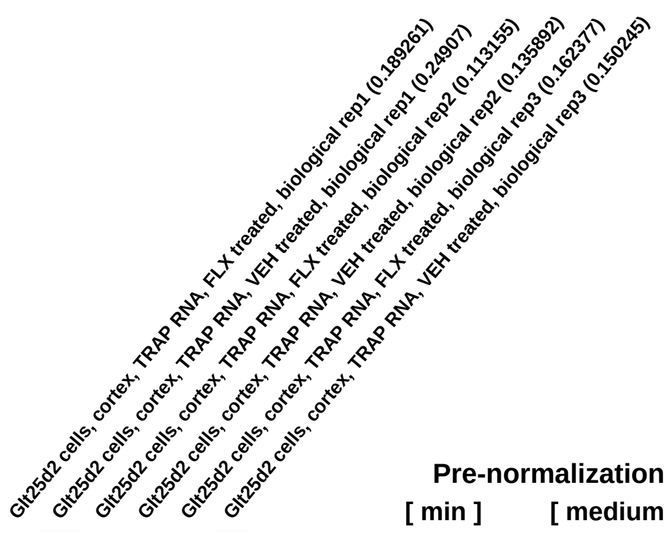

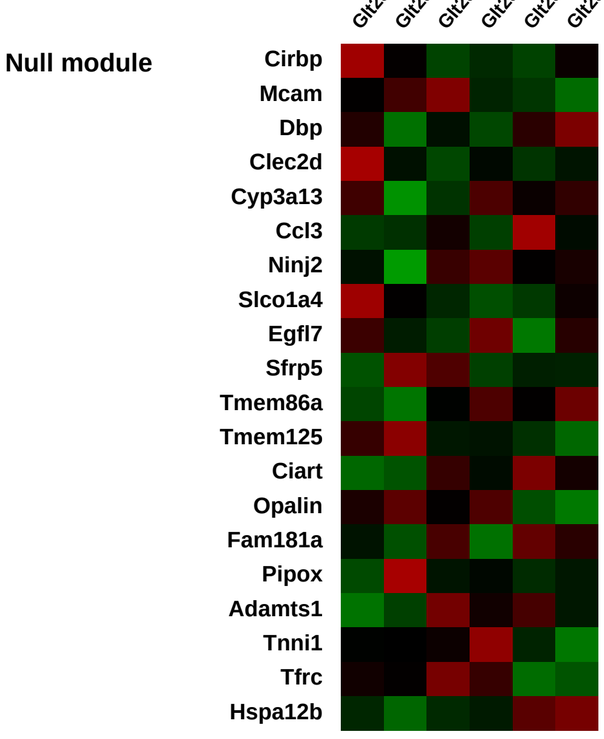

GEO Series "GSE8313" Expression Profiles

Num of samples in this series: 6

Scale of expression profile Z-scores

-3.0 -2.0 -1.0 0.0 1.0 2.0 3.0

GEO Link:	http://www.ncbi.nlm.nih.gov/geo/query/acc.cgi?acc=GSE8313
Status:	Public on Dec 23 2007
Title:	integrin alpha7 overexpression effects on skeletal muscle transcriptions
Organism:	Mus musculus
Experiment type:	Expression profiling by array
Platform:	GPL1261
Pubmed ID:	18045857
Summary & Design:	**Summary:** Analysis of integrin alpha7 transgenic mice skeletal muscle transcription profiles comparing to wild type controls. Integrin alpha7 is the major laminin binding integrin in muscle cells. Enhancing its expression has been demonstrated to alleviate pathology in a murine model of Duchenne muscular dystrophy. Results of this study provide insights into the effects of increasing integrin alpha7 expression on skeletal muscle transcription and physiology in vivo. This analysis also evaluates any potential possible side effects associate with enhancing integrin alpha7 in skeletal muscle. **Keywords:** transgenic mice comparision to wild type controls **Overall design:** Equal amount of total RNA from six animals of each genotype were pooled to generate a biological replicate. Total of three biological replicates were used. Together, 18 mice of each genotype were used in this analysis.

Background corr dist: KL-Divergence = 0.0494, L1-Distance = 0.0189, L2-Distance = 0.0004, Normal std = 0.5755

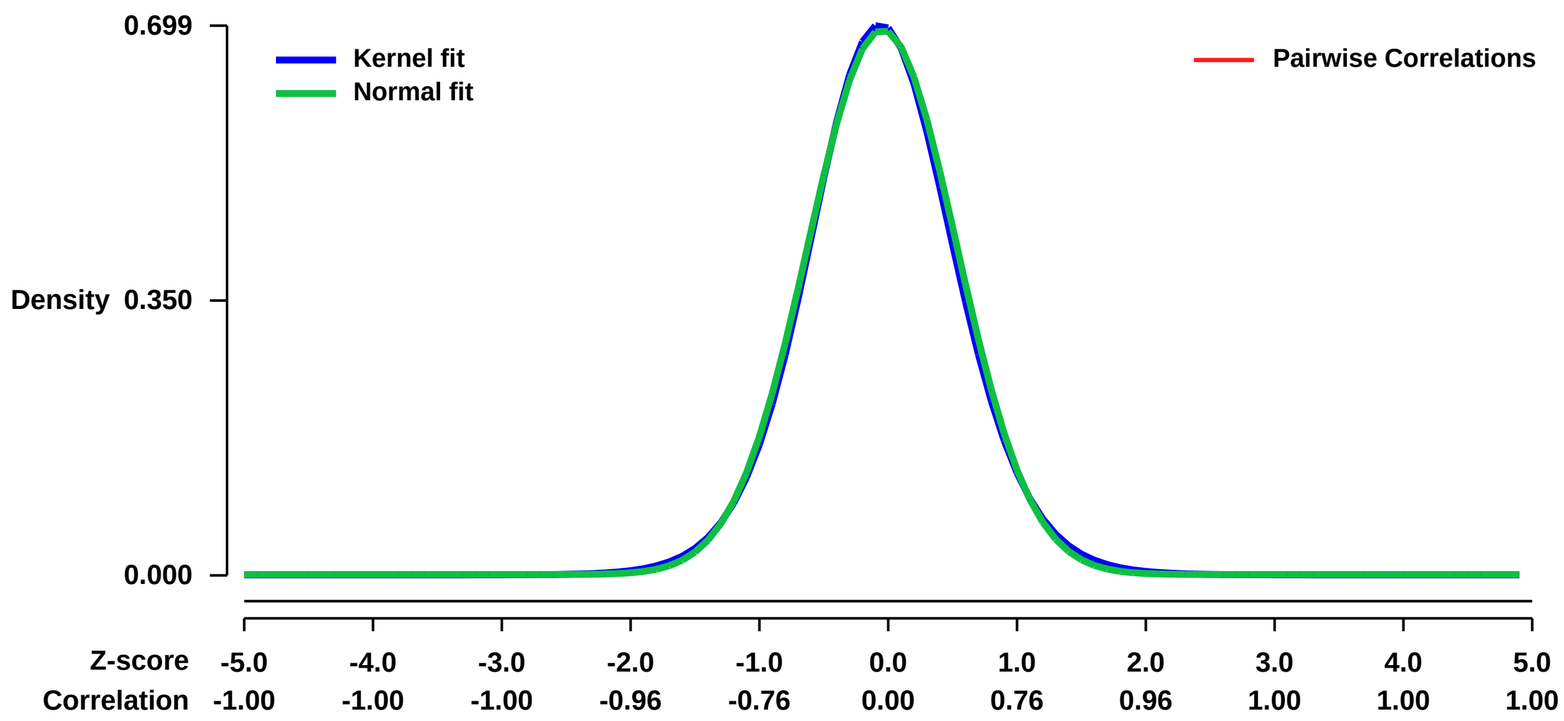

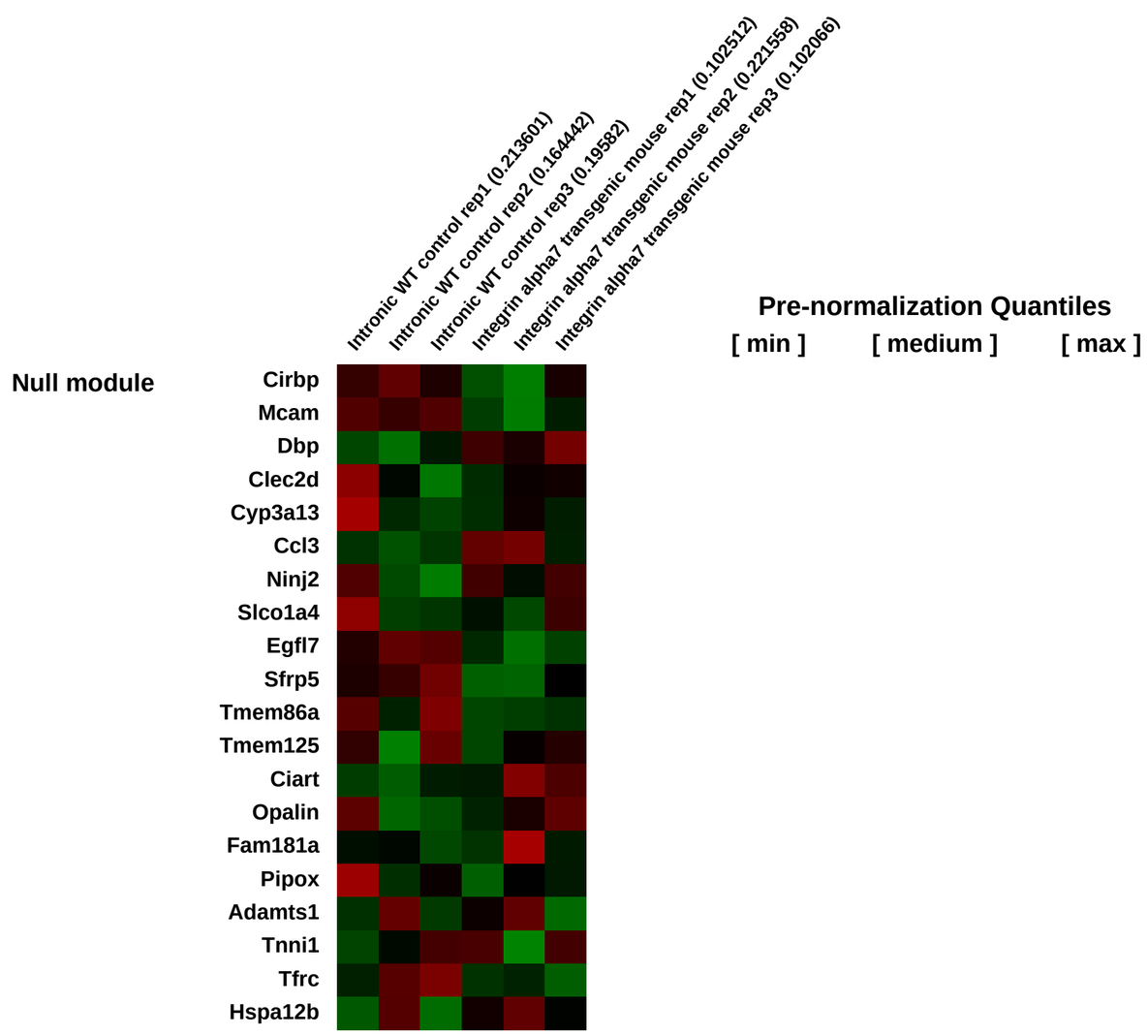

GEO Series "GSE38672" Expression Profiles

Num of samples in this series: 6

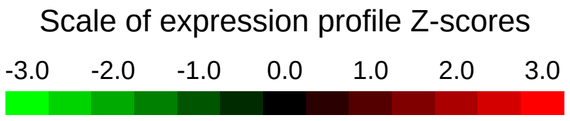

GEO Link:	**http://www.ncbi.nlm.nih.gov/geo/query/acc.cgi?acc=GSE38672**
Status:	**Public on Nov 16 2012**
Title:	**Deletion of miRNA processing enzyme Dicer in POMC-expressing cells leads to neurodegeneration and development of obesity**
Organism:	**Mus musculus**
Experiment type:	**Expression profiling by array**
Platform:	**GPL1261**
Pubmed ID:	
Summary & Design:	**Summary:** **The activity of the endoribonuclease Dicer is crucial to produce the mature form of most microRNAs (miRNAs). Recent studies indicate that lack of miRNAs in different neuronal types results in a range of anatomical and behavioural phenotypes. In the present study we aimed to investigate the developmental and metabolic consequences of miRNA ablation in hypothalamic POMC neurons studying mice with a conditional deletion of Dicer in this population of neurons (POMCDicerKO). These mice exhibited a progressive obese phenotype characterized by hyperphagia, increased adiposity, hyperleptinemia, defective glucose metabolism and alterations in the pituitary-adrenal axis. The development of the obese phenotype was paralleled by a POMC neuron degenerative process that was complete by 6 weeks of age. Furthermore, immunohistochemistry and gene expression studies in control C57Bl/6 adult mice showed that Dicer was expressed in relevant hypothalamic areas and neurons implicated in energy balance, and that its expression was regulated by nutrient availability. Collectively, our results highlight a crucial role for miRNAs in POMC neuron survival and the consequent development of neurodegenerative obesity.** **Overall design:** **Total RNA was extracted from hypothalamic microdissections of 2-week old control and POMCDicerKO mice using the RNeasy micro spin columns (Qiagen, Venlo, The Netherlands). Ten micrograms of total RNA were converted into cRNA, biotinylated, fragmented, and hybridized to GeneChip Mouse Genome 430 2.0 (Affymetrix, Santa Clara, CA). Six microarrays were hybridized with three independent samples from control and POMCDicerKO mice.**

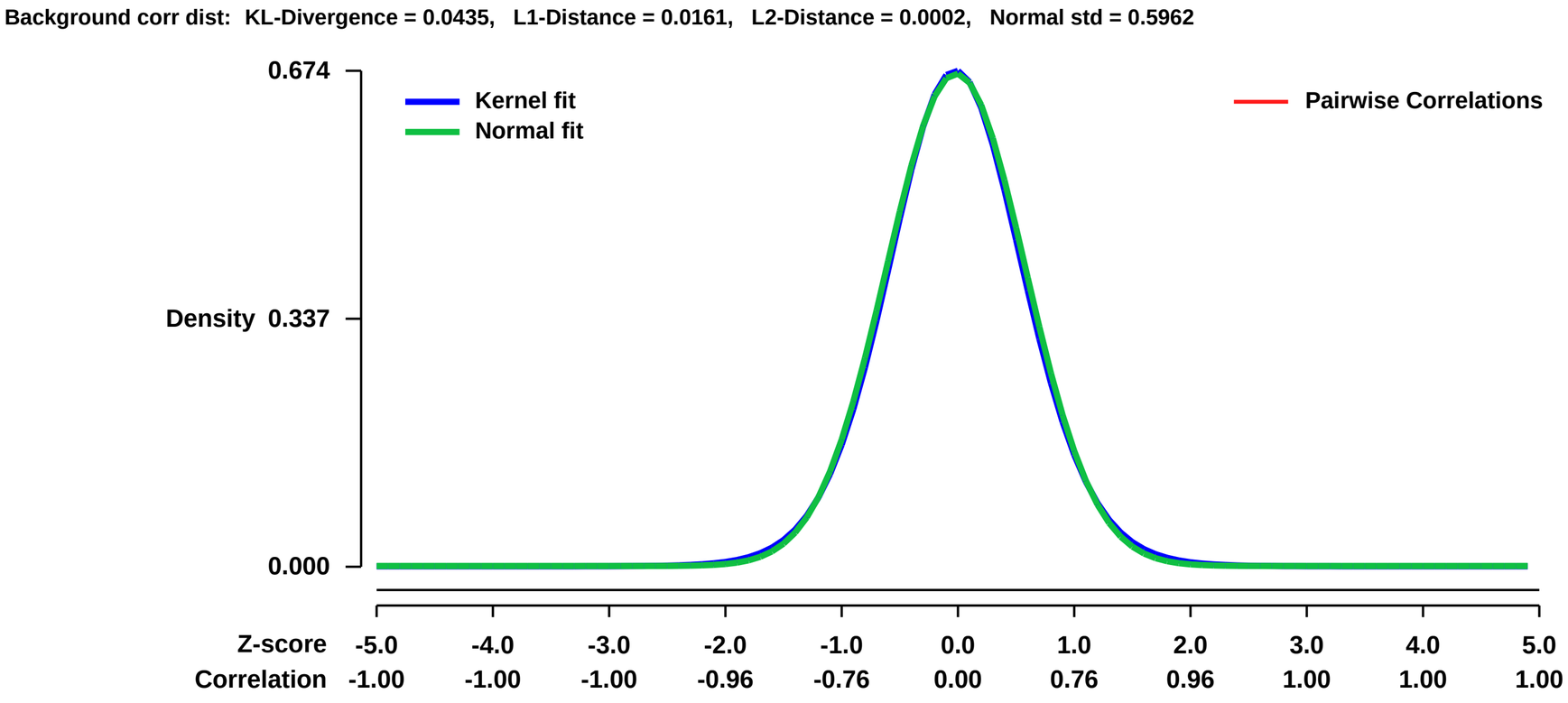

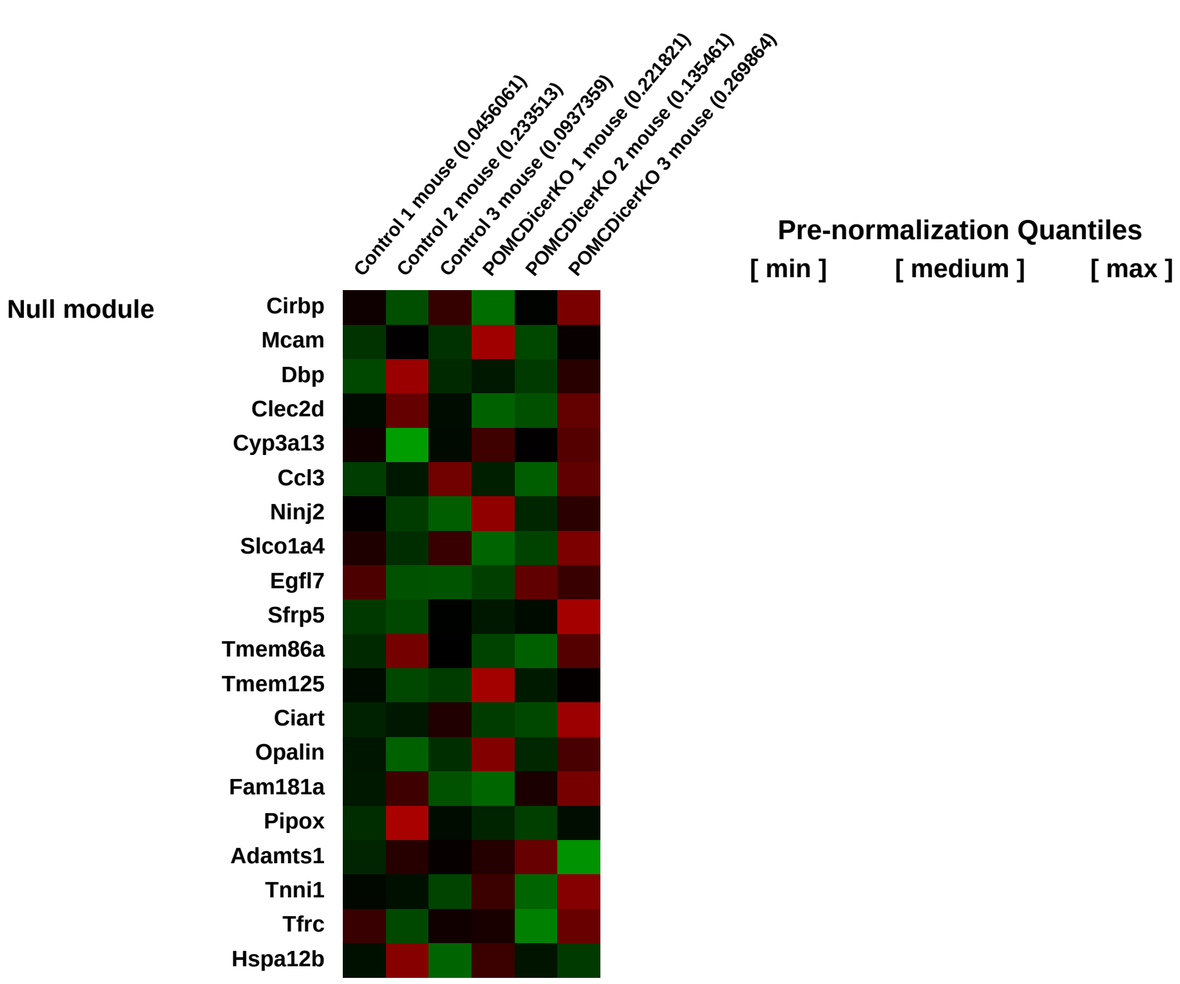

GEO Series "GSE3100" Expression Profiles

Num of samples in this series: 23

Scale of expression profile Z-scores

-3.0 -2.0 -1.0 0.0 1.0 2.0 3.0

GEO Link:	**http://www.ncbi.nlm.nih.gov/geo/query/acc.cgi?acc=GSE3100**
Status:	**Public on Mar 01 2006**
Title:	**Cystic Fibrosis Mouse Lung Profiles**
Organism:	**Mus musculus**
Experiment type:	**Expression profiling by array**
Platform:	**GPL1261**
Pubmed ID:	**16614460**
Summary & Design:	**Summary:** **Gene expression profiling with microarrays was used to identify genes differentially expressed in the lungs of B6 and BALB CF mice compared to non-CF littermates** **Keywords: disease state analysis** **Overall design:** **BALB/c and C57BL/6 mice (male and female) were examined in CF-/- and CF+/+ genotypes. 3 arrays of each combination of strain sex and CF status were analyzed (except for B6 male CF, which only had two replicates)**

Background corr dist: **KL-Divergence = 0.2285, L1-Distance = 0.0493, L2-Distance = 0.0056, Normal std = 0.3145**

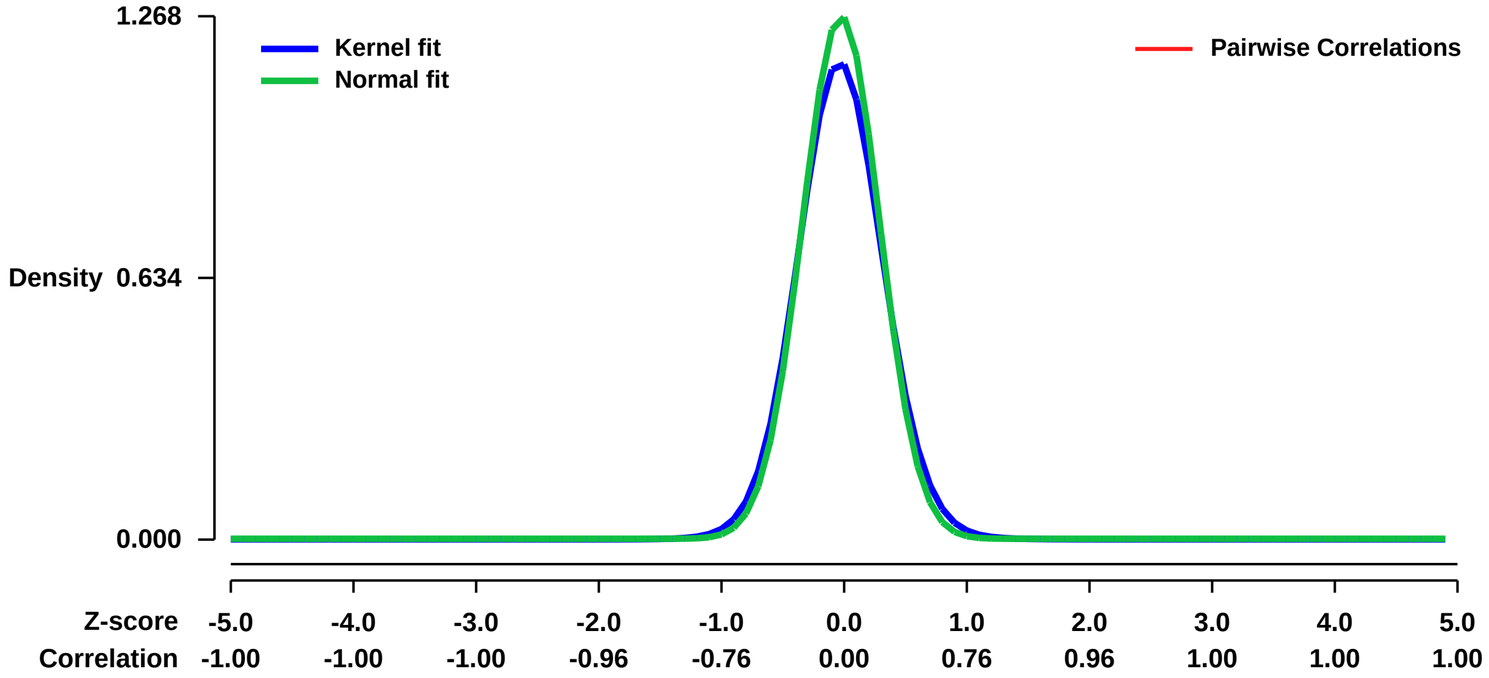

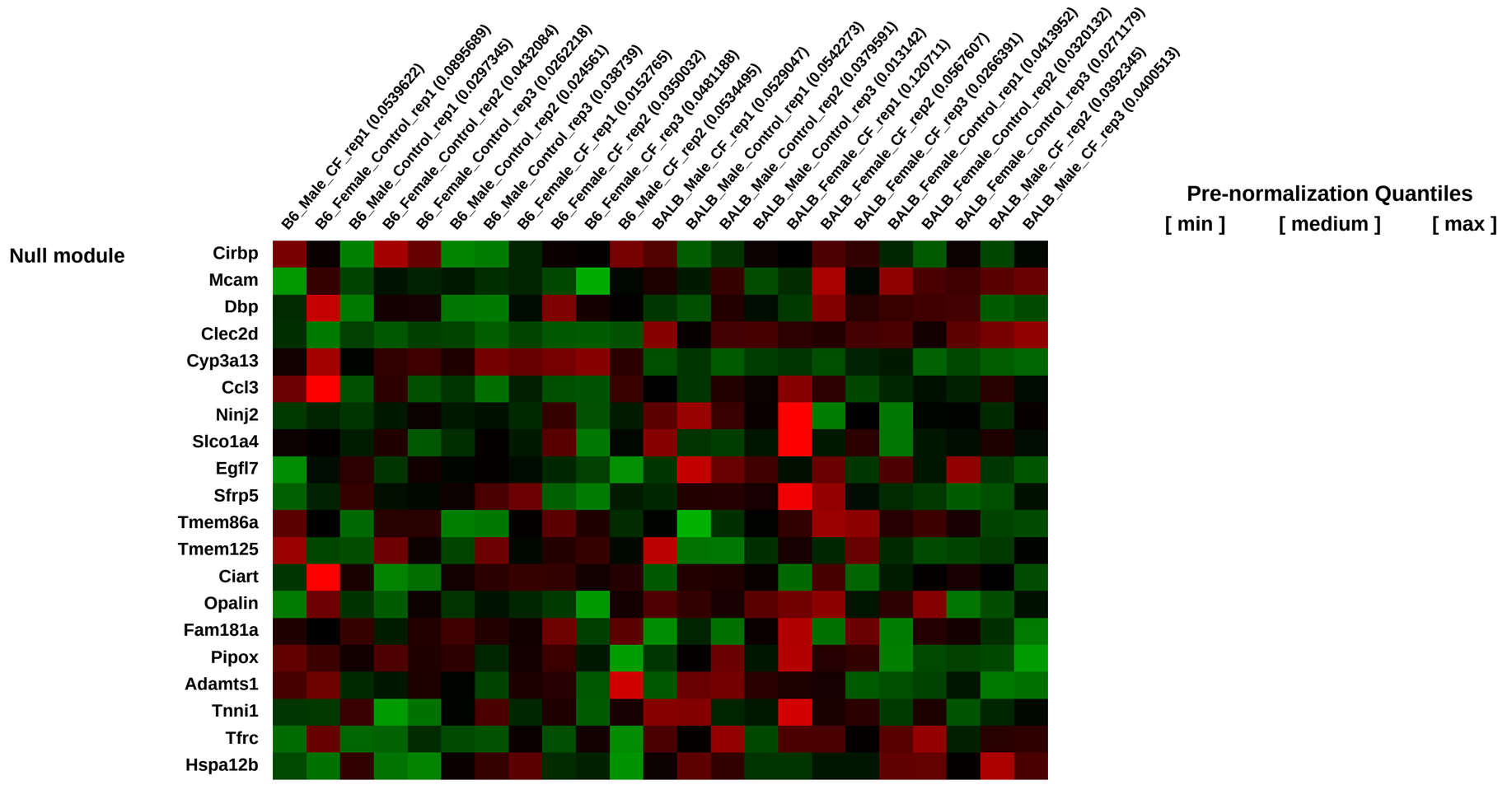

GEO Series "GSE19675" Expression Profiles

Num of samples in this series: 22

Scale of expression profile Z-scores

-3.0 -2.0 -1.0 0.0 1.0 2.0 3.0

GEO Link:	http://www.ncbi.nlm.nih.gov/geo/query/acc.cgi?acc=GSE19675
Status:	Public on Aug 02 2011
Title:	Negative regulation of the IFN/STAT signaling pathway by the Trim24 tumor suppressor protein through Rara inhibition
Organism:	Mus musculus
Experiment type:	Expression profiling by array
Platform:	GPL1261
Pubmed ID:	21768647
Summary & Design:	**Summary:** Recent genetic studies in mice have established a key role for the nuclear receptor coregulator Trim24 in liver tumor suppression and provided evidence that Trim24 suppresses hepatocarcinogenesis by inhibiting retinoic acid receptor alpha (Rara)-dependent transcription and cell proliferation. However, it is unknown which downstream targets of Rara regulated by Trim24 are critical for tumorigenesis. We report here that loss of Trim24 results in the overexpression of interferon (IFN)/STAT pathway genes in the liver, a process that occurs early in tumorigenesis and is more pronounced in tumors, despite the enhanced expression, late in the disease, of negative regulators such as Usp18, Socs1 and Socs2. Remarkably, Rara haplodeficiency, which was previously shown to suppress tumor development in Trim24-/- mice, also suppresses overexpression of the IFN/STAT pathway, thus providing evidence for a cross-pathway control that may be relevant to the transformation process. Biochemical studies revealed that Trim24 binds to the retinoic acid (RA)-responsive element in the Stat1 promoter in a RA-dependent manner and represses RA-induced transcription from this promoter. Together, these results identify Trim24 as a novel regulator of the IFN/STAT pathway and indicate that Trim24-mediated repression of the IFN/STAT signaling through Rara inhibition may play a critical role in preventing liver cancer. **Overall design:** Transcriptional profiling of mice at 5-weeks and 14-weeks of age.

Background corr dist: KL-Divergence = 0.1693, L1-Distance = 0.0423, L2-Distance = 0.0038, Normal std = 0.3544

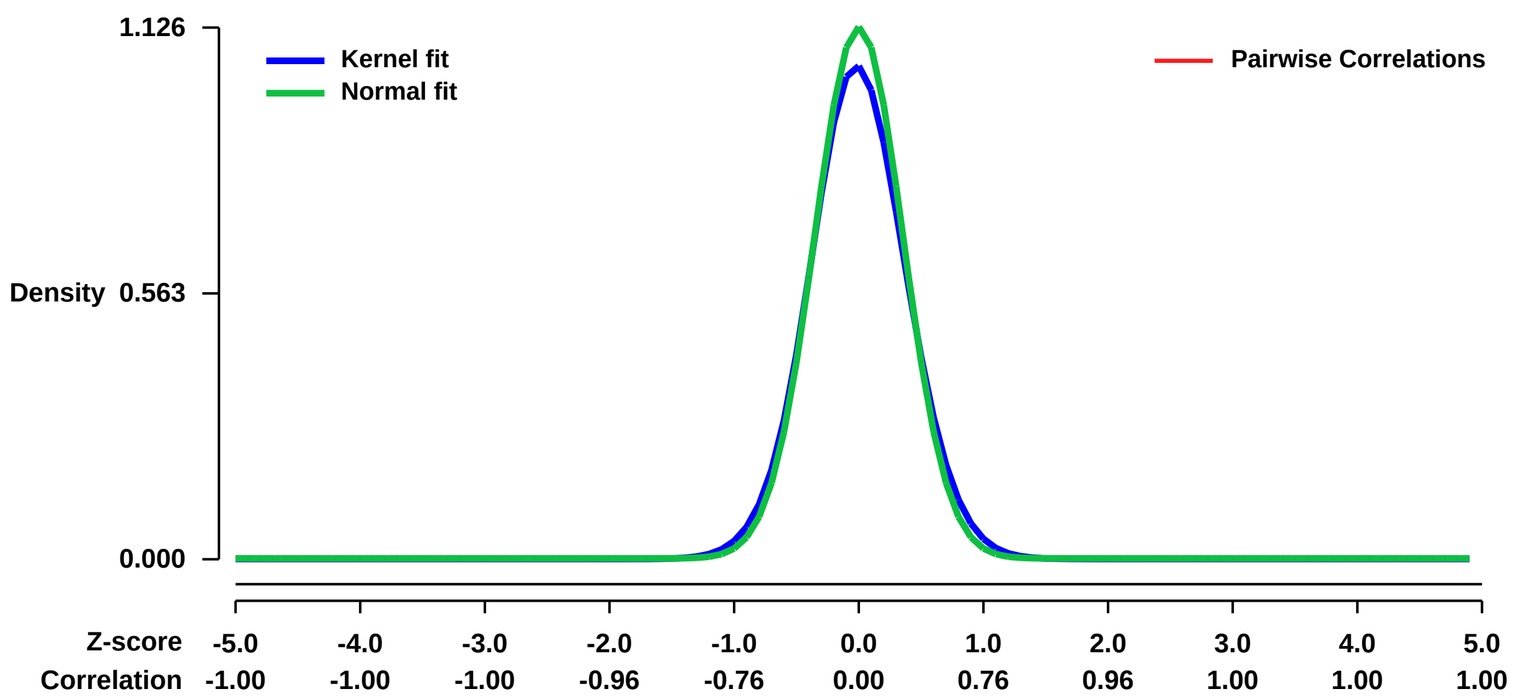

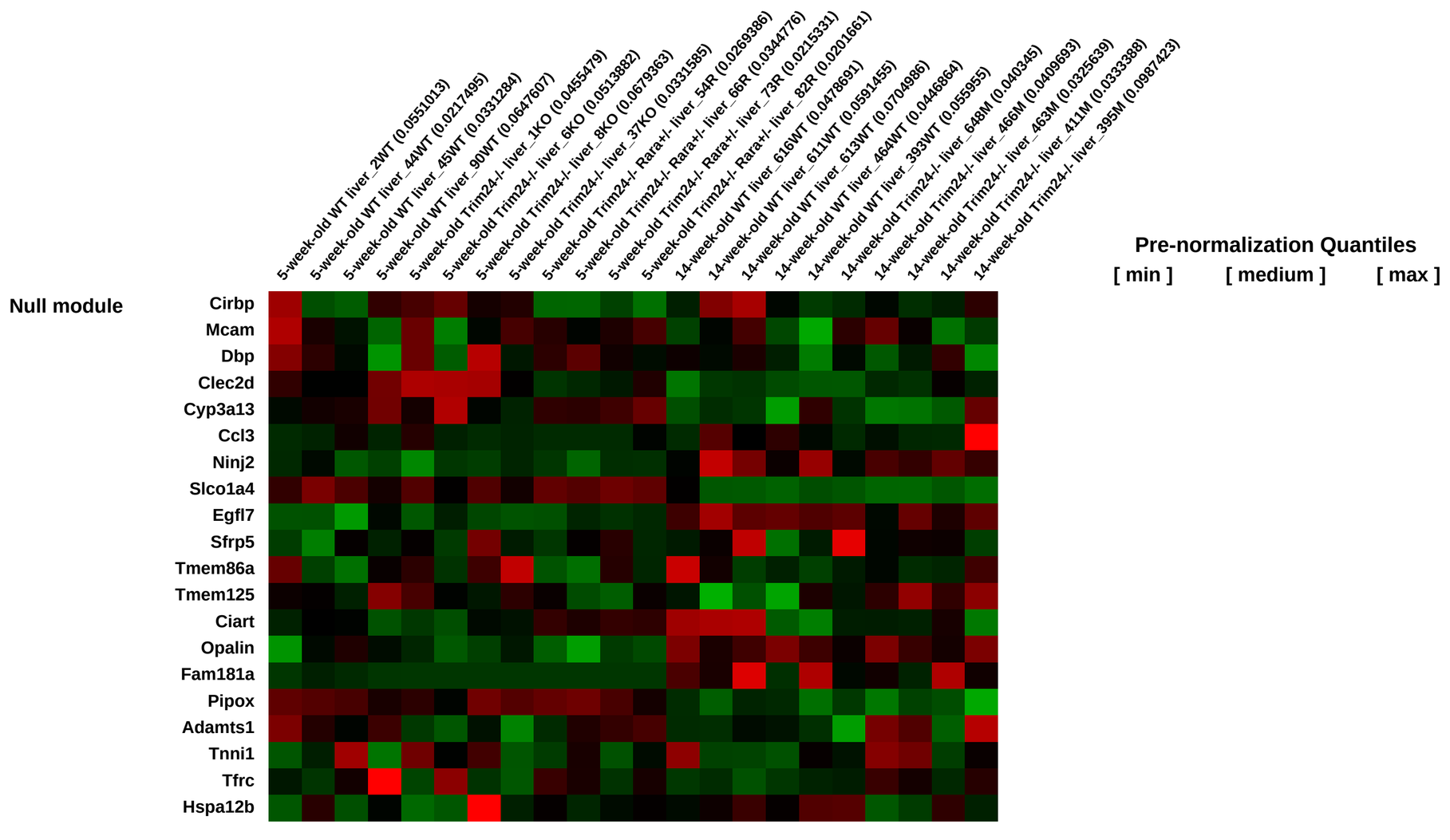

GEO Series "GSE13235" Expression Profiles

Num of samples in this series: 9

Scale of expression profile Z-scores

-3.0 -2.0 -1.0 0.0 1.0 2.0 3.0

GEO Link: http://www.ncbi.nlm.nih.gov/geo/query/acc.cgi?acc=GSE13235

Status: Public on Oct 17 2008

Title: Gene expression profile of mouse embryonic stem cells (D3-pOCT-mESC) grown in low concentrations of nitric oxide

Organism: Mus musculus

Experiment type: Expression profiling by array

Platform: GPL1261

Pubmed ID:

Summary & Design:

Summary:
In order to identify the genes regulated in mouse embryonic stem cells (mESC) by the effect of low concentrations of nitric oxide (NO), we analysed the transcriptome of cells treated with NO and compared it to those of cells cultured in the absence of leukemia inhibitory factor (LIF), and in the presence of LIF. We used the cell line D3-pOct4, which carries the enhanced Green Fluorescence Protein gene (eGFP) under the control of the Oct-4 promotor. This line is continuously maintained in the undifferentiated state in the presence of LIF, in comparison with the wild type line .

Overall design:
D3-pOct4 cells cultured in the presence of 1000 U/ml of LIF, in the absence of LIF, and in the absence of LIF supplemented with 2uM of diethylenetriamine nitric oxide adduct (DETA)/NO (Sigma) used as donor of nitric oxide. Treatments were maintained for seven days. RNA was extracted and analyzed by Bioanalyzer of Agilent. The cDNA microarray chip used was Mouse Genome 430_2.0 (Affymetrix) and the data were analyzed with GeneChip Operating System v1.4.0.036 using global scaling as the normalization method.

Background corr dist: KL-Divergence = 0.0684, L1-Distance = 0.0302, L2-Distance = 0.0016, Normal std = 0.5120

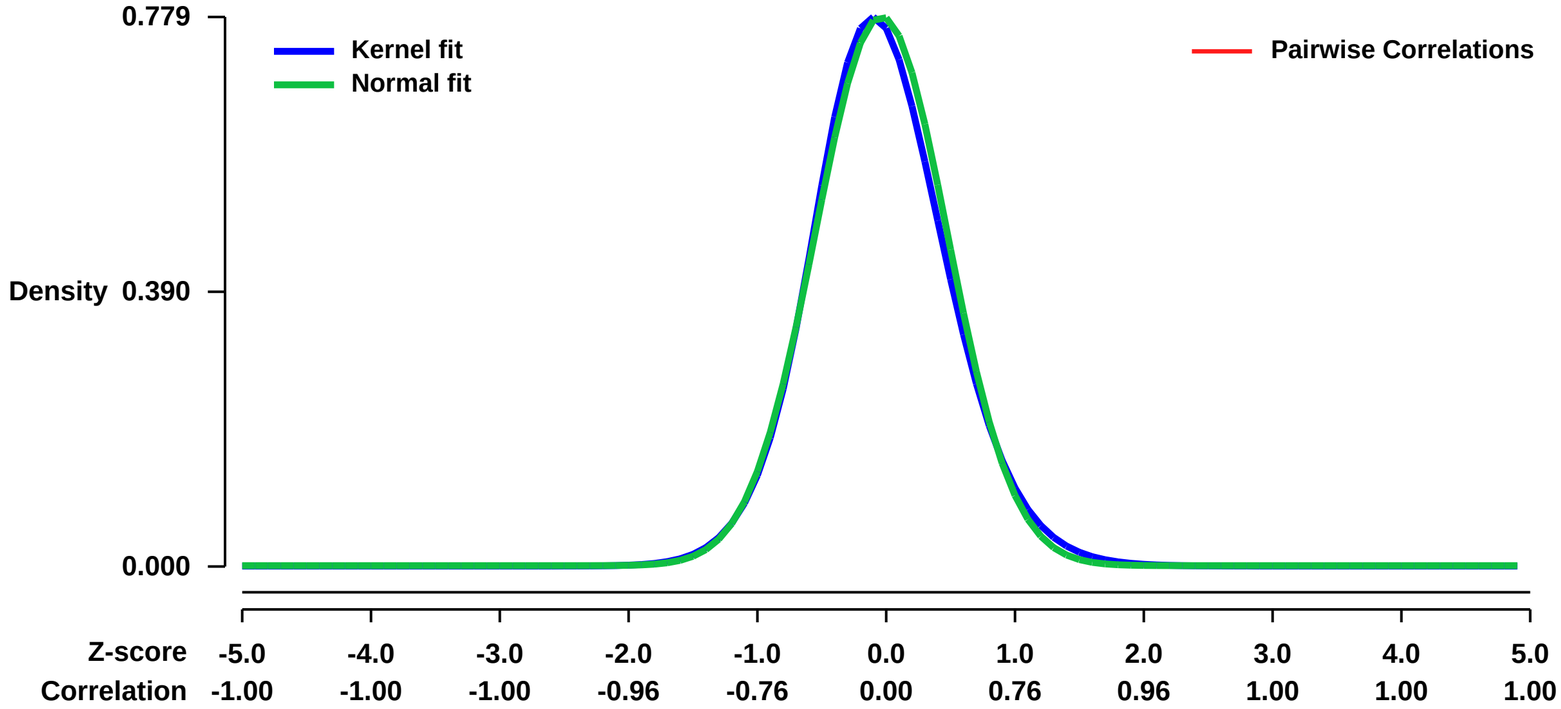

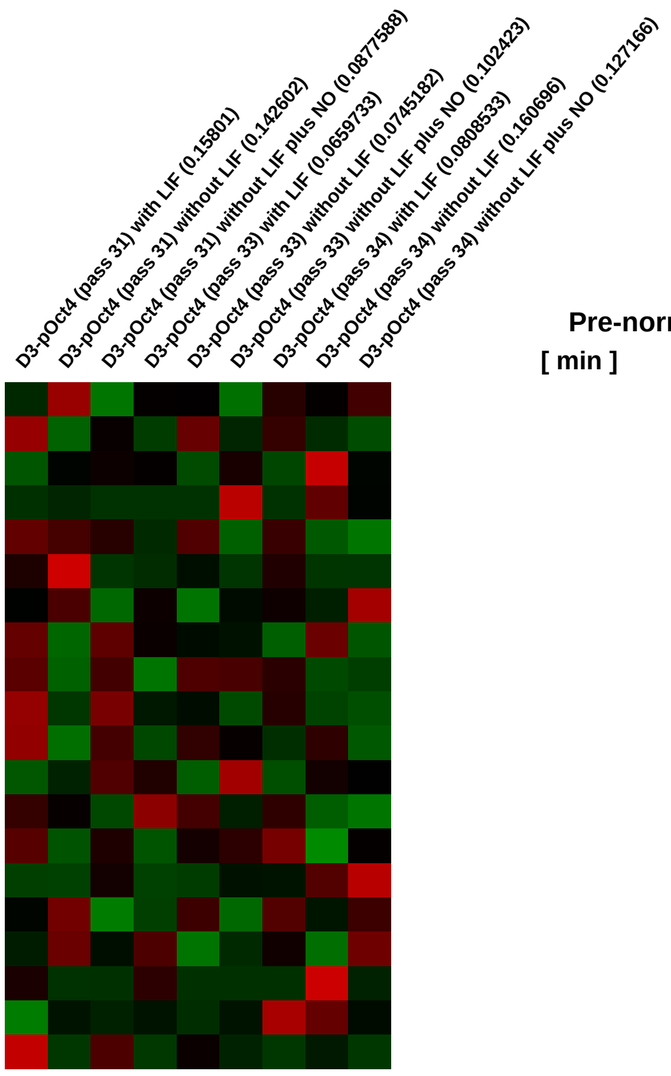

GEO Series "GSE11356" Expression Profiles

Num of samples in this series: 9

Scale of expression profile Z-scores

-3.0 -2.0 -1.0 0.0 1.0 2.0 3.0

GEO Link:	**http://www.ncbi.nlm.nih.gov/geo/query/acc.cgi?acc=GSE11356**
Status:	**Public on May 06 2008**
Title:	**Expression data from early and adult stages of mouse development**
Organism:	**Mus musculus**
Experiment type:	**Expression profiling by array**
Platform:	**GPL1261**
Pubmed ID:	
Summary & Design:	**Summary:** **DNA repair genes have been shown to be expressed in the early stages of mammalian development probably to reduce possible replication errors and genotoixc damages. Several birth defects and some cancers are due to inappropriate or defective DNA repair machinery indicating that a right activity of DNA repair genes in the early stages of fetal development are essential for an appropriate DNA function. Neuroblastoma (NB), an embryonal tumor deriving from neural crest cells (NCCs) is diagnosed in about 30% of patients within the first year of life. Moreover, several reports show that NB can be detected in foetus and in neonatal period.** **To assess gene expression profiling of DNA repair genes during early stage of development, we performed a genome-wide analysis of Neural Crest cells (NCCs) generating a gene expression database that can help to better understand the gene(s) involved in both genetic and cancer diseases. We found 11 genes involved in DNA repair activity during mouse embryo development overexpressed in early stages. Six out 11 were never been described in mouse embryology.** **Keywords: time course** **Overall design:** **Mouse embryos were collected at successive stages of early and adult development stages for RNA extraction and hybridization on Affymetrix microarrays. We sought to obtain homogeneous populations of NCCs by Laser Capture Microdissection (LCM) from embryos and adult in order to analyze DNA repair genes during mouse development. To that end, we collected cells at three time-points: at embryonal stage of 8.5 dpc: E8.5 (neural tube closure); at embryonal stage of 13.5dpc: E13.5 (dorsal root ganglion); at adult stage of 3 months postnatal: P90 (adrenal medulla).**

Background corr dist: KL-Divergence = 0.0700, L1-Distance = 0.0501, L2-Distance = 0.0047, Normal std = 0.5213

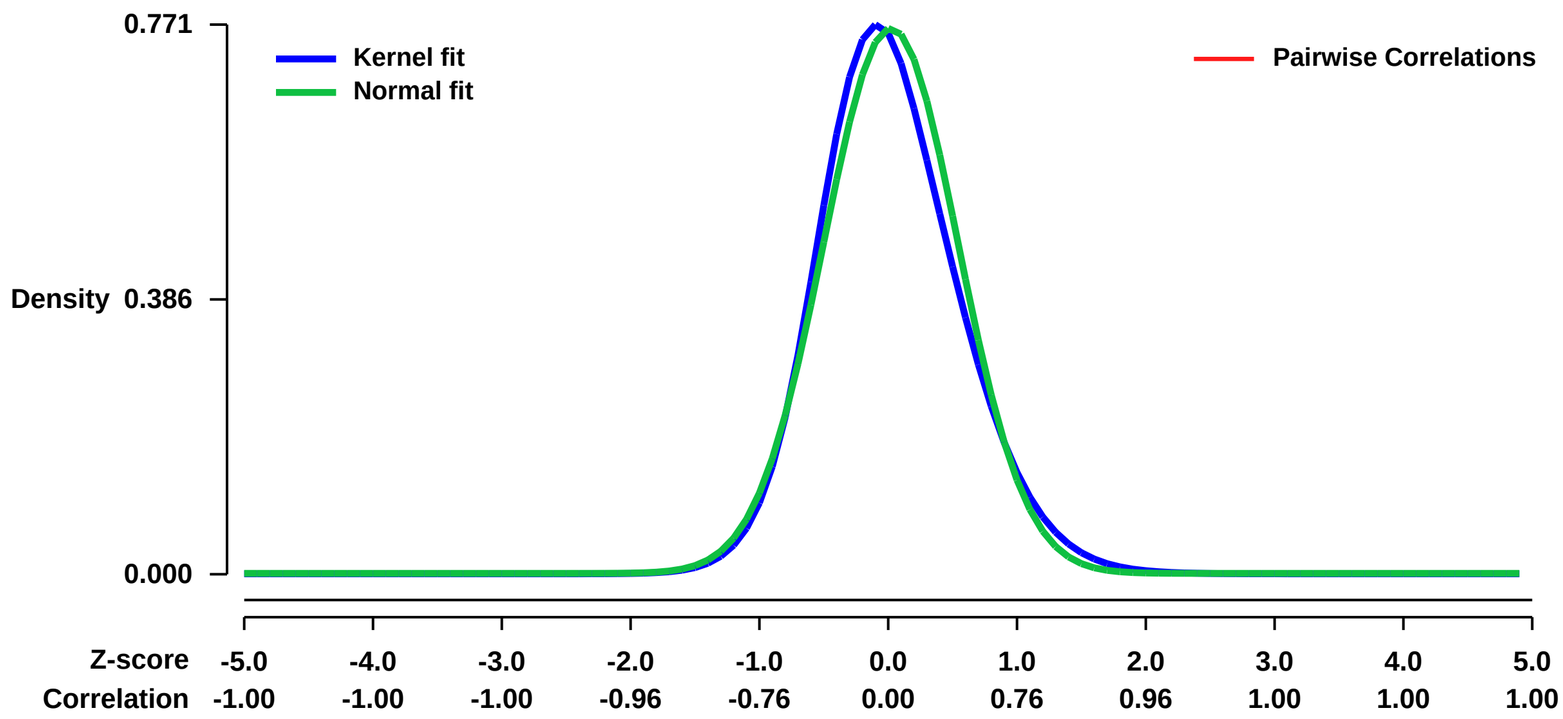

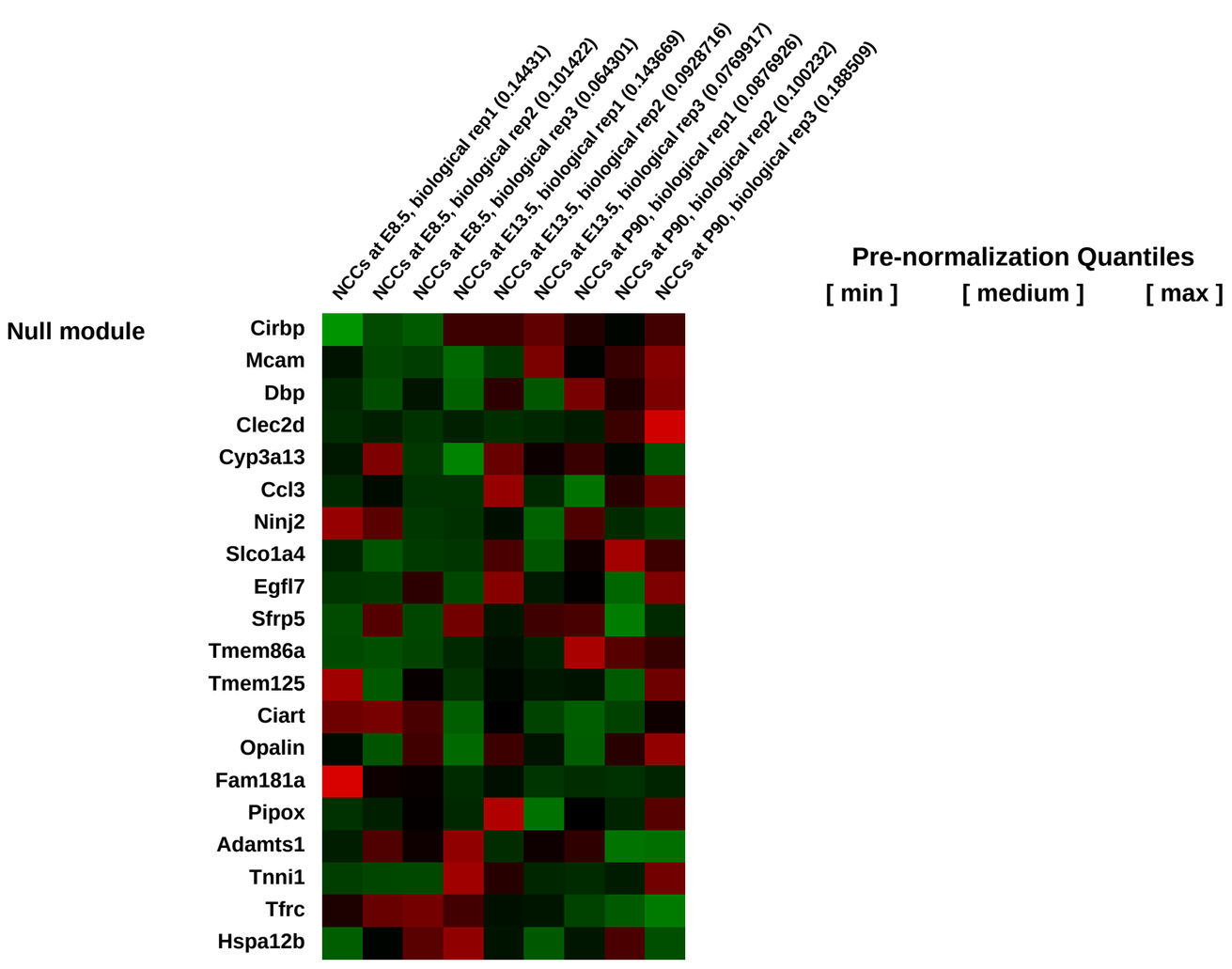

GEO Series "GSE18460" Expression Profiles

Num of samples in this series: 16

Scale of expression profile Z-scores

-3.0 -2.0 -1.0 0.0 1.0 2.0 3.0

GEO Link:	http://www.ncbi.nlm.nih.gov/geo/query/acc.cgi?acc=GSE18460
Status:	Public on Oct 08 2009
Title:	Lactobacillus acidophilus induces virus immune defense genes in murine dendritic cells by a TLR-2 dependent mechanism
Organism:	Mus musculus
Experiment type:	Expression profiling by array
Platform:	GPL1261
Pubmed ID:	20545783
Summary & Design:	**Summary:** Lactobacilli are probiotics that, among other health promoting effects, have been ascribed immunostimulating and virus preventive properties. Certain lactobacilli species have been shown to possess strong IL-12 inducing properties. As IL-12 production depends on the up-regulation of type I interferons, we hypothesized that the strong IL-12 inducing capacity of L. acidophilus NCFM in murine bone marrow derived DC is caused by an up-regulation of IFN-¿†, which subsequently stimulates the induction of IL-12 and the dsRNA binding toll like receptor (TLR)-3. The expression of the genes encoding IFN-¿†, IL-12, IL-10 and TLR-3 in DC upon stimulation with L. acidophilus NCFM was measured. L. acidophilus NCFM induced a much stronger expression of ifn-¿†, il-12 and il-10 compared to the synthetic dsRNA ligand Poly I:C, whereas the levels of expressed tlr-3 were similar. By the use of whole genome microarray gene expression, we investigated whether other genes related to the viral defence were up-regulated in DC upon stimulation with L. acidophilus NCFM and found that various virus defence related genes, both early and late, were among the strongest up-regulated genes. The IFN-¿† stimulating capability was also detected in another L. acidophilus strain, but was not a property of other probiotic bacteria tested (B. bifidum and E. coli nissle).The IFN-¿† inducing capacity was markedly reduced in TLR-2 -/- DCs, dependent on endocytosis and the major cause of the induction of il-12 and tlr-3 in L. acidophilus NCFM stimulated cells. Collectively, our results reveal that certain lactobacilli trigger the expression of viral defence genes in DC in a TLR-2 manner through induction of IFN- ¿†. **Overall design:** In the experiment Lactobacillus NCFM were added to murine dendritic cells and stimulated for 4, 10 or 18 hours. These were compared to control experiment at the same timepoints. Experiments were run in triplicates except for control 10h and control 18h which were only in duplicate, giving a total of 16 arrays.

Background corr dist: KL-Divergence = 0.0592, L1-Distance = 0.0699, L2-Distance = 0.0103, Normal std = 0.5549

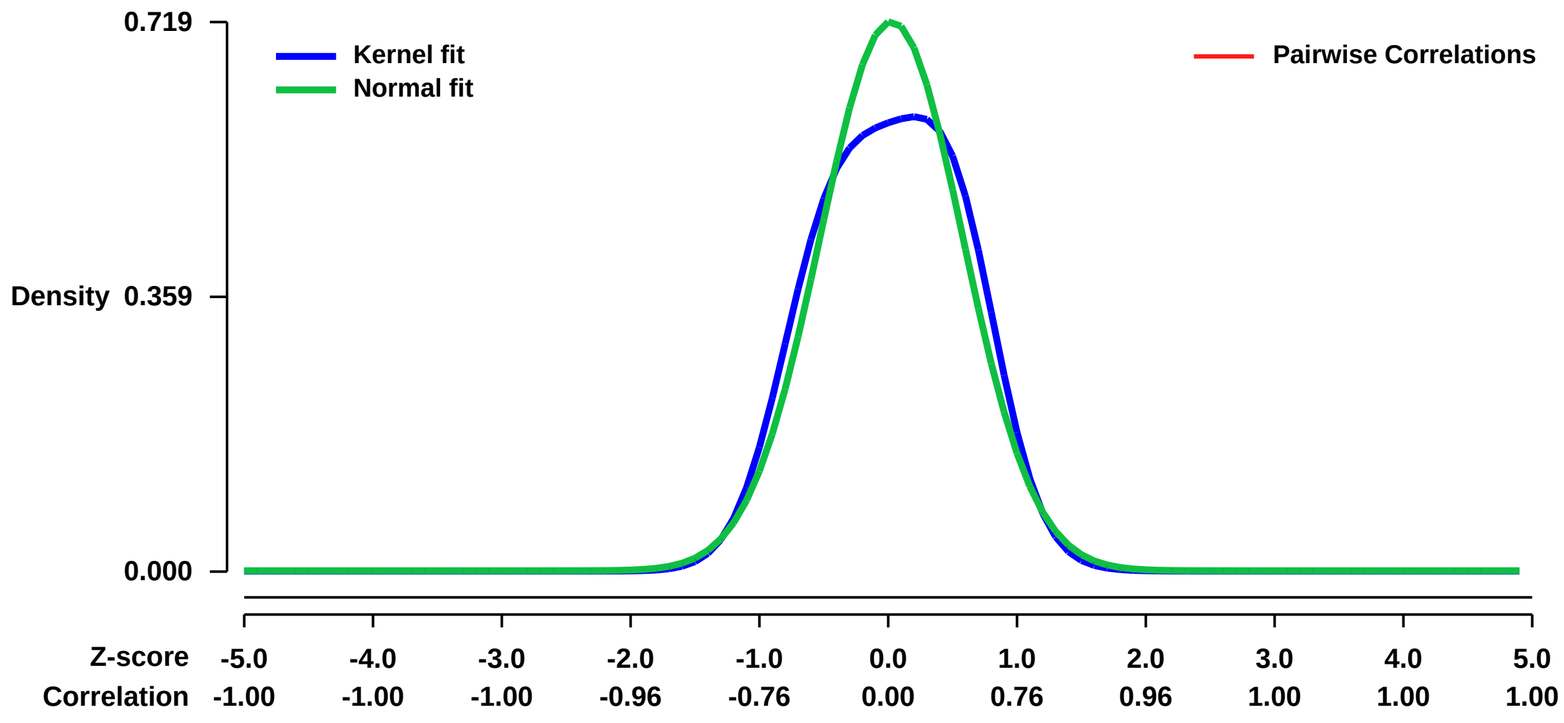

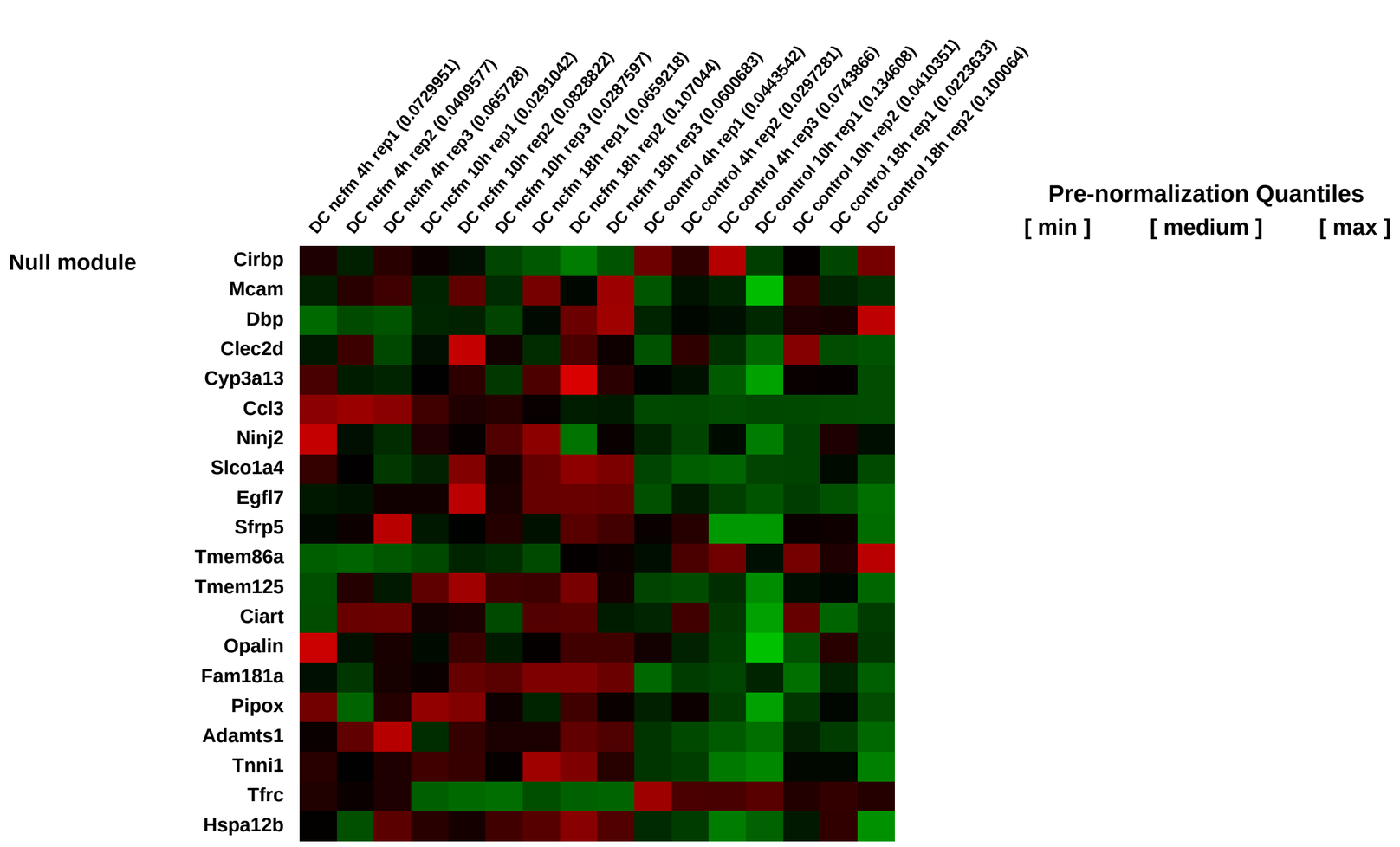

GEO Series "GSE27516" Expression Profiles

Num of samples in this series: 17

Scale of expression profile Z-scores

-3.0 -2.0 -1.0 0.0 1.0 2.0 3.0

GEO Link:	**http://www.ncbi.nlm.nih.gov/geo/query/acc.cgi?acc=GSE27516**
Status:	**Public on Mar 17 2011**
Title:	**Preclinical Models for Neuroblastoma: Establishing a Baseline for Treatment**
Organism:	**Mus musculus**
Experiment type:	**Expression profiling by array**
Platform:	**GPL1261**
Pubmed ID:	**21559450**
Summary & Design:	**Summary:** **Here we characterize and optimize both systems to increase their utility for preclinical studies. We show that TH-MYCN mice develop tumors in the paraspinal ganglia, but not in the adrenal, with cellular and gene expression patterns similar to human NB. In addition, we present a new ultrasound guided, non-invasive orthotopic xenograft method. This injection technique is rapid, provides accurate targeting of the injected cells and leads to efficient engraftment. We also demonstrate that tumors can be detected, monitored and quantified prior to visualization using ultrasound, MRI and bioluminescence. Finally we develop and test a â standard of careâ chemotherapy regimen. This protocol, which is based on current treatments for neuroblastoma, provides a baseline for comparison of new therapeutic agents.** **Overall design:** **A total of 17 samples are provided reprsenting TH-MYCN tumors derived from mice**

Background corr dist: **KL-Divergence = 0.2494, L1-Distance = 0.0536, L2-Distance = 0.0071, Normal std = 0.3045**

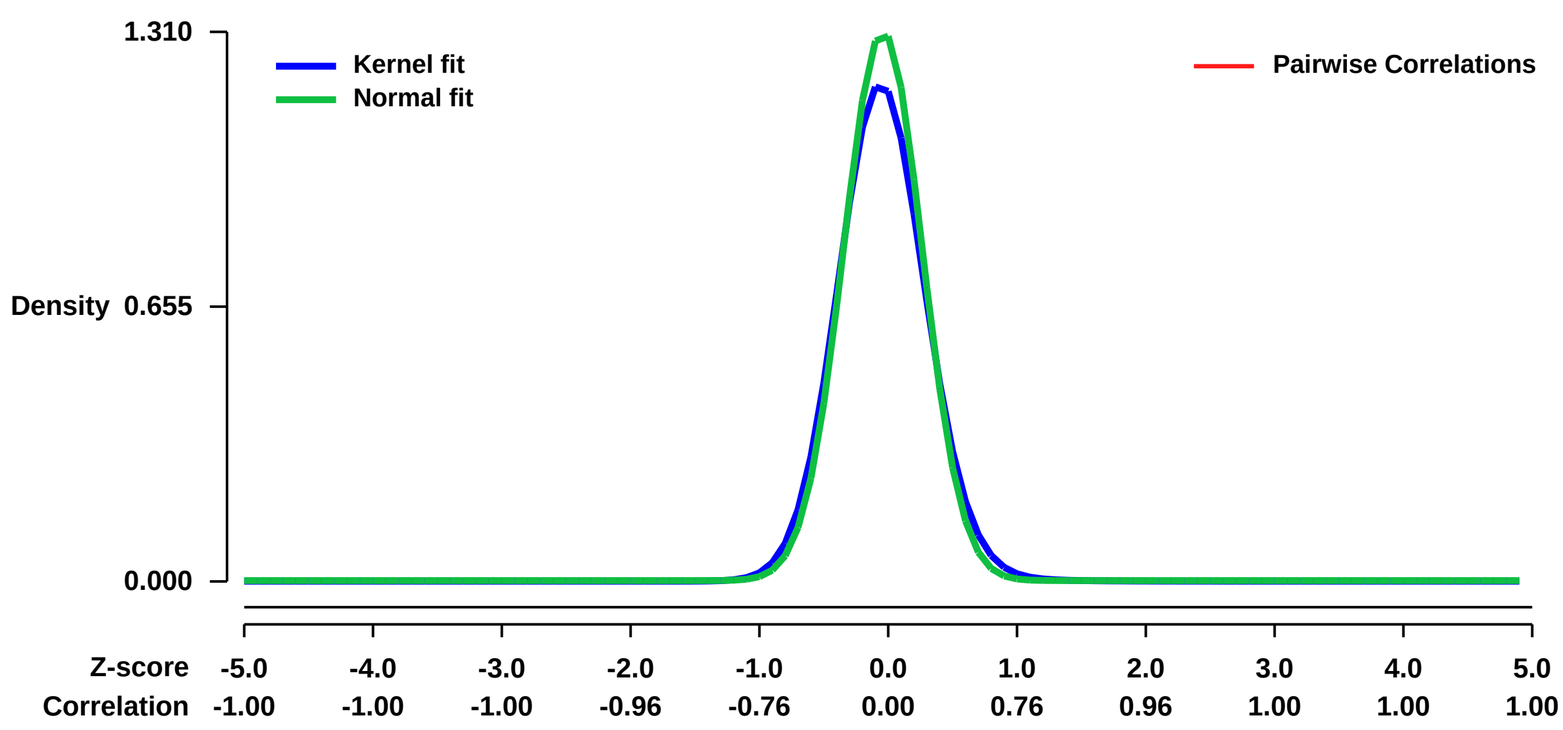

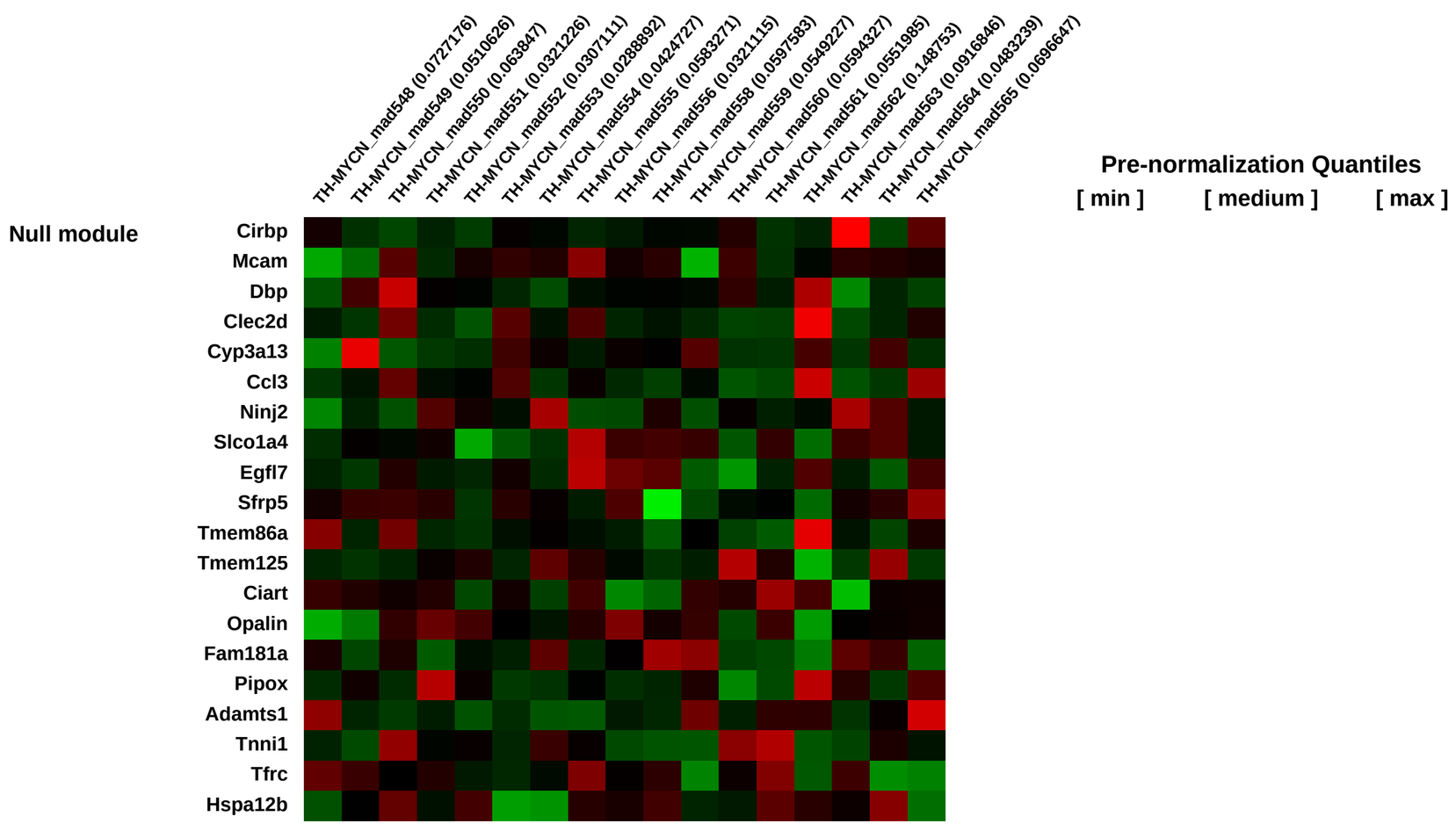

Pre-normalization Quantiles

[min] [medium] [max]

GEO Series "GSE48382" Expression Profiles

Num of samples in this series: 10

Scale of expression profile Z-scores

-3.0 -2.0 -1.0 0.0 1.0 2.0 3.0

GEO Link:	http://www.ncbi.nlm.nih.gov/geo/query/acc.cgi?acc=GSE48382
Status:	Public on Jul 01 2013
Title:	ChIp-Chip using RNAP II, CREB C/EBPb and cJun antibody in undifferentiated or differentiated keratinocytes (expression)
Organism:	Mus musculus
Experiment type:	Expression profiling by array
Platform:	GPL1261
Pubmed ID:	24244291
Summary & Design:	**Summary:** Combinatorial recruitment of CREB, C/EBPb and Jun determines activation of promoters upon keratinocyte differentiation Chromatin immunoprecipitation (ChIP) of RNAP II, CREB C/EBPb and cJun in undifferentiated or differentiated keratinocytes demonstrate recruitment of RNAP II to promoters bound by combination of specific transcription factors. Analysis of mRNA expression data from contrl keratinocytes or keratinovtyes where binding of transcription factors is disrupted demonstrate functional requirements for ceratin class of promoters **Overall design:** comparison of undifferentiated and differentated keratinocytes using mRNA expression data

Background corr dist: KL-Divergence = 0.0766, L1-Distance = 0.0223, L2-Distance = 0.0008, Normal std = 0.4867

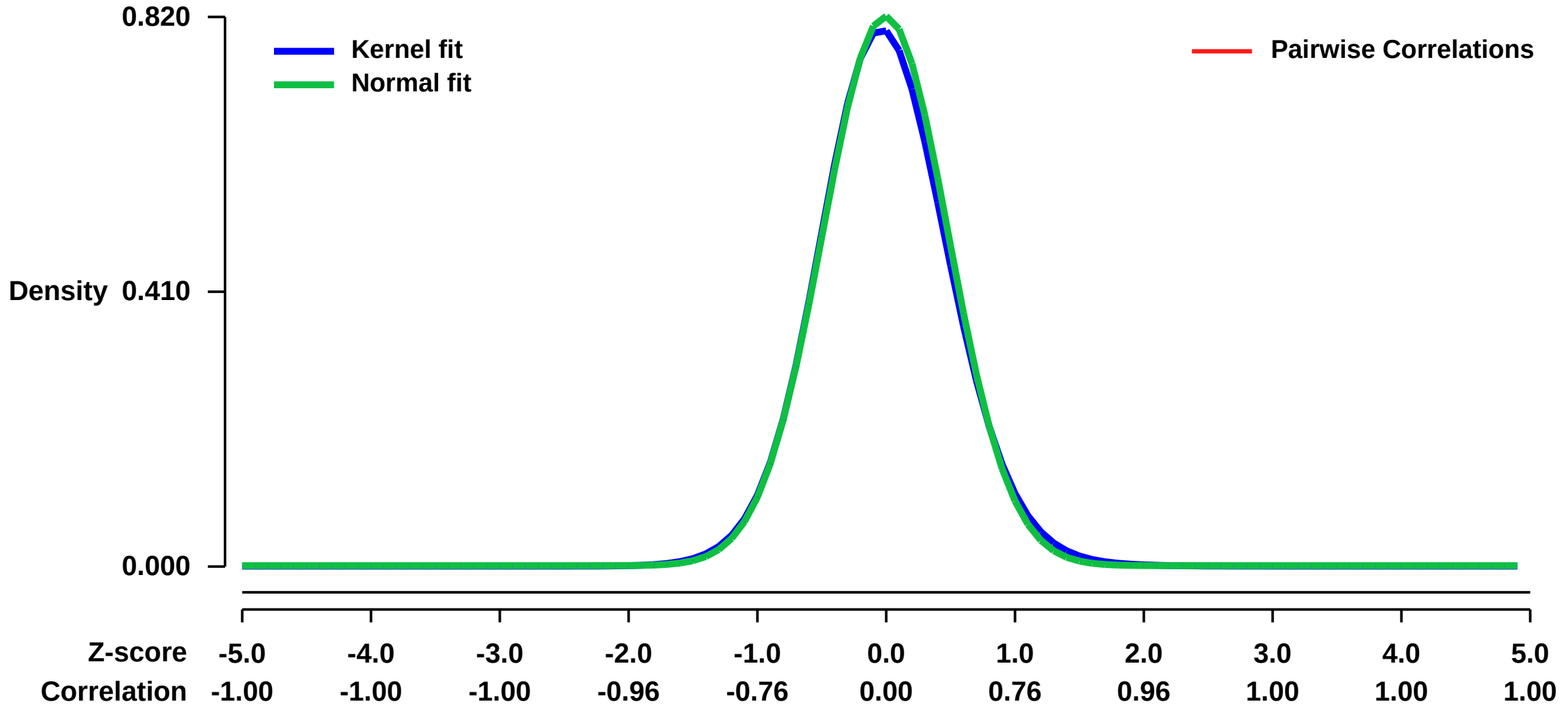

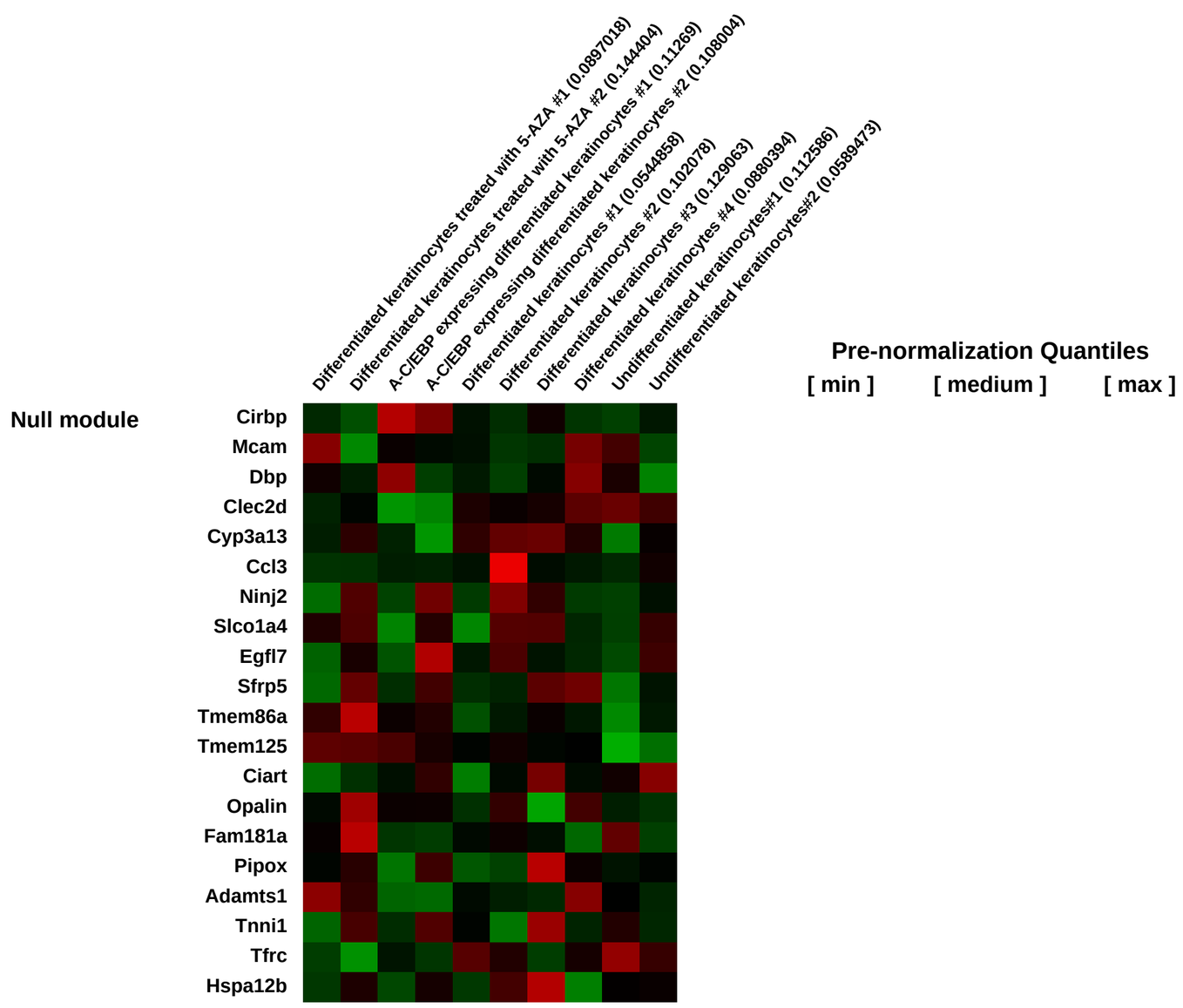

GEO Series "GSE11221" Expression Profiles

Num of samples in this series: 9

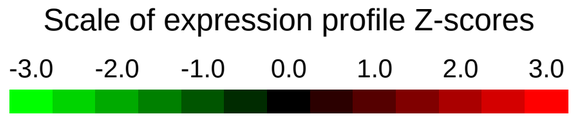

GEO Link:	http://www.ncbi.nlm.nih.gov/geo/query/acc.cgi?acc=GSE11221
Status:	Public on Apr 22 2008
Title:	Gene expression profiles of detrusor, stroma and urothelium isolated from SMGA (Actg2) transgenic neonatal bladders using LCM. (GUDMAP Series ID: 20)
Organism:	Mus musculus
Experiment type:	Expression profiling by array
Platform:	GPL1261
Pubmed ID:	
Summary & Design:	**Summary:** The long term objective is to create an encyclopedia of the expression levels of all genes in multiple components of the developing bladder. The central thesis is straightforward. The combination of microdissected and laser capture microdissection (LCM) plus microarray analysis offers a powerful, efficient and effective method for the creation of a global gene expression atlas of the developing urogenital system. Microarrays with essentially complete genome coverage can be used to quantitate expression levels of every gene. The ensuing rapid read-out provides an expression atlas that is more sensitive, more economical and more complete than would be possible by in situ hybridizations alone. The data submitted here represents the gene expression profiles of compartmental bladder tissues collected through laser capture microscopy. **Keywords:** Gene expression comparison from developing regions of the mouse postnatal day 1 and postnatal day 2 urogenital system. **Overall design:** Bladders were isolated from newborn SMGA/EGFP transgenic mice, embedded in OCT, frozen and sectioned (8 microns). Detrusor, stroma and urothelium were isloated using laser capture microscopy. The caps were frozen on dry ice and stored at -80 degrees C until RNA was extracted for gene expression analysis. Laser captured and total RNA isolated for gene expression analysis using the Affymetrix MOE430 microarray chip.

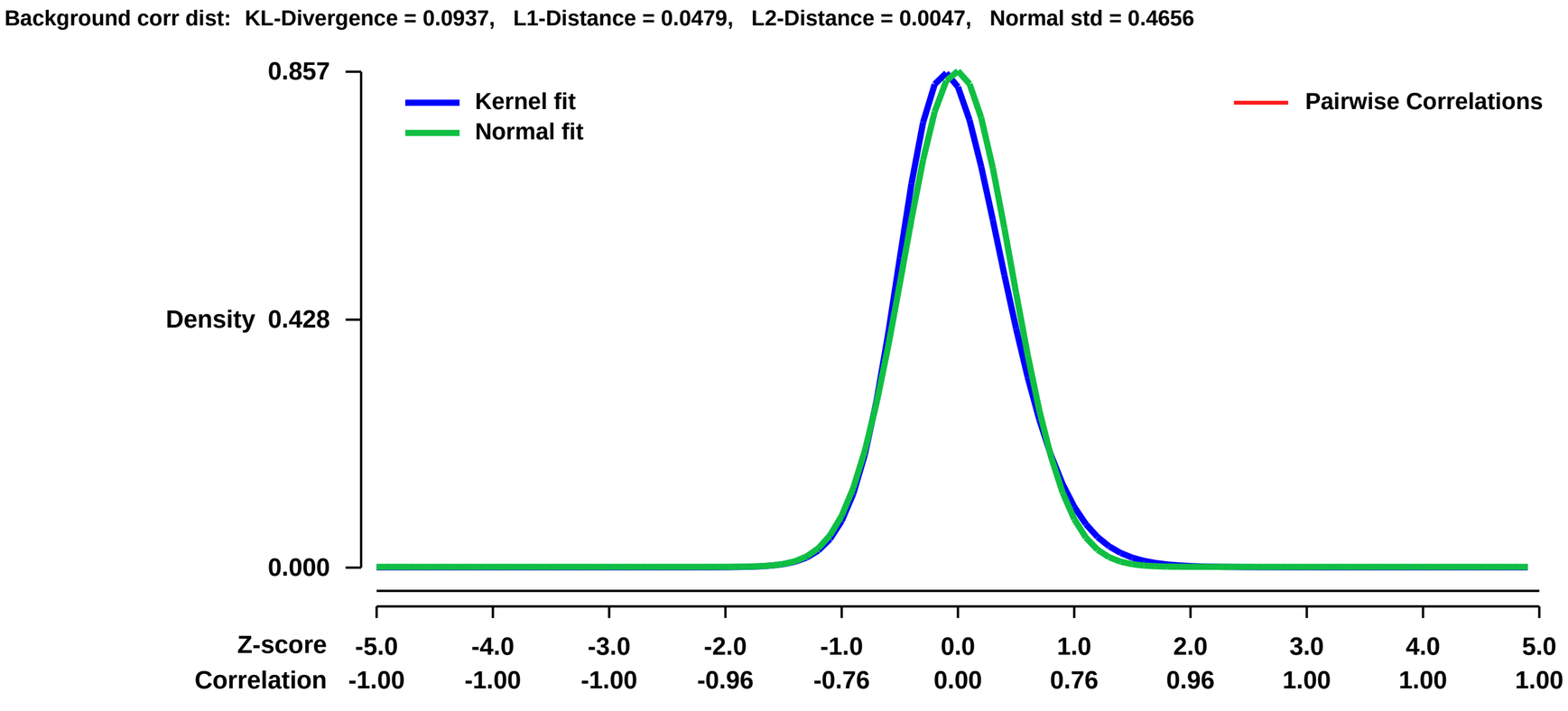

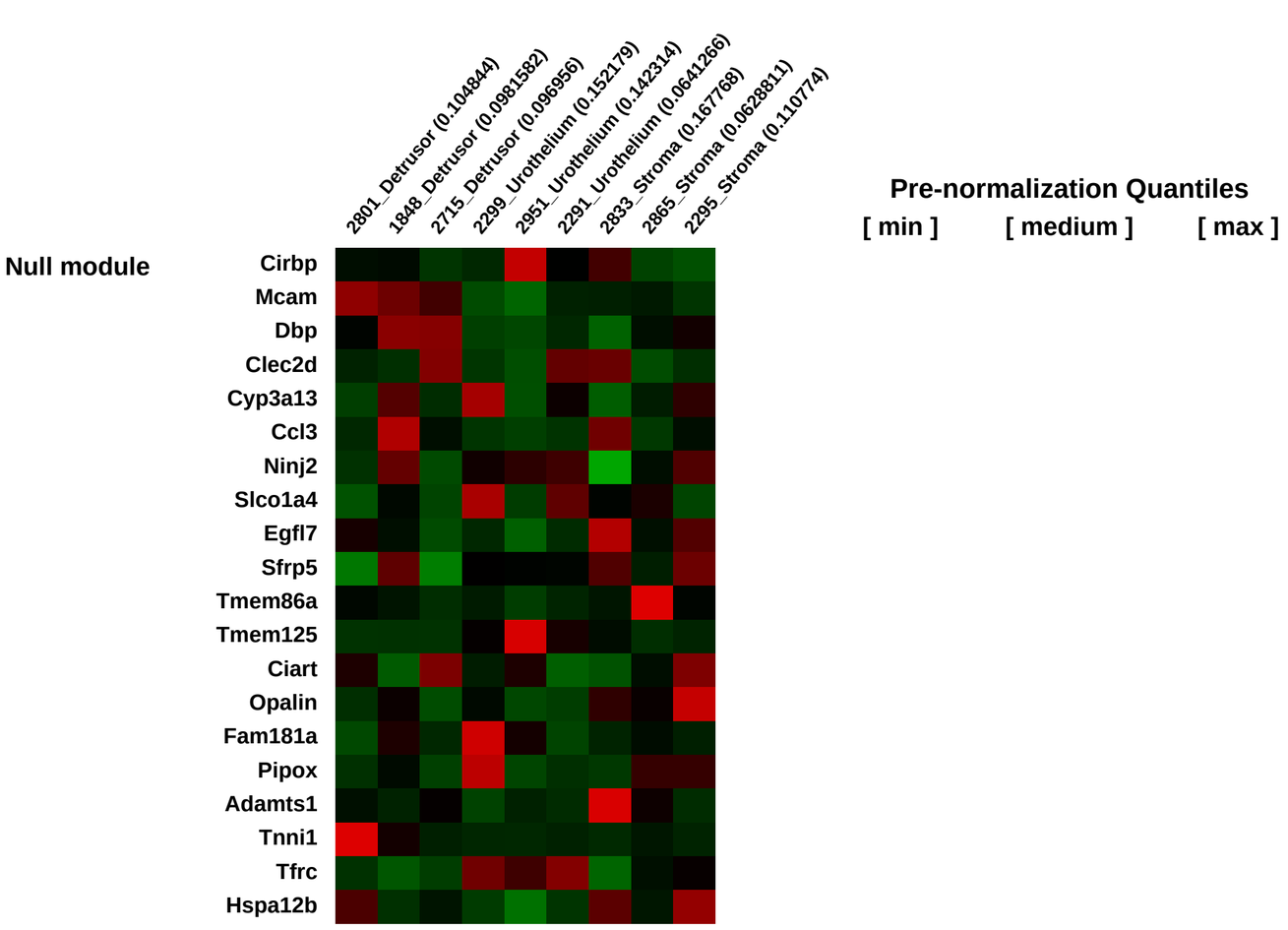

GEO Series "GSE57469" Expression Profiles

Num of samples in this series: 6

Scale of expression profile Z-scores

-3.0 -2.0 -1.0 0.0 1.0 2.0 3.0

GEO Link:	**http://www.ncbi.nlm.nih.gov/geo/query/acc.cgi?acc=GSE57469**
Status:	**Public on May 09 2014**
Title:	**Expression data from common myeloid progenitor cells (CMP) of C57BL6 mouse**
Organism:	**Mus musculus**
Experiment type:	**Expression profiling by array**
Platform:	**GPL1261**
Pubmed ID:	
Summary & Design:	**Summary:** **Common myeloid progenitor cells from murine bone marrow were sorted according to ROS content using FACS with H2-DCFDA staining.** **We compared gene expression profile between CMP with low-ROS levels and those with high-ROS levels.** **Overall design:** **We analysed function of ROS in differentiation step from CMP to MEP.**

Background corr dist: **KL-Divergence = 0.0403, L1-Distance = 0.0192, L2-Distance = 0.0004, Normal std = 0.6122**

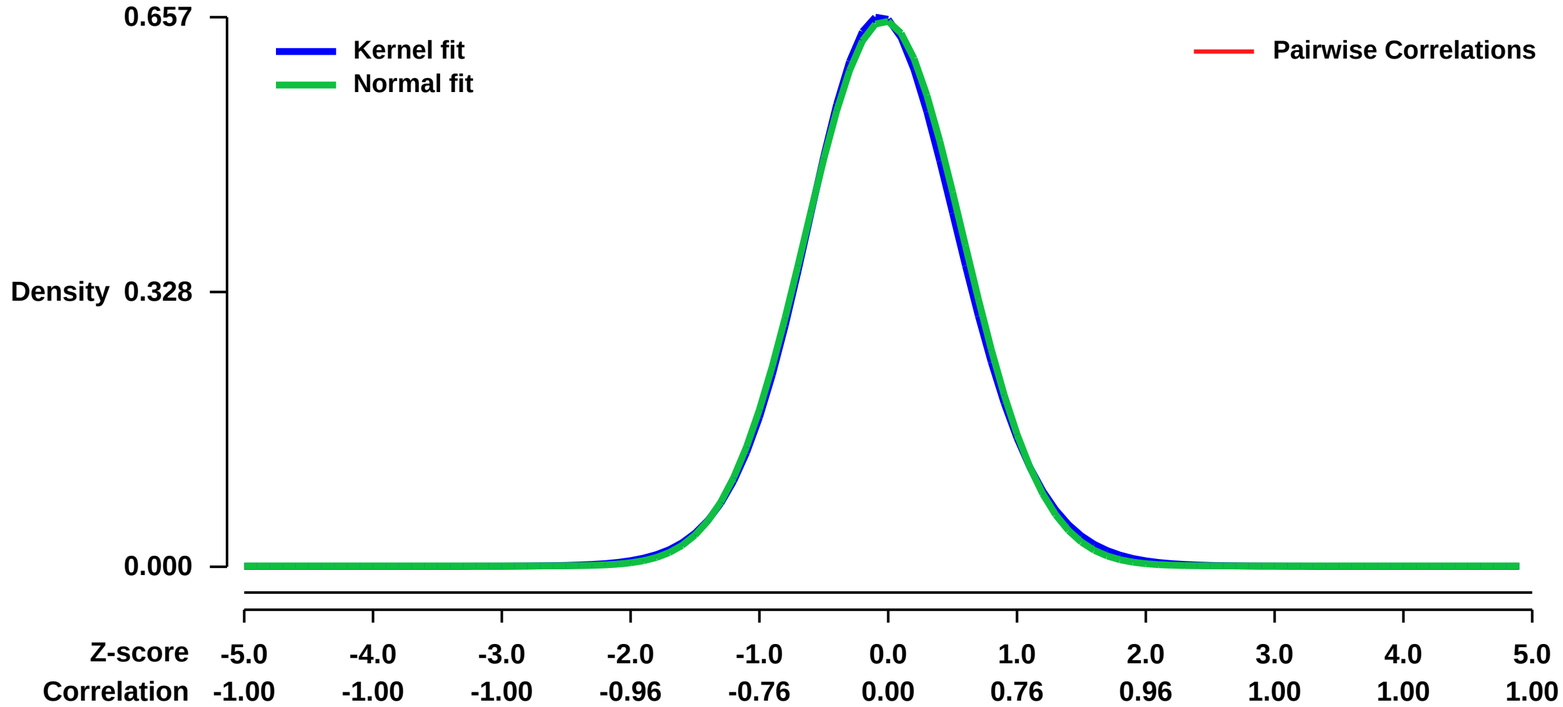

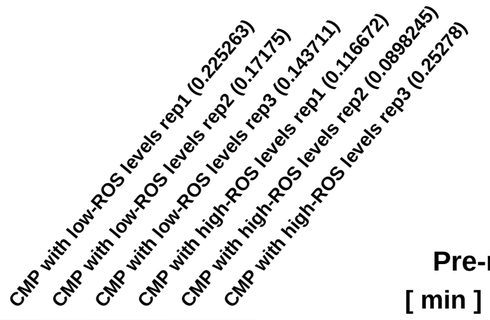

Pre-normalization Quantiles

[min] [medium] [max]

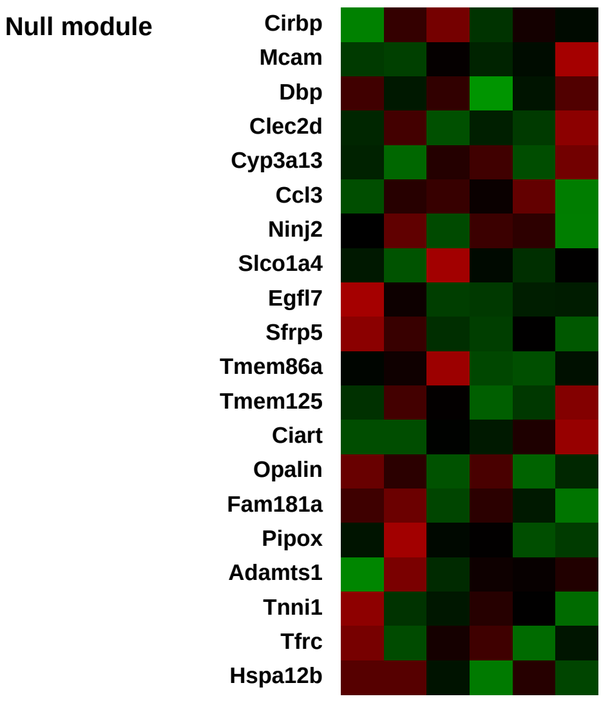

GEO Series "GSE19004" Expression Profiles

Num of samples in this series: 9

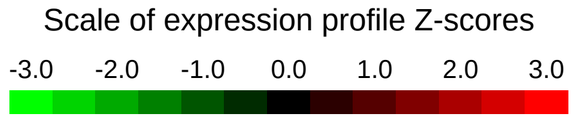

GEO Link:	**http://www.ncbi.nlm.nih.gov/geo/query/acc.cgi?acc=GSE19004**
Status:	**Public on Jul 01 2010**
Title:	**Mouse HCC model**
Organism:	**Mus musculus**
Experiment type:	**Expression profiling by array**
Platform:	**GPL1261**
Pubmed ID:	
Summary & Design:	**Summary:** **A mouse model of HCC has been developed based on the reported inactivation of the RB pathway in the majority of human HCC. This mouse model harbors floxed alleles of Rb and p130 genes, as well as germline mutation of the p107 gene. Various strategies to activate the activity of a Cre recombinase leads to the efficient deletion of the three genes in the liver of adult mice (TKO mice). Disruption of the RB pathway induces the rapid development of HCC. These HCCs share many similar features of human HCC.** **Overall design:** **The goal of this array is to assess genome wide expression of TKO HCCs. Gene expression of control livers (n=4) or TKO HCCs (n=5) was measured using the Affymetrix GeneChip Mouse Genome 430-2.0 arrays**

Background corr dist: **KL-Divergence = 0.0372, L1-Distance = 0.0331, L2-Distance = 0.0020, Normal std = 0.6133**

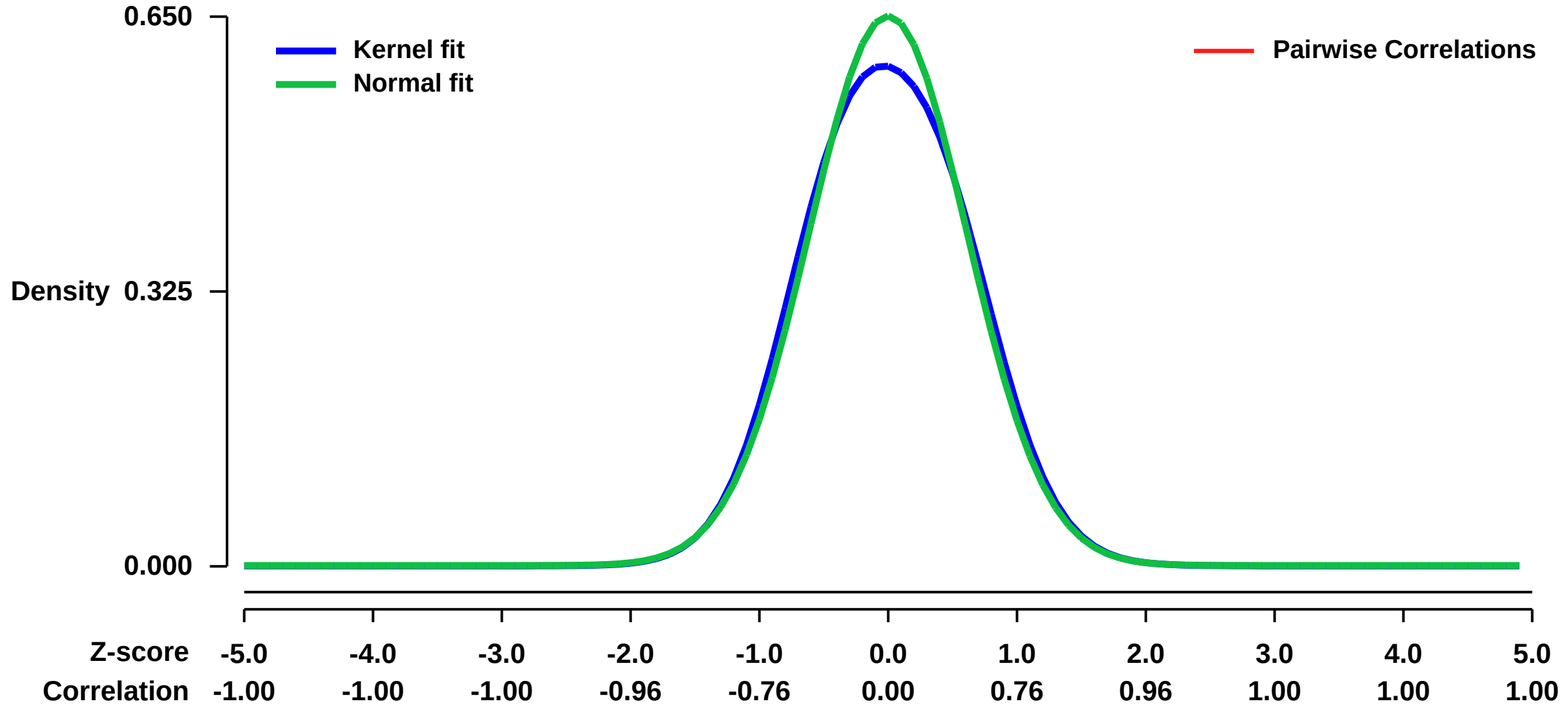

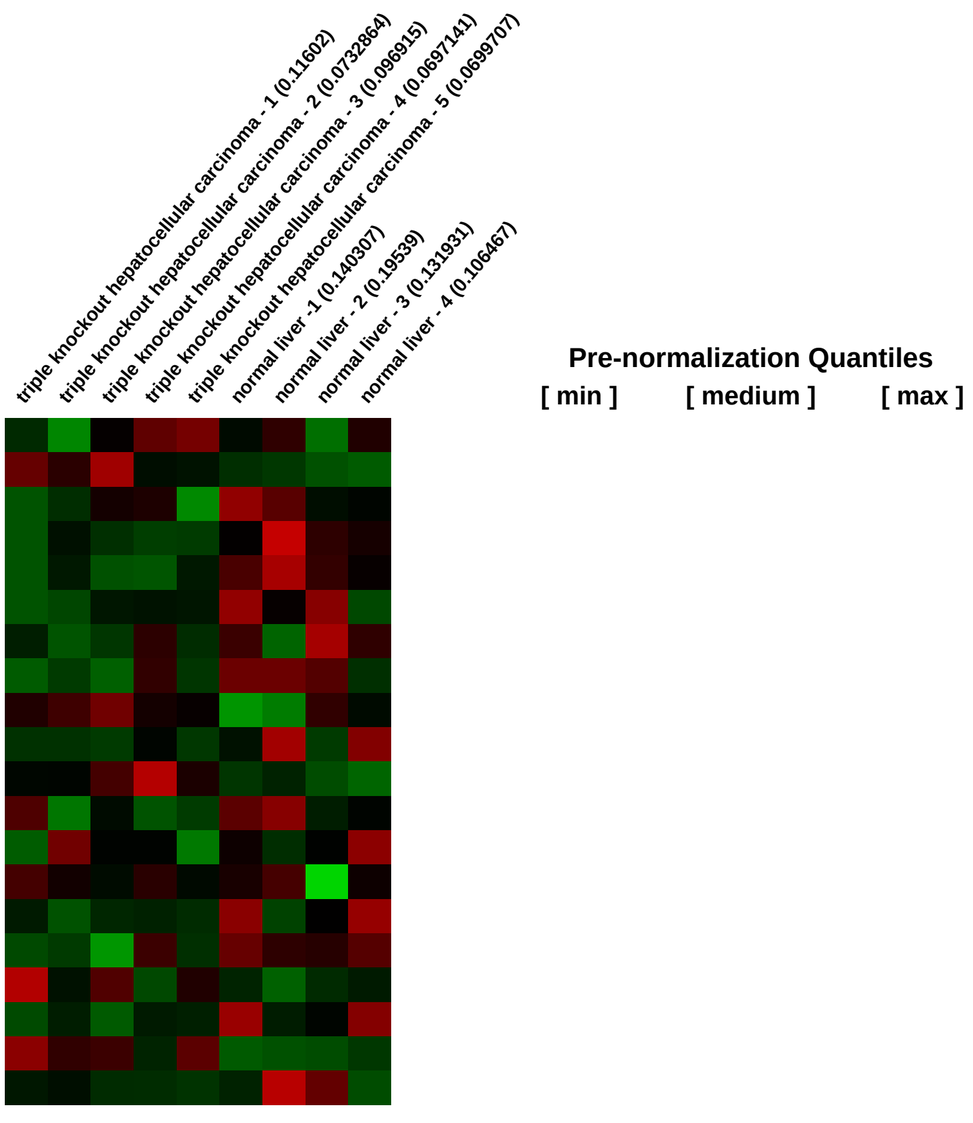

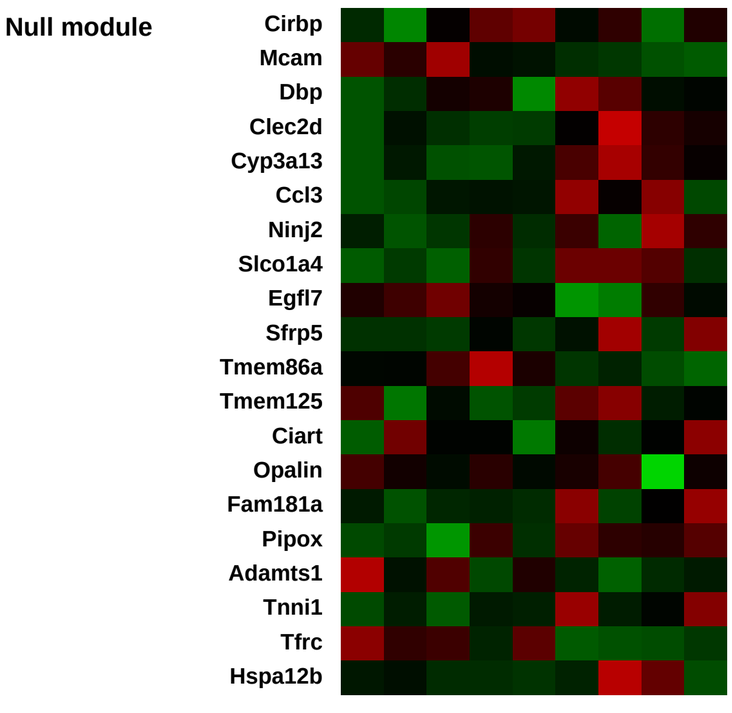

GEO Series "GSE1983" Expression Profiles

Num of samples in this series: 6

Scale of expression profile Z-scores

-3.0 -2.0 -1.0 0.0 1.0 2.0 3.0

GEO Link:	http://www.ncbi.nlm.nih.gov/geo/query/acc.cgi?acc=GSE1983
Status:	Public on Jul 01 2005
Title:	Transcriptional Profiling of the Metanephric Kidney
Organism:	Mus musculus
Experiment type:	Expression profiling by array
Platform:	GPL1261
Pubmed ID:	15917337
Summary & Design:	**Summary:** **In this study we identify molecules with highly restricted expression patterns during the initial stages of metanephric development, when the ureteric bud has entered the metanephric mesenchyme and initiated branching morphogenesis. Using the Affymetrix Mouse Genome 430 2.0 Array, we compare gene expression patterns in ureteric bud tips, stalks and metanephric mesenchymes from mouse E12.5 embryos. To identify conserved molecular pathways, we also analyze transcriptional profiles in rat E13.5 ureteric buds and metanephric mesenchymes using the Affymetrix Rat Genome U34 Set. Taken together, these data sets help to identify conserved and highly localized transcripts in the metanephric kidney.** **Keywords = Mus musculus** **Keywords = Rattus norvegicus** **Keywords = metanephric mesenchyme** **Keywords = ureteric bud** **Keywords = ureteric bud tips** **Keywords = ureteric bud stalks** **Keywords = molecular screen for spatially restricted transcripts** **Keywords: other** **Overall design:**

Background corr dist: **KL-Divergence = 0.0190, L1-Distance = 0.0266, L2-Distance = 0.0009, Normal std = 0.7646**

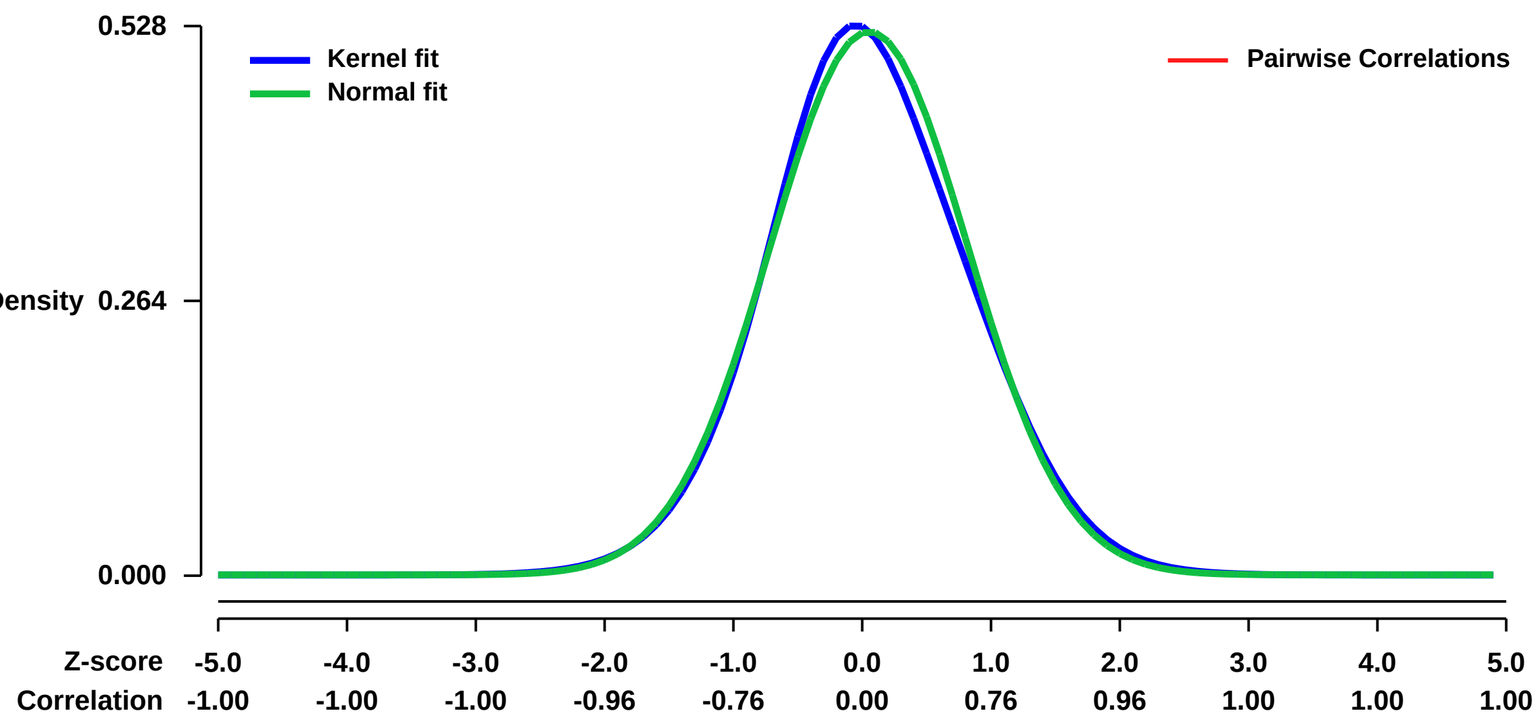

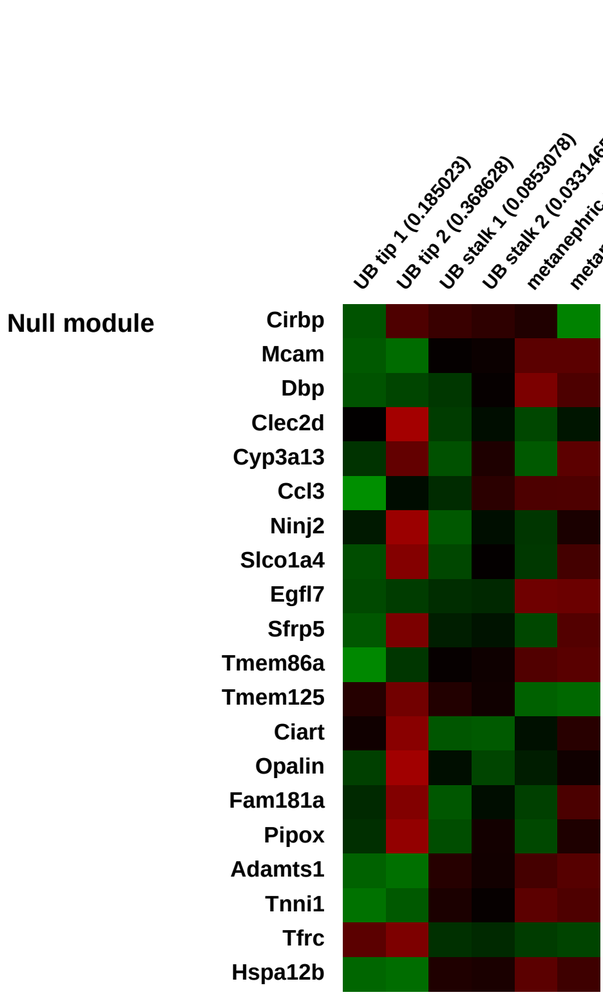

GEO Series "GSE21189" Expression Profiles

Num of samples in this series: 10

Scale of expression profile Z-scores

-3.0 -2.0 -1.0 0.0 1.0 2.0 3.0

GEO Link:	http://www.ncbi.nlm.nih.gov/geo/query/acc.cgi?acc=GSE21189
Status:	Public on May 01 2010
Title:	Mitochondrial DNA mutations induce supression of nuclear encoded mitochondrial Genes in skeletal muscle
Organism:	Mus musculus
Experiment type:	Expression profiling by array
Platform:	GPL1261
Pubmed ID:	20628647
Summary & Design:	**Summary:** To identify and analyze mtDNA mutation-responsive genes, a comparison of gastrocnemius muscle tissues from WT (control) and D257A mice was conducted. We examined changes in gene expression in the muscle associated with mtDNA mutations. **Overall design:** 5) Quality control measures were not used. No replicates were done. Dye swap was not used.

Background corr dist: KL-Divergence = 0.1134, L1-Distance = 0.0276, L2-Distance = 0.0014, Normal std = 0.4173

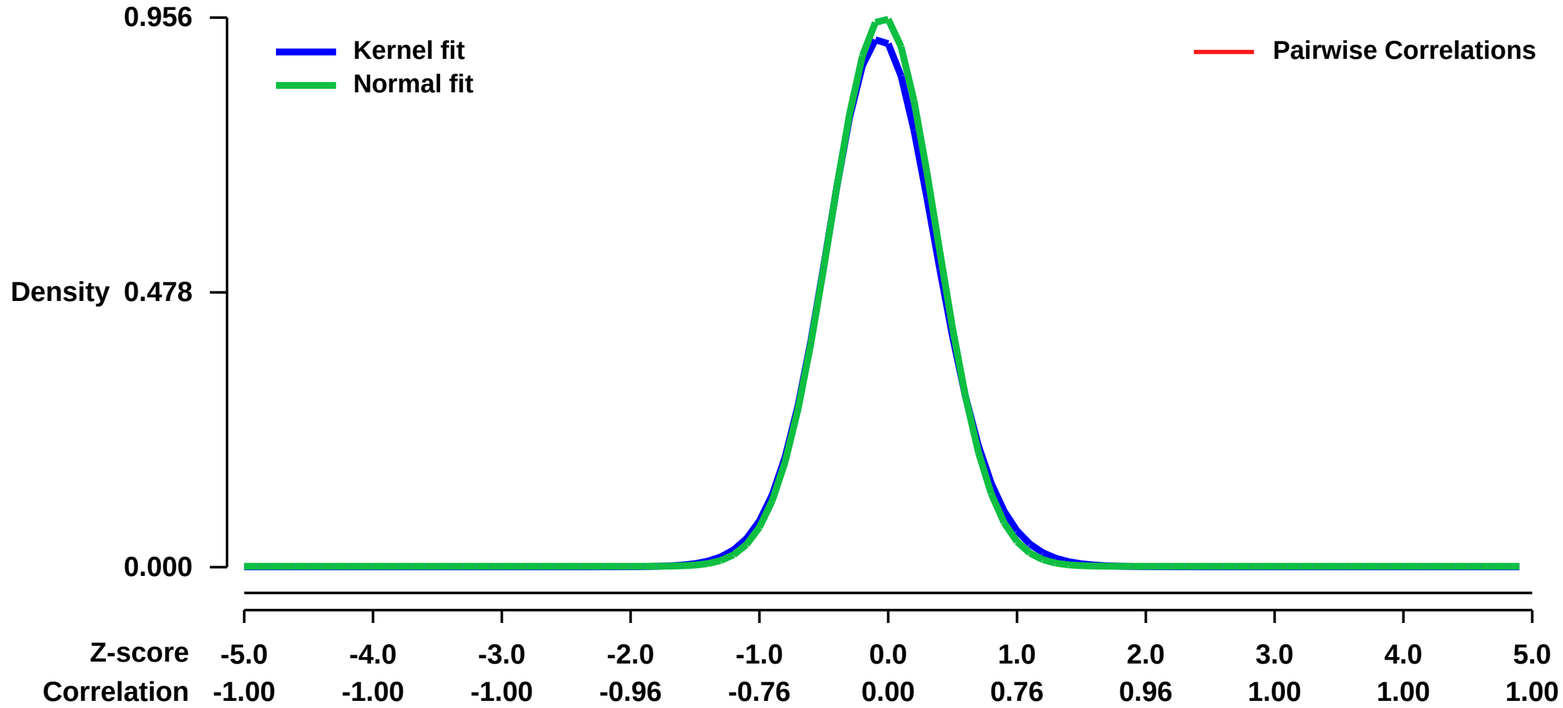

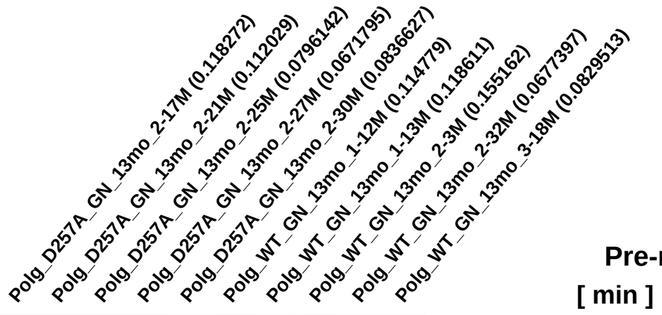

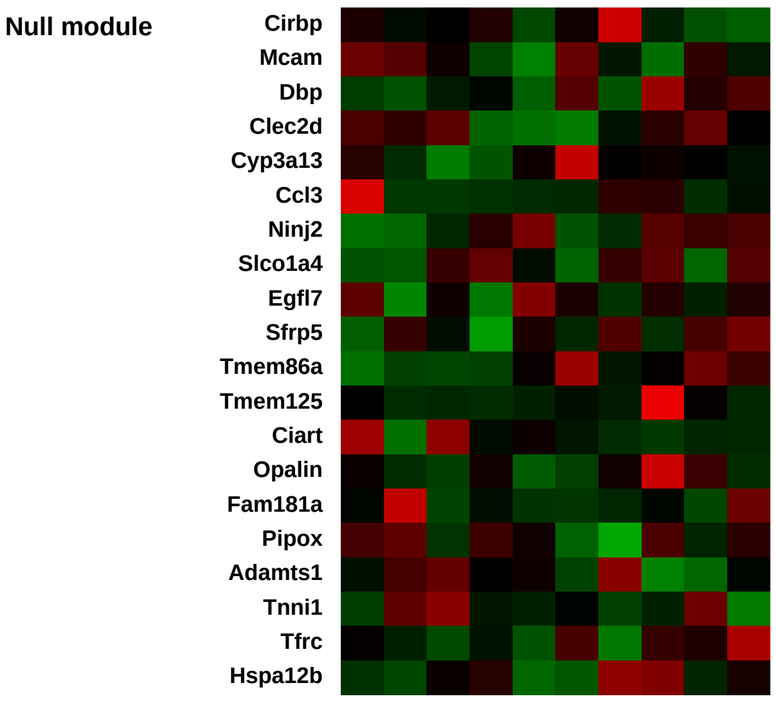

GEO Series "GSE19687" Expression Profiles

Num of samples in this series: 9

Scale of expression profile Z-scores

-3.0 -2.0 -1.0 0.0 1.0 2.0 3.0

GEO Link:	**http://www.ncbi.nlm.nih.gov/geo/query/acc.cgi?acc=GSE19687**
Status:	**Public on Dec 30 2009**
Title:	**shGFP- and shQk-transduced Ink4a/Arf-/- Pten-/- primary mouse astrocytes**
Organism:	**Mus musculus**
Experiment type:	**Expression profiling by array**
Platform:	**GPL1261**
Pubmed ID:	
Summary & Design:	**Summary:** **Identify potential QK-regulated mRNAs and linked pathways by comparing the transcriptional profiles of shGFP- and shQK-transduced Ink4a/Arf-/- Pten-/- primary mouse astrocytes** **Overall design:** **Ink4a/Arf-/- Pten-/- primary mouse astrocytes infected with shQk-1, shQk-2 and infected with shGFP as control**

Background corr dist: **KL-Divergence = 0.1127, L1-Distance = 0.0284, L2-Distance = 0.0014, Normal std = 0.4172**

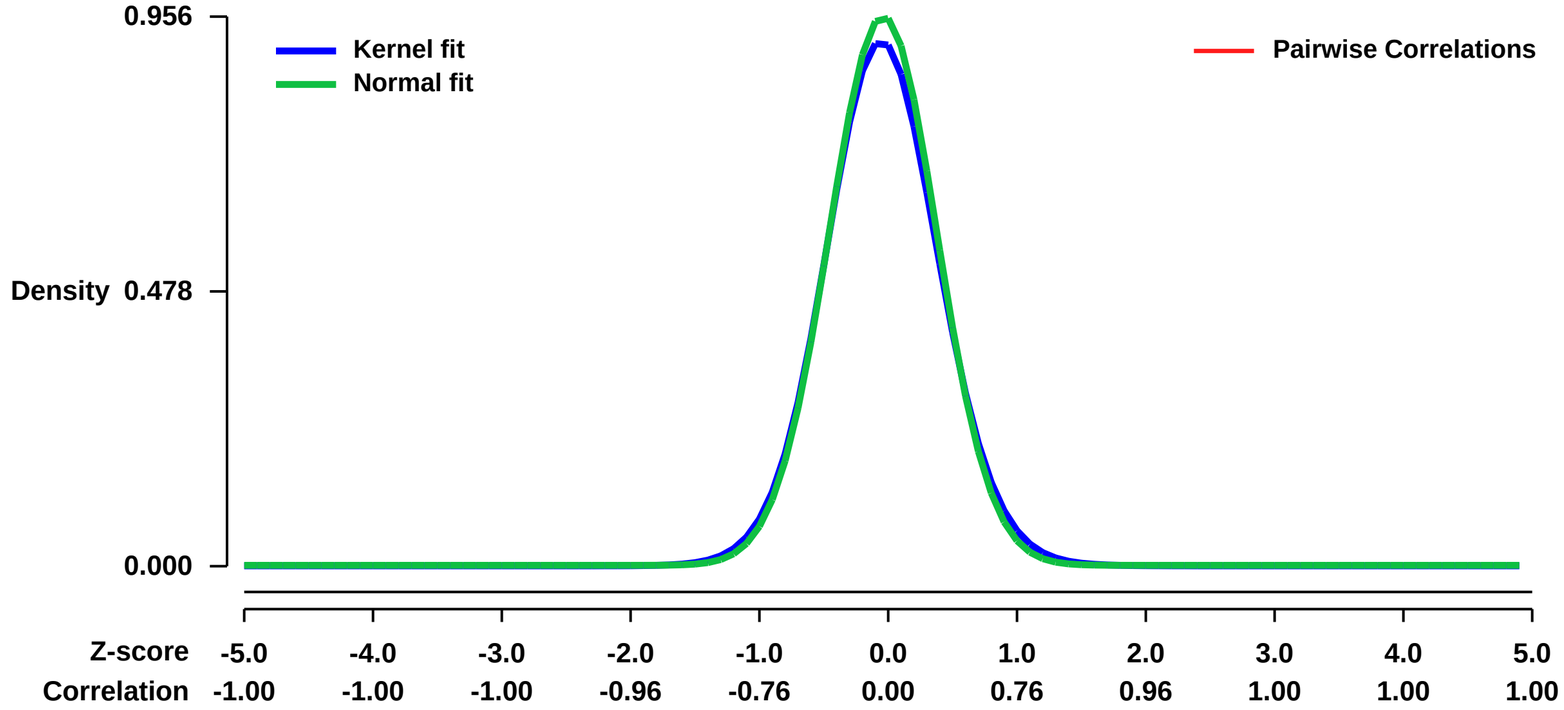

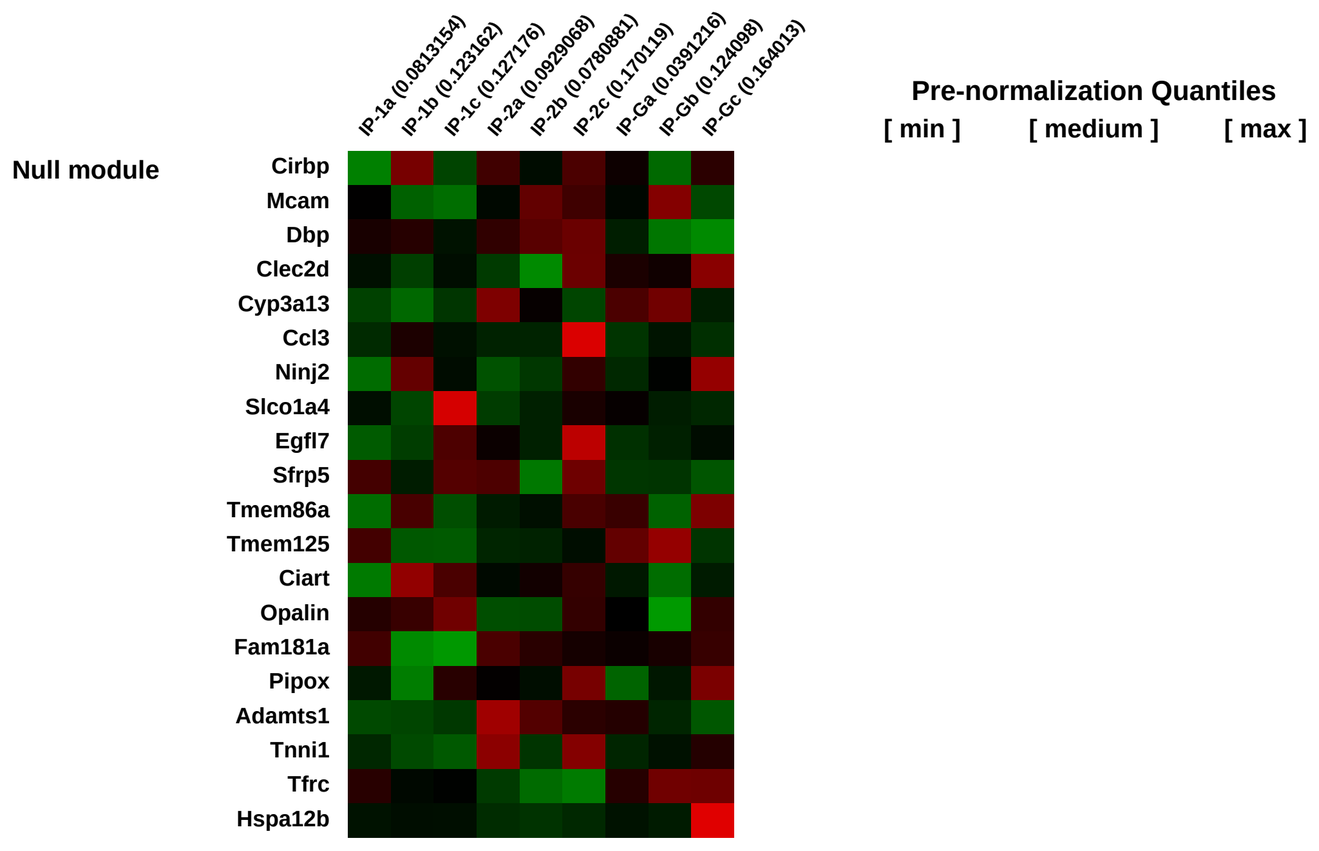

GEO Series "GSE17102" Expression Profiles

Num of samples in this series: 9

Scale of expression profile Z-scores

-3.0 -2.0 -1.0 0.0 1.0 2.0 3.0

GEO Link:	**http://www.ncbi.nlm.nih.gov/geo/query/acc.cgi?acc=GSE17102**
Status:	**Public on Jul 17 2009**
Title:	**Expression profiling of ntTS and TS cells**
Organism:	**Mus musculus**
Experiment type:	**Expression profiling by array**
Platform:	**GPL1261**
Pubmed ID:	
Summary & Design:	**Summary:** **Placental abnormalities occur frequently in cloned animals. To investigate gene expression profile of trophoblast cell lineage of somatic cell nuclear transferred (NT) embryos, we established TS cells from blastocysts produced by NT at the blastocyst stage.** **Overall design:** **Five independent TS cell lines derived from NT embryos were used in this study. Those included three lines from BDF1 background NT embryos and two lines from EGFP-Tg CD-1 background NT embryos. Two each of control lines, derived from native blastocysts of each background, were also used.**

Background corr dist: **KL-Divergence = 0.1104, L1-Distance = 0.0313, L2-Distance = 0.0019, Normal std = 0.4228**

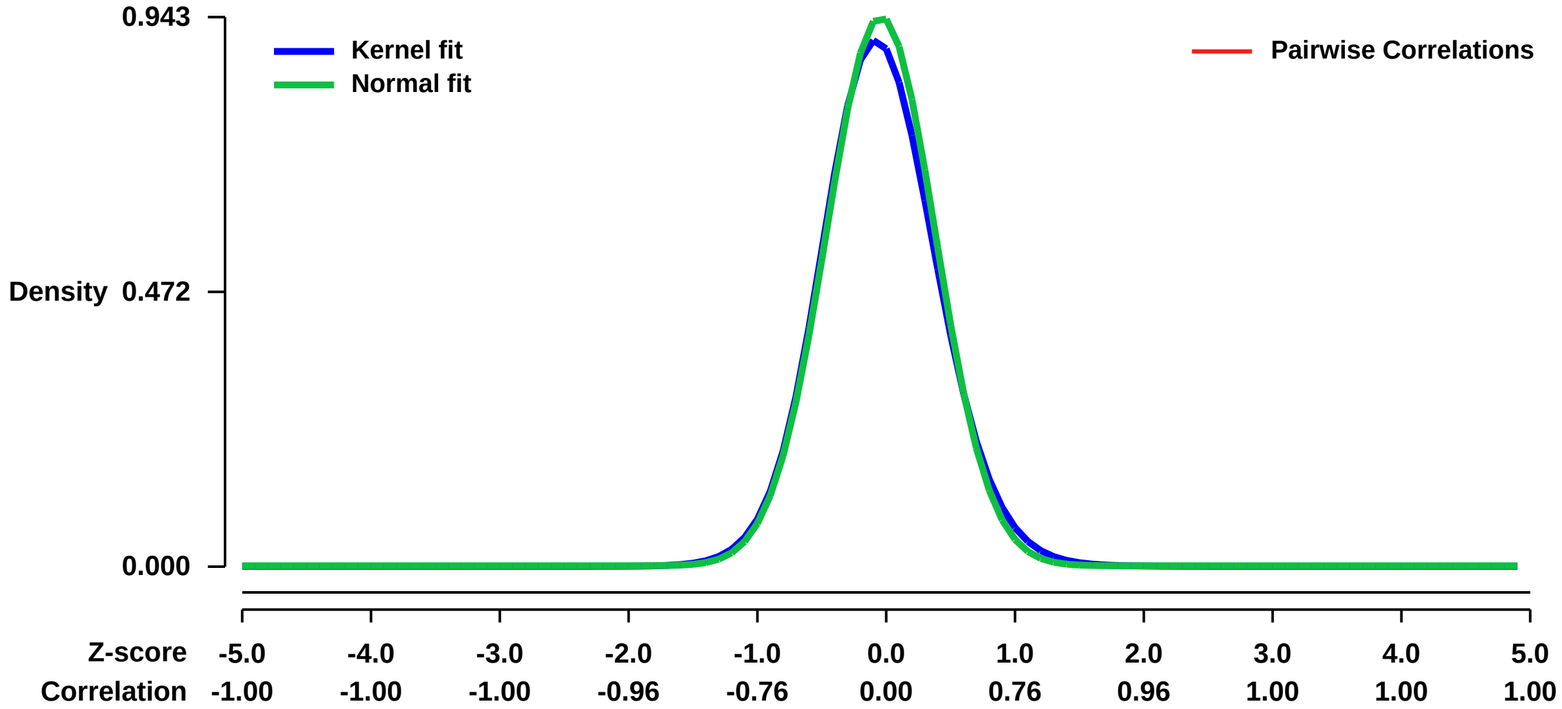

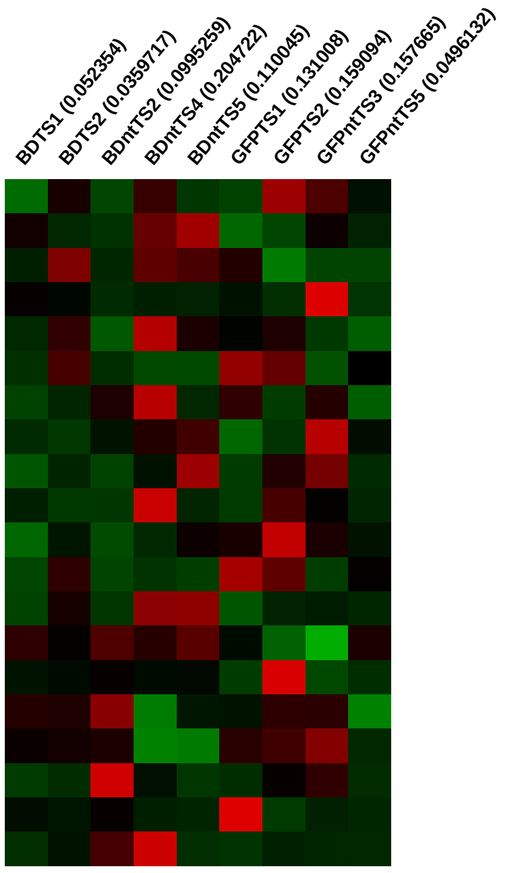

Null module

GEO Series "GSE14007" Expression Profiles

Num of samples in this series: 8

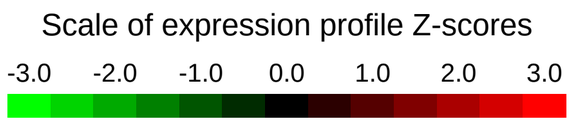

GEO Link:	**http://www.ncbi.nlm.nih.gov/geo/query/acc.cgi?acc=GSE14007**
Status:	**Public on Dec 23 2008**
Title:	**Gene expression of growth plate of mouse.**
Organism:	**Mus musculus**
Experiment type:	**Expression profiling by array**
Platform:	**GPL1261**
Pubmed ID:	
Summary & Design:	**Summary:** **The growth plate is histomorphologically classified into four zones {resting zone (RZ), proliferating zone (PZ), maturing zone (MZ) and hypertrophic zone (HZ)}. Gene expression profile analyses of 4 zones were performed using microarrays.** **Overall design:** **We performed global analysis of gene expression in tibias from nine-day-old mice. Chondrocytes layer was microdissected en-block from four anatomically distinct growth plate zones, and RNA expression was analyzed using microarrays.Chondrocytes from four anatomical zones were isolated from tibias of two mice. The eight samples were named after the mouse (1 or 2) and the growth plate zone, such as resting zone of 1st mouse (RZ01), 2nd mouse (RZ02), proliferation zone (PZ01, PZ02), maturing zone (MZ01, MZ02) and hypertrophic zone (HZ01, HZ02).**

Background corr dist: **KL-Divergence = 0.0621, L1-Distance = 0.0278, L2-Distance = 0.0013, Normal std = 0.5305**

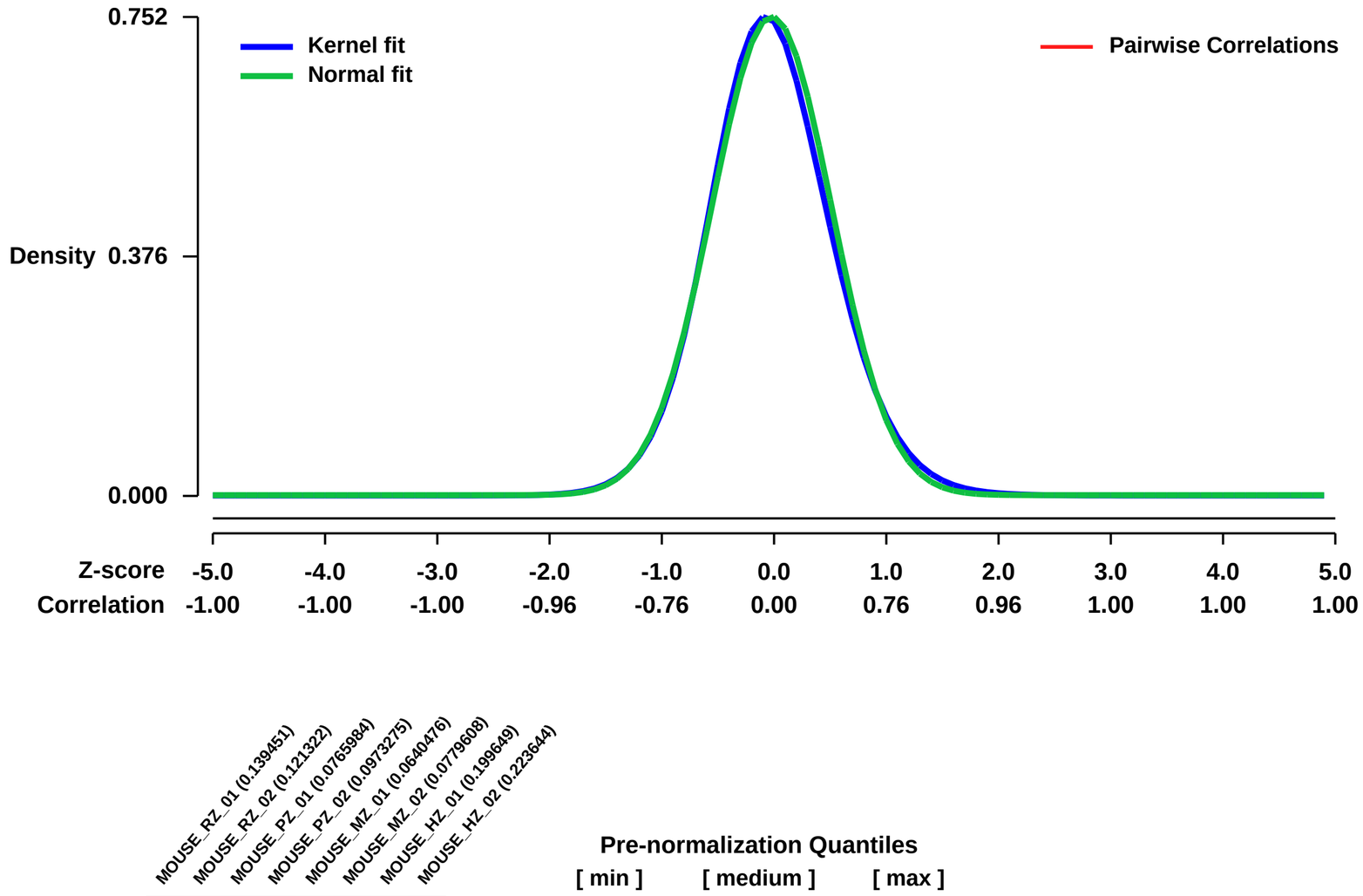

GEO Series "GSE16516" Expression Profiles

Num of samples in this series: 18

Scale of expression profile Z-scores

-3.0 -2.0 -1.0 0.0 1.0 2.0 3.0

GEO Link:	http://www.ncbi.nlm.nih.gov/geo/query/acc.cgi?acc=GSE16516
Status:	Public on Aug 07 2009
Title:	Distinct Self-renewal and Differentiation Phases in the Niche of Infrequently Dividing Hair Follicle Stem Cells
Organism:	Mus musculus
Experiment type:	Expression profiling by array
Platform:	GPL1261
Pubmed ID:	19664980
Summary & Design:	**Summary:** In homeostasis of adult vertebrate tissues, stem cells are thought to self-renew by infrequent and asymmetric divisions that generate another stem cell daughter and a progenitor daughter cell committed to differentiate. This model is based largely on in vivo invertebrate or in vitro mammal studies. Here we examine the dynamic behaviour of adult hair follicle stem cells in their normal setting by employing mice with repressible H2B-GFP expression to track cell divisions and Cre inducible mice to perform long-term single cell lineage tracing. We provide direct evidence for the infrequent stem cell division model in intact tissue. Moreover, we find that differentiation of progenitor cells occurs at different times and tissue locations than self-renewal of stem cells. Distinct fates of differentiation or self-renewal are assigned to individual cells in a temporal-spatial manner. We propose that large clusters of tissue stem cells behave as populations, whose maintenance involves unidirectional daughter-cell fate decisions. We used microarrays to expression profile the stem cell progeny generated at distinct differentiation and self-renewal stages. **Overall design:** We employed double transgenic mice, K5tTA x pTRE-H2B-GFP in which an epithelial Keratin 5 (K5) promoter drove repressible histone H2B-GFP expression. Repression is achieved by feeding the mice doxycycline for a period of time (chase), when the H2B-GFP dilutes in cells by 2-fold at division. This allowed us to quantify precise proliferation history in vivo, from the amount of H2B-GFP fluorescence retained in cells after chase. After various chase periods we sacrificed mice at different ages corresponding to distinct phases of hair cycle. We isolated skin cell suspensions from these mice and stained them for surface expression of stem cell niche bulge(Bu) markers CD34 and alpha 6-integrin. Fluorescence-activated cell sorting (FACS) revealed histograms with distinct peaks of 2-fold median H2B-GFP intensity corresponding to distinct divisions. For microarray, we FACS sorted bulge(Bu) and non-bulge(NonBu) cells based cell surface marker staining and their proliferation history with H2B-GFP intensity, after two doxycycline chase schemes (Postnatal Day 18-PD21 or PD22-PD25), then extract total RNA from each cell fractions. For microarrays 5 ng of high quality RNA (Bioanalyzer, Agilent) were amplified (Ovation Amplification; Nugene) in the Cornell Microarray Core Facility. GeneChip IVT labelling was followed by Gene Chip MOE 430 2.0 hybridization, GeneArray 3000 scanning, GCOS generation of present calls and signal values (Affymetrix).

Background corr dist: KL-Divergence = 0.2480, L1-Distance = 0.0547, L2-Distance = 0.0075, Normal std = 0.3038

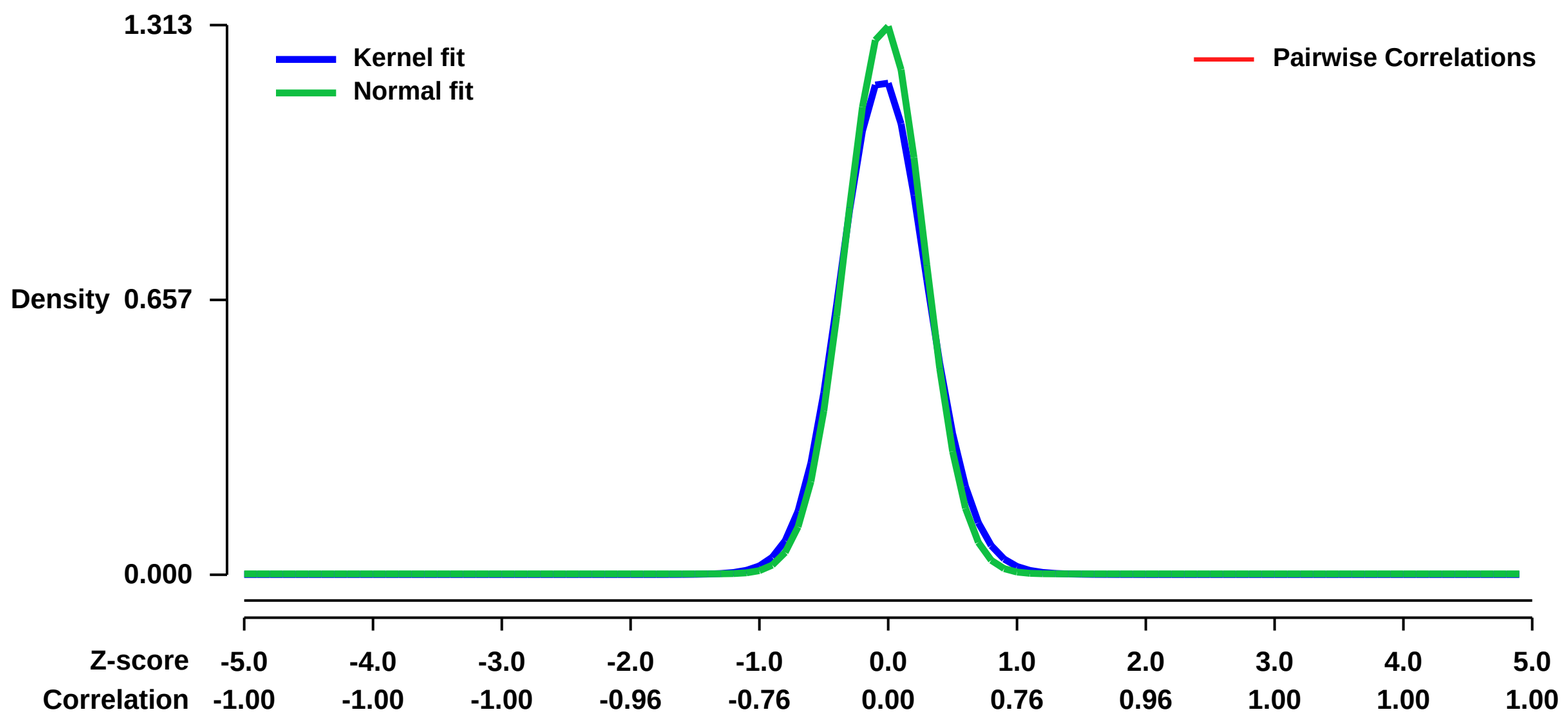

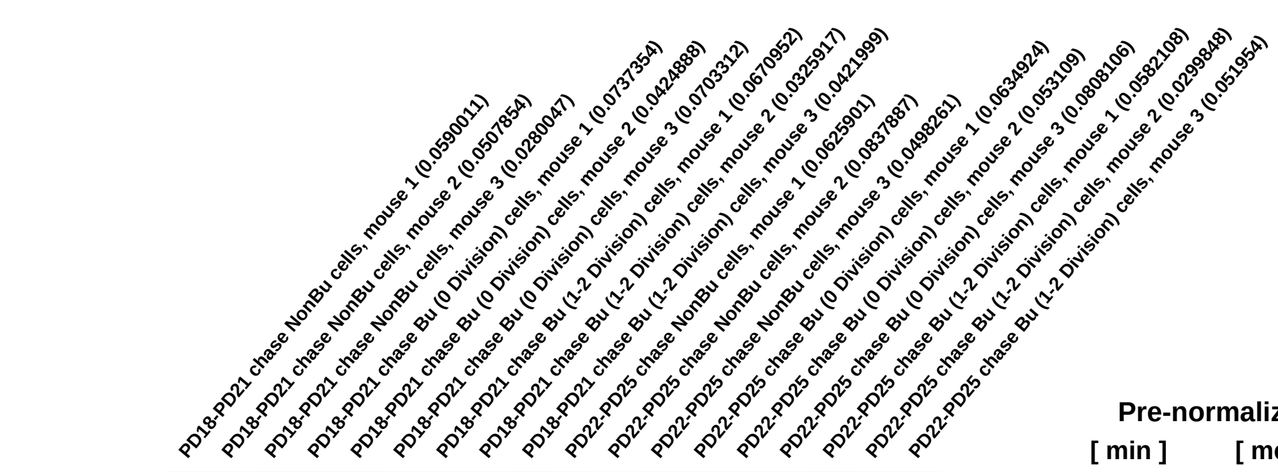

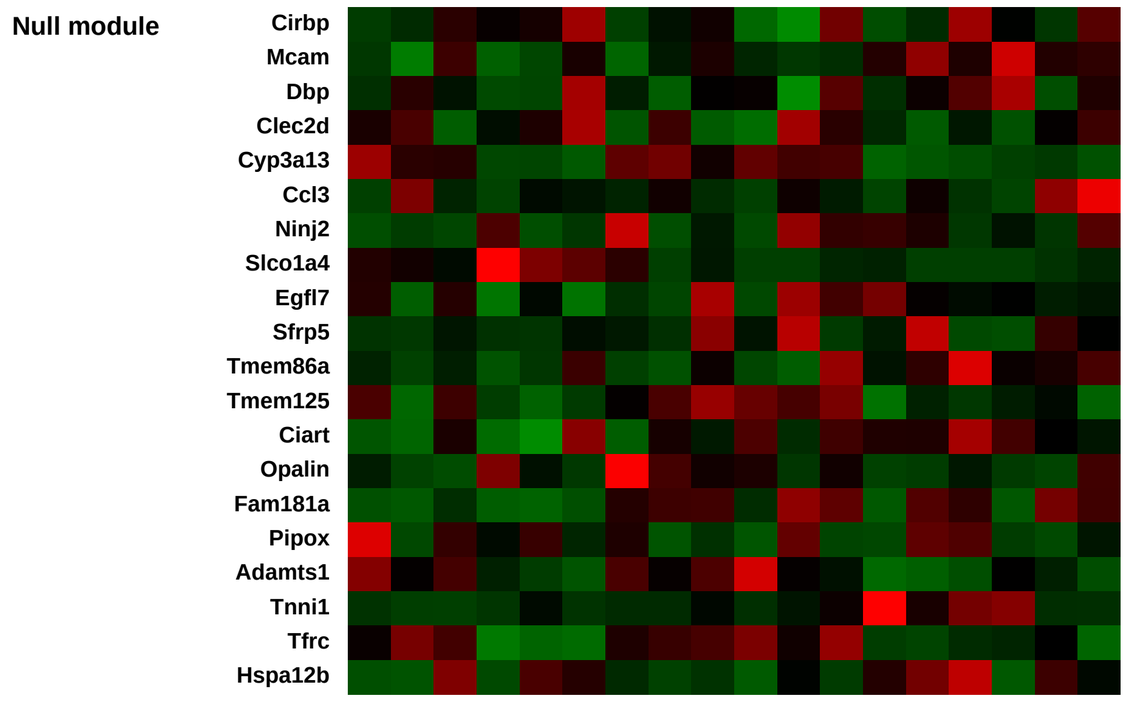

GEO Series "GSE39592" Expression Profiles

Num of samples in this series: 8

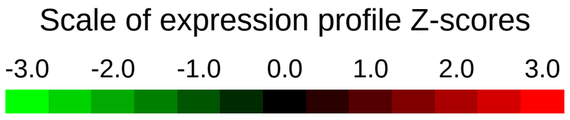

GEO Link:	**http://www.ncbi.nlm.nih.gov/geo/query/acc.cgi?acc=GSE39592**
Status:	**Public on Jul 24 2012**
Title:	**Expression data from cAMP-treated WT or IFN-gR1-deficient T cells**
Organism:	**Mus musculus**
Experiment type:	**Expression profiling by array**
Platform:	**GPL1261**
Pubmed ID:	
Summary & Design:	**Summary:** **cAMP inhibits TCR signaling, T cell proliferation, cytokine production and T cell function.** **We used microarrays to detail the global programme of gene expression in TCR-activated WT or IFN-gR1-deficient CD4+ T cells by db-cAMP.** **Overall design:** **CD4+ T cells were purified from spleens of WT or IFN-gR1-deficient mice by autoMACS, and activated with anti-CD3 plus anti-CD28 for 15 h. db-cAMP or vehicle control (med) was added into cultures for the last 3 h.**

Background corr dist: **KL-Divergence = 0.0621, L1-Distance = 0.0240, L2-Distance = 0.0007, Normal std = 0.5343**

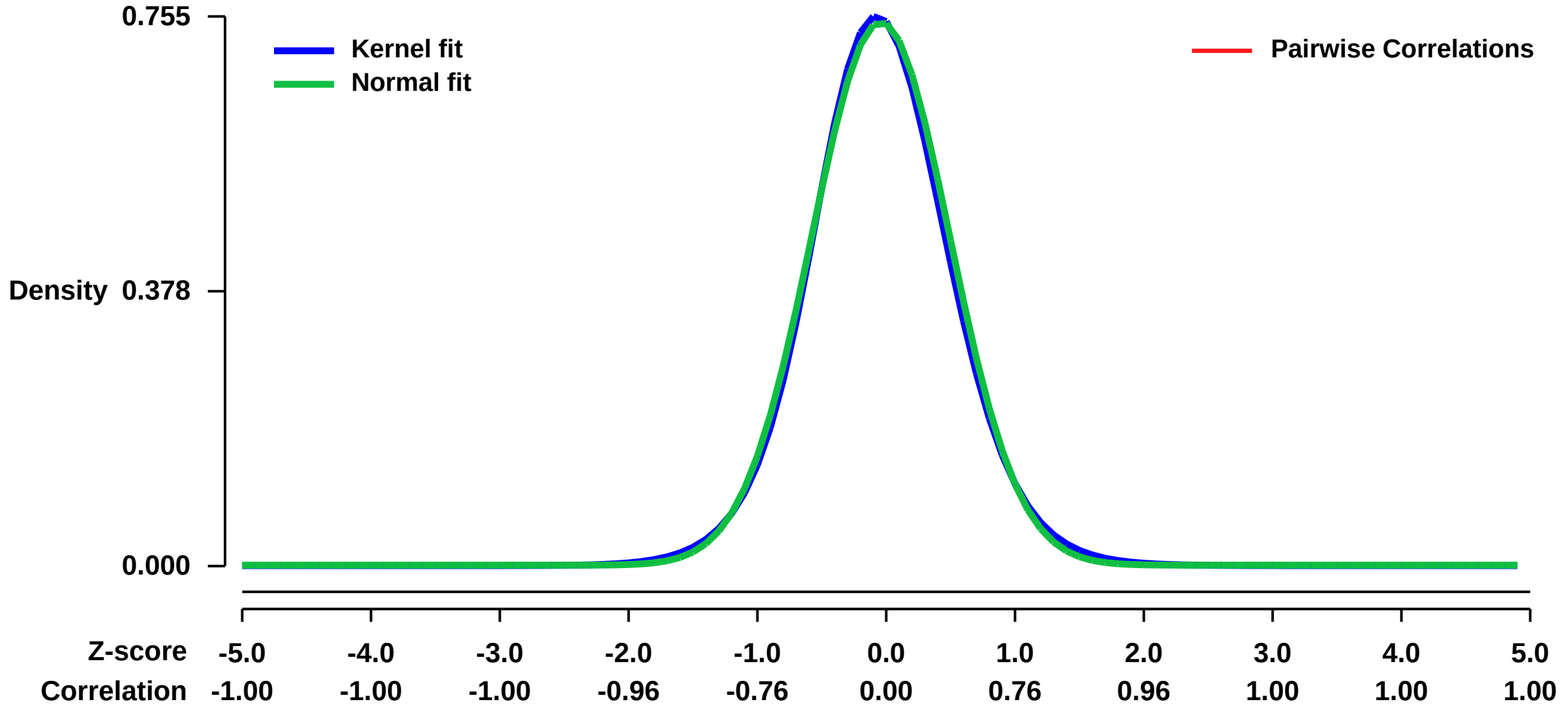

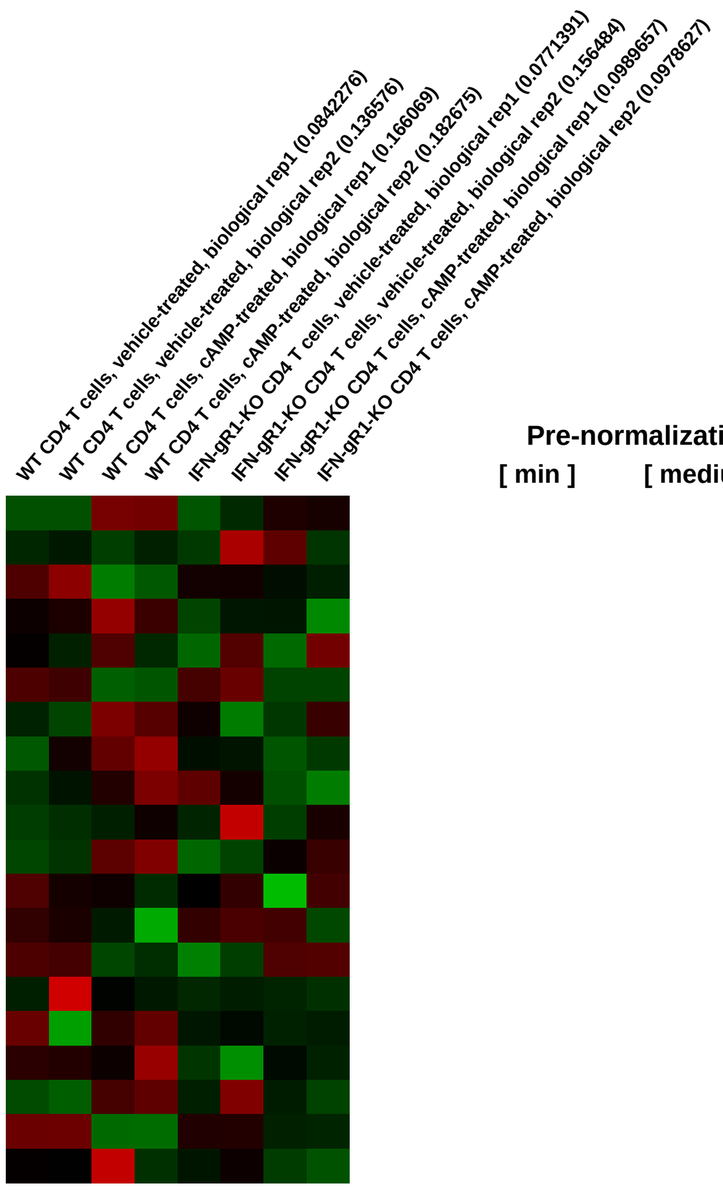

GEO Series "GSE51080" Expression Profiles

Num of samples in this series: 18

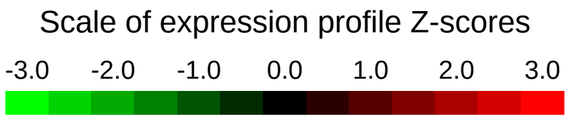

GEO Link:	**http://www.ncbi.nlm.nih.gov/geo/query/acc.cgi?acc=GSE51080**
Status:	**Public on Mar 01 2014**
Title:	**Expression data from exposure of BAT and WAT at 6 and 28 degrees C**
Organism:	**Mus musculus**
Experiment type:	**Expression profiling by array**
Platform:	**GPL1261**
Pubmed ID:	
Summary & Design:	**Summary:** **We run microarrays from three per group Sv129 female mice, ten weeks old, which were maintained at 28´°C (warm conditions) or 6´° C (cold stimulated) for ten days, while standard animal house temperature is 22 ´°C.** **After ten days, three types of tissue were collected: Brown Adipose Tissue (BAT), Mesenteric (visceral) White Adipose Tissue (MES) and Posterior Subcutaneous White Adipose Tissue (WAT)** **Overall design:** **Different adipose tissue depots were taken for RNA extraction and hybridization on Affymetrix microarrays. We sought to determine the differences between white and brown adipose tissues at different temperatures**

Background corr dist: **KL-Divergence = 0.0623, L1-Distance = 0.0392, L2-Distance = 0.0026, Normal std = 0.5381**

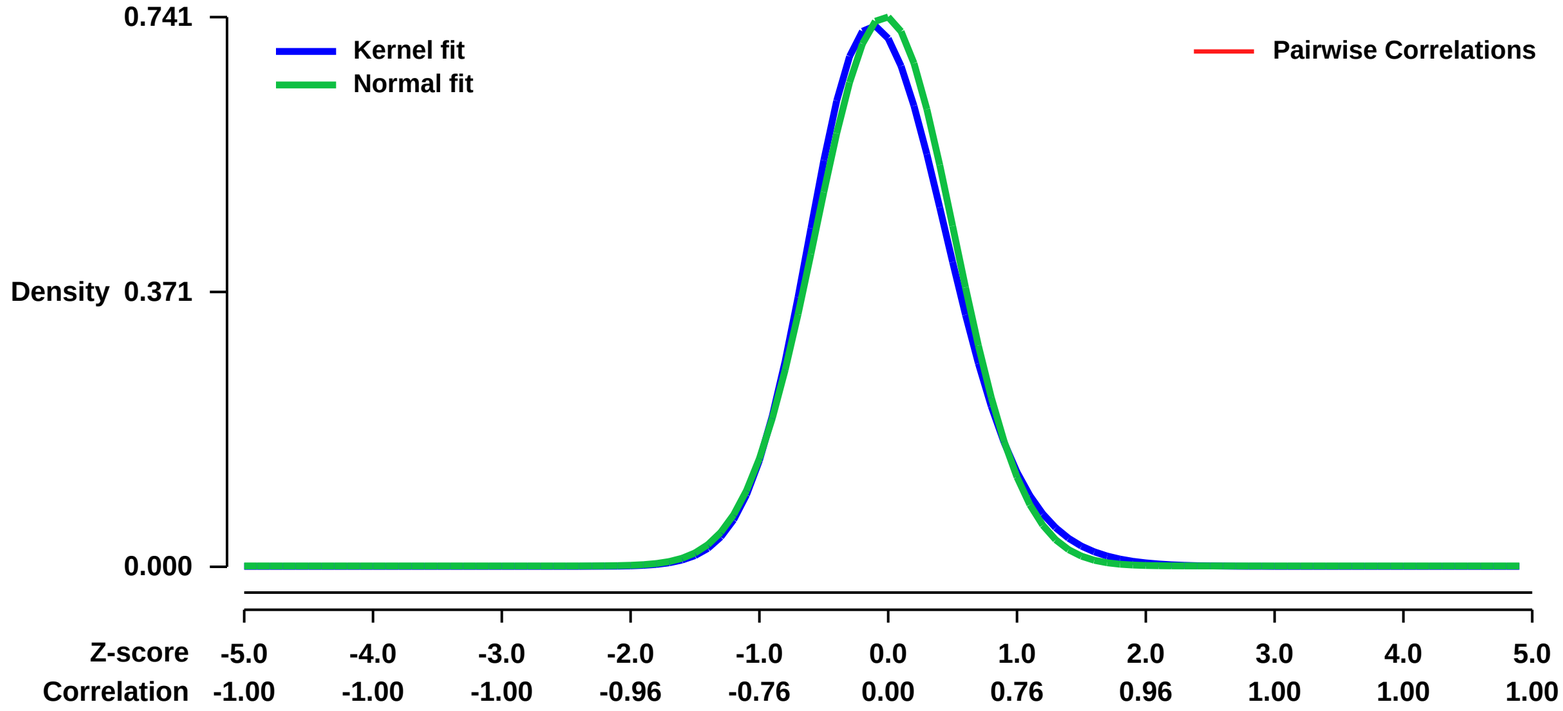

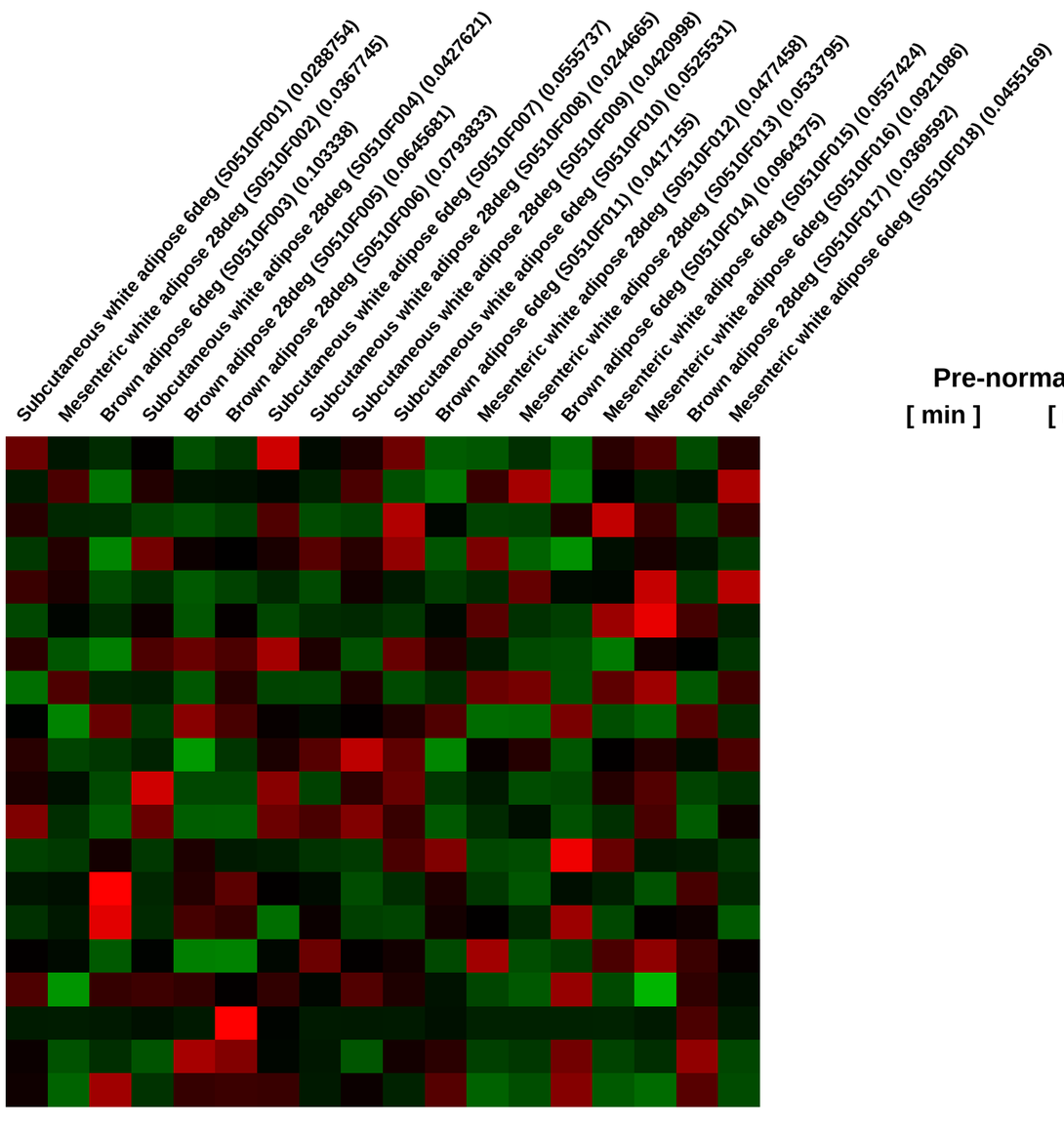

GEO Series "GSE42775" Expression Profiles

Num of samples in this series: 12

Scale of expression profile Z-scores

-3.0 -2.0 -1.0 0.0 1.0 2.0 3.0

GEO Link:	http://www.ncbi.nlm.nih.gov/geo/query/acc.cgi?acc=GSE42775
Status:	Public on Aug 13 2013
Title:	Gene expression microarray analysis on the medial prefrontal cortex of Schnurri-2 knockout and wild-type control mice
Organism:	Mus musculus
Experiment type:	Expression profiling by array
Platform:	GPL1261
Pubmed ID:	23389689
Summary & Design:	**Summary:** Schnurri-2 (Shn-2), an NF-kappa B site-binding protein, tightly binds to the enhancers of major histocompatibility complex (MHC) class I genes and inflammatory cytokines, which have been shown to harbor common variant single nucleotide polymorphisms associated with schizophrenia. Shn-2 knockout mice show behavioral abnormalities that strongly resemble those of schizophrenics. We performed gene expression microarray analysis of prefrontal cortices from Shn-2 knockout and wild-type control mice. **Overall design:** Prefrontal cortex RNA isolated from six Shn-2 knockout and six control wild-type mice were compared.

Background corr dist: KL-Divergence = 0.1296, L1-Distance = 0.0369, L2-Distance = 0.0026, Normal std = 0.3934

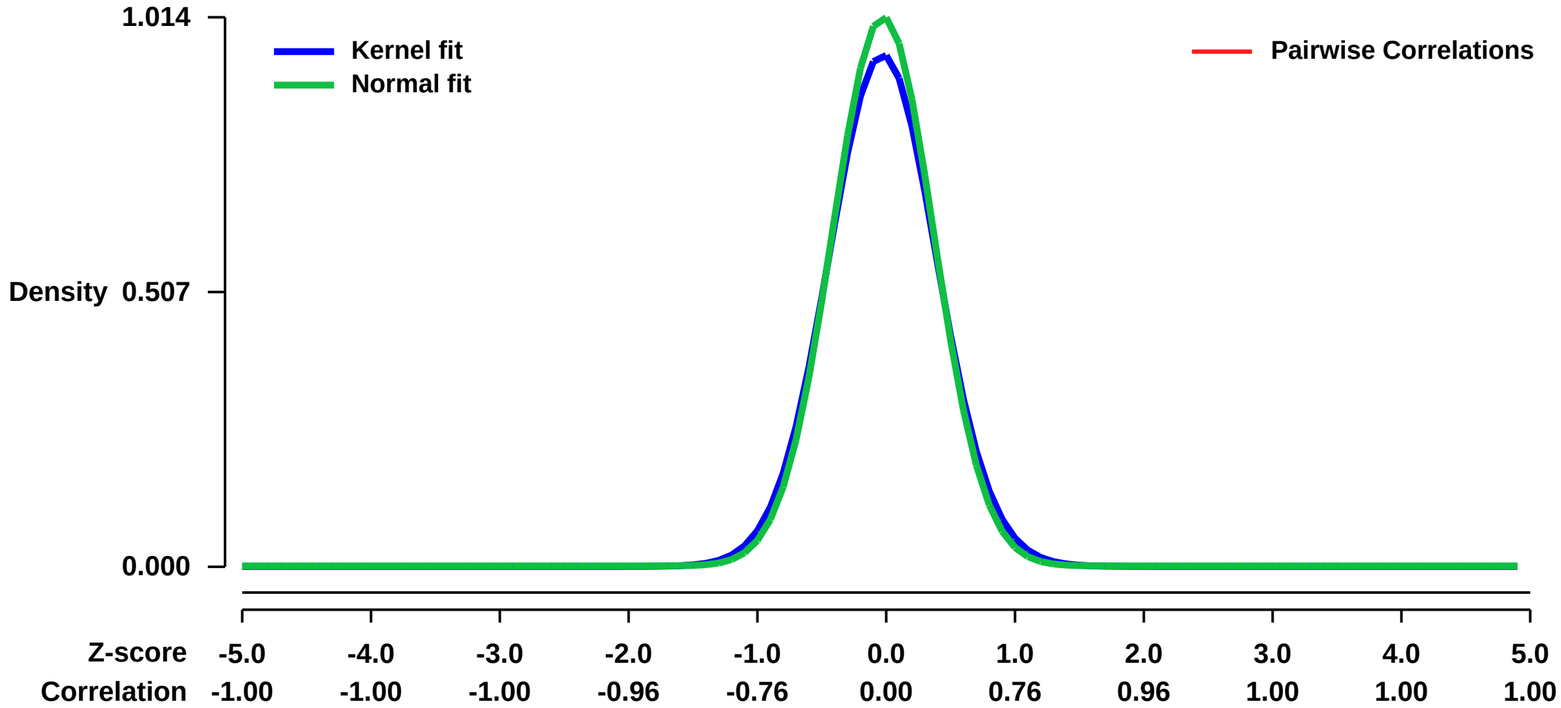

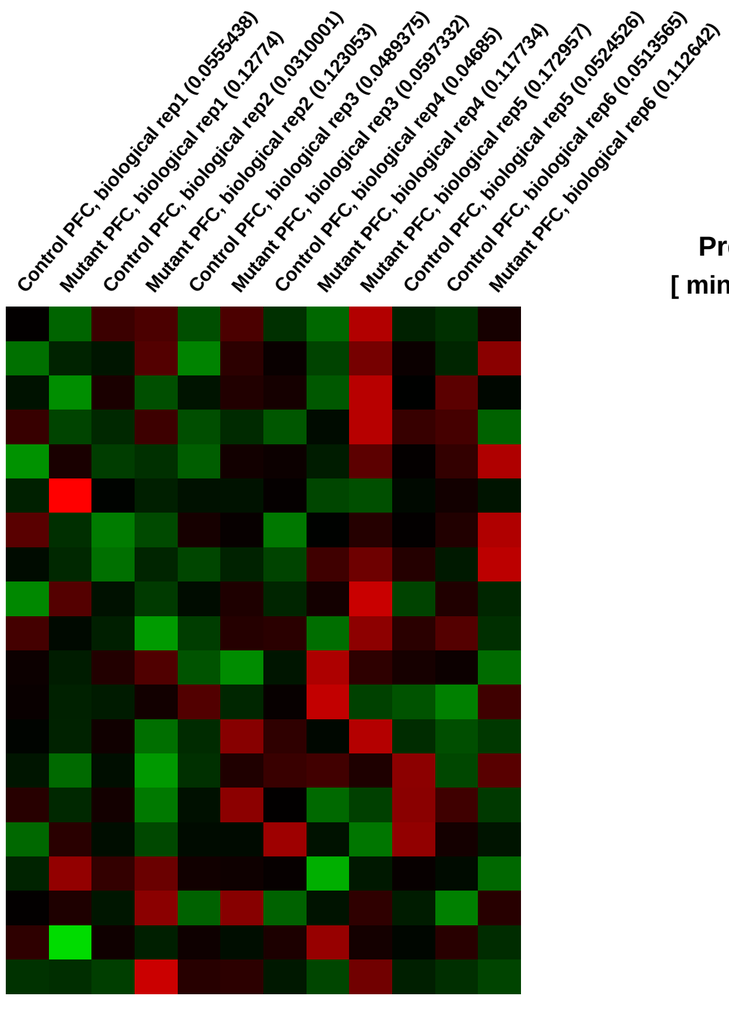

GEO Series "GSE14320" Expression Profiles

Num of samples in this series: 10

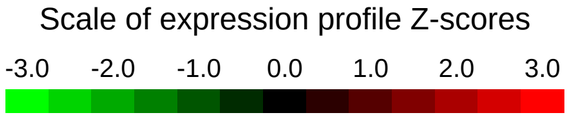

GEO Link:	http://www.ncbi.nlm.nih.gov/geo/query/acc.cgi?acc=GSE14320
Status:	Public on Jan 12 2009
Title:	Basal and kainate-induced gene expression in A-CREB mouse hippocampi
Organism:	Mus musculus
Experiment type:	Expression profiling by array
Platform:	GPL1261
Pubmed ID:	20395962
Summary & Design:	**Summary:** The cAMP responsive element binding protein (CREB) pathway has been involved in two major cascades of gene expression regulating neuronal function. The first one presents CREB as a critical component of the molecular switch that control longlasting forms of neuronal plasticity and learning. The second one relates CREB to neuronal survival and protection. To investigate the role of CREB-dependent gene expression in neuronal plasticity and survival in vivo, we generated bitransgenic mice expressing A-CREB, an artificial peptide with strong and broad inhibitory effect on the CREB family, in forebrain neurons in a regulatable manner. The expression of ACREB in hippocampal neurons impaired L-LTP, reduced intrinsic excitability and the susceptibility to induced seizures, and altered both basal and activity-driven gene expression. In the long-term, the chronic inhibition of CREB function caused severe loss of neurons in the CA1 subfield as well as in other brain regions. Our experiments confirmed previous findings in CREB deficient mutants and revealed new aspects of CREB-dependent gene expression in the hippocampus supporting a dual role for CREB-dependent gene expression regulating intrinsic and synaptic plasticity and promoting neuronal survival. manufacturer’s protocol. **Overall design:** Each sample contained total RNA from the hippocampi of a group of 3-4 three weeks old mice. We obtained duplicate samples for each experimental condition (in total 14 WT and 20 A-CREB mice where used in this experiment). Mouse Genome 430 2.0 genechips were hybridized, stained, washed and screened for quality according to the manufacturer’s protocol.

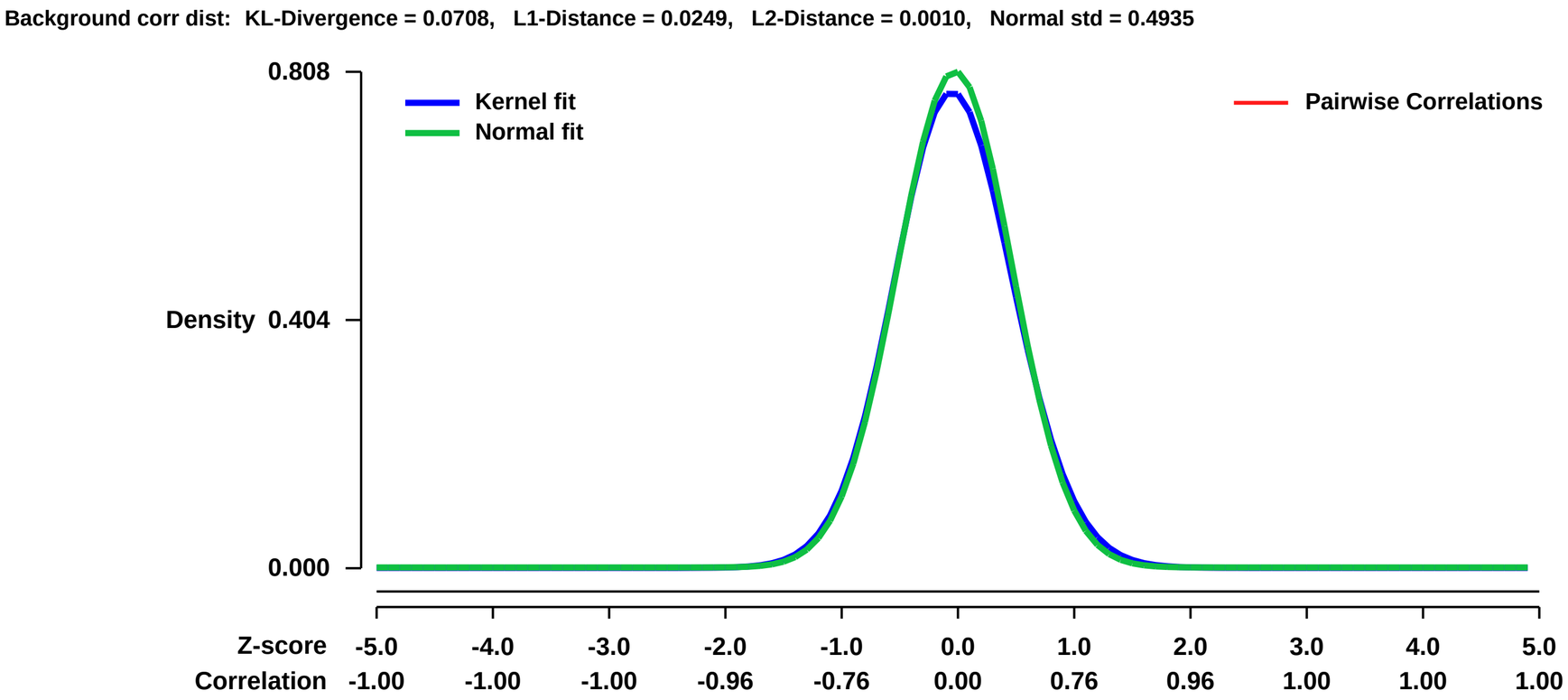

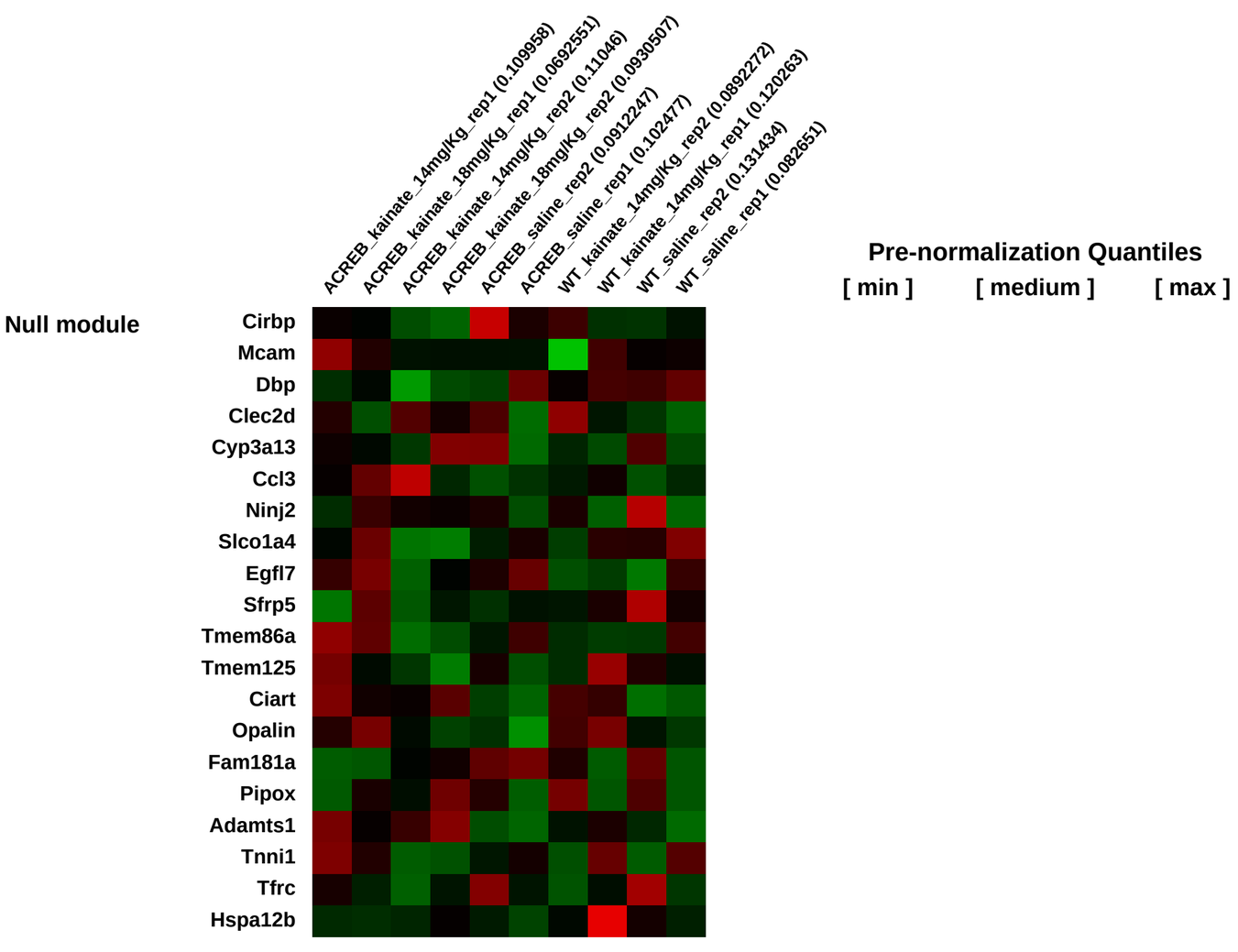

GEO Series "GSE42018" Expression Profiles

Num of samples in this series: 8

Scale of expression profile Z-scores

-3.0 -2.0 -1.0 0.0 1.0 2.0 3.0

GEO Link:	http://www.ncbi.nlm.nih.gov/geo/query/acc.cgi?acc=GSE42018
Status:	Public on Nov 07 2012
Title:	Cerebellar Granule Neuron Temporal-NFI Microarray Data
Organism:	Mus musculus
Experiment type:	Expression profiling by array
Platform:	GPL1261
Pubmed ID:	23407945
Summary & Design:	**Summary:** **Dendrite and synapse development are critical for establishing appropriate neuronal circuits, and disrupted timing of these events can alter connectivity leading to disordered neural function.** **In early postnatal development of cerebellar granule neurons (CGNs), the expression of many genes is temporally regulated. Further, NFI (Nuclear Factor I) proteins have been shown to play important roles in the regulation of gene expression in developing CGNs.** **To identify NFI-regulated genome-wide targets involved in late maturation of mouse CGNs, we performed two groups of microarray expression analysis: (1) temporal expression arrays using 1.5 and 6 day cultures of mouse CGNs representing immature and more mature CGNs, respectively, which identified 844 Temporal-Up or Down genes; and (2) NFI-regulated genes in 6 day CGN cultures that were infected at the time of plating with lentiviral vectors expressing either NFI dominant repressor (NFI-EnR) or EnR control protein. This identified 686 NFI-Up (NFI-EnR down-regulated) or NFI-Down (NFI-EnR up-regulated) genes.** **Overlap analysis identified 212 temporal genes that were regulated by NFI. These results indicated that NFI plays a pivotal role in the regulation of late CGN maturation.** **Overall design:** **For temporal arrays, mouse CGN progenitors were purified from P6 mouse cerebellum and cultured for either 1.5 or 6 days. Three biological replicates were analyzed for each time point. For NFI arrays, CGN progenitors from P6 mice were transduced upon plating with either NFI-EnR or EnR control lentivirus and cultured 6 days. Four pairs of biological replicates were performed.**

Background corr dist: KL-Divergence = 0.0420, L1-Distance = 0.0198, L2-Distance = 0.0006, Normal std = 0.5872

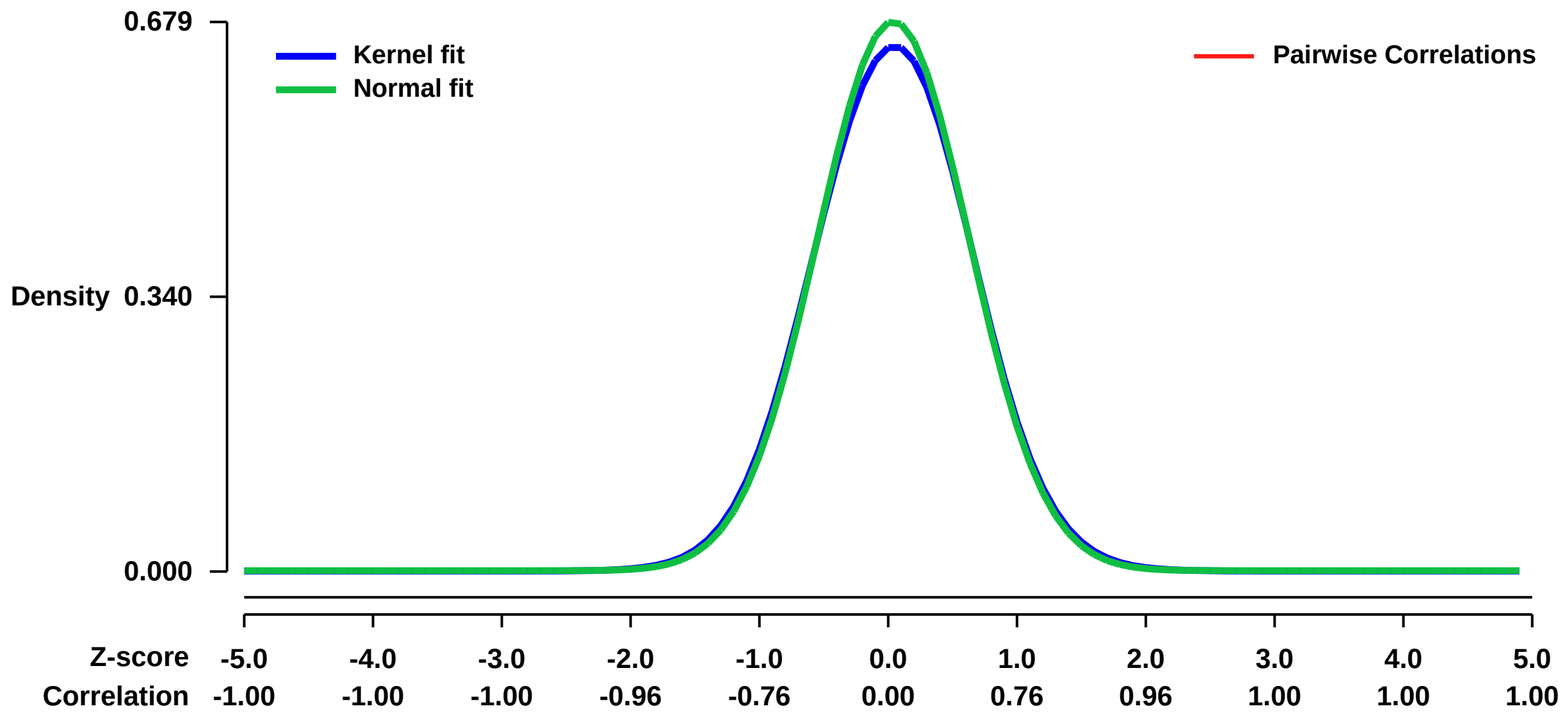

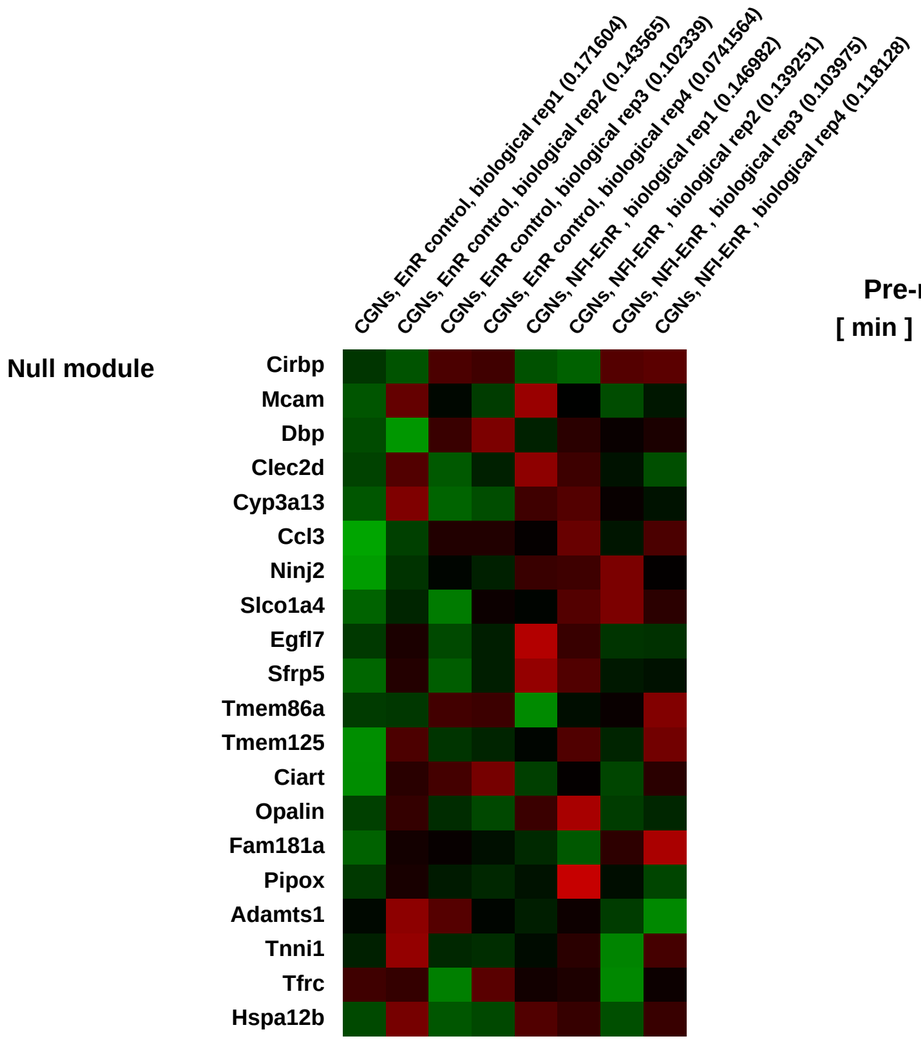

GEO Series "GSE7324" Expression Profiles

Num of samples in this series: 10

Scale of expression profile Z-scores

-3.0 -2.0 -1.0 0.0 1.0 2.0 3.0

GEO Link:	**http://www.ncbi.nlm.nih.gov/geo/query/acc.cgi?acc=GSE7324**
Status:	**Public on Mar 21 2007**
Title:	**Structural basis for recognition of SMRT/N-CoR by the MYND domain and its contribution to AML1/ETO's activity**
Organism:	**Mus musculus**
Experiment type:	**Expression profiling by array**
Platform:	**GPL1261**
Pubmed ID:	
Summary & Design:	**Summary:** **To examine the effects of disrupting the AML1/ETO MYND-SMRT interaction with the W692A substitution on AML1/ETO function, the global gene expression profile of mouse bone marrow LSK cells transduced with GFP was compared to that of cells transduced with either wild-type AML1/ETO or AML1/ETO harboring the W692A substitution in the MYND domain. Three independent biological replicates were assessed for both the control (GFP/MigR1) and AML1/ETO (intact MYND-SMRT interaction) conditions, whereas four independent biological replicates were assessed for the W692A (disrupted MYND-SMRT interaction) condition. The three GFP replicates were used to establish a baseline signal for comparison to both the AML1/ETO and W692A samples.** **Keywords: genetic modification** **Overall design:** **Global gene expression profiles of FACS-sorted Lin-Sca1+cKit+ mouse bone marrow cells transduced with empty vector (GFP-MigR1), AML1/ETO, or AML1/ETO with the W692A substitution (W692A).**

Background corr dist: **KL-Divergence = 0.0891, L1-Distance = 0.0209, L2-Distance = 0.0006, Normal std = 0.4614**

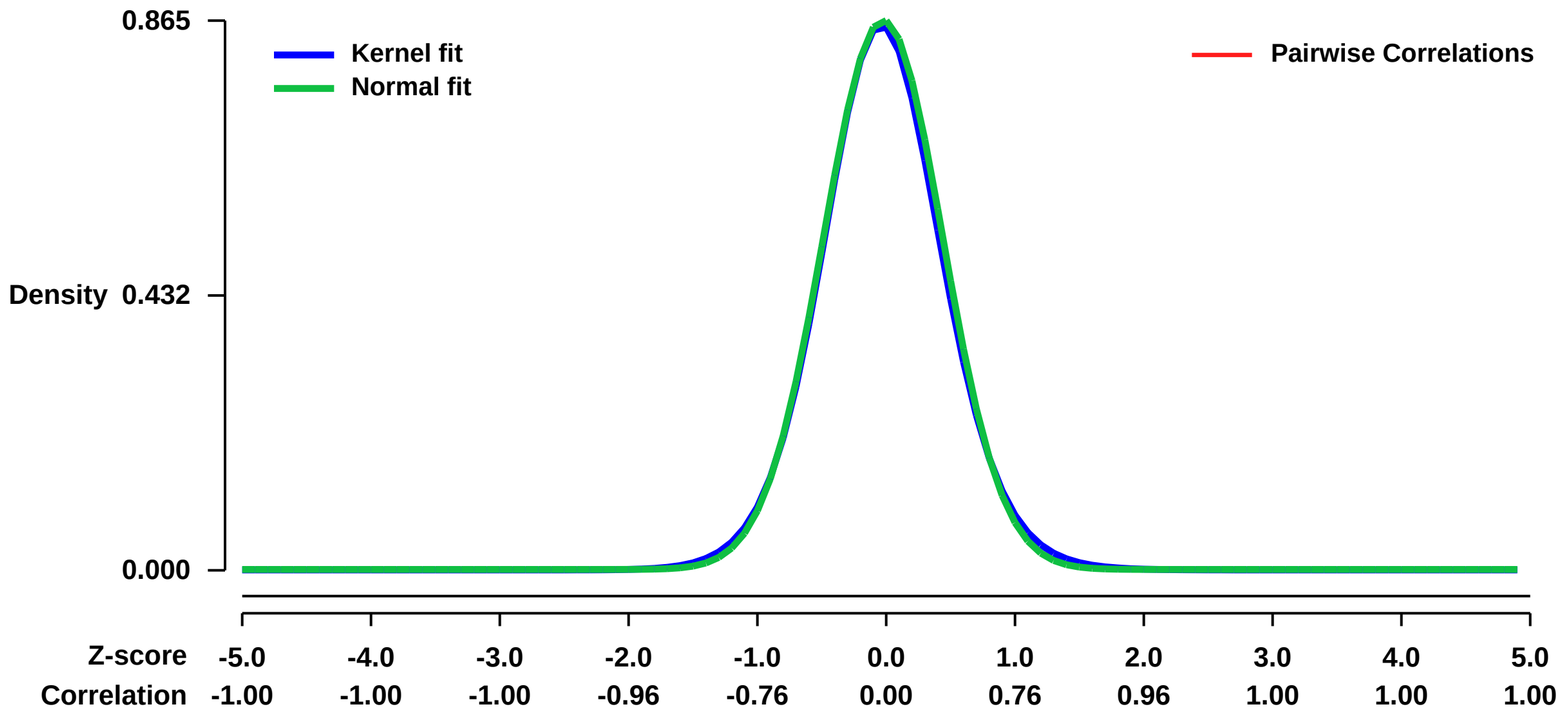

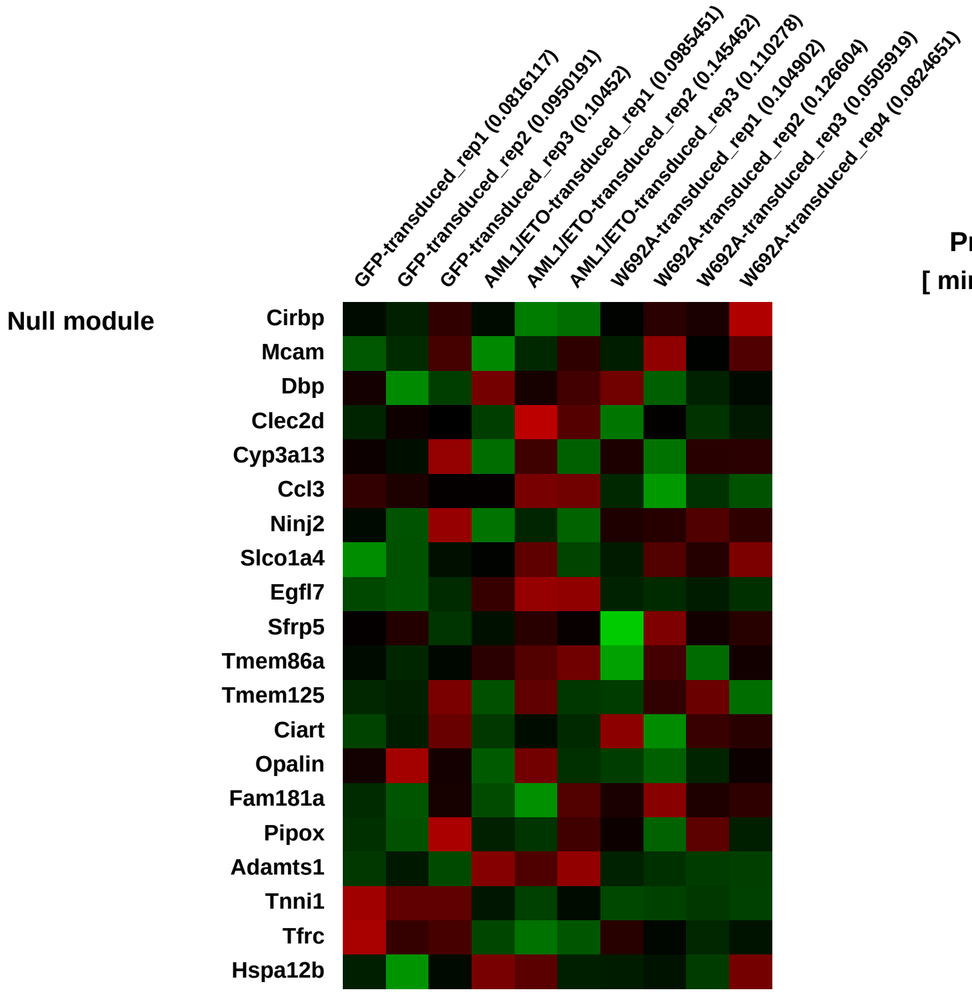

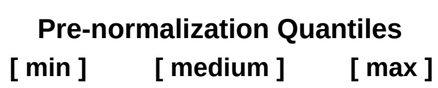

GEO Series "GSE8733" Expression Profiles

Num of samples in this series: 24

Scale of expression profile Z-scores

-3.0 -2.0 -1.0 0.0 1.0 2.0 3.0

GEO Link:	http://www.ncbi.nlm.nih.gov/geo/query/acc.cgi?acc=GSE8733
Status:	Public on Aug 10 2007
Title:	Folate deficiency enhances arsenic effects on ODC mouse skin gene expression
Organism:	Mus musculus
Experiment type:	Expression profiling by array
Platform:	GPL1261
Pubmed ID:	17928125
Summary & Design:	**Summary:** We demonstrate that expression of key markers of keratinocyte differentiation is suppressed by exposure to sodium arsenite. Folate deficiency exacerbates this effect. In addition, cancer-related cell movement genes, and growth and proliferation genes are altered. Several redox-sensitive transcription factors are implicated in mediating these gene expression changes due to arsenic treatment and folate deficiency. **Keywords: gene expression/microarray** **Overall design:** K6/ODC mice were maintained on either a folate deficient or folate sufficient diet and exposed to 0, 1, or 10 ppm sodium arsenite in the drinking water for 30 days. Total RNA was isolated from skin samples and gene expression analyzed using Affymetrix Mouse 430 2.0 GeneChips. Data from 24 samples, with four mice in each of the six treatment groups, were analyzed.

Background corr dist: KL-Divergence = 0.1869, L1-Distance = 0.0446, L2-Distance = 0.0043, Normal std = 0.3409

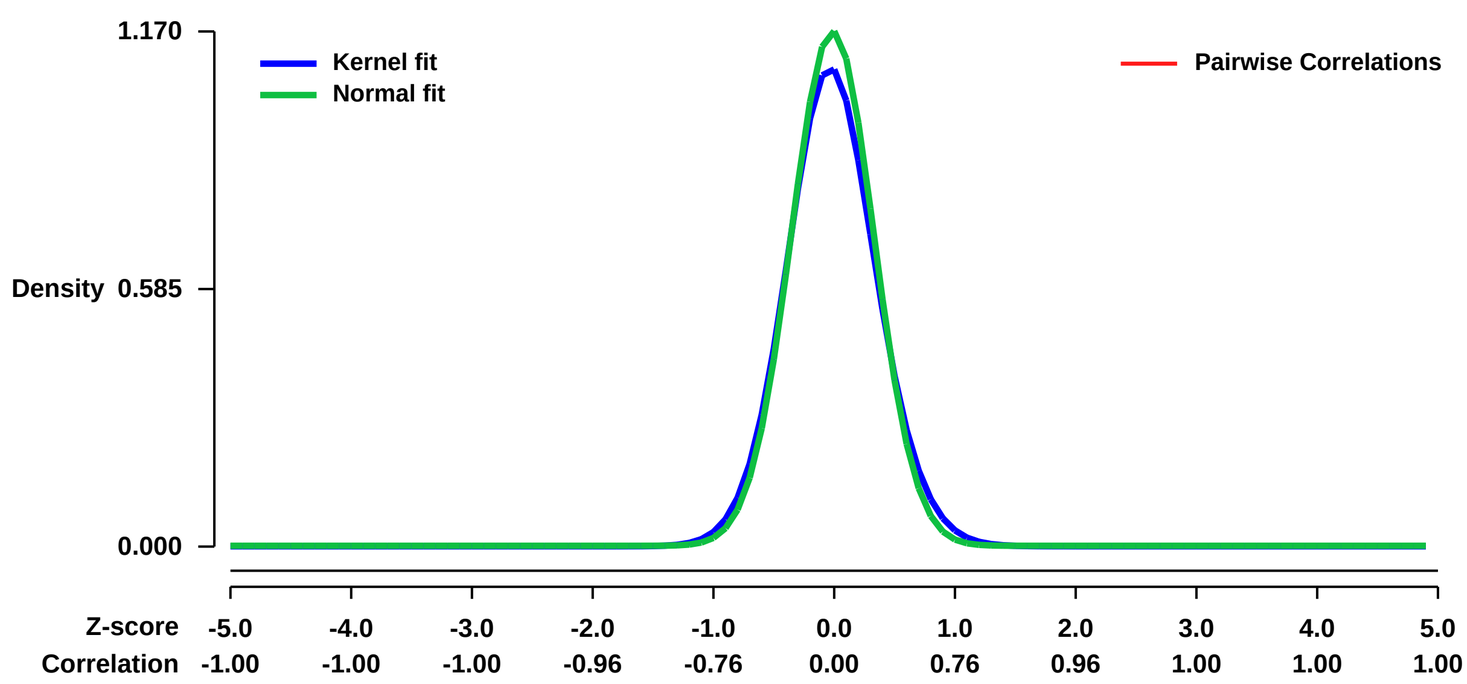

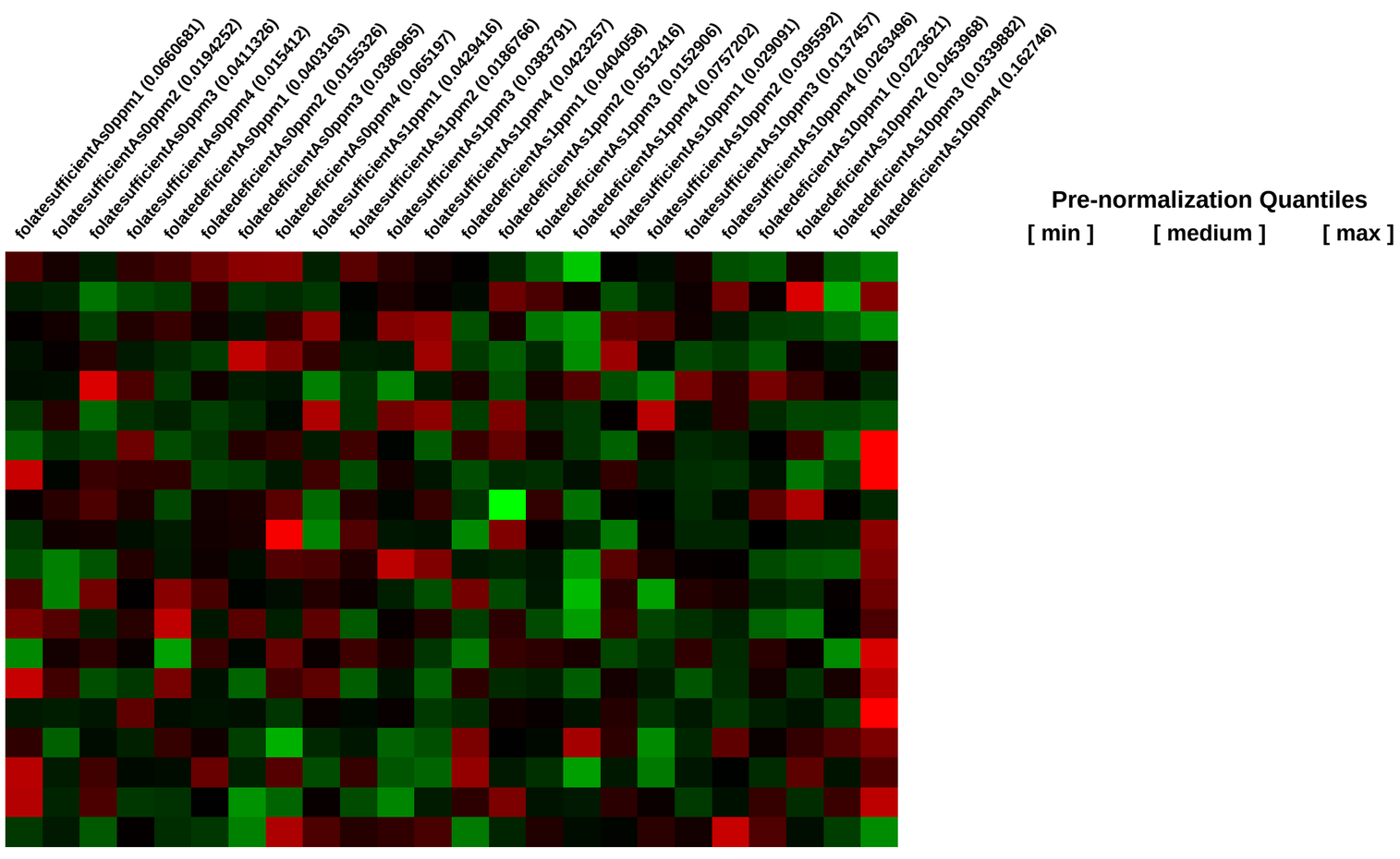

GEO Series "GSE35899" Expression Profiles

Num of samples in this series: 15

Scale of expression profile Z-scores

-3.0 -2.0 -1.0 0.0 1.0 2.0 3.0

GEO Link:	**http://www.ncbi.nlm.nih.gov/geo/query/acc.cgi?acc=GSE35899**
Status:	**Public on Feb 18 2014**
Title:	**Expression data from Mammospheres**
Organism:	**Mus musculus**
Experiment type:	**Expression profiling by array**
Platform:	**GPL1261**
Pubmed ID:	**24290754**
Summary & Design:	**Summary:** **The combined activation of Wnt/^ -catenin and MET/HGF is required for mammary cancer stem cell (MaCSC) maintenance. We generated mammospheres derived from tumors of mice harboring Wnt/Met signaling mutations on which we performed microarray analysis to evaluate gene expression signatures controlled by Wnt and MET pathways. We used the gene expression profiles to dissect the role and the functions of these pathways in MaCSCs.** **Overall design:** **We treated mammospheres with Wnt and MET pathway inhibitors alone or in combination. Samples treated with DMSO were used as vehicle control.**

Background corr dist: **KL-Divergence = 0.0642, L1-Distance = 0.0265, L2-Distance = 0.0012, Normal std = 0.5104**

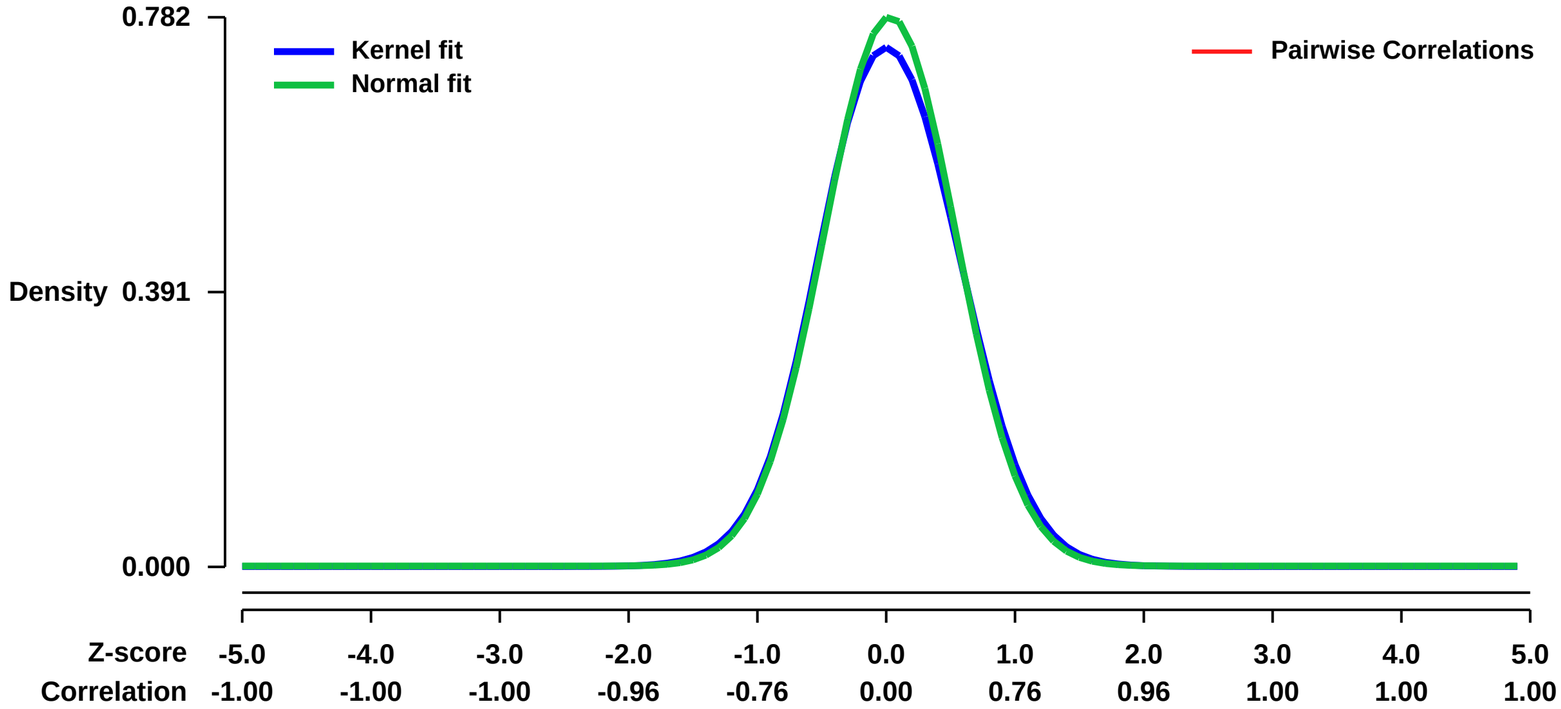

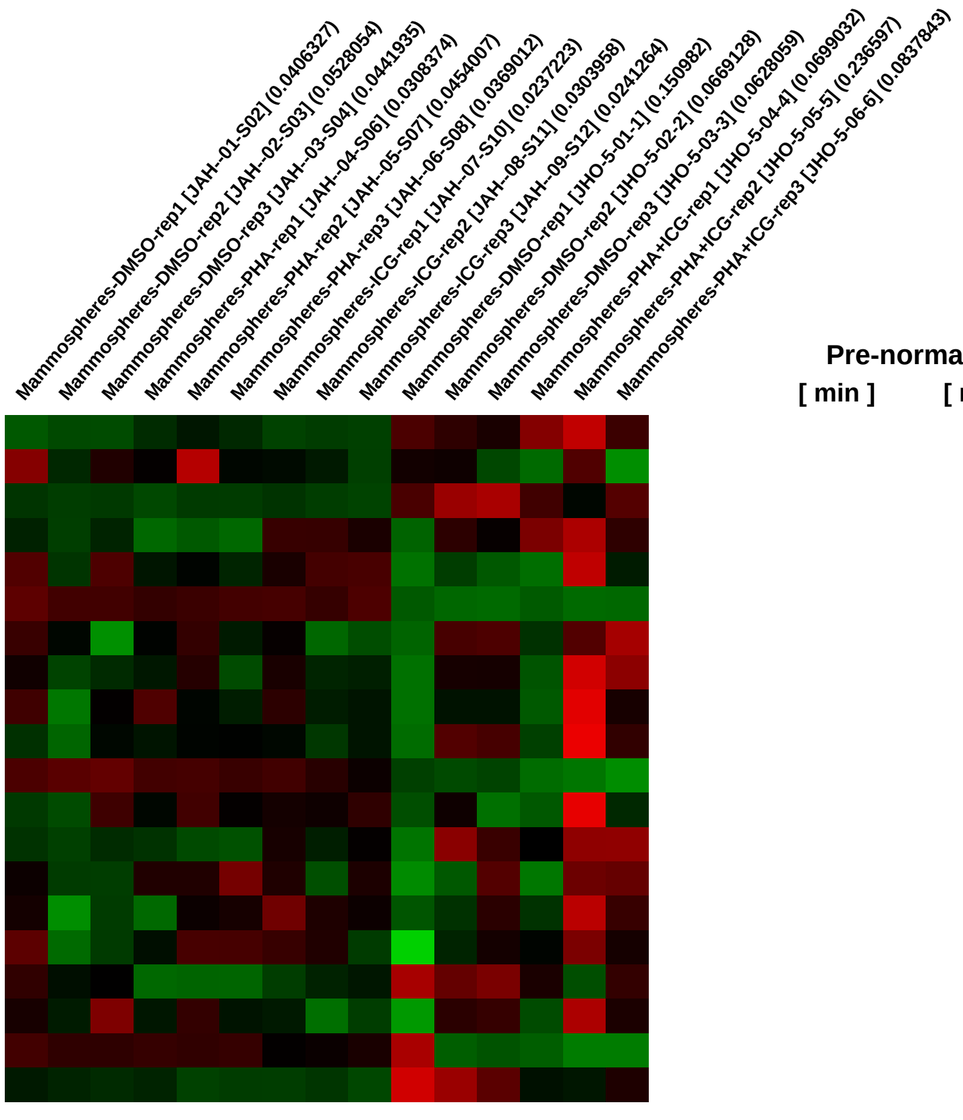

GEO Series "GSE9711" Expression Profiles

Num of samples in this series: 6

Scale of expression profile Z-scores

-3.0 -2.0 -1.0 0.0 1.0 2.0 3.0

GEO Link:	**http://www.ncbi.nlm.nih.gov/geo/query/acc.cgi?acc=GSE9711**
Status:	**Public on Jul 11 2008**
Title:	**Expression comparison between wild-type and transgenic mouse lenses**
Organism:	**Mus musculus**
Experiment type:	**Expression profiling by array**
Platform:	**GPL1261**
Pubmed ID:	
Summary & Design:	**Summary:** **The vertebrate ocular lens consists of two basic cell types: the lens fibers, highly specialized cells that make up the bulk of the lens and are the basis for its unique optical characteristics, and the epithelial cells that cover the anterior hemisphere and acts as a stem cell population for progenitors of new fibers. The forkhead transcription factor FoxE3 is essential for maintenance, proliferation and survival of the epithelial cells, and silencing of the FoxE3 gene coincides with the cell cycle arrest that marks initiation of fiber cell differentiation. Here we have used transgenic ectopic expression of murine Foxe3 in fiber cells to investigate the consequences of persistent Foxe3 expression during fiber differentiation. Microarray transcript profiling showed that ectopic Foxe3 caused a general increase in mRNAs which are normally enriched in epithelial cells, consistent with an epithelialization of the transgenic fibers.** **Keywords: Genetic modification** **Overall design:** **Whole lenses from P2 animals were dissected and genotyped. 12 lenses from each genotype were used for RNA extraction and hybridization to Affymetrix arrays. Total of 3 replicates/genotype.**

Background corr dist: KL-Divergence = 0.0358, L1-Distance = 0.0146, L2-Distance = 0.0002, Normal std = 0.6368

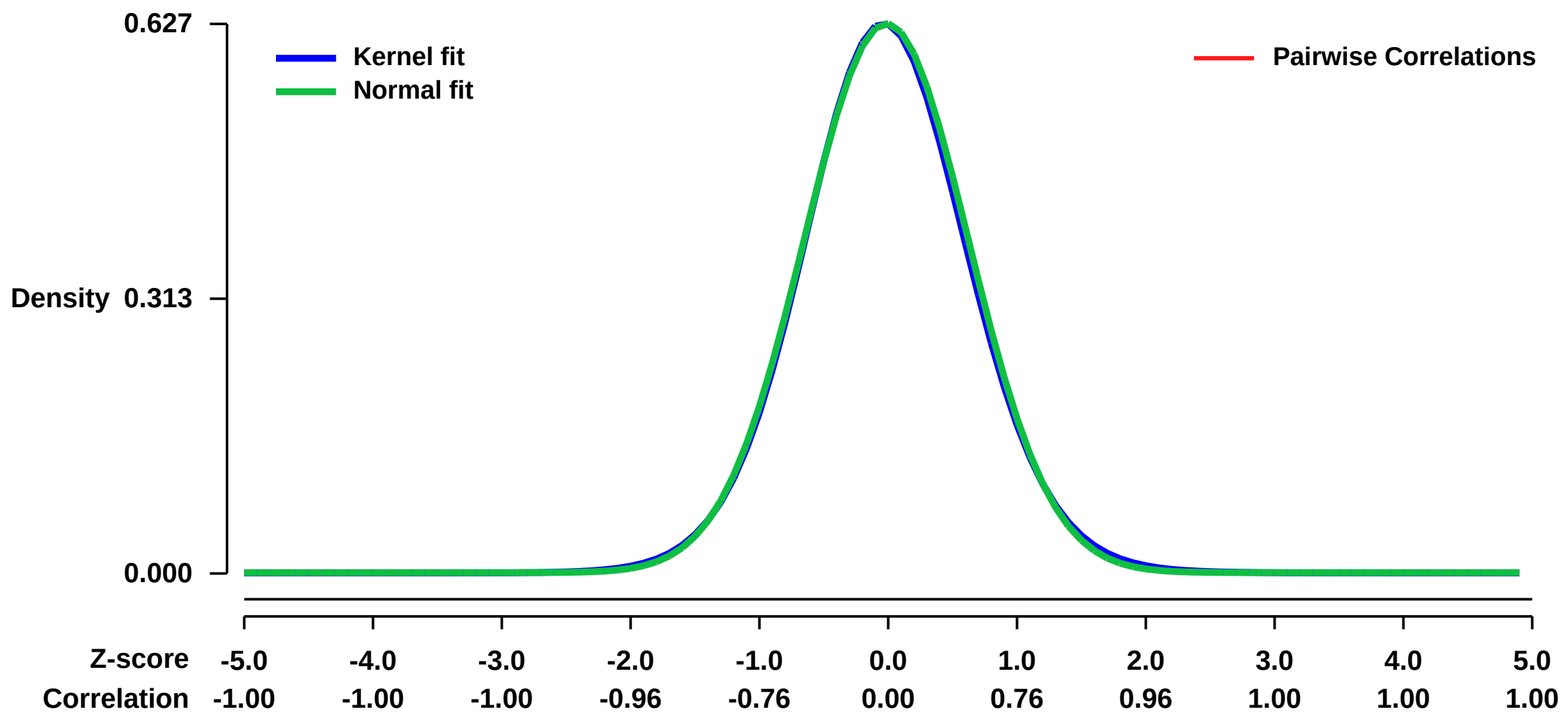

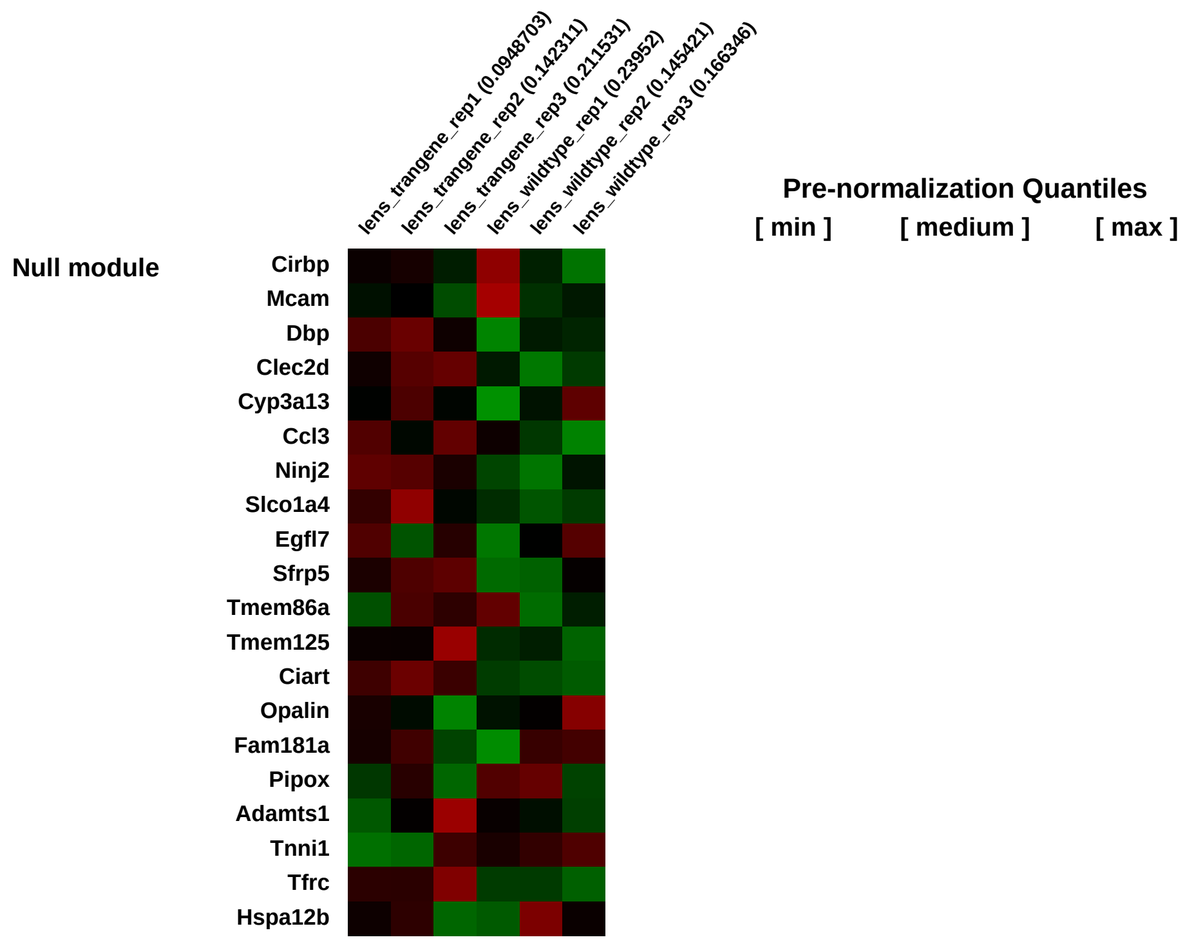

GEO Series "GSE24628" Expression Profiles

Num of samples in this series: 16

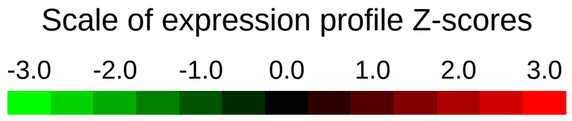

GEO Link:	**http://www.ncbi.nlm.nih.gov/geo/query/acc.cgi?acc=GSE24628**
Status:	**Public on Nov 01 2010**
Title:	**Subtypes of medulloblastoma have distinct developmental origins**
Organism:	**Mus musculus**
Experiment type:	**Expression profiling by array**
Platform:	**GPL1261**
Pubmed ID:	**21150899**
Summary & Design:	**Summary:** **Medulloblastoma encompasses a collection of clinically and molecularly diverse tumor subtypes that together comprise the most common malignant childhood brain tumor. These tumors are thought to arise within the cerebellum, with approximately 25% originating from granule neuron precursor cells (GNPCs) following aberrant activation of the Sonic Hedgehog pathway (hereafter, SHH-subtype). The pathological processes that drive heterogeneity among the other medulloblastoma subtypes are not known, hindering the development of much needed new therapies. Here, we provide evidence that a discrete subtype of medulloblastoma that contains activating mutations in the WNT pathway effector CTNNB1 (hereafter, WNT-subtype), arises outside the cerebellum from cells of the dorsal brainstem. We found that genes marking human WNT-subtype medulloblastomas are more frequently expressed in the lower rhombic lip (LRL) and embryonic dorsal brainstem than in the upper rhombic lip (URL) and developing cerebellum. Magnetic resonance imaging (MRI) and intra-operative reports showed that human WNT-subtype tumors infiltrate the dorsal brainstem, while SHH-subtype tumors are located within the cerebellar hemispheres. Activating mutations in Ctnnb1 had little impact on progenitor cell populations in the cerebellum, but caused the abnormal accumulation of cells on the embryonic dorsal brainstem that included aberrantly proliferating Zic1+ precursor cells. These lesions persisted in all mutant adult mice and in 15% of cases in which Tp53 was concurrently deleted, progressed to form medulloblastomas that recapitulated the anatomy and gene expression profiles of human WNT-subtype medulloblastoma. We provide the first evidence that subtypes of medulloblastoma have distinct cellular origins. Our data provide an explanation for the marked molecular and clinical differences between SHH and WNT-subtype medulloblastomas and have profound implications for future research and treatment of this important childhood cancer.** **Overall design:** **A total of 16 samples are analyzed, repsresenting 4 experimental groups: Ctnnb1 medulloblastoma (3 samples); Ptch1 medulloblastoma (6 samples); embryonic dorsal brainstem (4 samples); and postnatal granule neuron precursor cells (3 samples). Every sample was prepared from a different mouse.**

Background corr dist: **KL-Divergence = 0.1173, L1-Distance = 0.0431, L2-Distance = 0.0036, Normal std = 0.4305**

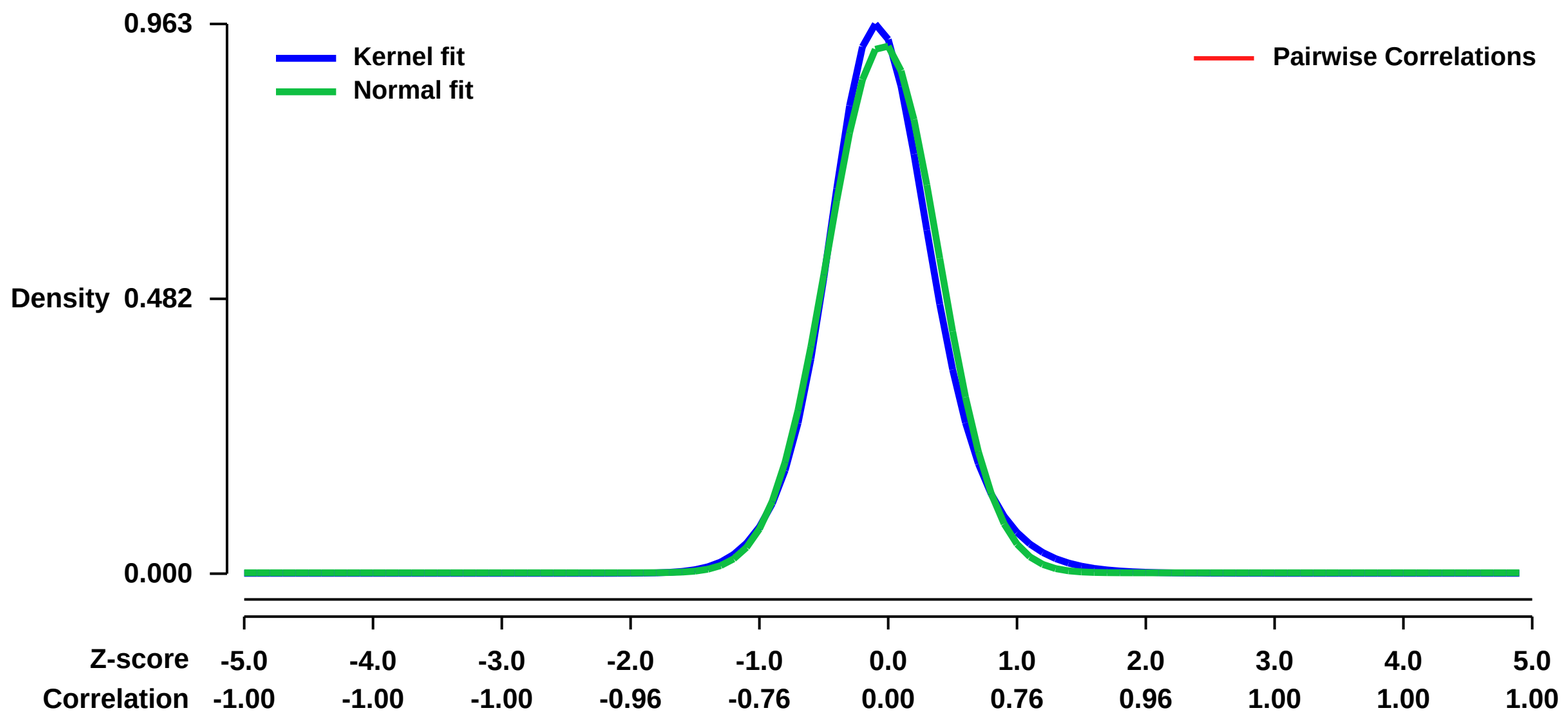

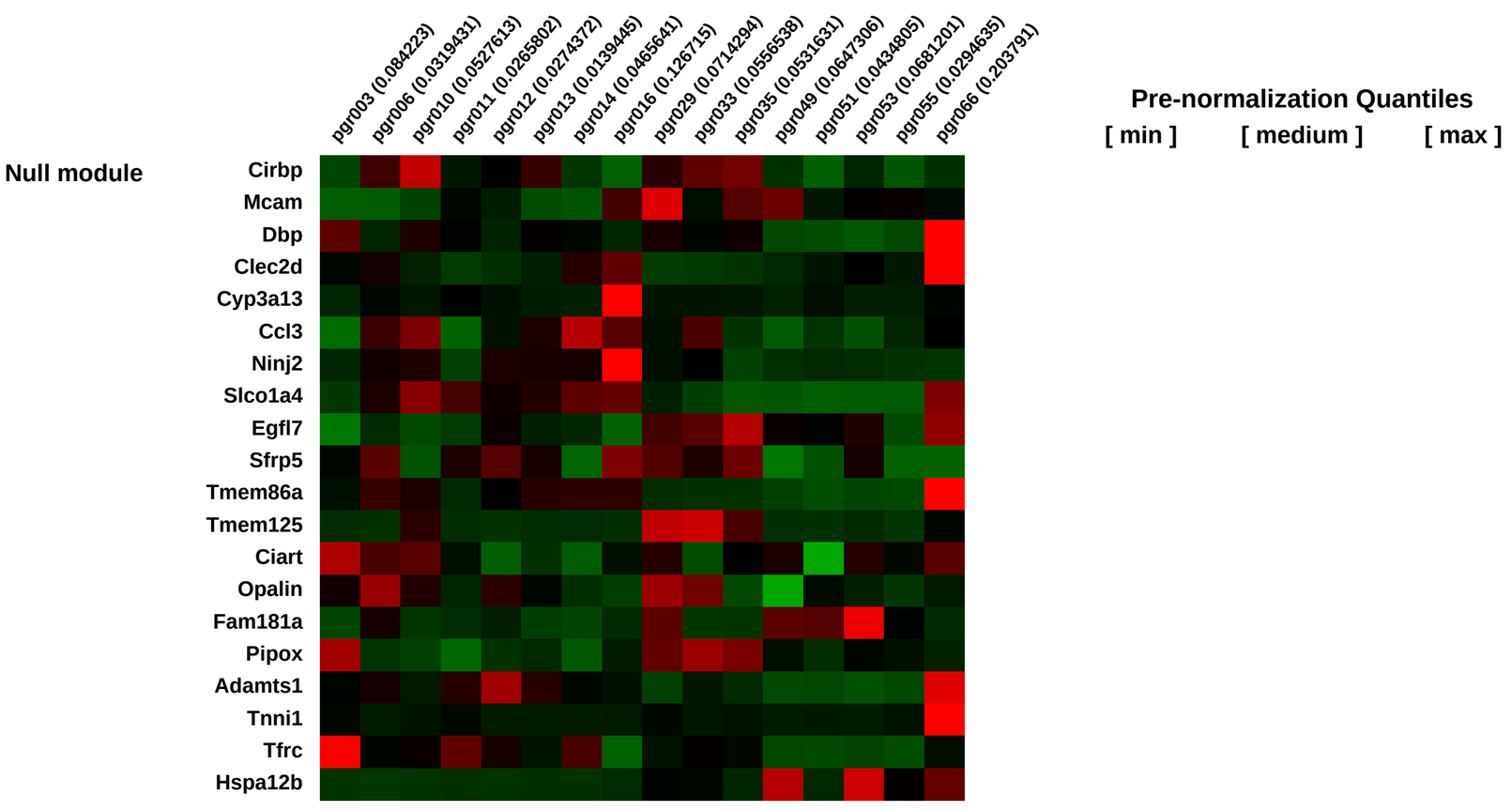

GEO Series "GSE20636" Expression Profiles

Num of samples in this series: 35

Scale of expression profile Z-scores

-3.0 -2.0 -1.0 0.0 1.0 2.0 3.0

GEO Link:	http://www.ncbi.nlm.nih.gov/geo/query/acc.cgi?acc=GSE20636
Status:	Public on Mar 06 2010
Title:	Expression data from OVE26 diabetic mouse kidney
Organism:	Mus musculus
Experiment type:	Expression profiling by array
Platform:	GPL1261
Pubmed ID:	
Summary & Design:	**Summary:** OVE26 mouse was chosen to study the progressive changes in renal gene expression because it displays the most advanced albuminuria mouse models that assembles advanced human diabetic nephropathy. OVE26 mice induce inflammatory gene expression changes consistent with advanced renal disease, associated with severe albuminuria and not reported in any other diabetic models. They provide the first opportunity in a model of diabetic nephropathy to assess the effect of induction of inflammatory proteins that have been implicated in renal injury. **Overall design:** Microarray expression was performed on whole kidney from control and diabetic mice at 2, 4 and 8 months of age and validated by rtPCR, in situ hybridization or immunohistochemistry.

Background corr dist: KL-Divergence = 0.0571, L1-Distance = 0.0288, L2-Distance = 0.0013, Normal std = 0.5364

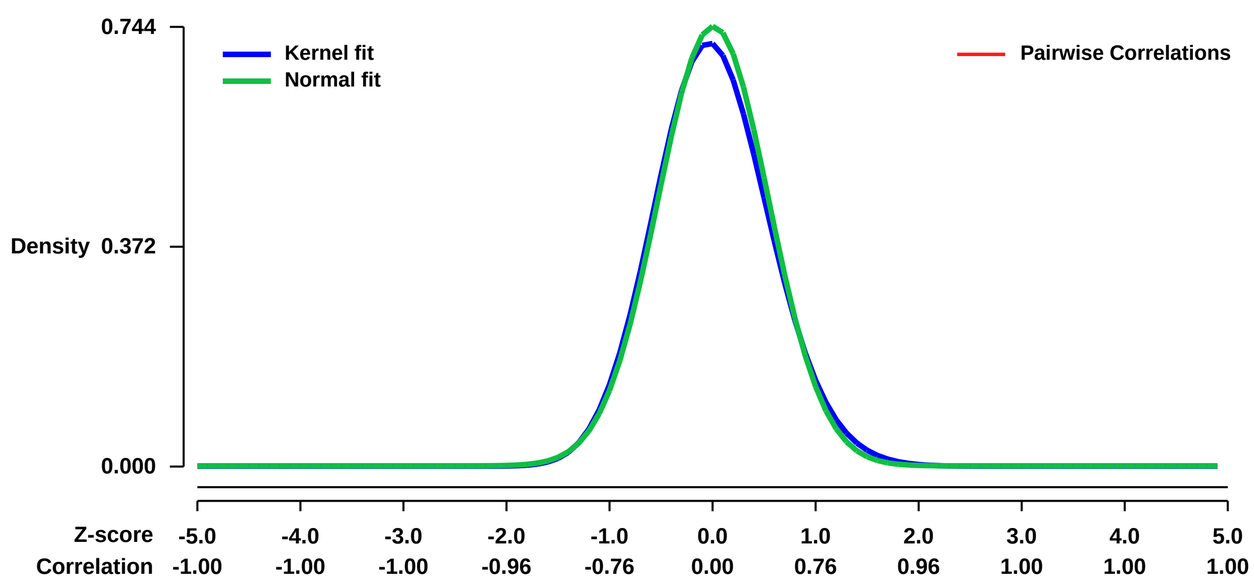

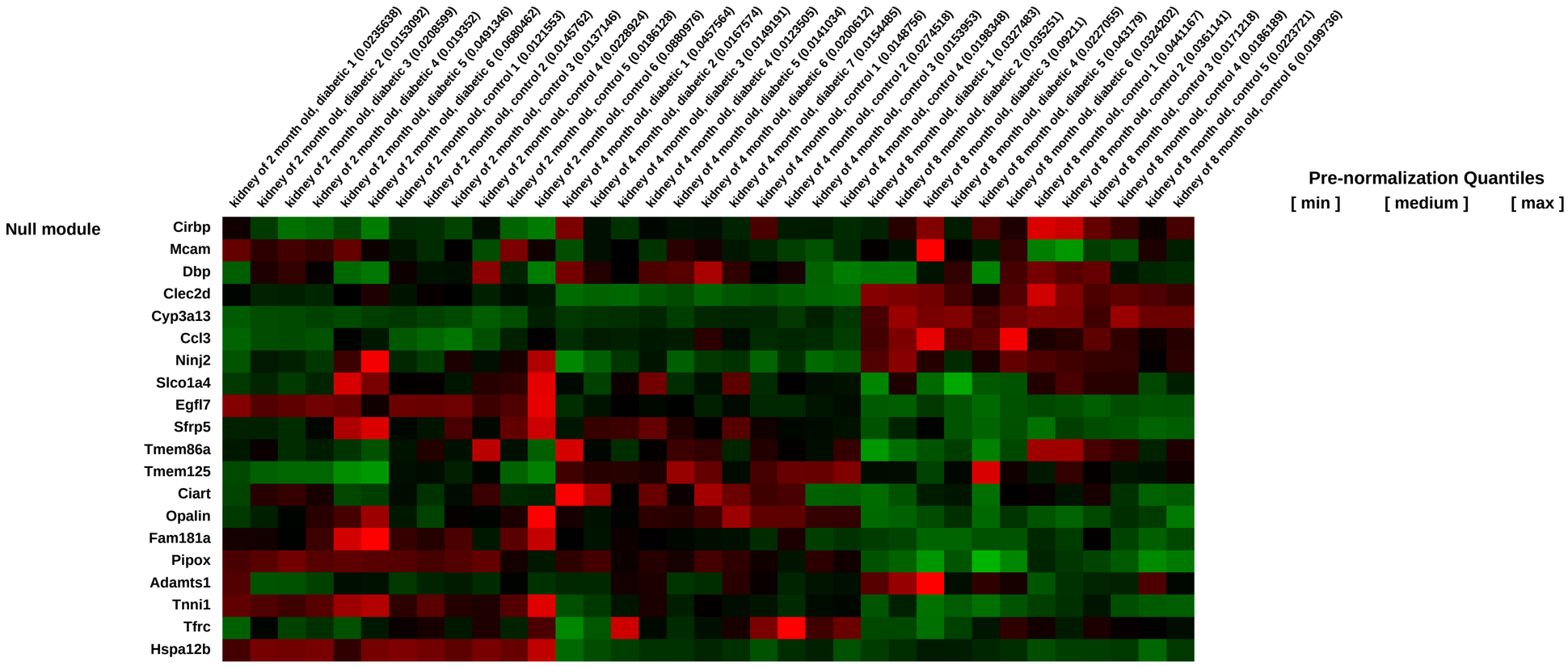

GEO Series "GSE40296" Expression Profiles

Num of samples in this series: 6

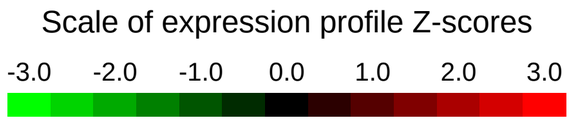

GEO Link:	http://www.ncbi.nlm.nih.gov/geo/query/acc.cgi?acc=GSE40296
Status:	Public on Aug 23 2012
Title:	Essential roles of the histone methyltransferase ESET in the epigenetic control of neural progenitor cells during development
Organism:	Mus musculus
Experiment type:	Expression profiling by array
Platform:	GPL1261
Pubmed ID:	22991445
Summary & Design:	**Summary:** In the developing brain, neural progenitor cells (NPCs) switch the differentiation competency via changing gene expression profiles that are governed partly by epigenetic control such as histone modification, although the precise mechanism is unknown. Here we found that ESET/Setdb1/KMT1E, a histone H3 Lys-9 (H3K9) methyltransferase, was highly expressed at early stages of brain development but down-regulated over time, and that ablation of ESET led to decreased H3K9 trimethylation and misregulation of genes, resulting in severe brain defects and early lethality. In the mutant brain, endogenous retrotransposons were derepressed, and non-neural gene expression was activated. Furthermore, early neurogenesis was most severely impaired, while astrocyte formation was enhanced. We conclude that there is an epigenetic role of ESET in temporal and tissue-specific gene regulation in the developing brain. We used microarrays to identify genes up- or down- regulated when ESET is ablated in the dorsal telencephalon. **Overall design:** We used 3 WT and 3 cKO male E14.5 embryo for each analysis

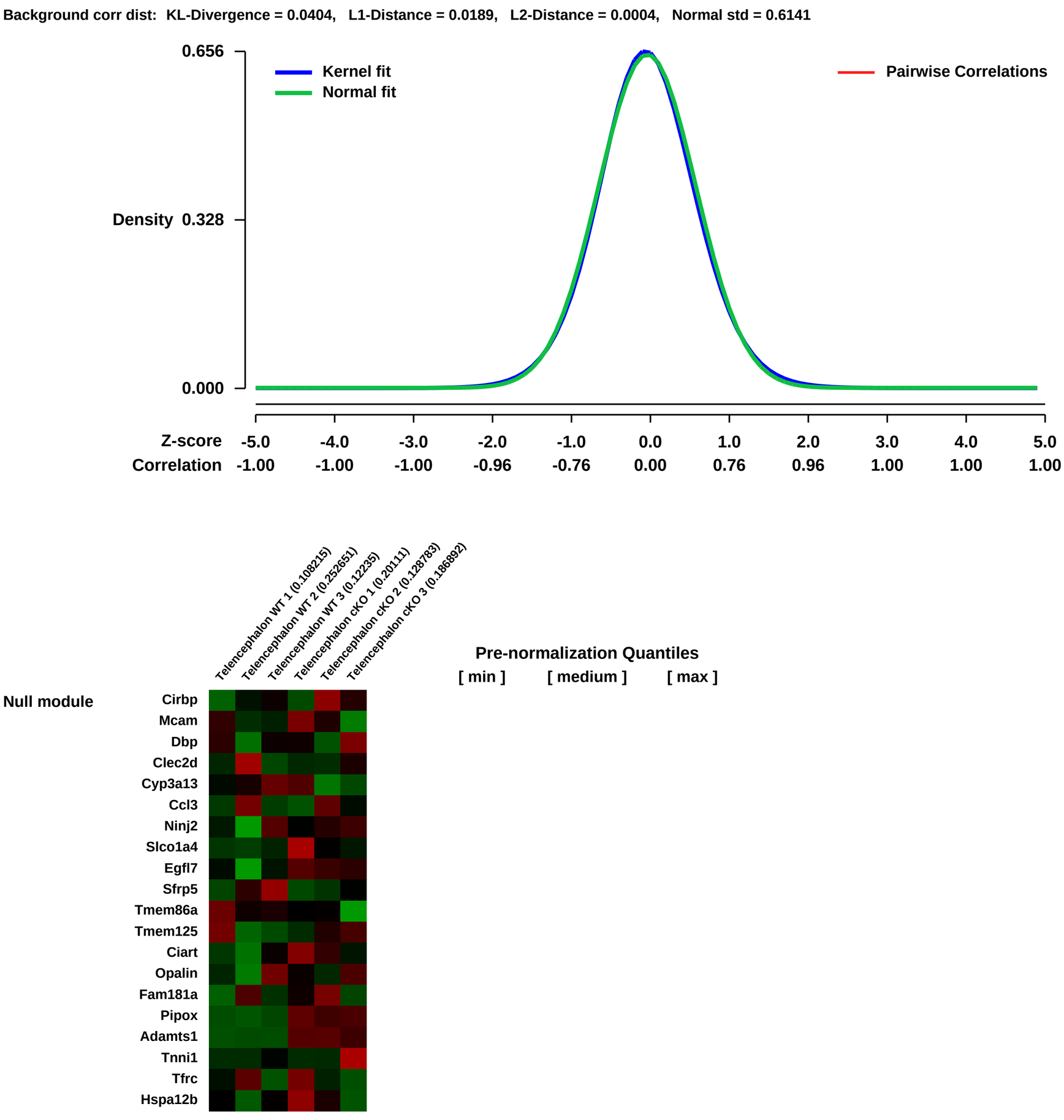

GEO Series "GSE21117" Expression Profiles

Num of samples in this series: 42

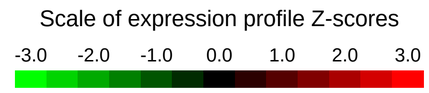

GEO Link:	http://www.ncbi.nlm.nih.gov/geo/query/acc.cgi?acc=GSE21117
Status:	Public on Jun 24 2011
Title:	Microarrays of macrophages infected with smooth or rough Brucella suis
Organism:	Mus musculus
Experiment type:	Expression profiling by array
Platform:	GPL1261
Pubmed ID:	21464087
Summary & Design:	**Summary:** The macrophage-Brucella interaction is critical for the establishment of a chronic Brucella infection. Smooth virulent B. suis strain 1330 (S1330) prevents macrophage cell death. However, rough attenuated B. suis strain VTRS1 induces strong macrophage cell death. To further investigate the mechanism of VTRS1-induced macrophage cell death, microarrays were used to analyze temporal transcriptional responses of murine macrophage-like J774. A1 cells infected with S1330 or VTRS1. **Overall design:** Murine J774.A1 macrophages were plated in T75 at 8 x 10^6 cells per flask one day prior to infection, and then infected with B. suis S1330 or VTRS1 at a MOI of 200:1. Total RNAs were isolated by TRIzol and further purified using Qiagen RNeasy Mini Kit (Qiagen, Valencia, CA) at 0, 1, 2, 4, 8, 24, and 48 h post infection. The RNA samples were stored at -80 ´”C until an Agilent 2100 BioAnalyzer (Agilent Technologies, Palo Alto, CA) was used to assess the concentrations and quality of RNA samples. Total RNA (20 ´µg) per sample was used for hybridization with Affymetrix mouse GeneChip 430 2.0 array. Preparation of cDNA, hybridization, quality controls and scanning of the GeneChip 430 2.0 arrays were performed according to the manufacturer’s protocol (Affymetrix, Santa Clara, CA) .

Background corr dist: KL-Divergence = 0.2179, L1-Distance = 0.0528, L2-Distance = 0.0072, Normal std = 0.3211

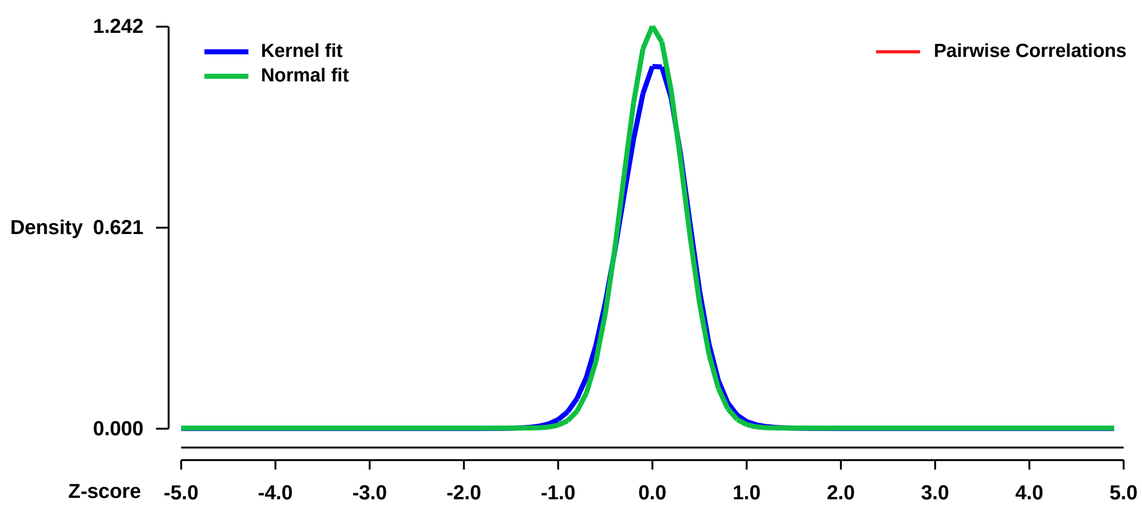

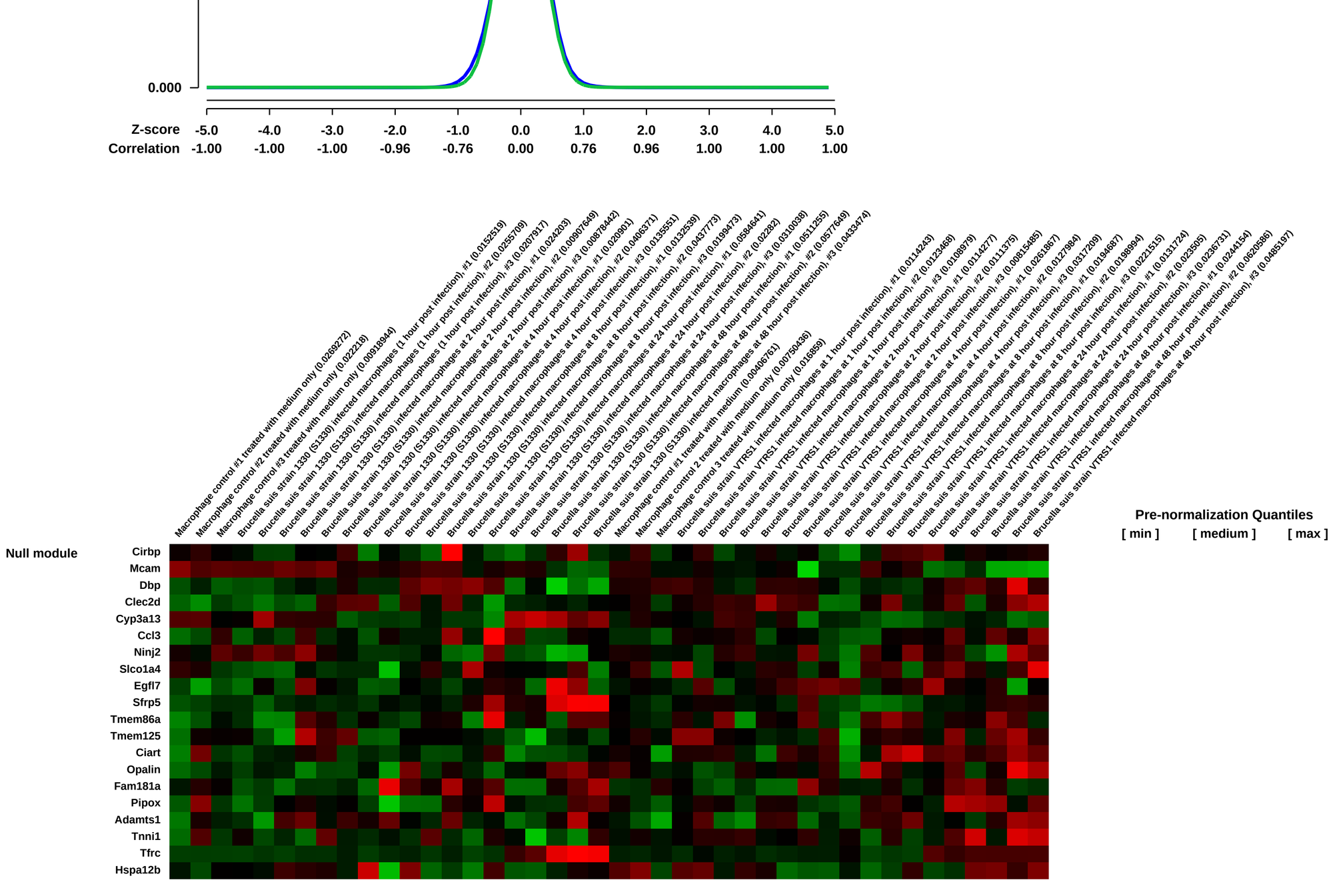

GEO Series "GSE18925" Expression Profiles

Num of samples in this series: 6

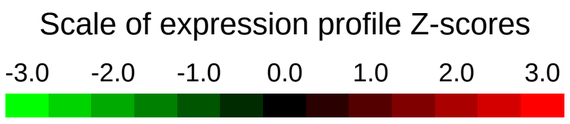

GEO Link:	http://www.ncbi.nlm.nih.gov/geo/query/acc.cgi?acc=GSE18925
Status:	Public on Dec 09 2011
Title:	Expression data from the liver of wild-type and Cnot3+/- mice: Fed vs Fasted
Organism:	Mus musculus
Experiment type:	Expression profiling by array
Platform:	GPL1261
Pubmed ID:	21897366
Summary & Design:	**Summary:** Decay of mRNAs initiates with shortening of the poly(A) tail. Although the CCR4-NOT complex participates in deadenylation, how it becomes activates remain obscure. We show that complete deficiency in CNOT3, subunit 3 of this complex, is lethal in mice, but that heterozygotes survive as lean mice with hepatic and adipose tissues containing reduced lipid levels. Cnot3+/- mice have enhanced metabolic rates and remain lean on high-fat diets. We further provide evidence suggesting that CNOT3, by changing its level in response to feeding conditions, affects the activity of the CCR4-NOT deadenylase against poly(A) tails of specific mRNAs coding for proteins involved in metabolism of carbohydrates and fats. Because the levels of CNOT3 protein were decreased under fasting conditions and increased upon refeeding and because CNOT3 could be a positive regulator of the CCR4-NOT deadenylase, we hypothesized that the levels of CCR4-NOT target mRNAs would be lower in fed mice than in fasted mice. We compared the gene expression profiles of fed and fasted wild-type mice. Microarray analysis revealed that approximately 1,200 mRNA transcripts were down-regulated in the livers of fed mice. Of these mRNAs, 68 corresponded to the genes up-regulated in the livers of Cnot3+/- mice and fasted wild-type mice. A large number of the 68 identified genes encoded proteins involved in metabolism, especially lipid metabolism and growth. **Overall design:** The livers were isolated from 8-week-old fed wild-type, fasted wild-type and fasted Cnot3+/- mice (n = 2 for each genotype).

Background corr dist: KL-Divergence = 0.0374, L1-Distance = 0.0187, L2-Distance = 0.0003, Normal std = 0.6293

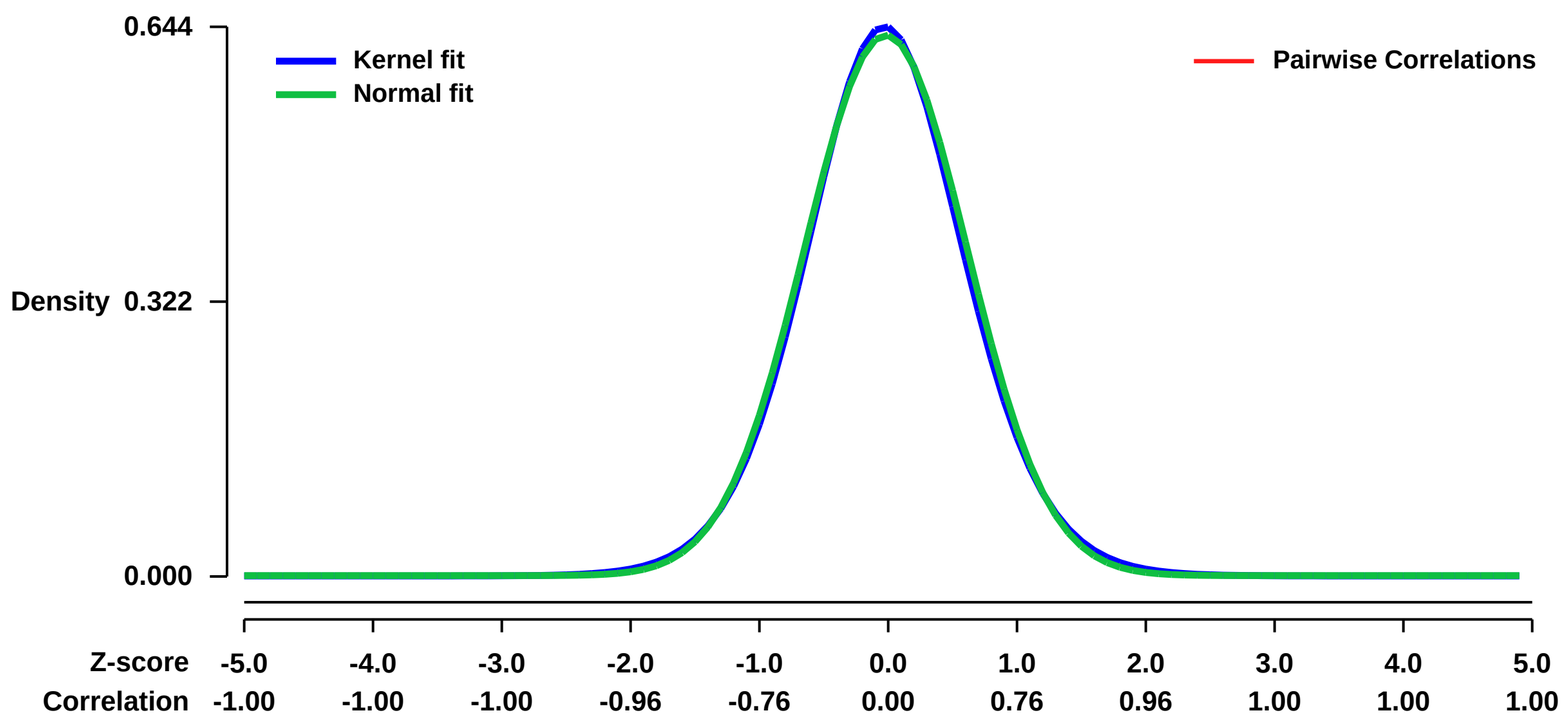

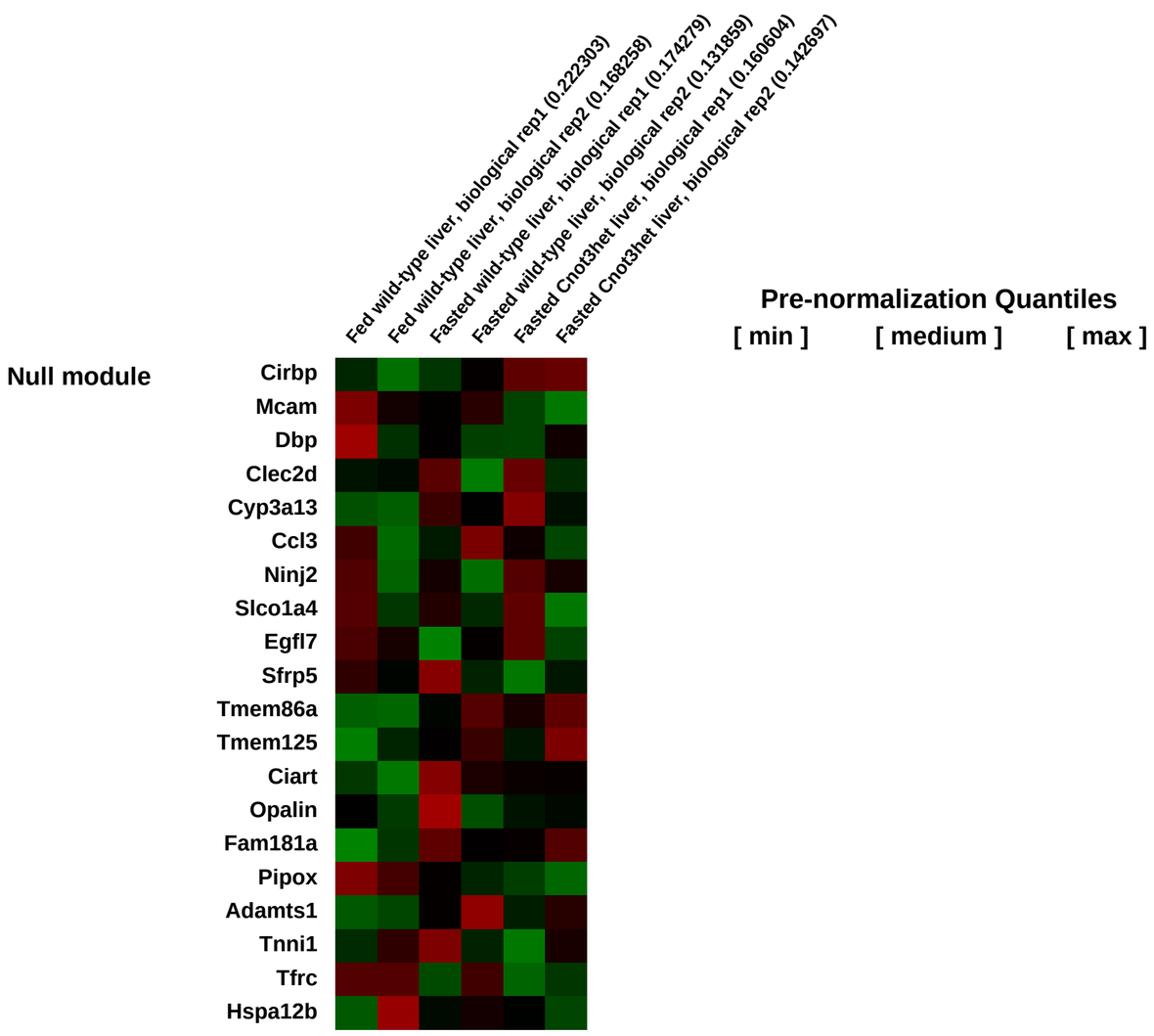

GEO Series "GSE21861" Expression Profiles

Num of samples in this series: 8

Scale of expression profile Z-scores

-3.0 -2.0 -1.0 0.0 1.0 2.0 3.0

GEO Link:	http://www.ncbi.nlm.nih.gov/geo/query/acc.cgi?acc=GSE21861
Status:	Public on Nov 15 2010
Title:	The transcription factors STAT5a/b negatively regulate cell proliferation through the activation of cdkn2b and cdkn1a expression
Organism:	Mus musculus
Experiment type:	Expression profiling by array
Platform:	GPL1261
Pubmed ID:	21038417
Summary & Design:	**Summary:** Although the cytokine-inducible transcription factors STAT5a/b promote proliferation of a wide range of cell types, there are cell- and context specific cases in which loss of STAT5a/b results in enhanced cell proliferation. Here we report that loss of STAT5a/b from mouse embryonic fibroblasts (MEFs) leads to enhanced proliferation, which was linked to reduced levels of the cell cycle inhibitor p15INK4B and p21CIP1. We further demonstrate that growth hormone through the transcription factor STAT5a/b enhances expression of the cdkn2B gene and that STAT5a binds to GAS sites within the promoter. We have recently demonstrated that ablation of STAT5a/b from liver results in hepatocellular carcinoma upon a CCl4 insult. We also established that in liver tissue, like in MEFs, STAT5a/b activates expression of the cdkn2B gene. Loss of STAT5a/b led to diminished p15INK4B and increased hepatocyte proliferation. This study for the first time demonstrates that cytokines through STAT5a/b can induce the expression of a key cell cycle inhibitor. These experiments therefore shed a light on the context-specific role of STAT5a/b as tumor suppressors. **Overall design:** Control and Stat5a/b-null embryonic fibroblasts (MEFs) cells were stimulated w/o a GH including two biological replications per group (Total four groups)

Background corr dist: KL-Divergence = 0.0201, L1-Distance = 0.0466, L2-Distance = 0.0026, Normal std = 0.8018

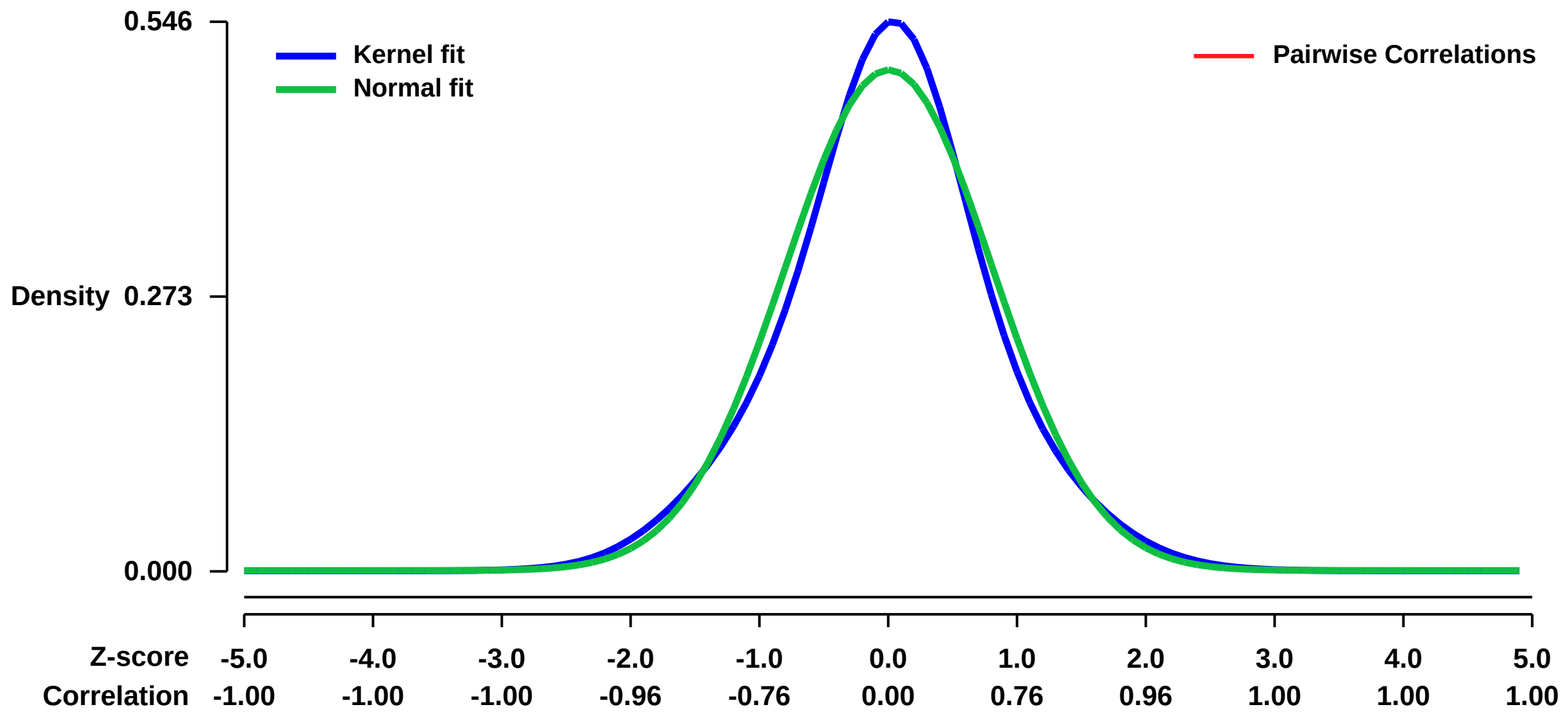

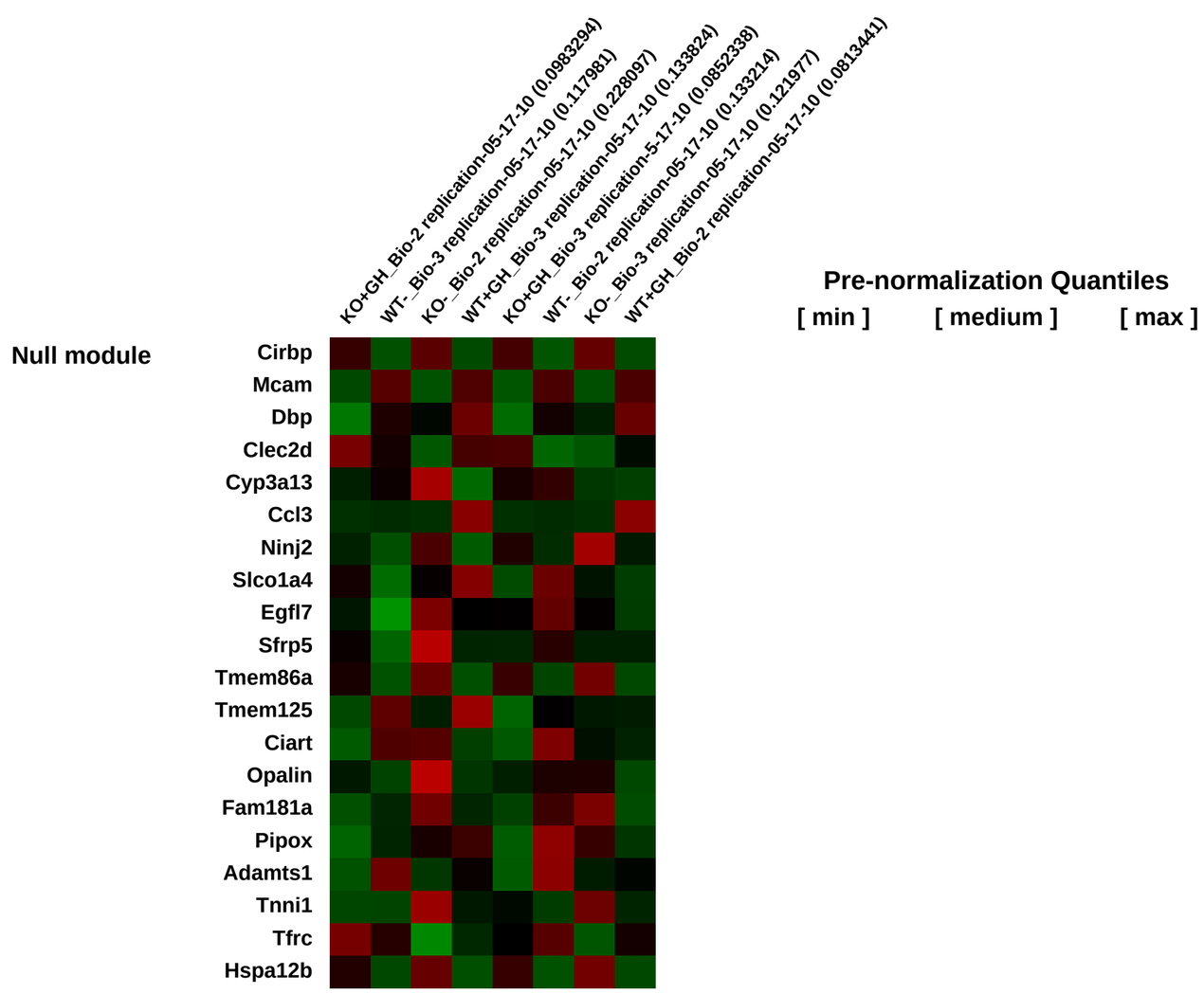

GEO Series "GSE6850" Expression Profiles

Num of samples in this series: 10

Scale of expression profile Z-scores

-3.0 -2.0 -1.0 0.0 1.0 2.0 3.0

GEO Link:	http://www.ncbi.nlm.nih.gov/geo/query/acc.cgi?acc=GSE6850
Status:	Public on Jun 15 2007
Title:	A dominant negative form of cJun affects genes that have opposing effects on lipid homeostasis in mice
Organism:	Mus musculus
Experiment type:	Expression profiling by array
Platform:	GPL1261
Pubmed ID:	17456467
Summary & Design:	**Summary:** cJun is a transcription factor activated by phosphorylation by SAPK/JNK MAP kinase pathway that has been linked to atherosclerosis. Adenovirus mediated gene transfer of a dominant negative form of cJun in C57BL/6 mice increased greatly the apolipoprotein E (ApoE) mRNA and plasma apoE levels and induced dyslipidmia, characterized by increased plasma cholesterol, triglyceride and VLDL levels and accumulation of discoidal HDL particles. Unexpectedly, infection of ApoE-/- mice with adenovirus expressing dn-cJun reduced by 50% plasma cholesterol, suggesting that the dn-cJun affected other genes that control plamsa cholesterol. To determine the molecular pathways implicated in this process we performed whole genome expression profiling using total RNA from the liver of infected ApoE-/- mice. **Keywords:** disease **Overall design:** We extracted total RNA from 5 ApoE-/- mice infected with an adenovirus expressing dominant negative cJun and 5 ApoE-/- mice infected with a control adenovirus expressing GFP. Each RNA sample was hybridized to a different Affymetrix 430 2.0 array.

Background corr dist: KL-Divergence = 0.1286, L1-Distance = 0.0328, L2-Distance = 0.0020, Normal std = 0.3960

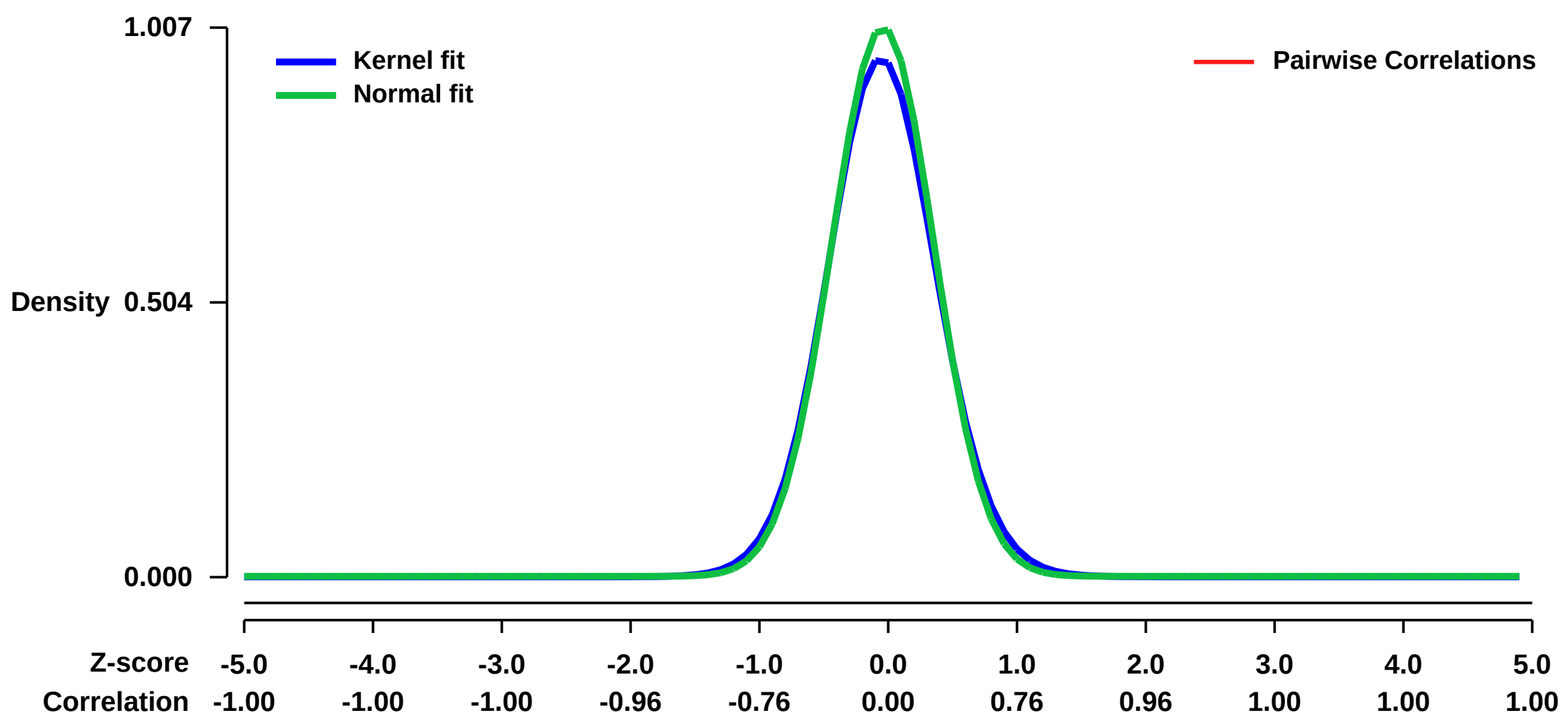

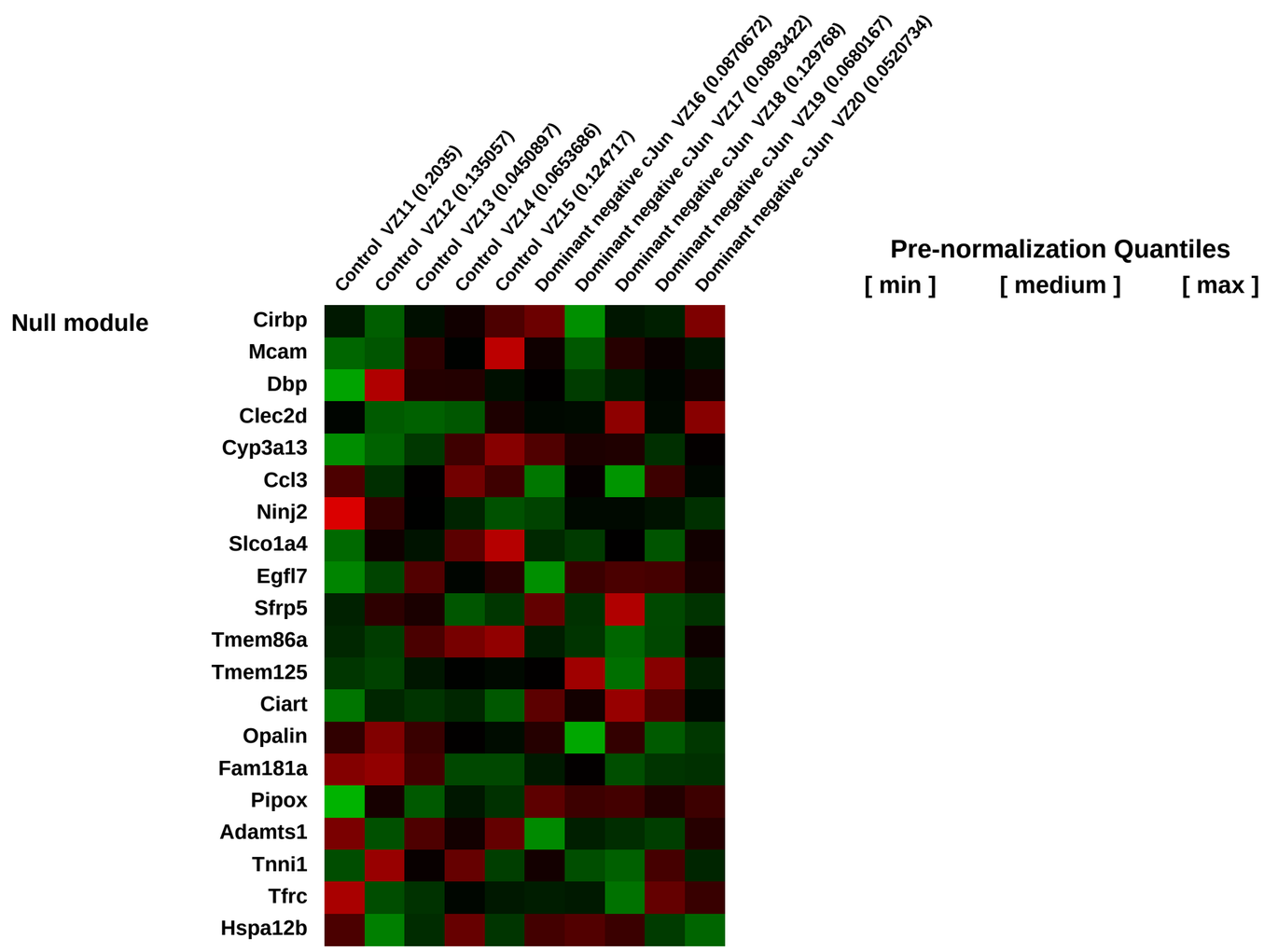

GEO Series "GSE29798" Expression Profiles

Num of samples in this series: 6

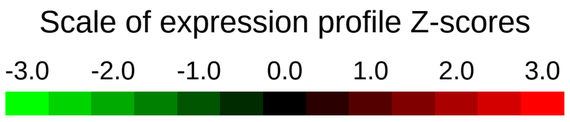

GEO Link:	http://www.ncbi.nlm.nih.gov/geo/query/acc.cgi?acc=GSE29798
Status:	Public on Feb 15 2012
Title:	A combined RNAi and localization approach for dissecting long noncoding RNAs reveals a function of Panct1 in ES cells
Organism:	Mus musculus
Experiment type:	Expression profiling by array
Platform:	GPL1261
Pubmed ID:	22327834
Summary & Design:	**Summary:** Long non-coding RNAs (lncRNAs) regulate diverse biological pathways. Unlike protein coding genes, where methods to comprehensibly study their functional roles in cellular systems are available, techniques to systematically investigate lncRNAs have largely remained unexplored. Here, we report a technology for combined Knockdown and Localization Analysis of Non-coding RNAs (c-KLAN) that merges phenotypic characterization and localization approaches to study lncRNAs. Using a library of endoribonuclease prepared short interfering RNAs (esiRNAs) coupled with a pipeline for synthesizing labeled riboprobes for RNA fluorescence in situ hybridization (FISH), we demonstrate the utility of c-KLAN by identifying a novel transcript Panct1 (Pluripotency associated non-coding transcript 1) that regulates embryonic stem cell identity. We postulate that c-KLAN should be generally useful in the discovery of lncRNAs implicated in various biological processes. **Overall design:** In this experiment, the levels of Panct1(AK156552) have been depleted by RNAi and the expression levels of all genes have been monitored 72 hours post transfection with esiRNAs against Panct1. An esiRNA against non-targeting Luciferase was used as a negative control.

Background corr dist: KL-Divergence = 0.0258, L1-Distance = 0.0248, L2-Distance = 0.0006, Normal std = 0.7131

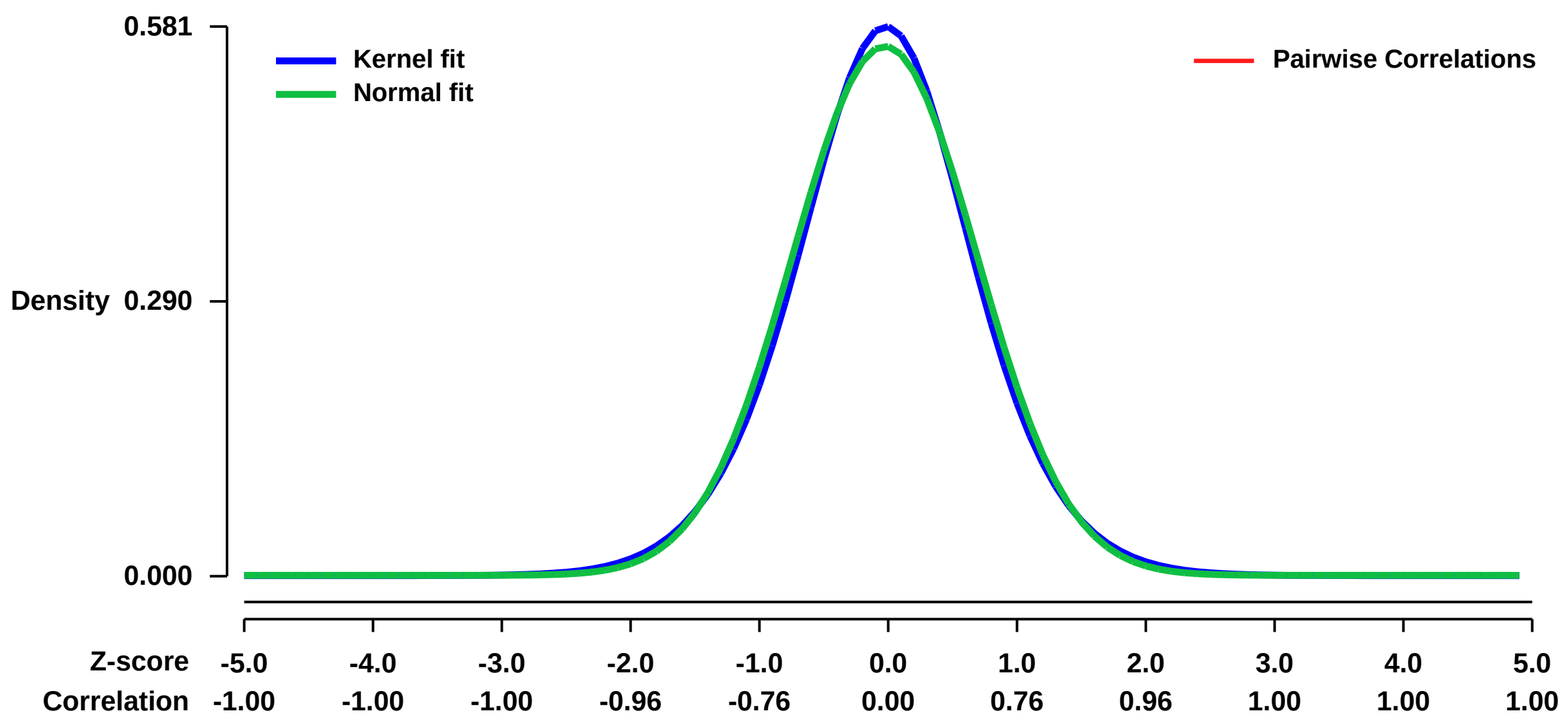

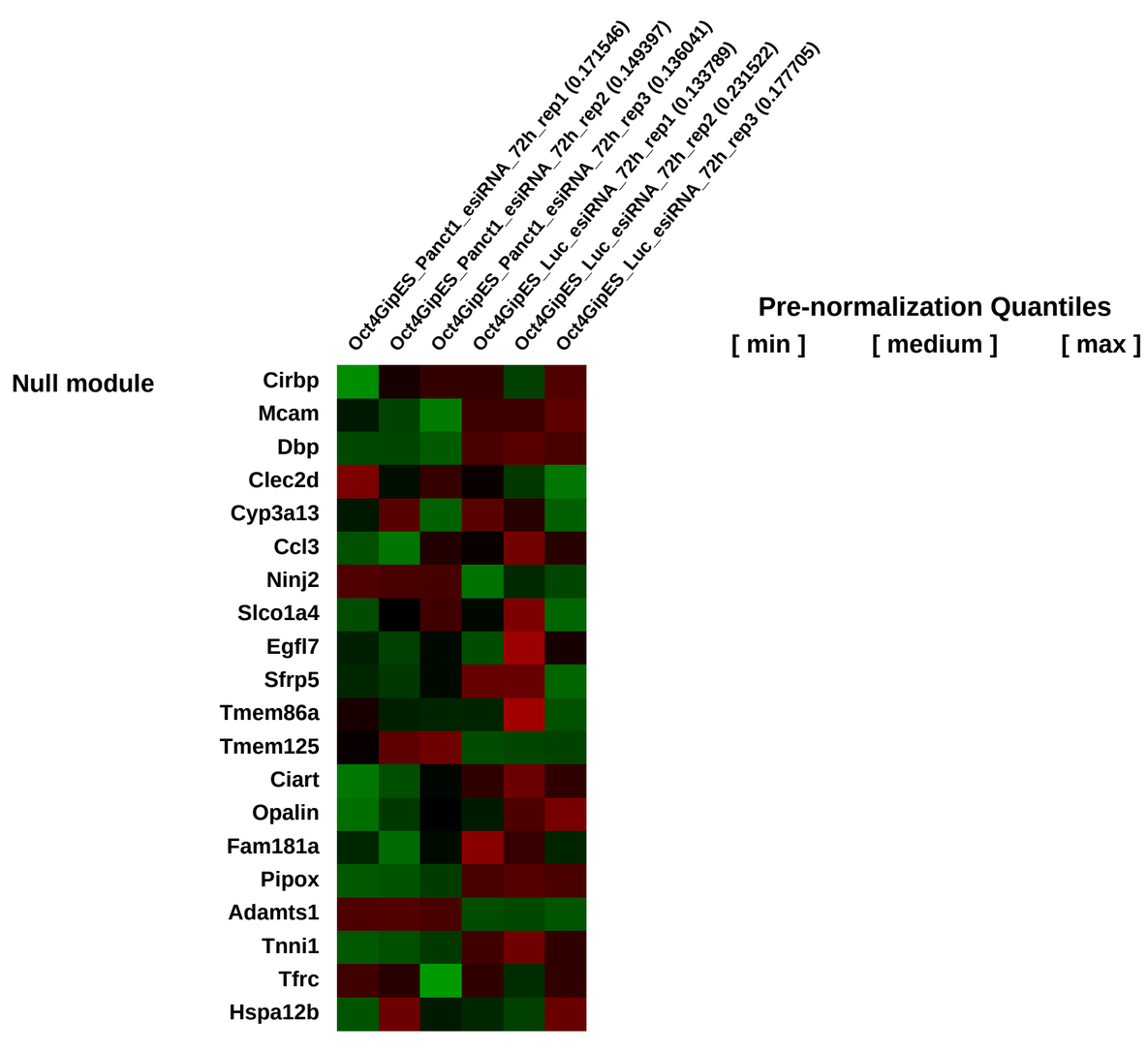

GEO Series "GSE11050" Expression Profiles

Num of samples in this series: 6

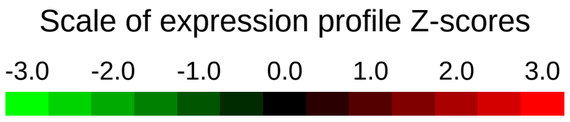

GEO Link:	**http://www.ncbi.nlm.nih.gov/geo/query/acc.cgi?acc=GSE11050**
Status:	**Public on May 01 2008**
Title:	**cross-hybridization of woodchuck HCCs using human, rat and mouse arrays**
Organism:	**Marmota monax**
Experiment type:	**Expression profiling by array**
Platform:	**GPL1261**
Pubmed ID:	
Summary & Design:	**Summary:** **Woodchucks that were infected with WHC virus developed HCCs. HCCs and surrounding tissues were removed and RNA was extracted from microarray study. Human, rat and mouse arrays were used due to the lack of a woodchuck array. Same procedures and parameters were used to conduct this experiment.** **Keywords: comparative study** **Overall design:** **3 woodchucks with HCCs were used. HCCs and their surrouding normal tissues were harvested. These 3 pairs of tissues were cross-species hybridized into a human, rat and mouse chip under same conditions. Data analysis were performed to compare the results.**

Background corr dist: **KL-Divergence = 0.0521, L1-Distance = 0.0349, L2-Distance = 0.0017, Normal std = 0.5843**

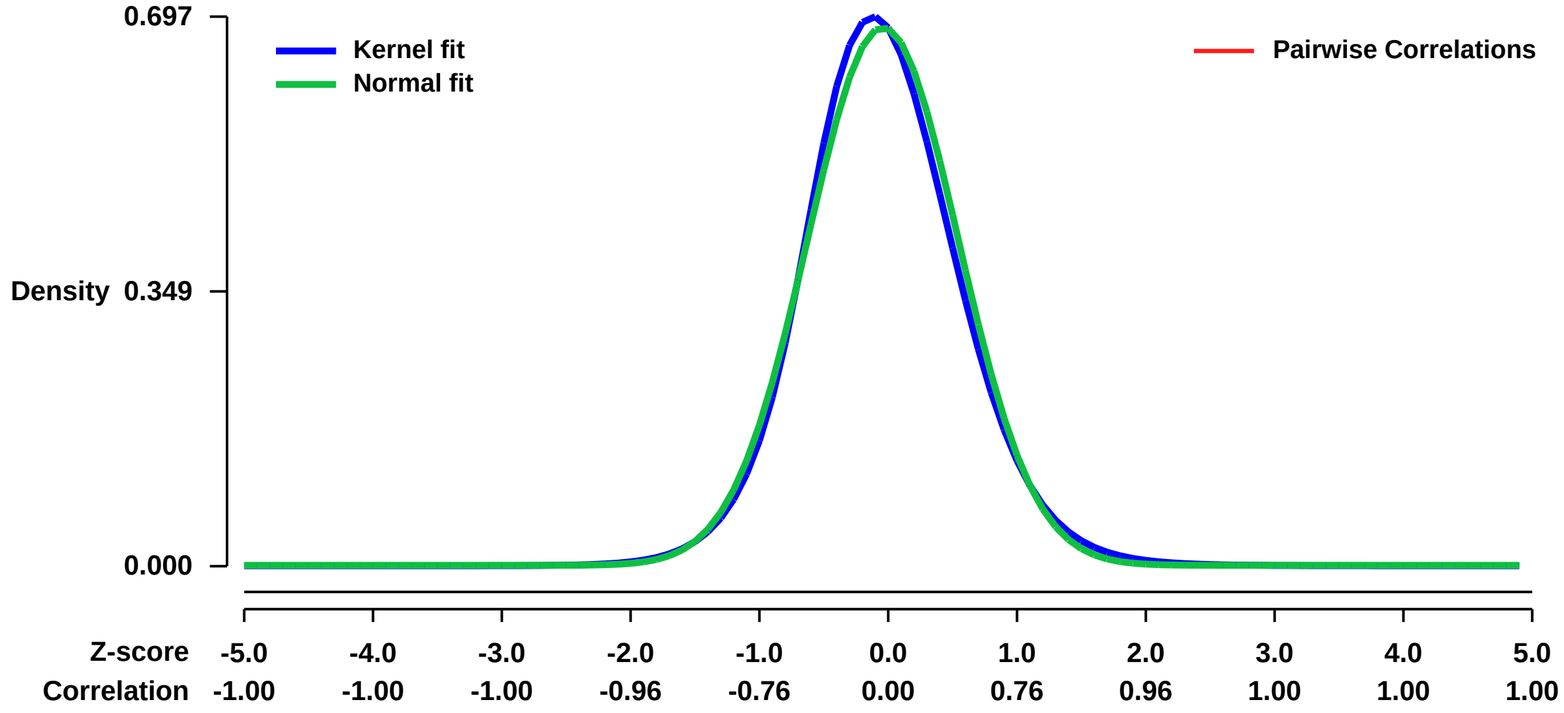

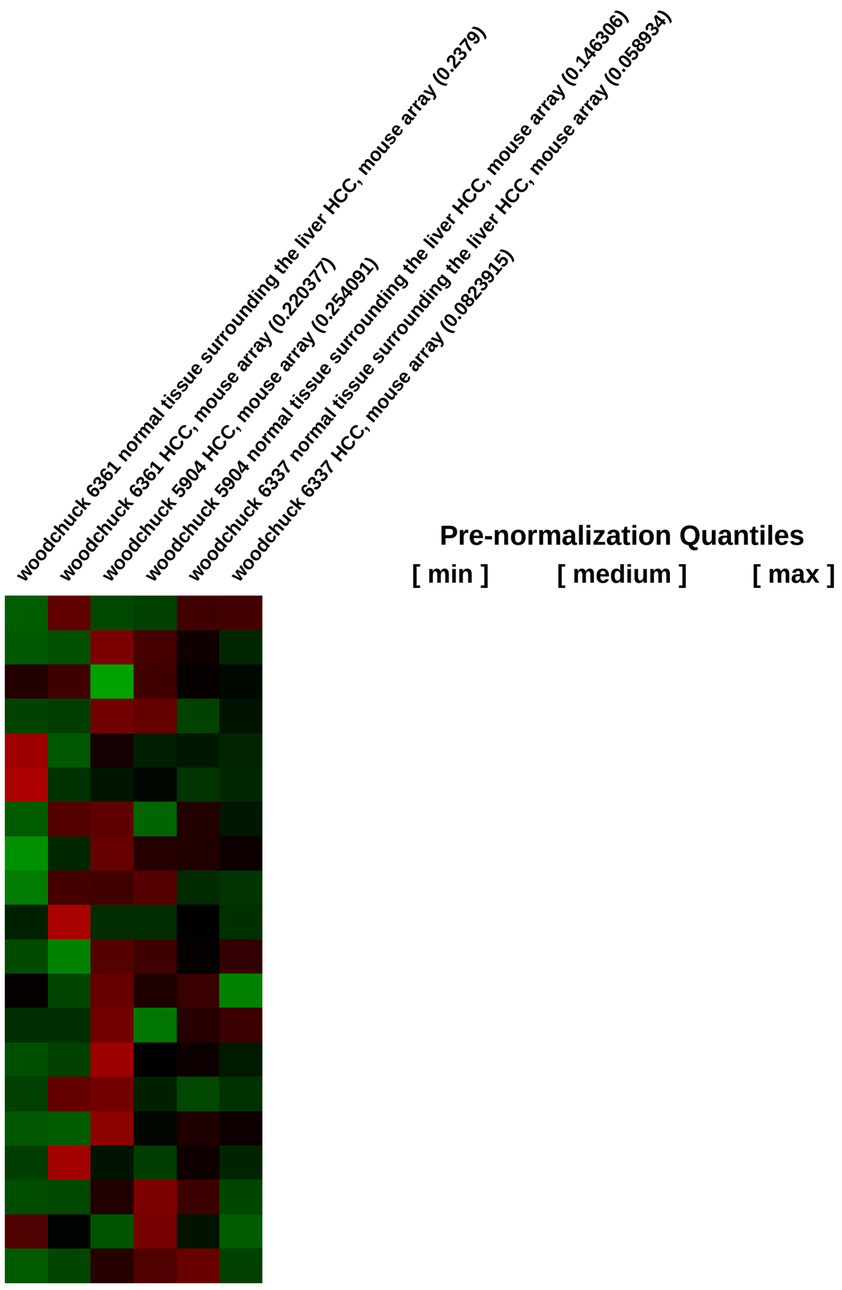

GEO Series "GSE31199" Expression Profiles

Num of samples in this series: 12

Scale of expression profile Z-scores

-3.0 -2.0 -1.0 0.0 1.0 2.0 3.0

GEO Link:	http://www.ncbi.nlm.nih.gov/geo/query/acc.cgi?acc=GSE31199
Status:	Public on Aug 16 2011
Title:	Down-regulation of cholesterol biosynthesis in forebrains of ERCC1-deficient mice
Organism:	Mus musculus
Experiment type:	Expression profiling by array
Platform:	GPL1261
Pubmed ID:	22245387
Summary & Design:	**Summary:** **Background: Several genetic defects of the nucleotide excision repair (NER) pathway, including deficiency of the Excision Repair Cross-Complementing rodent repair deficiency, complementation group 1 (ERCC1), result in pre-mature aging, impaired growth, microcephaly and delayed development of the cerebellum. Such a phenotype also occurs in ERCC1-knockout mice which survive for up to 4 weeks after birth. Therefore, we analyzed cerebellar and hippocamapal transcriptomes of these animals at 3 weeks of age to identify the candidate mechanisms underlying brain consequences of reduced ERCC1 activity.** **Results: In the cerebellum, the most prominent change was upregulation of genes that are associated with gliosis. Although Purkinje cell degeneration has been reported in some mouse strains with NER impairment, Purkinje cell transcriptome was mostly unaffected by the ERCC1 knockout. In the hippocampus, the gliosis response was minimal. Instead, there was an extensive downregulation of genes related to lipid metabolism including several enzymes of the cholesterol biosynthesis pathway as well as lipoproteins and plasma membrane proteins. Reduced expression of the cholesterol biosynthesis pathway genes was also present in the neocortex of adult mice whose ERCC1 gene was replaced by a mutant allele with a partial activity.** **Conclusions: Downregulation of forebrain cholesterol biosynthesis genes is a newly identified consequence of ERCC1 deficiency. Its presence in adult mice suggests that it is not a secondary consequence of brain growth impairment. Instead, reduced cholesterol biosynthesis may contribute to such an impairment as well as affect function of mature synapses.** **Overall design:** **We analyzed the hippocampus and cerebellum from three Ercc1-/- and three WT littermates using the Affymetrix Mouse Genome 430_2.0.** **Data was analyzed using the dChip DNA-Chip analyzer software .**

Background corr dist: KL-Divergence = 0.0135, L1-Distance = 0.0147, L2-Distance = 0.0002, Normal std = 0.7980

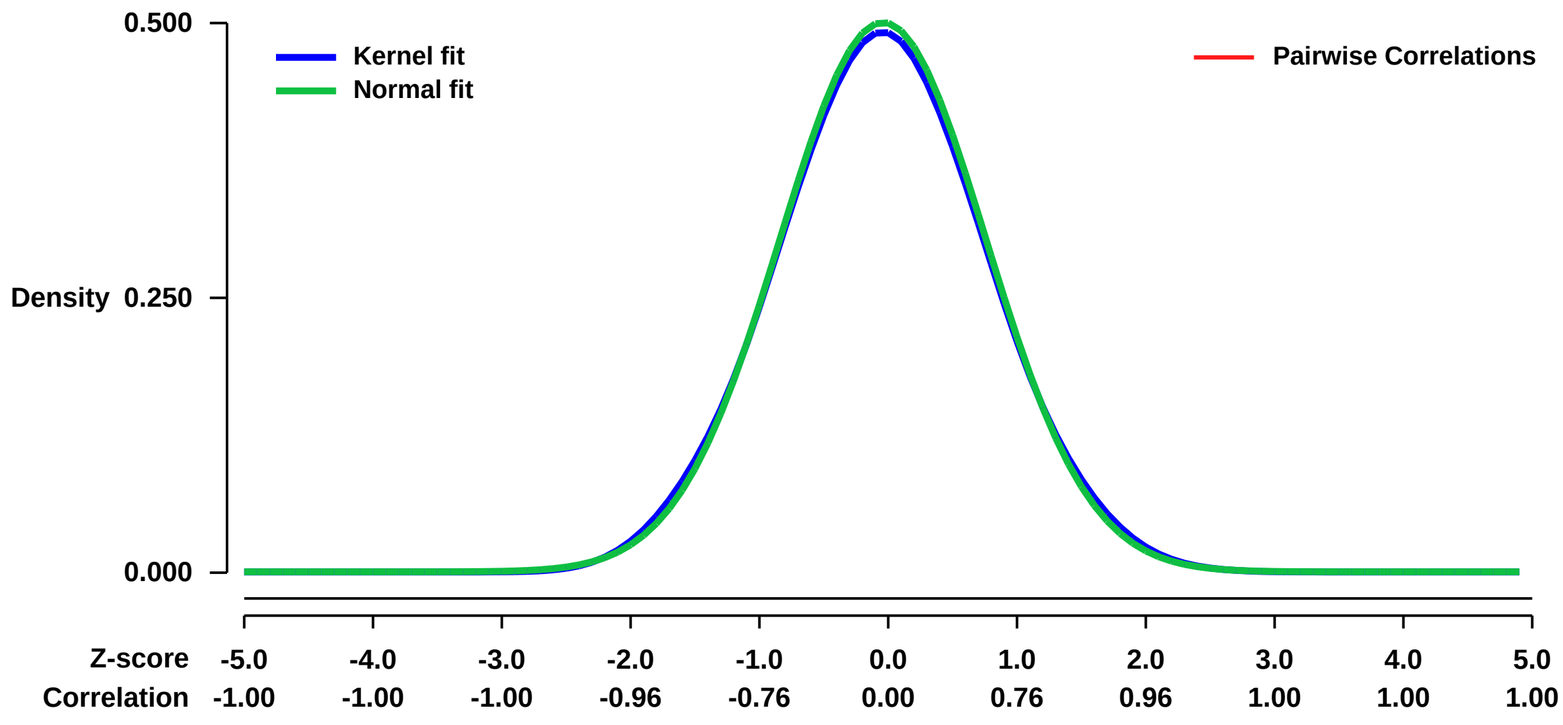

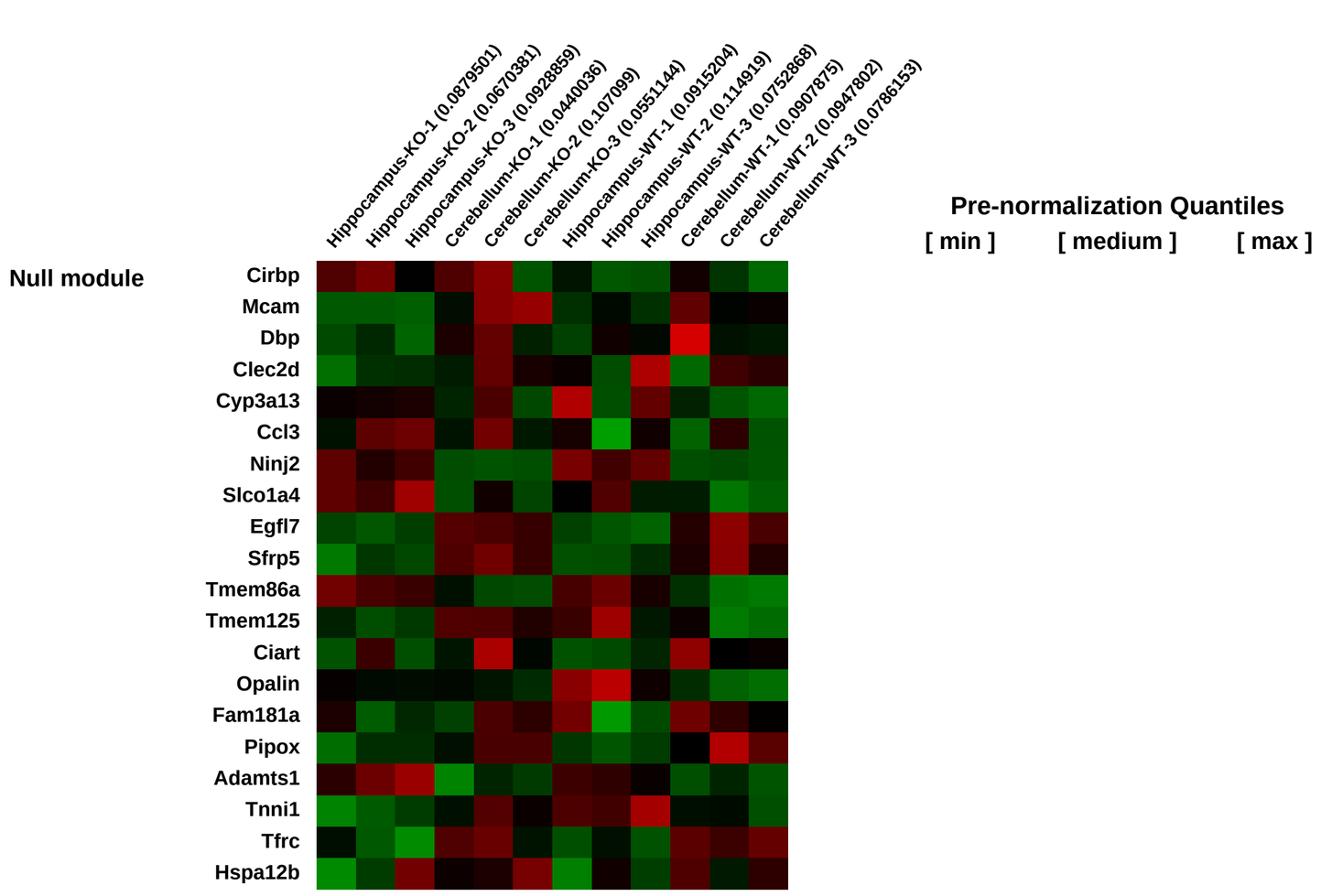

GEO Series "GSE55607" Expression Profiles

Num of samples in this series: 18

Scale of expression profile Z-scores

-3.0 -2.0 -1.0 0.0 1.0 2.0 3.0

GEO Link:	http://www.ncbi.nlm.nih.gov/geo/query/acc.cgi?acc=GSE55607
Status:	Public on Mar 06 2014
Title:	A mouse model of HIES reveals pro and anti-inflammatory functions of STAT3
Organism:	Mus musculus
Experiment type:	Expression profiling by array
Platform:	GPL1261
Pubmed ID:	24632714
Summary & Design:	**Summary:** Mutations of STAT3 underlie the autosomal dominant form of hyper-immunoglobulin E syndrome (HIES). STAT3 has critical roles in immune cells and thus, hematopoietic stem cell transplantation (HSCT), might be a reasonable therapeutic strategy in this disease. However, STAT3 also has critical functions in non-hematopoietic cells and dissecting the protean roles of STAT3 is limited by the lethality associated with germline deletion of Stat3. Thus, predicting the efficacy of HSCT for HIES is difficult. To begin to dissect the importance of STAT3 in hematopoietic and non-hematopoietic cells as it relates to HIES, we generated a mouse model of this disease. We found that these transgenic mice recapitulate multiple aspects of HIES, including elevated serum IgE and failure to generate Th17 cells. We found that these mice were susceptible to bacterial infection that was partially corrected by HSCT using wild type bone marrow, emphasizing the role played by the epithelium in the pathophysiology of HIES. **Overall design:** The effect of IL-6 and IL-10 on BM-DC gene expression was investigated in cell derived from wild type or mut-Stat3 mice

Background corr dist: KL-Divergence = 0.0380, L1-Distance = 0.0921, L2-Distance = 0.0112, Normal std = 0.7946

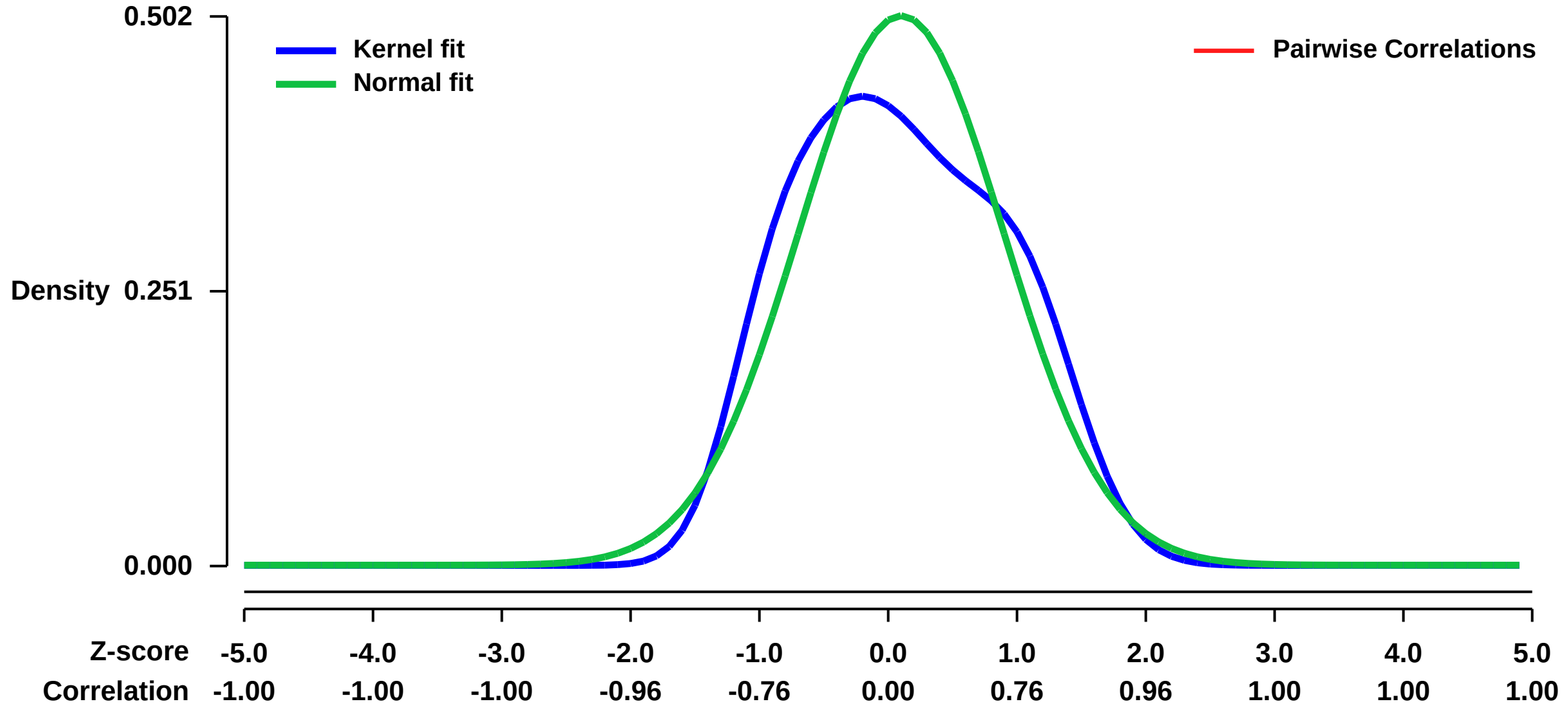

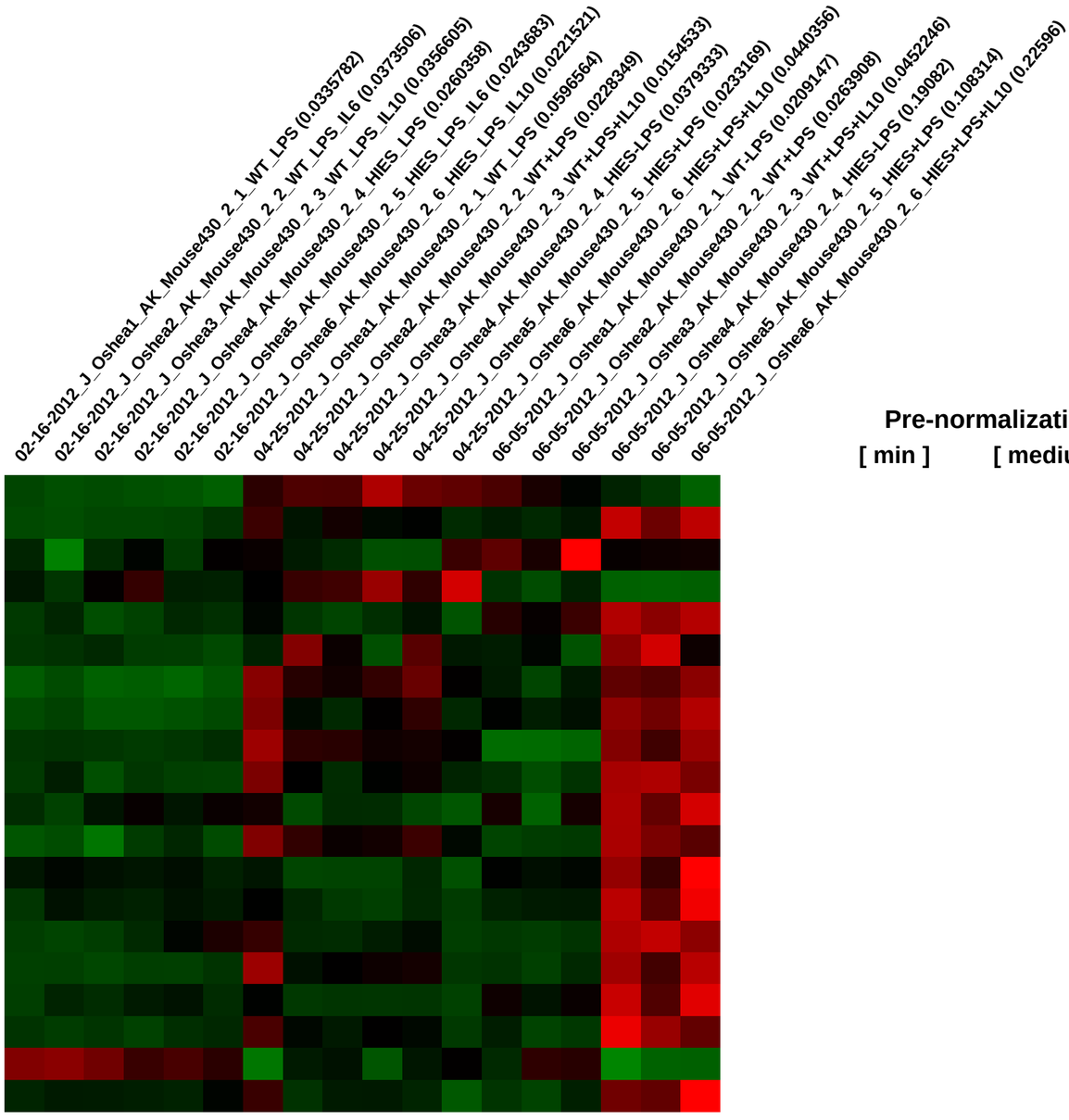

GEO Series "GSE16675" Expression Profiles

Num of samples in this series: 72

Scale of expression profile Z-scores

-3.0 -2.0 -1.0 0.0 1.0 2.0 3.0

GEO Link:	http://www.ncbi.nlm.nih.gov/geo/query/acc.cgi?acc=GSE16675
Status:	Public on Nov 17 2010
Title:	The influence of segmental copy number variation on tissue transcriptomes through development
Organism:	Mus musculus
Experiment type:	Expression profiling by array
Platform:	GPL1261
Pubmed ID:	21084671
Summary & Design:	**Summary:** A preliminary understanding of the phenotypic effect of copy number variation (CNV) of DNA segments is emerging. These rearrangements were demonstrated to influence, in a somewhat dose-dependent manner, the expression of genes mapping within. They were shown to also affect the expression of genes located on their flanks, sometimes at great distance. Here, we show by monitoring these effects at multiple life stages, that these controls over expression are effective throughout mouse development. Similarly, we observe that the more specific spatial expression patterns of CNV genes are maintained throughout life. However, we find that some brain-expressed genes appear to be under compensatory loops only at specific time-points, indicating that the influence of CNVs on these genes is modulated through development. We also observe that CNV genes are significantly enriched upon transcripts that show variable time-course of expression in different strains. Thus modifying the number of copy of a gene not only potentially alters its expression level, but possibly also its time of expression. **Keywords:** comparative genomic **Overall design:** Expression from brain and liver tissues from C57BL/6J, DBA2/J and 129S2 mouse strains at different developmental time points.

Background corr dist: KL-Divergence = 0.0580, L1-Distance = 0.0593, L2-Distance = 0.0060, Normal std = 0.5608

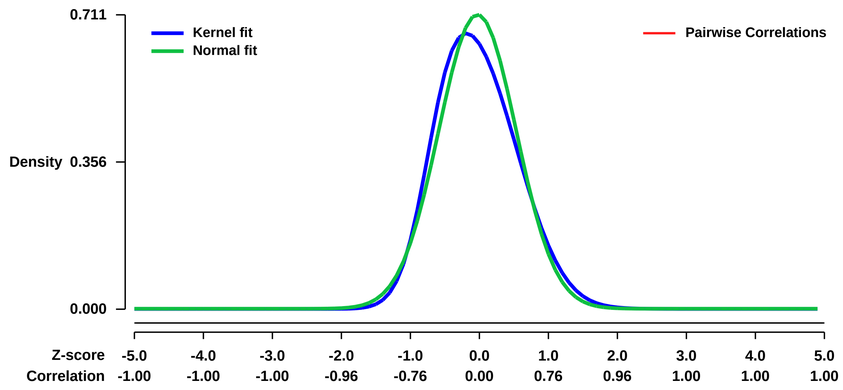

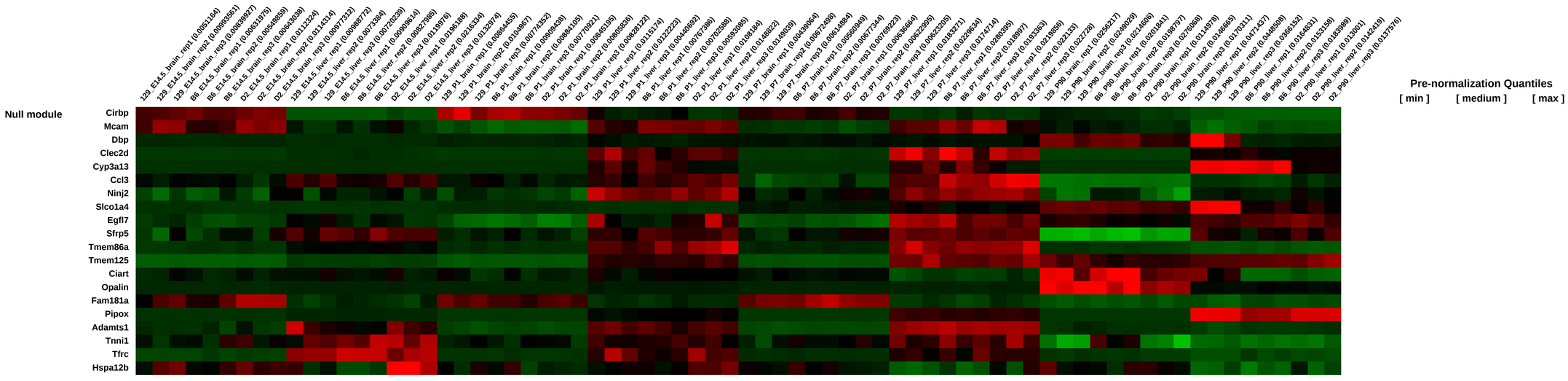

GEO Series "GSE11494" Expression Profiles

Num of samples in this series: 16

Scale of expression profile Z-scores

-3.0 -2.0 -1.0 0.0 1.0 2.0 3.0

GEO Link:	http://www.ncbi.nlm.nih.gov/geo/query/acc.cgi?acc=GSE11494
Status:	Public on Jul 01 2009
Title:	Innate immune response of murine nasal-associated lymphoid tissue (NALT) to Streptococcus pyogenes infection.
Organism:	Mus musculus
Experiment type:	Expression profiling by array
Platform:	GPL1261
Pubmed ID:	19243434
Summary & Design:	**Summary:** Streptococcus pyogenes is a major causative agent of tonsillitis or pharyngitis in children, which can lead to more invasive infections and noninfectious sequellae. S. pyogenes can persist in tonsils, while one-third of children treated with antibiotics continue to shed streptococci and have recurrent infections. Mouse nasal-associated lymphoid tissue (NALT) is functionally analogous to human oropharangeal lymphoid tissues. The innate immune responses of naˆflve cells from a mucosal site to S. pyogenes is not well described; therefore, we infected C57BL/6 mice intranasally with 108 CFU S. pyogenes. Transcriptional responses by NALT after S. pyogenes infection were analyzed by Affymetrix microarray and quantitative RT-PCR. Wild-type S. pyogenes induces transcription of both type I and IFN-gamma-responsive genes, pro-inflammatory genes, and acute phase response plasma proteins within 24h after infection. Invasion of NALT and the induction of the interferon response were not dependent on expression of anti-phagocytic M1 protein. However, infection with an attenuated, less invasive mutant indicated that a robust innate response by NALT is significantly influenced by intra-NALT bacterial load. Granulocytic populations of NALT, cervical lymph nodes and spleen were discriminated by characteristic surface and intracellular markers. Intranasal infection induces systemic release of neutrophils and a substantial influx of neutrophils into NALT at 24h, which decline by 48h after infection. Macrophages do not significantly increase in S. pyogenes-infected NALT. Intranasal infection of IFN-gamma -/- (GKO) C57BL/6 mice did not lead to systemic dissemination of wild type S. pyogenes, despite reduced expression of IFN-gamma-responsive mRNAs in NALT. Infected GKO mice had an unregulated influx of neutrophils into NALT compared to immunocompetant mice and mice treated with an anti-IFN-gamma antibody more rapidly cleared S. pyogenes from NALT. Thus, IFN-gamma-induced responses have a suppressive influence on early clearance of this pathogen from NALT. **Keywords:** disease state analysis **Overall design:** C57BL/6 mice (6-10 weeks old), 4 per group, were infected intranasally with log-phase Streptococcus pyogenes, 2 to 4 x 10^8 CFU per 15 ´µl of pyrogen-free PBS. Sham-infected mice were administered 15 ´µl of the same PBS. Mice were infected with wild type strain 90-226 (Cue 1998), a 90-226 strain containing an in-frame deletion of M1 protein (90-226 delta emm1) (Zimmerlein 2005) or an attenuated 90-226 which lacks both M1 and SCPA proteins (90-226att). NALT was collected from mice at 24h after infection and stored in RNAlater until RNA could be purified).

Background corr dist: KL-Divergence = 0.2816, L1-Distance = 0.0637, L2-Distance = 0.0111, Normal std = 0.2873

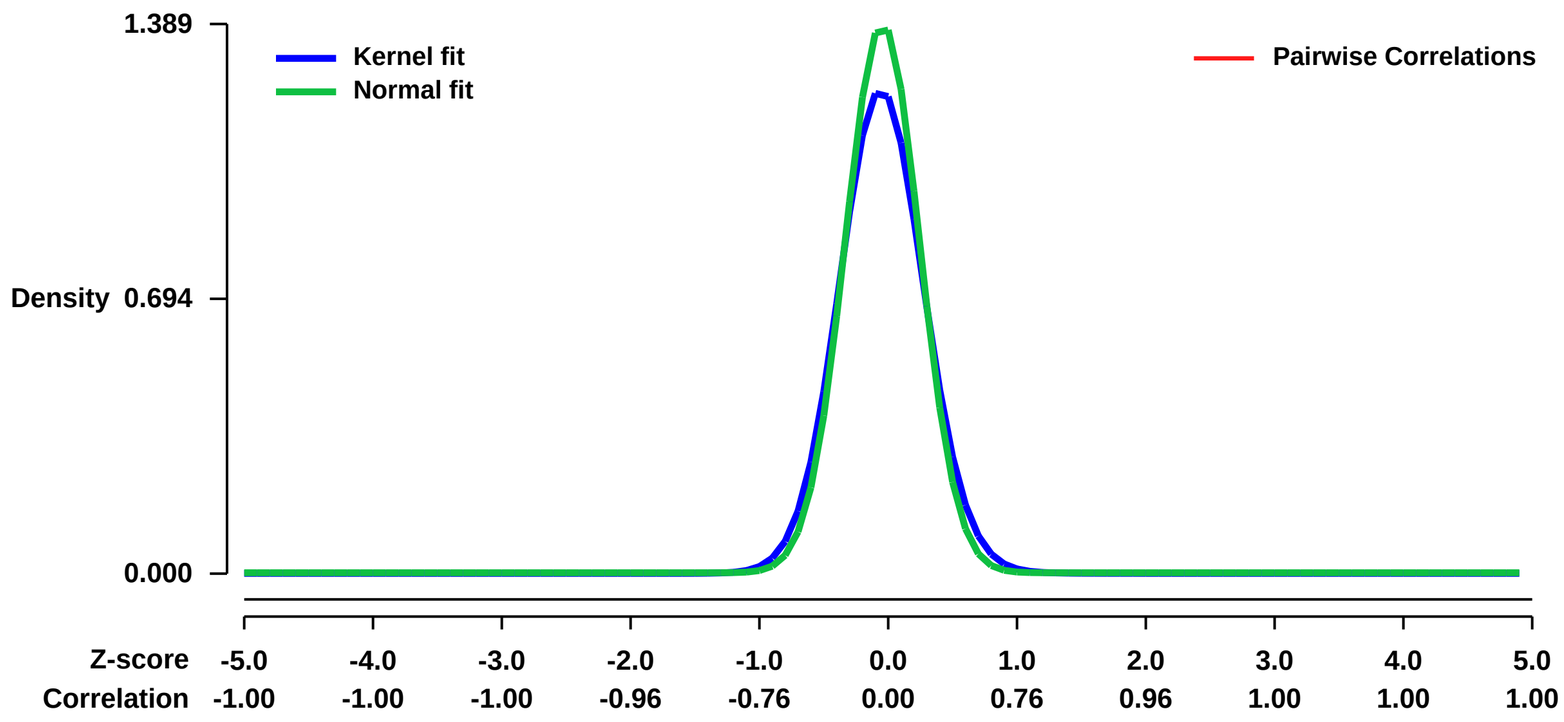

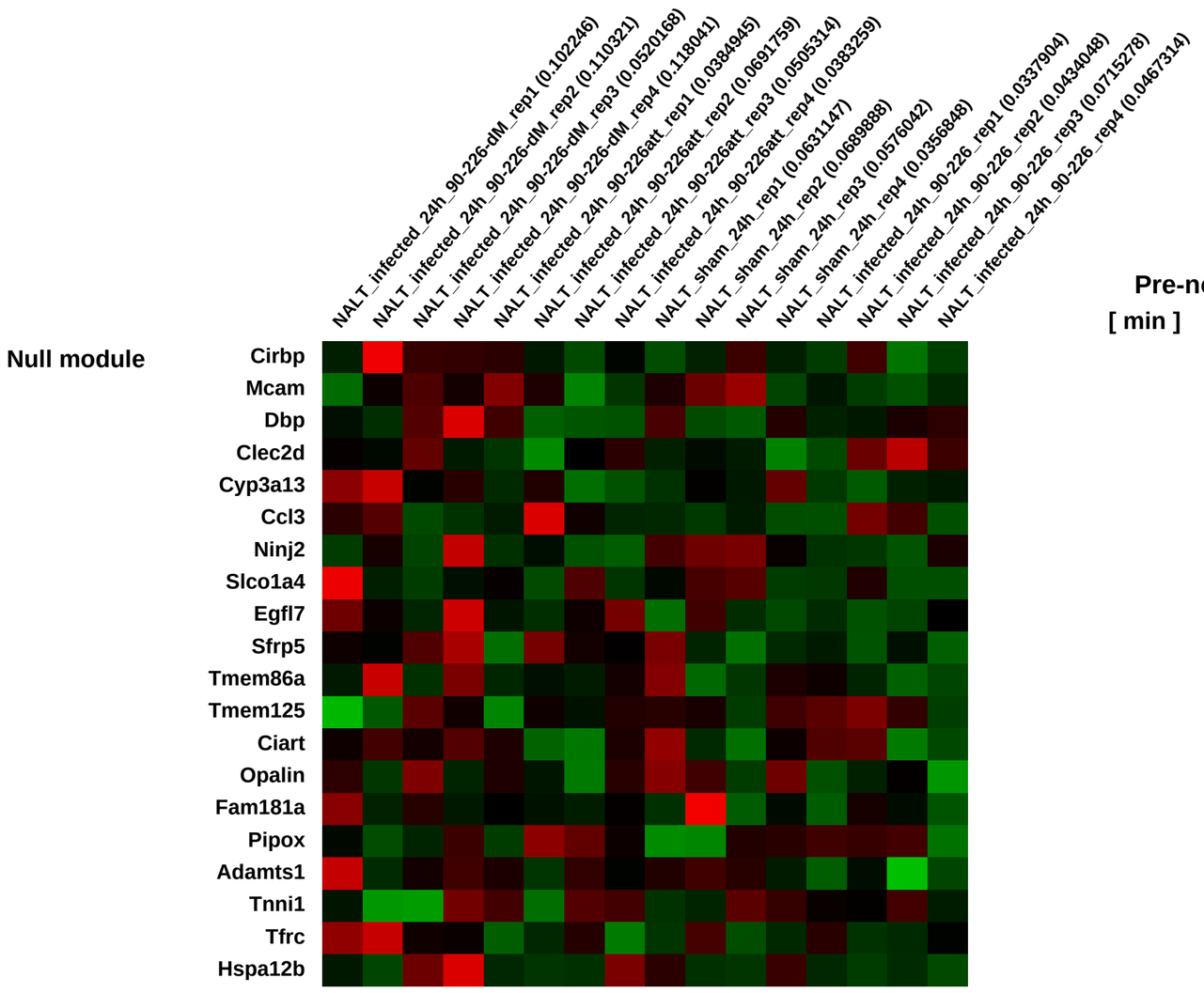

GEO Series "GSE11165" Expression Profiles

Num of samples in this series: 6

Scale of expression profile Z-scores

-3.0 -2.0 -1.0 0.0 1.0 2.0 3.0

GEO Link:	http://www.ncbi.nlm.nih.gov/geo/query/acc.cgi?acc=GSE11165
Status:	Public on Apr 15 2008
Title:	Genes regulated by GATA6 in the lung
Organism:	Mus musculus
Experiment type:	Expression profiling by array
Platform:	GPL1261
Pubmed ID:	18536717
Summary & Design:	**Summary:** Epithelial organs including the lung are known to possess regenerative abilities through activation of endogenous stem cell populations but the molecular pathways regulating stem cell expansion and regeneration are not well understood. Here we show that Gata6 regulates the temporal appearance and number of bronchioalveolar stem cells (BASCs) in the lung leading to the precocious appearance of BASCs and concurrent loss in epithelial differentiation in Gata6 null lung epithelium. This expansion of BASCs is the result of a dramatic increase in canonical Wnt signaling in lung epithelium upon loss of Gata6. Expression of the non-canonical Wnt receptor Fzd2 is down-regulated in Gata6 mutants and increased Fzd2 or decreased ¸†-catenin expression rescues, in part, the lung epithelial defects in Gata6 mutants. During lung epithelial regeneration, we show that canonical Wnt signaling is activated in the niche containing BASCs and forced activation of Wnt signaling leads to a dramatic increase in BASC numbers. Moreover, Gata6 is required for proper lung epithelial regeneration and postnatal loss of Gata6 leads to increased BASC expansion and decreased differentiation. Together, these data demonstrate that Gata6 regulated Wnt signaling controls the balance between stem/progenitor expansion and epithelial differentiation required for both lung development and regeneration. **Keywords:** gene targets in knockout mouse model **Overall design:** 3 replicates of each condition-wild-type and GATA6 null tissue. 6 total samples.

Background corr dist: KL-Divergence = 0.0496, L1-Distance = 0.0769, L2-Distance = 0.0084, Normal std = 0.7206

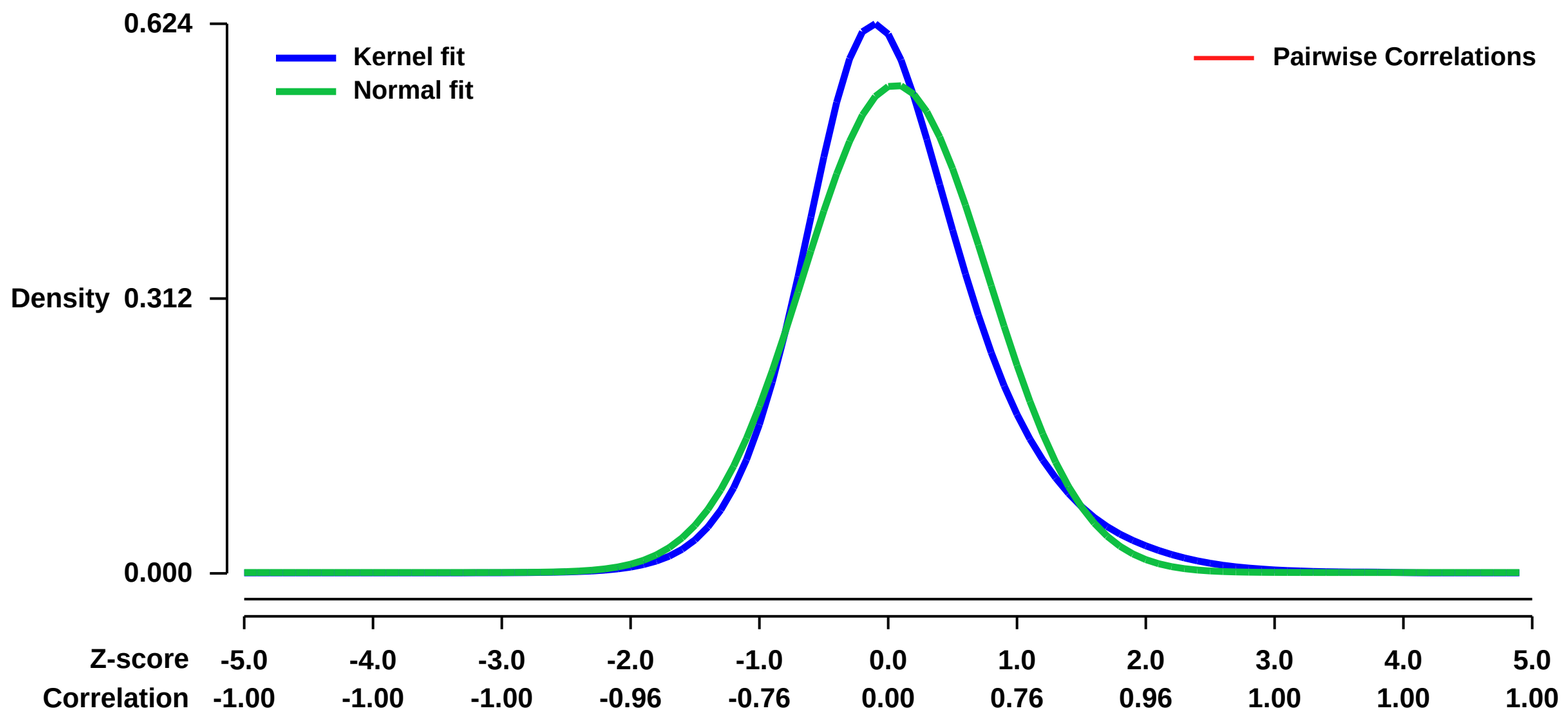

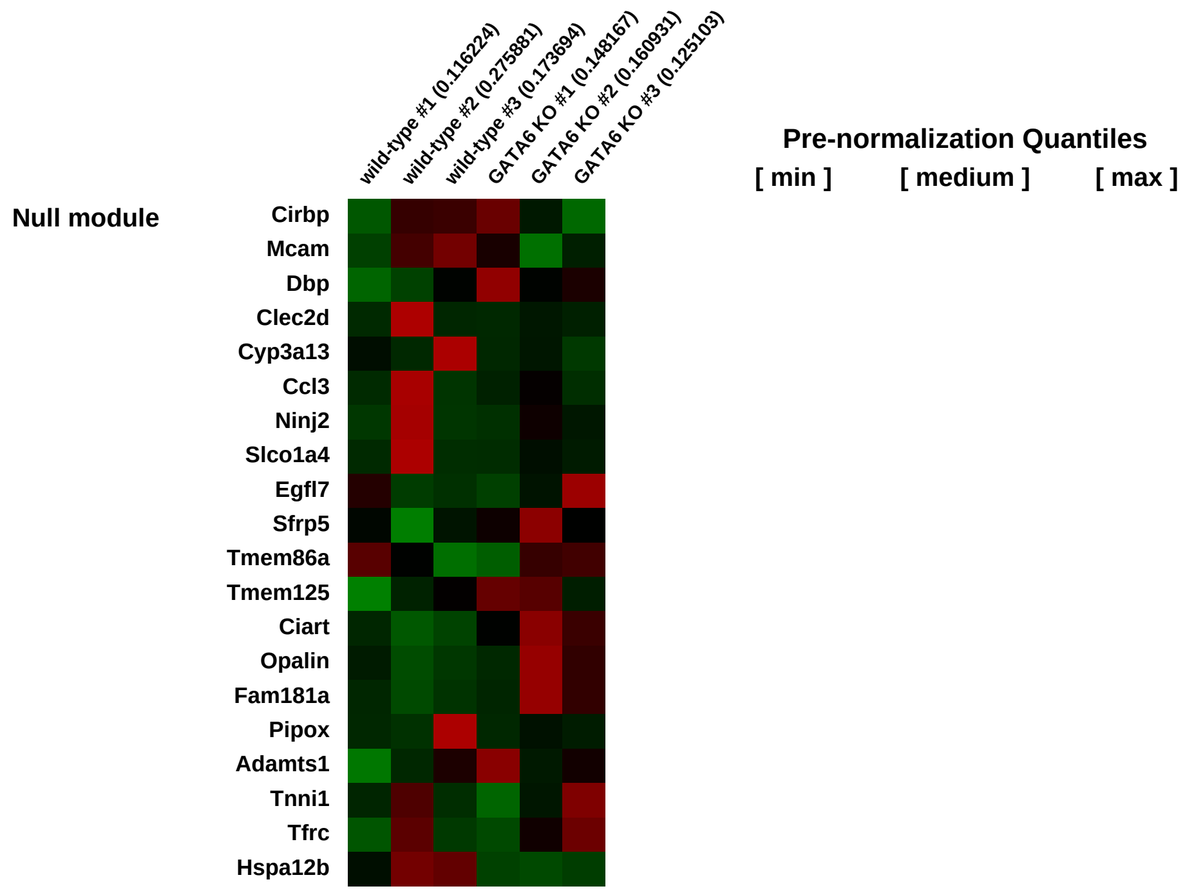

GEO Series "GSE47421" Expression Profiles

Num of samples in this series: 24

Scale of expression profile Z-scores

-3.0 -2.0 -1.0 0.0 1.0 2.0 3.0

GEO Link:	http://www.ncbi.nlm.nih.gov/geo/query/acc.cgi?acc=GSE47421
Status:	Public on Apr 05 2014
Title:	Ectopic Expression data of TLX1 in Hematopoietic Progenitors in TLX1 Transgenic Mice Deficient in DNA-PK
Organism:	Mus musculus
Experiment type:	Expression profiling by array
Platform:	GPL1261
Pubmed ID:	24586935
Summary & Design:	**Summary:** The noncluster homeodomain containing gene, HOX11/TLX1 (TLX1) is detected at the breakpoint of the t(10;14)(q24;q11) chromosome translocation in patients with T cell Acute Lymphoblastic leukemia (T-ALL). This translocation results in the inappropriate expression of TLX1 in T cells. The oncogenic potential of TLX1 was demonstrated in IgH´μTLX1Tg mice, which developed mature B cell lymphoma after a long latency period suggesting the requirement of additional mutations to initiate malignancy. To determine whether dysregulation of genes involved in the DNA damage response contributed to tumor progression, we crossed IgH´μTLX1Tg mice with PrkdcScid/Scid mice; To identify the molecular pathways dysregulated in the earliest stages of TLX1-induced transformation, we used Affimetrix microarrays to compare gene expression profiling of premaliganant thymocytes (6~8 weeks old): DN1, DN2 and DN3 stages from HOX11 transgenic PrkdcScid/Scid (HOXSCID) mice with the same stage thymocytes from the sex and age matched control PrkdcScid/Scid (SCID) mice. Expression analysis of IgH-TLX1TgPrkdcScid/Scid thymocytes revealed dysregulated expression of cell cycle, apoptotic, mitotic spindle and anaphase-promoting complex genes in double negative (DN) 2 and DN3 stage thymocytes. Moreover, DN1, DN2 and DN3 TLX1-expressing thymocytes showed downregulated expression of ribosomal and mitochondria ribosomal protein genes. **Overall design:** Four groups of double mutant IgH-HOX11TgPrkdcScid/Scid mice and four groups of control PrkdcScid/Scid mice were sacrificed at the age of 6~8 weeks and the fresh thymocytes were FACS sorted by markers CD25 and CD44 to DN1, DN2 and DN3 stages. To minimize the sample variability caused by individual differences among animals, about 2 ~5 the same phenotype, stage and sex thymocytes were pooled (total 104 ~ 105 cells) and used as one sample each for RNA extraction and hybridization on Affymetrix microarrays.

Background corr dist: KL-Divergence = 0.1395, L1-Distance = 0.0514, L2-Distance = 0.0045, Normal std = 0.4077

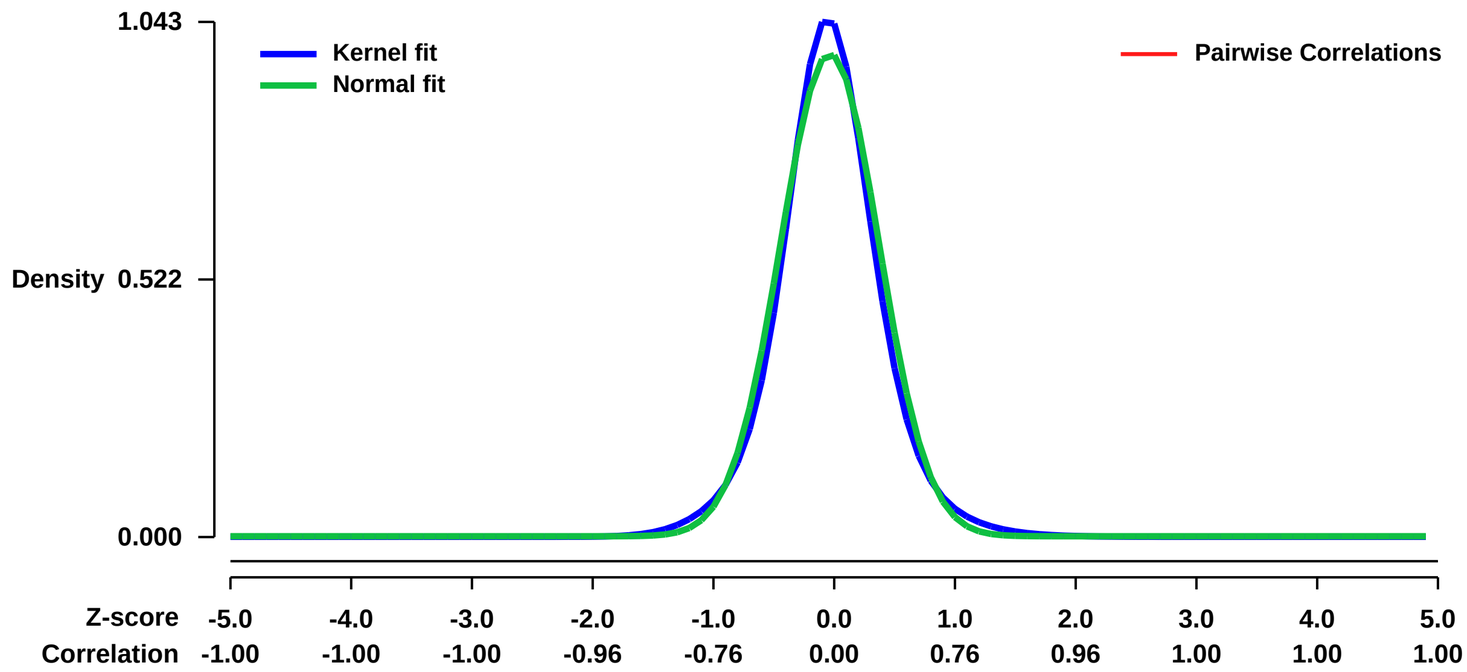

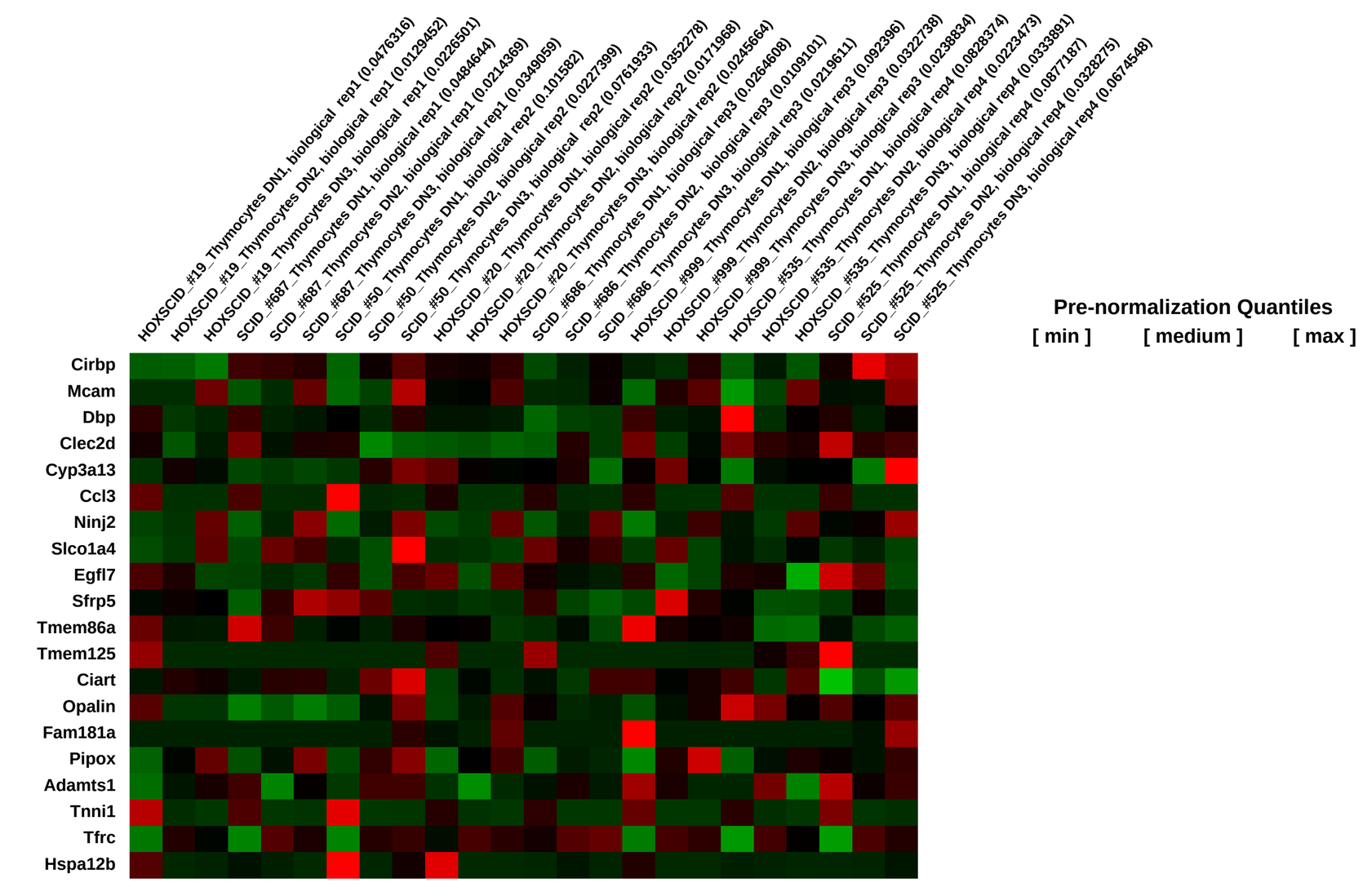

Pre-normalization Quantiles

[min] [medium] [max]

Null module

GEO Series "GSE40773" Expression Profiles

Num of samples in this series: 10

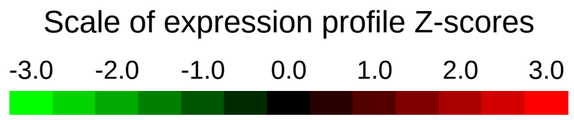

GEO Link:	**http://www.ncbi.nlm.nih.gov/geo/query/acc.cgi?acc=GSE40773**
Status:	**Public on Sep 12 2012**
Title:	**Dynamic changes in liver 5-hydroxymethylcytosine profiles upon non-genotoxic carcinogen exposure**
Organism:	**Mus musculus**
Experiment type:	**Expression profiling by array**
Platform:	**GPL1261**
Pubmed ID:	**23598998**
Summary & Design:	**Summary:** **29-32 days old male mice where either treated with Phenobarbital or untreated** **Overall design:** **Replicated control vs. pb treated study**

Background corr dist: **KL-Divergence = 0.0669, L1-Distance = 0.0246, L2-Distance = 0.0009, Normal std = 0.5027**

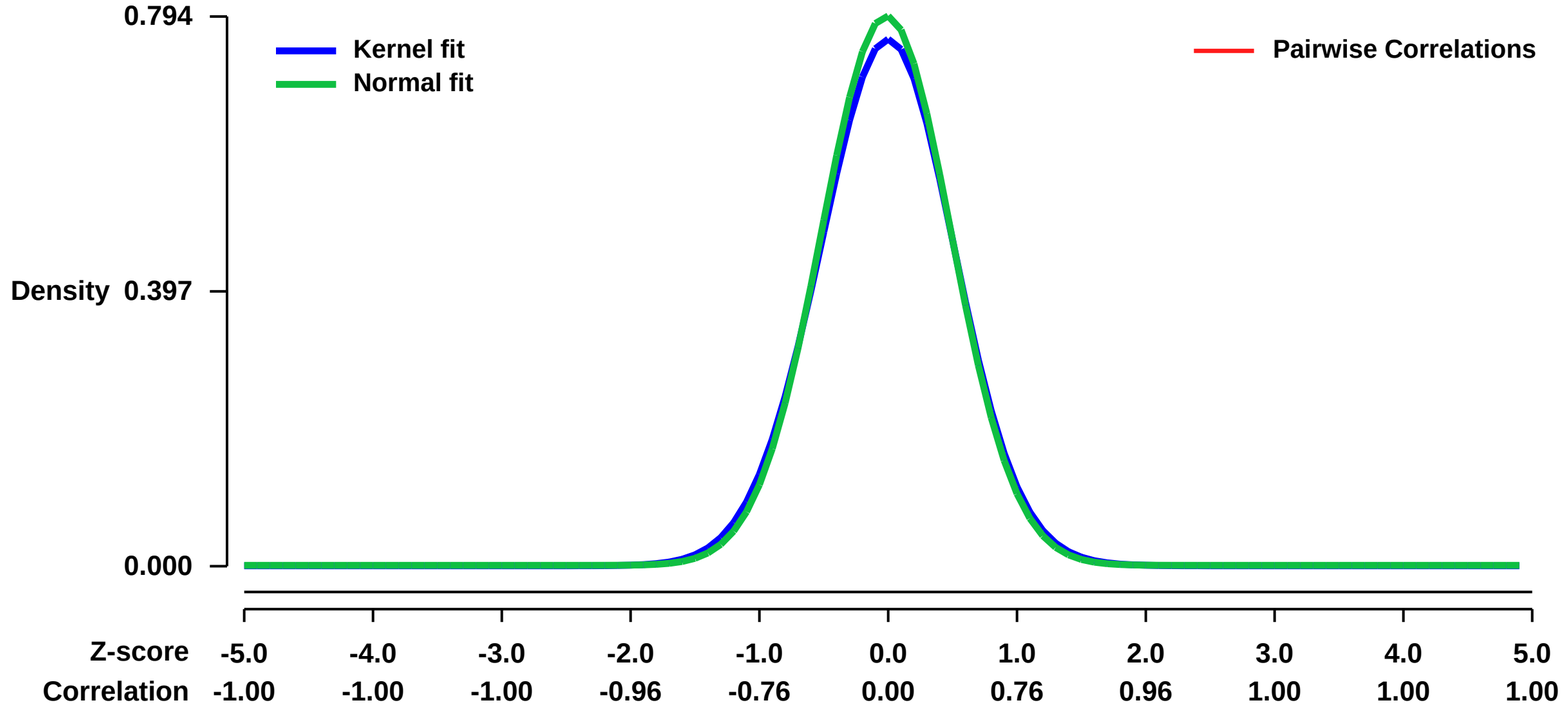

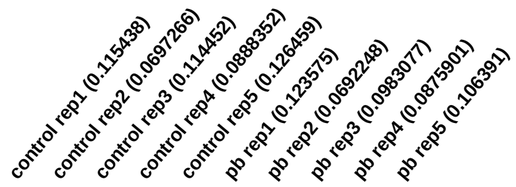

Pre-normalization Quantiles

[min] [medium] [max]

Null module

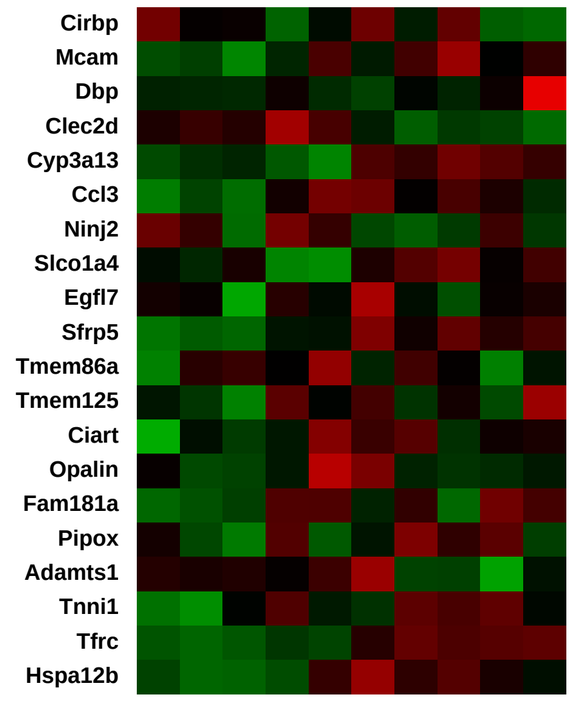

GEO Series "GSE52550" Expression Profiles

Num of samples in this series: 12

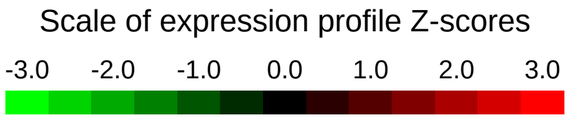

GEO Link:	http://www.ncbi.nlm.nih.gov/geo/query/acc.cgi?acc=GSE52550
Status:	Public on Dec 05 2013
Title:	Progressive loss of PGC-1alpha expression in aging muscle potentiates glucose intolerance and systemic inflammation
Organism:	Mus musculus
Experiment type:	Expression profiling by array
Platform:	GPL1261
Pubmed ID:	24280126
Summary & Design:	**Summary:** Decreased mitochondrial mass and function in muscle of diabetic patients is associated with low PGC-1alpha, a transcriptional coactivator of the mitochondrial gene program. To investigate whether reduced PGC-1alpha and oxidative capacity in muscle directly contributes to age-related glucose intolerance, we compared the genetic signatures and metabolic profiles of aging mice lacking muscle PGC-1alpha. Microarray analysis revealed that a significant proportion of PGC-1alpha-dependent changes in gene expression overlapped with age-associated effects, and aging muscle and muscle lacking PGC-1alpha shared gene signatures of impaired electron transport chain activity and TGFbeta signalling. **Overall design:** Gastrocnemius muscle mRNA from young (10 week old) and old (24 month old) wild-type and knock-out (muscle-specific PGC-1alpha, myogenin-cre) C57Bl/6N/6J/129 mice

Background corr dist: KL-Divergence = 0.1012, L1-Distance = 0.0285, L2-Distance = 0.0014, Normal std = 0.4339

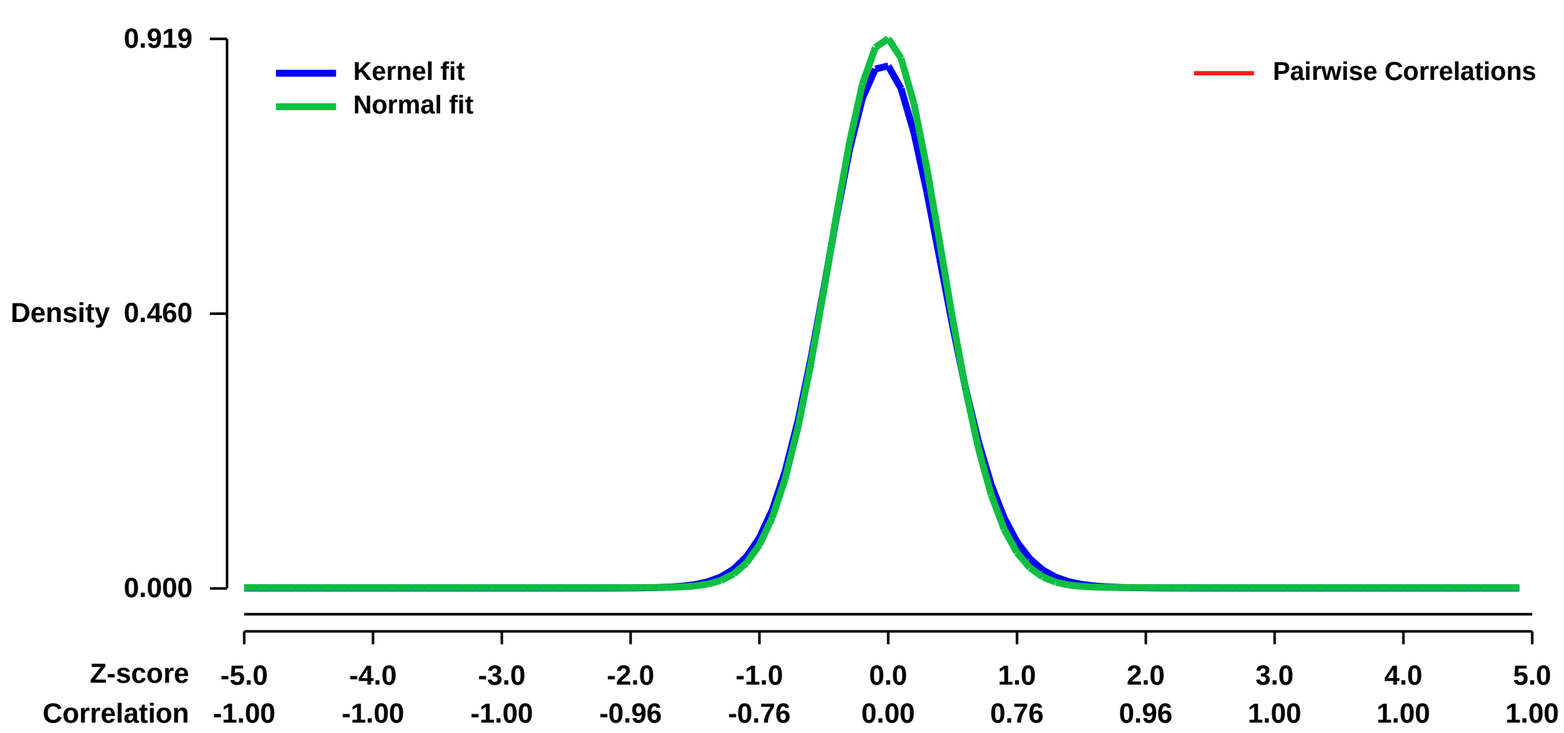

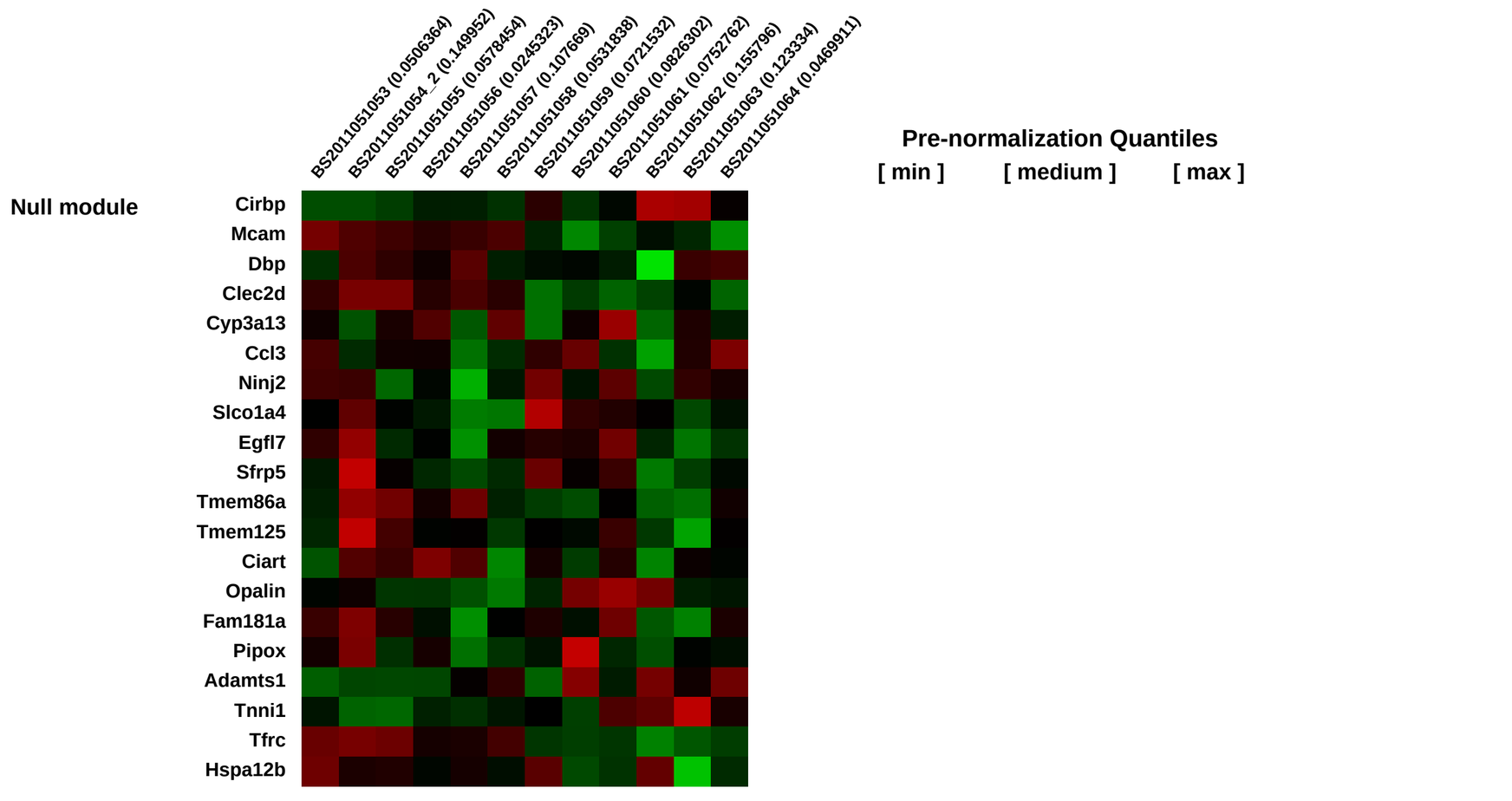

GEO Series "GSE31246" Expression Profiles

Num of samples in this series: 12

Scale of expression profile Z-scores

-3.0 -2.0 -1.0 0.0 1.0 2.0 3.0

GEO Link:	http://www.ncbi.nlm.nih.gov/geo/query/acc.cgi?acc=GSE31246
Status:	Public on Aug 08 2012
Title:	Expression data from SP and non-SP sorted anti-EpCAM treated A2C12 cells
Organism:	Mus musculus
Experiment type:	Expression profiling by array
Platform:	GPL1261
Pubmed ID:	
Summary & Design:	**Summary:** Targeted therapies against cancer stem cells which are enriched in side populations (SP) involves interruption of Wnt-signalling. Furthermore, EpCAM is a SP marker and modulator of Wnt-signalling. Therefore, the effects of an anti-EpCAM treatment on SP-cells and WNT/¸†-catenin signalling was studied. SP of the murine lung adenocarcinoma cell line A2C12 was obtained by fluorescence activated cell sorting and whole genome scans helped to define their molecular phenotype after anti-EpCAM antibody treatment. **Overall design:** Anti-EpCAM treated and untreated A2C12 cells were subjected to Hoechst 33342 dye exclusion assay and sorted to SP and non-SP fractions by FACS. Three biological replicates.

Background corr dist: KL-Divergence = 0.0751, L1-Distance = 0.0299, L2-Distance = 0.0015, Normal std = 0.4823

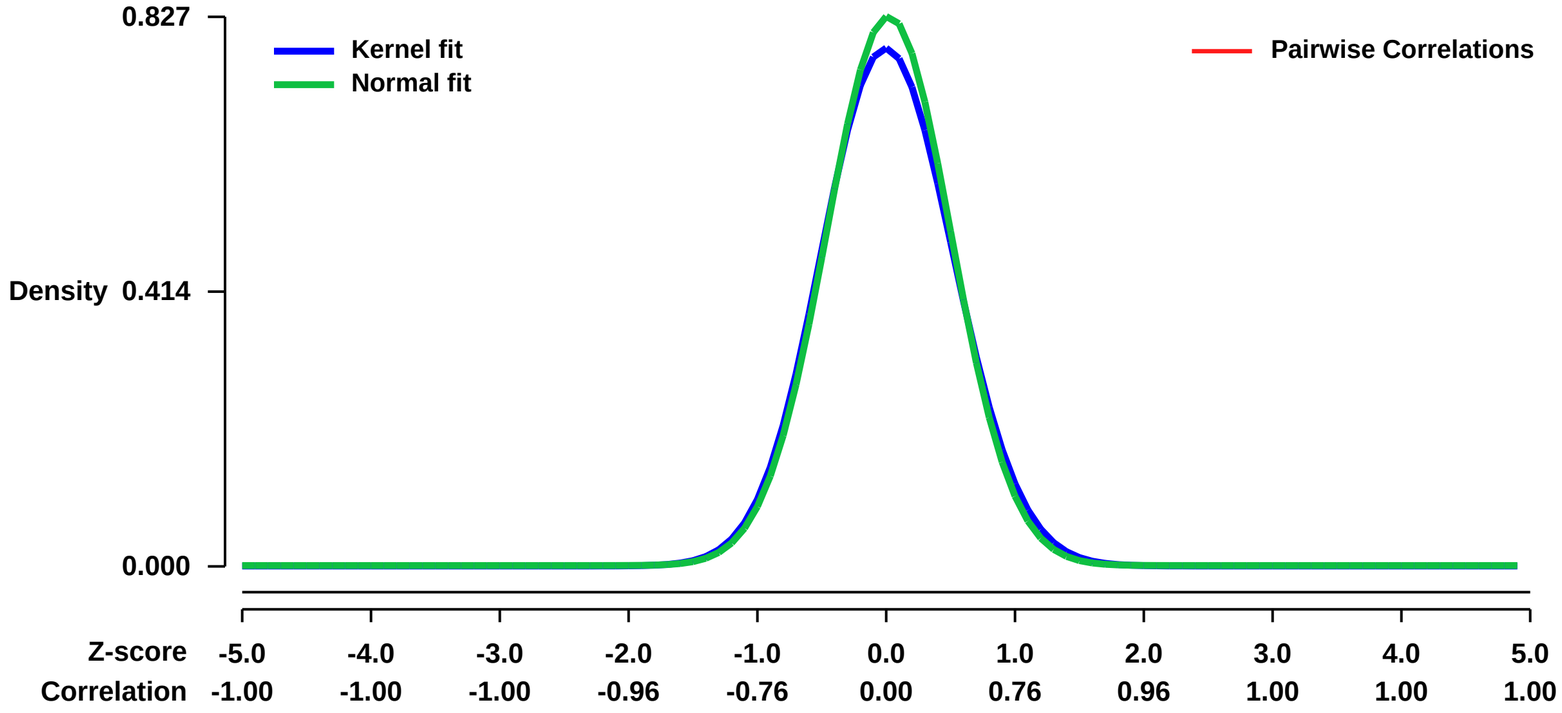

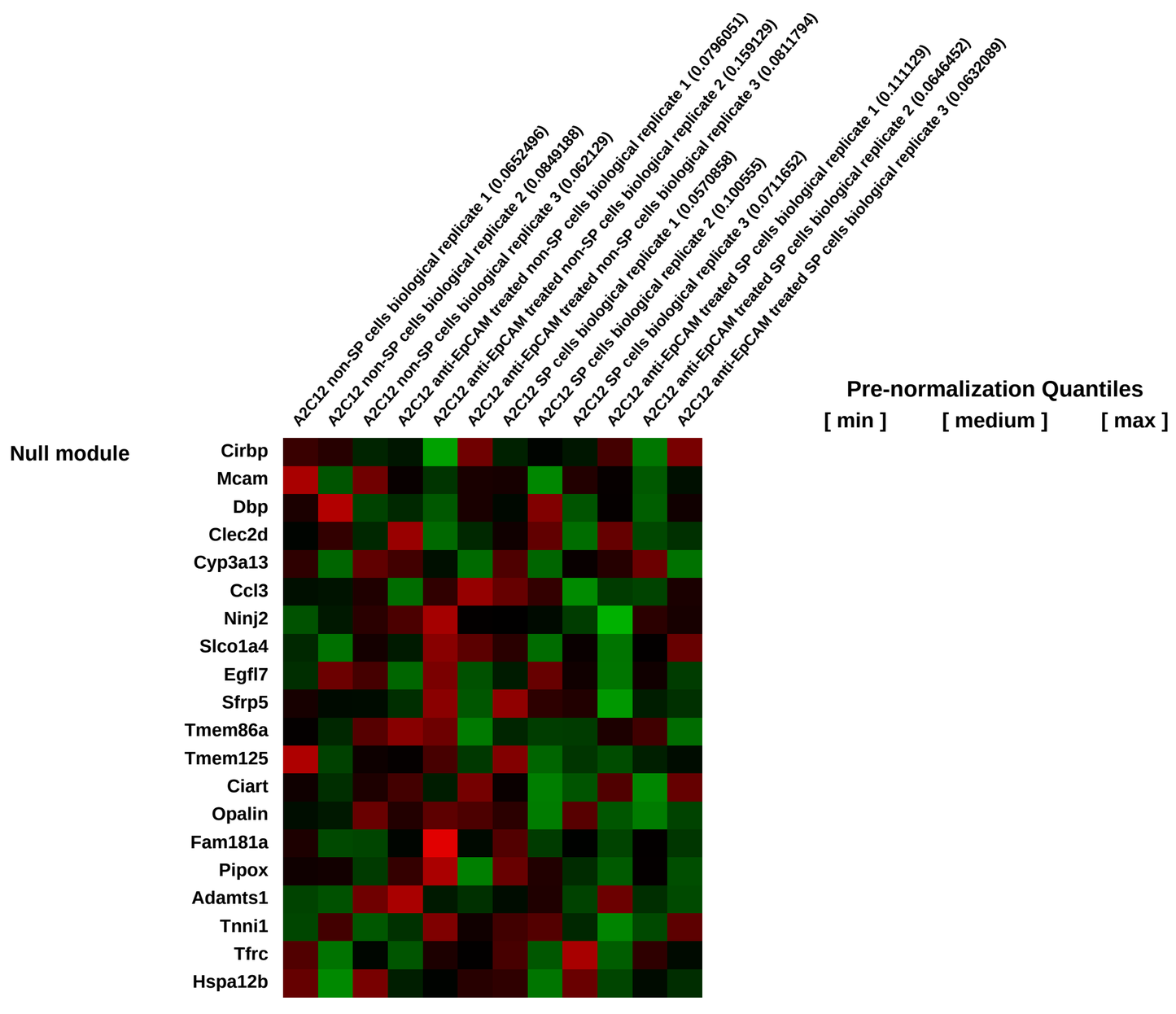

GEO Series "GSE4323" Expression Profiles

Num of samples in this series: 6

Scale of expression profile Z-scores

-3.0 -2.0 -1.0 0.0 1.0 2.0 3.0

GEO Link:	http://www.ncbi.nlm.nih.gov/geo/query/acc.cgi?acc=GSE4323
Status:	Public on Feb 04 2008
Title:	Gene expression changes in FORKO mice
Organism:	Mus musculus
Experiment type:	Expression profiling by array
Platform:	GPL1261
Pubmed ID:	17217615
Summary & Design:	**Summary:** To understand consequences of loss of FSH receptor, we used genetically altered mouse mutants with deletion of this receptor. Follitropin Receptor Knockout (FORKO) mice present various developmental and age-dependent abnormalities such as infertility, senescence and increased tumor incidences in addition to other phenotypes. To explore why the atrophic ovaries of FORKO mice develop ovarian anomalies later in life, we used expression profiling studies to gain a more comprehensive view of genes that are misregulated. Keywords: Comparison of Wildtype and FSH-Receptor Knock out Ovaries at 8 months of age. **Overall design:** Affymetrix 39 K GeneChip´fi Mouse Genome 430 2.0 Array has over 45000 probe sets which analyses 39000+ transcripts and variants from over 34000 well characterized mouse genes. A total of 1 ´µg of double-stranded cDNA was transcribed in vitro using the Bioarray High-Yield RNA Transcript Labeling Kit (Enzo, Farmingdale, NY) according to the manufacturer's instructions using biotinylated CTP and UTP (Enzo, Farmingdale, NY). Following 5-hr incubation at 37´ºC, the resultant biotin-labeled cRNA was purified with RNAeasy columns (Qiagen) and eluted in 40 ´µl of RNAse-free water. The concentration of biotin-labeled cRNA was determined by RNA bio-analyzer. Target cRNAs corresponding to either wild type ovary or FORKO ovarian tissue were hybridized to an individual GeneChip from an identical lot of Affymetrix 39 K GeneChip´fi Mouse Genome 430 2.0 array for 16 hr. GeneChip arrays were washed and stained using antibody-mediated signal amplification and the Affymetrix Fluidics Station's standard Eukaryotic GE Wash 2 protocol, using Affymetrix equipment and protocols (Affymetrix, Santa Clara, CA).

Background corr dist: KL-Divergence = 0.0459, L1-Distance = 0.0259, L2-Distance = 0.0008, Normal std = 0.5964

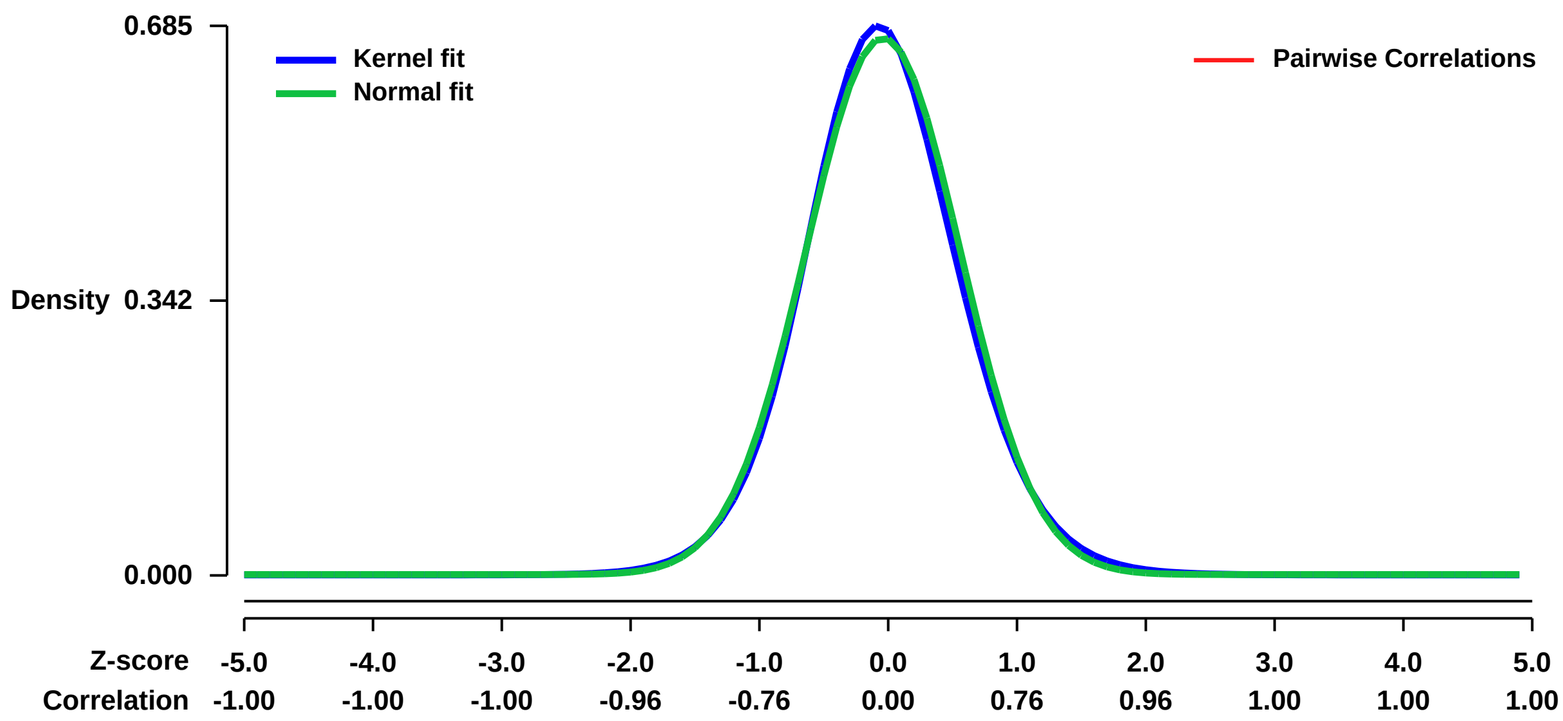

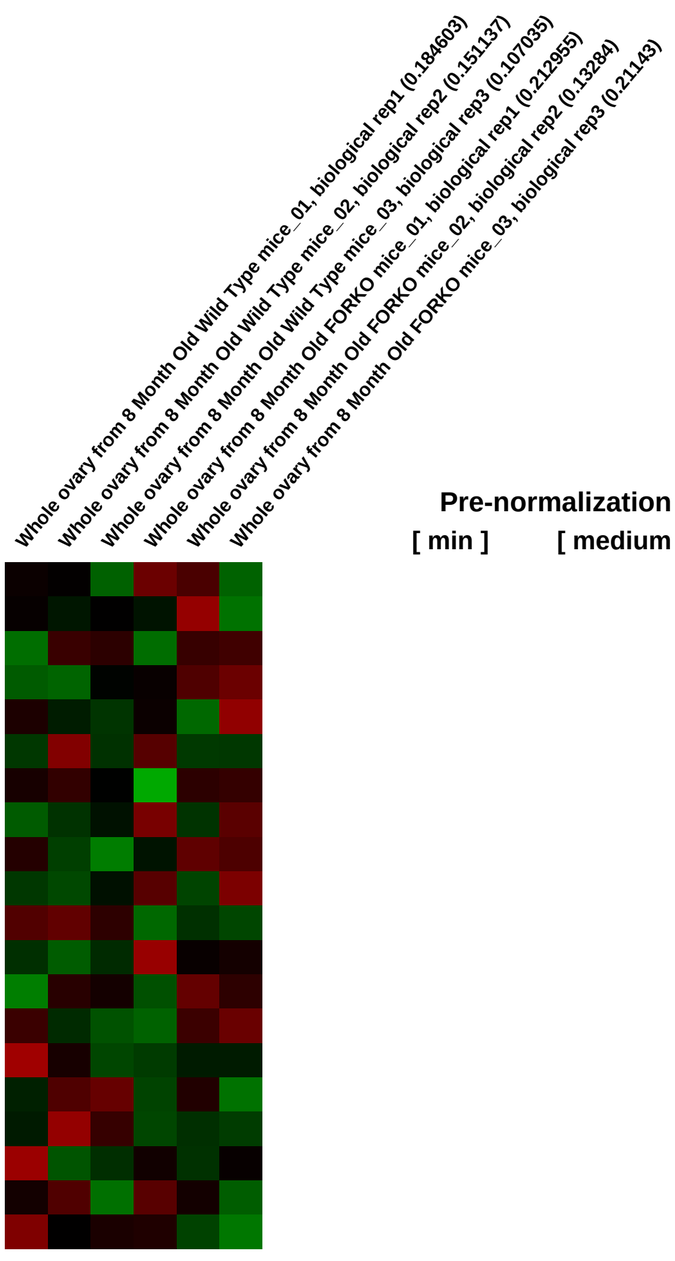

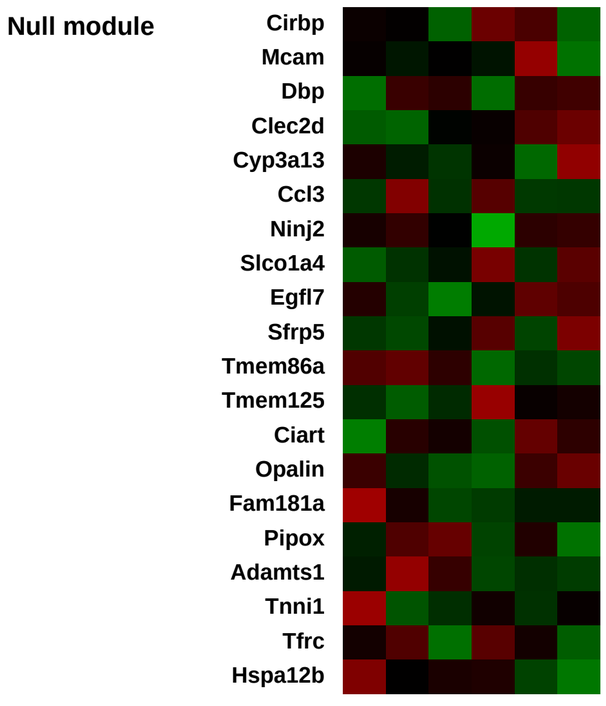

GEO Series "GSE16707" Expression Profiles

Num of samples in this series: 6

Scale of expression profile Z-scores

-3.0 -2.0 -1.0 0.0 1.0 2.0 3.0

GEO Link:	http://www.ncbi.nlm.nih.gov/geo/query/acc.cgi?acc=GSE16707
Status:	Public on Oct 01 2009
Title:	Long-term effect on the transcriptome of loss of Frizzled4 signaling in cerebellar endothelial cells
Organism:	Mus musculus
Experiment type:	Expression profiling by array
Platform:	GPL1261
Pubmed ID:	19837032
Summary & Design:	**Summary:** Transcriptional profiles of the cerebellar endothelial cells from P16 Fz4-/- animals were compared to their wild type littermate controls. The goal is to characterize the long-term effect on the transcriptome of loss of Fz4 signaling in cerebellar endothelial cells. **Overall design:** Endothelial cells were immuno-purification from P16 cerebellum using anti-PECAM antibody coated dynabeads. The cell immuno-purification procedure follows that described by Matsubara et al. (2000) and Su et al. (2003). 3 replicates of both wild type and Fz4-/- cerebellar endothelial cells were analyzed.

Background corr dist: KL-Divergence = 0.0281, L1-Distance = 0.0235, L2-Distance = 0.0006, Normal std = 0.6913

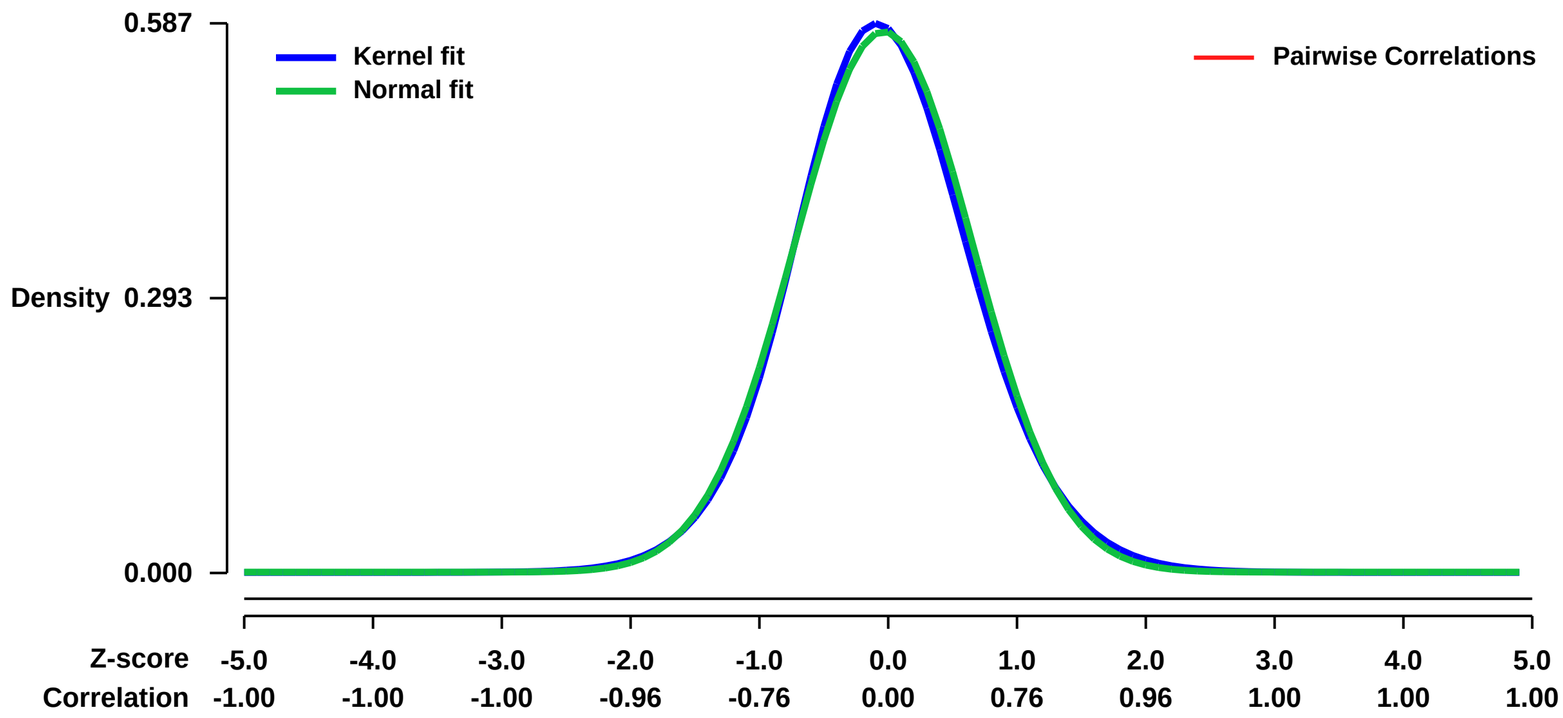

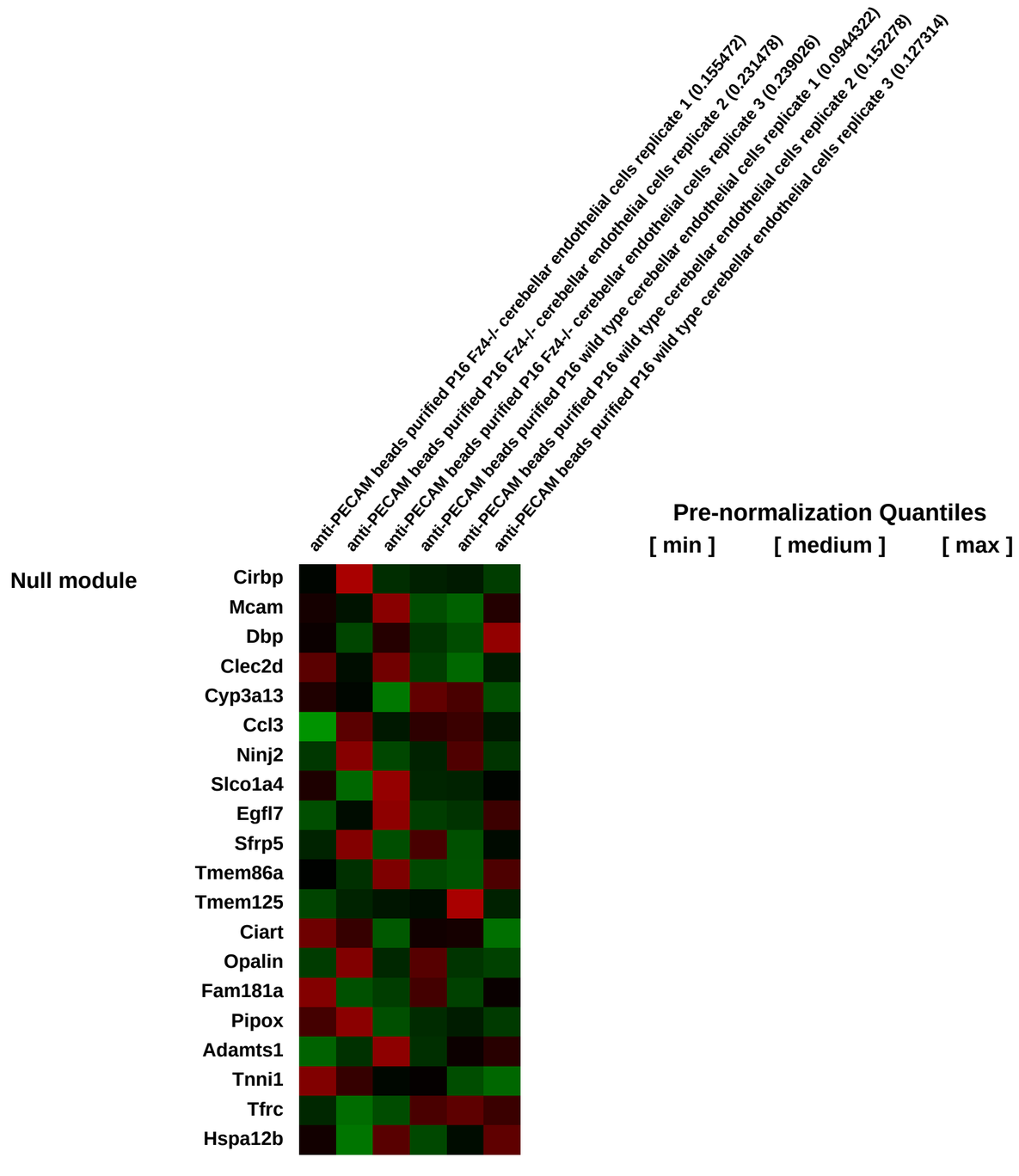

GEO Series "GSE5587" Expression Profiles

Num of samples in this series: 6

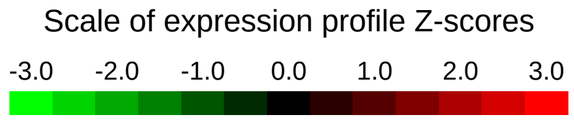

GEO Link:	http://www.ncbi.nlm.nih.gov/geo/query/acc.cgi?acc=GSE5587
Status:	Public on Aug 24 2006
Title:	tourt-affy-arabi-307860
Organism:	Mus musculus
Experiment type:	Expression profiling by array
Platform:	GPL1261
Pubmed ID:	17513727

Summary & Design:

Summary:
The Early Growth Response (Egr) family of transcription factors consists of 4 members (Egr1-4) that are expressed in a wide variety of cell types. A large body of evidence point to a role for Egr transcription factors in growth, survival, and differentiation. A major unanswered question is whether Egr transcription factors serve similar functions in diverse cell types by activating a common set of target genes. Signal transduction cascades in neurons and lymphocytes show striking parallels. Activation of either cell type activates the Ras-MAPK pathway and, in parallel, leads to increases in intracellular calcium stimulating the calcineurin-NFAT pathway. In both cell types, the strength of the activation signal affects the cellular outcomes and very strong stimuli lead to cell death. Notably both these pathways converge on the induction of Egr genes. We believe that downstream targets of Egr transcription factors in lymphocytes may also be activated by Egr factors in activated neurons. There is precedence for common target gene activation in these two cell types: apoptosis in both activated T cells and methamphetamine stimulated neurons occurs via FasL induction by NFAT transcription factors. We propose to use developing T lymphocytes (thymocytes) as a model system for discovery of Egr-dependent target genes for several reasons. First, we have observed a prominent survival defect in thymocytes from mice deficient in both Egr1 and Egr3 (1/3 DKO) and a partial differention block in the immature double negative (DN) stage. In addition, thymocytes are an easily manipulatable cell type, and the DN subpopulation affected in 1/3 DKO mice can be isolated to very high purity. We anticipate that 1/3 DKO thymocytes will provide an excellent experimental system that will provide insight into Egr-dependent transcription in neuronal development, activation, and death.

To identify Egr transcription factor target genes in developing thymocytes. Egr1/3 DKO mice show a profound defect in thymocyte survival and differentiation, but the target genes downstream of Egr1 and Egr3 are unknown. Using Egr1/3 double knockout and wild type littermate mice, we will compare gene expression profiles from DN thymocytes to identify genes that are deregulated in Egr1/3 DKO cells.

Egr1 and Egr3 expression is necessary for the proper survival and differentiation of developing thymocytes. We hypothesize that we will be able to identify crucial target genes of Egr1 and Egr3 by comparing gene expression profiles from wild type and 1/3 DKO thymocytes.

Egr1 and Egr3 are first expressed in the immature double negative (DN) thymocytes. We will isolate DN thymocytes by FACS sorting which allows isolation of cell populations of >99% purity. We will perform microarray analysis using the Mouse 430 2.0 gene array with thymocyte RNA samples from 3 wild type and 3 1/3 DKO mice (6 arrays total). Differentially regulated genes (up-regulated and down-regulated) will be identified from the list of genes with significantly altered expression greater than or equal to 2-fold by paired T test. Interesting genes will be validated by real-time PCR in wild type and 1/3 DKO thymocytes. Recognizing that both direct and indirect target genes may be identified in the list of differentially expressed genes, real-time PCR validated target genes will be further screened using chromatin immunoprecipitation coupled with PCR (ChIP-PCR) to determine whether Egr1 and/or Egr3 are bound to potential regulatory regions of the putative target genes.

Keywords: other

Overall design:

Background corr dist: **KL-Divergence = 0.0424, L1-Distance = 0.0270, L2-Distance = 0.0009, Normal std = 0.6121**

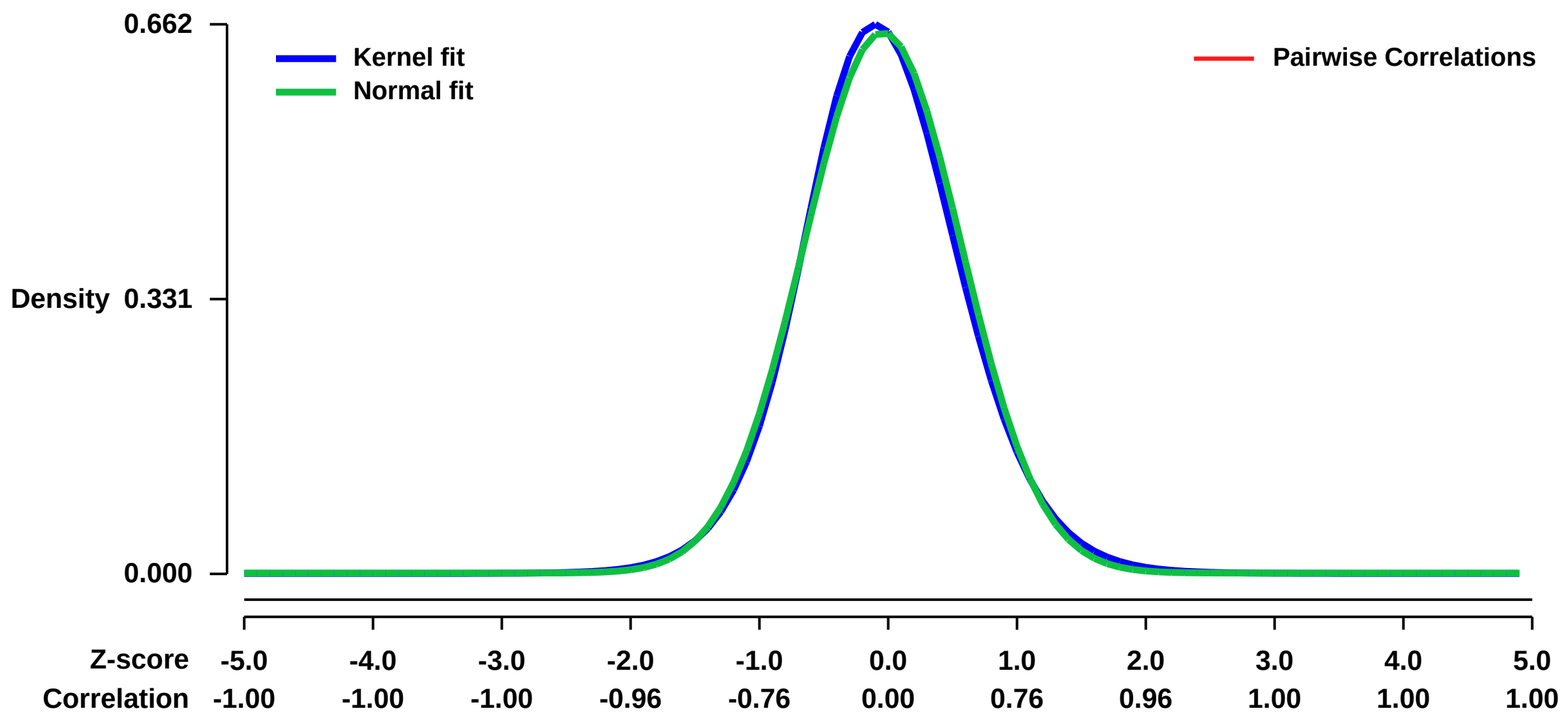

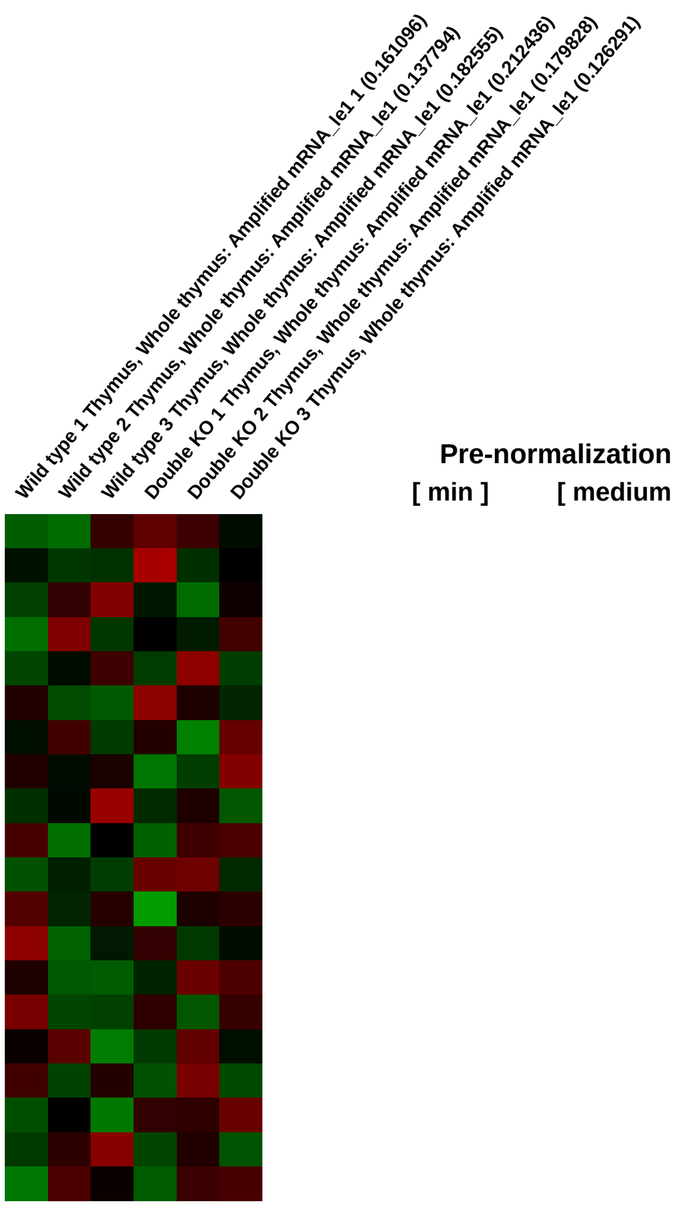

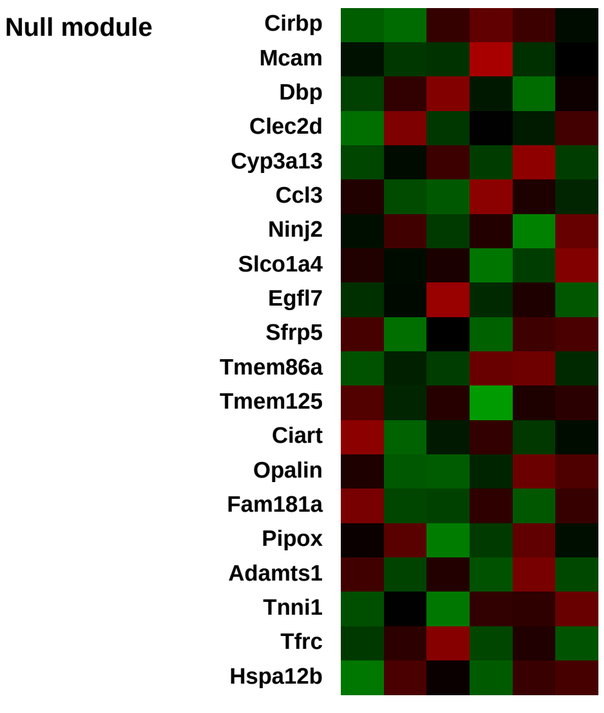

GEO Series "GSE45941" Expression Profiles

Num of samples in this series: 8

Scale of expression profile Z-scores

-3.0 -2.0 -1.0 0.0 1.0 2.0 3.0

GEO Link:	http://www.ncbi.nlm.nih.gov/geo/query/acc.cgi?acc=GSE45941
Status:	Public on Jan 30 2014
Title:	Transcription factor TFAP2C regulates major programs required for murine fetal germ cell maintenance and haploinsufficiency predisposes to teratomas in male mice
Organism:	Mus musculus
Experiment type:	Expression profiling by array
Platform:	GPL1261
Pubmed ID:	23967156
Summary & Design:	**Summary:** Maintenance and maturation of primordial germ cells is controlled by complex genetic and epigenetic cascades, and disturbances in this network lead to either infertility or malignant aberration. Transcription factor Tcfap2c / TFAP2C has been described to be essential for primordial germ cell maintenance and to be upregulated in several human germ cell cancers. Using global gene expression profiling, we identified genes deregulated upon loss of Tcfap2c in primordial germ cell-like cells. We show that loss of Tcfap2c affects many aspects of the genetic network regulating germ cell biology, such as downregulation maturation markers and induction of markers indicative of somatic differentiation, cell cycle, epigenetic remodeling, and pluripotency associated genes. Chromatin-immunoprecipitation analyses demonstrated binding of Tcfap2c to regulatory regions of deregulated genes (Sfrp1, Dmrt1, Nanos3, c-Kit, Cdk6, Cdkn1a, Fgf4, Klf4, Dnmt3b and Dnmt3l) suggesting that these genes are direct transcriptional targets of Tcfap2c in primordial germ cells. Since Tcfap2c deficient primordial germ cell like cells display cancer related deregulations in epigenetic remodeling, cell cycle and pluripotency control, the Tcfap2c-knockout allele was bred onto 129S2/Sv genetic background. There, mice heterozygous for Tcfap2c develop germ cell cancer with high incidence. Precursor lesions can be observed as early as E16.5 in developing testes displaying persisting expression of pluripotency markers. We further demonstrate, that mice with a heterozygous deletion of the Tcfap2c target gene Nanos3 are also prone to develop teratoma. These data highlight Tcfap2c as a critical and dose-sensitive regulator of germ cell fate. **Overall design:** **KO PGC:** Tcfap2c knock-out mouse primordial germ cells (PGCs), 2 biological rep

Background corr dist: KL-Divergence = 0.0560, L1-Distance = 0.0176, L2-Distance = 0.0004, Normal std = 0.5390

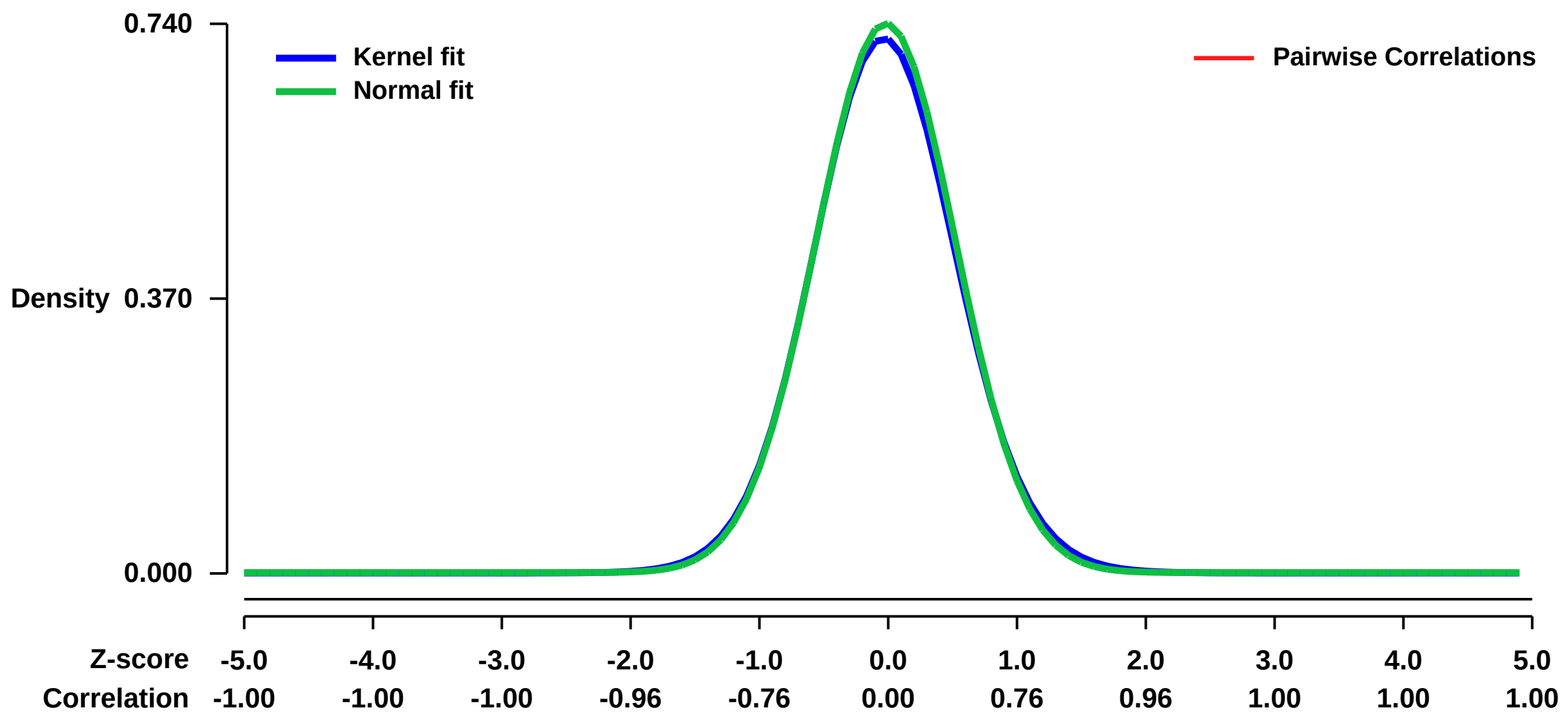

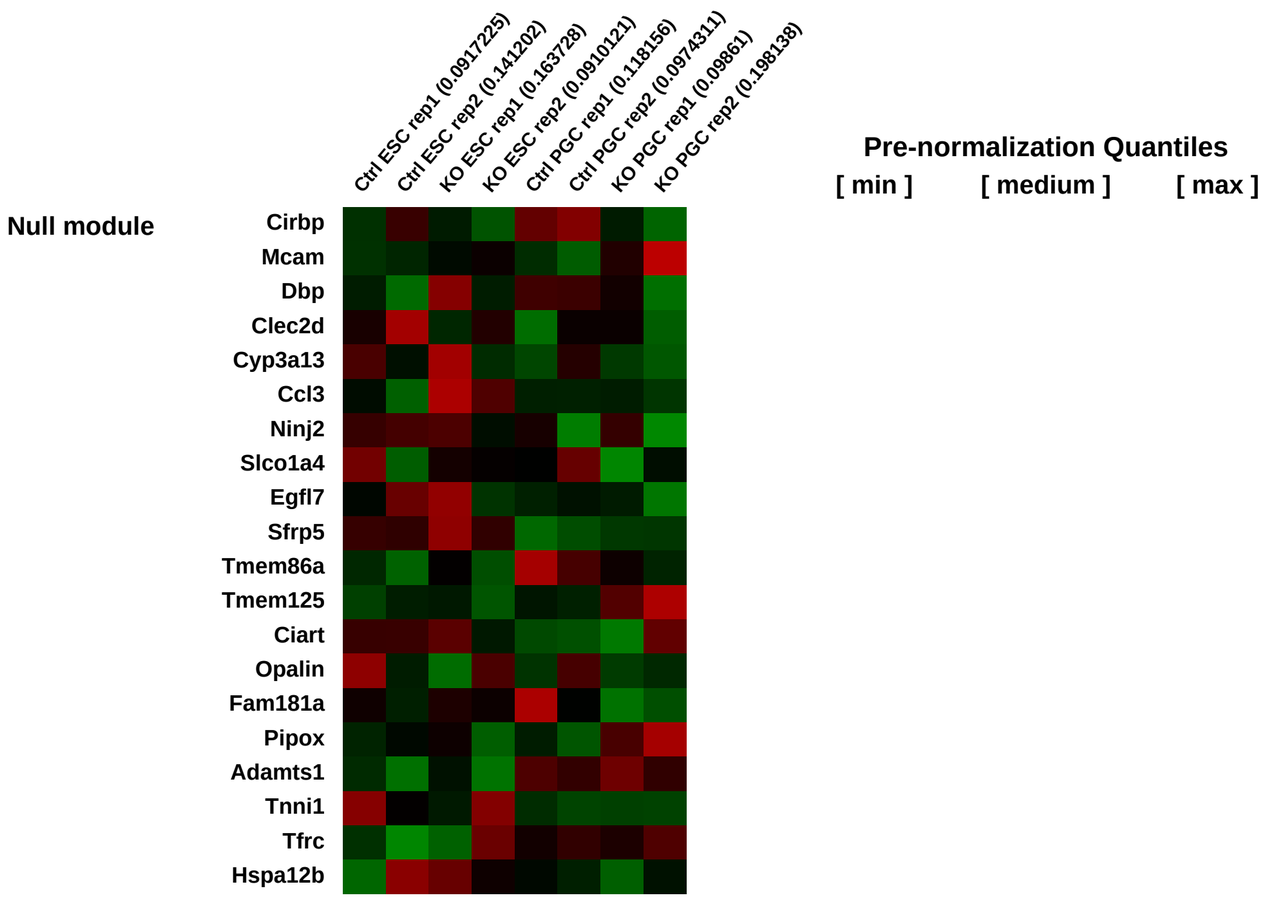

GEO Series "GSE21525" Expression Profiles

Num of samples in this series: 12

Scale of expression profile Z-scores

-3.0 -2.0 -1.0 0.0 1.0 2.0 3.0

GEO Link:	http://www.ncbi.nlm.nih.gov/geo/query/acc.cgi?acc=GSE21525
Status:	Public on Apr 27 2010
Title:	Expression data from testis of day-7 Sohlh1 knock-out mice
Organism:	Mus musculus
Experiment type:	Expression profiling by array
Platform:	GPL1261
Pubmed ID:	16564520
Summary & Design:	**Summary:** Sohlh1 and Sohlh2 encode a germ cell-specific basic helix-loop-helix transcriptional regulator critical in spermatogonial differentiation. Seven-day-old Sohlh1 or Sohlh2 knockout and wild-type testes were arrayed on the Affy 430 2.0 platform. **Overall design:** The following mice were analyzed at postnatal day 7: wild-type, Sohlh1-/-, and Sphlh2-/-. 4 samples/group.

Background corr dist: KL-Divergence = 0.1447, L1-Distance = 0.0339, L2-Distance = 0.0021, Normal std = 0.3785

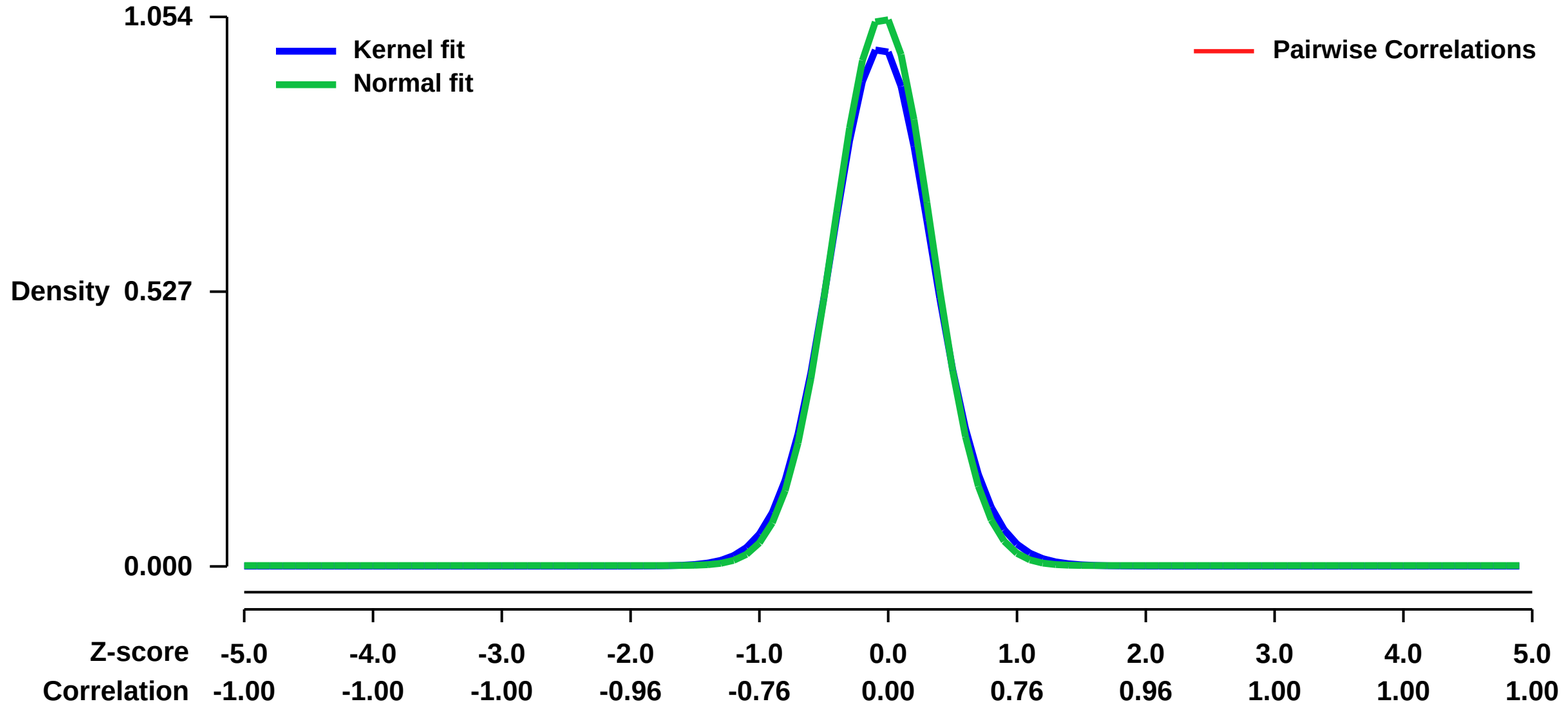

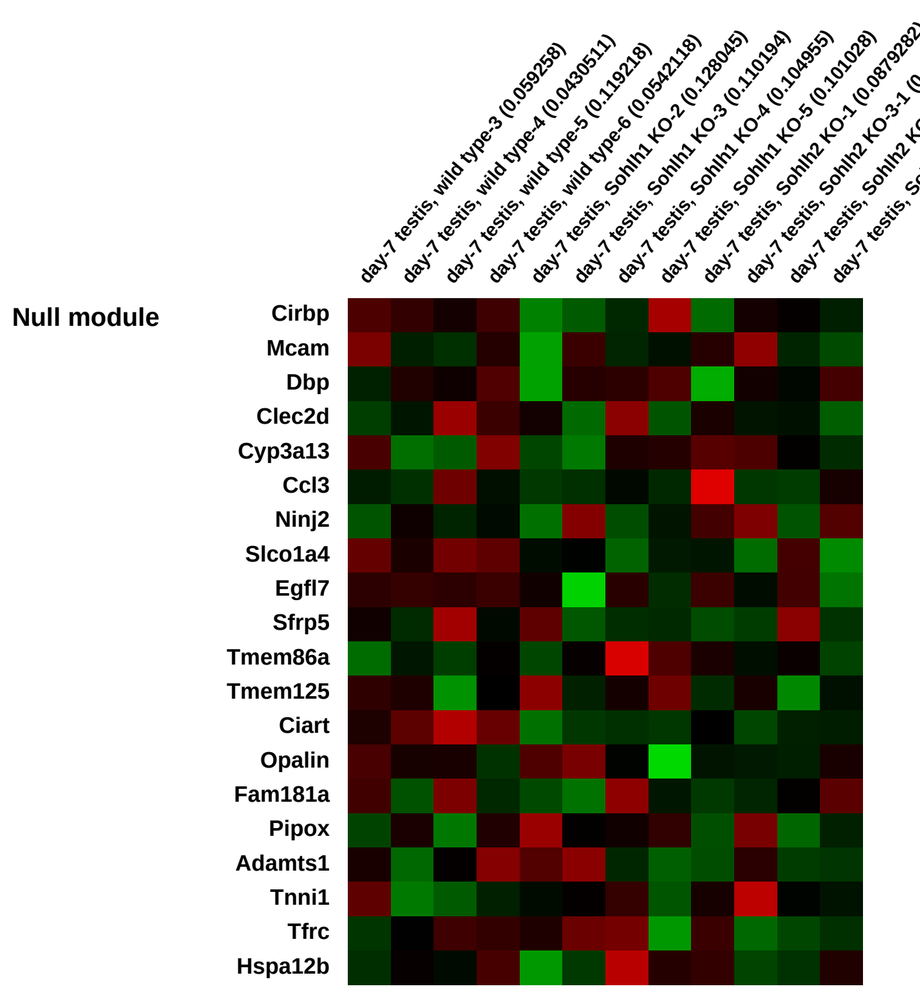

Pre-normalization Quantiles

[min] [medium] [max]

GEO Series "GSE5255" Expression Profiles

Num of samples in this series: 6

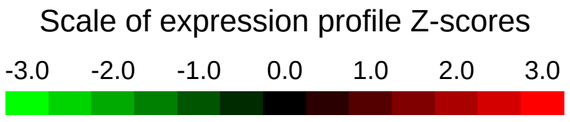

GEO Link:	http://www.ncbi.nlm.nih.gov/geo/query/acc.cgi?acc=GSE5255
Status:	Public on Jul 08 2006
Title:	Loss of BMPR2 Signaling in Smooth Muscle in Mouse Lung
Organism:	Mus musculus
Experiment type:	Expression profiling by array
Platform:	GPL1261
Pubmed ID:	17369292
Summary & Design:	**Summary:** Mice expressing a doxycycline-inducible dominant negative BMPR2 transgene expressed only in smooth muscle are activated for one or eight weeks, and compared to transactivator-only mice also fed doxycycline. All mice are 12 weeks of old at sacrifice. **Keywords: time course with SM22-rtTA x tetO7-BMPR2 transgene** **Overall design:** Each chip is a pool of three individual mice, to reduce variability. The transactivator-only mice are controls. The other mice all had elevated RV pressures at time of sacrifice. RNA was prepared from whole lung.

Background corr dist: **KL-Divergence = 0.0323, L1-Distance = 0.0268, L2-Distance = 0.0011, Normal std = 0.6609**

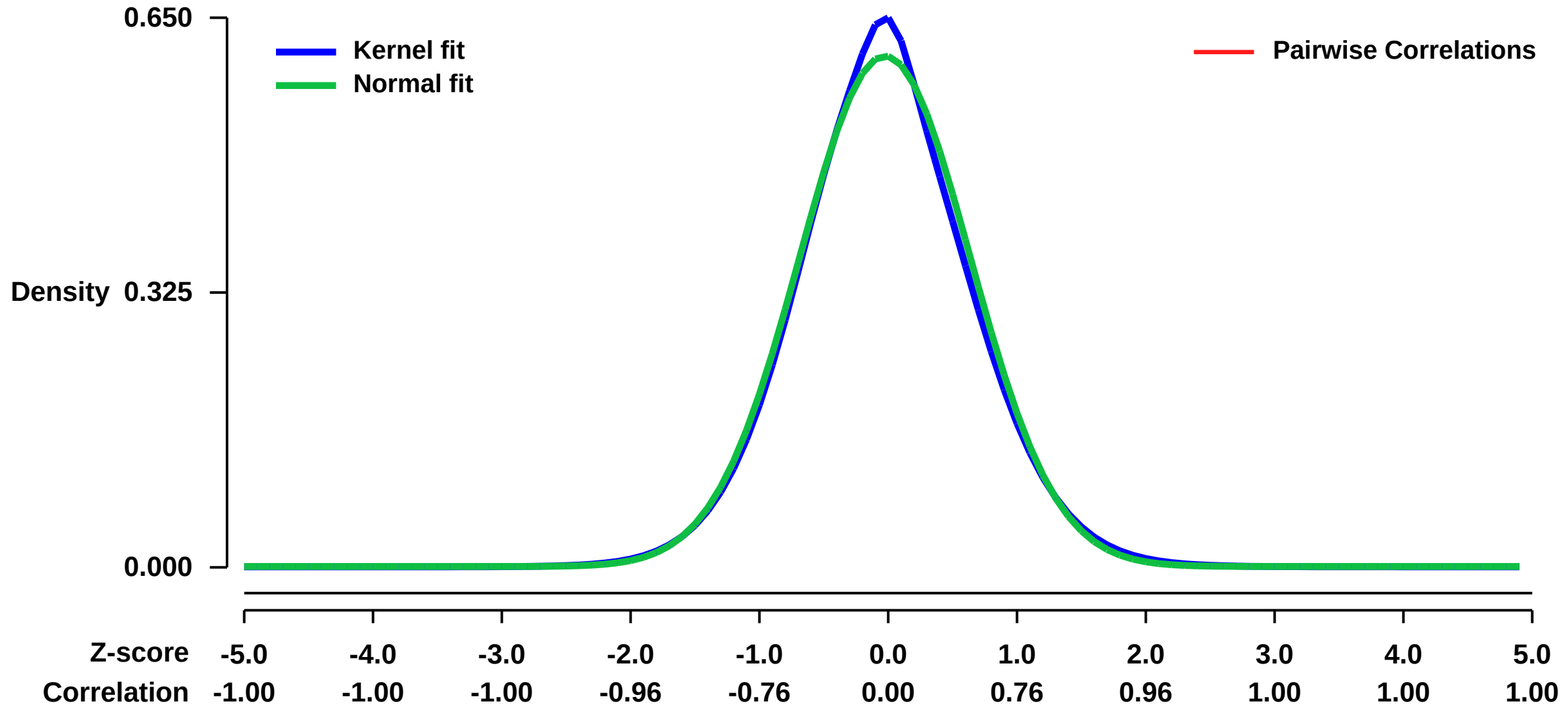

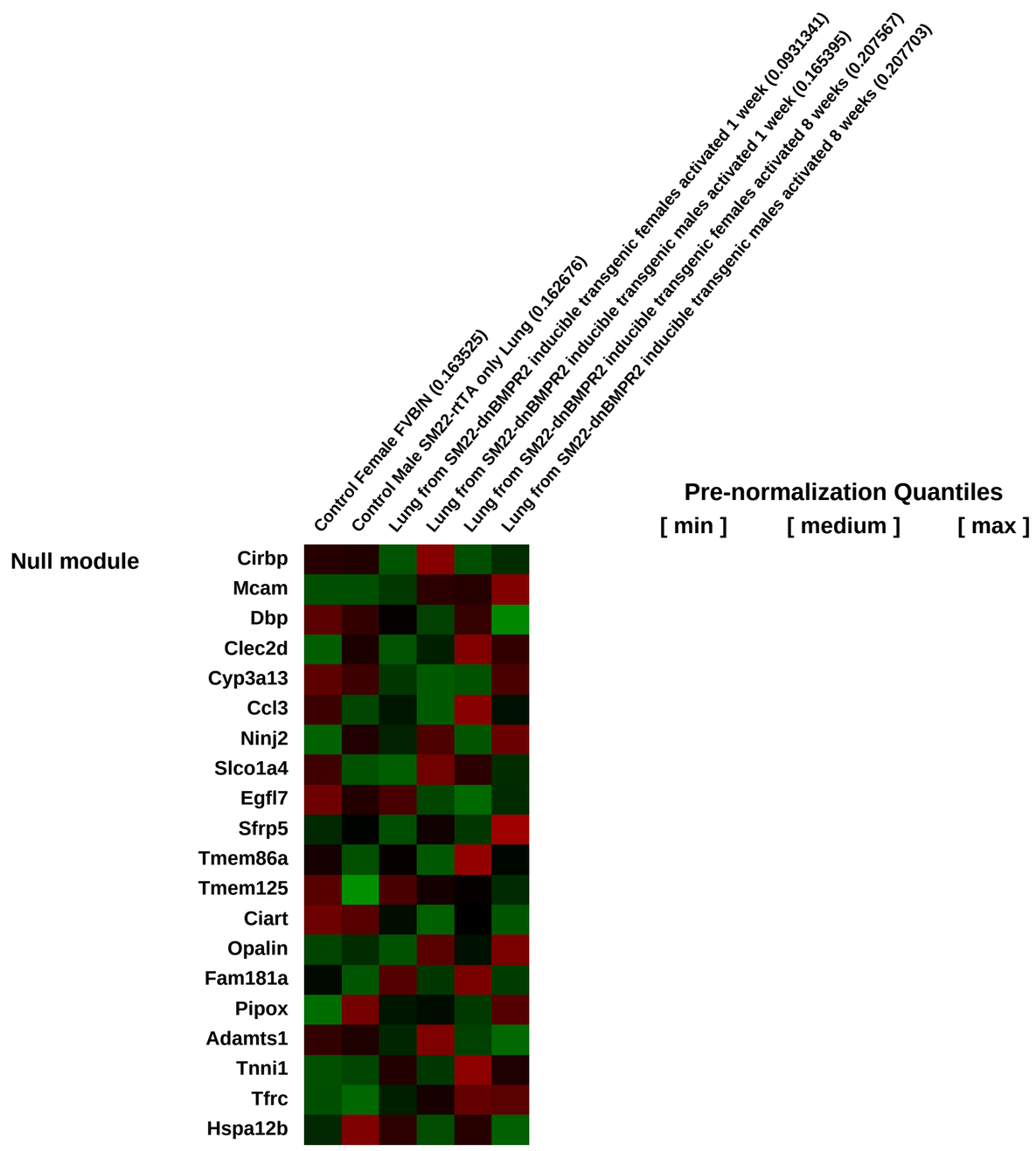

GEO Series "GSE21380" Expression Profiles

Num of samples in this series: 7

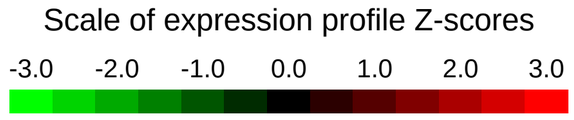

GEO Link:	http://www.ncbi.nlm.nih.gov/geo/query/acc.cgi?acc=GSE21380
Status:	Public on Apr 20 2010
Title:	Expression Data from in vivo Tfh vs GC Tfh vs non-Tfh
Organism:	Mus musculus
Experiment type:	Expression profiling by array
Platform:	GPL1261
Pubmed ID:	20525889
Summary & Design:	**Summary:** CD4 T cell help is critical for both the generation and maintenance of germinal centers, and T follicular helper (TFH) cells are the CD4 T cell subset required for this process. SAP (SH2D1A) expression in CD4 T cells is essential for germinal center development. However, SAP-deficient mice have only a moderate defect in TFH differentiation as defined by common TFH surface markers. CXCR5+ TFH cells are found within the germinal center as well as along the boundary regions of T/B cell zones. Here we show that germinal center associated T cells (GC TFH) can be identified by their co-expression of CXCR5 and the GL7 epitope, allowing for phenotypic and functional analysis of TFH and GC TFH populations. Here we show GC TFH are a functionally discrete subset of further polarized TFH cells, with enhanced B cell help capacity and a specialized ability to produce IL-4 in a TH2-independent manner. Strikingly, SAP-deficient mice have an absence of the GC TFH subset and SAP- TFH are defective in IL-4 and IL-21 production. We further demonstrate that SLAM (Slamf1, CD150), a surface receptor that utilizes SAP signaling, is specifically required for IL-4 production by GC TFH. GC TFH cells require IL-4 and IL-21 production for optimal help to B cells. These data illustrate complexities of SAP-dependent SLAM family receptor signaling, revealing a prominent role for SLAM receptor ligation in IL-4 production by germinal center CD4 T cells but not in TFH and GC TFH differentiation. **Overall design:** Analysis of in vivo follicular helper CD4 T cells (CXCR5high GL7low), versus germinal center follicular helper CD4 T cells (CXCR5hi GL7hi), versus non-follicular helper CD4 T cells (CXCR5low) eight days after viral infection.

Background corr dist: KL-Divergence = 0.0509, L1-Distance = 0.0348, L2-Distance = 0.0018, Normal std = 0.5824

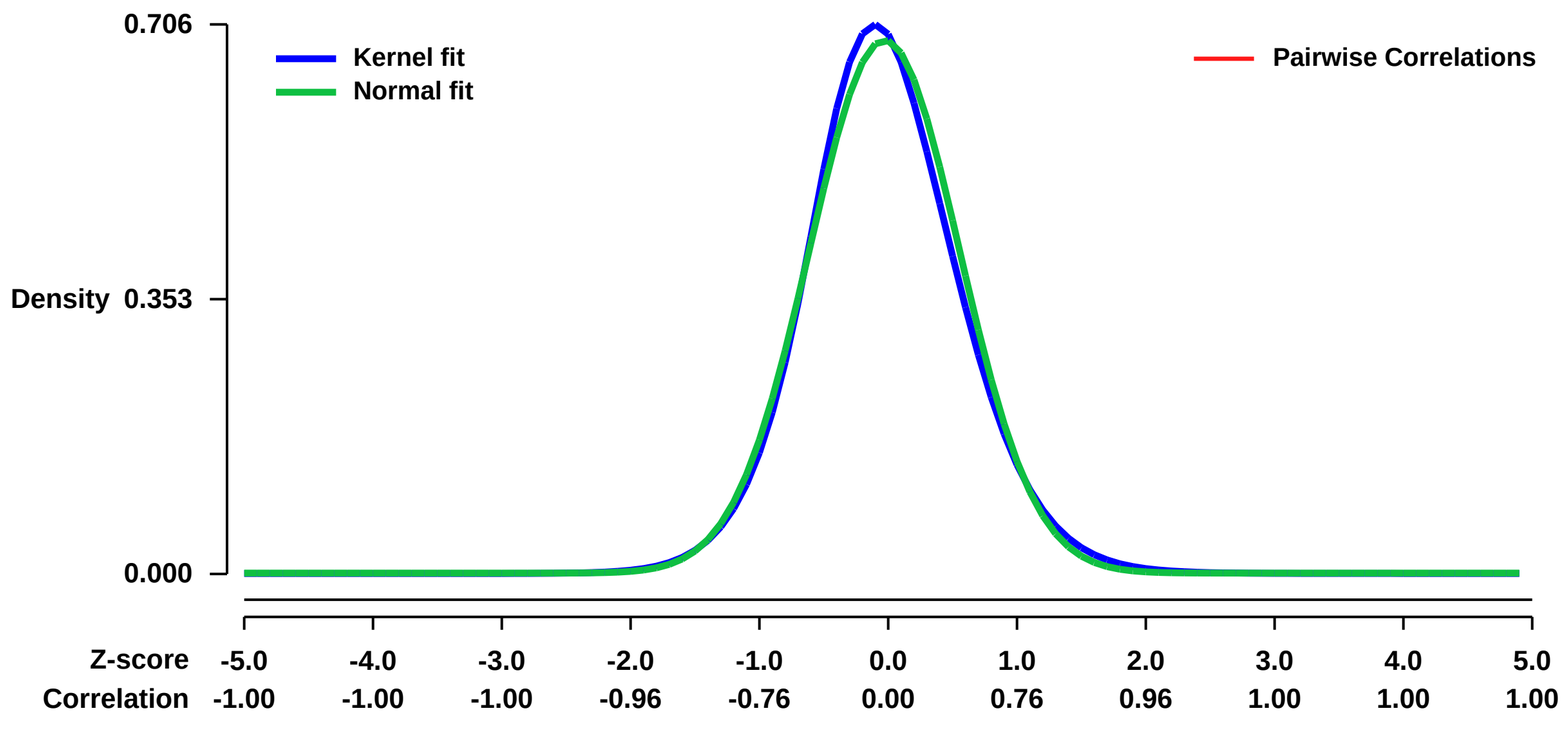

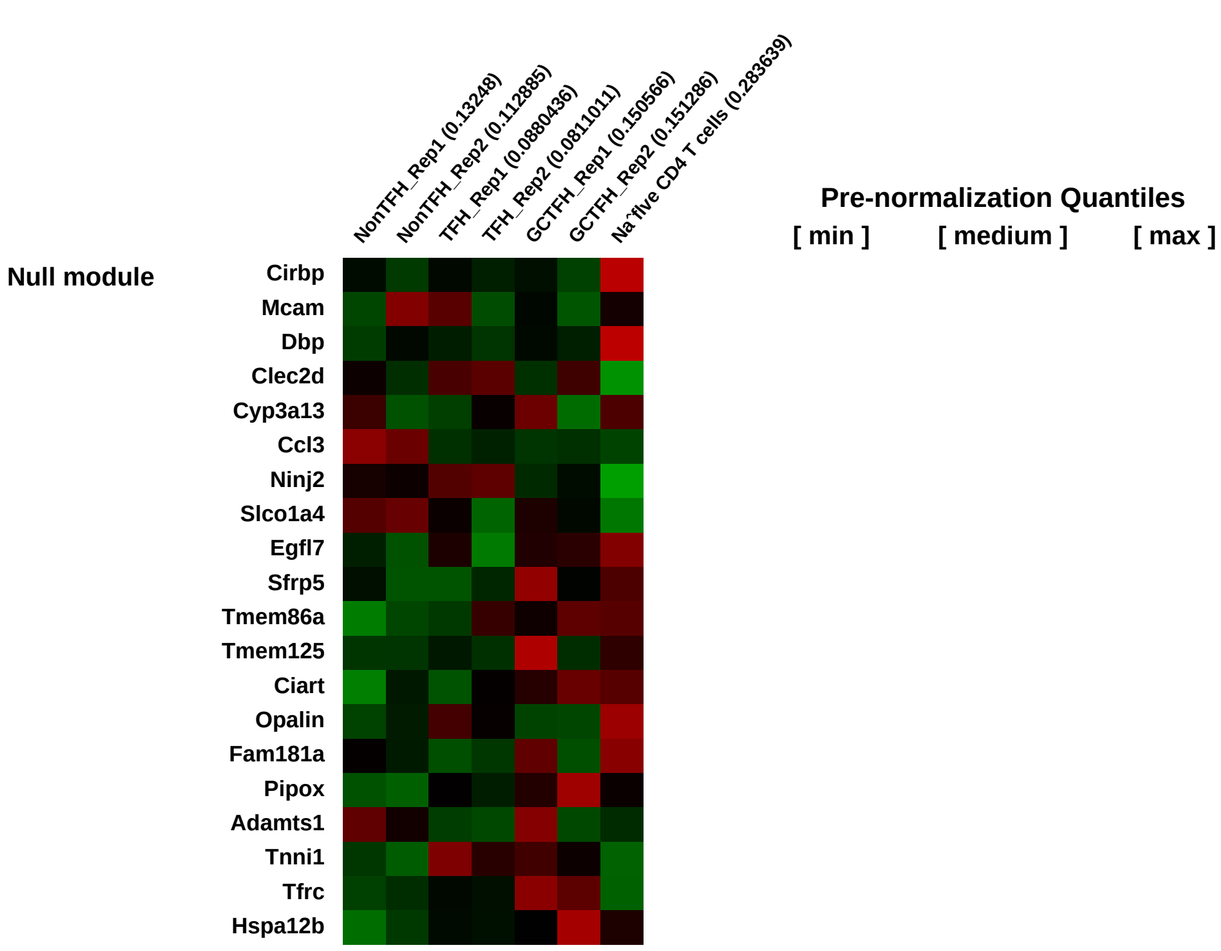

GEO Series "GSE13869" Expression Profiles

Num of samples in this series: 8

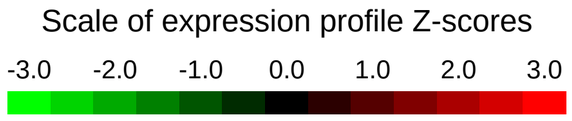

GEO Link:	**http://www.ncbi.nlm.nih.gov/geo/query/acc.cgi?acc=GSE13869**
Status:	**Public on Jan 24 2010**
Title:	**Transcriptome of the Nxnl1-/- mouse retina**
Organism:	**Mus musculus**
Experiment type:	**Expression profiling by array**
Platform:	**GPL1261**
Pubmed ID:	**20139892**
Summary & Design:	**Summary:** **Rod-derived Cone Viability Factor (RdCVF, alias nxnl1) is a retina-specific protein identified for its therapeutic potential in supporting cone survival during retinal degeneration.** **A nxnl1 knockout mouse model was created and the transcriptome used to demonstrate that the retina is compromised by the absence of nxnl1.** **Keywords: genetic modification, transcription-profile, retina** **Overall design:** **In total 9 samples were analyzed, they represent three different genotypes (wt/wt, ko/wt, ko/ko) that were tested in triplicate each.**

Background corr dist: **KL-Divergence = 0.0528, L1-Distance = 0.0188, L2-Distance = 0.0005, Normal std = 0.5499**

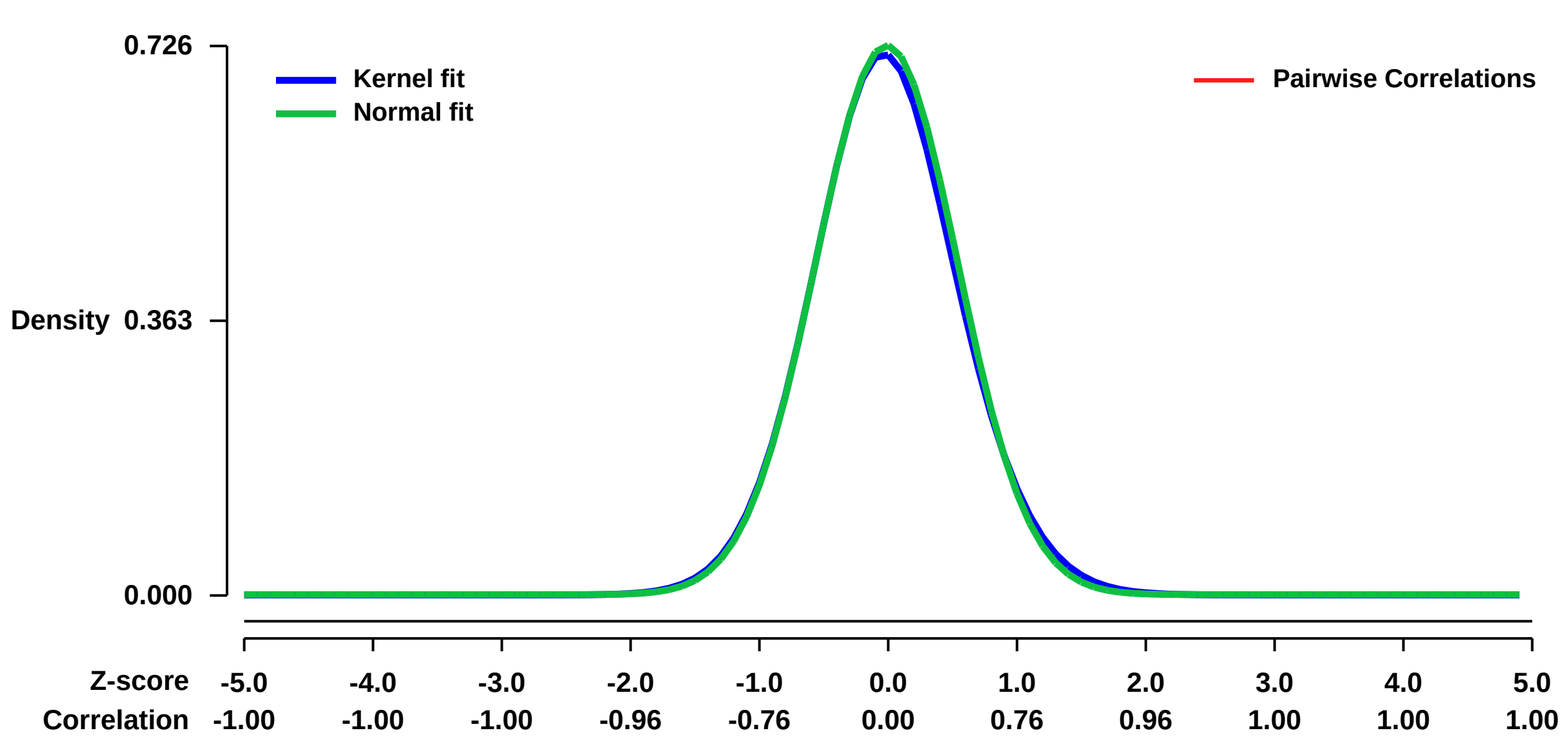

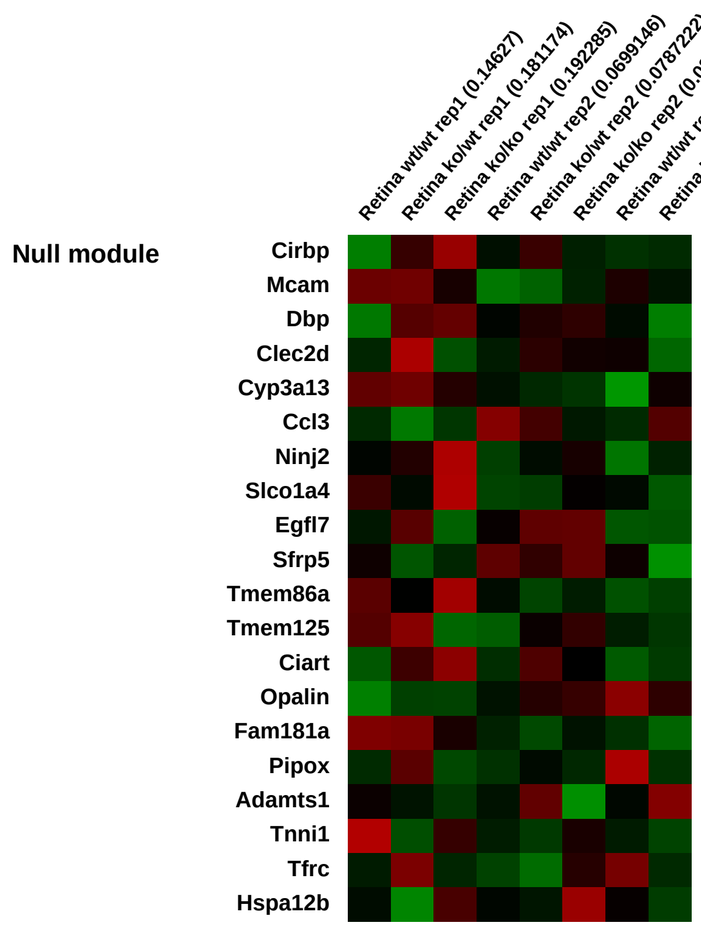

GEO Series "GSE23724" Expression Profiles

Num of samples in this series: 8

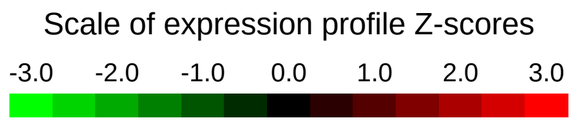

GEO Link:	http://www.ncbi.nlm.nih.gov/geo/query/acc.cgi?acc=GSE23724
Status:	Public on Aug 21 2010
Title:	Genes differentially regulated by the glucocorticoid receptor in developing skin of the GR knock out and wt embryos.
Organism:	Mus musculus
Experiment type:	Expression profiling by array
Platform:	GPL1261
Pubmed ID:	20880987
Summary & Design:	**Summary:** To understand the transcriptional program by which GR regulates skin development, we performed a microarray analysis using the skin of E18.5 GR-/- and GR+/+ mouse embryos. **Overall design:** RNA from four dorsal skin samples from GR-/- and GR+/+ E18.5 mouse embryos was collected and analyzed using Affymetrix Mouse Genome 430 2.0 GeneChips.

Background corr dist: KL-Divergence = 0.0611, L1-Distance = 0.0186, L2-Distance = 0.0004, Normal std = 0.5230

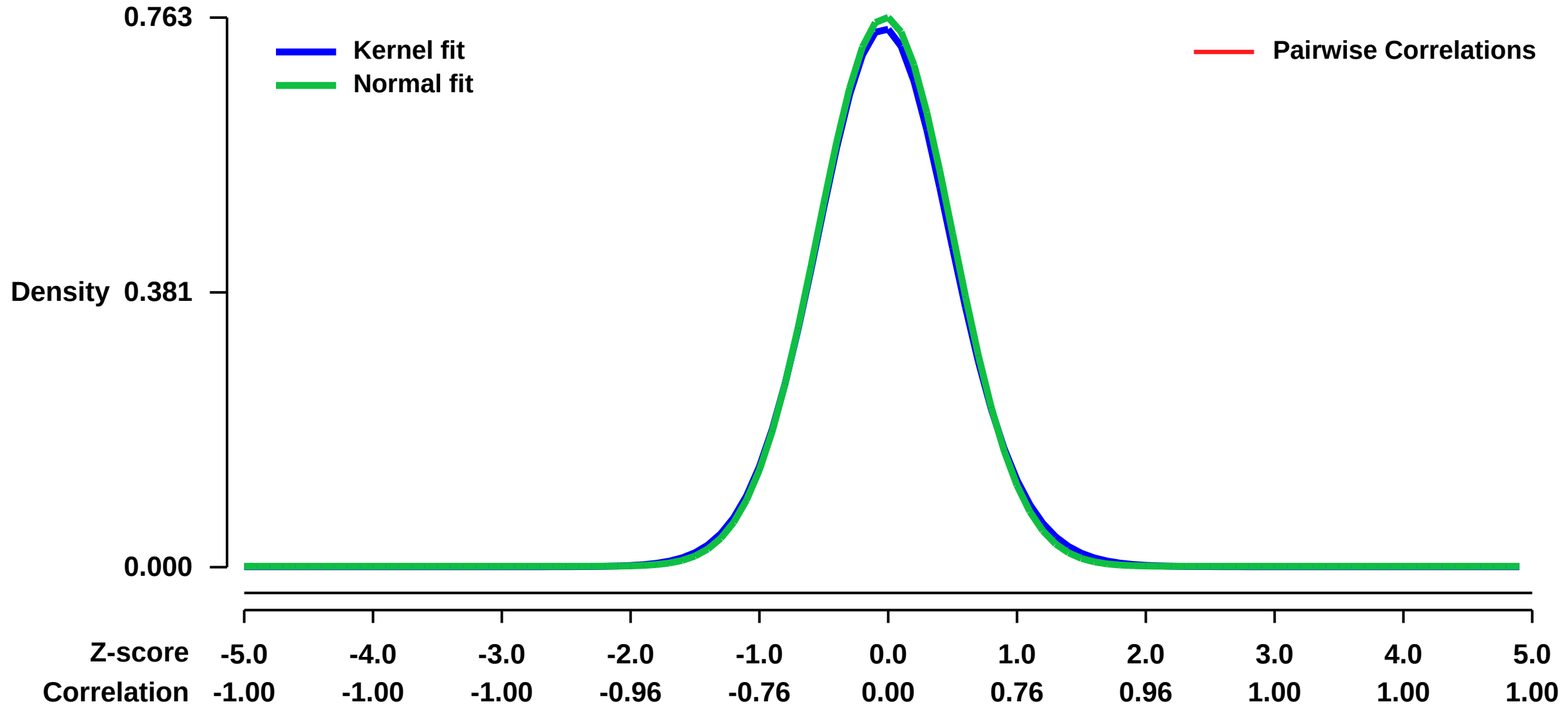

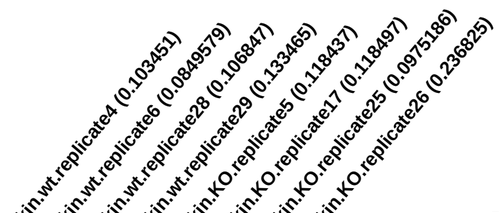

Pre-normalization Quantiles

[min] [medium] [max]

Null module

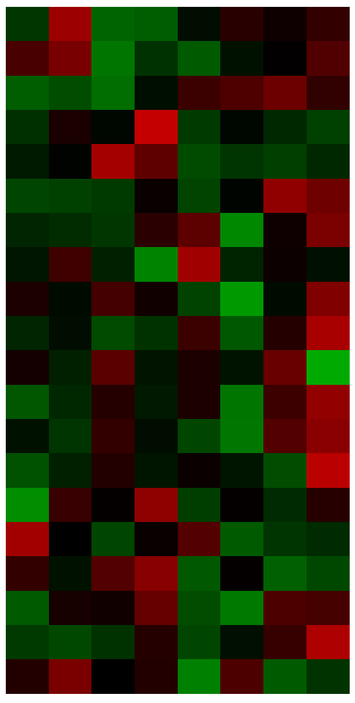

GEO Series "GSE23923" Expression Profiles

Num of samples in this series: 8

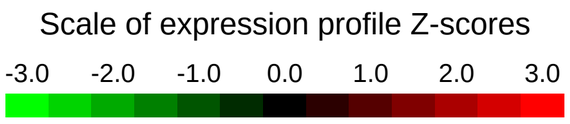

GEO Link:	http://www.ncbi.nlm.nih.gov/geo/query/acc.cgi?acc=GSE23923
Status:	Public on May 19 2011
Title:	Expression data from Rad21 knock-down in ES cells
Organism:	Mus musculus
Experiment type:	Expression profiling by array
Platform:	GPL1261
Pubmed ID:	21589869
Summary & Design:	**Summary:** The Cohesin complex has recently been described to regulate gene expression. We wanted to determine the gene expression profile specific in mouse ES cells after depletion of the Cohesin subunit Rad21. We used microarrays to detail the global programme of gene expression underlying depletion of Rad21 and identified distinct early development related genes up-regulated and many pluripotency related genes downregulated. **Overall design:** Rad21 was depleted in R1/E ES cells for 48h using esiRNAs against Rad21. An esiRNA against non-targeting Luciferase was used as a negative control

Background corr dist: KL-Divergence = 0.0270, L1-Distance = 0.0288, L2-Distance = 0.0015, Normal std = 0.6782

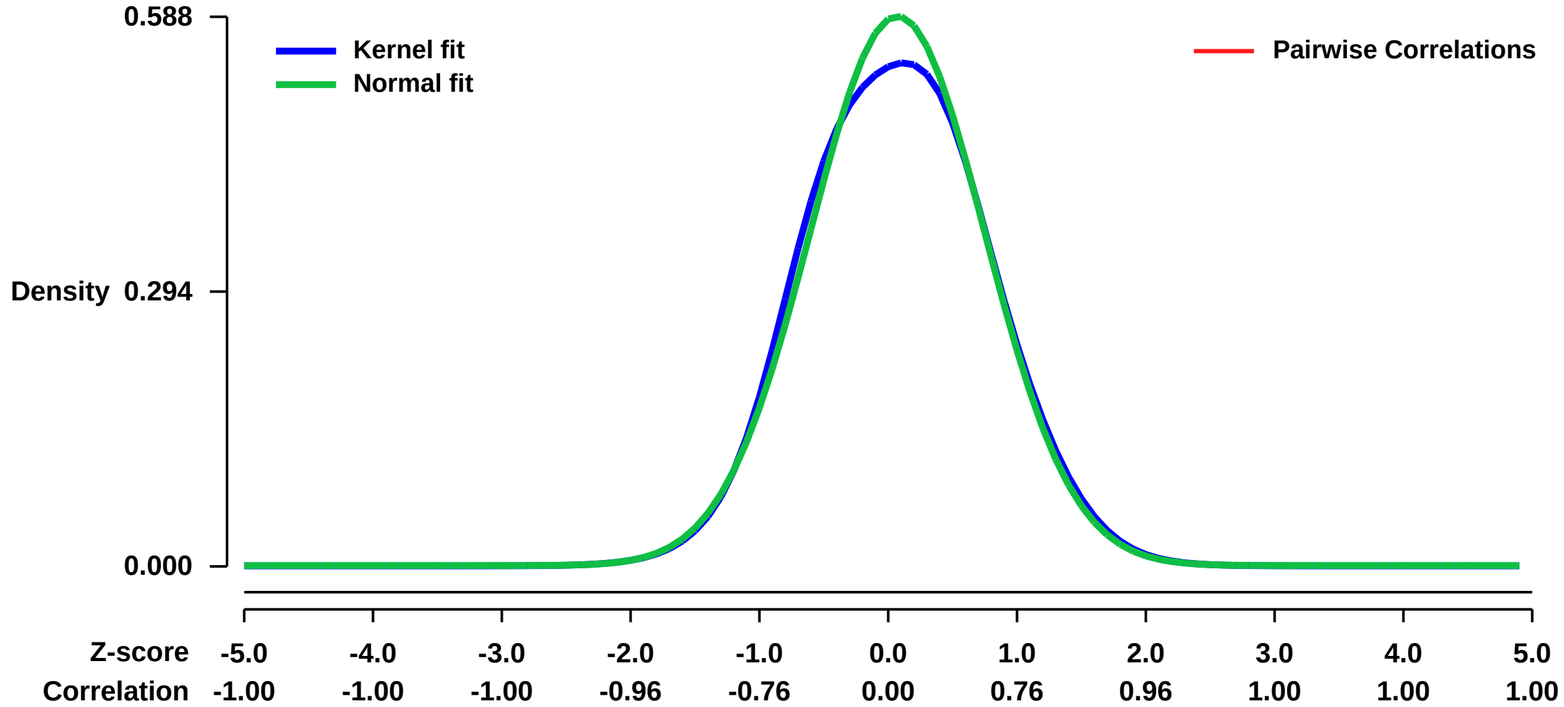

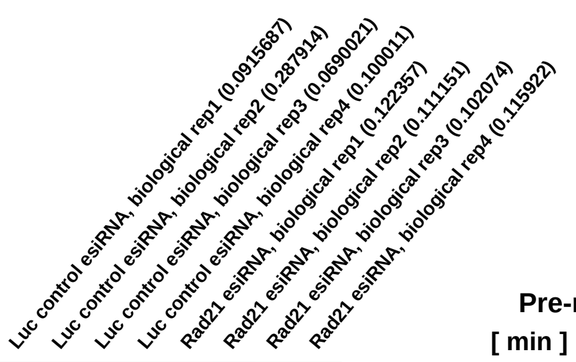

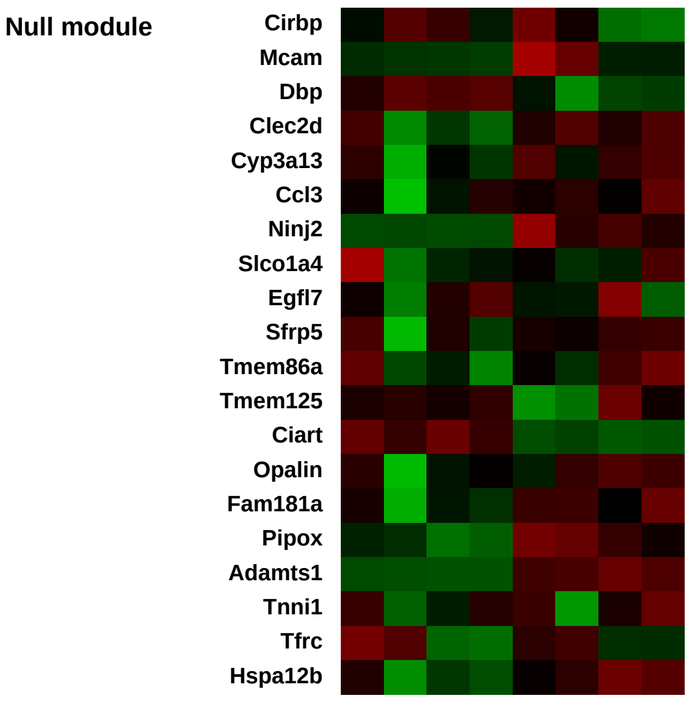

GEO Series "GSE32706" Expression Profiles

Num of samples in this series: 33

Scale of expression profile Z-scores

-3.0 -2.0 -1.0 0.0 1.0 2.0 3.0

GEO Link:	http://www.ncbi.nlm.nih.gov/geo/query/acc.cgi?acc=GSE32706
Status:	Public on Oct 08 2011
Title:	Comparative transcriptomics and metabolomic analysis of fenofibrate and fish oil treatments in mice
Organism:	Mus musculus
Experiment type:	Expression profiling by array
Platform:	GPL1261
Pubmed ID:	21954454
Summary & Design:	**Summary:** Elevated circulating triglycerides, which are considered a risk factor for cardiovascular disease, can be targeted by treatment with fenofibrate or fish oil. To gain insight into underlying mechanisms, we carried out a comparative transcriptomics and metabolomics analysis of the effect of 2 week treatment withfenofibrate and fish oil in mice. Plasma triglycerides were significantly decreased byfenofibrate (-49.1%) and fish oil (-21.8%), whereas plasma cholesterol was increased by fenofibrate (+29.9%) and decreased by fish oil (-32.8%). Levels of various phospholipid species were specifically decreased by fish oil, while levels of Krebs cycle intermediates were increased specifically by fenofibrate. Plasma levels of many amino acids were altered by fenofibrate and to a lesser extent by fish oil. Both fenofibrate and fish oil upregulated genes involved in fatty acid metabolism, and downregulated genes involved in blood coagulation and fibrinolysis. Significant overlap in gene regulation by fenofibrate and fish oil was observed, reflecting their property as high or low affinity agonist for PPAR$_{\alpha}$–, respectively. Fenofibrate specifically downregulated genes involved in complement cascade and inflammatory response. Fish oil specifically downregulated genes involved in cholesterol and fatty acid biosynthesis, and upregulated genes involved in amino acid and arachidonic acid metabolism. Taken together, the data indicate that despite being similarly potent towards modulating plasma free fatty acids, cholesterol and triglyceride levels, fish oil causes modest changes in gene expression likely via activation of multiple mechanistic pathways, whereas fenofibrate causes pronounced gene expression changes via a single pathway, reflecting the key difference between nutritional and pharmacological intervention. **Overall design:** Expression profiling of liver from mice fed control diet, fish oil or fenofibrate for 2 weeks.

Background corr dist: KL-Divergence = 0.4473, L1-Distance = 0.0814, L2-Distance = 0.0210, Normal std = 0.2363

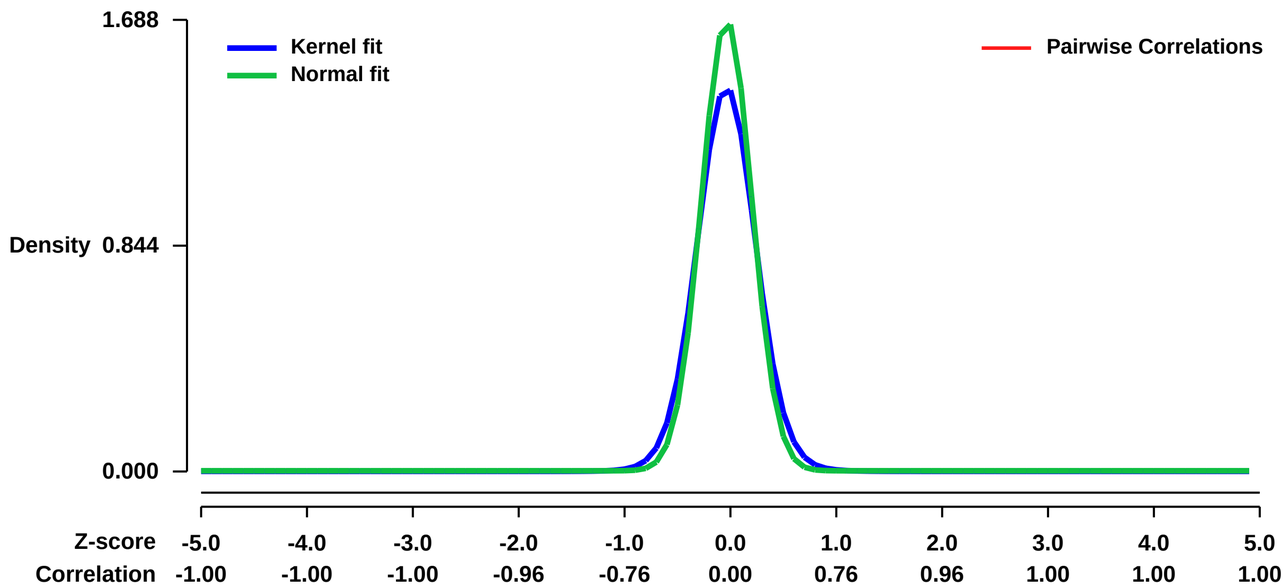

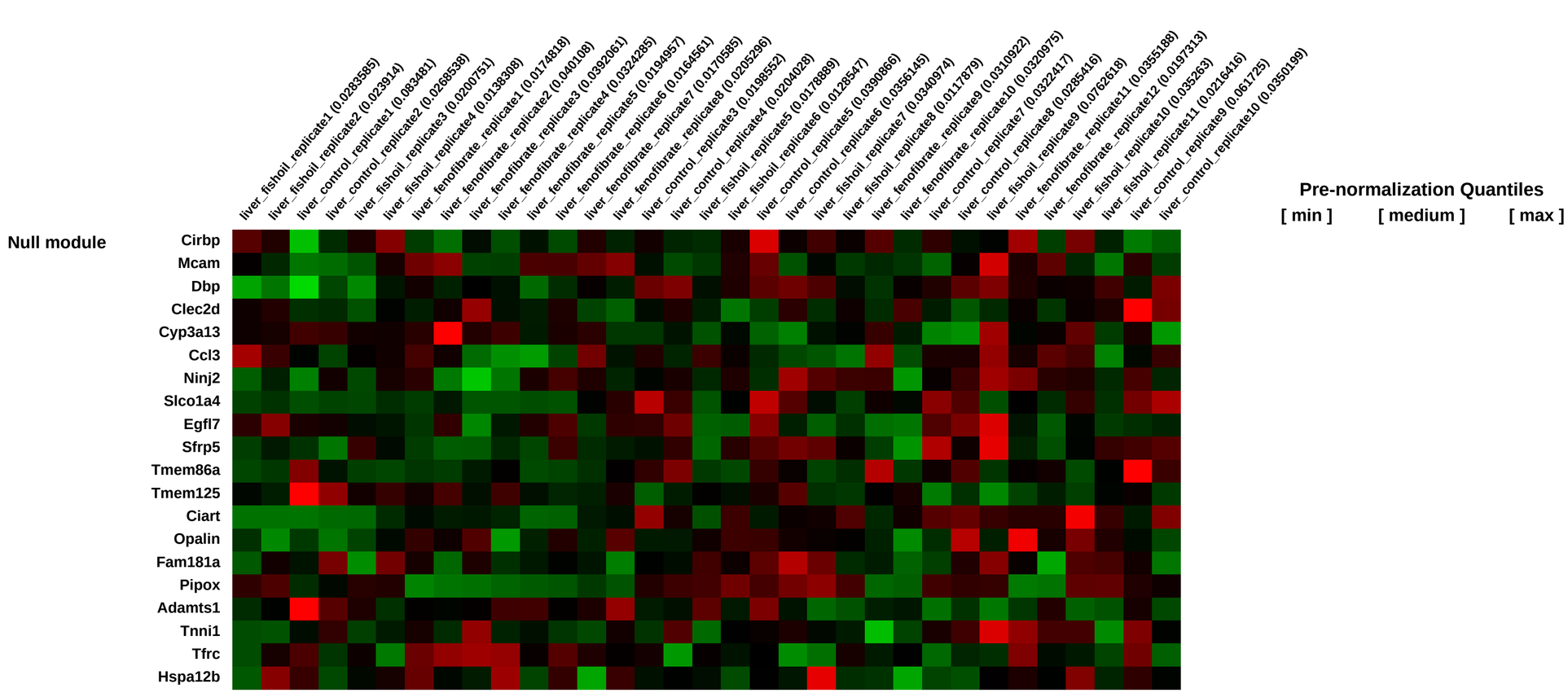

GEO Series "GSE51883" Expression Profiles

Num of samples in this series: 30

Scale of expression profile Z-scores

-3.0 -2.0 -1.0 0.0 1.0 2.0 3.0

GEO Link:	http://www.ncbi.nlm.nih.gov/geo/query/acc.cgi?acc=GSE51883
Status:	Public on Jan 28 2014
Title:	Effect of Mirn378 overexpression on gene expression during C2C12 myogenic and BMP2-induced osteogenic differentiation
Organism:	Mus musculus
Experiment type:	Expression profiling by array
Platform:	GPL1261
Pubmed ID:	
Summary & Design:	**Summary:** **Background: MicroRNAs (miRNAs) are a family of small, non-coding single-stranded RNA molecules involved in post-transcriptional regulation of gene expression. As such, they are believed to play a role in regulating the step-wise changes in gene expression patterns that occur during cell fate specification of multipotent stem cells. Here, we have studied whether terminal differentiation of C2C12 myoblasts is indeed controlled by lineage-specific changes in miRNA expression.** **Results: Using a previously generated RNA polymerase II (Pol-II) ChIP-on-chip dataset, we show differential Pol-II occupancy at the promoter regions of six miRNAs during C2C12 myogenic versus BMP2-induced osteogenic differentiation. Overexpression of one of these miRNAs, miR-378, enhances Alp activity, calcium deposition and mRNA expression of osteogenic marker genes in the presence of BMP2.** **Conclusions: Our results demonstrate a previously unknown role for miR-378 in promoting BMP2-induced osteogenic differentiation. #!#** **Overall design:** **Stable C2C12 cell lines C2C12-pMirn0 and C2C12-pMirn378 were generated by lentiviral transduction of C2C12 myoblasts with a Mirn378-overexpression construct and its parent vector, respectively. C2C12-pMirn0 and C2C12-pMirn378 cells were plated at 2.5 x 10^4 cells/cm2 (day -1), cultured for 1 day in DMEM 10%NCS, then (d0) treated with or without 300 ng/ml bone morphogenetic protein 2 (BMP2) for 6 days. RNA was extracted on d0, d3 and d6 and hybridized to GeneChip Mouse Genome 430 2.0 array (Affymetrix).**

Background corr dist: KL-Divergence = 0.1521, L1-Distance = 0.0728, L2-Distance = 0.0106, Normal std = 0.4058

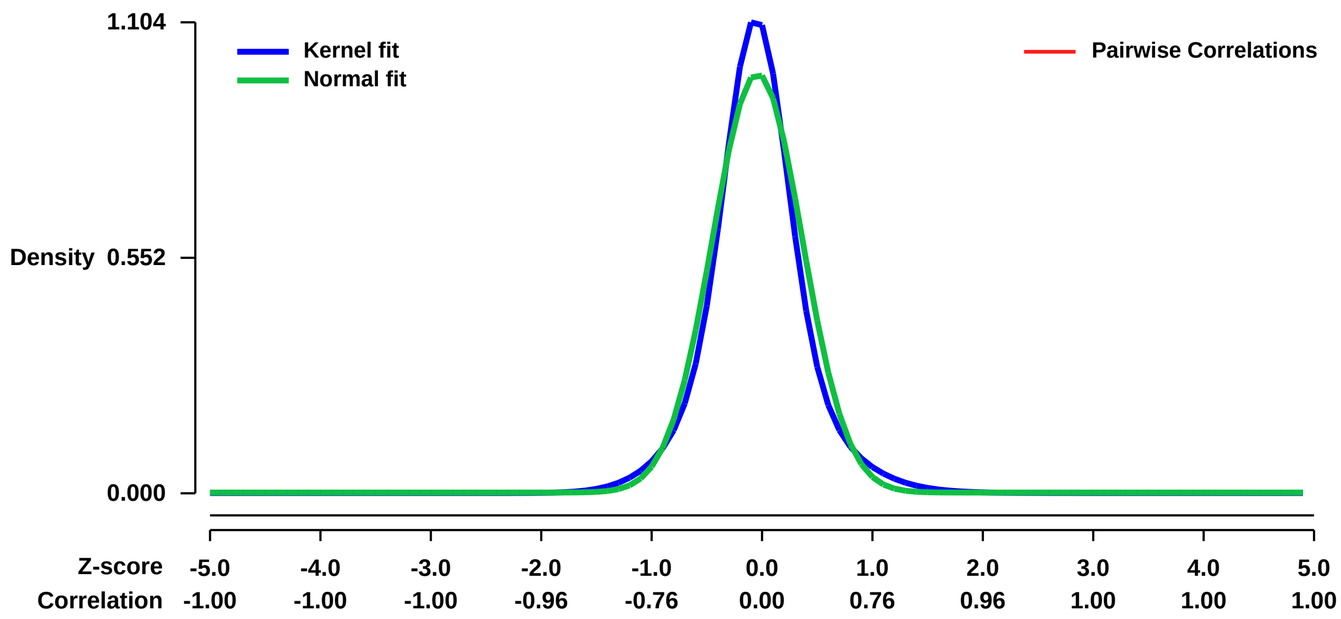

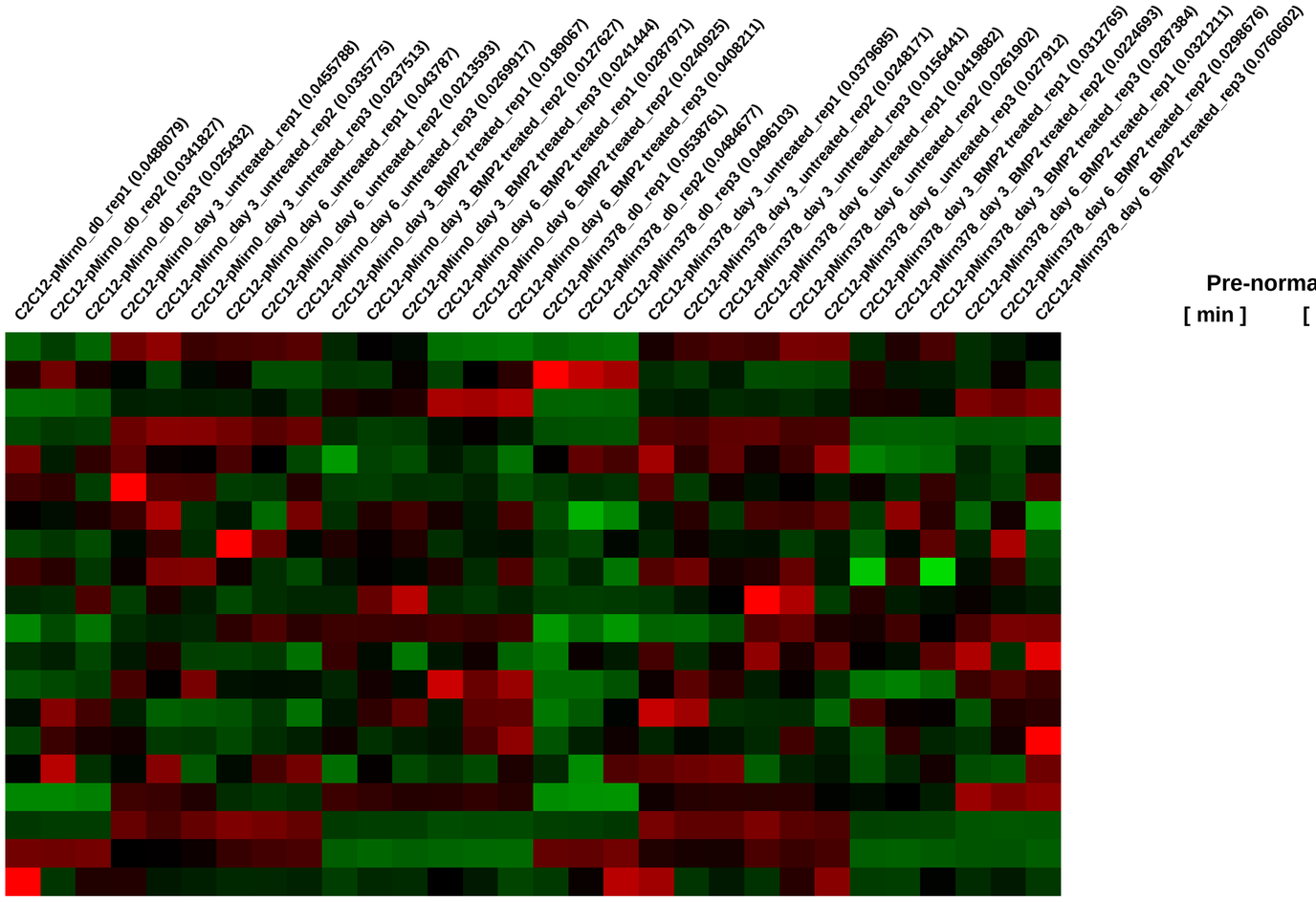

GEO Series "GSE16925" Expression Profiles

Num of samples in this series: 15

Scale of expression profile Z-scores

-3.0 -2.0 -1.0 0.0 1.0 2.0 3.0

GEO Link:	http://www.ncbi.nlm.nih.gov/geo/query/acc.cgi?acc=GSE16925
Status:	Public on Aug 03 2009
Title:	Expression data from mouse ES and iPS cells
Organism:	Mus musculus
Experiment type:	Expression profiling by array
Platform:	GPL1261
Pubmed ID:	19672241
Summary & Design:	**Summary:** Induced pluripotent stem (iPS) cells were produced from reprogramming of somatic cells, and they are shown to possess pluripotent properties similar to embryonic stem (ES) cells. Here we used microarrays to detail the global expression pattern among the ES cells and iPS cells, as well as the original mouse embryo fibroblast (MEF), to identify important players involved in the reprogramming process. **Overall design:** Mouse ES cell cultures, as well as selected iPS cell lines and the original MEF cells they were derived from, were used for RNA extraction and hybridization on Affymetrix microarrays. Three biological replicates for each sample were processed. GeneChips were processed and data were analyzed as previously described (Zeng et al., Dev Biol 20004).

Background corr dist: KL-Divergence = 0.0695, L1-Distance = 0.0886, L2-Distance = 0.0130, Normal std = 0.6146

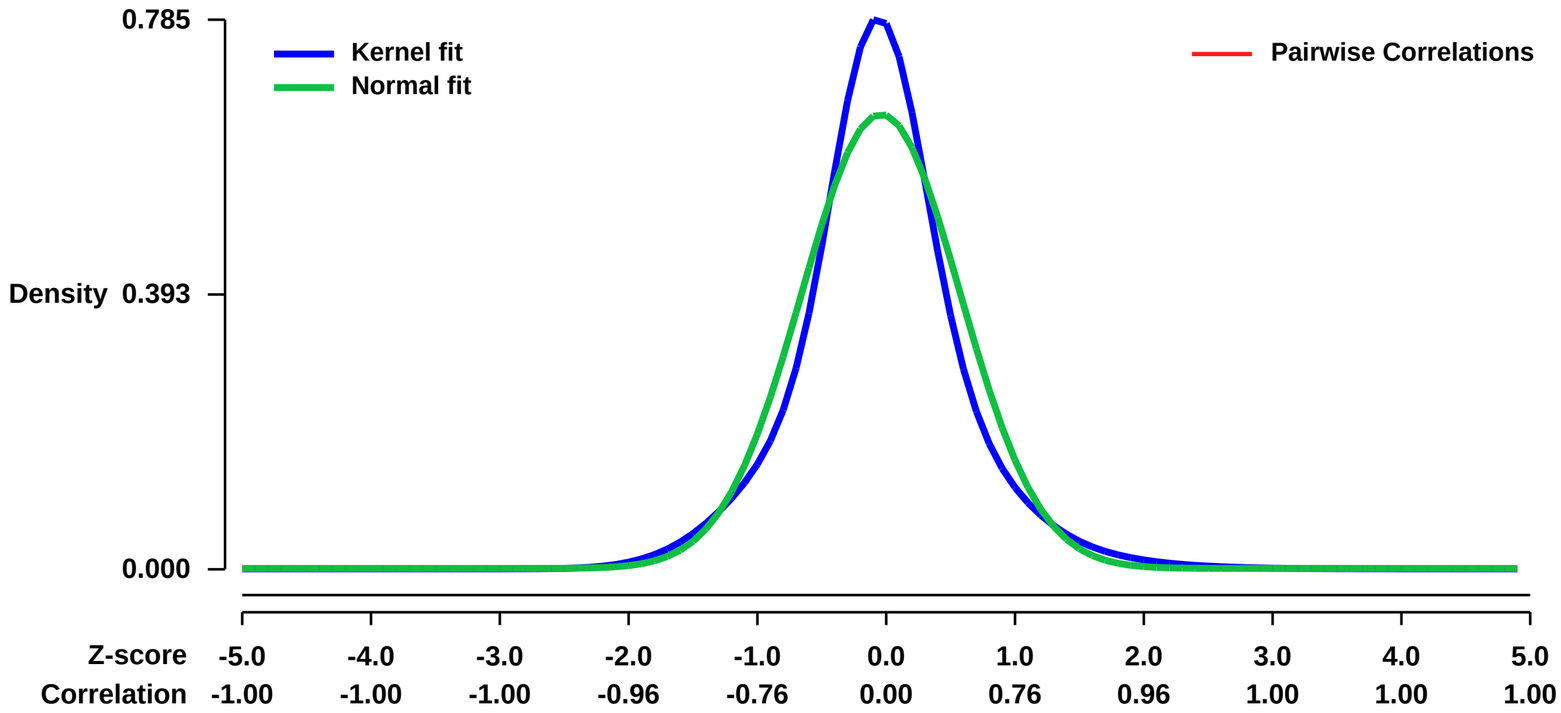

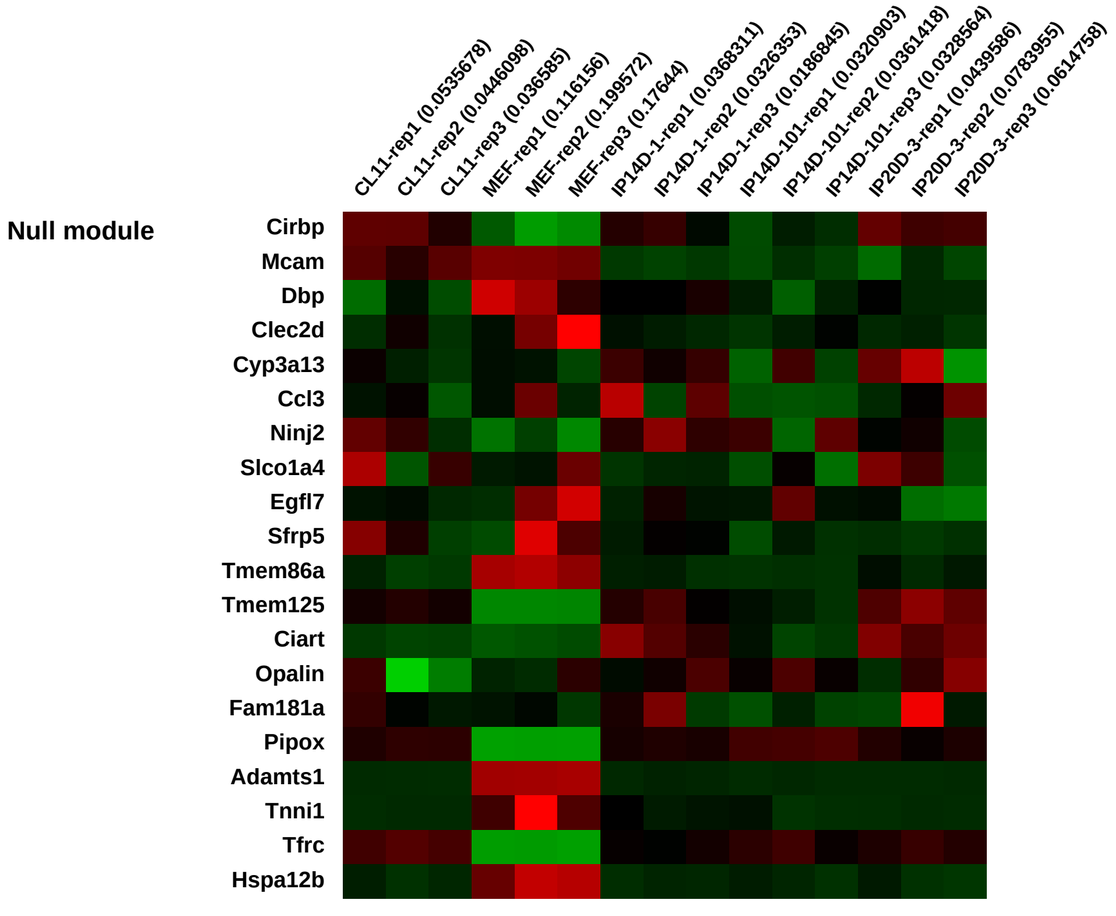

GEO Series "GSE48522" Expression Profiles

Num of samples in this series: 11

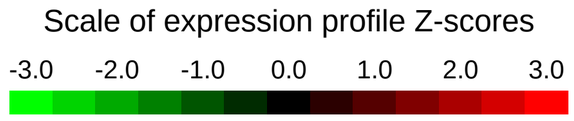

GEO Link:	http://www.ncbi.nlm.nih.gov/geo/query/acc.cgi?acc=GSE48522
Status:	Public on Jan 26 2014
Title:	Akt signalling leads to stem cell activation and promotes tumour development in epidermis.
Organism:	Mus musculus
Experiment type:	Expression profiling by array
Platform:	GPL1261
Pubmed ID:	24504902
Summary & Design:	**Summary:** A permantly active form of the oncogene Akt was expressed in the keratinocytes of the basal proliferative layer of the epidermis. Stem cells of the hair follicle expressing the cell surface marker CD34 were isolated. RNA form the CD34(+) and CD34(-) keratinocytes was extracted and and hybridized to Mouse Genome 430 2.0 Affymetrix arrays. **Overall design:** Gene expression was compared between CD34(+) hair follicle stem cells and CD34(-) cells isolates from the back skin of K5-myrAkt transgenic mice.

Background corr dist: KL-Divergence = 0.0750, L1-Distance = 0.0312, L2-Distance = 0.0018, Normal std = 0.4914

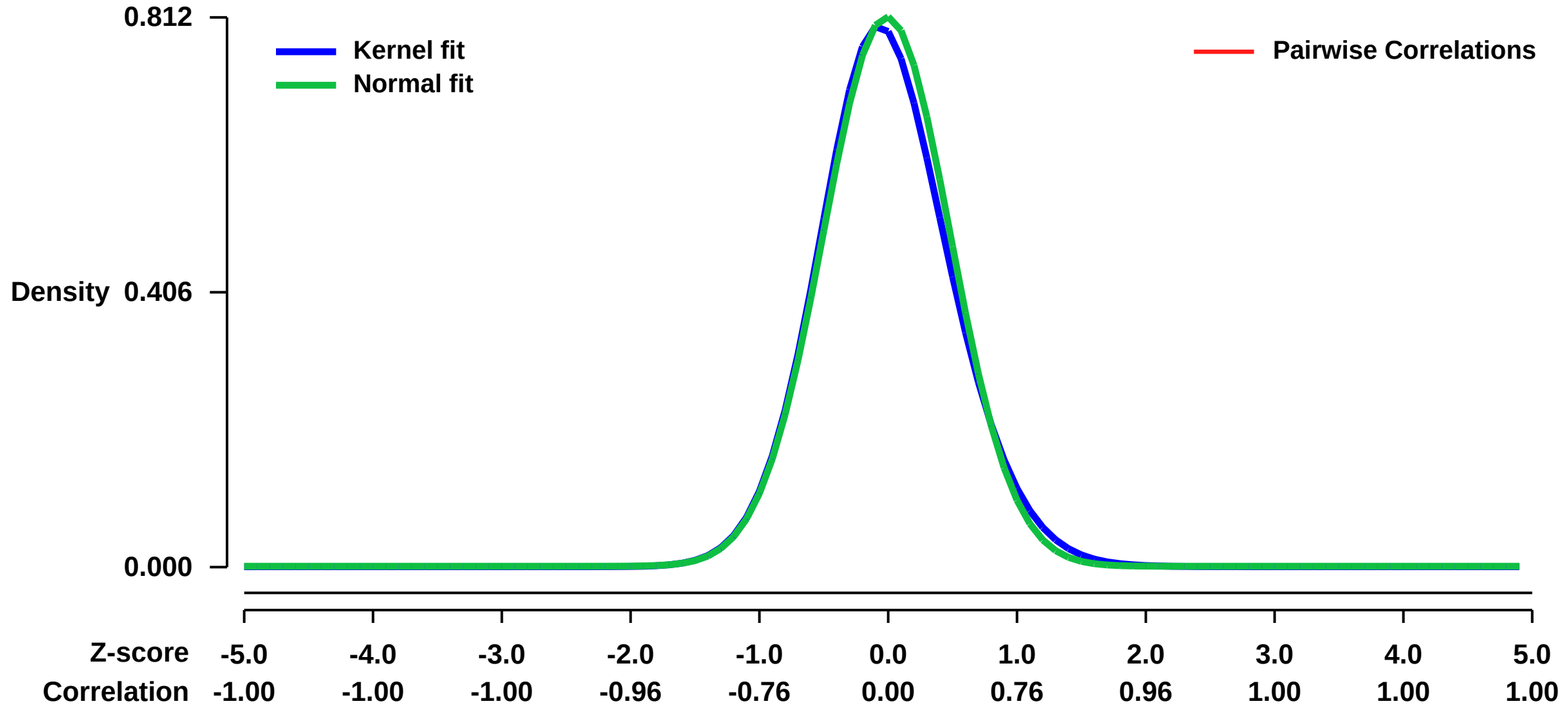

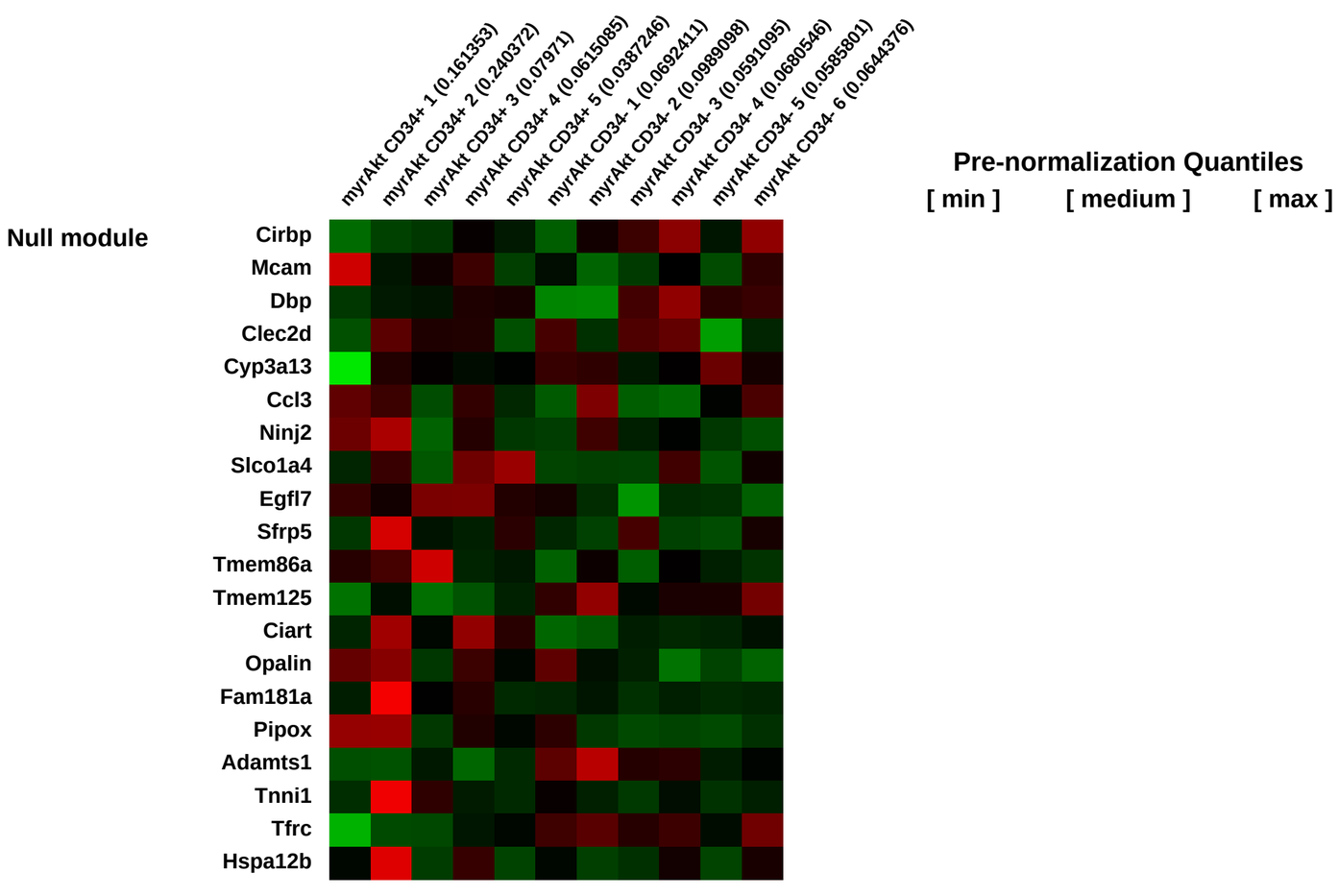

GEO Series "GSE43779" Expression Profiles

Num of samples in this series: 6

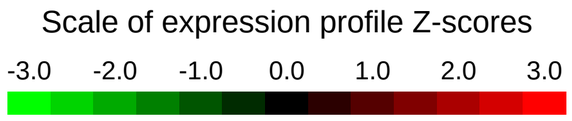

GEO Link:	**http://www.ncbi.nlm.nih.gov/geo/query/acc.cgi?acc=GSE43779**
Status:	**Public on Jan 28 2013**
Title:	**Expression data from 2-amino acetophenone (2-AA) treated mouse Skeletal muscle**
Organism:	**Mus musculus**
Experiment type:	**Expression profiling by array**
Platform:	**GPL1261**
Pubmed ID:	
Summary & Design:	**Summary:** **Metabolic responses begin promptly upon the initiation of infection, and progress as a series of coordinated events. Mitochondria may play a key role in the development of insulin resistance. Reduced energy production and mitochondrial dysfunctional may further favor infection, and be an important step in the establishment of chronic and persistent infections.** **We have used mouse skeletal muscle transcriptome data which have led to the hypothesis that 2-AA causes harm to the host by triggering mitochondrial dysfunction in skeletal muscle.** **Overall design:** **The gastrocnemius muscles were isolated from control and 4days 2-AA treated mouse for RNA extraction and hybridization on Affymetrix microarrays.**

Background corr dist: **KL-Divergence = 0.0223, L1-Distance = 0.0276, L2-Distance = 0.0011, Normal std = 0.7411**

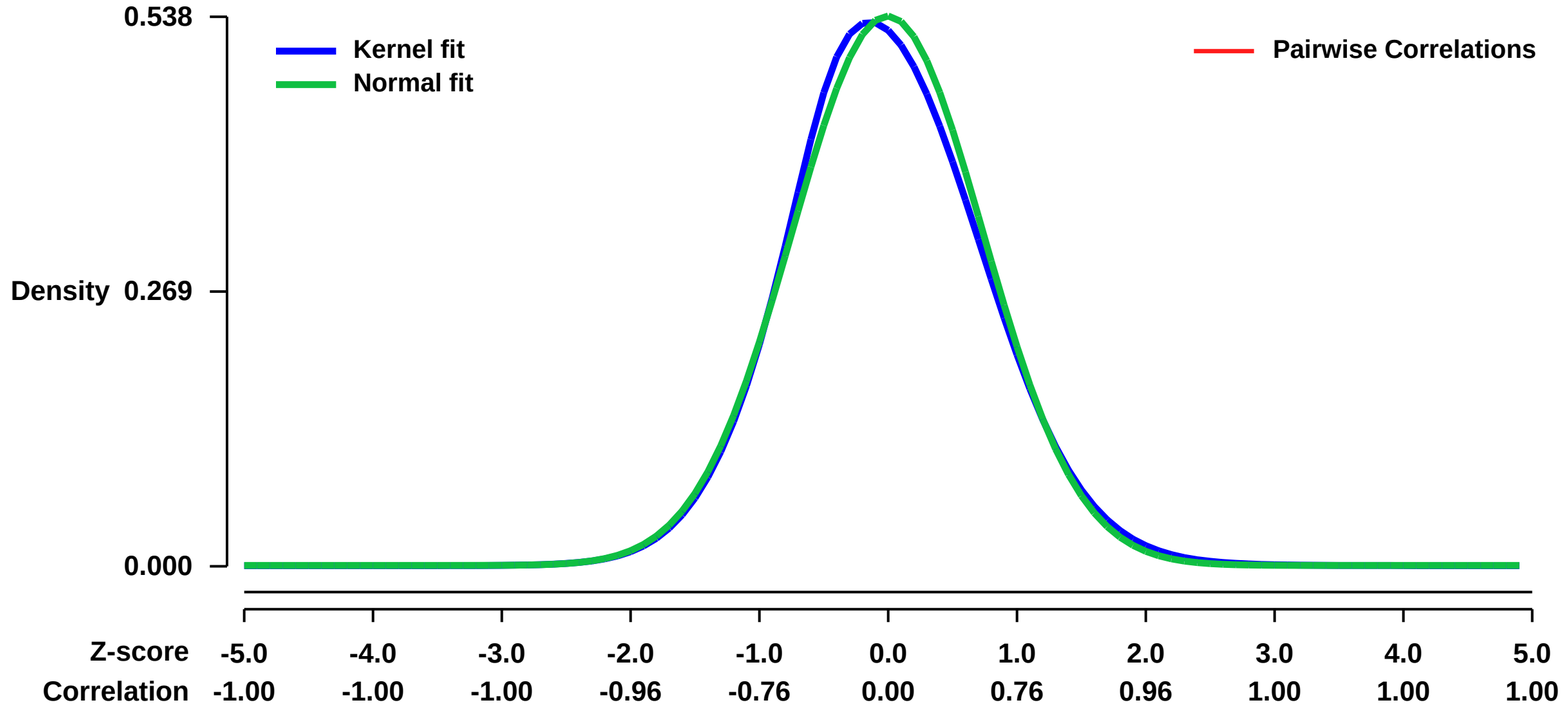

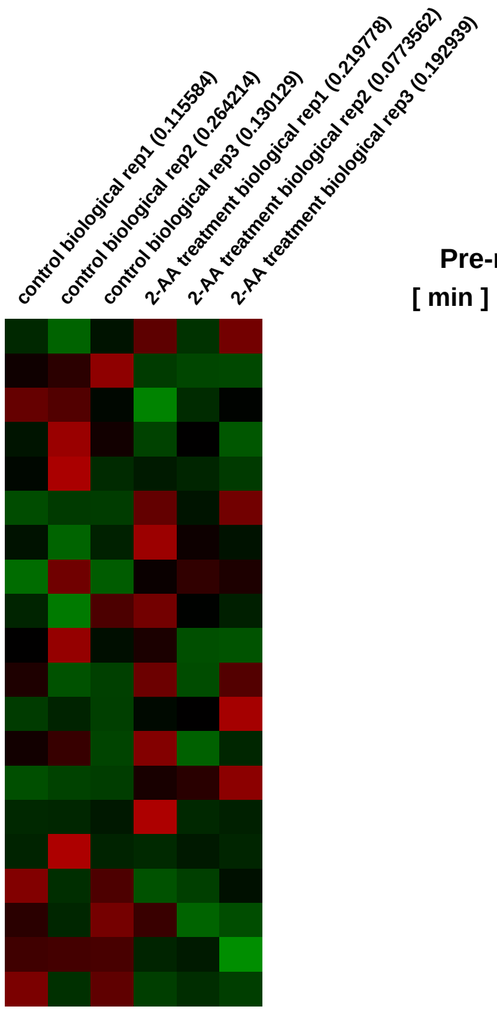

GEO Series "GSE35160" Expression Profiles

Num of samples in this series: 6

Scale of expression profile Z-scores

-3.0 -2.0 -1.0 0.0 1.0 2.0 3.0

GEO Link:	http://www.ncbi.nlm.nih.gov/geo/query/acc.cgi?acc=GSE35160
Status:	Public on Feb 01 2012
Title:	Functional analysis of the cytoprotective transcription factor Nrf2 in skin morphogenesis and disease: Identification of Nrf2 target genes
Organism:	Mus musculus
Experiment type:	Expression profiling by array
Platform:	GPL1261
Pubmed ID:	22383093
Summary & Design:	**Summary:** The Nrf2 transcription factor is a key player in the cellular stress response, which regulates the expression of important antioxidant enzymes and other cytoprotective proteins. We recently generated a novel transgenic mouse model to determine the function of Nrf2 in the skin. These mice revealed interesting phenotypic abnormalities, including hyperkeratosis and acanthosis. To gain insight into the underlying molecular mechanisms, we wanted to identify genes, which are differentially expressed in the skin of wild-type and mutant mice before the onset of phenotypic abnormalities. **Overall design:** RNA from whole skin of 3 single P2.5 K5cre-caNrf2 (tg/tg) and 3 single P2.5 K5cre-wt (tg/wt=control) mice were used

Background corr dist: KL-Divergence = 0.0365, L1-Distance = 0.0130, L2-Distance = 0.0001, Normal std = 0.6269

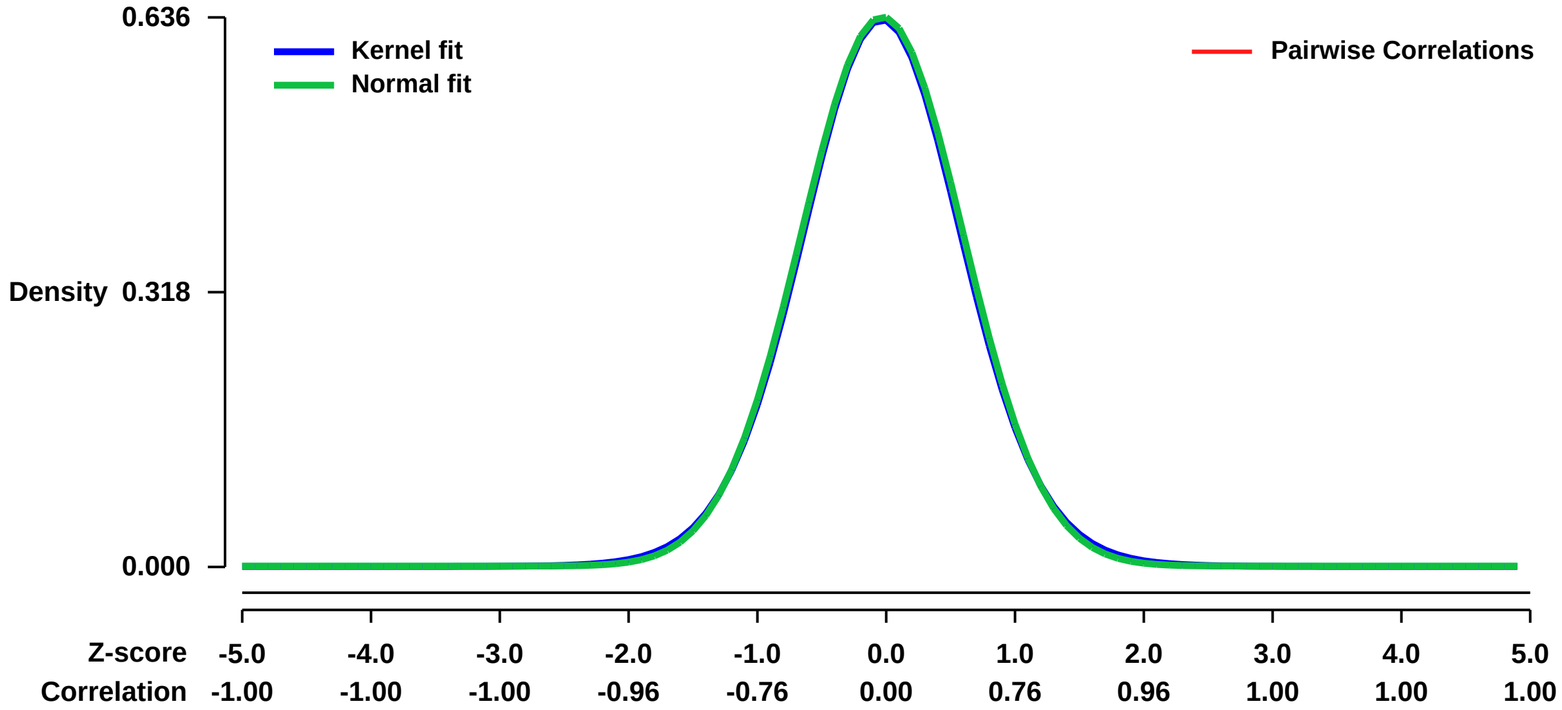

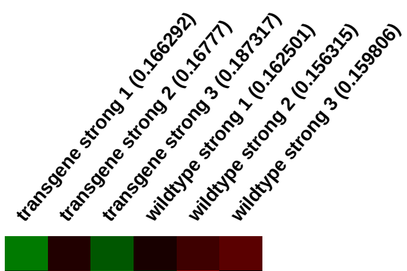

Pre-normalization Quantiles

[min] [medium] [max]

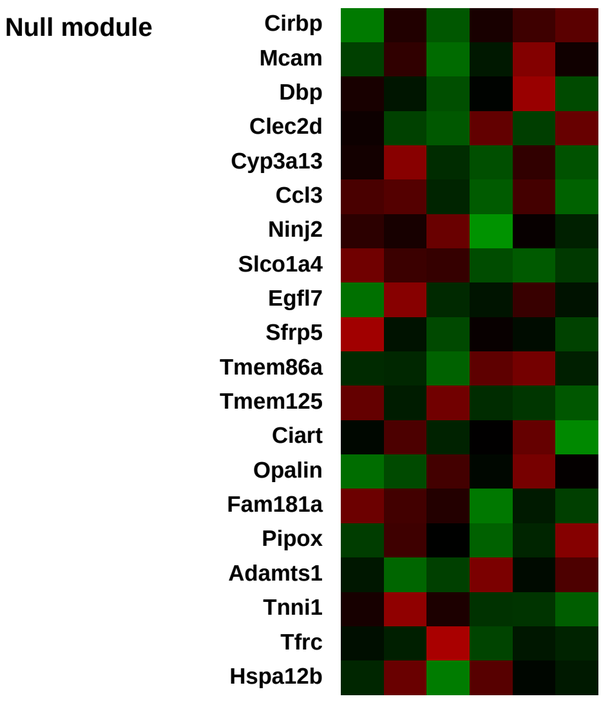

GEO Series "GSE7460" Expression Profiles

Num of samples in this series: 52

Scale of expression profile Z-scores

-3.0 -2.0 -1.0 0.0 1.0 2.0 3.0

GEO Link:	http://www.ncbi.nlm.nih.gov/geo/query/acc.cgi?acc=GSE7460
Status:	Public on Dec 04 2007
Title:	Contribution of Foxp3 to the Treg signature
Organism:	Mus musculus
Experiment type:	Expression profiling by array
Platform:	GPL1261
Pubmed ID:	18024188
Summary & Design:	**Summary:** The transcription factor Foxp3 is usually considered the master regulator for the CD4+CD25+ ""Treg"" lineage, which plays a key role in controlling immune and autoimmune responses, and is characterized by a unique transcriptional signature. We have performed a meta-analysis of this signature in Treg cells in several conditions to delineate the elements that can be ascribed to T cell activation, TGFbeta signaling, or Foxp3 itself. We find that these influences synergize to activate many of the signatureâ s components. Foxp3 and TGFbeta signaling have interconnected relationships, as Foxp3 is induced by TGFbeta while enhancing TGFbetaâ s positive feedback loop. Much of the Treg signature cannot be ascribed to Foxp3, as it contains gene clusters that are co-regulated, but cannot be transactivated, by Foxp3. This suggests that the Treg lineage is specified at a higher level of regulation, upstream of Foxp3, which does control some of the lineageâ s essential immunoregulatory attributes. **Keywords:** Cell population comparison **Overall design:** All gene expression profiles were obtained from highly purified T cell populations sorted by flow cytometry. To reduce variability, cells from multiple mice were pooled for sorting, and three replicates were generated for essentially all groups. RNA from 0.5-2.5 x 105 cells was amplified, labeled, and hybridized to Affymetrix M430v2 microarrays. Raw data were preprocessed with the RMA algorithm in GenePattern, and averaged expression values were used for analysis.

Background corr dist: KL-Divergence = 0.2827, L1-Distance = 0.0615, L2-Distance = 0.0101, Normal std = 0.2869

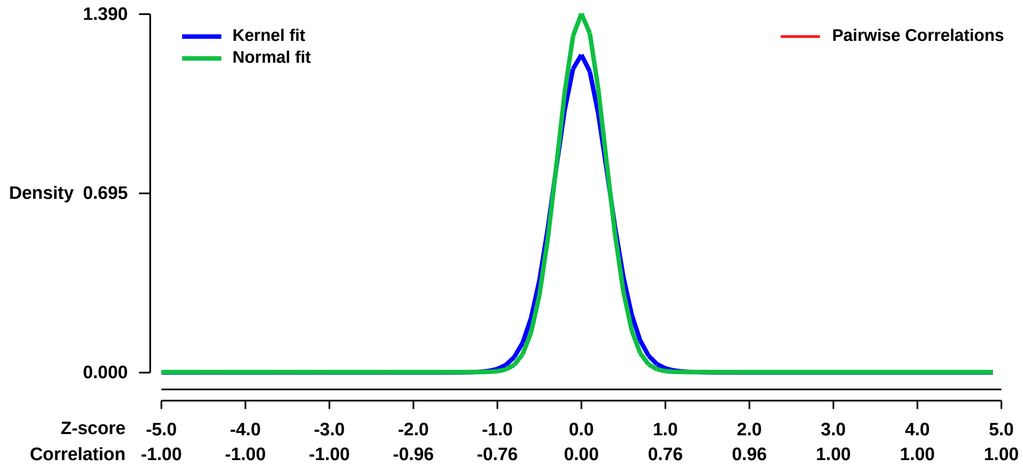

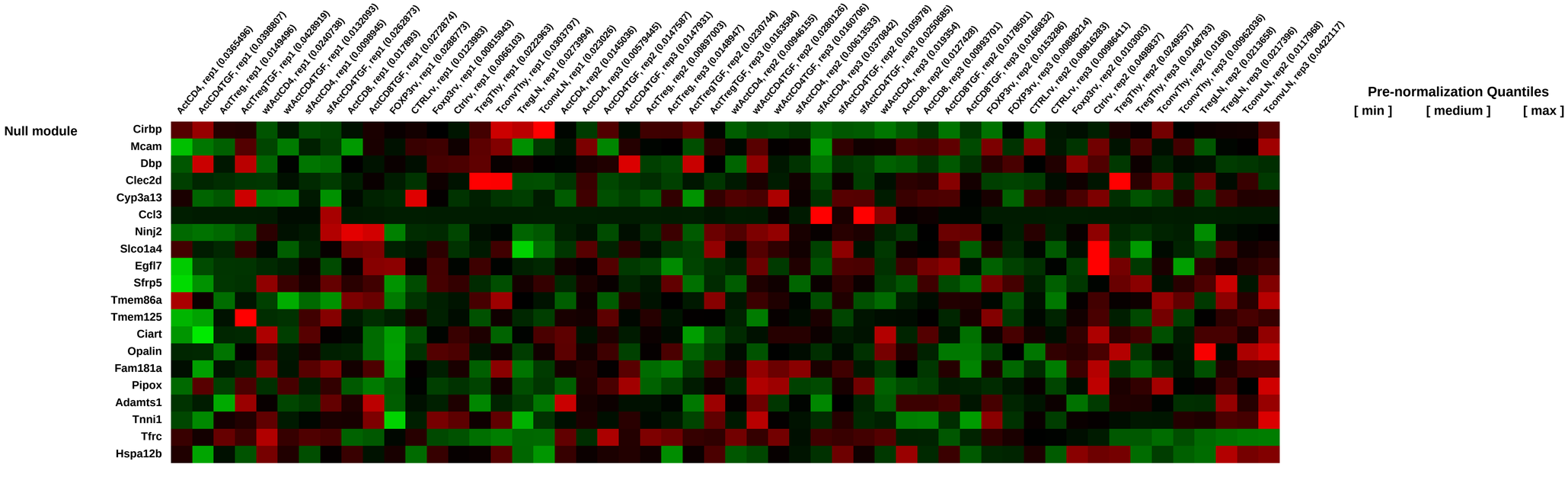

GEO Series "GSE48790" Expression Profiles

Num of samples in this series: 8

Scale of expression profile Z-scores

-3.0 -2.0 -1.0 0.0 1.0 2.0 3.0

GEO Link:	**http://www.ncbi.nlm.nih.gov/geo/query/acc.cgi?acc=GSE48790**
Status:	**Public on Jul 12 2013**
Title:	**Expression data from GTF2i mutated ES cells**
Organism:	**Mus musculus**
Experiment type:	**Expression profiling by array**
Platform:	**GPL1261**
Pubmed ID:	**23831514**
Summary & Design:	**Summary:** **Data present the expression analysis of different mouse ES cell line with altered expression of GTF2I.** **Overall design:** **We used microarrays to detail the global programme of gene expression underlying altered expression of GTF2I and identified distinct classes of deregulated genes**

Background corr dist: **KL-Divergence = 0.0303, L1-Distance = 0.0391, L2-Distance = 0.0018, Normal std = 0.6989**

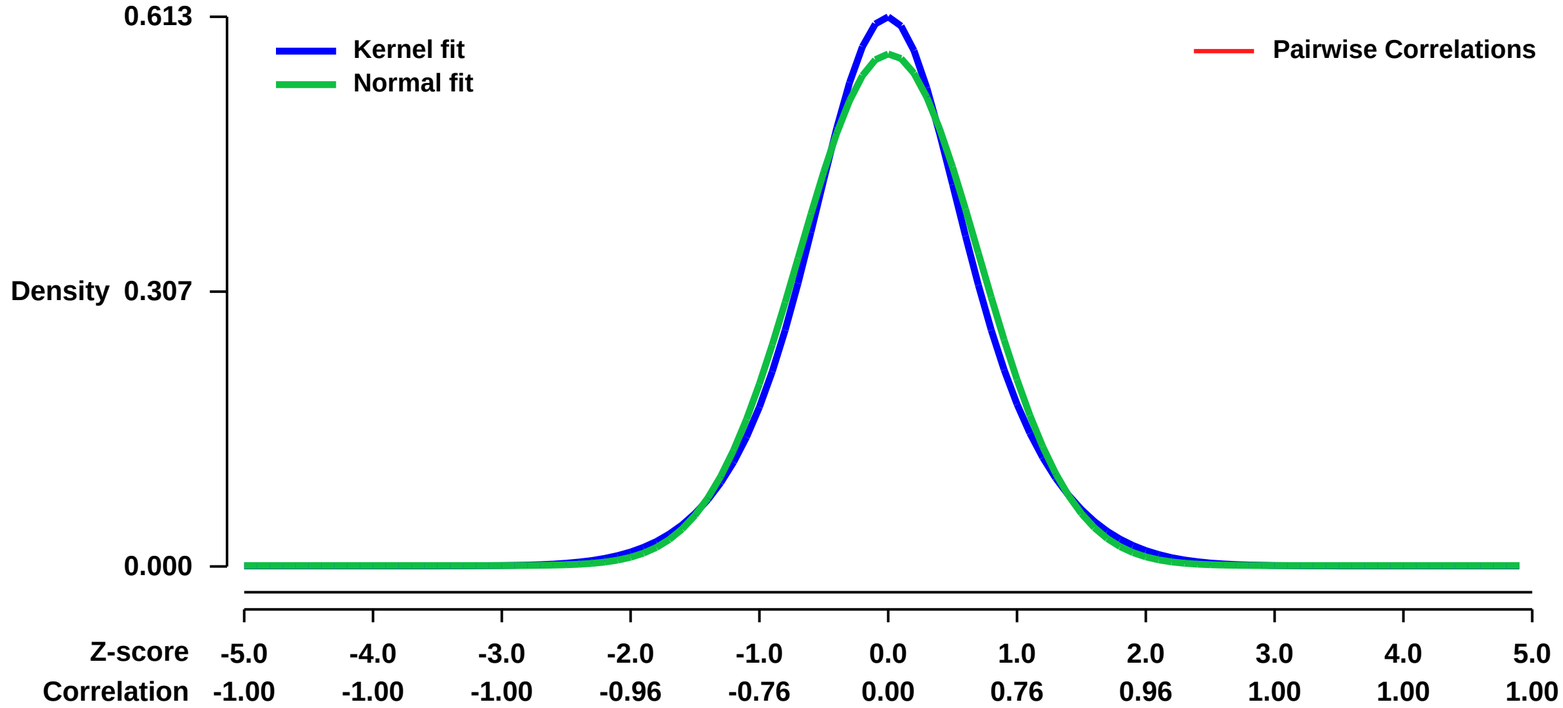

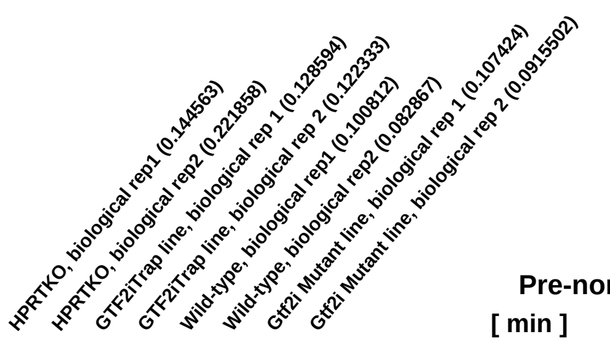

Pre-normalization Quantiles

[min] [medium] [max]

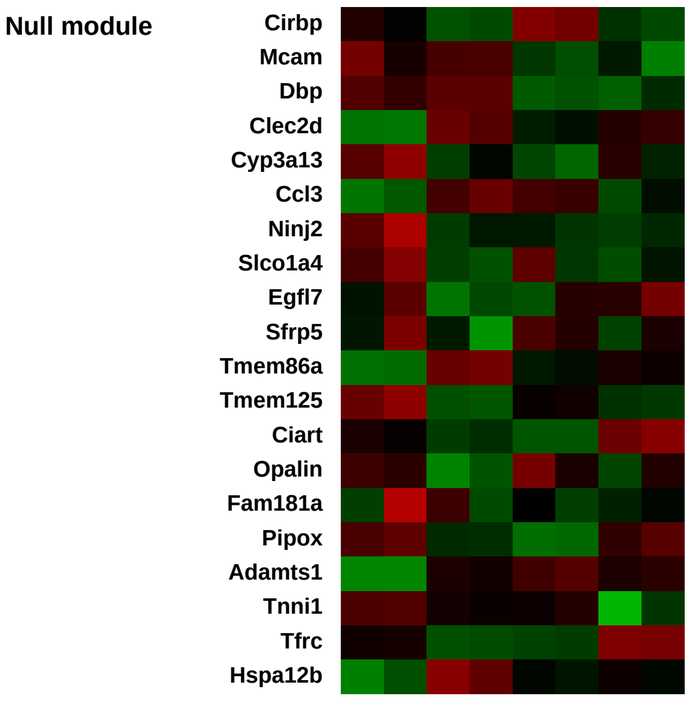

GEO Series "GSE8960" Expression Profiles

Num of samples in this series: 18

Scale of expression profile Z-scores

-3.0 -2.0 -1.0 0.0 1.0 2.0 3.0

GEO Link:	http://www.ncbi.nlm.nih.gov/geo/query/acc.cgi?acc=GSE8960
Status:	Public on Sep 01 2008
Title:	The TLR2/NOD2/RICK signaling axis regulates stimulus-specific IL-10 production
Organism:	Mus musculus
Experiment type:	Expression profiling by array
Platform:	GPL1261
Pubmed ID:	18549453
Summary & Design:	**Summary:** Recognition and response to gram-positive bacteria by macrophages and dendritic cells is mediated in part through TLR2. We found that that Streptococcus pneumoniae cell wall fragments, containing primarily peptidoglycan and teichoic acids, induced prodigious secretion of IL-10 from macrophages and dendritic cells and was dependent on TLR2 and NOD2, a cytoplasmic CARD-NACHT-LRR protein encoded by Card15. IL-10 secretion in response to cell walls was also dependent on RICK/RIP2, a kinase associated with NOD2, and MYD88 but independent of the ERK/p38 pathway. The reduction of IL-10 secretion by cell wall-activated NOD2-deficient myeloidâ derived cells translated into downstream effects on IL-10 target gene expression and elevations in subsets of pro-inflammatory cytokine expression normally restrained by autocrine/paracrine effects of IL-10. Since NOD2 is linked to aberrant immune responses in Crohnâ s Disease patients bearing mutations in CARD15, the temporal and quantitative effects of the TLR2/NOD/RICK pathway on IL-10 secretion may affect homeostatic control of immune responses to gram-positive bacteria. **Keywords:** immune response simulated pathogen response **Overall design:** KO mice were treated with a cel wall extract and evaluated for immune response 1 hr and 4 hrs after treatment

Background corr dist: KL-Divergence = 0.1989, L1-Distance = 0.0359, L2-Distance = 0.0026, Normal std = 0.3354

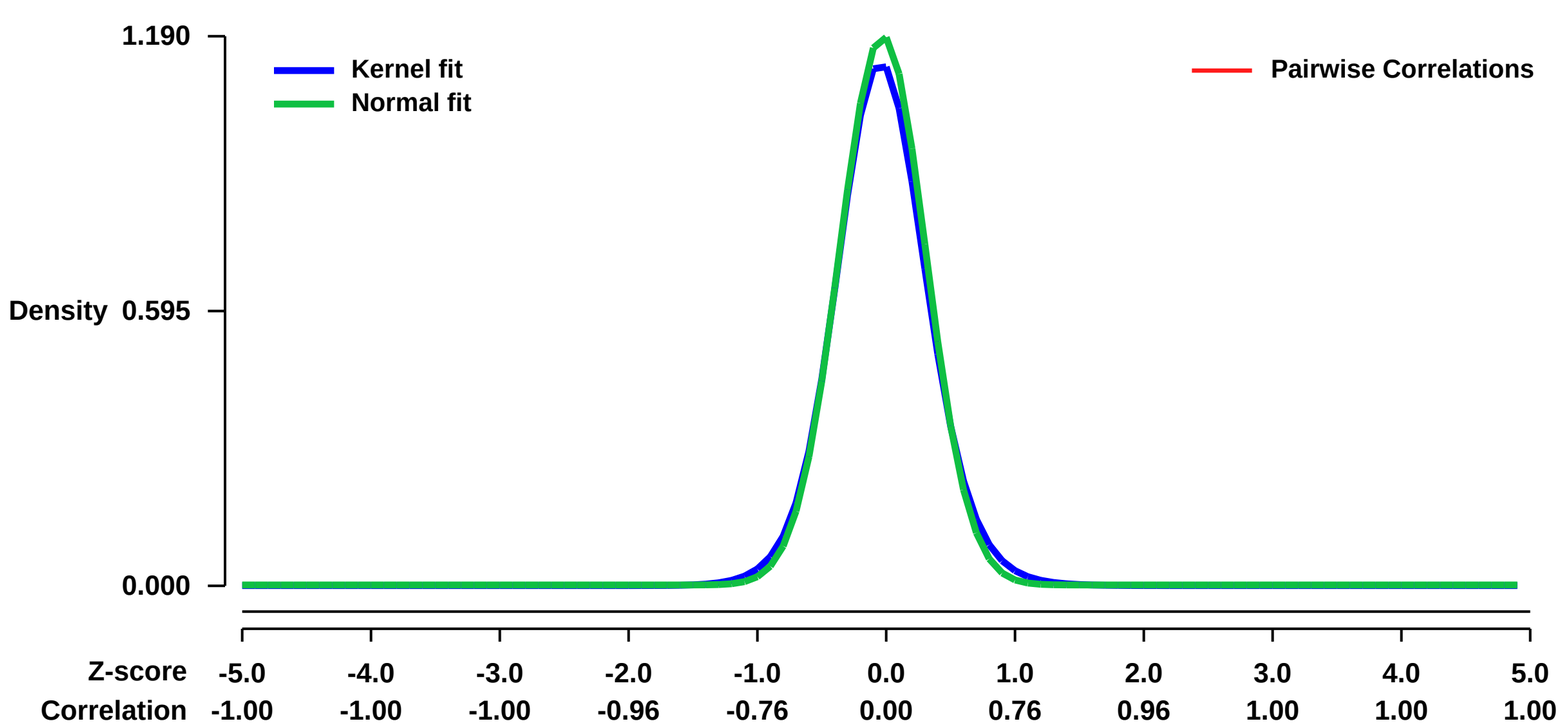

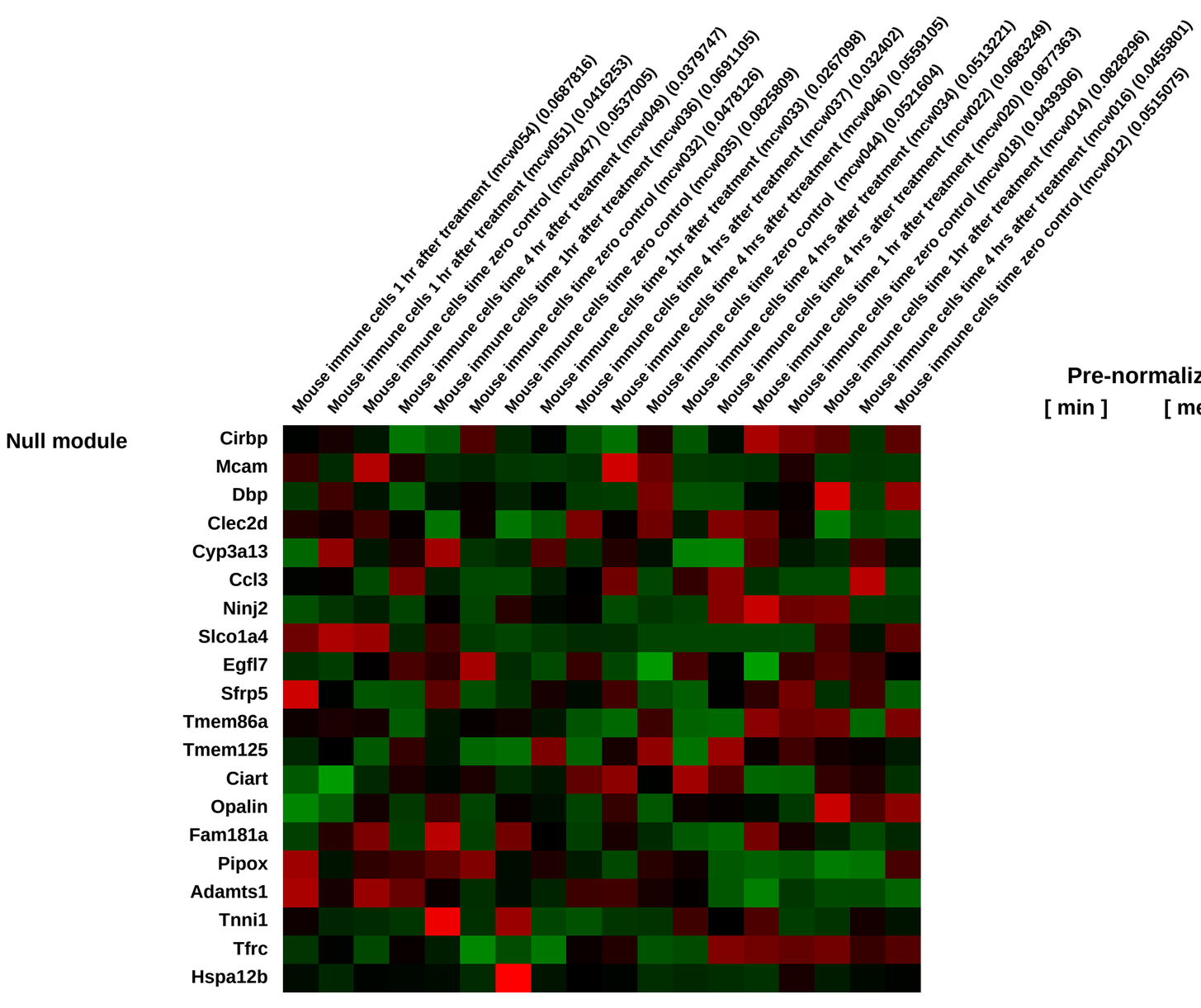

GEO Series "GSE10365" Expression Profiles

Num of samples in this series: 9

Scale of expression profile Z-scores

-3.0 -2.0 -1.0 0.0 1.0 2.0 3.0

GEO Link:	http://www.ncbi.nlm.nih.gov/geo/query/acc.cgi?acc=GSE10365
Status:	Public on Jan 29 2009
Title:	Expression Data from NKDxIL15tg and IL15 tg NK cells
Organism:	Mus musculus
Experiment type:	Expression profiling by array
Platform:	GPL1261
Pubmed ID:	18664585
Summary & Design:	**Summary:** NK cells from NKDxIL15tg mice spleens and bone marrow were purified by FACS. NK cells from IL15tg mice spleens were purified by FACS. Gene expression differences were analyzed to identify genes involved in NK cell development. Keywords: cell type comparison **Overall design:** Immature NK cells from NKDxIL15tg mice and mature NK cells from IL15tg mice were purified by FACS. RNA was made for target synthesis and hybridization to Affymetrix microarrays.

Background corr dist: KL-Divergence = 0.0614, L1-Distance = 0.0155, L2-Distance = 0.0003, Normal std = 0.5452

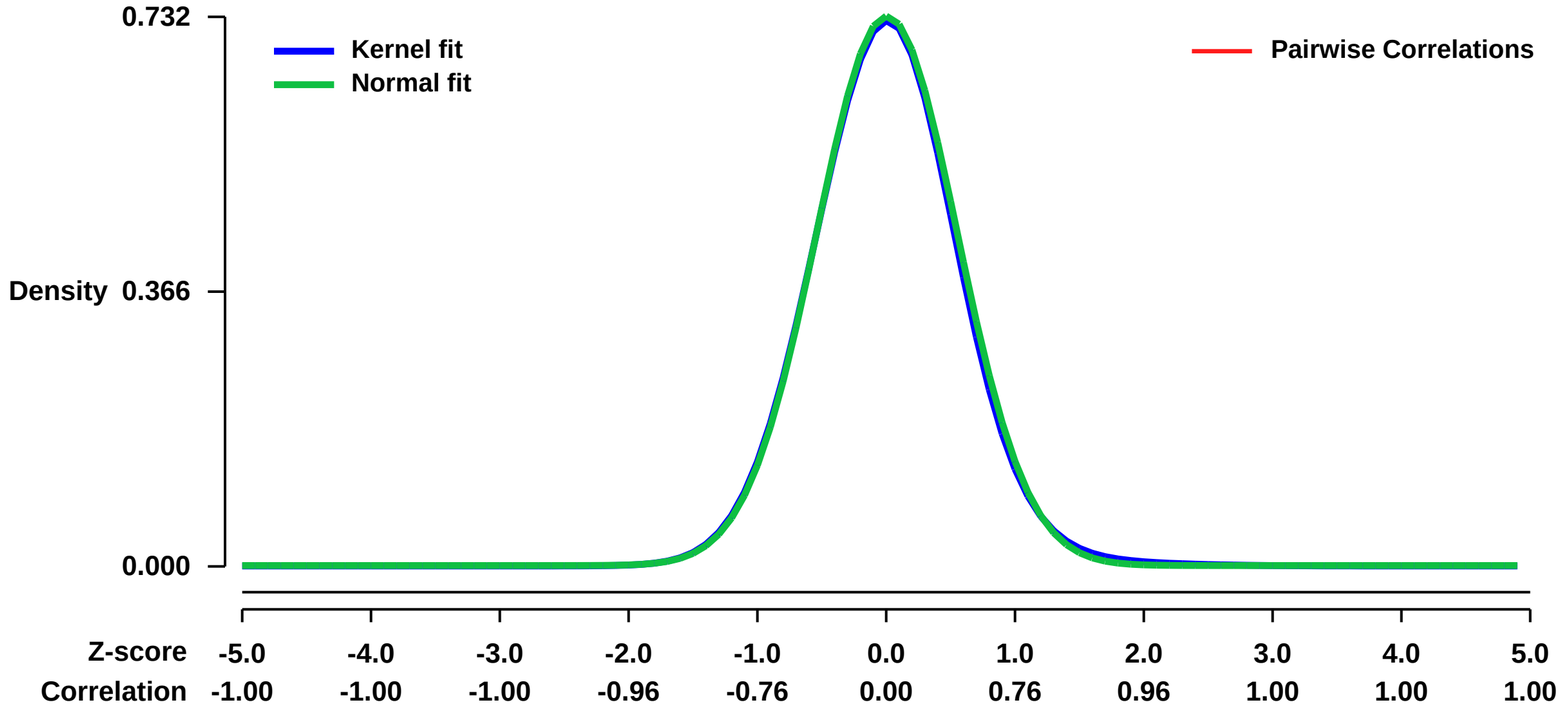

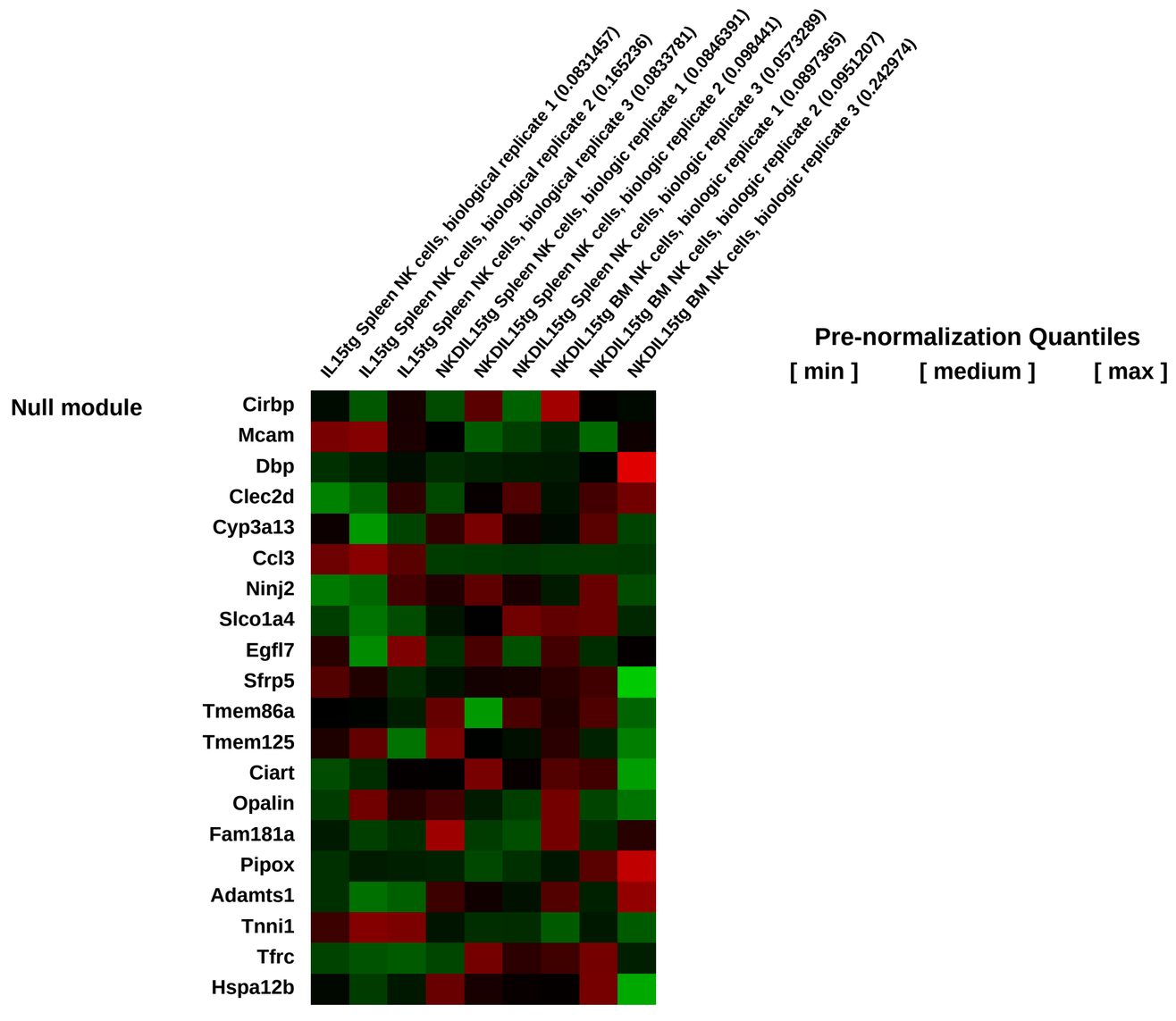

GEO Series "GSE17497" Expression Profiles

Num of samples in this series: 10

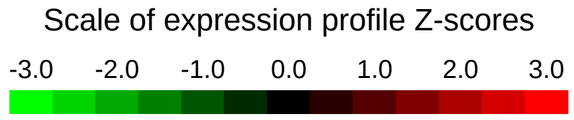

GEO Link:	http://www.ncbi.nlm.nih.gov/geo/query/acc.cgi?acc=GSE17497
Status:	Public on Aug 06 2009
Title:	Gene expression in murine acute lymphoblastic leukemia in vivo after allogeneic or syngeneic bone marrow transplantation
Organism:	Mus musculus
Experiment type:	Expression profiling by array
Platform:	GPL1261
Pubmed ID:	20602231
Summary & Design:	**Summary:** This study compared gene expression in murine bcr-abl positive acute lymphoblastic leukemia cells in vivo in allogeneic BMT recipients compared to syngneneic BMT recipients. **Overall design:** The goal of the experiment was to compare gene expression in leukemia cells that were in either an allogeneic transplant (5 samples) or syngeneic transplant (5 samples) immune environment in vivo. The bone marrow transplant model involved preparation of C57BL/6 recipients with total body irradiation and 5-fluoruracil. These recipients were then infused IV with either allogeneic C3.SW marrow and spleen cells or syngeneic C57BL/6 marrow and spleen cells. The leukemia cells were mixed in with the marrow and spleen cells. After a few weeks (2-3) the C57BL/6 leukemia cells were purified by flow cytometry and passed into other freshly transplanted animals. After three serial transplants the leukemia cells were flow purified and RNA prepared. Leukemia was C57BL/6 background (cells contain the human p210 bcr/abl oncogenic fusion gene and also have a deletion in the Ink4a/Arf locus, see: Biology of Blood and Marrow Transplantation. 14:622-630, 2008).

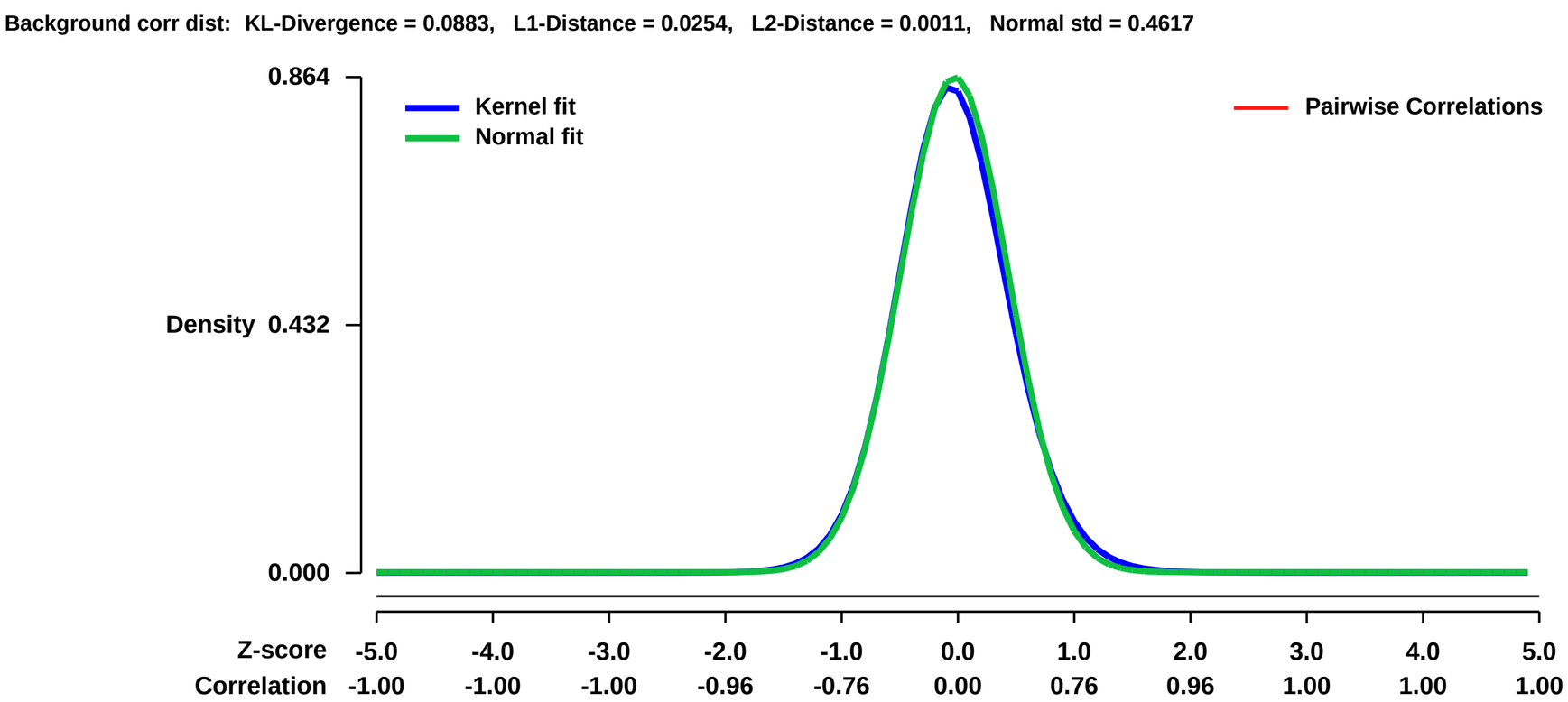

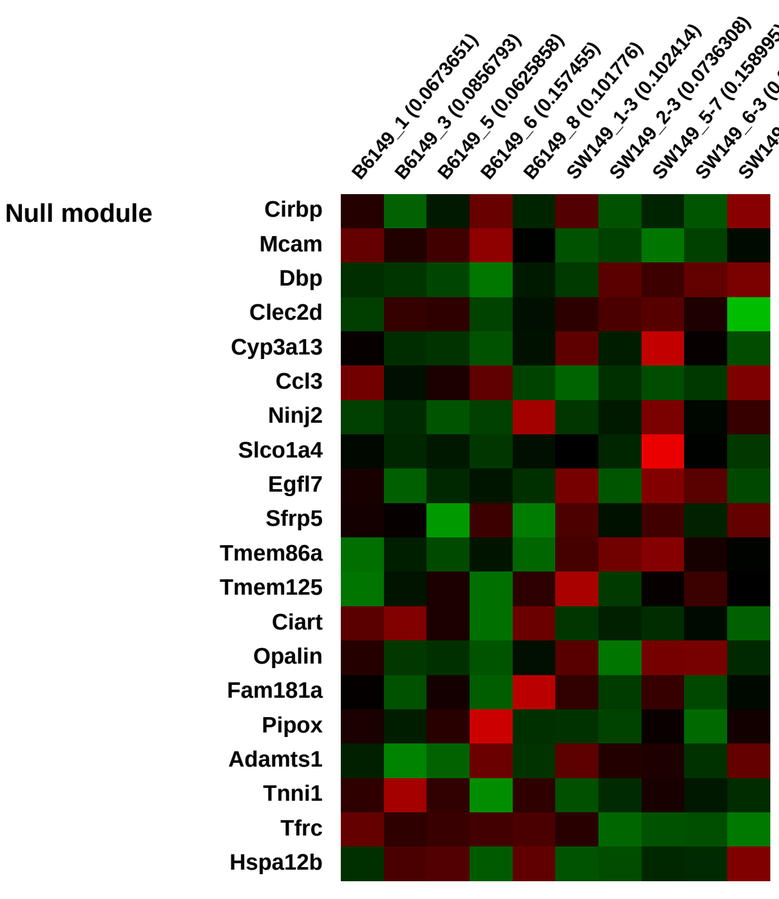

GEO Series "GSE3414" Expression Profiles

Num of samples in this series: 36

Scale of expression profile Z-scores

-3.0 -2.0 -1.0 0.0 1.0 2.0 3.0

GEO Link:	http://www.ncbi.nlm.nih.gov/geo/query/acc.cgi?acc=GSE3414
Status:	Public on May 01 2006
Title:	Immune Response to Nippostrongylus brasiliensis in the mouse lung
Organism:	Mus musculus
Experiment type:	Expression profiling by array
Platform:	GPL1261
Pubmed ID:	16926388
Summary & Design:	**Summary:** The goal of this experiment was to examine the innate immune response to helminth infection in the lung. Hookworms (like many other helminths) use an obligate migration pathway through the lung. Their infection has been characterized in the gut in detail, but early immune responses in the lung have not been fully characterized. **Keywords: Time Course** **Overall design:** SCID mice were used to examine the innate immune response. SCID mice have no functional B or T cells but a fully functional innate immune system. SCID and WT mice were infected with 500 L3 stage infectious Nippostrongylus brasiliensis SC and their lungs were removed at days 2,3,4,8 and 12 post infection.

Background corr dist: KL-Divergence = 0.5131, L1-Distance = 0.0975, L2-Distance = 0.0326, Normal std = 0.2221

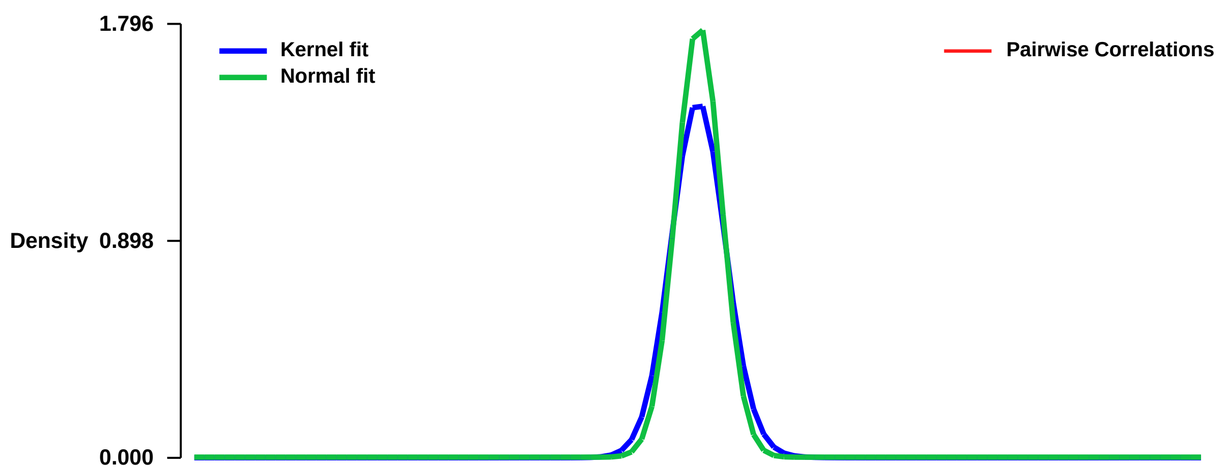

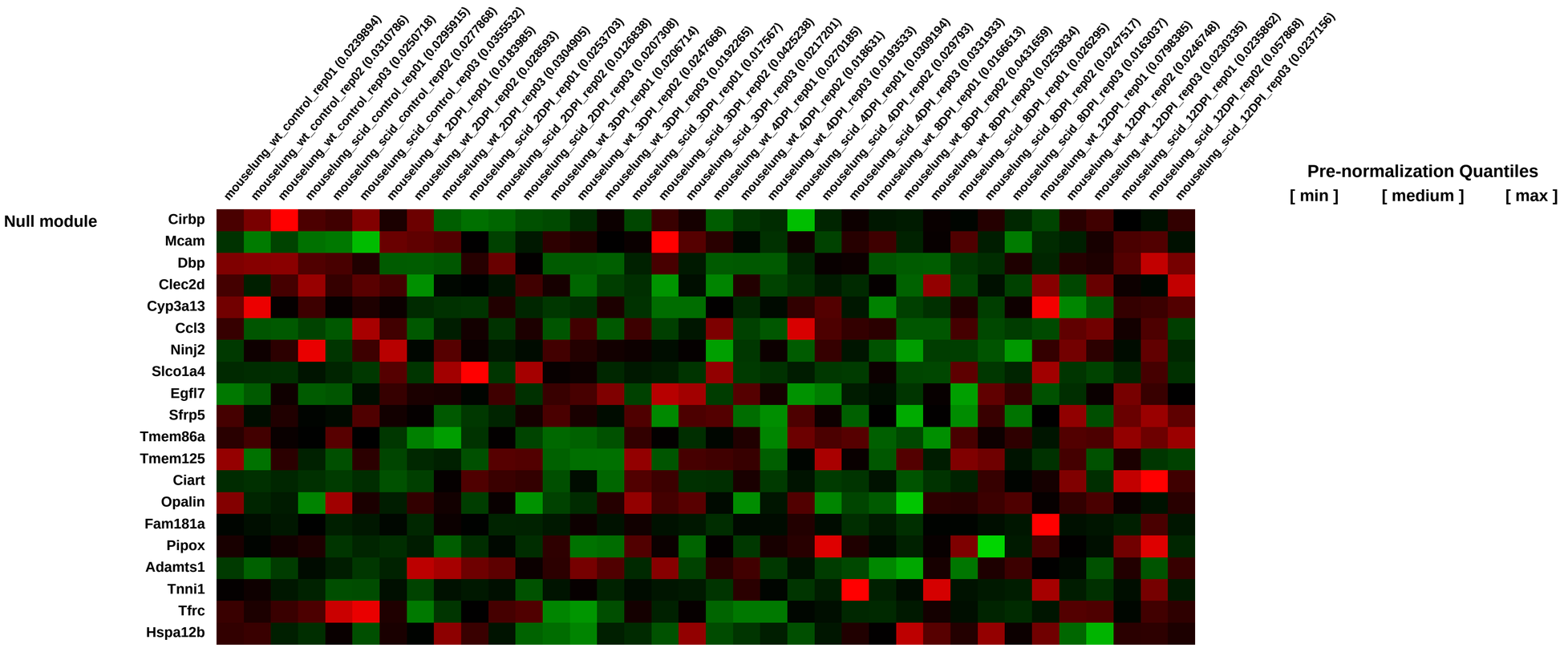

GEO Series "GSE58214" Expression Profiles

Num of samples in this series: 6

Scale of expression profile Z-scores

-3.0 -2.0 -1.0 0.0 1.0 2.0 3.0

GEO Link:	**http://www.ncbi.nlm.nih.gov/geo/query/acc.cgi?acc=GSE58214**
Status:	**Public on Jun 06 2014**
Title:	**Expression data from liver of Retnla transgenic (Tg) and non-transgenic (non-Tg) mice.**
Organism:	**Mus musculus**
Experiment type:	**Expression profiling by array**
Platform:	**GPL1261**
Pubmed ID:	
Summary & Design:	**Summary:** **We found that Retnla-Tg mice had significantly lower serum cholesterol levels than non-Tg mice on a high-fat diet (HFD). To explore the molecular mechanisms underlying the cholesterol-lowering effects of Retnla under hyperlipidemic conditions, we subjected age- and sex-matched Retnla-Tg and non-Tg mice to a HFD for 4 weeks.** **Using a microarray approach, we analyzed the hepatic gene expression profiles related to cholesterol metabolism, including catabolism, biosynthesis, and transport.** **Overall design:** **Total RNA was extracted from livers of Retnla-Tg and non-Tg mice after feeding with a HFD for four weeks, and transcriptional profiling was performed on individual samples using Affymetrix Mouse Genome chips (MG 430 2.0 array).**

Background corr dist: **KL-Divergence = 0.0480, L1-Distance = 0.0213, L2-Distance = 0.0005, Normal std = 0.5825**

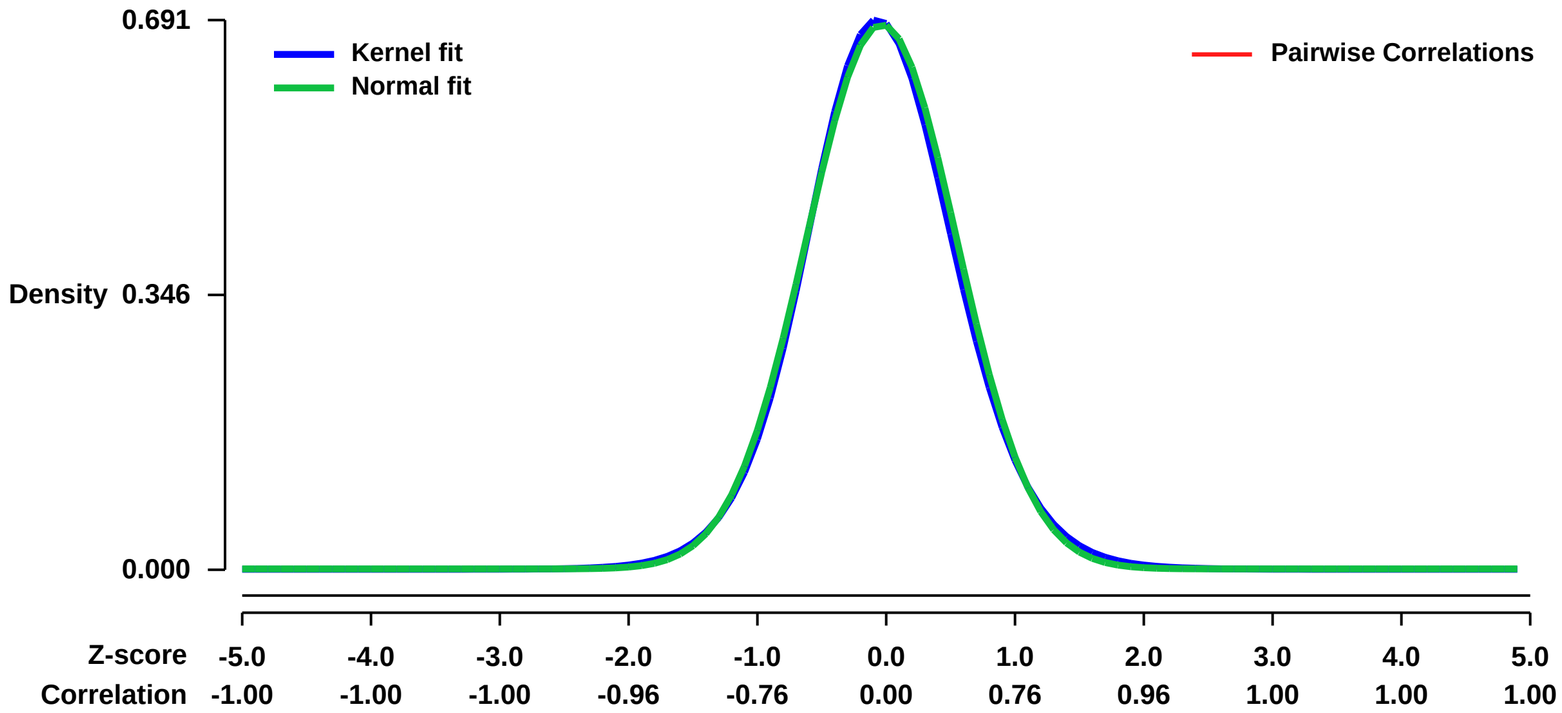

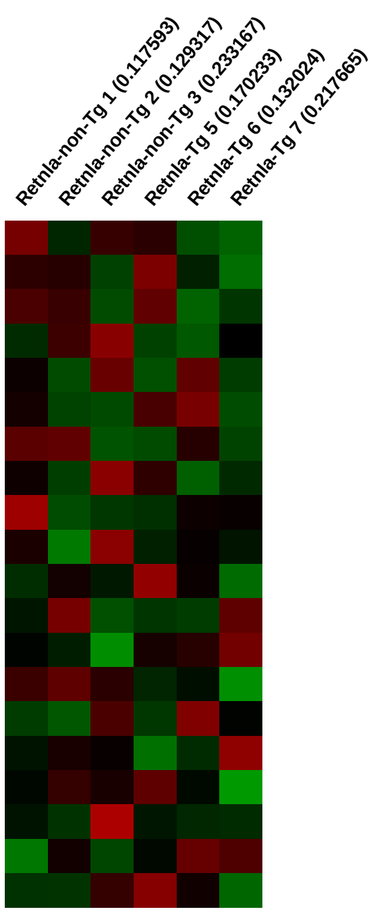

GEO Series "GSE20570" Expression Profiles

Num of samples in this series: 6

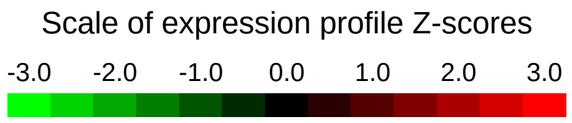

GEO Link:	**http://www.ncbi.nlm.nih.gov/geo/query/acc.cgi?acc=GSE20570**
Status:	**Public on Mar 02 2010**
Title:	**Gene profile of PTIP deletion in adult murine cardiac tissue**
Organism:	**Mus musculus**
Experiment type:	**Expression profiling by array**
Platform:	**GPL1261**
Pubmed ID:	

Summary & Design:

Summary:
Methylation of histone H3 lysine 4 (H3K4me) at actively expressed, cell type-specific genes is established during development by the Trithorax group of epigenetic regulators. In mammals, the Trithorax family includes KMT2A-D (MLL1-4), a family of SET domain proteins that function in large complexes to impart mono-, di-, and trimethylation at H3K4. Individual KMT2s and their co-factors are essential for embryonic development and the establishment of correct gene expression patterns, presumably by demarcating the active and accessible regions of the genome in a cell specific and heritable manner. Despite the importance of H3K4me marks in development, little is known about the importance of histone methylation in maintaining gene expression patterns in fully differentiated and non-dividing cell types. In this report, we utilized an inducible cardiac-specific Cre driver to delete the PTIP protein, a key component of a H3K4me complex, and ask whether this activity is still required to maintain the phenotype of terminally differentiated cardiomyocytes. Our results demonstrate that reducing the H3K4me3 marks is sufficient to alter gene expression patterns and significantly augment systolic heart function. These results clearly show that maintenance of H3K4me3 marks is necessary for the stability of the transcriptional program in differentiated cells. The array we performed allowed us to identify genes that are regulated by PTIP and histone methylation.

Overall design:
8-week-old littermate mice on a mixed C57B6 and B6129 background were utilized. Three mice were on a background with a PTIP floxed allele and a wild type PTIP allele (PTIP+1, PTIP+2, PTIP+3). Three mice had a transgene that expresses a modified estrogen receptor -Cre recombinase fusion protein under the control of a cardiac-specific driver (alpha myosin heavy chain, Jackson Lab stock #005650) and a floxed PTIP allele and a null PTIP (PTIPKO1, PTIPKO2, PTIPKO3). Both groups of mice were injected with tamoxifen at 8 weeks of age. Tamoxifen deletes the floxed PTIP allele in the PTIPKO mice. 5 days after tamoxifen injection, RNA was harvested from left ventricle (LV) apices in both groups. RNA was then sent to the University of Michigan microarray facility core for analysis.

Background corr dist: KL-Divergence = 0.0394, L1-Distance = 0.0187, L2-Distance = 0.0004, Normal std = 0.6171

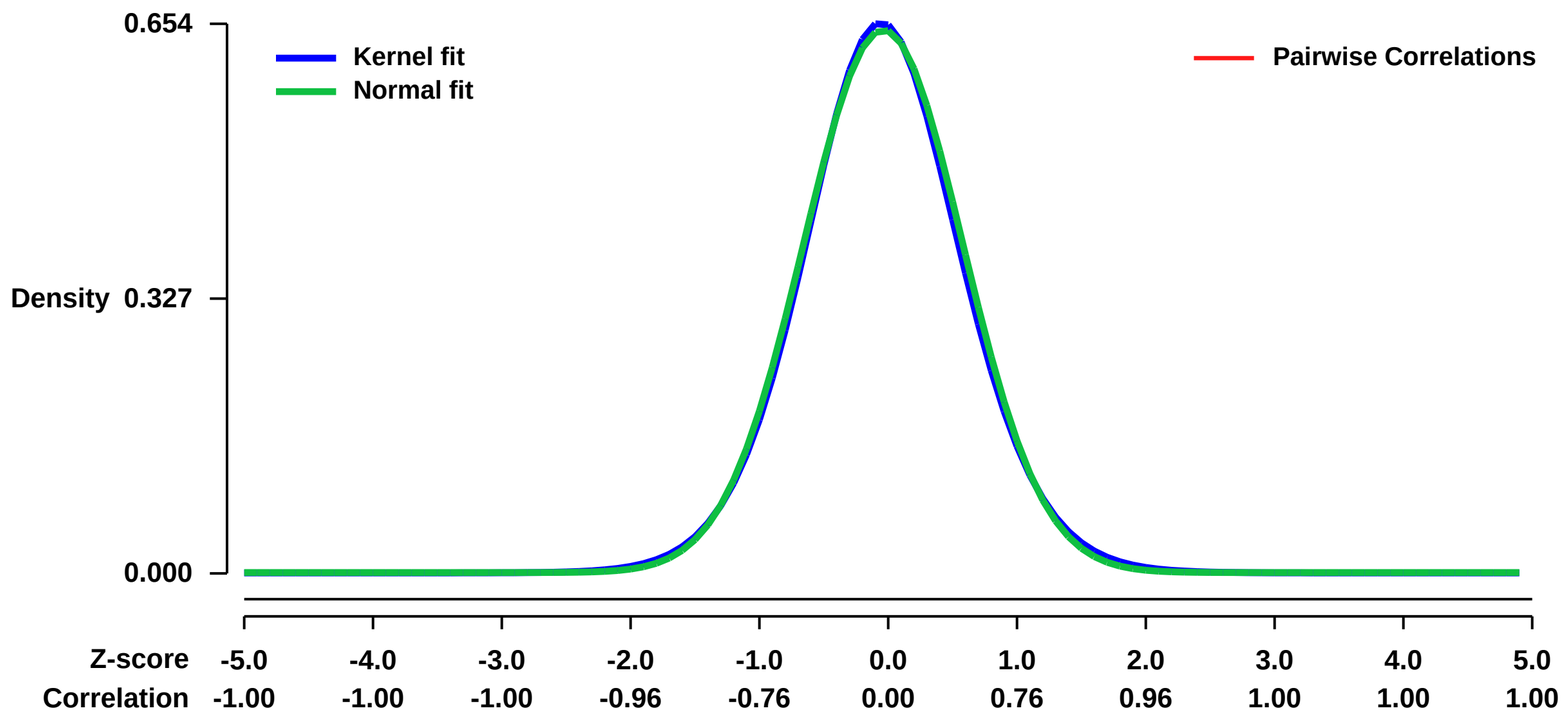

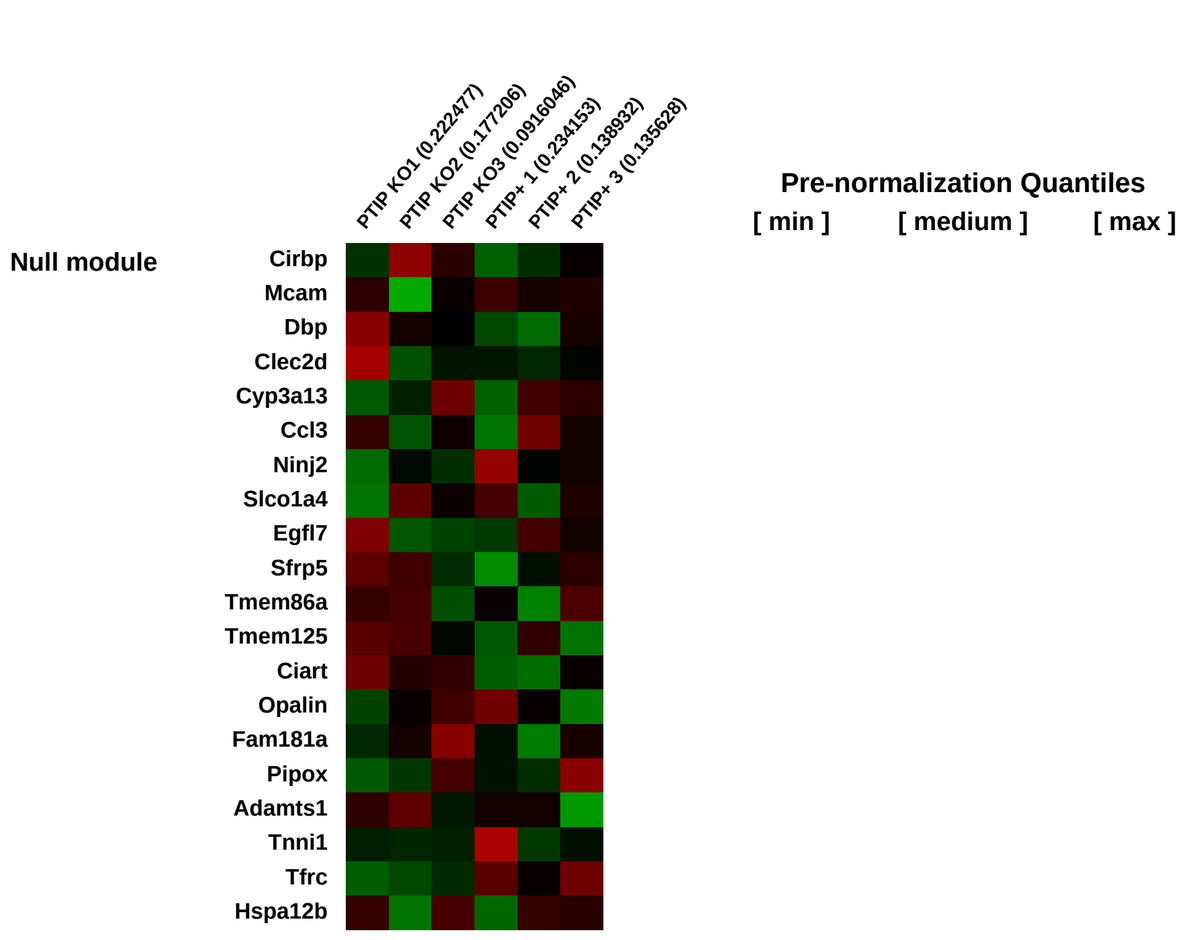

GEO Series "GSE42103" Expression Profiles

Num of samples in this series: 9

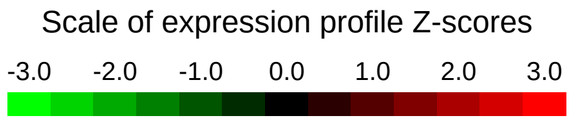

GEO Link:	**http://www.ncbi.nlm.nih.gov/geo/query/acc.cgi?acc=GSE42103**
Status:	**Public on Jan 01 2013**
Title:	**Dual Pten/p53 suppression enhances Notch signaling and sarcoma progression**
Organism:	**Mus musculus**
Experiment type:	**Expression profiling by array**
Platform:	**GPL1261**
Pubmed ID:	
Summary & Design:	**Summary:** **Soft tissue sarcomas (STS) are a heterogeneous group of tumors associated with poor clinical outcome. While a subset of STS are characterized by simple karyotypes and recurrent chromosomal translocations, the mechanisms driving cytogenetically complex sarcomas are largely unknown. Clinical evidence led us to partially inactivate Pten and p53 in the smooth muscle lineage of mice, which developed high-grade undifferentiated pleomorphic sarcomas (HGUPS), leiomyosarcomas (LMS) and carcinosarcomas (CS) that widely recapitulate the human disease, including the aberrant karyotype and metastatic behavior. Pten was found haploinsufficient whereas the wild-type allele of p53 invariably gained point mutations. Gene expression profile showed upregulated Notch signaling in Ptenâ /+p53â /+ tumors compared to Pten+/+p53â /+. Consistently, Pten silencing exacerbated the clonogenic and invasive potential of p53-deficient bone marrow-derived mouse mesenchymal stem cells and tumor cells, while activating the Notch pathway. Moreover, the increased oncogenic behavior of Ptenâ /+p53â /+ and shPten-transduced Pten+/+p53â /+ tumor cells was counteracted by treatment with a gamma secretase inhibitor (GSI), suggesting that the aggressiveness of those tumors can be attributed, at least in part, to enhanced Notch signaling. This study demonstrates a cooperative role for Pten and p53 suppression in complex karyotype sarcomas while establishing Notch as an important functional player in the crosstalk of these pathways during tumor progression. Our results highlight the importance of molecularly subclassifying high-grade sarcoma patients for targeted treatments.** **Compare Ptenâ /+p53â /+ to Pten+/+p53â /+ high-grade undifferentiated pleomorphic sarcomas (HGUPS)** **Overall design:** **Keywords: Differential gene expression.**

Background corr dist: KL-Divergence = 0.0618, L1-Distance = 0.0709, L2-Distance = 0.0081, Normal std = 0.5992

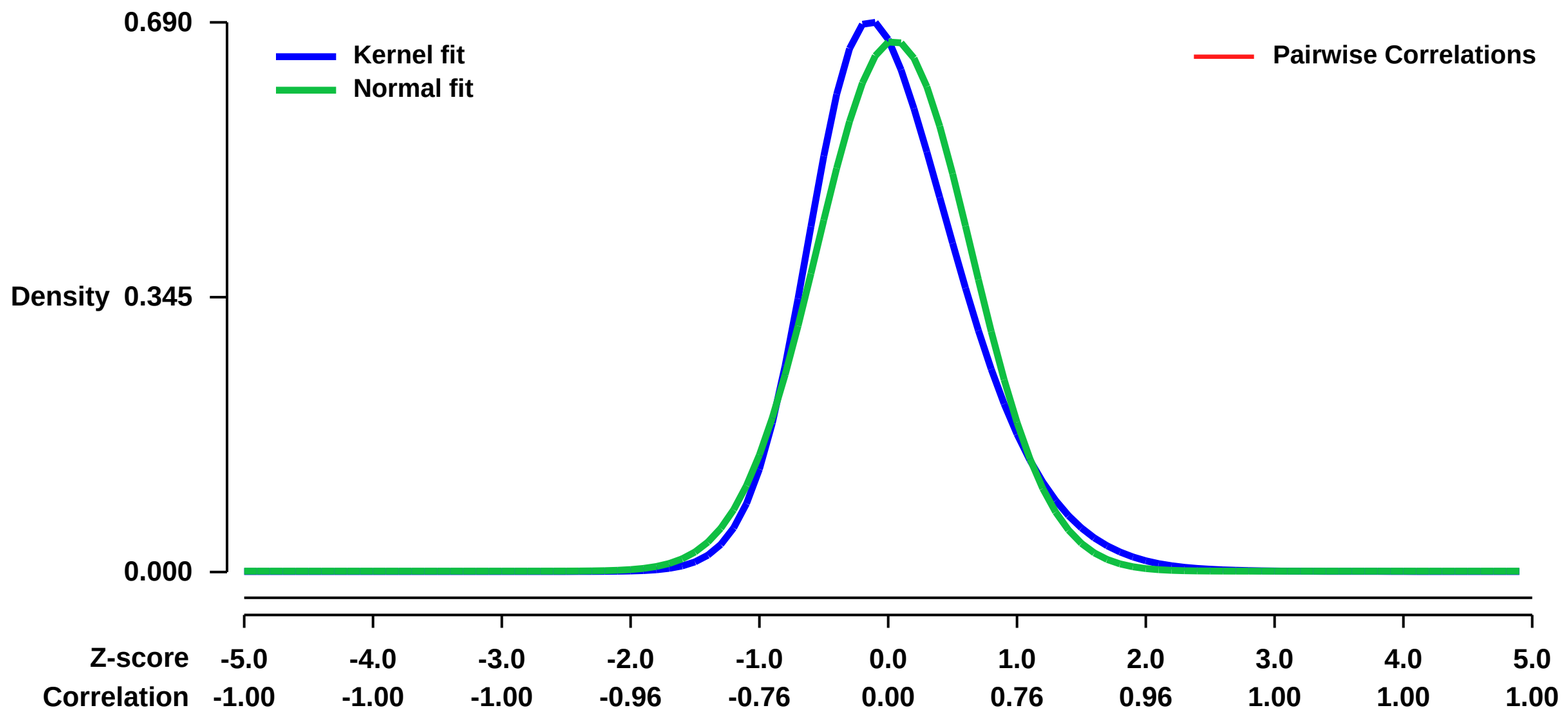

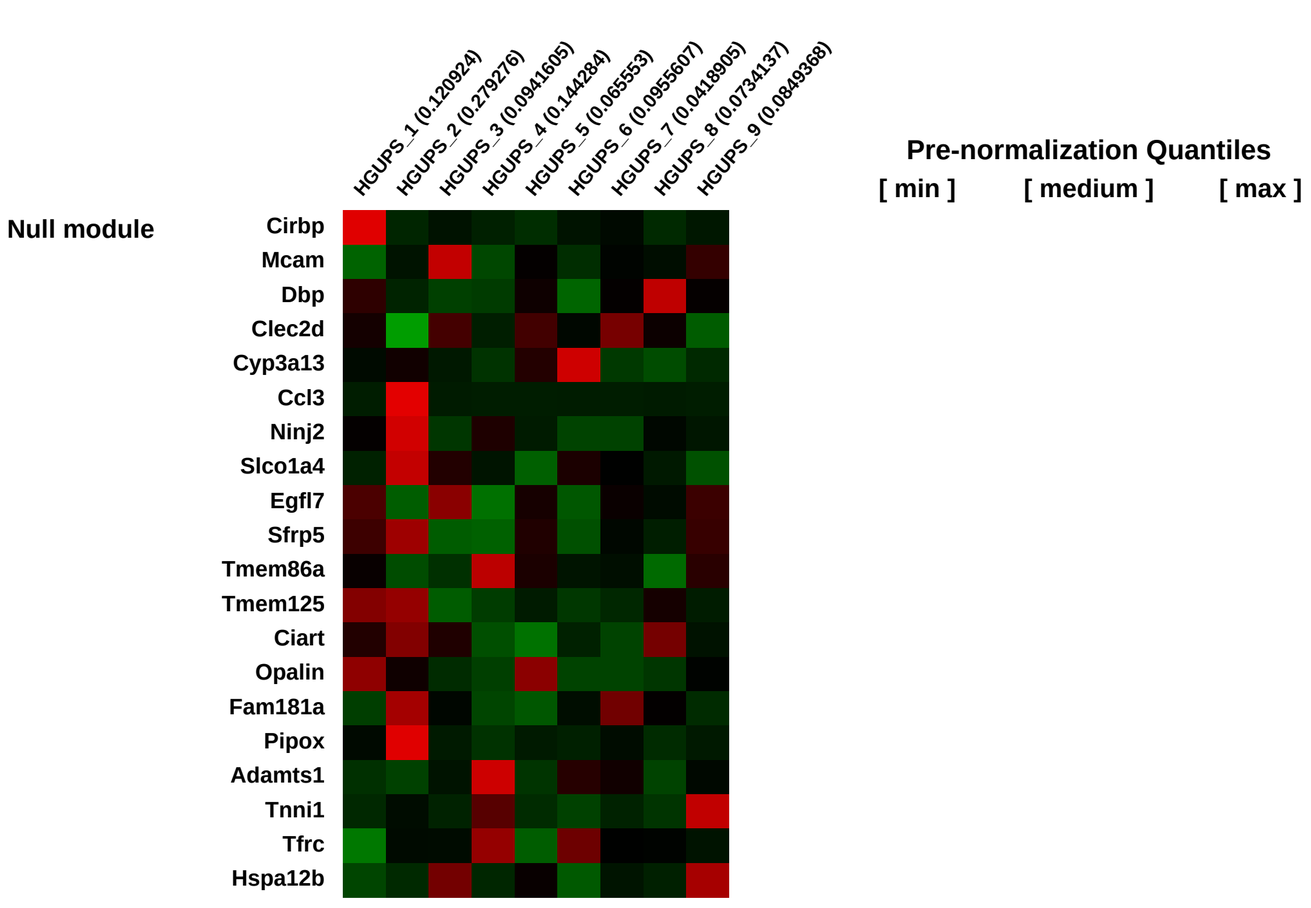

GEO Series "GSE19076" Expression Profiles

Num of samples in this series: 12

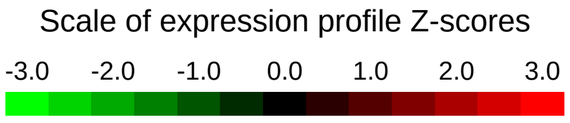

GEO Link:	http://www.ncbi.nlm.nih.gov/geo/query/acc.cgi?acc=GSE19076
Status:	Public on Dec 01 2009
Title:	Expression data from wild type, Ring1B-/-, Eed-/-, and Ring1B/Eed double deficient mouse ES cells
Organism:	Mus musculus
Experiment type:	Expression profiling by array
Platform:	GPL1261
Pubmed ID:	20123906
Summary & Design:	**Summary:** Polycomb complexes establish chromatin modifications for maintaining gene repression and are essential for embryonic development in mice. Here we use pluripotent embryonic stem (ES) cells to demonstrate an unexpected redundancy between Polycomb repressive complex 1 (PRC1) and PRC2 during the formation of differentiated cells. ES cells lacking the function of either PRC1 or PRC2 can differentiate into cells of the three germ layers, whereas simultaneous loss of PRC1 and PRC2 abrogates differentiation. On the molecular level the differentiation defect is caused by the derepression of a set of genes that is redundantly repressed by PRC1 and PRC2 in ES cells. Furthermore, we find that genomic repeats are Polycomb targets and show that in the absence of Polycomb complexes endogenous MLV elements can mobilize. This indicates a contribution of the PcG system to the defense against parasitic DNA and a potential role of genomic repeats in Polycomb mediated gene regulation. **Overall design:** RNA from wt and PcG mutant ES cells was extracted using Trizol and hybridized to an Affymetrix Mouse 430_2.0 chip. Labeling, hybridization and primary data analysis were performed by a commercial provider (Atlas Biolabs, Berlin). Before RNA extraction, the undifferentiated ES cell state was confirmed by colony morphology. All genotypes were hybridized in biological triplicates.

Background corr dist: KL-Divergence = 0.1022, L1-Distance = 0.0263, L2-Distance = 0.0012, Normal std = 0.4327

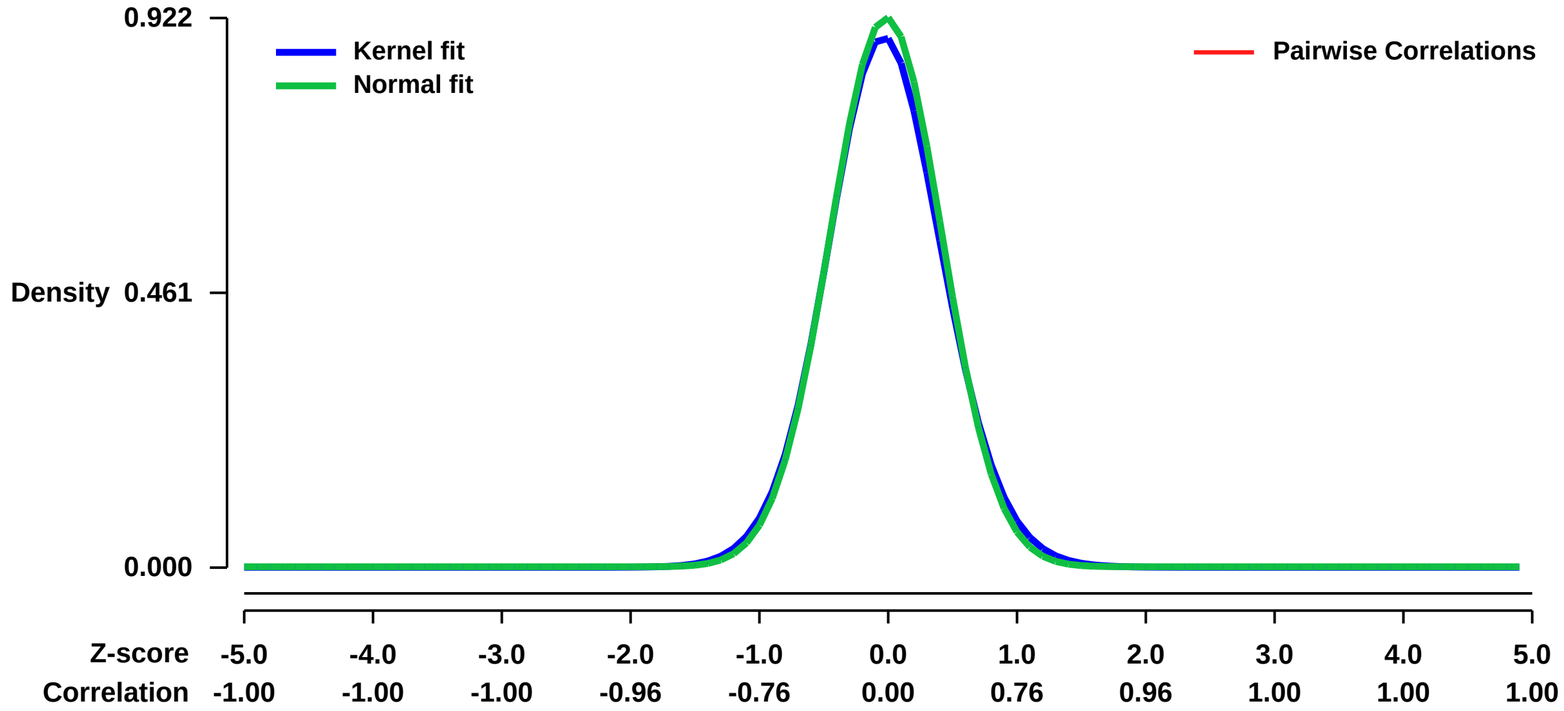

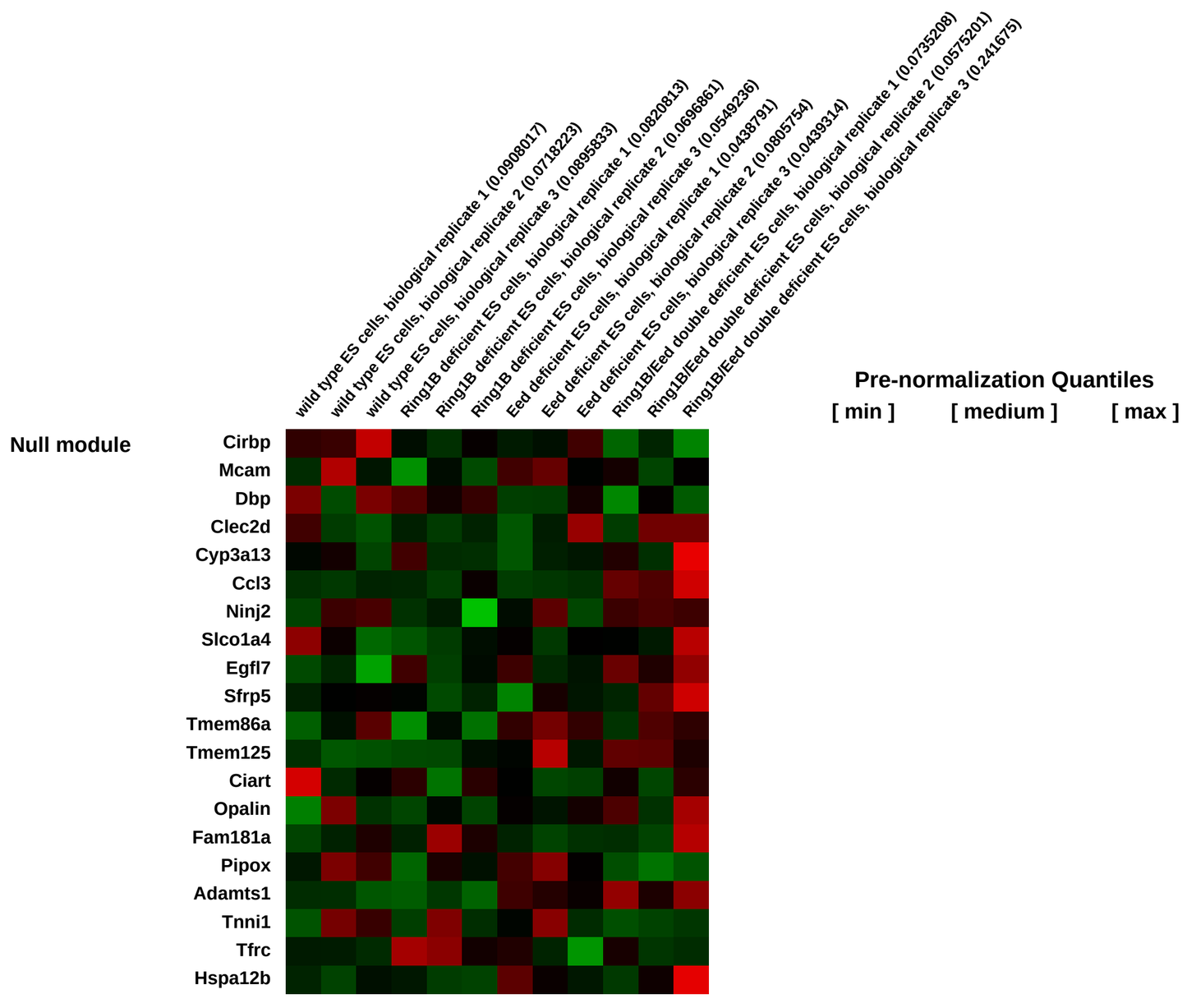

GEO Series "GSE6765" Expression Profiles

Num of samples in this series: 9

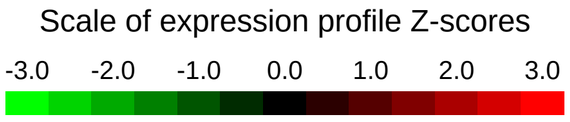

GEO Link:	http://www.ncbi.nlm.nih.gov/geo/query/acc.cgi?acc=GSE6765
Status:	Public on Jan 20 2007
Title:	Aeromonas caviae infection, 24 hours
Organism:	Mus musculus
Experiment type:	Expression profiling by array
Platform:	GPL1261
Pubmed ID:	20130691
Summary & Design:	**Summary:** Aeromonas caviae has been associated with human gastrointestinal disease. Strains of this species typically lack virulence factors (VFs) such as enterotoxins and hemolysins that are produced by other human pathogens of the Aeromonas genus. Microarray profiling of murine small intestinal extracts, 24 hours after oral infection with an A. caviae strain, provides evidence of a Th1 type immune response. A large number of gamma-interferon (¸‡-IFN) induced genes are up-regulated as well as several tumor necrosis factor-alpha (TNF-¸–) transcripts. A. caviae has always been considered an opportunistic pathogen because it lacks obvious virulence factors. This current effort suggests A. caviae colonizes murine intestinal tract and causes what has been described by others as a dysregulatory cytokine response leading to an irritable bowel-like syndrome. This response would explain why a number of diarrheal waterborne outbreaks have been attributed to A. caviae even though it lacks obvious enteropathogenic properties. **Keywords:** Aeromonas caviae, infection, disease mechanism, TH1 resposne **Overall design:** Biological replicates (n=5), controls are uninfected mice, test replicates are infected with organism

Background corr dist: KL-Divergence = 0.0980, L1-Distance = 0.0252, L2-Distance = 0.0010, Normal std = 0.4406

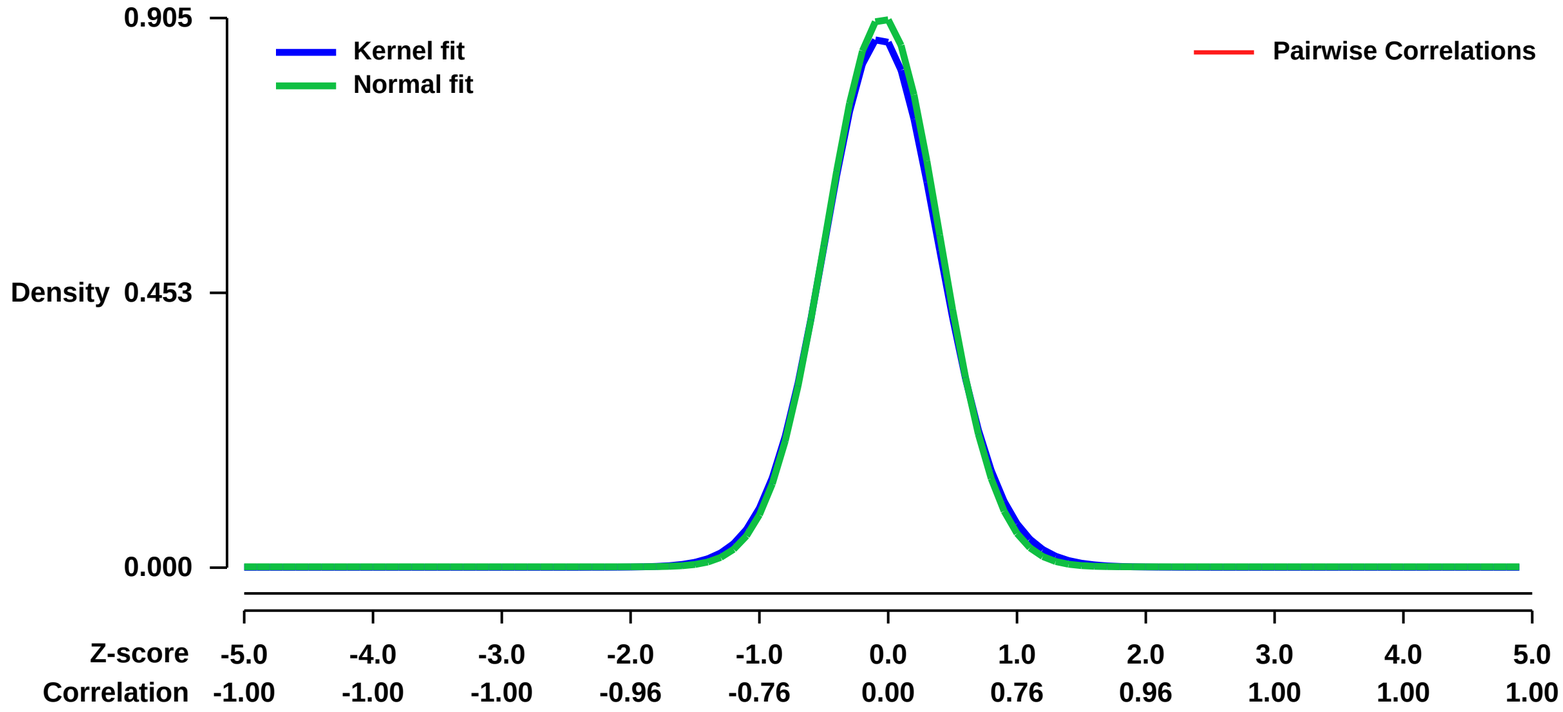

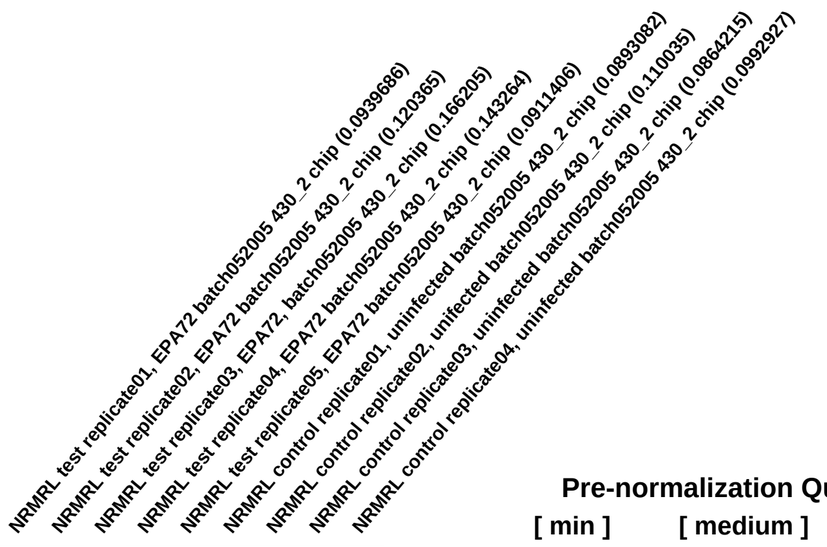

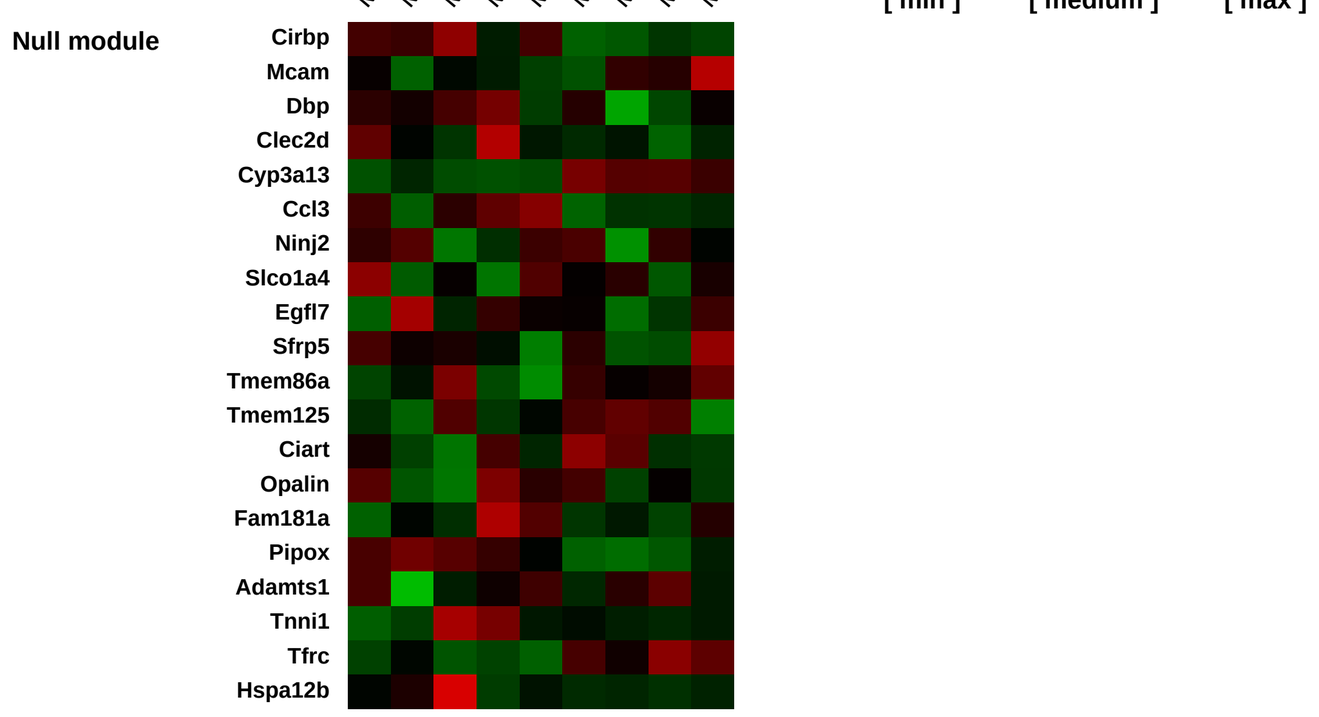

GEO Series "GSE17783" Expression Profiles

Num of samples in this series: 19

Scale of expression profile Z-scores

-3.0 -2.0 -1.0 0.0 1.0 2.0 3.0

GEO Link:	http://www.ncbi.nlm.nih.gov/geo/query/acc.cgi?acc=GSE17783
Status:	Public on Oct 01 2009
Title:	Analysis of gene expression in FACS-purified cortical projection neurons using Affymetrix 430 2.0 microarrays
Organism:	Mus musculus
Experiment type:	Expression profiling by array
Platform:	GPL1261
Pubmed ID:	19793993
Summary & Design:	**Summary:** 3 subtypes of cortical projection neurons were purified by fluorescence-activated cell sorting (FACS) at 4 different stages of development from mouse cortex. A detailed description of the data set is described in Arlotta, P et al (2005) and Molyneaux, BJ et al (2009). The hybridization cocktails used here were originally applied to the Affymetrix mouse 430A arrays and submitted as GEO accession number GSE2039. The same hybridization cocktails were then applied to the Affymetrix mouse 430 2.0 arrays, and those data are contained in this series. **Overall design:** Three subtypes of cortical neurons were purified by FACS at multiple stages of mouse brain development. The neuron subtypes are: corticospinal motor neurons (CSMN), callosal projection neurons (CPN), and corticotectal projection neurons (CTPN). The stages of development included embryonic day 18 (E18), postnatal day 3 (P3), postnatal day 6 (P6), and postnatal day 14 (P14). CSMN and CPN were analyzed at all four stages, while CTPN were only analyzed at P14. The replicates included in the data set are all true biological replicates with independent sample collection for each.

Background corr dist: KL-Divergence = 0.0948, L1-Distance = 0.0989, L2-Distance = 0.0187, Normal std = 0.5162

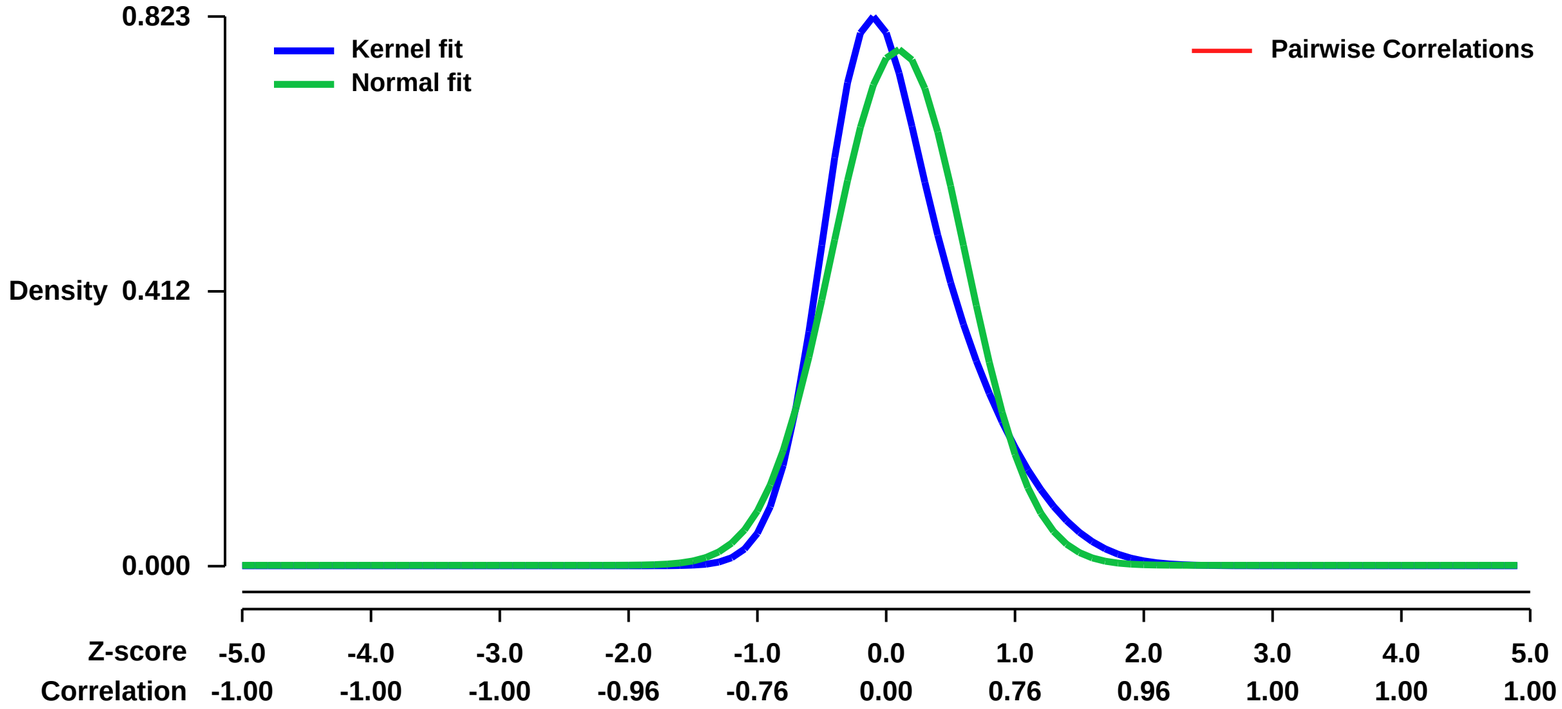

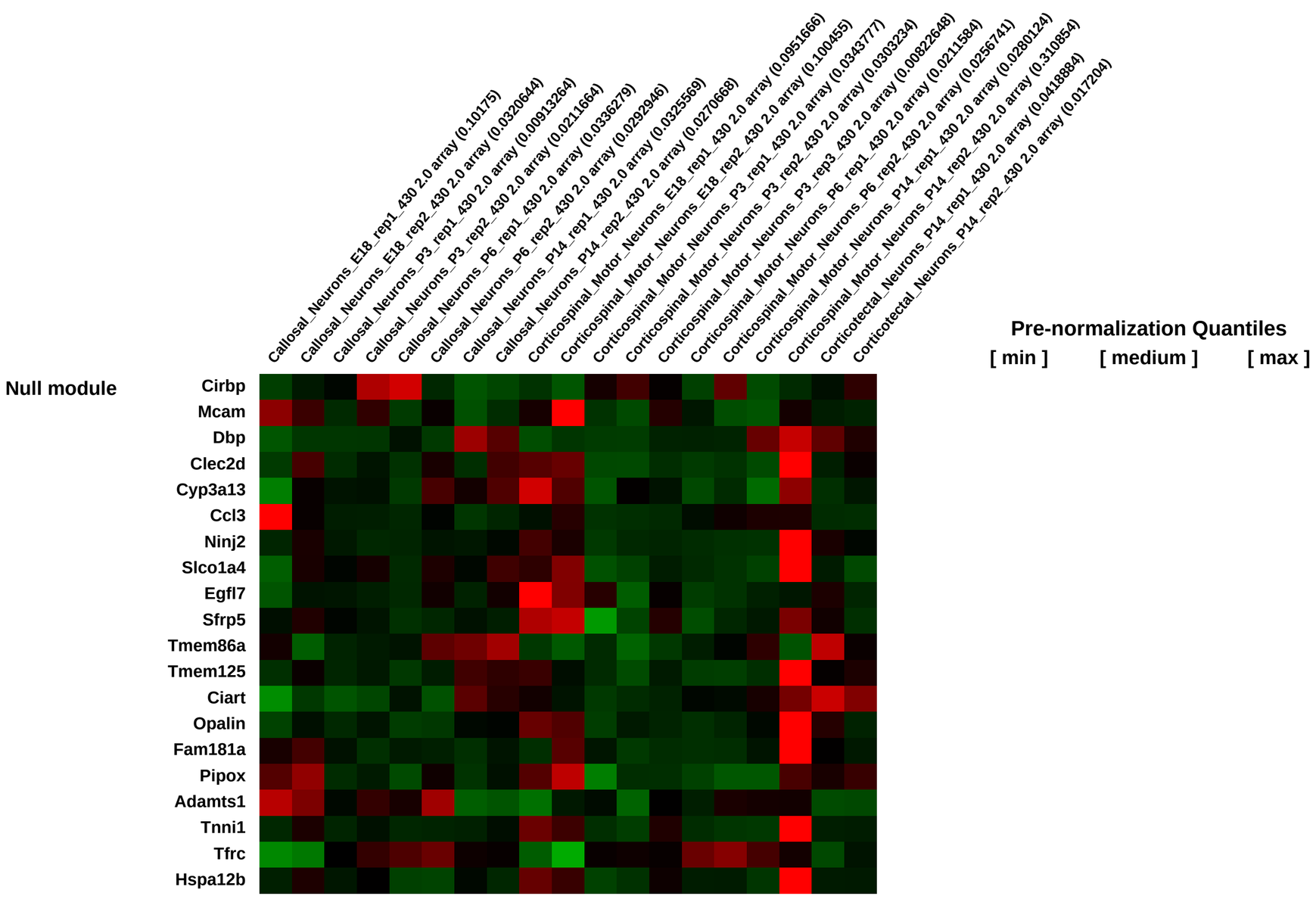

GEO Series "GSE23081" Expression Profiles

Num of samples in this series: 6

Scale of expression profile Z-scores

-3.0 -2.0 -1.0 0.0 1.0 2.0 3.0

GEO Link:	http://www.ncbi.nlm.nih.gov/geo/query/acc.cgi?acc=GSE23081
Status:	Public on Apr 20 2011
Title:	Identification of microRNA targets in the mammalian inner ear using a comprehensive transcriptome and proteome integrated approach
Organism:	Mus musculus
Experiment type:	Expression profiling by array
Platform:	GPL1261
Pubmed ID:	21483685
Summary & Design:	**Summary:** We have employed a novel approach for the identification of functionally important microRNA (miRNA)-target interactions using integrated miRNA, transcriptome and proteome profiles with advanced in silico analysis. By looking at both the transcript and protein levels of expression, a thorough coverage of miRNA regulation was obtained. Microdissected auditory and vestibular sensory epithelia were used as the model system, thus being the first time such a comparison was carried out in a neuroepithelial system. Moreover, this is one of only a few studies employing proteome screening for the identification of miRNA targets. Notably, this approach can be employed for the study of other tissues and organs. We detected the expression of 157 miRNAs in the inner ear sensory epithelia, with 53 miRNAs differentially expressed between the cochlea and vestibule. By searching for enrichment and depletion of miRNA targets in the transcript and protein datasets with a reciprocal or similar expression, respectively, as the regulatory miRNA, we identified functionally important miRNAs. Finally, the interaction between miR-135b and PSIP1-P75, a transcriptional coacitvator previously unknown in the inner ear, was identified and validated experimentally. We suggest that miR-135b may serve as a cellular effector, involved in regulating some of the differences between the cochlear and vestibular hair cells. **Overall design:** We investigated the mRNA expression profile of the cochlear and vestibular sensory epithelia from inner ears of postnatal day 2 mice using the Affymetrix GeneChip´fi 430 2Mouse Genome array. Cochlear and vestibular sensory epithelia were dissected from wild type C3H mice and collected separately. The vestibular epithelia consisted of the saccule, utricle and the lateral and anterior cristae. Both the cochlear and vestibular sensory epithelia were dissected with their underlying mesenchyma. Altogether three pools, three biological replicates, of each tissue type were collected consisting of cochlear or vestibular sensory epithelia dissected from 10 to 12 inner ears.

Background corr dist: KL-Divergence = 0.0241, L1-Distance = 0.0102, L2-Distance = 0.0001, Normal std = 0.7062

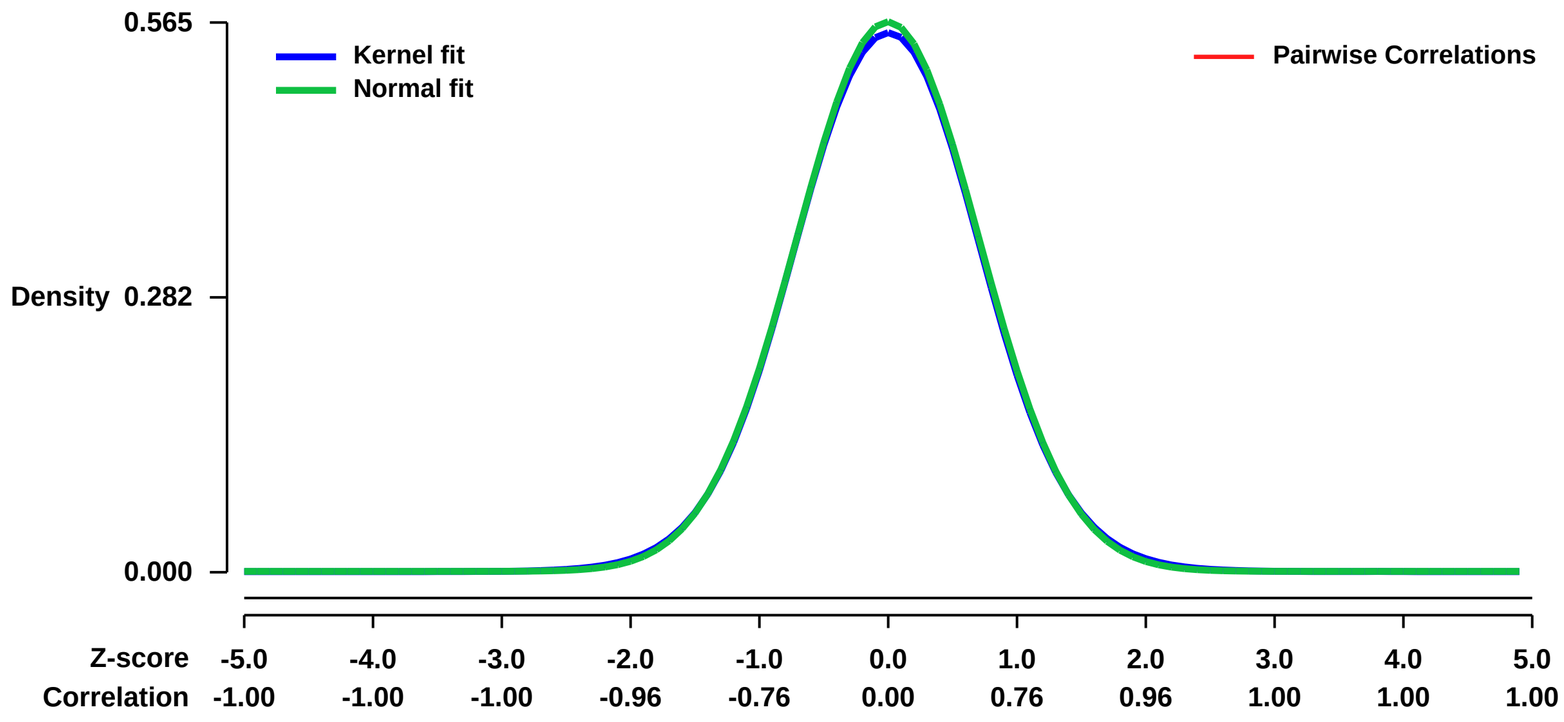

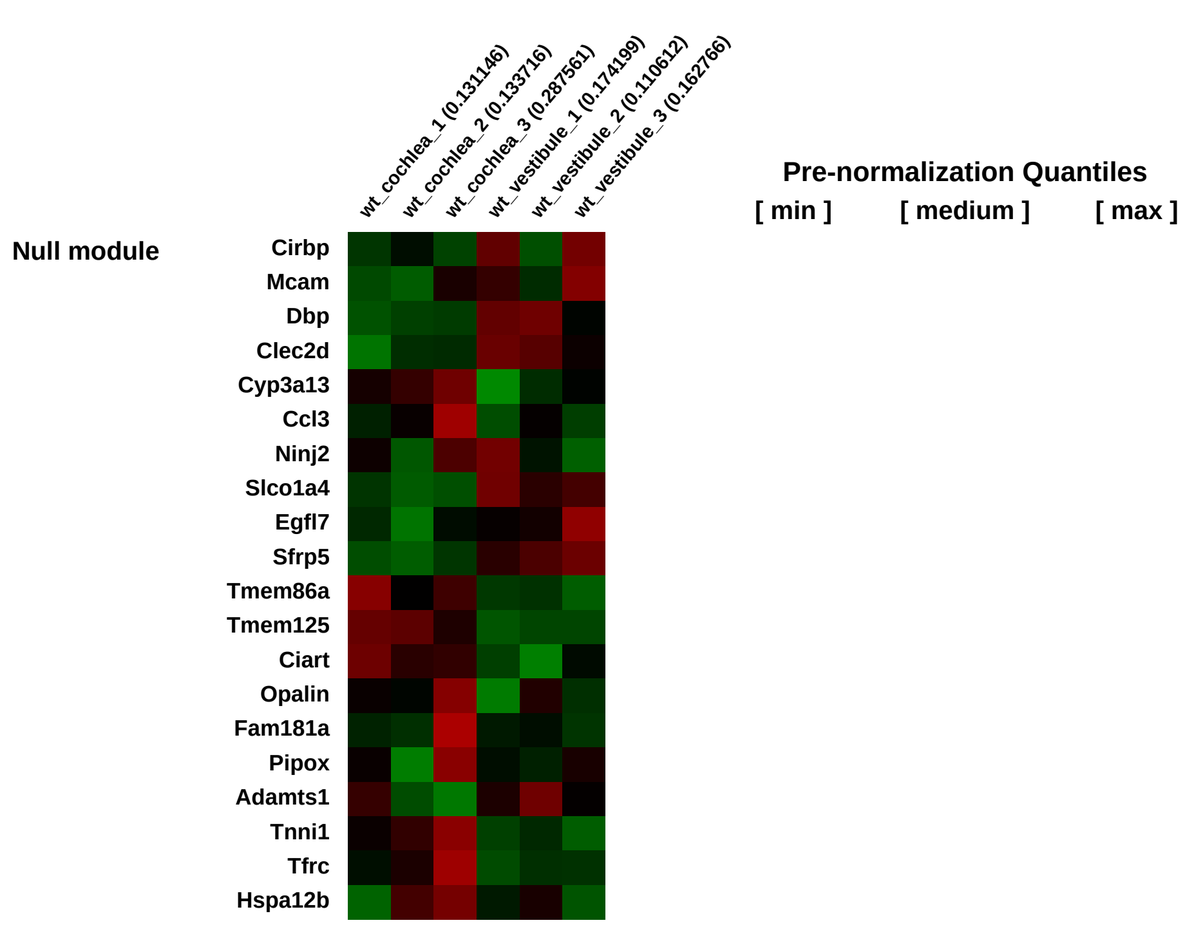

GEO Series "GSE31042" Expression Profiles

Num of samples in this series: 6

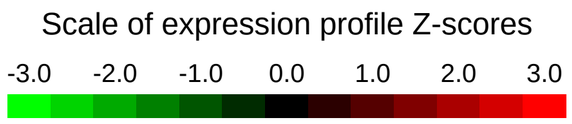

GEO Link:	**http://www.ncbi.nlm.nih.gov/geo/query/acc.cgi?acc=GSE31042**
Status:	**Public on Dec 30 2013**
Title:	**Expression data of mouse hematopoietic cells, Nr4a1/3 wild type and double mutant**
Organism:	**Mus musculus**
Experiment type:	**Expression profiling by array**
Platform:	**GPL1261**
Pubmed ID:	
Summary & Design:	**Summary:** **We investigate the cellular and molecular mechanisms of tumor suppression by NR4A1 and NR4A3, and show a cell intrinsic essential function in maintenance of hematopoietic stem cell (HSC) homeostasis. In the absence of Nr4a1/3, HSC lost quiescence, became highly proliferative leukemia-stem cell (LSC) that transplanted AML to recipient mice.´ We further revealed that loss of NR4A1/3 leads to deregulated expression of the key cell cycle regulator Cdkn1c (P57), c-Myc oncogene, and glucose metabolic genes leading to enhanced aerobic glycolysis or â Warburg effectâ in LSCs.´ Reintroduction of Nr4a1 in LSCs restored HSC quiescence, and reversed Nr4a1/3 deficiency induced P57 suppression and c-Myc overexpression. Collectively, we identify an essential role of Nr4a1/3 in coordinately regulating cell cycle entry and glucose metabolism to prevent uncontrolled stem cell proliferation and AML transformation. These results have major implications for designing therapeutic strategies in AML.** **Overall design:** **To identify NR4A-dependent molecular signaling pathways that may control HSC homeostasis, we performed genome-wide transcript profiling of Lin-Sca1+ (LS) cells from WT and DKO mice. For Affymetrix analysis, we generated three independent pools of RNA from sorted LS cells from 10-20 WT or DKO (2- to 3-week-old) mice per sample.**

Background corr dist: KL-Divergence = 0.0491, L1-Distance = 0.0294, L2-Distance = 0.0012, Normal std = 0.5845

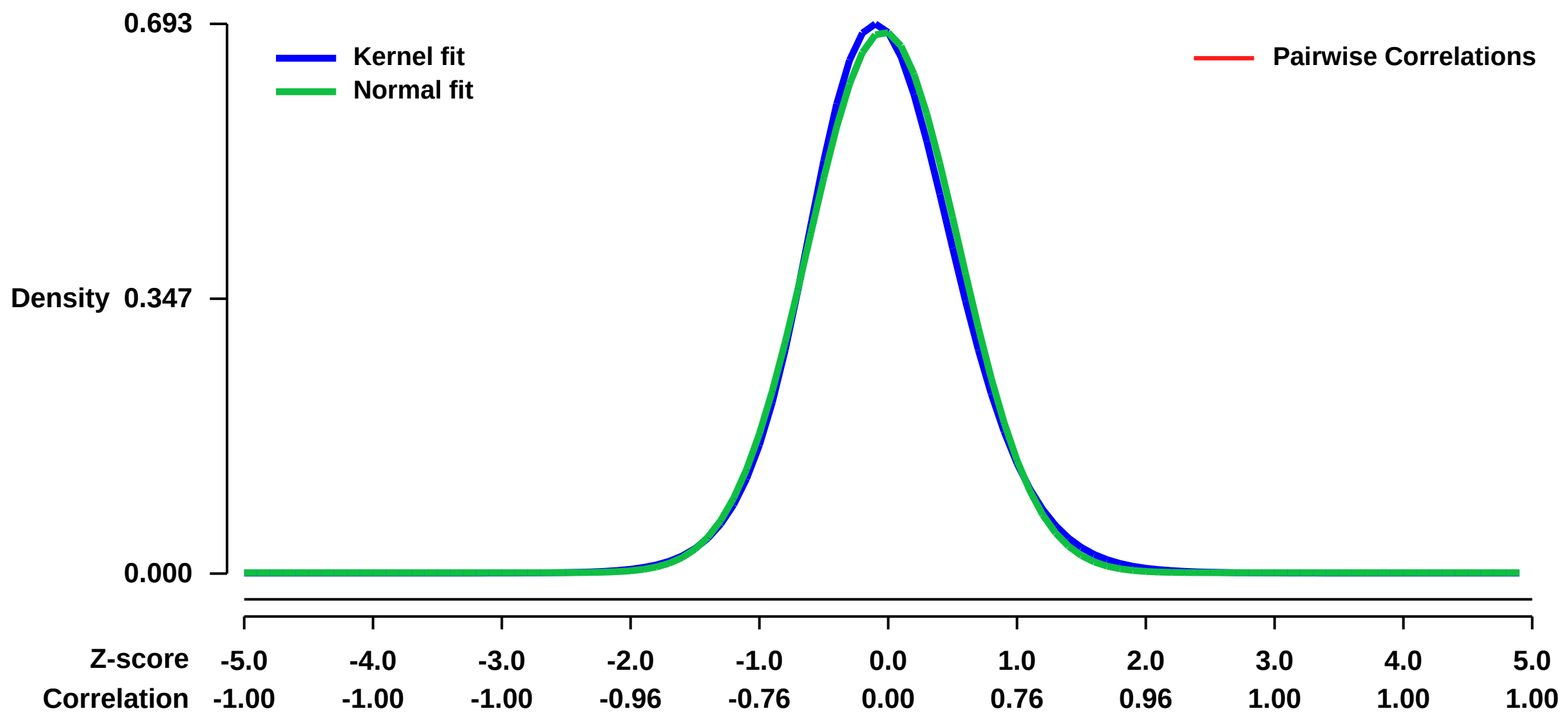

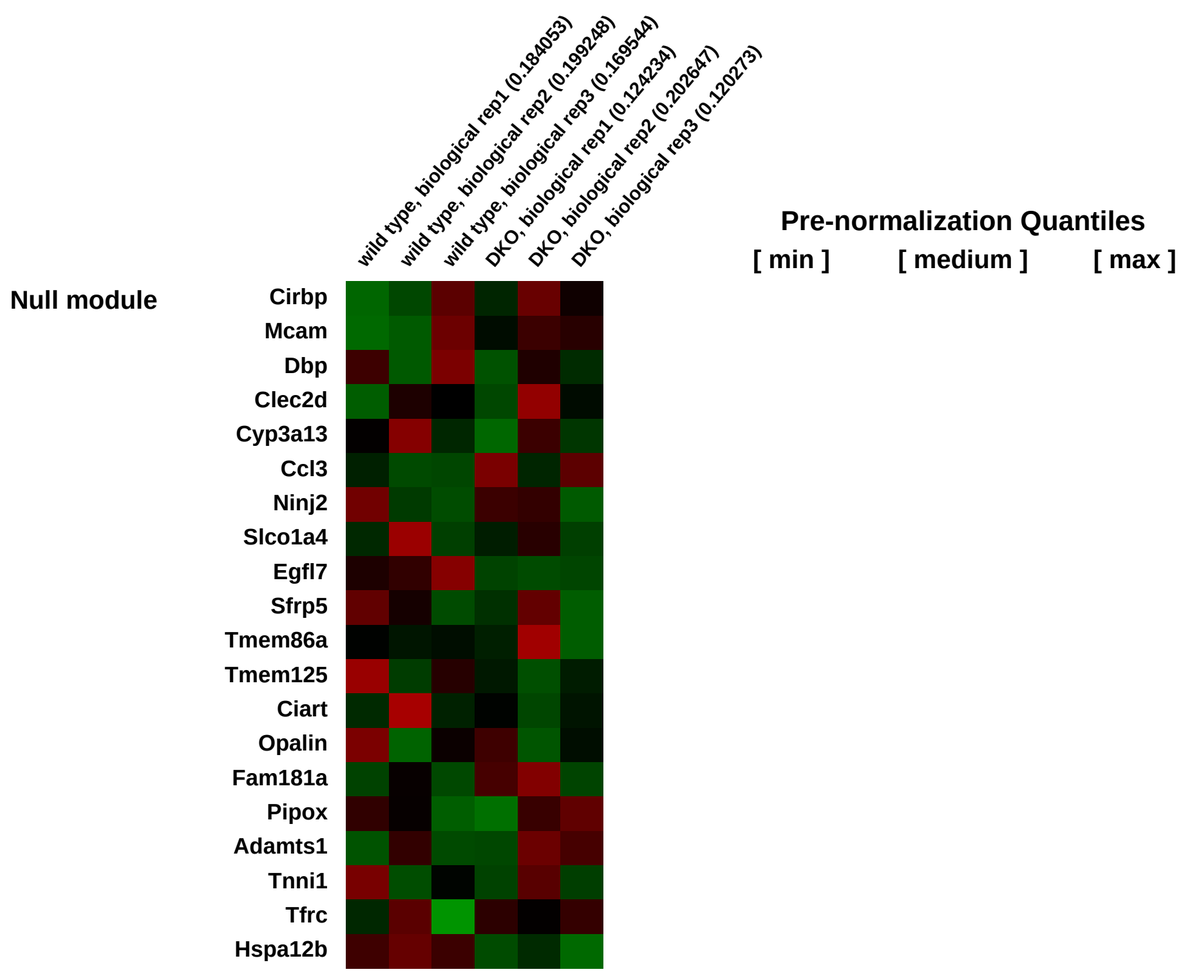

GEO Series "GSE30746" Expression Profiles

Num of samples in this series: 16

Scale of expression profile Z-scores

-3.0 -2.0 -1.0 0.0 1.0 2.0 3.0

GEO Link:	http://www.ncbi.nlm.nih.gov/geo/query/acc.cgi?acc=GSE30746
Status:	Public on Aug 05 2011
Title:	Expression data from murine Tet-off MLL-AF9/Ras acute myeloid leukemia cell lines following withdrawal of MLL-AF9
Organism:	Mus musculus
Experiment type:	Expression profiling by array
Platform:	GPL1261
Pubmed ID:	21828272
Summary & Design:	**Summary:** To explore oncogene addiction programs in a genetically defined leukemia context we developed an AML mouse model driven by a conditional MLL-AF9 allele together with oncogenic Ras, which enabled us to examine the consequences of MLL-AF9 inhibition in established disease. In order to produce a tightly regulated system that was easy to monitor, we constructed two retroviral vectors containing dsRed-linked MLL-AF9 under control of a tetracycline response element promoter, and KrasG12D or NrasG12D linked to the â Tet-offâ tet-transactivator, which activates TRE expression in a doxycycline repressible manner. Leukemias were generated by retroviral cotransduction of both vectors into hematopoietic stem and progenitor cells, which were transplanted into syngeneic mice. Cells harboring both constructs induced aggressive myelomonocytic leukemia. Five independent primary leukemia cell lines were established from bone marrow of terminal mice. Treatment of these lines with doxycycline rapidly turned off MLL-AF9 expression, and induced terminal myeloid differentiation and complete disease remission in vivo. To identify molecular mechanisms underlying addiction to MLL-AF9, we analyzed global gene expression changes following doxycycline-induced suppression of MLL-AF9. **Overall design:** Independent primary acute myeloid leukemia lines induced by cotransduction of Tet-off MLL-AF9 together with either KrasG12D or NrasG12D were grown in culture and treated with doxycycline for 6 days to inactivate MLL-AF9 expression. In addition, primary acute myeloid leukemia lines with constitutive MLL-AF9 and KrasG12D were included to control for the effects of doxycycline. Untreated and treated cells were harvested for RNA extraction and hybridization to Affymetrix arrays.

Background corr dist: KL-Divergence = 0.0602, L1-Distance = 0.0548, L2-Distance = 0.0054, Normal std = 0.5458

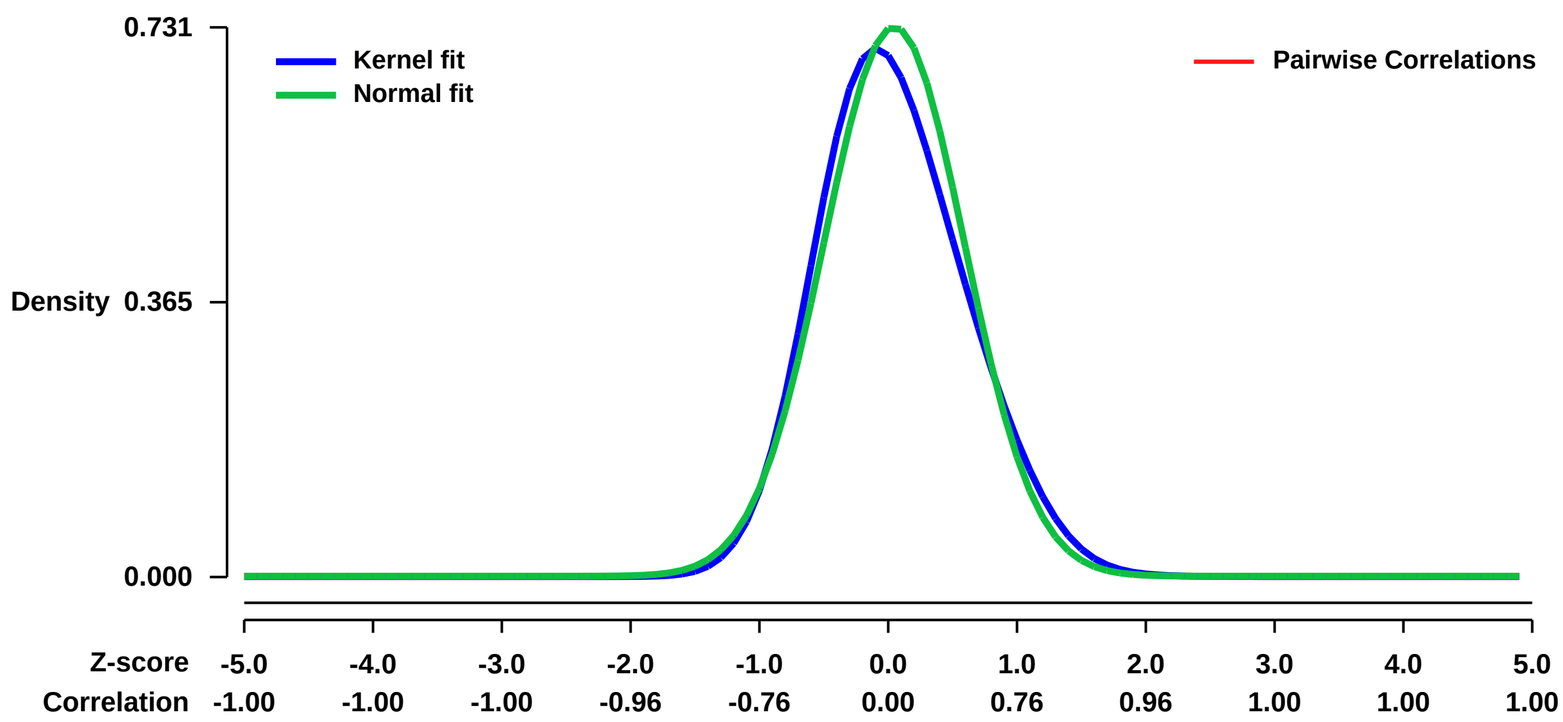

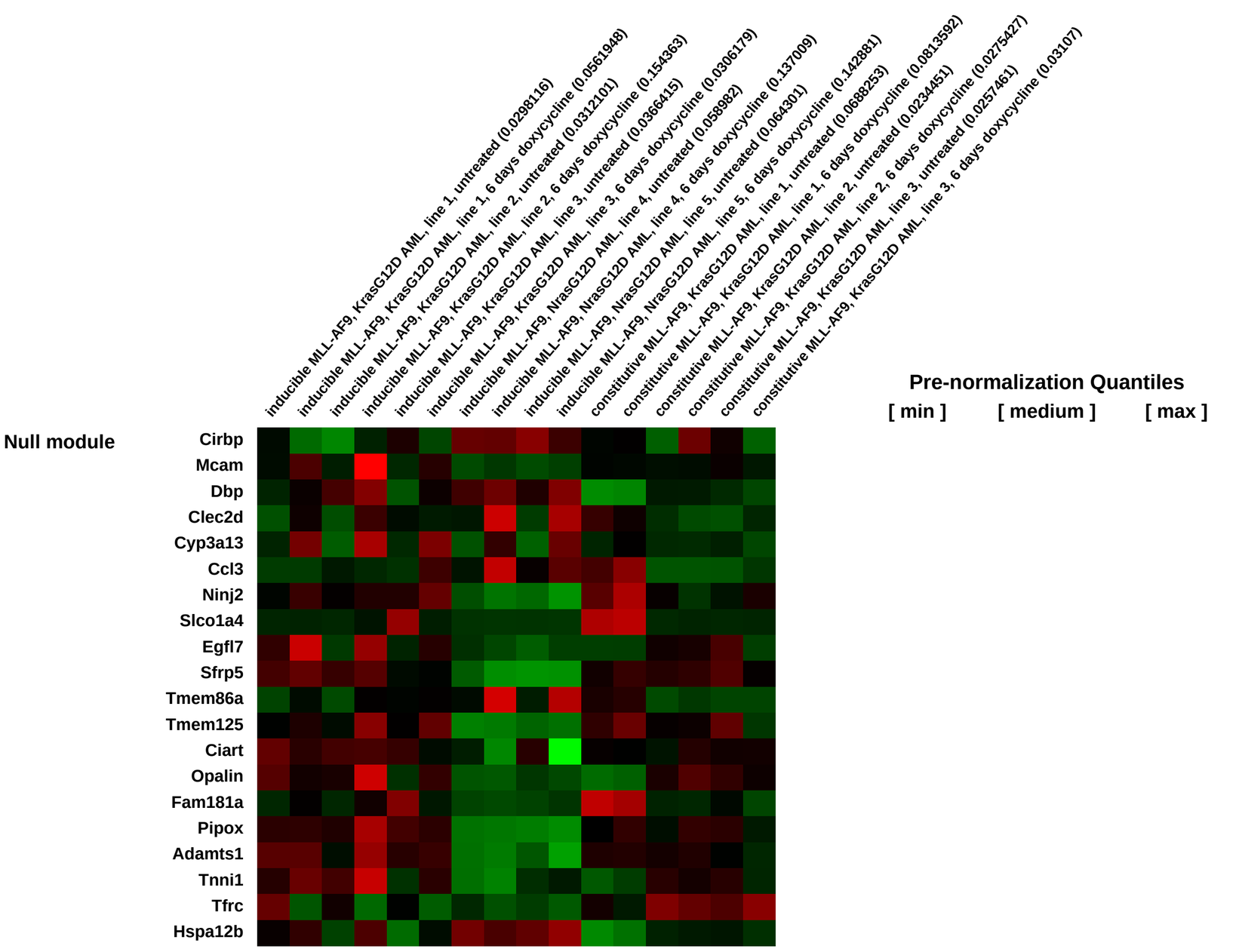

GEO Series "GSE11732" Expression Profiles

Num of samples in this series: 15

Scale of expression profile Z-scores

-3.0 -2.0 -1.0 0.0 1.0 2.0 3.0

GEO Link:	http://www.ncbi.nlm.nih.gov/geo/query/acc.cgi?acc=GSE11732
Status:	Public on Jun 12 2008
Title:	Runx transcriptional program for control of cell adhesion and survival
Organism:	Mus musculus
Experiment type:	Expression profiling by array
Platform:	GPL1261
Pubmed ID:	18560354
Summary & Design:	**Summary:** The Runx genes are important in development and cancer, where they can act either as oncogenes or tumour supressors. We compared the effects of ectopic Runx expression in established fibroblasts, where all three genes produce an indistinguishable phenotype entailing epithelioid morphology and increased cell survival under stress conditions. Gene array analysis revealed a strongly overlapping transcriptional signature, with no examples of opposing regulation of the same target gene. A common set of 50 highly regulated genes was identified after further filtering on regulation by inducible RUNX1-ER. This set revealed a strong bias toward genes with annotated roles in cancer and development, and a preponderance of targets encoding extracellular or surface proteins reflecting the marked effects of Runx on cell adhesion. **Keywords:** Comparative study of gene targets regulated by overexpression of the different Runx family members **Overall design:** 6 samples (expression of different Runx family members); 5 in duplicate, 1 single. 2 control samples (empty vector) in duplicate. Cultures of Runx expressing cells were grown to confluence, treated with ethanol +/- 4OHT tamoxifen for 24 hours and harvested for RNA extraction and hybridization on Affymetrix microarrays

Background corr dist: KL-Divergence = 0.1987, L1-Distance = 0.0453, L2-Distance = 0.0045, Normal std = 0.3323

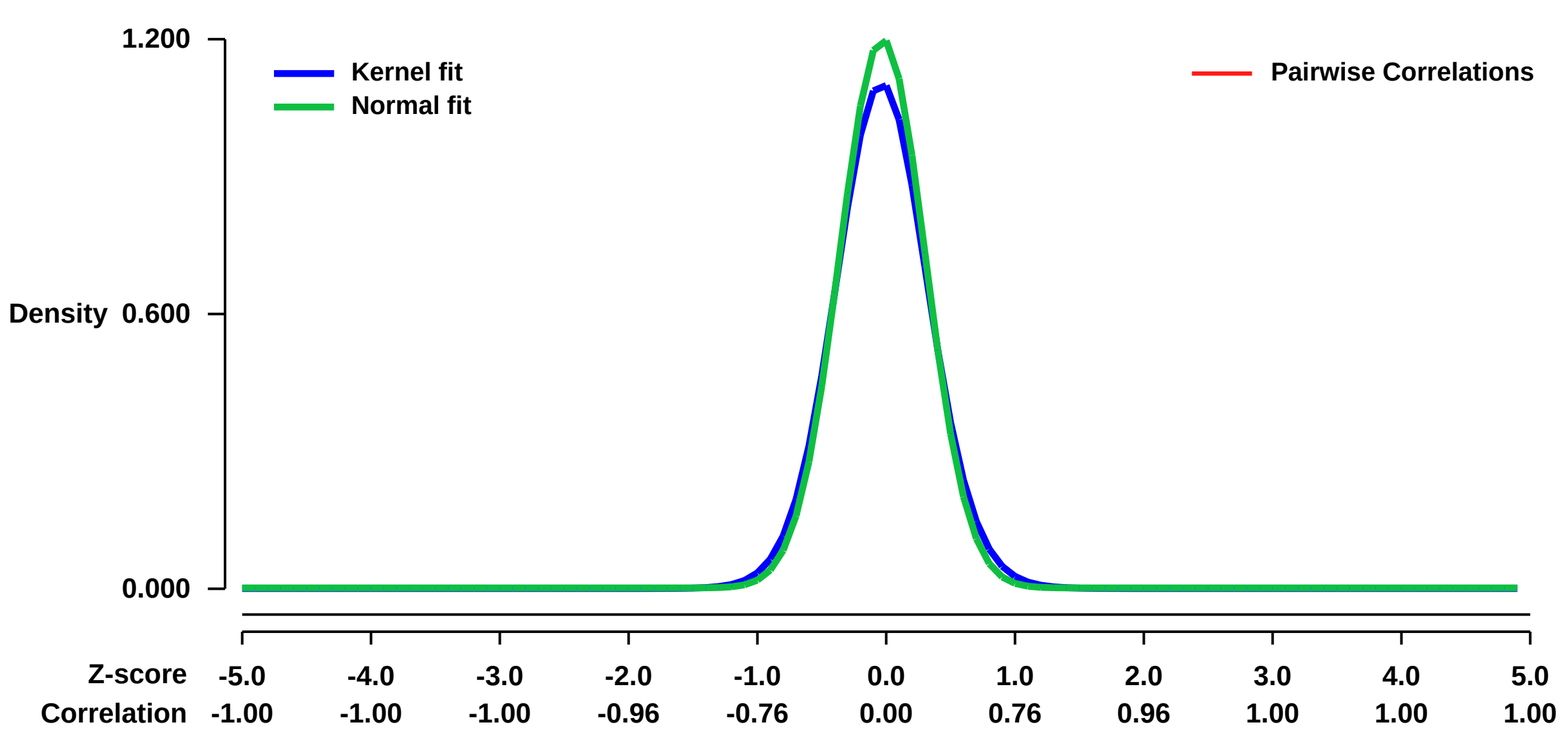

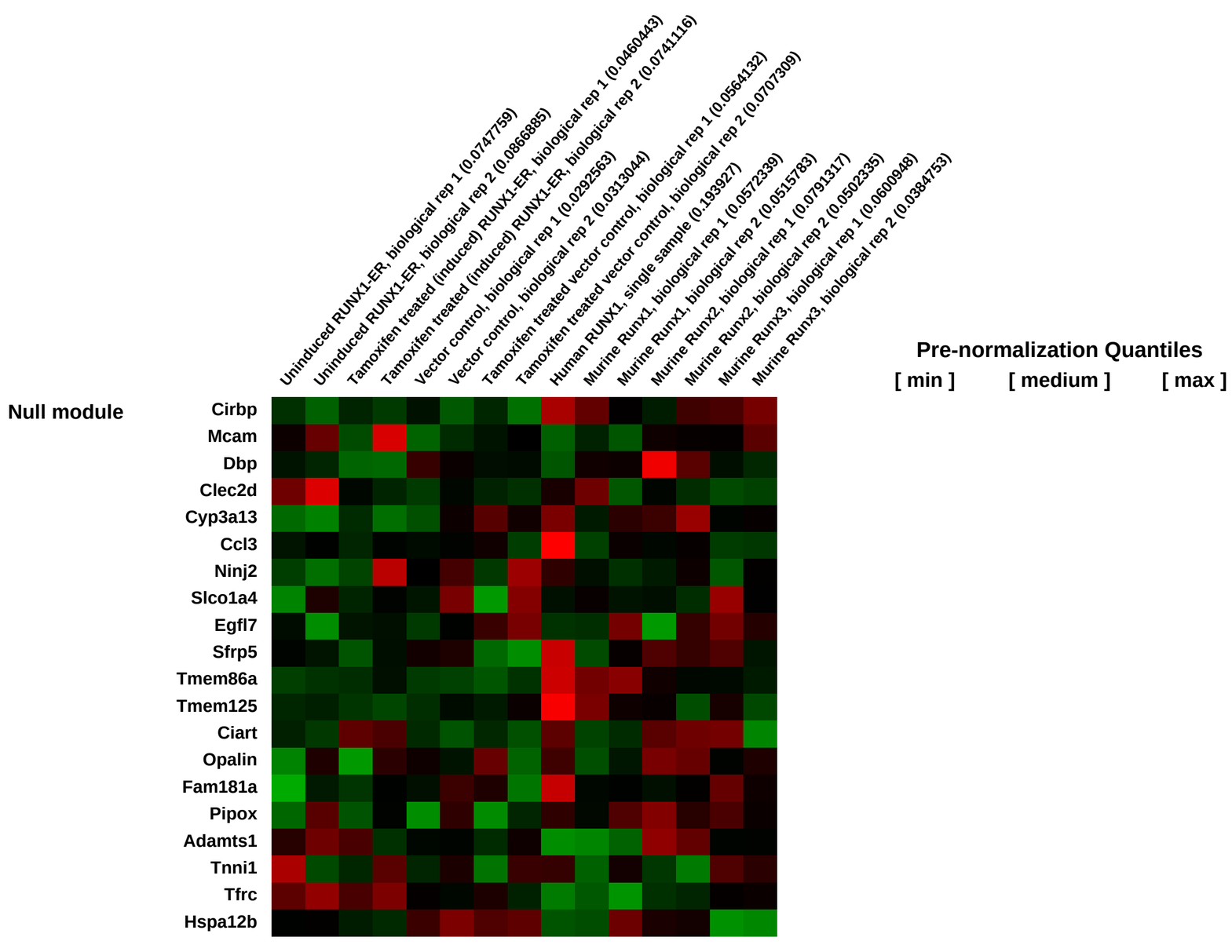

GEO Series "GSE48884" Expression Profiles

Num of samples in this series: 12

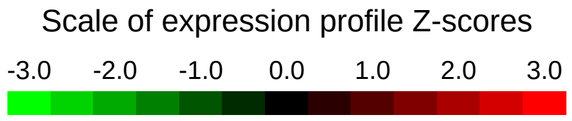

GEO Link:	http://www.ncbi.nlm.nih.gov/geo/query/acc.cgi?acc=GSE48884
Status:	Public on Jul 16 2013
Title:	Cyclin D1 determines estrogen depependent signaling in mouse mammary gland.
Organism:	Mus musculus
Experiment type:	Expression profiling by array
Platform:	GPL1261
Pubmed ID:	23864650
Summary & Design:	**Summary:** Ovariectomized virgin Ccnd1-/- and Ccnd1+/+ mice (5 weeks of age) were allowed to recuperate for 2 weeks. The mice were assigned to either replacement pellets containing E2 (0.75 mg, 60-day release) or pellet containing placebo. Mice were sacrificed at day 7 after pellet implantation. RNA extracted from mammary glands (3 each group) was labeled and used to probe Affymetrix 430_2.0 arrays. **Overall design:** Six separate control Ccnd1+/+ C57BL/6 were compared to six Ccnd1-/- C57BL/6 mice. 3 mice in each group treated with placebo and three mice treated with E2

Background corr dist: KL-Divergence = 0.0851, L1-Distance = 0.0269, L2-Distance = 0.0012, Normal std = 0.4687

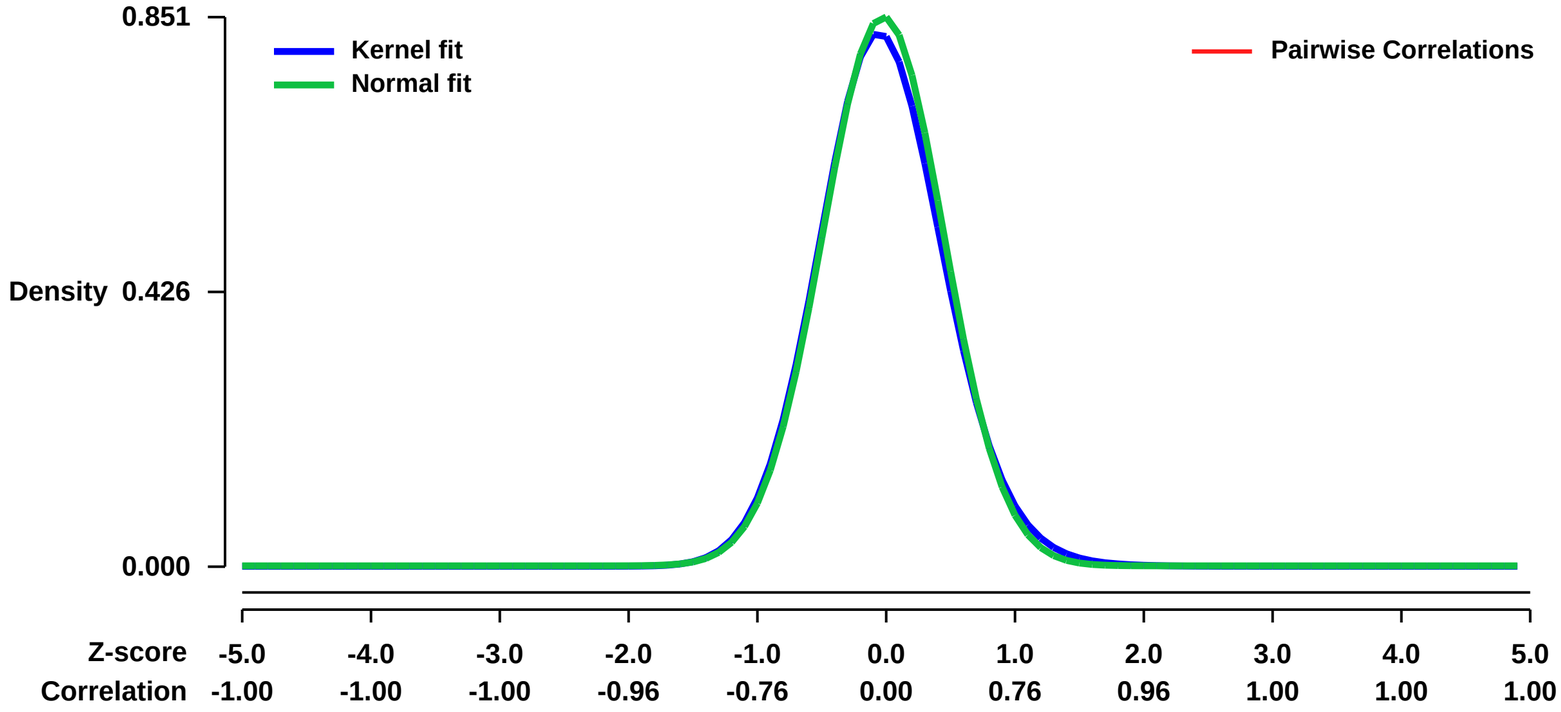

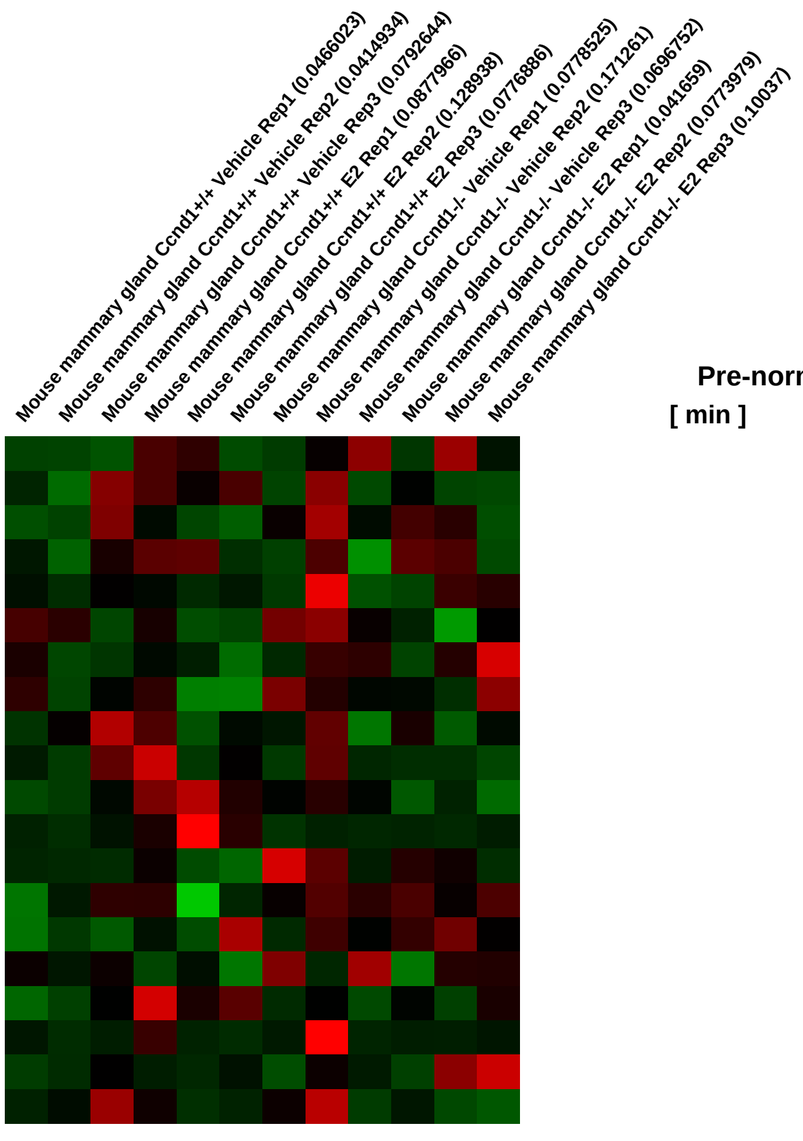

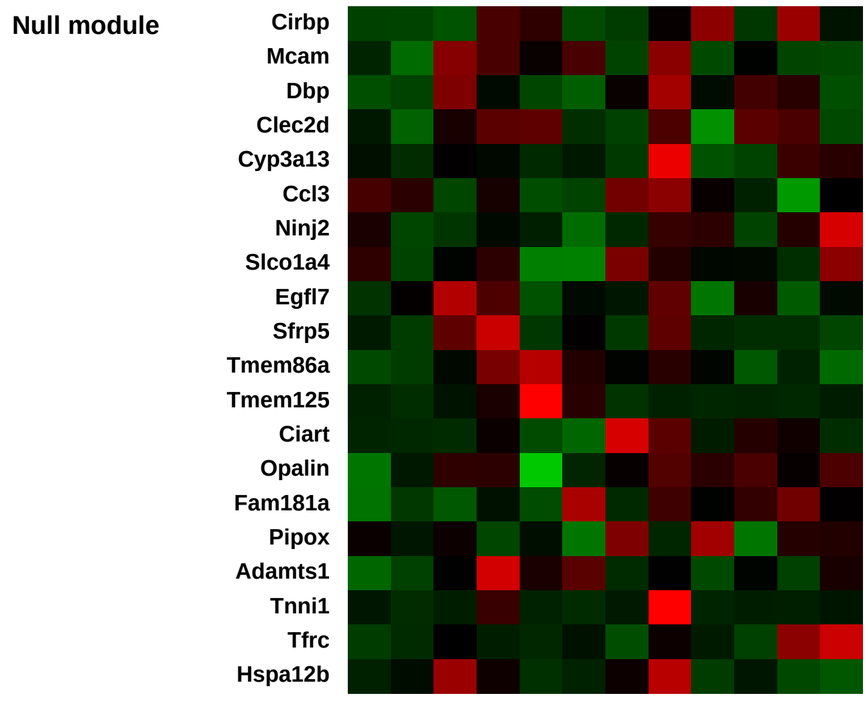

GEO Series "GSE31702" Expression Profiles

Num of samples in this series: 10

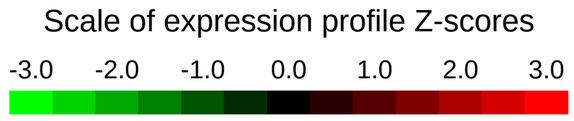

GEO Link:	http://www.ncbi.nlm.nih.gov/geo/query/acc.cgi?acc=GSE31702
Status:	Public on Aug 30 2011
Title:	CD4+ T cell gene expression in B6 vs B6.Sle1c2 mice
Organism:	Mus musculus
Experiment type:	Expression profiling by array
Platform:	GPL1261
Pubmed ID:	22711888
Summary & Design:	**Summary:** **Sle1c is a sublocus of the NZM2410-derived Sle1 major susceptibility locus. We have previously shown that Sle1c contributes to lupus pathogenesis by conferring CD4+ T cell-intrinsic hyperactivation and increased susceptibility to chronic graft-versus-host disease (cGVHD) that mapped to the centromeric portion of the locus. In this study, we have refined the centromeric sublocus to a 675Kb interval, termed Sle1c2. Recombinant congenic strains expressing Sle1c2 exhibited a T cell-intrinsic CD4+ T cell hyperactivation and cGVHD susceptibility, similar to mice with the parental Sle1c.** **We performed a microarray analysis on CD4+ T cells to gain insights into the transcriptional programs that regulate the hyperactivation conferred by Sle1c2.** **Overall design:** **CD4+ T cell cDNA was prepared from spenocytes from 5 mice from each strain and B6.Sle1c2 gene expression was compared to B6 gene expresion.**

Background corr dist: KL-Divergence = 0.0810, L1-Distance = 0.0213, L2-Distance = 0.0006, Normal std = 0.4784

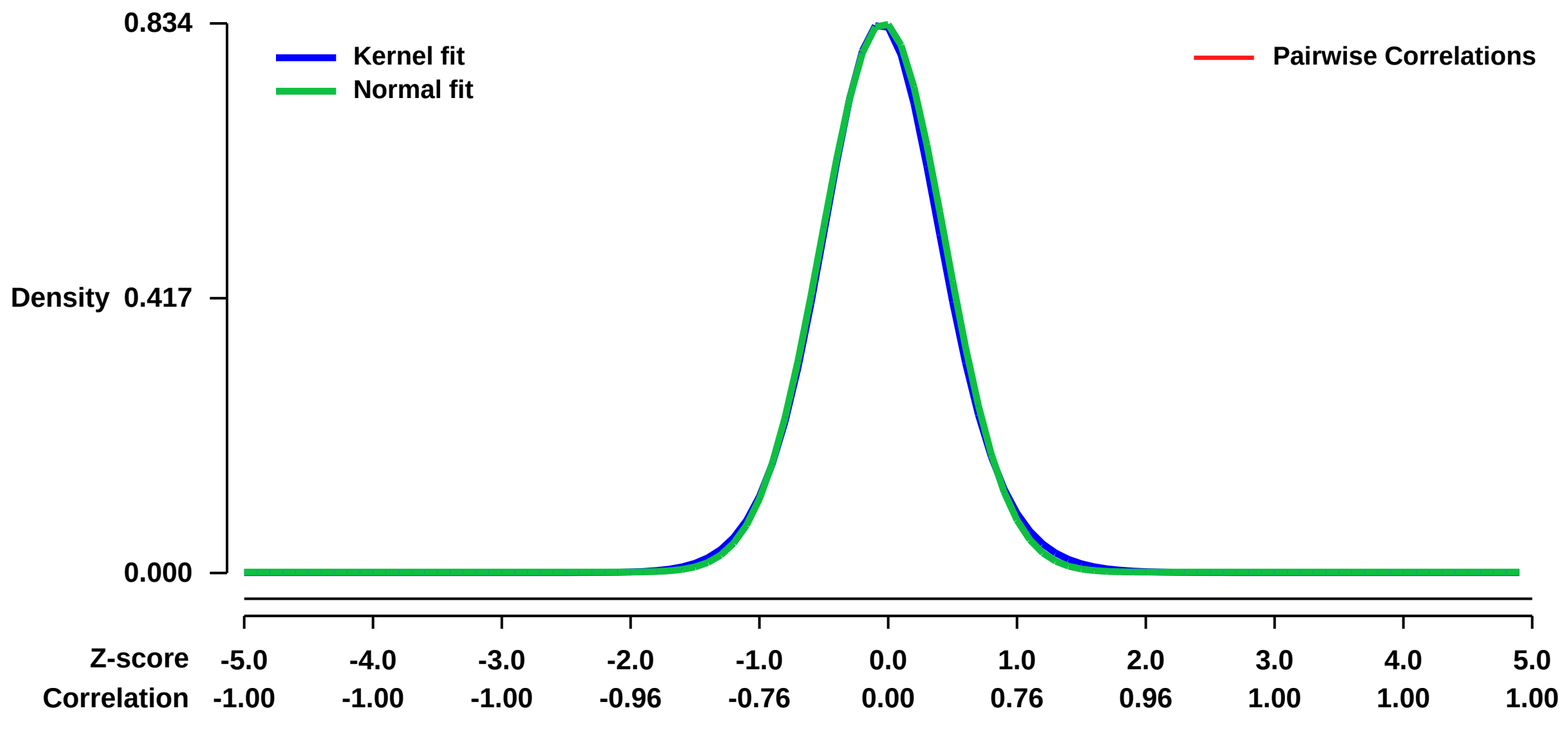

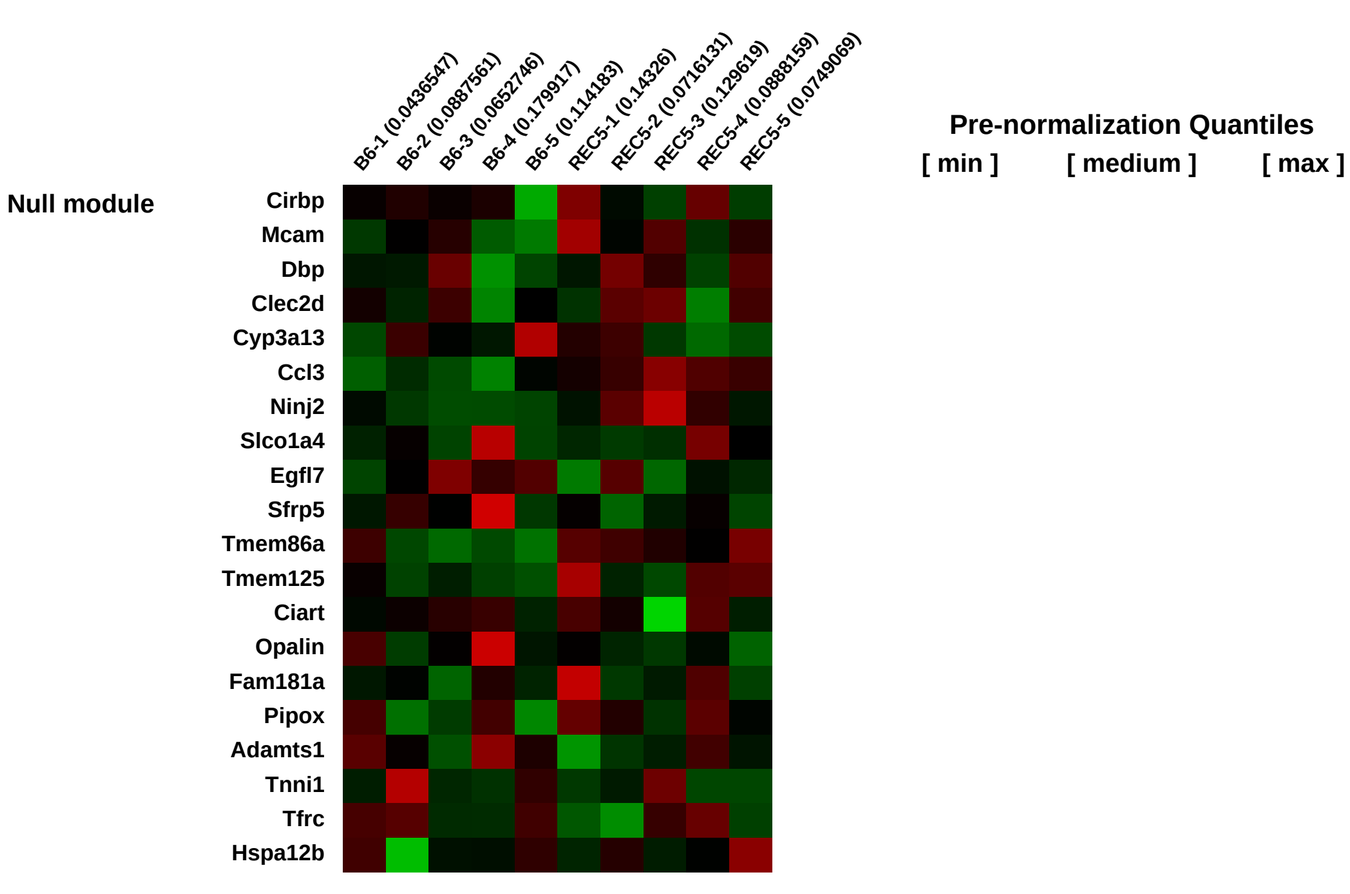

GEO Series "GSE4786" Expression Profiles

Num of samples in this series: 9

Scale of expression profile Z-scores

-3.0 -2.0 -1.0 0.0 1.0 2.0 3.0

GEO Link:	http://www.ncbi.nlm.nih.gov/geo/query/acc.cgi?acc=GSE4786
Status:	Public on May 01 2007
Title:	Caloric restriction suppresses apoptotic cell death in the mammalian cochlea and leads to prevention of presbycusis
Organism:	Mus musculus
Experiment type:	Expression profiling by array
Platform:	GPL1261
Pubmed ID:	16890326
Summary & Design:	**Summary:** Presbycusis is characterized by an age-related progressive decline of auditory function, and arises mainly from the degeneration of hair cells or spiral ganglion (SG) cells in the cochlea. Here we show that caloric restriction suppresses apoptotic cell death in the mouse cochlea and prevents late onset of presbycusis. Caloric restricted mice, which maintained body weight at the same level as that of young control (YC) mice, retained normal hearing and showed no cochlear degeneration. CR mice also showed significantly fewer TUNEL-positive staining cells and fewer cleaved caspase-3-positive staining cells relative to middle-age control (MC) mice. Microarray analysis revealed that CR down-regulated the expression of 28 proapoptotic genes, including Bak and Bim. Taken together, our findings suggest that loss of critical cells through apoptosis is an important mechanism of presbycusis in mammals, and that CR or staying lean can retard this process by suppressing apoptosis in the inner ear tissue. **Keywords:** Effect of aging, effect of caloric restriction, time course, disease state analysis **Overall design:** Quality control measures were not used. No replicates were done. Dye swap was not used.

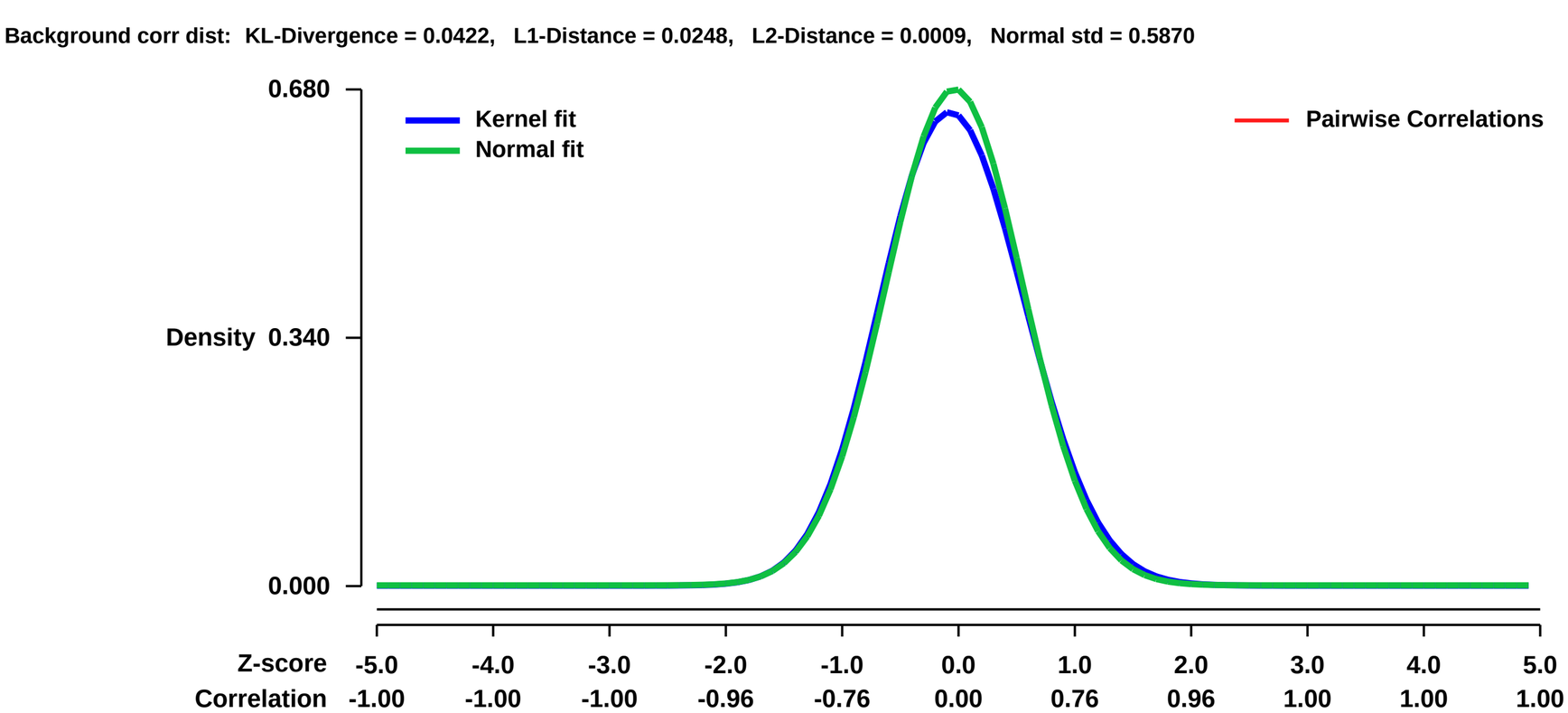

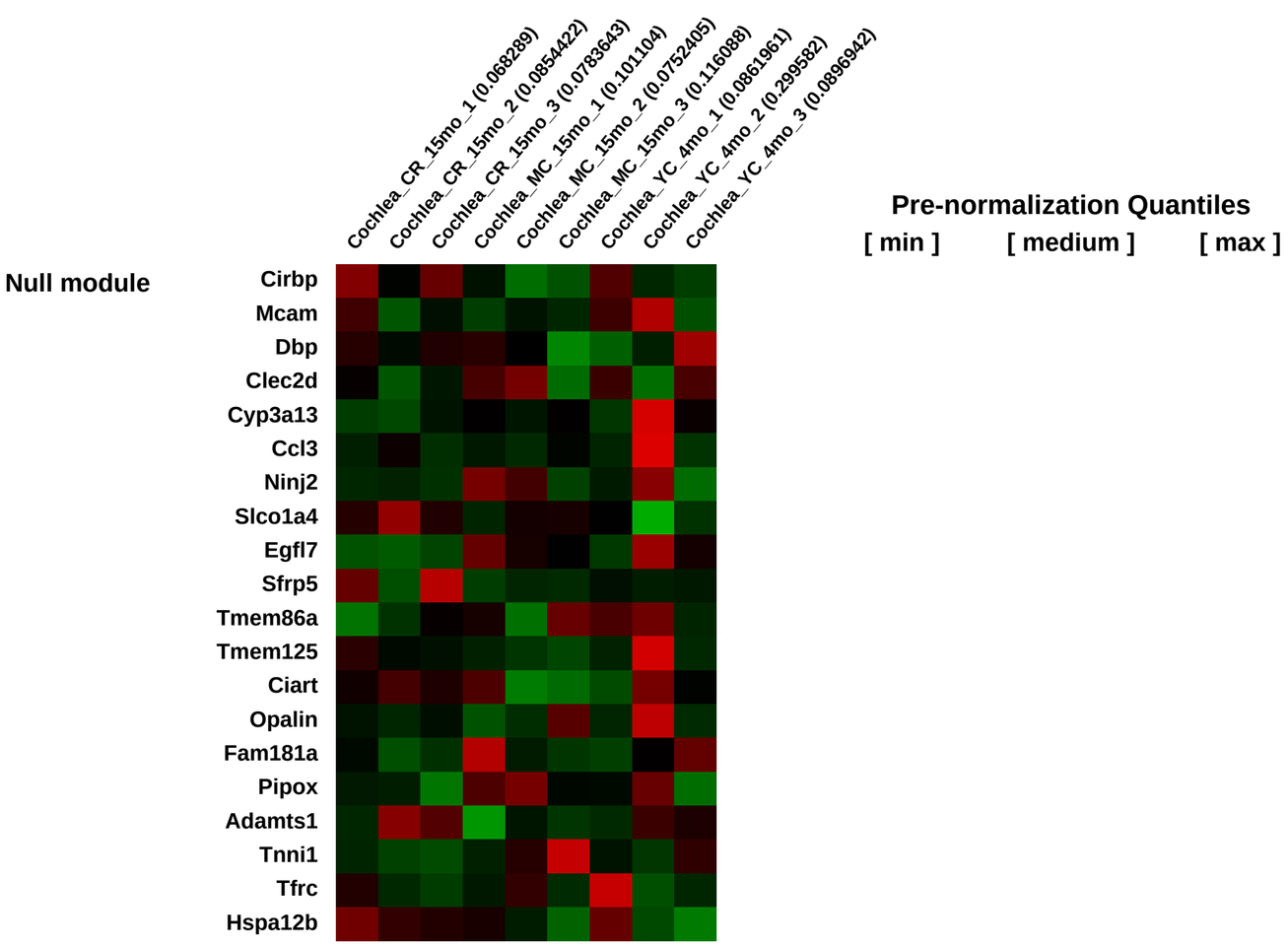

GEO Series "GSE12078" Expression Profiles

Num of samples in this series: 8

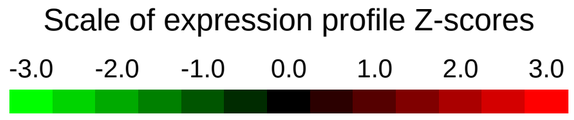

GEO Link:	**http://www.ncbi.nlm.nih.gov/geo/query/acc.cgi?acc=GSE12078**
Status:	**Public on Jul 18 2008**
Title:	**Ctr9 knockdown in mouse ES cells**
Organism:	**Mus musculus**
Experiment type:	**Expression profiling by array**
Platform:	**GPL1261**
Pubmed ID:	**19345177**
Summary & Design:	**Summary:** **To monitor global transcript changes after Paf1C depletion we transfected ESCs with esiRNA targeting Ctr9 and control esiRNA (Luc).** **Overall design:** **4 replicates of esiRNA tranfection controls (luciferase esiRNA) and 4 replicates of Ctr9 esiRNA tranfection samples**

Background corr dist: **KL-Divergence = 0.0399, L1-Distance = 0.0419, L2-Distance = 0.0022, Normal std = 0.6455**

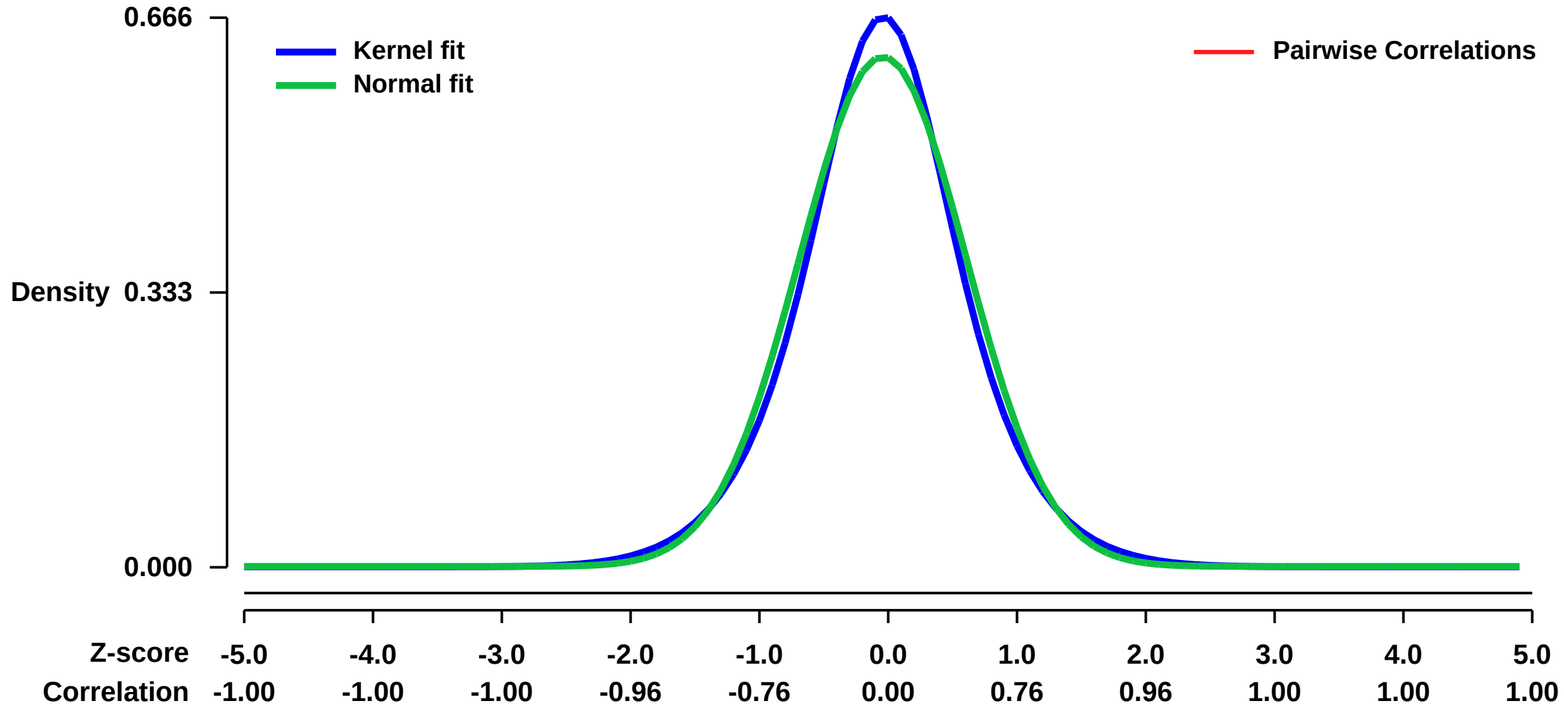

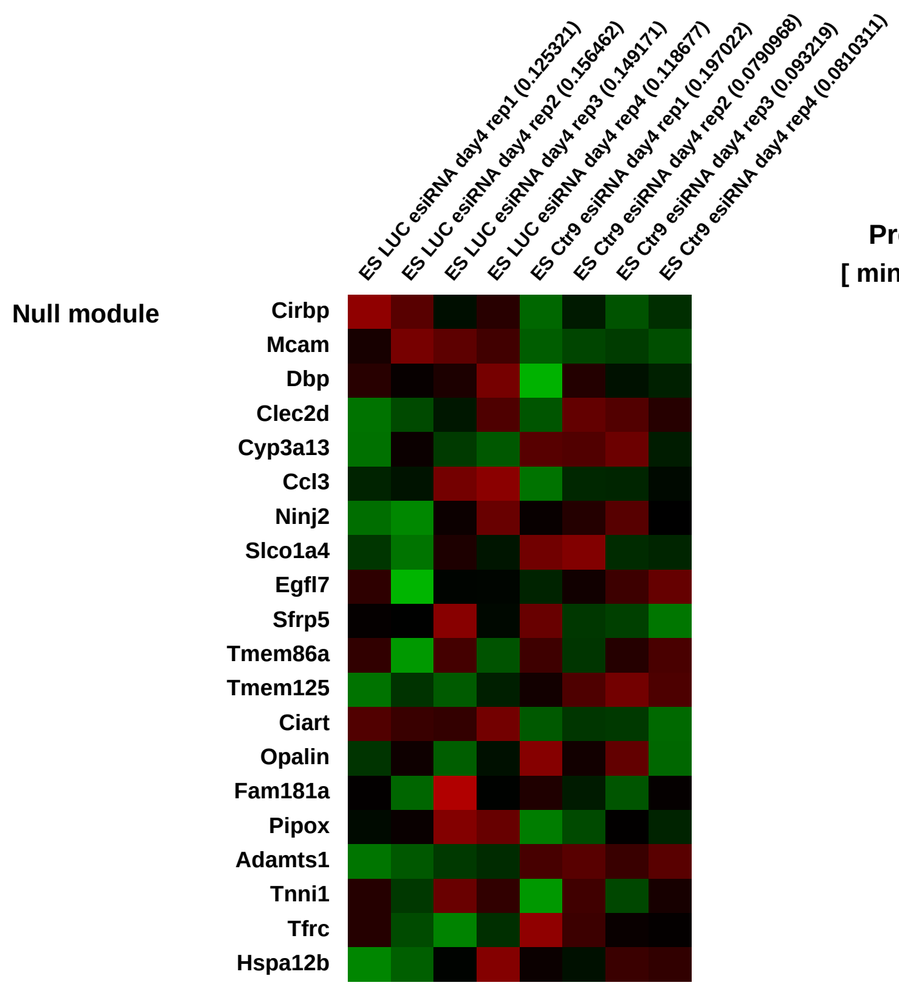

GEO Series "GSE26037" Expression Profiles

Num of samples in this series: 7

Scale of expression profile Z-scores

-3.0 -2.0 -1.0 0.0 1.0 2.0 3.0

GEO Link:	http://www.ncbi.nlm.nih.gov/geo/query/acc.cgi?acc=GSE26037
Status:	Public on Dec 14 2010
Title:	Gene expression analysis in the absence of Creb in Pomc-expressing neurons of the hypothalamus
Organism:	Mus musculus
Experiment type:	Expression profiling by array
Platform:	GPL1261
Pubmed ID:	21187319
Summary & Design:	**Summary:** Brain-derived serotonin favors appetite in mice following its binding to the Htr1a and Htr2b receptors in arcuate neurons of the hypothalamus. In this study, we identified that CREB is the transcriptional effector of brain-derived serotonin control of appetite in arcuate nuclei. **Overall design:** We isolated hypothalami of wild type and Creb-pomcCre-/- (deleted for Creb selectively in arcuate neurons of the hypothalamus) mice and performed microarray experiments.

Background corr dist: KL-Divergence = 0.0609, L1-Distance = 0.0175, L2-Distance = 0.0003, Normal std = 0.5248

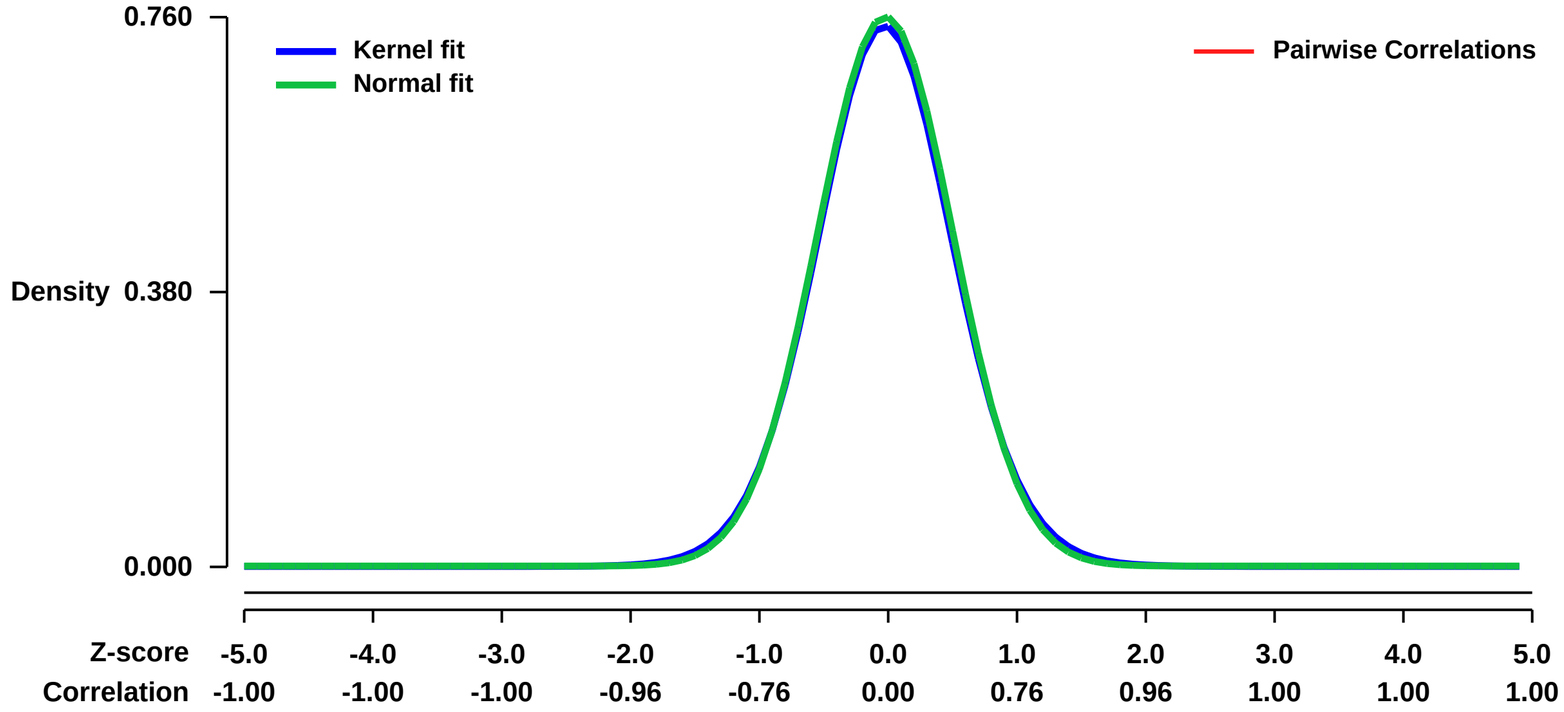

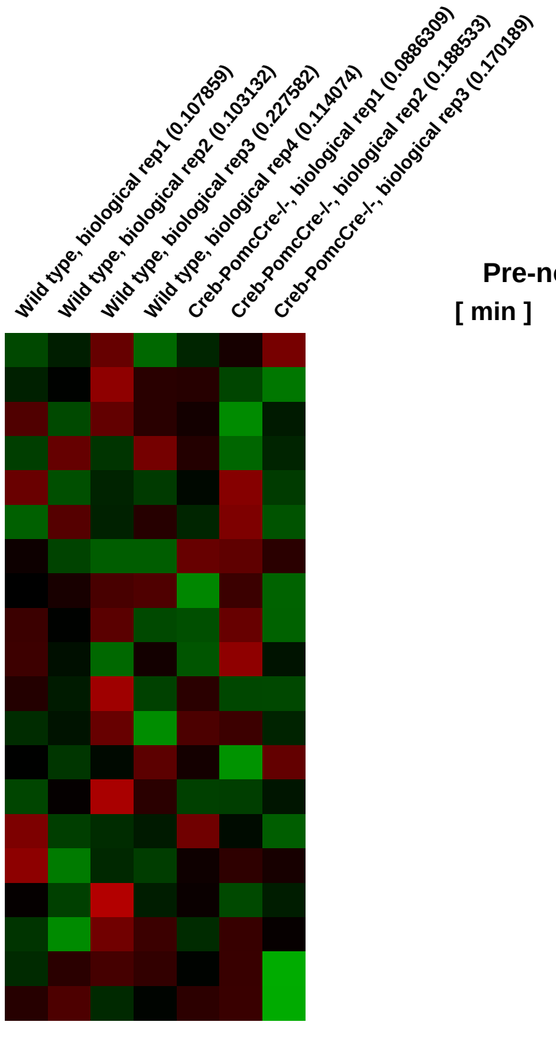

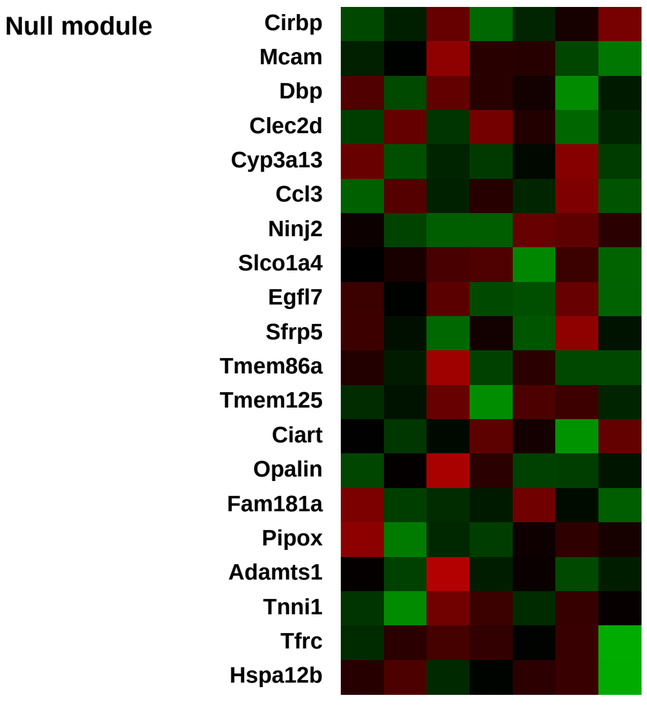

GEO Series "GSE32330" Expression Profiles

Num of samples in this series: 12

Scale of expression profile Z-scores

-3.0 -2.0 -1.0 0.0 1.0 2.0 3.0

GEO Link:	http://www.ncbi.nlm.nih.gov/geo/query/acc.cgi?acc=GSE32330
Status:	Public on Nov 30 2011
Title:	Expression data from C/EBP alpha induced transdifferentiation of pre-B cells into macrophages
Organism:	Mus musculus
Experiment type:	Expression profiling by array
Platform:	GPL1261
Pubmed ID:	21969581
Summary & Design:	**Summary:** Earlier work has shown that pre-B cells can be converted into macrophages by the transcription factor C/EBP? at very high frequencies. Using this system we have now performed a systematic analysis of the question whether during transdifferentiation the cells transiently reactivate progenitor restricted genes or even retrodifferentiate. A transcriptome analysis of transdifferentiating cells showed that most genes are continuously up or downregulated, acquiring a macrophage phenotype within 5 days. In addition, we observed the transient reactivation of a subset of immature myeloid markers, as well as low levels of the progenitor markers Kit and Flt3 and a few lineage inappropriate genes. However, we were unable to observe the re-expression of cell surface marker combinations that characterize hematopoietic stem and progenitor cells (HSPCs), including c-Kit and Flt3. This was the case even when C/EBPalpha was activated in pre-B cells under culture conditions that favor HSPC growth or when the transcription factor was activated in a time limited fashion. Together, our findings are consistent with the notion that the conversion from pre-B cells to macrophages is mostly direct and does not involve overt retrodifferentiation. Our microarray data indicate that most expression changes are direct, and that transdifferentiation does not involve retrodifferentiation. Our data also show that there is a low level transient activation of selected progenitor genes, as well as myeloid precursor genes. **Overall design:** Primary mouse pre-B cells were infected with an inducible form of C/EBPa and cells induced to transdifferentiate with beta Estradiol (b-Est) harvested at different time points to analyze expression profiles, using Affymetrix 430.2 arrays.

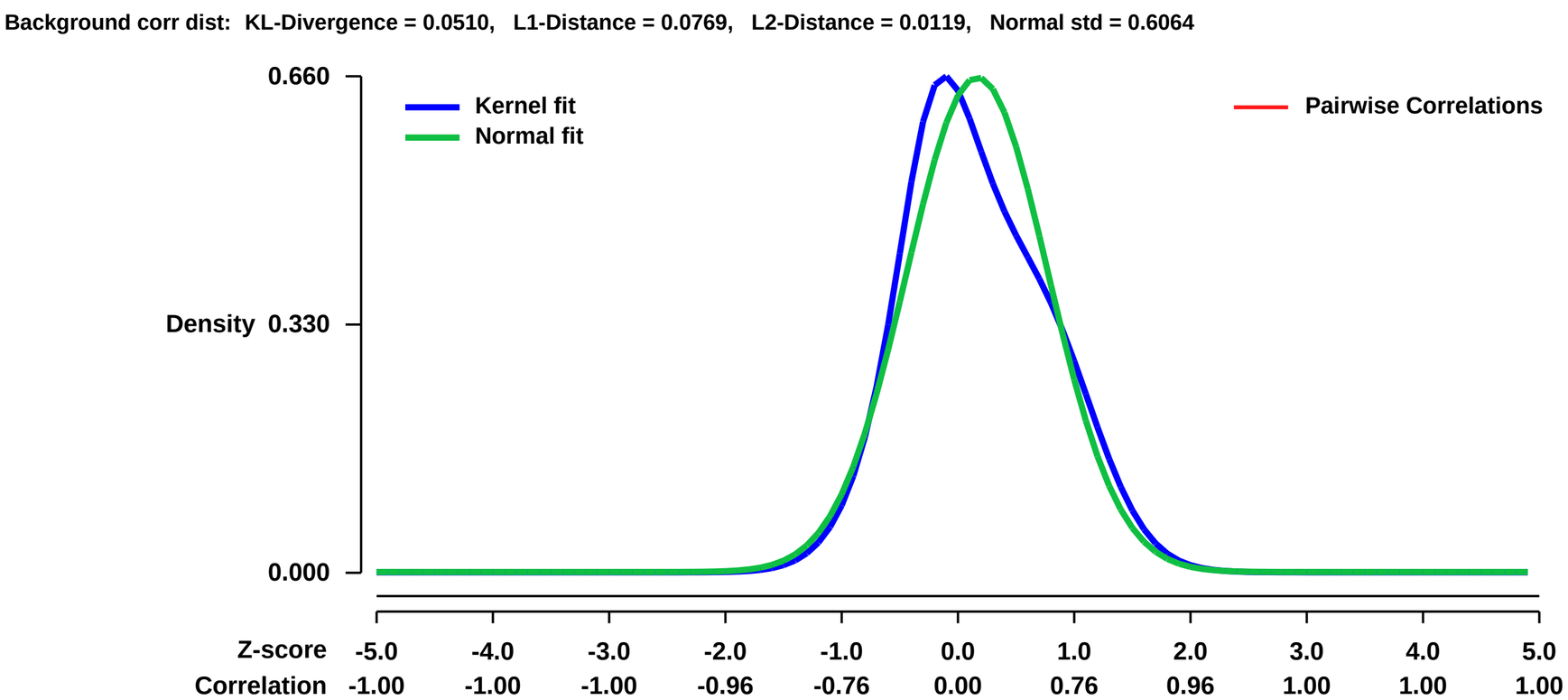

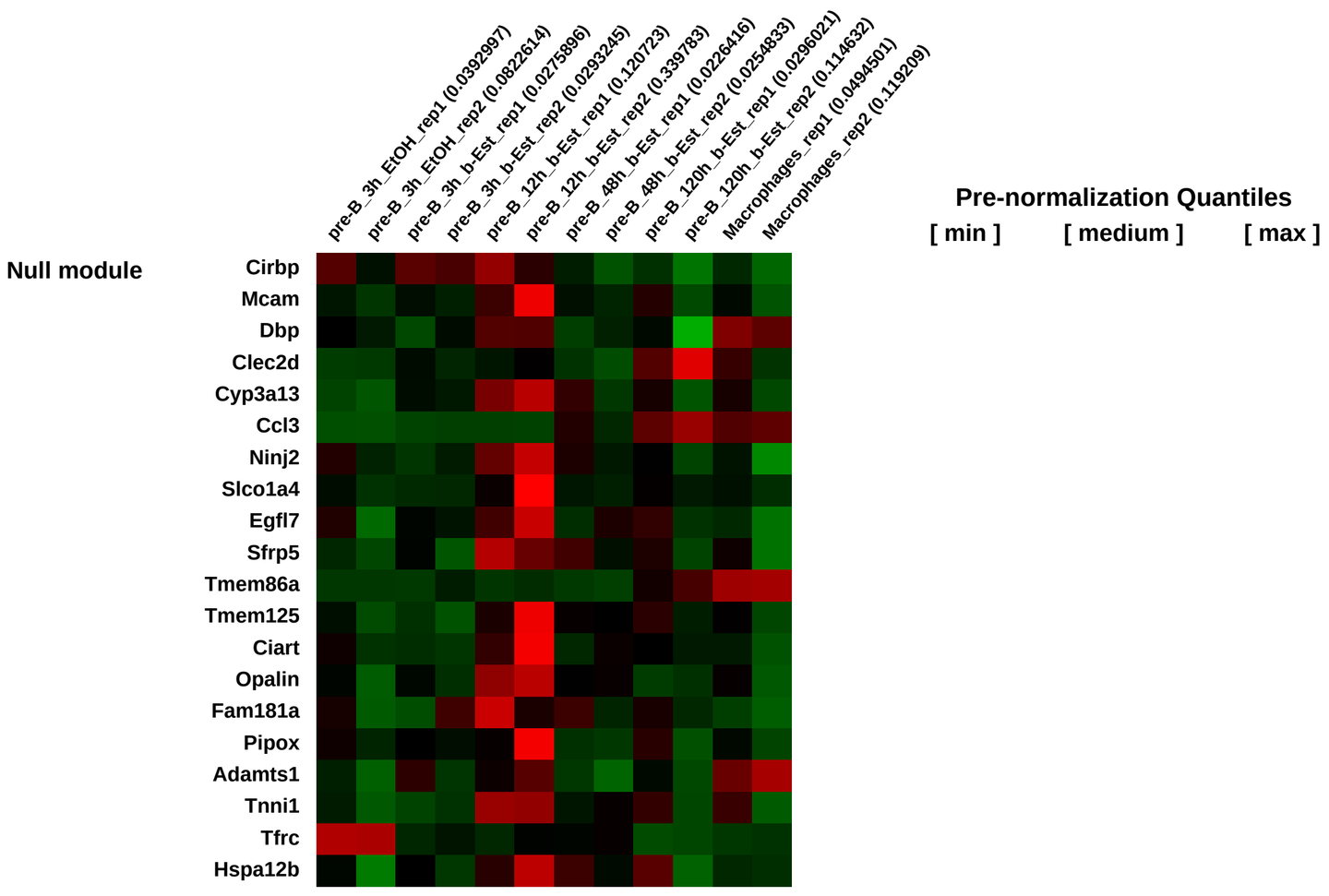

GEO Series "GSE15318" Expression Profiles

Num of samples in this series: 24

Scale of expression profile Z-scores

-3.0 -2.0 -1.0 0.0 1.0 2.0 3.0

GEO Link:	http://www.ncbi.nlm.nih.gov/geo/query/acc.cgi?acc=GSE15318
Status:	Public on Oct 01 2009
Title:	Cdcs1 a major colitis susceptibility locus in mice; subcongenic analysis reveals genetic complexity
Organism:	Mus musculus
Experiment type:	Expression profiling by array
Platform:	GPL1261
Pubmed ID:	19856416
Summary & Design:	**Summary:** Background and Aims: In the interleukin-10-deficient (Il10-/-) mouse model of IBD, 10 quantitative trait loci (QTL) have been shown to be associated with colitis susceptibility by linkage analyses on experimental crosses of highly susceptible C3H/HeJBir (C3Bir)-Il10-/- and partially resistant C57BL/6J (B6)-Il10-/- mice. The strongest locus (C3Bir-derived cytokine deficiency-induced colitis susceptibility [Cdcs]1 on Chromosome [Chr] 3) controlled multiple colitogenic subphenotypes and contributed the vast majority to the phenotypic variance in cecum and colon. This was demonstrated by interval-specific Chr 3 congenic mice wherein defined regions of Cdcs1 from C3Bir or B6 were bred into the IL-10-deficient reciprocal background and altered the susceptible or resistant phenotype. Furthermore, this locus likely acts by inducing innate hypo- and adaptive hyperresponsiveness, associated with impaired NF¸ B responses of macrophages. The aim of the present study was to dissect the complexity of Cdcs1 by further development and characterization of reciprocal Cdcs1 congenic strains and to identify potential candidate genes in the congenic interval. Material and Methods: In total, 15 reciprocal congenic strains were generated from Il10-/- mice of either C3H/HeJBir or C57BL/6J backgrounds by 10 cycles of backcrossing. Colitis activity was monitored by histological grading. Candidate genes were identified by fine mapping of congenic intervals, sequencing, microarray analysis and a high-throughput real-time RT-PCR approach using bone marrow-derived macrophages. Results: Within the originally identified Cdcs1-interval, three independent regions were detected that likely contain susceptibility-determining genetic factors (Cdcs1.1, Cdcs1.2, and Cdcs1.3). Combining results of candidate gene approaches revealed Fcgr1, Cnn3, Larp7, and Alpk1 as highly attractive candidate genes with polymorphisms in coding or regulatory regions and expression differences between susceptible and resistant mouse strains. Conclusions: Subcongenic analysis of the major susceptibility locus Cdcs1 on mouse chromosome 3 revealed a complex genetic structure. Candidate gene approaches revealed attractive genes within the identified regions with homologs that are located in human susceptibility regions for IBD. **Overall design:** Bone marrow derived macrophages (BMDM) of colitis susceptible C3Bir-Il10-/- and colitis resistant B6-Il10-/- as well as the Il10-/- reciprocal congenic strains CB-R1 (C3Bir genetic background carrying a long congenic chromosome 3 element containing Cdcs1 from B6, rendering this formerly susceptible background resistant) and BC-R3 (B6 genetic background that carries the Cdcs1-region of C3Bir) were cultured and stimulated with flagellin or left unstimulated. BMDM were obtained from 3 male mice per genotype and cultured in polystyrene 6-well culture plates. Before RNA-isolation, 3 wells per plate were stimulated with Cbir1 flagellin (and subsequently pooled for RNA isolation), the other 3 wells left unstimulated (and also pooled). In total, these experiments were replicated three times in order to perform microarray analyses in triplicates.

Background corr dist: KL-Divergence = 0.1423, L1-Distance = 0.0369, L2-Distance = 0.0028, Normal std = 0.3807

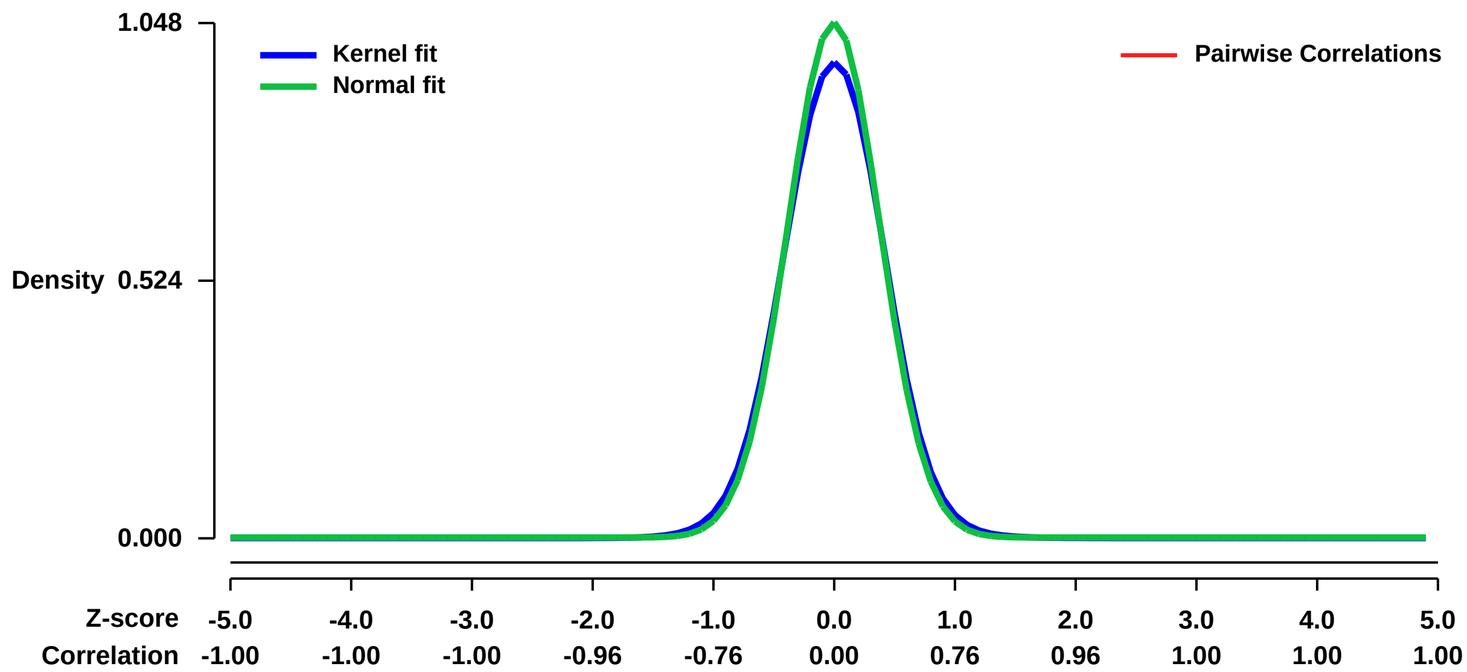

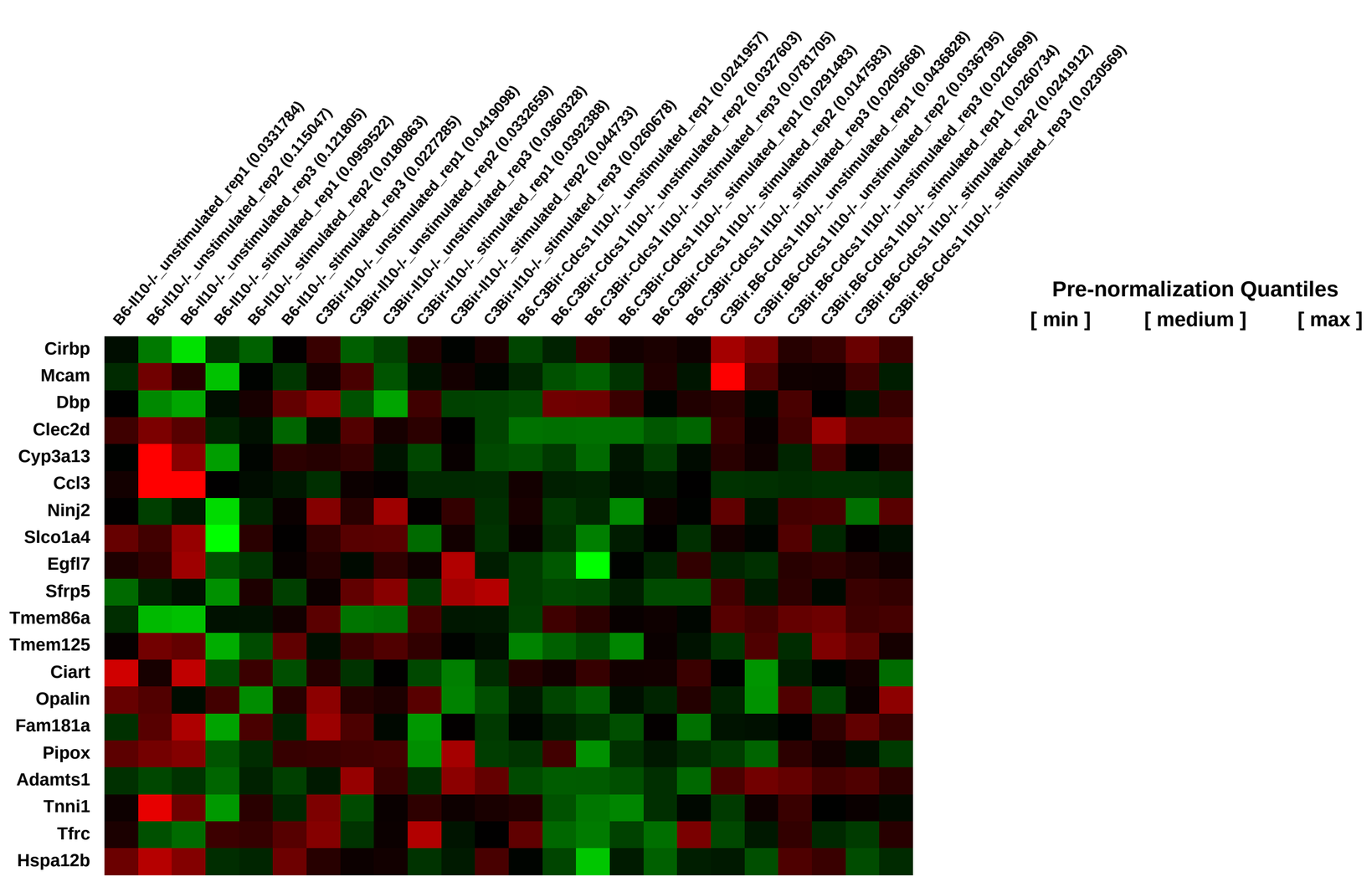

GEO Series "GSE7705" Expression Profiles

Num of samples in this series: 10

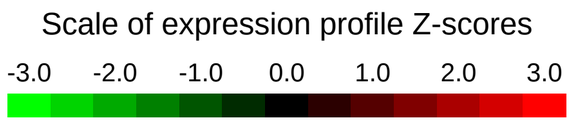

GEO Link:	**http://www.ncbi.nlm.nih.gov/geo/query/acc.cgi?acc=GSE7705**
Status:	**Public on May 01 2008**
Title:	**Microarray analysis of CD4+T cells in murine arthritis**
Organism:	**Mus musculus**
Experiment type:	**Expression profiling by array**
Platform:	**GPL1261**
Pubmed ID:	
Summary & Design:	**Summary:** **Although activated CD4+ T cell-driven overproduction of cytokines, especially TNF and IL1, is generally regarded as the major factor in the development of rheumatoid arthritis (RA), little is known about the precise role of CD4+ T cells in the initiation and progression of this disease. In this study, this issue was addressed using a time-course microarray analysis in a mouse model of RA, Il1rn deficient mice.No obvious cytokine gene expression changes reflecting T cell activation was observed in CD4+ T cells in the Il1rn deficient mice during the course of spontaneous arthritis. On the contrast, majority of dysregulated genes were those predominantly expressed in myeloid lineage cells, suggesting T cell reprogramming involvement in arthritis development. Distinct gene expression patterns were identified for different stages of disease, including downregulated expression of immunoglobulin heavy chain constant region genes and increased expression of inflammatory genes in the early phase, and downregulation of MHC class II genes in the late phase. The common changes occurred in both early and late phases included upregulation of Arl2bp and Mfap1, which are involved in the regulation of cytoskeletal dynamics.** **Keywords: Time course** **Overall design:** **Two KO mice and three WT mice for each time point (1 month and 4 month) were used for this study.**

Background corr dist: KL-Divergence = 0.0808, L1-Distance = 0.0282, L2-Distance = 0.0010, Normal std = 0.4856

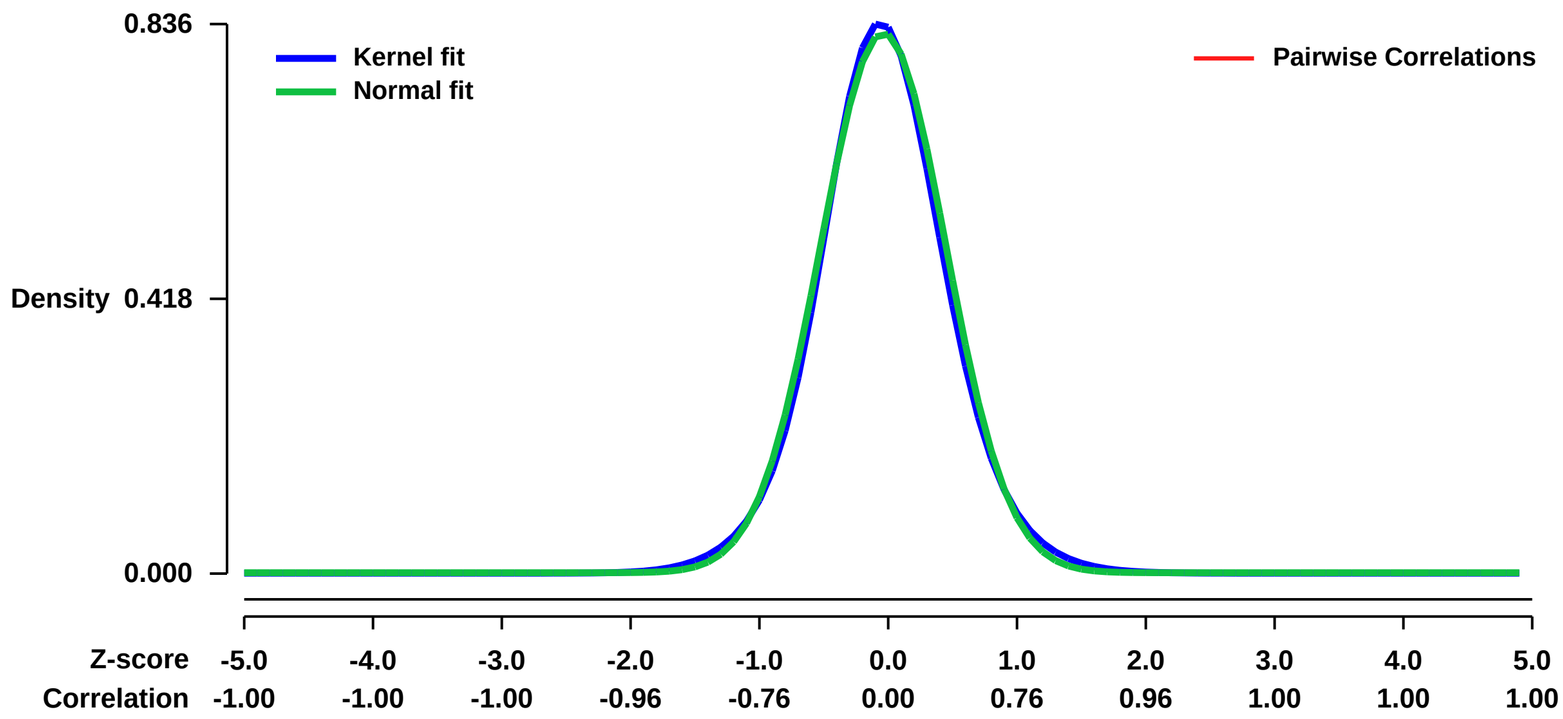

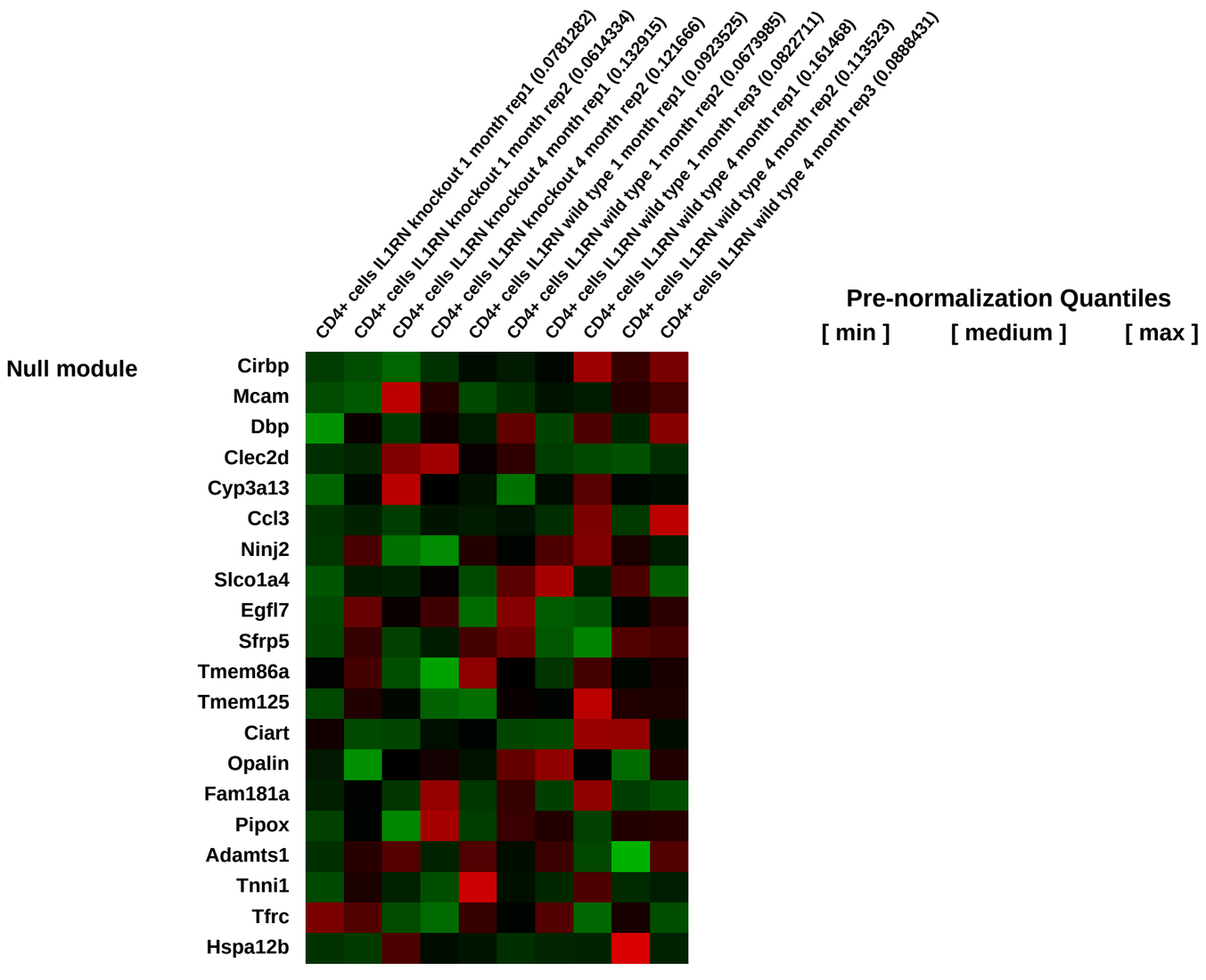

GEO Series "GSE10639" Expression Profiles

Num of samples in this series: 8

Scale of expression profile Z-scores

-3.0 -2.0 -1.0 0.0 1.0 2.0 3.0

GEO Link:	http://www.ncbi.nlm.nih.gov/geo/query/acc.cgi?acc=GSE10639
Status:	Public on Feb 28 2008
Title:	Differential expression of genes in pancreatic islets from high fat fed AKR/J and C57Bl/6J
Organism:	Mus musculus
Experiment type:	Expression profiling by array
Platform:	GPL1261
Pubmed ID:	18854371
Summary & Design:	**Summary:** Increased fat intake is associated with obesity and insulin resistance. In some individuals, a failure of pancreatic b-cells to increase insulin production in response to the high demands of obesity leads to diabetes. We sought to determine whether the impaired b- cell adaptation in obesity is associated with differential expression of genes involved in b-cell expansion and intermediary metabolism. Two strains of inbred mice prone to obesity, C57Bl/6J and AKR/J, were fed regular rodent chow or high-fat diet, after which islet morphology, secretory function and gene expression were assessed. AKR/J had lower blood glucose and higher insulin levels compared with C57Bl/6J mice on regular rodent chow or high fat diet. Insulin secretion was 3.2 fold higher in AKR/J than C57Bl/6J mice following intraperitoneal glucose injection. Likewise, glucose-stimulated insulin secretion from isolated islets was higher in AKR/J. Additionally, islet mass was 1.4 fold greater in AKR/J compared with C57Bl/6J. To elucidate the factors associated with the differences in insulin, we analyzed the gene expression profiles in pancreatic islets in AKR/J and C57Bl/6J mice. Of 14,000 genes examined, 220 were up-regulated and 286 were down-regulated in islets from diet-induced obese AKR/J mice compared with C57Bl/6J mice. Key genes involved in islet signaling and metabolism, e.g. glucagon like peptide-1 receptor, sterol Co-A desaturase 1 & 2 and fatty acid desaturase 2 were upregulated in obese AKR/J mice. The expression of multiple extracellular matrix proteins was also increased in AKR/J mice, suggesting a role in modulation of islet mass. Functional analyses of differentially regulated genes hold promise for elucidating factors linking obesity to alterations in islet function. **Keywords:** response to high fat diet **Overall design:** Microarray analyses were performed on quadruplicate RNA samples of pancreatic islets from AKR and Bl6 mice placed on high-fat diet for 3 months. Pancreases from two mice were combined to yield one sample of islet RNA. All protocols were conducted as described in the Affymetrix GeneChips Expression Analysis Technical Manual (Affymetrix, Santa Clara, CA) using 5 ¸…g total RNA and GeneChip Mouse Expression Arrays MOE 430 (Affymetrix).

Background corr dist: KL-Divergence = 0.0684, L1-Distance = 0.0758, L2-Distance = 0.0074, Normal std = 0.6701

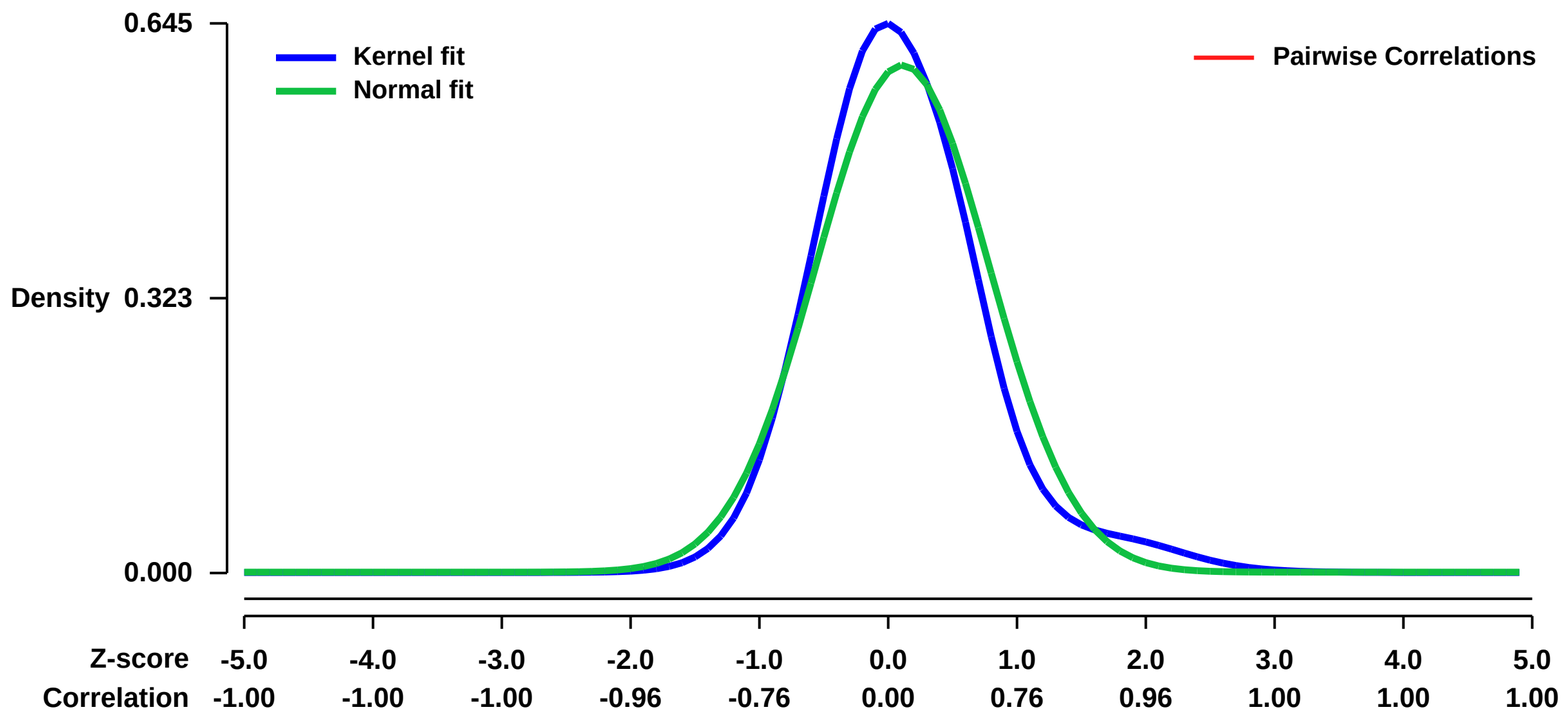

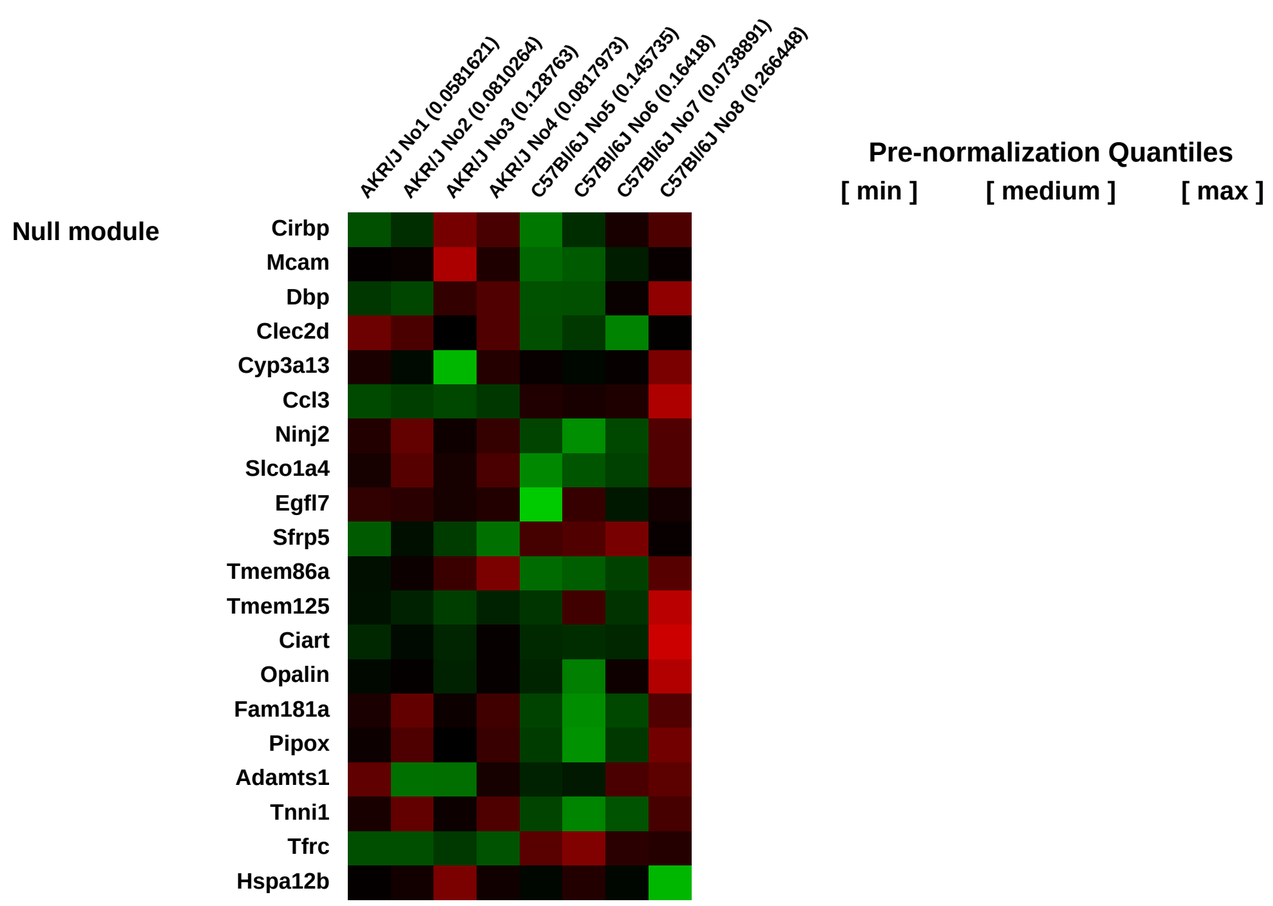

GEO Series "GSE35543" Expression Profiles

Num of samples in this series: 6

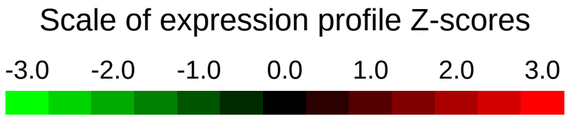

GEO Link:	http://www.ncbi.nlm.nih.gov/geo/query/acc.cgi?acc=GSE35543
Status:	Public on Dec 06 2012
Title:	Gene expression profiling of in vitro derived induced and natural FOXP3+ regulatory T cells and ex-iTreg cells in the mouse
Organism:	Mus musculus
Experiment type:	Expression profiling by array
Platform:	GPL1261
Pubmed ID:	23125413
Summary & Design:	**Summary:** Induced Treg (iTreg) cells are essential for tolerance and can be used therapeutically, yet their stability in vivo and mechanisms of suppression are unresolved. Here, we used a treatment model of colitis to examine the role of autologous IL-10 in iTreg cell function. Mice treated with IL-10+/+ iTreg cells in combination with IL-10â /â natural Treg (nTreg) cells survived and gained weight, even though iTreg cells were numerically disadvantaged and comprised just ~20% of all Treg cells in treated mice. Notably, ~85% of the transferred iTreg cells lost Foxp3 expression (ex-iTreg) but retained a portion of the iTreg transcriptome which failed to limit their pathogenic potential. The TCR repertoires of iTreg and ex-iTreg cells exhibited almost no overlap, which indicates that the two populations are clonally unrelated and maintained by different selective pressures. These data demonstrate a potent and critical role for iTreg cell produced IL-10 that can supplant the IL-10 produced by nTreg cells and compensate for the inherent instability of the iTreg population. **Overall design:** BALB/c Rag1-/- mice were treated with 500,00 WT nTreg cells plus 500,000 WT in-vitro-derived iTreg cells. After 125 days cells were sorted by flow cytometry from spleens and mesenteric lymph nodes from 14 treated mice. EGFP+ Thy1.1+ iTreg cells, EGFP+ Thy1.1â nTreg cells, and EGFPâ Thy1.1+ ex-iTreg cells were pooled and used to generate total RNA for each iTreg, nTreg, and ex-iTreg array set, which was labeled and hybridized to Affymetrix 430 2.0 GeneChips in accordance to the manufacturerâ s protocol. Two sets of arrays were performed, and the results were averaged. Both iTreg and nTreg array sets were compared to a) naˆflve CD4+EGFPâ Tconv cells from Foxp3EGFP. The subset of probe sets whose expression increased or decreased by twofold or more relative to Tconv cells as a common standard was identified and used for further analysis.

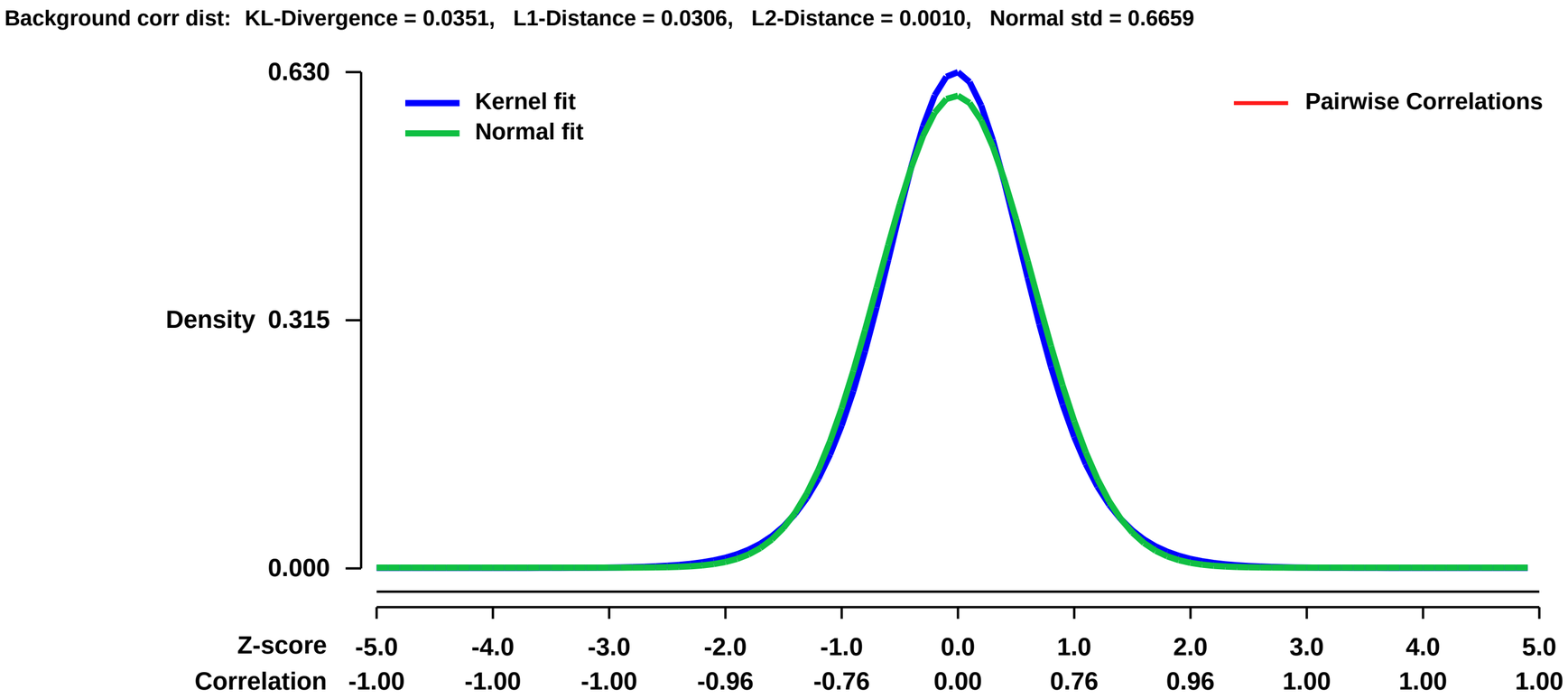

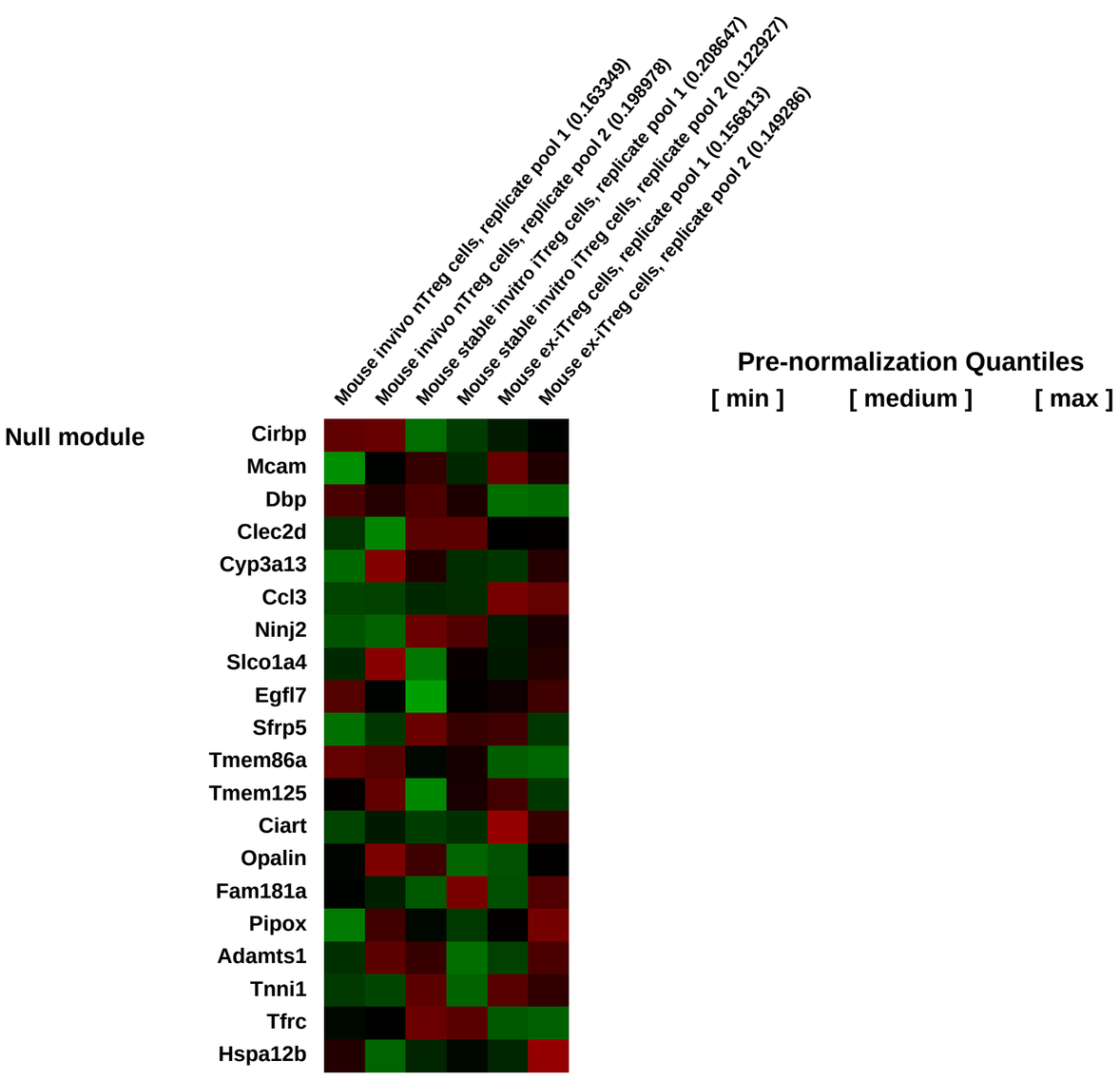

GEO Series "GSE6589" Expression Profiles

Num of samples in this series: 11

Scale of expression profile Z-scores

-3.0 -2.0 -1.0 0.0 1.0 2.0 3.0

GEO Link: http://www.ncbi.nlm.nih.gov/geo/query/acc.cgi?acc=GSE6589

Status: Public on Dec 23 2006

Title: Gene expression profiles of components isolated from developing kidney at E15.5 using LCM. (GUDMAP Series ID: 12)

Organism: Mus musculus

Experiment type: Expression profiling by array

Platform: GPL1261

Pubmed ID:

Summary & Design:

Summary:
The long term objective is to create an encyclopedia of the expression levels of all genes in multiple components of the developing kidney. The central thesis is straightforward. The combination of laser capture microdissection (LCM) plus microarray analysis offers a powerful, efficient and effective method for the creation of a global gene expression atlas of the developing kidney. Microarrays with essentially complete genome coverage can be used to quantitate expression levels of every gene in laser capture microdissected components of the developing kidney. The ensuing rapid read-out provides an expression atlas that is more sensitive, more economical and more complete than would be possible by in situ hybridizations alone.

Keywords: Comparison of kidney components.

Overall design:
At specific developmental time points we isolate discrete elements of the kidney by using laser capture microdissection and then define their gene expression profiles with microarrays.

Background corr dist: KL-Divergence = 0.1337, L1-Distance = 0.0480, L2-Distance = 0.0054, Normal std = 0.3999

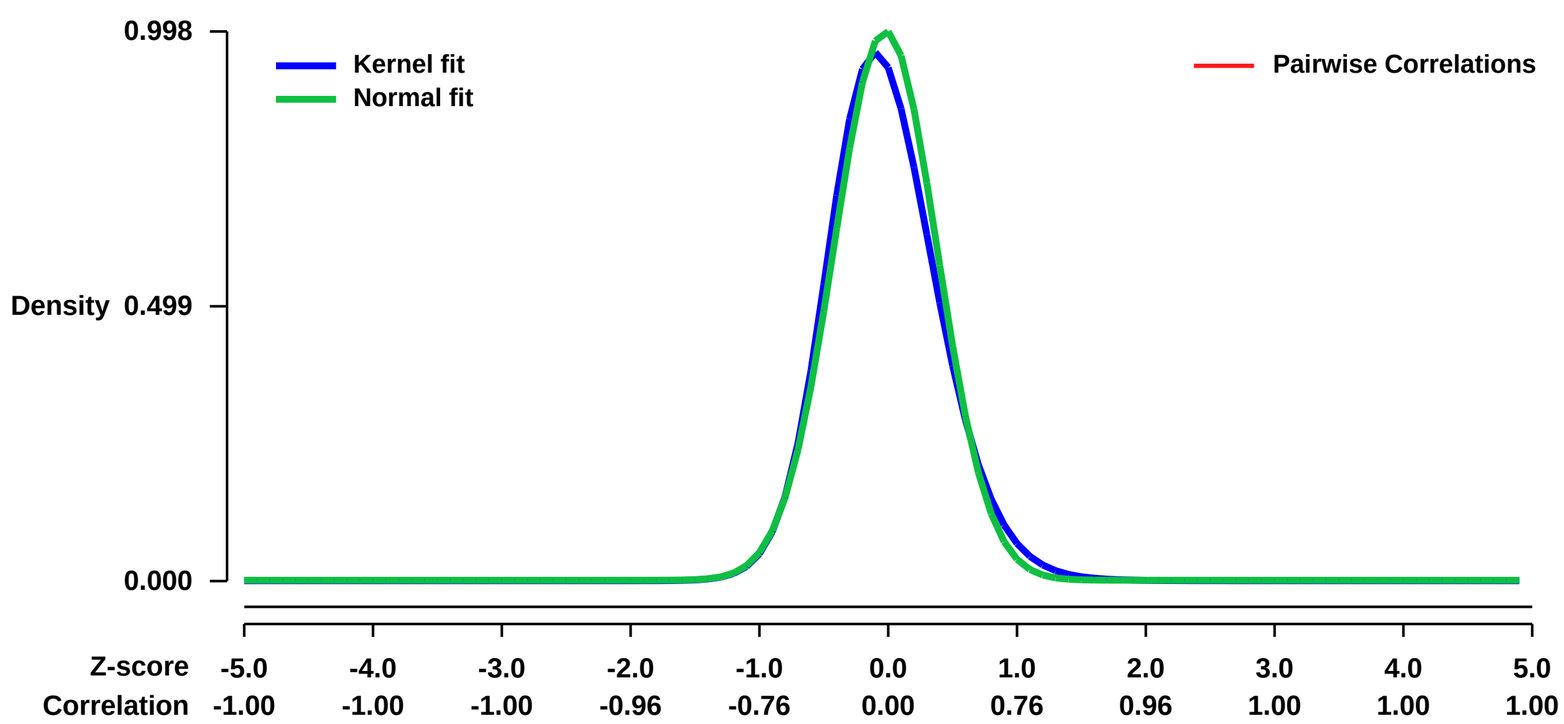

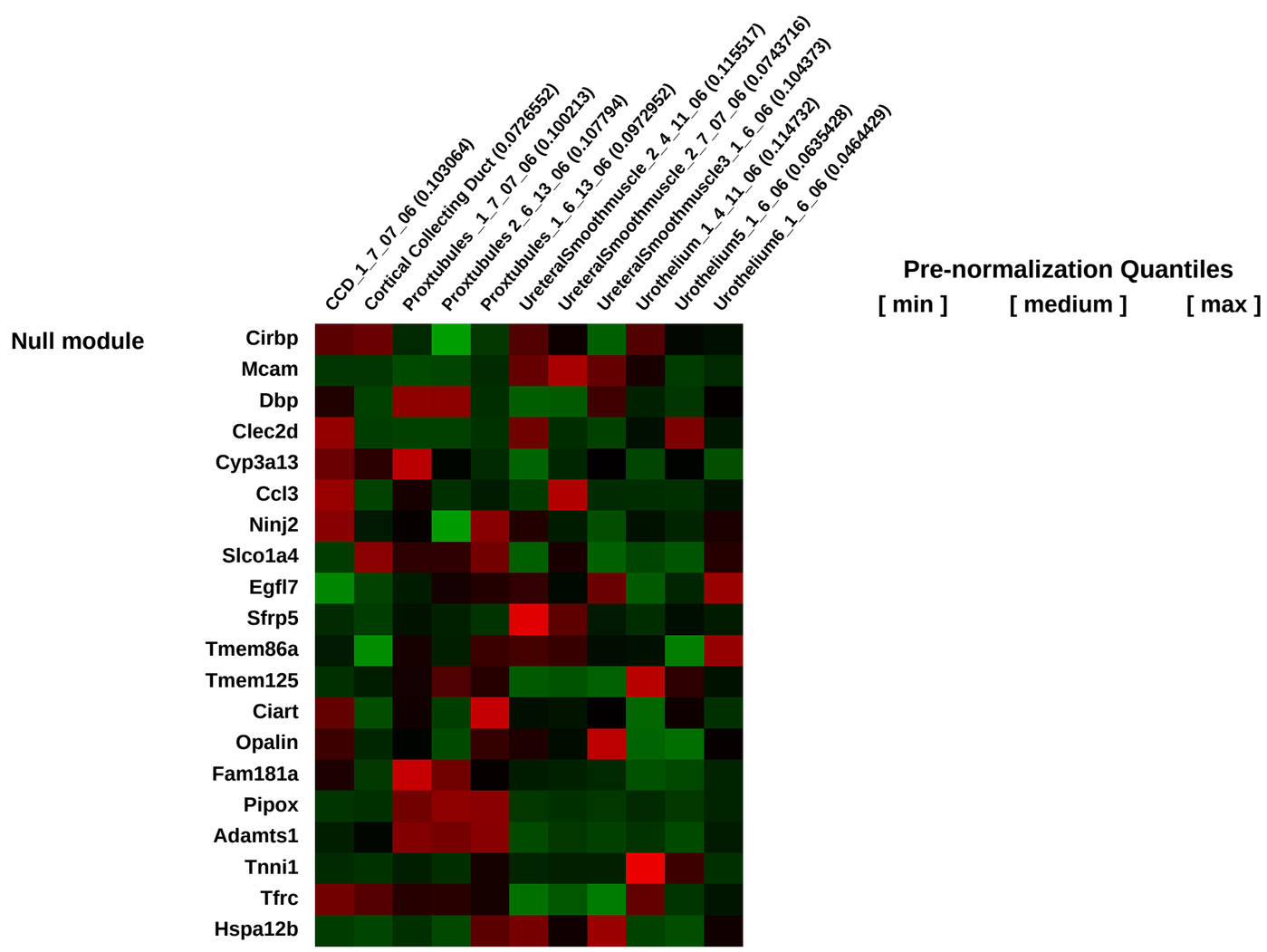

GEO Series "GSE17886" Expression Profiles

Num of samples in this series: 16

Scale of expression profile Z-scores

-3.0 -2.0 -1.0 0.0 1.0 2.0 3.0

GEO Link:	http://www.ncbi.nlm.nih.gov/geo/query/acc.cgi?acc=GSE17886
Status:	Public on Mar 22 2010
Title:	Gene expression data of BBB and BCB two-cell embryos
Organism:	Mus musculus
Experiment type:	Expression profiling by array
Platform:	GPL1261
Pubmed ID:	20107036
Summary & Design:	**Summary:** We constructed one-cell stage embryos by maternal pronuclear (mPN) transfer having B6 ooplasm, B6 paternal PN (pPN), and either B6 or C3H mPN (BBB and BCB, respectively). We collected embryos of each type that were either treated (BBB+a, BCB+a) or untreated with ¸–-amanitin (BBB, BCB) at the two-cell stage for microarray analysis. Comparison of the transcriptomes of these different kinds of embryos revealed genes for which expression differs according to maternal PN strain of origin, and the ¸–-amanitin data revealed which of these differences is due to gene transcription, as opposed to any transcription-independent differences attributable to ooplasm-derived maternal mRNA pools. **Overall design:** There are 4 replicates for each kind/treatment two-cell embryos (BBB, BCB, BBB+a, BCB+a).

Background corr dist: KL-Divergence = 0.0287, L1-Distance = 0.0723, L2-Distance = 0.0067, Normal std = 0.7860

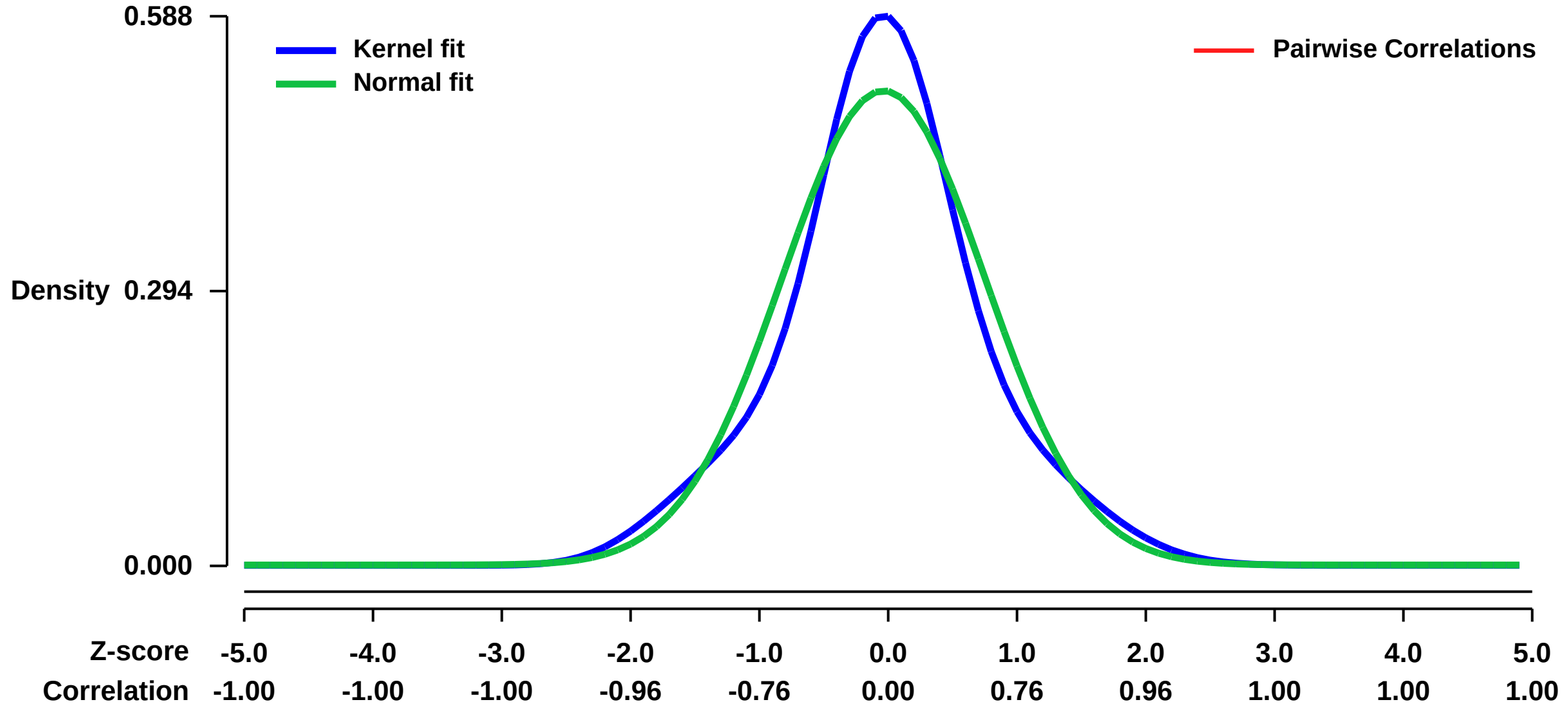

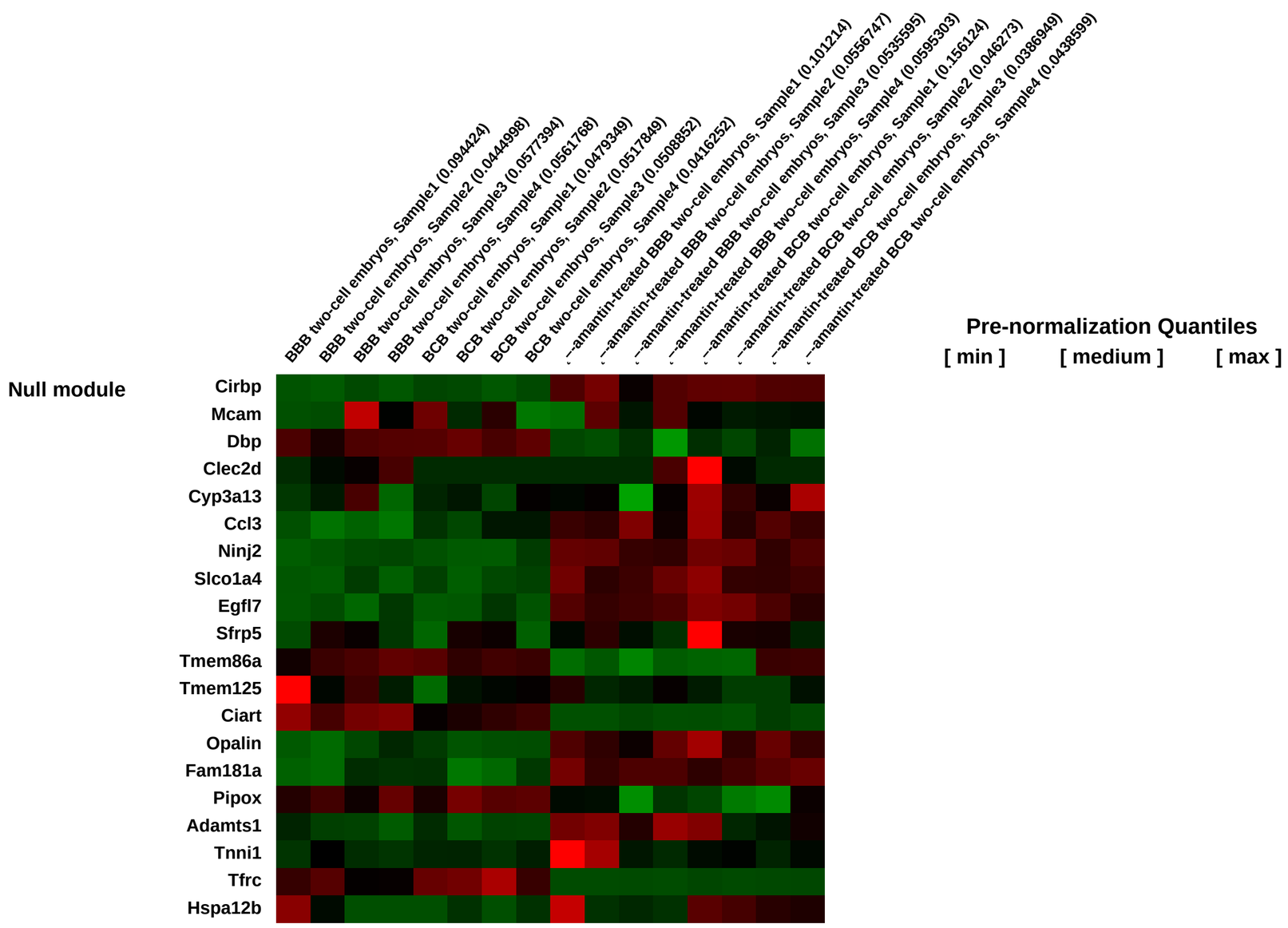

GEO Series "GSE24789" Expression Profiles

Num of samples in this series: 9

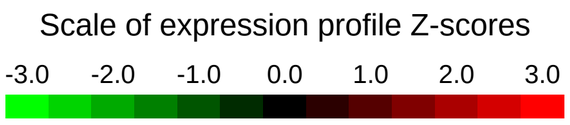

GEO Link:	http://www.ncbi.nlm.nih.gov/geo/query/acc.cgi?acc=GSE24789
Status:	Public on Mar 03 2011
Title:	Expression data from mouse ovarian surface epithelium cells at different stages of malignancy
Organism:	Mus musculus
Experiment type:	Expression profiling by array
Platform:	GPL1261
Pubmed ID:	21390237
Summary & Design:	**Summary:** Ovarian cancer is one of the most deadly cancers accounting for only 3% of diagnosed cancers, but is the fifth leading cause of cancer deaths among woman; however, the progression of ovarian cancer is poorly understood. To study and further understand the early events that lead to epithelial derived ovarian cancer, we previously developed a cell model of progressive ovarian cancer. Mouse ovarian surface epithelial (MOSE) cells have undergone spontaneous transformation in cell culture and represent pre-neoplastic, non-tumorigenic to an aggressive malignant phenotype. Microarray analysis was performed with RNA isolated from different stages of MOSE cells to examine changes in gene expression as MOSE cells transition from a pre-neoplastic to a malignant state. **Overall design:** RNA was isolated from MOSE early cell representing a pre-neoplastic, non-malignant stage, MOSE Intermediate cells representing a noeplastic, pre-invasive state, and MOSE Late cells representing a malignant, invasive stage. Three biological replicates were used to take into account variations within the heterogeneous cultures.

Background corr dist: KL-Divergence = 0.0820, L1-Distance = 0.0244, L2-Distance = 0.0010, Normal std = 0.4764

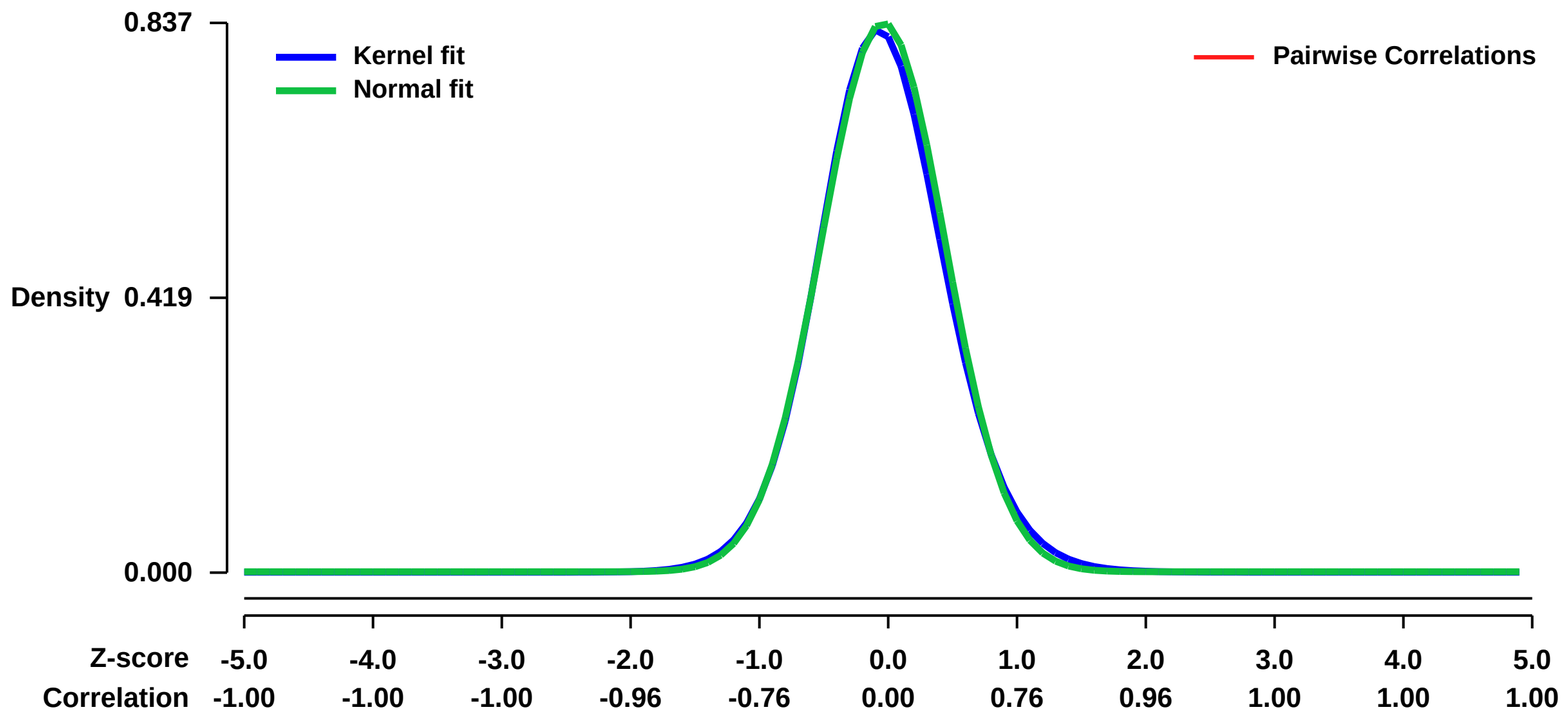

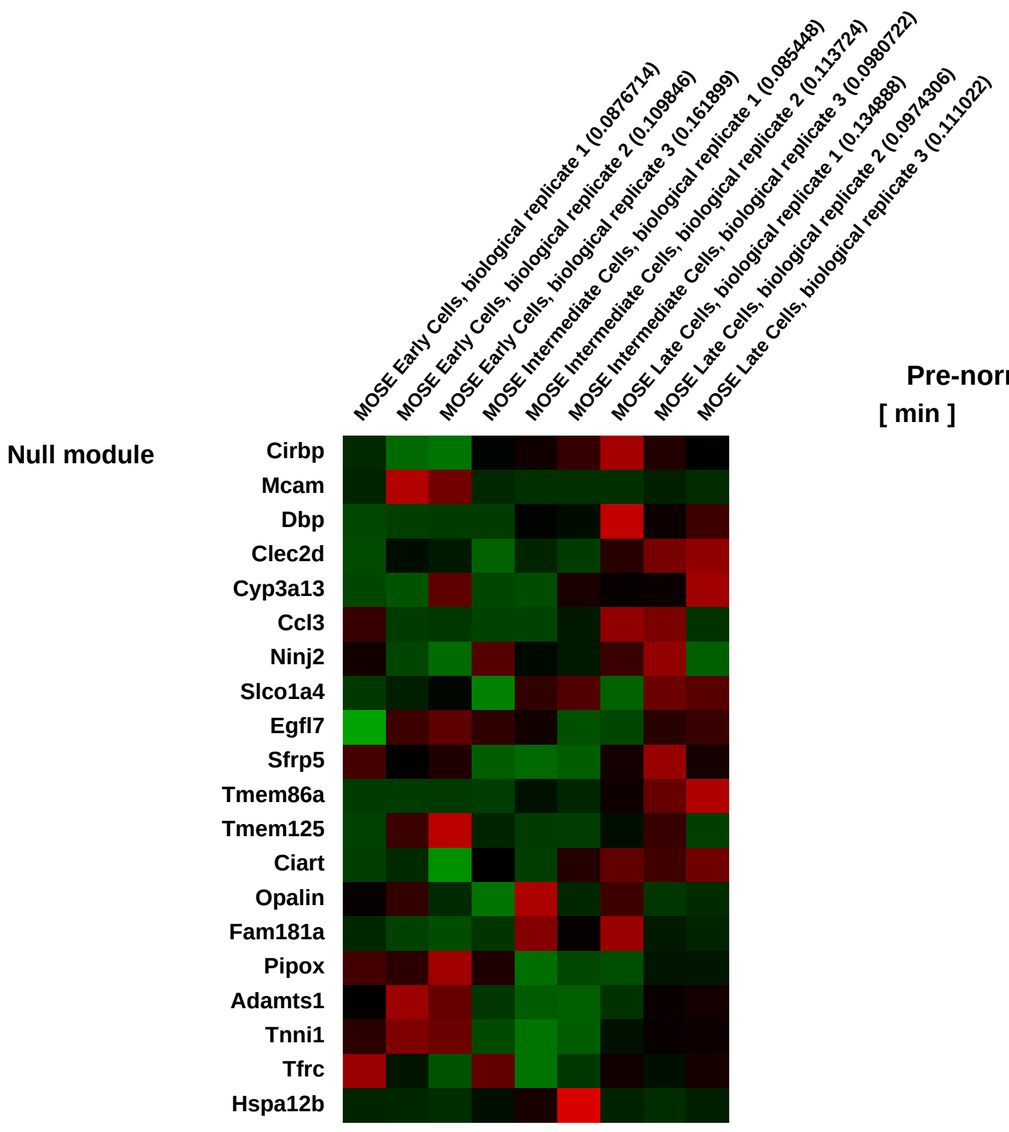

GEO Series "GSE56321" Expression Profiles

Num of samples in this series: 12

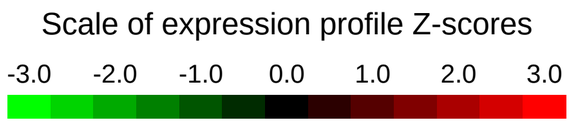

GEO Link:	http://www.ncbi.nlm.nih.gov/geo/query/acc.cgi?acc=GSE56321
Status:	Public on Mar 28 2014
Title:	SIRT4 KO livers microarray
Organism:	Mus musculus
Experiment type:	Expression profiling by array
Platform:	GPL1261
Pubmed ID:	24043310
Summary & Design:	**Summary:** Sirtuins are a family of protein deacetylases, deacylases, and ADP-ribosyltransferases that regulate life span, control the onset of numerous age-associated diseases, and mediate metabolic homeostasis. We have uncovered a novel role for the mitochondrial sirtuin SIRT4 in the regulation of hepatic lipid metabolism during changes in nutrient availability. We show that SIRT4 levels decrease in the liver during fasting and that SIRT4 null mice display increased expression of hepatic peroxisome proliferator activated receptor (PPAR) target genes associated with fatty acid catabolism. Accordingly, primary hepatocytes from SIRT4 knockout (KO) mice exhibit higher rates of fatty acid oxidation than wild-type hepatocytes, and SIRT4 overexpression decreases fatty acid oxidation rates. The enhanced fatty acid oxidation observed in SIRT4 KO hepatocytes requires functional SIRT1, demonstrating a clear cross talk between mitochondrial and nuclear sirtuins. Thus, SIRT4 is a new component of mitochondrial signaling in the liver and functions as an important regulator of lipid metabolism. **Overall design:** SIRT4 knockout (KO) and wild-type (WT) littermates (male; n 6 per genotype; 7- to 8-month-old littermates) were sacrificed after a 16-h overnight fast. Samples were individually hybridized on Affymetrix Mouse Genome 430 2.0 GeneChips by the Biopolymers Facility (Harvard Medical School).

Background corr dist: KL-Divergence = 0.1803, L1-Distance = 0.0453, L2-Distance = 0.0044, Normal std = 0.3452

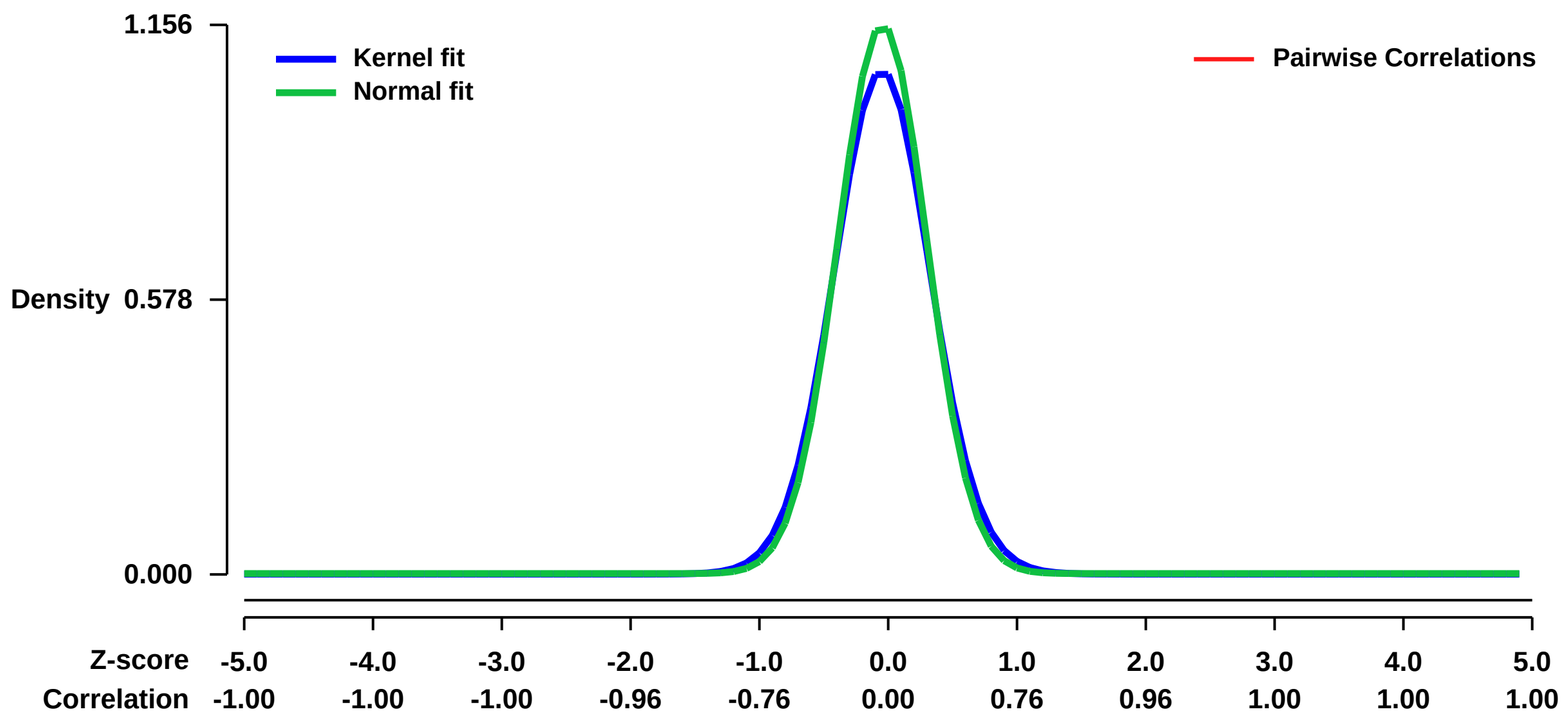

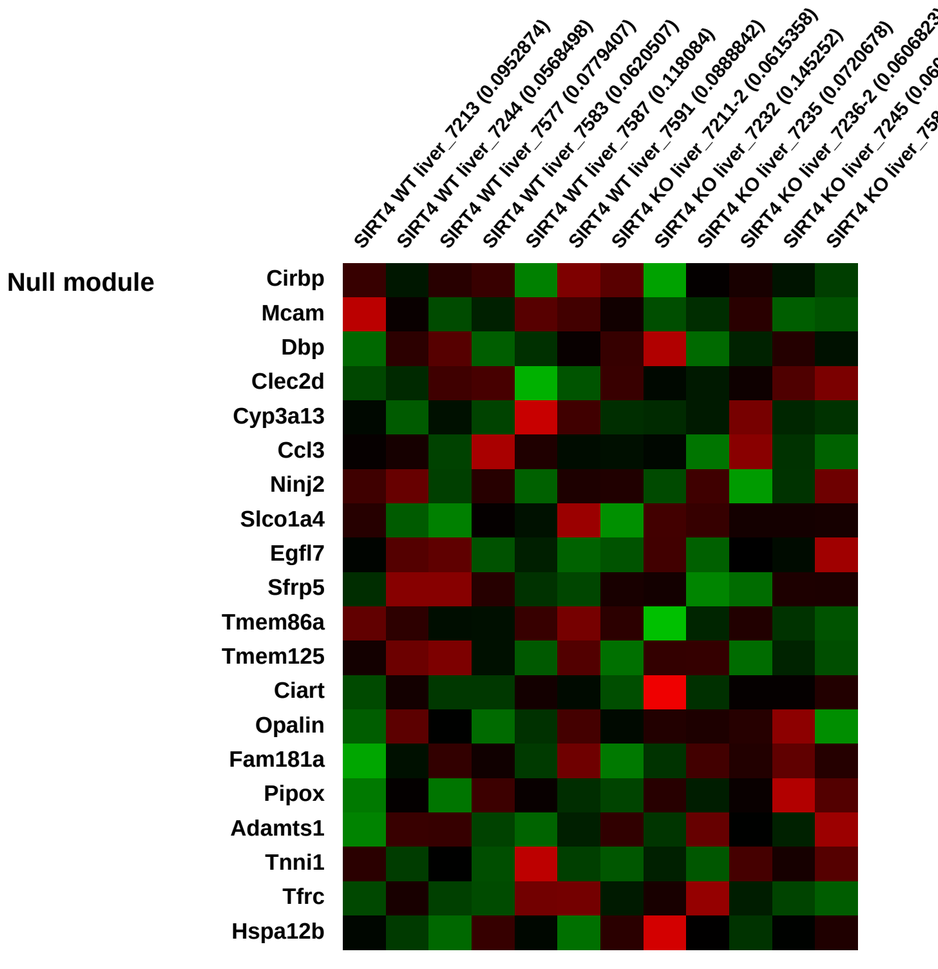

GEO Series "GSE5241" Expression Profiles

Num of samples in this series: 9

Scale of expression profile Z-scores

-3.0 -2.0 -1.0 0.0 1.0 2.0 3.0

GEO Link:	http://www.ncbi.nlm.nih.gov/geo/query/acc.cgi?acc=GSE5241
Status:	Public on Jan 31 2008
Title:	Liver toxicity of dichloroacetyl chloride and dichloroacetic anhydride in female MRL +/+ mice
Organism:	Mus musculus
Experiment type:	Expression profiling by array
Platform:	GPL1261
Pubmed ID:	18293905
Summary & Design:	**Summary:** Dichloroacetyl chloride (DCAC) is a metabolic intermediate of trichloroethene (TCE), an industrial chemical and ubiquitous environmental contaminant. TCE and its metabolites have been implicated in the induction of organ-specific and systemic autoimmunity, in the acceleration of autoimmune responses, and in the development of liver toxicity. In humans, effects of environmental toxicants are often multifactorial and detected only after long-term exposure. Therefore, we developed a small-animal model to determine mechanisms by which DCAC and related acylating agents affect liver disease. Autoimmune-prone female MRL +/+ mice were injected i.p. with 0.2 mmole/kg of DCAC or the acylating agent dichloroacetic anhydride (DCAA) in corn oil twice weekly for six weeks. We then determined changes in the liver transcriptome using microarray gene expression analysis. After exposure to DCAC or DCAA, we observed changes in liver gene expression consistent with inflammatory processes. Both toxicants up-regulated expression of acute phase response and inflammatory genes. Further, metallothionein genes were strongly up-regulated, indicating effects of the toxicants on zinc ion homeostasis and stress responses. In addition, DCAC and DCAA induced up-regulation of several genes indicative of tumorogenesis. Microarray gene expression analysis using a restricted set of genes could be a valuable tool to screen for early changes in liver function following suspected exposure to environmental toxicants. Keywords: Response to acylating agents; inflammatory response; disease state analysis. **Overall design:** Samples: Livers from three mice per group were independently processed. The integrity of the RNA samples was tested using an Agilent 2100 Bioanalyzer and RNA 6000 LabChip´fi kit (Agilent Technologies, Palo Alto, CA). Only RNA samples without signs of degradation were used. Comprehensive gene expression profiles were analyzed.

Background corr dist: KL-Divergence = 0.0831, L1-Distance = 0.0387, L2-Distance = 0.0023, Normal std = 0.5130

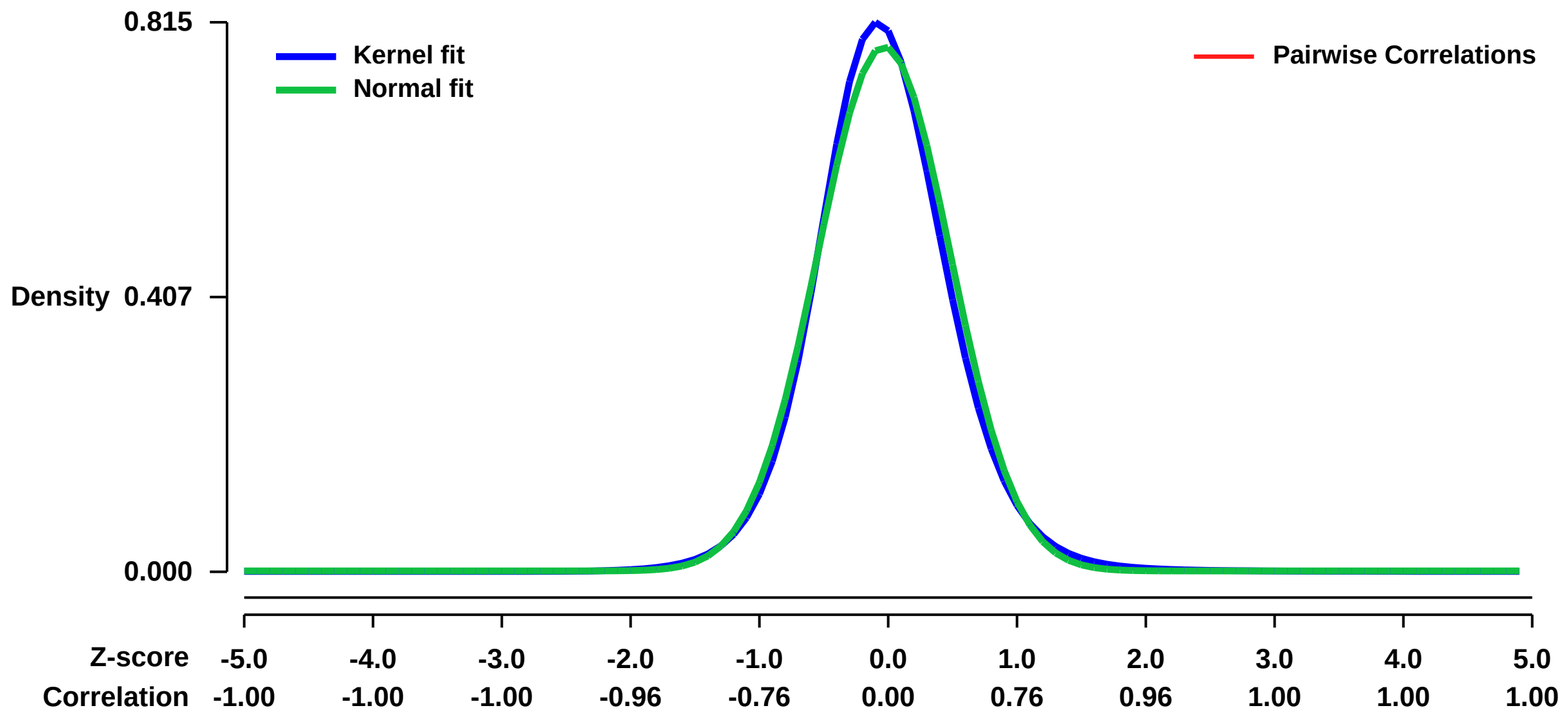

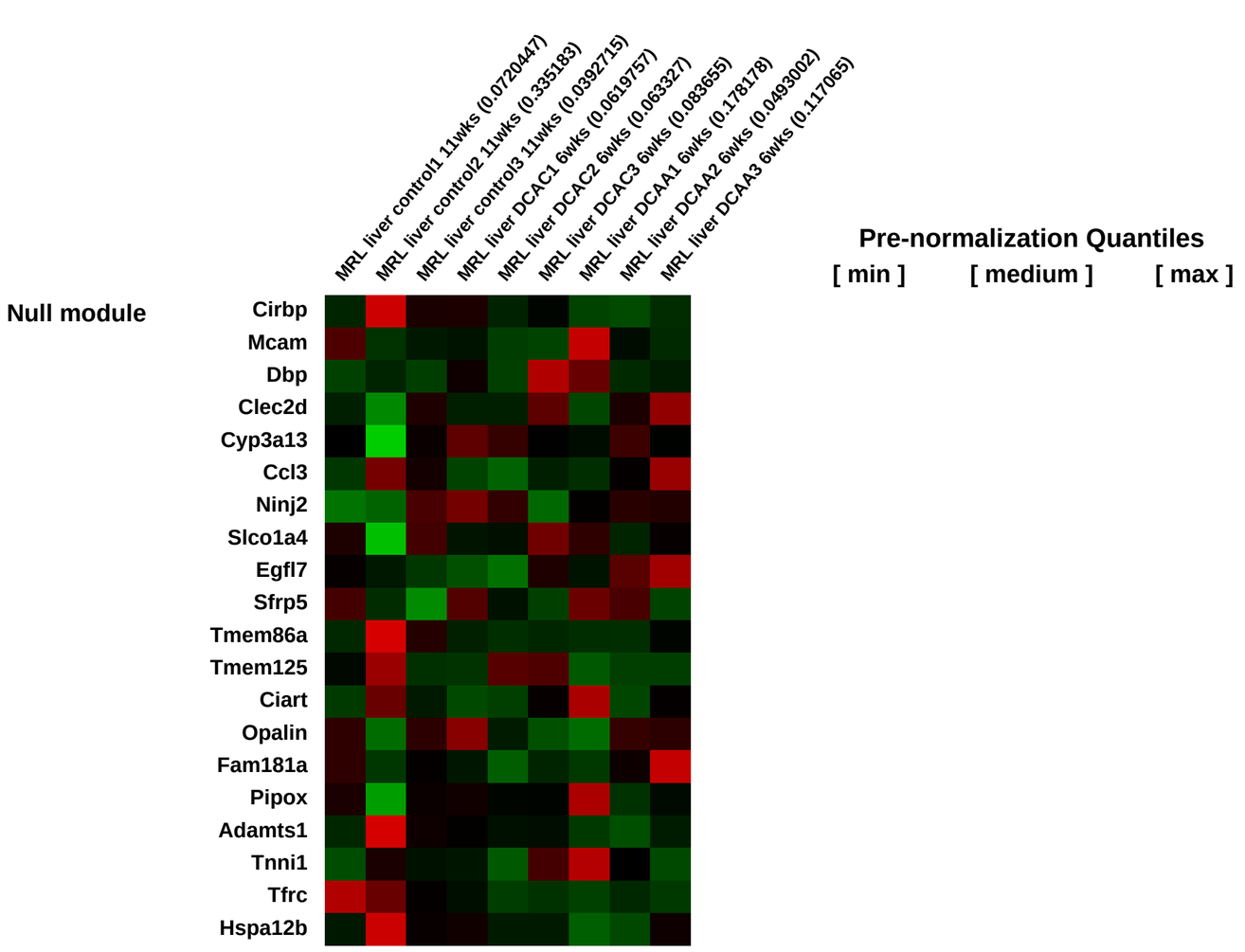

GEO Series "GSE31028" Expression Profiles

Num of samples in this series: 6

Scale of expression profile Z-scores

-3.0 -2.0 -1.0 0.0 1.0 2.0 3.0

GEO Link:	http://www.ncbi.nlm.nih.gov/geo/query/acc.cgi?acc=GSE31028
Status:	Public on Sep 02 2011
Title:	Genome-wide maps of histone modifications unwind in vivo chromatin states of the hair follicle lineage
Organism:	Mus musculus
Experiment type:	Expression profiling by array
Platform:	GPL1261
Pubmed ID:	21885018
Summary & Design:	**Summary:** Mouse hair follicles (HFs) undergo synchronized cycles. Cyclical regeneration and hair growth is fueled by stem cells (SCs). During the rest phase, the HF-SCs remain quiescent due to extrinsic inhibitory signals within the niche. As activating cues accumulate, HF-SCs become activated, proliferate, and grow downward to form transient-amplifying matrix progenitor cells. We used microarrays to detect the relative levels of global gene expression underlying the states of hair follicle stem cells and their transient-amplifying progeny before differentiation. **Overall design:** Quiescent hair follicle stem cells (qHF-SCs), activated hair follicle stem cells (aHF-SCs) and transient-amplifying matrix cells (HF-TACs) were FACS-purified for RNA extraction and hybridization on Affymetrix microarrays. To obtain homogeneous populations of expression profiles, we applied the FACS technique to purify SC and TACs according to their cell surface markers.

Background corr dist: KL-Divergence = 0.0298, L1-Distance = 0.0230, L2-Distance = 0.0006, Normal std = 0.6841

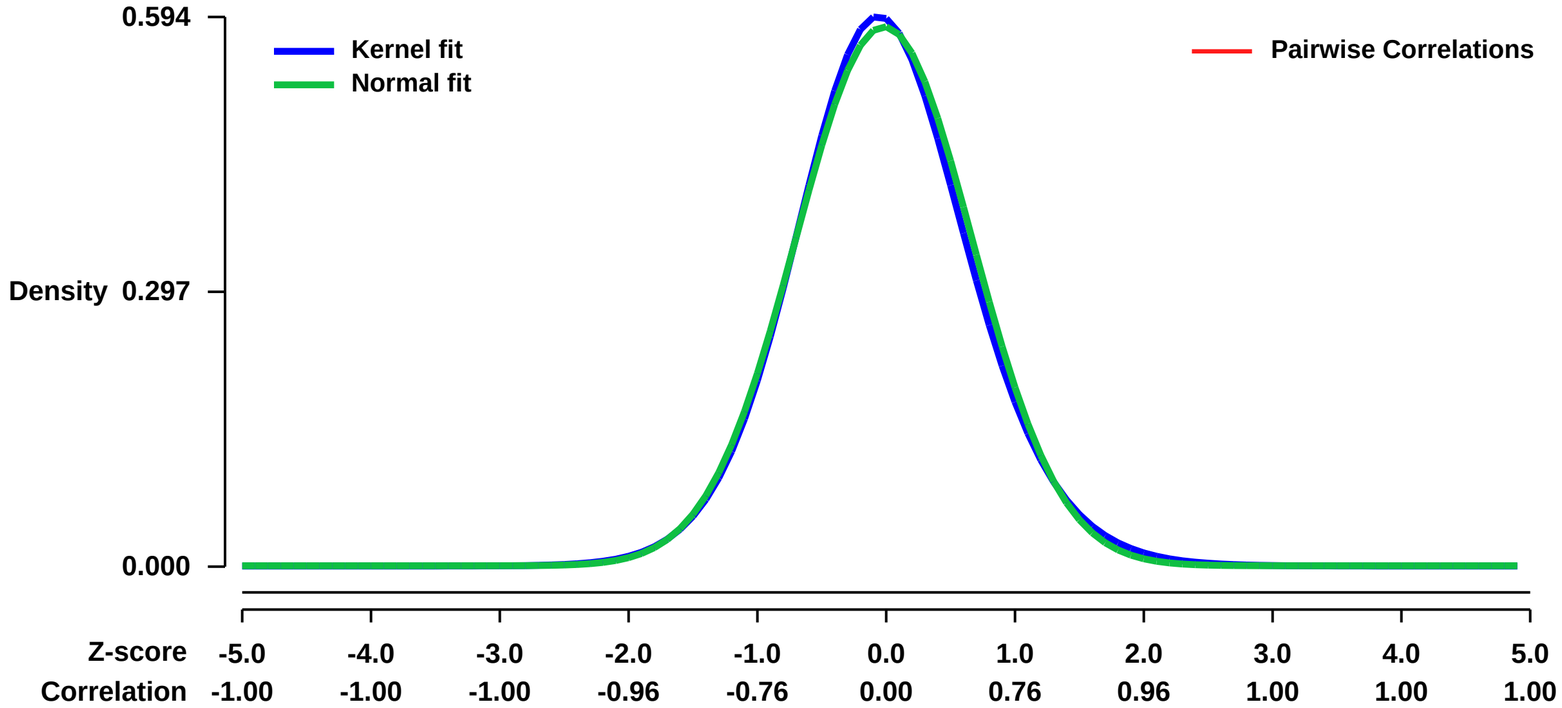

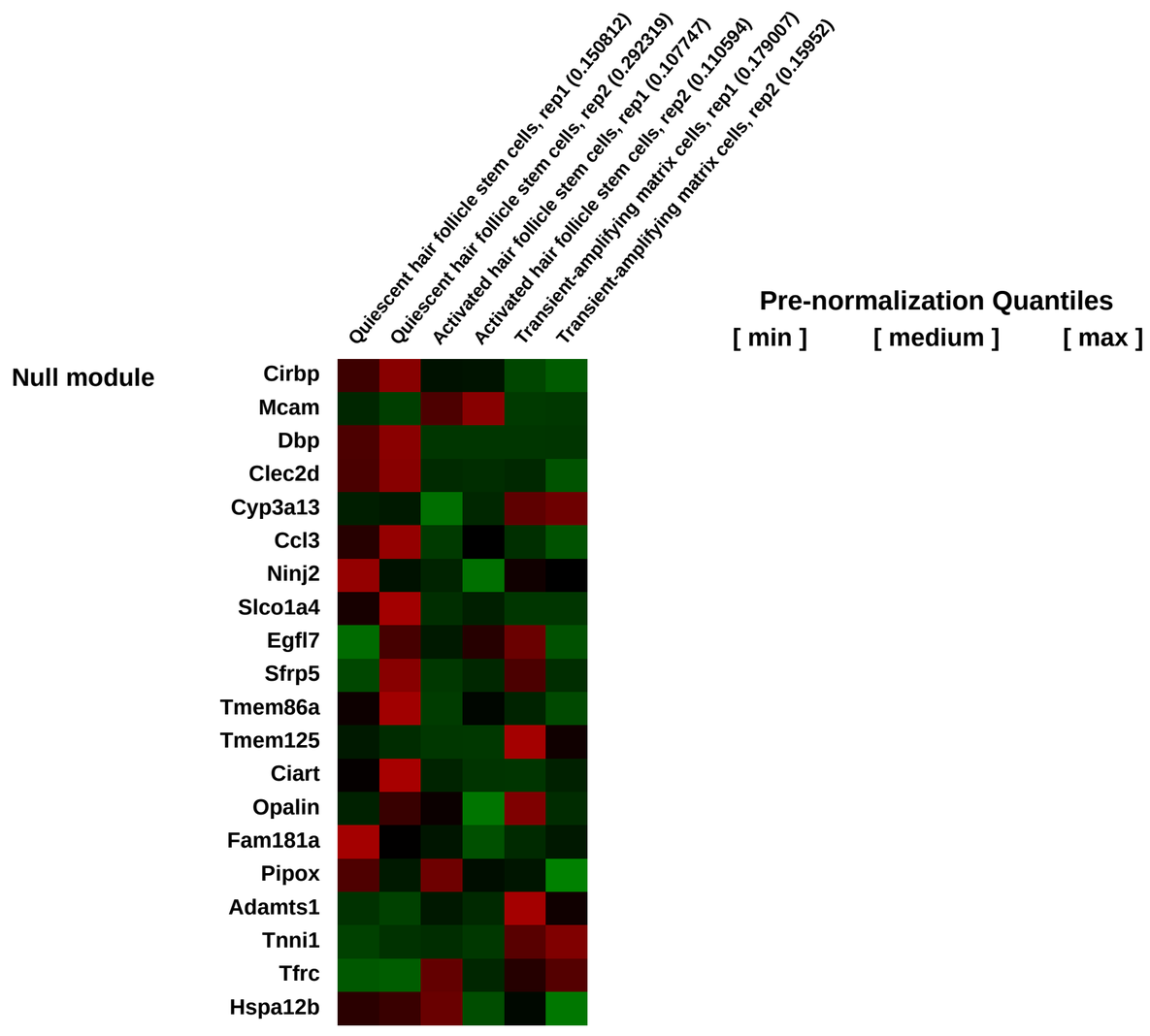

GEO Series "GSE46970" Expression Profiles

Num of samples in this series: 15

Scale of expression profile Z-scores

-3.0 -2.0 -1.0 0.0 1.0 2.0 3.0

GEO Link:	http://www.ncbi.nlm.nih.gov/geo/query/acc.cgi?acc=GSE46970
Status:	Public on Jun 18 2013
Title:	Gene expression of 4, 5, and 6 days differentiated Flk1+ WT ES cells, and of 6 days differentiated Flk1+ Runx1-/- and Tal-1-/- ES cells
Organism:	Mus musculus
Experiment type:	Expression profiling by array
Platform:	GPL1261
Pubmed ID:	19265543
Summary & Design:	**Summary:** **In order to identify genes that are activated in differentiating WT ESCs, but are missing in Tal-1-/- and Runx1-/- ESCs, and which might be involved in the generation of definitive hematopoietic progenitors and their specification thereafter, we performed microarray analyses on purified Flk-1+ cells, differentiated from these ESCs for 4, 5, and 6 days â in vitroâ .** **Overall design:** **Gene-expression profiling of three biological replicates was performed at days 4, 5, and 6 during the differentiation process of WT J1 ESCs (9 samples), and at day 6 during the differentiation process of either Runx1-/- J1 or Tal-1-/- J1 ESCs (3 samples each). Total RNA was extracted using the RNeasy Mini kit (Qiagen). The integrity and amount of isolated RNA was assessed for each sample using an Agilent 2100 Bioanalyzer (Agilent, Waldbronn, Germany) and a NanoDrop ND-1000 spectrophotometer (NanoDrop Technologies, Wilmington, DE). Complementary DNA was synthesized from 3-5 ¸…g total RNA, using reagents recommended in the technical manual GeneChip Expression Analysis (Affymetrix, Santa Clara, CA). The in vitro transcription, necessary for the synthesis of biotinylated complementary RNA (cRNA) was performed using the Enzo RNA Transcript Labeling kit (Affymetrix). Fifteen micrograms of fragmented cRNA of each sample were hybridized to nine Mouse Genome 430-2 arrays (Affymetrix). Hybridization was performed in a Hybridization Oven 640, and chips were washed and stained in the Fluidics Station 400 (both Affymetrix), according to procedure 2 as described in the technical manual. Finally, the arrays were scanned with a GeneChip Scanner 3000 using the GCOS software, both Affymetrix. All relevant GCOS data of quality checked microarrays were analyzed with High Performance Chip Data Analysis (HPCDA, unpublished), using the BioRetis database (www.bioretis-analysis.de), as described and validated previously (55). Used query parameters for database filtering process was described earlier several times (56). For hierarchical cluster analysis, we used the program Genes@Work (57) with gene vectors for normalization and Pearson w/mean for similarity measure. As cluster type, we used center of mass.**

Background corr dist: KL-Divergence = 0.1350, L1-Distance = 0.0345, L2-Distance = 0.0023, Normal std = 0.3999

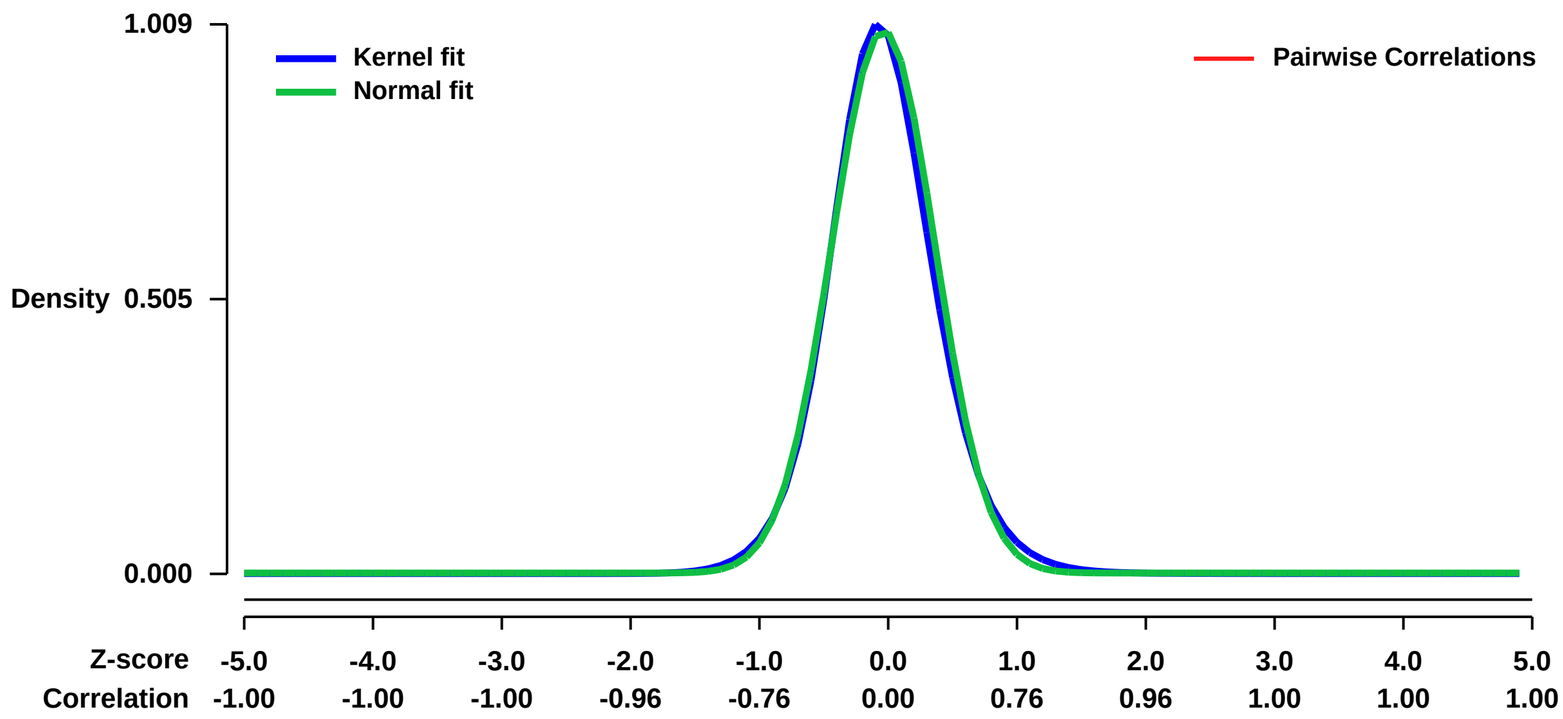

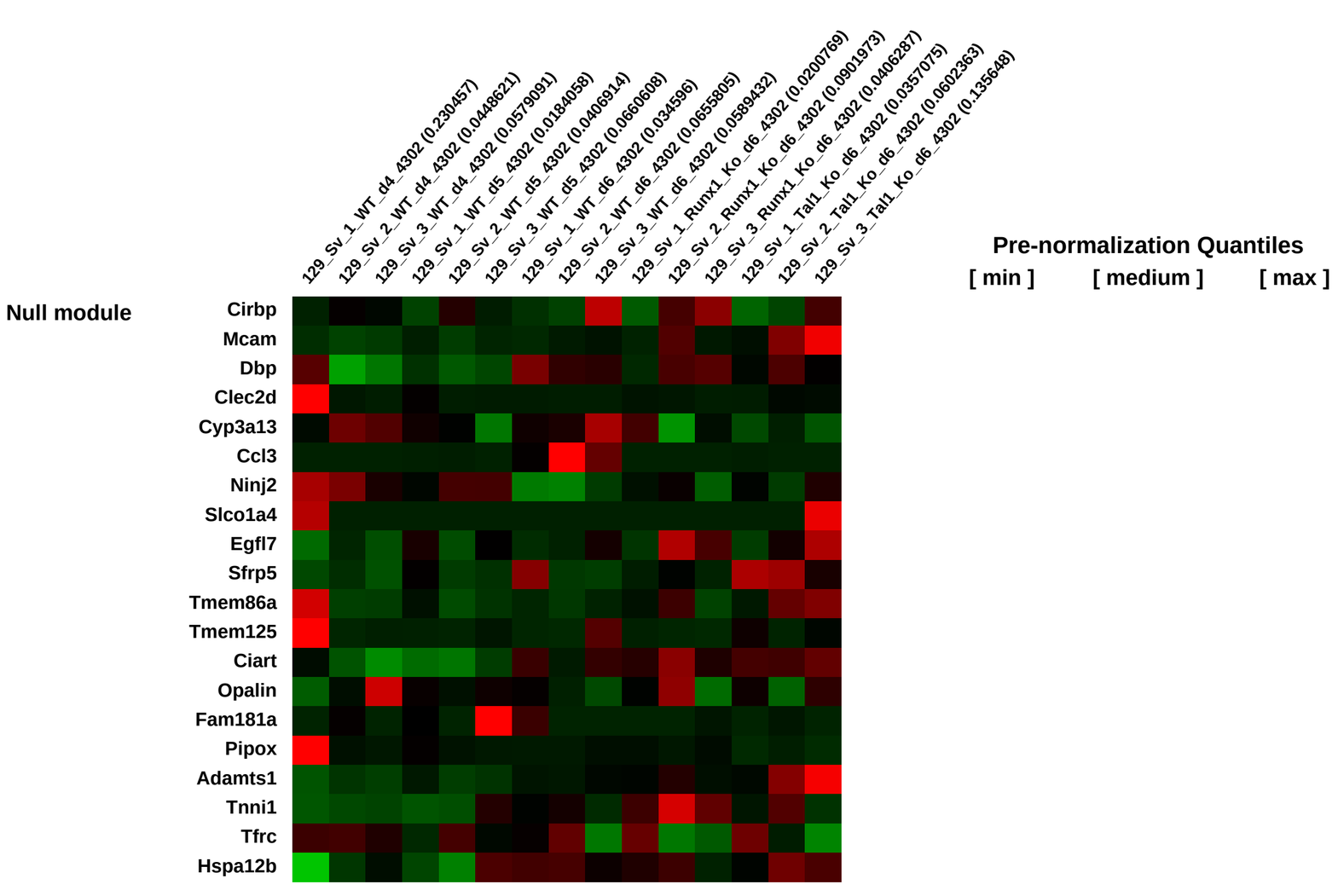

GEO Series "GSE56777" Expression Profiles

Num of samples in this series: 8

Scale of expression profile Z-scores

-3.0 -2.0 -1.0 0.0 1.0 2.0 3.0

GEO Link:	http://www.ncbi.nlm.nih.gov/geo/query/acc.cgi?acc=GSE56777
Status:	Public on May 14 2014
Title:	Expression data of E13.5 mouse Blood Brain Barrier and lung endothelial cells
Organism:	Mus musculus
Experiment type:	Expression profiling by array
Platform:	GPL1261
Pubmed ID:	24828040
Summary & Design:	**Summary:** Following the identification of a critical time window of Blood Brain Barrier formation in the mouse embryo, we aimed to identify genes important for barriergenesis. To this end, we isolated cortical and lung E13.5 endothelial cells and compared expression between the two populations. The working hypothesis was that endothelial cells which are actively building a barrier would have a uniqe pattern of gene expression that would be detectable in comparison to a non-barrier endothelial population that is also active in vasculogenesis. **Overall design:** E13.5 Tie2-GFP embryos were micro-dissected for cortex and lungs. Cortex tissue was carefully cleared of the meninges and choroid plexus. FACS purification of GFP positive cells and GeneChip analysis was applied . All material from a single litter (10-13 embryos) was pooled and considered as a biological replicate. n=4 litters.

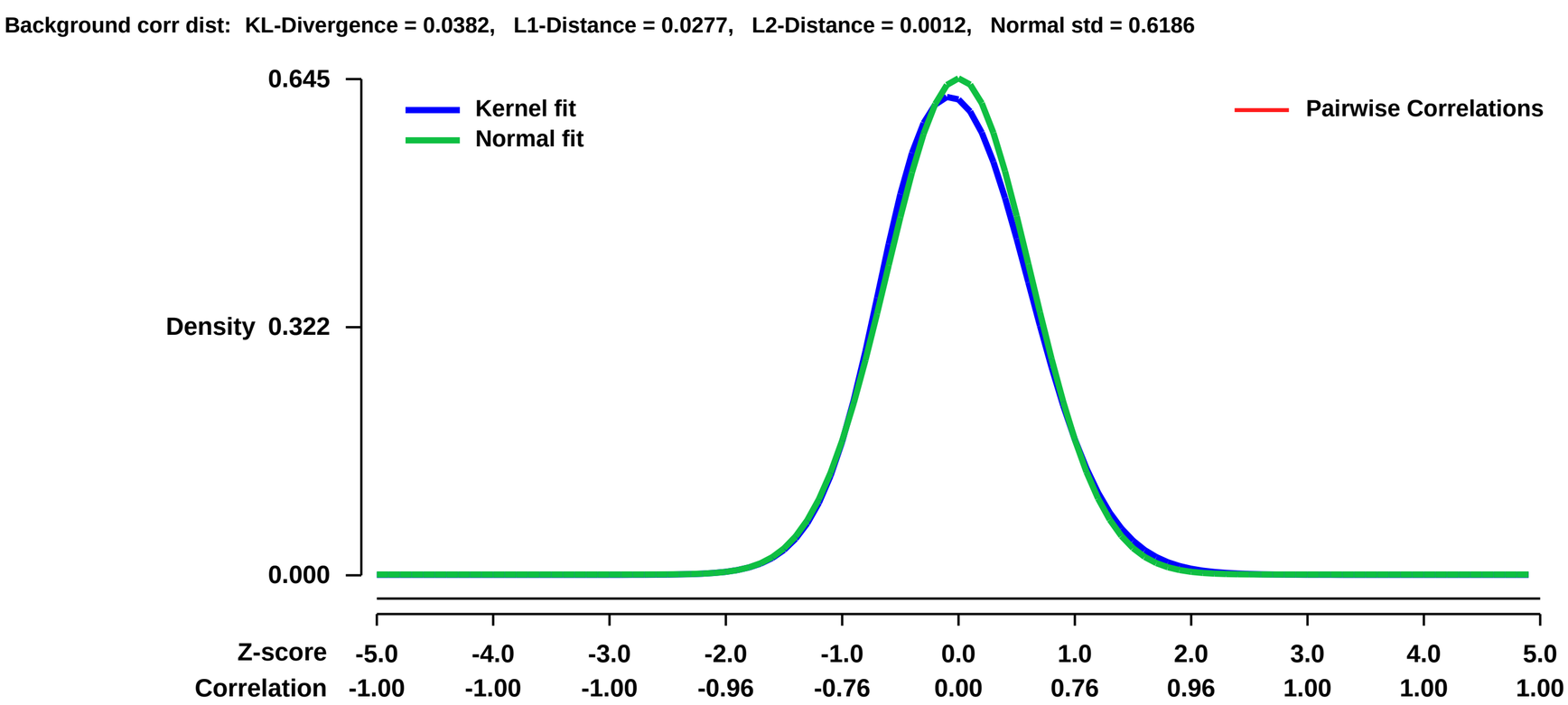

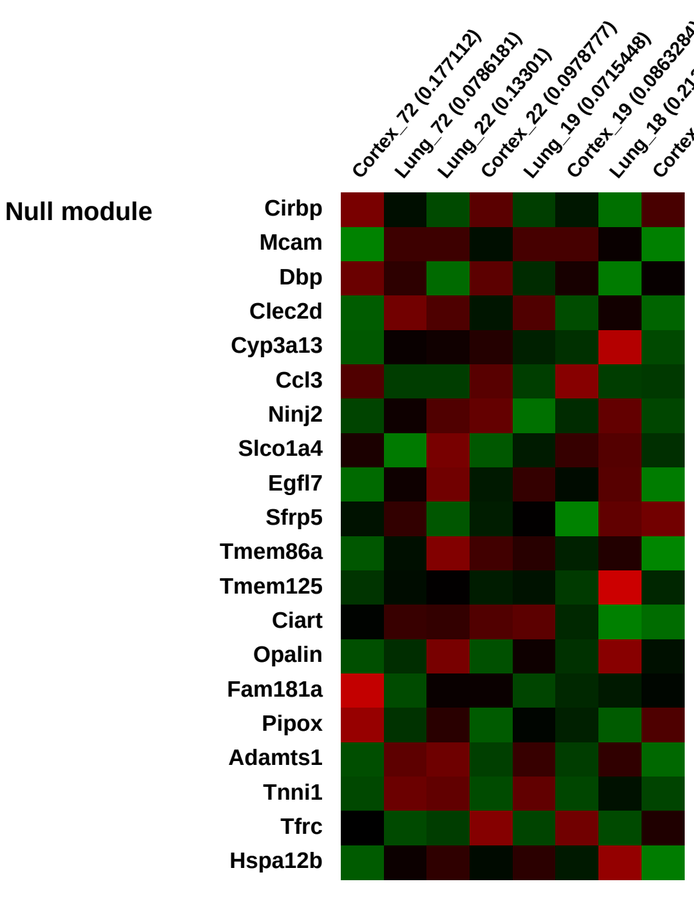

GEO Series "GSE24512" Expression Profiles

Num of samples in this series: 29

Scale of expression profile Z-scores

-3.0 -2.0 -1.0 0.0 1.0 2.0 3.0

GEO Link:	http://www.ncbi.nlm.nih.gov/geo/query/acc.cgi?acc=GSE24512
Status:	Public on Mar 15 2012
Title:	Expression variation in the mouse retina
Organism:	Mus musculus
Experiment type:	Expression profiling by array
Platform:	GPL1261
Pubmed ID:	21779340
Summary & Design:	**Summary:** Expression analysis of multiple mouse strains across two developmental timepoints to determine both strain specific and temporal expression of genes in the mouse retina **Overall design:** A total of 29 retinas were collected from 15 mice of each strain at similar time points during the day. Equimolar amounts of RNA isolated from ten retinas were pooled into three separate pools from each strain and time point, then hybridized to Affymetrix Mouse 420A 2.0 GeneChip arrays.

Background corr dist: KL-Divergence = 0.1455, L1-Distance = 0.0524, L2-Distance = 0.0048, Normal std = 0.3969

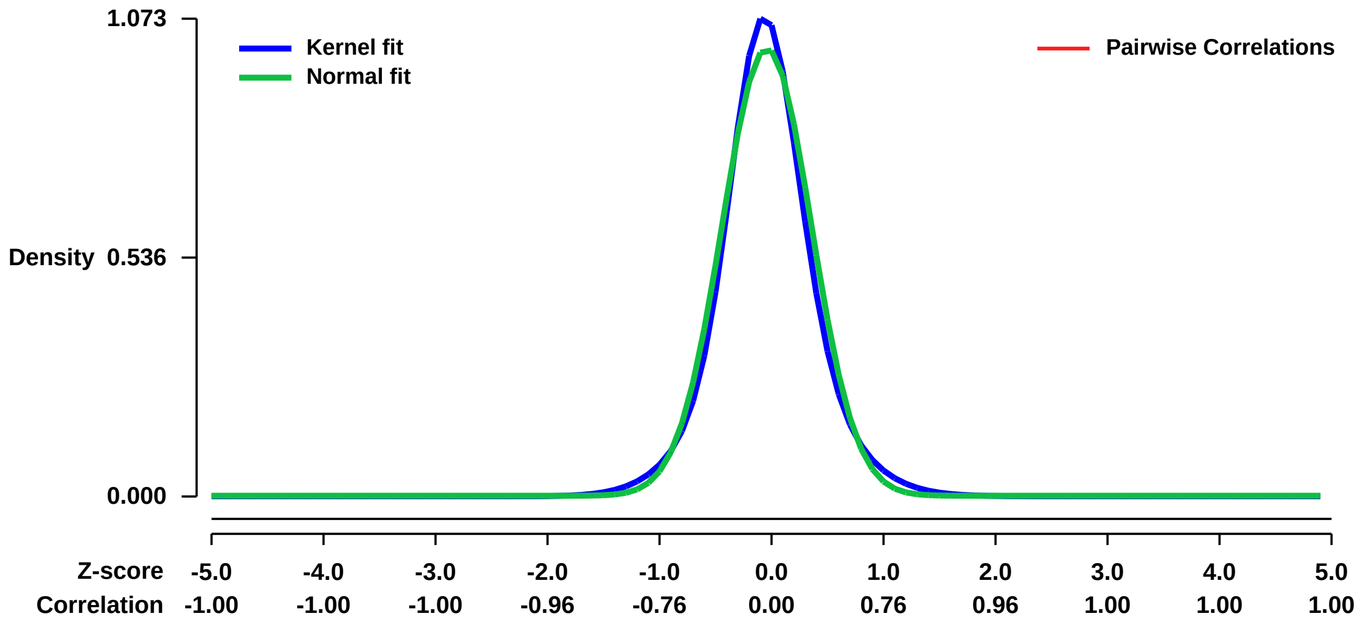

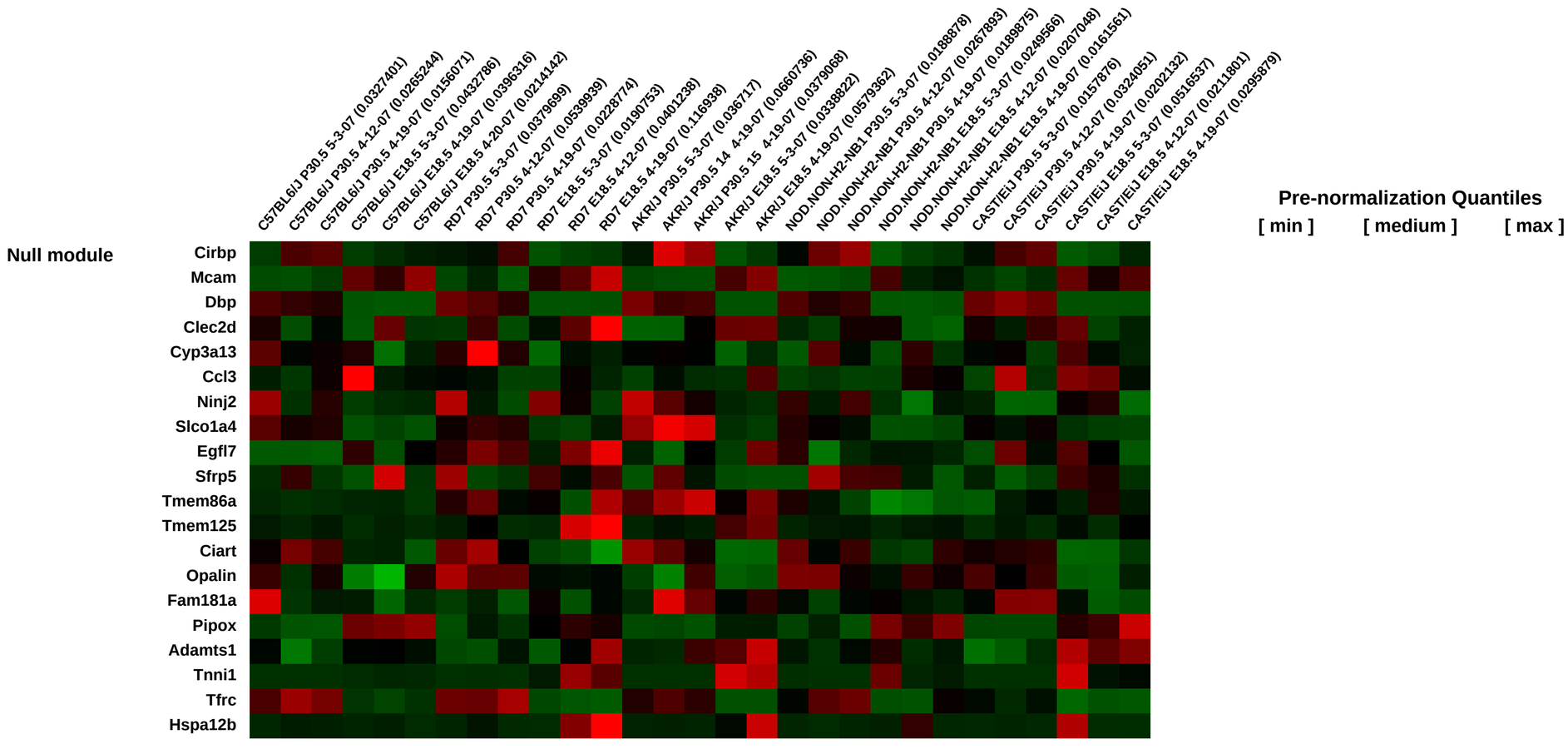

GEO Series "GSE18587" Expression Profiles

Num of samples in this series: 9

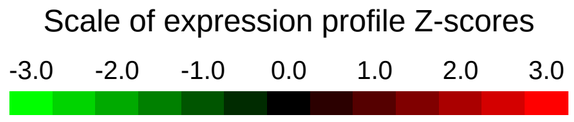

GEO Link:	http://www.ncbi.nlm.nih.gov/geo/query/acc.cgi?acc=GSE18587
Status:	Public on Sep 21 2011
Title:	Specific modulation of mucosal immune response, tolerance and proliferation in mice colonized with A. muciniphila
Organism:	Mus musculus
Experiment type:	Expression profiling by array
Platform:	GPL1261
Pubmed ID:	21904534

Summary & Design:

Summary:
Epithelial cells of the mammalian intestine are covered with a mucus layer that prevents direct contact with intestinal microbes but also constitutes a substrate for mucus-degrading bacteria. To study the effect of mucus degradation on the host response, germ-free mice were colonized with Akkermansia muciniphila. This anaerobic bacterium belonging to the Verrucomicrobia is specialized in the degradation of mucin, the glycoprotein present in mucus, and found in high numbers in the intestinal tract of human and other mammalian species. Efficient colonization of A. muciniphila was observed with highest numbers in the cecum, where most mucin is produced. In contrast, following colonization by Lactobacillus plantarum, a facultative anaerobe belonging to the Firmicutes that ferments carbohydrates, similar cell-numbers were found at all intestinal sites. Whereas A. muciniphila was located closely associated with the intestinal cells, L. plantarum was exclusively found in the lumen. The global transcriptional host response was determined in intestinal biopsies and revealed a consistent, site-specific, and unique modulation of about 750 genes in mice colonized by A. muciniphila and over 1500 genes after colonization by L. plantarum. Pathway reconstructions showed that colonization by A. muciniphila altered mucosal gene expression profiles toward increased expression of genes involved in immune responses and cell fate determination, while colonization by L. plantarum led to up-regulation of lipid metabolism. These indicate that the colonizers induce host responses that are specific per intestinal location. In conclusion, we propose that A. muciniphila modulates pathways involved in establishing homeostasis for basal metabolism and immune tolerance toward commensal microbiota.

Keywords: Analysis of target gene regulation by using microarrays

Overall design:
Adult germ-free female NMRI-KI mice (45 â 65 days) were used for bacterial mono-association. Two bacterial strains were used in this study, A. muciniphila MucT (ATTC BAA-835) and L. plantarum WCFS1 (NCIMB 8826). A. muciniphila was grown anaerobically in a basal mucin based medium and L. plantarum was grown anaerobically at 37´°C in Man-Rogosa-Sharpe broth (MRS; Le Pont de Claix, France). After 7 days of colonization, mice were killed by cervical dislocation and terminal ileum, cecum and ascending colon specimens were sampled.

Background corr dist: KL-Divergence = 0.0560, L1-Distance = 0.0627, L2-Distance = 0.0089, Normal std = 0.5753

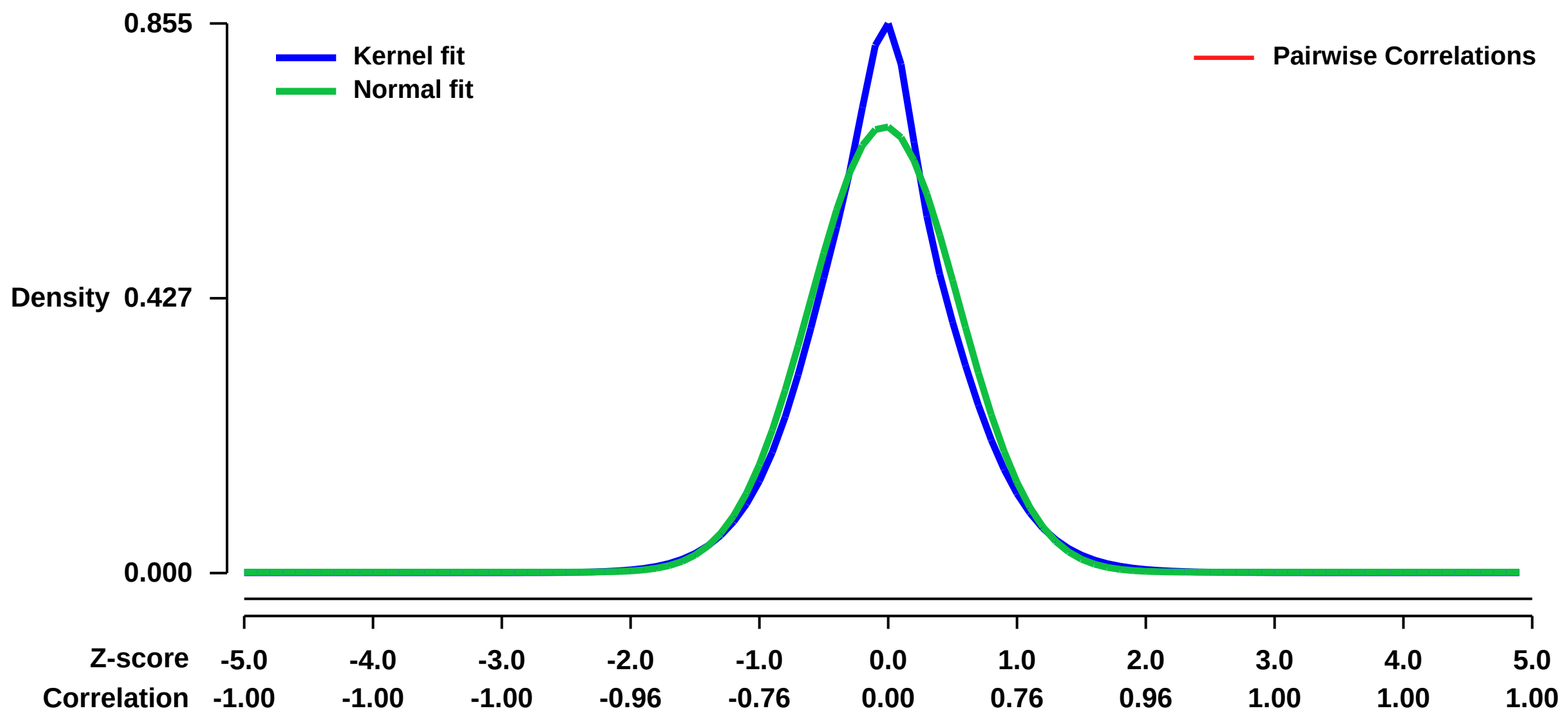

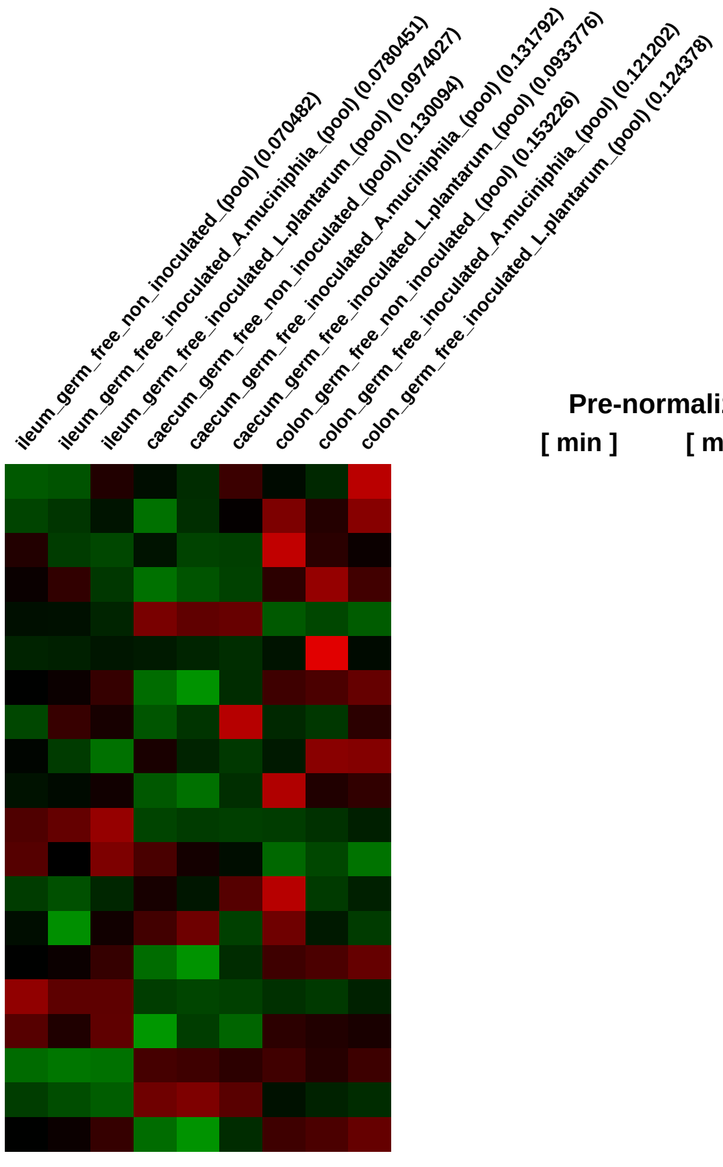

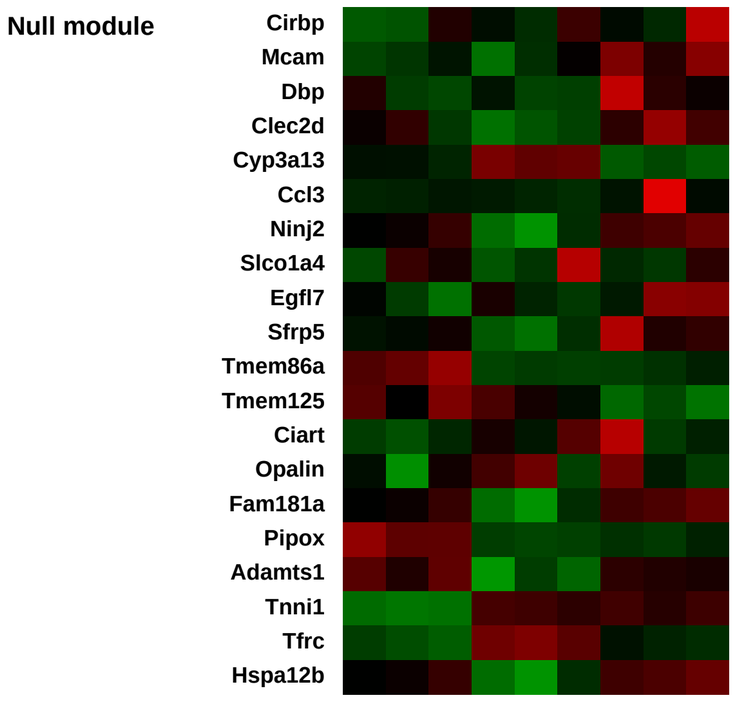

GEO Series "GSE9123" Expression Profiles

Num of samples in this series: 8

Scale of expression profile Z-scores

-3.0 -2.0 -1.0 0.0 1.0 2.0 3.0

GEO Link:	http://www.ncbi.nlm.nih.gov/geo/query/acc.cgi?acc=GSE9123
Status:	Public on Sep 22 2007
Title:	transcription factor PlagL2 regulates steps in chylomicron metabolism
Organism:	Mus musculus
Experiment type:	Expression profiling by array
Platform:	GPL1261
Pubmed ID:	17983586
Summary & Design:	**Summary:** Enterocytes assemble dietary lipids into chylomicron particles that are taken up by intestinal lacteal vessels and peripheral tissues. Although chylomicrons are known to assemble in part within membrane secretory pathways, the modifications required for efficient vascular uptake are unknown. We report that the transcription factor Pleomorphic adenoma gene-like 2 (PLAGL2) is essential for this aspect of dietary lipid metabolism. PlagL2-/- mice die from post-natal wasting owing to failure of fat absorption. Lipids modified in the absence of PlagL2 exit from enterocytes but fail to enter interstitial lacteal vessels. Dysregulation of enterocyte genes closely linked to intracellular membrane transport identified candidate regulators of critical steps in chylomicron assembly. PlagL2 thus regulates essential and poorly understood aspects of dietary lipid absorption and its deficiency represents an authentic animal model with implications for amelioration of obesity or the metabolic syndrome. **Keywords:** gene expression profiling analysis **Overall design:** Total RNA was extracted from 4 knockout and 4 wild-type mouse small intestines at 18.5 dpc using the Macherey-Nagel Nucleospin kit. cRNA synthesis and labeling, hybridization to Affymetrix (Santa Clara, CA) MOE430 2.0 expression arrays, and data acquisition occurred on the Affymetrix GeneChip Instrument System.

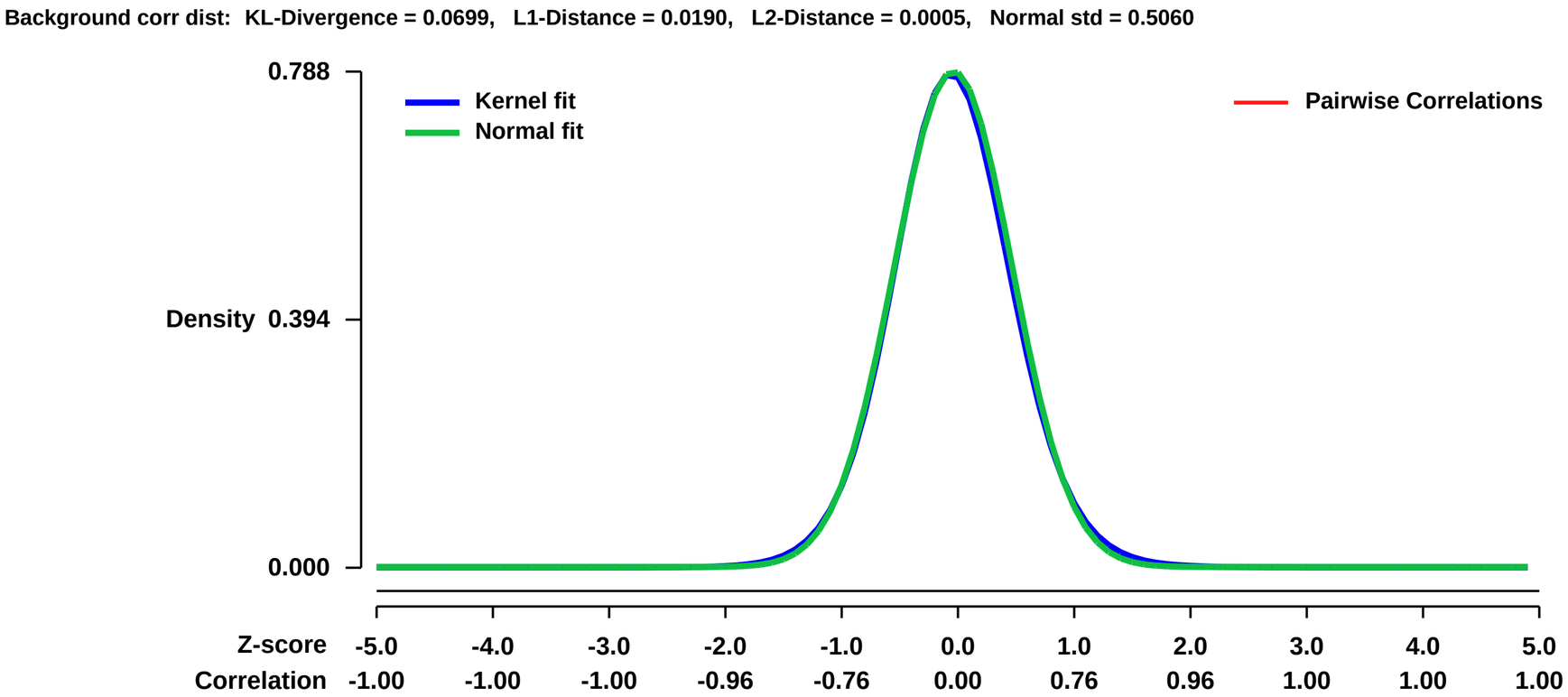

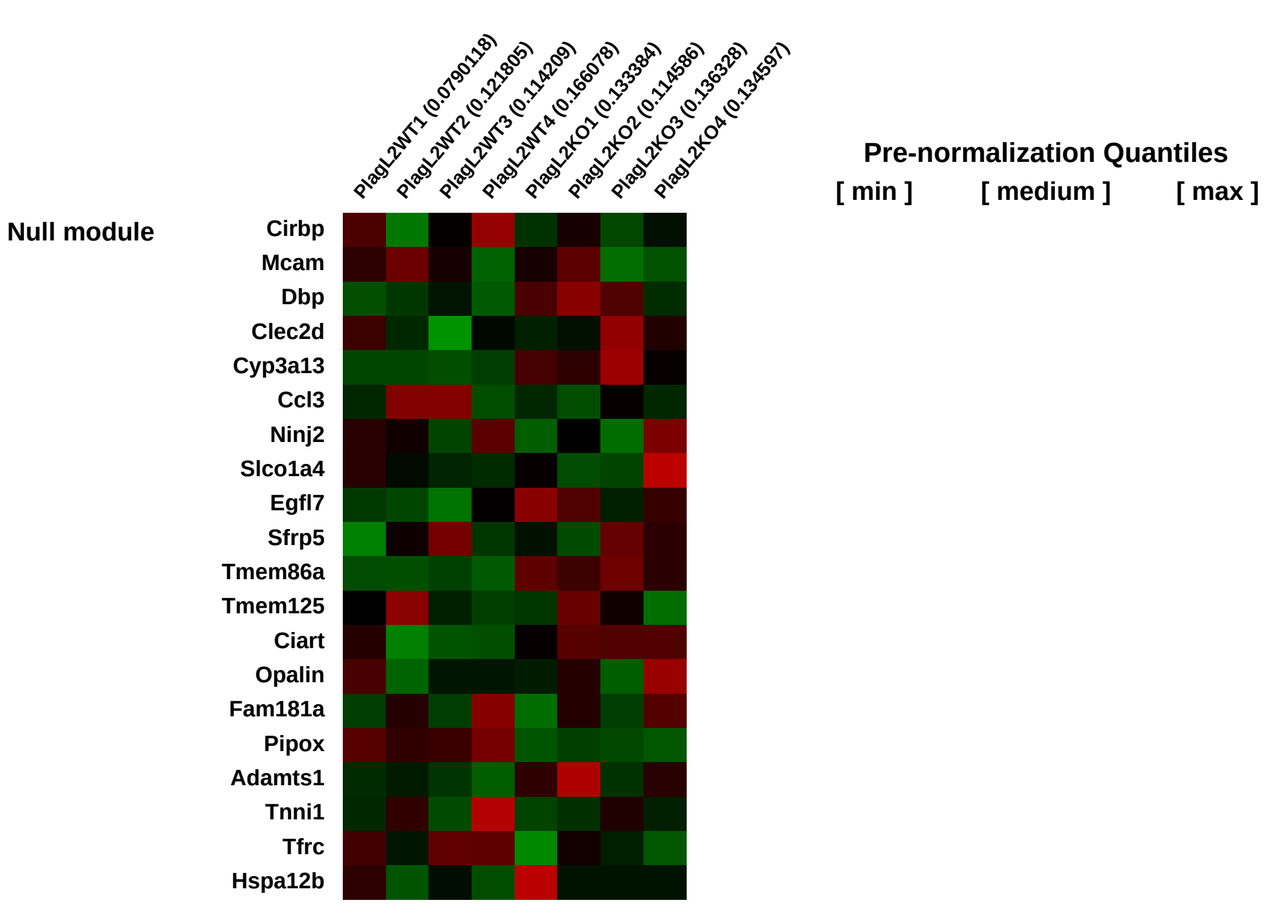

GEO Series "GSE15293" Expression Profiles

Num of samples in this series: 37

Scale of expression profile Z-scores

-3.0 -2.0 -1.0 0.0 1.0 2.0 3.0

GEO Link:	http://www.ncbi.nlm.nih.gov/geo/query/acc.cgi?acc=GSE15293
Status:	Public on Mar 09 2010
Title:	Gene expression profiling of temporal lobes of wfs1 deficient mice
Organism:	Mus musculus
Experiment type:	Expression profiling by array
Platform:	GPL1261
Pubmed ID:	19293327
Summary & Design:	**Summary:** Aim of present study was to describe the changes induced deletion of the Wfs1 gene in the temporal lobe of mice. Mutant mice were backcrossed to two different genomic backgrounds in order to exclude confounding foreign genomic background influence. Samples from temporal lobes were analyzed by using Affymetrix Genechips, expression profiles were functionally annotated by using GSEA and Ingenuity Pathway Analysis. We found that Wfs1 mutant mice are significantly smaller (20.9 ´– 1.6 g) than their wild-type counterparts (31.0 ´– 0.6g, p < 0.0001). Interestingly, genechip analysis identified growth hormone transcripts up-regulated and functional analysis found appropriate pathways activated. Moreover, we found significant increase in the level of IGF1 in the plasma of wfs1 mutant mice. Taken together, wfs1 mutation induces growth retardation whereas the growth hormone pathway is activated. Further studies are needed to describe biochemical and molecular details of the growth hormone axis in the wfs1 mutant mice. **Overall design:** 37 samples, two genotypes (wild type and mutant), in two different genetic background (C57B6 and 129S6)

Background corr dist: KL-Divergence = 0.3637, L1-Distance = 0.0766, L2-Distance = 0.0180, Normal std = 0.2576

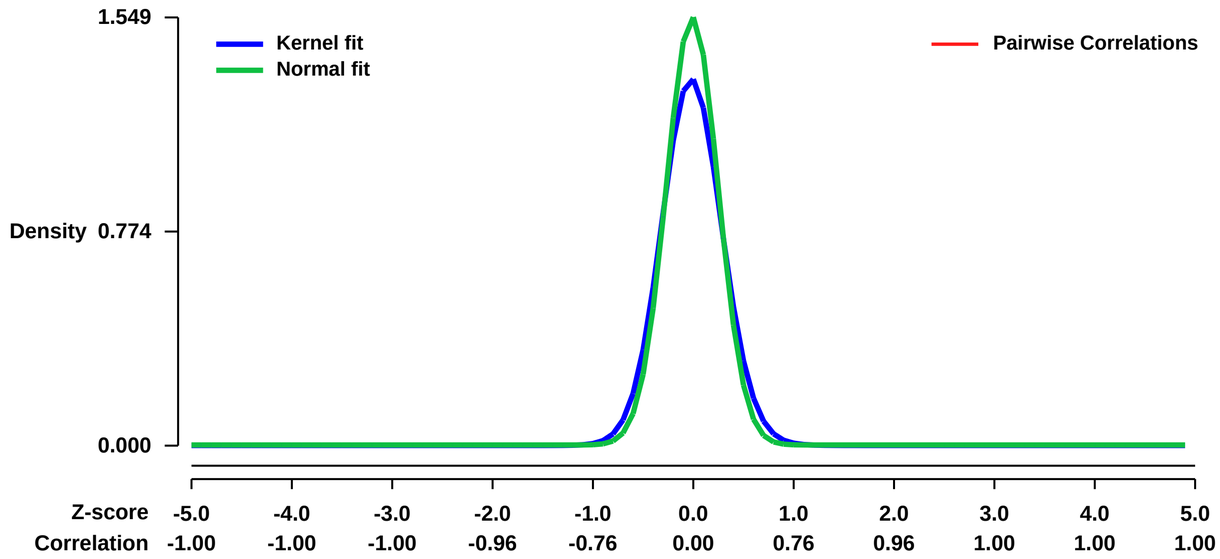

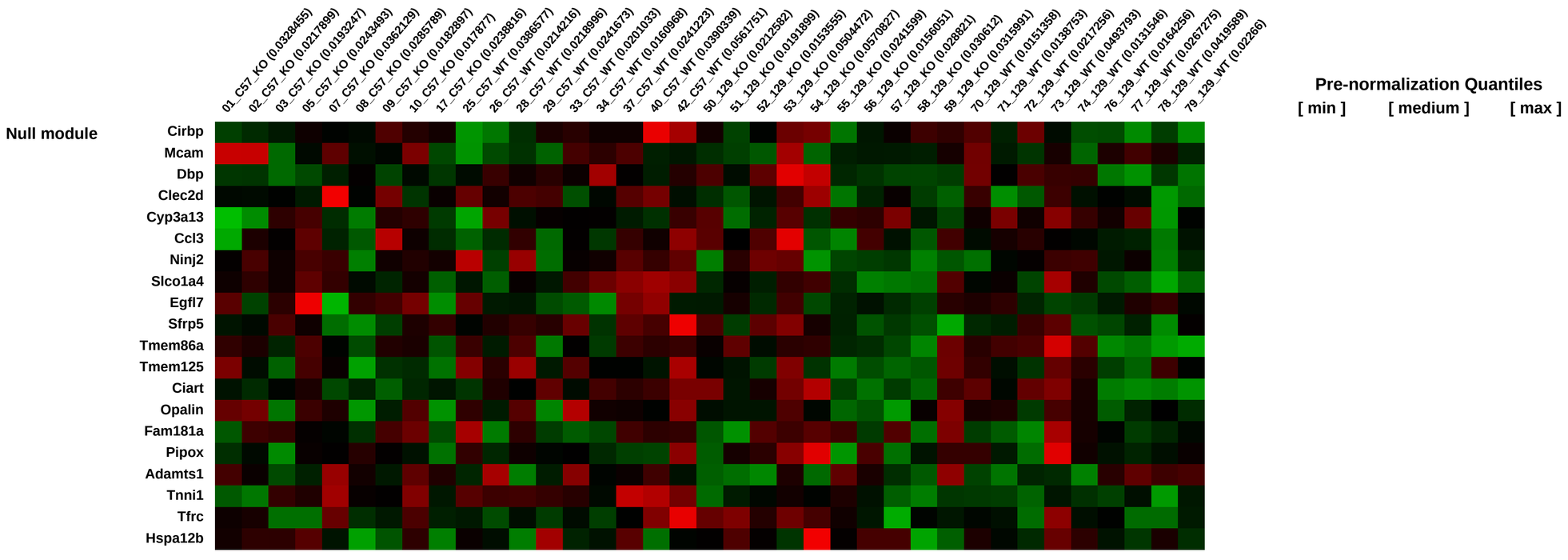

GEO Series "GSE31744" Expression Profiles

Num of samples in this series: 8

Scale of expression profile Z-scores

-3.0 -2.0 -1.0 0.0 1.0 2.0 3.0

GEO Link:	**http://www.ncbi.nlm.nih.gov/geo/query/acc.cgi?acc=GSE31744**
Status:	**Public on Aug 31 2011**
Title:	**Comparison of Flk-1+/PDGFRa+(Flk-1PRa+(DP)) population from Etv2Het vs Etv2KO ES cells**
Organism:	**Mus musculus**
Experiment type:	**Expression profiling by array**
Platform:	**GPL1261**
Pubmed ID:	**21911838**
Summary & Design:	**Summary:** **Screening for genes regulated by Etv2 within Flk-1+/PDGFRa+ ES derived mesoderm.Microarray analysis performed to screen for the candidate genes regulated by Etv2. TT2 ES cells differentiated on OP9 feeder cells were sorted using Flk-1 and PDGFRa antibodies.Gene expressions from these two populations were compared.** **Overall design:** **Extract RNA from sorted Flk-1+/PDGFRa+ populations from Etv2Het vs KO cells. To obtain primitive mesoderm cells TT2 ES cells of corresponding genotypes were differentiated on OP9 cells for 4 days. Flk-1+/PDGFRa+ populations were sorted from Etv2 Het vs. KO cells for RNA extraction.**

Background corr dist: **KL-Divergence = 0.0220, L1-Distance = 0.0195, L2-Distance = 0.0005, Normal std = 0.7076**

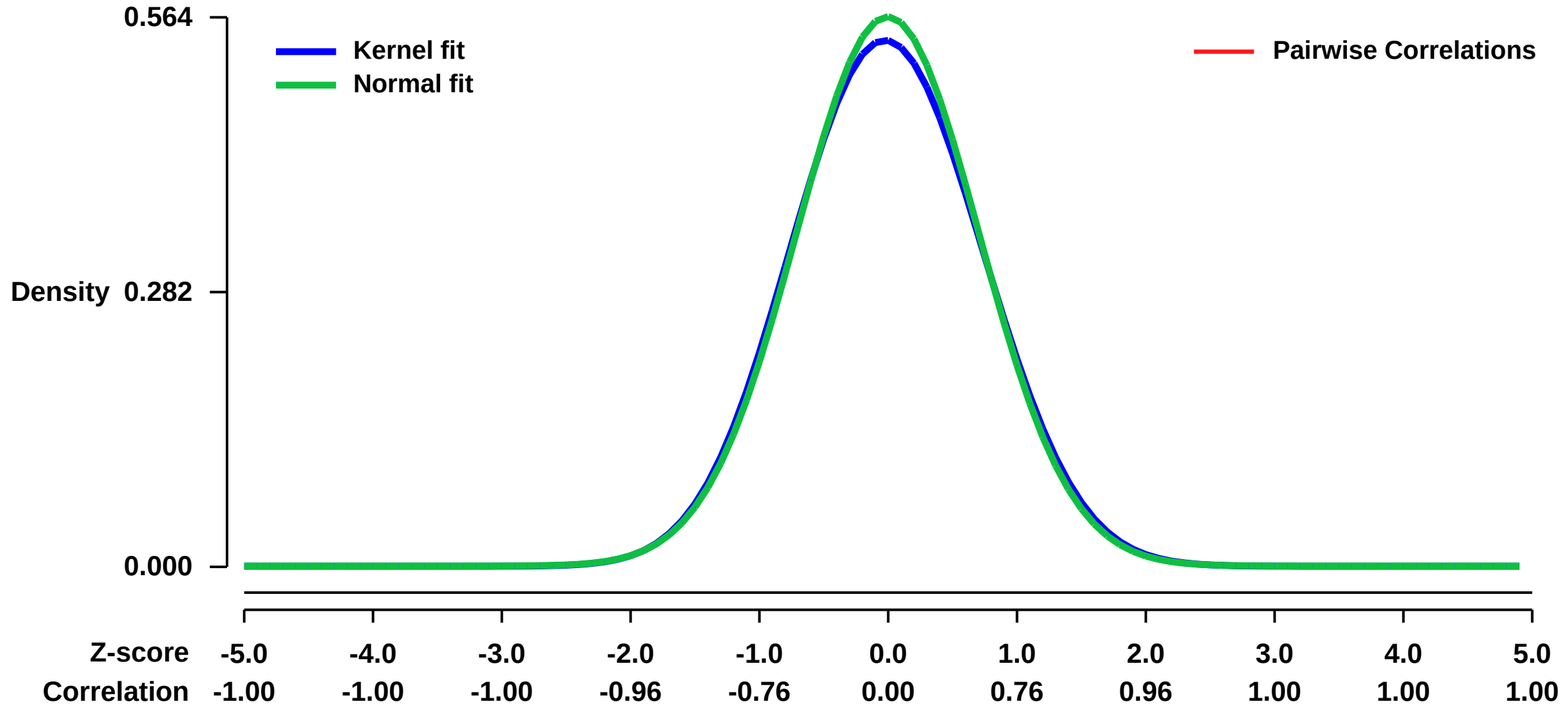

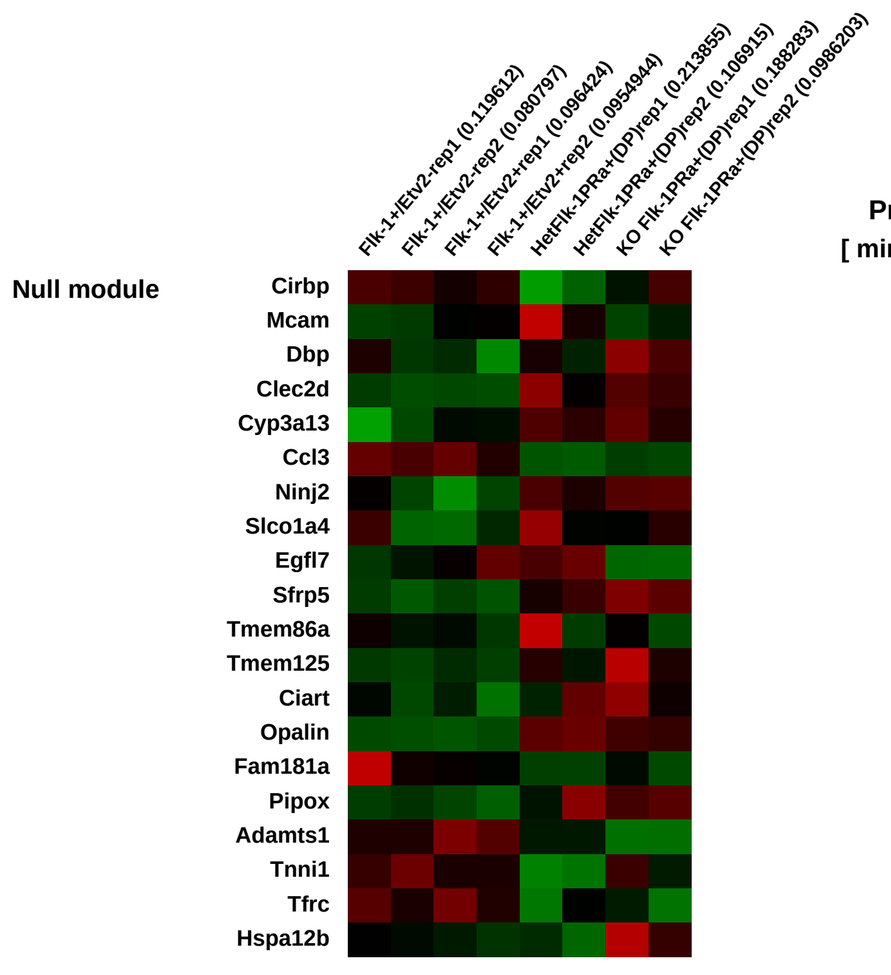

GEO Series "GSE40443" Expression Profiles

Num of samples in this series: 6

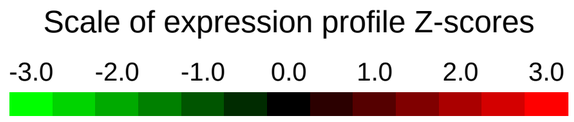

GEO Link:	**http://www.ncbi.nlm.nih.gov/geo/query/acc.cgi?acc=GSE40443**
Status:	**Public on Aug 30 2012**
Title:	**iTreg cells compared to WT Total Treg**
Organism:	**Mus musculus**
Experiment type:	**Expression profiling by array**
Platform:	**GPL1261**
Pubmed ID:	**22966001**
Summary & Design:	**Summary:** **iTreg cells from Tbmc mLN mice treated with one week of 1% Oral Ova were compared to Total Treg from WT mice.** **Overall design:** **CD4+ Foxp3+ cells were also sorted from WT Foxp3 GFP Balb/c mice.**

Background corr dist: **KL-Divergence = 0.0492, L1-Distance = 0.0369, L2-Distance = 0.0020, Normal std = 0.5956**

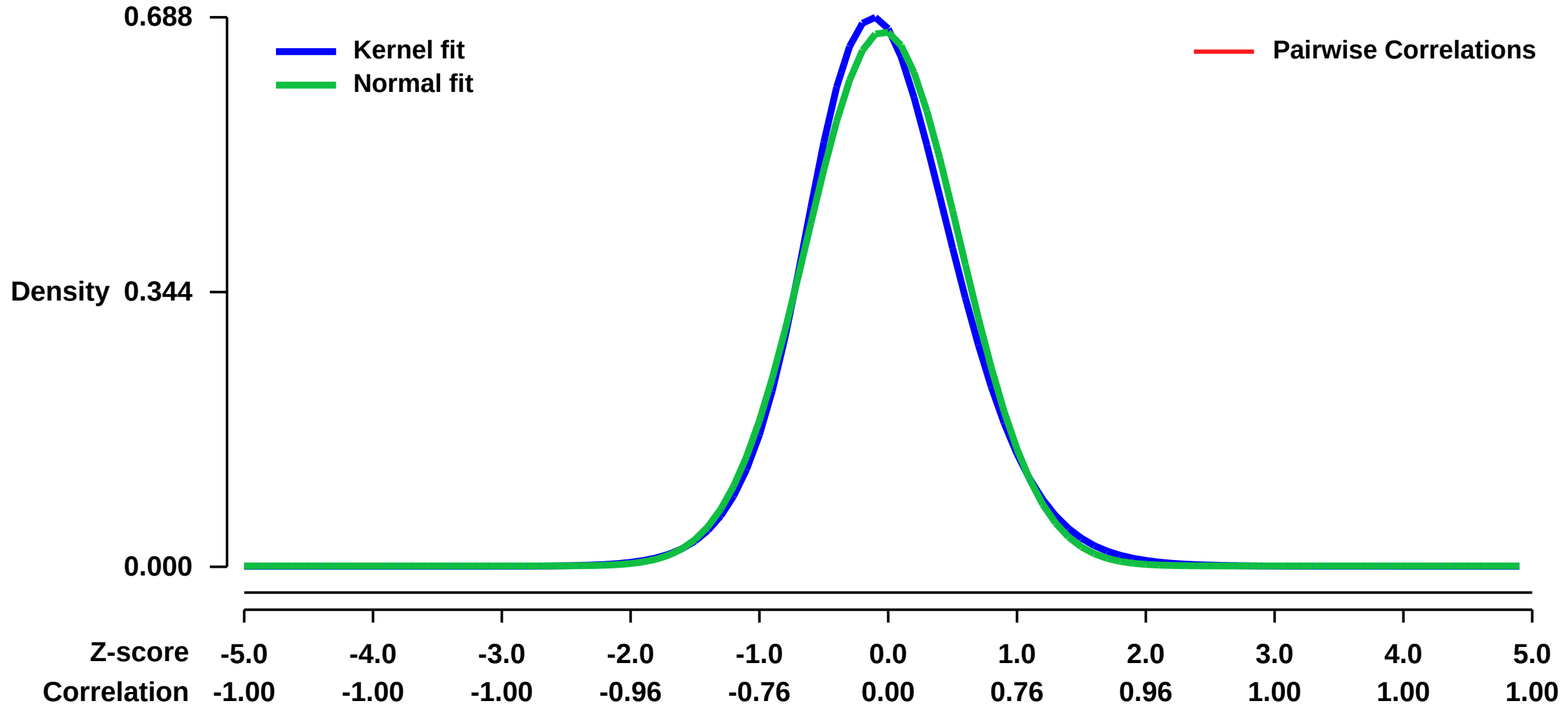

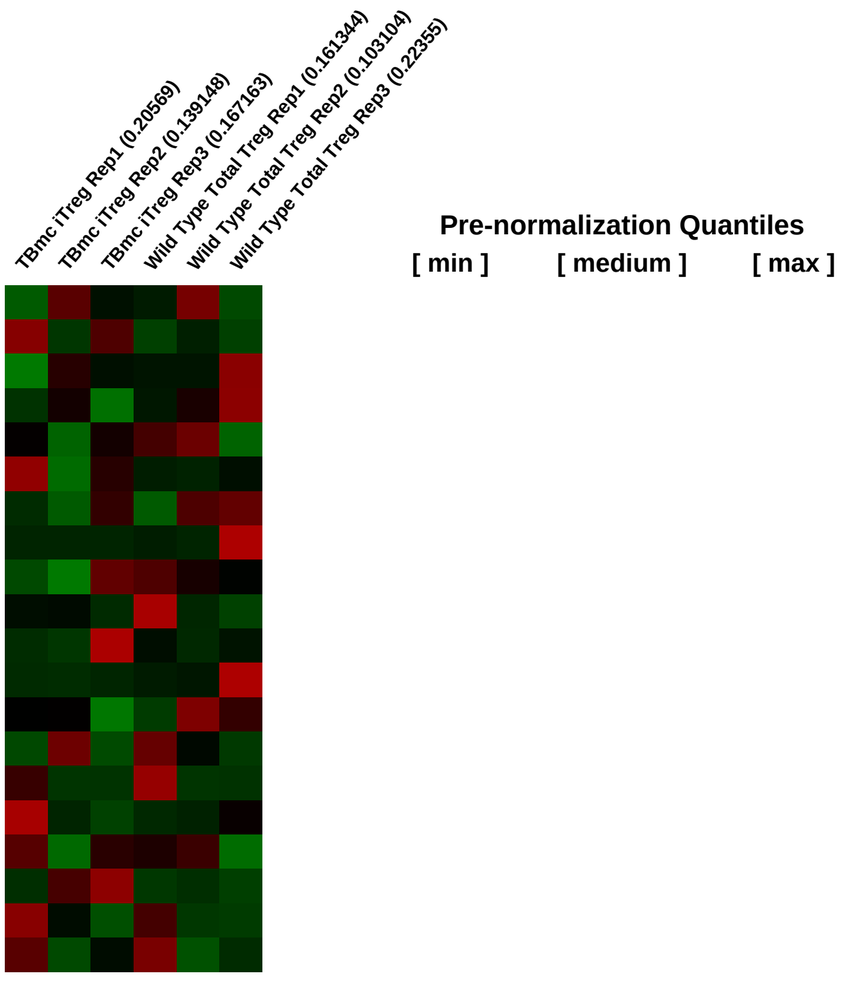

GEO Series "GSE22824" Expression Profiles

Num of samples in this series: 24

Scale of expression profile Z-scores

-3.0 -2.0 -1.0 0.0 1.0 2.0 3.0

GEO Link:	http://www.ncbi.nlm.nih.gov/geo/query/acc.cgi?acc=GSE22824
Status:	Public on Jan 01 2011
Title:	Gene expression in retina and LGN of wild type and Chrnb2-/- mice
Organism:	Mus musculus
Experiment type:	Expression profiling by array
Platform:	GPL1261
Pubmed ID:	21547082
Summary & Design:	**Summary:** Mice lacking the beta 2 subunit (Chrnb2) of the neuronal nicotinic acetylcholine receptor display altered retinal waves and disorganized projections of the retinal ganglion cells to the lateral geniculate nucleus (LGN). mRNA populations from retinas and LGN from Chrnb2-/-and wild type (C57BL/6J) mice were compared at 4 days postnatal, when RGC segregation to the LGN begins in WT mice. Retinal mRNAs were also compared at adulthood. Using microarray hybridization, we identified transcripts which are differentially expressed between Chrnb2-/- and wild type animals in these two tissues at these two ages. **Overall design:** mRNA was isolated from retina and LGN of three male littermates each of WT and Chrnb2-/- mice at P4. mRNA from retinas of two adult male littermates of each type was also examined.

Background corr dist: KL-Divergence = 0.0272, L1-Distance = 0.0235, L2-Distance = 0.0007, Normal std = 0.6813

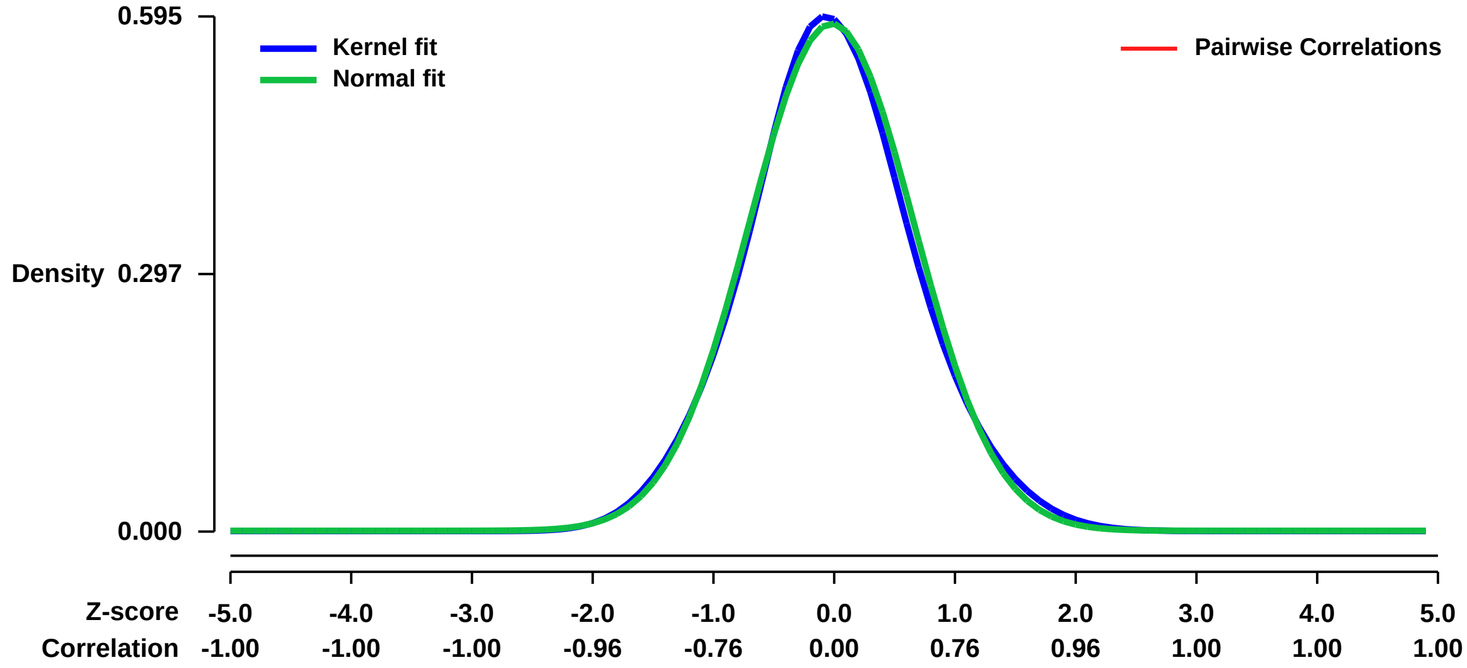

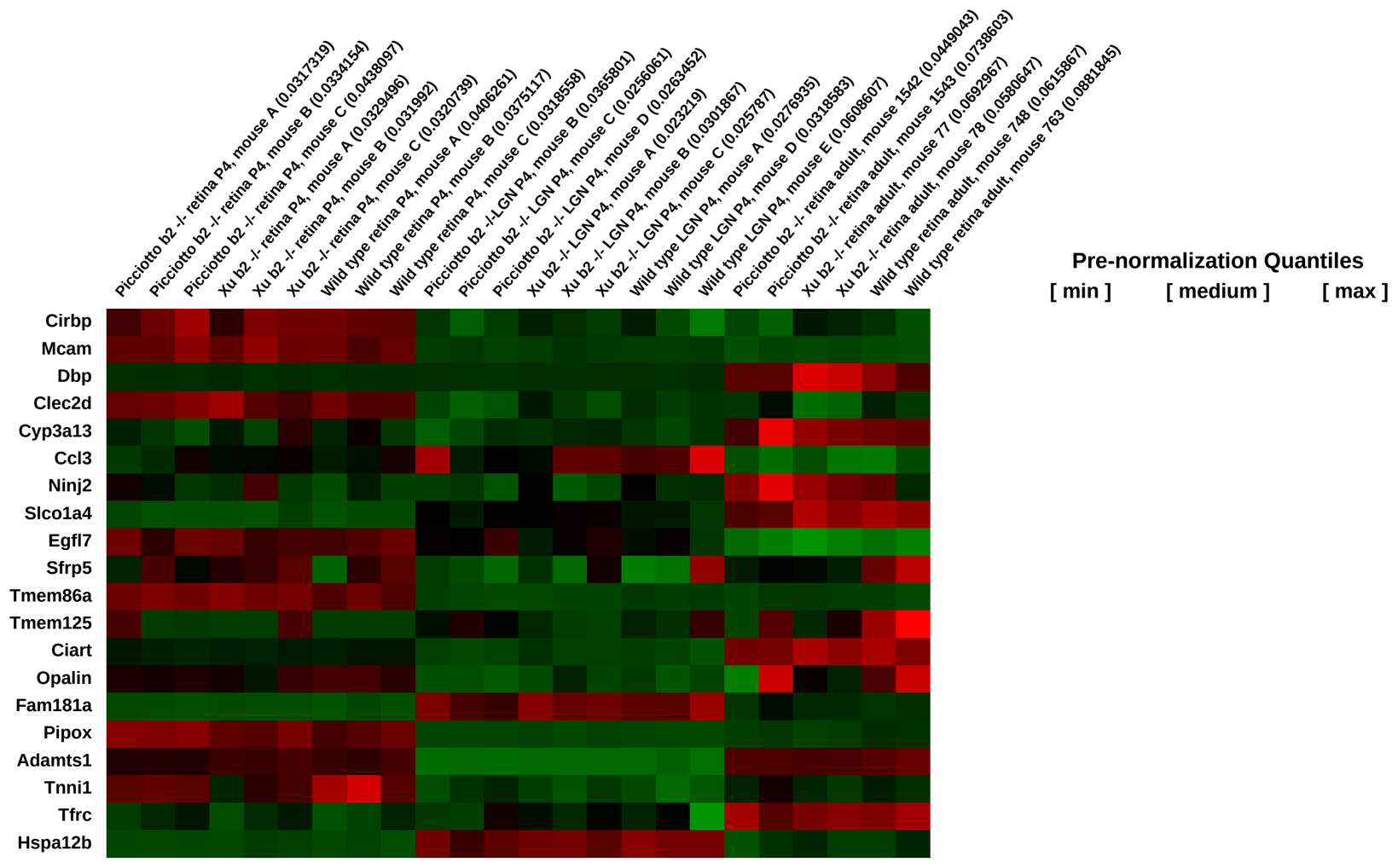

GEO Series "GSE7012" Expression Profiles

Num of samples in this series: 13

Scale of expression profile Z-scores

-3.0 -2.0 -1.0 0.0 1.0 2.0 3.0

GEO Link:	http://www.ncbi.nlm.nih.gov/geo/query/acc.cgi?acc=GSE7012
Status:	Public on May 01 2007
Title:	Identif. of oscillatory genes in somitogenesis from functional genomic analysis of C2C12 myoblast line
Organism:	Mus musculus
Experiment type:	Expression profiling by array
Platform:	GPL1261
Pubmed ID:	17362910
Summary & Design:	**Summary:** During somitogenesis, oscillatory expression of genes in the notch and wnt signaling pathways plays a key role in regulating segmentation. These oscillations in expression levels are elements of a species-specific developmental mechanism. To date, the periodicity and components of the human clock remain unstudied. Here we show that a human mesenchymal stem/stromal cell (MSC) model can be induced to display oscillatory gene expression. We observed that the known cycling gene HES1 oscillated with a 5 hour period, consistent with available data on the rate of somitogenesis in humans. We also observed cycling of Hes1 expression in mouse C2C12 myoblasts with a period of 2 hours, consistent with previous in vitro and embryonic studies. Furthermore, we used microarray and quantitative PCR (Q-PCR) analysis to identify additional genes that display oscillatory expression both in vitro and in mouse embryos. We confirmed oscillatory expression of the notch pathway gene Maml3 and the wnt pathway gene Nkd2 by whole mount in situ hybridization analysis and Q-PCR. Expression patterns of these genes were disrupted in Wnt3atm1Amc mutants but not in Dll3pu mutants. Our results demonstrate that human and mouse in vitro models can recapitulate oscillatory expression observed in embryo and that a number of genes in multiple developmental pathways display dynamic expression in vitro. **Keywords: time series** **Overall design:** Synchronization of C2C12 myoblasts was carried out as follows: T-25 cm flasks were set up in parallel. These cells were grown to 90% confluence in DMEM supplemented with 5% FBS then incubated in DMEM with only 0.2% FBS for 24 hours, and returned to DMEM supplemented with FBS. Samples were collected every 30 min. for 8 hours.

Background corr dist: KL-Divergence = 0.1130, L1-Distance = 0.0298, L2-Distance = 0.0017, Normal std = 0.4214

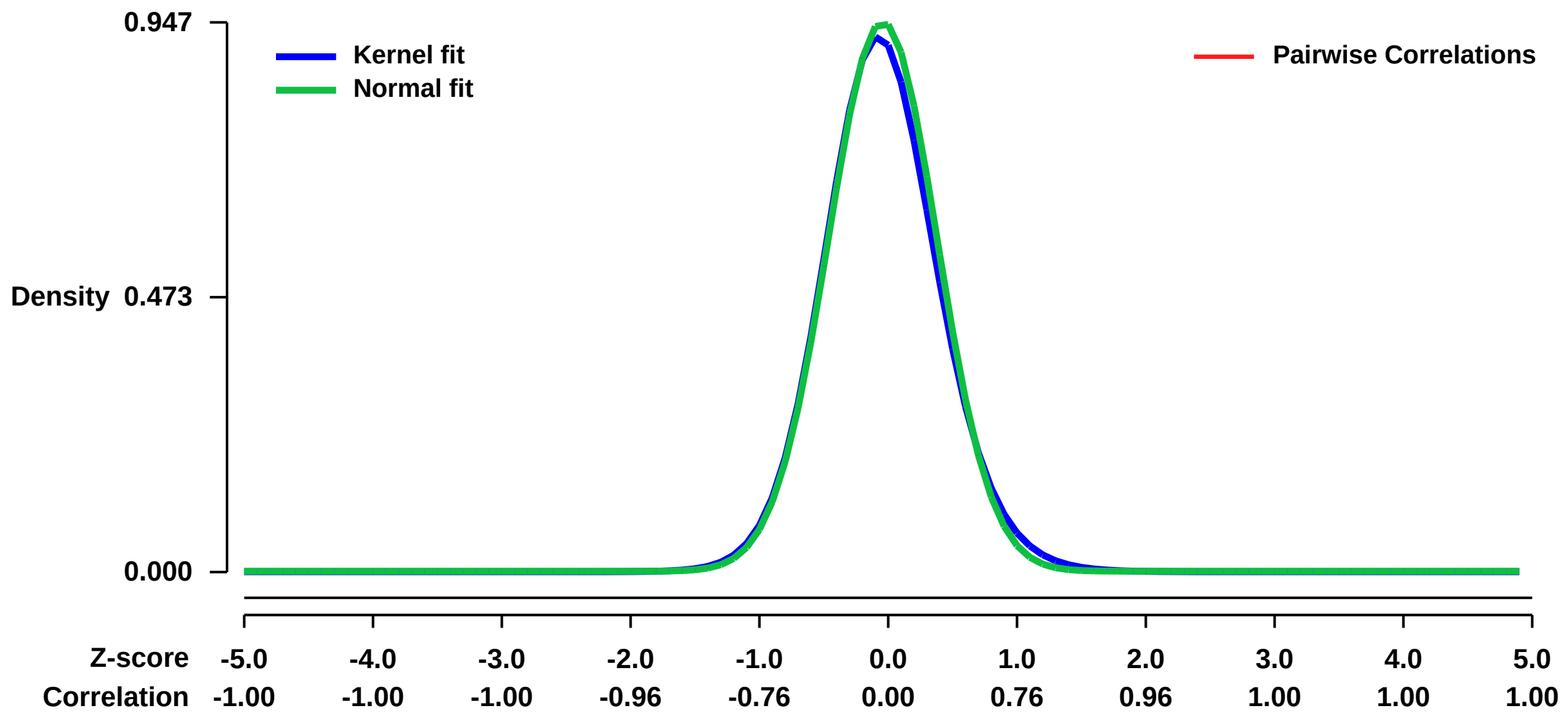

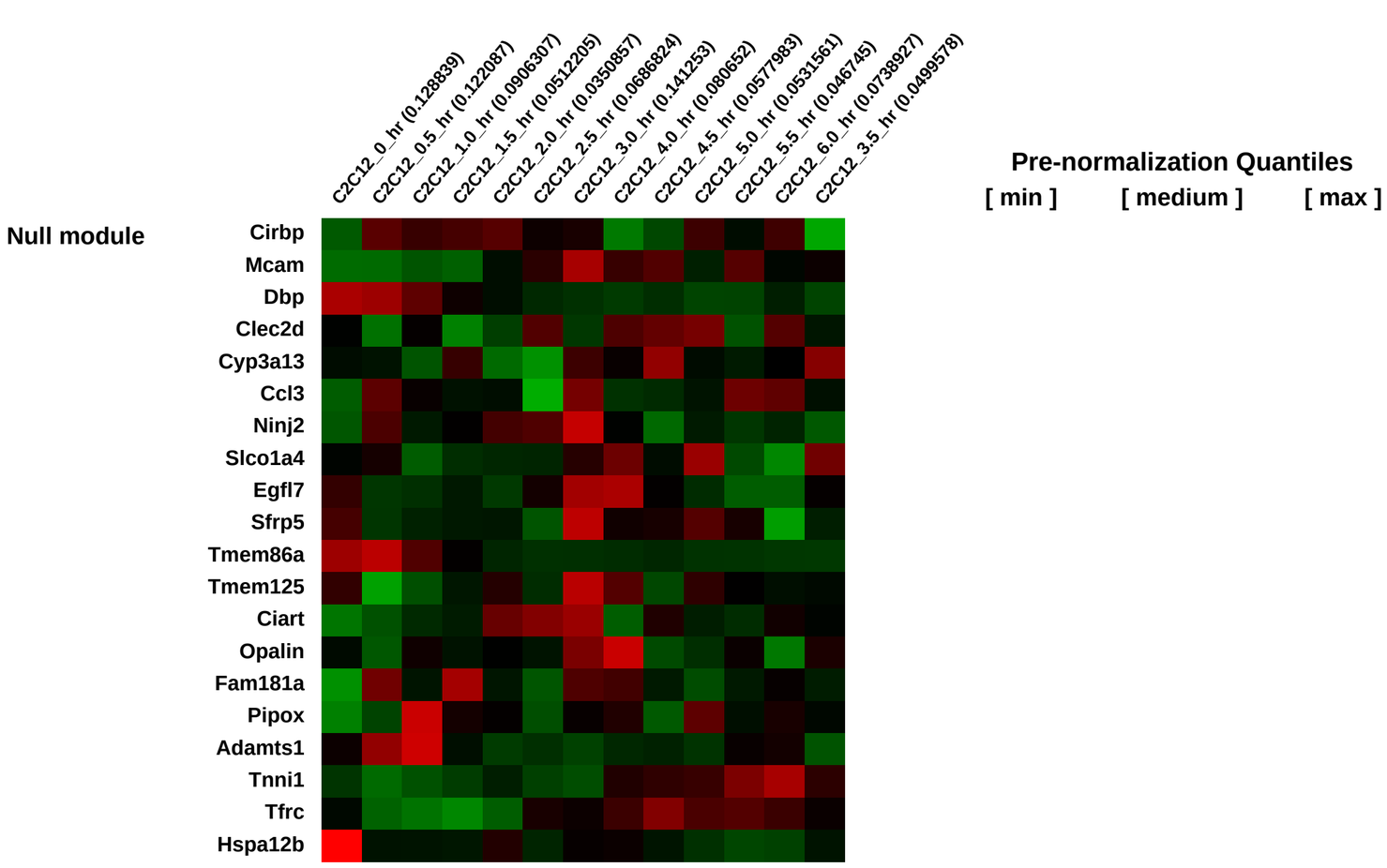

GEO Series "GSE43825" Expression Profiles

Num of samples in this series: 31

Scale of expression profile Z-scores

-3.0 -2.0 -1.0 0.0 1.0 2.0 3.0

GEO Link:	http://www.ncbi.nlm.nih.gov/geo/query/acc.cgi?acc=GSE43825
Status:	Public on Dec 31 2013
Title:	Gene expression profiles from mammary tissue of control mice, small K5¸ N¸†cat hyperplasia, large K5¸ N¸†cat hyperplasia and K5¸ N¸†cat tumor
Organism:	Mus musculus
Experiment type:	Expression profiling by array
Platform:	GPL1261
Pubmed ID:	
Summary & Design:	**Summary:** Basal-like breast cancer is a heterogeneous disease characterised by the expression of basal cell markers, no oestrogen or progesterone receptor expression and a lack of HER2 overexpression. Recent studies have linked activation of the Wnt/beta-catenin pathway to basal-like breast cancer. Transgenic mice expressing N-terminally truncated stabilised beta-catenin in the mammary basal/myoepithelial cell layer (K5deltaNbetacat strain) develop mammary hyperplasias that progress to invasive carcinomas. Histological and microarray analyses of these lesions have revealed their high similarity to a subset of basal-like human breast tumours with squamous differentiation. As in human basal-like carcinomas, the Myc pathway was found to be activated in the mammary lesions of K5deltaNbetacat mice. Mammosphere and transplantation assays showed that a basal cell population with stem/progenitor characteristics was amplified in K5deltaNbetacat mouse preneoplastic glands. Myc deletion from the mammary basal layer of K5deltaNbetacat mice abolished both basal cell regenerative capacity and tumorigenesis. These results show that Myc is essential for beta-catenin-induced stem cell amplification and tumorigenesis and that basal stem/progenitor cells may be at the origin of a subset of basal-like breast tumours. **Overall design:** mammary tissue from K5¸ N¸†cat mice were dissected at successive stages of development (small hyperplasia (n=5), large hyperplasia (n=5), tumor (n=11) and control (n=4)) for RNA extraction and hybridization on Affymetrix microarrays

Background corr dist: KL-Divergence = 0.0953, L1-Distance = 0.0371, L2-Distance = 0.0022, Normal std = 0.4542

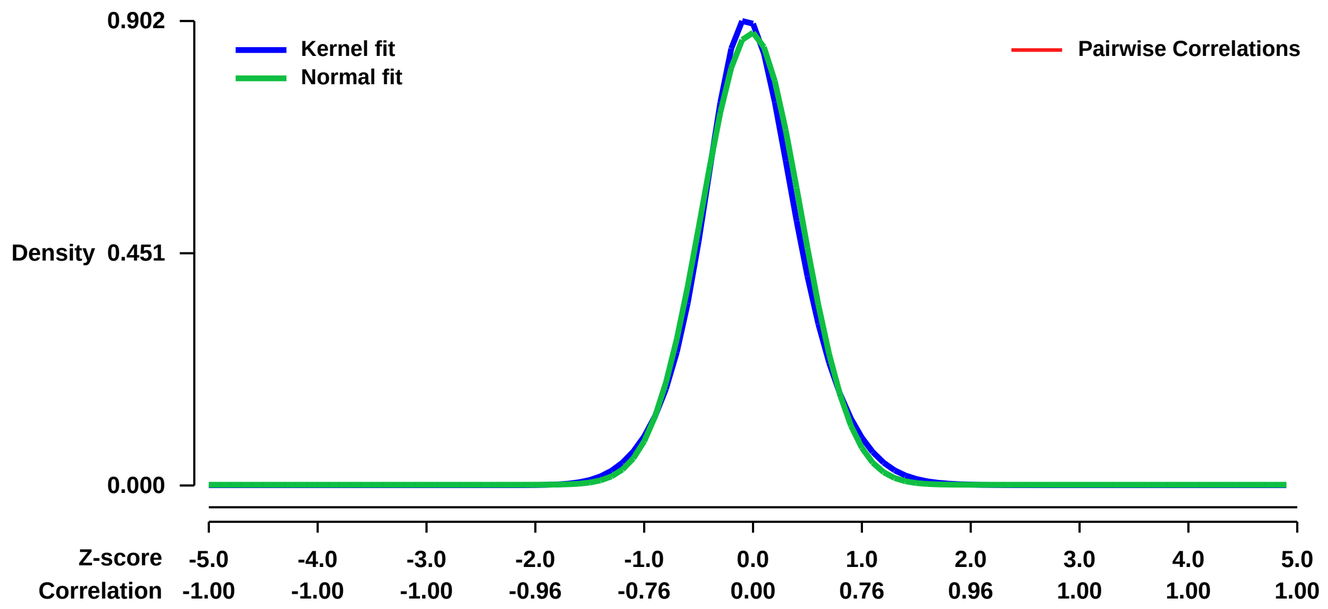

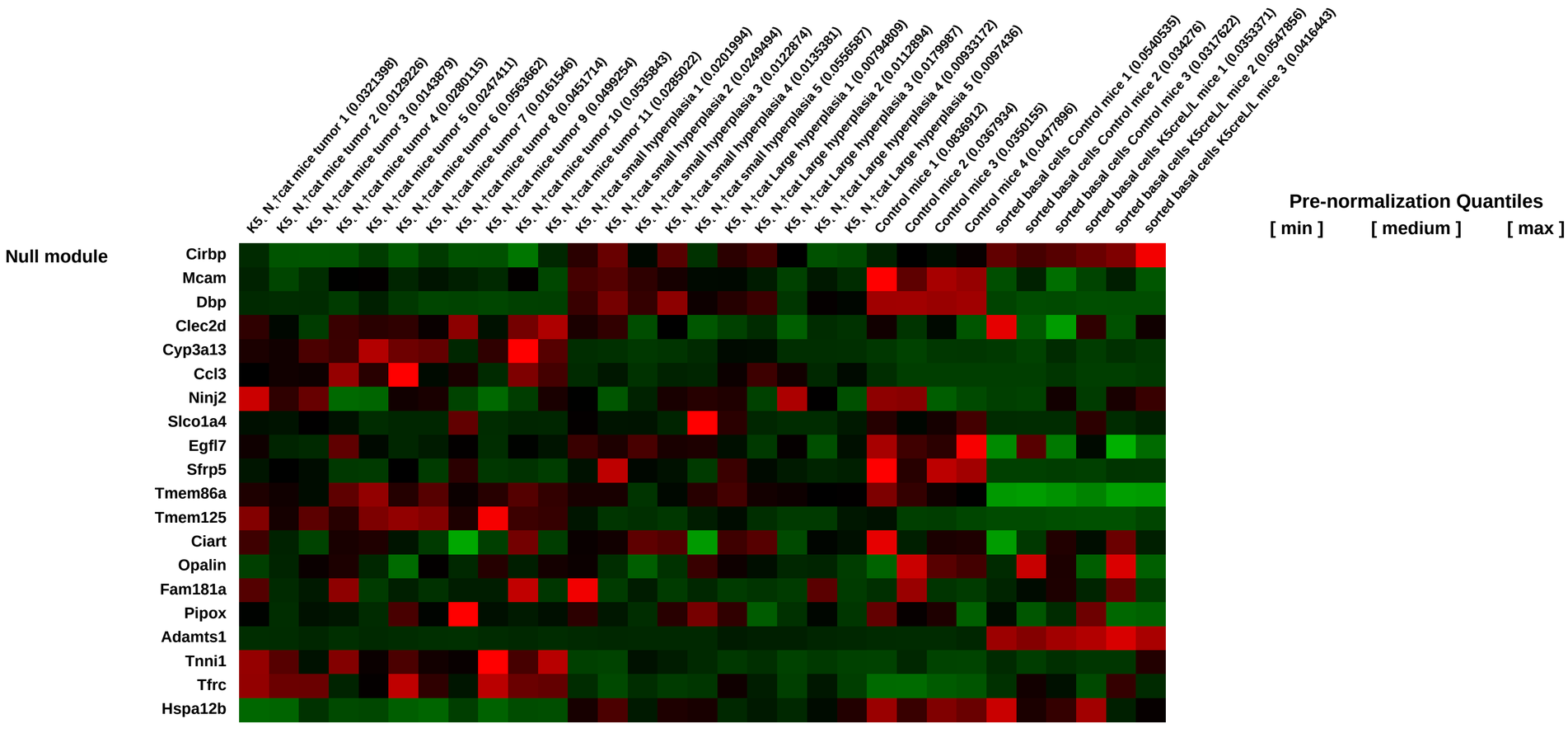

GEO Series "GSE4518" Expression Profiles

Num of samples in this series: 12

Scale of expression profile Z-scores

-3.0 -2.0 -1.0 0.0 1.0 2.0 3.0

GEO Link:	http://www.ncbi.nlm.nih.gov/geo/query/acc.cgi?acc=GSE4518
Status:	Public on Mar 21 2007
Title:	Divergent and Convergent Effects on Gene Expression and Function in Acute versus Chronic Endothelial Activation
Organism:	Mus musculus
Experiment type:	Expression profiling by array
Platform:	GPL1261
Pubmed ID:	17566077
Summary & Design:	**Summary:** Activation of the vascular endothelium with cytokines such as TNF is widely used to study the role of the vasculature in proinflammatory disease. To gain insight into mechanisms of prolonged vascular endothelial activation we compared changes in gene expression induced by continuous activation in stable tmTNFalpha expressing cells with changes due to acute TNFalpha challenge in vitro. Affymetrix Genechip´fi analysis was performed on RNA from control, acute and continuous TNFalpha-activated endothelial cells. Only 36% of the significant changes in gene expression were convergent between the acute and continuously activated endothelial cells in comparison to the control. From the divergently regulated genes, for example the cytokine ENA-78 was specifically induced in chronically activated cells, while E-Selectin, a cell adhesion molecule, was upregulated only in acutely activated endothelial cells. Antioxidant SOD gene induction was noted in acute activation while NADPH oxidase was selectively upregulated in continuous activated endothelium in accordance with significant ROS induction occurred only in these cells. In addition, the anti-angiogenic genes PAI-1 and thrombospondin were upregulated only in acutely activated endothelium, consistent with reduced angiogenic activity observed in acute versus chronically activated endothelial cells in vitro. These data suggest that continuous activation of endothelial cells leads to specific expression and functional changes, consistent with alterations observed in dysfunctional endothelium exposed to or involved in chronic inflammation. **Keywords: Expression profiling** **Overall design:** This experiment compares the response of endothelial cells from newborn mice that were either stably transfected with a non-cleavable transmembrane mutant form of murine TNFalpha, or treated with soluble TNFalpha (20ng/ml) for 4 hours. Each treatment was compared to mock-transfected control cells. Four replicates for each condition were used. Five micrograms of total RNA was assayed per Genechip using standard Affymetrix protocols.

Background corr dist: KL-Divergence = 0.1479, L1-Distance = 0.0409, L2-Distance = 0.0037, Normal std = 0.3783

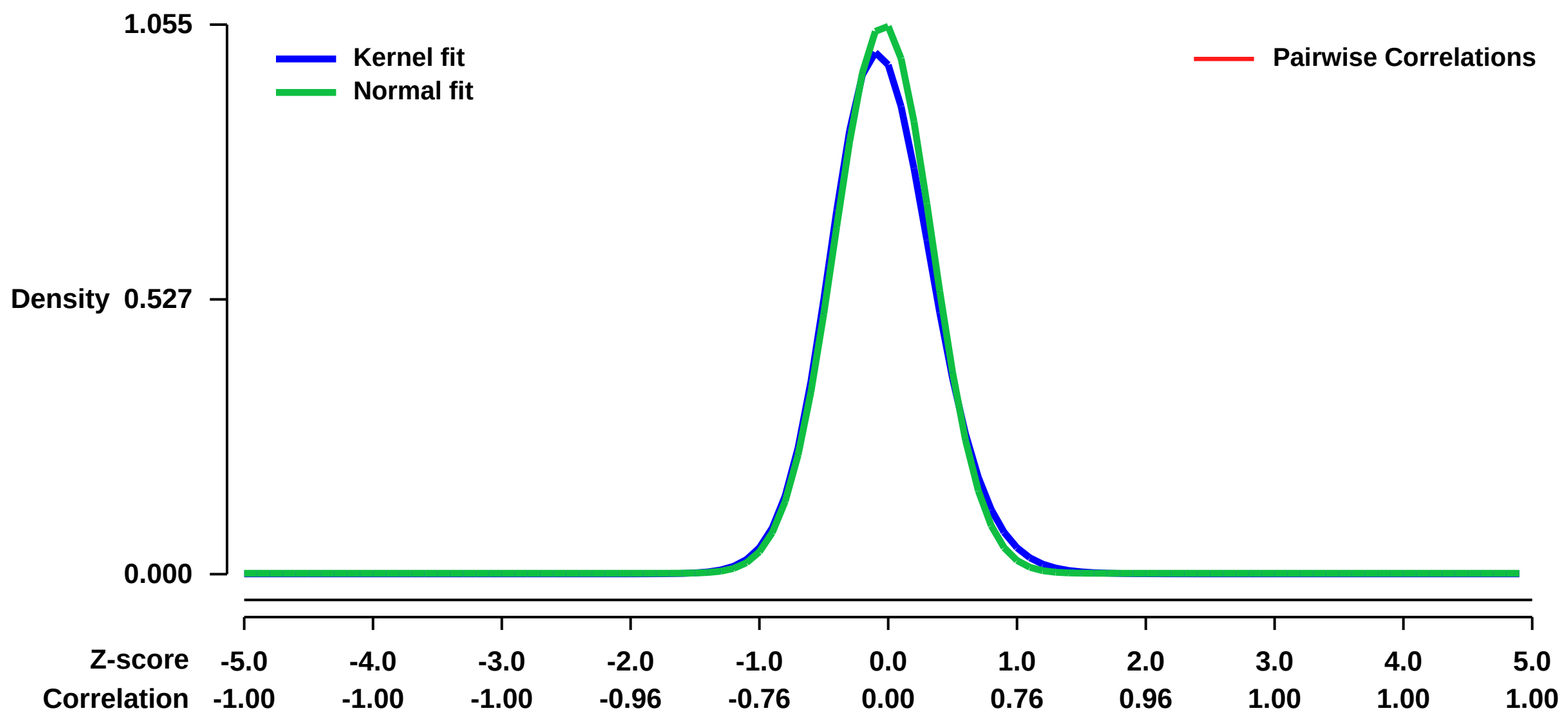

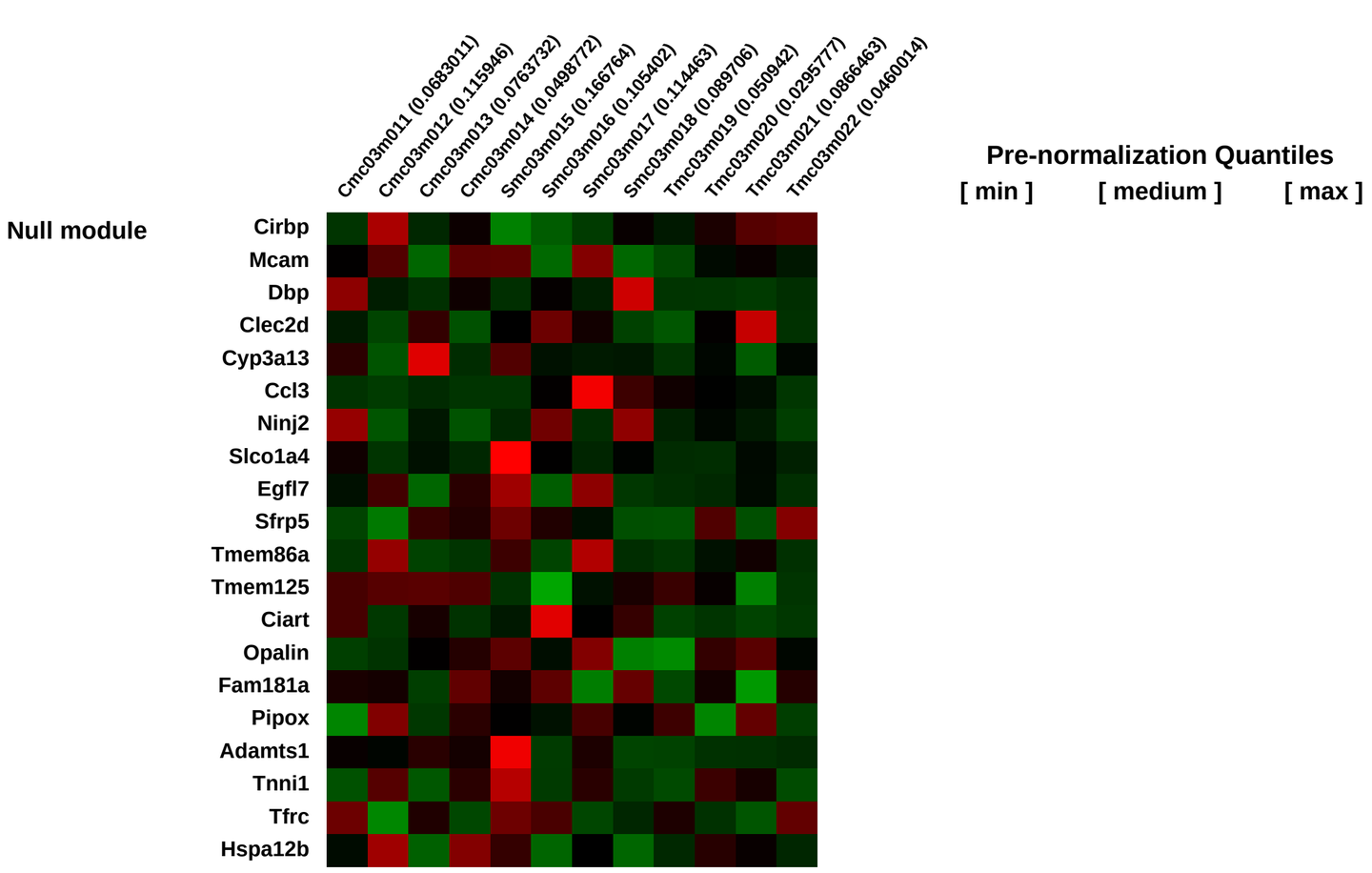

GEO Series "GSE26461" Expression Profiles

Num of samples in this series: 6

Scale of expression profile Z-scores

-3.0 -2.0 -1.0 0.0 1.0 2.0 3.0

GEO Link:	http://www.ncbi.nlm.nih.gov/geo/query/acc.cgi?acc=GSE26461
Status:	Public on Dec 01 2012
Title:	Epigenetic regulation of type 1 diabetes in nonobese diabetic mice
Organism:	Mus musculus
Experiment type:	Expression profiling by array
Platform:	GPL1261
Pubmed ID:	23383062
Summary & Design:	**Summary:** **Background: Epigenetic alteration of the genome has been shown to provide palliative effects in mouse models of certain human autoimmune disorders. We have investigated whether chromatin remodeling could provide protection against autoimmune diabetes in nonobese diabetic (NOD) mice. Treatment of female mice during the transition from prediabetic to diabetic stage (18-24 weeks of age) with the well-characterized histone deacetylase inhibitor, Trichostatin A (TSA) effectively reduced the incidence of diabetes and abrogated the ability of splenocytes to adoptively transfer the disease into immunodeficient NOD.scid mice. Protection against diabetes was accompanied by histone hyperacetylation in pancreas and spleen, increased frequency of CD4+ CD62L+ cells in the spleen, reduction in cellular infiltration of islets, restoration of normoglycemia and glucose-induced insulin release by beta cells. In vitro activation of splenic T lymphocytes derived from protected mice resulted in enhanced expression of IFN-gamma mRNA and protein without altering the expression of Il4, Il17, Il18, Inos, and Tnfa genes nor the secretion of IL-2, IL-4, IL-17 and TNF-alpha proteins. Consistently, expression of the transcription factor involved in Ifng transcription, Tbet/Tbx21 but not Gata3 and Rorgt, respectively required for the transcription of Il4 and Il17, was upregulated in activated splenocytes of protected mice. These data indicate that abrogation of autoimmune diabetes is associated with the selective upregulation of certain inducible genes in T lymphocytes.** **Microarray analysis was performed to determine the changes in global gene expression underlying abrogation of autoimmune diabetes by TSA-mediated epigenetic modulation and identified a distinct group of genes down-regulated during this process.** **Overall design:** **Female NOD mice were treated with Trichostatin A (500 ´¡g/Kg body weight) between 18-24 weeks of age or left untreated.**

Background corr dist: KL-Divergence = 0.0144, L1-Distance = 0.0197, L2-Distance = 0.0006, Normal std = 0.7962

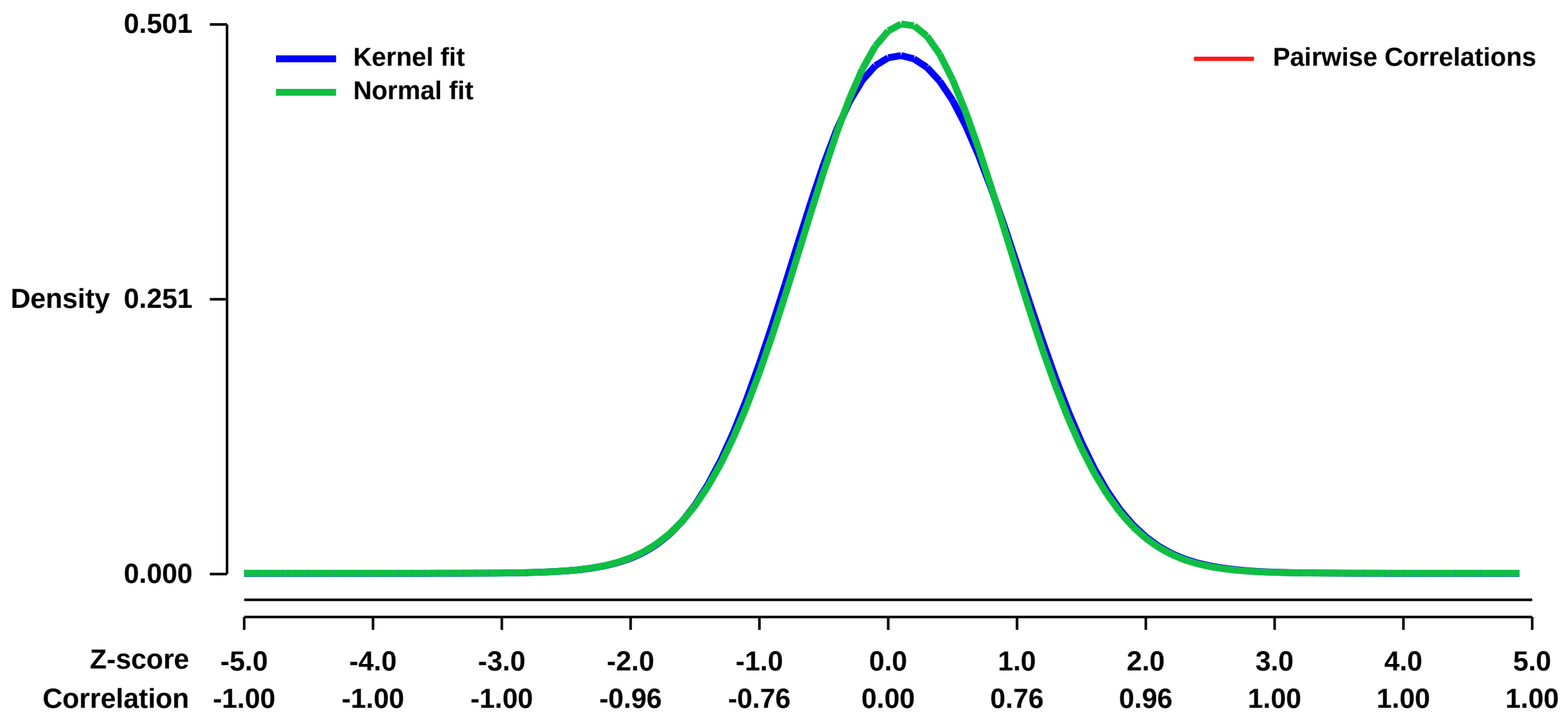

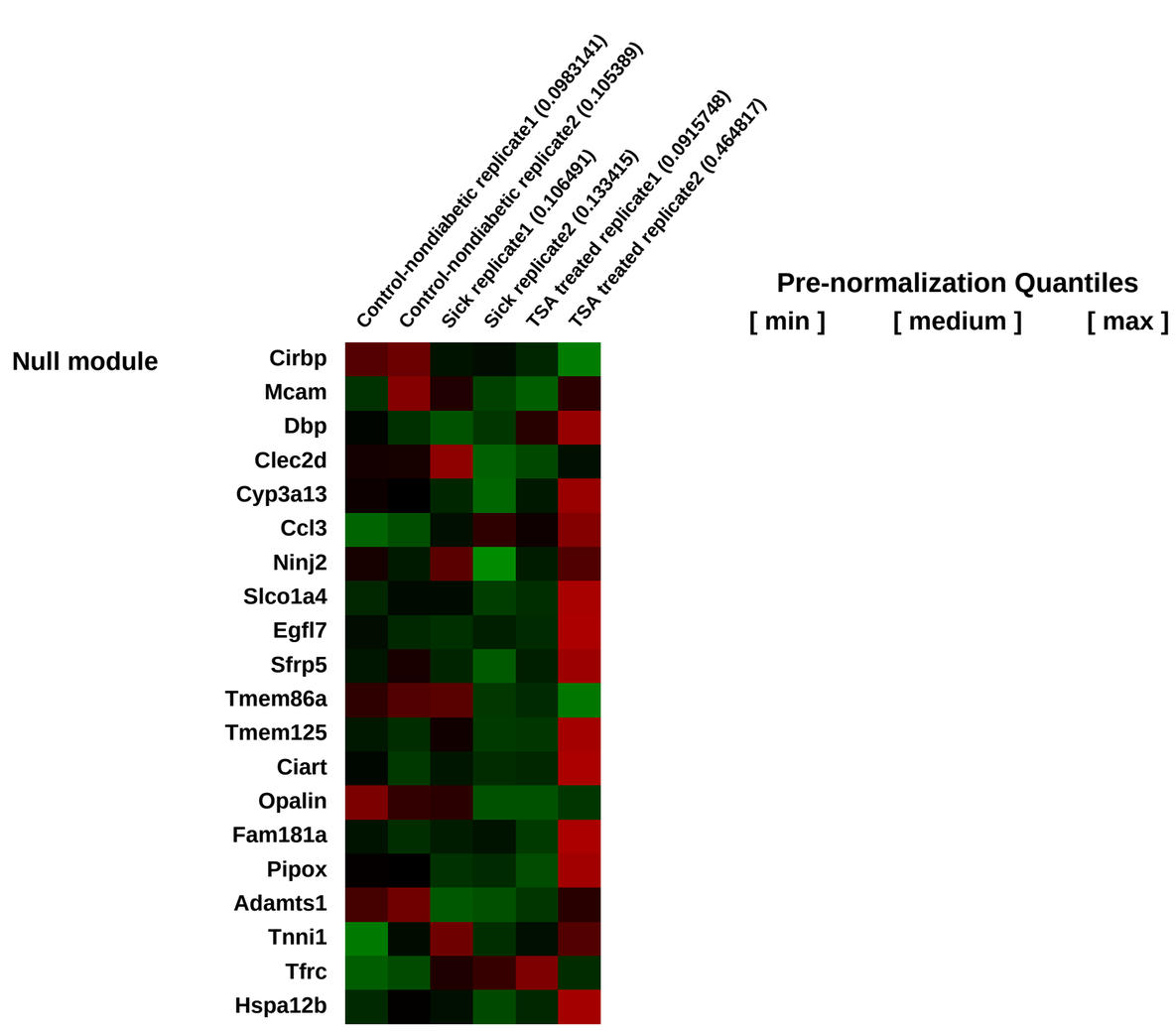

GEO Series "GSE7381" Expression Profiles

Num of samples in this series: 6

Scale of expression profile Z-scores

-3.0 -2.0 -1.0 0.0 1.0 2.0 3.0

GEO Link:	**http://www.ncbi.nlm.nih.gov/geo/query/acc.cgi?acc=GSE7381**
Status:	**Public on Apr 12 2007**
Title:	**Expression profiling of back skin of Get1 and control mice at e18.5**
Organism:	**Mus musculus**
Experiment type:	**Expression profiling by array**
Platform:	**GPL1261**
Pubmed ID:	**16949565**
Summary & Design:	**Summary:** **Defective permeability barrier is an important feature of many skin diseases and causes mortality in premature infants. To investigate the control of barrier formation, we characterized the epidermally expressed Grainyhead-like epithelial transactivator (Get-1)/Grhl3, a conserved mammalian homologue of Grainyhead, which plays important roles in cuticle development in Drosophila. Get-1 interacts with the LIM-only protein LMO4, which is co-expressed in the developing mammalian epidermis. The epidermis of Get-1(-/-) mice showed a severe barrier function defect associated with impaired differentiation of the epidermis, including defects of the stratum corneum, extracellular lipid composition and cell adhesion in the granular layer. The Get-1 mutation affects multiple genes linked to terminal differentiation and barrier function, including most genes of the epidermal differentiation complex. Get-1 therefore directly or indirectly regulates a broad array of epidermal differentiation genes encoding structural proteins, lipid metabolizing enzymes and cell adhesion molecules. Although deletion of the LMO4 gene had no overt consequences for epidermal development, the epidermal terminal differentiation defect in mice deleted for both Get-1 and LMO4 is much more severe than in Get-1(-/-) mice with striking impairment of stratum corneum formation. These findings indicate that the Get-1 and LMO4 genes interact functionally to regulate epidermal terminal differentiation.** **Keywords: knockout and wildtype mice comparison** **Overall design:** **The same region of the mouse back skin was excised from three Get1 +/+ and three Get1 â /â mice at e18.5.**

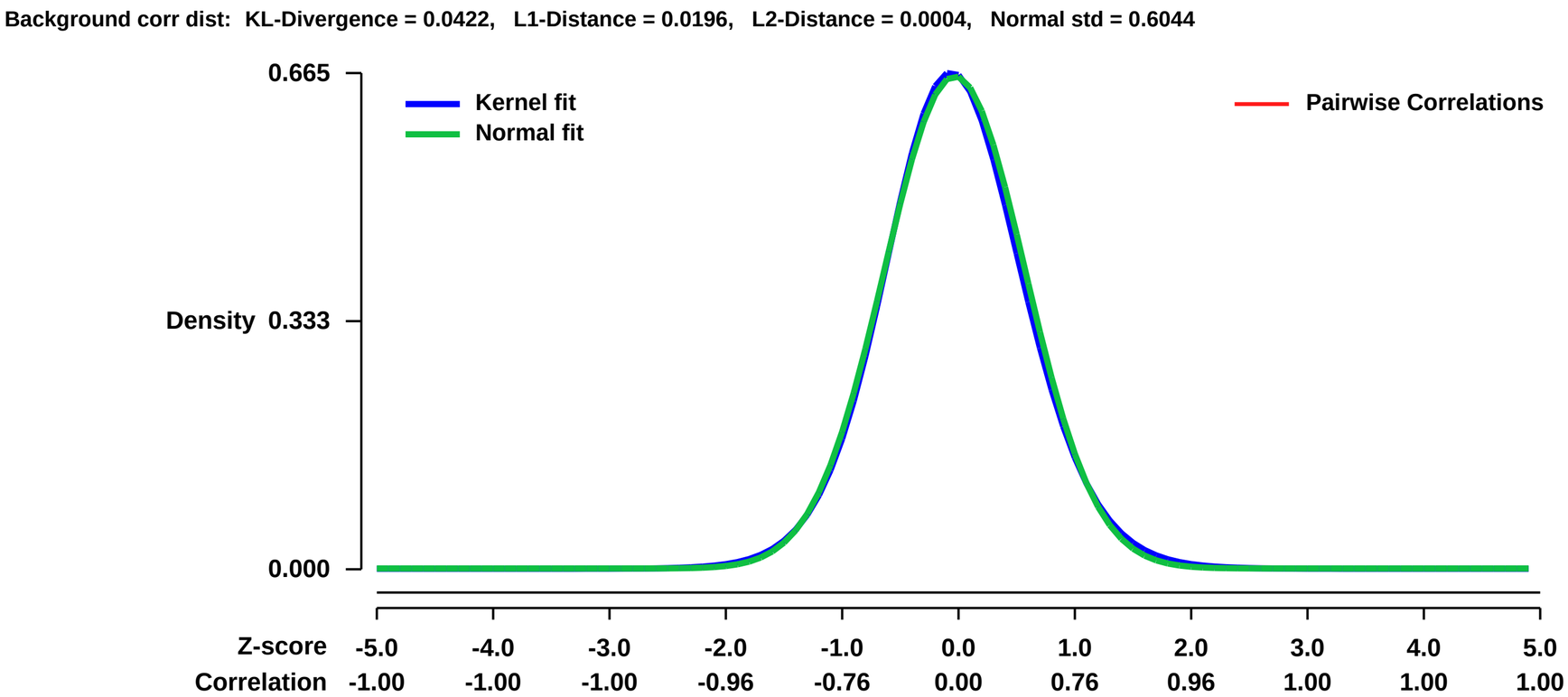

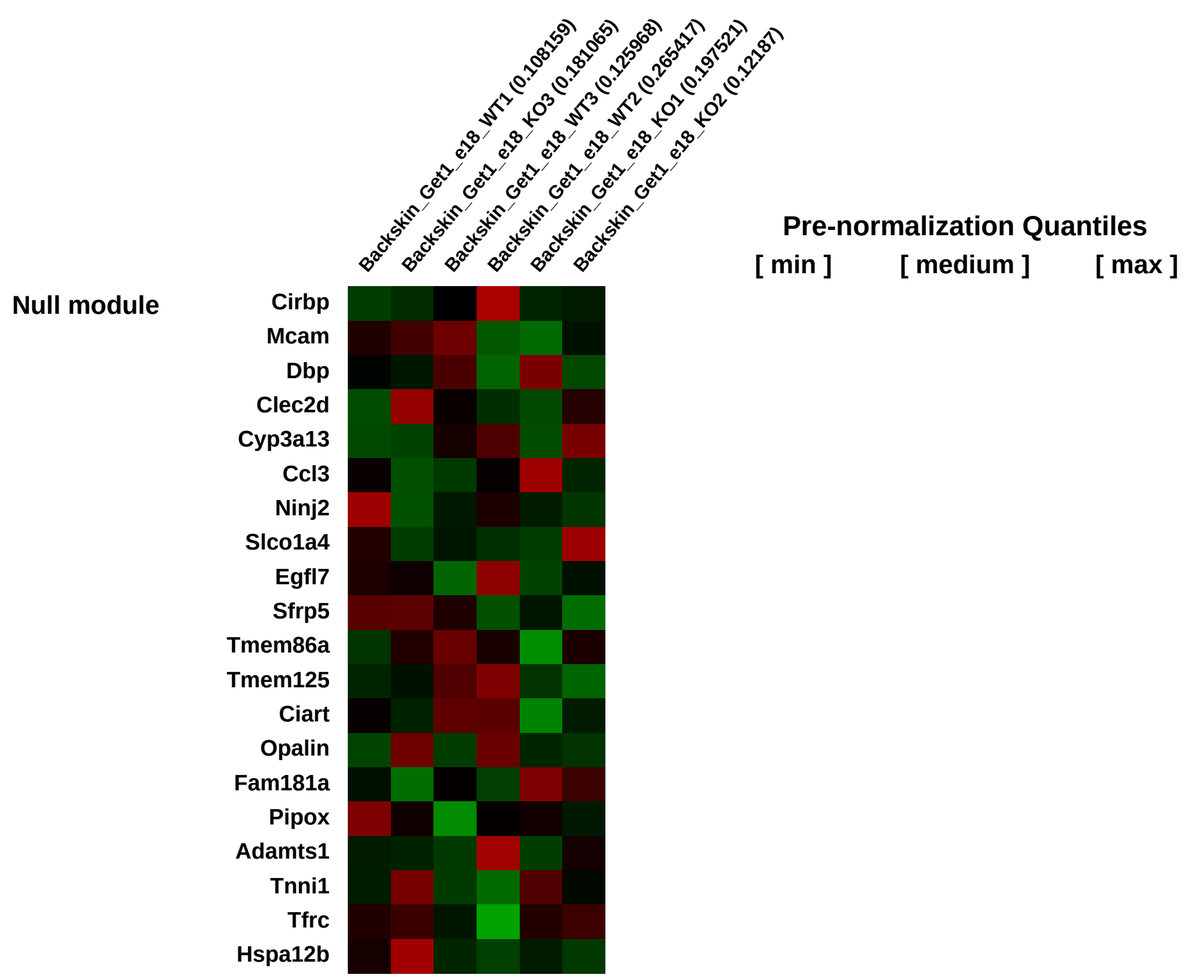

GEO Series "GSE30852" Expression Profiles

Num of samples in this series: 6

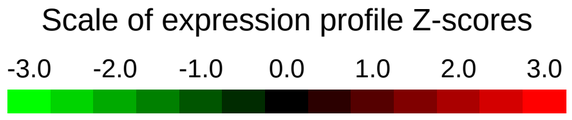

GEO Link:	http://www.ncbi.nlm.nih.gov/geo/query/acc.cgi?acc=GSE30852
Status:	Public on Sep 02 2011
Title:	Expression data from Bmi1 mutant versus wild-type lung cells
Organism:	Mus musculus
Experiment type:	Expression profiling by array
Platform:	GPL1261
Pubmed ID:	21885022
Summary & Design:	**Summary:** **Bmi1 is an important stem cell regulator in multiple tissues, including the lung.** **We used microarrays to analyze the dysregulation of gene expression in the absence of Bmi1 in the lung, to identify pathways important in Bmi1-dependent lung stem cell regulation** **Overall design:** **Primary lung cells (CD31-negative, CD45-negative) were FACS-isolated from Bmi1 wild-type or mutant mice; RNA was then extracted, amplified, and analyzed using Affymetrix Mouse Genome 430 2.0 Arrays.**

Background corr dist: **KL-Divergence = 0.0439, L1-Distance = 0.0208, L2-Distance = 0.0005, Normal std = 0.5988**

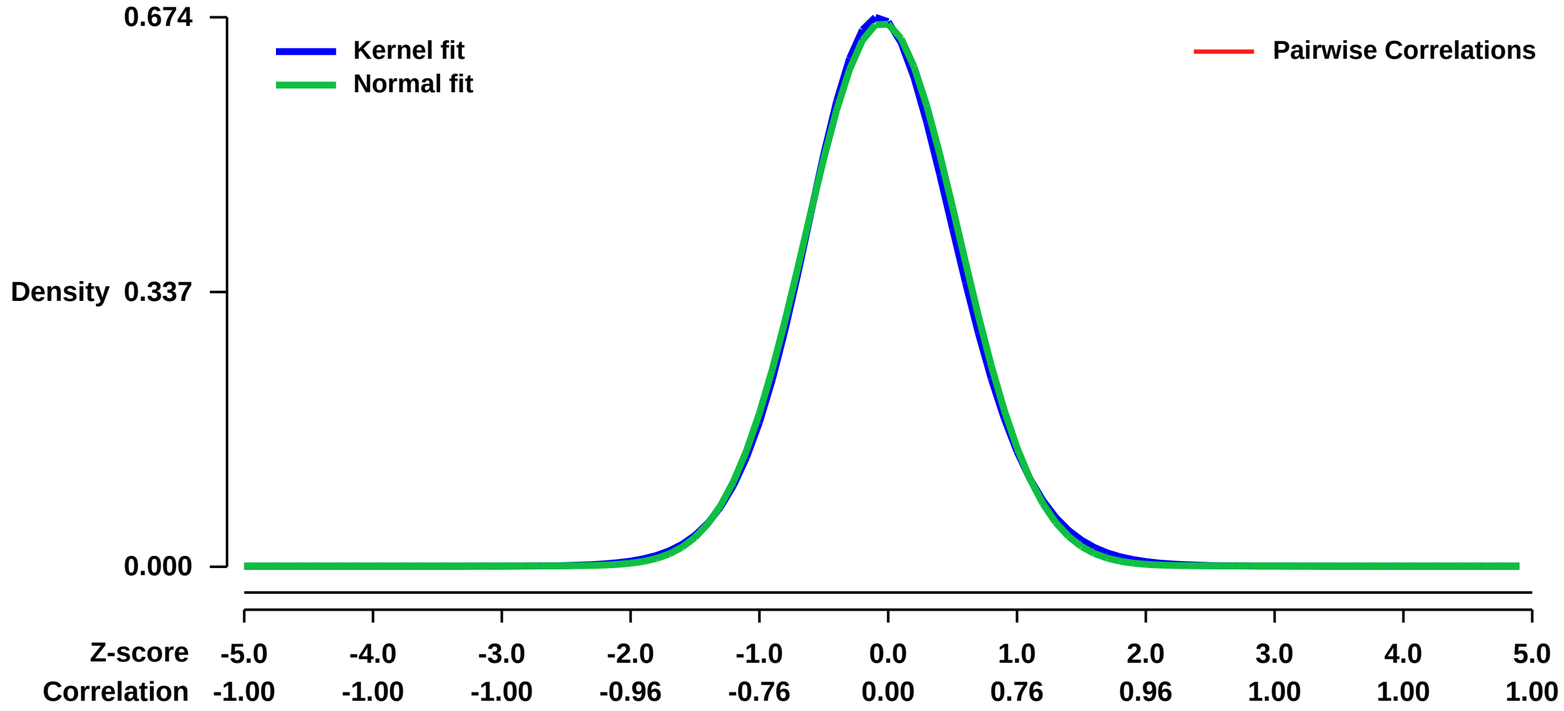

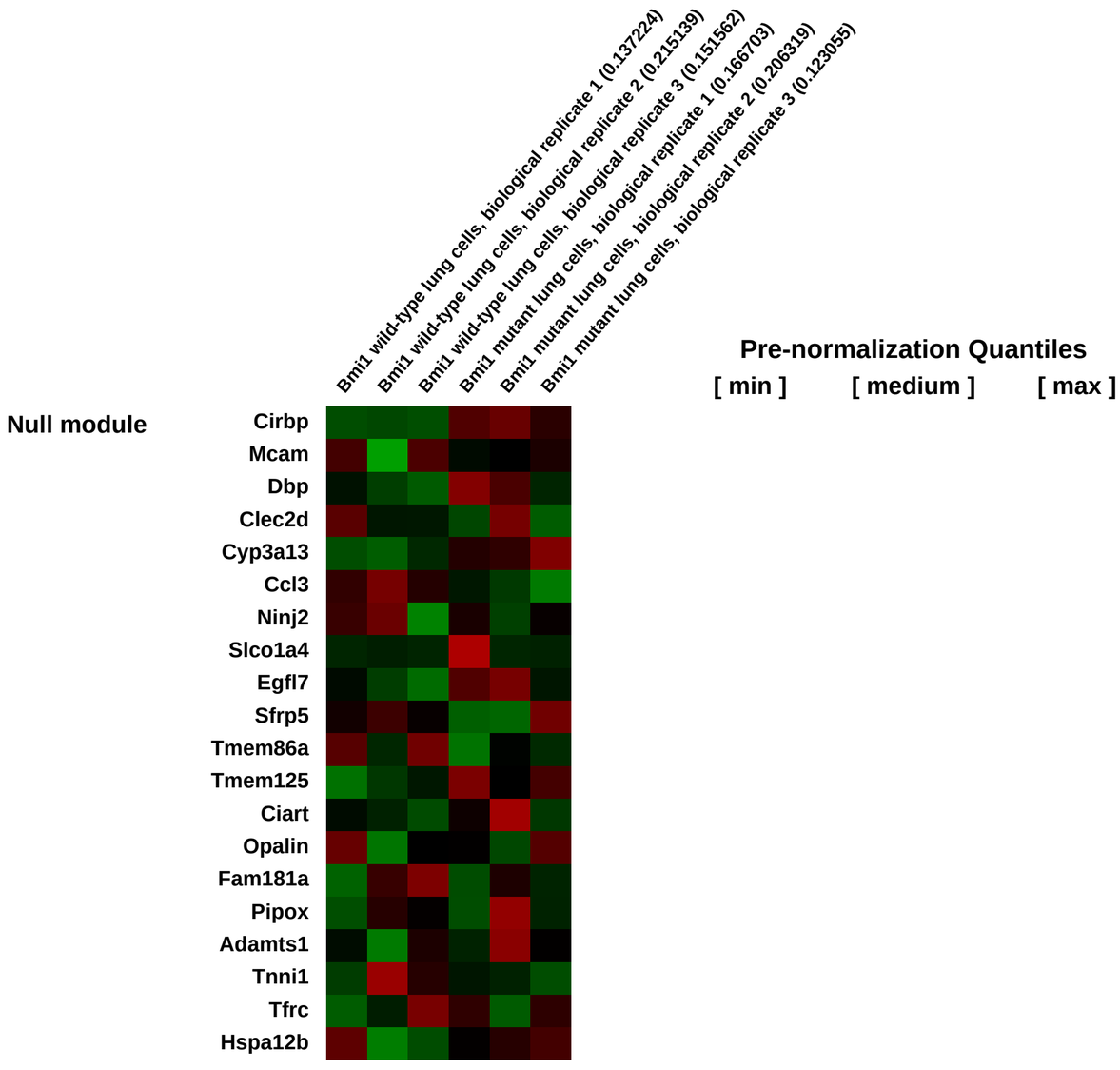

GEO Series "GSE10516" Expression Profiles

Num of samples in this series: 6

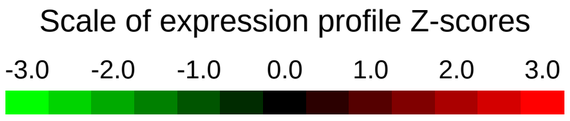

GEO Link:	**http://www.ncbi.nlm.nih.gov/geo/query/acc.cgi?acc=GSE10516**
Status:	**Public on Feb 15 2008**
Title:	**Identification of genes controlled by LMX1B in the developing mouse hindlimb bud**
Organism:	**Mus musculus**
Experiment type:	**Expression profiling by array**
Platform:	**GPL1261**
Pubmed ID:	**18351676**
Summary & Design:	**Summary:** **A control vs. genetic knockout experiment aimed at determining what RNAs are upregulated or downregulated in e11.5 mouse proximal limb tissue lacking the Lmx1b gene. Because Lmx1b is required for dorsal-ventral patterning of the limb, this screen gives insight into what putative downstream targets of Lmx1b contribute to dorsal-ventral patterning.** **Keywords: Genetic allele comparison** **Overall design:** **The proximal portion of e11.5 hindlimb buds (~500um) was used for RNA extraction. Each array was hybridized with pooled cRNAs from both hindlimb buds of three embryos (6 hindlimbs/sample).**

Background corr dist: **KL-Divergence = 0.0438, L1-Distance = 0.0172, L2-Distance = 0.0003, Normal std = 0.5963**

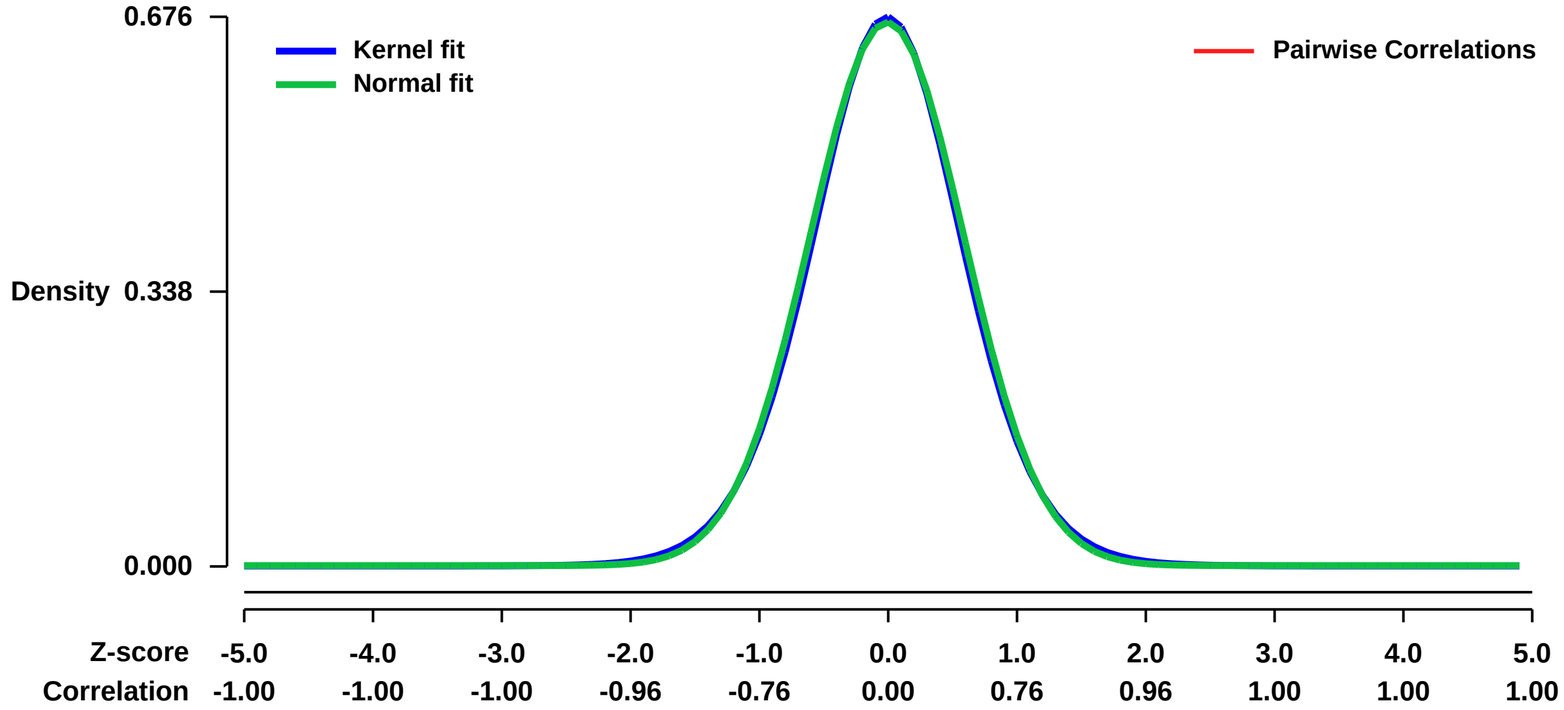

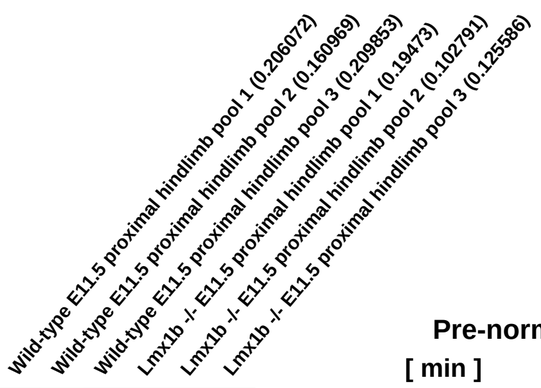

Pre-normalization Quantiles

[min] [medium] [max]

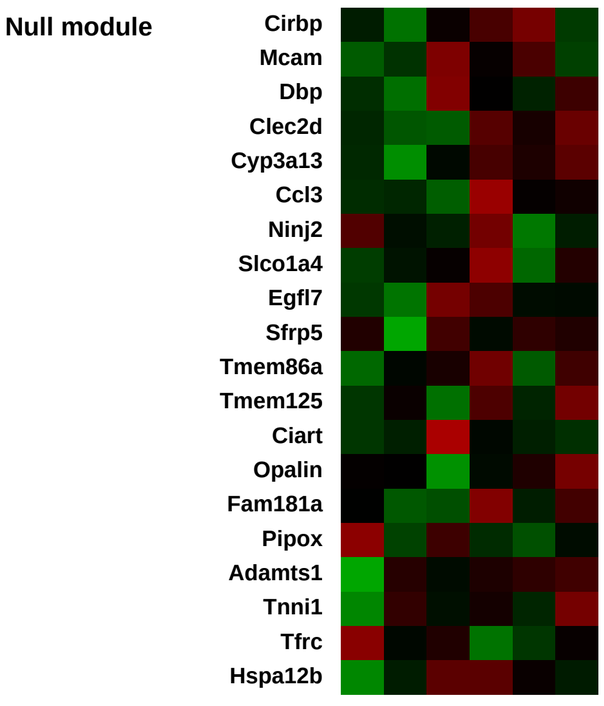

GEO Series "GSE18326" Expression Profiles

Num of samples in this series: 8

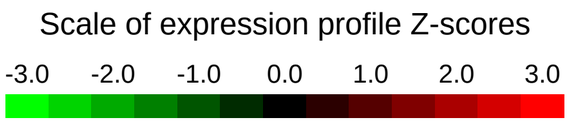

GEO Link:	http://www.ncbi.nlm.nih.gov/geo/query/acc.cgi?acc=GSE18326
Status:	Public on Nov 29 2009
Title:	Role of FoxO3 in adult neural stem cell maintenance in mice
Organism:	Mus musculus
Experiment type:	Expression profiling by array
Platform:	GPL1261
Pubmed ID:	19896443
Summary & Design:	**Summary:** In the nervous system, neural stem cells (NSC) are necessary for the generation of new neurons and for cognitive function. Here we show that FoxO3, a member of a transcription factor family known to extend lifespan in invertebrates, regulates the NSC pool. We find that adult FoxO3-/- mice have fewer NSC in vivo than wild type counterparts. NSC isolated from adult FoxO3-/- mice have decreased self-renewal and an impaired ability to generate different neural lineages. Identification of the FoxO3-dependent gene expression profile in NSC suggests that FoxO3 regulates the NSC pool by inducing a program of genes that preserves quiescence, prevents premature differentiation, and controls oxygen metabolism. The ability of FoxO3 to prevent the premature depletion of NSC might have important implications for counteracting brain aging in long-lived species. **Overall design:** mRNA expression from secondary neurospheres cultured from cells taken from mouse forebrains was compared between FoxO3+/+ (wildtype) and FoxO3-/- (null mutant) mice from the FVB/N background.

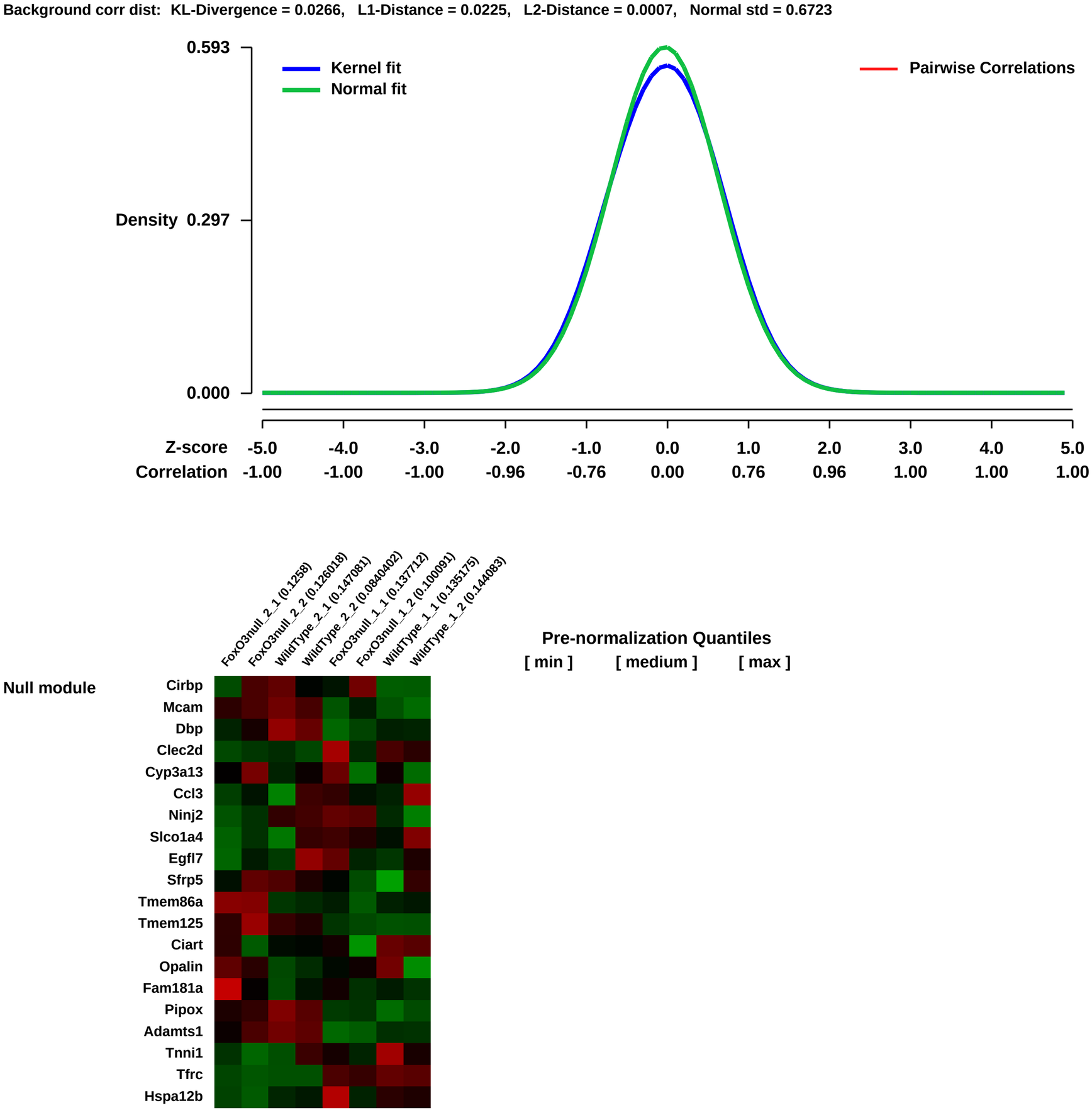

GEO Series "GSE38074" Expression Profiles

Num of samples in this series: 39

Scale of expression profile Z-scores

-3.0 -2.0 -1.0 0.0 1.0 2.0 3.0

GEO Link:	http://www.ncbi.nlm.nih.gov/geo/query/acc.cgi?acc=GSE38074
Status:	Public on Aug 23 2012
Title:	Scaling proprioceptor gene transcription by retrograde NT3 signaling
Organism:	Mus musculus
Experiment type:	Expression profiling by array
Platform:	GPL1261
Pubmed ID:	23029089
Summary & Design:	**Summary:** Transcriptional analysis of identified DRG subpopulations. Cell-type specific intrinsic programs instruct neuronal subpopulations before target-derived factors influence later neuronal maturation. Retrograde neurotrophin signaling controls neuronal survival and maturation of dorsal root ganglion (DRG) sensory neurons, but how these potent signaling pathways intersect with transcriptional programs established at earlier developmental stages remains poorly understood. Here we determine the consequences of genetic alternation of NT3 signaling on genome-wide transcription programs in proprioceptors, an important sensory neuron subpopulation involved in motor reflex behavior. We find that the expression of many proprioceptor-enriched genes is dramatically altered by genetic NT3 elimination, independent of survival-related activities. Combinatorial analysis of gene expression profiles with proprioceptors isolated from mice expressing surplus muscular NT3 identifies an anticorrelated gene set with transcriptional levels scaled in opposite directions. Voluntary running experiments in adult mice further demonstrate the maintenance of transcriptional adjustability of genes expressed by DRG neurons, pointing to life-long gene expression plasticity in sensory neurons. **Overall design:** We combined a mouse line expressing GFP under the control of the TrkC promoter (BAC transgene approach) with various NT3 signaling mutants in order to identify the transcriptional changes in identified subpopulations of dorsal root ganglia (DRG) neurons. Sorted cells were processed for RNA extraction and hybridization on Affymetrix microarrays. Analysis was performed a postnatal (p) day p0. Subsequent analysis focused on the transcriptional profile of DRG neuron subpopulations at specific lumbar levels. Additional work addressed the transcriptional changes in whole DRG in adult mice with and without physical exercise.

Background corr dist: KL-Divergence = 0.0769, L1-Distance = 0.0455, L2-Distance = 0.0046, Normal std = 0.4814

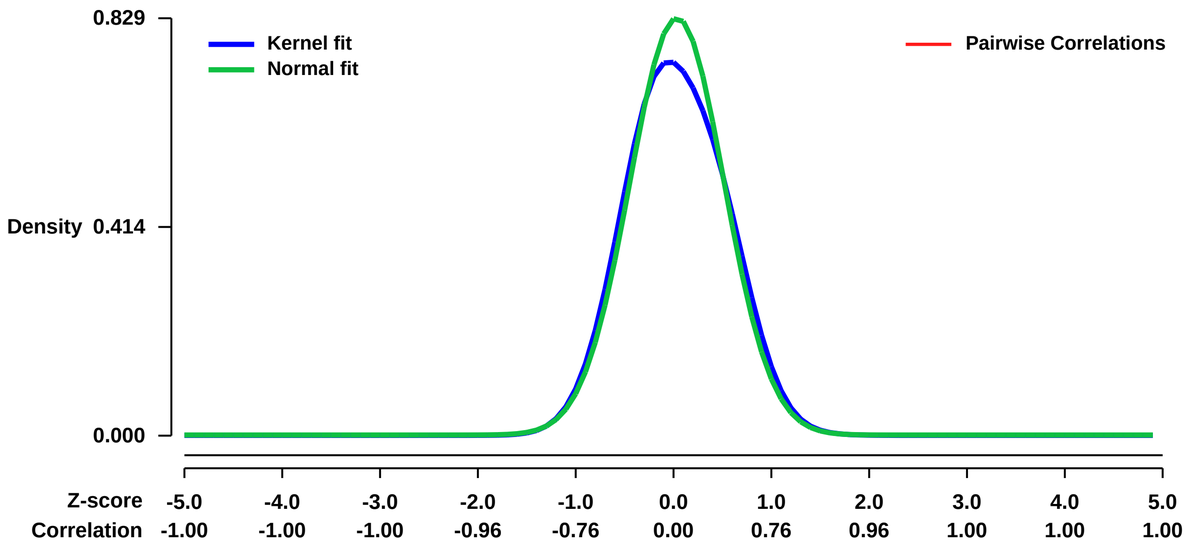

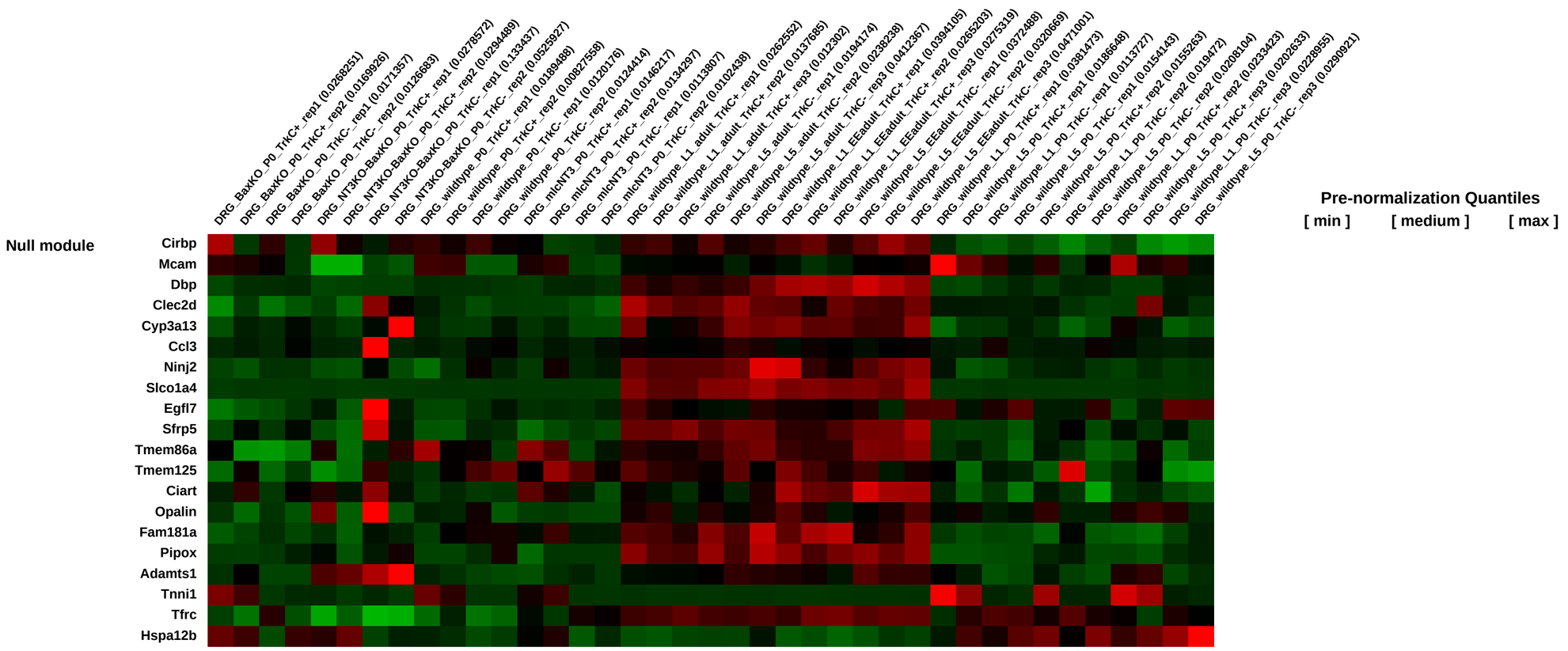

GEO Series "GSE5128" Expression Profiles

Num of samples in this series: 18

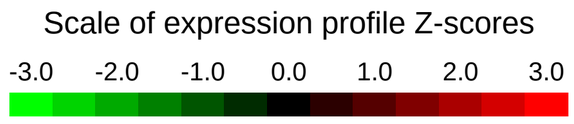

GEO Link:	http://www.ncbi.nlm.nih.gov/geo/query/acc.cgi?acc=GSE5128
Status:	Public on Sep 01 2006
Title:	Gene Expression Biomarkers for Predicting Liver Tumors in Two-Year Rodent Bioassays
Organism:	Mus musculus
Experiment type:	Expression profiling by array
Platform:	GPL1261
Pubmed ID:	17114358
Summary & Design:	**Summary:** Two-year rodent bioassays play a central role in evaluating both the carcinogenic potential of a chemical and generating quantitative information on the dose-response behavior for chemical risk assessments. The bioassays involved are expensive and time-consuming, requiring nearly lifetime exposures (two years) in mice and rats and costing $2 to $4 million per chemical. Since there are approximately 80,000 chemicals registered for commercial use in the United States and 2,000 more are added each year, applying animal bioassays to all chemicals of concern is clearly impossible. To efficiently and economically identify carcinogens prior to widespread use and human exposure, alternatives to the two-year rodent bioassay must be developed. In this study, animals were exposed for 13 weeks to two chemicals that were positive for liver tumors in the two-year rodent bioassay, two chemicals that were negative for liver tumors, and two vehicle controls. Gene expression analysis was performed on the livers of the animals to assess the potential for identifying gene expression biomarkers that can predict tumor formation in a two-year bioassay following a 13 week exposure. **Keywords: toxicology, chemical carcinogenesis, liver** **Overall design:** Five week old female B6C3F1 mice were exposed for 13 weeks to the following treatments: 1) 1,5-Naphthalenediamine, CAS No. 2243-62-1, feed, 2000 ppm, positive liver carcinogen; 2) 2,3-Benzofuran, CAS No. 271-89-6, gavage, 240 mg/kg, positive liver carcinogen; 3) N-(1-naphthyl)ethylenediamine dihydrochloride, CAS No. 1465-25-4, feed, 2000 ppm, negative liver carcinogen; 4) Pentachloronitrobenzene, CAS No. 82-68-8, feed, 8187 ppm, negative liver carcinogen; 5) Feed control; 6) Corn oil gavage control. Feed animals were exposed 7 days/week and gavage animals were exposed 5 days/week (5 ml/kg). Microarray analysis was performed on the livers of three mice per treatment group.

Background corr dist: KL-Divergence = 0.0940, L1-Distance = 0.0565, L2-Distance = 0.0073, Normal std = 0.4505

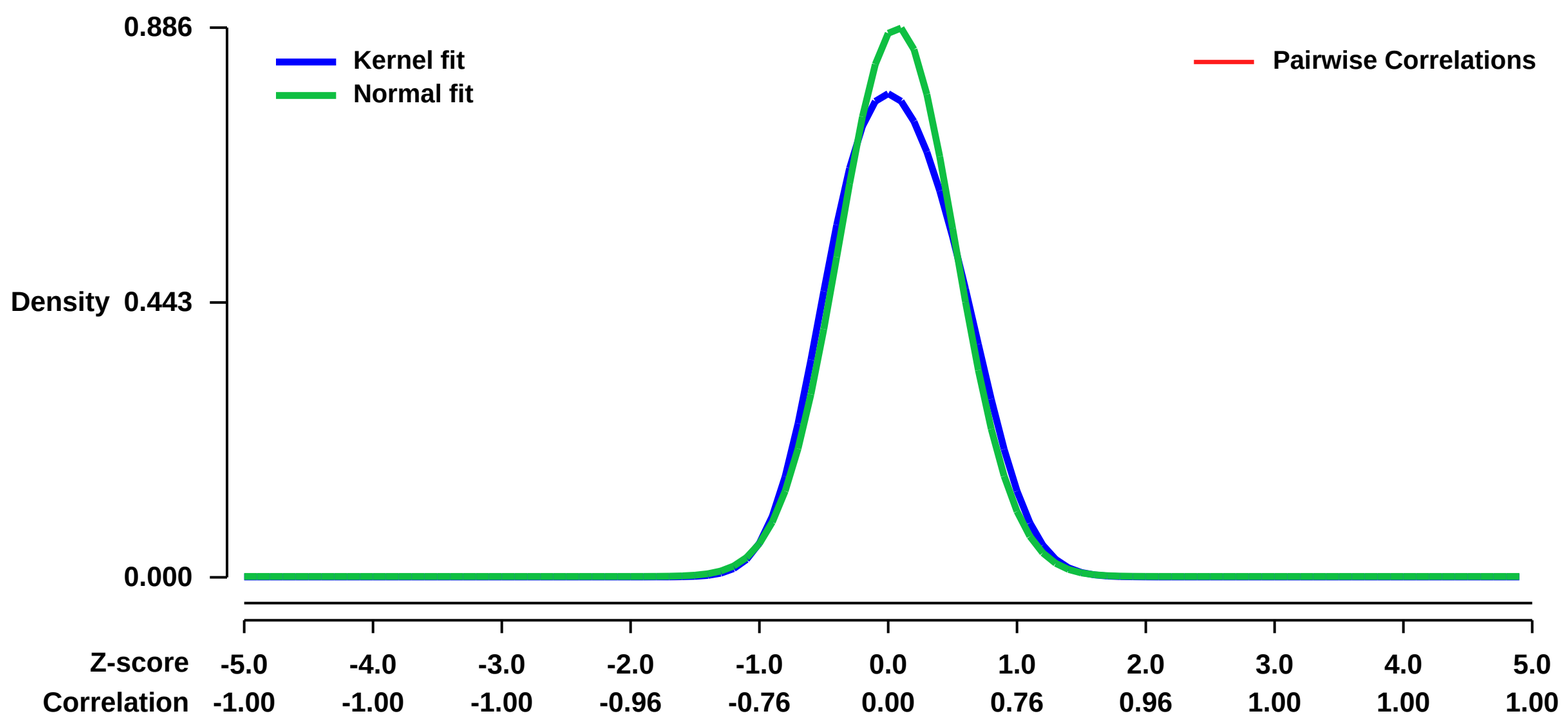

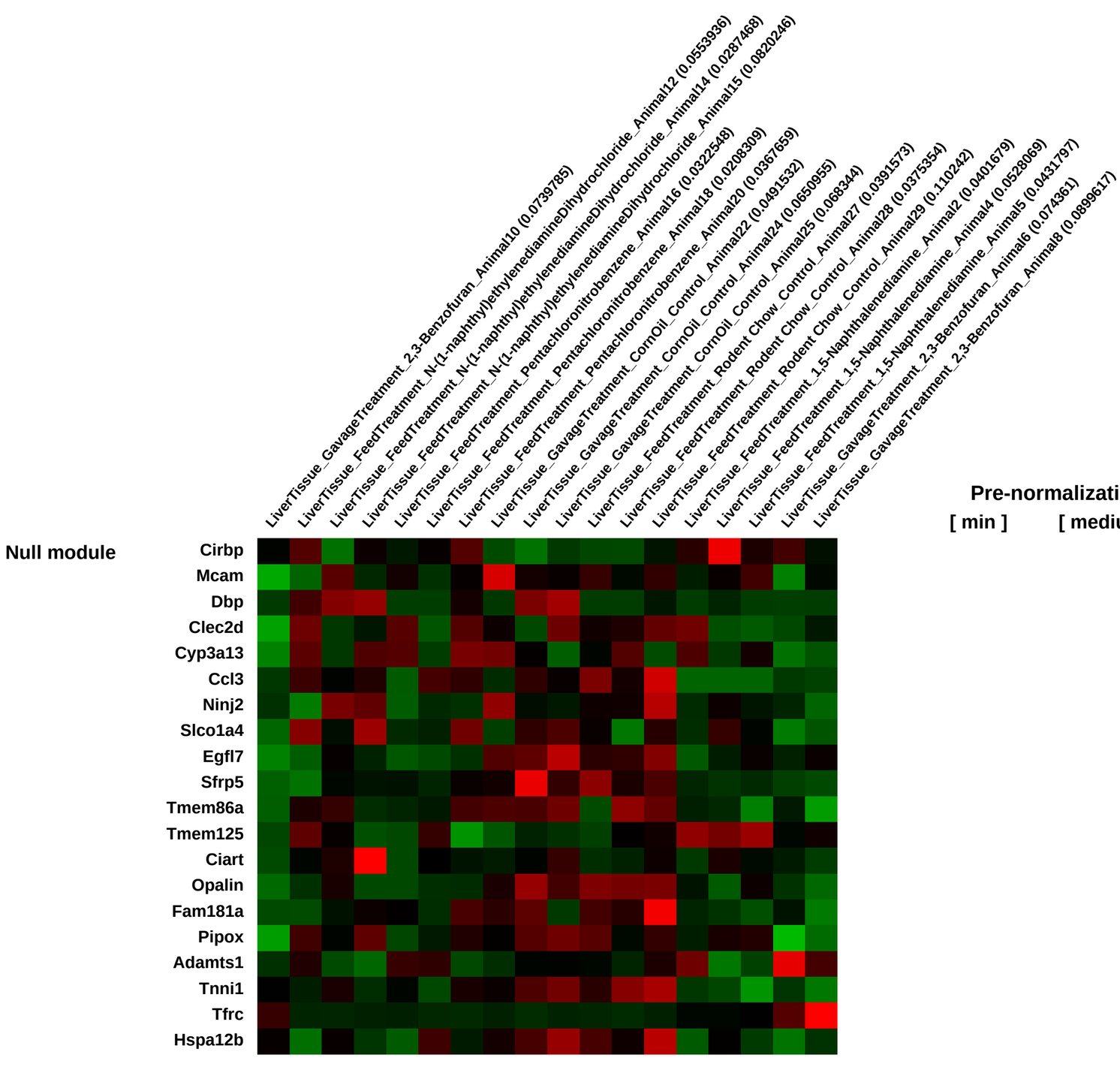

GEO Series "GSE12618" Expression Profiles

Num of samples in this series: 6

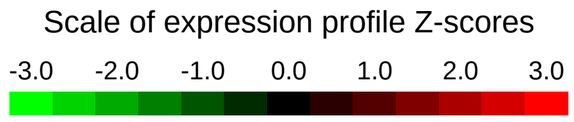

GEO Link:	**http://www.ncbi.nlm.nih.gov/geo/query/acc.cgi?acc=GSE12618**
Status:	**Public on Jan 16 2009**
Title:	**Gene expression profiles of E13 bladder compartments. (GUDMAP Series ID: 24)**
Organism:	**Mus musculus**
Experiment type:	**Expression profiling by array**
Platform:	**GPL1261**
Pubmed ID:	
Summary & Design:	**Summary:** **The long term objective is to create an encyclopedia of the expression levels of all genes in multiple components of the developing bladder. The central thesis is straightforward. The combination of microdissected tissues and FACS sorted cells plus microarray analysis offers a powerful, efficient and effective method for the creation of a global gene expression atlas of the developing urogenital system. Microarrays with essentially complete genome coverage can be used to quantitate expression levels of every gene. The ensuing rapid read-out provides an expression atlas that is more sensitive, more economical and more complete than would be possible by in situ hybridizations alone. The data submitted here delineates the gene expression profiles of the mesenchymal and epithelial compartments of the e13 mouse bladder.** **Keywords: Mouse embryonic day 13 bladder mesenchyme and epithelium.** **Overall design:** **FVB/N mice were time mated. At embryonic day 13 mice were euthanized by decapitation and the bladders were microdissected, cut just above the ureters, and treated with 20 ´µM EDTA for 20 minutes. Mesenchymal and epithelial compartments were then separated by rimming the bladder with a needle and harvested in RLT. Total RNA was isolated for gene expression analysis using the Affymetrix MOE430 microarray chip**

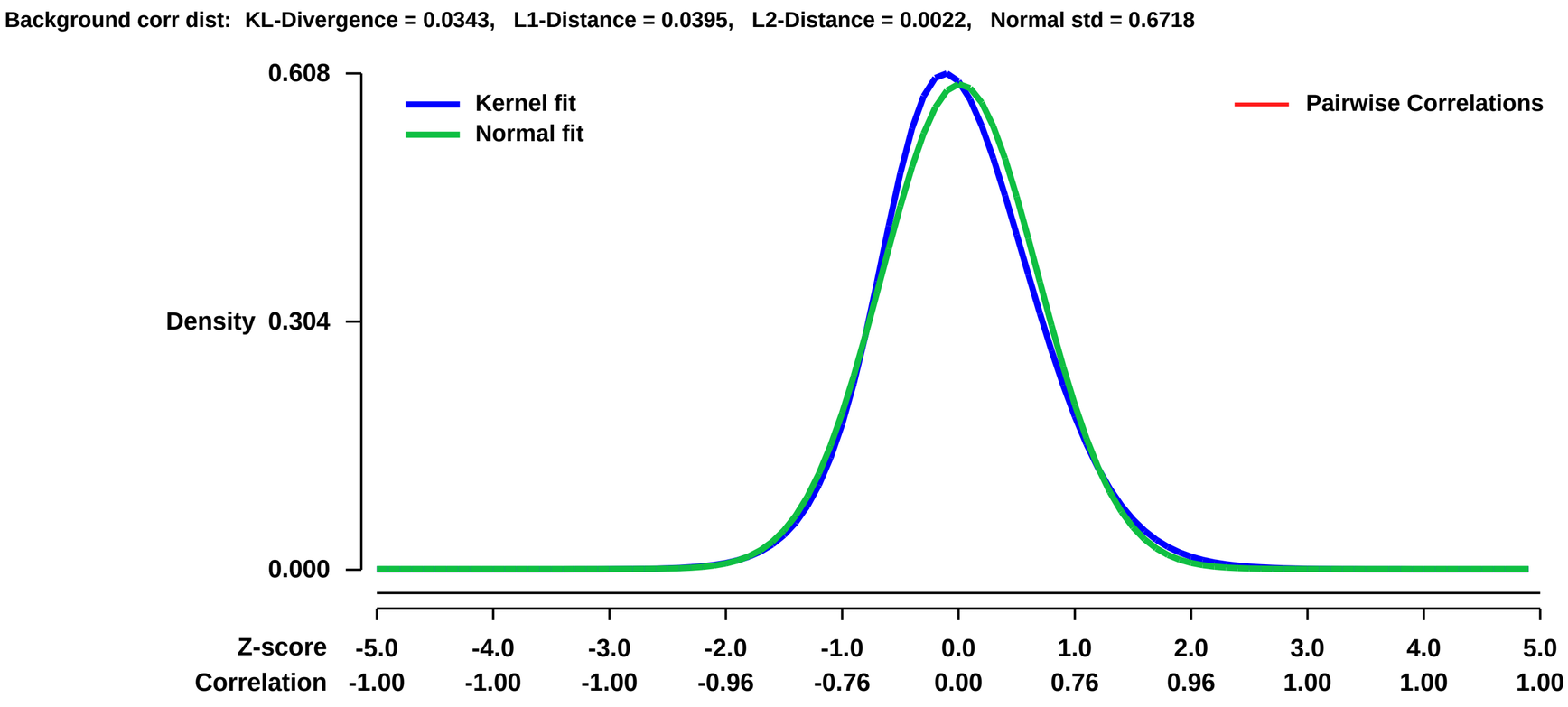

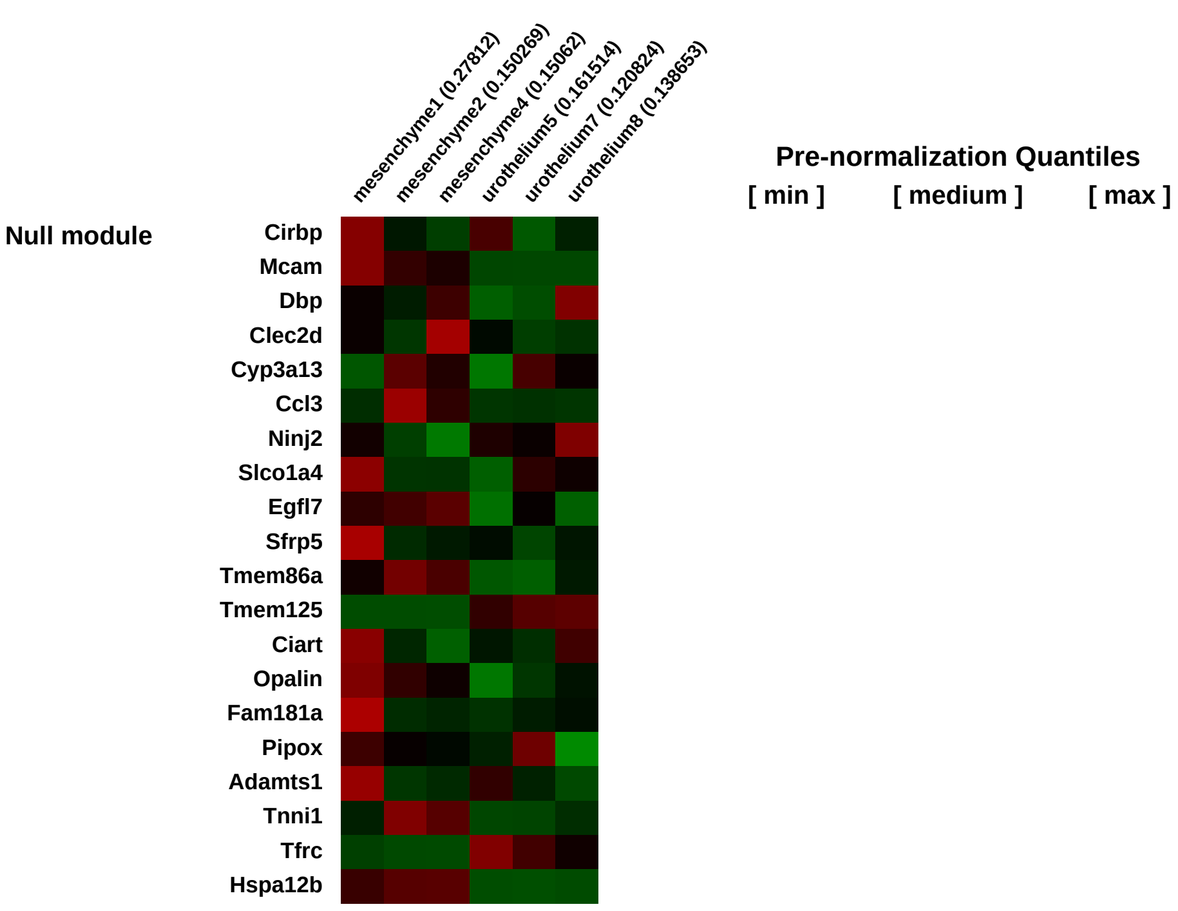

GEO Series "GSE15161" Expression Profiles

Num of samples in this series: 26

Scale of expression profile Z-scores

-3.0 -2.0 -1.0 0.0 1.0 2.0 3.0

GEO Link:	http://www.ncbi.nlm.nih.gov/geo/query/acc.cgi?acc=GSE15161
Status:	Public on Apr 10 2009
Title:	Expression data from retroviral vector-infected immortalized mouse embryonic fibroblasts (MEFs)
Organism:	Mus musculus
Experiment type:	Expression profiling by array
Platform:	GPL1261
Pubmed ID:	19483725
Summary & Design:	**Summary:** Cultured cancer cells exhibit substantial phenotypic heterogeneity when measured in a variety of ways such as sensitivity to drugs or the capacity to grow under various conditions. Among these, the ability to exhibit anchorage-independent cell growth (colony forming capacity in semisolid media) has been considered to be fundamental in cancer biology because it has been connected with tumor cell aggressiveness in vivo such as tumorigenic and metastatic potentials, and also utilized as a marker for in vitro transformation. Although multiple genetic factors for anchorage-independence have been identified, the molecular basis for this capacity is still largely unknown. To investigate the molecular mechanisms underlying anchorage-independent cell growth, we have used genome-wide DNA microarray studies to develop an expression signature associated with this phenotype. Using this signature, we identify a program of activated mitochondrial biogenesis associated with the phenotype of anchorage-independent growth and importantly, we demonstrate that this phenotype predicts potential for metastasis in primary breast and lung tumors. **Keywords:** c-Myc or v-Src retroviral vector-infected immortalized mouse embryonic fibroblasts. **Overall design:** Expression data of c-Myc and v-Src transformed MEFs was used to validate an expression signature generated from human cultured breast cancer cell lines with anchorage-independent growth ability.

Background corr dist: KL-Divergence = 0.2660, L1-Distance = 0.0442, L2-Distance = 0.0043, Normal std = 0.2972

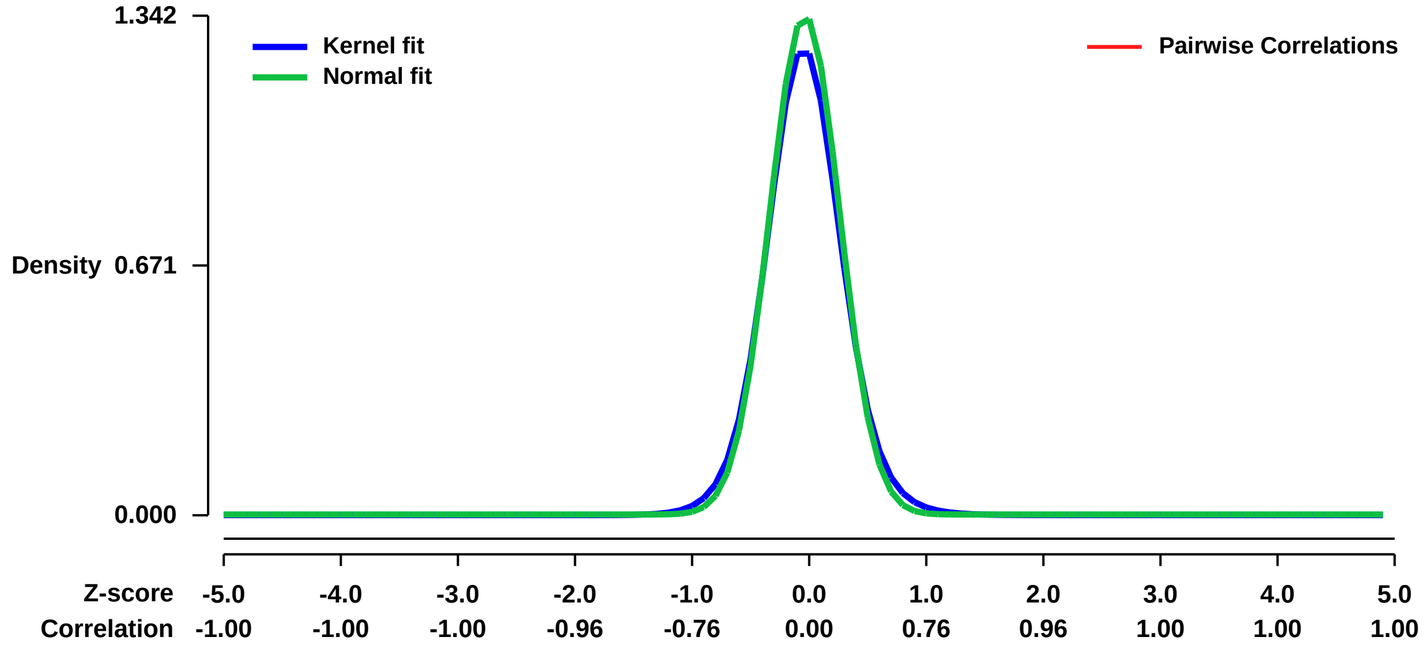

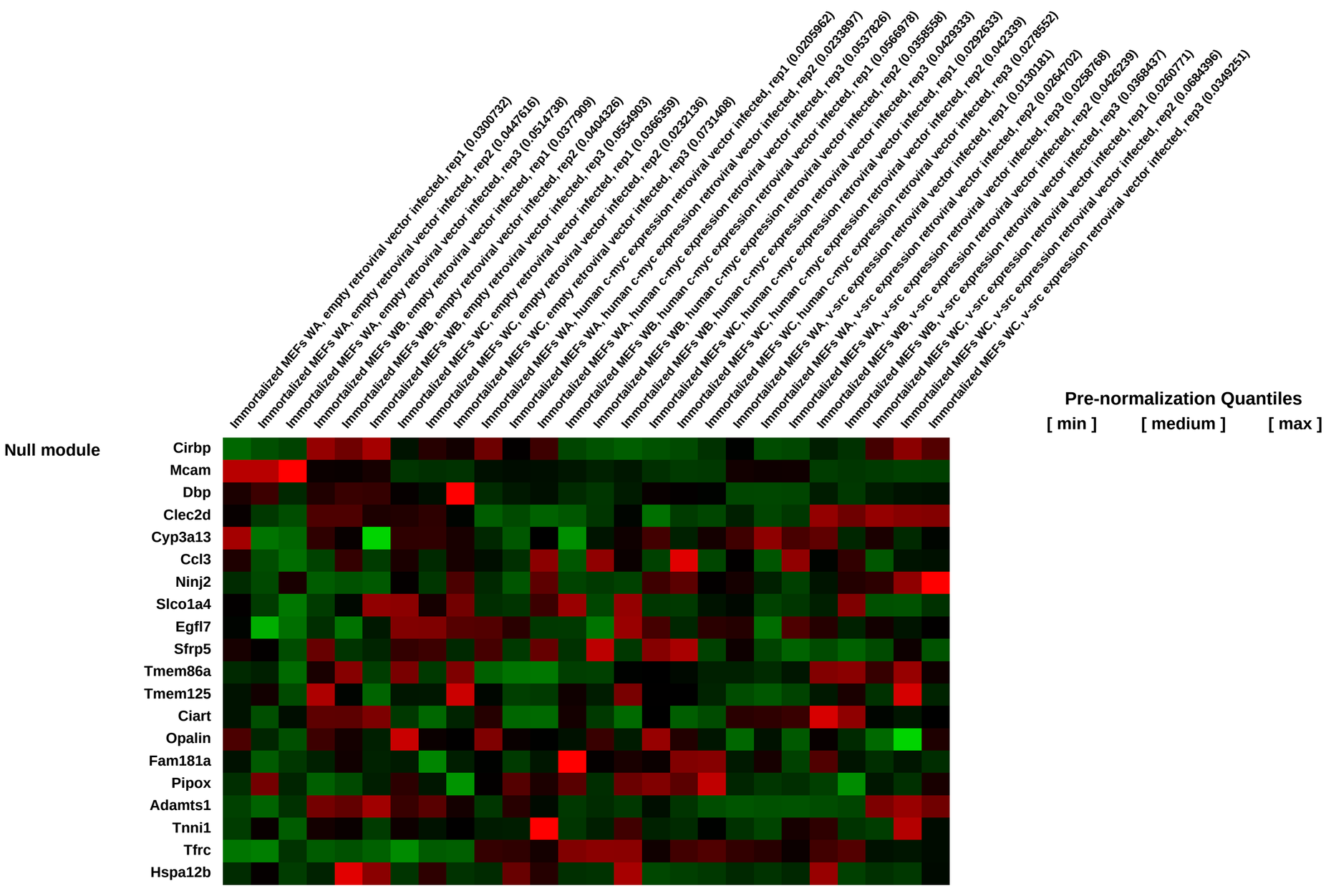

GEO Series "GSE7596" Expression Profiles

Num of samples in this series: 6

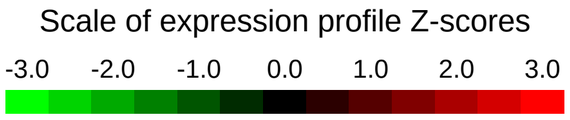

GEO Link:	http://www.ncbi.nlm.nih.gov/geo/query/acc.cgi?acc=GSE7596
Status:	Public on Feb 15 2008
Title:	AKT regulates de novo induction of Foxp3
Organism:	Mus musculus
Experiment type:	Expression profiling by array
Platform:	GPL1261
Pubmed ID:	18283119
Summary & Design:	**Summary:** The CD4+Foxp3+ regulatory T cells play an essential role in maintaining tolerance via their suppressive function on conventional T cells. The intracellular signaling pathways that regulate Foxp3 expression are largely unknown. In this study we describe a novel inhibitory role for AKT in regulating de novo induction of Foxp3 both in vivo and in vitro. A constitutively active allele of AKT significantly diminished TGF-ˆ¢ induced Foxp3 induction via a rapamycin-sensitive pathway, establishing a role for the AKT-mTOR axis in Treg cells. Moreover, the observed impairment in Foxp3 induction was paralleled by a selective downmodulation of the imparted Treg transcriptional signature highlighting the importance of the balance of intracellular signals in Treg differentiation . Our results provide a basis for further elucidation of molecular mechanisms that regulate Foxp3 induction and identify AKT as an important negative regulator of this process. **Keywords: Cell population comparison** **Overall design:** All gene expression profiles were obtained from highly purified T cell populations sorted by flow cytometry. To reduce variability, cells from multiple mice were pooled for sorting, and three replicates were generated for all groups. RNA from 0.5-2.5 x 105 cells was amplified, labeled, and hybridized to Affymetrix M430v2 microarrays. Raw data were preprocessed with the RMA algorithm in GenePattern, and averaged expression values were used for analysis.

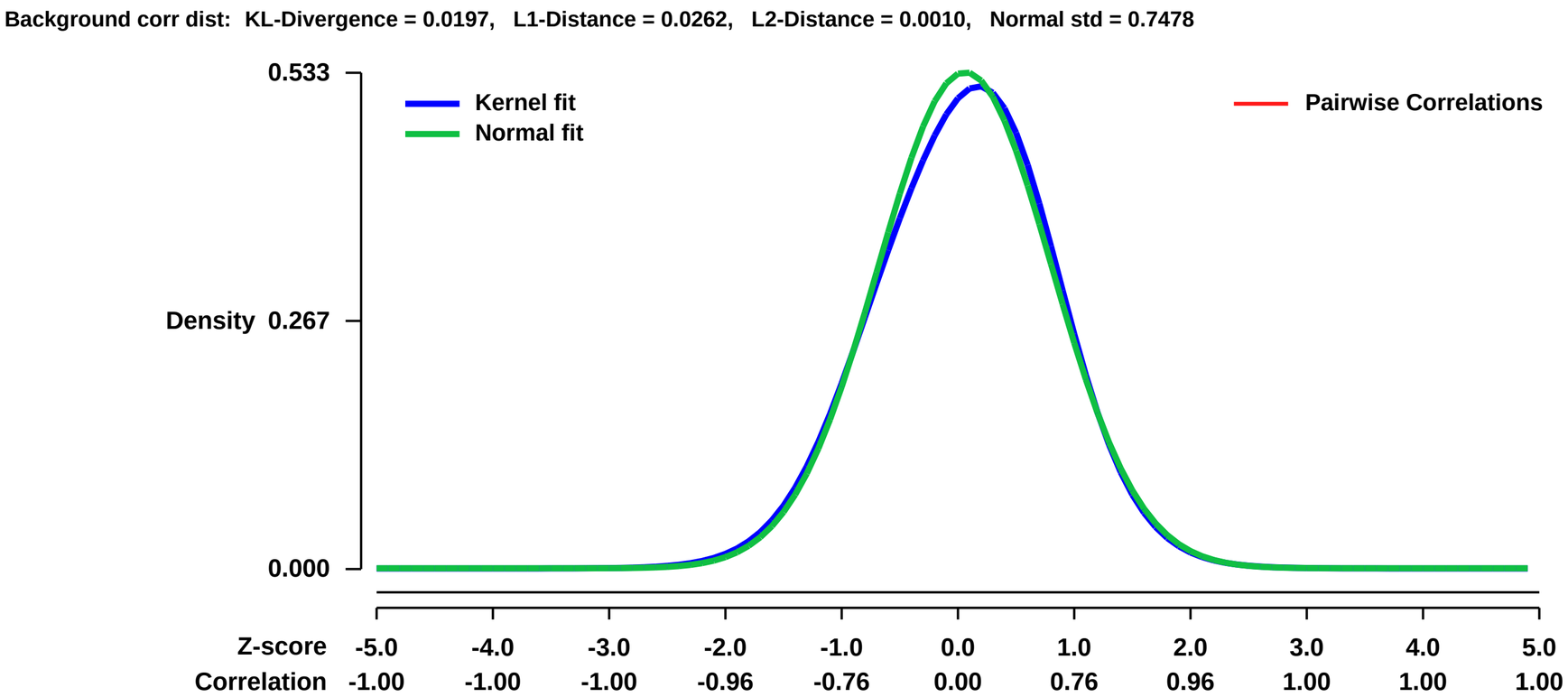

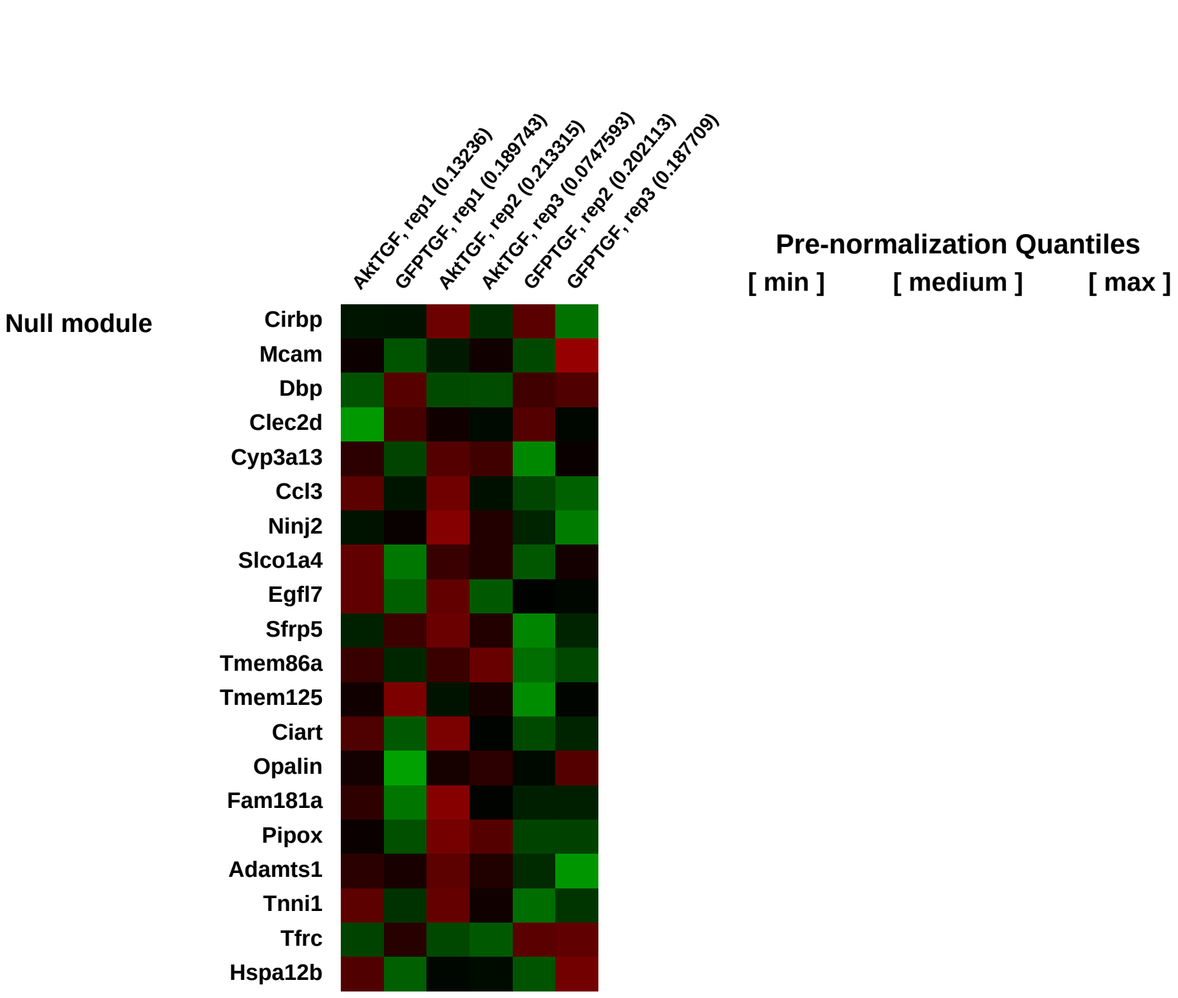

GEO Series "GSE9442" Expression Profiles

Num of samples in this series: 71

Scale of expression profile Z-scores

-3.0 -2.0 -1.0 0.0 1.0 2.0 3.0

GEO Link: http://www.ncbi.nlm.nih.gov/geo/query/acc.cgi?acc=GSE9442
Status: Public on Dec 07 2007
Title: Molecular correlates of sleep deprivation in the brain of three inbred mouse strains in an around-the-clock experiment
Organism: Mus musculus
Experiment type: Expression profiling by array
Platform: GPL1261
Pubmed ID: 18077435

Summary & Design:

Summary:
These studies adress differential changes in gene expression between sleep deprived and control mice. We profiled gene expression at four time points across the 24H Light/Dark cycle to take into account circadian influences and used three different inbred strains to understand the influence of genetic background.

Keywords: brain, circadian, genetic background, sleep deprivation

Overall design:
Experiments were performed on male mice (AKR/J (A), C57BL/6J (B), DBA/2J (D)), 12-13 weeks of age, purchased from Jackson Laboratory. Animals were housed in a light/dark cycle of 24 hrs with water and food available ad libitum. Mice of the 3 inbred strains were sleep deprived for 6h starting at light onset (ZT0), at the middle of the light (ZT6), at the beginning of the dark (ZT12), or at the middle of the dark (ZT18) period, and sacrificed together with their home-cage controls (n=9 / strain =3 / time =4 / condition =2; total =216 mice).

Background corr dist: KL-Divergence = 0.5365, L1-Distance = 0.0827, L2-Distance = 0.0223, Normal std = 0.2191

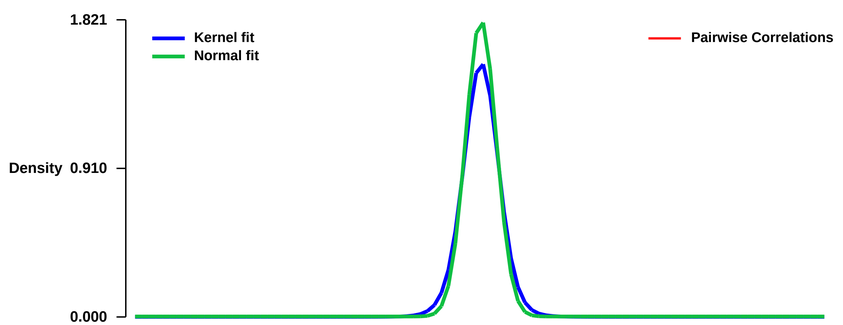

Z-score	-5.0	-4.0	-3.0	-2.0	-1.0	0.0	1.0	2.0	3.0	4.0	5.0
Correlation	-1.00	-1.00	-1.00	-0.96	-0.76	0.00	0.76	0.96	1.00	1.00	1.00

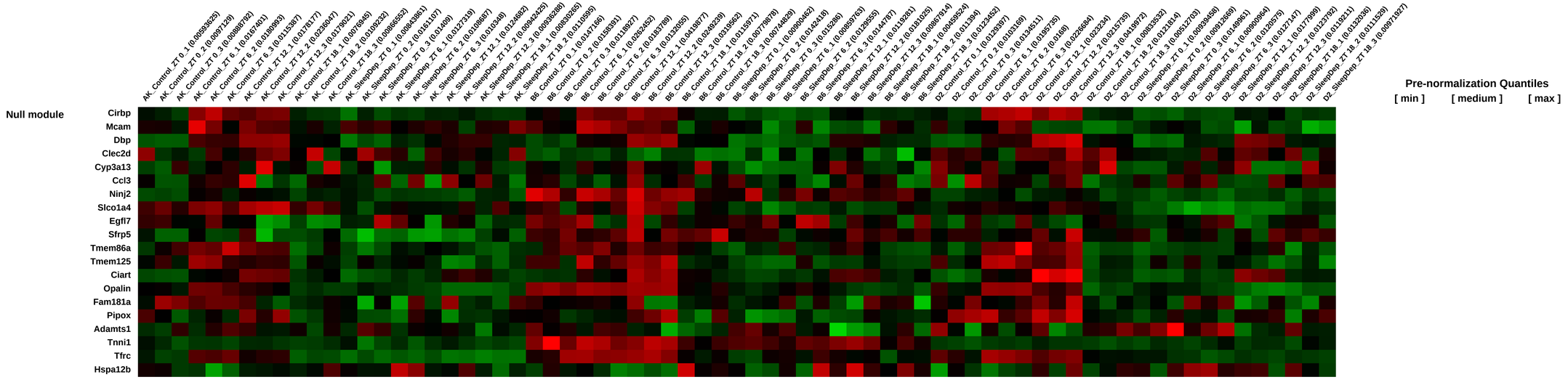

GEO Series "GSE22040" Expression Profiles

Num of samples in this series: 9

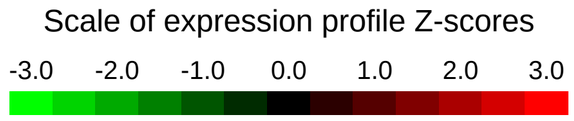

GEO Link:	**http://www.ncbi.nlm.nih.gov/geo/query/acc.cgi?acc=GSE22040**
Status:	**Public on Dec 01 2010**
Title:	**Gene expression data from somites of E9.5 mouse embryos**
Organism:	**Mus musculus**
Experiment type:	**Expression profiling by array**
Platform:	**GPL1261**
Pubmed ID:	
Summary & Design:	**Summary:** **We used microarrays to identify Pax3 targets during myogenesis in the mouse embryo** **Overall design:** **Mouse embryos were genotyped Pax3GFP/+ or Pax3PAX3-FKHR/GFP and dissected at E9.5 under a fluorescent binocular. Somites were dissected from the interlimb region and the more hypaxial domain separated from the neural tube and the epaxial extremity of the somites. GFP positive cells were then sorted by flow cytometry before RNA extraction and hybridization on Affymetrix microarrays. We also sorted GFP negative cells.**

Background corr dist: **KL-Divergence = 0.0785, L1-Distance = 0.0184, L2-Distance = 0.0003, Normal std = 0.4841**

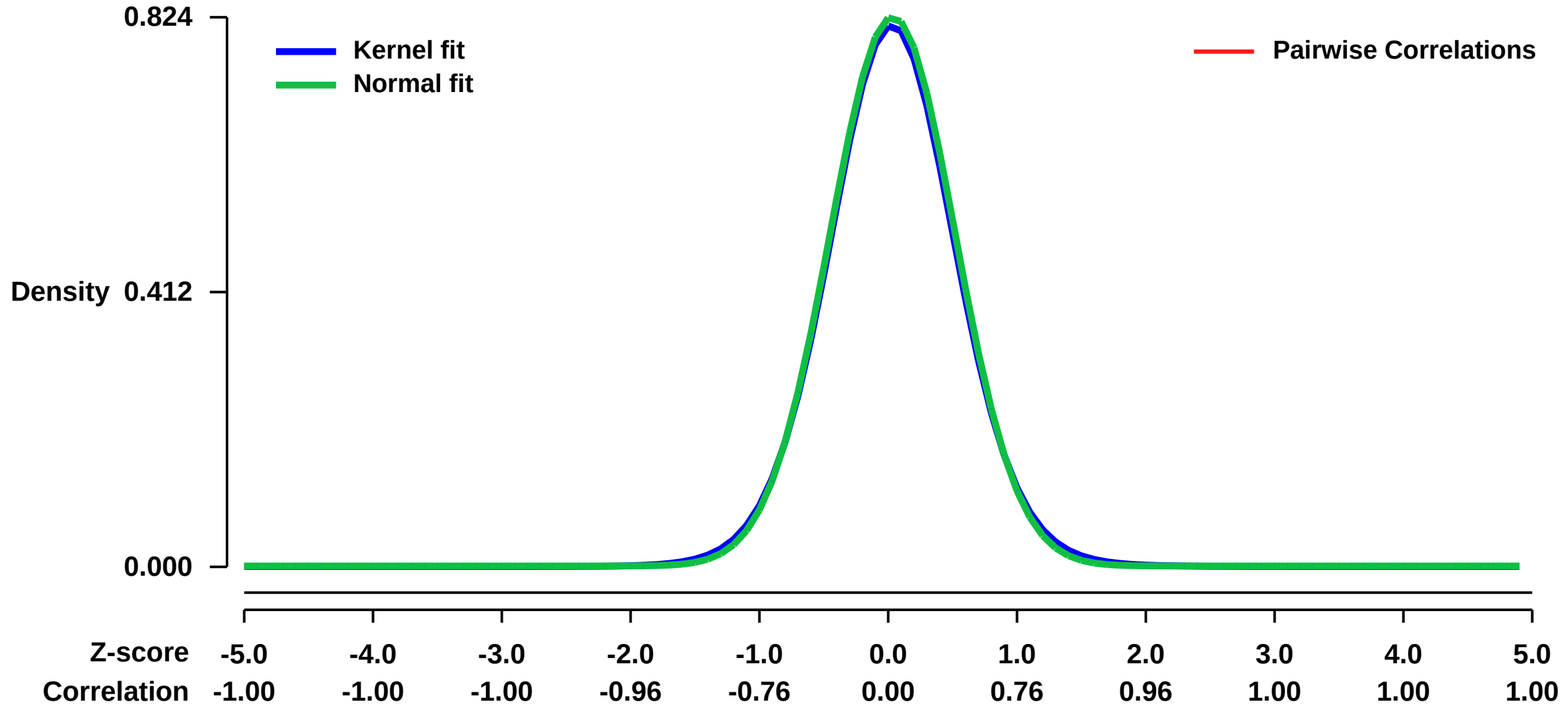

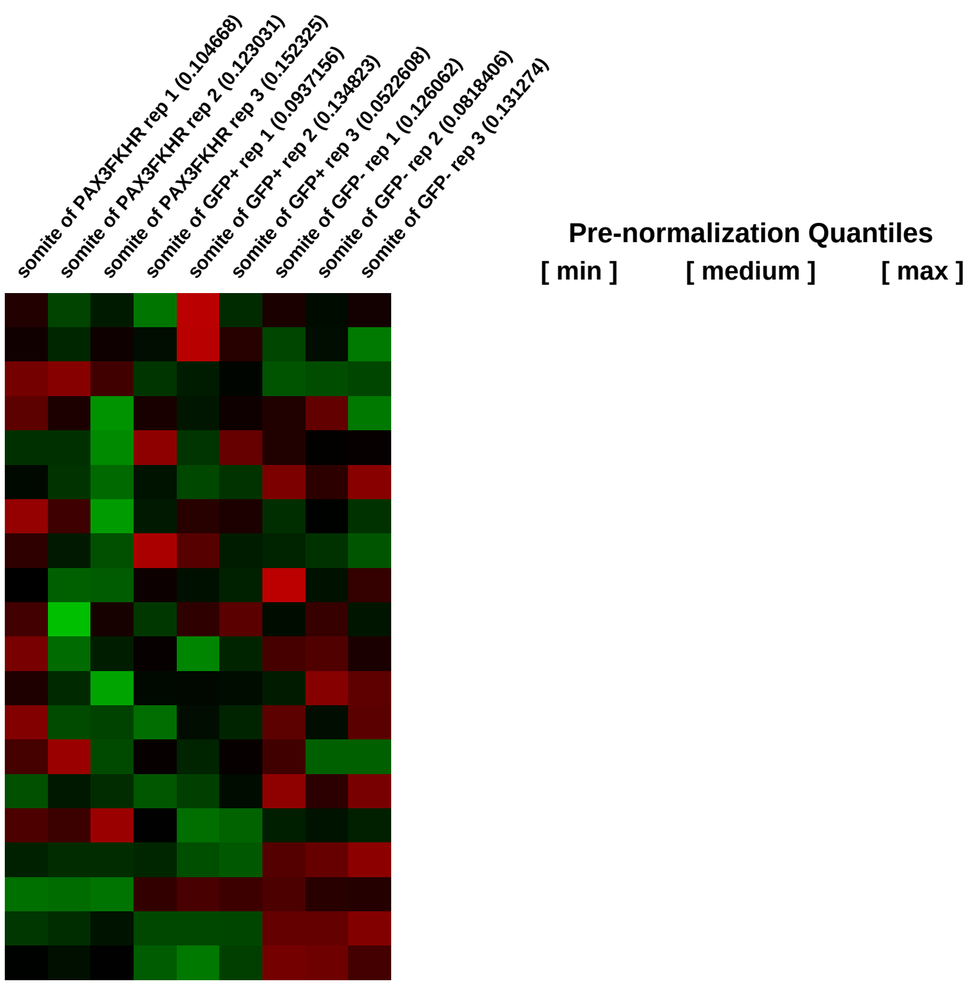

GEO Series "GSE13044" Expression Profiles

Num of samples in this series: 59

Scale of expression profile Z-scores

-3.0 -2.0 -1.0 0.0 1.0 2.0 3.0

GEO Link: http://www.ncbi.nlm.nih.gov/geo/query/acc.cgi?acc=GSE13044
Status: Public on Oct 07 2008
Title: Gene expression profiling in the lung and liver of low and high dose Perfluorooctanoic Acid exposed mouse fetuses
Organism: Mus musculus
Experiment type: Expression profiling by array
Platform: GPL1261
Pubmed ID: 17681415

Summary & Design:

Summary:
Exposure to PFOA during gestation altered the expression of genes related to fatty acid catabolism in both the fetal liver and lung. In the fetal liver, the effects of PFOA were robust and also included genes associated with lipid transport, ketogenesis, glucose metabolism, lipoprotein metabolism, cholesterol biosynthesis, steroid metabolism, bile acid biosynthesis, phospholipid metabolism, retinol metabolism, proteosome activation, and inflammation. These changes are consistent with activation of PPAR alpha. Non-PPAR alpha related changes were suggested as well.

Keywords: gene expression, microarray,PFOA, mouse, fetus, liver

Overall design:
Please note that each dose experiment had separate concurrent controls.

Background corr dist: KL-Divergence = 0.0397, L1-Distance = 0.0327, L2-Distance = 0.0022, Normal std = 0.6008

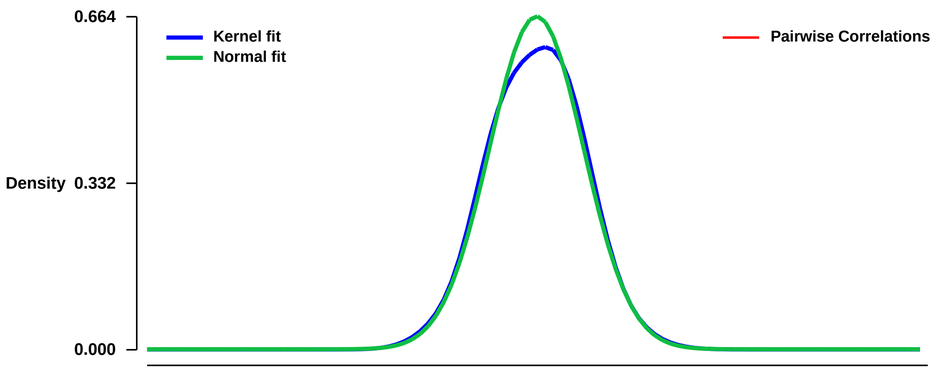

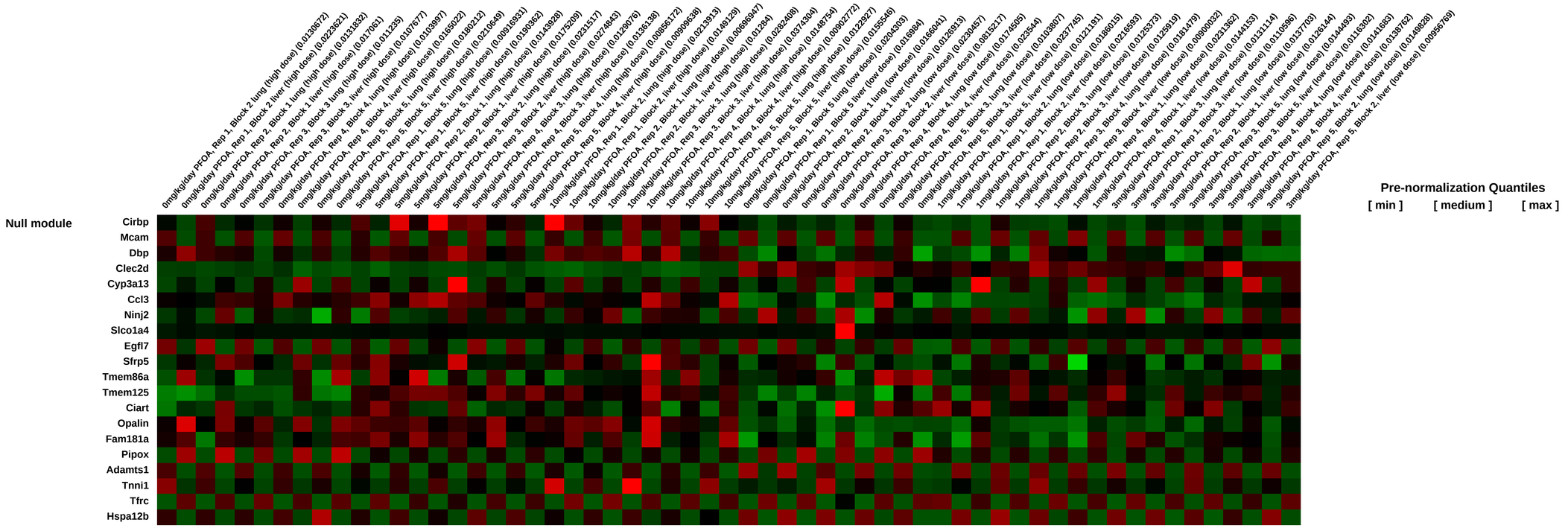

GEO Series "GSE6846" Expression Profiles

Num of samples in this series: 6

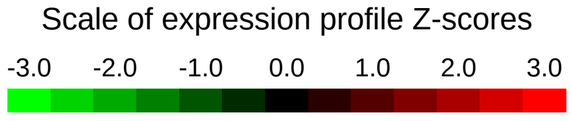

GEO Link:	http://www.ncbi.nlm.nih.gov/geo/query/acc.cgi?acc=GSE6846
Status:	Public on Aug 24 2007
Title:	Gene Expression and Biological Processes Influenced By Deletion of Stat3 in pulmonary Alveolar Type II Cells
Organism:	Mus musculus
Experiment type:	Expression profiling by array
Platform:	GPL1261
Pubmed ID:	18070348
Summary & Design:	**Summary:** Deletion of Stat3 induced genes influencing protein metabolism, transport, chemotaxis and apoptosis and decreased the expression of genes mediating lipid synthesis and metabolism. Srebf1 and 2, key regulators of fatty acid and steroid biosynthesis, were decreased in Stat3D/D mice. Stat3 influenced both pro- and anti-apoptotic pathways, regulating and maintaining the balance between a subset of pro- and anti-apoptotic genes that determine cell death or survival. Akt, a known target of Stat3, participates in many Stat3 mediated pathways including Jak-Stat signaling, apoptosis, the MAPK signaling, cholesterol and fatty acid biosynthesis. Deletion of Stat3 from type II epithelial cells altered the expression of genes regulating diverse cellular processes, including cell growth and apoptosis, lipid biosynthesis and metabolism. Stat3 regulates cell formation through a complex regulatory network that likely enhances alveolar epithelial cell survival and surfactant/lipid synthesis, necessary for the protection of the lung during injury. Keywords: genotype comparison **Overall design:** To better understand the roles and molecular mechanisms by which Stat3 influences gene expression in lung, the effect of cell-selective deletion of Stat3 (Stat3D/D) on genome wide mRNA expression profiles was determined in murine type II alveolar epithelial cells. Differentially expressed genes were identified from Affymetrix Murine GeneChips analysis and subjected to gene ontology classification promoter analysis, pathway mapping and literature mining.

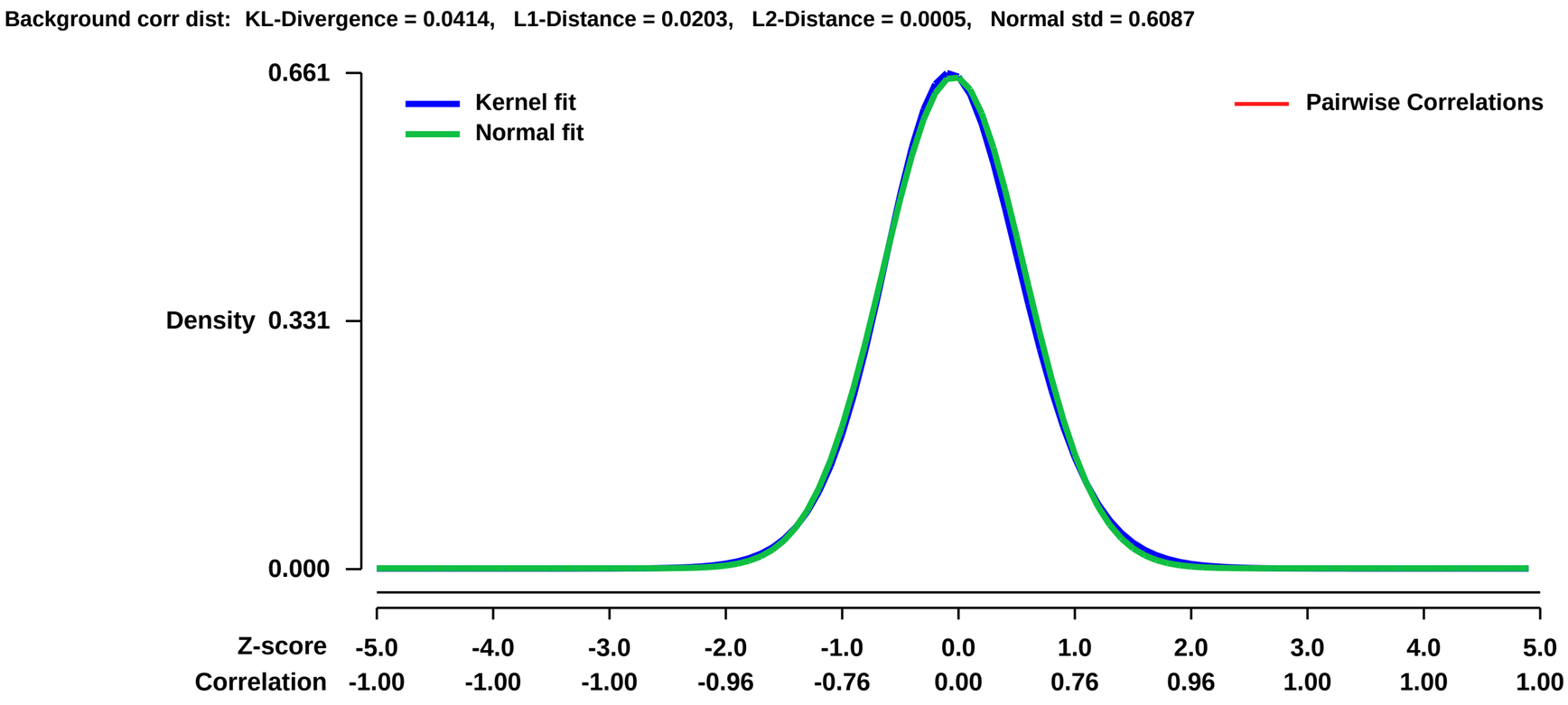

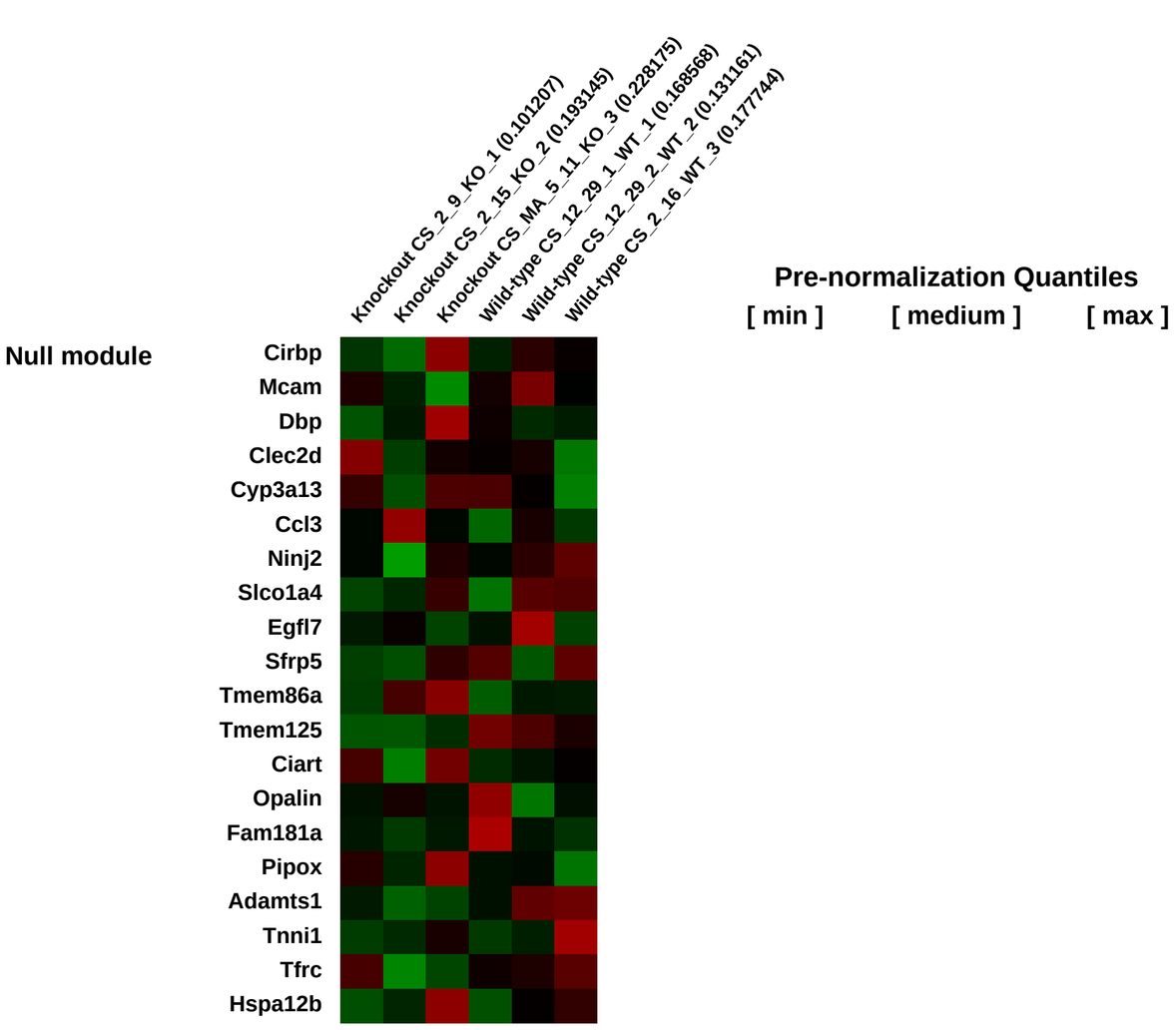

GEO Series "GSE42135" Expression Profiles

Num of samples in this series: 42

Scale of expression profile Z-scores

-3.0 -2.0 -1.0 0.0 1.0 2.0 3.0

GEO Link: http://www.ncbi.nlm.nih.gov/geo/query/acc.cgi?acc=GSE42135
Status: Public on Nov 09 2012
Title: Expression data from preimplantation mouse embryos
Organism: Mus musculus
Experiment type: Expression profiling by array
Platform: GPL1261
Pubmed ID:
Summary & Design:

Summary:
Landmark events occur in a coordinated manner during preimplantation development of the mammalian embryo, yet the regulatory network that orchestrates these events remains largely unknown.

We delineated the regulons of Oct4, Sall4, and Nanog using morpholino (MO)-mediated gene knockdowns followed by microarray analysis of pooled embryos.

Overall design:
1-cell fertilized mouse embryos were injected with a morpholino and were collected at either 20 hours or at 44 hours after microinjection.

Background corr dist: KL-Divergence = 0.2010, L1-Distance = 0.0369, L2-Distance = 0.0032, Normal std = 0.3366

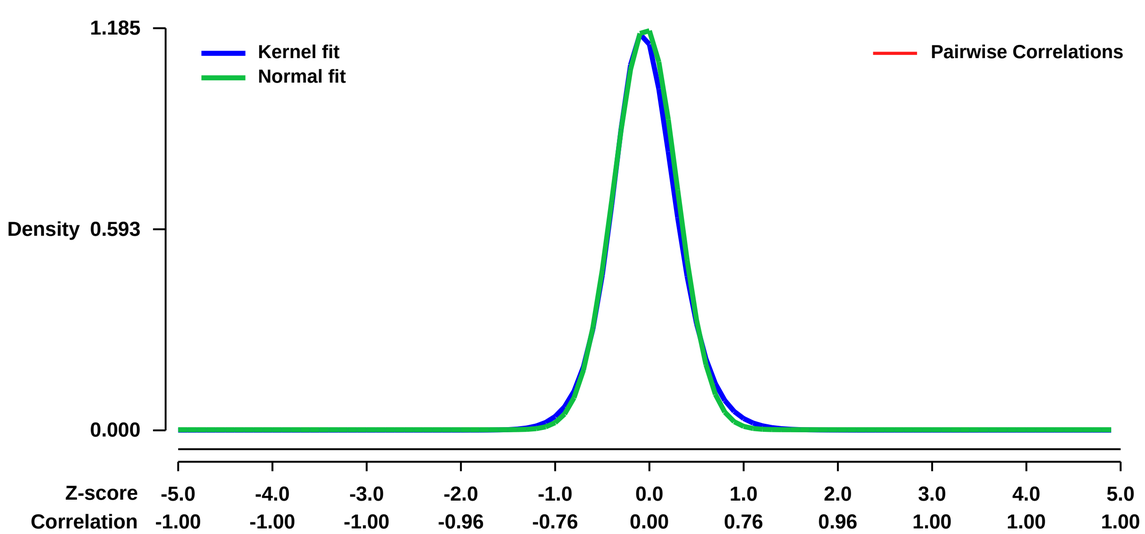

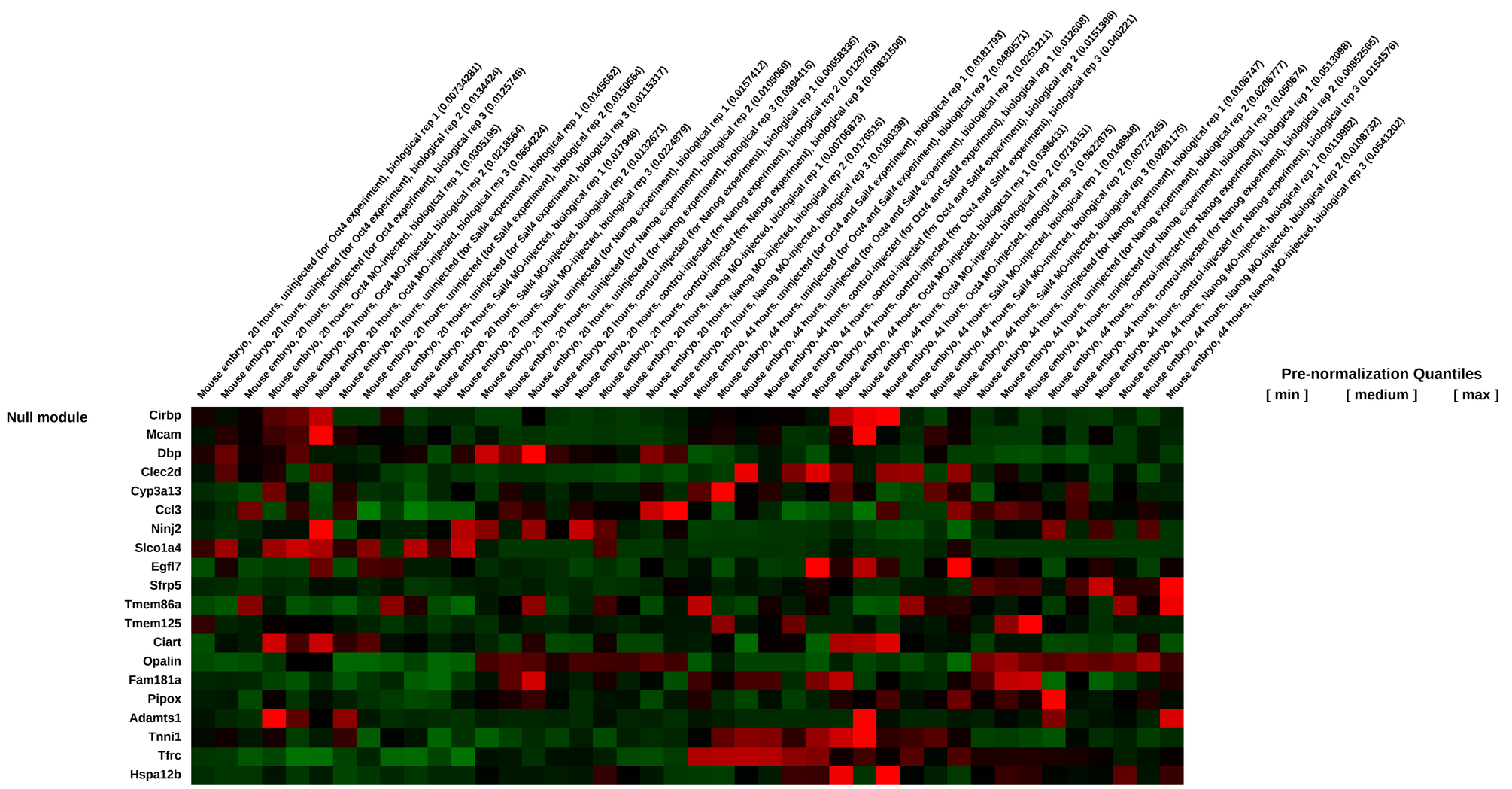

GEO Series "GSE5425" Expression Profiles

Num of samples in this series: 6

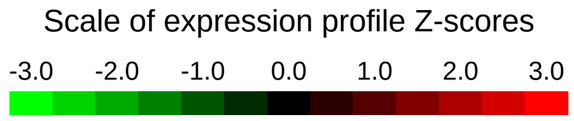

GEO Link:	**http://www.ncbi.nlm.nih.gov/geo/query/acc.cgi?acc=GSE5425**
Status:	**Public on Aug 02 2006**
Title:	**Spinal cord and dorsal root ganglion gene expression**
Organism:	**Mus musculus**
Experiment type:	**Expression profiling by array**
Platform:	**GPL1261**
Pubmed ID:	**16824496**
Summary & Design:	**Summary:** **We used microarrays to test the fundamental quantitative differences between central and peripheral nervous system transcriptomes.** **Keywords: repeat** **Overall design:** **3 independent SC and 3 independent DRG samples were analyzed. Each sample contained material from 4 age-matched male C57B/6 mice.**

Background corr dist: **KL-Divergence = 0.0201, L1-Distance = 0.0458, L2-Distance = 0.0024, Normal std = 0.8355**

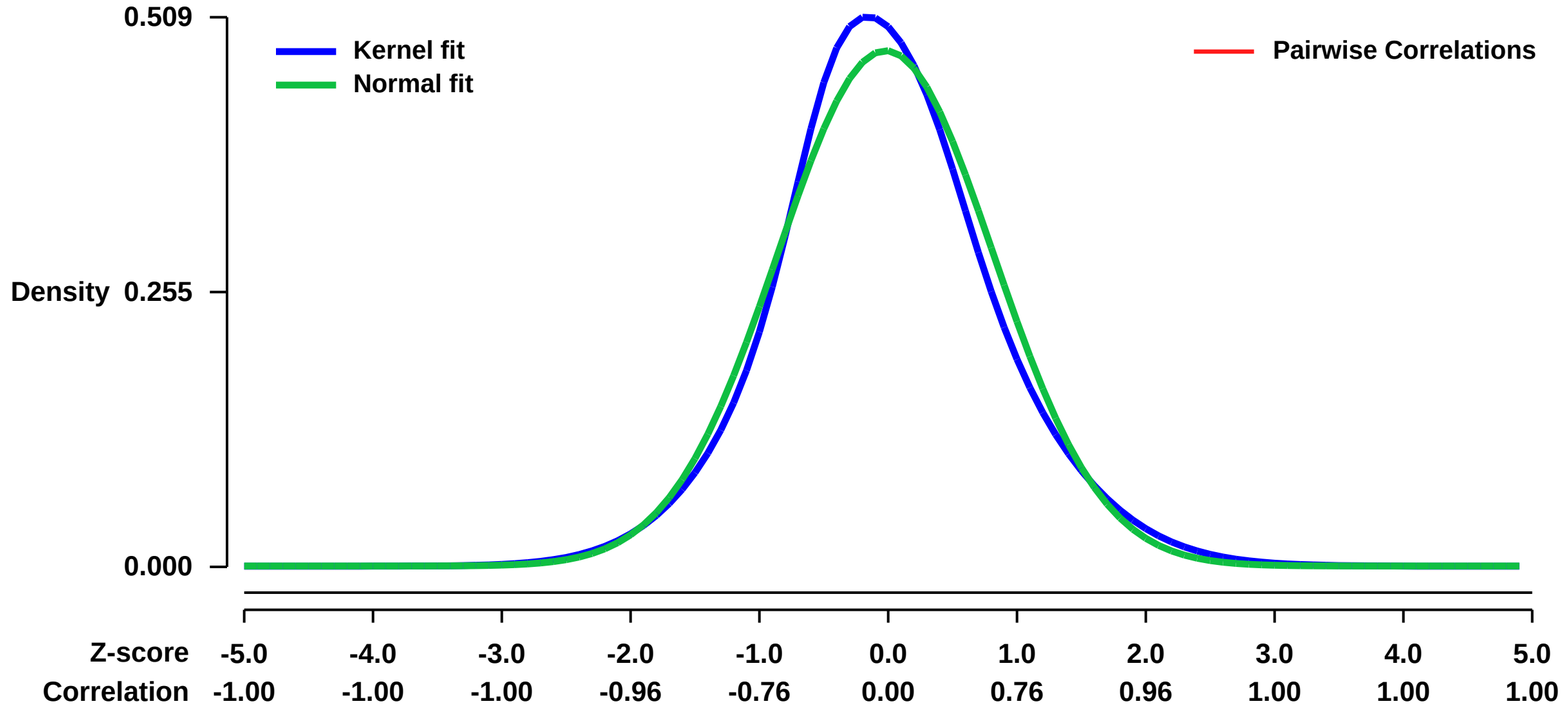

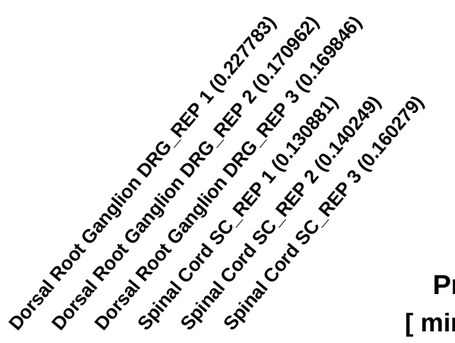

Pre-normalization Quantiles

[min] [medium] [max]

Null module

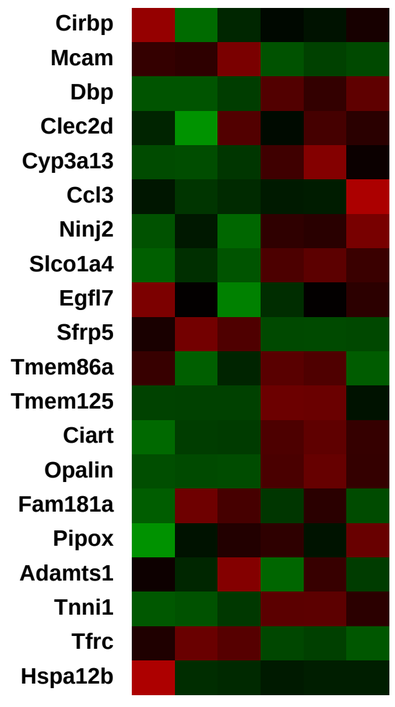

GEO Series "GSE29975" Expression Profiles

Num of samples in this series: 6

Scale of expression profile Z-scores

-3.0 -2.0 -1.0 0.0 1.0 2.0 3.0

GEO Link:	http://www.ncbi.nlm.nih.gov/geo/query/acc.cgi?acc=GSE29975
Status:	Public on Jun 28 2011
Title:	Expression data from FOG1+/- (or FOG1+/+) and FOG1 ki/ki mouse megakaryocyte (Meg)
Organism:	Mus musculus
Experiment type:	Expression profiling by array
Platform:	GPL1261
Pubmed ID:	21989988
Summary & Design:	**Summary:** The transcription co-factor FOG1 interacts with the chromatin remodeling complex NuRD to mediate gene activation and gene repression during hematopoiesis. We have generated mice with a targeted mutation in the endogenous Fog1 locus that results in an N-ternimal mutation in FOG1 that disrupts the interaction with NuRD. We used gene expression microarrays to explore the global transcriptional programs regulated by FOG1 and NuRD in megakaryocytic cells to aid in understanding its role during hematopoiesis. **Overall design:** Bovine serum albumin (BSA) gradient centrifugation was used to isolate maturated megakaryocutes from mouse

Background corr dist: KL-Divergence = 0.0481, L1-Distance = 0.0629, L2-Distance = 0.0077, Normal std = 0.6379

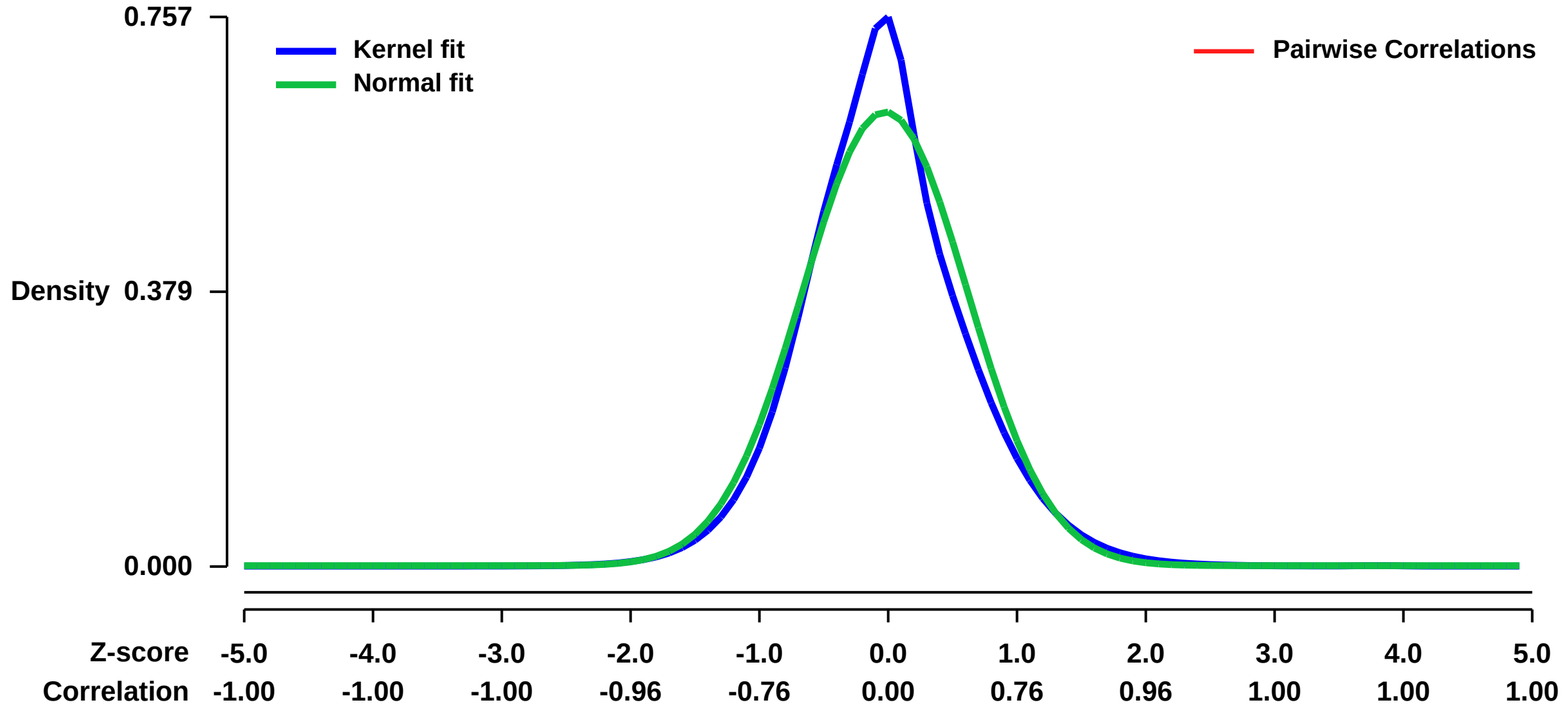

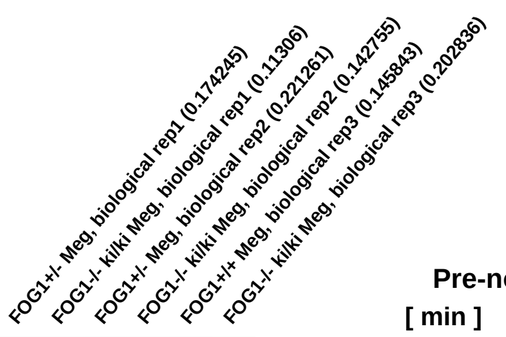

Pre-normalization Quantiles

[min] [medium] [max]

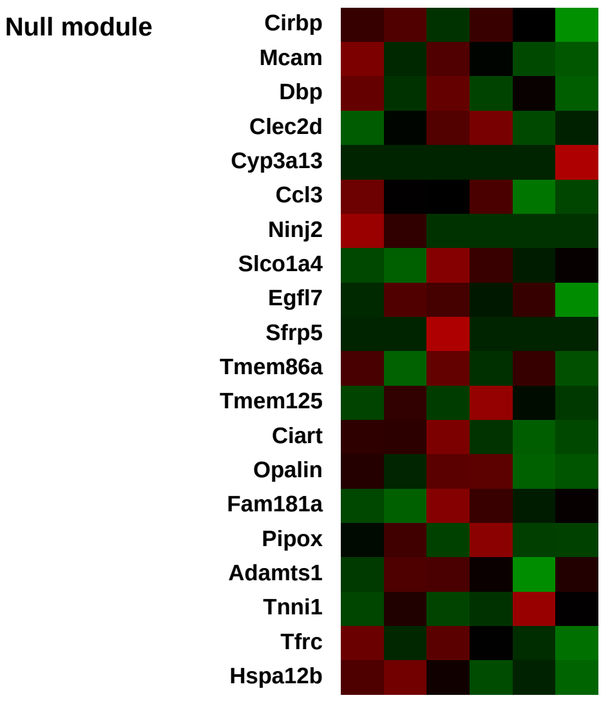

GEO Series "GSE6275" Expression Profiles

Num of samples in this series: 36

Scale of expression profile Z-scores

-3.0 -2.0 -1.0 0.0 1.0 2.0 3.0

GEO Link: http://www.ncbi.nlm.nih.gov/geo/query/acc.cgi?acc=GSE6275
Status: Public on Nov 14 2006
Title: ernst-affy-mouse-264940
Organism: Mus musculus
Experiment type: Expression profiling by array
Platform: GPL1261
Pubmed ID:

Summary & Design:

Summary:
Inherited mutations of calcium ion channels exhibit neurological defects, such as epilepsy, ataxia, and migraine, and these phenotypes are shared among humans and mouse models. Absence epilepsy and ataxic phenotypes are present in the calcium channelopathy mutants stargazer (stg-gamma2 subunit), tottering (tg-alpha1 subunit), and lethargic (lh-beta4 subunit). These mutations of high-voltage-activated (HVA) calcium channel subunits initiate increases in membrane excitability of low-voltage-activated (LVA) calcium channels in thalamic neurons, thus enhancing LVA currents. Elevated LVA currents, produced from T-type calcium channels, induce rhythmic thalamocortical burst firing and spike-wave seizures. The changes in gene expression originating from the different mutations result in similar T-type channel function; however, the network of gene modifications causing altered molecular plasticity and the emergence of pathological phenotypes remain unknown. We would like to understand how loss of 3 different subunits of a calcium ion channel differentially alter gene expression in the brain. Characterizing the gene expression profiles of the mutant stg, tg, and lh mice will provide evidence of the epileptic and ataxic mechanisms, which may identify potential therapeutic targets.

We will compare the gene expression profiles among adult mutant stg, tg, and lh mice, which display the ataxic and epileptic phenotypes, along with their wildtype, litter-mate controls, in the cerebellum and brain (without cerebellum).

We propose that the neuronal dysfunction associated with the ataxic and epileptic phenotypes develops from a common network of interacting gene alterations within the mutant stg, tg, and lh brain. The changes dictated by the initial mutations leading to the ataxic and epileptic phenotypes are hypothesized to be localized to the cerebellum and the remaining areas of the brain, including the thalamus and cortex, respectively.

Adult mutant stg, tg, and lh mice, between 2 and 5 months of age, along with wildtype, litter-mate controls, will be sacrificed. Two brain regions responsible for two phenotypes will be examined. The cerebellum (ataxia) will be dissected from remainder of the forebrain (generalized epilepsy). Each tissue set will be collected in triplicate (3 separate mice per set) to account for biological variance, and total RNA isolated via standard Trizol procedure (Invitrogen) and purified with the RNeasy cleanup kit (Qiagen). RNA samples will be stored at -80 C until sent for analysis using the Affymetrix GeneChip Mouse Genome 430 2.0 whole genome array.

Keywords: other

Overall design:

Background corr dist: KL-Divergence = 0.1864, L1-Distance = 0.0710, L2-Distance = 0.0102, Normal std = 0.3729

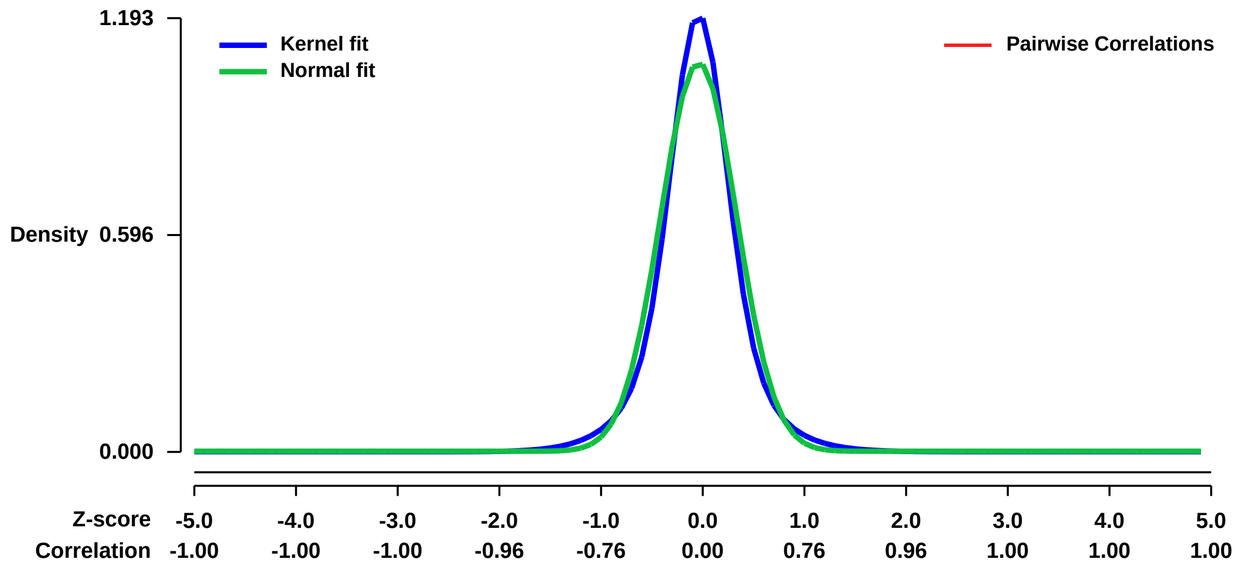

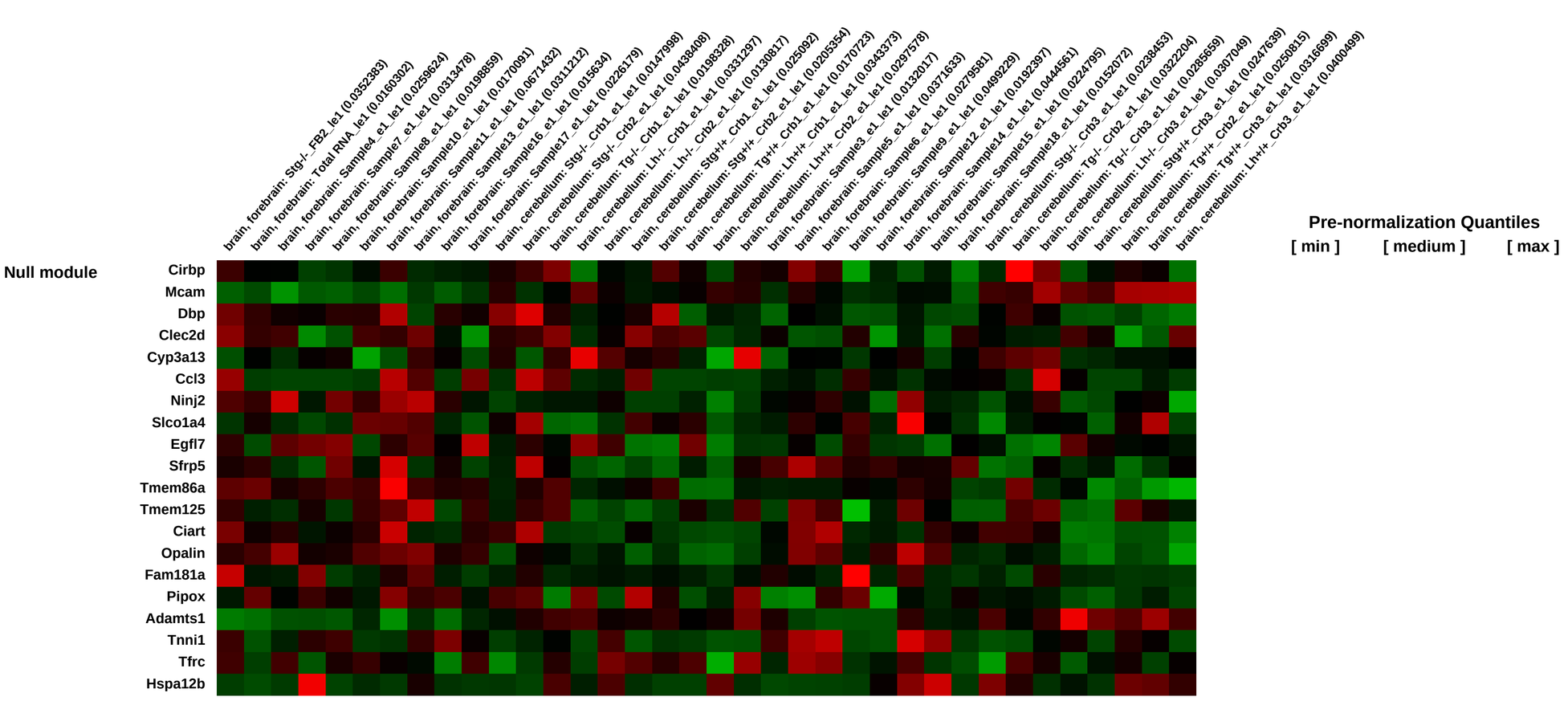

GEO Series "GSE11400" Expression Profiles

Num of samples in this series: 8

Scale of expression profile Z-scores

-3.0 -2.0 -1.0 0.0 1.0 2.0 3.0

GEO Link:	http://www.ncbi.nlm.nih.gov/geo/query/acc.cgi?acc=GSE11400
Status:	Public on Jun 01 2008
Title:	Gene Expression Data in R26Pax3 palates
Organism:	Mus musculus
Experiment type:	Expression profiling by array
Platform:	GPL1261
Pubmed ID:	18483623
Summary & Design:	**Summary:** We used microarrays to detail the global programme of gene expression underlying palate development by persistent expression in R26Pax3 mice and identified distinct classes of up-regulated and down-regulated genes during this process. **Keywords: palate development** **Overall design:** Palatal shelves were dissected at E14.5 for RNA extraction and hybridization on Affymetrix microarrays. Wild type and R26Pax3/Pax3 littermates were used.

Background corr dist: KL-Divergence = 0.0896, L1-Distance = 0.0231, L2-Distance = 0.0008, Normal std = 0.4557

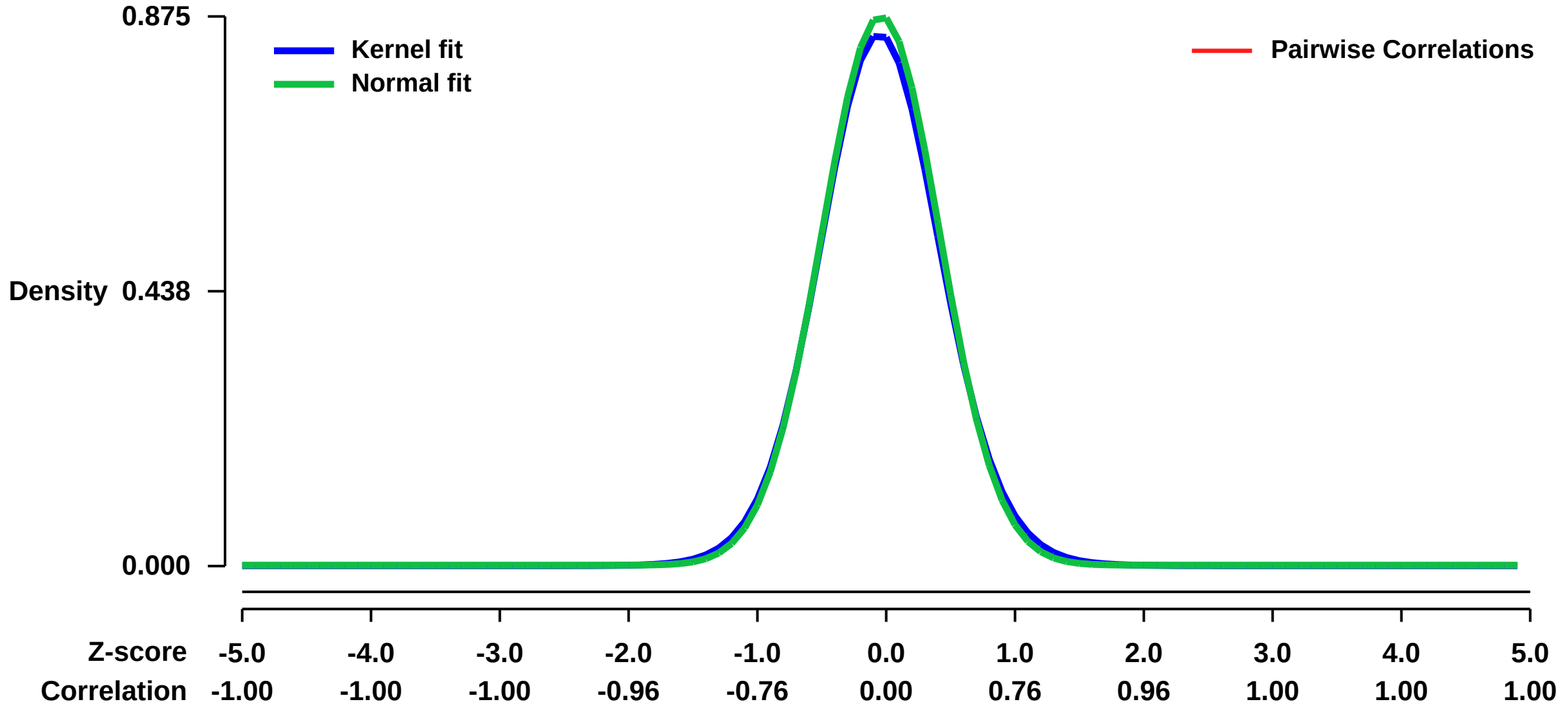

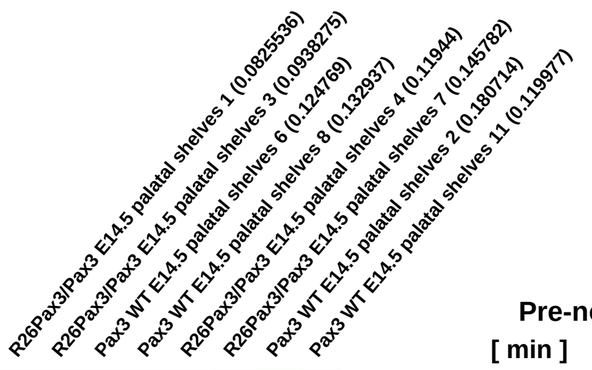

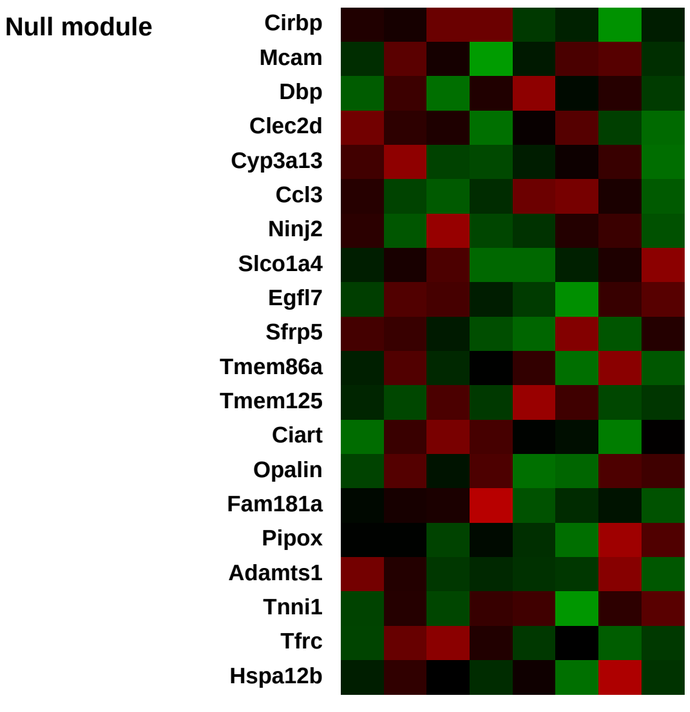

GEO Series "GSE52358" Expression Profiles

Num of samples in this series: 8

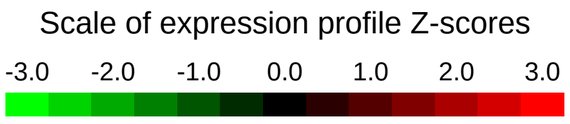

GEO Link:	**http://www.ncbi.nlm.nih.gov/geo/query/acc.cgi?acc=GSE52358**
Status:	**Public on Jun 18 2014**
Title:	**Gene expression profiling of the tongue bud from Alk5 mutant mouse models**
Organism:	**Mus musculus**
Experiment type:	**Expression profiling by array**
Platform:	**GPL1261**
Pubmed ID:	
Summary & Design:	**Summary:** **The overall goal of this project is to investigate the role of TGF-beta signaling in tissue-tissue interactions between myogenic precursors of craniofacial muscles and cranial neural crest cells (CNCCs). Here, we conducted gene expression profiling of the tongue bud from mice at embryonic day E13.5 with a CNCC-specific conditional inactivation of the TGF-beta receptor type 1 gene Alk5. These mice provide a model of microglossia as well as disrupted extraocular and masticatory muscle development, which are congenital birth defects commonly observed in several syndromic conditions.** **Overall design:** **To investigate the adverse effects of dysfunctional TGF-beta signaling on tissue-tissue interactions between CNCCs and myogenic precursors of craniofacial muscles, we analyzed tongue bud tissue of mice with a CNCC-specific conditional inactivation of Alk5 (Wnt1-Cre; Alk5 fl/fl). We performed microarray analyses of the tongue bud of Alk5 fl/fl control mice and Wnt1-Cre; Alk5 fl/fl mutant mice, collected at embryonic day E13.5 (n=4 per group).**

Background corr dist: **KL-Divergence = 0.0605, L1-Distance = 0.0184, L2-Distance = 0.0004, Normal std = 0.5241**

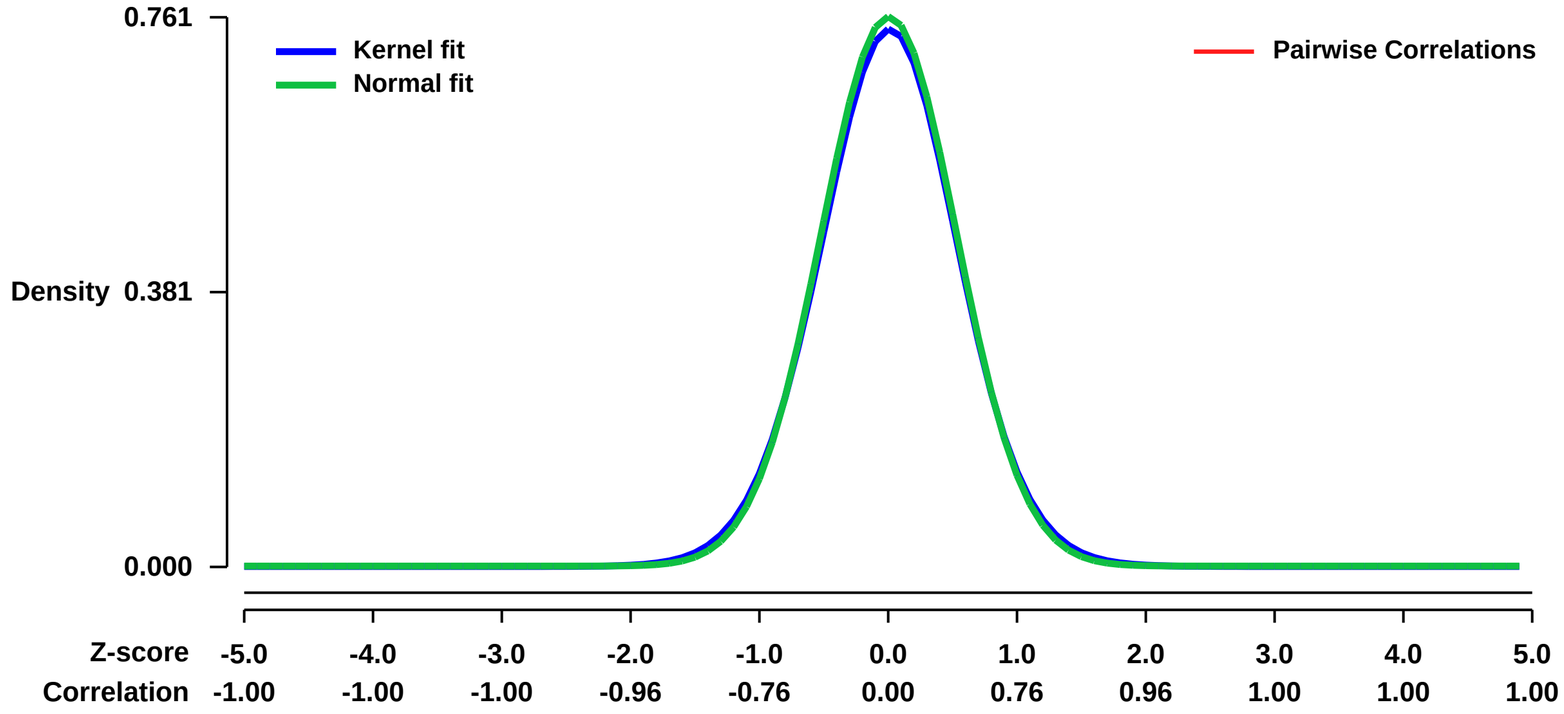

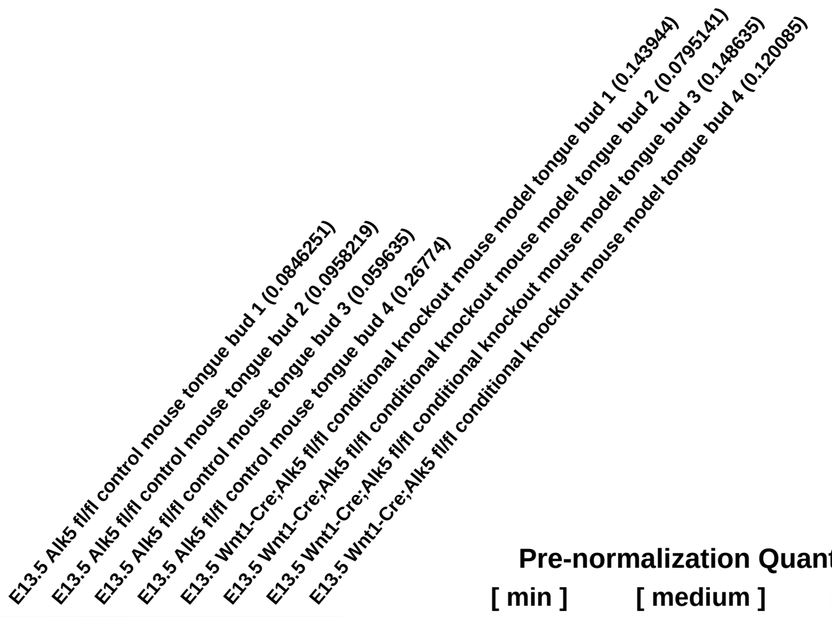

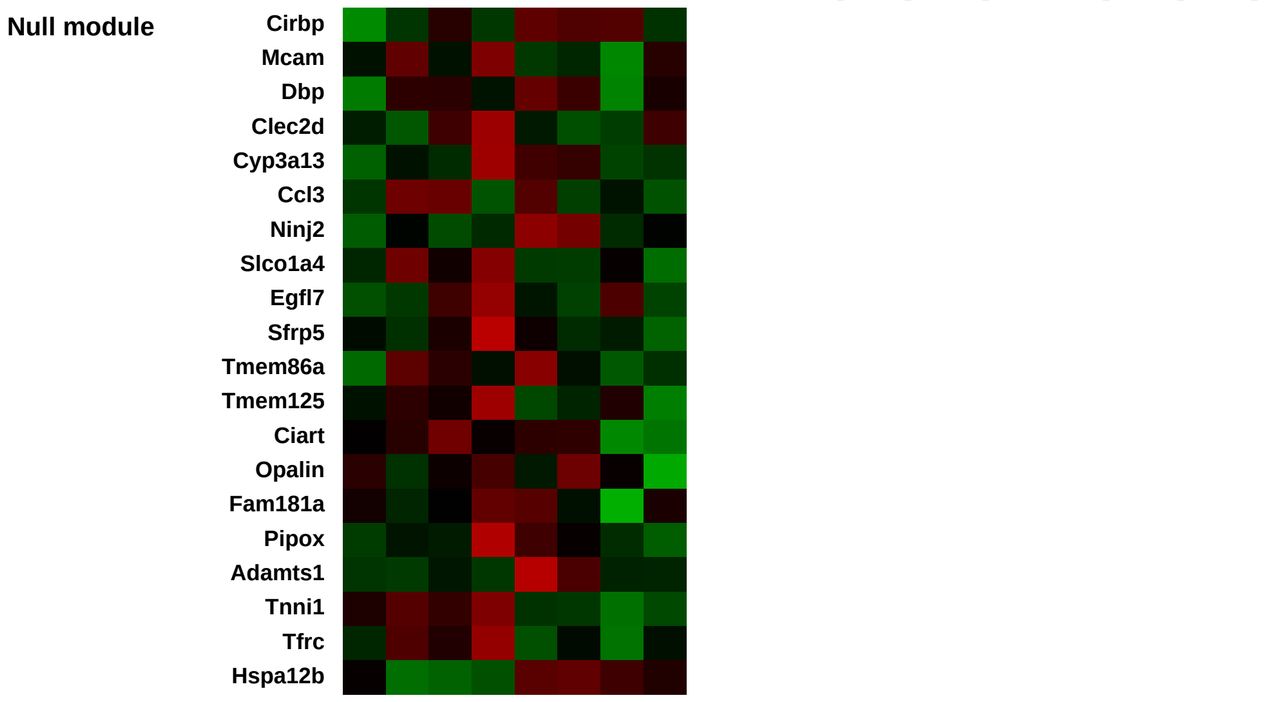

GEO Series "GSE4756" Expression Profiles

Num of samples in this series: 8

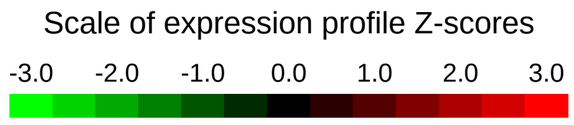

GEO Link:	**http://www.ncbi.nlm.nih.gov/geo/query/acc.cgi?acc=GSE4756**
Status:	**Public on May 02 2006**
Title:	**ruiz-affy-mouse-243540**
Organism:	**Mus musculus**
Experiment type:	**Expression profiling by array**
Platform:	**GPL1261**
Pubmed ID:	

Summary & Design:

Summary:
The retinal degeneration slow gene (rds/peripherin), is essential for normal photoreceptor (rods and cones) outer segment structure in the neurosensory retina. Our rds animal model, are stable transgenic mice that carry a null mutation (complete lost of function) in the rds gene. Those animals become blind, mimicking a human form of retinitis pigmentosa. In our experience we have observed dramatic levels of photoreceptor rescue after subretinal injection of those animals with a ciliary neurotrophic factor (CNTF) inserted into a recombinant Adeno-associate virus (rAAV) vector. However, this cell rescue is accompanied by changes in photoreceptor nuclear morphology, attenaution of the electroretinogram and evetually Apoptosis. By using Microarray analysis we hope to identify genes whose expression or lack thereof brings the cell to the brink of suicide. Identification of these genes will suggest therapeutic targets for the future.

We will determine gene expression patterns in the retina of rds mice non-injected and injected with CNTF/rAAV virus after 60 days of injection.

Our working hypothesis is that the injected CNTF/rAAV vector induces the expression of genes that somehow partially restores the photoreceptor morphology of rds mice. Paradoxically, it also has a negative effect on the phisiology of these cells (ERG). The up or down regulation of genes in different areas of the neurosensory retina collected by Laser Capture Microdissection will give us an insight on the relevance of candidate genes responsible for this phenomenon.

We will use rds mice at age P25 and inject their rigth eye with CNTF/AVV virus (2.68x e13 particles/ml) and use the left eye as a control. Injection is performed via subretinal. Retinas will be collected at age P90 post injection. RNA will be extracted and processed accordingly for MIcroarray analysis.

Keywords: dose response

Overall design:

Background corr dist: KL-Divergence = 0.0571, L1-Distance = 0.0213, L2-Distance = 0.0006, Normal std = 0.5396

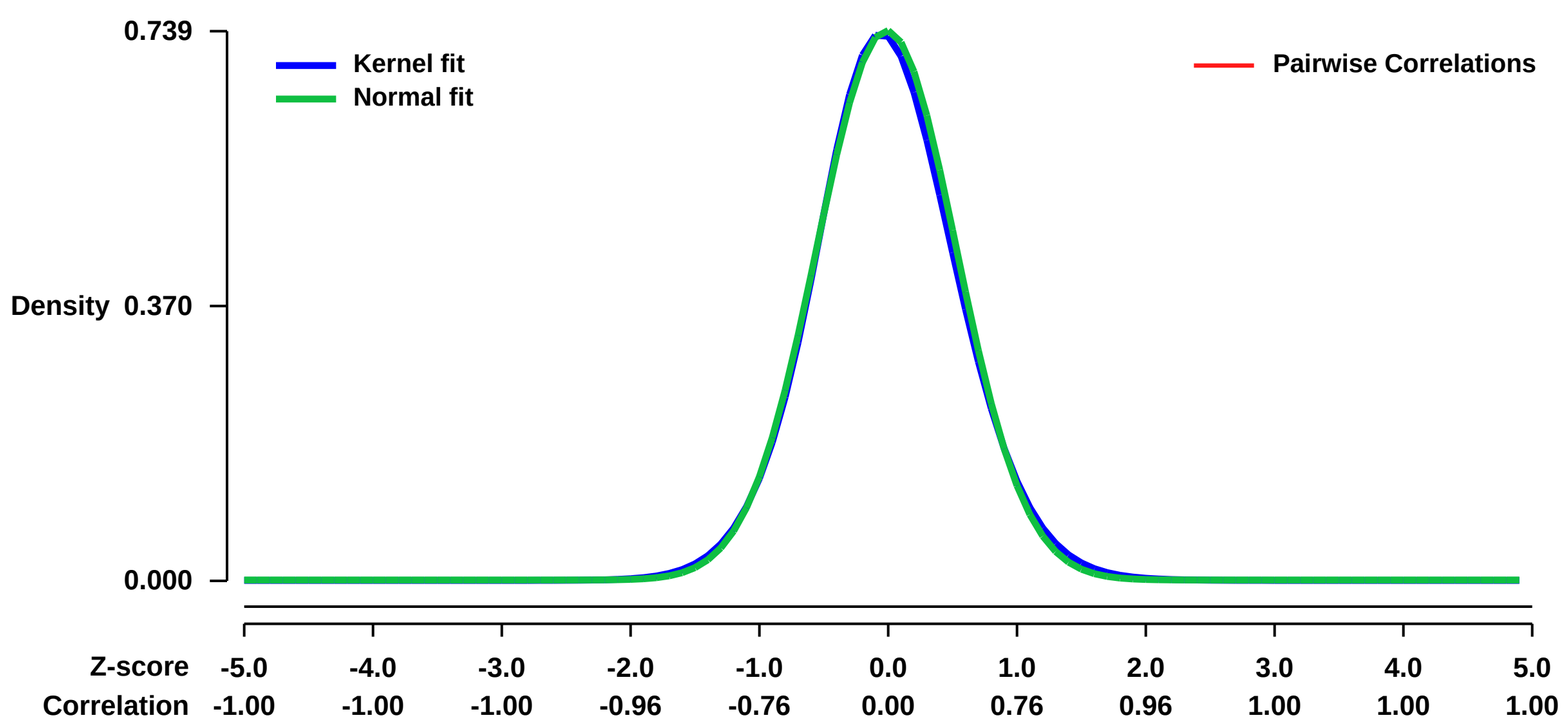

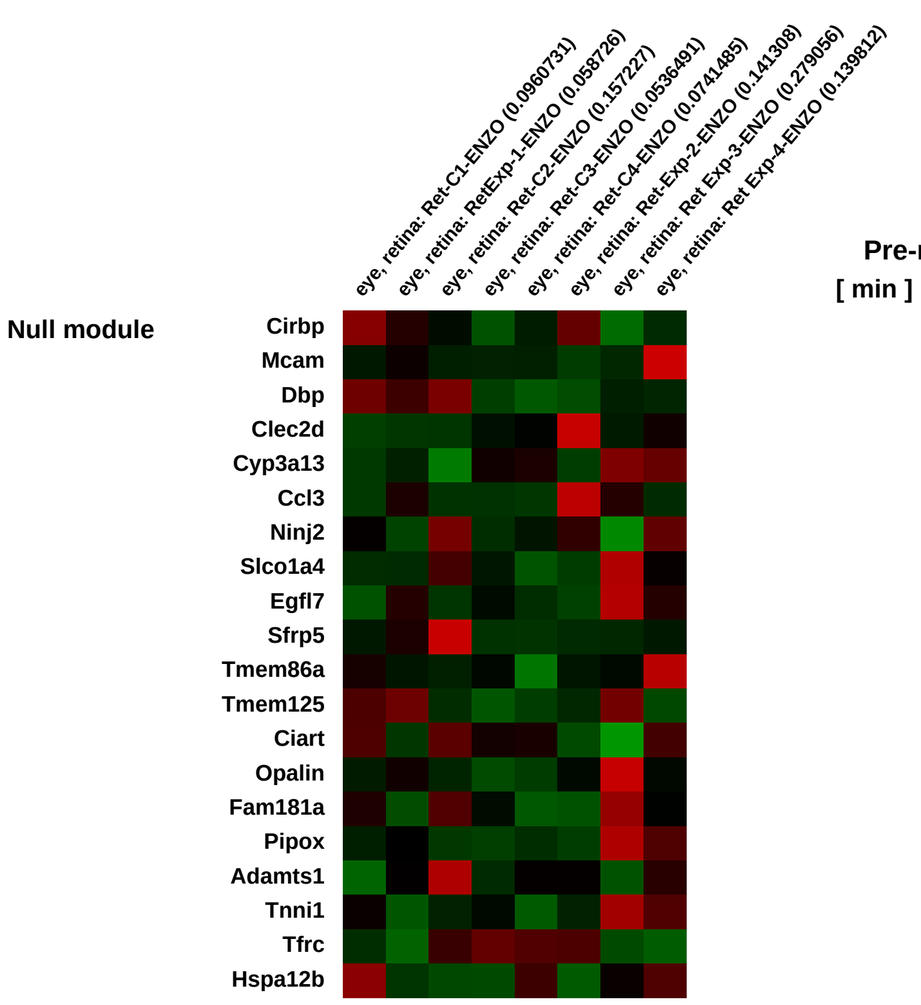

GEO Series "GSE13225" Expression Profiles

Num of samples in this series: 6

Scale of expression profile Z-scores

-3.0 -2.0 -1.0 0.0 1.0 2.0 3.0

GEO Link:	http://www.ncbi.nlm.nih.gov/geo/query/acc.cgi?acc=GSE13225
Status:	Public on Nov 30 2008
Title:	(AKR/J x FVB/NJ)F1 versus (DBA/2J x FVB)F1 spleen expression data
Organism:	Mus musculus
Experiment type:	Expression profiling by array
Platform:	GPL1261
Pubmed ID:	19118016
Summary & Design:	**Summary:** F1 hybrids from (AKR/J x FVB/NJ) and (DBA/2J x FVB/NJ) outcrosses display a 20-fold difference in mammary tumor metastatic capacity, due to differences in inherited polymorphisms. Expression studies were performed to determine whether polymorphism-driven gene expression signatures predictive of outcome could be generated from normal tissues **Keywords: Basal transcription profiles** **Overall design:** Spleen from adult F1 animals from (AKR/J x FVB/NJ) and (DBA/2J x FVB/NJ) outcrosses was collected and arrayed on Affymetrics chip to identify basal differences in gene expression between the different genotypes

Background corr dist: KL-Divergence = 0.0222, L1-Distance = 0.0130, L2-Distance = 0.0002, Normal std = 0.7145

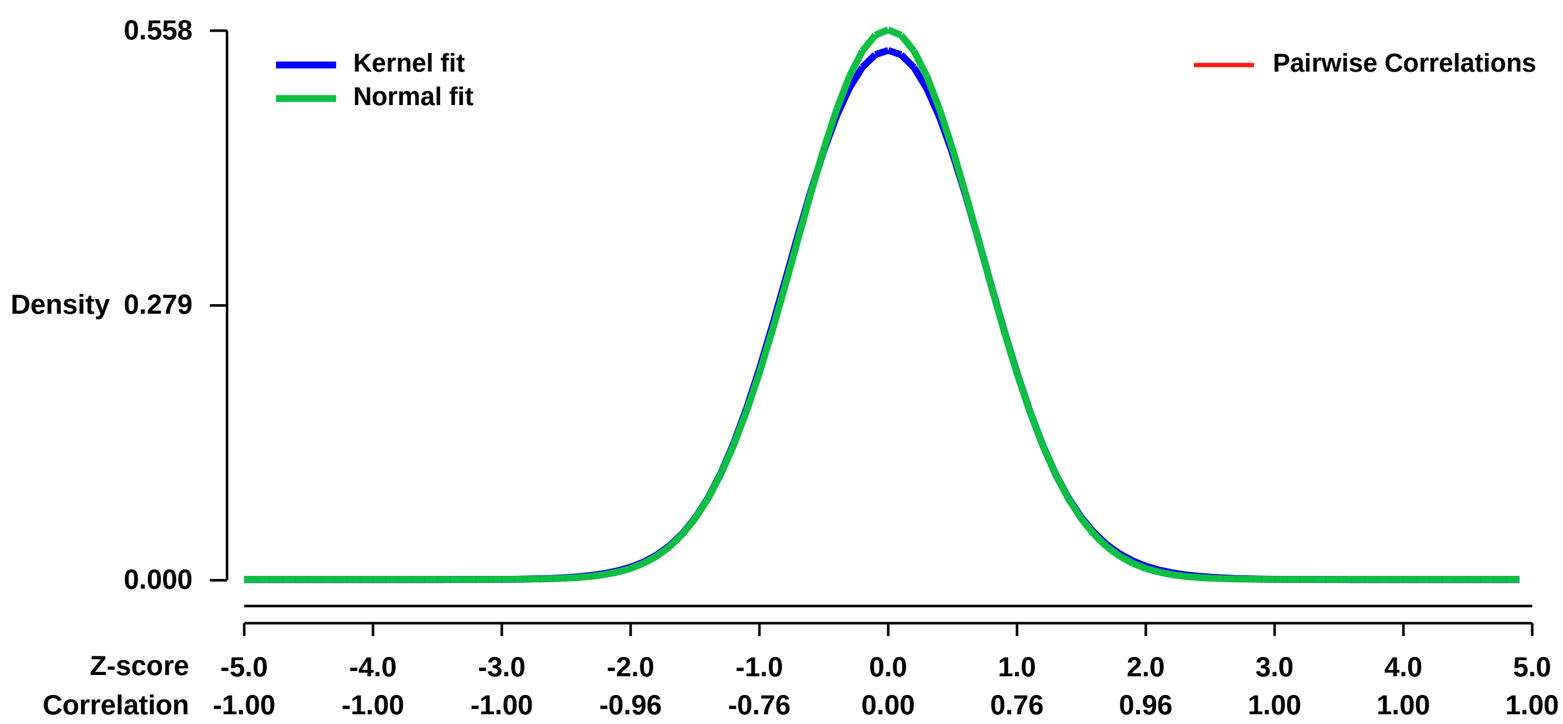

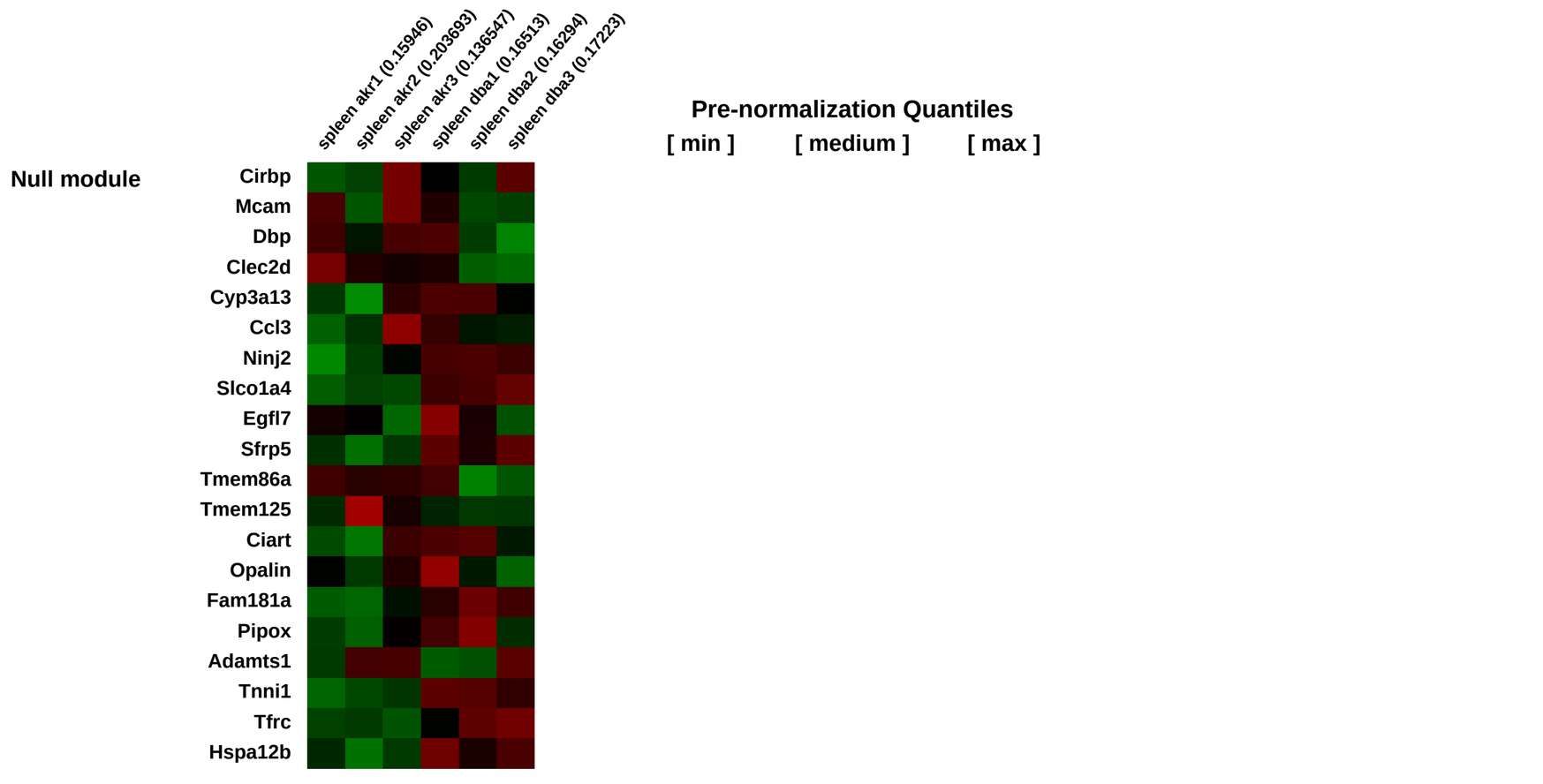

GEO Series "GSE32311" Expression Profiles

Num of samples in this series: 11

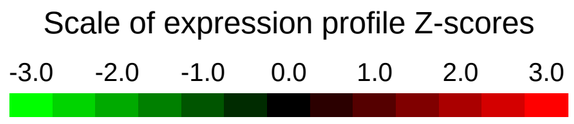

GEO Link:	http://www.ncbi.nlm.nih.gov/geo/query/acc.cgi?acc=GSE32311
Status:	Public on Nov 13 2011
Title:	Harnessing of the Nucleosome Remodeling Deacetylase complex controls lymphocyte development and prevents leukemogenesis
Organism:	Mus musculus
Experiment type:	Genome binding/occupancy profiling by high throughput sequencing
Platform:	GPL1261
Pubmed ID:	22080921
Summary & Design:	**Summary:** Cell fate decisions depend on the interplay between chromatin regulators and transcription factors. Here we show that activity of the Mi-2u Nucleosome Remodeling and Deacetylase (NuRD) complex is controlled by the Ikaros family of lymphoid-lineage determining proteins. Ikaros, an integral component of the NuRD complex in lymphocytes, tethers this complex to active lymphoid differentiation genes, but keeps it in a functionally-poised state. Loss in Ikaros DNA binding activity causes a local increase in Mi-2u chromatin remodeling, histone deacetylation and suppression of lymphoid gene expression. The NuRD complex also redistributes to transcriptionally-poised non-Ikaros gene targets, involved in proliferation and metabolism, inducing their re-activation. Thus release of NuRD from Ikaros regulation blocks lymphocyte maturation and mediates progression to a leukemic state by engaging functionally-opposing epigenetic mechanisms and genetic networks. We used microarrays to detail the global programme of gene expression of mouse DP thymocyte after Ikaros inactivation with dominant negative of Ik at different stage. **Overall design:** 8 samples (mouse DP thymocytes from wt, and different stage after Ikaros inactivation) are analyzed Mouse Microarray Expression platforms, Affymetrix Mouse 430 2.0. Examination of different histone modifications and binding sites for Ikaros, Mi2beta in wild type DP thymocytes, and Ikaros knockout thymocytes.

Background corr dist: KL-Divergence = 0.0614, L1-Distance = 0.0258, L2-Distance = 0.0011, Normal std = 0.5185

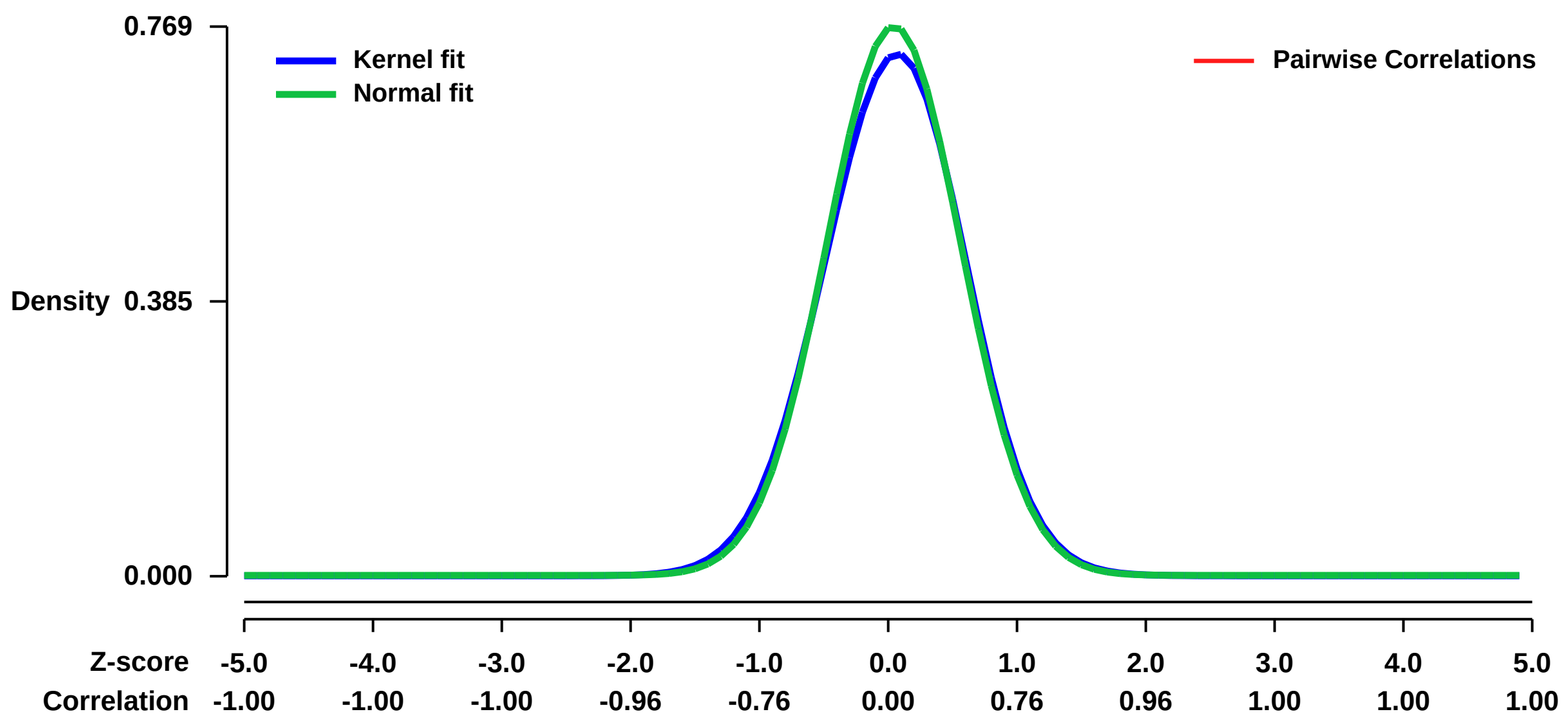

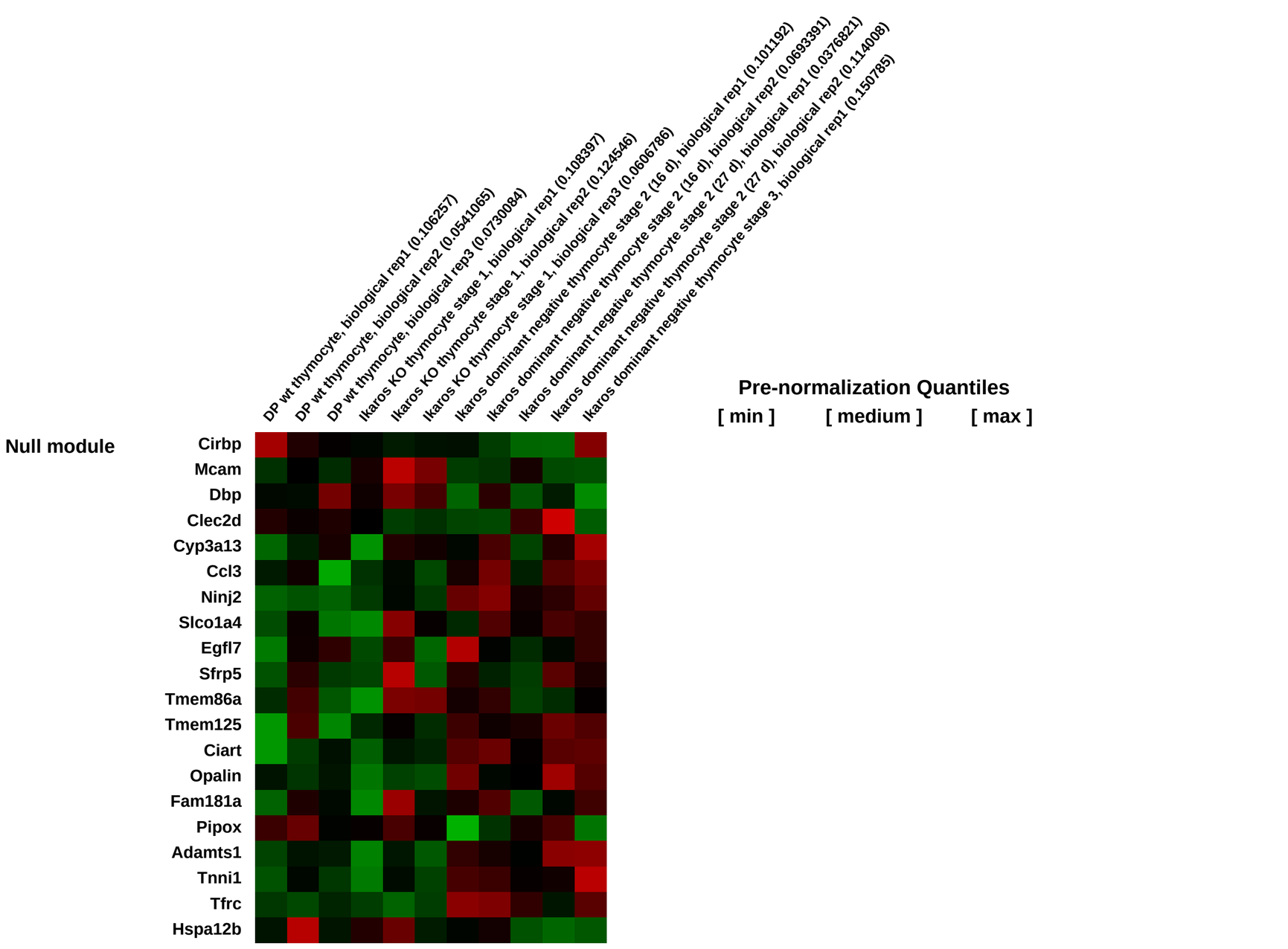

GEO Series "GSE5657" Expression Profiles

Num of samples in this series: 20

Scale of expression profile Z-scores

-3.0 -2.0 -1.0 0.0 1.0 2.0 3.0

GEO Link:	**http://www.ncbi.nlm.nih.gov/geo/query/acc.cgi?acc=GSE5657**
Status:	**Public on Feb 06 2007**
Title:	**Effect of X-linked hypophosphatemia (the Hyp mutation) on gene expression in the mid-shaft of the mouse femur**
Organism:	**Mus musculus**
Experiment type:	**Expression profiling by array**
Platform:	**GPL1261**
Pubmed ID:	
Summary & Design:	**Summary:** **The pathophysiology of the osteomalacia in X-linked hypophosphatemia is uncertain. In this project, genomic DNA microarrays were used to identify novel genes with abnormal mRNA expression levels in mice with the dominant Hyp mutation of the Phex gene. Femoral shafts from five-week-old C57BL/6J mice, male and female, normal and Hyp (hemizygous male and heterozygous female), were flushed with saline to remove the marrow. RNA was extracted from each bone, pooled between two mice for each array, processed to cRNA, and hybridized to Affymetrix Mouse 430 2.0 GeneChip microarrays with probe sets for 45,101 genes. Twenty microarrays (40 mice) were done with 5 arrays for each treatment group (normal male, Hyp male, normal female and Hyp female). For each gene, factorial analysis of variance was performed for the main effects of genotype (normal vs. Hyp), sex (male vs. female), and genotype-by-sex interaction. The mRNA levels for 54 % of the genes on each array were scored as present. At P < 0.01, 2,635 genes were significant for genotype, 1,488 for sex, and 509 for genotype-by-sex interaction. There were two probes sets for the Phex gene. Probe 1450445, at the 3â end of the coding sequence, was low in normal samples (246 ´– 37 (10), mean ´– SEM (n)) and absent in Hyp samples. Probe 1421979, at the far 3â end of the untranslated region of the cDNA, 3,000 base pairs from the coding sequence, was high in normal mice (3,915 ´– 315 (10); 8x brighter than the average gene), undetectable in Hyp males, and 725 ´– 93 (5) in Hyp females. Both probe sets were scored as absent in kidney tissue. In Hyp bone, male and female, there was significant down-regulation of markers of osteoblasts and bone matrix synthesis with significant up-regulation of markers of blood vessel formation and cytoskeleton. No prominent skeletal gene was up-regulated in Hyp to attempt to compensate for the low skeletal mineralization. The genes with significant genotype-by-sex interaction did not show a marked fold difference between male and female Hyp mice. In conclusion, male and female Hyp mice showed similar depression of mRNA levels of genes related to bone synthesis in the femoral shaft. There was a high signal level from probes for a sequence in the 3â untranslated region of the Phex gene of normal, but not Hyp, mice, suggesting the need for further study of the molecular organization of this gene.** **Keywords: 2x2 factorial design with complete blocks** **Overall design:** **Equal amounts of RNA from two mice, matched for genotype and sex were pooled to create each sample for microarray analysis. Four treatment groups were done: (1) Normal male mice, (2) Hyp male mice, (3) normal female mice, and (4) Hyp female mice. Five replicates were done with each replicate containing one sample from each of the four treatment groups for a total of 20 independent samples (40 mice total). Each replicate was matched for littermates and parallel processing.**

Background corr dist: KL-Divergence = 0.2840, L1-Distance = 0.0582, L2-Distance = 0.0087, Normal std = 0.2875

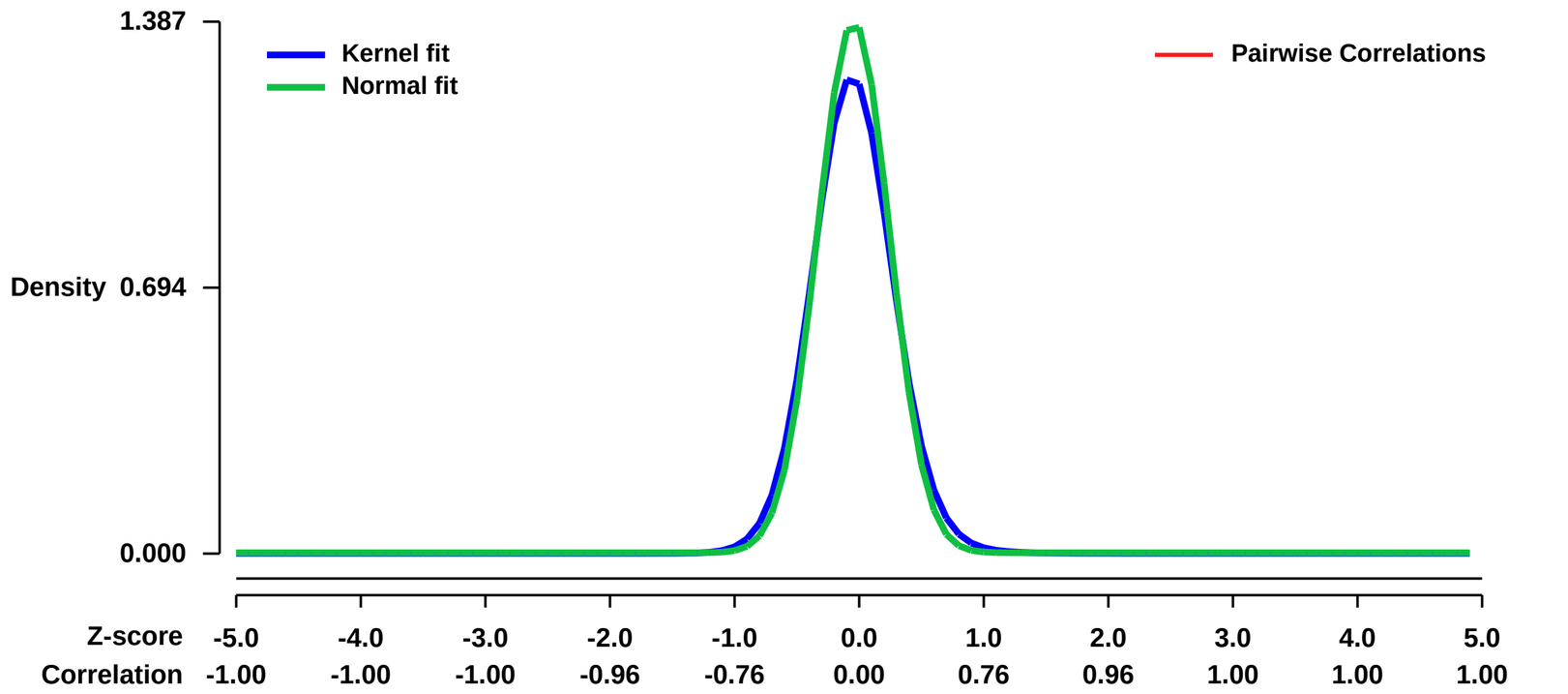

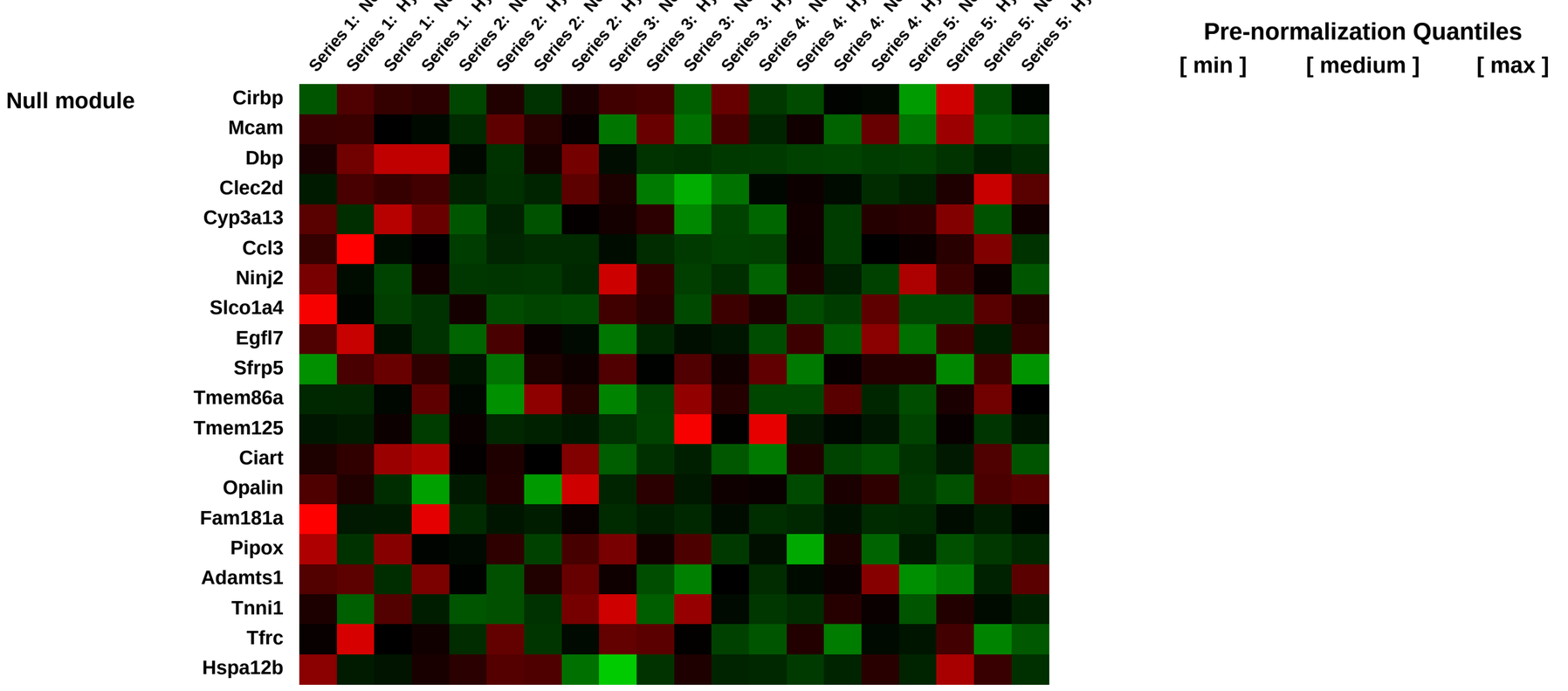

GEO Series "GSE29082" Expression Profiles

Num of samples in this series: 6

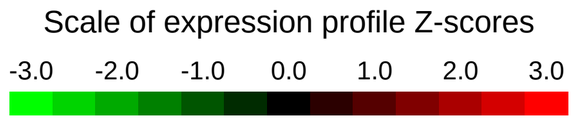

GEO Link:	http://www.ncbi.nlm.nih.gov/geo/query/acc.cgi?acc=GSE29082
Status:	Public on Sep 13 2011
Title:	Gene expression analysis of non-cerebellar portion of Gb5-deficient mice brain
Organism:	Mus musculus
Experiment type:	Expression profiling by array
Platform:	GPL1261
Pubmed ID:	21883221
Summary & Design:	**Summary:** Gb5 is a divergent, evolutionarily-conserved, member of the heterotrimeric G protein b subunit family that is expressed principally in brain and neuronal tissue. Among Gb isoforms, Gb5 is unique in its ability to heterodimerize with members of the R7 subfamily of the regulator of G protein signaling (RGS) proteins that contain G protein-g like (GGL) domains. Previous studies employing Gb5 knockout mice have shown that Gb5 is an essential stabilizer of GGL domain-containing RGS proteins and regulates the deactivation of retinal phototransduction and the proper functioning of retinal bipolar cells. The purpose of this study is to better understand the functions of Gb5 in the brain outside the visual system by employing molecular biology, immunohistochemistry and confocal imaging technologies. We show here that mice lacking Gb5 have a markedly abnormal neurologic phenotype that includes neurobehavioral developmental delay, wide-based gait, motor learning and coordination deficiencies, and hyperactivity. Using immunohistochemical analysis and a green fluorescent reporter of Purkinje cell maturation we show that the phenotype of Gb5-deficient mice includes, in part, delayed development of the cerebellar cortex, an abnormality that likely contributes to the neurobehavioral phenotype. Multiple neuronally-expressed genes are dysregulated in non-cerebellar portion of Gb5 KO mice. **Overall design:** Brain tissues(non-cerebellar portion of brain) from WT and KO with three biological replications of mice were collected, frozen in liquid nitrogen, and stored at -70 ´℃

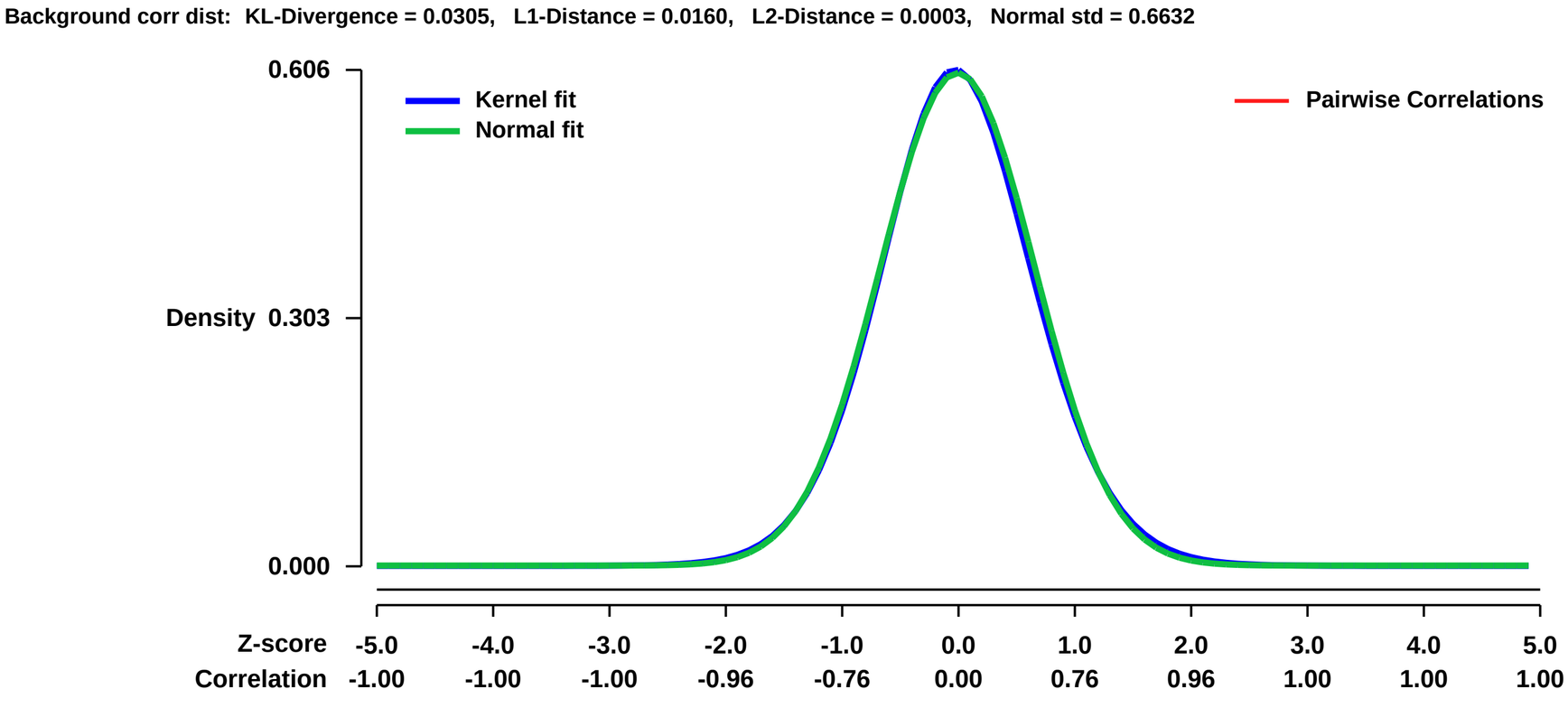

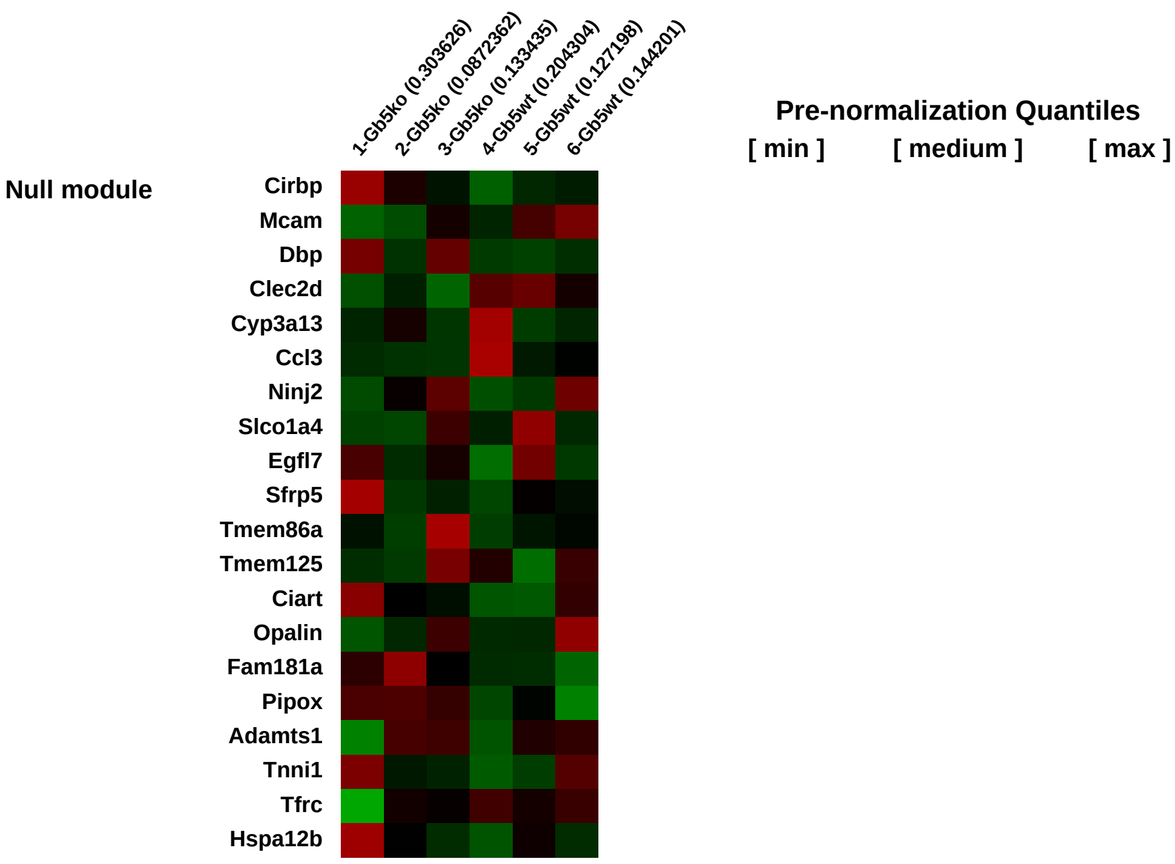

GEO Series "GSE16073" Expression Profiles

Num of samples in this series: 6

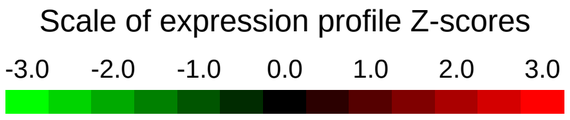

GEO Link:	http://www.ncbi.nlm.nih.gov/geo/query/acc.cgi?acc=GSE16073
Status:	Public on Oct 22 2009
Title:	Expression Data from Pten Null Fibroblasts
Organism:	Mus musculus
Experiment type:	Expression profiling by array
Platform:	GPL1261
Pubmed ID:	19847259
Summary & Design:	**Summary:** The tumor stroma is believed to contribute to some of the most malignant characteristics of epithelial tumors. However, signaling between stromal and tumor cells is complex and remains poorly understood. Here we show that genetic inactivation of Pten in stromal fibroblasts of mouse mammary glands accelerated the initiation, progression and malignant transformation of mammary epithelial tumors. Global gene expression profiling in mammary stromal cells identified a Pten-specific signature associated with massive extra-cellular matrix (ECM) remodeling, innate immune cell infiltraion and increased angiogenesis. Execution of this transcriptional program was mediated, in part, by the induction, phosphorylation and recruitment of Ets2 to target promoters. Remarkably, Ets2 inactivation in Pten stroma-deleted tumors was sufficient to decrease tumor growth and progression. These findings identify the Pten-Ets2 axis as a critical stroma-specific signaling pathway that suppresses mammary epithelial tumors. **Overall design:** Wild type and Pten null primary mammary fibroblasts isolated from 8 week old female mice were cultured, RNA was extracted and Affymetrix gene expression arrays were performed.

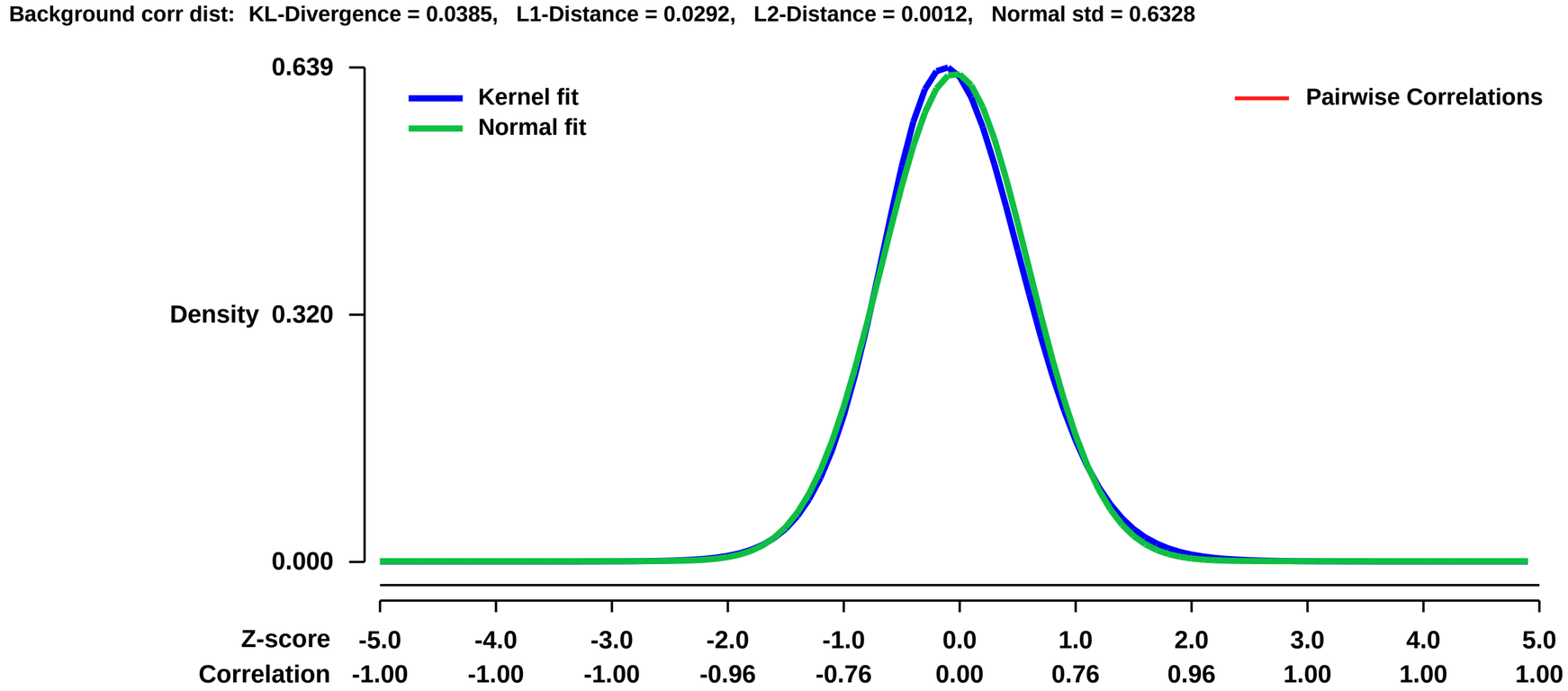

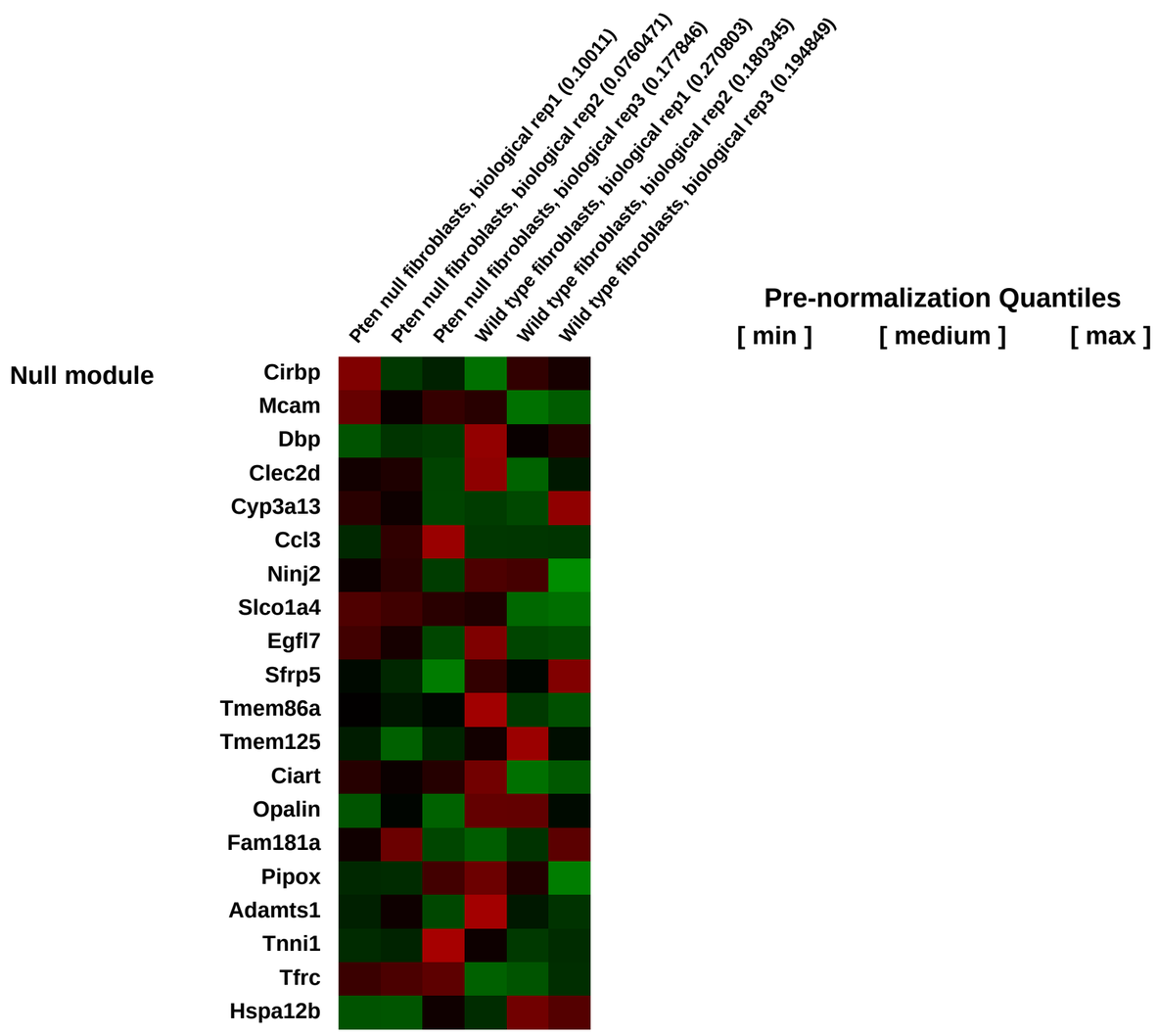

GEO Series "GSE21761" Expression Profiles

Num of samples in this series: 43

Scale of expression profile Z-scores

-3.0 -2.0 -1.0 0.0 1.0 2.0 3.0

GEO Link:	http://www.ncbi.nlm.nih.gov/geo/query/acc.cgi?acc=GSE21761
Status:	Public on Aug 09 2010
Title:	A large intergenic non-coding RNA induced by p53 mediates global gene repression in the p53 transcriptional response
Organism:	Mus musculus
Experiment type:	Expression profiling by array
Platform:	GPL1261
Pubmed ID:	20673990
Summary & Design:	**Summary:** Recently, more than a thousand large intergenic non-coding RNAs (lincRNAs) have been reported. These RNAs are evolutionarily conserved in mammalian genomes and thus presumably function in diverse biological processes. Here, we report the identification of lincRNAs that are regulated by p53. One of these lincRNAs (lincRNA-p21) serves as a repressor in p53-dependent transcriptional responses. Inhibition of lincRNA-p21 affects the expression of hundreds of gene targets enriched for genes normally repressed by p53. The observed transcriptional repression by lincRNA-p21 is mediated through the physical association with hnRNP-K. This interaction is required for proper genomic localization of hnRNP-K at repressed genes and regulation of p53 mediated apoptosis. We propose a model whereby transcription factors activate lincRNAs that serve as key repressors by physically associating with repressive complexes and modulating their localization to sets of previously active genes. **Overall design:** [4] RAS profiling: For p53 restoration, cultured tumor cell lines were incubated with 500nM 4-hydroxytamoxifen for the indicated times.

Background corr dist: KL-Divergence = 0.0959, L1-Distance = 0.0350, L2-Distance = 0.0024, Normal std = 0.4436

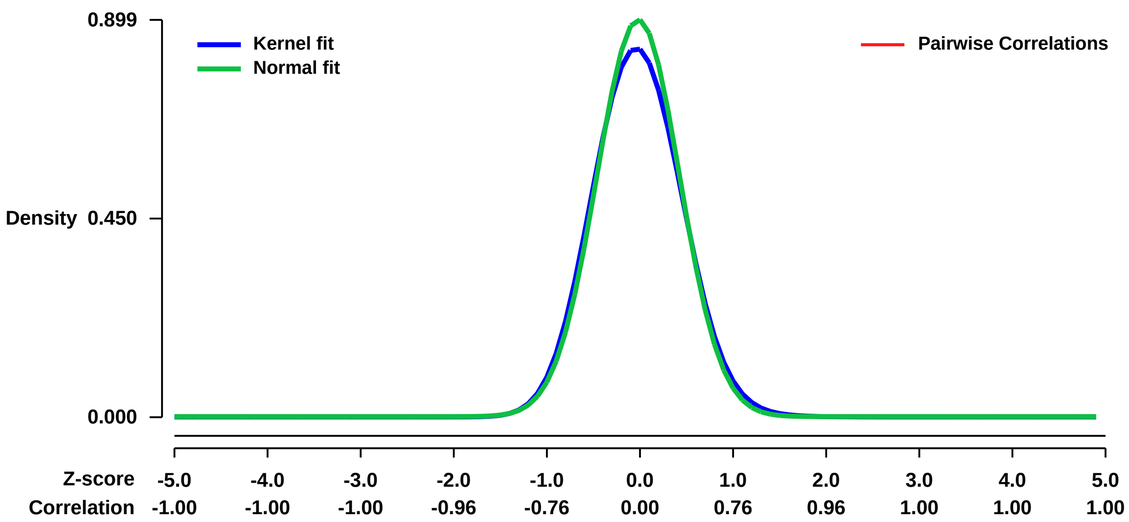

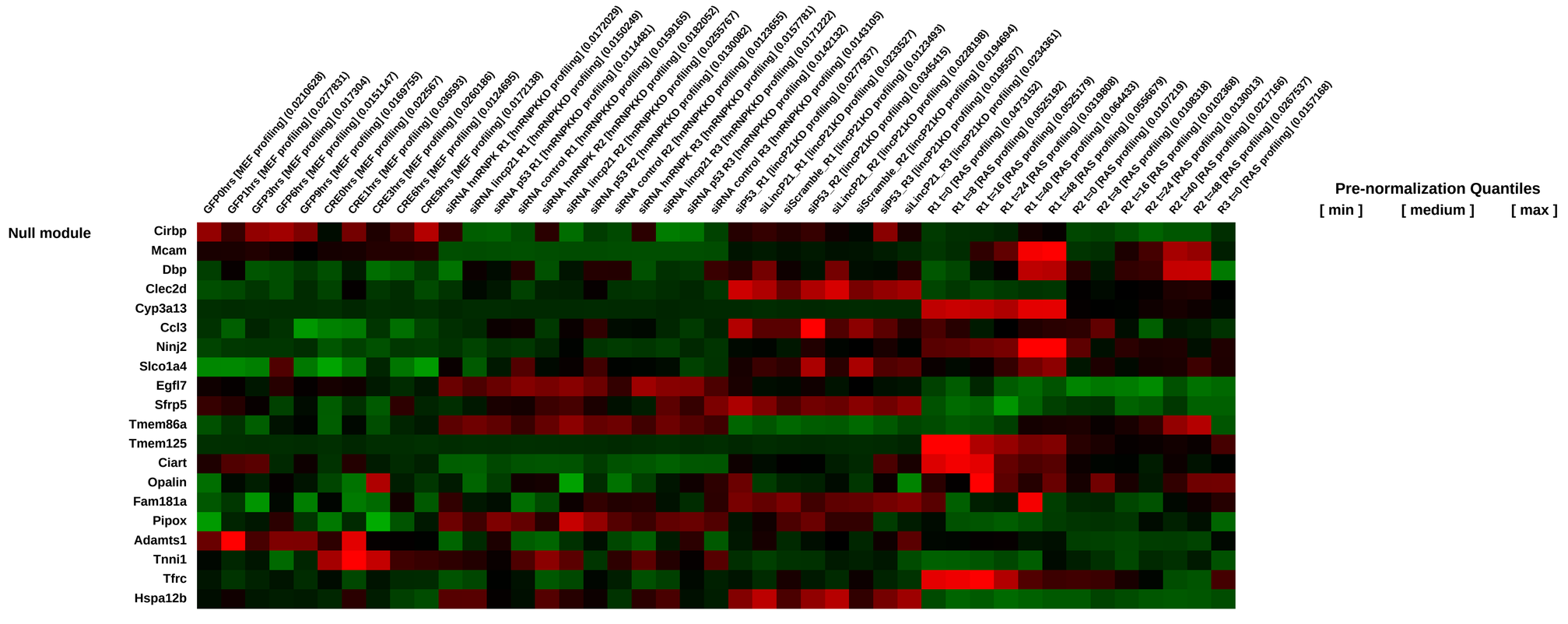

GEO Series "GSE35785" Expression Profiles

Num of samples in this series: 10

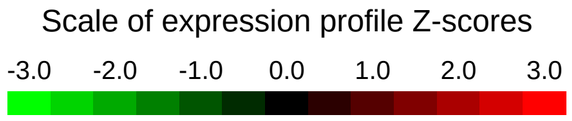

GEO Link:	http://www.ncbi.nlm.nih.gov/geo/query/acc.cgi?acc=GSE35785
Status:	Public on Apr 27 2012
Title:	mRNA expression data from AG-haESC, E14 and MEF
Organism:	Mus musculus
Experiment type:	Expression profiling by array
Platform:	GPL1261
Pubmed ID:	22541431
Summary & Design:	**Summary:** Haploid cells are amenable for genetic analysis because they contain only one set of chromosomes.Here,we report the derivation of haESCs from androgenetic blastocysts. These cells, which we designated AG-haESCs, express classical ESC markers, are pluripotent, and contribute to various tissues including the germline upon injection into diploid blastocysts. We used microarrays to compare the gene expression levels among androgenetic haploid embryonic stem cell lines(AG-haESC) E14 and male mouse embryonic fibroblasts (MEFs) and identified that most paternally imprinted genes were down-regulated and the maternally imprinted genes were up-regulated. **Overall design:** To avoid the influence of diploidized cells on the expression profile, we collected samples from FACS of cells at G1/G0 stage by staining Hochest 33342. We used E14,which was a male embryonic stem cell lines, and MEFs isloated from male individuals as control. Gene expression profiles of all the cell lines were analysed on an Affymetrix GeneChip 430 2.0 array.

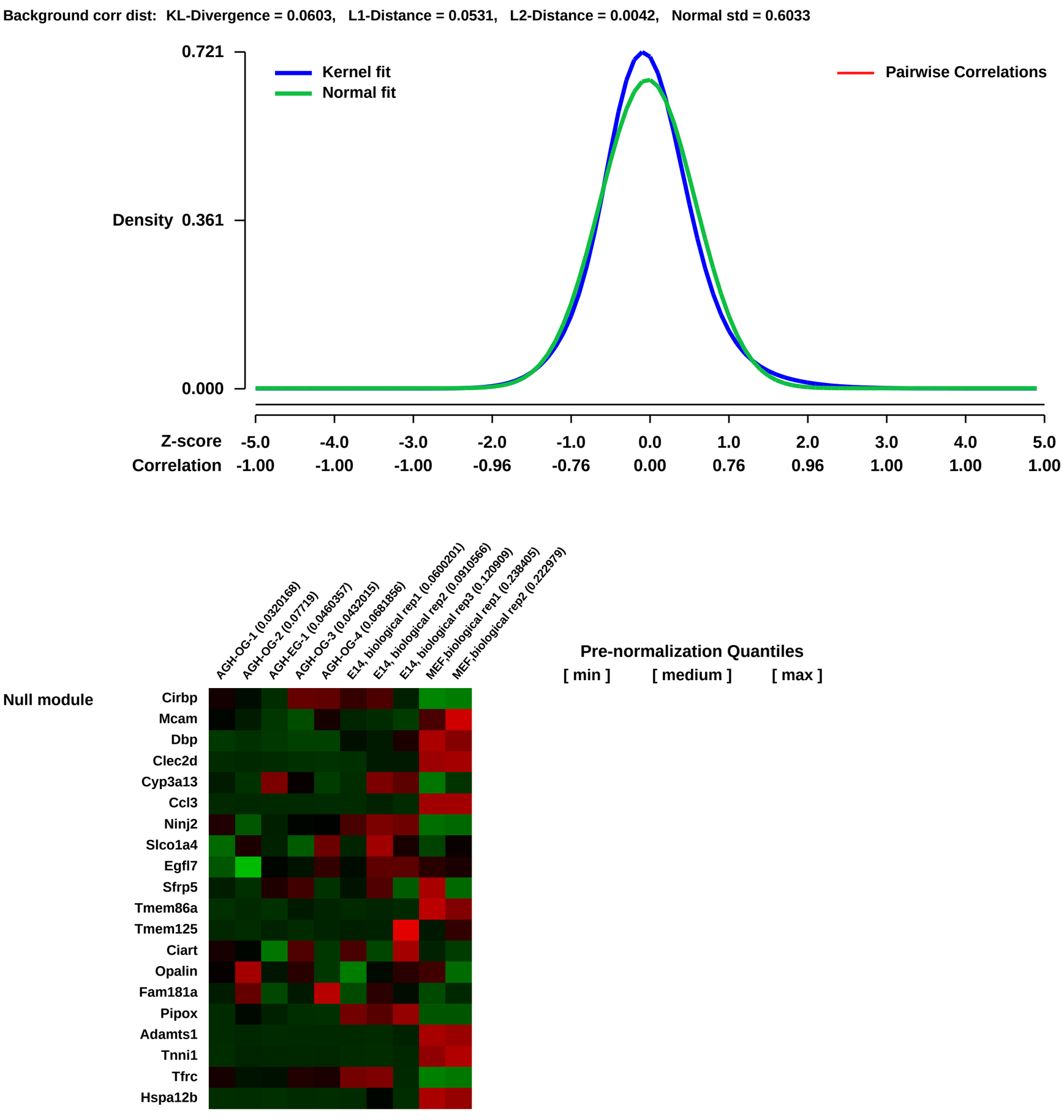

GEO Series "GSE20100" Expression Profiles

Num of samples in this series: 15

Scale of expression profile Z-scores

-3.0 -2.0 -1.0 0.0 1.0 2.0 3.0

GEO Link:	http://www.ncbi.nlm.nih.gov/geo/query/acc.cgi?acc=GSE20100
Status:	Public on Jul 01 2010
Title:	Expression data from primary MEF lacking either HDAC1, HDAC2 or both
Organism:	Mus musculus
Experiment type:	Expression profiling by array
Platform:	GPL1261
Pubmed ID:	20194438
Summary & Design:	**Summary:** Previously published data suggested some redundant functions between HDAC1 and HDAC2 in mouse. To test this hypothesis, we used microarrays to have a genome wide analysis at the transcription level of primary MEFs lacking HDAC1, HDAC2. **Overall design:** MEF HDAC1 F/F were were transduced with two different retroviruses: one virus expresses the Tamoxifen-inducible cre recombinase Cre-ERT2 and the second virus expresses either a small hairpin micro-RNA against HDAC2 or a scrambled version. HDAC1F/F MEFs expressing either a scrambled micro-RNA or a micro-RNA against HDAC2 can be induced by addition of Tamoxifen to delete HDAC1, thereby generating four different genotypes: WT, HDAC1 KO, HDAC2 knockdown (Kd) and HDAC1/2 KO/Kd.

Background corr dist: KL-Divergence = 0.0906, L1-Distance = 0.0823, L2-Distance = 0.0115, Normal std = 0.5232

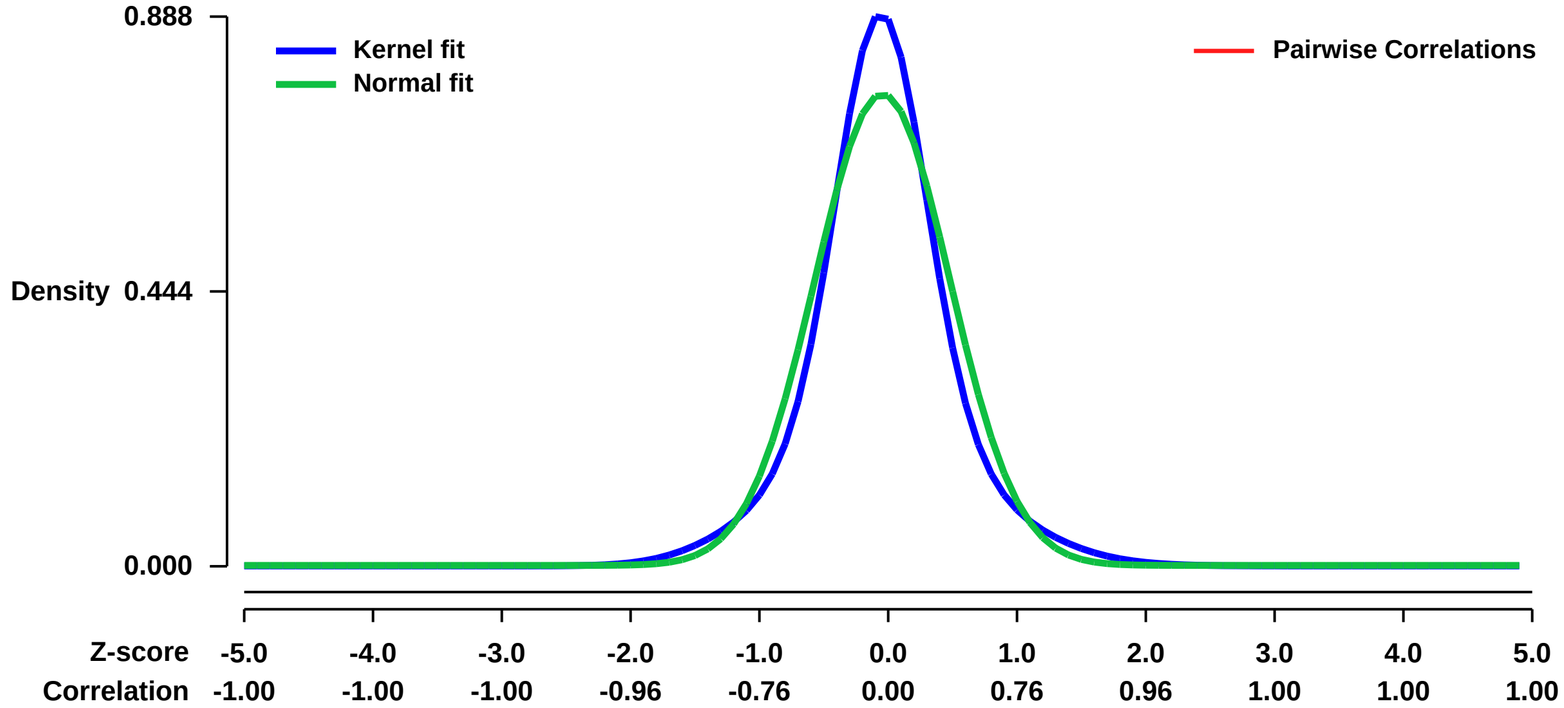

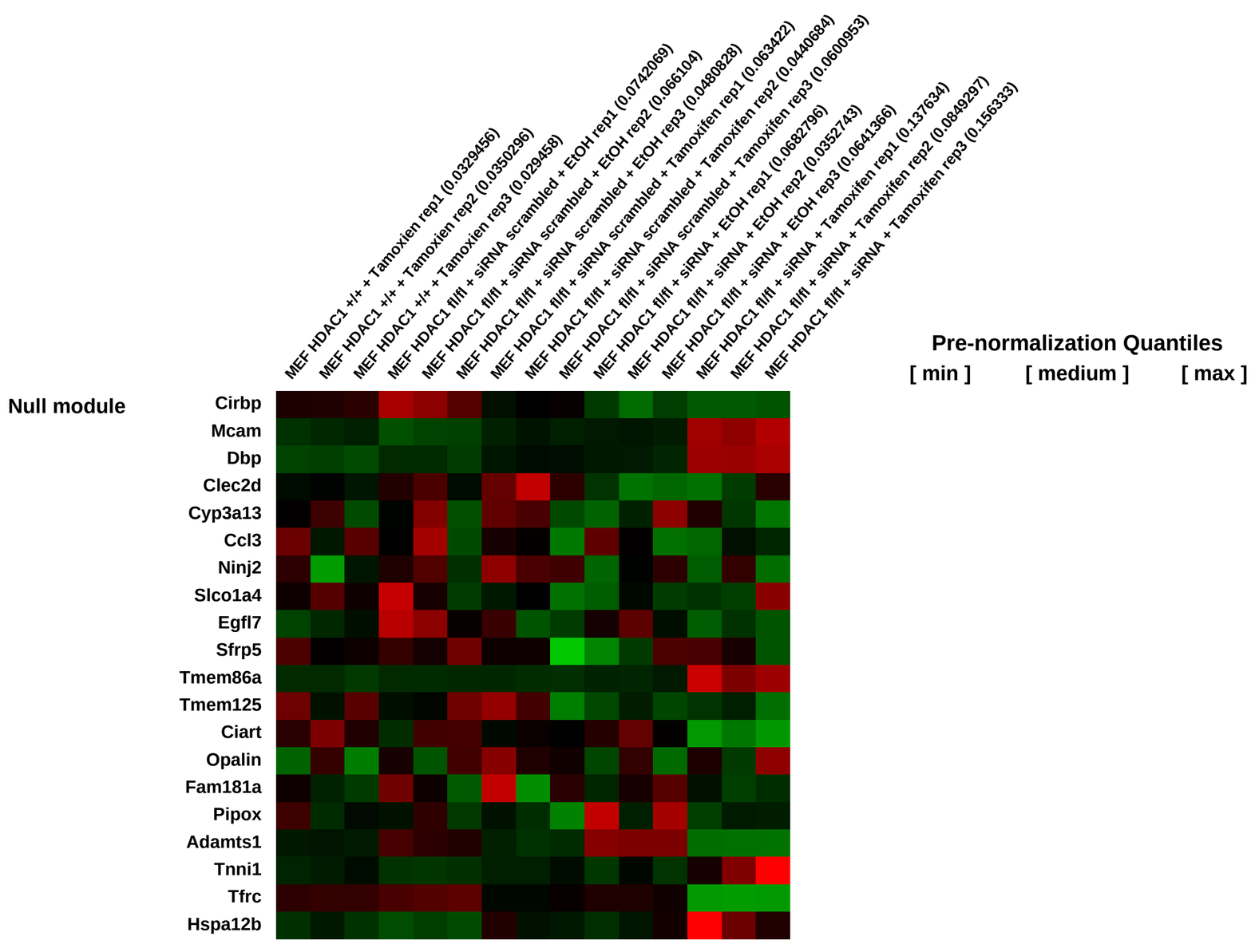

GEO Series "GSE21156" Expression Profiles

Num of samples in this series: 6

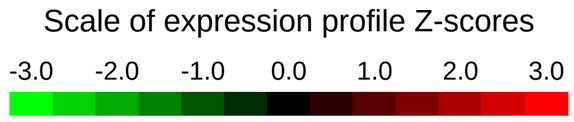

GEO Link:	http://www.ncbi.nlm.nih.gov/geo/query/acc.cgi?acc=GSE21156
Status:	Public on Apr 02 2010
Title:	Expression data from rostral forebrains of wild-type and Fezf1-/- Fezf2-/- mice
Organism:	Mus musculus
Experiment type:	Expression profiling by array
Platform:	GPL1261
Pubmed ID:	20431123
Summary & Design:	**Summary:** Zinc-finger genes Fezf1 and Fezf2 encode transcriptional repressors. Fezf1 and Fezf2 are expressed in the early neural stem/progenitor cells and control neuronal differentiation in mouse dorsal telencephalon. We compared gene expression profiles of rostral forebrains, which contain the telencephalon and the rostral part of the diencephalon, from embryonic day (E) 9.5, E10.5, and E12.5 wild-type control and Fezf1-/- Fezf2 -/- mouse embryos. **Overall design:** The forebrain rostral to the caudal limit of the lateral ventricles was isolated manually from E9.5, E10.5, and E12.5 wild-type and Fezf1-/- Fezf2-/- mice. Total RNAs were isolated by Separsol-RNA I and were used for microarray analyses.

Background corr dist: KL-Divergence = 0.0250, L1-Distance = 0.0333, L2-Distance = 0.0012, Normal std = 0.7381

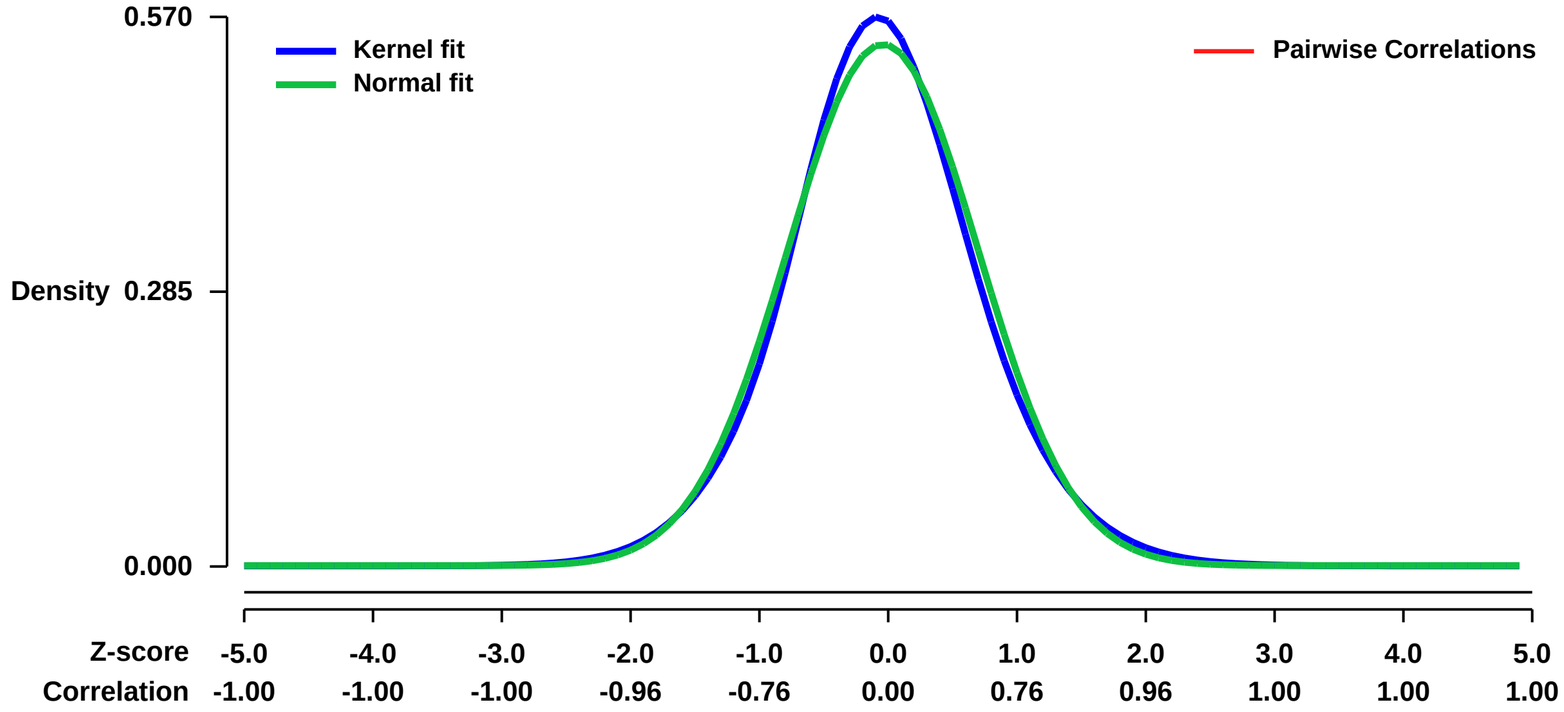

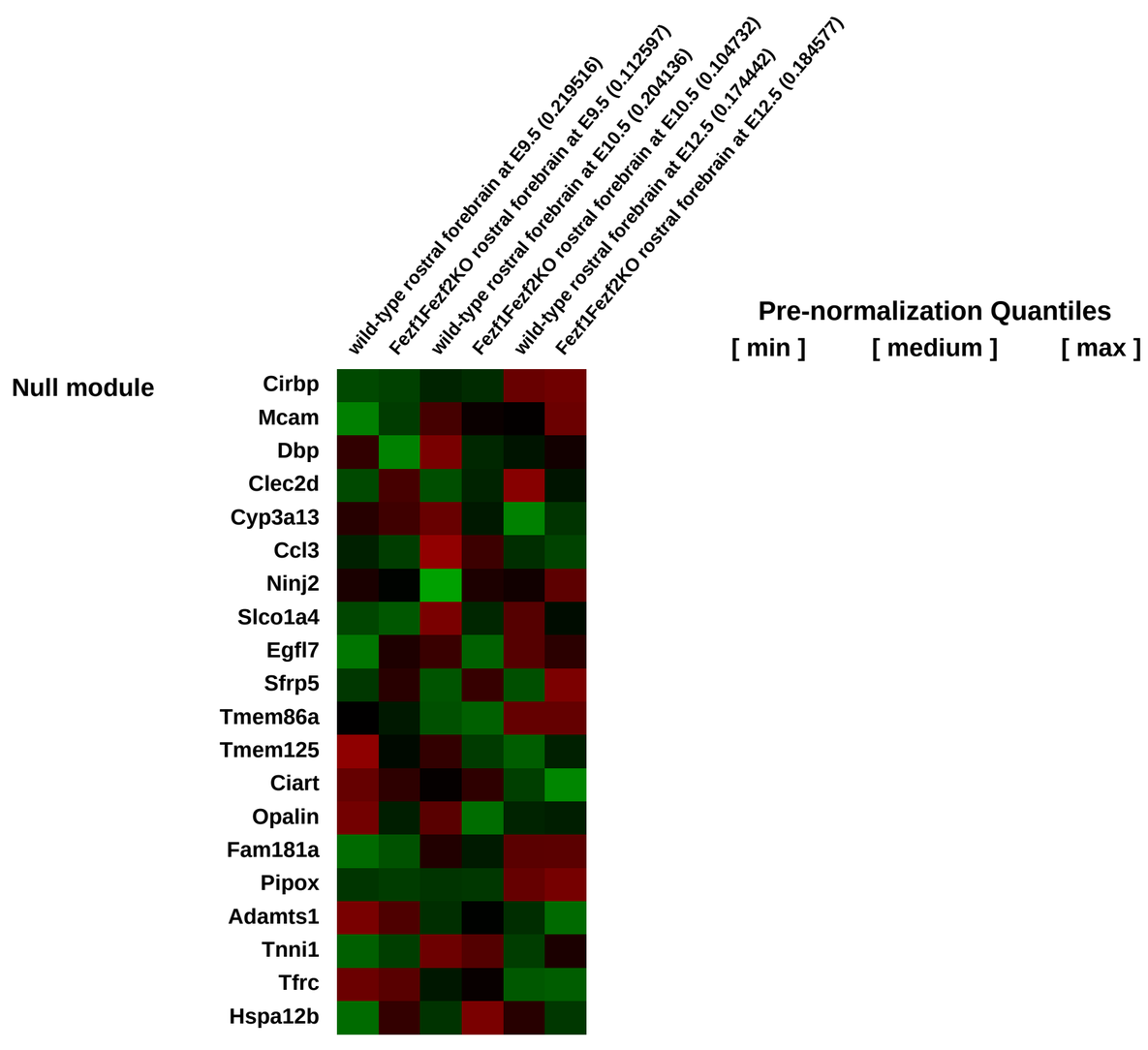

GEO Series "GSE20620" Expression Profiles

Num of samples in this series: 22

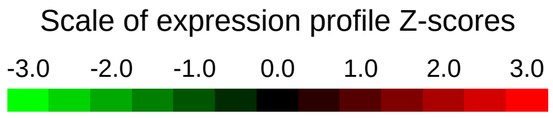

GEO Link:	http://www.ncbi.nlm.nih.gov/geo/query/acc.cgi?acc=GSE20620
Status:	Public on Aug 31 2010
Title:	Global analysis of gene expression by SV40 T antigen in mouse embryo fibroblasts
Organism:	Mus musculus
Experiment type:	Expression profiling by array
Platform:	GPL1261
Pubmed ID:	20692676
Summary & Design:	**Summary:** SV40 large T antigen (TAg) contributes to cell transformation, in part, by targeting two well characterized tumor suppressors, pRb and p53. TAg expression affects the transcriptional circuits controlled by Rb and by p53. We have performed a microarray analysis to examine the global change in gene expression induced by wild-type TAg and TAg-mutants, in an effort to link changes in gene expression to specific transforming functions. For this analysis we have used MEFs expressing TAg or infected by SV40. Our analysis indicates that TAg can induce interferon-stimulated genes in MEFs and that this induction depends upon the LXCXE motif and p53 binding. **Overall design:** Two independent wild-type MEFs and three independent MEF cell lines expressing TAg and the mutants were used. Additionally, three independent mock and SV40 infections were conduted in MEFs. Total RNA was isolated from with the RNeasy kit. Total RNA was processed by the Genomics and Proteomics Core Laboratories at the University of Pittsburgh and hybridized to the Affymetrix GeneChip Mouse Genome 430 2.0 array. MAS 5.0 was used to obtain the present/absent calls and CEL files were normalized by RMA to obtain log2 expression values.

Background corr dist: KL-Divergence = 0.1241, L1-Distance = 0.0433, L2-Distance = 0.0041, Normal std = 0.4128

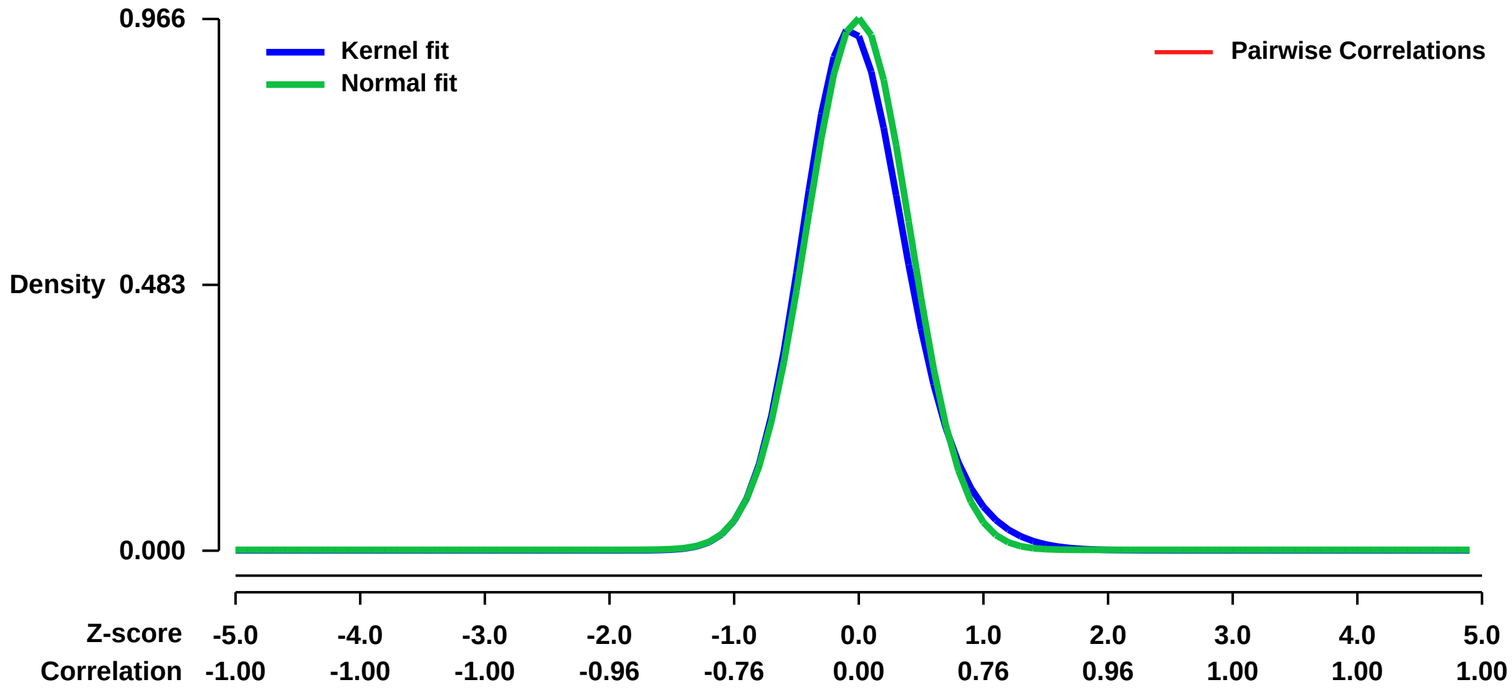

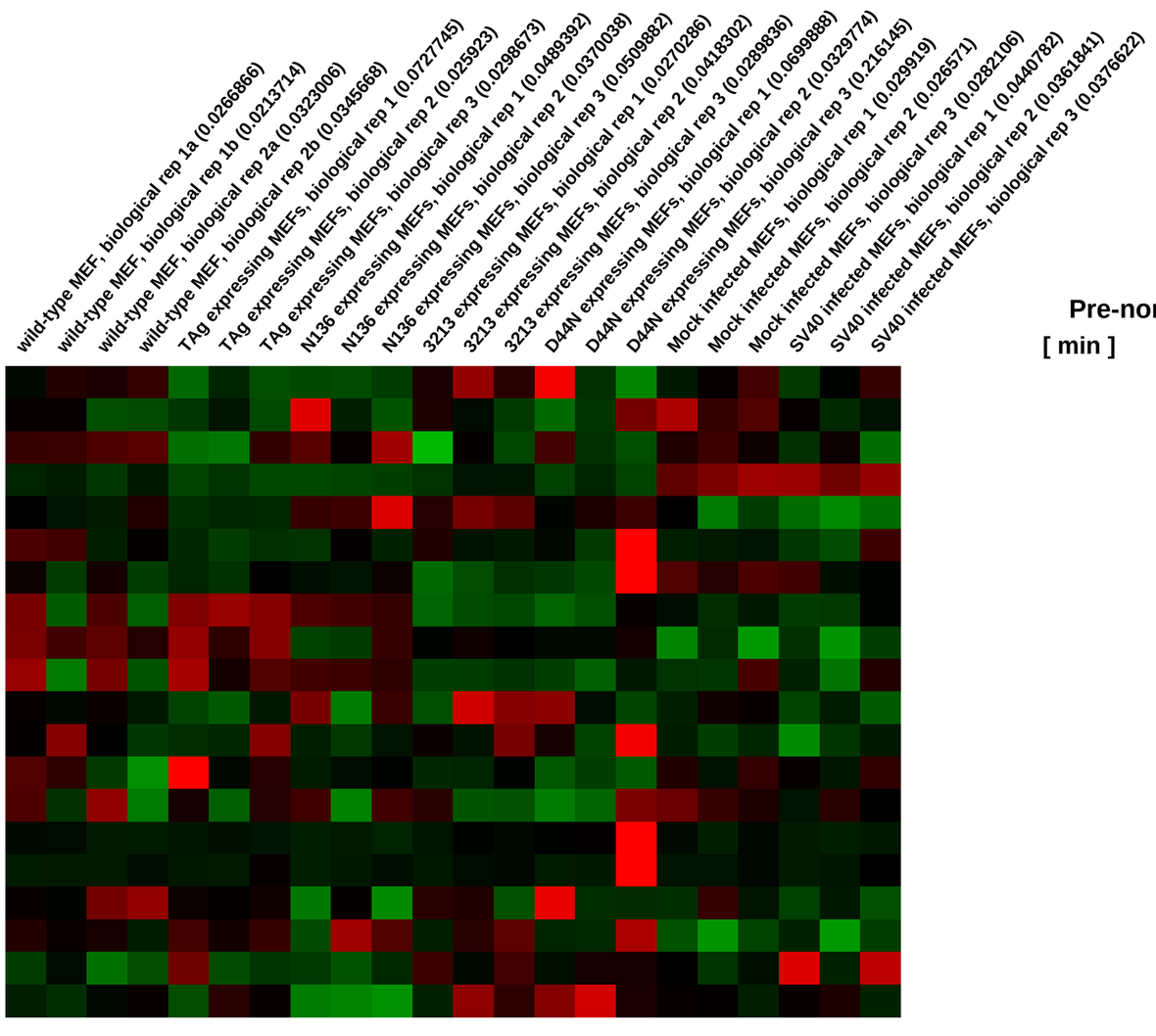

GEO Series "GSE30655" Expression Profiles

Num of samples in this series: 35

Scale of expression profile Z-scores

-3.0 -2.0 -1.0 0.0 1.0 2.0 3.0

GEO Link:	http://www.ncbi.nlm.nih.gov/geo/query/acc.cgi?acc=GSE30655
Status:	Public on Jul 14 2014
Title:	Mice Lacking the ¸†2 Adrenergic Receptor Have a Unique Genetic Profile Before and After Focal Brain Ischemia
Organism:	Mus musculus
Experiment type:	Expression profiling by array
Platform:	GPL1261
Pubmed ID:	
Summary & Design:	**Summary:** The role of the beta2 adrenergic receptor (¸†2AR) after stroke is unclear as pharmacological manipulations of the ¸†2AR have produced contradictory results. We previously showed that mice deficient in the ¸†2AR (¸†2KO) had smaller infarcts compared to wild-type mice (FVB) after middle cerebral artery occlusion (MCAO), a model of stroke. To elucidate mechanisms of this neuroprotection, we evaluated changes in gene expression using microarrays comparing differences before and after MCAO, and differences between genotypes. Genes associated with inflammation and cell death were enriched after MCAO in both genotypes, and we identified several genes not previously shown to increase following ischemia (Ccl9, Gem, and Prg4). In addition to networks that were similar between genotypes, one network with a central node of G protein-coupled receptor and including biological functions carbohydrate metabolism, small molecule biochemistry and inflammation was identified in FVB mice but not in ¸†2KO mice. Analysis of differences between genotypes revealed 11 genes differentially expressed by genotype in all conditions. We demonstrate greater Glo1 protein levels and lower Pmaip/Noxa mRNA levels in ¸†2KO mice. As both genes are implicated in NF¸"B signaling, we measured p65 activity and tumor necrosis factor alpha (TNF¸–) levels 24h after MCAO. MCAO-induced p65 activation and post-ischemic TNF¸– production were both greater in FVB compared to ¸†2KO mice. These results suggest that loss of ¸†2AR signaling results in a neuroprotective phenotype in part due to decreased NF¸"B signaling, decreased inflammation, and decreased apoptotic signaling in the brain. **Overall design:** A total of 15 naˆflve samples were analyzed, with 7-8 of each genotype, wild-type (FVB) and beta2 adrenergic receptor deficient (B2) mice. The naive samples were normalized independently of the MCAO and sham surgery samples.

Background corr dist: KL-Divergence = 0.0829, L1-Distance = 0.0426, L2-Distance = 0.0038, Normal std = 0.4716

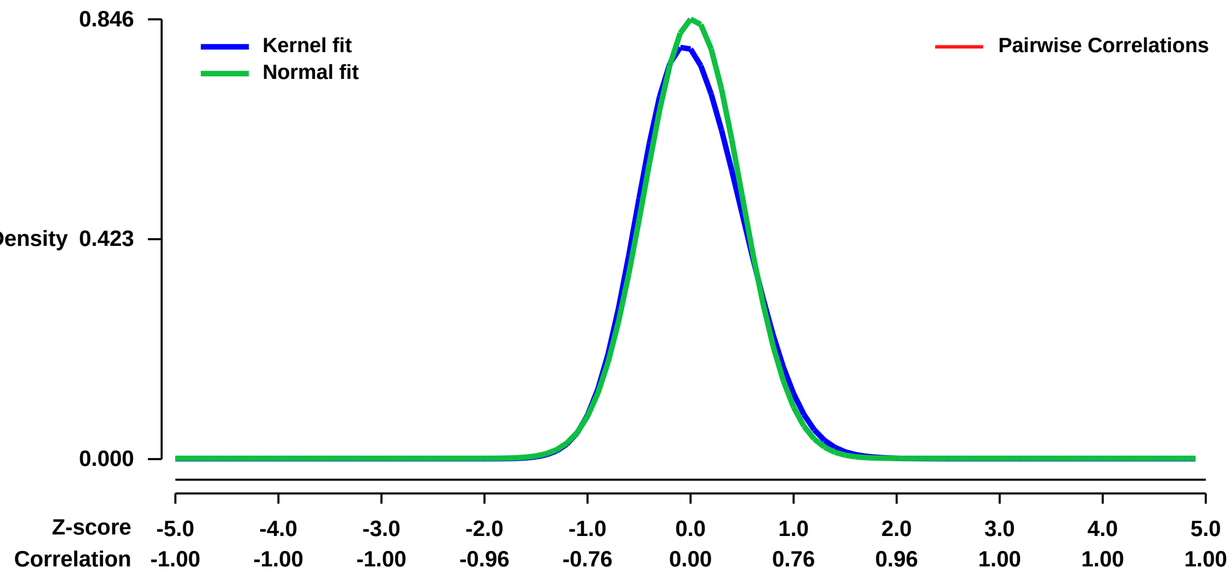

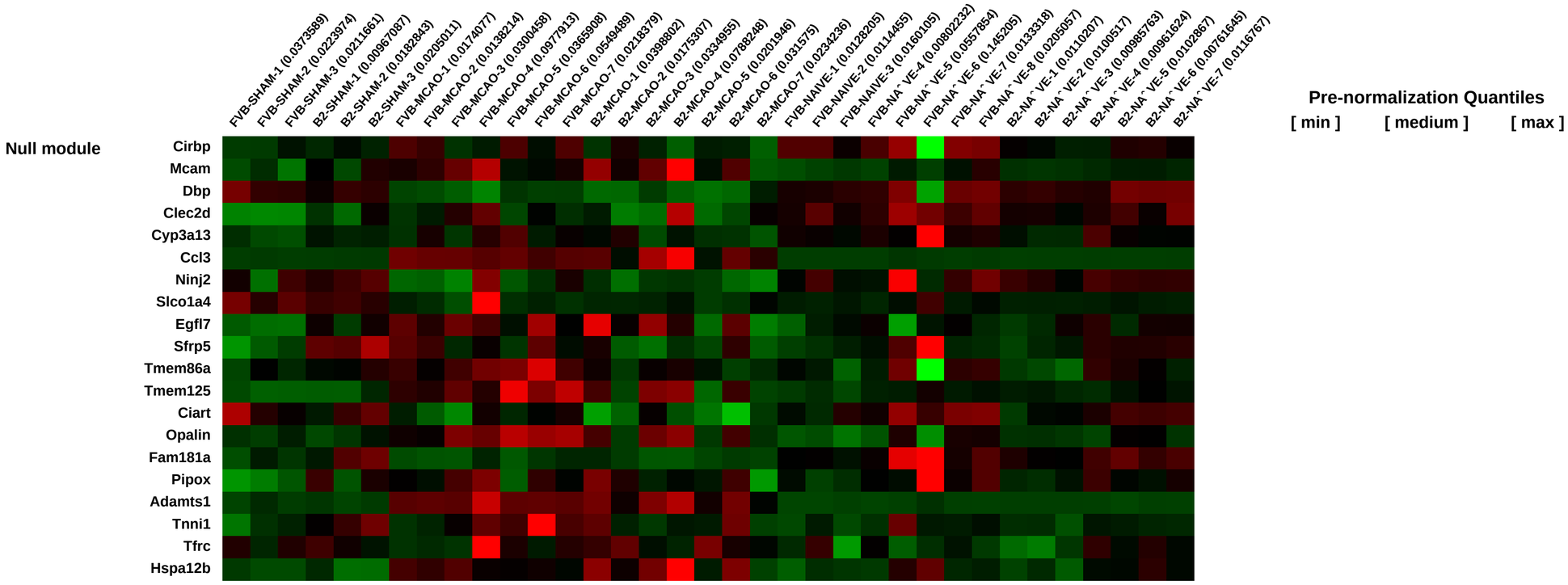

GEO Series "GSE33860" Expression Profiles

Num of samples in this series: 28

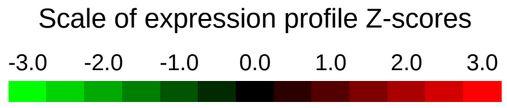

GEO Link:	http://www.ncbi.nlm.nih.gov/geo/query/acc.cgi?acc=GSE33860
Status:	Public on Nov 21 2012
Title:	Profile of testicular polysomal gene expression regulated by Gonadotropin Regulated Testicular RNA helicase in adult mice
Organism:	Mus musculus
Experiment type:	Expression profiling by array
Platform:	GPL1261
Pubmed ID:	
Summary & Design:	**Summary:** The down-regulation of known genes concerned with spermatogenesis at polysomal sites in GRTH KO and their association with GRTH in WT coupled with early findings of minor or unchanged total mRNAs and abolition of their protein expression in KO, underscore the relevance of GRTH in translation. Studies showed the association of GRTH bound polysome genes with the ubiquitin-proteasome-heat shock protein signaling network pathway and NF¸"B/TP53/TGFB1 signaling networks were derived from the differentially expressed gene analysis. **Overall design:** Microarray differential gene expression analysis was performed using polysome-bound RNA isolated from testes of wild type (WT) and GRTH KO mice.

Background corr dist: KL-Divergence = 0.1161, L1-Distance = 0.0416, L2-Distance = 0.0039, Normal std = 0.4234

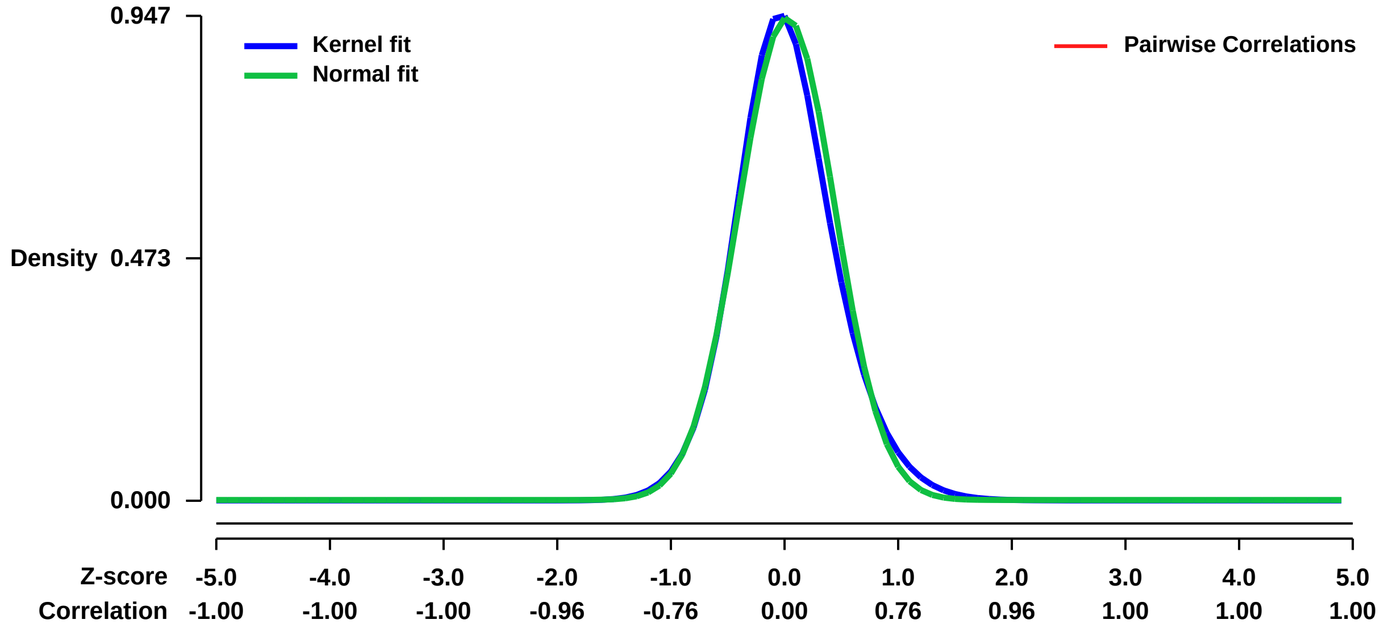

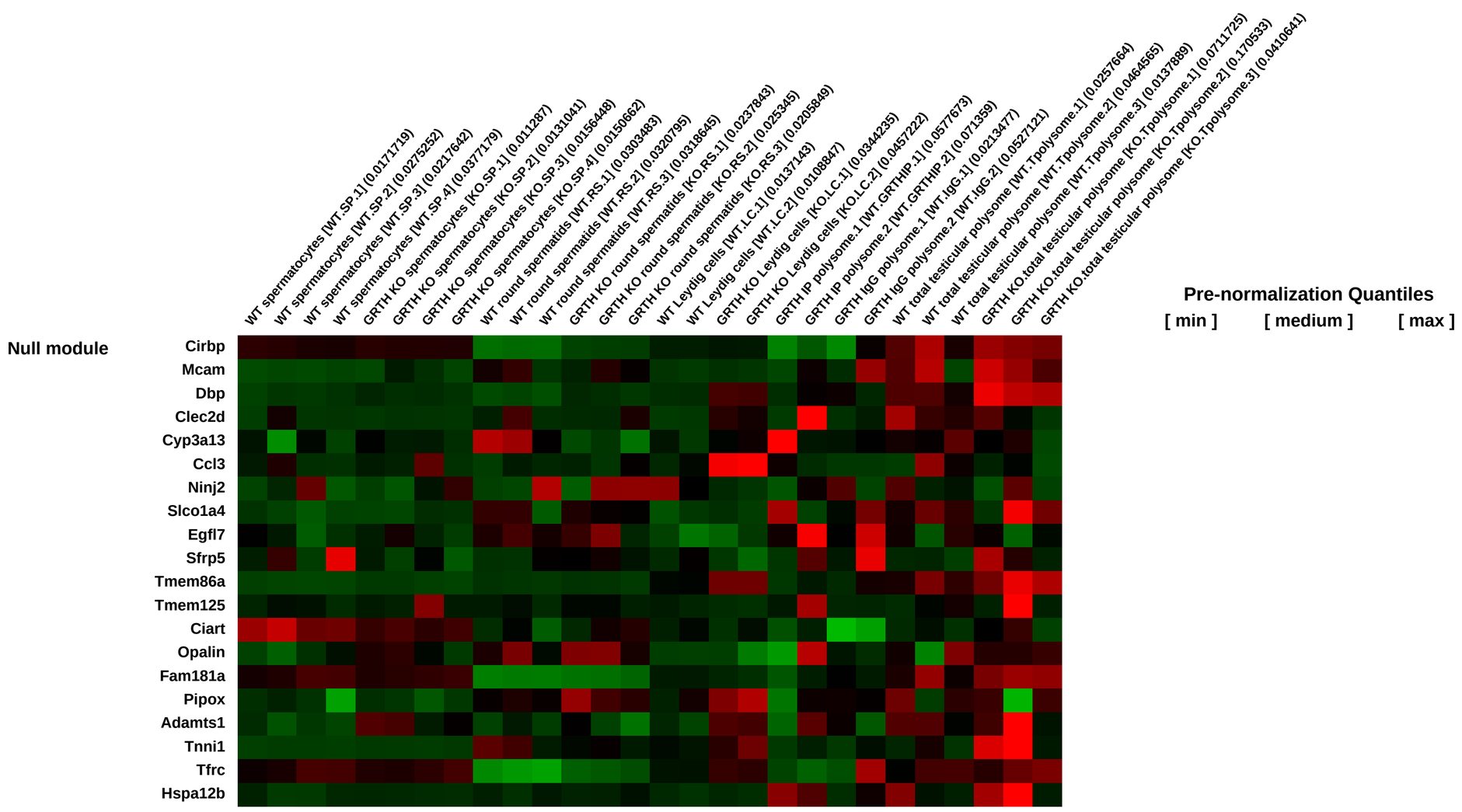

GEO Series "GSE15794" Expression Profiles

Num of samples in this series: 6

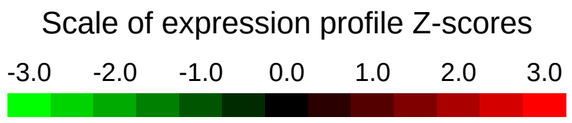

GEO Link:	**http://www.ncbi.nlm.nih.gov/geo/query/acc.cgi?acc=GSE15794**
Status:	**Public on Apr 25 2009**
Title:	**Gene expression profiles of E13 bladder neck/urethral compartments. (GUDMAP Series ID: 25)**
Organism:	**Mus musculus**
Experiment type:	**Expression profiling by array**
Platform:	**GPL1261**
Pubmed ID:	
Summary & Design:	**Summary:** **The long term objective is to create an encyclopedia of the expression levels of all genes in multiple components of the developing bladder. The central thesis is straightforward. The combination of micro dissected tissues and FACS sorted cells plus microarray analysis offers a powerful, efficient and effective method for the creation of a global gene expression atlas of the developing urogenital system. Microarrays with essentially complete genome coverage can be used to quantitate expression levels of every gene. The ensuing rapid read-out provides an expression atlas that is more sensitive, more economical and more complete than would be possible by in situ hybridizations alone. The data submitted here delineates the gene expression profiles of the mesenchymal and epithelial compartments of the E13 mouse bladder neck/urethral compartment.** **Overall design:** **FVB/N mice were time mated. At embryonic day 13 mice were euthanized by decapitation and the bladders were microdissected and cut just below the ureters. Since the EDTA dissociation was ineffective, the bladder neck and urethra were collected and treated with 1 mg/ml trypsin in Tyrode's solution for 20 minutes at 37˚C. The layers were separated using a fine needle and rimming. The samples were placed in RLT and stored at -80˚C. RNA was prepared and the Epicentre 2-round amplification scheme described under the Lessard Group Protocols on the GUDMAP pages were performed. The amplified RNA was examined with the Affymetrix GeneChip Mouse Genome 430 2.0 Array.**

Background corr dist: KL-Divergence = 0.0453, L1-Distance = 0.0594, L2-Distance = 0.0048, Normal std = 0.7260

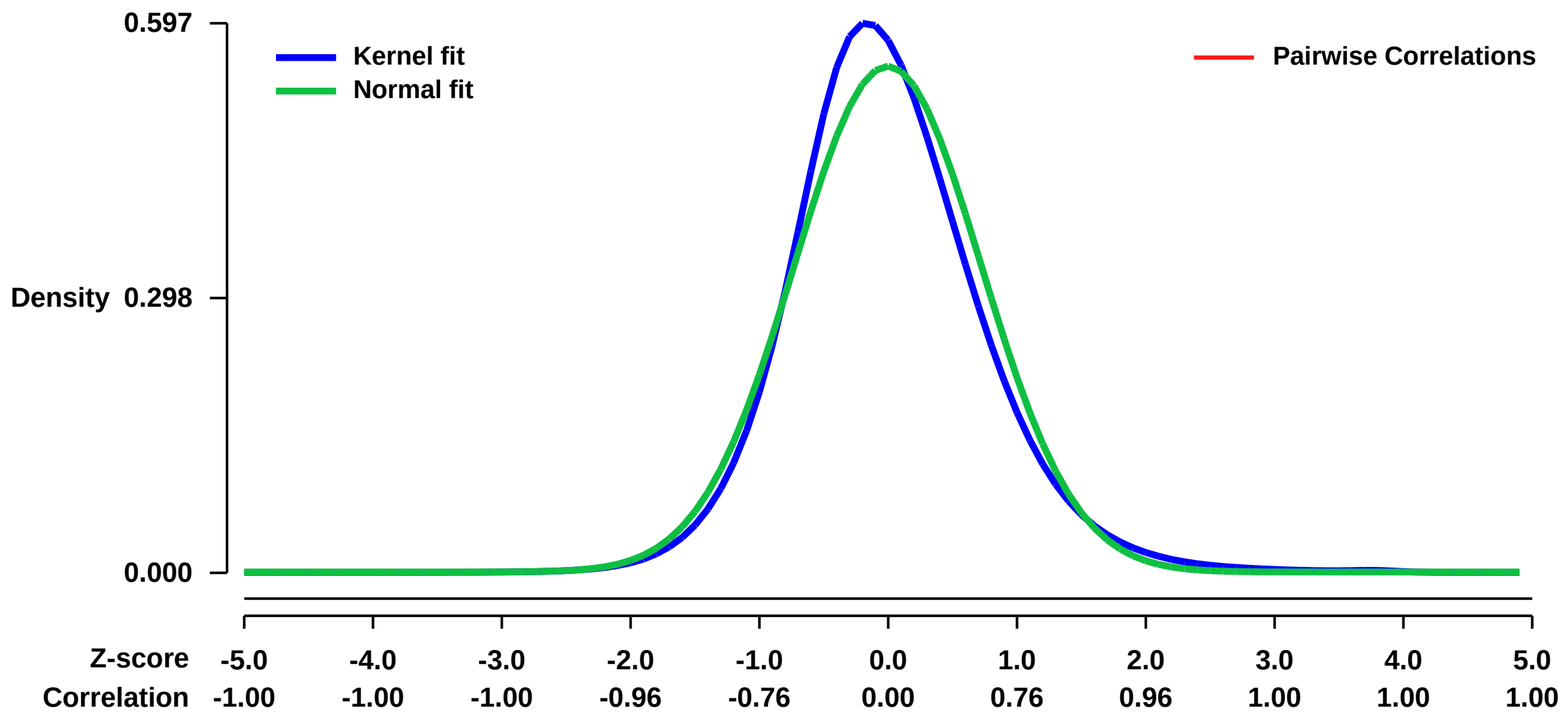

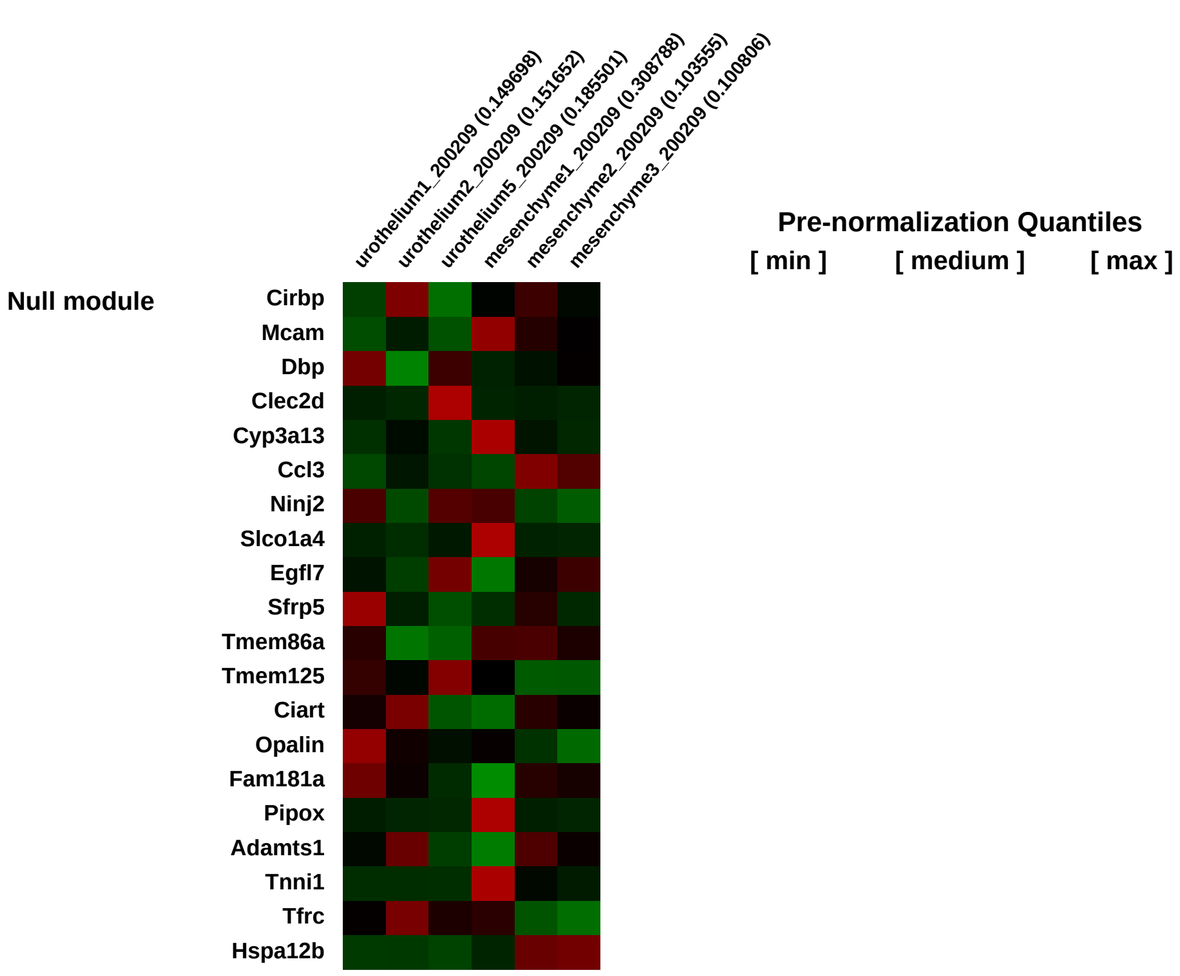

GEO Series "GSE11677" Expression Profiles

Num of samples in this series: 8

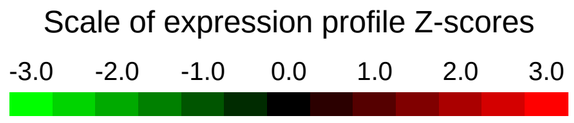

GEO Link:	http://www.ncbi.nlm.nih.gov/geo/query/acc.cgi?acc=GSE11677
Status:	Public on Aug 15 2008
Title:	Gene expression profiles of age-associated clonal expansions of CD8 memory T cells
Organism:	Mus musculus
Experiment type:	Expression profiling by array
Platform:	GPL1261
Pubmed ID:	18728183
Summary & Design:	**Summary:** Many aged individuals develop monoclonal expansions of CD8 T cells. These expansions are derived from a CD8 memory T cell that outcompetes neighboring CD8 T cells. The molecular alterations within clonal expansions that confer this competitive advantage relative to other CD8 T cells remains unknown. These microarray experiments were designed to identify genes differentially expressed in age-associated expansions of CD8 memory T cells relative to polyclonal CD8 memory T cells found in the same aged mice. Subsequent analysis of these data identified two major types of clonal expansions, distinguished by expression level of integrin a4 mRNA and protein. Based on this classification, Expansion_rep1 belongs to the integrin a4 high subtype of clonal expansions. In contrast, reps 2, 4, and 5 belong to the integrin a4 low subtype of clonal expansions. Given the divergent biological properties of these two subtypes of clonal expansions, we have focused genes differentially expressed between Expansion_rep 2, 4, and 5 and their paired PolyclonalAged samples. **Keywords:** Cell type comparison of gene expression **Overall design:** A total of 8 samples were analyzed for gene expression using the Affymetrix mouse genome 430 2.0 microarray platform. The experimental samples of interest were age-associated clonal expansions of CD8 memory T cells. We purified four clonal expansions from four independent, aged mice (indicated as ""Expansion"" rep1 2, 3, 4). For each clonal expansion of CD8 memory T cells that was purified, there was a paired control in which polyclonal CD8 memory T cells were harvested from the same aged mouse (denoted as ""PolyclonalAged"" rep1, 2, 3, 4). These paired samples allow one to consider gene expression changes from mice which have undergone the same age-associated changes in biology. The predominant comparison this study focused on was changes in gene expression between age-associated clonal expansions of CD8 memory T cells and their paired, polyclonal CD8 memory T cells. A total of 4 of these pairs were collected.

Background corr dist: KL-Divergence = 0.0783, L1-Distance = 0.0370, L2-Distance = 0.0026, Normal std = 0.4898

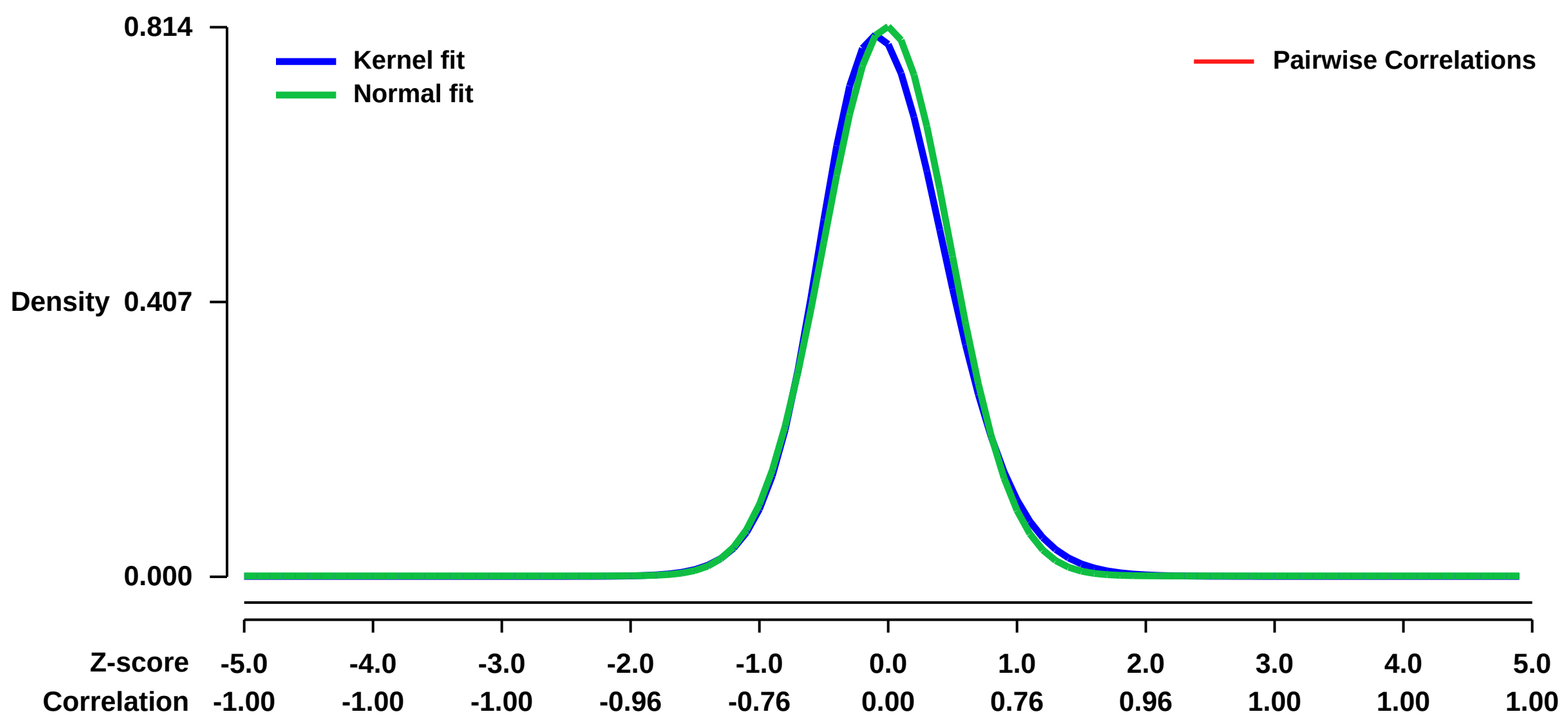

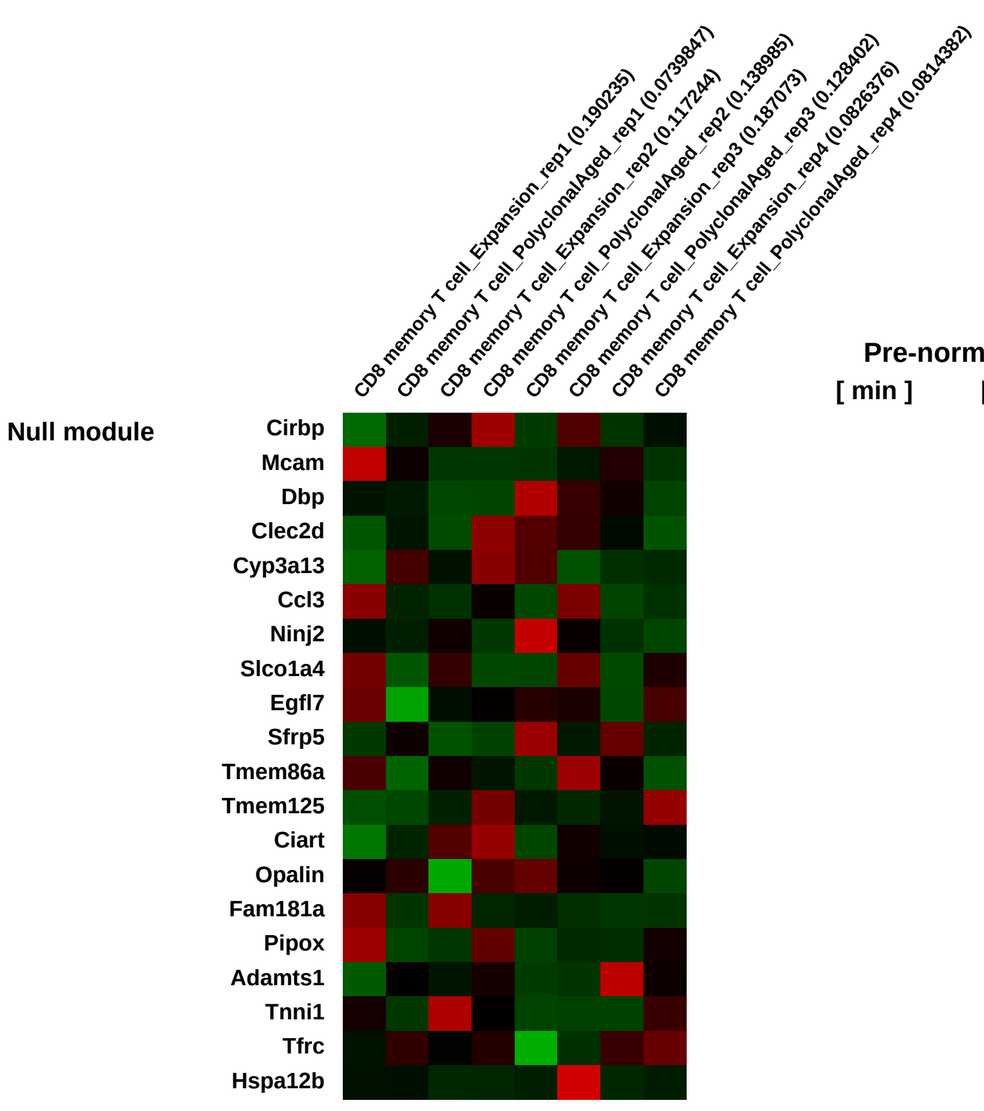

GEO Series "GSE21711" Expression Profiles

Num of samples in this series: 6

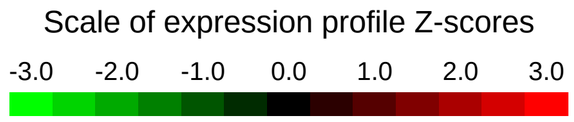

GEO Link:	http://www.ncbi.nlm.nih.gov/geo/query/acc.cgi?acc=GSE21711
Status:	Public on May 07 2010
Title:	Effect of cholera toxin or forskolin on mouse bone marrow-derived dendritic cells
Organism:	Mus musculus
Experiment type:	Expression profiling by array
Platform:	GPL1261
Pubmed ID:	20479237
Summary & Design:	**Summary:** Bone marrow-derived dendritic cells from C57BL/6 mice were treated with 1 ug/ml cholera toxin, 10 uM forskolin or control medium for 2 h. **Overall design:** drug treatment groups

Background corr dist: KL-Divergence = 0.0361, L1-Distance = 0.0260, L2-Distance = 0.0007, Normal std = 0.6542

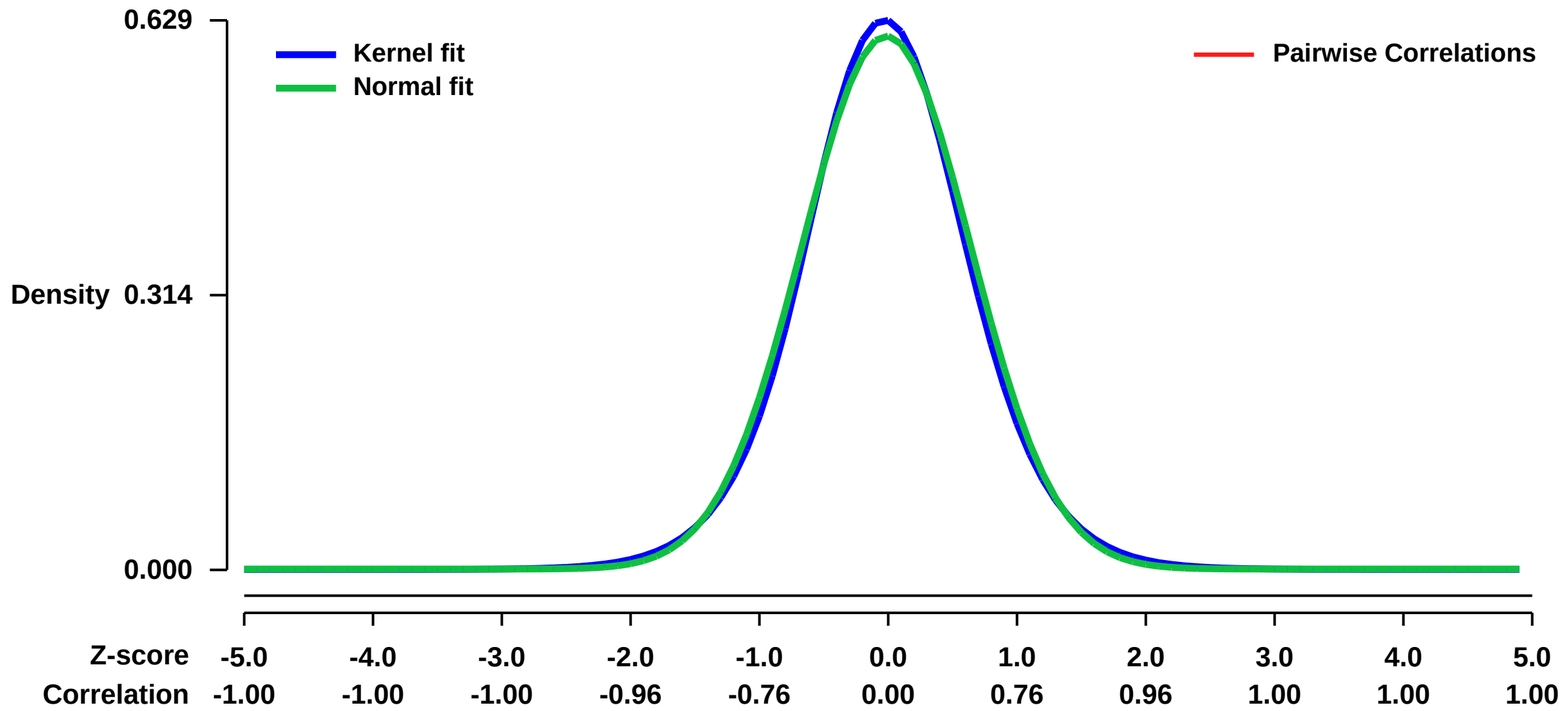

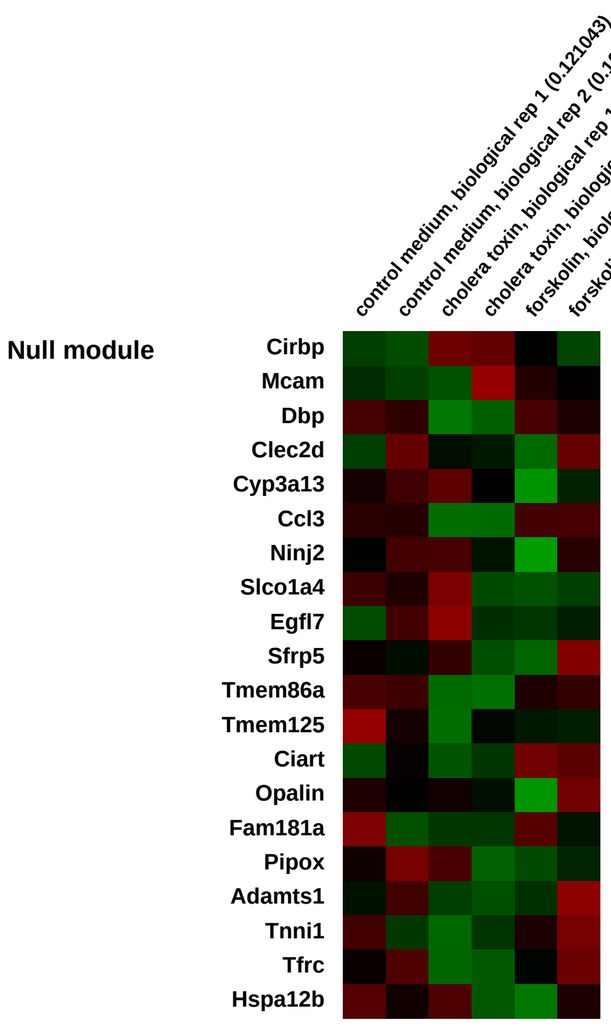

GEO Series "GSE11259" Expression Profiles

Num of samples in this series: 9

Scale of expression profile Z-scores

-3.0 -2.0 -1.0 0.0 1.0 2.0 3.0

GEO Link:	http://www.ncbi.nlm.nih.gov/geo/query/acc.cgi?acc=GSE11259
Status:	Public on Aug 01 2008
Title:	Role of epithelial to mesenchymal transition (EMT) in spontaneous breast cancer metastasis
Organism:	Mus musculus
Experiment type:	Expression profiling by array
Platform:	GPL1261
Pubmed ID:	18773493
Summary & Design:	**Summary:** Epithelial-mesenchymal transition (EMT) has been linked to cancer progression and metastatic propensity. The 4T1 tumor is a clinically relevant model of spontaneous breast cancer metastasis. Here we characterize 4T1-derived cell lines for EMT, in vitro invasiveness and in vivo metastatic ability. Contrary to expectations, the 67NR cells, which form primary tumors but fail to metastasize, express vimentin and N-cadherin, but not E-cadherin. 4T1 cells, however, express E-cadherin, are highly migratory and invasive, and metastasize to multiple sites. The 66cl4 metastatic cells display mixed epithelial and mesenchymal markers, but are less migratory and invasive than 67NR cells. These findings demonstrate that the metastatic ability of breast cancer cells does not correlate with genotypic and phenotypic properties of EMT per se, and suggest that other processes may govern metastatic capability. Gene expression analysis also has not identified differences in EMT markers, but has identified several candidate genes that may influence metastatic ability. **Keywords:** cell type comparison **Overall design:** Female BALB/c mice were injected with 1x10^6 viable cells (3 mice with 4T1/CMVLUC, 3 mice with 66cl4/CMVLUC, and 3 mice with 67NR/CMVLUC) into the right fourth mammary gland. 15 days after injection primary tumors were excised, and total RNA for microarray hybridization was isolated from the tumor part of laser capture microdissected sections.

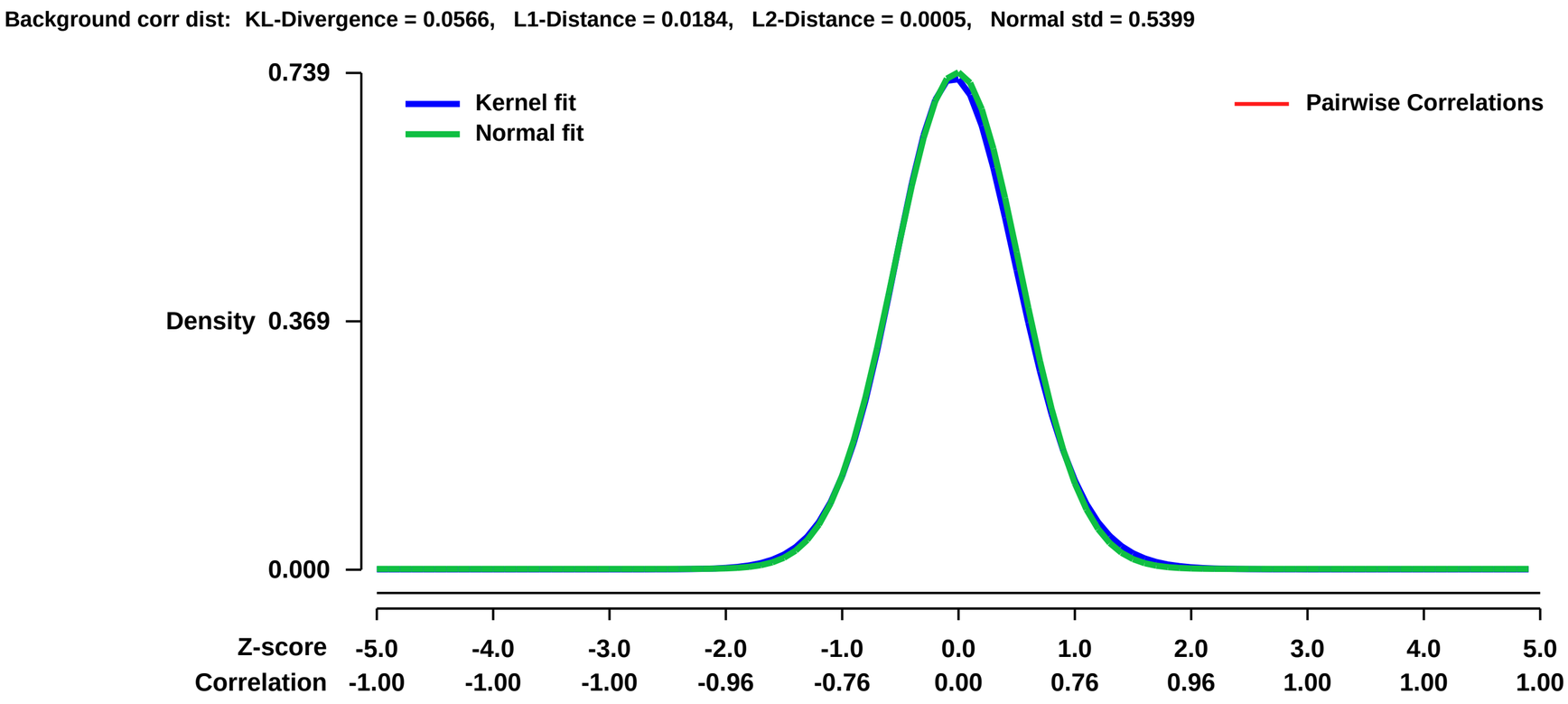

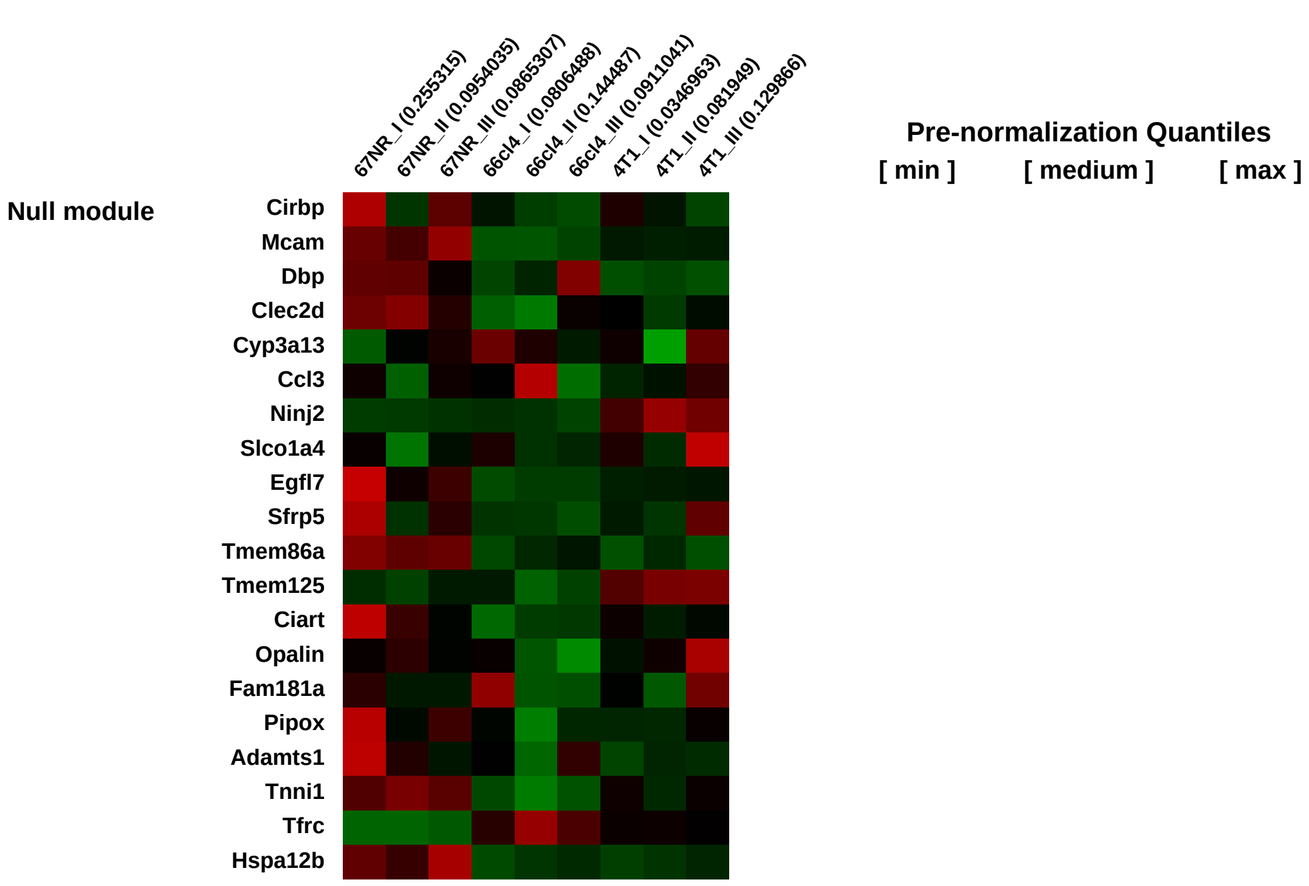

GEO Series "GSE58368" Expression Profiles

Num of samples in this series: 15

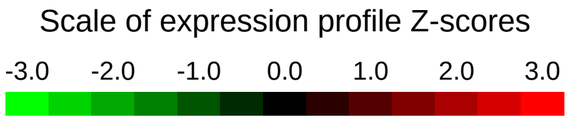

GEO Link:	**http://www.ncbi.nlm.nih.gov/geo/query/acc.cgi?acc=GSE58368**
Status:	**Public on Jun 11 2014**
Title:	**Linking Notch signaling to ischemic stroke**
Organism:	**Mus musculus**
Experiment type:	**Expression profiling by array**
Platform:	**GPL1261**
Pubmed ID:	
Summary & Design:	**Summary:** **Using a hitherto uncharacterized knockout mouse model of Notch 3, a Notch signaling receptor paralogue highly expressed in vascular SMCs, we uncover a striking susceptibility to ischemic stroke upon challenge. Cellular and molecular analyses of vascular SMCs derived from these animals associate Notch 3 activity to the expression of specific gene targets, whereas genetic rescue experiments unambiguously link Notch 3 function in vessels to the ischemic phenotype.** **Overall design:** **Microarray Studies. Biotinylated cRNA samples from freshly sorted brain SMCs (four Notch 3 +/â mice and five Notch 3 â /â mice) were fragmented before hybridization (15 ¿…g each) onto mouse 430 2.0 Affymetrix chips. The chips were washed, stained by using strepavidin-phycoerytrin, and scanned the next day as described in ref. 24. For data normalization, all probe sets were scaled to a target intensity of 150. Microarray data analysis was performed by using Rosetta Resolver. All cells were from 10- to 12-week-old male mice. Gene Ontology Analyses. PANTHER software was used to define over- and underrepresented functions in the list of signature genes found by microarray analysis (25). P values were calculated by using binomial statistics.**

Background corr dist: **KL-Divergence = 0.0540, L1-Distance = 0.0336, L2-Distance = 0.0015, Normal std = 0.5673**

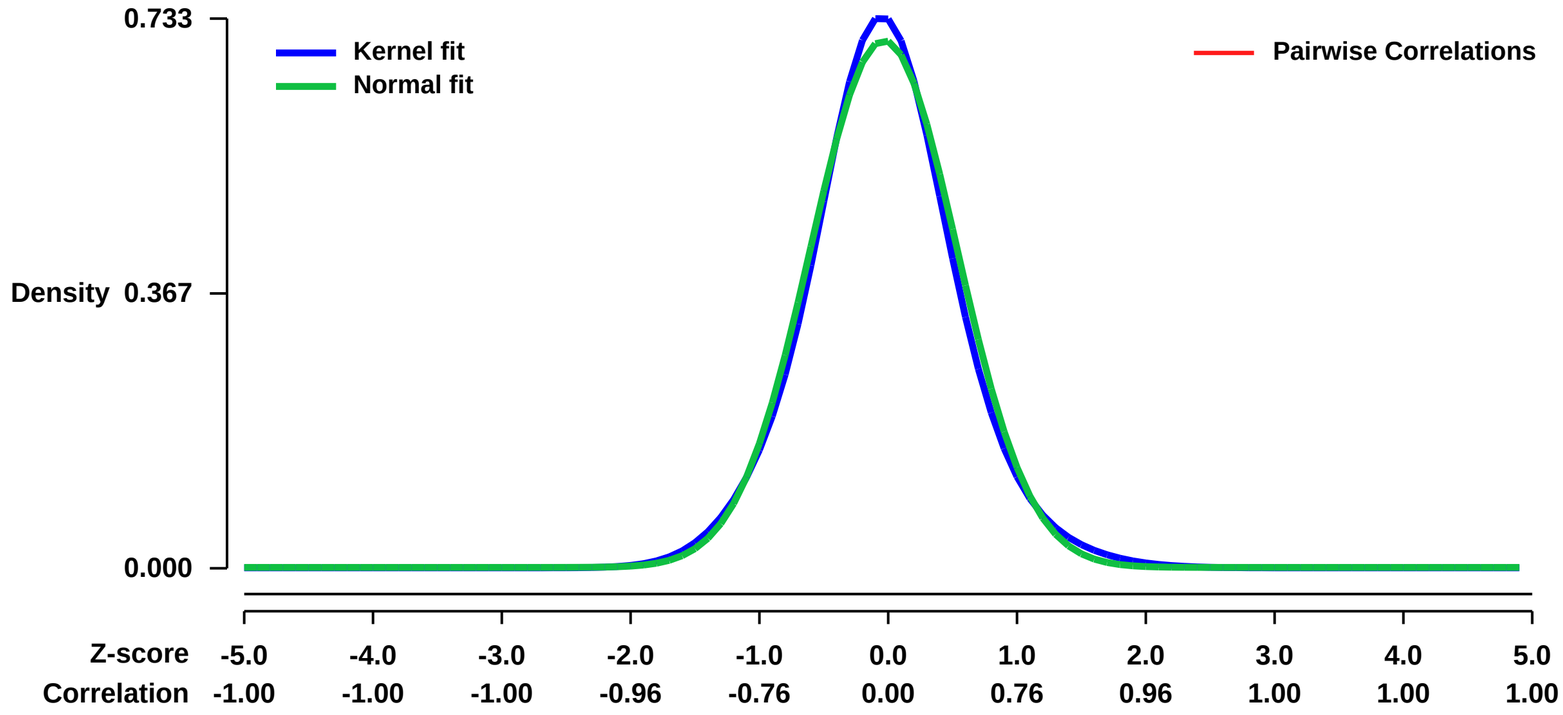

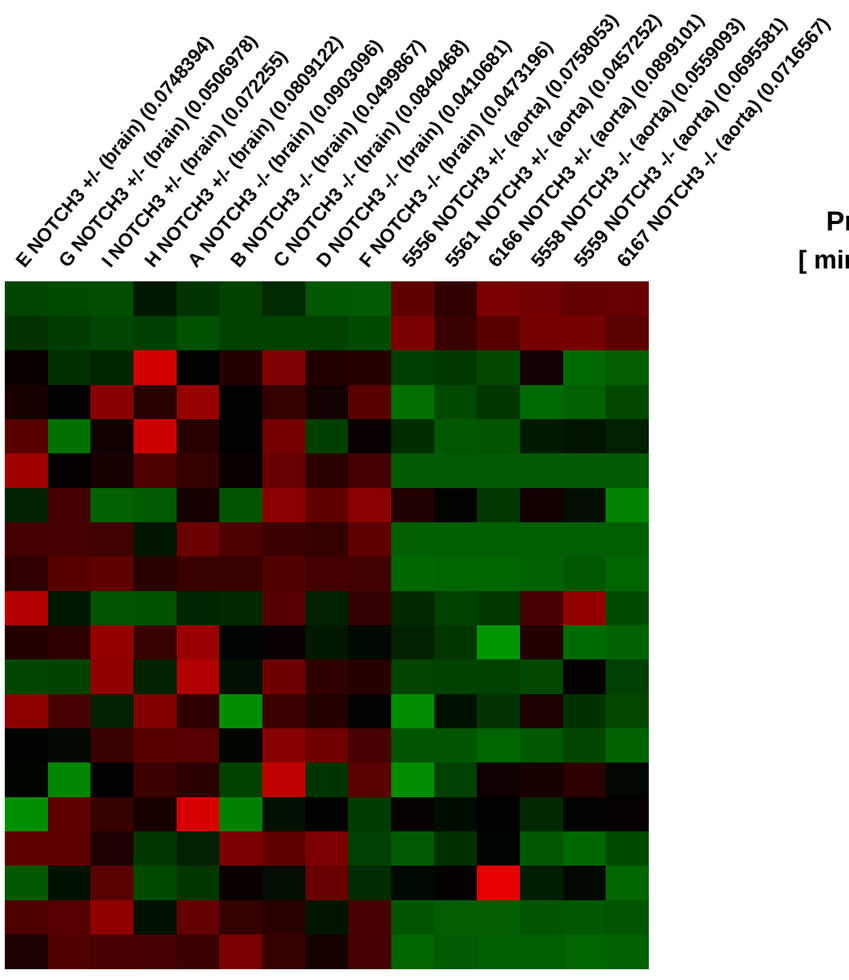

GEO Series "GSE20844" Expression Profiles

Num of samples in this series: 7

Scale of expression profile Z-scores

-3.0 -2.0 -1.0 0.0 1.0 2.0 3.0

GEO Link:	http://www.ncbi.nlm.nih.gov/geo/query/acc.cgi?acc=GSE20844
Status:	Public on Feb 22 2011
Title:	Differential Expression of Ove26(Diabetic) vs FVB(Nondiabetic) mice
Organism:	Mus musculus
Experiment type:	Expression profiling by array
Platform:	GPL1261
Pubmed ID:	20627935
Summary & Design:	**Summary:** **Objective â Previous studies showed that genetic deletion or pharmacological blockade of the Receptor for Advanced Glycation Endproducts (RAGE) prevents the early structural changes in the glomerulus associated with diabetic nephropathy (DN). To overcome limitations of mouse models that lack the progressive glomerulosclerosis observed in humans, we studied the contribution of RAGE to DN in the OVE26 type 1 mouse, a model of progressive glomerulosclerosis and decline of renal function.** **Research Design and Methods â We bred OVE26 mice with homozygous RAGE knock out (RKO) mice and examined structural changes associated with DN and used inulin clearance studies and albumin:creatinine measurements to assess renal function. Affymetrix Mouse 430.2 microarrays were used to measure the differential expression of OVE26vsFVB(WT) mice. Transcriptional changes in the TGF-¸†1 and Plasminogen activator inhibitor 1 gene products were measured by pcr to investigate mechanisms underlying accumulation of mesangial matrix in OVE26 mice.** **Results - Deletion of RAGE in OVE26 mice reduced nephromegaly, mesangial sclerosis, cast formation, glomerular basement membrane thickening, podocyte effacement, and albuminuria. The significant 29% reduction in glomerular filtration rate observed in OVE26 mice was completely prevented by deletion of RAGE. Increased transcription of the genes for Plasminogen activator inhibitor 1, TGF-¸†1, TGF-¸† induced, ¸–1- (IV) collagen observed in OVE26 renal cortex significantly reduced in OVE26 RKO kidney cortex. ROCK1 activity was significantly lower in OVE26 RKO compared to OVE26 kidney cortex.** **Conclusions - These data provide compelling evidence for critical roles for RAGE in the pathogenesis of DN and suggest that strategies targeting RAGE in long-term diabetes may prevent loss of renal function.** **Overall design:** **The differential gene expression of OVE26 (diabetics) vs FVB (nodiabetic WT) mice was measured using Affymetrix Mouse 430.2 arrays.**

Background corr dist: KL-Divergence = 0.0600, L1-Distance = 0.0188, L2-Distance = 0.0005, Normal std = 0.5319

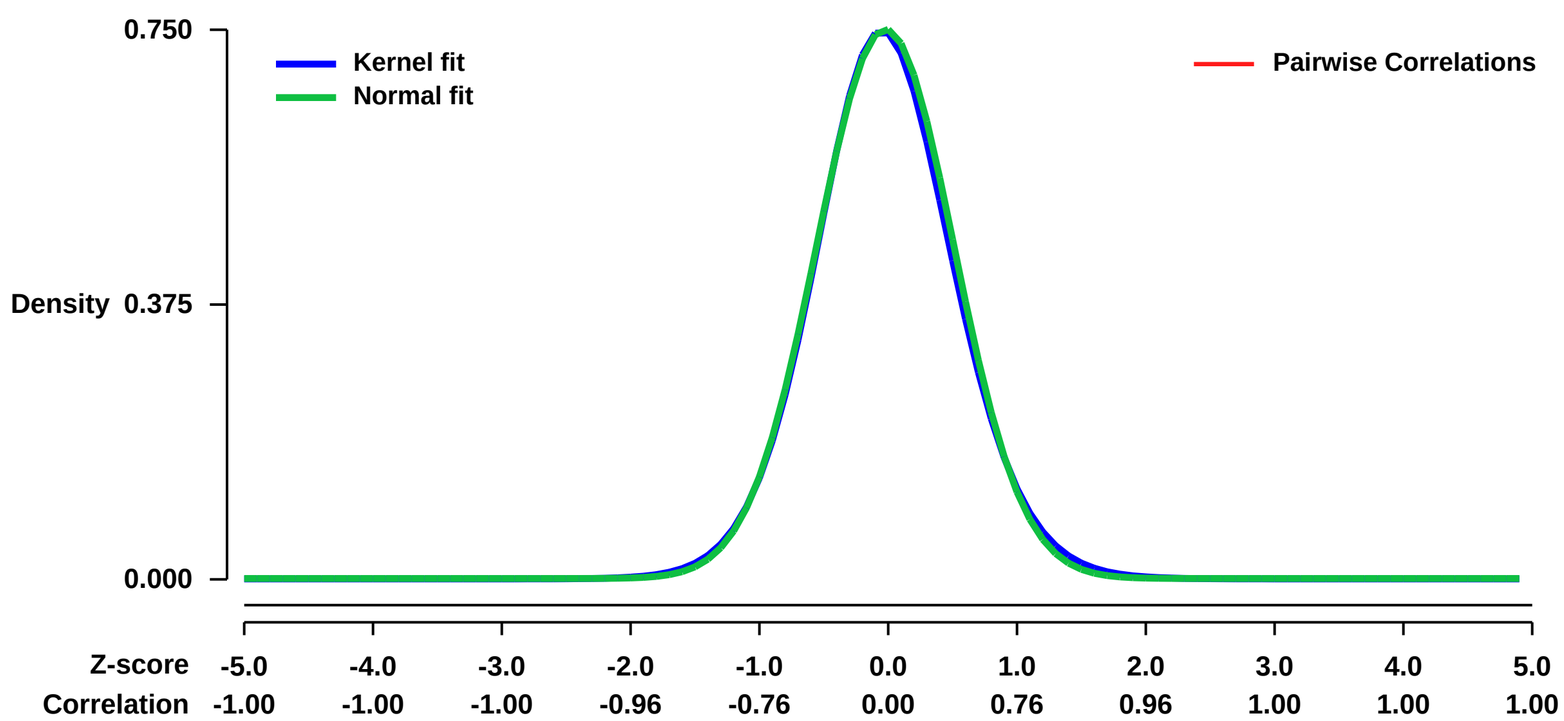

GEO Series "GSE25828" Expression Profiles

Num of samples in this series: 8

Scale of expression profile Z-scores

-3.0 -2.0 -1.0 0.0 1.0 2.0 3.0

GEO Link:	http://www.ncbi.nlm.nih.gov/geo/query/acc.cgi?acc=GSE25828
Status:	Public on Sep 01 2011
Title:	Pten deficiency cooperates with KrasG12D to activate NFkB pathway promoting the development of malignant pancreatic ductal adenocarcinoma
Organism:	Mus musculus
Experiment type:	Expression profiling by array
Platform:	GPL1261
Pubmed ID:	21984975
Summary & Design:	**Summary:** Almost all human pancreatic ductal adenocarcinomas (PDACs) are driven by oncogenic Kras and the progression of the disease is characterized by the serial appearance of certain genetic lesions. Mouse models have convincingly shown that Kras mutation induces classical PanIN lesions that can progress to PDAC in the appropriate tumor suppressor background. However, the cooperative mechanism between mutant Kras-dependent signaling surrogates and other oncogenic pathways remains to be fully elucidated in order to devise better therapeutic strategy. Mounting evidence PTEN/PI3K perturbation on PDAC tumorigenesis, we observed frequent PTEN inactivation at both genomic and histopathological levels in primary human PDAC samples. The importance of PTEN/PI3K pathway during the development of PDAC was further supported by genetic studies demonstrating that Pten deficiency in cooperation with Kras activation accelerated the formation of invasive PDAC. Mechanistically, combined Kras mutation and Pten inactivation leads to NFkB activation and subsequent induction of cytokine pathways, accompanied with strong stromal activation and immune cell infiltration. Therefore, PTEN/PI3K pathway dictates the activity of NFkB network and serves as a major surrogate during Kras-mediated pancreatic tumorigenesis. **Overall design:** Primary pancreatic ductal epithelial cell cultures were established from 6 week old Pdx1-Cre;LSL-KrasG12D L/+ (n=3) or Pdx1-Cre;LSL-KrasG12D L/+;Pten L/+ (n=5) mice. Total RNA was collected from early passage cells.

Background corr dist: KL-Divergence = 0.0859, L1-Distance = 0.0232, L2-Distance = 0.0009, Normal std = 0.4654

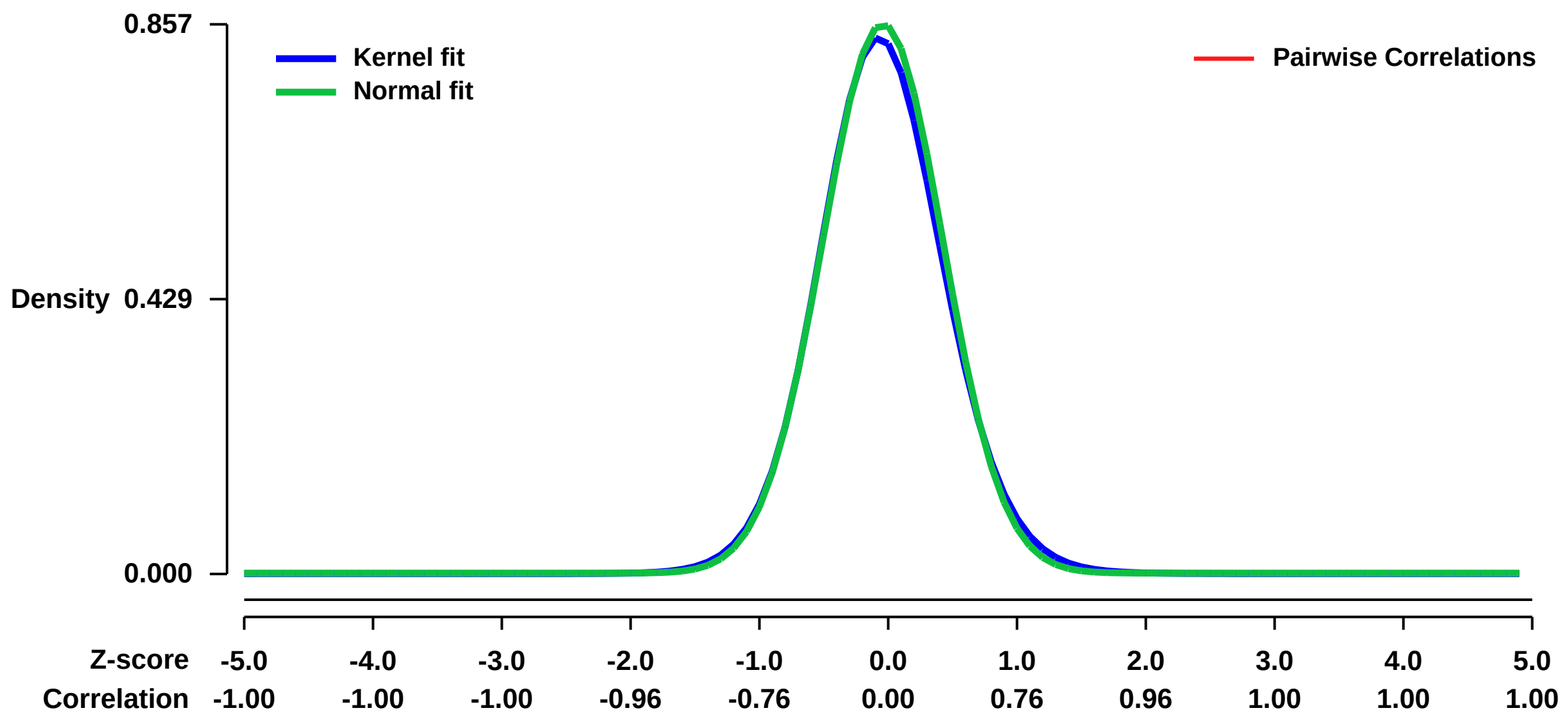

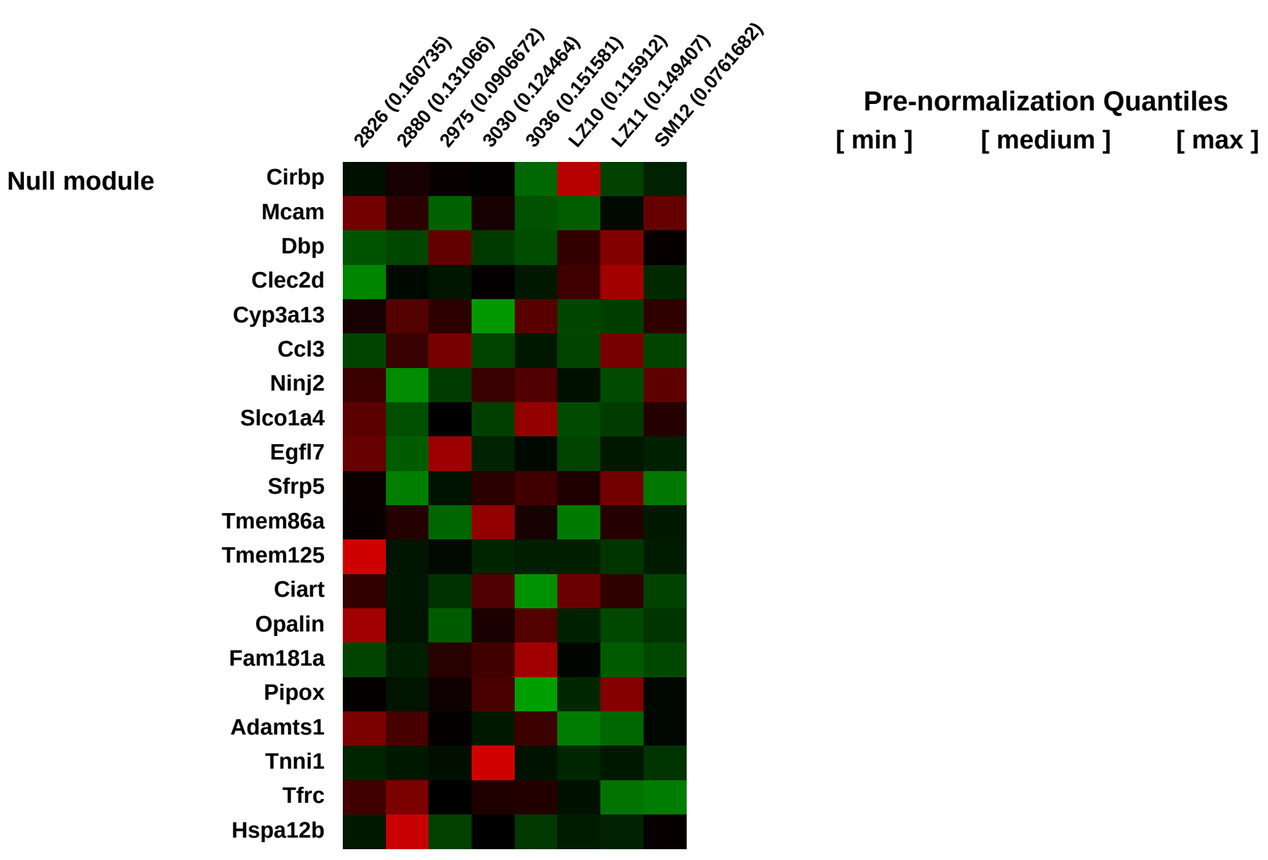

GEO Series "GSE34002" Expression Profiles

Num of samples in this series: 9

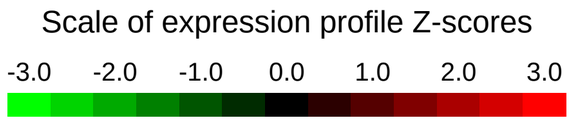

GEO Link:	http://www.ncbi.nlm.nih.gov/geo/query/acc.cgi?acc=GSE34002
Status:	Public on Apr 16 2013
Title:	Identification of differential expressed genes between P-RPCs, ESC-RPCs and Dkk1 treated ESC-RPCs through genome-wide transcript profiling
Organism:	Mus musculus
Experiment type:	Expression profiling by array
Platform:	GPL1261
Pubmed ID:	23524971
Summary & Design:	**Summary:** Tumor formation constitutes a major obstacle to the clinical application of embryonic stem cells (ESCs). As P-RPCs could successfully integrate into host eyes without development of teratomas or NOG, we sought to identify differentially expressed genes between P-RPCs and ESC-RPCs through genome-wide transcript profiling. Inhibition of Wnt signaling by DKK1 promotes the commitment of ESC-RPCs to more mature retinal cells and reduces the occurrence of NOG to 3%. DKK1-treated ESC-RPCs efficiently integrate to the host retina, form synaptic connections and restore visual function. Here, we report that further differentiation of ESC-derived neural progenitors into retinal progenitor cells (ESC-RPCs) completely eliminates teratomas in ocular transplantation. However, tumor-like neural overgrowth (NOG) occurs in 61% of transplanted eyes. **Overall design:** ESC-RPCs were divided into two groups according to the differentiation stages for RNA extraction and hybridization on Affymetrix microarrays. Normal control ESC-RPCs (N) were represented the homogeneous populations of early stage expression profiles of immature ESC-RPCs. DKK1 treated ESC-RPCs (D) were represented the homogeneous populations of late stage expression profiles of further differetiated mature ESC-RPCs. To sought the pathways involved in the proliferation and oncogenesis of ESC-RPCs, the newborn C57 mice reitinal progenitor cells (R) were applied as negative control. Each group above had three independent biological repeats.

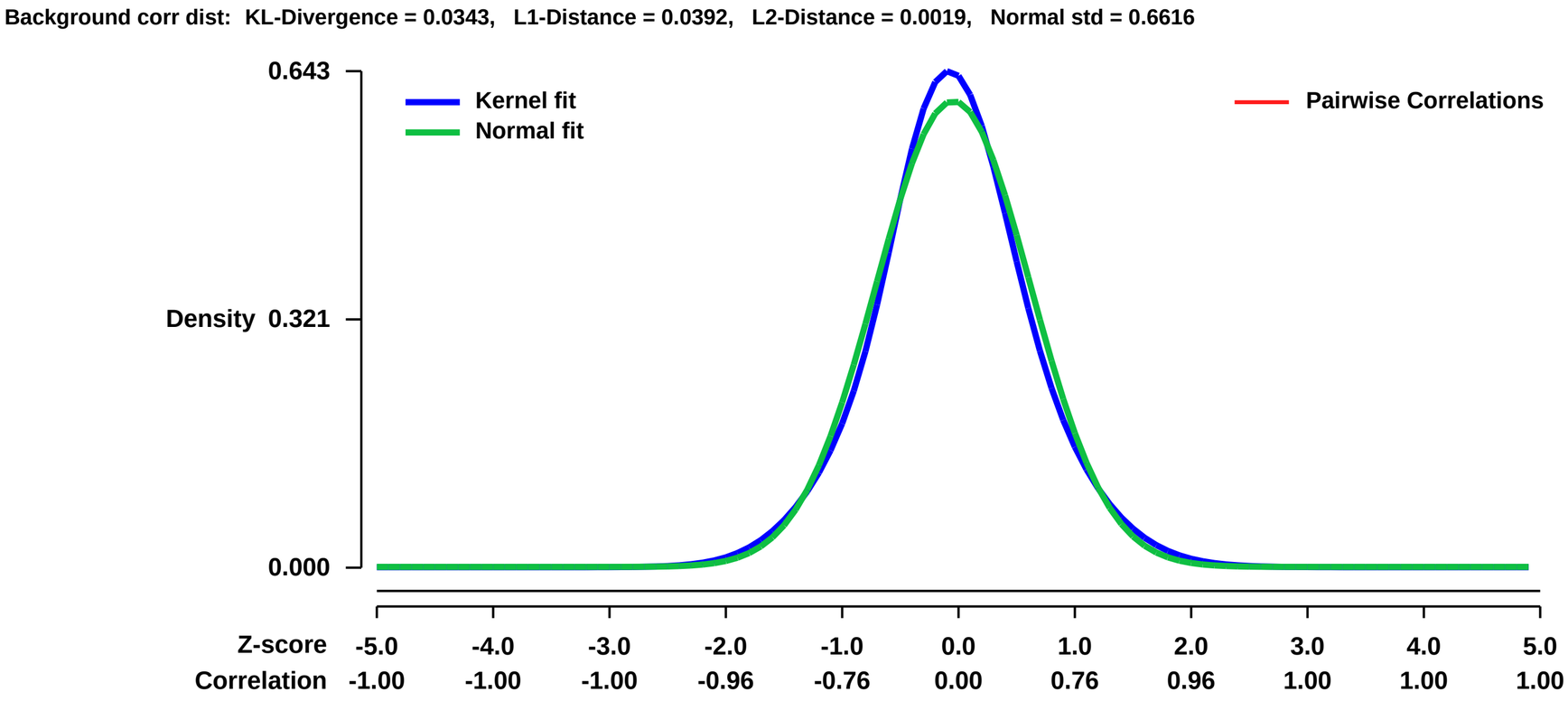

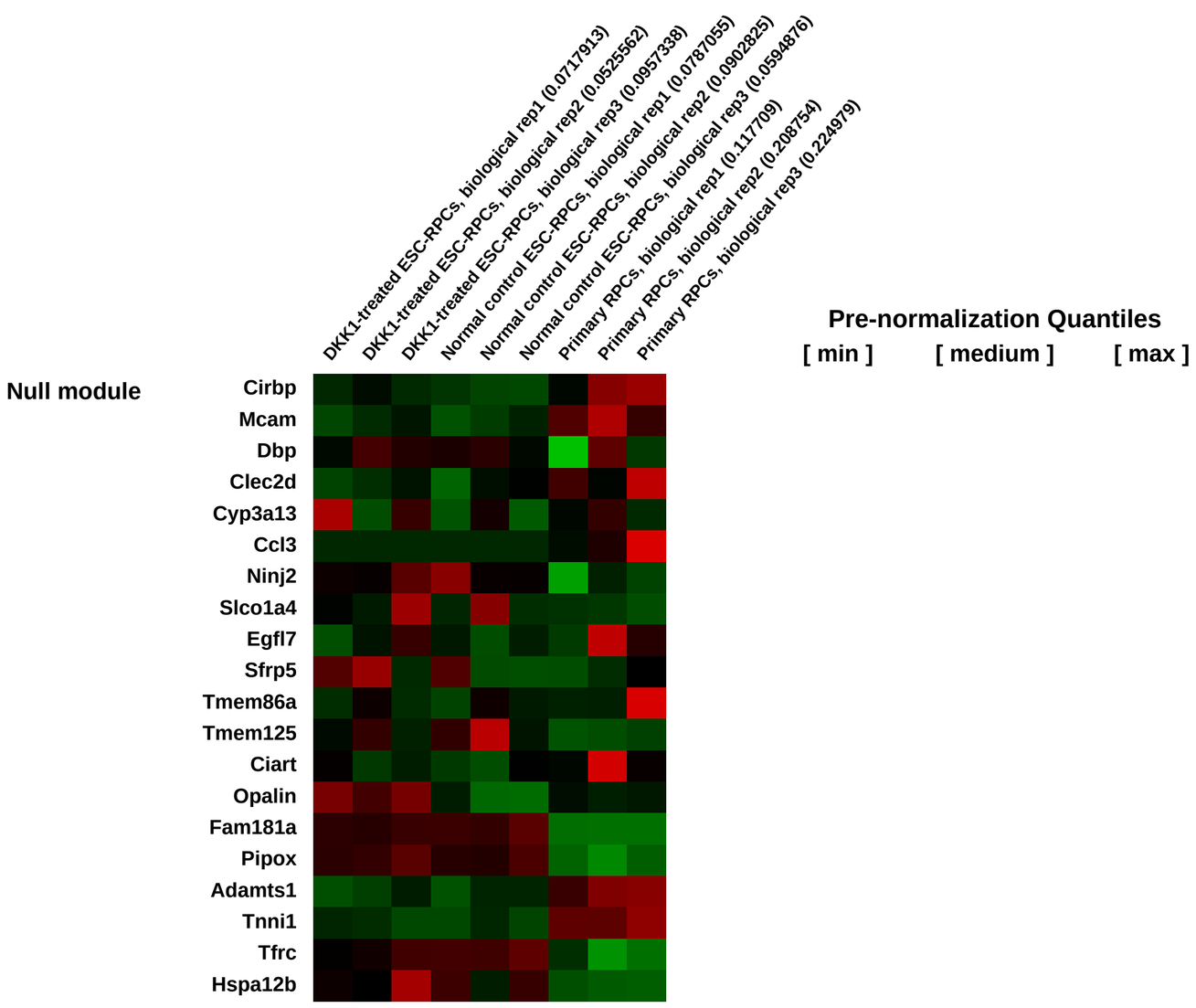

GEO Series "GSE9533" Expression Profiles

Num of samples in this series: 35

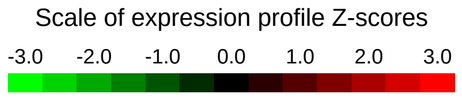

GEO Link:	http://www.ncbi.nlm.nih.gov/geo/query/acc.cgi?acc=GSE9533
Status:	Public on May 22 2008
Title:	PPARalpha-mediated effects of dietary lipids on intestinal barrier gene expression
Organism:	Mus musculus
Experiment type:	Expression profiling by array
Platform:	GPL1261
Pubmed ID:	18489776

Summary & Design:

Summary:
Background: The selective absorption of nutrients and other food constituents in the small intestine is mediated by a group of transport proteins and metabolic enzymes, often collectively called â intestinal barrier proteinsâ . An important receptor that mediates the effects of dietary lipids on gene expression is the peroxisome proliferator-activated receptor alpha (PPARˆ–), which is abundantly expressed in enterocytes. In this study we examined the effects of acute nutritional activation of PPARˆ– on expression of genes encoding intestinal barrier proteins. To this end we used triacylglycerols composed of identical fatty acids in combination with gene expression profiling in wild-type and PPARˆ–-null mice. Treatment with the synthetic PPARˆ– agonist WY14643 served as reference.

Results: We identified 74 barrier genes that were PPARˆ–-dependently regulated 6 hours after activation with WY14643. For eicosapentaenoic acid (EPA), docosahexaenoic acid (DHA) and oleic acid (OA) these numbers were 46, 41, and 19, respectively. The overlap between EPA-, DHA-, and WY14643-regulated genes was considerable, whereas OA treatment showed limited overlap. Functional implications inferred form our data suggested that nutrient-activated PPARˆ– regulated transporters and phase I/II metabolic enzymes were involved in a) fatty acid oxidation, b) cholesterol, glucose, and amino acid transport and metabolism, c) intestinal motility, and d) oxidative stress defense.

Conclusion: We identified intestinal barrier genes that were PPARˆ–-dependently regulated after acute activation by fatty acids.This knowledge provides a better understanding of the impact dietary fat has on the barrier function of the gut, identifies PPARˆ– as an important factor controlling this key function, and underscores the importance of PPARˆ– for nutrient-mediated gene regulation in intestine.

Keywords: metabolic state analysis

Overall design:
Pure bred wild-type (129S1/SvImJ) and PPARˆ–-null (129S4/SvJae) mice were treated for 6 hours with the synthetic triacylglycerols triolein [oleic acid (OA, C18:1)], trieicosapentaenoin [eicosapentaenoic acid (EPA, C20:5)] or tridocosahexaenoin [ocosahexaenoic acid (DHA, C22:6)], or the potent PPARˆ– agonist WY14,643. Two weeks before the start of the experiment, mice were put on a modified AIN76A diet, in which corn oil was replaced by olive oil. At the day of the experiment mice were fasted for four hours. At 9 AM mice were dosed by oral gavage with 400 ´µl of a 0.1% WY14643 suspension in 0.5% carboxymethyl cellulose, or 400 ´µl of the synthetic triacylglycerols. Six hours after the gavage the mice were anaesthetized, small intestines were removed, flushed with ice-cold PBS and remaining fat and pancreatic tissue was carefully removed. Total RNA was then isolated. RNA of 4-5 biological replicates was hybridized to Affymetrix 430-2.0 plus arrays. Five microgram total RNA was labelled according to the ENZO-protocol, fragmented and hybridized according to Affymetrix's protocols.

Background corr dist: **KL-Divergence = 0.3720, L1-Distance = 0.0584, L2-Distance = 0.0087, Normal std = 0.2574**

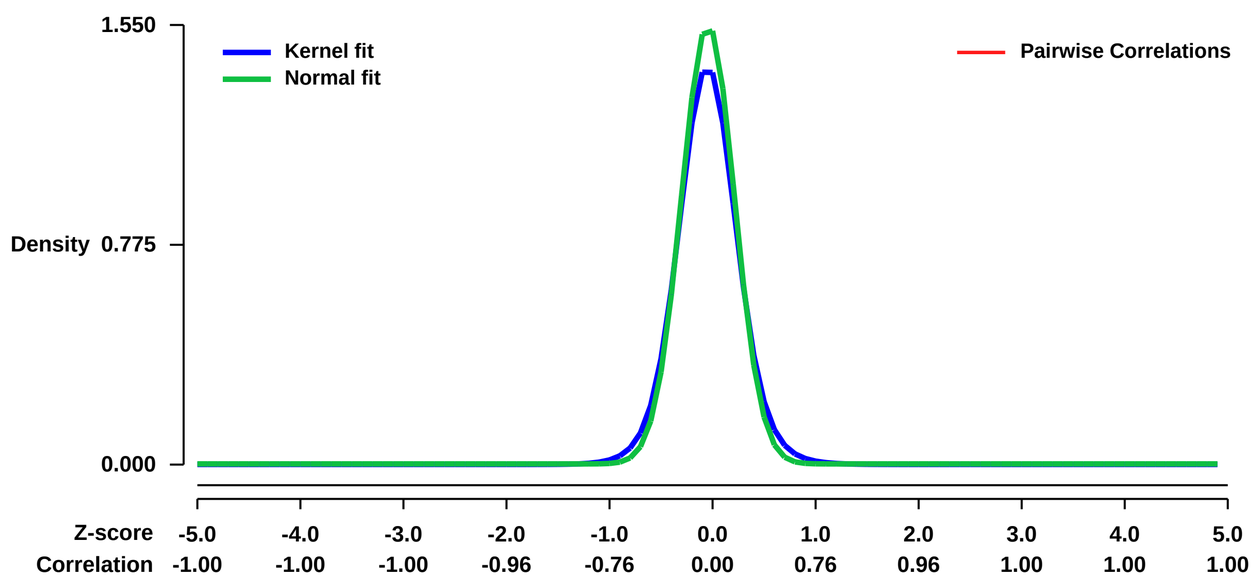

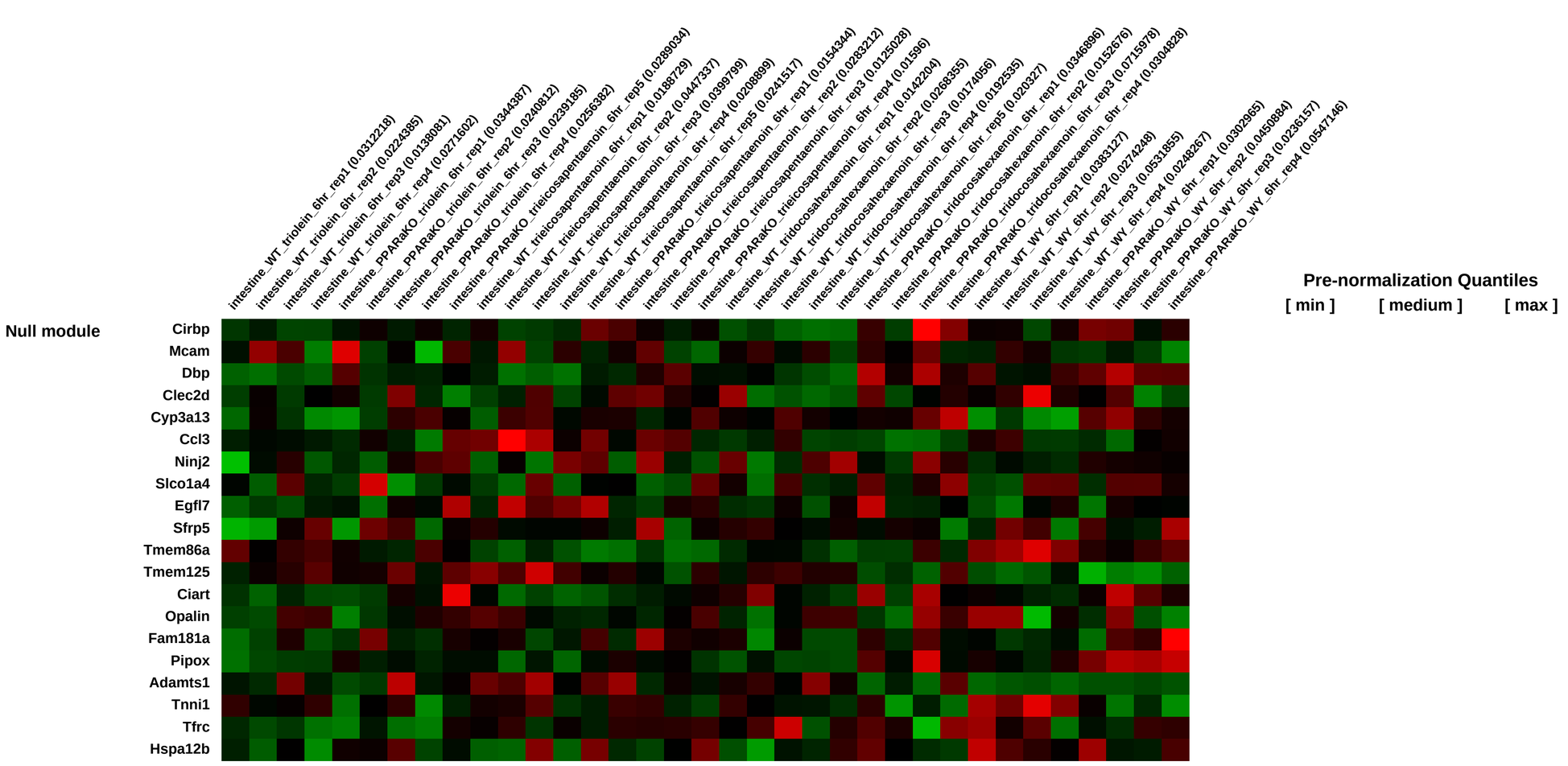

GEO Series "GSE17879" Expression Profiles

Num of samples in this series: 6

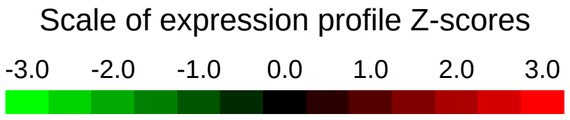

GEO Link:	http://www.ncbi.nlm.nih.gov/geo/query/acc.cgi?acc=GSE17879
Status:	Public on Aug 31 2009
Title:	Activin/Nodal signaling in mouse embryonic stem cells
Organism:	Mus musculus
Experiment type:	Expression profiling by array
Platform:	GPL1261
Pubmed ID:	20427282
Summary & Design:	**Summary:** Members of the transforming growth factor (TGF)-¸† superfamily play essential roles in the pluripotency, self-renewal, and differentiation of embryonic stem cells. While bone morphogenic proteins maintain pluripotency of undifferentiated mouse ES cells, the role of Activin/Nodal signaling is less clear. To determine the target genes of Activin/Nodal-Smad2 signaling in undifferentiated embryonic stem cells, changes in gene expression were examined following stimulation with recombinant Activin (2 hours) or after inhibition of Activin/Nodal with SB431542 (24 hours) using defined media culture conditions with LIF and 20 ng/mL BMP4. SB431542 is a specific inhibitor of ALK4/5/7 receptors and antagonizes both Activin and Nodal signaling. Via western analysis, Activin stimulation increased pSmad2 in ES cells after 2 hours, and treatment with SB431542 for 24 hours virtually eliminated pSmad2. Total Smad2 expression remained unchanged through these manipulations. RNA from cells treated with Activin or SB431542 was extracted by standard methods with Qiagen RNeasy columns. The RNA was analyzed with the Mouse Genome 430A Array from Affymetrix. Samples were performed in duplicate, and RNA from cells treated with Activin or SB431542 was compared to untreated embryonic stem cells. **Overall design:** RNA from cells treated with Activin or SB431542 was extracted by standard methods with Qiagen RNeasy columns. The RNA was analyzed with the Mouse Genome 430A Array from Affymetrix. Samples were performed in duplicate, and RNA from cells treated with Activin or SB431542 was compared to untreated embryonic stem cells.

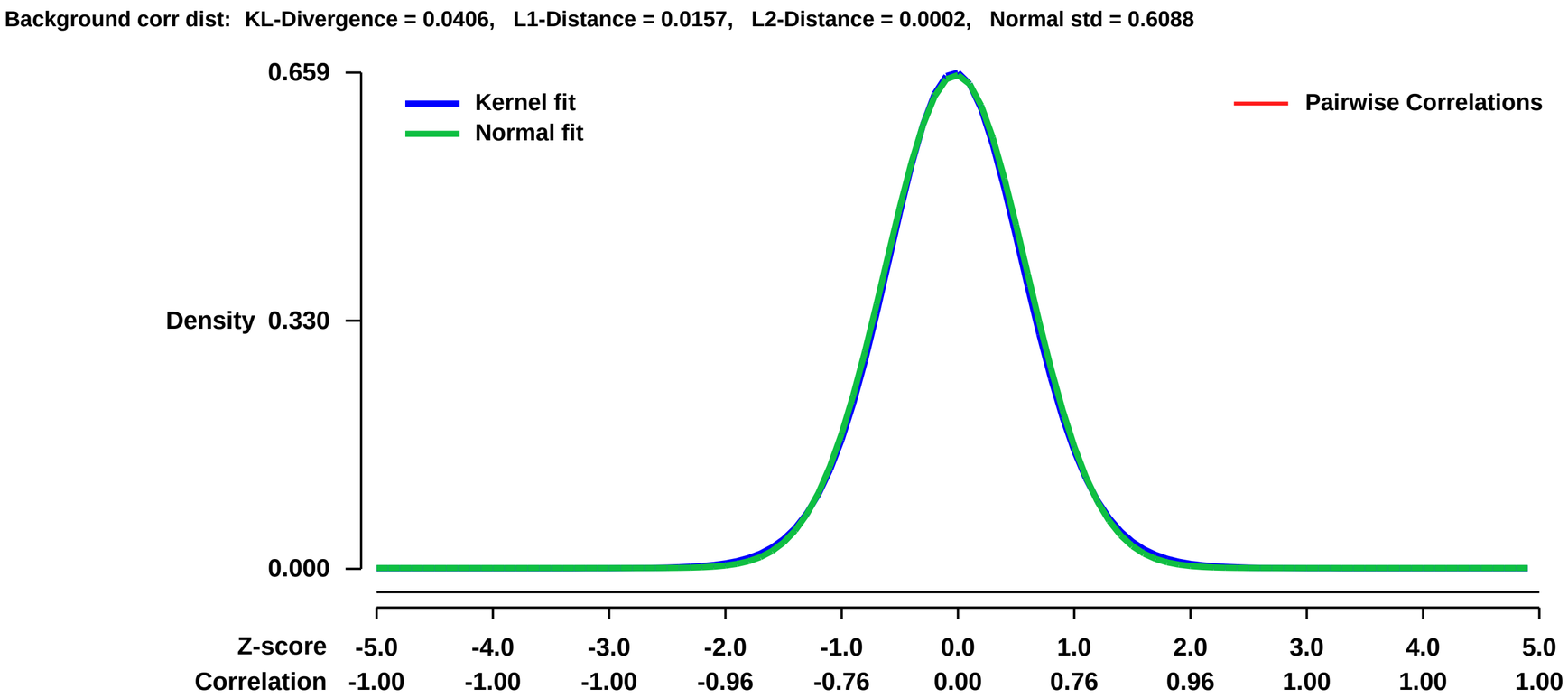

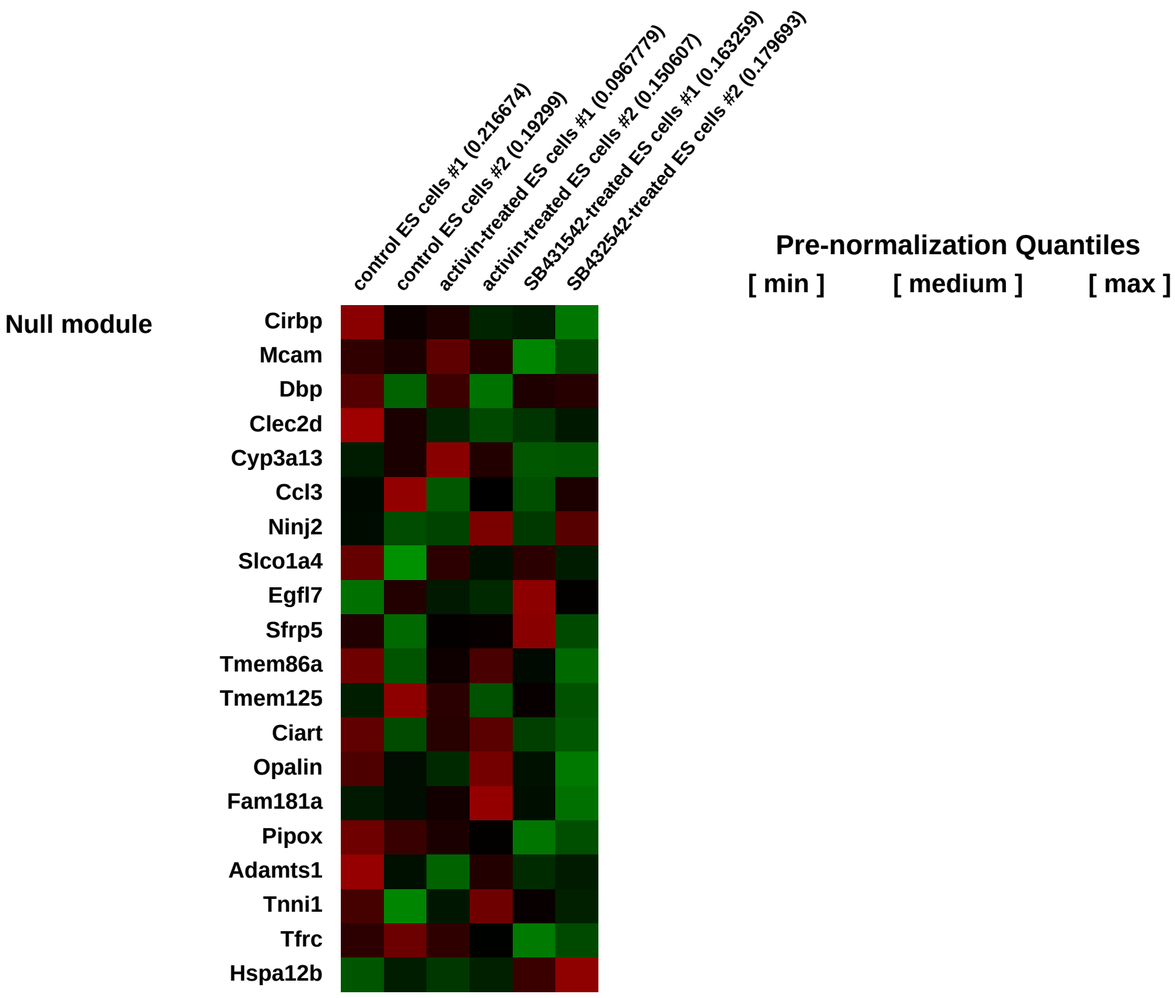

GEO Series "GSE6632" Expression Profiles

Num of samples in this series: 6

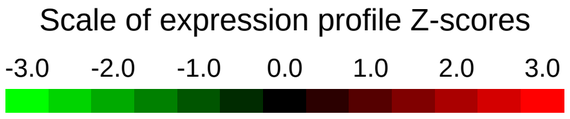

GEO Link:	http://www.ncbi.nlm.nih.gov/geo/query/acc.cgi?acc=GSE6632
Status:	Public on Oct 06 2007
Title:	Hepatocellular carcinoma follows loss of liver-gender specificity in mice
Organism:	Mus musculus
Experiment type:	Expression profiling by array
Platform:	GPL1261
Pubmed ID:	18089782
Summary & Design:	**Summary:** We are investigating hepatic transcriptional responses associated with castration and tumorigenic hepatitis induced by Helicobacter hepaticus infection in mature male A/JCr mice Microarray data demonstrated a global loss of gender-dimorphic gene expression regulation in mice with chronic hepatitis and liver cancer Keywords: dose **Overall design:** Male A/JCr mice were inoculated with H. hepaticus or vehicle at 4 weeks; some underwent castration at 1 year, and all were necropsied at 21 months

Background corr dist: KL-Divergence = 0.0381, L1-Distance = 0.0232, L2-Distance = 0.0006, Normal std = 0.6377

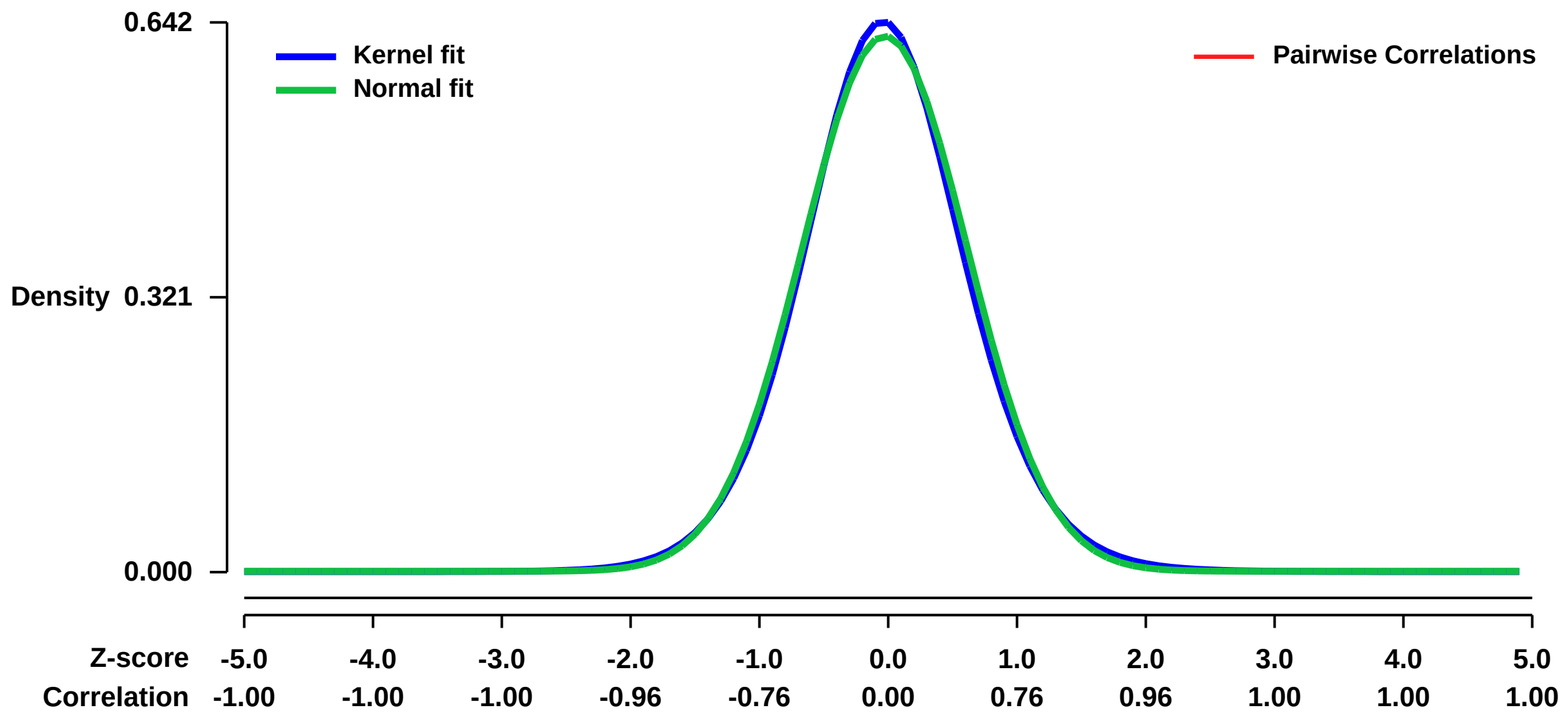

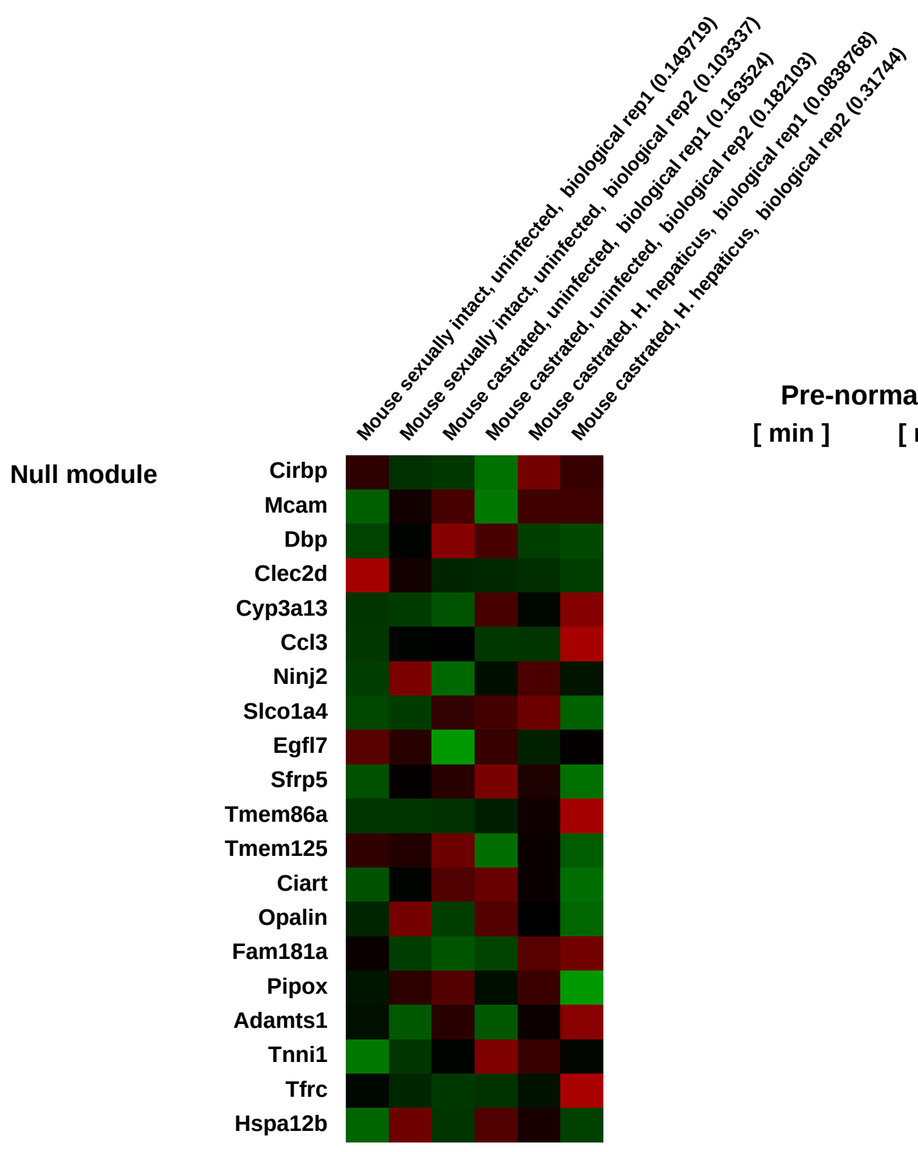

GEO Series "GSE8407" Expression Profiles

Num of samples in this series: 17

Scale of expression profile Z-scores

-3.0 -2.0 -1.0 0.0 1.0 2.0 3.0

GEO Link:	http://www.ncbi.nlm.nih.gov/geo/query/acc.cgi?acc=GSE8407
Status:	Public on Aug 01 2007
Title:	Elucidation of the phenotypic, functional and molecular topography of a myeloerythroid progenitor cell hierarchy
Organism:	Mus musculus
Experiment type:	Expression profiling by array
Platform:	GPL1261
Pubmed ID:	18371379
Summary & Design:	**Summary:** The major myeloid blood cell lineages, including erythrocytes, platelets, granulocytes and macrophages, are generated from hematopoietic stem cells (HSC) by differentiation through a series of increasingly more committed progenitor cells. Precise phenotypic identification and functional characterization of such intermediate progenitors has important consequences for understanding fundamental differentiation processes and is clinically relevant since such events become dysregulated in various disease settings, including leukemia. While previous studies have suggested a hierarchy for myeloid differentiation involving a common progenitor through which all myeloid lineages are derived, several recent studies have suggested that such a developmental intermediate might not be an absolute requirement. Here, we evaluated the functional in vitro and in vivo potentials of a range of prospectively isolated myeloid precursors with differential expression of CD150, Endoglin and CD41. Our studies reveal a complex hierarchy of myeloerythroid progenitors with distinct and developmentally restricted lineage potentials. Global gene expression signatures of these cellular subsets revealed expression patterns consistent with their functional capacities, while hierarchical clustering analysis provides details on their lineage relationships. These data challenge existing models of hematopoietic differentiation, by suggesting that progenitors of the innate and adaptive immune system in the adult separate late, and to a large extent, following the divergence of megakaryocytic/erythroid potential. **Keywords:** global gene expression profiling of prospectively isolated murine bone marrow progenitor subset by usage of affymetrix **Overall design:** RNA was extracted from purified adult BM subsets using RNeasy mRNA purification kit (Qiagen). Subsequent handling was performed at the SweGene Affymetrix unit at Lund University (http://www.swegene.org/microarray). Briefly, RNA (arrays in triplicate for all progenitor fractions except for pre MegE for which 5 arrays were produced) was labeled and amplified according to AffymetrixTM; Small Sample Labelling Protocol v.2, with the exception that the second round of in vitro transcription (IVT) was performed using AffymetrixTM GeneChipTM Expression 3â amplification kit. Hybridization and washing was performed according to AffymetrixTM GeneChipTM Expression analysis technical manual. Chips were scanned using an AffymetrixTM GeneChipTM Scanner 3000 and scaled to a median intensity of 100. For subsequent analysis, probe level expression values were extracted using RMA (Irizarry et al., 2003) and subsequent analyses was performed using dChip software (http://biosun1.harvard.edu/complab/dchip/) following filtering (0.5<SD/mean<1,000).

Background corr dist: KL-Divergence = 0.0647, L1-Distance = 0.0781, L2-Distance = 0.0127, Normal std = 0.5494

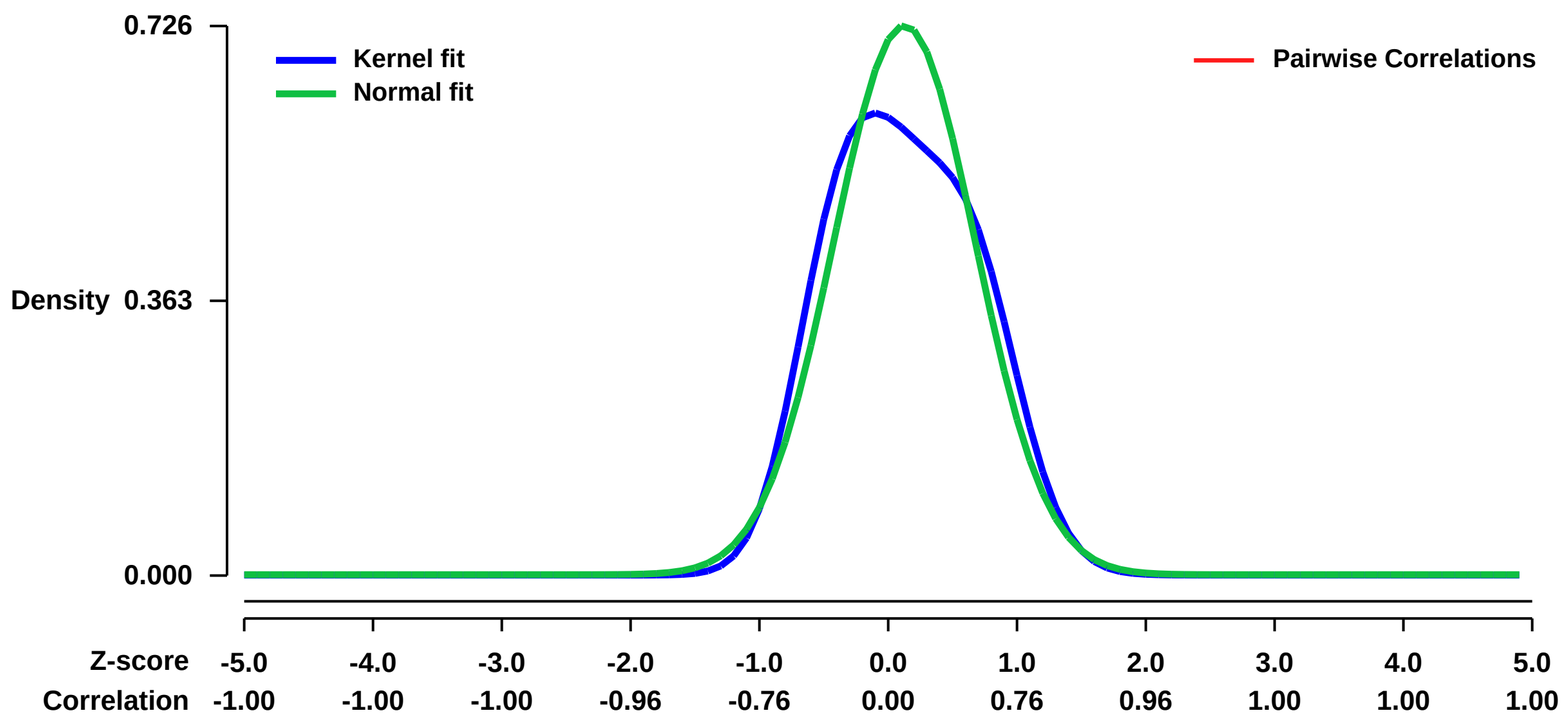

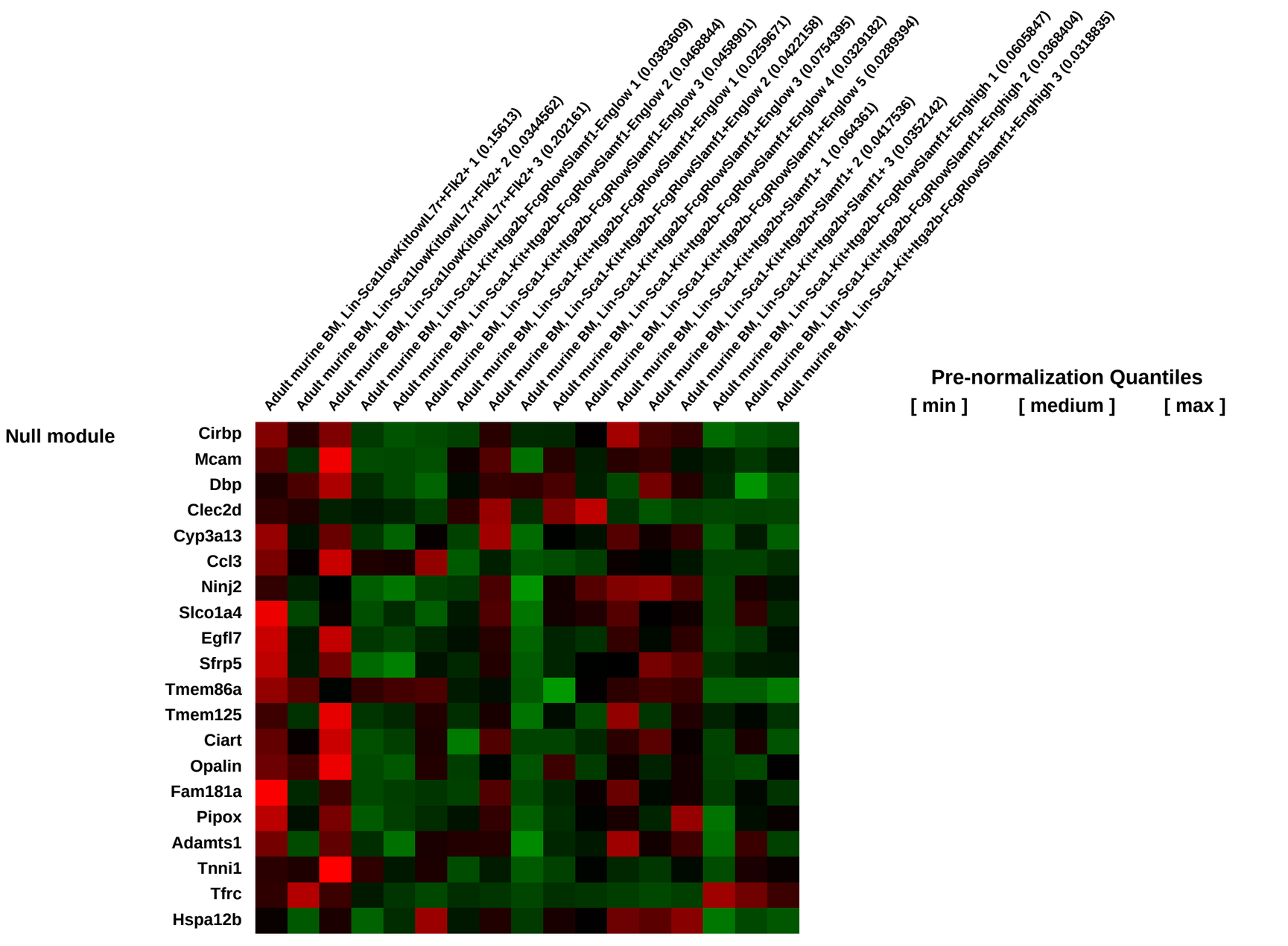

GEO Series "GSE20944" Expression Profiles

Num of samples in this series: 18

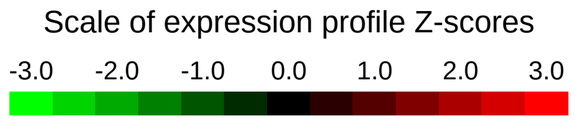

GEO Link:	http://www.ncbi.nlm.nih.gov/geo/query/acc.cgi?acc=GSE20944
Status:	Public on Oct 09 2010
Title:	Impact of dietary fatty acids on gene expression of liver-specific knockout of cytochrome P450 reductase
Organism:	Mus musculus
Experiment type:	Expression profiling by array
Platform:	GPL1261
Pubmed ID:	21098682

Summary & Design:

Summary:
In the present study, we explored the hypothesis that the fatty liver phenotype and associated gene expression changes associated with the specific deletion of the POR gene in adult mouse liver could be abrogated by supplementation of the mouse diet with the very long chain highly unsaturated fatty acids, arachidonic acid (C20:4ˇ 6), eicosapentaenoic acid (C20:5ˇ 3) and docosahexaenoic acid (C22:6ˇ 3). We expected the fatty liver phenotype would not be reduced by the polyunsaturated fatty acids linoleic (C18:2ˇ 6) or linolenic acid (C18:3ˇ 3), since these accumulated in the fatty livers of LivPORKO animals. This proved to be the case. However, we also made two surprising observations. First, control animals fed a diet enriched in PUFA had fatty livers and gene expression profiles similar to animals fed a lard diet, which was deficient in both PUFA and HUFA. Second, while a diet enriched in HUFA did result in reduced steatosis in livers of the LivPOKO animals, fat accumulation was still elevated relative to controls. Array analyses indicated most differences in gene expression were related to fatty acid metabolism and could explain differences in fat accumulation in LivPORKO livers with dietary treatment.

Overall design:
Generation of the founder line with hepatic ablation of POR is described in Wu, et al. ((2003) Genesis 36, 177-181). Male test animals used in this study had the genotype Alb-Cre+/-/POR-lox+/+ and were called LivPORKOs. For each series of experiments, mice were placed on one of three synthetic diets upon weaning. Siblings of the same genotype were randomized between dietary groups. Upon weaning (four weeks after birth) male mice of each genotype were placed on one of the test diets for eight weeks. Synthetic diets used base diet AIN-93G and contained 18.7% protein, 64.7% carbohydrate, 5% fiber, 6% fat, 0.025% cholesterol, 0.008% sodium cholate, and 3.97 kcal per gram. The added fats were as follows: 6% lard (lard diet); 6% canola oil (canola diet); or 3.27% ARASCO oil (Martek Biosciences Corp.) and 2.73% menhadin oil (fish/fungal diet). After 8 weeks on the test diets (12 weeks of age) the animals were fasted for four hours prior to sacrifice. Liver samples were placed in mRNAlater´fi for mRNA analysis and immediately frozen and stored at -80´℃. To reduce variability between arrays, three RNA samples from individual mice of the same genotype/diet group were pooled using equivalent RNA amounts for each animal. Three microarrays on three pools were done per genotype/diet. The quality of RNA was analyzed using an Agilent 2100 Bioanalyzer. Three micrograms of RNA was reverse transcribed to make cDNA. Hybridization of cDNA, washing, and scanning of the Affymetrix GeneChip Mouse Genome 430 2.0 (containing 45,101 probe sets representing over 34,000 mouse genes) was performed according to standard Affymetrix protocol.

Background corr dist: KL-Divergence = 0.2208, L1-Distance = 0.0574, L2-Distance = 0.0081, Normal std = 0.3174

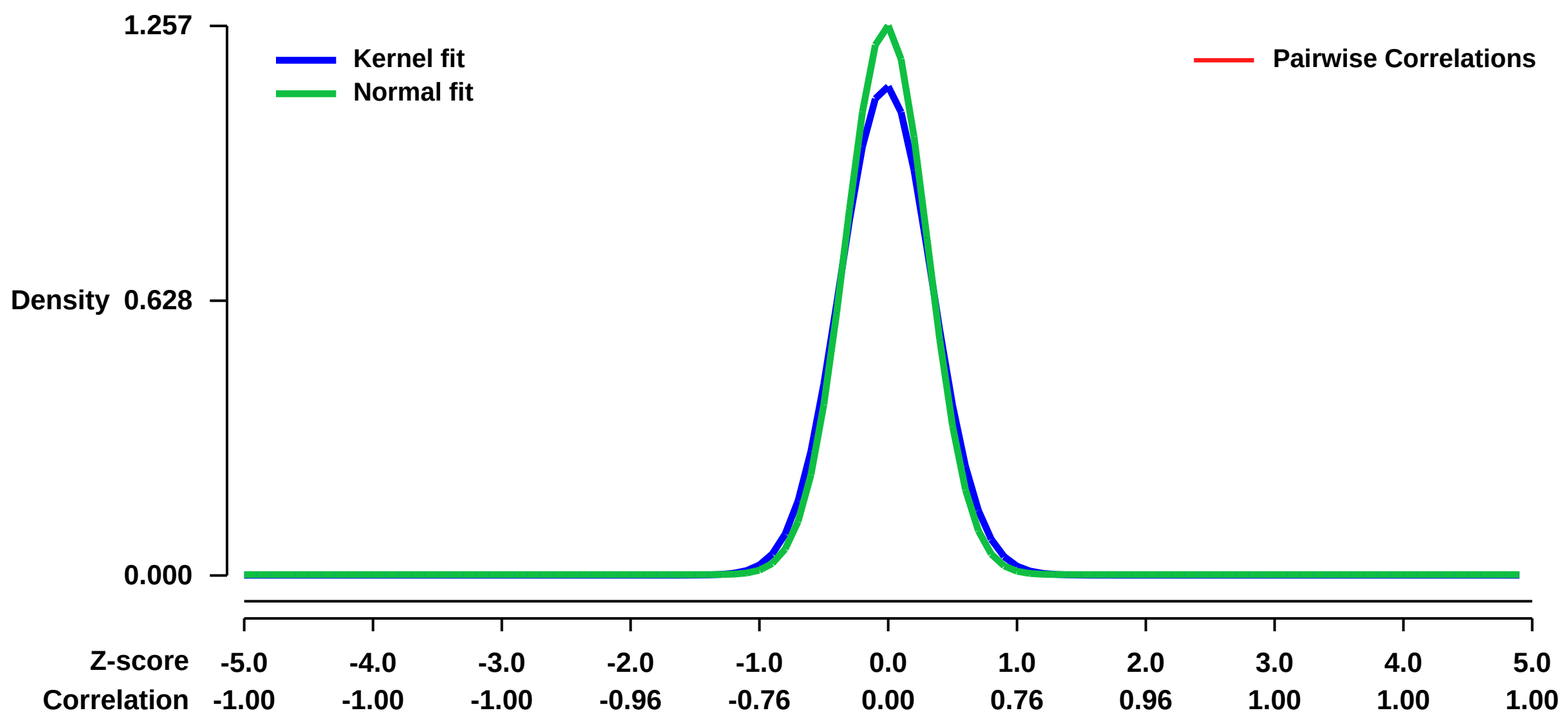

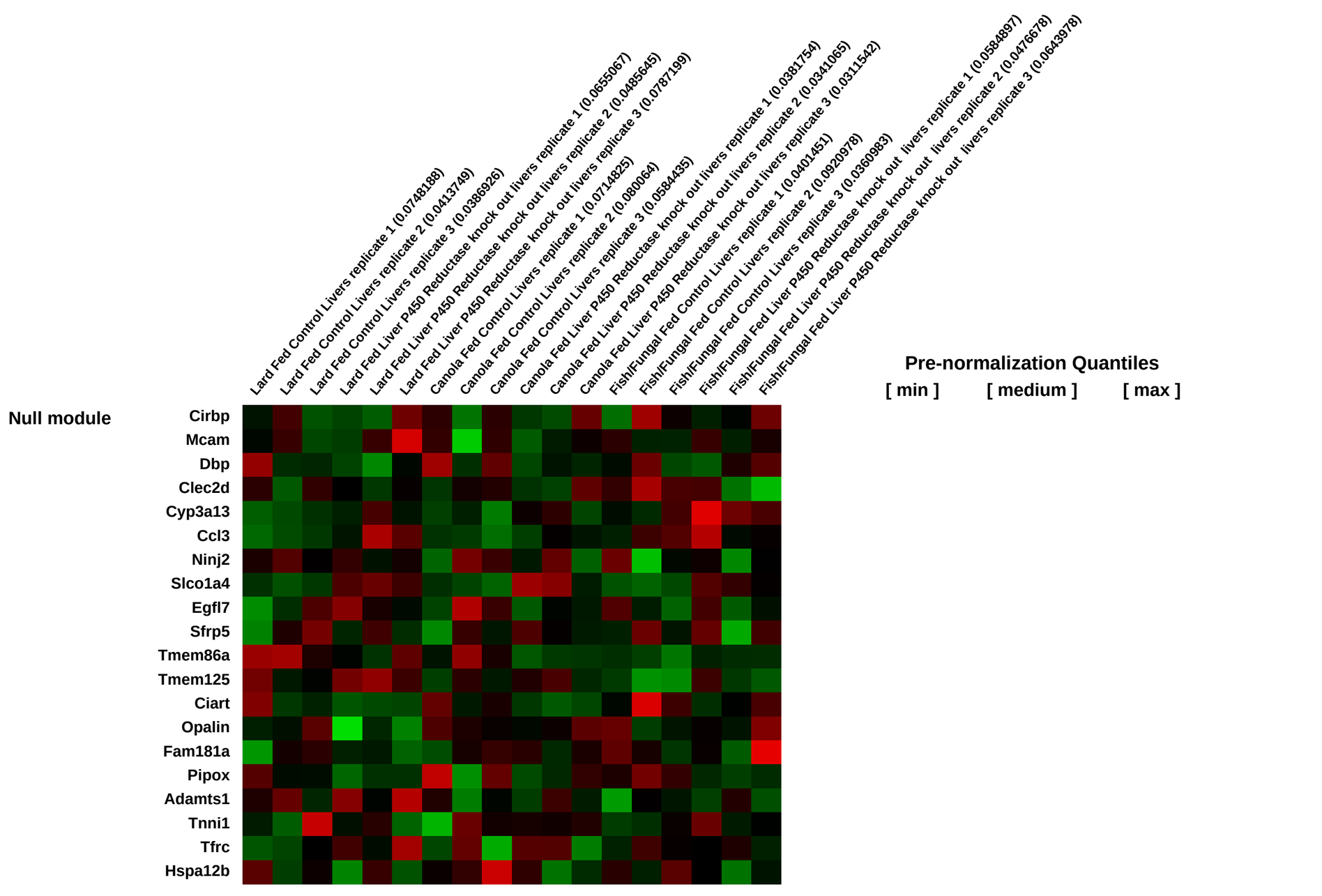

GEO Series "GSE41095" Expression Profiles

Num of samples in this series: 6

Scale of expression profile Z-scores

-3.0 -2.0 -1.0 0.0 1.0 2.0 3.0

GEO Link:	http://www.ncbi.nlm.nih.gov/geo/query/acc.cgi?acc=GSE41095
Status:	Public on Sep 25 2012
Title:	Maternal diabetes alters transcriptional programs in the developing embryo.
Organism:	Mus musculus
Experiment type:	Expression profiling by array
Platform:	GPL1261
Pubmed ID:	19538749
Summary & Design:	**Summary:** Exposure to maternal diabetes during pregnancy alters transcriptional profiles in the developing embryo. The enrichment, within the set of de-regulated genes, of those encoding transcriptional regulatory molecules provides support for the hypothesis that maternal diabetes affects specific developmental programs. We compared E10.5 cntrol embryos to E10.5 embryos from diabetic pregnancies in the FVB mouse strain. **Overall design:** Diabetes was induced in 7-9 week old female FVB mice by streptozotocin. Dams whose blood glucose levels exceeded 250 mg/dl were set up for mating. Embryos were dissected at E10.5 and total RNA was isolated. Equal amounts of RNA prepared from 3 individual embryos were pooled into one sample; each embryo was from a different pregnancy. Three pools were constructed for a total of nine embryos from diabetic pregnancies, and independently three pools for control embryos.

Background corr dist: KL-Divergence = 0.0201, L1-Distance = 0.0326, L2-Distance = 0.0011, Normal std = 0.7805

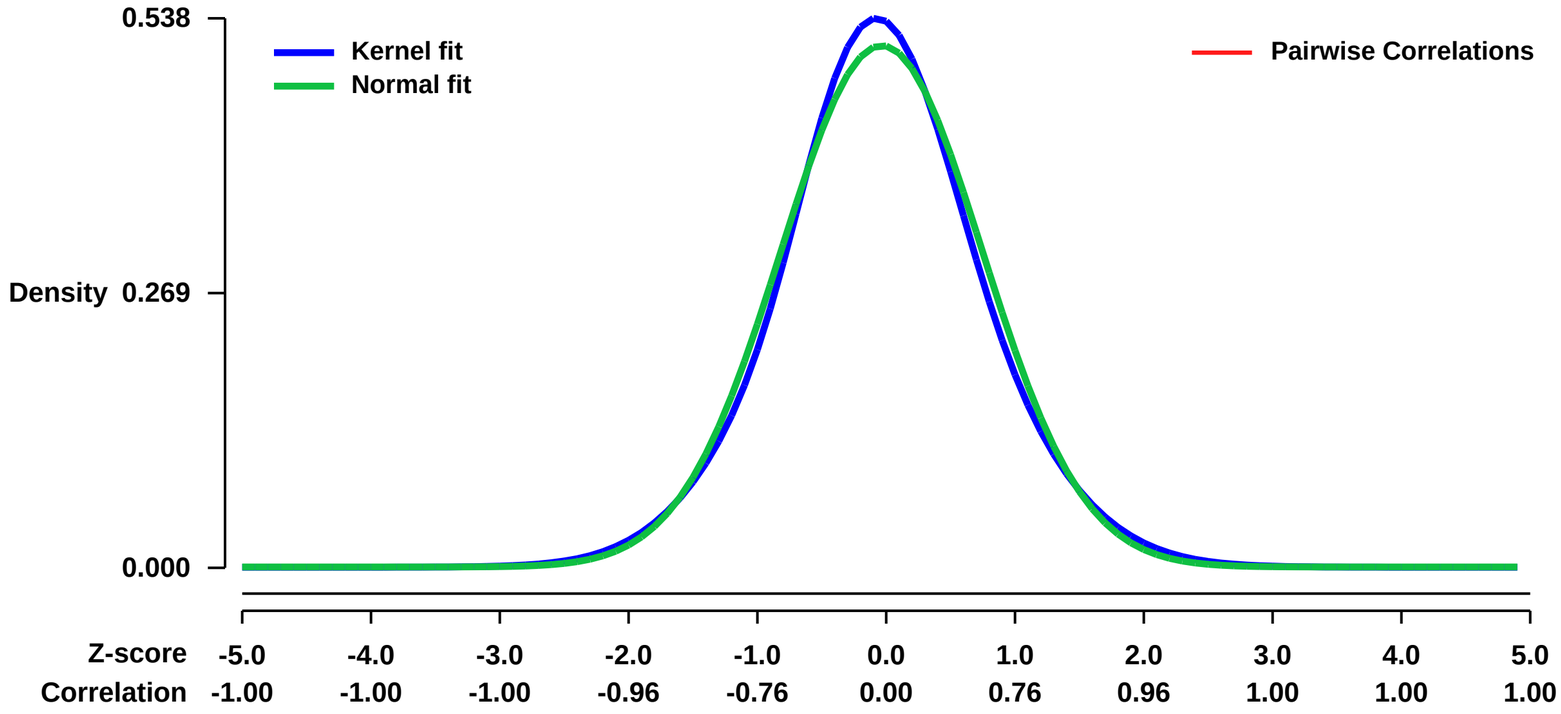

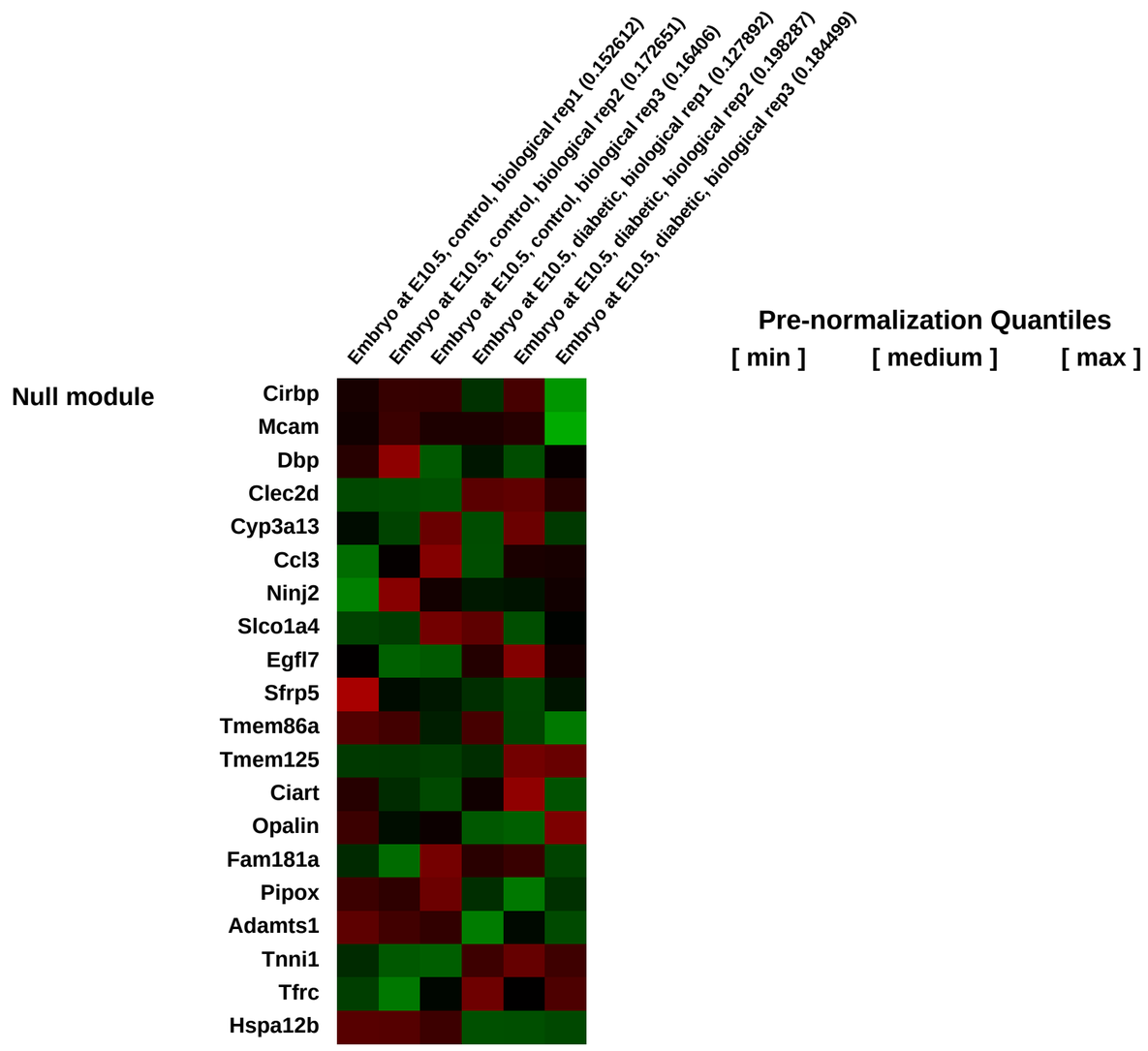

GEO Series "GSE32095" Expression Profiles

Num of samples in this series: 24

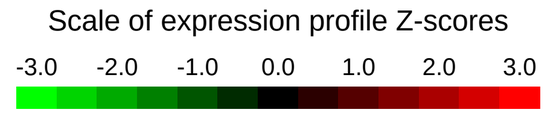

GEO Link:	**http://www.ncbi.nlm.nih.gov/geo/query/acc.cgi?acc=GSE32095**
Status:	**Public on Feb 22 2012**
Title:	**GPR120 mediates high-fat diet induced obesity**
Organism:	**Mus musculus**
Experiment type:	**Expression profiling by array**
Platform:	**GPL1261**
Pubmed ID:	**22343897**
Summary & Design:	**Summary:** **Analysis of GPR120 which play roles for the fatty acid sensor in adipose tissue. Results provide insight into the transcriptional effects caused by the loss of the GPR120 proteins and provide further insight into their functions.** **Overall design:** **GPR120 KO mice and the corresponding wild-type with normal diet(ND) or high fat diet(HFD), were subjected to Affymetrix Mus musculus microarrays. Epididymal adipose tissue and liver were analyzed in triplicates.**

Background corr dist: **KL-Divergence = 0.1001, L1-Distance = 0.0645, L2-Distance = 0.0080, Normal std = 0.4859**

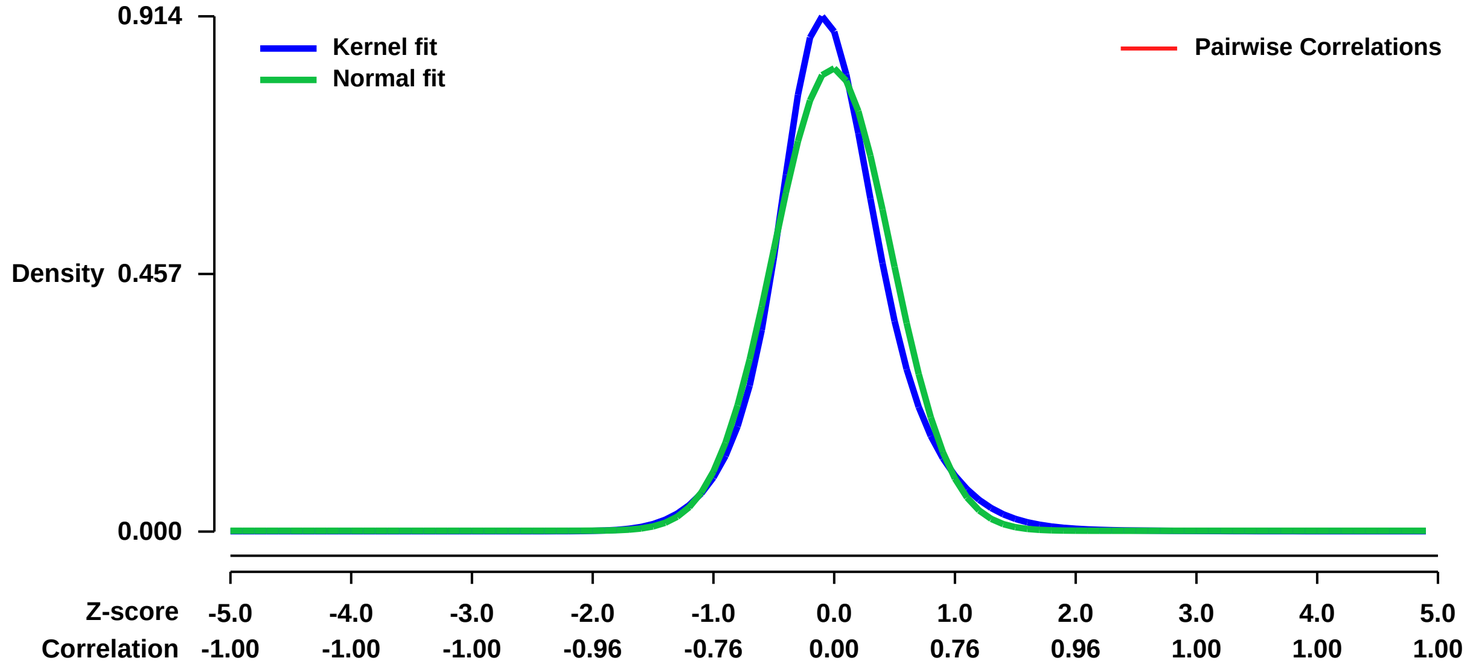

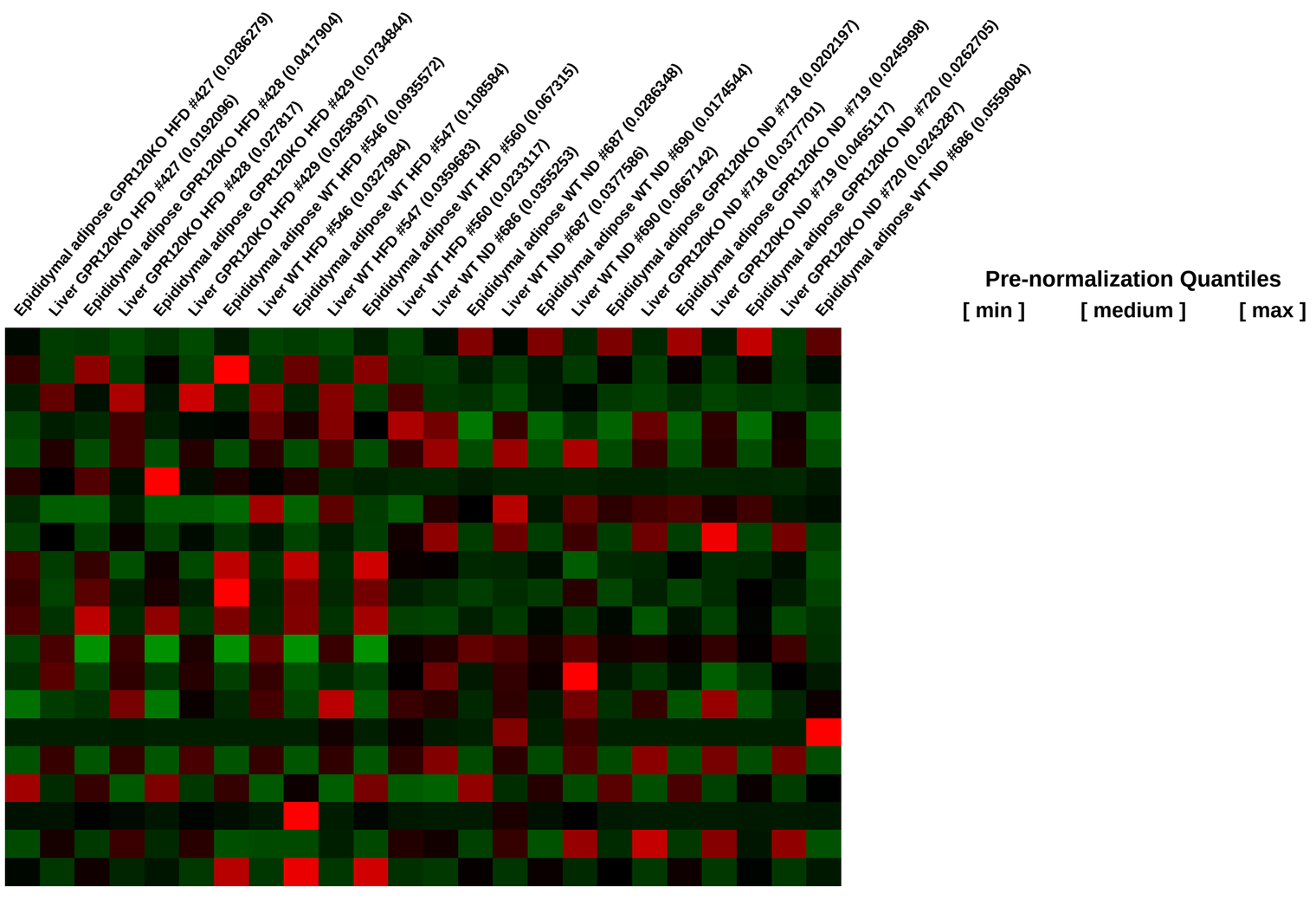

GEO Series "GSE44651" Expression Profiles

Num of samples in this series: 12

Scale of expression profile Z-scores

-3.0 -2.0 -1.0 0.0 1.0 2.0 3.0

GEO Link:	http://www.ncbi.nlm.nih.gov/geo/query/acc.cgi?acc=GSE44651
Status:	Public on Jul 03 2013
Title:	Laser Capture Microdissection isolation of preovulatory granulosa cells from WT and bERKO ovaries
Organism:	Mus musculus
Experiment type:	Expression profiling by array
Platform:	GPL1261
Pubmed ID:	23580569
Summary & Design:	**Summary:** Determining the spatial and temporal expression of genes involved in the ovulatory pathway is critical for the understanding of the role of each estrogen receptor in the modulation of folliculogenesis and ovulation. Estrogen receptor (ER) ¸† is highly expressed in ovarian granulosa cells and mice lacking ER¸† (¸†ERKO) are subfertile due to inefficient ovulation. Previous work has focused on isolated granulosa cells or cultured follicles and while informative, provides confounding results due to the heterogeneous cell types present including granulosa, theca and oocytes and exposure to in vitro conditions. Herein, we isolated preovulatory granulosa cells from WT and ER¸†-null mice using laser capture microdissection to examine the genomic transcriptional response downstream of PMSG (mimicking FSH) and PMSG/hCG (mimicking LH) stimulation. This allows for a direct comparison of in vivo granulosa cells at the same stage of development from both WT and ER¸†-null ovaries. ER¸†-null granulosa cells showed altered expression of genes known to be regulated by FSH (Akap12 and Runx2) as well as not previously reported (Arnt2 and Pou5f1) in WT granulosa cells. Our analysis also identified 304 genes not previously associated with ER¸† in granulosa cells. LH responsive genes including Abcb1b and Fam110c show reduced expression in ER¸†-null granulosa cells; however novel genes including Rassf2 and Megf10 were also identified as being downstream of LH signaling in granulosa cells. Collectively, our data suggests that granulosa cells from ER¸†-null ovaries may not be appropriately differentiated and are unable to respond properly to gonadotropin stimulation We used microarray to compare the gene expression profiles of wiltype (WT) and Erb-null (bERKO) preovulatory granulosa cells as they respond to either PMSG or PMSG+hCG treatments. **Overall design:** Laser microdissection was used to collect a purified population of granulosa cells only from preovulatory follicles. We chose to compre the response to PMSG or PMSG+hCG of granulosa cells collected from either WT and bERKO preovulatory follicles. We chose to collect cells 48h after mice were treated with PMSG to compare the gene expression profile ot preovulatory granulosa cells. We also studied the response of these cells to LH (or hCG) as we collected cells 4h after mice were treated with hCG (peak of transcriptional response to hCG).

Background corr dist: KL-Divergence = 0.1242, L1-Distance = 0.0379, L2-Distance = 0.0031, Normal std = 0.4079

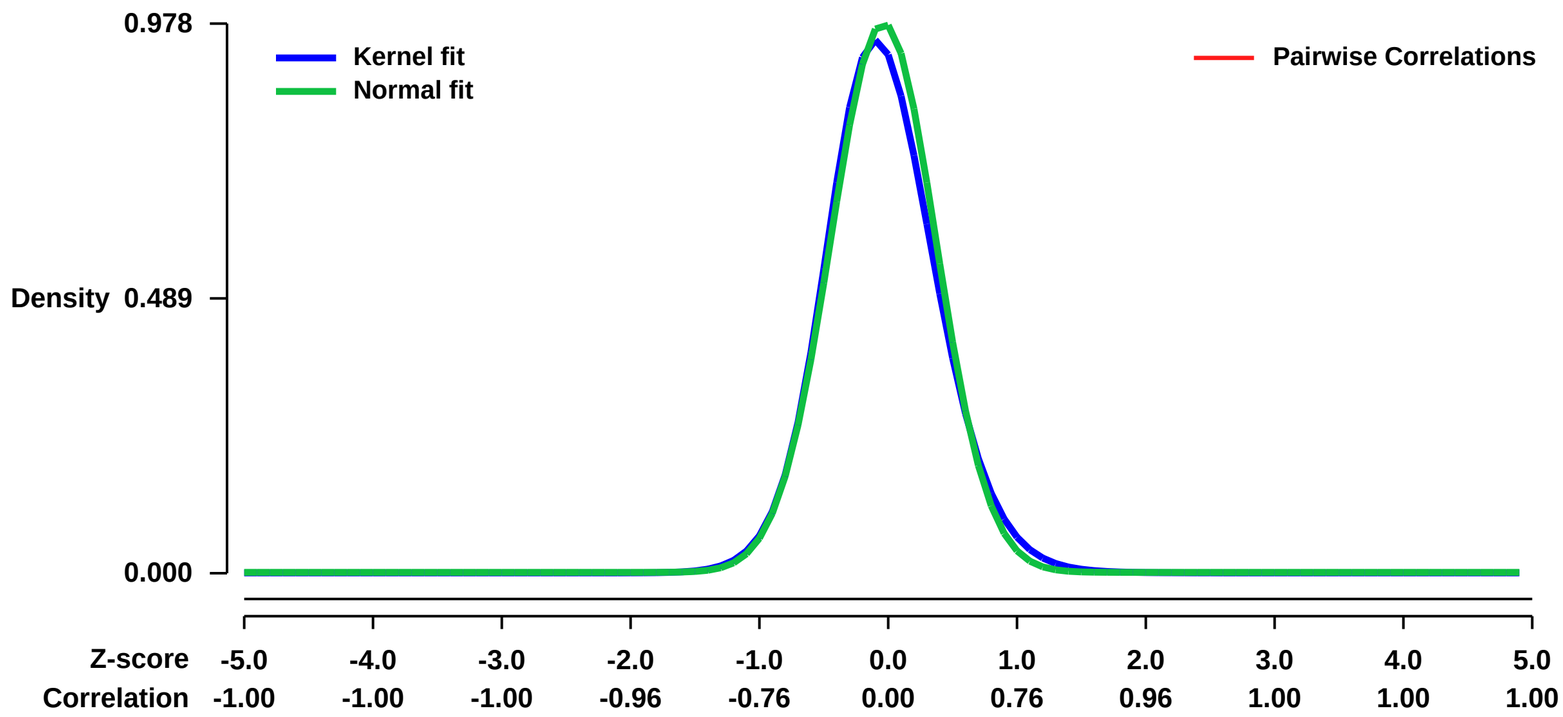

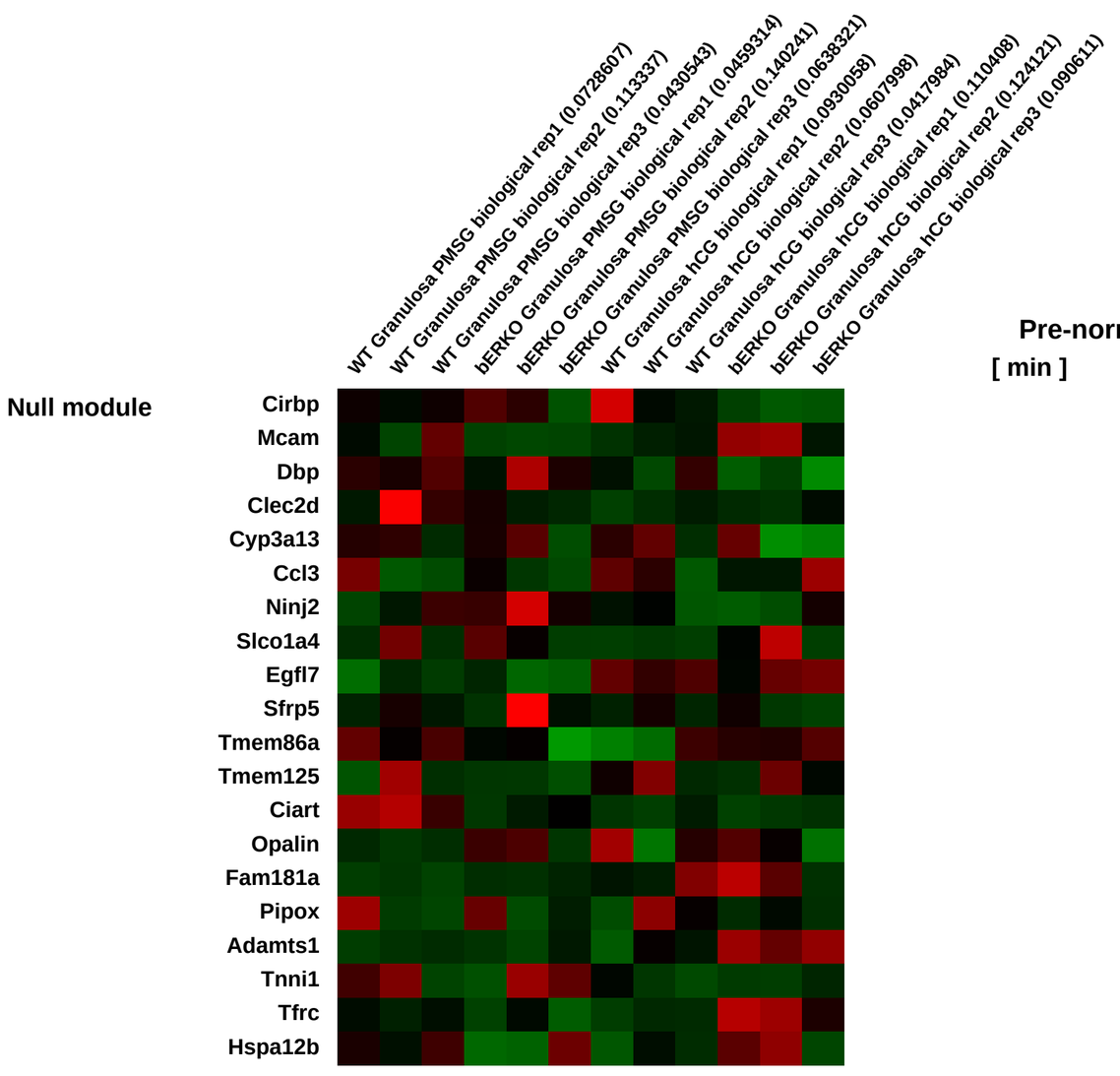

GEO Series "GSE6290" Expression Profiles

Num of samples in this series: 37

Scale of expression profile Z-scores

-3.0 -2.0 -1.0 0.0 1.0 2.0 3.0

GEO Link:	http://www.ncbi.nlm.nih.gov/geo/query/acc.cgi?acc=GSE6290
Status:	Public on Nov 18 2006
Title:	Gene expression profiles of components isolated from developing kidney at E11.5, E12.5 & E15.5 using LCM. (GUDMAP Series ID: 10)
Organism:	Mus musculus
Experiment type:	Expression profiling by array
Platform:	GPL1261
Pubmed ID:	19501082
Summary & Design:	**Summary:** The long term objective is to create an encyclopedia of the expression levels of all genes in multiple components of the developing kidney. The central thesis is straightforward. The combination of laser capture microdissection (LCM) plus microarray analysis offers a powerful, efficient and effective method for the creation of a global gene expression atlas of the developing kidney. Microarrays with essentially complete genome coverage can be used to quantitate expression levels of every gene in laser capture microdissected components of the developing kidney. The ensuing rapid read-out provides an expression atlas that is more sensitive, more economical and more complete than would be possible by in situ hybridizations alone. **Keywords:** Comparison of kidney components. **Overall design:** At different developmental time points we isolate discrete elements of the kidney by using laser capture microdissection and then define their gene expression profiles with microarrays.

Background corr dist: KL-Divergence = 0.3783, L1-Distance = 0.0765, L2-Distance = 0.0180, Normal std = 0.2563

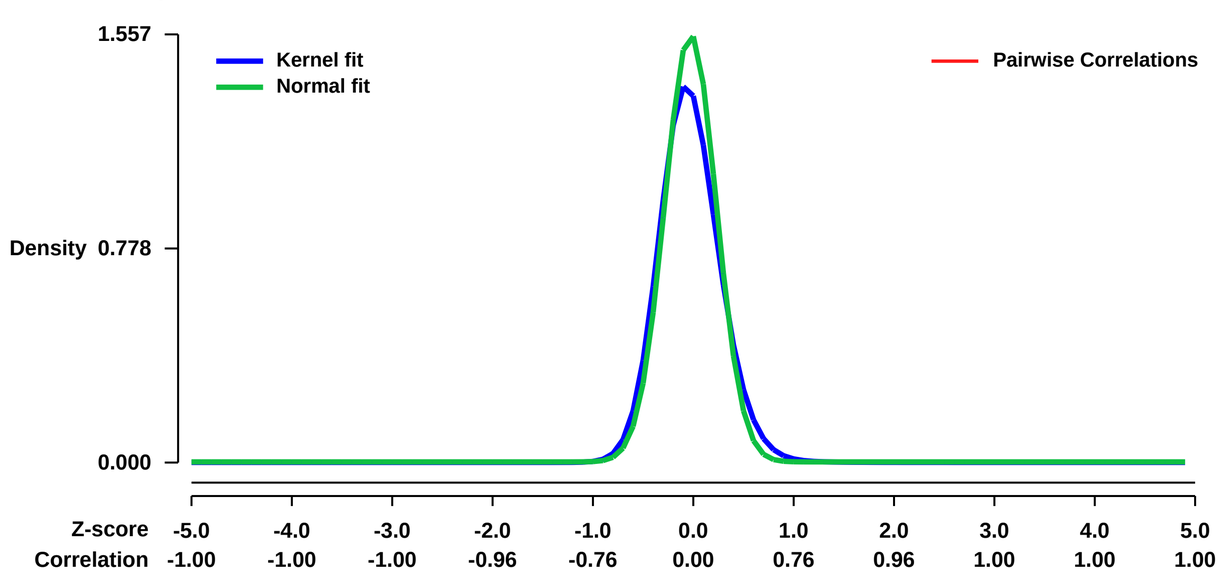

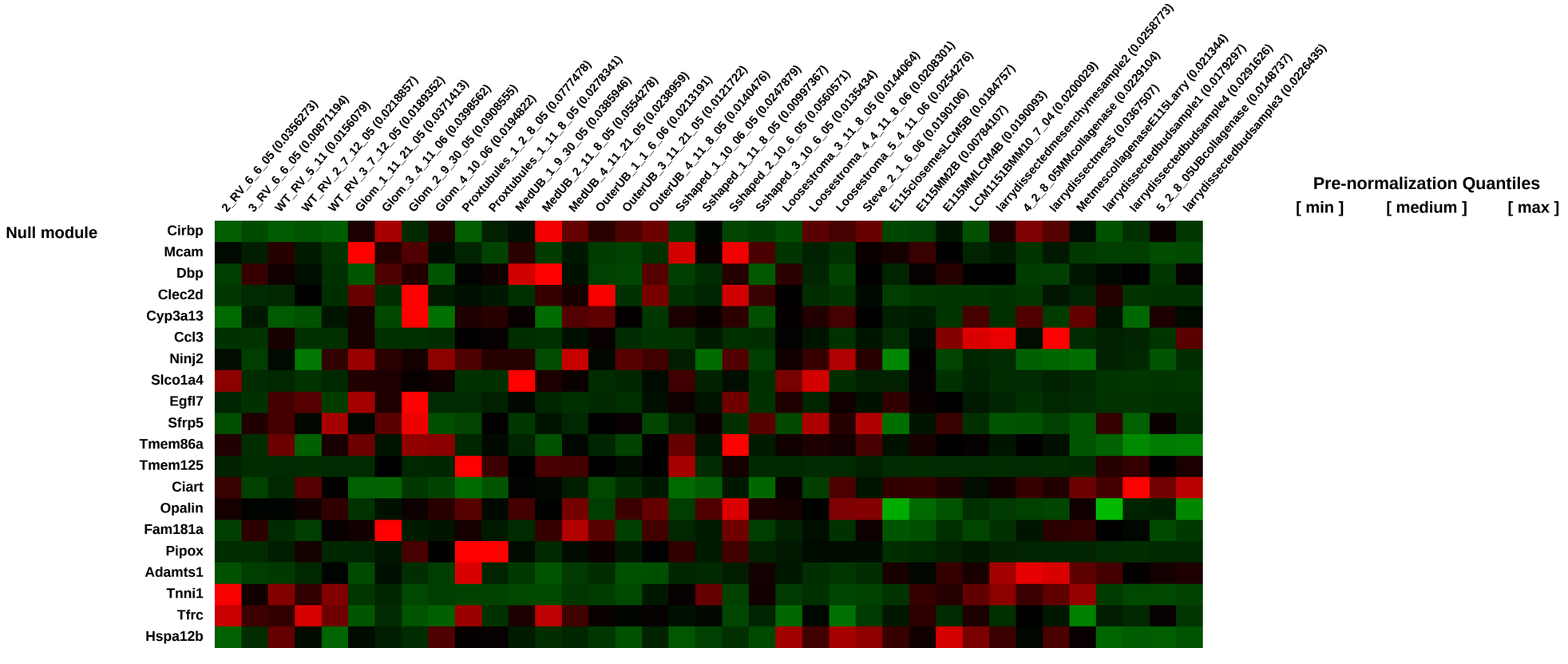

GEO Series "GSE18064" Expression Profiles

Num of samples in this series: 12

Scale of expression profile Z-scores

-3.0 -2.0 -1.0 0.0 1.0 2.0 3.0

GEO Link:	http://www.ncbi.nlm.nih.gov/geo/query/acc.cgi?acc=GSE18064
Status:	Public on Aug 31 2010
Title:	Comparison of MBT/Pas and BALB/cByJ MEFs response after infection with Rift Valley Fever virus
Organism:	Mus musculus
Experiment type:	Expression profiling by array
Platform:	GPL1261
Pubmed ID:	20937849
Summary & Design:	**Summary:** The Rift Valley Fever (RVF) is an arthropod-borne disease present in several countries of Africa and Middle East. It is caused by RVF virus which can infect both humans and animals. In humans, it leads to various manifestations including hepatitis, encephalitis and death, while in domestic animals it usually causes miscarriage in pregnant females and it is often fatal for the newborn. Not all people or animal infected by the virus present the same disease. Some patients exhibit unapparent or moderate febrile reactions, while others develop severe symptoms. This observation suggests that host genetic factors play a role in controlling the outcome of infection. In this work, we compare the response of two different inbred strains of mice, MBT/Pas and BALB/cByJ, to infection with RVF virus. These strains exhibit different profiles of susceptibility to RVF virus infection. Indeed, MBT/Pas mice rapidly develop high viraemia and die soon after infection, while BALB/cByJ mice have a lower viraemia and die later. Interestingly, mouse embryonic fibroblasts (MEFs) obtained from MBT/Pas foetuses allows higher viral production than BALB/cByJ MEFs. **Keywords:** expression profiling **Overall design:** The experiment was designed to include ARN samples from MBT/Pas and BALB/cByJ MEFs infected with the Rift Valley Fever (RVF) virus, and their respective mock-infected controls; each one of those in triplicate. Therefore, we have used 12 different samples for the study, divided as follows: 3 samples of RVF virus-infected BALB/cByJ MEFs, 3 samples of mock-infected BALB/cByJ MEFs, 3 samples of RVF virus-infected MBT/Pas MEFs and 3 samples of mock-infected MBT/Pas MEFs. Each RNA was extracted from a different culture well.

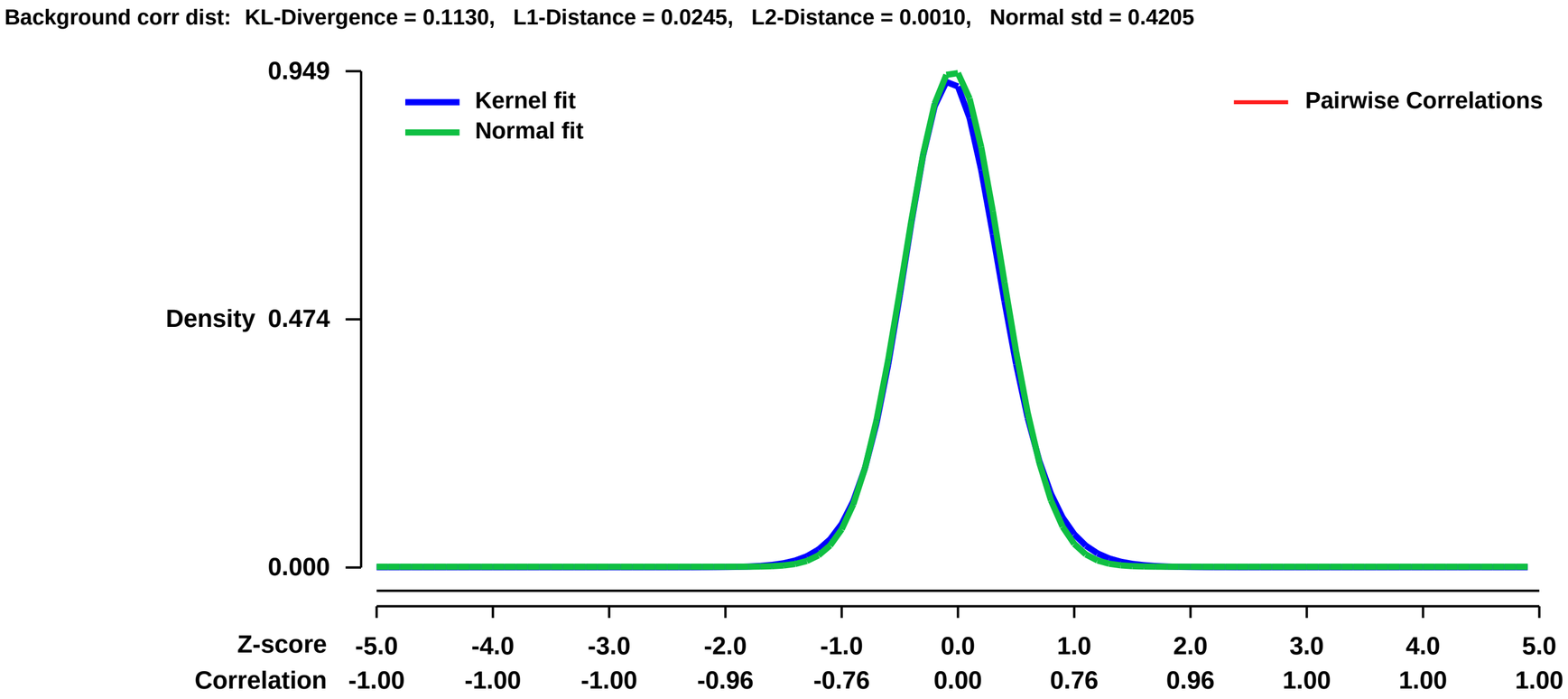

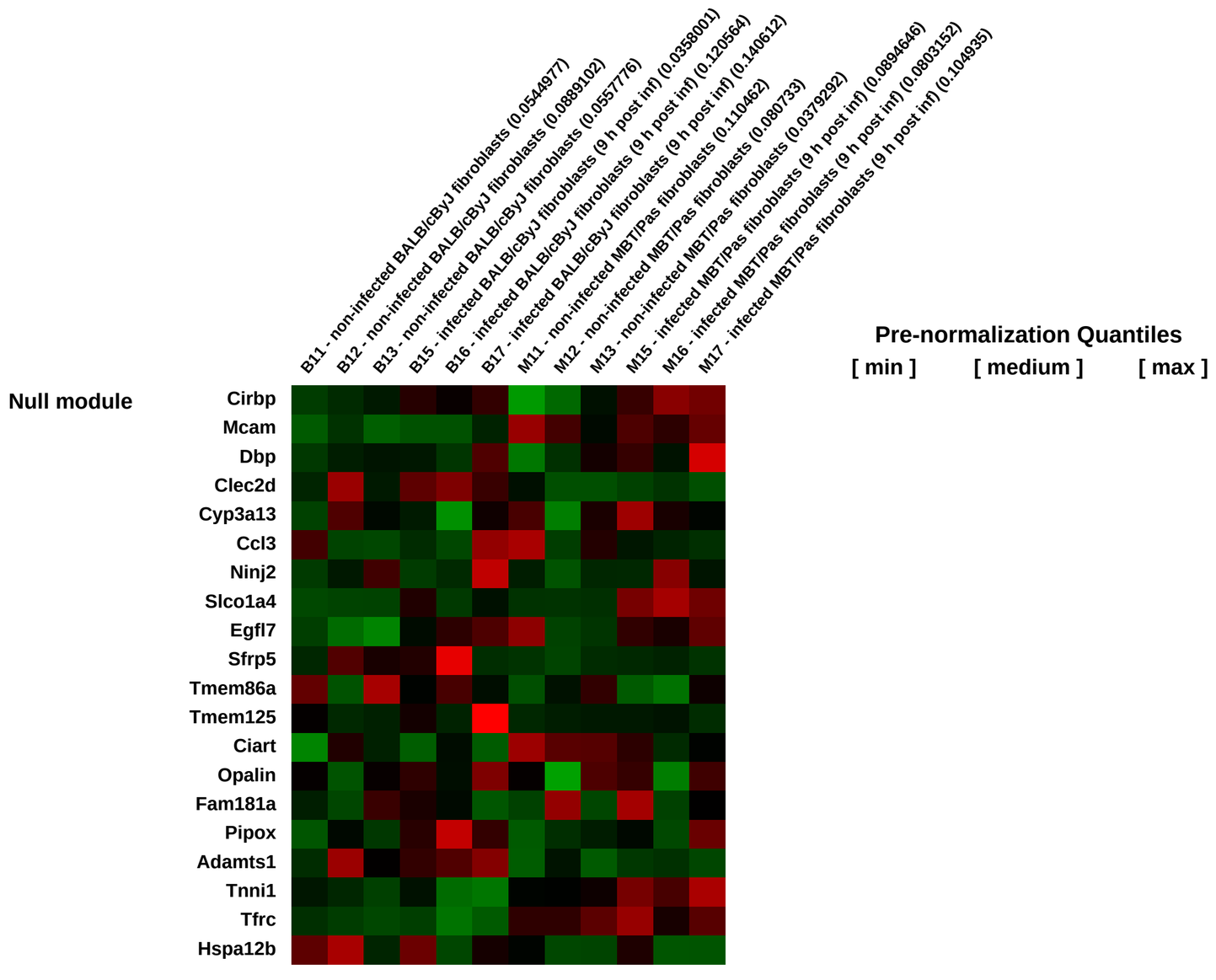

GEO Series "GSE31561" Expression Profiles

Num of samples in this series: 36

Scale of expression profile Z-scores

-3.0 -2.0 -1.0 0.0 1.0 2.0 3.0

GEO Link:	http://www.ncbi.nlm.nih.gov/geo/query/acc.cgi?acc=GSE31561
Status:	Public on Feb 19 2013
Title:	Transcriptional analysis of organ-specific toxicity induced by a panPPAR agonist in mice: Identification of organ-specific toxicity biomarkers
Organism:	Mus musculus
Experiment type:	Expression profiling by array
Platform:	GPL1261
Pubmed ID:	23272042
Summary & Design:	**Summary:** In this study, we aim to identify candidate biomarkers which may be useful as surrogate indicators of toxicity for pre-clinical development of panPPAR-agonist drug candidates. Gene expression microarray, histopathology and clinical chemistry data were generated from liver, heart, kidney and skeletal muscles of three groups of mice administered with three different dosages of an experimental pan-peroxisome proliferator-activated receptor (pan-PPAR) agonist, PPM-201, for 14 days. The histopathology and clinical chemistry data were compared with the gene expression analysis and candidate biomarker genes were identified. **Overall design:** Nine wild type mice (strain: C57BL/6J) were randomly divided into three groups - Group-I, II and III. PPM-201 in the vehicle base was administered daily for 14 days at 6 mg/kg body weight dose rate to each mouse in Group-II and at 20mg/kg body weight dose rate to each mouse in Group-III while the mice in Group-I received only the vehicle base. On 15th day, the mice were sacrificed to harvest blood, heart, skeletal muscle, liver and kidney tissues for clinical chemistry, microarray and histopathology analysis. In the clinical chemistry analysis, alanine aminotransferase (ALT, U/L), aspartate aminotransferase (AST, U/L), creatinine kinase (CK, U/L), blood urea nitrogen (BUN, mmol/L), creatinine (umol/L) and lactate dehydrogenase (LDH, U/L) were measured from the blood of each mouse. Two sections of liver, two sections of kidney, one or two sections of skeletal muscle, and one section of heart were prepared from each mouse, stained with hematoxylin and eosin (H&E), and examined by a veterinary pathologist. RNA was extracted and processed as per the established protocol from heart, skeletal muscle, liver and kidney tissue samples of all the 9 mice for profiling with Affymetrix Mouse Genome 430 2.0 Array and in total 36 chips were prepared. Using various quality control measures, the data was analysed for its quality. As it was found to be good in quality, the data from all the 36 chips were used for further analysis. The results from histopathology and clinical chemistry analysis were compared with the gene expression to determine if the dosages selected for the study were associated with findings in target organs.

Background corr dist: KL-Divergence = 0.0965, L1-Distance = 0.0540, L2-Distance = 0.0060, Normal std = 0.4768

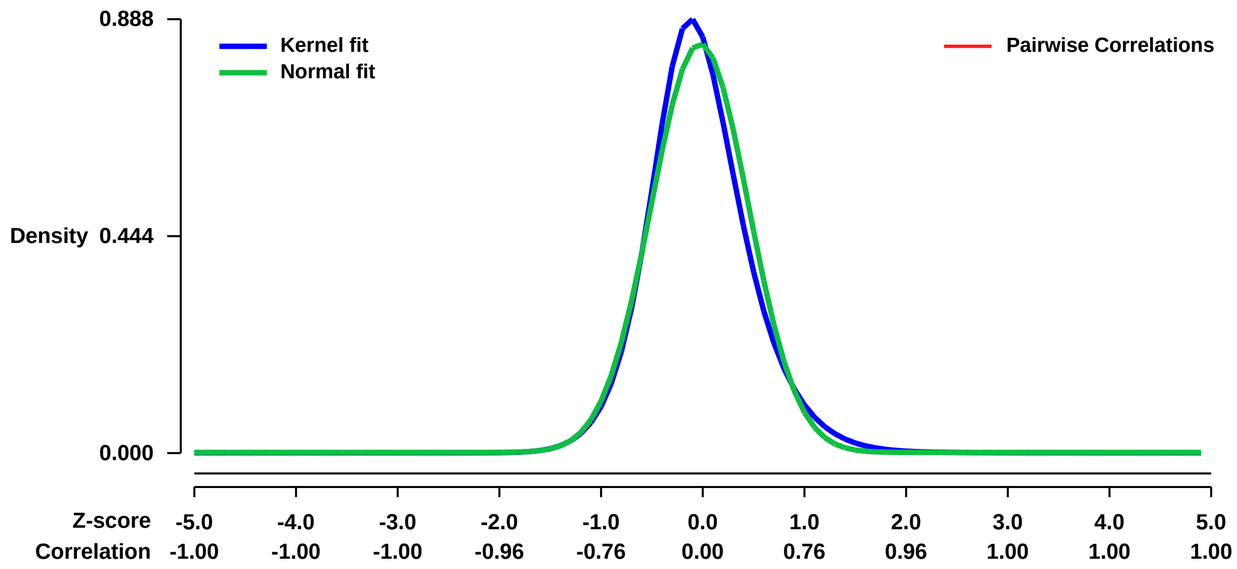

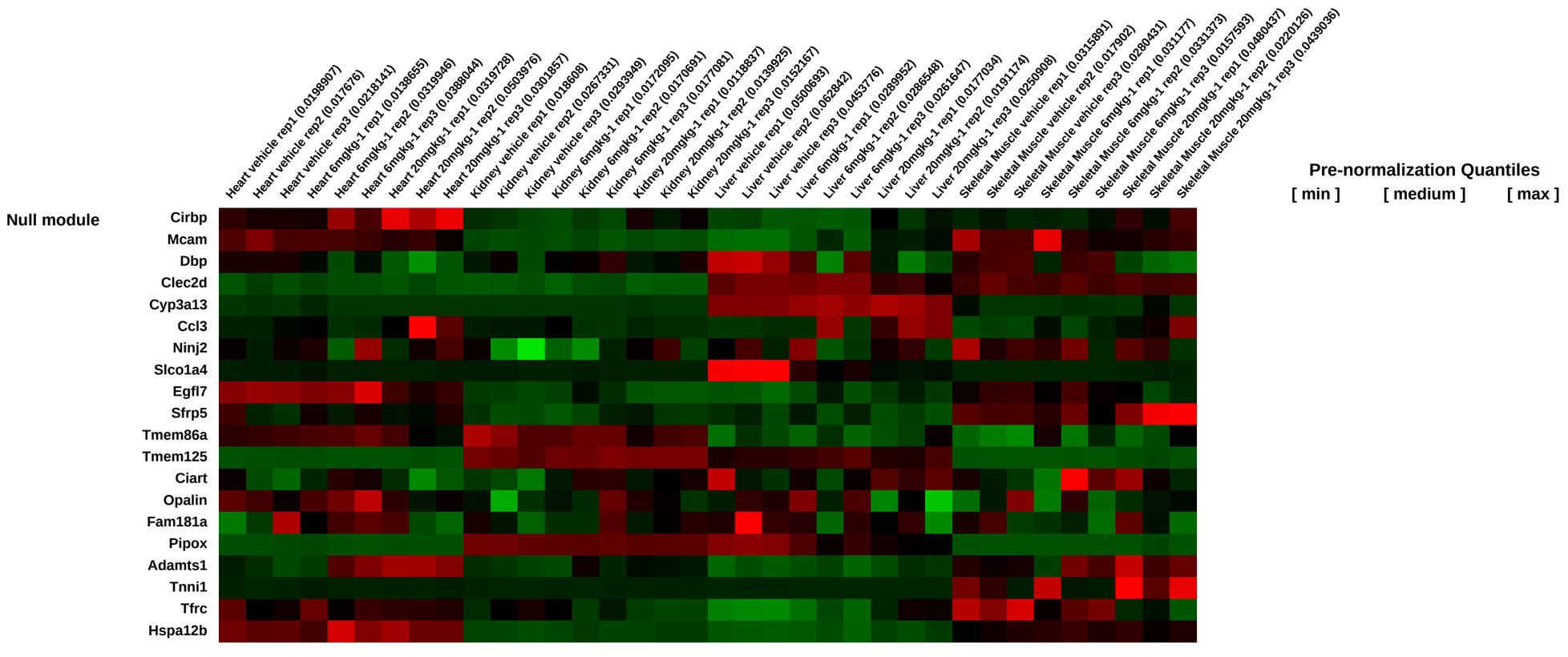

GEO Series "GSE6591" Expression Profiles

Num of samples in this series: 15

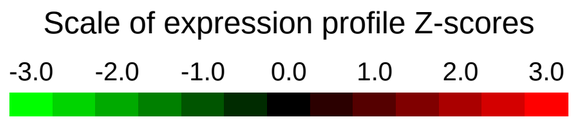

GEO Link:	http://www.ncbi.nlm.nih.gov/geo/query/acc.cgi?acc=GSE6591
Status:	Public on Aug 31 2007
Title:	Comparative analysis of gene expression in C57BL/6J and DBA/2J aging lungs.
Organism:	Mus musculus
Experiment type:	Expression profiling by array
Platform:	GPL1261
Pubmed ID:	17726092
Summary & Design:	**Summary:** We hypothesize that gene expression in the aging lungs of these two strains of mice are divergent thus contributing to the disparity in the phenotypes. More specifically, (1) Aging DBA/2J mice compared to aging C57BL/6 mice are known to be accelerated in their lung physiology and morphometry; (2) C57BL/6J are known to have longer natural longevity than DBA/2J mice. In order to test these hypotheses at the gene expression level, we utilized microarray analysis to examine transcriptional differences between aging lungs of both strains of mice. **Keywords: comparative expression profiling** **Overall design:** This study utilizes microarray analysis to test these hypotheses. Three sets of lungs were harvested from both strains at each time point (C57BL/6J: 2, 18, AND 26 mos; DBA/2J: 2 and 18 mos). RNA was isolated and used for global gene expression profiling (Affymetrix Mouse 430 2.0 array). Statistically significant gene expression was determined as a minimum 6 counts of 9 pairwise comparisons, minimum 1.5-fold change, and p < 0.05. Further, Absolute | FC - FC SEM | >= 1.5.

Background corr dist: KL-Divergence = 0.1652, L1-Distance = 0.0405, L2-Distance = 0.0034, Normal std = 0.3584

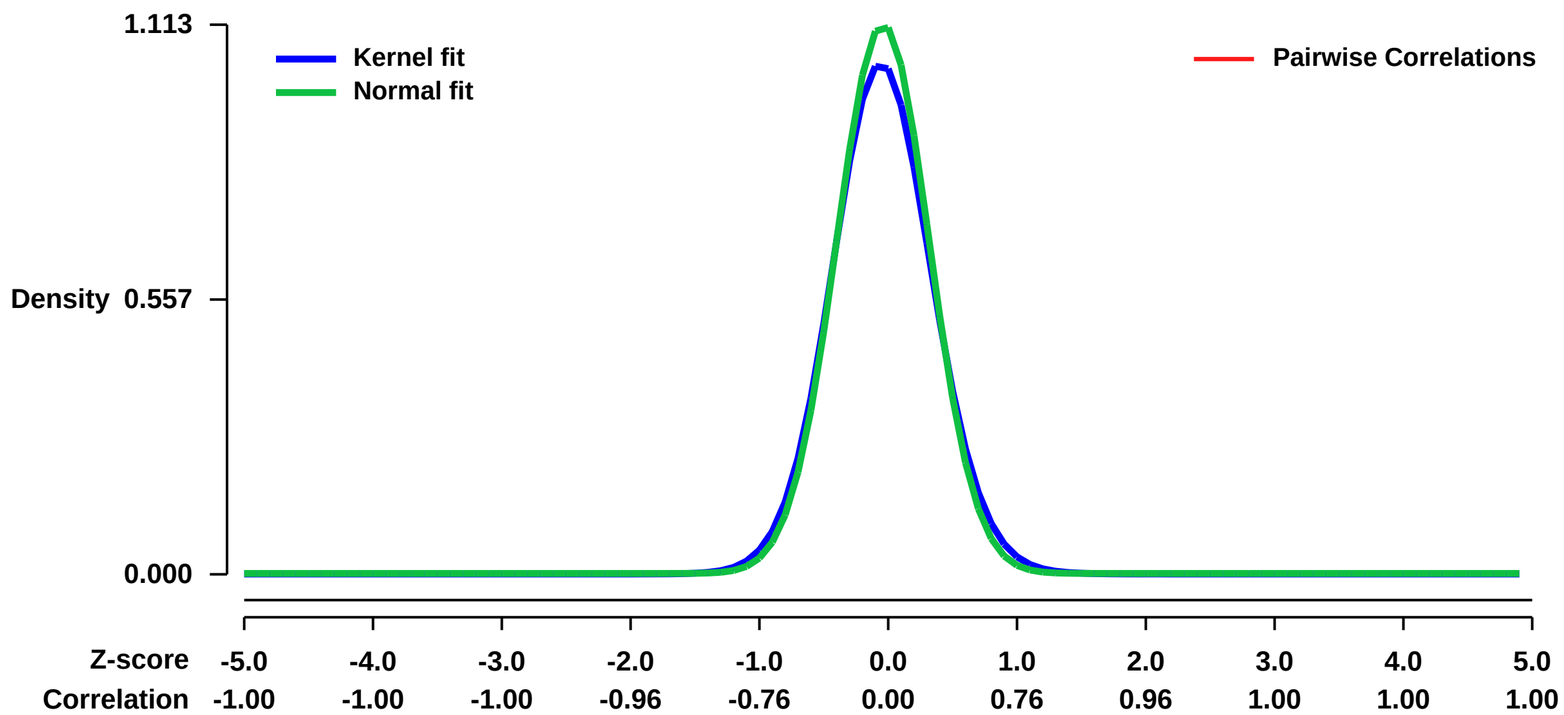

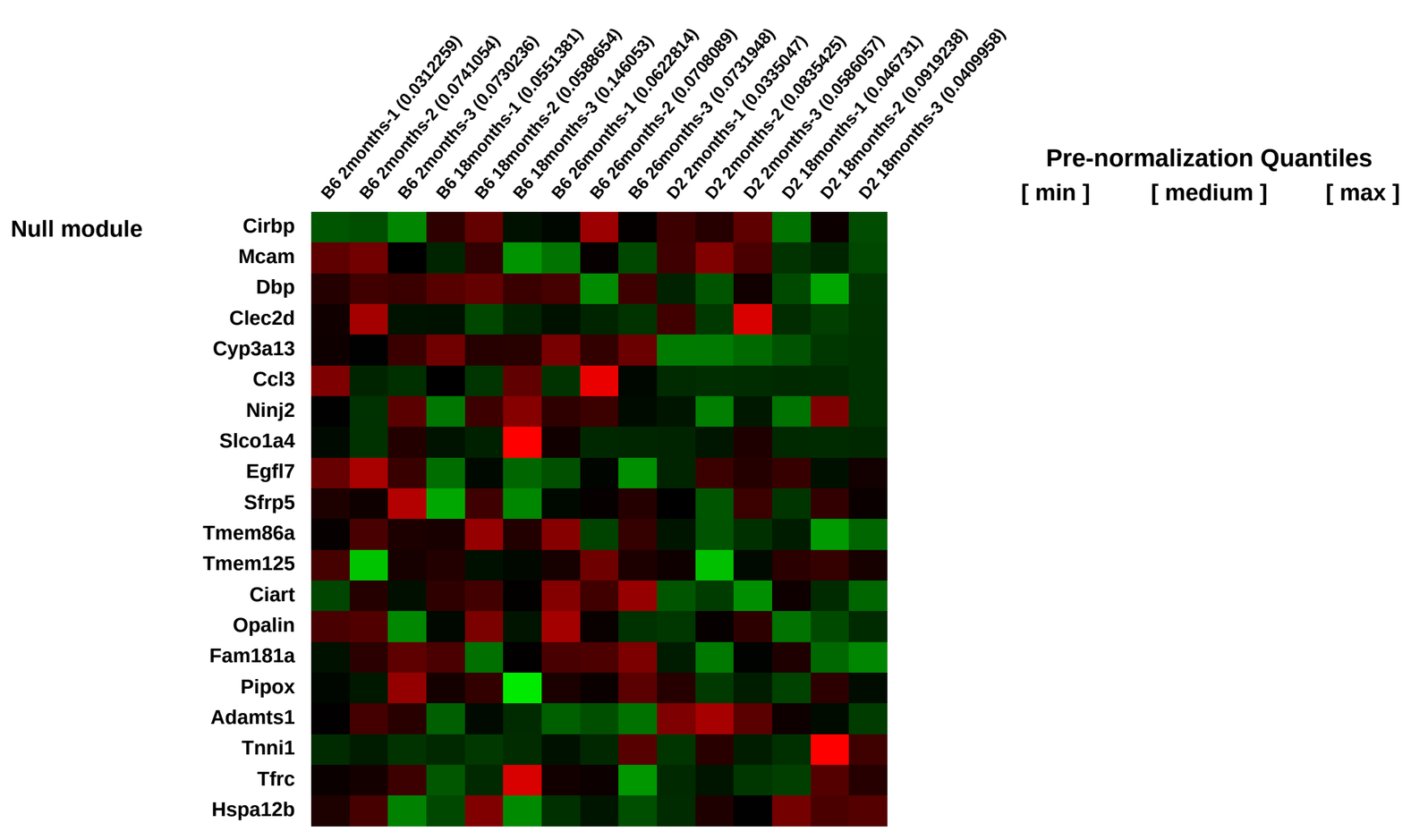

GEO Series "GSE11628" Expression Profiles

Num of samples in this series: 12

Scale of expression profile Z-scores

-3.0 -2.0 -1.0 0.0 1.0 2.0 3.0

GEO Link:	**http://www.ncbi.nlm.nih.gov/geo/query/acc.cgi?acc=GSE11628**
Status:	**Public on Dec 31 2009**
Title:	**Wnt & LIF signalling in mESC**
Organism:	**Mus musculus**
Experiment type:	**Expression profiling by array**
Platform:	**GPL1261**
Pubmed ID:	
Summary & Design:	**Summary:** **The molecular processes underlying the properties of ESC are yet unknown even when it's well established that LIF/STAT3 is neccesary for the maintenance of pluripotency. Other pathways as Wnt are may be implicated in the regulation of the biological mechanisms in mESC. Work model: D3-ES cultivated with or without LIF and treated with chronic (7 days) low doses (50nM) of GSK3 ¸† inhibitor (lithium).** **We used microarrays to detail the global profile of gene expression to identified different groups of up and down-regulated genes in the work model.** **Overall design:** **mESC cultivated as it has been defined in the work model were prepared for RNA extraction and hybridization on Affymetrix microarrays. We analyzed 3 independent experiments per replicate, and we did three replicates per sample.**

Background corr dist: **KL-Divergence = 0.0952, L1-Distance = 0.0254, L2-Distance = 0.0010, Normal std = 0.4504**

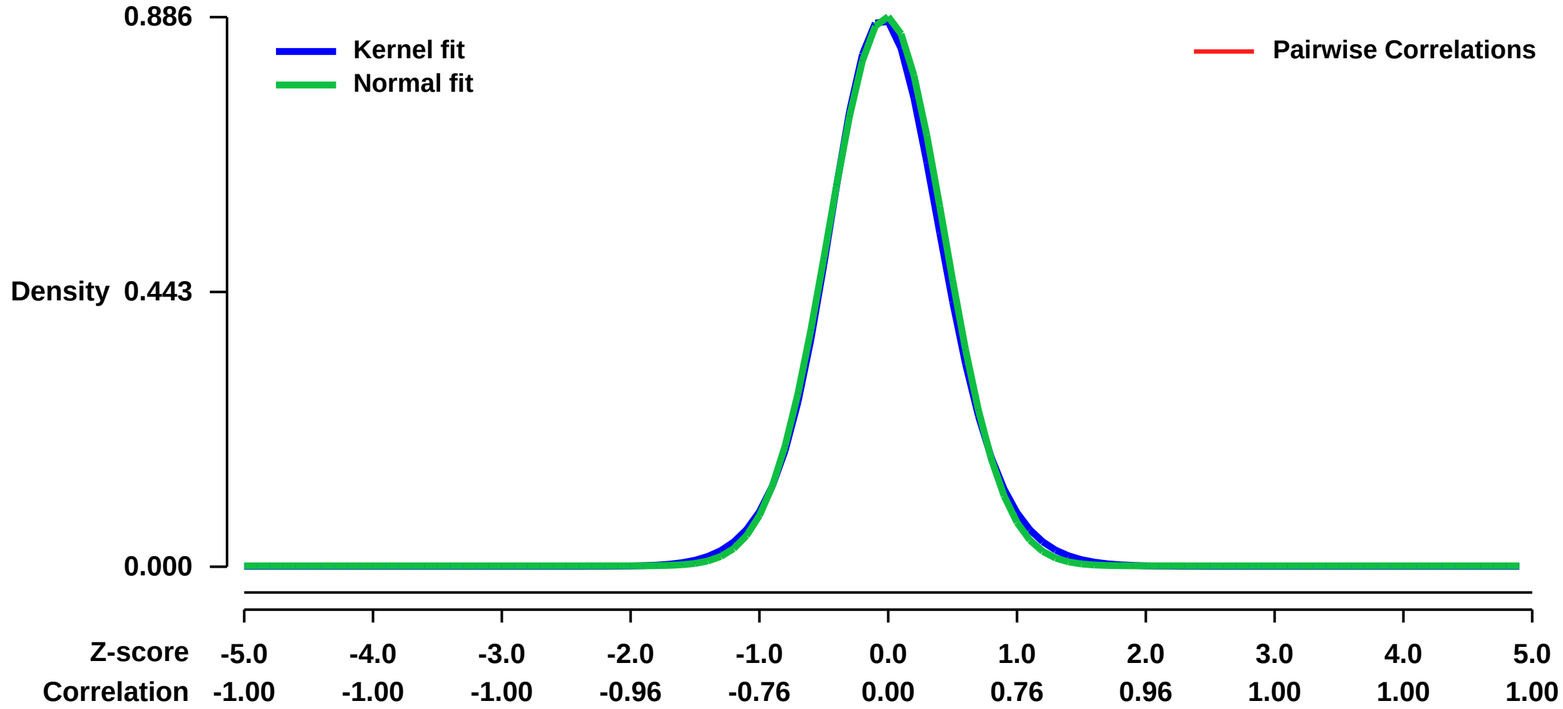

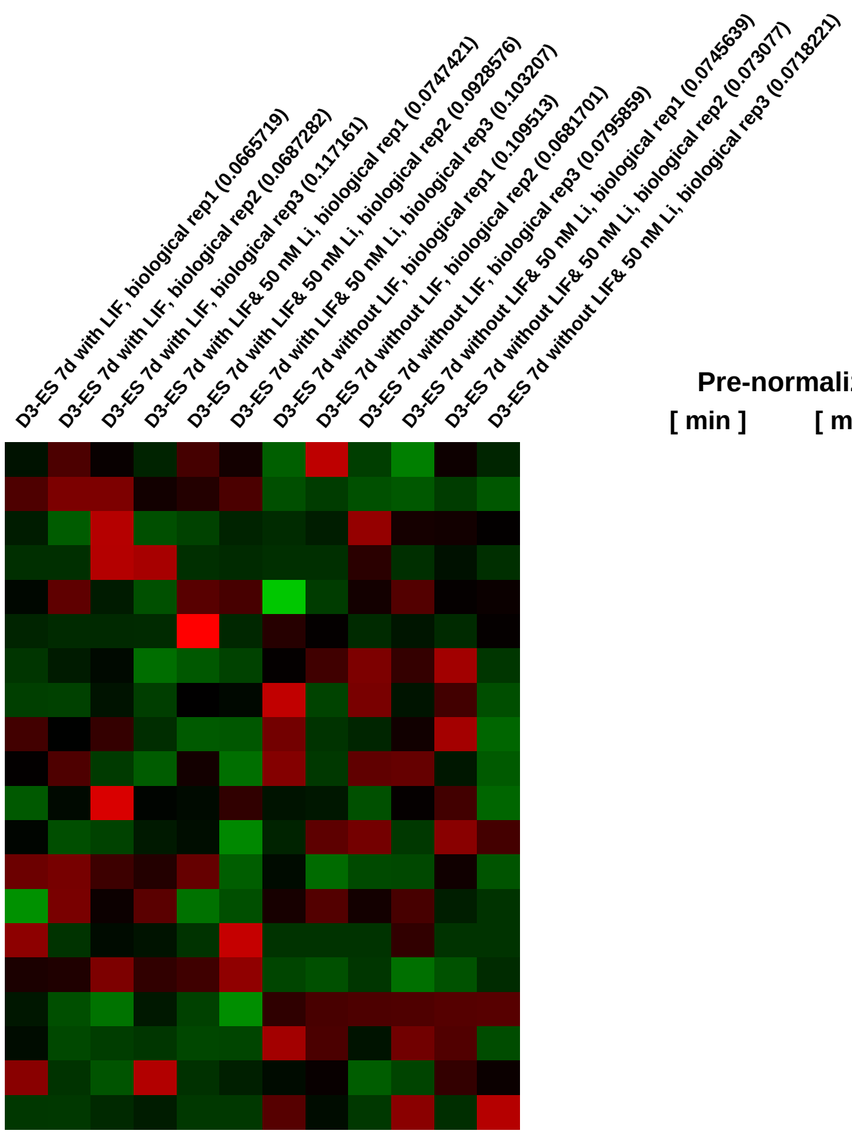

GEO Series "GSE7798" Expression Profiles

Num of samples in this series: 16

Scale of expression profile Z-scores

-3.0 -2.0 -1.0 0.0 1.0 2.0 3.0

GEO Link:	http://www.ncbi.nlm.nih.gov/geo/query/acc.cgi?acc=GSE7798
Status:	Public on Jun 01 2007
Title:	Osteoclastic estrogen receptor alpha mediates the osteoprotective estrogen action through Fas ligand signaling
Organism:	Mus musculus
Experiment type:	Expression profiling by array
Platform:	GPL1261
Pubmed ID:	17803905
Summary & Design:	**Summary:** Estrogen clearly prevents osteoporotic bone loss by attenuating bone resorption. The molecular basis of how this is accomplished, however, remains elusive. Here we report a critical role of osteoclastic ERa in mediating estrogen action on bone in females. We selectively ablated ERa in differentiated osteoclasts (ERa dOc/dOc). ERa dOc/dOc females, but not males, exhibited clear trabecular bone loss, similar to the osteoporotic bone phenotype in post-menopausal women. Recovery of bone loss by estrogen treatment of the ovariectomized ERa dOc/dOc females was ineffective in the trabecular areas of the long bones and lumbar vertebral bodies. Osteoclastic apoptosis, induced by estrogen, occurred simultaneously with up-regulation of Fas ligand (FasL) expression in intact trabecular bones of ERa +/+mice, but not in ERa dOc/dOc mice. ERa was also required for similar effects of estrogen and tamoxifen in cultured osteoclasts. These findings suggest that the osteoprotective actions of estrogen and SERMS are mediated at least in part through osteoclastic ERa in trabecular bone; and the life span of mature osteoclasts is regulated through activation of the Fas/FasL system. **Keywords:** Study about estrogen response of osteoclast-specific estrogen receptor alpha mice **Overall design:** Wild type and osteoclast-specific Estrogen Receptor alpha knock-out mice were ovariectomized. The number of both genotypes of mice was eight. The mice of each genotypes were divided to vehicle control and estrogen treated group. Four hours after chemical treatment, the distal 5 mm of the left femurs were harvested after sacrificing by cervical dislocation and total RNAs were purified for Affymetix GeneChip microarray analysis without pooling. Therefore, this experiment consists of four groups with four replicates per group.

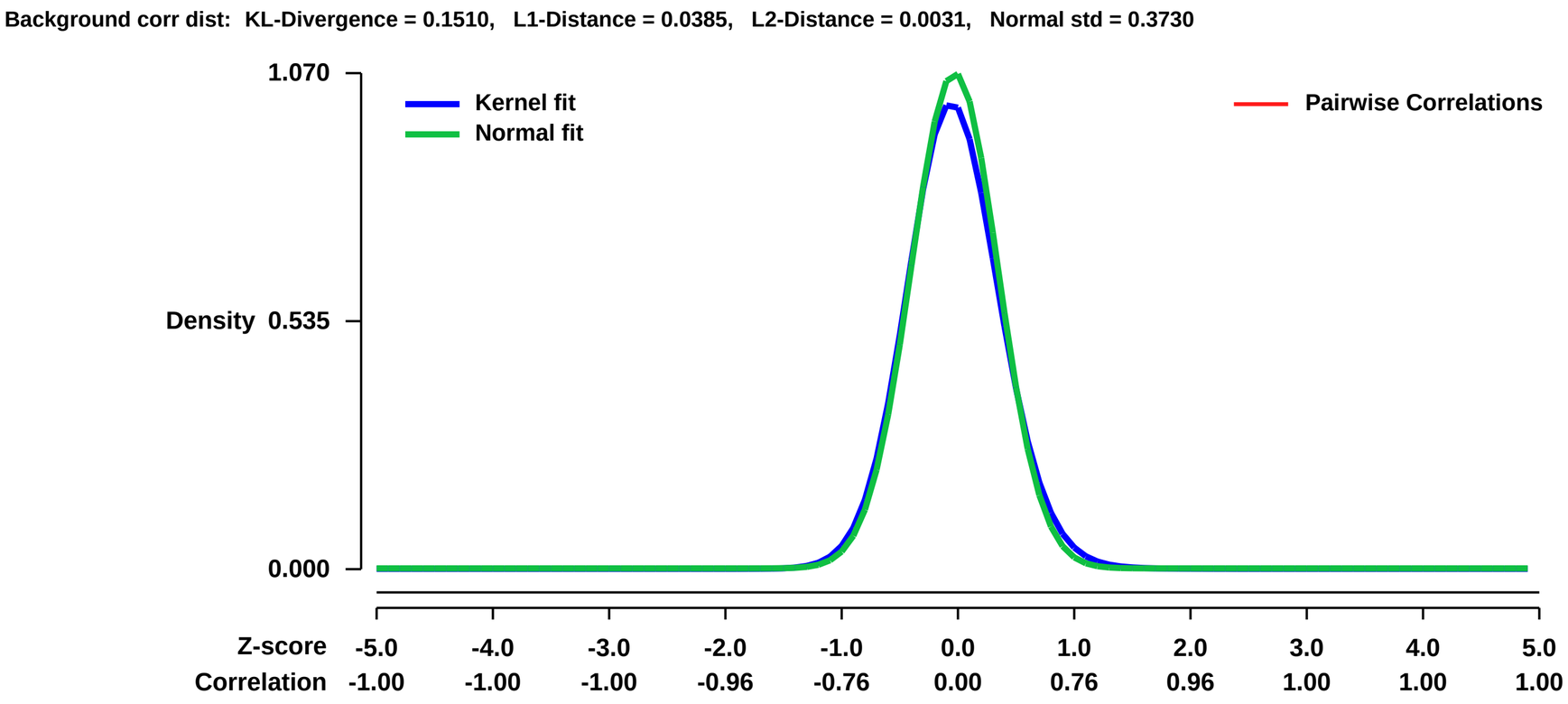

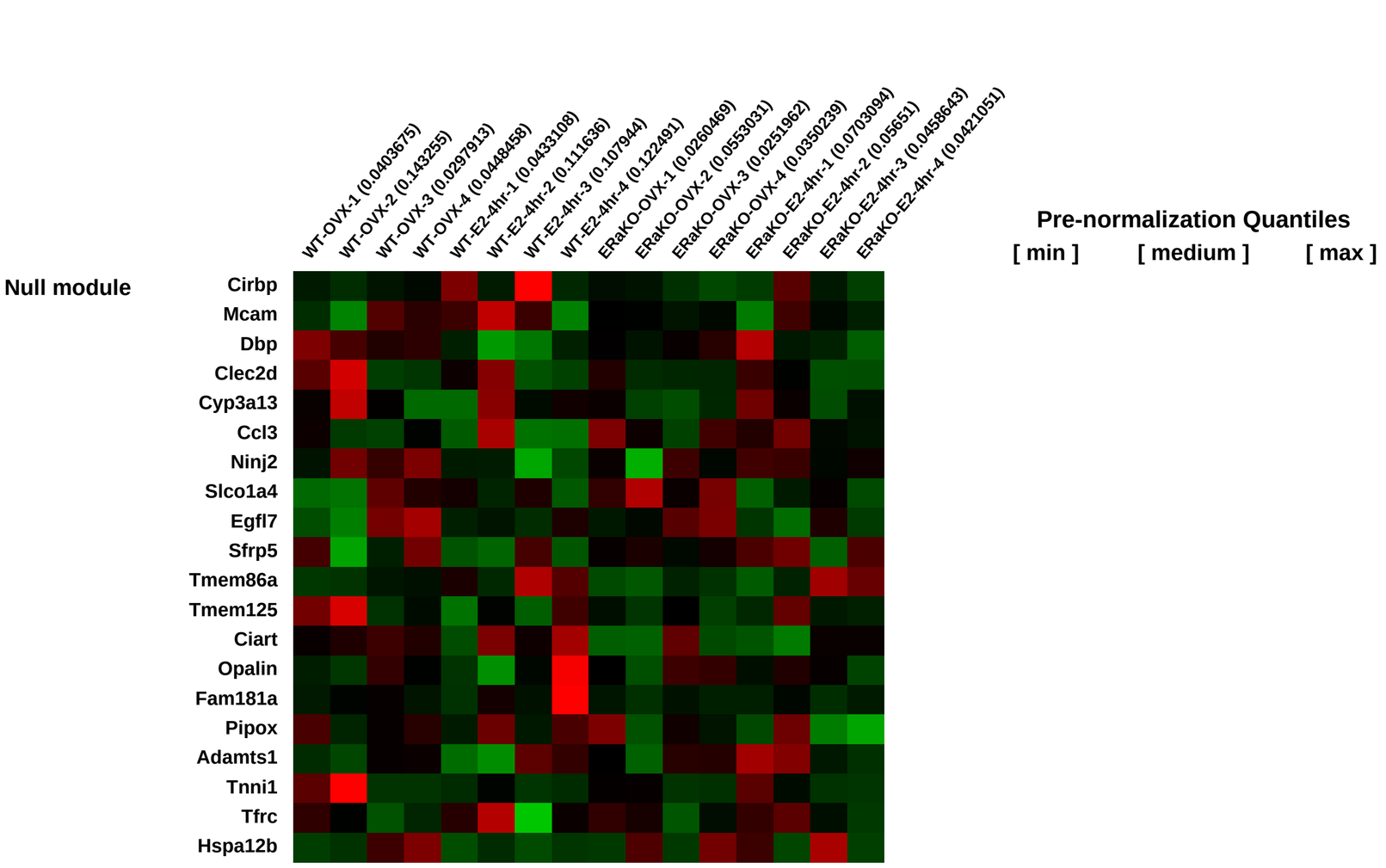

GEO Series "GSE8312" Expression Profiles

Num of samples in this series: 6

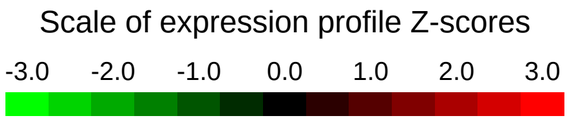

GEO Link:	http://www.ncbi.nlm.nih.gov/geo/query/acc.cgi?acc=GSE8312
Status:	Public on Dec 23 2007
Title:	Enhancing integrin alpha7 expression effect on myoblast transcription
Organism:	Mus musculus
Experiment type:	Expression profiling by array
Platform:	GPL1261
Pubmed ID:	18045857
Summary & Design:	**Summary:** Analysis of C2C12 myoblast induced with tetracycline to enhance integrin alpha7 expression. Integrin alpha7 is the major laminin binding integrin in muscle cells. Enhancing its expression has been demonstrated to alleviate pathology in a murine model of Duchenne muscular dystrophy. Results of this study provide insights into the effects of increasing integirn alpha7 expression on muscle cells and possible side effects associate with enhancing integrin alpha7 in muscle cells. **Keywords:** comparitive of integrin lapha7 induced and non-induced c2C12 myobalst **Overall design:** Triplicate biological smaples for each condition(induced and non-induced) C2C12 myoblast were used.

Background corr dist: KL-Divergence = 0.0480, L1-Distance = 0.0208, L2-Distance = 0.0005, Normal std = 0.5830

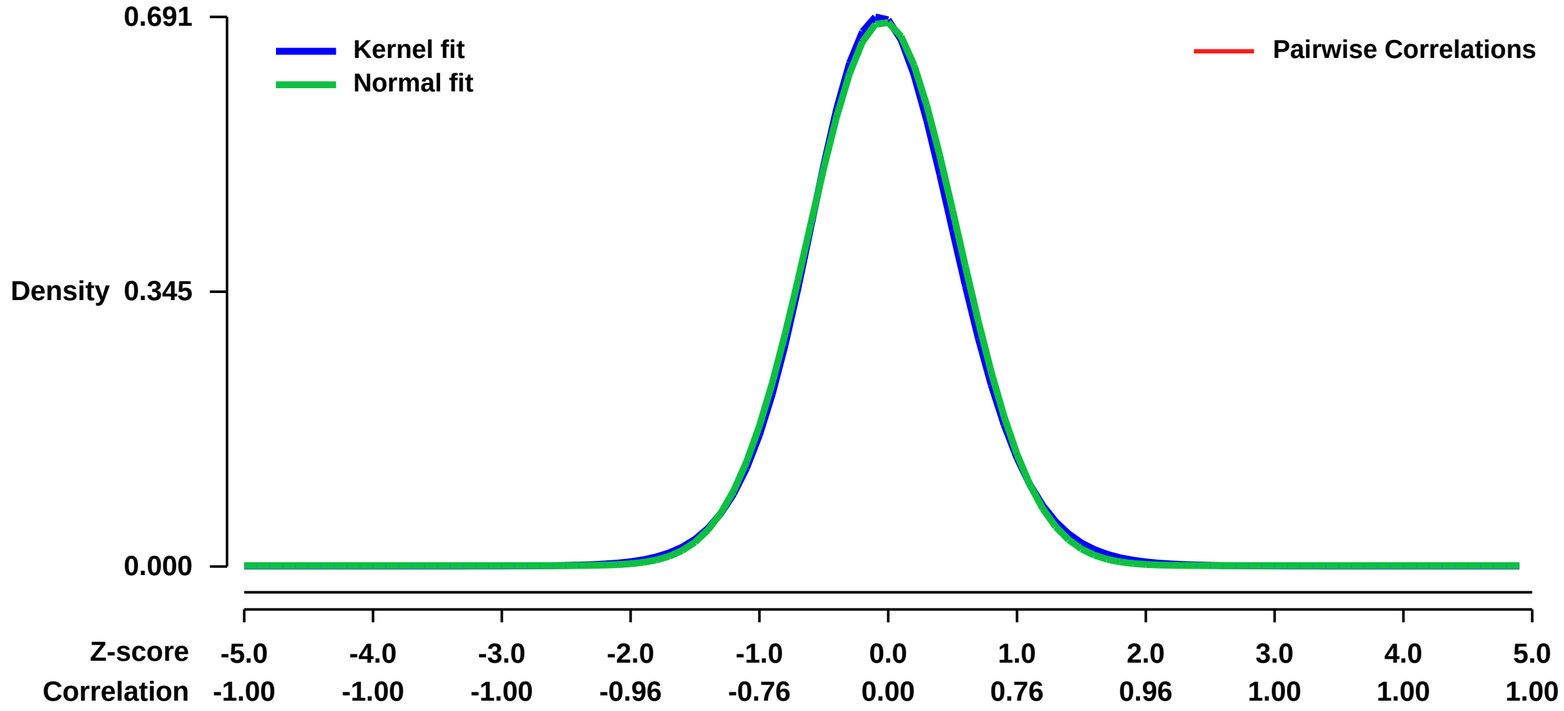

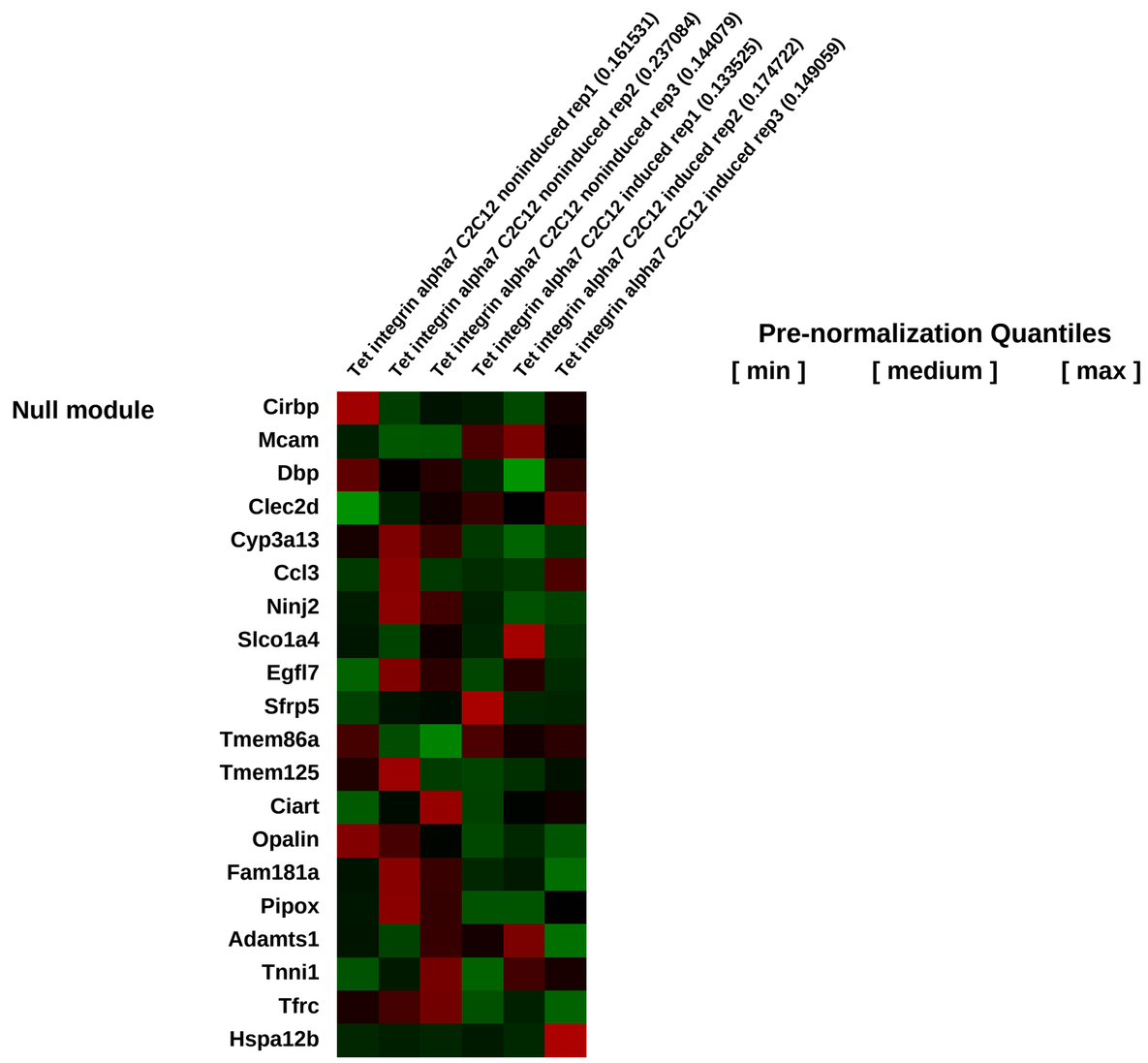

GEO Series "GSE46185" Expression Profiles

Num of samples in this series: 6

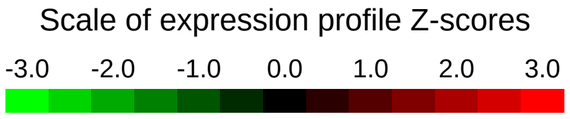

GEO Link:	http://www.ncbi.nlm.nih.gov/geo/query/acc.cgi?acc=GSE46185
Status:	Public on Apr 19 2013
Title:	Genome-wide gene expression profiling revealed a critical role for GATA3 in the maintenance of the Th2 cell identity
Organism:	Mus musculus
Experiment type:	Expression profiling by array
Platform:	GPL1261
Pubmed ID:	23824597
Summary & Design:	**Summary:** Functionally polarized CD4+ T helper (Th) cells such as Th1, Th2 and Th17 cells are central to the regulation of acquired immunity. However, the molecular mechanisms governing the maintenance of the polarized functions of Th cells remain unclear. GATA3, a master regulator of Th2 cell differentiation, initiates the expressions of Th2 cytokine genes and other Th2-specific genes. GATA3 also plays important roles in maintaining Th2 cell function and in continuous chromatin remodeling of Th2 cytokine gene loci. However, it is unclear whether continuous expression of GATA3 is required to maintain the expression of various other Th2-specific genes. In this report, genome-wide DNA gene expression profiling revealed that GATA3 expression is critical for the expression of a certain set of Th2-specific genes. We demonstrated that GATA3 dependency is reduced for some Th2-specific genes in fully developed Th2 cells compared to that observed in effector Th2 cells, whereas it is unchanged for other genes. Moreover, effects of a loss of GATA3 expression in Th2 cells on the expression of cytokine and cytokine receptor genes were examined in detail. A critical role of GATA3 in the regulation of Th2-specific gene expression is confirmed in in vivo generated antigen-specific memory Th2 cells. Therefore, GATA3 is required for the continuous expression of the majority of Th2-specific genes involved in maintaining the Th2 cell identity. **Overall design:** Mock-transfected and GATA3 siRNA-transfected Th2 and Th2-4th cells are profiled for mRNA expression

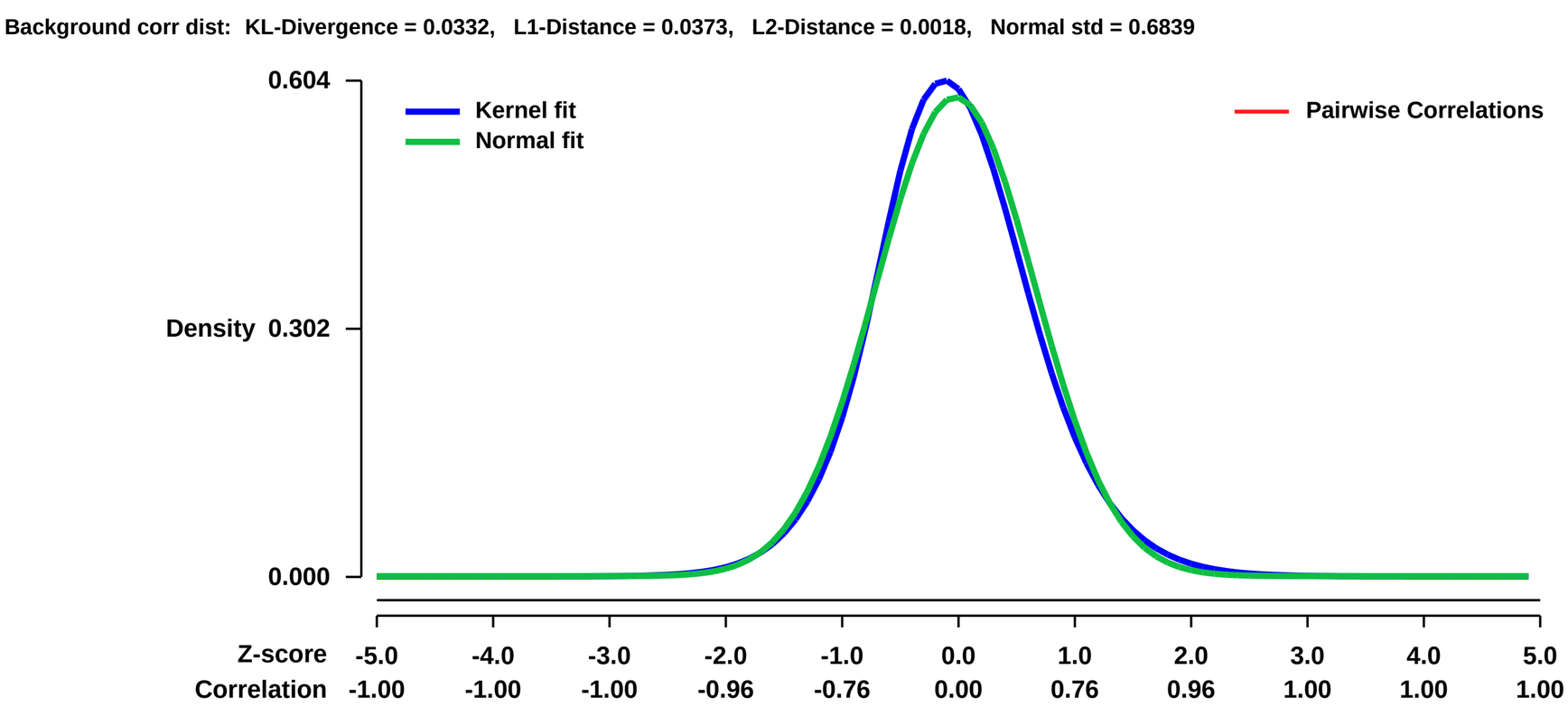

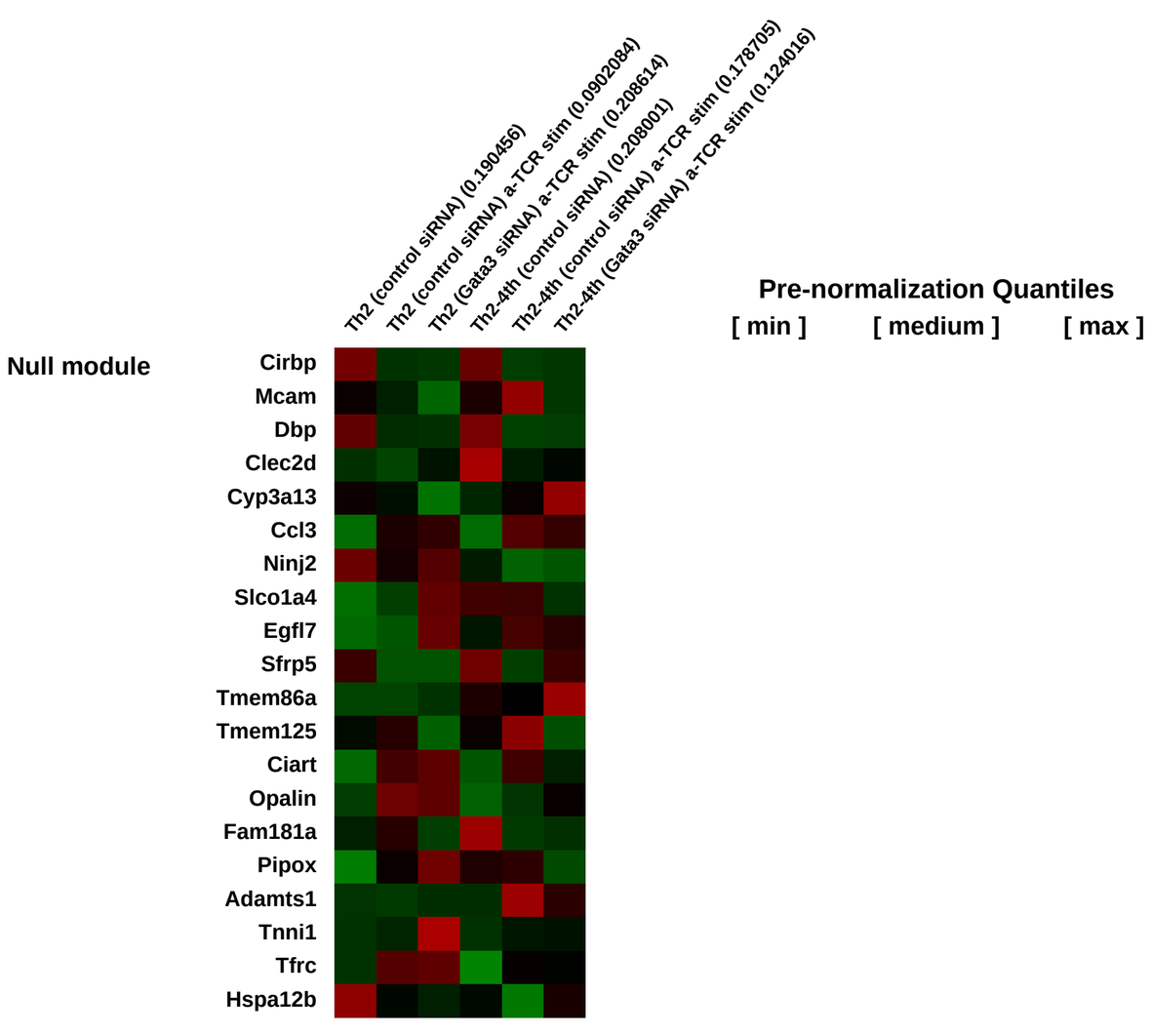

GEO Series "GSE8357" Expression Profiles

Num of samples in this series: 6

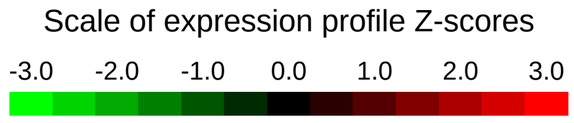

GEO Link:	**http://www.ncbi.nlm.nih.gov/geo/query/acc.cgi?acc=GSE8357**
Status:	**Public on Dec 31 2007**
Title:	**Functional analysis of exon 2 of p130Cas in fibroblasts derived from exon 2-specific knockout mice.**
Organism:	**Mus musculus**
Experiment type:	**Expression profiling by array**
Platform:	**GPL1261**
Pubmed ID:	

Summary & Design:

Summary:
p130Cas (Cas, Crk-associated substrate) is an adaptor molecule composed of an N-terminal Src homology 3 (SH3) domain, a substrate domain (SD), and a C-terminal Src binding domain (SBD). The SH3 domain of Cas has been shown to associate with various signaling molecules, including focal adhesion kinase (FAK), but its role in cellular function remains unclear. To address this issue, we established and analyzed primary fibroblasts derived from mice expressing a truncated Cas lacking the exon 2 encoding the SH3 domain (Cas exon 2â /â). In comparison to wild-type (Cas exon 2+/+) cells, Cas exon 2â /â primary fibroblasts showed delayed migration in wound healing and reduced spreading on fibronectin (FN), which would be due to reduced complex formation of Cas exon 2â /â with FAK and CrkII and also to impaired localization of Cas exon 2â /â to focal adhesions on FN. In addition, to analyze downstream signaling pathway regulated by Cas exon 2, we compared gene expression profiles between Cas exon 2+/+ and Cas exon 2â /â cells by a microarray analysis. Interestingly, we found that Cas exon 2-deficiency upregulated expression of CXC Chemokine Receptor-4 (CXCR4), CC Chemokine Receptor-5 (CCR5), and thrombospondin 4, which are implicated in cell motility and adhesion. These results define the role of Cas SH3-encoding exon in cell motility, FAK/Cas/CrkII complex formation, recruitment of Cas to focal adhesions, and regulation of cell adhesion-associated gene expression in primary fibroblasts.

Keywords: SH3-encoding exon, p130Cas

Overall design:
RNA samples extracted from Cas exon 2+/+, Cas exon 2+/â , and Cas exon 2â /â fibroblasts (12.5dpc, two embryos for each genotype) were labeled and hybridized on Affymetrix microarray. Gene expression patterns of Cas exon 2â /â fibroblasts were compared with those of Cas exon 2+/+ and Cas exon 2+/â cells.

Background corr dist: **KL-Divergence = 0.0415, L1-Distance = 0.0221, L2-Distance = 0.0005, Normal std = 0.6121**

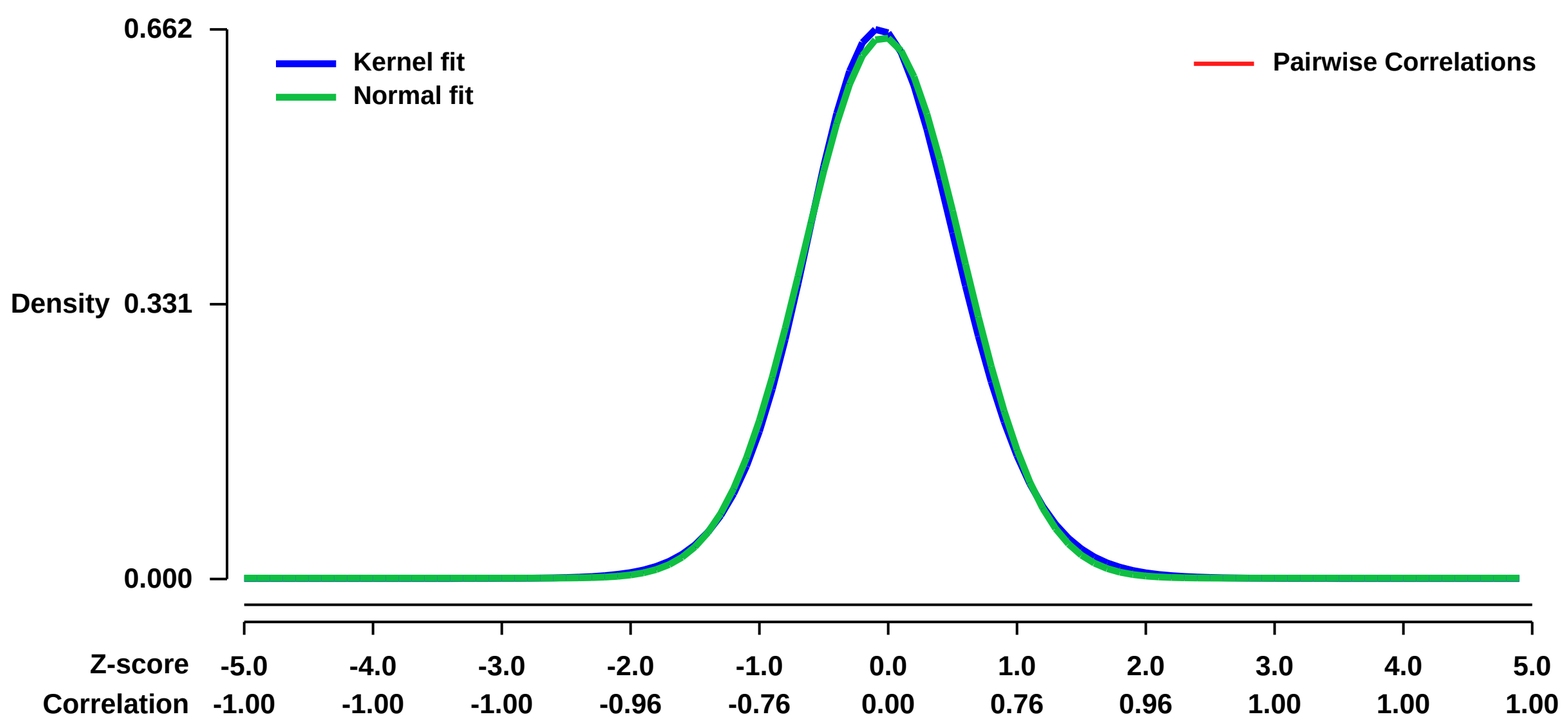

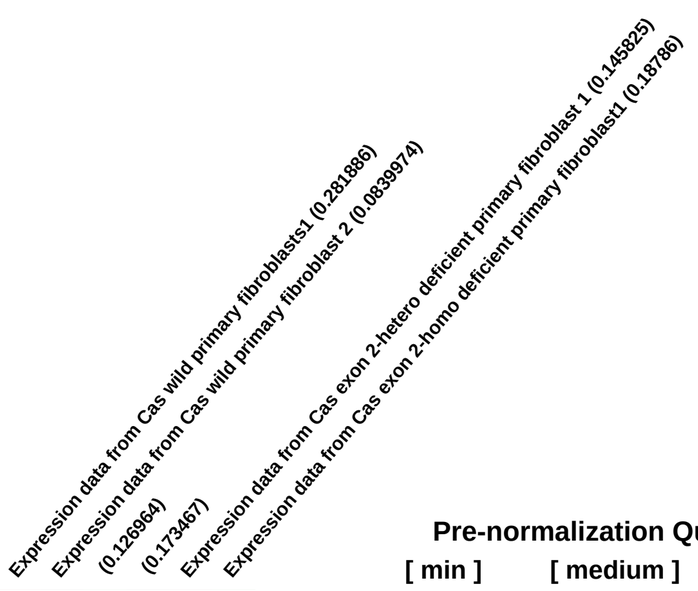

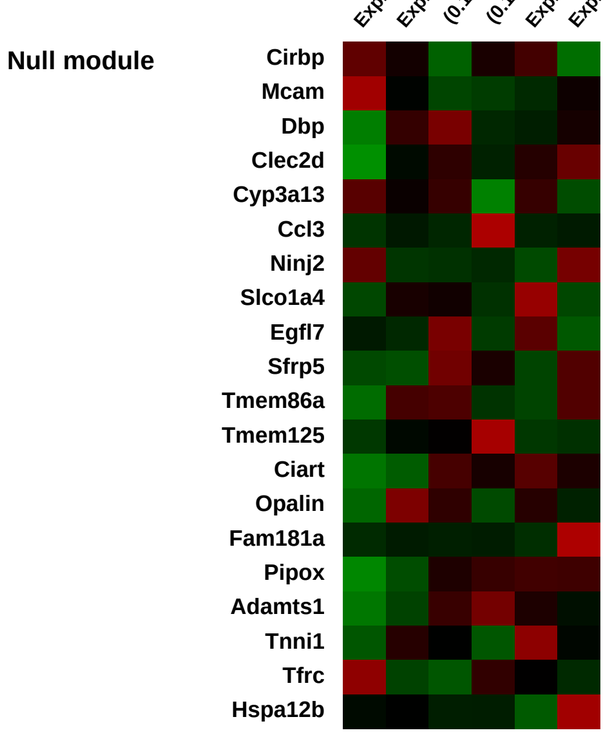

GEO Series "GSE32277" Expression Profiles

Num of samples in this series: 33

Scale of expression profile Z-scores

-3.0 -2.0 -1.0 0.0 1.0 2.0 3.0

GEO Link: http://www.ncbi.nlm.nih.gov/geo/query/acc.cgi?acc=GSE32277

Status: Public on Apr 30 2012

Title: Kras is required for pancreatic tumor maintenance through regulation of hexosamine biosynthesis and the non-oxidative pentose phosphate pathway

Organism: Mus musculus

Experiment type: Expression profiling by array

Platform: GPL1261

Pubmed ID: 22541435

Summary & Design:

Summary:
The maintenance of advanced malignancies relies on continued activity of driver oncogenes, although their rate-limiting role is highly context-dependent with respect to tumor types and associated genetic alterations. Oncogenic Kras mutation is the signature event in human pancreatic ductal adenocarcinoma (PDAC), serving a critical role in tumor initiation. Here, an inducible KrasG12D-driven p53 mutant PDAC mouse model establishes that advanced PDAC remains strictly dependent on continued KrasG12D expression and that KrasG12D serves a vital role in the control of tumor metabolism, through stimulation of glucose uptake and channeling of glucose intermediates through the hexosamine biosynthesis pathway (HBP) and the pentose phosphate pathway (PPP). Notably, these studies reveal that oncogenic Kras regulates ribose biogenesis. Unlike canonical models of PPP-mediated ribose biogenesis, we demonstrate that oncogenic Kras drives intermediates from enhanced glycolytic flux into the non-oxidative arm of the PPP, thereby decoupling ribose biogenesis from NADPNADPH-mediated redox control. Together, this work provides in vivo mechanistic insights into how oncogenic Kras promotes metabolic reprogramming in native tumors and illuminates potential metabolic targets that can be exploited for therapeutic benefit in Kras-driven PDAC.

Overall design:
Primary pancreatic tumor lines were established from p48Cre tetO_LKrasG12D ROSA_rtTAL+ p53L+ mice. Five independent tumor lines (iKras1-5) were used for pancreatic injection into nude mice to generate orthotopic tumors. The mice were kept on doxycycline for 2 weeks until obvious tumor formation. Half of the animals were pulled off doxycycline for 24 hours. Tumors with over 75% cellularity were collected for total RNA prepartion. For in vitro expression profiles, the same five tumor lines were cultured in the presence or absence of doxycycline for 24 hours and total cellular RNA was prepared. For control samples, two independent tumor lines from LSL-KrasG12D p53L+ tumors were cultured in the presence or absence of doxycycline for 24 hours and total cellular RNA was prepared.

Background corr dist: KL-Divergence = 0.1319, L1-Distance = 0.0356, L2-Distance = 0.0021, Normal std = 0.4008

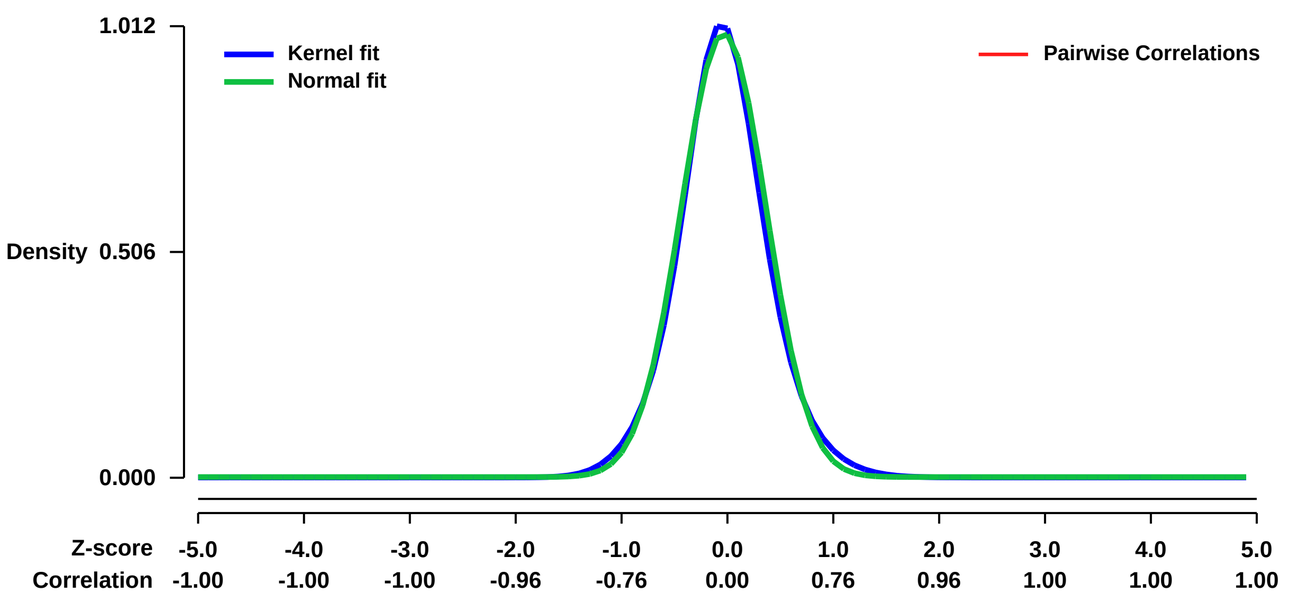

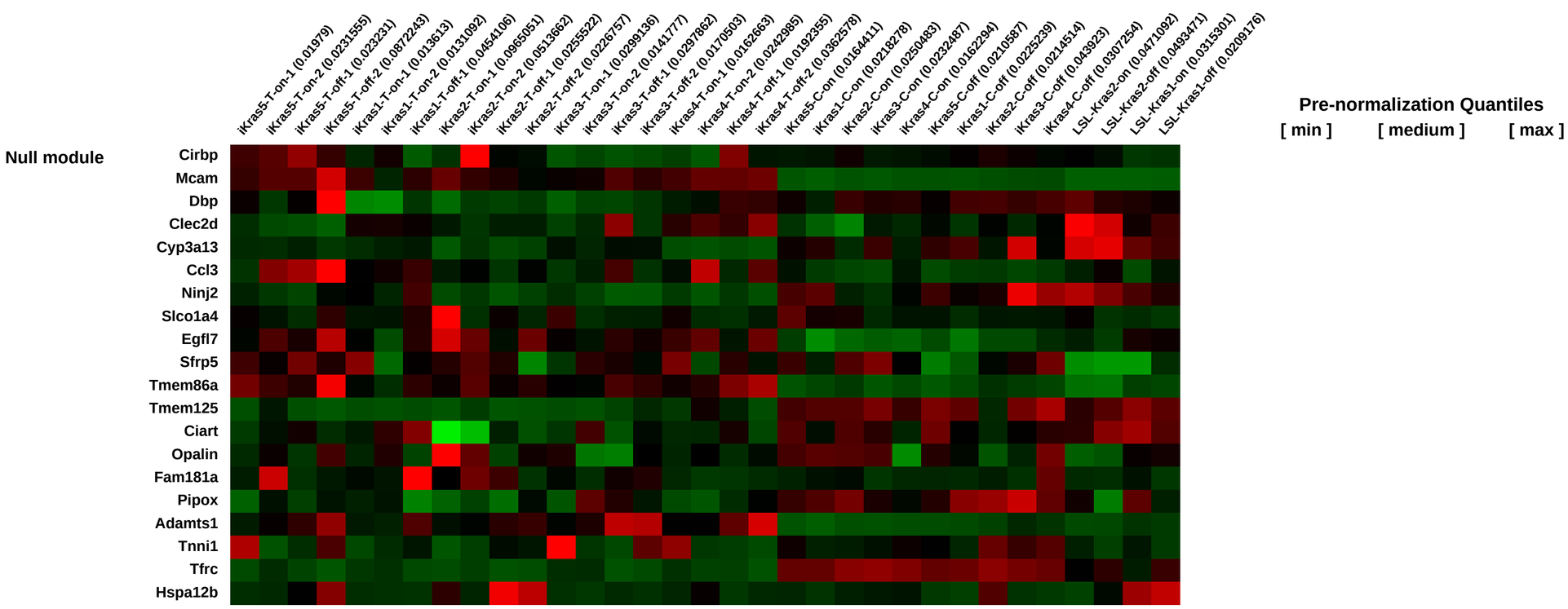

GEO Series "GSE34423" Expression Profiles

Num of samples in this series: 40

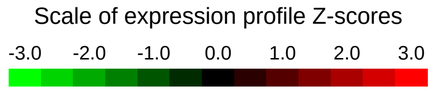

GEO Link:	http://www.ncbi.nlm.nih.gov/geo/query/acc.cgi?acc=GSE34423
Status:	Public on Dec 14 2011
Title:	Phenobarbital mediates an epigenetic switch at the constitutive androstane receptor (CAR) target gene Cyp2b10 in the liver of B6C3F1 mice [Expression array].
Organism:	Mus musculus
Experiment type:	Expression profiling by array
Platform:	GPL1261
Pubmed ID:	21455306
Summary & Design:	**Summary:** Evidence suggests that epigenetic perturbations are involved in the adverse effects associated with some drugs and toxicants, including certain classes of non-genotoxic carcinogens. Such epigenetic changes (altered DNA methylation and covalent histone modifications) may take place at the earliest stages of carcinogenesis and their identification holds great promise for biomedical research. Here, we evaluate the sensitivity and specificity of genome-wide epigenomic and transcriptomic profiling in phenobarbital (PB)-treated B6C3F1 mice, a well-characterized rodent model of non-genotoxic liver carcinogenesis. Methylated DNA Immunoprecipitation (MeDIP)-coupled microarray profiling of 17,967 promoter regions and 4,566 intergenic CpG islands was combined with genome-wide mRNA expression profiling to identify liver tissue-specific PB-mediated DNA methylation and transcriptional alterations. Only a limited number of significant anti-correlations were observed between PB-induced transcriptional and promoter-based DNA methylation perturbations. However, the constitutive androstane receptor (CAR) target gene Cyp2b10 was found to be concomitantly hypomethylated and transcriptionally activated in a liver tissue-specific manner following PB treatment. Furthermore, analysis of active and repressive histone modifications using chromatin immunoprecipitation revealed a strong PB-mediated epigenetic switch at the Cyp2b10 promoter. Our data reveal that PB-induced transcriptional perturbations are not generally associated with broad changes in the DNA methylation status at proximal promoters and suggest that the drug-inducible CAR pathway regulates an epigenetic switch from repressive to active chromatin at the target gene Cyp2b10. This study demonstrates the utility of integrated epigenomic and transcriptomic profiling for elucidating early mechanisms and biomarkers of non-genotoxic carcinogenesis. **Overall design:** 29â 32 days old male B6C3F1/Crl (C57BL/6 â x C3H/He â) mice were obtained from Charles River Laboratories (Germany). Animals were allowed to acclimatise for 5 days prior to being randomly divided into two treatment groups (n = 10) and phenobarbital (Sigma 04710, 0.05% (w/v) in drinking water) was administered to one group through ad libitum access to drinking water for 28 days. Mice were checked daily for activity and behavior and sacrificed on the last day of dosing (day 28). Blood was withdrawn for PK analysis and target (liver) and non-target (kidney) tissues removed, split into several sections, frozen in liquid nitrogen and stored at â 80´℃ for subsequent analyses. Total RNA from liver and kidney was purified and processed for Affymetrix gene expression profiling while genomic DNA was prepared for promoter array based methylome analysis using the Methylated DNA immunoprecipitation (MeDIP) procedure. Remaining tissue material was used for chromatin immunoprecipitation (ChIP) to analyze histone modifications at individual promoters. Plasma samples were also collected to evaluate phenobarbital exposure in individual animals by LC-MS.

Background corr dist: KL-Divergence = 0.0734, L1-Distance = 0.0729, L2-Distance = 0.0087, Normal std = 0.5583

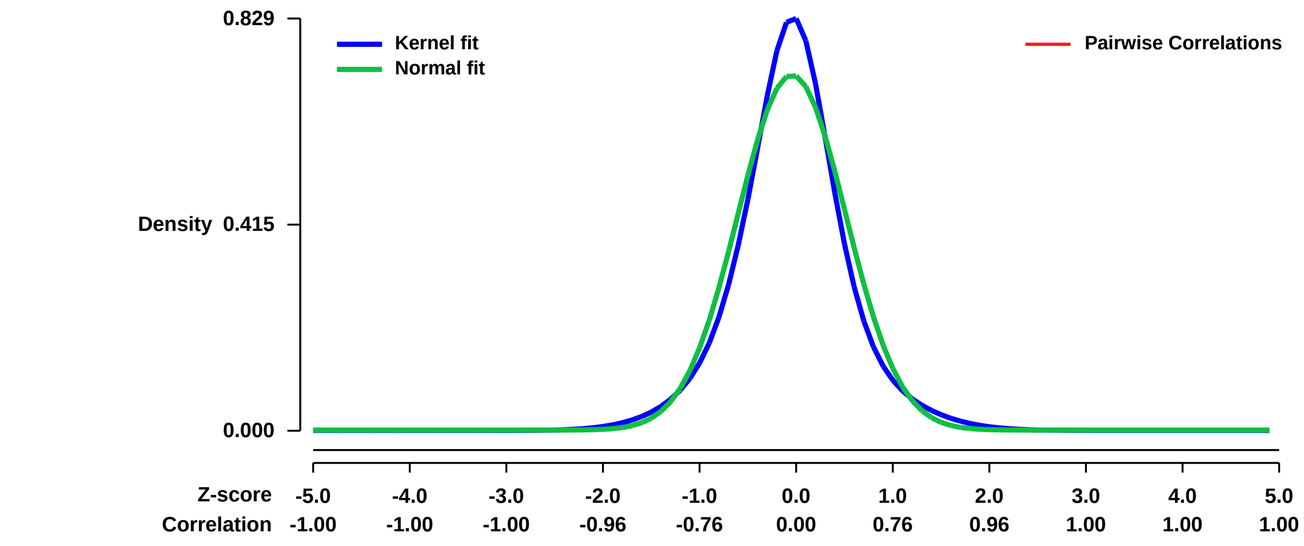

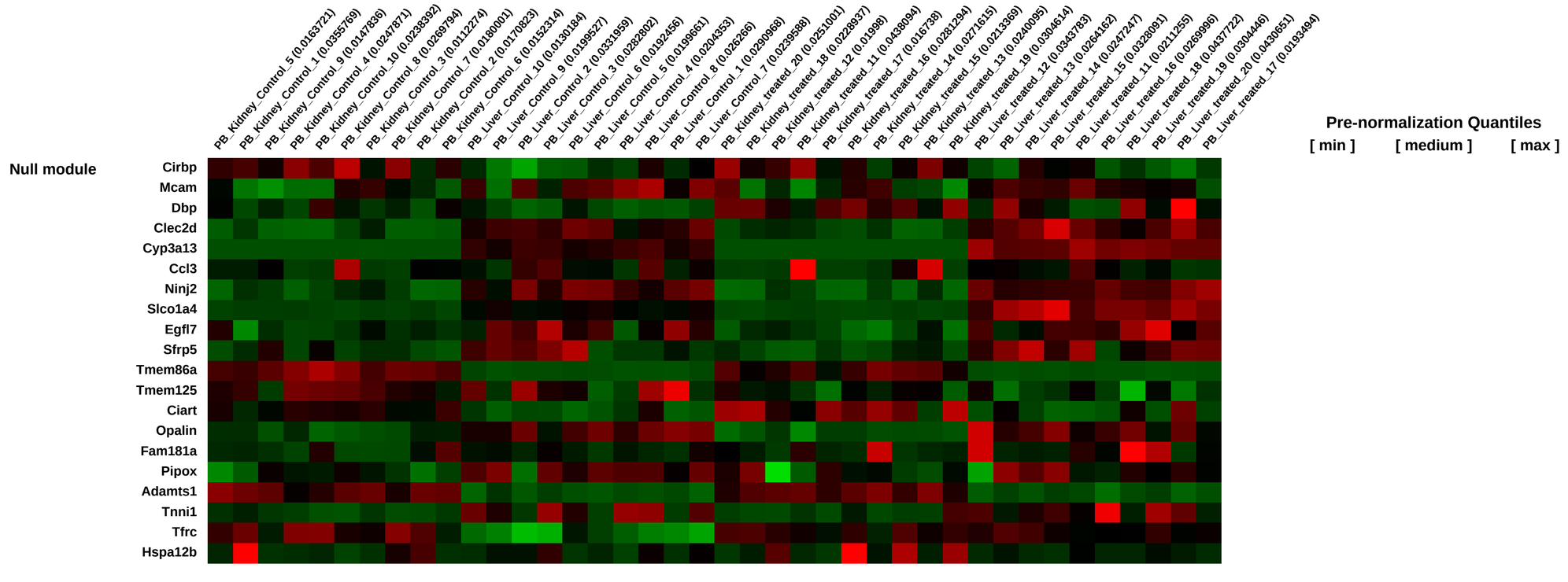

GEO Series "GSE10113" Expression Profiles

Num of samples in this series: 12

Scale of expression profile Z-scores

-3.0 -2.0 -1.0 0.0 1.0 2.0 3.0

GEO Link:	http://www.ncbi.nlm.nih.gov/geo/query/acc.cgi?acc=GSE10113
Status:	Public on Dec 28 2009
Title:	Comparison of gene expression pattern between Wild-type and Hypb knockout embryo yolk sacs
Organism:	Mus musculus
Experiment type:	Expression profiling by array
Platform:	GPL1261
Pubmed ID:	20133625
Summary & Design:	**Summary:** This study aimed at exploring the physiological function of mammalian HYPB by means of knockout mouse model. Homogenous disruption of mouse Hypb gene leads to embryonic lethality at E10.5-E11.5. Severe vascular defects were observed in the Hypb-/- embryos, yolk sac and placenta.In the mutant embryo and yolk sac, disorganized and abnormally dilated capillaries cannot be remodeled into large blood vessels or intricate networks. Thus, our results suggest that the mammalian HYPB HMT plays an important role in embryonic vascularization. **Keywords:** knockout, mouse embryo development, angiogenesis, yolk sac, E9.0, E10.5 **Overall design:** To systematically examine and compare gene expression patterns between Hypb+/+ and Hypb-/- embryos at the global genome-level, we use the Affymetrix GeneChip´fi mouse genome 430 2.0 arrays. We choose to use E9.0 and E10.5 yolk sacs for analysis because at E9.0 this early stage Hypb-/- embryos did not show severe visible mutant phenotype, and at E10.5 this antemortem stage Hypb-/- embryos show mang lethal mutant phenotypes. For comparison, four independently derived yolk sacs were pooled for each genotype of the two development stages, and three biological repeats were performed.

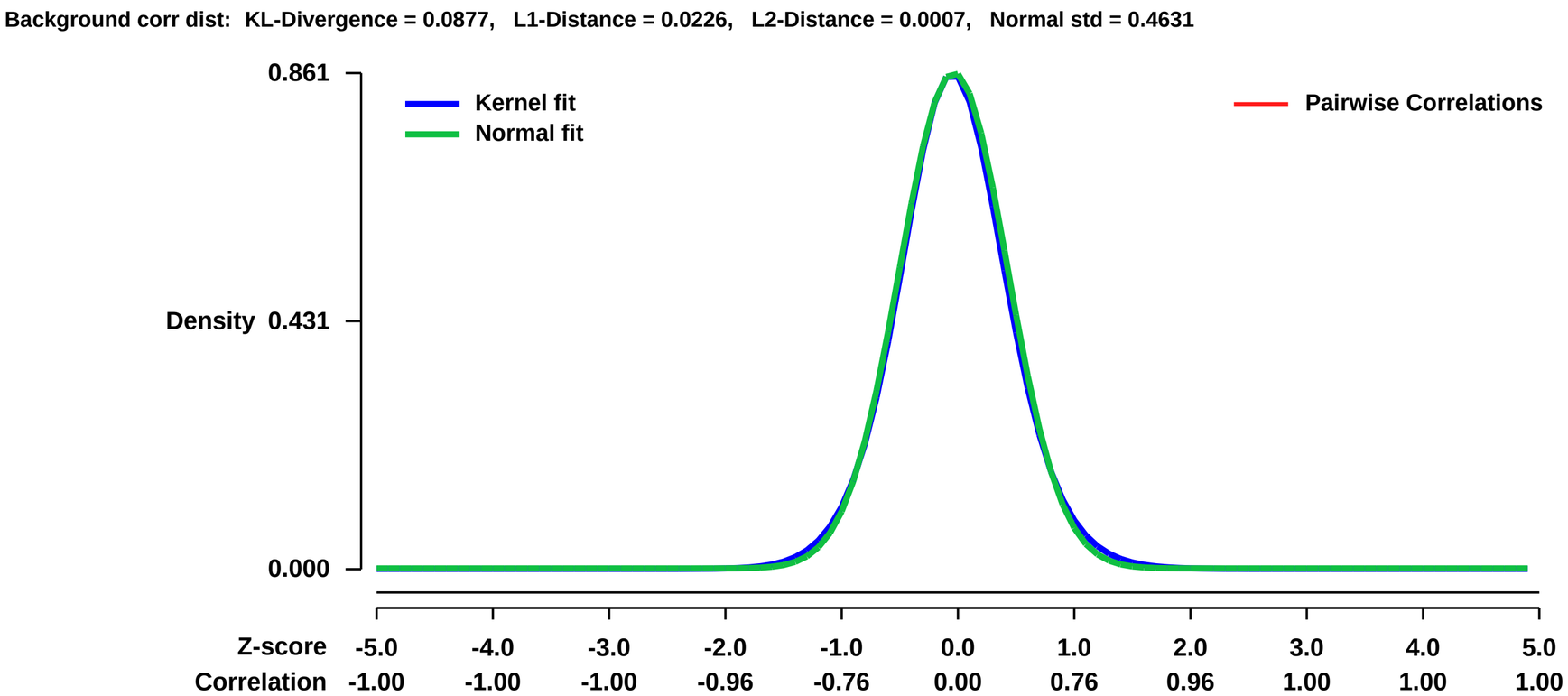

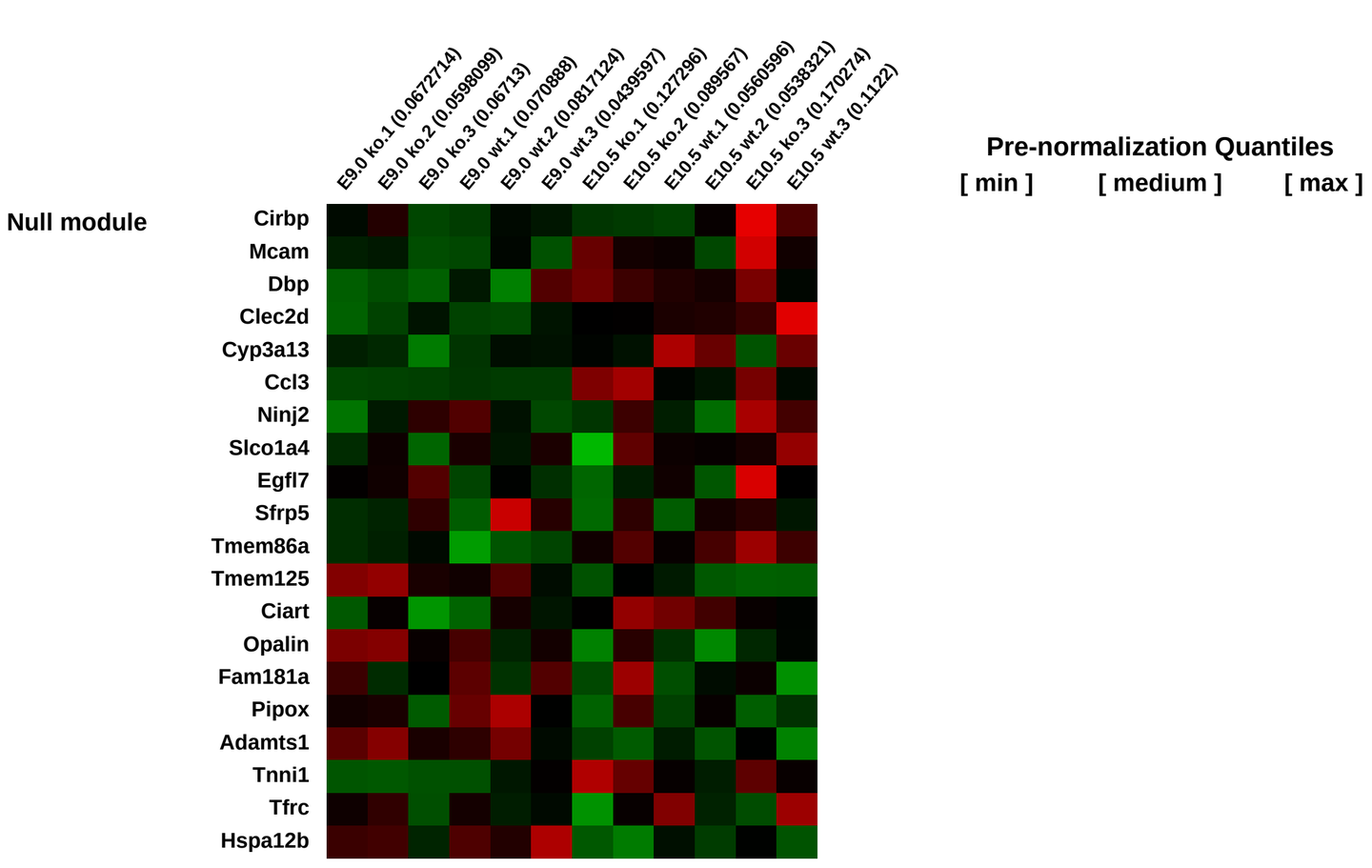

GEO Series "GSE9338" Expression Profiles

Num of samples in this series: 42

Scale of expression profile Z-scores

-3.0 -2.0 -1.0 0.0 1.0 2.0 3.0

GEO Link: http://www.ncbi.nlm.nih.gov/geo/query/acc.cgi?acc=GSE9338
Status: Public on Jan 19 2008
Title: Expression data from Mus musculus subspecies and their F1 hybrids for 3 tissues (brain, liver, testis)
Organism: Mus musculus domesticus
Experiment type: Expression profiling by array
Platform: GPL1261
Pubmed ID: 17947435

Summary & Design:

Summary:
We have studied different subspecies of the house mouse (M. m. musculus, M. m. domesticus and M. m. castaneus) and their reciprocal F1 hybrids to estimate the within-locus mode of inheritance for subspecies differences in gene expression in three tissues (brain, liver, testis) of male mice. This study investigates mode of inheritance in crosses at a larger taxonomic distance than have been previously systematically investigated. We found the vast majority of transcripts to be additively expressed with only a few transcripts showing dominance or overdominance in expression, except for one direction of one cross, which showed large mis-expression in the testis.

Keywords: comparative whole transcripome analysis

Overall design:
Wild-derived inbred lines of M. m. musculus, M. m. domesticus and M. m. castaneus were used to generate reciprocal crosses of M. m. musculus x M. m. domesticus and M. m. musculus x M. m. castaeneus. The gene expression profile of 2 males each of the hybrids and the pure parental subspecies were analyzed by using the Affymetrix GeneChip 430 2.0 to obtain evidence about the within-locus mode of inheritance of genes. First, we studied all transcripts that are differentially expressed between the parental subspecies and assessed additivity vs. nonadditivity of expression of these transcripts in the F1 hybrids. Second, we investigated those transcripts which do not differ in expression between the parental lines, but which are expressed differently in the F1 hybrids relative to both of their parents.

Background corr dist: KL-Divergence = 0.0697, L1-Distance = 0.0890, L2-Distance = 0.0131, Normal std = 0.6057

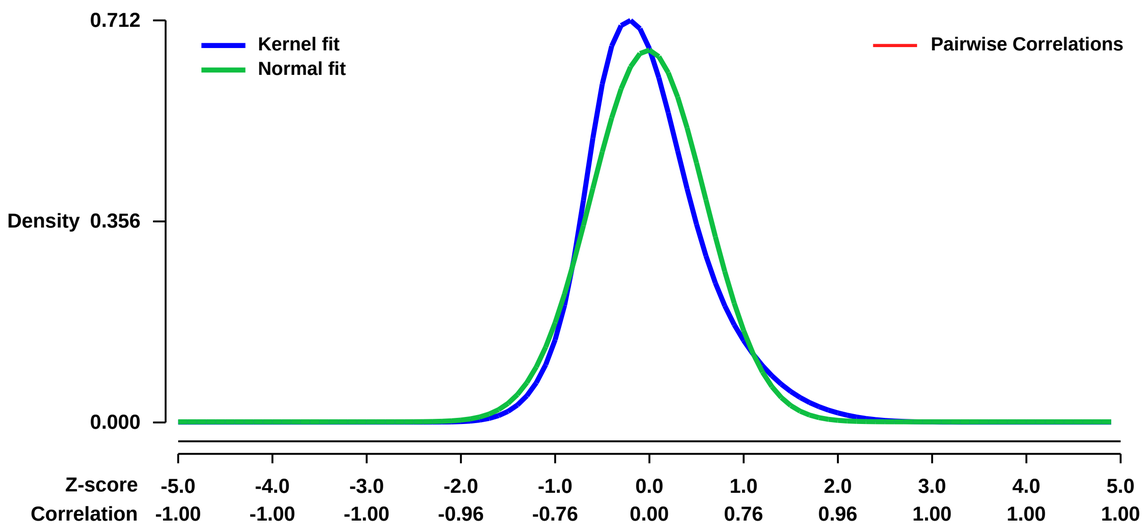

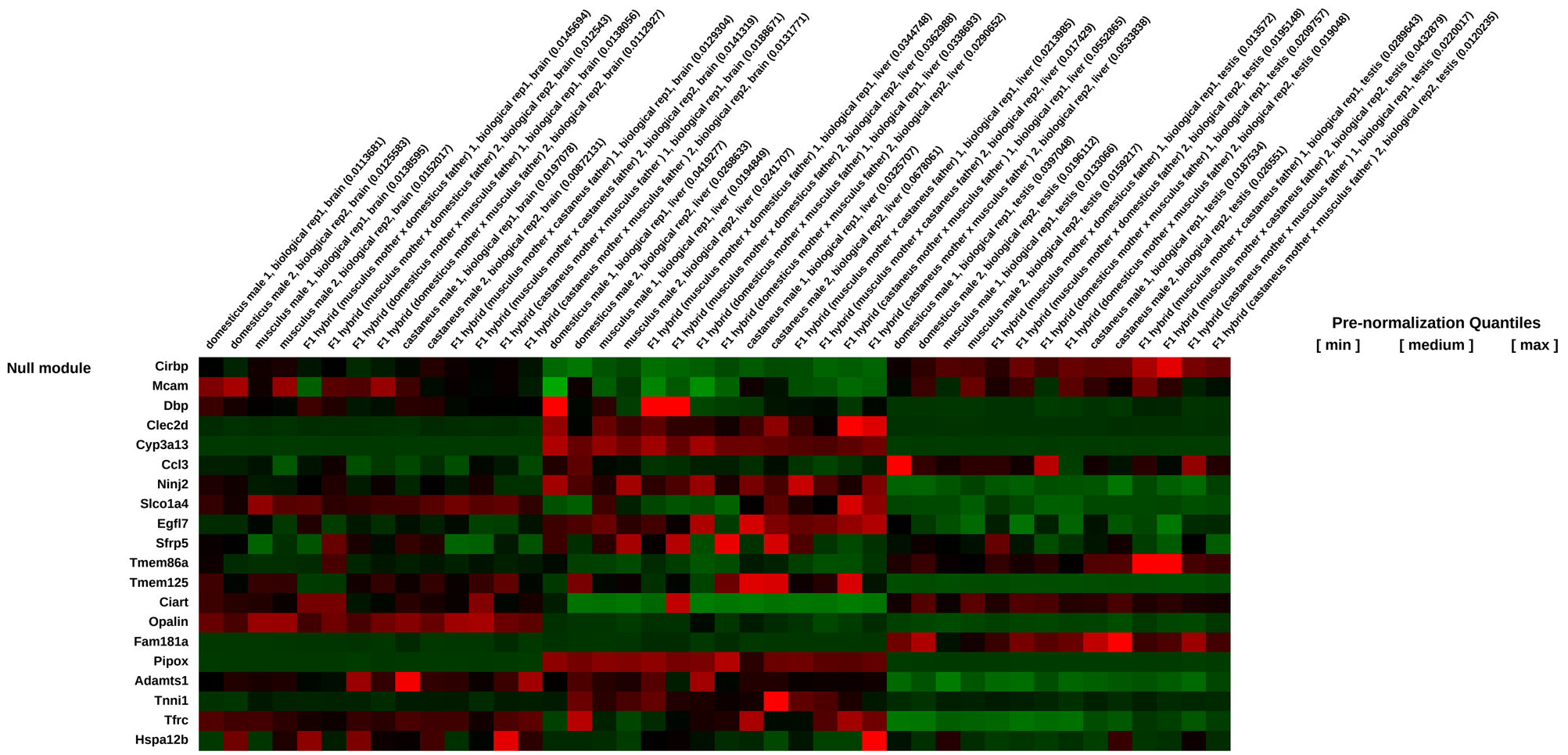

GEO Series "GSE47065" Expression Profiles

Num of samples in this series: 8

Scale of expression profile Z-scores

-3.0 -2.0 -1.0 0.0 1.0 2.0 3.0

GEO Link:	http://www.ncbi.nlm.nih.gov/geo/query/acc.cgi?acc=GSE47065
Status:	Public on May 18 2013
Title:	Gene expression profiling of IR-/-, IGF-1R-/- (dKO) newborn epidermis.
Organism:	Mus musculus
Experiment type:	Expression profiling by array
Platform:	GPL1261
Pubmed ID:	23906066
Summary & Design:	**Summary:** Analysis of newborn mouse epidermis lacking the expression of Insulin receptor (IR) and Insulin like growth factor 1 receptor (IGF-1R). Results show that IR/IGF-1R signalling control epidermal morphogenesis. **Overall design:** RNA was isolated from newborn mouse epidermis.Gene expression profiling was on on Affymetrix 430-2.0 platform.

Background corr dist: KL-Divergence = 0.0742, L1-Distance = 0.0224, L2-Distance = 0.0008, Normal std = 0.4920

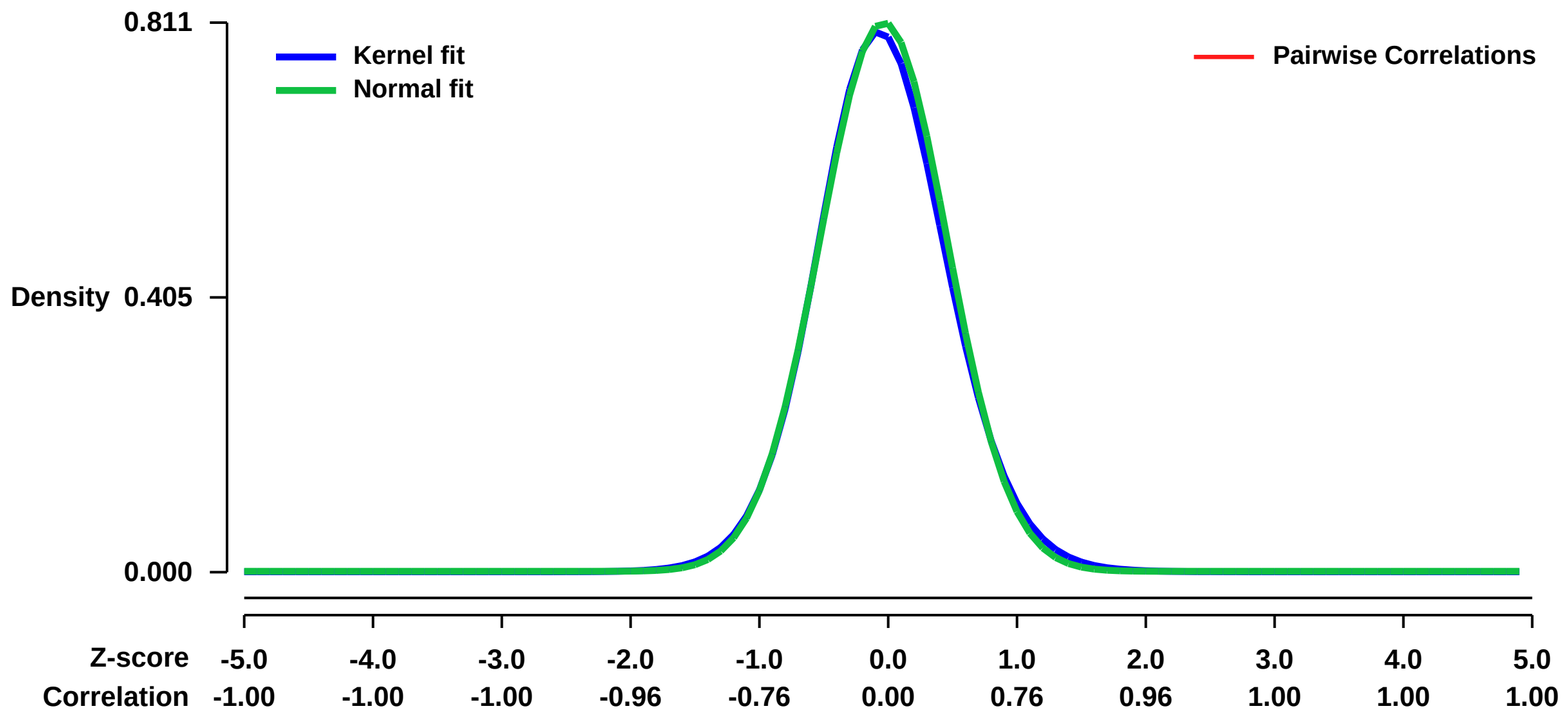

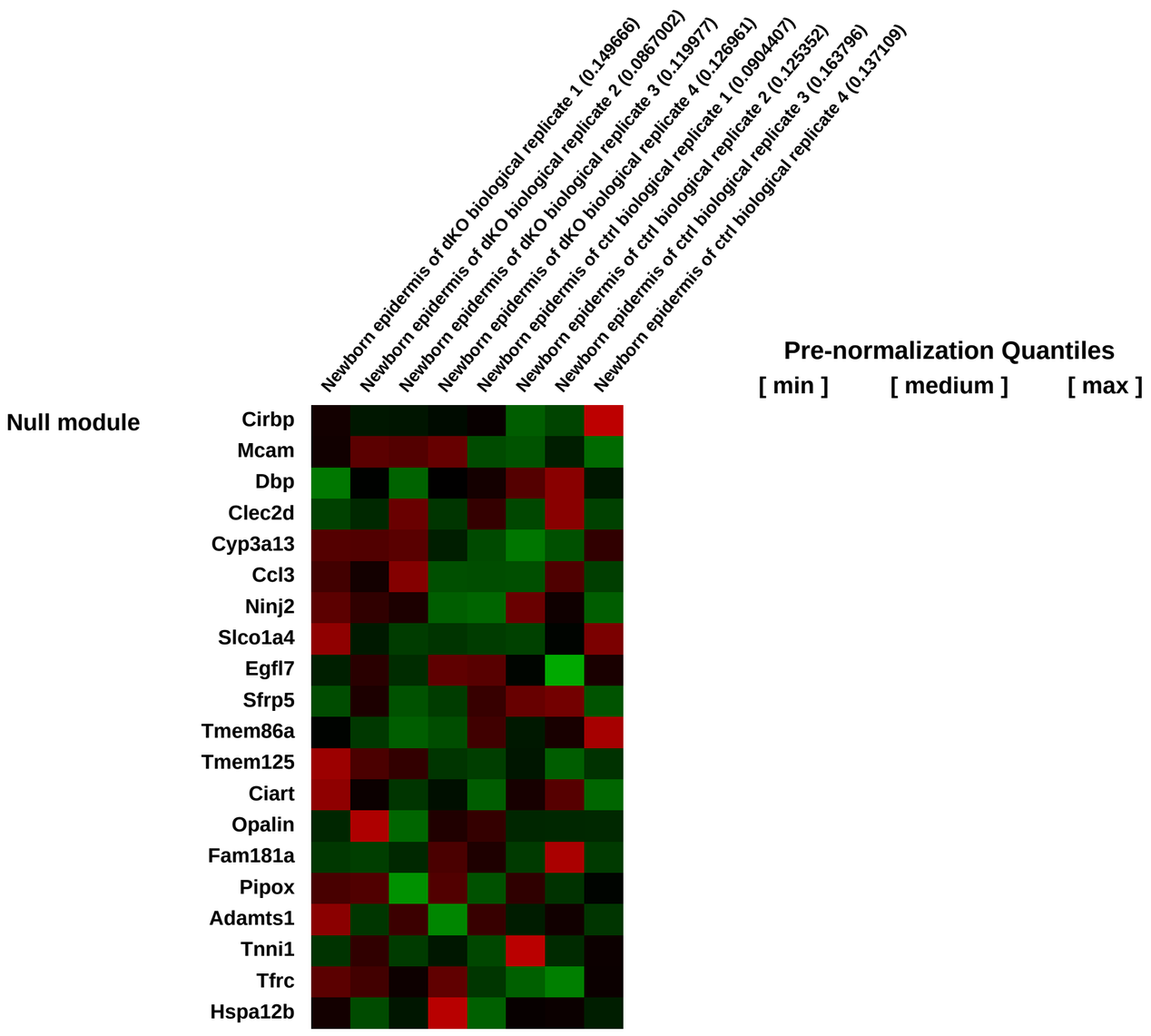

GEO Series "GSE4734" Expression Profiles

Num of samples in this series: 61

Scale of expression profile Z-scores

-3.0 -2.0 -1.0 0.0 1.0 2.0 3.0

GEO Link:	http://www.ncbi.nlm.nih.gov/geo/query/acc.cgi?acc=GSE4734
Status:	Public on Mar 05 2007
Title:	Mouse brain region gene expression (430 2.0 Array)
Organism:	Mus musculus
Experiment type:	Expression profiling by array
Platform:	GPL1261
Pubmed ID:	17324278
Summary & Design:	**Summary:** Gene expression patterns were determined from five brain regions (bed nucleus of the stria terminalis, hippocampus, hypothalamus, periaqueductal gray, and pituitary gland) in six mouse strains (129S6/SvEvTac, A/J, C57BL/6J, C3H/HeJ, DBA/2J, and FVB/NJ). At least two replicate samples per brain region/strain were analyzed using Affymetrix Mouse Genome 430 2.0 arrays. **Keywords:** mouse strain and brain region comparison **Overall design:** six mouse strains and five brain regions were analyzed

Background corr dist: KL-Divergence = 0.1388, L1-Distance = 0.0659, L2-Distance = 0.0086, Normal std = 0.4122

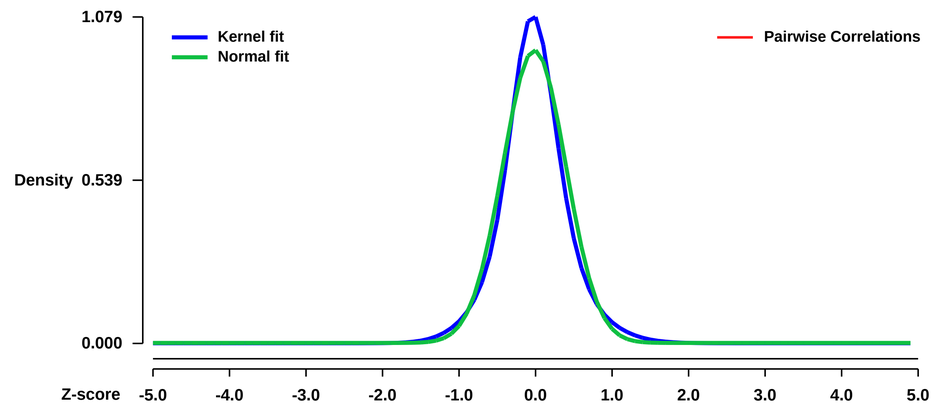

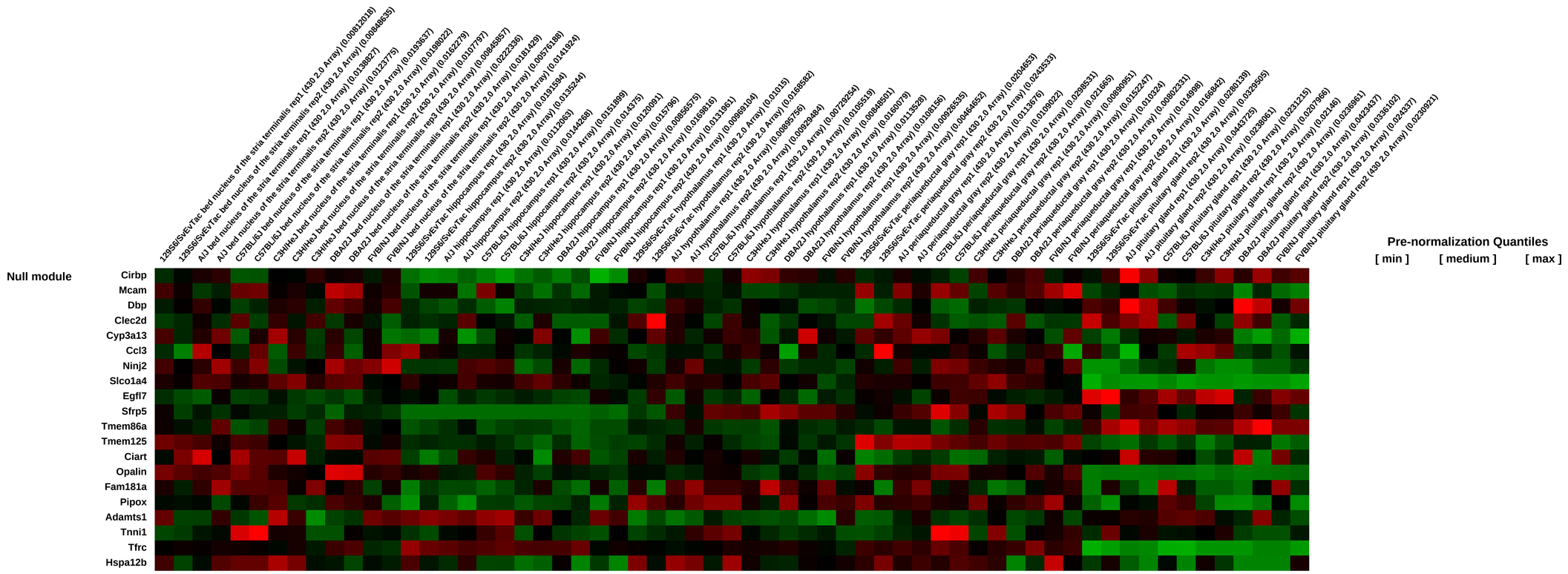

GEO Series "GSE36415" Expression Profiles

Num of samples in this series: 14

Scale of expression profile Z-scores

-3.0 -2.0 -1.0 0.0 1.0 2.0 3.0

GEO Link:	http://www.ncbi.nlm.nih.gov/geo/query/acc.cgi?acc=GSE36415
Status:	Public on Mar 08 2013
Title:	Effect of NF-kappaB activation in bone marrow stromal cells co-cultured with CLL cells
Organism:	Mus musculus
Experiment type:	Expression profiling by array
Platform:	GPL1261
Pubmed ID:	23328482
Summary & Design:	**Summary:** Tumor cell survival critically depends on heterotypic communication with benign cells in the microenvironment. Here we describe a novel survival signaling pathway activated in stromal cells by contact to B-cells from chronic lymphocytic leukemia (CLL) patients. The expression of PKC-¸†II and the subsequent activation of NF-¸”B in bone marrow stromal cells is a prerequisite to support the survival of malignant B-cells. PKC-¸† knockout mice are insusceptible to CLL-transplantations, underscoring the in vivo significance of the PKC-¸†II-NF-¸”B signaling pathway in the tumor microenvironment. Upregulated stromal PKC-¸†II in biopsies from CLL, breast- and pancreatic-cancer patients suggest that this pathway may commonly be activated in a variety of malignancies. We used microarrays to determine Nemo/ IKK-gamma dependent gene expression changes in bone marrow stromal cells (BMSCs) induced by co-culturing with leukemic B-cells (CLL) **Overall design:** We compared mouse BMSC cells from Nemo knockout cells (Nemo+CRE) and Nemo wild type cells (Nemo-CRE) co-cultured for 5 days with leukemic B-cells microarray analysis on Affymetrix MG-430_2.0 arrays..

Background corr dist: KL-Divergence = 0.0724, L1-Distance = 0.0218, L2-Distance = 0.0007, Normal std = 0.4965

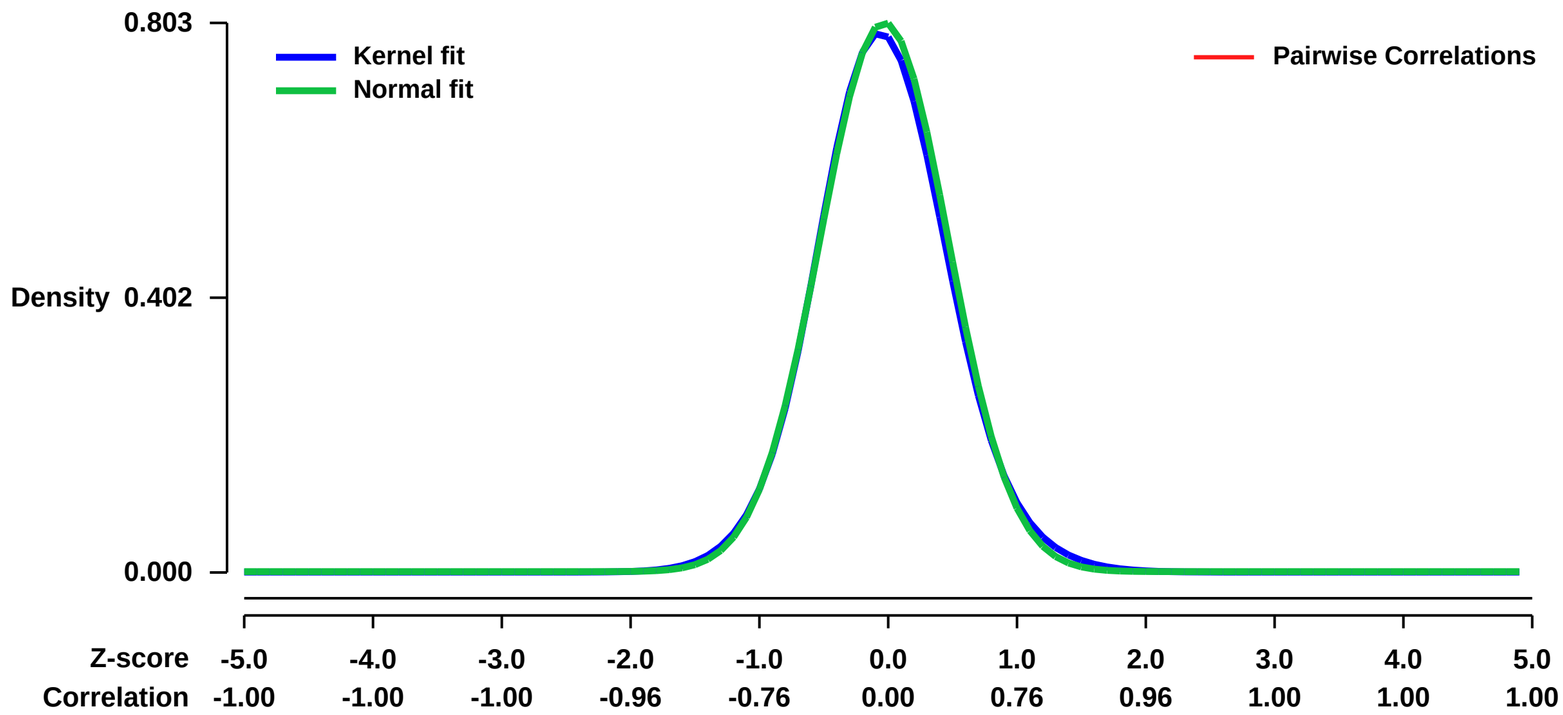

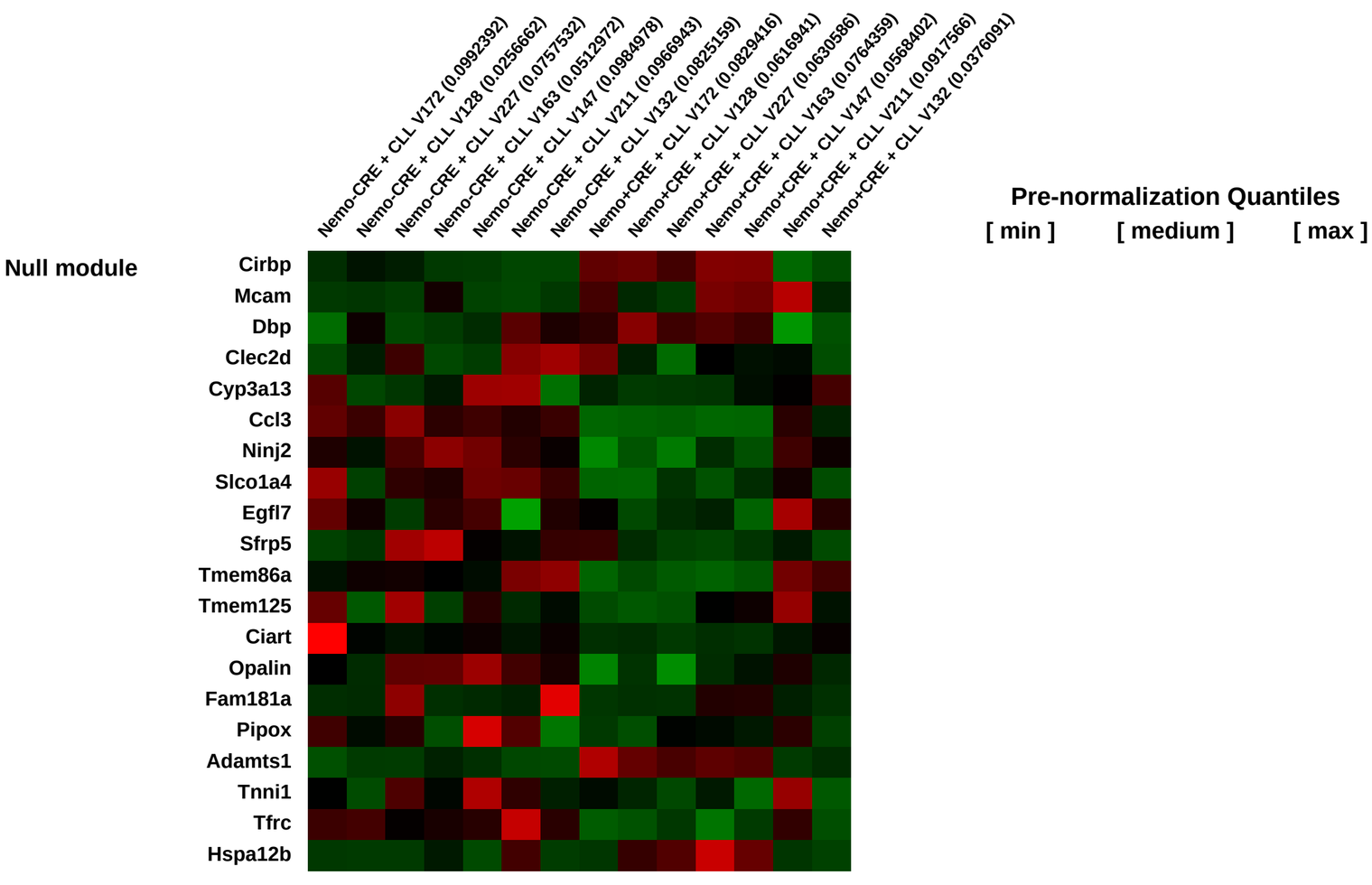

GEO Series "GSE7683" Expression Profiles

Num of samples in this series: 12

Scale of expression profile Z-scores

-3.0 -2.0 -1.0 0.0 1.0 2.0 3.0

GEO Link:	http://www.ncbi.nlm.nih.gov/geo/query/acc.cgi?acc=GSE7683
Status:	Public on Jul 04 2007
Title:	Microarray of Dexamethasone-treated primary chondrocytes identifies downstream targets of glucocorticoid signalling
Organism:	Mus musculus
Experiment type:	Expression profiling by array
Platform:	GPL1261
Pubmed ID:	17603917
Summary & Design:	**Summary:** **Background: Glucocorticoids (GCs) are widely used anti-inflammatory drugs. While useful in clinical practice, patients taking GCs often suffer from skeletal side effects including growth retardation and decreased bone quality in adults. On a physiological level, GCs have been implicated in the regulation of chondrogenesis and osteoblast differentiation, as well as maintaining homeostasis in cartilage and bone. We identified the glucocorticoid receptor (GR) as a potential regulator of chondrocyte hypertrophy in a microarray screen of primary limb bud mesenchyme micromass cultures. Some targets of GC regulation in chondrogenesis are known, but the global effects of pharmacological GC doses on chondrocyte gene expression have not been comprehensively evaluated.** **Results: This study systematically identifies a spectrum of GC target genes in embryonic growth plate chondrocytes treated with synthetic GR agonist, dexamethasone (DEX), at 6 and 24 hrs. Conventional analysis of this data set and gene set enrichment analysis (GSEA) was performed. Transcripts associated with metabolism were enriched in the DEX condition along with extracellular matrix genes. In contrast, a subset of growth factors and cytokines were negatively correlated with DEX treatment. Comparing DEX-induced gene expression data to developmental changes in gene expression in micromass cultures revealed an additional layer of complexity in which DEX maintains the expression of certain chondrocyte marker genes while inhibiting factors that promote vascularization and ultimately ossification of the cartilaginous template.** **Conclusions: Together, these results provide insight into the mechanisms and major molecular classes functioning downstream of DEX in primary chondrocytes monolayers. In addition, comparison of our data with microarray studies of DEX treatment in other cell types demonstrated that the majority of DEX effects are tissue-specific. This study provides novel insights into the effects of pharmacological GC on chondrocyte gene transcription and establishes the basis for subsequent functional studies.**
	Keywords: Time course and pharmacological treatment
	Overall design:

Background corr dist: KL-Divergence = 0.0700, L1-Distance = 0.0295, L2-Distance = 0.0011, Normal std = 0.5113

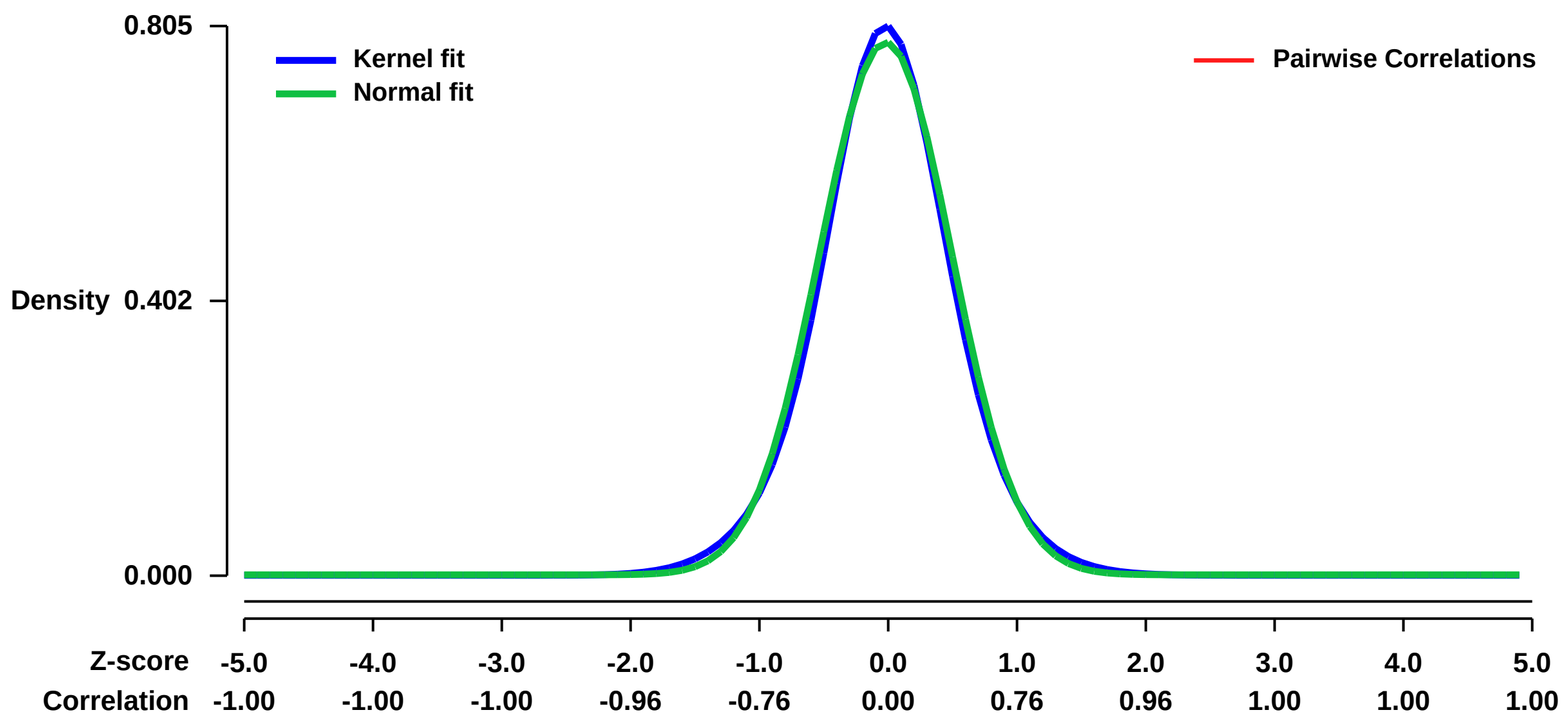

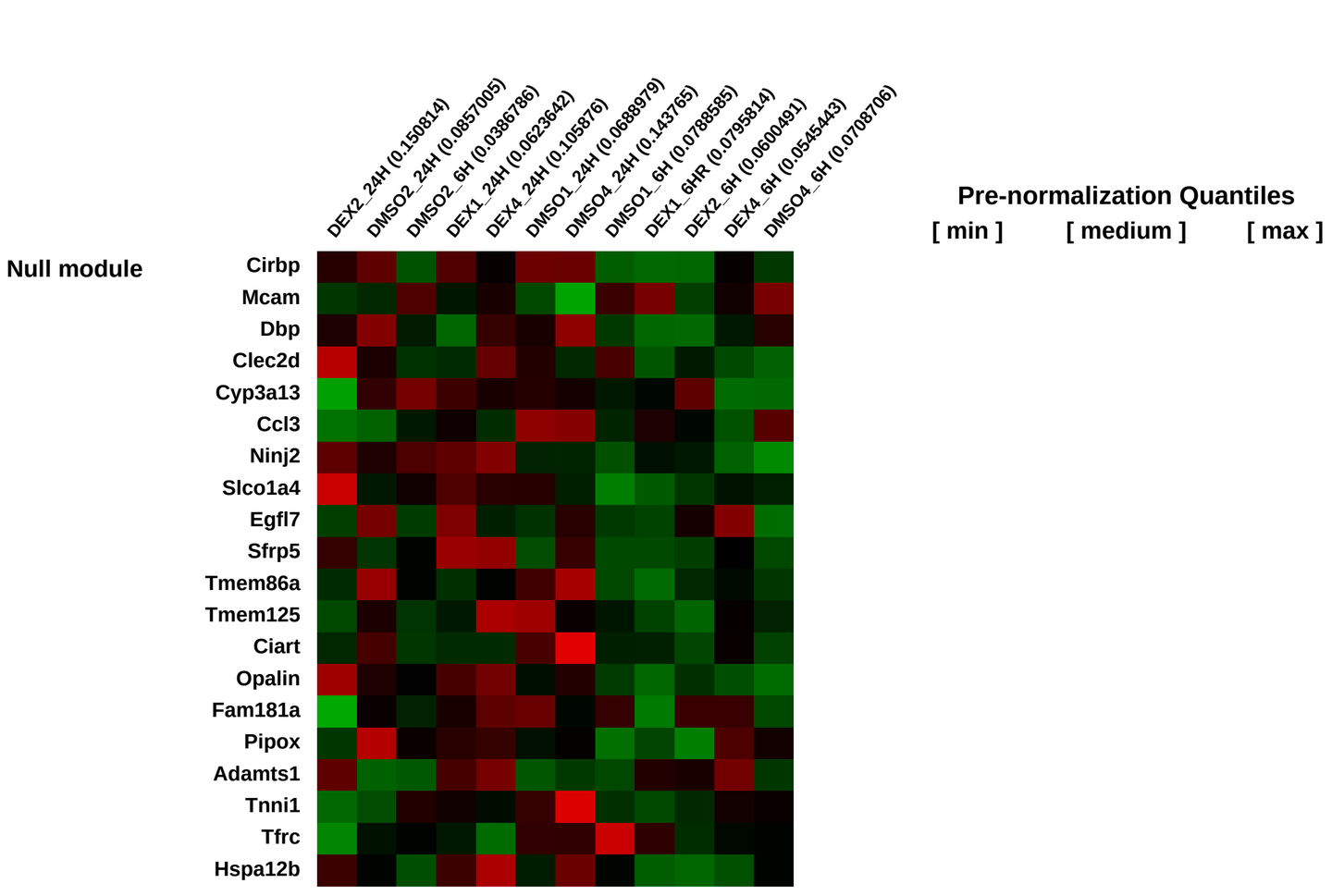

GEO Series "GSE30980" Expression Profiles

Num of samples in this series: 6

Scale of expression profile Z-scores

-3.0 -2.0 -1.0 0.0 1.0 2.0 3.0

GEO Link:	http://www.ncbi.nlm.nih.gov/geo/query/acc.cgi?acc=GSE30980
Status:	Public on May 21 2014
Title:	Gene profiling on mandibular arches (MdPA1) from Tbx1+/+ and Tbx1-/- mouse embryos
Organism:	Mus musculus
Experiment type:	Expression profiling by array
Platform:	GPL1261
Pubmed ID:	24705356
Summary & Design:	**Summary:** Velo-cardio-facial syndrome/DiGeorge syndrome/22q11.2 deletion syndrome (22q11DS) patients have a submucous cleft palate, velo-pharyngeal insufficiency associated with hypernasal speech, facial muscle hypotonia and feeding difficulties. Inactivation of both alleles of mouse Tbx1, encoding a T-box transcription factor, deleted on 22q11.2, results in a cleft palate and a reduction or loss of branchiomeric muscles. To identify genes downstream of Tbx1 for myogenesis, gene profiling was performed on mandibular arches (MdPA1) from Tbx1+/+ and Tbx1-/- mouse embryos. **Overall design:** To obtain enough RNA for microarray hybridization experiments, dissected mandibular arches from three Tbx1+/+ and three Tbx1-/- E10.5 embryos were pooled according to genotype, with three microarrays performed in total per genotype. The tissue was homogenized in Buffer RLT (QIAGEN). Total RNA was isolated with the RNeasy Micro Kit according to the manufacturerâ s protocol. Quality and quantity of total RNA was determined using an Agilent 2100 Bioanalyzer (Agilent) and an ND-1000 Spectrophotometer (NanoDrop), respectively. Biotinylated single-stranded cDNA targets were amplified from 100 nanograms (ng) starting total RNA using the Ovation RNA Amplification System V2 and FL- Ovation cDNA Biotin Module V2 (NuGEN). A total of 3.75 ¸…g of cDNA from the last step was hybridized to the GeneChip Test3 array (Affymetrix) to test the quality of the labeled target. Nucleic acid samples that passed quality control were then hybridized to the GeneChip Mouse Genome 430 2.0 Arrays (Affymetrix). Hybridization, washing, staining and scanning were performed in the Genomics Core at Einstein (http://www.einstein.yu.edu/genetics/CoreFacilities.aspx?id=23934) according to the Affymetrix manual.

Background corr dist: KL-Divergence = 0.0413, L1-Distance = 0.0184, L2-Distance = 0.0004, Normal std = 0.6119

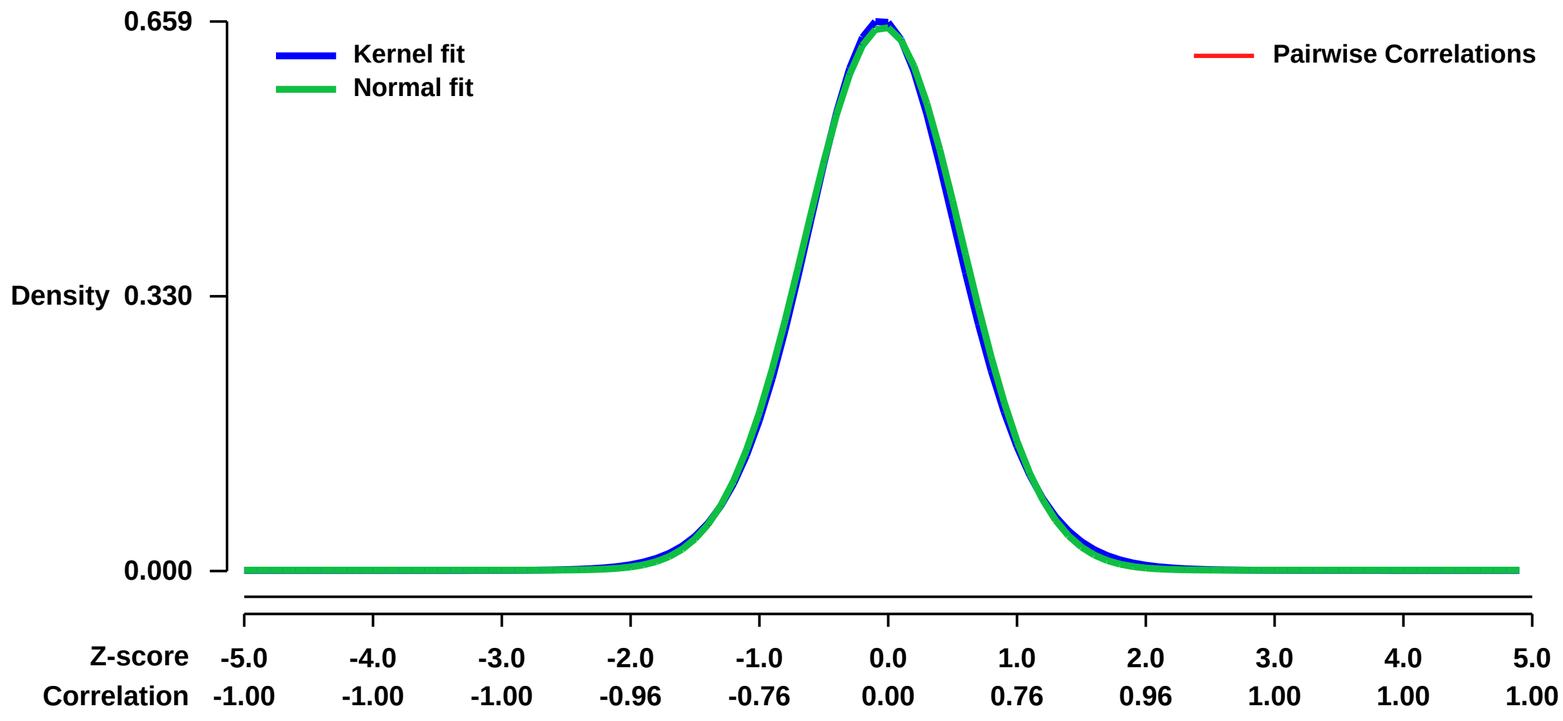

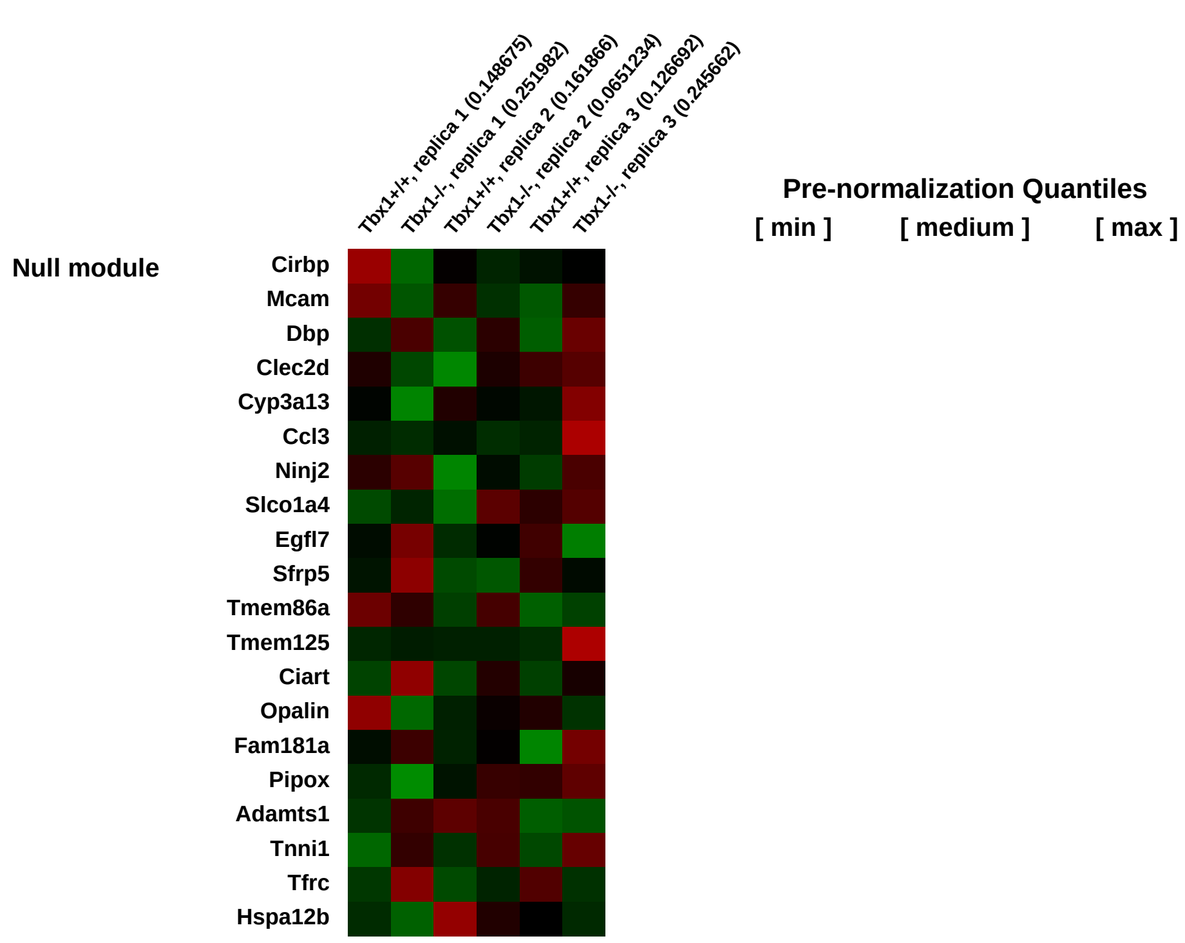

GEO Series "GSE24289" Expression Profiles

Num of samples in this series: 6

Scale of expression profile Z-scores

-3.0 -2.0 -1.0 0.0 1.0 2.0 3.0

GEO Link:	**http://www.ncbi.nlm.nih.gov/geo/query/acc.cgi?acc=GSE24289**
Status:	**Public on Sep 22 2011**
Title:	**Expression data from differentiating ES cells expressing miR-200c and miR-141**
Organism:	**Mus musculus**
Experiment type:	**Expression profiling by array**
Platform:	**GPL1261**
Pubmed ID:	
Summary & Design:	**Summary:** **ES cells express the miR-200 family which becomes down-regulated during the course of differentiation in serum. We generated an ES cell line which expresses miR-200c and miR-141 upon addition of doxycycline.** **Microarrays were used to gain a global picture of differentiation when miR-200c and miR-141 expression were maintained throughout differentiation through the addition of doxycycline.** **Overall design:** **A2.miR200c ES cells, which express miR-200c/miR-141 upon addition of doxycycline, were differentiated as embryoid bodies in six petri dishes. Half of the samples were treated with doxycycline on both days 2 and 4 of differentiation, and RNA was collected from all samples on days 3, 4, and 5.**

Background corr dist: **KL-Divergence = 0.0303, L1-Distance = 0.0253, L2-Distance = 0.0007, Normal std = 0.6791**

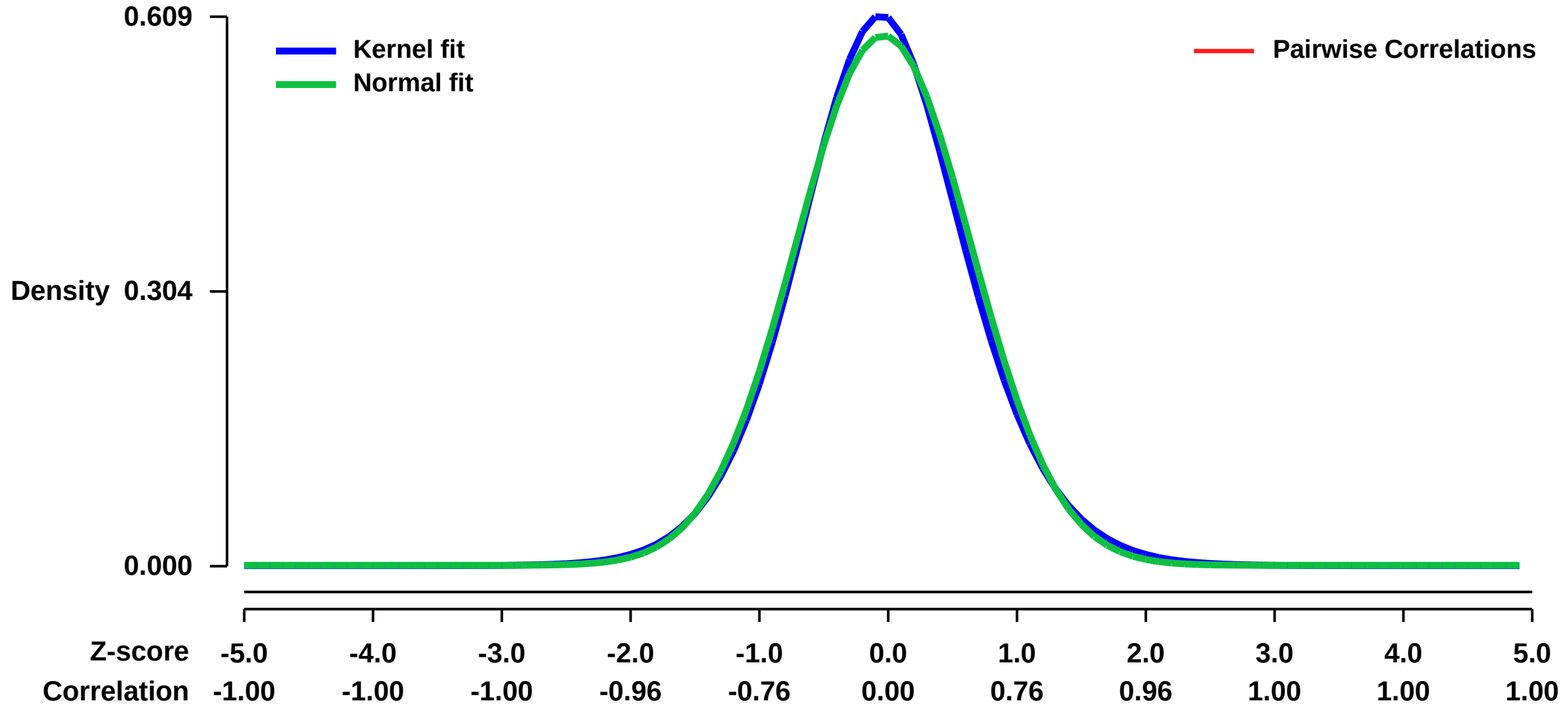

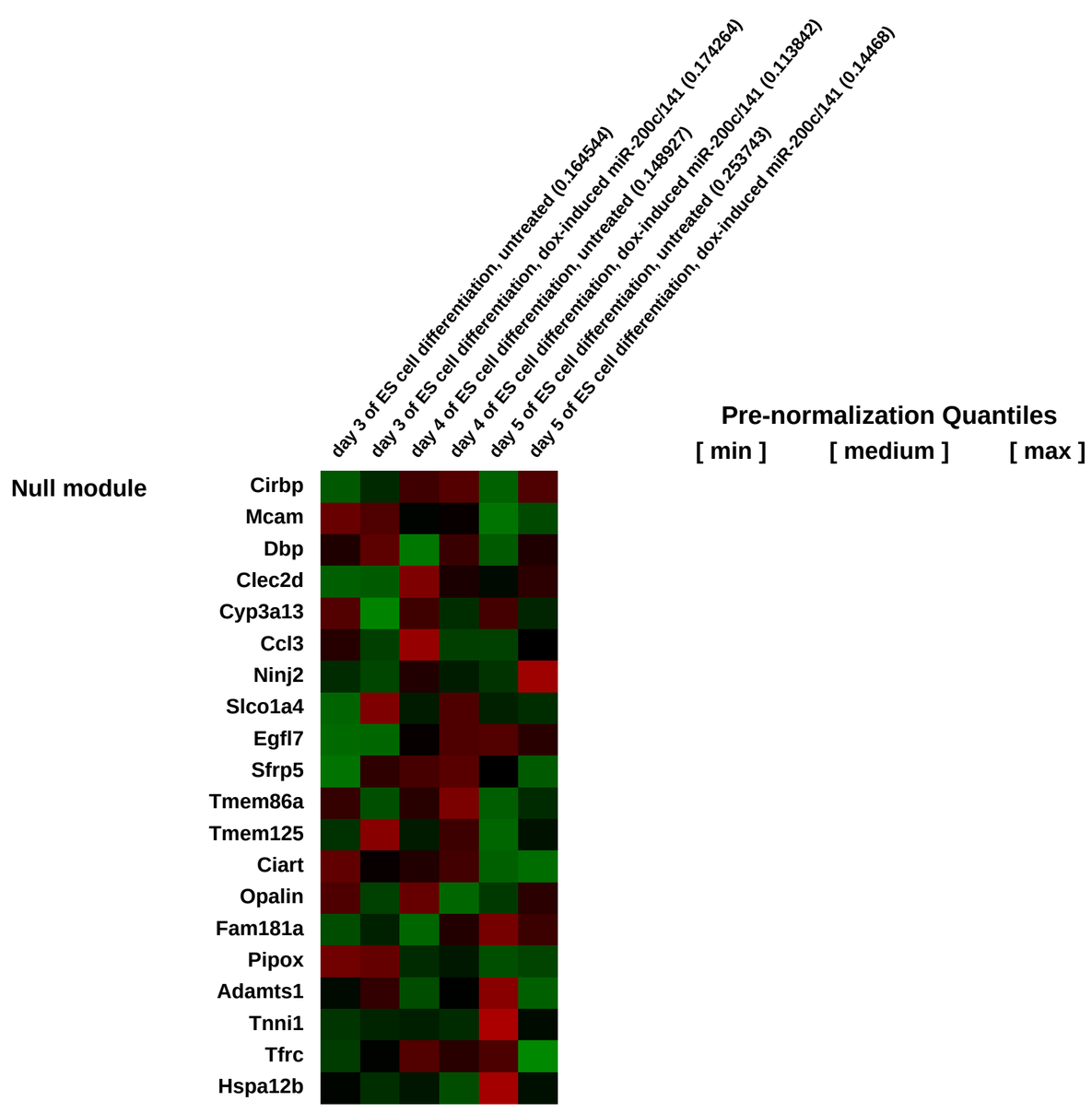

GEO Series "GSE21836" Expression Profiles

Num of samples in this series: 8

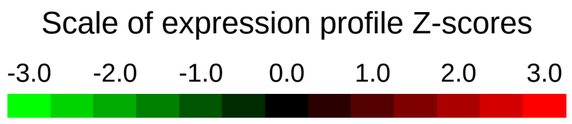

GEO Link:	http://www.ncbi.nlm.nih.gov/geo/query/acc.cgi?acc=GSE21836
Status:	Public on May 15 2010
Title:	Tob1 is a Constitutively Expressed Repressor of Liver Regeneration
Organism:	Mus musculus
Experiment type:	Expression profiling by array
Platform:	GPL1261
Pubmed ID:	20513747
Summary & Design:	**Summary:** How proliferative and inhibitory cell signals integrate to control liver regeneration remains poorly understood. A screen for antiproliferative factors repressed after liver injury identified Tob1, a member of the PC3/BTG1 family of mitoinhibitory molecules as a target for further evaluation. Tob1 protein decreases after 2/3 hepatectomy in mice secondary to post-transcriptional mechanisms. Deletion of Tob1 increases hepatocyte proliferation and accelerates restoration of liver mass after hepatectomy. Down-regulation of Tob1 is required for normal liver regeneration and Tob1 controls hepatocyte proliferation in a dose-dependent fashion. Tob1 associates directly with both Caf1 and the Cyclin/cdk complex to modulate kinase activity. In addition, Tob1 has significant effects on the transcription of critical cell cycle components, including E2F targets and genes involved in p53 signaling. These studies provide direct evidence that levels of an inhibitory factor control the rate of liver regeneration. Our data identify Tob1 as a crucial check-point molecule that acts by by modulating levels and activity of cell cycle proteins. **Overall design:** Samples from wild type and Tob1 null mice as normal adults and 24 hours after 2/3 hepatectomy are used. Each experimental point used data from two chips, each having a different set of three pooled animals. In summary we had 8 chips: 2 for WT time 0, 2 for WT time 24, 2 for KO time 0, 2 for KO time 24.

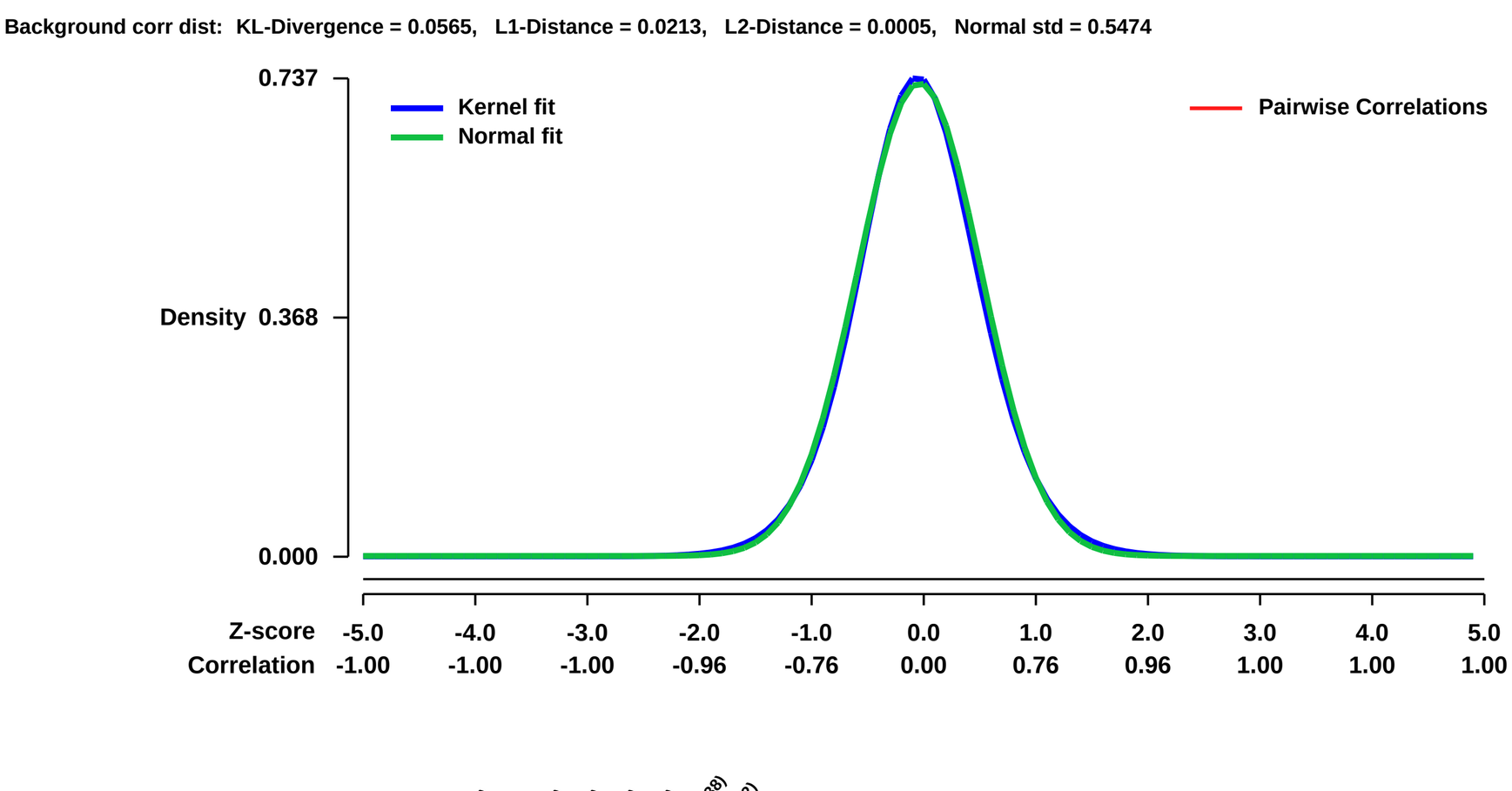

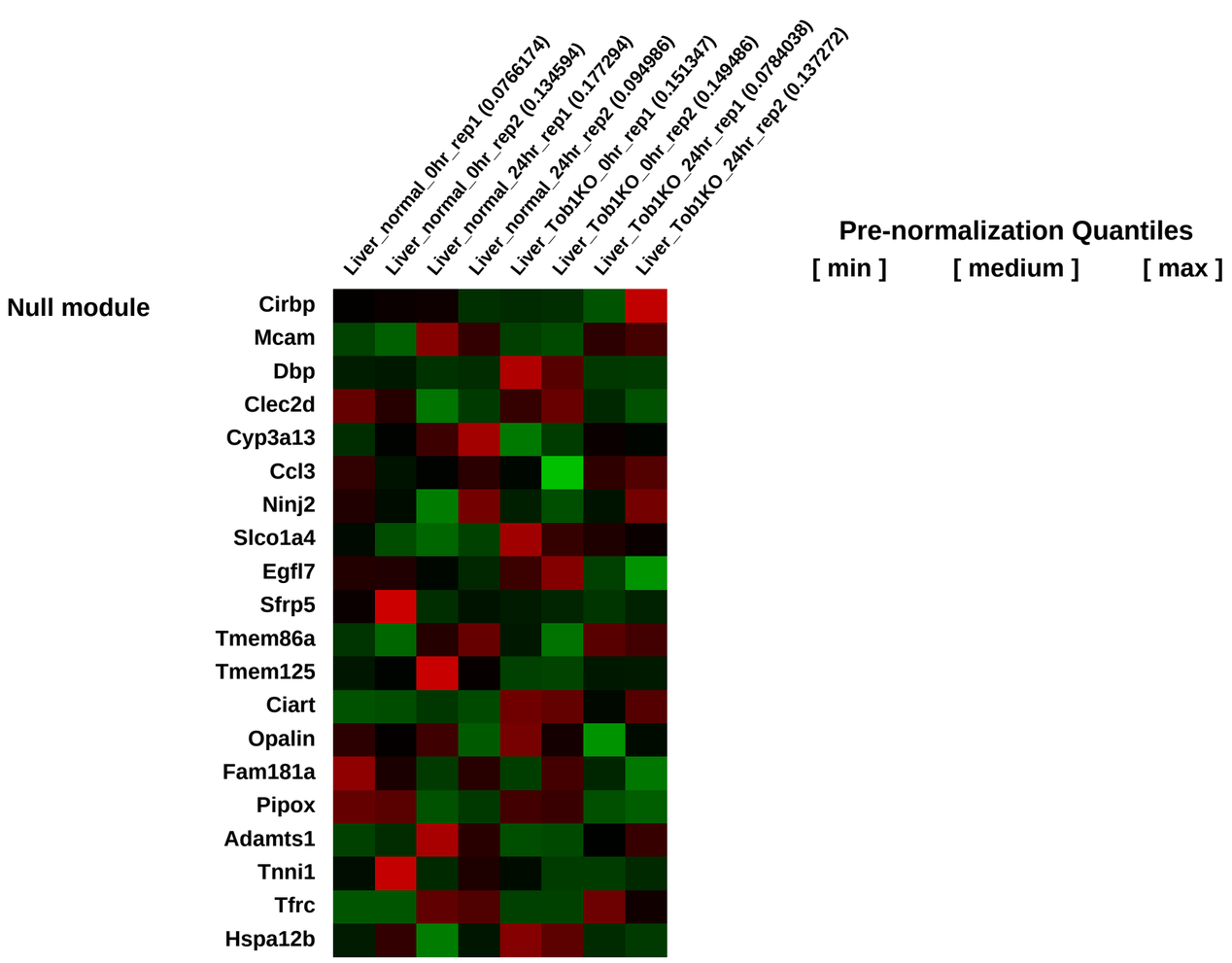

GEO Series "GSE5041" Expression Profiles

Num of samples in this series: 8

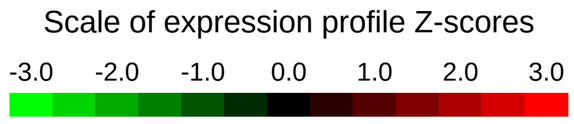

GEO Link:	http://www.ncbi.nlm.nih.gov/geo/query/acc.cgi?acc=GSE5041
Status:	Public on Jul 06 2006
Title:	Expression of the brown fat thermogenic gene program requires PGC-1alpha
Organism:	Mus musculus
Experiment type:	Expression profiling by array
Platform:	GPL1261
Pubmed ID:	16679291
Summary & Design:	**Summary:** To investigate the specific role of PGC-1 coactivators in brown fat cells, we generated immortal preadipocyte lines from the brown adipose tissue of mice lacking PGC-1alpha. We could then efficiently knockdown PGC-1beta expression by shRNA expression. Loss of PGC-1alpha did not alter brown fat differentiation but severly reduced the induction of thermogenic genes. In order to assess the specific requirement for PGC-1$_c$– in the global transcriptional response to cAMP, we used Affymetrix arrays to compare the sets of genes induced in response to a 4 hr dbcAMP treatment in differentiated wt and KO cells. This analysis revealed that 88 genes were induced more than 3-fold in the wt cells; of these, 54 (61% of total) were similarly increased in both wt and KO. However, 28 genes (32% of total) were decreased by at least 50% in the KO cells compared to wt cells. These data were confirmed by quantitative PCR for a subset of genes. These data indicate that PGC-1$_c$– is required for proper expression of approximately one third of the genes induced in response to cAMP in brown fat cells, but this set of sensitive genes is enriched in those involved in adaptative thermogenesis. **Keywords: thermogenic gene program** **Overall design:** WT and PGC-1alpha KO brown preadipocytes were differentiated into mature brown adipocytes for seven days. Cells were then treated with dibutyryl cAMP for four hours. Two replicates were made for each condition: WT non treated, WT treated with cAMP, KO non treated, KO treated with cAMP.

Background corr dist: KL-Divergence = 0.0435, L1-Distance = 0.0186, L2-Distance = 0.0004, Normal std = 0.5959

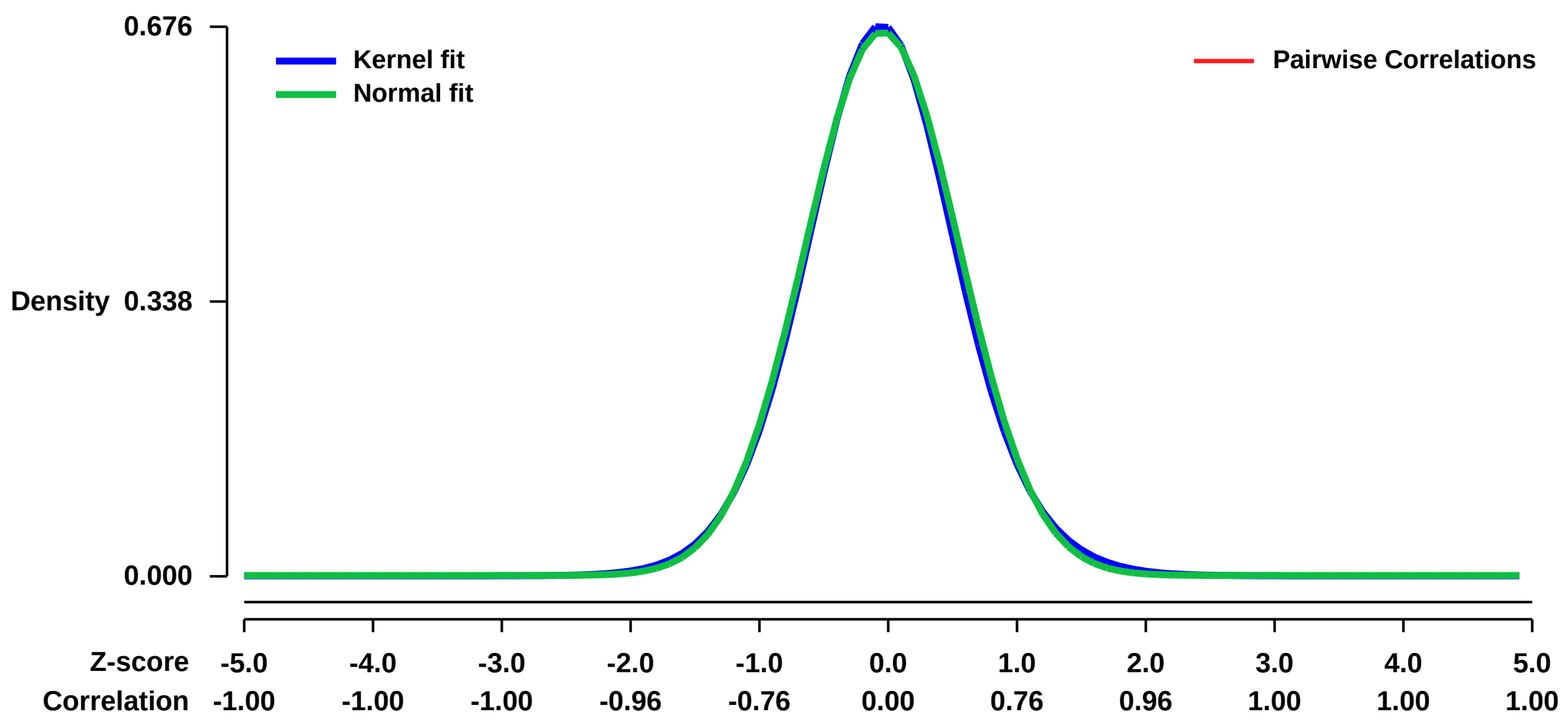

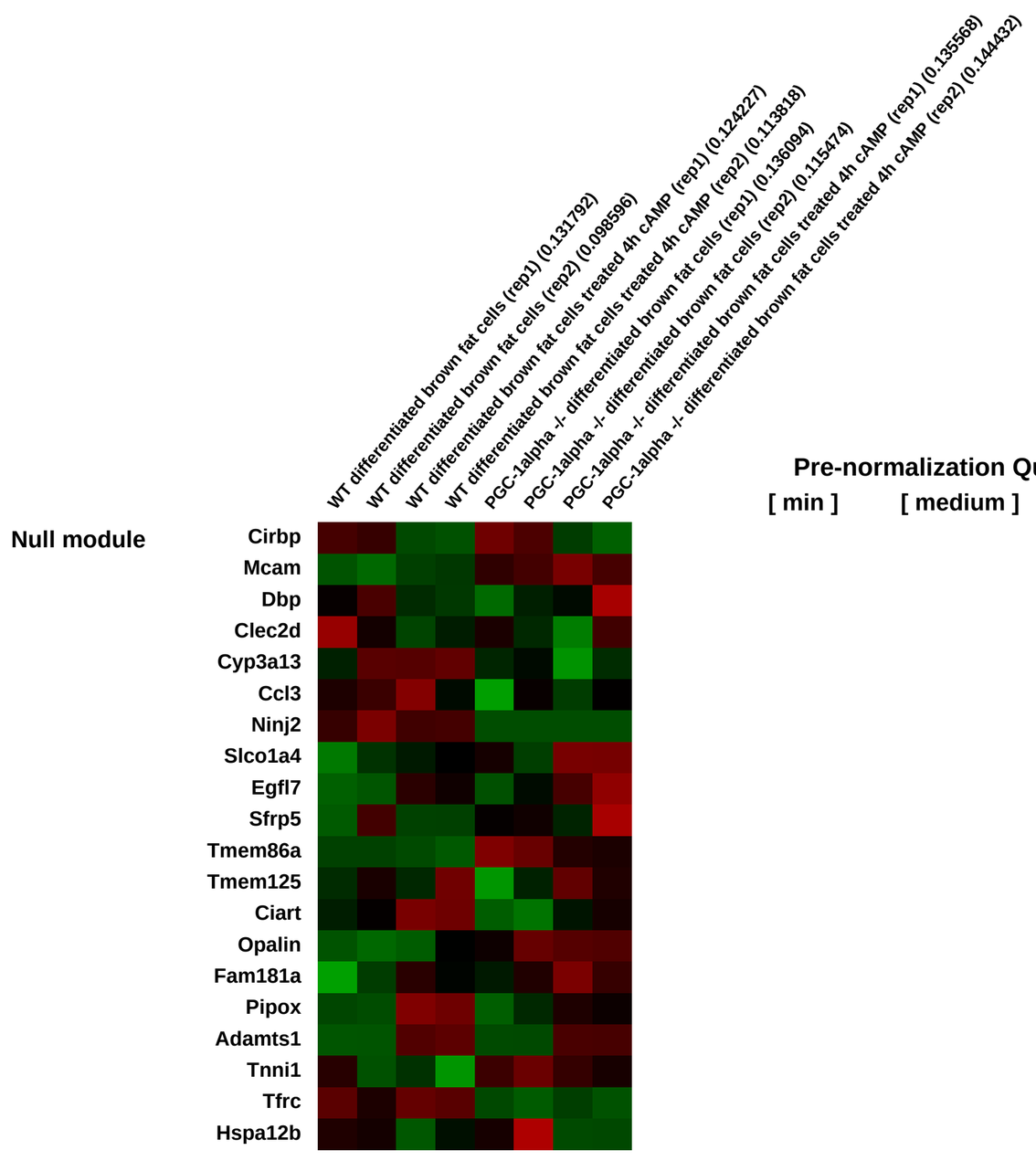

GEO Series "GSE23908" Expression Profiles

Num of samples in this series: 31

Scale of expression profile Z-scores

-3.0 -2.0 -1.0 0.0 1.0 2.0 3.0

GEO Link:	http://www.ncbi.nlm.nih.gov/geo/query/acc.cgi?acc=GSE23908
Status:	Public on Dec 20 2010
Title:	Expression analysis of Wv/Wv fetal gonads
Organism:	Mus musculus
Experiment type:	Expression profiling by array
Platform:	GPL1261
Pubmed ID:	21148109
Summary & Design:	**Summary:** Following sex determination, XY and XX gonads develop into a testis and an ovary, respectively. Depending on the sex of the gonad, resident germ cells will subsequently be committed to either spermatogenesis or oogenesis. In this study we took advantage of the Wv/Wv mouse genetic model, in which gonads are almost devoided of germ cells, to uncover gene expression underlying fetal germ cell development. **Overall design:** Male and Female gonads were collected at 12, 14 and 16 days post coitum (dpc) from wild-type and Wv/Wv mouse embryos. Total RNAs were extracted and hybridized on Affymetrix microarrays. Expression signals from male and female gonads or from wild-type and mutant gonads were compared to identify sexually dimorphic genes as well as genes expressed in germ cell during fetal gonad development.

Background corr dist: KL-Divergence = 0.0515, L1-Distance = 0.0758, L2-Distance = 0.0094, Normal std = 0.6178

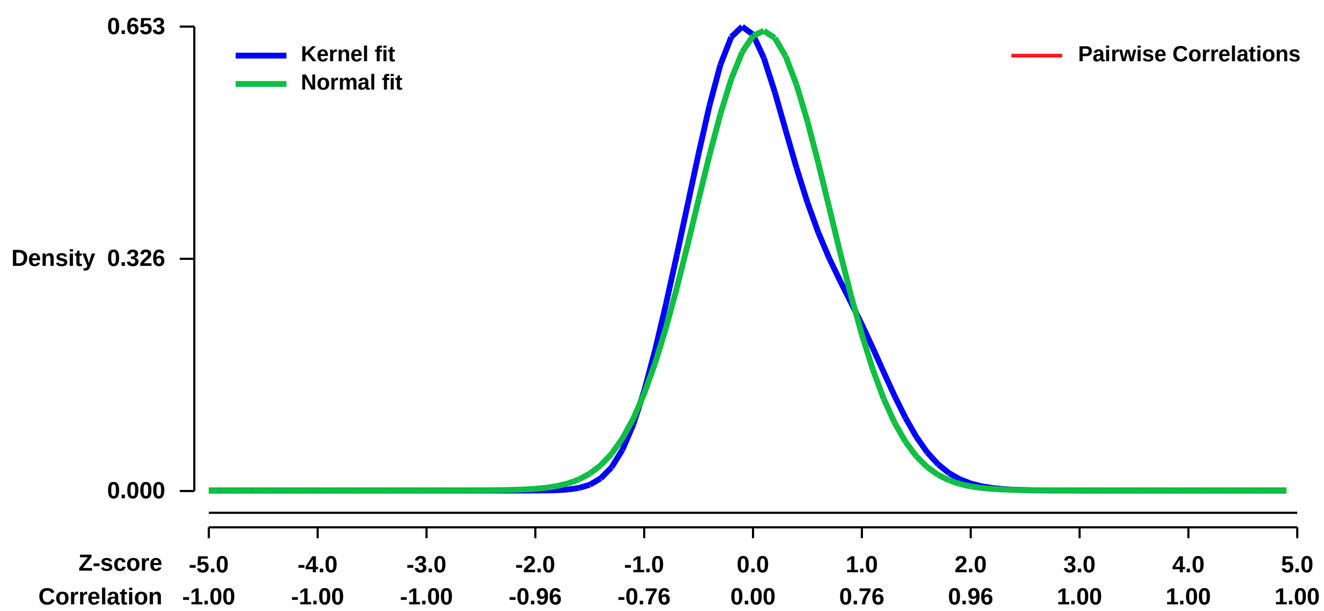

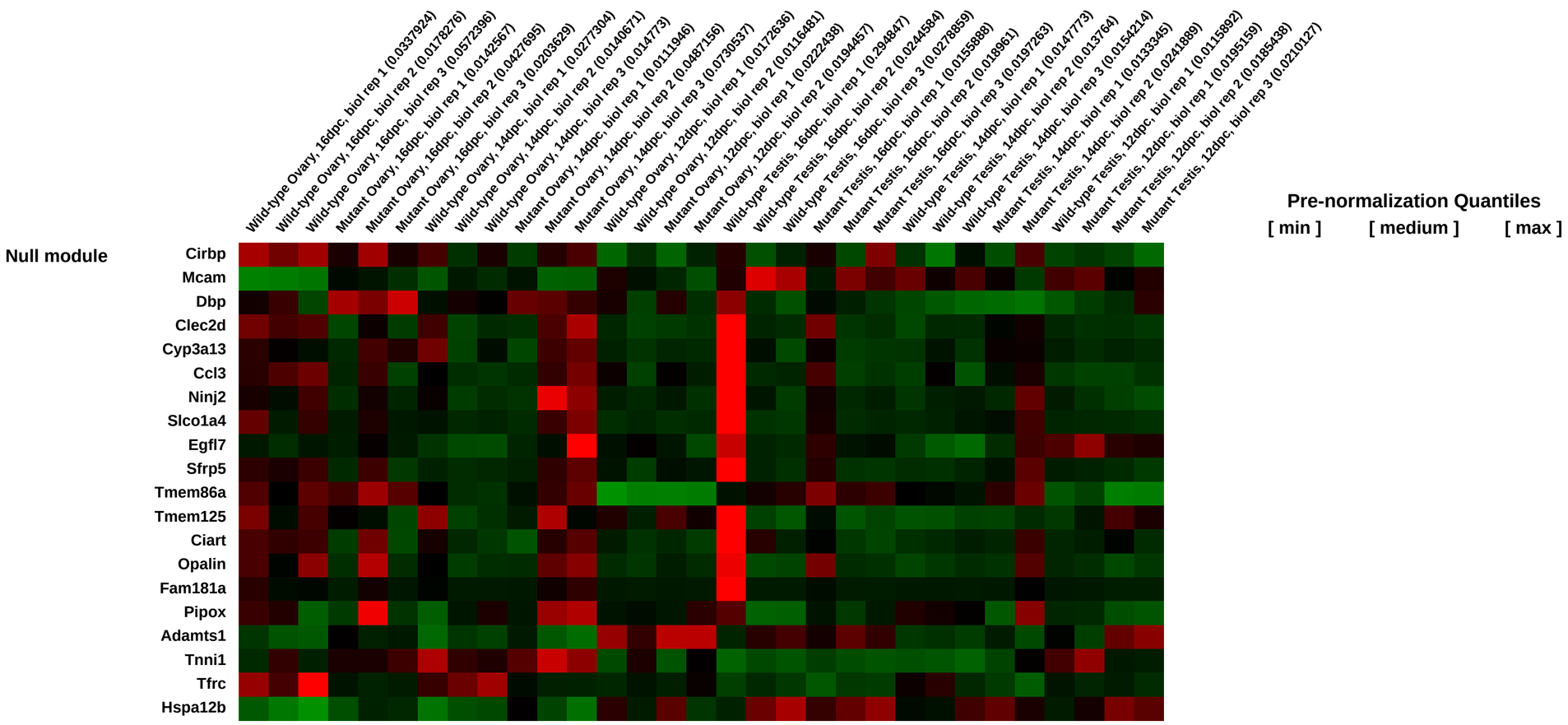

GEO Series "GSE36384" Expression Profiles

Num of samples in this series: 12

Scale of expression profile Z-scores

-3.0 -2.0 -1.0 0.0 1.0 2.0 3.0

GEO Link:	http://www.ncbi.nlm.nih.gov/geo/query/acc.cgi?acc=GSE36384
Status:	Public on Dec 31 2012
Title:	ZNF335 regulates stem cell proliferation and neuronal differentiation via Trithorax complex and REST/NRSF [gene expression]
Organism:	Mus musculus
Experiment type:	Expression profiling by array
Platform:	GPL1261
Pubmed ID:	23178126
Summary & Design:	**Summary:** The progression from stem cell to differentiated neuron is associated with extensive chromatin remodeling that controls gene expression, but the mechanisms that connect chromatin to gene expression are not well defined. Here we show that mutation of ZNF335 causes severe human microcephaly (""small brain""), small somatic size, and neonatal death. Germline Znf335 null mutations are embryonically lethal in mice, whereas RNA-interference studies and postmortem human studies show that Znf335 is essential for neural progenitor self-renewal, neurogenesis, and neuronal differentiation. Znf335 is a component of a vertebrate-specific, trithorax H3K4 methylation complex, while global ChIP-seq and mRNA expression studies show that Znf335 is a previously unsuspected, direct regulator of REST/NRSF, a master regulator of neural gene expression and neural cell fate, as well as other essential neural-specific genes. Our results reveal ZNF335 as an essential link between H3K4 complexes and REST/NRSF, and provide the first direct evidence that this pathway regulates human neurogenesis and neuronal differentiation. **Overall design:** ShRNA knockdown cells were FACS sorted and analyzed for changes in gene expression

Background corr dist: KL-Divergence = 0.0259, L1-Distance = 0.0379, L2-Distance = 0.0021, Normal std = 0.6957

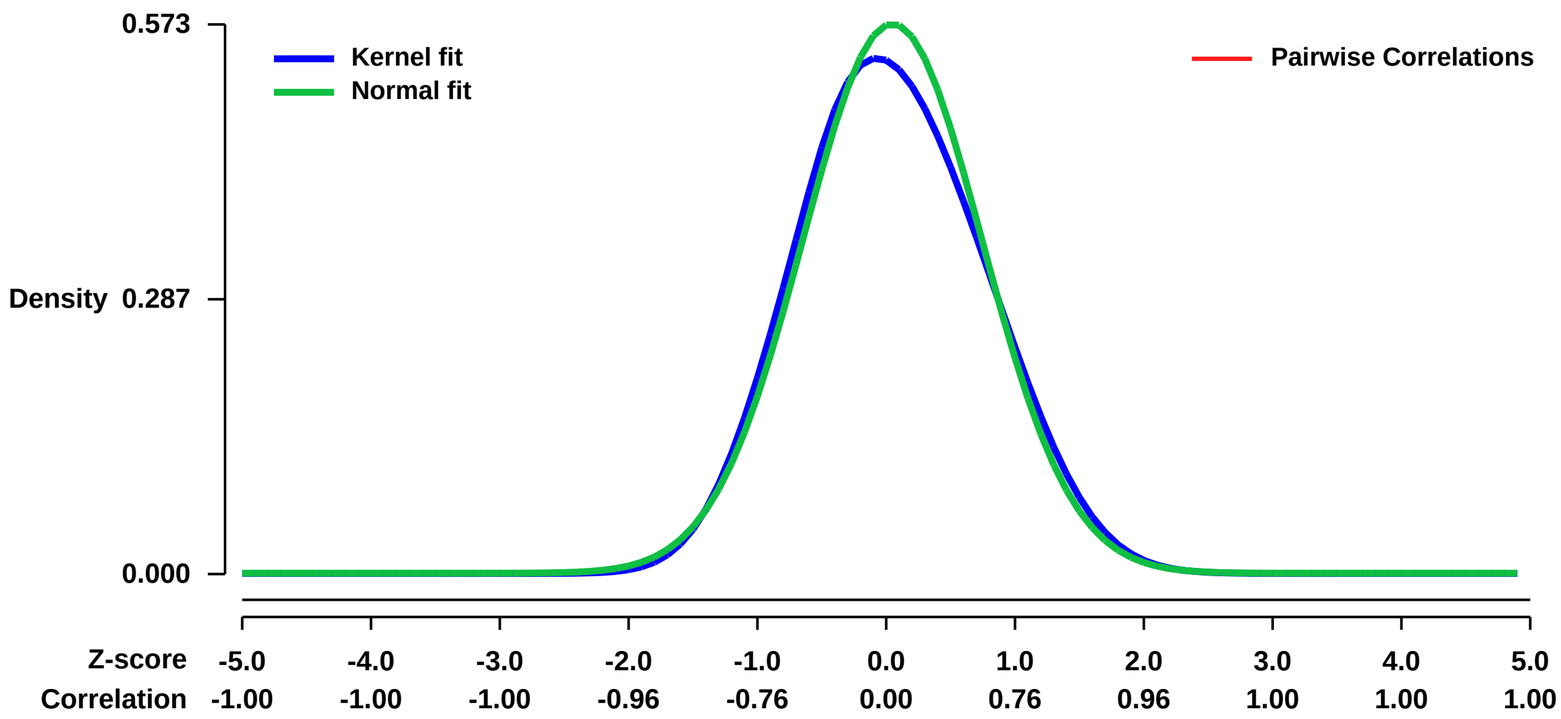

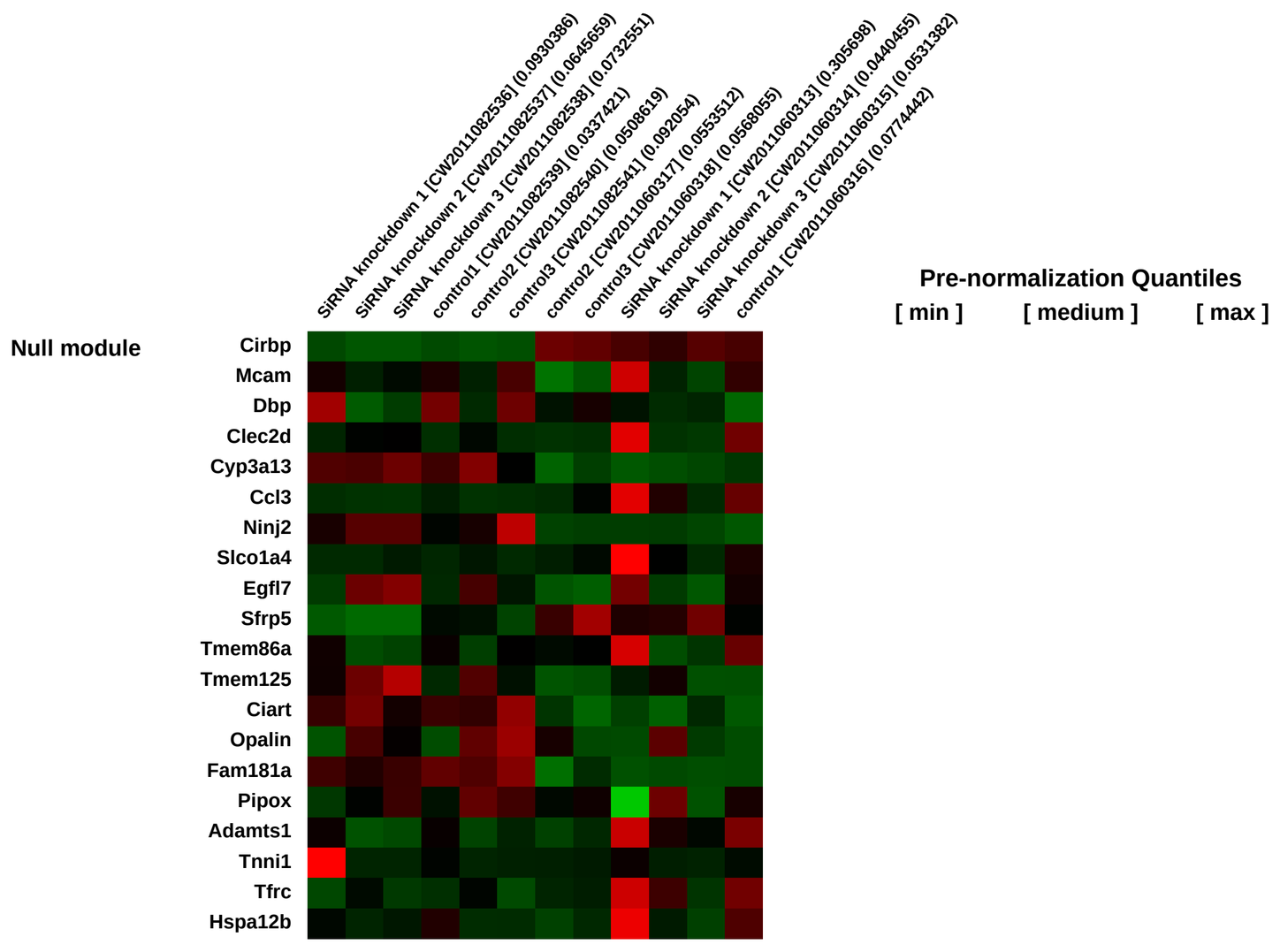

GEO Series "GSE20152" Expression Profiles

Num of samples in this series: 8

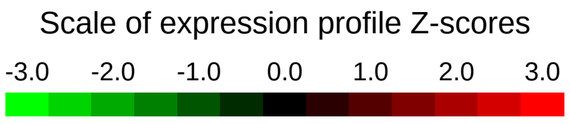

GEO Link:	http://www.ncbi.nlm.nih.gov/geo/query/acc.cgi?acc=GSE20152
Status:	Public on Jan 15 2011
Title:	The role of SphK1 in hTNF$_{\epsilon}$– induced inflammation
Organism:	Mus musculus
Experiment type:	Expression profiling by array
Platform:	GPL1261
Pubmed ID:	20644167
Summary & Design:	**Summary:** The study analyzes analyzes gene expression changes in the ankle joint in mouse TNFa overexpression models with or without sphingosine kinase 1 activity. SphK1 is a sphingolipid enzyme that converts sphingosine to bioactive sphingosine-1-phosphate (S1P). Recent data suggest a potential relationship between SphK1 and TNF$_{\epsilon}$– and have implicated SphK1/S1P in the development and progression of inflammation. Here we further study the relationship of TNF$_{\epsilon}$– and SphK1 using an in vivo model. Transgenic hTNF$_{\epsilon}$– mice, which develop a spontaneous arthritis (limited to paws) at 20 weeks, were crossed with SphK1 activity null mice (SphK1-/-) to study the development of inflammatory arthritis in the functional absence of SphK1. Results show that hTNF/SphK1-/- have significantly less severity and progression of arthritis and bone erosions as measured through micro-CT images. Additionally, less COX-2 protein, mTNF$_{\epsilon}$– transcript levels and fewer Th 17 cells were detected in the joints of hTNF/SphK1-/- compared to hTNF/SphK1+/+ mice. Microarray analysis of the ankle joint showed that hTNF/SphK1-/- mice have increased transcript levels of IL-6 and SOCS3 compared to hTNF/SphK1+/+ mice. Finally, fewer mature osteoclasts were detected in the ankle joints of hTNF/SphK1-/- mice compared to hTNF/SphK1+/+ mice. These data show that SphK1 plays a role in hTNF$_{\epsilon}$– induced inflammatory arthritis, potentially through a novel pathway involving IL-6 and SOCS3. **Overall design:** Two wild-type replicates; three replicates of human TNFa transgene overexpression and normal sphingosine kinase 1; three replicates of human TNFa transgene overexpression and sphingosine kinase 1 null.

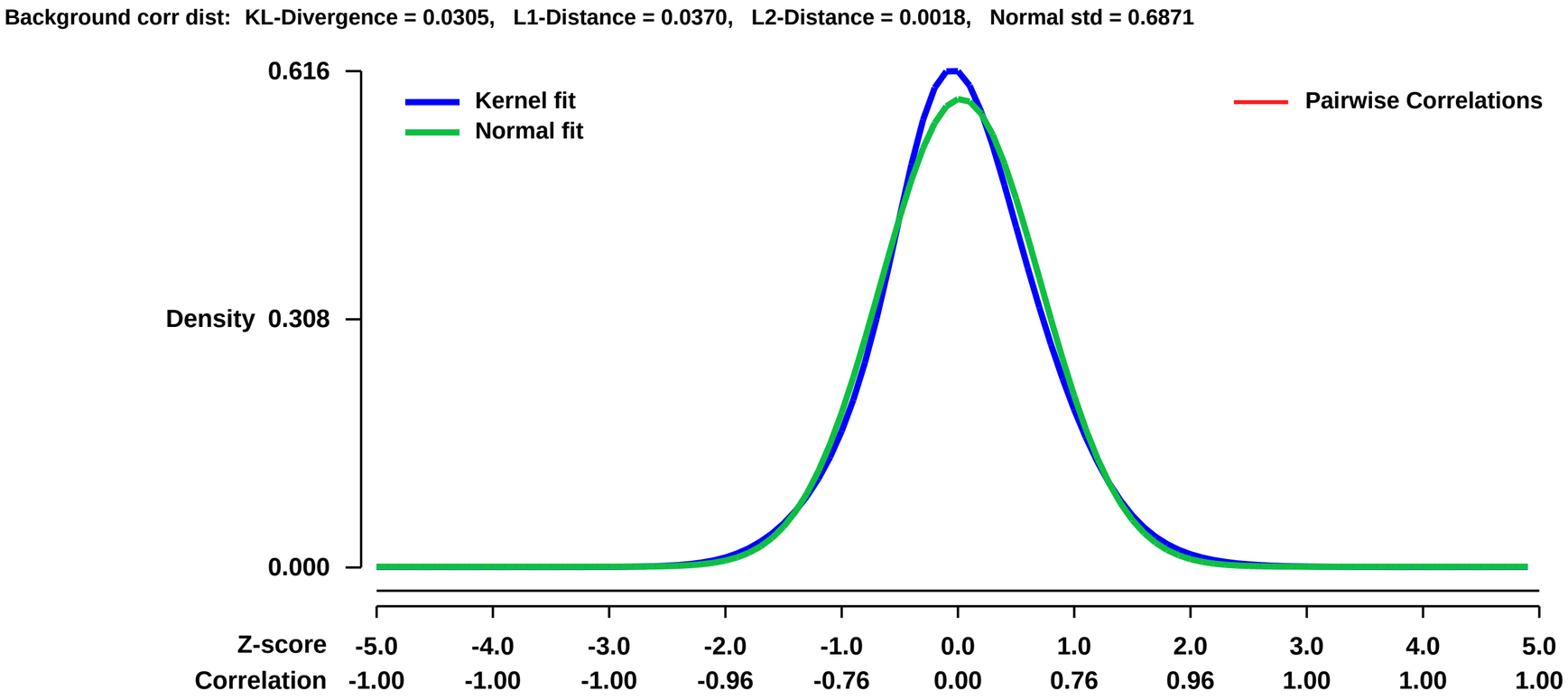

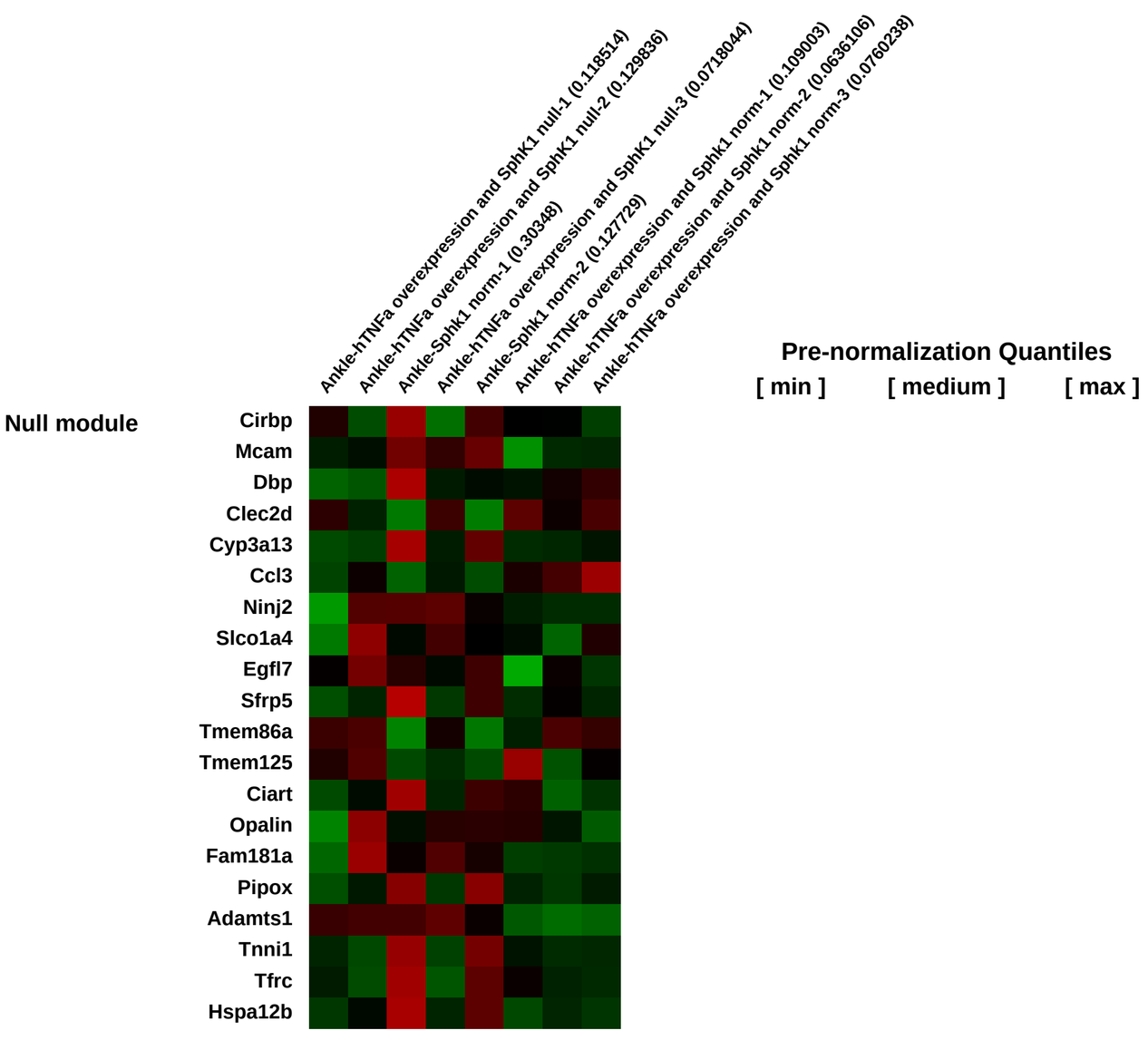

GEO Series "GSE15729" Expression Profiles

Num of samples in this series: 15

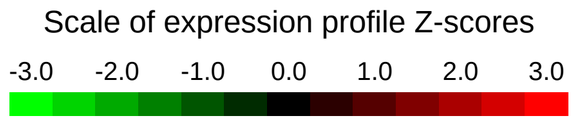

GEO Link:	http://www.ncbi.nlm.nih.gov/geo/query/acc.cgi?acc=GSE15729
Status:	Public on Mar 01 2010
Title:	Gene Expression of ApoE Null and ApoE Null/RAGE Diabetic and Non-diabetic Mice
Organism:	Mus musculus
Experiment type:	Expression profiling by array
Platform:	GPL1261
Pubmed ID:	20133903

Summary & Design:

Summary:
The multi-ligand Receptor for AGE (RAGE) contributes to atherosclerosis in apolipoprotein (ApoE) null mice in both the non-diabetic and diabetic states. Previous studies using soluble RAGE, the extracellular ligand-binding domain of RAGE, or homozygous RAGE null mice showed that blockade or deletion of RAGE resulted in marked reduction in atherosclerotic lesion area and complexity compared to control animals. In parallel, significant down-regulation of inflammatory mediators and matrix metalloproteinases was evident in ApoE null mice aortas devoid of RAGE compared to those of ApoE null RAGE-expressing mice. Although these findings suggested that RAGE triggered pro-atherogenic mechanisms via regulation of inflammatory gene expression, these studies did not reveal the broader pathways by which RAGE contributed to atherosclerosis in ApoE null mice.

Therefore, we performed Affymetrix gene expression arrays on aortas of non-diabetic and diabetic ApoE null mice expressing RAGE or devoid of RAGE at nine weeks of age, as this reflected a time point at which frank atherosclerotic lesions were not yet present, but, that we would be able to identify the genes likely involved in diabetes- and RAGE-dependent atherogenesis. The comparisons were as follows: 1. diabetic ApoE null relative to non-diabetic ApoE null; 2. non-diabetic ApoE null / RAGE null relative to non-diabetic ApoE null; 3. diabetic ApoE null / RAGE null relative to non-diabetic ApoE null / RAGE null; and 4. diabetic ApoE null / RAGE null relative to diabetic ApoE null aorta.

Our data reveal that there is very little overlap of the genes which are differentially expressed both in the onset of diabetes in ApoE null mice, and in the effect of RAGE deletion in diabetic ApoE null mice. We next performed a Pathway-Express analysis to determine the pathways that were most associated with the onset of diabetes in ApoE null mice and the effect of RAGE gene deletion in diabetic ApoE null mice. Rigorous statistical analysis was undertaken and revealed that the transforming growth factor-¿† pathway (tgf-¿†) and focal adhesion pathways might be expected to play a significant role in both the mechanism by which diabetes facilitates the formation of atherosclerotic plaques in ApoE null mice, and the mechanism by which deletion of RAGE ameliorates this effect. We focused on three genes of the tgf-¿† family which were found to be up-regulated in diabetic vs. non-diabetic ApoE null aorta, and which were reduced by deletion of RAGE. These included: thrombospondin1 (Thbs1), transforming growth factor-¿†2 (tgf-¿†2) and rho-associated kinase (ROCK1). Real-time quantitative polymerase chain reaction and Western blotting experiments were performed, as well as ROCK1 activity assays in mouse aorta, and validated the findings of the Affymetrix gene array. Further, confocal microscopy revealed that a principal cell type in the ApoE null aorta expressing these factors was the vascular smooth muscle cell. Our data suggest the novel finding that the observed reduction of accelerated atherosclerosis in diabetic ApoE null / RAGE null vs. diabetic ApoE null mice occurs, all or in part, through the ROCK1 branch of the TGF-¿† pathway. We have inferred a detailed mechanism for this process.

Taken together, these data suggest that suppression of ROCK1 activity in the atherosclerosis-vulnerable vessel wall, especially in diabetes, but in non-diabetes as well, may underlie the beneficial effects of RAGE antagonism and genetic deletion in murine models. These findings highlight logical and novel targets for therapeutic intervention in cardiovascular disease and diabetes.

Overall design:
There were 4 mice in each group initially. However there are only 3 non-diabetic ApoE null / RAGE null mice in the final experimental sample in group 3 due to a failure to generate cRNA from that sample. All samples were normalized to remove chip-dependent regularities using the RMA method. Chips and controls at each combination of genotype and disease sate were normalized together. The statistical significance of differential expression was calculated using the empirical Bayesian LIMMA (LInear Model for MicroArrays) method A cut-off B>0 was used for the statistical significance of gene expression.

Background corr dist: KL-Divergence = 0.1445, L1-Distance = 0.0344, L2-Distance = 0.0024, Normal std = 0.3840

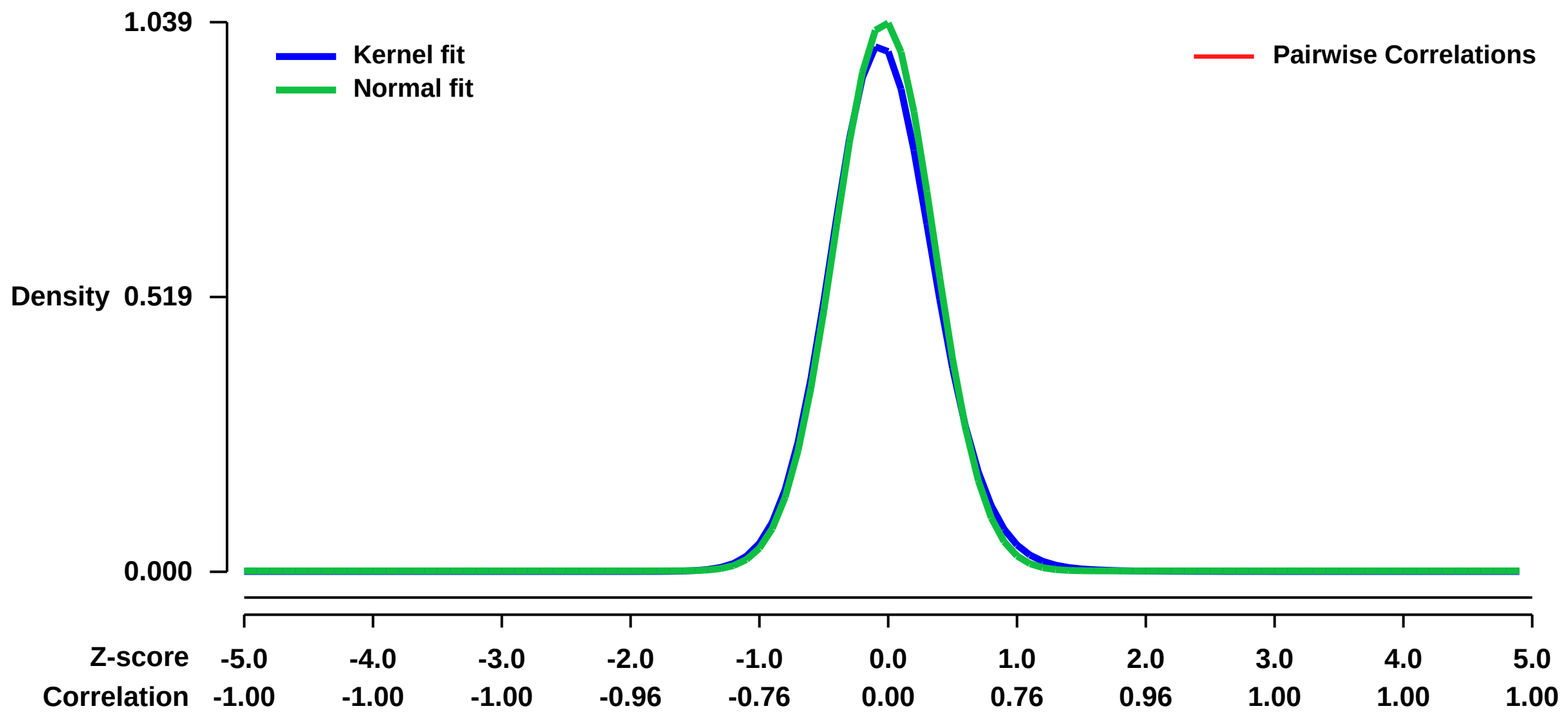

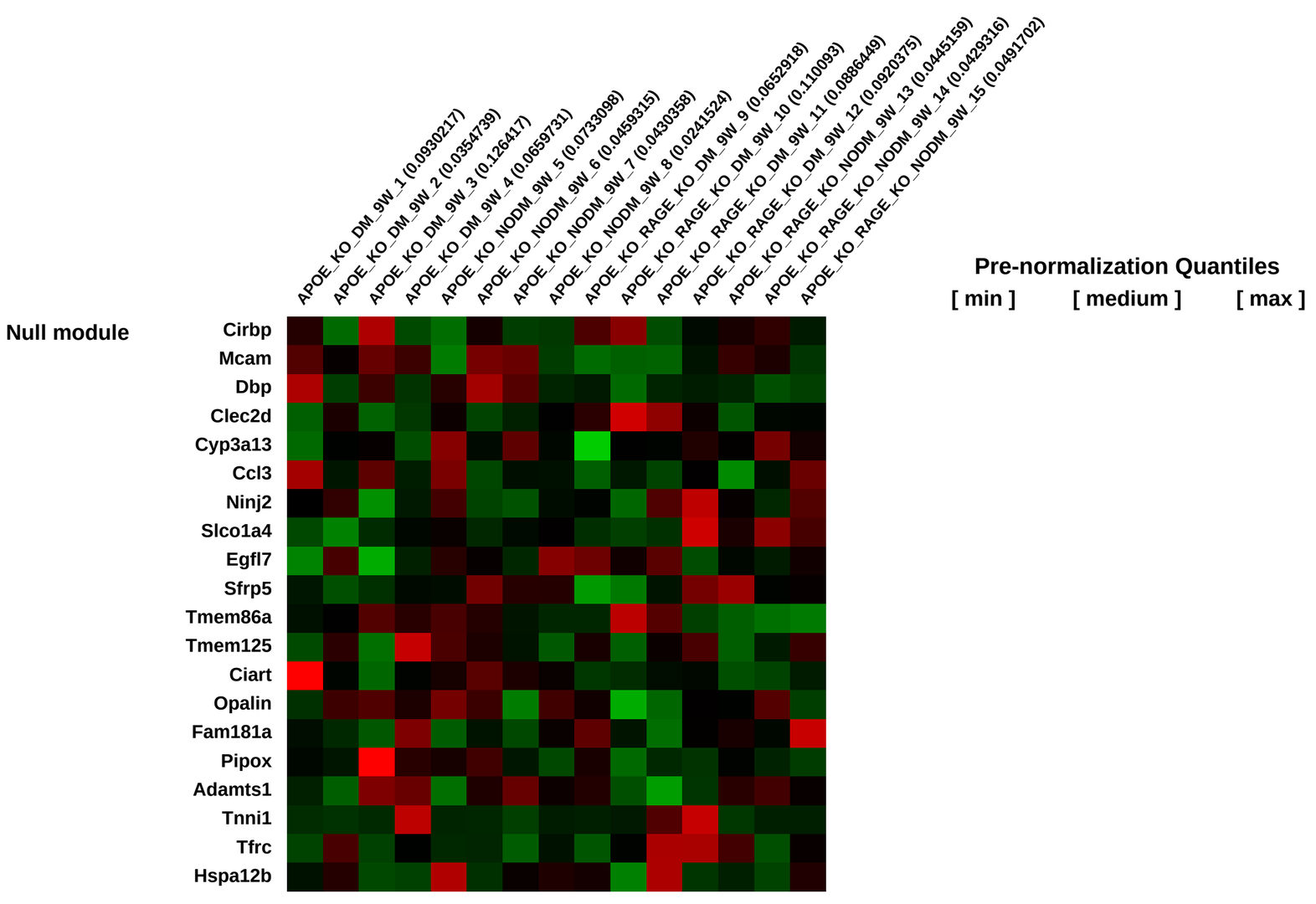

GEO Series "GSE39375" Expression Profiles

Num of samples in this series: 10

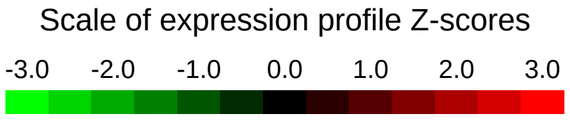

GEO Link:	http://www.ncbi.nlm.nih.gov/geo/query/acc.cgi?acc=GSE39375
Status:	Public on Sep 01 2012
Title:	Polysome profiling in liver identifies dynamic regulation of endoplasmic reticulum translatome by obesity and fasting
Organism:	Mus musculus
Experiment type:	Other
Platform:	GPL1261
Pubmed ID:	22927828
Summary & Design:	**Summary:** Obesity-associated metabolic complications are generally considered to emerge from abnormalities in carbohydrate and lipid metabolism, whereas the status of protein metabolism is not well studied. Here, we performed comparative polysome and associated transcriptional profiling analyses to study the dynamics and functional implications of endoplasmic reticulum (ER)-associated protein synthesis in the mouse liver under conditions of obesity and nutrient deprivation. **Overall design:** lean wild type and genetically obese (ob/ob) mice with or without overnight fasting were sacrificed with their liver tissues removed. ER-associated polysomes were purified and analyzed by microarray.

Background corr dist: KL-Divergence = 0.1087, L1-Distance = 0.0301, L2-Distance = 0.0017, Normal std = 0.4250

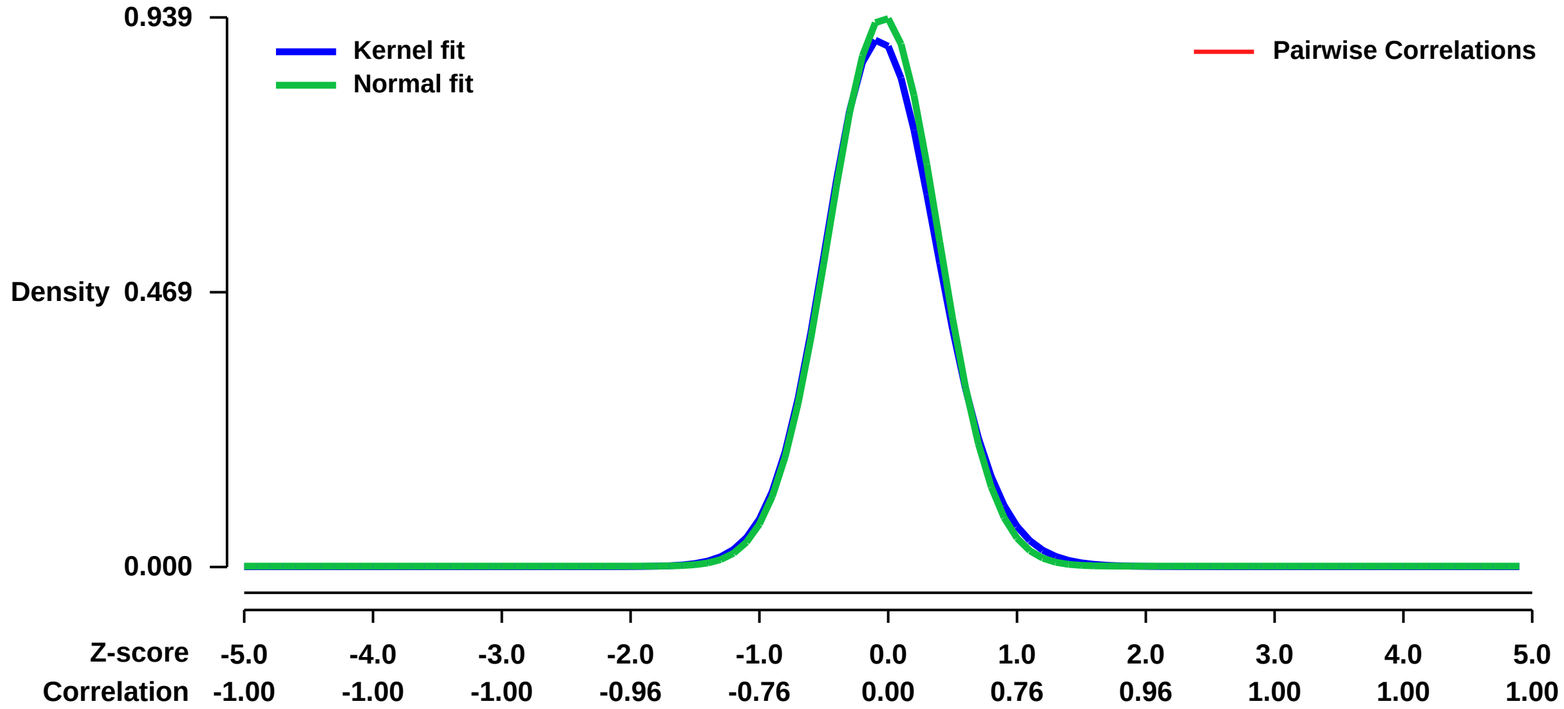

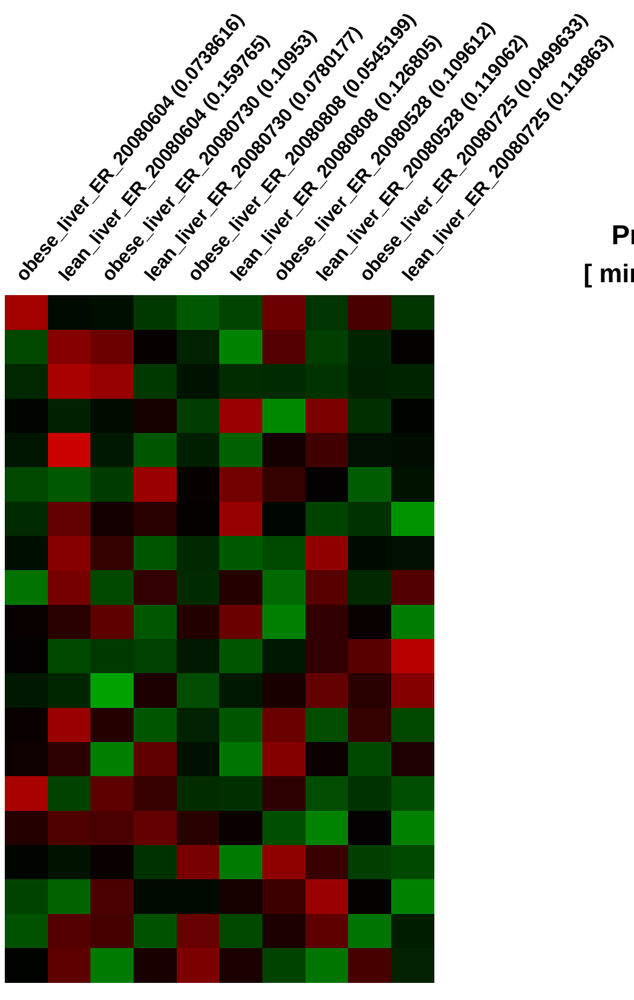

GEO Series "GSE40286" Expression Profiles

Num of samples in this series: 10

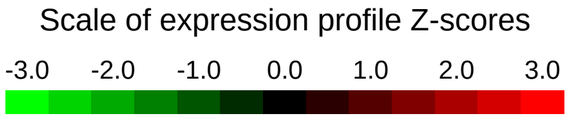

GEO Link:	http://www.ncbi.nlm.nih.gov/geo/query/acc.cgi?acc=GSE40286
Status:	Public on Oct 01 2012
Title:	The Mediator MED23 plays opposing roles in directing smooth muscle cell and adipocyte differentiation
Organism:	Mus musculus
Experiment type:	Expression profiling by array
Platform:	GPL1261
Pubmed ID:	22972934
Summary & Design:	**Summary:** We examined how MED23 regulates SRF-targeted genes by comparing WT and Med23 KO mouse embryonic fibroblasts (MEFs) in the presence or absence of serum-stimulation (for 30 and 90 min). To investigate whether MAL antagonizes MED23 in the adipocyte lineage program, we compared the gene expression changes resulting from Mal overexpression (oxMal) and Med23 deficiency (siMed23) in 10T1/2 cell. **Overall design:** In MEF cells, we examined SRF-dependent gene expression in three time points (0, 30, 90min) and two conditions (WT and KO). In 10T1/2 cells, we used three treatment conditions (Mal overexpression, Med23 knockdown, and treatment of both Mal overexpression and Med23 knockdown) with control (no treatment).

Background corr dist: KL-Divergence = 0.0284, L1-Distance = 0.0534, L2-Distance = 0.0049, Normal std = 0.7021

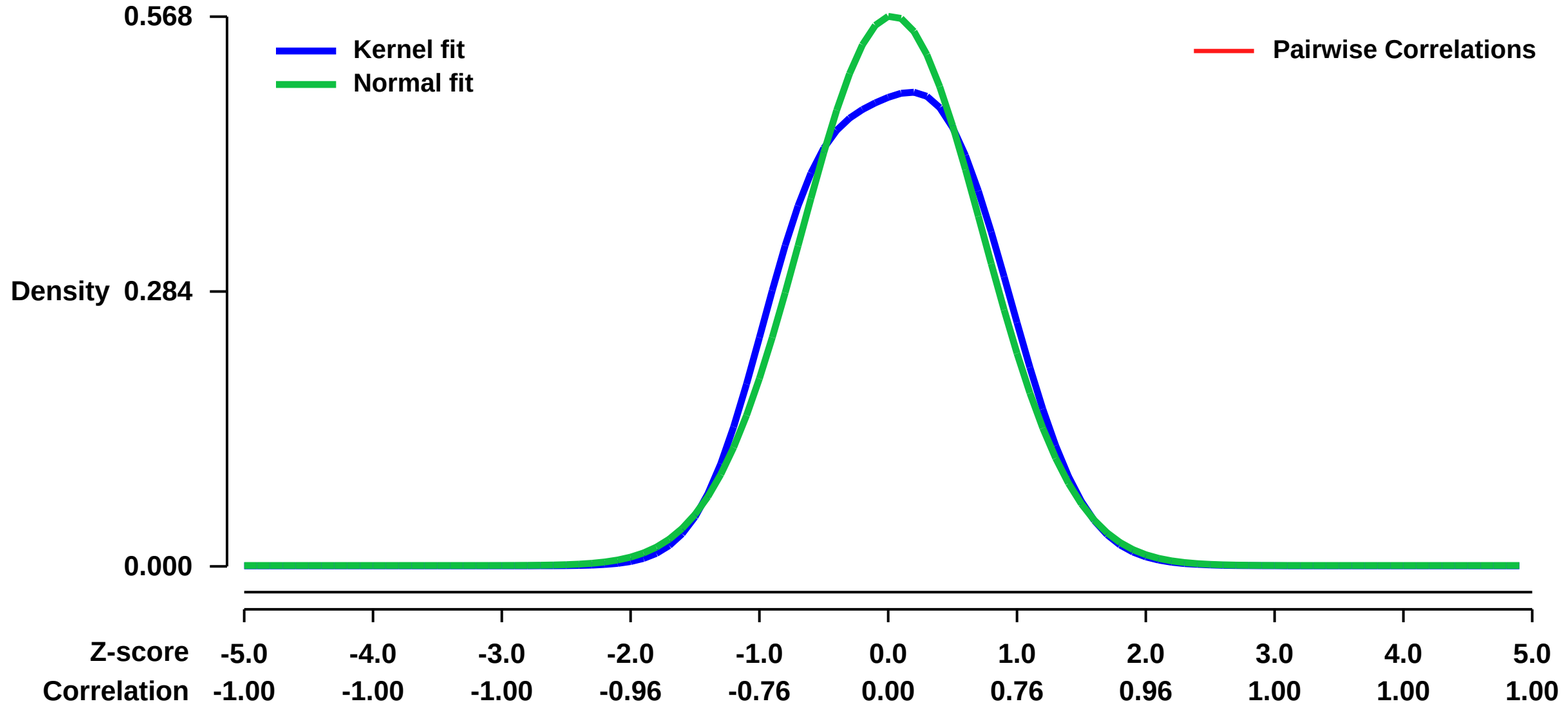

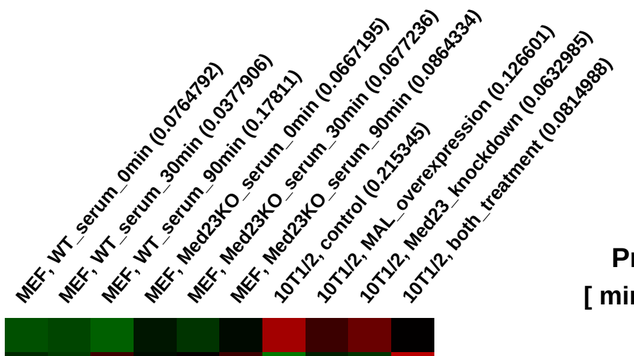

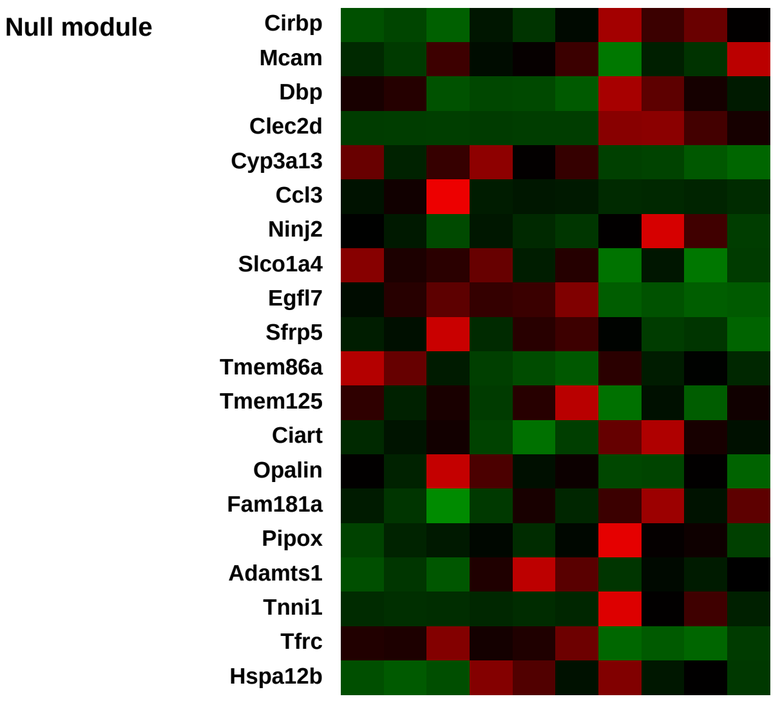

GEO Series "GSE44355" Expression Profiles

Num of samples in this series: 10

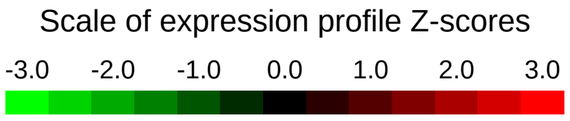

GEO Link:	**http://www.ncbi.nlm.nih.gov/geo/query/acc.cgi?acc=GSE44355**
Status:	**Public on Jul 04 2013**
Title:	**Expression data from Adriamycin-treated Emu-myc; Suv39h1-/- B-cell lymphoma**
Organism:	**Mus musculus**
Experiment type:	**Expression profiling by array**
Platform:	**GPL1261**
Pubmed ID:	**23945590**
Summary & Design:	**Summary:** **Oncogene-induced senescence (OIS), a terminal cell cycle block countering (pre)neoplastic lesions, is characterised on the molecular level by trimethylated histone H3 lysine 9 (h3K9me3), a transcriptionally repressive chromatin mark linked to silencing of S-phase-promoting genes. Whether H3K9-governed chromatin remodelling influences anticancer treatment-induced senescence (TIS) and whether functional control of this mark impacts on treatment outcome is not known. We used global gene expression profiling by microarrays to gain insight into the molecular responses of Emu-myc; Suv39h1-/- B-cell lymphoma cells to senescence-inducing anticancer agent Adriamycin (ADR).** **Overall design:** **Primary lymphoma cells isolated from lymph nodes of Emu-Myc; Suv39h1-/- mice were used. In this model, the c-Myc oncogene is constitutively expressed in the cells of the B-cell lineage, leading to spontaneous development of aggressive B-cell lymphomas. Adriamycin (ADR), a cytostatic drug used as a standard part of several lymphoma treatment regimens, is known to massively induce TIS in Suv39h1-proficient lymphomas, protected from apoptosis by Bcl-2 over expression (Myc;Bcl2). In order to discern the impact of Suv39h1 to TIS induction under these conditions, we analysed here transcriptional profiles of matched pairs of Emu-myc;Suv39h1-/-;Bcl2 lymphomas, untreated or treated for 5 days with ADR.**

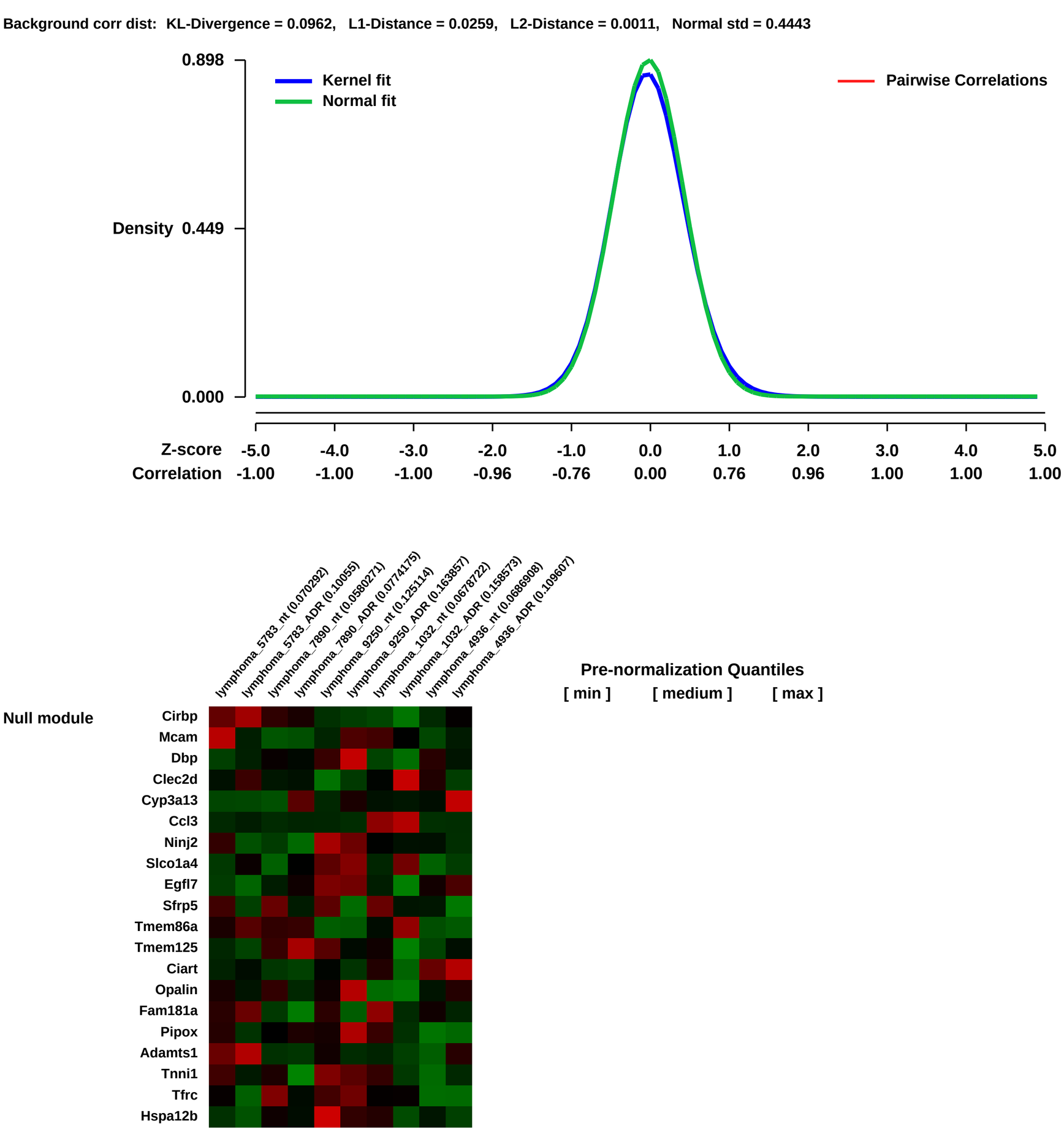

GEO Series "GSE36330" Expression Profiles

Num of samples in this series: 18

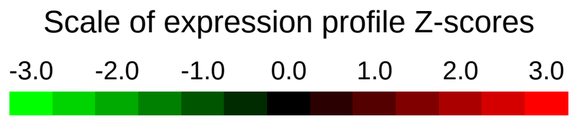

GEO Link:	**http://www.ncbi.nlm.nih.gov/geo/query/acc.cgi?acc=GSE36330**
Status:	**Public on Mar 08 2012**
Title:	**Comparison of exercise and pregnancy-induced cardiac hypertrophy**
Organism:	**Mus musculus**
Experiment type:	**Expression profiling by array**
Platform:	**GPL1261**
Pubmed ID:	**22860109**
Summary & Design:	**Summary:** **Comparative analysis of mouse cardiac left ventricle gene expression: voluntary wheel exercise and pregnancy-induced cardiac hypertrophy** **Overall design:** **We performed microarray analysis on RNA from left ventricles of mice in non-pregnant diestrus cycle, mid-pregnancy (MP), late-pregnancy (LP), and immediate post-partum (0PP). These were compared to 7days (7EX) and 21 days (21EX) of voluntary wheel running exercise.**

Background corr dist: **KL-Divergence = 0.2289, L1-Distance = 0.0576, L2-Distance = 0.0082, Normal std = 0.3127**

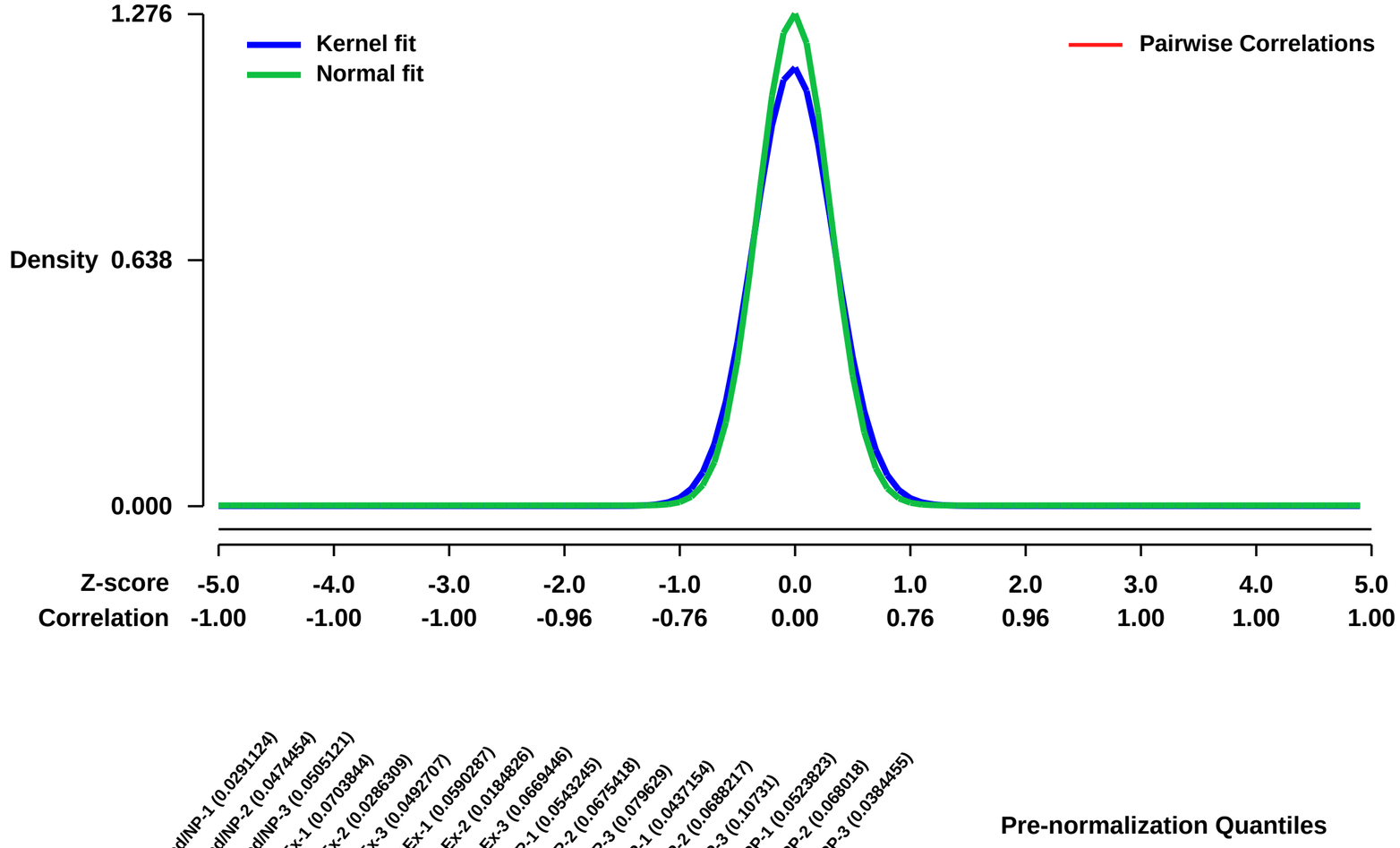

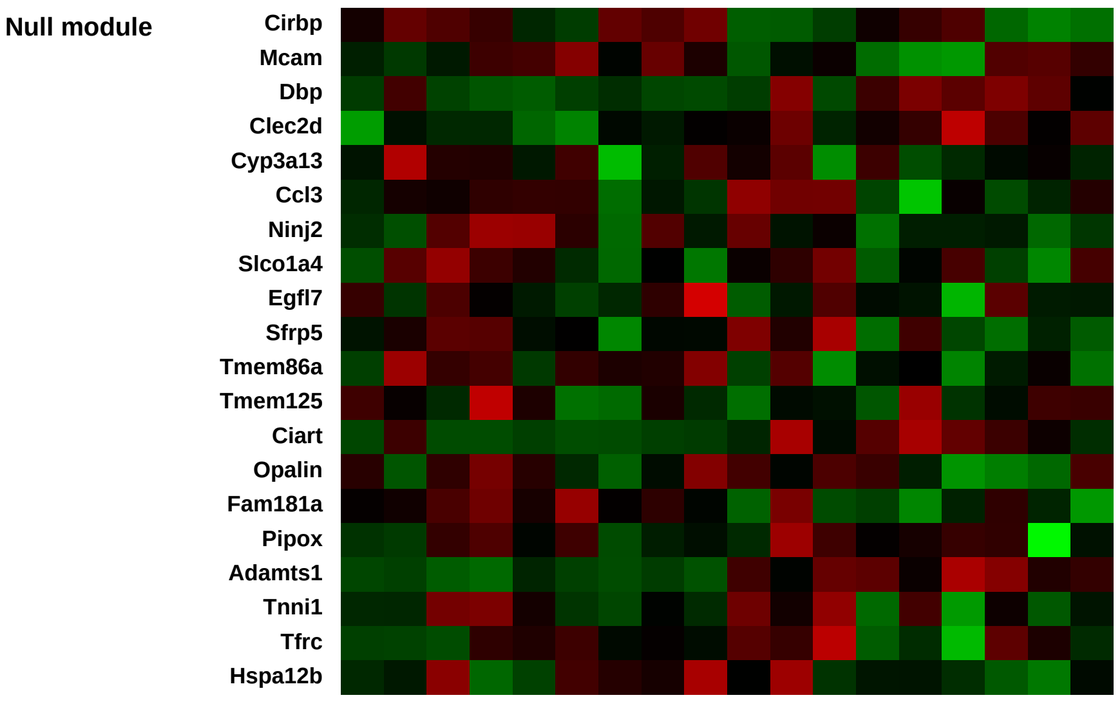

GEO Series "GSE27881" Expression Profiles

Num of samples in this series: 16

Scale of expression profile Z-scores

-3.0 -2.0 -1.0 0.0 1.0 2.0 3.0

GEO Link:	http://www.ncbi.nlm.nih.gov/geo/query/acc.cgi?acc=GSE27881
Status:	Public on Jul 20 2011
Title:	Effect of ablation of Max gene expression on ES cells cultured under conventional or 2i/Nam condition.
Organism:	Mus musculus
Experiment type:	Expression profiling by array
Platform:	GPL1261
Pubmed ID:	21726832
Summary & Design:	**Summary:** c-Myc is one of key players that are crucially involved in maintaining the undifferentiated state and the self-renewal of ESCs. To understand the mechanism by which c-Myc helps preserve these prominent characteristics of ESCs, we generated null-ES cells for the Max gene, which encodes the best characterized partner protein for all Myc family proteins. Although Myc/Max complexes have been widely regarded as crucial regulators of the ESC status, our data reveal that ESCs do not absolutely require these complexes in so-called ground state or related conditons and that this requirement is restricted to conventional ES culture conditions without using a MAPK inhibitor. **Overall design:** Simply Dox-treated or Nanog (WT or D67G mutant)-rescued Max-null ESCs which were cultured under conventional culture condition and 2i/Nam-treated completely Max-null ES cells from which Dox-regulatable cDNA was removed were used for RNA source. Samples from Dox-untreated Max-null ESCs cultured under conventional culture condition were used as reference samples for Dox-treated cells and Nanog-rescued cells, while a sample from wild-type ESCs cultured under 2i/Nam condition was used as a reference sample for completely Max-null ES cells cultured with 2i/Nam.

Background corr dist: KL-Divergence = 0.0755, L1-Distance = 0.0470, L2-Distance = 0.0046, Normal std = 0.4865

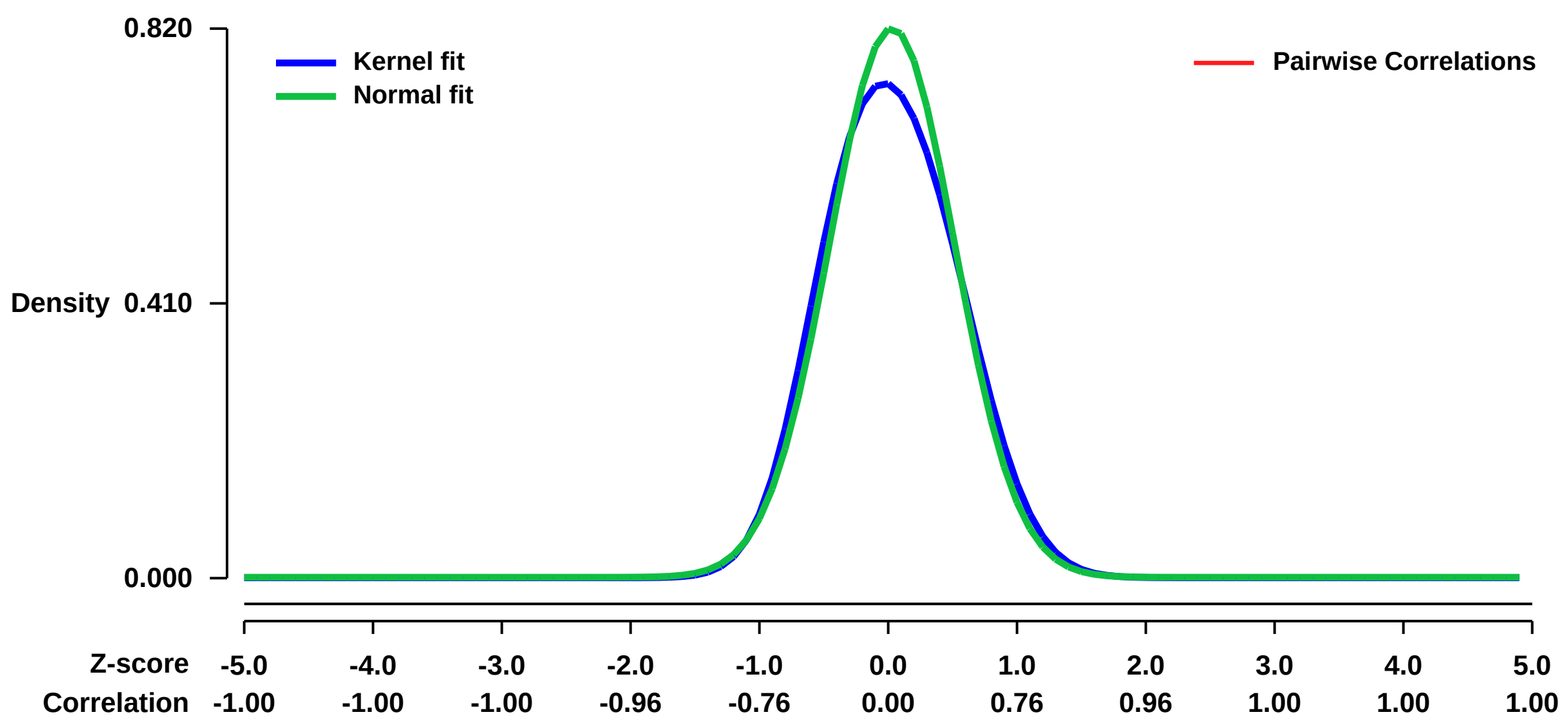

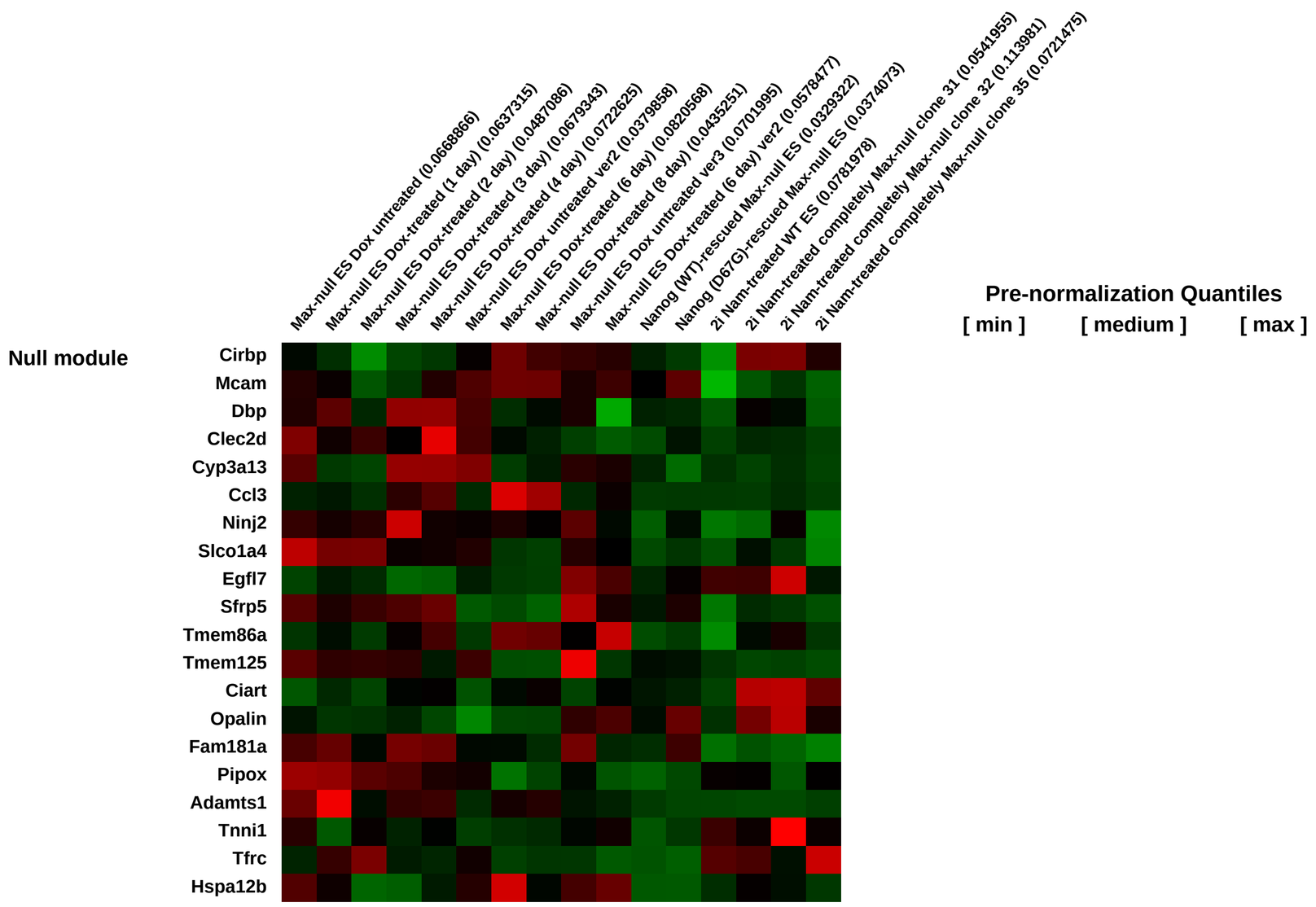

GEO Series "GSE33341" Expression Profiles

Num of samples in this series: 227

Details of this dataset are not shown due to large number of samples and the page size limit.

Find details in http://www.ncbi.nlm.nih.gov/geo/query/acc.cgi?acc=GSE33341

Background corr dist: KL-Divergence = 0.2132, L1-Distance = 0.0887, L2-Distance = 0.0240, Normal std = 0.3326

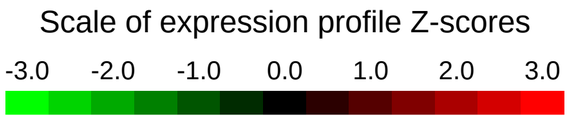

GEO Series "GSE59437" Expression Profiles

Num of samples in this series: 30

Scale of expression profile Z-scores

-3.0 -2.0 -1.0 0.0 1.0 2.0 3.0

GEO Link:	http://www.ncbi.nlm.nih.gov/geo/query/acc.cgi?acc=GSE59437
Status:	Public on Jul 16 2014
Title:	Expression data from mouse tissue Angiotensin II treated for 0,1,3,7days
Organism:	Mus musculus
Experiment type:	Expression profiling by array
Platform:	GPL1261
Pubmed ID:	
Summary & Design:	**Summary:** Angiotensin II (Ang II) mediated signaling plays a key role in the development of hypertension associated target organ damages. However, the gene expression changes regulated by Ang II in the early stage of acute cerebral, cardiac, renal, vascular injury remain unclear. we investigated Ang IIâ mediated gene expression alteration associated with the development of early cerebral, cardiac, renal, vascular injury by microarray assay in a mouse model. **Overall design:** All mice were euthanized by an overdose of pentobarbital on days 1, 3 and 7 of Angiotensin II treatment. Total RNA was isolated with TRIzol (Invitrogen) from brains, hearts, kidneys and vessels (n=1-3 per group) at each time point according to manufacturerâ s instructions. Gene expression profiling was performed using Affymetrix GeneChip mouse Genome 430 2.0 array according to the manufacturerâ s instructions (Affymetrix, Inc., Santa Clara, CA). On the GeneChip Mouse Genome 430 2.0 Array, over 45,000 probe sets analyze the expression level of over 39,000 transcripts and variants from over 34,000 well characterized mouse genes.

Background corr dist: KL-Divergence = 0.0645, L1-Distance = 0.0519, L2-Distance = 0.0054, Normal std = 0.5458

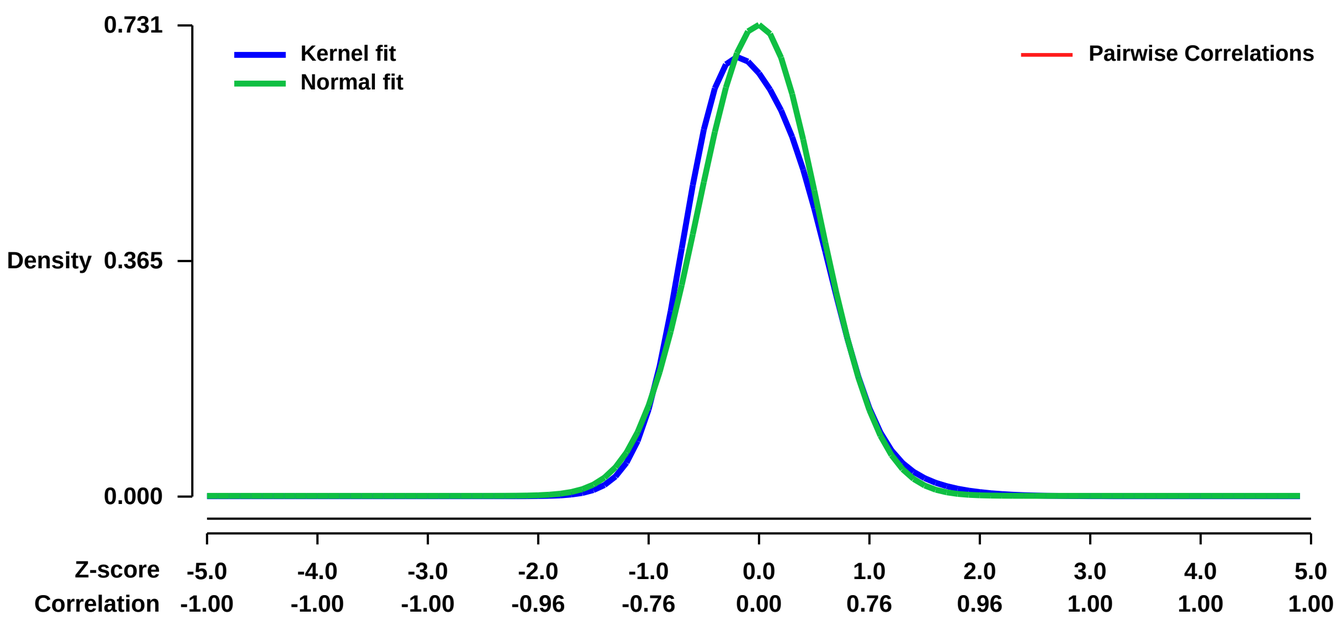

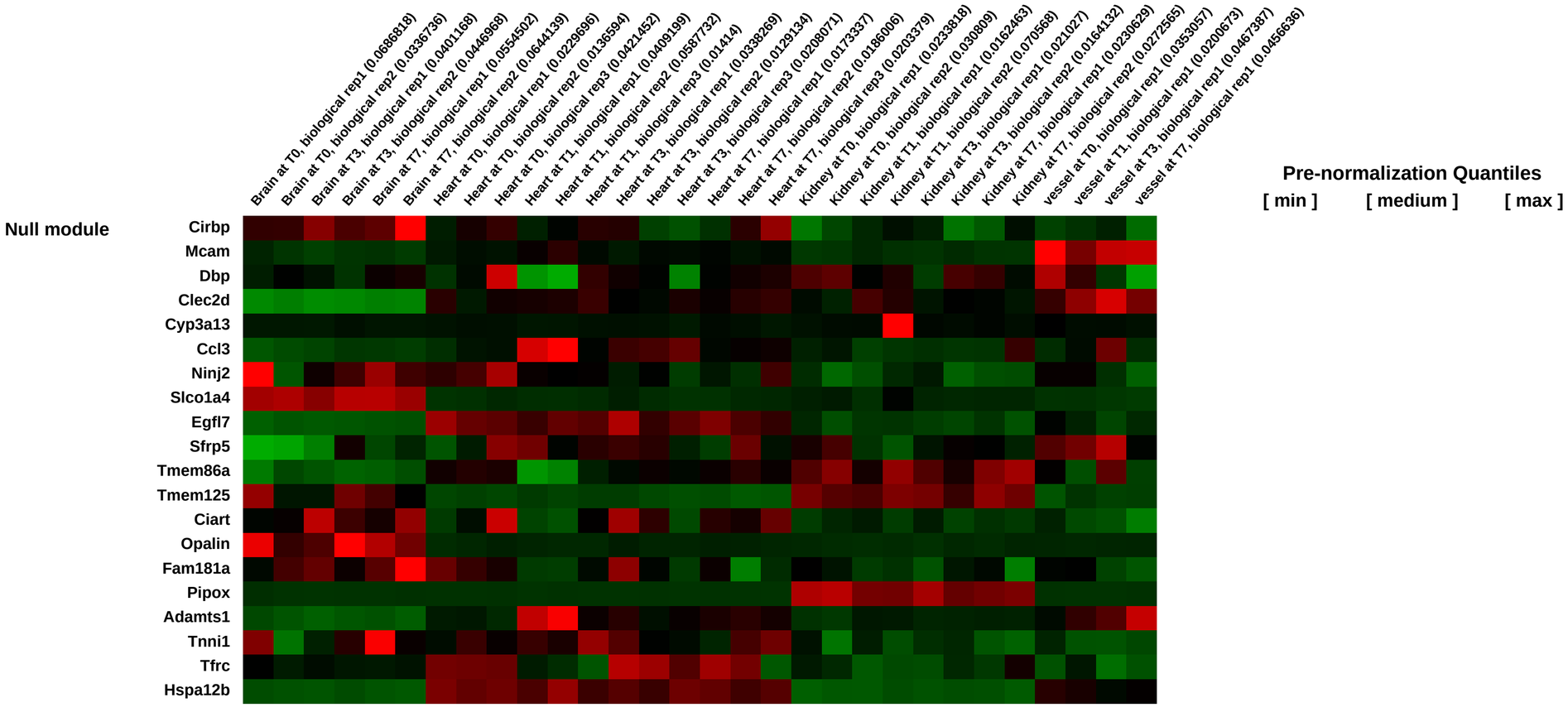

GEO Series "GSE26745" Expression Profiles

Num of samples in this series: 24

Scale of expression profile Z-scores

-3.0 -2.0 -1.0 0.0 1.0 2.0 3.0

GEO Link:	http://www.ncbi.nlm.nih.gov/geo/query/acc.cgi?acc=GSE26745
Status:	Public on Jul 21 2011
Title:	Comparison of total and polyribosome-associated mRNA levels in male Fmr1 KO mice and male WT littermates
Organism:	Mus musculus
Experiment type:	Expression profiling by array
Platform:	GPL1261
Pubmed ID:	21784246
Summary & Design:	**Summary:** The Fragile X Mental Retardation Protein, FMRP, is thought to regulate the translation of a specific set of neuronal mRNAs on polyribosomes. Therefore, we prepared polyribosomes on sucrose gradients and purified mRNA specifically from these fractions, as well as the total mRNA levels, to determine whether a set of mRNAs might be changed in its % association with polyribosomes in the absence of FMRP in the KO mouse model. No significant differences were found, other than the Fmr1 transcript itself, in total mRNA levels or % polyribosome association that withstood multiple test correction, in P7 Fmr1 KO mouse cerebral cortex compared with WT littermates.. **Overall design:** We prepared polyribosomes on sucrose gradients from 6 littermate pairs of Fmr1 KO and WT littermates (FVB background, P7 males, cerebral cortex) and purified RNA from both polyribosomal fractions and input to the gradient, reflecting total mRNA levels for comparison.

Background corr dist: KL-Divergence = 0.1111, L1-Distance = 0.0459, L2-Distance = 0.0033, Normal std = 0.4392

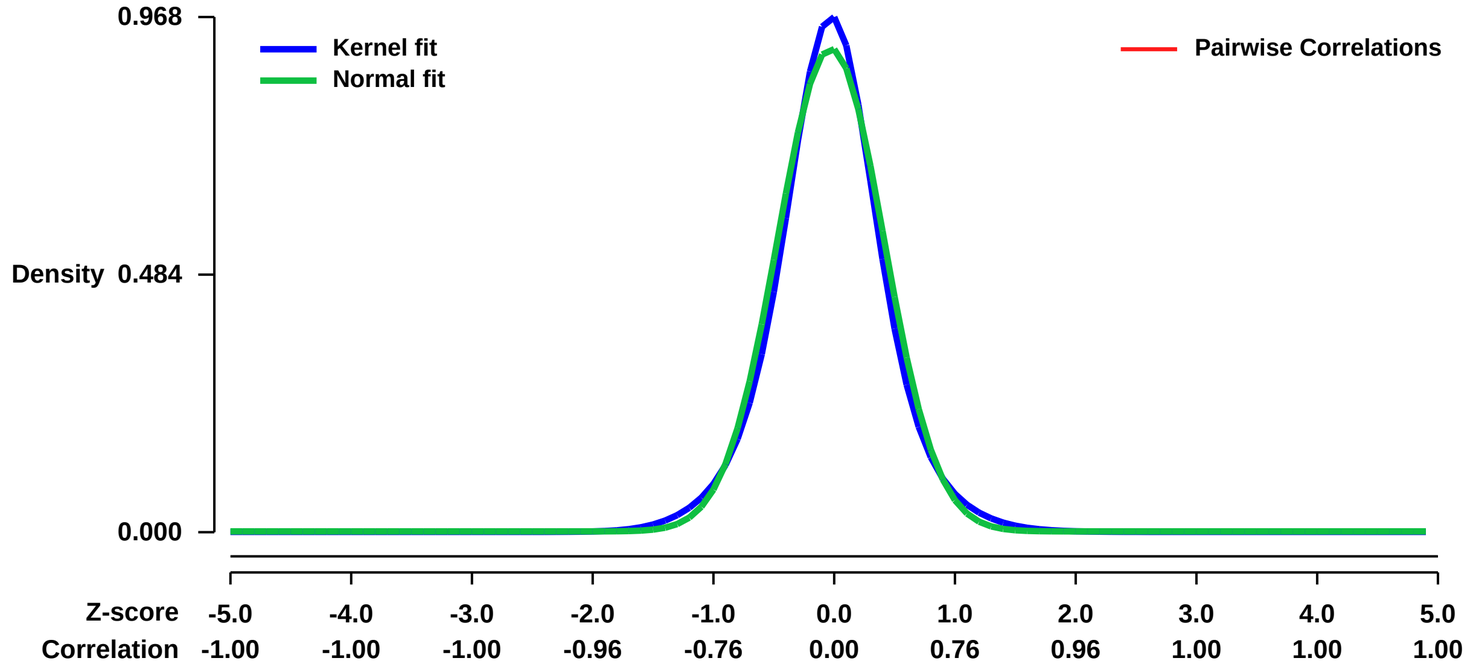

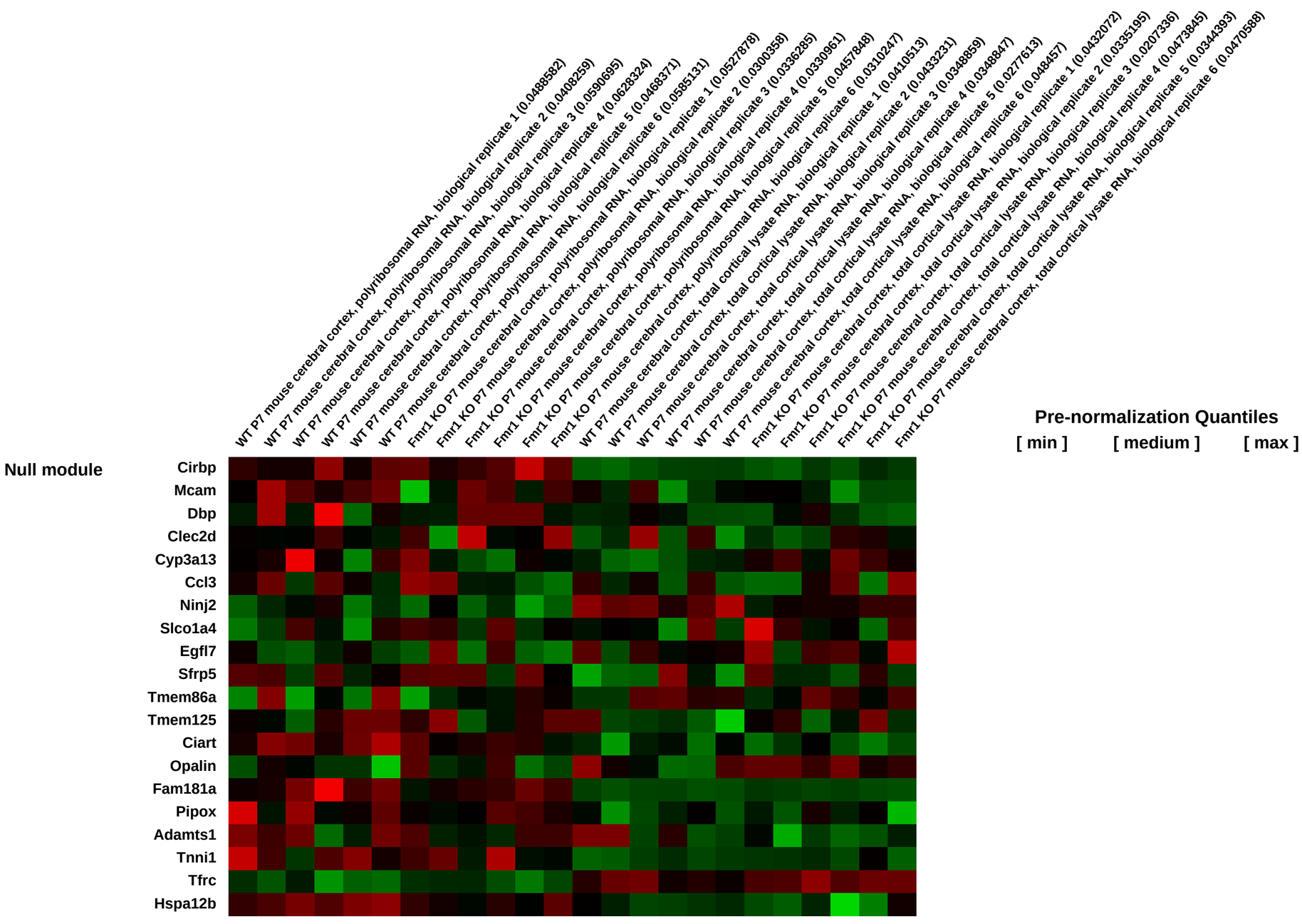

GEO Series "GSE6674" Expression Profiles

Num of samples in this series: 15

Scale of expression profile Z-scores

-3.0 -2.0 -1.0 0.0 1.0 2.0 3.0

GEO Link:	**http://www.ncbi.nlm.nih.gov/geo/query/acc.cgi?acc=GSE6674**
Status:	**Public on Dec 01 2007**
Title:	**Gene expression program of AM-14 B cells stimulated through the B cell receptor (BCR) and/or Toll-like receptors (TLR)**
Organism:	**Mus musculus**
Experiment type:	**Expression profiling by array**
Platform:	**GPL1261**
Pubmed ID:	**18025183**
Summary & Design:	**Summary:** **We have previously shown that rheumatoid factors (RF) produced by Fas-deficient autoimmune-prone mice typically bind autologous IgG2a with remarkably low affinity. Nevertheless, B cells representative of this RF population proliferate vigorously in response IgG2a/chromatin immune complexes through a mechanism dependent on the sequential engagement of the BCR and Toll-like receptor 9 (TLR9). To more precisely address the role of both receptors in this response, we analyzed the signaling pathways activated in AM14 B cells stimulated with these complexes. We found that the BCR not only serves to direct the chromatin complex to an internal compartment where it can engage TLR9 but also transmits a suboptimal signal that in combination with the signals emanating from TLR9 leads to NF?B activation and proliferation. Importantly, engagement of both receptors leads to the upregulation of a group of gene products, not induced by the BCR or TLR9 alone, that include IL-2. These data indicate that autoreactive B cells, stimulated by a combination of BCR and TLR9 ligands, acquire functional properties that may contribute to the activation of additional cells involved in the autoimmune disease process.** **Keywords: cell stimulation** **Overall design:** **15 Samples, 3 replicates for each treatment**

Background corr dist: KL-Divergence = 0.1169, L1-Distance = 0.0268, L2-Distance = 0.0011, Normal std = 0.4129

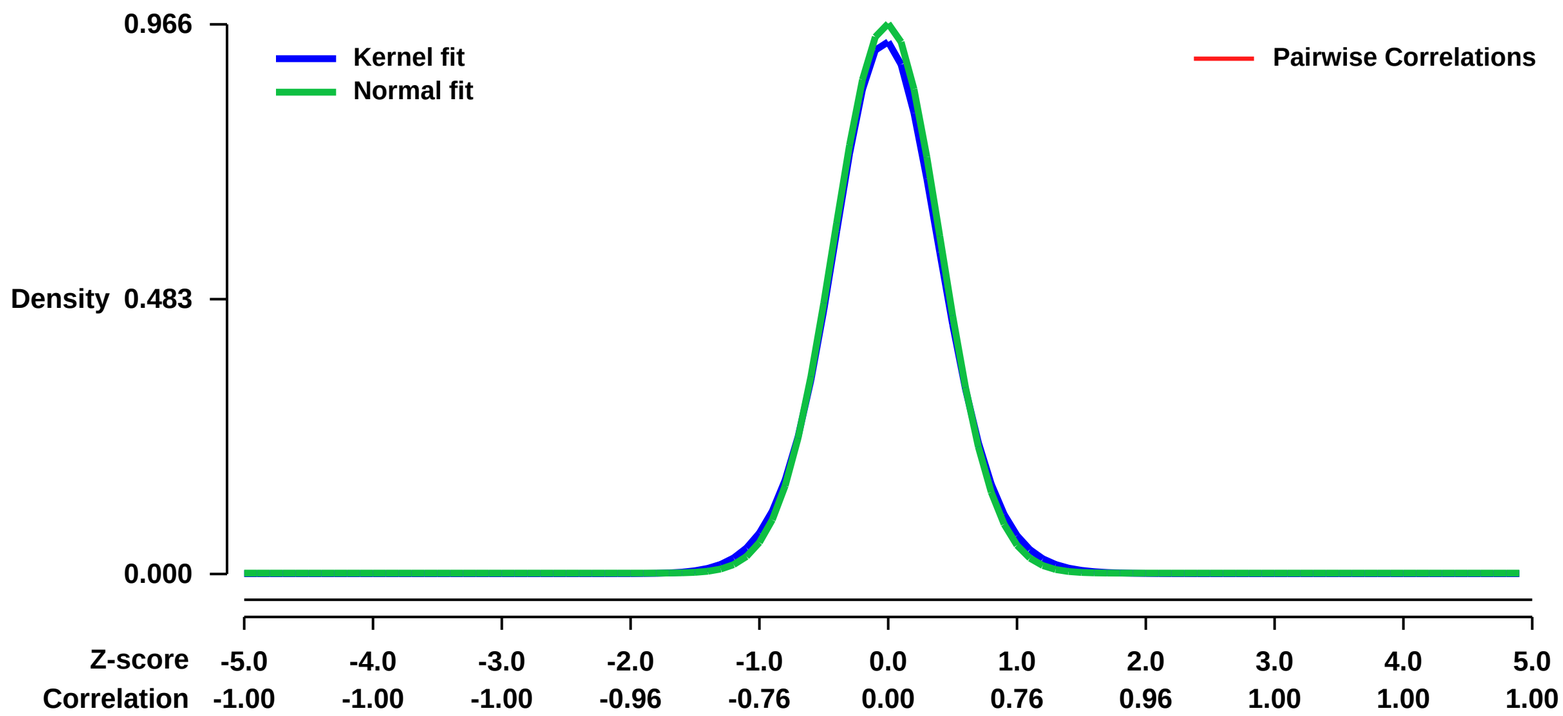

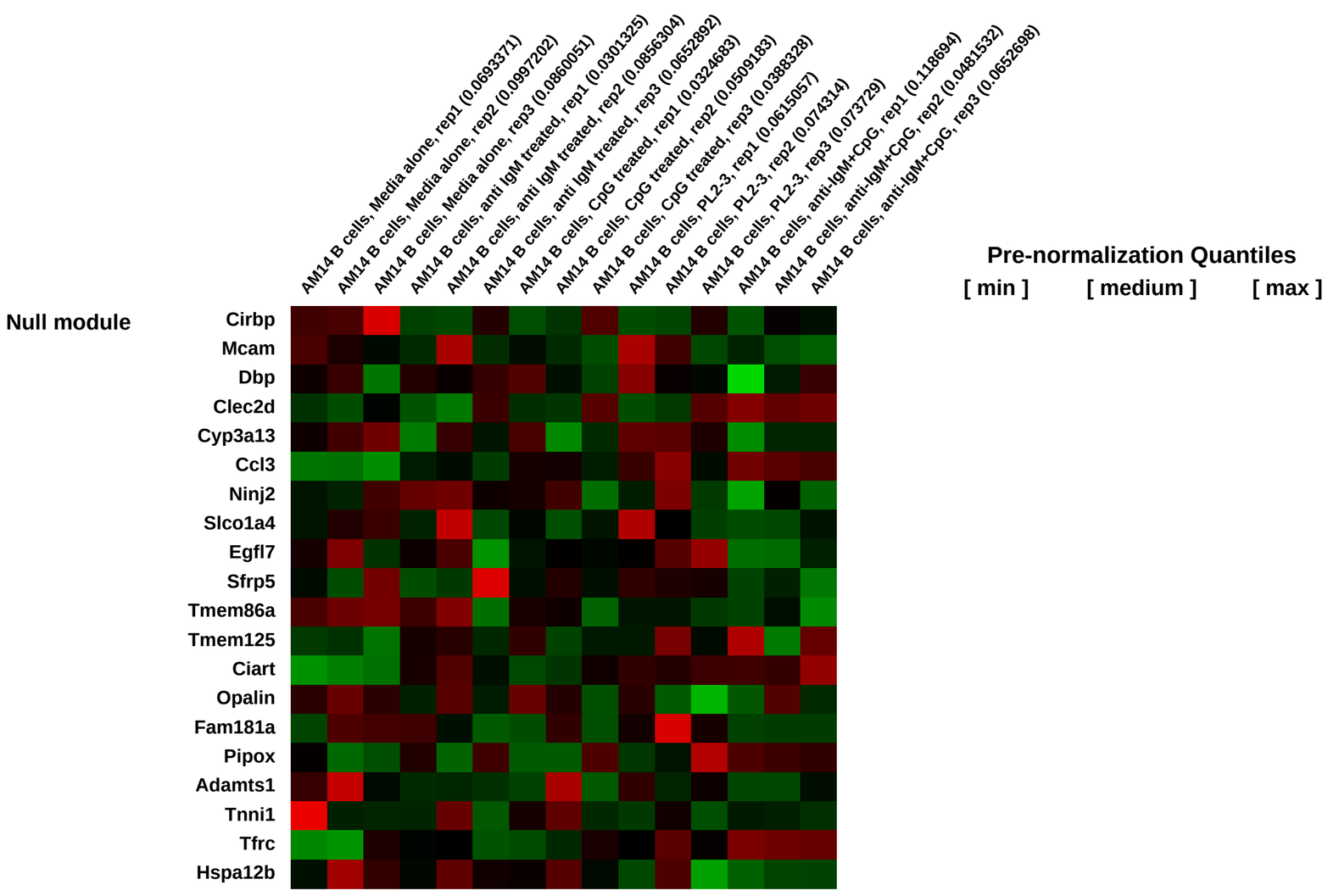

Pre-normalization Quantiles

[min] [medium] [max]

GEO Series "GSE56345" Expression Profiles

Num of samples in this series: 9

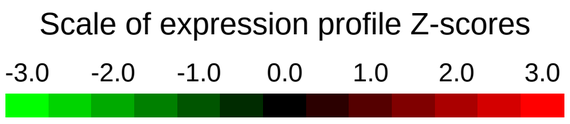

GEO Link:	http://www.ncbi.nlm.nih.gov/geo/query/acc.cgi?acc=GSE56345
Status:	Public on Mar 29 2014
Title:	Therapeutic potential of spleen tyrosine kinase inhibition for treatment of high-risk precursor B-cell acute lymphoblastic leukemia
Organism:	Mus musculus
Experiment type:	Expression profiling by array
Platform:	GPL1261
Pubmed ID:	24828076
Summary & Design:	**Summary:** **This study revealed pathogenic role of pre-BCR-independent SYK activation in high-risk B-ALL.** **Intensified and central nervous system (CNS)-directed chemotherapy has significantly improved outcomes for pediatric B-acute lymphoblastic leukemia (B-ALL), but confers significant late-effect morbidities. Moreover, many patients suffer relapses, underscoring the need to develop novel, molecularly targeted B-ALL therapies. Using a mouse model, we showed that leukemic B-cells require pre-B-cell receptor (pre-BCR)-independent spleen tyrosine kinase (SYK) signaling in vivo. In diagnostic samples from human B-ALL patients, SYK and downstream targets were phosphorylated regardless of pre-BCR expression or genetic subtype. Two small molecule SYK inhibitors, fostamatinib and BAY61-3606, attenuated growth of 69 B-ALL samples, including high-risk (HR) subtypes. Orally administered fostamatinib significantly reduced high disease burden after xenotransplantation of HR B-ALL samples into immune-deficient mice, and decreased leukemia dissemination into spleen, liver, kidneys and the CNS of recipients. Thus, SYK activation sustains growth of multiple HR B-ALL subtypes, suggesting that SYK inhibitors may improve outcomes for HR and relapsed B-ALL.** **Overall design:** **B-cell leukemia samples (3) from a mutant mouse model were compared to sorted or cultured preB or proB cells from normal mice using Affymetrix GeneChip arrays.**

Background corr dist: KL-Divergence = 0.0709, L1-Distance = 0.0252, L2-Distance = 0.0009, Normal std = 0.5061

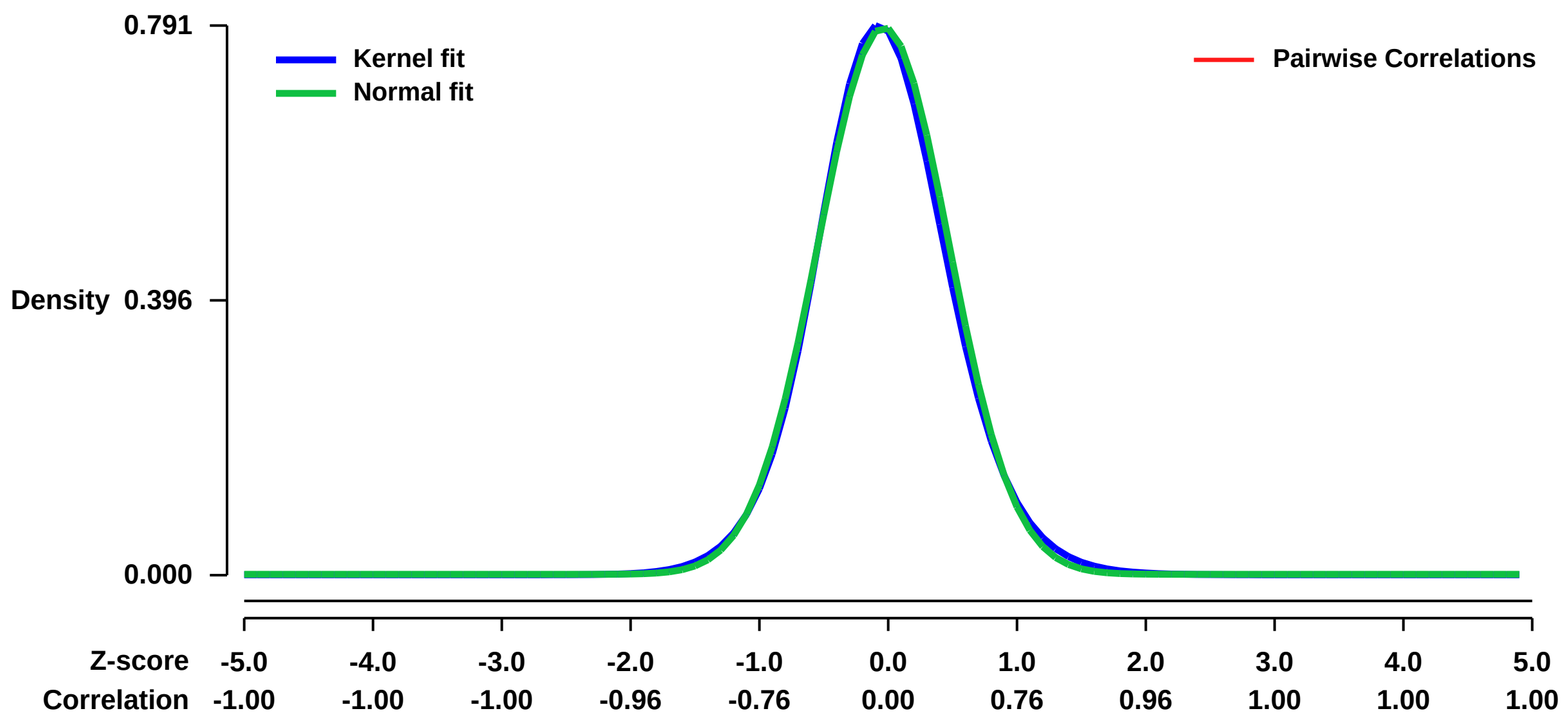

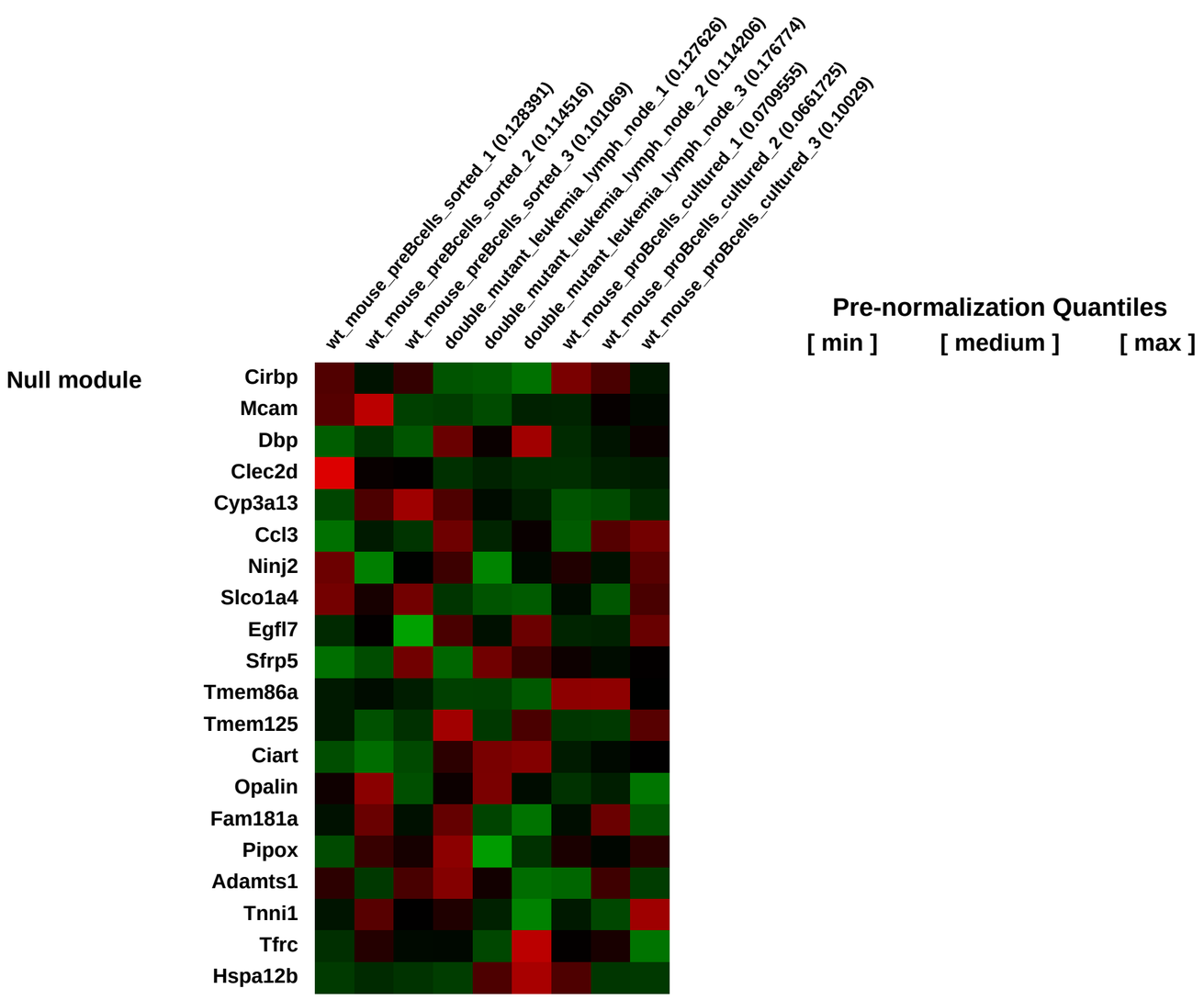

GEO Series "GSE5841" Expression Profiles

Num of samples in this series: 6

Scale of expression profile Z-scores

-3.0 -2.0 -1.0 0.0 1.0 2.0 3.0

GEO Link:	http://www.ncbi.nlm.nih.gov/geo/query/acc.cgi?acc=GSE5841
Status:	Public on Nov 19 2010
Title:	Differential gene expression in mouse skNAC knockout heart at E11.5
Organism:	Mus musculus
Experiment type:	Expression profiling by array
Platform:	GPL1261
Pubmed ID:	21071677
Summary & Design:	**Summary:** Targeted deletion of skNAC in mice resulted in early embryonic lethality with cardiac defects. In order to investigate the molecular mechanism of the cardiac defect, we designed the microarray comparing gene expression of the mutant E11.5 heart to wild type E11.5 heart. **Keywords: genetic modification in mouse** **Overall design:** 3 for each genotypes, comparing Littermates of E11.5, total RNA (500ng) from ventricles, Affymetrix GeneChip Mouse Genome 430 2.0 Array

Background corr dist: KL-Divergence = 0.0415, L1-Distance = 0.0183, L2-Distance = 0.0004, Normal std = 0.6077

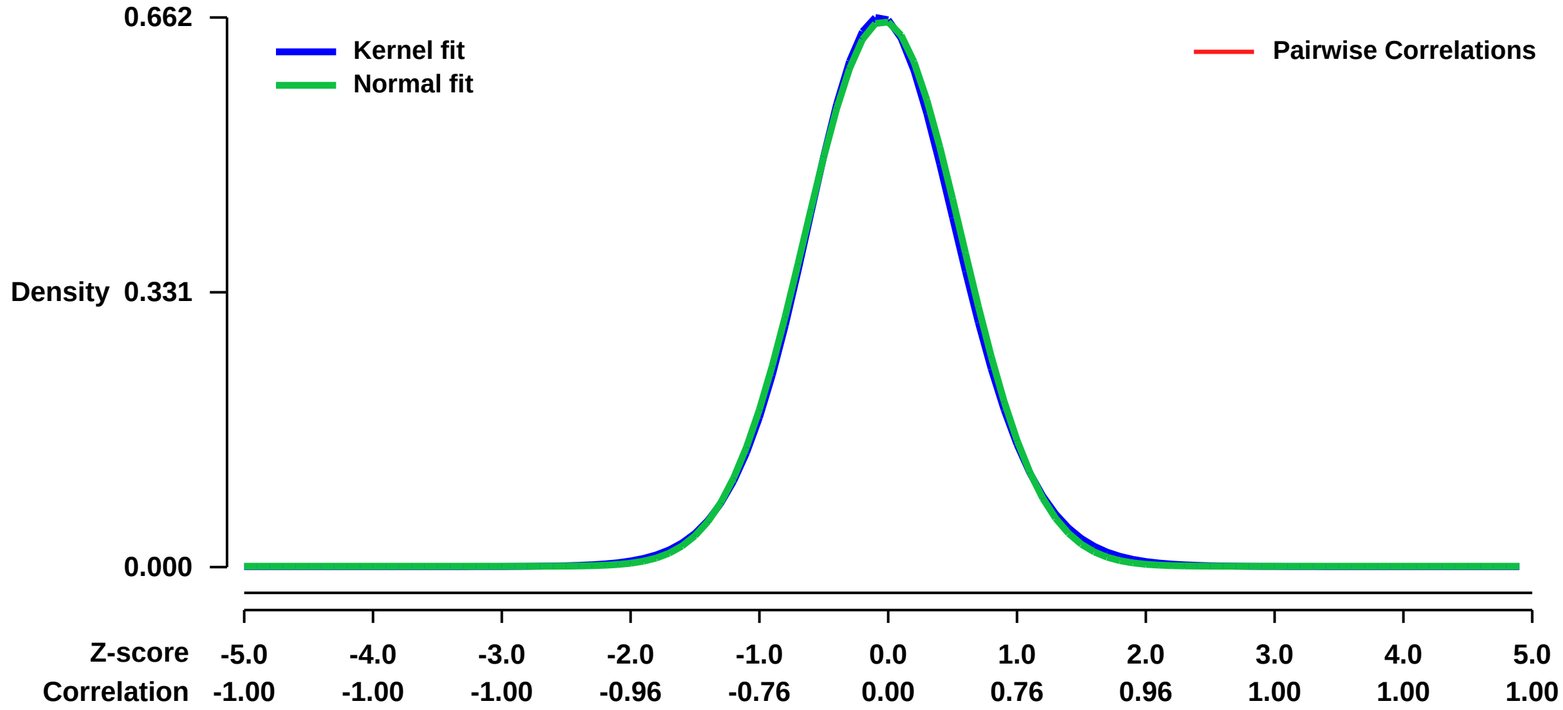

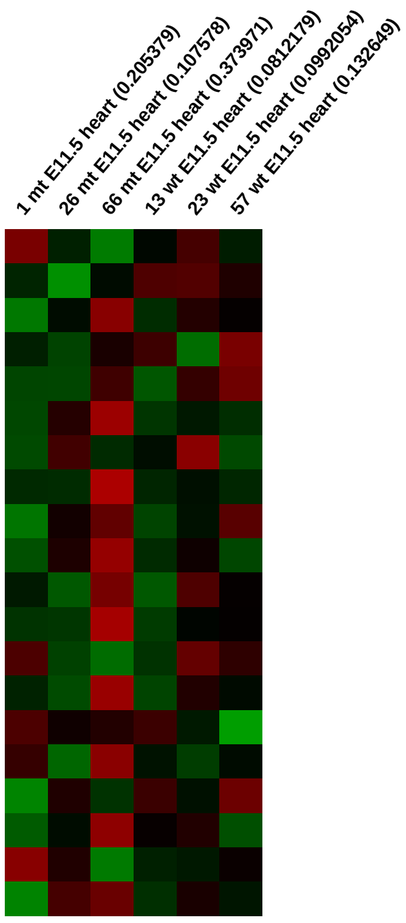

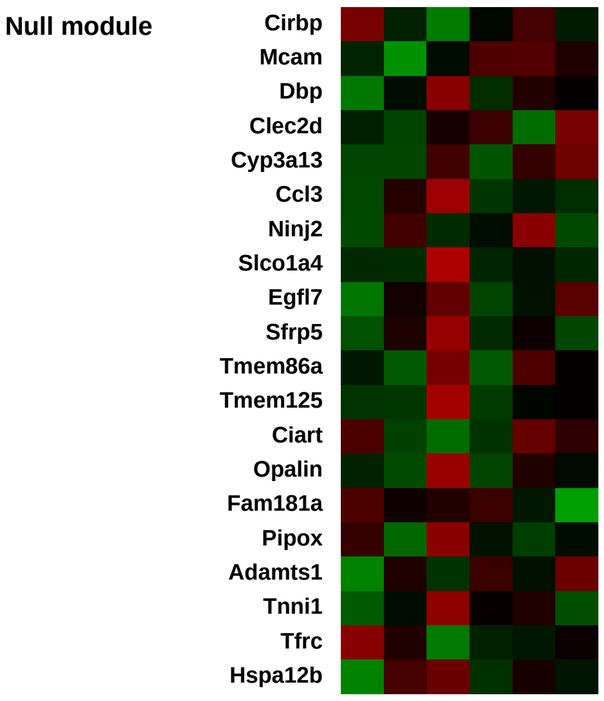

GEO Series "GSE28664" Expression Profiles

Num of samples in this series: 17

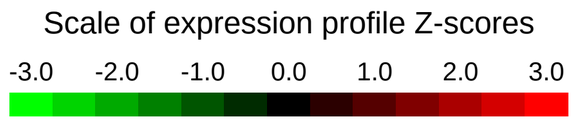

GEO Link:	http://www.ncbi.nlm.nih.gov/geo/query/acc.cgi?acc=GSE28664
Status:	Public on Sep 04 2011
Title:	Akt1 is critical in Maintaining the Blood-Testis Barrier Following Exposure to the Neonatal Goitrogen, 6-N-Propylthiouracil (PTU)
Organism:	Mus musculus
Experiment type:	Expression profiling by array
Platform:	GPL1261
Pubmed ID:	
Summary & Design:	**Summary:** Akt1 plays a protective role in the postnatal C57BL6 mouse testis following lactational exposure to the neonatal goitrogen, propylthiouracil (PTU). To elucidate the transcriptional profile mediating this phenotypic effect, we monitored changes in testicular gene expression at postnatal days (PNDs) 15 and 25 in Akt1+/+, Akt1+/-, and Akt1-/- testes following exposure to 0.01% PTU allowing us to determine changes in gene expression due to 1.) genotype effects; 2.) exposure effects; and 3.) genotype-by-exposure interactions. Early PTU-dependent gene changes included genes involved in lipid metabolism, spermatid differentiation, meiosis and adhesion. Early Akt1-dependent effects were associated with germ cell development, spermatid development and differentiation, and sperm motility. By PND25, the Akt1 gene-environment interaction had pronounced effects on genes associated with Sertoli cell (SC) differentiation and claudin-associated junctional formation suggesting delayed formation of the blood-testis barrier (BTB). To confirm these observations, biotin tracer experiments demonstrated a permeable blood-testis barrier in PTU-exposed PKBalpha/Akt1-/- tubules as late as PND25 compared to PTU-exposed Akt1+/+ seminiferous tubules. Transmission electron microscopy demonstrated altered SC morphology, aberrant SC localization, and disorganized actin bundle formation. Taken together, loss of Akt1 coupled with postnatal exposure to the neonatal goitrogen, PTU, in the testis contributes to a transcriptional profile associated with impaired integrity of the blood-testis barrier. In summary, the Akt1-/- mouse represents a potentially important model to study BTB formation and reassembly in response to male reproductive toxicants and the various signaling networks which mediate these responses. **Overall design:** The microarray analysis employed a balanced factorial design, with one chip created for each of three mice under each experimental condition: mouse genotype (Akt1+/+, Akt1+/-, and Akt1-/-), exposure (PTU and Control), and age (sacrificed at PND15 and 25), with a total of 36 mice and 36 chips. MoGene 1.0 st v1 arrays were used for the samples from PND 15 and Mouse Genome 430 2.0 arrays were used for the samples from PND 25. One chip, PTU-exposed, Akt1-/-, PND25, was determined to not be of high quality and was not included in the analysis or provided here.

Background corr dist: KL-Divergence = 0.0331, L1-Distance = 0.0207, L2-Distance = 0.0005, Normal std = 0.6440

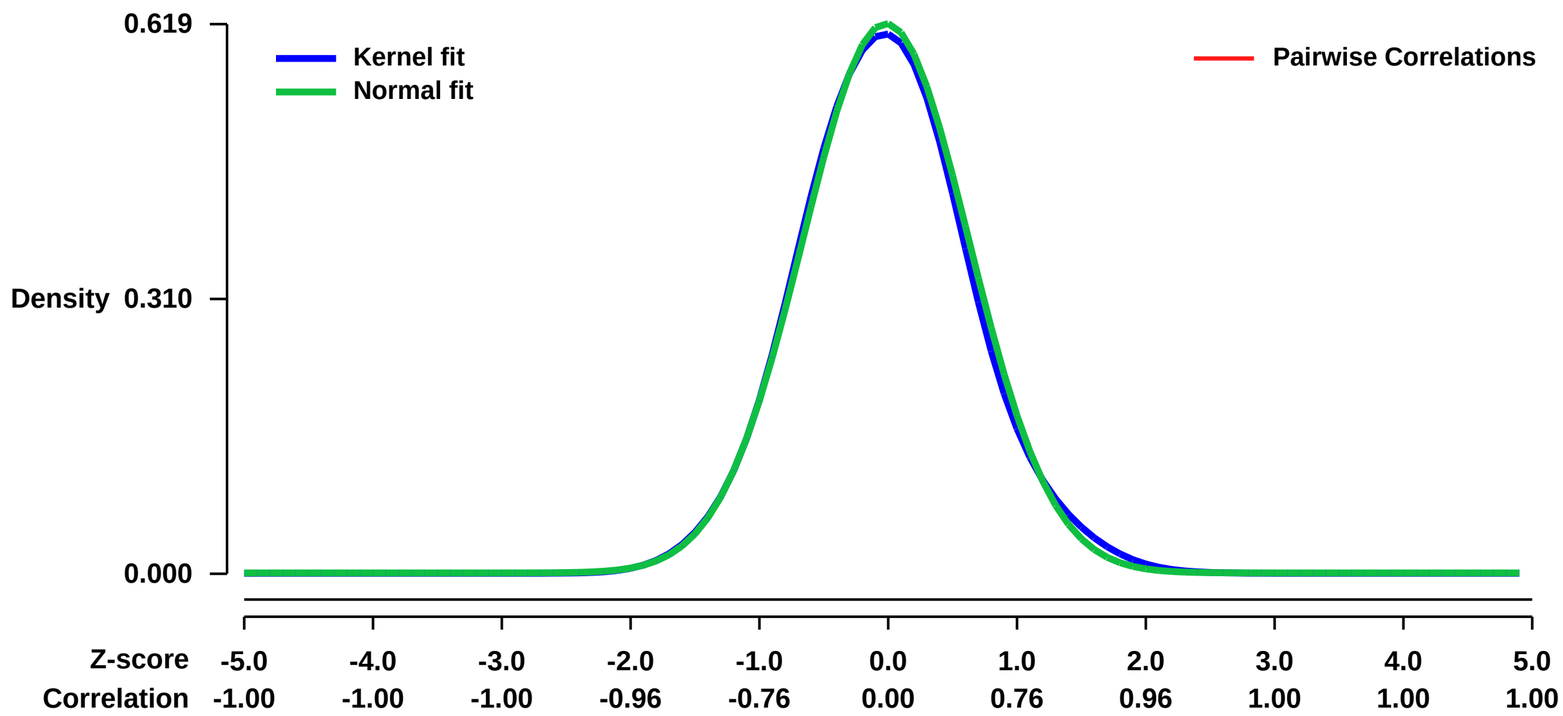

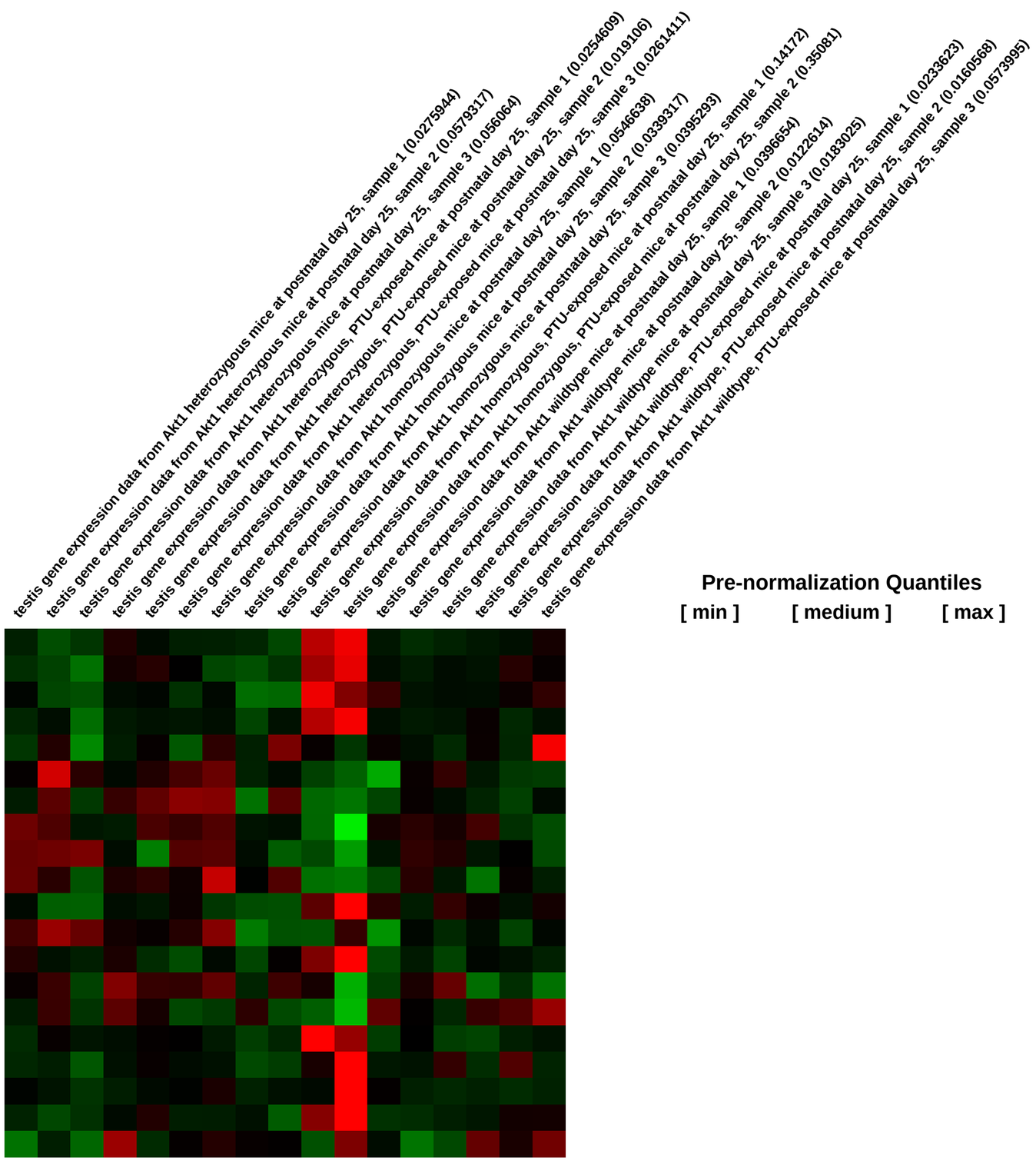

GEO Series "GSE35436" Expression Profiles

Num of samples in this series: 6

Scale of expression profile Z-scores

-3.0 -2.0 -1.0 0.0 1.0 2.0 3.0

GEO Link:	http://www.ncbi.nlm.nih.gov/geo/query/acc.cgi?acc=GSE35436
Status:	Public on Sep 29 2012
Title:	Genome-wide analysis of mouse macrophages stimulated with IL-4 (Biogel and thioglycollate macrophages) (Affymetrix)
Organism:	Mus musculus
Experiment type:	Expression profiling by array
Platform:	GPL1261
Pubmed ID:	23293084
Summary & Design:	**Summary:** Analysis of alternative activation of macrophages at gene expression level. The study forms part of a wider study where we compare the effects of IL-4 in different human and mouse macrophages. Our results support the notion that in vitro culture conditions greatly affect the macrophage response to IL-4. Total RNA obtained from Thioglycollate and Biogel elicited peritoneal macrophages exposed to 20 ng/ml of IL-4 for 18 hours. **Overall design:** Biogel and thioglycollate elicited macrophages were stimulated with the Th2 cytokine IL-4, for RNA extraction and hybridization on Affymetrix microarrays.

Background corr dist: KL-Divergence = 0.0230, L1-Distance = 0.0244, L2-Distance = 0.0009, Normal std = 0.7147

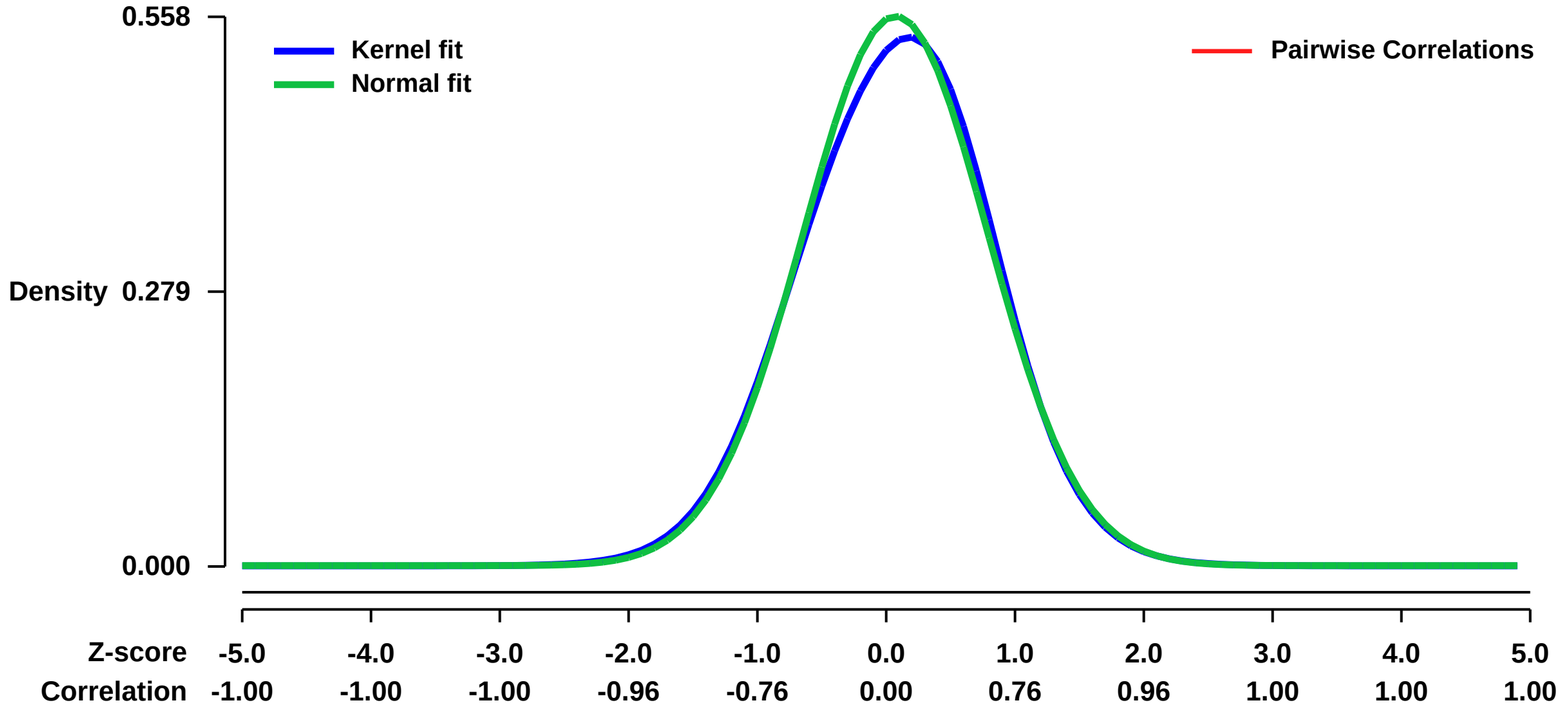

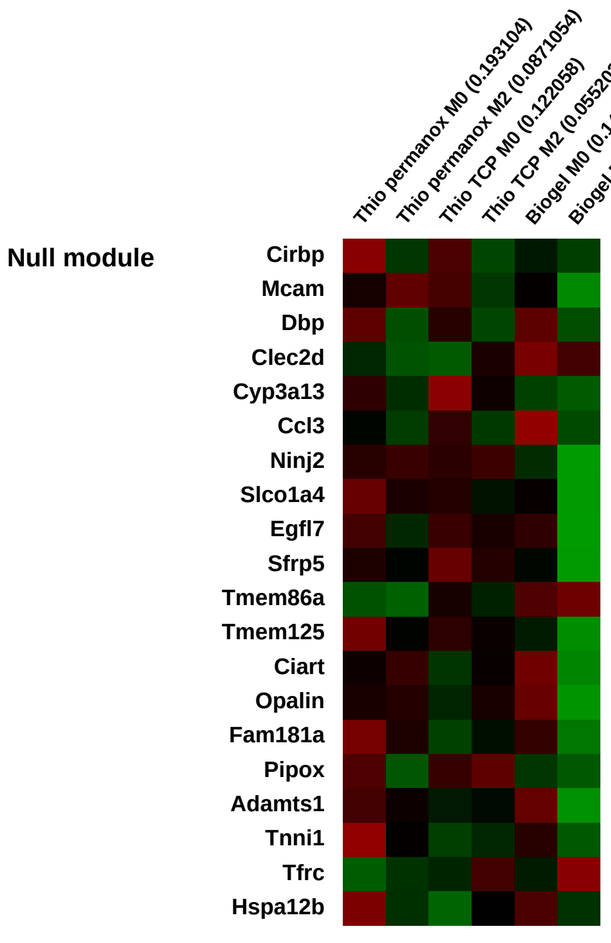

GEO Series "GSE51432" Expression Profiles

Num of samples in this series: 15

Scale of expression profile Z-scores

-3.0 -2.0 -1.0 0.0 1.0 2.0 3.0

GEO Link:	http://www.ncbi.nlm.nih.gov/geo/query/acc.cgi?acc=GSE51432
Status:	Public on May 28 2014
Title:	¸†-Cryptoxanthin suppresses inflammatory gene expression in diet-induced nonalcoholic steatohepatitis in mice
Organism:	Mus musculus
Experiment type:	Expression profiling by array
Platform:	GPL1261
Pubmed ID:	24858832
Summary & Design:	**Summary:** To evaluate the effect of ¸†-cryptoxanthin on diet-induced NASH, we fed a high-cholesterol and high-fat diet (CL diet) with or without 0.003% ¸†-cryptoxanthin to C56BL/6J mice for 12 weeks. After feeding, ¸†-cryptoxanthin attenuated fat accumulation, increases in Kupffer and activated stellate cells, and fibrosis in CL diet-induced NASH in the mice. Comprehensive gene expression analysis showed that although ¸†-cryptoxanthin histochemically reduced steatosis, it was more effective in inhibiting inflammatory gene expression change in NASH. ¸†-Cryptoxanthin reduced the alteration of expression of genes associated with cell death, inflammatory responses, infiltration and activation of macrophages and other leukocytes, quantity of T cells, and free radical scavenging. However, it showed little effect on the expression of genes related to cholesterol and other lipid metabolism. The expression of markers of M1 and M2 macrophages, T helper cells, and cytotoxic T cells was significantly induced in NASH and reduced by ¸†-cryptoxanthin. ¸†-Cryptoxanthin suppressed the expression of lipopolysaccharide (LPS)-inducible and/or TNF¸–-inducible genes and the antioxidant enzyme glutathione peroxidase 1 in NASH. Thus, ¸†-cryptoxanthin suppresses inflammation and the resulting fibrosis probably by primarily suppressing the increase and activation of macrophages and other immune cells. Reducing oxidative stress is likely to be a major mechanism of inflammation and injury suppression in the livers of mice with NASH. **Overall design:** Eight-week old male C57BL/6J mice were fed for 12 weeks on a CRF-1 standard chow (control), a high-cholesterol and high-fat diet (CL diet; 38.23% CRF-1, 60% cocoa butter, 1.25% cholesterol, 0.5% sodium cholate) or a CL diet containing 0.003% ¸†-cryptoxanthin.

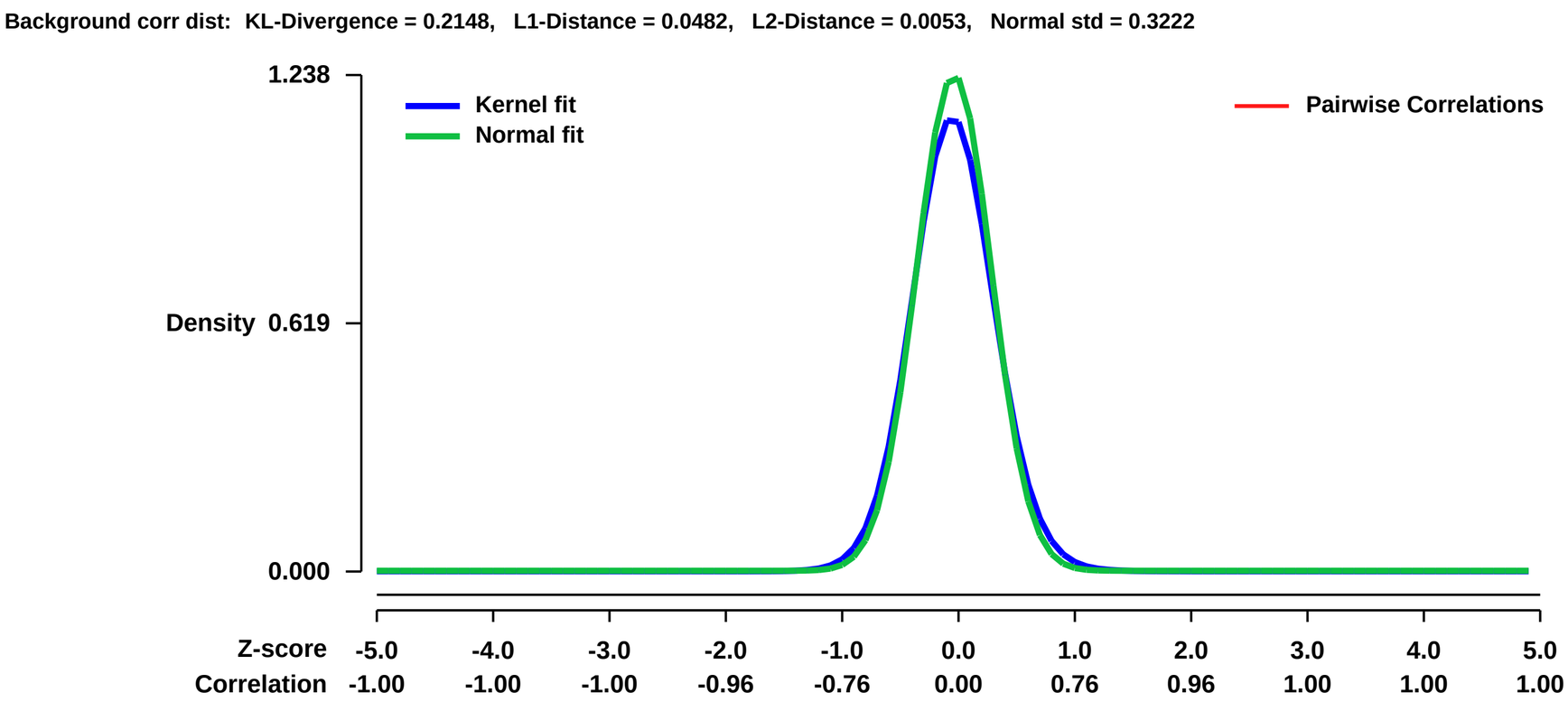

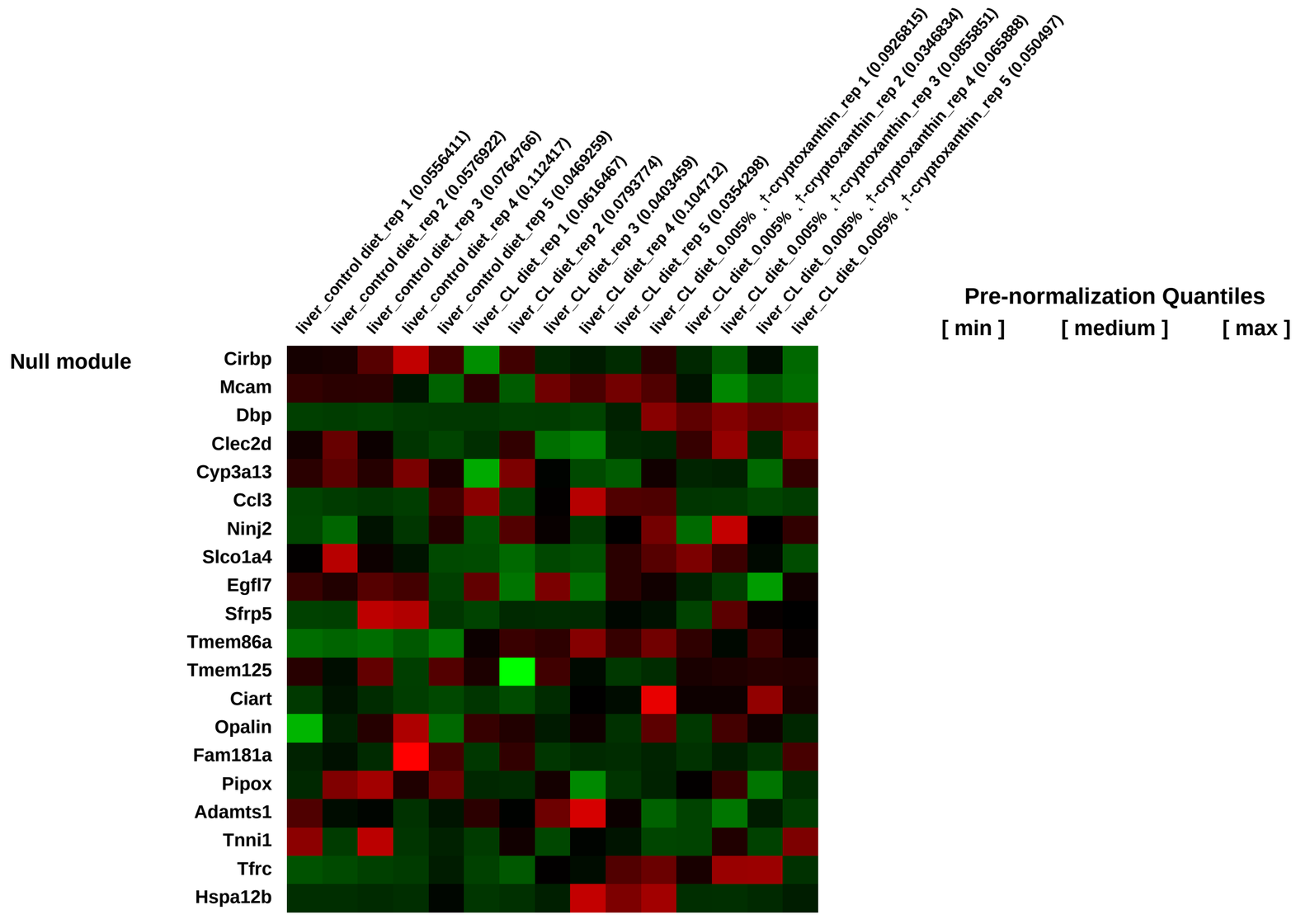

GEO Series "GSE25636" Expression Profiles

Num of samples in this series: 8

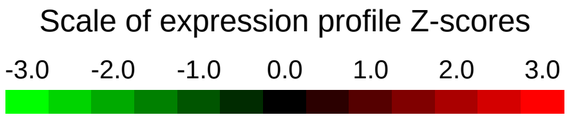

GEO Link:	http://www.ncbi.nlm.nih.gov/geo/query/acc.cgi?acc=GSE25636
Status:	Public on Jul 10 2012
Title:	A mouse model of deregulation of the malt1 oncogene recapitulates the pathogenesis of human malt lymphoma [MouseSca1 dataset]
Organism:	Mus musculus
Experiment type:	Expression profiling by array
Platform:	GPL1261
Pubmed ID:	22689981
Summary & Design:	**Summary:** Attempts at modeling chromosomal translocations involving MALT1 gene, hallmarks of human mucosa-associated lymphoid tissue (MALT) lymphoma, have failed to reproduce the disease in mice. Here we describe a transgenic model in which MALT1 expression was targeted to mouse hematopoietic stem/progenitor cells. In Sca1-MALT1 mice, MALT1 deregulation activated the NF-kappaB pathway in Sca1+ cells, promoting selective B-cell differentiation and mature lymphocyte accumulation in extranodal tissues, progressively leading to the development of clonal B-cell lymphomas. These tumors recapitulated the histopathological features of human MALT lymphomas, presenting typical lymphoepithelial lesions and plasmacytic differentiation. Transcriptional profiling of Sca1-MALT1 murine lymphomas revealed overlapping molecular signatures with human MALT lymphomas, including MALT1-mediated NFkappaB activation, pro-inflammatory signaling and XBP1-induced plasmacytic differentiation. Moreover, murine Malt1 showed proteolytic activity by cleaving Bcl10 in Sca1-MALT1 lymphomas. Our novel technological approach has allowed modeling human MALT lymphoma in mice, which represent unique tools study MALT lymphoma biology and evaluate anti-MALT1 therapies. **Keywords:** Genetic modification, wt vs. transgenic, MALT1 expression **Overall design:** 8 sorting purified Sca1+Lin- samples were analized of which 5 were from Sca1-MALT1 transgenic mice and 3 were from WT mice.

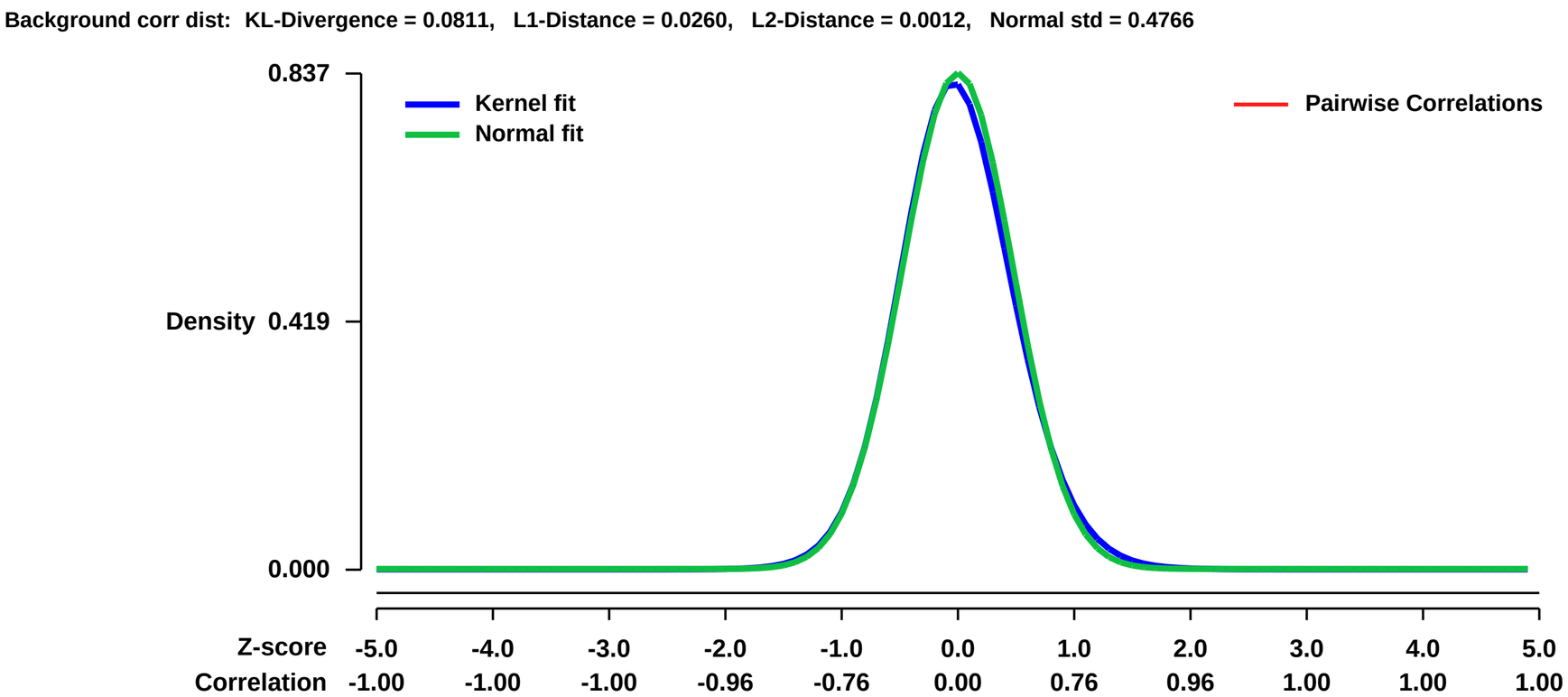

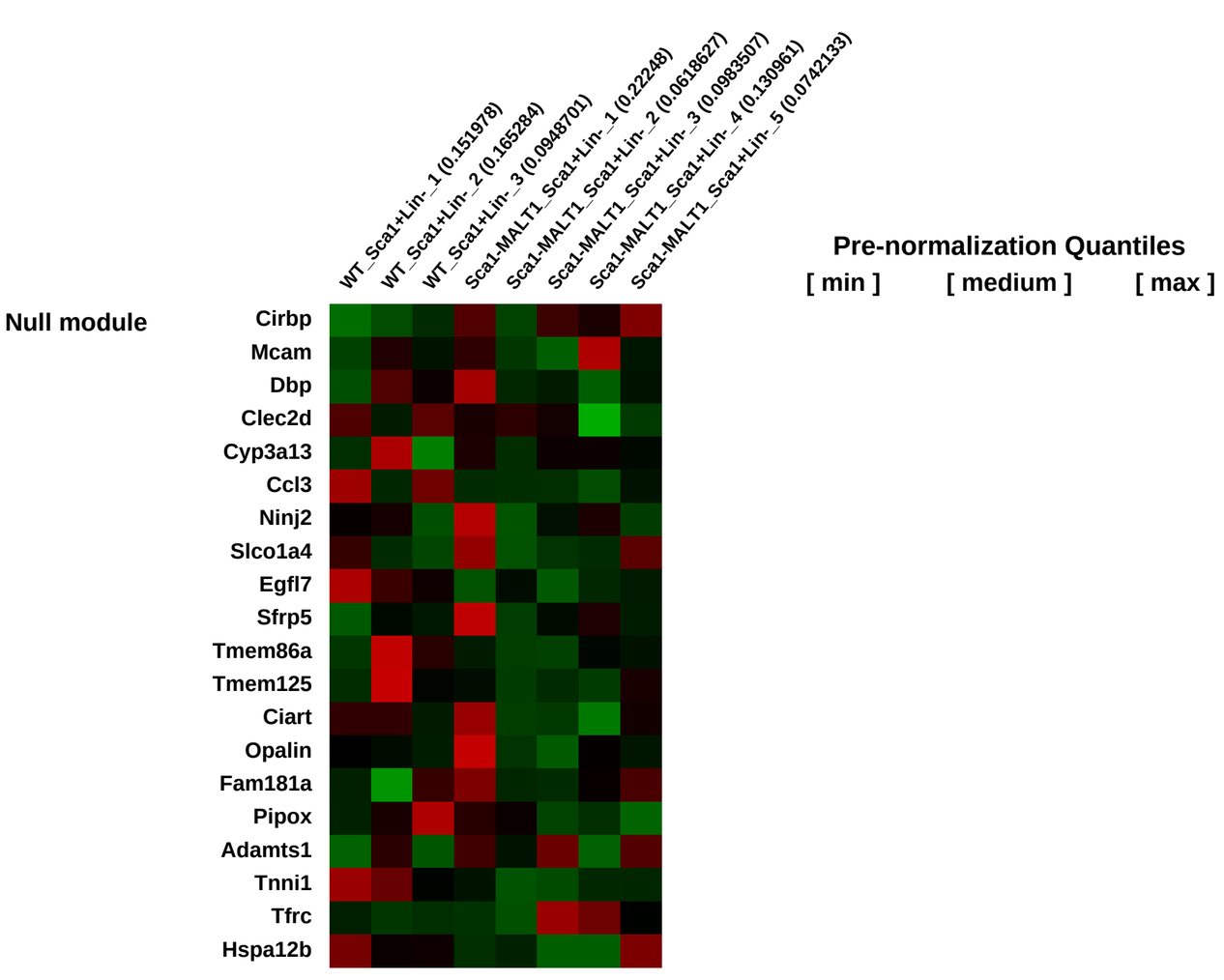

GEO Series "GSE15330" Expression Profiles

Num of samples in this series: 27

Scale of expression profile Z-scores

-3.0 -2.0 -1.0 0.0 1.0 2.0 3.0

GEO Link:	http://www.ncbi.nlm.nih.gov/geo/query/acc.cgi?acc=GSE15330
Status:	Public on Apr 03 2009
Title:	Gene expression data from mouse hematopoietic cells, Ikaros wt and null mutant
Organism:	Mus musculus
Experiment type:	Expression profiling by array
Platform:	GPL1261
Pubmed ID:	19345118
Summary & Design:	**Summary:** Regulation of lineage potential and transcriptional priming by Ikaros. New insight is provided into a bivalent regulation of lineage priming in the HSC and its lympho-myeloid restricted progeny the LMPP by the lymphoid lineage-determining factor Ikaros Whereas Ikaros is responsible for the activation of a cascade of lymphoid expression programs and for the establishment of lymphoid potential from the HSC to the LMPP it is also responsible for the repression of stem cell and erythroid genetic programs that are incompatible with further lineage restrictions emanating from the LMPP Keywords: Ikaros null versus wt **Overall design:** Ikaros null versus wt

Background corr dist: KL-Divergence = 0.1031, L1-Distance = 0.0552, L2-Distance = 0.0075, Normal std = 0.4330

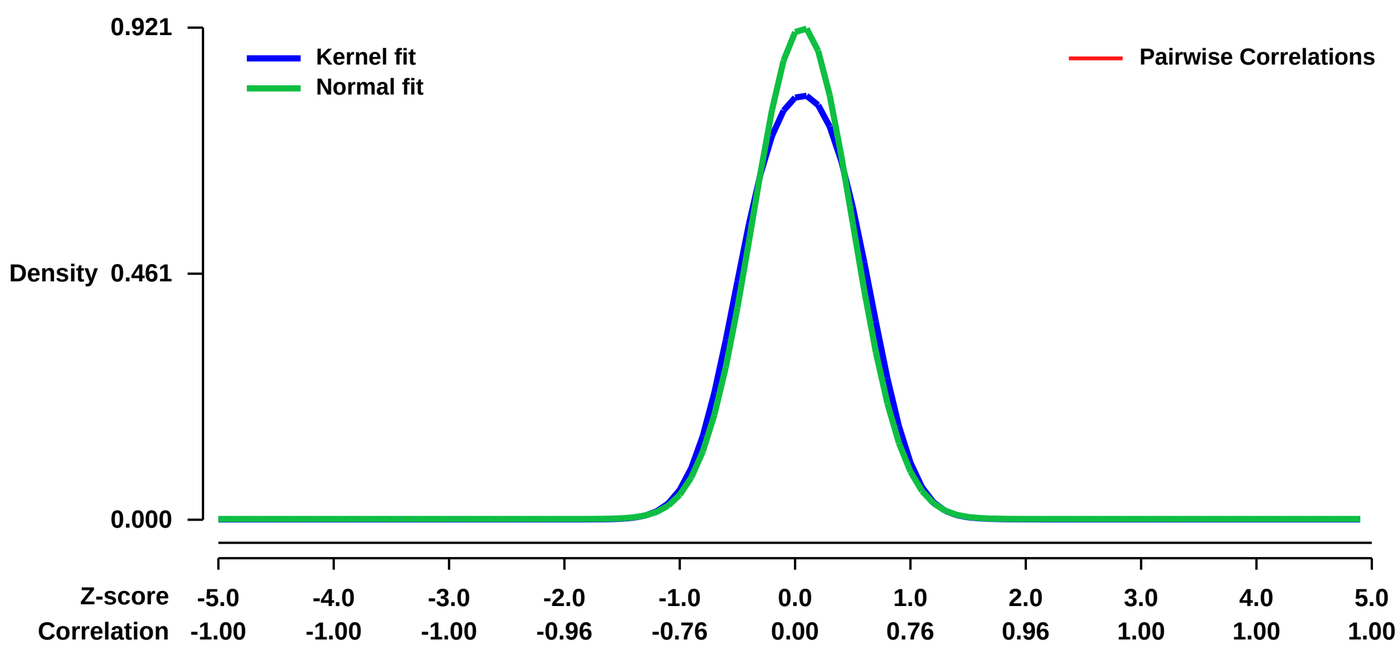

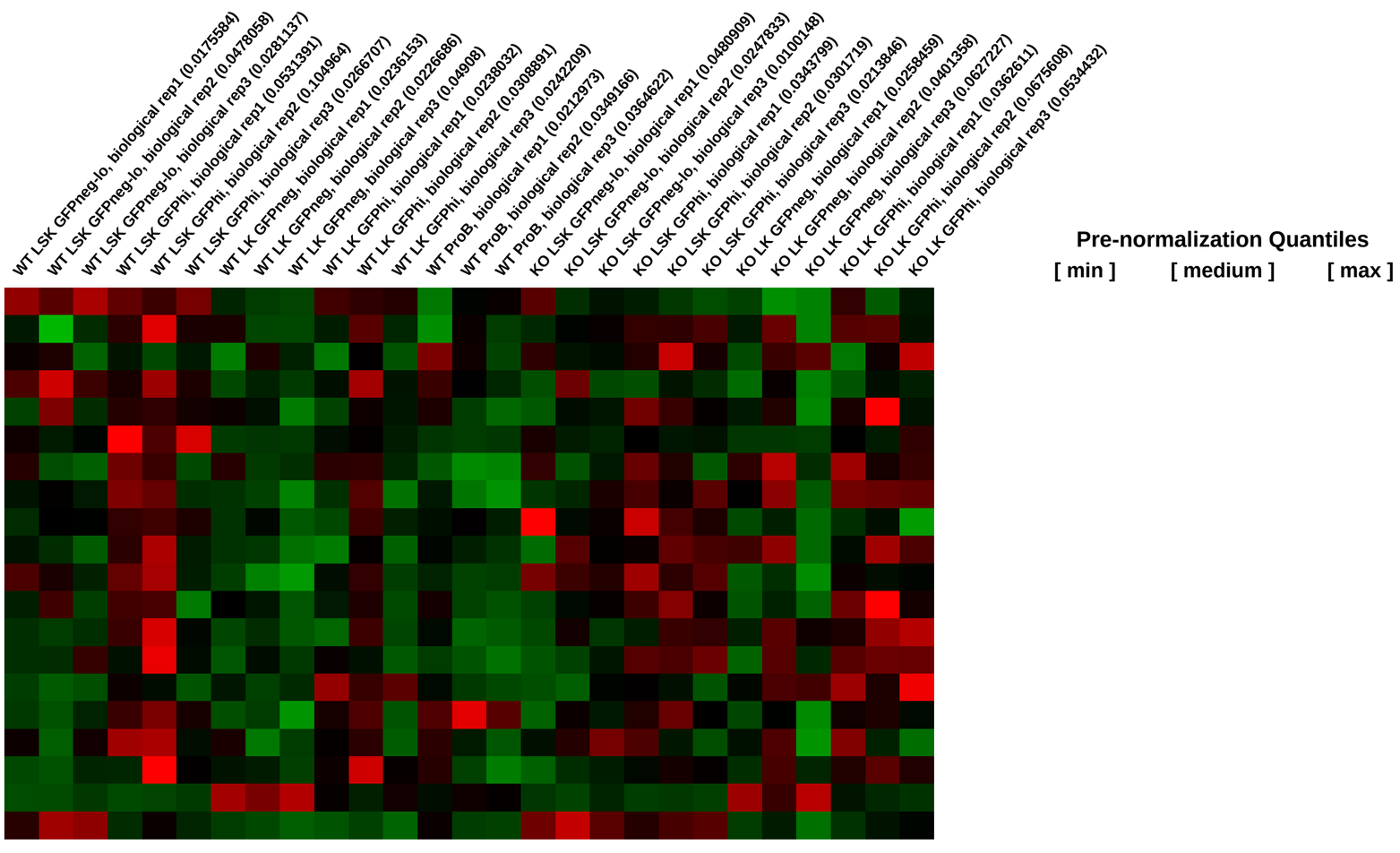

GEO Series "GSE30012" Expression Profiles

Num of samples in this series: 6

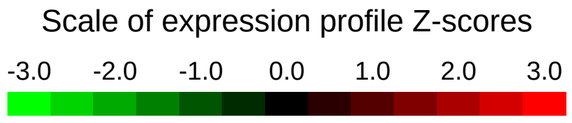

GEO Link:	**http://www.ncbi.nlm.nih.gov/geo/query/acc.cgi?acc=GSE30012**
Status:	**Public on Jun 18 2011**
Title:	**A latent pro-survival function for the mir-290-295 cluster in mouse embryonic stem cells.**
Organism:	**Mus musculus**
Experiment type:	**Expression profiling by array**
Platform:	**GPL1261**
Pubmed ID:	
Summary & Design:	**Summary:** **MicroRNAs (miRNAs) post-transcriptionally regulate the expression of thousands of distinct mRNAs. While some regulatory interactions help to maintain basal cellular functions, others are likely relevant in more specific settings, such as response to stress. Here we describe such a role for the mir-290-295 cluster, the dominant miRNA cluster in mouse embryonic stem cells (mESCs). Examination of a target list generated from bioinformatic prediction, as well as expression data following miRNA loss, revealed strong enrichment for apoptotic regulators, two of which we validated directly: Caspase 2, the most highly conserved mammalian caspase, and Ei24, a p53 transcriptional target. Consistent with these predictions, mESCs lacking miRNAs were more likely to initiate apoptosis following genotoxic exposure to gamma irradiation or doxorubicin. Knockdown of either candidate partially rescued this pro-apoptotic phenotype, as did transfection of members of the mir-290-295 cluster. These findings were recapitulated in a specific mir-290-295 deletion line, confirming that they reflect miRNA functions at physiological levels. In contrast to the basal regulatory roles previously identified, the pro-survival phenotype shown here may be most relevant to stressful gestations, where pro-oxidant metabolic states induce DNA damage. Similarly, this cluster may mediate chemotherapeutic resistance in a neoplastic context, making it a useful clinical target.** **Overall design:** **Three replicates of mouse embryonic stem cells with Dicer (CTRL) compared to three replicates of mouse embryonic stem cells lacking Dicer (CRE)**

Background corr dist: KL-Divergence = 0.0342, L1-Distance = 0.0179, L2-Distance = 0.0003, Normal std = 0.6434

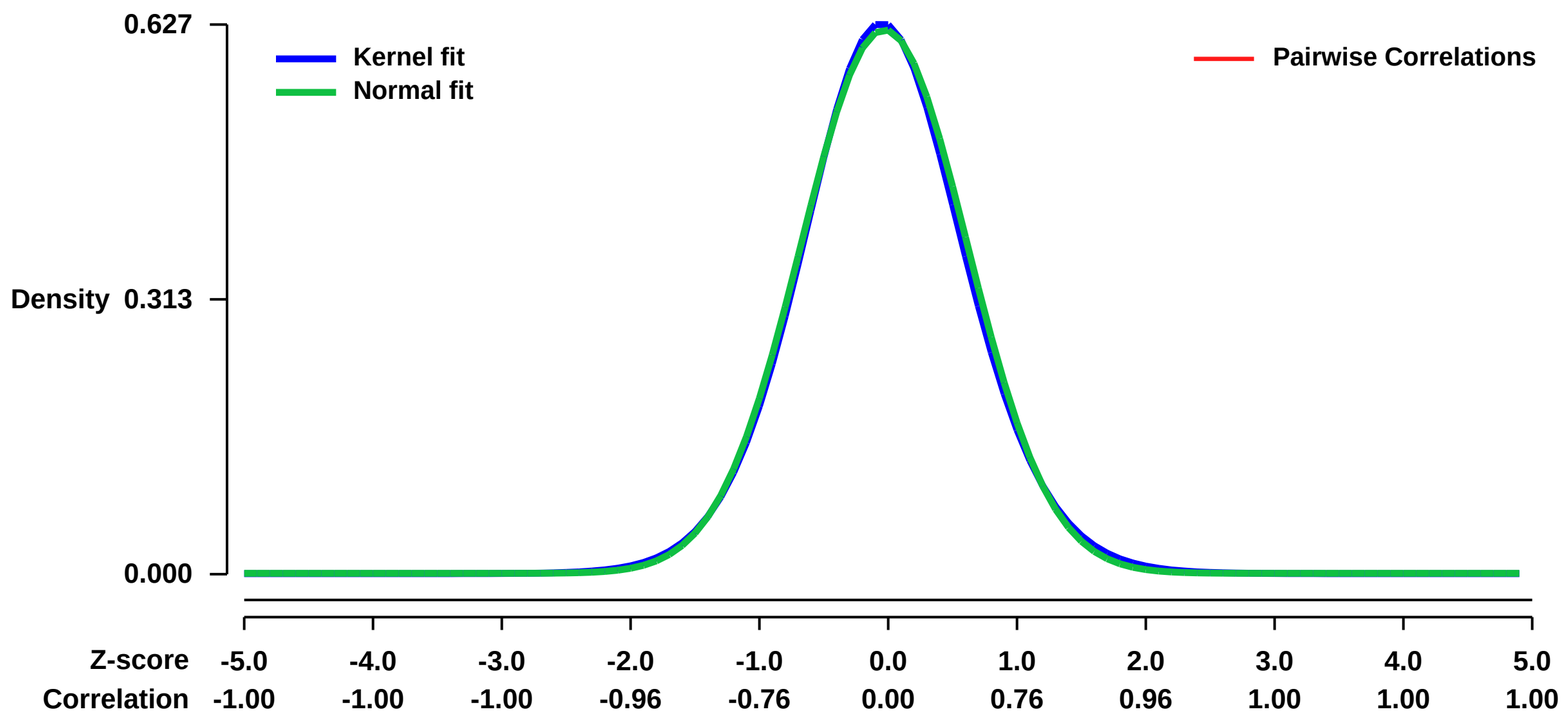

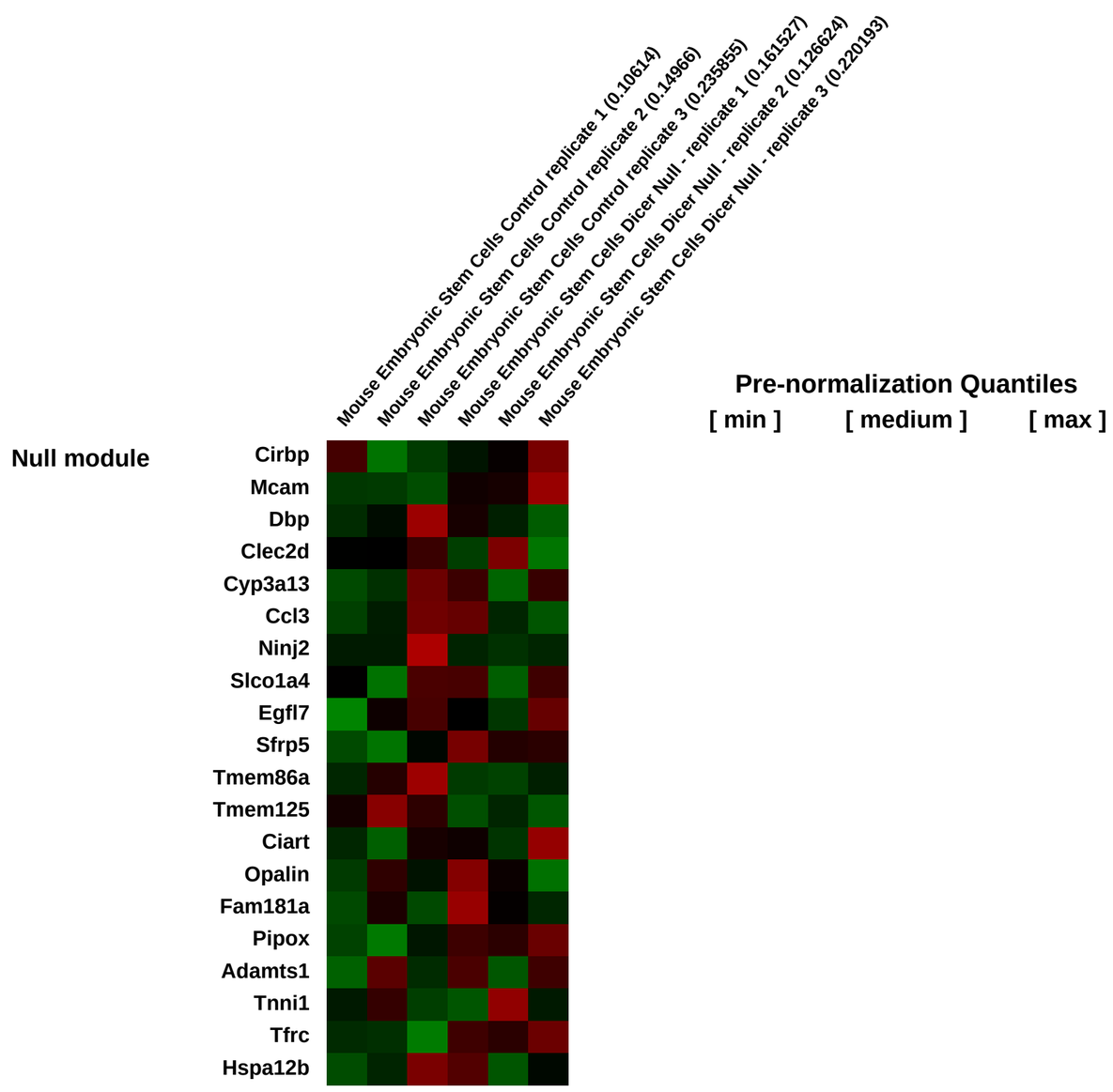

GEO Series "GSE47872" Expression Profiles

Num of samples in this series: 6

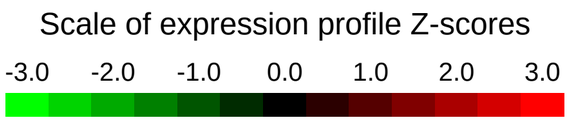

GEO Link:	http://www.ncbi.nlm.nih.gov/geo/query/acc.cgi?acc=GSE47872
Status:	Public on Mar 26 2014
Title:	Integrated analysis identifies key determinants of embryonic stem cell identity and homeostasis
Organism:	Mus musculus
Experiment type:	Expression profiling by array
Platform:	GPL1261
Pubmed ID:	24711389
Summary & Design:	**Summary:** Despite RNAi-based screens to uncover genes controlling embryonic stem cell (ESC) identity, the pluripotency network remains poorly characterized, as does the precise molecular mechanisms underlying the balance between self-renewal and differentiation. Here we carried out a systematic meta-analysis of published gene expression data to rank-order genes based on their likelihood of regulating ESC identity. Not only did our analysis correctly rank known pluripotency-associated genes atop the list, but it also helped unearth many novel determinants of ESC identity including several components of functionally distinct complexes, as determined using RNAi. We focus on our top-hit Nucleolin, and characterize its mechanistic role in the maintenance of ESC homeostasis by shielding from differentiation-inducing redox imbalance-induced oxidative stress. Notably, we identify a conceptually novel mechanism involving a Nucleolin-dependent bistable switch regulating the homeostatic balance between self-renewal and differentiation in ESCs. Our gene ranks represent a rich and valuable resource for uncovering novel ESC regulators. **Overall design:** Microarray gene expression profiling in E14Tg2a mESCs after transfection with indicated siRNAs: Ncl siRNA #1 (Invitrogen, 17975-MSS206961) Ncl siRNA #2 (Invitrogen, 17975-MSS275939), and Control siRNA duplex targeting firefly luciferase.

Background corr dist: KL-Divergence = 0.0151, L1-Distance = 0.0201, L2-Distance = 0.0004, Normal std = 0.8200

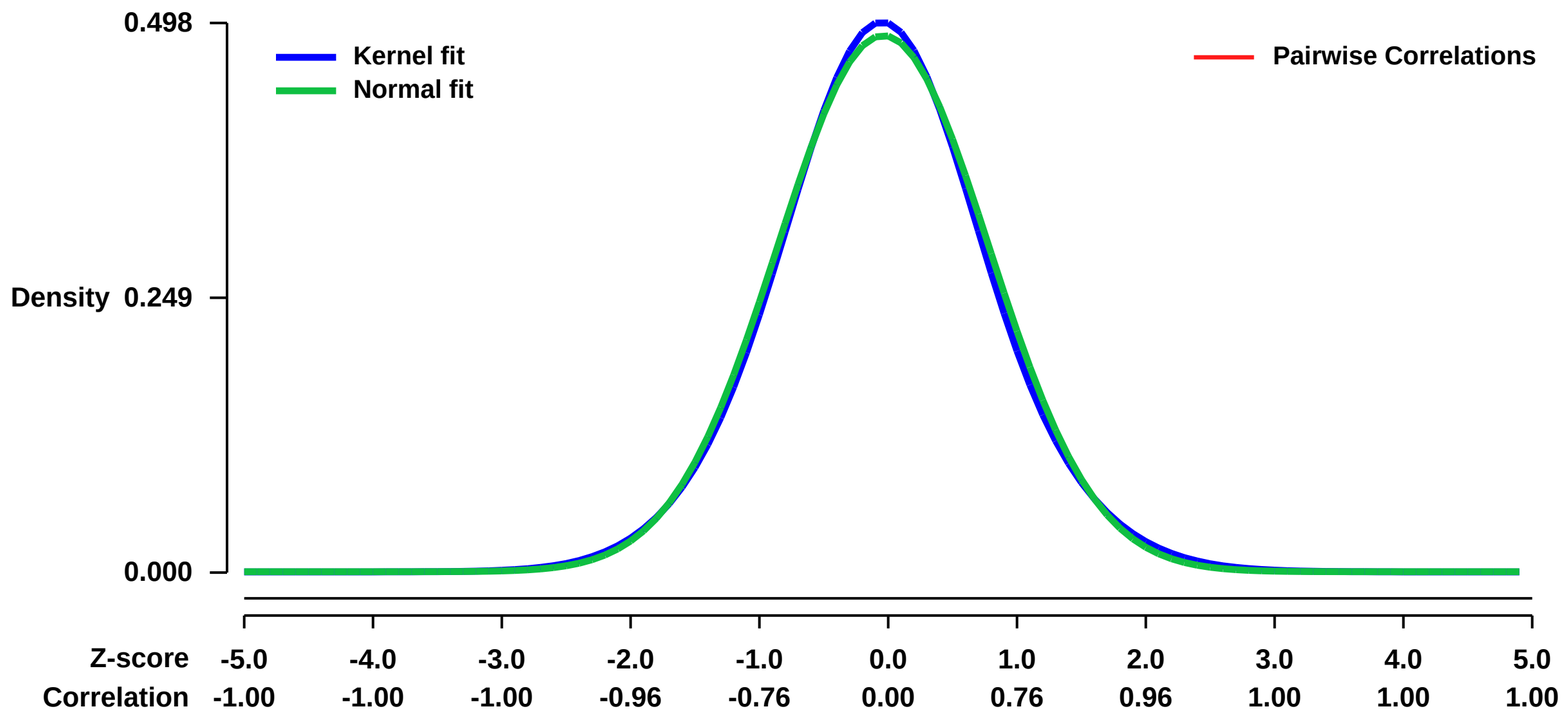

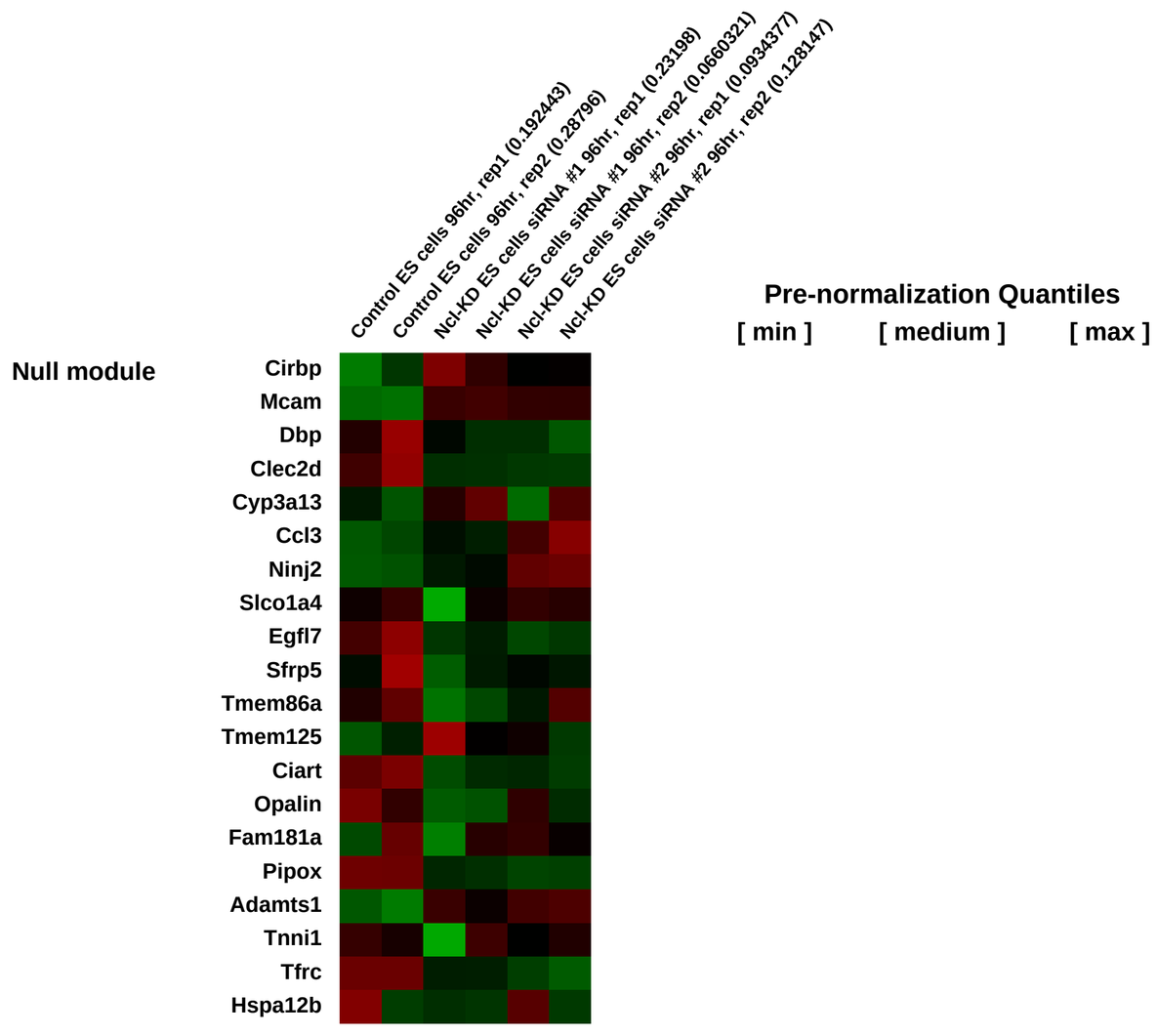

GEO Series "GSE20366" Expression Profiles

Num of samples in this series: 23

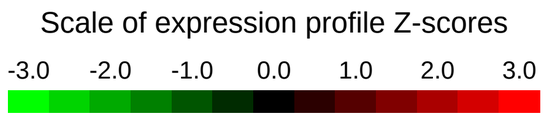

GEO Link:	http://www.ncbi.nlm.nih.gov/geo/query/acc.cgi?acc=GSE20366
Status:	Public on Mar 02 2010
Title:	Genomic definition of multiple ex vivo Treg sub-phenotypes
Organism:	Mus musculus
Experiment type:	Expression profiling by array
Platform:	GPL1261
Pubmed ID:	20231436
Summary & Design:	**Summary:** Regulatory T (Treg) cells that express the FoxP3 transcription factor are essential for lymphoid homeostasis and immune tolerance to self. Other non-immunological functions of Treg cells, such as controlling metabolic function in adipose tissue, are also emerging. Treg cells originate primarily in the thymus, but can also be elicited from conventional T cells by in vivo exposure to low-dose antigen or homeostatic expansion, or by activation in the presence of TGF¸† in vitro. Treg cells are characterized by a distinct transcriptional signature controlled in part, but not solely, by FoxP3. For a better perspective on transcriptional control in Treg cells, we compared gene expression profiles of a broad panel of Treg cells from various origins or anatomical locations. Treg cells generated by different means form different sub-phenotypes identifiable by particular combinations of transcripts, none of which fully encompass the entire Treg signature. Molecules involved in Treg effector function, chemokine receptors, and the transcription factors that control them are differentially represented in these subphenotypes. Treg cells from the gut proved dissimilar to cells elicited by exposure to TGF¸†, but instead they resembled a CD103+Klrg1+ subphenotype preferentially generated in response to lymphopenia. **Overall design:** All gene expression profiles were obtained from highly purified T cell populations sorted by flow cytometry. To reduce variability, cells from multiple mice were pooled for sorting, and replicates or triplicates were generated for all groups. RNA from 1-5 x 104 cells was amplified, labeled, and hybridized to Affymetrix M430v2 microarrays. Raw data were preprocessed with the RMA algorithm in GenePattern, and averaged expression values were used for analysis.

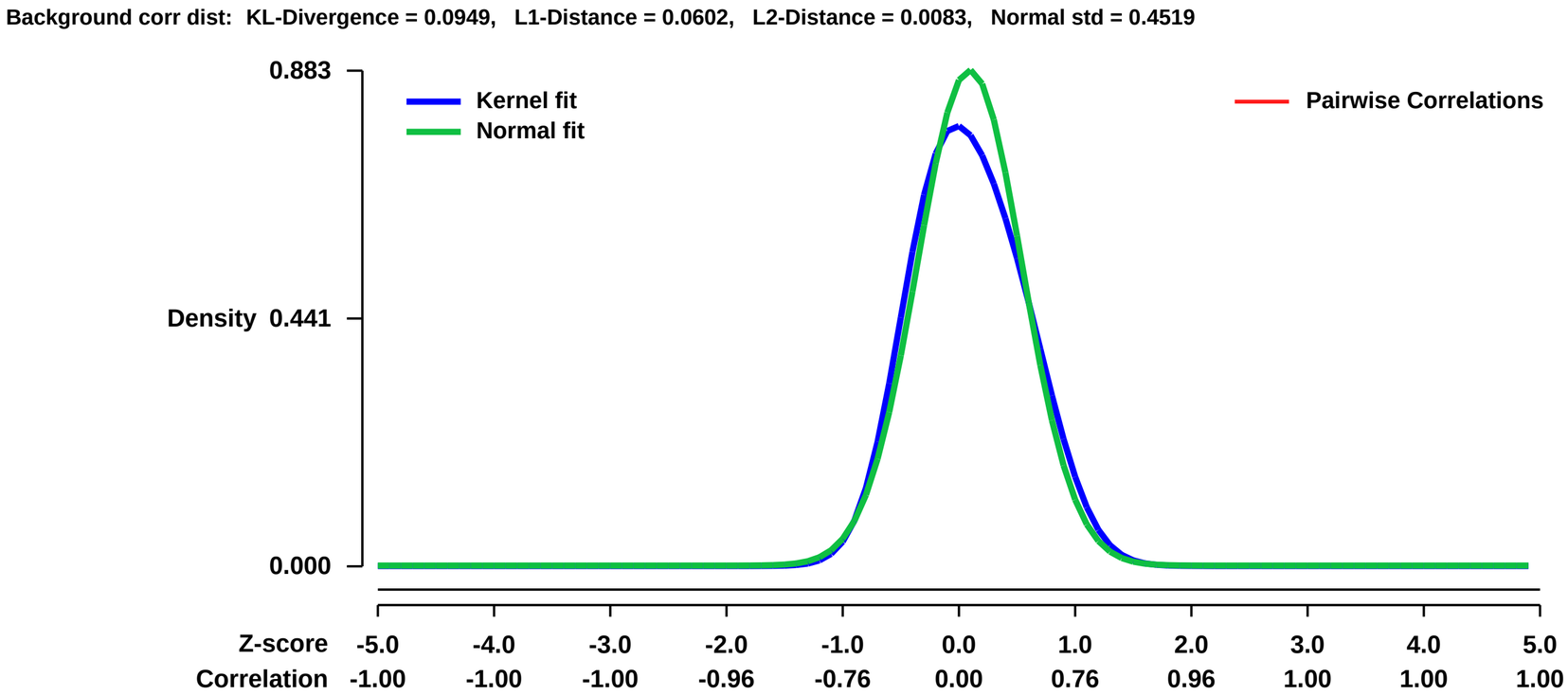

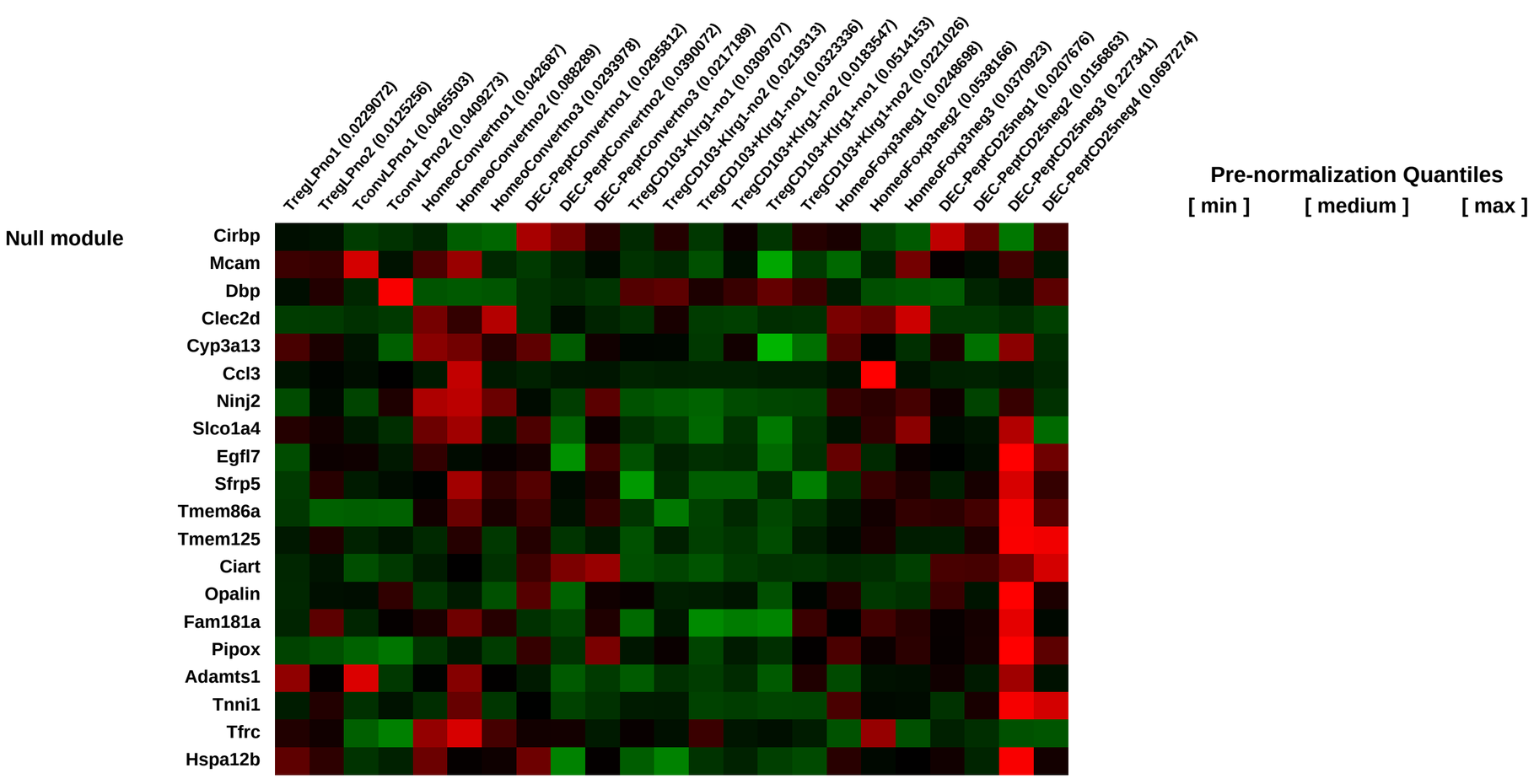

GEO Series "GSE36392" Expression Profiles

Num of samples in this series: 9

Scale of expression profile Z-scores

-3.0 -2.0 -1.0 0.0 1.0 2.0 3.0

GEO Link:	http://www.ncbi.nlm.nih.gov/geo/query/acc.cgi?acc=GSE36392
Status:	Public on Mar 10 2012
Title:	Expression data from pulmonary Type 2 Myeloid (T2M) cells, Eosinophils, Neutrophils, and Macrophages, from IL-25 treated 4get mice
Organism:	Mus musculus
Experiment type:	Expression profiling by array
Platform:	GPL1261
Pubmed ID:	22543263
Summary & Design:	**Summary:** Many symptoms associated with allergic asthma result from the sequelae of type 2 inflammation. Interleukin (IL)-25 promotes type 2 inflammatory responses, and T2M cells represent an IL-4 and IL-13 producing granulocytic IL-25 responsive population. We used microarrays to characterize the gene expression profile of T2M cells, and compared T2M cells to other inflammatory subsets (eosinophils, neutrophils, and macrophages) in the lungs of mice with IL-25-induced pulmonary inflammation. **Overall design:** We analyzed 3 T2M replicates and 2 replicates each of the other inflammatory subsets.

Background corr dist: KL-Divergence = 0.0426, L1-Distance = 0.0583, L2-Distance = 0.0056, Normal std = 0.6219

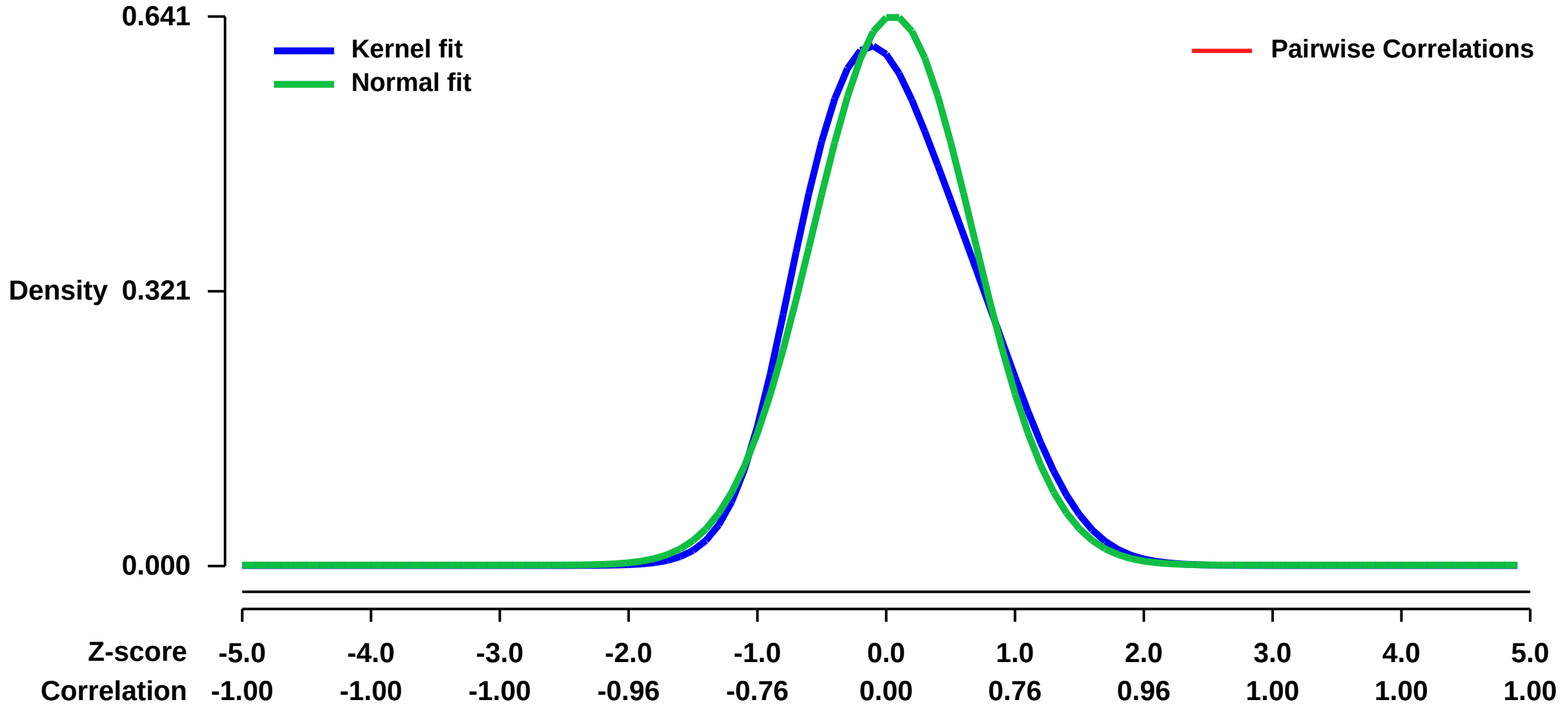

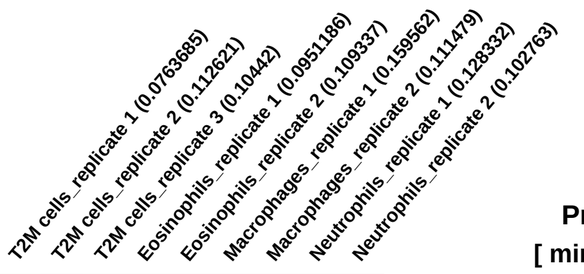

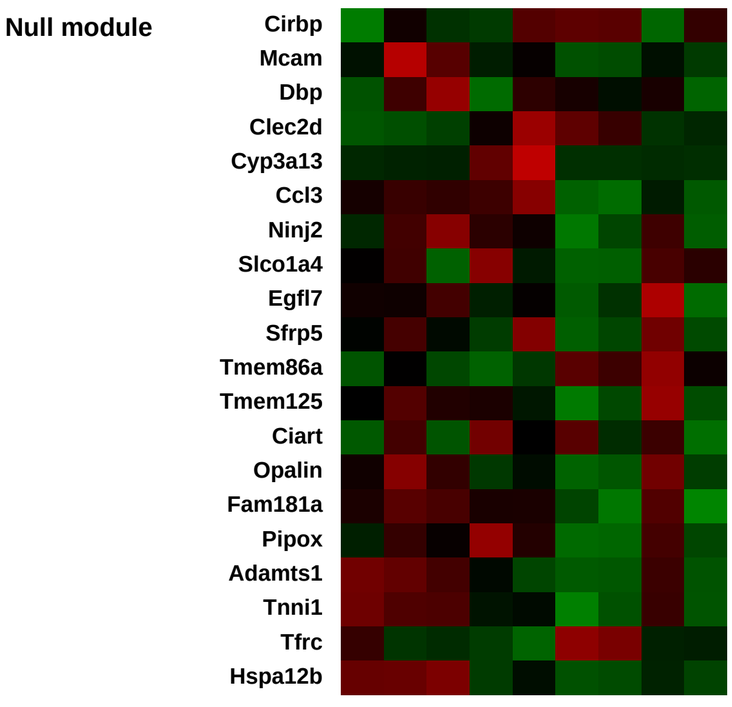

GEO Series "GSE18858" Expression Profiles

Num of samples in this series: 242

Details of this dataset are not shown due to large number of samples and the page size limit.

Find details in http://www.ncbi.nlm.nih.gov/geo/query/acc.cgi?acc=GSE18858

Background corr dist: KL-Divergence = 0.6578, L1-Distance = 0.0680, L2-Distance = 0.0123, Normal std = 0.2032

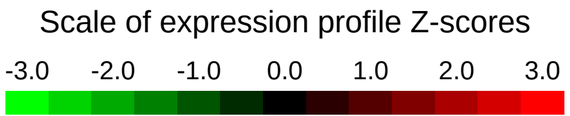

GEO Series "GSE32199" Expression Profiles

Num of samples in this series: 6

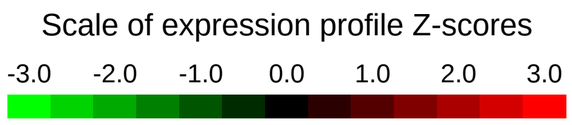

GEO Link:	http://www.ncbi.nlm.nih.gov/geo/query/acc.cgi?acc=GSE32199
Status:	Public on Nov 10 2011
Title:	BMP and Activin treatment of mouse extraembryonic endoderm (XEN) cells
Organism:	Mus musculus
Experiment type:	Expression profiling by array
Platform:	GPL1261
Pubmed ID:	22027433
Summary & Design:	**Summary:** XEN cells are derived from the primitive endoderm of mouse blastocysts. In culture and in chimeras they exhibit properties of parietal endoderm. However, BMP signaling promotes XEN cells to form an epithelium and differentiate into visceral endoderm (VE). Of the several different subtypes of VE described, BMP induces a subtype that is most similar to the VE adjacent to the trophoblast-derived extraembryonic ectoderm. The experiment was performed to gain insight into genes regulated by BMP and activin in XEN cells, and also to more precisely define the VE subtypes formed in culture. **Overall design:** IM8A1 XEN cells were treated for 6 days with BMP2 (20 ng/ml, R&D Systems), activin A (30 ng/ml, Peprotech), both, or neither in GMEM + 10% fetal bovine serum.

Background corr dist: KL-Divergence = 0.0437, L1-Distance = 0.0276, L2-Distance = 0.0009, Normal std = 0.6099

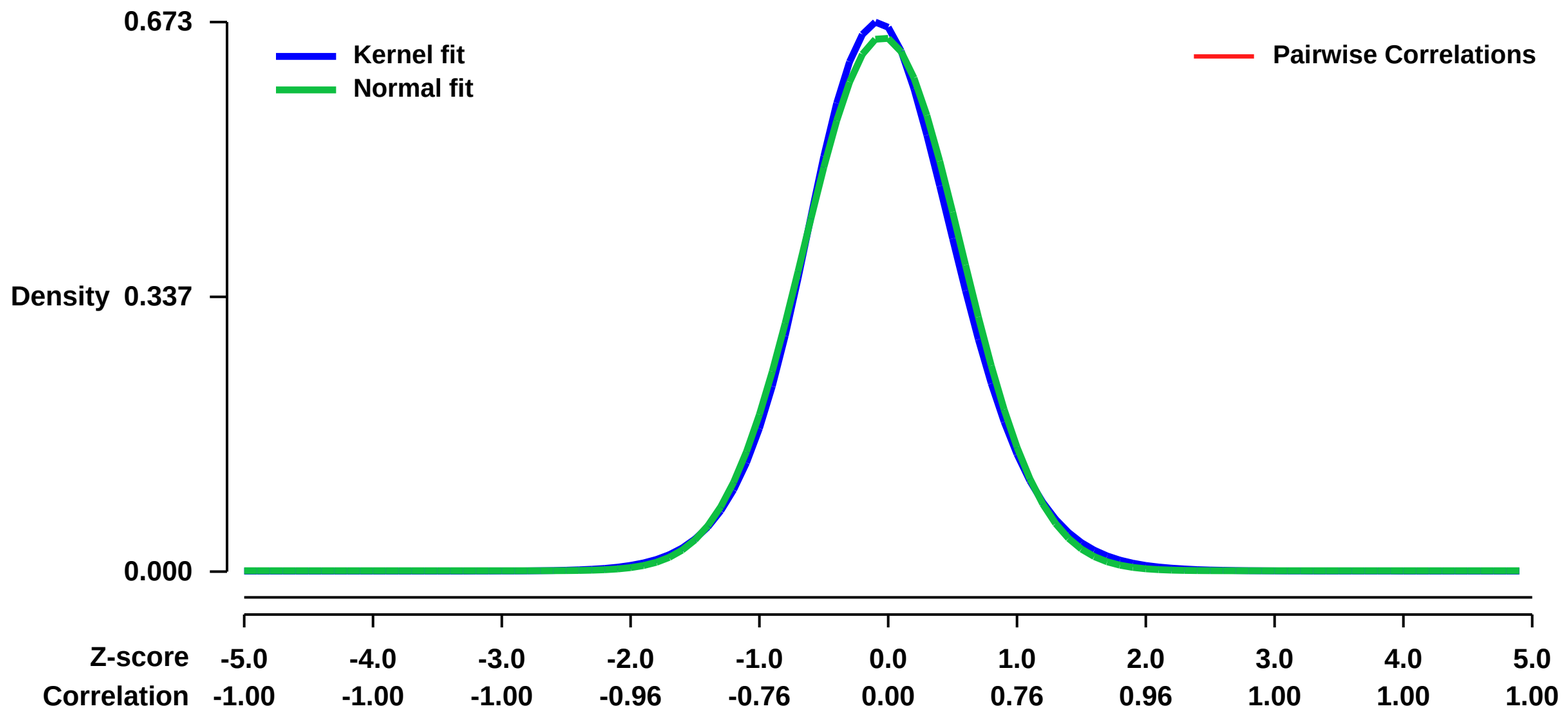

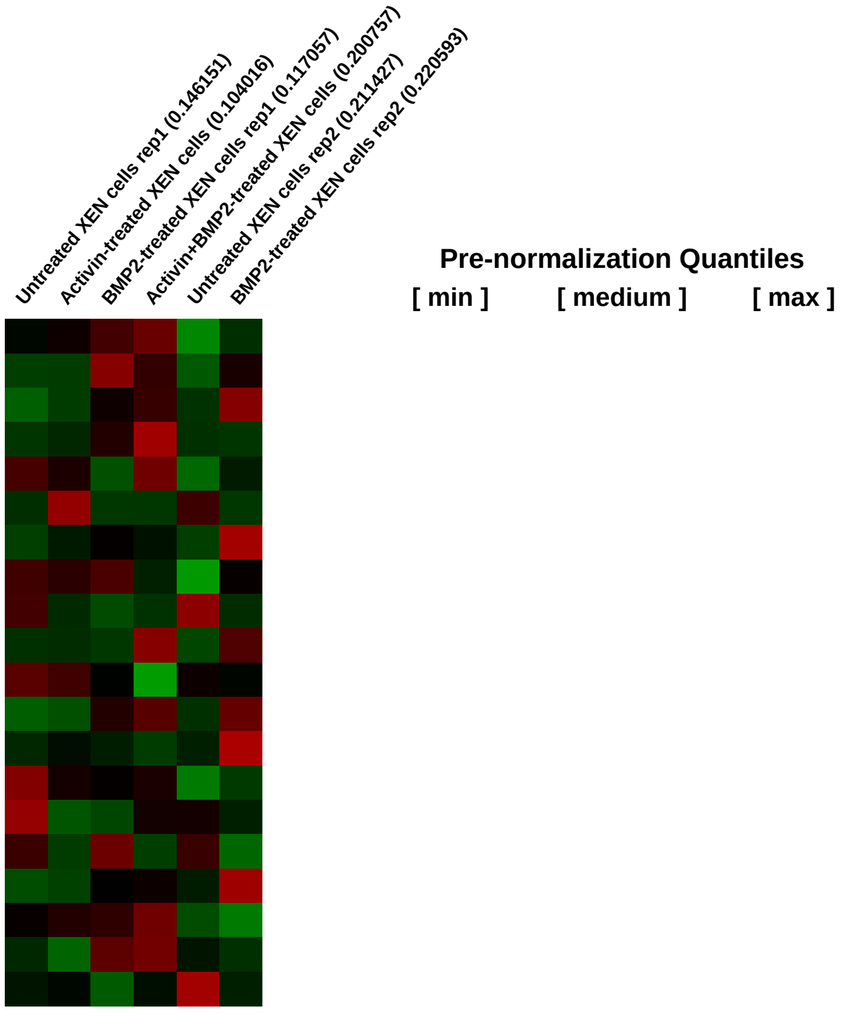

GEO Series "GSE18211" Expression Profiles

Num of samples in this series: 12

Scale of expression profile Z-scores

-3.0 -2.0 -1.0 0.0 1.0 2.0 3.0

GEO Link:	**http://www.ncbi.nlm.nih.gov/geo/query/acc.cgi?acc=GSE18211**
Status:	**Public on Nov 09 2009**
Title:	**New candidate gene identification for controlling mammalian gonadal sex determination**
Organism:	**Mus musculus**
Experiment type:	**Expression profiling by array**
Platform:	**GPL1261**
Pubmed ID:	**19864314**
Summary & Design:	**Summary:** **Mammalian gonadal sex determination is dependent on proper expression of sex determining genes in fetal gonadal somatic support cells (i.e., pre-granulosa and pre-Sertoli cells in XX and XY gonads, resp.). We used a unique transgenic mouse strain combined with microarray profiling to identify all the differentially expressed transcripts in XX and XY isolated somatic support cells during critical stages of gonadal development and differentiation.** **Overall design:** **XX and XY somatic support cells (SSC) were isolated by flow cytometry from embryonic day (E) 11.5 and E12.5 mouse gonads. Total RNA was isolated from pools of isolated cells; 3 pools per sex and each timepoint.**

Background corr dist: **KL-Divergence = 0.1005, L1-Distance = 0.0254, L2-Distance = 0.0015, Normal std = 0.4337**

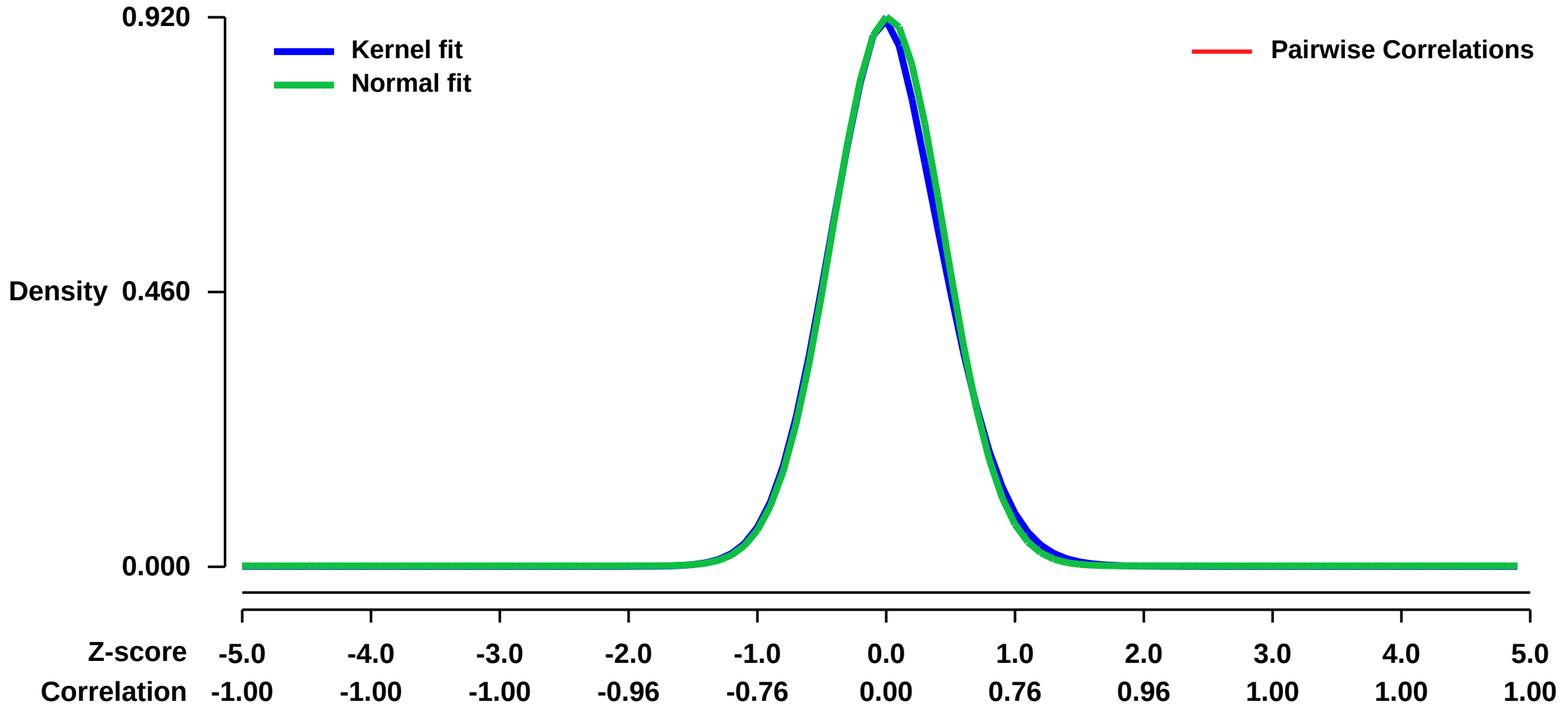

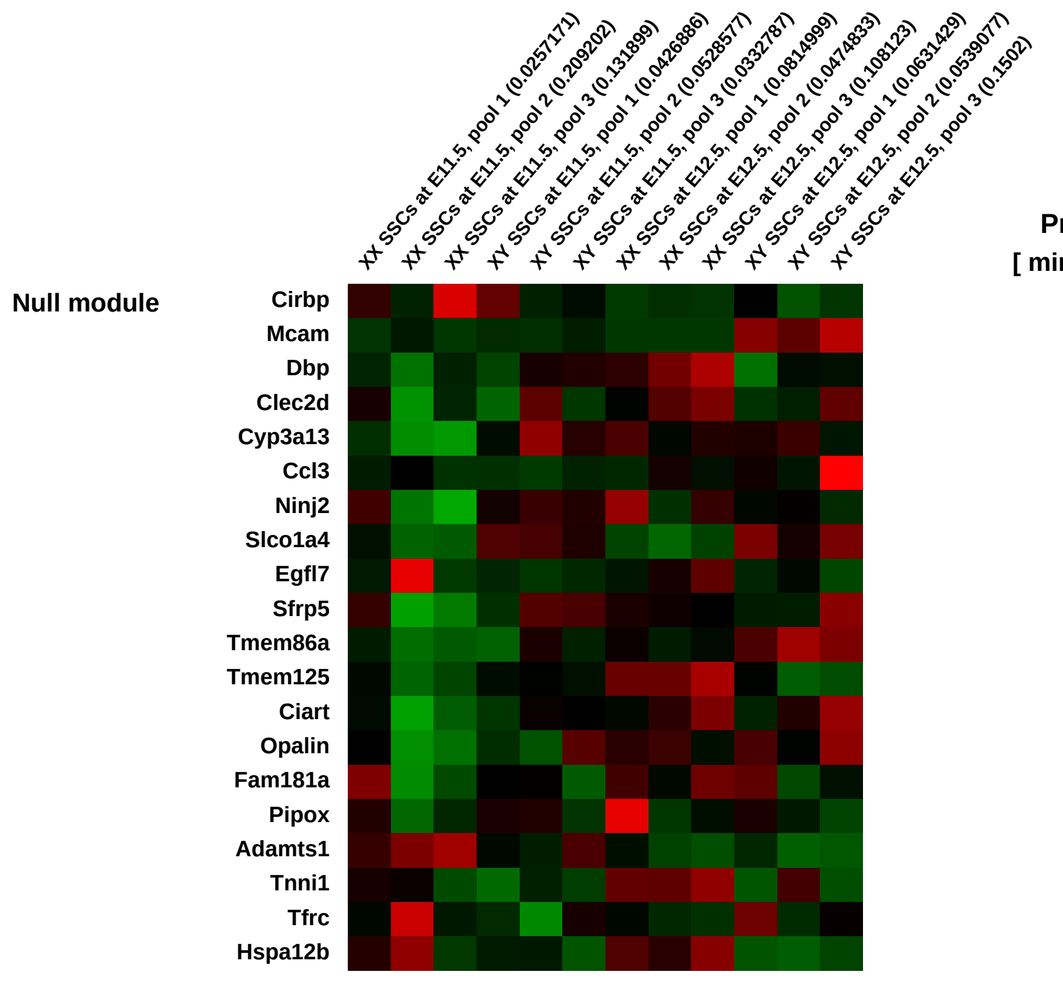

GEO Series "GSE13948" Expression Profiles

Num of samples in this series: 21

Scale of expression profile Z-scores

-3.0 -2.0 -1.0 0.0 1.0 2.0 3.0

GEO Link:	http://www.ncbi.nlm.nih.gov/geo/query/acc.cgi?acc=GSE13948
Status:	Public on Dec 16 2008
Title:	Antagonism of microRNA-122 in mice by systemically administered LNA-antimiR
Organism:	Mus musculus
Experiment type:	Expression profiling by array
Platform:	GPL1261
Pubmed ID:	18158304
Summary & Design:	**Summary:** **Antagonism of microRNA-122 in mice by systemically administered LNA-antimiR leads to up-regulation of a large set of predicted target mRNAs in the liver** **MicroRNA-122 (miR-122) is an abundant liver-specific miRNA, implicated in fatty acid and cholesterol metabolism as well as hepatitis C viral replication. Here, we report that a systemically administered 16-nt, unconjugated LNA (locked nucleic acid)-antimiR oligonucleotide complementary to the 5' end of miR-122 leads to specific, dose-dependent silencing of miR-122 and shows no hepatotoxicity in mice. Antagonism of miR-122 is due to formation of stable heteroduplexes between the LNA-antimiR and miR-122 as detected by northern analysis. Fluorescence in situ hybridization demonstrated uptake of the LNA-antimiR in mouse liver cells, which was accompanied by markedly reduced hybridization signals for mature miR-122 in treated mice. Functional antagonism of miR-122 was inferred from a low cholesterol phenotype and de-repression within 24 h of 199 liver mRNAs showing significant enrichment for miR-122 seed matches in their 3' UTRs. Expression profiling extended to 3 weeks after the last LNA-antimiR dose revealed that most of the changes in liver gene expression were normalized to saline control levels coinciding with normalized miR-122 and plasma cholesterol levels. Combined, these data suggest that miRNA antagonists comprised of LNA are valuable tools for identifying miRNA targets in vivo and for studying the biological role of miRNAs and miRNA-associated gene-regulatory networks in a physiological context.** **Keywords: compound treatment** **Overall design:** **Female NMRI mice were treated at day 2 with either 25mg/kg antimiR-122 (SPC3372) or vehicle (saline). Mice were sacrificied at day 3, 9 and 23 and liver RNA assayed. Three biological replicates for each of the six groups.**

Background corr dist: KL-Divergence = 0.2960, L1-Distance = 0.0653, L2-Distance = 0.0117, Normal std = 0.2812

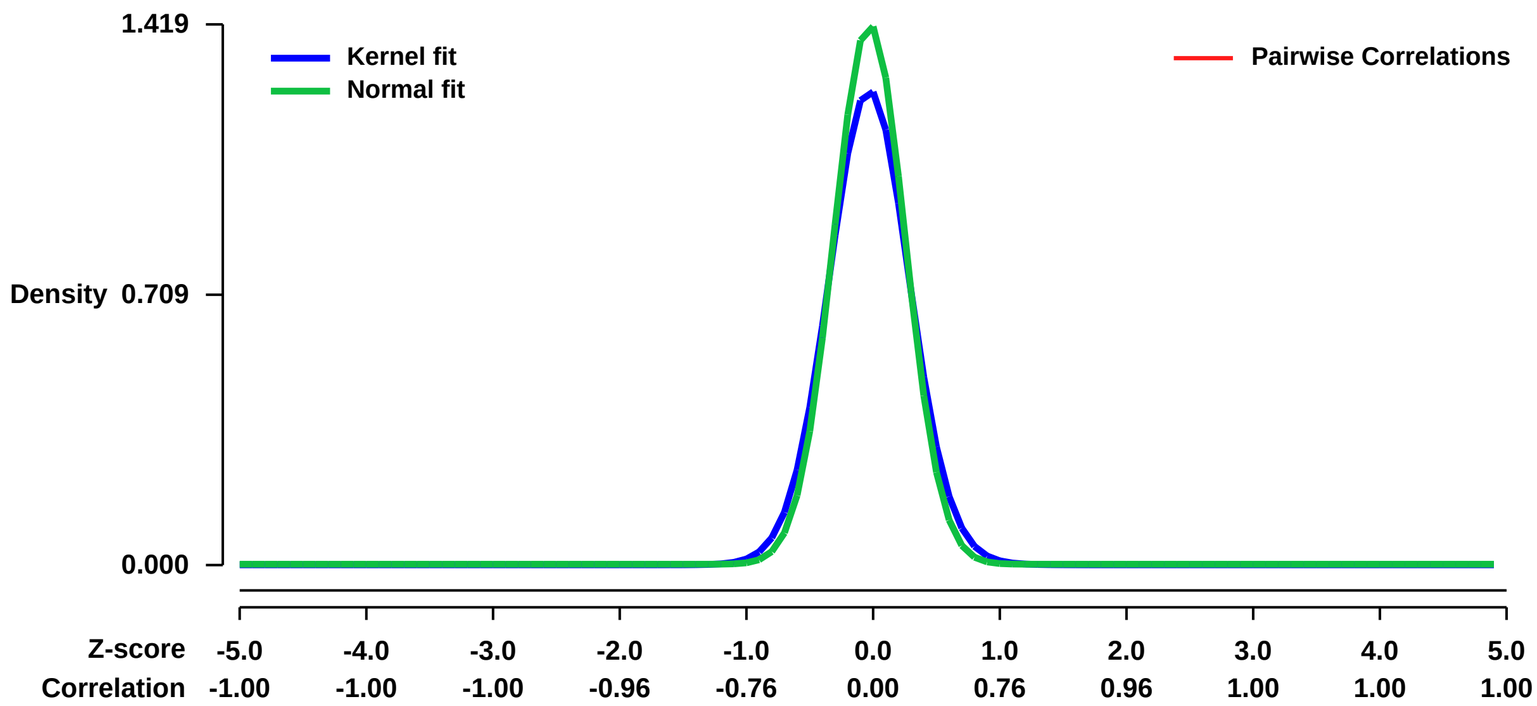

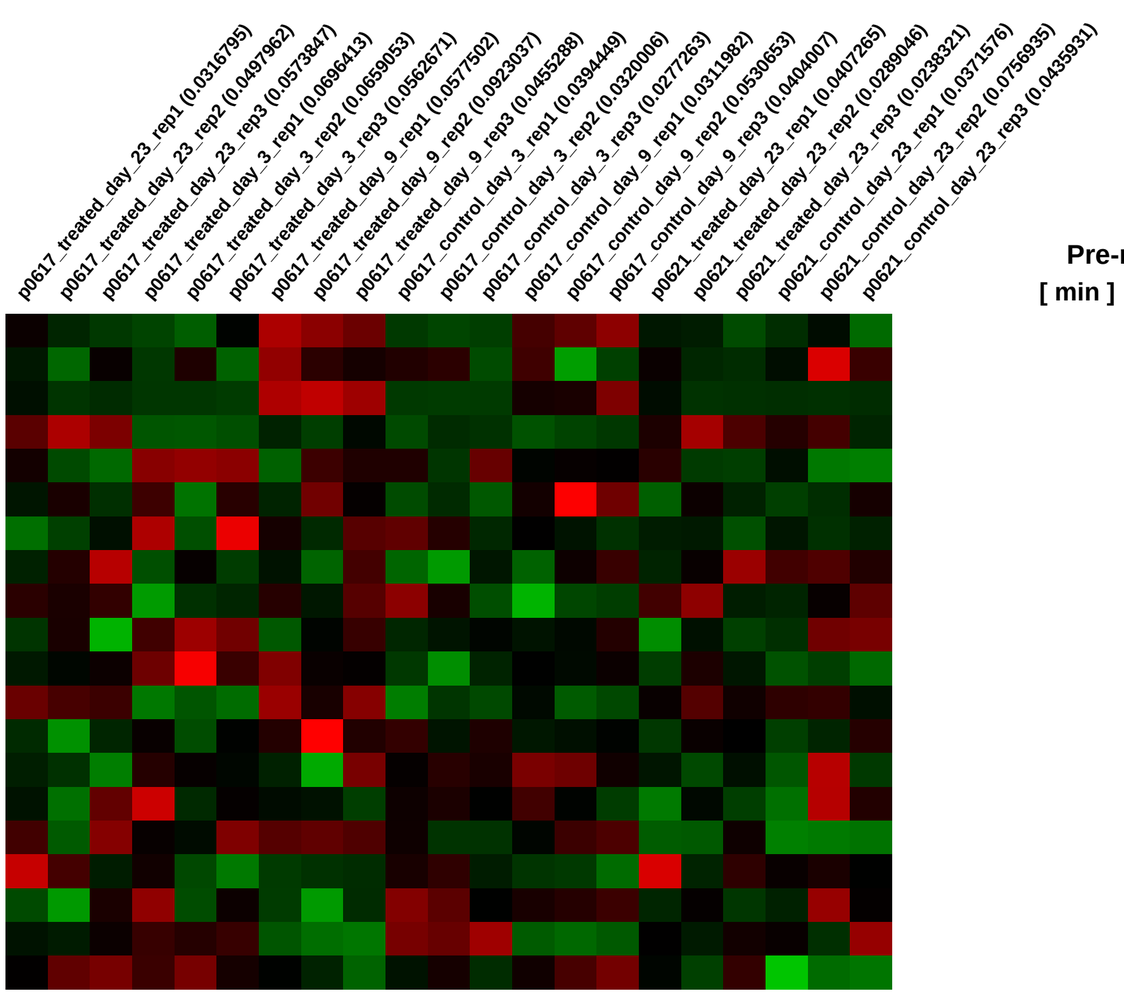

GEO Series "GSE7831" Expression Profiles

Num of samples in this series: 14

Scale of expression profile Z-scores

-3.0 -2.0 -1.0 0.0 1.0 2.0 3.0

GEO Link:	http://www.ncbi.nlm.nih.gov/geo/query/acc.cgi?acc=GSE7831
Status:	Public on Dec 13 2007
Title:	Expression data from immature pDC and pDC activated with CpG 1826 and influenza virus PR8
Organism:	Mus musculus
Experiment type:	Expression profiling by array
Platform:	GPL1261
Pubmed ID:	18029397
Summary & Design:	**Summary:** CpG 1826 binds to Toll-like receptor (TLR)9, whereas influenza virus PR8 activates pDC via TLR7. Differential stimulation of pDCs is expected to result in unique activation mechanism(s) leading to a different phenotypically and functionally matured pDC We used microarrays to detail the global programme of gene expression underlying the maturation process of pDC activated with CpG 1826 and influenza virus PR8. We identified a distinct expression profile of upregulated immunomediators. Keywords: time course **Overall design:** Sorted pDCs were cultured for 1h and 4hs in medium control or with 5 ´µg/ml CpG 1826 or 300 HAU/ml purified influenza A/PR/8 virus. The first experiment (e1) included pDC in media and stimulated with CpG for 4h. In two other independent experimental batches (e2 and e3), we obtained samples of sorted pDC cultured in medium alone (med), and with CpG or PR8 (flu) for 1h and 4h. RNA extraction was performed using the RNeasy Kit (Qiagen) and hybridization on Affymetrix microarrays was performed using standard protocols. We sought to obtain homogeneous populations of pDCs at different time points under defined activation conditions in order to decipher the temporal resolution of expression profiles during the process of their maturation.

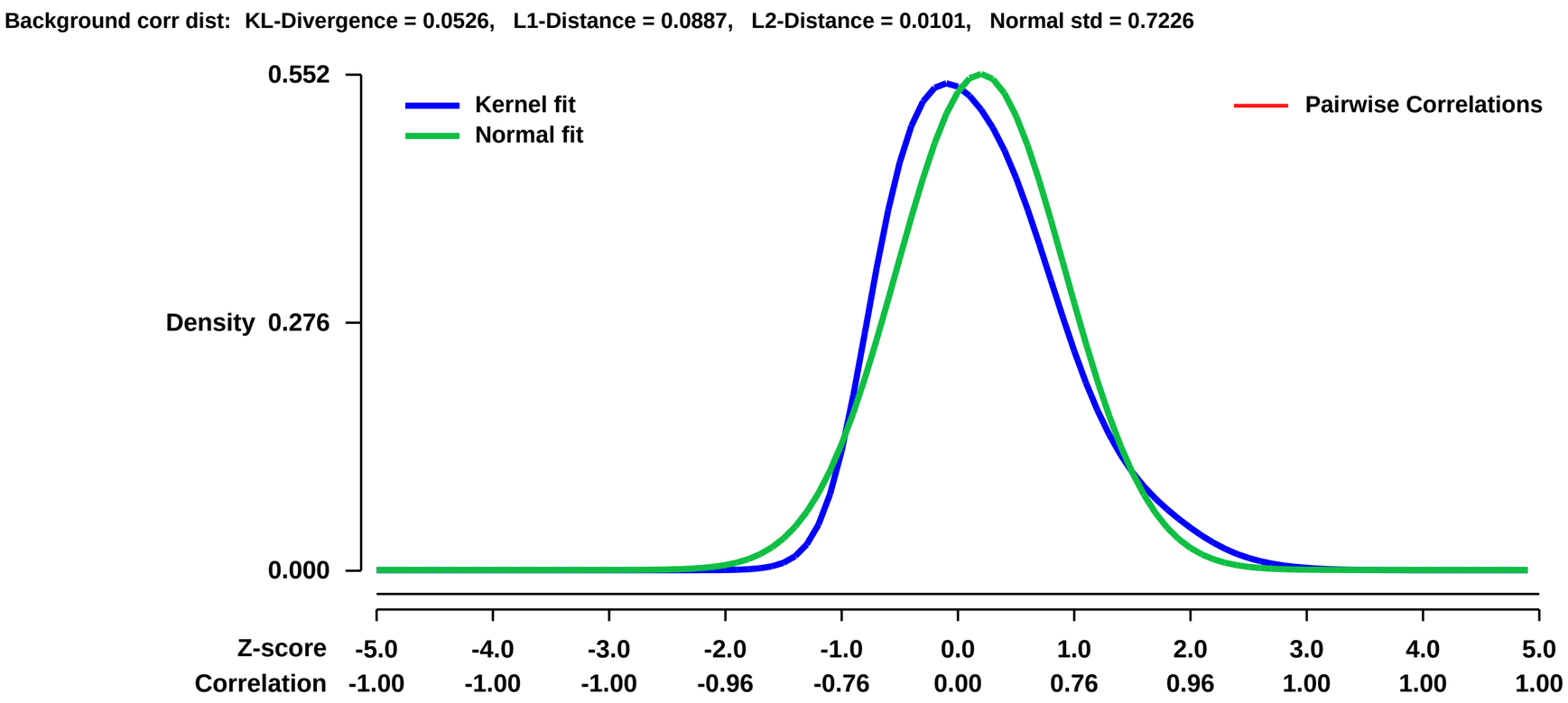

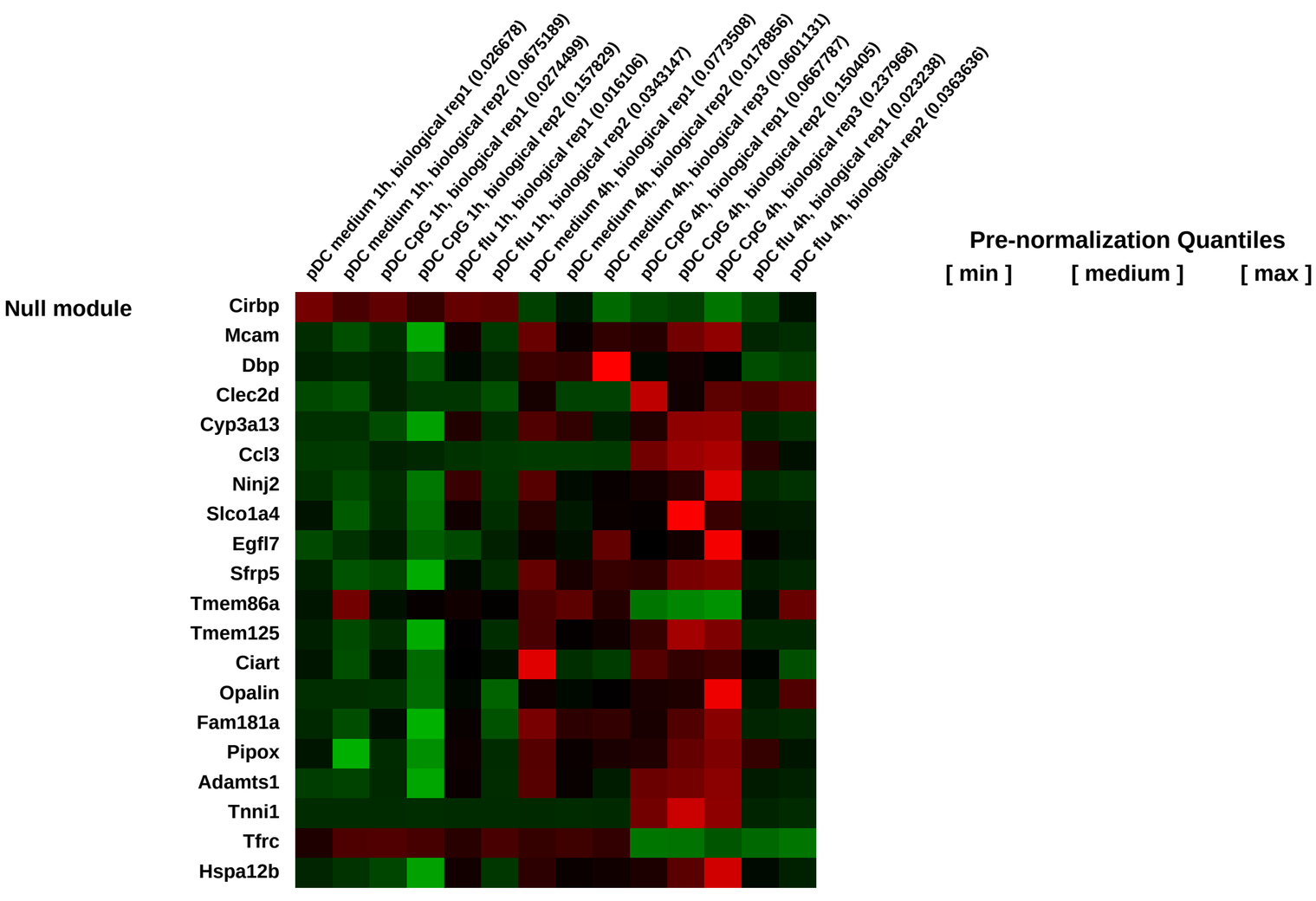

GEO Series "GSE29048" Expression Profiles

Num of samples in this series: 8

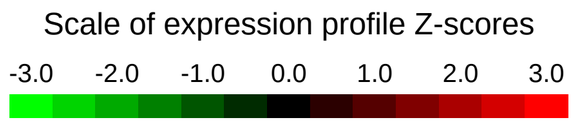

GEO Link:	http://www.ncbi.nlm.nih.gov/geo/query/acc.cgi?acc=GSE29048
Status:	Public on Jan 12 2012
Title:	Expression Profiling Identifies Novel Gene Targets and Functions for Pdx1 in the Duodenum of Mature Mice
Organism:	Mus musculus
Experiment type:	Expression profiling by array
Platform:	GPL1261
Pubmed ID:	22135308
Summary & Design:	**Summary:** Transcription factor pancreatic and duodenal homeobox 1 (Pdx1) plays an essential role in the pancreas to regulate its development and maintain proper islet function. However, less is known about the function of Pdx1 in the small intestine. We aim to investigate the role of Pdx1 in mature proximal small intestine by profiling the expression of genes differentially regulated in response to Pdx1 inactivation restricted to the intestinal epithelium in mice. **Overall design:** Pdx1 was conditionally inactivated in the intestinal epithelium of Pdx1flox/flox;VilCre mice, by crossing mutant mice homozygous for loxP site-flanked Pdx1 alleles with transgenic mice expressing Cre recombinase under the control of the mouse villin 1 gene promoter. Total RNA was isolated from the first five centimeters of the small intestine from adult Pdx1flox/flox;VilCre and littermate control mice. Microarray analysis was performed to investigate genome-wide transcriptional profiles in the proximal small intestine.

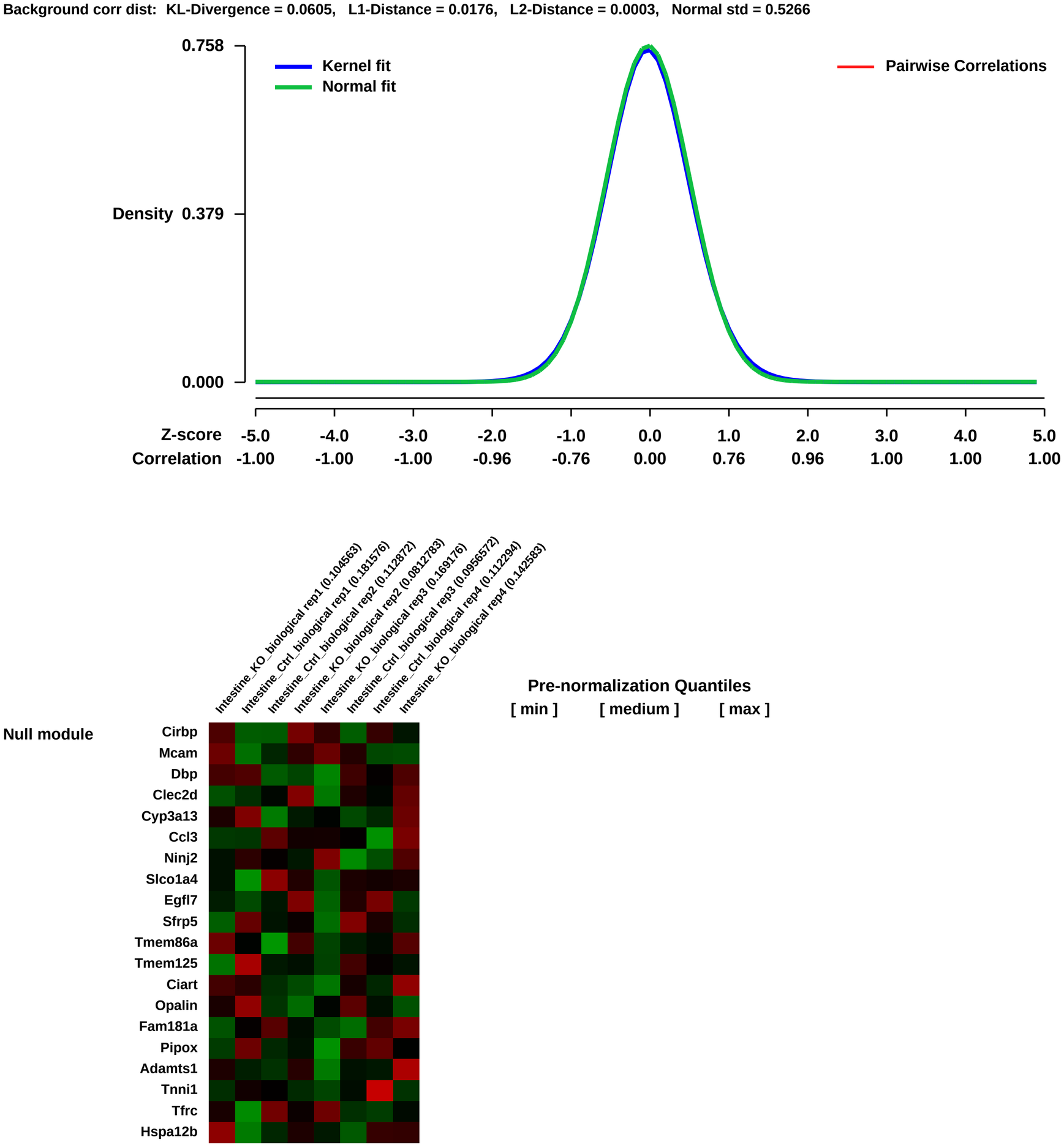

GEO Series "GSE42883" Expression Profiles

Num of samples in this series: 12

Scale of expression profile Z-scores

-3.0 -2.0 -1.0 0.0 1.0 2.0 3.0

GEO Link:	**http://www.ncbi.nlm.nih.gov/geo/query/acc.cgi?acc=GSE42883**
Status:	**Public on Jan 15 2013**
Title:	**Gene expression data following Neurogenin 1 expression in mouse embryonic stem cells**
Organism:	**Mus musculus**
Experiment type:	**Expression profiling by array**
Platform:	**GPL1261**
Pubmed ID:	
Summary & Design:	**Summary:** **To study the early gene expression events involved in neurogenesis, we expressed the bHLH neural determination factor neurogenin 1 in mouse embryonic stem cells.** **We used microarray to examine the program of gene expression at 24, 48, 72 hours of transgene expression.** **Overall design:** **RNAs from uninduced and induced cells were isolated at 24, 48, and 72 hours of differentiation and subjected to microarray analysis.**

Background corr dist: **KL-Divergence = 0.0734, L1-Distance = 0.0365, L2-Distance = 0.0022, Normal std = 0.5043**

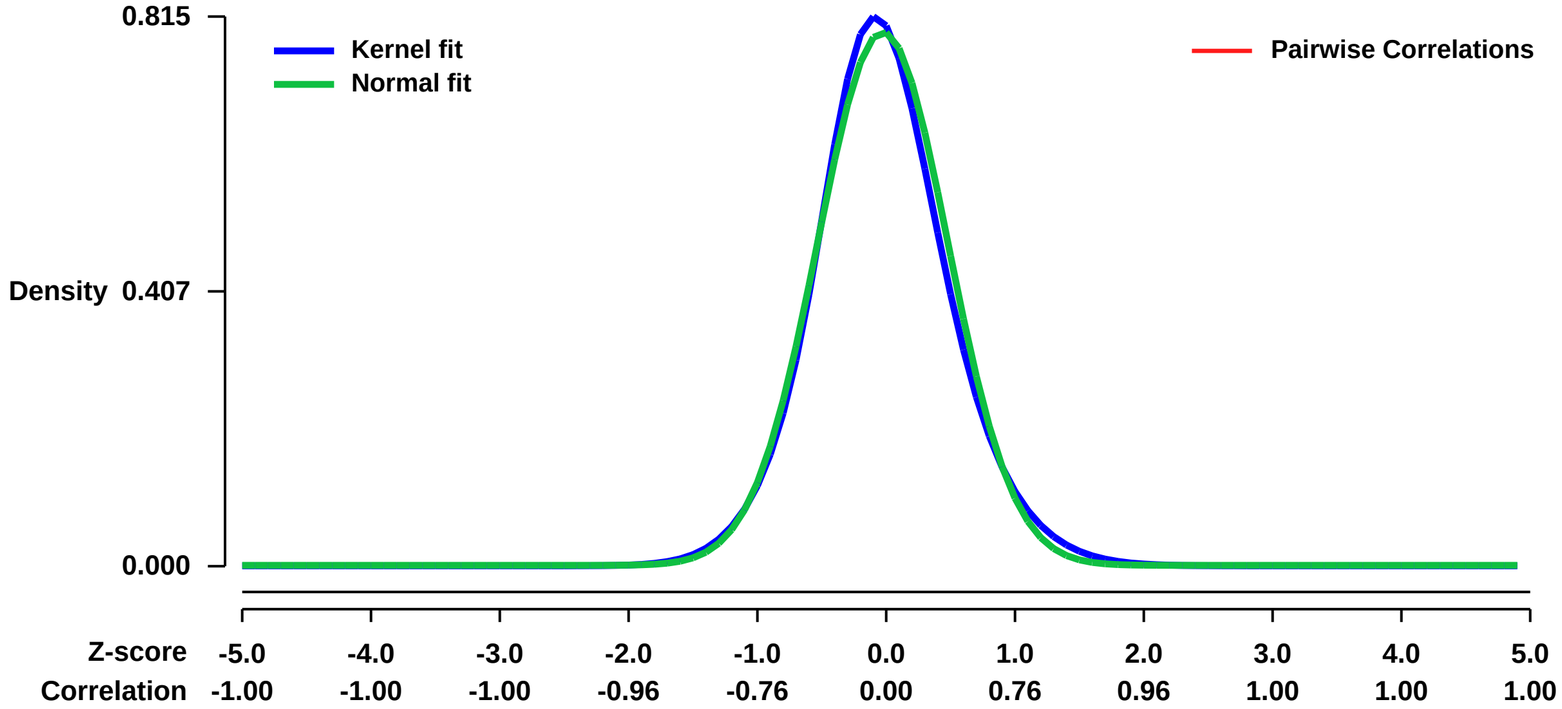

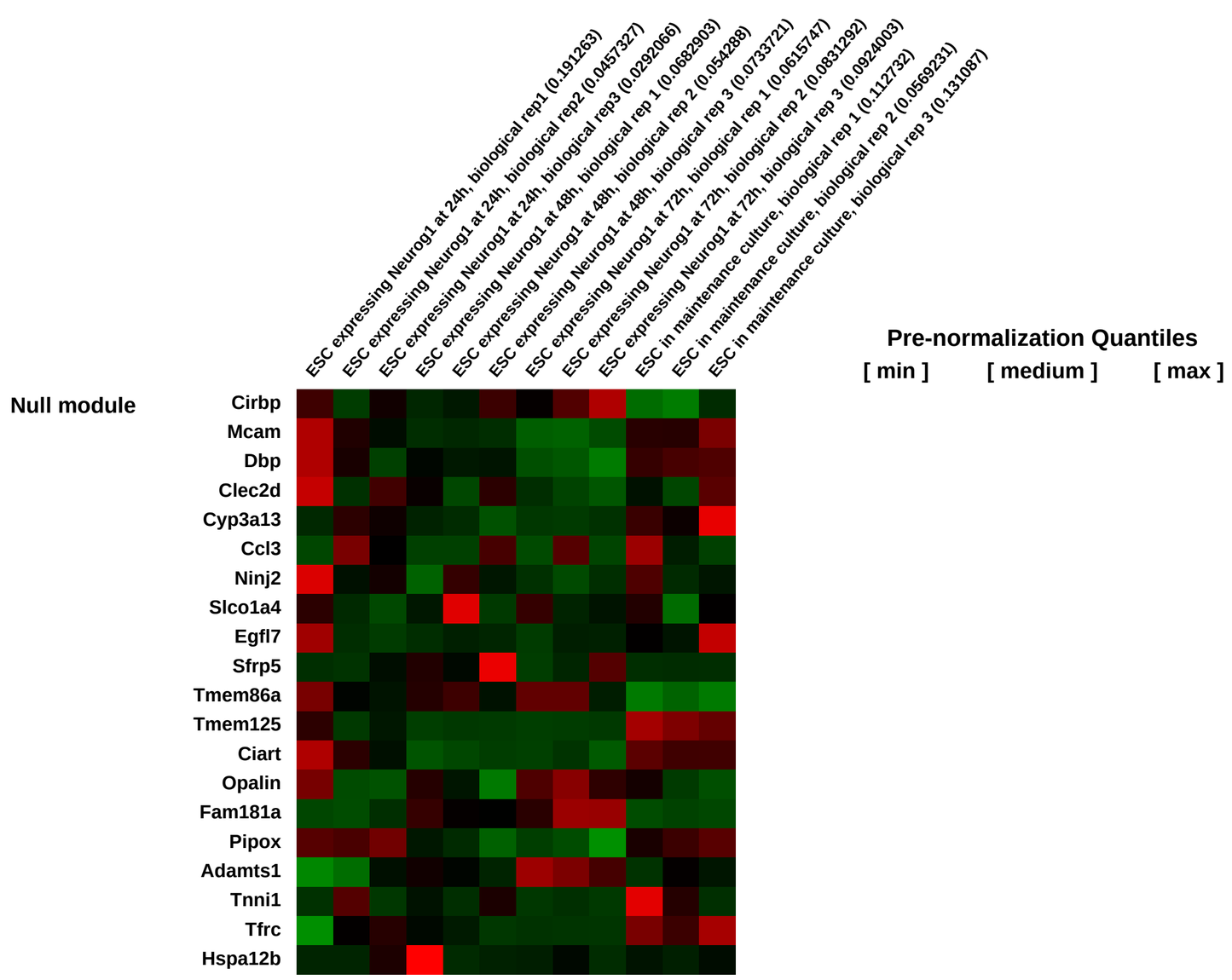

GEO Series "GSE54653" Expression Profiles

Num of samples in this series: 6

Scale of expression profile Z-scores

-3.0 -2.0 -1.0 0.0 1.0 2.0 3.0

GEO Link:	**http://www.ncbi.nlm.nih.gov/geo/query/acc.cgi?acc=GSE54653**
Status:	**Public on May 07 2014**
Title:	**Expression data from quiescent and activated neural stem cells from the adult mouse V-SVZ niche**
Organism:	**Mus musculus**
Experiment type:	**Expression profiling by array**
Platform:	**GPL1261**
Pubmed ID:	
Summary & Design:	**Summary:** **RNA was purified from GFAP::GFP+CD133+ and GFAP::GFP+CD133+EGFR+ cells isolated from the adult mouse V-SVZ niche (GFAP::GFP mice, Jackson Mice Stock number 003257)** **Overall design:** **6 samples consisting of two conditions of three biological replicates each were analyzed**

Background corr dist: **KL-Divergence = 0.0262, L1-Distance = 0.0342, L2-Distance = 0.0016, Normal std = 0.7186**

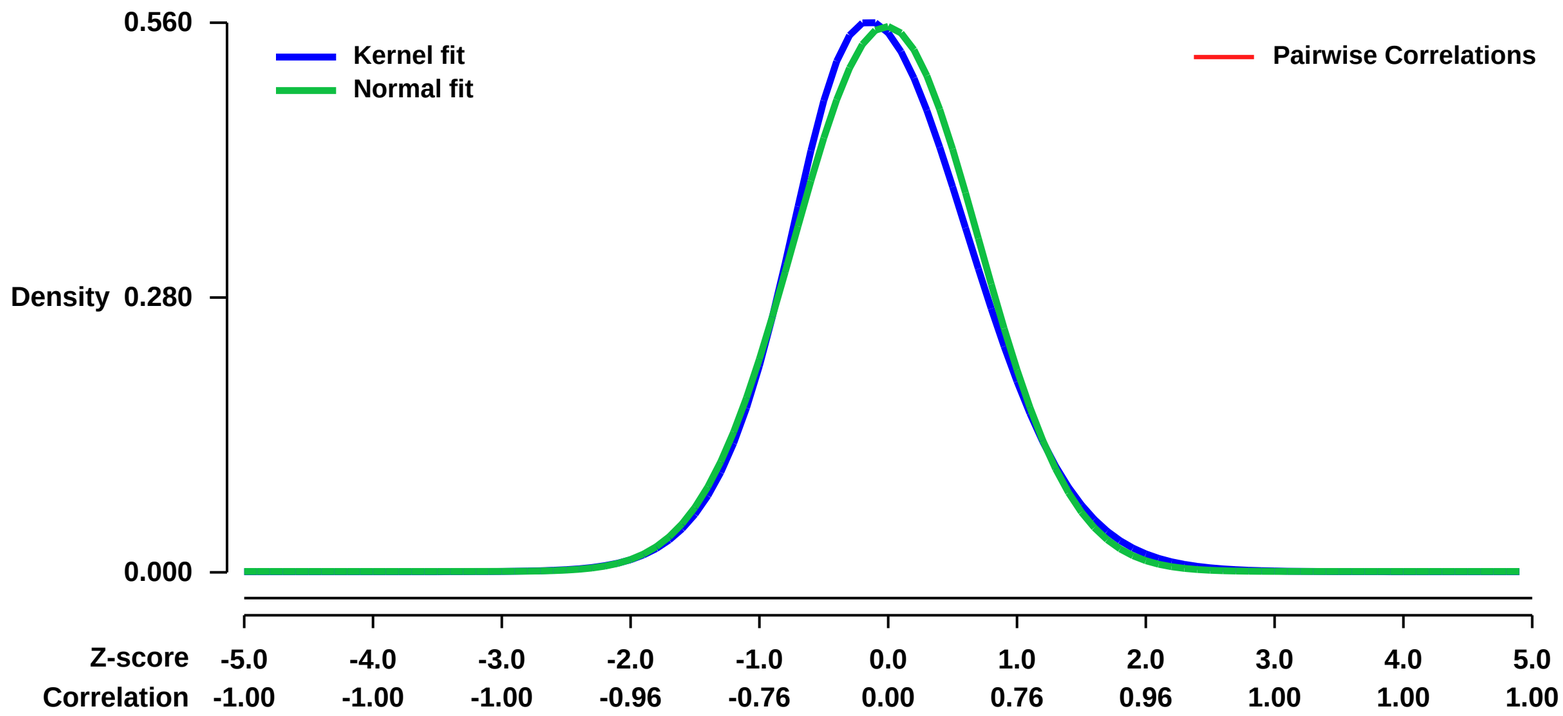

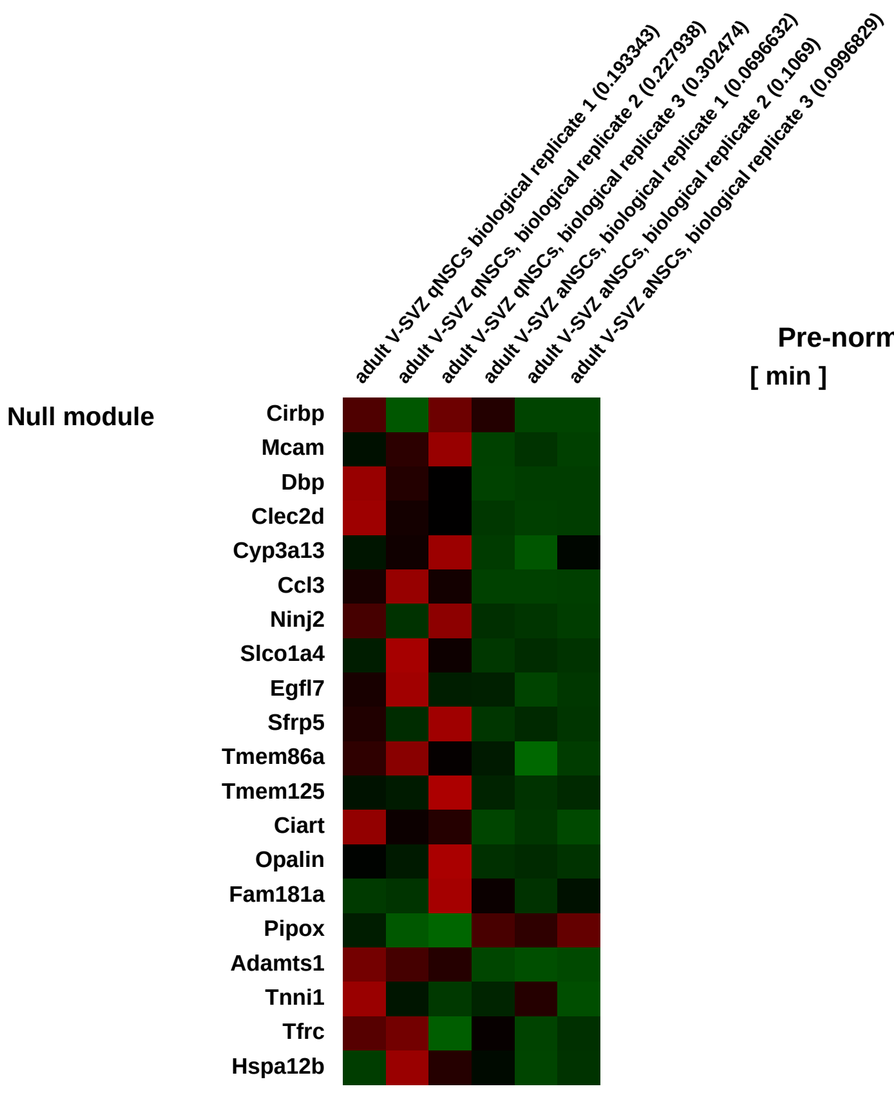

GEO Series "GSE10175" Expression Profiles

Num of samples in this series: 6

Scale of expression profile Z-scores

-3.0 -2.0 -1.0 0.0 1.0 2.0 3.0

GEO Link:	http://www.ncbi.nlm.nih.gov/geo/query/acc.cgi?acc=GSE10175
Status:	Public on Jan 16 2008
Title:	Comparison of gene expression in the epidermis of Tcfap2c mutant and control skin at embryonic day 16.5
Organism:	Mus musculus
Experiment type:	Expression profiling by array
Platform:	GPL1261
Pubmed ID:	18353300
Summary & Design:	**Summary:** The development of the epidermis, a stratified squamous epithelium, is dependent on the regulated differentiation of keratinocytes. Differentiation begins with the initiation of stratification, a process tightly controlled through proper gene expression. AP-2‚Ä° is expressed in skin and previous research suggested a pathway where p63 gene induction results in increased expression of AP-2‚Ä° which in turn is responsible for induction of K14. This study uses a conditional gene ablation model to further explore the role of AP-2‚Ä° in skin development. Mice deficient for AP-2‚Ä° exhibited delayed expression of p63, K14, and K1, key genes required for development and differentiation of the epidermis. In addition, microarray analysis of E16.5 skin revealed delayed expression of additional late epidermal differentiation genes: filaggrin, repetin and secreted Ly6/Plaur domain containing 1, in mutant mice. The genetic delay in skin development was further confirmed by a functional delay in the formation of an epidermal barrier. These results document an important role for AP-2‚Ä° in skin development, and reveal the existence of regulatory factors that can compensate for AP-2‚Ä° in its absence. **Keywords:** genetic modification **Overall design:** Skin samples were collected from 3 Tcfap2c and 3 control animals at embryonic day 16.5.

Background corr dist: KL-Divergence = 0.0410, L1-Distance = 0.0179, L2-Distance = 0.0003, Normal std = 0.6117

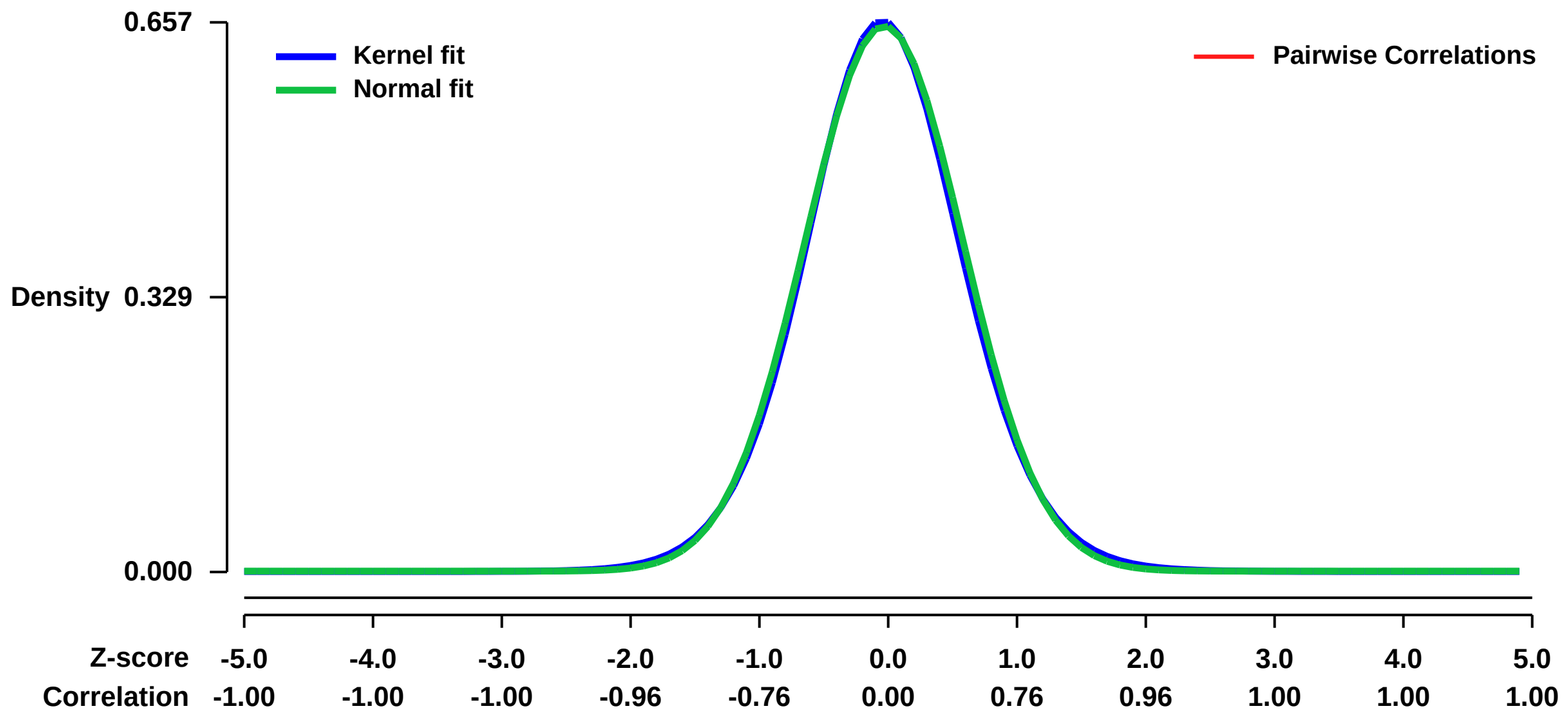

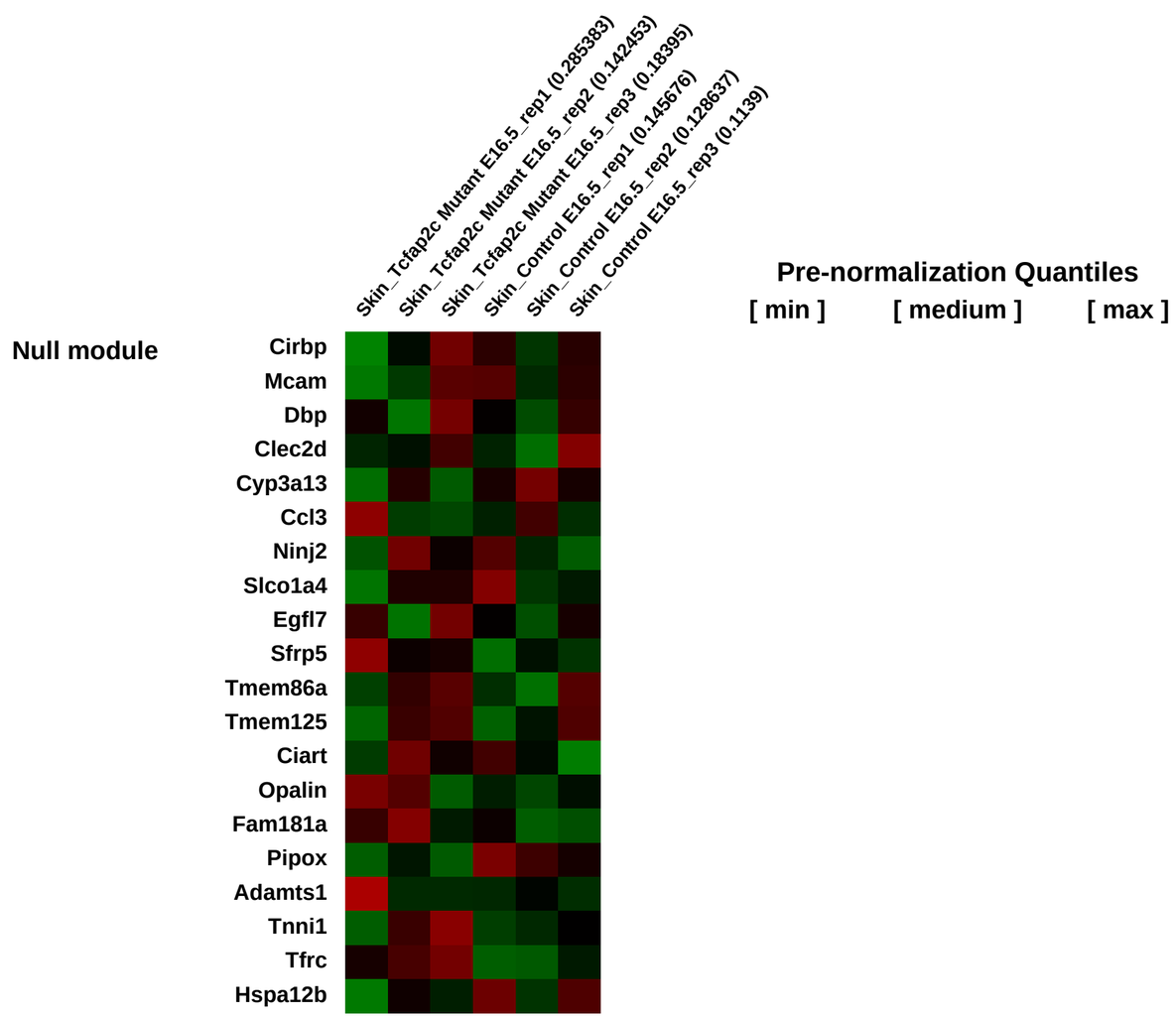

GEO Series "GSE15724" Expression Profiles

Num of samples in this series: 9

Scale of expression profile Z-scores

-3.0 -2.0 -1.0 0.0 1.0 2.0 3.0

GEO Link:	http://www.ncbi.nlm.nih.gov/geo/query/acc.cgi?acc=GSE15724
Status:	Public on Jul 02 2009
Title:	Gene expression in mouse tracheal basal cells
Organism:	Mus musculus
Experiment type:	Expression profiling by array
Platform:	GPL1261
Pubmed ID:	19625615
Summary & Design:	**Summary:** Epithelial basal cells (BCs) are an important stem cell population of the airways. We purified BCs from a KRT5-GFP transgenic mouse line and used Affymetrix arrays to compare there gene expression to that of non-BC epithelium. **Overall design:** Three populations of cells were obtained by FACS: 1. KRT5-GFP-, lectin- columnar epithelium. 2. KRT5-GFP-, lectin+ BCs. 3. KRT5-GFP+, lectin+ BCs. Three biological replicates of each sample were hybridized to Affymetrix microarray.

Background corr dist: KL-Divergence = 0.0768, L1-Distance = 0.0258, L2-Distance = 0.0012, Normal std = 0.4878

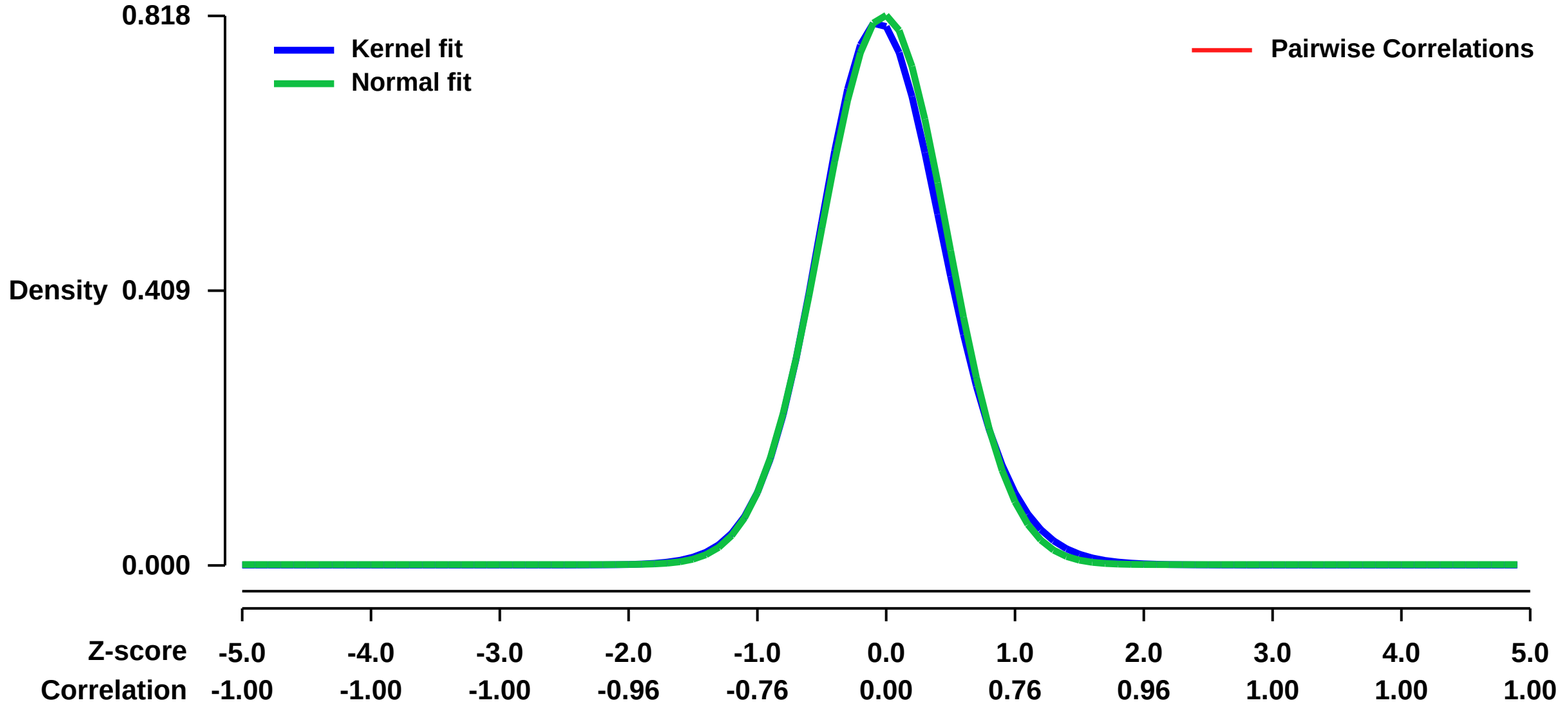

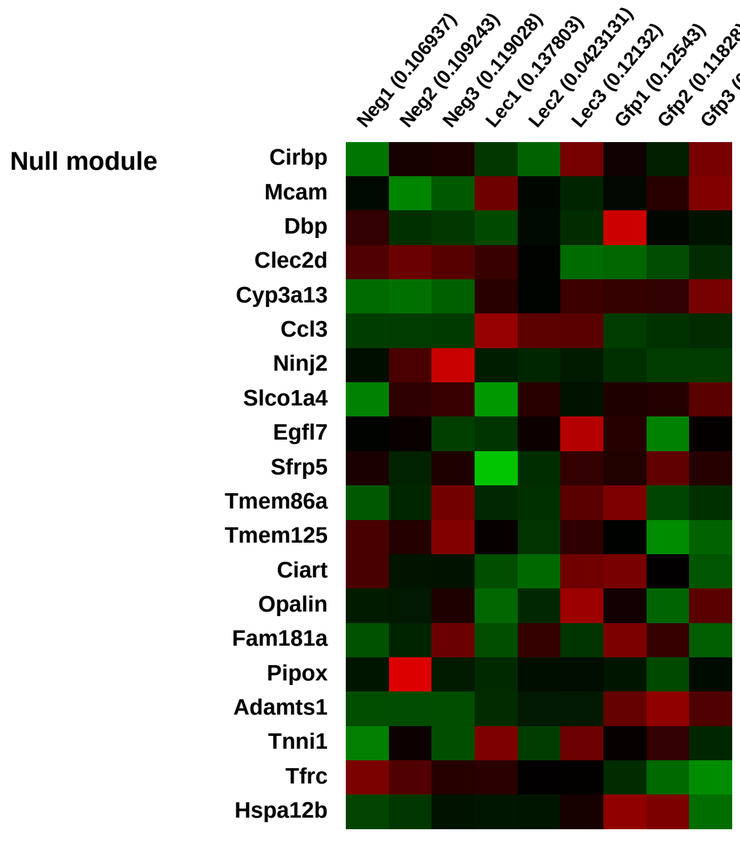

GEO Series "GSE45051" Expression Profiles

Num of samples in this series: 18

Scale of expression profile Z-scores

-3.0 -2.0 -1.0 0.0 1.0 2.0 3.0

GEO Link:	**http://www.ncbi.nlm.nih.gov/geo/query/acc.cgi?acc=GSE45051**
Status:	**Public on Jun 01 2013**
Title:	**Gene expression profile of liver from adult and neonatal Balb/c mice after listeriosis**
Organism:	**Mus musculus**
Experiment type:	**Expression profiling by array**
Platform:	**GPL1261**
Pubmed ID:	
Summary & Design:	**Summary:** **Expression profiling by microarray was used with a murine listeriosis model to better understand increased susceptibility of preterm neonates to infection.** **We used DNA microarray to identify genes that were differentially expressed in liver of adult and neonatal Balb/c mice after listeriosis infection.** **Overall design:** **A murine listeriosis model was established. The methods for culturing and counting the Listeria monocytogenes (strain CNL 85/163) had been described in previous publications. The Listeria was injected intraperitoneally using a 1-mL U-100 insulin syringe with a 30 gauge needle. Doses of Listeria monocytogenes used were based on work by our laboratory showing that similar bacterial colony counts were obtained with 4.2 x 10^5 total Listeria per adult mouse and 150 Listeria per gram for 3 to 5 day old neonatal mice. In neonatal mice, great care was taken to void deep intraperitoneal injection towards the viscera, or across the central abdominal vessels. At specified time points, liver was removed upon animal sacrifice and immediately flash frozen in liquid nitrogen and stored at -80 degrees Centigrade. Three adult mice and three neonatal mice were used at each time point.**

Background corr dist: KL-Divergence = 0.1508, L1-Distance = 0.0278, L2-Distance = 0.0014, Normal std = 0.3783

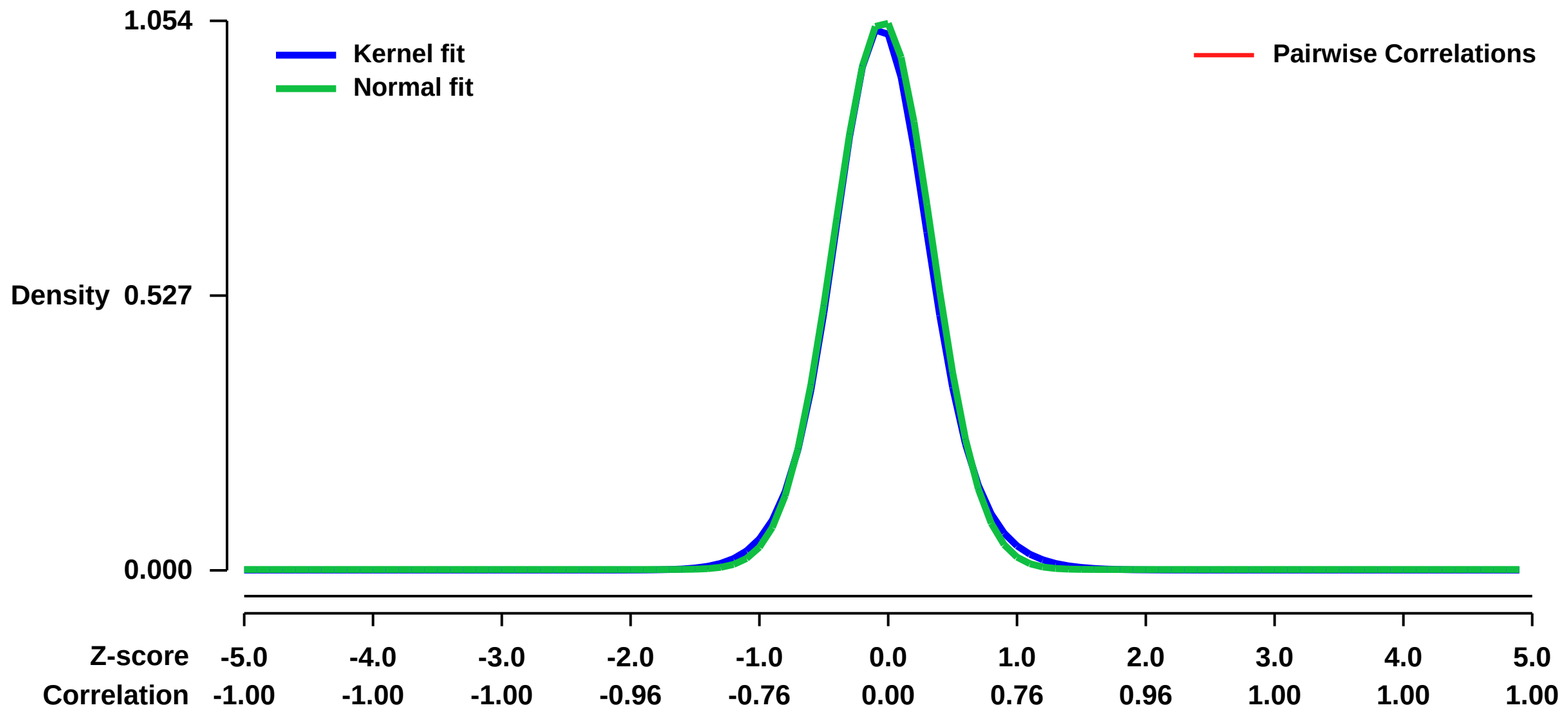

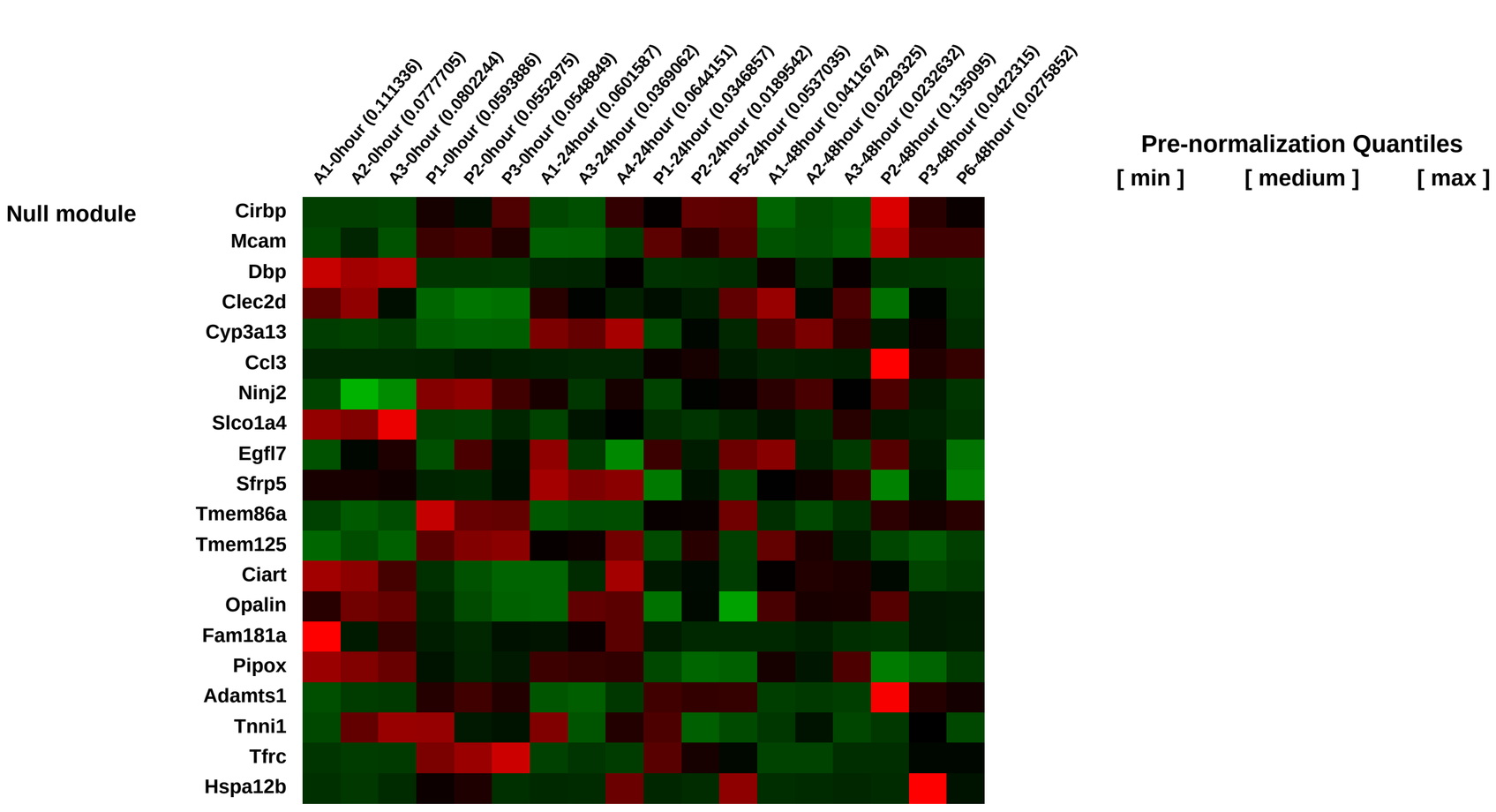

GEO Series "GSE19753" Expression Profiles

Num of samples in this series: 29

Scale of expression profile Z-scores

-3.0 -2.0 -1.0 0.0 1.0 2.0 3.0

GEO Link:	http://www.ncbi.nlm.nih.gov/geo/query/acc.cgi?acc=GSE19753
Status:	Public on Jan 15 2010
Title:	Mad2-induced chromosome instability leads to lung tumor relapse after oncogene withdrawal
Organism:	Mus musculus
Experiment type:	Expression profiling by array
Platform:	GPL1261
Pubmed ID:	20173739
Summary & Design:	**Summary:** Inhibition of an initiating oncogene often leads to extensive tumor cell death, a phenomenon known as oncogene addiction. This has led to the search for compounds that specifically target and inhibit oncogenes as anti-cancer agents. Whether chromosomal instability (CIN) generated as a result of deregulation of the mitotic checkpoint pathway, a frequent characteristic of solid tumors, has any effect on oncogene addiction, however, has not been explored systematically. We show here that induction of chromosome instability by overexpression of the mitotic checkpoint gene Mad2 does not affect the regression of Kras driven lung tumors upon Kras inhibition. However, tumors that experience transient Mad2 overexpression and consequent chromosome instability recur at dramatically elevated rates. The recurrent tumors are highly aneuploid and have varied activation of pro-proliferative pathways. Thus, early CIN may be responsible for tumor relapse after seemingly effective anti-cancer treatments. **Overall design:** Lung tumor tissue from TI-K (CCSP-rtTA;TRE-KrasV12), TI-KM (CCSP-rtTA; TRE-KrasV12; TRE-Mad2), recurrence (TI-KM) or normal lung tissue (CCSP-rtTA) was subjected to RNA extraction and individual samples hybridized to array platform MOE430A 2.0 Affymetrix.

Background corr dist: KL-Divergence = 0.1767, L1-Distance = 0.0485, L2-Distance = 0.0056, Normal std = 0.3528

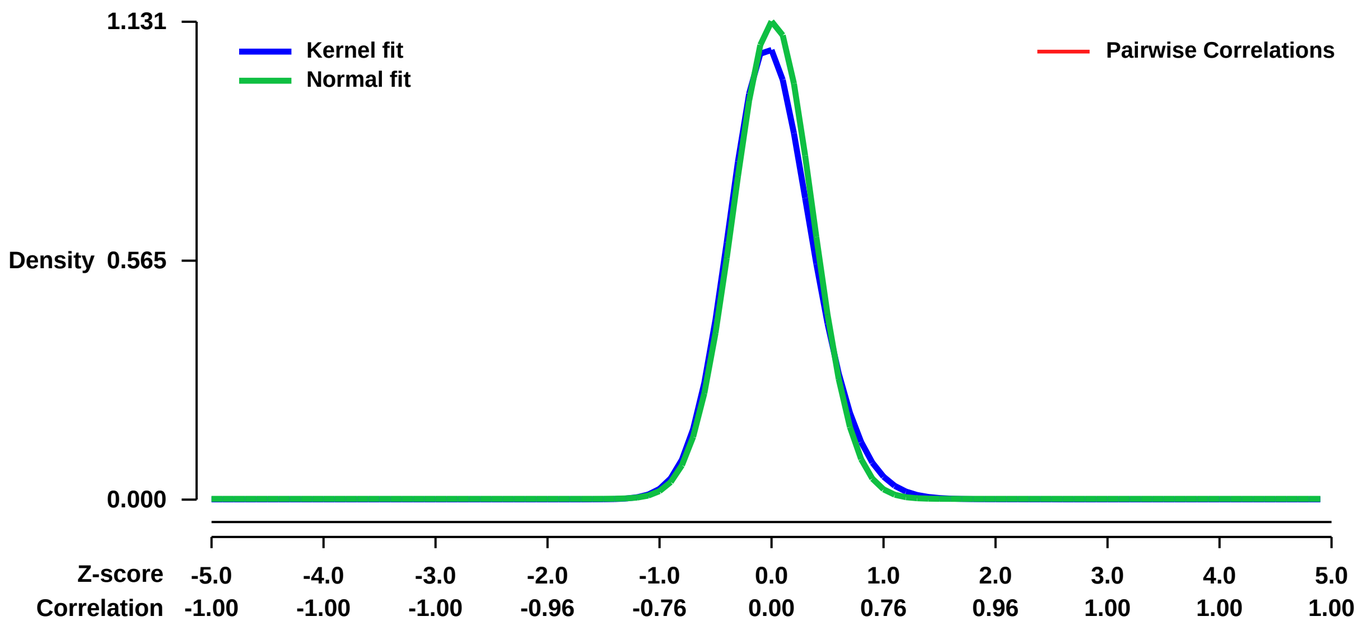

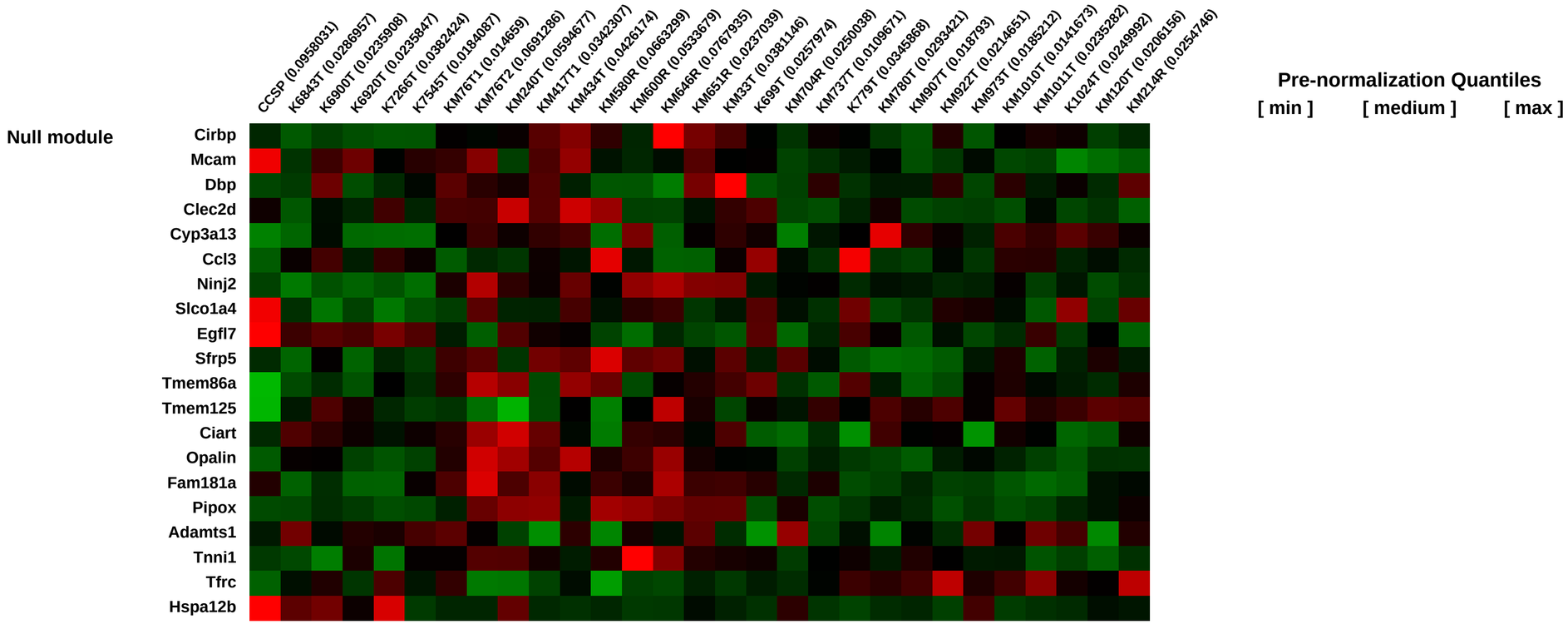

GEO Series "GSE31849" Expression Profiles

Num of samples in this series: 18

Scale of expression profile Z-scores

-3.0 -2.0 -1.0 0.0 1.0 2.0 3.0

GEO Link:	**http://www.ncbi.nlm.nih.gov/geo/query/acc.cgi?acc=GSE31849**
Status:	**Public on Sep 08 2011**
Title:	**Genome-wide activity-dependent MeCP2 phosphorylation regulates nervous system development and function [cultured cortical neurons]**
Organism:	**Mus musculus**
Experiment type:	**Expression profiling by array**
Platform:	**GPL1261**
Pubmed ID:	
Summary & Design:	**Summary:** **To examine potential differences in activity-dependent gene expression, we analyzed mRNA expression in cultured neurons isolated from Wild-type vs MeCP2 S421A mice at 0 (unstimulated), 1 or 6 hours after membrane depolarization by exposure to high extracellular KCl (55mM)** **All mice were male littermates from one of three litters.** **Overall design:** **We isolated RNA from dissociated cortical cultures (E16+7DIV) isolated from Wild-Type or MeCP2 S421A knock-in mice littermates. Cells were either left unstimulated or depolarized for 1 or 6 hours by addition of 55mM KCl to the media. mRNA expression was analyzed using the Affymetrix GeneChip Mouse Expression Set 430 2.0 microarray platform.**

Background corr dist: **KL-Divergence = 0.1022, L1-Distance = 0.0832, L2-Distance = 0.0119, Normal std = 0.4971**

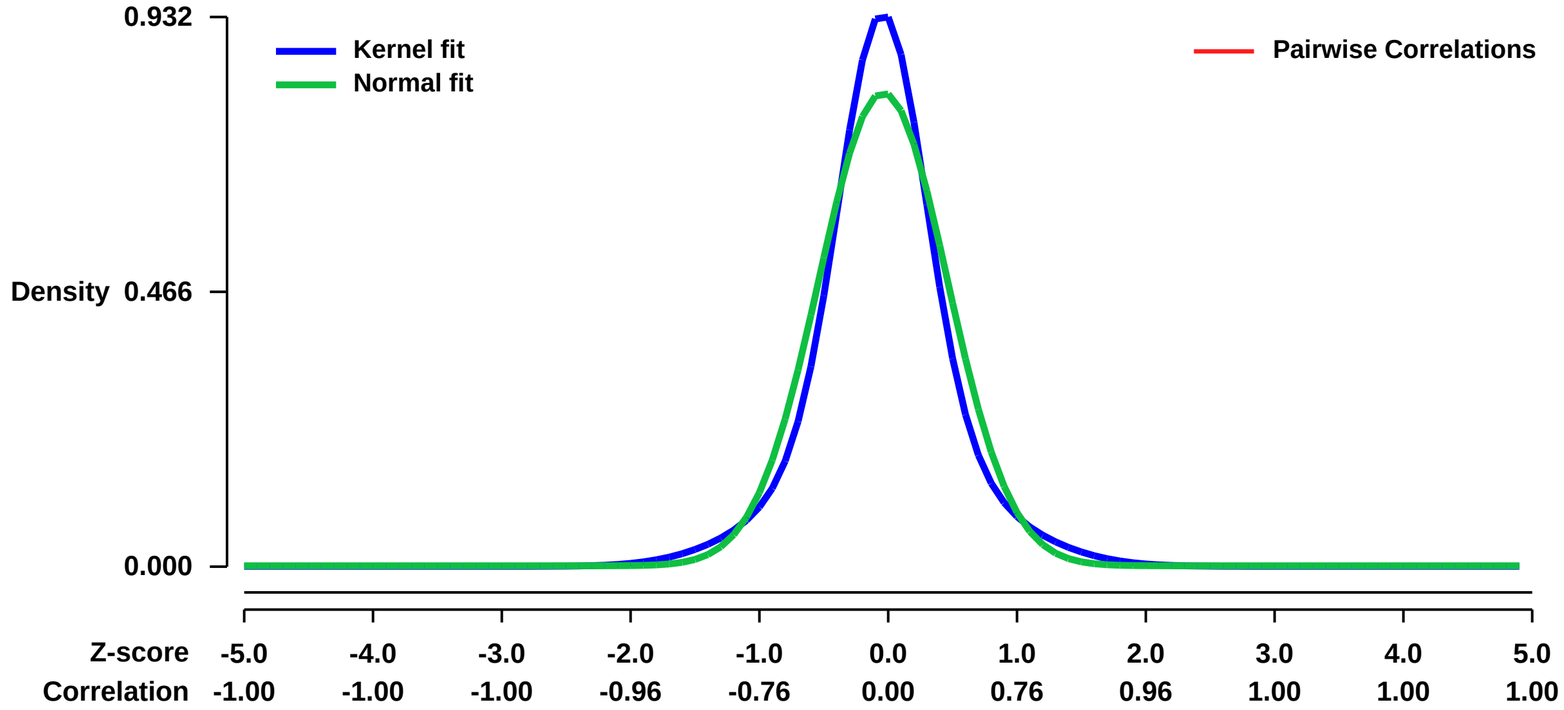

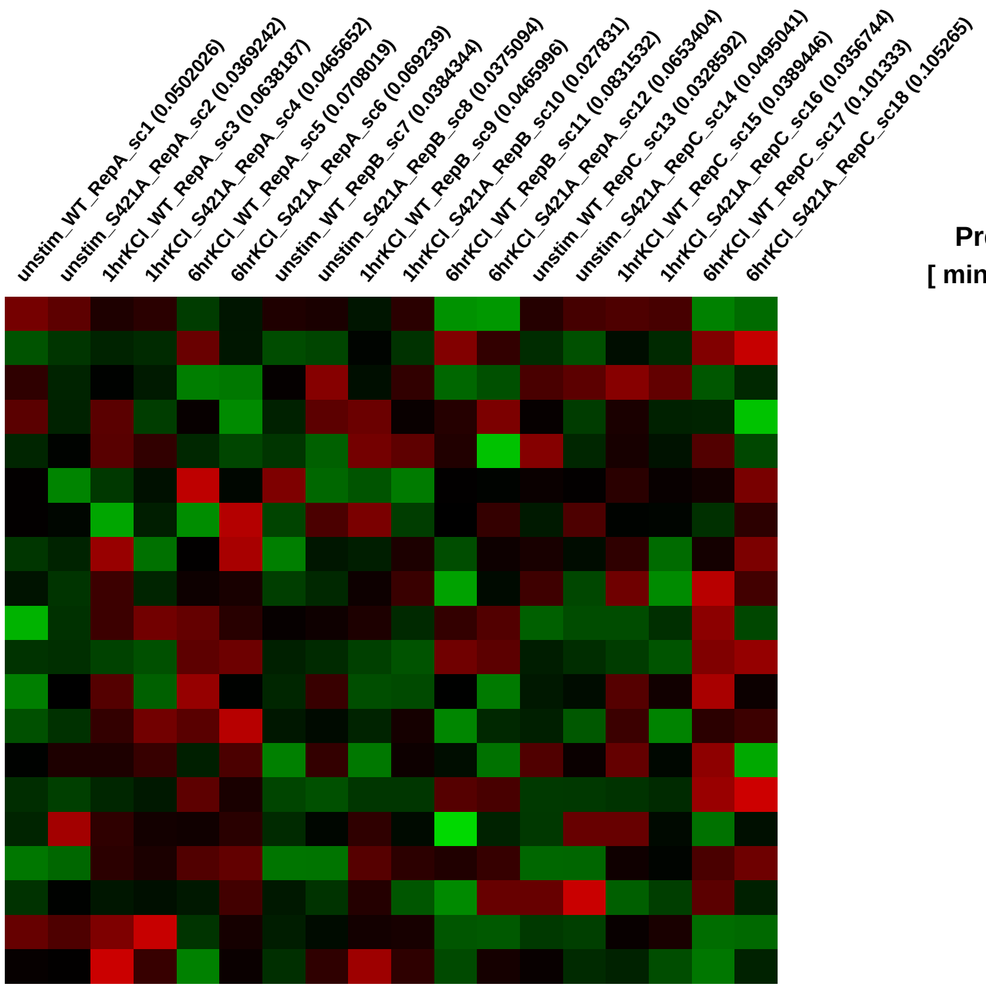

GEO Series "GSE13306" Expression Profiles

Num of samples in this series: 17

Scale of expression profile Z-scores

-3.0 -2.0 -1.0 0.0 1.0 2.0 3.0

GEO Link:	http://www.ncbi.nlm.nih.gov/geo/query/acc.cgi?acc=GSE13306
Status:	Public on Nov 16 2008
Title:	Retinoic Acid Enhances Foxp3 Induction Indirectly by Relieving Inhibition from CD4(+)CD44(hi) Cells.
Organism:	Mus musculus
Experiment type:	Expression profiling by array
Platform:	GPL1261
Pubmed ID:	19006694
Summary & Design:	**Summary:** CD4(+)Foxp3(+) regulatory T (Treg) cells originate primarily from thymic differentiation, but conversion of mature T lymphocytes to Foxp3 positivity can be elicited by several means, including in vitro activation in the presence of TGF-beta. Retinoic acid (RA) increases TGF-beta-induced expression of Foxp3, through unknown molecular mechanisms. We showed here that, rather than enhancing TGF-beta signaling directly in naive CD4(+) T cells, RA negatively regulated an accompanying population of CD4(+) T cells with a CD44(hi) memory and effector phenotype. These memory cells actively inhibited the TGF-beta-induced conversion of naive CD4(+) T cells through the synthesis of a set of cytokines (IL-4, IL-21, IFN-gamma) whose expression was coordinately curtailed by RA. This indirect effect was evident in vivo and required the expression of the RA receptor alpha. Thus, cytokine-producing CD44(hi) cells actively restrain TGF-beta-mediated Foxp3 expression in naive T cells, and this balance can be shifted or fine-tuned by RA. **Overall design:** All gene expression profiles were obtained from highly purified T cell populations sorted by flow cytometry. To reduce variability, cells from multiple mice were pooled for sorting, and replicates were generated for essentially all groups. RNA from 0.5-3 x 105 cells was amplified, labeled, and hybridized to Affymetrix M430v2 microarrays. Raw data were preprocessed with the RMA algorithm in GenePattern, and averaged expression values were used for analysis.

Background corr dist: KL-Divergence = 0.0519, L1-Distance = 0.0522, L2-Distance = 0.0058, Normal std = 0.5629

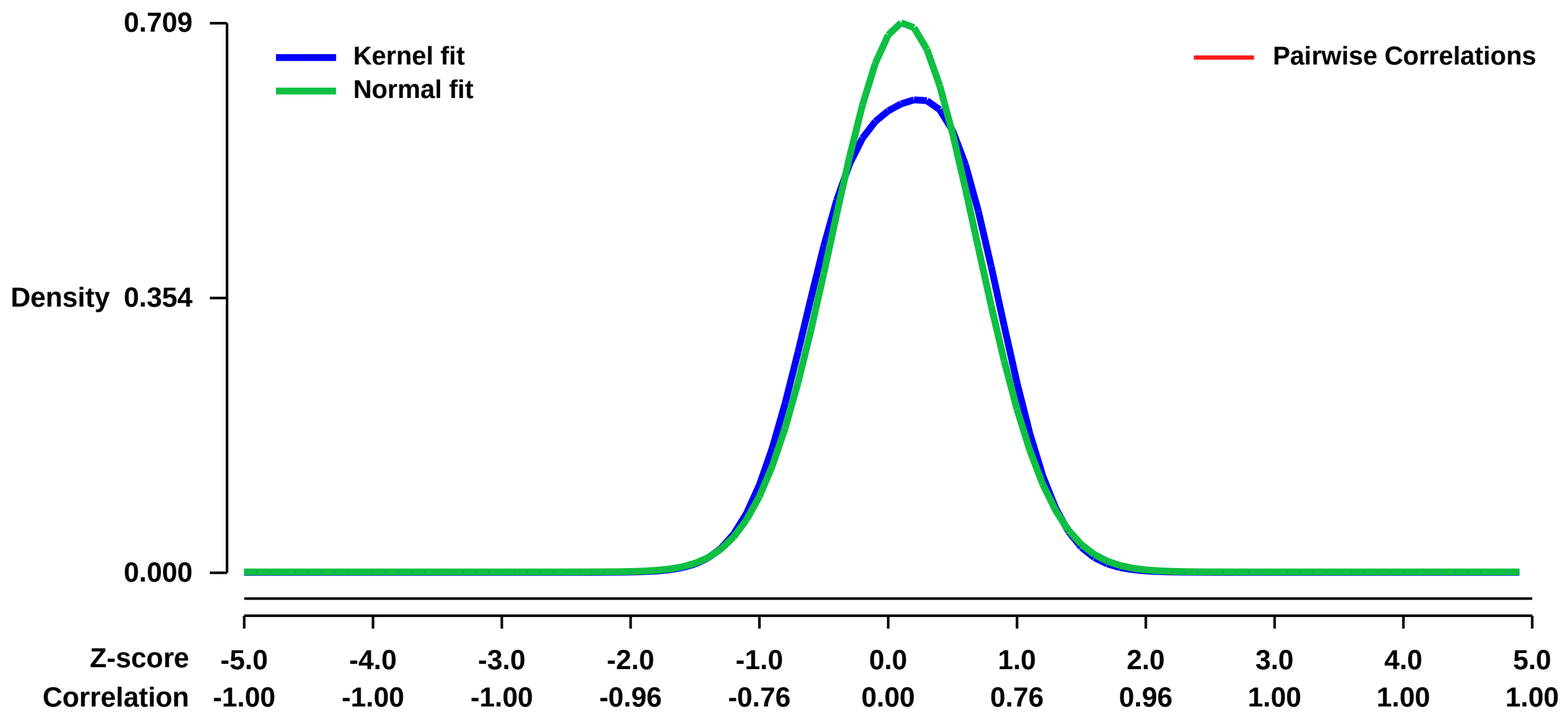

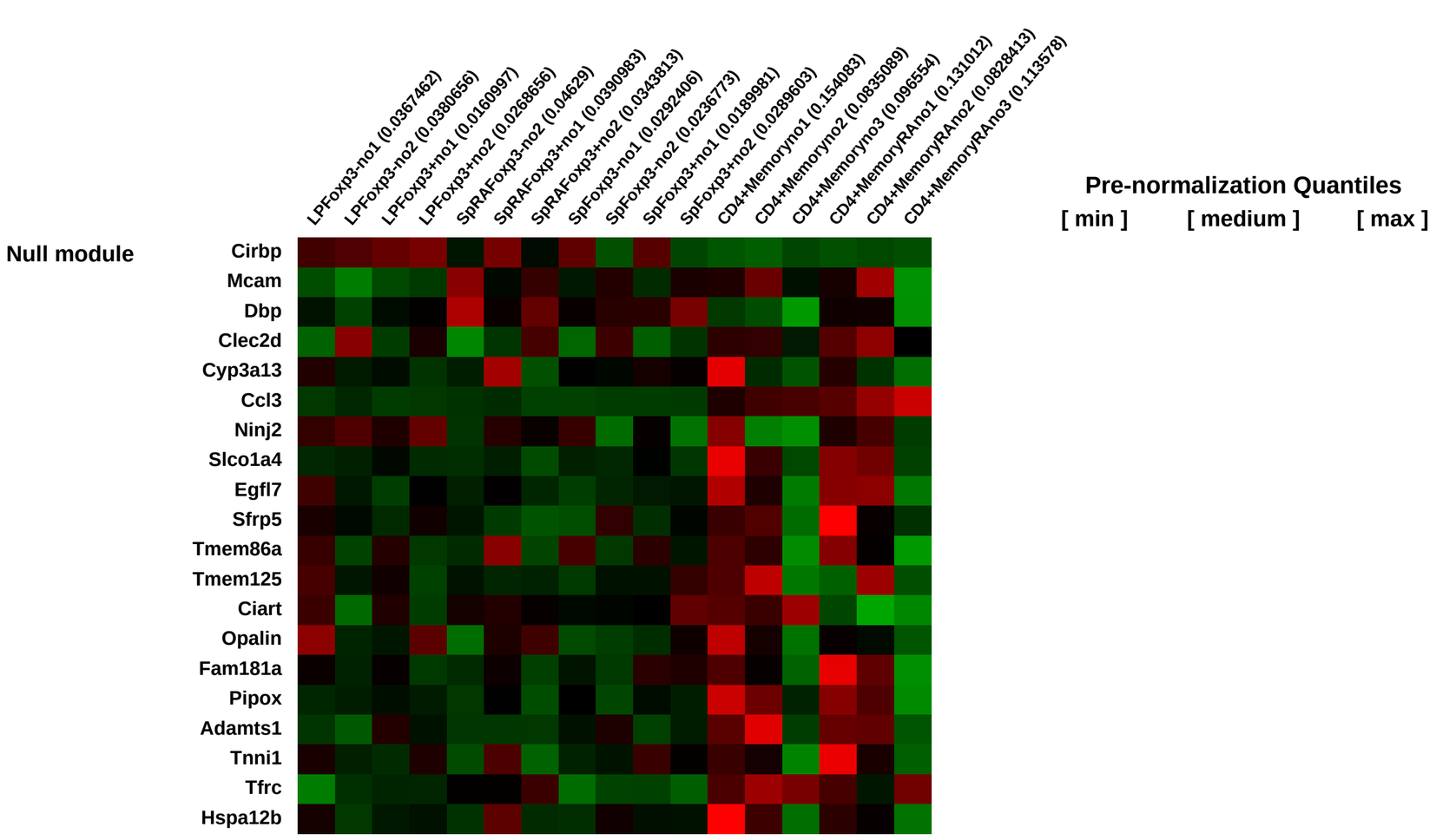

GEO Series "GSE43775" Expression Profiles

Num of samples in this series: 32

Scale of expression profile Z-scores

-3.0 -2.0 -1.0 0.0 1.0 2.0 3.0

GEO Link:	http://www.ncbi.nlm.nih.gov/geo/query/acc.cgi?acc=GSE43775
Status:	Public on Aug 04 2013
Title:	Induction of the mouse germ cell fate by transcription factors in vitro [exp1]
Organism:	Mus musculus
Experiment type:	Expression profiling by array
Platform:	GPL1261
Pubmed ID:	23913270
Summary & Design:	**Summary:** The germ cell lineage ensures the continuity of life through the generation of male and female gametes, which unite to form a totipotent zygote. We have established a culture system that recapitulates the mouse germ-cell specification pathway: Using cytokines, embryonic stem cells (ESCs)/induced pluripotent stem cells (iPSCs) are induced into epiblast-like cells (EpiLCs) and then into primordial germ cell-like cells (PGCLCs) with capacity both for spermatogenesis and oogenesis, creating an opportunity for understanding and regulating mammalian germ cell development in both sexes in vitro. Here we show that, without cytokines, simultaneous over-expression of three transcription factors (TFs), Blimp1 (also known as Prdm1), Prdm14 and Tfap2c (also known as AP2‚‡), directs EpiLCs, but not ESCs, swiftly and highly efficiently into a PGC state with endogenous transcription circuitry. The induction of the PGC state on EpiLCs minimally requires Prdm14 but not Blimp1 or Tfap2c. The TF-induced PGC state reconstitutes key transcriptome and epigenetic reprogramming in PGCs, but bypasses a mesodermal program that accompanies PGC specification in vivo and in vitro by cytokines including BMP4. Importantly, the TF-induced PGC-like cells robustly contribute to spermatogenesis and fertile offspring. Our findings provide not only a novel insight into the transcriptional logic that creates a germ cell state, but also a foundation for the TF-based reconstitution and regulation of mammalian gametogenesis. **Overall design:** Aim of this analysis is characterization of transcription factor-induced primordial germ cells (TF-PGCLCs) compared with cytokine-induced primordial germ cells (Ck-PGCLCs) (Hayashi et al., 2011, Cell), epiblast-like cells (EpiLCs) (Hayashi et al., 2011, Cell), and embryonic stem cells (ESCs) and identification of genes differentially expressed among them. TF-PGCLCs induced by multiple combinations of TFs (Blimp1 (B), Prdm14 (P14), and Tfap2c (A) (BP14A), BP14, P14A, P14) on day 2 and 4 (for BP14A cells) of the induction were also compared. Parental clone without exogenous TFs cultured with doxycycline, are also included as a negative control. Ck-PGCLCs day 2 and day 4 samples, which are previously unreported, EpiLCs and ESCs used in this study were also included. Overexpression of exogenous three TFs in ESCs yields stella-ECFP (SC) positive cells, which were sorted and included in the analysis. cDNA samples, prepared from approximately 20,000 cells, were amplified with a quantitative global PCR method (Kurimoto et al., 2006, Nucleic Acids Research). Two biological duplicates for each cell type were analyzed. Samples from GSE30056 were also included and reanalysed (GSM1070855-GSM1070864).

Background corr dist: KL-Divergence = 0.3312, L1-Distance = 0.0604, L2-Distance = 0.0096, Normal std = 0.2698

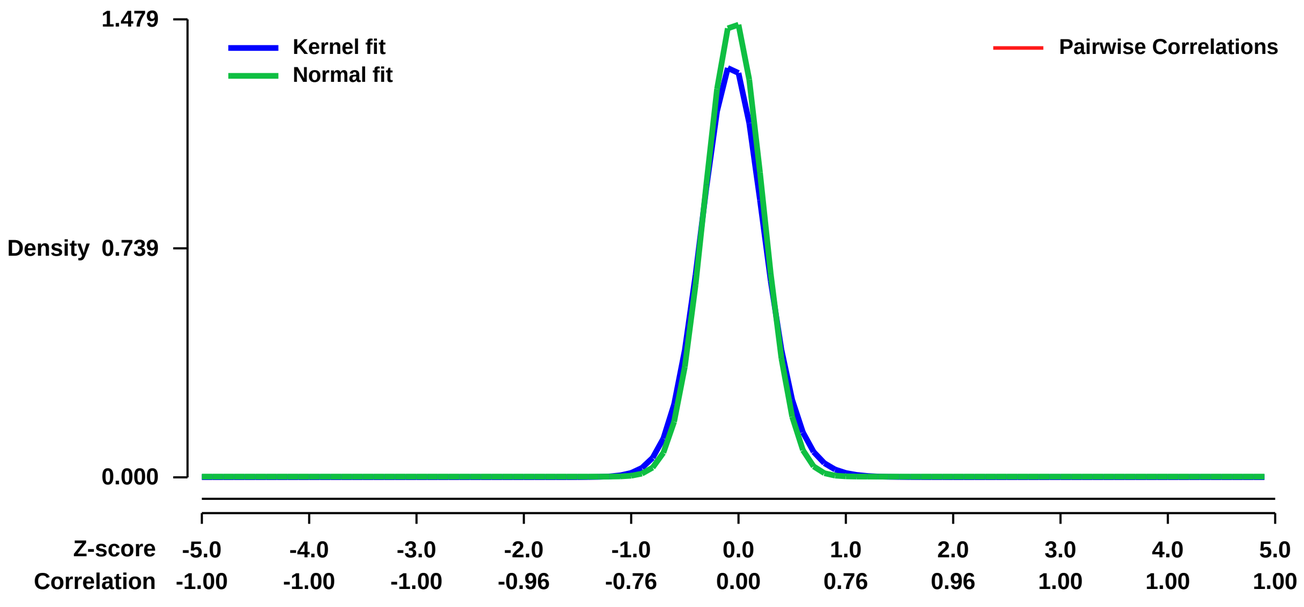

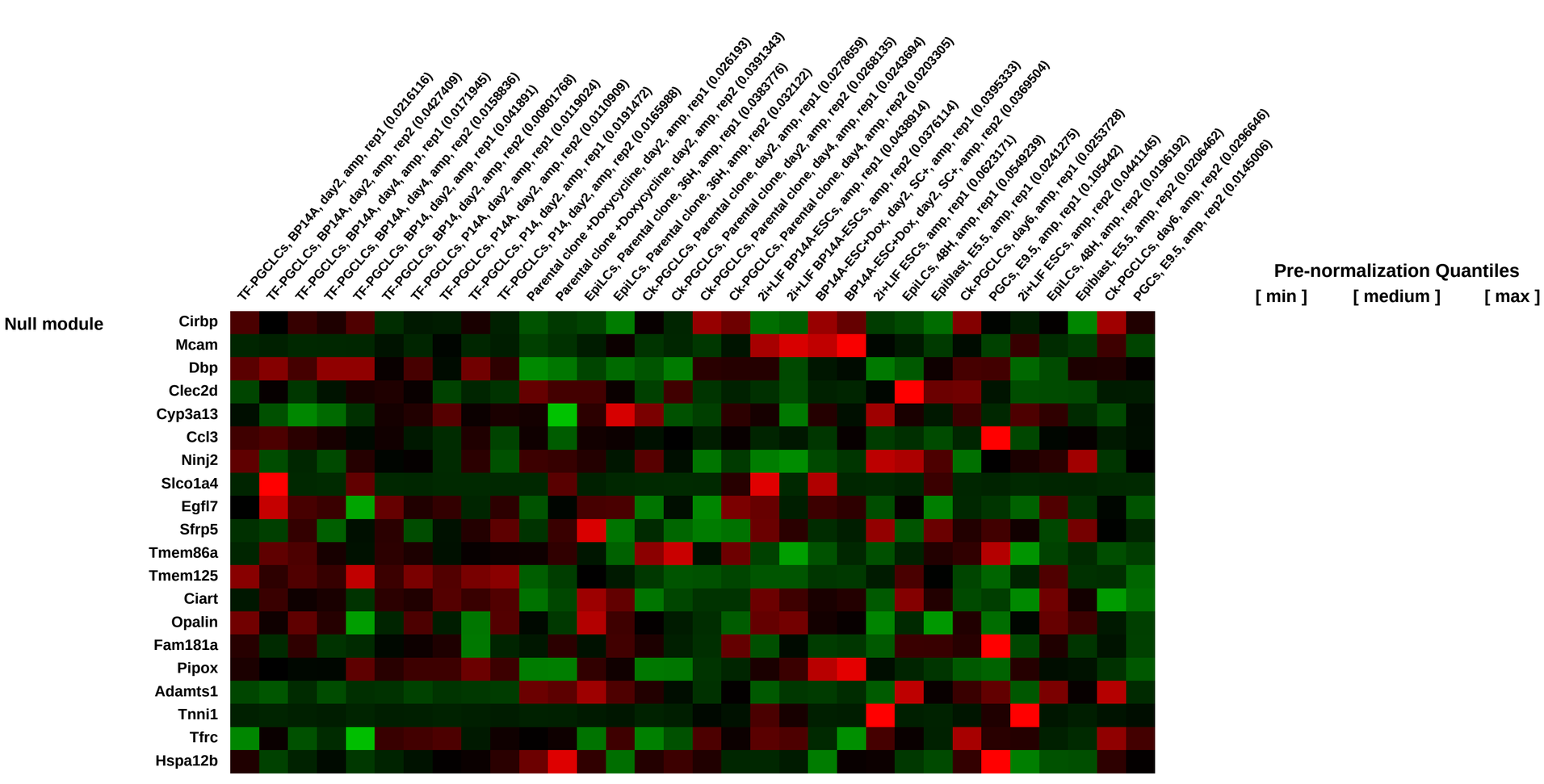

GEO Series "GSE46722" Expression Profiles

Num of samples in this series: 6

Scale of expression profile Z-scores

-3.0 -2.0 -1.0 0.0 1.0 2.0 3.0

GEO Link:	http://www.ncbi.nlm.nih.gov/geo/query/acc.cgi?acc=GSE46722
Status:	Public on Jul 01 2013
Title:	Expression data from adult LSK Hes1-GFP positive and adult LSK Hes1-GFP negative
Organism:	Mus musculus
Experiment type:	Expression profiling by array
Platform:	GPL1261
Pubmed ID:	23791481
Summary & Design:	**Summary:** Notch signaling defines a conserved, fundamental pathway, responsible for determination in metazoan development and is widely recognized as an essential component of lineage specific differentiation and stem cell self-renewal in many tissues including the hematopoietic system. Until recently, the majority of studies in the hematopoietic system focused on Notch signaling in lymphocyte differentiation and knowledge of individual Notch receptor roles in early hematopoiesis has been limited due to a paucity of genetic tools available To fate-map Notch receptor expression and pathway activity in the hematopoietic system we used tamoxifen-inducible CreER knock-in mice for individual Notch receptors in combination to a novel Notch reporter strain (Hes1GFP) and a conditional gain of function allele of Notch2 receptor (Rosa-lsl-ICN2). **Overall design:** Bone marrow lineage negative, cKit+, Sca1+ cells were sorted from Hes-GFP mice for RNA extraction and hybridization on Affymetrix microarrays

Background corr dist: KL-Divergence = 0.0508, L1-Distance = 0.0373, L2-Distance = 0.0021, Normal std = 0.5892

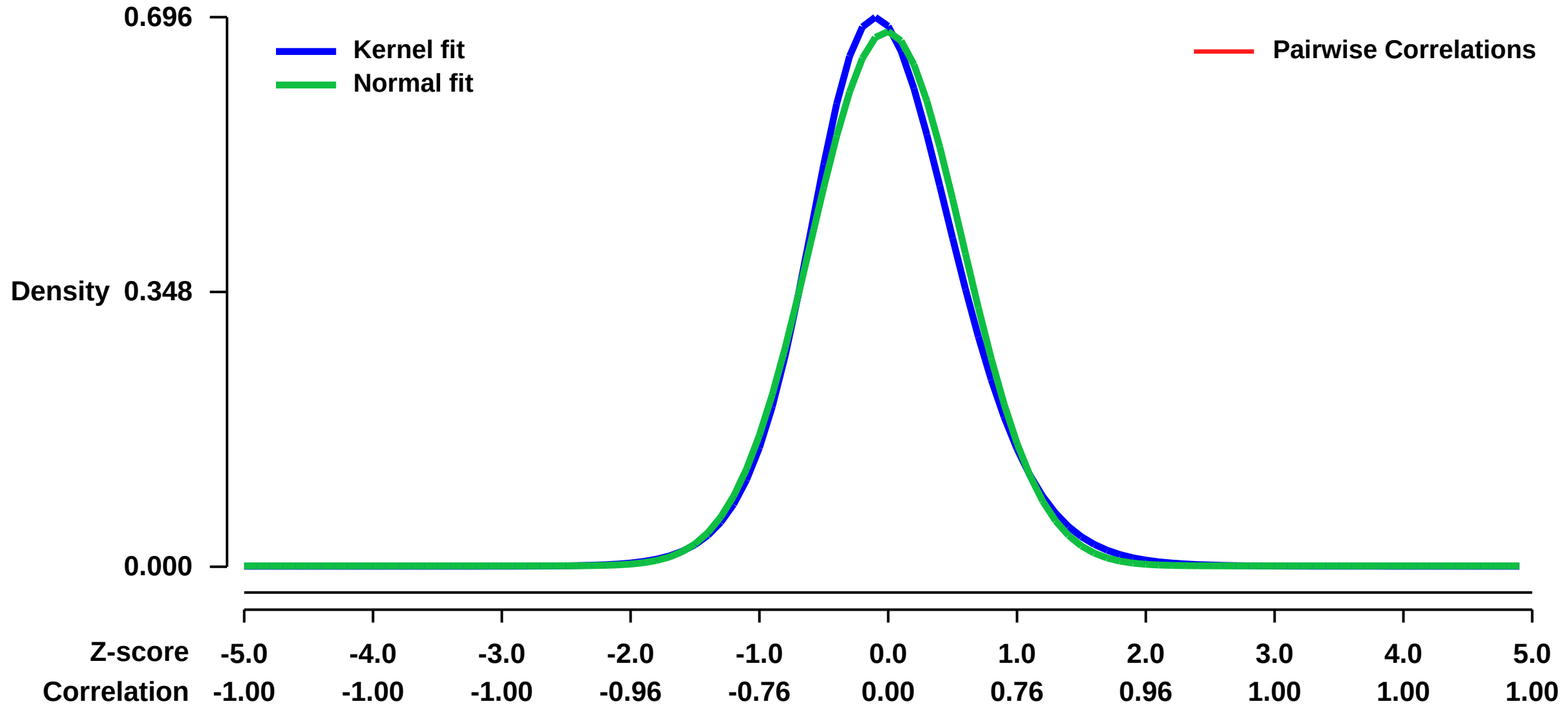

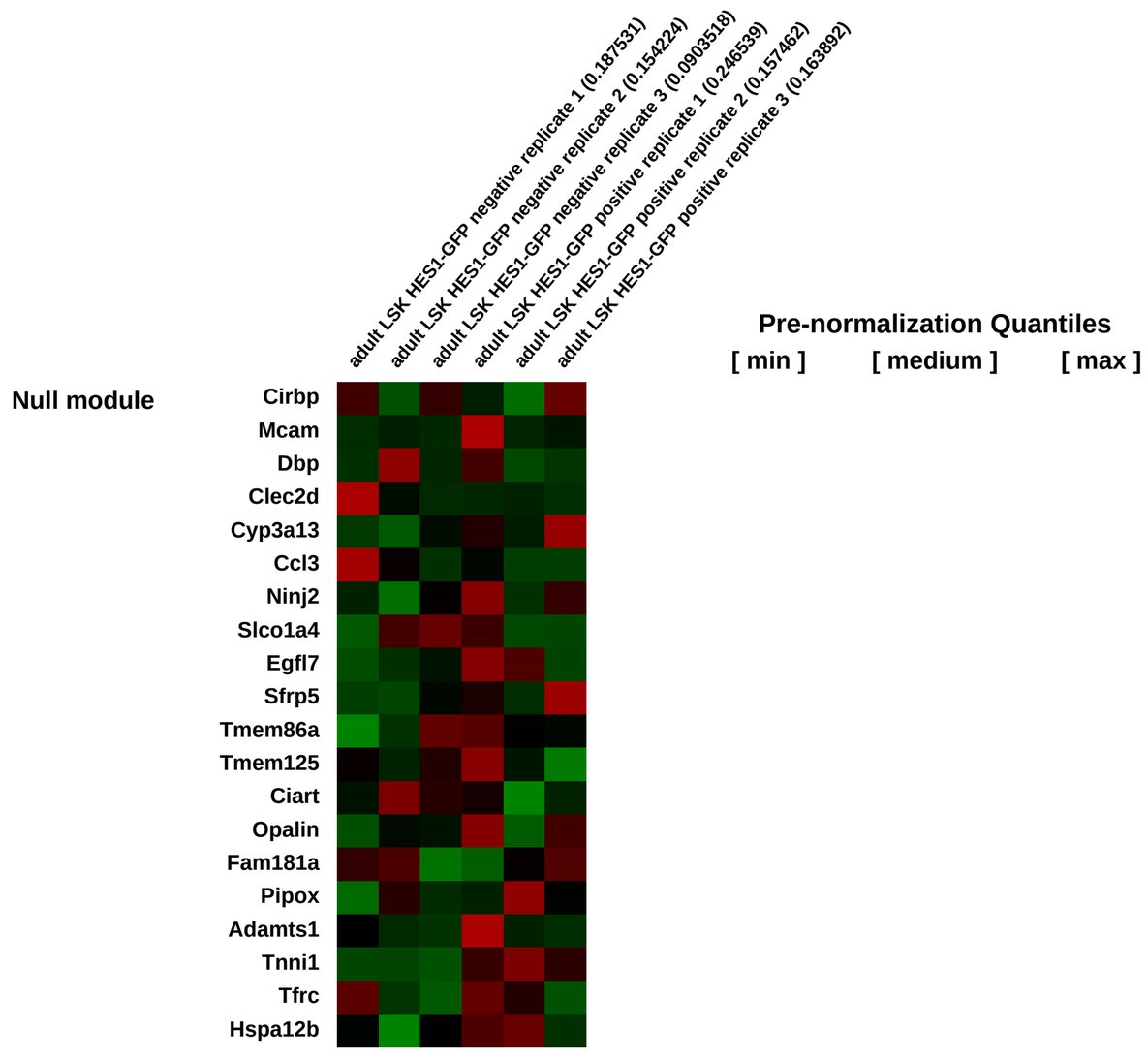

GEO Series "GSE38693" Expression Profiles

Num of samples in this series: 8

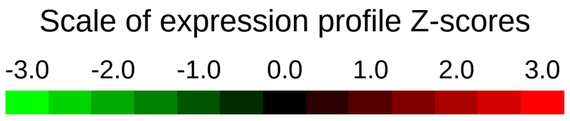

GEO Link:	**http://www.ncbi.nlm.nih.gov/geo/query/acc.cgi?acc=GSE38693**
Status:	**Public on Jun 14 2012**
Title:	**c-JUN REPROGRAMS SCHWANN CELLS OF INJURED NERVES TO GENERATE A REPAIR CELL ESSENTIAL FOR REGENERATION**
Organism:	**Mus musculus**
Experiment type:	**Expression profiling by array**
Platform:	**GPL1261**
Pubmed ID:	
Summary & Design:	**Summary:** **The striking PNS regenerative response to injury rests on the plasticity of adult Schwann cells and their ability to transit between differentiation states, a highly unusual feature in mammals. Using mice with inactivation of Schwann cell c-Jun, we show that the injury response involves c-Jun dependent natural reprograming of differentiated cells to generate a distinct Schwann cell state specialized to promote regeneration. Transected distal stumps of c-Jun mutants show 172 disregulated genes, resulting in abnormal expression of growth factors, adhesion molecules and cytoskeletal changes that lead to neuronal death, inhibition of axon growth and striking failures of functional repair after injury. These observations provide a molecular basis for understanding Schwann cell plasticity and nerve regeneration. They offer conclusive support for the notion that Schwann cells control repair in the PNS, using dedicated transcriptional controls to generate a distinct repair cell, a transition that shows similarities to transdifferentiation seen in other systems.** **Overall design:** **Total RNA was purified from a 10mm segment of the distal stump and uninjured contralateral nerve from c-Jun mutants and control mice 7 days after nerve cut. For each condition (injured/uninjured) and genotype (control/ knock-out) 2 independent samples (replicates) were generated from pooled nerves of 4/6 mice resulting in a total of 8 samples: CTRL.cut.R1, CTRL.cut.R2, CTRL.uncut.R1, CTRL.uncut.R2, KO.cut.R1, KO.cut.R2, KO.uncut.R1,KO.uncut.R2.**

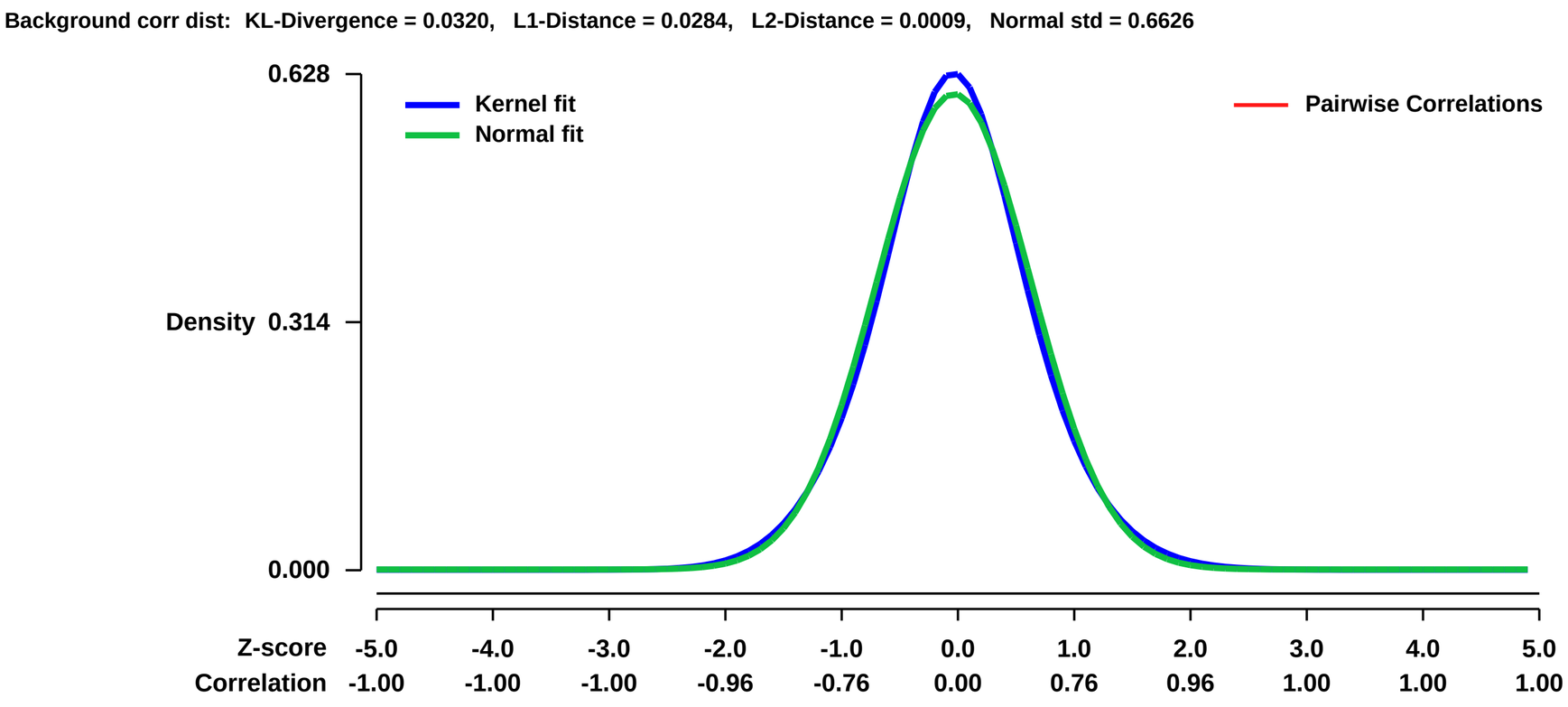

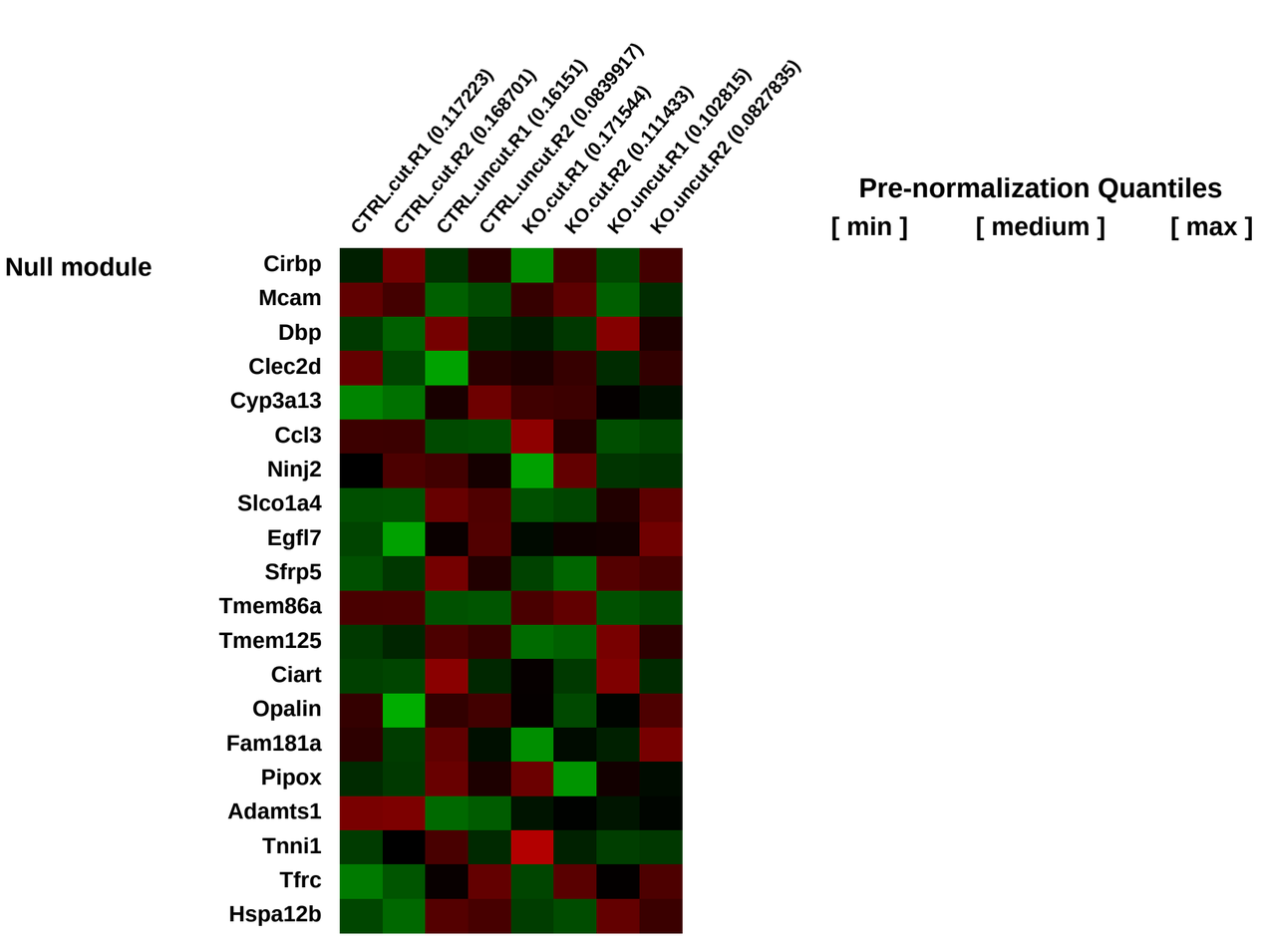

GEO Series "GSE45465" Expression Profiles

Num of samples in this series: 39

Scale of expression profile Z-scores

-3.0 -2.0 -1.0 0.0 1.0 2.0 3.0

GEO Link:	http://www.ncbi.nlm.nih.gov/geo/query/acc.cgi?acc=GSE45465
Status:	Public on Mar 25 2013
Title:	Dynamic changes in liver 5-hydroxymethylcytosine profiles upon non-genotoxic carcinogen exposure [Replicated control vs. pb treated study]
Organism:	Mus musculus
Experiment type:	Expression profiling by array
Platform:	GPL1261
Pubmed ID:	23598998
Summary & Design:	**Summary:** Dynamic changes in the mouse liver DNA methylome associated with short (1 day) and prolonged (7, 28 and 91 days) exposure to the rodent liver non-genotoxic carcinogen (NGC), phenobarbital (PB). **Overall design:** Replicated control vs. pb treated study

Background corr dist: KL-Divergence = 0.2219, L1-Distance = 0.0499, L2-Distance = 0.0058, Normal std = 0.3176

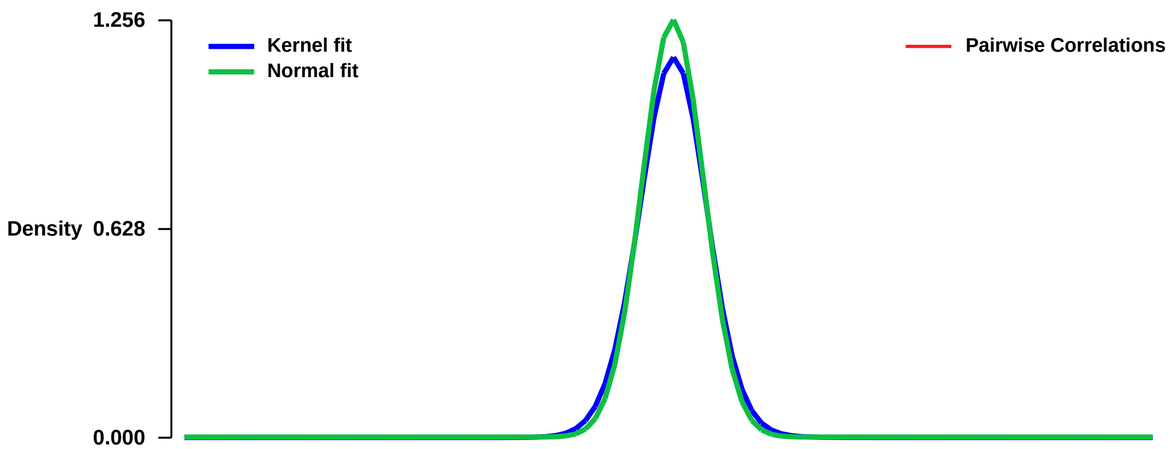

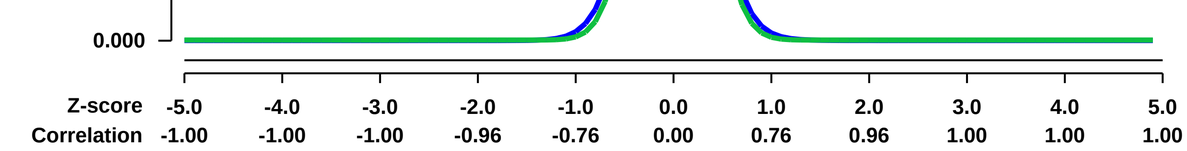

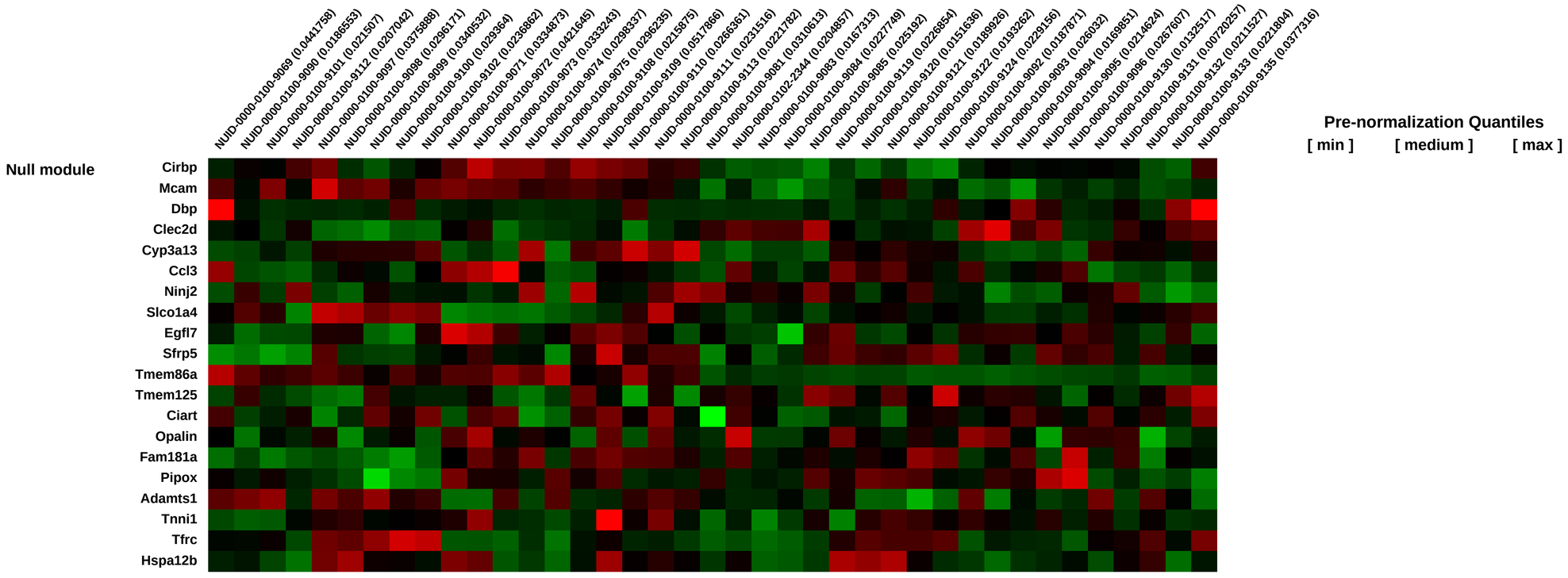

GEO Series "GSE45592" Expression Profiles

Num of samples in this series: 16

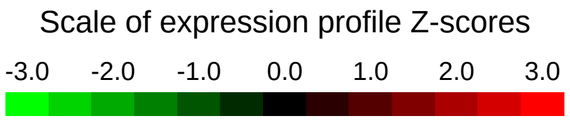

GEO Link:	http://www.ncbi.nlm.nih.gov/geo/query/acc.cgi?acc=GSE45592
Status:	Public on May 01 2013
Title:	Dicer deficiency reveals microRNAs predicted to control gene expression in developing adrenal cortex [array]
Organism:	Mus musculus
Experiment type:	Expression profiling by array
Platform:	GPL1261
Pubmed ID:	23518926
Summary & Design:	**Summary:** MicroRNAs (miRNAs) are small, endogenous, non-protein coding RNAs that are an important means of post-transcriptional gene regulation. Deletion of Dicer, a key miRNA processing enzyme, is embryonic lethal in mice, and tissue-specific Dicer deletion results in developmental defects. Using a conditional knockout model, we generated mice lacking Dicer in the adrenal cortex. These Dicer knockout (KO) mice exhibited perinatal mortality and failure of the adrenal cortex during late gestation between embryonic day 16.5 (E16.5) and E18.5. Further study of Dicer KO adrenals demonstrated a significant loss of Sf1 expressing cortical cells that was histologically evident as early as E16.5 coincident with an increase in p21 and cleaved-caspase 3 staining in the cortex. However, peripheral cortical proliferation persisted in KO adrenals as assessed by anti-PCNA staining. To further characterize the embryonic adrenals from Dicer KO mice, we performed microarray analyses for both gene expression and miRNA on purified RNA isolated from control and KO adrenals of E15.5 and E16.5 embryos. Consistent with the absence of Dicer and the associated loss of miRNA-mediated mRNA degradation, we observed an up-regulation of a small subset of adrenal transcripts in Dicer KO mice, most notably the transcripts coded by the genes Nr6a1 and Acvr1c. Indeed, several miRNAs, including let-7, miR-34c, and miR-21 that are predicted to target these genes for degradation, were also markedly down-regulated in Dicer KO adrenals. Together these data suggest a role for miRNA mediated regulation of a subset of genes that are essential for normal adrenal growth and homeostasis. **Overall design:** Adrenals from control and Dicer KO litter mates were pooled separately from 4 individual litters, resulting in a total of 4 control (cre-) and 4 Dicer KO biological replicates at both E15.5 and E16.5.

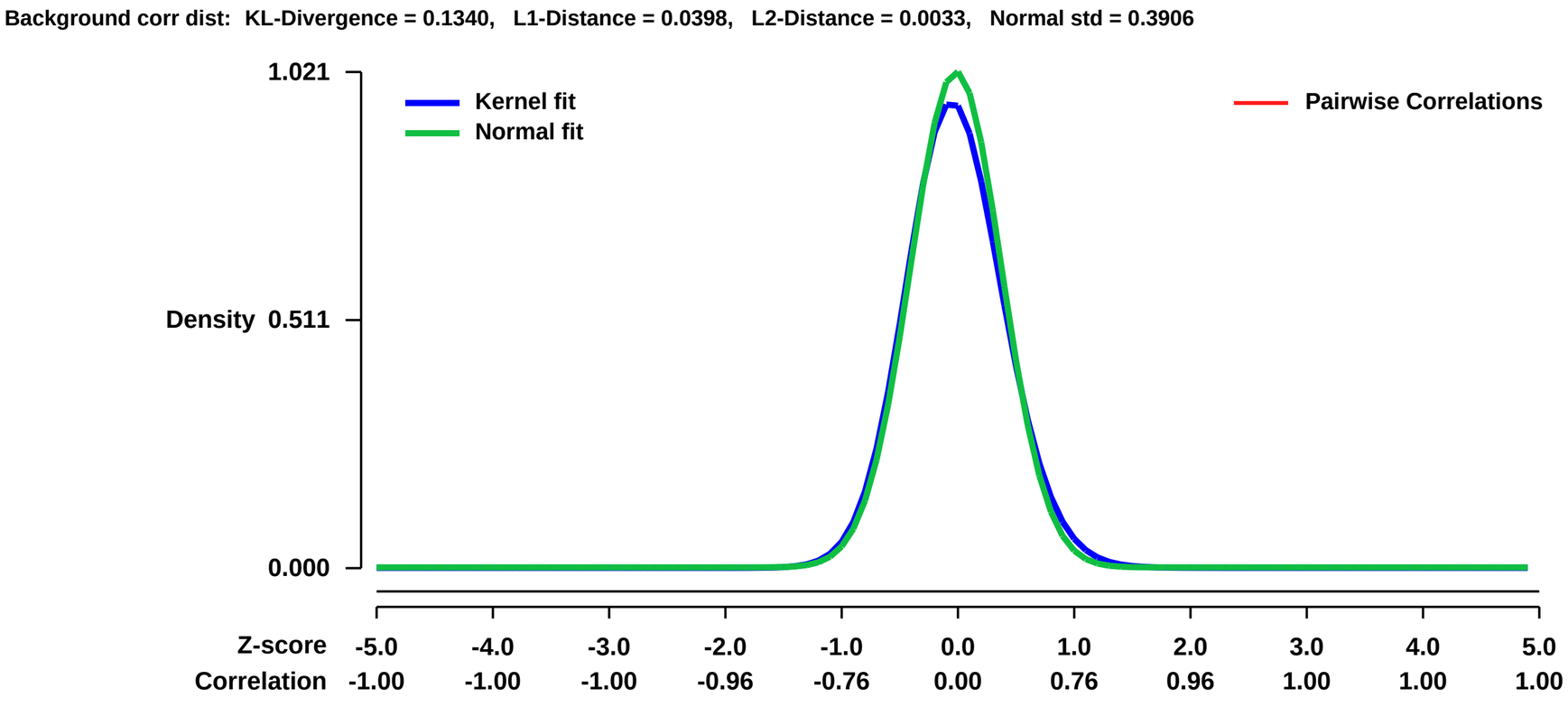

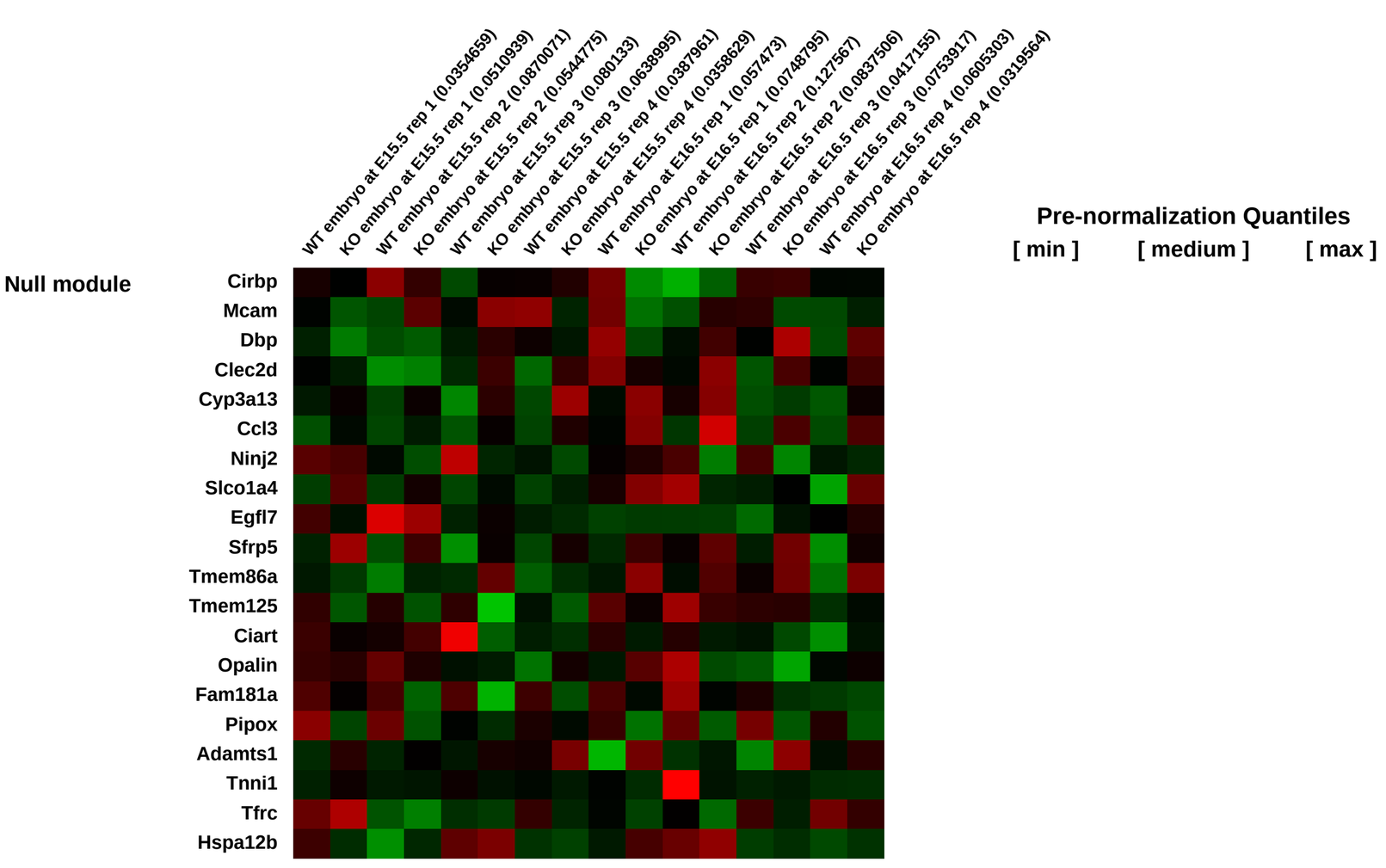

GEO Series "GSE12609" Expression Profiles

Num of samples in this series: 8

Scale of expression profile Z-scores

-3.0 -2.0 -1.0 0.0 1.0 2.0 3.0

GEO Link:	http://www.ncbi.nlm.nih.gov/geo/query/acc.cgi?acc=GSE12609
Status:	Public on Aug 30 2008
Title:	Transcription factor Arx null brains (fulp-affy-mouse-364520)
Organism:	Mus musculus
Experiment type:	Expression profiling by array
Platform:	GPL1261
Pubmed ID:	18799476
Summary & Design:	**Summary:** Arx is a paired-box homeodomain transcription factor and the vertebrate ortholog to the Drosophila aristaless (al) gene. Mutations in Arx are associated with a variety of human diseases, including X-linked infantile spasm syndrome (OMIM: 308350), X-linked myoclonic epilepsy with mental retardation and spasticity (OMIM: 300432), X-linked lissencephaly with ambiguous genitalia (OMIM: 300215), X-linked mental retardation 54 (OMIM: 300419), and agenesis of the corpus callosum with abnormal genitalia (OMIM: 300004). Arx-deficient mice exhibit a complex, pleiotrophic phenotype, including decreased proliferation of neuroepithelial cells of the cortex, dysgenesis of the thalamus and olfactory bulbs, and abnormal nonradial migration of GABAergic interneurons. It has been suggested that deficits in interneuron specification, migration, or function lead to loss of inhibitory neurotransmission, which then fails to control excitatory activity and leads to epilepsy or spasticities. Given that Arx mutations are associated with developmental disorders in which epilepsy and spasticity predominate and that Arx-deficient mice exhibit deficits in interneuron migration, understanding the function of Arx in interneuron migration will prove crucial to understanding the pathology underlying interneuronopathies. Yet, downstream transcriptional targets of Arx, to date, remain unidentified. The aim of this project is to identify bona fide transcriptional targets for the Arx, a transcription factor required for normal migration of interneurons from the ganglionic eminences to the cortex, and to investigate the functions of these genes in the Arx-dependent pathway regulating nonradial neuronal migration. We hypothesize that the genes regulated by the Arx transcription factor will play a critical role in the nonradial migration of interneurons and that the results of this study will provide novel insights into the molecular mechanisms of nonradial neuronal migration, in particular, and possibly the molecular and biochemical pathogenesis underlying epilepsy, mental retardation, infantile spasm syndromes, and other so-called interneuronopathies; We have recently generated a transgenic mouse with a floxed Arx allele (Arxflox). We have generated conditional knockouts in which Arx is removed specifically from the brain by mating Arxflox mice with transgenic mice expressing Cre behind the neural tube-specific transcriptional regulatory elements of the POU domain, class 3, transcription factor 4 promoter. Preliminary analyses of these mice suggest that conditional knockout mice recapitulate the nonradial migration defects associated with conventional knockout mice. We will compare the gene expression profiles of ganglion eminences (GEs; the anatomical source for nonradially migrating interneurons) from male Arxflox mice that express Pou3f-Cre to those from male mice without Arxflox allele. Animals will be prepared and sacrificed following our institutional protocol. Tissue will be rapidly dissected from E14.5 (the temporal peak of interneuron migration) GEs (MGE and LGE from both left and right hemispheres). Preliminary experiments suggest that the amounts of RNA that can be isolated from a pair of GEs is in the range of 2000-3500 ng, which should be sufficient for microarray analysis following linear amplification of RNA. The GEs from each animal will be combined, snap frozen in liquid nitrogen, and stored at -80 C until RNA is extracted. Total RNA will be extracted using Trizol followed by RNA purification with the RNeasy cleanup kit. We will be providing total RNA samples from four wildtype and four transgenic animals (true biological replicates) from three separate litters to mitigate any expression differences resulting from mouse to mouse or litter to litter variation. #!# **Overall design:**

Background corr dist: KL-Divergence = 0.0873, L1-Distance = 0.0223, L2-Distance = 0.0008, Normal std = 0.4610

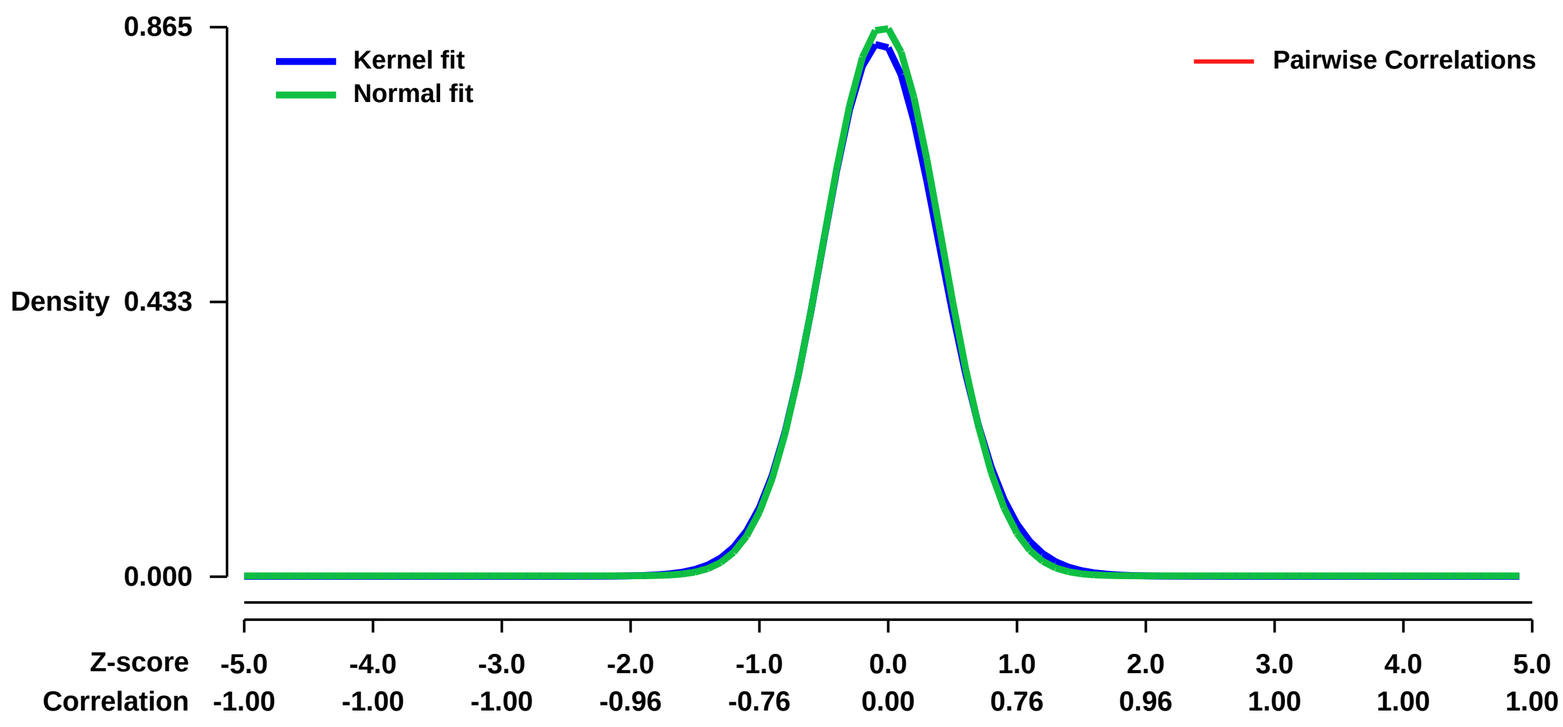

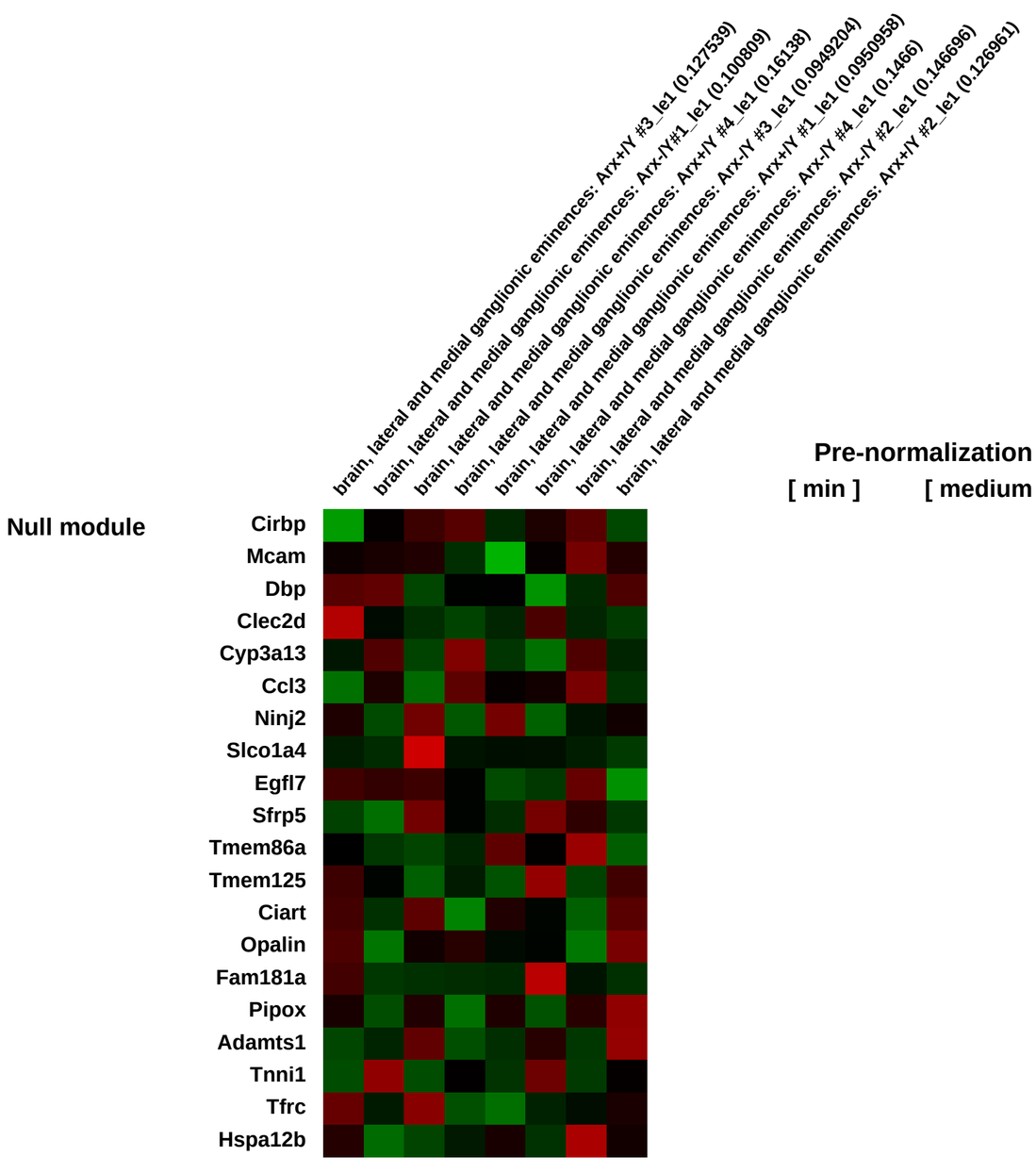

GEO Series "GSE45222" Expression Profiles

Num of samples in this series: 27

Scale of expression profile Z-scores

-3.0 -2.0 -1.0 0.0 1.0 2.0 3.0

GEO Link:	http://www.ncbi.nlm.nih.gov/geo/query/acc.cgi?acc=GSE45222
Status:	Public on Nov 27 2013
Title:	Reversible mRNA and miRNA expression patterns in the transcriptome of Rasless fibroblasts
Organism:	Mus musculus
Experiment type:	Non-coding RNA profiling by array
Platform:	GPL1261
Pubmed ID:	24156637
Summary & Design:	**Summary:** Analysis of the transcriptional profiles of mRNA and microRNA in Rasless fibroblasts. 4-Hydroxy-tamoxifen (4-OHT) treatment triggers removal of K-Ras expression in [H-Ras-/-;N-Ras-/-;K-Raslox/lox;RERTert/ert] mouse fibroblasts (named K-Raslox) generating â Raslessâ MEFs which are unable to proliferate, but recover proliferative ability after ectopic expression of constitutively active downstream kinases such as BRAF and MEK1. Using Affymetrix microarrays, we compared the transcriptional profiles of Rasless fibroblasts to those of K-Raslox (MEFs lacking only H-Ras and N-Ras). We also compared the transcriptional profile of Rasless cells with those of BRAF and MEK1-transfected Rasless cells which recovered proliferative ability. Re-entry of the Rasless cells into cell cycle progression through ectopic expression of activated BRAF or MEK1 resulted in full reversion of most transcriptional alterations identified in cells lacking the three canonical Ras proteins. **Overall design:** Regarding the miRNA expression study, the experimental samples analyzed included (i) 4 samples samples K-Raslox (used as Control): 2 biological replicates, technical duplicates each; (ii) 8 samples Rasless: the same cells after treatment with 4-OHT for 6 days (2 biological replicates, technical duplicates each) and 12 days (2 biological replicates, technical duplicates each); (iii) 4 samples BRAF-rescued, including 2 biological replicates, technical duplicates each; (iv) 4 samples MEK1-rescued,including 2 biological replicates, technical duplicates each, and (v) 4 samples Puromycin-resistant empty vector, containing 2 biological replicates, technical duplicates each. The miRNA expression study contains a total of 24 samples.

Background corr dist: KL-Divergence = 0.1968, L1-Distance = 0.0489, L2-Distance = 0.0056, Normal std = 0.3334

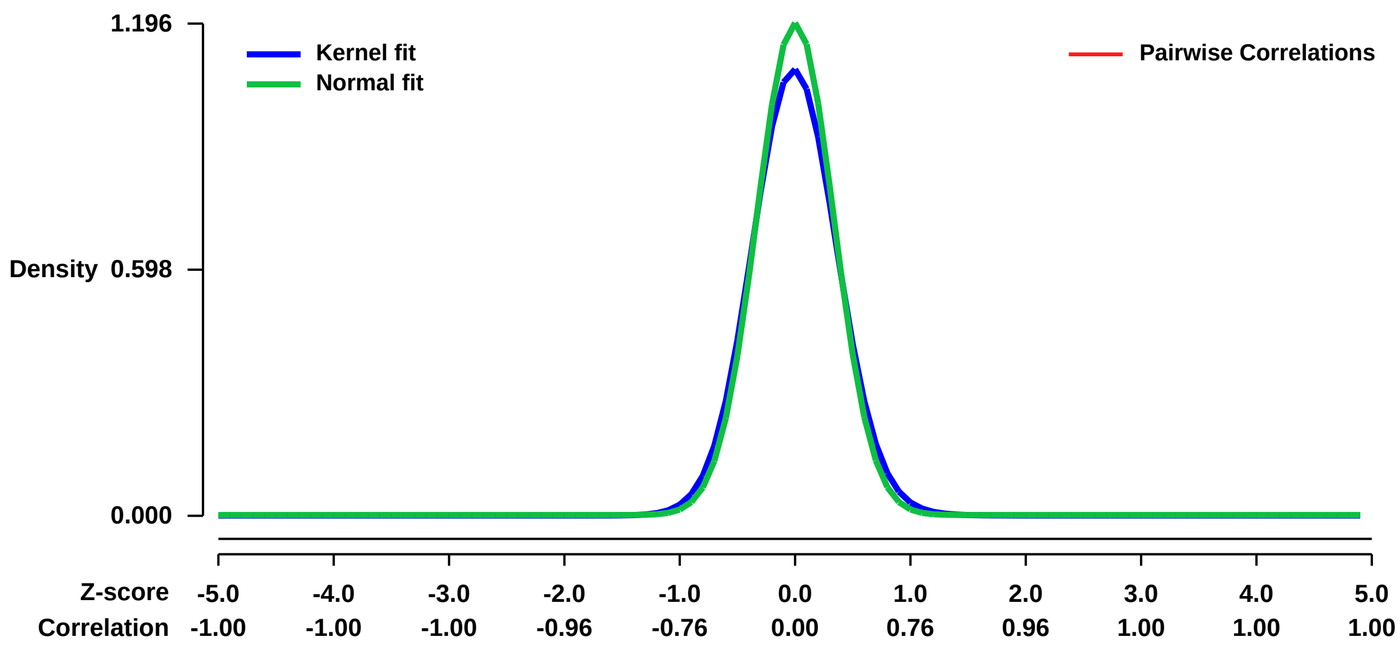

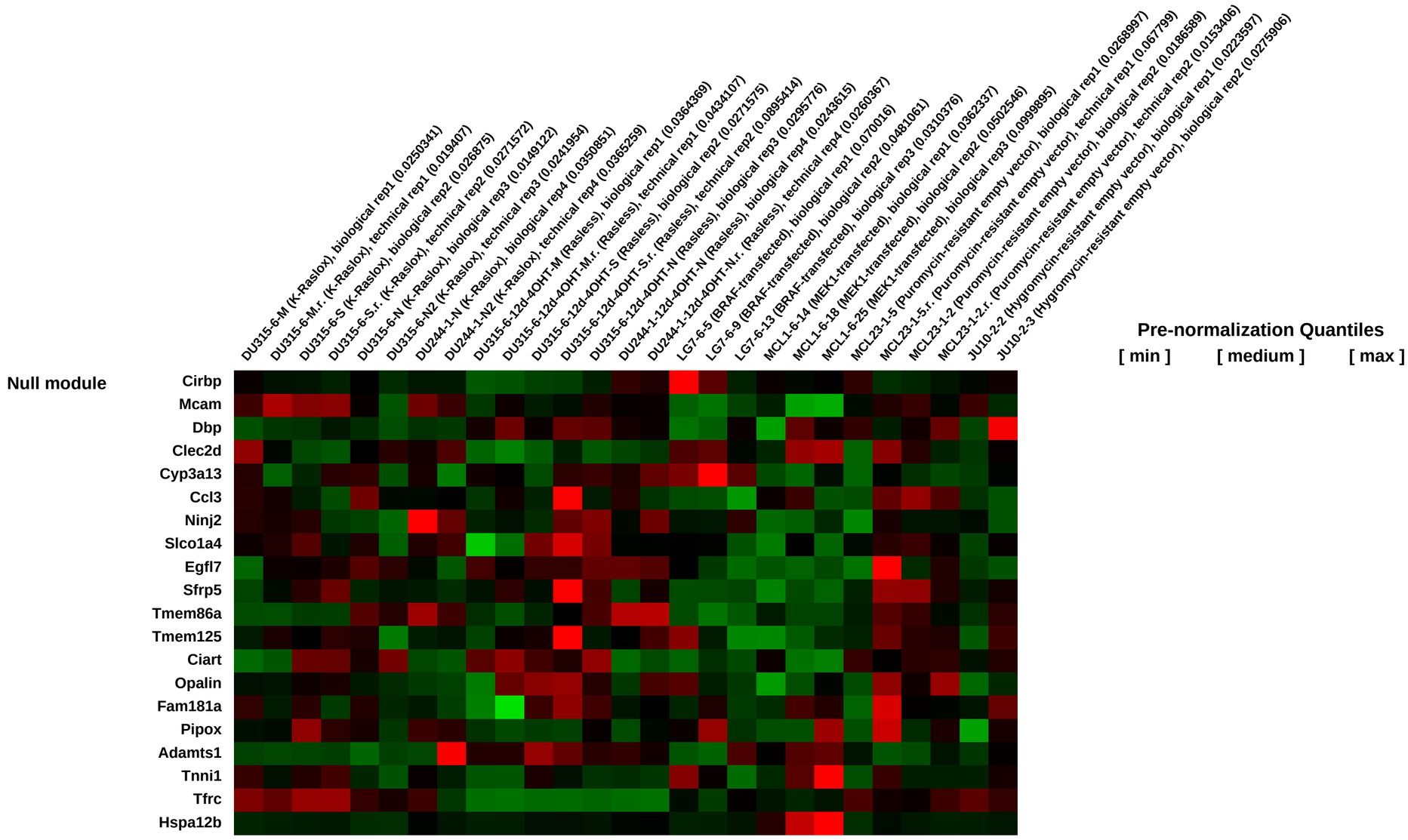

GEO Series "GSE53951" Expression Profiles

Num of samples in this series: 10

Scale of expression profile Z-scores

-3.0 -2.0 -1.0 0.0 1.0 2.0 3.0

GEO Link:	http://www.ncbi.nlm.nih.gov/geo/query/acc.cgi?acc=GSE53951
Status:	Public on Jan 10 2014
Title:	Gene expression after type-I interferon treatment in primary neurons, primary fibroblasts and L929 cells
Organism:	Mus musculus
Experiment type:	Expression profiling by array
Platform:	GPL1261
Pubmed ID:	24453359
Summary & Design:	**Summary:** Microarray expression profilling of mouse primary mixed cortical/hippocampal neurons, primary fibroblasts and L929 cells to compare ISGs signature in disctinct cell types **Overall design:** Primary mixed cortical/hippocampal neurons, primary fibroblasts (MEFs) and L929 cells were mock-treated or treated with 5U/mL of IFN-beta and RNA was harvested after 24 hours. For neurons and fibroblast, 2 samples were analyzed for each condition.

Background corr dist: KL-Divergence = 0.0405, L1-Distance = 0.0863, L2-Distance = 0.0101, Normal std = 0.7845

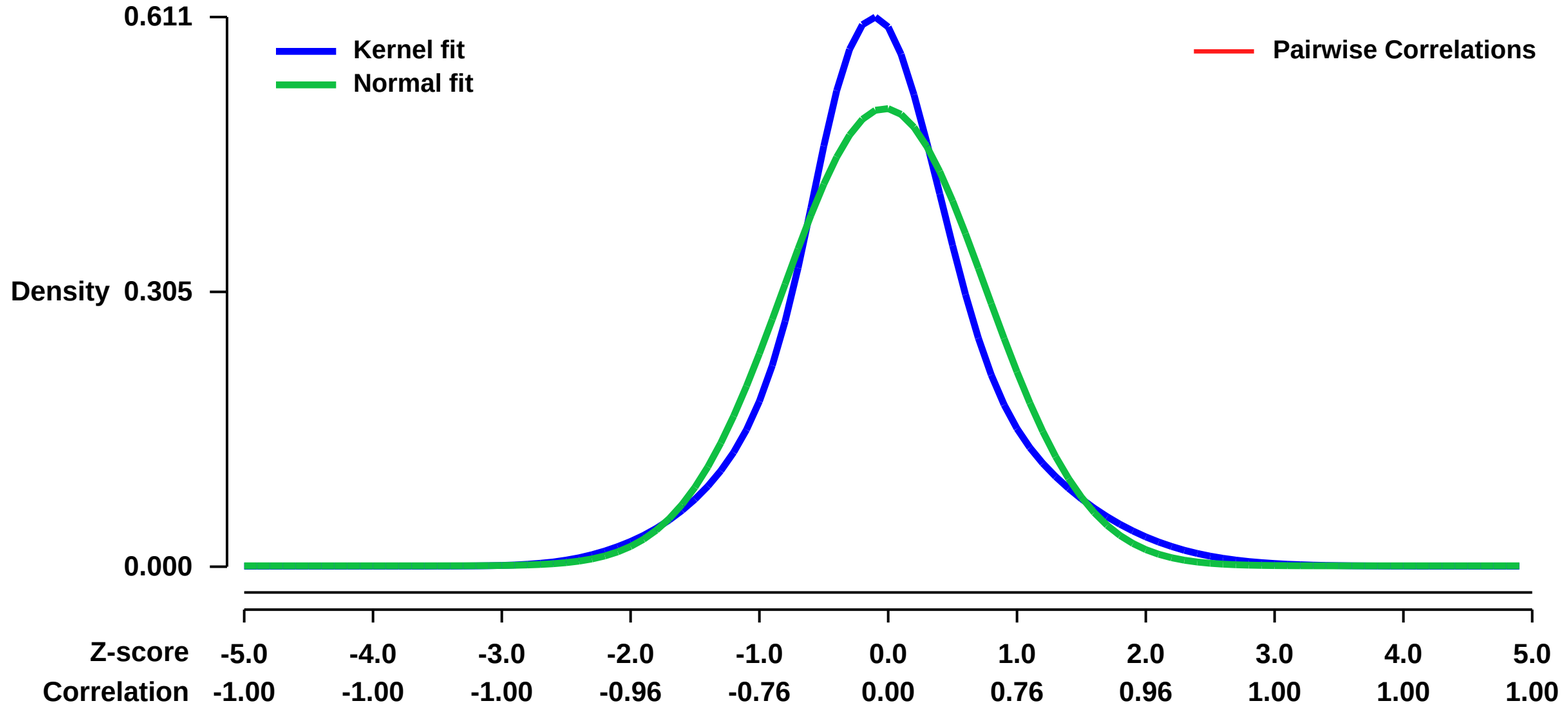

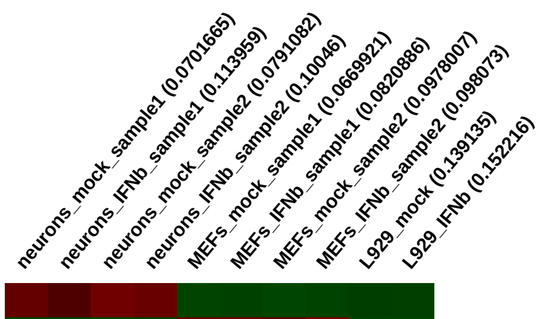

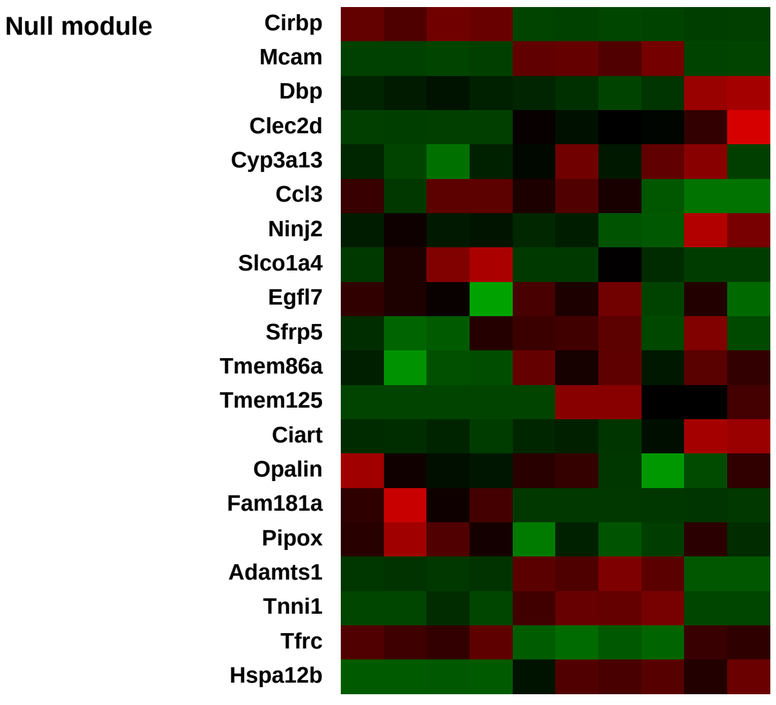

GEO Series "GSE6514" Expression Profiles

Num of samples in this series: 90

GEO Link:	http://www.ncbi.nlm.nih.gov/geo/query/acc.cgi?acc=GSE6514
Status:	Public on Feb 11 2007
Title:	Gene expression in the mouse brain during spontaneous sleep and prolonged wakefulness
Organism:	Mus musculus
Experiment type:	Expression profiling by array
Platform:	GPL1261
Pubmed ID:	17698924
Summary & Design:	**Summary:** These studies address temporal changes in gene expression during spontaneous sleep and extended wakefulness in the mouse cerebral cortex, a neuronal target for processes that control sleep; and the hypothalamus, an important site of sleep regulatory processes. We determined these changes by comparing expression in sleeping animals sacrificed at different times during the lights on period, to that in animals sleep deprived and sacrificed at the same diurnal time. Keywords: gene expression, temporal changes, brain, behavior, sleep, **Overall design:** Experiments were performed on male mice (C57/BL6), 10 weeks of age ´–1 week. Animals were housed in a light/dark cycle of 12 hrs, in a pathogen free, temperature- and humidity-controlled room (22´°C and 45-55%, respectively) with water available ad libitum. Food was accessible for 12 hrs only during the active period. Animals were subjected to 14 days of acclimatization during which a nighttime feeding pattern was established. This was done to avoid differential food intake between mice that were subsequently sleep deprived during the lights on period and those allowed to sleep. Mice were sacrificed following 3, 6, 9 and 12 hrs of total sleep deprivation (n=5 at each time point). Deprivation was initiated at lights-on, and performed through gentle handling. Sleeping animals, which were left undisturbed, were sacrificed at the same diurnal time points as sleep deprived mice (n=5 at each time point). An additional control group of mice were sacrificed at time zero, i.e., at the time of lights-on (n=5). All mice were behaviorally monitored using the AccuScan infrared monitoring system that detects movement when the mouse crosses electronic beams (Columbus Instruments). Mice were sacrificed by cervical dislocation. Brain sectioning was performed according to the mouse brain atlas of Franklin and Paxinos . The primary and secondary motor areas (M1 and M2) of the cerebral cortex and broadly defined regions and zones of the hypothalamus were sampled. RNA was isolated with Trizol (Invitrogen) and further purified using RNeasy columns (Qiagen) as per the manufacturer's instructions.

Scale of expression profile Z-scores

-3.0 -2.0 -1.0 0.0 1.0 2.0 3.0

Background corr dist: KL-Divergence = 0.4027, L1-Distance = 0.0528, L2-Distance = 0.0064, Normal std = 0.2506

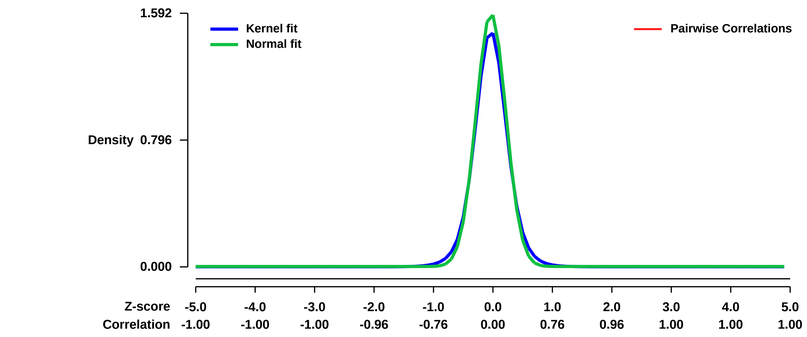

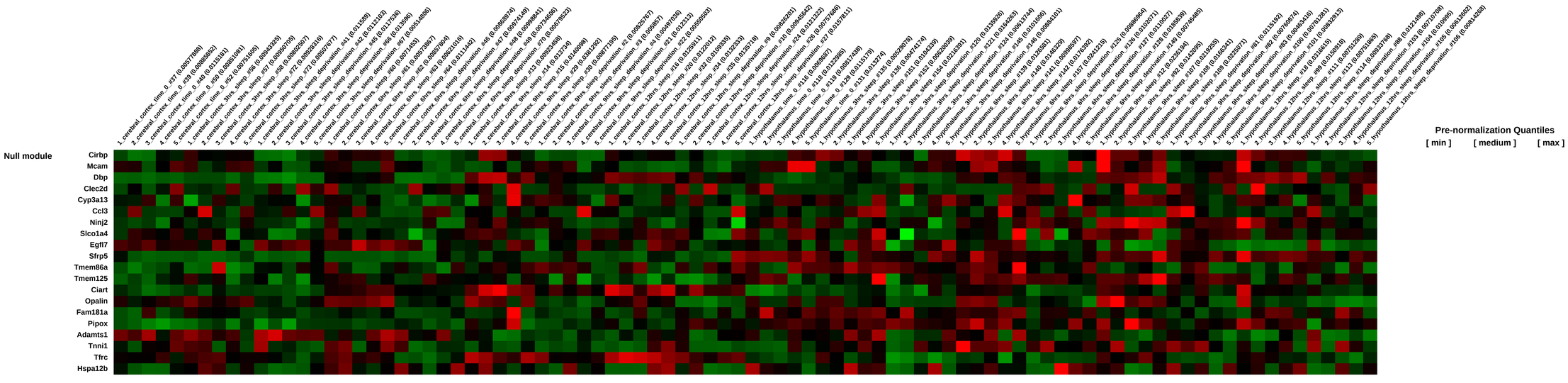

GEO Series "GSE16902" Expression Profiles

Num of samples in this series: 21

Scale of expression profile Z-scores

-3.0 -2.0 -1.0 0.0 1.0 2.0 3.0

GEO Link:	**http://www.ncbi.nlm.nih.gov/geo/query/acc.cgi?acc=GSE16902**
Status:	**Public on Jul 02 2009**
Title:	**Expression data from mouse gastric tumor models**
Organism:	**Mus musculus**
Experiment type:	**Expression profiling by array**
Platform:	**GPL1261**
Pubmed ID:	**20015407**
Summary & Design:	**Summary:** **Transgenic mice with prostaglandin E2 pathway in stomach develops gastric tumors. Simultaneous activation of both Wnt pathway and prostaglandin E2 pathway causes gastric adenocarcinoma. Combination of prostaglandin E2 pathway activation and suppression of BMP pathway leads to the development of gastric hamartomas.** **We used microarrays to find the mechanism of these tumor development and to evaluate whether these mouse models recapitulate human gastric tumors.** **Overall design:** **Glandular stomach from three C57BL/6 wild-type, five K19-Wnt1 transgenic, three K19-C2mE, five K19-Wnt1/C2mE, two K19-Nog, and three K19-Nog/C2mE transgenic mice were used. All mice were female at 18-65 weeks of age.**

Background corr dist: **KL-Divergence = 0.0934, L1-Distance = 0.0243, L2-Distance = 0.0010, Normal std = 0.4487**

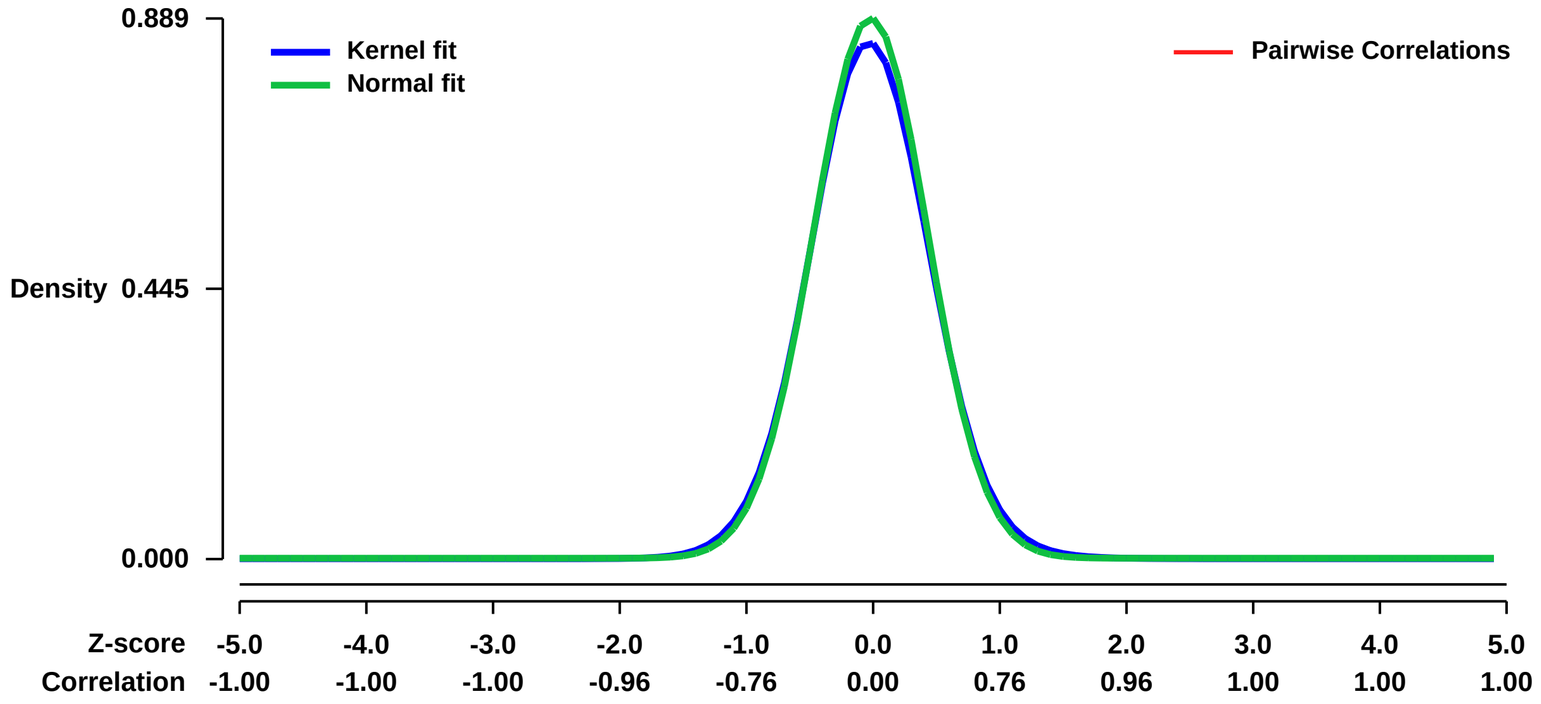

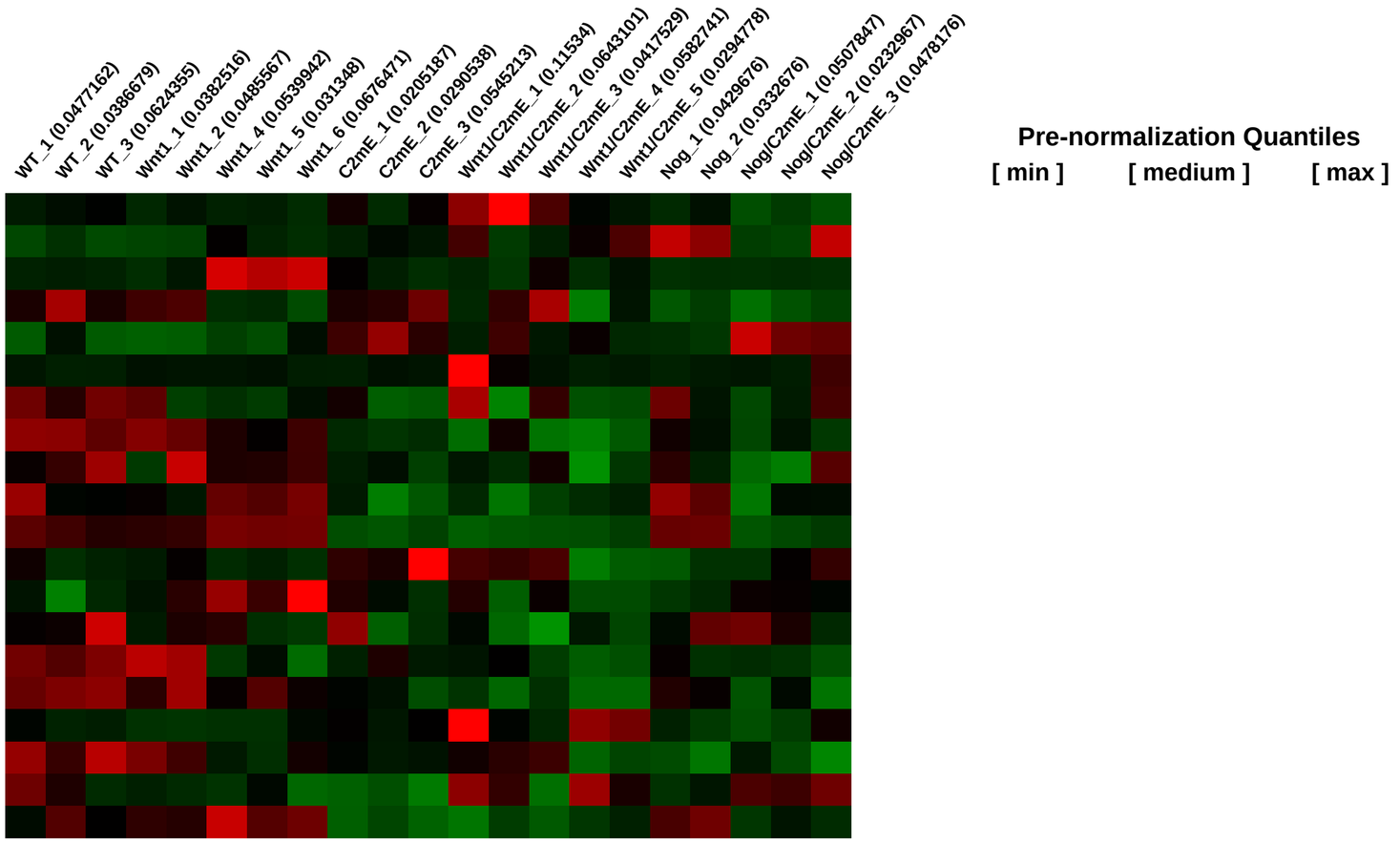

GEO Series "GSE53946" Expression Profiles

Num of samples in this series: 6

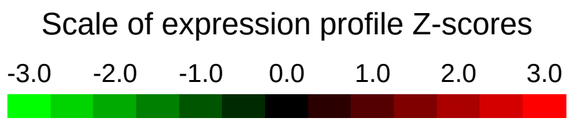

GEO Link:	http://www.ncbi.nlm.nih.gov/geo/query/acc.cgi?acc=GSE53946
Status:	Public on Jan 10 2014
Title:	Affymetrix gene expression of Transitional Type-1 B-cells from Wild-type (CBA), Xid and Btk KO mice
Organism:	Mus musculus
Experiment type:	Expression profiling by array
Platform:	GPL1261
Pubmed ID:	16764821
Summary & Design:	**Summary:** Splenic Transitional Type-1 B-cells from CBA wild-type mice, X-linked immunodeficiency mice and Bruton's tyrosine kinase knock-out mice. Two replicates where run on Affymetrix 420 2.0 arrays for CBA wild-type, Xid samples and the Btk KO samples. Bruton's tyrosine kinase (Btk) is a cytoplasmic tyrosine kinase important for B-lymphocyte maturation. Mutations in Btk give rise to the primary immunodeficiency disease X-linked agammaglobulinemia (XLA) in man and X-linked immunodeficiency (Xid) in mice. Recent studies have subdivided the mouse immature, or transitional, B-cells into two distinct subsets according to their respective surface markers. Transitional type 1 (T1) and transitional type 2 (T2) cells are also located in distinct anatomic locations. Based on a limited number of markers it has previously been reported that the earliest phenotypic sign of Btk deficiency is manifested at the T2 stage in mice. Here, we report on distinct genome-wide transcriptomic signature differences found in T1 B-lymphocytes from Btk-defective compared to normal mice and demonstrate that Btk deficiency is visible already at this stage. **Overall design:** 2 replicates of T1 B-cells from CBA (WT), Xid samples and the Btk KO samples

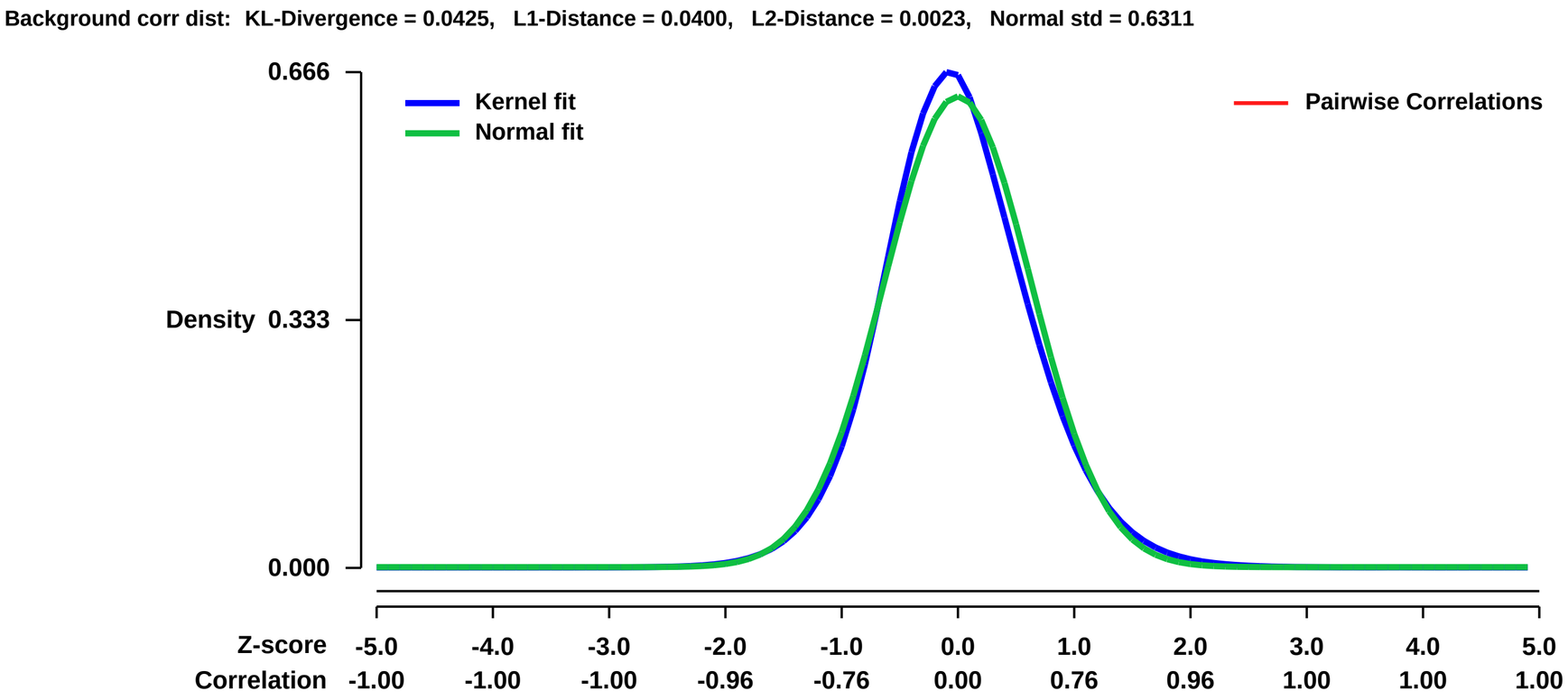

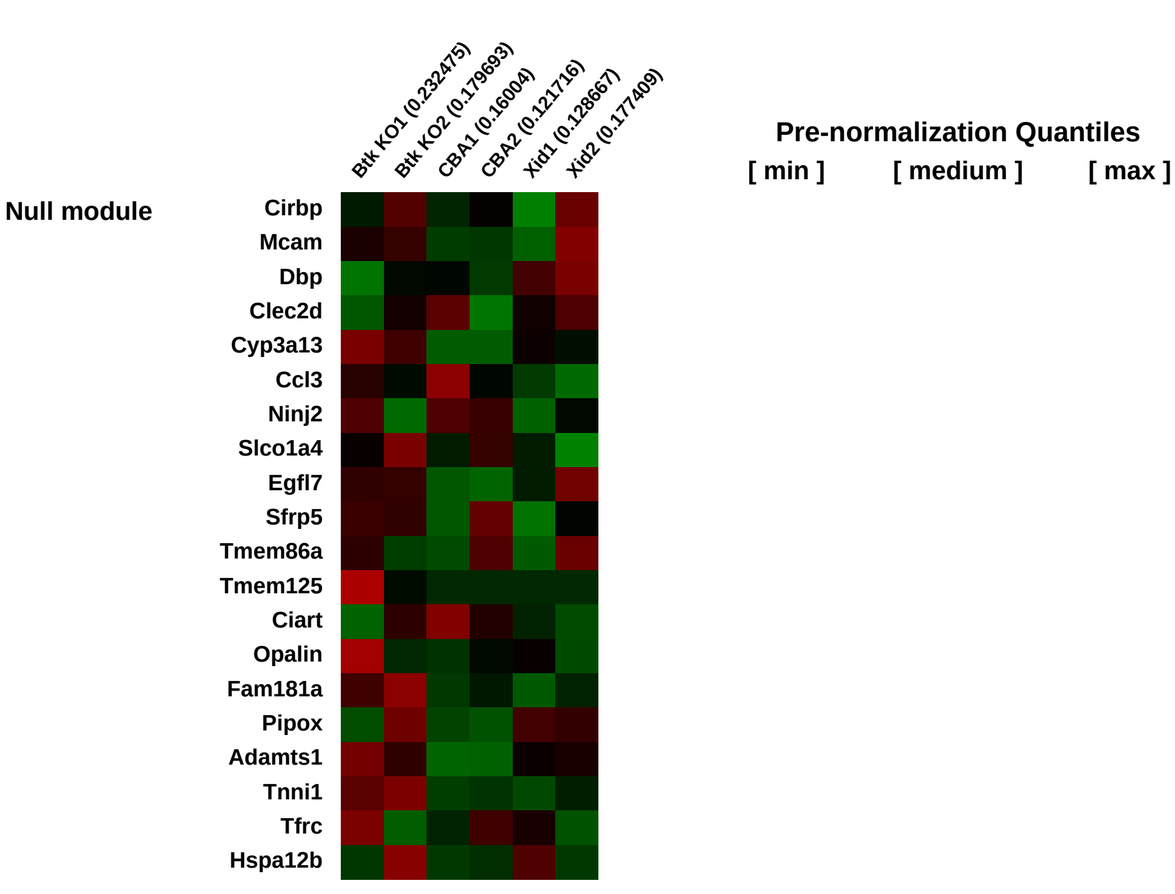

GEO Series "GSE41789" Expression Profiles

Num of samples in this series: 45

Scale of expression profile Z-scores

-3.0 -2.0 -1.0 0.0 1.0 2.0 3.0

GEO Link:	http://www.ncbi.nlm.nih.gov/geo/query/acc.cgi?acc=GSE41789
Status:	Public on Nov 01 2013
Title:	Senescence gene signature of radiation fibrosis
Organism:	Mus musculus
Experiment type:	Expression profiling by array
Platform:	GPL1261
Pubmed ID:	24052614
Summary & Design:	**Summary:** Radiation lung injury is characterized by early inflammation and late fibrosis. The causes underlying the chronic, progressive nature of radiation injury are poorly understood. Here, we report that the gene expression of irradiated lung tissue correlates with that observed in the lungs in aged animals. We demonstrate that NOX4 expression and superoxide elaboration is increased in irradiated lungs and pneumocytes in a dose dependent fashion. We used microarrays to detail the global programme of gene expression and report that irradiated lung tissue correlates with that observed in the lungs in aged animals. **Overall design:** Female C57Bl/Ncr mice, aged 10 weeks were treated with/ without radiation to the thorax with a X-RAD 320 x-ray irradiator at a dose rate of 2.61 Gy/minute. An age-matched cohort of mice received no IR while additional cohorts received 5 Gy in a single dose, 17.5 Gy in a single dose. RNA was extracted and hybridization done on Affymetrix Mouse430_2 microarrays.

Background corr dist: KL-Divergence = 0.2852, L1-Distance = 0.0589, L2-Distance = 0.0090, Normal std = 0.2862

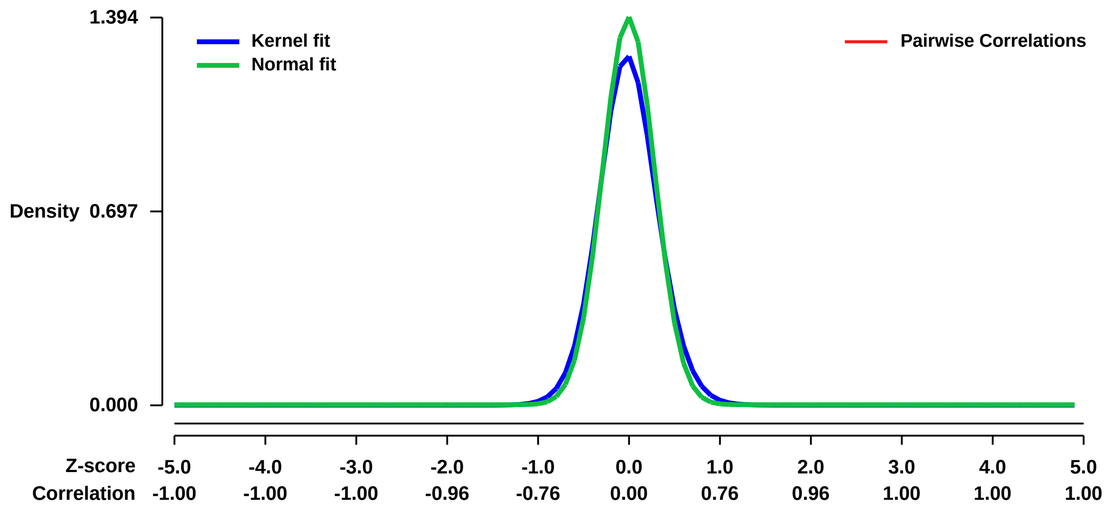

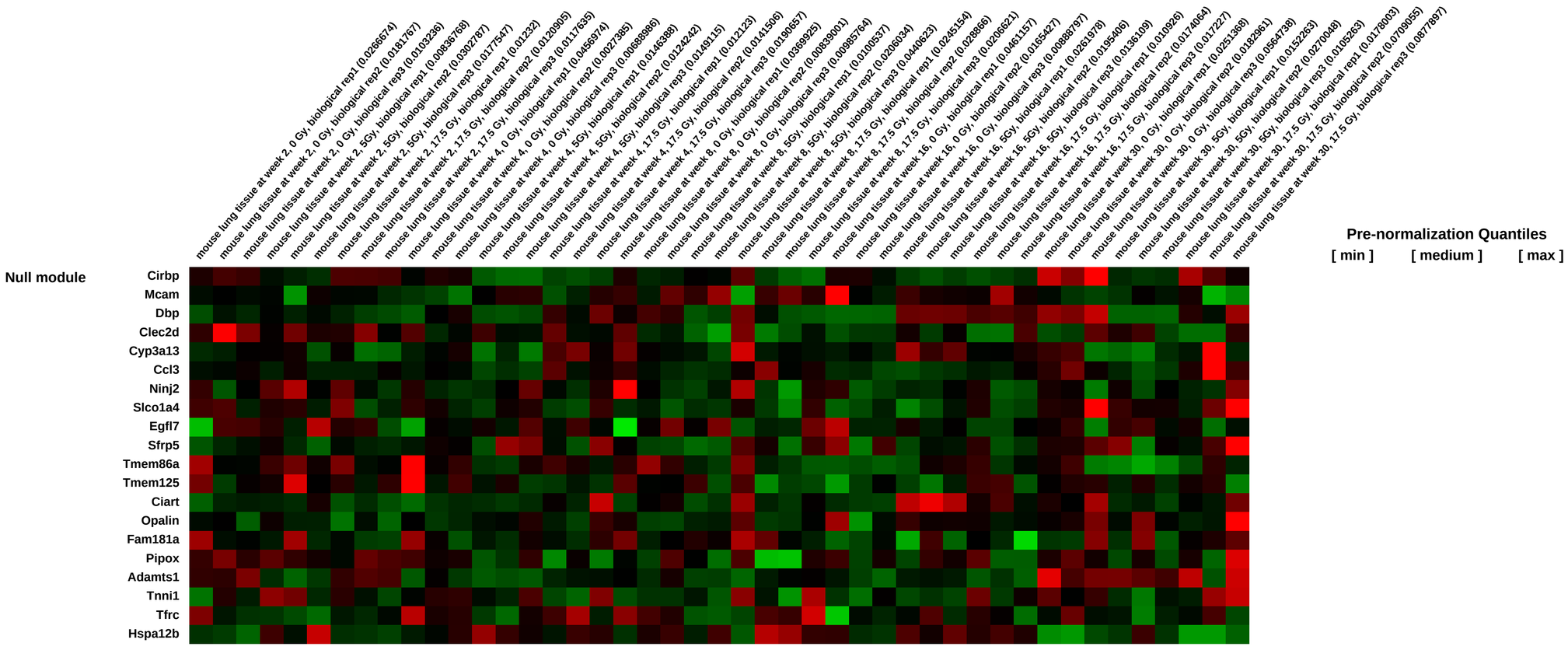

GEO Series "GSE46606" Expression Profiles

Num of samples in this series: 30

Scale of expression profile Z-scores

-3.0 -2.0 -1.0 0.0 1.0 2.0 3.0

GEO Link:	http://www.ncbi.nlm.nih.gov/geo/query/acc.cgi?acc=GSE46606
Status:	Public on May 04 2013
Title:	Transcriptional regulation of germinal center B and plasma cell fates by dynamical control of IRF4 (expression)
Organism:	Mus musculus
Experiment type:	Expression profiling by array
Platform:	GPL1261
Pubmed ID:	23684984
Summary & Design:	**Summary:** Temporal analysis of B cell activation in vitro using CD40L and IL-2/4/5 cytokines in wild type Irf4+/+ B cells or in mutant Irf4-/- B cells harboring a tet-inducible allele of Irf4. IRF4 expression was restored, or not, in the Irf4-/- background by culturing in the presence of low or high concentrations of doxycycline. The results provide insight in the role of IRF4 expression levels in coordinating different programs of B cell differentiation. **Overall design:** Resting mature peripheral primary B cells were enriched from the spleens of Irf4+/+ or Irf4-inducible mice on the Irf4-/- background. We sought to compare gene expression profiles of wild type and Irf4 mutant B cells in response to mitogens that promote the differentiation of the B cells into plasma cells and cells that have undergone class switch recombination. Day 0 samples represent RNA analysis of unstimulated cells, whereas Day 1 and Day 3 samples represent analysis of stimulated cells in culture. For stimulation, cells were cultured with insect cell purified CD40L and IL-2/4/5 cytokines for the indicated days. In the case of doxycycline-mediated rescue of IRF4 expression, doxycycline was added at predefined low and high concentrations that yield low or high numbers of plasma cells, respectively (see Molecular Systems Biology 7:495). Each replicate represents analysis of B cells from an individual mouse. Of the three replicates in each group, two were performed in parallel and one was performed at a different time. All cells were lysed using Trizol and total RNA was purified according to manufacturer's suggestions. The high quality of the RNA was confirmed using Agilent Bioanalyzer 2100 system. 250ng of RNA was then processed into biotinylated cRNA according to standard procedures and used to hybridize to Affymetrix 430 2.0 arrays. Signal intensities were normalized using the D-Chip algorithm (PM-only model) and the output was used to quantify differential gene expression between groups.

Background corr dist: KL-Divergence = 0.0934, L1-Distance = 0.0402, L2-Distance = 0.0024, Normal std = 0.4712

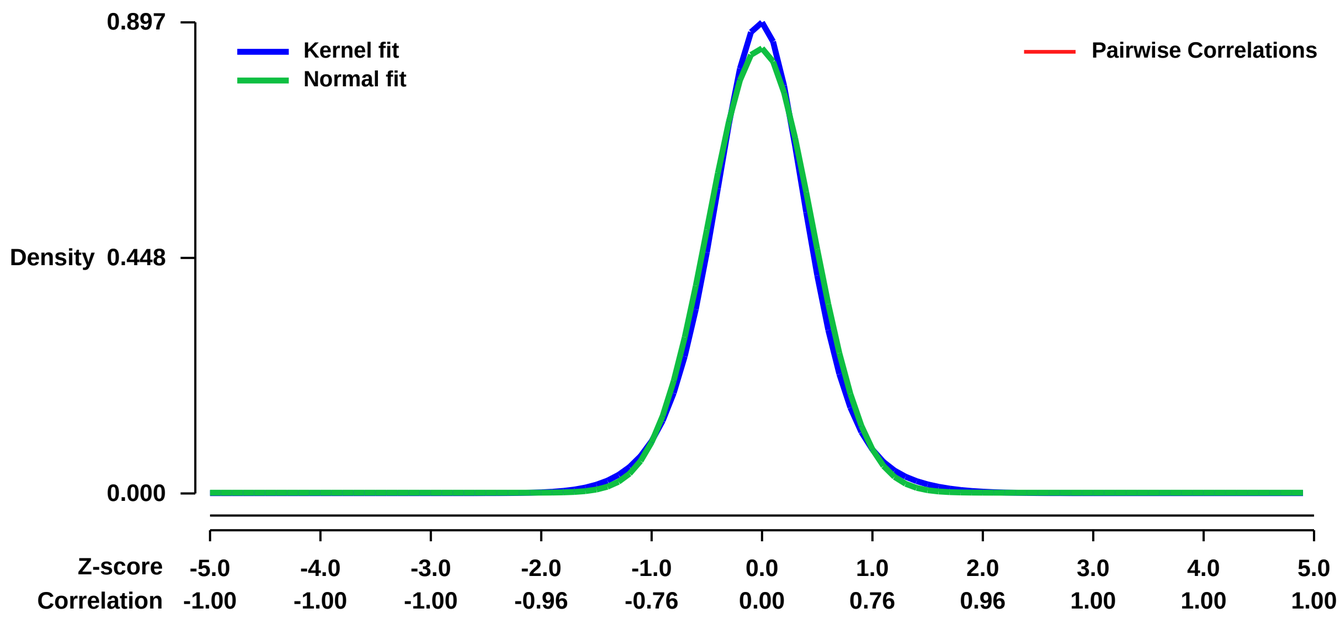

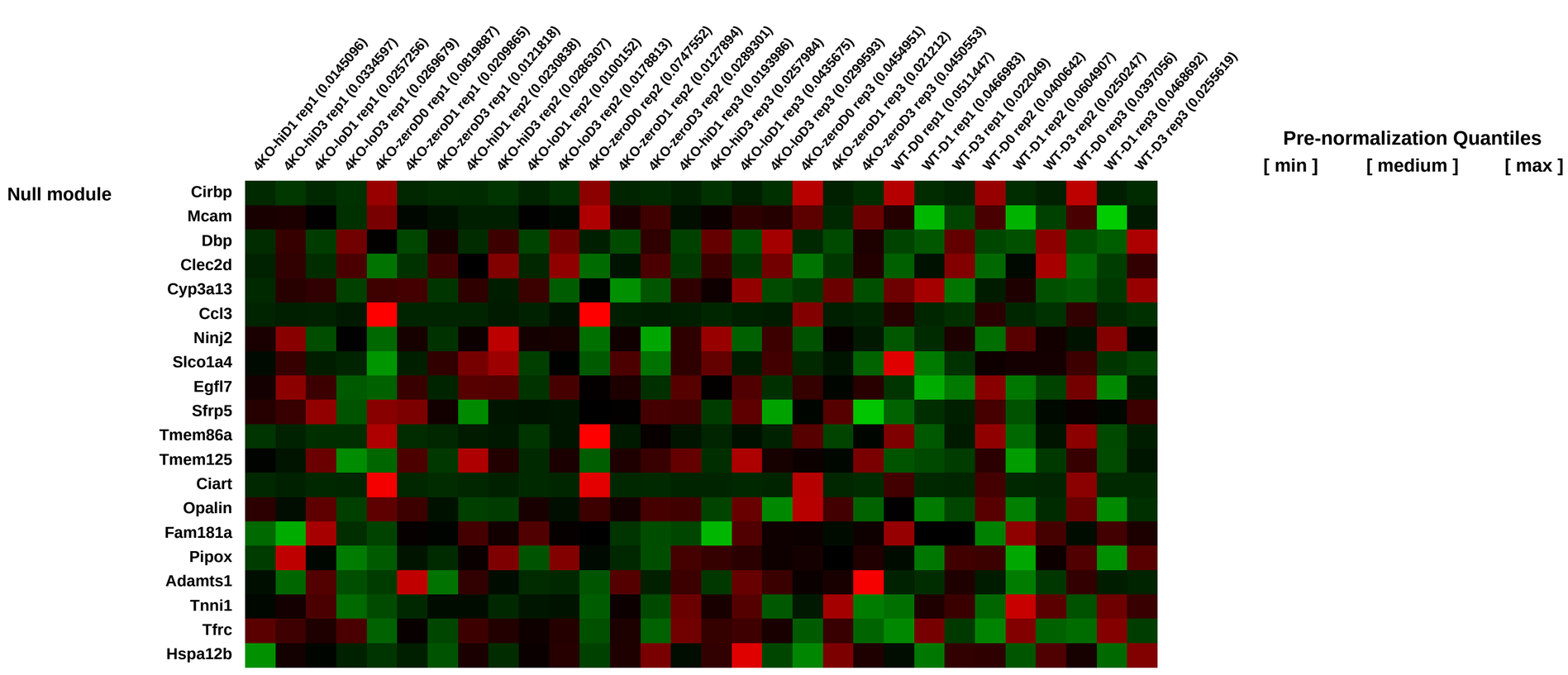

GEO Series "GSE32903" Expression Profiles

Num of samples in this series: 12

Scale of expression profile Z-scores

-3.0 -2.0 -1.0 0.0 1.0 2.0 3.0

GEO Link:	http://www.ncbi.nlm.nih.gov/geo/query/acc.cgi?acc=GSE32903
Status:	Public on Jan 09 2012
Title:	Smad4 and Trim33 dependend nodal/activin responsive genes in differentiated mouse ESCs
Organism:	Mus musculus
Experiment type:	Expression profiling by array
Platform:	GPL1261
Pubmed ID:	22196728
Summary & Design:	**Summary:** In differentiated mouse ESCs, most of the nodal/activin responsive genes are dependent on both Smad4 and Trim33, some are solely dependent on Smad4, and some are dependent on Trim33. **Overall design:** Ebs at Day2.5 from WT, Smad4 null, and Trim33 knock-down ESCs, were treated with activin or SB 431542 for 2 h.

Background corr dist: KL-Divergence = 0.0926, L1-Distance = 0.0220, L2-Distance = 0.0007, Normal std = 0.4528

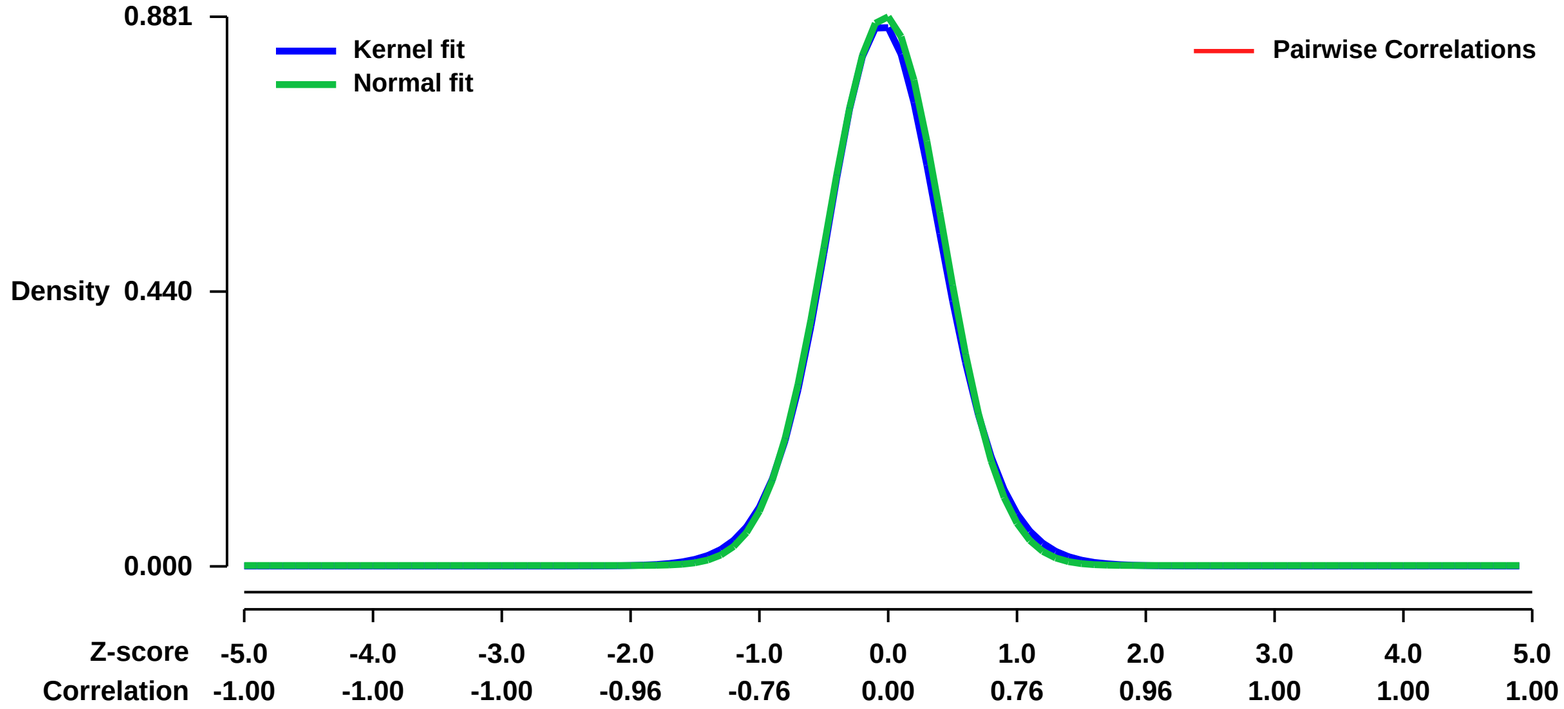

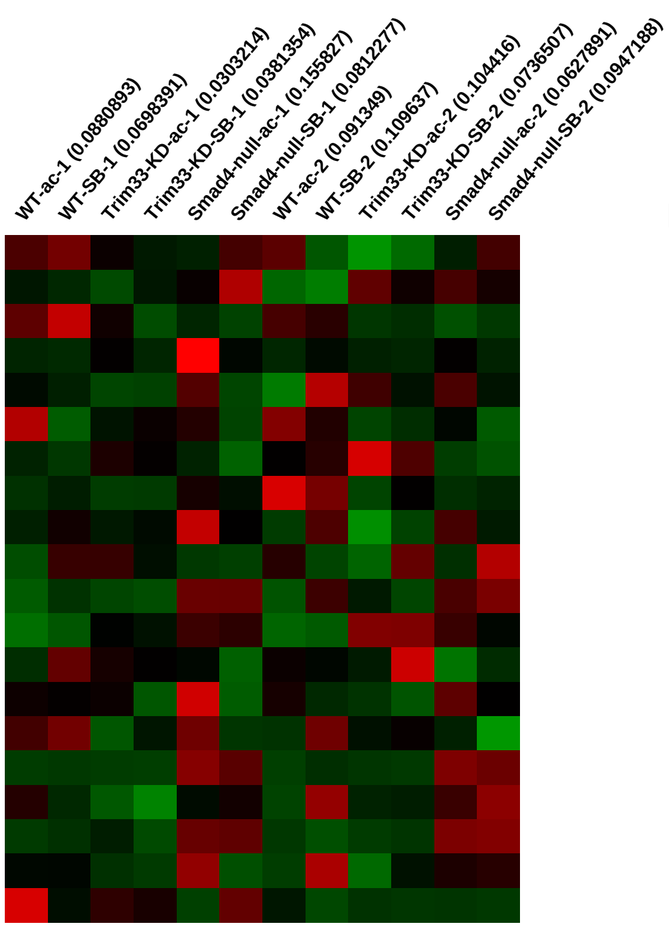

GEO Series "GSE5037" Expression Profiles

Num of samples in this series: 18

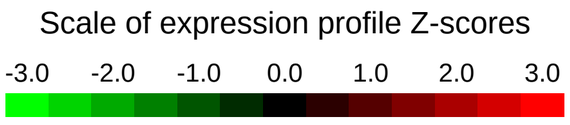

GEO Link:	**http://www.ncbi.nlm.nih.gov/geo/query/acc.cgi?acc=GSE5037**
Status:	**Public on Jun 09 2006**
Title:	**zhang-affy-mouse-217286**
Organism:	**Mus musculus**
Experiment type:	**Expression profiling by array**
Platform:	**GPL1261**
Pubmed ID:	
Summary & Design:	**Summary:**

In our original grant we proposed to use the NR3B-null mouse model to study the role of NR3B subunit in motor neuron function. We have now successfully generated NR3B null mice. Interestingly, NR3B-null mice invariably die at age P4-P8. Our preliminary examination indicates that the motor strength of these mice is severely impaired prior to death. As we continue to explore the cause of death in NR3B null mice, we propose to conduct gene profiling experiments to search for transcription changes in the brain related to ablation of the NR3B gene. We have used the facility provided by the NINDS/NIMH Microarray Consortium to identify genes that show abnormal expression patterns in these mice. We would like to compare these changes with that opccured in SOD1 mice, a mouse model of motor neuron diseases. Analysis of these genes will help to identify changes in networks and pathways that may cause the death of NR3B-null mice. These studies will further help to elucidate the functional role of NR3B in motor neurons.

We will compare samples from motor neurons of wild type and SOD1 mice to identify genes that show abnormal expression patterns, which may be implicated in the death of SOD1 mice and shared with the same changes in NR3B-null mice.

We hypothesize that genes with their transcription level changing significantly by ablation of NR3B will be associated with the molecular mechanism underlying the death of motor neurons in NR3B null mice.

As NR3B is expressed primarily in the motor neurons of hindbrain and spinal cord, we have first collected and analyzed the spinal cord samples from NR3B null mice and wild-type controls in P4, an age of disease onset. We like to compare motor neuron and spinal cord smaples from SOD1 mice at the age prior to the disease onset. Total RNA from total 12 samples will be purified from ~200 motor neurons obtained by Laser Capture Microdissection and the total spinal cord. Extracted RNAs will be subjected to one or two rounds of amplification and the obtained cRNA will be biotinylated. The purified cRNA will be sent to the NINDS/NIMH Microarray Consortium be used to hybridize the GeneChip Mouse Genome 430 2.0 Array. The hybridization, scanning, and initial data analysis of these GeneChips will be conducted by the Consortium staff. We will analyze the collected data further after data collection. We will first identify genes that show significant changes between wild-type and SOD1 mice and then compare that with the result from NR3B null mice.

Keywords: dose response

Overall design:

Background corr dist: **KL-Divergence = 0.0803, L1-Distance = 0.0825, L2-Distance = 0.0124, Normal std = 0.5517**

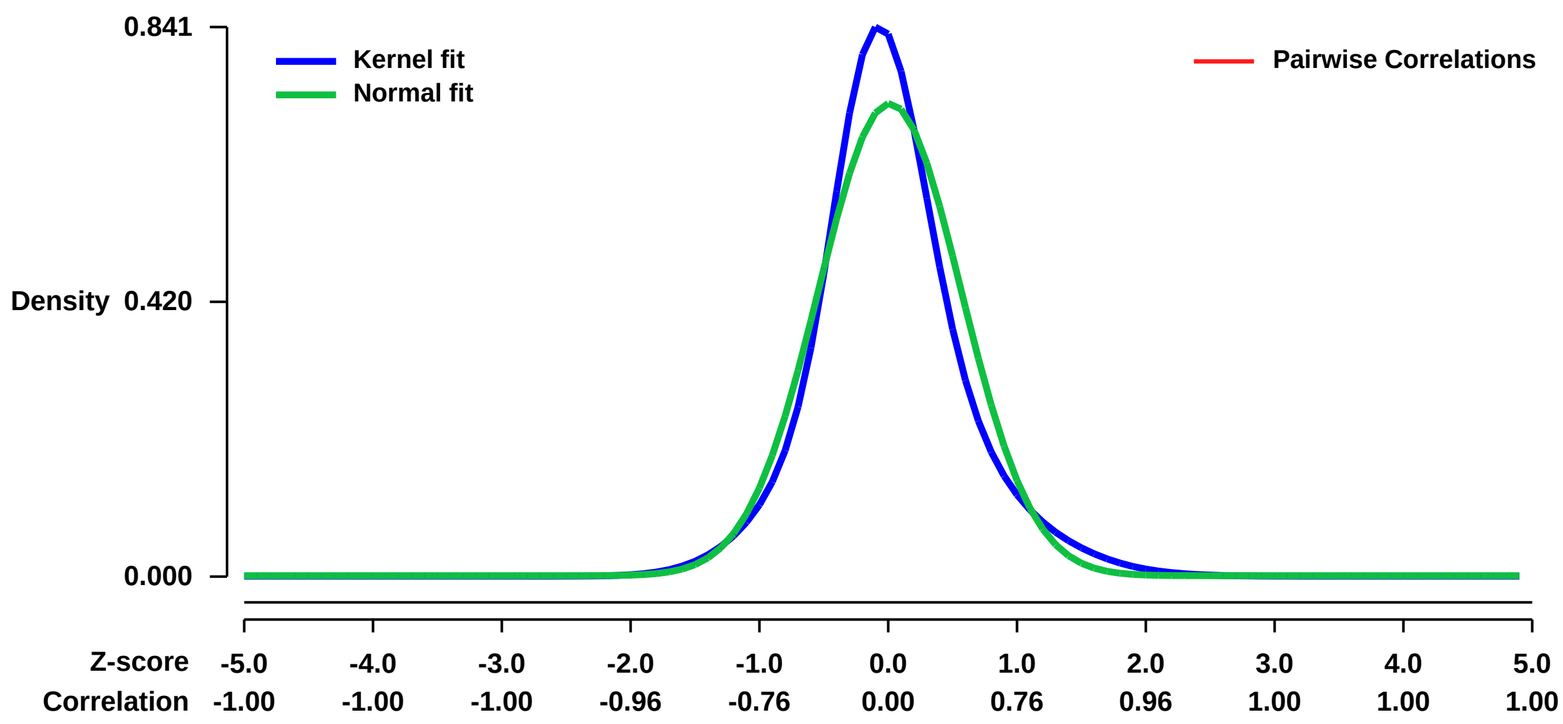

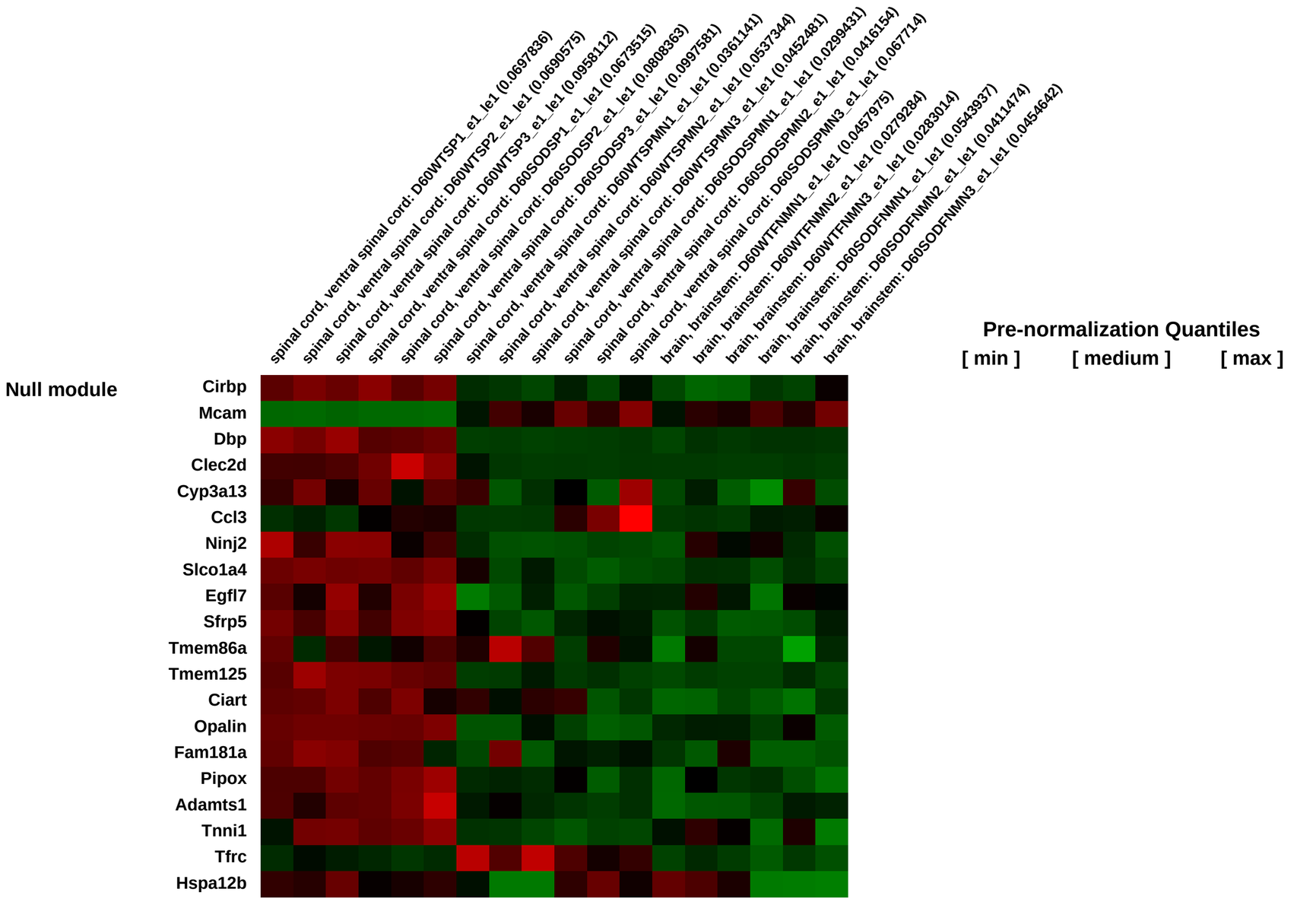

GEO Series "GSE13223" Expression Profiles

Num of samples in this series: 6

Scale of expression profile Z-scores

-3.0 -2.0 -1.0 0.0 1.0 2.0 3.0

GEO Link:	http://www.ncbi.nlm.nih.gov/geo/query/acc.cgi?acc=GSE13223
Status:	Public on Nov 30 2008
Title:	(AKR/J x FVB/NJ)F1 versus (DBA/2J x FVB)F1 bone marrow expression data
Organism:	Mus musculus
Experiment type:	Expression profiling by array
Platform:	GPL1261
Pubmed ID:	19118016
Summary & Design:	**Summary:** F1 hybrids from (AKR/J x FVB/NJ) and (DBA/2J x FVB/NJ) outcrosses display a 20-fold difference in mammary tumor metastatic capacity, due to differences in inherited polymorphisms. Expression studies were performed to determine whether polymorphism-driven gene expression signatures predictive of outcome could be generated from normal tissues **Keywords: Basal transcription profiles** **Overall design:** Bone Marrow from adult F1 animals from (AKR/J x FVB/NJ) and (DBA/2J x FVB/NJ) outcrosses was collected and arrayed on Affymetrics chip to identify basal differences in gene expression between the different genotypes

Background corr dist: KL-Divergence = 0.0268, L1-Distance = 0.0196, L2-Distance = 0.0004, Normal std = 0.6966

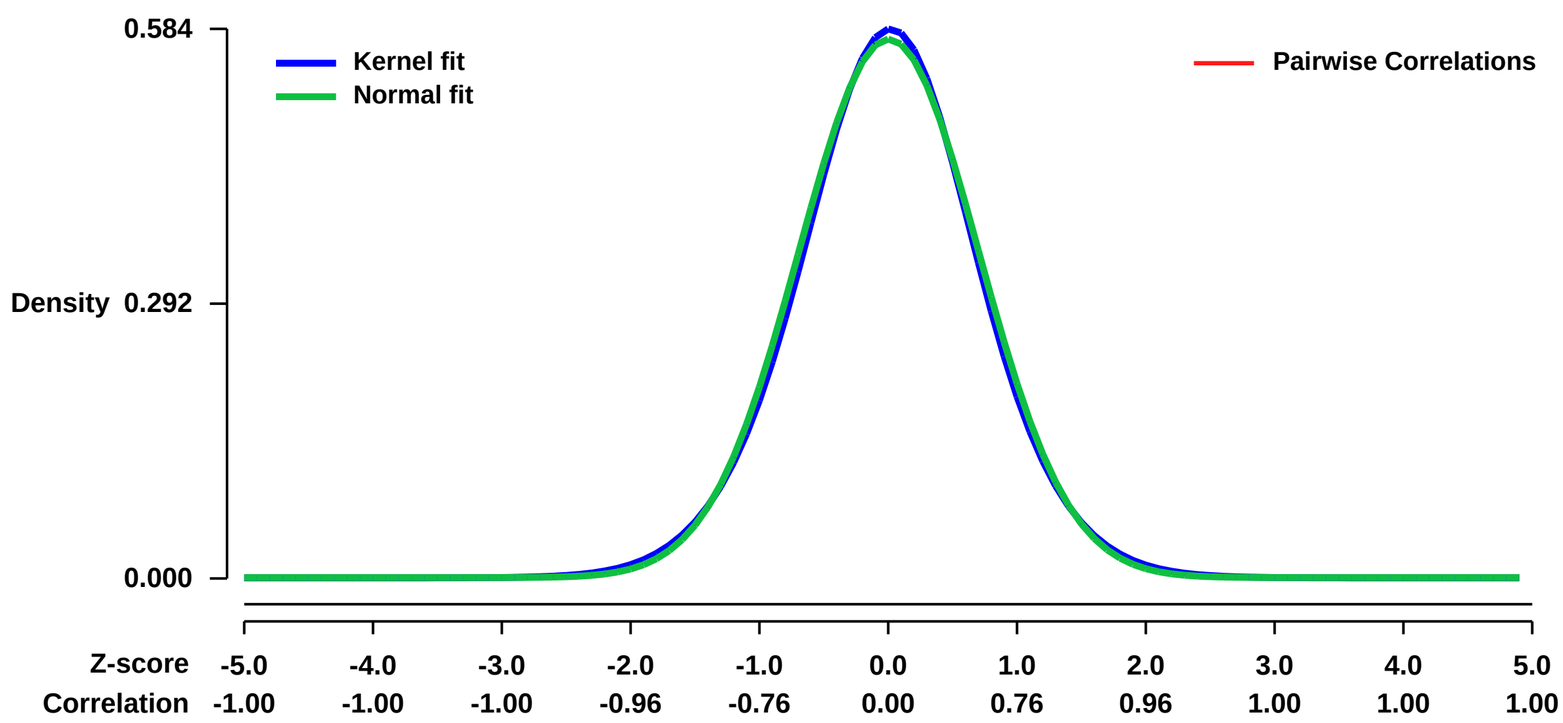

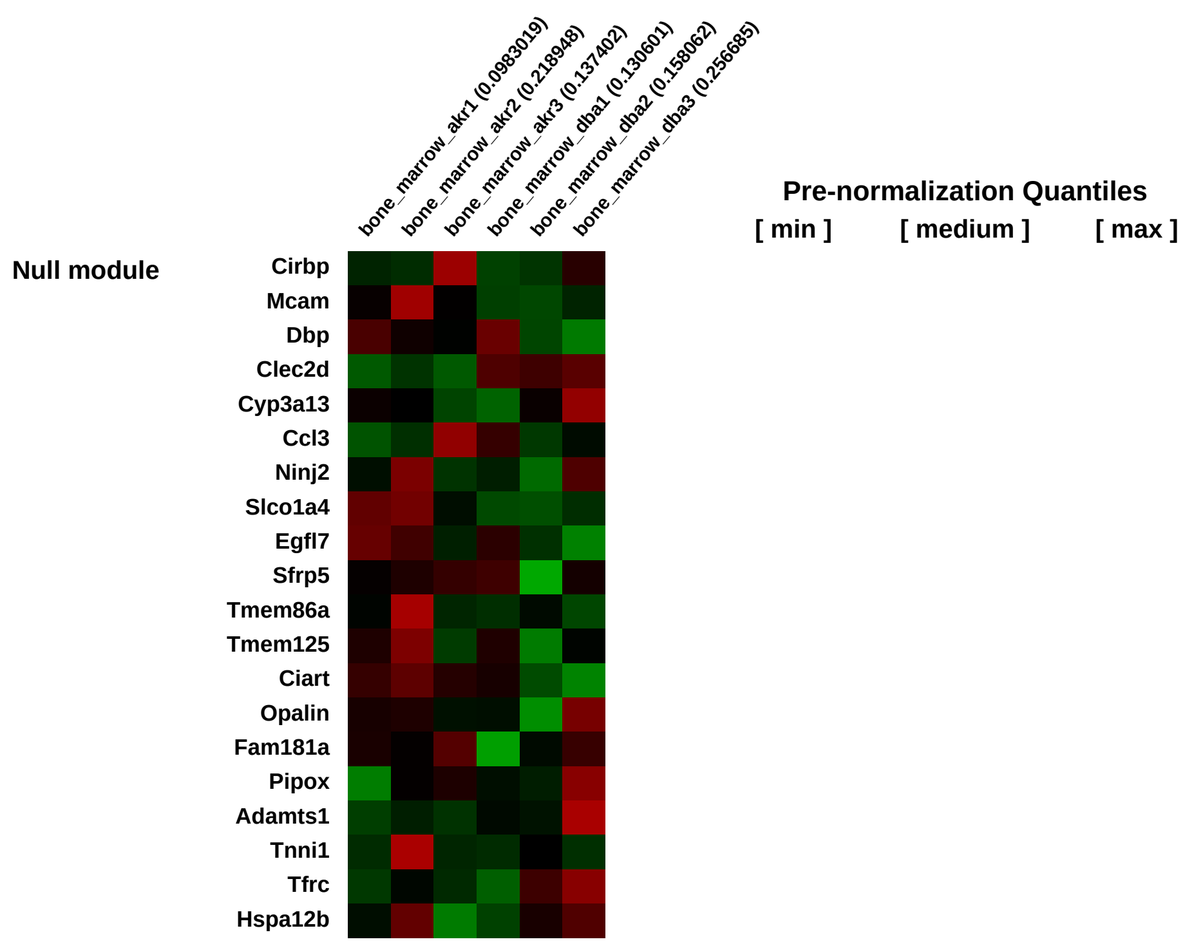

GEO Series "GSE16777" Expression Profiles

Num of samples in this series: 38

Scale of expression profile Z-scores

-3.0 -2.0 -1.0 0.0 1.0 2.0 3.0

GEO Link:	http://www.ncbi.nlm.nih.gov/geo/query/acc.cgi?acc=GSE16777
Status:	Public on Jun 25 2009
Title:	Discrimination of Tumorigenic Triazole Conazoles from Phenobarbital by Transcriptional Analyses of Mouse Liver
Organism:	Mus musculus
Experiment type:	Expression profiling by array
Platform:	GPL1261
Pubmed ID:	19363144
Summary & Design:	**Summary:** The goal of this study was to apply transcriptional analyses to hepatic tissues from mice exposed to PB, propiconazole (Pro) or triadimefon (Tri) at tumorigenic exposure levels to reveal similarities and differences in response among these treatments.The goal of this study was to apply transcriptional analyses to hepatic tissues from mice exposed to PB, propiconazole (Pro) or triadimefon (Tri) at tumorigenic exposure levels to reveal similarities and differences in response among these treatments. **Overall design:** Briefly, male CD-1 mice received propiconazole (2500 ppm), tridimefon (1800 ppm), or phenobarbital (850 ppm) in the feed or, control feed for periods of 4 and 30 days. This resulted in an average daily intake of 349.6 ´– 46.7 of propiconazole, 257.1 ´– 33.5 of tridimefon or 97.2 ´– 5.9 mg/kg/day of phenobarbital.

Background corr dist: KL-Divergence = 0.1403, L1-Distance = 0.0497, L2-Distance = 0.0055, Normal std = 0.3850

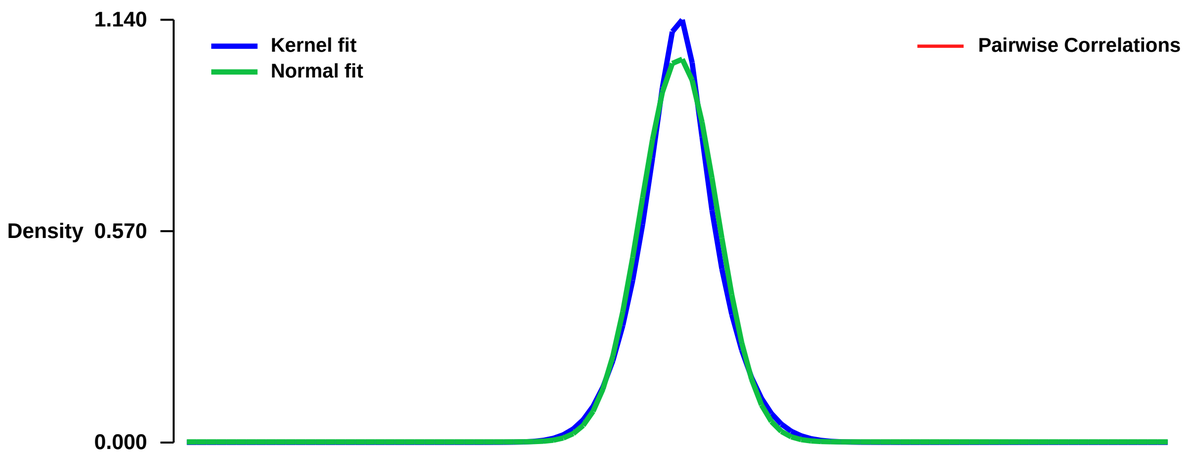

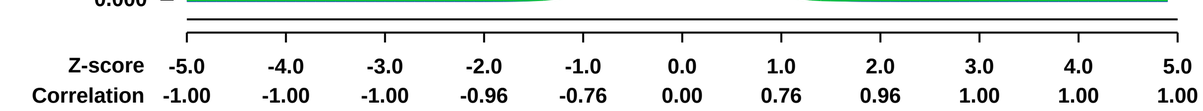

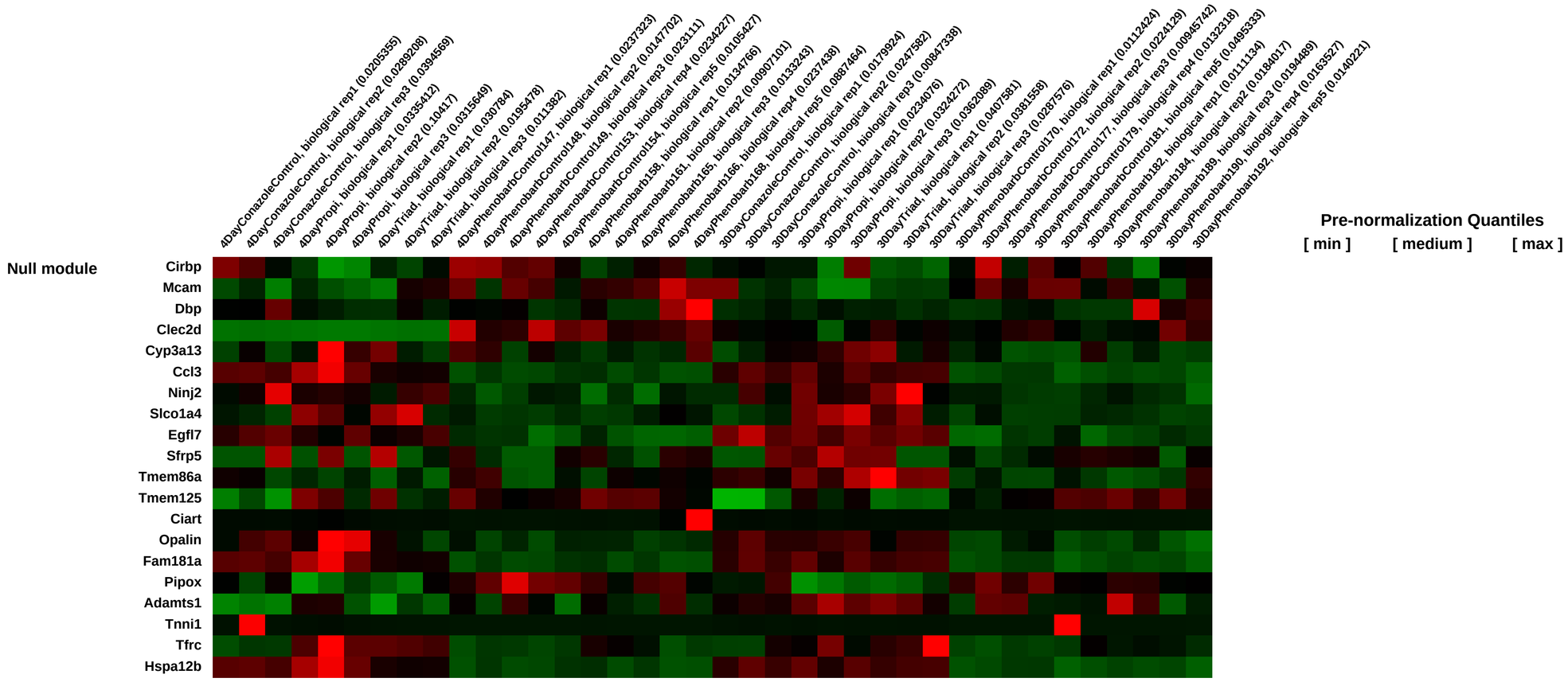

GEO Series "GSE20696" Expression Profiles

Num of samples in this series: 8

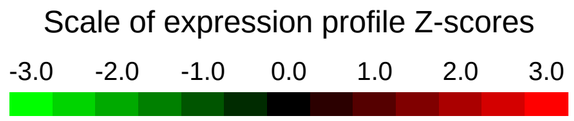

GEO Link:	**http://www.ncbi.nlm.nih.gov/geo/query/acc.cgi?acc=GSE20696**
Status:	**Public on Sep 30 2010**
Title:	**Expression profiling of 3T3-L1 adipogenesis**
Organism:	**Mus musculus**
Experiment type:	**Expression profiling by array**
Platform:	**GPL1261**
Pubmed ID:	**20887899**
Summary & Design:	**Summary:** **3T3-L1 pre-adipocyte cells were grown to confluence and induced to differentiate in adipogeneic media.** **Overall design:** **Two technical replicates from four time points relative to induction of adipogenesis (day 0)**

Background corr dist: **KL-Divergence = 0.0408, L1-Distance = 0.0317, L2-Distance = 0.0012, Normal std = 0.6378**

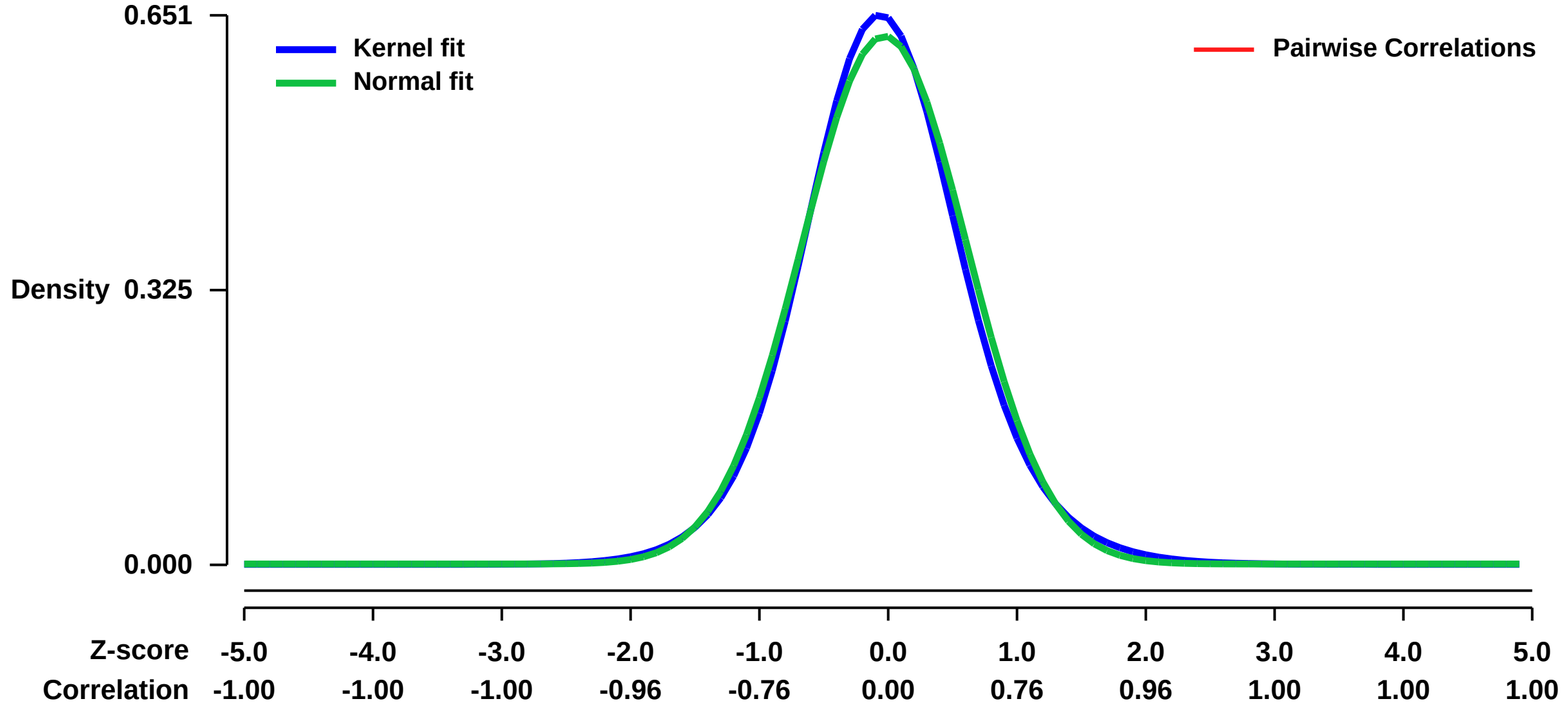

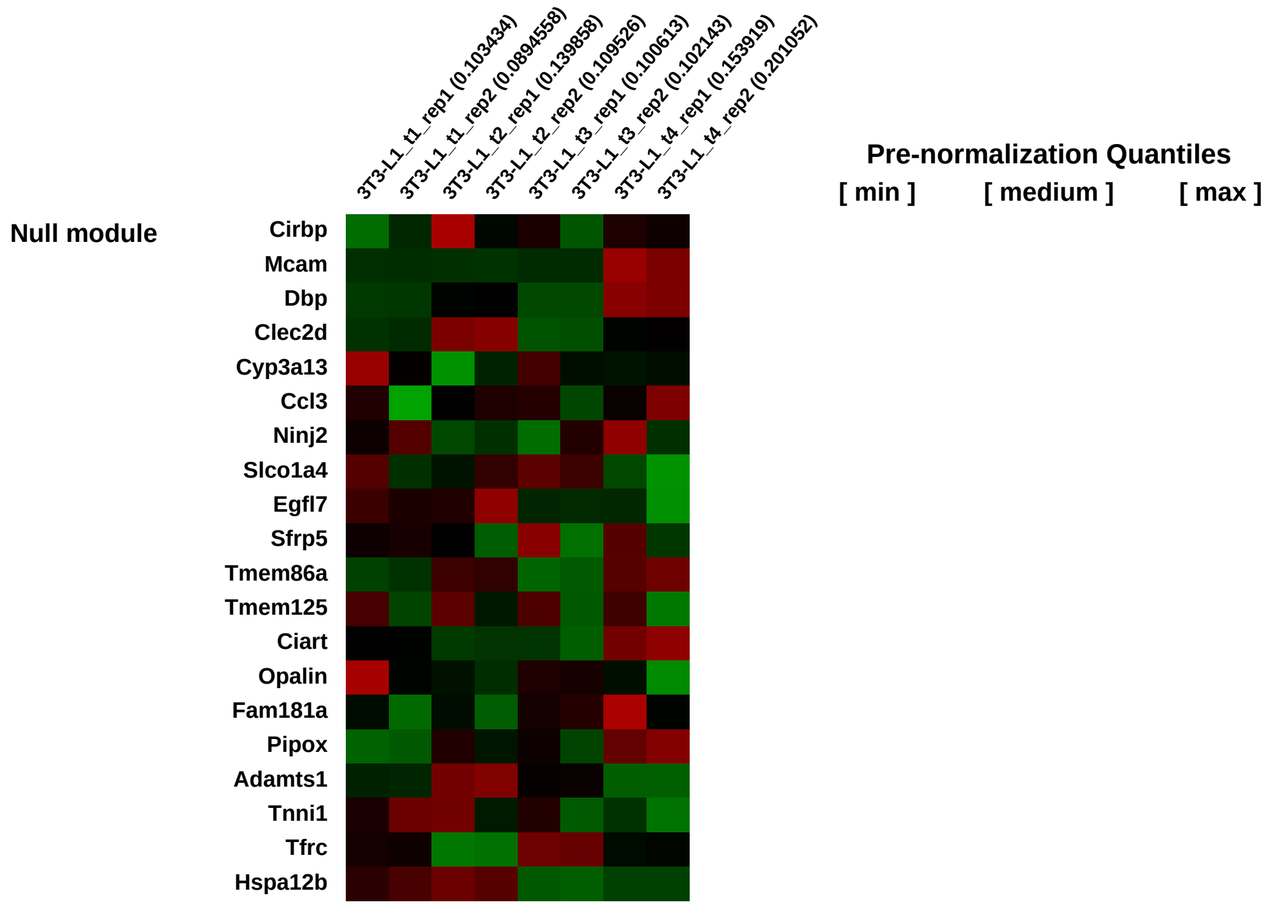

GEO Series "GSE32624" Expression Profiles

Num of samples in this series: 6

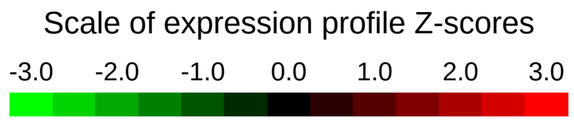

GEO Link:	http://www.ncbi.nlm.nih.gov/geo/query/acc.cgi?acc=GSE32624
Status:	Public on Dec 06 2011
Title:	Functional and epigenetic studies reveal multistep differentiation and plasticity of in vitro and in vivo follicular T helper cells.
Organism:	Mus musculus
Experiment type:	Expression profiling by array
Platform:	GPL1261
Pubmed ID:	22018472
Summary & Design:	**Summary:** Follicular T helper cells (Tfh) are critical for providing help to B cells for germinal center (GC) formation. Mutations affecting SAP prevent GC formation due to defective T:B cell interactions, yet effects on Tfh cell differentiation remain unclear. We describe the in vitro differentiation of functionally competent â Tfh-likeâ cells that expressed IL-21, Tfh markers, and Bcl6, and rescued GC formation in SAP-deficient hosts substantially better than other T helper (Th) cells. SAP-deficient Tfh-like cells appeared virtually indistinguishable from wildtype, yet failed to support GCs in vivo. Interestingly, both Tfh-like and in vivo-derived Tfh cells could produce effector cytokines in response to polarizing conditions. Moreover, other Th cell populations could be reprogrammed to obtain Tfh characteristics. ChIP-Seq analyses revealed positive epigenetic markings on Tbx21, Gata3 and Rorc in Tfh-like and ex vivo Tfh cells, and Bcl6 in other Th cells, supporting the concept of plasticity between Tfh and other Th populations. We describe the in vitro differentiation of functionally competent IL-21-producing cells with Tfh-like properties. Importantly, transfer of low numbers of these cells induced GC formation in SAP-deficient hosts more effectively than other in vitro differentiated Th cells, suggesting they represent bona fide Tfh cell precursors. We have chosen the name â Tfh-likeâ cells for these in vitro differentiated IL-21 producing cells as they exhibit Tfh characteristics, but do not reside within B cell follicles. SAP-deficient Tfh-like cells were virtually indistinguishable from WT, yet nonetheless, failed to effectively contribute to Tfh cells and rescue GC formation in vivo. Evaluation of cytokine production as well as epigenetic chromatin modifications of genes encoding Th cell-specific transcription factors from either in vitro-generated Tfh-like cells or Tfh cells isolated directly ex vivo provided evidence for plasticity between Tfh-like and other Th cell populations. Our results provide insight into the requirements for differentiation and plasticity of Tfh cells, which are critical for the generation of effective long-term humoral immunity. **Overall design:** RNA was prepared from subconfluent asynchronously proliferating cells using TRIZOL and purified by RNeasy MinElute Cleanup kit (Qiagen). Hybridization to Affymetrix GeneChip Mouse Genome 430 2.0 arrays was used to generate gene expression profiles of WT Tfh-like and SAP-deficient Tfh-like cells.

Background corr dist: KL-Divergence = 0.0264, L1-Distance = 0.0124, L2-Distance = 0.0001, Normal std = 0.6898

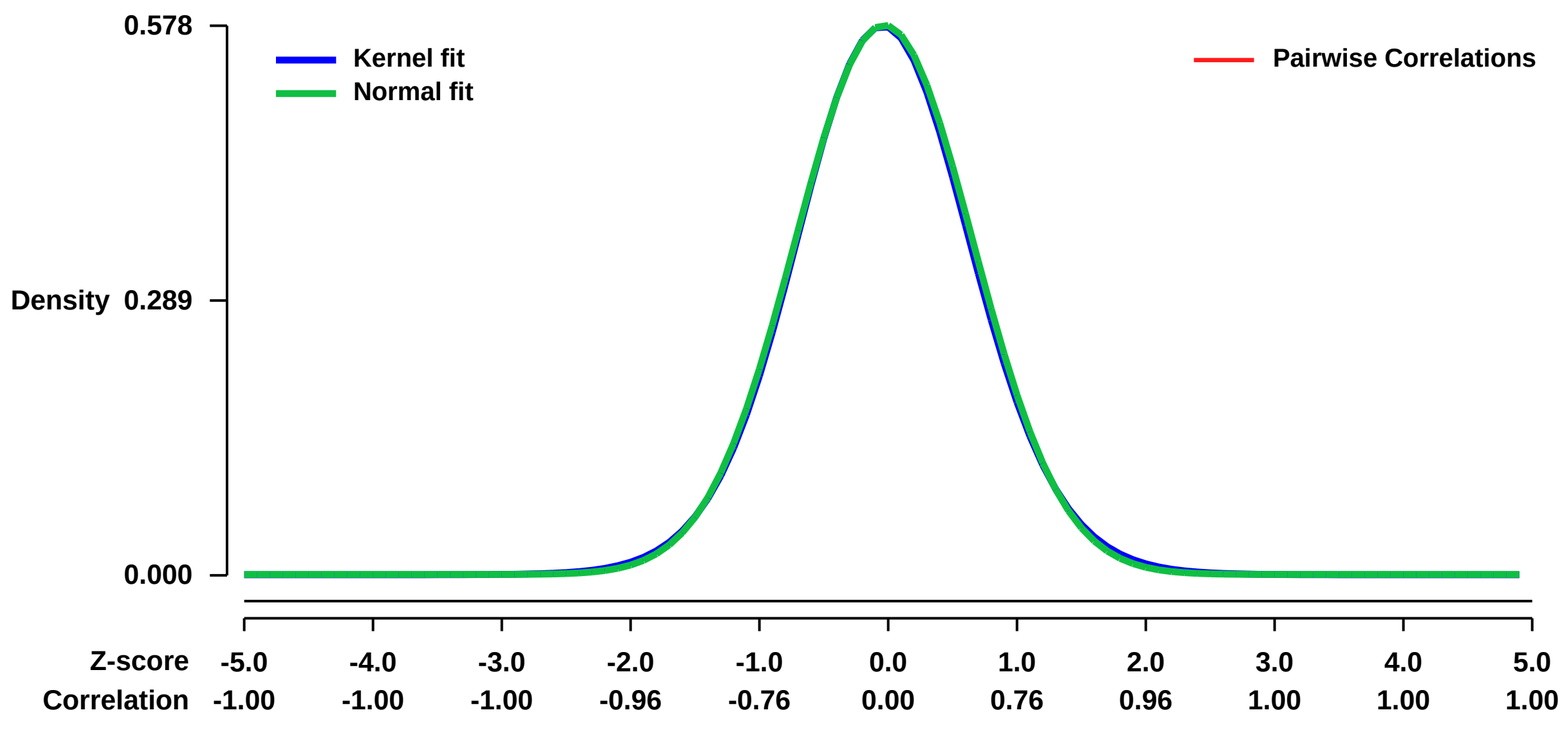

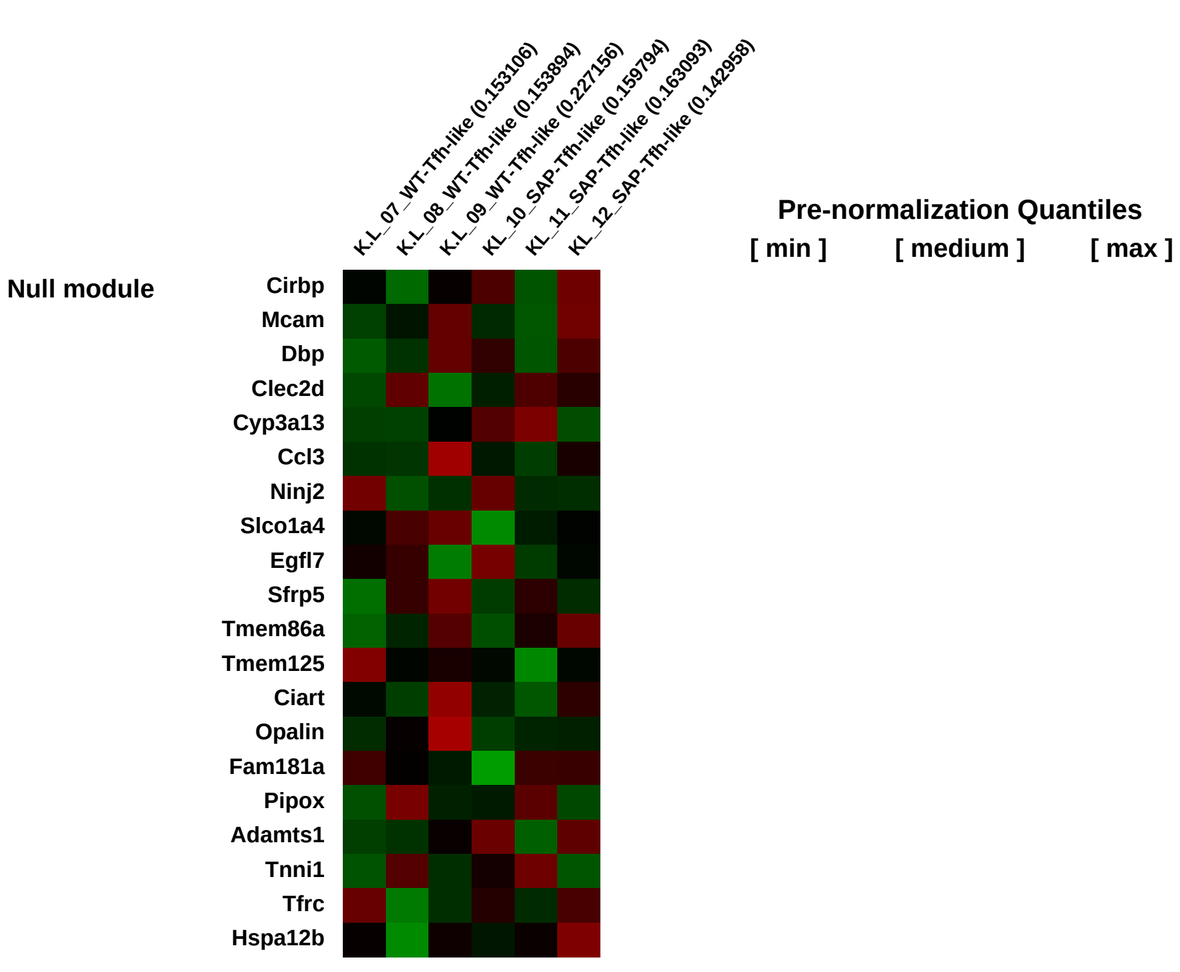

GEO Series "GSE32966" Expression Profiles

Num of samples in this series: 24

Scale of expression profile Z-scores

-3.0 -2.0 -1.0 0.0 1.0 2.0 3.0

GEO Link:	http://www.ncbi.nlm.nih.gov/geo/query/acc.cgi?acc=GSE32966
Status:	Public on Oct 13 2011
Title:	Dermal reprogramming through epidermal activation of beta-catenin
Organism:	Mus musculus
Experiment type:	Expression profiling by array
Platform:	GPL1261
Pubmed ID:	22031549
Summary & Design:	**Summary:** Hair follicle formation depends on reciprocal epidermal-dermal interactions and occurs during skin development, but not in adult life. This suggests that the properties of dermal fibroblasts change during postnatal development. To examine this, we used a PdgfraEGFP mouse line to isolate GFP-positive fibroblasts from neonatal skin, adult telogen and anagen skin and adult skin in which ectopic hair follicles had been induced (EF skin) by transgenic epidermal activation of beta-catenin. We also isolated epidermal cells from each mouse. The gene expression profile of EF epidermis was most similar to that of anagen epidermis, consistent with activation of beta-catenin signalling. In contrast, adult dermis with ectopic hair follicles more closely resembled neonatal dermis than adult telogen or anagen dermis. In particular, genes associated with mitosis were upregulated and extracellular matrix-associated genes were downregulated in neonatal and EF fibroblasts. We confirmed that sustained epidermal beta-catenin activation stimulated fibroblasts to proliferate to reach the high cell density of neonatal skin. In addition, the extracellular matrix was comprehensively remodelled, with mature collagen being replaced by collagen subtypes normally present only in developing skin. The changes in proliferation and extracellular matrix composition originated from a specific subpopulation of fibroblasts located beneath the sebaceous gland. Our results show that adult dermis is an unexpectedly plastic tissue that can be reprogrammed to acquire the molecular, cellular and structural characteristics of neonatal dermis in response to cues from the overlying epidermis. **Overall design:** We have isolated the following populations of cells from mouse back skin by flow cytometry: 1A) GFP+ WT neonatal dermal fibroblasts, 1B) ItgA6+ WT neonatal epidermal keratinocytes, 2A) GFP+ WT telogen dermal fibroblasts, 2B) ItgA6+ WT telogen epidermal keratinocytes, 3A) GFP+ D2 transient activation (anagen) dermal fibroblasts, 3B) ItgA6+ D2 transient activation (anagen) epidermal keratinocytes, 4A) GFP+ D2 sustained activation (ectopic follicles) dermal fibroblasts, 4B) ItgA6+ D2 sustained activation (ectopic follicles) epidermal keratinocytes

Background corr dist: KL-Divergence = 0.1707, L1-Distance = 0.0413, L2-Distance = 0.0039, Normal std = 0.3594

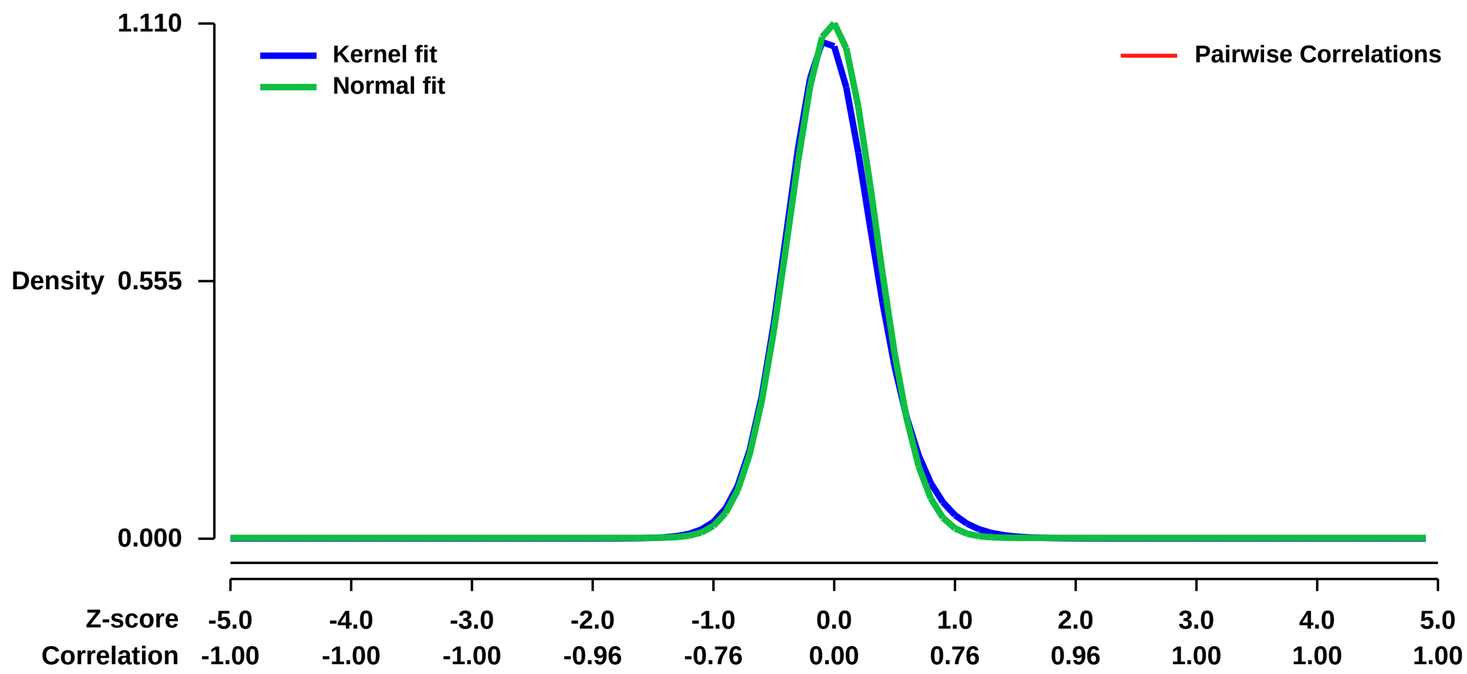

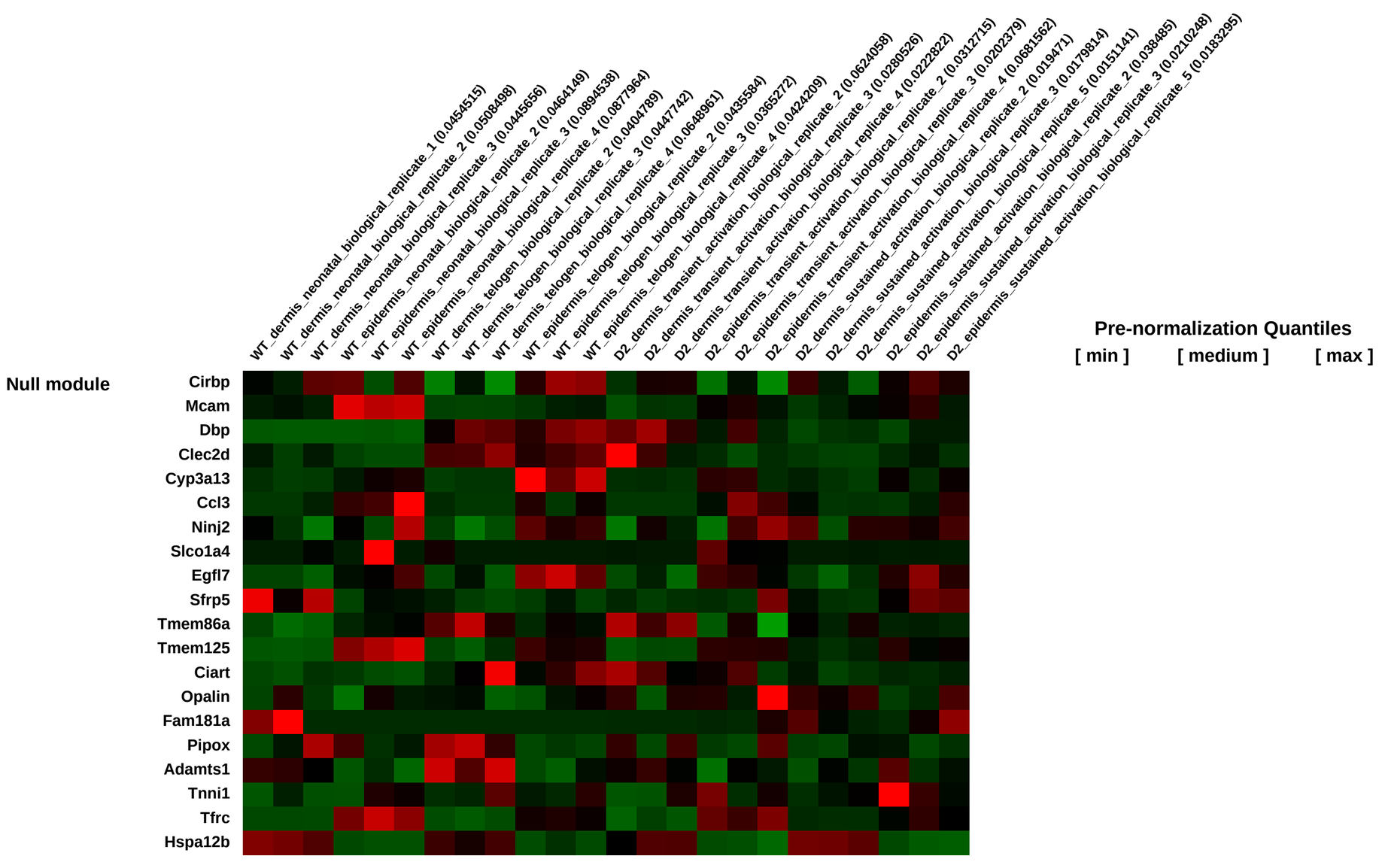

GEO Series "GSE33942" Expression Profiles

Num of samples in this series: 12

Scale of expression profile Z-scores

-3.0 -2.0 -1.0 0.0 1.0 2.0 3.0

GEO Link:	**http://www.ncbi.nlm.nih.gov/geo/query/acc.cgi?acc=GSE33942**
Status:	**Public on Feb 29 2012**
Title:	**Role of PKD2 in TCR-induced transcriptional reprogramming of naˆflve T cells**
Organism:	**Mus musculus**
Experiment type:	**Expression profiling by array**
Platform:	**GPL1261**
Pubmed ID:	**23525088**
Summary & Design:	**Summary:** **Comparison of transcriptional profile of TCR stimulated P14-TCR wild-type and P14-PKD2 null murine lymph node cells** **Overall design:** **Lymph node cells from 3 biological replicates (3 wild-type and 3 PKD2 null mice) were isolated and left unstimulated or stimulated for 4 hours with antigenic peptide (gp33-41) prior to RNA extraction and hybridization to Affymetrix microarray.**

Background corr dist: **KL-Divergence = 0.0765, L1-Distance = 0.0838, L2-Distance = 0.0107, Normal std = 0.5803**

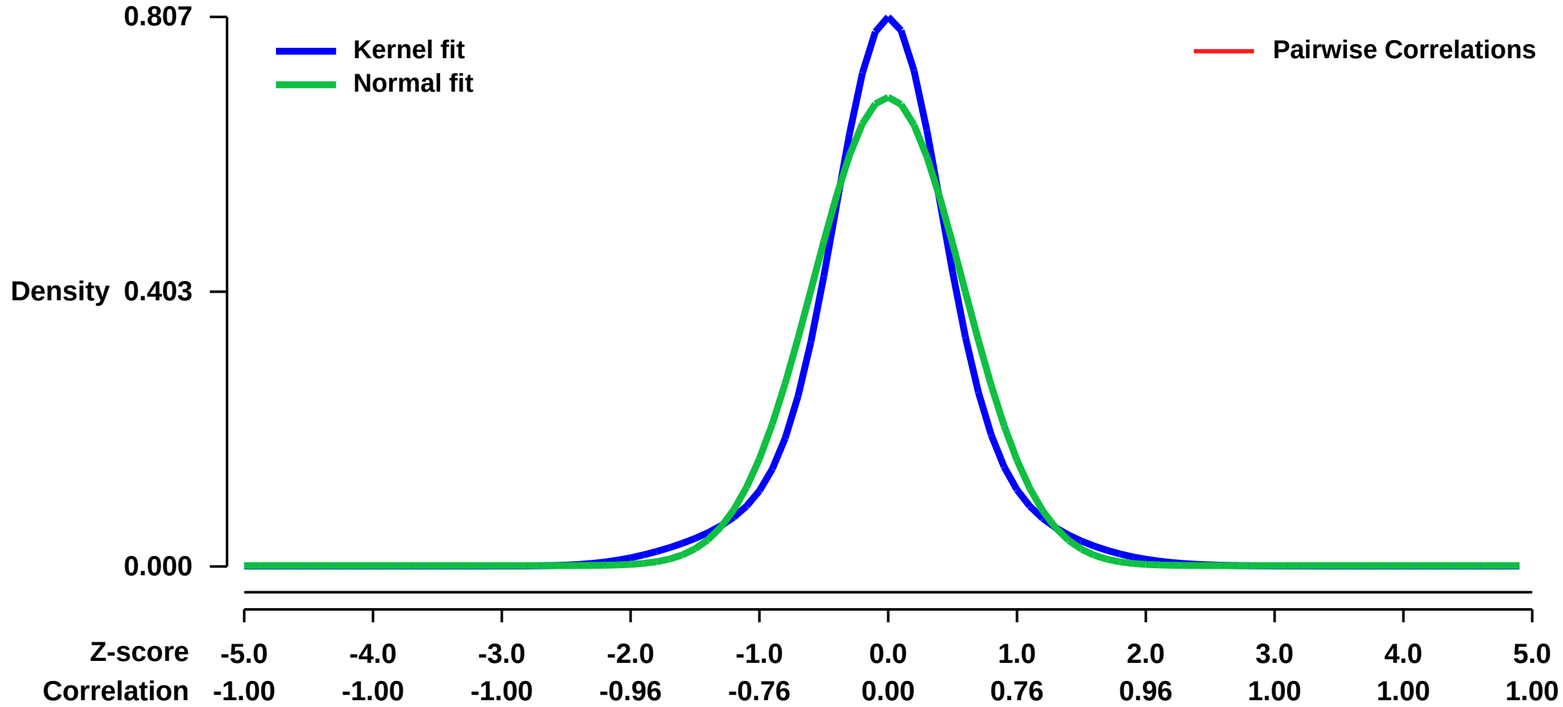

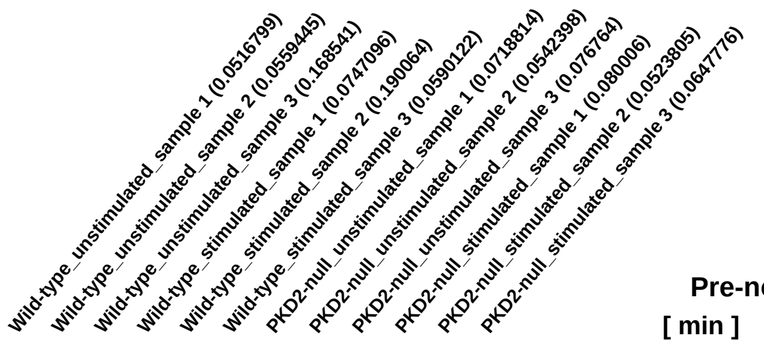

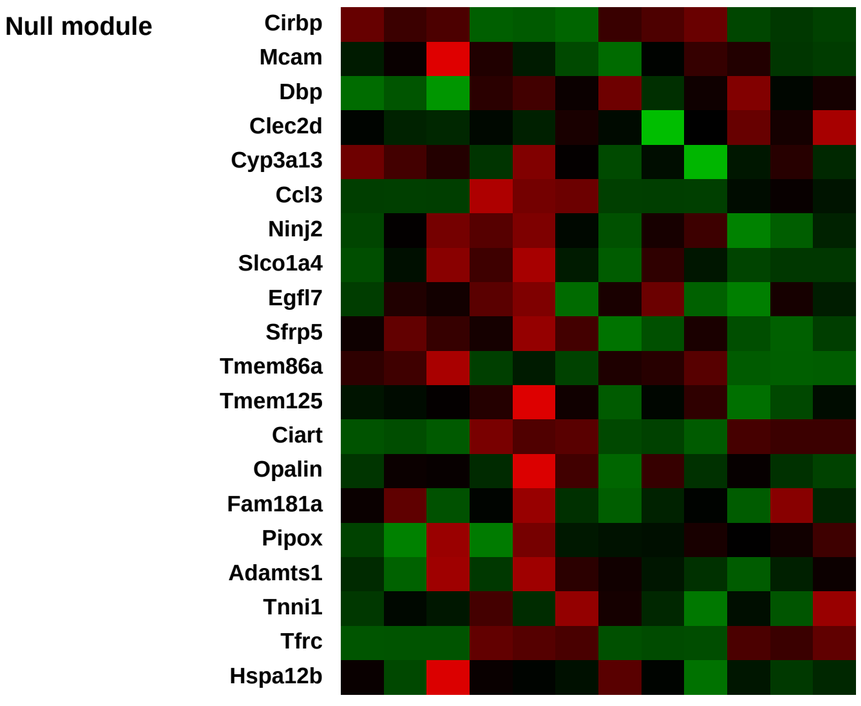

GEO Series "GSE10659" Expression Profiles

Num of samples in this series: 6

Scale of expression profile Z-scores

-3.0 -2.0 -1.0 0.0 1.0 2.0 3.0

GEO Link:	http://www.ncbi.nlm.nih.gov/geo/query/acc.cgi?acc=GSE10659
Status:	Public on Mar 17 2008
Title:	AFFYMETRIX ANALYSIS OF E9.5 RFC MOUSE KO EMBRYOS REVEALS ALTERED EXPRâ N OF GENES IN THE CUBILIN-MEGALIN COMPLEX
Organism:	Mus musculus
Experiment type:	Expression profiling by array
Platform:	GPL1261
Pubmed ID:	18400109
Summary & Design:	**Summary:** The reduced folate carrier (RFC1) is an integral membrane protein and facilitative anion exchanger that mediates delivery of 5-methyltetrahydrofolate into mammalian cells. Adequate maternal-fetal transport of folate is necessary for normal embryogenesis. Targeted inactivation of the murine RFC1 gene results in post-implantation embryo lethality, but daily folic acid supplementation of pregnant dams prolongs survival of homozygous embryos until mid-gestation. At E10.5 RFC1-/- embryos are developmentally delayed relative to wildtype littermates, have multiple malformations, including neural tube defects, and die due to failure of chorioallantoic fusion. The mesoderm is sparse and disorganized, and there is a marked absence of erythrocytes in yolk sac blood islands. Affymetrix microarray analysis and quantitative RT-PCR validation of the relative gene expression profiles in E9.5 RFC1-/- vs. RFC1+/+ embryos indicates a dramatic downregulation of multiple genes involved in erythropoiesis, and upregulation of several genes that form the cubilin-megalin multiligand endocytic receptor complex. Megalin protein expression disappears from the visceral yolk sac of RFC1-/- embryos, and cubilin protein is widely misexpressed. Inactivation of RFC1 impacts the expression of several ligands and interacting proteins in the cubilin-amnionless-megalin complex that are involved in the maternal-fetal transport of folate, vitamin B12, and other nutrients, lipids and morphogens required for normal embryogenesis. Comparison of RFC KO, wildtype normal embryos vs. RFC KO, nullizygous affected embryos Keywords: reduced folate carrier knockout, folate receptor, cubilin, megalin, embryos, gene expression, neural tube defect, chorioallantoic fusion **Overall design:** 6 samples RFC KO mouse embryos, E9.5, folic acid treated: 3 Control, Wildtype, normal; 3 Affected, Nullizygous, CR/chorioallantoic defect; as paired-littermates with one normal and one affected embryo per set from each of three separate litters for RNA extraction and hybridization on Affymetrix microarrays.

Background corr dist: KL-Divergence = 0.0372, L1-Distance = 0.0154, L2-Distance = 0.0002, Normal std = 0.6268

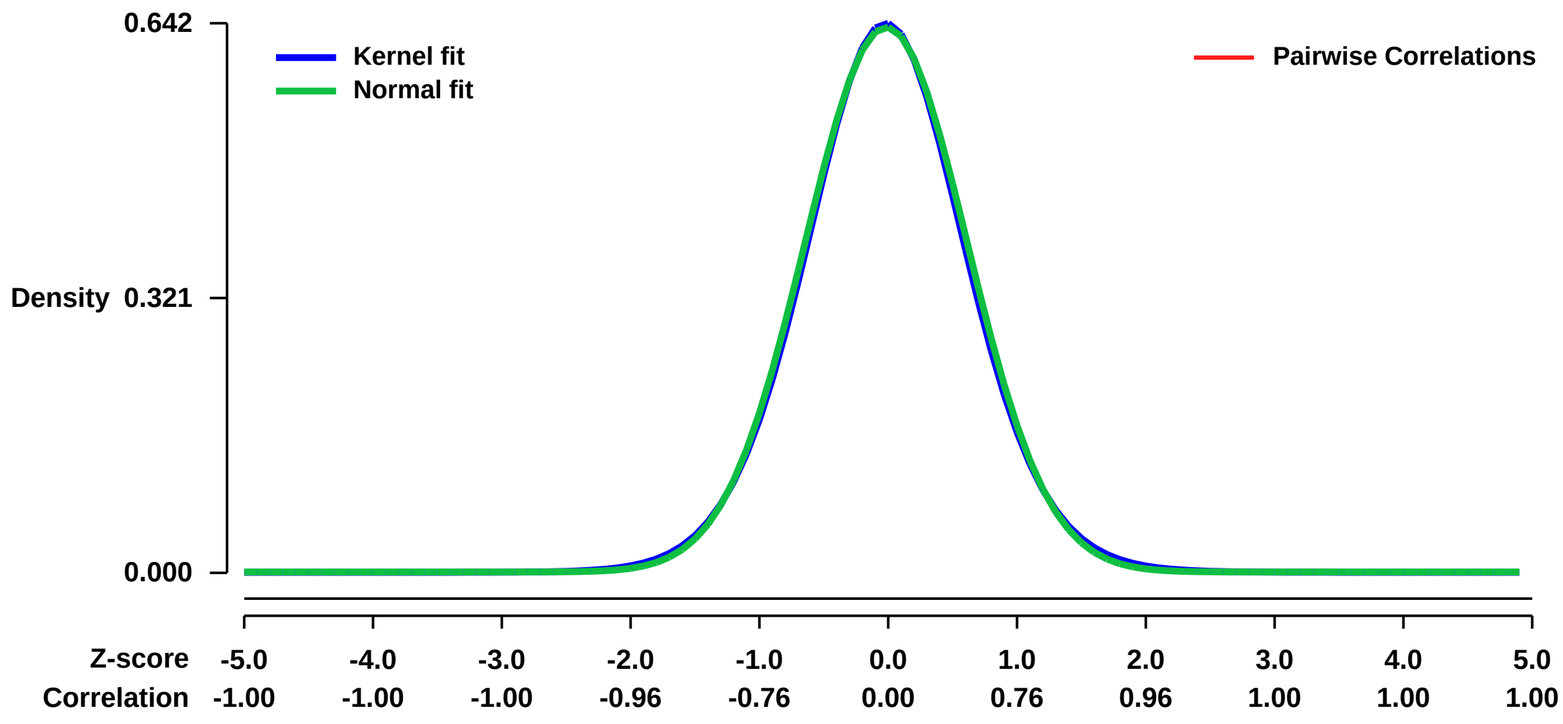

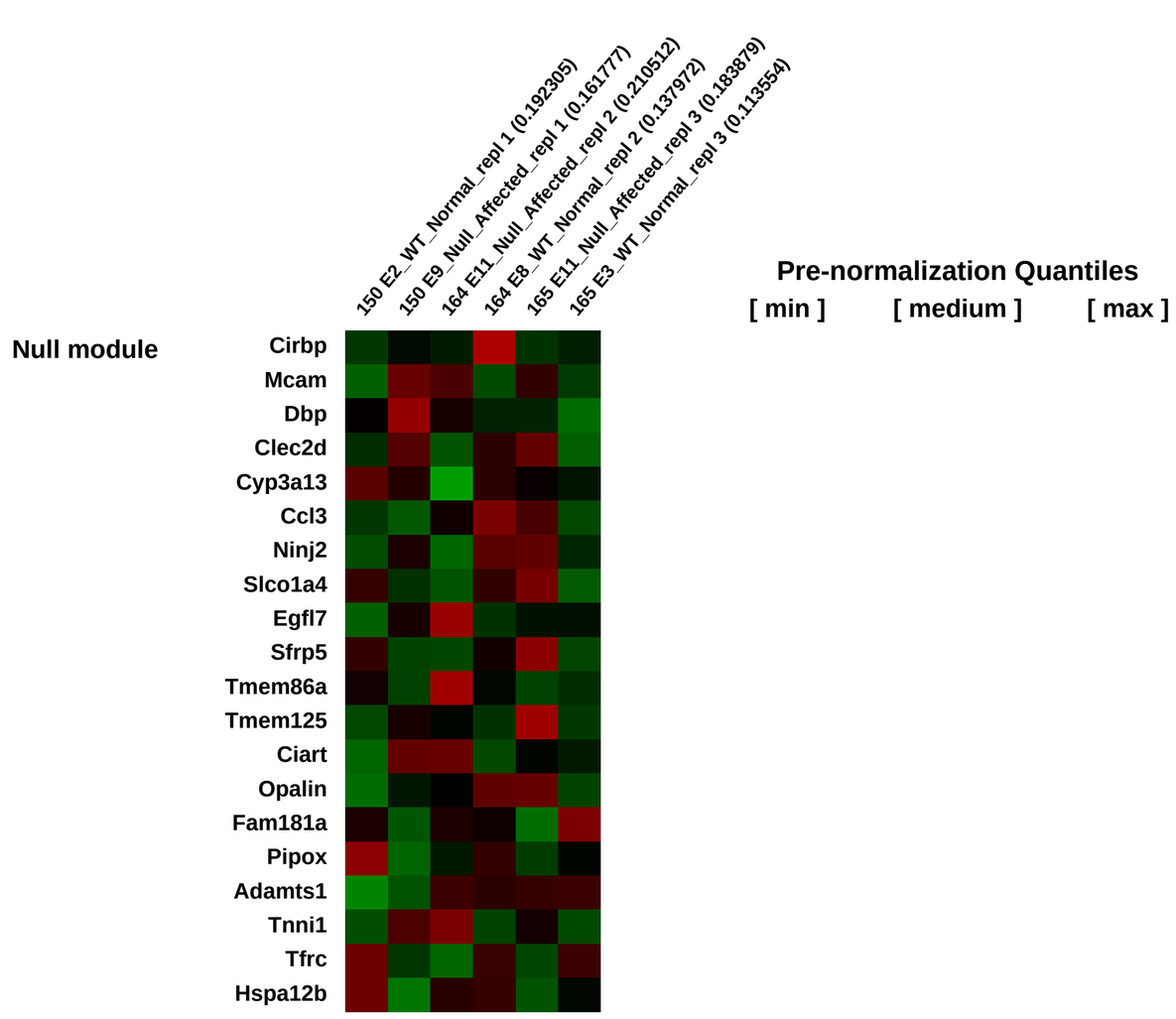

GEO Series "GSE20684" Expression Profiles

Num of samples in this series: 12

Scale of expression profile Z-scores

-3.0 -2.0 -1.0 0.0 1.0 2.0 3.0

GEO Link:	http://www.ncbi.nlm.nih.gov/geo/query/acc.cgi?acc=GSE20684
Status:	Public on Aug 25 2010
Title:	The gene encoding the hematopoietic stem cell regulator CCN3 (NOV) is under direct cytokine control through the transcription factors STAT5a/b.
Organism:	Mus musculus
Experiment type:	Expression profiling by array
Platform:	GPL1261
Pubmed ID:	20720003
Summary & Design:	**Summary:** Cytokines control the biology of hematopoietic stem and progenitor cells in part through the transcription factors STAT5a/b. CCN3/NOV has been reported as a positive regulator of hematopoietic stem and progenitor cells. We report microarray analyses of Lineage- Sca-1+ c-Kit+ (KSL) cells in the presence and absence of STAT5a/b. Expression of the ccn3 gene was induced over 100-fold in control, but not STAT5a/b-null cells, upon stimulation with a cocktail containing IL-3, IL-6, SCF, TPO and Flt3 ligand. Among the cytokines, IL-3 elevated ccn3 mRNA level in Lineage- c-Kit+ (KL) cells and 32D cells. ChIP assays using 32D cells revealed IL-3-induced binding of STAT5a/b to a GAS site in the ccn3 gene promoter. This is the first report to link two molecules with importance in the regulation of HSCs, CCN3 and STAT5a/b. We report that the regulation and expression of the ccn3 gene is directly controlled by IL-3 through the transcription factors STAT5a/b. **Overall design:** Six Control and Six Stat5a/b-null KSL cells, including three biological replications, were unstimulated or stimulated with a cocktail containing IL-3, IL-6, SCF, TPO and FL.

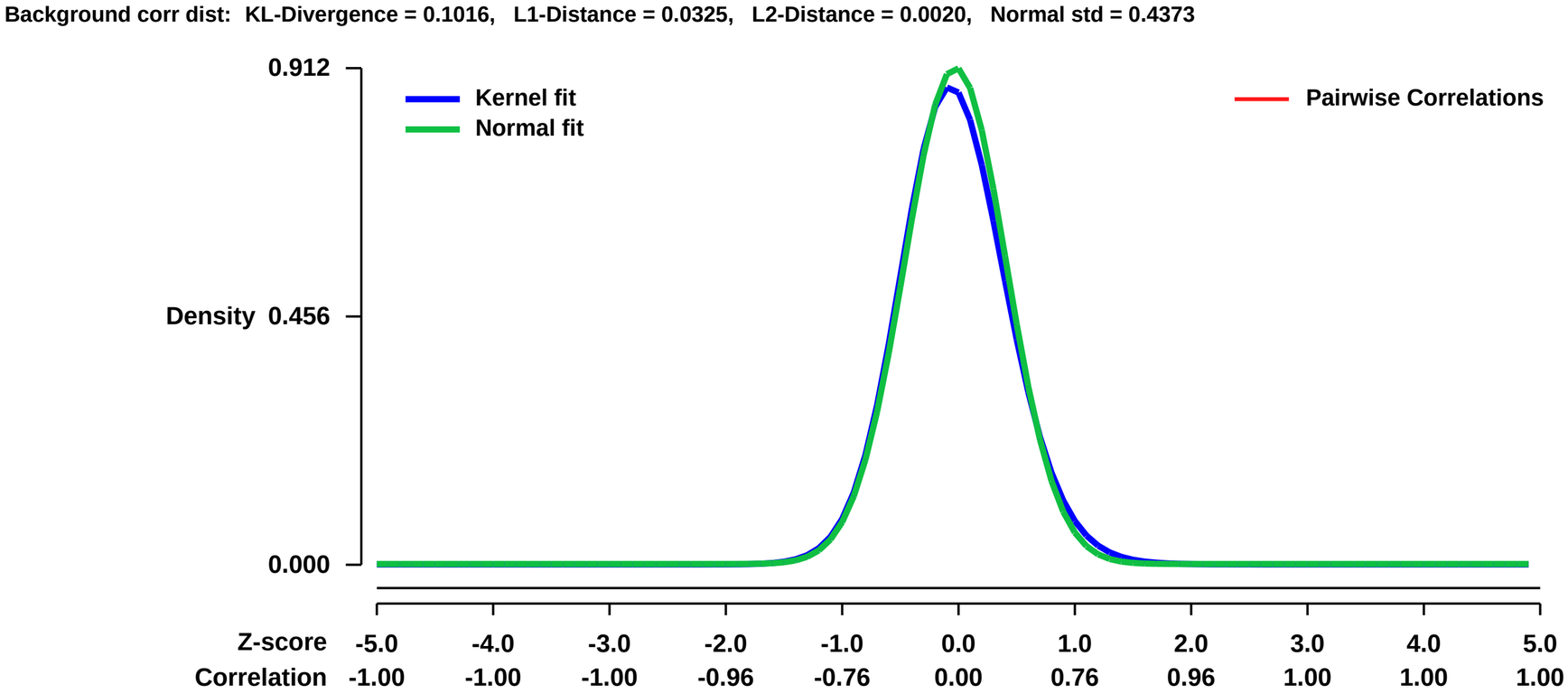

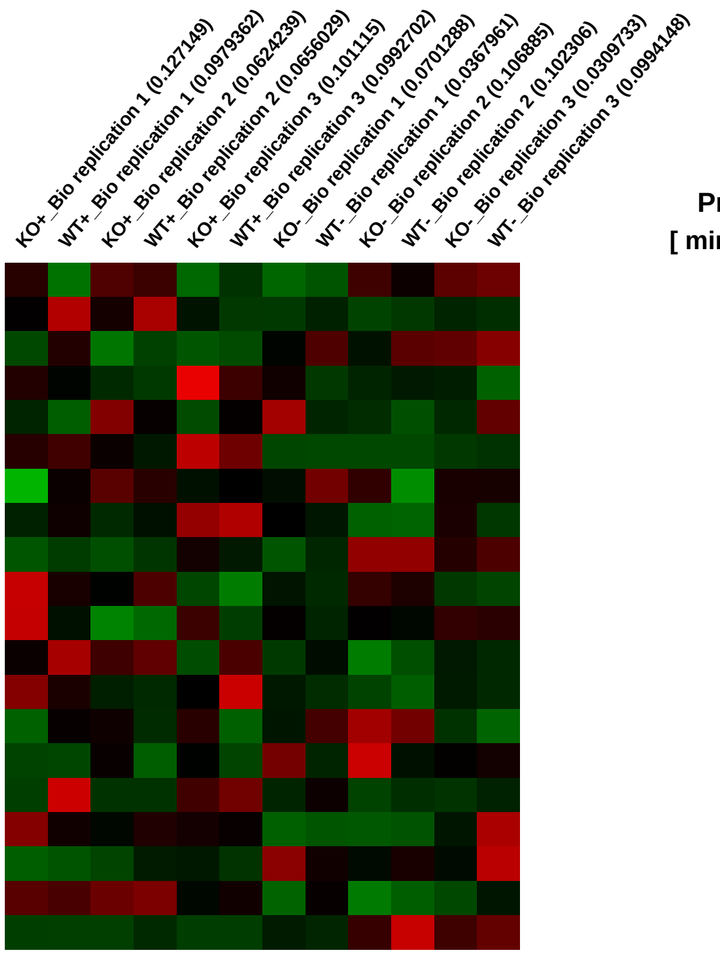

GEO Series "GSE16454" Expression Profiles

Num of samples in this series: 24

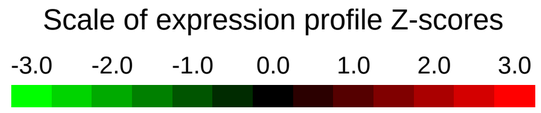

GEO Link:	http://www.ncbi.nlm.nih.gov/geo/query/acc.cgi?acc=GSE16454
Status:	Public on Dec 17 2009
Title:	Gene expression data from small intestines
Organism:	Mus musculus
Experiment type:	Expression profiling by array
Platform:	GPL1261
Pubmed ID:	20016602
Summary & Design:	**Summary:** Rb and E2F are thought to play antagonistic roles in celll proliferation. However, this model is based mostly from in vitro cell culture systems. We used small intestines to test this model in vivo. We found that deletion of E2f1-3 in the small intestine of mice suppressed the ectopic expression of E2F targets and cell proliferation caused by Rb-deficiency. Surprisingly, E2f1-3 deletion failed to arrest the proliferation of intestinal cells containing an intact Rb gene, and instead led to E2F target derepression and apoptosis. **Overall design:** Total RNA of crypts and villi from wild-type, Rb-/-, E2f1-/-, E2f2-/-, E2f3-/-, E2f1-/-, E2f2-/-, and E2f3-/- small intestines. Small intestines were harvested 7 days after mice were injected intraperitoneally with beta-napthoflavone.

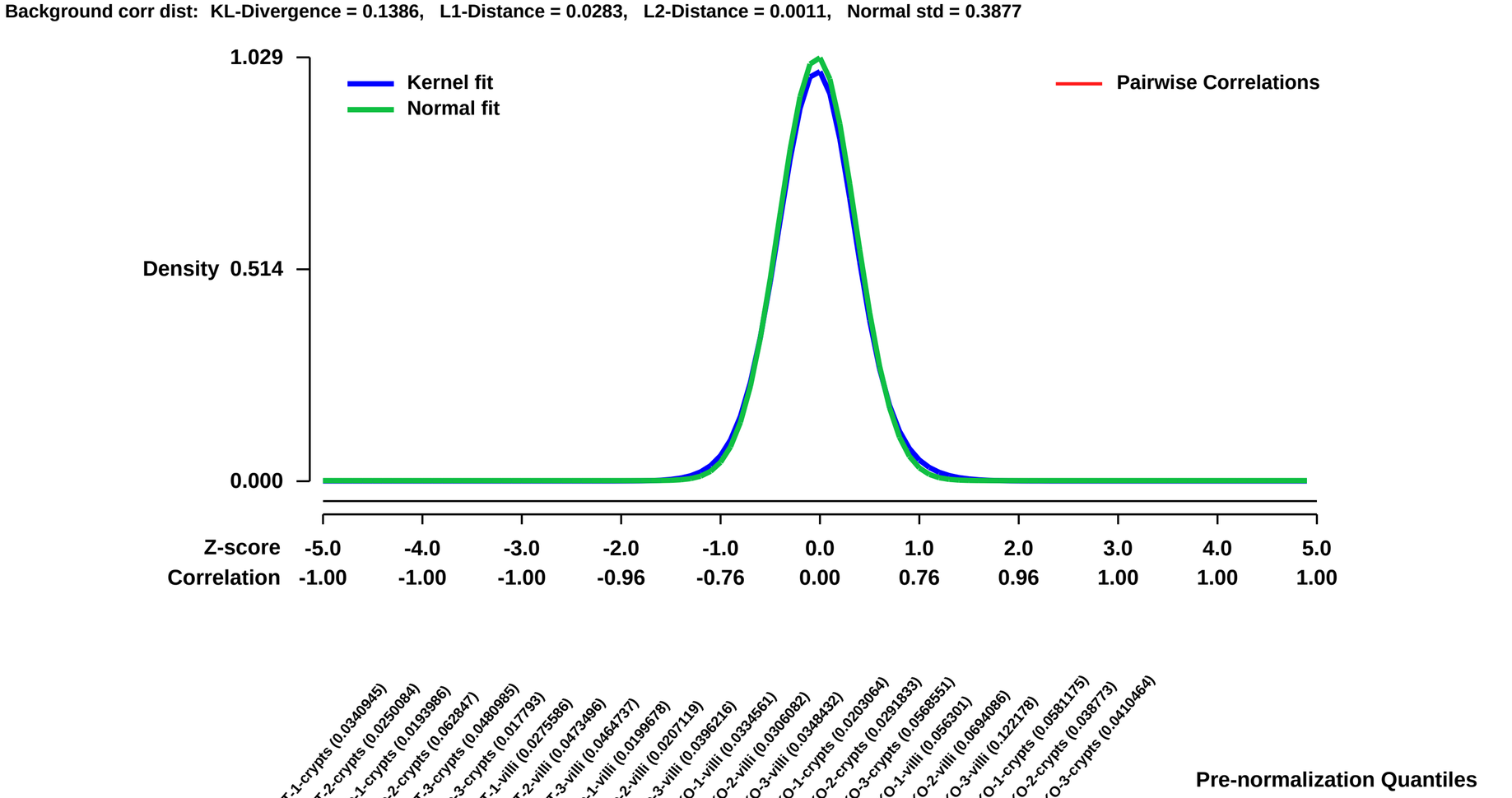

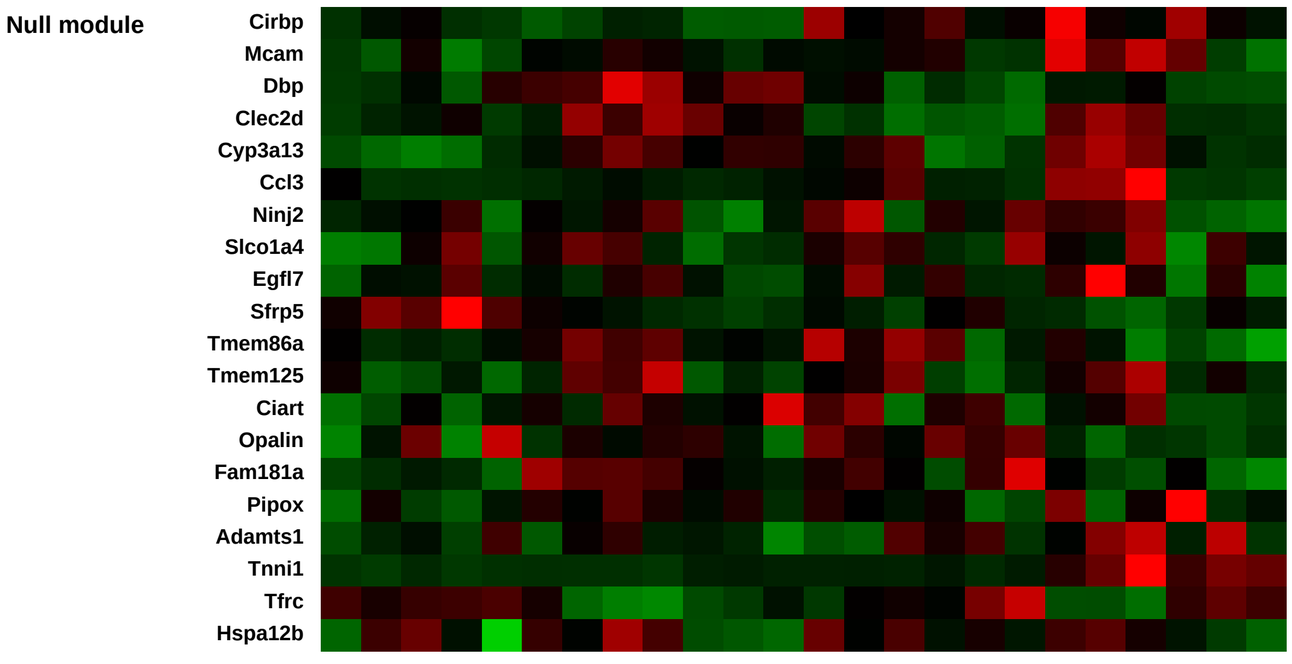

GEO Series "GSE42049" Expression Profiles

Num of samples in this series: 8

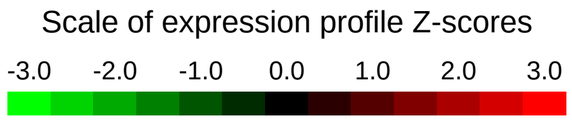

GEO Link:	http://www.ncbi.nlm.nih.gov/geo/query/acc.cgi?acc=GSE42049
Status:	Public on Oct 04 2013
Title:	TWEAK-treated time course in CAKI cells grown as xenografts
Organism:	Homo sapiens
Experiment type:	Expression profiling by array
Platform:	GPL1261
Pubmed ID:	23974006
Summary & Design:	**Summary:** Tumor necrosis factor-related weak inducer of apoptosis, TWEAK, is a TNF superfamily member that mediates signaling through its receptor fibroblast growth factor inducible-14, Fn14. In tumor cell lines, TWEAK induces proliferation, survival and NF-kappaB signaling and gene expression that promote tumor growth and suppress antitumor immune responses. Anti-TWEAK antibody, RG7212, inhibits tumor growth in vivo with decreases in pathway activation markers and modulation of tumor, blood and spleen immune cell composition. Candidate response prediction markers, including Fn14, have been identified in mouse models. Phase I pharmacodynamic data from patients are consistent with preclinical results. TWEAK:Fn14 signaling is upregulated in human cancer and pathway activation induces tumor proliferation and survival signaling. Blockade with anti-TWEAK mAb, RG7212, inhibits tumor growth in multiple models in mice. TWEAK induces changes that suppress anti-tumor immune responses and RG7212 blocks these effects resulting in changes in tumor immune cell composition and decreases in cytokines that promote immunosuppression. Antitumor efficacy in mice was observed in a range of Fn14 expressing models with pathway activation and expressing either wild-type or mutant p53, BRAF or KRAS suggesting both a patient selection strategy and potential broad clinical applicability. Preclinical mechanism of action hypotheses are supported by Phase I clinical data, with decreases in proliferation markers and increased tumor T cell infiltration. **Overall design:** CAKI cells impanted as xenografts in Athymic, Nu/Nu nude mice, treated with anti-TWEAK antibody (TW212) or Vehicle for 24 hours. Four replicates for each condition were performed. RNA was extracted from xenografts, processed and hybridized to human and mouse chips.

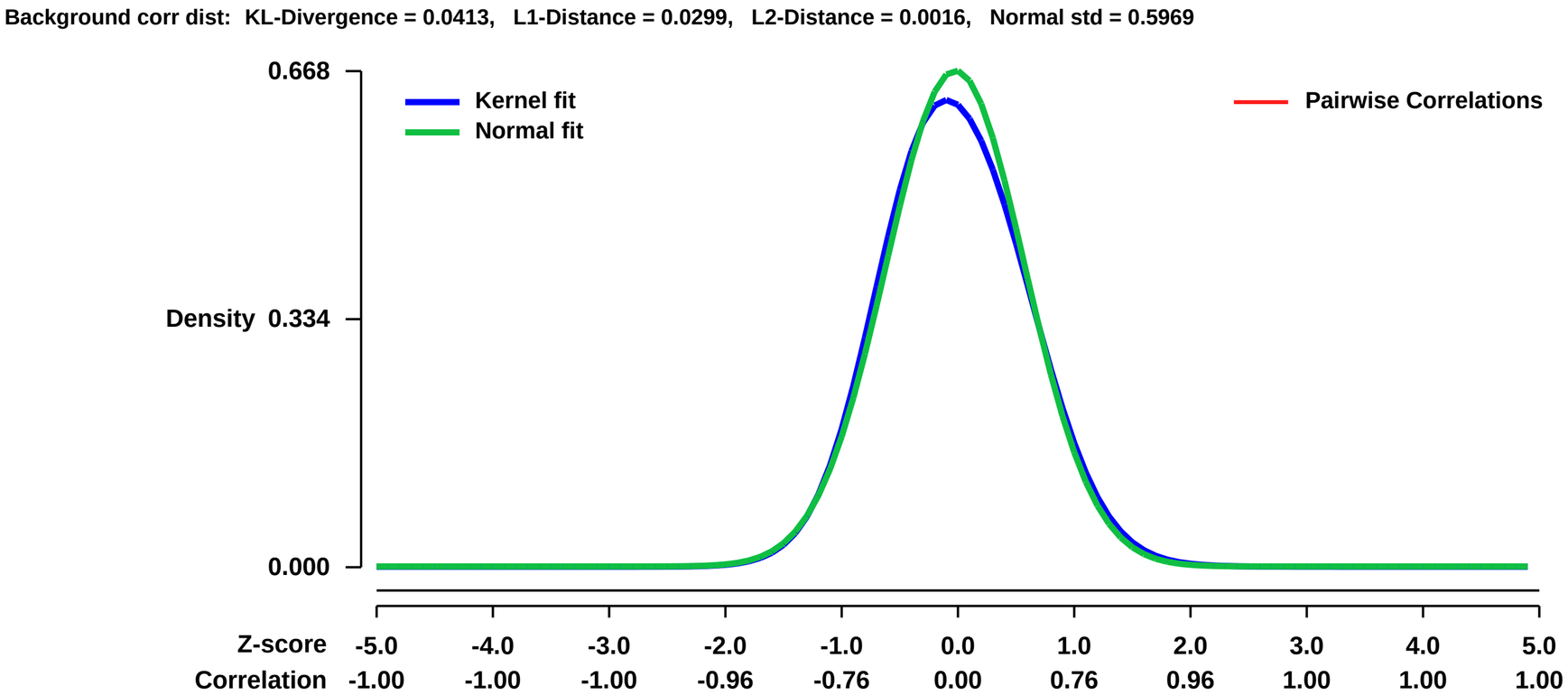

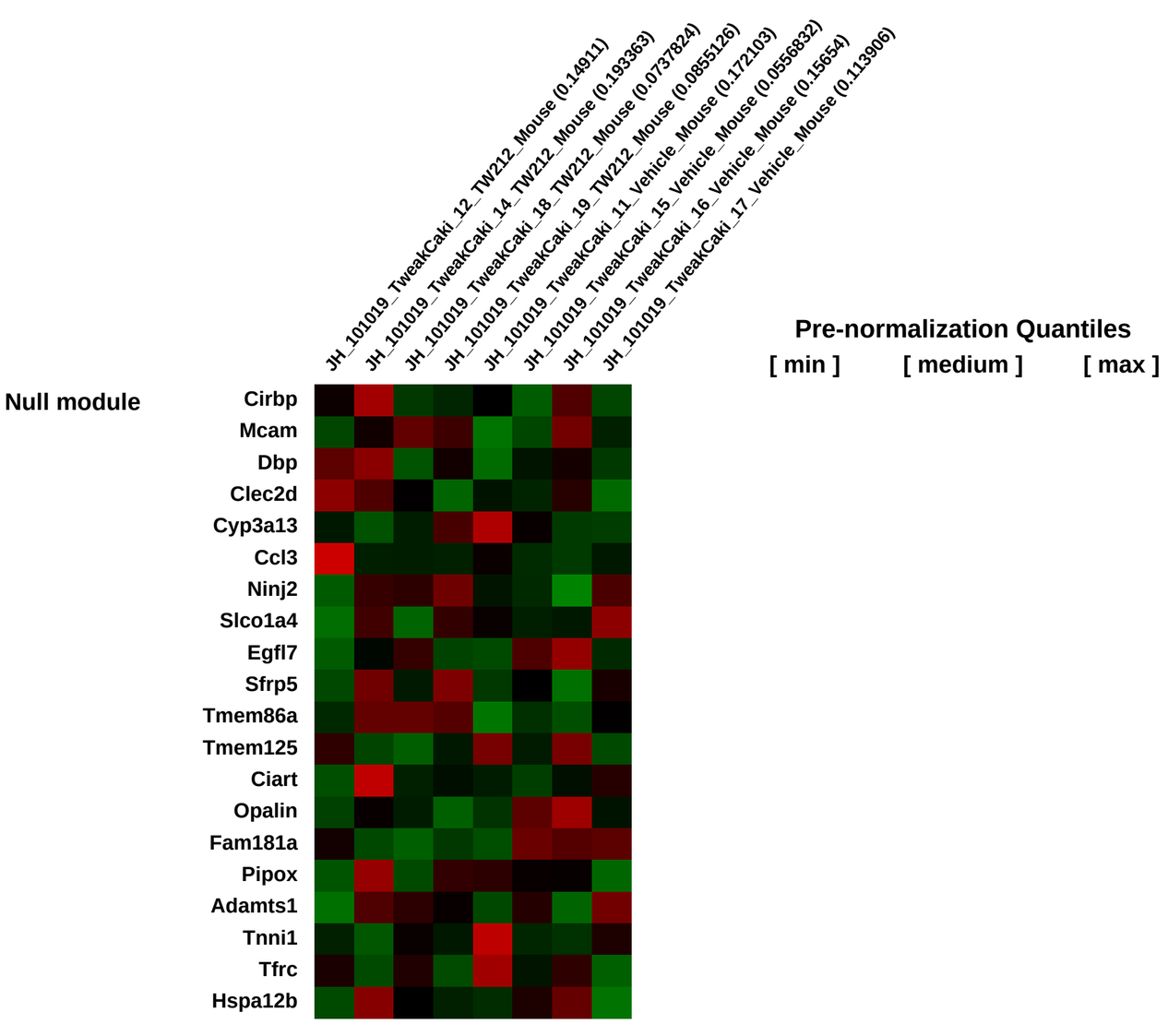

GEO Series "GSE7781" Expression Profiles

Num of samples in this series: 12

Scale of expression profile Z-scores

-3.0 -2.0 -1.0 0.0 1.0 2.0 3.0

GEO Link:	http://www.ncbi.nlm.nih.gov/geo/query/acc.cgi?acc=GSE7781
Status:	Public on Dec 25 2007
Title:	Impaired heart function in Apelin gene-deficient mice
Organism:	Mus musculus
Experiment type:	Expression profiling by array
Platform:	GPL1261
Pubmed ID:	17673668
Summary & Design:	**Summary:** The endogenous peptide Apelin is crucial for maintaining heart function in pressure overload and aging **Keywords: knockout** **Overall design:** Heart samples from Apelin knockout mice with pressure overload and sham control together with the wild-type mice with pressure overload and sham were compared

Background corr dist: KL-Divergence = 0.1597, L1-Distance = 0.0386, L2-Distance = 0.0030, Normal std = 0.3634

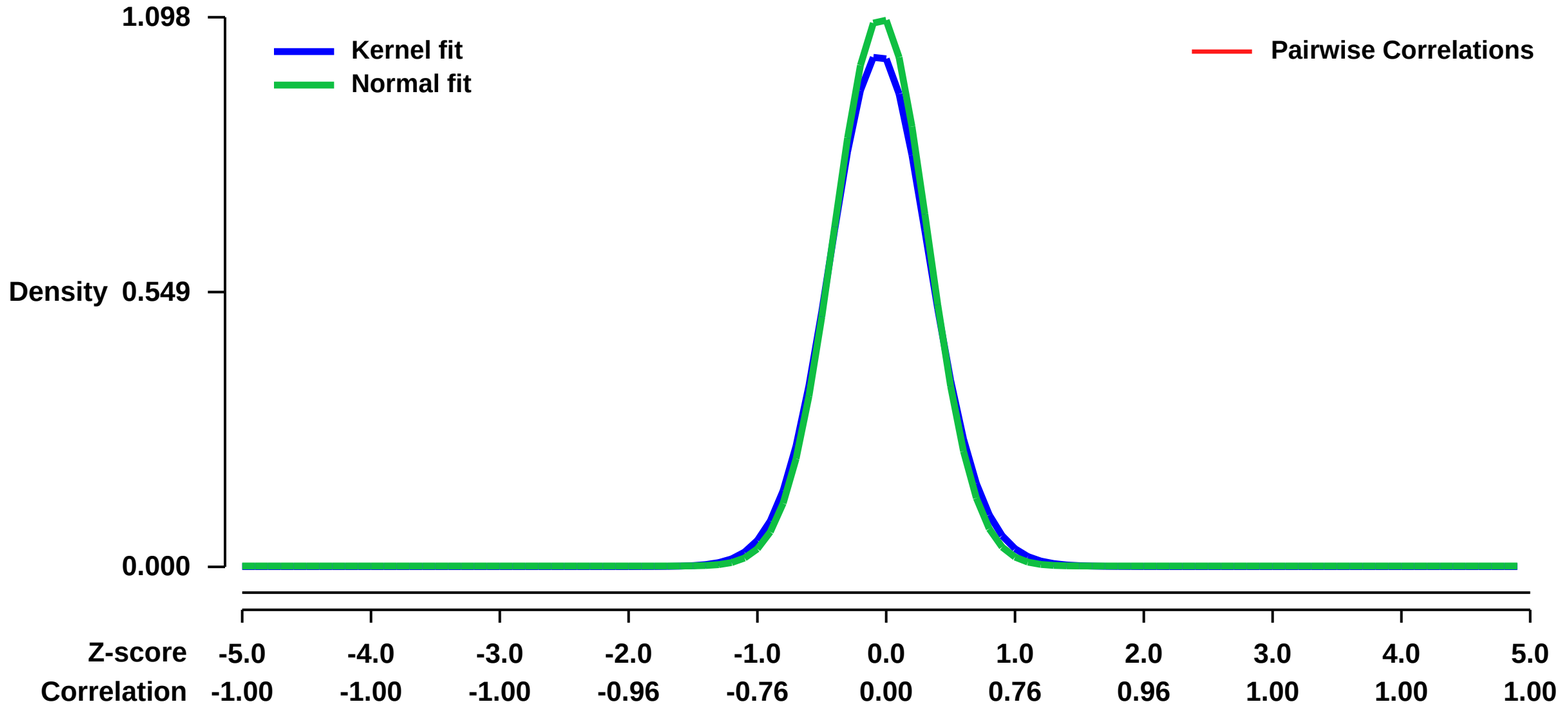

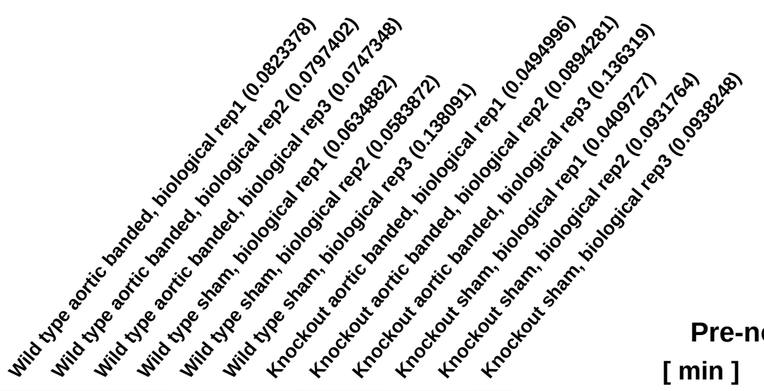

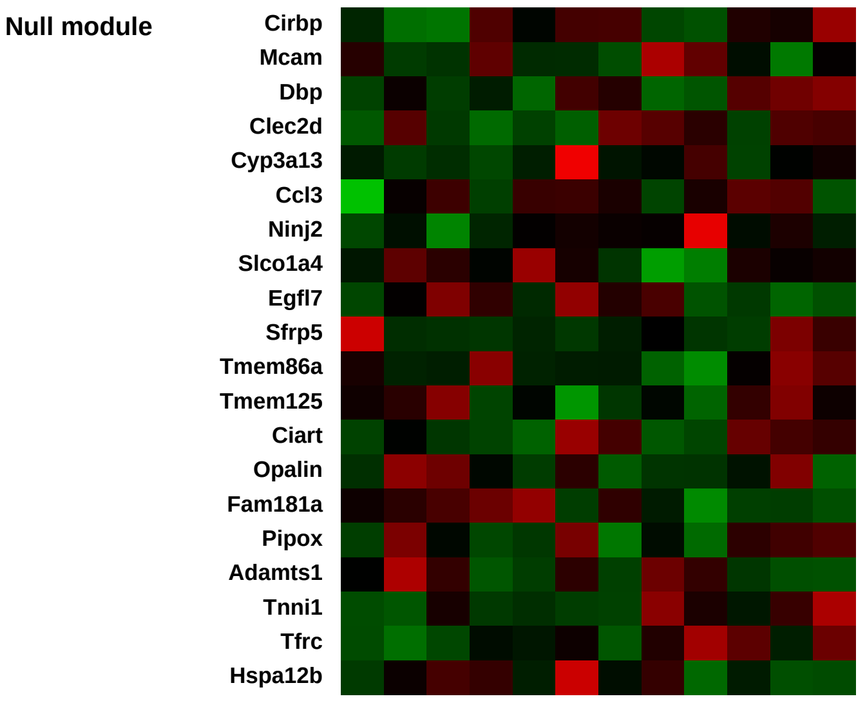

GEO Series "GSE6785" Expression Profiles

Num of samples in this series: 9

Scale of expression profile Z-scores

-3.0 -2.0 -1.0 0.0 1.0 2.0 3.0

GEO Link: http://www.ncbi.nlm.nih.gov/geo/query/acc.cgi?acc=GSE6785

Status: Public on Dec 15 2010

Title: Activation and Function of Alternatively and Classically Activated MH-S Alveolar Macrophages

Organism: Mus musculus

Experiment type: Expression profiling by array

Platform: GPL1261

Pubmed ID:

Summary & Design:

Summary:
Alveolar macrophages (AMs), the tissue dwelling monocytes of the lungs, are the first to encounter the menagerie of items that pass the mechanical barriers of the nose and throat. AMs must be able to mount an effective immune response against invading pathogens as well as maintain homeostasis in the lungs to avoid excessive inflammatory responses. In vivo data suggests that AMs can take on different phenotypes depending on the conditions of simulation. Limited progress has been made in defining the mechanisms responsible for these phenotypic issues largely due to logistical difficulties in isolating a sufficient number of cells from the lungs that have not been activated by the isolation protocol. To circumvent these logistical issues, an in vitro cell culture model was developed to study AM biology with specific emphasis on the generation of alternatively activated alveolar macrophages (AAAMs). Utilizing the BALB/c AM cell line MH-S it was determined that LPS could be used to generate classically activated AMs (CAAMs) and that IL-4 was effective in producing AAAMs. We examined the full transcriptome of AAAMs and CAAMs using microarray technology in an attempt to confirm previously described AAAM expression patterns and to identify new molecules associated with AM phenotypic change. AAAMs up-regulated an entirely distinct group of transcripts including genes encoding Arg1, Ym1 and a number of repair and remodeling genes whereas CAAMs up-regulated proinflammatory cytokines such as IL-1, IL-6 and IL-12. Additional novel markers are identified in this study to better characterize CAAMs and AAAMs in the lung.

Keywords: Characterization of Cell Type Based on Activation Stimulus

Overall design:
MH-S Cells (ATCC CRL-2019) were stimulated with either 50 ng/ml IL-4 or 1´µg/ml LPS and analyzed 12 hours later by whole genome DNA microarray analysis.

Background corr dist: KL-Divergence = 0.0806, L1-Distance = 0.0211, L2-Distance = 0.0007, Normal std = 0.4772

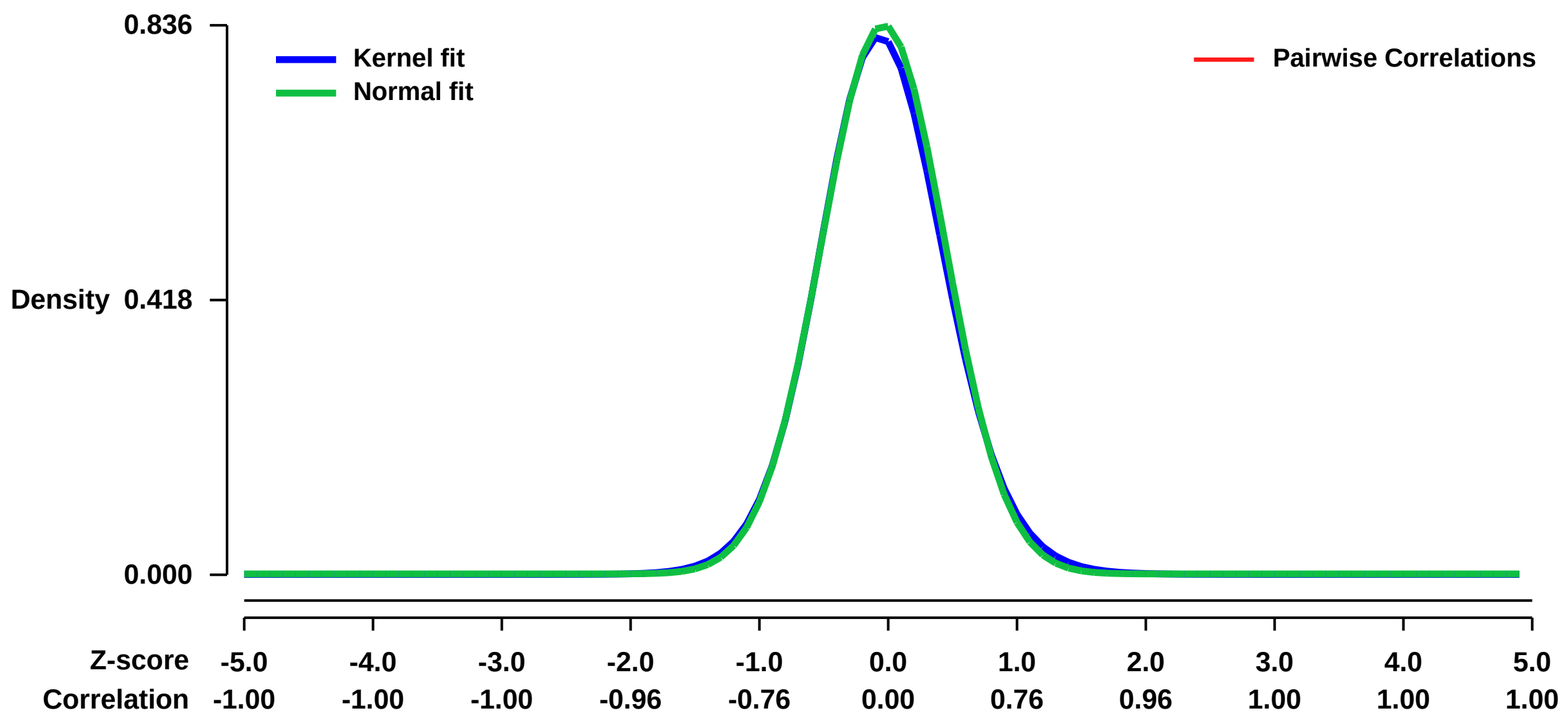

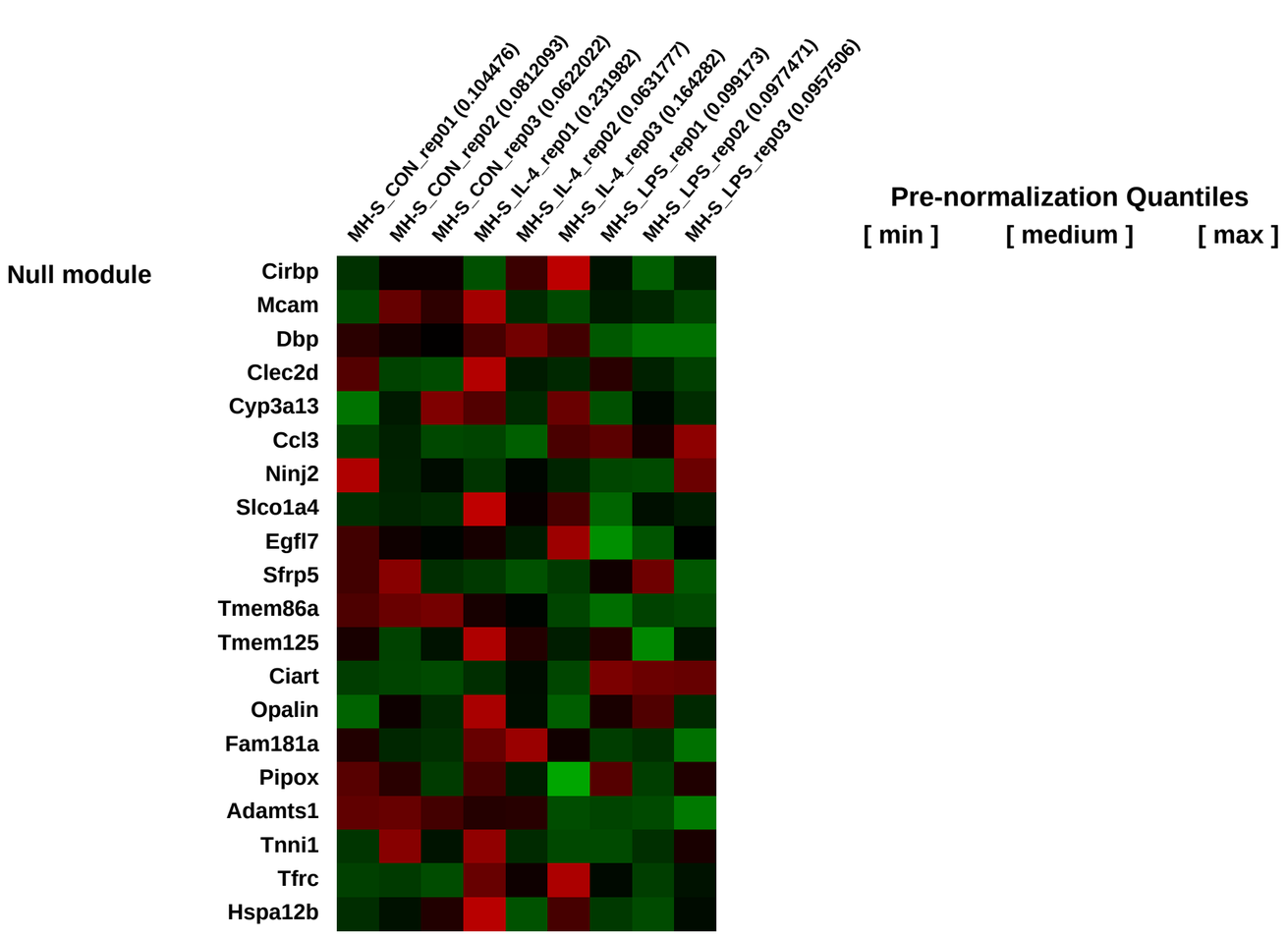

GEO Series "GSE54774" Expression Profiles

Num of samples in this series: 12

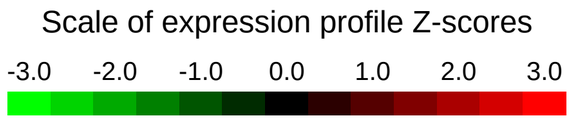

GEO Link:	http://www.ncbi.nlm.nih.gov/geo/query/acc.cgi?acc=GSE54774
Status:	Public on Jun 01 2014
Title:	Expression data from mice on a high fat, high carbohydrate diet treated with exenatide
Organism:	Mus musculus
Experiment type:	Expression profiling by array
Platform:	GPL1261
Pubmed ID:	
Summary & Design:	**Summary:** The present study was constructed to confirm previous findings that mice on a high fat diet (HFD) treated by subcutaneous injection with exenatide (EXE) at 3´¡g/kg once daily for 6 weeks develop exocrine pancreatic injury (Rouse et al. 2014). The present study included 12 weeks of EXE exposure at multiple concentrations (3, 10, or 30 ¸…g/kg) with multiple endpoints (histopathology evaluations, immunoassay for cytokines, immunostaining of the pancreas, serum chemistries and measurement of trypsin, amylase, and, lipase, and gene expression profiles). Time- and dose-dependent exocrine pancreatic injury was observed in mice associated with EXE exposure in a HFD environment. The time- and dose-dependent morphological changes identified in the pancreas involved acinar cell injury and death (autophagy, apoptosis, necrosis, and atrophy), cell adaptations (hypertrophy and hyperplasia), and cell survival (regeneration) accompanied with varying degrees of inflammatory response leading to secondary injury in pancreatic blood vessels, ducts, and adipose tissues. Gene expression profiles supported the presence of increased signaling for cell survival and altered lipid metabolism. The potential for EXE to cause acute or early chronic pancreatic injury was identified in a HFD environment. In human disease, the influence of pancreatitis risk factors or pre-existing chronic pancreatitis on this injury potential requires further investigation. **Overall design:** Male C57BL/6 mice 6 to 8 weeks of age were purchased from Harlan Laboratories (Frederick, MD). Mice were housed individually in an environmentally controlled room (18´℃â 21´℃, 40%â 70% relative humidity) with a twelve-hour light/dark cycle. Mice were initially fed Certified Purina Rodent Chow #5002 (Ralston Purina Co., St. Louis, MO) providing 63% of calories through carbohydrates, 24% from protein, and 13% from fat. Per the experimental design, mice were subsequently placed on a Teklad Custom Research Diet, TD.06415 (Harlan, Frederick, MD), providing 45% of calories through fats (36% saturated, 47% monounsaturated, 17% polyunsaturated), 36% from carbohydrates, and 19% from protein. Water and food were available ad libitum. Thorough out the experiment all mice were weighed weekly and dosing adjusted accordingly for each mouse. A cohort of eighty 6 to 8 week-old male C57BL6 mice were received from Harlan Laboratories. The cohort represented experimental time point of 12 weeks. The cohort was further divided into 4 exenatide (EXE) treatment groups (0, 3, 10, or 30 ¸…g/kg) of 20 mice each. Initially, all mice were placed on HFD for six weeks without additional treatment and were then maintained on HFD for an additional 12 weeks while receiving daily subcutaneous injections of saline or EXE (Creative Peptides, Shirley, NY; 3, 10, or 30¸…g/kg). At the 12 week timepoint, twenty-four hours following their final dose, the mice from the treatment cohort were anesthetized with isoflurane and euthanized by exsanguination with collection of blood for serum harvest. The pancreas from 12 mice in each cohort was preserved in 10% formalin for histology processing. The pancreas from 5 mice in each cohort was placed in RNAlater (Life Technologies, Grand Island, NY) for subsequent RNA extraction and the pancreas from 3 mice in each cohort was immediately frozen in liquid nitrogen and then stored at -80´℃. Pancreas tissue was resected, preserved in RNALater, and stored at -80 C. After thawing, 2.5 mg of each sample were processed using miRNeasy Mini Kits (Cat # 217004) (Qiagen, Valencia, CA). Samples were homogenized in 700 uL of Qiazol Lysis Reagent (Qiagen), for 5 minutes at 50 hz in a TissueLyser LT (Qiagen), and processed using the automated purification of total RNA on a Qiacube (Qiagen), using the â Purification of total RNA, including small RNAs, from animal tissues & cells (aqueous phase), version 2 (April 2010)â standard protocol, as described in the miRNeasy Mini Handbook (1073008 07/2012) & http://www.qiagen.com/QIAcube/Standard/ProtocolView.aspx?StandardProtocolID=847.Mean yield per 2.5 mg of pancreas tissue was approximately 35 ug, determined by NanoDrop spectrophotometer (Thermo Scientific, Wilmington, DE). Average RIN values were approximately 5.4 +/- 1.4, as assayed by a 2100 Bioanalyzer Instrument (Agilent Technologies, Santa Clara, CA), using an Agilent RNA 6000 Nano Kit (cat # 5067-1511). This RIN mean was consistent with our previous experiences in RNA extraction from murine pancreatic tissue. The isolated RNA was labeled and gene expression analysis performed by Expression Analysis, Inc. (Durham, NC). The 3 samples with the highest RIN from each treatment group were used to probe treatment effect on gene expression. Total RNA samples (100 ng) were converted into cDNA using Ovation WGA FFPE System (NuGEN, Part No. 6200). The second strand cDNA is then purified with Agencourt RNAClean beads and followed by SPIA amplification. Amplified SPIA cDNA product is purified using Agencourt RNAClean beads and quantitated using a NanoDrop ND-8000 spectrophotometer. Target preparation was performed using 4 ¸…g of amplified cDNA and the NuGEN FL-Ovation cDNA Biotin Module V2. Fragmented and biotin-labeled target was hybridized to Affymetrix GeneChip Mouse Genome 430 2.0 microarrays. Raw gene expression data were first analyzed using ArrayTrack bioinformatics tool with robust multichip average algorithm and quantile normalization. Differentially expressed genes were defined by $p < 0.05$ and fold change > 1.3 in Welch t-test comparing treatment and control groups. Expression data were then imported to Ingenuity Pathway Analysis (IPA) tool for further analyses of pathway, biofunction, and toxicity using general and pancreas-specific knowledge bases.

Background corr dist: KL-Divergence = 0.1265, L1-Distance = 0.0189, L2-Distance = 0.0006, Normal std = 0.4217

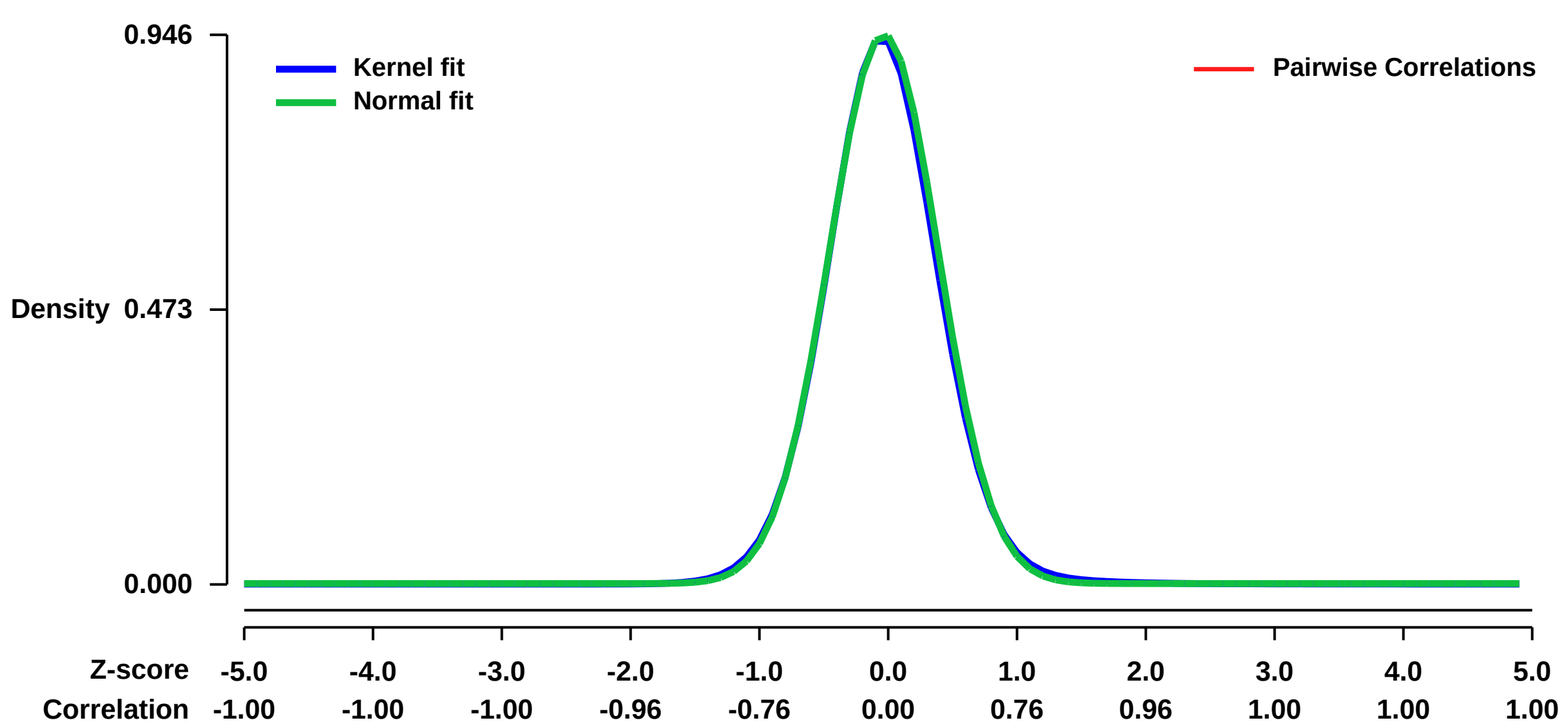

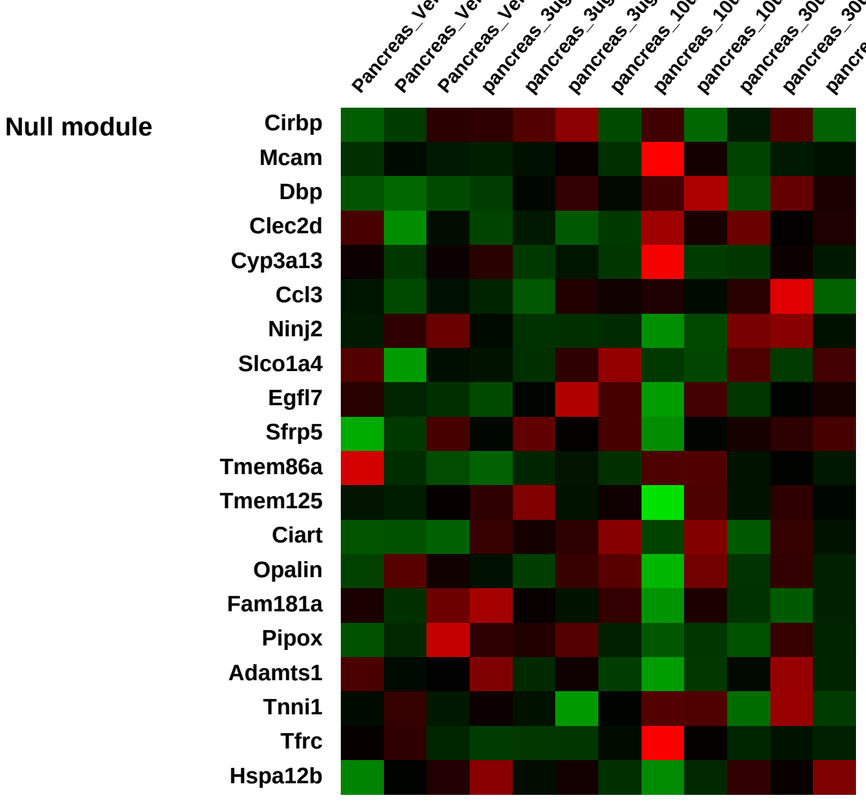

GEO Series "GSE15624" Expression Profiles

Num of samples in this series: 12

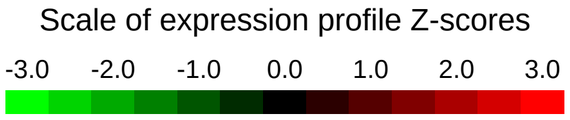

GEO Link:	http://www.ncbi.nlm.nih.gov/geo/query/acc.cgi?acc=GSE15624
Status:	Public on Apr 10 2009
Title:	Regulation of T cell gene expression by Halofuginone (HF)
Organism:	Mus musculus
Experiment type:	Expression profiling by array
Platform:	GPL1261
Pubmed ID:	19498172
Summary & Design:	**Summary:** T cell differentiation to the Th17 effector subset requires stimulation through the T cell and co-stimulatory receptors, together with cytokine stimulation by TGFb and IL-6. The small molecule halofuginone (HF) inhibits Th17 cell development and induces a pattern of stress-regulated gene expression that mimics amino acid starvation. We used global transcript profiling to ask how halofuginone modulates gene expression induced during T cell activaiton and Th17 differentiation Keywords: T cell activation/ differentiation timecourse **Overall design:** Purified mouse CD4+ CD25- T cells were activated under Th17 polarizing cytokine conditions and treated with either halofuginone or its inactive derivative, MAZ1310, for 3- or 6-hours.

Background corr dist: KL-Divergence = 0.0801, L1-Distance = 0.0252, L2-Distance = 0.0011, Normal std = 0.4730

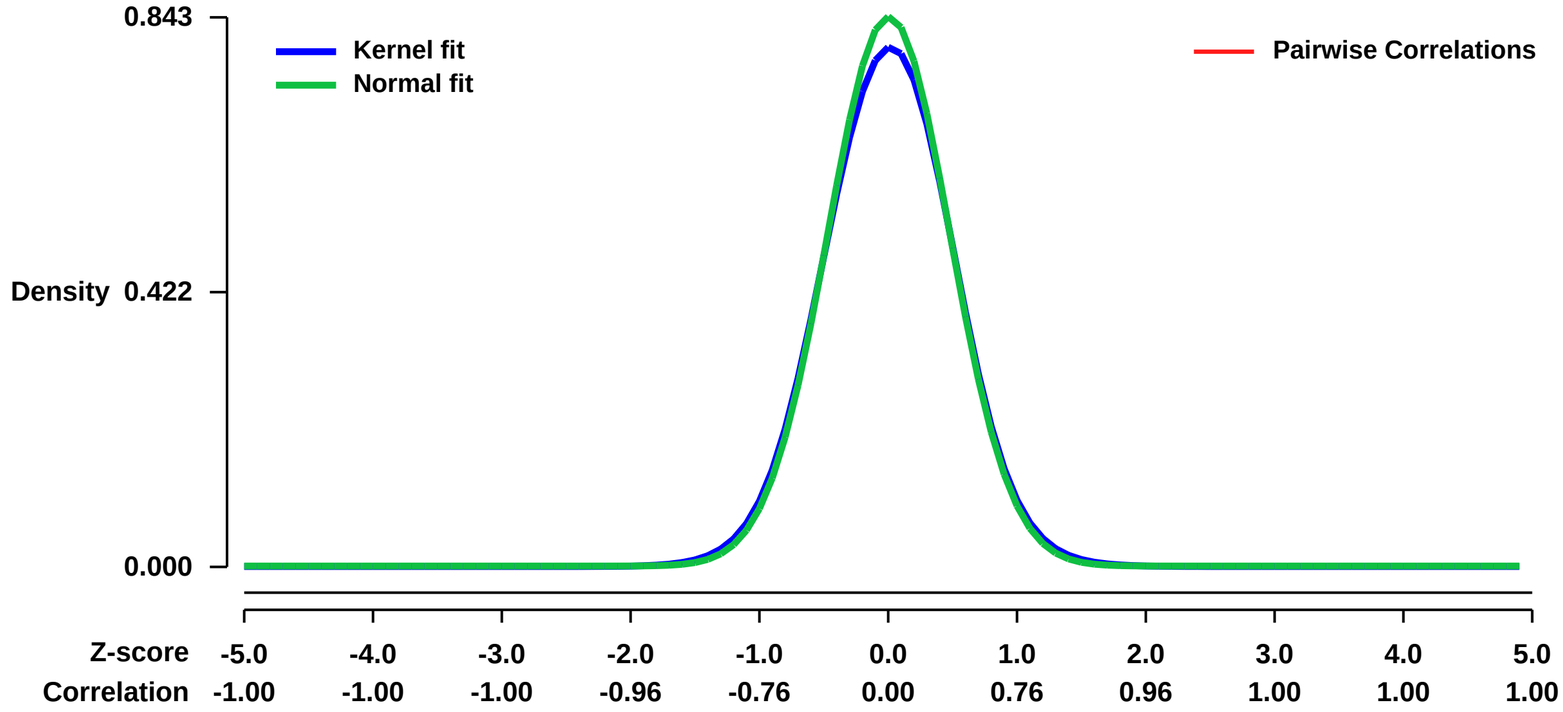

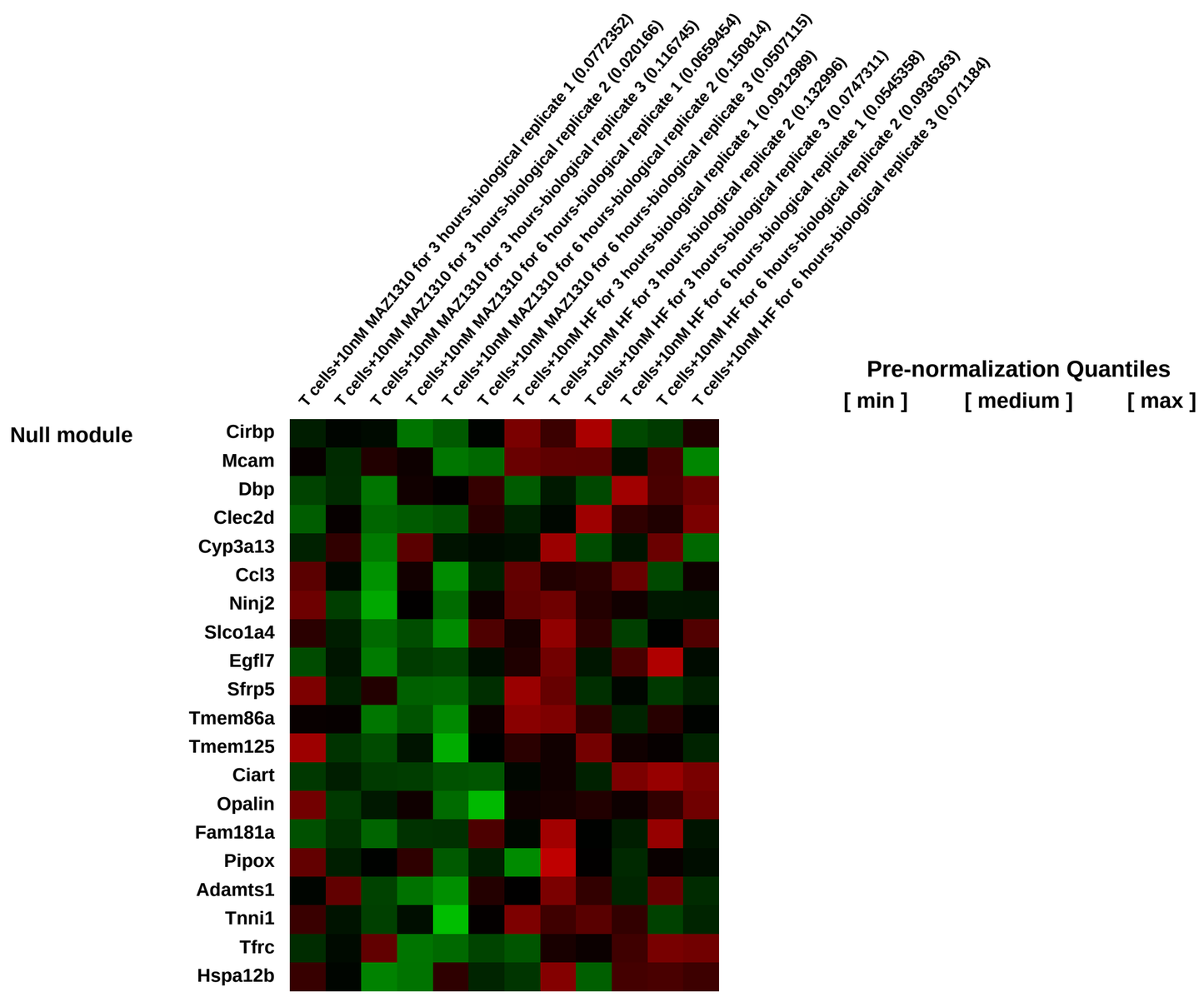

GEO Series "GSE20513" Expression Profiles

Num of samples in this series: 12

Scale of expression profile Z-scores

-3.0 -2.0 -1.0 0.0 1.0 2.0 3.0

GEO Link:	http://www.ncbi.nlm.nih.gov/geo/query/acc.cgi?acc=GSE20513
Status:	Public on Jun 15 2010
Title:	Expression data from (bezafibrate treated-wild type, Clock mutant, and PPARalpha-null) mouse liver
Organism:	Mus musculus
Experiment type:	Expression profiling by array
Platform:	GPL1261
Pubmed ID:	20400680
Summary & Design:	**Summary:** A functional interaction between peroxisome proliferator-activated receptor alpha (PPARalpha) and components of the circadian clock has been suggested; however, it remains to be clarified whether those transcriptional factors interact with each other to regulate the expression of their target genes. In this study, we used a ligand of PPARalpha, bezafibrate, to search the PPARalpha-regulated genes that express in a CLOCK-dependent circadian manner. Microarrays analyses using hepatic RNA isolated from bezafibrate treated-wild type, Clock mutant (Clk/Clk), and PPARalpha-null mice revealed that 136 genes are transcriptionally regulated by PPARalpha in a CLOCK-dependent manner. **Overall design:** To examine the PPARalpha-regulated genes that express in a CLOCK-dependent manner in mice, we performed oligonucleotide microarray analysis at ZT14, when CLOCK/BMAL1 transcriptional activity is maximal, using RNA isolated from wild-type (n = 3), Clock mutant (n = 3), and PPARalpha-null mice (n = 3) treated with bezafibrate for 5 days, and control wild-type mice (n = 3). Livers were collected and frozen in liquid nitrogen. Total RNA (250 ng) was extracted using RNAiso.

Background corr dist: KL-Divergence = 0.0812, L1-Distance = 0.0202, L2-Distance = 0.0004, Normal std = 0.4749

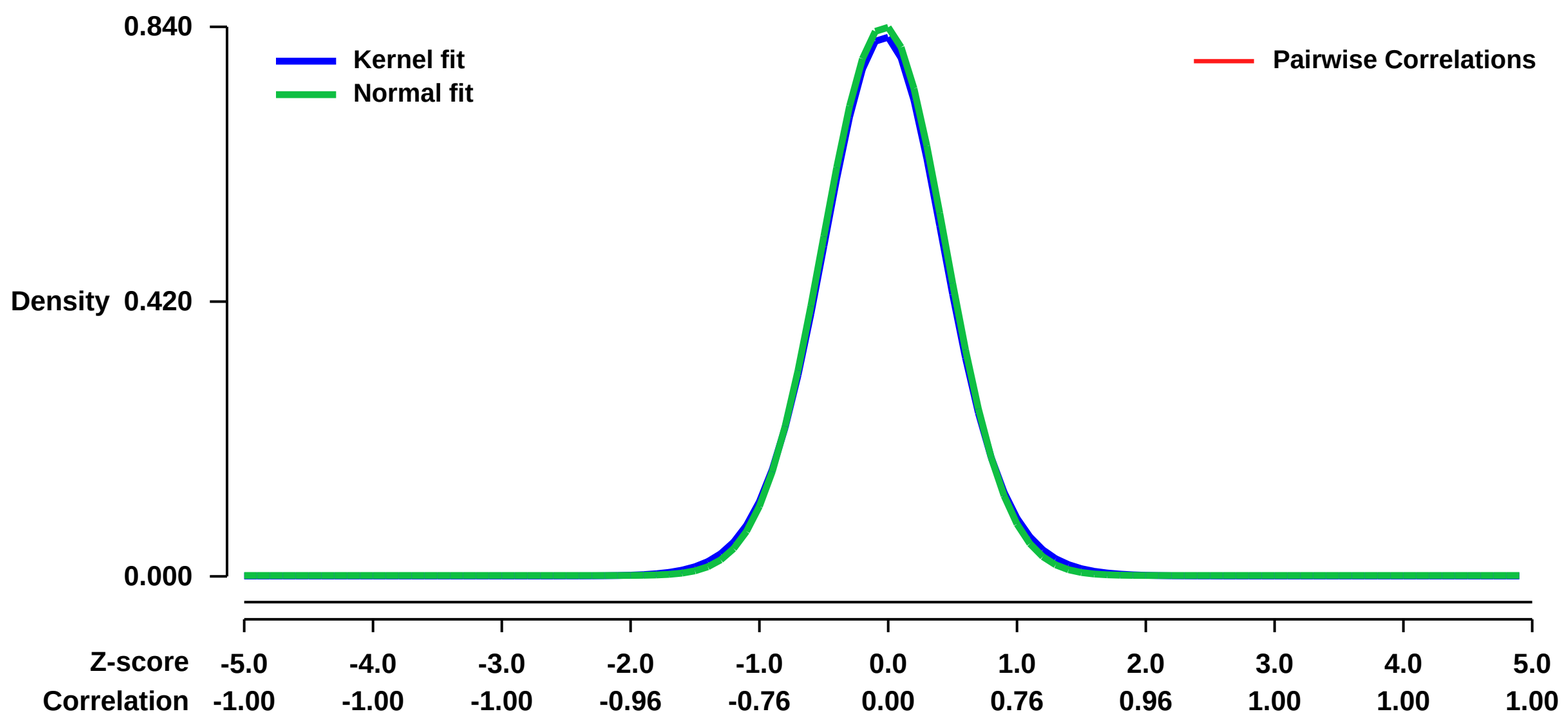

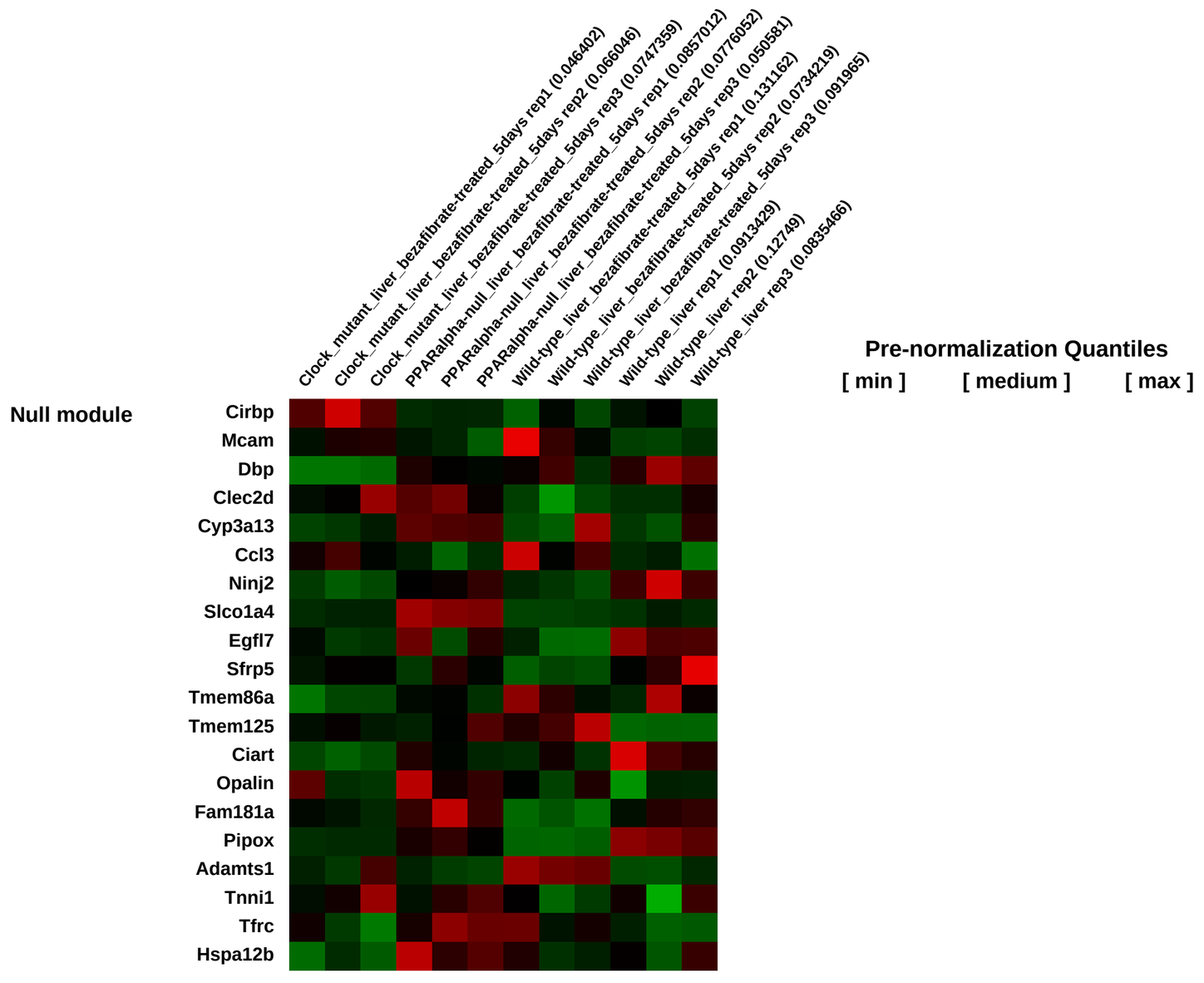

GEO Series "GSE10904" Expression Profiles

Num of samples in this series: 6

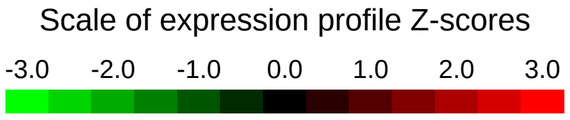

GEO Link:	http://www.ncbi.nlm.nih.gov/geo/query/acc.cgi?acc=GSE10904
Status:	Public on Apr 30 2008
Title:	Expression data from wildtype and alb/cre liver-conditional Pdss2 knockout mutant mice
Organism:	Mus musculus
Experiment type:	Expression profiling by array
Platform:	GPL1261
Pubmed ID:	18437205
Summary & Design:	**Summary:** Utilizing M. musculus as a model of mitochondrial dysfunction provides insight into cellular adaptations which occur as a consequence of genetic alterations causative of human disease. We characterized genome-wide expression profiles of liver-conditional knockout mice for Pdss2 compared with loxP controls. Our goal was to detect concordant changes among clusters of genes that comprise defined metabolic pathways utilizing gene set enrichment analysis. Keywords: Wildtype vs mutant comparison as a method for studying contributors to disease processes. **Overall design:** Liver from three biological replicates each of wildtype and coenzyme Q biosynthetic mutant M. musculus were used as sources of total RNA for hybridization to Affymetrix whole-genome microarrays. Comparison of the data was intended to reveal metabolic pathway alterations downstream of the mutation.

Background corr dist: KL-Divergence = 0.0183, L1-Distance = 0.0199, L2-Distance = 0.0005, Normal std = 0.7615

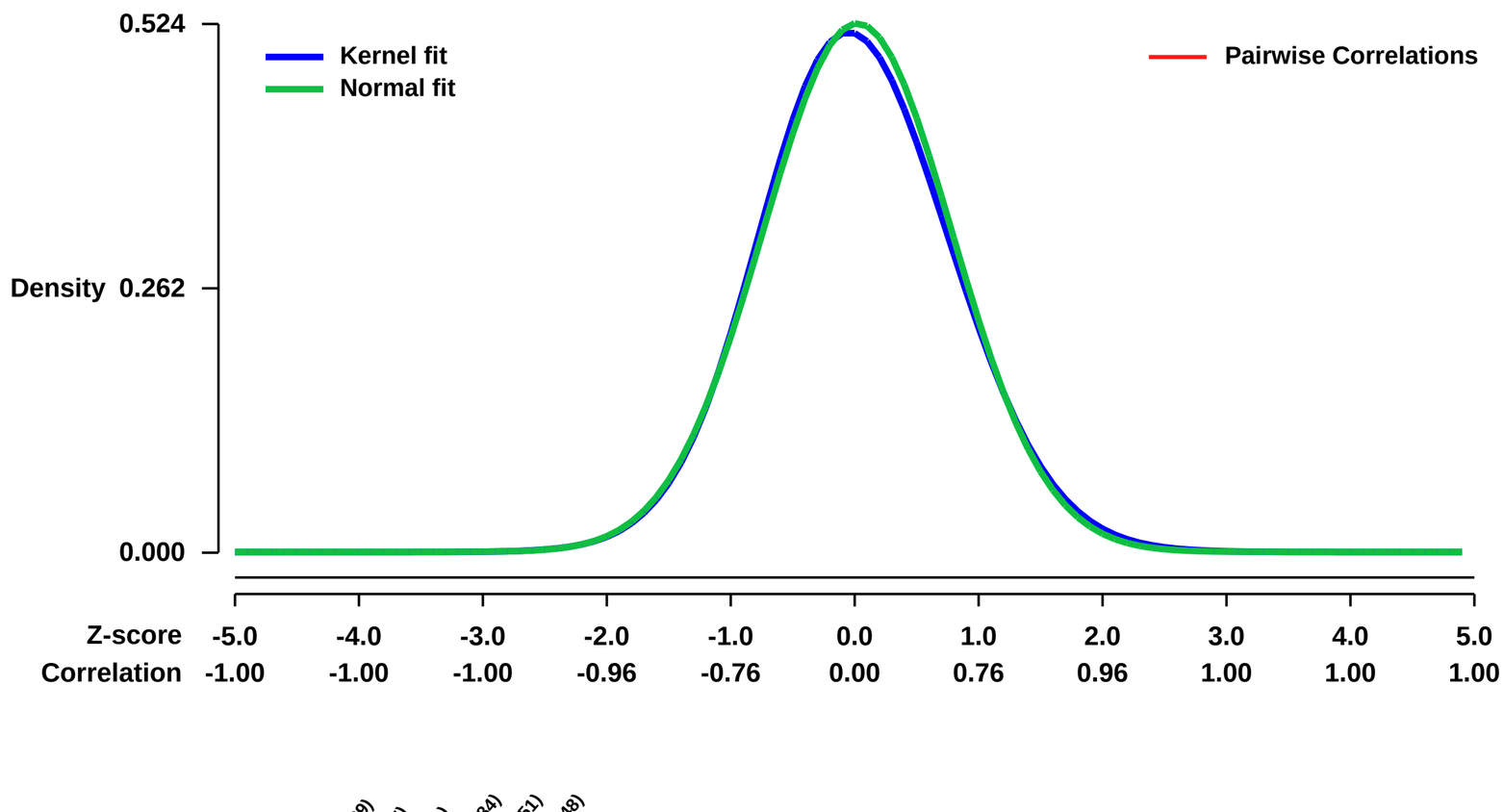

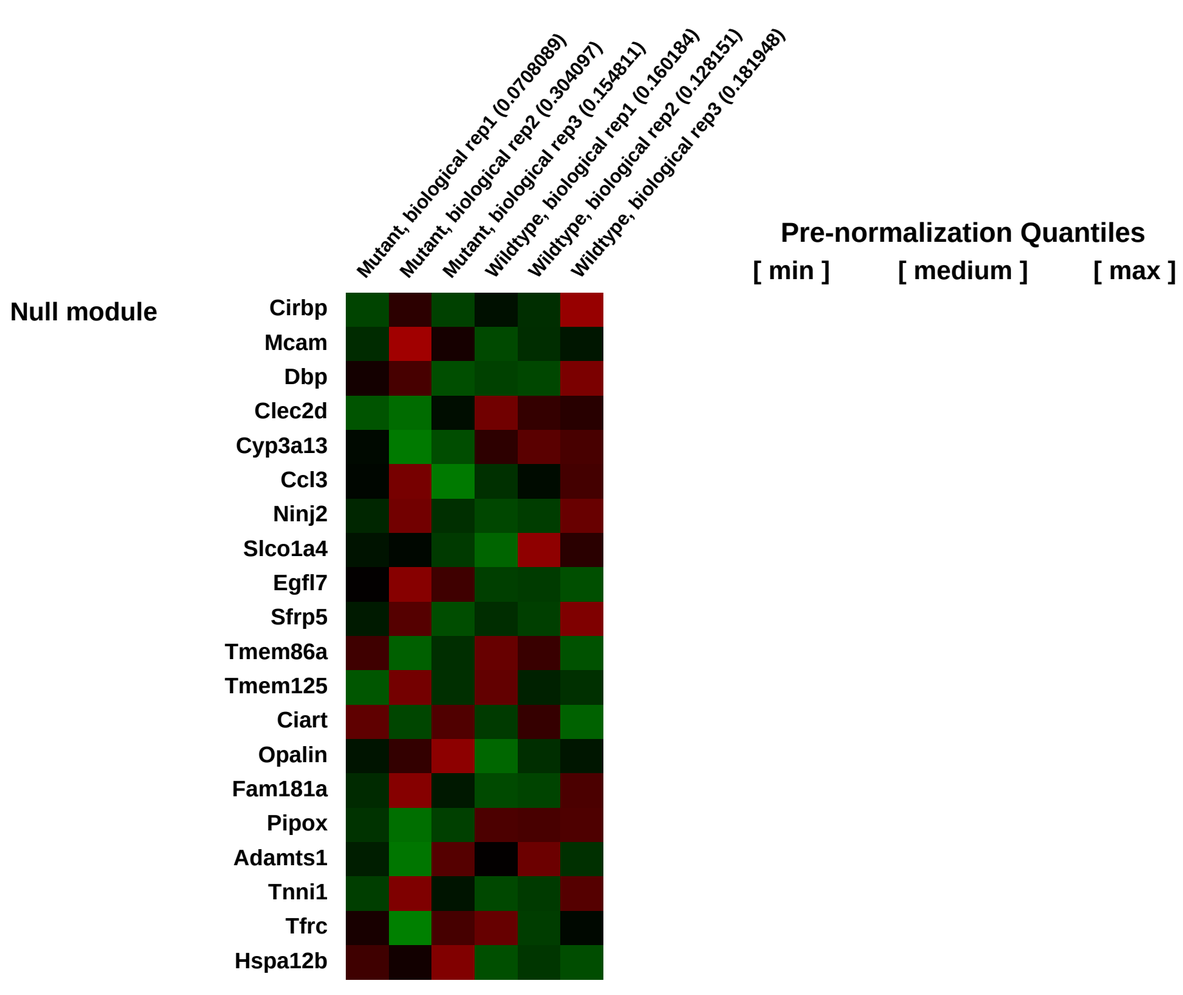

GEO Series "GSE46211" Expression Profiles

Num of samples in this series: 18

Scale of expression profile Z-scores

-3.0 -2.0 -1.0 0.0 1.0 2.0 3.0

GEO Link:	http://www.ncbi.nlm.nih.gov/geo/query/acc.cgi?acc=GSE46211
Status:	Public on Oct 01 2013
Title:	Gene expression profiling of anterior and posterior palatal tissue from Tgfbr2 mutant mouse models
Organism:	Mus musculus
Experiment type:	Expression profiling by array
Platform:	GPL1261
Pubmed ID:	24496627
Summary & Design:	**Summary:** The overall goal of this project is to investigate the role of TGF-beta signaling in epithelial cells as it pertains to the orientation of muscle fibers in the soft palate during embryogenesis. Here, we first conducted gene expression profiling of the anterior and posterior portions of the palate from wild-type mice. In addition, we also conducted gene expression profiling of the posterior palate in mutant mice with an epithelium-specific conditional inactivation of the Tgfbr2 gene. The latter mice provide a model of submucosal cleft palate, which is a congenital birth defect commonly observed in many syndromic conditions. **Overall design:** To investigate the adverse effects of dysfunctional TGF-Beta signaling on tissue-tissue interaction between the palatal epithelium and myofibers during palatogenesis, we analyzed mice with an epithelial cell-specific conditional inactivation of Tgfbr2 (Tgfbr2fl/fl;K14-Cre). We performed microarray analyses of anterior palatal tissue and posterior palatal tissue of E15.5 Tgfbr2fl/fl control mice (n=5, each region), and posterior palatal tissue of Tgfbr2fl/fl;K14-Cre mutant mice, collected at embryonic day 15.5 (n=5). Control samples and mutant samples are from separate litters.

Background corr dist: KL-Divergence = 0.1225, L1-Distance = 0.0338, L2-Distance = 0.0021, Normal std = 0.4035

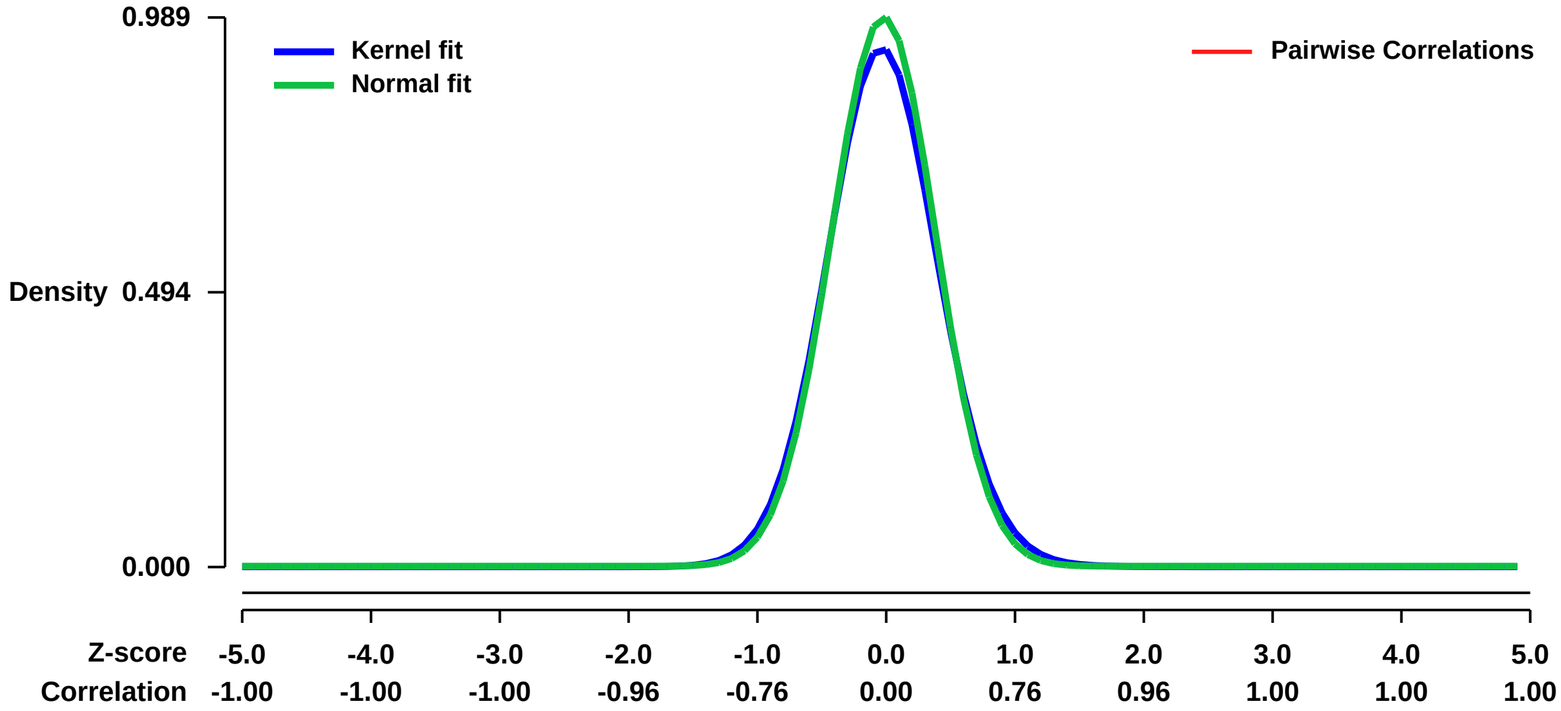

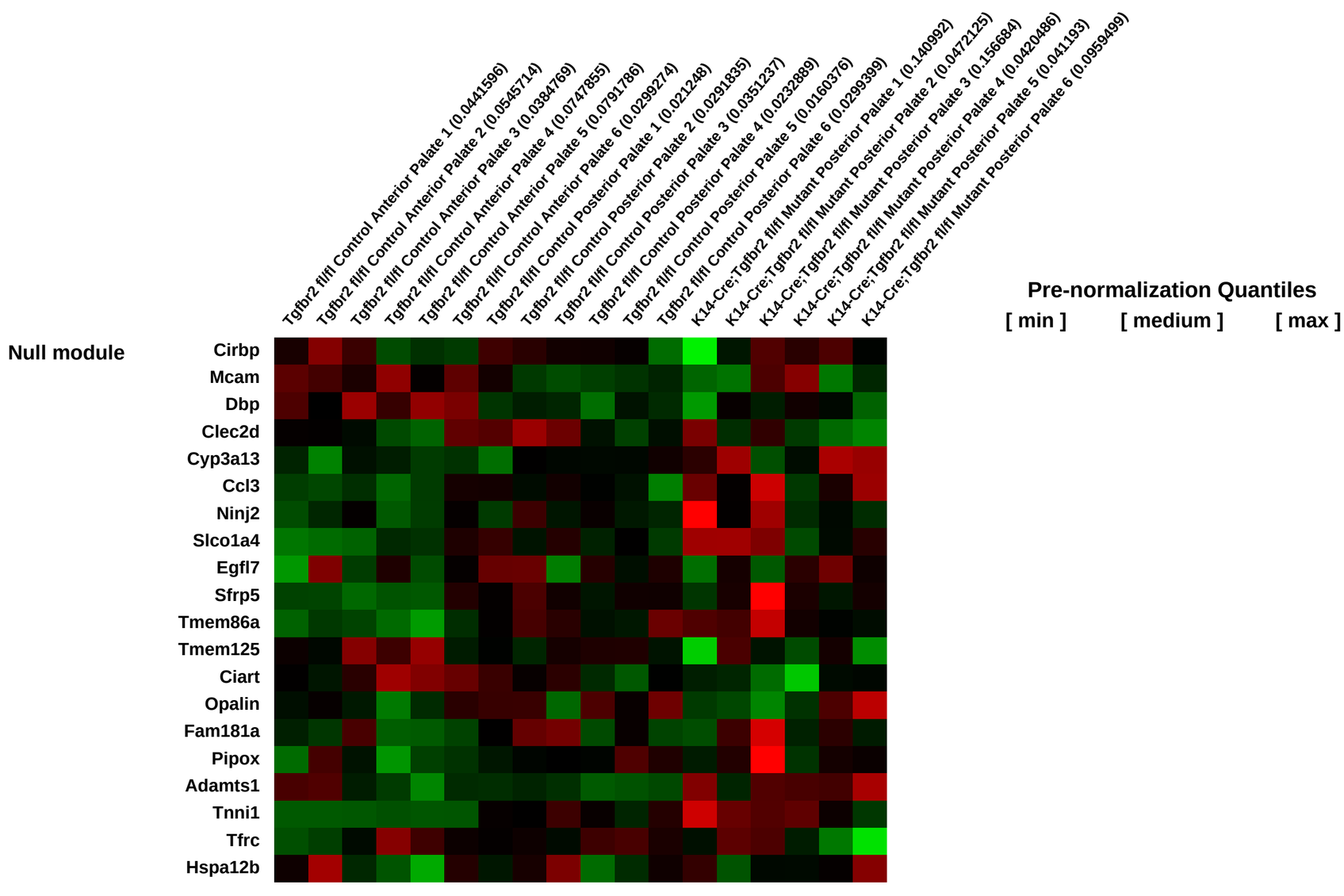

GEO Series "GSE45005" Expression Profiles

Num of samples in this series: 12

Scale of expression profile Z-scores

-3.0 -2.0 -1.0 0.0 1.0 2.0 3.0

GEO Link:	http://www.ncbi.nlm.nih.gov/geo/query/acc.cgi?acc=GSE45005
Status:	Public on Jul 31 2013
Title:	Expression data from renal cortex of ICR-derived Glomerulonephritis (ICGN) mice and ICR mice
Organism:	Mus musculus
Experiment type:	Expression profiling by array
Platform:	GPL1261
Pubmed ID:	23989031
Summary & Design:	**Summary:** ICR-derived glomerulonephritis (ICGN) mice is a novel inbred strain of mice with a hereditary nephrotic syndrome. Deletion mutation of tensin 2 (Tns2), a focal adhesion molecule, has been suggested to be responsible for nephrotic syndrome in ICGN mice, however, existence of other associative factors has been suggested. To identify additional associative factors and to better understand onset mechanism of nephrotic syndrome in ICGN mice, comprehensive gene expression analysis using DNA microarray was conducted. Immune-related pathways were markedly altered in ICGN mice kidney as compared with ICR mice. Furthermore, gene expression level of complement component 1, s subcomponent (C1s), whose human homologue has been reported to associate with lupus nephritis, was markedly low in ICGN mice kidney. **Overall design:** RNA from renal cortex of 4- and 8-week-old ICGN and ICR mice was extracted and processed for hybridization on Affymetrix microarrays (N=3).

Background corr dist: KL-Divergence = 0.1065, L1-Distance = 0.0253, L2-Distance = 0.0010, Normal std = 0.4277

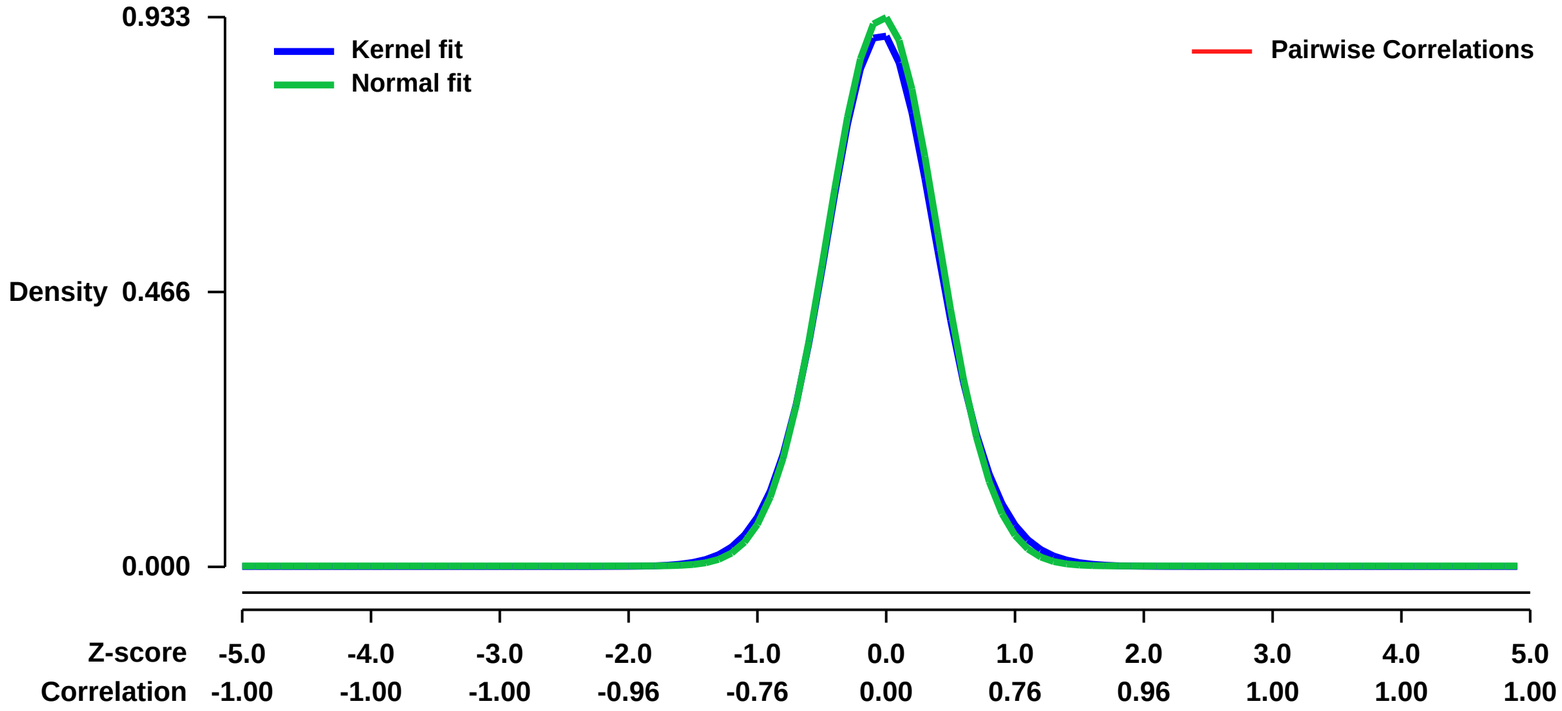

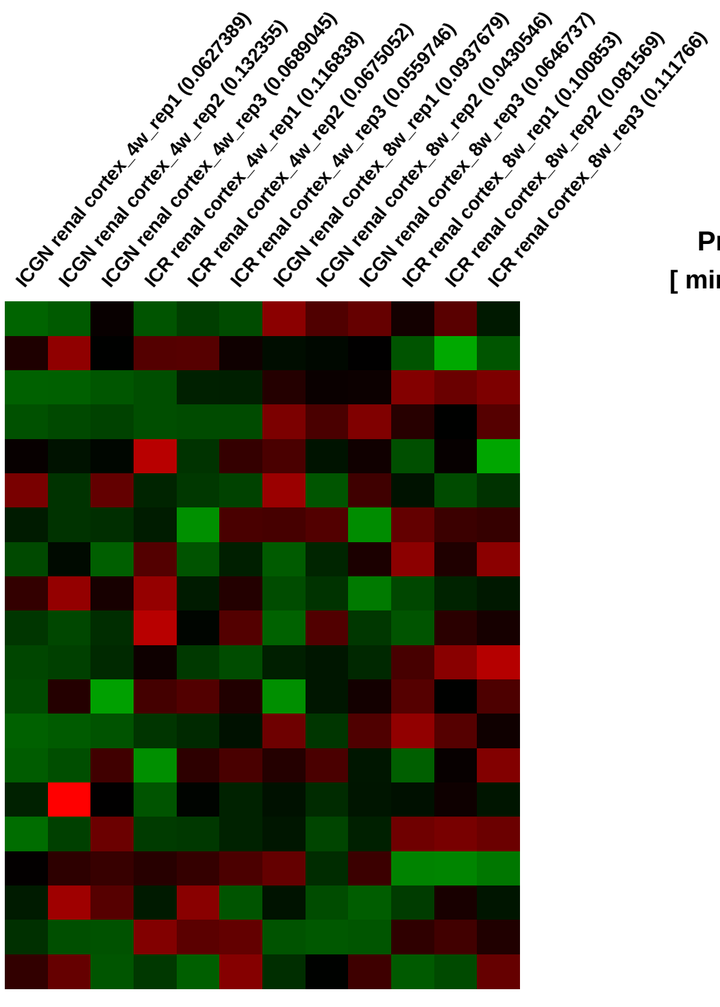

GEO Series "GSE54349" Expression Profiles

Num of samples in this series: 6

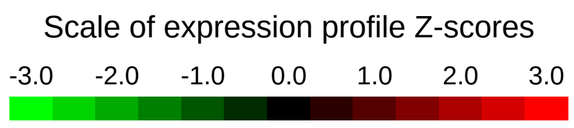

GEO Link:	**http://www.ncbi.nlm.nih.gov/geo/query/acc.cgi?acc=GSE54349**
Status:	**Public on Jan 24 2014**
Title:	**Expression data from colon and livers of mice**
Organism:	**Mus musculus**
Experiment type:	**Expression profiling by array**
Platform:	**GPL1261**
Pubmed ID:	

Summary & Design:

Summary:
Here we describe our unprecedented approach in proposing parsley (PAR) as a nutraceutical intervention in inflammatory bowel disease (IBD) using a mouse model of dextran sodium sulphate (DSS)-induced colitis, following a multi-integrated-omics analysis. PAR supplementation (n=7) significantly improved colon shortening and increased the disease activity index compared to the DSS group (n=7). The colonic transcriptome revealed the down-regulation of inflammatory cytokines, and the hepatic transcriptome and metabolome revealed the up-regulation of fatty acid synthesis genes, thereby improving body weight loss. Down-regulated cancer markers were observed in the hepatic transcriptome and proteome. A global plasma metabolite analysis indicated shifts in the citric cycle and urea cycle, implicating improved impaired glycolysis and oxidative stress. Our integration of three omics analyses highlighted the involvement of the methionine-recycling pathway and PARâ s role in decreasing the risk of IBD. This pioneering use of multi-integrated-omics in the evaluation of nutrientsâ effects on physiology is expected to be widely useful and informative, shaping the future of nutritional research.

Here we describe our unprecedented approach in proposing parsley (PAR) as a nutraceutical intervention in inflammatory bowel disease (IBD) using a mouse model of dextran sodium sulphate (DSS)-induced colitis, following a multi-integrated-omics analysis. PAR supplementation (n=7) significantly improved colon shortening and increased the disease activity index compared to the DSS group (n=7). The colonic transcriptome revealed the down-regulation of inflammatory cytokines, and the hepatic transcriptome and metabolome revealed the up-regulation of fatty acid synthesis genes, thereby improving body weight loss. Down-regulated cancer markers were observed in the hepatic transcriptome and proteome. A global plasma metabolite analysis indicated shifts in the citric cycle and urea cycle, implicating improved impaired glycolysis and oxidative stress. Our integration of three omics analyses highlighted the involvement of the methionine-recycling pathway and PARâ s role in decreasing the risk of IBD. This pioneering use of multi-integrated-omics in the evaluation of nutrientsâ effects on physiology is expected to be widely useful and informative, shaping the future of nutritional research.

Overall design:
Total hepatic and colonic RNA from each respective group were pooled (n=7). The microarray analysis was carried as out as described by Jia et al. 8 Mouse Genome 430 2.0 Array GeneChips (Affymetrix, Santa Clara, CA) containing over 30,000 gene probe sets were used for genome-wide expression profiling.

Background corr dist: KL-Divergence = 0.0145, L1-Distance = 0.0248, L2-Distance = 0.0008, Normal std = 0.8186

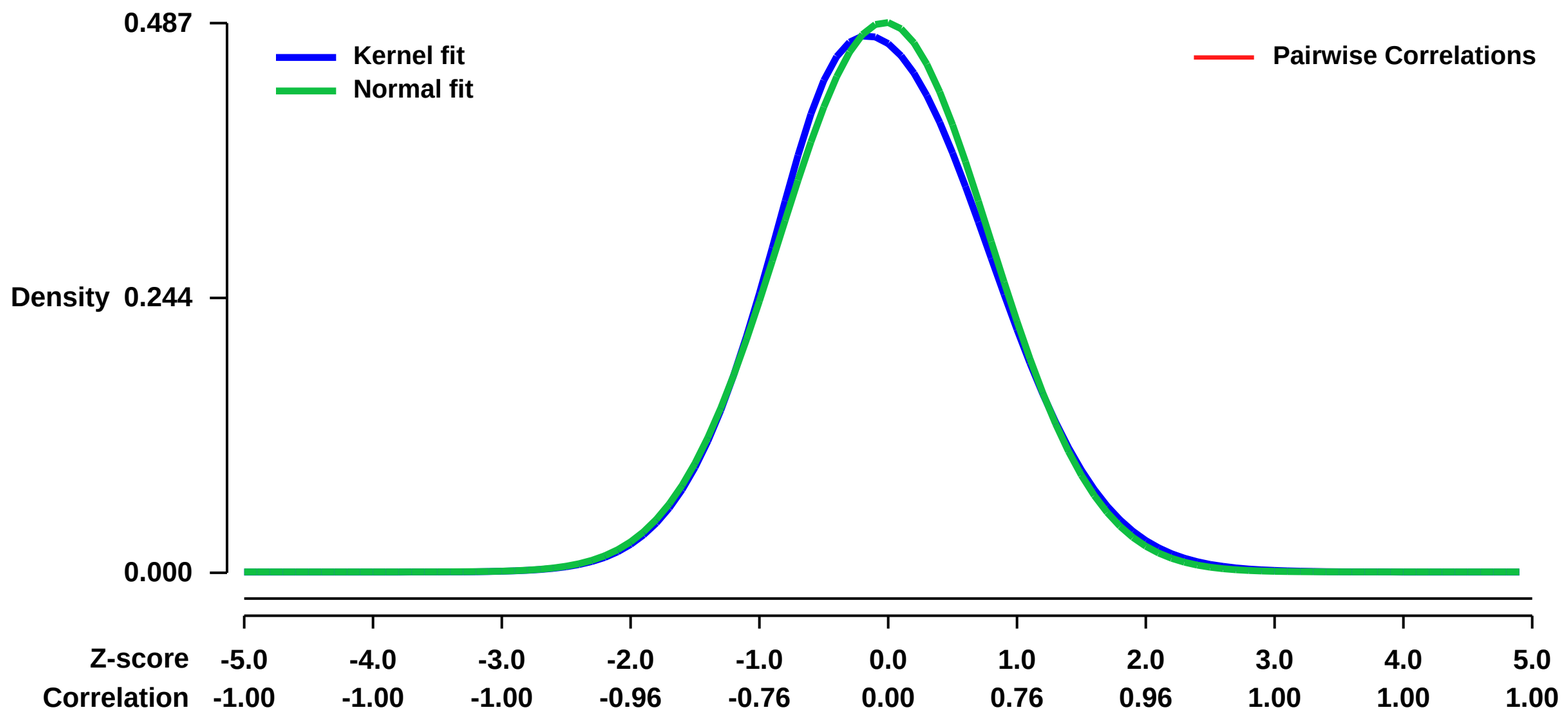

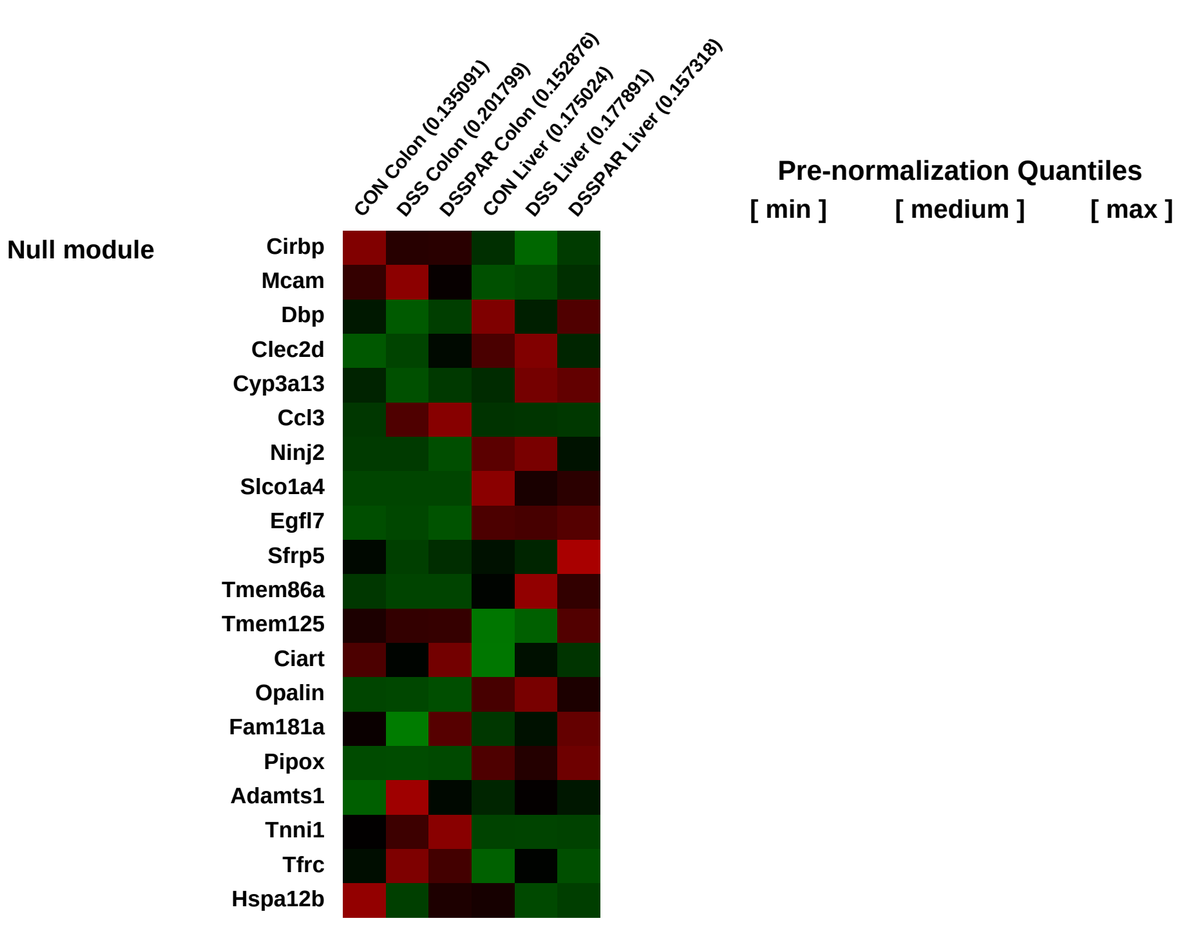

GEO Series "GSE35318" Expression Profiles

Num of samples in this series: 12

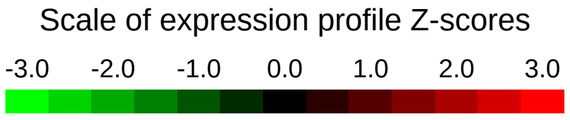

GEO Link:	**http://www.ncbi.nlm.nih.gov/geo/query/acc.cgi?acc=GSE35318**
Status:	**Public on Jul 10 2012**
Title:	**p38a-dependent gene expression in dendritic cells**
Organism:	**Mus musculus**
Experiment type:	**Expression profiling by array**
Platform:	**GPL1261**
Pubmed ID:	**22615377**
Summary & Design:	**Summary:** **Gene expression in wild-type and p38a-knockout dendritic cells (DCs) were compared. Lymph node dendritic cells were isolated from mice, and left unstimulated and stimulated with Pam3CSK4, a toll-like receptor 2 agonist.** **C57BL/6 wild-type mice, and dendritic cell-specific p38a-knockout mice on a C57BL/6 background were used for isolation of primary DCs.** **Overall design:** **Gene expression 0, 2, and 4 h after stimulation was analyzed with each time point in duplicate.**

Background corr dist: **KL-Divergence = 0.1423, L1-Distance = 0.0306, L2-Distance = 0.0017, Normal std = 0.3824**

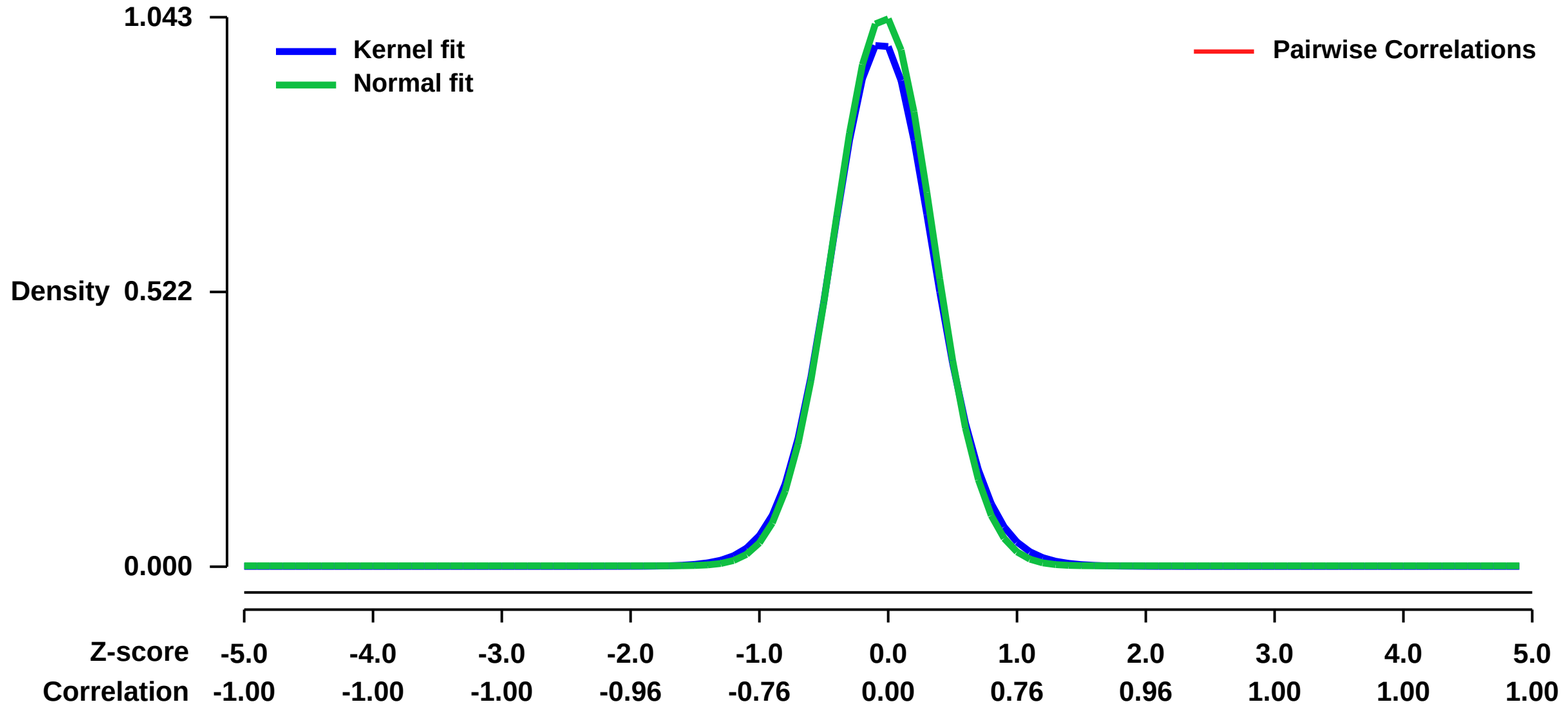

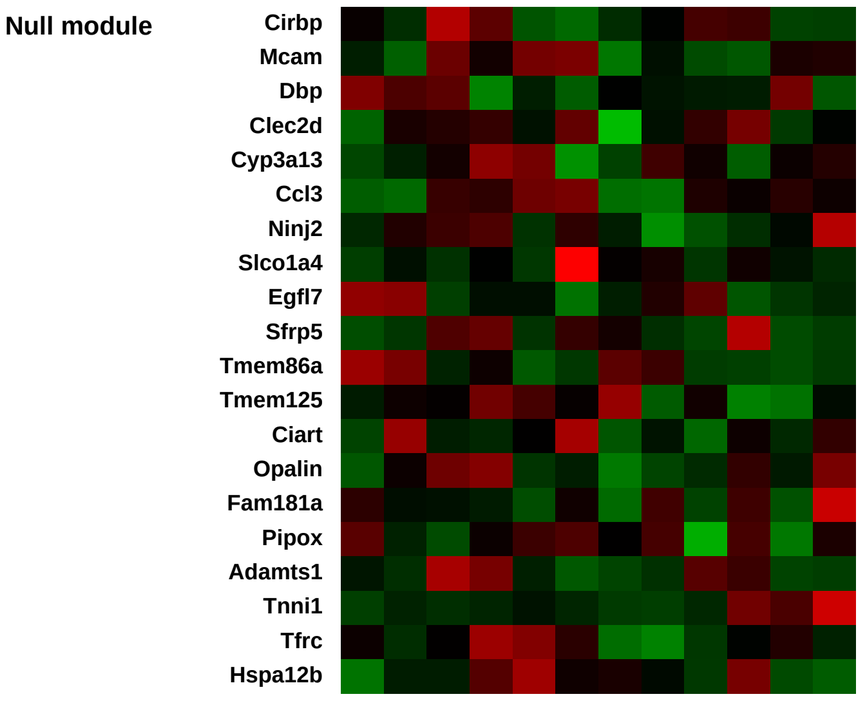

GEO Series "GSE39273" Expression Profiles

Num of samples in this series: 6

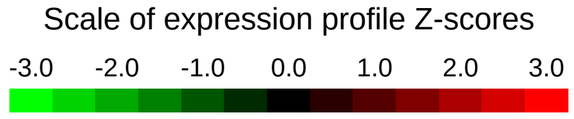

GEO Link:	**http://www.ncbi.nlm.nih.gov/geo/query/acc.cgi?acc=GSE39273**
Status:	**Public on Jan 11 2013**
Title:	**Effect of transgenic human IL8 on gene expression in mouse colon cancer tumors**
Organism:	**Mus musculus**
Experiment type:	**Expression profiling by array**
Platform:	**GPL1261**
Pubmed ID:	**23041326**
Summary & Design:	**Summary:** **mRNA expression in colon cancer tumores** **of CBA/C57BL/6 transgenic mice** **bearing a BAC which contains the human IL8 gene and promoter** **was compared to that of CBA/C57BL/6 controls.** **Overall design:** **B. human IL8 transgenic CBA/C57BL/6 mice (n=3).**

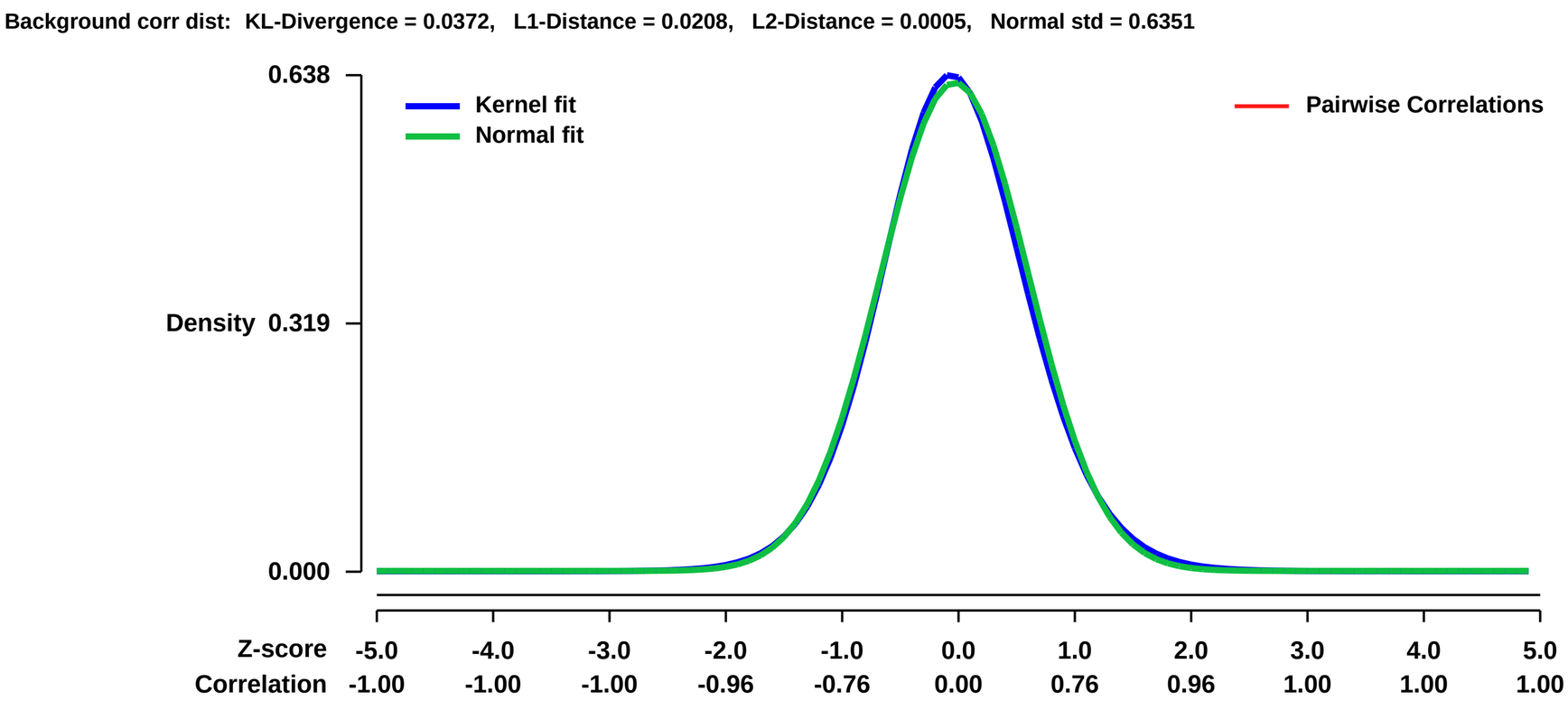

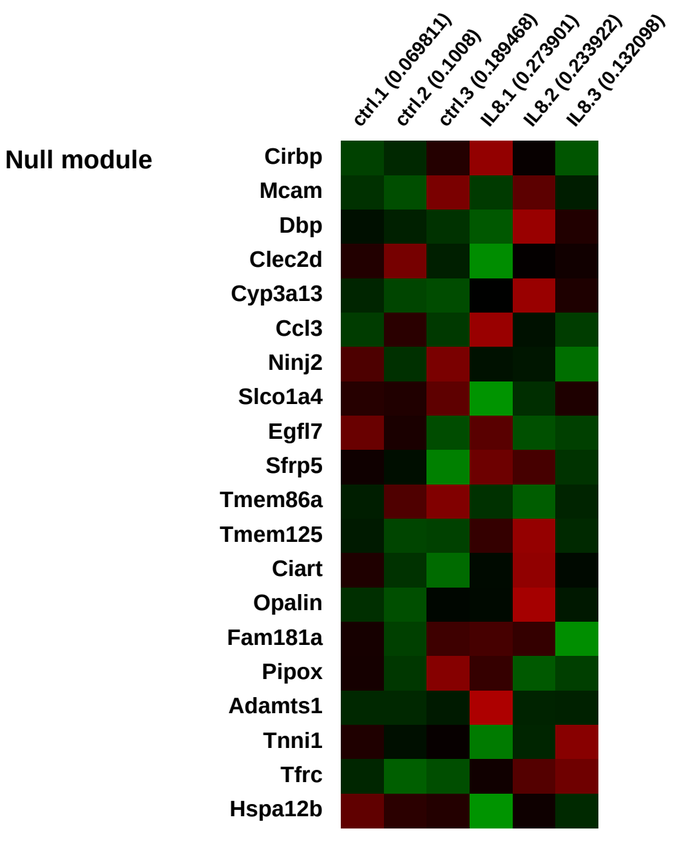

GEO Series "GSE33513" Expression Profiles

Num of samples in this series: 6

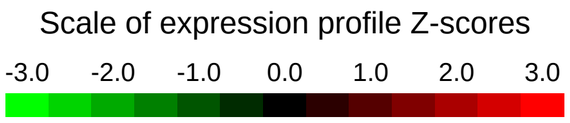

GEO Link:	http://www.ncbi.nlm.nih.gov/geo/query/acc.cgi?acc=GSE33513
Status:	Public on Dec 06 2011
Title:	T cell factor 1 is a gatekeeper for T-cell specification in response to Notch signaling
Organism:	Mus musculus
Experiment type:	Expression profiling by array
Platform:	GPL1261
Pubmed ID:	22109558
Summary & Design:	**Summary:** Although transcriptional programs associated with T-cell specification and commitment have been described, the functional hierarchy and the roles of key regulators in structuring/ orchestrating these programs remain unclear. Activation of Notch signaling in uncommitted precursors by the thymic stroma initiates the T-cell differentiation program. One regulator first induced in these precursors is the DNA binding protein Tcf-1, a T-cell specific mediator of Wnt signaling. Yet the specific contribution of Tcf-1 to early T-cell development and the signals inducing it in these cells remain unclear. Here we assign functional significance to Tcf-1 as a gatekeeper of T-cell fate. We show that Tcf-1 is directly activated by Notch signals. Tcf-1 is required at the earliest phase of Tcell determination for progression beyond the early thymic progenitor (ETP) stage. The global expression profile of Tcf-1 deficient progenitors indicates that basic processes of DNA metabolism are downregulated in its absence and the blocked T-cell progenitors become abortive and die by apoptosis. Our data thus add an important functional relationship to the roadmap of T-cell development. We used microarrays to detail the global programme of gene expression of mouse ETP thymocyte after Ikaros inactivation with dominant negative of Ik at different stage. **Overall design:** 6 samples (mouse ETP thymocytes from wt, and Tcf1 inactivation) are analyzed Mouse Microarray Expression platforms, Affymetrix Mouse 430 2.0,

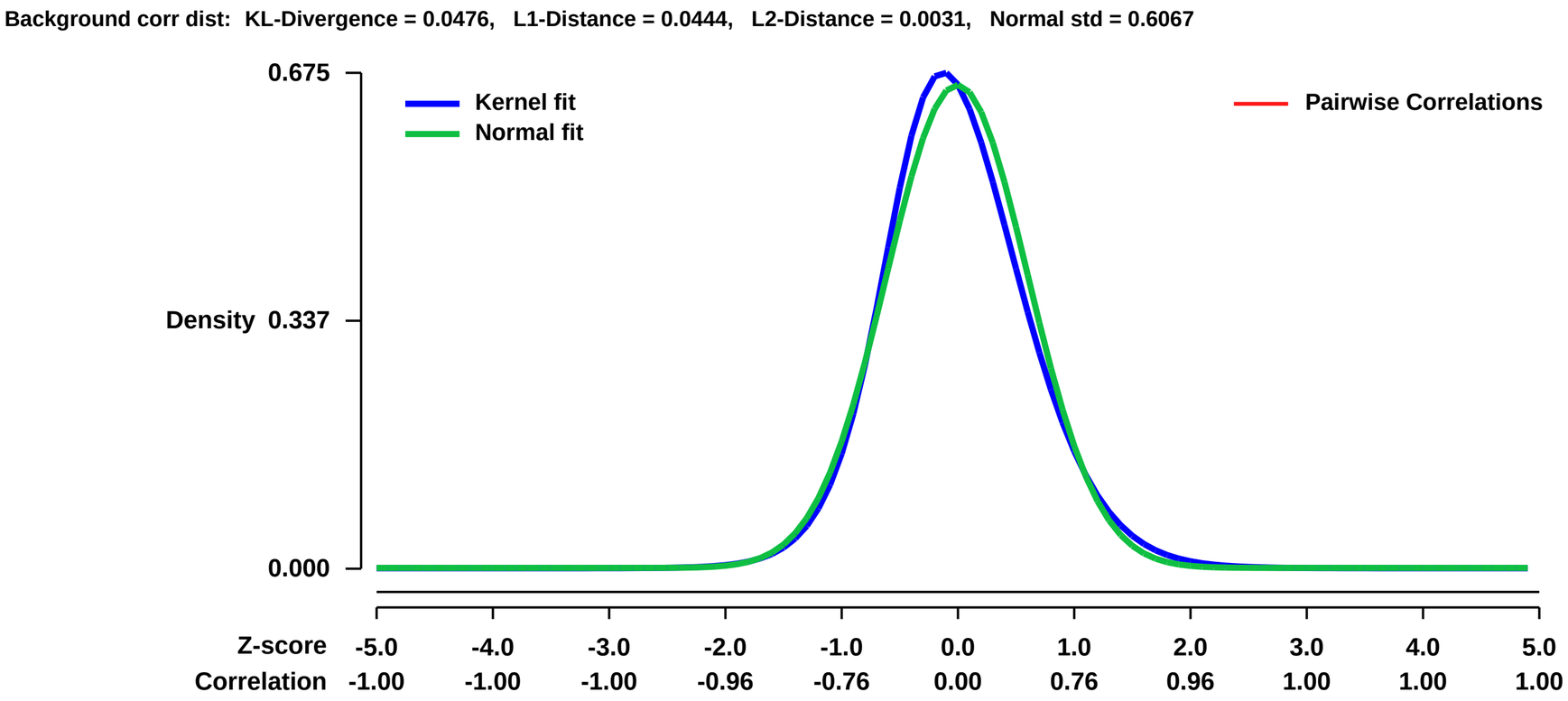

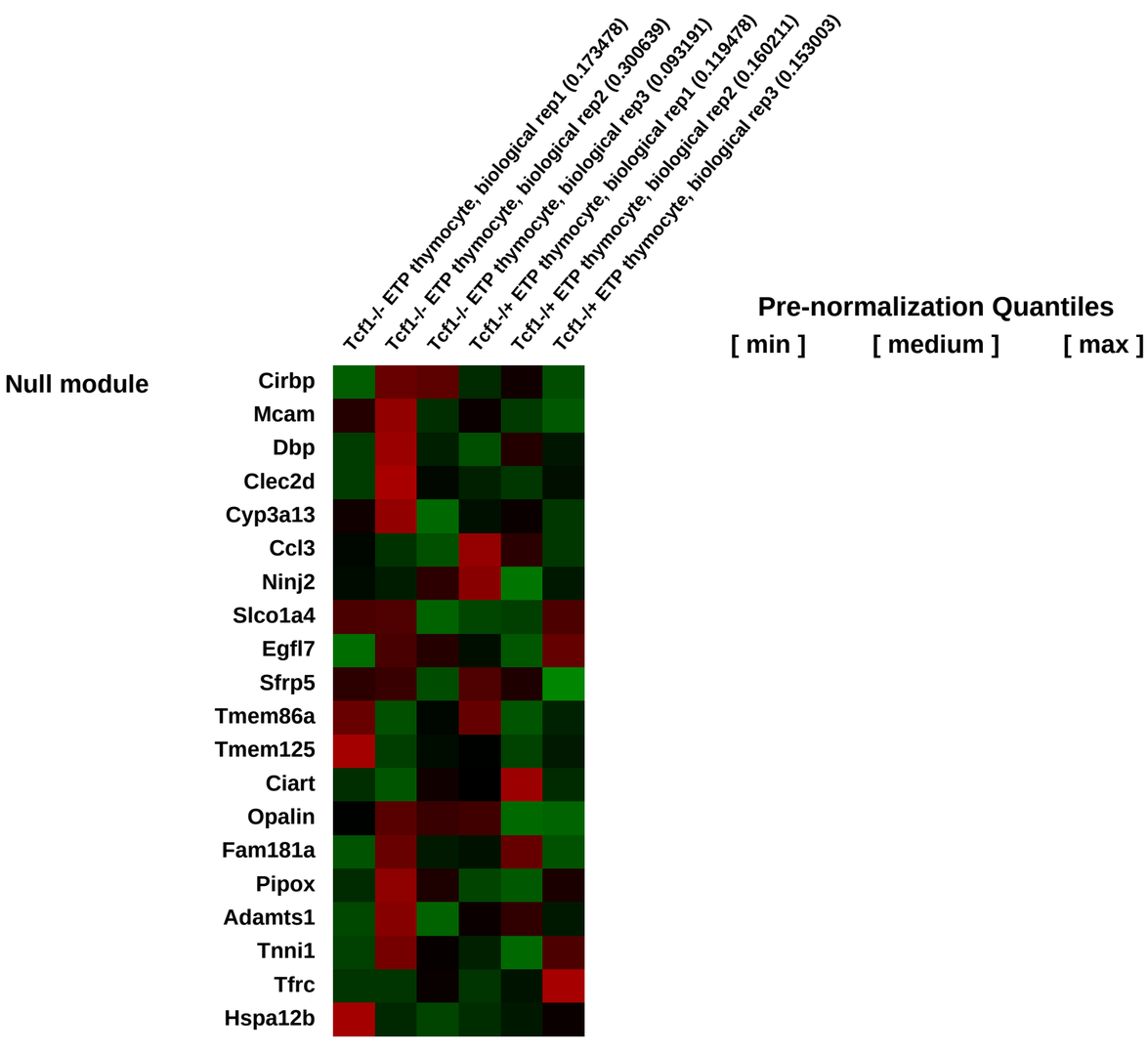

GEO Series "GSE17825" Expression Profiles

Num of samples in this series: 18

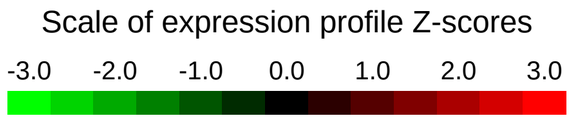

GEO Link:	http://www.ncbi.nlm.nih.gov/geo/query/acc.cgi?acc=GSE17825
Status:	Public on Sep 01 2009
Title:	Murine fracture healing
Organism:	Mus musculus
Experiment type:	Expression profiling by array
Platform:	GPL1261
Pubmed ID:	18752025
Summary & Design:	**Summary:** Time-point expression analysis of fractures calluses at 1, 3, and 5 days post-fracture in young and old BALB/c mice. **Overall design:** Femur fractures were generated on female c57Bl6 mice in triplicate: 8 month old retired breeders (old mice) and 6 week old mice (young mice) were used. 1, 3, and 5 days post-fracture, fracture calluses were dissected and total RNA isolated. Expression profiling was performed using Affymetrix's Mouse Genome 430 2.0 array.

Background corr dist: KL-Divergence = 0.0962, L1-Distance = 0.0386, L2-Distance = 0.0030, Normal std = 0.4412

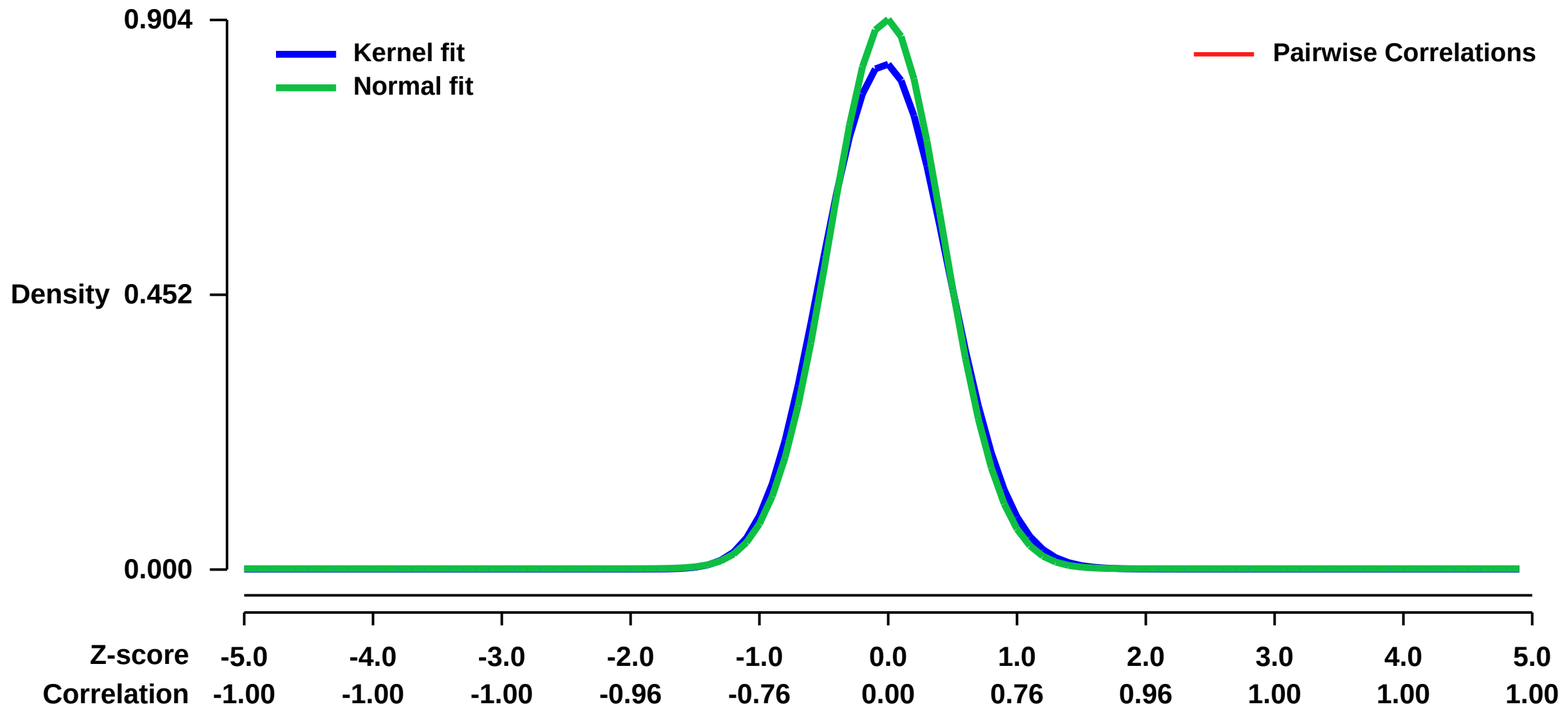

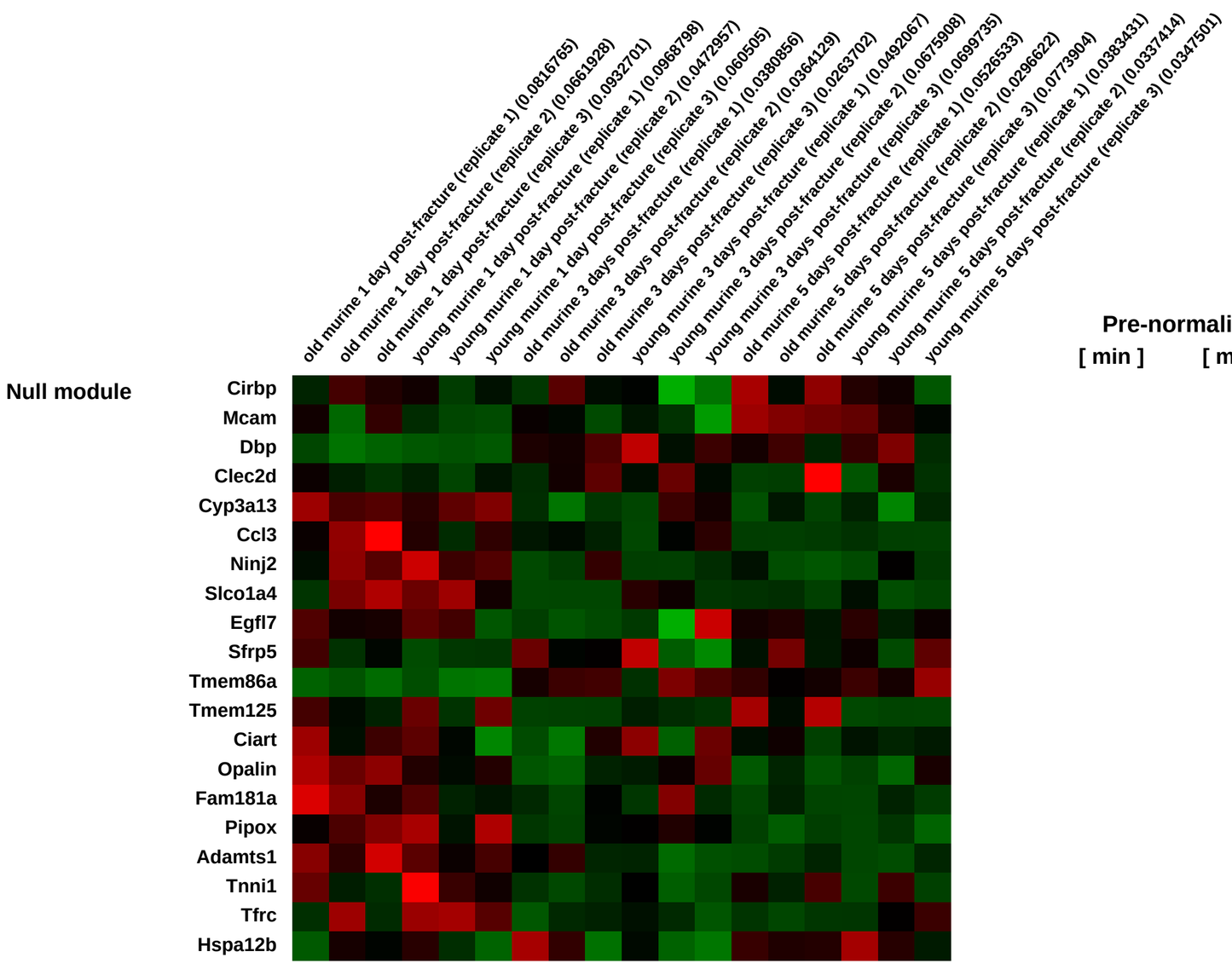

GEO Series "GSE22841" Expression Profiles

Num of samples in this series: 12

Scale of expression profile Z-scores

-3.0 -2.0 -1.0 0.0 1.0 2.0 3.0

GEO Link:	http://www.ncbi.nlm.nih.gov/geo/query/acc.cgi?acc=GSE22841
Status:	Public on Nov 10 2011
Title:	Discrete subsets of myogenic and mesenchymal precursors give rise to soft tissue sarcomas of distinct lineage differentiation
Organism:	Mus musculus
Experiment type:	Expression profiling by array
Platform:	GPL1261
Pubmed ID:	22135462
Summary & Design:	**Summary:** This work examines sarcoma formation within discrete subsets of KRAS(G12V)-expressing p16p19null myogenic and mesenchymal cells found normally in skeletal muscle. We show that prospectively isolated skeletal muscle precursor cells (SMPs) within the satellite cell pool can serve as cancer cells-of-origin for mouse rhabdomyosarcomas (soft tissue sarcomas with features of myogenic differentiation). Alternatively, non-myogenic progenitors (ScaPCs) induce sarcomas lacking myogenic differentiation markers. **Overall design:** We used Affymetrix whole mouse genome 430 2.0 microarrays to gain deeper insights into the molecular underpinnings of the three types of KRAS; p16p19null mouse soft-tissue sarcomas (originating from SMPs, ScaPCs and CD45-MAC1-TER119-Sca1-CXCR4- cells). Four replicates of each type.

Background corr dist: KL-Divergence = 0.1135, L1-Distance = 0.0242, L2-Distance = 0.0008, Normal std = 0.4203

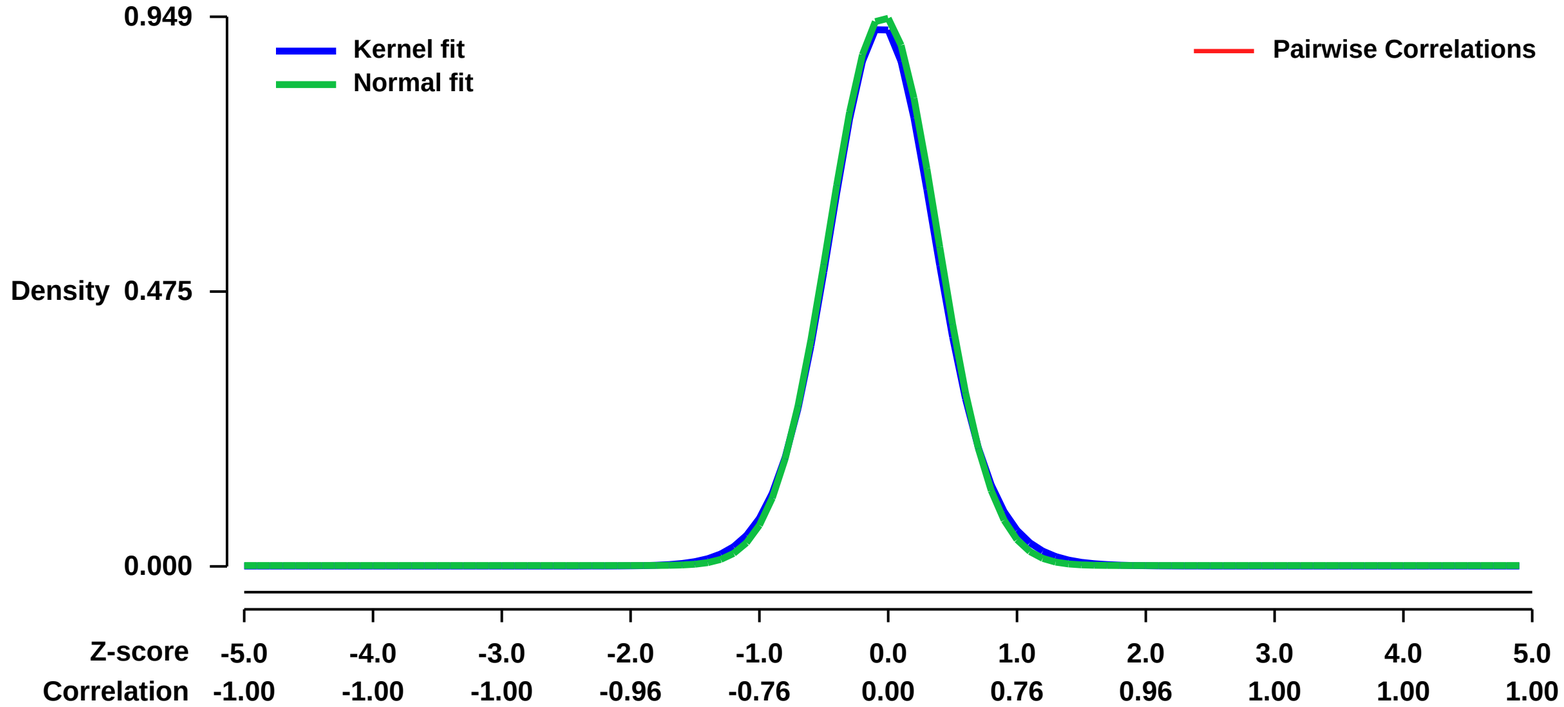

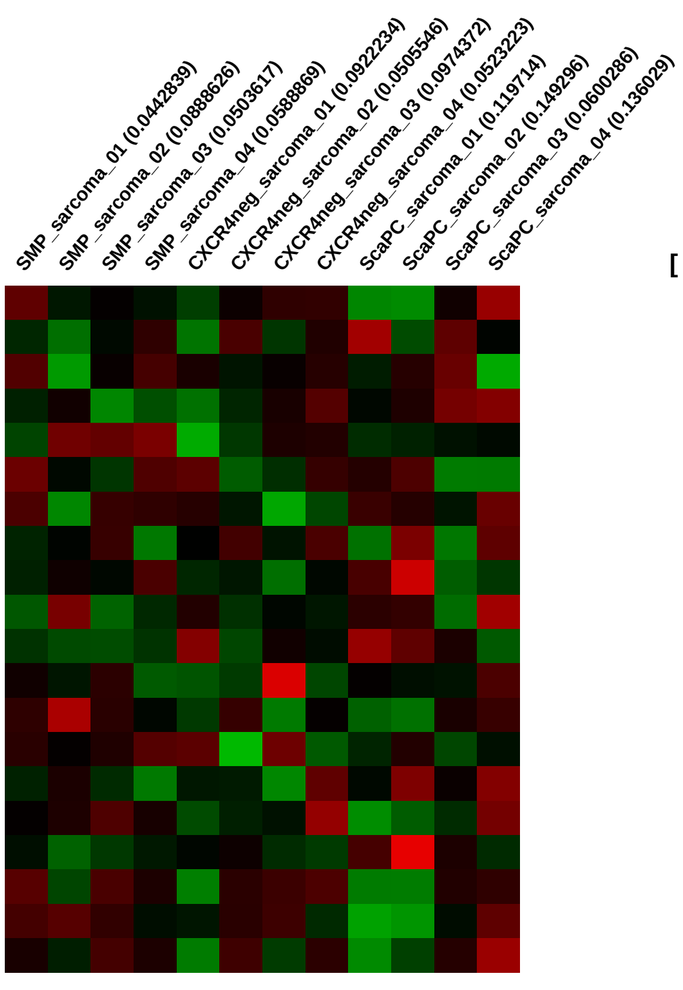

GEO Series "GSE41083" Expression Profiles

Num of samples in this series: 6

Scale of expression profile Z-scores

-3.0 -2.0 -1.0 0.0 1.0 2.0 3.0

GEO Link:	http://www.ncbi.nlm.nih.gov/geo/query/acc.cgi?acc=GSE41083
Status:	Public on Jul 01 2013
Title:	Expression data after irradiating mMSCs for 2 hours with broadband terahertz source
Organism:	Mus musculus
Experiment type:	Expression profiling by array
Platform:	GPL1261
Pubmed ID:	23378916
Summary & Design:	**Summary:** We report that terahertz (THz) irradiation of mouse mesenchymal stem cells with a pulsed broadband (centered at 10 THz) source, or a single-frequency, 2.52 THz, (SF) laser source, both with weak average power (<1mW/cm2), results in specific heterogenic changes in gene expression. The insignificant differential expression of heat shock and stress related genes as well as our temperature measurements imply a non-thermal response. The microarray survey and RT-PCR experiments demonstrate that at different irradiation conditions distinct groups of genes are activated. Stem cells irradiated for 12 hours with the broadband THz source exhibit an accelerated differentiation toward adipose phenotype, while the 2-hour (broadband or SF) irradiation affects genes transcriptionally active in pluripotent stem cells. Phenotypic and gene expression differences suggest that the THz effect depends on irradiation parameters such as duration and type of THz source, and on the level of stem cell differentiation. Computer simulations of the core promoters of two pluripotency markers reveal association between gene upregulation and propensity for DNA breathing. We propose that THz radiation has potential for non-contact control of cellular gene expression. **Overall design:** Growing in petri dish mouse mesenchymal stem cell cultures are irradiated for 2 hours with pulsed ultrafast (35 fs) broadband (centered at ~10 THz) source. Three independent biological experiments were conducted. In each experiment, a control mMSC culture was placed adjacent to the irradiated sample, and the temperature was kept at 26-27´”C for both the control and the irradiated sample. Immediately after completing the irradiation, total RNA was extracted from the irradiated sample and the control, and microarrays were used to identify differential changes in gene expression between the irradiated sample and its respective control. In each experiment, the mMSC cultures were synchronized to be at the same differentiation time point immediately before the irradiation.

Background corr dist: KL-Divergence = 0.0358, L1-Distance = 0.0162, L2-Distance = 0.0002, Normal std = 0.6337

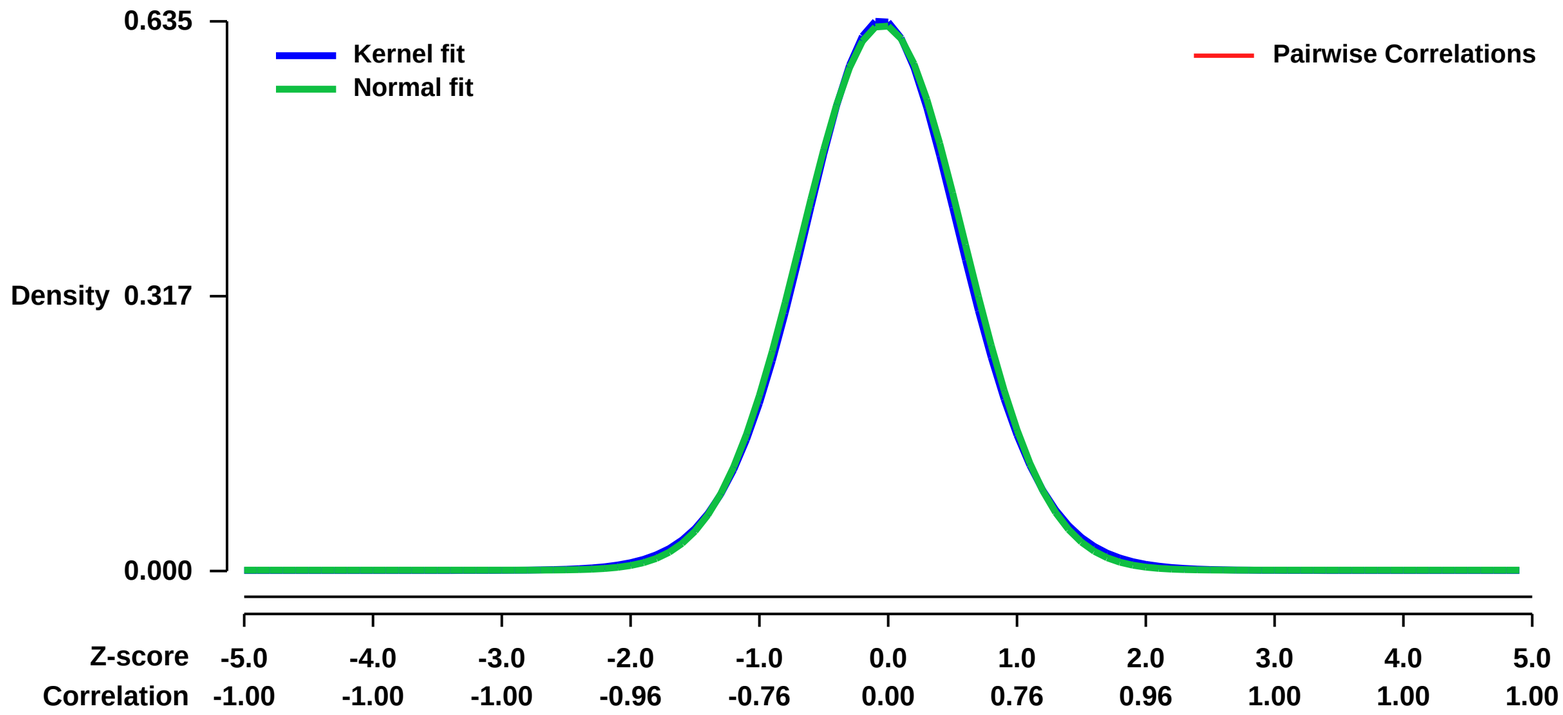

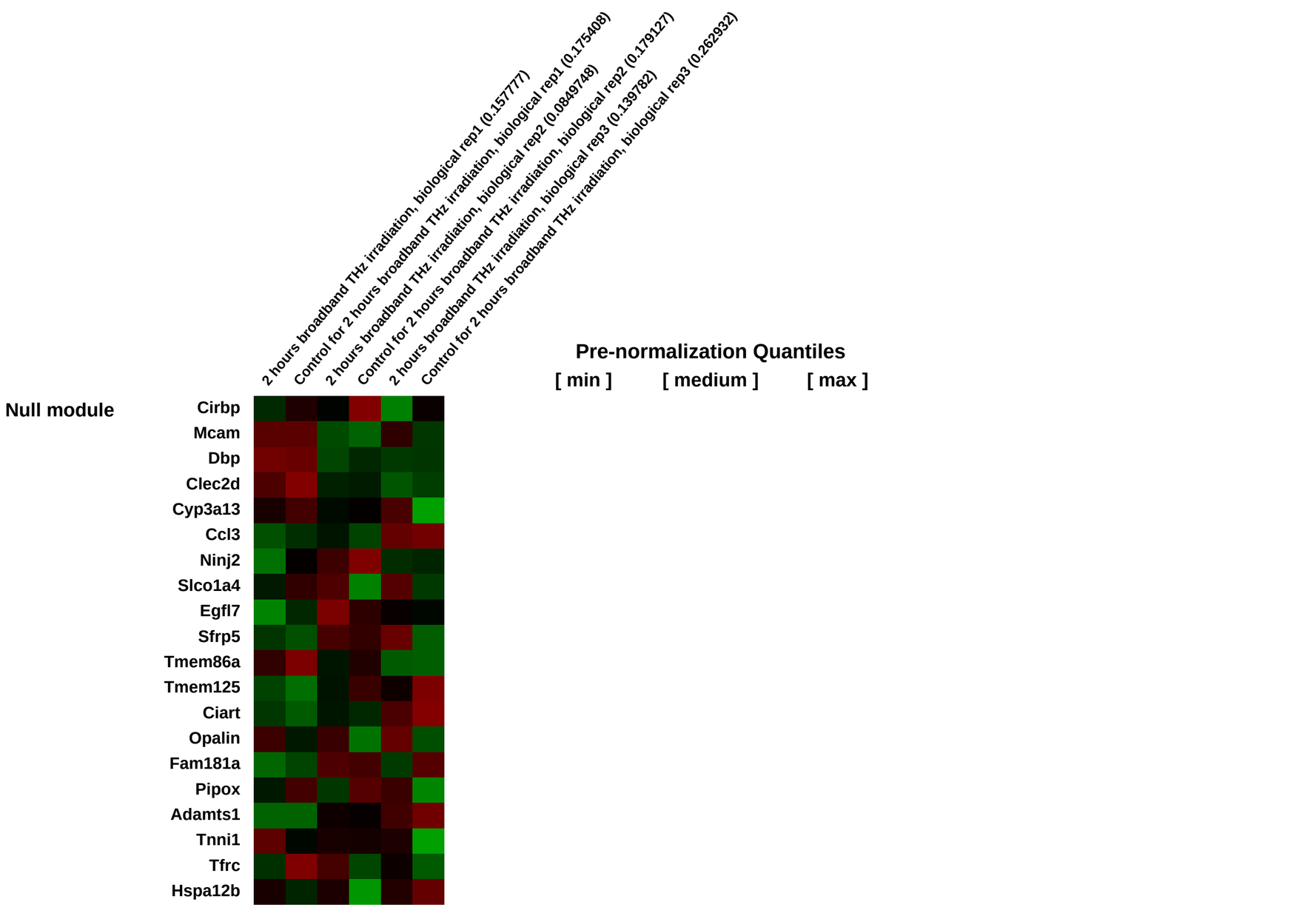

GEO Series "GSE5236" Expression Profiles

Num of samples in this series: 8

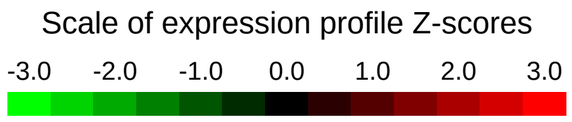

GEO Link:	http://www.ncbi.nlm.nih.gov/geo/query/acc.cgi?acc=GSE5236
Status:	Public on Aug 18 2007
Title:	Expression of the human Cathepsin L inhibitor hurpin in mice: skin alterations and increased carcinogenesis.
Organism:	Mus musculus
Experiment type:	Expression profiling by array
Platform:	GPL1261
Pubmed ID:	17697143
Summary & Design:	**Summary:** Aim of this study was to identify gene expression differences in the skin of hurpin (=headpin=serpinB13) transgenic mice in comparison to wildtype mice. **Keywords: genetic modification** **Overall design:** Gender: mixed (male and female)

Background corr dist: KL-Divergence = 0.0629, L1-Distance = 0.0182, L2-Distance = 0.0004, Normal std = 0.5201

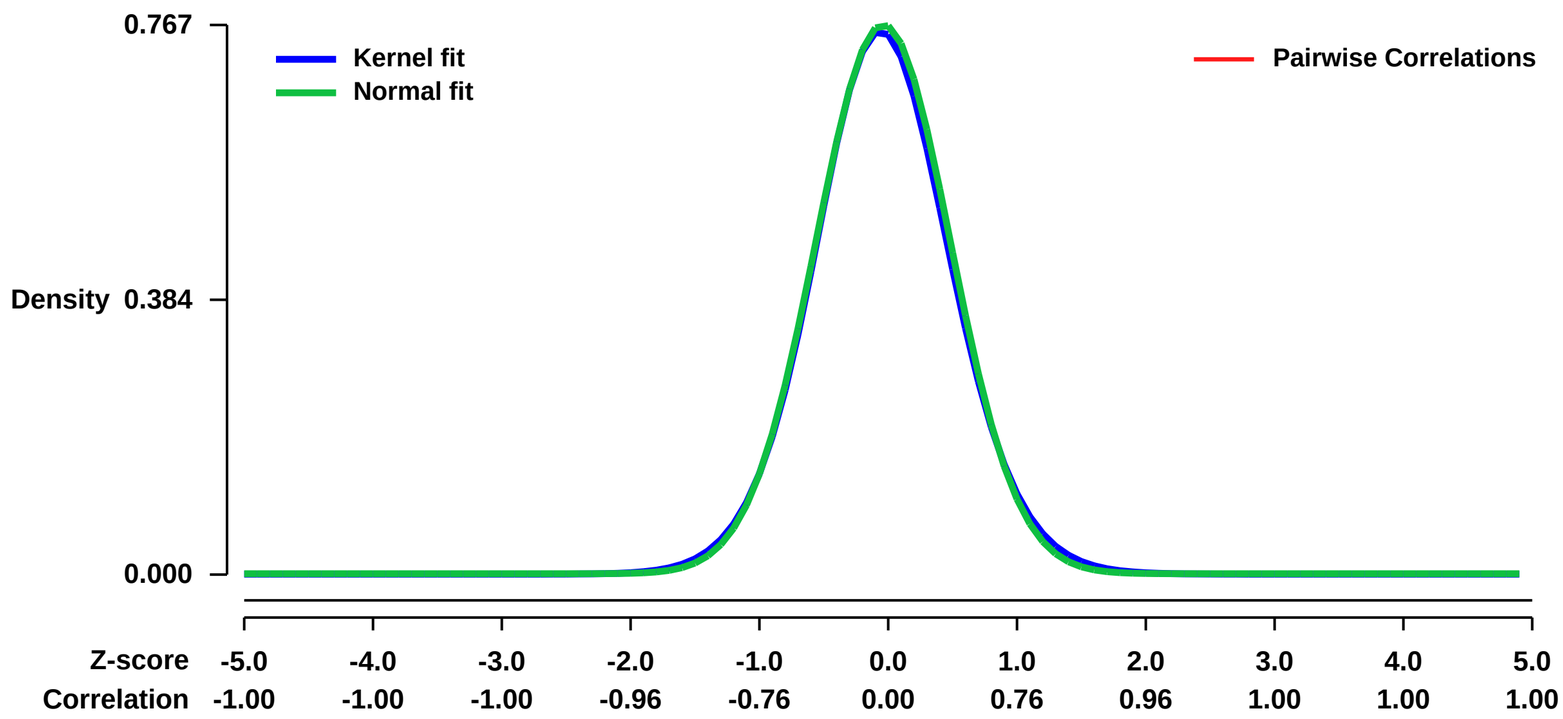

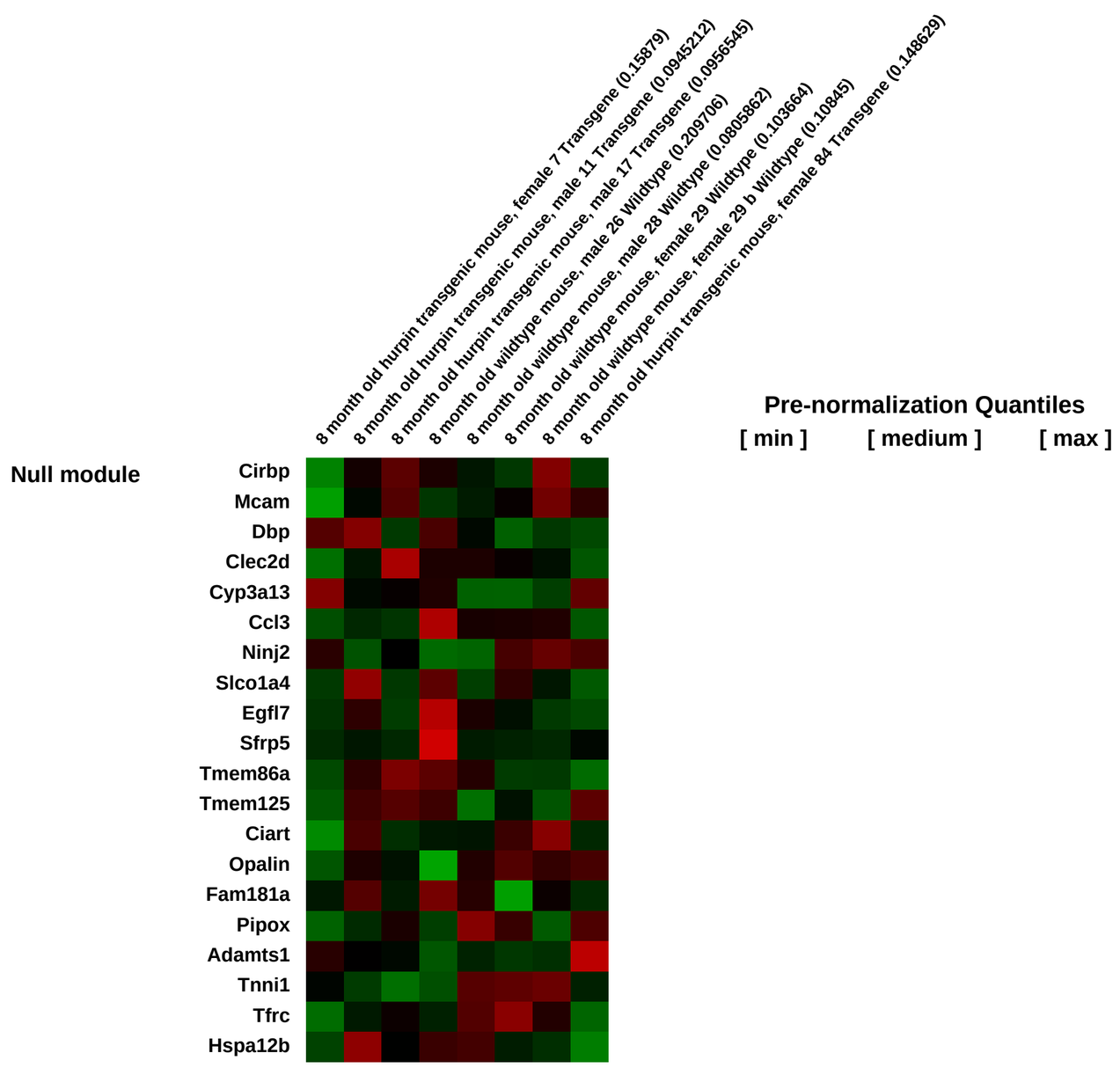

GEO Series "GSE24465" Expression Profiles

Num of samples in this series: 6

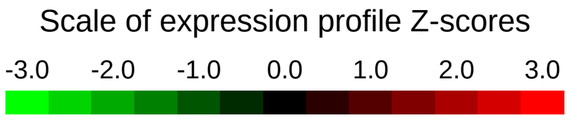

GEO Link:	**http://www.ncbi.nlm.nih.gov/geo/query/acc.cgi?acc=GSE24465**
Status:	**Public on Sep 29 2011**
Title:	**Mesenchymal Nuclear factor I B regulates cell proliferation and epithelial differentiation during lung maturation**
Organism:	**Mus musculus**
Experiment type:	**Expression profiling by array**
Platform:	**GPL1261**
Pubmed ID:	
Summary & Design:	**Summary:** **We generated Nfibf/f mice and then cross with Dermo1-Cre mice to obtain Nfibf/f, Dermo1-Cre mice. In these Nfibf/f, Dermo1-Cre mice, there are defects in sacculation and epithelial cell differentiation. We performed micoarray analysis to find the genes which are possibley regulated by NFI-B and related to lung maturation during lung development.** **Overall design:** **We used microarrays to performing transcriptional profiling of Nfibf/f, Dermo1-Cre and Nfibf/f lungs at E18.5**

Background corr dist: **KL-Divergence = 0.0391, L1-Distance = 0.0205, L2-Distance = 0.0004, Normal std = 0.6225**

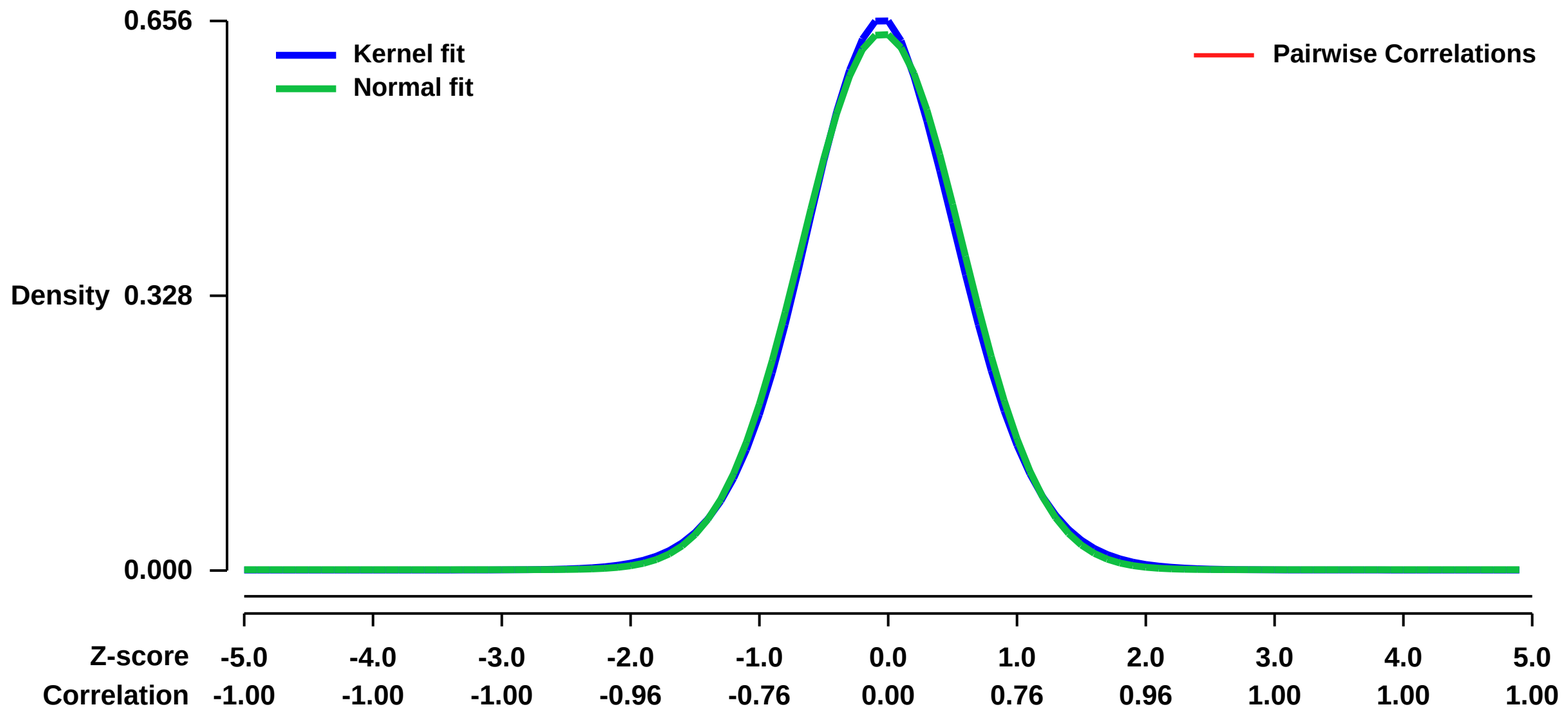

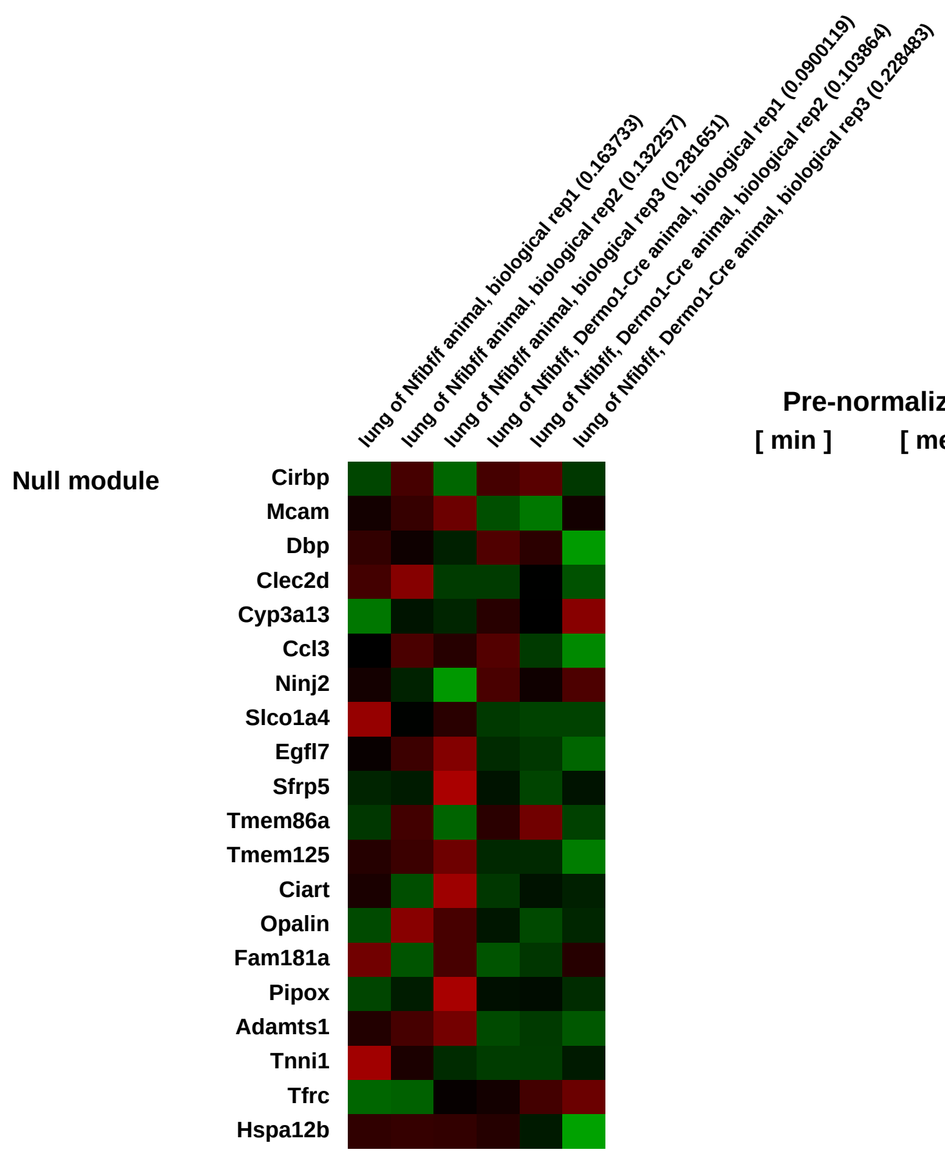

GEO Series "GSE25766" Expression Profiles

Num of samples in this series: 6

Scale of expression profile Z-scores

-3.0 -2.0 -1.0 0.0 1.0 2.0 3.0

GEO Link:	http://www.ncbi.nlm.nih.gov/geo/query/acc.cgi?acc=GSE25766
Status:	Public on Dec 03 2010
Title:	Cardiac gene expression profiling of heart failure treatment with the anti-ischemic drug ranolazine
Organism:	Mus musculus
Experiment type:	Expression profiling by array
Platform:	GPL1261
Pubmed ID:	21711241
Summary & Design:	**Summary:** Heart failure is a leading cause of cardiovascular mortality with limited options for treatment. We analyzed whether the anti-ischemic drug ranolazine could retard the progression of heart failure in an experimental model of heart failure induced by 6 months of chronic pressure overload. The study showed that 2 months of ranolazine treatment improved cardiac function of aortic constricted C57BL/6J (B6) mice with symptoms of heart failure as assessed by echocardiography. The microarray gene expression study of heart tissue from failing hearts relative to ranolazine-treated and healthy control hearts identified heart failure-specific genes that were normalized during treatment with the anti-ischemic drug ranolazine. **Overall design:** Microarray gene expression profiling was performed with heart tissue isolated from three study groups: (i) untreated 10 month-old C57BL/6J (B6) mice with heart failure induced by 6 months of abdominal aortic constriction (AAC), (ii) 10 month-old B6 mice with 6 months of AAC and two months of treatment with the anti-ischemic drug ranolazine (200 mg/kg), and (iii) age-matched, untreated, sham-operated B6 control mice.

Background corr dist: KL-Divergence = 0.0360, L1-Distance = 0.0242, L2-Distance = 0.0006, Normal std = 0.6490

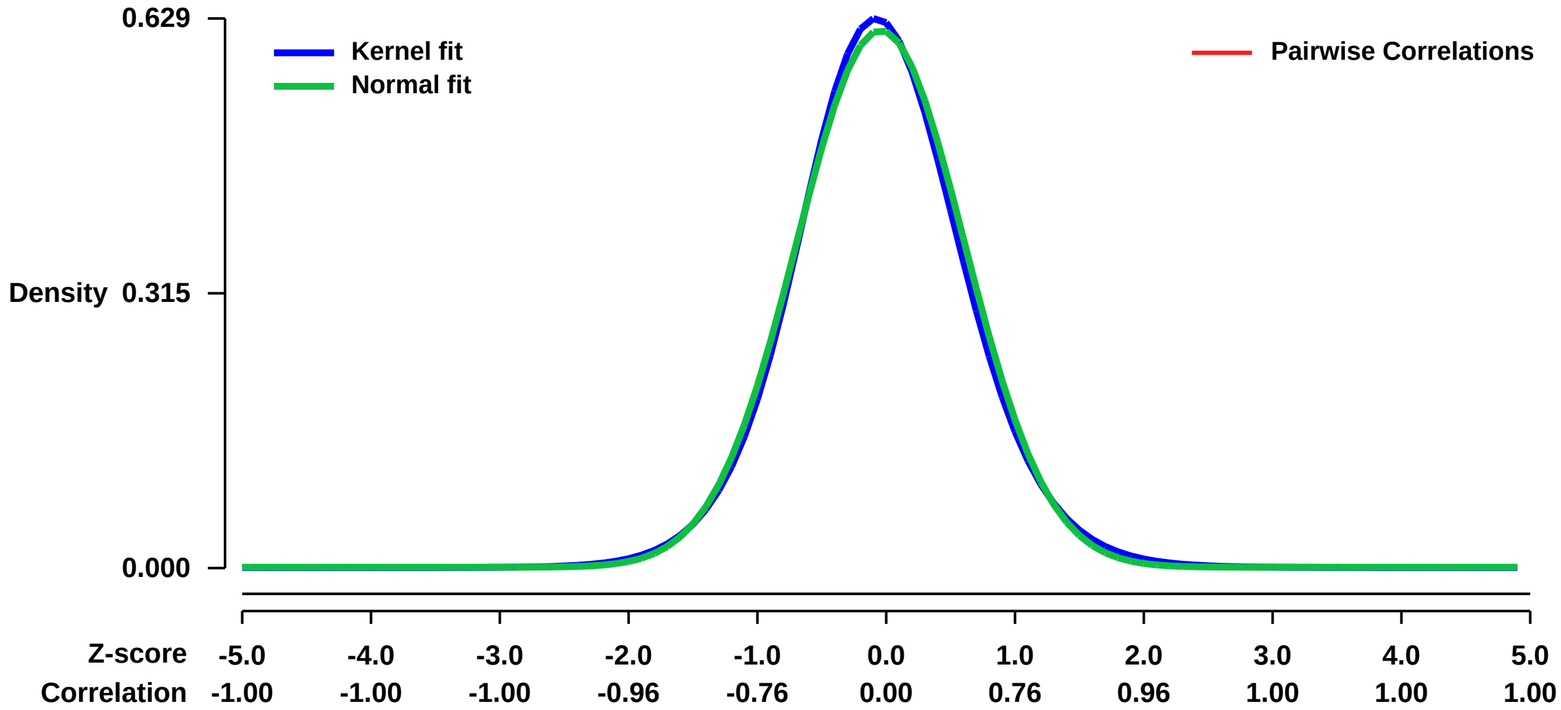

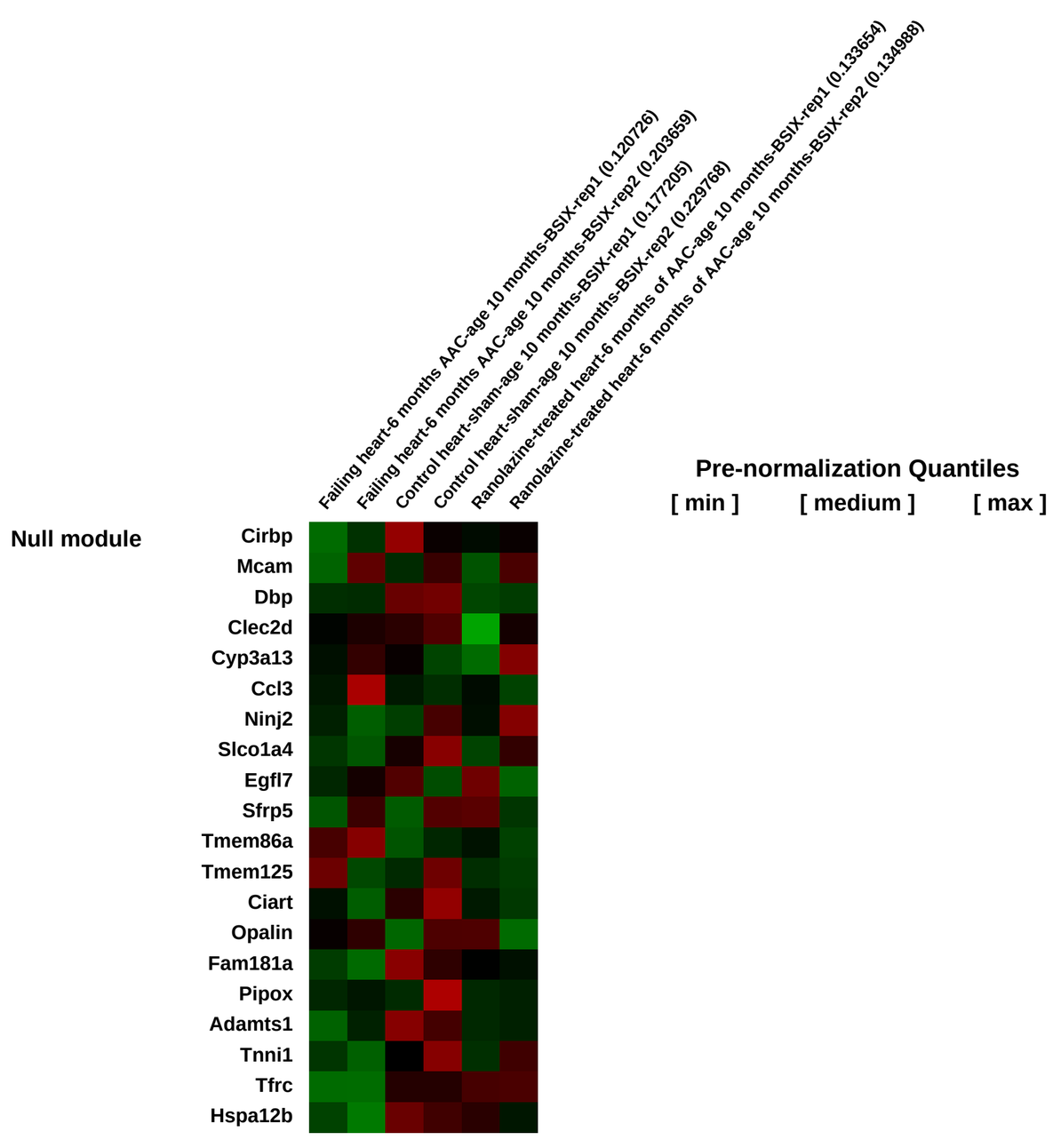

GEO Series "GSE13707" Expression Profiles

Num of samples in this series: 20

Scale of expression profile Z-scores

-3.0 -2.0 -1.0 0.0 1.0 2.0 3.0

GEO Link:	http://www.ncbi.nlm.nih.gov/geo/query/acc.cgi?acc=GSE13707
Status:	Public on Nov 22 2008
Title:	Effect of an anti-myostatin antibody on skeletal muscle gene expression in mice
Organism:	Mus musculus
Experiment type:	Expression profiling by array
Platform:	GPL1261
Pubmed ID:	19141683
Summary & Design:	**Summary:** More than 2,000 genes appear to be upregulated or downregulated in skeletal muscle of mice with constitutive knockout of myostatin (Steelman et al., FASEB J 20:580-2, 2006). This study was done to determine whether inhibition of myostatin activity in mature mice has similar effects on the pattern of gene expression. **Keywords: Differential expression in treated and control mice** **Overall design:** Ten samples from JA16 antibody-treated mice were compared with 10 samples from saline-treated mice

Background corr dist: KL-Divergence = 0.1434, L1-Distance = 0.0544, L2-Distance = 0.0058, Normal std = 0.4029

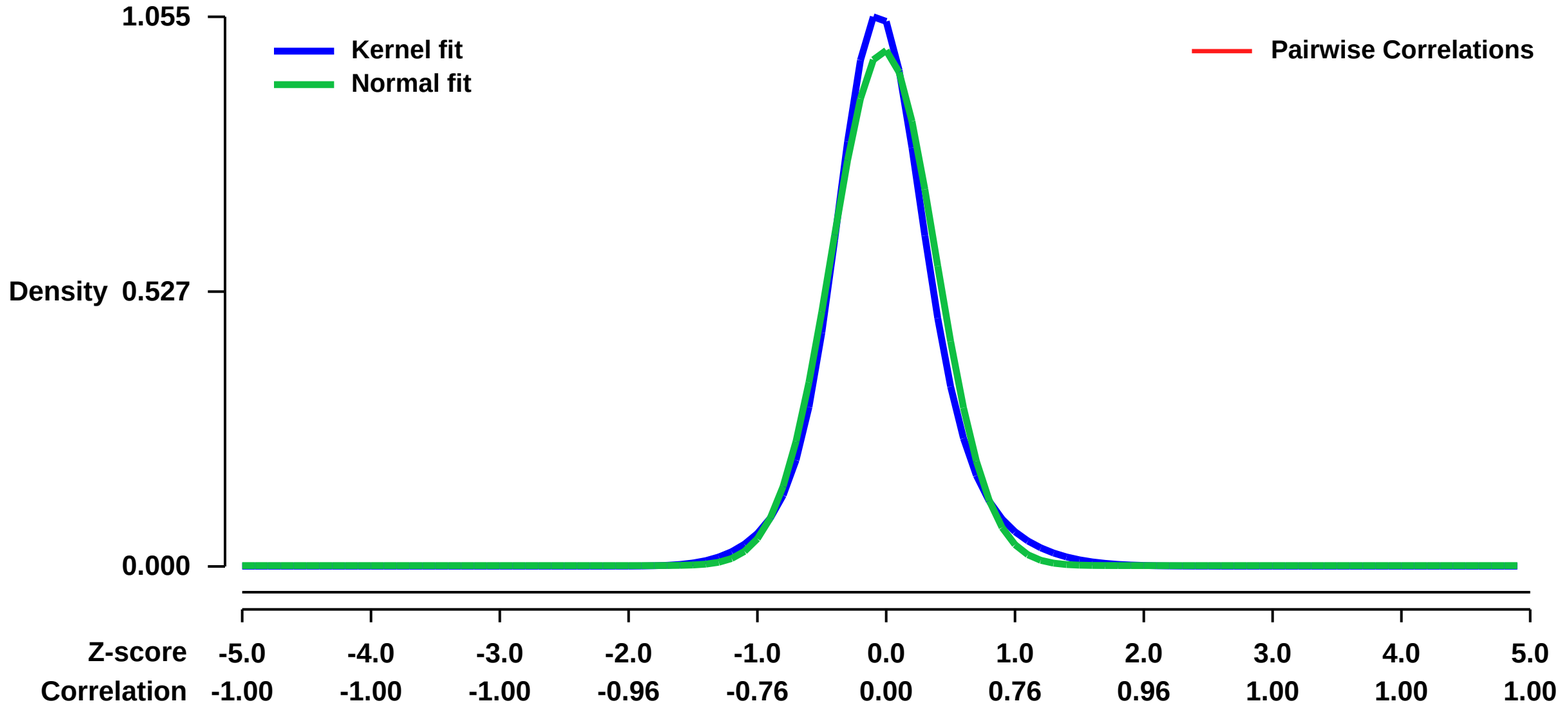

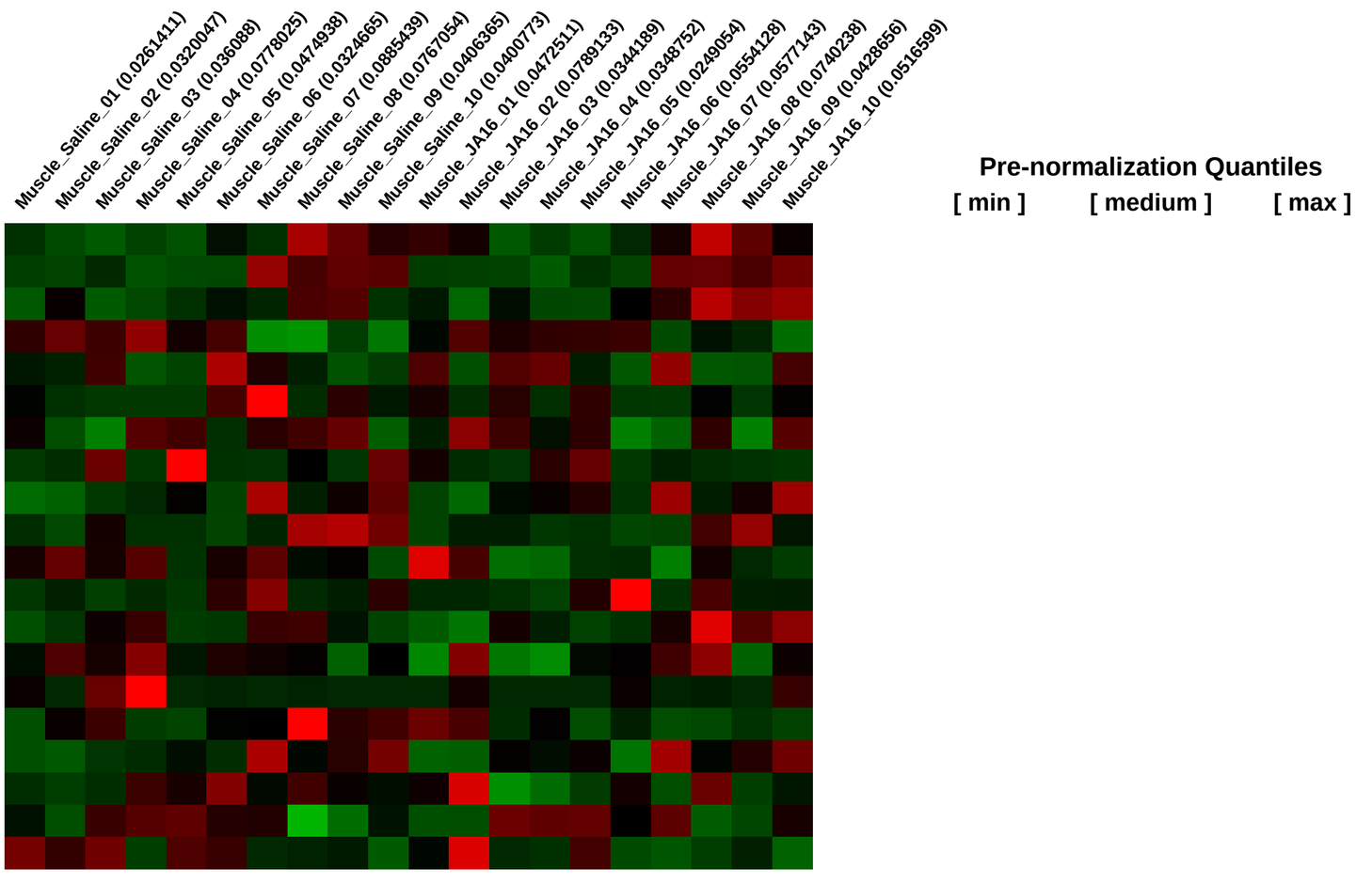

GEO Series "GSE16486" Expression Profiles

Num of samples in this series: 9

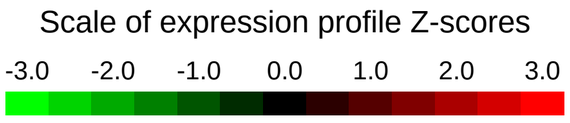

GEO Link:	http://www.ncbi.nlm.nih.gov/geo/query/acc.cgi?acc=GSE16486
Status:	Public on Jun 08 2009
Title:	Gene expression data from gastrocnemius muscle (m.Gas) in young adult mice
Organism:	Mus musculus
Experiment type:	Expression profiling by array
Platform:	GPL1261
Pubmed ID:	20403060
Summary & Design:	**Summary:** This study examined the effects of castration and testosterone replacement on global differential gene transcription in the gastrocnemius muscle (m.Gas) in young adult mice over 14-days. **Overall design:** Each of the 3 treatment groups was composed of 3 independent biological replicates, totaling 9 arrays. Equal amounts of the highest quality total RNA (4 ´µg) from three animals were pooled for each biological replicate, totaling the use of 27 animals in the 9-array experiment. The balanced design of this study enabled the use of a 1-way ANOVA, which was used to statistically determine which of the >34,000 genes (>45,000 probes) were differentially expressed between groups. The three pair-wise comparisons were: Castration vs. Sham (castration (C) effect); Testosterone vs. Castration (testosterone replacement (T) effect); and Testosterone vs. Sham (overall effects).

Background corr dist: KL-Divergence = 0.0262, L1-Distance = 0.0463, L2-Distance = 0.0036, Normal std = 0.7084

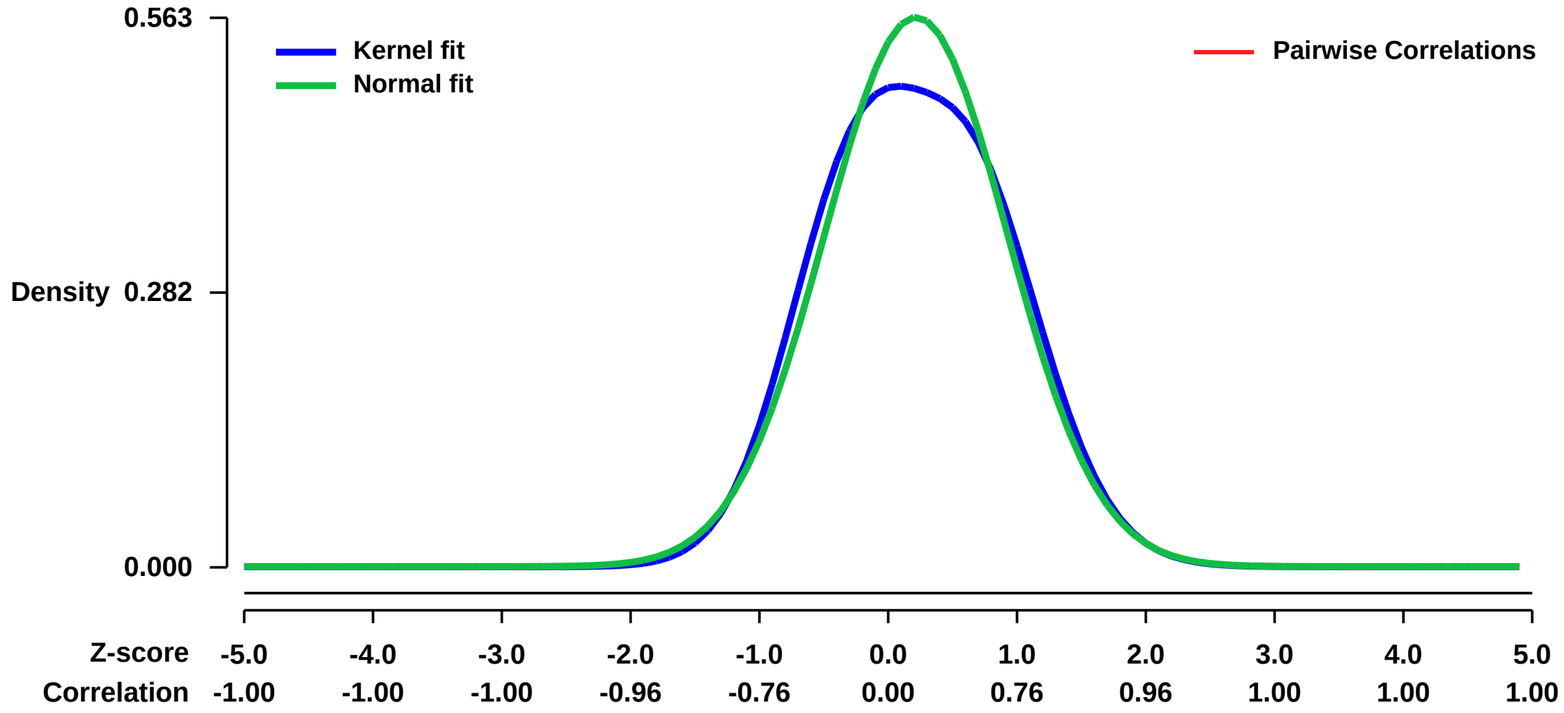

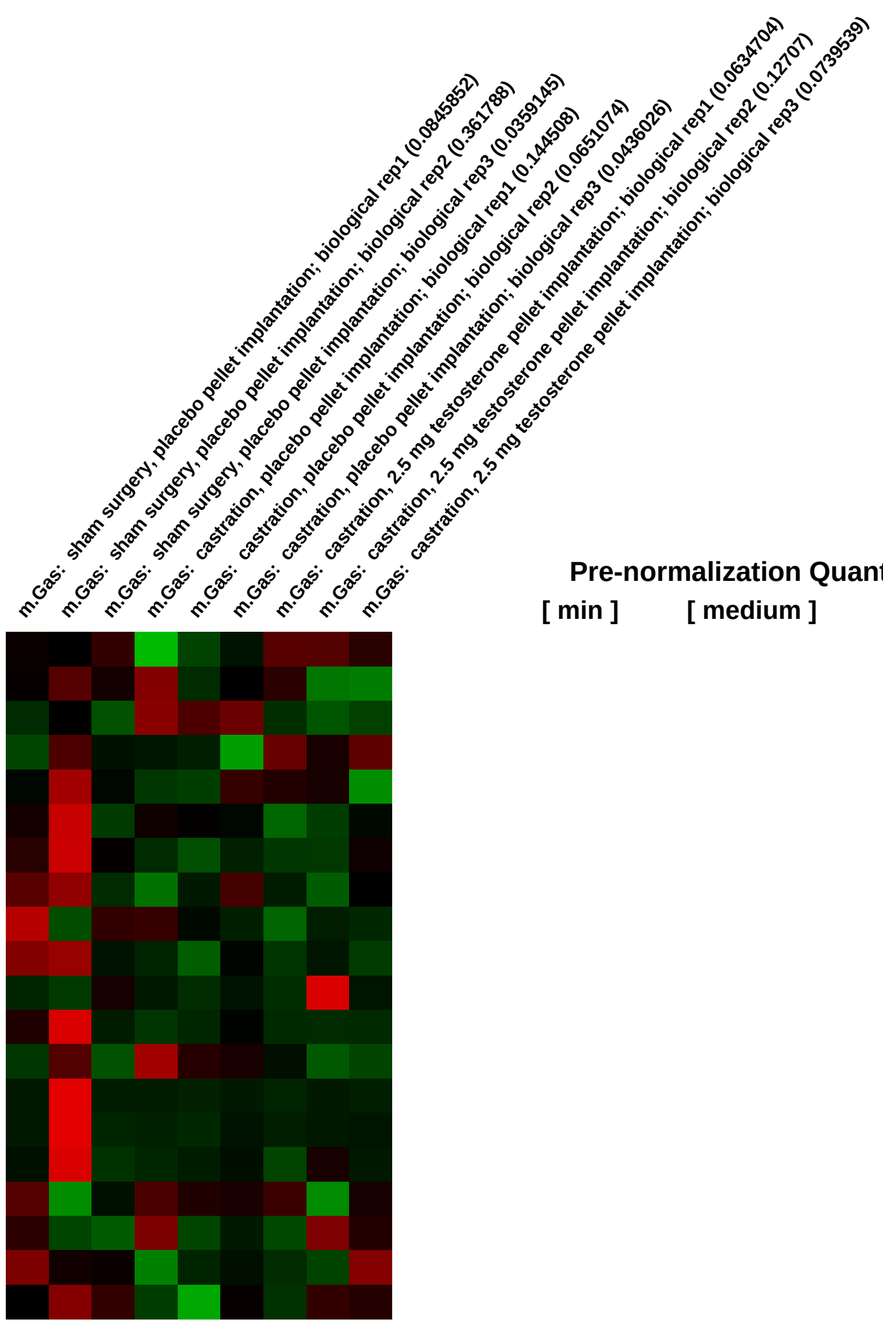

GEO Series "GSE23009" Expression Profiles

Num of samples in this series: 16

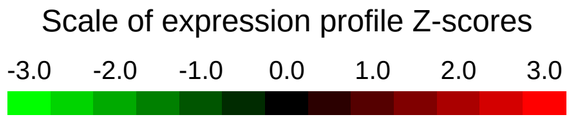

GEO Link:	**http://www.ncbi.nlm.nih.gov/geo/query/acc.cgi?acc=GSE23009**
Status:	**Public on Nov 10 2010**
Title:	**Effect of intra-cytoplasmic sperm injection (ICSI) on gene expression and development of mouse preimplantation embryos**
Organism:	**Mus musculus**
Experiment type:	**Expression profiling by array**
Platform:	**GPL1261**
Pubmed ID:	**20889529**
Summary & Design:	**Summary:** **Background: In vitro culture of preimplantation mouse embryos is associated with changes in gene expression. It is however not known if the method of fertilization affects the global pattern of gene expression. Method: We compared gene expression and development of mouse blastocysts produced by intra-cytoplasmic sperm injection and cultured in Whittenâ s medium (ICSIWM) or KSOM medium with amino acids (ICSIKSOMaa) with control blastocysts flushed out of the uterus on post coital day 3.5 (In vivo). Global pattern of gene expression was assessed using the Affymetrix 430 2.0 chip. In addition we compared gene expression in embryos generated in IVF or ICSI using WM. Results: Blastocysts resulting from ICSI fertilization have a reduction in the number of trophoblastic and inner cell mass cells compared to in vivo generated embryos. Approximately 1000 genes are different between ICSI blastocyst and in vivo blastocysts; proliferation, apoptosis and morphogenetic pathways are the most common pathways altered after in vitro culture. Unexpectedly, only 41 genes were statistically different between embryo cultured in suboptimal conditions (WM) or optimal conditions (KSOMaa). Conclusion: The method of fertilization plays a more important role in shaping the transcriptome of the developing mouse embryo than the culture media used.** **Overall design:** **16 samples were used in 4 treatment groups (4 replicate samples per treatment)**

Background corr dist: KL-Divergence = 0.0884, L1-Distance = 0.0402, L2-Distance = 0.0032, Normal std = 0.4589

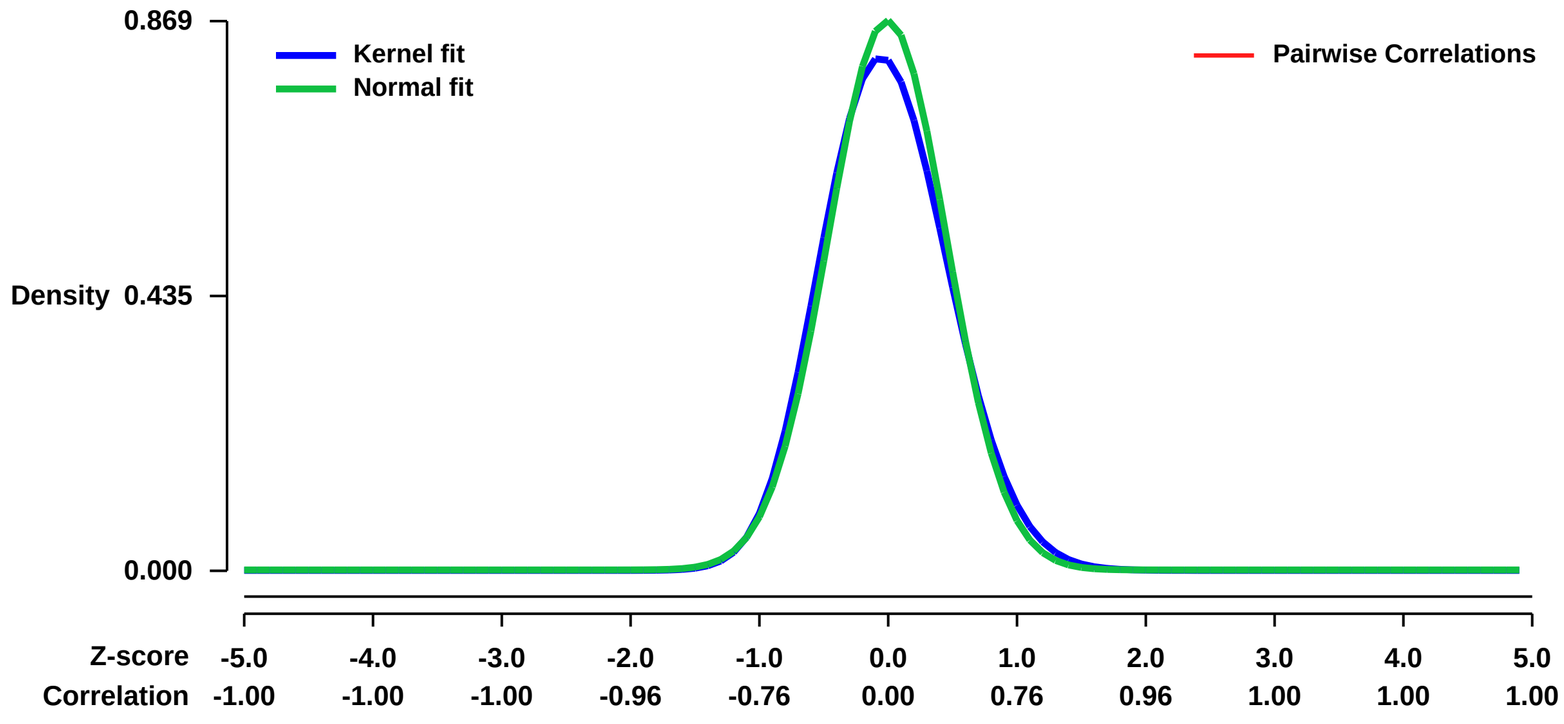

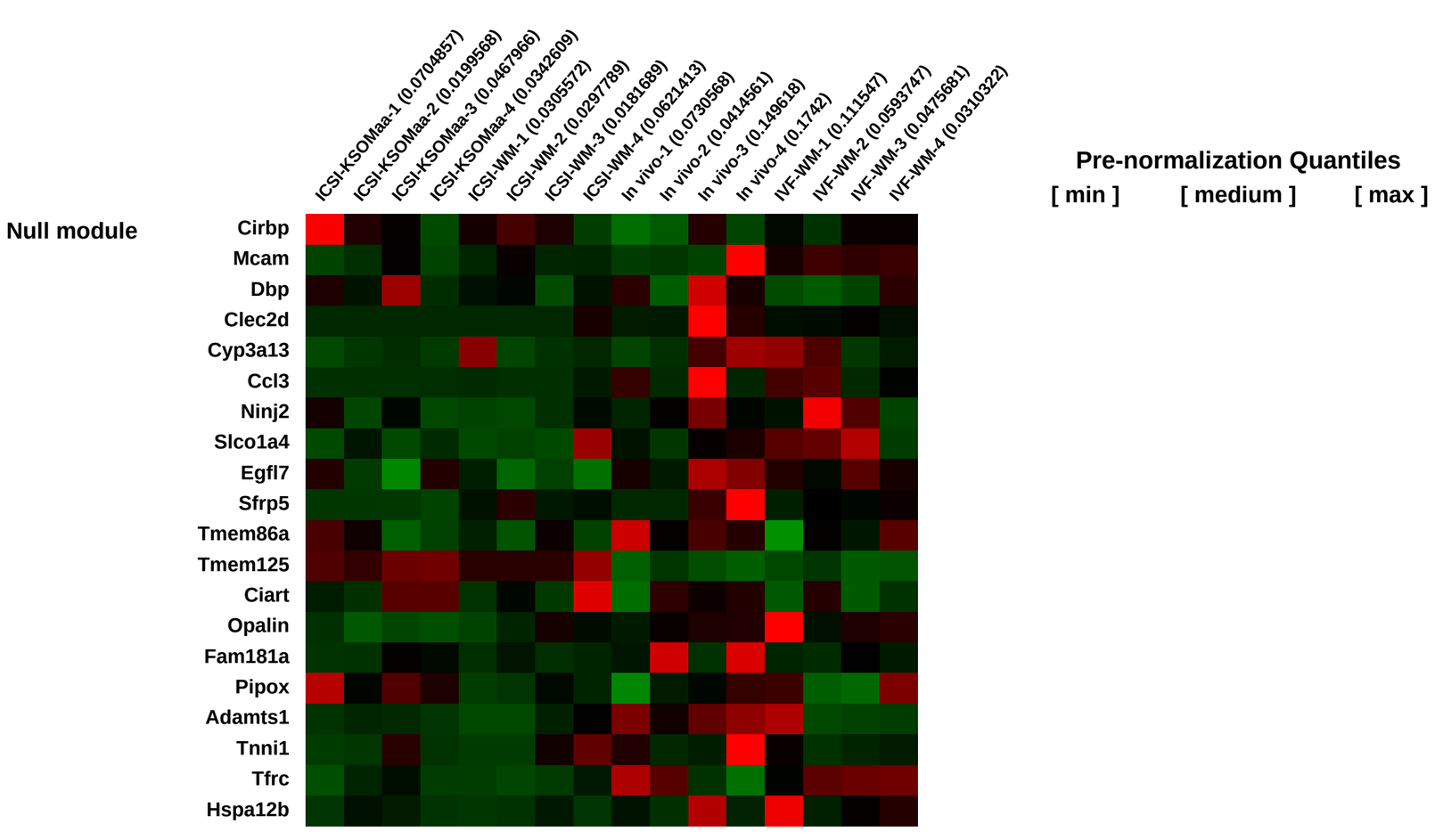

GEO Series "GSE47777" Expression Profiles

Num of samples in this series: 8

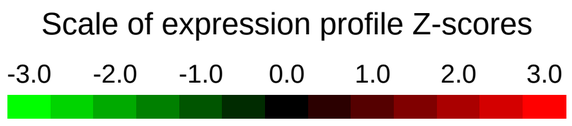

GEO Link:	http://www.ncbi.nlm.nih.gov/geo/query/acc.cgi?acc=GSE47777
Status:	Public on Jun 30 2013
Title:	Whole genome expression data comparison between WT and Cebpg-/- MEFs.
Organism:	Mus musculus
Experiment type:	Expression profiling by array
Platform:	GPL1261
Pubmed ID:	23775115
Summary & Design:	**Summary:** C/EBP‚† is an important regulator of oncogene-induced senescence (OIS). Here we show that C/EBP‚‡, a heterodimeric partner of C/EBP‚† whose biological functions are not well understood, inhibits cellular senescence. Cebpg-/- MEFs proliferated poorly, entered senescence prematurely, and expressed a pro-inflammatory gene signature, including elevated levels of senescence-associated secretory phenotype (SASP) genes whose induction by oncogenic stress requires C/EBP‚†. The senescence-suppressing activity of C/EBP‚‡ required its ability to heterodimerize with C/EBP‚†. Covalently linked C/EBP‚† homodimers (‚†~‚†) inhibited the proliferation and tumorigenicity of RasV12-transformed NIH3T3 cells, activated SASP gene expression, and recruited the CBP co-activator in a Ras-dependent manner, whereas ‚‡~‚† heterodimers lacked these capabilities and efficiently rescued proliferation of Cebpg-/- MEFs. C/EBP‚† depletion partially restored growth of C/EBP‚‡-deficient cells, indicating that the increased levels of C/EBP‚† homodimers in Cebpg-/- MEFs inhibit proliferation. The proliferative functions of C/EBP‚‡ are not restricted to fibroblasts, as hematopoietic progenitors from Cebpg-/- bone marrow also displayed impaired growth. Furthermore, high CEBPG expression correlated with poorer clinical prognoses in several human cancers, and C/EBP‚‡ depletion decreased proliferation and induced senescence in lung tumor cells. Our findings demonstrate that C/EBP‚‡ neutralizes the cytostatic activity of C/EBP‚† through heterodimerization, which prevents senescence and suppresses basal transcription of SASP genes. **Overall design:** Mouse embryonic fibroblasts were isolated at E13.5 and propagated. At passage 3 cells were plated with equal density and collected 48 hours later.

Background corr dist: KL-Divergence = 0.0549, L1-Distance = 0.0186, L2-Distance = 0.0005, Normal std = 0.5405

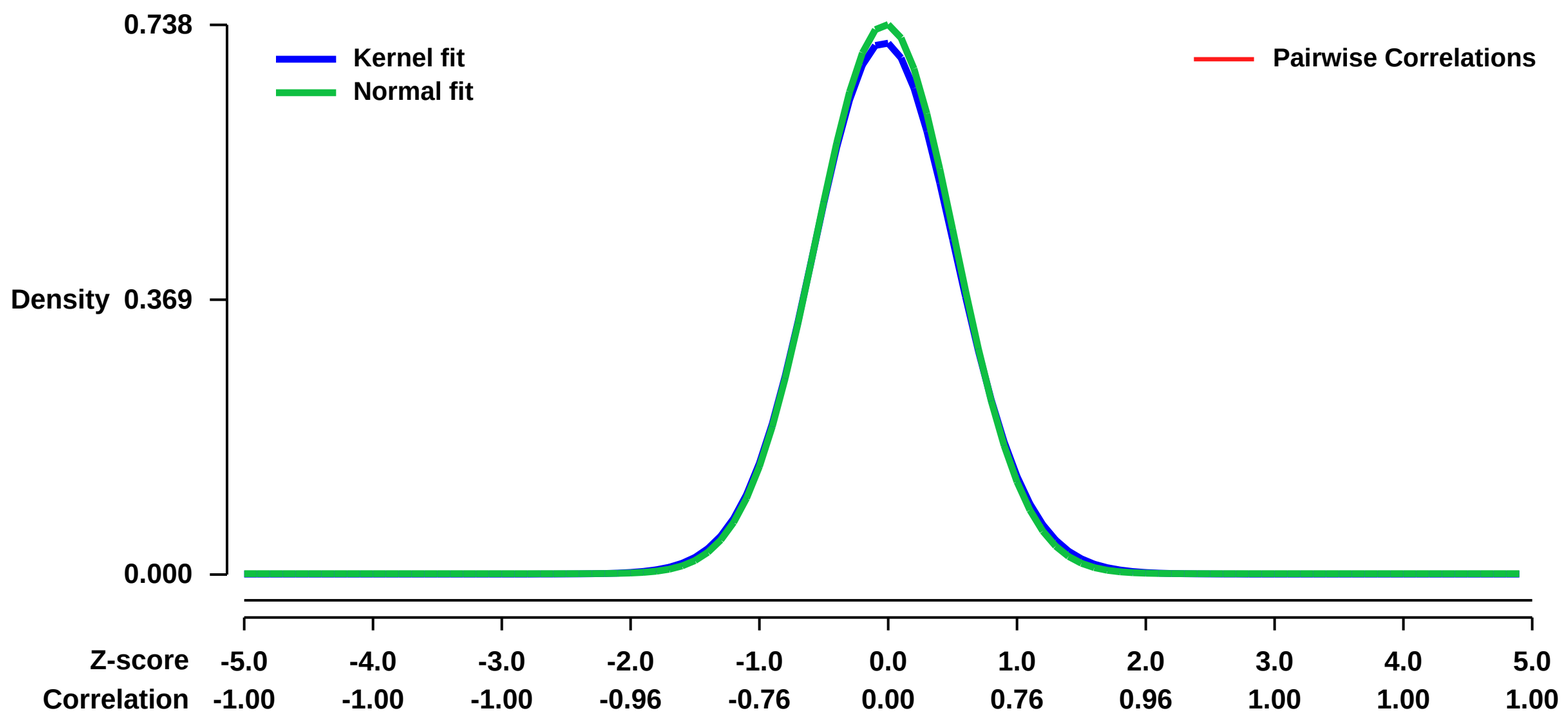

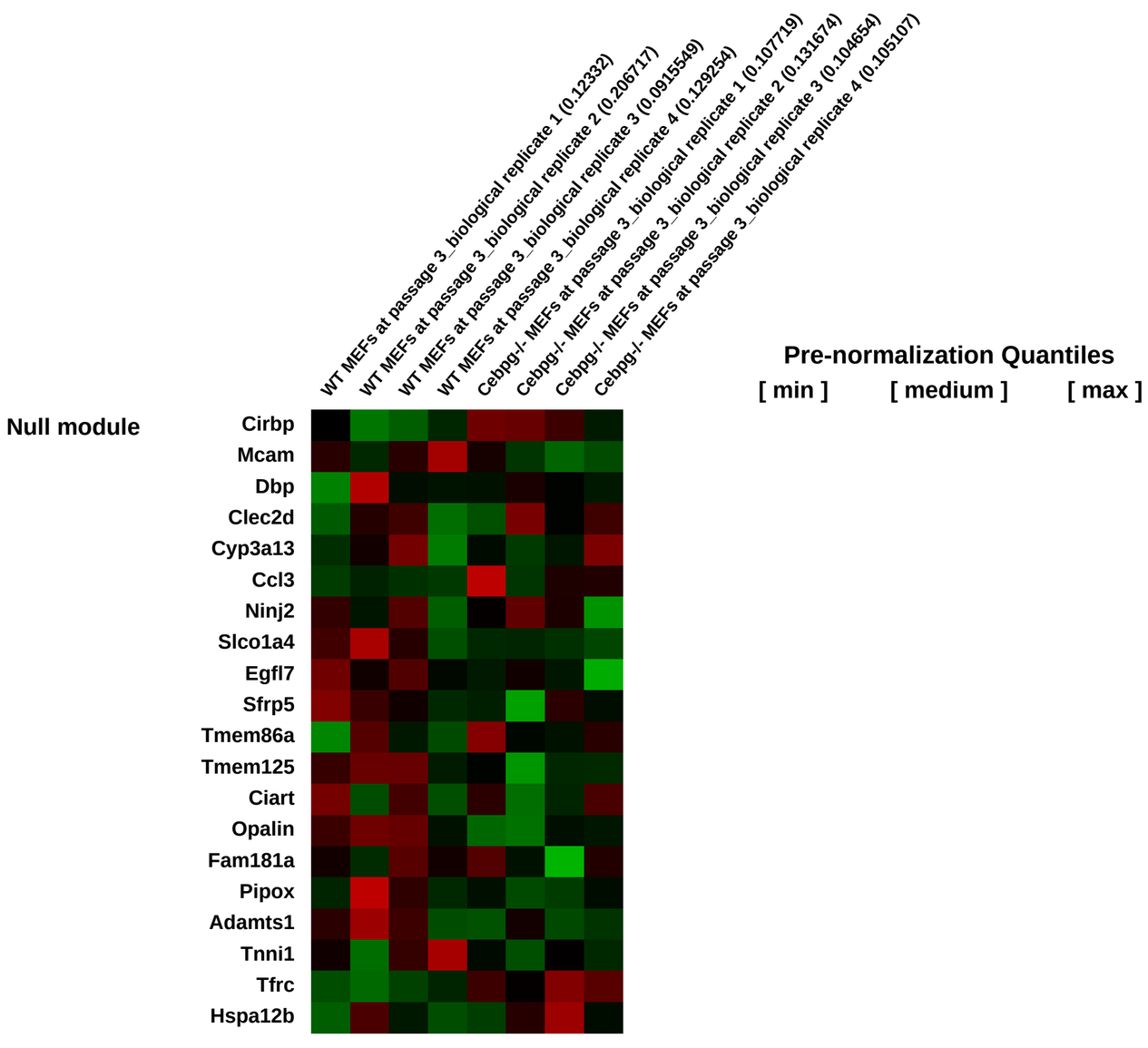

GEO Series "GSE33688" Expression Profiles

Num of samples in this series: 12

Scale of expression profile Z-scores

-3.0 -2.0 -1.0 0.0 1.0 2.0 3.0

GEO Link:	http://www.ncbi.nlm.nih.gov/geo/query/acc.cgi?acc=GSE33688
Status:	Public on Mar 14 2012
Title:	Genome-wide analyses reveal the extent of opportunistic STAT5 binding that does not yield transcriptional activation of neighboring genes
Organism:	Mus musculus
Experiment type:	Expression profiling by array
Platform:	GPL1261
Pubmed ID:	22319210
Summary & Design:	**Summary:** Stat5+/- mice were bred into the C57BL/6 background. Stat5+/- mice were intercrossed and mouse embryonic fibroblasts (MEFs) were isolated from 12.5-13.5-day WT or Stat5-/- fetuses. The retroviral-expression vector carrying a wild-type Stat5A gene based on an MSCV-IRES-GFP backbone (gift from Richard Moriggl, Ludwig-Boltzmann Institute, Vienna, Austria) was infected into Stat5-/- MEFs. FACS was used to select GFP+ cells. After 5 hours starvation in serum free medium with 0.1% of BSA, MEFs were treated with growth hormone for 2 hours. Total cellular RNA from each group of the MEFs was extracted with TRIzol reagent (Invitrogen) according to the manufacturer's instructions. Microarray analyses were performed using Affymetrix Mouse Genome 430 2.0 GeneChips (Affymetrix, Santa Clara, CA) (six groups, biological replicates for each group). Expression values were determined with GeneChip Operating Software (GCOS) v1.1.1 software. RMA signals were summarized using GeneSpring GX 10.0.1 (Agilent) and normalized by quantile normalization. All data analysis was performed with GeneSpring software GX 10.01. **Overall design:** Total 6 groups (S5, S5-GH, WT, WT_GH, KO, KO_GH), biological duplicate replication for each group

Background corr dist: KL-Divergence = 0.0547, L1-Distance = 0.0851, L2-Distance = 0.0113, Normal std = 0.6302

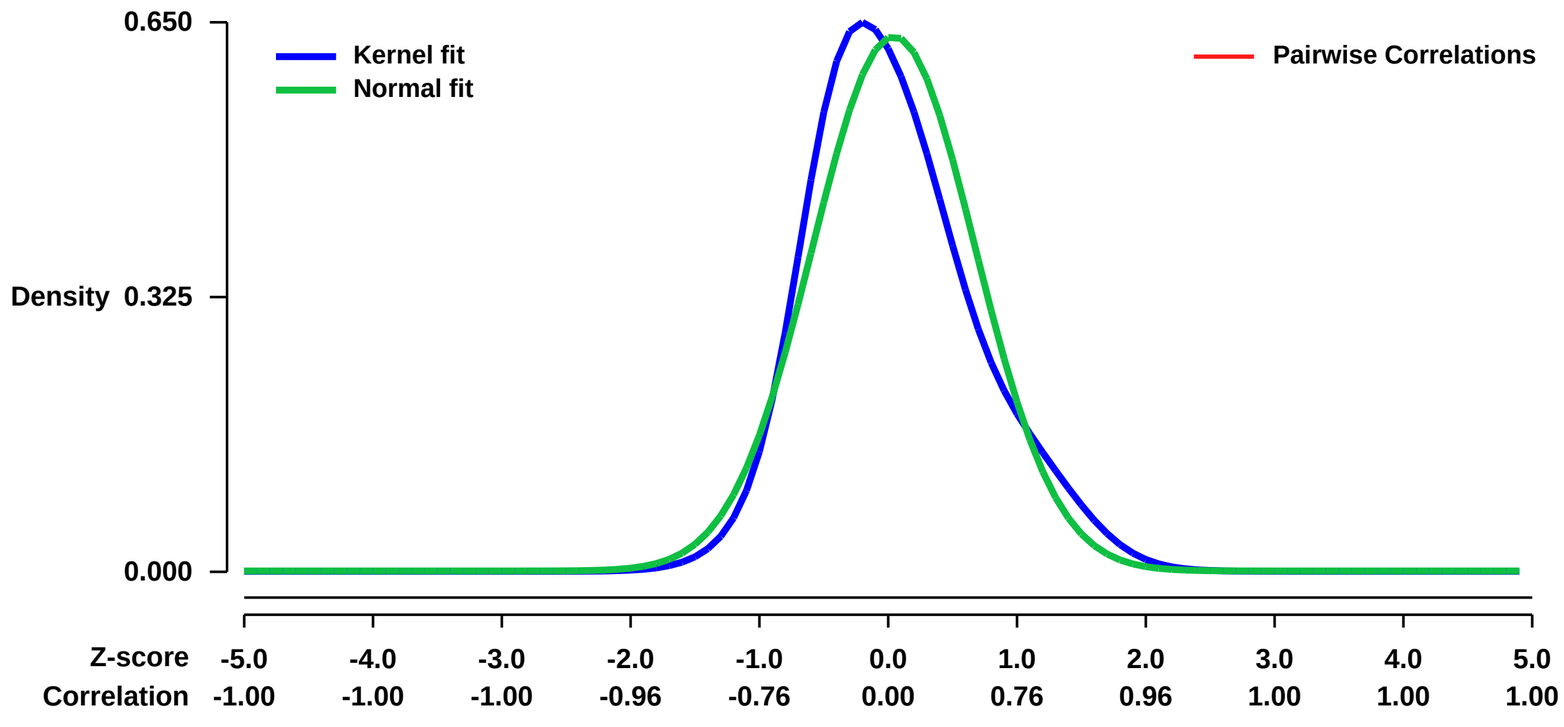

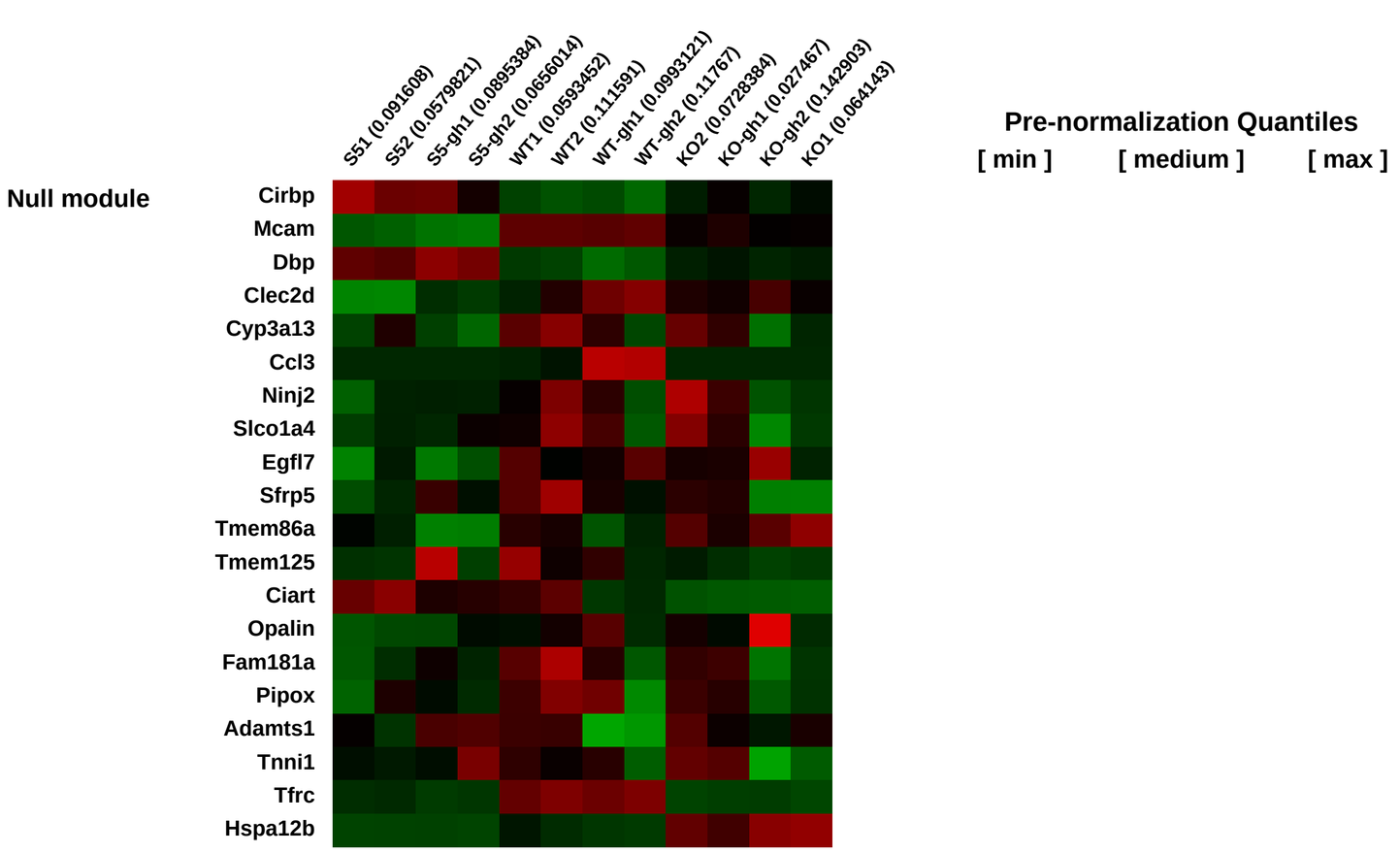

GEO Series "GSE11484" Expression Profiles

Num of samples in this series: 6

Scale of expression profile Z-scores

-3.0 -2.0 -1.0 0.0 1.0 2.0 3.0

GEO Link:	http://www.ncbi.nlm.nih.gov/geo/query/acc.cgi?acc=GSE11484
Status:	Public on Nov 15 2008
Title:	Gene expression analysis of ctrl_islets versus VhlhKO_islets
Organism:	Mus musculus
Experiment type:	Expression profiling by array
Platform:	GPL1261
Pubmed ID:	19056893
Summary & Design:	**Summary:** Understanding the nature of the various glucose-derived signals for insulin secretion (both triggering and amplifying) is essential for gaining insight into the functional failure of the beta-cells in diabetes and the development of drugs for correcting this problem. The beta-cells uniquely couple changes in cellular metabolism to electrical activity and thus insulin release. In mice, beta-cell specific deletion of the von Hippel-Lindau (VHL) tumor suppressor protein leads to the activation of a HIF transcription program that includes genes involved in glycolysis, suppression of mitochondrial activity and lactate production. This reprogramming of cellular metabolism results in abnormal insulin secretion properties. **Overall design:** Three batches of isolated islets from each genotype where used for RNA isolation and Affymetrix measurements.

Background corr dist: KL-Divergence = 0.0441, L1-Distance = 0.0255, L2-Distance = 0.0008, Normal std = 0.6009

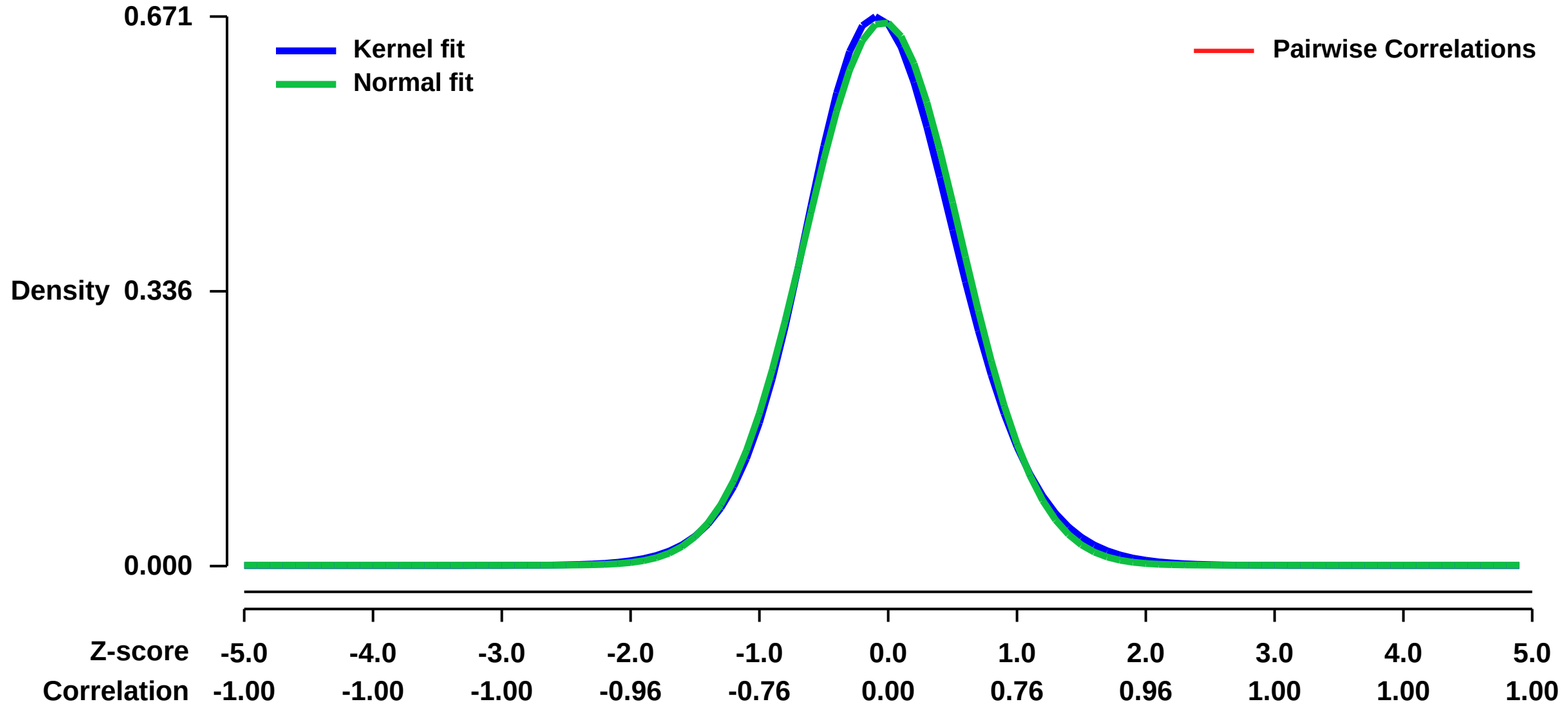

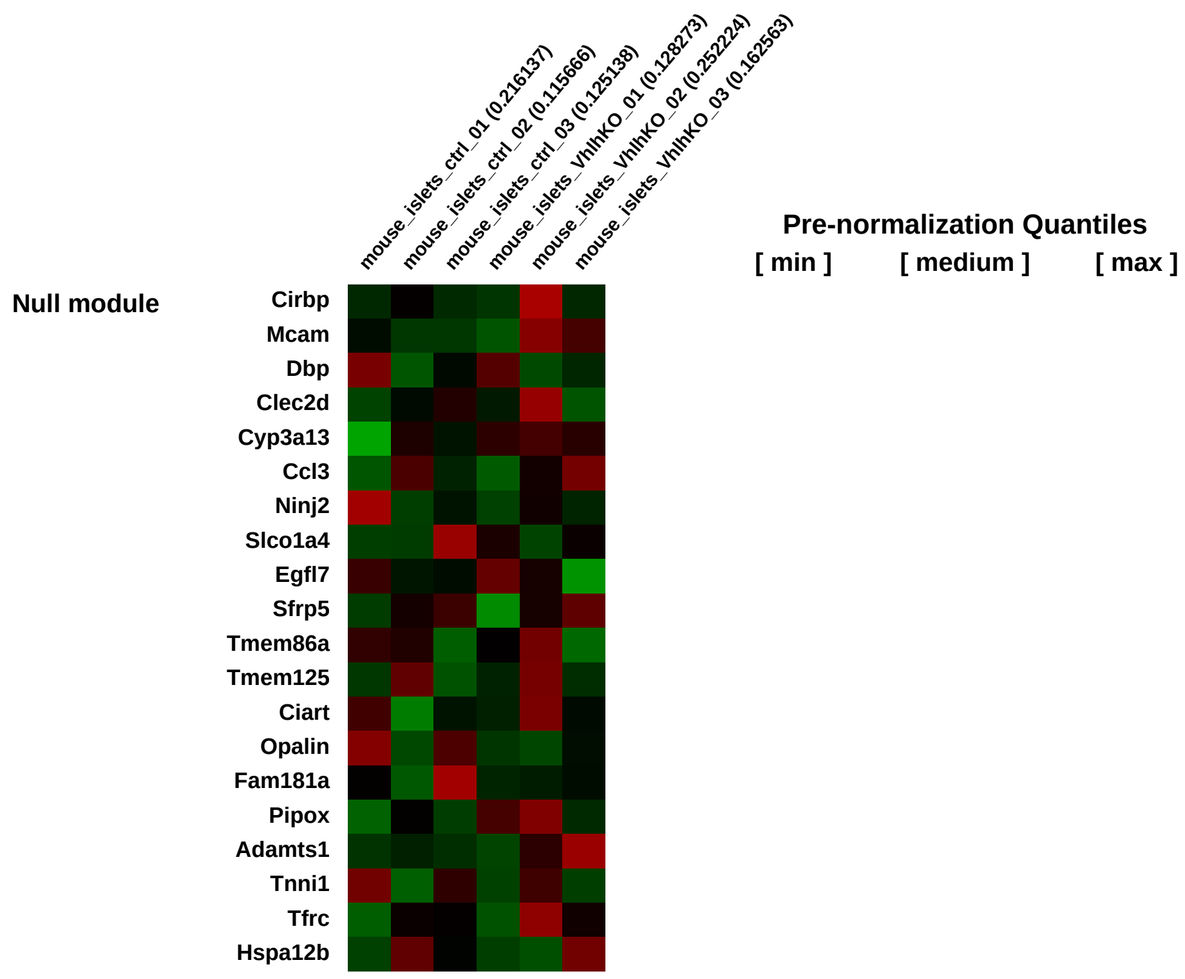

GEO Series "GSE21063" Expression Profiles

Num of samples in this series: 24

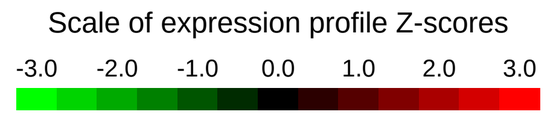

GEO Link:	http://www.ncbi.nlm.nih.gov/geo/query/acc.cgi?acc=GSE21063
Status:	Public on Mar 24 2011
Title:	NFATc1 controls the survival, function and suppressive capacity of B lymphocytes upon B cell receptor stimulation
Organism:	Mus musculus
Experiment type:	Expression profiling by array
Platform:	GPL1261
Pubmed ID:	21464221
Summary & Design:	**Summary:** Triggering of B cell receptors (BCR) induces a massive synthesis of NFATc1 in splenic B cells. By inactivating the Nfatc1 gene and re-expressing NFATc1 we show that NFATc1 levels are critical for the survival of splenic B cells upon BCR stimulation. NFATc1 ablation led to decreased BCR-induced Ca++ flux and proliferation of splenic B cells, increased apoptosis and suppressed germinal centre formation and immunoglobulin class switch by T cell-independent antigens. By controlling IL-10 synthesis in B cells, NFATc1 supported the proliferation and IL-2 synthesis of T cells in vitro and appeared to contribute to the mild clinical course of Experimental Autoimmune Encephalomyelitis in mice bearing NFATc1-/- B cells. These data indicate NFATc1 as a key factor controlling B cell function. **Overall design:** Splenic mice cells were isolated from mice bearing NFATc1 deficient B-cells and from control mice, stimulated with anti-IgM for 0h, 3h, 8h and 16h, respectively and isolated using Milteny beads to enrich the B cell population. This experiment was performed in 3 biological replicates.

Background corr dist: KL-Divergence = 0.1823, L1-Distance = 0.0423, L2-Distance = 0.0030, Normal std = 0.3613

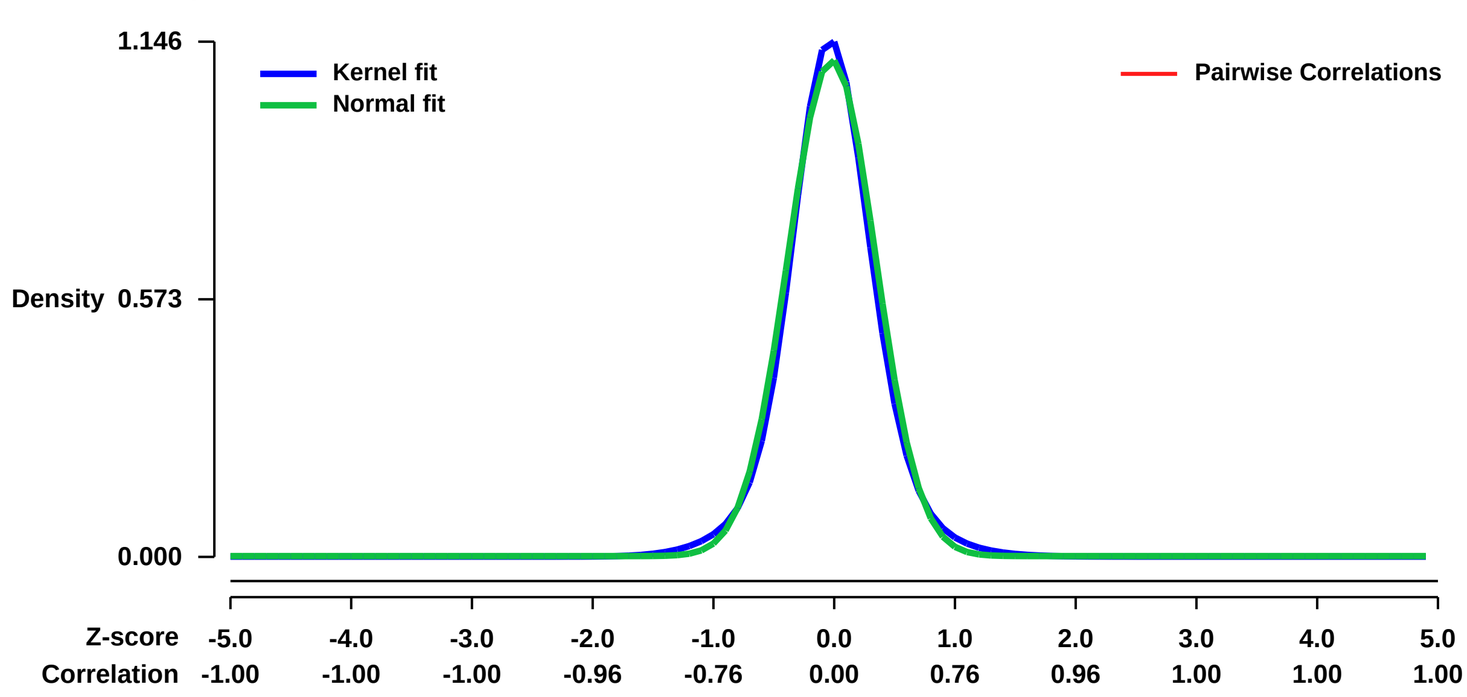

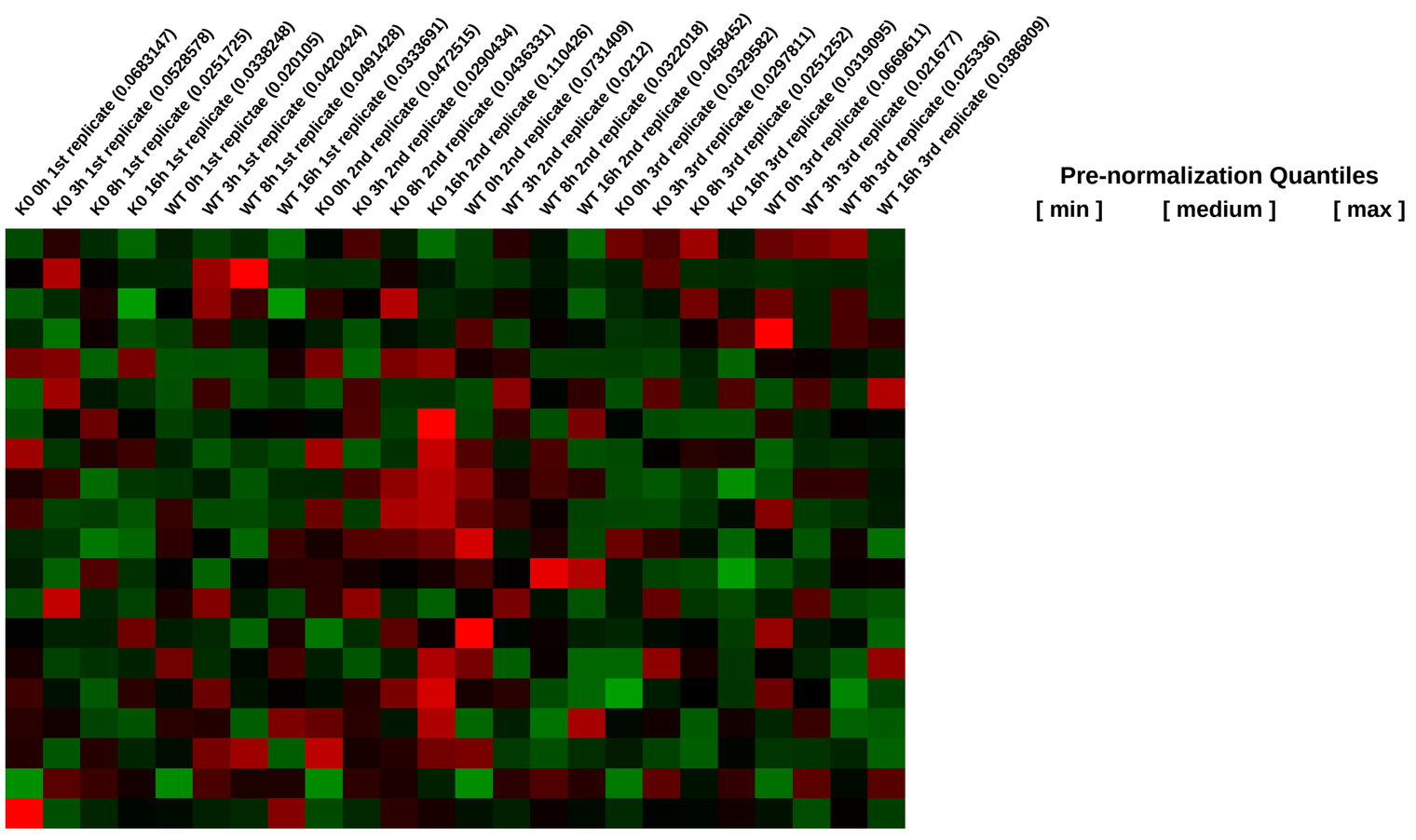

GEO Series "GSE26600" Expression Profiles

Num of samples in this series: 94

GEO Link: http://www.ncbi.nlm.nih.gov/geo/query/acc.cgi?acc=GSE26600
Status: Public on Jan 10 2013
Title: Cycad Genotoxin Methylazoxymethanol (MAM) Modulates Cellular Pathways Involved in Cancer and Neurodegenerative Disease
Organism: Mus musculus
Experiment type: Expression profiling by array
Platform: GPL1261
Pubmed ID: 21731631

Summary & Design:

Summary:
Methylazoxymethanol (MAM), the genotoxic metabolite of the cycad azoxyglucoside cycasin, induces genetic alterations in bacteria, yeast, plants, insects and mammalian cells, but adult nerve cells are thought to be unaffected. We show that the brains of young adult mice treated with a single systemic dose of MAM display DNA damage (O6-methylguanine lesions) that peaks at 48 hours and decline to near-normal levels at 7 days post-treatment. By contrast, at this time, MAM-treated mice lacking the gene encoding the DNA repair enzyme O6-methylguanine DNA methyltransferase (MGMT), showed persistent O6-methylguanine DNA damage. The DNA damage was linked to cell-signaling pathways that are perturbed in cancer and neurodegenerative disease. These data are consistent with the established carcinogenic and developmental neurotoxic properties of MAM in rodents, and they support the proposal that cancer and neurodegeneration share common signal transduction pathways. They also strengthen the hypothesis that early life exposure to the MAM glucoside cycasin has an etiological association with a declining, prototypical neurodegenerative disease seen in Guam, Japan, and New Guinea populations that formerly used the neurotoxic cycad plant for medicine and/or food. Exposure to environmental genotoxins may have relevance to the etiology of related tauopathies, notably, Alzheimerâ s disease, as well as cancer.

Overall design:
Mouse brains from eleven-week-old male C57BL6 wild-type and Mgmt-/- mice were exposed to either MAM or Vehicle for 6 hr, 24 hr, 48 hr, 168 hr. Five or six mice per group for a total of 94 mice.

Background corr dist: KL-Divergence = 0.1906, L1-Distance = 0.0481, L2-Distance = 0.0054, Normal std = 0.3949

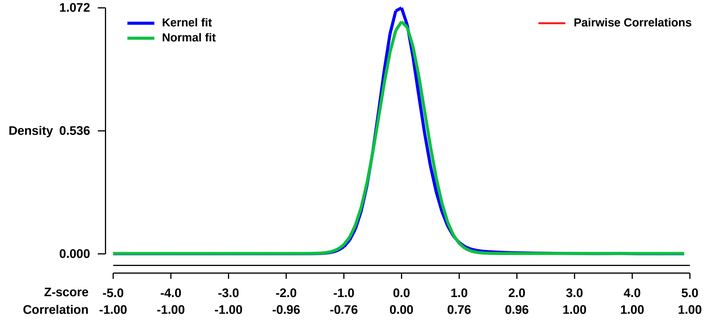

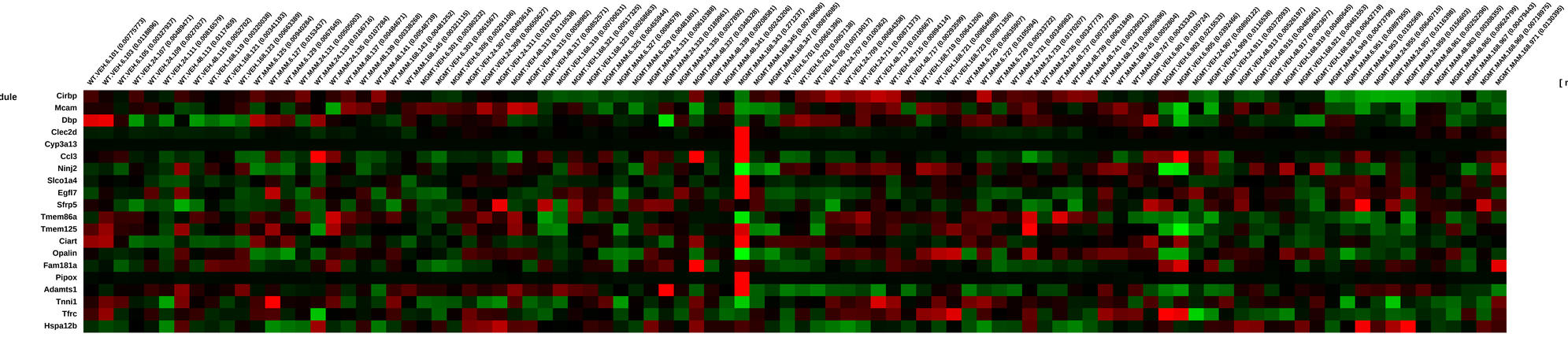

GEO Series "GSE7694" Expression Profiles

Num of samples in this series: 12

Scale of expression profile Z-scores

-3.0 -2.0 -1.0 0.0 1.0 2.0 3.0

GEO Link:	http://www.ncbi.nlm.nih.gov/geo/query/acc.cgi?acc=GSE7694
Status:	Public on Jun 11 2007
Title:	Cannabinoid receptor double knockout mice (Cnr1 -/- /Cnr2 -/-) in CHS model
Organism:	Mus musculus
Experiment type:	Expression profiling by array
Platform:	GPL1261
Pubmed ID:	17556587
Summary & Design:	**Summary:** We evaluated cutaneous contact hypersensitivity (CHS) in Cnr1-/-/Cnr2-/- animals using the obligate contact allergen 2,4-dinitrofluorobenzene (DNFB), which generates a specific cutaneous T-cell mediated allergic response upon repeated allergen contact. Allergic contact dermatitis affects about 5% of men and 11% of women in industrialized countries and is one of the leading causes for occupational diseases. In an animal model for cutaneous contact hypersensitivity we show that mice lacking both known cannabinoid receptors display exacerbated allergic inflammation. In contrast, fatty acid amide hydrolase deficient mice, which have increased levels of the endocannabinoid anandamide, displayed reduced allergic responses in the skin. Cannabinoid receptor antagonists exacerbated whereas receptor agonists attenuated allergic inflammation. These results demonstrate a protective role of the endocannabinoid system in contact allergy in the skin, and suggest a novel target for therapeutic intervention. Keywords: Strain (Wt versus Ko) and disease state (DNFB treated versus control). **Overall design:** Three wildtype mice (Wt) and three Cnr1-/-/Cnr2-/- (Ko) mice were used. Contact hypersensitivity was determined always at the right ears, which therefore were treated with DNFB (Tr). Left ears of mice were kept untreated and served as control ears (C). A total of 12 hybridizations were performed (2 strains x 2 treatments X 3 biological replicates) in this experiment.

Background corr dist: KL-Divergence = 0.0647, L1-Distance = 0.0516, L2-Distance = 0.0039, Normal std = 0.5463

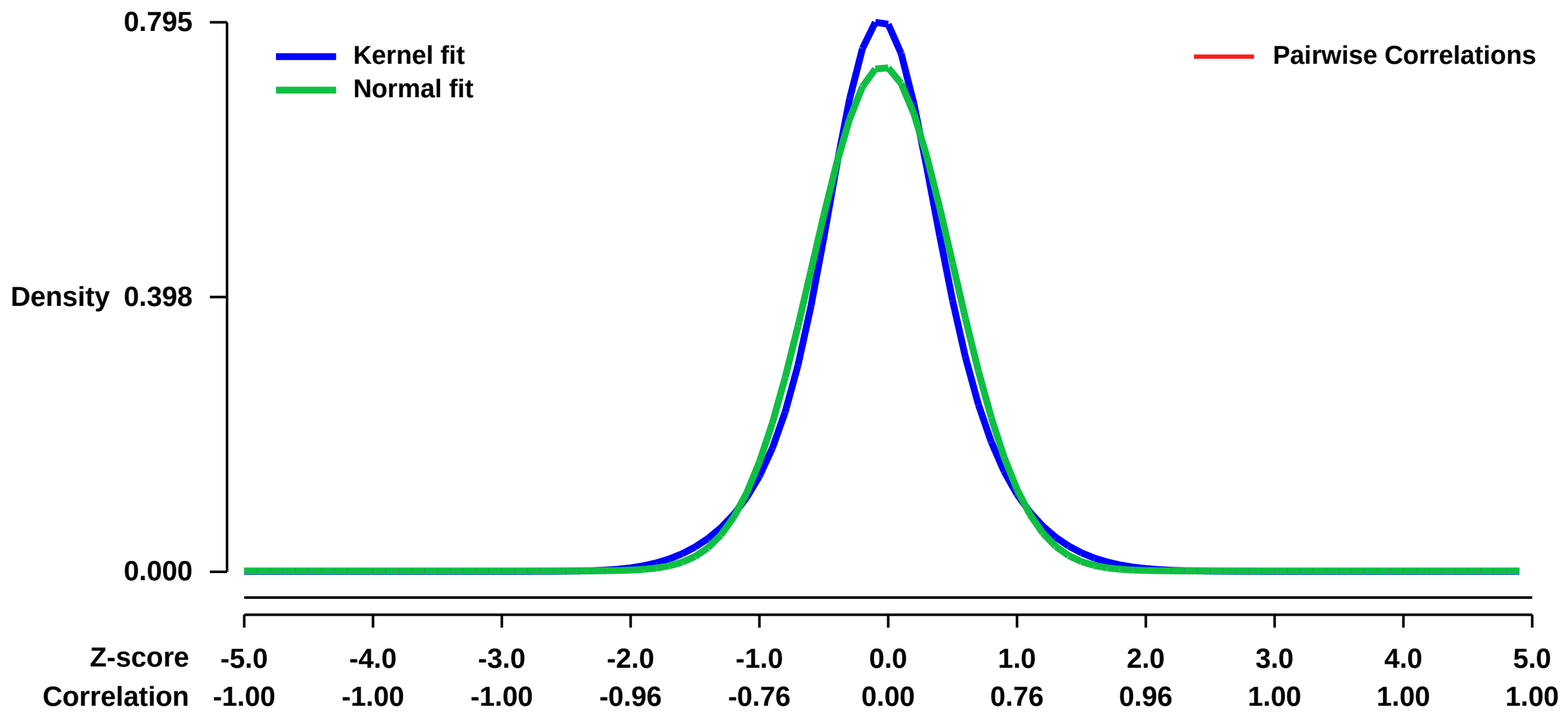

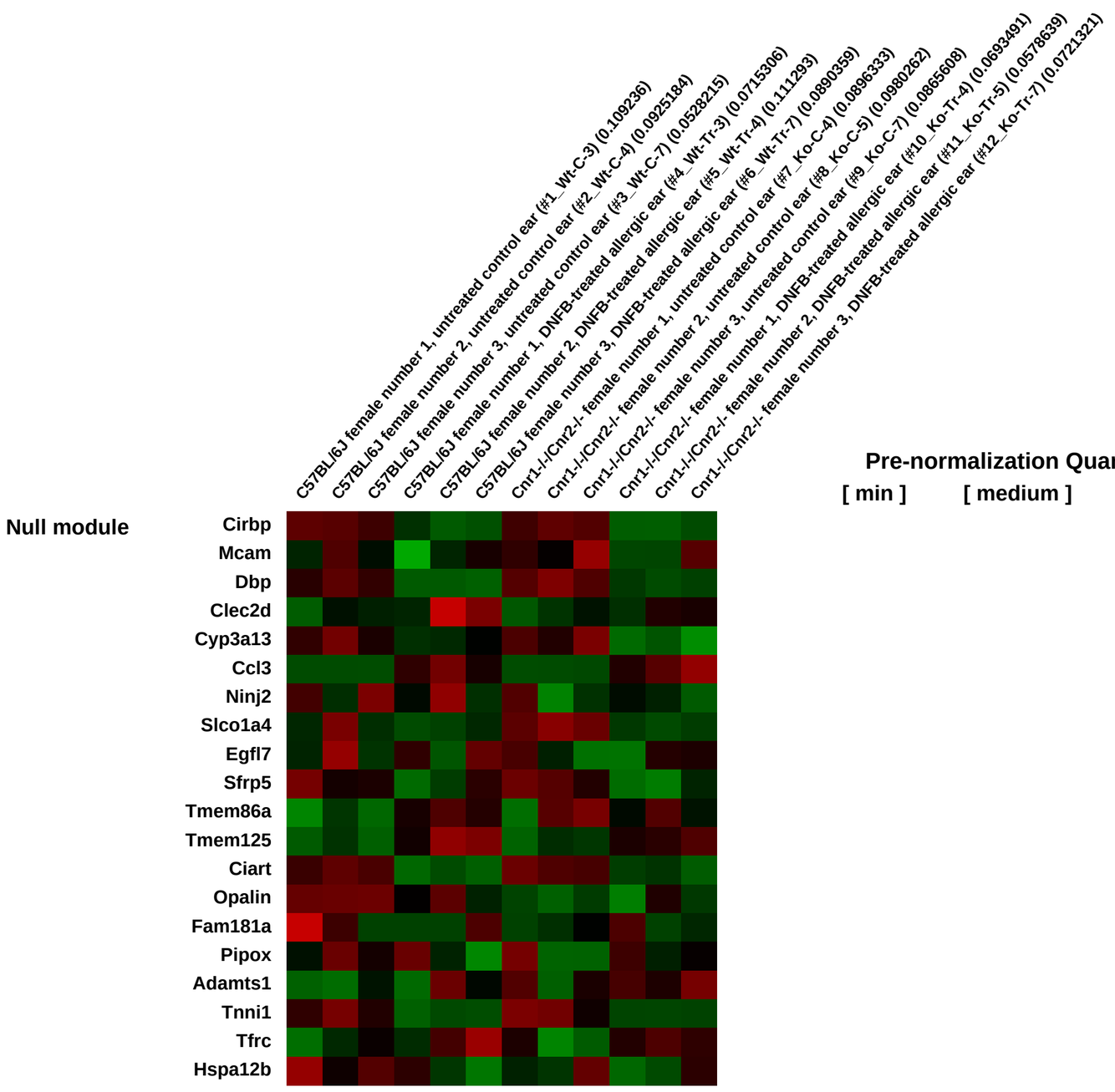

GEO Series "GSE35396" Expression Profiles

Num of samples in this series: 24

Scale of expression profile Z-scores

-3.0 -2.0 -1.0 0.0 1.0 2.0 3.0

GEO Link:	http://www.ncbi.nlm.nih.gov/geo/query/acc.cgi?acc=GSE35396
Status:	Public on Jul 26 2012
Title:	Selective knockout of NeuroD1 in the retina and pineal gland
Organism:	Mus musculus
Experiment type:	Expression profiling by array
Platform:	GPL1261
Pubmed ID:	22784109
Summary & Design:	**Summary:** NeuroD1 encodes a basic helix-loop-helix transcription factor involved in the development of neural and endocrine structures. NeuroD1 mRNA is highly abundant in the adult mammalian pineal gland and exhibits a developmental expression pattern similar to the retina. This is consistent with the common evolutionary origin of pinealocytes and retinal photoreceptors. Pinealocytes and retinal photoreceptors express a shared set of phototransduction genes and submammalian pinealocytes are photosensitive. In contrast to the retina, the pineal gland is a relatively homogeneous structure, composed 95% of pinealocytes. This makes the pineal gland a particularly useful model for understanding photoreceptor cell biology. The loss of NeuroD1 in the retina results in progressive photoreceptor degeneration and the molecular mechanisms underlying this retinal degeneration phenotype remain unknown. Similarly, the role that NeuroD1 plays in the pineal gland is unknown. To determine the function of NeuroD1 in the pineal gland and retina, a Cre/loxP recombination strategy was used to selectively target a NeuroD1 floxed allele and generate NeuroD1 conditional knockout (cKO) mice. Tissue specificity was conferred using Cre recombinase expressed under the control of the promoter of Crx, a transcription factor selectively expressed in the pineal gland and retina. Pineal and retinal tissues from two-month-old NeuroD1 cKO and control animals were used in microarray studies to identify candidate genes responsible for the photoreceptor degeneration phenotype. **Overall design:** The Cre/loxP recombination strategy was used to target a NeuroD1 floxed allele and generate NeuroD1 conditional knockout mice (NeuroD1floxed::Crx-Cre+/-). NeuroD1 floxed mice (NeuroD1floxed::Crx-Cre-/-) served as the controls. Pineal glands and retinas from two-month-old control and conditional knockout mice were collected at ZT6 and ZT20. 3 pools of 6 pineal glands per genotype and respective time of day were collected for each sample. Similarly, 3 pools of 6 retinas each were also collected. RNA from each pool was extracted and hybridized on the Affymetrix Mouse 430 2.0 array.

Background corr dist: KL-Divergence = 0.0411, L1-Distance = 0.0557, L2-Distance = 0.0049, Normal std = 0.6303

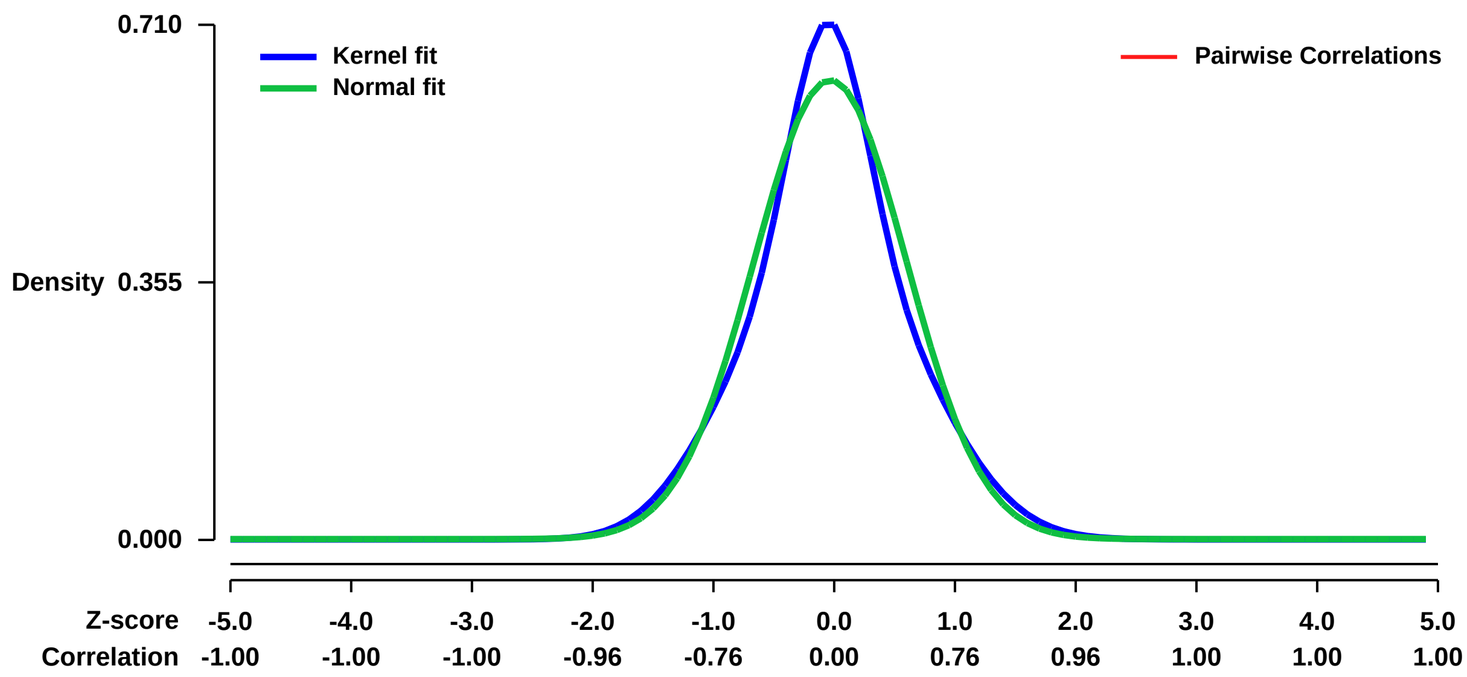

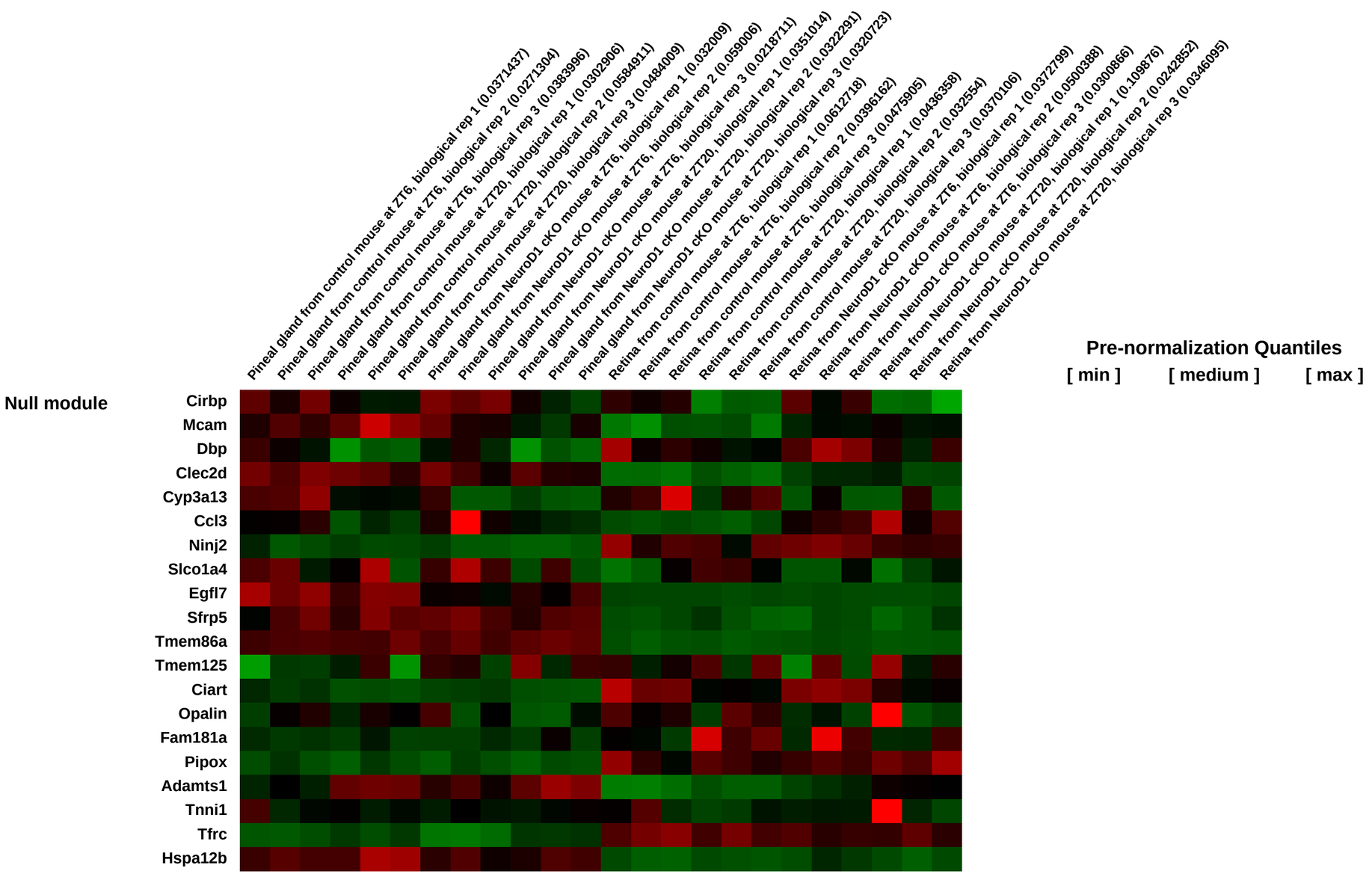

GEO Series "GSE11358" Expression Profiles

Num of samples in this series: 8

Scale of expression profile Z-scores

-3.0 -2.0 -1.0 0.0 1.0 2.0 3.0

GEO Link:	http://www.ncbi.nlm.nih.gov/geo/query/acc.cgi?acc=GSE11358
Status:	Public on May 17 2008
Title:	Histones associated with downregulated genes are hypo-acetylated in Huntingtonâ s disease models
Organism:	Mus musculus
Experiment type:	Expression profiling by array
Platform:	GPL1261
Pubmed ID:	17409194
Summary & Design:	**Summary:** Transcriptional dysregulation plays a major role in the pathology of Huntington's disease (HD). However, the mechanisms causing selective downregulation of genes remain unknown. Histones regulate chromatin structure and thereby control gene expression; recent studies have demonstrated a therapeutic role for histone deacetylase (HDAC) inhibitors in polyglutamine diseases. This study demonstrates that despite no change in overall acetylated histone levels, histone H3 is hypo-acetylated at promoters of downregulated genes in R6/2 mice, ST14a and STHdh cells, as demonstrated by in vivo chromatin immunoprecipitation. In addition, HDAC inhibitor treatment increases association of acetylated histones with downregulated genes and corrects mRNA abnormalities. In contrast, there is a decrease in mRNA levels in wild-type cells following treatment with a histone acetyltransferase inhibitor. Although changes in histone acetylation correlate with decreased gene expression, histone hypo-acetylation may be a late event, as no hypo-acetylation is observed in 4-week-old R6/2 mice. Nevertheless, treatment with HDAC inhibitors corrects mRNA abnormalities through modification of histone proteins and may prove to be of therapeutic value in HD. **Keywords:** cell type comparison and disease state analysis **Overall design:** The processed images of the arrays were analyzed for quality control, we found all the samples to be of equal very good quality, with an average of 40.5% ´– 1.44% Present calls with a range of 38% to 42.4%, (the background, noise, spike in controls, housekeeping genes presented a variability over the 8 samples less than 7% pre-normalization). In addition, 31.55% of the probe sets were called Present or Marginal in all the 8 samples and 44.6% were called Absent in all the 8 samples, showing a good consistency of the quality between the samples and between the groups compared.

Background corr dist: KL-Divergence = 0.0500, L1-Distance = 0.0375, L2-Distance = 0.0017, Normal std = 0.6073

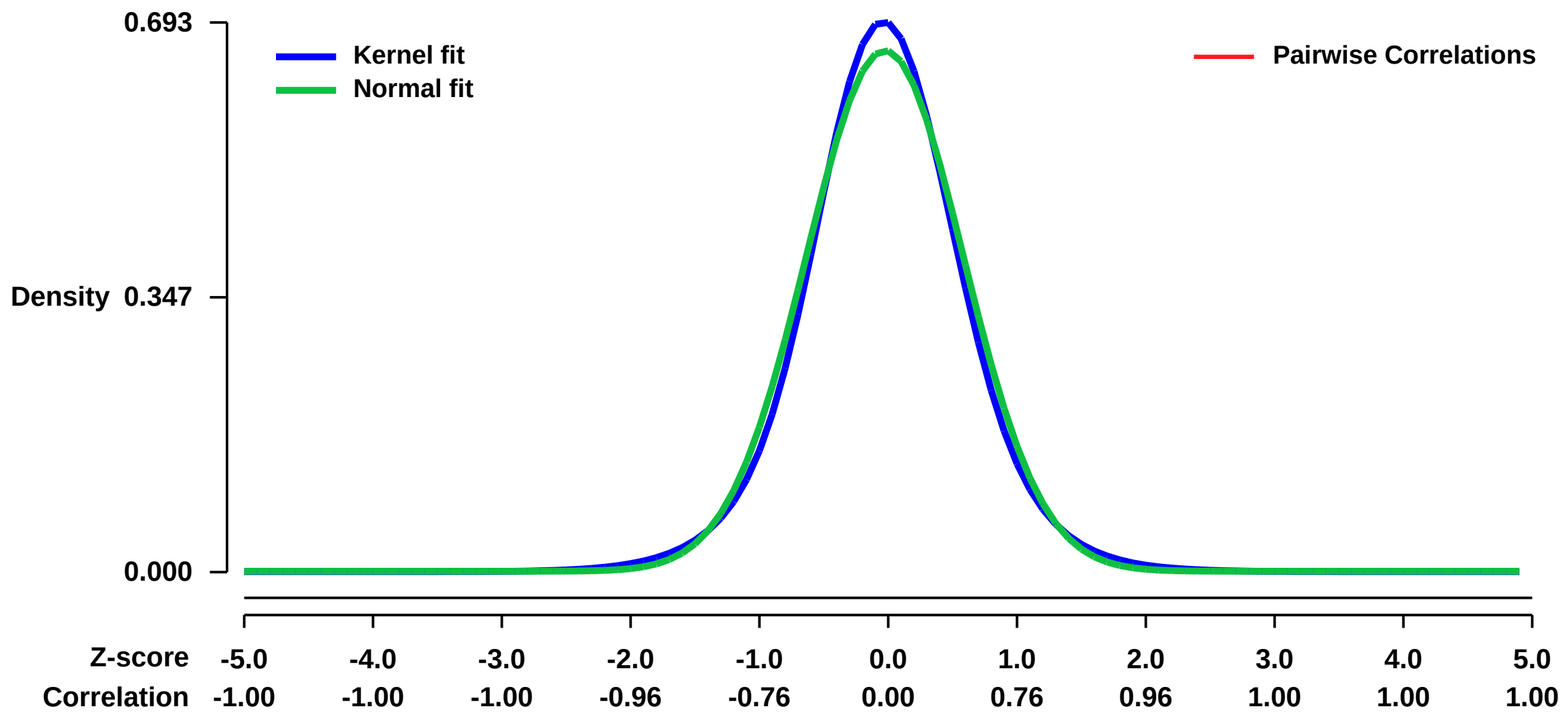

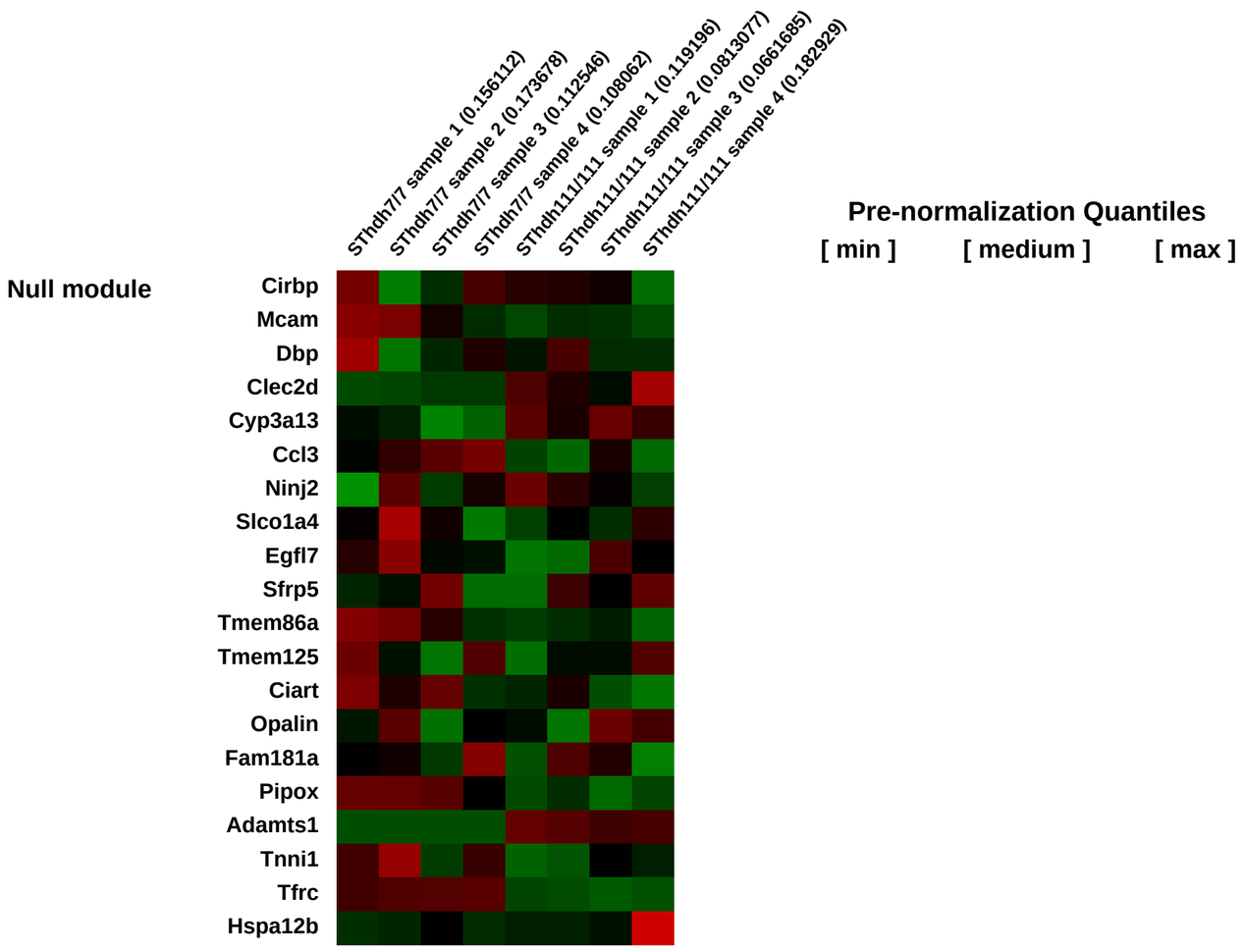

GEO Series "GSE15062" Expression Profiles

Num of samples in this series: 21

Scale of expression profile Z-scores

-3.0 -2.0 -1.0 0.0 1.0 2.0 3.0

GEO Link:	http://www.ncbi.nlm.nih.gov/geo/query/acc.cgi?acc=GSE15062
Status:	Public on Nov 23 2009
Title:	Mouse aorta smooth muscle cells differentiate into lymphoid tissue organizers upon combined TNFR1/LTBR NF-kB signaling
Organism:	Mus musculus
Experiment type:	Expression profiling by array
Platform:	GPL1261
Pubmed ID:	20139359
Summary & Design:	**Summary:** Mouse aorta smooth muscle cells (SMCs) express TNF receptor superfamily member 1A (TNFR1) and lymphotoxin ˆ receptor (LTˆ R). Circumstantial evidence has linked the SMC LTˆ R to tertiary lymphoid organogenesis in diseased aortae of hyperlipidemic mice. Here, we explored potential roles of TNFR1 and LTˆ R activation in cultured SMCs. TNFR1 signaling by TNF activated the classical RelA NF-¸”B pathway, whereas LTˆ R signaling by agonistic anti LTˆ R antibody activated both the classical RelA and alternative RelB NF-¸”B pathways. Addition of both agonists synergized to enhance p100 inhibitor processing to the p52 subunit of NF-¸”B and promoted its nuclear translocation suggesting RelA-RelB cross-talk in transcription regulation. Correspondingly, microarrays showed that simultaneous TNFR1 and LTˆ R activation when compared to activation of single receptors was followed by markedly elevated levels of mRNAs encoding leukocyte homeostatic chemokines CCL2, CCL5, CXCL1, and CX3CL1. Furthermore, SMCs acquired prototypical features of mesenchymal cells known as lymphoid tissue organizers (LTOs), which control tertiary lymphoid organogenesis in autoimmune diseases, through hyperinduction of CCL7, CCL9, CXCL13, CCL19, CXCL16, VCAM-1, and ICAM-1. Experiments with ltbr-/- SMCs suggested that the LTˆ R-RelB activation component of NF-¸”B signaling was obligatory to generate the LTO phenotype. TNFR1-LTˆ R crosstalk also resulted in augmented synthesis and prolonged secretion of lymphorganogenic chemokine proteins into the culture medium. Thus, combined TNFR1-LTˆ R signaling triggers SMC transdifferentiation into a phenotype that strikingly resembles LTOs. LTO-like SMCs may adopt a thus far unrecognized role in diseased arteries, i.e. to coordinate tertiary lymphoid organogenesis in atherosclerosis, aortic aneurysm, and transplant vasculopathy. **Overall design:** Smooth muscle cells in tissue culture were stimulated with agonists and subsequently microarray, RT-PCR, and protein assays / analyses were performed

Background corr dist: KL-Divergence = 0.1735, L1-Distance = 0.0370, L2-Distance = 0.0025, Normal std = 0.3524

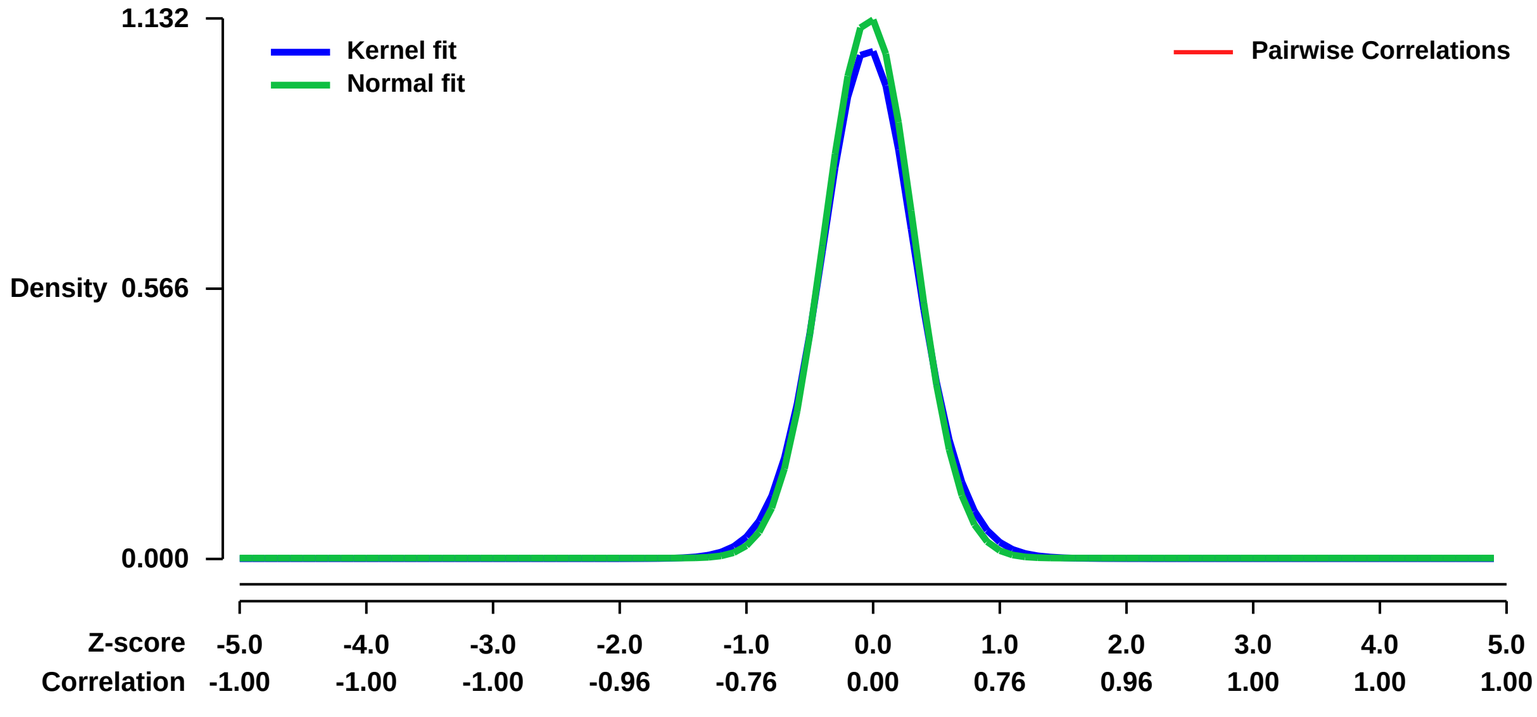

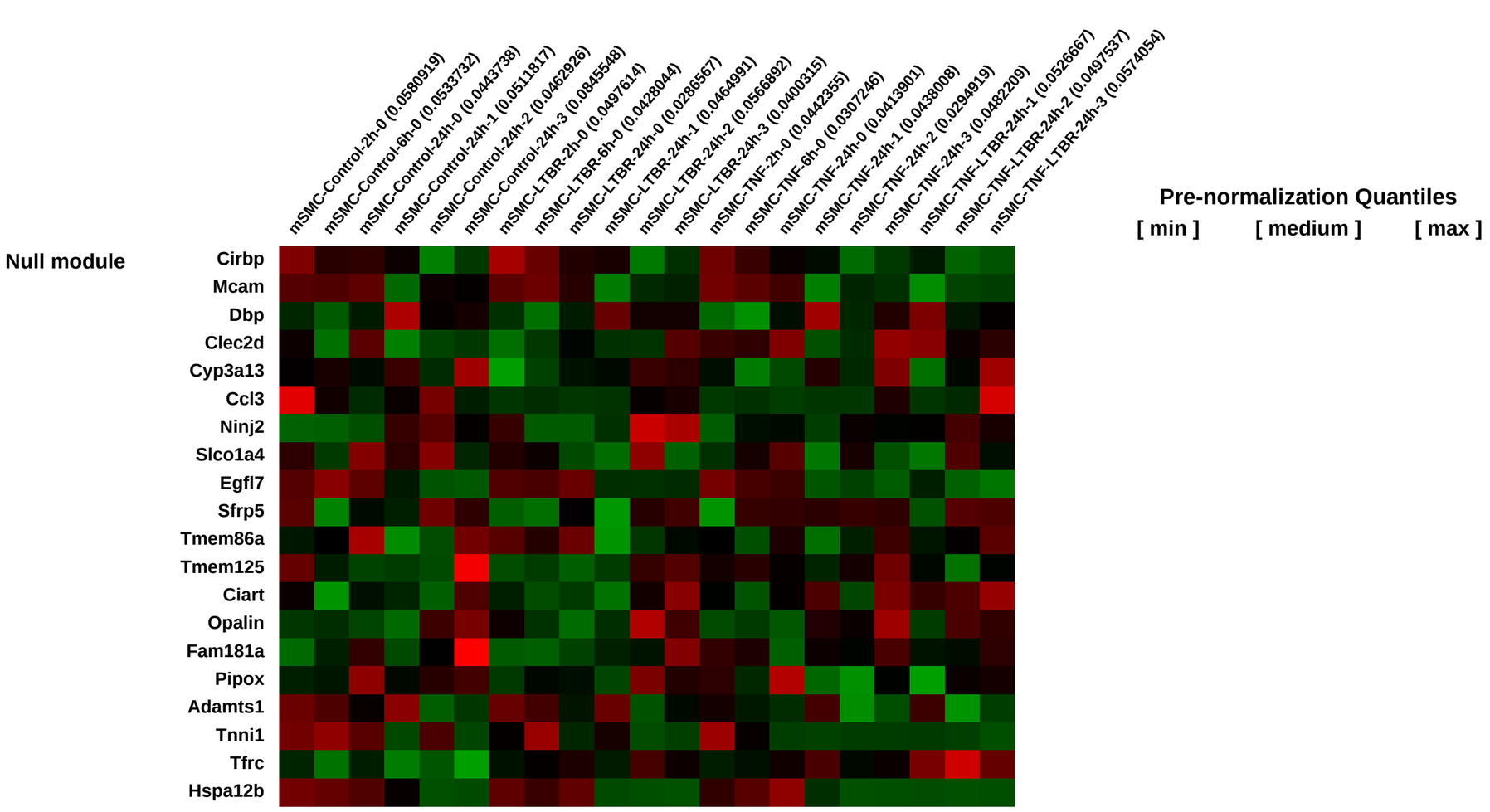

GEO Series "GSE20325" Expression Profiles

Num of samples in this series: 6

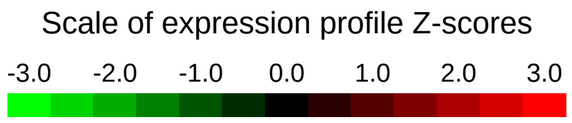

GEO Link:	http://www.ncbi.nlm.nih.gov/geo/query/acc.cgi?acc=GSE20325
Status:	Public on Mar 28 2011
Title:	Stabilization of ^ -catenin during murine Kidney Development
Organism:	Mus musculus
Experiment type:	Expression profiling by array
Platform:	GPL1261
Pubmed ID:	21436291
Summary & Design:	**Summary:** We define a pathogenic role for a ^ -catenin-activated genetic pathway in murine renal dysplasia. Cre-mediated stabilization of ^ -catenin in the ureteric cell lineage prior to the onset of kidney development increased ^ -catenin levels and caused renal aplasia or severe hypodysplasia. A genome-wide analysis of mRNA expression in dysplastic tissue identified down-regulation of genes required for ureteric branching and up regulation of Tgf^ 2 and Dkk1. **Overall design:** Hoxb7-Cre:EGFP mice (Zhao, et al. (2004) Dev Biol 276:403-415) were crossed with mice containing loxP sites flanking exon 3 of the ^ -catenin allele (^ -catdelta3/delta3) (Harada,et al. (2002) Cancer Res 62:1971-1977) to generate ^ -catenin gain-of-function mutant mice specific to the uteric bud, termed ^ -catGOF-UB .Eighteen ^ -catGOF-UB mutant kidneys and 9 WT kidneys were micro-dissected at E12.5. Mutant kidneys were divided into three random pools (n=3) consisting of 6 kidneys each and mRNA expression assessed by microarray.

Background corr dist: KL-Divergence = 0.0416, L1-Distance = 0.0228, L2-Distance = 0.0006, Normal std = 0.6103

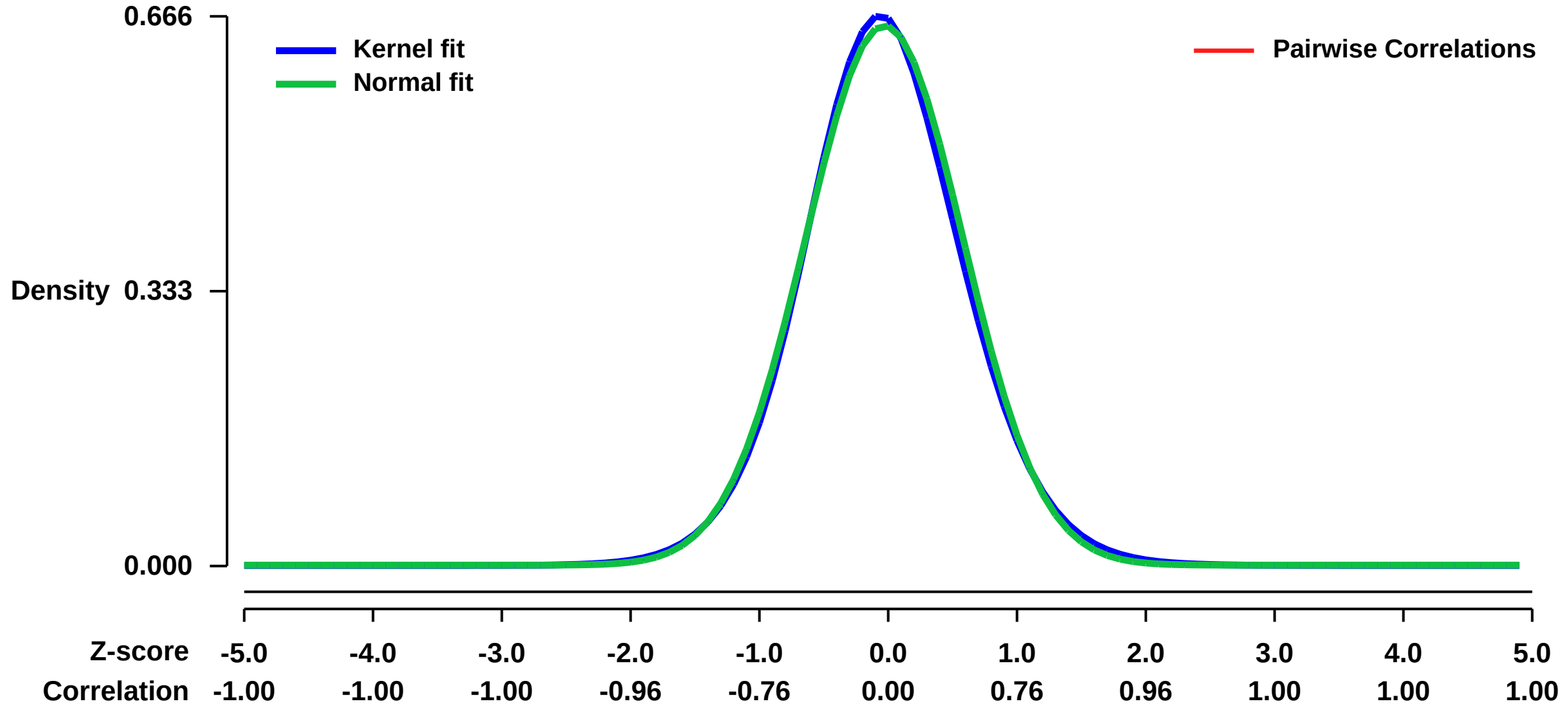

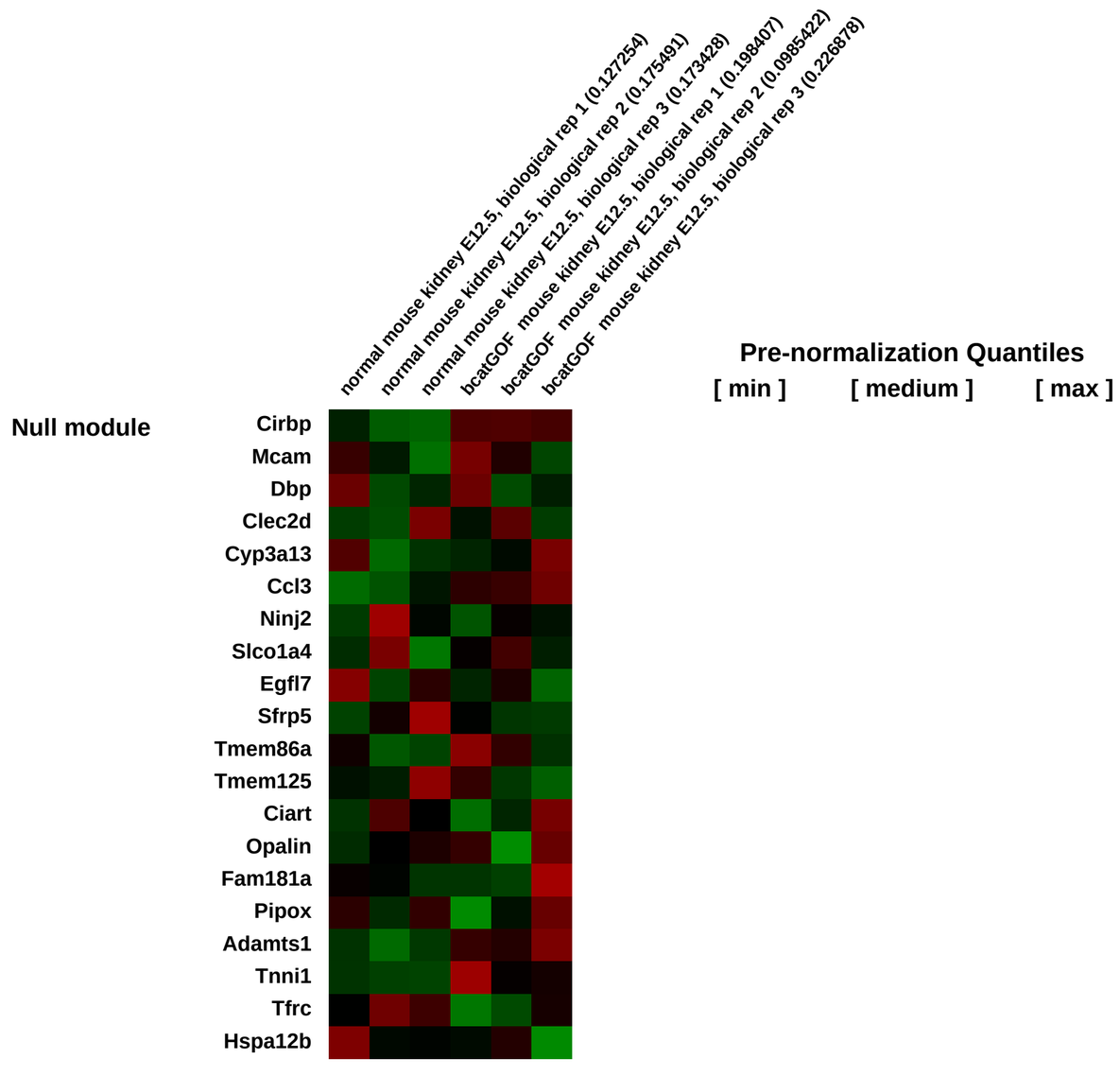

GEO Series "GSE43261" Expression Profiles

Num of samples in this series: 38

Scale of expression profile Z-scores

-3.0 -2.0 -1.0 0.0 1.0 2.0 3.0

GEO Link:	http://www.ncbi.nlm.nih.gov/geo/query/acc.cgi?acc=GSE43261
Status:	Public on Dec 31 2013
Title:	Fluoxetine resistance in mice is associated with attenuated progression of a stereotyped dentate gyrus gene expression program
Organism:	Mus musculus
Experiment type:	Expression profiling by array
Platform:	GPL1261
Pubmed ID:	24465494
Summary & Design:	**Summary:** Selective serotonin reuptake inhibitors (SSRIs) such as fluoxetine are the most common treatment for major depression. However, approximately 50% of depressed patients fail to achieve an effective treatment response. Understanding how gene expression systems relate to treatment responses may be critical for understanding antidepressant resistance. Transcriptome profiling allows for the simultaneous measurement of expression levels for thousands of genes and the opportunity to utilize this information to determine mechanisms underlying antidepressant treatment responses. However, the best way to relate this immense amount of information to treatment resistance remains unclear. We take a novel approach to this question by examining dentate gyrus transcriptomes from the perspective of a stereotyped fluoxetine-induced gene expression program. Expression programs usually represent stereotyped changes in expression levels that occur as cells transition phenotypes. Fluoxetine will shift transcriptomes so they lie somewhere between a baseline state and a full-response at the end of the program. The position along this fluoxetine-induced gene expression program (program status) was measured using principal components analysis (PCA). The same expression program was initiated in treatment-responsive and resistant mice but treatment response was associated with further progression along the fluoxetine-induced gene expression program. The study of treatment-related differences in gene expression program status represents a novel way to conceptualize differences in treatment responses at a transcriptome level. Understanding how antidepressant-induced gene expression program progression is modulated represents an important area for future research and could guide efforts to develop novel augmentation strategies for antidepressant treatment resistant individuals. **Overall design:** 38 samples, 2 dentate regions (dorsal/ventral), 3 groups (control, antidepressant resistant (4 mice), antidepressant responsive (7 mice), untreated (8 mice).

Background corr dist: KL-Divergence = 0.3830, L1-Distance = 0.0689, L2-Distance = 0.0133, Normal std = 0.2529

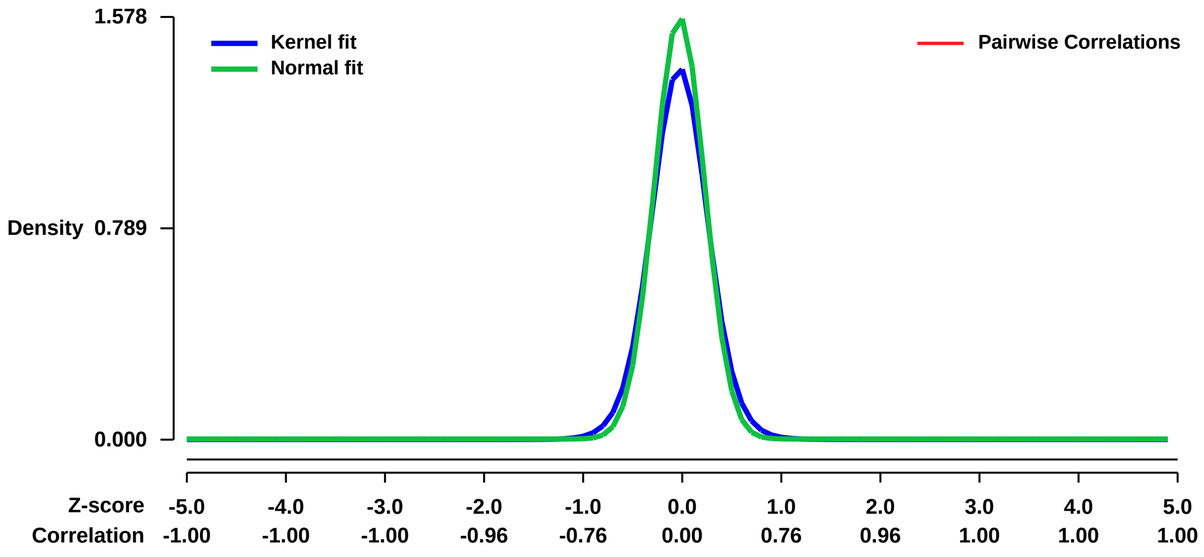

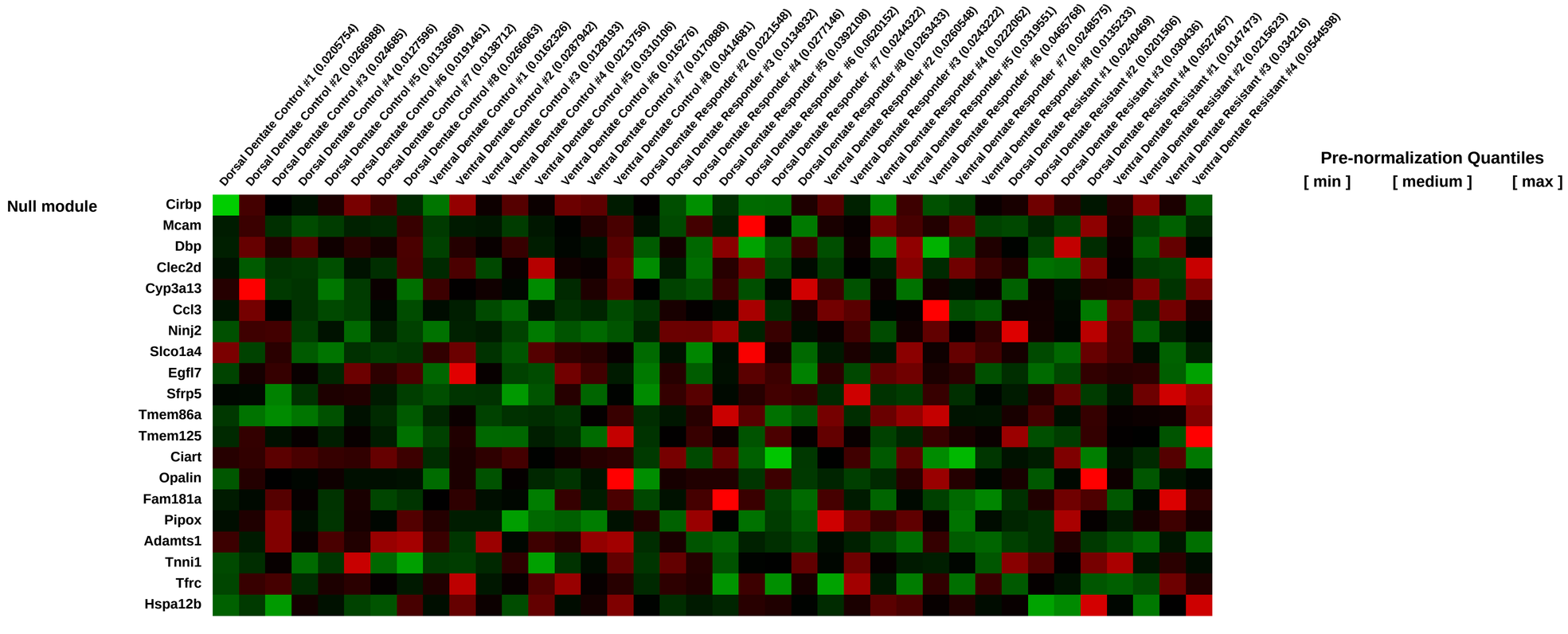

GEO Series "GSE43928" Expression Profiles

Num of samples in this series: 12

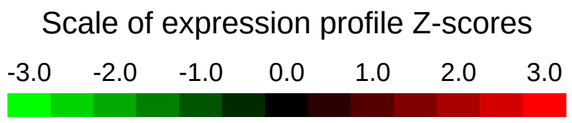

GEO Link:	http://www.ncbi.nlm.nih.gov/geo/query/acc.cgi?acc=GSE43928
Status:	Public on Sep 11 2013
Title:	Expression data from TNF-stimulated mouse glomeruli
Organism:	Mus musculus
Experiment type:	Expression profiling by array
Platform:	GPL1261
Pubmed ID:	23869211
Summary & Design:	**Summary:** The specific contribution of the two TNF-receptors Tnfr1 and Tnfr2 to TNF-induced inflammation in the glomerulus is unknown. In mice, TNF exposure induces glomerular expression of inflammatory mediators like adhesion molecules and chemokines in vivo, and glomerular accumulation of leukocytes. To examine Tnfr-specific inflammatory responses in intrinsic glomerular cells but not infiltrating leukocytes we performed microarray gene expression profiling on intact glomeruli isolated from wild-type and Tnfr-deficient mice following TNF exposure in vitro. **Overall design:** Glomeruli were isolated from male C57BL/6J wild-type and Tnfr-deficient mice applying a magnetic bead-based isolation technique. Isolated intact glomeruli were stimulated with TNF for 12 hours in vitro for subsequent RNA extraction and hybridization on Affymetrix microarrays.

Background corr dist: KL-Divergence = 0.0686, L1-Distance = 0.0204, L2-Distance = 0.0006, Normal std = 0.5034

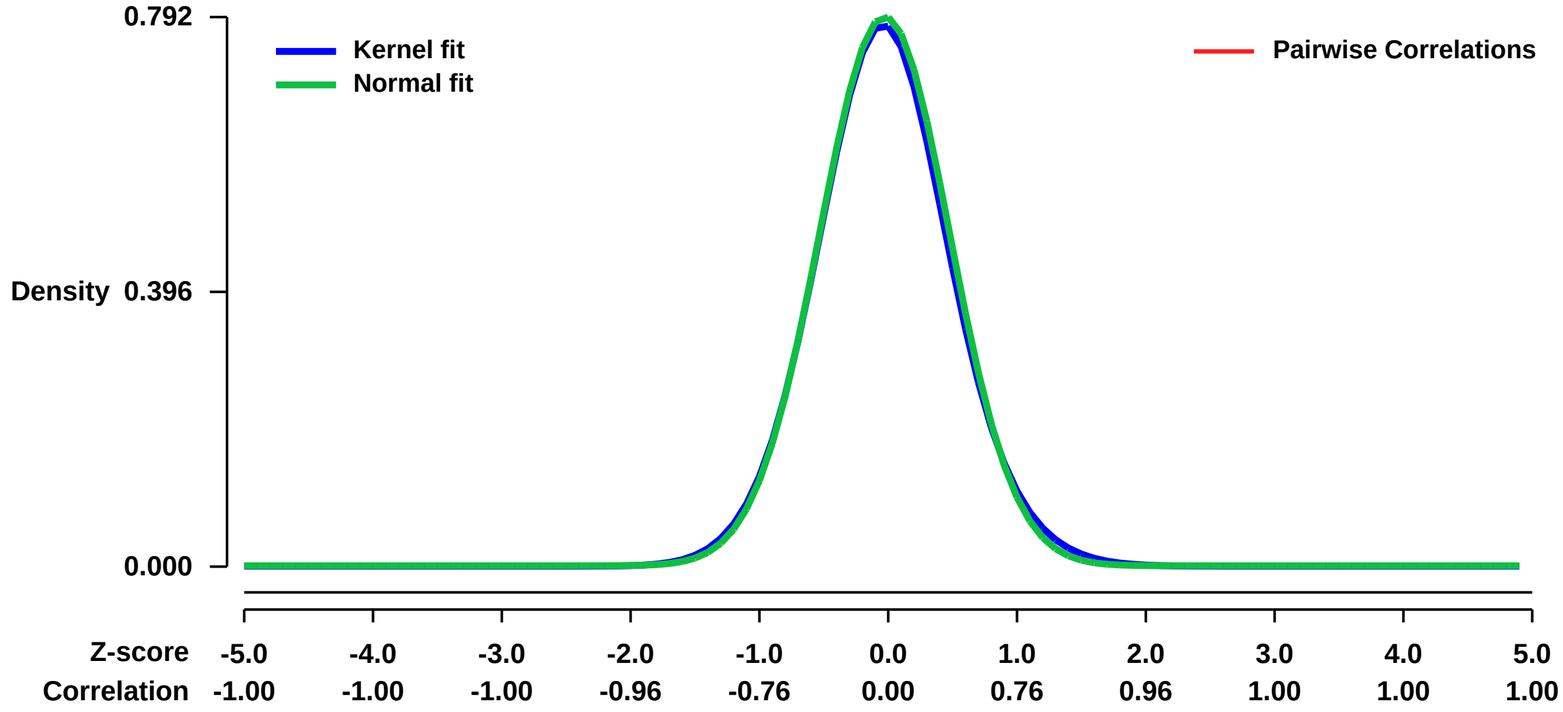

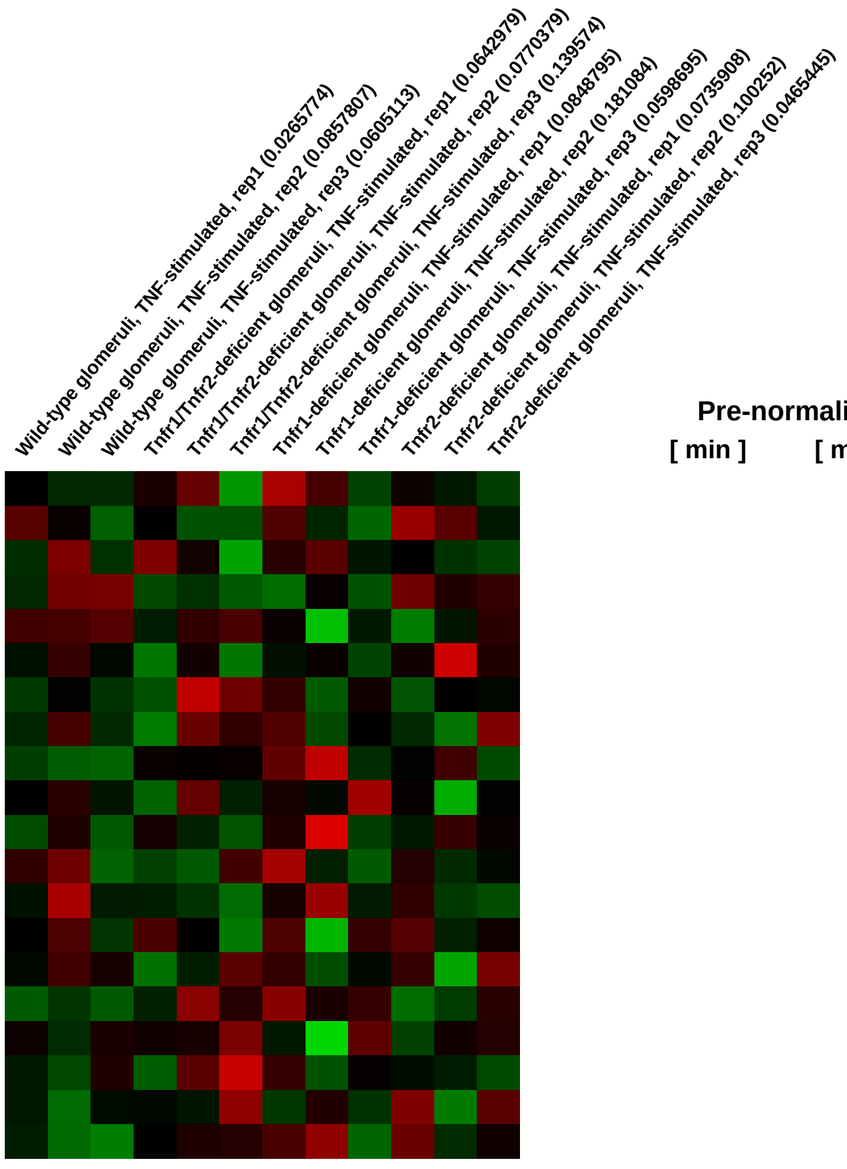

GEO Series "GSE41907" Expression Profiles

Num of samples in this series: 7

Scale of expression profile Z-scores

-3.0 -2.0 -1.0 0.0 1.0 2.0 3.0

GEO Link:	http://www.ncbi.nlm.nih.gov/geo/query/acc.cgi?acc=GSE41907
Status:	Public on Dec 01 2012
Title:	Transcriptional regulation of myoblasts in HMGA2 KO mice
Organism:	Mus musculus
Experiment type:	Expression profiling by array
Platform:	GPL1261
Pubmed ID:	23177649
Summary & Design:	**Summary:** We sought to identify critical factors regulating muscle stem cell activation and commitment, and determined through loss-of-function analyses that HMGA2 (high mobility group AT-hook 2) is a key regulator of myogenesis both in vitro and in vivo. **Overall design:** mRNAs were isolated from Hmga2 -/- and Hmga2 +/+ mice myoblasts, and a microarray experiment was performed.

Background corr dist: KL-Divergence = 0.0533, L1-Distance = 0.0165, L2-Distance = 0.0003, Normal std = 0.5505

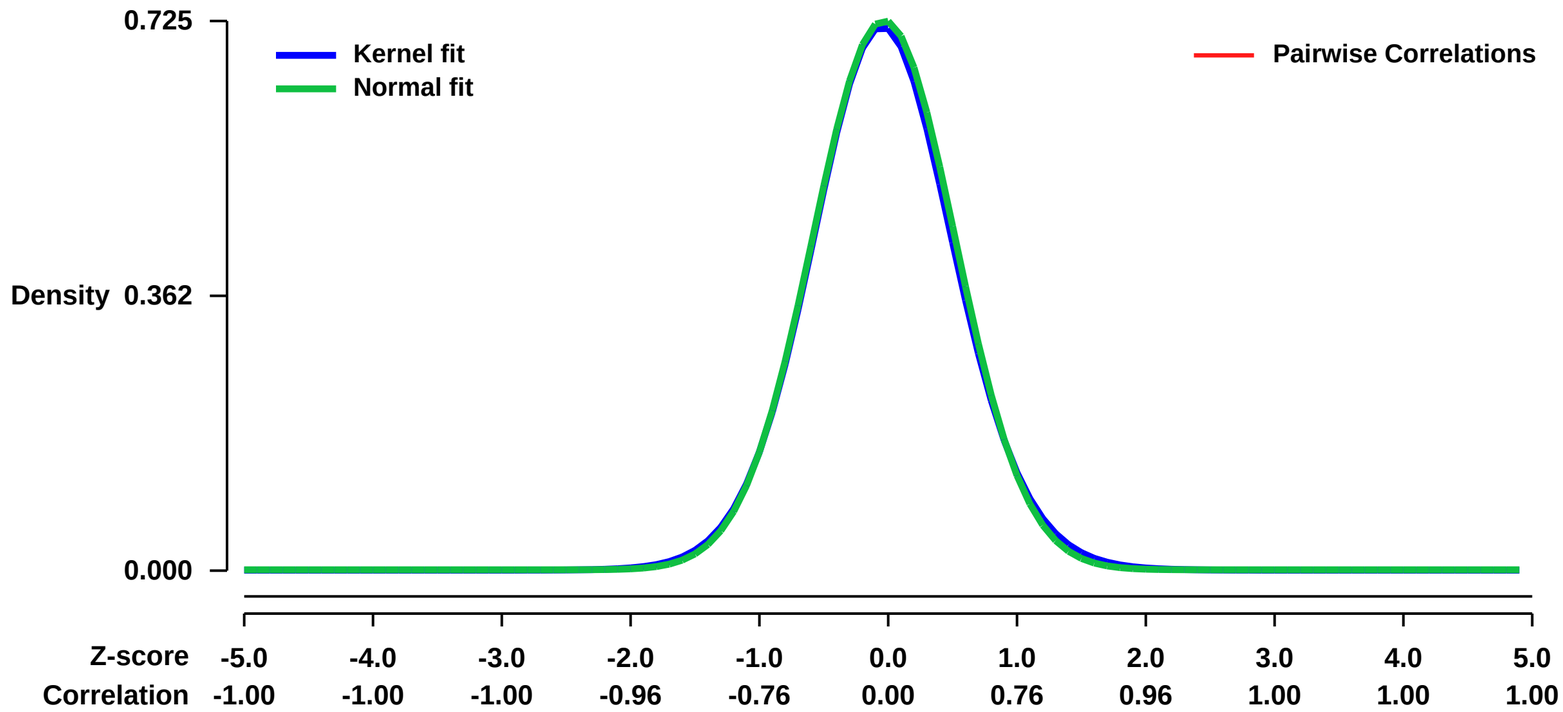

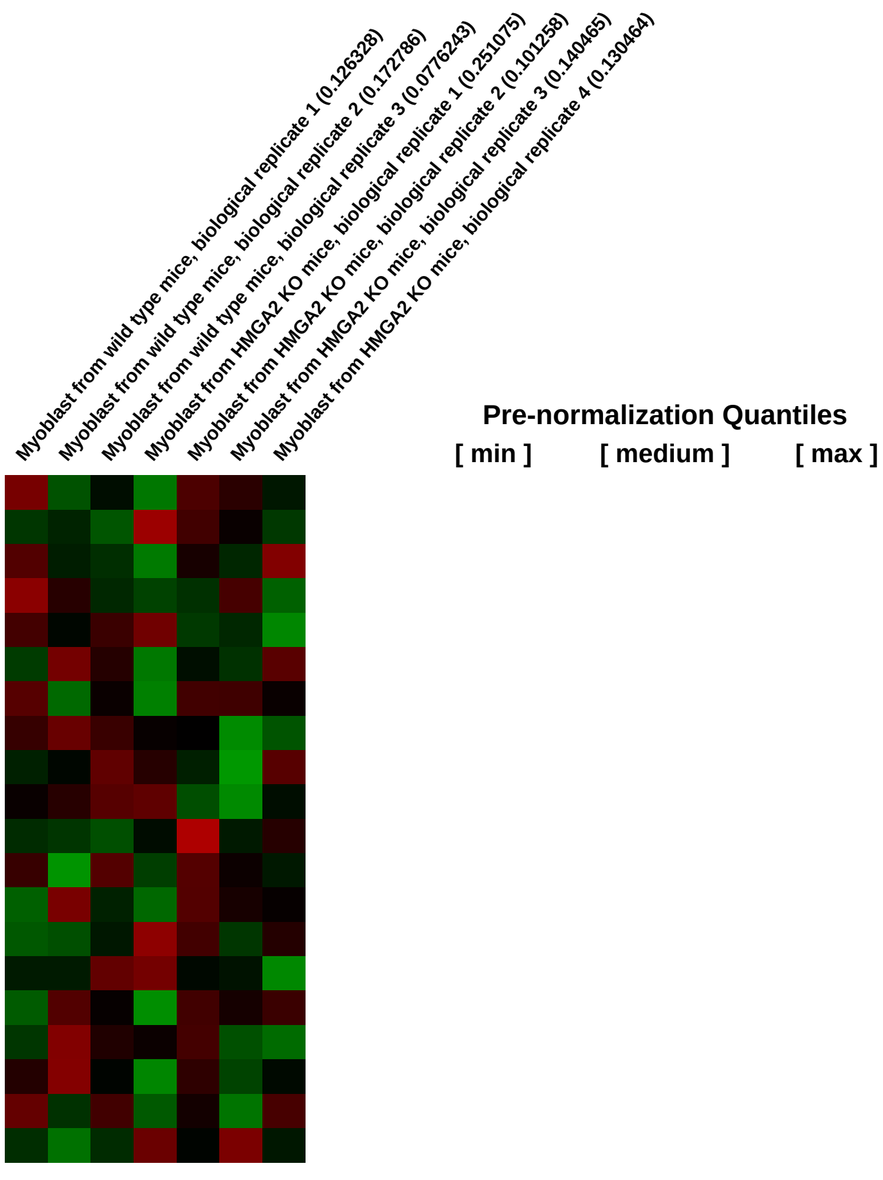

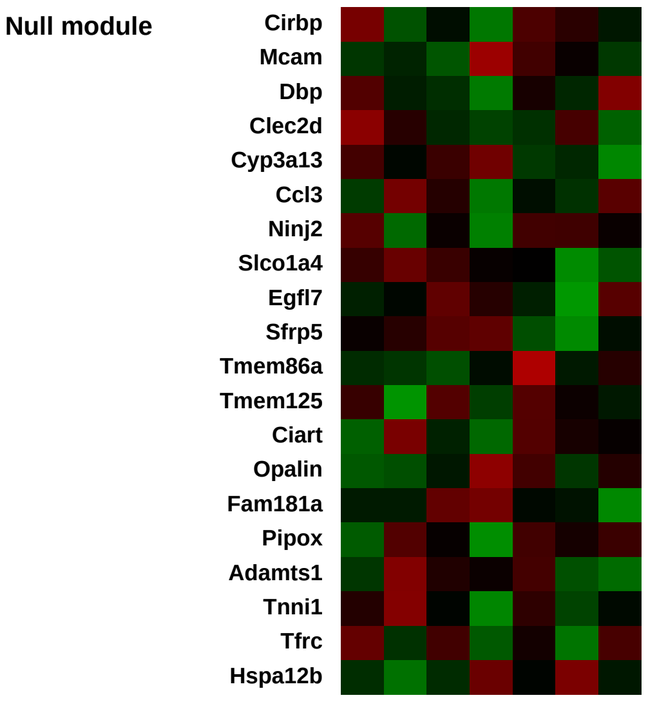

GEO Series "GSE58484" Expression Profiles

Num of samples in this series: 15

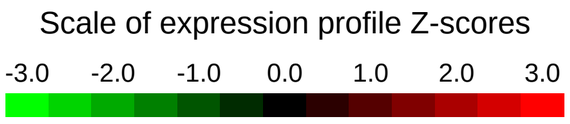

GEO Link:	**http://www.ncbi.nlm.nih.gov/geo/query/acc.cgi?acc=GSE58484**
Status:	**Public on Jun 14 2014**
Title:	**Expression data from mus musculus subjected to traumatic brain injury (TBI) for treatment with cyclophosphamide**
Organism:	**Mus musculus**
Experiment type:	**Expression profiling by array**
Platform:	**GPL1261**
Pubmed ID:	
Summary & Design:	**Summary:** **We inflicted TBI to wildetype (wt) mice in order to establish whether the anti-inflammatory agent cyclophosphamide can be used therapeutically.** **Cyclophosphamide was found to regulate distinct inflammatory cells such as activated microglia separate from invading phagocytes and dendritic cells. Cyclophosphamide postinjury selectively reduces antigen-presenting dendritic cells. Findings show feasibility of drug development to interfere with brain inflammation.** **Overall design:** **TBI was carried out in injured wt B6 mice for postinjury treatment with cyclophospamide i.p. using saline as a control substance for comparison with injured but untreated mice. Total RNA was prepared from injured cerebral neocortex after three days. RNA samples were also from uninjured wt mice as reference for hybridization on Affymetrix microarrays.**

Background corr dist: **KL-Divergence = 0.1498, L1-Distance = 0.0359, L2-Distance = 0.0025, Normal std = 0.3731**

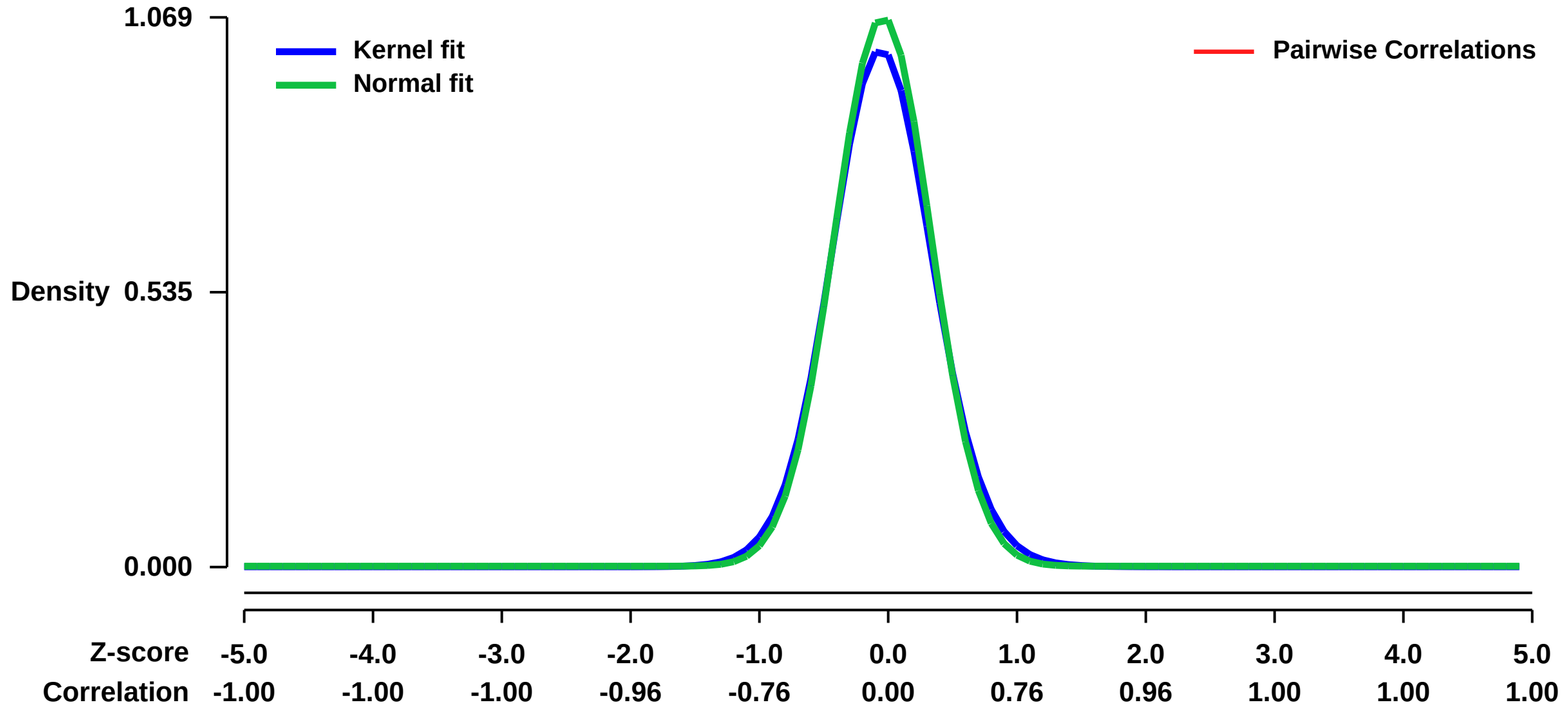

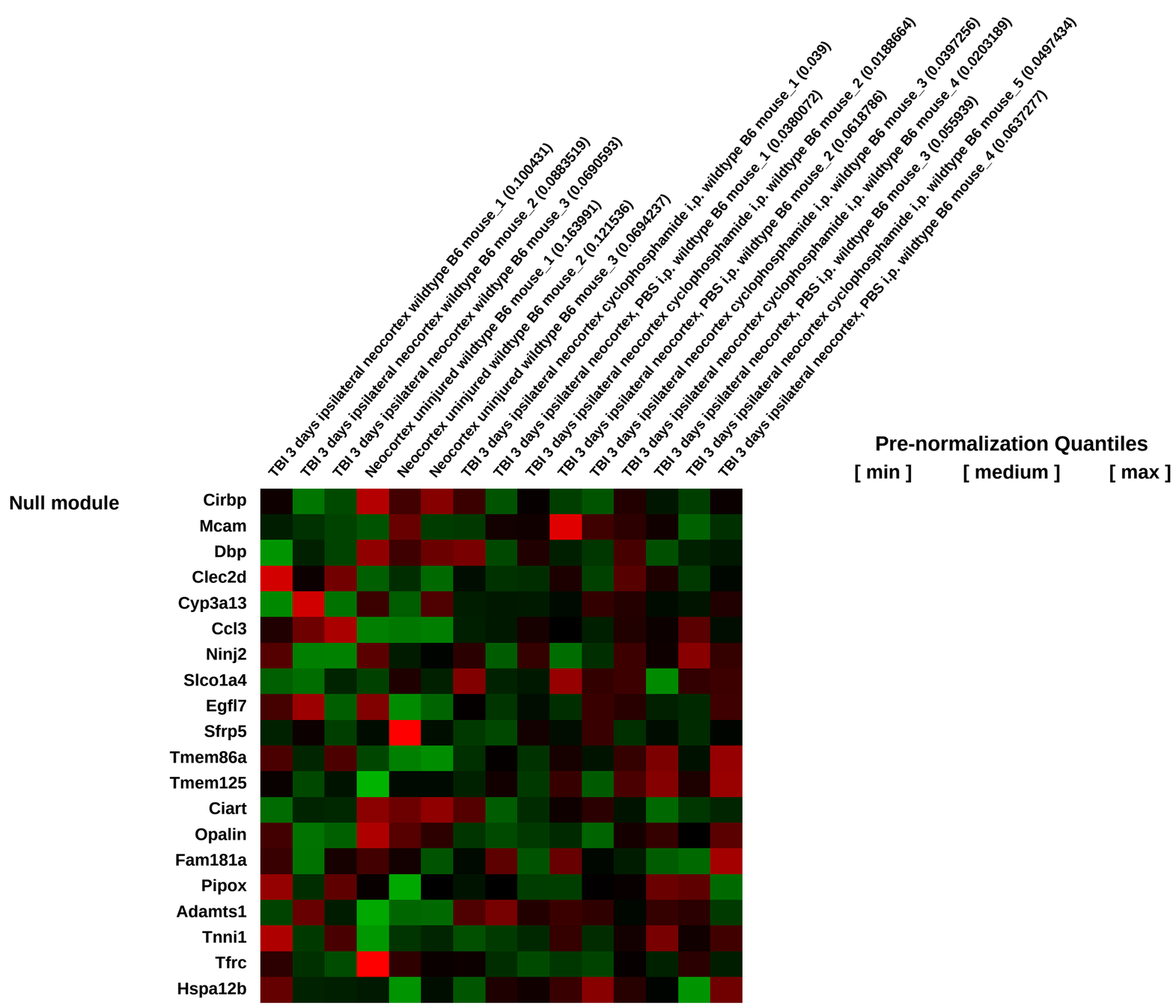

GEO Series "GSE2527" Expression Profiles

Num of samples in this series: 6

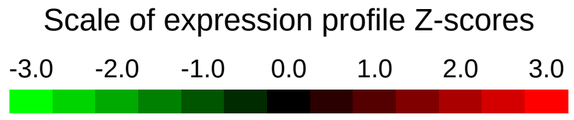

GEO Link:	http://www.ncbi.nlm.nih.gov/geo/query/acc.cgi?acc=GSE2527
Status:	Public on May 06 2005
Title:	Gata-1 Knock Down - Wild Type Megakaryocyte Gene Expression
Organism:	Mus musculus
Experiment type:	Expression profiling by array
Platform:	GPL1261
Pubmed ID:	15860665
Summary & Design:	**Summary:** **Hematopoietic progenitor cells were isolated from 13.5 day mouse fetal livers by lineage depletion and expanded for three days. Fetal livers were isolated from both wild type and Gata-1 knock embryos. Gata-1 knock embryos contain a deletion of the Gata-1 promoter sequence that results in undetectable levels of Gata-1 protein specifically in the megakaryocyte lineage. Following progenitor outgrowth megakaryocytes were enriched in a differentiation media for three days and isolated on a discontinuous BSA gradient. The resulting megakaryocytes were >90% pure as determined by acetylcholinesterase staining. These cells were lysed in Trizol and the resulting RNA was used for hybridization.** **Keywords = Gata-1** **Keywords = Megakaryocytes** **Keywords: other** **Overall design:**

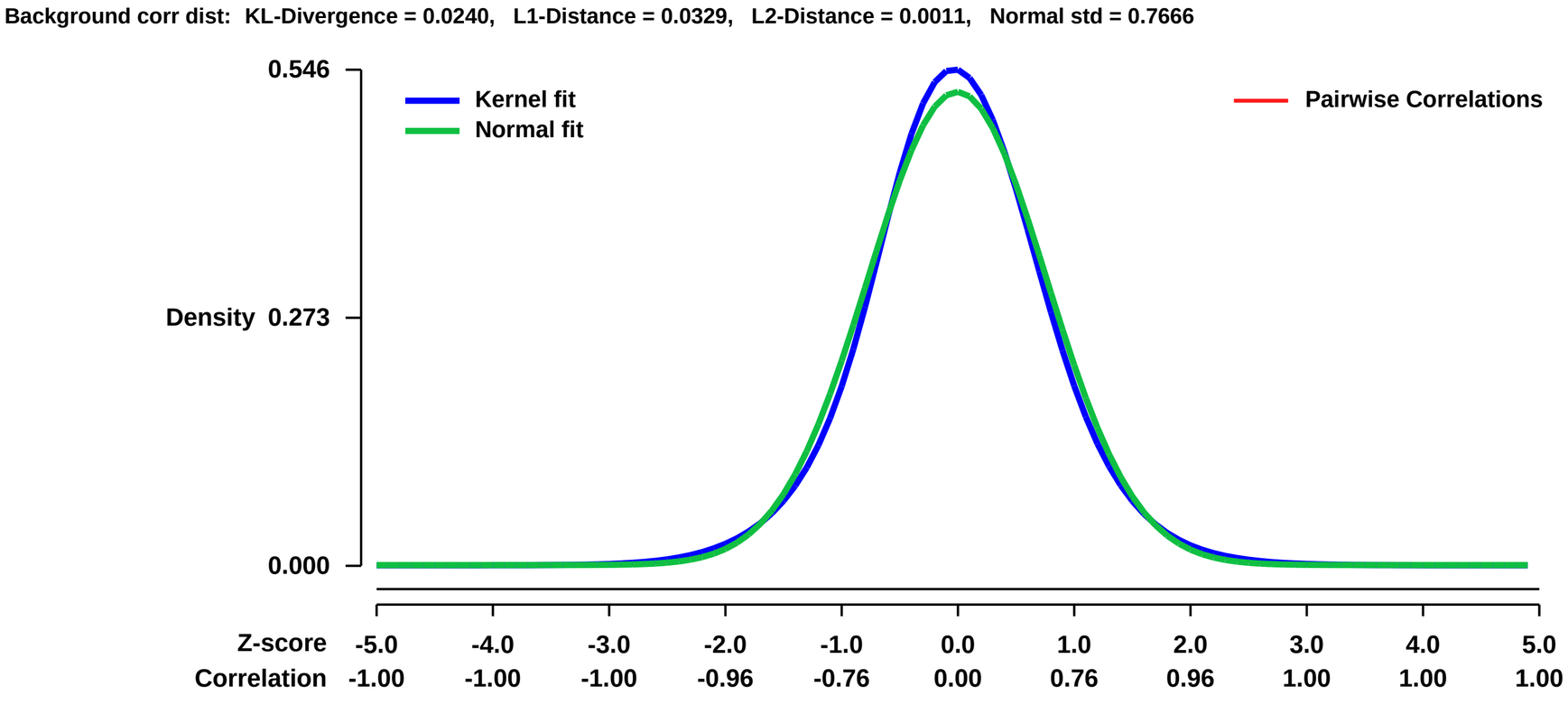

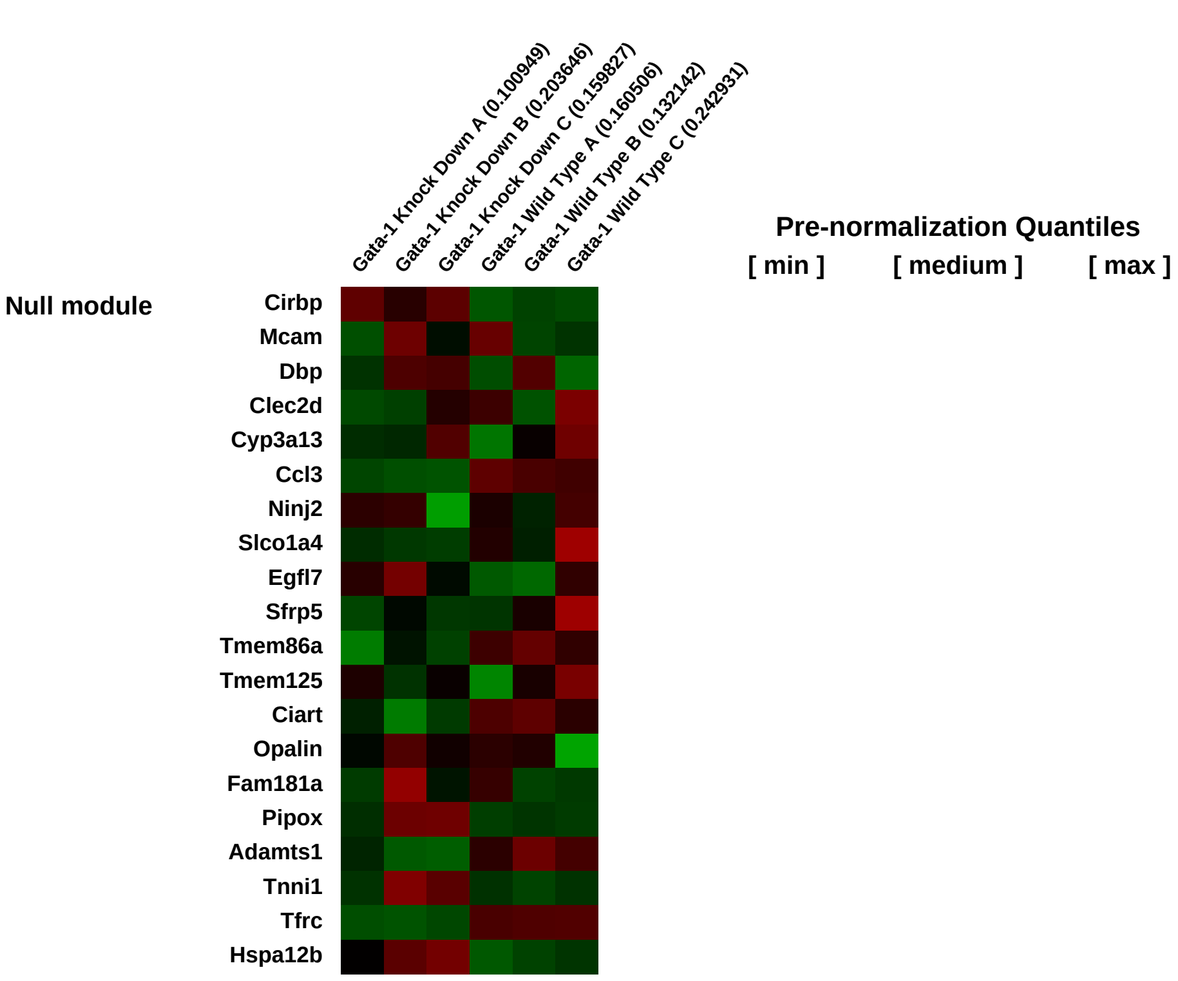

GEO Series "GSE35106" Expression Profiles

Num of samples in this series: 9

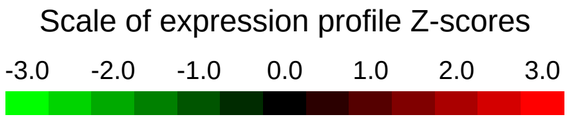

GEO Link:	http://www.ncbi.nlm.nih.gov/geo/query/acc.cgi?acc=GSE35106
Status:	Public on Jan 14 2012
Title:	Polysome-bound mRNA during oocyte maturation
Organism:	Mus musculus
Experiment type:	Expression profiling by array
Platform:	GPL1261
Pubmed ID:	21460039
Summary & Design:	**Summary:** Oocyte maturation, fertilization, and early embryonic development occur in the absence of gene transcription. Therefore, it is critical to understand at a global level the post-transcriptional events that are driving these transitions. Here, we have used a systems approach by combining polysome mRNA profiling and bioinformatics to identify RNA binding motifs in mRNAs that either enter or exit the polysome pool during mouse oocyte maturation. Association of mRNA with the polysomes correlates with active translation. **Overall design:** Forty-eight hours (h) after PMSG injection, mice were stimulated with hCG for 0, 4, or 14 h, and GV-, MI- and MII-stage oocytes were collected. Polysome-bound mRNAs were purified, reverse-transcribed and linearly amplified with the WT-Ovation FFPE RNA Amplification System V2 (NuGEN). 5´µg cDNA were fragmented and hybridized with Affymetrix Mouse Genome 430.2 array chips. Experiments were done using 3 independent sample sets.

Background corr dist: KL-Divergence = 0.1068, L1-Distance = 0.0773, L2-Distance = 0.0124, Normal std = 0.4711

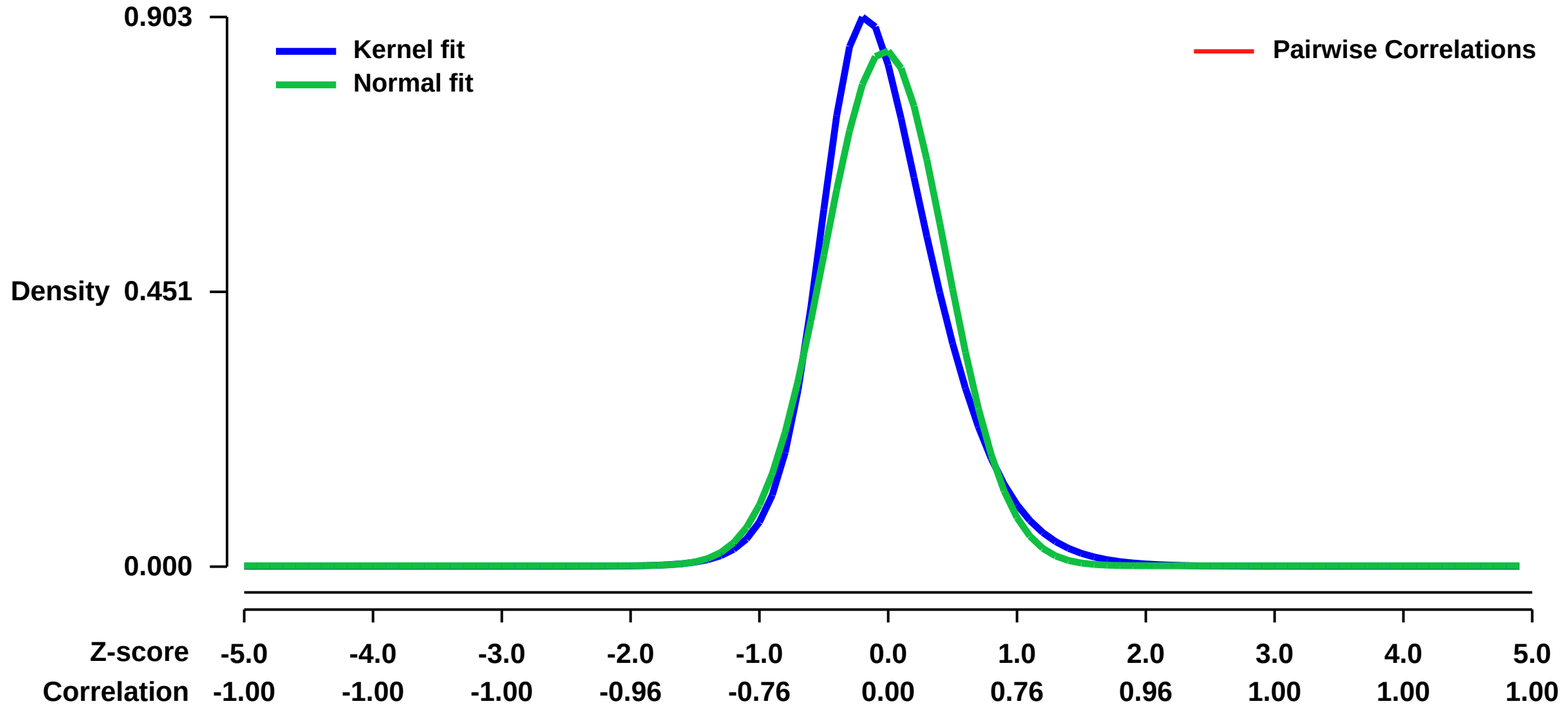

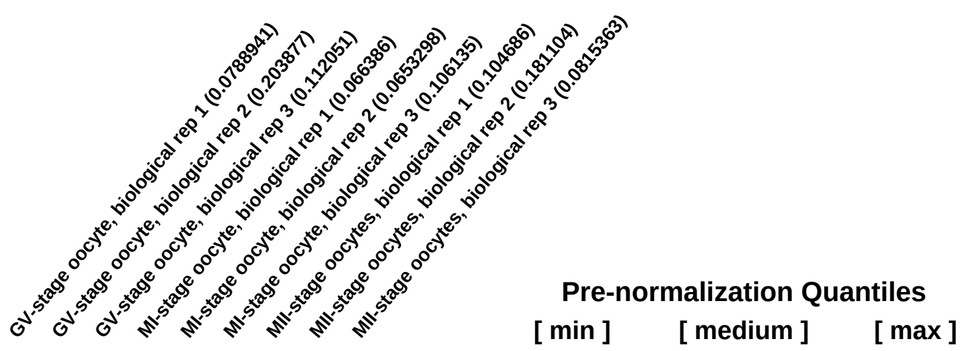

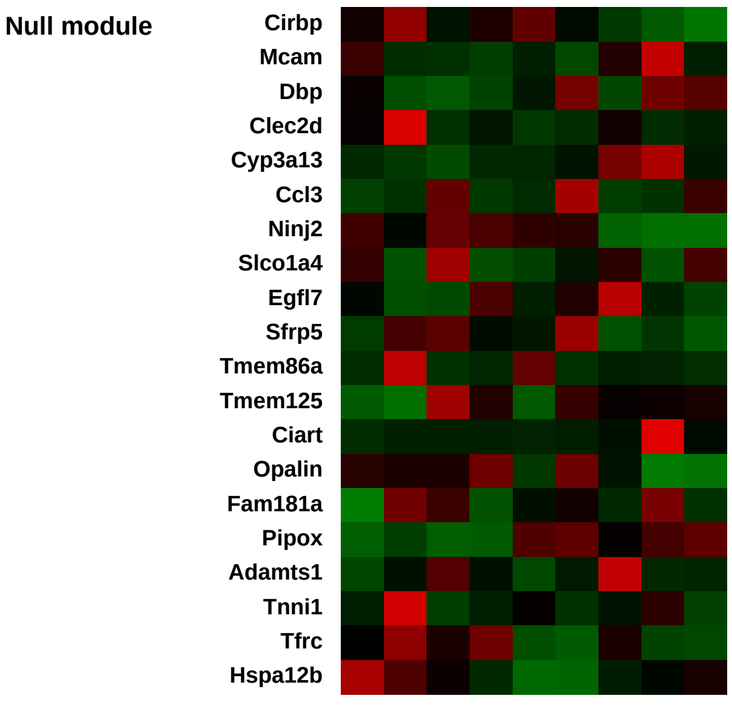

GEO Series "GSE11044" Expression Profiles

Num of samples in this series: 6

Scale of expression profile Z-scores

-3.0 -2.0 -1.0 0.0 1.0 2.0 3.0

GEO Link:	**http://www.ncbi.nlm.nih.gov/geo/query/acc.cgi?acc=GSE11044**
Status:	**Public on Apr 29 2008**
Title:	**Differential H3K4 methylation identifies developmentally poised hematopoietic genes**
Organism:	**Mus musculus**
Experiment type:	**Genome binding/occupancy profiling by genome tiling array**
Platform:	**GPL1261**
Pubmed ID:	
Summary & Design:	**Summary:** **We assess the concordance of histone H3 lysine 4 dimethylation (H3K4me2) and trimethylation (H3K4me3) on a genome-wide scale in erythroid development by analyzing pluripotent, multipotential and unipotent cell types. Although H3K4me2 and H3K4me3 are concordant at most genes, multipotential hematopoietic cells have a subset of genes that are differentially methylated (H3K4me2+/me3-). These genes are transcriptionally silent, highly enriched in lineage-specific hematopoietic genes, and uniquely susceptible to differentiation-induced H3K4 demethylation. Self-renewing embryonic stem cells, which restrict H3K4 methylation to genes that contain CpG islands (CGIs), lack H3K4me2+/me3- genes. These data reveal distinct epigenetic regulation of CGI and non-CGI genes during development and indicate an interactive relationship between DNA sequence and differential H3K4 methylation in lineage-specific differentiation.** **Keywords: comparison of different cell lines** **Overall design:** **Multipotential and erythroid-differentiated hematopoietic cells were compared. Expression was measured using Affymetrix microarrays. H3K4me2 and H3K4me3 enrichment was assessed using Agilent tiling arrays.**

Background corr dist: KL-Divergence = 0.0291, L1-Distance = 0.0366, L2-Distance = 0.0019, Normal std = 0.6955

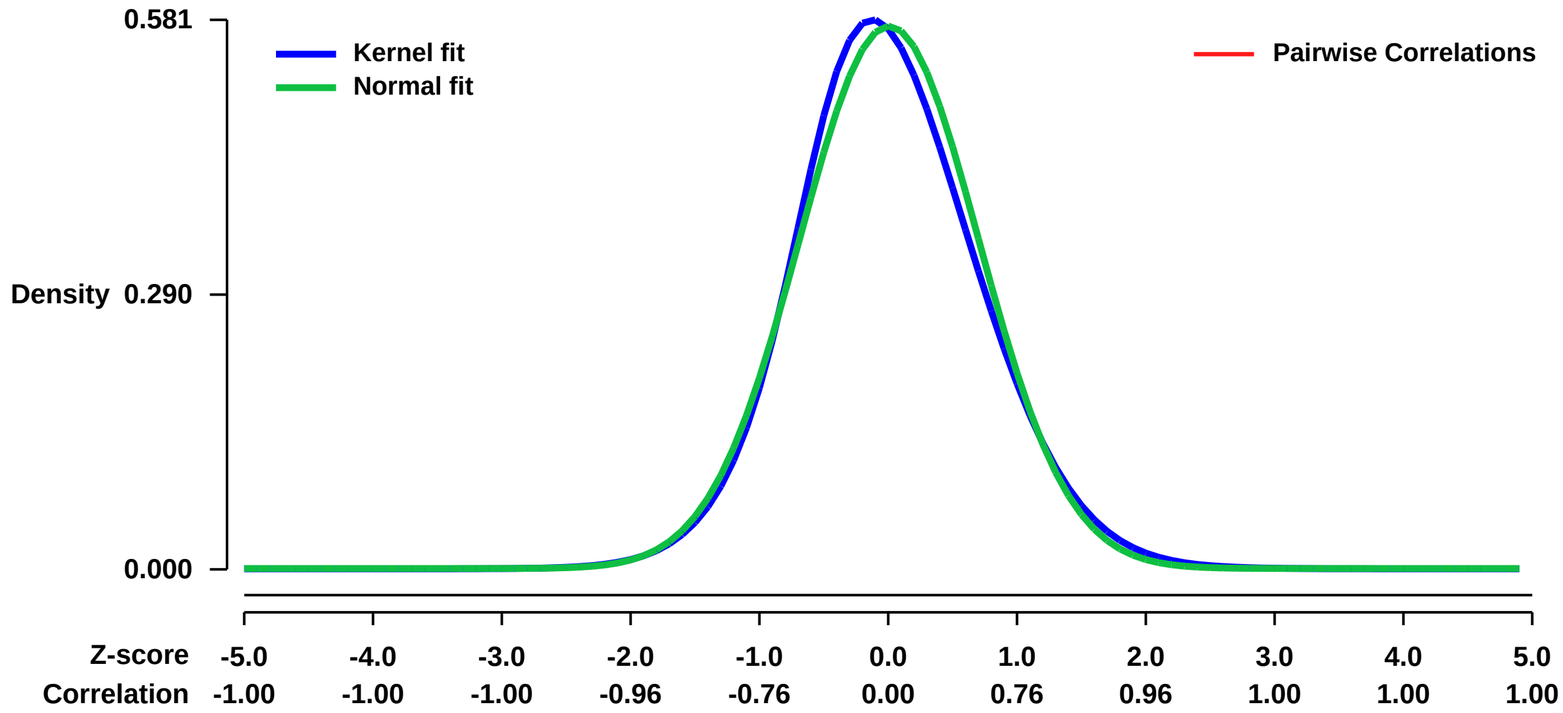

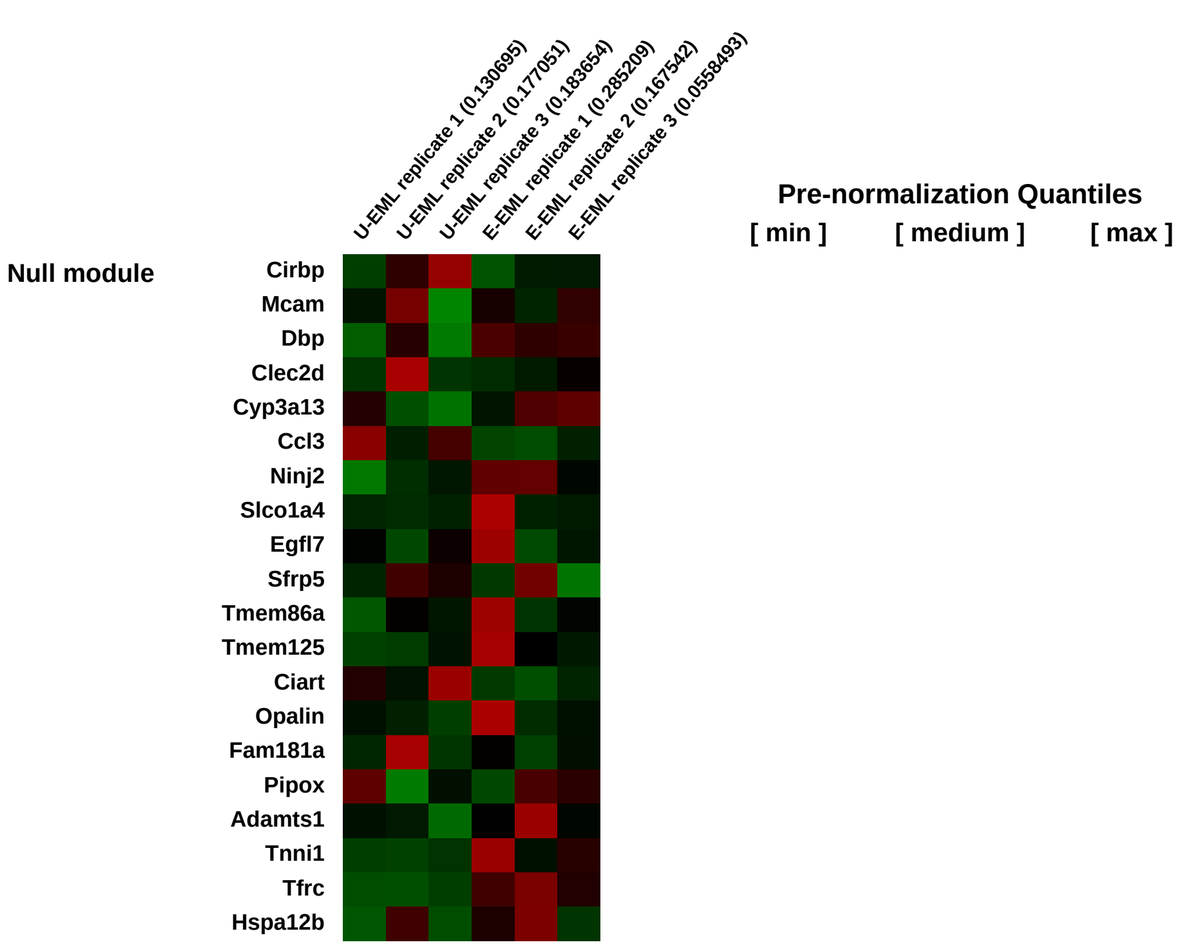

GEO Series "GSE24291" Expression Profiles

Num of samples in this series: 6

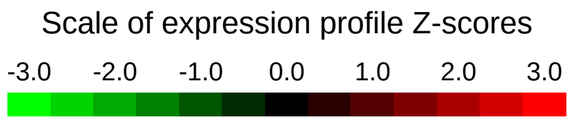

GEO Link:	http://www.ncbi.nlm.nih.gov/geo/query/acc.cgi?acc=GSE24291
Status:	Public on Sep 22 2011
Title:	Expression data from differentiating ES cells expressing Snail during Wnt inhibition
Organism:	Mus musculus
Experiment type:	Expression profiling by array
Platform:	GPL1261
Pubmed ID:	21394833
Summary & Design:	**Summary:** ES cells differentiated in the presence of the Wnt inhibitor DKK1 fail to express the transcription factor Snail and undergo EMT. We generated an ES cell line, A2.snail, that induced Snail expression upon addition of doxycycline addition. Microarrays were used to gain a global picture of ES cell differentiation at early timepoints after Snail was expressed during Wnt inhibition. **Overall design:** A2.snail ES cells, which express Snail upon addition of doxycycline, were differentiated as embryoid bodies in differentiation media and DKK1. Total RNA was harvested from control (no doxycycline) and Snail-induced (doxycycline at day 2) cultures at 6, 12, and 24 hours after doxycycline addition (corresponding to days 2.25, 2.5, and 3 of differentiation).

Background corr dist: KL-Divergence = 0.0278, L1-Distance = 0.0167, L2-Distance = 0.0003, Normal std = 0.6839

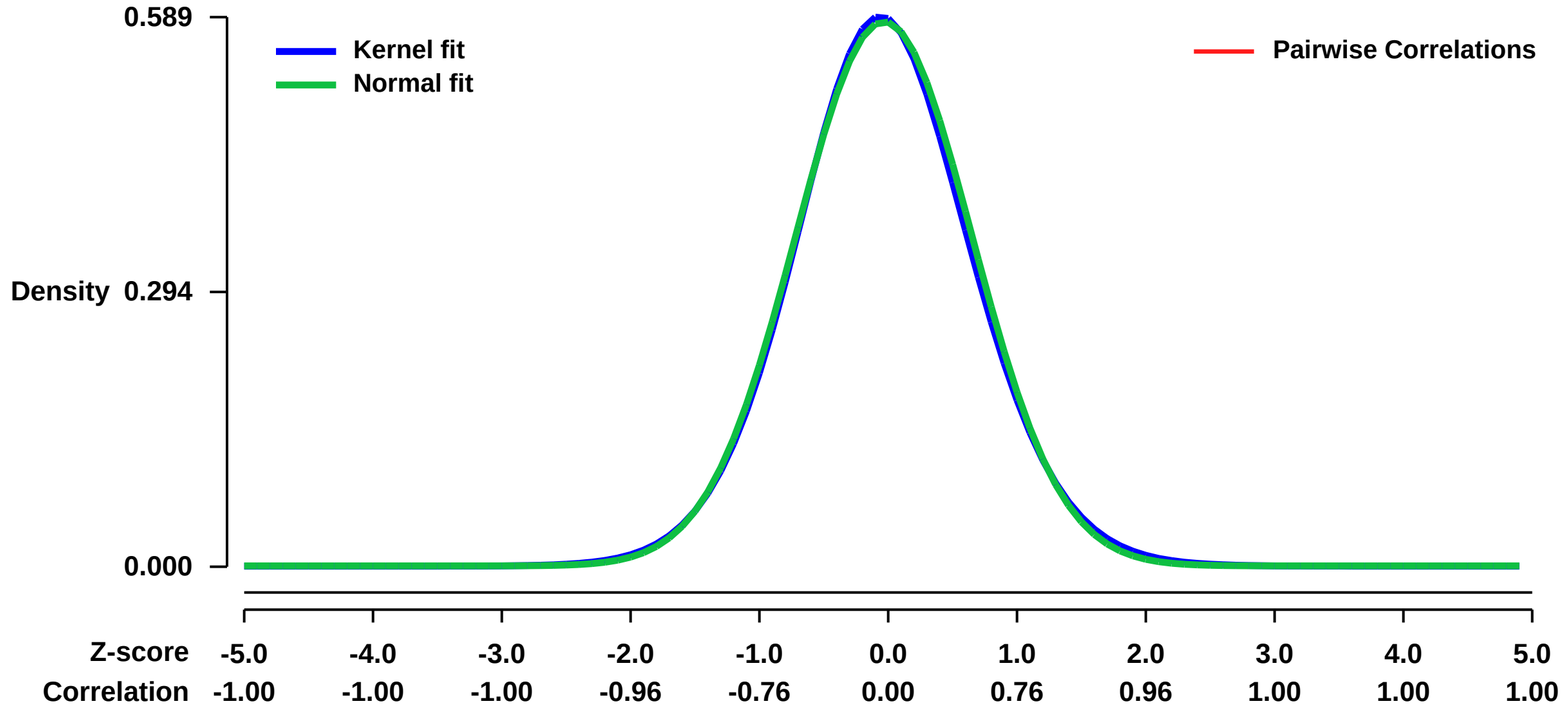

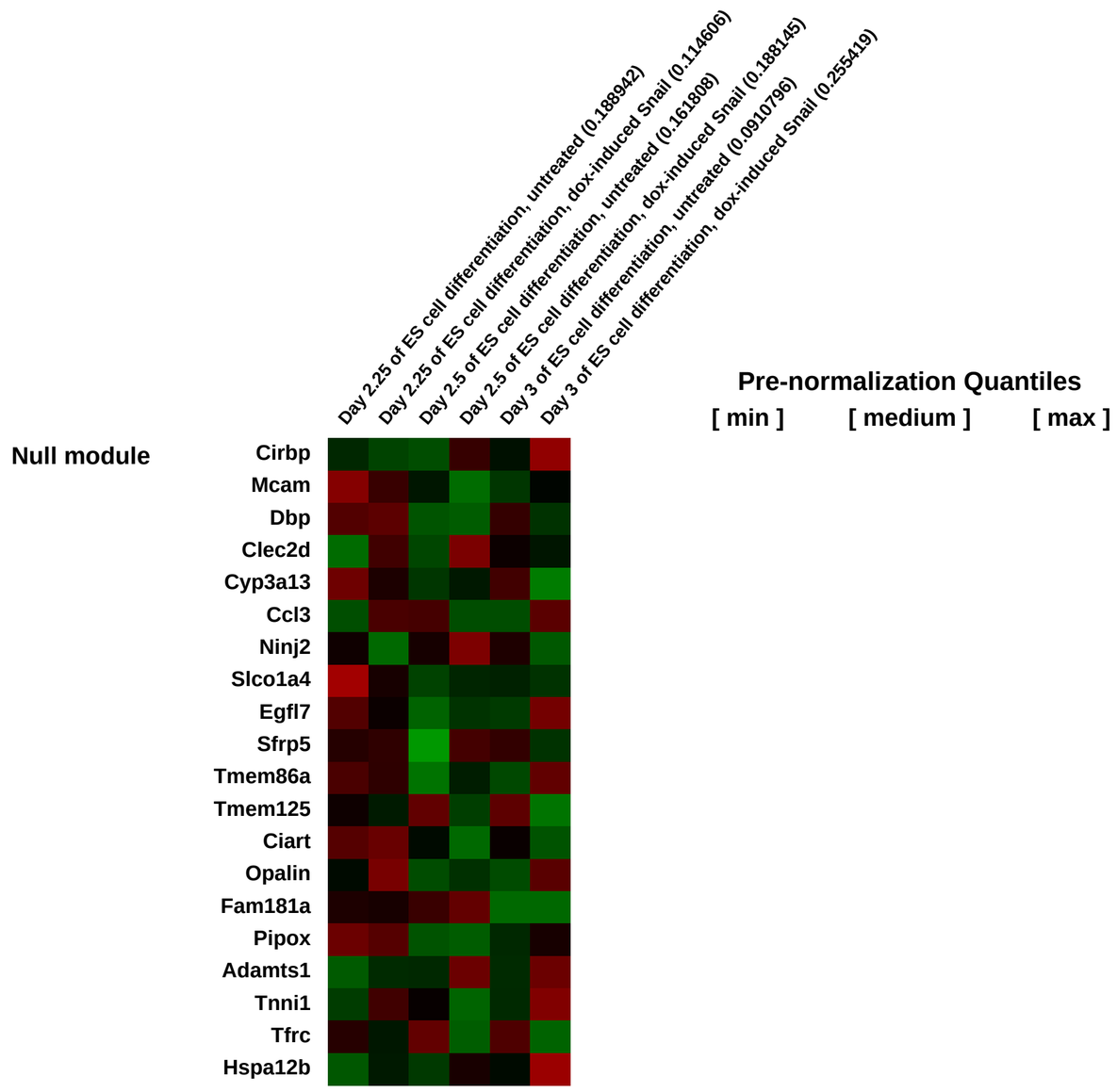

GEO Series "GSE8621" Expression Profiles

Num of samples in this series: 12

Scale of expression profile Z-scores

-3.0 -2.0 -1.0 0.0 1.0 2.0 3.0

GEO Link:	http://www.ncbi.nlm.nih.gov/geo/query/acc.cgi?acc=GSE8621
Status:	Public on Aug 10 2007
Title:	LPS tolerance in macrophages
Organism:	Mus musculus
Experiment type:	Expression profiling by array
Platform:	GPL1261
Pubmed ID:	18086374
Summary & Design:	**Summary:** Among the multiple mechanisms that control the intensity and duration of macrophage activation, the development of a state of refractoriness to a second stimulation in cells treated with LPS has long been recognized. Release of inhibitory cytokines and alterations in intracellular signaling pathways may be involved in the development of LPS tolerance. Although a number of molecules have been implicated, a detailed picture of the molecular changes in LPS tolerance is still missing. We have used a genome-wide gene expression analysis approach to (i) define which fraction of LPS target genes are subject to tolerance induction and (ii) identify genes that are expressed at high levels in tolerant macrophages. Our data show that in LPS tolerant macrophages the vast majority of LPS-induced gene expression is abrogated. The extent of tolerance induction varies for individual genes, and a small subset appears to be excepted. Compared to other negative control mechanisms of macrophages, e.g. IL-10-induced deactivation, LPS-tolerance inhibits a much wider range of transcriptional targets. Some previously described negative regulators of TLR-signaling (e.g. IRAK-M) were confirmed as expressed at higher levels in LPS-tolerant macrophages. In addition, we discuss other potential players in LPS tolerance identified in this group of genes. **Keywords:** pre and restimulation with LPS, tolerance induction **Overall design:** Cells were either prestimulated (1_X) or not (0_X) for 18h with 100 ng/ml LPS. Media was exchanged and after 2h rest, cells either restimulated (X_1) or not (X_0) with again 100 ng/ml LPS. This resulted in 4 experimental conditions: 0_0, 0_1, 1_0 and 1_1. There were 3 biological replicates done, resulting in 12 arrays altogether.

Background corr dist: KL-Divergence = 0.0499, L1-Distance = 0.0755, L2-Distance = 0.0102, Normal std = 0.6205

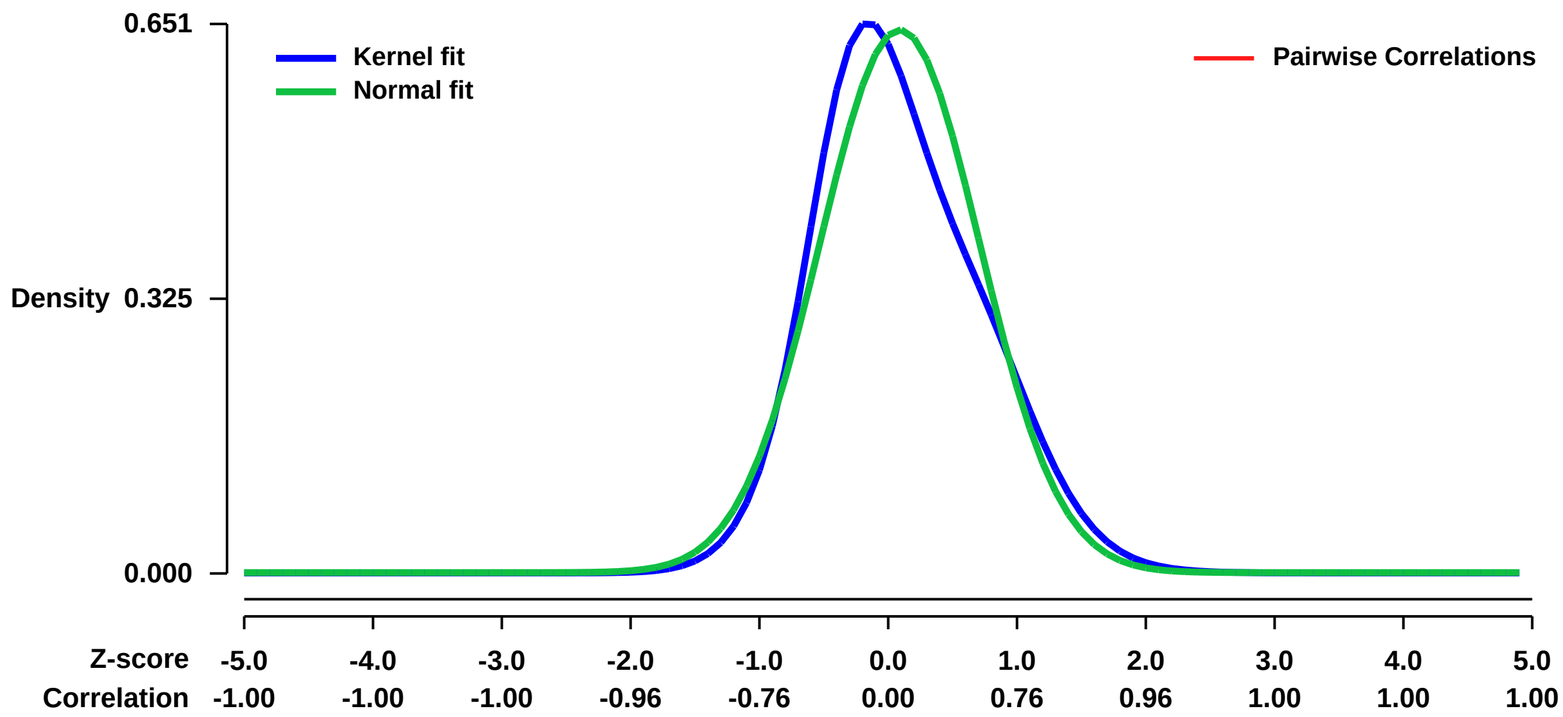

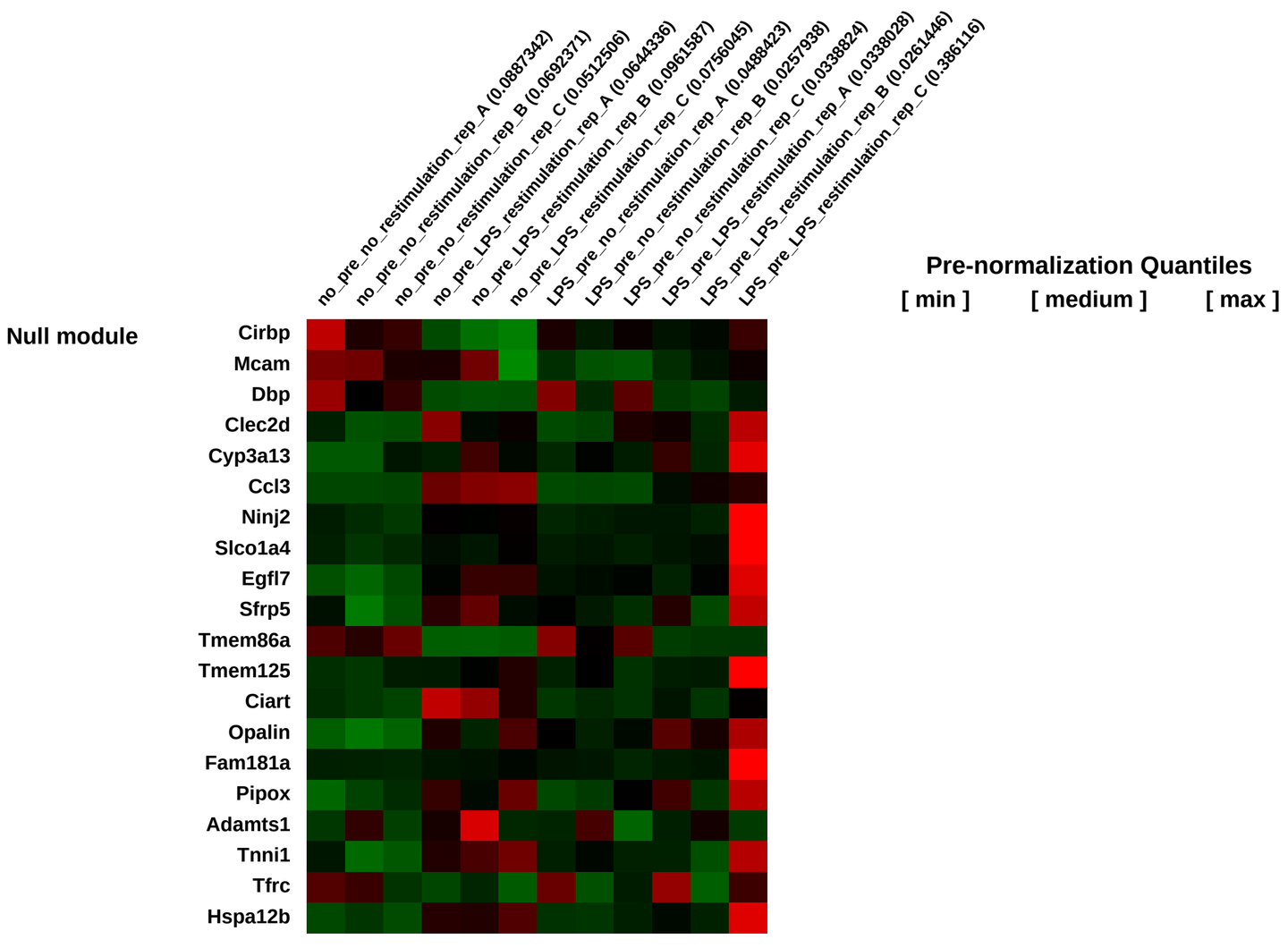

GEO Series "GSE30192" Expression Profiles

Num of samples in this series: 6

Scale of expression profile Z-scores

-3.0 -2.0 -1.0 0.0 1.0 2.0 3.0

GEO Link:	http://www.ncbi.nlm.nih.gov/geo/query/acc.cgi?acc=GSE30192
Status:	Public on Jan 01 2012
Title:	Effect of 5-azacytidine on gene expression in C2C12 myoblasts
Organism:	Mus musculus
Experiment type:	Expression profiling by array
Platform:	GPL1261
Pubmed ID:	21795504
Summary & Design:	**Summary:** Mesenchymal progenitor cells can be differentiated in vitro into myotubes that exhibit many characteristic features of primary mammalian skeletal muscle fibers. However, in general, they do not show the functional excitation-contraction coupling or the striated sarcomere arrangement typical of mature myofibers. Epigenetic modifications have been shown to play a key role in regulating the progressional changes in transcription necessary for muscle differentiation. In this study, we demonstrate that treatment of murine C2C12 mesenchymal progenitor cells with 10 ´µM of the DNA methylation inhibitor 5-azacytidine (5AC) promotes myogenesis, resulting in myotubes with enhanced maturity as compared to untreated myotubes. Specifically, 5AC treatment resulted in the upregulation of muscle genes at the myoblast stage while at later stages nearly 50 % of the 5AC-treated myotubes displayed a mature, well-defined sarcomere organization as well as spontaneous contractions that coincided with action potentials and intracellular calcium transients. Both the percentage of striated myotubes and their contractile activity could be inhibited by 20 nM TTX, 10 ´µM ryanodine and 100 ´µM nifedipine, suggesting that action potential-induced calcium transients are responsible for these characteristics. Our data suggest that genomic demethylation induced by 5AC overcomes an epigenetic barrier that prevents untreated C2C12 myotubes from reaching full maturity. **Overall design:** C2C12 cells were plated at 1500 cells/cm2 (day -1), cultured for 1 day in DMEM 10%NCS, then treated (d0) with or without 10uM 5-azacytidine (5AC) for an additional 3 days. RNA was extracted on day 3 and hybridized to GeneChip Mouse Genome 430 2.0 array (Affymetrix).

Background corr dist: KL-Divergence = 0.0286, L1-Distance = 0.0590, L2-Distance = 0.0044, Normal std = 0.7900

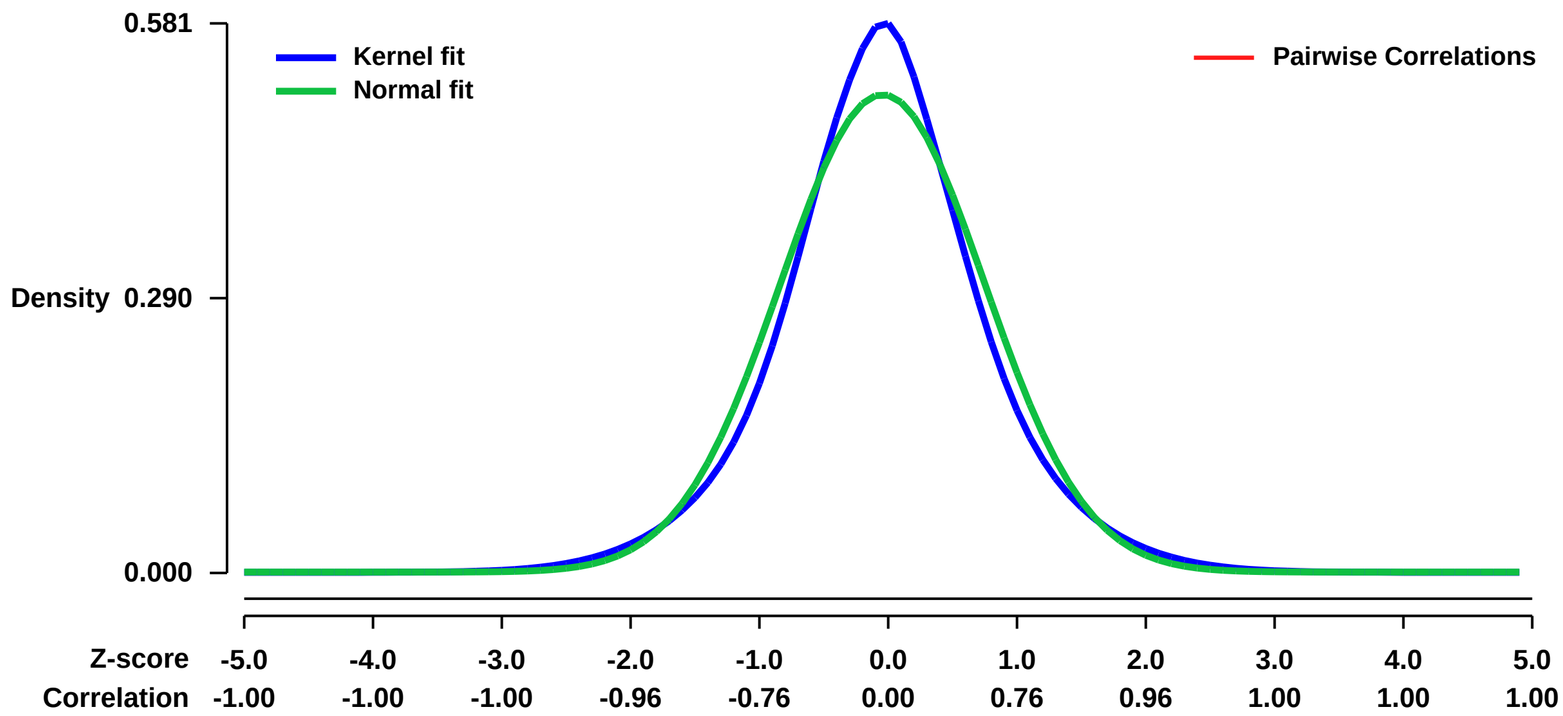

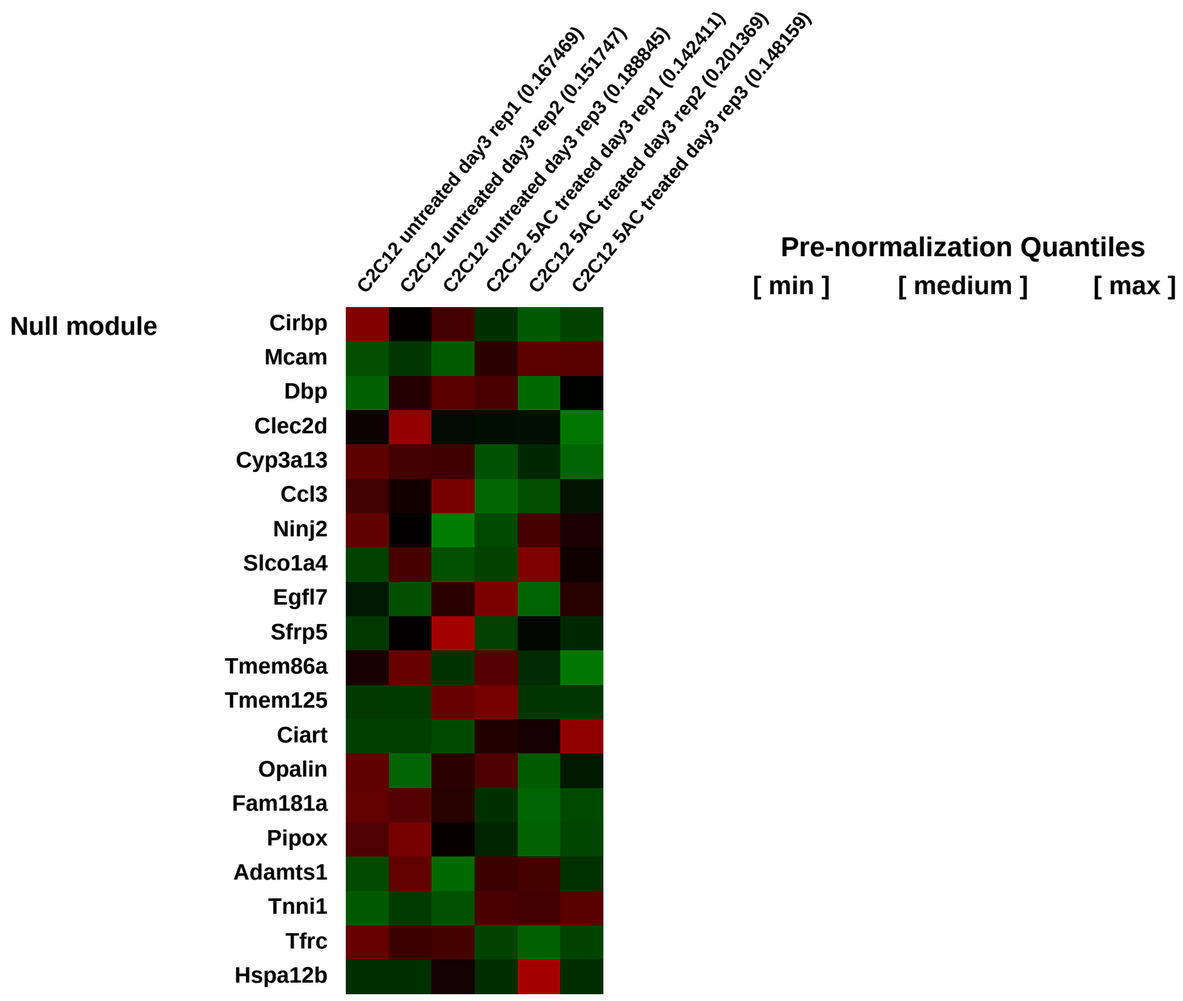

GEO Series "GSE6686" Expression Profiles

Num of samples in this series: 13

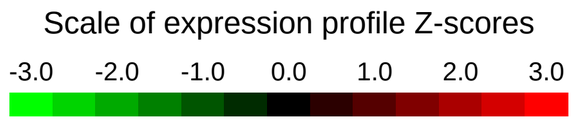

GEO Link:	**http://www.ncbi.nlm.nih.gov/geo/query/acc.cgi?acc=GSE6686**
Status:	**Public on Jul 05 2007**
Title:	**Gene expression profiles in skeletal muscle after gene transfer by electroporation**
Organism:	**Mus musculus**
Experiment type:	**Expression profiling by array**
Platform:	**GPL1261**
Pubmed ID:	**17598924**
Summary & Design:	**Summary:** **Abstract** **Background: Gene transfer by electroporation (electro gene transfer) to muscle results in high level long term transgenic expression, showing great promise for treatment of e.g. protein deficiency syndromes.** **However little is known about the effects of electro gene transfer on muscle fibres. We have therefore investigated transcriptional changes through gene expression profile analyses, as well as morphological changes evaluated by histological analysis. Electro gene transfer was obtained using a combination of a short high voltage pulse (HV, 1000 V/cm, 100 @s) followed by a long low voltage pulse (LV, 100 V/cm, 400 ms); a pulse combination optimised for efficient and safe gene transfer. Muscles were transfected with green fluorescent protein (GFP) and excised at 4 hours, 48 hours or 3 weeks after treatment.** **Results: Differentially expressed genes were investigated by microarray analysis, and descriptive statistics were performed to evaluate the effects of 1) electroporation, 2) DNA injection, and 3) time after treatment.** **The biological significance of the results was assessed by gene annotation and supervised cluster analysis. Generally, electroporation caused down-regulation of structural proteins e.g. sarcospan and catalytic en-zymes such as phosphoenolpuryvate carboxykinase. Injection of DNA induced down-regulation of intracellular transport proteins e.g. sentrin. The effects on muscle fibres were transient as the expression profiles 3 weeks after treatment were closely related with the control muscles. Most interestingly, no changes in the expression of proteins involved in inflammatory responses or muscle regeneration was detected, indicating limited muscle damage and regeneration. Histological analysis revealed structural changes with loss of cell integrity and striation pattern in some fibres after DNA+HV+LV treatment, while electroporation alone caused minor loss of striation pattern but preservation of cell integrity.** **Conclusion: The small and transient changes found in the gene expression profiles are of great importance, as this demonstrates that electro gene transfer is safe with minor effects on the muscle host cells. These findings are essential for introducing the electro gene transfer to muscle for clinical use. Indeed the HV+LV pulse combination used have been optimised to ensure highly efficient and safe electro gene transfer.** **Keywords: Electro gene transfer, microarray, affymetrix, gene therapy, skeletal muscle, mouse, time course** **Overall design:** **A total number of mice 13.**

Background corr dist: KL-Divergence = 0.1115, L1-Distance = 0.0333, L2-Distance = 0.0022, Normal std = 0.4264

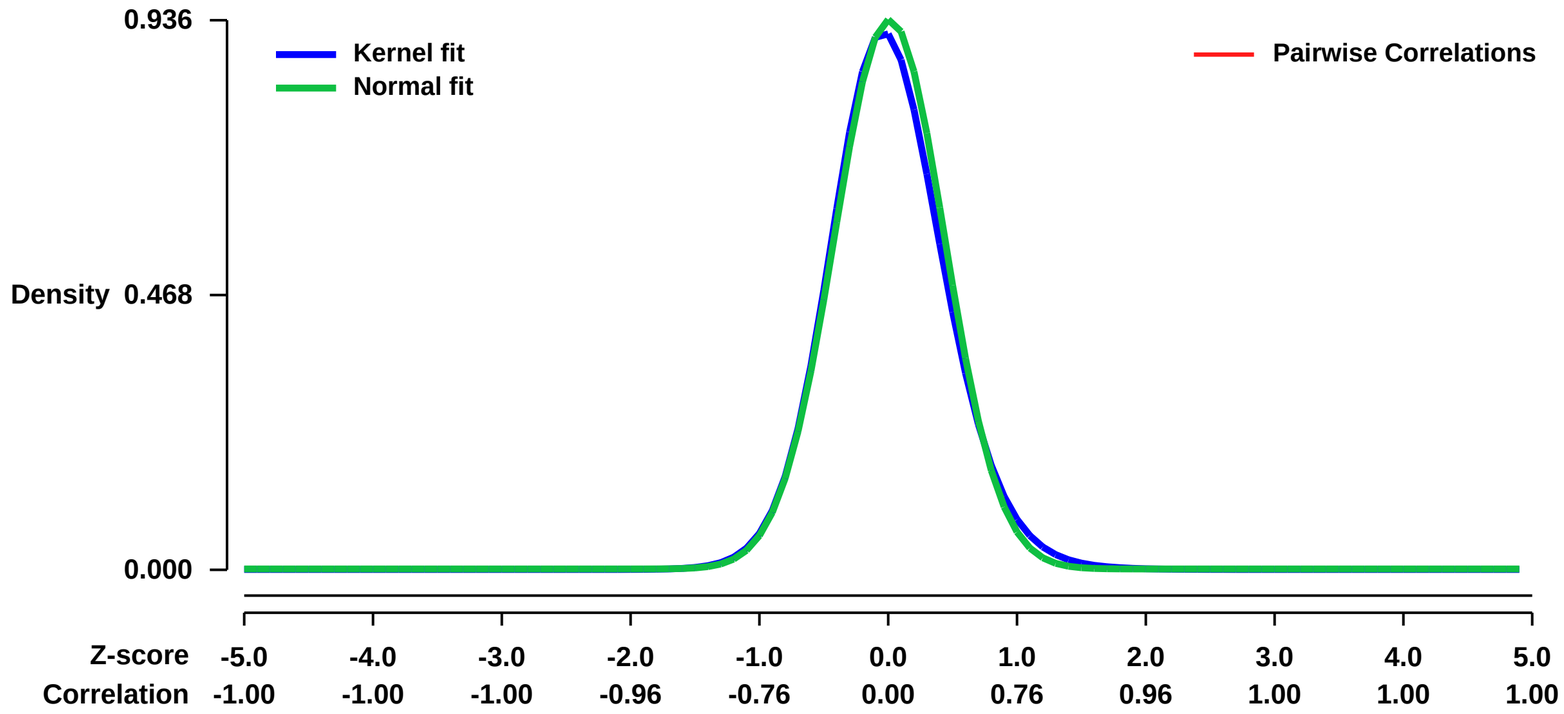

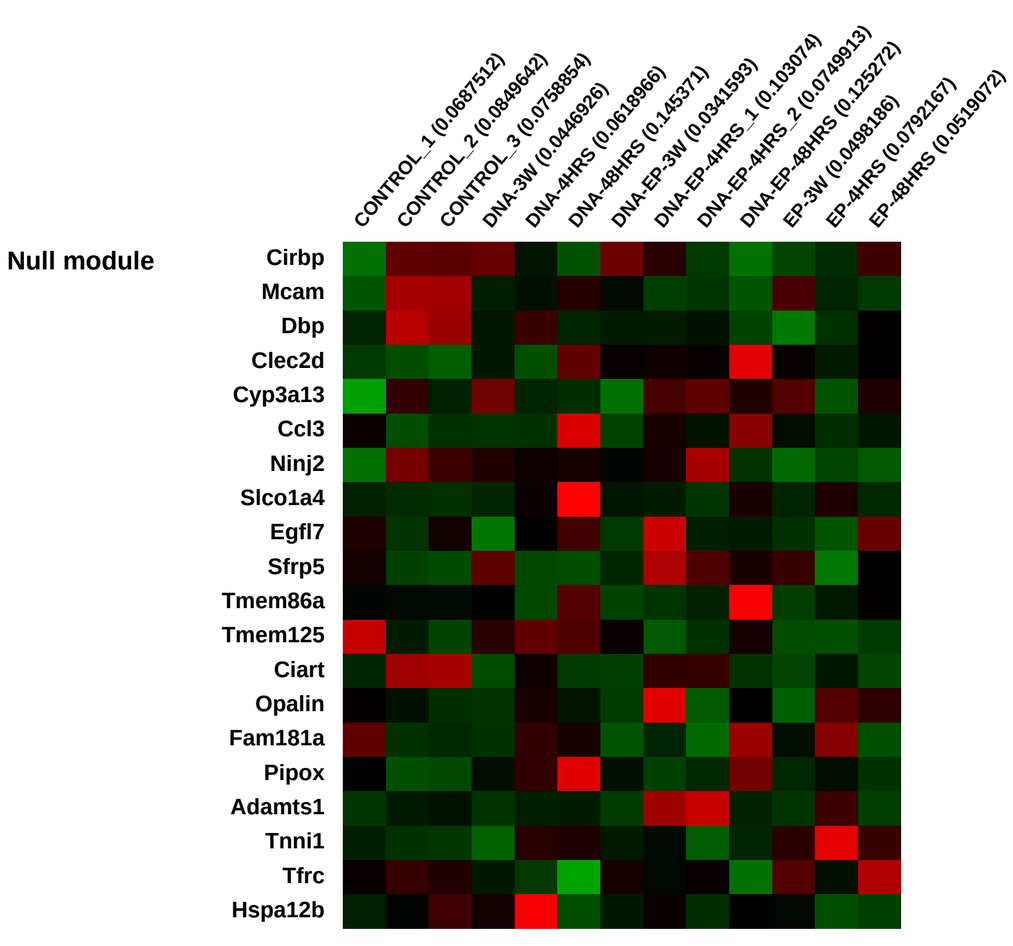

GEO Series "GSE32078" Expression Profiles

Num of samples in this series: 12

Scale of expression profile Z-scores

-3.0 -2.0 -1.0 0.0 1.0 2.0 3.0

GEO Link:	http://www.ncbi.nlm.nih.gov/geo/query/acc.cgi?acc=GSE32078
Status:	Public on Sep 14 2011
Title:	Differential gene expression profiles during embryonic heart development in diabetic mice pregnancy
Organism:	Mus musculus
Experiment type:	Expression profiling by array
Platform:	GPL1261
Pubmed ID:	23287646
Summary & Design:	**Summary:** Congenital heart defects (CHD) are one of the most common defects in offspring of diabetic mothers. There is a clear association between maternal diabetes and CHD; however the underlying molecular mechanism remains unknown. We hypothesized that maternal diabetes affects with the expression of early developmental genes that regulate the essential developmental processes of the heart, thereby resulting in the pathogenesis of CHD. We analyzed genome-wide expression profiling in the developing heart of embryos from diabetic and control mice by using the oligonucleotide microarray. Microarray analysis revealed that a total of 878 genes exhibited more than 1.5 fold changes in expression level in the hearts of experimental embryos in either E13.5 or E15.5 compared with their respective controls. Expression pattern of genes that is differentially expressed in the developing heart was further examined by the real-time reverse transcriptase-polymerase chain reaction. Several genes involved in a number of molecular signaling pathways such as apoptosis, proliferation, migration and differentiation in the developing heart were differentially expressed in embryos of diabetic pregnancy. It is concluded that altered expression of several genes involved in heart development may contribute to CHD in offspring of diabetic mothers. **Overall design:** Embryos with heart malformations from diabetic mice were used as the experimental samples. At least three or four embryos each from three or four different litters of diabetic or control groups were used for each microarray experiment (n = 3). Total RNA was extracted from the pooled embryonic heart tissues at E13.5 and E15.5 of diabetic and control groups using RNeasy micro kit (Qiagen, CA, USA). RNA was quantified by Nanodrop 1000 (Thermo Scientific, MA, USA) and its quality was determined using a Bioanalyzer (Agilent, CA, USA). For each sample, 100 ng of total RNA was used for the 3â IVT Express assay according to Origen Labs SOP (Origen Labs, Singapore). The extracted total RNA was transcribed into cDNA, which was then used as a template to synthesize biotin-labeled aRNA (amplified RNA). The aRNA was then fragmented and hybridized to Affymetrix Mouse Genome 430 2.0 array(Affymetrix, CA, USA) for 16 hours at 45´”C with rotation at 60 rpm. Arrays were then washed and stained using the FS450_0004 fluidics protocol on 3 fluidics stations and scanned using an Affymetrix 3000 7G scanner (Affymetrix, CA, USA). The scanned images were inspected for hybridization efficiency. The raw data (CEL) files generated from GCOS (GeneChip Operating Software, Affymetrix, CA, USA) were imported into Expression Console (EC) 1.1 (Affymetrix, CA, USA) to perform the Mas5 normalization and generate the quality control (QC) metrics.

Background corr dist: KL-Divergence = 0.1298, L1-Distance = 0.0323, L2-Distance = 0.0018, Normal std = 0.3944

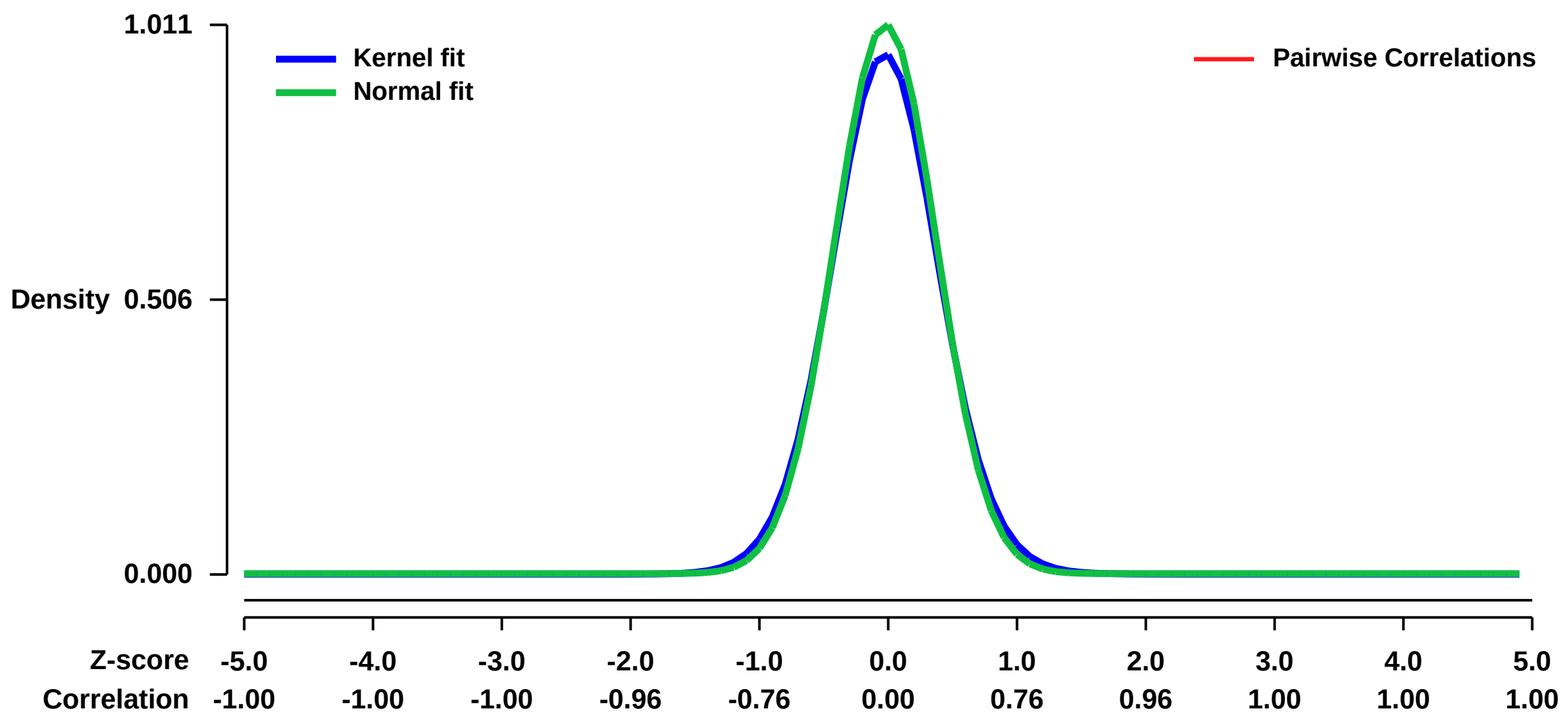

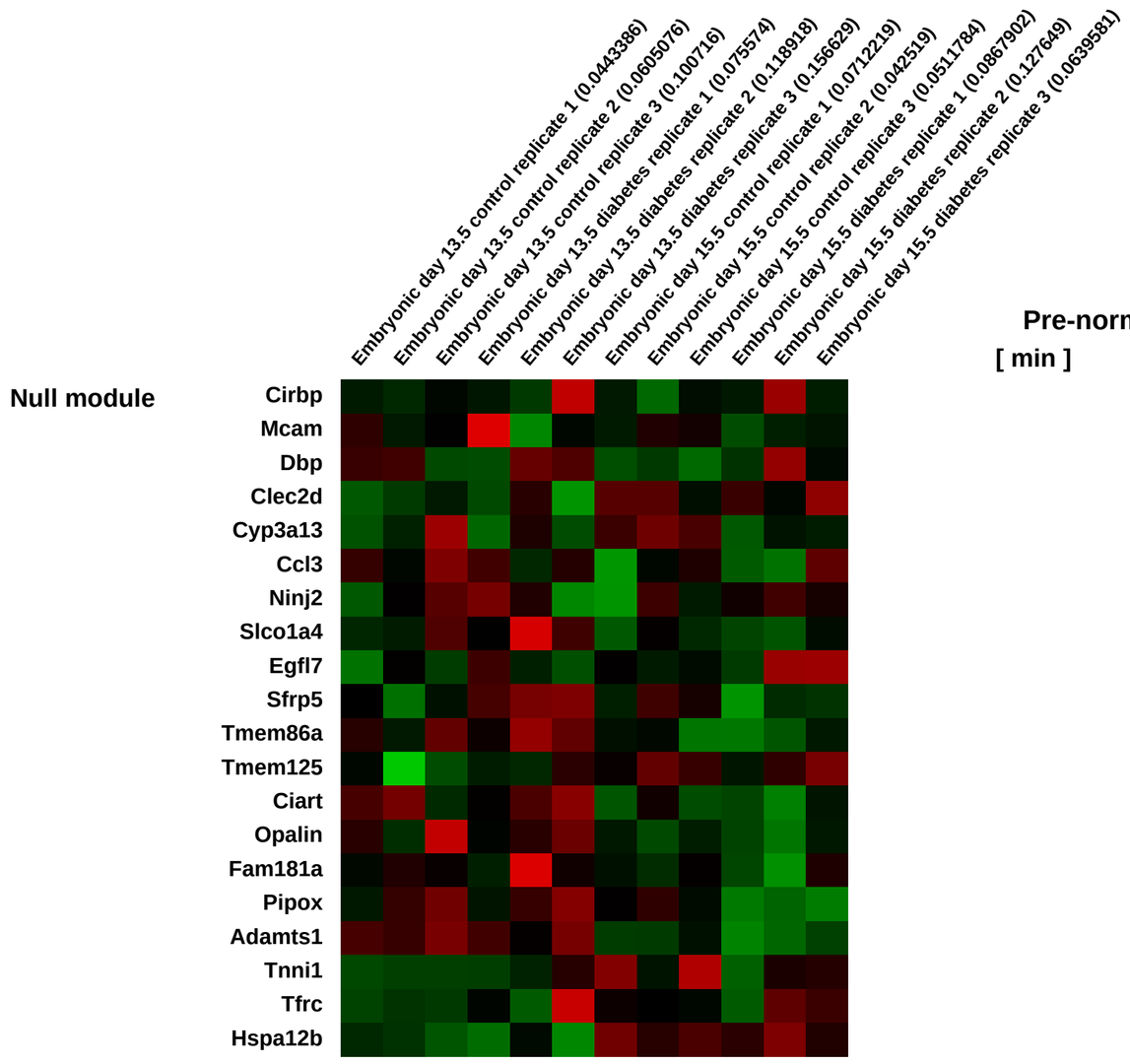

GEO Series "GSE26446" Expression Profiles

Num of samples in this series: 8

Scale of expression profile Z-scores

-3.0 -2.0 -1.0 0.0 1.0 2.0 3.0

GEO Link:	http://www.ncbi.nlm.nih.gov/geo/query/acc.cgi?acc=GSE26446
Status:	Public on Jul 20 2011
Title:	Expression data from Rbp2f/f and Rbp2-/- ES cells before and after differentiation
Organism:	Mus musculus
Experiment type:	Expression profiling by array
Platform:	GPL1261
Pubmed ID:	21788502
Summary & Design:	**Summary:** Aberrations in epigenetic processes, such as histone methylation, can lead to cancer. Retinoblastoma Binding Protein 2 (RBP2)(also called JARID1A or KDM5A) can demethylate tri- and di-methylated lysine 4 in histone H3, which are epigenetic marks for transcriptionally active chromatin, whereas the MEN1 tumor suppressor promotes H3K4 methylation. Previous studies suggested that inhibition of RBP2 contributed to tumor suppression by pRB. Here we show RBP2 loss promotes cellular differentiation in vitro. We use mouse expression array 430 2.0 array to profile gene expression patterns of Rbp2f/f and Rbp2-/- ES cells in ES cell medium and after 6 days in ES cell medium without LIF. **Overall design:** Subconfluent Rbp2f/f and Rbp2-/- ES cells in ES cell medium and after 6 days in ES cell medium without LIF were harvested for RNA isolation using RNeasy mini kit with on-column DNase digestion (Qiagen). Gene expression profiling was performed using Affymetrix GeneChip mouse genome 430 2.0 arrays. Duplicate samples were used

Background corr dist: KL-Divergence = 0.0611, L1-Distance = 0.0239, L2-Distance = 0.0008, Normal std = 0.5304

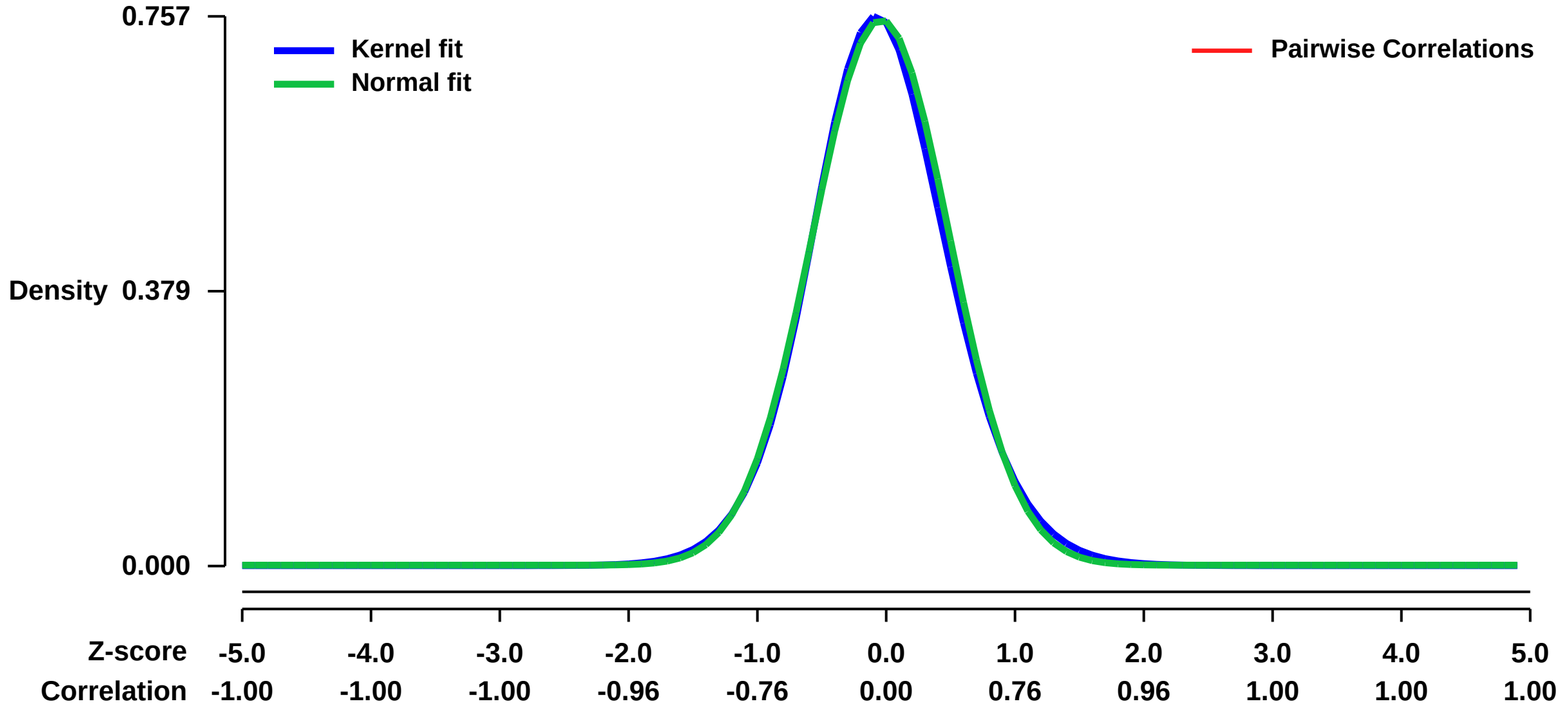

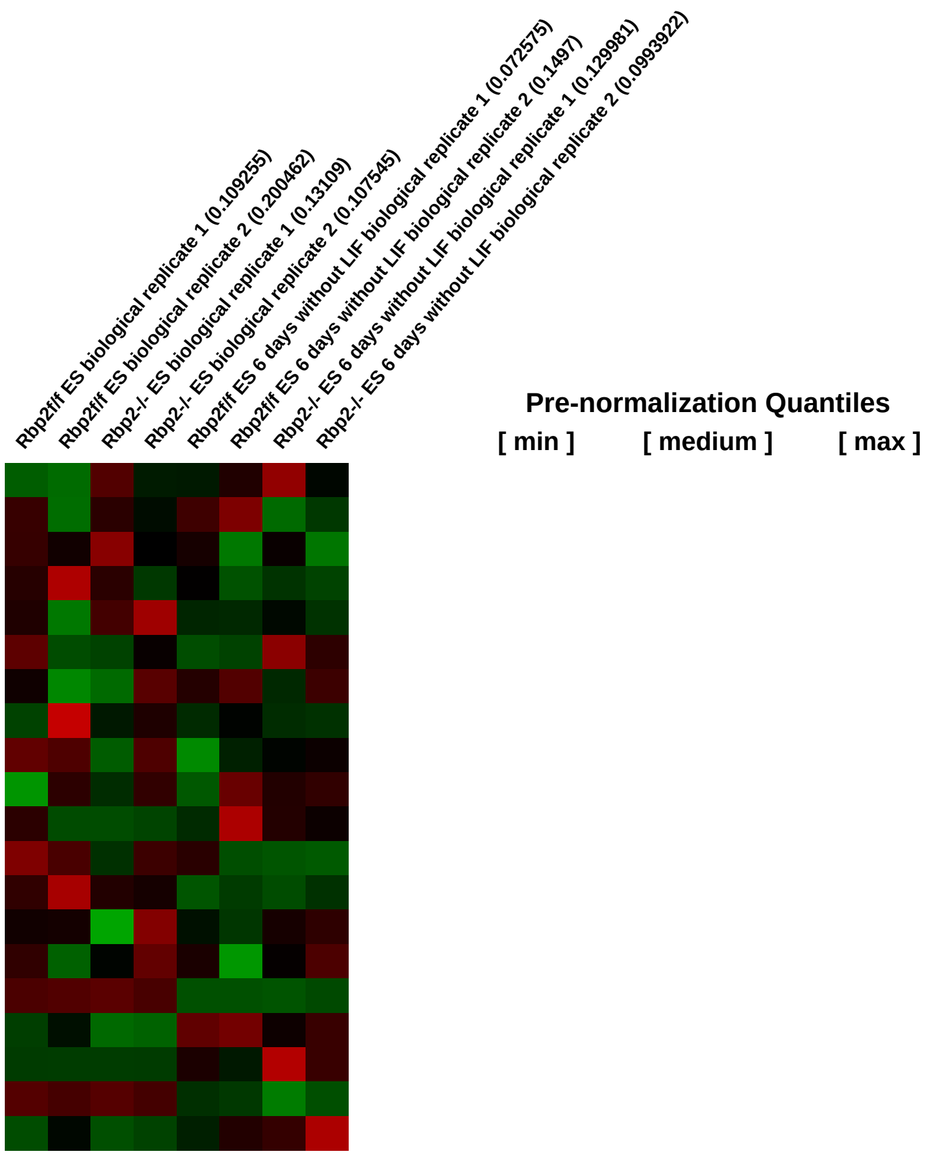

GEO Series "GSE27159" Expression Profiles

Num of samples in this series: 8

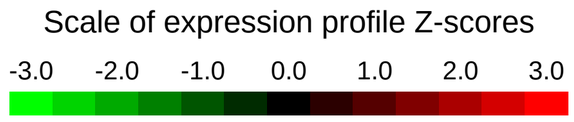

GEO Link:	**http://www.ncbi.nlm.nih.gov/geo/query/acc.cgi?acc=GSE27159**
Status:	**Public on Apr 30 2012**
Title:	**Expression profiling of the murine neural crest precursor cell line, JoMa1**
Organism:	**Mus musculus**
Experiment type:	**Expression profiling by array**
Platform:	**GPL1261**
Pubmed ID:	
Summary & Design:	**Summary:** **JoMa1 cells are pluripotent precursor cells, derived from the neural crest of mice transgenic for tamoxifen-inducible c-Myc. Following transfection with a cDNA encoding for MYCN, cells become immortlized even in the absence of tamoxifen.** **Overall design:** **The expression profile of JoMa1 cells was compared to cell lines derived from tumors induced by JoMa1 transfected with MYCN.**

Background corr dist: **KL-Divergence = 0.0379, L1-Distance = 0.0219, L2-Distance = 0.0005, Normal std = 0.6256**

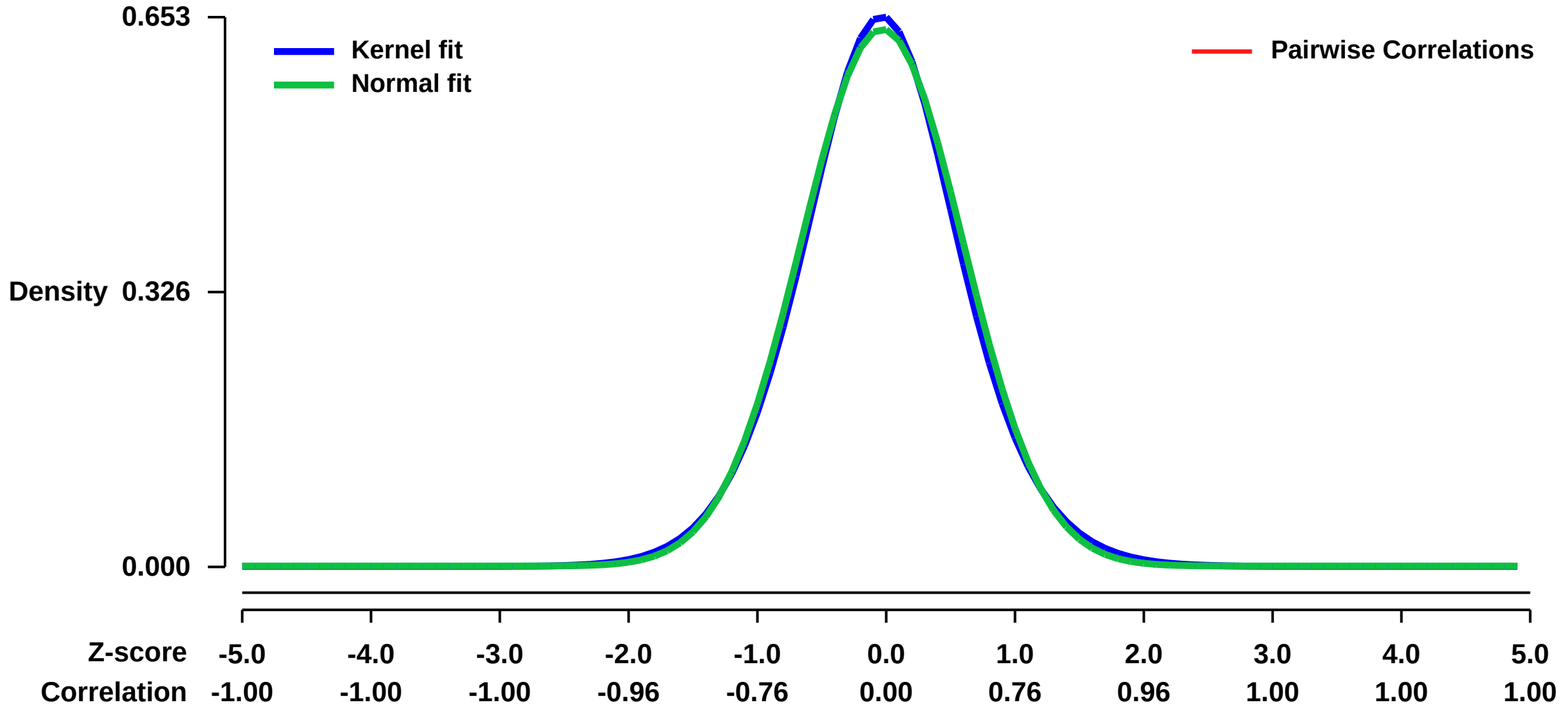

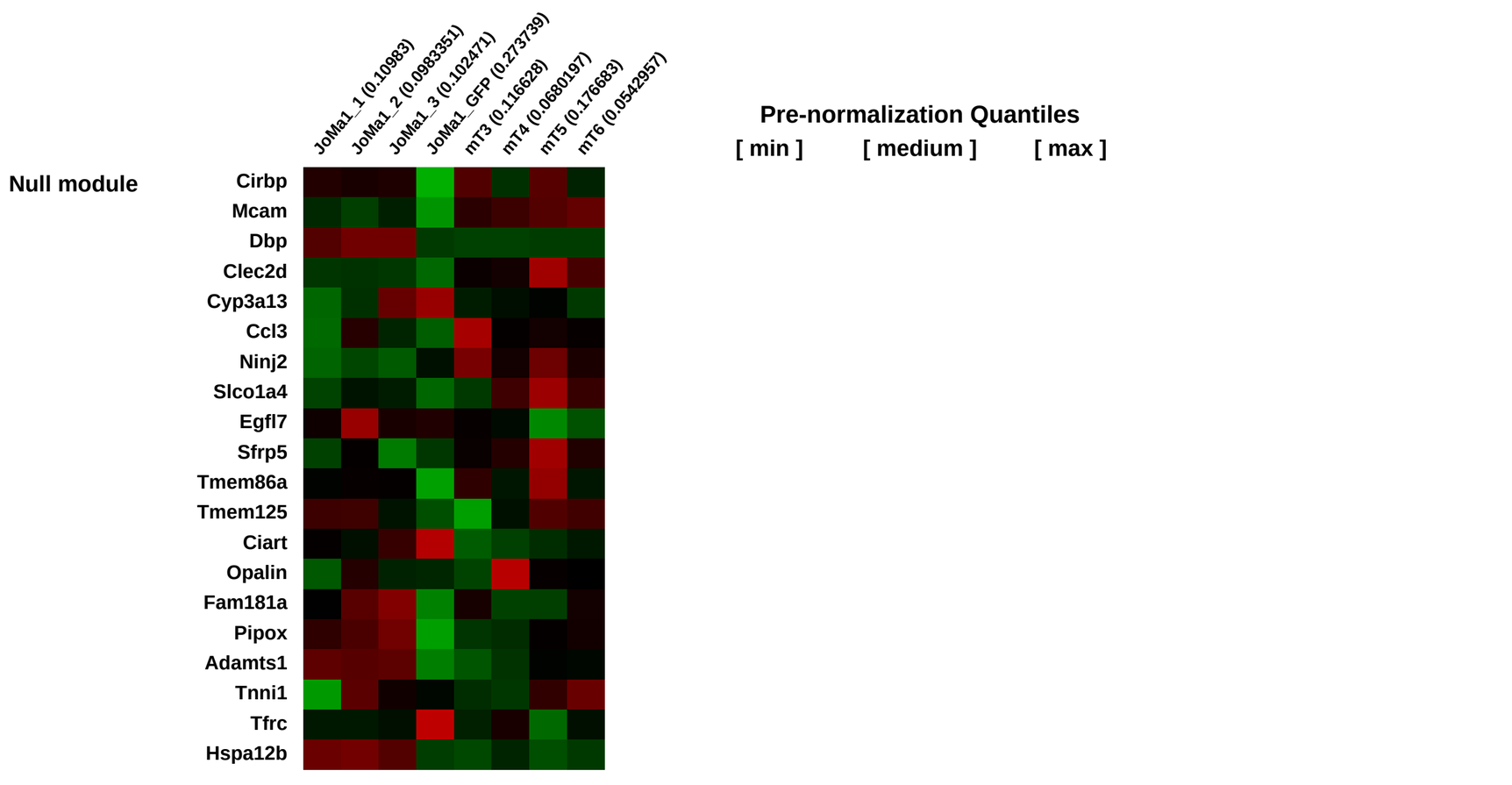

GEO Series "GSE6998" Expression Profiles

Num of samples in this series: 32

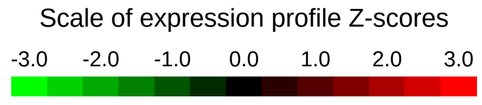

GEO Link:	http://www.ncbi.nlm.nih.gov/geo/query/acc.cgi?acc=GSE6998
Status:	Public on Feb 09 2007
Title:	Expression profiling of developmental and regenerating liver in mice
Organism:	Mus musculus
Experiment type:	Expression profiling by array
Platform:	GPL1261
Pubmed ID:	17227769
Summary & Design:	Summary: Normal adult liver is uniquely capable of renewal and repair after injury. Whether this response represents simple hyperplasia of various liver elements or requires recapitulation of the genetic program of the developing liver is not known. To study these possibilities, we examined transcriptional programs of adult liver after partial hepatectomy and contrasted these with developing embryonic liver. Principal component analysis demonstrated that the time series of gene expression during liver regeneration does not segregate according to developmental transcription patterns. Gene ontology analysis revealed that liver restoration after hepatectomy and liver development differ dramatically with regard to transcription factors and chromatin structure modification. In contrast, the tissues are similar with regard to proliferationassociated genes. Consistent with these findings, realtime polymerase chain reaction showed transcription factors known to be important in liver development are not induced during liver regeneration. These three lines of evidence suggest that at a transcriptional level, restoration of liver mass after injury is best described as hepatocyte hyperplasia and not true regeneration. We speculate this novel pattern of gene expression may underlie the unique capacity of the liver to repair itself after injury. Keywords: time course Overall design: Each experimental time point is represented by two separate samples, each consisting of at least 3 pooled tissues from different animals. For example, 6 hepatectomies were performed for the 1 hour post-hepatectomy time point. Time 0 is used as control.

Background corr dist: KL-Divergence = 0.0534, L1-Distance = 0.0220, L2-Distance = 0.0006, Normal std = 0.5487

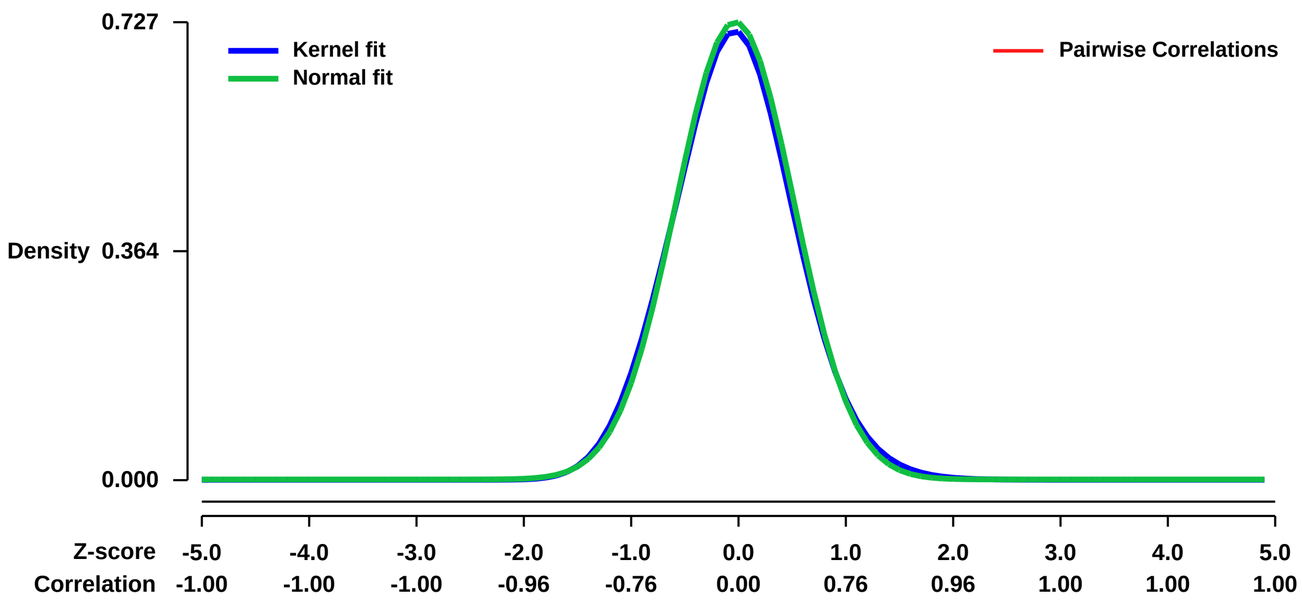

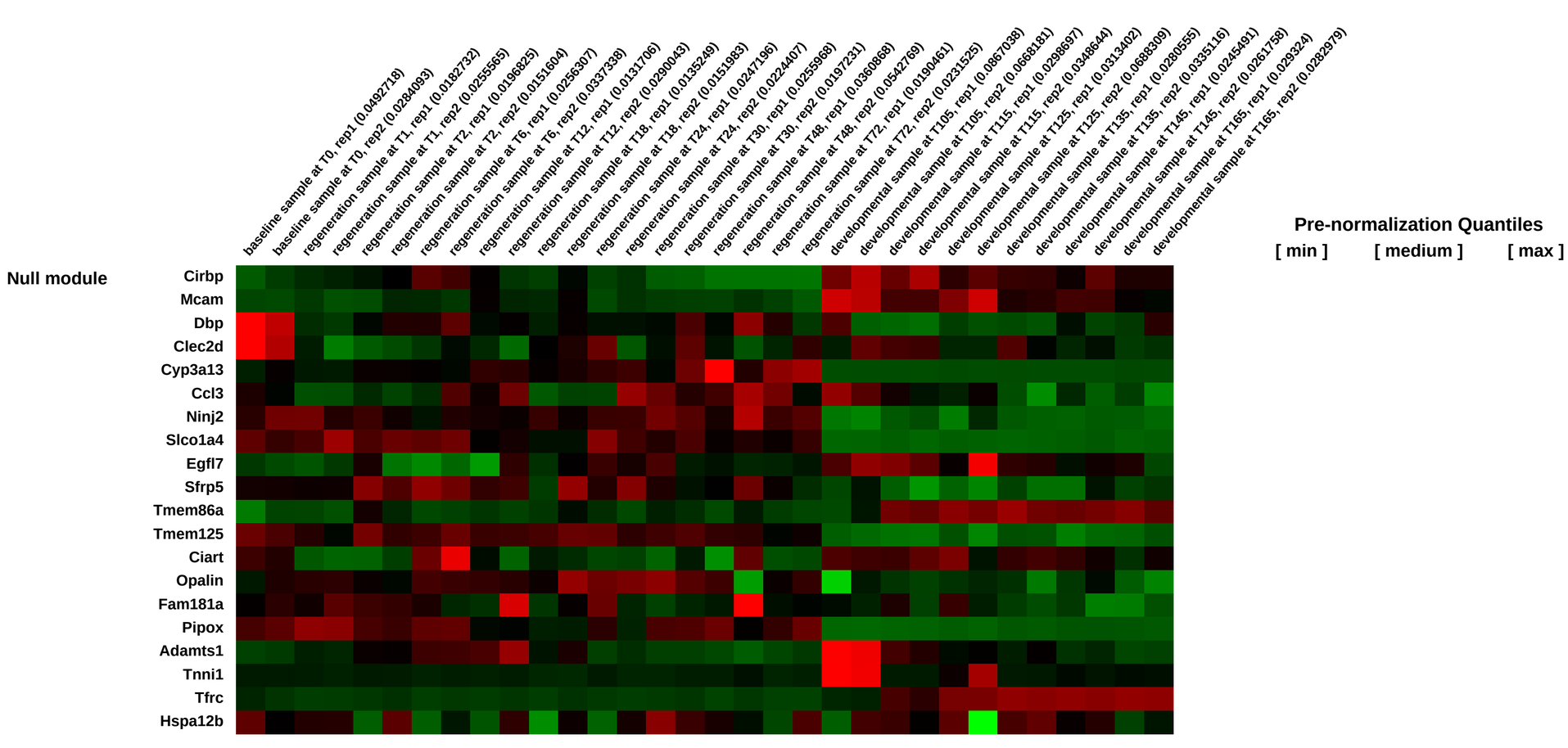

GEO Series "GSE26695" Expression Profiles

Num of samples in this series: 20

Scale of expression profile Z-scores

-3.0 -2.0 -1.0 0.0 1.0 2.0 3.0

GEO Link:	http://www.ncbi.nlm.nih.gov/geo/query/acc.cgi?acc=GSE26695
Status:	Public on Jan 24 2011
Title:	Transcriptomic response of murine liver to severe injury and hemorrhagic shock: Affymetrix portion of dual platform
Organism:	Mus musculus
Experiment type:	Expression profiling by array
Platform:	GPL1261
Pubmed ID:	21828244
Summary & Design:	**Summary:** A dual platform microarray analysis was used to characterize the temporal transcriptomic response in the mouse liver following trauma and hemmorhagic shock **Overall design:** Mice were divided into five groups, anesthetized and surgically treated to simulate a time course and trauma severity model: non-manipulated animals (C), minor trauma (MT), 1.5 hour of hemorrhagic shock and severe trauma (HS/T), 1.5 hour HS/T followed by 1 hour resuscitation (HS/T+1.0R), 1.5 hour HS/T followed by 4.5 hours resuscitation (HS/T+4.5R)

Background corr dist: KL-Divergence = 0.2191, L1-Distance = 0.0407, L2-Distance = 0.0035, Normal std = 0.3217

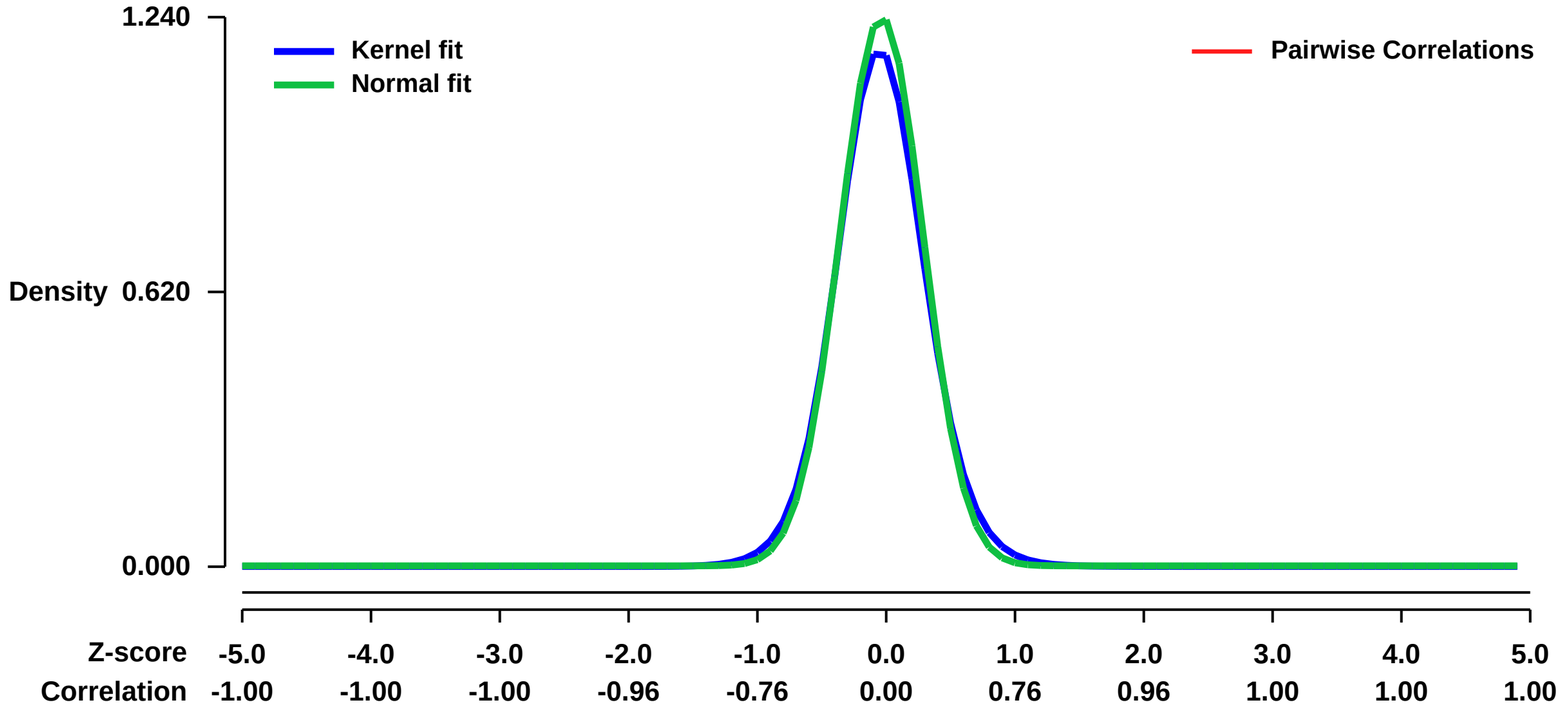

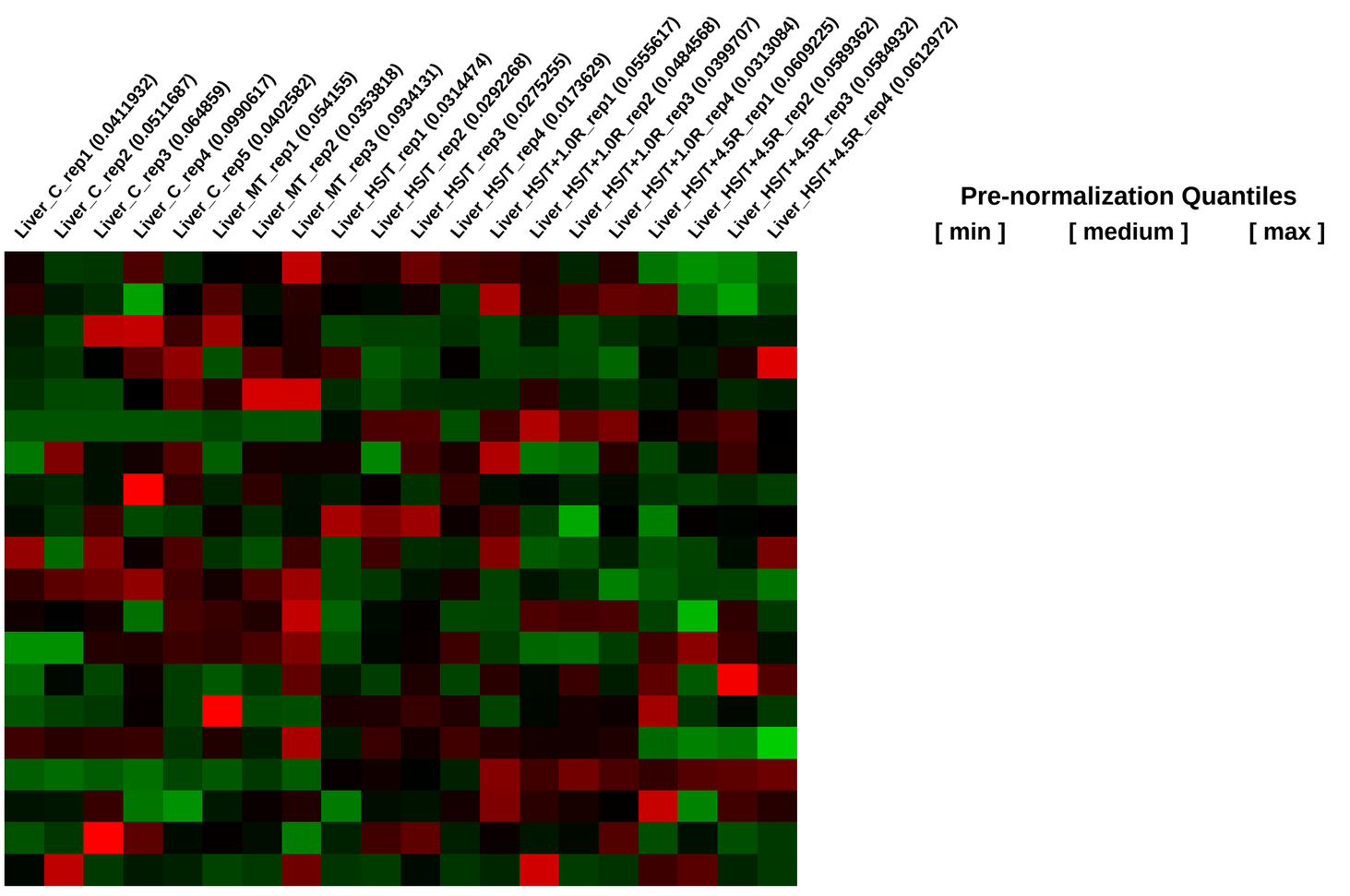

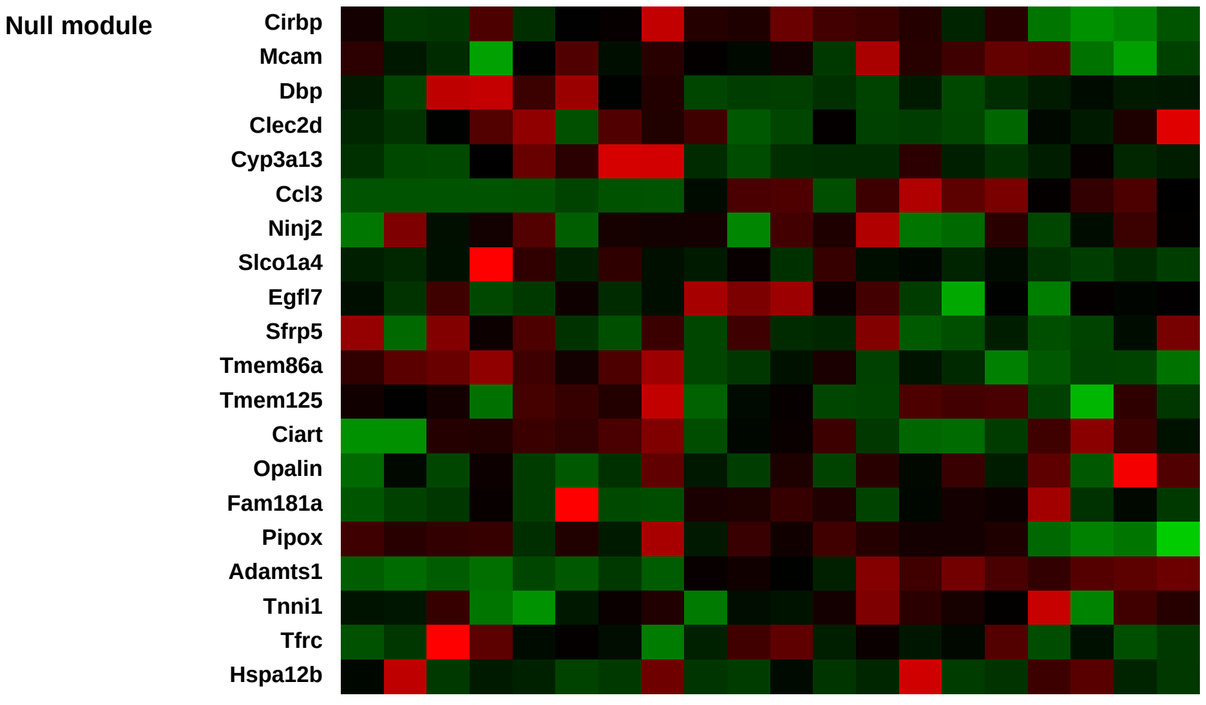

GEO Series "GSE23738" Expression Profiles

Num of samples in this series: 17

Scale of expression profile Z-scores

-3.0 -2.0 -1.0 0.0 1.0 2.0 3.0

GEO Link:	http://www.ncbi.nlm.nih.gov/geo/query/acc.cgi?acc=GSE23738
Status:	Public on Aug 22 2010
Title:	Global changes of expression patterns of vaccinia virus infected lungs of C57BL/6 mice.
Organism:	Mus musculus
Experiment type:	Expression profiling by array
Platform:	GPL1261
Pubmed ID:	20943971
Summary & Design:	**Summary:** Vaccinia virus infection of mouse lungs produces a focal infection within the lung remaining at the large bronchi throughout the course of infection. Animals die of respiratory failure with little edema and few infiltrating immune cells. It is well established that poxviruses control the host immune system by encoding multiple host defense pathway antagonists. The goal of this study was to examine the local response to infection within the lung given that the virus controls the host immune response. **Overall design:** The global changes exhibited over the course of a lung infection with vaccinia virus were analyzed by arrays of lungs harvested from 1 to 5 day post infection using Affymetrix Mouse 430A 2.0 arrays.

Background corr dist: KL-Divergence = 0.2052, L1-Distance = 0.0397, L2-Distance = 0.0033, Normal std = 0.3305

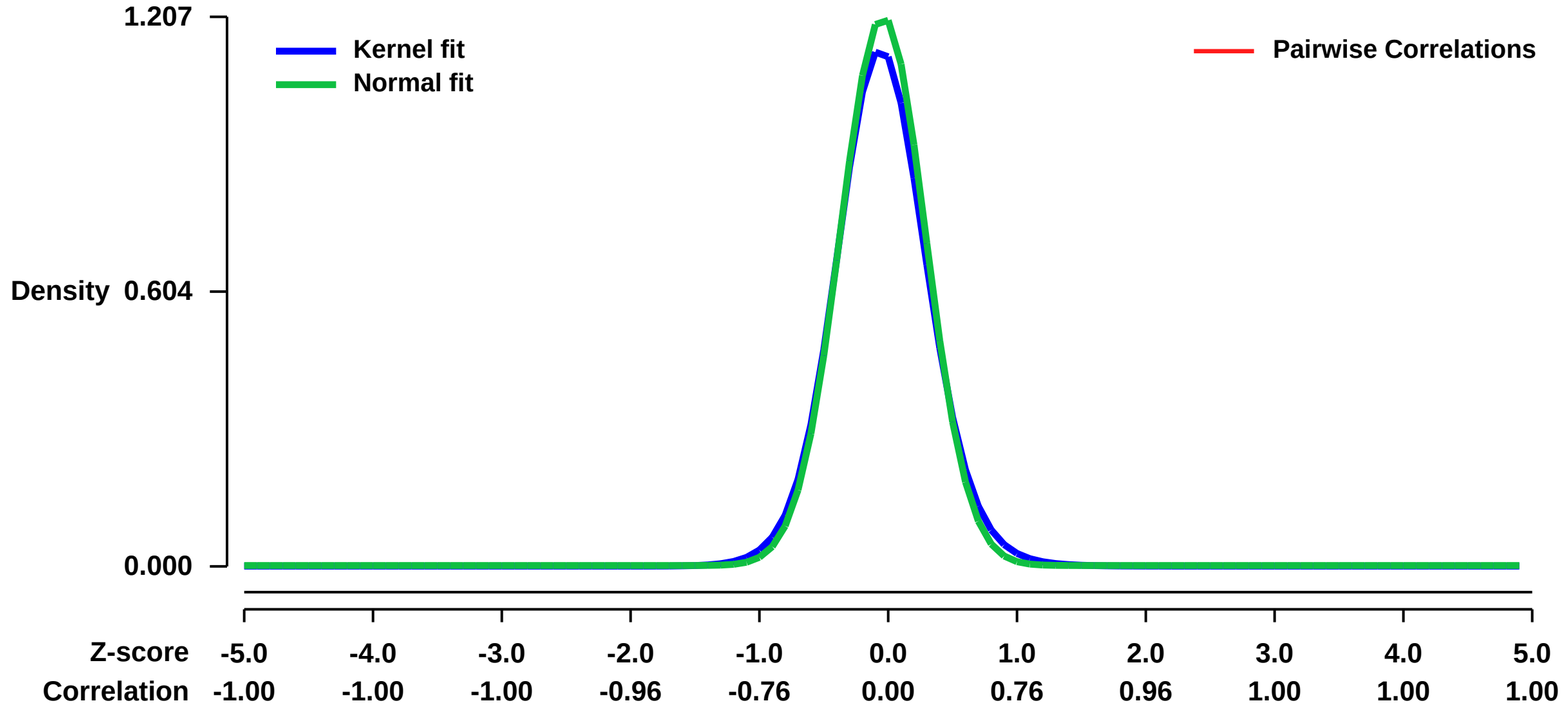

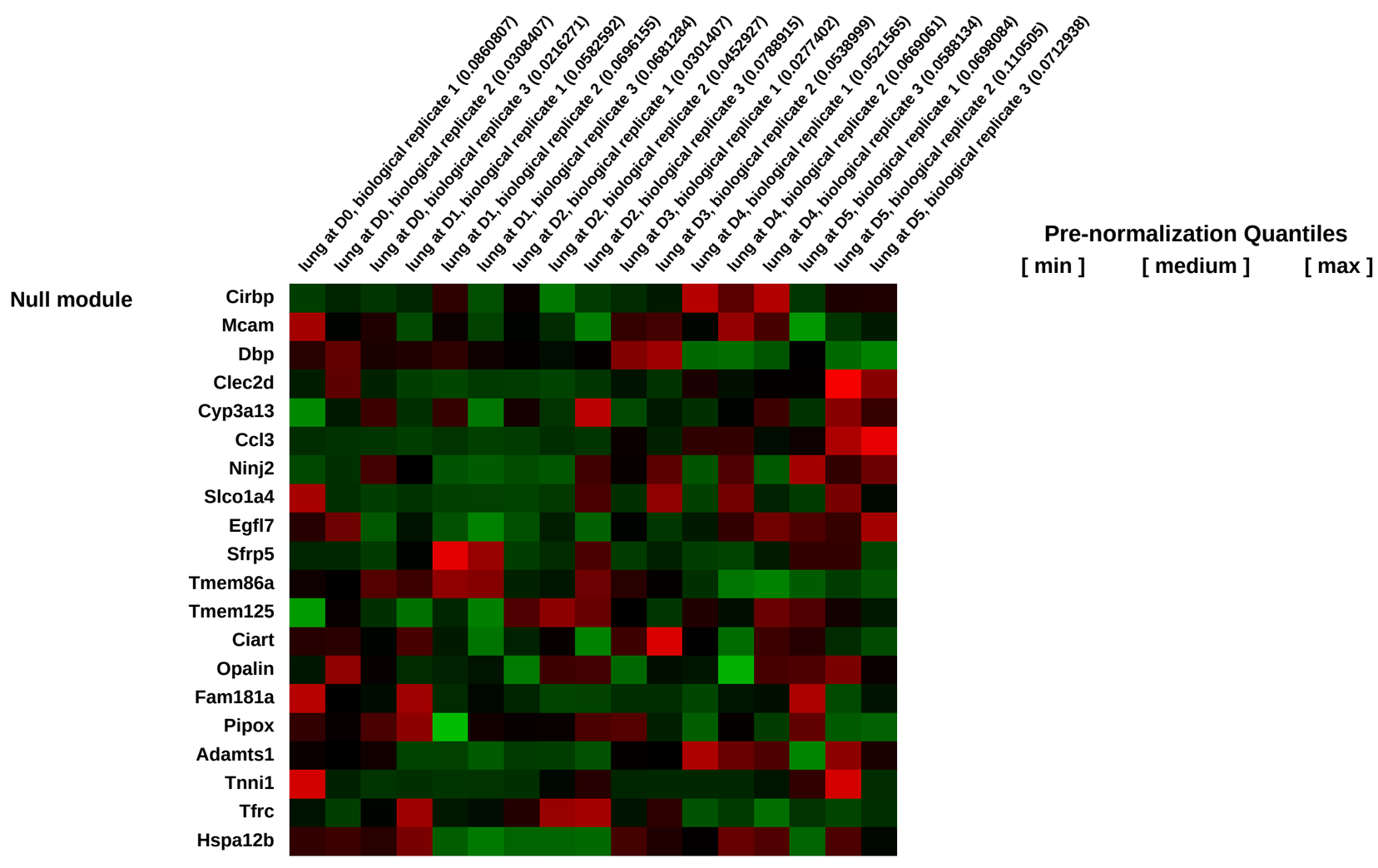

GEO Series "GSE21272" Expression Profiles

Num of samples in this series: 44

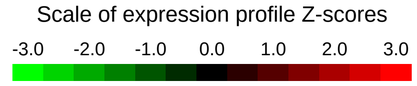

GEO Link:	http://www.ncbi.nlm.nih.gov/geo/query/acc.cgi?acc=GSE21272
Status:	Public on Oct 21 2010
Title:	Time Course Gene Expression Microarray Analysis of a Mouse B-cell Line (CH12.LX) Activated with Lipopolysaccharide and Treated with 2,3,7,8-Tetrachlorodibenzo-p-dioxin
Organism:	Mus musculus
Experiment type:	Expression profiling by array
Platform:	GPL1261
Pubmed ID:	20819909
Summary & Design:	**Summary:** The objective of the study was to characterize gene expression cascade involved in the suppression of B-cell activation and differentiation by 2,3,7,8-tetrachlorodibenzo-p-dixoxin (TCDD). The underlying hypothesis was that multiple nodes in the B-cell differentiation network are directly or indirectly regulated by TCDD through its receptor, the AHR. **Overall design:** The mouse B-cell line (CH12.LX) was plated at 1X10^5 cells/ml at time 0 and activated with lipopolysaccharide (LPS, Salmonella typhosa). The cells were then treated with either dimethyl sulfoxide (DMSO, 0.01%) or 10 nM 2,3,7,8-tetrachlorodibenzo-p-dixoxin (TCDD). The cells were harvested at 0, 8, 12, 24, 36, and 48 hrs post-treatment. At the 0 hr time point, cells were untreated. A total of 4 experimental replicates per time point per treatment group were included with the cells for each replicate treated and harvested on separate days. Single color Affymetrix Mouse 430 2.0 arrays were used.

Background corr dist: KL-Divergence = 0.2971, L1-Distance = 0.0472, L2-Distance = 0.0048, Normal std = 0.2838

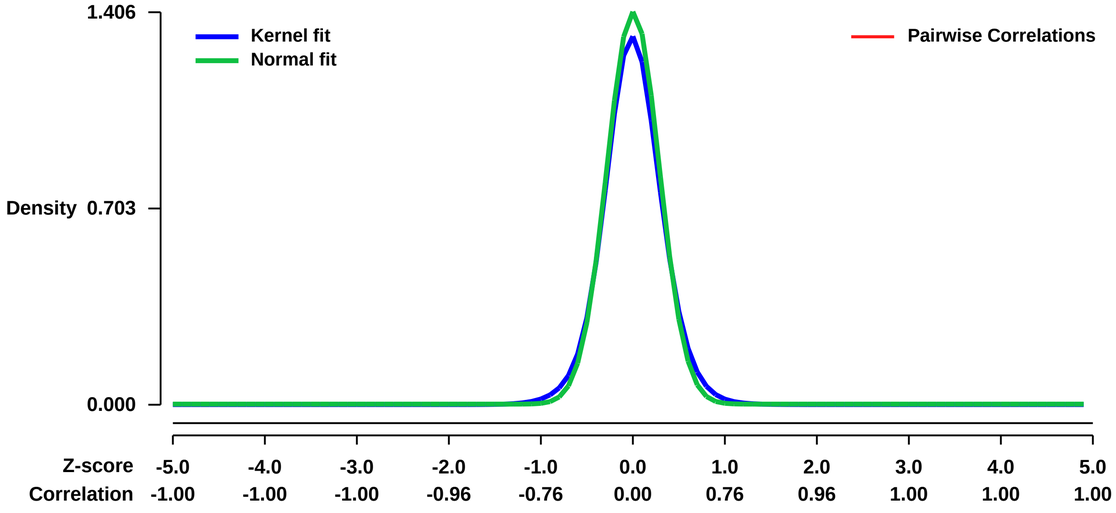

Z-score	-5.0	-4.0	-3.0	-2.0	-1.0	0.0	1.0	2.0	3.0	4.0	5.0
Correlation	-1.00	-1.00	-1.00	-0.96	-0.76	0.00	0.76	0.96	1.00	1.00	1.00

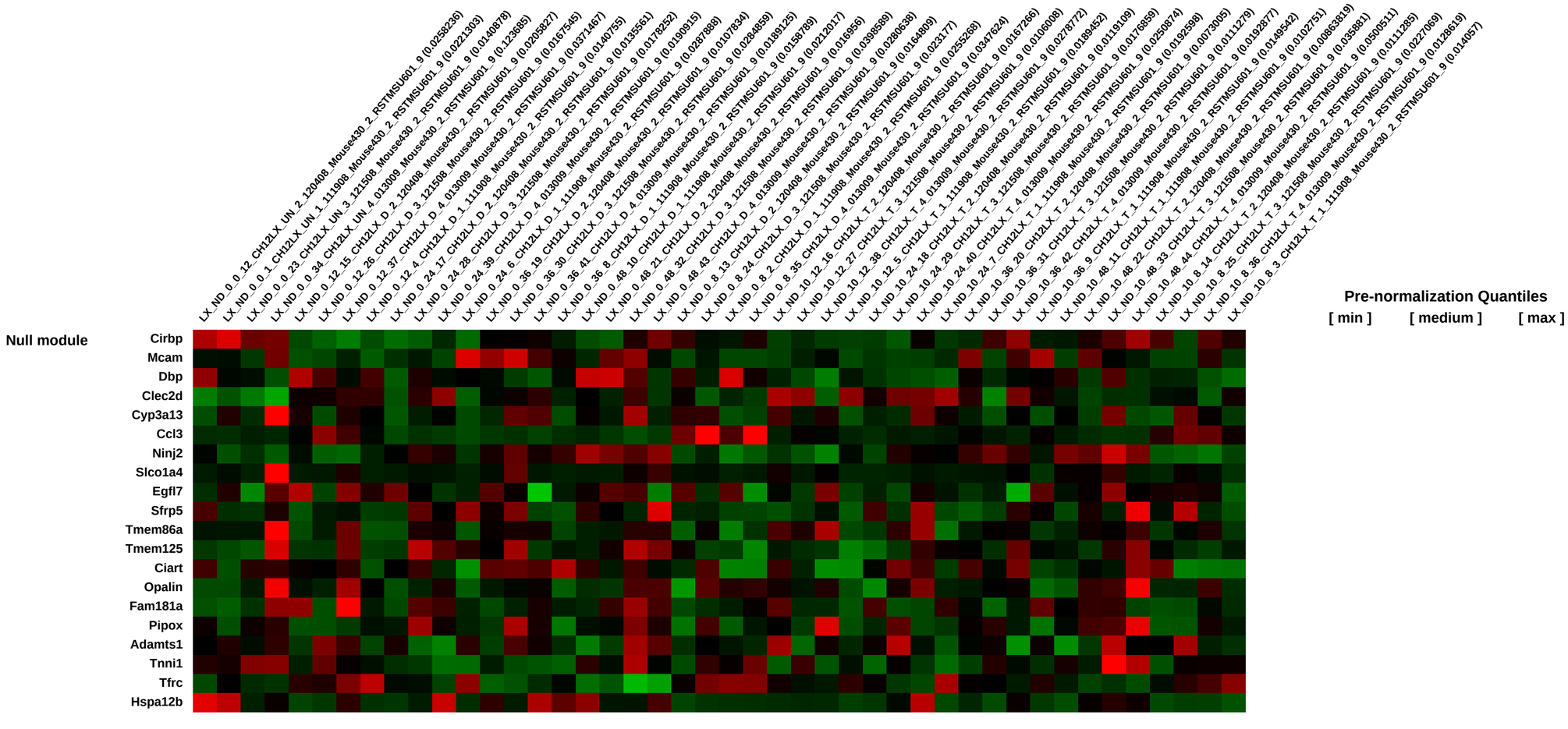

GEO Series "GSE46496" Expression Profiles

Num of samples in this series: 9

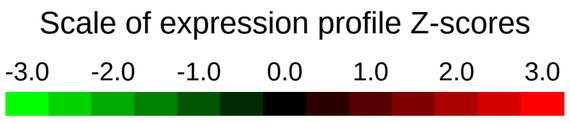

GEO Link:	http://www.ncbi.nlm.nih.gov/geo/query/acc.cgi?acc=GSE46496
Status:	Public on Jun 07 2013
Title:	Atrial Identity Is Determined by A COUP-TFII Regulatory Network (RNA)
Organism:	Mus musculus
Experiment type:	Expression profiling by array
Platform:	GPL1261
Pubmed ID:	23725765
Summary & Design:	**Summary:** Atria and ventricles exhibit distinct molecular profiles that produce structural and functional differences between the two cardiac compartments. However, factors that determine these differences remain largely undefined. Cardiomyocyte-specific COUP- TFII ablation produces ventricularized atria that exhibit ventricle-like action potentials, increased cardiomyocyte size, and development of extensive T-tubules. We used microarrays to examine the molecular profile of cardiomyocyte-specific COUP-TFII knockout adult atria in comparison with that of normal atria. **Overall design:** We extracted RNA from mutant right atria, control right atria and control ventricles from 2 months old adult mice, followed by gene expression profiling using Affymetrix microarrays.

Background corr dist: KL-Divergence = 0.0268, L1-Distance = 0.0394, L2-Distance = 0.0028, Normal std = 0.6869

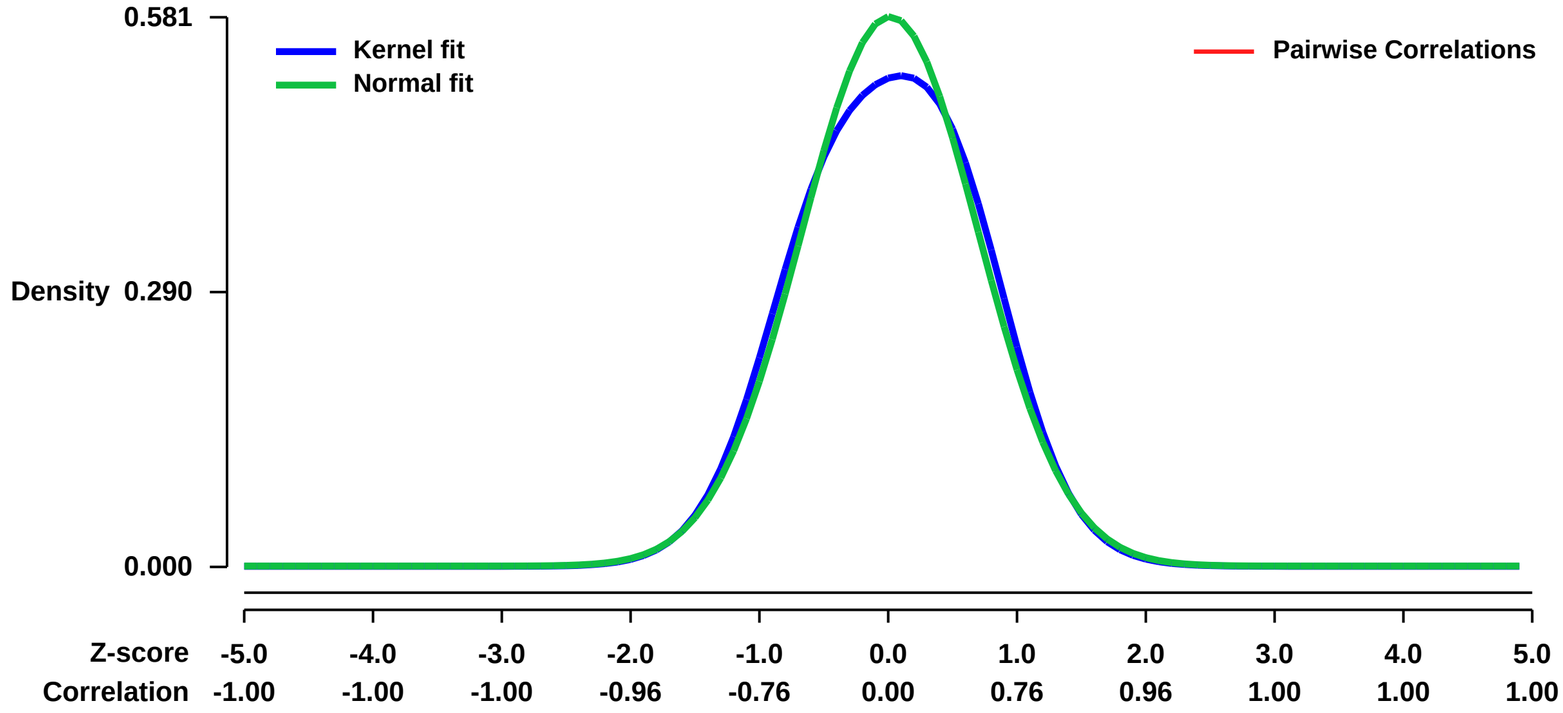

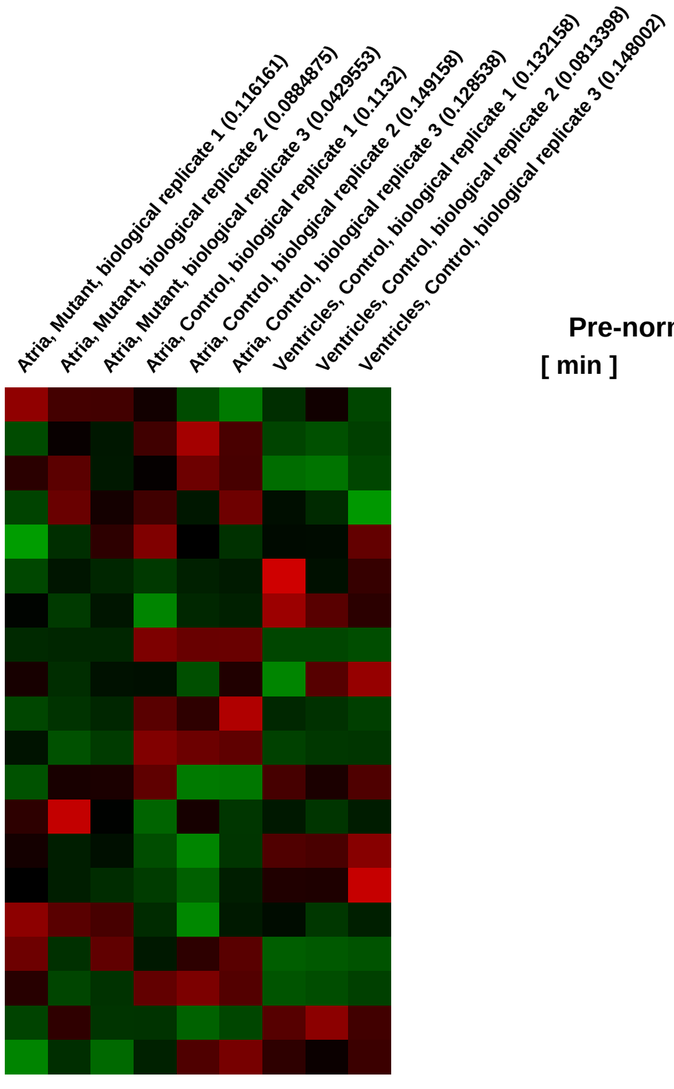

GEO Series "GSE11291" Expression Profiles

Num of samples in this series: 60

Scale of expression profile Z-scores

-3.0 -2.0 -1.0 0.0 1.0 2.0 3.0

GEO Link:	http://www.ncbi.nlm.nih.gov/geo/query/acc.cgi?acc=GSE11291
Status:	Public on Jun 10 2008
Title:	Effect of age, calorie restriction and resveratrol on gene expression in mouse heart, brain, and skeletal muscle
Organism:	Mus musculus
Experiment type:	Expression profiling by array
Platform:	GPL1261
Pubmed ID:	18523577
Summary & Design:	**Summary:** Resveratrol in high doses has been shown to extend lifespan in some studies in invertebrates and to prevent early mortality in mice fed a high-fat diet. We fed mice from middle age (14-months) to old age (30-months) either a control diet, a low dose of resveratrol (4.9 mg kg-1 day-1), or a calorie restricted (CR) diet and examined genome-wide transcriptional profiles. We report a striking transcriptional overlap of CR and resveratrol in heart, skeletal muscle and brain. Both dietary interventions inhibit gene expression profiles associated with cardiac and skeletal muscle aging. Gene expression profiling suggests that both CR and resveratrol may retard some aspects of aging through alterations in chromatin structure and transcription. Resveratrol, at doses that can be readily achieved in humans, fulfills the definition of a dietary compound that mimics some aspects of CR. Keywords: aging intervention study **Overall design:** Heart, neocortex tissue, and gastrocnemius muscle was collected from young and old mice at 5 and 30 months of age, respectively; mice were subjected to either a calorie restricted diet or a control diet supplemented with resveratrol

Background corr dist: KL-Divergence = 0.0995, L1-Distance = 0.0458, L2-Distance = 0.0038, Normal std = 0.4744

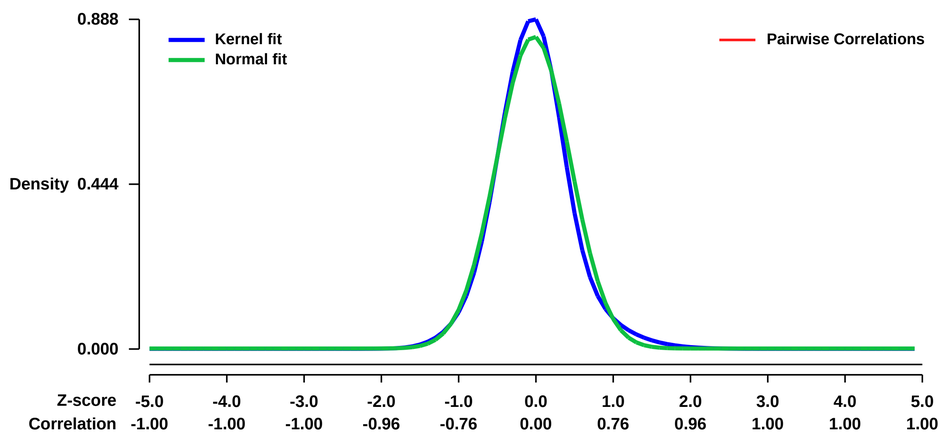

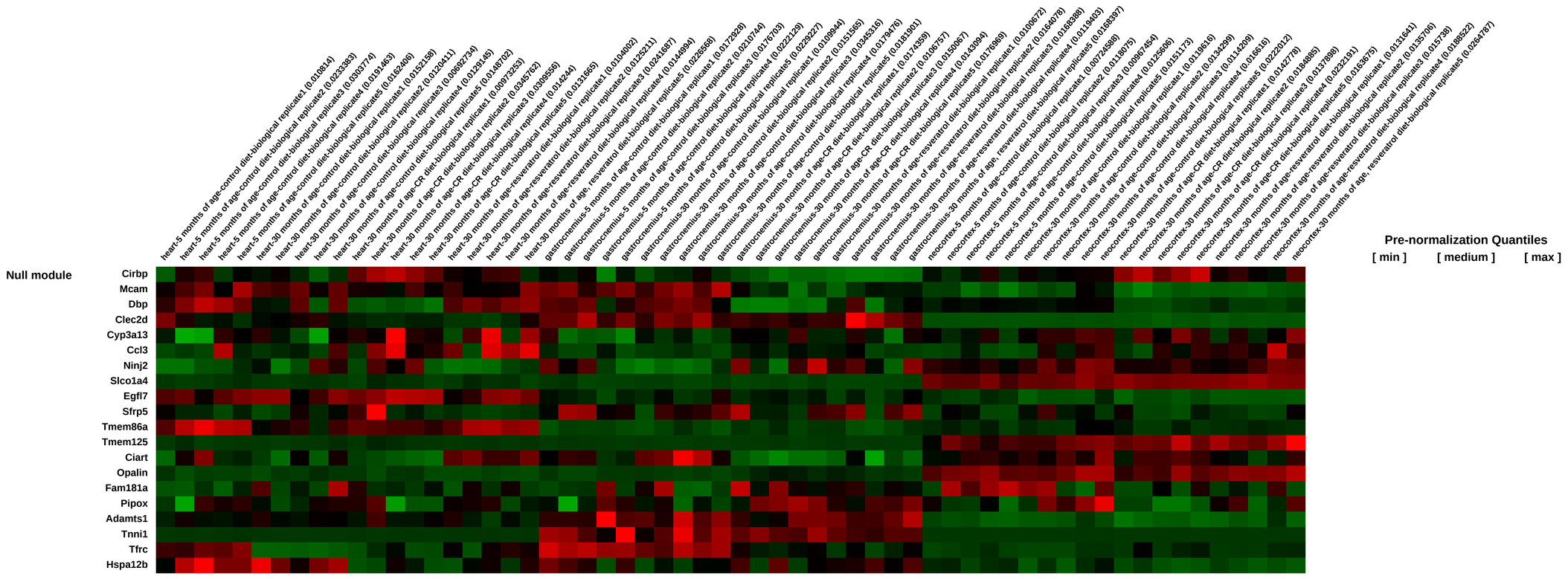

GEO Series "GSE40655" Expression Profiles

Num of samples in this series: 6

Scale of expression profile Z-scores

-3.0 -2.0 -1.0 0.0 1.0 2.0 3.0

GEO Link:	http://www.ncbi.nlm.nih.gov/geo/query/acc.cgi?acc=GSE40655
Status:	Public on Sep 07 2012
Title:	Novel Foxo1-dependent Transcriptional Programs Control Treg Cell Function [Affymetrix gene expression data]
Organism:	Mus musculus
Experiment type:	Expression profiling by array
Platform:	GPL1261
Pubmed ID:	23135404
Summary & Design:	**Summary:** Regulatory T (Treg) cells characterized by expression of the transcription factor forkhead box P3 (Foxp3) maintain immune homeostasis by suppressing self-destructive immune responses1-4. Foxp3 operates as a late acting differentiation factor controlling Treg cell homeostasis and function5, whereas the early Treg cell lineage commitment is regulated by the Akt kinase and the forkhead box O (Foxo) family of transcription factors6-10. However, whether Foxo proteins act beyond the Treg cell commitment stage to control Treg cell homeostasis and function remains largely unexplored. Here we show that Foxo1 is a pivotal regulator of Treg cell function. Treg cells express high amounts of Foxo1, and display reduced T-cell receptor-induced Akt activation, Foxo1 phosphorylation, and Foxo1 nuclear exclusion. Mice with Treg cell-specific deletion of Foxo1 develop a fatal inflammatory disorder similar in severity to Foxp3-deficient mice, but without the loss of Treg cells. Genome-wide analysis of Foxo1 binding sites reveals ~300 Foxo1-bound target genes, including the proinflammatory cytokine Ifng, that do not appear to be directly regulated by Foxp3. These findings demonstrate that the evolutionarily ancient Akt-Foxo1 signaling module controls a novel genetic program indispensable for Treg cell function. **Overall design:** Regulatory T cells were FACS sorted in WT mice (2 reps), Foxo1 KO mice (2 reps), mice expressing a constitutively active form of Foxo1 (1 rep), and Foxo1 KO mice expressing constitutively active Foxo1. We identified genes differentially expressed in WT vs. KO mice and assessed whether expression was recovered in the KO in presence of constitutively active Foxo1

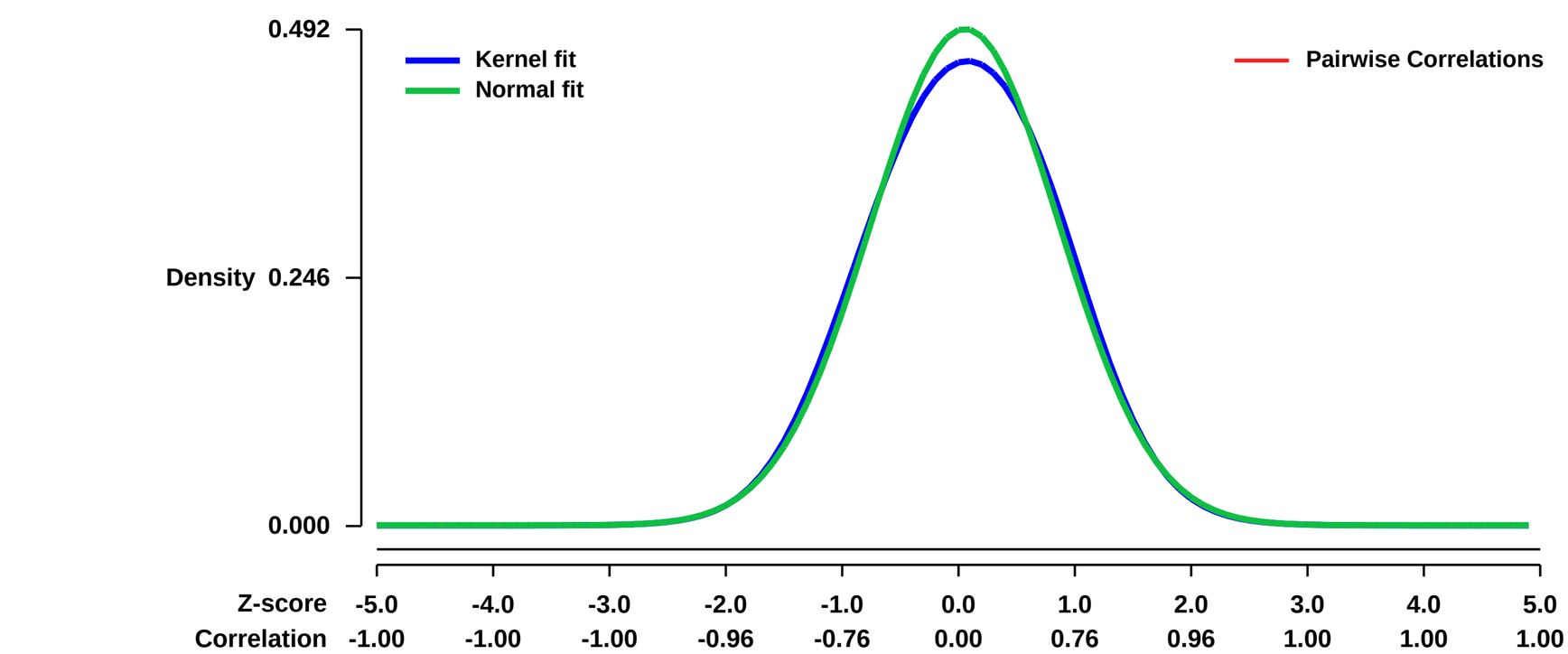

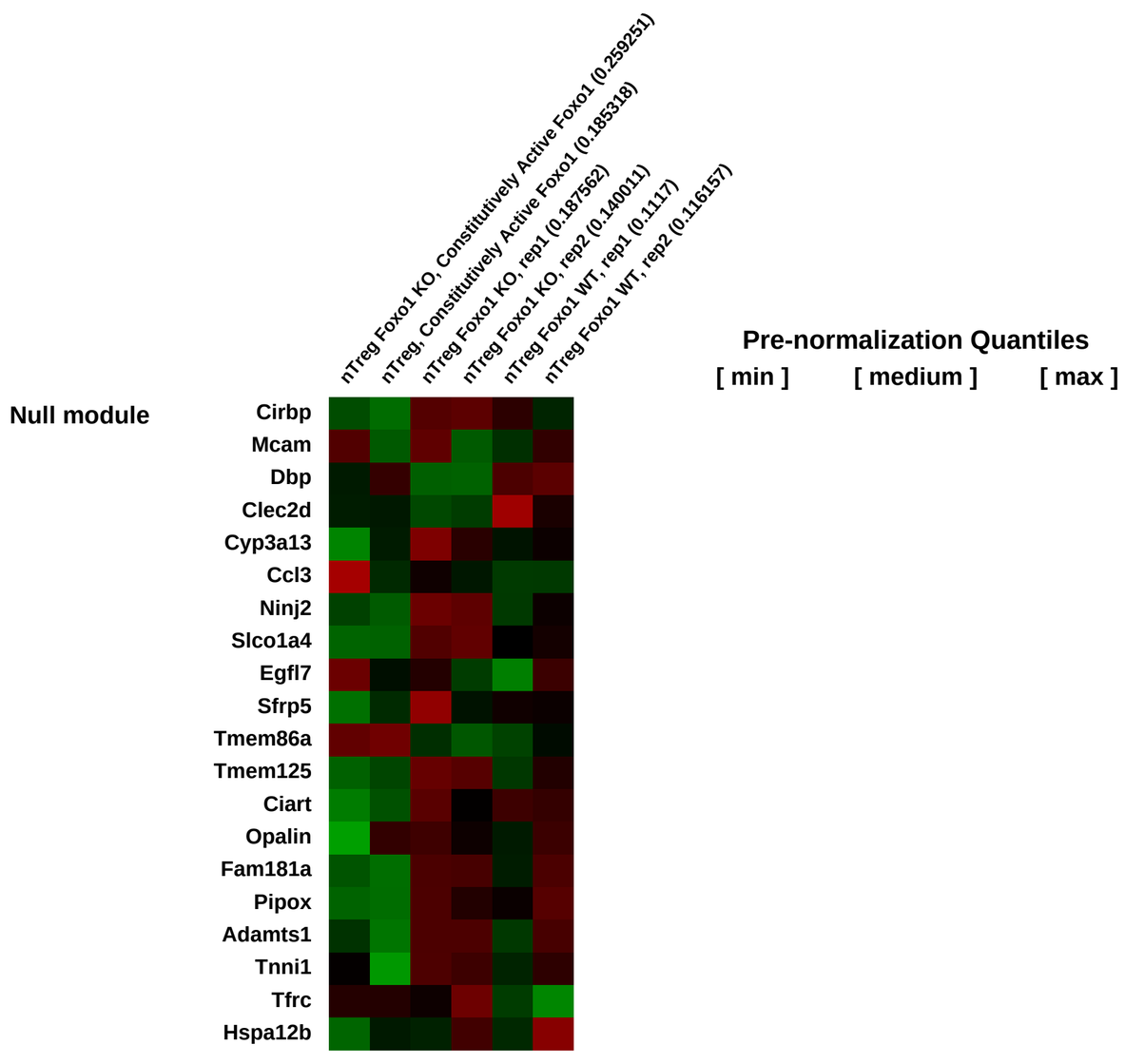

GEO Series "GSE12073" Expression Profiles

Num of samples in this series: 12

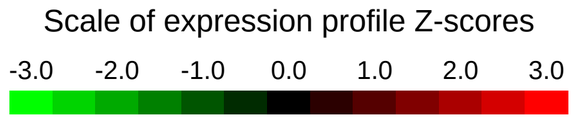

GEO Link:	**http://www.ncbi.nlm.nih.gov/geo/query/acc.cgi?acc=GSE12073**
Status:	**Public on Aug 20 2008**
Title:	**Expression data from transgenic Aire expressing pancreatic islets**
Organism:	**Mus musculus**
Experiment type:	**Expression profiling by array**
Platform:	**GPL1261**
Pubmed ID:	**18780794**
Summary & Design:	**Summary:** **The aim of this study was to determine the effect of transgenic Aire expression on the transcriptional profile of a tissue that normally does not express Aire: pancreatic islets. The transcriptional profile of transgenic RIP-Aire27 islets was compared to non-transgenic littermate islets as well as to archival NOD thymic medullary epithelial cells (MEC) data. All data were from non-obese diabetic (NOD) mice** **Keywords: RIP-Aire transgenic vs non-transgenic comparison** **Overall design:** **3-wk-old individual male RIP-Aire27 or non-transgenic littermates islets were isolated by gradient purification followed by hanpicking under a microscope for subsequent RNA purification, labeling and hybridization to Affymetrix arrays.**

Background corr dist: **KL-Divergence = 0.0336, L1-Distance = 0.0527, L2-Distance = 0.0050, Normal std = 0.6590**

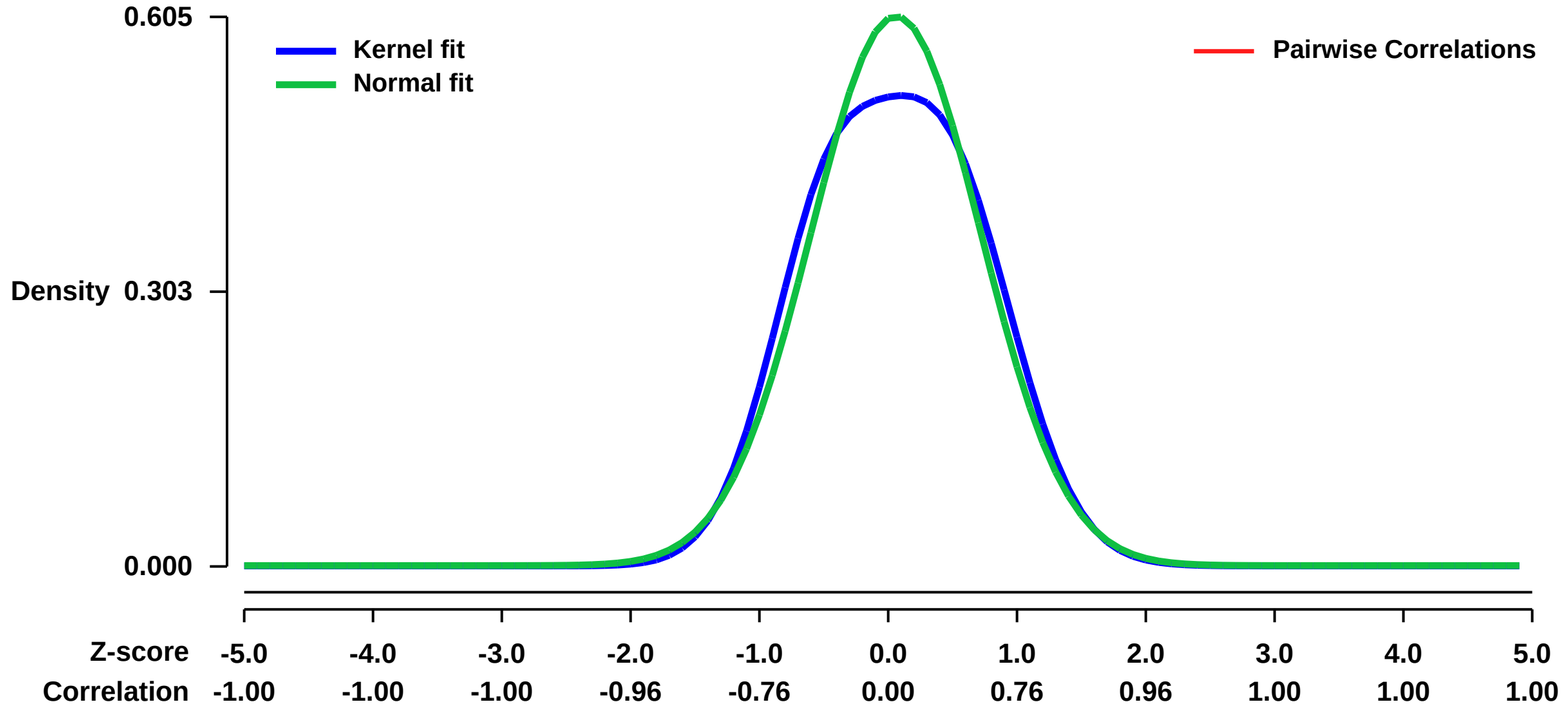

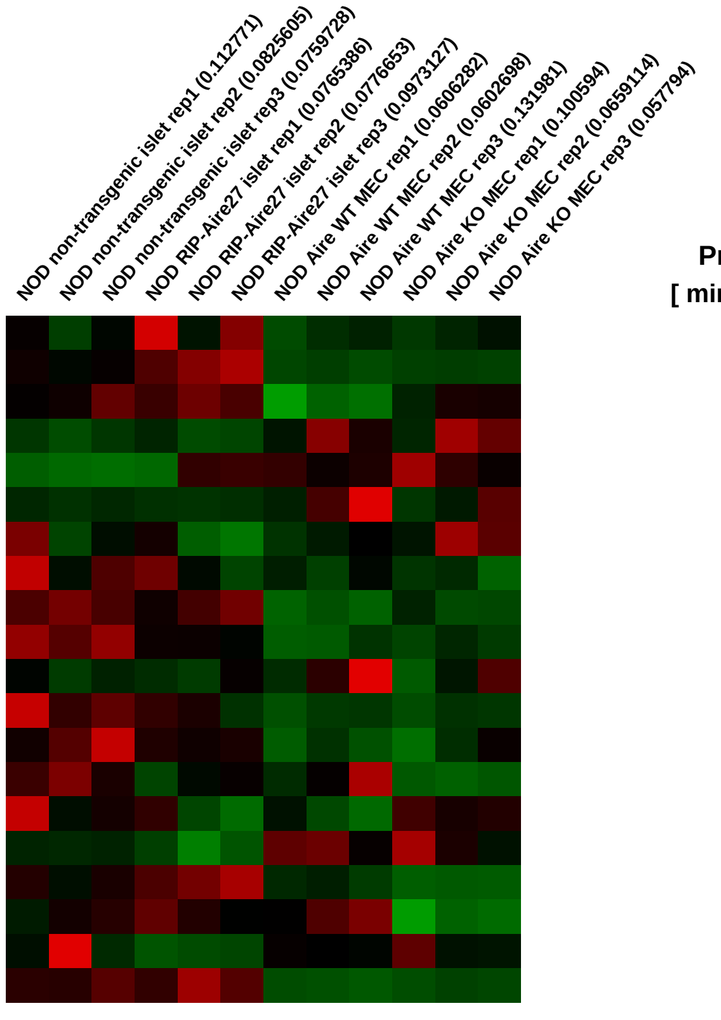

GEO Series "GSE35435" Expression Profiles

Num of samples in this series: 6

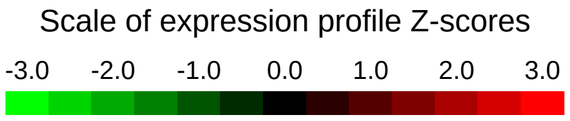

GEO Link:	http://www.ncbi.nlm.nih.gov/geo/query/acc.cgi?acc=GSE35435
Status:	Public on Sep 29 2012
Title:	Genome-wide analysis of mouse macrophages stimulated with IL-4 (bone marrow macrophages) (Affymetrix)
Organism:	Mus musculus
Experiment type:	Expression profiling by array
Platform:	GPL1261
Pubmed ID:	23293084
Summary & Design:	**Summary:** Analysis of alternative activation of macrophages at gene expression level. The study forms part of a wider study where we compare the effects of IL-4 in different human and mouse macrophages. Our results support the notion that in vitro culture conditions greatly affect the macrophage response to IL-4. Total RNA obtained from bone marrow derived macrophages upon exposure to 20 ng/ml of IL-4 for 18 hours. **Overall design:** Bone marrow derived macrophages were stimulated with the Th2 cytokine IL-4, for RNA extraction and hybridization on Affymetrix microarrays.

Background corr dist: KL-Divergence = 0.0170, L1-Distance = 0.0428, L2-Distance = 0.0029, Normal std = 0.8007

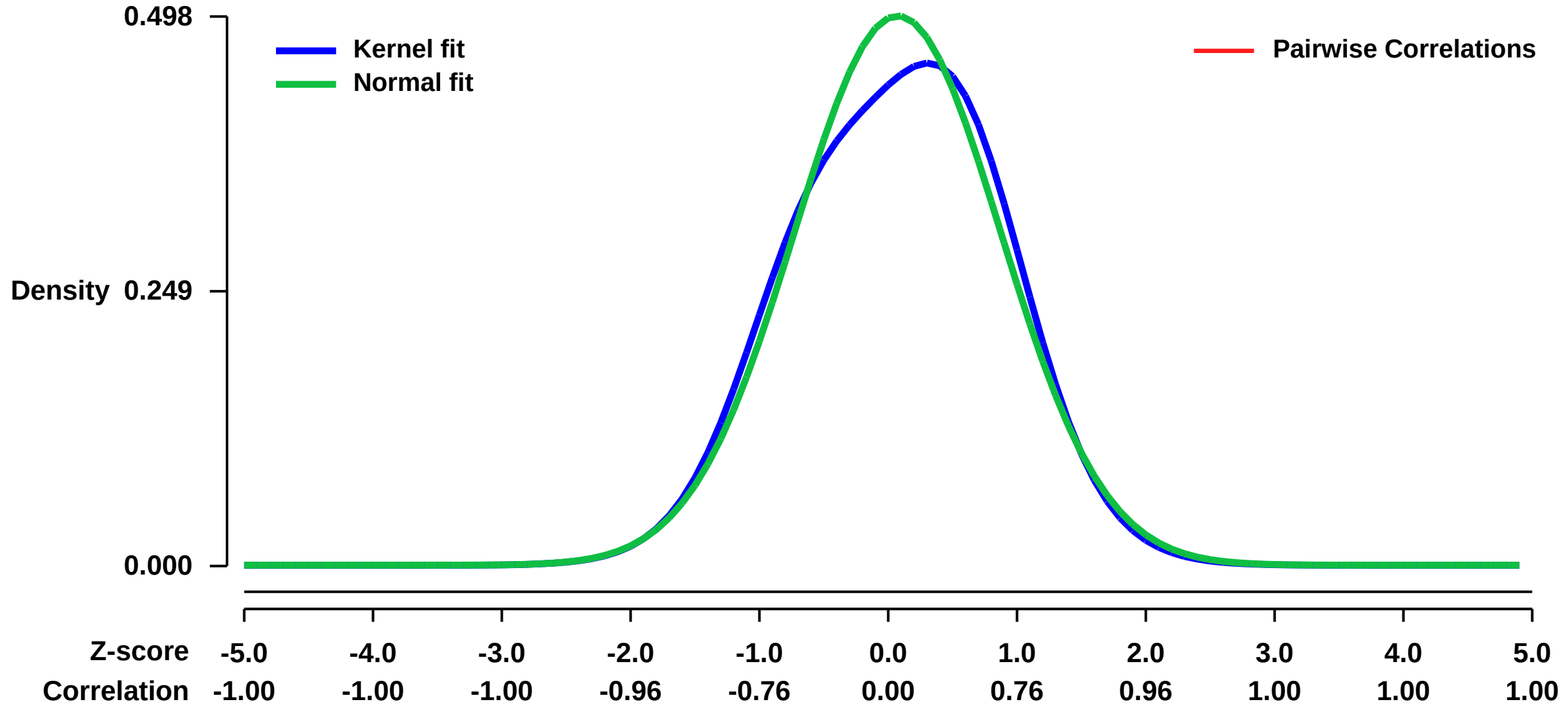

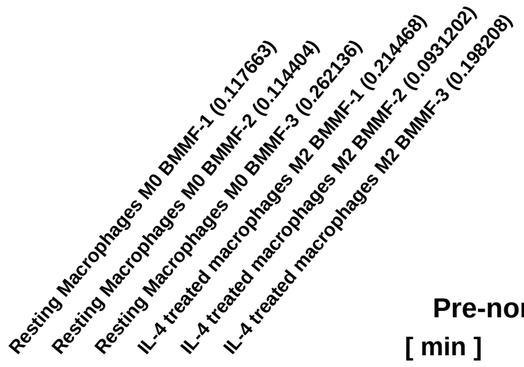

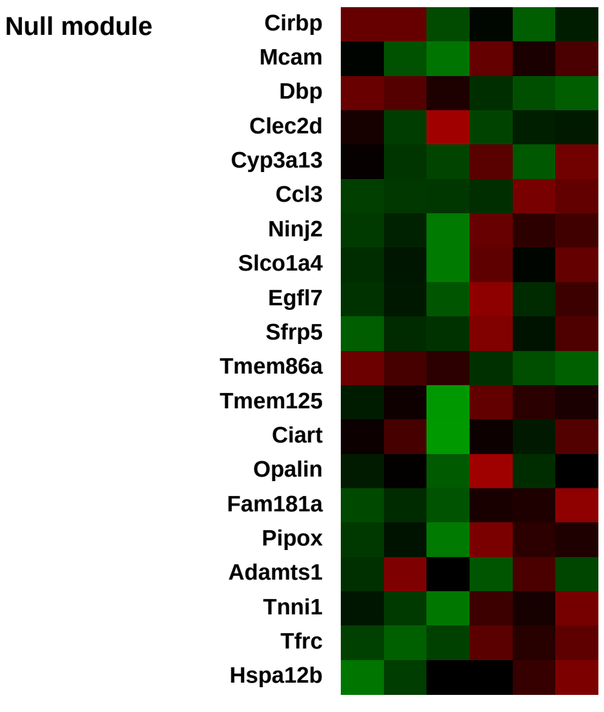

GEO Series "GSE27329" Expression Profiles

Num of samples in this series: 24

Scale of expression profile Z-scores

-3.0 -2.0 -1.0 0.0 1.0 2.0 3.0

GEO Link:	http://www.ncbi.nlm.nih.gov/geo/query/acc.cgi?acc=GSE27329
Status:	Public on Nov 30 2012
Title:	Genome-Wide Analysis of Gene Program Activation by Defined Cardiac Transcription Factor Tbx5, Gata4 and Myocardin
Organism:	Mus musculus
Experiment type:	Expression profiling by array
Platform:	GPL1261
Pubmed ID:	23144723
Summary & Design:	**Summary:** **Background: Cardiac transcription factors are master regulators during heart development. Recently, some were shown to transdifferentiate noncardiac mesoderm cells and cardiac fibroblasts into cardiomyocytes. However, the individual roles of each transcription factors in activating cardiac gene program have not been elucidated. We examined cardiac-specific and genome-wide gene expression in fibroblasts induced with cardiac transcription factors Nkx2.5 (N), Tbx5 (T), Gata4 (G), Myocardin (M) alone or different combinations.** **Methodology/Principal Findings: We applied different combinations of human Nkx2.5 (N), Tbx5 (T), Gata4 (G) and Myocardin (M) lentiviruses into 10T1/2 fibroblasts. Immunostaining and quantitative reverse transcription polymerase chain reaction (qRT-PCR) showed that N, T, G or M alone did not induce expression of cardiac marker genes ¸–-myosin heavy chain (¸–MHC) and cardiac troponin T (cTnT). Only T+M and T+G+M combinations induced ¸–MHC and cTnT expression. Microarray-based gene ontology analysis revealed that T alone inhibited most genes involved in cardiac-related processes and activated genes involved in Wnt receptor signaling pathway and in aberrant processes. M alone inhibited genes involved in Wnt receptor signaling pathway and activated genes involved in cardiac-related processes and in aberrant processes. G alone inhibited genes involved in ectoderm development. T+G+M combination was the most effective activator of genes associated with cardiac-related processes including muscle cell differentiation, sarcomere, striated muscle contraction, regulation of heart contraction, and glucose metabolism and fatty acid oxidation (two significant forms of cardiomyocyte energy metabolism). And unlike T, M, G alone or T+M, T+G+M did not activate genes associated with aberrant processes.** **Conclusions: Tbx5, Gata4 and Myocardin play different roles in activating cardiac gene program and in avoiding aberrant gene program activation. The combination of T+G+M activated cardiac gene program and avoided aberrant gene program activation.** **Overall design:** **Two weeks after doxycline induction, total RNA was isolated from 10T1/2-tTA cells infected with different combinations of Tbx5, Gata4, and Myocardin lentiviruses. Biological triplicated.**

Background corr dist: KL-Divergence = 0.1953, L1-Distance = 0.0380, L2-Distance = 0.0026, Normal std = 0.3365

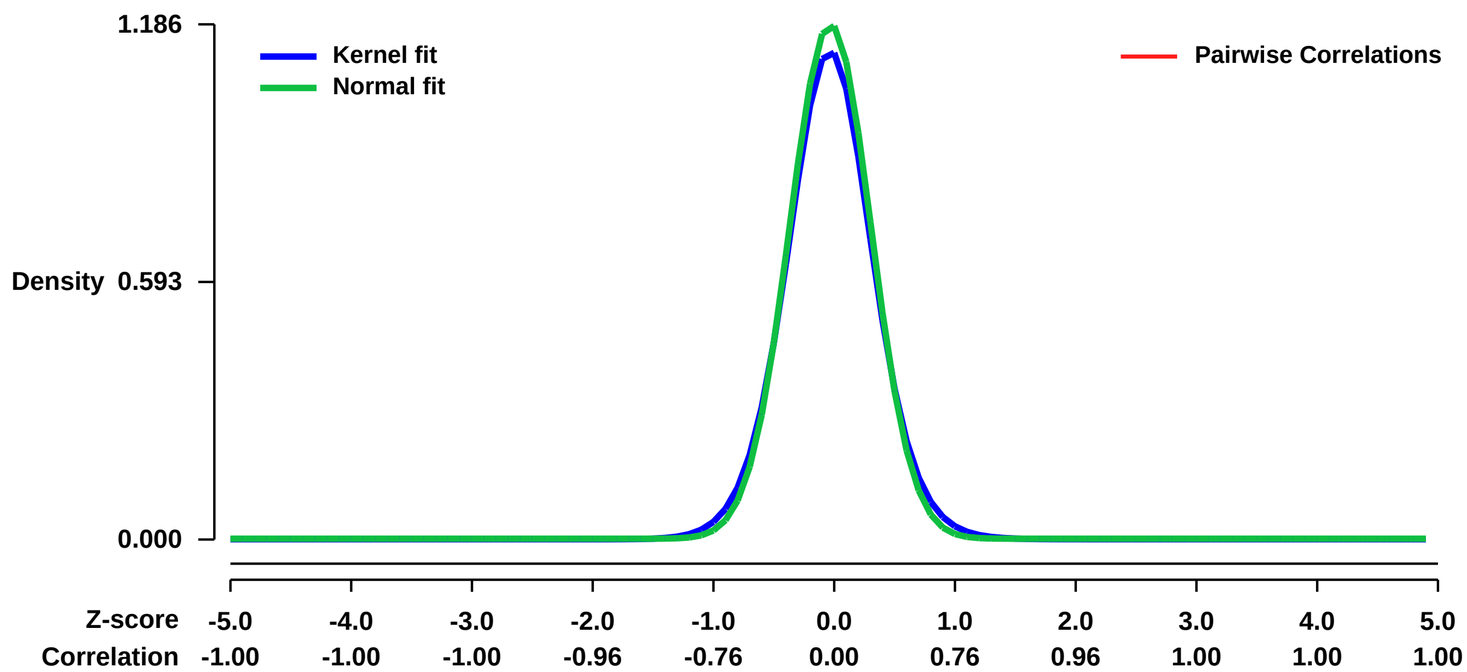

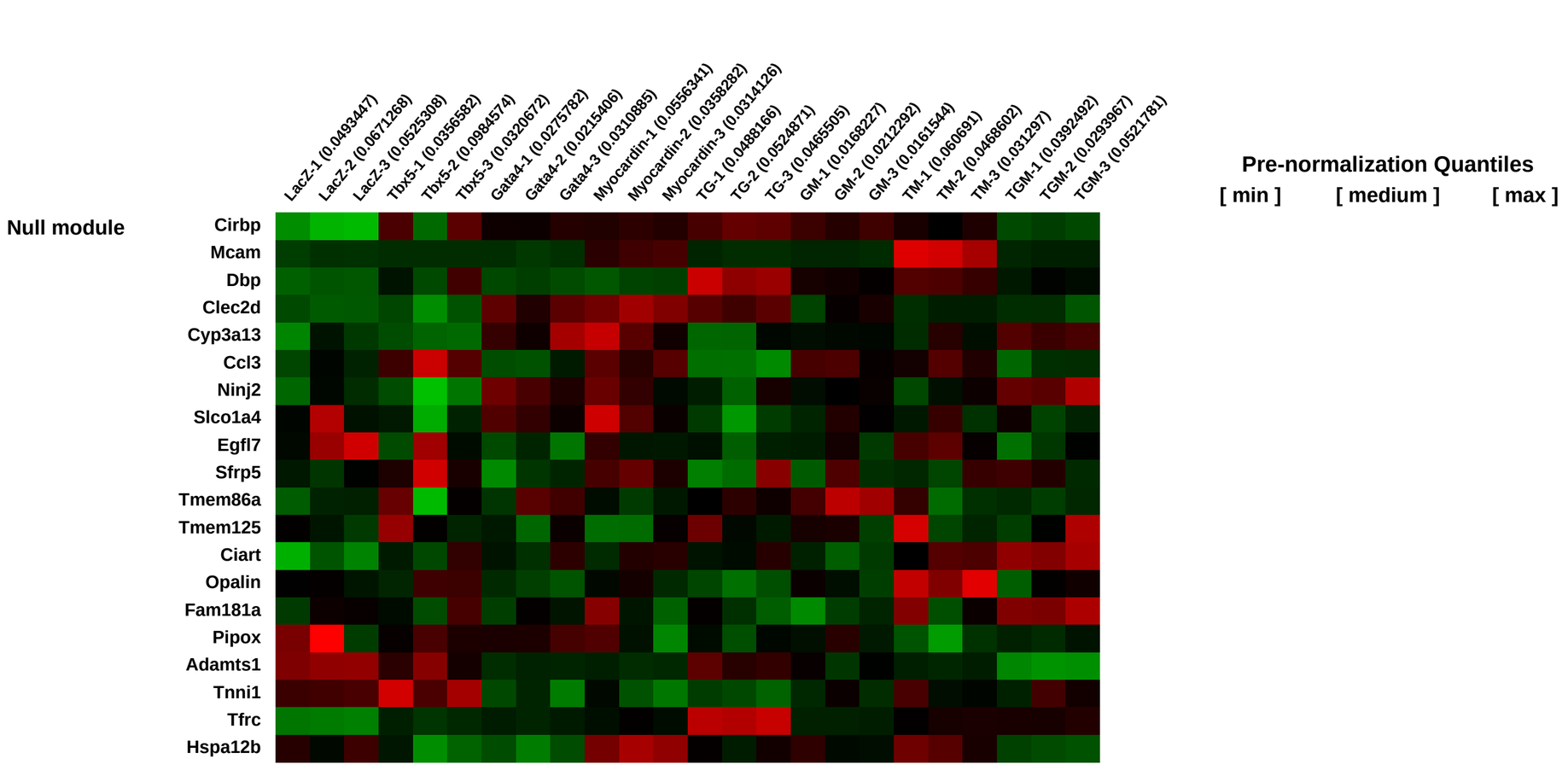

GEO Series "GSE14678" Expression Profiles

Num of samples in this series: 6

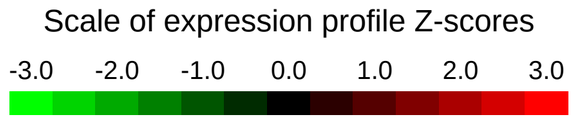

GEO Link:	**http://www.ncbi.nlm.nih.gov/geo/query/acc.cgi?acc=GSE14678**
Status:	**Public on Feb 26 2009**
Title:	**Expression Profile of Skeletal Muscle from Young and Aged C57B1/6 Mice**
Organism:	**Mus musculus**
Experiment type:	**Expression profiling by array**
Platform:	**GPL1261**
Pubmed ID:	
Summary & Design:	**Summary:** **Our laboratory wanted to define the transcription profile of aged skeletal muscle. For this reason, we performed a triplicate microarray study on young (3 weeks) and aged (24 months) gatrocnemius muscle from wild-type C57B16 Mice** **Keywords: other** **Overall design:** **this experiment include 2 samples and 6 replicates**

Background corr dist: **KL-Divergence = 0.0496, L1-Distance = 0.0330, L2-Distance = 0.0015, Normal std = 0.5866**

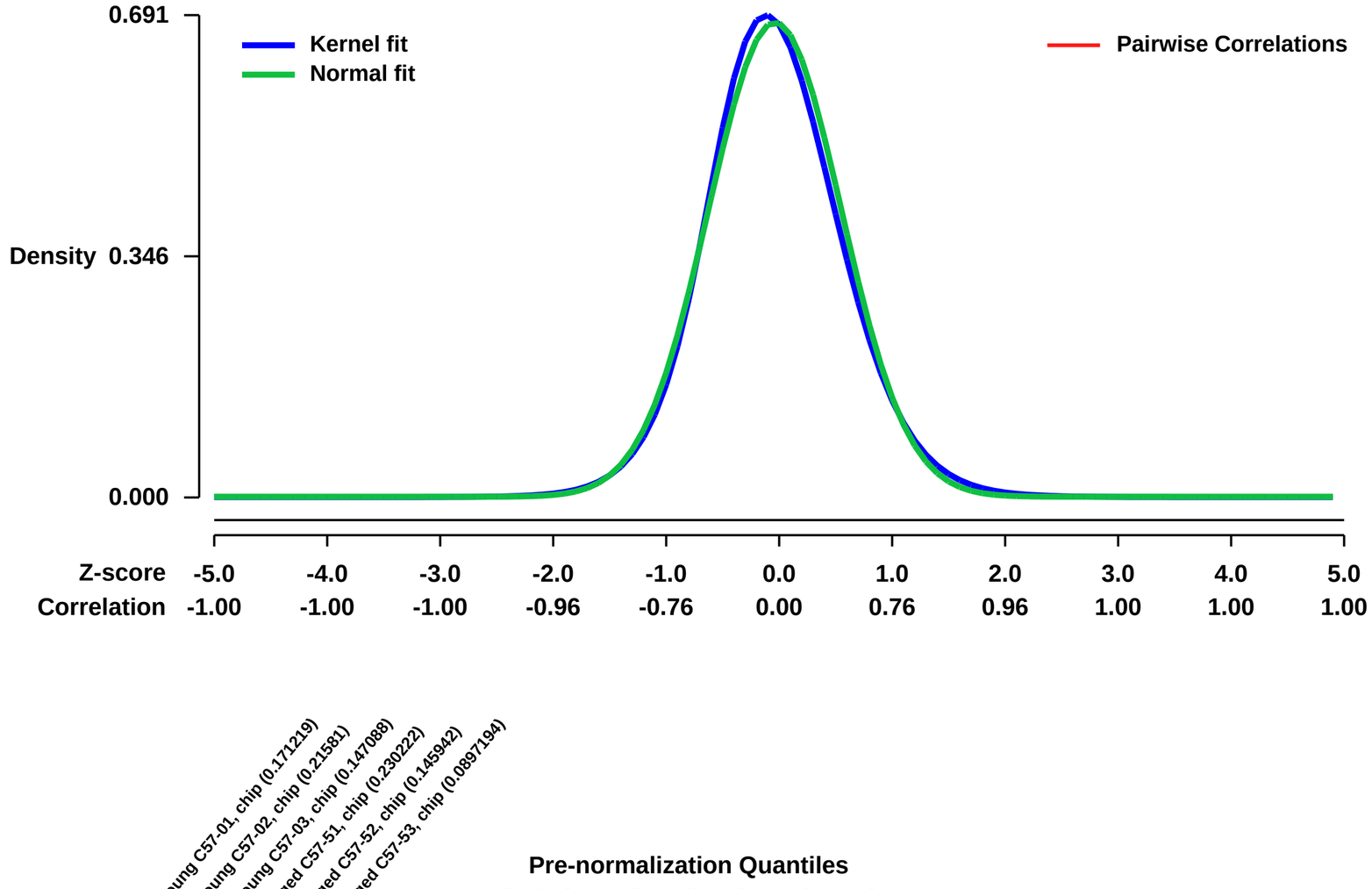

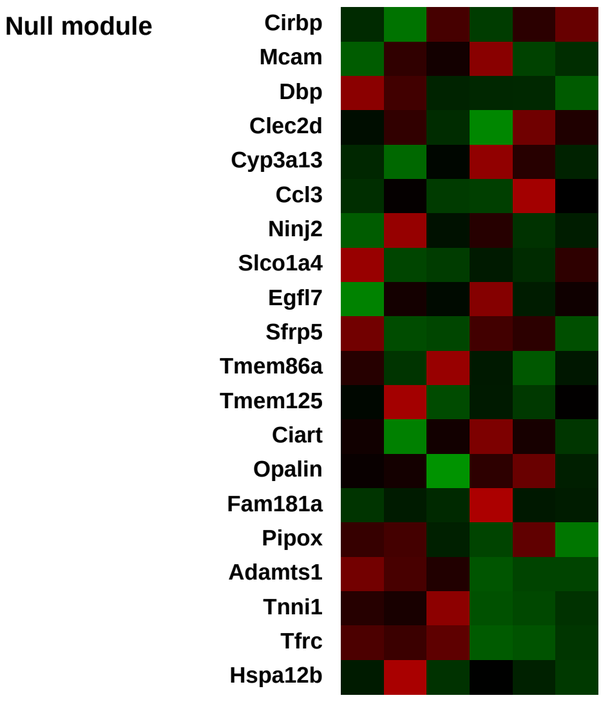

GEO Series "GSE42688" Expression Profiles

Num of samples in this series: 8

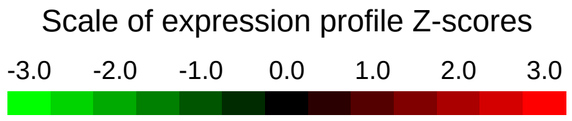

GEO Link:	**http://www.ncbi.nlm.nih.gov/geo/query/acc.cgi?acc=GSE42688**
Status:	**Public on Dec 04 2012**
Title:	**Gene expression analysis of male and female embryonic day 14 genital tubercle (GUDMAP Series ID: 45).**
Organism:	**Mus musculus**
Experiment type:	**Expression profiling by array**
Platform:	**GPL1261**
Pubmed ID:	
Summary & Design:	**Summary:** **The long term objective is to create an encyclopedia of the expression levels of all genes in multiple components of the developing urogenital system. The central thesis is straightforward. The combination of microdissected and laser capture microdissection (LCM) plus Microarray analysis offers a powerful, efficient and effective method for the creation of a global gene expression atlas of the developing urogenital system. Microarrays with essentially complete genome coverage can be used to quantitate expression levels of every gene. The ensuing rapid read-out provides an expression atlas that is more sensitive, more economical and more complete than would be possible by in situ hybridizations alone. The data submitted here represents the gene expression profiles of the embryonic day 14 genital tubercle of the male and the female.** **Overall design:** **The genital tubercle region from E14 (TS22) FVB/N males and females were microdissected and total RNA isolated for gene expression analysis using the Affymetrix MOE430 microarray chip.**

Background corr dist: KL-Divergence = 0.0489, L1-Distance = 0.0248, L2-Distance = 0.0008, Normal std = 0.5759

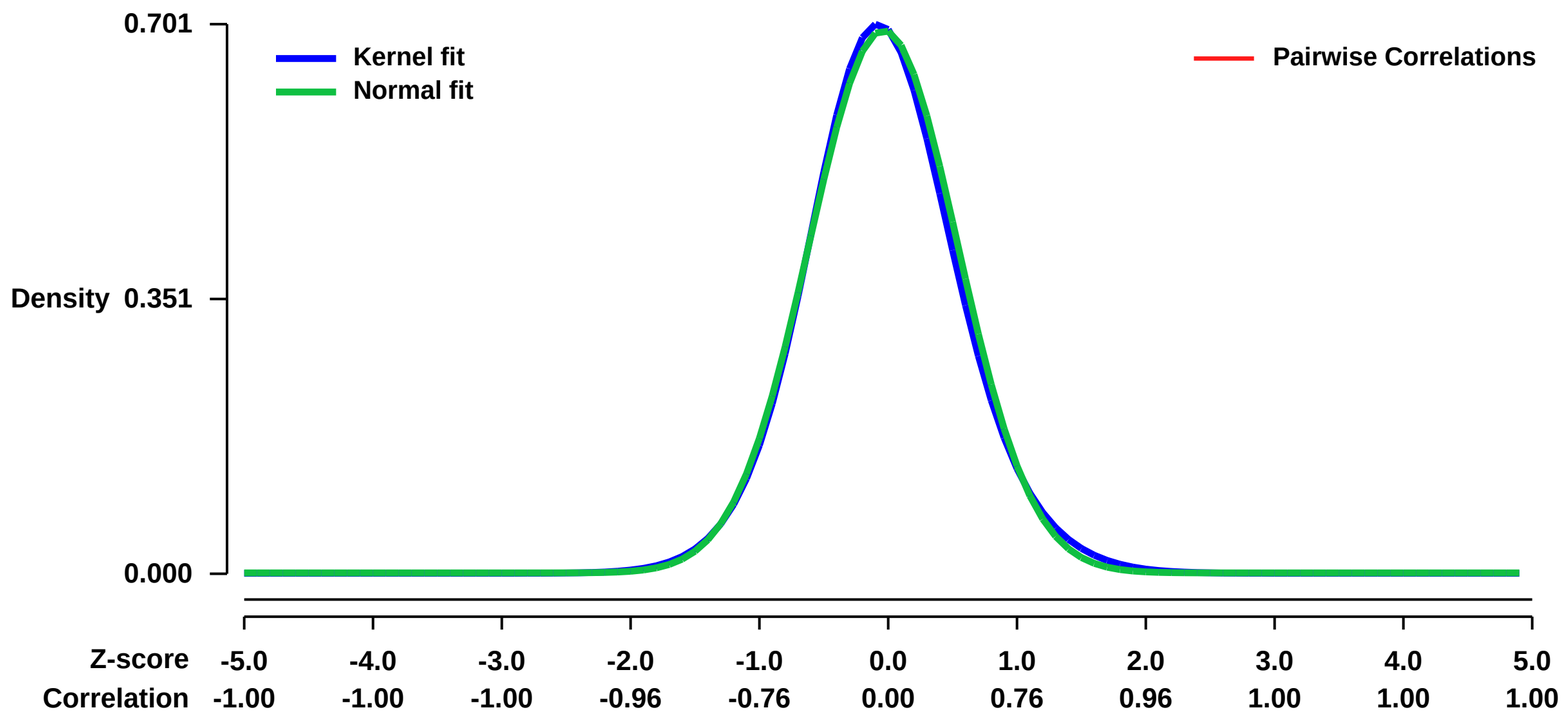

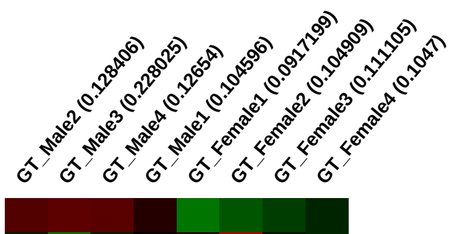

Pre-normalization Quantiles

[min] [medium] [max]

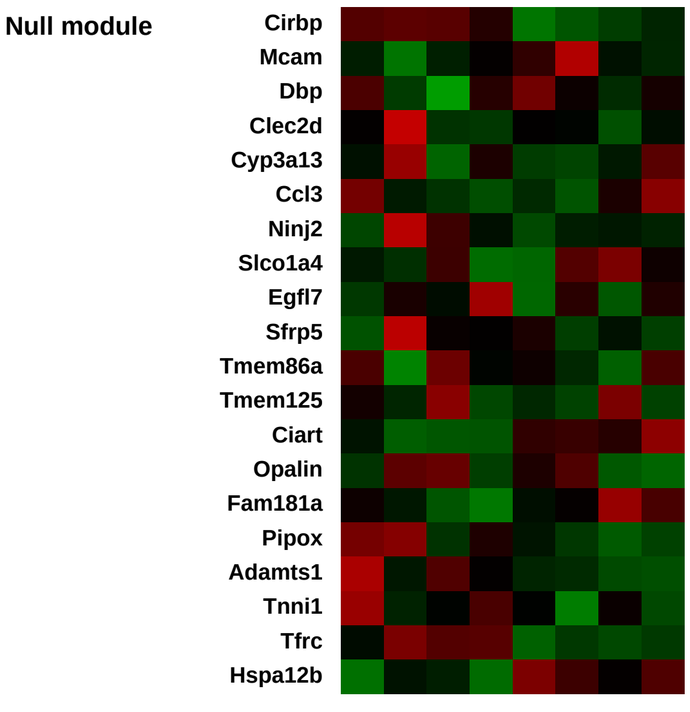

GEO Series "GSE31453" Expression Profiles

Num of samples in this series: 13

Scale of expression profile Z-scores

-3.0 -2.0 -1.0 0.0 1.0 2.0 3.0

GEO Link:	http://www.ncbi.nlm.nih.gov/geo/query/acc.cgi?acc=GSE31453
Status:	Public on Aug 07 2012
Title:	Genome-wide analysis of gene expression patterns in the liver tumors of mir-122 knockout mice
Organism:	Mus musculus
Experiment type:	Expression profiling by array
Platform:	GPL1261
Pubmed ID:	22820290
Summary & Design:	**Summary:** To invesigate the physiological roles of mir-122 in hepatocarcinogenesis, we performed expression profiling of the liver tumors of mir-122 knockout mice and the liver tissues of the control B6/129 mice. **Overall design:** Total RNA was extracted from three tumors of mir-122 knockout mice and liver tissues of two control mice of 11 months of age; five tumors of mir-122 knockout mice and the liver tissues of three control mice of 14 months of age. Gene expression was quantified by robust multi-array analysis (RMA) using the Genomic Suite software from Partek.

Background corr dist: KL-Divergence = 0.0913, L1-Distance = 0.0362, L2-Distance = 0.0026, Normal std = 0.4497

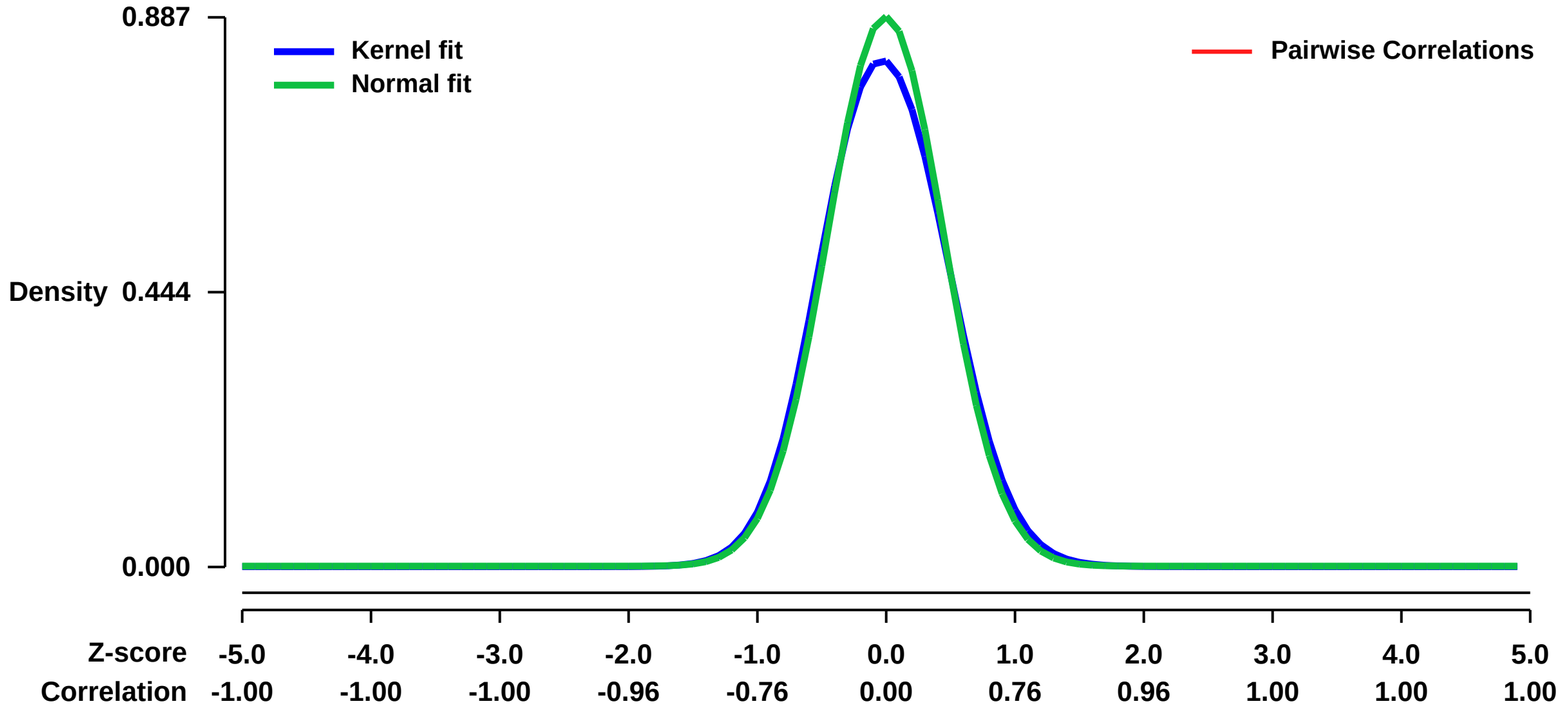

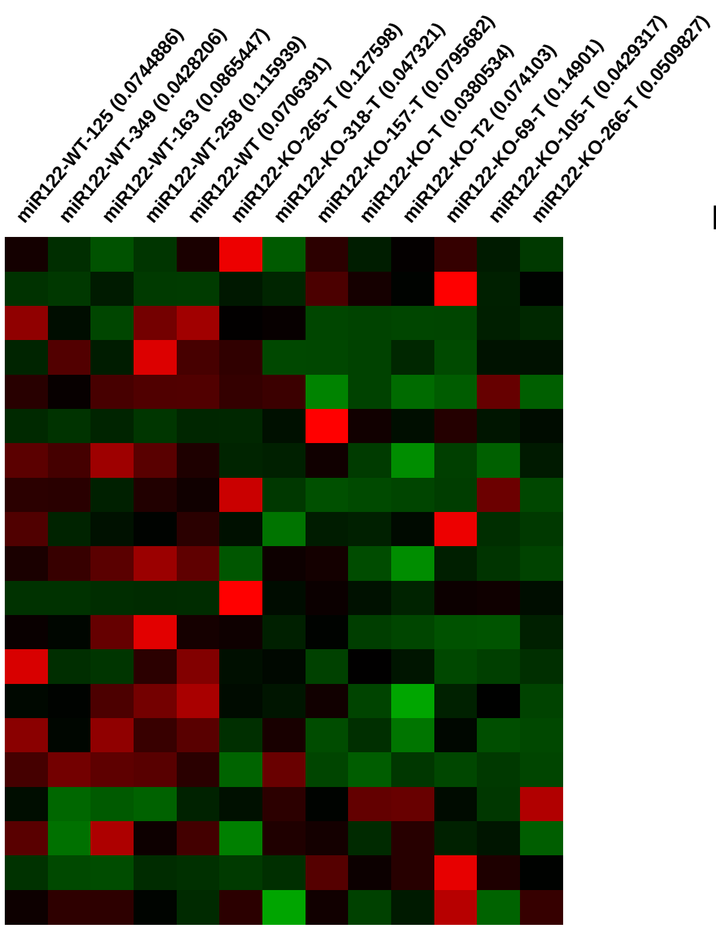

GEO Series "GSE9443" Expression Profiles

Num of samples in this series: 24

Scale of expression profile Z-scores

-3.0 -2.0 -1.0 0.0 1.0 2.0 3.0

GEO Link:	http://www.ncbi.nlm.nih.gov/geo/query/acc.cgi?acc=GSE9443
Status:	Public on Dec 07 2007
Title:	Gene expression in brain Homer1a-expressing cells after sleep deprivation
Organism:	Mus musculus
Experiment type:	Expression profiling by array
Platform:	GPL1261
Pubmed ID:	18077435
Summary & Design:	**Summary:** To gain insight into the molecular changes of sleep need, this study addresses gene expression changes in a subpopulation of neurons selectively activated by sleep deprivation. Whole brain expression analyses after 6h sleep deprivation clearly indicate that Homer1a is the best index of sleep need, consistently in all mouse strains analyzed. Transgenic mice expressing a FLAG-tagged poly(A)-binding protein (PABP) under the control of Homer1a promoter were generated. Because PABP binds the poly(A) tails of mRNA, affinity purification of FLAG-tagged PABP proteins from whole brain lysates, is expected to co-precipitate all mRNAs from neurons expressing Homer1a. Three other activity-induced genes (Ptgs2, Jph3, and Nptx2) were identified by this technique to be over-expressed after sleep loss. All four genes play a role in recovery from glutamate-induced neuronal hyperactivity. The consistent activation of Homer1a suggests a role for sleep in intracellular calcium homeostasis for protecting and recovering from the neuronal activation imposed by wakefulness. **Keywords:** sleep deprivation, neuronal subpopulation transcriptome **Overall design:** Experiments were performed on male mice, 12 weeks of age +/- 1 week. Animals were housed in polycarbonate cages (31x18x18cm) in an experimental room with an ambient temperature varying from 23˚° to 25˚℃ under a 12:12 hrs light/dark cycle. Food and water were available ad libitum. At light onset mice were either sleep deprived by gentle handling (n=10) or left undisturbed (n=10) for 6 hrs. Animals were then randomly sacrificed by cervical dislocation. Total RNA from the whole brain was isolated for control (n=4) and sleep deprived (n=4) using a commercial RNA extraction kit (RNeasy Lipid Tissue Kit, Quiagen). Specific Homer1a-expressing cells polyA RNAs were immunoprecipitated following the total brain crosslinking (1% formaldehyde perfusion) for sleep deprived (n=6) and control (n=6) animals. The total RNA from the pull-down supernatants were also harvested (n=4). To test for transcriptional changes after sleep deprivation Homer1a-expressing cells, we proceeded in 2 steps: (1) identify probe sets enriched in the pull-down extracts, (2) among those probe sets compare sleep deprivation to control condition in both pull-down (6 vs. 6 chip comparison) and whole-brain (4 vs. 4 chip comparison) extracts. 4728 probe sets were significantly enriched at 5% FDR when pull-downs were compared to both supernatant and whole-brain extracts.

Background corr dist: KL-Divergence = 0.0432, L1-Distance = 0.0441, L2-Distance = 0.0032, Normal std = 0.6010

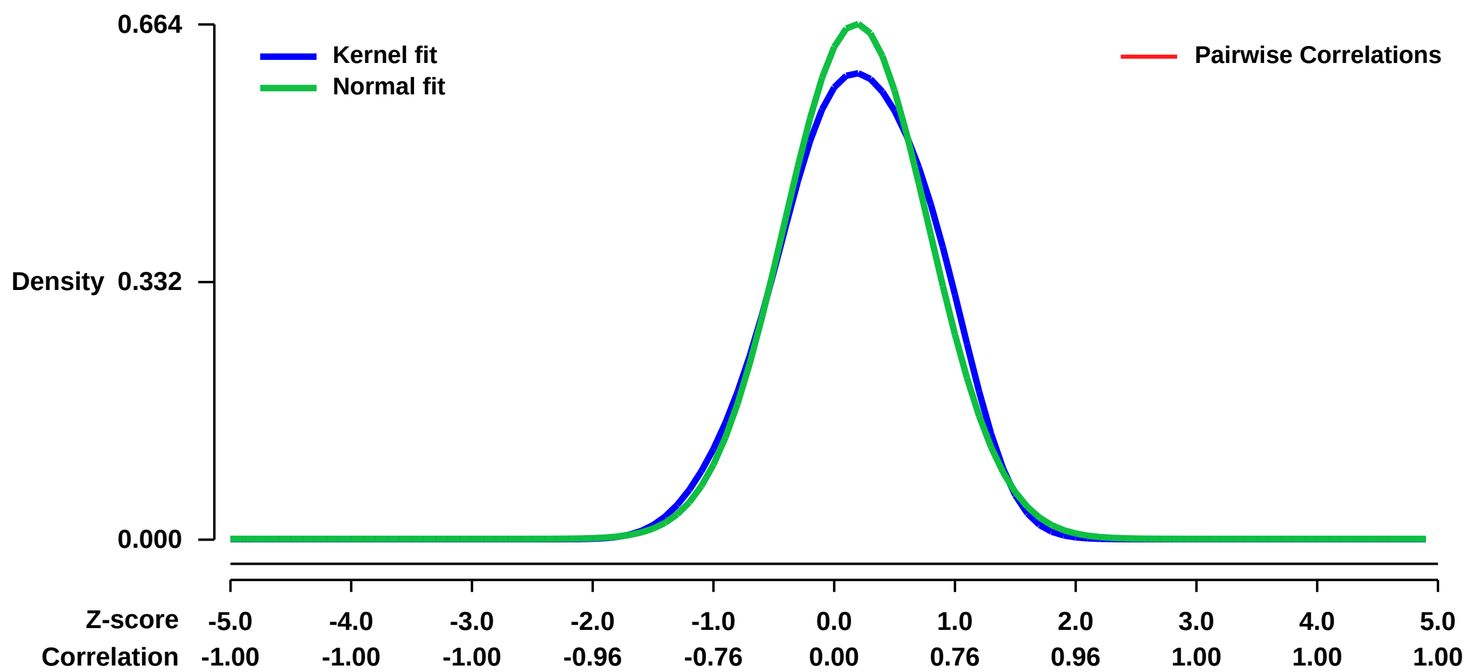

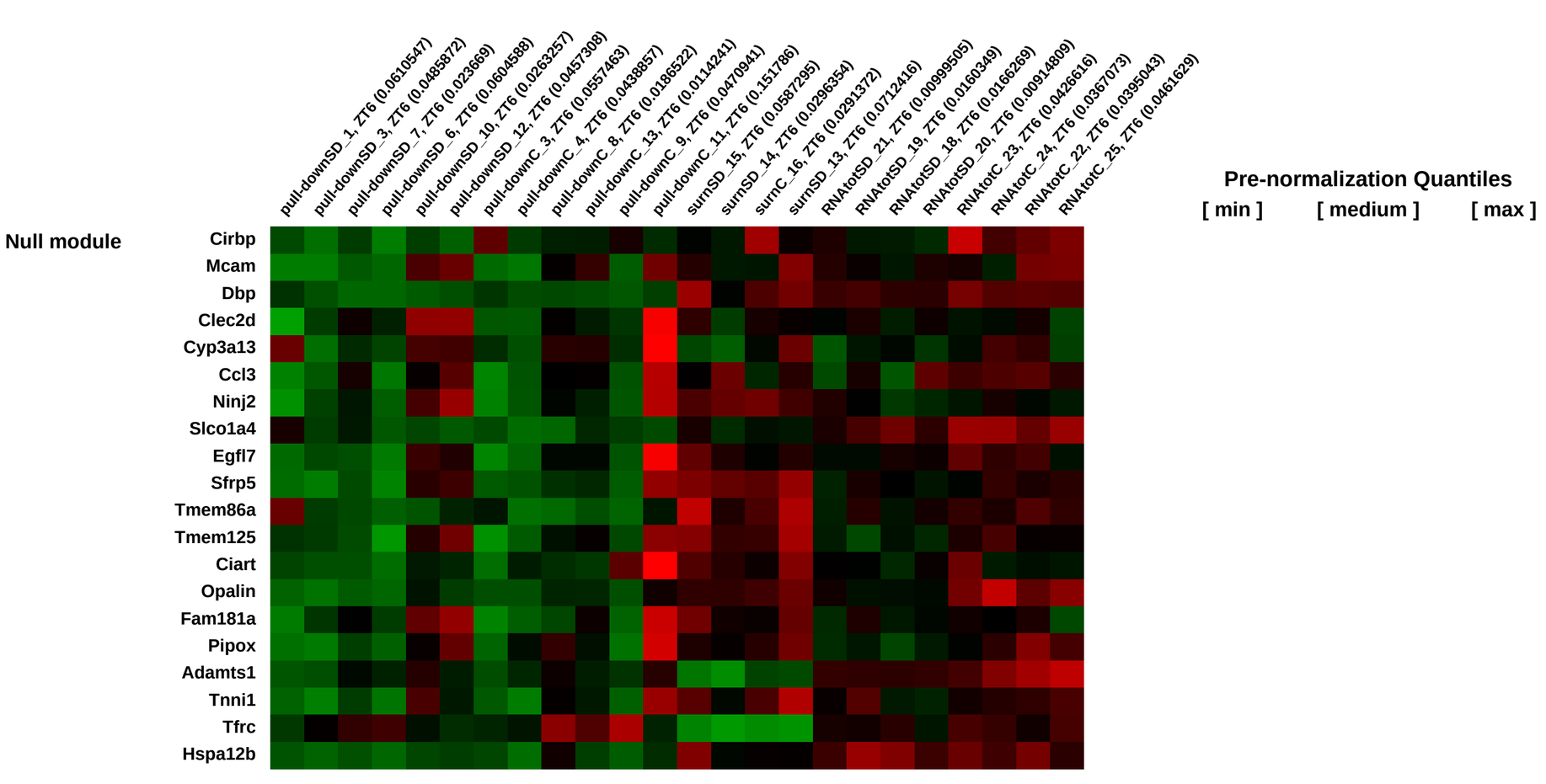

GEO Series "GSE8512" Expression Profiles

Num of samples in this series: 207

Details of this dataset are not shown due to large number of samples and the page size limit.

Find details in http://www.ncbi.nlm.nih.gov/geo/query/acc.cgi?acc=GSE8512

Background corr dist: KL-Divergence = 0.6663, L1-Distance = 0.0976, L2-Distance = 0.0324, Normal std = 0.1991

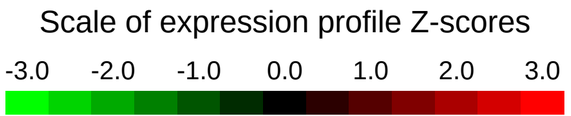

GEO Series "GSE33156" Expression Profiles

Num of samples in this series: 18

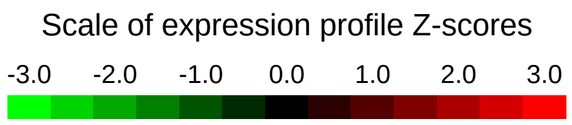

GEO Link:	http://www.ncbi.nlm.nih.gov/geo/query/acc.cgi?acc=GSE33156
Status:	Public on Jan 01 2013
Title:	Hedgehog signaling in T cell differentiation
Organism:	Mus musculus
Experiment type:	Expression profiling by array
Platform:	GPL1261
Pubmed ID:	23408837
Summary & Design:	**Summary:** **Despite Hedgehogâ s influence on T-cell activation and proliferation, the transcriptional targets of Gli2 in lymphocytes are not known. We therefore examined the Hedgehog-dependent transcriptional response of resting and early-stage activated T-cells in order to define their transcriptional response to Hedgehog pathway activation.** **We have established transgenic models where transcription of target genes by Gli2 is either constitutively activated or repressed in cells of the T-lineage. Gli2 has an N-terminal repressor domain and a C-terminal activator domain. Lck-Gli2¸ N2 (Gli2A) mice carry a transgene encoding a truncated form of Gli2 that acts as a permanent transcriptional activator of Hh target genes. Conversely, Lck-Gli2¸ C2 (Gli2R) mice express a repressor of Gli2-dependent transcription, which by binding to Gli binding sites inhibits physiological Hh-dependent transcription, and hence Hh signal transduction, in the cell. These transgenes are driven by the Lck promoter and are only expressed in T-lineage cells** **Overall design:** **Purified fresh, resting CD4 cells (unstimulated) and from CD4 cells stimulated with anti-CD3/CD28 for 6h (stimulated) were analysed in order to obtain transcriptional profiles before and during the early stages of T-cell activation.**

Background corr dist: KL-Divergence = 0.0709, L1-Distance = 0.0778, L2-Distance = 0.0097, Normal std = 0.5606

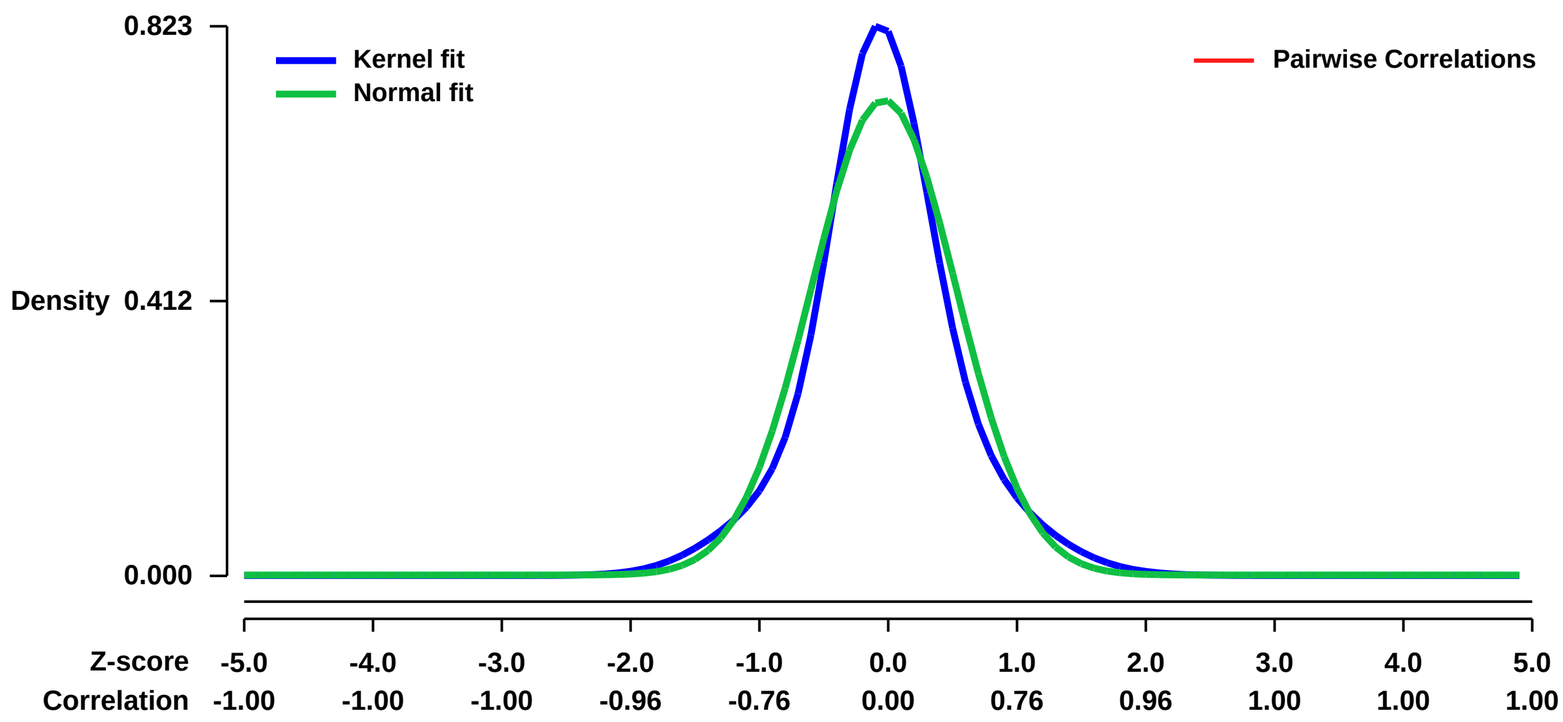

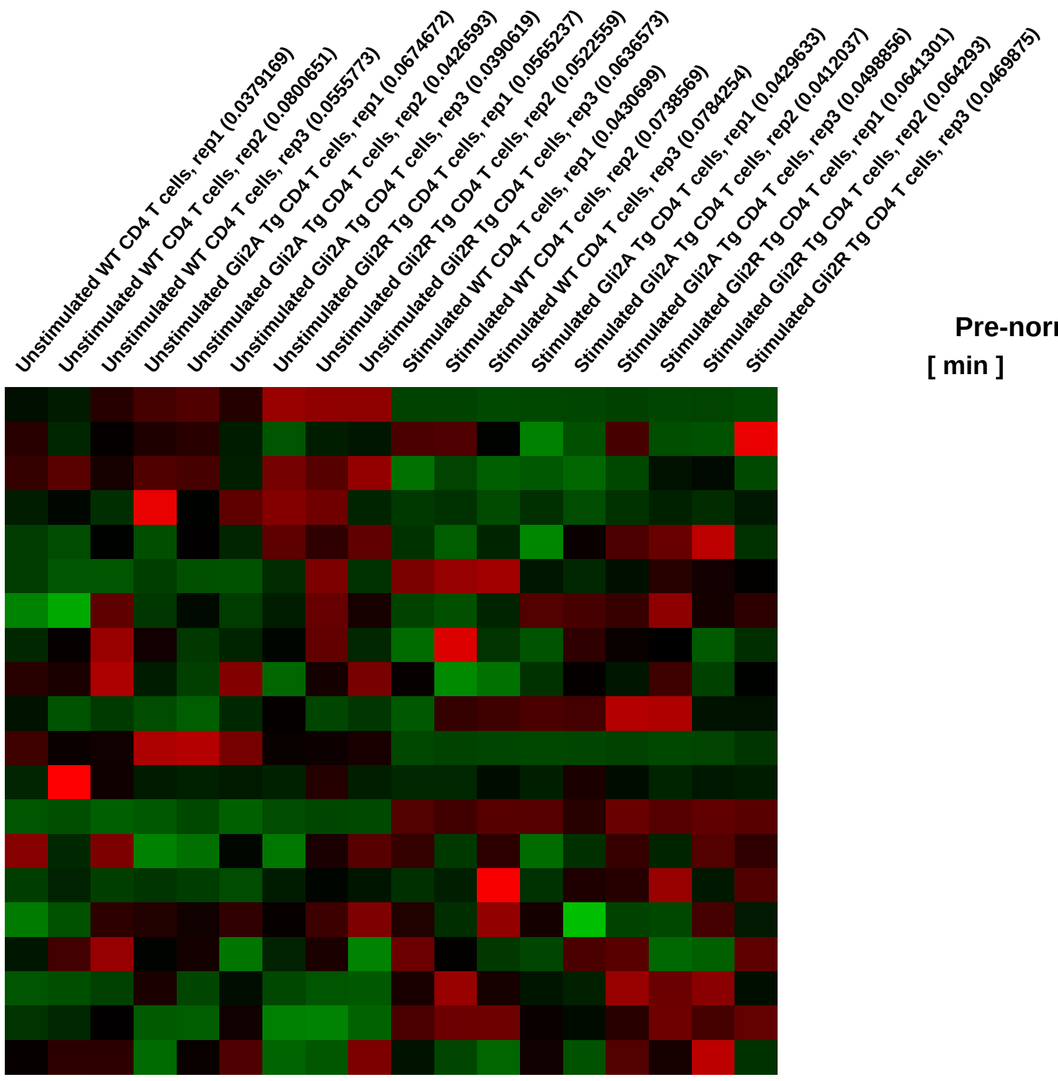

GEO Series "GSE4928" Expression Profiles

Num of samples in this series: 8

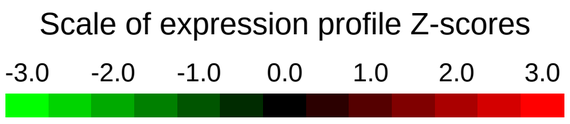

GEO Link:	http://www.ncbi.nlm.nih.gov/geo/query/acc.cgi?acc=GSE4928
Status:	Public on May 27 2006
Title:	Gene expression profile in isolated E13 gonadal somatic support cells and E13 gonads.
Organism:	Mus musculus
Experiment type:	Expression profiling by array
Platform:	GPL1261
Pubmed ID:	16839824
Summary & Design:	**Summary:** Gonadal sex determining (GSD) genes that initiate fetal ovarian and testicular development and differentiation are expressed in the cells of the urogenital ridge that differentiate as somatic support cells (SSCs), i.e., granulosa cells of the ovary and Sertoli cells of the testis. To identify potential new mammalian GSD genes, we analyzed the gene expression differences between XX and XY SSCs cells isolated from the gonads of embryonic day (E) 13 mouse fetuses carrying an EGFP reporter transgene expressed specifically in SSCs. In addition, genome wide expression differences between XX and XY E13 whole gonads were examined. Newly identified differentially expressed transcripts are potential GSD genes involved in unexplained human sex reversal cases. **Keywords:** microarray, mouse fetal gonadal somatic support cells, sex determination **Overall design:** Two seperate RNA samples were obtained from E13 XX and XY sorted EGFP+ cells, and two seperate RNA samples were obtained from E13 XX and XY pooled gonads. Approximately 20ng of total RNA from each sample was used to generate biotin-labelled cDNA. Approximately 2.5ug biotin labelled cDNA of each sample was used for each Mouse Genome 430v2.0 GeneChip array (Affymetrix). Significantly differentially expressed transcripts were identified using R/maanova. Statistical significance was determined at a false discovery rate value of equal to or less than 1%.

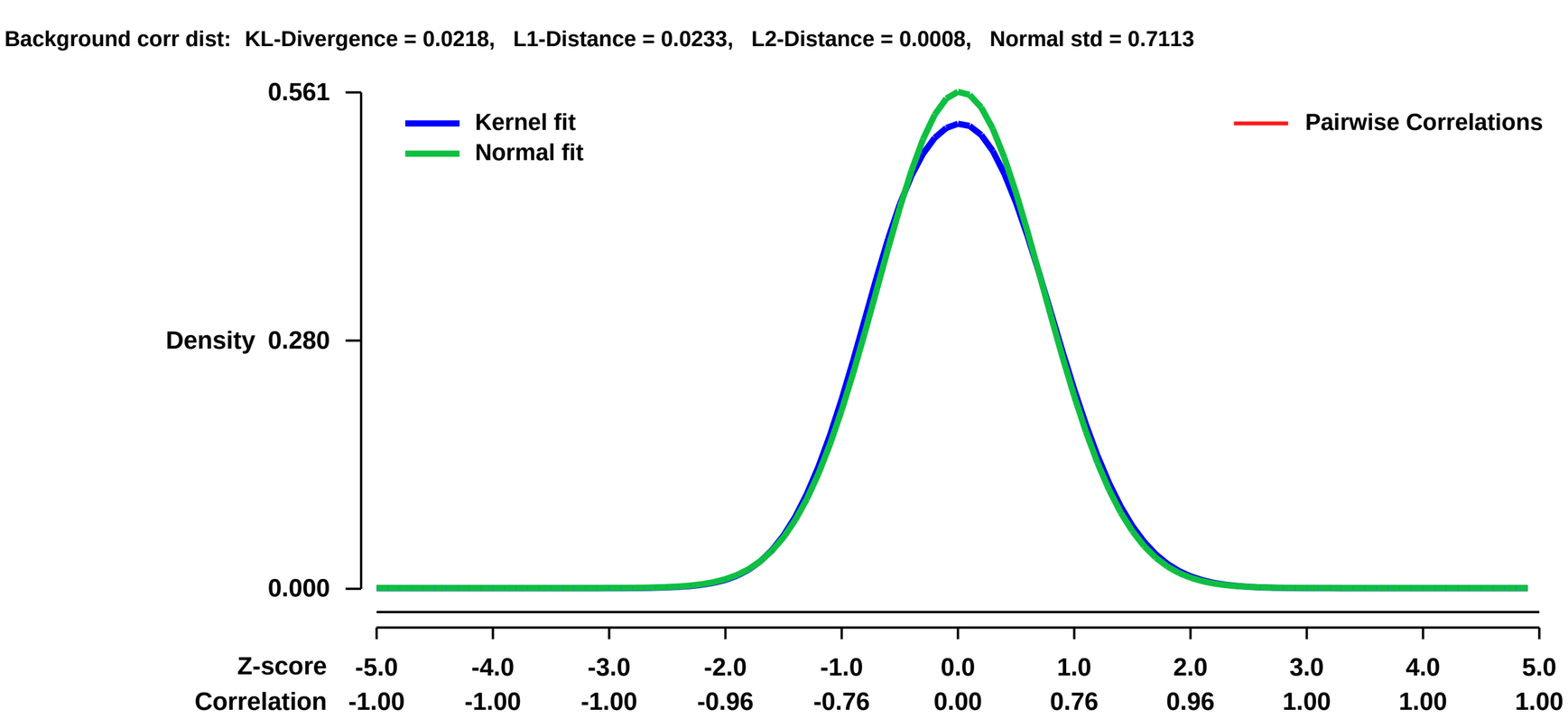

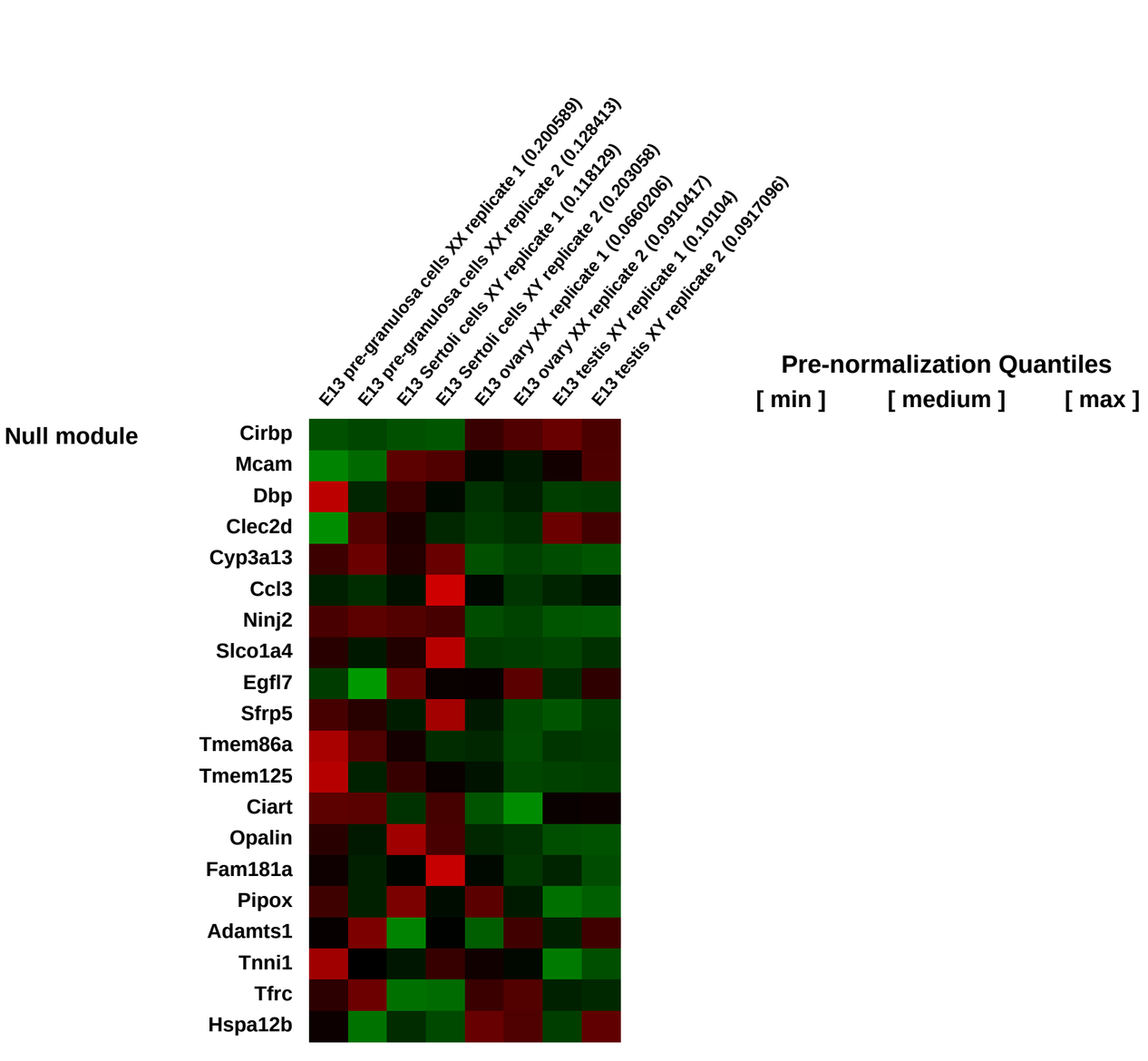

GEO Series "GSE55238" Expression Profiles

Num of samples in this series: 28

Scale of expression profile Z-scores

-3.0 -2.0 -1.0 0.0 1.0 2.0 3.0

GEO Link:	http://www.ncbi.nlm.nih.gov/geo/query/acc.cgi?acc=GSE55238
Status:	Public on Feb 21 2014
Title:	Host Responses to Sepsis Vary in Different Low-Lethality Murine Models
Organism:	Mus musculus
Experiment type:	Expression profiling by array
Platform:	GPL1261
Pubmed ID:	
Summary & Design:	**Summary:** **The CS and CLP murine models of intra-abdominal sepsis have unique transcriptomic respones 2 hrs, 1 and 3 days after sepsis** **Overall design:** **Infection protocol: Used the Cecal Ligation and Puncture (CLP) model and Cecal Slurry (CS) method in young mice.**

Background corr dist: **KL-Divergence = 0.0772, L1-Distance = 0.0719, L2-Distance = 0.0112, Normal std = 0.5033**

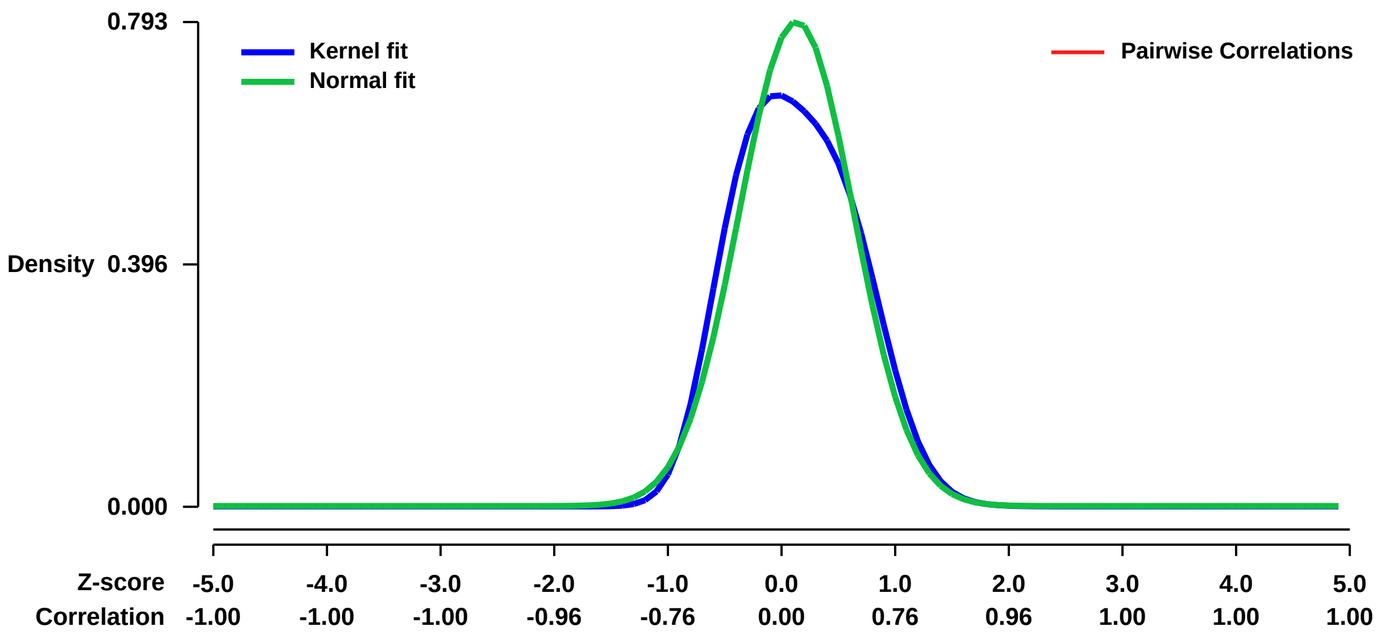

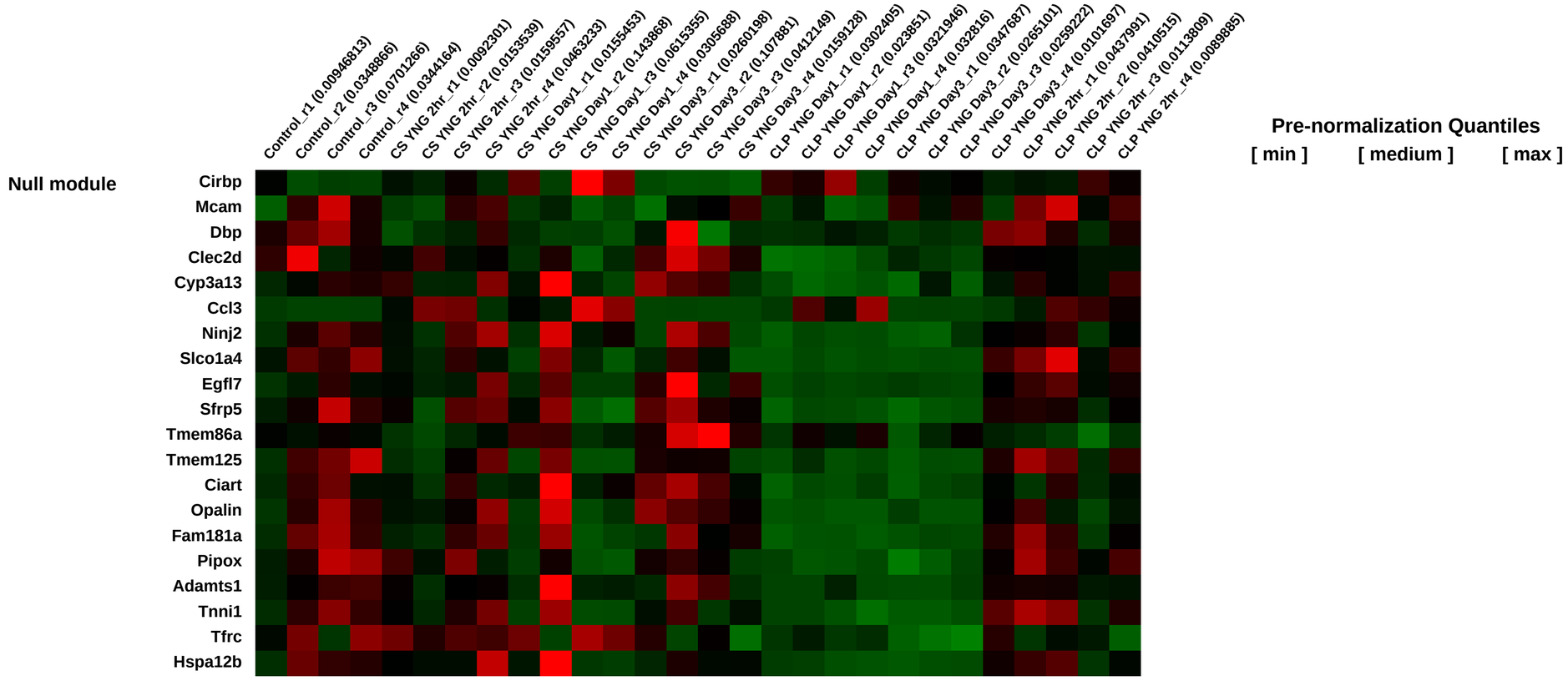

GEO Series "GSE17096" Expression Profiles

Num of samples in this series: 20

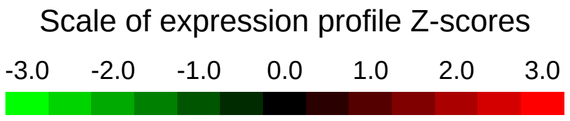

GEO Link:	http://www.ncbi.nlm.nih.gov/geo/query/acc.cgi?acc=GSE17096
Status:	Public on Dec 09 2011
Title:	mRNA composition of IRP1 mRNPs in mouse tissues
Organism:	Mus musculus
Experiment type:	Expression profiling by array
Platform:	GPL1261
Pubmed ID:	21940823
Summary & Design:	**Summary:** Affymetrix microarrays were used to determine the mRNA composition of mRNPs obtained by immunoprecipitation with IRP1 (iron regulatory protein 1). **Overall design:** All the microarray procedures were conducted at the EMBL Genomics Core Facility using standard Affymetrix protocols. In brief, approximately 120ng of immunoprecipitated RNA was used as input to a two-step amplification procedure to generate biotin-labeled RNA fragments for hybridization to the Affymetrix GeneChip Mouse Genome 430 2.0 array (Eukaryotic Sample and Array Processing manual 701024 Rev.3). Intensity values for the hybridizations were obtained either using RMA, calculations done in bioconductor (www.bioconductor.org) or MAS5, calculated using Affymetrix GCOS package. MAS5 calculated intensities were further quantile normalized using bioconductor.

Background corr dist: KL-Divergence = 0.0791, L1-Distance = 0.0942, L2-Distance = 0.0182, Normal std = 0.5457

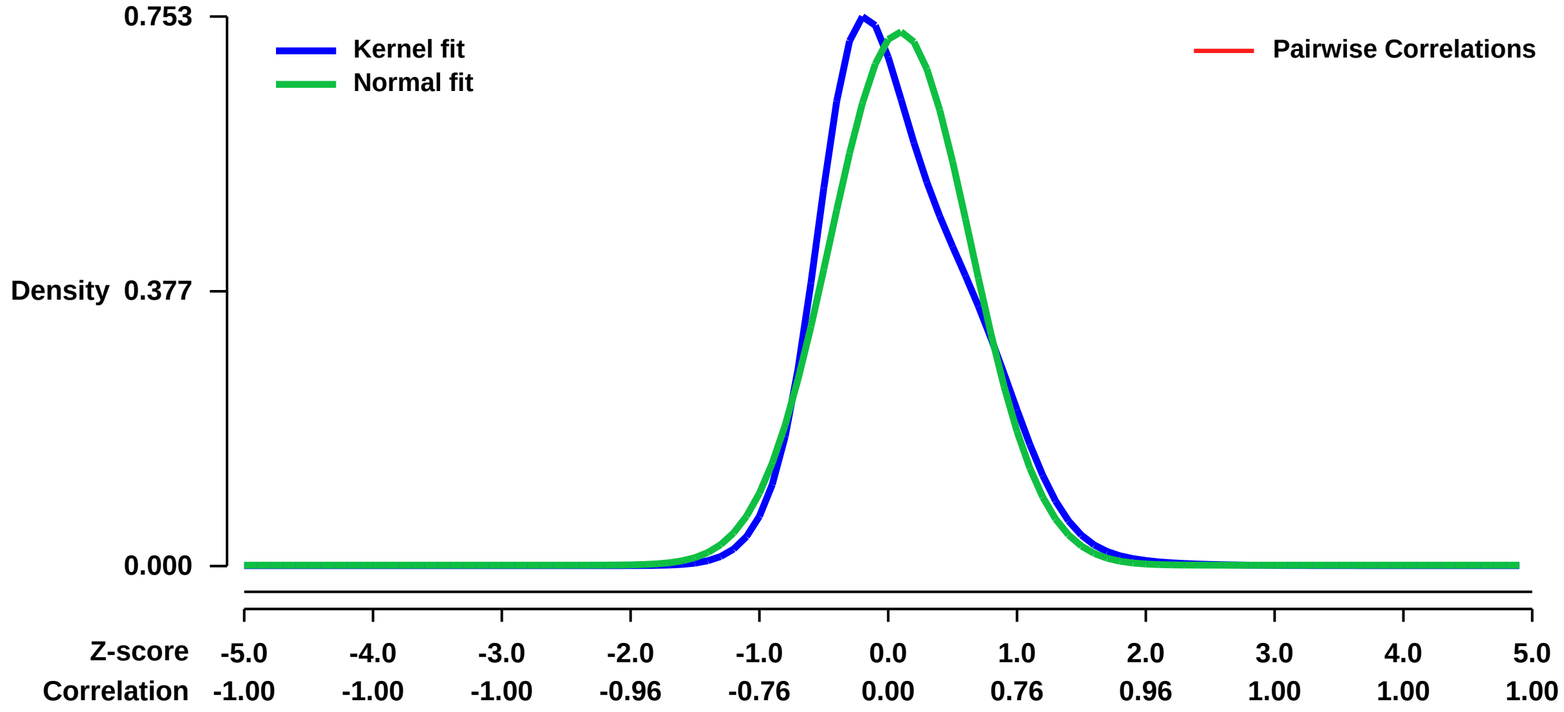

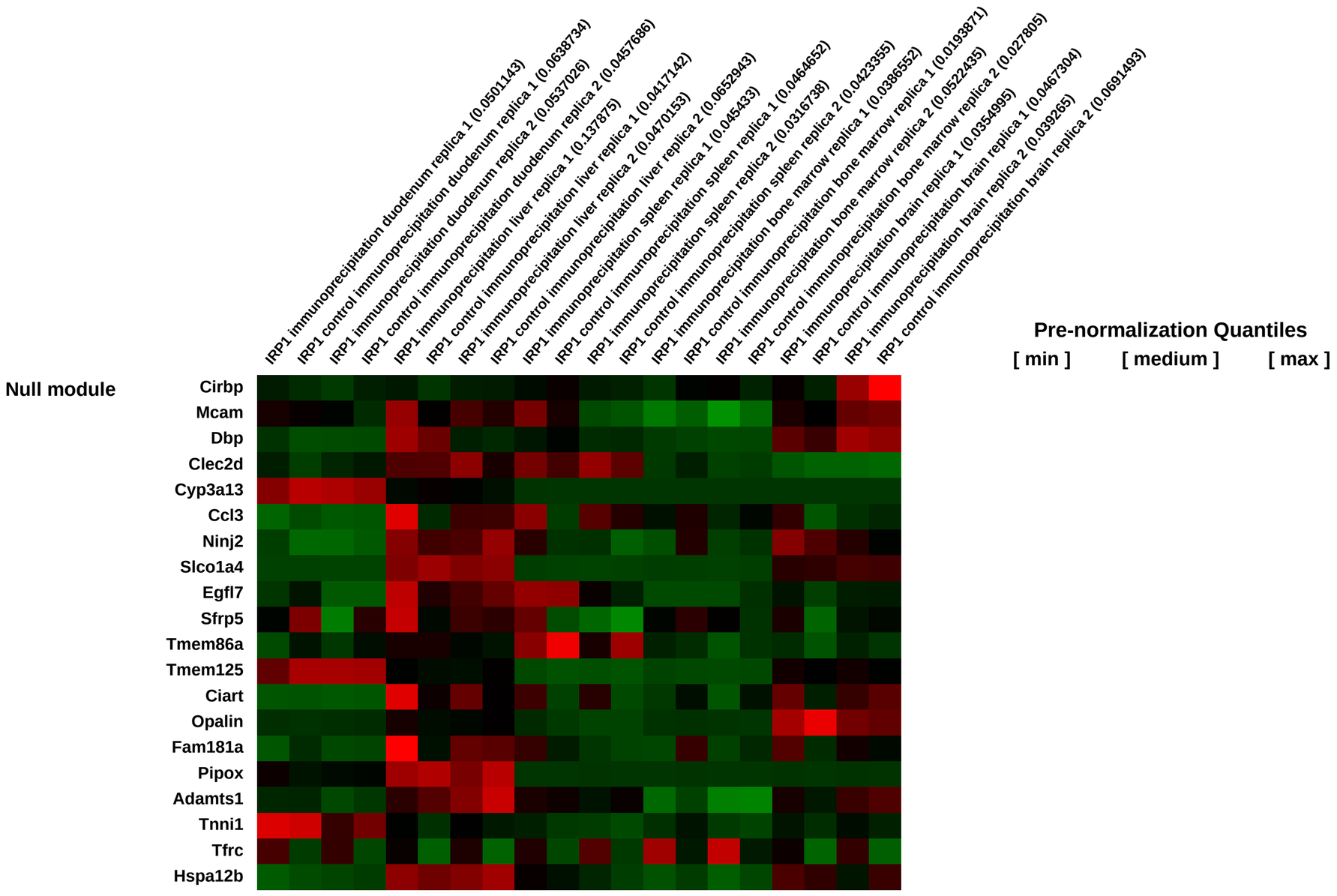

GEO Series "GSE24928" Expression Profiles

Num of samples in this series: 9

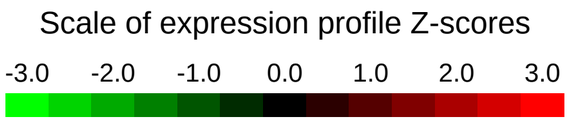

GEO Link:	http://www.ncbi.nlm.nih.gov/geo/query/acc.cgi?acc=GSE24928
Status:	Public on Dec 06 2010
Title:	Gene expression change induced by bisphenol A in mouse urogenital sinus
Organism:	Mus musculus
Experiment type:	Expression profiling by array
Platform:	GPL1261
Pubmed ID:	21123812
Summary & Design:	**Summary:** **Bisphenol A (BPA), an endocrine-disrupting chemical (EDC), is a well-known, ubiquitous estrogenic chemical. To investigate the effects of fetal exposure to low-dose BPA on the development of the prostate, we first examined the alterations of in situ sex steroid hormonal environment in the mouse urogenital sinus (UGS).** **Next, to investigate the BPA-specific gene alterations related to increases of the E2 levels and aromatase activity, we performed comprehensive gene expression analysis using Affymetrix GeneChip in the BPA-treated or DES-treated male UGS at embryonic day 17th and postnatal day 1st.** **Overall design:** **Pregnant female C57BL/6 mice were exposed to BPA (20 ¸…g/kg/day) or synthetic estrogen Diethylstilbestrol (DES: 0.2 ¸…g/kg/day), which were dissolved in tocopherol-stripped corn oil, on embryonic day 13 (E13) to E16. Between E17 and postnatal day 1 (P1), all animals were terminated by an overdose of isoflurane followed by cervical dislocation. Fetuses were collected at E17, E18, P0, and P1. The bladder and urethra were removed and dissected to isolate UGS and collected in RNA later. To isolate pure UGS, other tissues such as the bladder, urethra, Wolffian duct (WD), seminal vesicle (SV), and Mullerian duct (MD) were removed from both the male and female urogenital tracts. The histopathology of the mouse UGS was then examined by hematoxylin and eosin staining. Total RNA was extracted using the Qiagen mini RNA Easy kit. Each RNAs were linearly amplified and hybridized to Affymetrix GeneChip.**

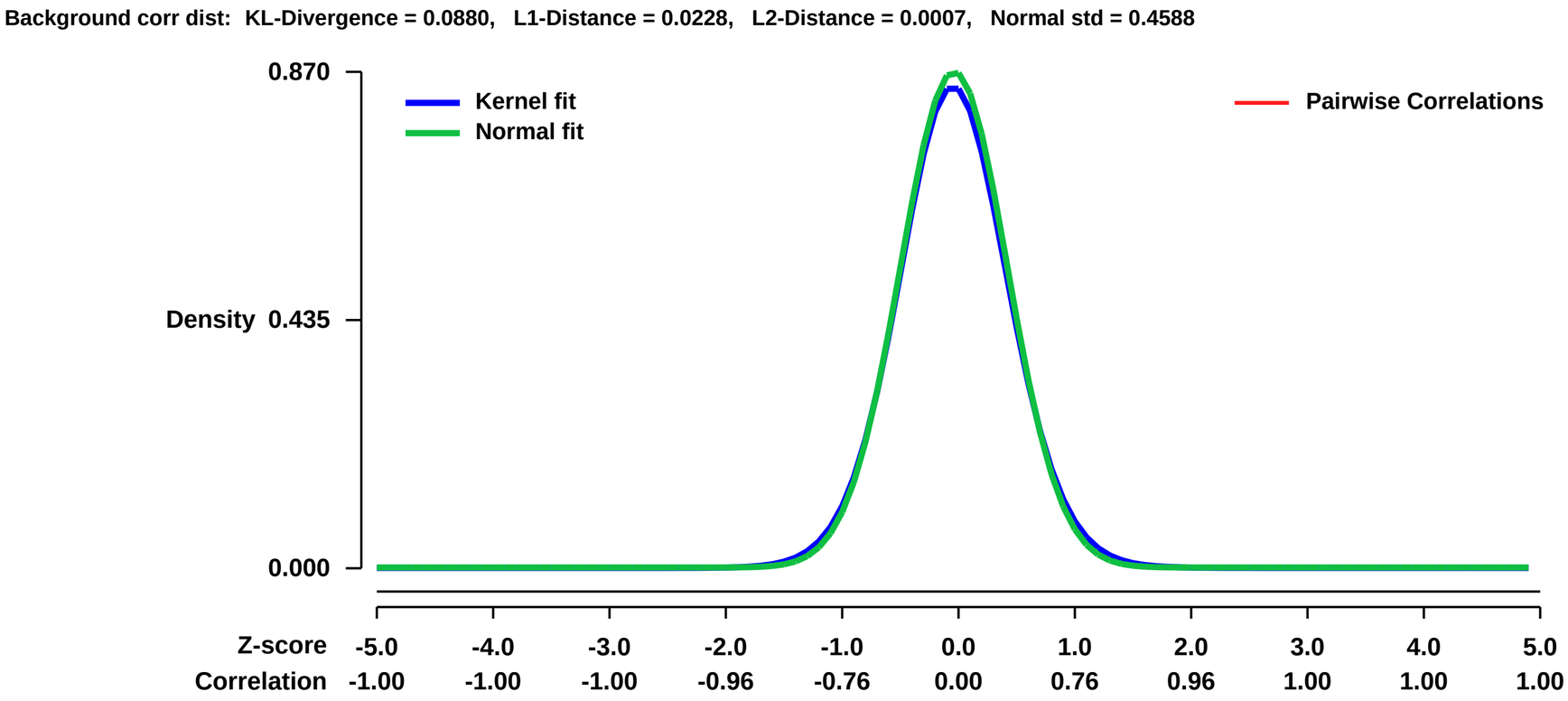

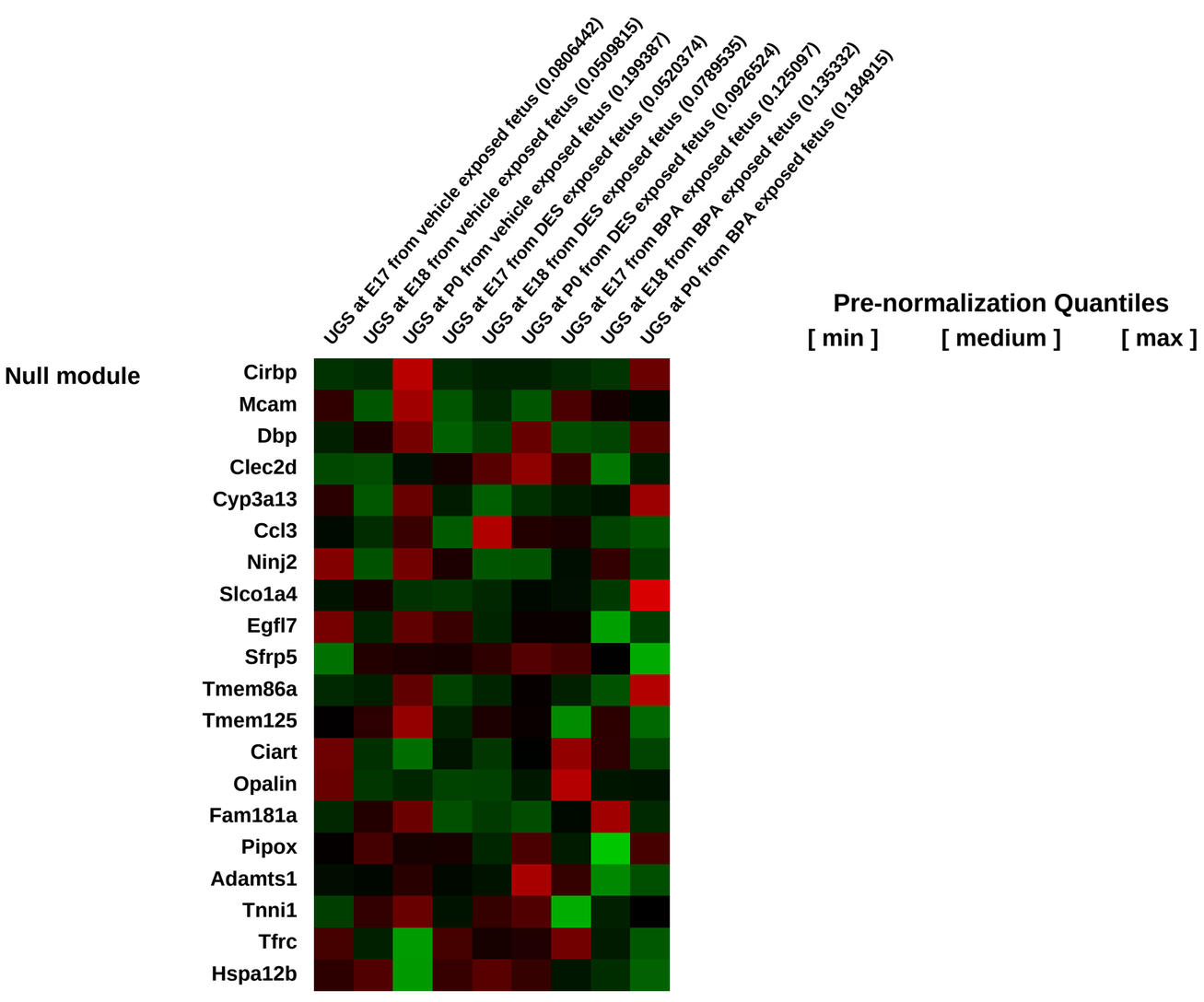

GEO Series "GSE18010" Expression Profiles

Num of samples in this series: 29

Scale of expression profile Z-scores

-3.0 -2.0 -1.0 0.0 1.0 2.0 3.0

GEO Link:	http://www.ncbi.nlm.nih.gov/geo/query/acc.cgi?acc=GSE18010
Status:	Public on Oct 01 2009
Title:	Pathogenicity of a disease-associated human IL-4 receptor allele in experimental asthma
Organism:	Mus musculus
Experiment type:	Expression profiling by array
Platform:	GPL1261
Pubmed ID:	19770271
Summary & Design:	**Summary:** Polymorphisms in the interleukin-4 receptor ¸– chain (IL-4R¸–) have been linked to asthma incidence and severity, but a causal relationship has remained uncertain. In particular, a glutamine to arginine substitution at position 576 (Q576R) of IL-4R¸– has been associated with severe asthma, especially in African Americans. We show that mice carrying the Q576R polymorphism exhibited intense allergen-induced airway inflammation and remodeling. The Q576R polymorphism did not affect proximal signal transducer and activator of transcription (STAT) 6 activation, but synergized with STAT6 in a gene targetâ and tissue-specific manner to mediate heightened expression of a subset of IL-4â and IL-13â responsive genes involved in allergic inflammation. Our findings indicate that the Q576R polymorphism directly promotes asthma in carrier populations by selectively augmenting IL-4R¸–â dependent signaling. **Keywords: Cell population analysis** **Overall design:** To determine potential mechanisms underlying the trophic effects of the R576 allele on airway inflammation and remodeling, we first compared the gene expression profile in the lungs of doxycycline-treated B6.129Il4raR576/R576/IL-13tg mice versus B6.129Il4raR576/R576 littermates that lacked the IL-13tg (n = 11 and 5, respectively). We similarly compared the gene expression profile in the lungs of doxycycline-treated B6.Il4raQ576/Q576/IL-13tg mice versus tg-negative littermates (n = 8 and 5, respectively). Lastly, we directly compared the gene expression profiles in the doxycycline-treated B6.129Il4raR576/R576/IL-13tg versus B6.Il4raQ576/Q576/IL-13tg mice.

Background corr dist: KL-Divergence = 0.1125, L1-Distance = 0.0457, L2-Distance = 0.0045, Normal std = 0.4194

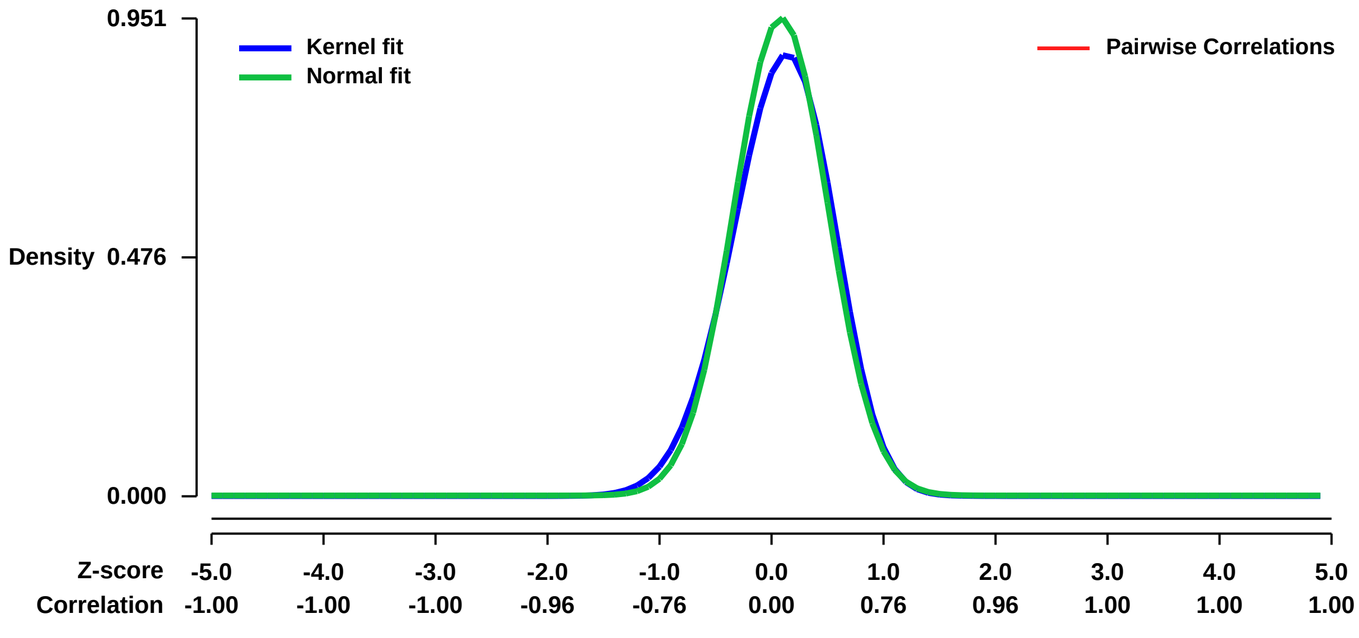

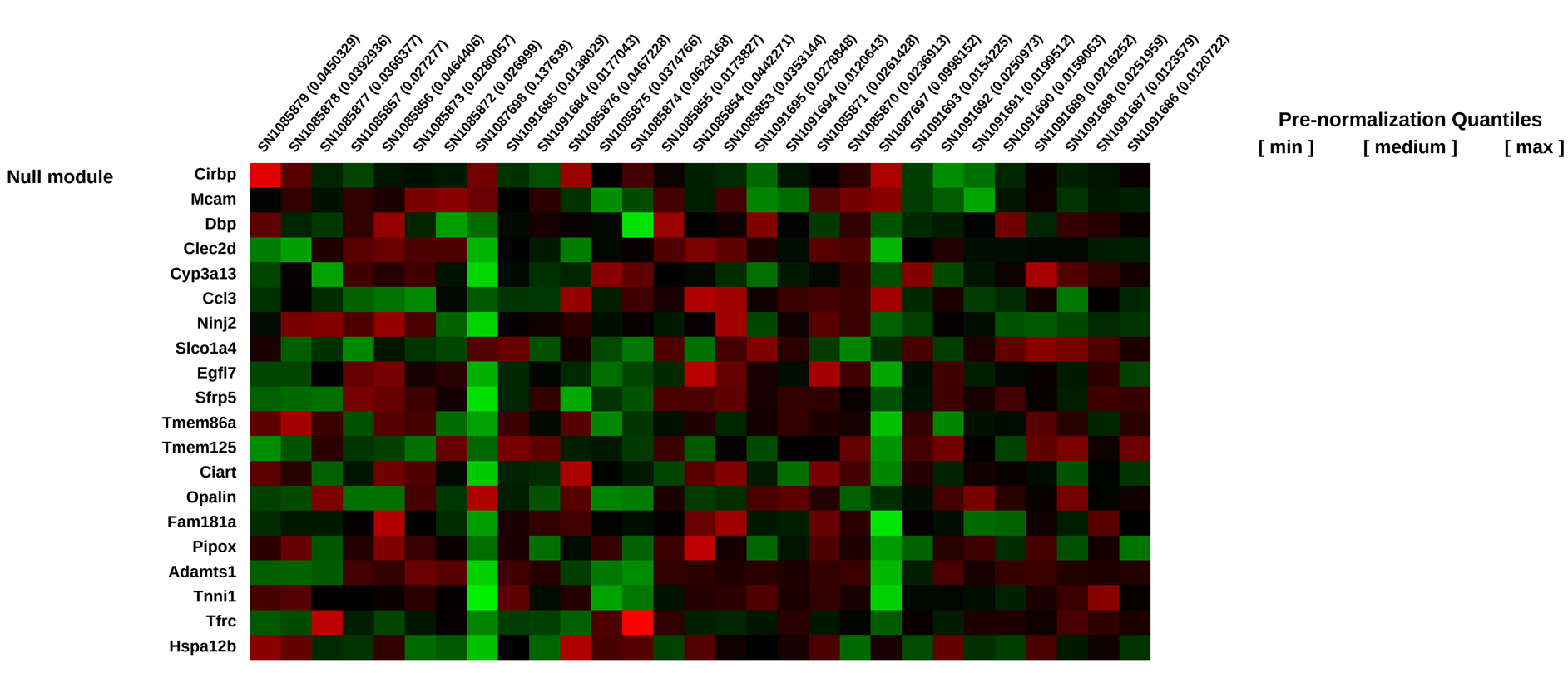

GEO Series "GSE51608" Expression Profiles

Num of samples in this series: 6

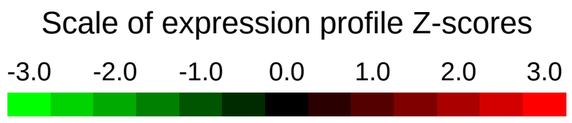

GEO Link:	http://www.ncbi.nlm.nih.gov/geo/query/acc.cgi?acc=GSE51608
Status:	Public on Oct 24 2013
Title:	Expression profiling of Ebf2- and Ebf2- stromal cells in mouse bone marrow
Organism:	Mus musculus
Experiment type:	Expression profiling by array
Platform:	GPL1261
Pubmed ID:	23184664
Summary & Design:	**Summary:** To identify the true molecular features of the Ebf2+ cells, we performed microarray analysis of freshly sorted CD45-TER119-Ebf2+ and Ebf2- cells. This allowed for the detection of 1968 genes that were 2-fold differentially expressed in Ebf2+ and Ebf2- cells. Among these, 1075 genes were upregulated and 893 genes including Ebf2, were downregulated in the Ebf2- as compared to the Ebf2+ cells. These include Nov, Fmod, Ndn, Dcn, Ctgf, Angiopoietin like-1(Angptl1), Fn1 and Jag1, some of which has been reported to be expressed in culture-selected MSCs. Furthermore, consistent with antigen expression analysis by FACS, the Ebf2+ cells highly expressed transcripts of Pdgfra, Pdgfrb, Sca1/Ly6a, Thy1 and Itga7 and Itgav, that have been suggested to be linked to MSCs. Nestin was mainly expressed in the Ebf2+ cells whereas it was hardly detectable in the Ebf2- cells. Altogether, molecularly, the Ebf2+ cells displayed features of a MSC. Ebf2 expression is not restricted to committed osteoblast progenitor cells but rather marks a multipotent mesenchymal progenitor cell population in adult mouse BM. These cells do not appear to be completely overlapping with the previous reported MSC populations. The findings provide new insights into the in vivo cellular identity and molecular properties of BM mesenchymal stem and progenitor cells. **Overall design:** RNA was extracted from 1,000 or 2000 purified adult bone marrow cells using the RNAeasy microkit. RNA was labeled and amplified by dual amplification and hybridized to Affymetrix microarray MOE430_2, according to AffymetrixTM GeneChip Expression Analysis Technical Manual. Probe level expression values were calculated using the RMA algorithm.

Background corr dist: KL-Divergence = 0.0181, L1-Distance = 0.0273, L2-Distance = 0.0011, Normal std = 0.7703

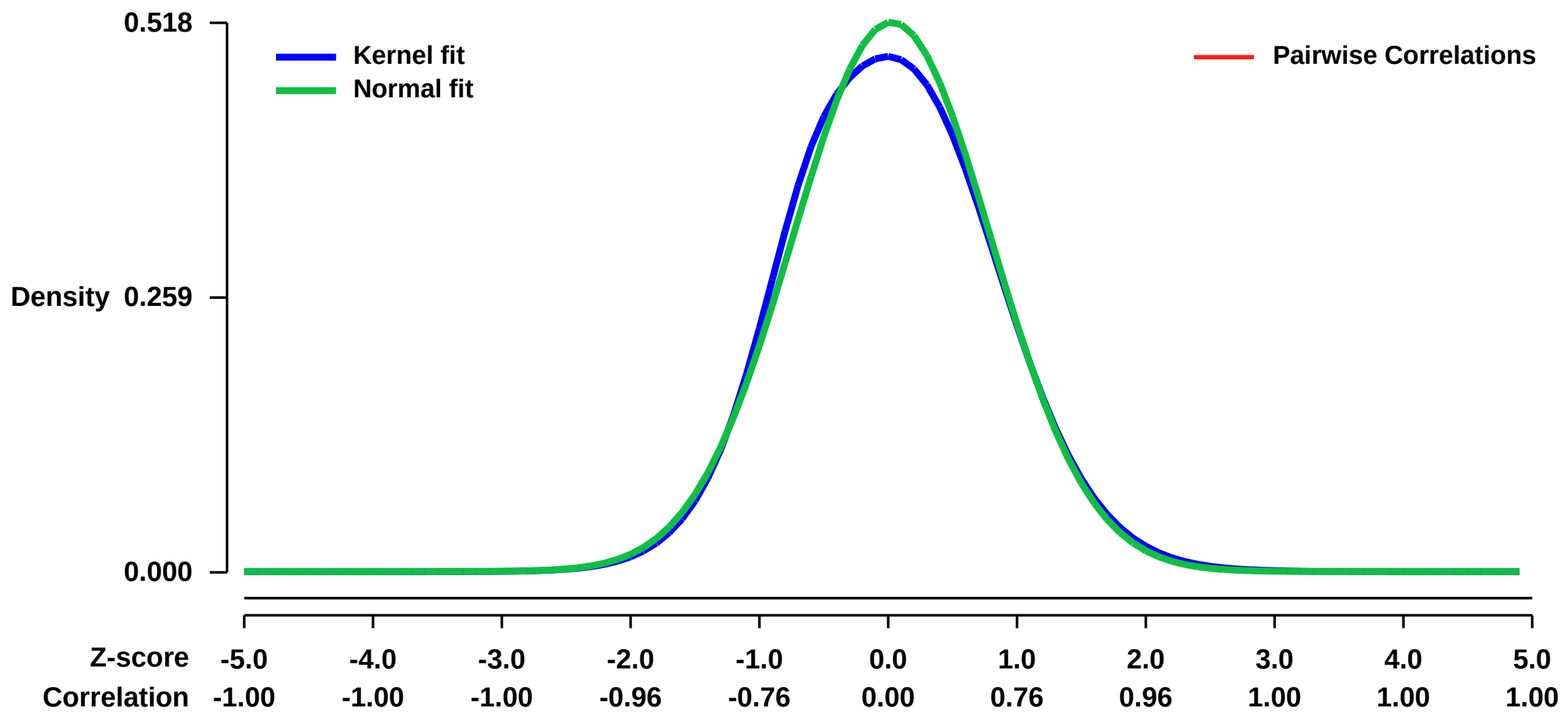

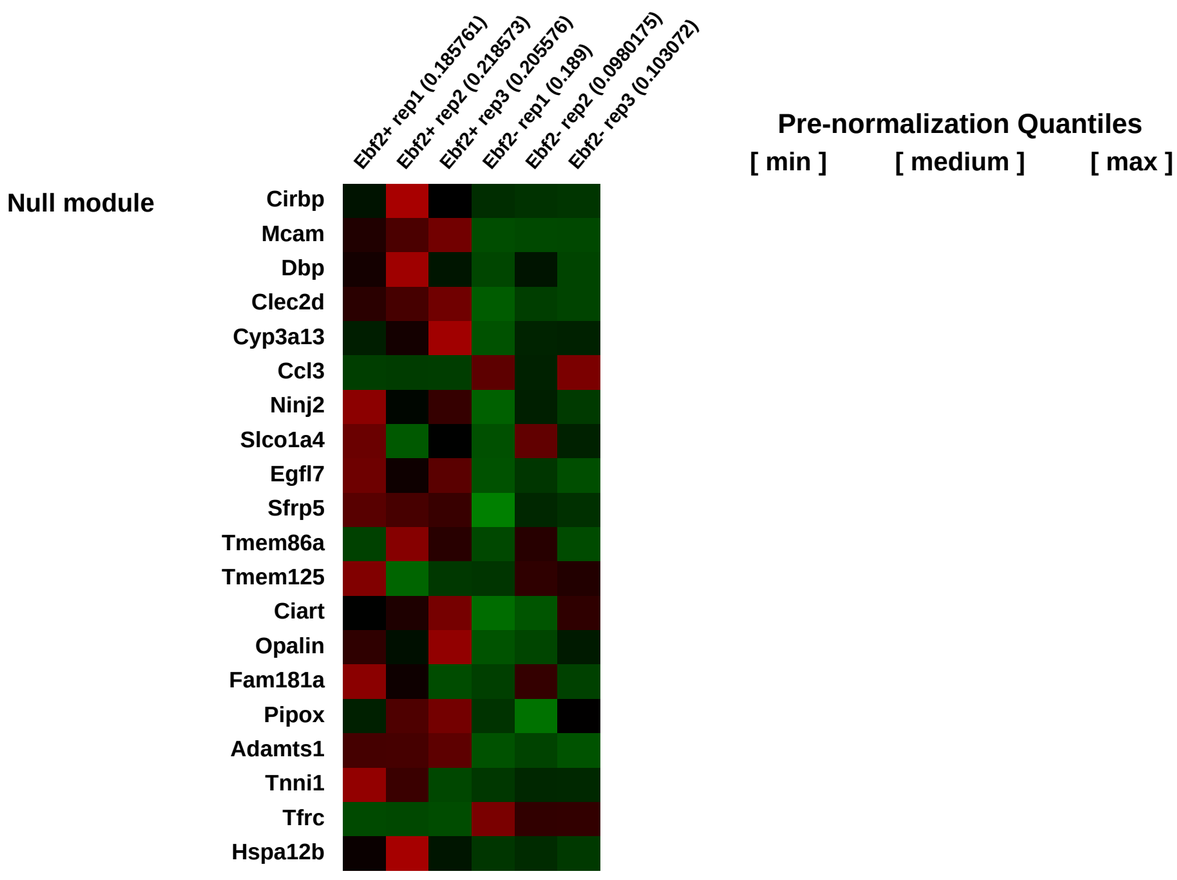

GEO Series "GSE20918" Expression Profiles

Num of samples in this series: 6

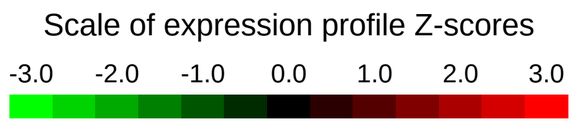

GEO Link:	http://www.ncbi.nlm.nih.gov/geo/query/acc.cgi?acc=GSE20918
Status:	Public on Sep 06 2010
Title:	GENE EXPRESSION ALTERATIONS IN ADULT UTP14b (jsd) MICE BY CONDITIONAL KNOCKOUT OF ANDROGEN RECEPTOR IN SERTOLI CELLS
Organism:	Mus musculus
Experiment type:	Expression profiling by array
Platform:	GPL1261
Pubmed ID:	20650881
Summary & Design:	**Summary:** Spermatogenesis is dependent primarily on testosterone action on the Sertoli cells. Although the identification of testosterone-regulated target genes in Sertoli cells has been approached using microarray analysis to compare gene expression in mice with androgen receptor (AR) elimination in the Sertoli cells (SCARKO) and wild type mice, the analysis has been complicated by alteration of germ cell composition of the testis when pubertal or adult mice were used and differences in Sertoli-cell gene expression from those in adult when prepubertal mice were used. Since the testicular cell components of adult jsd (Utp14bjsd ,juvenile spermatogonial depletion) mice and SCARKO-jsd mice are essentially identical, consisting of only type A spermatogonia and somatic cells, comparisons of gene expression profiles between jsd and SCARKO-jsd testes would identify AR regulated genes in adult Sertoli cells, with minimum effects of cell number changes. Microarray analysis identified 161 genes as downregulated and 202 genes as upregulated in the SCARKO-jsd mice compared to jsd mice. Some of the genes identified in the previous studies, including Rhox5, Drd4, and Fhod3, were also AR-regulated in the jsd testes but others, such as proteases and components of junctional complexes, were not androgen regulated in our model. Surprisingly, a set of germ-cell-specific genes preferentially expressed in differentiated spermatogonia and meiotic cells, including Meig1, Sycp3, and Ddx4, were all upregulated about 2-fold in SCARKO-jsd testes, demonstrating that, although there was no significant differentiation to spermatocytes in SCARKO-jsd mice, AR-regulated genes in Sertoli cells are involved in the regulation of spermatogonial differentiation. Further gene ontogeny analysis revealed possible sets of genes whose expression changes may be involved in the disruption of Sertoli cell organization in SCARKO-jsd testes. **Overall design:** Comparisons of gene expression profiles between the testis of jsd mice (n=3) and SCARKO-jsd mice (n=3).

Background corr dist: KL-Divergence = 0.0295, L1-Distance = 0.0137, L2-Distance = 0.0002, Normal std = 0.6682

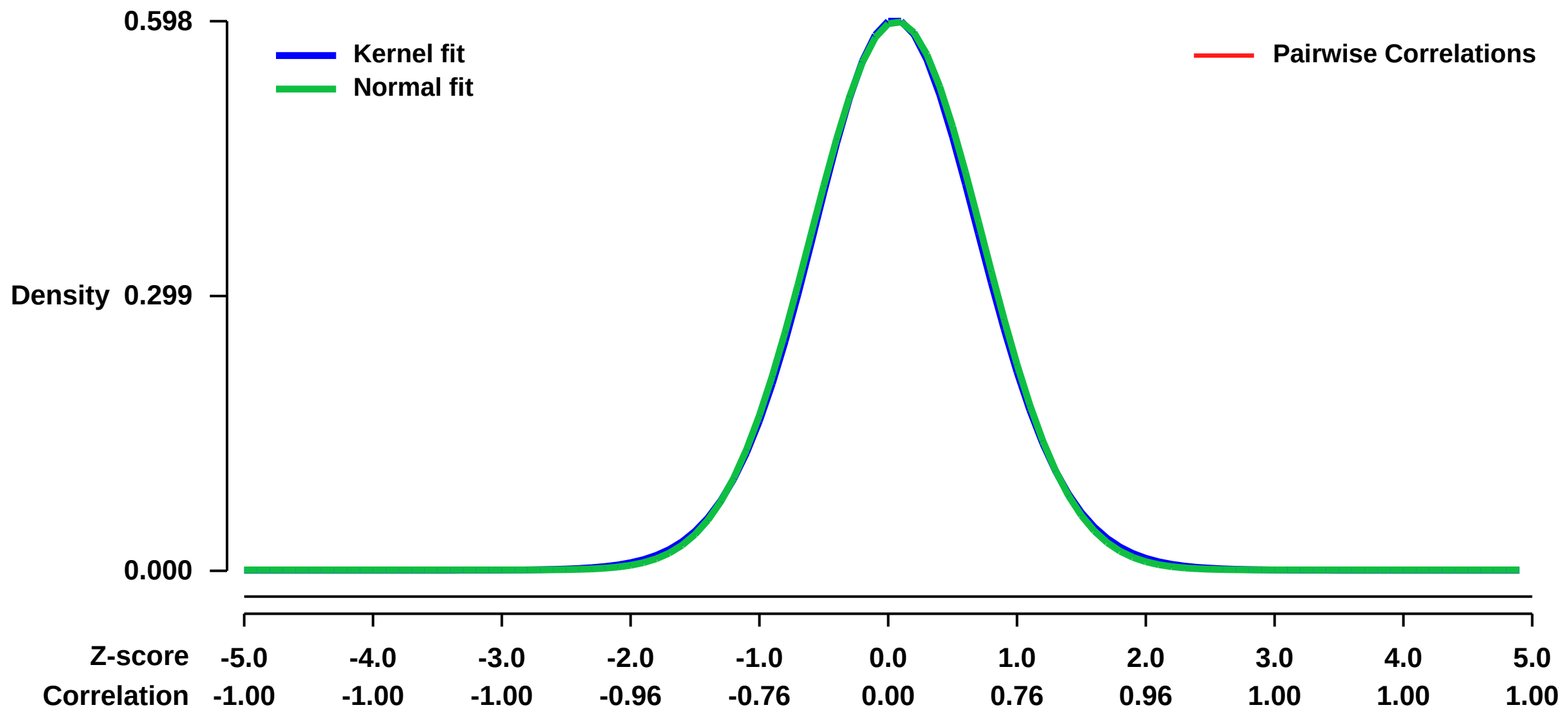

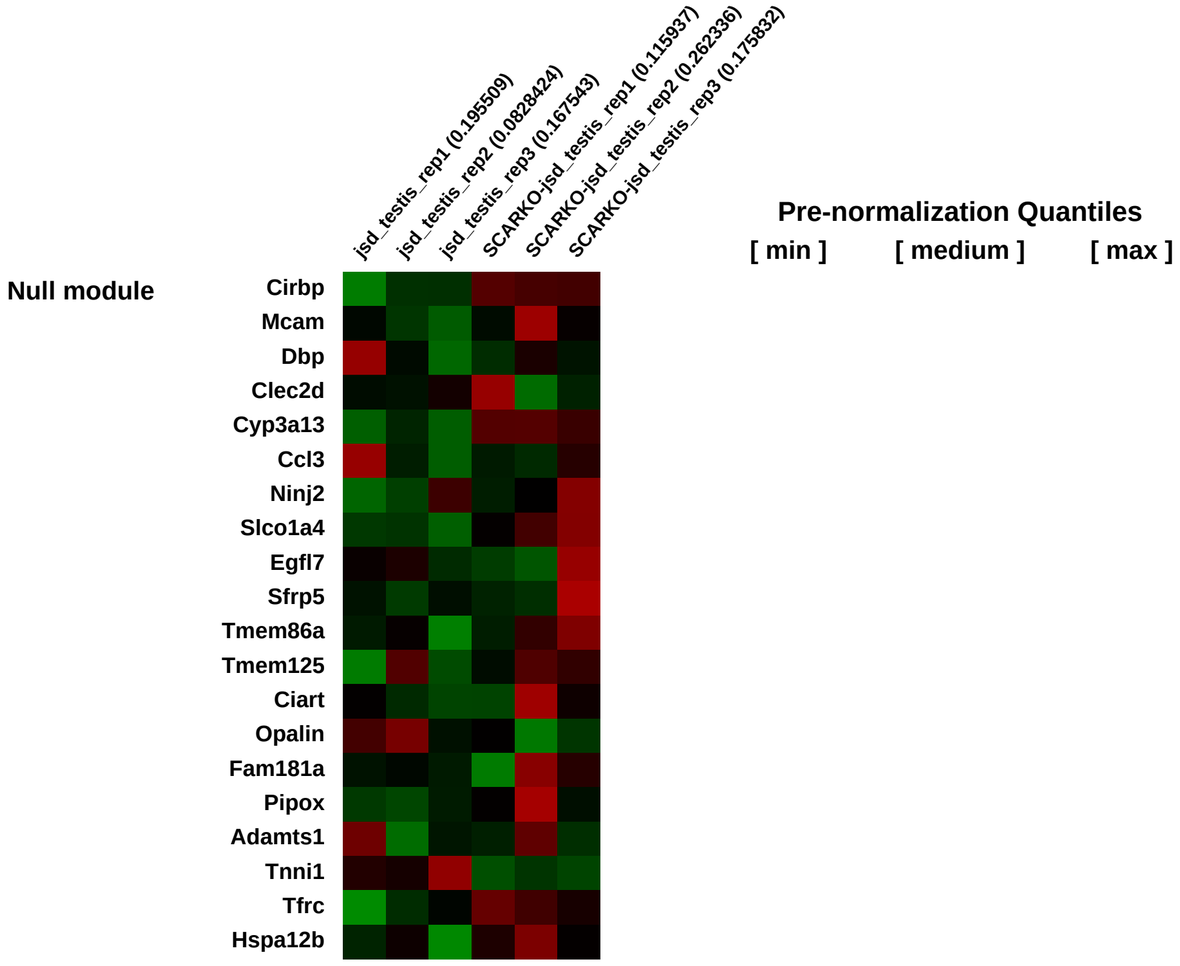

GEO Series "GSE7764" Expression Profiles

Num of samples in this series: 10

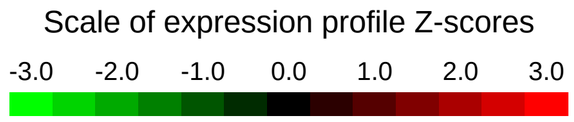

GEO Link:	http://www.ncbi.nlm.nih.gov/geo/query/acc.cgi?acc=GSE7764
Status:	Public on May 15 2007
Title:	mRNA expression profiles of resting and IL-15 activated murine NK cells
Organism:	Mus musculus
Experiment type:	Expression profiling by array
Platform:	GPL1261
Pubmed ID:	17540585
Summary & Design:	**Summary:** Murine NK cells were compared at rest and following 24 hours of IL-15 stimulation for their mRNA expression profiles on the Affymetrix MOE430_2 microarray platform. Additional comparators included resting bulk splenocytes. **Keywords: mRNA, mouse, NK cell, IL-15** **Overall design:** Three pairs of flow sorted murine NK cells (C57Bl/6) were analzyed at rest or after 24 hours of IL-15 stimulation. Three biological replicates of each condition (resting or IL-15) are included in this anlaysis. In addition, bulk resting splenocytes were used (2 biological replicates with 2 chip replicates for a total of 4 replicates).

Background corr dist: **KL-Divergence = 0.0707, L1-Distance = 0.0425, L2-Distance = 0.0029, Normal std = 0.5268**

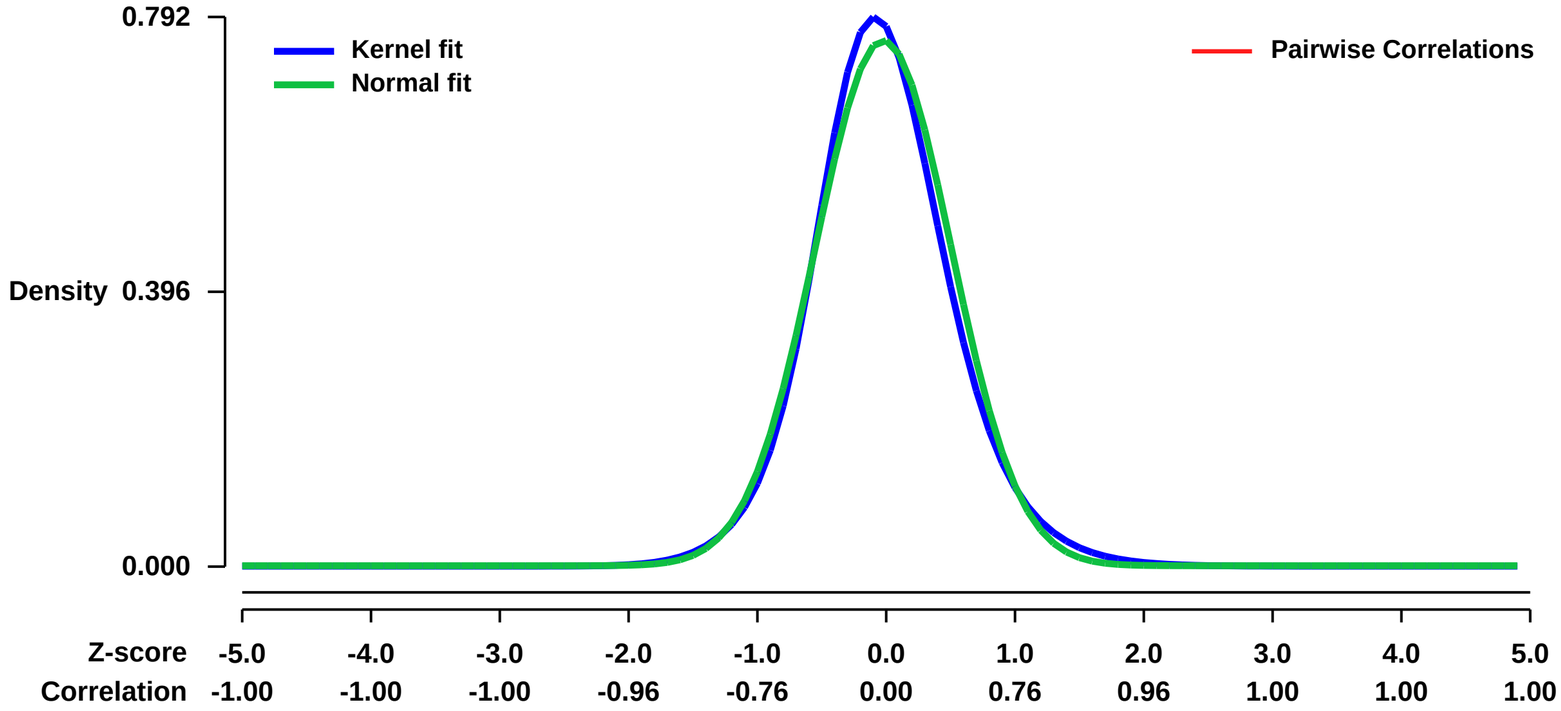

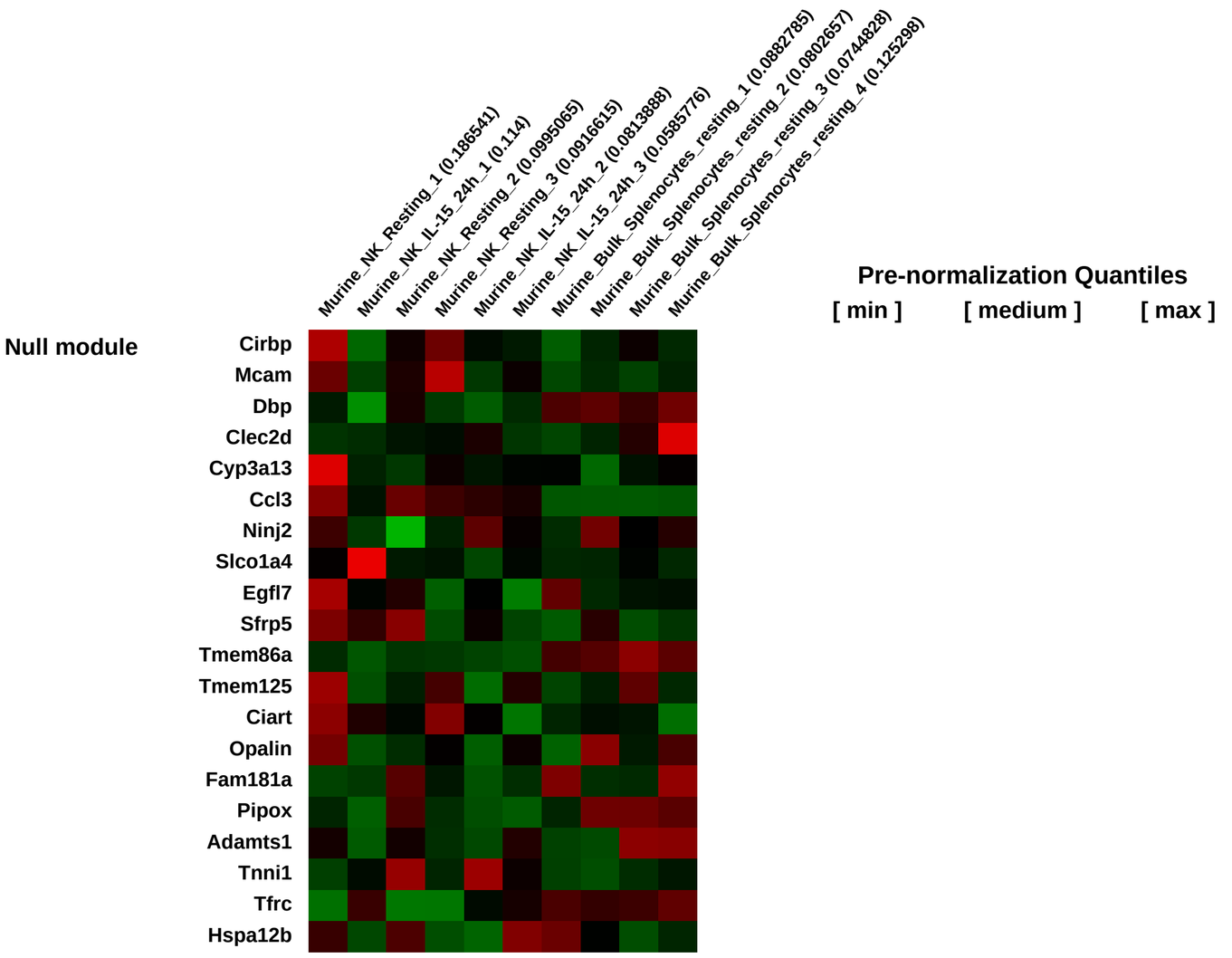

GEO Series "GSE31972" Expression Profiles

Num of samples in this series: 6

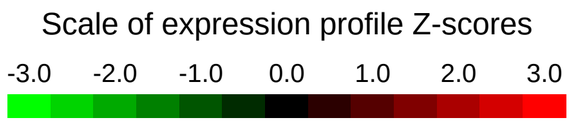

GEO Link:	**http://www.ncbi.nlm.nih.gov/geo/query/acc.cgi?acc=GSE31972**
Status:	**Public on Dec 07 2011**
Title:	**Transcriptional profiling of ICAM-positive and -negative cells from the mouse olfactory epithelium**
Organism:	**Mus musculus**
Experiment type:	**Expression profiling by array**
Platform:	**GPL1261**
Pubmed ID:	
Summary & Design:	**Summary:** **We used trasncriptional profiling of fluorescent activated cell sorting (FACS) purified ICAM1-positive and negative cells from the olfactory epithelium (OE) of three-week old mice to identify genes enriched in the horizontal basal cells.** **Overall design:** **The olfactory epithelia from P21-P25 CD1 mice (Charles River Laboratories, Wilmington, MA), were isolated, dissociated, and then purified by FACS using a FITC-conjugated antibody for ICAM1 (CD54). ICAM1-positive and negative cell populations were collected and compared. RNA was purified with TRIzol reagent (Invitrogen, Carlsbad, CA), subjected to two rounds of amplification, labeled, and hybridized to Affymetrix Mouse Genome 430.2 GeneChip microarrays (Affymetrix Inc., Santa Clara, CA, USA) using Affymetrix reagents and protocols (http://www.affymetrix.com). There were three experimental replicates, each consisting of the ICAM1 (+) and ICAM1 (-) FACS purified cell populations from individual litters of mice that were dissected/dissociated/FACS-purified using an ICAM1-FITC conjugated antibody; one microarray was used for each ICAM1 (+) and ICAM1 (-) sample for a total of six microarrays. Microarray data were normalized using GCRMA.**

Background corr dist: **KL-Divergence = 0.0145, L1-Distance = 0.0398, L2-Distance = 0.0017, Normal std = 0.8821**

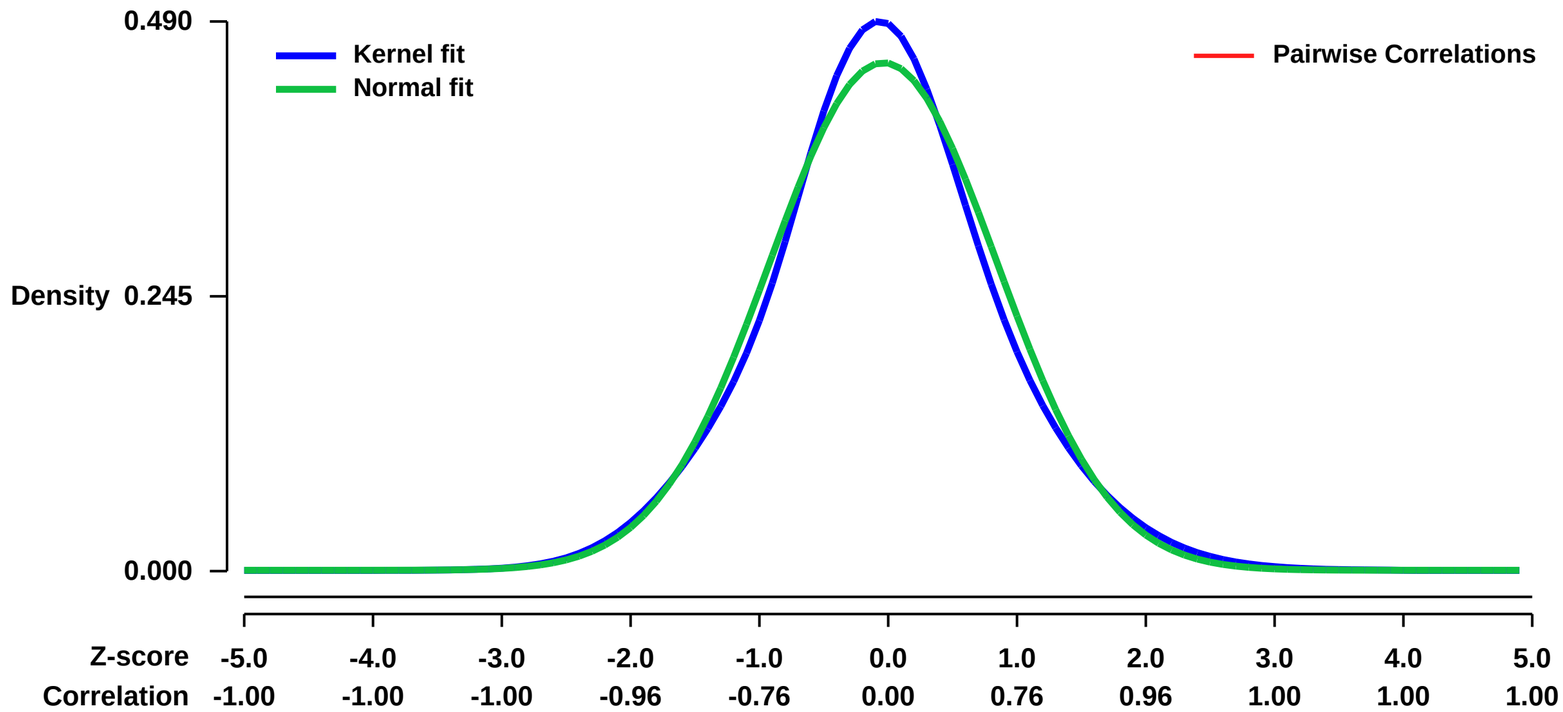

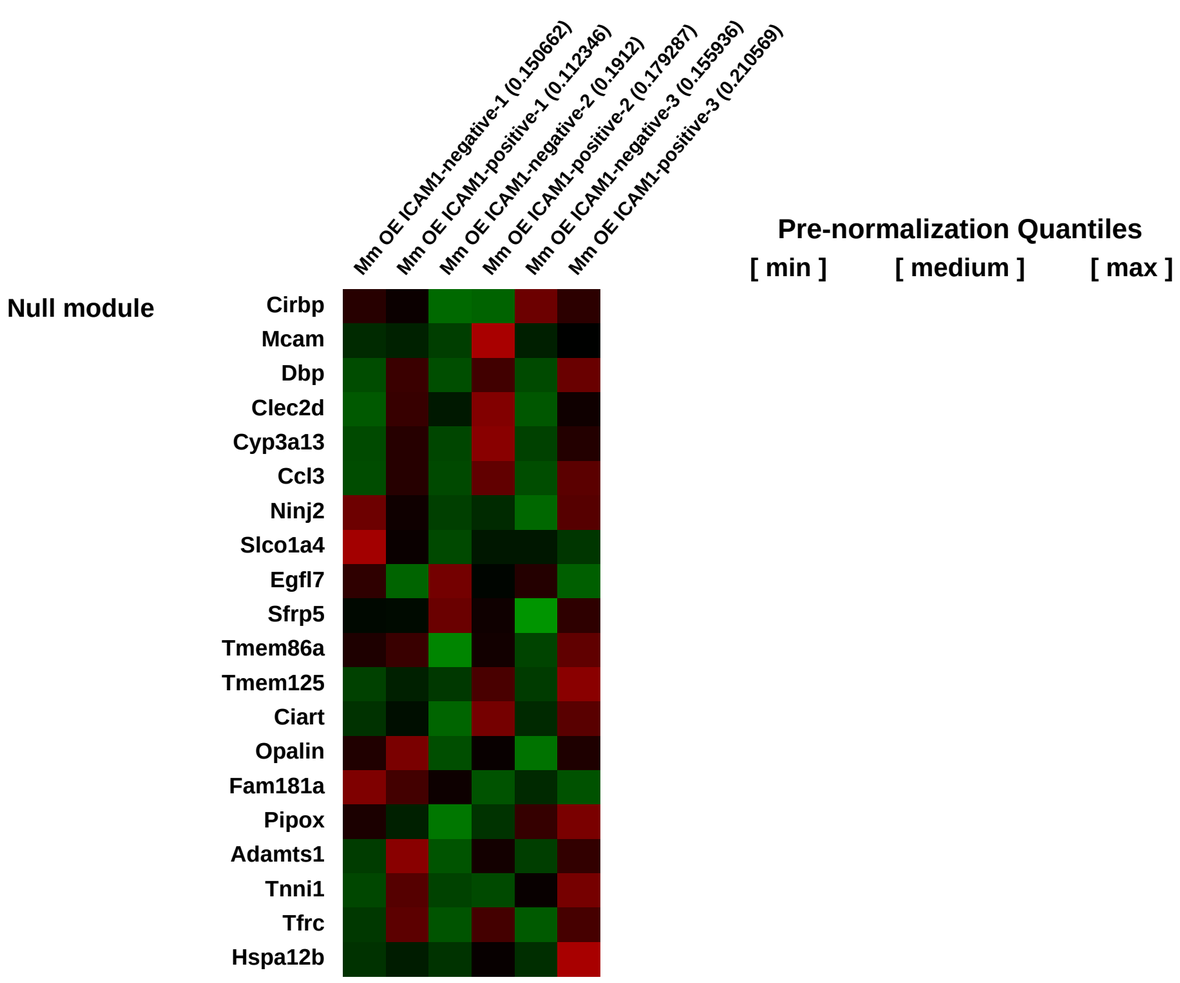

GEO Series "GSE24695" Expression Profiles

Num of samples in this series: 9

Scale of expression profile Z-scores

-3.0 -2.0 -1.0 0.0 1.0 2.0 3.0

GEO Link:	http://www.ncbi.nlm.nih.gov/geo/query/acc.cgi?acc=GSE24695
Status:	Public on Oct 15 2010
Title:	Transcription Factor Redundancy Ensures Induction of the Antiviral State
Organism:	Mus musculus
Experiment type:	Expression profiling by array
Platform:	GPL1261
Pubmed ID:	20943654
Summary & Design:	**Summary:** **Transcriptional response to virus infection in mice lacking type I and type III signaling** **The transcriptional response to virus infection is thought to be predominantly induced by interferon (IFN) signaling. Here we demonstrate that, in the absence of IFN signaling, an IFN-like transcriptome is still maintained. This transcriptional activity is mediated from IFN-stimulated response elements (ISREs) that bind to both the IFN stimulated gene factor 3 (ISGF3) as well as to IFN response factor 7 (IRF7). Through a combination of both in vitro biochemistry and in vivo transcriptional profiling, we have dissected what constitutes IRF-specific, ISGF3-specific, or universal ISREs. Taken together, the data presented here suggests that IRF7 can induce an IFN-like transcriptome in the absence of type-I or -III signaling and therefore provides a level of redundancy to cells to ensure the induction of the antiviral state.** **Overall design:** **Human: Analysis of IRF7 transcriptome in U3A cell line was performed in duplicates.**

Background corr dist: **KL-Divergence = 0.0750, L1-Distance = 0.0207, L2-Distance = 0.0006, Normal std = 0.4869**

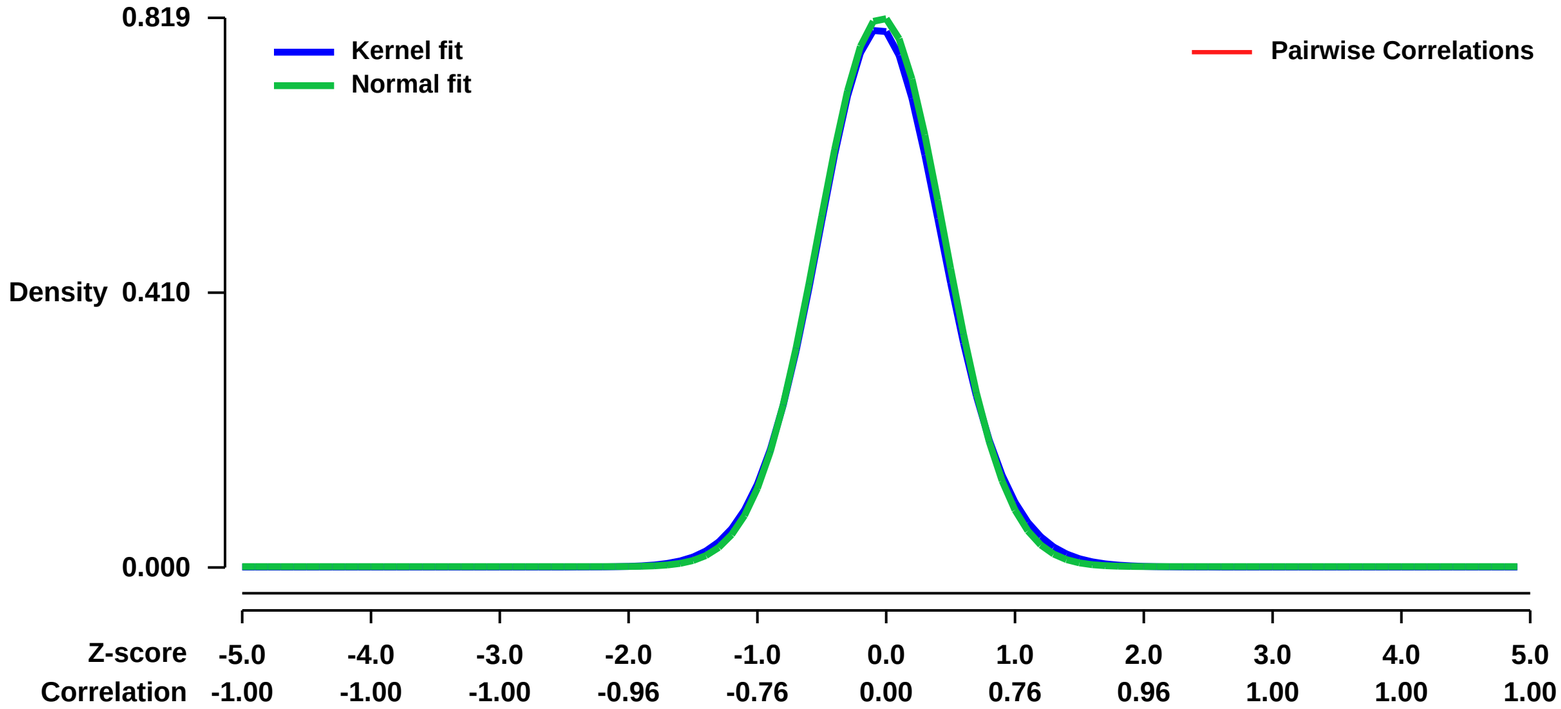

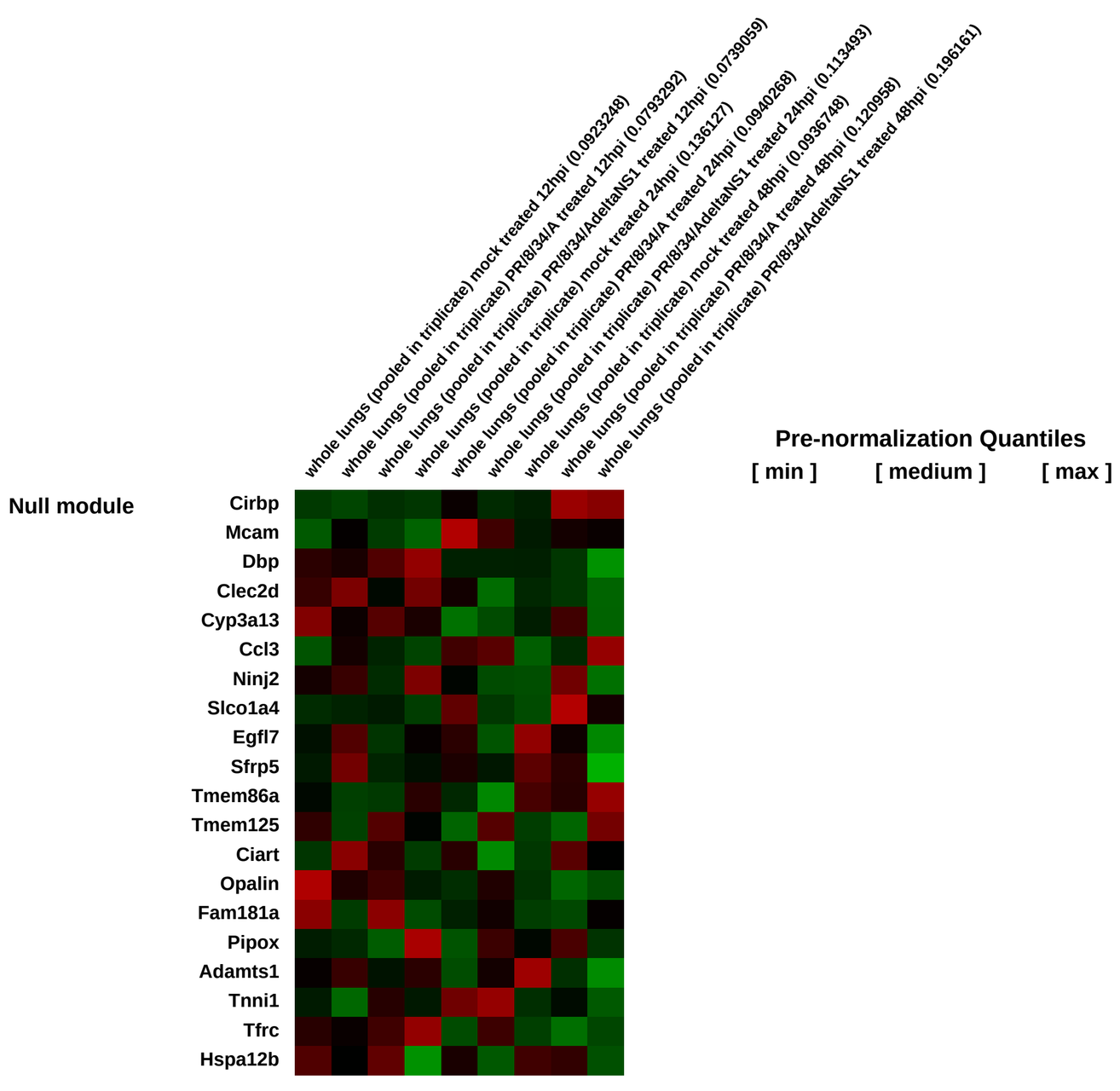

GEO Series "GSE10895" Expression Profiles

Num of samples in this series: 8

Scale of expression profile Z-scores

-3.0 -2.0 -1.0 0.0 1.0 2.0 3.0

GEO Link:	**http://www.ncbi.nlm.nih.gov/geo/query/acc.cgi?acc=GSE10895**
Status:	**Public on Nov 06 2008**
Title:	**Expression study of liver smaples of 2-days old Mfp2 knockout mice as compared to wild type**
Organism:	**Mus musculus**
Experiment type:	**Expression profiling by array**
Platform:	**GPL1261**
Pubmed ID:	**18773970**
Summary & Design:	**Summary:** **Study on gene expression in multifunctional protein 2 deficient mice. Liver samples of two days old mice in normal conditions are used. In total 8 arrays were hybridized corresponding to 4 KO mice and 4 WT mice Results: Cholesterol synthesis is induced and ppar alpha targets also differentially expressed between KO and WT.** **Keywords: Knockout gene expression study; genetic modification** **Overall design:** **Liver samples, 4 KO mice and 4 WT mice**

Background corr dist: **KL-Divergence = 0.0772, L1-Distance = 0.0214, L2-Distance = 0.0006, Normal std = 0.4812**

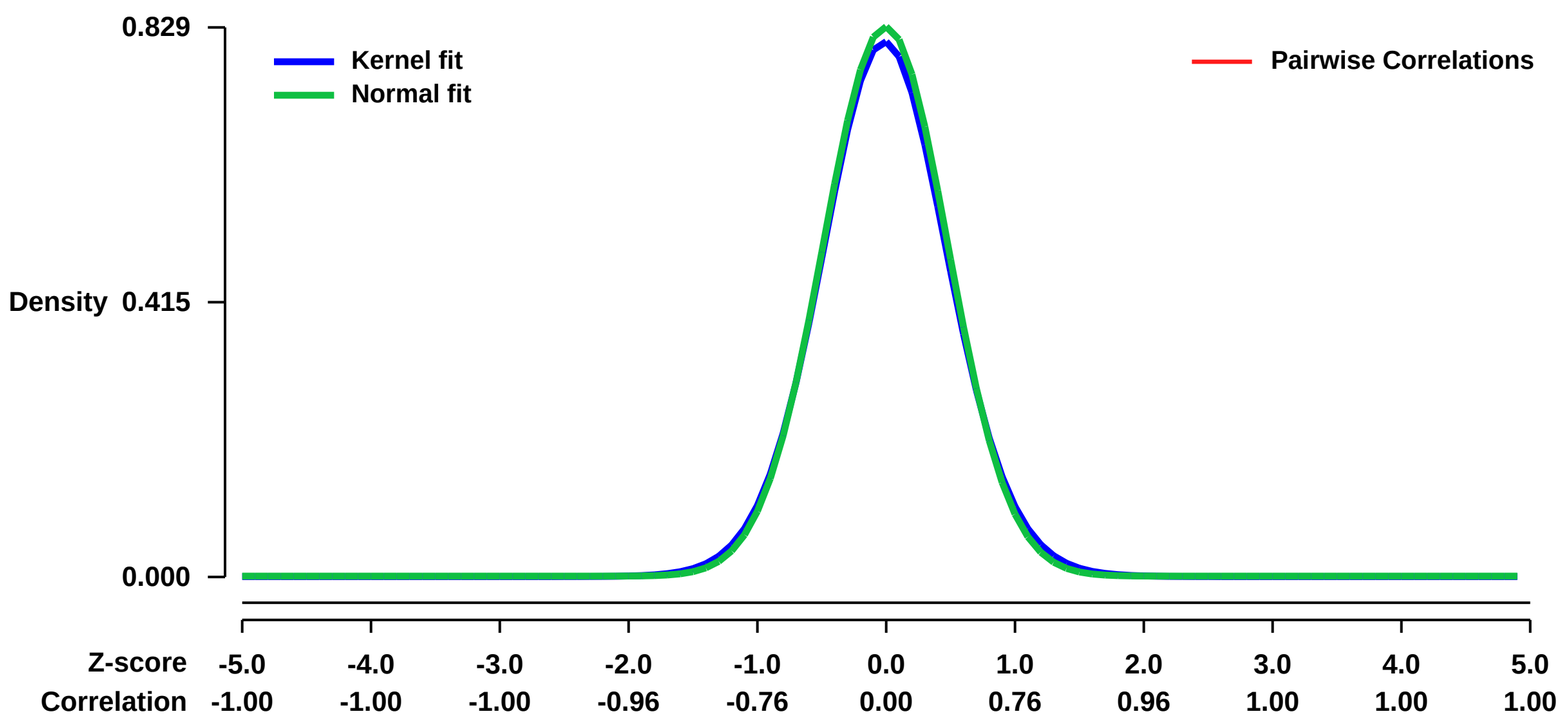

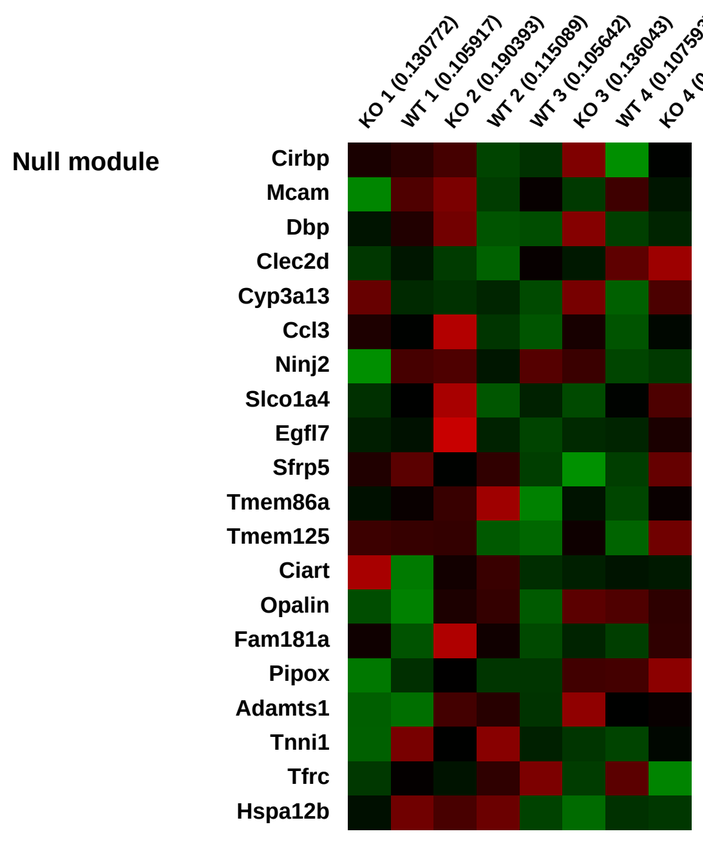

GEO Series "GSE9038" Expression Profiles

Num of samples in this series: 24

Scale of expression profile Z-scores

-3.0 -2.0 -1.0 0.0 1.0 2.0 3.0

GEO Link:	http://www.ncbi.nlm.nih.gov/geo/query/acc.cgi?acc=GSE9038
Status:	Public on Aug 23 2011
Title:	Gene expression profiles of striatum and cerebellum from knock-in mouse model of Huntington's disease
Organism:	Mus musculus
Experiment type:	Expression profiling by array
Platform:	GPL1261
Pubmed ID:	21840924
Summary & Design:	**Summary:** Huntingtonâ s disease (HD) involves marked early neurodegeneration in the striatum whereas the cerebellum is relatively spared despite the ubiquitous expression of full-length mutant huntingtin, implying that inherent tissue-specific differences determine susceptibility to the HD CAG mutation. To understand this tissue specificity, we compared early mutant huntingtin-induced gene expression changes in striatum to those in cerebellum in young Hdh CAG knock-in mice, prior to onset of evident pathological alterations. Endogenous levels of full-length mutant huntingtin caused qualitatively similar, but quantitatively different gene expression changes in the two brain regions. Importantly, the quantitatively different responses in striatum and cerebellum in mutant mice were well accounted for by the intrinsic molecular differences in gene expression between striatum and cerebellum in wild-type animals. Tissue-specific gene expression changes in response to the HD mutation, therefore, appear to reflect the different inherent capacities of these tissues to buffer qualitatively similar effects of mutant huntingtin. These findings highlight a role for intrinsic quantitative tissue differences in contributing to HD pathogenesis, and likely to other neurodegenerative disorders exhibiting tissue-specificity, thereby guiding the search for effective therapeutic interventions. **Overall design:** Total RNA was isolated from striatum and cerebellum of Hdh CAG knock-in mice (HdhQ111/HdhQ111) and wild-type mice (Hdh+/Hdh+, 3~10 weeks) for gene expression profiling using Affymetrix MG430 2.0 arrays.

Background corr dist: KL-Divergence = 0.0382, L1-Distance = 0.0736, L2-Distance = 0.0076, Normal std = 0.7672

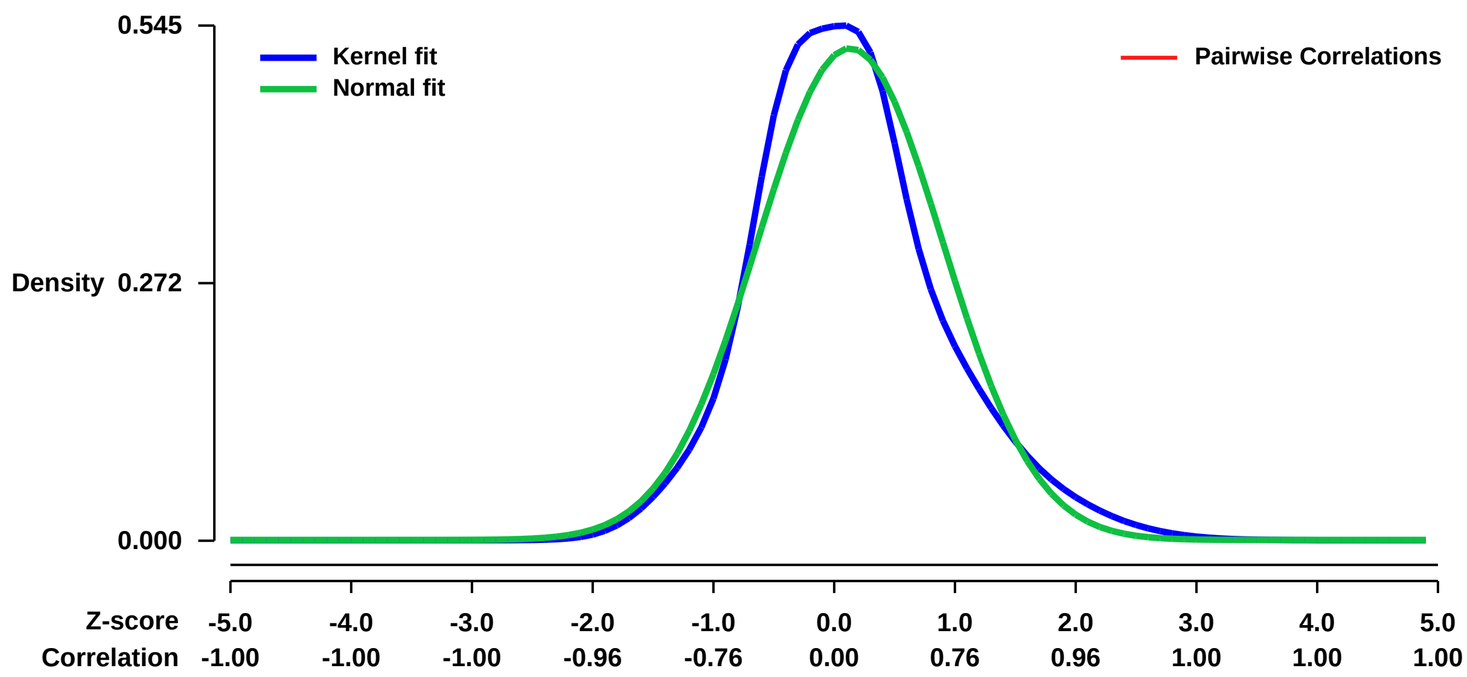

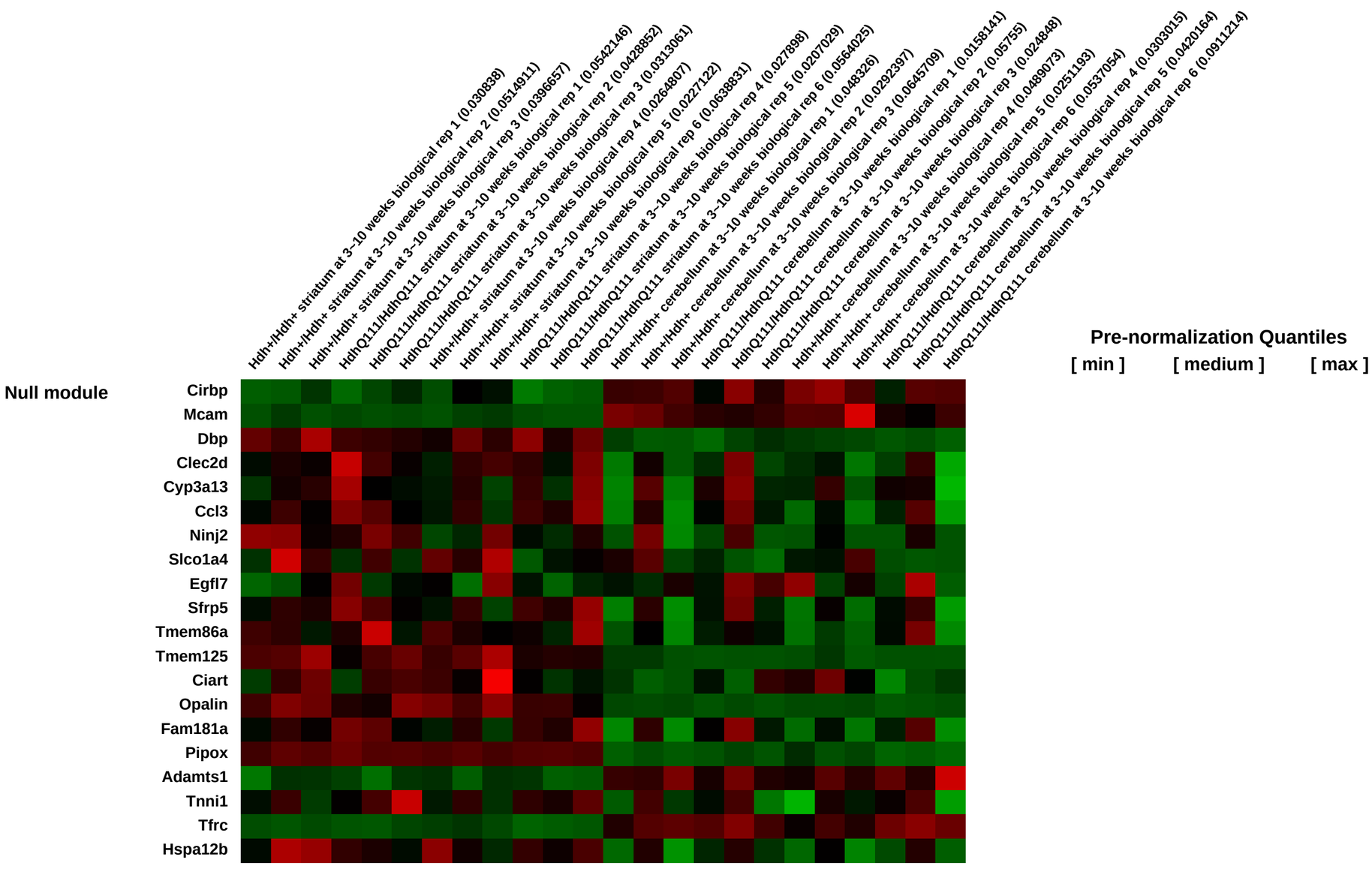

GEO Series "GSE29688" Expression Profiles

Num of samples in this series: 12

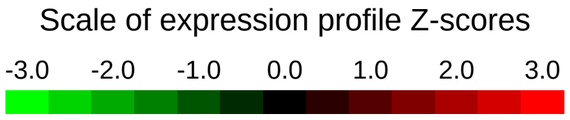

GEO Link:	**http://www.ncbi.nlm.nih.gov/geo/query/acc.cgi?acc=GSE29688**
Status:	**Public on May 30 2012**
Title:	**Tumor-stroma interaction between RCC cell lines and lung stroma in mouse xenografts**
Organism:	**Mus musculus**
Experiment type:	**Expression profiling by array**
Platform:	**GPL1261**
Pubmed ID:	**22665059**
Summary & Design:	**Summary:** **The leading cause of death in human patients with metastatic renal cell carcinoma (RCC) and malignant cancer in general is the dissemination of the primary tumor to secondary sites. The mechanisms by which RCC colonize the lung microenvironment during metastasis remain largely unknown. To investigate the mechanisms of lung colonization by tumor cells, we grafted human RCC cells with different lung metastatic activities in mice. Gene expression profiling of the mouse lung stromal compartment revealed a gene signature enriched for neutrophil-specific functions, induced preferentially by poorly metastatic cells. Analysis of the gene expression patterns in tumor cells and clinical specimens showed an inverse correlation between metastatic activity and the levels of a number of chemokines, including CXL5 ad IL8. Enforced depletion of CXCL5 and IL8 in tumor cells allowed us to establish a functional link between lung neutrophil infiltration, the secretion of chemokines by cancer cells and metastatic activity. Finally, we showed that human neutrophils displayed a higher cytotoxic activity toward poorly metastatic cells relative to highly metastatic cells. Together, these results support a model in which neutrophils recruited to the lung by tumor-secreted chemokines build an antimetastatic barrier and loss of those neutrophil chemokines in tumor cells is a critical rate-limiting step during lung metastatic seeding.** **Overall design:** **Total 12 samples are analysed from two cell lines (SN12C and LM2) and Normal tissue. There are four biological replicates for each cell line and four biological replicates from normal lung tissue (as reference).**

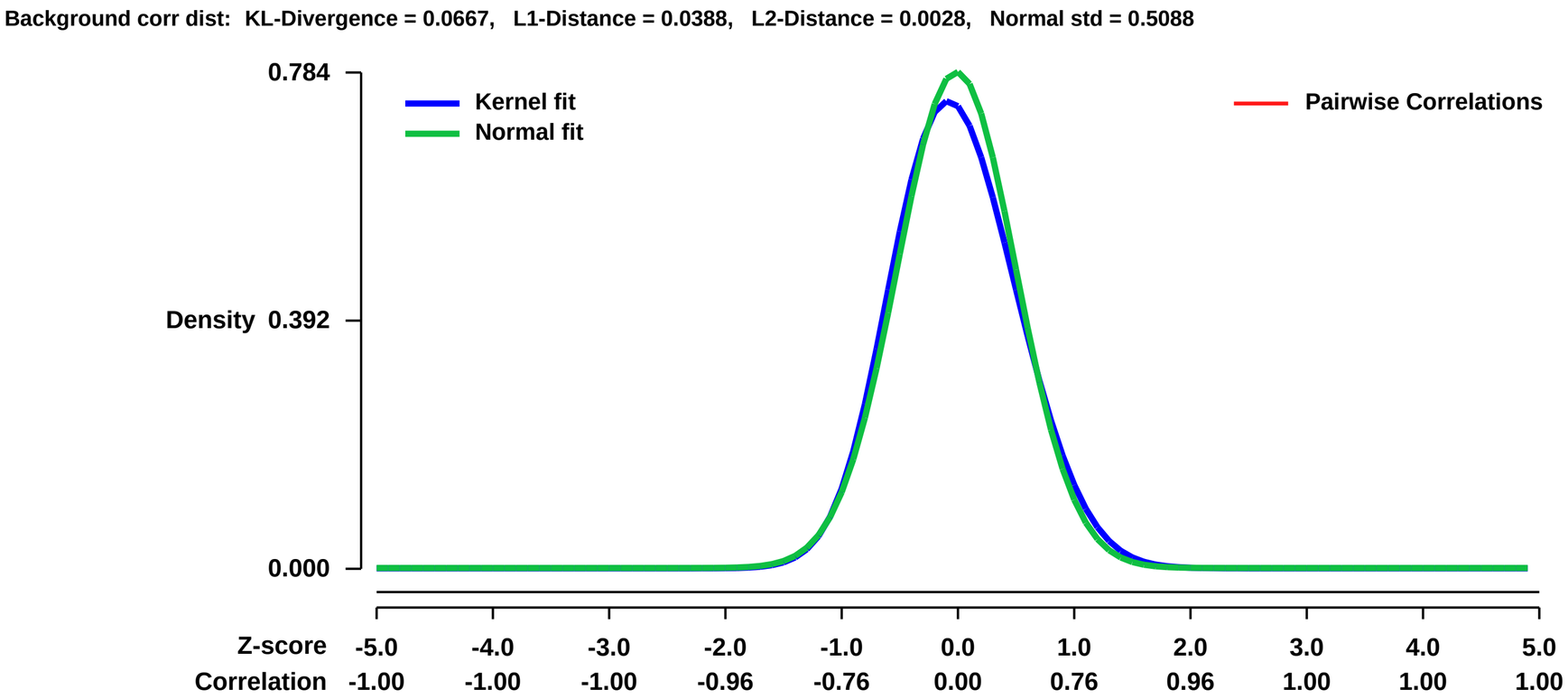

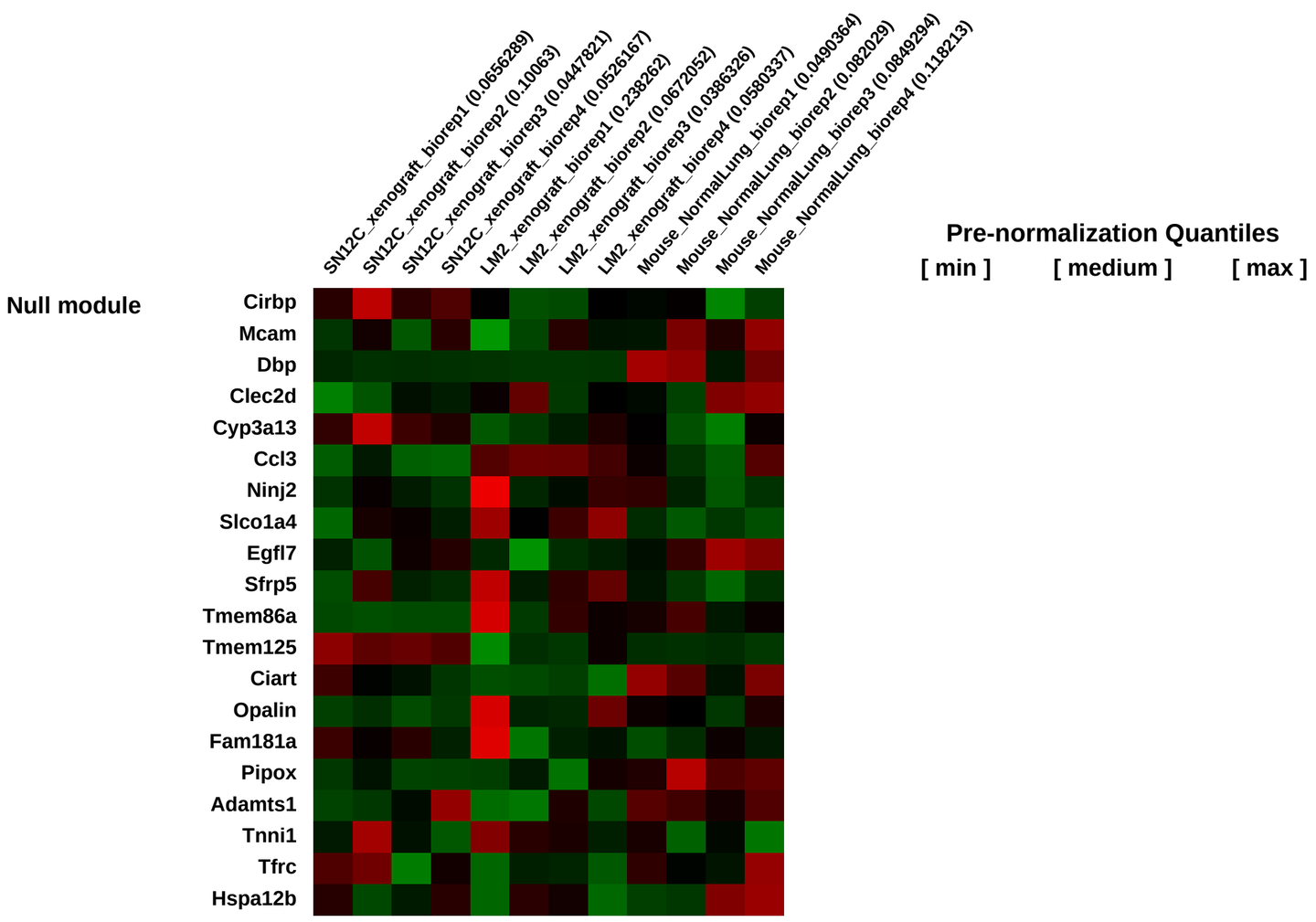

GEO Series "GSE12467" Expression Profiles

Num of samples in this series: 6

Scale of expression profile Z-scores

-3.0 -2.0 -1.0 0.0 1.0 2.0 3.0

GEO Link:	http://www.ncbi.nlm.nih.gov/geo/query/acc.cgi?acc=GSE12467
Status:	Public on Feb 20 2009
Title:	Differentially regulated genes in control and c-myc N-myc deficient LT-HSCs
Organism:	Mus musculus
Experiment type:	Expression profiling by array
Platform:	GPL1261
Pubmed ID:	19041778
Summary & Design:	**Summary:** Analysis of HSCs from control and c-myc N-myc deficient long-term hematopoietic stem cells. HSCs lacking both c-myc and N-myc display increased apoptosis rates. Data provide insight into the molecular changes occuring upon complete loss of Myc activity, clarifying the resulting apoptotic mechanism and the role of Myc family proteins in HSCs. **Overall design:** LT-HSC (Lin-Sca1+CD150+CD48-) cells were sorted from the BM of MxCre c-myc flox2 N-myc flox2 (experimental) and c-myc flox2 N-myc flox2 (control) mice 3 days after the last pI-pC injection. Each condition was analysed in triplicates, with each replicate consisting of a pool of 3 dKO mice or 2 control mice.

Background corr dist: KL-Divergence = 0.0377, L1-Distance = 0.0208, L2-Distance = 0.0005, Normal std = 0.6297

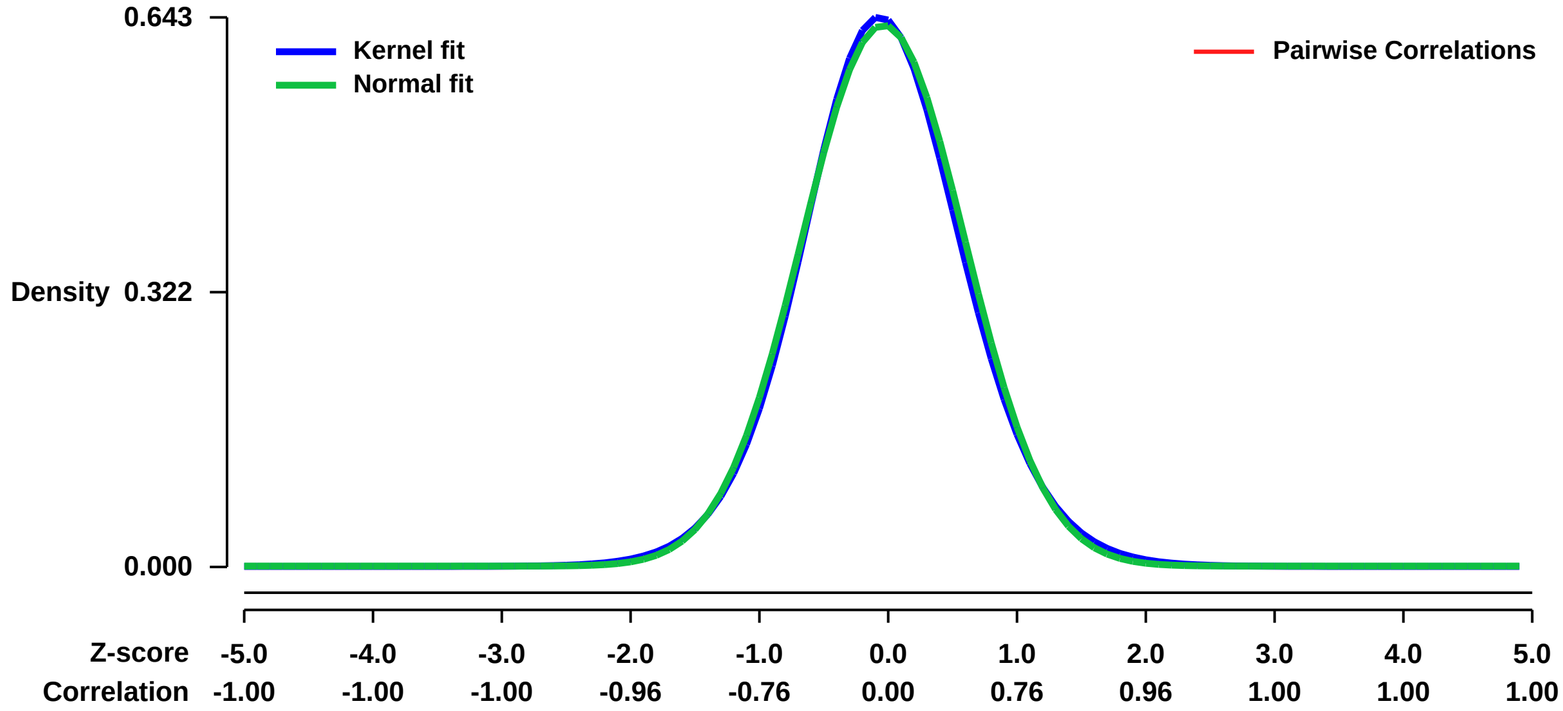

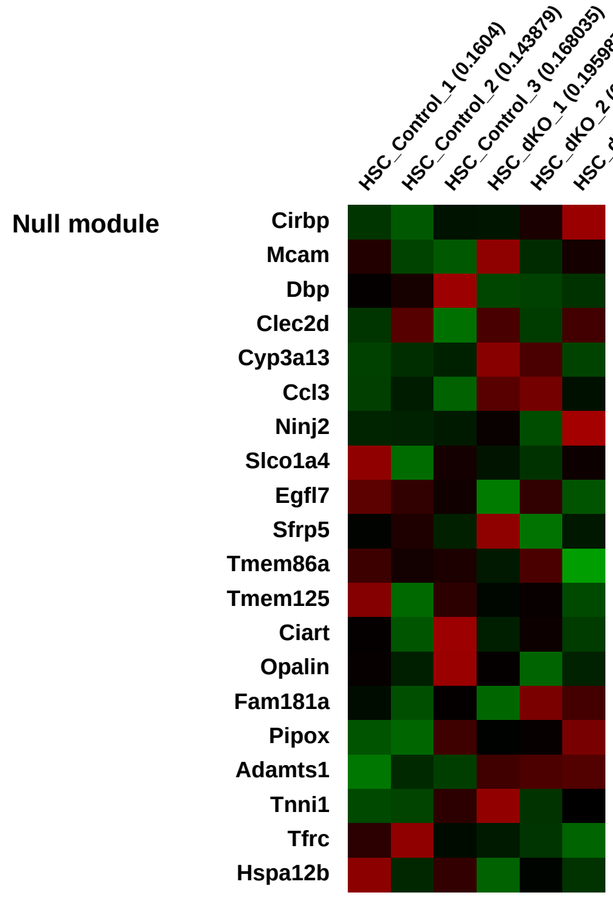

GEO Series "GSE27901" Expression Profiles

Num of samples in this series: 23

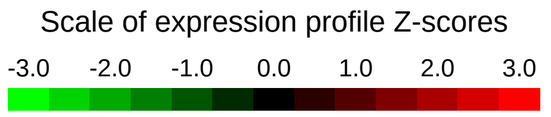

GEO Link:	http://www.ncbi.nlm.nih.gov/geo/query/acc.cgi?acc=GSE27901
Status:	Public on May 13 2011
Title:	Transactivation-deficient p53 Mutants in Ras-induced Cellular Senescence
Organism:	Mus musculus
Experiment type:	Expression profiling by array
Platform:	GPL1261
Pubmed ID:	21565614
Summary & Design:	**Summary:** As a critical cellular stress sensor, p53 mediates a variety of defensive processes including cell-cycle arrest, apoptosis, and senescence to prevent propagation of hyperproliferative cells or cells with a damaged genome, hence the formation of neoplasia. Transactivation of downstream genes plays an important while sometimes controversial role in regulating these cellular processes. To evaluate the dependence on transcriptional activation in p53â s activities, we generated genetically-modified mouse lines carrying mutations in the transactivation domains (TADs) of p53. These transactivatio-deficient mutants serve as unique reagents to probe the dependence on robust transactivation in p53-mediated cellular functions, as well as the underneath mechanisms. To identify genes differentially regulated by these p53 mutants, we performed gene expression profiling analysis on mouse embryonic fibroblast cells (MEFs) from these mice in the context of oncogenic Ras-induced premature cellular senescence. **Overall design:** Mouse embryonic fibroblasts (MEFs) with different p53 genotypes were infected with retroviral H-Ras V12, which induces premature cellular senescence in p53 wild-type MEFs but not in p53 null MEFs. 5 genotypic groups of MEFs were used in the study: (i) p53L25Q/W26S, or ""25,26"", in which the first TAD (transactivation domain) of p53 is disrupted by the mutation, 5 biological samples; (ii) p53W53Q/F54S, or ""53,54"", in which the second TAD of p53 is disrupted by the mutation, 3 biological samples; (iii) p53L25Q/W26S/W53Q/F54S, or ""QM"", in which both TADs or p53 are disrupted, 3 biological samples; (iv) p53 wild-type, or ""WT"", 6 biological samples; (v) p53 null, or ""Null"", 6 biological samples.

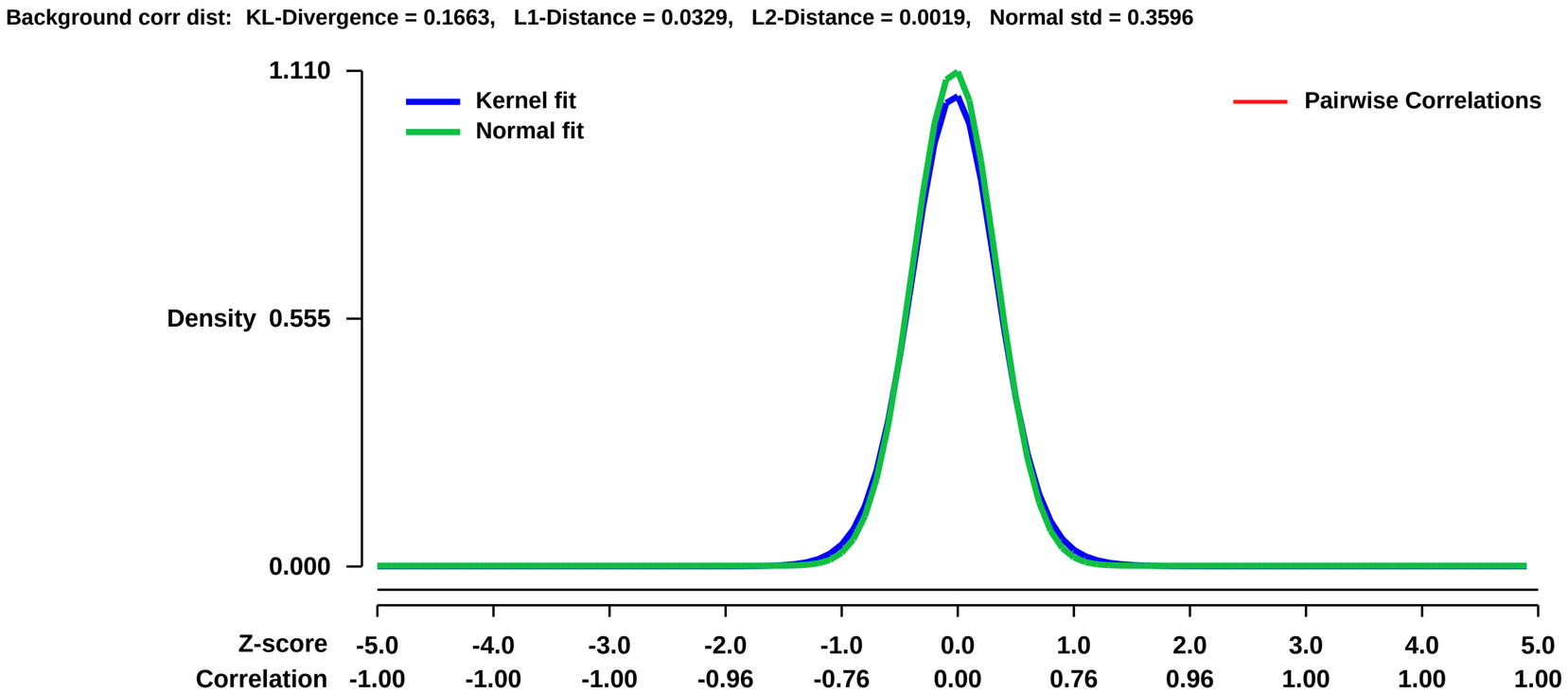

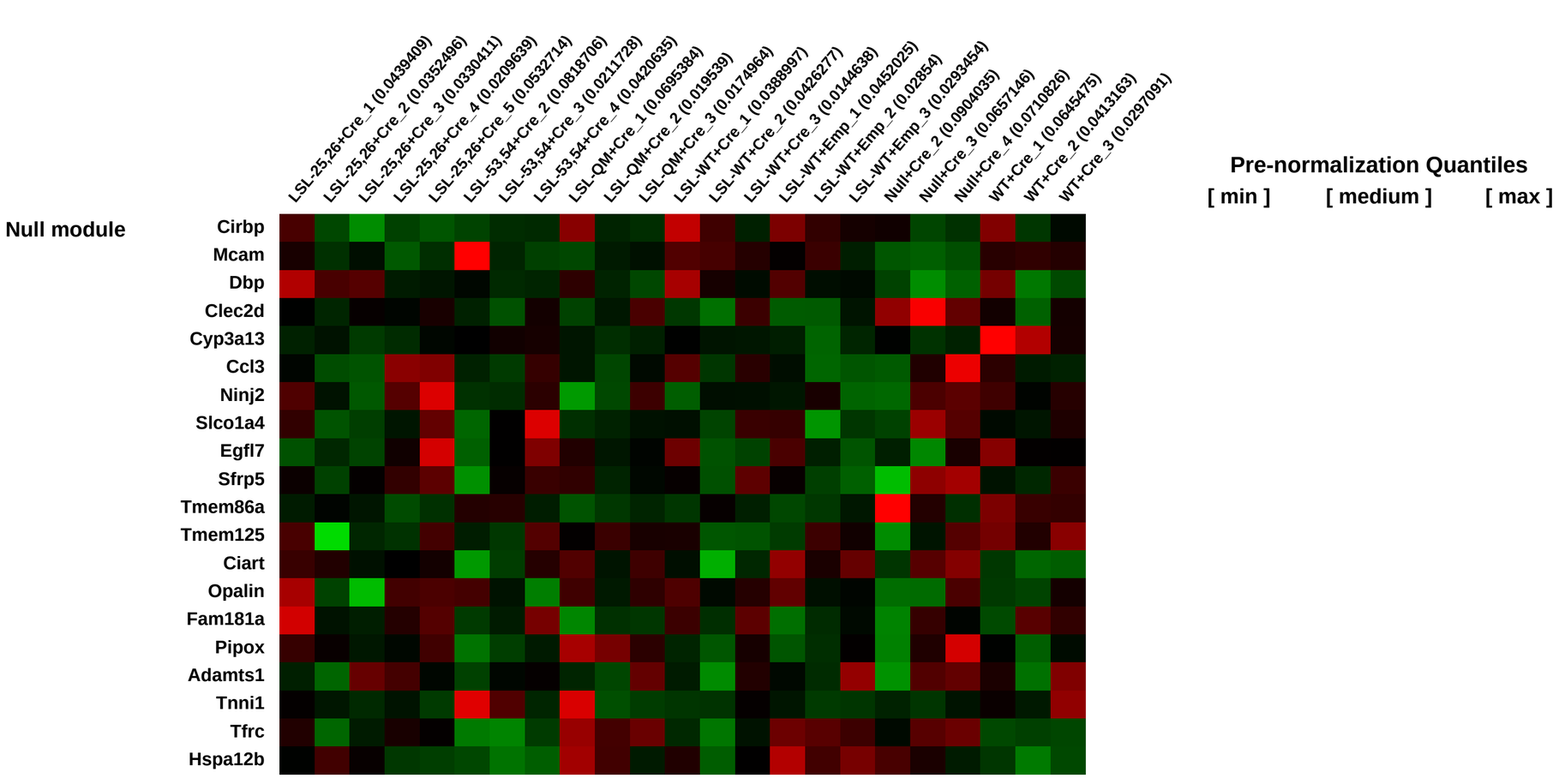

GEO Series "GSE31638" Expression Profiles

Num of samples in this series: 15

Scale of expression profile Z-scores

-3.0 -2.0 -1.0 0.0 1.0 2.0 3.0

GEO Link:	http://www.ncbi.nlm.nih.gov/geo/query/acc.cgi?acc=GSE31638
Status:	Public on Aug 31 2011
Title:	Expression data from primary hepatocytes knocking down or overexpressing IRE1a
Organism:	Mus musculus
Experiment type:	Expression profiling by array
Platform:	GPL1261
Pubmed ID:	21911379
Summary & Design:	**Summary:** The ER-resident protein kinase/endoribonuclease IRE1 is activated through trans-autophosphorylation in response to protein folding overload in the ER lumen and maintains ER homeostasis by triggering a key branch of the unfolded protein response. Here we show that mammalian IRE1a in liver cells is also phosphorylated by a kinase other than itself in response to metabolic stimuli. Glucagon stimulated protein kinase PKA, which in turn phosphorylated IRE1a at Ser724, a highly conserved site within the kinase activation domain. Blocking Ser724 phosphorylation impaired the ability of IRE1a to augment the upregulation by glucagon signaling of the expression of gluconeogenic genes. Moreover, hepatic IRE1a was highly phosphorylated at Ser724 by PKA in mice with obesity, and silencing hepatic IRE1a markedly reduced hyperglycemia and glucose intolerance. Hence, these results suggest that IRE1a integrates signals from both the ER lumen and the cytoplasm in the liver and is coupled to the glucagon signaling in the regulation of glucose metabolism. We used DNA microarray to analyze the transcriptomic change upon IRE1a overexpression or IRE1a depletion in primary hepatocytes, to study the changes related to IRE1a **Overall design:** Primary hepatocytes were infected with the desired adenoviruses (Ad-EGFP, Ad-WT, Ad-S724A, Ad-shCON, Ad-shIRE1a#2) or treated with glucagon. Total cellular RNA was isolated with TRIzol (Invitrogen) and subjected to analysis by Affymetrix Mouse Genome 430 2.0 Arrays. Three experiments were independently conducted.

Background corr dist: KL-Divergence = 0.1161, L1-Distance = 0.0361, L2-Distance = 0.0027, Normal std = 0.4128

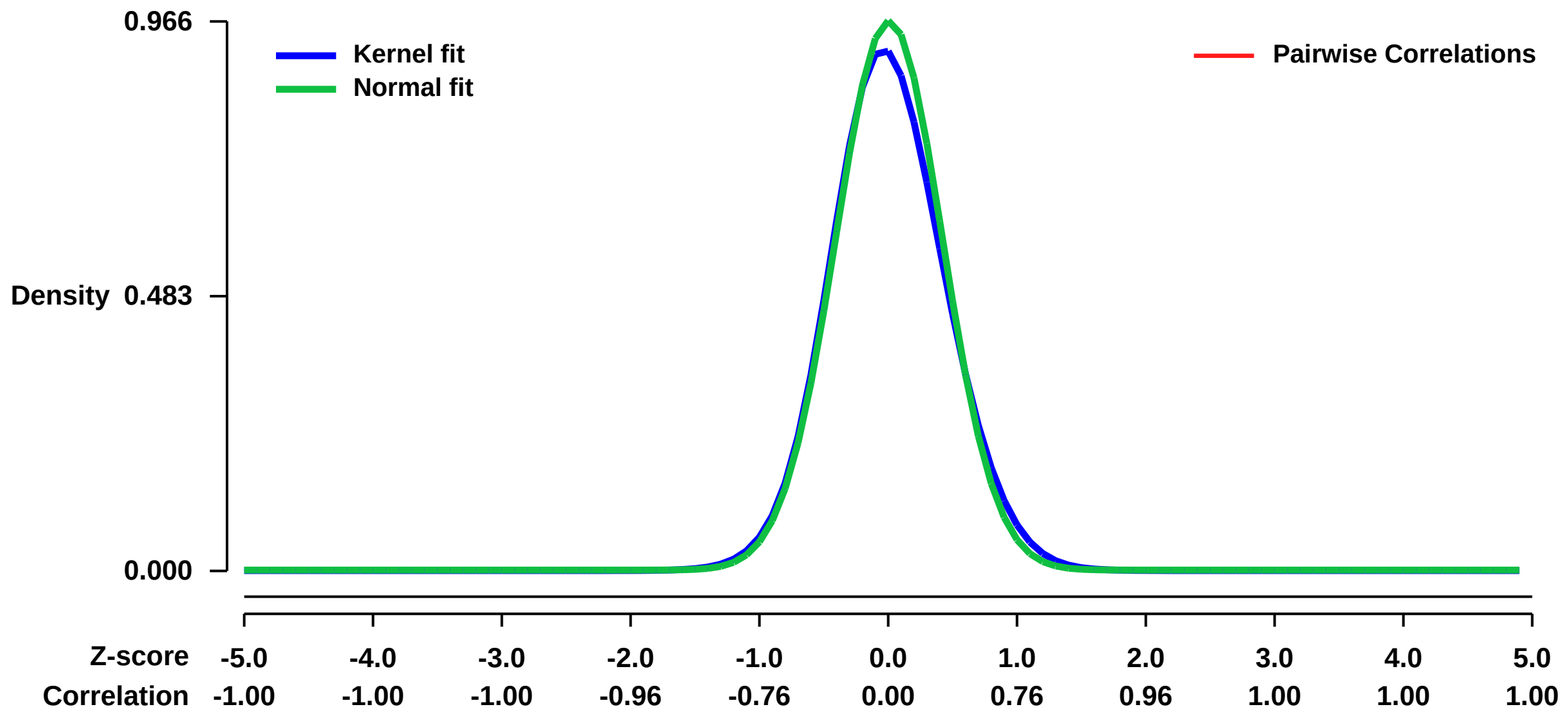

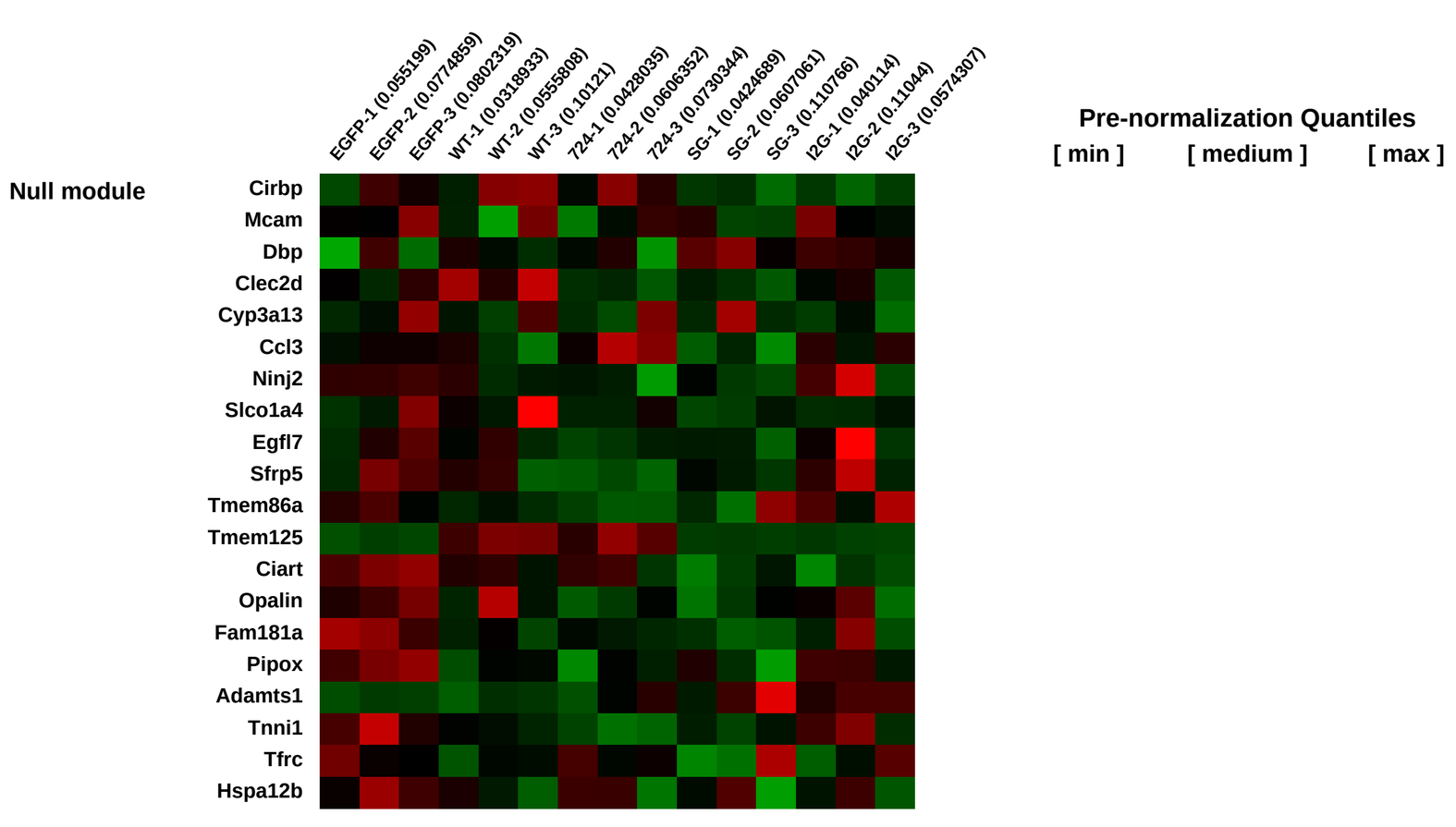

GEO Series "GSE48204" Expression Profiles

Num of samples in this series: 6

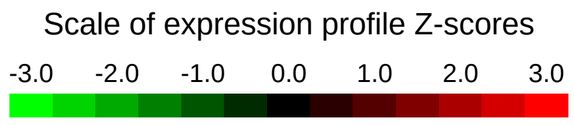

GEO Link:	http://www.ncbi.nlm.nih.gov/geo/query/acc.cgi?acc=GSE48204
Status:	Public on Jul 26 2013
Title:	Gene expression in epithelial, EMT (epithelial-mesenchymal transition) and MET (mesenchymal-epithelial transition) cells
Organism:	Mus musculus
Experiment type:	Expression profiling by array
Platform:	GPL1261
Pubmed ID:	23878399
Summary & Design:	**Summary:** NMuMG is an epithelial cell line that can be induced into EMT by TGF-¸† treatment or MET by TGF-¸† withdrawl. During EMT, several marker genes were downregulated/upregulated, which is consistent with its mesenchymal phenotype. Transcription factors that are regulated during EMT and its reverse process MET are candidate genes for the regulations of the EMT marker genes. **Overall design:** NMuMG cells treated with vehicle, TGF-¸† for 11 days, or 11days of TGF-¸† treatment followed by TGF-¸† withdrawl for another 13 days. RNA from these 3 conditions of NMuMG were extracted and subject to microarray analysis

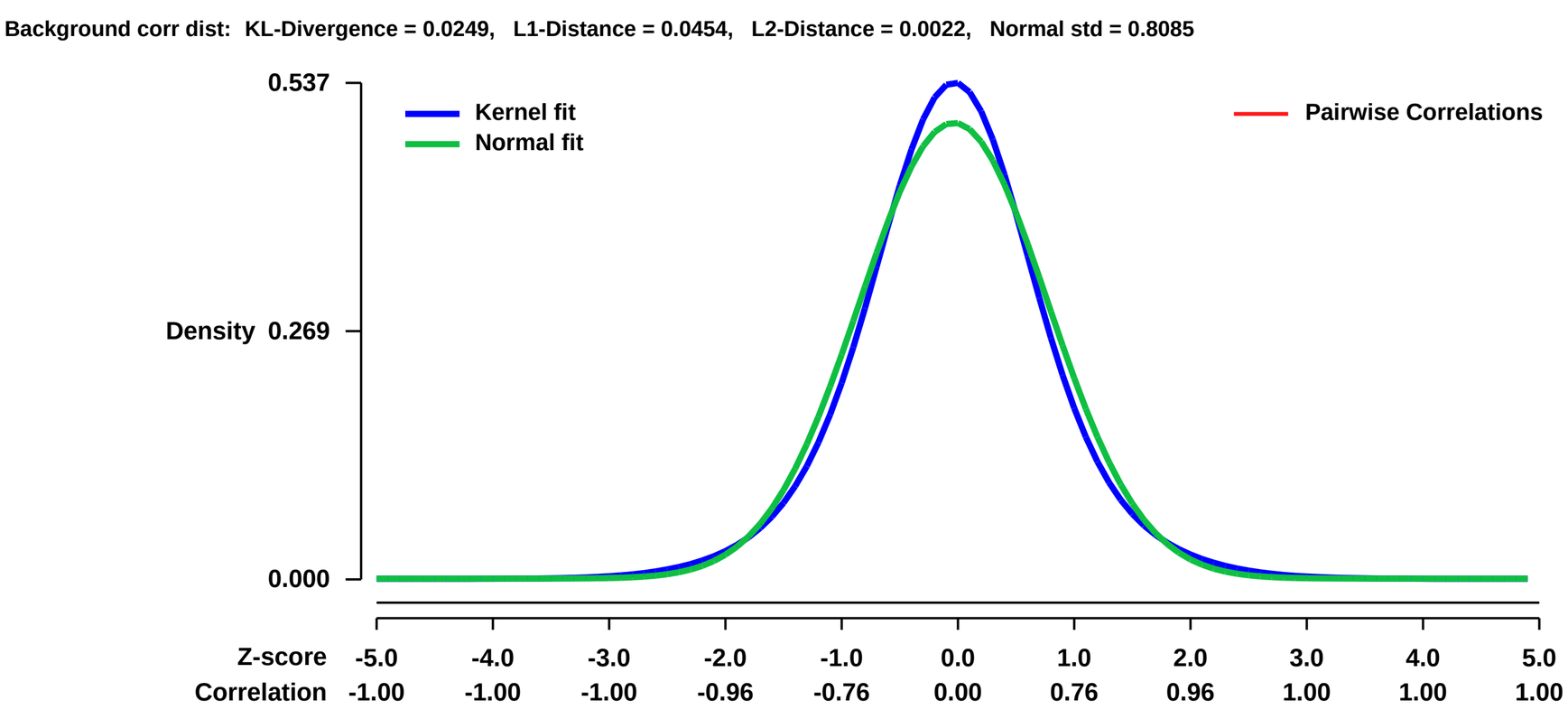

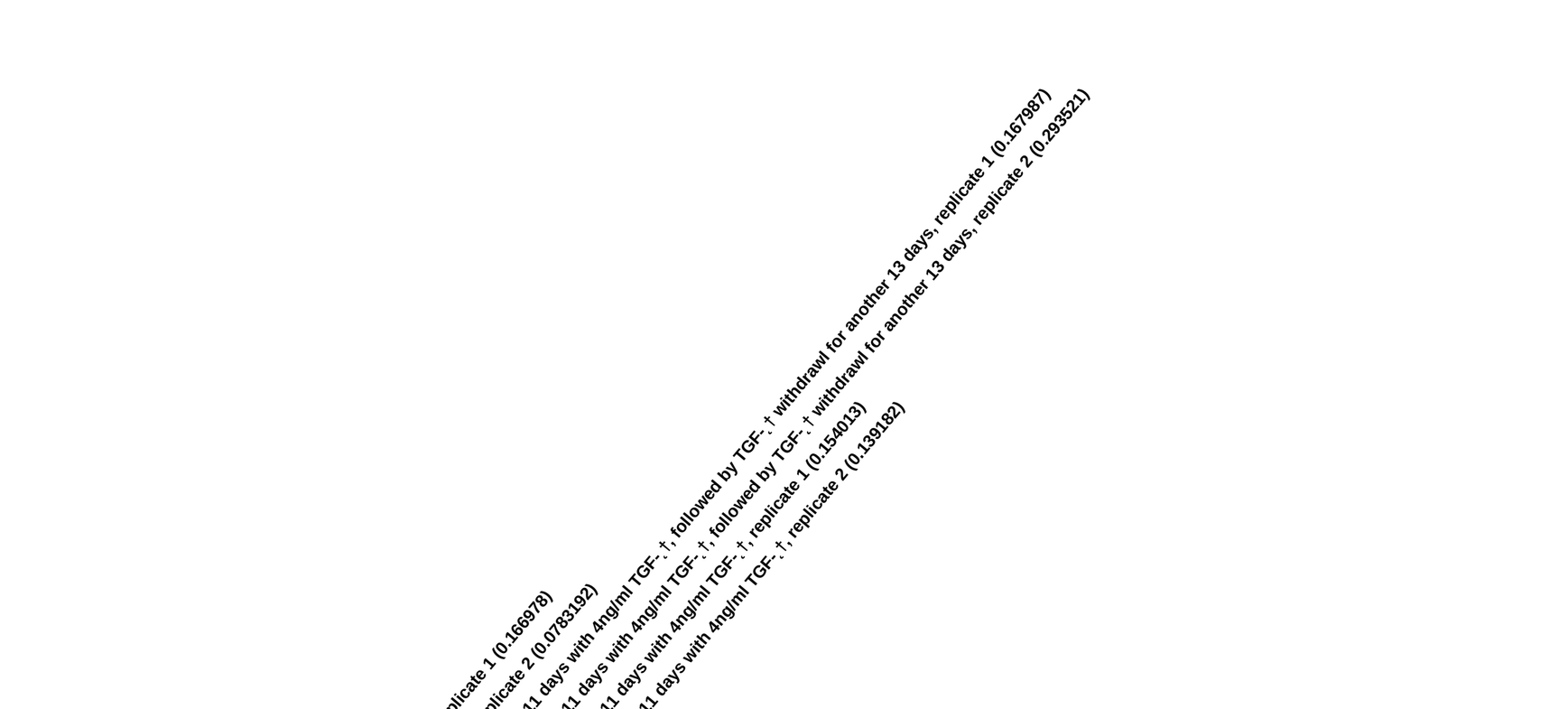

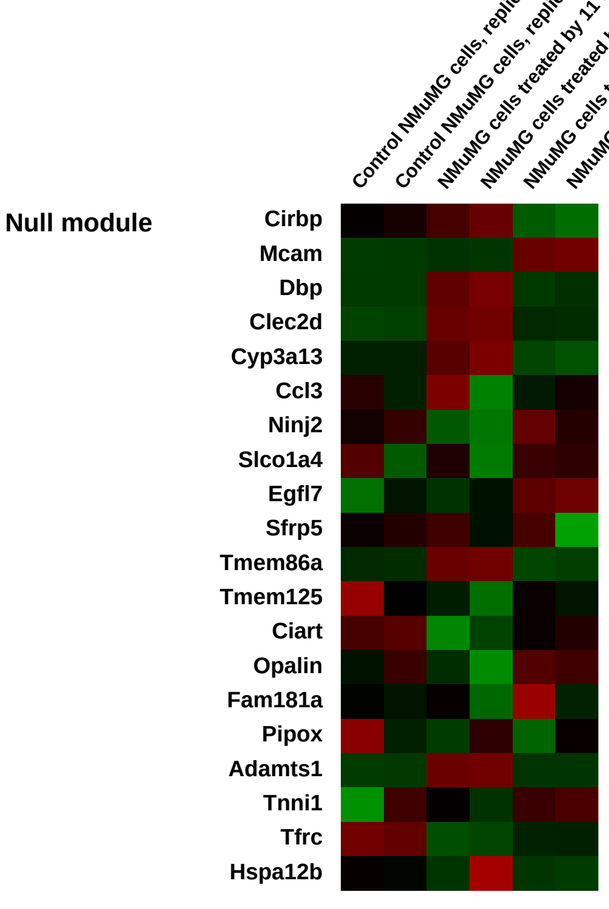

GEO Series "GSE5671" Expression Profiles

Num of samples in this series: 18

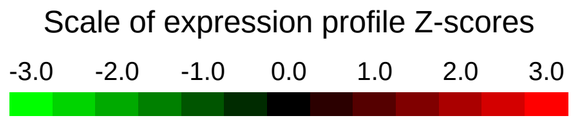

GEO Link:	http://www.ncbi.nlm.nih.gov/geo/query/acc.cgi?acc=GSE5671
Status:	Public on Aug 30 2007
Title:	Cardiac differentiation of embryonic stem cells recapitulates embryonic cardiac development.
Organism:	Mus musculus
Experiment type:	Expression profiling by array
Platform:	GPL1261
Pubmed ID:	18246200
Summary & Design:	**Summary:** Mouse embryonic stem cells can differentiate in vitro into spontaneously contracting cardiomyocytes. The main objective of this study was to investigate cardiogenesis in cultures of differentiating embryonic stem cells (ESCs) and to determine how closely it mimics in vivo cardiac development. We identified and isolated a population of cardiac progenitor cells (CPCs) through the use of a reporter DNA construct that allowed the expression of a selectable marker under the control of the Nkx2.5 enhancer. We proceeded to characterize these CPCs by examining their capacity to differentiate into cardiomyocytes and to proliferate. We then performed a large-scale temporal microarray expression analysis in order to identify genes that are uniquely upregulated or downregulated in the CPC population. We determined that the transcriptional profile of the mESC derived CPCs was consistent with pathways known to be active during embryonic cardiac development. We conclude that in vitro differentiation of mESCs recapitulates the early steps of mouse cardiac development. **Keywords:** embryonic stem cell, differentiation, cardiac progenitor, cardiogenesis **Overall design:** The Spotfire DecisionSite software package was used for the identification of uniquely upregulated or downregulated (at least 1.5 times increase or decrease in the expression value) probe sets in the CPC population when compared to the rest of the cells in the differentiating EBs. Probe sets that were considered unique for the CPC population were found to be commonly upregulated or downregulated during all four days of analysis. Probe sets that exhibited an increasing or decreasing pattern of expression with at least 1.5 times increase or decrease in the expression values of day 5 CPCs and day 8 CPCs were also reported. Probe sets of the CPC population that exhibited upregulation or downregulation by at least 1.5 times when compared to the mESC derived cardiomyocytes were also reported. The final analysis included probe sets that exhibited a different temporal pattern of expression in the CPC population when compared to the rest of the cells along the four days of differentiation. Specifically in order to identify these probe sets gene expression curve over time was modeled flexibly

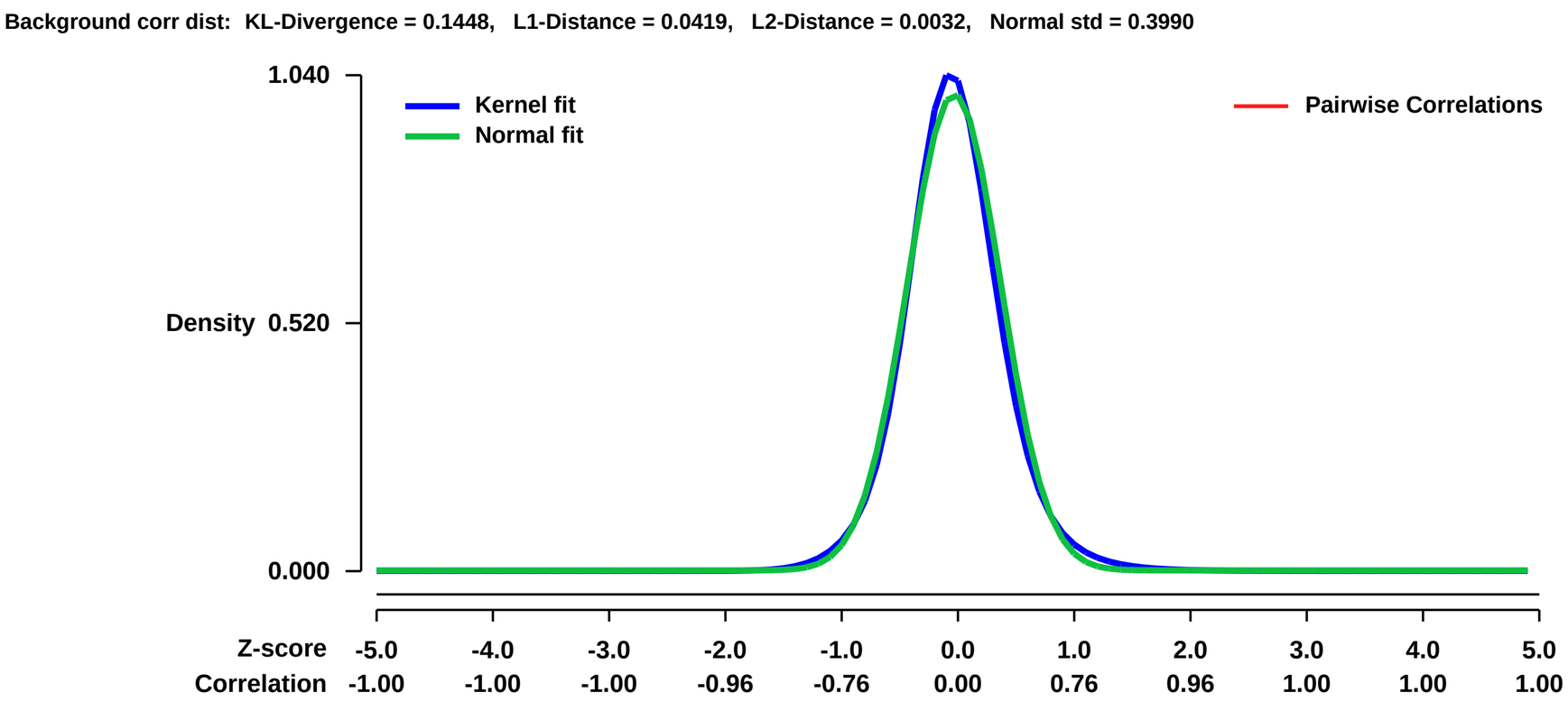

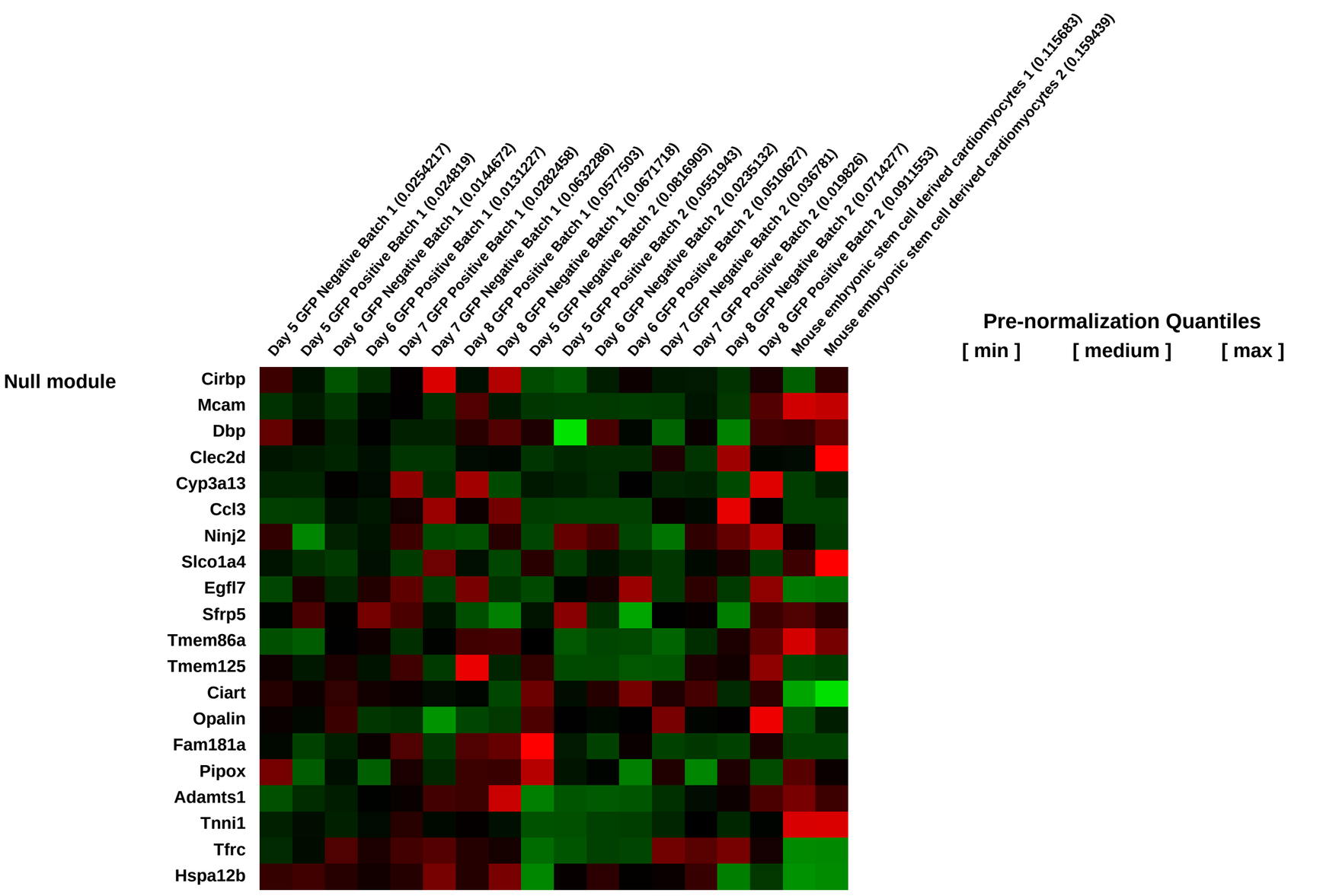

GEO Series "GSE41342" Expression Profiles

Num of samples in this series: 26

Scale of expression profile Z-scores

-3.0 -2.0 -1.0 0.0 1.0 2.0 3.0

GEO Link:	http://www.ncbi.nlm.nih.gov/geo/query/acc.cgi?acc=GSE41342
Status:	Public on Nov 01 2012
Title:	Data from a time course study of gene expression in a mouse model of osteoarthritis
Organism:	Mus musculus
Experiment type:	Expression profiling by array
Platform:	GPL1261
Pubmed ID:	23382930
Summary & Design:	**Summary:** The purpose of this study was to characterize the histologic development of OA in a mouse model where OA is induced by destabilization of the medial meniscus (DMM model) and to identify genes regulated during different stages of the disease, using RNA isolated from the joint â organâ and analyzed using microarrays.427 genes from the microarrays passed consistency and significance filters. There was an initial up-regulation at 2 and 4 weeks of genes involved in morphogenesis, differentiation, and development, including growth factor and matrix genes, as well as transcription factors including Atf2, Creb3l1, and Erg. Most genes were off or down-regulated at 8 weeks with the most highly down-regulated genes involved in cell division and the cytoskeleton. Gene expression increased at 16 weeks, in particular extracellular matrix genes including Prelp, Col3a1 and fibromodulin.The results support a phasic development of OA with early matrix remodelling and transcriptional activity followed by a more quiescent period that is not maintained. **Overall design:** RNA was pooled prior to microarray analysis such that 3 randomly selected samples from each surgical group and time point were pooled to create each biological replicate. Because 9 mice were used for each experimental group, a total of three biological replicates per group were analyzed using the Affymetrix Mouse Genome 430 2.0 oligonucleotide arrays as described. One replicate pool, which was from week two DMM mice, did not meet the RNA integrity level needed for microarray analysis; thus, this pool was not analyzed further, leaving two pools for the week two DMM mice.

Background corr dist: KL-Divergence = 0.1052, L1-Distance = 0.0242, L2-Distance = 0.0007, Normal std = 0.4325

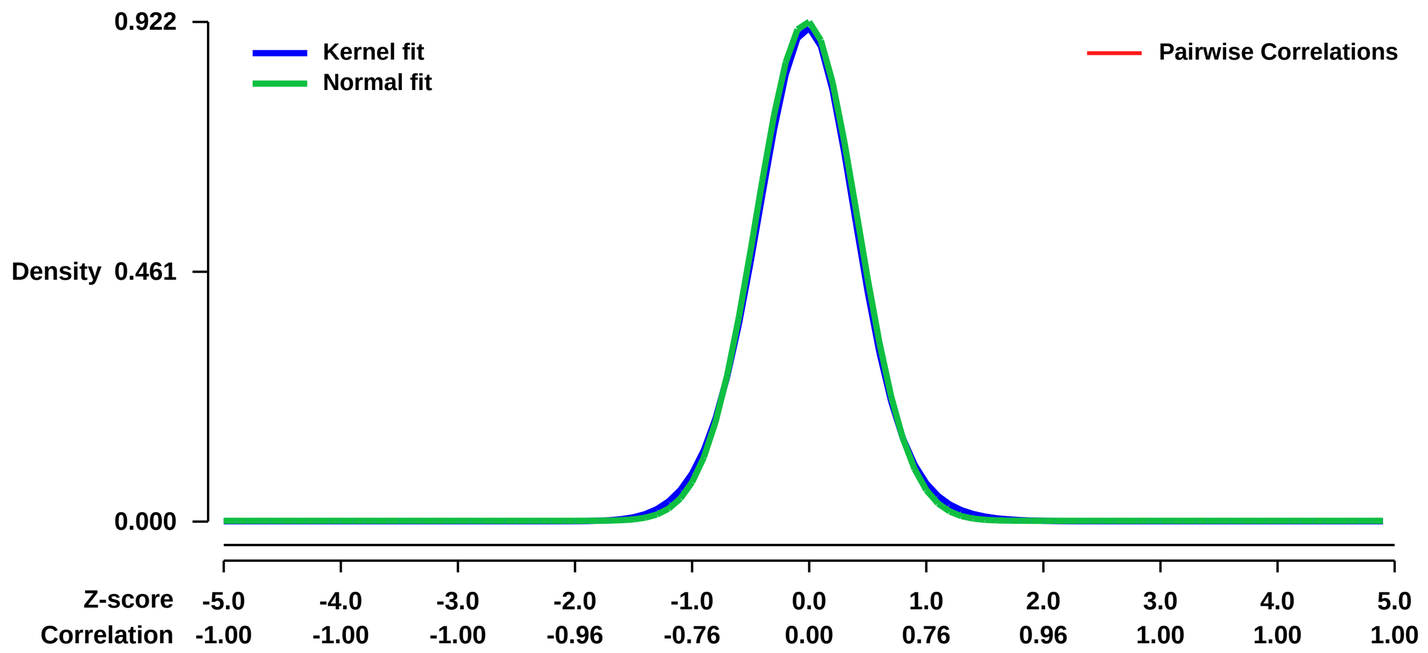

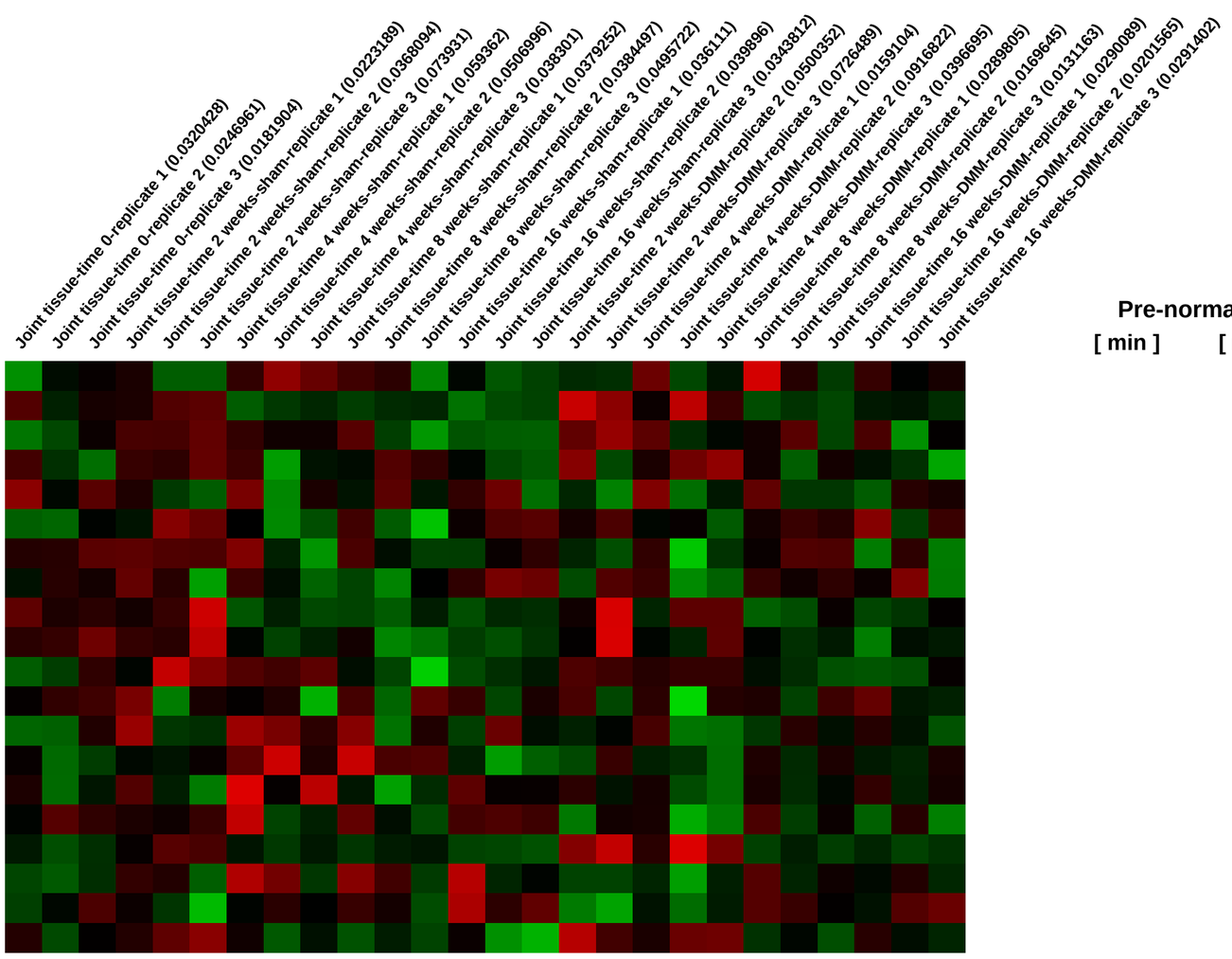

GEO Series "GSE13963" Expression Profiles

Num of samples in this series: 15

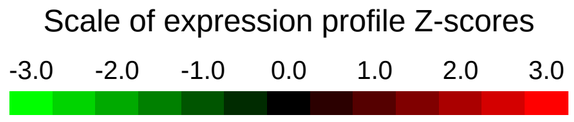

GEO Link:	http://www.ncbi.nlm.nih.gov/geo/query/acc.cgi?acc=GSE13963
Status:	Public on Mar 07 2011
Title:	Molecular characterization of lung dysplasia induced by c-raf-1
Organism:	Mus musculus
Experiment type:	Expression profiling by array
Platform:	GPL1261
Pubmed ID:	19529782
Summary & Design:	**Summary:** **Background: Lung cancer is a multistage process with poor prognosis and high morbidity. Importantly, the genetics of dysplasia, a facultative cancer, at the edge of malignant transformation is unknown.** **Results: We employed laser microdissection to harvest dysplastic as opposed to transgenic but otherwise morphologically unaltered epithelium and compared findings to non-transgenic lung. We then employed microarrays to search genome wide for gene regulatory networks. A total of 120 and 287 genes were significantly regulated, respectively. Dysplasia was exclusive associated with up-regulation of genes coding for cell growth and proliferation, cell-to-cell signalling and interaction, lipid metabolism, development, and cancer. Likewise, when dysplasia was compared with non-transgenic cells up-regulation of cancer associated genes, tight junction proteins, xenobiotic defence and developmental regulators was observed. We additionally confirmed regulation of some genes by immunohistochemistry and therefore demonstrate good concordance between gene regulation and coded protein.** **Conclusion: Our study identified transcriptional networks at successive stages of tumor-development, i.e. from histological unaltered but transgenic lungs to nuclear atypia. Our animal model revealed interesting and novel candidate genes and pathways that provide clues on the mechanism forcing respiratory epithelium into dysplasia and subsequently cancer, some of which might also be useful in the molecular imaging and flagging of early stages of disease.** **Overall design:** **In our study, we used predominately 5 month old mice to gain information at an early stage of tumor development where isolated foci of transformed cells in distinct areas of the lung are visible. By use of laser microdissection pressure catapulting (LMPC) dysplastic cells in well defined lesions [18] could be isolated. Dysplastic lesions were than compared with transgenic but otherwise normal cells or tumor cells. We applied whole genome microarrays to determine differentially expressed genes as to identify the gene regulatory networks associated with dysplasia and, as will be reported in a second part of our study, the subsequent malignant transformation. Overall, our study revealed interesting and novel genes and pathways that may contribute to the early stages of lung cancer development many of which are worthy for their exploration as candidate biomarkers and for molecular imaging of early stages of disease.**

Background corr dist: **KL-Divergence = 0.0972, L1-Distance = 0.0370, L2-Distance = 0.0020, Normal std = 0.4603**

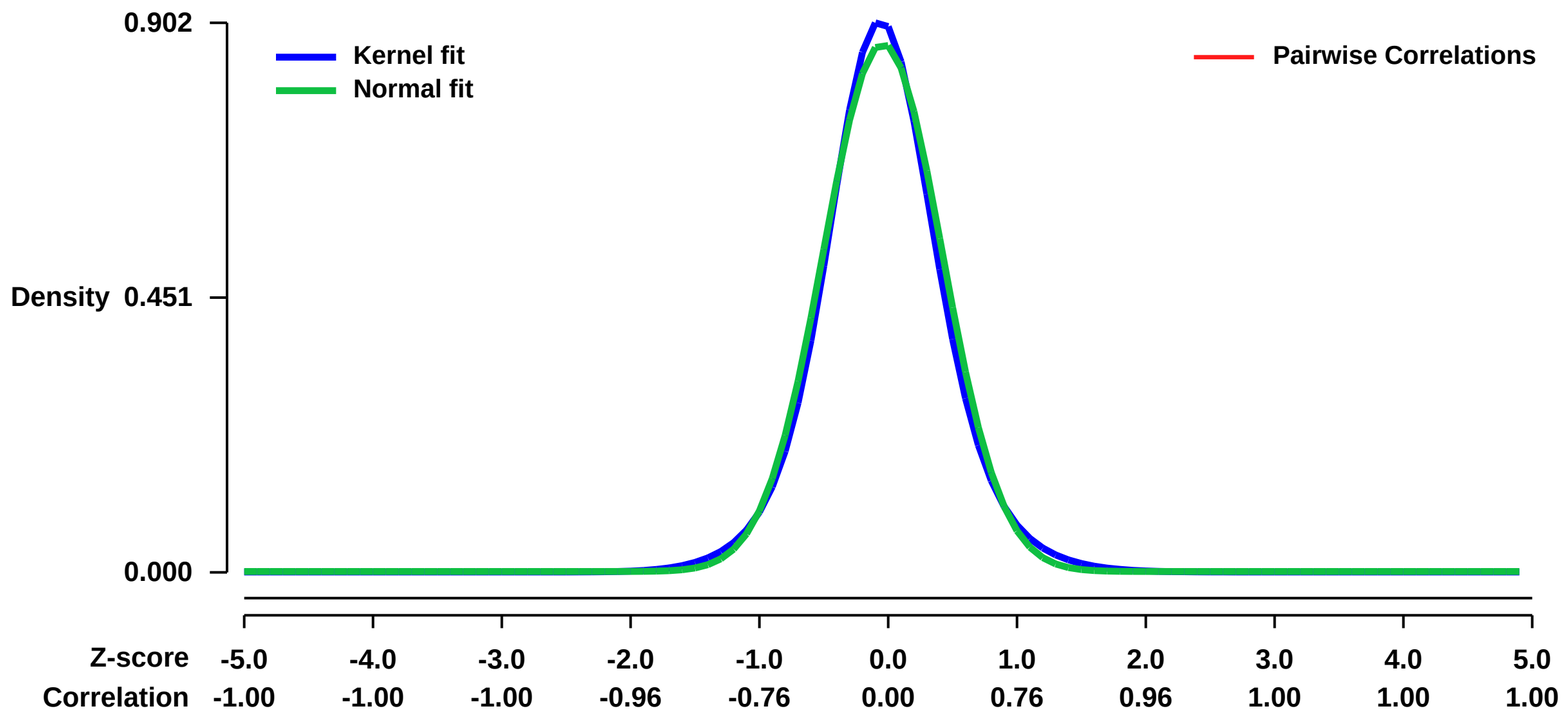

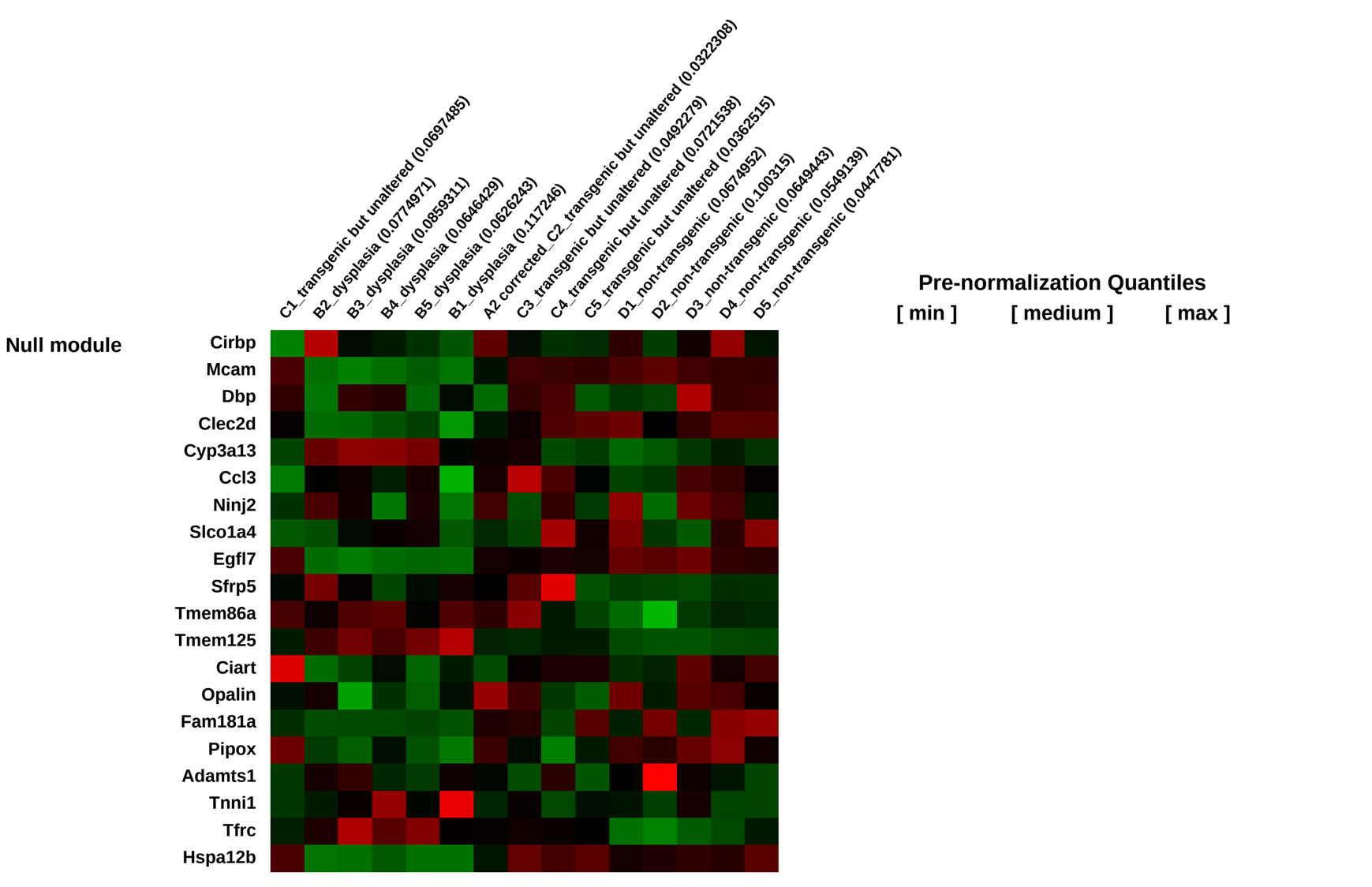

GEO Series "GSE22871" Expression Profiles

Num of samples in this series: 30

Scale of expression profile Z-scores

-3.0 -2.0 -1.0 0.0 1.0 2.0 3.0

GEO Link:	http://www.ncbi.nlm.nih.gov/geo/query/acc.cgi?acc=GSE22871
Status:	Public on Oct 01 2010
Title:	Expression data from wild-type and PPARalpha-null mice exposed to perfluorooctane sulfonate (PFOS)
Organism:	Mus musculus
Experiment type:	Expression profiling by array
Platform:	GPL1261
Pubmed ID:	20936131
Summary & Design:	**Summary:** Perfluorooctane sulfonate (PFOS) is a perfluoroalkyl acid (PFAA) and a persistent environmental contaminant found in the tissues of humans and wildlife. Although blood levels of PFOS have begun to decline, health concerns remain because of the long half-life of PFOS in humans. Like other PFAAs, such as perfluorooctanoic acid (PFOA), PFOS is an activator of peroxisome proliferator-activated receptor-alpha (PPARˌ–) and exhibits hepatocarcinogenic potential in rodents. PFOS is also a developmental toxicant in rodents where, unlike PFOA, itâ s mode of action is independent of PPARˌ–. Wild-type (WT) and PPARˌ–-null (Null) mice were dosed with 0, 3, or 10 mg/kg/day PFOS for 7 days. Animals were euthanized, livers weighed, and liver samples collected for histology and preparation of total RNA. Gene profiling was conducted using Affymetrix 430_2 microarrays. In WT mice, PFOS induced changes that were characteristic of PPARˌ– transactivation including regulation of genes associated with lipid metabolism, peroxisome biogenesis, proteasome activation, and inflammation. PPARˌ–-independent changes were indicated in both WT and Null mice by altered expression of genes related to lipid metabolism, inflammation, and xenobiotic metabolism. Such results are similar to prior studies done with PFOA and are consistent with modest activation of the constitutive androstane receptor (CAR) and possibly PPARˌ‡ and/or PPARˌ†/ˌ·. Unique treatment-related effects were also found in Null mice including altered expression of genes associated with ribosome biogenesis, oxidative phosphorylation and cholesterol biosynthesis. Of interest was up-regulation of Cyp7a1, a gene which is under the control of various transcription regulators. Hence, in addition to its ability to modestly activate PPARˌ–, PFOS induces a variety of â off-targetâ effects as well. **Overall design:** PPARalpha-null and wild-type male mice at 6-9 months of age were dosed by gavage for 7 consecutive days with either 0, 3, or 10 mg/kg PFOS (potassium salt) in 0.5% Tween 20. Five biological replicates consisting of individual animals were included in each dosage group. Data were compared to results previously published by our group for PFOA and Wy-14,643, a commonly used agonist of PPARalpha (Rosen et al., Toxicol Pathol. 36:592-607, 2008; GSE9796)

Background corr dist: KL-Divergence = 0.2576, L1-Distance = 0.0583, L2-Distance = 0.0086, Normal std = 0.2982

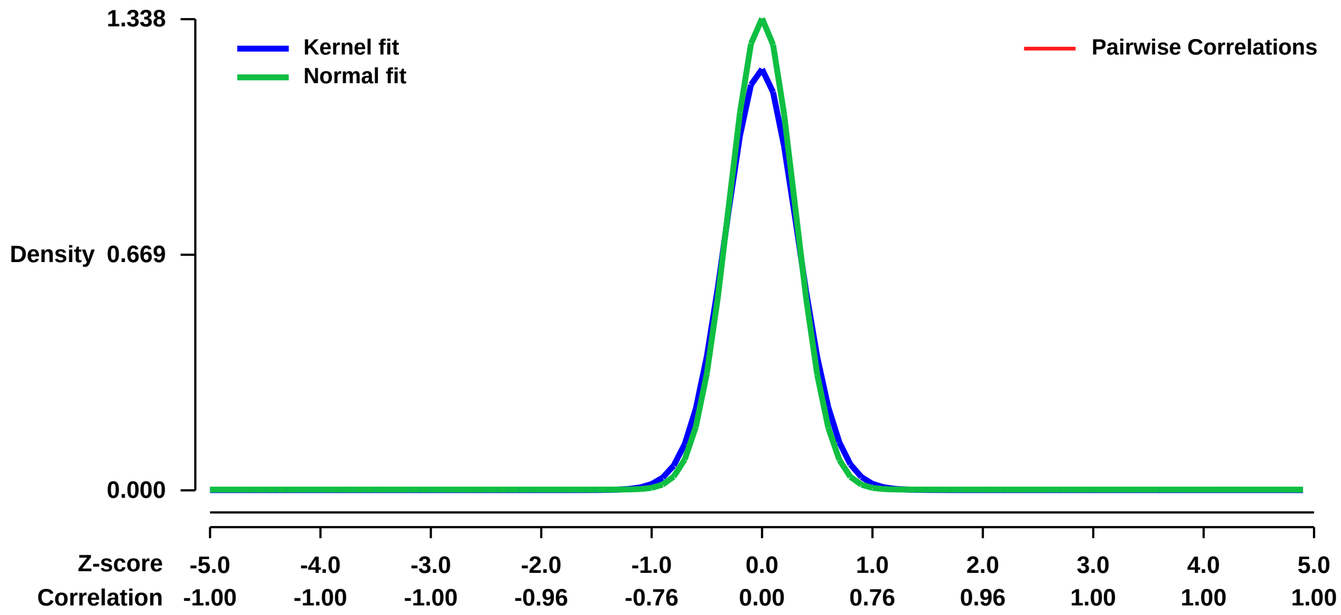

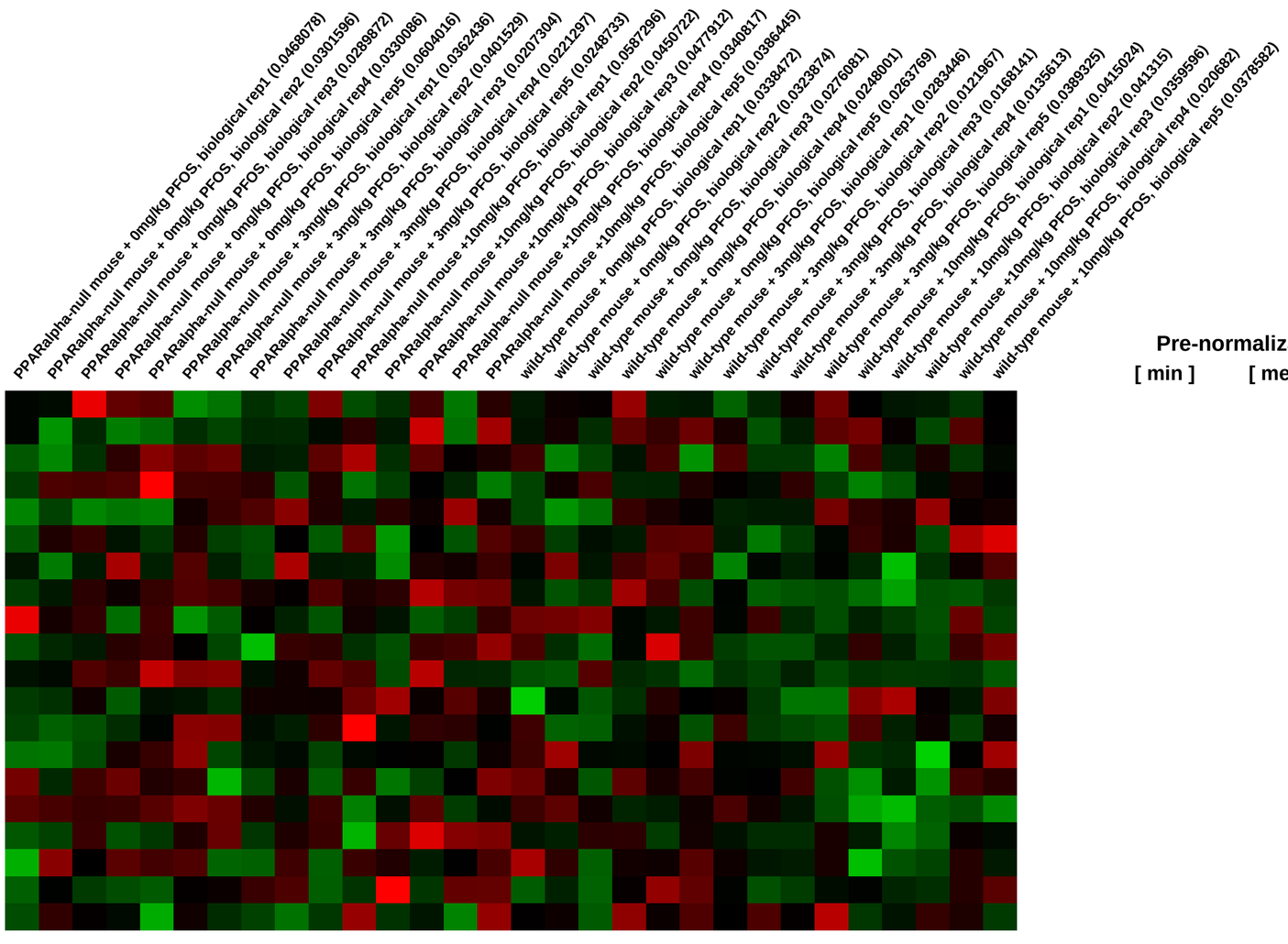

GEO Series "GSE11120" Expression Profiles

Num of samples in this series: 10

Scale of expression profile Z-scores

-3.0 -2.0 -1.0 0.0 1.0 2.0 3.0

GEO Link:	http://www.ncbi.nlm.nih.gov/geo/query/acc.cgi?acc=GSE11120
Status:	Public on Apr 09 2009
Title:	Assessment of Thermotolerance in preshocked hsp70(-/-) and (+/+) cells
Organism:	Mus musculus
Experiment type:	Expression profiling by array
Platform:	GPL1261
Pubmed ID:	21246580
Summary & Design:	**Summary:** From preliminary experiments, HSP70 deficient MEF cells display moderate thermotolerance to a severe heatshock of 45.5 degrees after a mild preshock at 43 degrees, even in the absence of hsp70 protein. We would like to determine which genes in these cells are being activated to account for this thermotolerance. **Keywords: thermal stress, heat shock response, knockout, cell culture, hsp70** **Overall design:** Two cell lines are analyzed - hsp70 knockout and hsp70 rescue cells. 6 microarrays from the (-/-)knockout cells are analyzed (3 Pretreated vs 3 unheated controls). For the (+/+) rescue cells, 4 microarrays are used (2 pretreated and 2 unheated controls). Cells were plated at 3k/well in a 96 well plate, covered with a gas permeable sealer and heat shocked at 43degrees for 30 minutes at the 20 hr time point. The RNA was harvested at 3hrs after heat treatment.

Background corr dist: KL-Divergence = 0.0655, L1-Distance = 0.0343, L2-Distance = 0.0022, Normal std = 0.5187

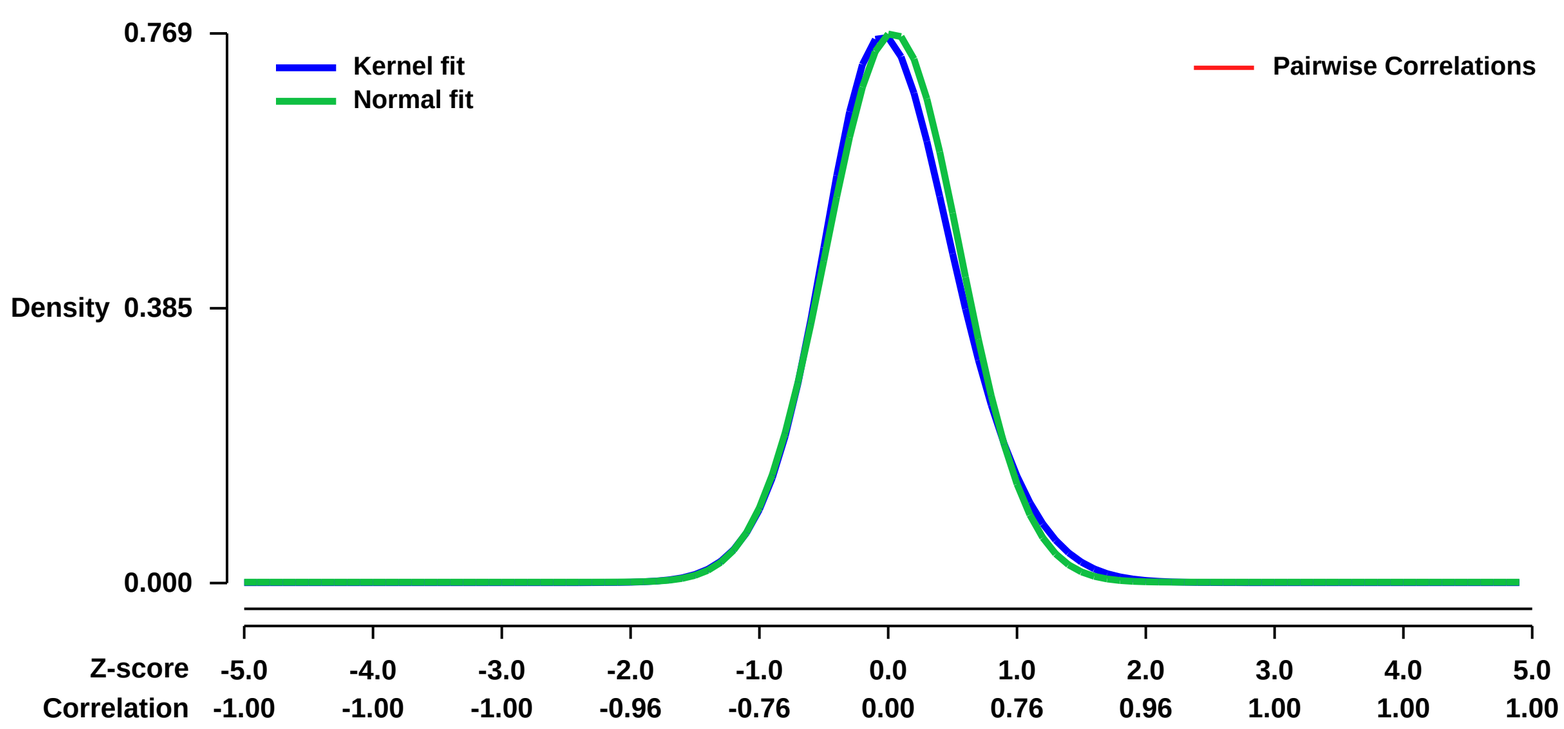

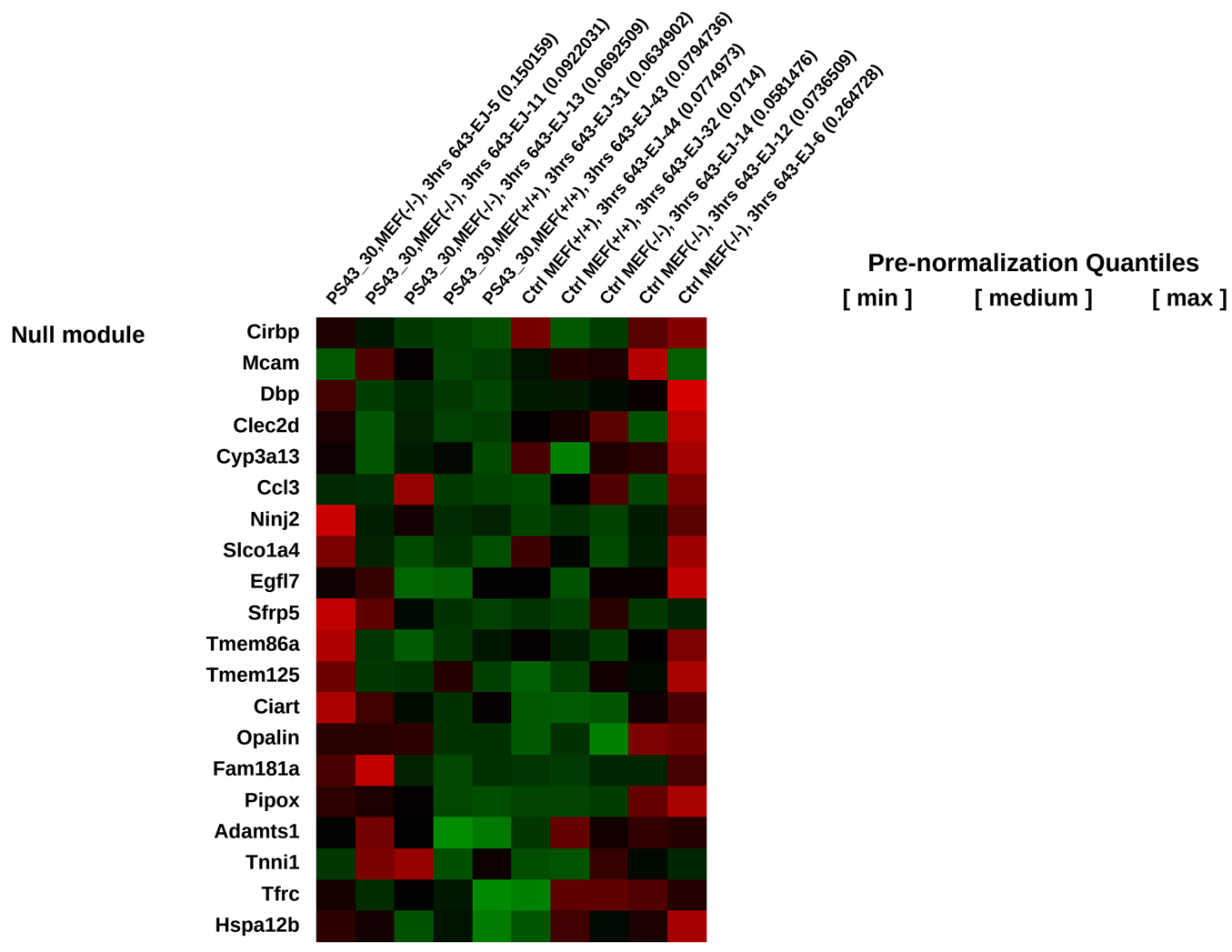

GEO Series "GSE34755" Expression Profiles

Num of samples in this series: 6

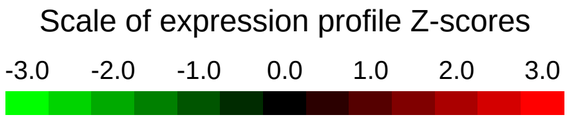

GEO Link:	**http://www.ncbi.nlm.nih.gov/geo/query/acc.cgi?acc=GSE34755**
Status:	**Public on May 01 2014**
Title:	**Gene expression changes induced by Evi1 withdrawal in Evi1 dependent myeloid clone C6**
Organism:	**Mus musculus**
Experiment type:	**Expression profiling by array**
Platform:	**GPL1261**
Pubmed ID:	
Summary & Design:	**Summary:** **The transcription factor Evi1 is essential for the formation and maintenance of hematopoietic stem cells, and induces clonal dominance with malignant progression upon constitutive activation by chromosomal rearrangements or transgene integration events. To understand the immediate and adaptive response of primary murine hematopoietic cells to the transcriptional upregulation of Evi1, we developed an inducible lentiviral vector system with a robust expression switch. We found that Evi1 delays differentiation and promotes survival in myeloid culture conditions, orchestrating a battery of genes involved in stemness (Aldh1a1, Ly6a [Sca1], Abca1, Epcam, among others). Importantly, Evi1 suppresses Cyclins and Cyclin-dependent kinases (Cdk), while it upregulates Cdk inhibitors, inducing quiescence in various proliferation-inducing cytokine conditions and operating in a strictly dose-dependent manner. Hematopoietic cells with persisting Evi1-induction tend to adopt a relatively low expression level. We thus classify Evi1 as a dormancy-inducing oncogene, likely requiring epigenetic and genetic compensation for cell expansion and malignant progression.** **Overall design:** **Evi1 dependent myeloid clone C6 cells expressing a Doxycyclin inducible codon-optimized murine Evi1 were harvested at day 2 after DOX withdrawal and compared to C6 cells under Doxycyclin 1 ug/ml**

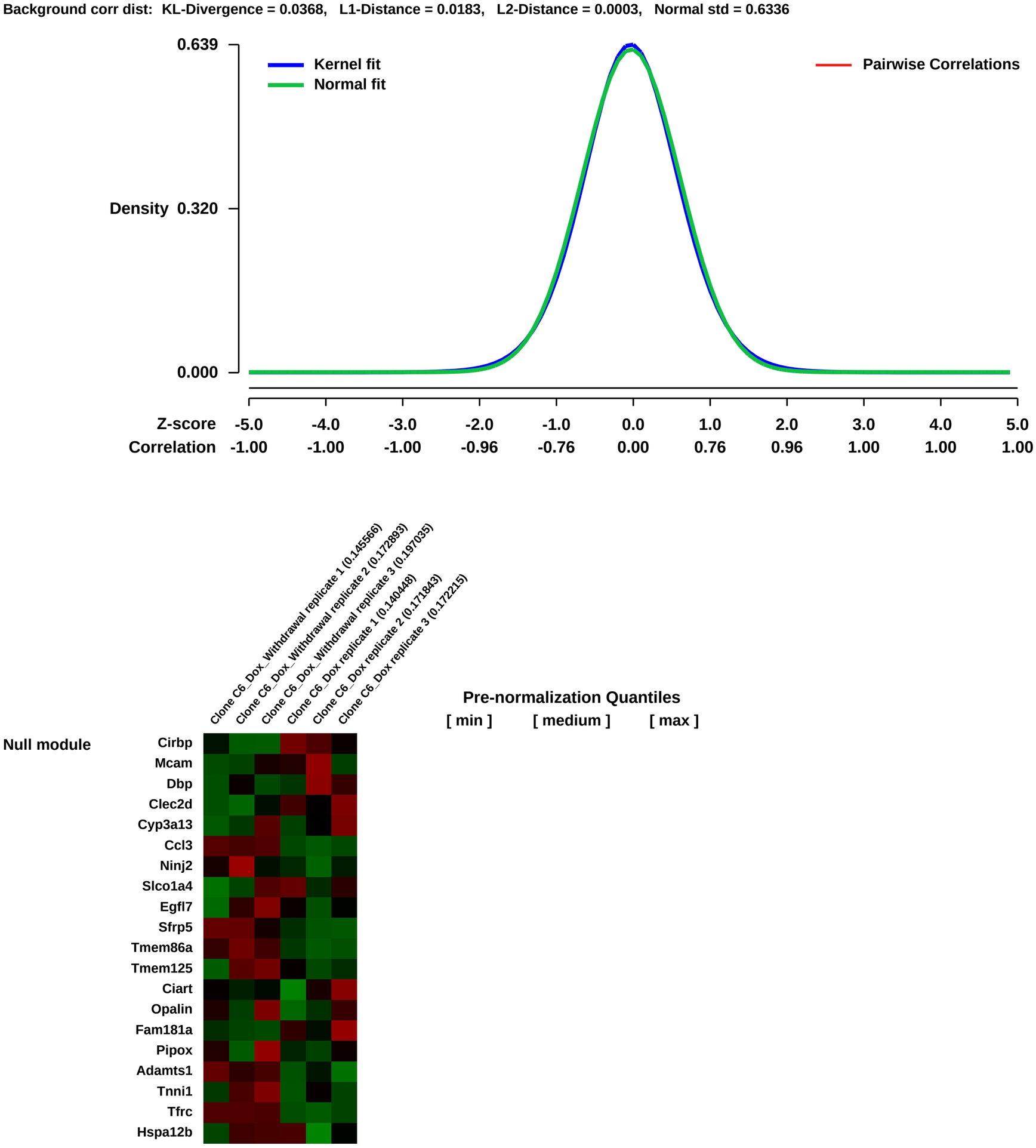

GEO Series "GSE30855" Expression Profiles

Num of samples in this series: 6

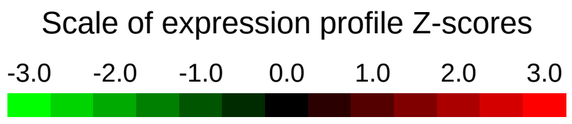

GEO Link:	http://www.ncbi.nlm.nih.gov/geo/query/acc.cgi?acc=GSE30855
Status:	Public on Sep 01 2011
Title:	Establishment of Enhancer Repertoires that Orchestrate the Myeloid and Lymphoid Cell Fates (gene expression dataset 1)
Organism:	Mus musculus
Experiment type:	Expression profiling by array
Platform:	GPL1261
Pubmed ID:	21903424
Summary & Design:	**Summary:** Recent studies have documented genome-wide binding patterns of transcriptional regulators and their associated epigenetic marks in hematopoietic cell lineages. In order to determine how epigenetic marks are established and maintained during developmental progression, we have generated long-term cultures of hematopoietic progenitors by enforcing the expression of the E-protein antagonist Id2. Hematopoietic progenitors that express Id2 are multipotent and readily differentiate upon withdrawal of Id2 expression into committed B lineage cells, thus indicating a causative role for E2A in promoting the B cell fate. Genome-wide analyses revealed that a substantial fraction of lymphoid and myeloid enhancers are pre-marked by H3K4me1 in multipotent progenitors. However, H3K4me1 levels at a subset of enhancers are elevated during developmental progression, resulting in evolving enhancer repertoires that we propose orchestrate the myeloid and B cell fates. **Overall design:** To characterize Id2-HPCs, we performed microarray analysis using RNA derived from cultured E2A-deficient cells, EBF-deficient cells and Id2-HPCs. Id2-HPC cells were cultured in IMDM medium supplemented with 10% FCS/2% PSG/¸†-me and IL7, Flt3-ligand, and SCF cytokines on S17 feeder cells in a humidified incubator at 37 degrees C with 5% CO2. Id2-HPC expanded cells were depleted of small (<1-5%) numbers of CD19-, CD25- and CD11b-positive cells by auto-MACS. E2A -/- and EBF -/- cells were cultured in IMDM supplemented with 10% FCS/2% PSG/¸†-me on S17 feeder cells in the presence of IL-7, Flt3-ligand, and SCF cytokines in a humidified incubator at 37 degree C with 5% CO2.

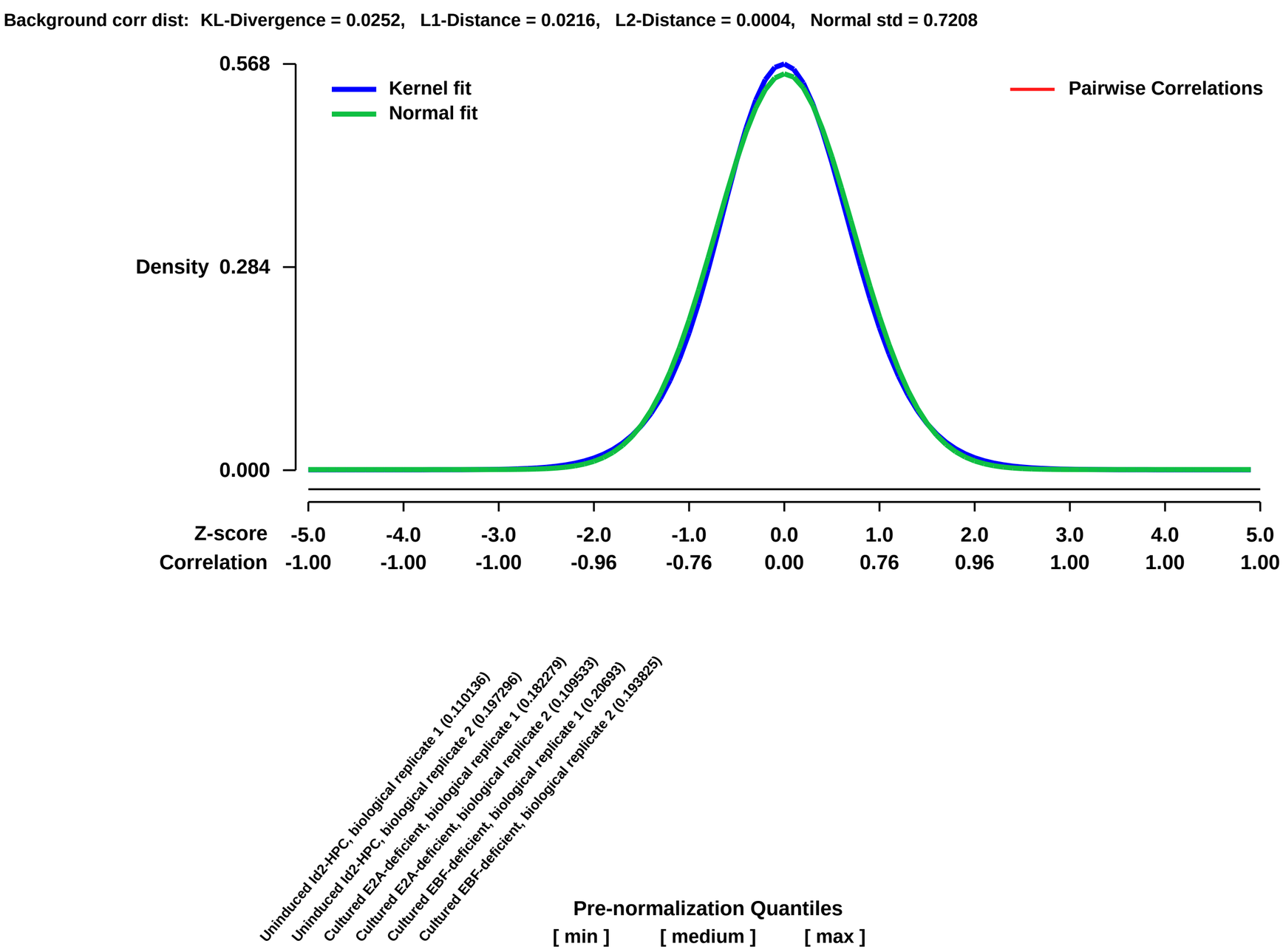

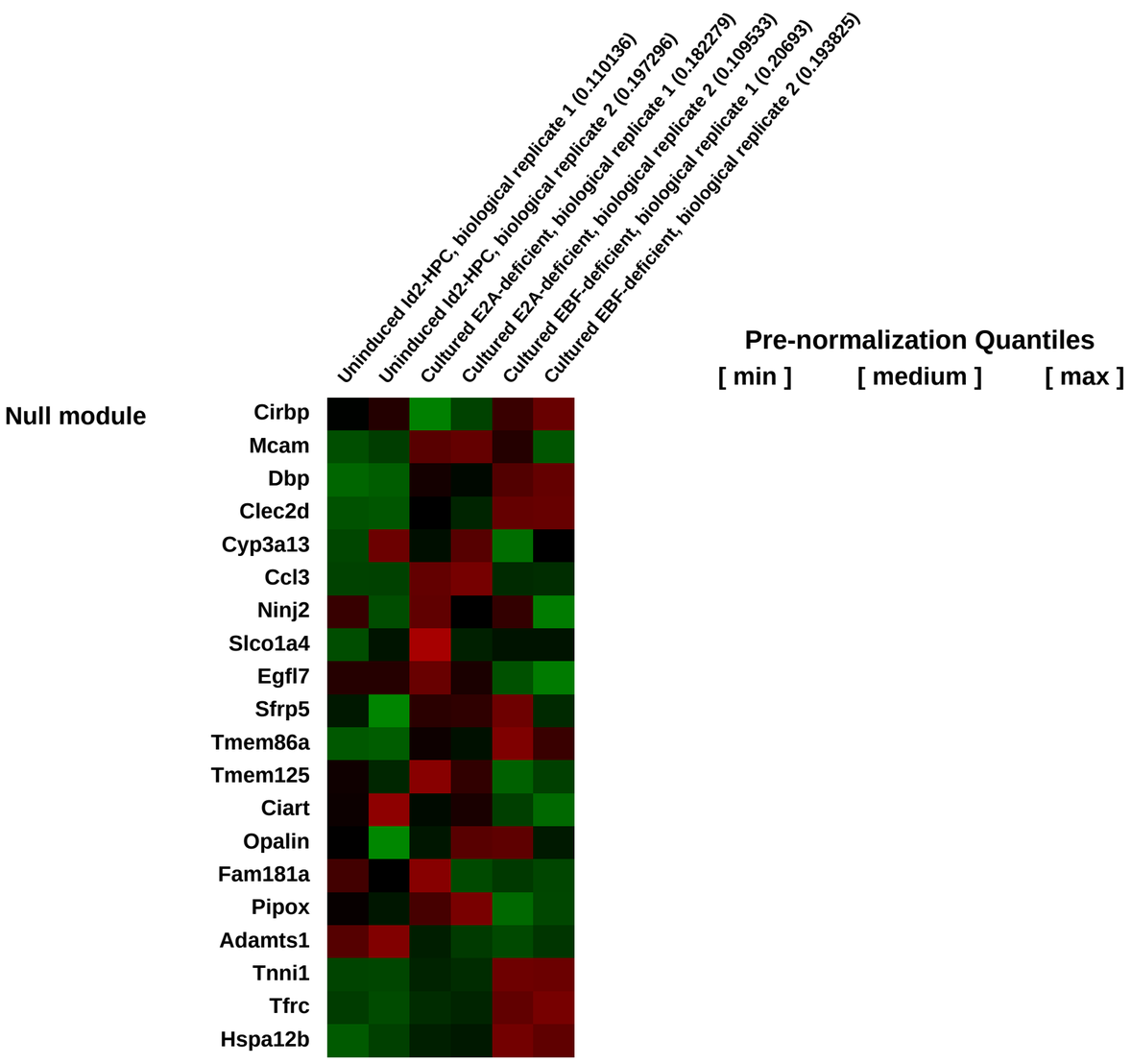

GEO Series "GSE21018" Expression Profiles

Num of samples in this series: 6

Scale of expression profile Z-scores

-3.0 -2.0 -1.0 0.0 1.0 2.0 3.0

GEO Link:	**http://www.ncbi.nlm.nih.gov/geo/query/acc.cgi?acc=GSE21018**
Status:	**Public on Aug 22 2010**
Title:	**Cooperation of IRF-4 and IRF-8 deficiencies in the development of hematological malignancies**
Organism:	**Mus musculus**
Experiment type:	**Expression profiling by array**
Platform:	**GPL1261**
Pubmed ID:	
Summary & Design:	**Summary:** **We found that mice deficient in both IRF-4 and IRF-8 develop from a very early age a more aggressive CML-like disease than mice deficient in IRF-8 alone. IRF-4 deficiency dramatically enhanced the effect of IRF-8 deficiency on expansion of granulocyte-monocyte progenitors (GMPs). All mice deficient in both IRF-4 and IRF-8 eventually develop and succumb to a B-lymphoblastic leukemia/lymphoma at approximately 25 weeks of age. The results demonstrate that IRF-4 and IRF-8 deficiencies can cooperate in the development of both myeloid and lymphoid tumors.** **To gain insights into how loss of IRF-4 affects the transcriptional program underlying leukemogenesis, we analyzed the genome-wide transcription profiles of GMPs from WT, IRF-8 KO and IRF-4/8 DKO mice. Microarray analysis revealed genes differentially expressed in IRF-4/8 DKO and IRF-8 KO GMPs, including genes that are involved in cell growth regulation and/or tumorigenesis.** **Overall design:** **Total RNA was extracted from GMPs (Lin-/IL-7R-/Sca1-/Kit+/CD34+/FcRII/IIIhi) of wild type, IRF8 KO and IRF4/8 DKO mice (two samples each group) using the Qiagen RNAeasy Micro kit. Affymetrix Mouse Genome 430 2.0 microarray with 45,000 probe sets was used at the BIDMC Genomics Center. Hybridization data were normalized and expression values were determined using the PM/MM difference model by dChip 1.3 (DNA-Chip analyzer).**

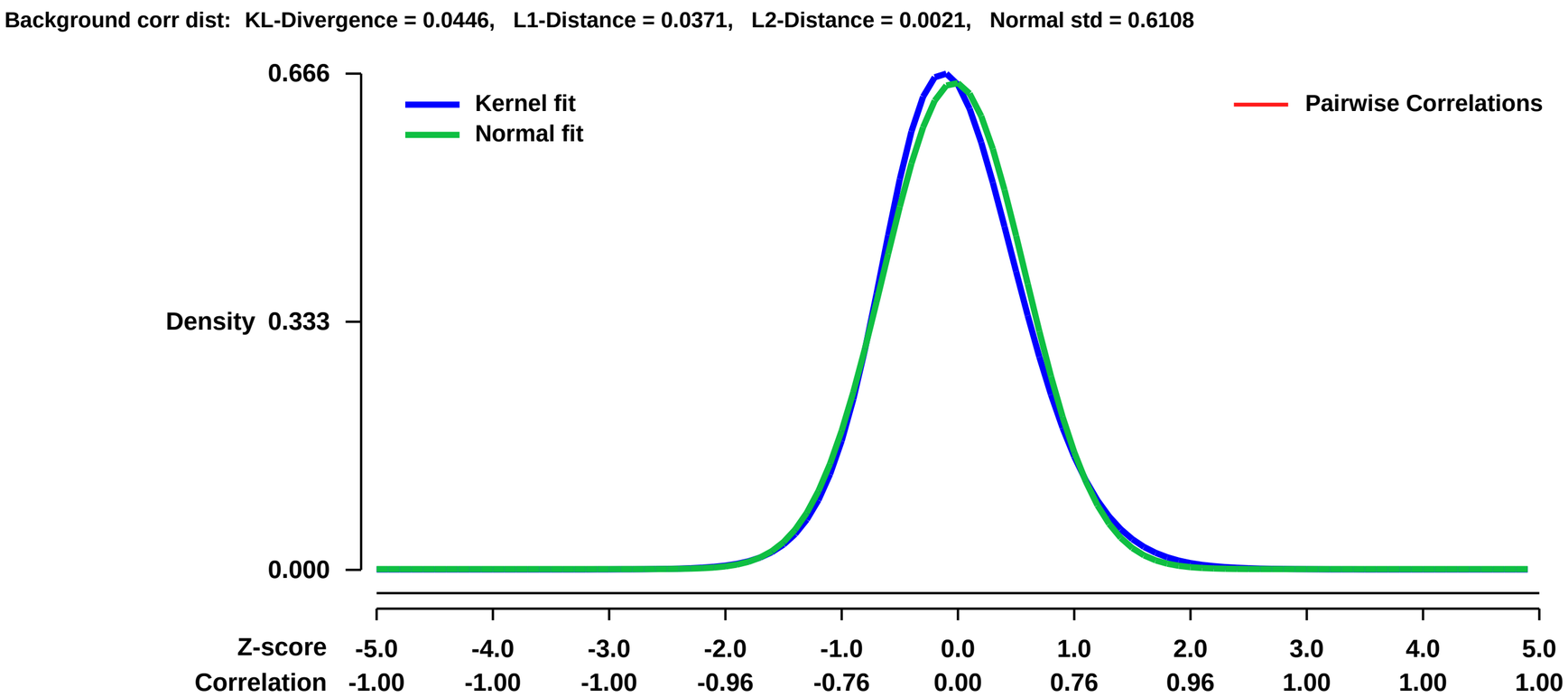

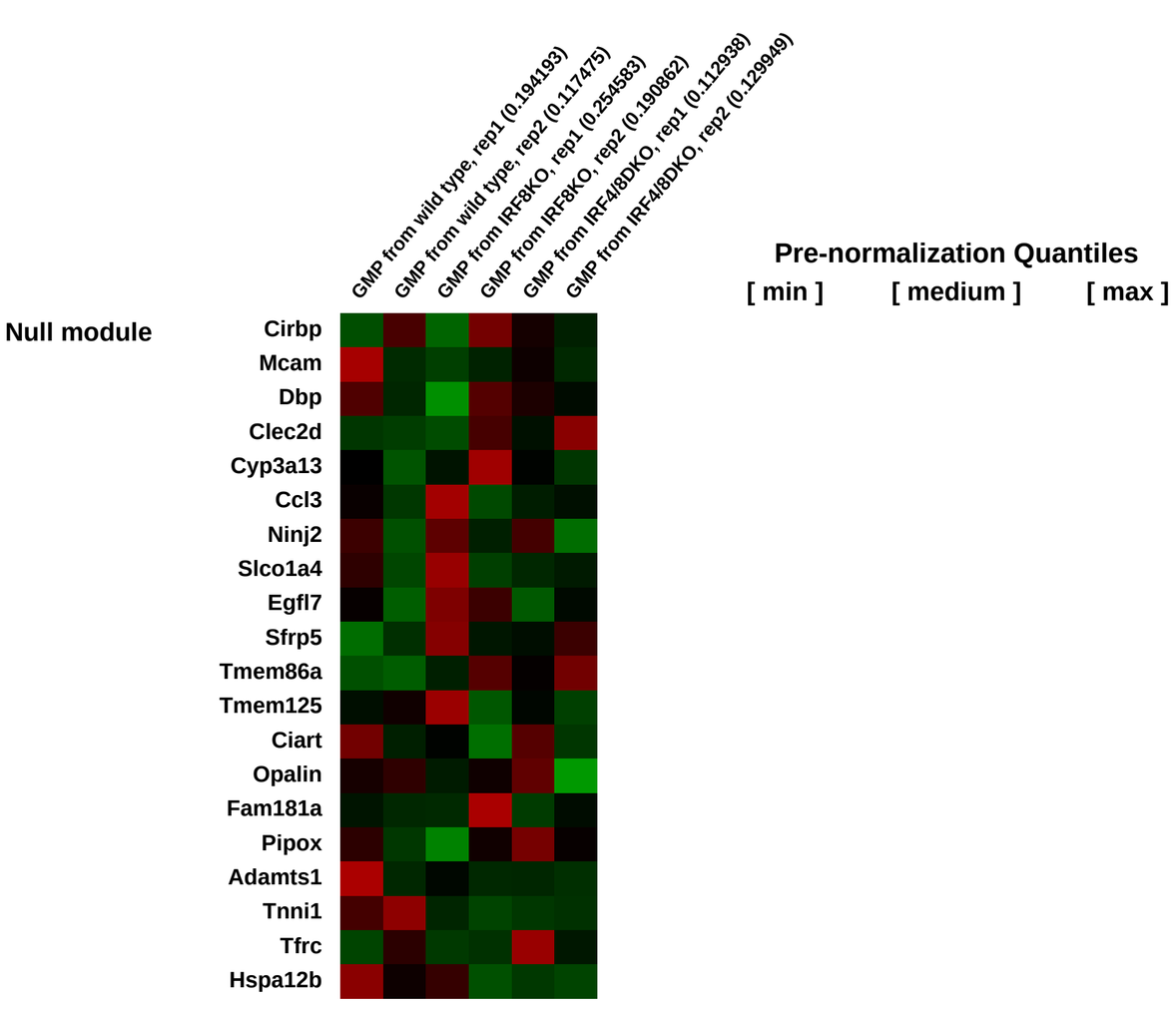

GEO Series "GSE17462" Expression Profiles

Num of samples in this series: 8

Scale of expression profile Z-scores

-3.0 -2.0 -1.0 0.0 1.0 2.0 3.0

GEO Link:	http://www.ncbi.nlm.nih.gov/geo/query/acc.cgi?acc=GSE17462
Status:	Public on Aug 01 2009
Title:	Expression data from Bmi1-overexpressing Ink4a-Arf-null hepatoblasts
Organism:	Mus musculus
Experiment type:	Expression profiling by array
Platform:	GPL1261
Pubmed ID:	
Summary & Design:	**Summary:** Forced expression of Bmi1 accelerated the self-renewal of hepatic stem/progenitor cells and eventually induced their transformation in an in vivo transplant model. The Ink4a/Arf locus, which encodes a cyclin-dependent kinase inhibitor, p16Ink4a, and a tumor suppressor, p19Arf, is a pivotal target of Bmi1. Therefore, it would be of importance to understand the contribution of the Ink4a/Arf locus to Bmi1 oncogenic functions in cancer and search for as-yet-unknown Bmi1 target genes other than Ink4a/Arf. We used microarrays to explore novel candidate downstream targets for Bmi1 in hepatic stem/progenitor cells **Overall design:** Purified Dlk-positive hepatoblasts at day 28 of culture were subjected to RNA extraction and hybridization on Affymetrix microarrays. Data were obtained for quadrant samples from four independent experiments.

Background corr dist: KL-Divergence = 0.0597, L1-Distance = 0.0375, L2-Distance = 0.0025, Normal std = 0.5470

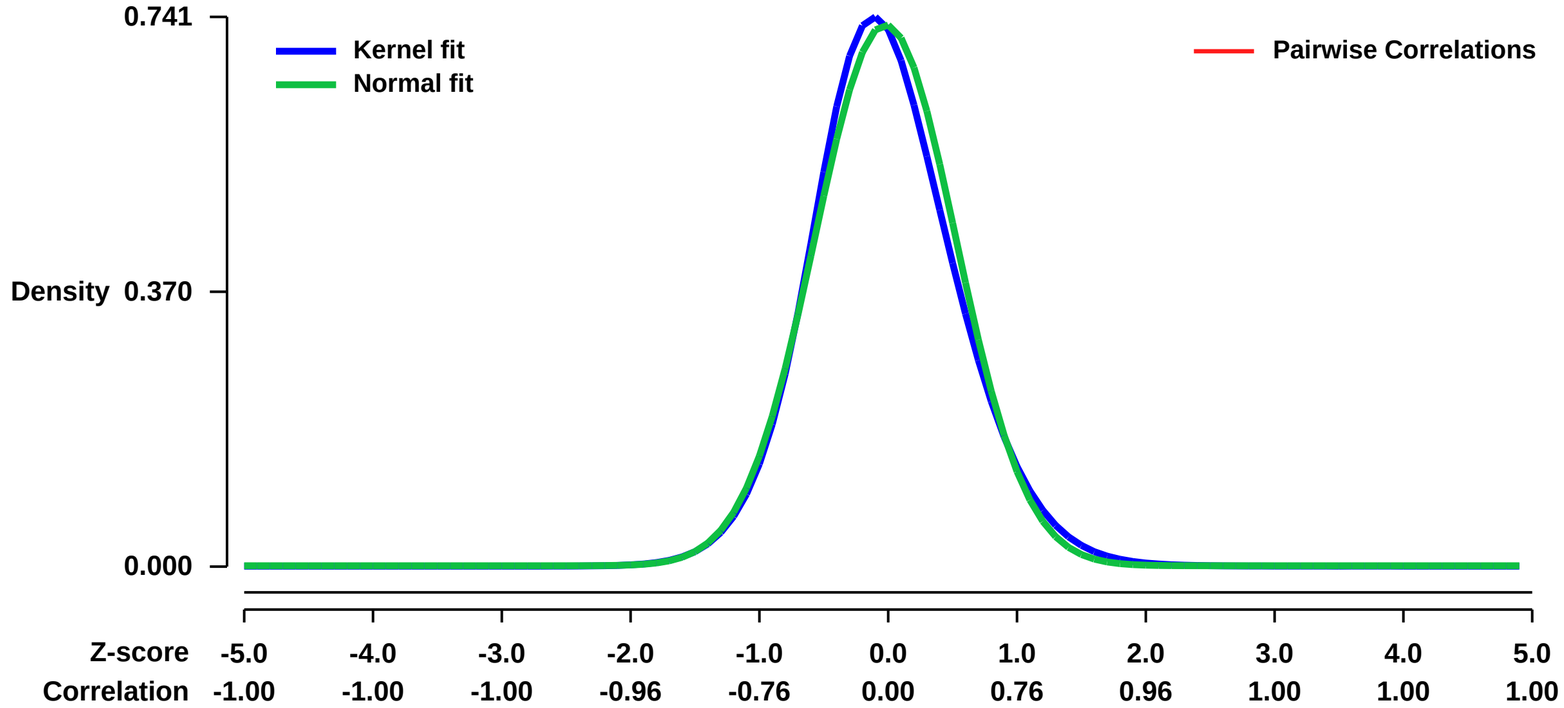

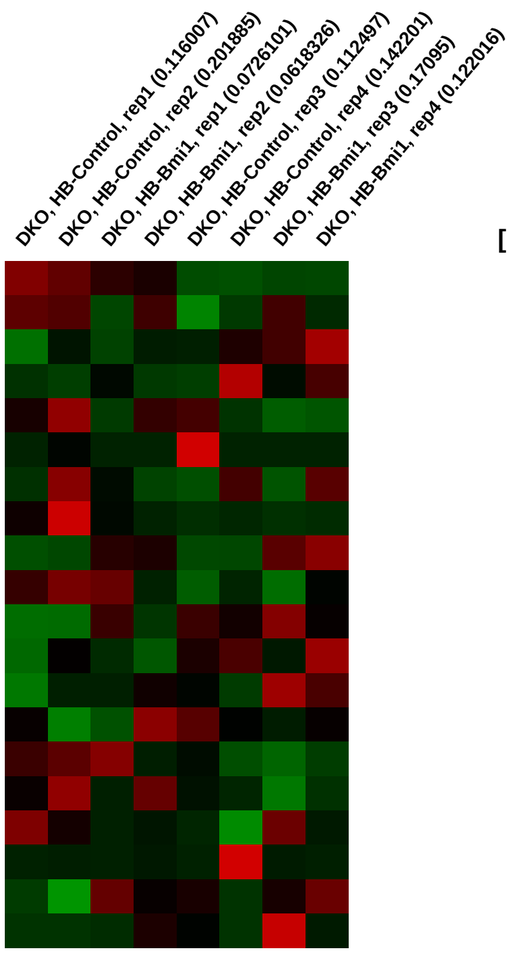

GEO Series "GSE56236" Expression Profiles

Num of samples in this series: 12

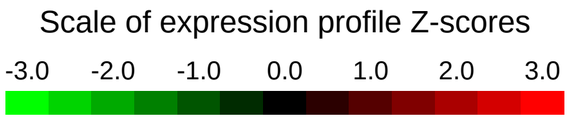

GEO Link:	**http://www.ncbi.nlm.nih.gov/geo/query/acc.cgi?acc=GSE56236**
Status:	**Public on Jul 14 2014**
Title:	**Glomerular transcriptomic analysis of the influence of Genetic background effect during anti-GBM glomerulonephritis in mice**
Organism:	**Mus musculus**
Experiment type:	**Expression profiling by array**
Platform:	**GPL1261**
Pubmed ID:	
Summary & Design:	**Summary:** **We analyzed the impact of the genetic background during experimental passive non-accelerated anti-glomerular basement membrane glomerulonephritis (anti-GBM-GN) (an equivalent to nephrotoxic nephritis) in two different mouse genetic backgrounds (C57BL6/J vs 129S2svPAS/crl).** **Glomerular extracts have been made at an early time point (e.g day 4 of the induction of the glomerulonephritis). RNA have been extracted following standard procedures.** **Overall design:** **3 mice per group have been compared. 3 Control mice from each background. And 3 anti-GBM-GN challenged mice from each Genetic background, corresponding to 12 samples in total.**

Background corr dist: **KL-Divergence = 0.0993, L1-Distance = 0.0856, L2-Distance = 0.0127, Normal std = 0.5345**

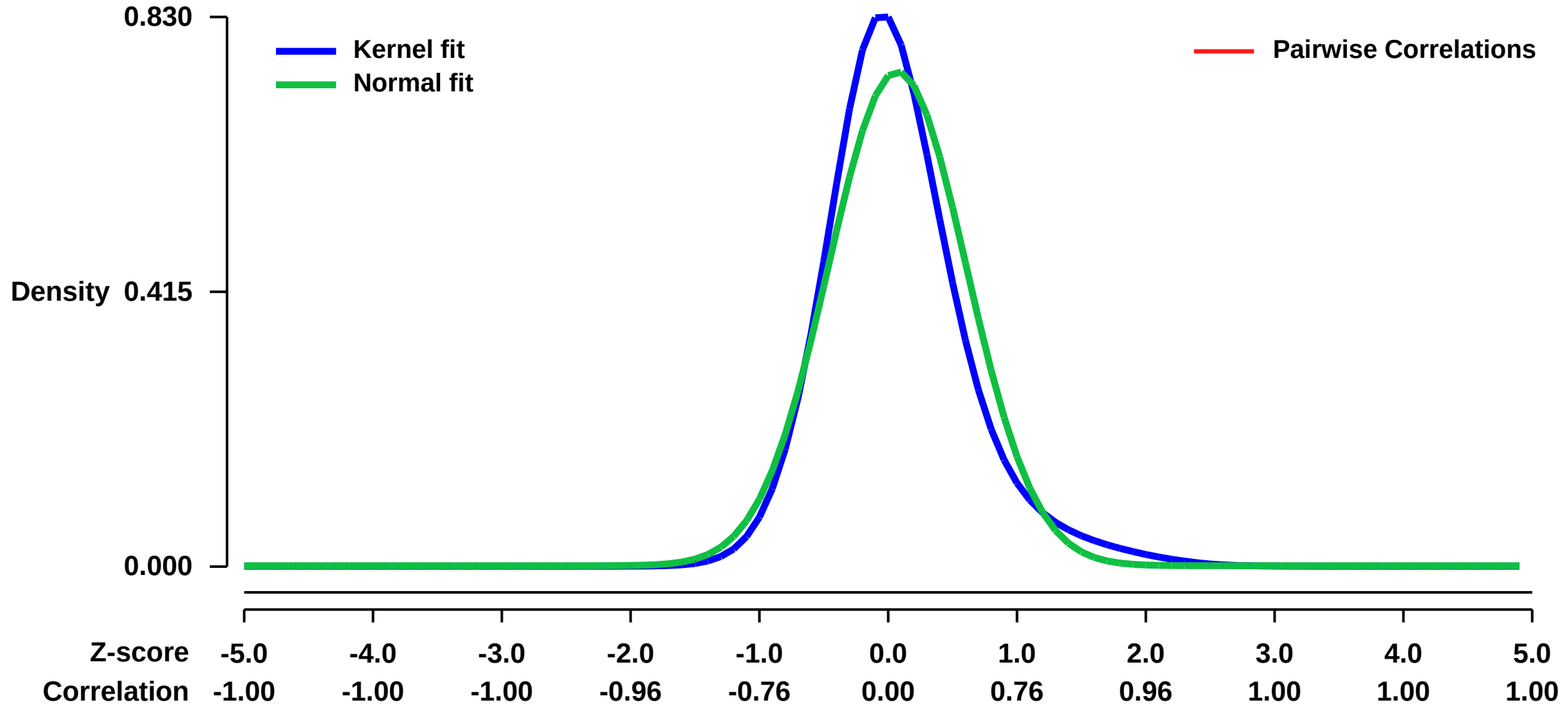

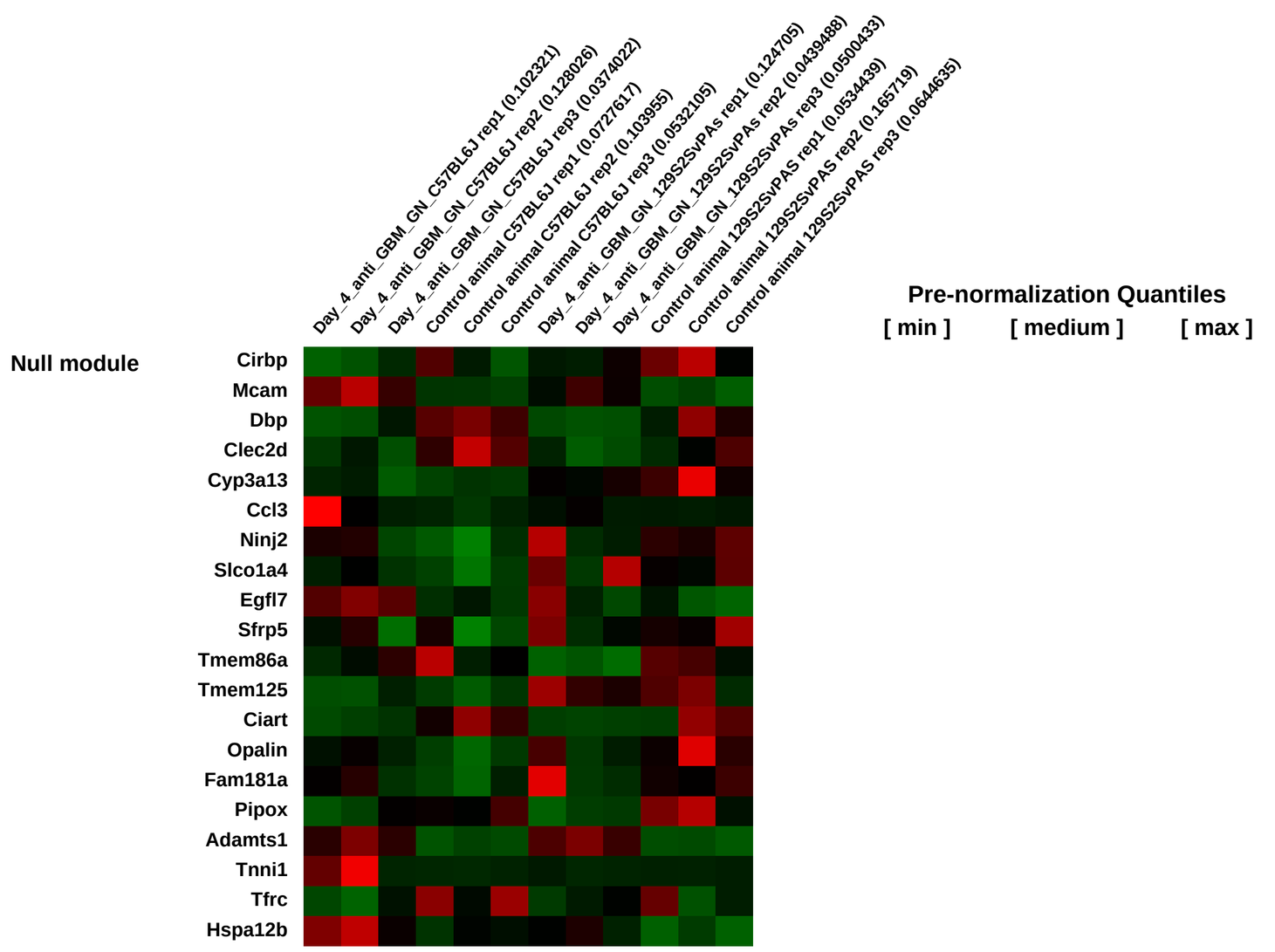

GEO Series "GSE55855" Expression Profiles

Num of samples in this series: 6

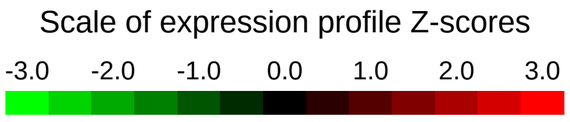

GEO Link:	**http://www.ncbi.nlm.nih.gov/geo/query/acc.cgi?acc=GSE55855**
Status:	**Public on Mar 13 2014**
Title:	**Effect of CSF1R inhibition in tumor macrophages on gene expression in metastatic epithelial cells**
Organism:	**Mus musculus**
Experiment type:	**Expression profiling by array**
Platform:	**GPL1261**
Pubmed ID:	
Summary & Design:	**Summary:** **Metastasis is the primary cause of mortality in breast cancer patients. Tumor associated macrophages (TAMs) are active collaborators in mediating several steps of the tumor metastatic cascade, but the molecular details governing this collaboration remain ill-defined. Colony Stimulating Factor 1 (CSF1), a factor critical for macrophage differentiation and survival, functions to recruit TAMs to the primary tumor site, and anti-CSF1 therapies are in clinical trials.In this study, we tested the effect of inhibiting CSF1 signaling in macrophages on gene expression in metastatic tumor cells in mouse models of breast cancer metastasis. Tumor cells were sorted from lung metastases from control and CSF1R inhibitor treated mice. Several pro-tumor processes were significantly affected by CSF1R inhibitor treatment, including angiogenesis and tumor cell proliferation. In addition, a 29 gene signature derived from this data could retrospectively predict survival in a cohort of luminal B breast cancer patients. Collectievly, our results highlight the utility of employing CSF1R inhibitors for the treatment of metastatic breast cancer.** **Overall design:** **GFP tagged MVT1 metastatic mammary tumor cells were injected intravenously into FVB/N mice. Mice were gavaged with the CSF1R inhibitor GW2580 or vehicle starting one week post injection. GFP tagged tumor cells were sorted from metastatic tumor bearing lungs 1 and 2 weeks post injection from 2 vehicle treated mice for each. These are denoted 1_week_WT and 2_week_WT respectively. GFP tagged tumor cells were simultaneously sorted from mice gavaged with GW2580. These samples are denoted 2_week_GW. RNA was extracted and gene expression profiling was performed using the Affymetrix Mouse Genome 430 2.0 Array platform.**

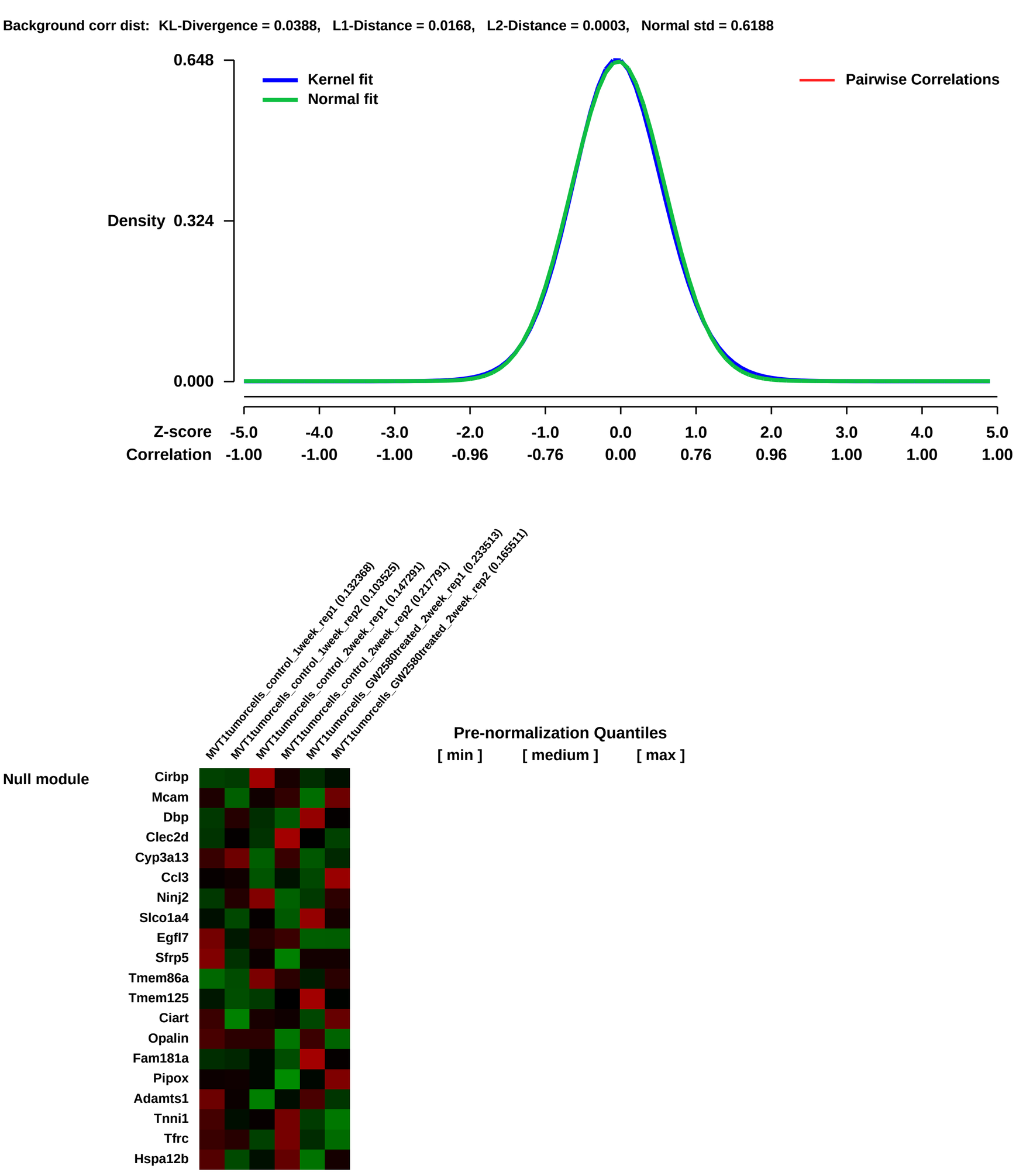

GEO Series "GSE34206" Expression Profiles

Num of samples in this series: 8

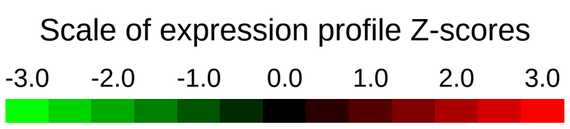

GEO Link:	http://www.ncbi.nlm.nih.gov/geo/query/acc.cgi?acc=GSE34206
Status:	Public on Dec 07 2011
Title:	Gene regulation in macrophages from irradiated tumors
Organism:	Mus musculus
Experiment type:	Expression profiling by array
Platform:	GPL1261
Pubmed ID:	22761754
Summary & Design:	**Summary:** Tumors engender an environment dominated by M2 differentiated tumor macrophages that support tumor invasion, metastases and escape from immune control. In this study, we demonstrate that following radiation therapy of tumors in mice there is an influx of tumor macrophages that polarize towards wound repair and immune suppression. To investigate changes in the phenotype of tumor macrophages following radiation therapy, we FACS sorted tumor macrophages from Panc02 tumors. We have previously shown that we can distinguish mature tumor macrophages from immature myeloid and MDSC populations by expression of Gr1 and IA (MHC class II). To isolate these sub-populations, we first gated CD11b+ cells in the untreated or irradiated tumors, then sorted the CD11b+IA+ macrophage population and the CD11b+Gr1hi MDSC population. Cytospins of the sorted populations demonstrates that the CD11b+Gr1hi MDSC predominantly have a granulocyte morphology and the CD11b+IA+ cells have a macrophage morphology in both the untreated and irradiated tumors. RNA was purified from CD11b+IA+ macrophages from untreated or irradiated tumors 1 day or 7 days following radiation therapy and Gene Expression Microarray analysis was performed. **Overall design:** There are untreated and irradiated samples at time points 1 day and 7 days following radiation therapy. The experiment was repeated in entirety, generating a second gene array sample for each. For analysis, the untreated samples of 1 day and 7 days were grouped together.

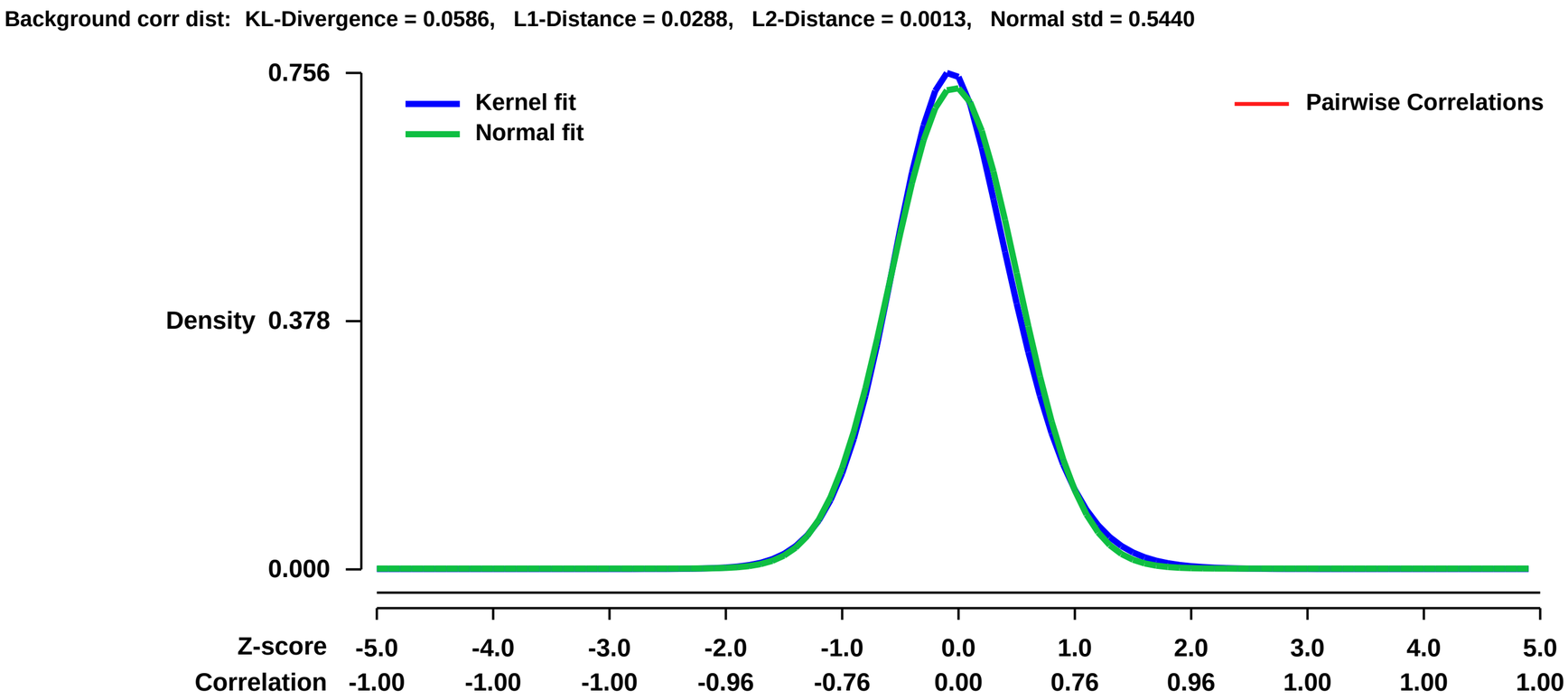

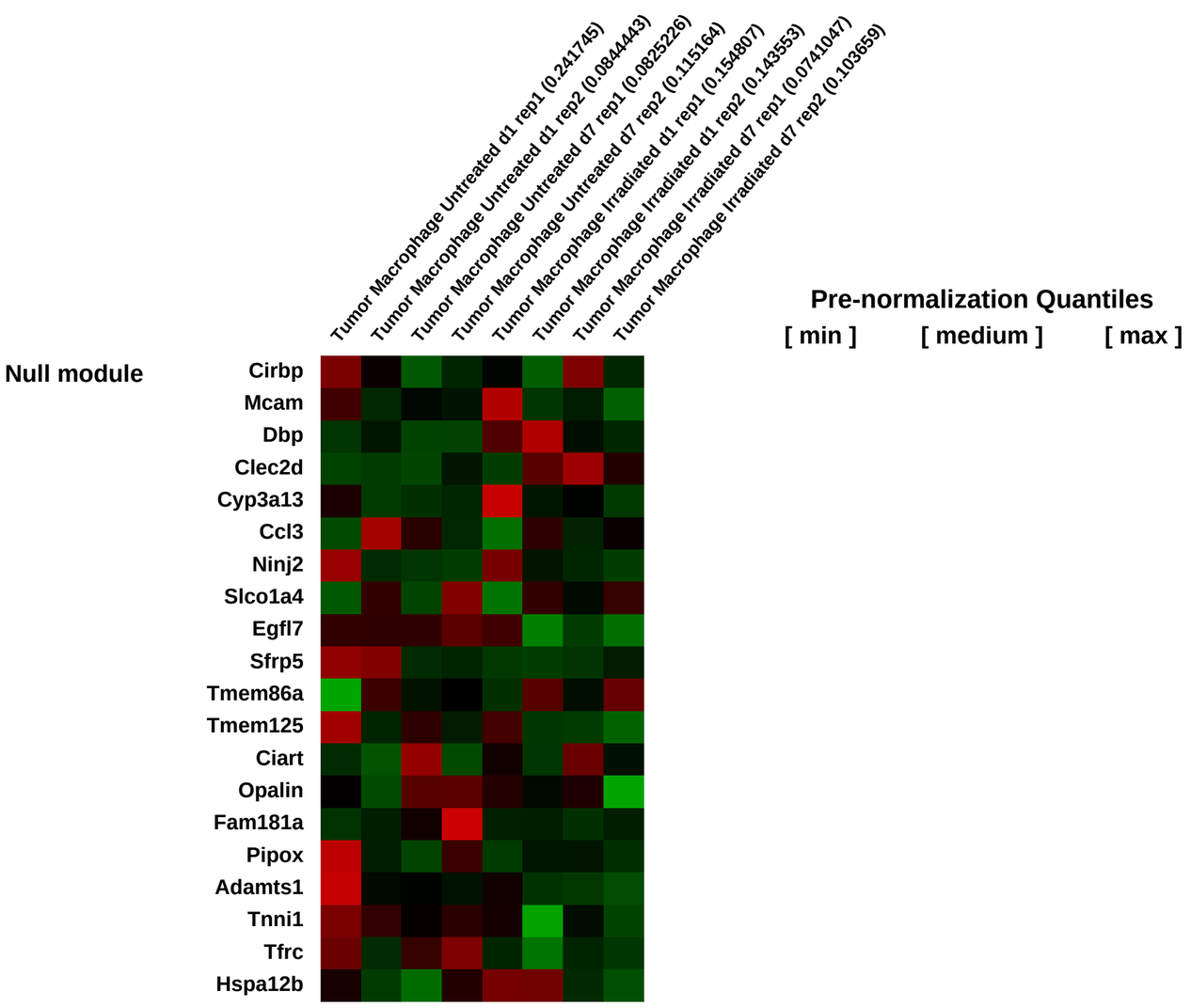

GEO Series "GSE15458" Expression Profiles

Num of samples in this series: 8

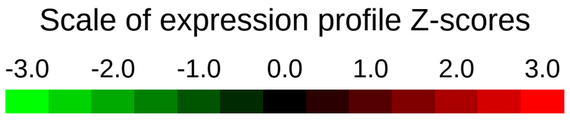

GEO Link:	**http://www.ncbi.nlm.nih.gov/geo/query/acc.cgi?acc=GSE15458**
Status:	**Public on Jun 30 2009**
Title:	**Effect of v-erbA on T3-responsive genes in AML-12 hepatocytes**
Organism:	**Mus musculus**
Experiment type:	**Expression profiling by array**
Platform:	**GPL1261**
Pubmed ID:	

Summary & Design:

Summary:
The v-erbA oncogene belongs to a superfamily of transcription factors called nuclear receptors, which includes the thyroid hormone receptors (TRs) responsible for mediating the effects of thyroid hormone (T3). Nuclear receptors bind to specific DNA sequences in the promoter region of target genes and v-erbA is known to exert a dominant negative effect on the activity of the TRs. The repressor activity of v-erbA has been linked to the development of hepatocellular carcinoma (HCC) in a mouse model. We have used microarray analysis to identify genes differentially expressed in hepatocytes in culture (AML12 cells) stably transfected with v-erbA and exposed to T3. We have found that v-erbA can negatively regulate expression of T3-responsive genes known to have a protective function against tumor development. We have also identified a number of v-erbA- (but not T3-) responsive genes that are known to be involved in carcinogenesis and which may play a role in the development of HCC.

Overall design:
AML12 control cells and v-erbA-transfected AML12 cells were exposed to 10 nM T3 for 3h or 24h. Using microarray analysis, we compared gene expression in the presence and absence of v-erbA and identified T3-regulated genes differentially expressed in the presence of v-erbA.

Background corr dist: **KL-Divergence = 0.0342, L1-Distance = 0.0167, L2-Distance = 0.0003, Normal std = 0.6313**

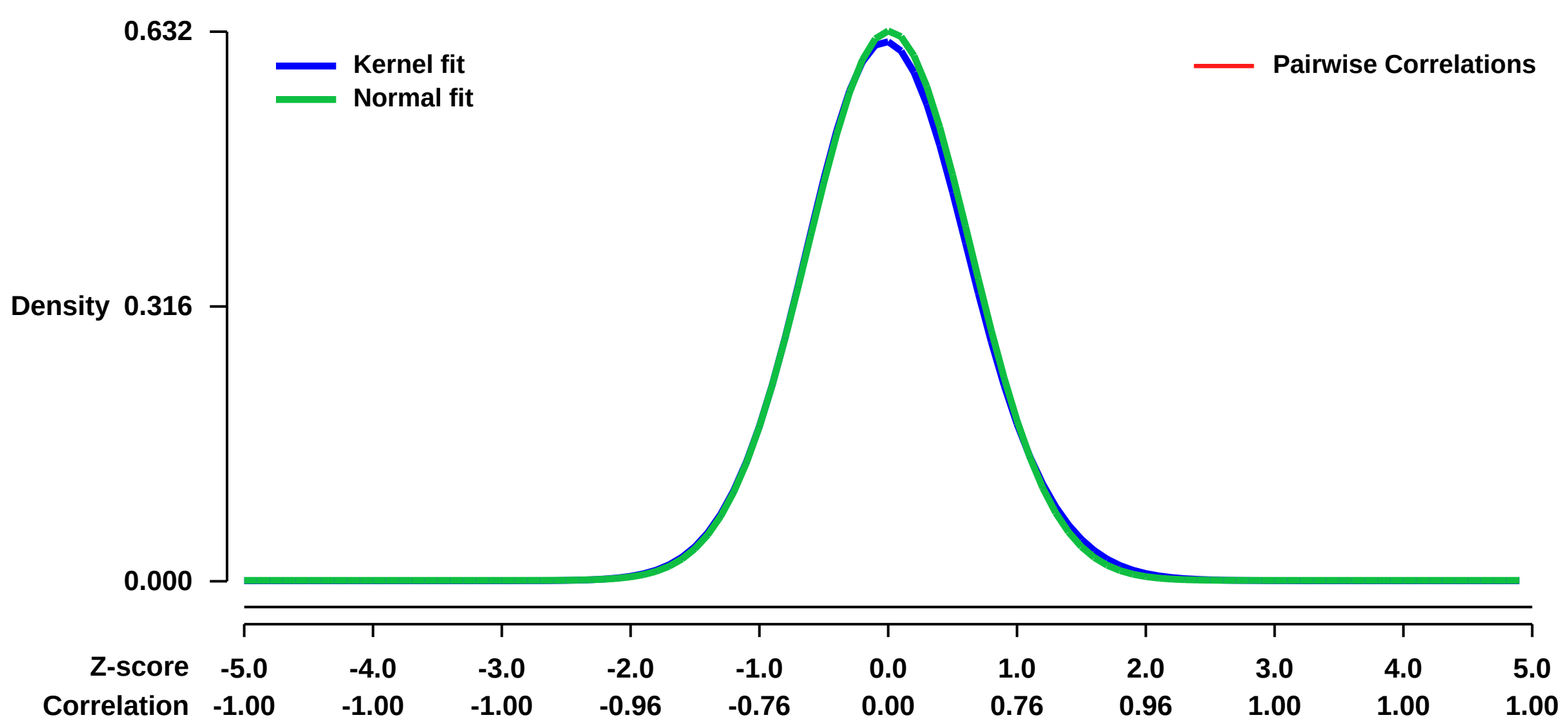

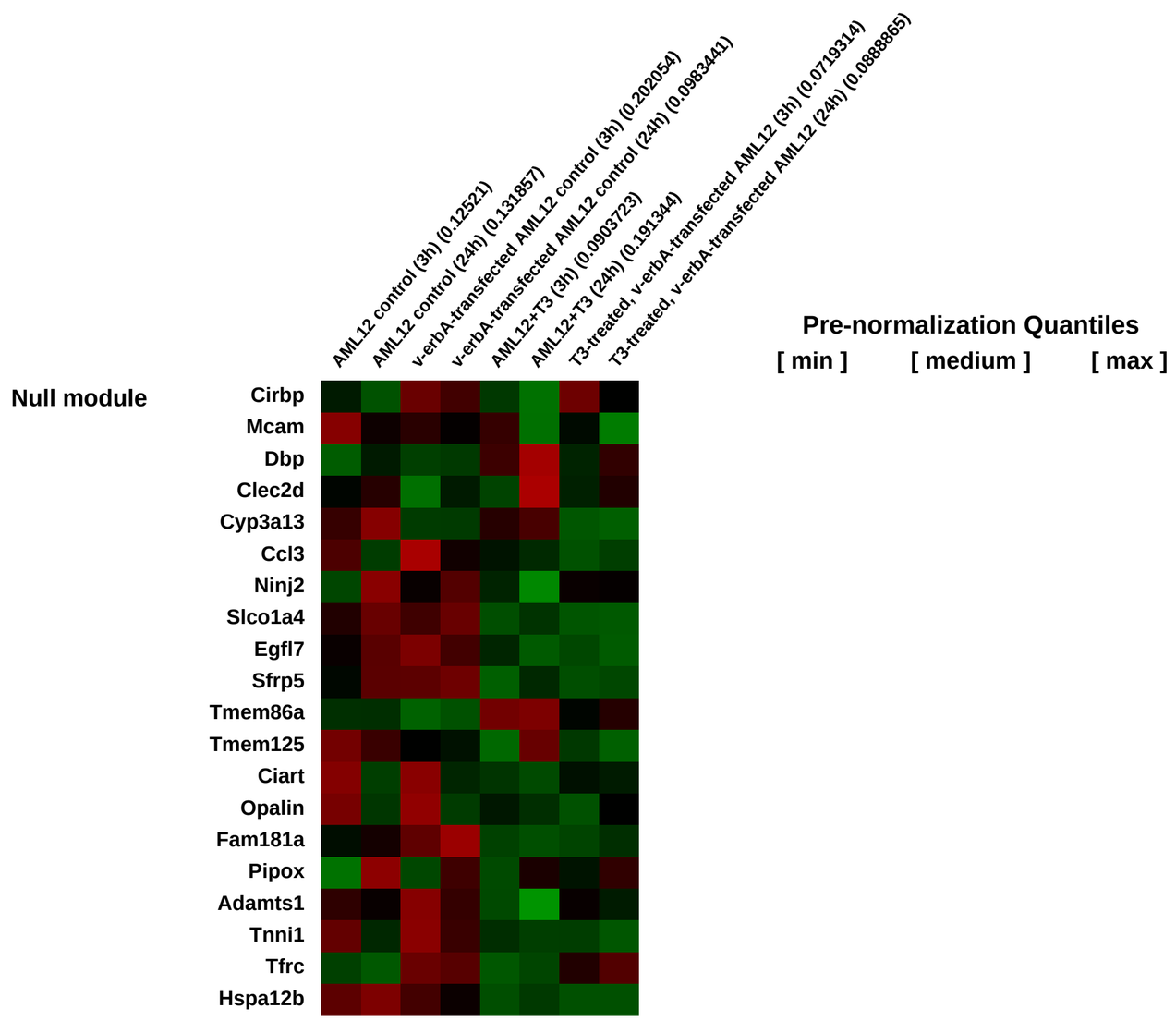

GEO Series "GSE38044" Expression Profiles

Num of samples in this series: 6

Scale of expression profile Z-scores

-3.0 -2.0 -1.0 0.0 1.0 2.0 3.0

GEO Link:	http://www.ncbi.nlm.nih.gov/geo/query/acc.cgi?acc=GSE38044
Status:	Public on Mar 13 2013
Title:	Gene activation by Rag-mediated DNA double-strand breaks in G1-phase murine pre-B cells
Organism:	Mus musculus
Experiment type:	Expression profiling by array
Platform:	GPL1261
Pubmed ID:	23496831
Summary & Design:	**Summary:** The objective is to identify genes that are differentially expressed following the introduction of DNA double-strand breaks (DSBs) by the Rag proteins in murine pre-B cells. Cells lacking Artemis are used since the Rag-induced DSBs will not be repaired, and thus, will provide a continuous stimulus to the cell. **Overall design:** Murine v-abl-transformed pre-B cells were treated with 3 uM STI571 for 48 hours. Cell types included RAG-2-deficient (3 biological replicates) and Artemis-deficient (3 biological replicates) G1-phase pre-B cells. Each sample was hybridized once using Affymetrix Mouse Genome 2.0 GeneChip arrays (Mouse 430 v2, Affymetrix, Santa Clara, CA). Data were analyzed using the RAG-2-deficient samples as the controls.

Background corr dist: KL-Divergence = 0.0469, L1-Distance = 0.0246, L2-Distance = 0.0007, Normal std = 0.5897

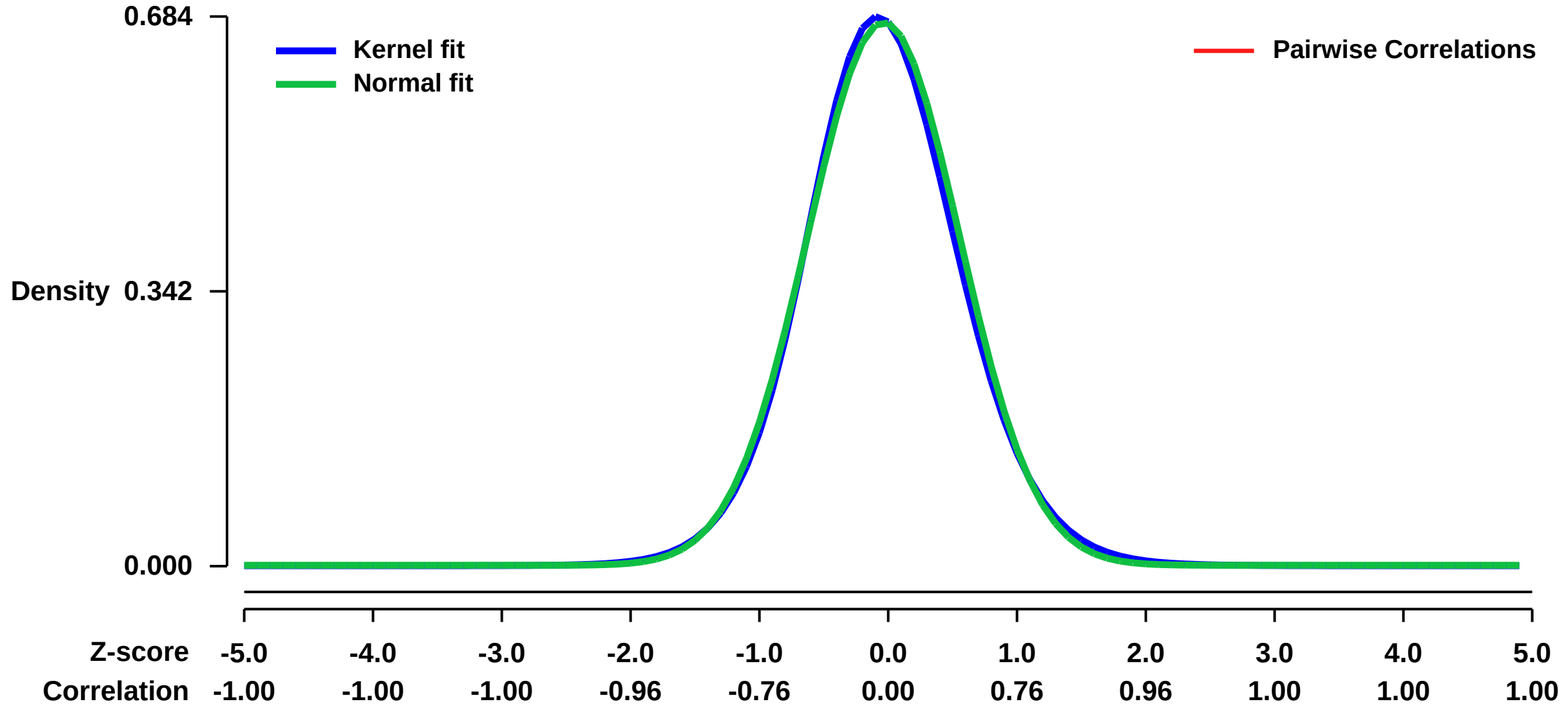

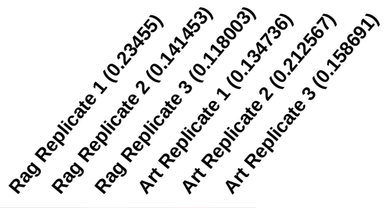

Pre-normalization Quantiles

[min] [medium] [max]

Null module

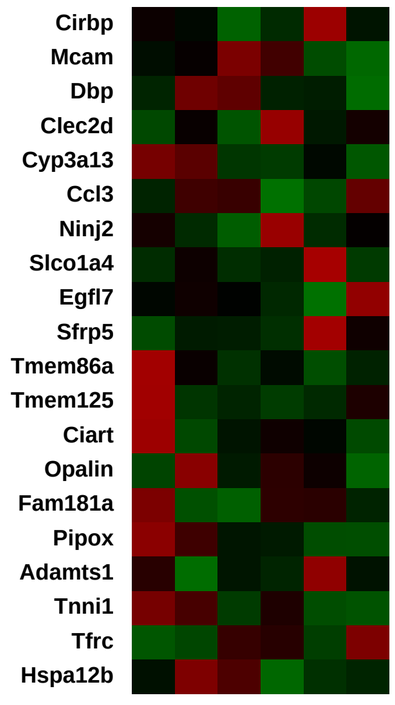

GEO Series "GSE23972" Expression Profiles

Num of samples in this series: 6

Scale of expression profile Z-scores

-3.0 -2.0 -1.0 0.0 1.0 2.0 3.0

GEO Link:	http://www.ncbi.nlm.nih.gov/geo/query/acc.cgi?acc=GSE23972
Status:	Public on Sep 03 2010
Title:	Ikaros deficient mouse thymic lymphomas
Organism:	Mus musculus
Experiment type:	Expression profiling by array
Platform:	GPL1261
Pubmed ID:	20829372
Summary & Design:	**Summary:** This dataset comprises expression profiles from 3 thymic lymphomas from Ikaros deficient mice (IkL/L model, see Dumortier et al, Mol. Cell. Biol. 26, 209-220, 2006 for a description of the tumor model) and 3 thymic lymphomas from IkL/L mice that harbor a mutation of the Notch1 gene (deletion of floxed sequences comprising the promoter and exon 1 with the CD4-Cre transgene). The results from this experimpent is that the expression of Notch target genes was unexpectedly not altered in the tumors with the Notch1 deletion. This result is explained by the activation of a cryptic 3' Notch1 promoter in the deleted tumors, which leads to constitutive Notch1 activation. These results are described in the following publication: R Jeannet, J Mastio, B Macias-Garcia, A Oravecz, T Ashworth, AS Geimer-Lelay, B Jost, S Le Gras, J Ghysdael, T Gridley, T Honjo, F Radtke, J Aster, S Chan and P Kastner. Oncogenic activation of the Notch1 gene in mouse T-cell leukemia by deletion of its promoter. Blood, in press (2010) **Overall design:** Primary thymic tumors from 3 IkL/L Notch1+/+ CD4-Cre+ mice (aged 18-20 weeks) were compared to similar tumors from 3 IkL/L Notch1f/f CD4-Cre+ mice (aged 8-10 weeks).

Background corr dist: KL-Divergence = 0.0466, L1-Distance = 0.0348, L2-Distance = 0.0017, Normal std = 0.6050

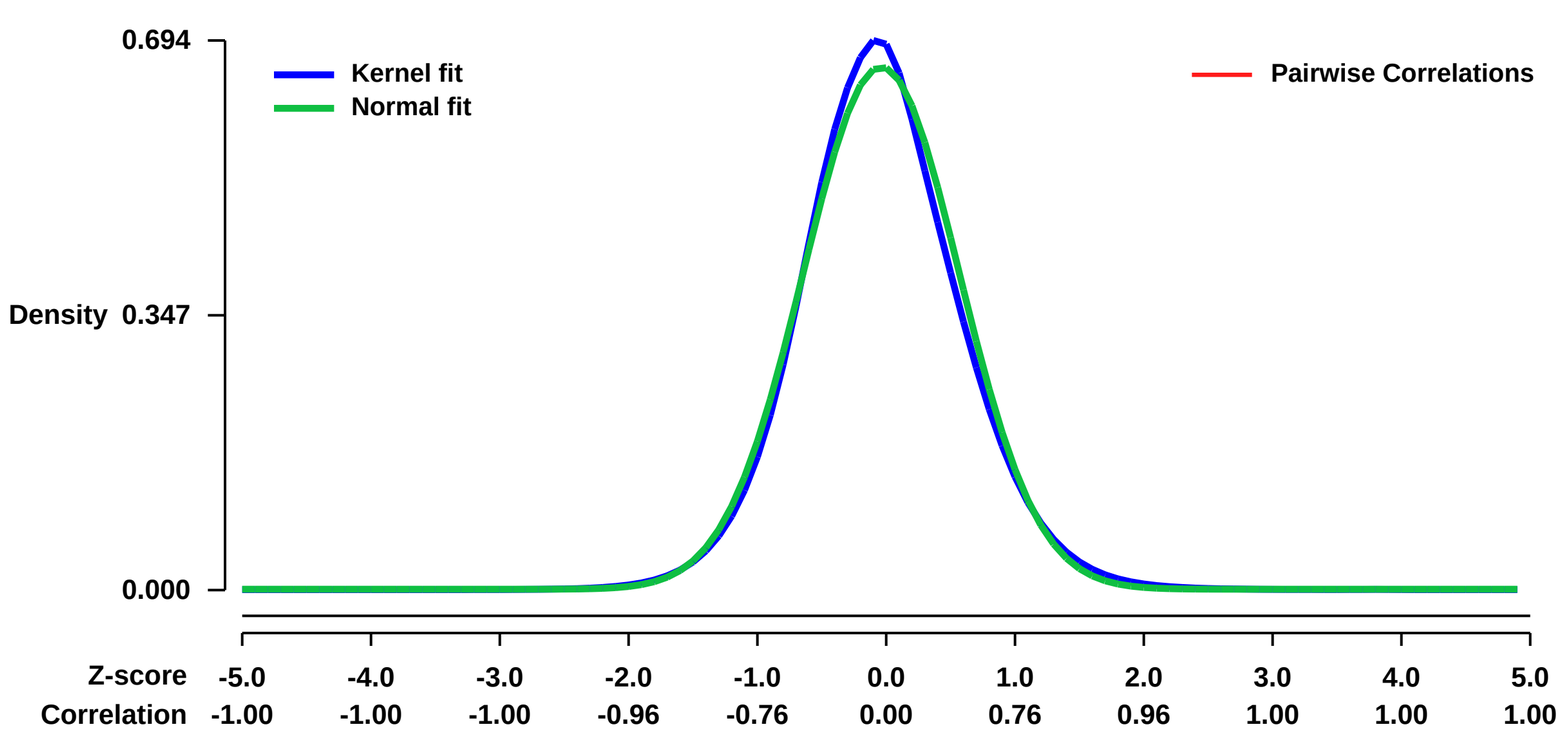

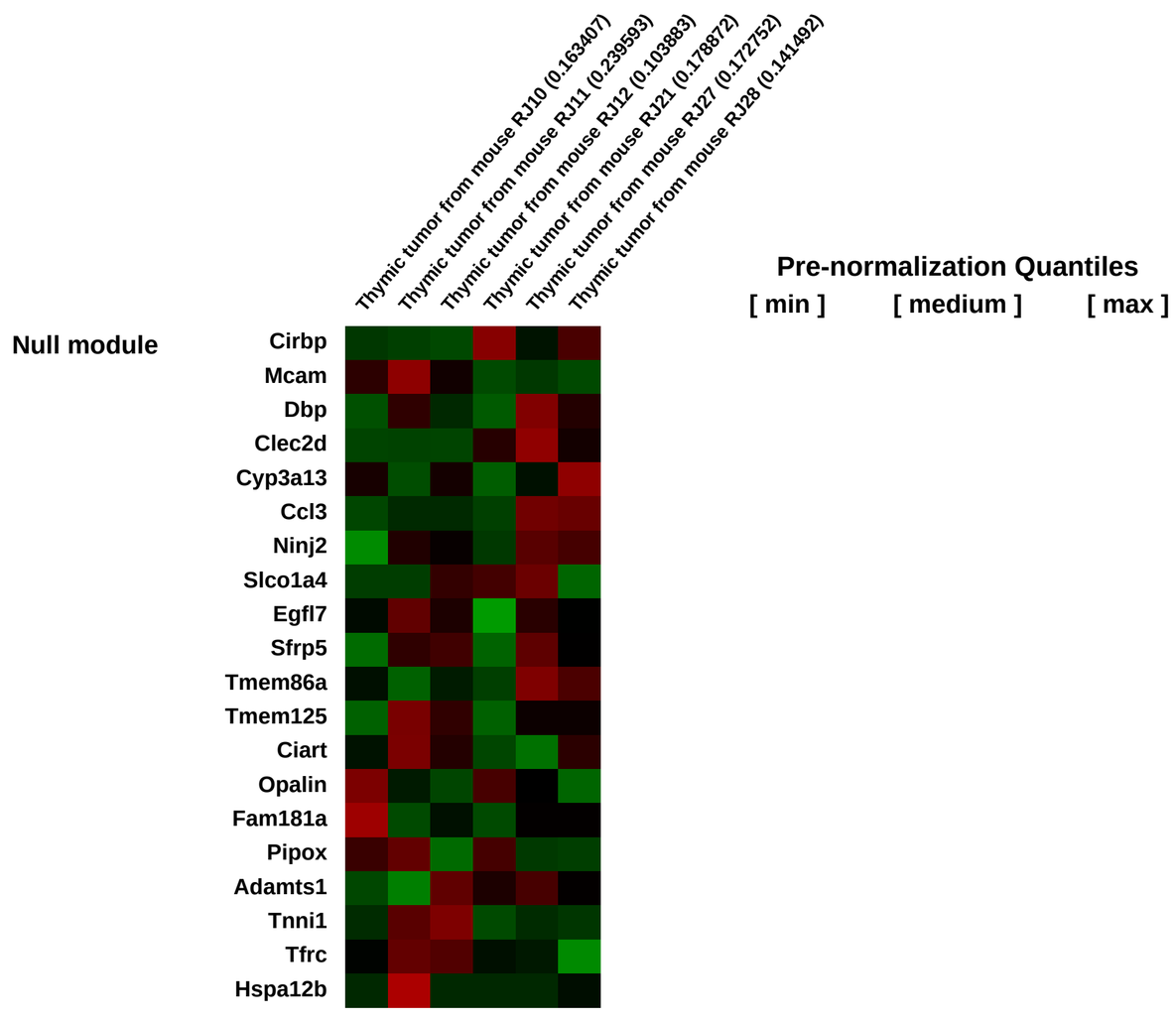

GEO Series "GSE15733" Expression Profiles

Num of samples in this series: 6

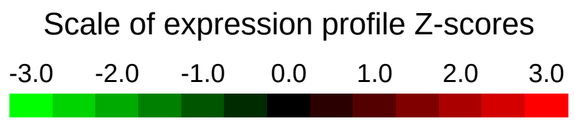

GEO Link:	http://www.ncbi.nlm.nih.gov/geo/query/acc.cgi?acc=GSE15733
Status:	Public on Apr 21 2009
Title:	Professional memory CD4+ T lymphocytes preferentially reside and rest in the bone marrow
Organism:	Mus musculus
Experiment type:	Expression profiling by array
Platform:	GPL1261
Pubmed ID:	19265543
Summary & Design:	**Summary:** CD4+ T lymphocytes are key to immunological memory, but little is known about the lifestyle of memory CD4+ T lymphocytes. We showed that in the memory phase of specific immune responses to antigens, most of the memory CD4+ T lymphocytes relocated into the bone marrow (BM) within 3-8 weeks after their generation, a process involving integrin a2. Antigen-specific memory CD4+ T lymphocytes expressed Ly-6C to a high degree, unlike most splenic CD44hiCD62L- CD4+ T lymphocytes. In adult mice, more than 80% of Ly-6Chi CD44hiCD62L- memory CD4+ T lymphocytes were in the BM. In the BM, they are located next to IL-7-expressing VCAM-1+ stroma cells, and were in a resting state. Upon challenge with antigen, they rapidly expressed cytokines and CD154 and induced the production of high-affinity antibodies, indicating their functional activity in vivo and marking them as professional memory T helper cells **Overall design:** Lists of differentially regulated genes were created using High Performance Chip Data Analysis (HPCDA) with Bioretis database (http://www.bioretis-analysis.de). To see the list of significant genes, go to Bioretis database, register and with your username and password log into the database. Then check under Account, User Details the two boxes Public Chip Rights and Public Analyses. Then select under Comparison, View single results in the window Select an existing Analysis the analysis SPL_294. To find the list of significant genes, click an next, then on Choose an existing parameterset and select first a default increase parameterset (be shure that on row ""t-Test EG vs. BG *"" in the first 4 left columns <0.05 is included and check the box ""* use Bonferroni correction""). Then click on Search only and you will get the list of differentially ^›ncreased genes. Perform the same procedure with a default parameterset for decrease genes. You can get instruction/help about Bioretis database before Login on sheet introduction.

Background corr dist: KL-Divergence = 0.0403, L1-Distance = 0.0415, L2-Distance = 0.0025, Normal std = 0.6448

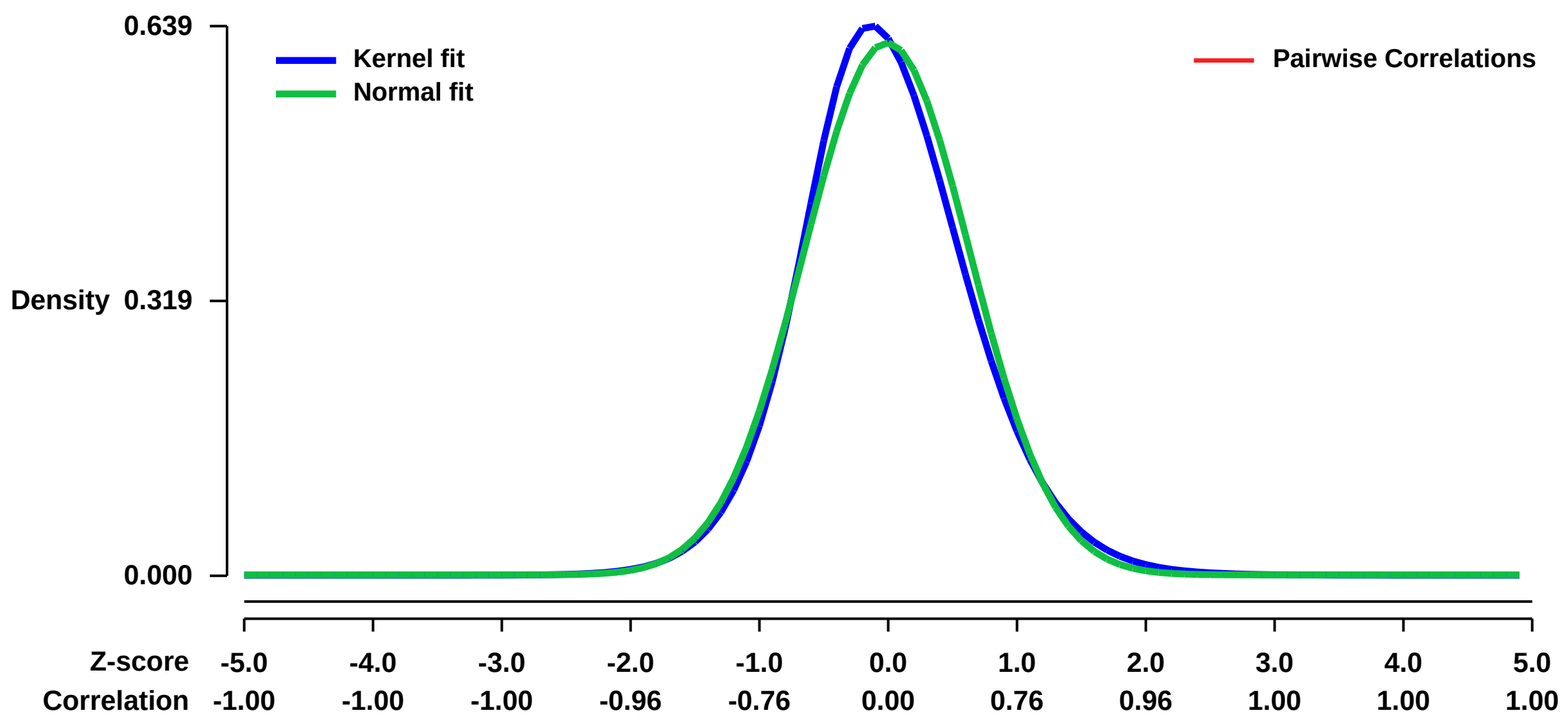

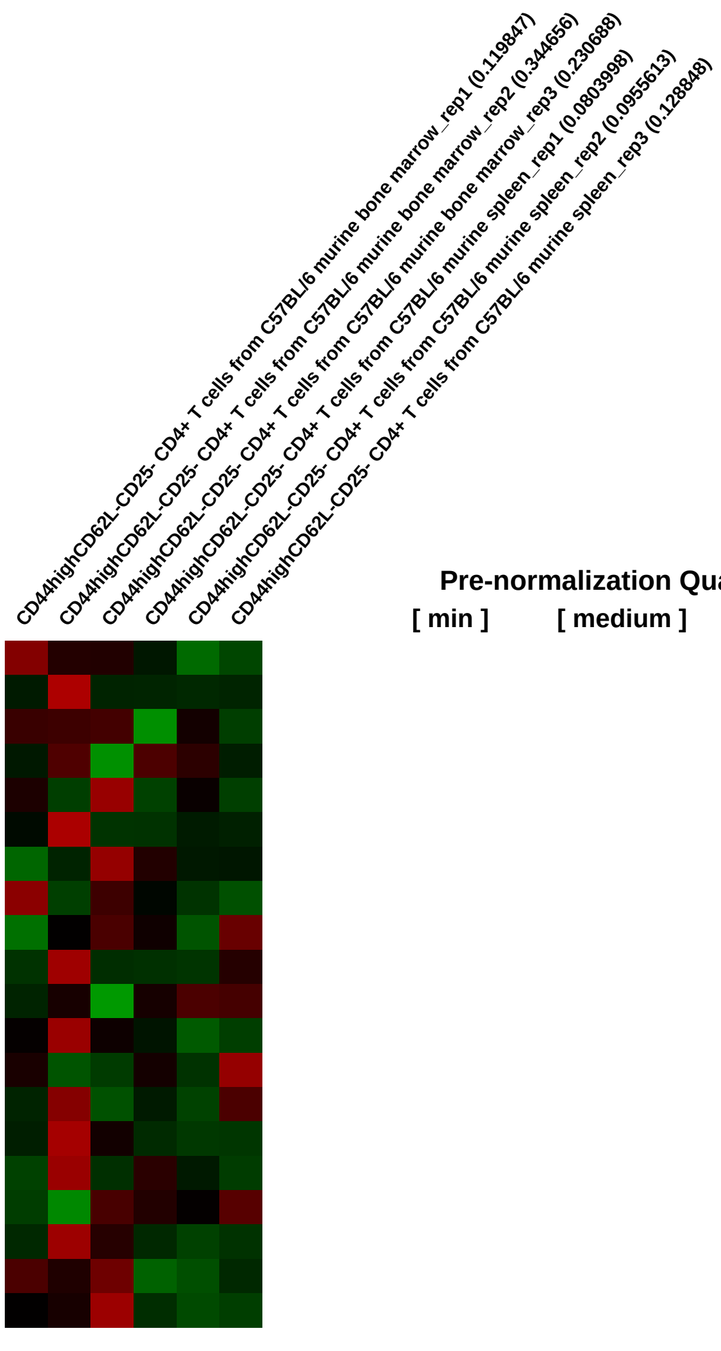

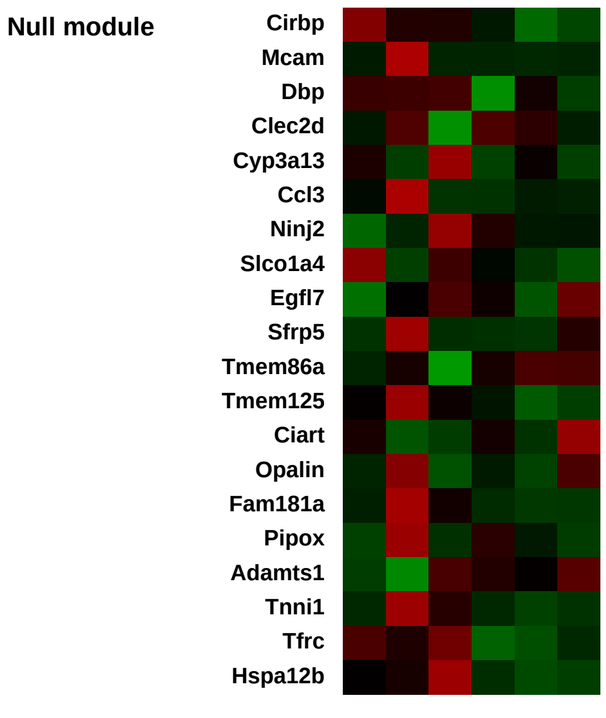

GEO Series "GSE50439" Expression Profiles

Num of samples in this series: 15

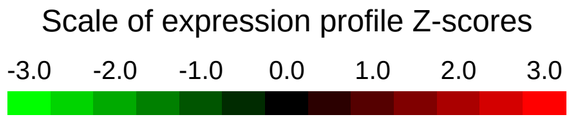

GEO Link:	**http://www.ncbi.nlm.nih.gov/geo/query/acc.cgi?acc=GSE50439**
Status:	**Public on Mar 01 2014**
Title:	**Examining efficiency of enrichment of kidney pericyte-specific messages by TRAP (Translating Ribosome Affinity Purification)**
Organism:	**Mus musculus**
Experiment type:	**Expression profiling by array**
Platform:	**GPL1261**
Pubmed ID:	**24652793**
Summary & Design:	**Summary:** **The long term goal is to define the transcriptional changes that accompany pericyte-to-myofibroblast transition in fibrotic kidney disease. Medullary pericytes are identified by their expression of a eGFPL10a fusion protein whose expression is driven by a Col1a1 promoter. Pericyte-specific RNA is generated by eGFP-affinity purification of polysomes from medullary lysates and then subject to microarray analysis.** **Overall design:** **Col1a1-eGFPL10a mice were subject to Sham or unilateral ureteral obstruction surgery. Sham kidneys were collected at day 0, and UUO kidneys were collected at day 2 or day 5 for TRAP.**

Background corr dist: **KL-Divergence = 0.1276, L1-Distance = 0.0385, L2-Distance = 0.0032, Normal std = 0.4031**

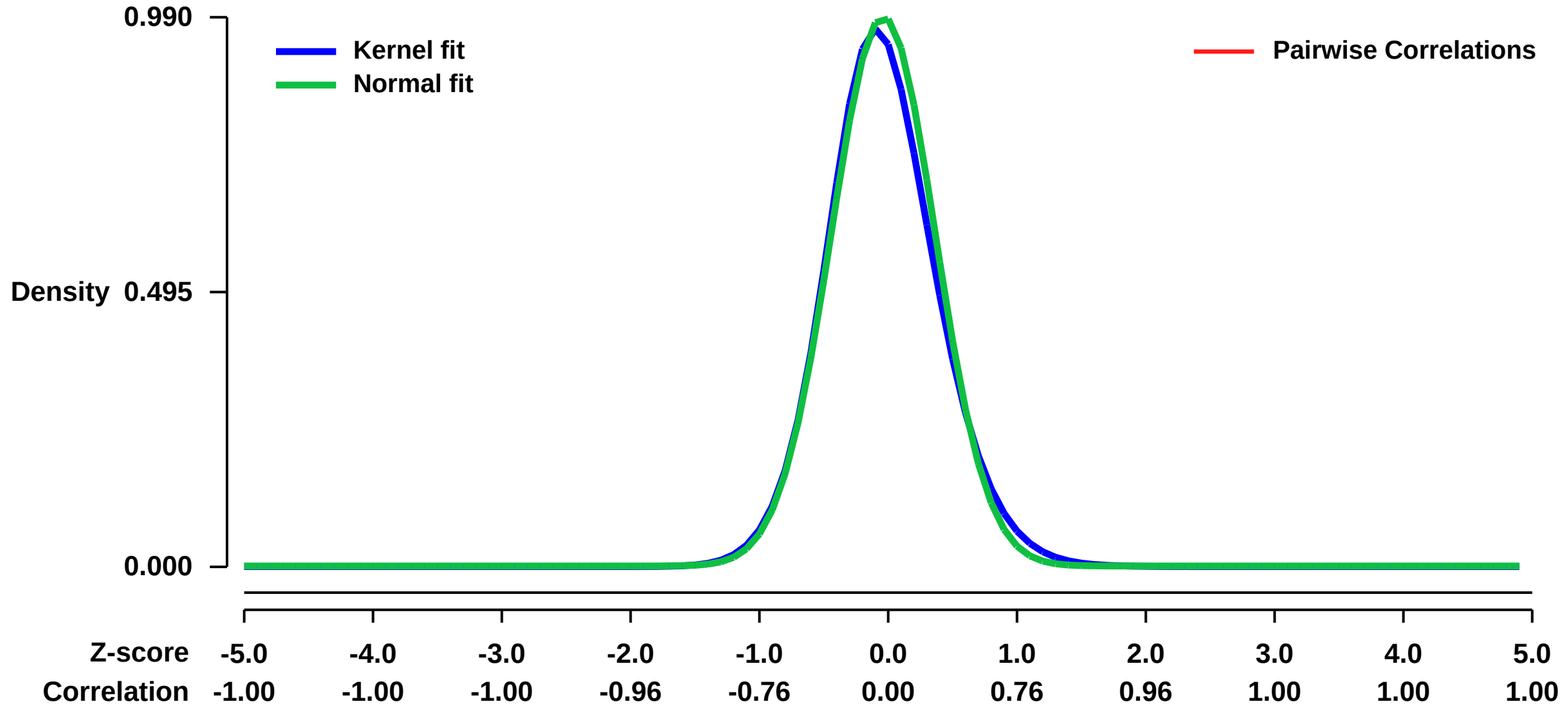

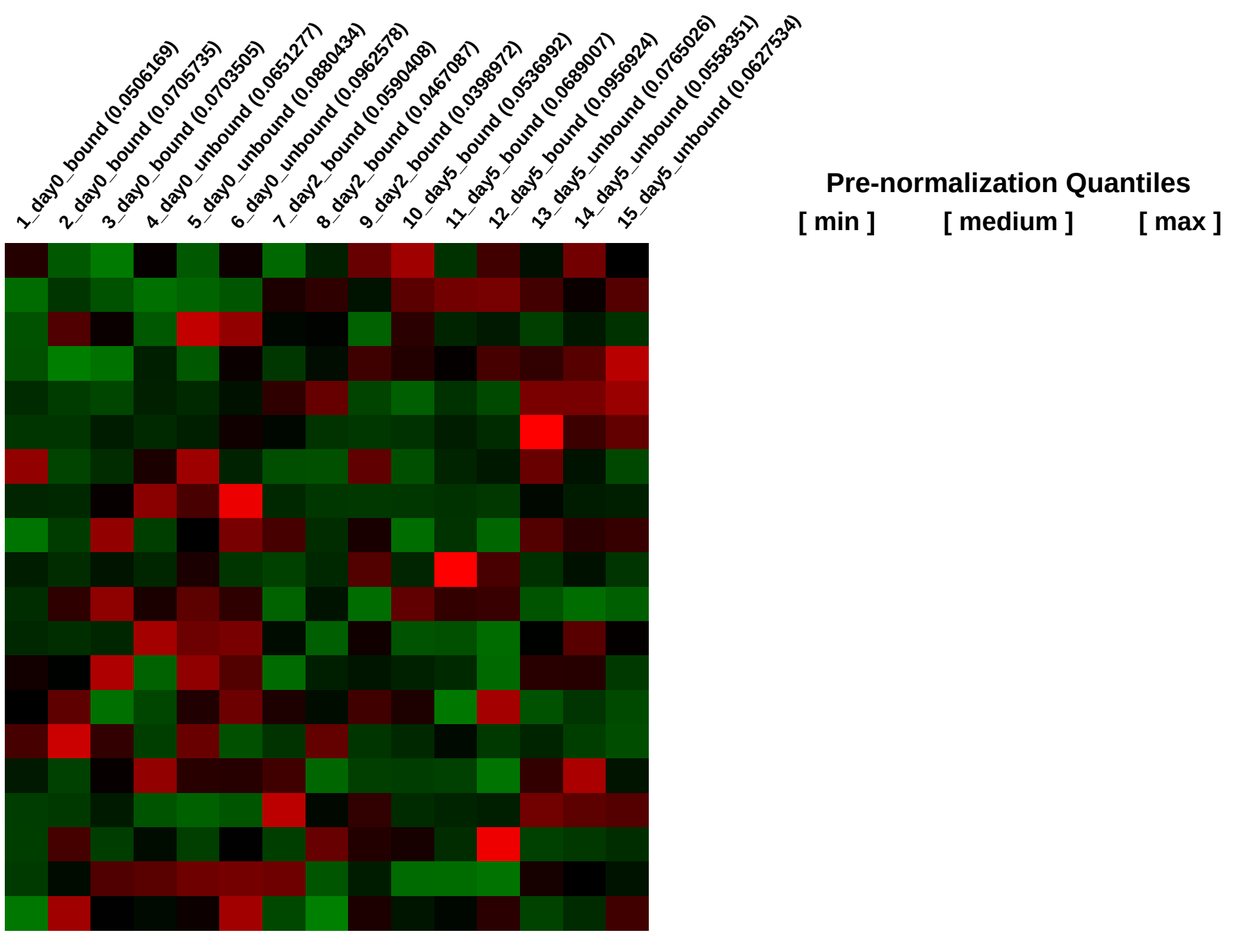

GEO Series "GSE11443" Expression Profiles

Num of samples in this series: 6

Scale of expression profile Z-scores

-3.0 -2.0 -1.0 0.0 1.0 2.0 3.0

GEO Link:	**http://www.ncbi.nlm.nih.gov/geo/query/acc.cgi?acc=GSE11443**
Status:	**Public on May 17 2008**
Title:	**Choroid plexus function in B10.pl WT mice versus B10.PL RAG-/- mice (carri-affy-mouse-302760)**
Organism:	**Mus musculus**
Experiment type:	**Expression profiling by array**
Platform:	**GPL1261**
Pubmed ID:	
Summary & Design:	**Summary:** **Previous work has led us to examine the differences in the choroid plexus function in B10.pl WT mice versus B10.PL RAG-/- mice. We believe that there is a difference between those that are normal functioning and those that are lymphocyte deficient.** **To determine the gene expression profile of the choroid plexus in wild type mice as compared to those that are lymphocyte deficient.** **We hypothesize that there is altered expression in the genes that mediate cellular adhesion in choroid plexus from wild type mice as compared to those that are lymphocyte deficient.** **8-10 week old animals (age and sex matched) were injected with Evan's blue post anesthetization. After waiting an hour the animals were euthanized and their brains were extracted and placed in RNALater for 24 hours. The brains were then sliced sagitally**
	Keywords: RAG mutant, choroid plexus
	Overall design:

Background corr dist: KL-Divergence = 0.0359, L1-Distance = 0.0301, L2-Distance = 0.0012, Normal std = 0.6517

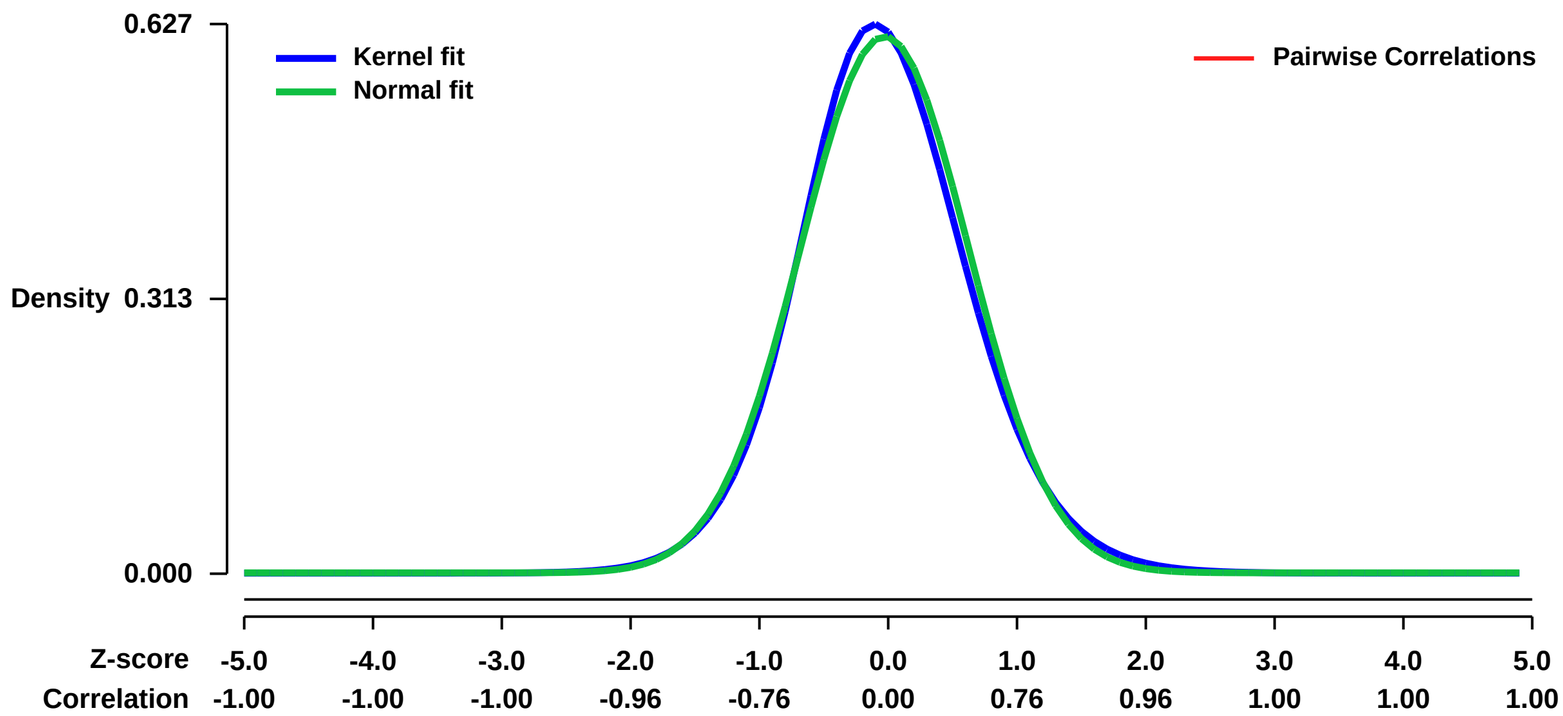

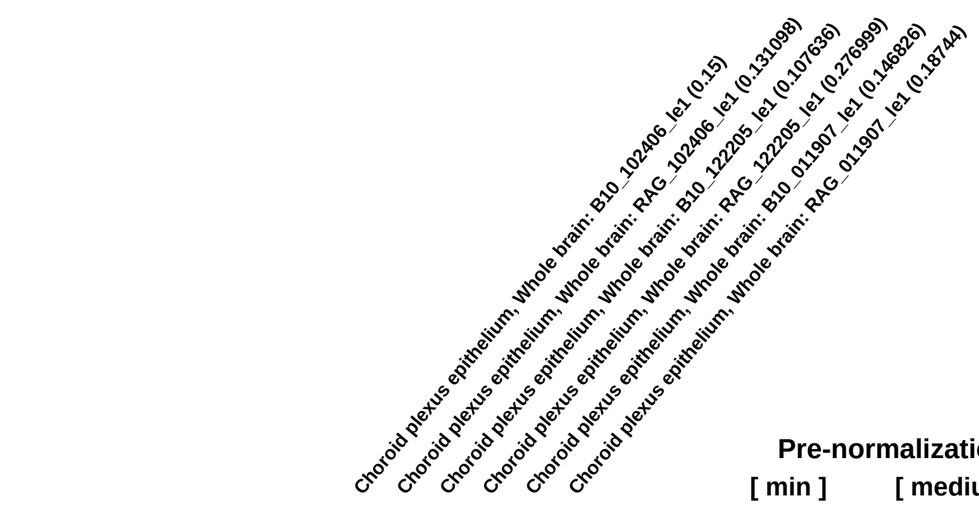

Pre-normalization Quantiles

[min] [medium] [max]

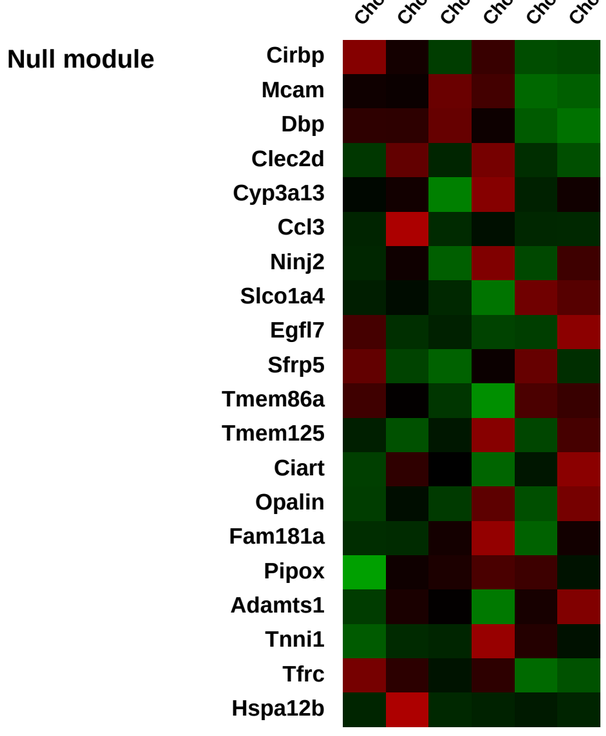

GEO Series "GSE19997" Expression Profiles

Num of samples in this series: 9

Scale of expression profile Z-scores

-3.0 -2.0 -1.0 0.0 1.0 2.0 3.0

GEO Link:	http://www.ncbi.nlm.nih.gov/geo/query/acc.cgi?acc=GSE19997
Status:	Public on Apr 09 2010
Title:	POU4F1 is associated with t(8;21) AML and contributes directly to its unique transcriptional signature
Organism:	Mus musculus
Experiment type:	Expression profiling by array
Platform:	GPL1261
Pubmed ID:	20376082
Summary & Design:	**Summary:** POU4F1 is associated with t(8;21) acute myeloid leukemia (AML) and contributes directly to its unique transcriptional signature **Overall design:** To identify targets of POU4F1, we performed gene expression profiling, comparing Pou4f1+/+ or Pou4f1-/- fetal liver cells to cells overexpressing POU4F1 and identified 140 differentially expressed genes.

Background corr dist: KL-Divergence = 0.0360, L1-Distance = 0.0369, L2-Distance = 0.0026, Normal std = 0.6235

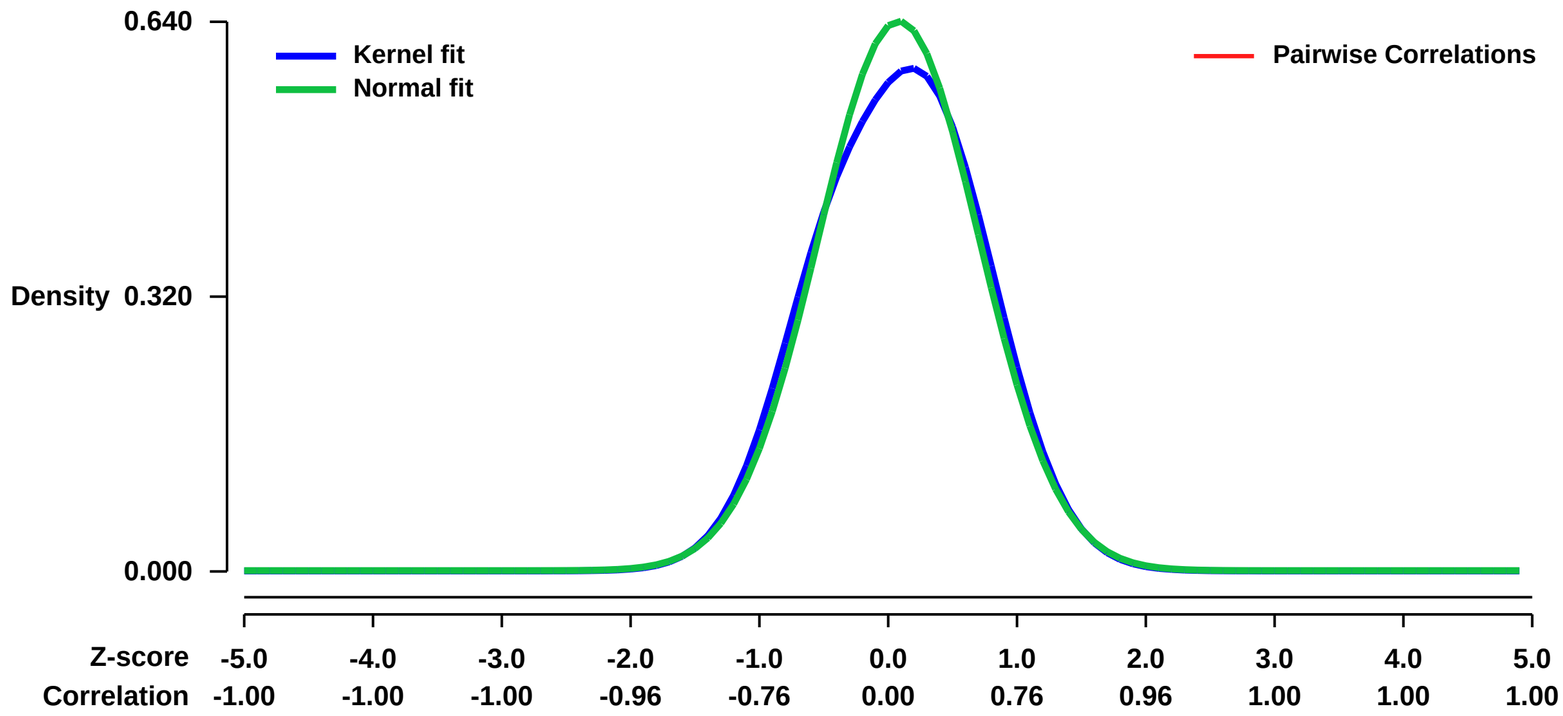

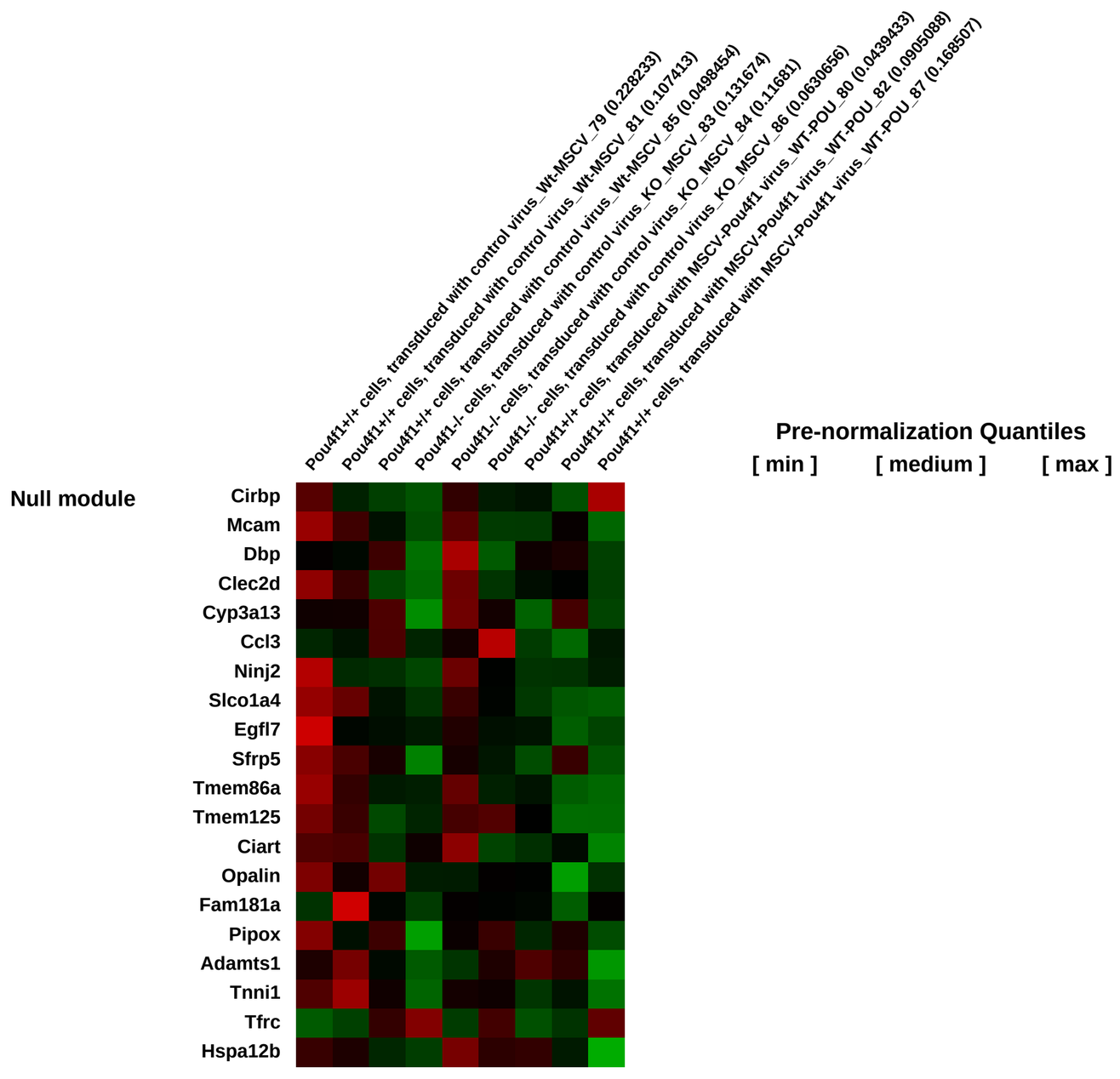

GEO Series "GSE25640" Expression Profiles

Num of samples in this series: 12

Scale of expression profile Z-scores

-3.0 -2.0 -1.0 0.0 1.0 2.0 3.0

GEO Link:	http://www.ncbi.nlm.nih.gov/geo/query/acc.cgi?acc=GSE25640
Status:	Public on Nov 29 2010
Title:	Expression data from wild type or FIZZ2 knockout murine lungs
Organism:	Mus musculus
Experiment type:	Expression profiling by array
Platform:	GPL1261
Pubmed ID:	21602491
Summary & Design:	**Summary:** To study the possible fibrotic role of FIZZ2, bleomycin was used to induce pulmonary fibrosis in wild type and FIZZZ2 knockout mice, lungs were then harvested and processed for RNA isolation. We used microarrays to detail the global gene expression regulated by FIZZ2 during fibrotic process. **Overall design:** Bleomycin/saline treated wild type or FIZZ2 knockout lungs at day 21 post injection were harvested for RNA isolation and hybridization on Affymetrix microarrays

Background corr dist: KL-Divergence = 0.0807, L1-Distance = 0.0207, L2-Distance = 0.0005, Normal std = 0.4759

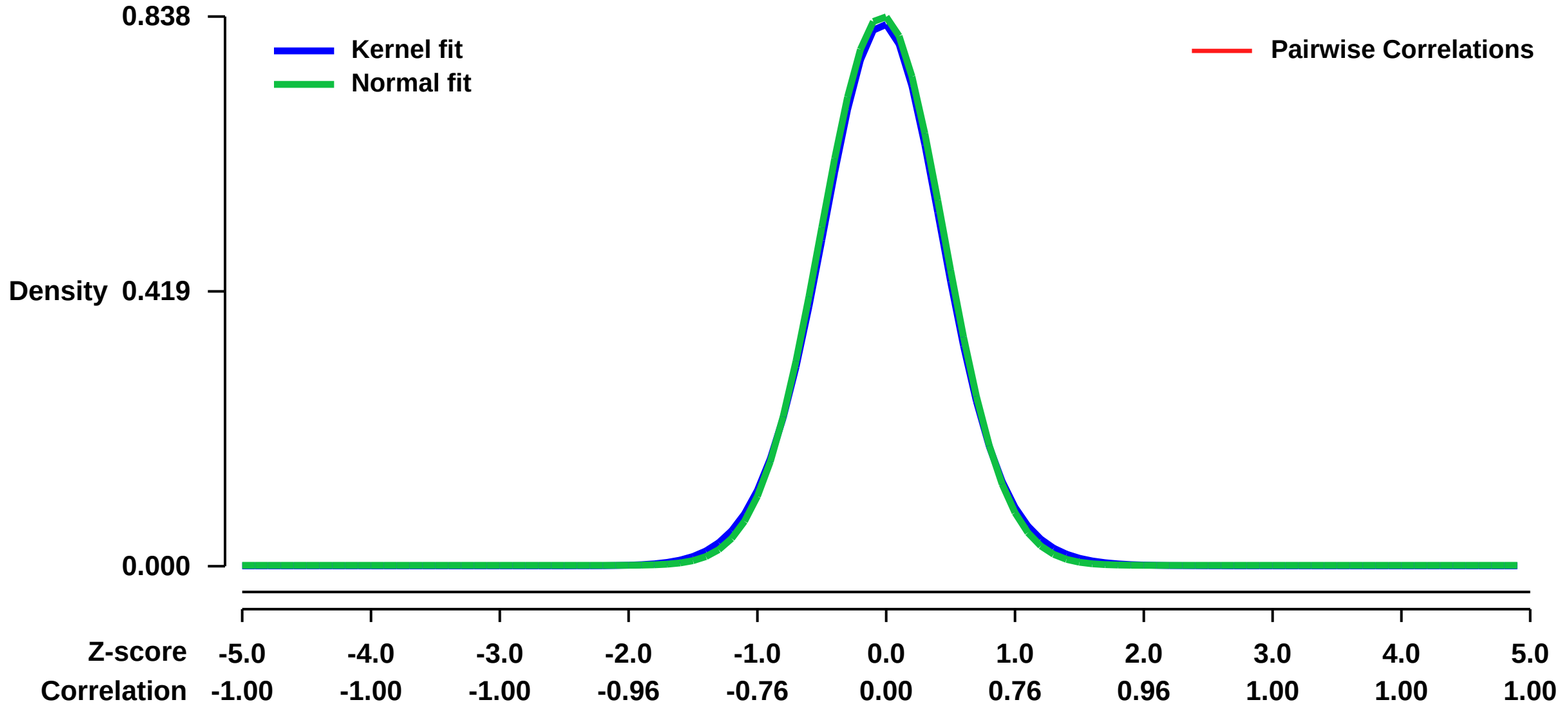

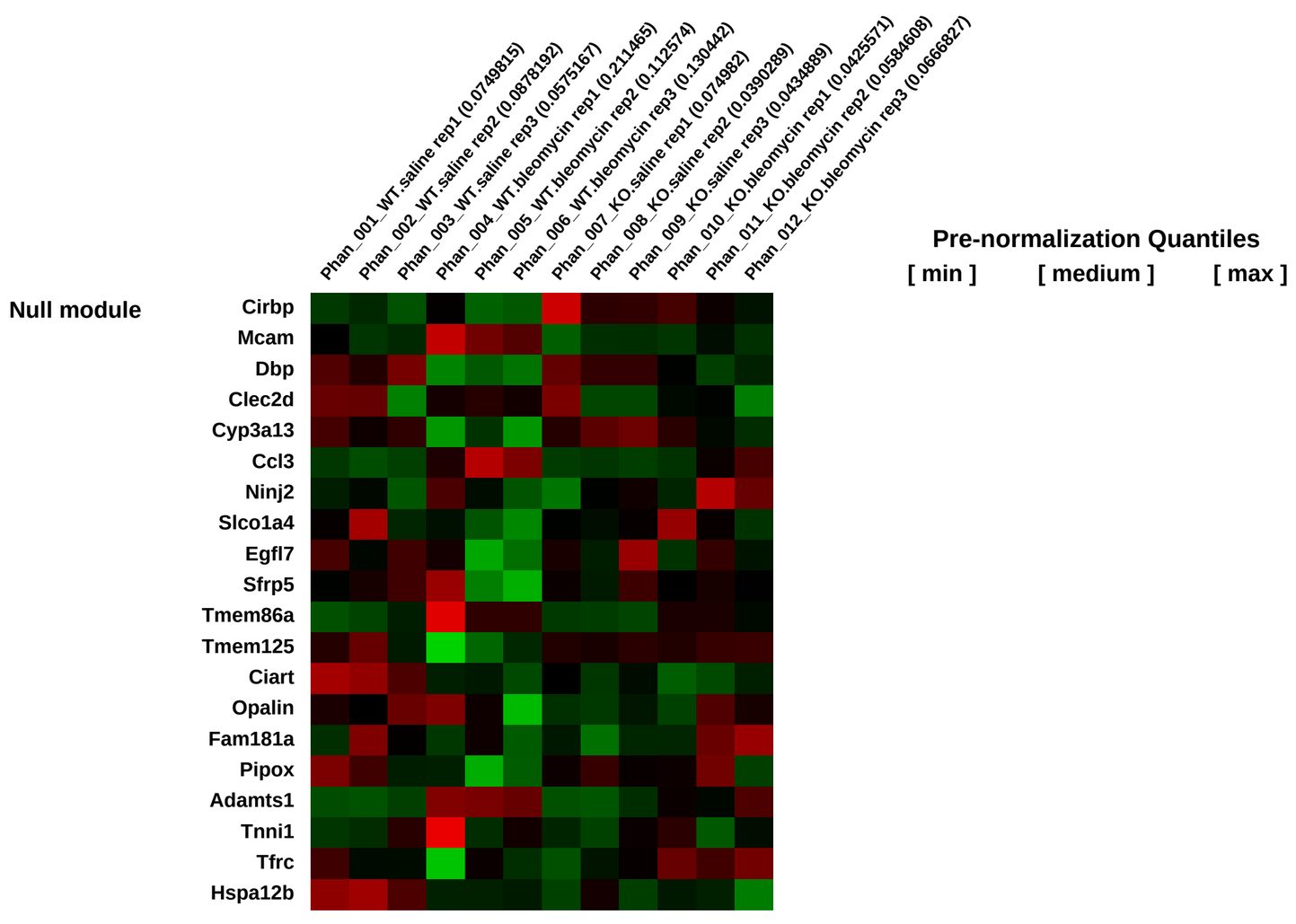

GEO Series "GSE44663" Expression Profiles

Num of samples in this series: 6

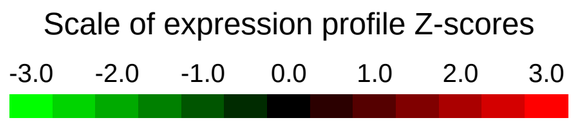

GEO Link:	**http://www.ncbi.nlm.nih.gov/geo/query/acc.cgi?acc=GSE44663**
Status:	**Public on Feb 26 2013**
Title:	**Expression data from adult mouse mesenteric arteries**
Organism:	**Mus musculus**
Experiment type:	**Expression profiling by array**
Platform:	**GPL1261**
Pubmed ID:	
Summary & Design:	**Summary:** **Vascular smooth muscle cells require beta1 integrin for survival. Following the induced deletion of smooth muscle beta1 integrin, smooth muscle cells undergo apoptosis and arteries become fibrotic. This microarray study on mesenteric arteries 2 weeks after the initiation of beta1 integrin deletion specifically in smooth muscle cells of the adult mouse aimed to examine early changes in expression following deletion.** **Overall design:** **Mesenteric arteries from three wild type mixed background and three beta1 integrin smooth muscle knockout mixed background mice are examined.**

Background corr dist: **KL-Divergence = 0.0392, L1-Distance = 0.0238, L2-Distance = 0.0007, Normal std = 0.6246**

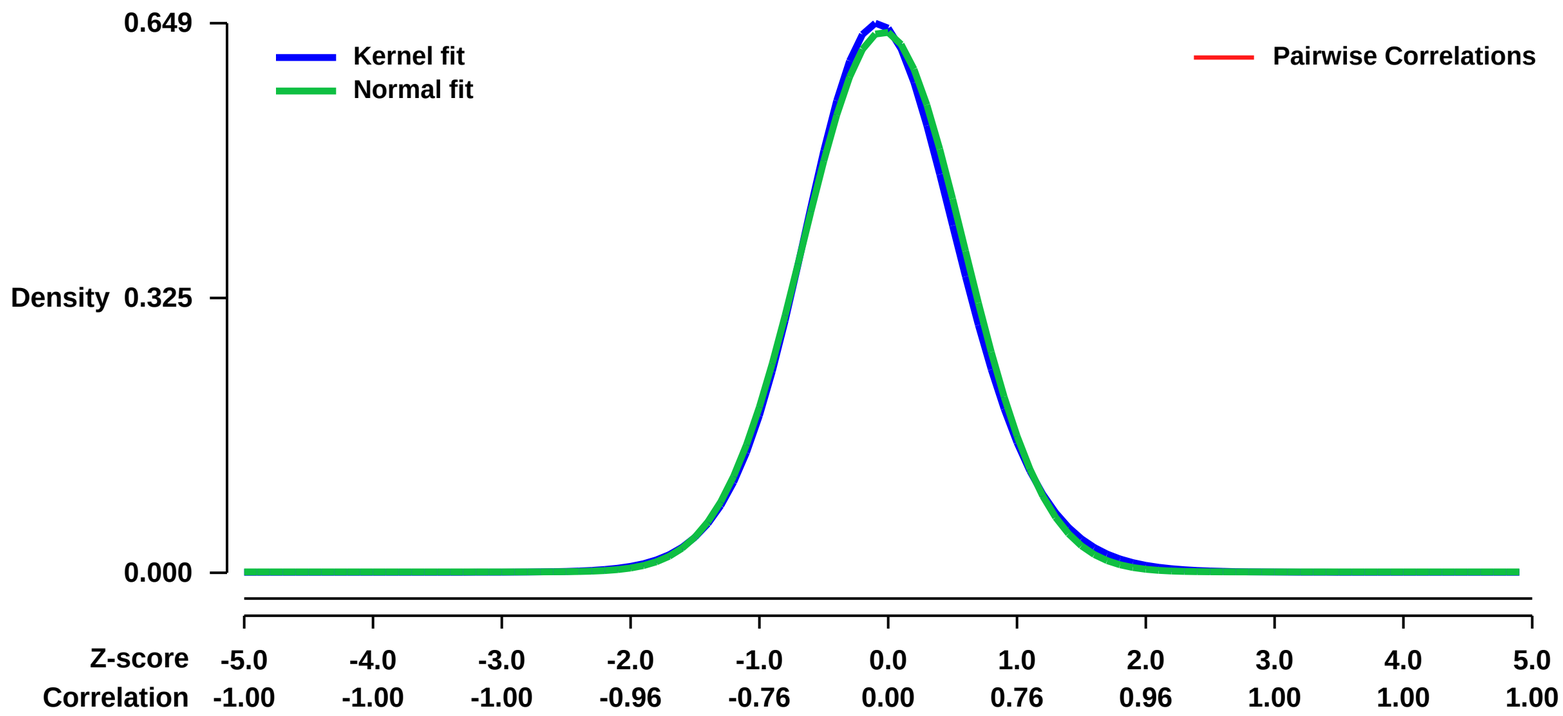

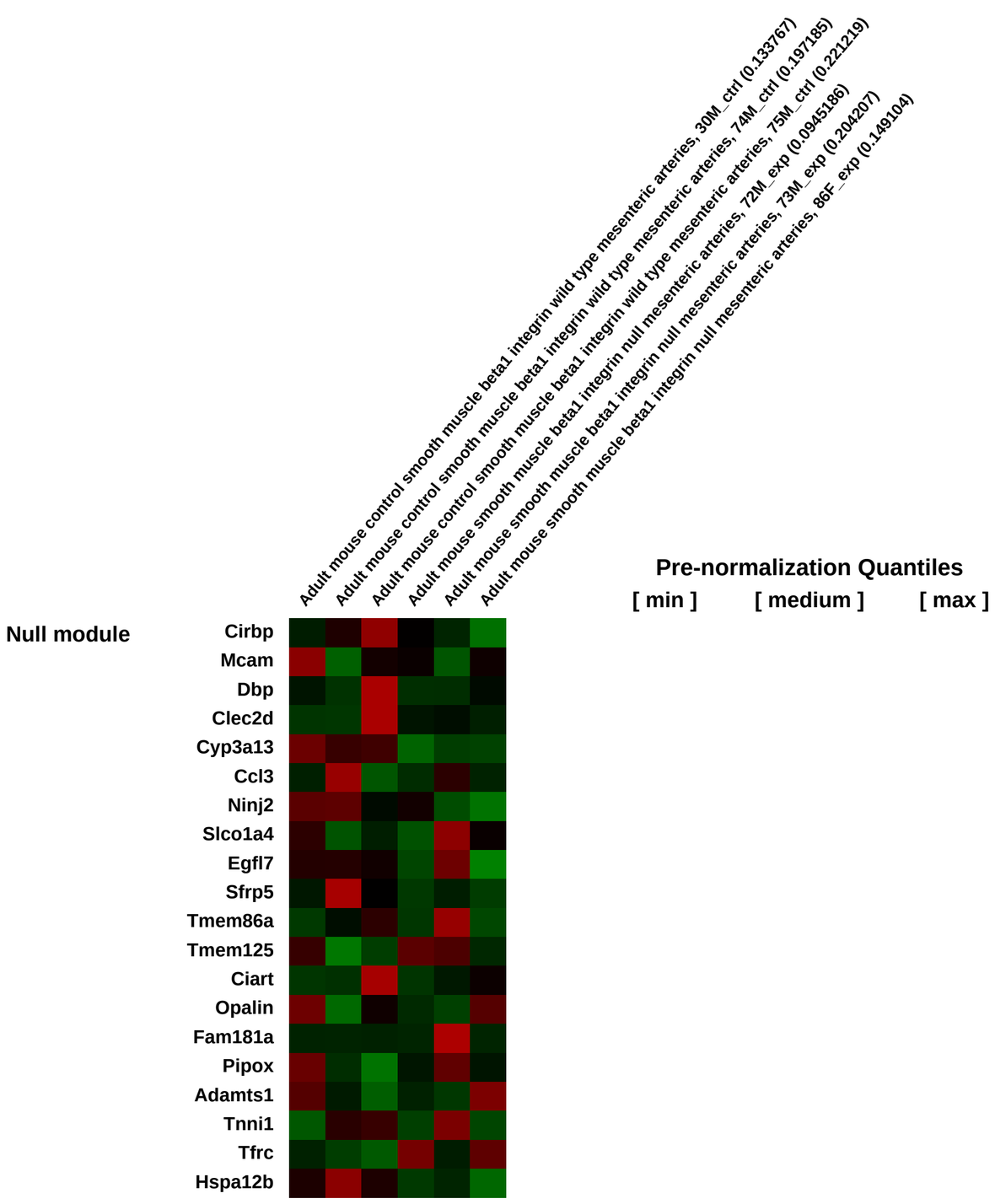

GEO Series "GSE27563" Expression Profiles

Num of samples in this series: 93

Scale of expression profile Z-scores

-3.0 -2.0 -1.0 0.0 1.0 2.0 3.0

GEO Link: http://www.ncbi.nlm.nih.gov/geo/query/acc.cgi?acc=GSE27563
Status: Public on Mar 01 2011
Title: Expression data from murine PBCs from mice with advanced mammary tumors and their tumor-free counterparts.
Organism: Mus musculus
Experiment type: Expression profiling by array
Platform: GPL1261
Pubmed ID: 21781289

Summary & Design:

Summary:
Female MMTV/c-MYC transgenic mice expressed the c-MYC proto-oncogene or a more stable point mutation variant (T58A) of the gene under the control of the hormone-responsive MMTV long terminal repeat (LTR) in an FVB/NJ background (Jackson Laboratories, Bar Harbor, ME). The hormones released during pregnancy and lactation have been shown to enhance expression of the oncogene. Thus, the mice were maintained in a continuous breeding program. Mice were monitored twice weekly for tumor development by palpation and tumors were measured twice weekly. Once the tumors reached 3cm3 the animals were sacrificed and tissue was obtained to confirm the tumors by histological analysis. As a control, female mice of the same age and background strain were maintained in the same facility and under the same breeding conditions as their transgenic counterparts.

Overall design:
Blood (50-250 ˆµL, based on weight of the mouse) was collected from MMTV/c-MYC female mice and controls at regular intervals (approximately once per month) and again prior to euthanization (average age 431 days).

Background corr dist: KL-Divergence = 0.2402, L1-Distance = 0.0631, L2-Distance = 0.0109, Normal std = 0.3116

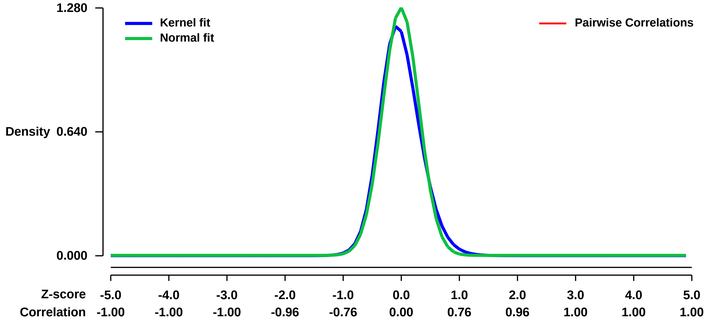

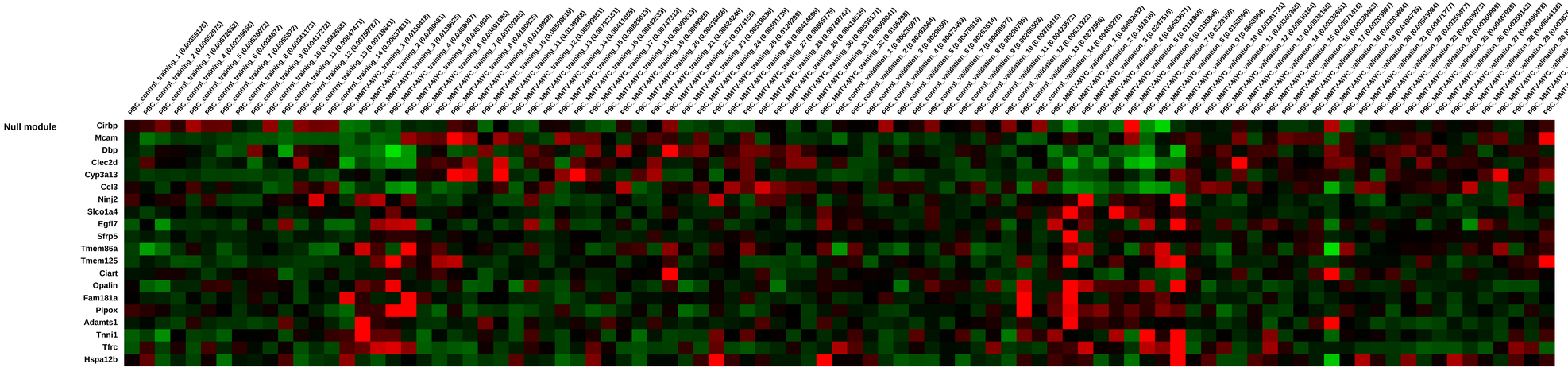

GEO Series "GSE28515" Expression Profiles

Num of samples in this series: 66

Scale of expression profile Z-scores

-3.0 -2.0 -1.0 0.0 1.0 2.0 3.0

GEO Link: http://www.ncbi.nlm.nih.gov/geo/query/acc.cgi?acc=GSE28515

Status: Public on Dec 01 2011

Title: Effect of acute ethanol on medidal prefrontal cortex across BXD genetic mapping panel and progenitors.

Organism: Mus musculus

Experiment type: Expression profiling by array

Platform: GPL1261

Pubmed ID: 22511924

Summary & Design:

Summary:
In order to elucidate the molecular mechanisms underlying individual variation in sensitivity to ethanol we profiled the prefrontal cortex transcriptomes of two inbred strains that exhibit divergent responses to acute ethanol, the C57BL6/J (B6) and DBA/2J (D2) strains, as well as 27 members of the BXD recombinant inbred panel, which was derived from a B6 x D2 cross. With this dataset we were able to identify several gene co-expression networks that were robustly altered by acute ethanol across the BXD panel. These ethanol-responsive gene-enriched networks were heavily populated by genes regulating synaptic transmission and neuroplasticity, and showed strong genetic linkage to discreet chromosomal loci. Network-based measurements of node importance identified several hub genes as established regulators of ethanol response phenotypes, while other hubs represent novel candidate modulators of ethanol responses.

Overall design:
Animals were injected intraperitoneally (IP) with saline or 1.8 g/kg of ethanol. As part of a parallel study of ethanol induced anxiolysis, all mice underwent behavioral testing that included 15 minutes of restraint in a 50 mL conical tube followed by 10 minutes in a light-dark chamber. Mice were killed by cervical dislocation four hours following IP injection. Immediately thereafter, brains were extracted and chilled for 1 minute in iced phosphate buffer before being microdissected into 8 constituent regions, including the medial prefrontal cortex. Samples were randomly assigned to batch groups prior to total RNA extraction, cRNA synthesis and hybridization. Each microarray represent a pooling of 4-5 animals.

Background corr dist: KL-Divergence = 0.4180, L1-Distance = 0.0881, L2-Distance = 0.0251, Normal std = 0.2427

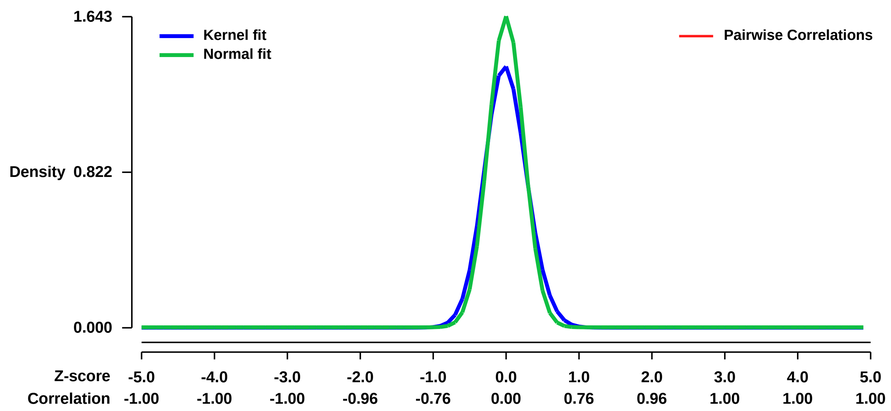

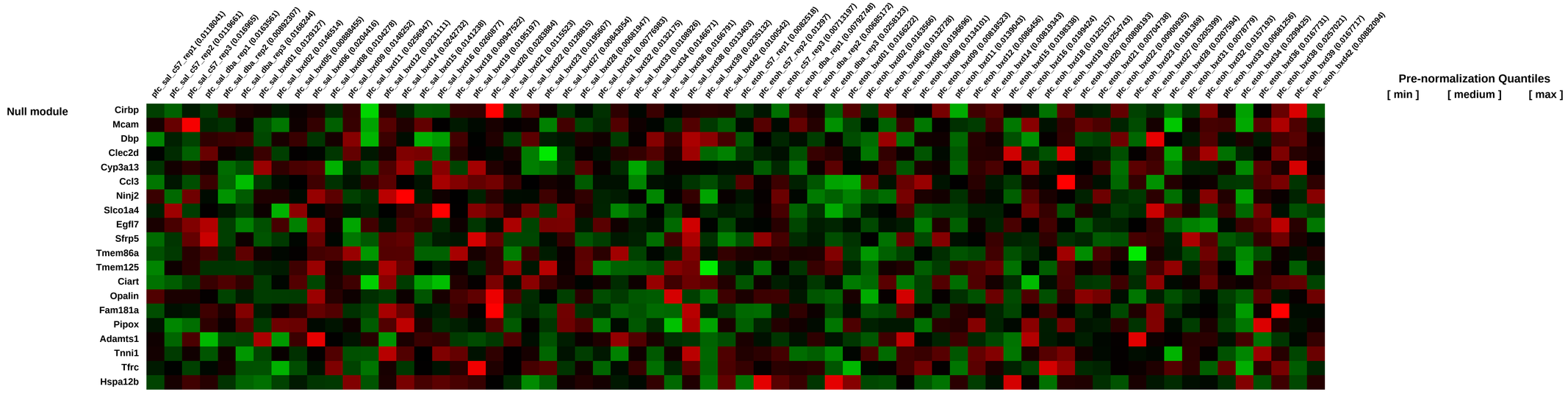

GEO Series "GSE27720" Expression Profiles

Num of samples in this series: 6

Scale of expression profile Z-scores

-3.0 -2.0 -1.0 0.0 1.0 2.0 3.0

GEO Link:	http://www.ncbi.nlm.nih.gov/geo/query/acc.cgi?acc=GSE27720
Status:	Public on Jan 06 2012
Title:	AMPK stimulation and PGC-1 alpha suppression in peroxisome deficient hepatocytes favor catabolic over anabolic carbohydrate metabolism
Organism:	Mus musculus
Experiment type:	Expression profiling by array
Platform:	GPL1261
Pubmed ID:	22002056
Summary & Design:	**Summary:** These arrays contain data from the livers of 10 week old L-Pex5 -/- male mice **Overall design:** 6 arrays, 3 biological replicates

Background corr dist: KL-Divergence = 0.0148, L1-Distance = 0.0326, L2-Distance = 0.0017, Normal std = 0.8076

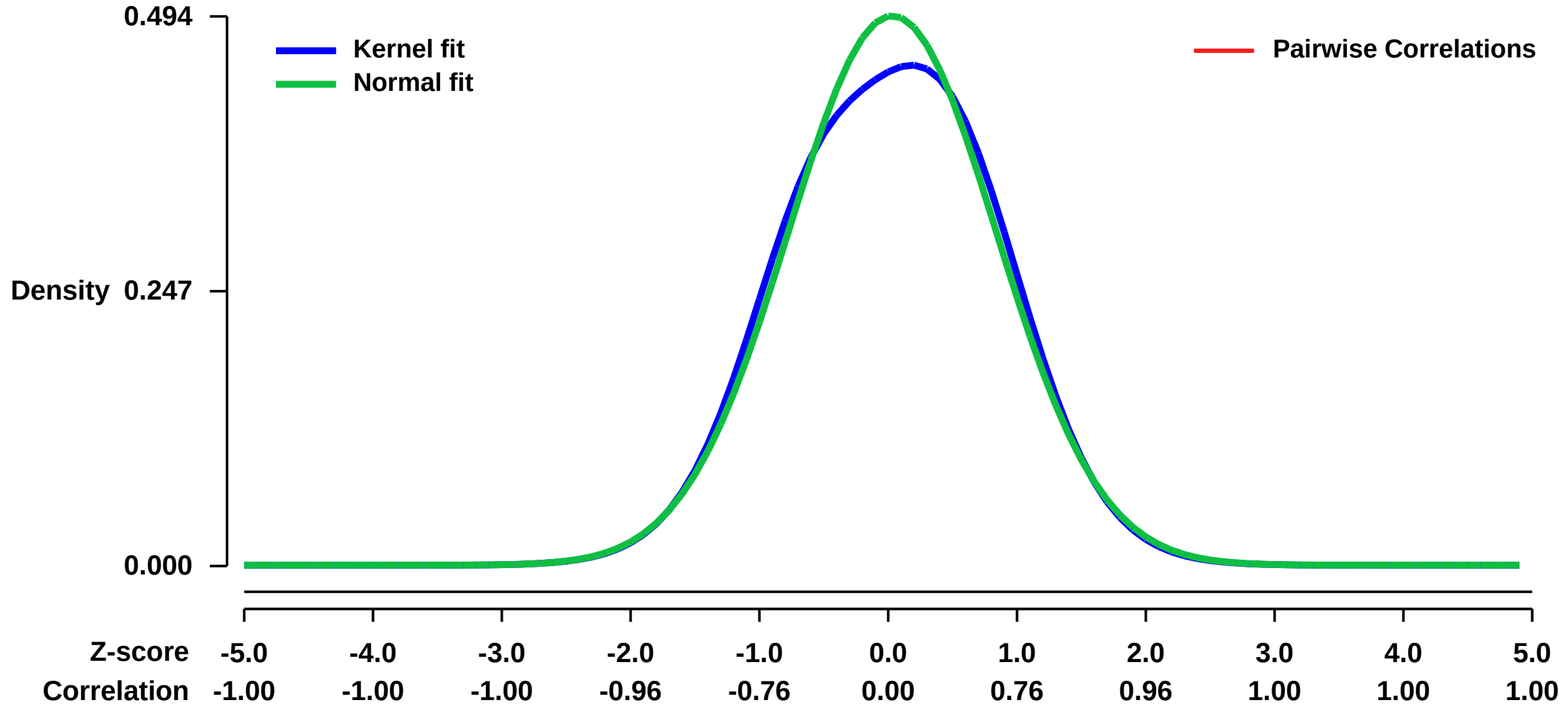

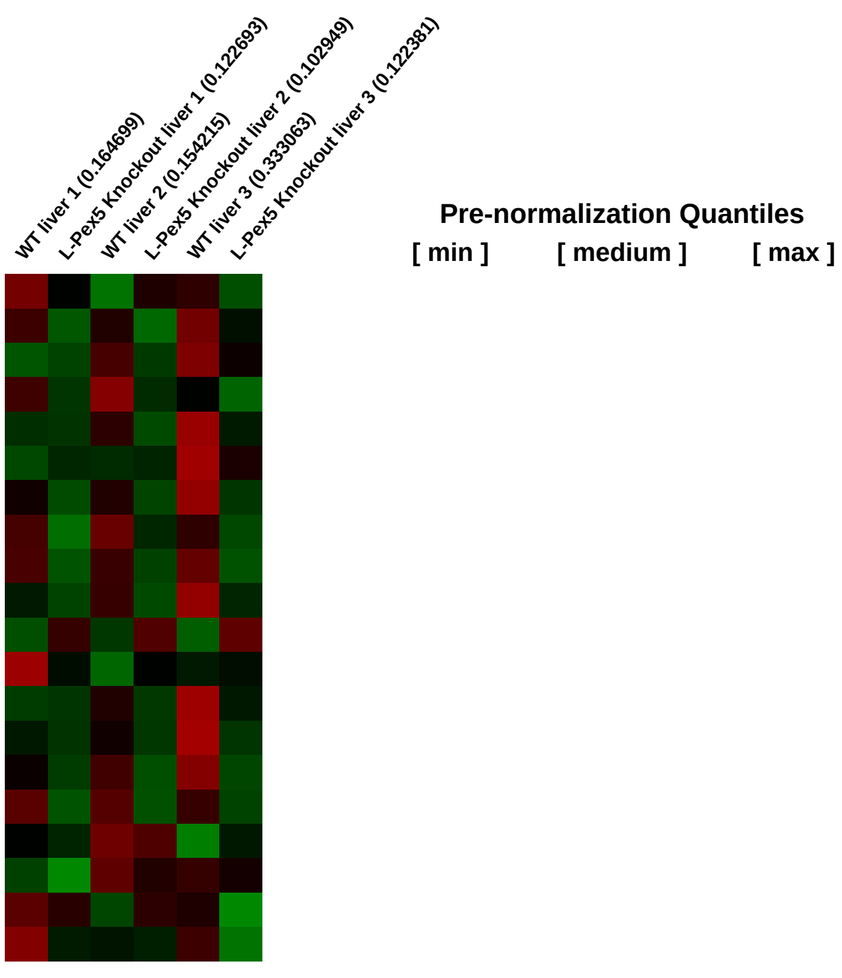

GEO Series "GSE45618" Expression Profiles

Num of samples in this series: 6

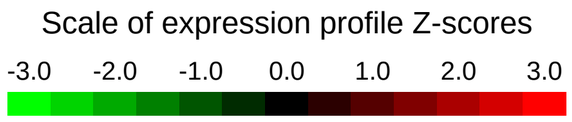

GEO Link:	http://www.ncbi.nlm.nih.gov/geo/query/acc.cgi?acc=GSE45618
Status:	Public on Mar 29 2013
Title:	Expression analysis of BL6 murine megakaryocyte progenitors from bone marrow and fetal Liver
Organism:	Mus musculus
Experiment type:	Expression profiling by array
Platform:	GPL1261
Pubmed ID:	
Summary & Design:	**Summary:** About 10% of Down syndrome (DS) infants are born with a myeloproliferative disorder (DS-TMD) that spontaneously resolves within the first few months of life. About 20-30% of these infants subsequently develop acute megakaryoblastic leukemia (DS-AMKL). In order to understand differences that may exist between fetal and bone marrow megakaryocyte progenitor cell populations we flow sorted megakaryocyte progenitor cells and performed microarray expression analysis. kewywords: Mouse megakaryocyte progenitors **Overall design:** Expression data of flow cytometrically isolated murine megakaryocyte progenitor cells (lin-, Sca-1-, c-kit+, CD150+, CD41+) from C57/BL6 murine fetal liver and bone marrow

Background corr dist: KL-Divergence = 0.0460, L1-Distance = 0.0371, L2-Distance = 0.0020, Normal std = 0.6078

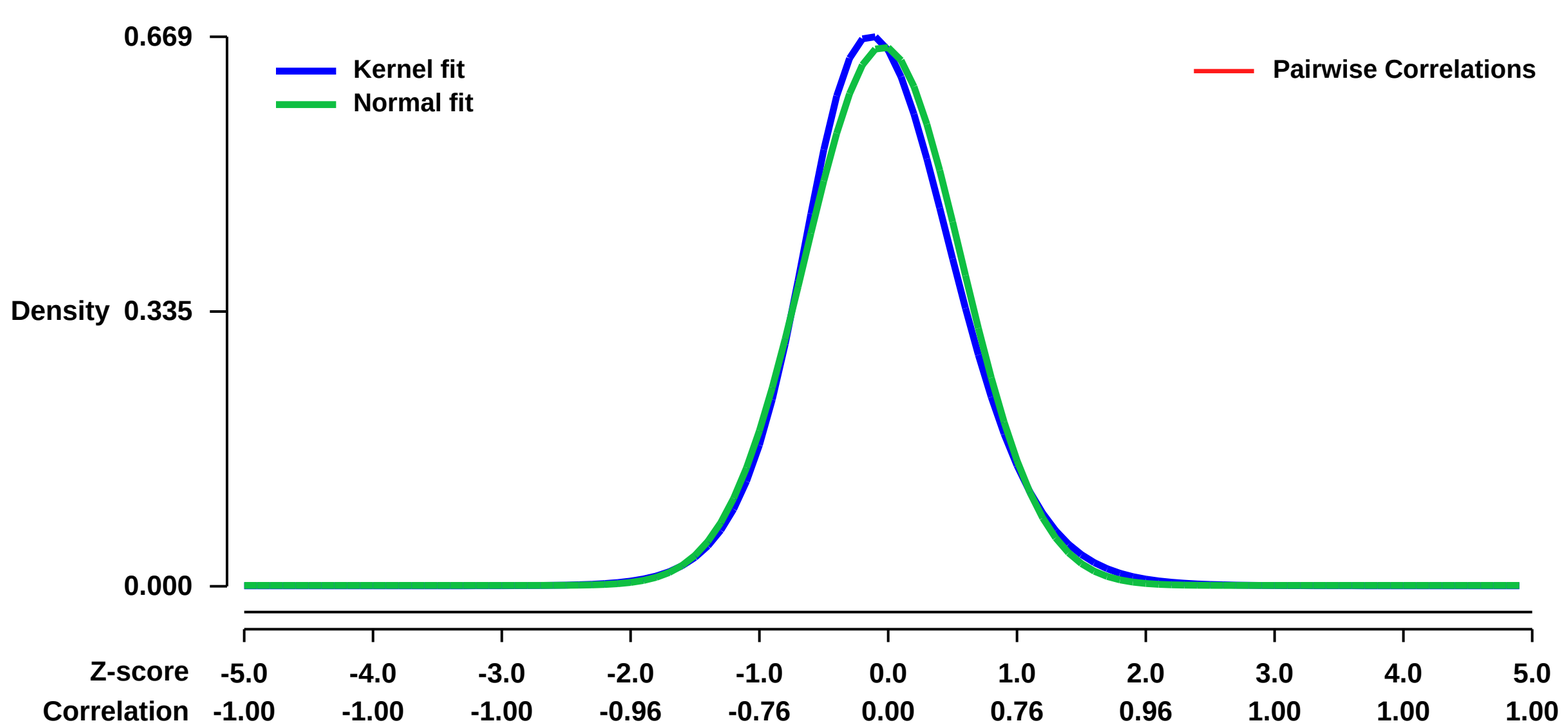

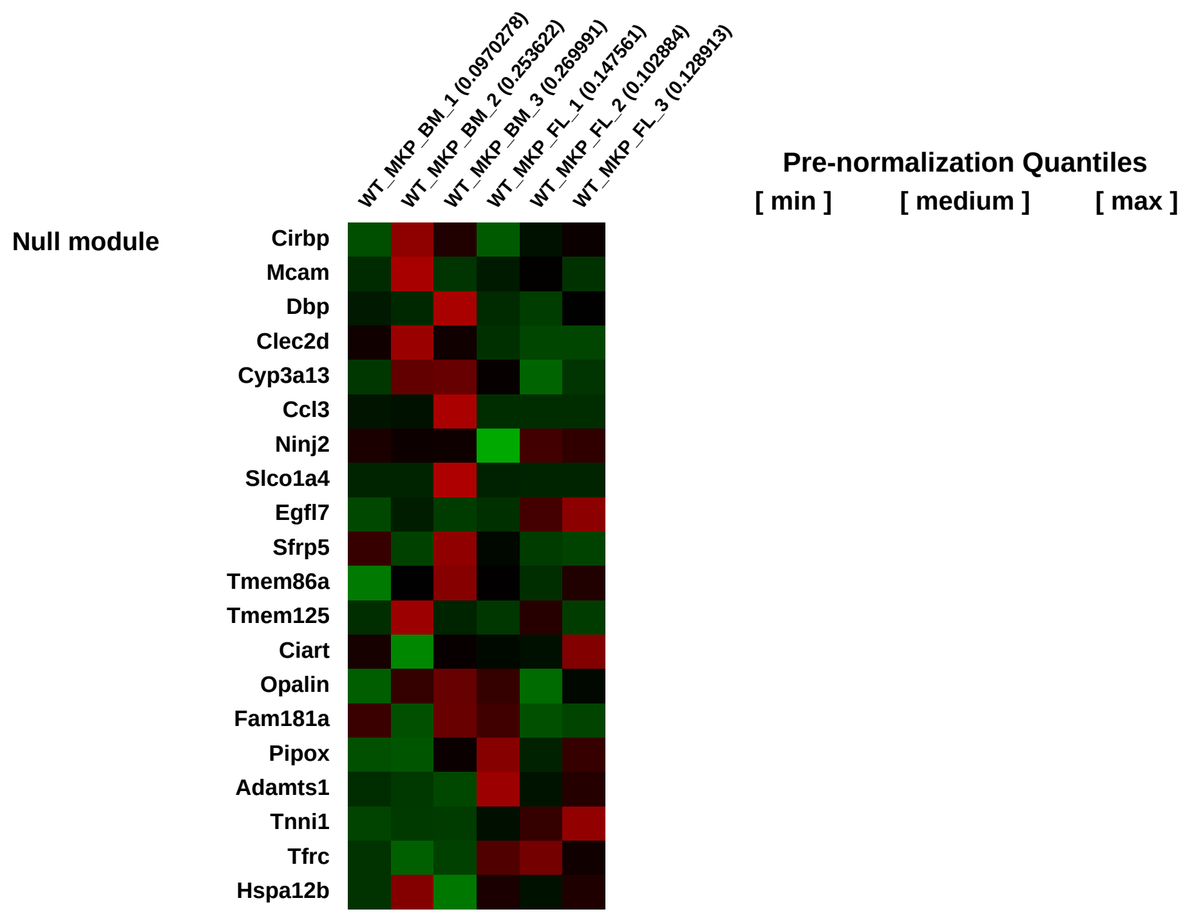

GEO Series "GSE7875" Expression Profiles

Num of samples in this series: 16

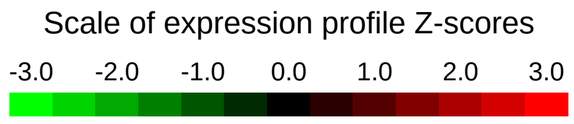

GEO Link:	http://www.ncbi.nlm.nih.gov/geo/query/acc.cgi?acc=GSE7875
Status:	Public on Oct 03 2007
Title:	Deletion of PKBalpha/Akt1 affects thymic development
Organism:	Mus musculus
Experiment type:	Expression profiling by array
Platform:	GPL1261
Pubmed ID:	17912369
Summary & Design:	**Summary:** The thymus constitutes the primary lymphoid organ for the majority of T cells. The phosphatidyl-inositol 3 kinase (PI3K) signaling pathway is involved in lymphoid development. Defects in single components of this pathway prevent thymocytes from progressing beyond early T cell developmental stages. Protein kinase B (PKB) is the main effector of the PI3K pathway. To determine whether PKB mediates PI3K signaling in early T cell development, we characterized PKB knockout thymi. Our results reveal a significant thymic hypocellularity in PKBalpha-/- neonates and an accumulation of early thymocyte subsets in PKBalpha-/- adult mice. The latter finding is specifically attributed to the lack of PKBalpha within the lymphoid component of the thymus. Microarray analyses show that the absence of PKBalpha in early thymocyte subsets modifies the expression of genes known to be involved in pre-TCR signaling, in T cell activation, and in the transduction of interferon-mediated signals. This report highlights the specific requirements of PKBalpha for thymic development. **Keywords:** Genetic modification **Overall design:** Early thymocyte subsets (DN3 and ISP8) were sorted by FACS from 4 PKBalpha-/- / PKBalpha+/+ mouse littermate pairs. The same number of DN3 or ISP8 cells was sorted (7 000 to 25 000 cells) within a PKBalpha-/- / PKBalpha+/+ pair. Four replicates per condition were then analysed (4xPKBalpha-/- DN3, 4xPKBalpha+/+ DN3, 4xPKBalpha-/- ISP8, 4xPKBalpha+/+ ISP8). Total RNA was extracted using PicoPureTM RNA isolation kit (Arcturus, Sunnyvale, CA, USA) and RNA quality was controlled using the 2100 Bioanalyser (Agilent Technologies, Santa Clara, CA, USA). Total RNA was amplified and labeled using the Affymetrix 2-cycle 3â labelling kit according to manufacturerâ s instructions. After fragmentation, 10 ug cRNA was hybridised to mouse genome 430 2.0 GeneChips (Affymetrix, Santa Clara, CA). The supplementary file represents the expression values estimated using the GC-RMA function provided by Refiner 3.1 (Genedata, Basel, Switzerland) for each of the samples.

Background corr dist: KL-Divergence = 0.1420, L1-Distance = 0.0394, L2-Distance = 0.0024, Normal std = 0.3992

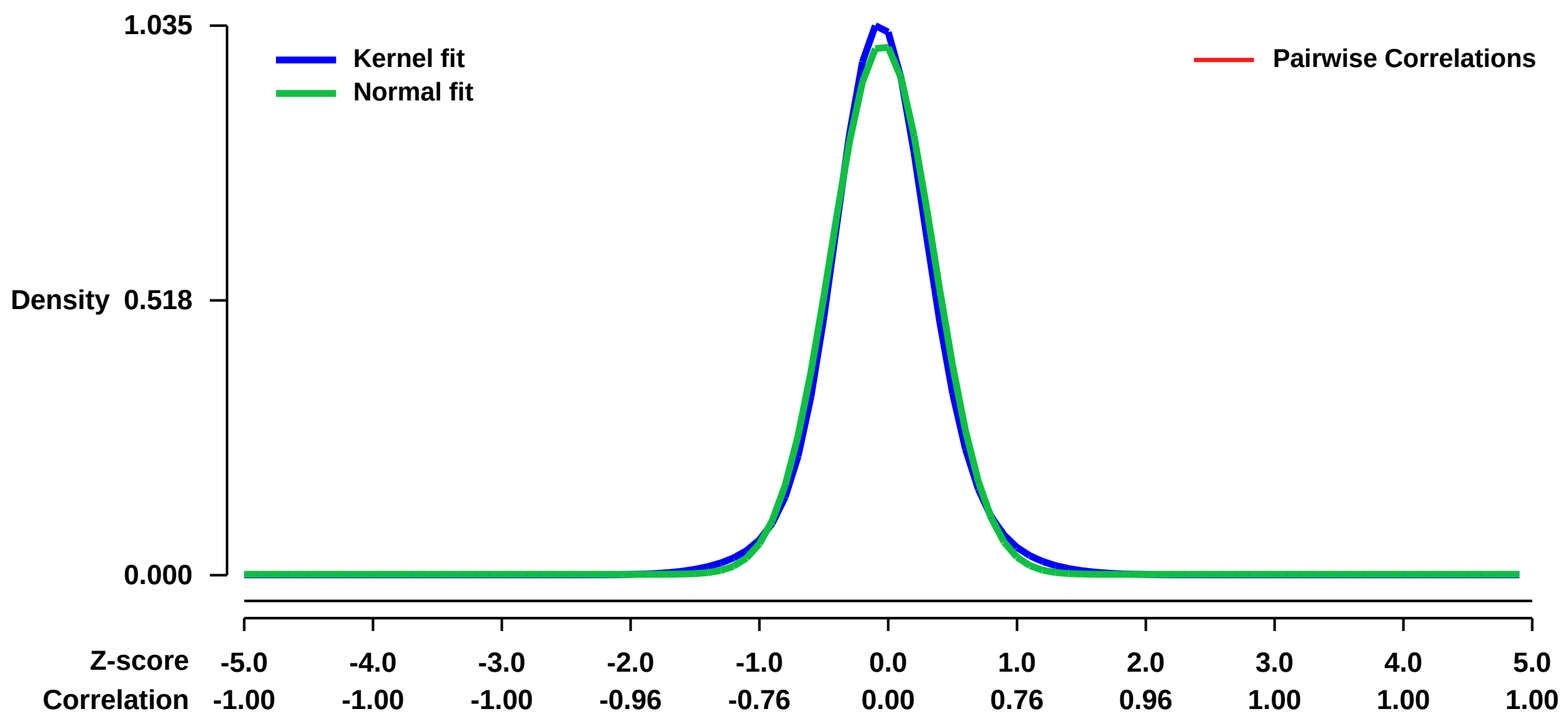

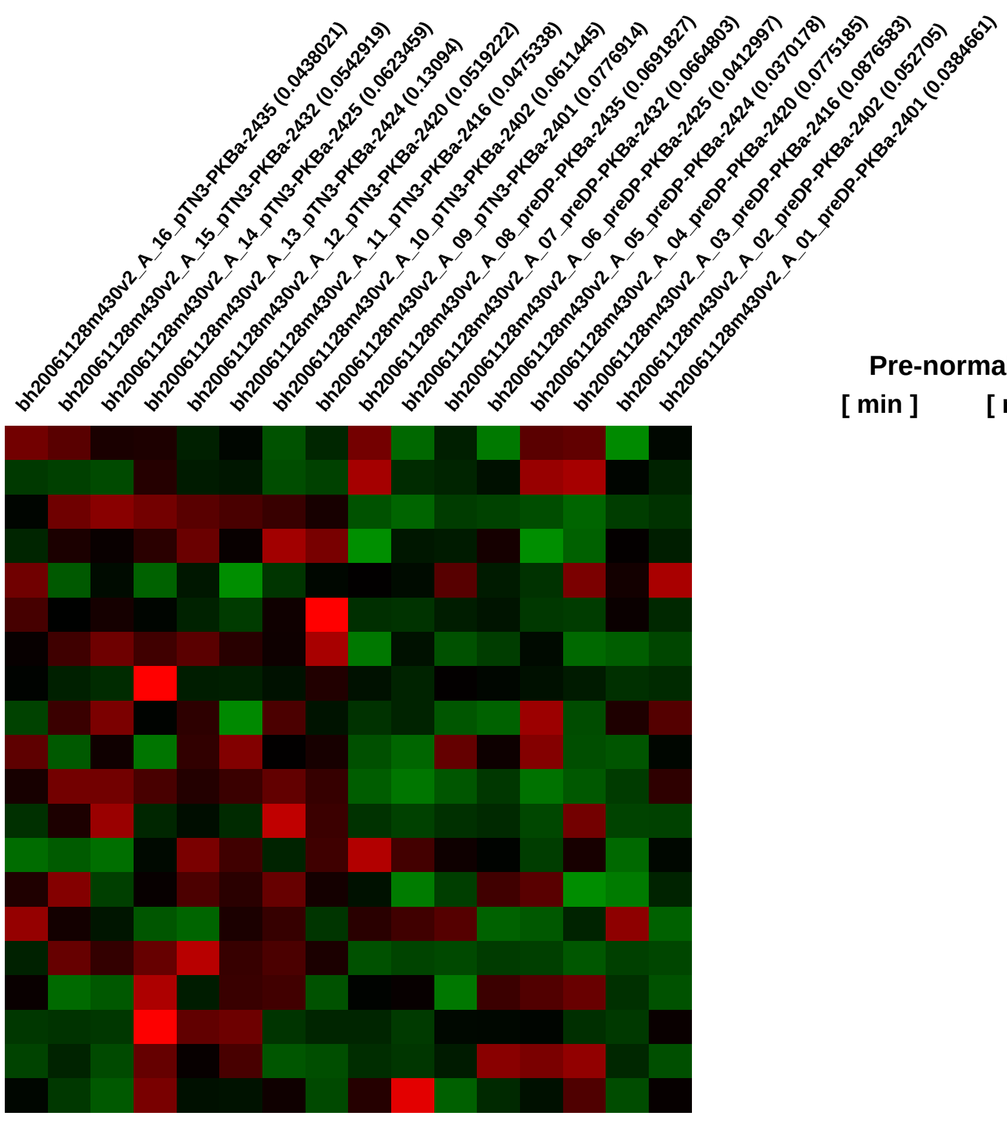

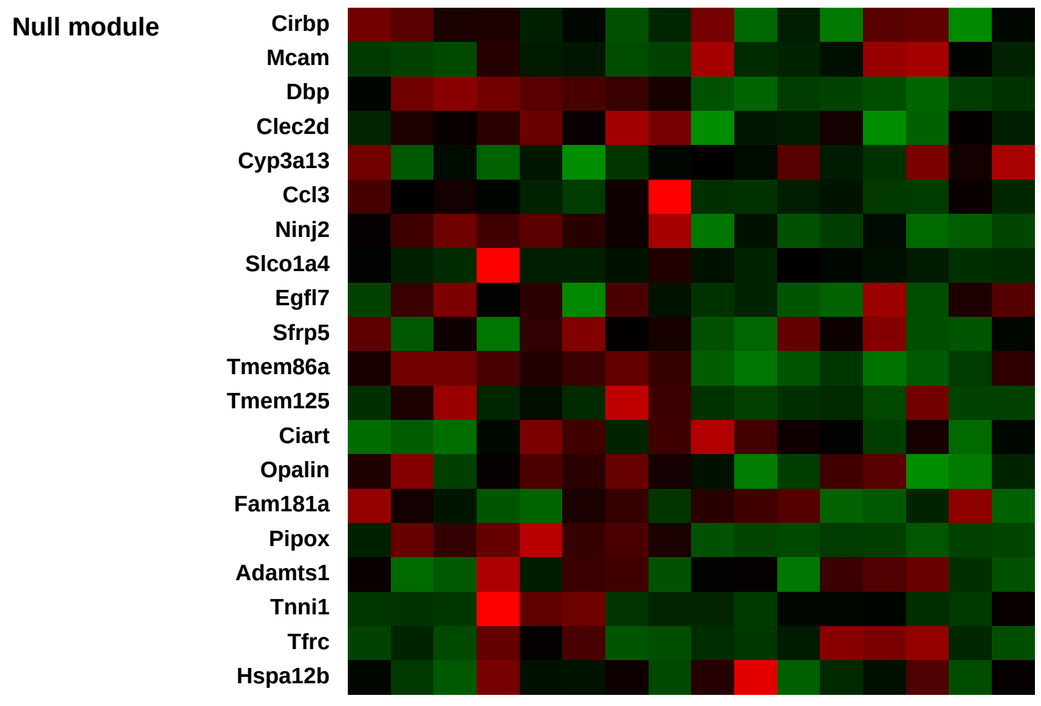

GEO Series "GSE11804" Expression Profiles

Num of samples in this series: 12

Scale of expression profile Z-scores

-3.0 -2.0 -1.0 0.0 1.0 2.0 3.0

GEO Link:	http://www.ncbi.nlm.nih.gov/geo/query/acc.cgi?acc=GSE11804
Status:	Public on Jun 18 2008
Title:	Pharmacological regulation of skeletal muscle gene expression
Organism:	Mus musculus
Experiment type:	Expression profiling by array
Platform:	GPL1261
Pubmed ID:	18674809
Summary & Design:	**Summary:** Exercise activates serine/threonine kinase AMPK and transcriptional factor PPARdelta that re-model metabolism and endurance capacity of skeletal muscle. Whether and how synthetic activation of these molecules regulated muscle gene signature is unknown. We have conducted skeletal muscle microarrays from mice treated with AMPK agoinst (AICAR), PPARdelta agonist (GW1516) or the combination of the two drugs to investigate the individual and interactive effects of the two on muscle genes. Keywords: Pharmacology study **Overall design:** C57Bl/6J mice were treated with Vehicle, AICAR, GW1516 and the combination of two drugs for 6 days, followed by collection of quadriceps for gene expression analysis.

Background corr dist: KL-Divergence = 0.1790, L1-Distance = 0.0427, L2-Distance = 0.0040, Normal std = 0.3470

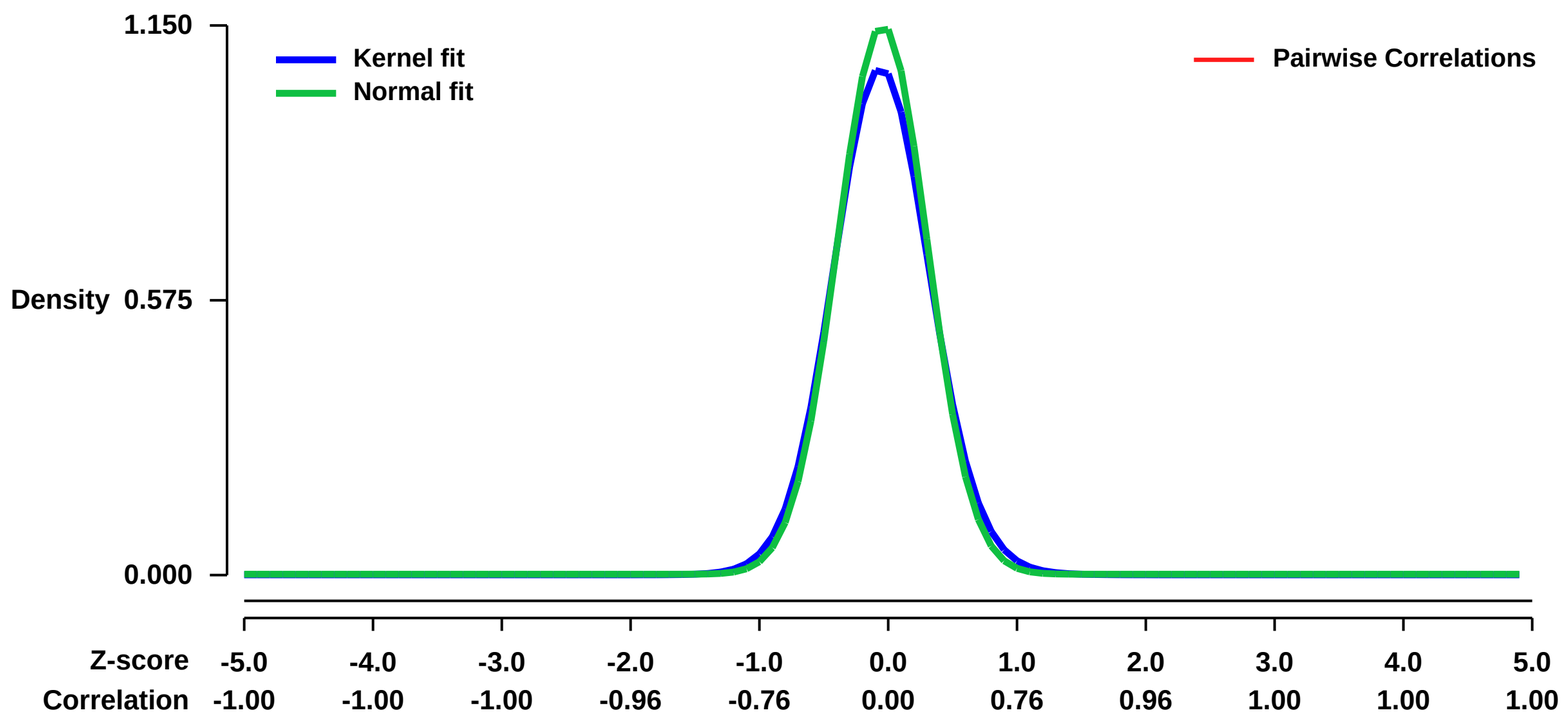

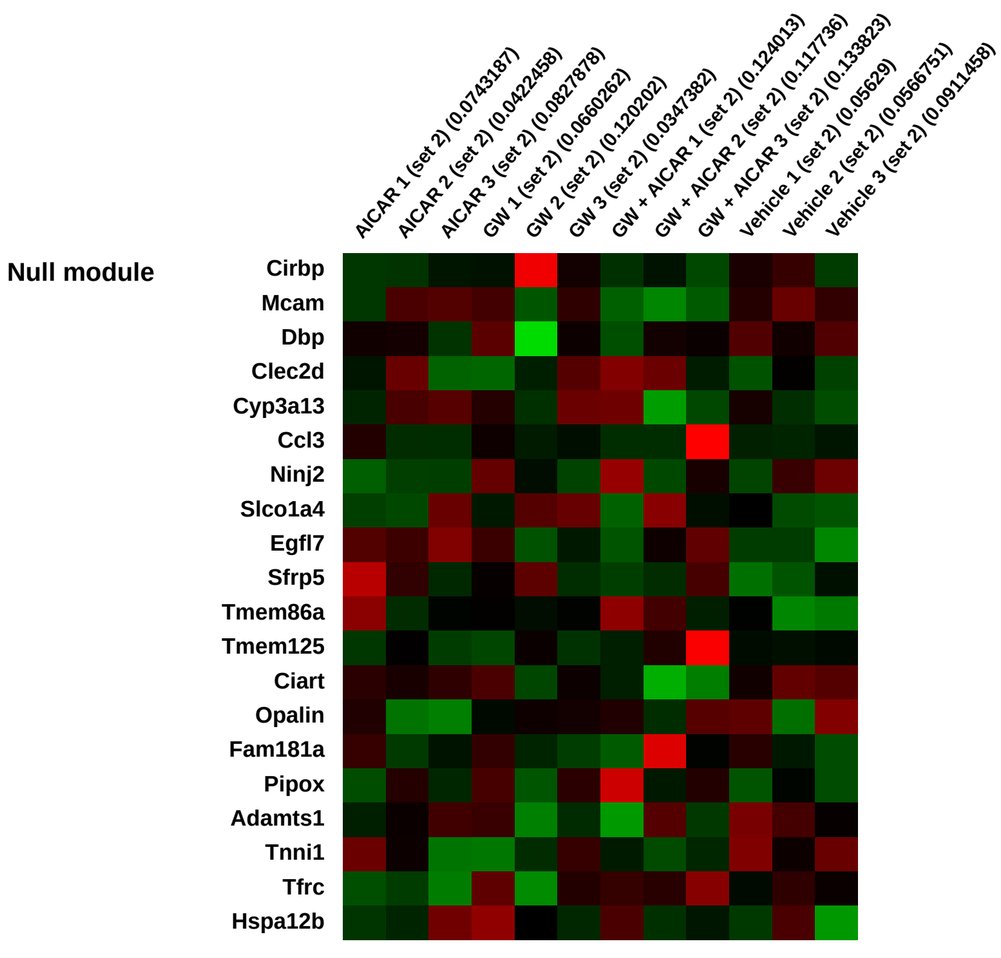

GEO Series "GSE10644" Expression Profiles

Num of samples in this series: 18

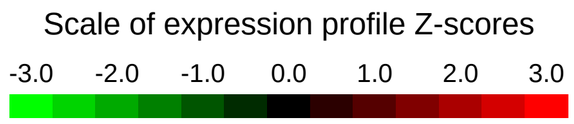

GEO Link:	http://www.ncbi.nlm.nih.gov/geo/query/acc.cgi?acc=GSE10644
Status:	Public on Sep 15 2008
Title:	Characteristic Transcriptional Profiling of Rhythmic mRNA Expression in the Murine Distal Colon
Organism:	Mus musculus
Experiment type:	Expression profiling by array
Platform:	GPL1261
Pubmed ID:	18848557
Summary & Design:	**Summary:** To identify a cohort of rhythmically expressed genes in the murine Distal Colon,microarrays were used to measure gene expression over a 24-hour light/dark cycle.The rhythmic transcripts were classified according to expression patterns, functions and association with physiological and pathophysiological processes of the colon including motility, colorectal cancer formation and inflammatory bowel disease. **Keywords: time series** **Overall design:** Mice were maintained for 2 weeks on a 12 hour light/dark (LD) cycle (lights on 7 AM, lights off 7 PM) prior to all experiments. For the reference experiment, mice had ad libitum access to food. Samples were collected every four hours, at 0400, 0800, 1200, 1600, 2000 and 2400, starting 1 hour after the lights went on. Total RNA was isolated by modified guanidinium thicyanate-phenol-chloroform extraction method and was treated with DNase I (Promega, Madison, WI) at 37 oC for 30 minutes.Hybridizations and Scaning were done as per Affymetrix techniques. Three MOE 430 plus 2.0 chips were used per time point.

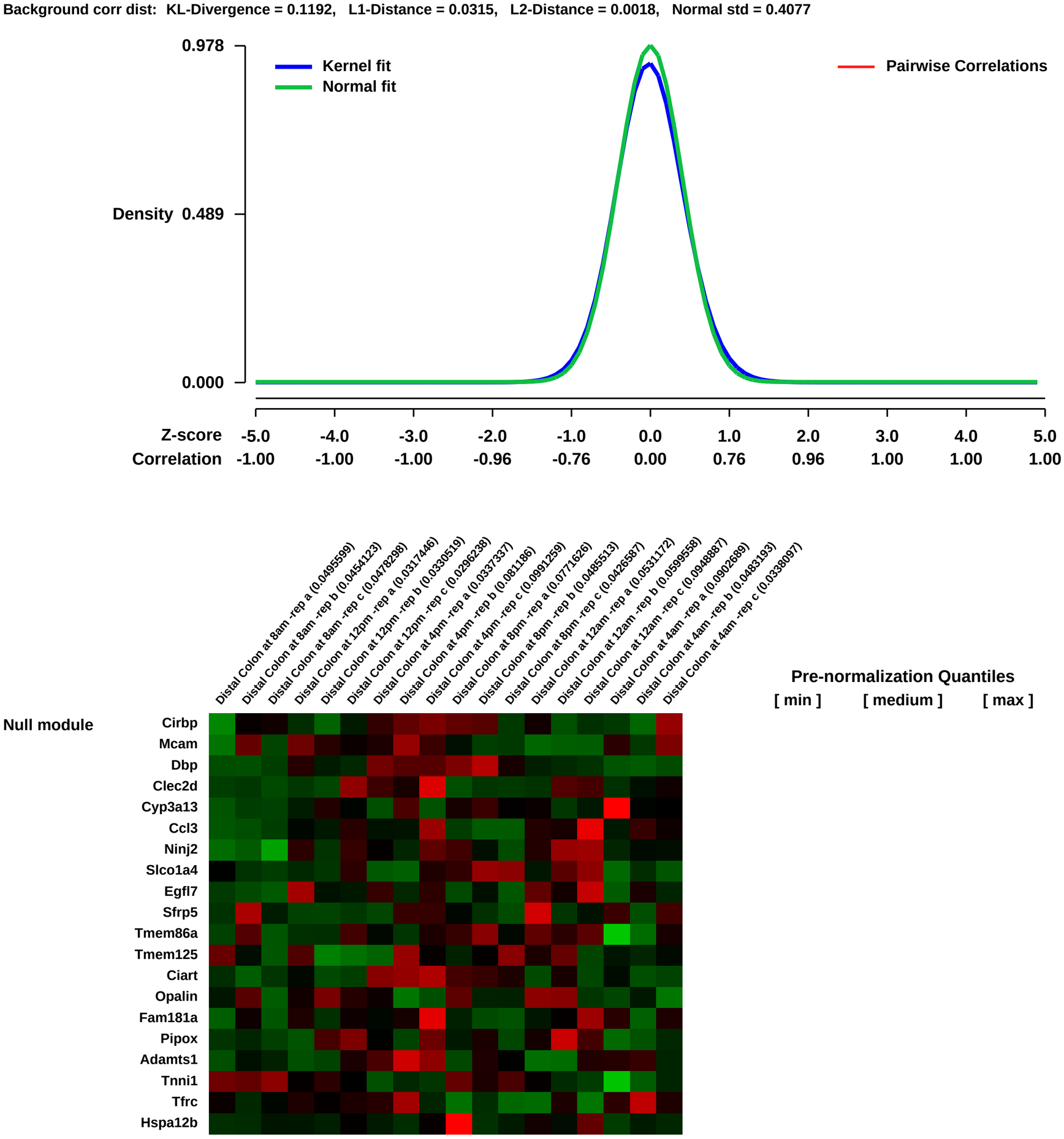

GEO Series "GSE19925" Expression Profiles

Num of samples in this series: 6

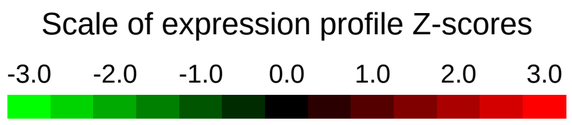

GEO Link:	http://www.ncbi.nlm.nih.gov/geo/query/acc.cgi?acc=GSE19925
Status:	Public on Dec 18 2010
Title:	Gene expression profile of the mammary stroma in Rarb -/- mice compared to their wild type littermates
Organism:	Mus musculus
Experiment type:	Expression profiling by array
Platform:	GPL1261
Pubmed ID:	21187396
Summary & Design:	**Summary:** Inactivation of RAR-b, which has been reported as a tumor suppressing gene by numerous studies, results in protective effect against the tumorigenesis induced by activated ErbB2. Moreover, tissue recombination indicates that the RAR-b deficient-microenvironment, rather than the RAR-b status of mammary epithelial cells, plays a key-determining role in the initiation and progression of the mammary carcinoma. Ablation of RAR-b extensively modulates the remodeling of stroma during tumor progression through suppressing the activation and transdifferetiation of myofibroblasts. RNA microarray has been employed to identify the gene expression signature in the mammary stroma of our RAR-b null animals. We want to find out the underlining mechanism of the protective effects resulted from Rarb abliton. **Overall design:** A global gene expression profile of mouse mammary stroma was obtained on total RNA from the cleared mammary fat pads (stroma) of both RAR-b KO (n=3) and their wild type (n=3) littermates at the age of four weeks.

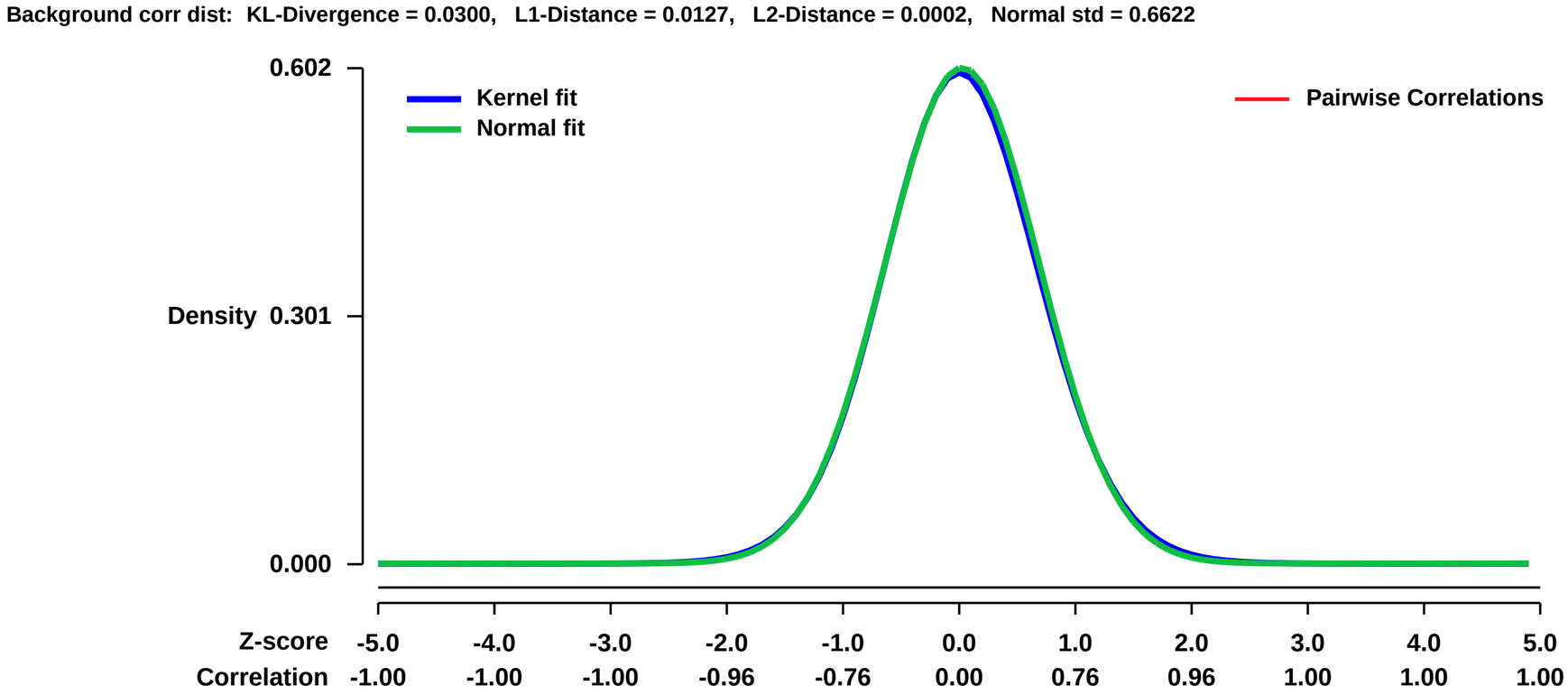

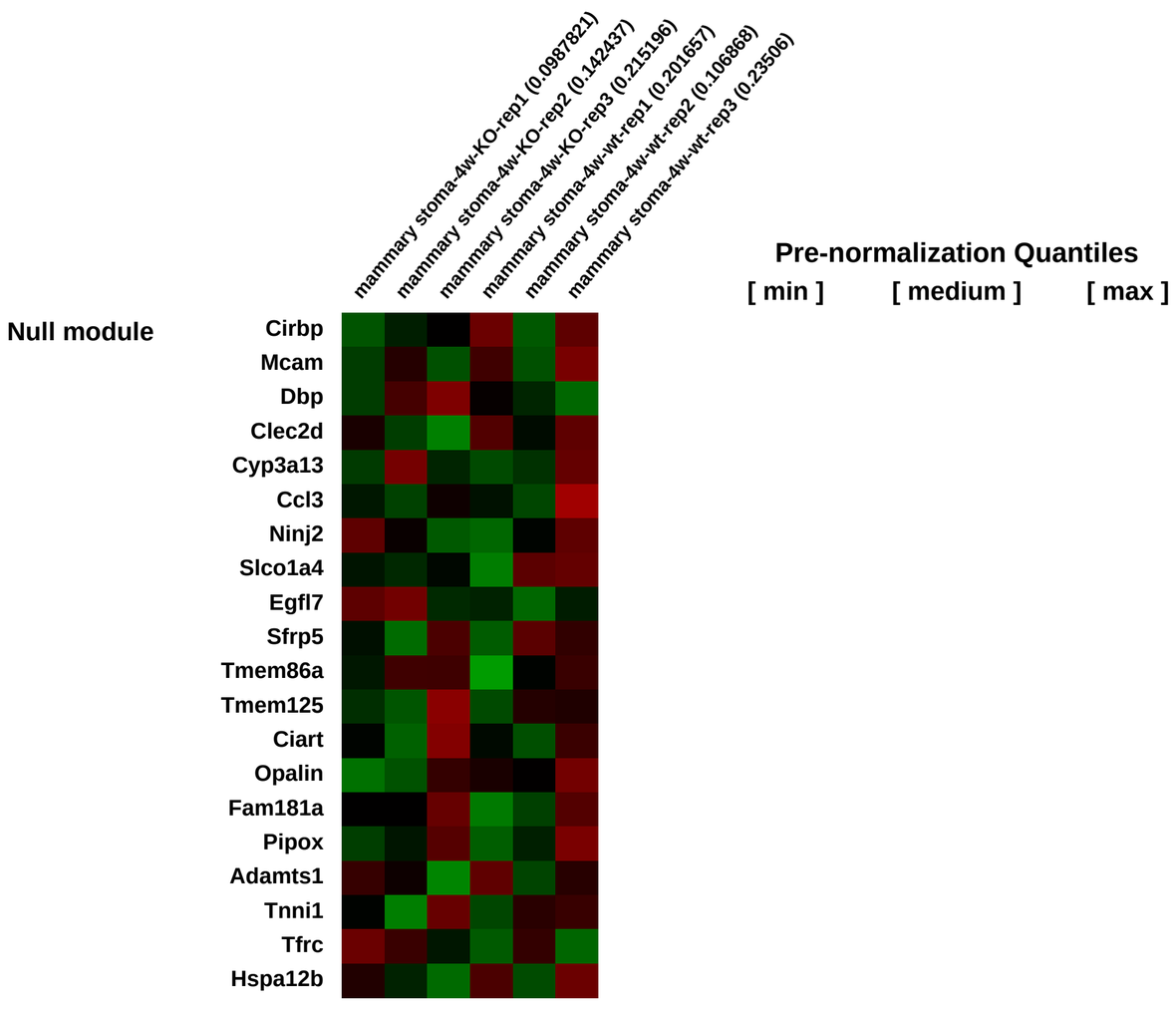

GEO Series "GSE6482" Expression Profiles

Num of samples in this series: 9

Scale of expression profile Z-scores

-3.0 -2.0 -1.0 0.0 1.0 2.0 3.0

GEO Link:	**http://www.ncbi.nlm.nih.gov/geo/query/acc.cgi?acc=GSE6482**
Status:	**Public on Jan 01 2007**
Title:	**mECK36: a cell and animal model of virally induced Kaposi's sarcoma**
Organism:	**Mus musculus**
Experiment type:	**Expression profiling by array**
Platform:	**GPL1261**
Pubmed ID:	**17349582**
Summary & Design:	**Summary:** **Transfection of a Kaposi's sarcoma (KS) herpesvirus (KSHV) Bacterial Artificial Chromosome (KSHVBac36) into mouse bone marrow endothelial lineage cells generated a cell (mECK36) that induced KS-like tumors in mice. mECK36 formed KSHV-harboring vascularized spindle-cell sarcomas that were LANA+ and displayed a KSHV and host transcriptomes reminiscent of KS tumors.** **Keywords: Cell type comparison** **Overall design:** **There are three biological replicates per sample. Tumors (mKS) were compared the the human KS signature. mECK36 and mEC-V were compared to putative BM lineage cells.**

Background corr dist: **KL-Divergence = 0.0664, L1-Distance = 0.0251, L2-Distance = 0.0010, Normal std = 0.5172**

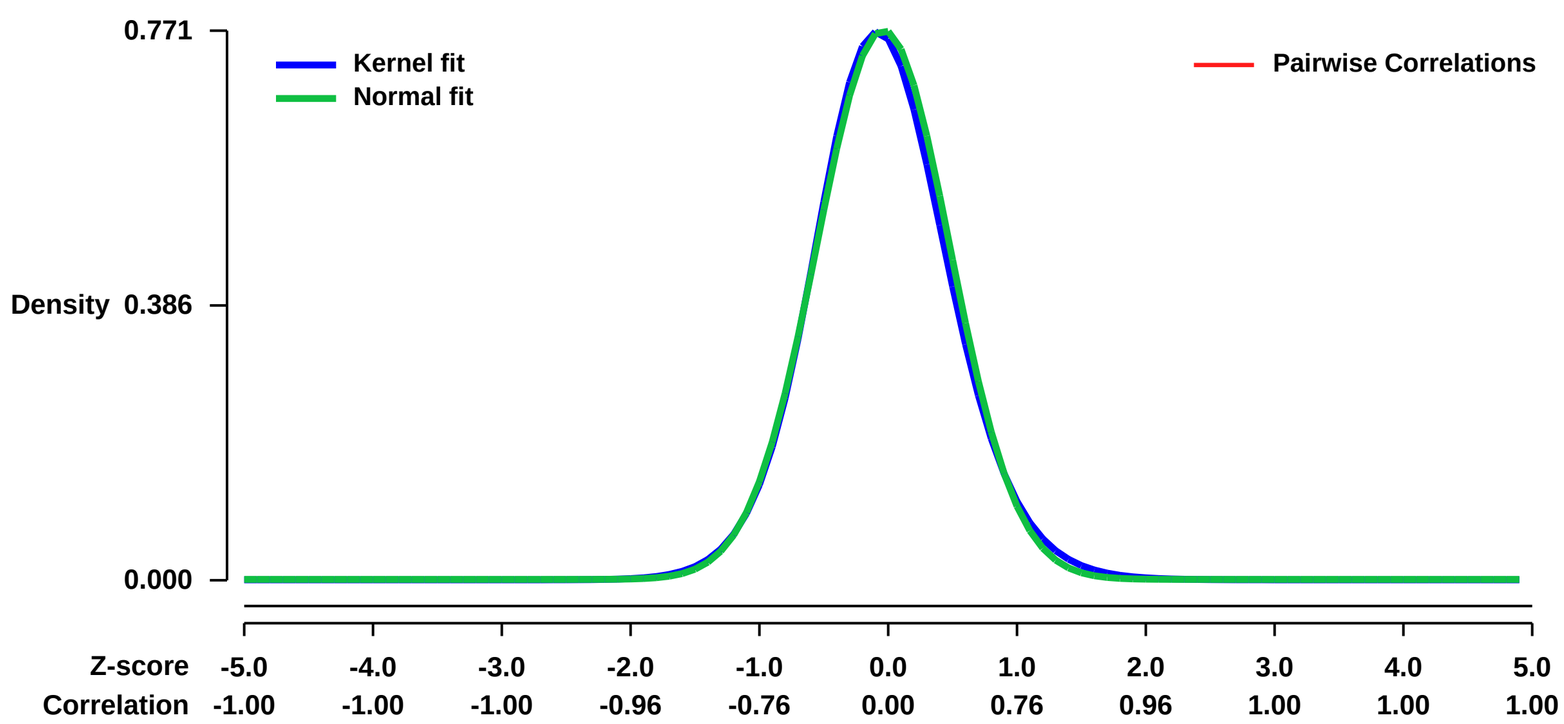

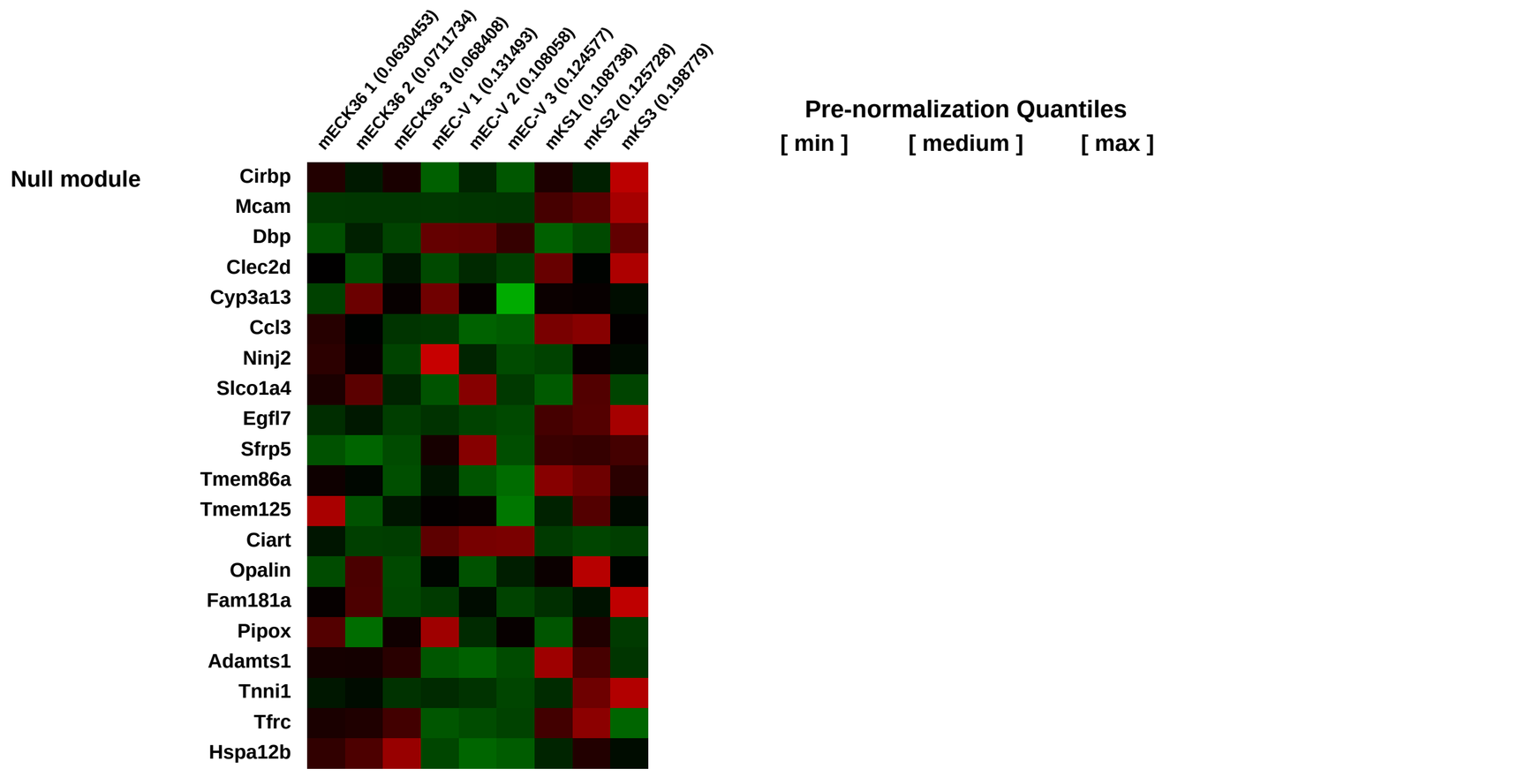

GEO Series "GSE52220" Expression Profiles

Num of samples in this series: 6

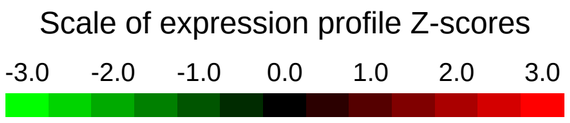

GEO Link:	http://www.ncbi.nlm.nih.gov/geo/query/acc.cgi?acc=GSE52220
Status:	Public on Nov 09 2013
Title:	Expression data from E11.5 mouse branchial arch 1 (BA1) - comparison between Ezh2lox/lox and Wnt1Cre Ezh2lox/lox embryos
Organism:	Mus musculus
Experiment type:	Expression profiling by array
Platform:	GPL1261
Pubmed ID:	24496623
Summary & Design:	**Summary:** Conditional ablation of Ezh2 in the neural crest lineage results in loss of the neural crest-derived mesenchymal derivatives. In this data sheet we determine gene expression analysis in Ezh2lox/lox and Wnt1Cre Ezh2lox/lox in E11.5 mouse BA1 cells. **Overall design:** Conditional ablation of Ezh2 in the neural crest lineage was achieved by crossing Wnt1creEzh2lox/wt mice with Ezh2lox/lox mouse lines. We analyzed a total of 6 samples including 3 biological replicates from Ezh2lox/lox embryos and 3 biological replicates from Wnt1cre Ezh2lox/lox embryos.

Background corr dist: KL-Divergence = 0.0375, L1-Distance = 0.0159, L2-Distance = 0.0002, Normal std = 0.6257

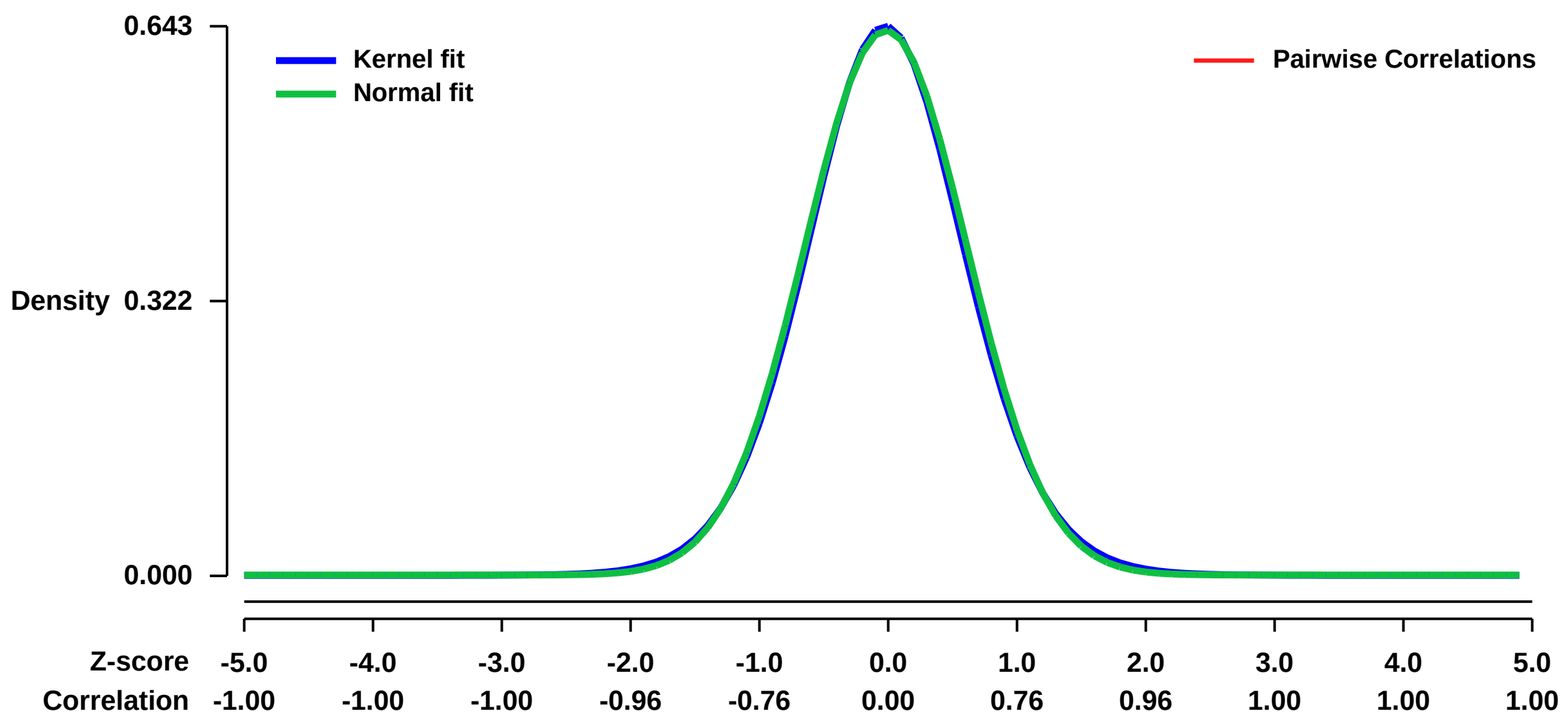

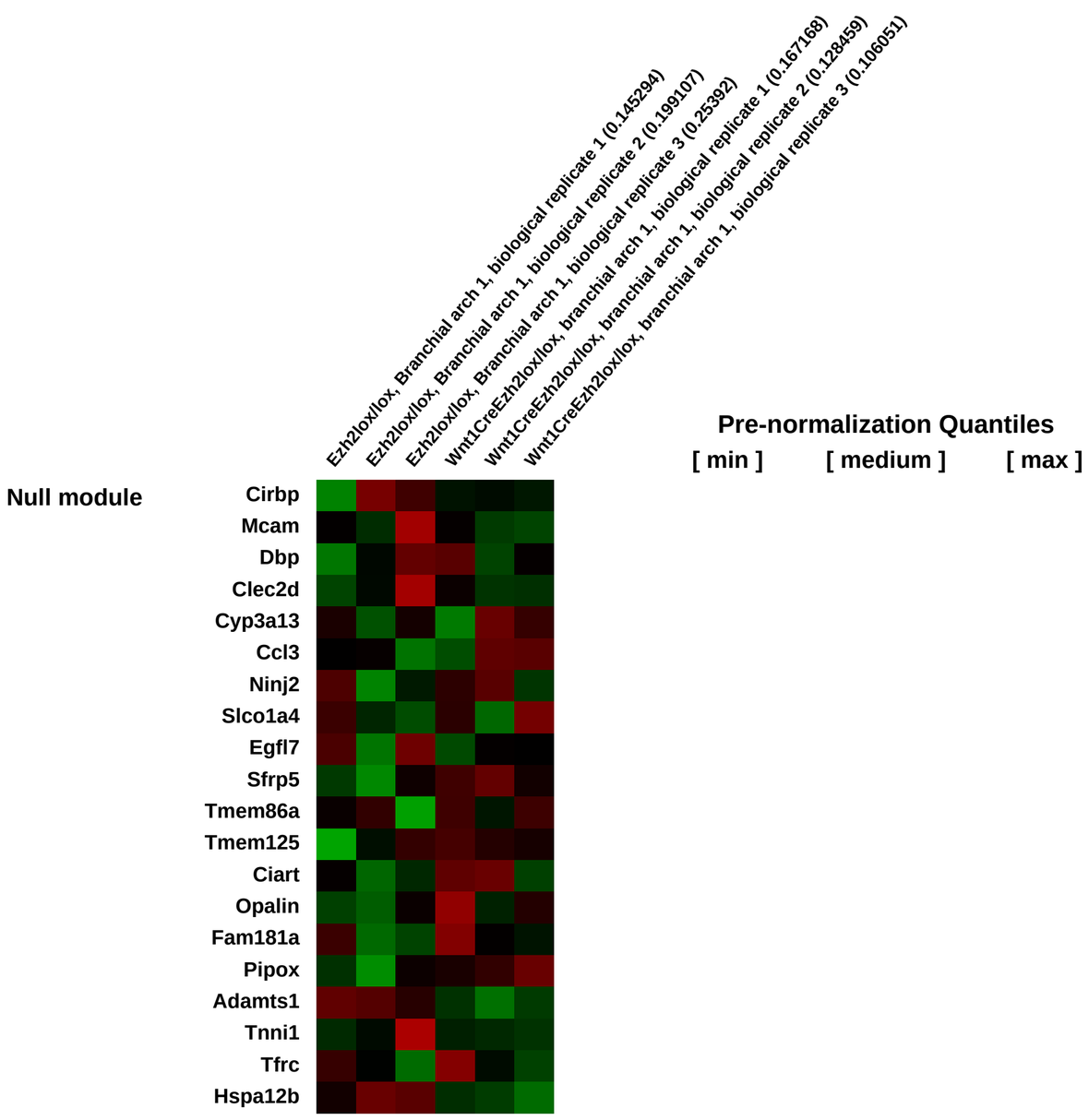

GEO Series "GSE10273" Expression Profiles

Num of samples in this series: 9

Scale of expression profile Z-scores

-3.0 -2.0 -1.0 0.0 1.0 2.0 3.0

GEO Link:	**http://www.ncbi.nlm.nih.gov/geo/query/acc.cgi?acc=GSE10273**
Status:	**Public on Jan 26 2008**
Title:	**Convergent molecular pathways that induce immunoglobulin light-chain recombination**
Organism:	**Mus musculus**
Experiment type:	**Expression profiling by array**
Platform:	**GPL1261**
Pubmed ID:	**18280186**
Summary & Design:	**Summary:** **Productive rearrangement of the immunoglobulin heavy chain locus triggers a major developmental checkpoint that promotes limited clonal expansion of pre-B cells, culminating in cell cycle arrest and rearrangement of the kappa (¸”) or lambda (¸») light-chain loci. B lineage cells lacking the related transcription factors IRF-4 and IRF-8 undergo a developmental arrest at the cycling pre-B cell stage and are blocked for light-chain recombination. Using Irf-4,8-/- pre-B cells we demonstrate that two pathways converge to synergistically drive light-chain rearrangement, a process that is not simply activated by cell cycle exit. One pathway is directly dependent on IRF-4, whose expression is elevated by pre-BCR signaling. IRF-4 targets the ¸” 3â† and ¸» enhancers to increase locus accessibility and positions a kappa allele away from pericentromeric heterochromatin. The other pathway is triggered by attenuation of IL-7 signaling and results in activation of the ¸” intronic enhancer via binding of the transcription factor, E2A. Intriguingly, IRF-4 regulates the expression of CXCR4 and promotes the migration of pre-B cells in response to the chemokine CXCL12. We propose that IRF-4 coordinates the two pathways regulating light-chain recombination by positioning pre-B cells away from IL-7 expressing stromal cells.** **We used microarrys to identify the changes in gene expression under different levels of the cytokine IL-7 and after rescue of genetic defect.** **Keywords: growth conditions and rescue** **Overall design:** **IRF4,8 null pre-B cells were cultures in the indicated conditions prior to RNA isolation and hybridization to Affymetrix arrays.**

Background corr dist: KL-Divergence = 0.0485, L1-Distance = 0.0228, L2-Distance = 0.0005, Normal std = 0.5808

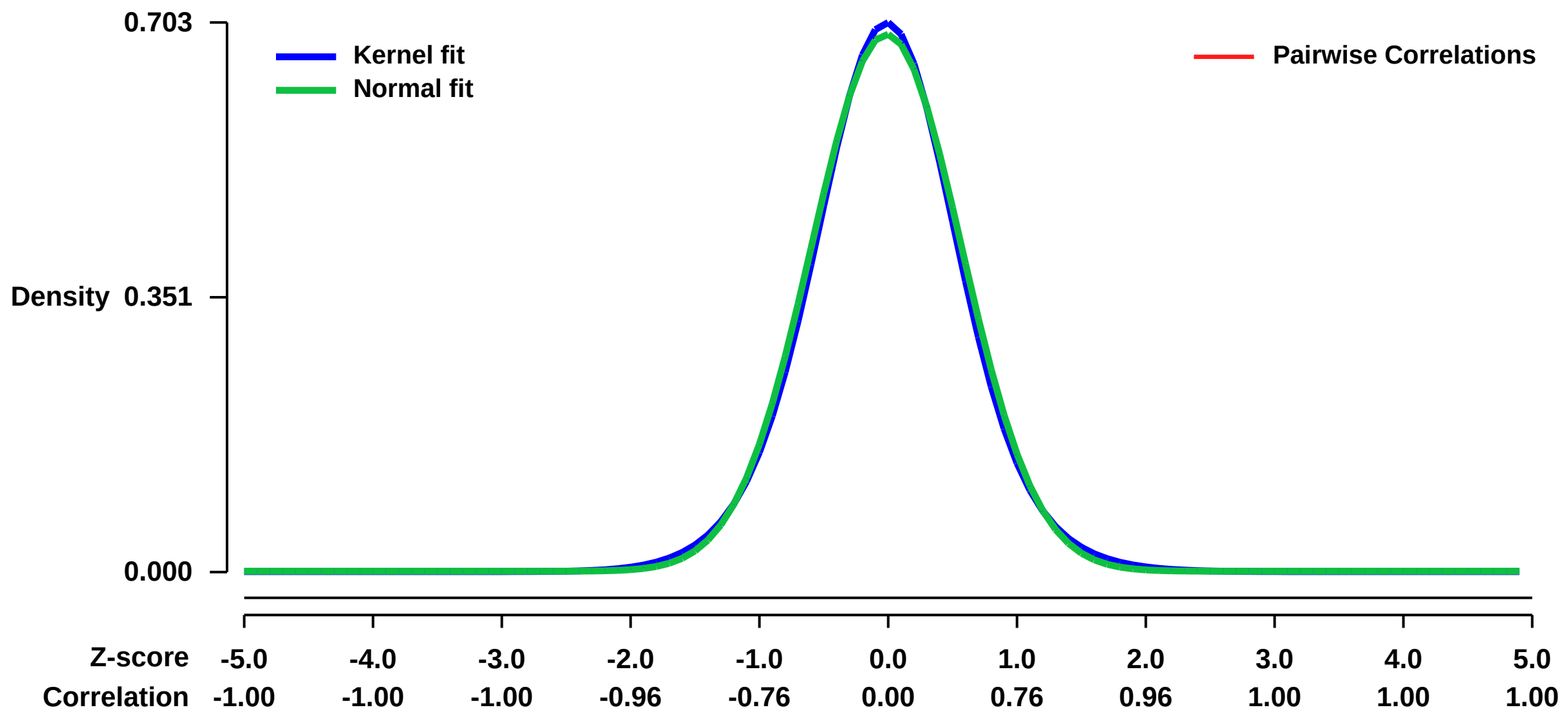

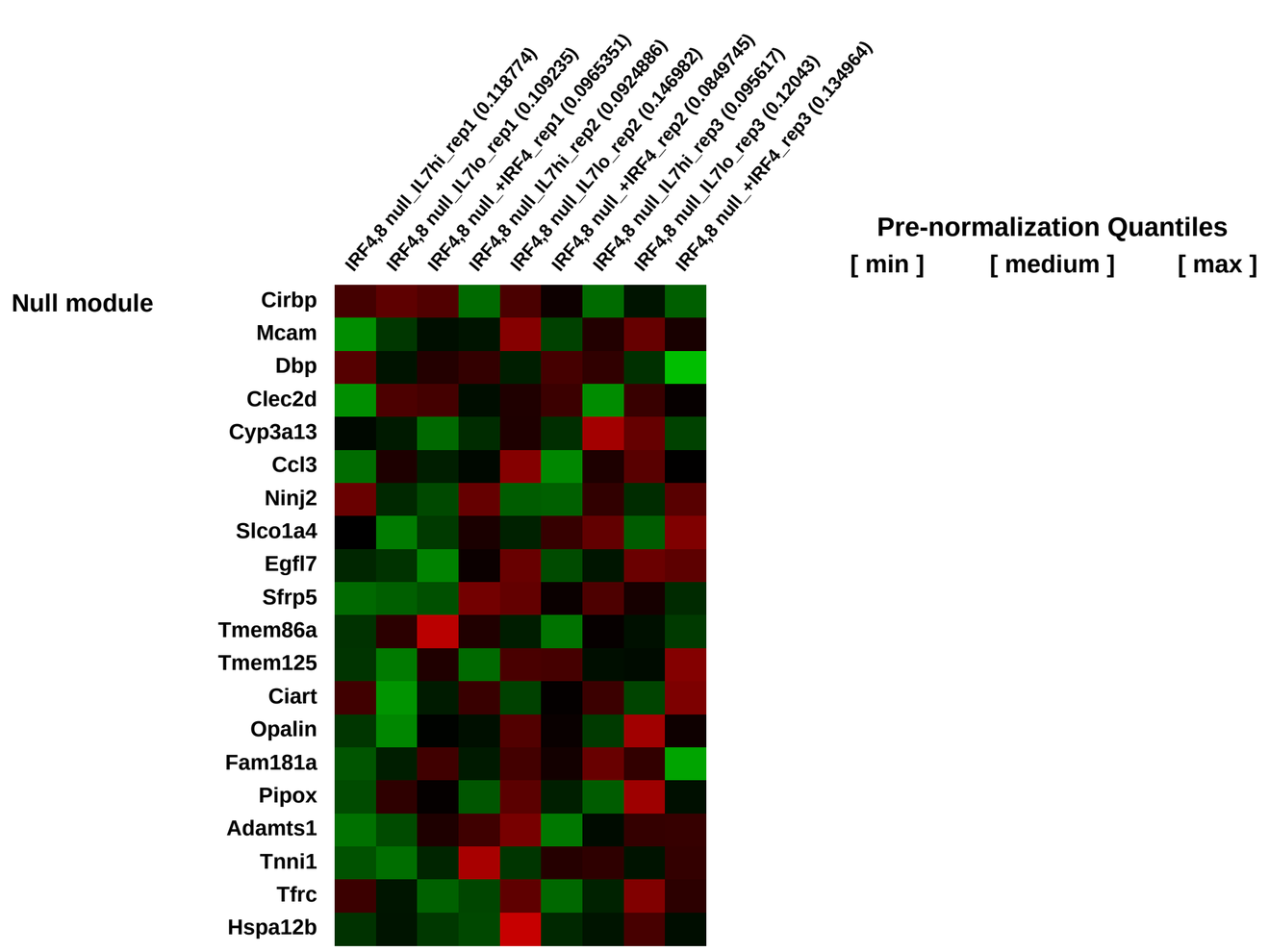

GEO Series "GSE14499" Expression Profiles

Num of samples in this series: 26

Scale of expression profile Z-scores

-3.0 -2.0 -1.0 0.0 1.0 2.0 3.0

GEO Link:	http://www.ncbi.nlm.nih.gov/geo/query/acc.cgi?acc=GSE14499
Status:	Public on Jan 23 2009
Title:	Effect of BDNF on the APP transgenic mouse model of Alzheimer’s disease
Organism:	Mus musculus
Experiment type:	Expression profiling by array
Platform:	GPL1261
Pubmed ID:	19198615
Summary & Design:	**Summary:** We examined transgenic (TG) mice expressing human APP695 bearing the double Swedish (671KM>NL) and Indiana (717V>F) amyloid precursor protein (APP) mutations. Lentiviral vectors constitutively expressing BDNF-GFP under control of the CMV/^ -actin hybrid promoter or GFP alone were injected into the entorhinal cortices of TG mice bilaterally at age 6 months, a time point by which neuropathological degeneration and cell loss are established. Age-matched wild-type littermates underwent sham surgery or injection of lentivirus expressing GFP into the entorhinal cortices bilaterally. **Keywords: Treatment effect** **Overall design:** 26 Samples total: 4 biological replicates of APP transgenic mice BDNF treated, 4 biological replicates of APP transgenic mice GFP treated, 3 biological replicates of non-trangenic mice sham lesion and 2 biological replicates of non-transgenic mice GFP treated for both tissues: Entorhinal cortex and hippocampus.

Background corr dist: KL-Divergence = 0.1592, L1-Distance = 0.0299, L2-Distance = 0.0015, Normal std = 0.3705

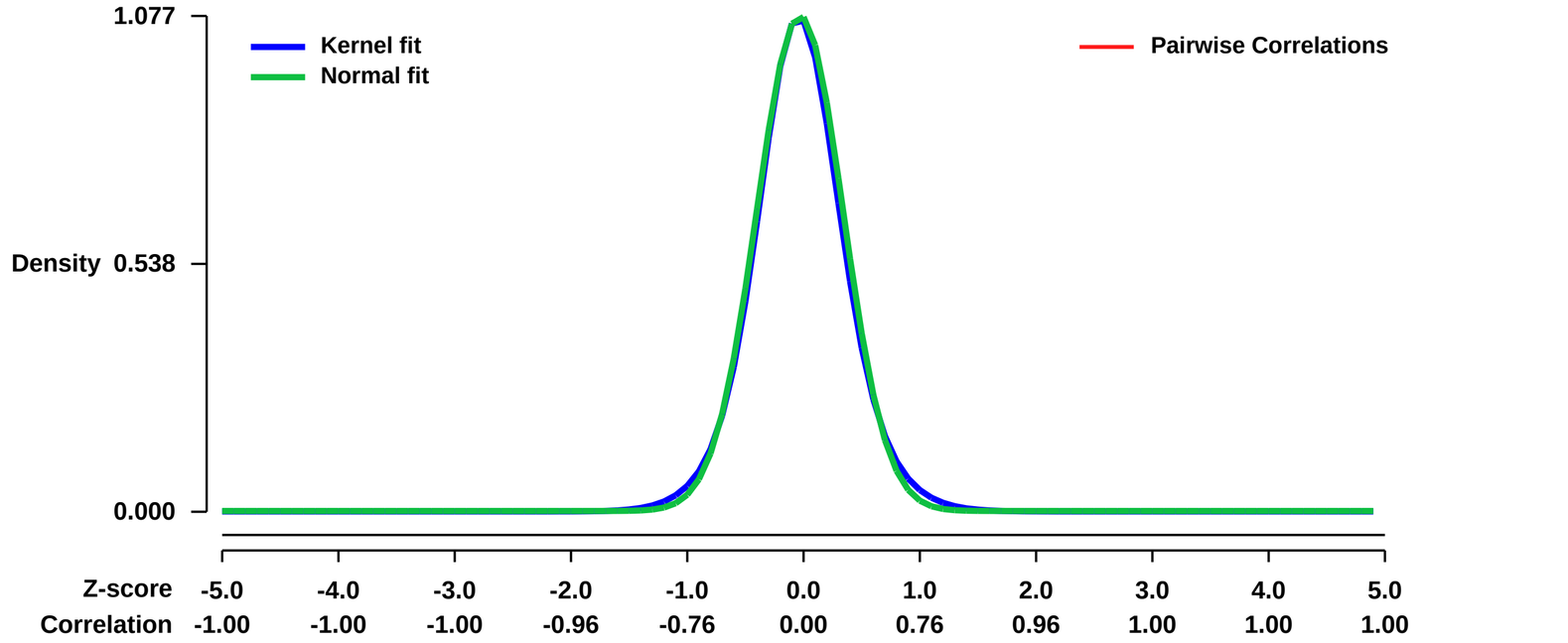

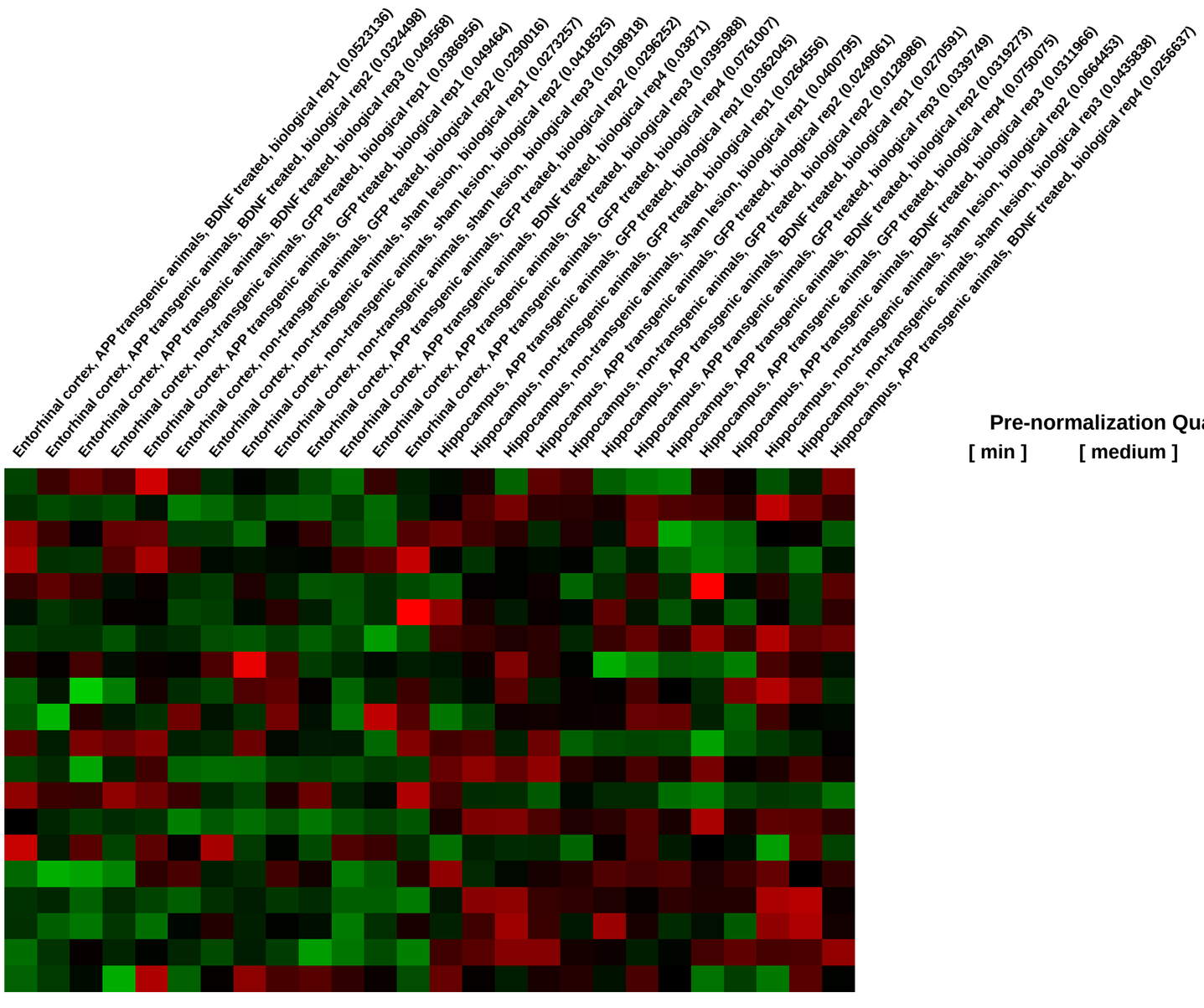

GEO Series "GSE8322" Expression Profiles

Num of samples in this series: 12

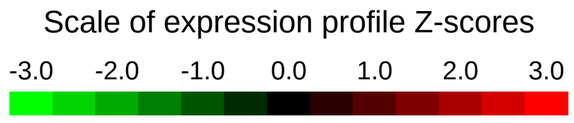

GEO Link:	http://www.ncbi.nlm.nih.gov/geo/query/acc.cgi?acc=GSE8322
Status:	Public on Mar 06 2008
Title:	Identification of MCIP1 as an ATF6-inducible ER Stress Response Gene in the Heart by Gene Expression Profiling
Organism:	Mus musculus
Experiment type:	Expression profiling by array
Platform:	GPL1261
Pubmed ID:	18319259

Summary & Design:

Summary:
We recently found that the endoplasmic reticulum (ER) stress response (ERSR) is activated in surviving cardiac myocytes in a mouse model of in vivo myocardial infarction. ATF6 is an ER stress-activated transcription factor that induces ERSR genes, some of which encode proteins that may protect against ischemic damage. However, few ERSR genes have been identified in the heart, and there have been no gene expression profiling studies of ATF6-inducible genes, in vivo. We previously generated transgenic (TG) mice that express tamoxifen-activated ATF6, ATF6-MER, in the heart; ATF6-MER conferred tamoxifen-dependent ATF6 activation and protection from ischemic damage. To understand of the mechanism of ATF6-mediated cardioprotection, gene expression profiling of ATF6-MER TG mouse hearts was performed. Activated ATF6 changed expression levels of 1,162 genes in the heart; of the 775 ATF6-inducible genes, only 23 are known ERSR genes. One of the genes not expected to be induced by ATF6 is modulatory calcinuerin-interacting protein-1 (MCIP1). MCIP1 is induced in a calcineurin/NFAT-dependent manner during myocardial hypertrophy and it can feedback inhibit cardiomyocyte growth. We found that MCIP1 expression in cultured cardiomyocytes was increased by the prototypical ER stresser, tunicamycin (TM), or by simulated ischemia. Moreover, infecting cardiomyocytes with adenovirus encoding activated ATF6 induced MCIP1 expression and inhibited myocyte growth in response to the alpha 1-adrenergic agonist, phenylephrine. These results suggest that MCIP1 can be induced in the heart by ER stresses, such as ischemia. Moreover, b integrating hypertrophy and ER stress, MCIP-modulated myocyte growth may help rejuvenate nascent ER protein folding, which could contribute to protection from ischemic damage.

Keywords: Gene expression analysis of the effect of activating ATF6 in the hearts of transgenic mice upon treatment with tamoxifen.

Overall design:
12 mice were analyzed in this study. Four treatment groups were included in this study: transgenic ATF6-MER mice treated with tamoxifen, transgenic ATF6-MER mice treated with vehicle, nontransgenic littermates treated with tamoxifen, and nontransgenic littermates treated with vehicle. Each treatment group included 3 separate biological replicate samples. Each mouse sampled was male, C57/BL6, ~30 weeks old. Each mouse was treated, then the mouse was sacrificed, the heart was extracted, and left ventricle was isolated. Total RNA was isolated from the left ventricle, and used for hybridization onto an Affymetrix mus 430 2.0 full-genome chip. Each heart was hybridized onto its own chip.

Background corr dist: KL-Divergence = 0.1158, L1-Distance = 0.0244, L2-Distance = 0.0009, Normal std = 0.4173

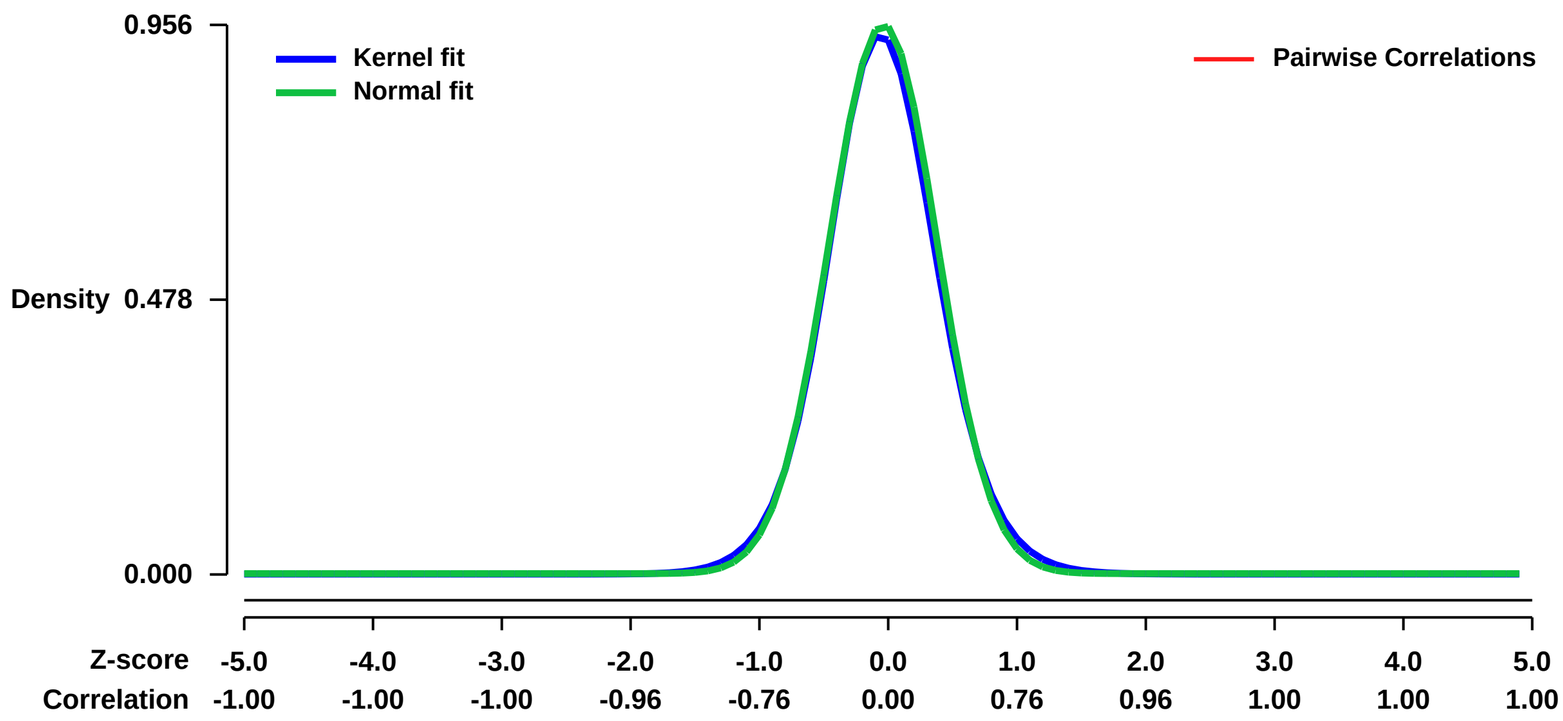

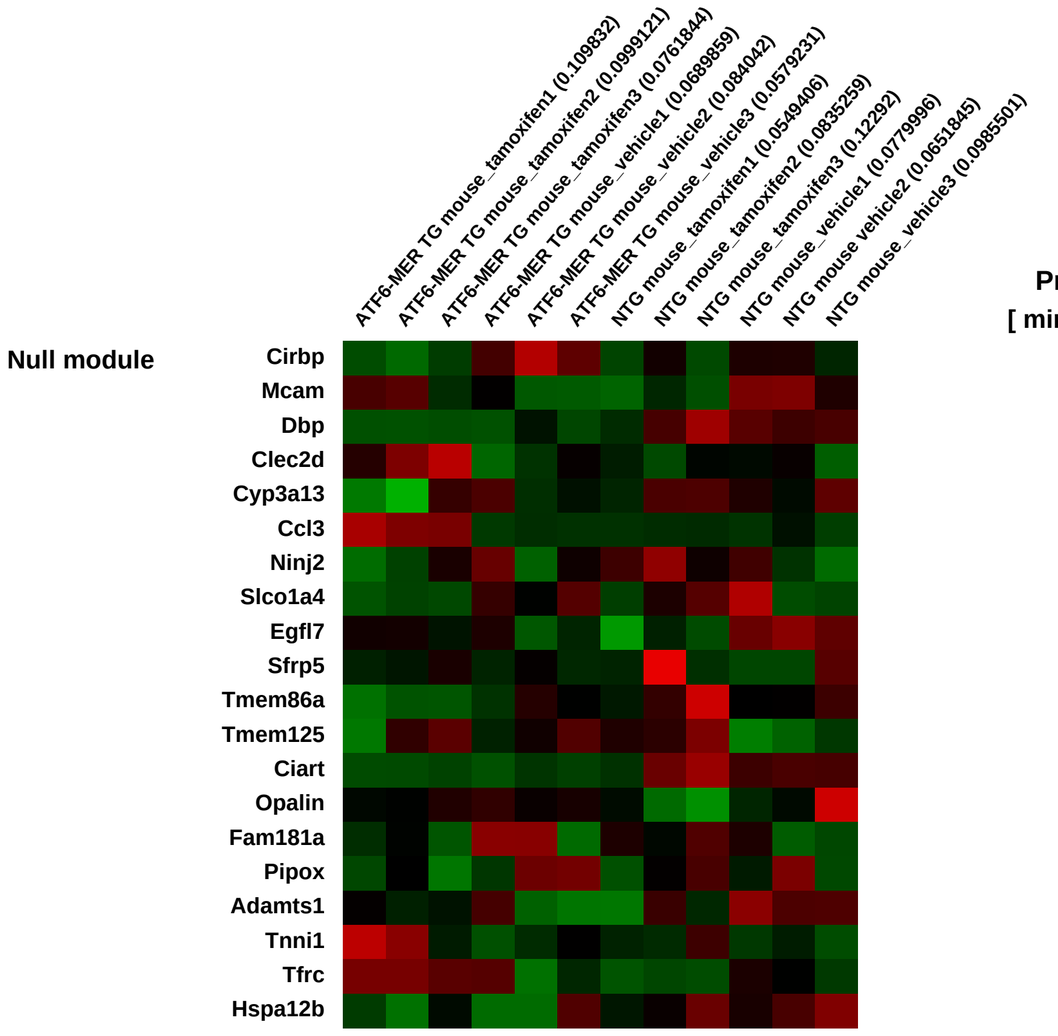

GEO Series "GSE4816" Expression Profiles

Num of samples in this series: 12

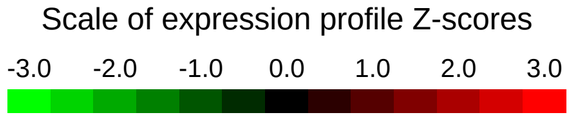

GEO Link:	**http://www.ncbi.nlm.nih.gov/geo/query/acc.cgi?acc=GSE4816**
Status:	**Public on May 12 2006**
Title:	**Gene expression profiles of the P1 bladder isolated from SMAA or SMAGA (Acta2 or Actg2) transgenic and wild type mice. (GUDMAP Series ID: 2)**
Organism:	**Mus musculus**
Experiment type:	**Expression profiling by array**
Platform:	**GPL1261**
Pubmed ID:	
Summary & Design:	**Summary:** **The long term objective is to create an encyclopedia of the expression levels of all genes in multiple components of the developing bladder. The central thesis is straightforward. The combination of laser capture microdissection (LCM) plus microarray analysis offers a powerful, efficient and effective method for the creation of a global gene expression atlas of the developing bladder. Microarrays with essentially complete genome coverage can be used to quantitate expression levels of every gene in laser capture microdissected components of the developing bladder. The ensuing rapid read-out provides an expression atlas that is more sensitive, more economical and more complete than would be possible by in situ hybridizations alone. As a first step we sought to determine if expression of the reporter gene (EGFP or EYFP) used to identify smooth muscle cells altered the gene expression profile of the bladder.** **Keywords: Comparison of postnatal day 1 bladders.** **Overall design:** **Postnatal day 1 bladders were isolated from transgenic and wild-type mice to determine the effects of transgene expression on the gene expression profile in the bladder.**

Background corr dist: KL-Divergence = 0.1519, L1-Distance = 0.0383, L2-Distance = 0.0029, Normal std = 0.3705

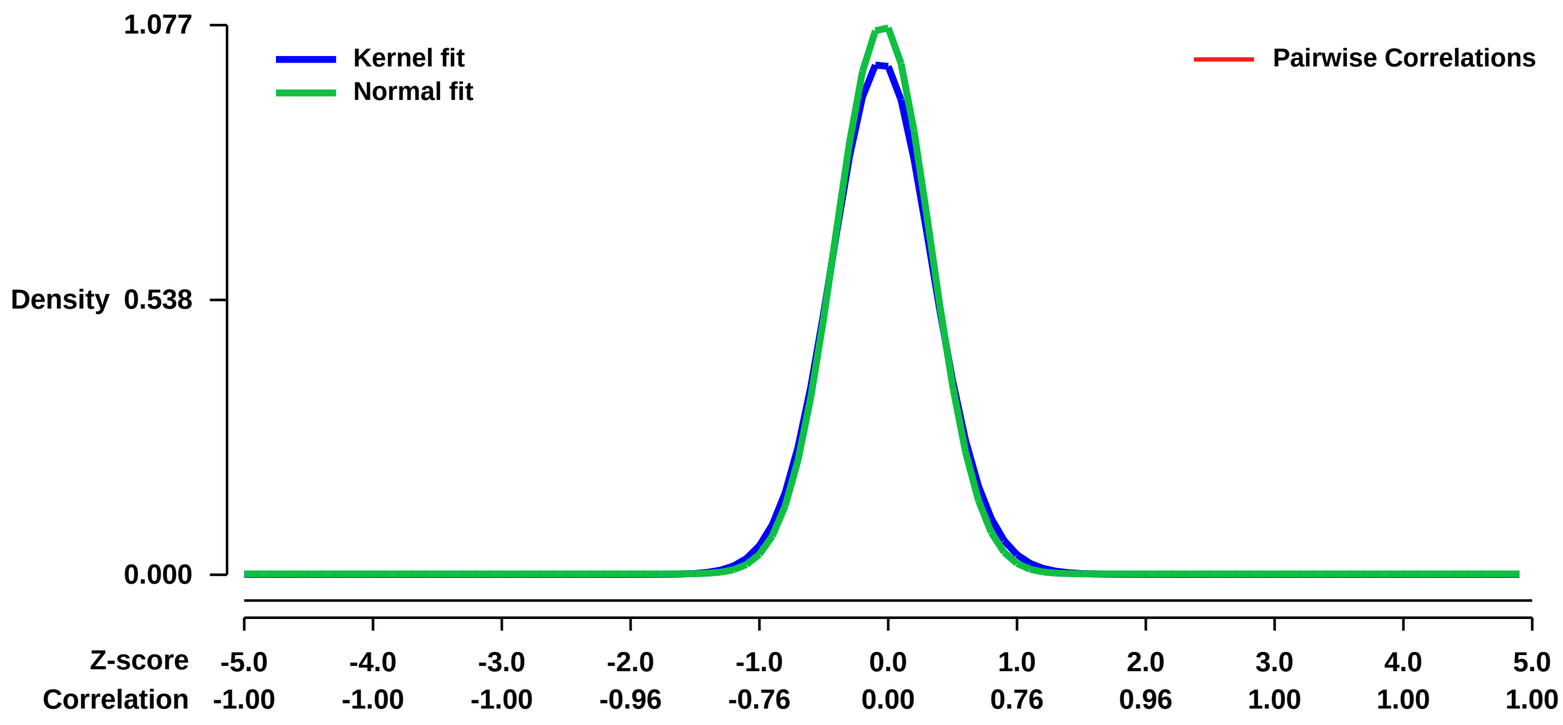

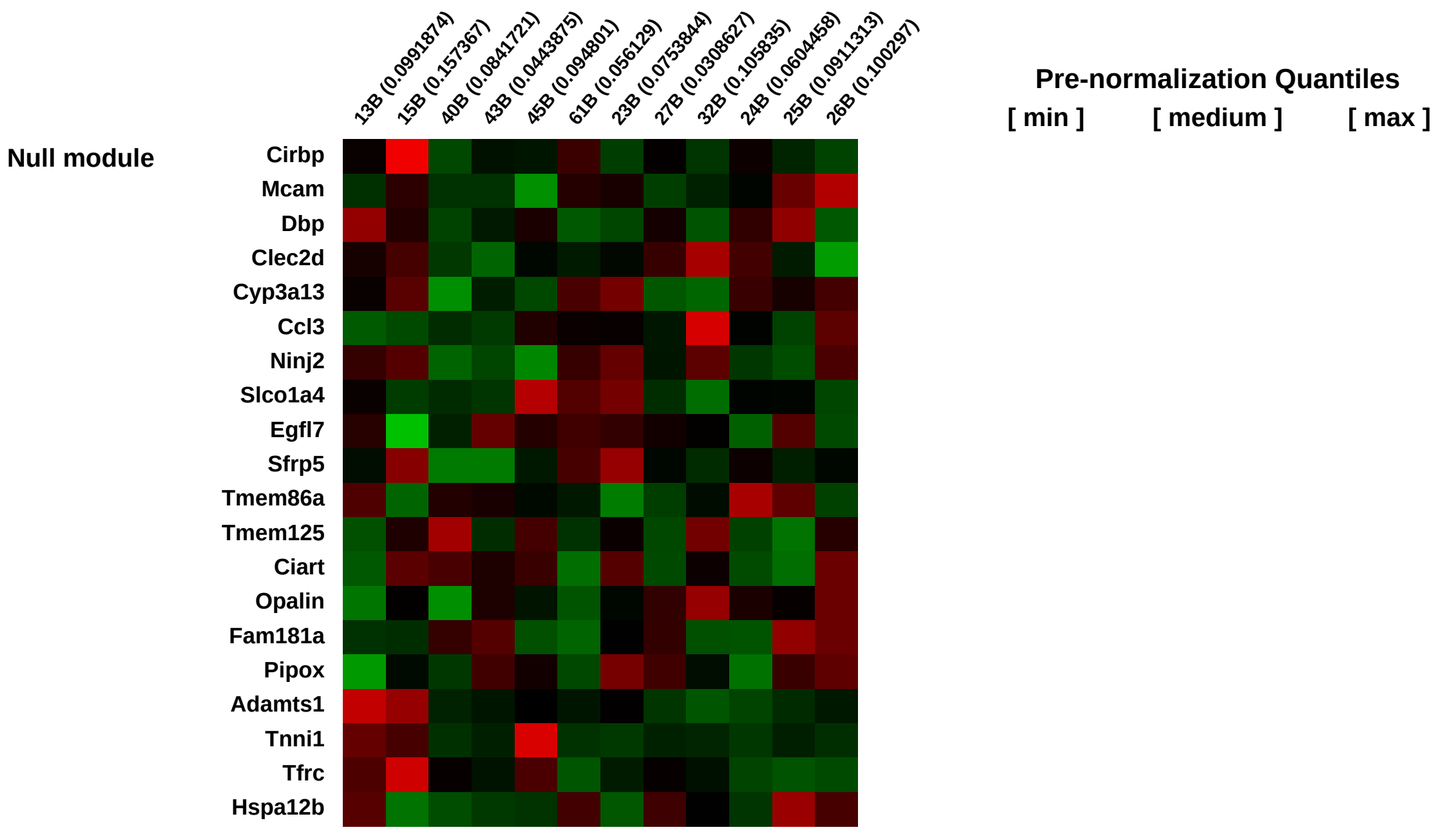

GEO Series "GSE19616" Expression Profiles

Num of samples in this series: 16

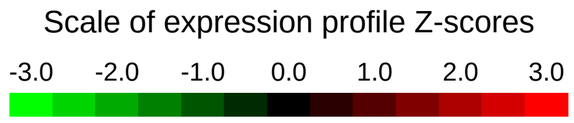

GEO Link:	http://www.ncbi.nlm.nih.gov/geo/query/acc.cgi?acc=GSE19616
Status:	Public on Jul 20 2010
Title:	Gene expression profiling of mouse p53-deficient epidermal carcinoma defines molecular determinants of human cancer malignancy (testing dataset)
Organism:	Mus musculus
Experiment type:	Expression profiling by array
Platform:	GPL1261
Pubmed ID:	20630075
Summary & Design:	**Summary:** The epidermal specific ablation of Trp53 gene leads to the spontaneous development of aggressive tumors in mice through a process that is accelerated by the simultaneous ablation of Rb gene. Since alterations of p53-dependent pathway are common hallmarks of aggressive, poor prognostic human cancers, these mouse models can recapitulate the molecular features of some of these human malignancies. To evaluate this possibility, gene expression microarray analysis was performed in mouse samples. The mouse tumors display increased expression of cell cycle and chromosomal instability associated genes. Remarkably, they are also enriched in human embryonic stem cell gene signatures, a characteristic feature of human aggressive tumors. Using cross-species comparison and meta-analytical approaches, we also observed that spontaneous mouse tumors display robust similarities with gene expression profiles of human tumors bearing mutated TP53, or displaying poor prognostic outcome, from multiple body tissues. We have obtained a 20-gene signature whose genes are overexpressed in mouse tumors and can identify human tumors with poor outcome from breast cancer, astrocytoma and multiple myeloma. This signature was consistently overexpressed in additional mouse tumors using microarray analysis. Two of the genes of this signature, AURKA and UBE2C, were validated in human breast and cervical cancer as potential biomarkers of malignancy. Our analyses demonstrate that these mouse models are promising preclinical tools aimed to search for malignancy biomarkers and to test targeted therapies of prospective use in human aggressive tumors and/or with p53 mutation or inactivation. **Overall design:** Control skin was compared with skin tumors arising in k14Cre;p53loxP/loxP and k14Cre;p53loxP/loxP;pRbloxP/loxP animals, giving a mouse p53-tumor signature

Background corr dist: KL-Divergence = 0.1802, L1-Distance = 0.0477, L2-Distance = 0.0056, Normal std = 0.3576

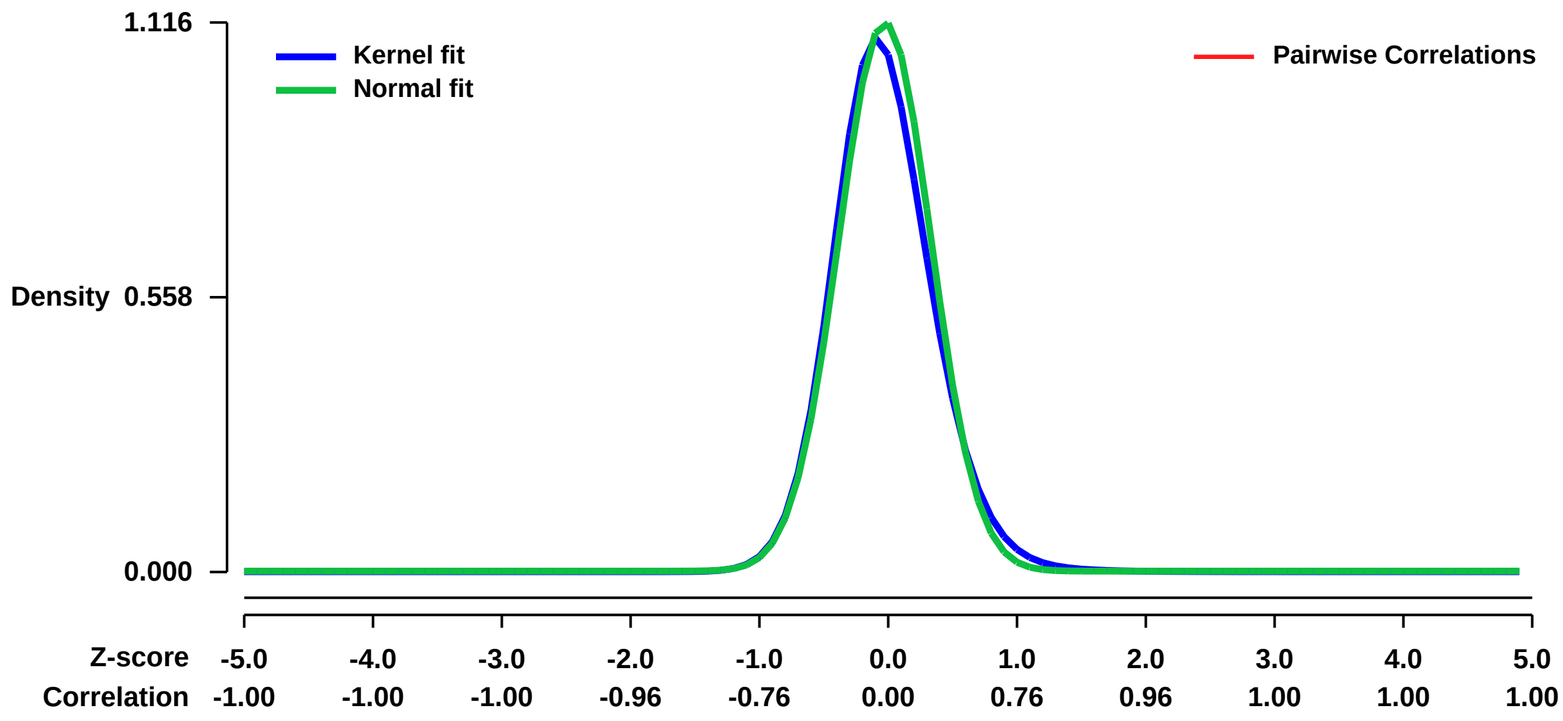

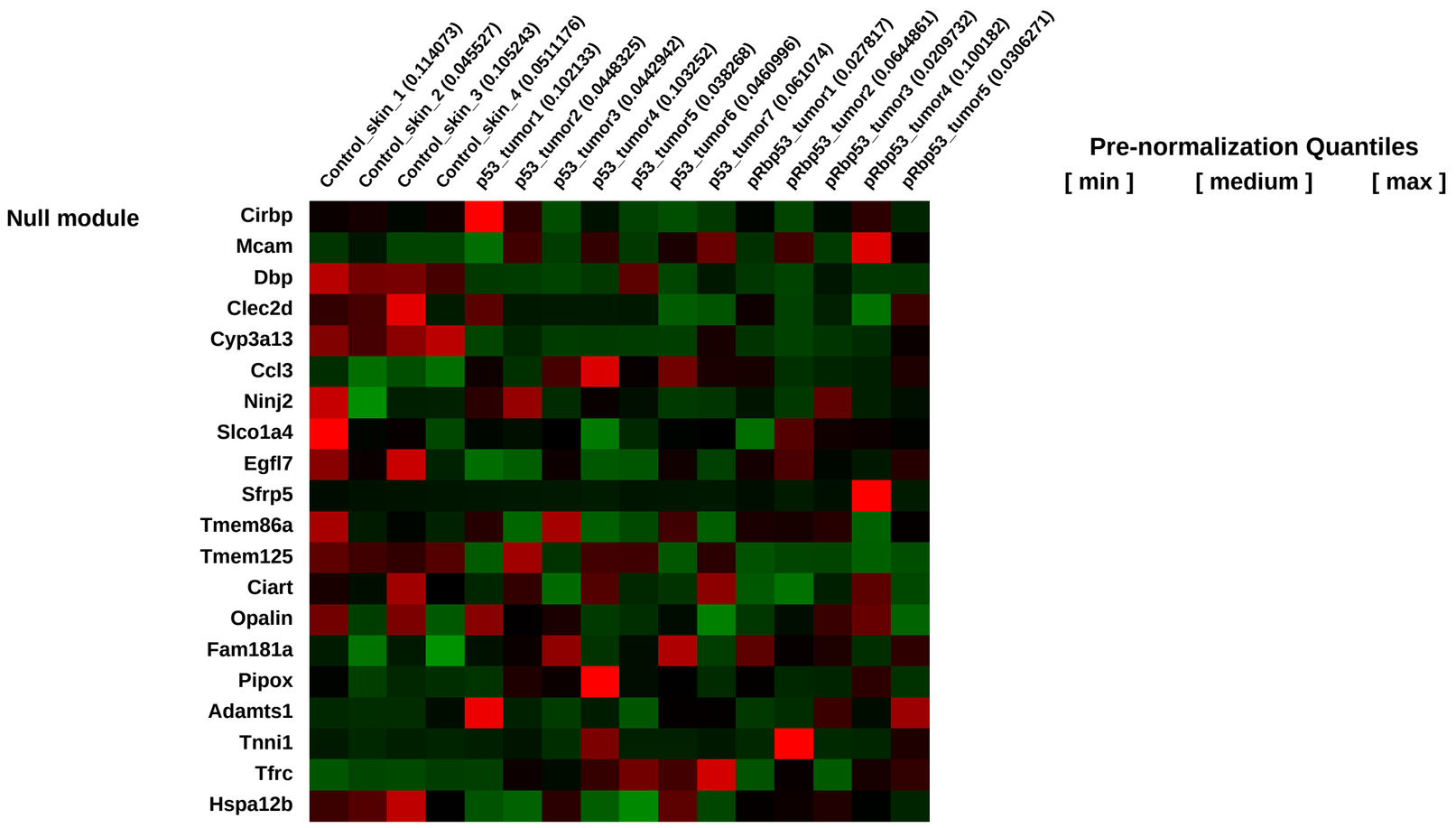

GEO Series "GSE7430" Expression Profiles

Num of samples in this series: 12

Scale of expression profile Z-scores

-3.0 -2.0 -1.0 0.0 1.0 2.0 3.0

GEO Link:	http://www.ncbi.nlm.nih.gov/geo/query/acc.cgi?acc=GSE7430
Status:	Public on Apr 04 2007
Title:	Investigate the role of Wnt/beta-catenin signaling in development of the exocrine pancreas
Organism:	Mus musculus
Experiment type:	Expression profiling by array
Platform:	GPL1261
Pubmed ID:	17222338
Summary & Design:	**Summary:** beta-catenin is an essential mediator of canonical Wnt signaling and a central component of the cadherin-catenin epithelial adhesion complex. Dysregulation of beta-catenin expression has been described in pancreatic neoplasia. Newly published studies have suggested that beta-catenin is critical for normal pancreatic development although these reports reached somewhat different conclusions. In addition, the molecular mechanisms by which loss of beta-catenin affects pancreas development are not well understood. The goals of this study then were; 1] to further investigate the role of beta-catenin in pancreatic development using a conditional knockout approach and 2] to identify possible mechanisms by which loss of beta-catenin disrupts pancreatic development. A Pdx1-cre mouse line was used to delete a floxed beta-catenin allele specifically in the developing pancreas, and embryonic pancreata were studied by immunohistochemistry and microarray analysis. **Keywords:** Time course **Overall design:** In the study, we hybridized RNA from Embryonic day 14.6 and 16.5 pancreas of wild type (WT) control and Pdx1Cre/+; beta-cateninflox/flox´ beta-catenin null in the pancreas) embryonic pancreas to Affymetrix MOE430 2.0 GeneChipˆ´fi arrays containing 45,101 well characterized mouse genes/ESTs.

Background corr dist: KL-Divergence = 0.0780, L1-Distance = 0.0340, L2-Distance = 0.0021, Normal std = 0.4802

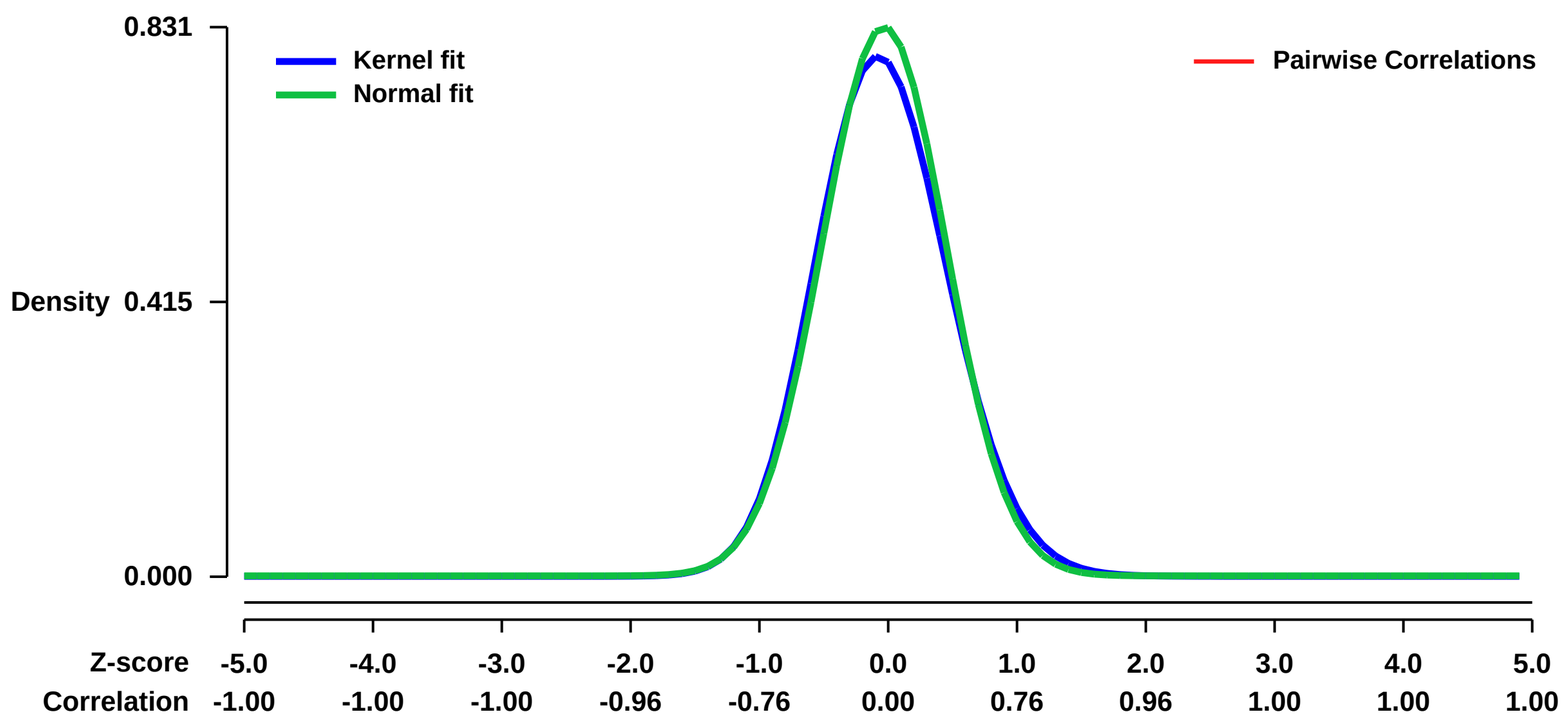

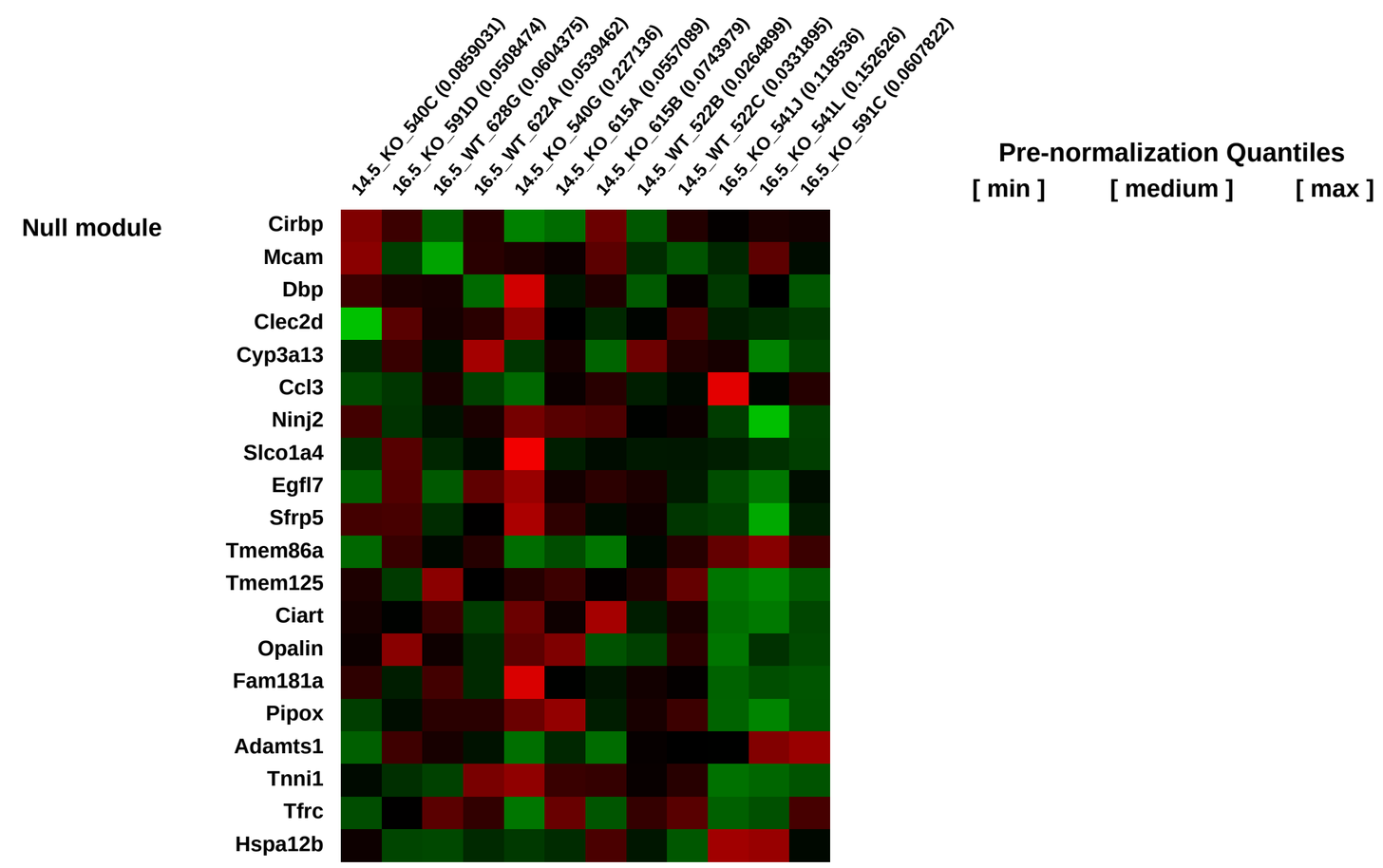

GEO Series "GSE43242" Expression Profiles

Num of samples in this series: 10

Scale of expression profile Z-scores

-3.0 -2.0 -1.0 0.0 1.0 2.0 3.0

GEO Link:	**http://www.ncbi.nlm.nih.gov/geo/query/acc.cgi?acc=GSE43242**
Status:	**Public on Jan 21 2014**
Title:	**Effect of osteoblast-specific constitutive activation of beta-catenin or deletion of FoxO1 on gene expression in mice**
Organism:	**Mus musculus**
Experiment type:	**Expression profiling by array**
Platform:	**GPL1261**
Pubmed ID:	**24429522**
Summary & Design:	**Summary:** **The gene expression of mice with osteoblast-specific beta-catenin activation or FoxO1 deactivation are each compared to that of Wt.** **Overall design:** **C. Osteoblast specific FoxO1 deleted mice (n=3)**

Background corr dist: **KL-Divergence = 0.1216, L1-Distance = 0.0309, L2-Distance = 0.0017, Normal std = 0.4052**

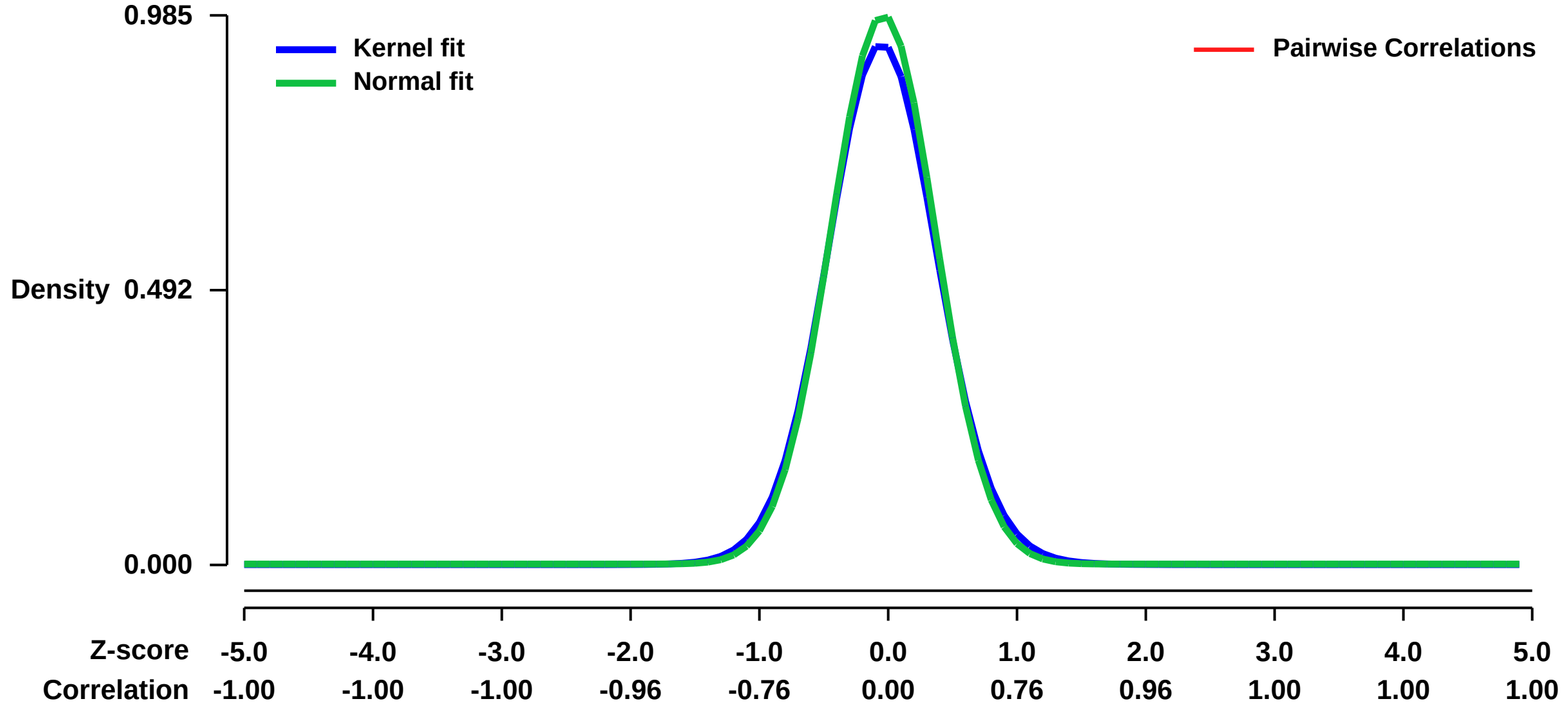

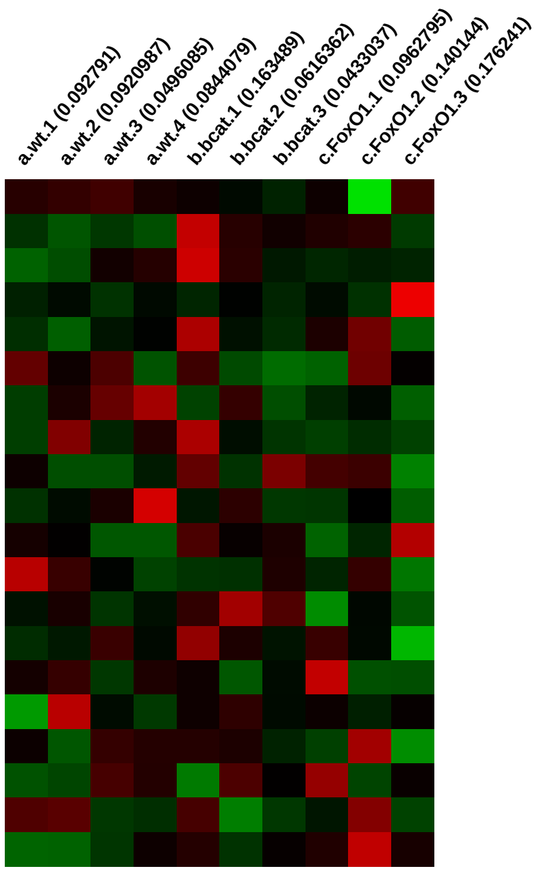

GEO Series "GSE51686" Expression Profiles

Num of samples in this series: 9

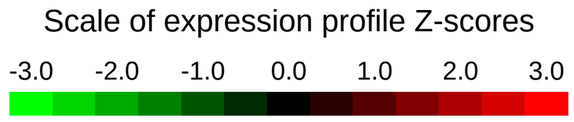

GEO Link:	**http://www.ncbi.nlm.nih.gov/geo/query/acc.cgi?acc=GSE51686**
Status:	**Public on Oct 25 2013**
Title:	**Fracture healing in osteoporotic mice**
Organism:	**Mus musculus**
Experiment type:	**Expression profiling by array**
Platform:	**GPL1261**
Pubmed ID:	
Summary & Design:	**Summary:** **Genome-wide comparative gene expression analysis of callus tissue of osteoporotic mice (Col1a1-Krm2 and Lrp5-/-) and wild-type were performed to identify candidate genes that might be responsible for the impaired fracture healing observed in Col1a1-Krm2 and Lrp5-/- mice.** **Overall design:** **To investigate bone healing in osteoporosis, we performed fracture healing studies in wild-type mice (C57BL/6 genetic background) and the low bone mass strains Col1a1-Krm2 and Lrp5-/- (Schulze et al., 2010; Kato et al., 2002). Osteotomy was set in femora of female mice and stabilized by a semi-rigid fixator to allow fast bone healing (R^¶ntgen et al., 2010). 21 days post surgery we analyzed the fracture calli by biochemical/histological methods, as well as micro-computed tomography, and observed impaired fracture healing in Col1a1-Krm2 and Lrp5-/- mice in comparison to wild-type. To identify genes that may be responsible for the impaired healing in osteoporotic mice, we performed microarray analysis of three independent callus samples of each genotype. The callus tissue was taken 10 days after surgery, because extensive bone formation took place at this point.**

Background corr dist: KL-Divergence = 0.0680, L1-Distance = 0.0239, L2-Distance = 0.0009, Normal std = 0.5035

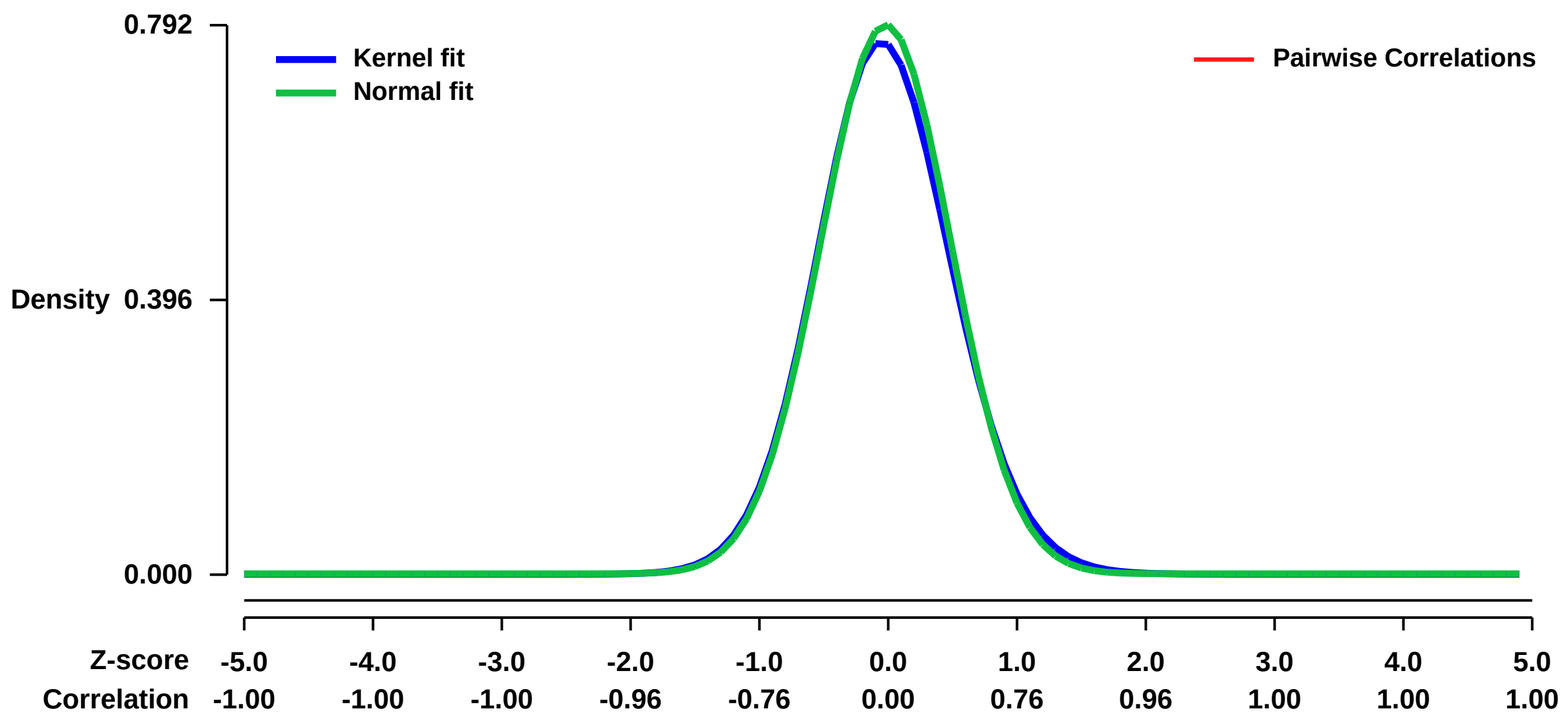

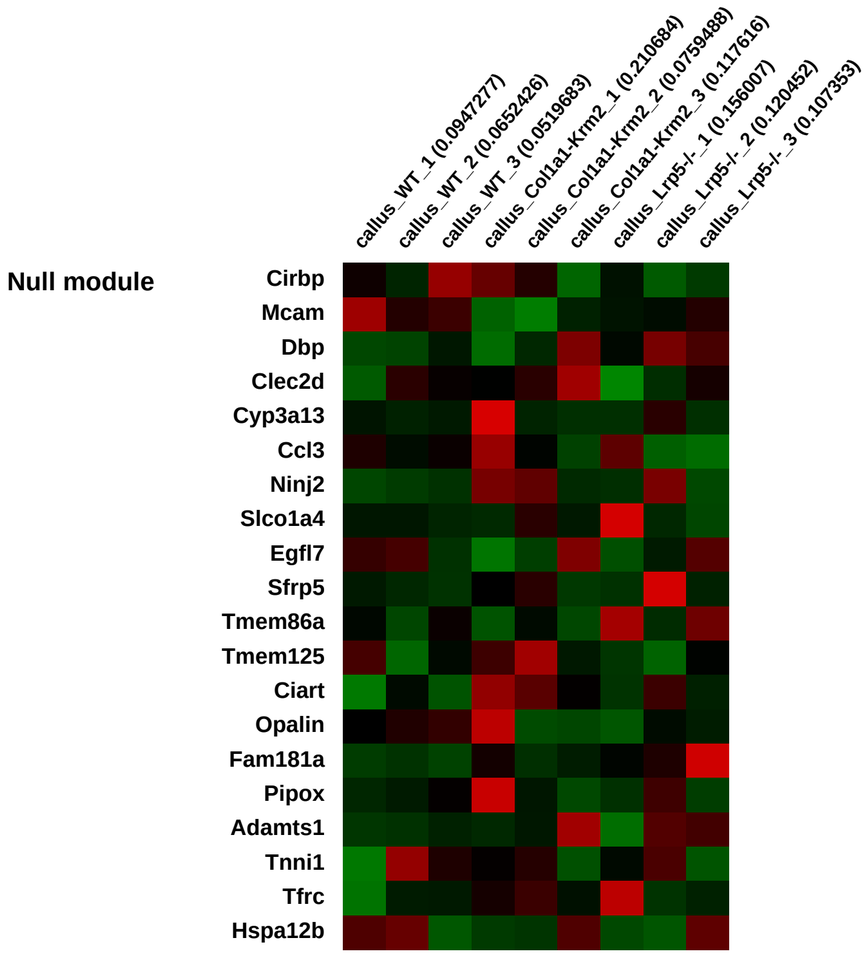

GEO Series "GSE45619" Expression Profiles

Num of samples in this series: 6

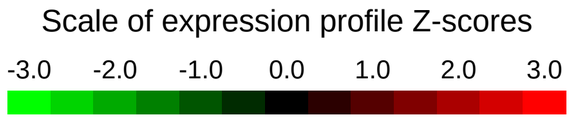

GEO Link:	**http://www.ncbi.nlm.nih.gov/geo/query/acc.cgi?acc=GSE45619**
Status:	**Public on Mar 29 2013**
Title:	**Expression analysis of GATA1s murine megakaryocyte progenitors from bone marrow and fetal Liver**
Organism:	**Mus musculus**
Experiment type:	**Expression profiling by array**
Platform:	**GPL1261**
Pubmed ID:	
Summary & Design:	**Summary:** **About 10% of Down syndrome (DS) infants are born with a myeloproliferative disorder (DS-TMD) that spontaneously resolves within the first few months of life. About 20-30% of these infants subsequently develop acute megakaryoblastic leukemia (DS-AMKL). In order to understand differences that may exist between fetal and bone marrow megakaryocyte progenitor cell populations we flow sorted megakaryocyte progenitor cells and performed microarray expression analysis.** **kewywords: Mouse megakaryocyte progenitors** **Overall design:** **Expression data of flow cytometrically isolated murine megakaryocyte progenitor cells (lin-, Sca-1-, c-kit+, CD150+, CD41+) from GATA1s fetal liver and bone marrow**

Background corr dist: **KL-Divergence = 0.0282, L1-Distance = 0.0322, L2-Distance = 0.0012, Normal std = 0.7067**

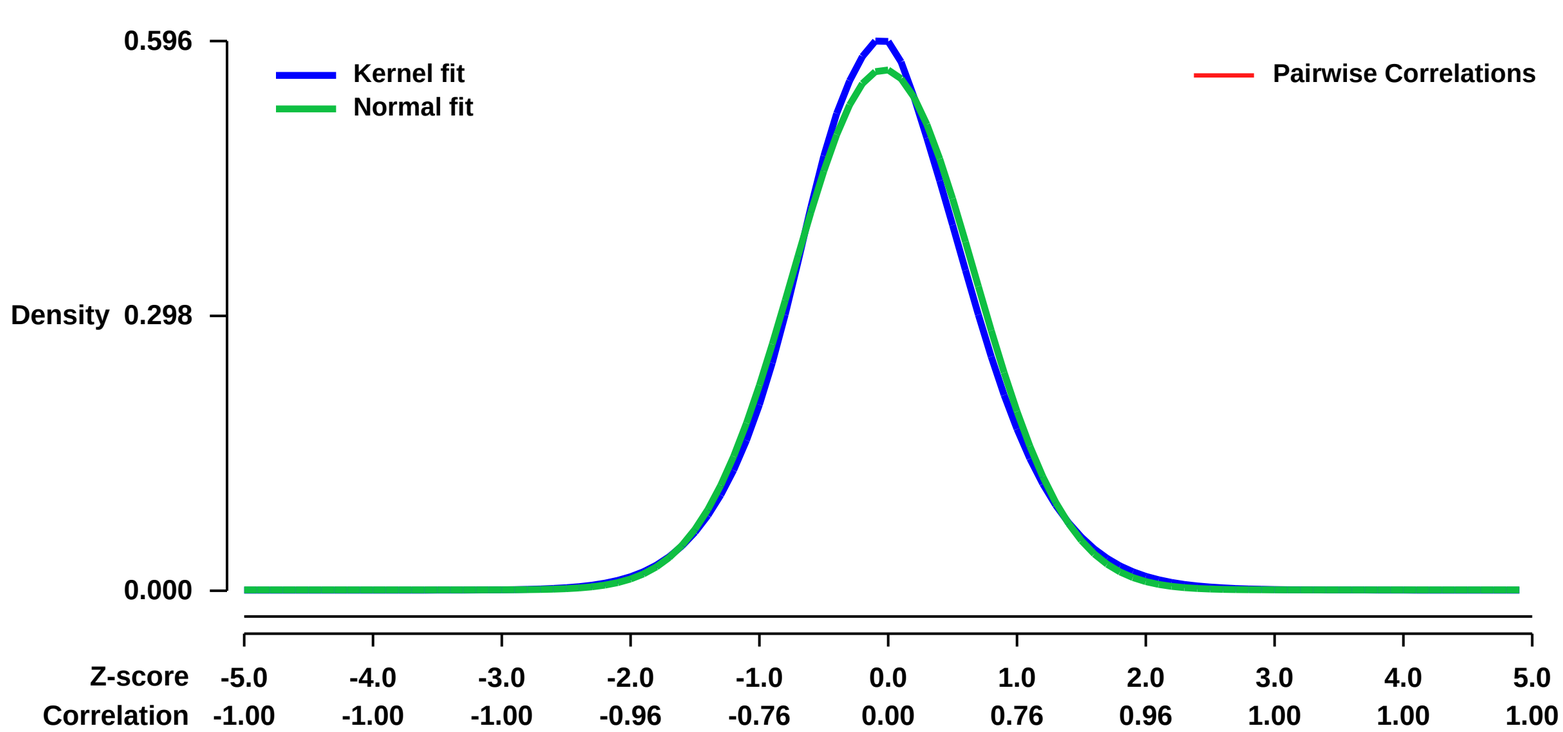

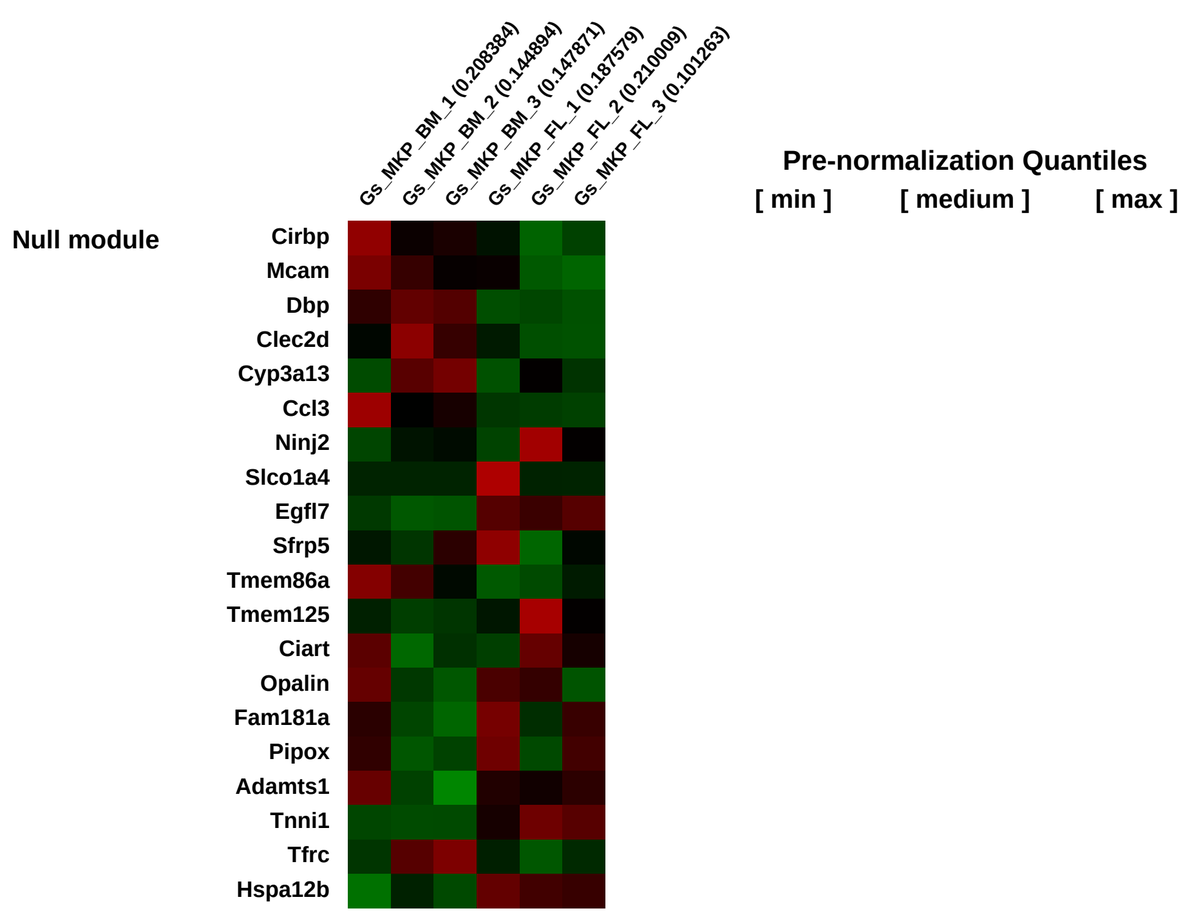

GEO Series "GSE9441" Expression Profiles

Num of samples in this series: 36

Scale of expression profile Z-scores

-3.0 -2.0 -1.0 0.0 1.0 2.0 3.0

GEO Link:	http://www.ncbi.nlm.nih.gov/geo/query/acc.cgi?acc=GSE9441
Status:	Public on Dec 07 2007
Title:	The effect of sleep deprivation on gene expression in the brain and the liver of three inbred mouse strains
Organism:	Mus musculus
Experiment type:	Expression profiling by array
Platform:	GPL1261
Pubmed ID:	18077435
Summary & Design:	**Summary:** These studies adress differential changes in gene expression between 6h sleep deprived and control mice in the brain and the liver. We profiled gene expression in three different inbred strains to understand the influence of genetic background. **Keywords: brain, genetic background, sleep deprivation** **Overall design:** Experiments were performed on male mice (C57BL/6J (B6), AKR/J (AK), DBA/2J (D2)), 12-13 weeks of aged, purchased from Jackson Laboratory. Animals were housed in a light/dark cycle of 24 hrs with water and food available ad libitum. Mice of the 3 inbred strains were sleep deprived for 6h starting at light onset (ZT0) and sacrificed together with their home-cage controls at ZT6 (n=9 / strain =3 / condition =2 / tissues =2; total = 108 mice).

Background corr dist: KL-Divergence = 0.0092, L1-Distance = 0.0360, L2-Distance = 0.0014, Normal std = 0.9491

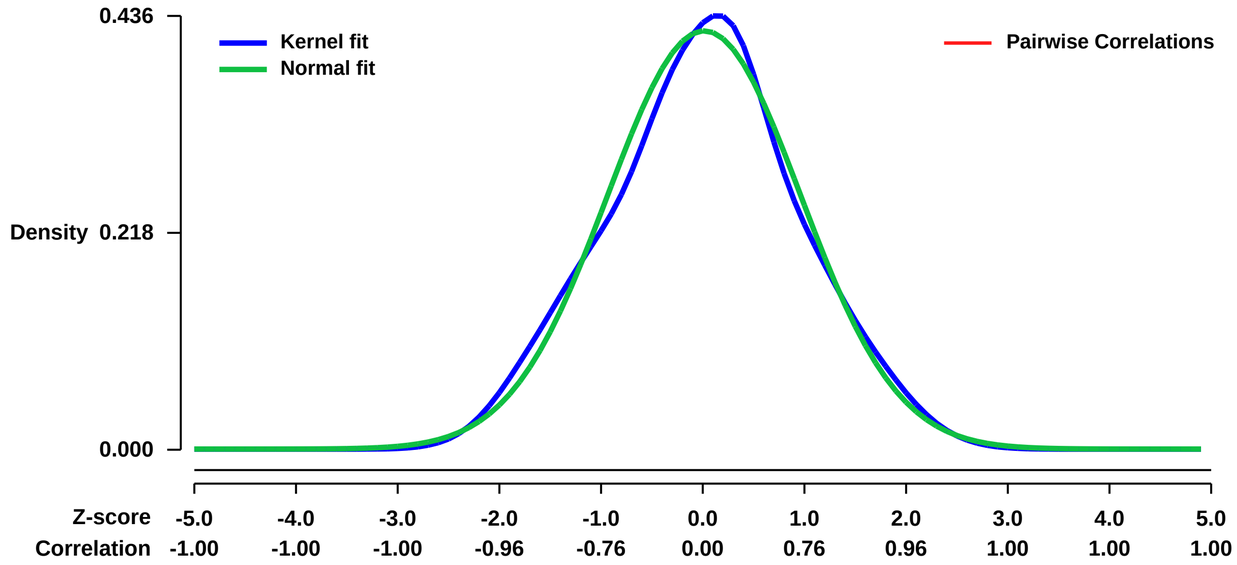

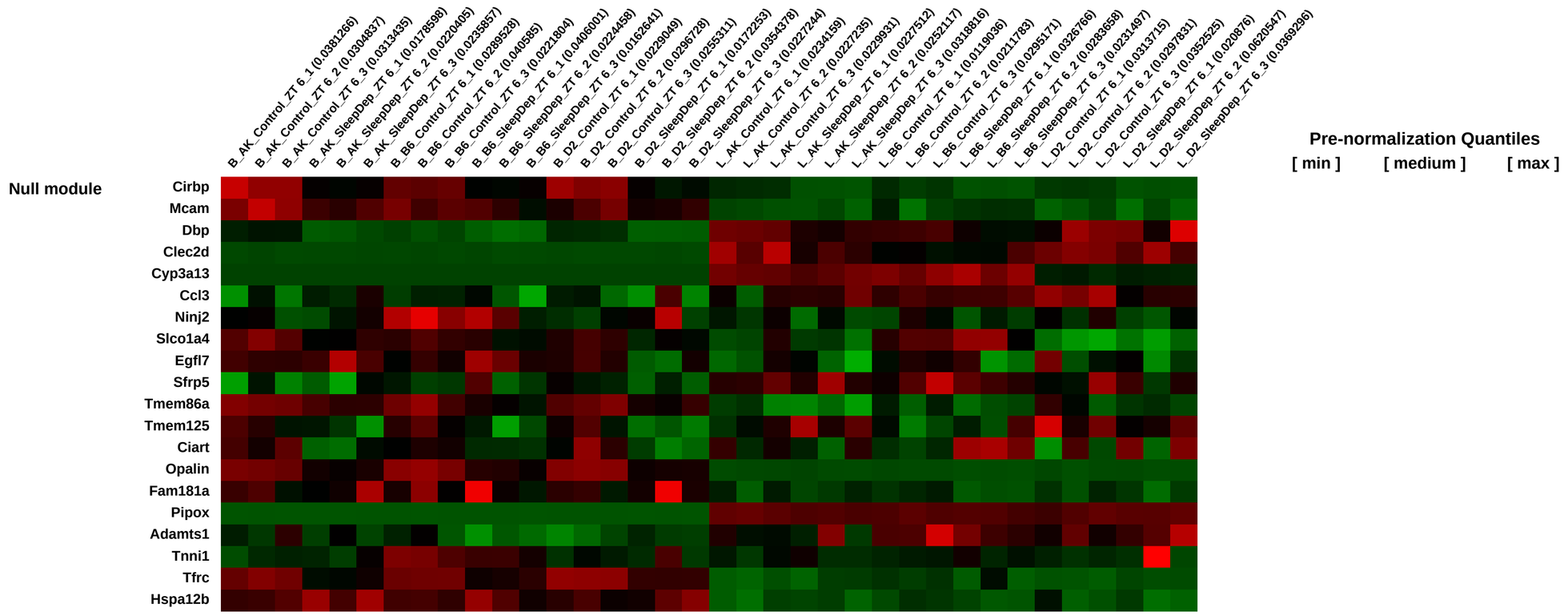

GEO Series "GSE28823" Expression Profiles

Num of samples in this series: 12

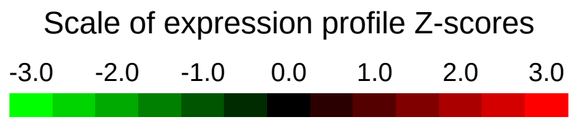

GEO Link:	http://www.ncbi.nlm.nih.gov/geo/query/acc.cgi?acc=GSE28823
Status:	Public on Feb 14 2012
Title:	Expression data from ZMYM2-FGFR1-induced T-cell lymphomas in a mouse model
Organism:	Mus musculus
Experiment type:	Expression profiling by array
Platform:	GPL1261
Pubmed ID:	21527531
Summary & Design:	**Summary:** The ZMYM2-FGFR1 (formerly known as ZNF198-FGFR1) fusion kinase induces stem cell leukemia-lymphoma syndrome (SCLL), a hematological malignancy characterized by rapid transformation to acute myeloid leukemia and T-lymphoblastic lymphoma. We previously developed a mouse model of ZMYM2-FGFR1 (Ren et al. 2009, Blood). To further investigate mechanisms of oncogenesis and progression, we undertook a global gene expression analysis of leukemic T-cells from the animal model compared with Thy1+DP+ (CD4+CD8+) cells isolated from normal Balb/c thymuses, as well as lukemic stem cells (LSK, GFP+Lin-Sca-1+c-kit+ cells) sorted from the leukemic mice versus hematopoietic stem cells (HSC, Lin-Sca-1+c-kit+ cells) sorted from normal BALB/c bone marrow cells. We found high expressions of Notch1 and its downstream target genes in T-cell lymphomas that arise in a murine model of ZMYM2-FGFR1 SCLL. Our functional studies demonstrate the importance of Notch signaling in the etiology of SCLL and suggest that targeting this pathway could provide a novel strategy for molecular therapies to treat SCLL patients.´ **Overall design:** RNA was isolated from HSC (Lin-Sca-1+c-kit+) sorted from normal BALB/c bone marrow cells and lukemic stem cells (LSK, GFP+ Lin-Sca-1+c-kit+ cells) sorted from the leukemic mice bone marrow or spleen cells. To minimize biological variability, each HSC sorting experiment used BM cells from 5 normal female Balb/c. LSC were obtained from BM or spleen cells from 2-3 leukemic mice. Gene expression profiles of T-lymphoma and Thy1+DP+ (CD4+CD8+) cells were obtained from three independently sorted Thy1+DP+ cell samples (each sample was derived from thymuses from 3 normal Balb/c mice). The T-lymphoma samples were derived from third serial transplanted disease mice, where >90% of cells were GFP+Thy1+DP+. To investigate whether the sorting process influenced gene expression, one T-lymphoma sample was sorted for GFP+Thy1+DP+ cells. RNA was amplified using a GeneChip Two-Cycle Target Labeling and Control Reagents kit (Affymetrix), and cRNA was hybridized to the Affymetrix Mouse430 2.0 arrays.

Background corr dist: KL-Divergence = 0.0837, L1-Distance = 0.0437, L2-Distance = 0.0038, Normal std = 0.4838

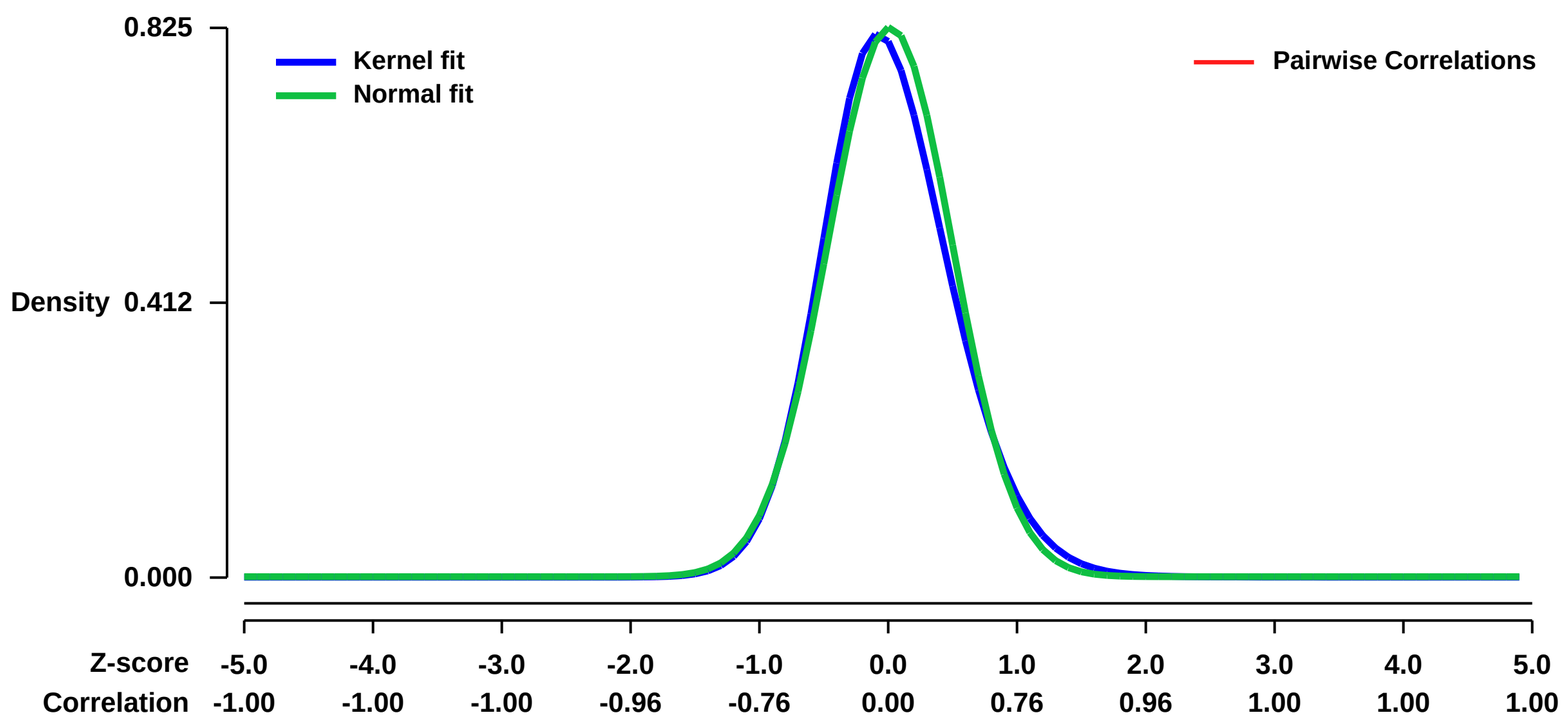

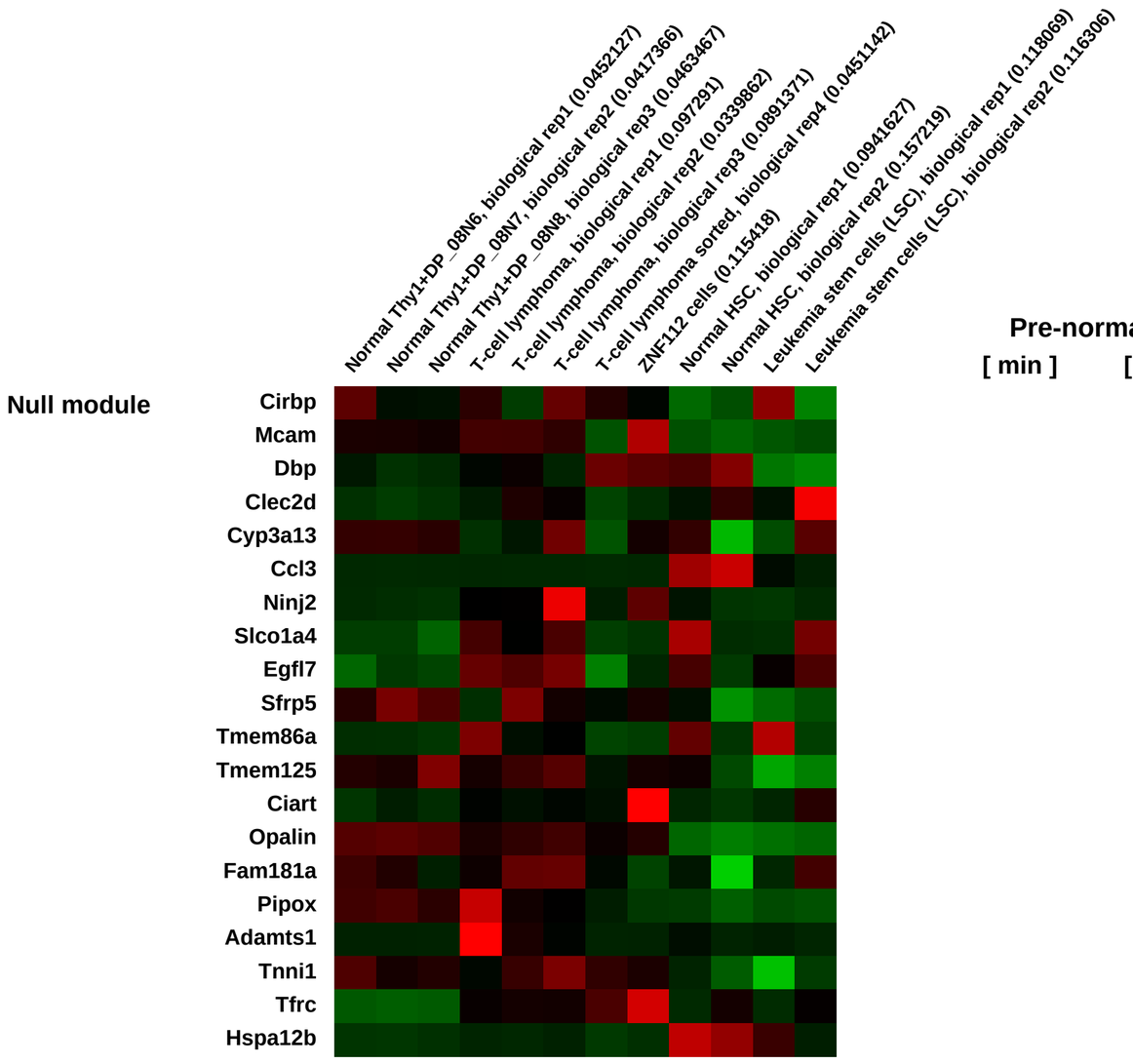

GEO Series "GSE7219" Expression Profiles

Num of samples in this series: 12

Scale of expression profile Z-scores

-3.0 -2.0 -1.0 0.0 1.0 2.0 3.0

GEO Link:	http://www.ncbi.nlm.nih.gov/geo/query/acc.cgi?acc=GSE7219
Status:	Public on Mar 05 2008
Title:	NIK/NF-kappaB2 regulated gene products.
Organism:	Mus musculus
Experiment type:	Expression profiling by array
Platform:	GPL1261
Pubmed ID:	18566401
Summary & Design:	**Summary:** This study aims at identifying genes that are NIK/NF-kappaB2 responsive in murine dendritic cells matured in vivo. Keywords: NIK/NF-kappaB2 responsive genes in dendritic cells after TLR/CD40 signaling **Overall design:** This study isolated dendritic cells from the spleens of Alymphoplasia or heterozygeous littlermates (wild type). Mice were eiter not treated as a reference or treated I.P. with 25 micrograms of LPS and 100 micrograms of agonistic anti-CD40 antibody. DCs were isolated 6 hours after treatment allowing in vivo maturation via both TLR and CD40 signals. DCs from 3 mice per group were pooled. Experiment was performed in triplicate.

Background corr dist: KL-Divergence = 0.0960, L1-Distance = 0.0692, L2-Distance = 0.0095, Normal std = 0.4840

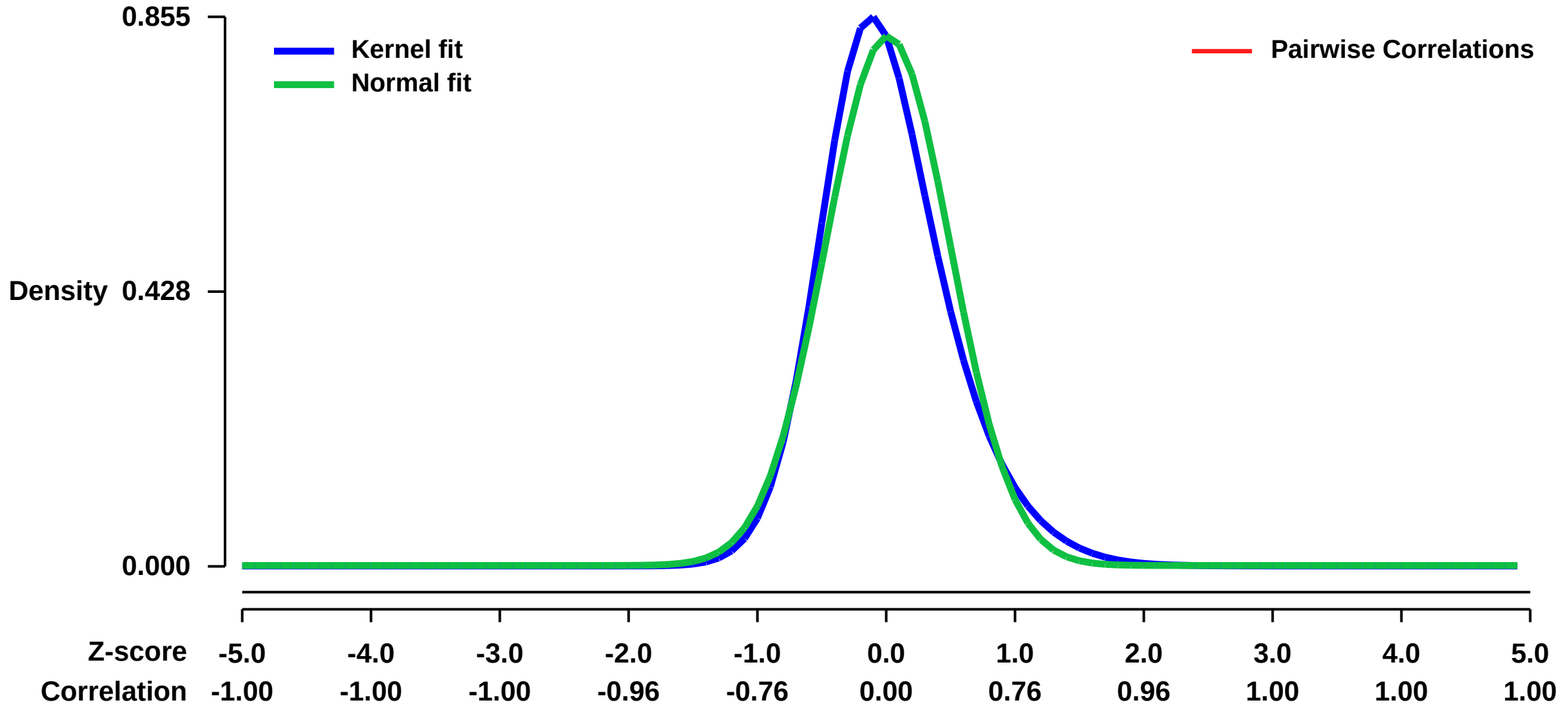

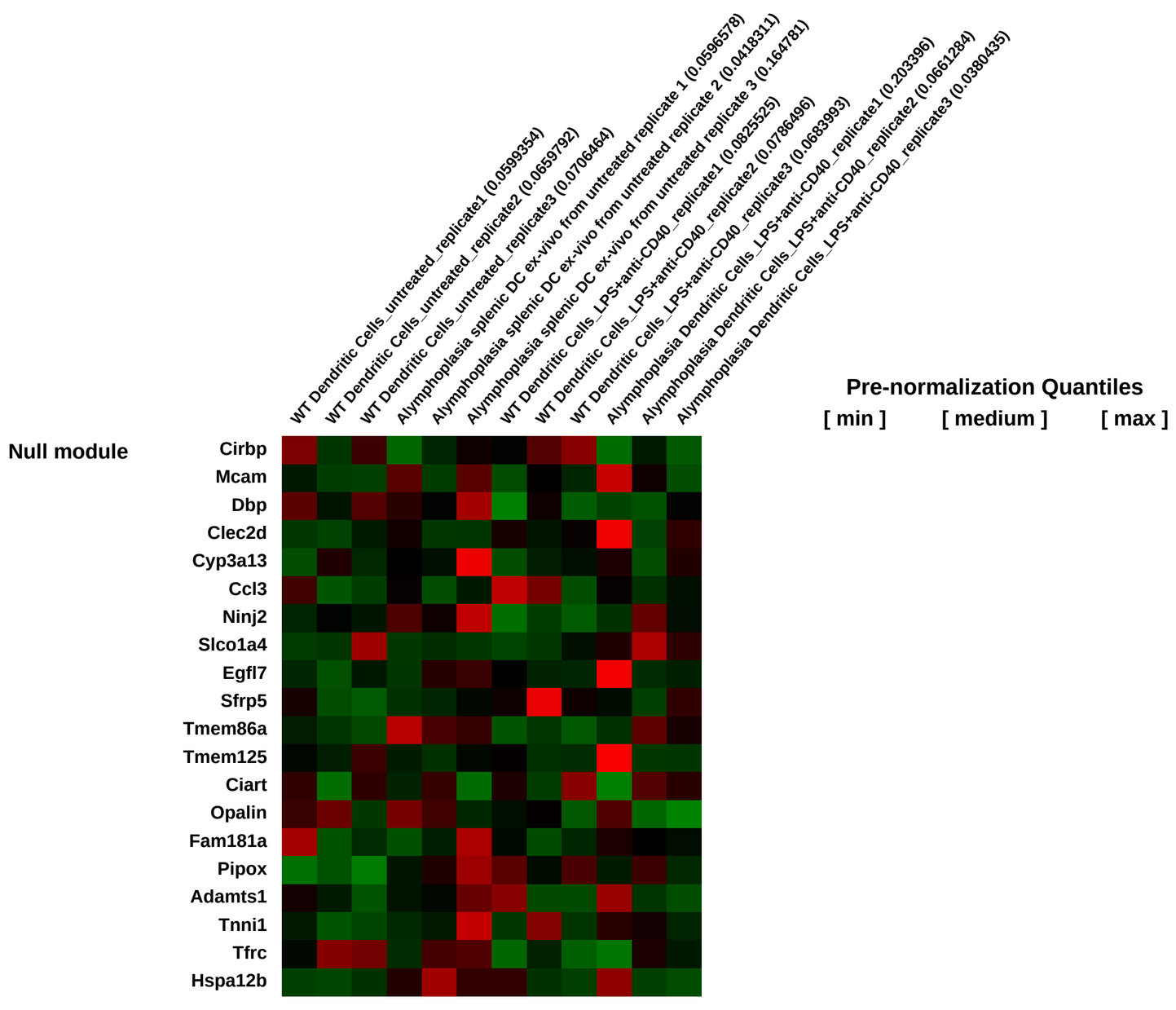

GEO Series "GSE22094" Expression Profiles

Num of samples in this series: 12

Scale of expression profile Z-scores

-3.0 -2.0 -1.0 0.0 1.0 2.0 3.0

GEO Link:	http://www.ncbi.nlm.nih.gov/geo/query/acc.cgi?acc=GSE22094
Status:	Public on Jul 01 2010
Title:	Bone marrow transcriptomal differences between wild type, Fancc-deficient, Fancg-deficient, and doubly deficient (Fancc/Fancg) mice.
Organism:	Mus musculus
Experiment type:	Expression profiling by array
Platform:	GPL1261
Pubmed ID:	20606166
Summary & Design:	**Summary:** Seeking to challenge the current dogma that the nuclear core-complex proteins function in an entirely epistatic manner, Dr. Clapp's group developed a new double-knockout mouse nullizygous for Fancc and Fancg. Because the hematopoietic phenotype was more severe than single knockout mice, we reasoned that transcriptomal differences would exist and lead to the identification of molecular defects unique to each FA gene. **Overall design:** RNA was purified from unfractionated and uncultured bone marrow cells from three types of Fanconi anemia gene knockout mice: nullizygous for Fancc, Fancg, or both Fancc and Fancg.. Three wild type C57Bl/6 mice served as controls. Each of three marrow samples provided one RNA sample (the RNA samples were not pooled).

Background corr dist: KL-Divergence = 0.1250, L1-Distance = 0.0337, L2-Distance = 0.0021, Normal std = 0.3997

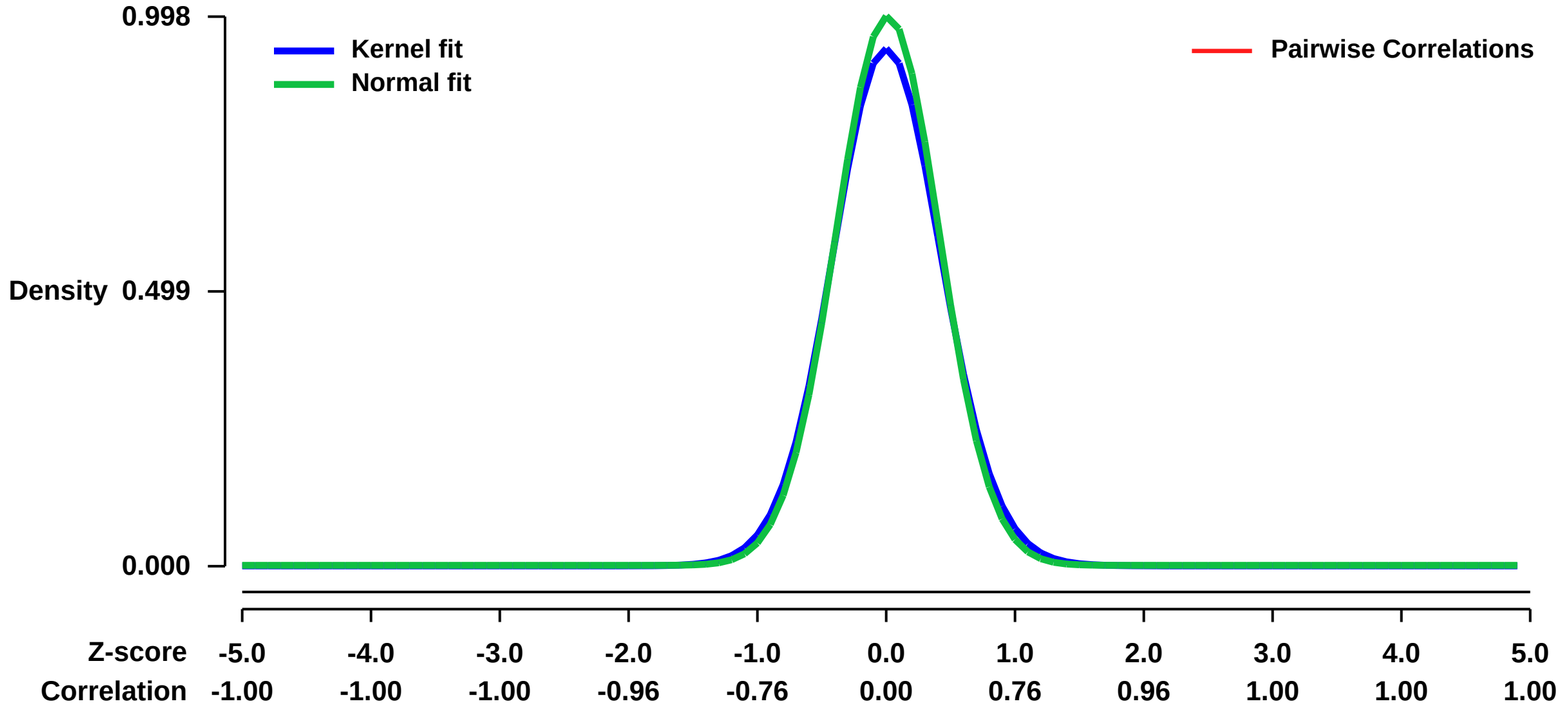

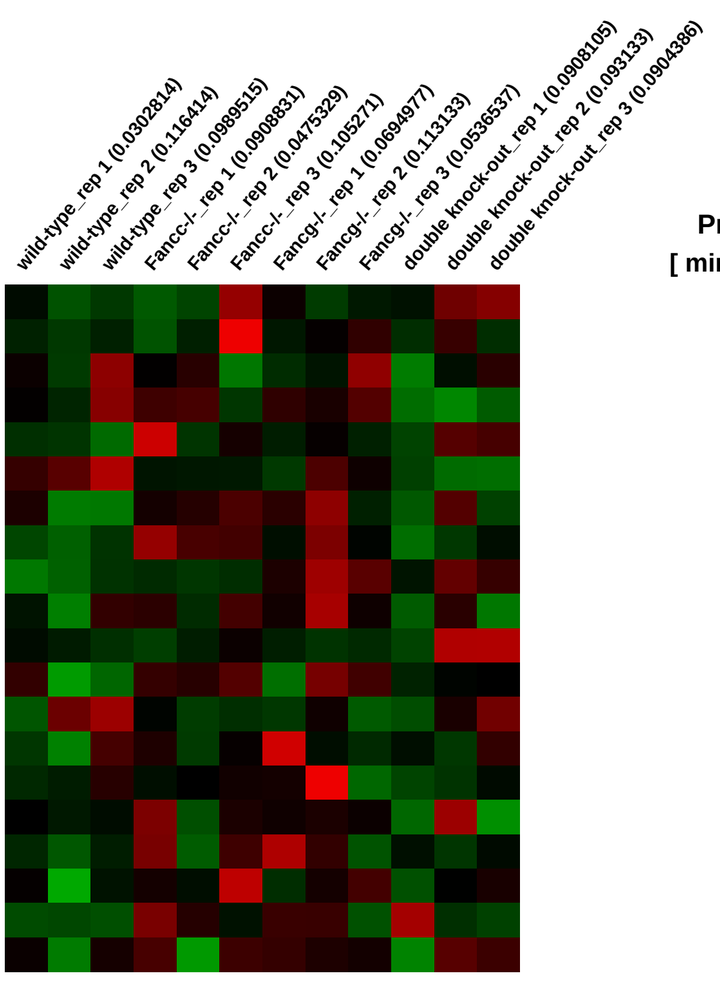

GEO Series "GSE4718" Expression Profiles

Num of samples in this series: 6

Scale of expression profile Z-scores

-3.0 -2.0 -1.0 0.0 1.0 2.0 3.0

GEO Link:	http://www.ncbi.nlm.nih.gov/geo/query/acc.cgi?acc=GSE4718
Status:	Public on Apr 27 2006
Title:	Improved DNA methylation analysis via enrichment of demethylated cells expressing an X-inactivated GFP transgene
Organism:	Mus musculus
Experiment type:	Methylation profiling by array
Platform:	GPL1261
Pubmed ID:	17068962
Summary & Design:	**Summary:** **The demethylating drug 5-aza-2â -deoxycytidine (5-aza-2dC) is frequently used to investigate the** **effect of global DNA demethylation on gene expression in cultured mammalian cells. Here, we utilize a novel method that uses the reactivation of an X-inactivated GFP transgene as a marker to enrich for cells that have undergone drug-induced demethylation. By combining it with microarray gene expression profiling, we demonstrate the methodâ s utility in identifying genes activated by global DNA demethylation.** **Keywords: 5-aza-2'-deoxycytidine; methylation; dermal fibroblast; X-linked GFP** **Overall design:** **Laboratory. Male transgenic animals were bred to wildtype BL6 female mice to obtain females that were heterozygous for the transgene. Dermal fibroblasts were obtained from explant cultures of neonatal female mice from these crosses. The cells were then sorted using FACS to obtain only GFP-nonexpressing cells. These cells represent the population with the GFP transgene on the inactive X chromosome. The GFP-silent cells were treated with the demethylating drug 5-aza-2'-deoxycytidine. This drug does not affect all cells and uses a passive form of demethylation that results in a heterogenous population of unaffected and demethylated cells. A portion of the cells affected by demethylation activate the inactive GFP transgene by demethylating the inactive X chromosome. The GFP-active and GFP-inactive cells were sorted by FACS and assayed by microarray to determine what genes were affected by demethylation. Also the microarray results indicated if sorting for GFP-active cells enriches for cells affected by the drug.**

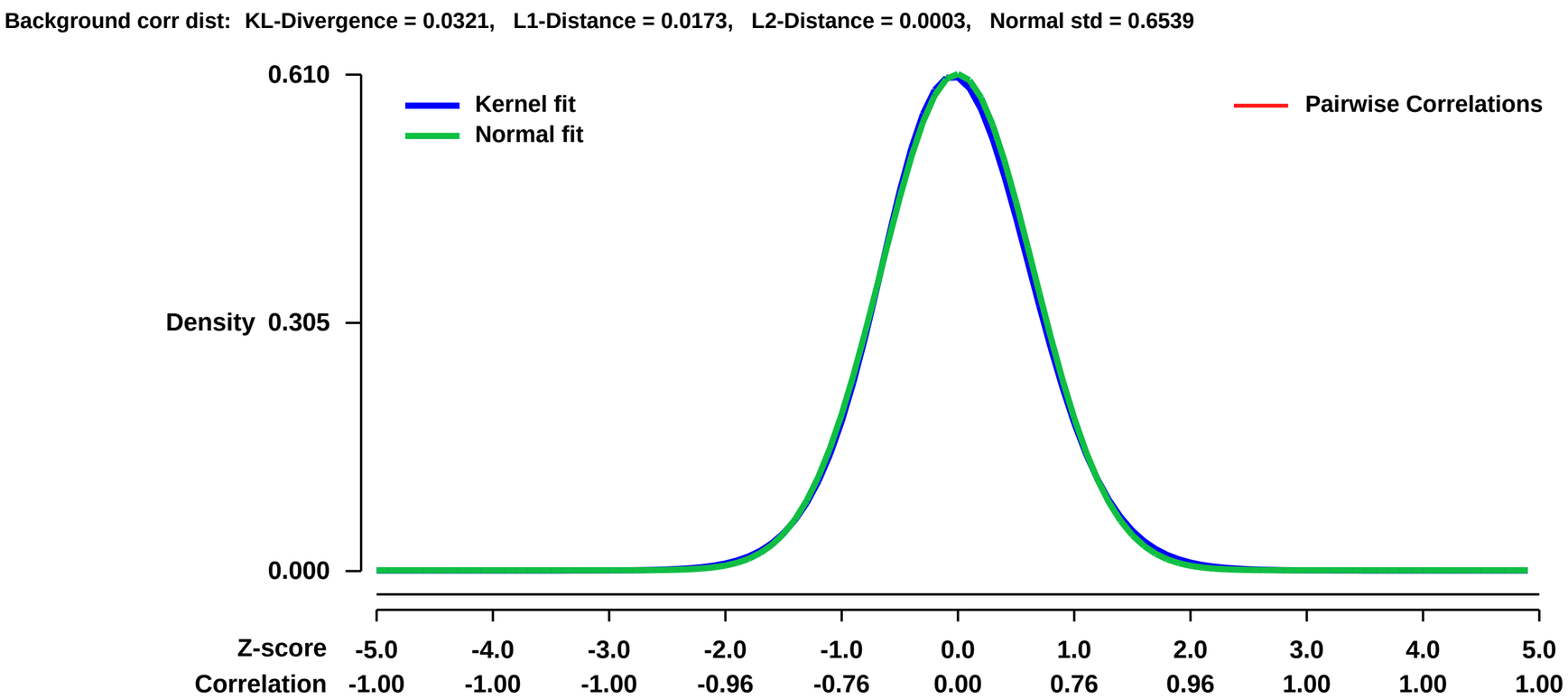

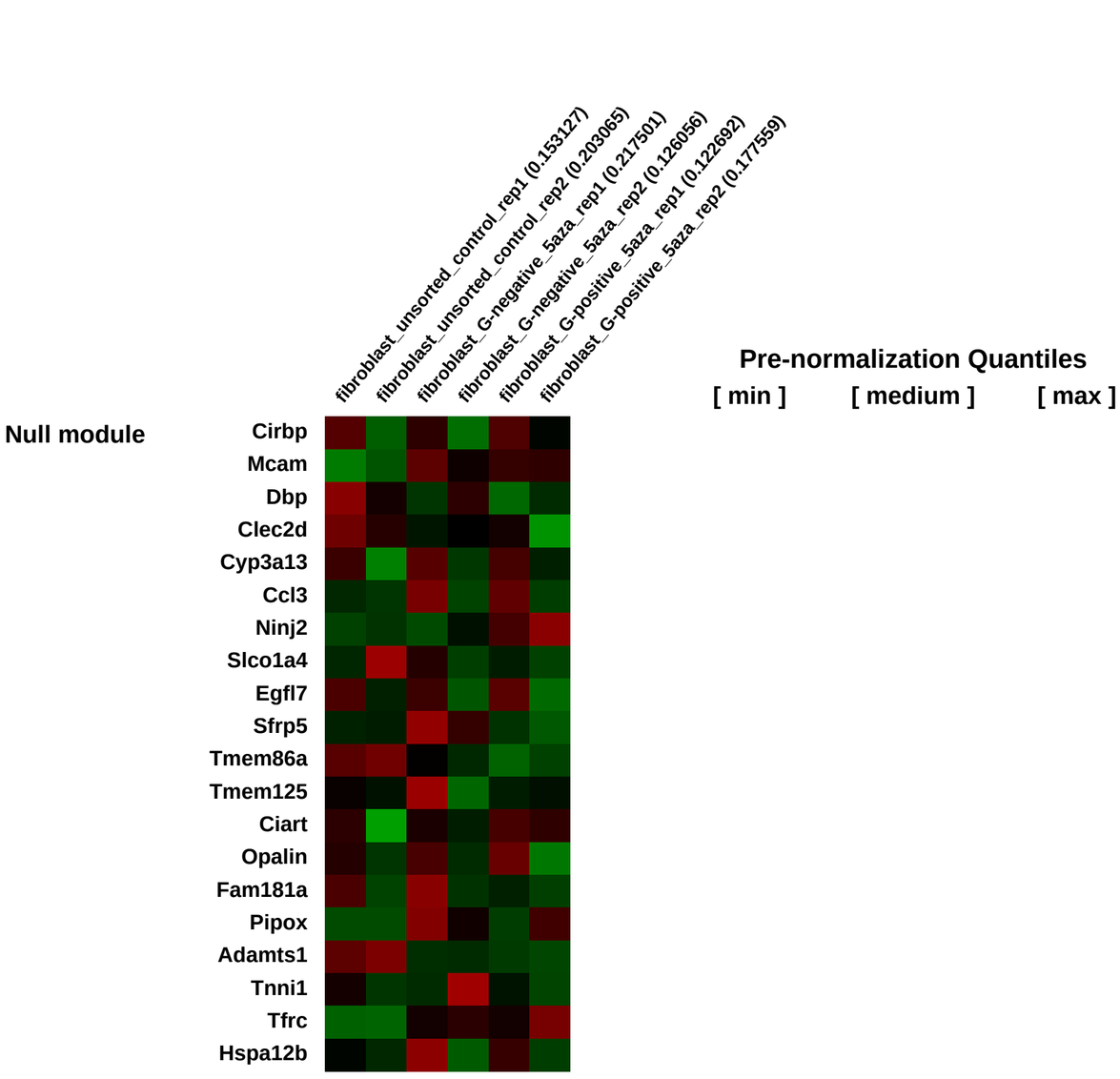

GEO Series "GSE27092" Expression Profiles

Num of samples in this series: 6

Scale of expression profile Z-scores

-3.0 -2.0 -1.0 0.0 1.0 2.0 3.0

GEO Link:	http://www.ncbi.nlm.nih.gov/geo/query/acc.cgi?acc=GSE27092
Status:	Public on Mar 13 2011
Title:	Expression data from P14 TCR cytotoxic T cells overexpressing HDAC7 phosphorylation deficient mutant
Organism:	Mus musculus
Experiment type:	Expression profiling by array
Platform:	GPL1261
Pubmed ID:	21399638
Summary & Design:	**Summary:** The present study reports an unbiased analysis of the cytotoxic T cell serine-threonine phosphoproteome using high resolution mass spectrometry. Approximately 2,000 phosphorylations were identified in CTLs of which approximately 450 were controlled by TCR signaling. A significantly overrepresented group of molecules identified in the phosphoproteomic screen were transcription activators, co-repressors and chromatin regulators. A focus on the chromatin regulators revealed that CTLs have high expression of the histone deacetylase HDAC7 but continually phosphorylate and export this transcriptional repressor from the nucleus. HDAC7 dephosphorylation results in its nuclear accumulation and suppressed expression of genes encoding key cytokines, cytokine receptors and adhesion molecules that determine CTL function. The screening of the CTL phosphoproteome thus reveals intrinsic pathways of serine-threonine phosphorylation that target chromatin regulators in CTLs and determine the CTL functional program. We used Affymetrix microarray analysis to explore the molecular basis for the role of HDAC7 in CTLs and the impact of GFP-HDAC7 phosphorylation deficient mutant expression on the CTL transcriptional profile. **Overall design:** In vitro generated P14 TCR cytotoxic T cells were retrovirally infected with a construct encoding GFP-HDAC7 phosphorylation deficient mutant, sorted in base of GFP expression (GFP positive and GFP negative) and processed for microarray analysis in three biological replicas.

Background corr dist: KL-Divergence = 0.0166, L1-Distance = 0.0217, L2-Distance = 0.0007, Normal std = 0.7816

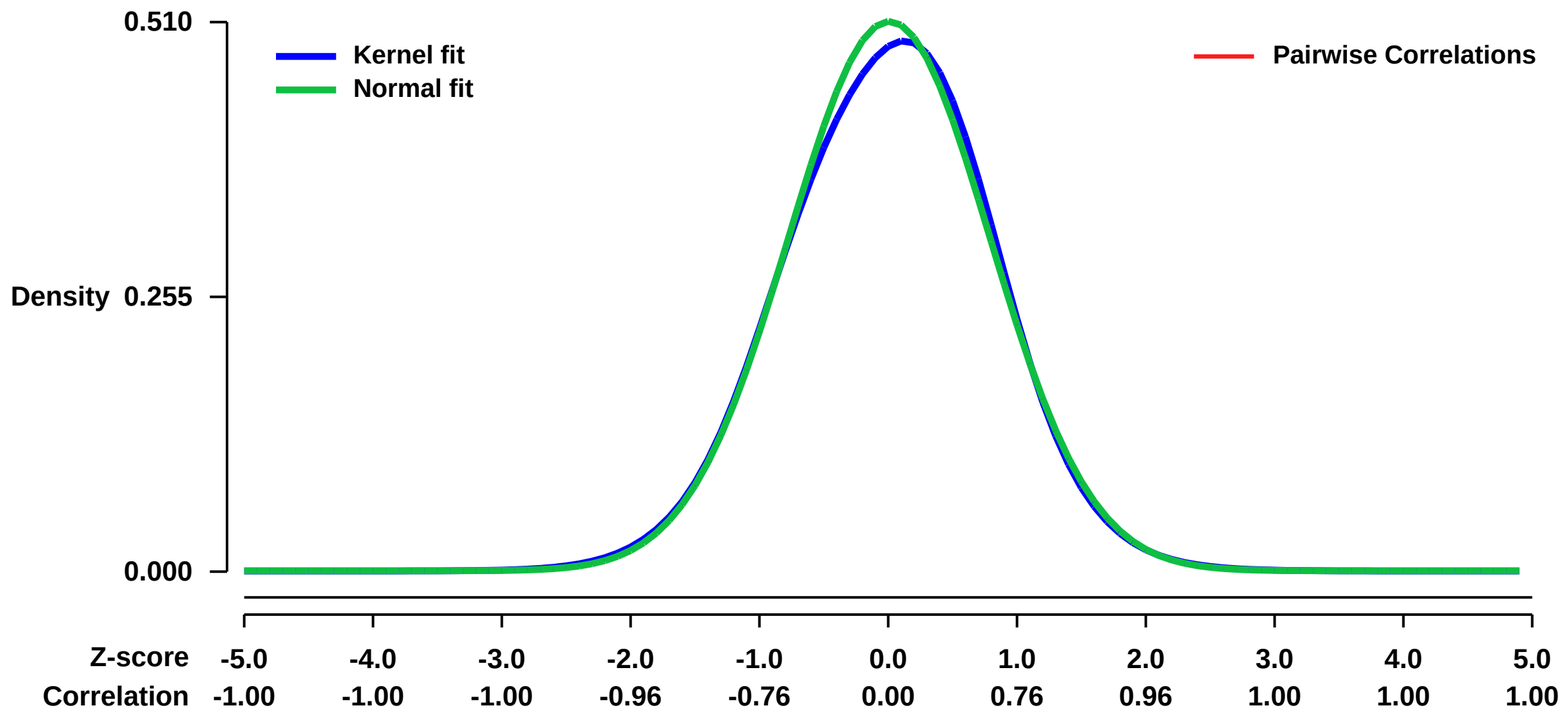

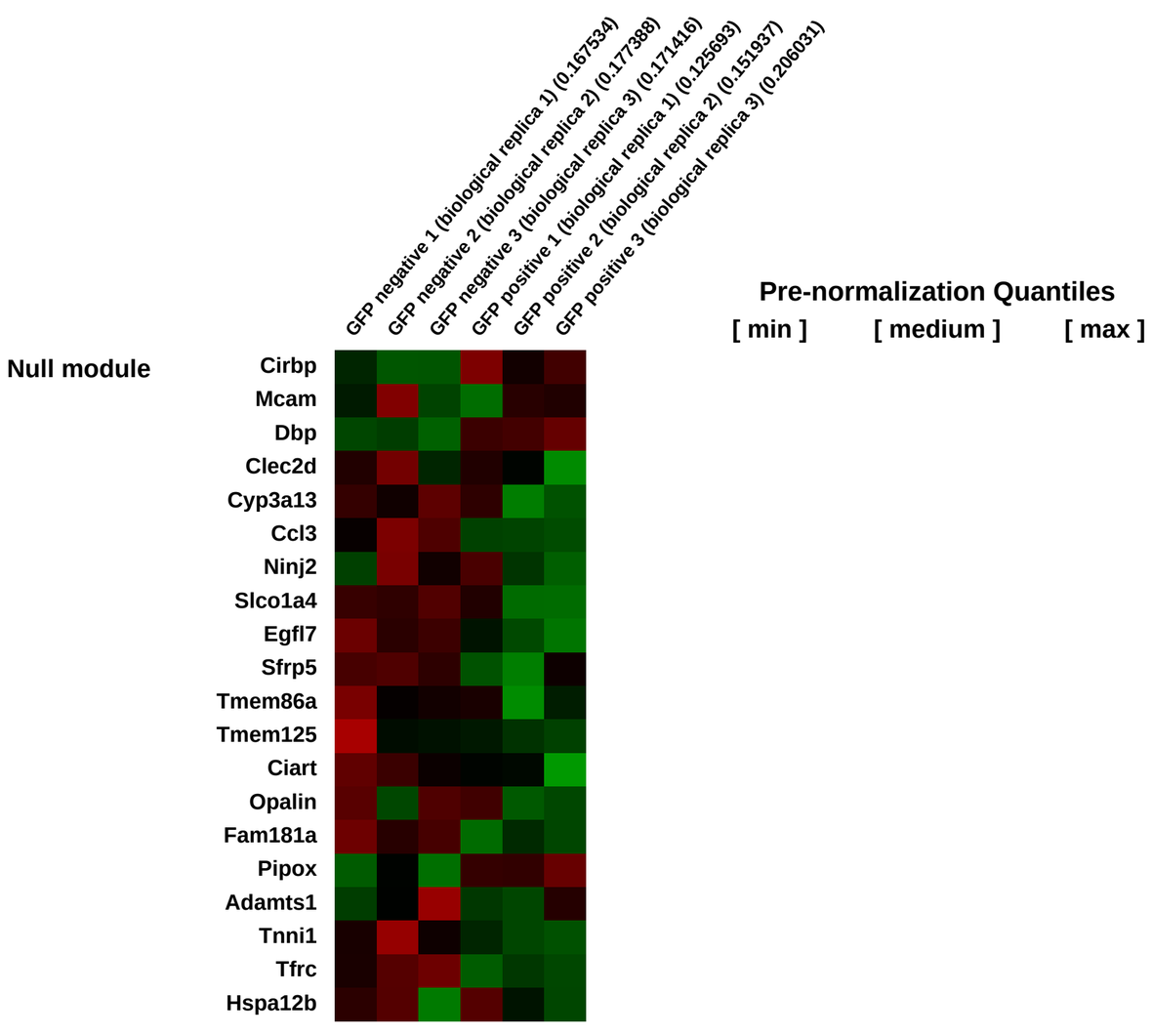

GEO Series "GSE8690" Expression Profiles

Num of samples in this series: 36

Scale of expression profile Z-scores

-3.0 -2.0 -1.0 0.0 1.0 2.0 3.0

GEO Link: http://www.ncbi.nlm.nih.gov/geo/query/acc.cgi?acc=GSE8690
Status: Public on Jul 31 2008
Title: Microarray analysis identifies distinct subpopulations of arthritic mice deficient for interleukin 1 receptor antagonist
Organism: Mus musculus
Experiment type: Expression profiling by array
Platform: GPL1261
Pubmed ID:

Summary & Design:

Summary:
Rheumatoid arthritis (RA) is a heterogeneous disease with clinical and biological polymorphisms. However, little is known about baseline molecular variations among individual RA patients. The purpose of this study was to address this issue using F2 intercross mice generated from arthritis-prone BALB/c and arthritis-resistant DBA/1 mice deficient for interleukin 1 receptor antagonist (Il1rn). Two distinct subpopulations of arthritic mice were identified in the 38 mice studied. One subgroup of diseased mice was characterized by myeloid cell dominant inflammation, whereas the other was mainly associated with increased anti-apoptotic activities of inflammatory cells.

Keywords: disease state analysis

Overall design:
Thirteen F2 mice, 18 with arthritis and 18 without, were included in this study. Total RNAs were extracted from individual spleens for Affymmetrix mouse genome array analysis. Normalized data were hierarchically clustered to identify subpopulations of arthritic mice.

Background corr dist: KL-Divergence = 0.3922, L1-Distance = 0.0716, L2-Distance = 0.0152, Normal std = 0.2501

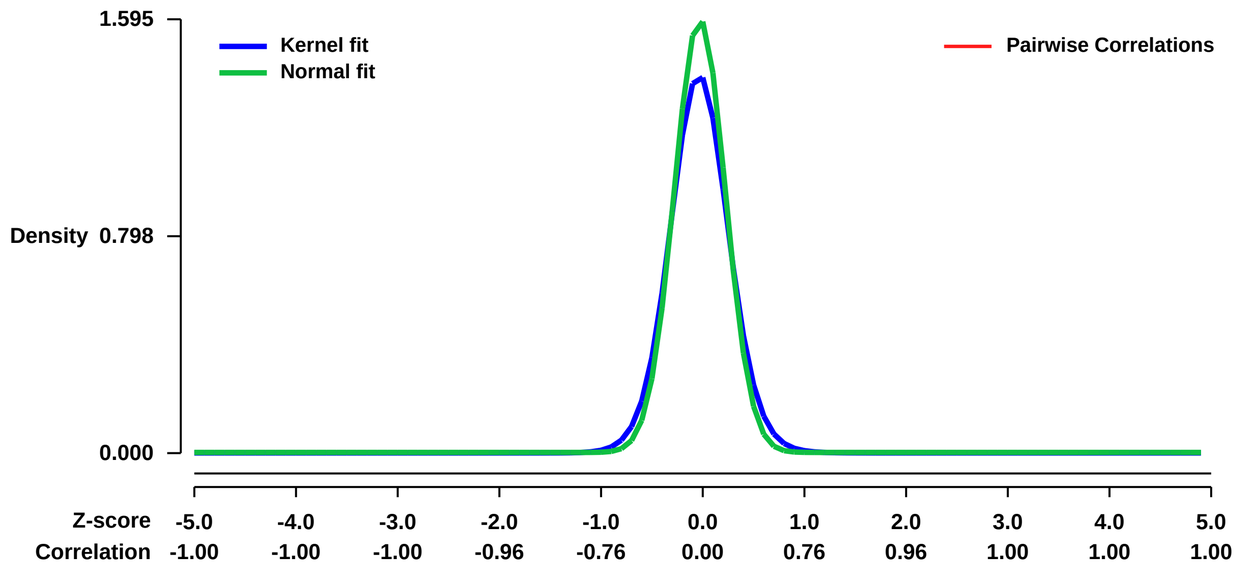

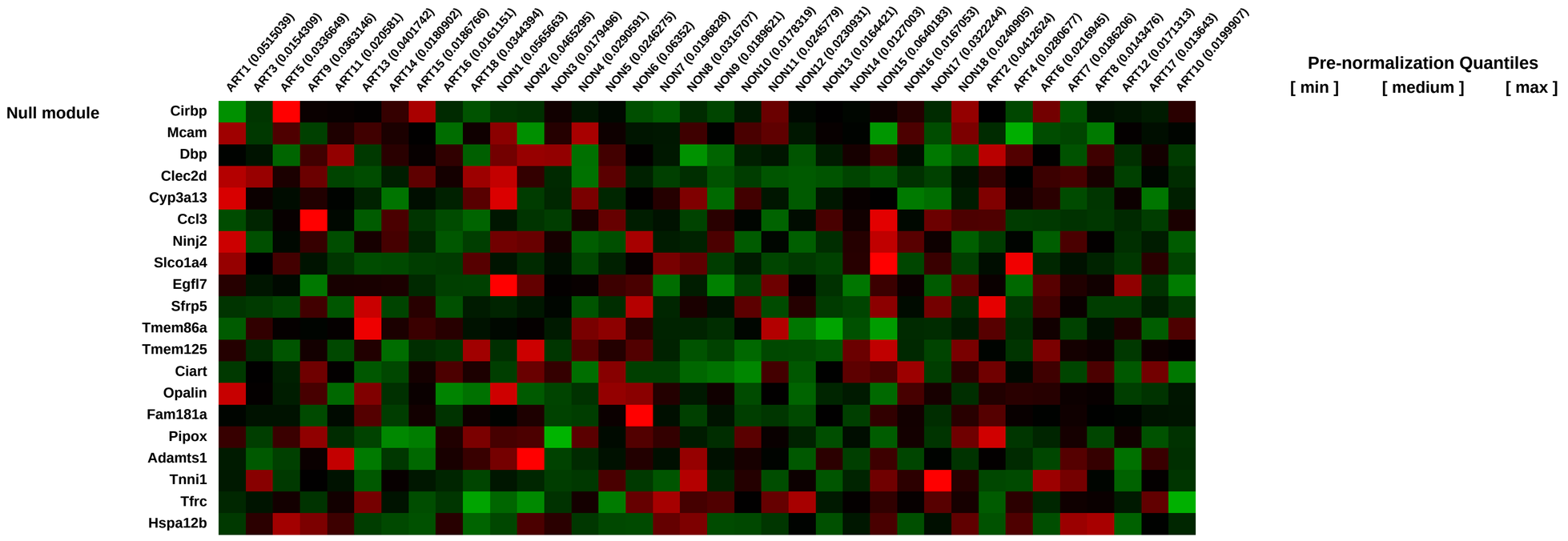

GEO Series "GSE43899" Expression Profiles

Num of samples in this series: 12

Scale of expression profile Z-scores

-3.0 -2.0 -1.0 0.0 1.0 2.0 3.0

GEO Link:	http://www.ncbi.nlm.nih.gov/geo/query/acc.cgi?acc=GSE43899
Status:	Public on Aug 30 2013
Title:	Co-ordinate inhibiton of autism candidate genes by topoisomerase inhibitors [array]
Organism:	Mus musculus
Experiment type:	Expression profiling by array
Platform:	GPL1261
Pubmed ID:	23995680
Summary & Design:	**Summary:** Topoisomerases are necessary for the expression of neurodevelopmental genes, and are mutated in some patients with autism spectrum disorder (ASD). We have studied the effects of inhibitors of Topoisomerase 1 (Top1) and Topoisomerase 2 (Top2) enzymes on mouse cortical neurons. We find that topoisomerases selectively inhibit long genes (>100kb), with little effect on all other gene expression. Using ChIPseq against RNA Polymerase II (Pol2) we show that the Top1 inhibitor topotecan blocks transcriptional elongation of long genes specifically. Many of the genes inhibited by topotecan are candidate ASD genes, leading us to propose that topoisomerase inhibition might contribute to ASD pathology. **Overall design:** 9) cultured mouse cortical neurons treated with topotecan with or without subsequent drug washout, vs vehicle-treated controls.

Background corr dist: KL-Divergence = 0.0306, L1-Distance = 0.0234, L2-Distance = 0.0007, Normal std = 0.6443

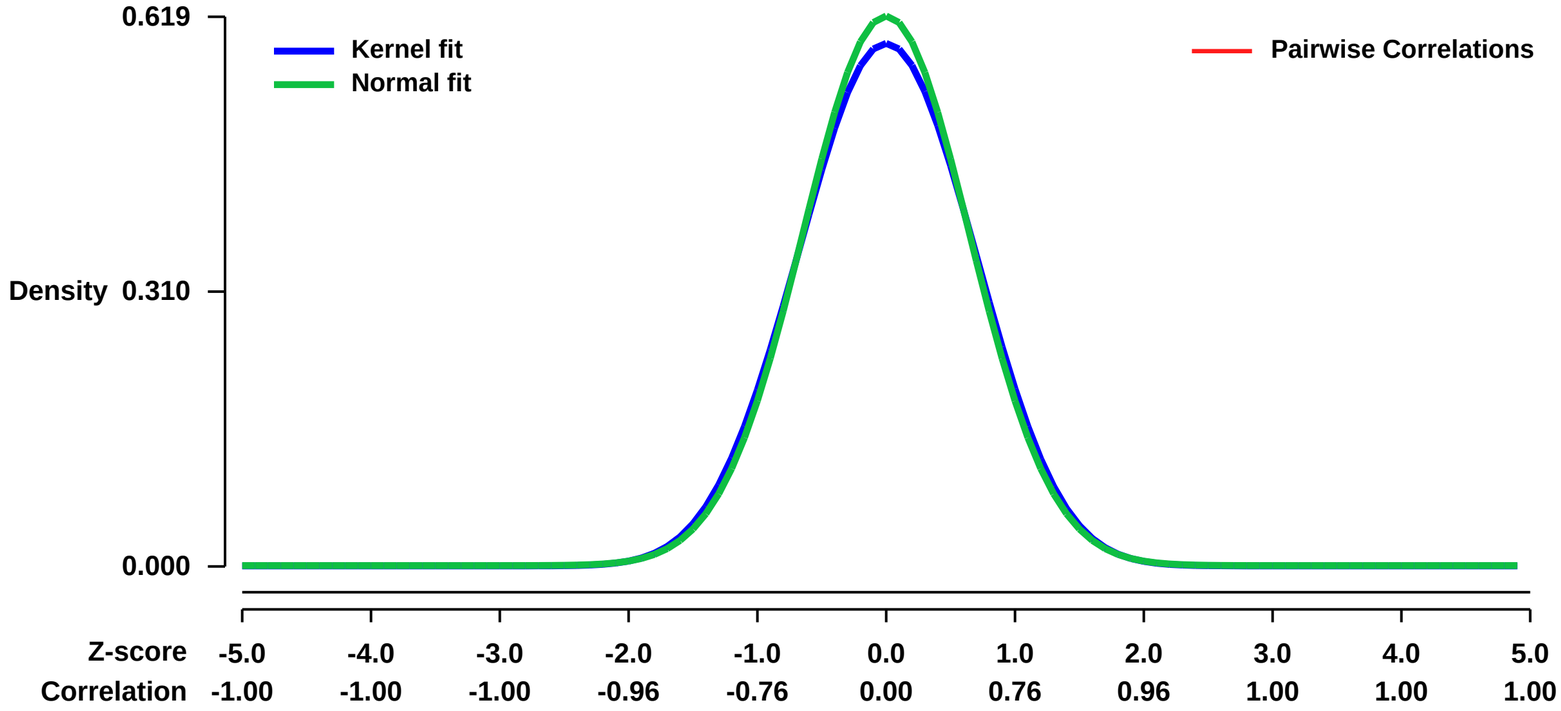

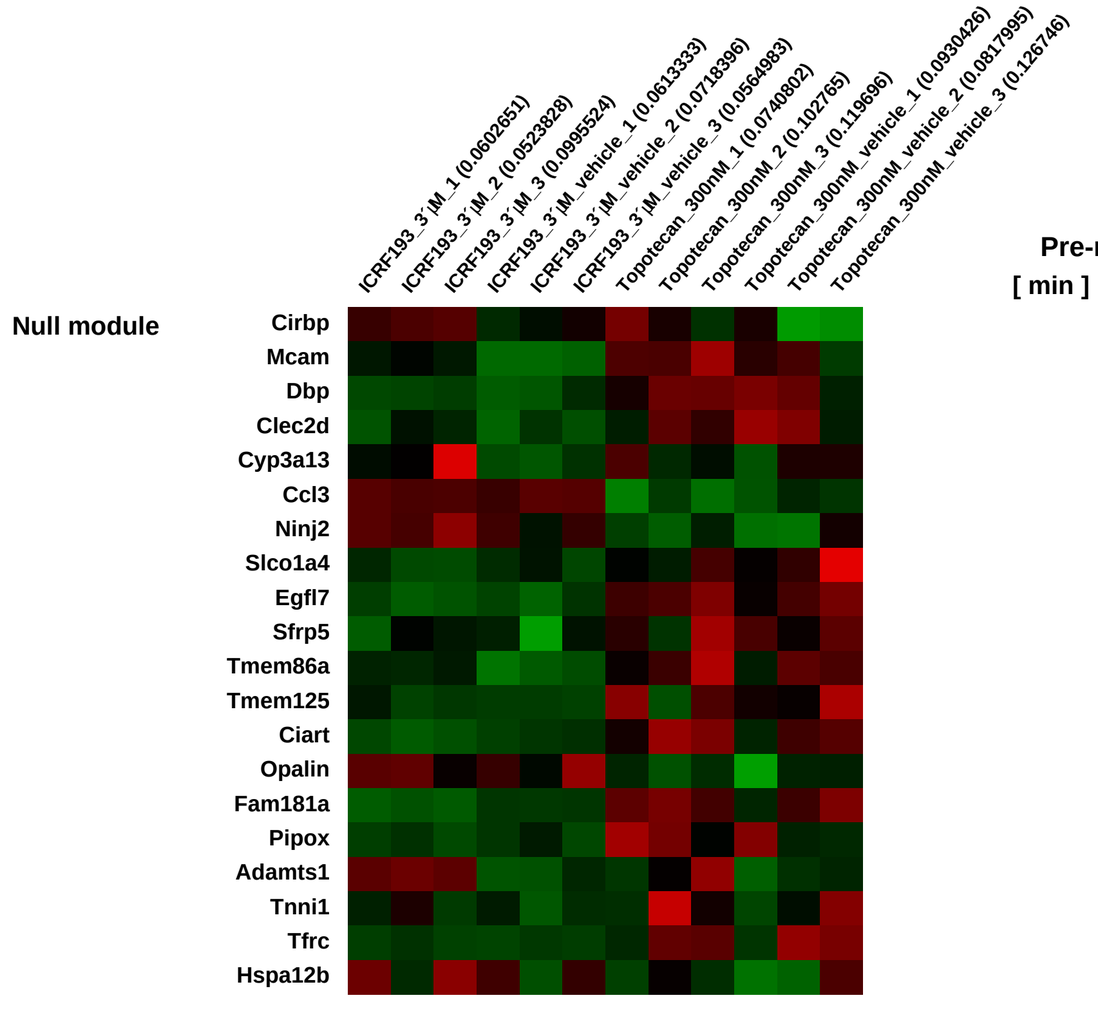

GEO Series "GSE4712" Expression Profiles

Num of samples in this series: 21

Scale of expression profile Z-scores

-3.0 -2.0 -1.0 0.0 1.0 2.0 3.0

GEO Link:	http://www.ncbi.nlm.nih.gov/geo/query/acc.cgi?acc=GSE4712
Status:	Public on Oct 24 2006
Title:	Edema Toxin-treated Macrophage Study
Organism:	Mus musculus
Experiment type:	Expression profiling by array
Platform:	GPL1261
Pubmed ID:	16846716
Summary & Design:	**Summary:** Edema toxin (EdTx), which is a combination of edema factor and a binding moiety (protective antigen), is produced by Bacillus anthracis, the etiological agent of anthrax. EdTx is an adenylyl cyclase enzyme that converts adenosine triphosphate to adenosine-3â ,5â -monophosphate, resulting in interstitial edema seen in anthrax patients. We used GeneChip analysis to examine global transcriptional profiles of EdTx-treated RAW 264.7 murine macrophage-like cells at 3 and 6 hr. **Keywords: Toxin response** **Overall design:** RAW 264.7 cells were treated with EdTx (2.5 ´µg/ml of protective antigen and 0.625 ´µg/ml of Edema factor), PA (2.5 ´µg/ml), or LPS (1 ng/mL) for 0, 3, and 6 hr. Each experiment was performed in triplicate, generating a total of 21 arrays (biological replciates).

Background corr dist: KL-Divergence = 0.2004, L1-Distance = 0.0429, L2-Distance = 0.0041, Normal std = 0.3331

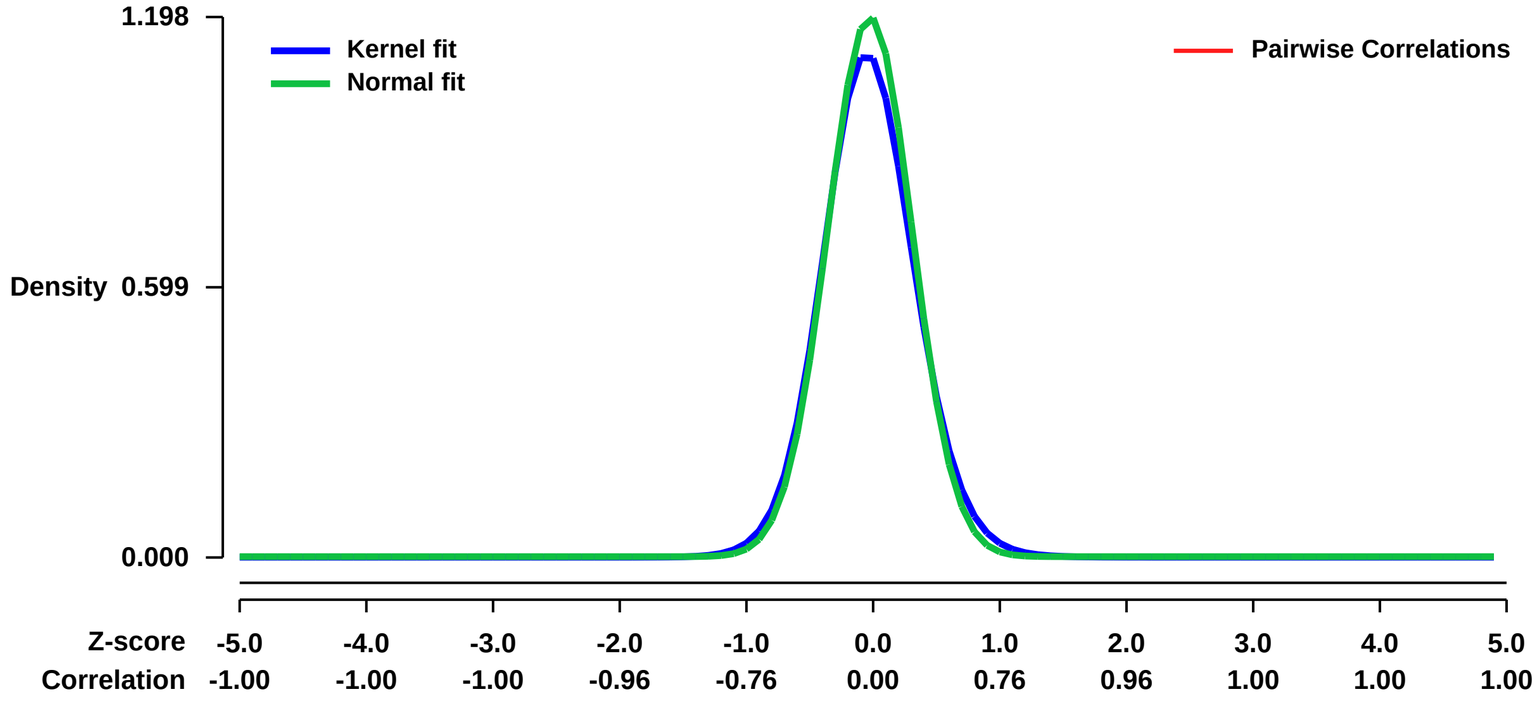

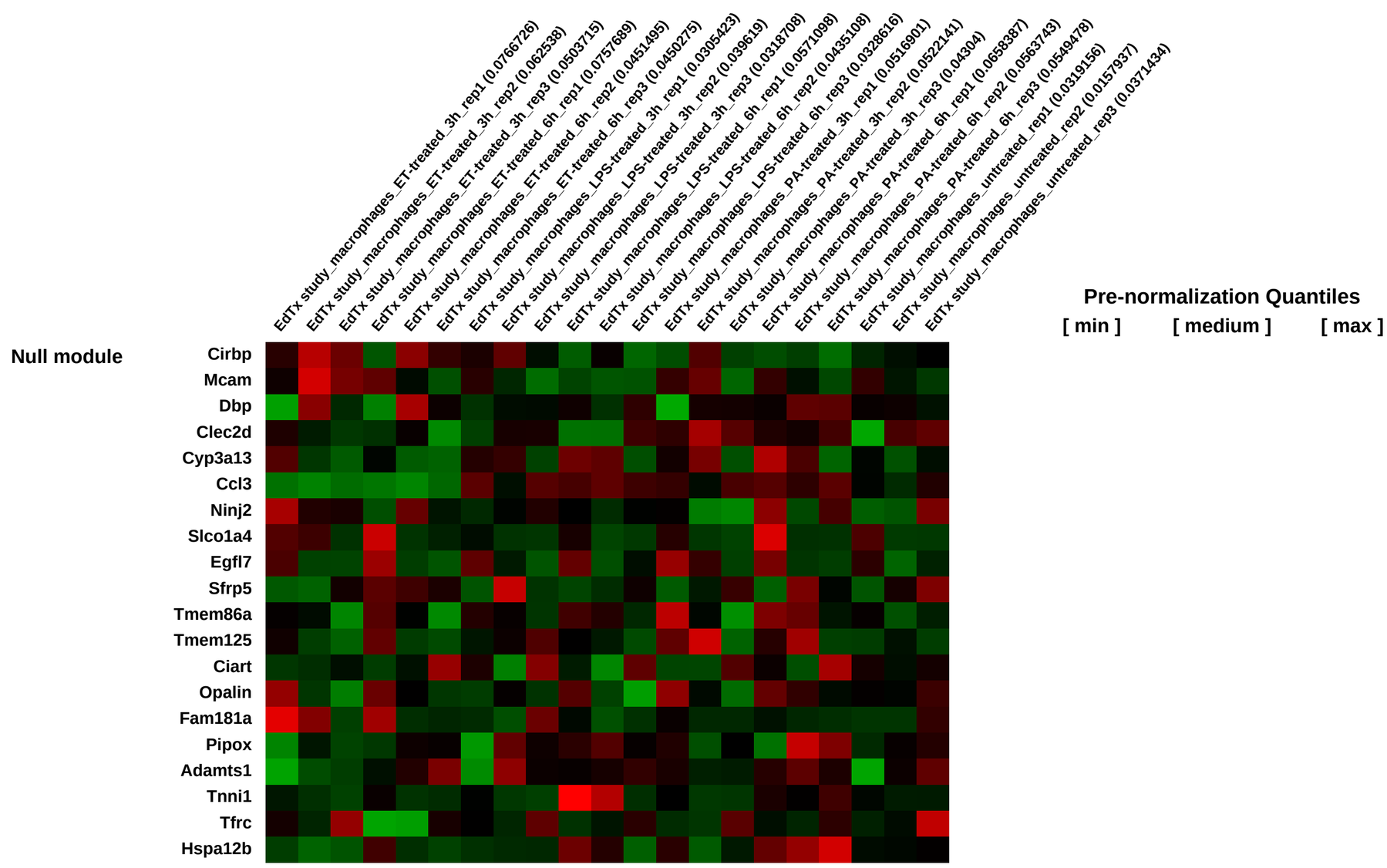

GEO Series "GSE18660" Expression Profiles

Num of samples in this series: 10

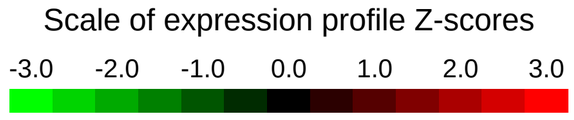

GEO Link:	http://www.ncbi.nlm.nih.gov/geo/query/acc.cgi?acc=GSE18660
Status:	Public on Jan 03 2011
Title:	Modulation of calcium activated potassium channels induces cardiogenesis of pluripotent stem cells and enrichment of pacemaker- like cells
Organism:	Mus musculus
Experiment type:	Expression profiling by array
Platform:	GPL1261
Pubmed ID:	20956206
Summary & Design:	**Summary:** **Background: Ion channels are key determinants for the function of excitable cells but little is known about their role and involvement during cardiac development. Earlier work identified Ca2+-activated potassium channels of small and intermediate conductance (SKCas) as important regulators of neural stem cell fate. Here, we have investigated their impact on the differentiation of pluripotent cells towards the cardiac lineage. Methods and Results: We have applied the SKCa-activator EBIO on embryonic stem cells and identified this particular ion channel family as a new critical target involved in the generation of cardiac pacemaker-like cells: SKCa-activation led to rapid remodeling of the actin cytoskeleton, inhibition of proliferation, induction of differentiation and diminished teratoma formation. Time-restricted SKCa-activation induced cardiac mesoderm and commitment to the cardiac lineage as shown by gene regulation, protein and functional electrophysiological studies. In addition, the differentiation into cardiomyocytes was modulated in a qualitative fashion, resulting in a strong enrichment of pacemaker-like cells. This was accompanied by induction of the sino-atrial gene program and in parallel by a loss of the chamber-specific myocardium. In addition, SKCa activity induced activation of the Ras-Mek-Erk signaling cascade, a signaling pathway involved in the EBIO-induced effects.** **Conclusions: SKCa-activation drives the fate of pluripotent cells towards the cardiac lineage and preferentially into pacemaker-like cardiomyocytes. This provides a novel strategy for the enrichment of cardiomyocytes and in particular, the generation of a specific subtype of cardiomyocytes, pacemaker-like cells, without genetic modification.** **Overall design:** **- EBIO-treated differentiated ES cells sample 2 (EBIO_day5+10_2)**

Background corr dist: KL-Divergence = 0.0149, L1-Distance = 0.0633, L2-Distance = 0.0051, Normal std = 0.9657

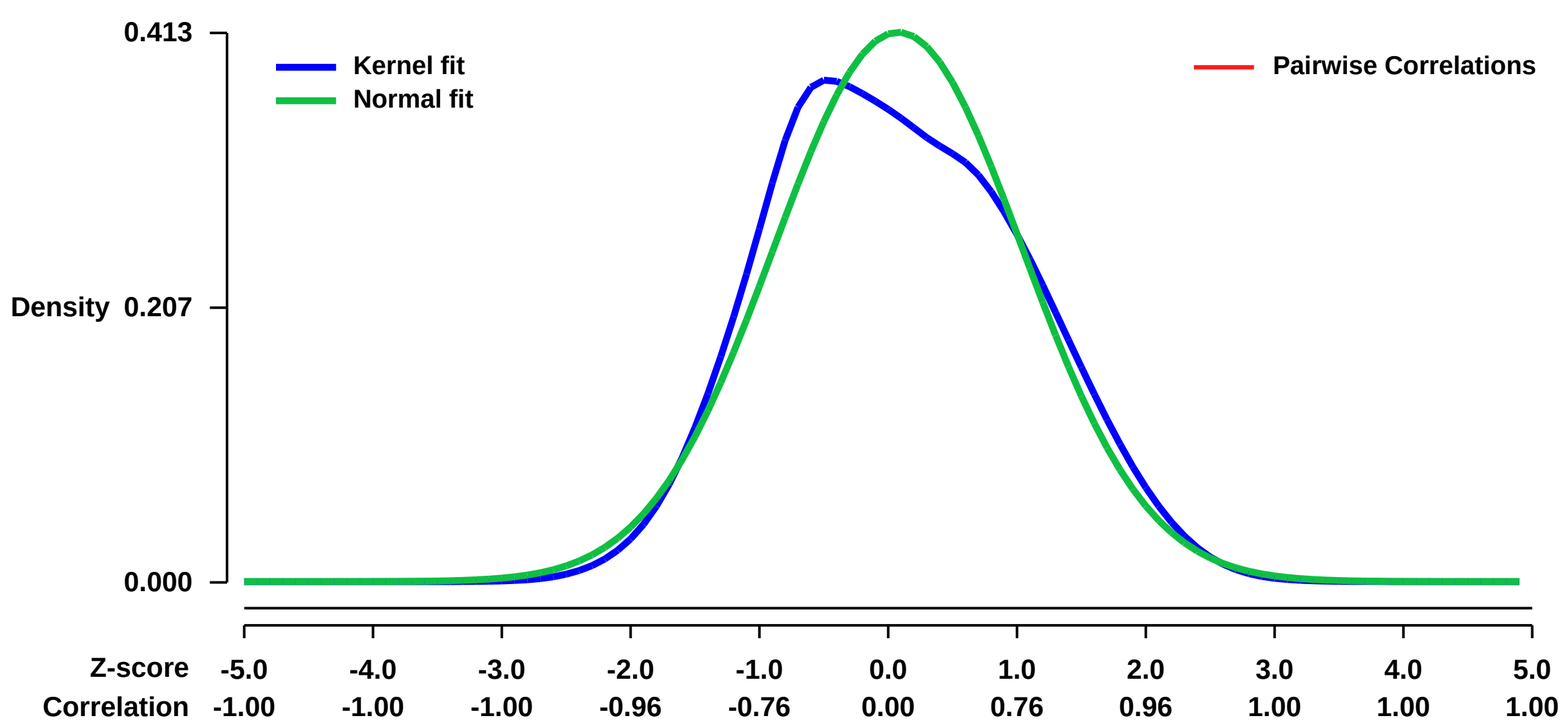

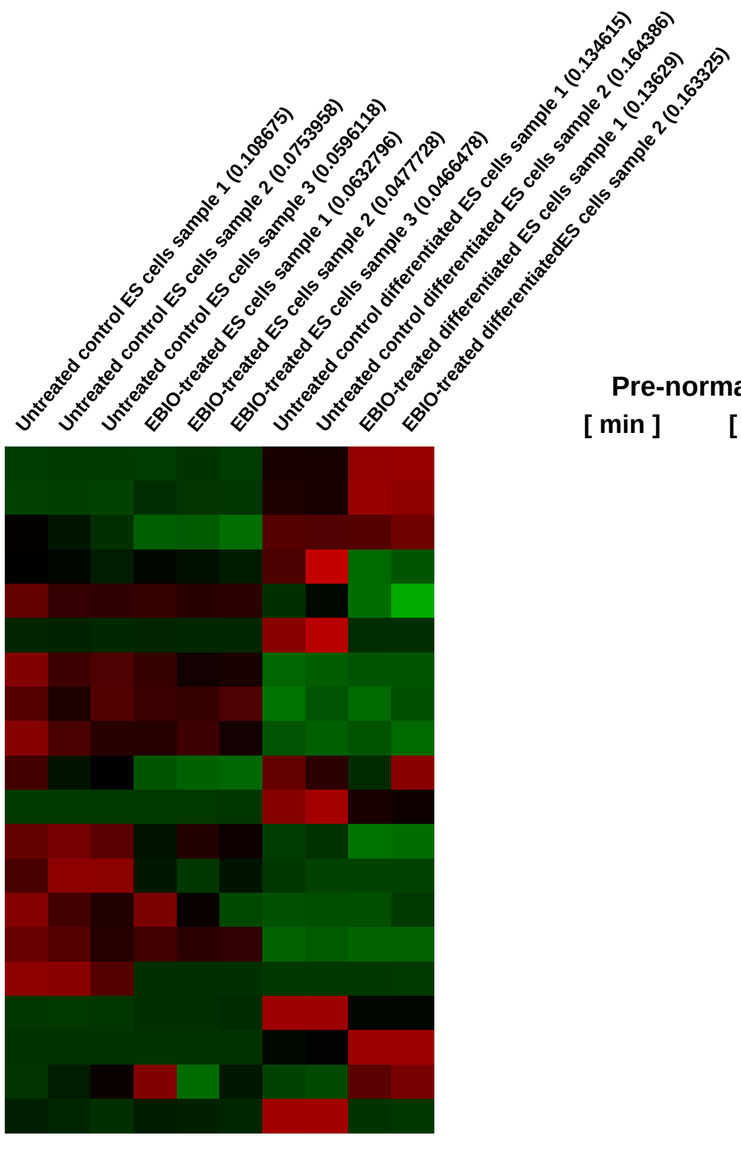

GEO Series "GSE13583" Expression Profiles

Num of samples in this series: 6

Scale of expression profile Z-scores

-3.0 -2.0 -1.0 0.0 1.0 2.0 3.0

GEO Link:	http://www.ncbi.nlm.nih.gov/geo/query/acc.cgi?acc=GSE13583
Status:	Public on Jan 22 2009
Title:	Expression data from liver of the KRAP deficient mice
Organism:	Mus musculus
Experiment type:	Expression profiling by array
Platform:	GPL1261
Pubmed ID:	19156225
Summary & Design:	**Summary:** KRAP (Ki-ras-induced actin-interacting protein) is a cytoskeleton-associated protein and a ubiquitous protein among tissues, originally identified as a cancer-related molecule. KRAP-deficient (KRAP-/-) mice show enhanced metabolic rate, decreased adiposity, improved glucose tolerance, hypoinsulinemia and hypoleptinemia. KRAP-/- mice are also protected against high-fat diet-induced obesity and insulin resistance despite of hyperphagia. **Overall design:** Total RNA was extracted from livers of three pairs of littermates (KO1 vs. WT1, KO2 vs. WT2 and KO3 vs. WT3) fed normal chow.

Background corr dist: KL-Divergence = 0.0485, L1-Distance = 0.0224, L2-Distance = 0.0006, Normal std = 0.5811

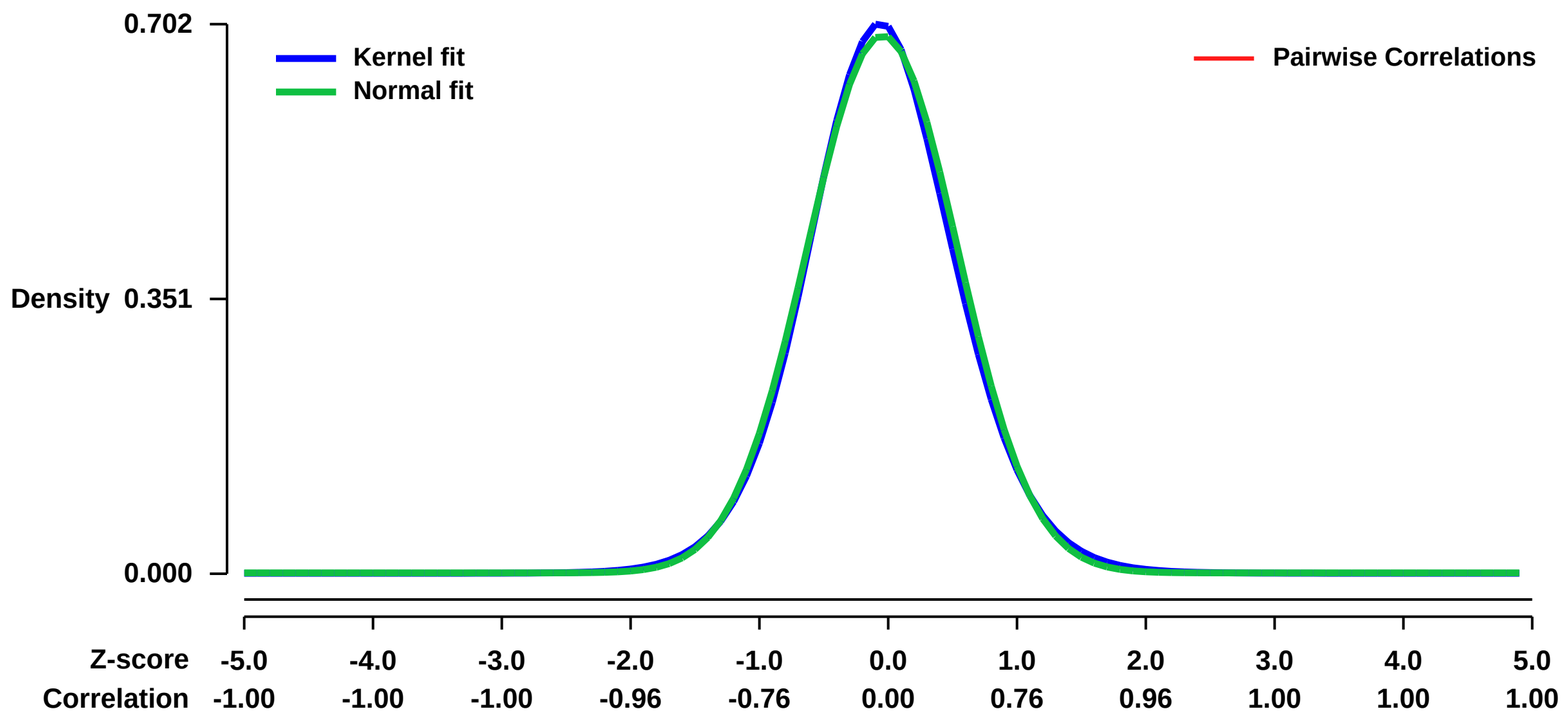

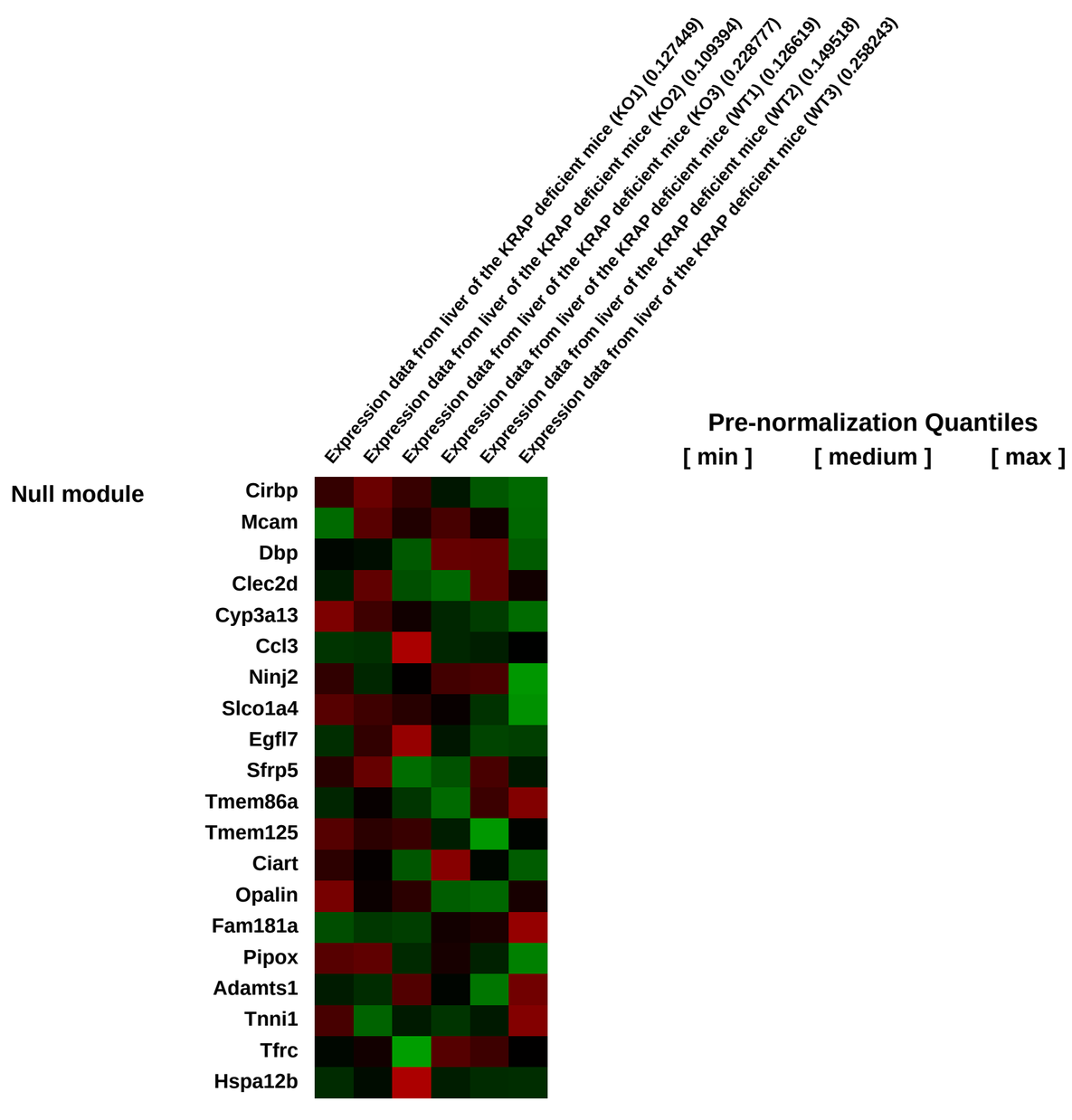

GEO Series "GSE4523" Expression Profiles

Num of samples in this series: 6

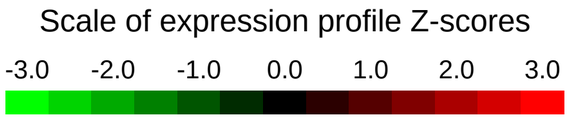

GEO Link:	http://www.ncbi.nlm.nih.gov/geo/query/acc.cgi?acc=GSE4523
Status:	Public on Mar 29 2006
Title:	Expression Studies of Melanotransferrin in Mouse Brain
Organism:	Mus musculus
Experiment type:	Expression profiling by array
Platform:	GPL1261
Pubmed ID:	17449903
Summary & Design:	**Summary:** Melanotransferrin (MTf) or melanoma tumor antigen p97 is an iron (Fe)-binding transferrin homolog expressed highly on melanomas and at lower levels on normal tissues. It has been suggested that MTf is involved in a variety of processes such as Fe metabolism and cellular differentiation. Considering the crucial role of Fe in many metabolic pathways e.g., DNA synthesis, it is important to understand the function of MTf. To define the roles of MTf, a MTf knockout (MTf -/-) mouse model was developed. Examination of the MTf -/- mice demonstrated no phenotypic differences compared to wild-type littermates. However, microarray analysis showed differential expression of molecules involved in proliferation such as Mef2a, Tcf4, Gls and Apod in MTf -/- mice compared to MTf +/+ littermates, suggesting a role for MTf in proliferation and tumorigenesis. **Keywords:** Melanotransferrin, knockout mouse, comparative genomic hybridization **Overall design:** Six 17.5 week old female mice comprising four MTf -/- and two MTf +/+ from the same litter were used. Total RNA was isolated from brain tissue and processed as per standard Affymetrix protocol to obtain final cRNA products that were hybridized to the mouse GeneChip´fi 430 2.0. The mouse GeneChip´fi 430 2.0 consists of greater than 39,000 transcripts and variants from over 34,000 well characterized mouse genes. On completion of hybridization and washing, microarray chips were scanned with the Affymetrix GeneChip´fi Scanner 3000 (Millenium Sciences).

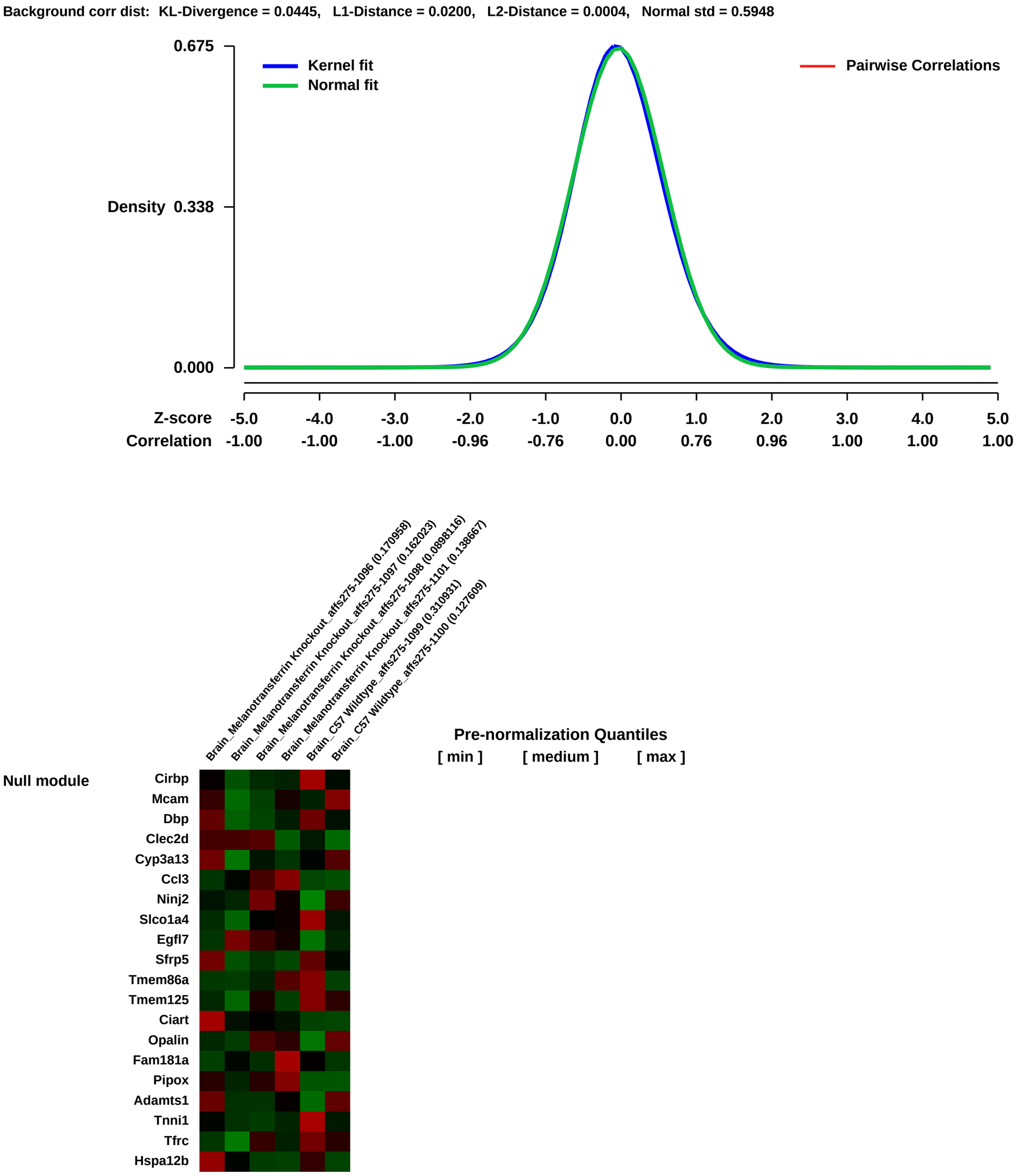

GEO Series "GSE9061" Expression Profiles

Num of samples in this series: 6

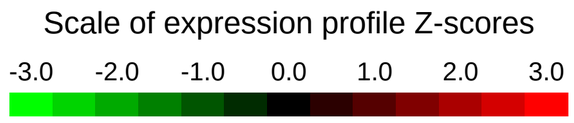

GEO Link:	**http://www.ncbi.nlm.nih.gov/geo/query/acc.cgi?acc=GSE9061**
Status:	**Public on Aug 24 2011**
Title:	**Dap12-deficient mouse brain (1 month)**
Organism:	**Mus musculus**
Experiment type:	**Expression profiling by array**
Platform:	**GPL1261**
Pubmed ID:	
Summary & Design:	**Summary:** **Polycystic lipomembranous osteodysplasia with sclerosing leukoencephalopathy (PLOSL) is an inherited brain and bone disease. It manifests as dementia and bone fractures. The PLOSL phenotype is caused by loss-of-function mutations in one of the two genes encoding the components of the DAP12/TREM2 receptor complex. The DAP12/TREM2 complex is expressed in cells of the myeloid lineage, including microglia in the central nervous system (CNS). The molecular mechanisms producing the CNS phenotype of PLOSL remain largely unknown. To gain insight into dysfunctional CNS pathways behind PLOSL, we performed genome-wide expression analysis of Dap12 (Tyrobp)-deficient mouse brain. In Dap12-deficient mice, we observed alterations in several pathways involved in synaptic function. In agreement with the myelin loss in PLOSL patients, we also saw changes in transcript levels of genes encoding myelin components.** **Keywords: knockout response** **Overall design:** **Transcript profiles of the midbrain (diencephalon and basal ganglia) of three Dap12-knockout and three heterozygous mice were analyzed.**

Background corr dist: KL-Divergence = 0.0275, L1-Distance = 0.0302, L2-Distance = 0.0012, Normal std = 0.7023

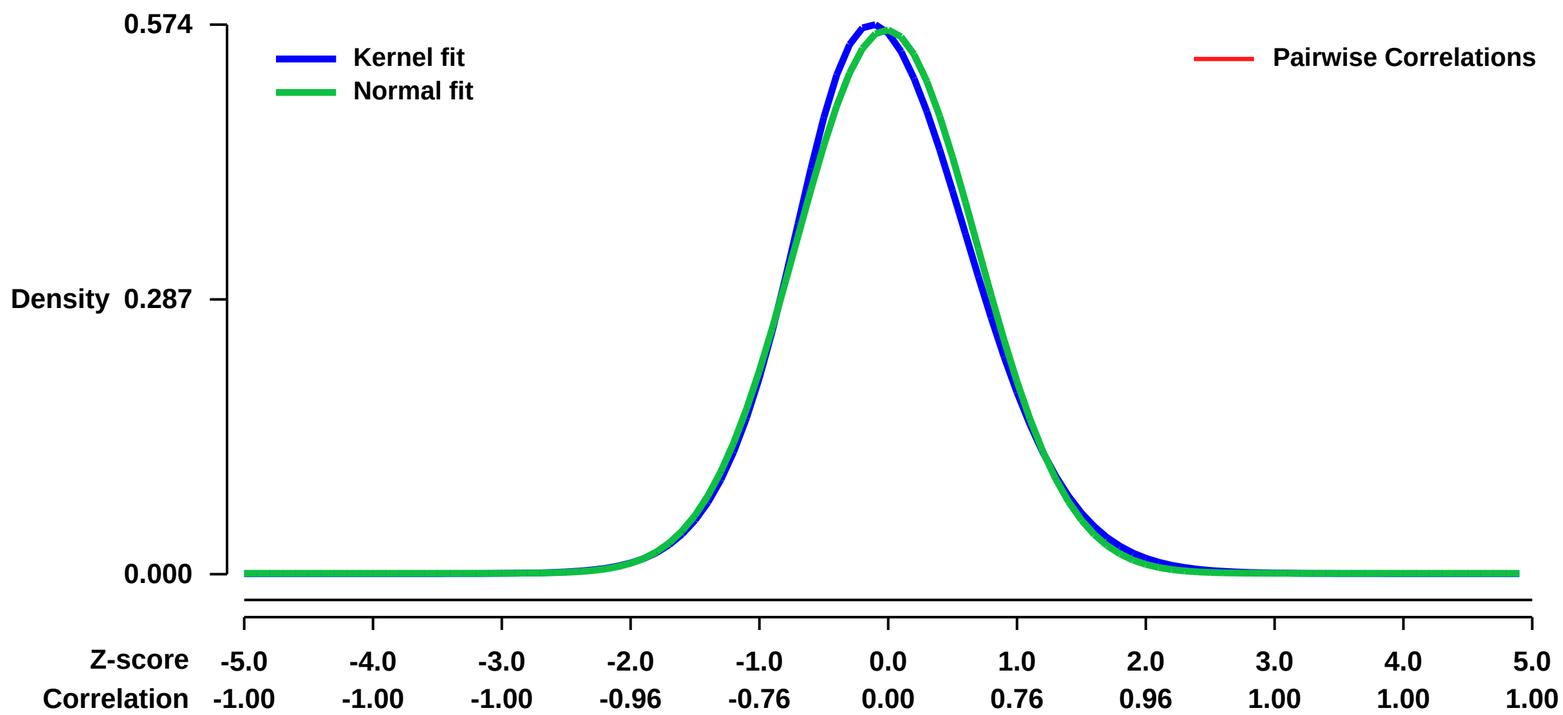

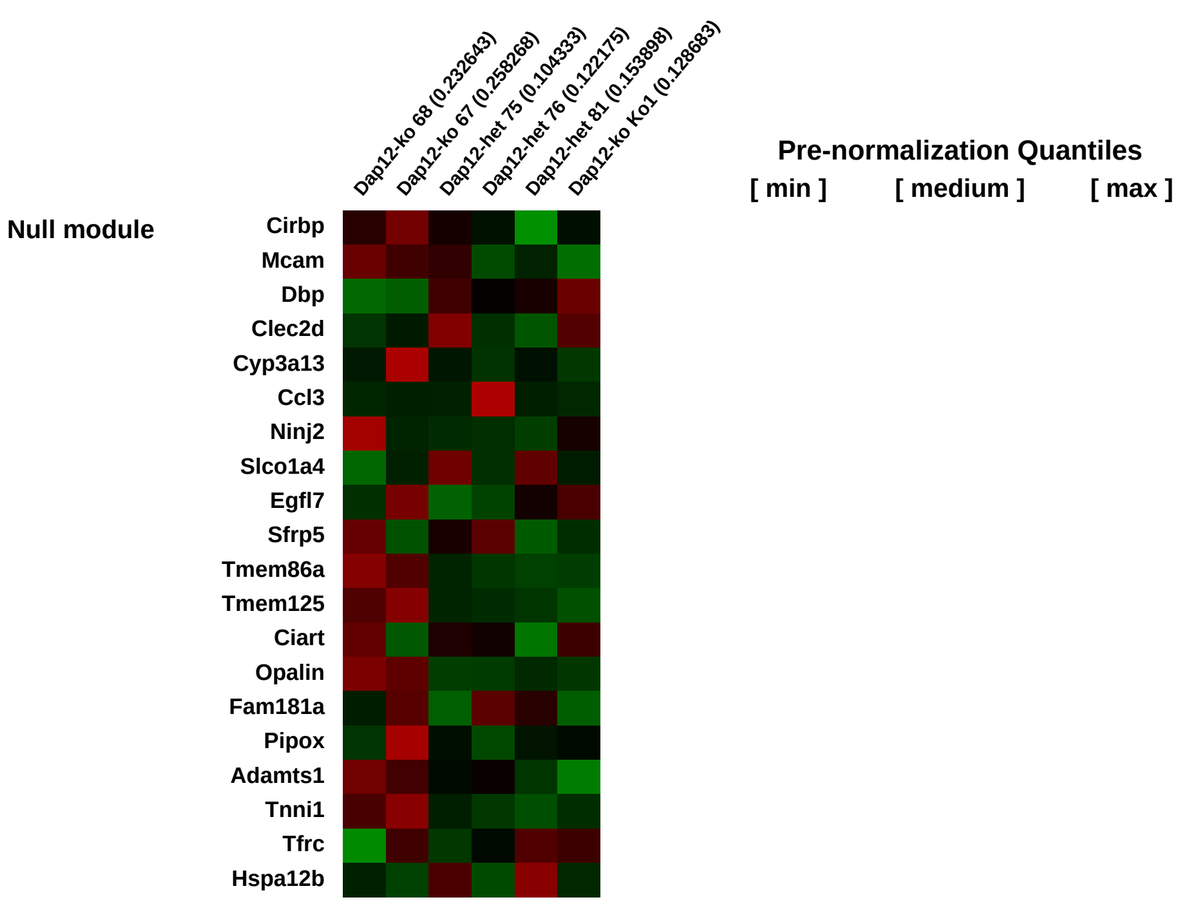

GEO Series "GSE18148" Expression Profiles

Num of samples in this series: 6

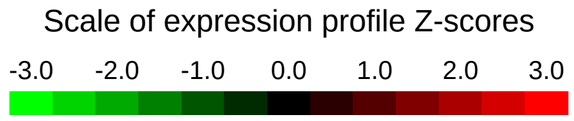

GEO Link:	http://www.ncbi.nlm.nih.gov/geo/query/acc.cgi?acc=GSE18148
Status:	Public on Sep 19 2009
Title:	Microarray analysis of Cbfb-deficient regulatory T cells
Organism:	Mus musculus
Experiment type:	Expression profiling by array
Platform:	GPL1261
Pubmed ID:	19800266
Summary & Design:	**Summary:** **Gene expression profiles of Cbfb-deficient and control Treg cells were compared.** **Abstract: Naturally arising regulatory T (Treg) cells express the transcription factor FoxP3, which critically controls the development and function of Treg cells. FoxP3 interacts with another transcription factor Runx1 (also known as AML1). Here we showed that Treg cell-specific deficiency of Cbf‚†, a cofactor for all Runx proteins, or that of Runx1, but not Runx3, induced lymphoproliferation, autoimmune disease, and hyper-production of IgE. Cbfb-deleted Treg cells exhibited impaired suppressive function in vitro and in vivo, with altered gene expression profiles including attenuated expression of FoxP3 and high expression of interleukin-4. The Runx complex bound to more than 3000 gene loci in Treg cells, including the Foxp3 regulatory regions and the Il4 silencer. In addition, knockdown of RUNX1 showed that RUNX1 is required for the optimal regulation of FoxP3 expression in human T cells. Taken together, our results indicate that the Runx1-Cbf‚† heterodimer is indispensable for in vivo Treg cell function, in particular, suppressive activity and optimal expression of FoxP3.** **Overall design:** **CD4+CD25hi cells, most of which were Foxp3+ Treg cells, were isolated from Cbfb-flox/flox: Foxp3-ires-Cre (n = 3) and control Cbfb-flox/wt: Foxp3-ires-Cre (n = 3) mice. Total RNA was extracted from those purified Cbfb-deficient or control Treg cells.**

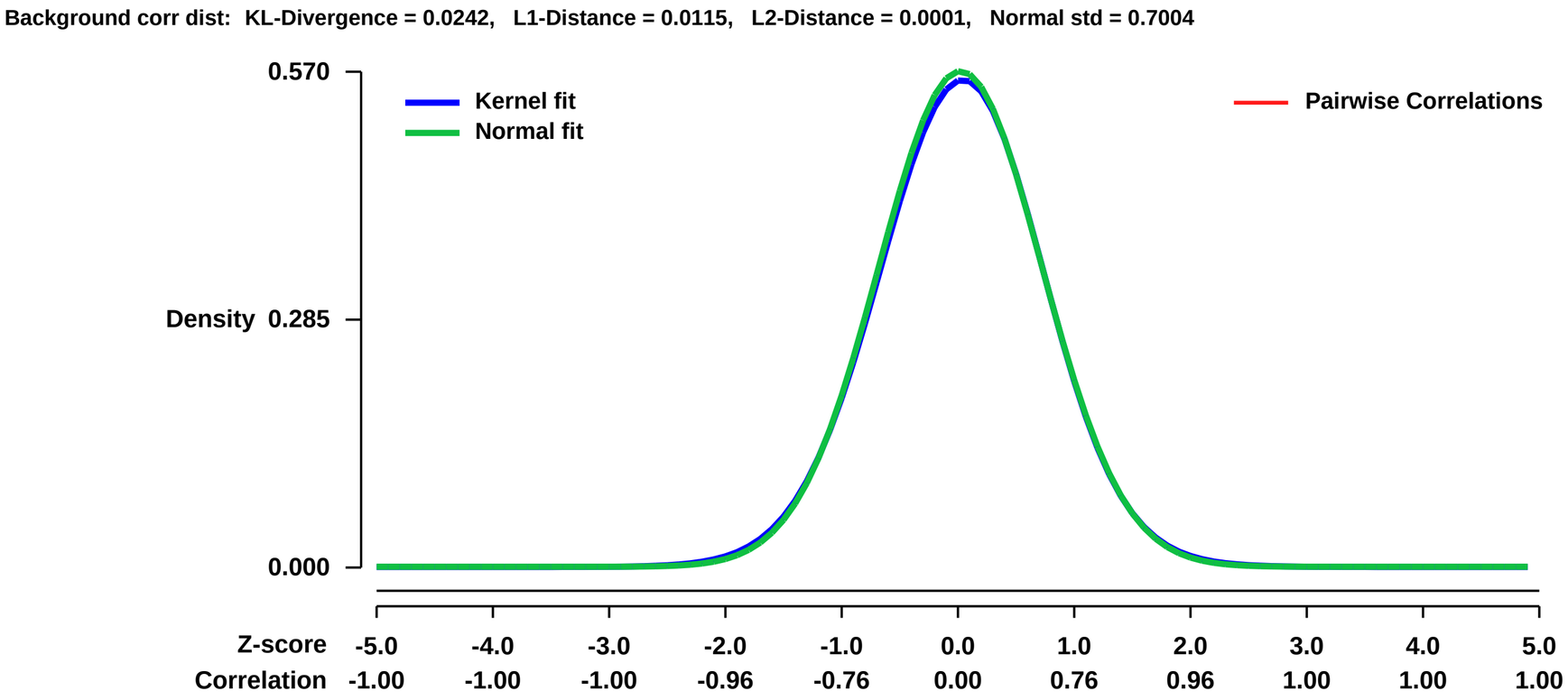

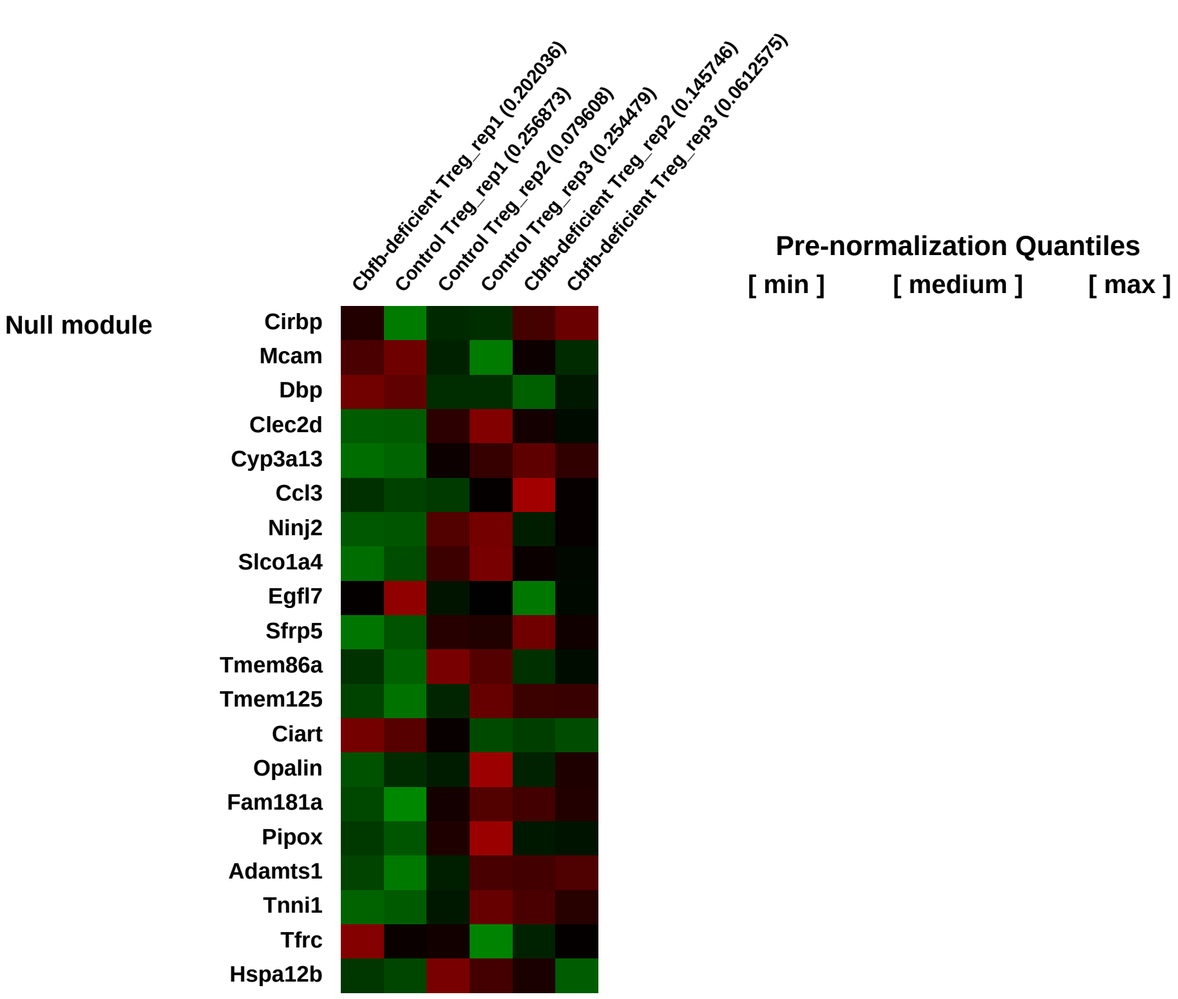

GEO Series "GSE21278" Expression Profiles

Num of samples in this series: 48

Scale of expression profile Z-scores

-3.0 -2.0 -1.0 0.0 1.0 2.0 3.0

GEO Link:	http://www.ncbi.nlm.nih.gov/geo/query/acc.cgi?acc=GSE21278
Status:	Public on May 04 2010
Title:	A genomic atlas of mouse hypothalamic development
Organism:	Mus musculus
Experiment type:	Expression profiling by array
Platform:	GPL1261
Pubmed ID:	20436479
Summary & Design:	**Summary:** The hypothalamus is a central regulator of many behaviors essential for survival such as temperature regulation, food intake and circadian rhythms. However, the molecular pathways that mediate hypothalamic development are largely unknown. To identify genes expressed in developing mouse hypothalamus, microarray analysis at 12 different developmental time points was performed. Developmental in situ hybridization was conducted for 1,045 genes dynamically expressed by microarray analysis. In this way, we identified markers that stably labeled each major hypothalamic nucleus over the entire course of neurogenesis, and thus constructed a detailed molecular atlas of the developing hypothalamus. As proof of concept for the utility of this data, we used these markers to analyze the phenotype of mice where Sonic Hedgehog (Shh) was selectively deleted from hypothalamic neuroepithelium, demonstrating an essential role for Shh in anterior hypothalamic patterning. Our results serve as a resource for functional investigations of hypothalamic development, connectivity, physiology, and dysfunction. **Overall design:** Affymetrix MOE430 microarrays were used to analyze the expression patterns of mouse hypothalamic and preoptic area tissues. The results were compared across the variables of Strain, Sex and Age.

Background corr dist: KL-Divergence = 0.1534, L1-Distance = 0.0326, L2-Distance = 0.0023, Normal std = 0.3769

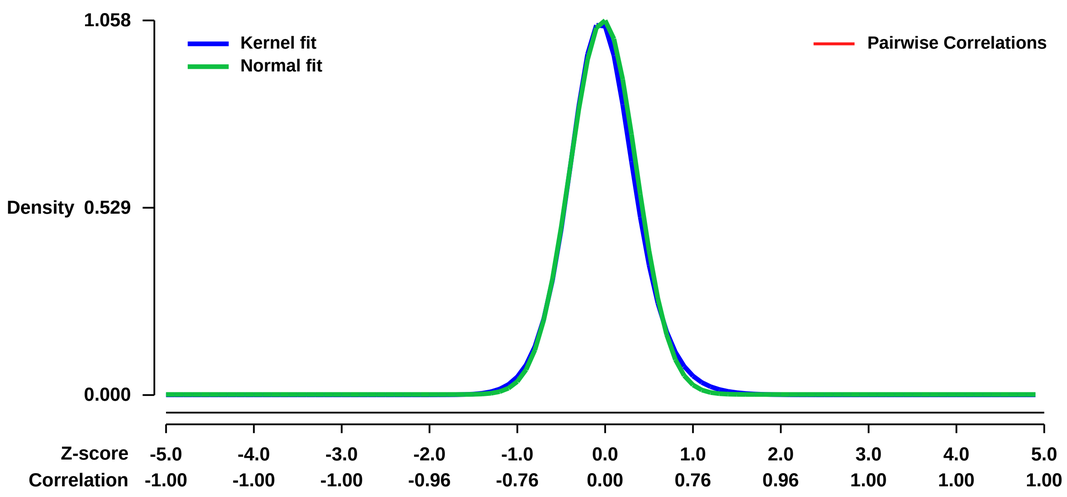

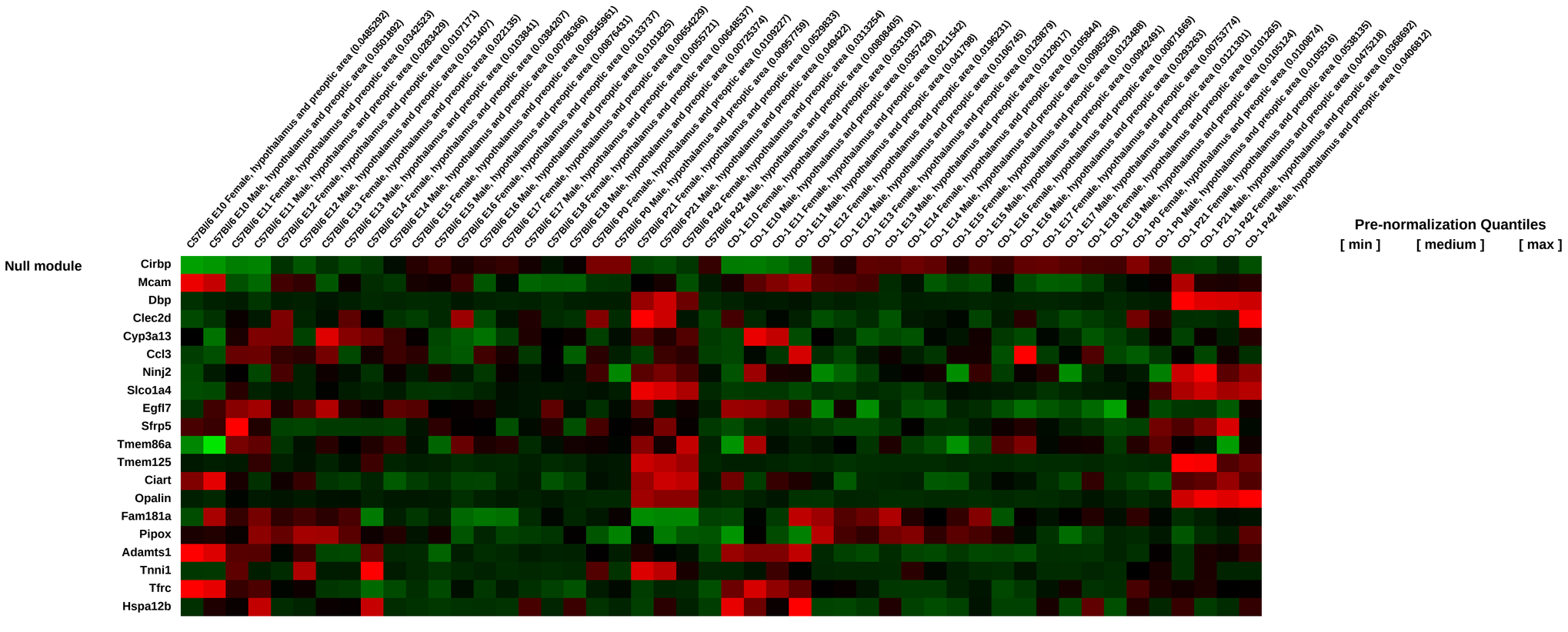

GEO Series "GSE21193" Expression Profiles

Num of samples in this series: 10

Scale of expression profile Z-scores

-3.0 -2.0 -1.0 0.0 1.0 2.0 3.0

GEO Link:	http://www.ncbi.nlm.nih.gov/geo/query/acc.cgi?acc=GSE21193
Status:	Public on Jul 22 2010
Title:	The effects of subchronic arsenate exposure on gene expression in the mouse lung
Organism:	Mus musculus
Experiment type:	Expression profiling by array
Platform:	GPL1261
Pubmed ID:	20667999
Summary & Design:	**Summary:** Eight week old female C57BL/6 mice were exposed to arsenate in drinking water (50 ppm) for a period of twelve weeks (n = 5). Control animals received distilled deionized water (n = 5). Lung tissue was dissected and used for RNA isolation and gene expression microarray analysis. **Overall design:** Eight week old female C57BL/6 mice were exposed to arsenate in drinking water (50 ppm) for a period of twelve weeks (n = 5). Control animals received distilled deionized water (n = 5). Lung tissue was dissected and used for RNA isolation and gene expression microarray analysis.

Background corr dist: KL-Divergence = 0.0535, L1-Distance = 0.0371, L2-Distance = 0.0023, Normal std = 0.5581

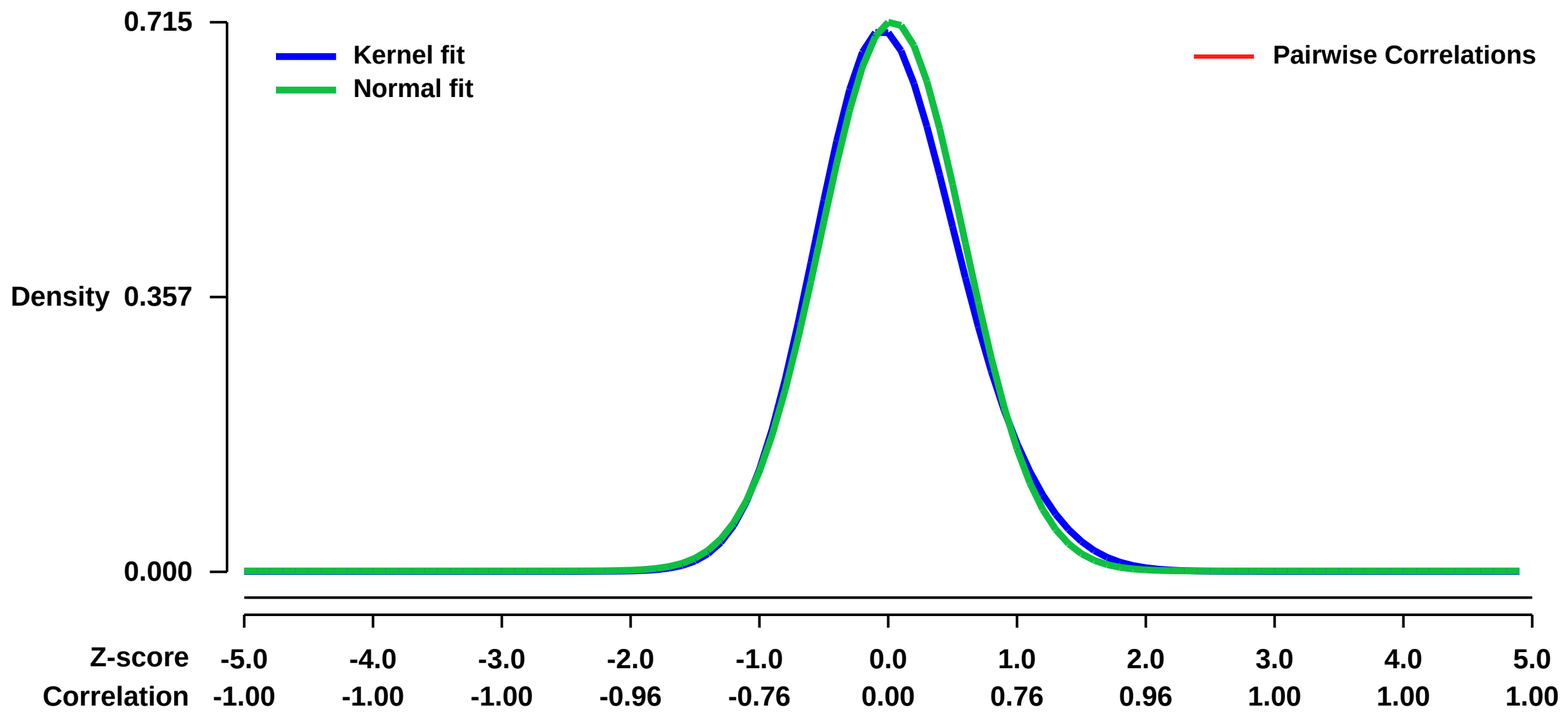

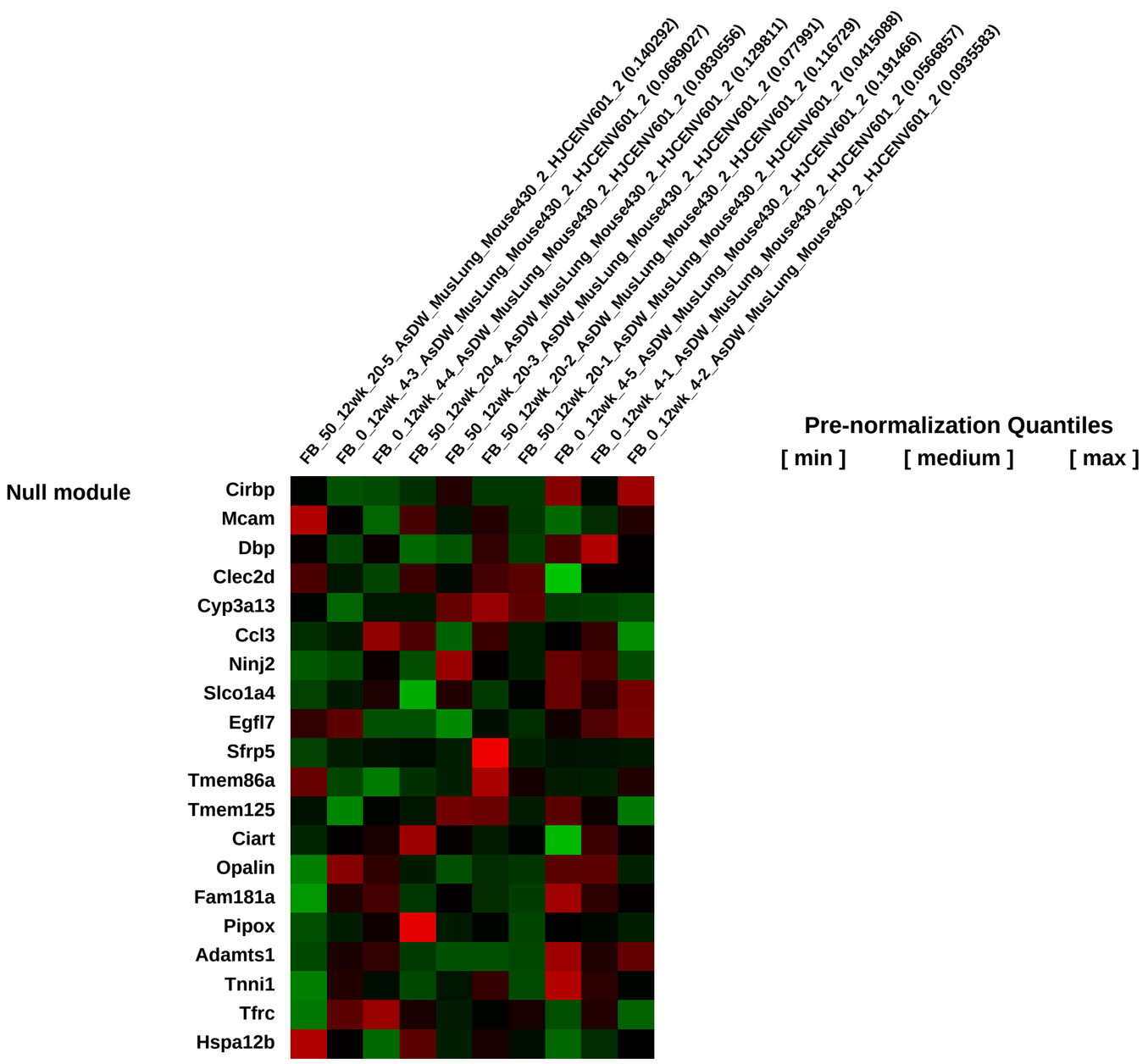

GEO Series "GSE7258" Expression Profiles

Num of samples in this series: 17

Scale of expression profile Z-scores

-3.0 -2.0 -1.0 0.0 1.0 2.0 3.0

GEO Link:	http://www.ncbi.nlm.nih.gov/geo/query/acc.cgi?acc=GSE7258
Status:	Public on Feb 20 2008
Title:	Expression data of bronchoalveolar lavage cells from control or urethane treated AJ mice
Organism:	Mus musculus
Experiment type:	Expression profiling by array
Platform:	GPL1261
Pubmed ID:	18172294
Summary & Design:	**Summary:** AJ mouse is susceptible to lung carcinogenesis from urethane treatment and is a good model for human adenocarcinoma. We completed a study using microarray analysis of bronchoalveolar lavage cells from control or urethane treated mice. A unique macrophage expression signature in the lung tumor microenvironment was able to correctly classify the lavage samples. **Keywords:** AJ mouse control and urethane treatment carcinogenesis protocol **Overall design:** RNA from bronchoalveolar lavage cells of age matched untreated AJ mice controls (C) or from urethane treated (T) AJ mice was prepared. Datasets were accurately classified using a unique macrophage gene expression signature derived from the tumor microenvironment.

Background corr dist: KL-Divergence = 0.1136, L1-Distance = 0.0400, L2-Distance = 0.0032, Normal std = 0.4166

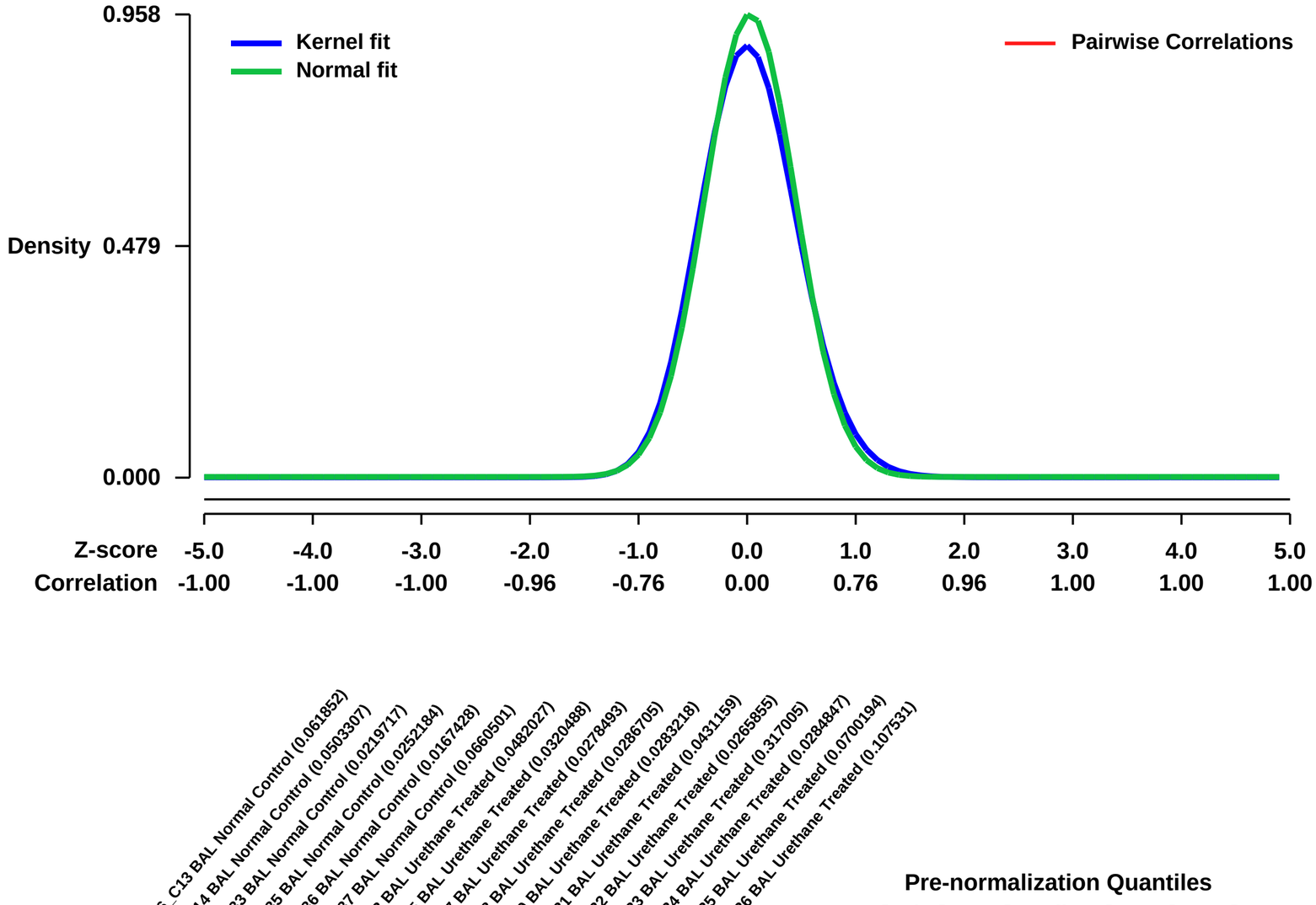

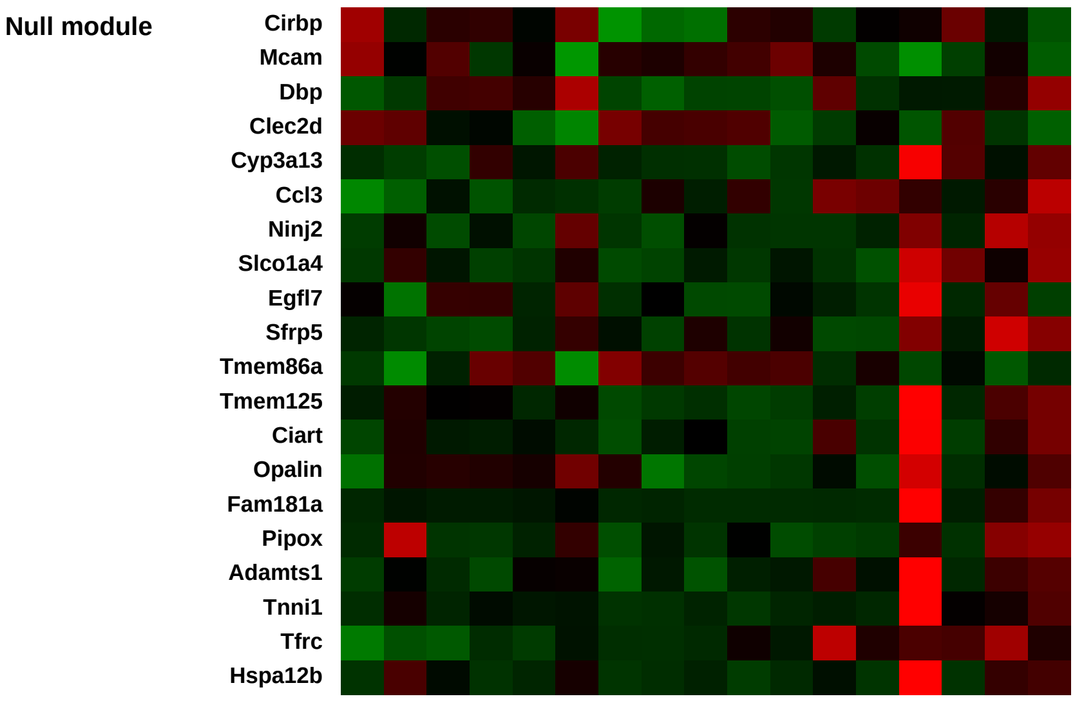

GEO Series "GSE39770" Expression Profiles

Num of samples in this series: 10

Scale of expression profile Z-scores

-3.0 -2.0 -1.0 0.0 1.0 2.0 3.0

GEO Link:	http://www.ncbi.nlm.nih.gov/geo/query/acc.cgi?acc=GSE39770
Status:	Public on Aug 01 2012
Title:	Expression data from embryonic stem cells following siRNA transfection of UPS members [Differentiation_ES]
Organism:	Mus musculus
Experiment type:	Expression profiling by array
Platform:	GPL1261
Pubmed ID:	23103054
Summary & Design:	**Summary:** While transcriptional regulation of stem cell self-renewal and differentiation has been extensively studied, only a small number of studies have addressed the roles for post-translational modifications in these processes. A key mechanism of post-translational modification is ubiquitination by the ubiquitin-proteasome system (UPS). Using UPS-targeted RNAi screens, we identify novel regulators of pluripotency and differentiation. We focus on two of these proteins, the deubiquitinating enzyme, Psmd14, and the E3 ligase, Fbxw7, and characterize their importance in ES cell pluripotency and cellular reprogramming. **Overall design:** Embryonic stem cells were reverse transfected with siRNA, and differentiated for 48hrs in conditions with retinoic acid, 48 hrs post transfection cells were isloated for RNA extraction and hybridization on Affymetrix microarrays

Background corr dist: KL-Divergence = 0.0856, L1-Distance = 0.0226, L2-Distance = 0.0006, Normal std = 0.4634

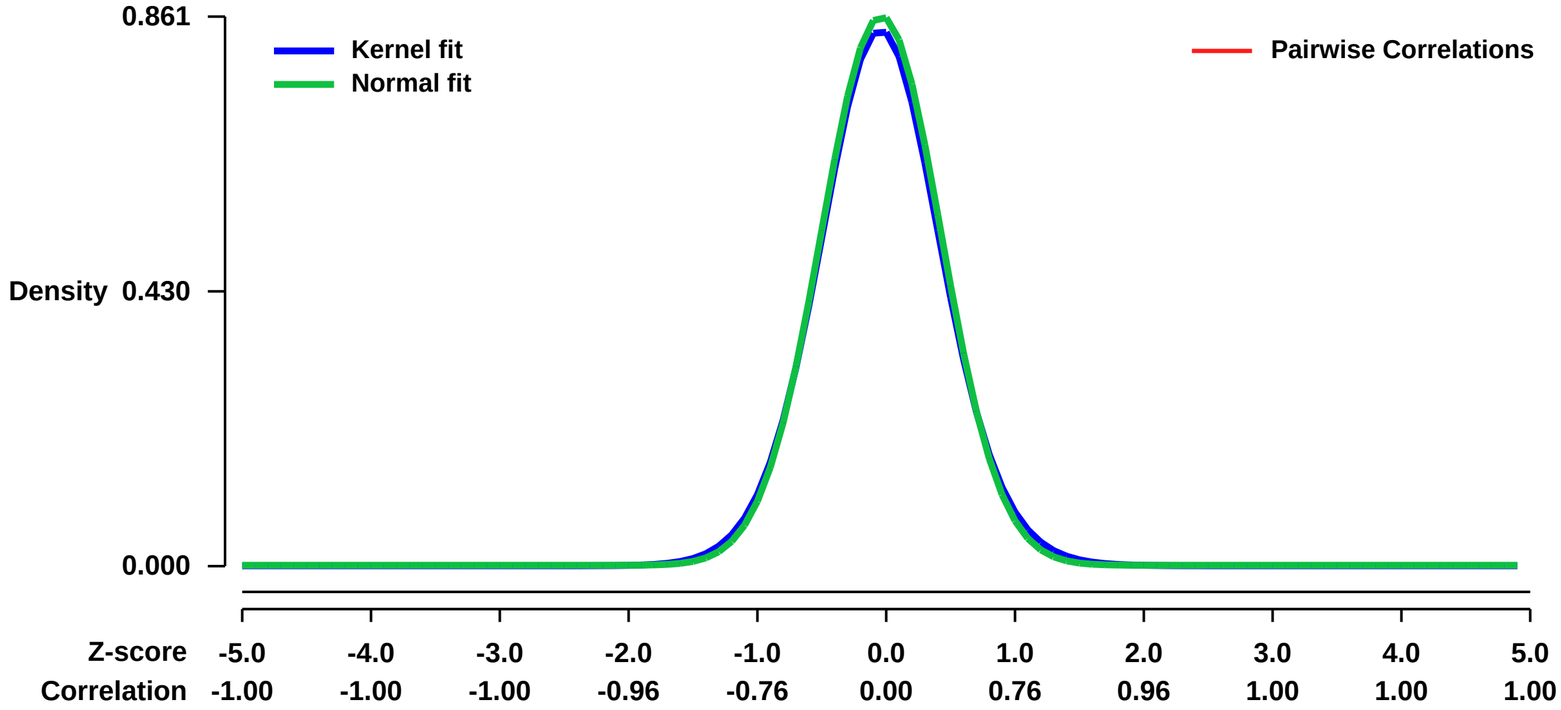

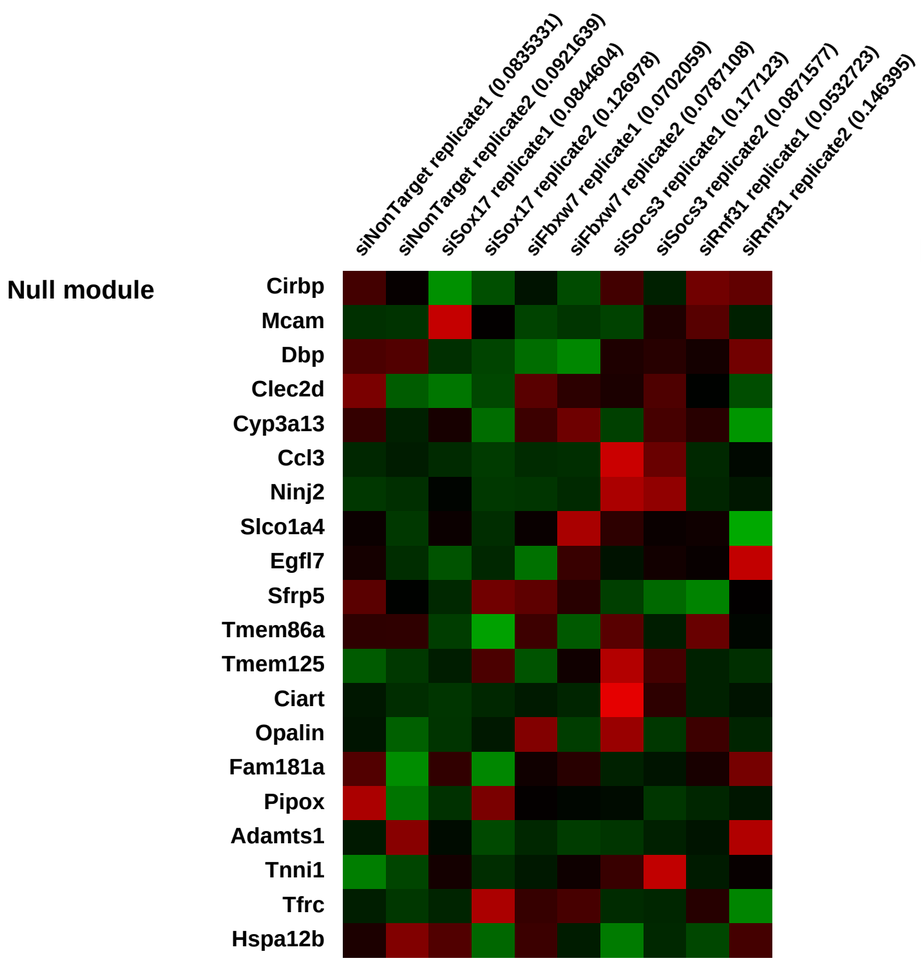

GEO Series "GSE16377" Expression Profiles

Num of samples in this series: 6

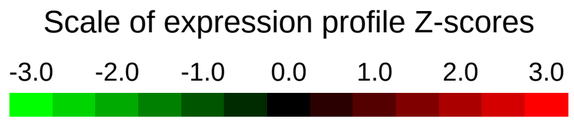

GEO Link:	**http://www.ncbi.nlm.nih.gov/geo/query/acc.cgi?acc=GSE16377**
Status:	**Public on Jun 01 2010**
Title:	**wild type mouse lung control vs. high fat diet**
Organism:	**Mus musculus**
Experiment type:	**Expression profiling by array**
Platform:	**GPL1261**
Pubmed ID:	
Summary & Design:	**Summary:** **To study the effects of a high fat diet on the mouse lung transcrptional profile.** **Overall design:** **6 samples were analyzed. 3 wild type mice on a control diet (lung samples) vs. 3 wild type mice on a high fat diet (lung samples).**

Background corr dist: **KL-Divergence = 0.0411, L1-Distance = 0.0234, L2-Distance = 0.0007, Normal std = 0.6141**

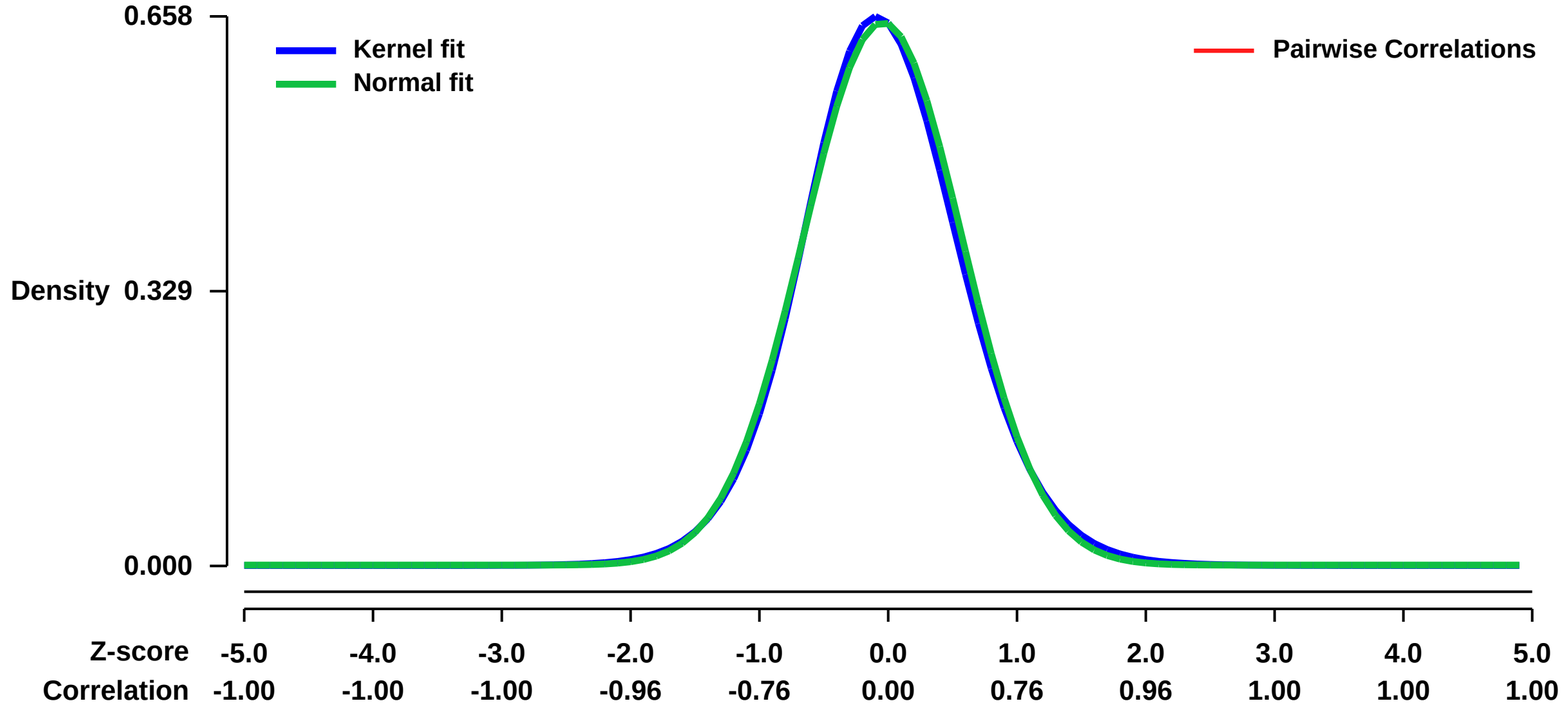

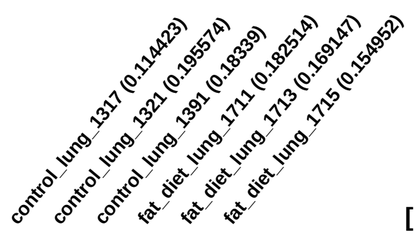

Pre-normalization Quantiles

[min] [medium] [max]

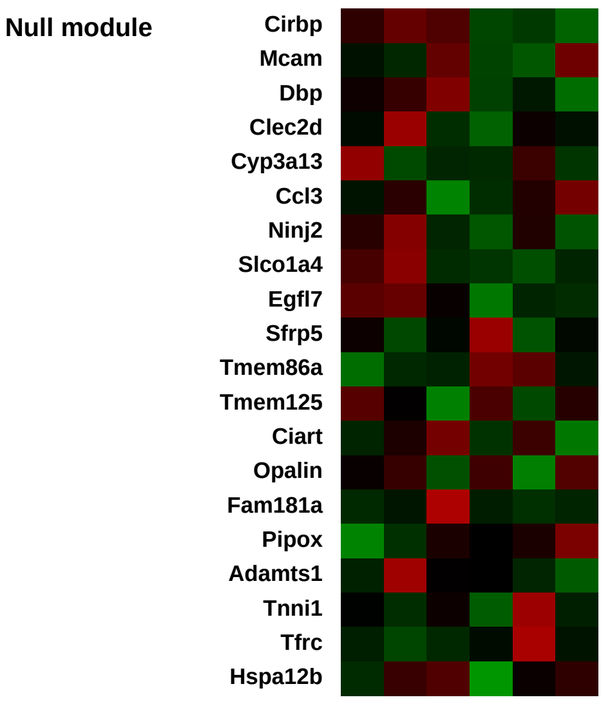

GEO Series "GSE6623" Expression Profiles

Num of samples in this series: 12

Scale of expression profile Z-scores

-3.0 -2.0 -1.0 0.0 1.0 2.0 3.0

GEO Link:	http://www.ncbi.nlm.nih.gov/geo/query/acc.cgi?acc=GSE6623
Status:	Public on Jan 25 2007
Title:	FoxO are critical mediators of hematopoietic stem cell resistance to physiologic oxidative stress
Organism:	Mus musculus
Experiment type:	Expression profiling by array
Platform:	GPL1261
Pubmed ID:	17254970
Summary & Design:	**Summary:** To investigate the role of FoxO transcription factors as mediators of hematopoietic stem cell resistance to oxidative stress. **Keywords: Hematopoietic stem cells, myeloid progenitors, oxidative stress, ROS, Affymetrix Mouse Genome 430 2.0** **Overall design:** Study the effect of the deficiency of FoxO1, FoxO3, and FoxO4 in murine bone marrow hematopoietic stem cells and myeloid progenitors on expression of genes involved in reactive oxygen species (ROS) metabolism.

Background corr dist: **KL-Divergence = 0.0999, L1-Distance = 0.0390, L2-Distance = 0.0024, Normal std = 0.4543**

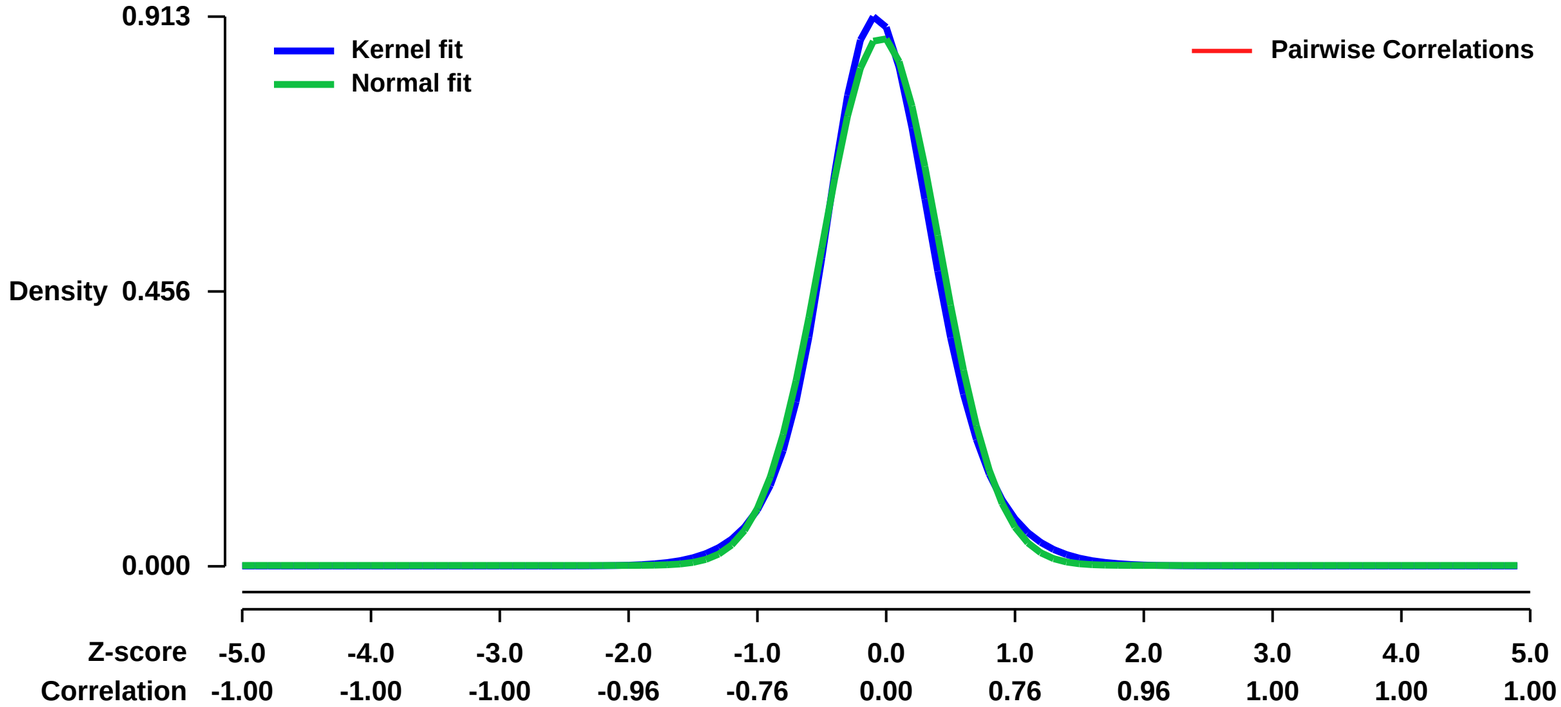

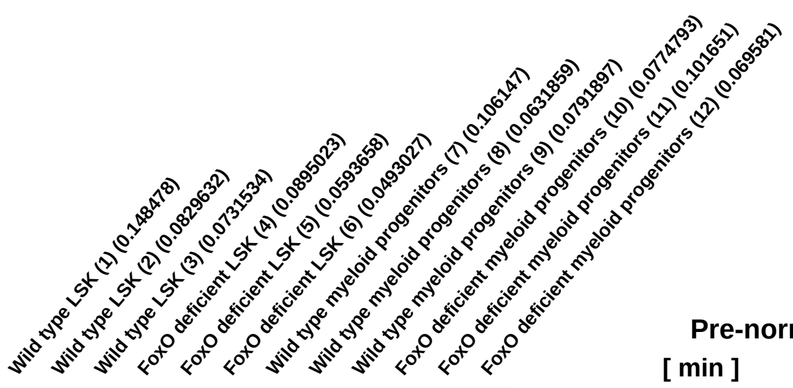

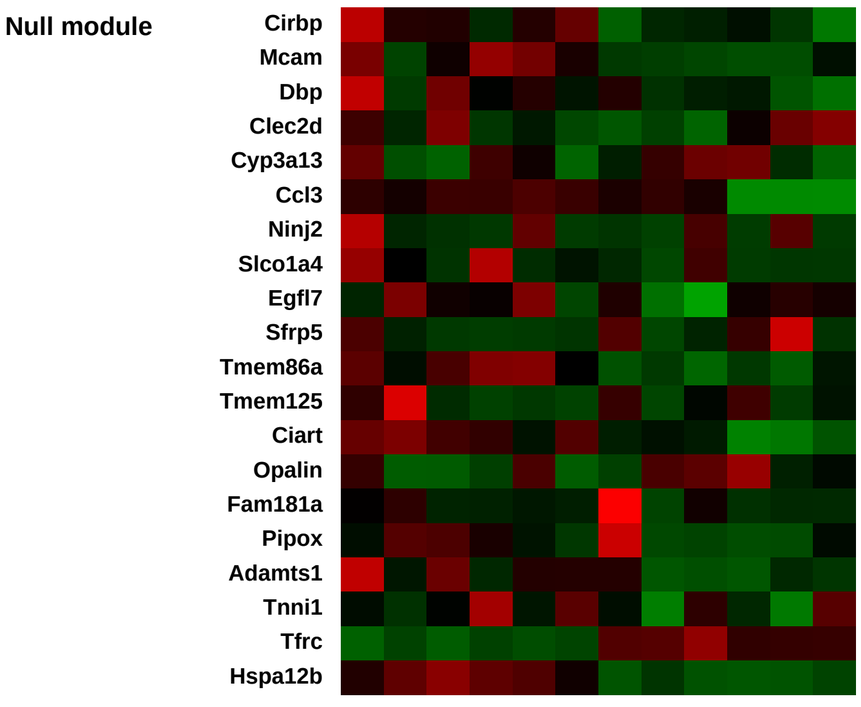

GEO Series "GSE36513" Expression Profiles

Num of samples in this series: 8

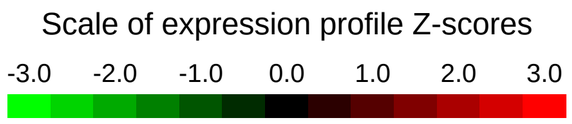

GEO Link:	http://www.ncbi.nlm.nih.gov/geo/query/acc.cgi?acc=GSE36513
Status:	Public on Feb 18 2013
Title:	Long noncoding RNA as regulatory switch of protein turnover
Organism:	Mus musculus
Experiment type:	Expression profiling by array
Platform:	GPL1261
Pubmed ID:	24521543
Summary & Design:	**Summary:** Long intervening noncoding RNAs (lincRNAs) are prevalent genes with poorly understood functions. Here we discover a pathway of lincRNA-regulated proteolysis. The enhancer-like lincRNA HOTTIP extends the half-life of its binding protein WDR5, a subunit of the MLL H3K4 methylase complex, resulting in increased chromatin occupancy and gene activation. LincRNA-mediated stabilization requires direct RNA-protein interaction in a long RNA context, and blocks turnover at a step after target protein poly-ubiquitination. We elucidate the lincRNA binding interface on WDR5. A WDR5 mutant that selectively abrogates lincRNA binding becomes unstable, and is defective in gene activation, maintenance of histone H3 lysine 4 trimethylation, and embryonic stem cell self renewal. The ability to modulate protein turnover may allow lincRNAs to control the lifespan of molecular interactions at chromatin and elsewhere, broadening their scope in epigenetics and cell fate control. **Overall design:** Gene expression analysis: To establish a differentiation signature for mouse V6.5 ES cells infected with anti mouse WDR5 shRNA, rescued with doxycycline inducible WDR5 WT or WDR5 F266A, total RNA was isolated in biologic duplicate from cells in different conditions and hybridized to Affymetrix Mouse 430 2.0 arrays.

Background corr dist: KL-Divergence = 0.0512, L1-Distance = 0.0247, L2-Distance = 0.0007, Normal std = 0.5684

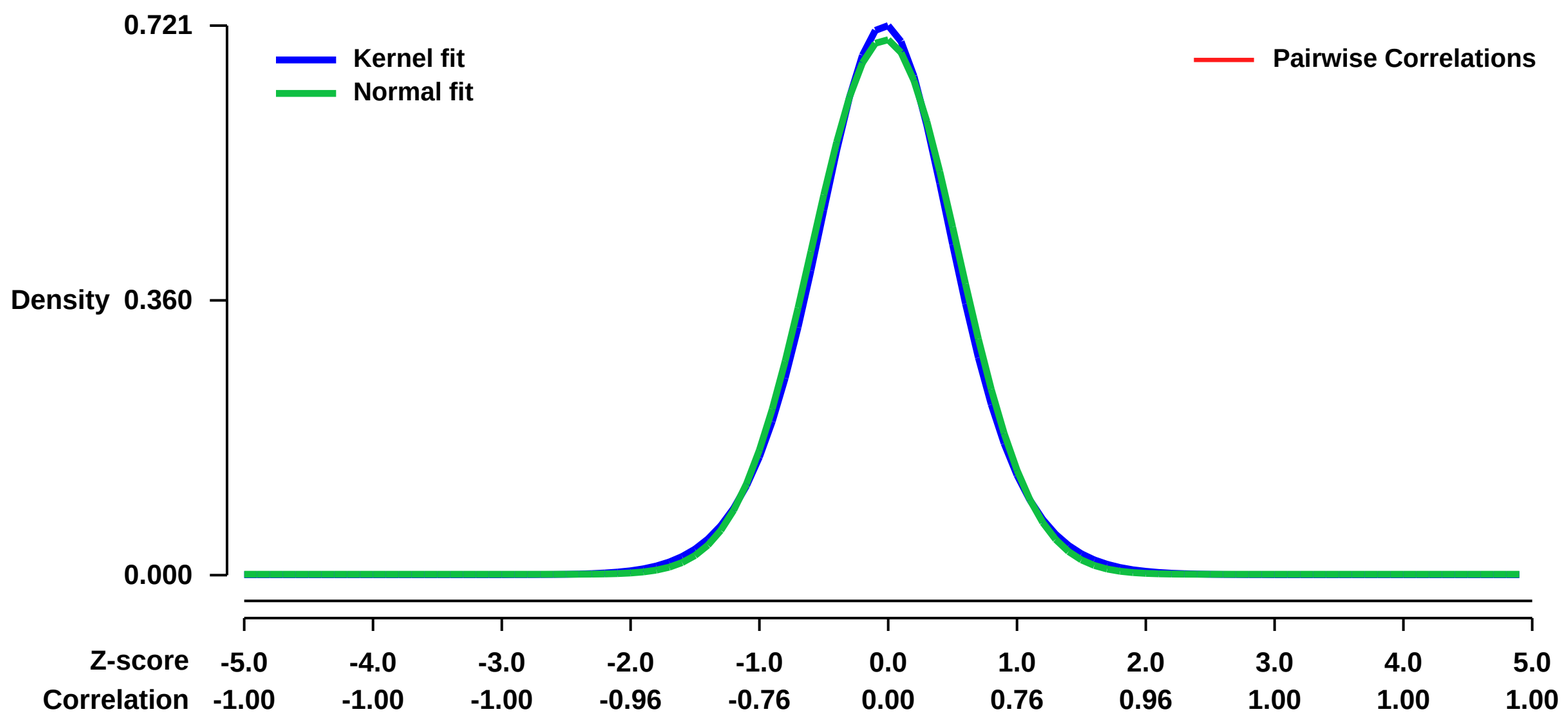

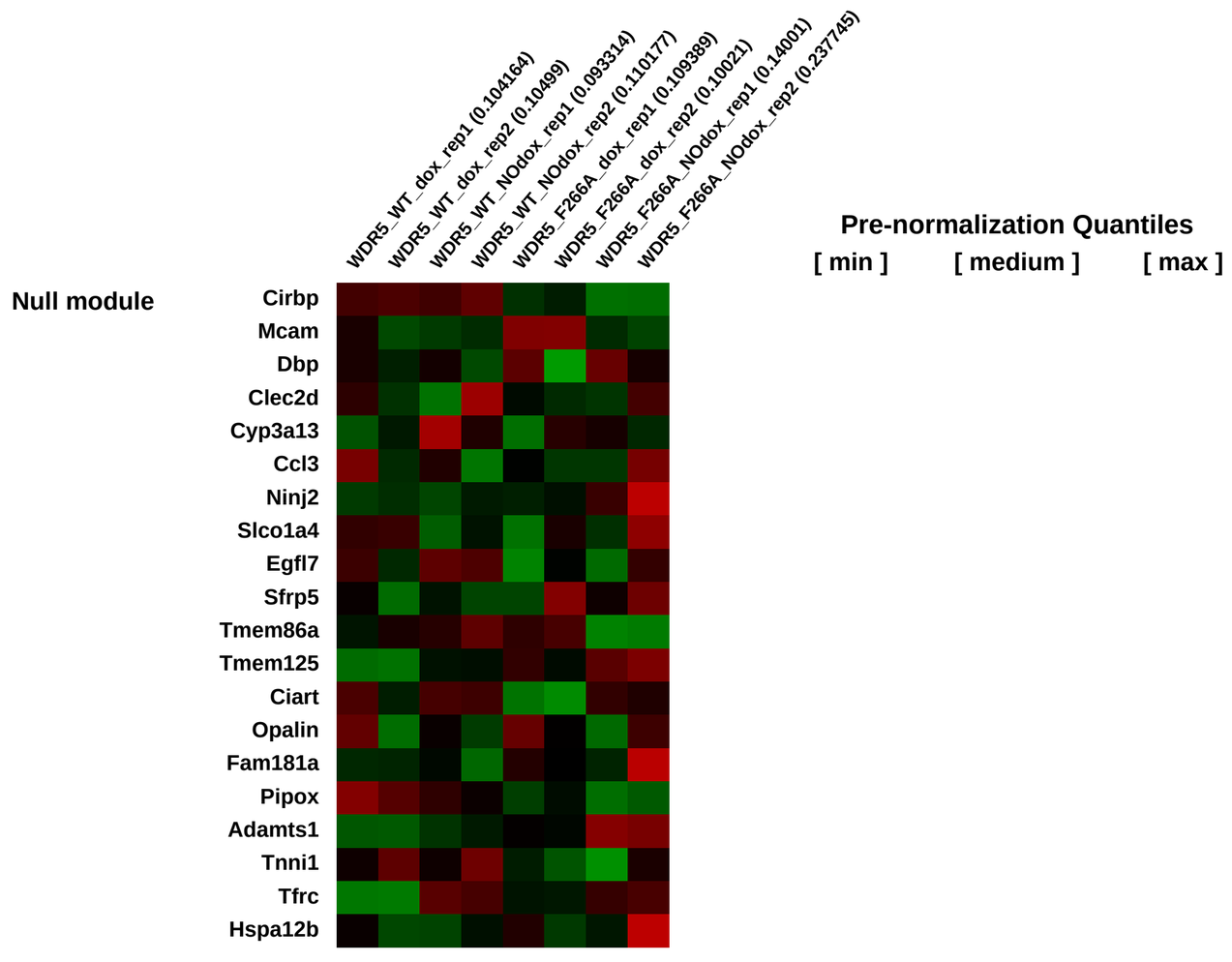

GEO Series "GSE31776" Expression Profiles

Num of samples in this series: 10

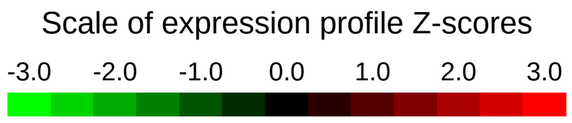

GEO Link:	**http://www.ncbi.nlm.nih.gov/geo/query/acc.cgi?acc=GSE31776**
Status:	**Public on Nov 01 2012**
Title:	**Microarray analysis of T-cell death-associated gene 8 (TDAG8)-mediated gene expression in mouse Lewis lung carcinoma (LLC) cells.**
Organism:	**Mus musculus**
Experiment type:	**Expression profiling by array**
Platform:	**GPL1261**
Pubmed ID:	
Summary & Design:	**Summary:** **We previously identified an extracellular pH-sensing G protein-coupled receptor T cell death associated gene 8 (TDAG8) as an extracellular pH sensor of tumor cells that promotes cell growth/survival in vitro and tumor development in vivo. To determine genes regulated by TDAG8 in vitro, mouse Lewis lung carcinoma (LLC) cells stably expressing TDAG8 (TDAG8-LLC cells) and control vector (control LLC cells) were cultured under acidic conditions. Transcriptome microarray analysis using Affymetrix GeneChip Mouse Genome 430 2.0 Arrays was performed with total RNA prepared from these cells.** **Overall design:** **To determine genes regulated by TDAG8 in vitro, mouse Lewis lung carcinoma (LLC) cells stably expressing TDAG8 (TDAG8-LLC cells) and control vector (control LLC cells) were cultured under acidic conditions. Transcriptome microarray analysis using Affymetrix GeneChip Mouse Genome 430 2.0 Arrays was performed with a mixture of equal amounts of total RNA samples from four independent cell cultures.**

Background corr dist: **KL-Divergence = 0.0916, L1-Distance = 0.0241, L2-Distance = 0.0008, Normal std = 0.4588**

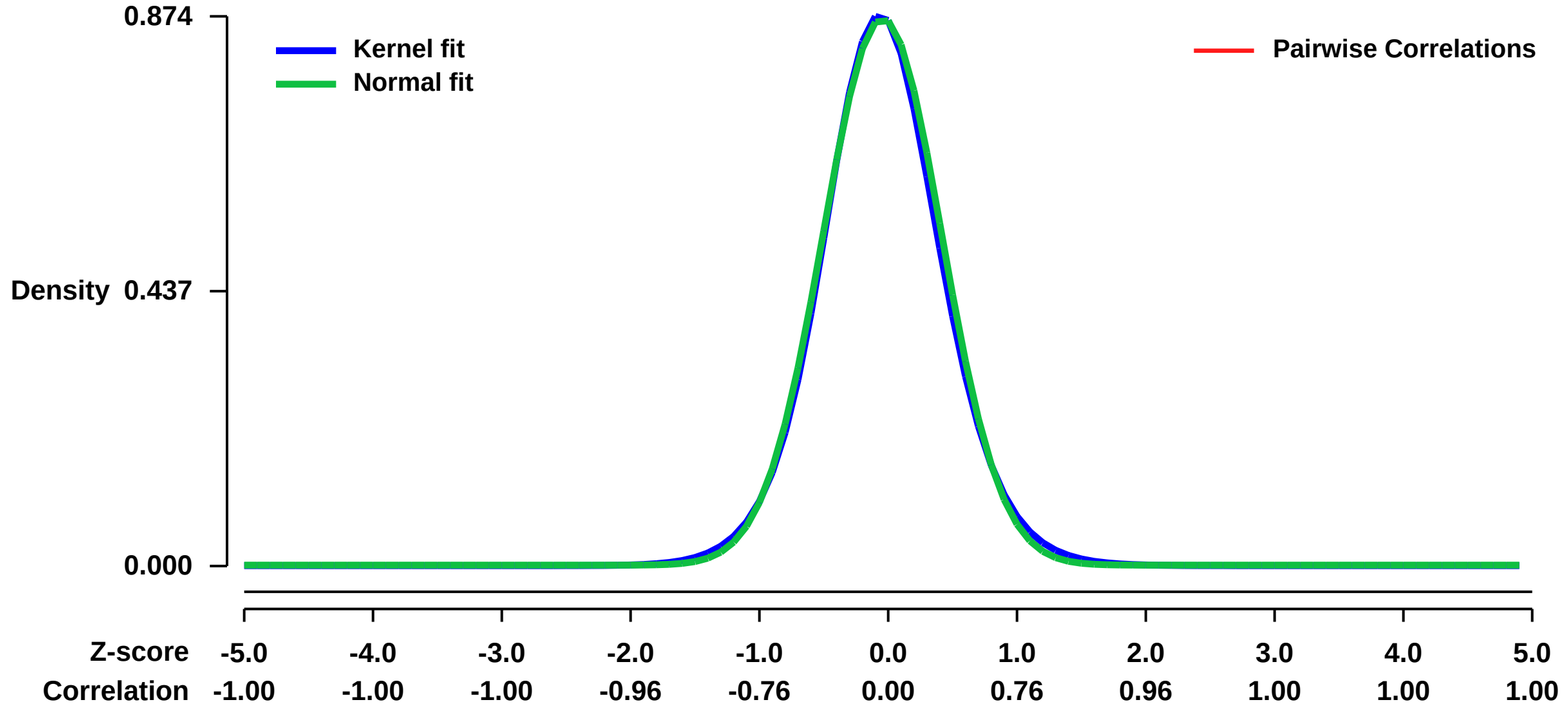

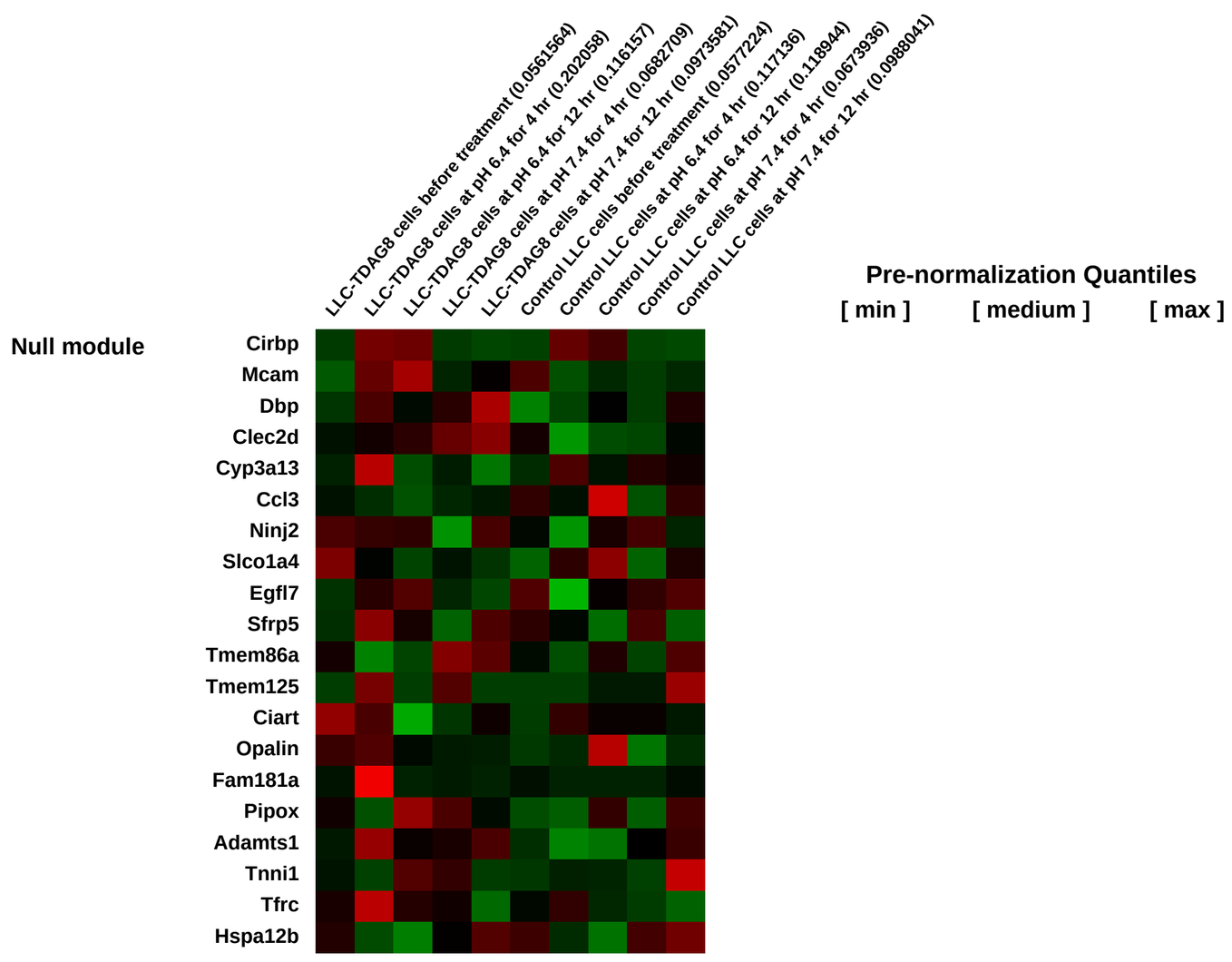

GEO Series "GSE3843" Expression Profiles

Num of samples in this series: 8

Scale of expression profile Z-scores

-3.0 -2.0 -1.0 0.0 1.0 2.0 3.0

GEO Link:	http://www.ncbi.nlm.nih.gov/geo/query/acc.cgi?acc=GSE3843
Status:	Public on Dec 22 2005
Title:	Targeted disruption of glycerol kinase gene in mice: expression analysis in liver
Organism:	Mus musculus
Experiment type:	Expression profiling by array
Platform:	GPL1261
Pubmed ID:	16368706
Summary & Design:	**Summary:** Glycerol kinase deficiency (GKD) is an X-linked inborn error of metabolism with metabolic and neurologic crises. Liver shows the highest level of glycerol kinase (GK) activity in humans and mice. Absence of genotype-phenotype correlations in patients with GKD indicate the involvement of modifier genes, including other network partners. To understand the molecular pathogenesis of GKD, we performed microarray analysis on liver mRNA from neonatal glycerol kinase (Gyk) knockout (KO) and wild type (WT) mice. Unsupervised learning revealed the overall gene expression profile of the KO mice was different from that of WT. Real time PCR confirmed differences for selected genes. Functional gene enrichment analysis was used to find 56 increased and 37 decreased gene functional categories. Pathway Assist analysis identified changes in gene expression levels of genes involved in organic acid metabolism indicating that GK was part of the same metabolic network which correlates well with the patients with GKD having metabolic acidemia during their episodic crises. Network component analysis (NCA) showed that transcription factors SREBP-1c, ChREBP, HNF-4alpha, and PPAR-alpha, had increased activity in the Gyk KO mice compared with WT mice; while SREBP-2 was less active in the Gyk KO mice. These studies show that Gyk deletion causes alterations in gene expression of genes in several regulatory networks and is the first time NCA has been used to expand on microarray data from a mouse knockout model of a human disease. **Keywords:** Glycerol kinase (Gyk) knockout mouse; mouse model of human Glycerol Kinase Deficiency; Gyk KO versus WT liver expression analysis; Affymetrix mus 430 2.0 GeneChip **Overall design:** Male WT and KO mouse pups were sacrificed on day of life (dol) 3 and each liver was harvested. Total RNA from 4 KO and 4 WT livers was isolated individually. cDNA was synthesized from the poly(A)+ mRNA in the total RNA, Biotin-tagged and fragmented to an average strand length of 100 bases (range 35-200 bases). Ten ´µg of each cRNA was hybridized onto an Affymetrix mus 430 2.0 GeneChip to analyze differences in liver gene expression between KO and WT mice. Day of life three was chosen because the mice are phenotypically symptomatic with statistically different parameters for hypoglycemia, acidosis; low bicarbonate and decreased base excess. On day of life 2 they are not significantly different from wild type in all of these important clinical phenotypes.

Background corr dist: KL-Divergence = 0.0646, L1-Distance = 0.0186, L2-Distance = 0.0005, Normal std = 0.5135

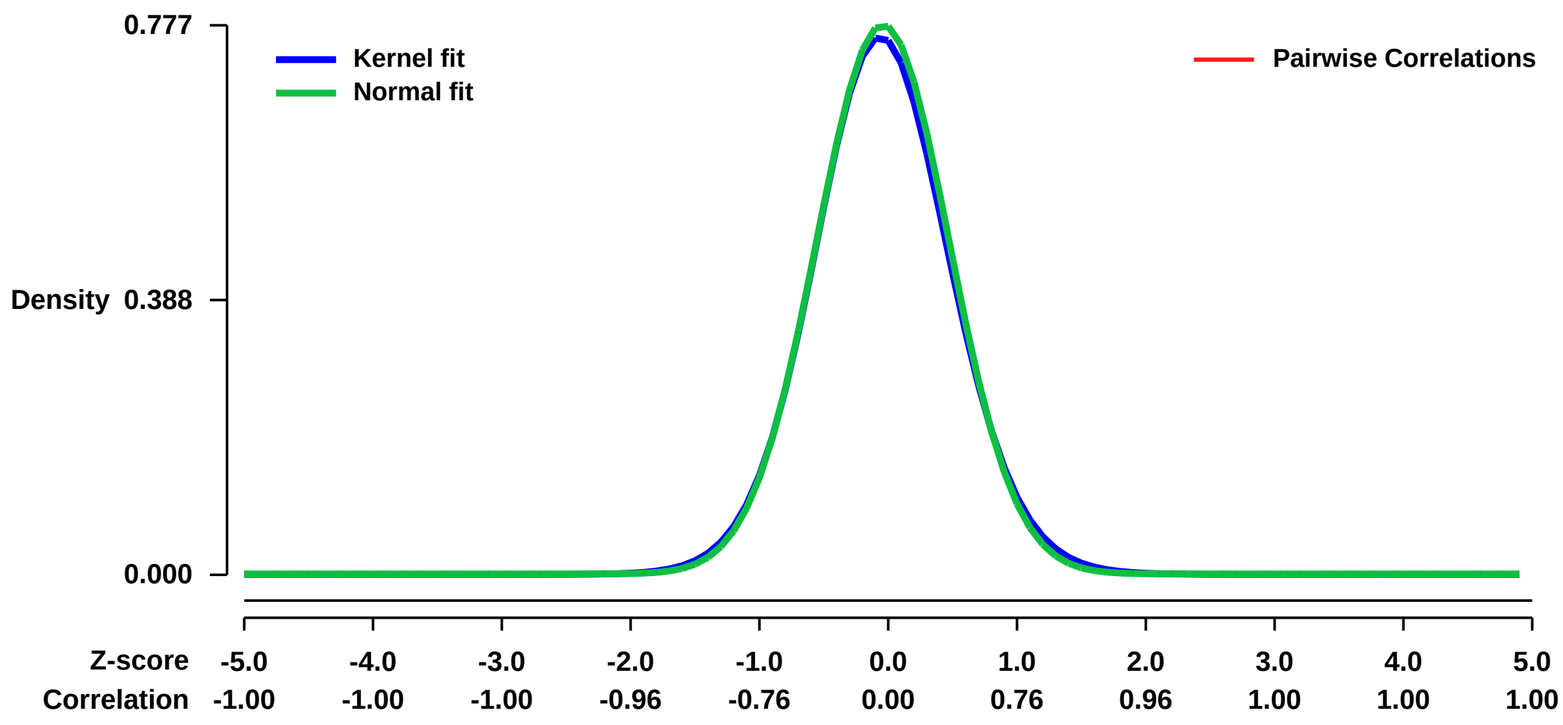

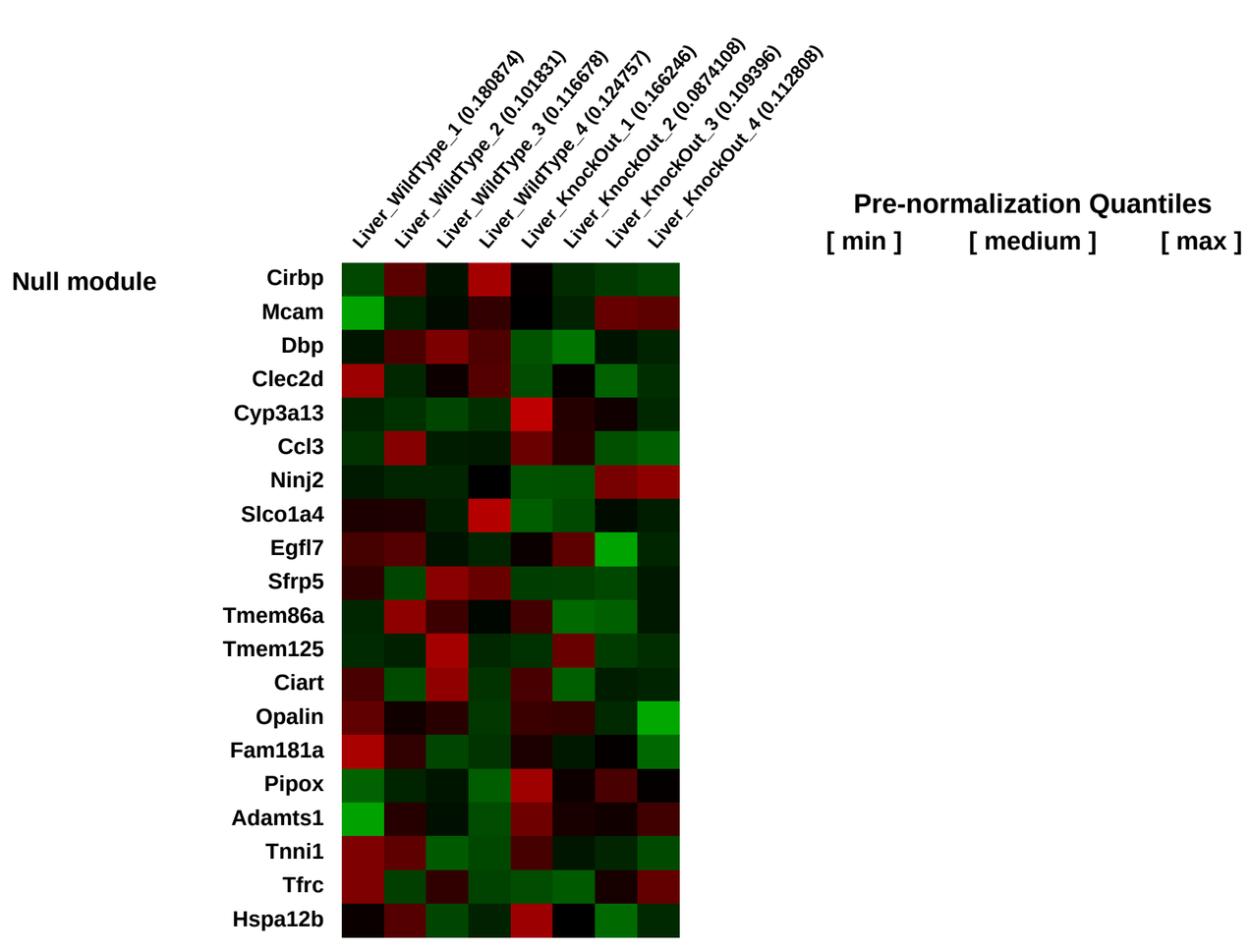

GEO Series "GSE38375" Expression Profiles

Num of samples in this series: 27

Scale of expression profile Z-scores

-3.0 -2.0 -1.0 0.0 1.0 2.0 3.0

GEO Link:	http://www.ncbi.nlm.nih.gov/geo/query/acc.cgi?acc=GSE38375
Status:	Public on Jul 01 2012
Title:	Interleukin-27 priming of T cells controls Interleukin-17-production in trans via induction of Programmed cell death ligand 1
Organism:	Mus musculus
Experiment type:	Expression profiling by array
Platform:	GPL1261
Pubmed ID:	
Summary & Design:	**Summary:** Interleukin (IL)-27 is a key immunosuppressive cytokine that counters T helper 17 (Th17) cell-mediated pathology. To identify mechanisms by which IL-27 might exert its immunosuppressive effect, we analyzed genes in T cells rapidly induced by IL-27. We found that IL-27 priming of naˆflve T cells upregulated expression of programmed death ligand 1 (PD-L1) in a signal transducer and activator of transcription (STAT)1-dependent manner. When co-cultured with naˆflve CD4+ T cells, IL-27-primed T cells inhibited the differentiation of Th17 cells in trans through a PD-1-PD-L1 interaction. In vivo, co-administration of naˆflve TCR transgenic T cells (2D2 T cells) with IL-27-primed T cells expressing PD-L1 inhibited the development of Th17 cells and protected from severe autoimmune encephalomyelitis. Thus, these data identify a suppressive activity of IL-27, by which CD4+ T cells can restrict differentiation of Th17 cells in trans. **Overall design:** The roles of IL-6 and IL-27 in naˆflve CD4+ T cells was investigated by comparing global gene expression by Affymetrix Mouse Genome 430 2.0 Arrays. The functional outcome of STAT proteins was further evaluated by profiling gene expression changes between WT and STAT-deficient T cells in naˆflve CD4+ T cells with specific stimulation. All condition were done in biological triplicate.

Background corr dist: KL-Divergence = 0.2235, L1-Distance = 0.0477, L2-Distance = 0.0049, Normal std = 0.3169

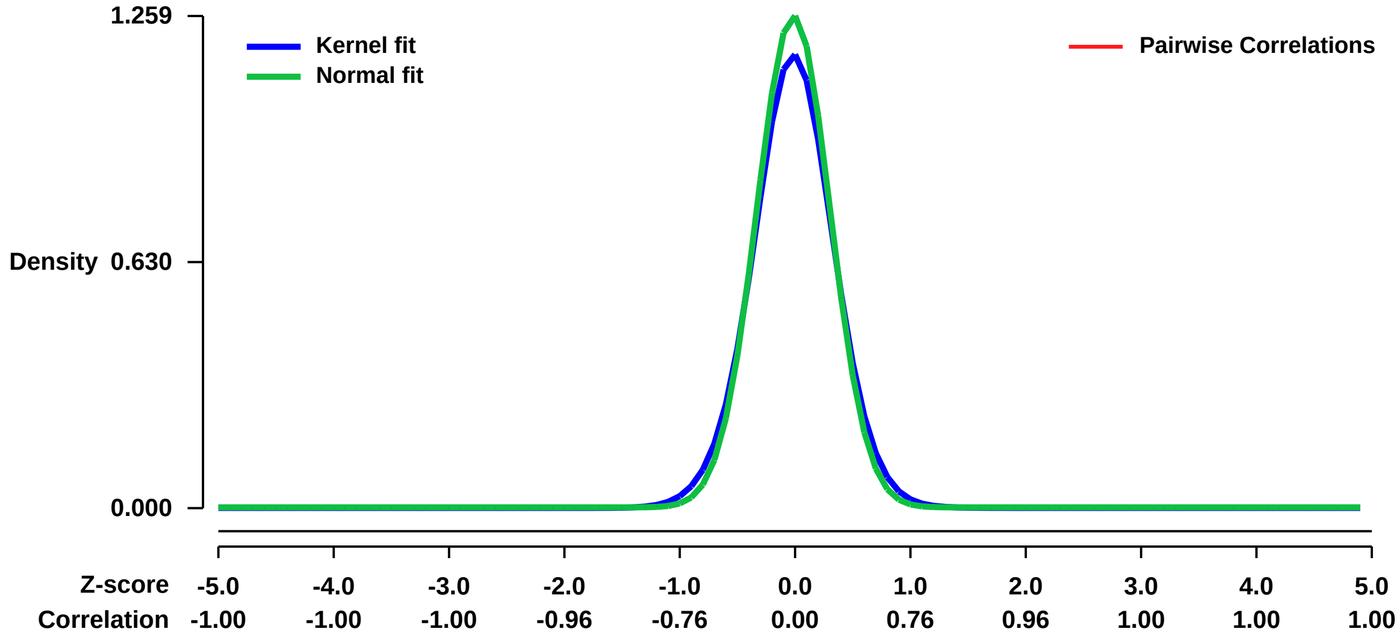

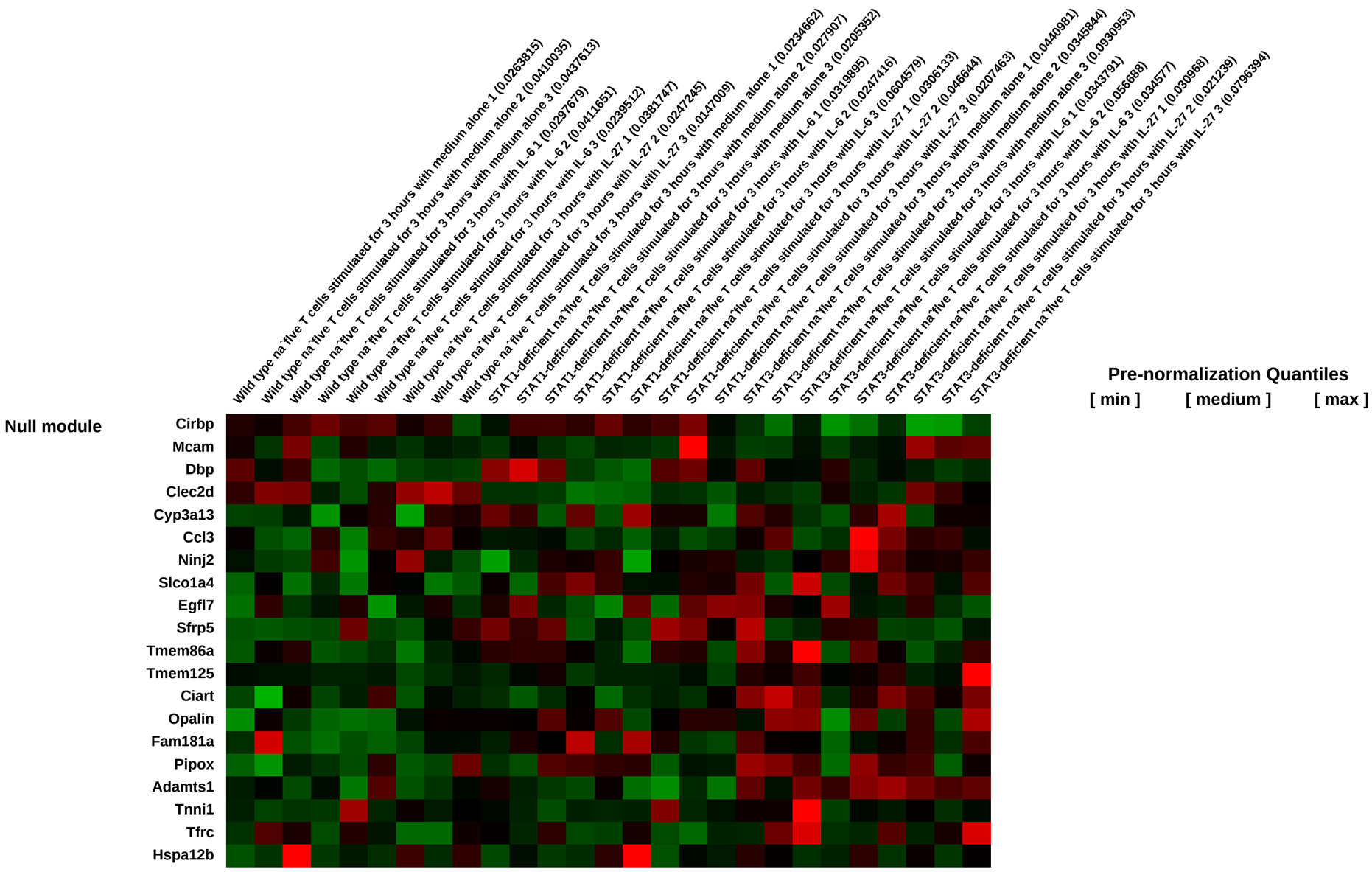

GEO Series "GSE20562" Expression Profiles

Num of samples in this series: 20

Scale of expression profile Z-scores

-3.0 -2.0 -1.0 0.0 1.0 2.0 3.0

GEO Link:	http://www.ncbi.nlm.nih.gov/geo/query/acc.cgi?acc=GSE20562
Status:	Public on Jan 01 2011
Title:	Expression data in mouse liver exposed to low dose-rate radiation
Organism:	Mus musculus
Experiment type:	Expression profiling by array
Platform:	GPL1261
Pubmed ID:	20954861
Summary & Design:	**Summary:** Expression profiles in mouse liver exposed to long-term gamma-irradiation were examined to assess in vivo effects of low dose-rate radiation. Three groups of male C57BL/6J mice were exposed to whole body irradiation at dose-rates of 17-20 mGy/day, 0.86-1.0 mGy/day or 0.042-0.050 mGy/day for 401-485 days (cumulative doses were approximately 8 Gy, 0.4 Gy or 0.02 Gy, respectively). Expression profiles were produced for RNA isolated from irradiated individual animals and for pooled RNA from sham-irradiated 3 animals for control. The expression levels of 6 irradiated animals for each dose were compared individually with those of 2 pooled controls (3 irradiated samples to one pooled control in first and second experiments). **Overall design:** The experiments were conducted twice at similar dose-rates. In the first experiment, three groups of 8 weeks old male C57BL/6J mice were exposed to whole body irradiation at dose-rates of either 16.6 mGy/day (H1), 0.858 mGy/day (M1) or 0.042 mGy/day (L1) for 485 days (cumulative doses were 8030 mGy, 416 mGy or 20.6 mGy, respectively). In the second experiment, the doe-rates were slightly elevated as 20.0 mGy/day (H2), 1.000 mGy/day (M2) or 0.050 mGy/day (L2) for 401 days (doses were 8015 mGy, 401 mGy or 20 mGy, respectively). A group of control unirradiated mice were set for each experiment (C1, C2).

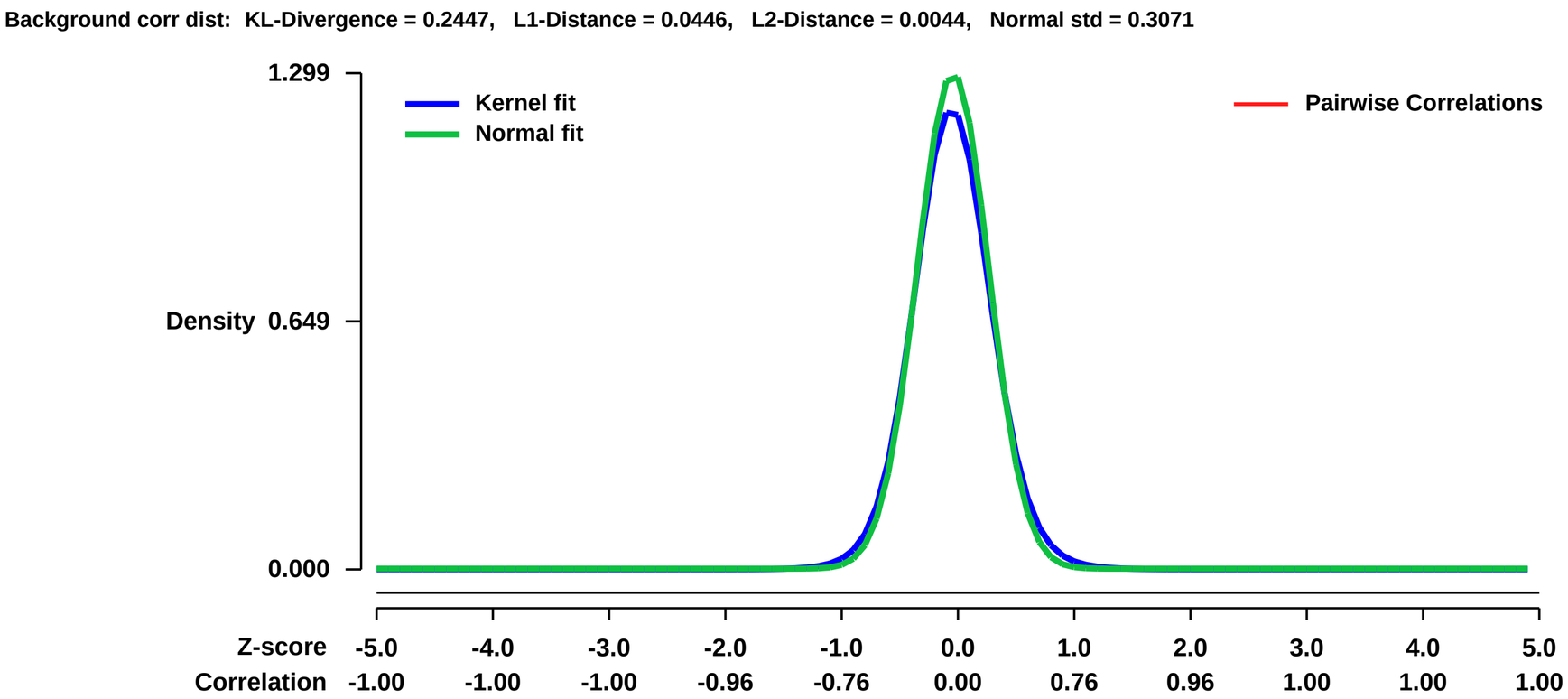

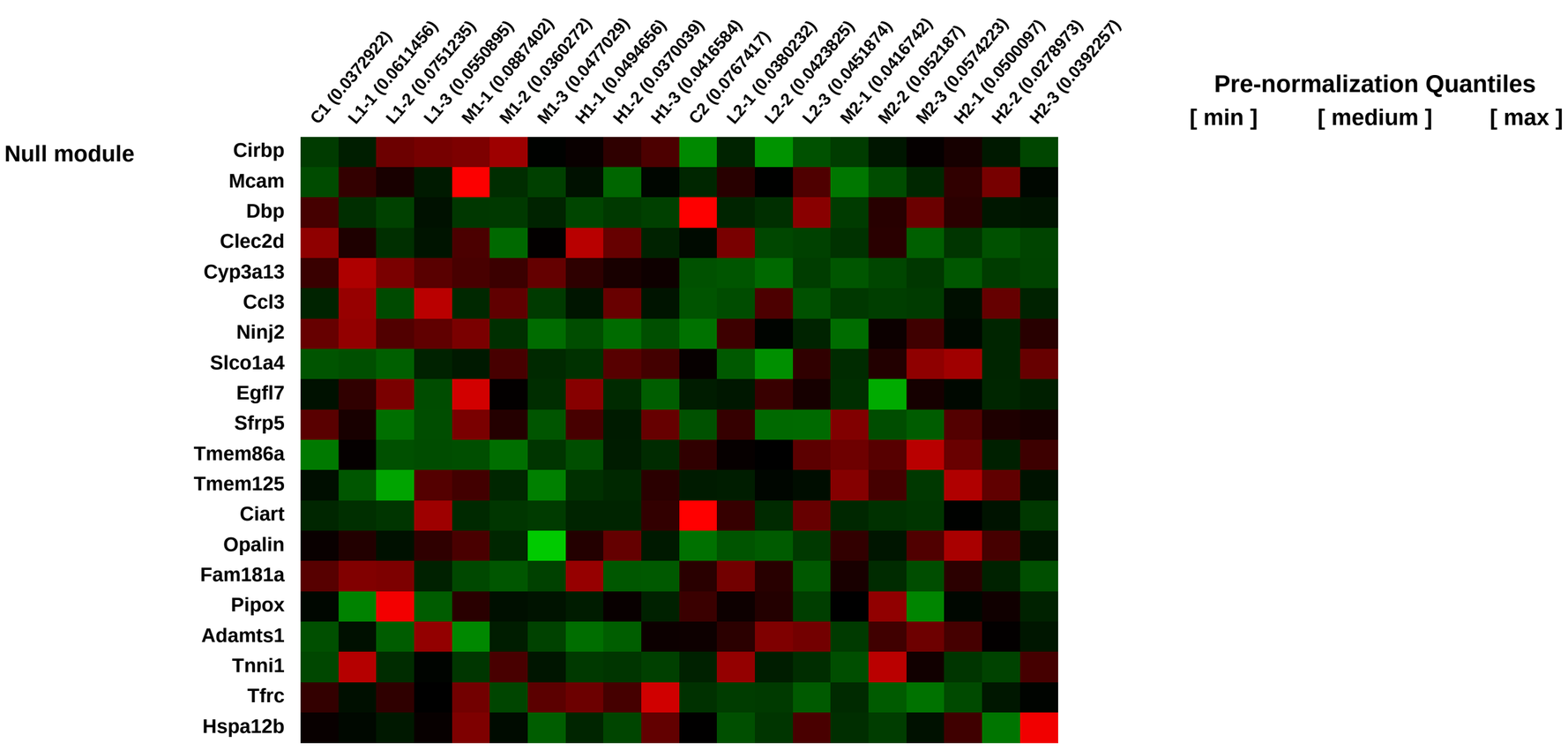

GEO Series "GSE16533" Expression Profiles

Num of samples in this series: 20

Scale of expression profile Z-scores

-3.0 -2.0 -1.0 0.0 1.0 2.0 3.0

GEO Link:	http://www.ncbi.nlm.nih.gov/geo/query/acc.cgi?acc=GSE16533
Status:	Public on Jun 10 2010
Title:	Expression data from lenses triply deficient for E2F1, E2F2, and E2F3 transcription factors
Organism:	Mus musculus
Experiment type:	Expression profiling by array
Platform:	GPL1261
Pubmed ID:	21185283
Summary & Design:	**Summary:** The E2F family consists of transcriptional repressors and activators that control cell proliferation. In the classic paradigm of cell cycle regulation, the three activators, E2F1, E2F2 and E2F3, are invariably depicted as the final components of a CDK/Rb signaling cascade that executes the transcriptional program necessary to commit cells to enter S phase. Unexpectedly, we find through analysis of Affymetrix expression array data that mature lens epithelial cells deficient for E2F1-3 fail to repress cell cycle-regulated genes (and other targets of E2F) and that this corresponds with subsequent apoptosis and cellular collapse in the lens. **Overall design:** Murine lenses were collected at two stages of development for RNA extraction and hybridization on Affymetrix microarrays. Our aim was to determine key events that lead to cellular collapse of lenses triply deficient for E2F1, E2F2, and E2F3 in neonates.

Background corr dist: KL-Divergence = 0.1098, L1-Distance = 0.0404, L2-Distance = 0.0035, Normal std = 0.4188

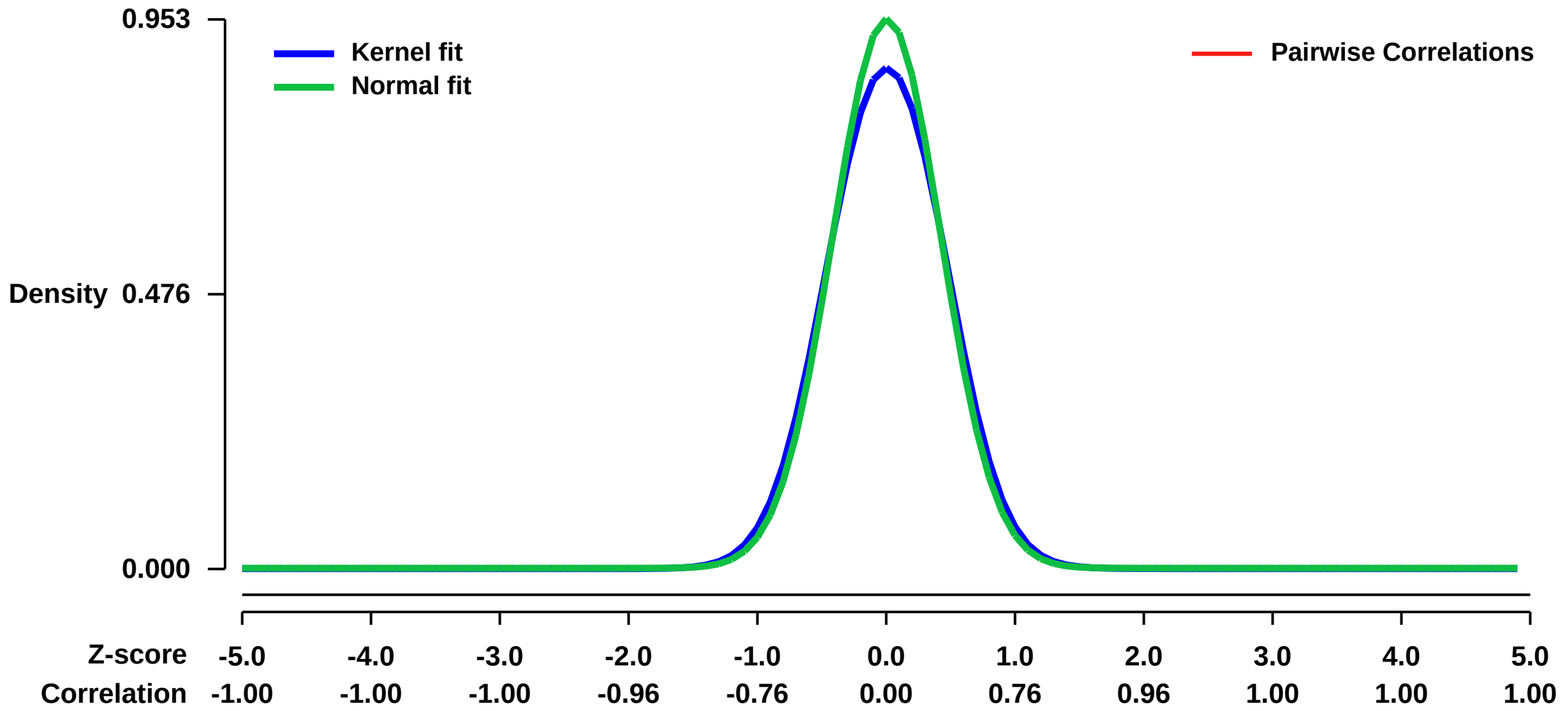

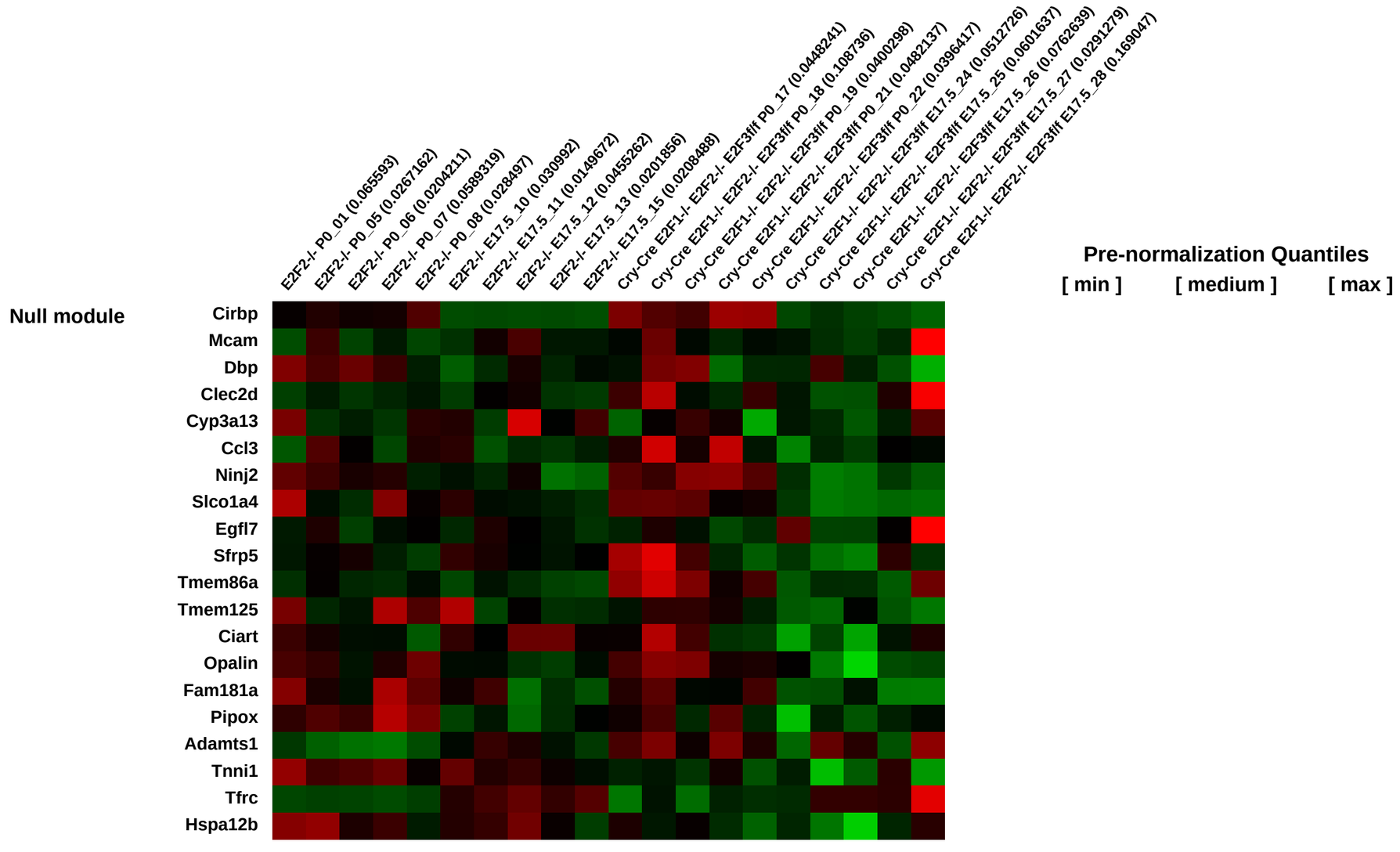

GEO Series "GSE11775" Expression Profiles

Num of samples in this series: 12

Scale of expression profile Z-scores

-3.0 -2.0 -1.0 0.0 1.0 2.0 3.0

GEO Link:	http://www.ncbi.nlm.nih.gov/geo/query/acc.cgi?acc=GSE11775
Status:	Public on Aug 28 2009
Title:	Foxp3-deficient Treg cells do not revert into conventional Effector CD4+ T cells but constitute a unique cell subset
Organism:	Mus musculus
Experiment type:	Expression profiling by array
Platform:	GPL1261
Pubmed ID:	21642545
Summary & Design:	**Summary:** Gene expression profiles were compared between regulatory T cells (Treg) and Effector CD4+ T cells in healthy B6 mice and sick mice with scurfy mutation. We used microarrays to elucidate the molecular mechanisms underlying the suppression function of the Treg cells. Keywords: Cell type comparison **Overall design:** To identify candidate genes that might be related to the suppressive activity, the Treg cells expressing functional and mutant Foxp3 transcription factor were compared

Background corr dist: KL-Divergence = 0.0455, L1-Distance = 0.0525, L2-Distance = 0.0051, Normal std = 0.5931

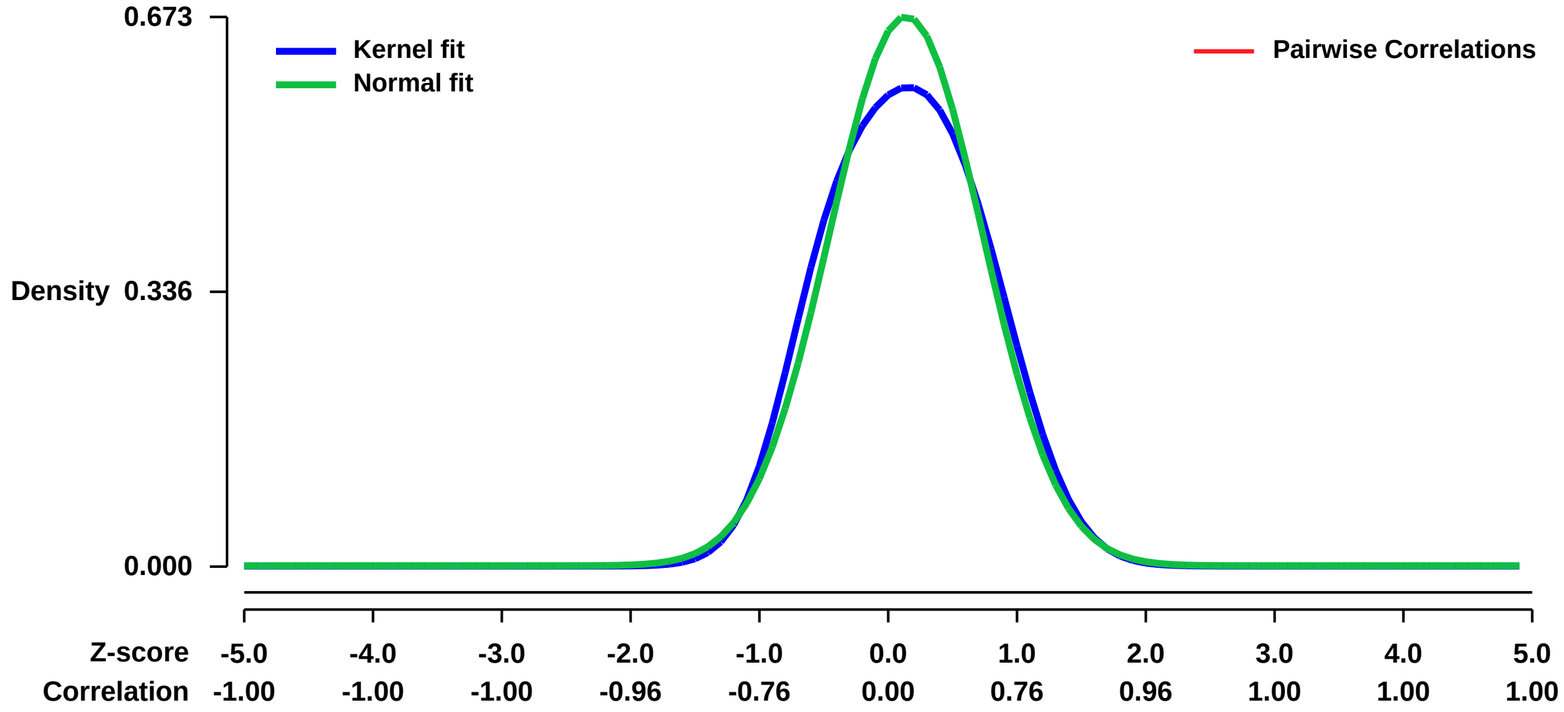

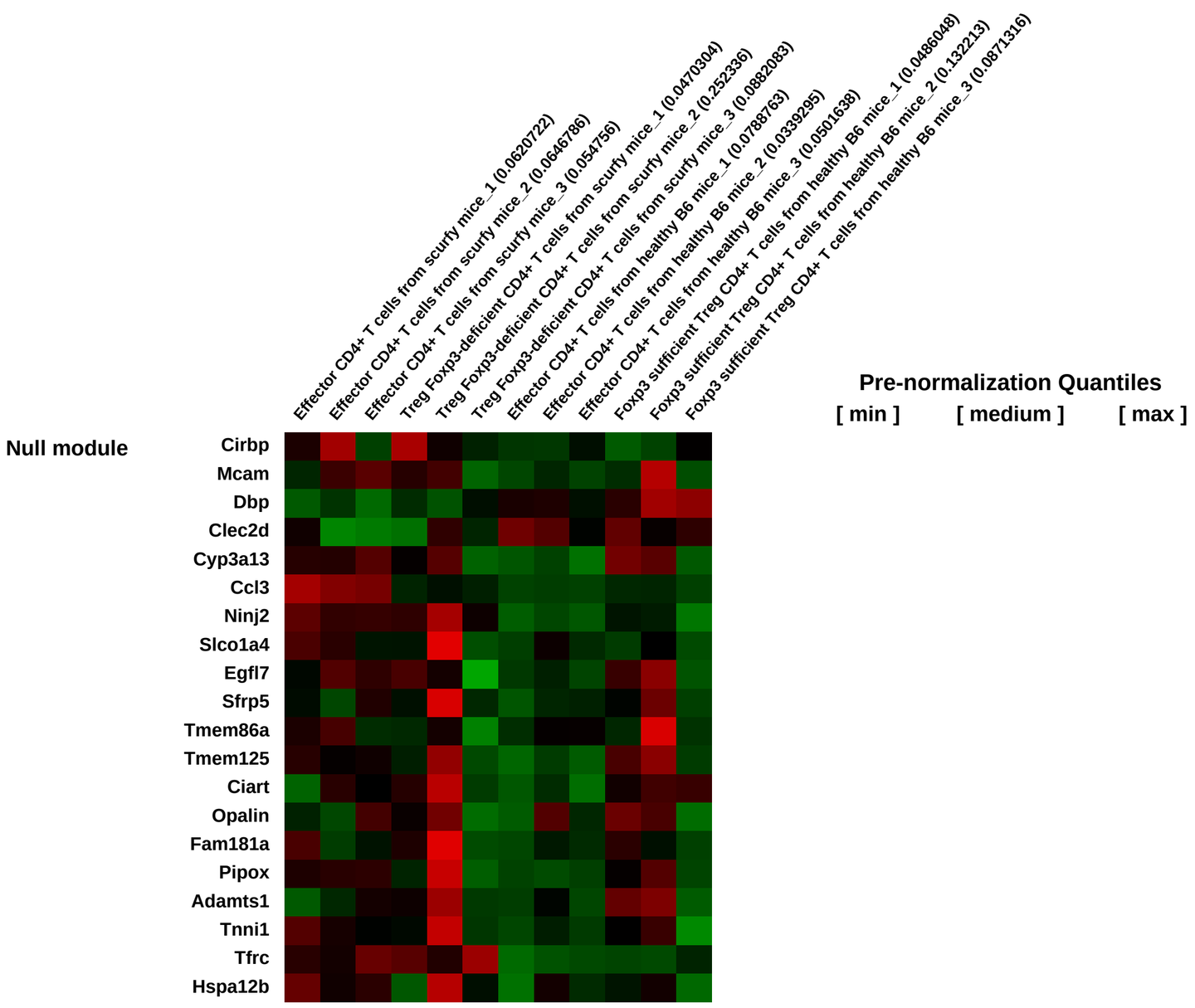

GEO Series "GSE10813" Expression Profiles

Num of samples in this series: 12

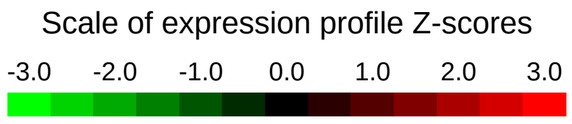

GEO Link:	http://www.ncbi.nlm.nih.gov/geo/query/acc.cgi?acc=GSE10813
Status:	Public on Feb 01 2009
Title:	The in vitro expanded CD8+ T cells and its controls
Organism:	Mus musculus
Experiment type:	Expression profiling by array
Platform:	GPL1261
Pubmed ID:	18664279
Summary & Design:	**Summary:** CD8+ NKT cells are naturally occurring but rare T cells that express both T cell and natural killer (NK) cell markers. These cells may play key roles in establishing tolerance to self antigens; however, the mechanism of action and the molecular profiles of these cells are poorly characterized due to their extremely low frequencies. We developed a highly efficient in vitro conversion/expansion protocol for such cells and extensively characterized their functional and molecular phenotypes using a variety of genomic and immunological techniques. We used microarrays to elucidate the molecular mechanisms underlying the suppression function of the converted CD8+ NKT cells. **Keywords: Cell type comparison** **Overall design:** To identify candidate genes that might be related to the suppressive activity, the CD8+ NKT cells with potent suppressive activity were compared to three different control cells: 1) CD4+ T cells (with very weak suppression) cultured under the same condition as a control for culture condition, 2) naˆflve CD8 T cells as the baseline expression level, and 3) CD8+ T cells activated using conventional activation protocols. The last two cell populations do not possess suppressive activity. This data set allows us to examine a number of different questions

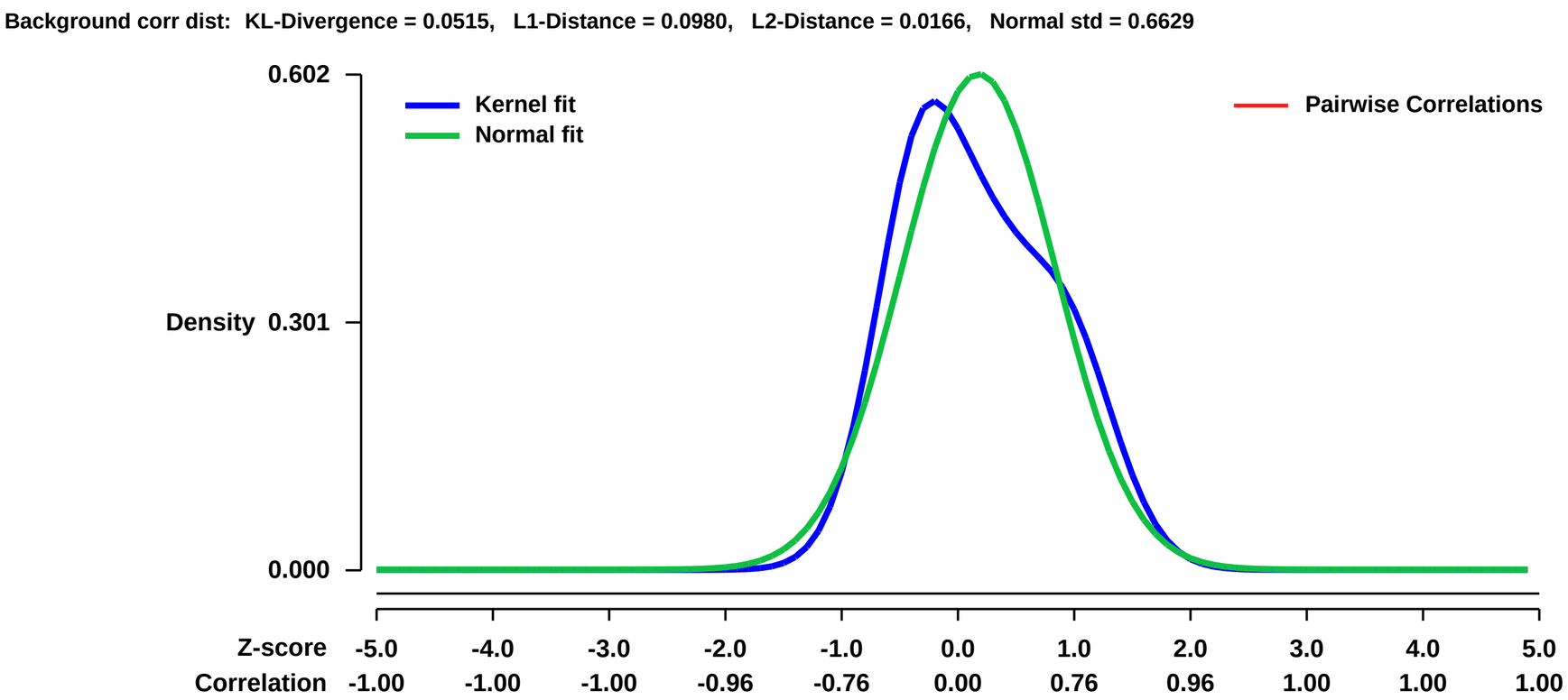

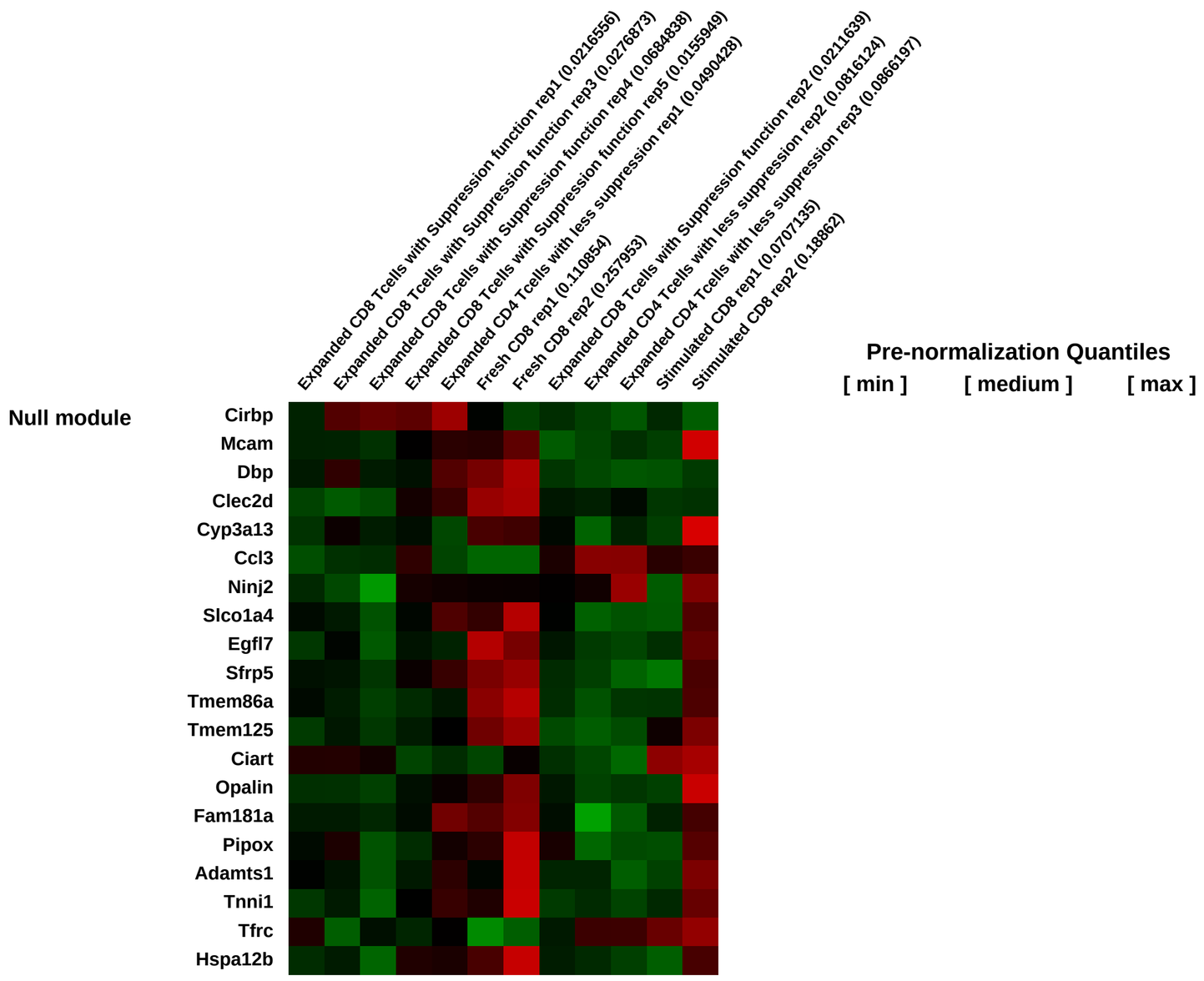

GEO Series "GSE17985" Expression Profiles

Num of samples in this series: 8

Scale of expression profile Z-scores

-3.0 -2.0 -1.0 0.0 1.0 2.0 3.0

GEO Link:	http://www.ncbi.nlm.nih.gov/geo/query/acc.cgi?acc=GSE17985
Status:	Public on Mar 05 2010
Title:	Gene expression profile of Dicer-deficient oocytes
Organism:	Mus musculus
Experiment type:	Expression profiling by array
Platform:	GPL1261
Pubmed ID:	20116252
Summary & Design:	**Summary:** Small RNAs, such as miRNAs and siRNAs, are involved in gene regulation in a variety of systems, including mouse oocytes. Dicer is a ribonuclease III enzyme essential for miRNA and siRNA biosynthesis. In an effort to uncover the function of small RNAs during oocyte growth, we specifically deleted Dicer in growing oocytes and analyzed the global pattern of gene expression in these Dicer-deficient oocytes. **Overall design:** Germinal vesicle-intact, fully grown oocytes were collected from eCG-primed wild-type or Dicer-deficient female mice and freed of attached cumulus cells by pipetting. Twenty oocytes per mouse were used for RNA extraction and hybridization on the MOE430 v2 Affymetrix microarray platform. Oocytes from four wild-type and four Dicer-knockout mice were analyzed.

Background corr dist: KL-Divergence = 0.0463, L1-Distance = 0.0174, L2-Distance = 0.0004, Normal std = 0.5715

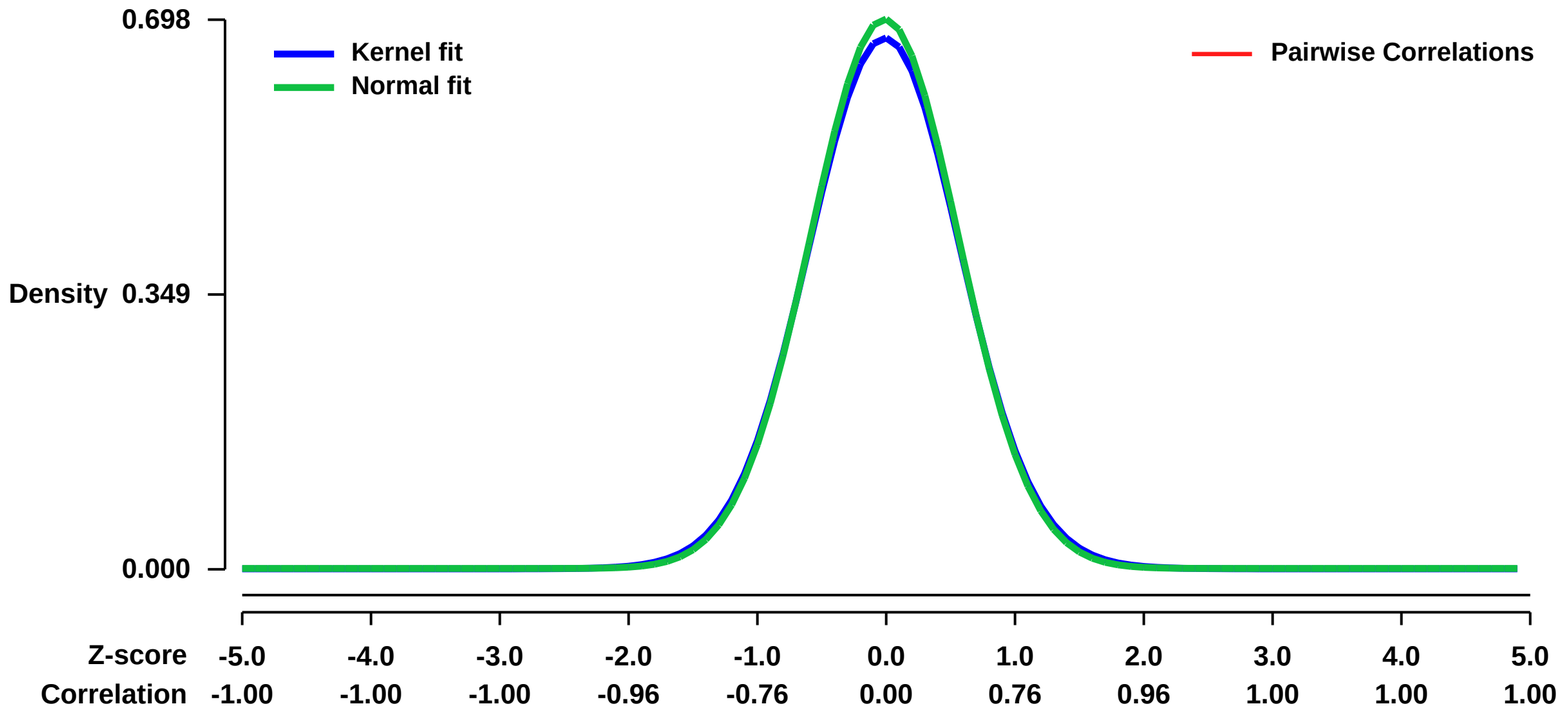

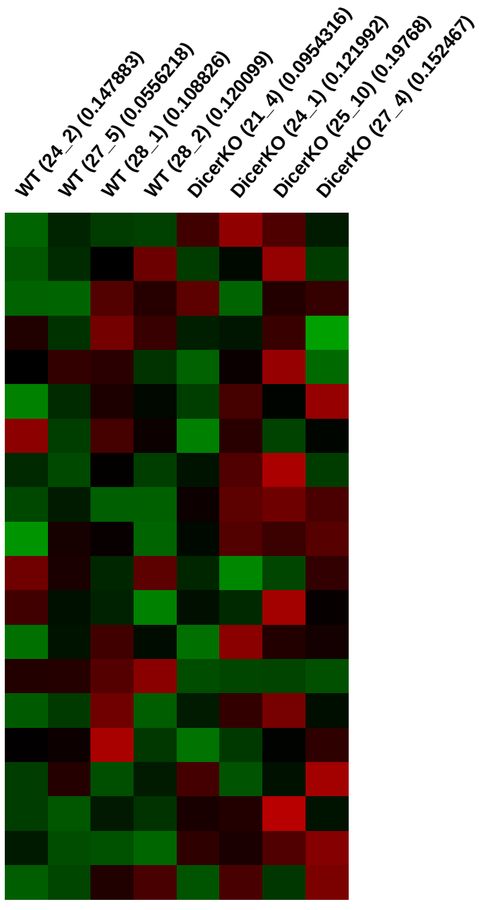

GEO Series "GSE25926" Expression Profiles

Num of samples in this series: 15

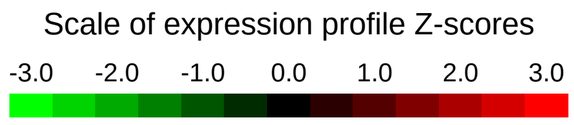

GEO Link:	http://www.ncbi.nlm.nih.gov/geo/query/acc.cgi?acc=GSE25926
Status:	Public on Mar 18 2011
Title:	Comparative transcriptome profiling of Amyloid Precursor Protein APP family members in the adult cortex
Organism:	Mus musculus
Experiment type:	Expression profiling by array
Platform:	GPL1261
Pubmed ID:	21435241
Summary & Design:	**Summary:** **The ˛†-amyloid precursor protein APP and the related APLPs, undergo complex proteolytic processing giving rise to several fragments. Whereas it is well established that A˛† accumulation is a central trigger for Alzheimer disease (AD), the physiological role of APP family members and their diverse proteolytic products is still largely unknown. The secreted APPs˛– ectodomain has been shown to be involved in neuroprotection and synaptic plasticity. The ˛‡-secretase generated APP intracellular domain AICD, functions as a transciptional regulator in heterologous reporter assays, although its role for endogenous gene regulation has remained controversial. To gain further insight into the molecular changes associated with knockout phenotypes and to elucidate the physiological functions of APP family members including their proposed role as transcriptional regulators we performed a DNA microarray transcriptome profiling of the frontal cortex of adult wild type, APP-/-, APLP2-/- and APPs˛– knockin (KI) mice, APP˛–/˛–, expressing solely the secreted APPs˛– ectodomain. Biological pathways affected by the lack of APP family members included regulation of neurogenesis, regulation of transcription and regulation of neuron projection development. Comparative analysis of transcriptome changes and qPCR validation identified co-regulated gene sets. Interestingly, these included heat shock proteins and plasticity related genes that were down-regulated in knock-out cortices. In contrast, we failed to detect significant differences in expression of previously proposed AICD target genes including Bace1, Kai1, Gsk3b, p53, Tip60 and Vglut2. Only Egfr was slightly up-regulated in APLP2-/- mice. Comparison of APP-/- and APP˛–/˛– with wild-type mice revealed a high proportion of co-regulated genes indicating an important role of the C-terminus for cellular signaling. Finally, comparison of APLP2-/- on different genetic backgrounds revealed that background related transcriptome changes may dominate over changes due to the knockout of a single gene. Shared transcriptome profiles corroborated closely related physiological functions of APP family members in the adult central nervous system. As expression of proposed AICD target genes was not altered in adult cortex, this may indicate that these genes are not affected by lack of APP under resting conditions or only in a small subset of cells.** **Overall design:** **Prefrontal cortices of adult male mice (24 - 28 weeks) of the following genotypes were analyzed: WT (n=3), APP-/- (n=3), APP˛–/˛– (n=3), APLP2-/- (n=3), APLP2(R1)-/- (n=3). WT, APP-/-, APP˛–/˛–, APLP2-/- had been backcrossed for six generations to C57BL/6 mice. APLP2(R1)-/- harbors the identical knockout allele as APLP2-/- but was back-crossed only once.**

Background corr dist: KL-Divergence = 0.1865, L1-Distance = 0.0462, L2-Distance = 0.0047, Normal std = 0.3406

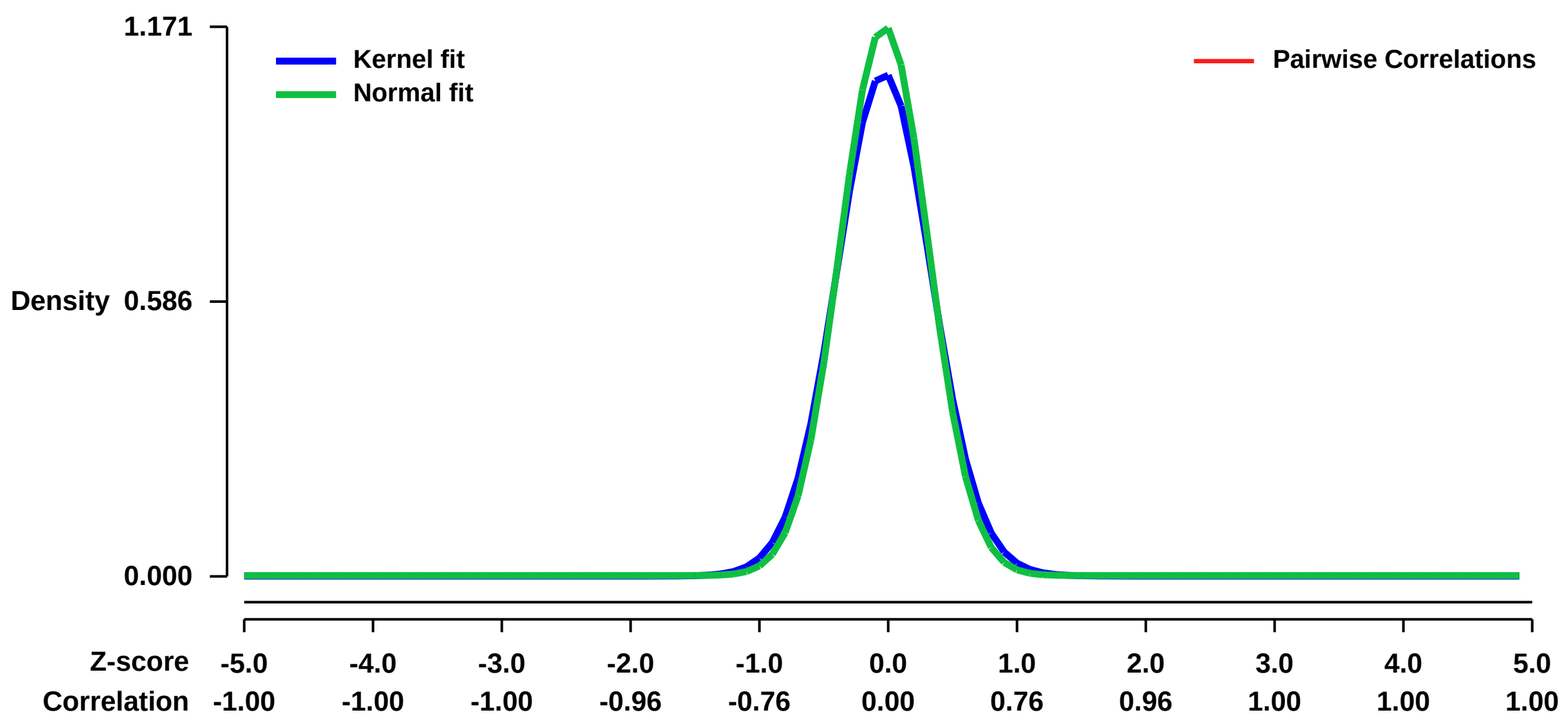

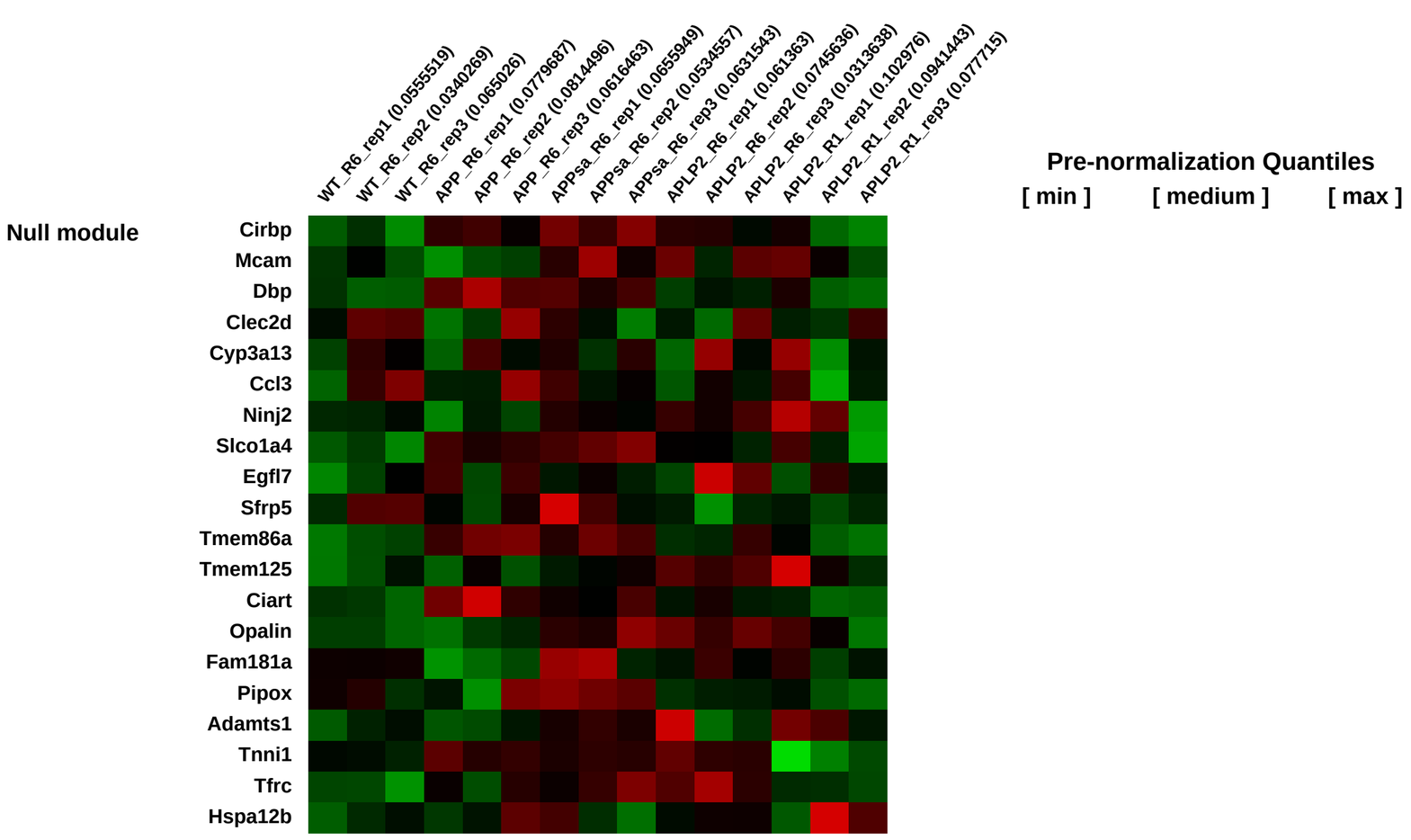

GEO Series "GSE43373" Expression Profiles

Num of samples in this series: 130

Details of this dataset are not shown due to large number of samples and the page size limit.

Find details in http://www.ncbi.nlm.nih.gov/geo/query/acc.cgi?acc=GSE43373

Background corr dist: KL-Divergence = 0.1128, L1-Distance = 0.0557, L2-Distance = 0.0090, Normal std = 0.4228

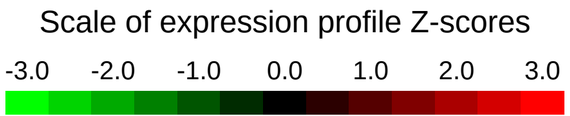

GEO Series "GSE52075" Expression Profiles

Num of samples in this series: 9

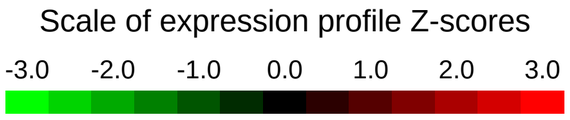

GEO Link:	http://www.ncbi.nlm.nih.gov/geo/query/acc.cgi?acc=GSE52075
Status:	Public on Nov 11 2013
Title:	Expression data of the endothelial-to-hematopoietic transition in E8.5 concepti
Organism:	Mus musculus
Experiment type:	Expression profiling by array
Platform:	GPL1261
Pubmed ID:	24326267
Summary & Design:	**Summary:** During development a specialised subset of endothelial cells, the haemogenic endothelium, undergo an endothelial-to-haematopoietic transition. This process critically involves the transcription factor Runx1. Here we have isolated a specific subpopulation of endothelial cells using a Runx1 enhancer-reporter transgenic mouse line (23GFP). We have compared the gene expression profile of this population to non-23GFP expressing endothelial cells and CD41 expressing haematopoietic progenitor cells to assess whether 23GFP expression marks a biologically distinct subset of endothelium. We used affymetrix microarrays to detail the global programme of gene expression underlying the different populations and identified a distinct expression profile of the 23GFP expressing endothelium. **Overall design:** 23GFP transgenic mouse embryos were dissected free of the ectoplacental cone at embryonic day E8.5, pooled, and sorted into 23GFP- and 23GFP+ endothelial (VE-Cad+ Ter119- CD45- CD41-) and CD41+ haematopoietic cells (VE-Cad+ Ter119-CD45-CD41+23GFP+) cells by FACS. Triplicate samples for each cell population were analysed. cDNA synthesis, fragmentation, and hybridisation were performed by the Stanford Protein and Nucleic Acid Facility.

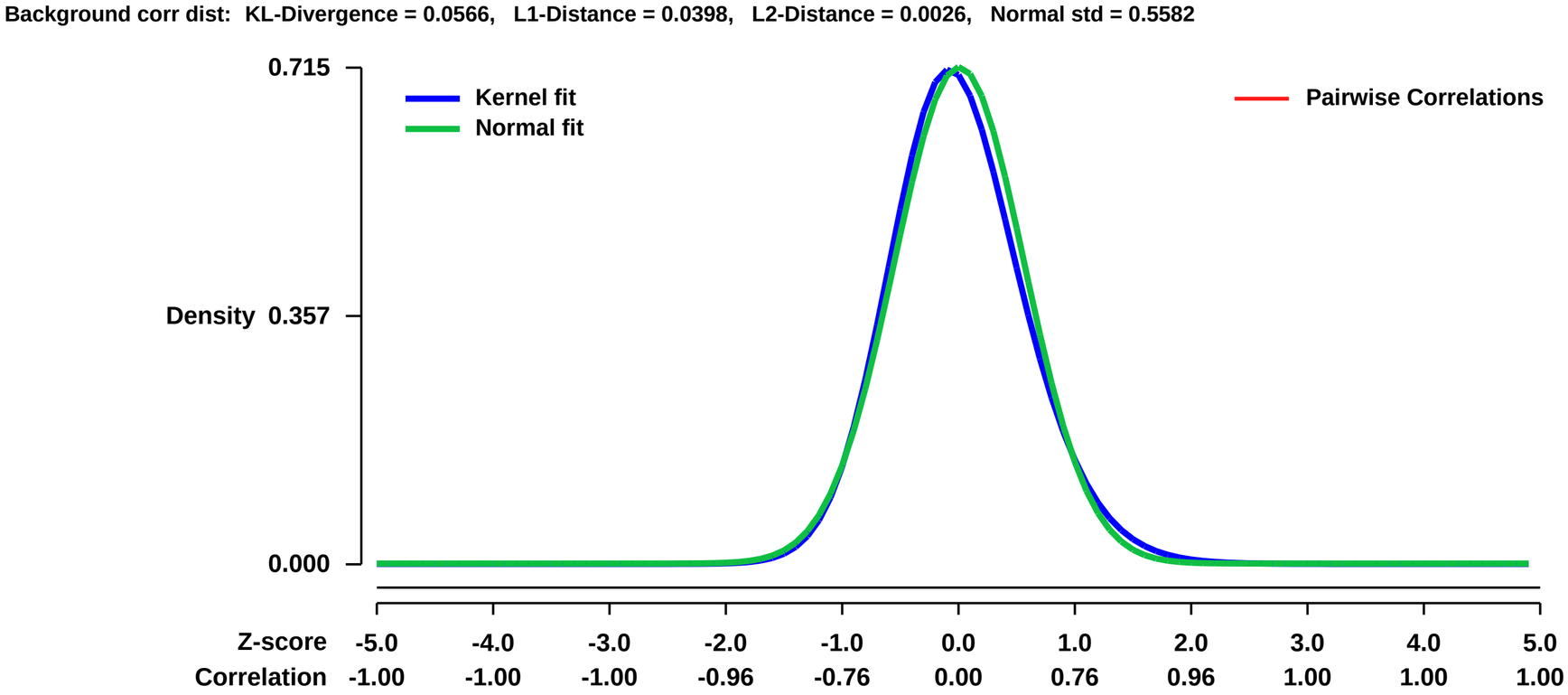

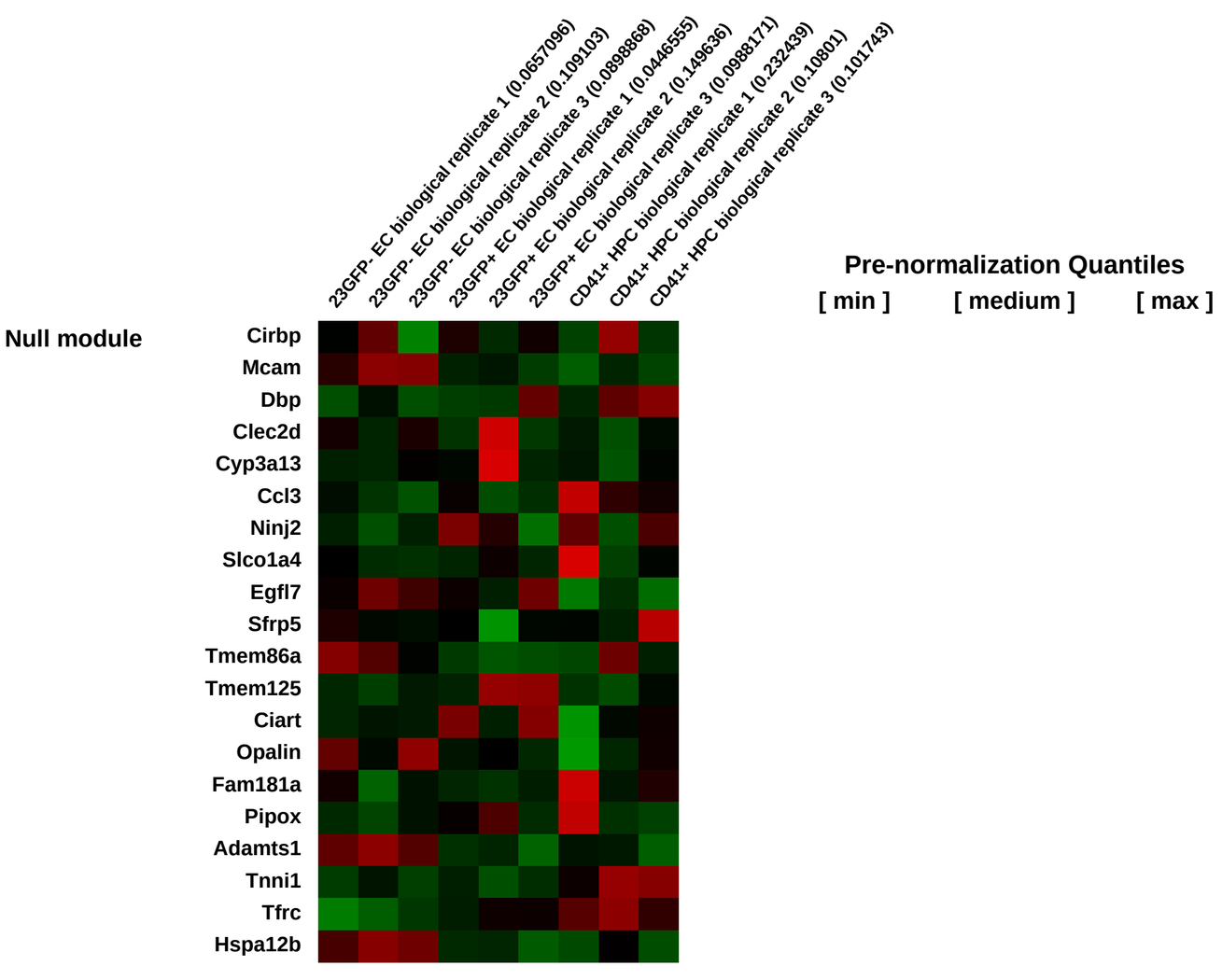

GEO Series "GSE24451" Expression Profiles

Num of samples in this series: 6

Scale of expression profile Z-scores

-3.0 -2.0 -1.0 0.0 1.0 2.0 3.0

GEO Link:	http://www.ncbi.nlm.nih.gov/geo/query/acc.cgi?acc=GSE24451
Status:	Public on Nov 26 2010
Title:	Knockout of the Acyl CoA binding protein (ACBP) in mice - expression profile from the liver of 21 days old ACBP-/- and +/+ mice.
Organism:	Mus musculus
Experiment type:	Expression profiling by array
Platform:	GPL1261
Pubmed ID:	21106527
Summary & Design:	**Summary:** The ACBP knockout were created by targeted disruption of the gene in mice. The expression profiling was performed on liver tissue from ACBP-/- (KO) and +/+ (WT) mice at the age of 21 days, which in our study is the time immediately before weaning. The mice used for this experiment were taken directly away from their mother. Thus, having free access to chow and breast milk until sacrificed at 8-11am **Overall design:** 15 ACBP-/- and 15 +/+ control mice divided into 6 groups (KO1, KO2, KO3, WT1, WT2 and WT3) with 5 individuals in each group were used for this study.

Background corr dist: KL-Divergence = 0.0405, L1-Distance = 0.0171, L2-Distance = 0.0003, Normal std = 0.6111

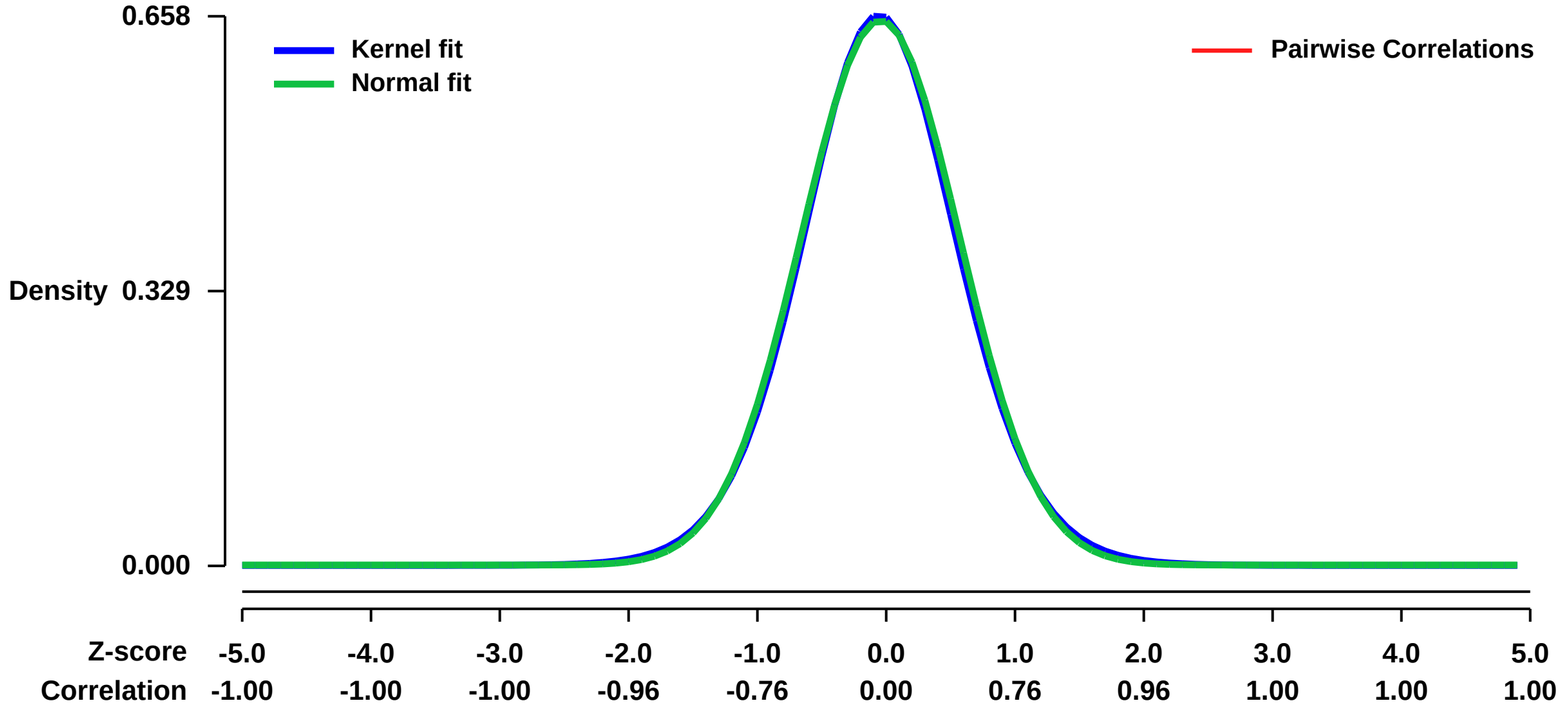

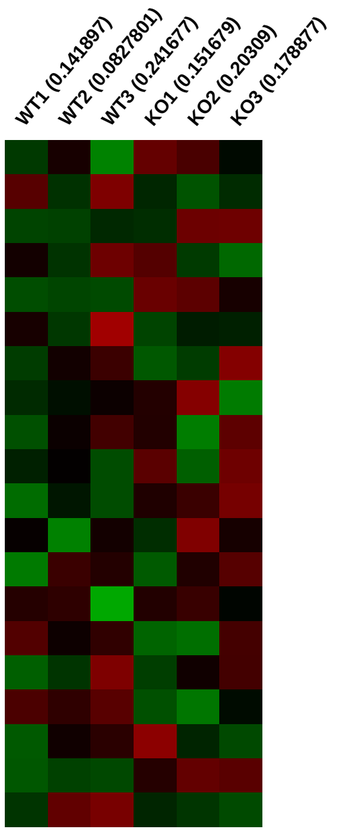

GEO Series "GSE24295" Expression Profiles

Num of samples in this series: 7

Scale of expression profile Z-scores

-3.0 -2.0 -1.0 0.0 1.0 2.0 3.0

GEO Link:	http://www.ncbi.nlm.nih.gov/geo/query/acc.cgi?acc=GSE24295
Status:	Public on Sep 23 2010
Title:	Gene expression in epithelial and non-epithelial cells of renal origin
Organism:	Mus musculus
Experiment type:	Expression profiling by array
Platform:	GPL1261
Pubmed ID:	20978075
Summary & Design:	**Summary:** We aimed to define epithelial-specific genes in the kidney. In the developing mouse kidney at E12.5 epithelial cells are restricted to the ureteric bud, while mesenchymal cells surrounding the ureteric bud are non-epithelial. The mouse renal epithelial cell line mIMCD-3 was used to represent kidney epithelia in vitro. Gene expression was analyzed using Affymetrix microarrays in ureteric bud stalks, ureteric bud tips, and mIMCD-3 cells and compared to metanephric mesenchyme. **Overall design:** Affymetrix Mouse Genome 430 2.0 microarrays from mouse E12.5 ureteric bud tips, ureteric bus stalks, and metanephric mesenchymes had previously been published (GEO deposition: GDS1583) (Schmidt-Ott, K. M., Yang, J., Chen, X., Wang, H., Paragas, N., Mori, K., Li, J. Y., Lu, B., Costantini, F., Schiffer, M. et al. (2005). Novel regulators of kidney development from the tips of the ureteric bud. J Am Soc Nephrol 16, 1993-2002.). We added a new microarray analysis from a subclone of mIMCD-3 cells and recalculated expression values in the complete dataset by robust multichip analysis.

Background corr dist: KL-Divergence = 0.0216, L1-Distance = 0.0311, L2-Distance = 0.0012, Normal std = 0.7597

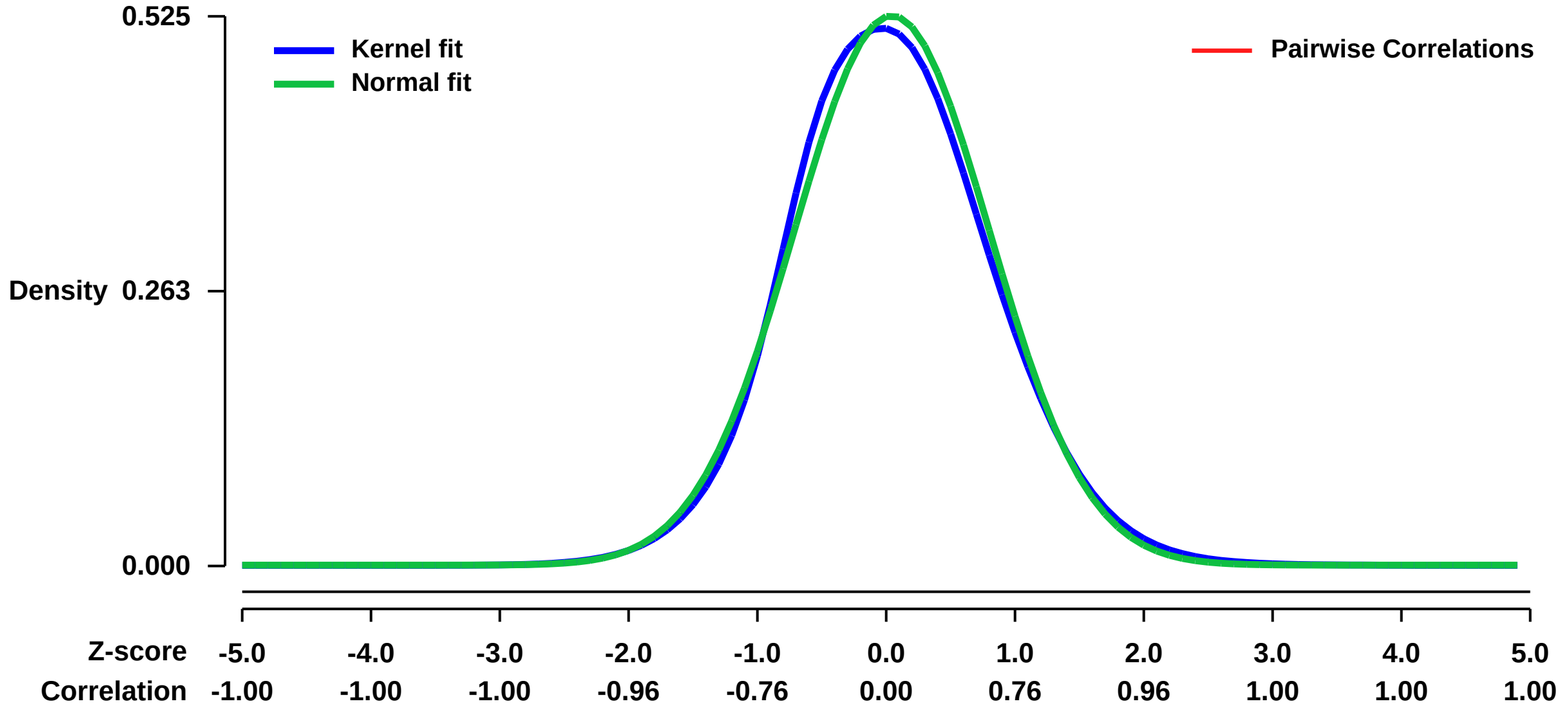

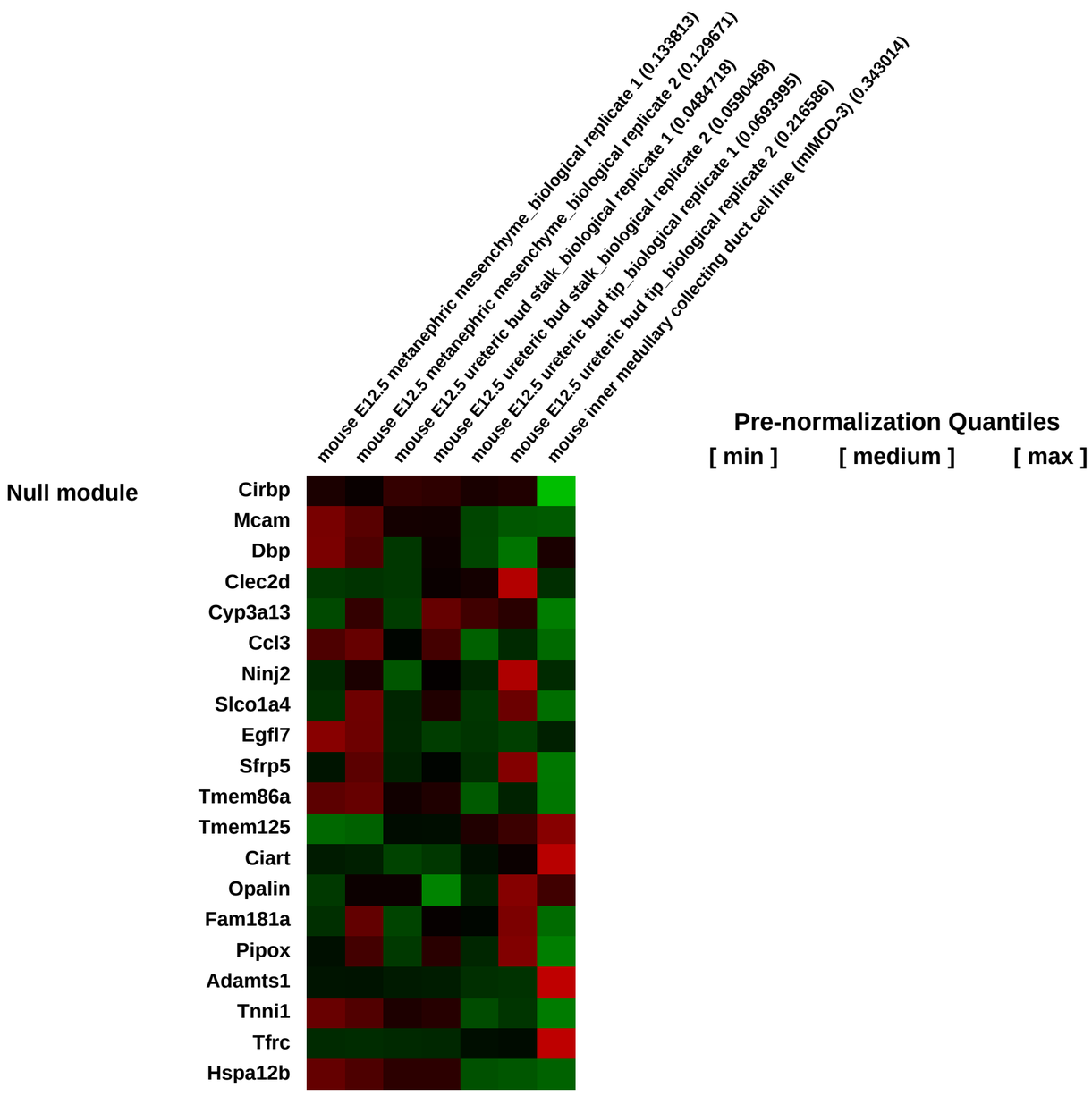

GEO Series "GSE48811" Expression Profiles

Num of samples in this series: 20

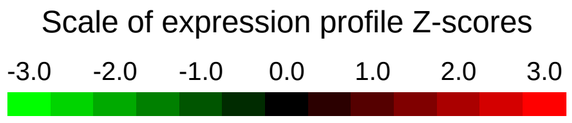

GEO Link:	**http://www.ncbi.nlm.nih.gov/geo/query/acc.cgi?acc=GSE48811**
Status:	**Public on Dec 31 2013**
Title:	**Visceral obesity in murine pregnancy**
Organism:	**Mus musculus**
Experiment type:	**Expression profiling by array**
Platform:	**GPL1261**
Pubmed ID:	
Summary & Design:	**Summary:** **Maternal obesity is linked with increased adverse outcomes for mother and fetus. However, the metabolic impact of excessive fat accumulation within the altered hormonal context of pregnancy is not well understood. We used a murine model of obesity, the high fat diet-fed C57BL/6J mouse to determine adipose tissue-mediated molecular mechanisms driving metabolic dysfunction throughout pregnancy. Remarkably, obese mice exhibited a normalization of visceral fat accumulation at late-stage pregnancy (-53%, P<0.001 E18.5) to achieve levels comparable in mass (per gram of body weight) to that of non pregnant, control diet fed mice. Moreover, whilst obese pregnant mice showed a marked glucose intolerance and apparent insulin resistance at mid-stage pregnancy (E14.5), glucose homeostasis converged with that of lean pregnant mice at late-stage pregnancy, suggesting an unexpected amelioration of the worsening metabolic dysfunction in obese pregnant mice.** **Transcriptomic analysis of the late-stage visceral fat indicated reduced de novo lipogenic drive (Me1, Fasn, Scd1, Dgat2), retinol metabolism (Rdh11, Rbp4) and inflammation (Mcp1, Tnf$_{\epsilon}$–) in obese pregnant mice that was confirmed functionally by their lower adipose proinflammatory macrophage density. Elevated expression of estrogen receptor a (ER$_{\epsilon}$–) in visceral adipose tissue was identified as potential unifying mechanism for the transcriptional changes and reduced adiposity of late stage obese pregnancy. Support for a role for ER$_{\epsilon}$– was provided by experiments showing that the ER$_{\epsilon}$– selective agonist PPT suppressed lipogenesis in primary mouse adipocytes and suppressed Me1, Fasn, SCD1 and Dgat2 mRNA levels in mature female human ChubS7 clonal fat cells. Our data reveal a novel role for elevated visceral adipocyte estrogen signaling as a protective mechanism against visceral fat hypertrophy and inflammation in late pregnancy.** **Overall design:** **Pregnant high fat, pregnant control fat, non pregnant high fat, non pregnant control fat. Five biologial replictes each (20 samples).**

Background corr dist: KL-Divergence = 0.0815, L1-Distance = 0.0212, L2-Distance = 0.0006, Normal std = 0.4777

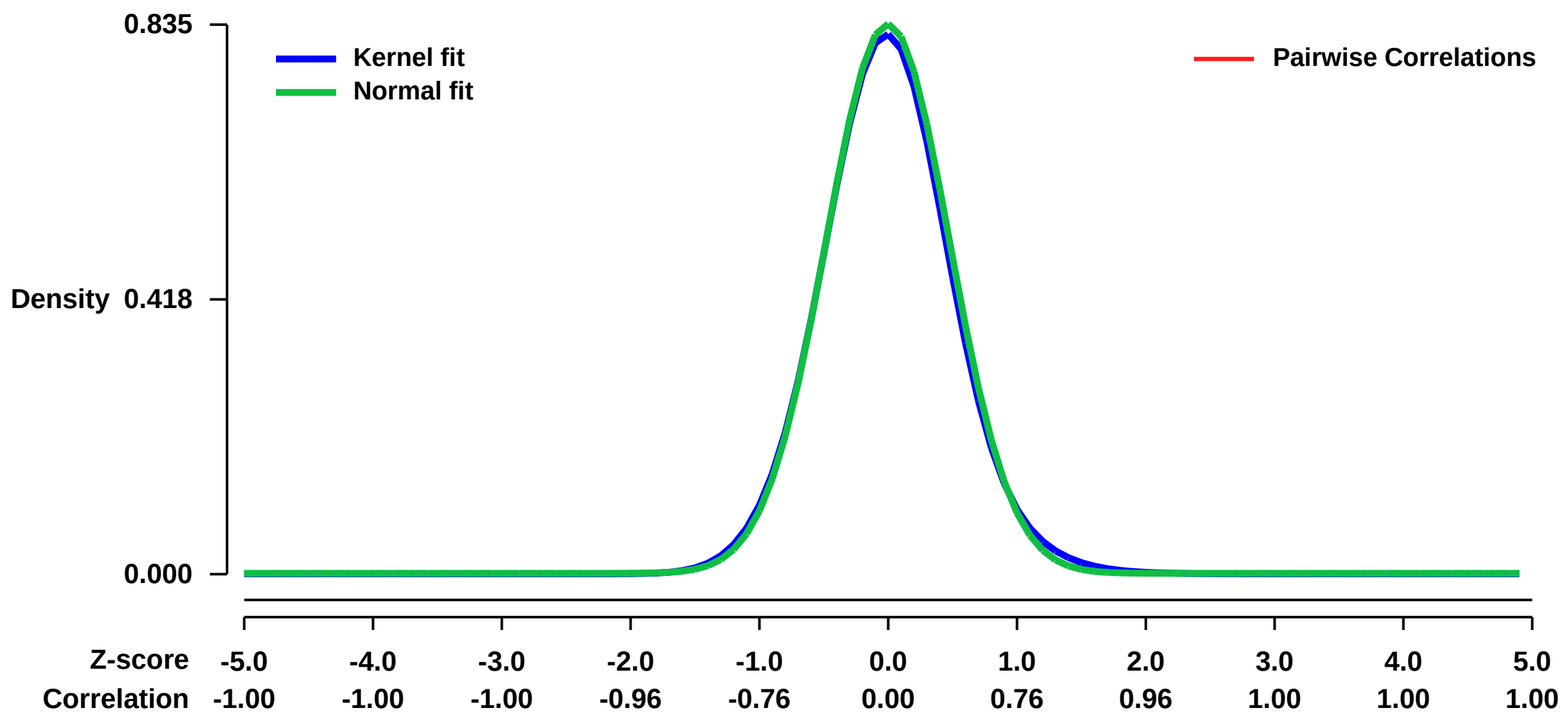

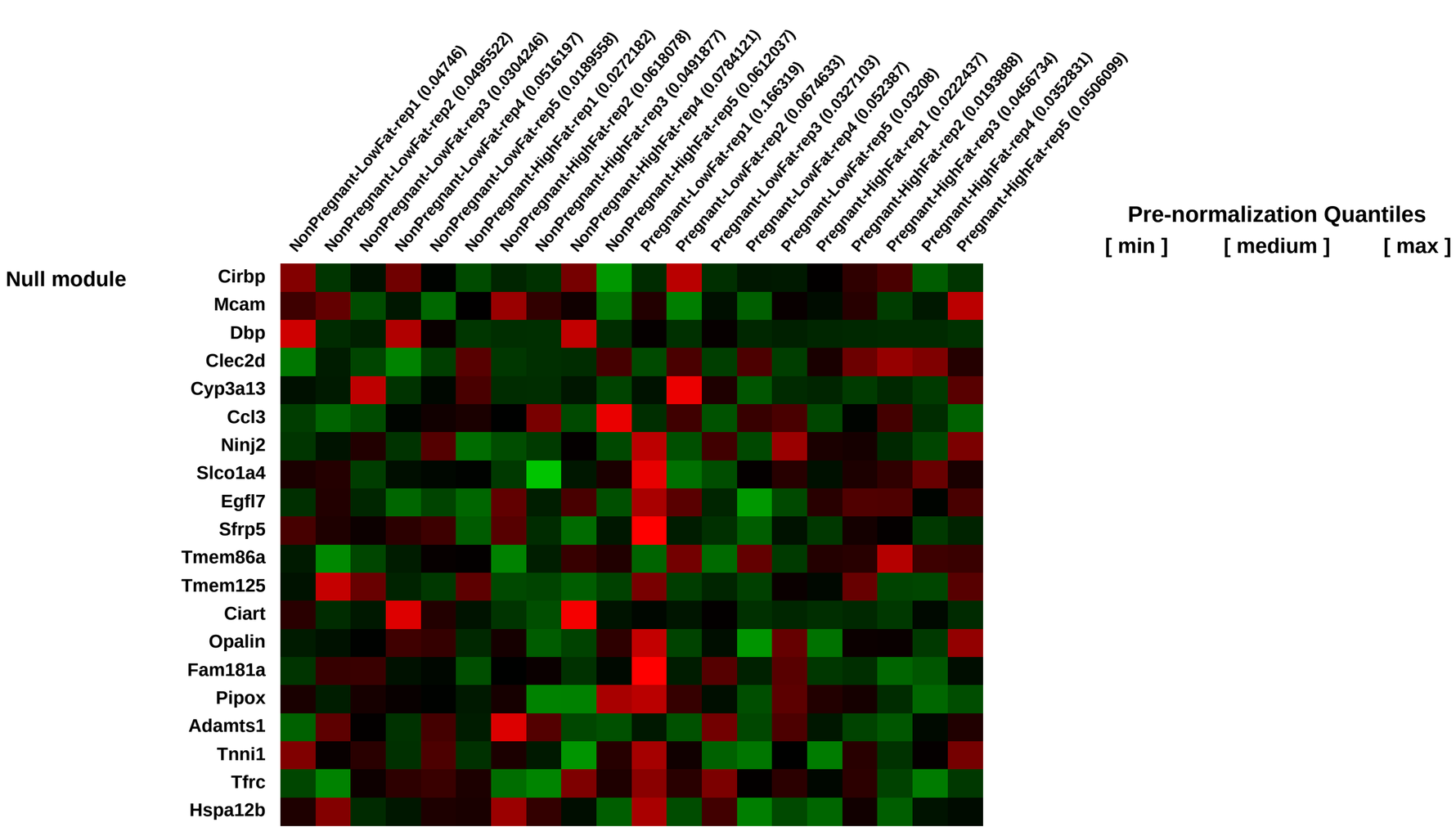

GEO Series "GSE37563" Expression Profiles

Num of samples in this series: 6

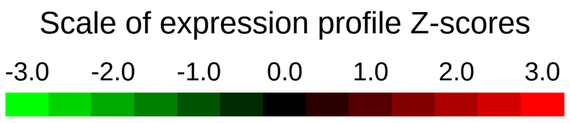

GEO Link:	http://www.ncbi.nlm.nih.gov/geo/query/acc.cgi?acc=GSE37563
Status:	Public on Sep 05 2012
Title:	In vivo gene expression data from wild type and CTLA-4 KO 5C.C7 T cells
Organism:	Mus musculus
Experiment type:	Expression profiling by array
Platform:	GPL1261
Pubmed ID:	22753941
Summary & Design:	**Summary:** CTLA-4 is thought to inhibit effector T cells both intrinsically, by competing with CD28 for B7 ligands, and extrinsically, through the action of regulatory T cells. We studied in vivo responses of normal and CTLA-4-deficient antigen-specific murine effector CD4+ T cells. In order to do these studies in a physiological model of immunity to foreign antigen, we transferred small numbers of congenically marked RAG2-deficient 5C.C7 T cells with either a normal or knockout allele of CTLA-4 into normal syngeneic B10.A recipient mice. The T cells were then activated by immunization with MCC peptide and LPS. To look for transcriptional signatures of negative regulation of T cell responses by CTLA-4, we used microarray analysis to compare transcripts in wild type and CTLA-4 KO 5C.C7 T cells four days after immunization. This is the first instance in which differences are observed in extent of accumulation of wild type and CTLA-4 KO 5C.C7 T cells. #!# **Overall design:** To compare the gene expression profile between wild type and CTLA-4 KO adoptively transferred T cells 4 days after immunization.

Background corr dist: KL-Divergence = 0.0451, L1-Distance = 0.0197, L2-Distance = 0.0004, Normal std = 0.5927

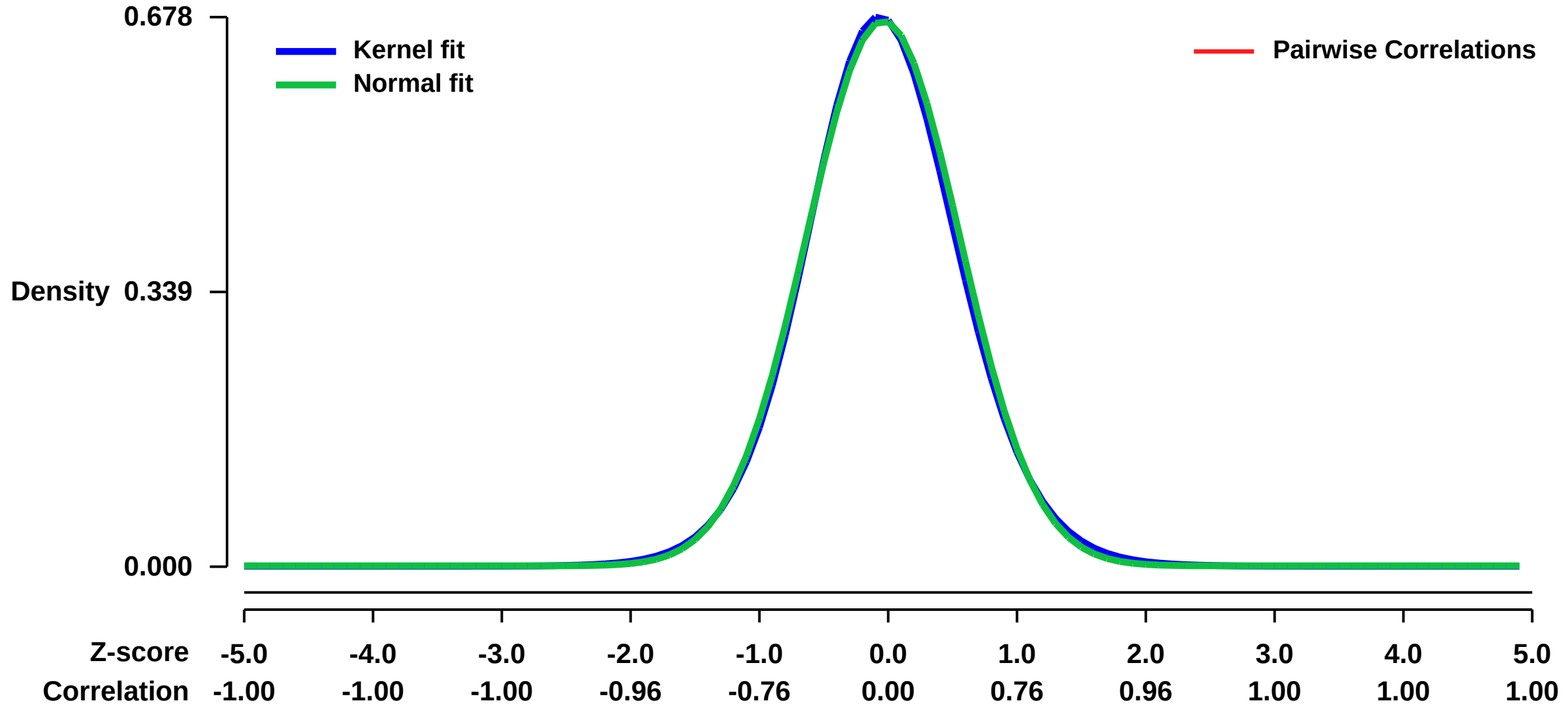

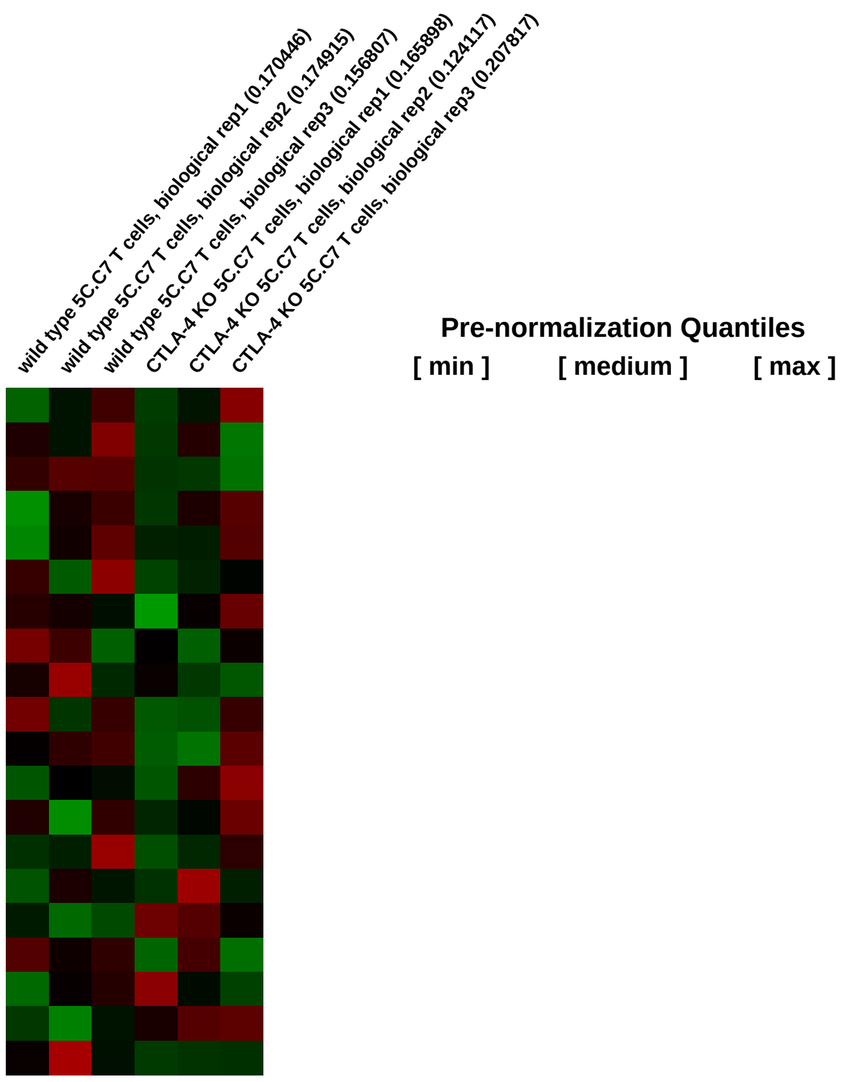

GEO Series "GSE35299" Expression Profiles

Num of samples in this series: 8

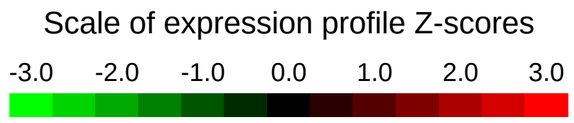

GEO Link:	**http://www.ncbi.nlm.nih.gov/geo/query/acc.cgi?acc=GSE35299**
Status:	**Public on Jan 01 2013**
Title:	**Implantation Failure of Blastocysts Derived from Oocyte-directed Connexin 43 depleted Mice is Associated with Impaired Ribosomal and Translational Machinery Gene Exp**
Organism:	**Mus musculus**
Experiment type:	**Expression profiling by array**
Platform:	**GPL1261**
Pubmed ID:	
Summary & Design:	**Summary:** **Oocyte quality is a well- established determinant of embryonic fate. However, the molecular participants and biological markers that affect and predict adequate embryonic development are largely elusive. We have previously reported that oocyte- directed Connexin 43 (Cx43) depletion leads to embryo implantation defects, although both the morphology of the oocyte and processes presiding embryo implantation appear to undergo normally. In the context of previous data determining Cx43 indispensability to oocyte and embryonic development, we show here that the timing of Cx43 depletion from the oocyte and the ovarian follicle is crucial in determining the severity of subsequent embryonic defects. Specifically, we show that the implantation defects of blastocysts resulting from oocyte- directed Cx43-depleted follicles (depletion occurs at day 3 postnatal), is not due to maternal luteal insufficiency but rather depends solely on the defective blastocysts. Gene expression microarray analysis revealed global defects in the expression of ribosomal proteins, translation initiation factors and other genes associated with cellular biosynthetic and metabolic processes in these defective oocytes and specifically blastocysts. We therefore propose that timely expression of Cx43 in the oocyte and ovarian follicles is a major determinant of oocyte developmental competence, by determining the ability of the resulting blastocyst to facilitate biomass expansion and undergo adequate embryo implantation** **Overall design:** **To study the effect of CX43 on the transcriptom of the pre implantation stages, we compared CX43 KO oocytes to the WT oocytes in three different stages of the very early development. First comparison MII oocytes, second comparison blastocysts, third comparison implantation site.**

Background corr dist: KL-Divergence = 0.0632, L1-Distance = 0.0559, L2-Distance = 0.0053, Normal std = 0.5652

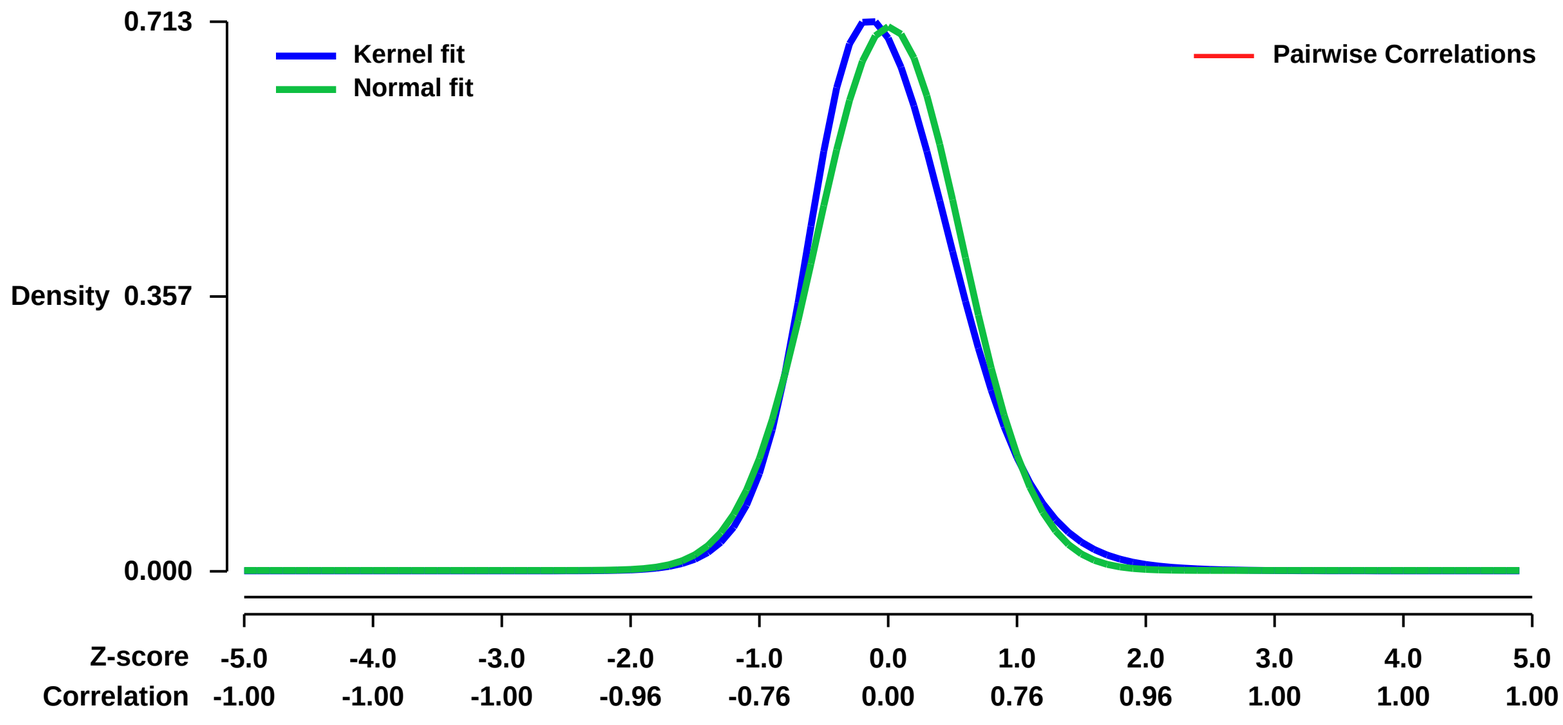

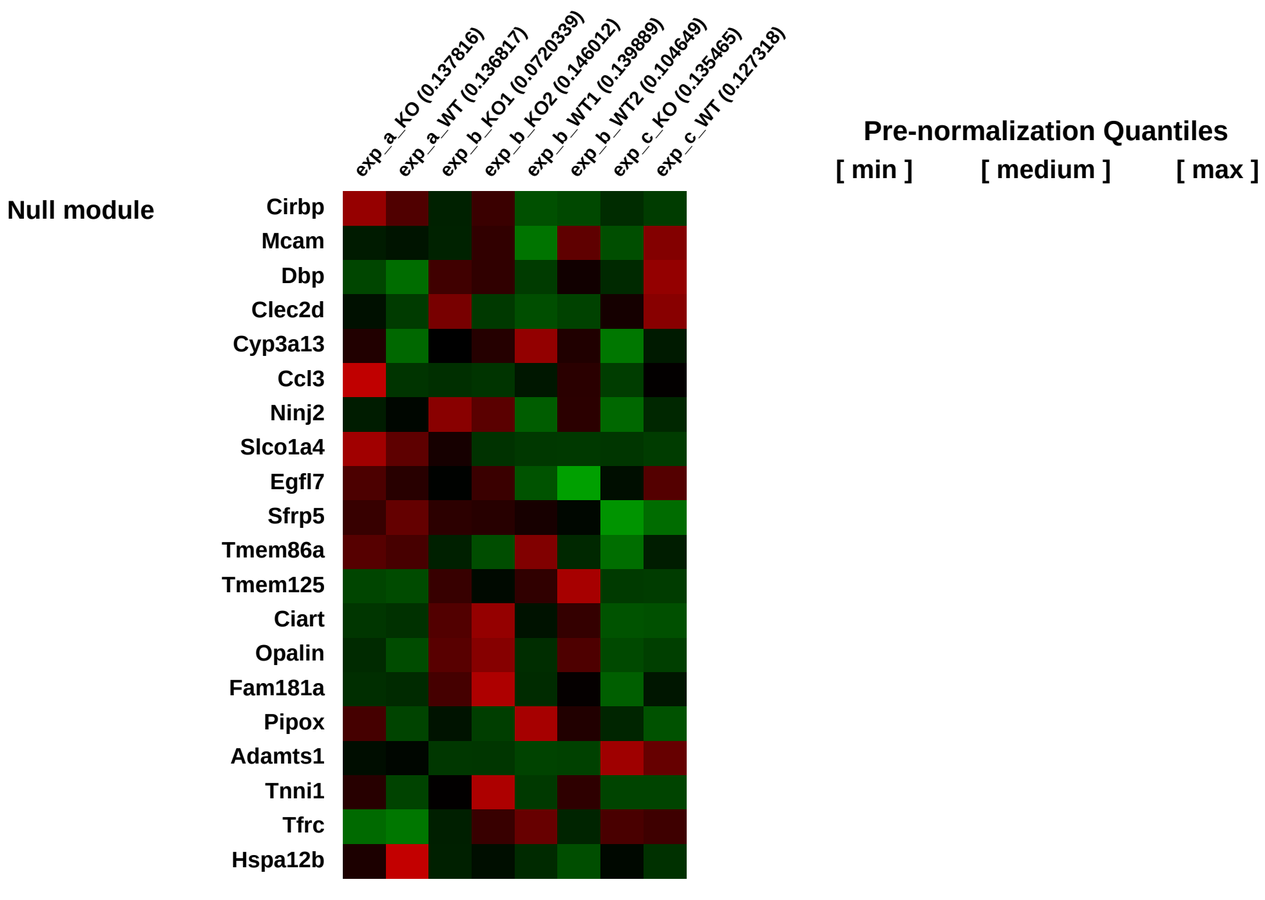

GEO Series "GSE6882" Expression Profiles

Num of samples in this series: 10

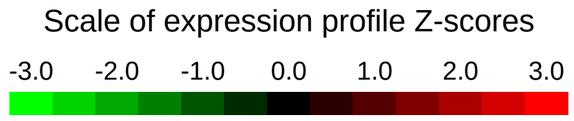

GEO Link:	http://www.ncbi.nlm.nih.gov/geo/query/acc.cgi?acc=GSE6882
Status:	Public on Feb 05 2007
Title:	Embryonic Ovary Developmental Time Course
Organism:	Mus musculus
Experiment type:	Expression profiling by array
Platform:	GPL1261
Pubmed ID:	15496517
Summary & Design:	**Summary:** Time course of gene expression in the murine embryonic ovary from the time of the indifferent gonad (11.5dpc) to birth (18.5dpc) **Keywords: Time course** **Overall design:** Independent embryonic ovary preps were used for array analysis. Duplicates were provided for each sample.

Background corr dist: KL-Divergence = 0.0405, L1-Distance = 0.0692, L2-Distance = 0.0059, Normal std = 0.7288

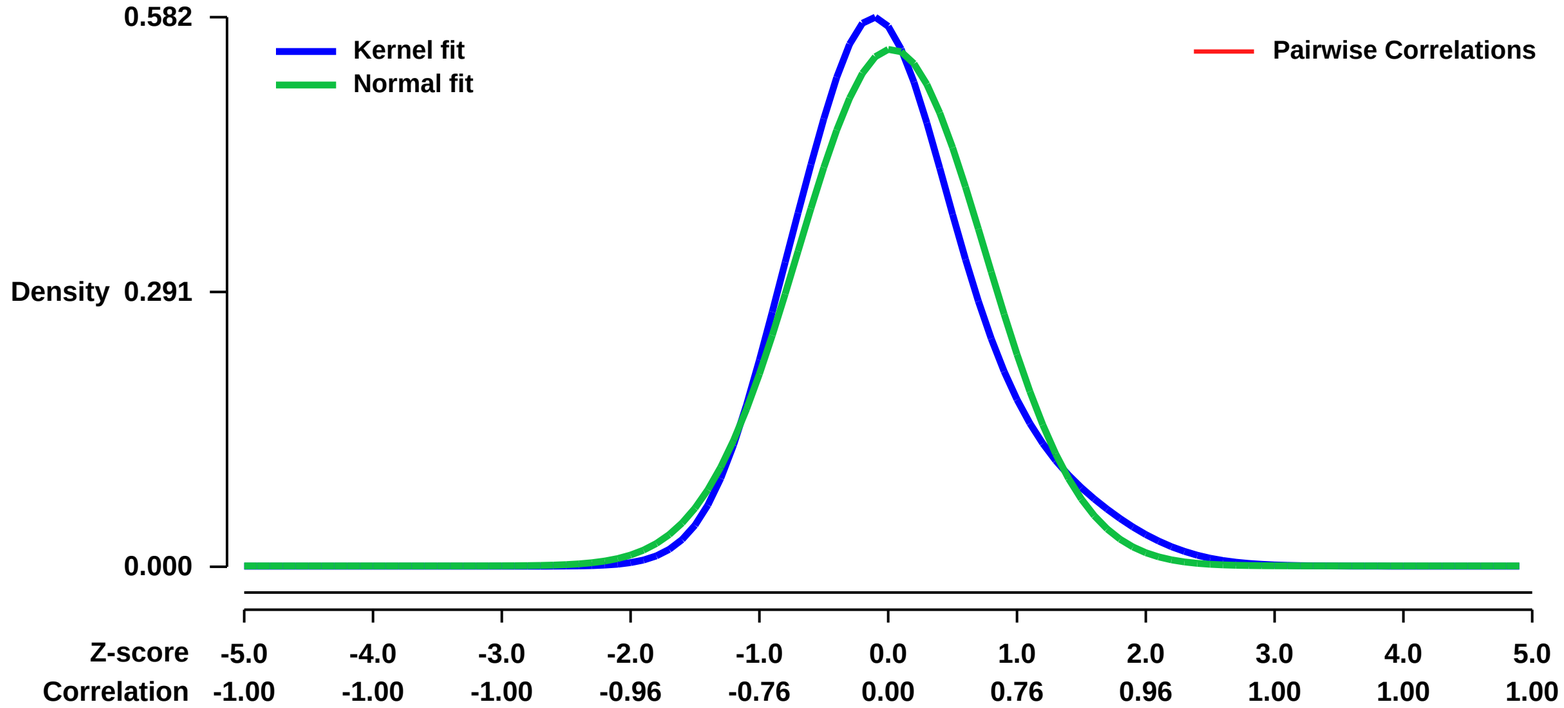

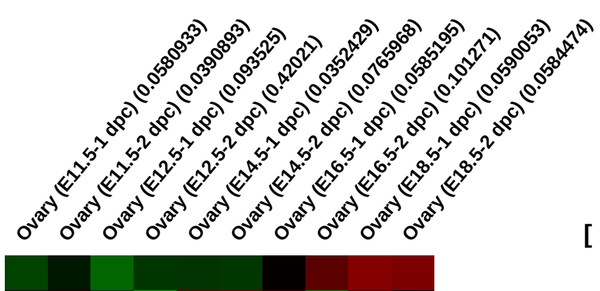

Pre-normalization Quantiles

[min] [medium] [max]

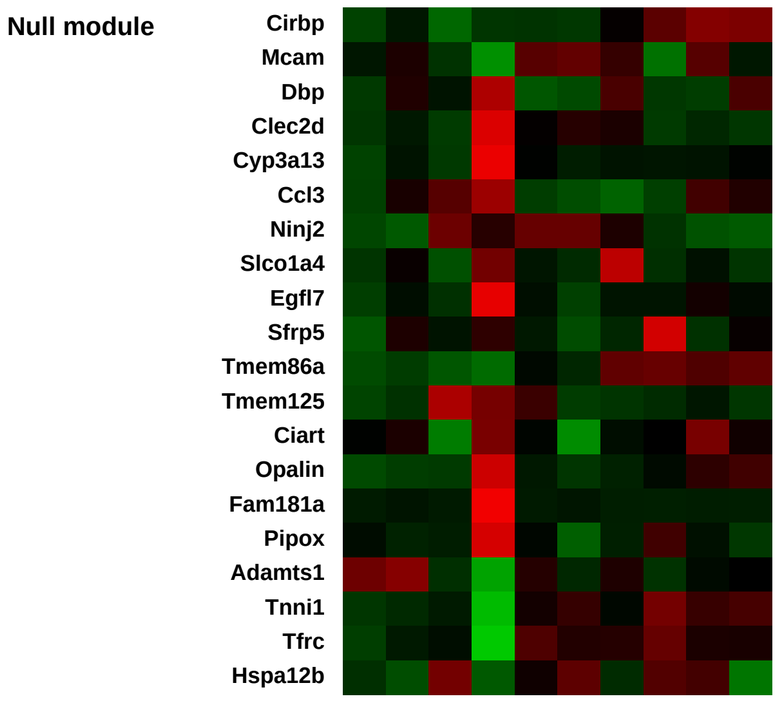

GEO Series "GSE33031" Expression Profiles

Num of samples in this series: 6

Scale of expression profile Z-scores

-3.0 -2.0 -1.0 0.0 1.0 2.0 3.0

GEO Link:	http://www.ncbi.nlm.nih.gov/geo/query/acc.cgi?acc=GSE33031
Status:	Public on Dec 01 2011
Title:	PU.1 restricts adult hematopoietic stem cell proliferation via cell specific autoregulation
Organism:	Mus musculus
Experiment type:	Expression profiling by array
Platform:	GPL1261
Pubmed ID:	23395001
Summary & Design:	**Summary:** To guarantee blood supply throughout adult life hematopoietic stem cells (HSCs) need to carefully balance between self-renewing cell divisions and quiescence. Identification of genes controlling HSC self-renewal is of utmost importance given that HSCs are the only stem cells with broad clinical applications. Transcription factor PU.1 is one of the major regulators of myeloid and lymphoid development. Recent reports suggest that PU.1 mediates its functions via gradual expression level changes rather than binary on/off states. So far, this has not been considered in any study of HSCs and thus, PU.1â s role in HSC function has remained largely unclear. Here we demonstrate using hypomorphic mice with an engineered disruption of an autoregulatory feedback loop that decreased PU.1 levels resulted in loss of key HSC functions, all of which could be fully rescued by restoration of proper PU.1 levels via a human PU.1 transgene. Mechanistically, we found excessive HSC cell divisions and altered expression of cell cycle regulators whose promoter regions were bound by PU.1 in normal HSCs. Adequate PU.1 levels were maintained by a mechanism of direct autoregulation restricted to HSCs through a physical interaction of a -14kb enhancer with the proximal promoter. Our findings identify PU.1 as novel regulator controling the switch between cell division and quiescence in order to prevent exhaustion of HSCs. Given that even moderate level changes greatly impact stem cell function, our data suggest important therapeutic implications for leukemic patients with reduced PU.1 levels. Moreover, we provide first proof, that autoregulation of a transcription factor, PU.1, has a crucial function in vivo. We anticipate that our concept of how autoregulation forms an active chromosomal conformation will impact future research on transcription factor networks regulating stem cell fate. **Overall design:** HSCs of Pu.1 knock-in (PU.1ki/ki) mice were used for RNA extraction and hybridization on Affymetrix microarrays. We compared these microarray samples with the corresponding wild type.

Background corr dist: KL-Divergence = 0.0424, L1-Distance = 0.0588, L2-Distance = 0.0056, Normal std = 0.6556

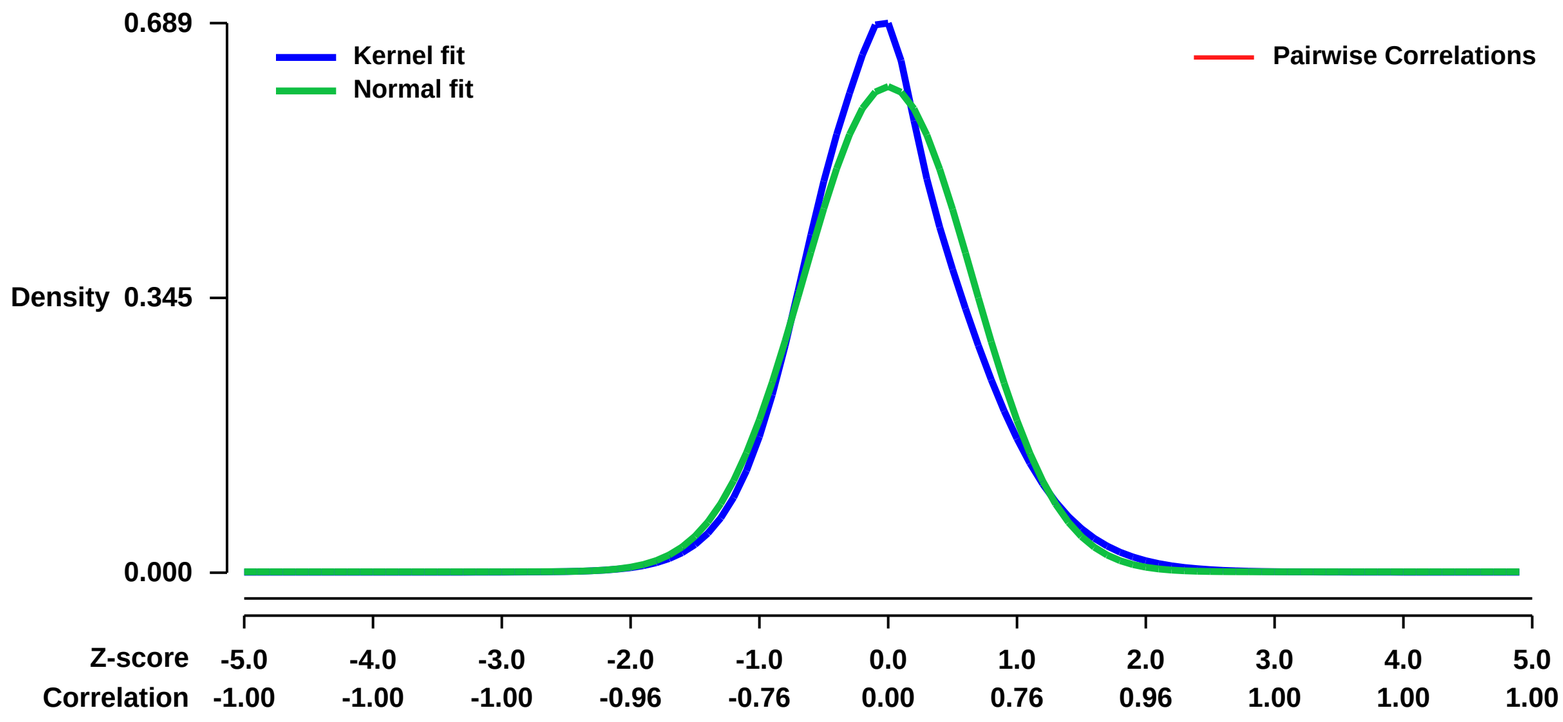

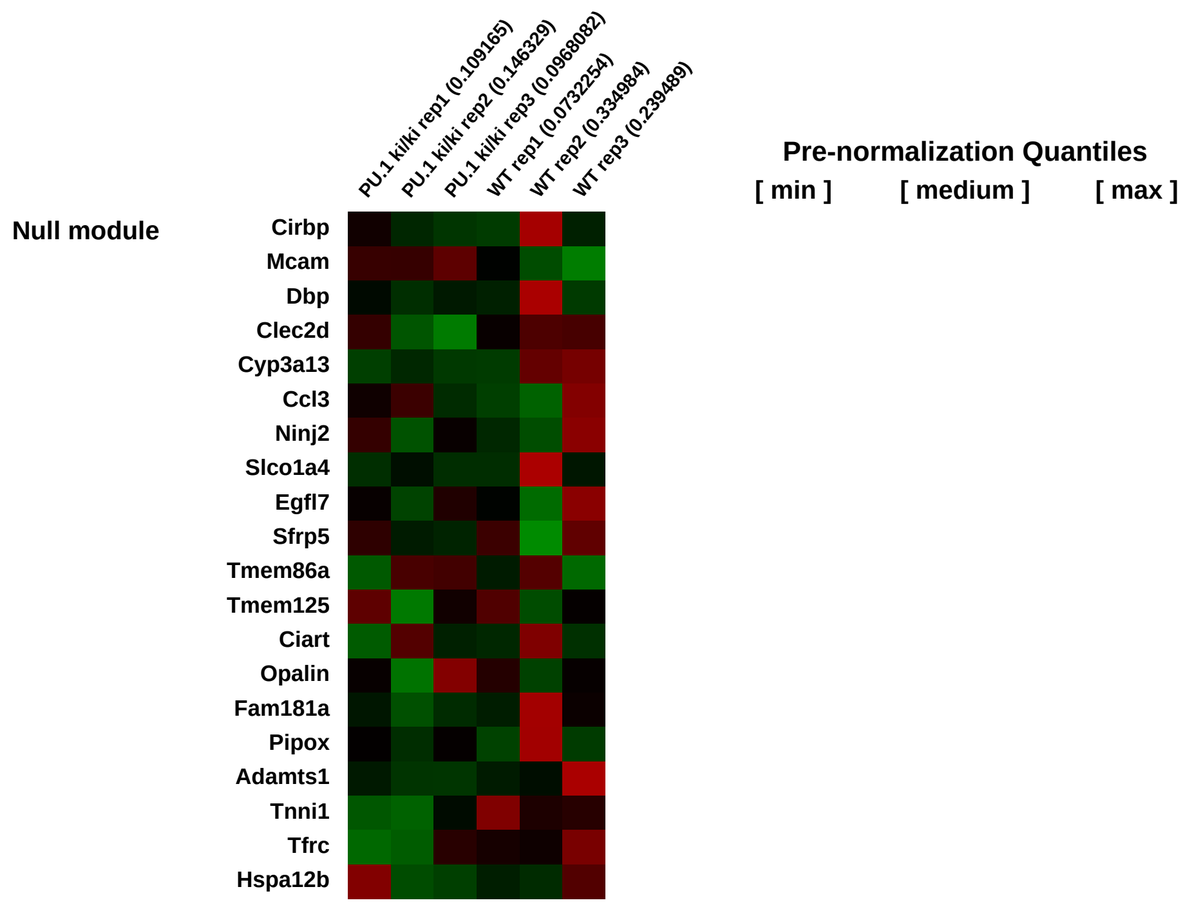

GEO Series "GSE6466" Expression Profiles

Num of samples in this series: 7

Scale of expression profile Z-scores

-3.0 -2.0 -1.0 0.0 1.0 2.0 3.0

GEO Link: http://www.ncbi.nlm.nih.gov/geo/query/acc.cgi?acc=GSE6466

Status: Public on Dec 08 2006

Title: Gene expression profiles of P1 and adult bladders isolated from SMGA (Actg2) transgenic mice. (GUDMAP Series ID: 11)

Organism: Mus musculus

Experiment type: Expression profiling by array

Platform: GPL1261

Pubmed ID:

Summary & Design:

Summary:
The long term objective is to create an encyclopedia of the expression levels of all genes in multiple components of the developing bladder. The central thesis is straightforward. The combination of microdissected and laser capture microdissection (LCM) plus microarray analysis offers a powerful, efficient and effective method for the creation of a global gene expression atlas of the developing urogenital system. Microarrays with essentially complete genome coverage can be used to quantitate expression levels of every gene. The ensuing rapid read-out provides an expression atlas that is more sensitive, more economical and more complete than would be possible by in situ hybridizations alone. The data submitted here represents the gene expression profiles of the adult and postnatal day 1 bladder.

Keywords: Gene expression comparison between postnatal day 1 and adult bladders

Overall design:
Bladders, from postnatal day 1 and adult transgenic mice in which EGFP is driven by a SMGA promoter/EGFP, were isolated by dissection and total RNA was extracted and underwent 2-round amplification (Epicentre´fi Biotechnologies) for gene expression analysis using the Affymetrix MOE430 microarray chip

Background corr dist: KL-Divergence = 0.0589, L1-Distance = 0.0444, L2-Distance = 0.0030, Normal std = 0.6024

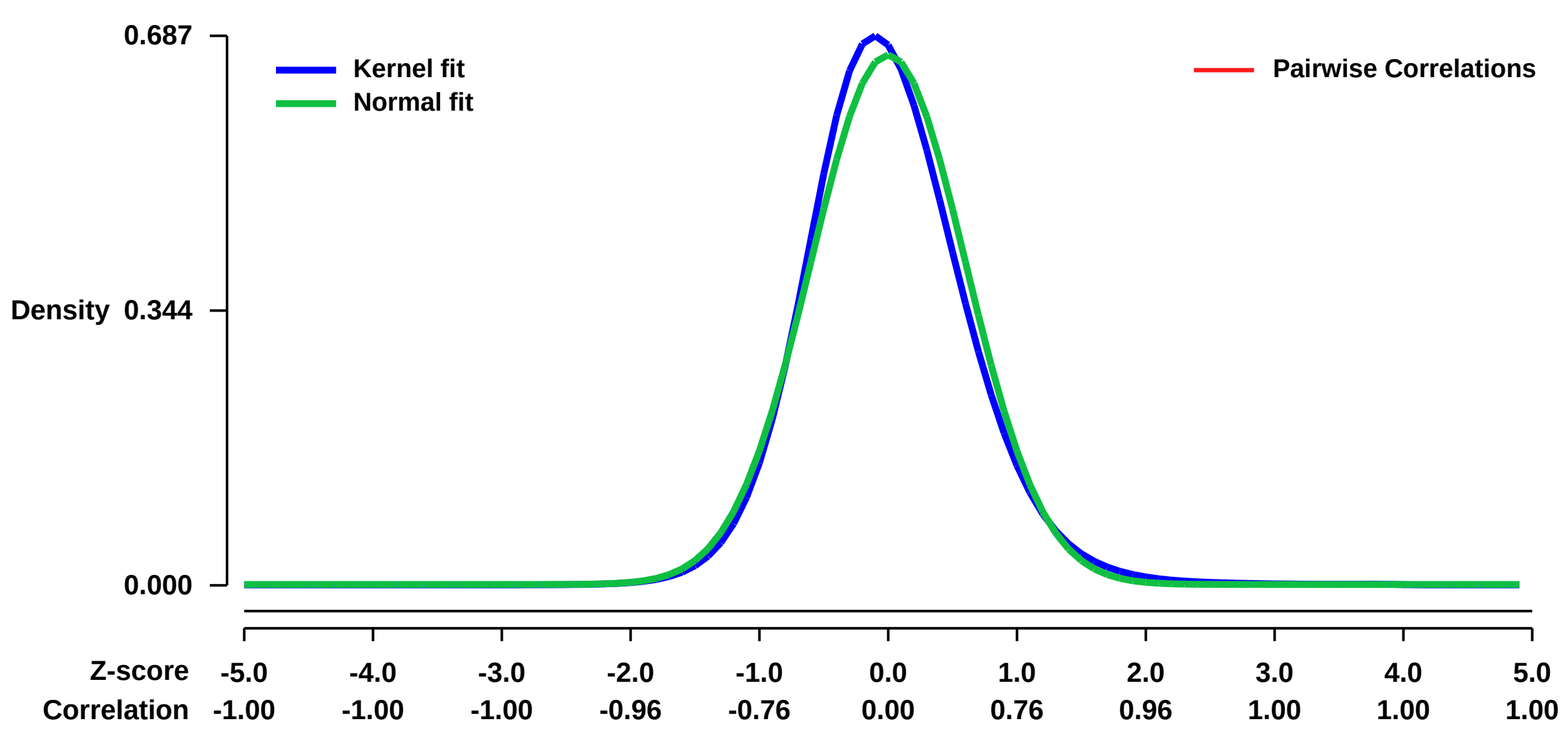

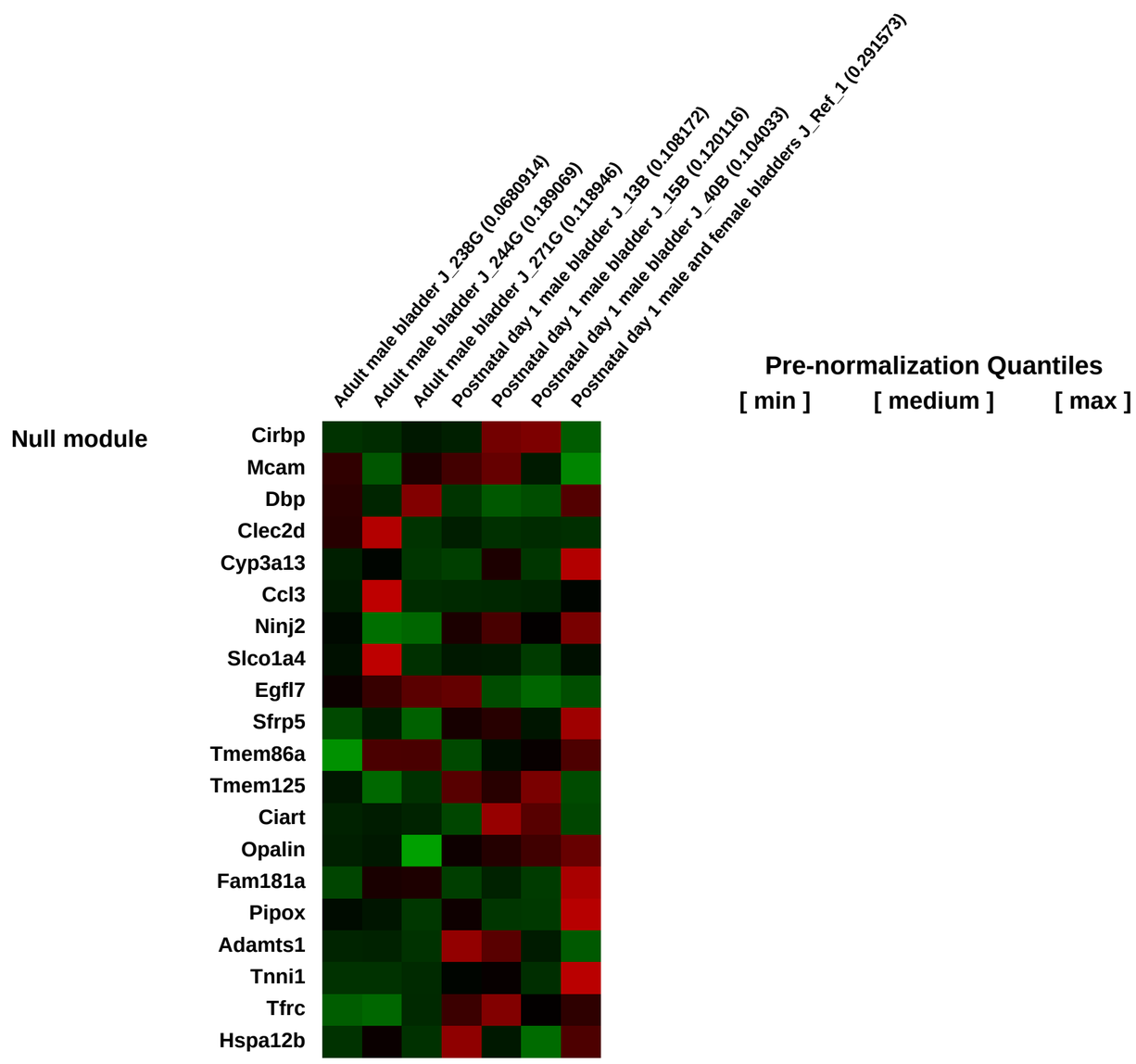

GEO Series "GSE46646" Expression Profiles

Num of samples in this series: 12

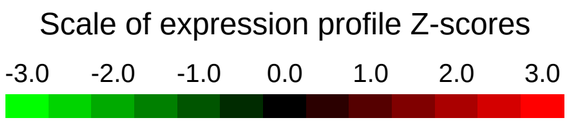

GEO Link:	http://www.ncbi.nlm.nih.gov/geo/query/acc.cgi?acc=GSE46646
Status:	Public on Dec 13 2013
Title:	IQGAP2 knockout model of hepatocellular carcinoma
Organism:	Mus musculus
Experiment type:	Expression profiling by array
Platform:	GPL1261
Pubmed ID:	23951254
Summary & Design:	**Summary:** Whole body knockout mice lacking IQ-motif containing GTPase-activating protein 2 (IQGAP2) develop spontaneous hepatocellular carcinoma (HCC) at the age of 12 months and older (Schmidt et al., 2008). Hepatic transcript expression profiles were obtained for IQGAP2 knockout and wild-type control mice of two age groups, 6- and 24-month-old. Liver samples from 24-month-old IQGAP2 knockout mice were HCC tumors, livers from all other groups were tumor-free. Results provide insights into the potential role of IQGAP2 as a liver-specific tumor suppressor. **Overall design:** Transcript profiles of four groups of mouse livers (N = 3 in each group) were compared using Affymetrix GeneChip´fi Mouse Genome 430 2.0 Array. The groups included livers from 6- and 24-month-old wild-type (WT) mice and 6- and 24-month-old (KO) Iqgap2-/- mice.

Background corr dist: KL-Divergence = 0.1090, L1-Distance = 0.0294, L2-Distance = 0.0016, Normal std = 0.4252

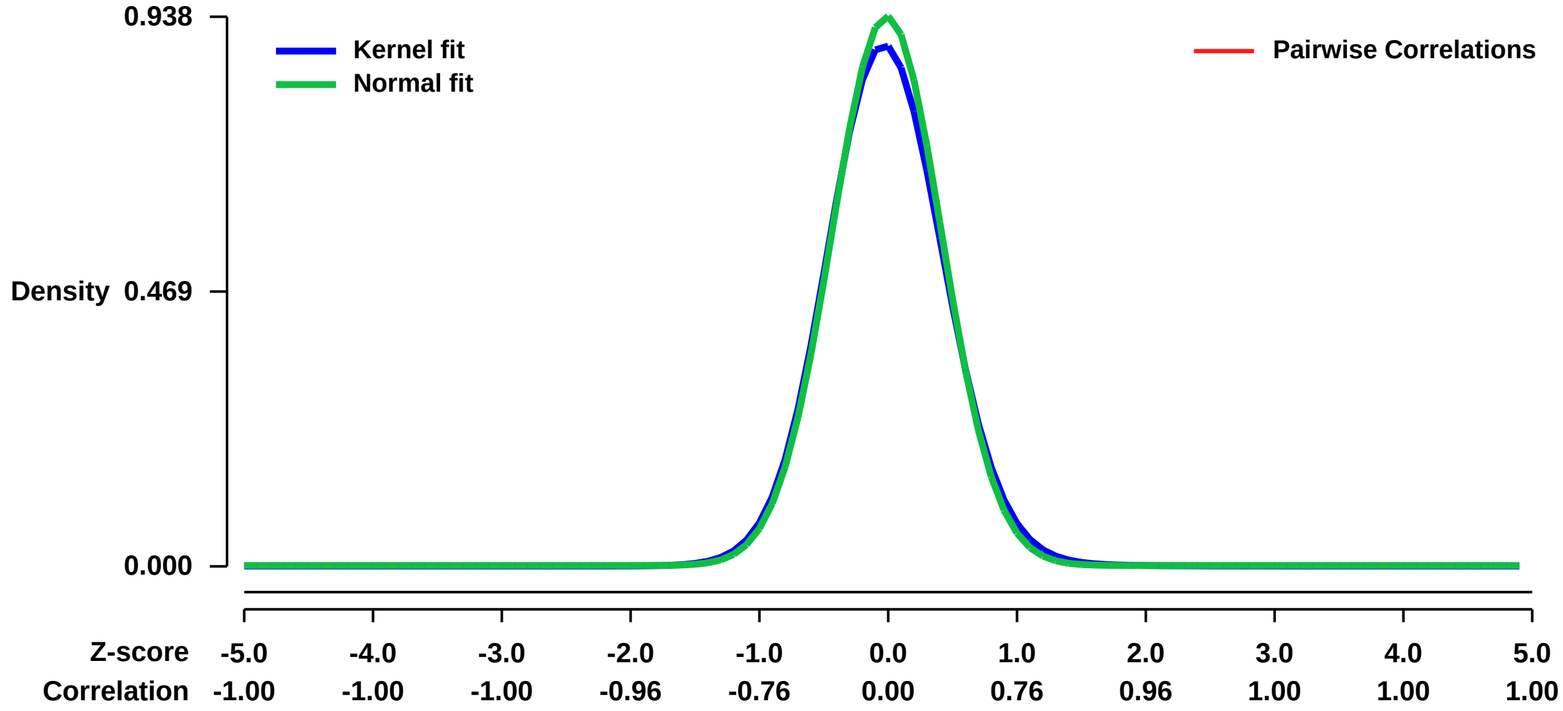

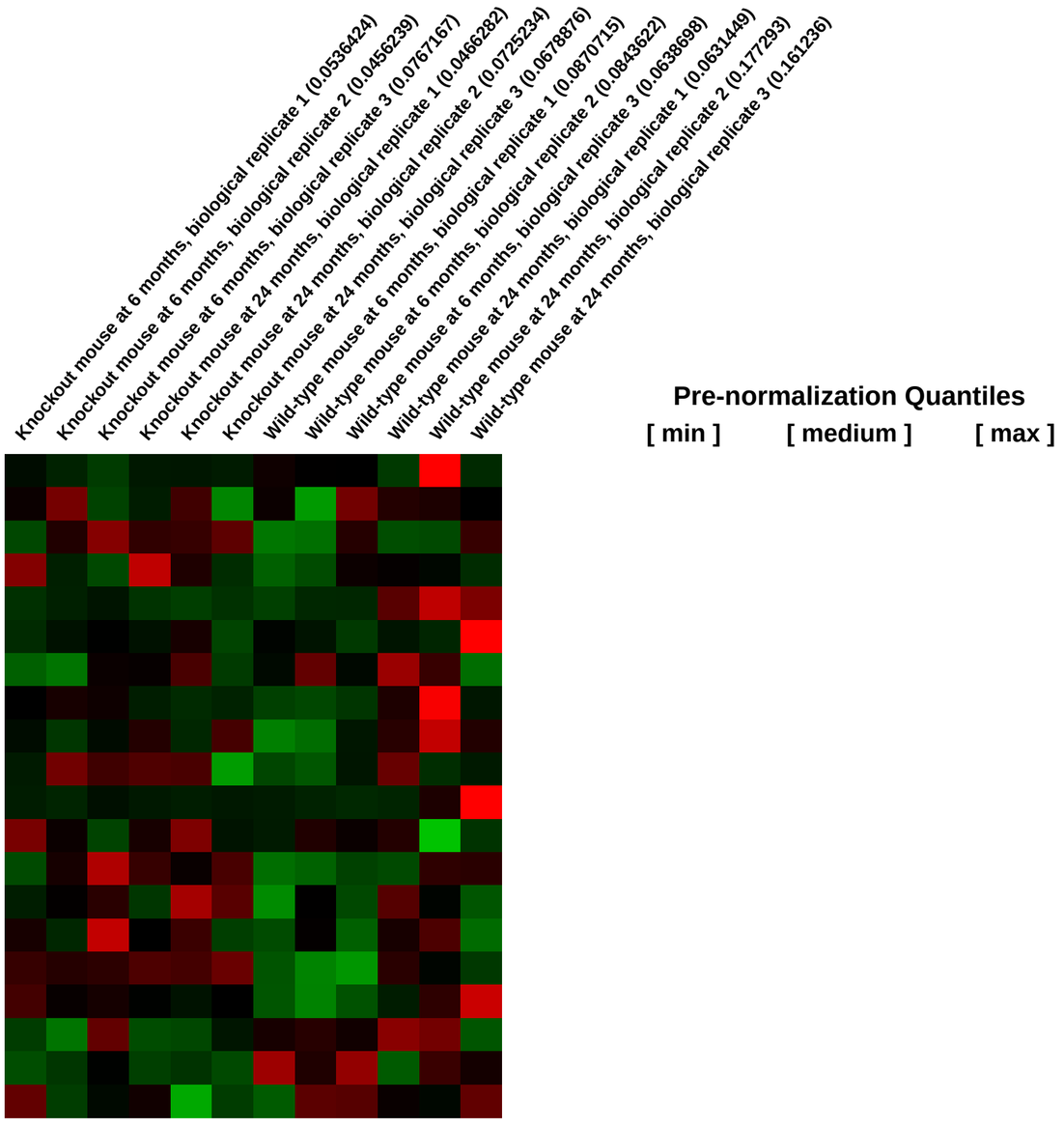

GEO Series "GSE7050" Expression Profiles

Num of samples in this series: 18

Scale of expression profile Z-scores

-3.0 -2.0 -1.0 0.0 1.0 2.0 3.0

GEO Link:	http://www.ncbi.nlm.nih.gov/geo/query/acc.cgi?acc=GSE7050
Status:	Public on Feb 17 2007
Title:	Stabilization of b-catenin induces lymphomas
Organism:	Mus musculus
Experiment type:	Expression profiling by array
Platform:	GPL1261
Pubmed ID:	17317856
Summary & Design:	**Summary:** Activation of b-catenin has been causatively linked to the etiology of colon cancer. Conditional stabilization of this molecule in pro-T-cells promotes thymocyte development without the requirement for preTCR signaling. We show here that activated b-catenin stalls the developmental transition from the double-positive (DP) to the single-positive (SP) thymocyte stage and predisposes DP thymocytes to transformation. b-Catenin induced thymic lymphomas have a leukemic arrest at the early DP stage. Lymphomagenesis requires Rag activity, which peaks at this developmental stage, as well as additional secondary genetic events. A consistent secondary event is the transcriptional upregulation of c-Myc, whose activity is required for transformation since its conditional ablation abrogates lymphomagenesis. In contrast, the expression of Notch receptors as well as targets is reduced in DP thymocytes with stabilized b-catenin and remains low in the lymphomas indicating that Notch activation is not required or selected for in b-catenin induced lymphomas. Thus, b-catenin activation may provide a mechanism for the induction of T-ALL that does not depend on Notch activation. **Keywords:** Lckcre, CD4Cre-Ctnnbex3, lymphoma, gene expression **Overall design:** This study was used to compare gene expression patterns of LckCre mice, CD4Cre-Ctnnbex3 mice before and after T-cell transformation. 5 independent Lckcre (control), 5 independent CD4Cre-Ctnnbex3 mice and 8 independent mice with lymphomas were used. Thymocytes or tumor masses were collected from Lckcre, CD4Cre-Ctnnbex3 mice. Total RNA isolation and purification followed by synthesis of dscDNA, Biotinylated cRNA and purification of Biotinylated cRNA. Then the hybridization to Affymetrix â Mouse Expression Array 430 Genechipsâ was done. Data was analysed by dchip.

Background corr dist: KL-Divergence = 0.0954, L1-Distance = 0.0327, L2-Distance = 0.0019, Normal std = 0.4425

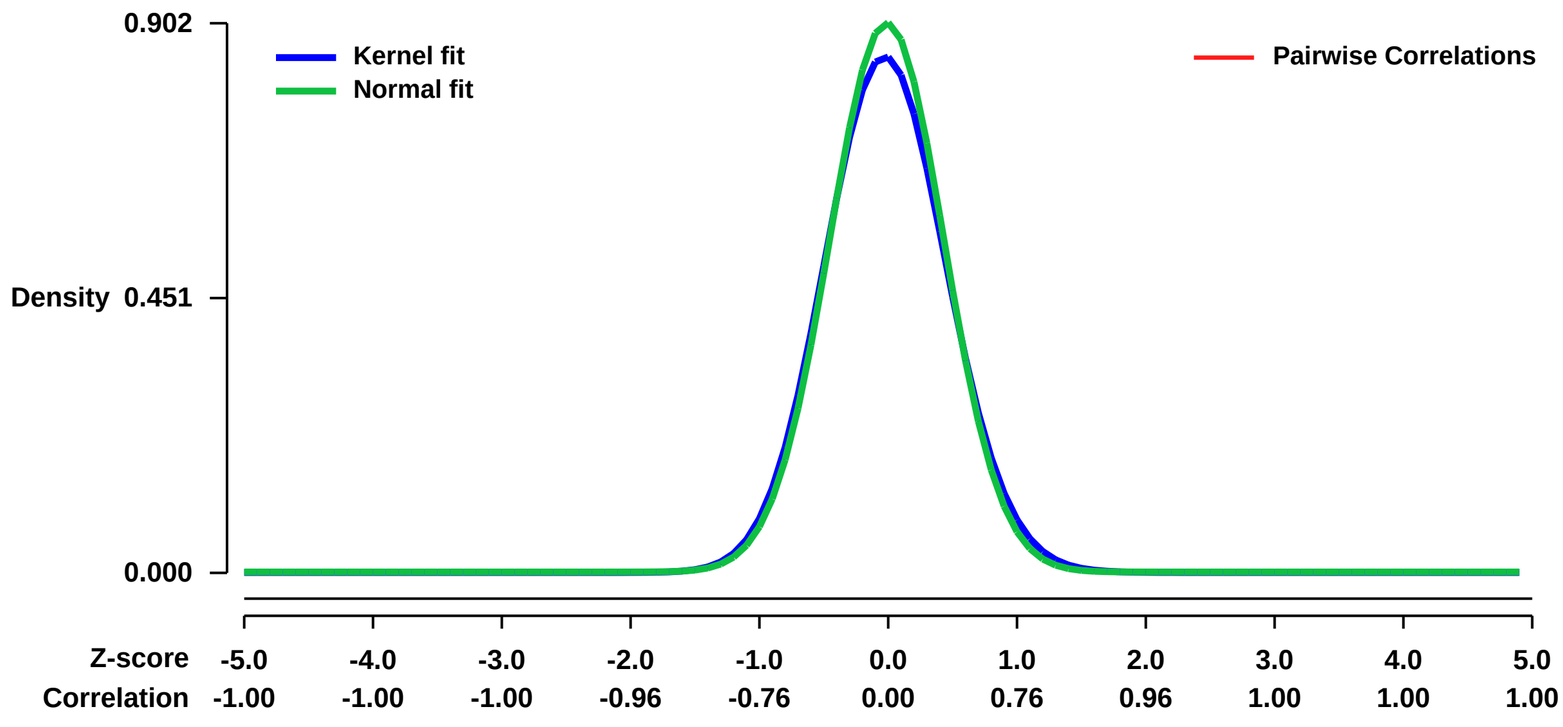

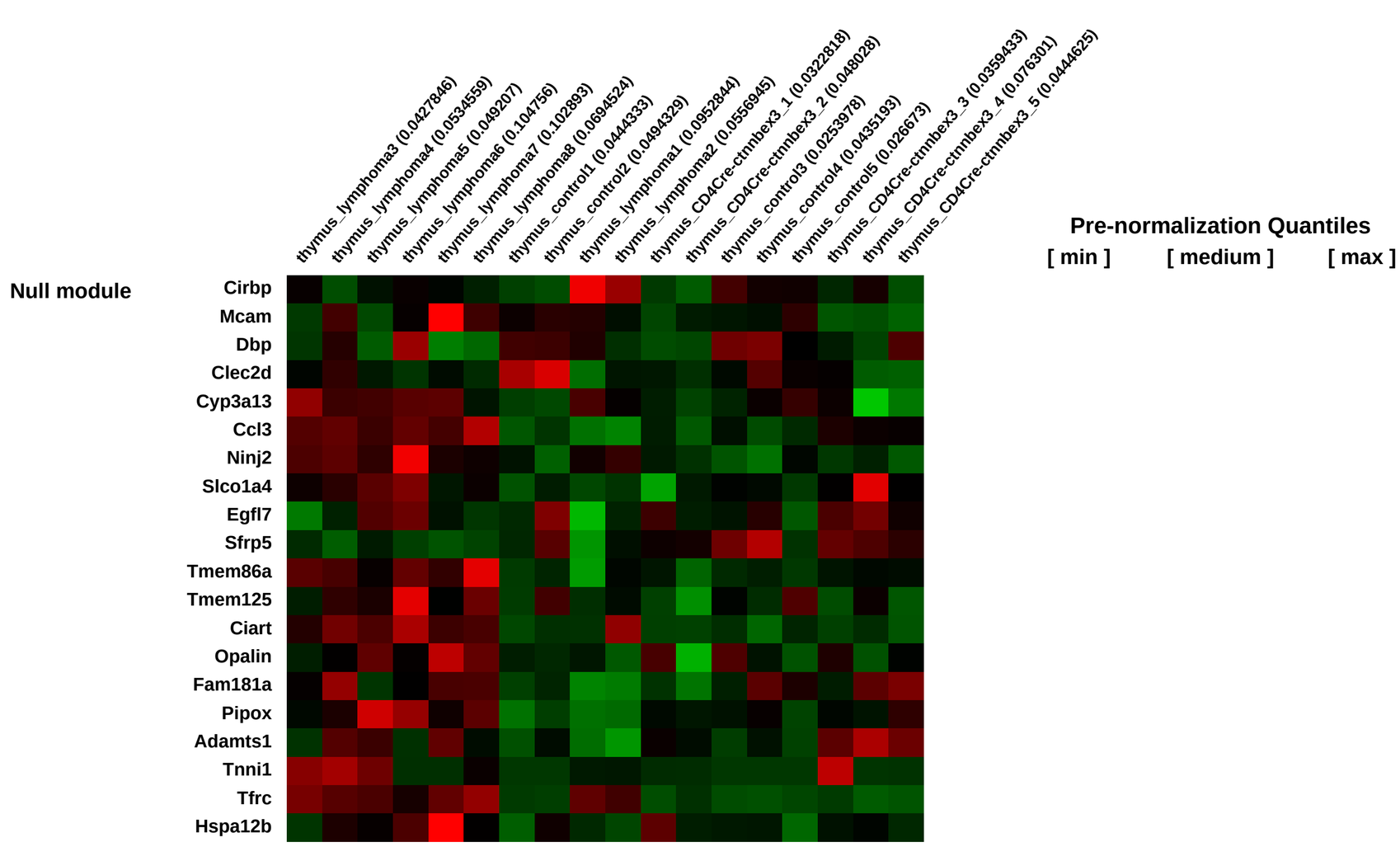

GEO Series "GSE17256" Expression Profiles

Num of samples in this series: 8

Scale of expression profile Z-scores

-3.0 -2.0 -1.0 0.0 1.0 2.0 3.0

GEO Link:	http://www.ncbi.nlm.nih.gov/geo/query/acc.cgi?acc=GSE17256
Status:	Public on Dec 04 2009
Title:	Comparison of gene expression profiles between human and mouse monocyte subsets [mouse data]
Organism:	Mus musculus
Experiment type:	Expression profiling by array
Platform:	GPL1261
Pubmed ID:	19965649
Summary & Design:	**Summary:** Human and mouse blood each contain two monocyte subsets. Here, we investigated the extent of their similarity using a microarray approach. Approximately 300 genes in human and 550 genes in mouse were differentially expressed between subsets. More than 130 of these gene expression differences were conserved between mouse and human monocyte subsets. We confirmed numerous differences at the cell surface protein level. Despite overall conservation, some molecules were conversely expressed between the two speciesâ subsets, including CD36, CD9, and TREM-1. Furthermore, other differences existed, including a prominent PPAR‹ signature in mouse monocytes absent in human. Overall, human and mouse monocyte subsets are far more broadly conserved than currently recognized. Thus, studies in mice may indeed yield relevant information regarding the biology of human monocyte subsets. However, differences between the species deserve consideration in models of human disease studied in the mouse. **Overall design:** The two major subsets of monocytes (Ly-6C+ and Ly-6Clo) from 12-week old C57Bl/6 mice were sorted and the RNA extracted and hybridized to Affymetrix GeneChip´fi 430 2.0 arrays. We pooled leukocytes from 5 mice for each sort and sorted 4 separate times for 4 biological replicates. The two major monocyte subsets (CD16- and CD16+) were isolated from venous heparinized blood from apparently healthy human volunteers using MACS technology with all reagents and tools from Miltenyi Biotec. Three separate donors were hybridized three different times to Affymetrix U133 Plus 2.0 array.

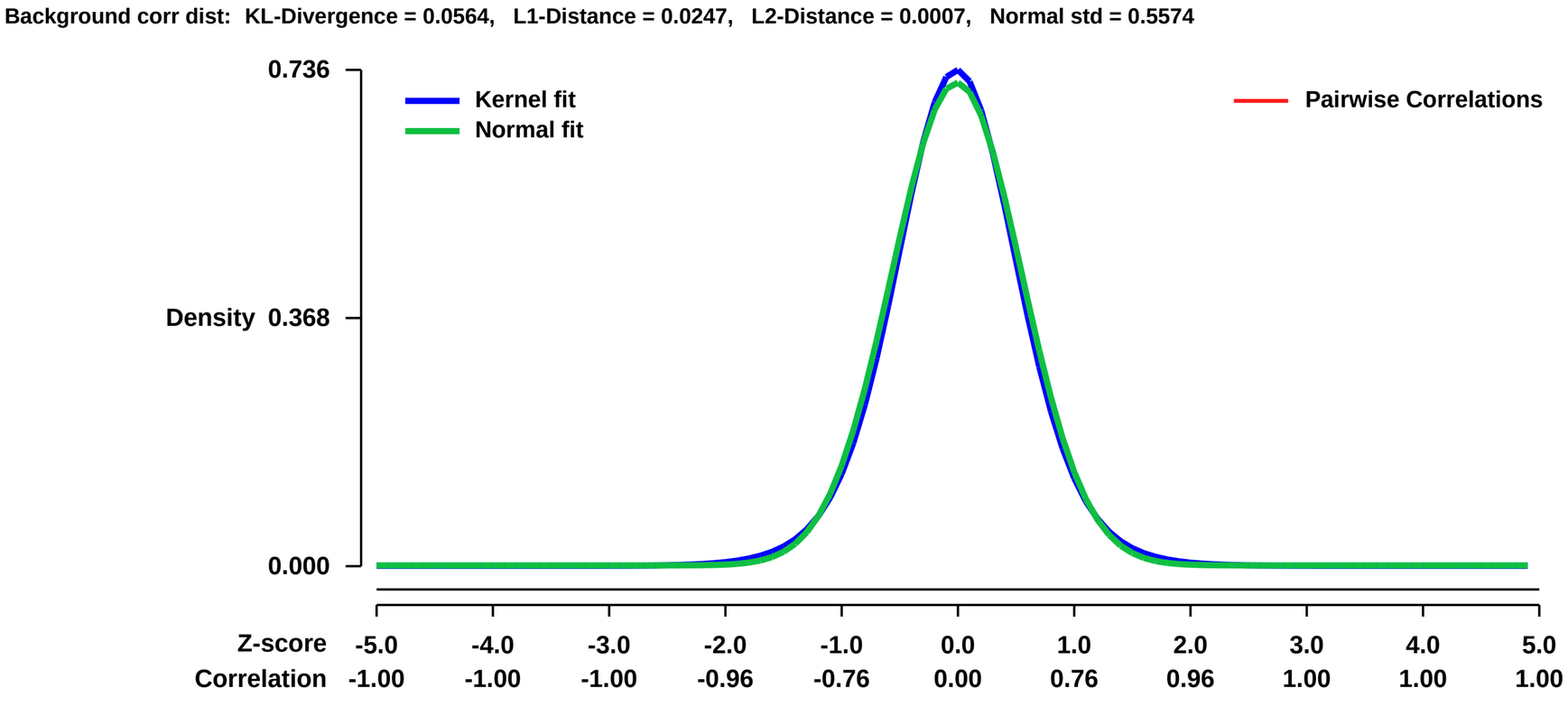

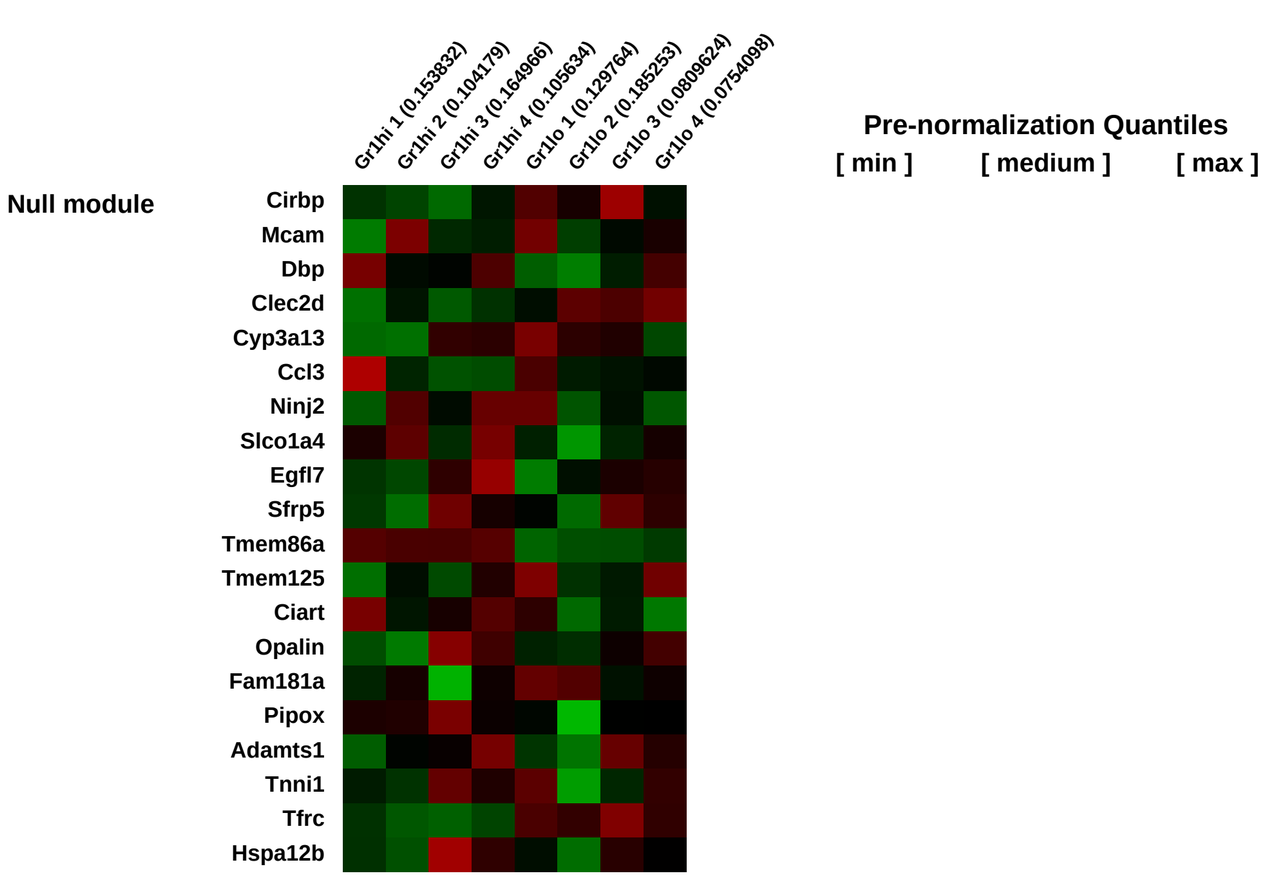

GEO Series "GSE40609" Expression Profiles

Num of samples in this series: 28

Scale of expression profile Z-scores

-3.0 -2.0 -1.0 0.0 1.0 2.0 3.0

GEO Link:	http://www.ncbi.nlm.nih.gov/geo/query/acc.cgi?acc=GSE40609
Status:	Public on Sep 06 2012
Title:	Murine PDAC cell lines
Organism:	Mus musculus
Experiment type:	Expression profiling by array
Platform:	GPL1261
Pubmed ID:	
Summary & Design:	**Summary:** Expression profiles of 28 murine pancreatic cancer cell lines isolated from a KrasG12D-based mouse model of pancreatic cancer **Overall design:** mRNA of 28 low passaged murine pancreatic cancer cell lines was extracted and hybridized to Affymetrix microarrays

Background corr dist: KL-Divergence = 0.2861, L1-Distance = 0.0675, L2-Distance = 0.0126, Normal std = 0.2853

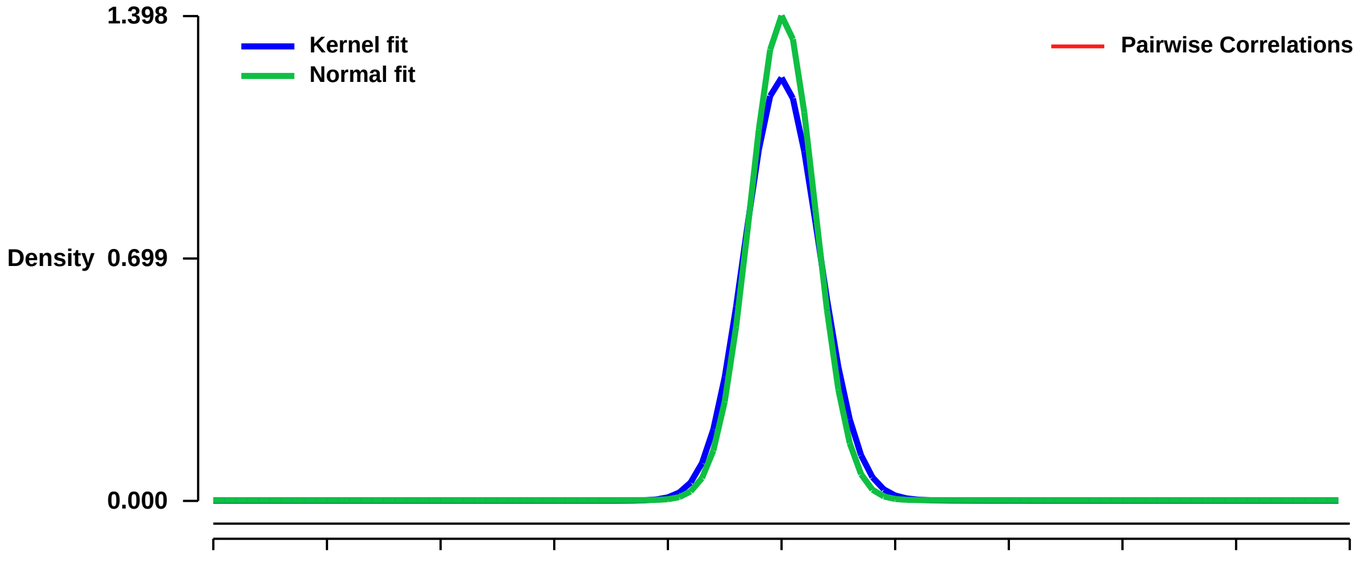

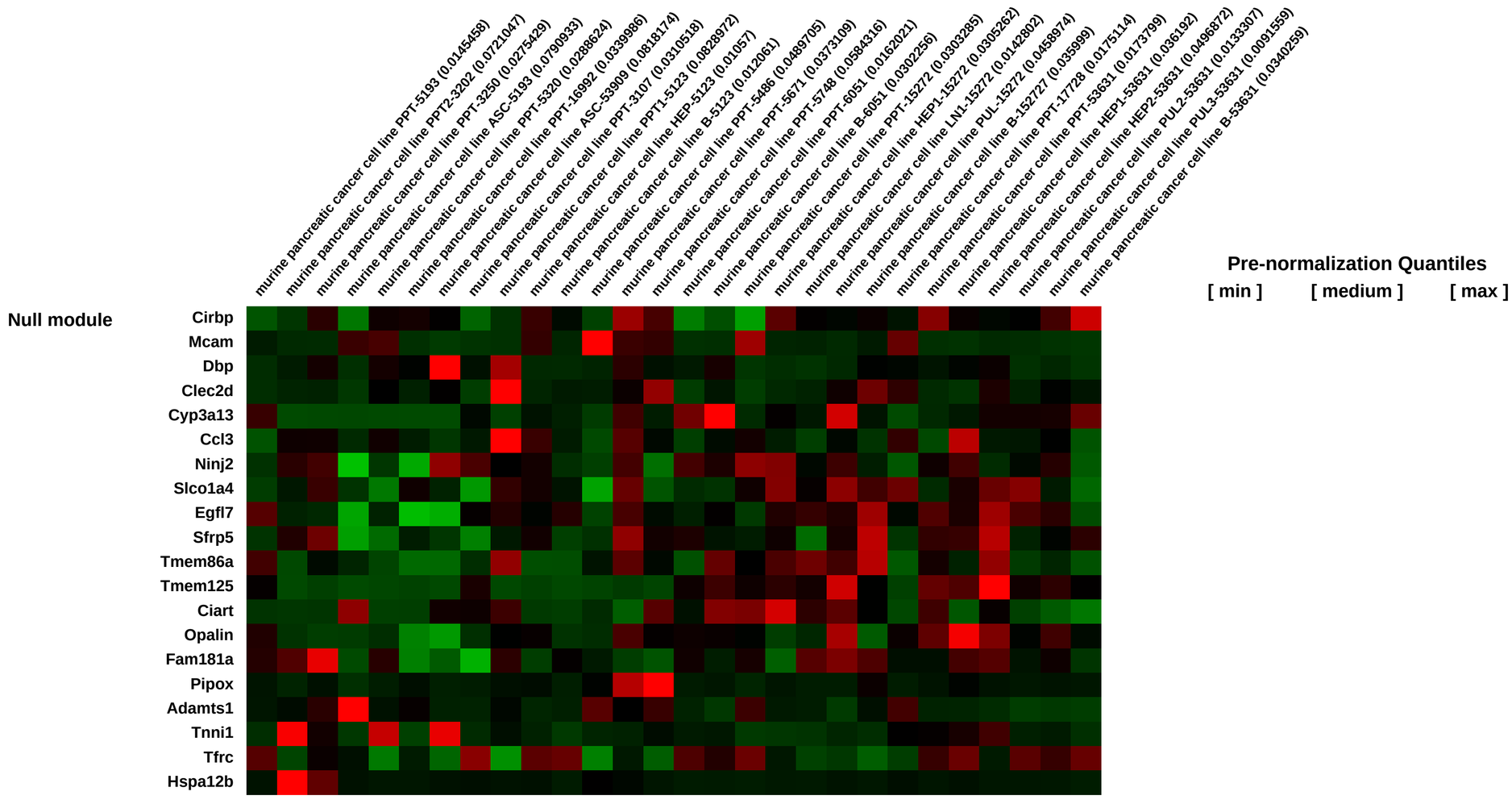

GEO Series "GSE17840" Expression Profiles

Num of samples in this series: 9

Scale of expression profile Z-scores

-3.0 -2.0 -1.0 0.0 1.0 2.0 3.0

GEO Link:	http://www.ncbi.nlm.nih.gov/geo/query/acc.cgi?acc=GSE17840
Status:	Public on Oct 31 2009
Title:	Hedgehog is an anti-inflammatory epithelial signal for the intestinal lamina propria
Organism:	Mus musculus
Experiment type:	Expression profiling by array
Platform:	GPL1261
Pubmed ID:	20206176
Summary & Design:	**Summary:** Epithelial Hedgehog (Hh) ligands regulate several aspects of fetal intestinal organogenesis and emerging data implicate the Hh pathway in inflammatory signaling in adult colon. We investigated the effects of chronic Hh inhibition in vivo and profiled molecular pathways acutely modulated by Hh signaling in the intestinal mesenchyme. **Overall design:** E18.5 intestinal mesenchyme was isolated and cultured. Mesenchyme was treated with Sonic (Shh) or Indian (Ihh) hedgehog ligand or Vehicle (control) acutely to identify targets regulated by Hh signaling in intestinal mesenchyme.

Background corr dist: KL-Divergence = 0.0739, L1-Distance = 0.0254, L2-Distance = 0.0010, Normal std = 0.4855

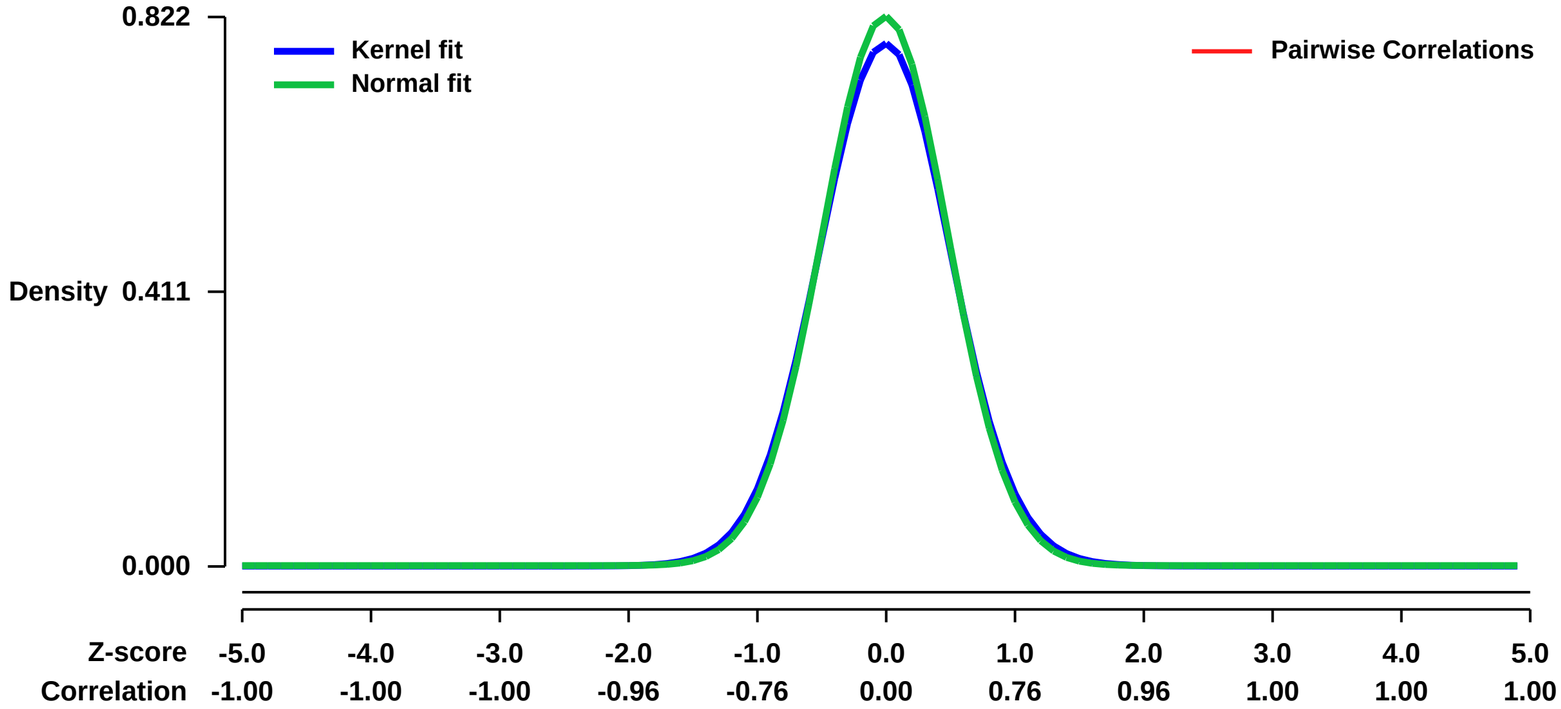

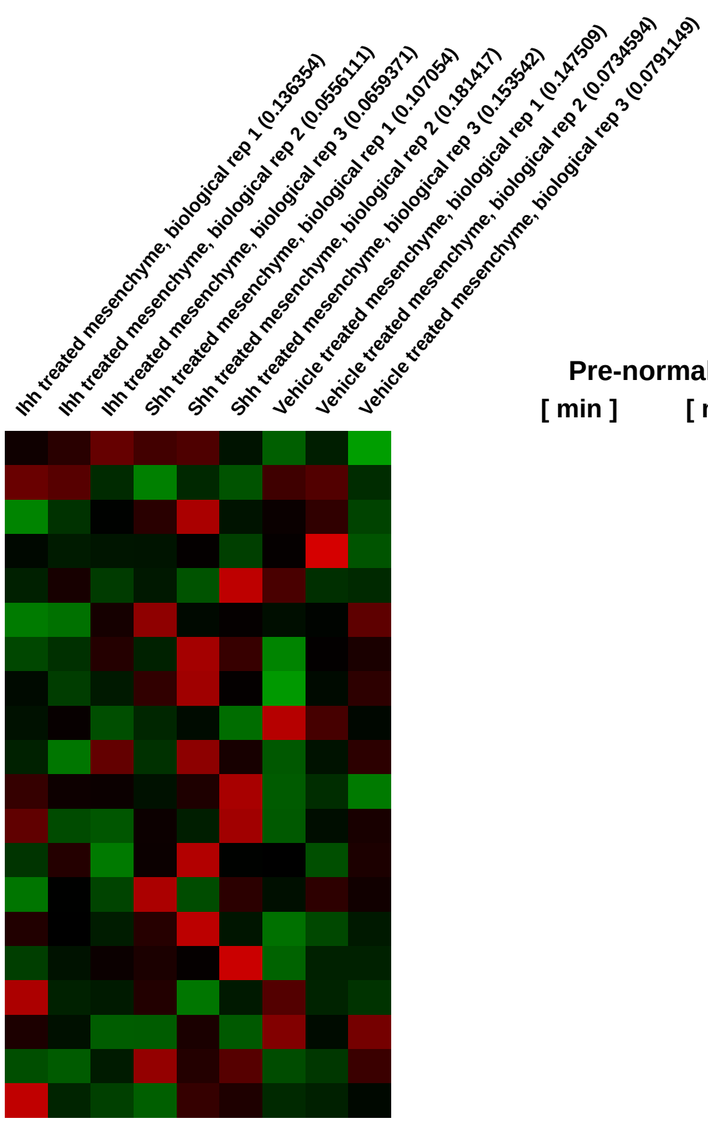

GEO Series "GSE2869" Expression Profiles

Num of samples in this series: 8

Scale of expression profile Z-scores

-3.0 -2.0 -1.0 0.0 1.0 2.0 3.0

GEO Link: http://www.ncbi.nlm.nih.gov/geo/query/acc.cgi?acc=GSE2869
Status: Public on Jul 06 2005
Title: Rosenfeld-5R01NS034934-14
Organism: Mus musculus
Experiment type: Expression profiling by array
Platform: GPL1261
Pubmed ID:

Summary & Design:

Summary:
Using targeted gene deletion, we have firmly established that the Class IV POU domain transcription factor Brn-3.2 controls a developmental program regulating axon pathfinding in the mouse visual system. We have isolated and identified downstream gene targets of Brn-3.2, using Representational Difference Analysis (RDA), on cDNA populations derived from wildtype and Brn-3.2-/- retina at the appropriate embryonic stage. One of these candidate genes, the Homeodomain Interacting Protein Kinase 2 (HIPK2), is postulated to be a transcriptional coregulator, based on its in vitro interactions with repressor homeodomain proteins of the NK class, as well as other components of repressor complexes. HIPK2 has also been shown to be involved in post-translational modification of two major transcriptional regulators, p53 and CtBP. Expression of a dominant-negative form of HIPK2 in sensory neurons affects the innervation patterns of their target tissues, suggesting an axon pathfinding defect.

The aim of this project is to identify targets for the Homeodomain Interacting Protein Kinase 2 (HIPK2), that we isolated as a downstream gene target of the class IV POU domain transcription factor Brn-3.2, and to investigate their function in the Brn-3.2 dependent pathway regulating axon pathfinding.

We hypothesize that the genes regulated by HIPK2 will play a critical role in axon pathfinding and that the results of this study will provide novel insights into the molecular mechanisms of axon pathfinding, and possibly neural plasticity and regeneration, and therefore, be of great interest to the field of neurobiology in general.

In order to uncover potential biological role(s) of HIPK2 in neural development, and particularly axon pathfinding, we generated transgenic mouse models for in vivo studies. Our preliminary observations in transgenic mice, indicate that a form of the molecule expected to act as a dominant-negative and designed to be expressed in sensory neurons, affects the innervation patterns of their target tissues, suggesting an axon pathfinding defect. We plan to take advantage of this model to identify genes regulated by HIPK2, and which are likely to be involved in axon pathfinding. To this end, we will compare gene expression profiles in sensory neurons isolated wild-type and transgenic mice. In our experimental paradigm, the trigeminal ganglion represents the ideal sensory structure in which to perform such an analysis: 1) High levels of transgene can be expressed in the trigeminal ganglion, as assessed by the expression of LacZ from the bicistronic construct which contains IRES-LacZ downstream of a dominant negative form of HIPK2. 2) The trigeminal ganglion can be dissected at embryonic day 13.5, when the phenotype is apparent, with ease and free of contamination from surrounding tissues. 3) The amounts of RNA that can be isolated from a single ganglion are in the range of 200-300 ng, which should be sufficient for microarray analysis following linear amplification of RNA. One series will be carried out with transgenic embryos and a control series will be carried out with wildtype littermates. Animals will be prepared and sacrificed by a standard protocol. Tissue will be rapidly dissected from E13.5 trigeminal ganglion, frozen in liquid nitrogen, and stored at -80C until RNA is extracted. RNA will be prepared using RNeasy Micro Kit. We will be providing 4 tissue samples for each of the wildtype and transgenic animals to mitigate any expression differences resulting from mouse to mouse variation.

Keywords: other

Overall design:
as above

Background corr dist: KL-Divergence = 0.0910, L1-Distance = 0.0235, L2-Distance = 0.0008, Normal std = 0.4529

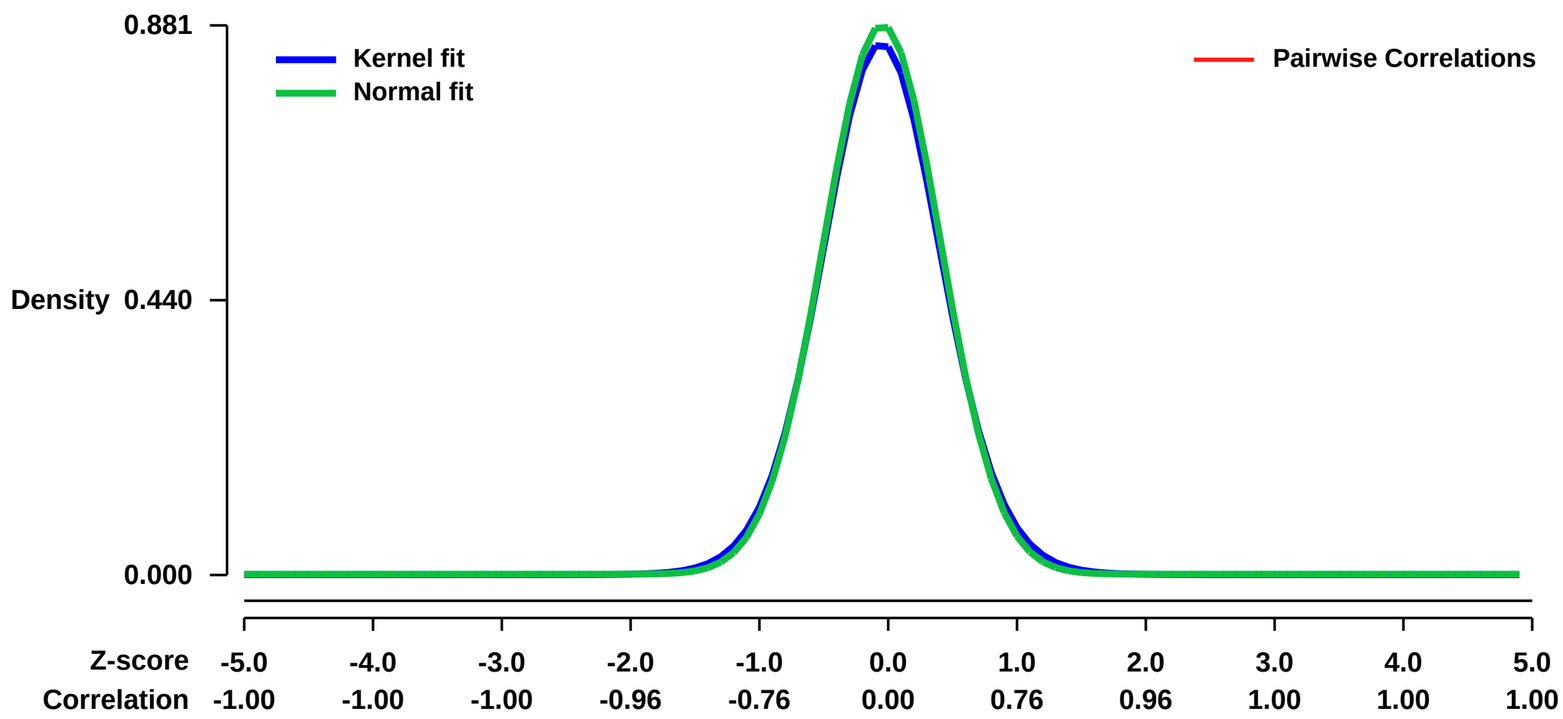

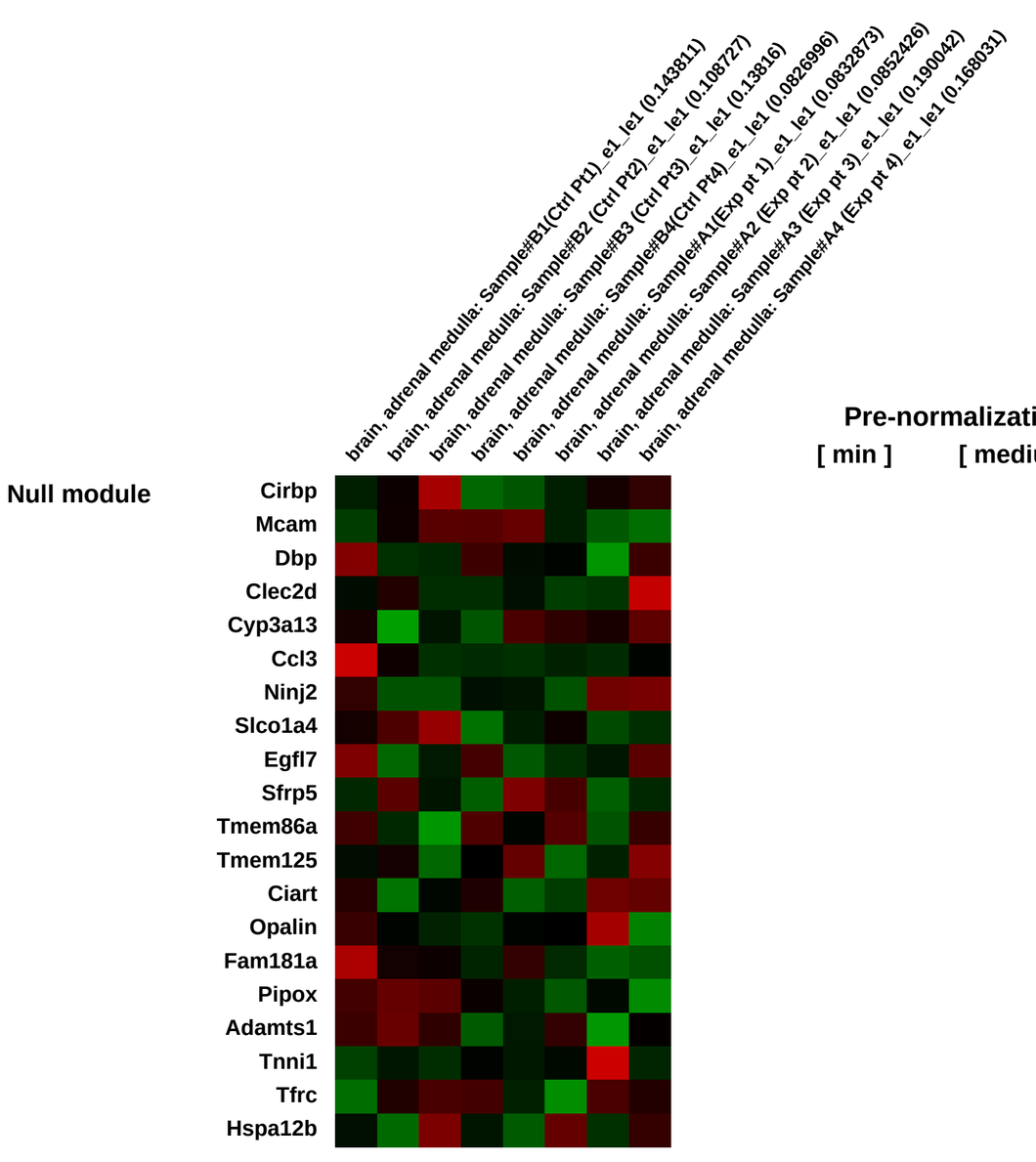

GEO Series "GSE14059" Expression Profiles

Num of samples in this series: 6

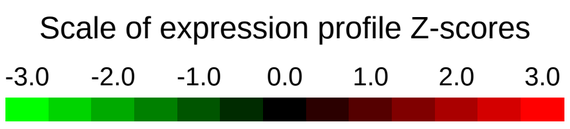

GEO Link:	**http://www.ncbi.nlm.nih.gov/geo/query/acc.cgi?acc=GSE14059**
Status:	**Public on Apr 01 2009**
Title:	**Gene expression profiles of heterozygous periphilin knockout mice compared to wt littermates**
Organism:	**Mus musculus**
Experiment type:	**Expression profiling by array**
Platform:	**GPL1261**
Pubmed ID:	
Summary & Design:	**Summary:** **Periphilin is a protein which is involved in multiple processes in vivo, including terminal differentiation of keratinozytes as well as cell-cycle and cancer related functions. Here we generated mice with a targeted disruption of the periphilin-1 gene to explore its physiological role from an organismic perspective. In accordance with a ubiquitous expression of periphilin in the murine embryo, the homozygous deficiency of periphilin is lethal in early embryogenesis. We therefore characterized mice with a disruption of only one periphilin allele. As heterozygous periphilin knockout mice show no obvious histological alterations and have no apparent behavioural phenotypes, we compared whole transcriptome RNA expression profiles of total brain tissue of periphilin+/- knockout mice and wild type littermates for an in-depth analysis of heterozygous animals. In periphilin+/- knockout mice, 3 probe sets were indicative of significant differential expression (p â∕0.05, SLR â¥ 1 which is equivalent to 2 fold). Two of these probe sets (1438864_at and 1439170_at) refer to unannotated or unclassifiable genes. According to the NetAffxâ¢ Analysis Center, the third probe set (1447831_s_at) is assigned to myotubularin related protein 7 (Mtmr7). The probe set, however, lies upstream of the Mtmr7 gene (Ensembl gene ENSMUSG00000039431), and its signal is therefore not representative for the Mtmr7 gene. Quantitative RT-PCR (qRT-PCR) analysis with a primer set specific for Mtmr7 confirmed that its expression is not altered in periphilin+/- knockout mice (relative expression compared to wild type: 0.924; p = 0.419). In summary, none of more than 45.000 covered transcripts is differentially expressed in periphilin+/- knockout mice in comparison to wild type littermates.** **Overall design:** **Whole brains of three male 2-months-old periphilin+/-knockout mice and three C57BL/6-wild type littermates**

Background corr dist: KL-Divergence = 0.0487, L1-Distance = 0.0187, L2-Distance = 0.0004, Normal std = 0.5774

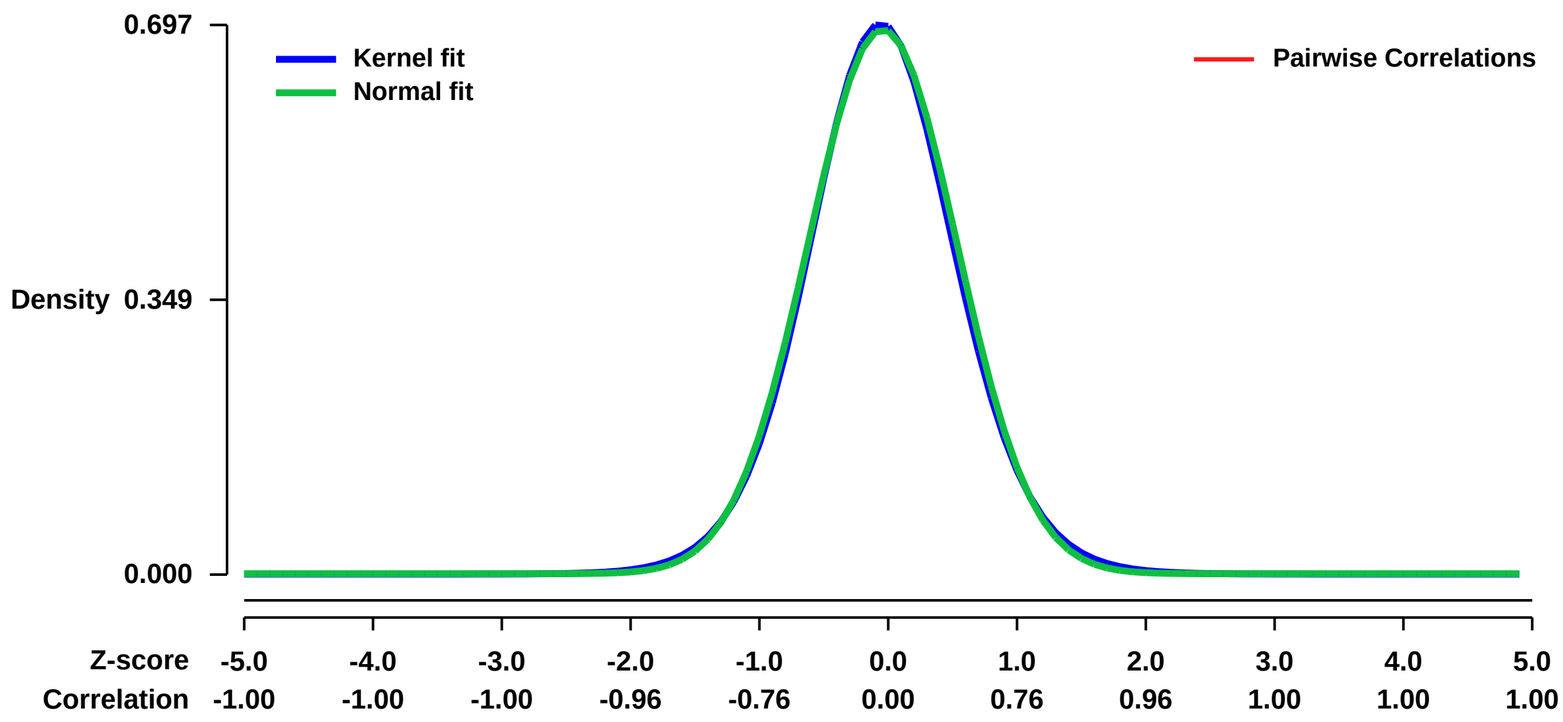

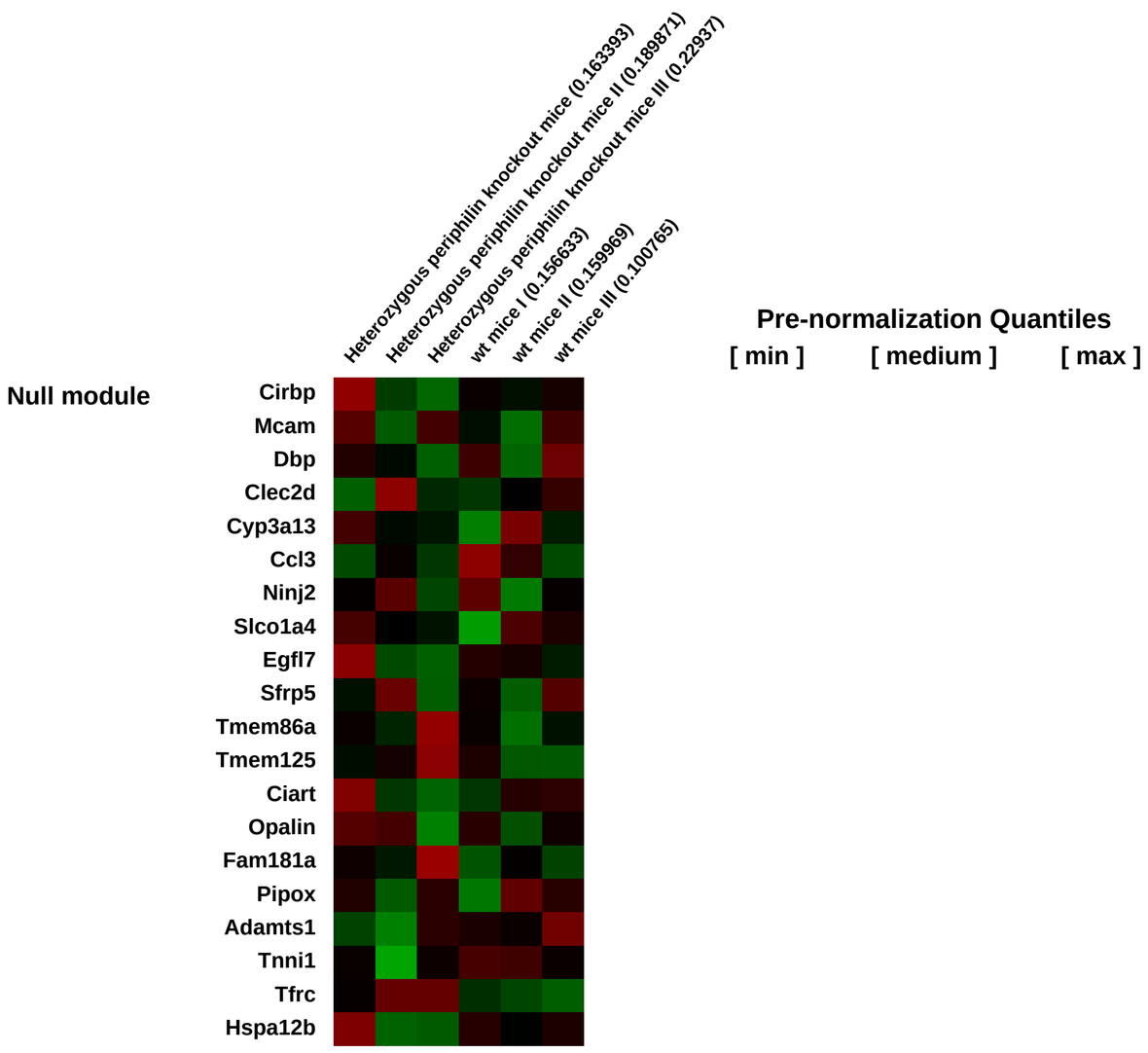

GEO Series "GSE40230" Expression Profiles

Num of samples in this series: 15

Scale of expression profile Z-scores

-3.0 -2.0 -1.0 0.0 1.0 2.0 3.0

GEO Link:	http://www.ncbi.nlm.nih.gov/geo/query/acc.cgi?acc=GSE40230
Status:	Public on Aug 27 2012
Title:	Expression data from primary and secondary CD4 T cell effectors responding towards influenza A virus infection
Organism:	Mus musculus
Experiment type:	Expression profiling by array
Platform:	GPL1261
Pubmed ID:	22927425
Summary & Design:	**Summary:** How secondary CD4 T cell effectors, derived from resting memory cells, differ from primary cells, derived from naˆflve precursors, and how such differences impact recall responses to pathogens is unknown. We used microarrays to detail the global programme of gene expression underlying differences between primary and secondary CD4 T cell effectors purified from the spleen, dLN, and lung on day 7 following A/PR8/34 influenza infection. **Overall design:** Congenic naˆflve or in vivo influenza primed memory HNT TCR trangenic CD4 T cells were sort purifed from the spleens, dLNs, and lungs of infected mice on day 7 post infection for RNA extraction and hybridization on Affymetrix microarrays. We sought to obtain only CD4 T cell populations that had entered into the immune response by also sorting and collecting only those cells that had divided at least 5 times by CFSE analysis.

Background corr dist: KL-Divergence = 0.0525, L1-Distance = 0.0533, L2-Distance = 0.0050, Normal std = 0.5678

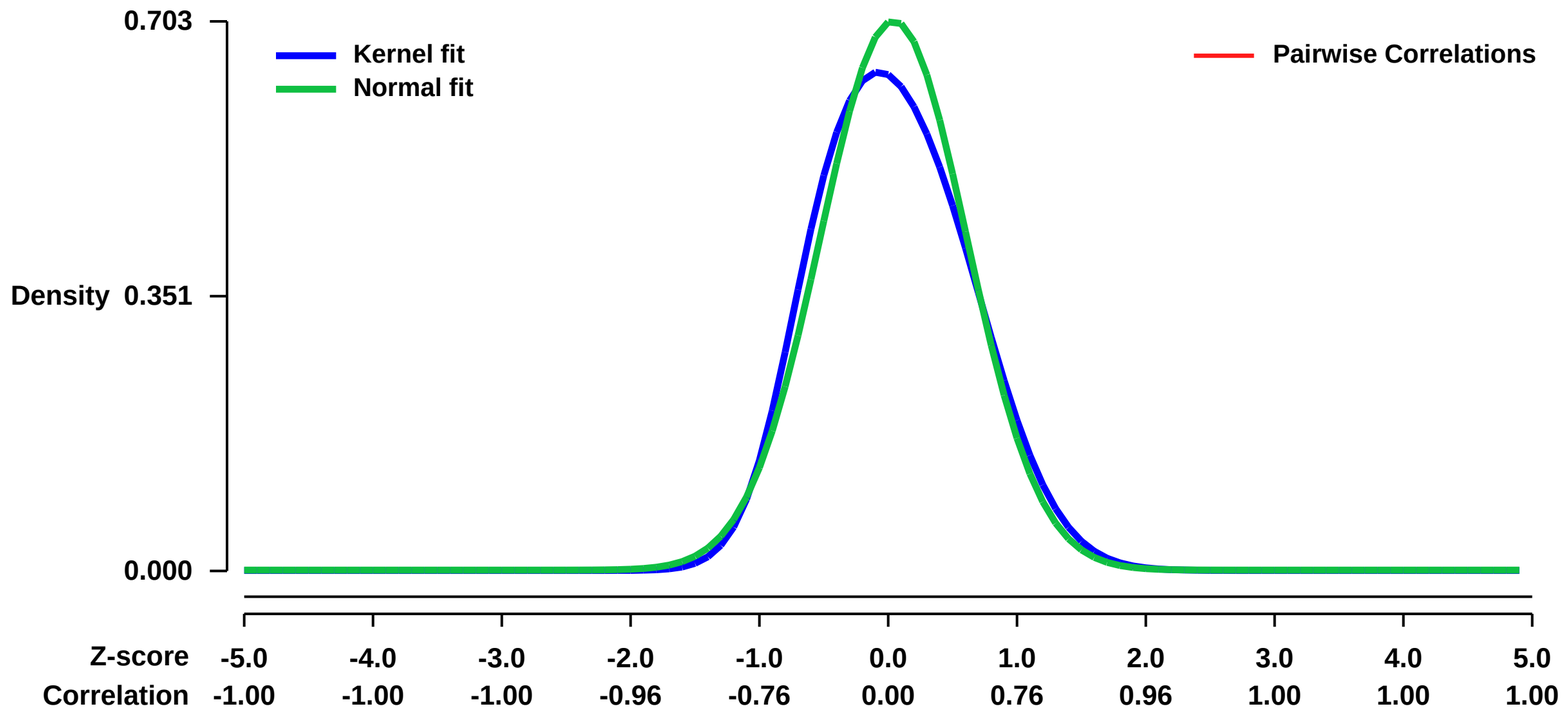

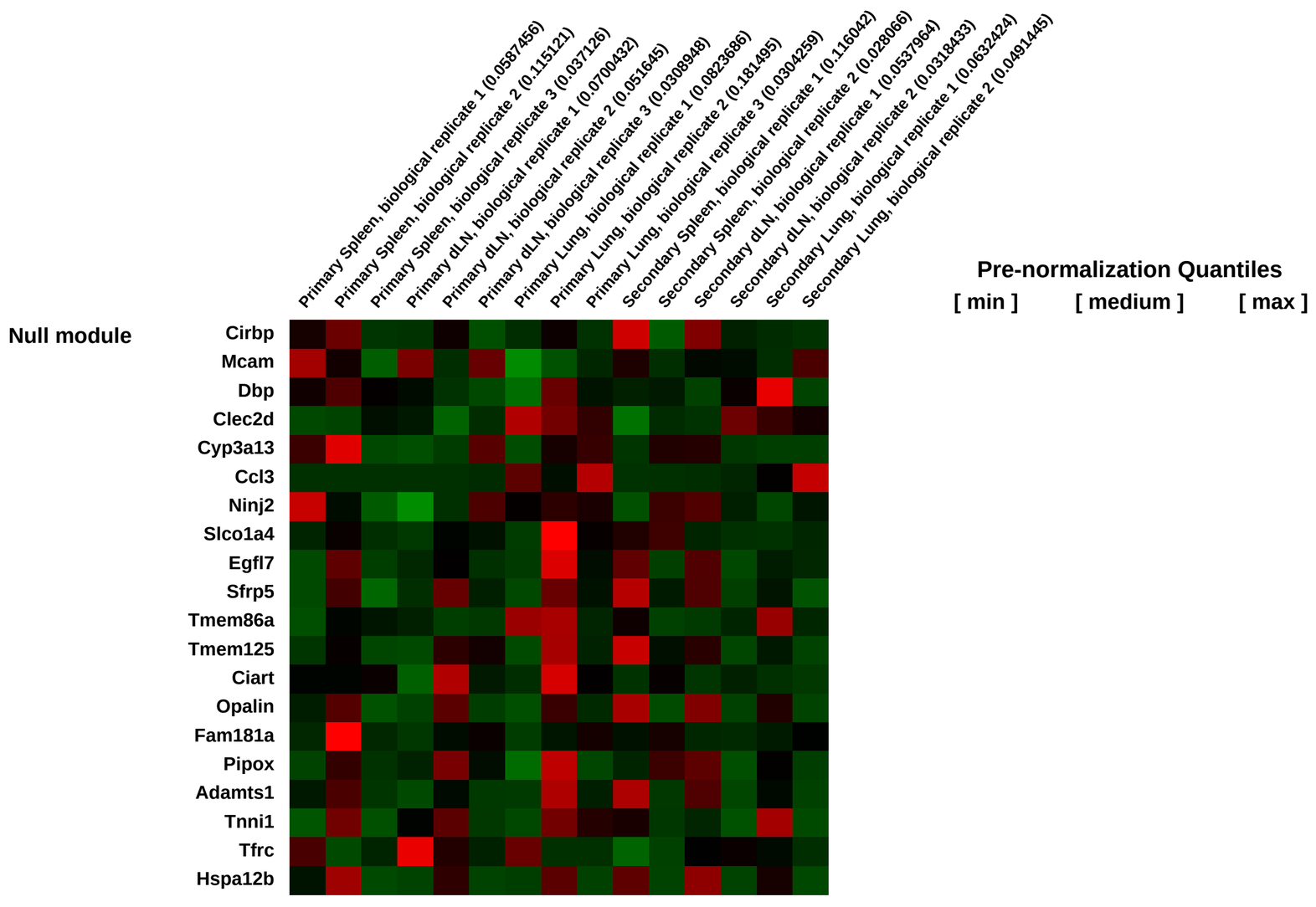

GEO Series "GSE25100" Expression Profiles

Num of samples in this series: 6

Scale of expression profile Z-scores

-3.0 -2.0 -1.0 0.0 1.0 2.0 3.0

GEO Link:	http://www.ncbi.nlm.nih.gov/geo/query/acc.cgi?acc=GSE25100
Status:	Public on Nov 04 2010
Title:	Expression data from CD19-positive splenic B cells isolated from 1-month old ID4+/-TCL1-tg and ID4+/+TCL1-tg mice
Organism:	Mus musculus
Experiment type:	Expression profiling by array
Platform:	GPL1261
Pubmed ID:	21098398
Summary & Design:	**Summary:** The function of ID4 in CLL development was studied in vivo using TCL1 transgenic mouse model that develop leukemia similar to human CLL. TCL1 mice with ID4 single knockout gene have accelerated CLL progression. Results from the animal study suggest ID4 as a tumor suppressor gene that might regulate cell proliferation and apoptosis in B lymphocytes. **Overall design:** Gene expression in CD19-positive splenic B cells collected from 1-month old ID4+/-TCL1-tg and ID4+/+TCL1-tg mice was compared by microarray, the goal is to find ID4-regulated genes involved in CLL development.

Background corr dist: KL-Divergence = 0.0420, L1-Distance = 0.0183, L2-Distance = 0.0003, Normal std = 0.6059

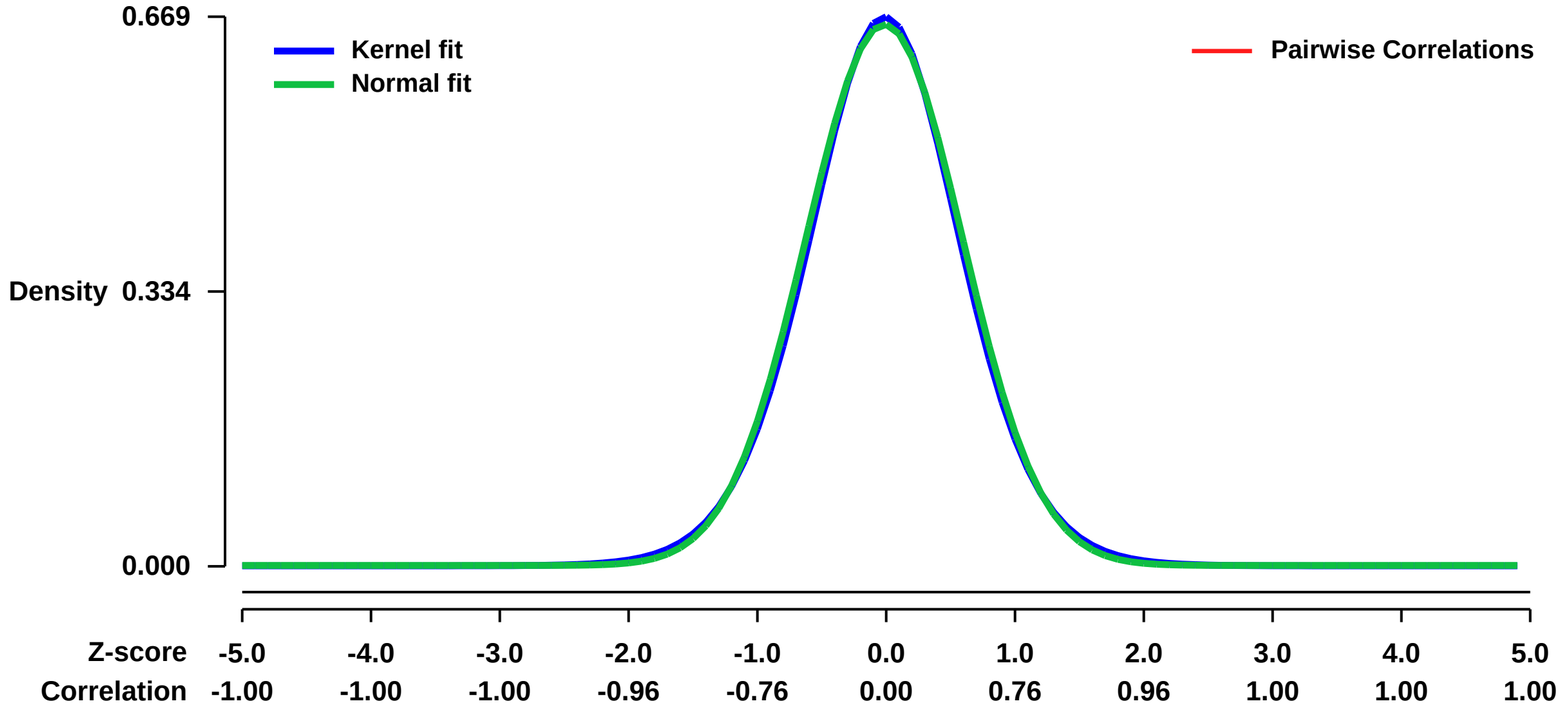

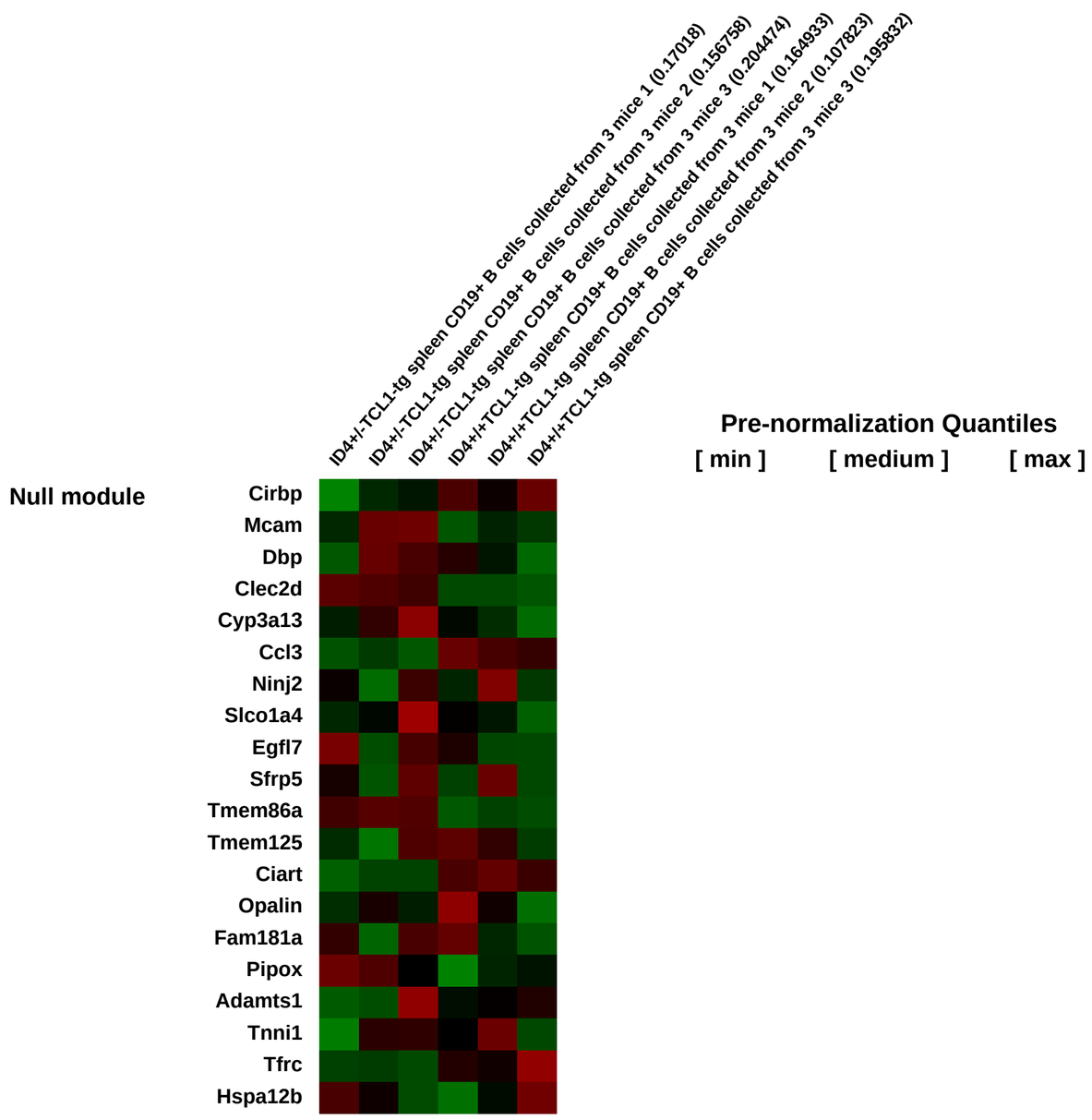

GEO Series "GSE11222" Expression Profiles

Num of samples in this series: 42

Scale of expression profile Z-scores

-3.0 -2.0 -1.0 0.0 1.0 2.0 3.0

GEO Link: http://www.ncbi.nlm.nih.gov/geo/query/acc.cgi?acc=GSE11222
Status: Public on Apr 23 2008
Title: Placental and decidual timecourse samples normalized and modeled with an undissected e17 sample
Organism: Mus musculus
Experiment type: Expression profiling by array
Platform: GPL1261
Pubmed ID: 18340042

Summary & Design:

Summary:
We used full genome microarrays to profile the full lifetime of the mouse placenta from embryonic day 8.5 (e8.5), at the time of chorioallantoic fusion, until postnatal day 0 (P0). For these samples, at each stage the fetal placenta and maternal decidual tissues were dissected and profiled separately (See series 1).

For this experiment (Series 2), placental and decidual timecourse samples were normalized and modeled with two undissected (including placental and decidual tissue) e17 placentas to allow for scaling of values for comparison to the undissected placenta samples used in the publicly available mouse GeneAtlas dataset

Keywords: time course

Overall design:
Mouse placentas were obtained from timed pregnant female mice at each timepoint, and fetal tissues were used to confirm embryo staging. For all dissected samples, fetal placenta and maternal decidual tissues were dissected and pooled separately for each litter prior to RNA extraction and hybridization on Affymetrix microarrays.

Background corr dist: KL-Divergence = 0.1507, L1-Distance = 0.0356, L2-Distance = 0.0027, Normal std = 0.3773

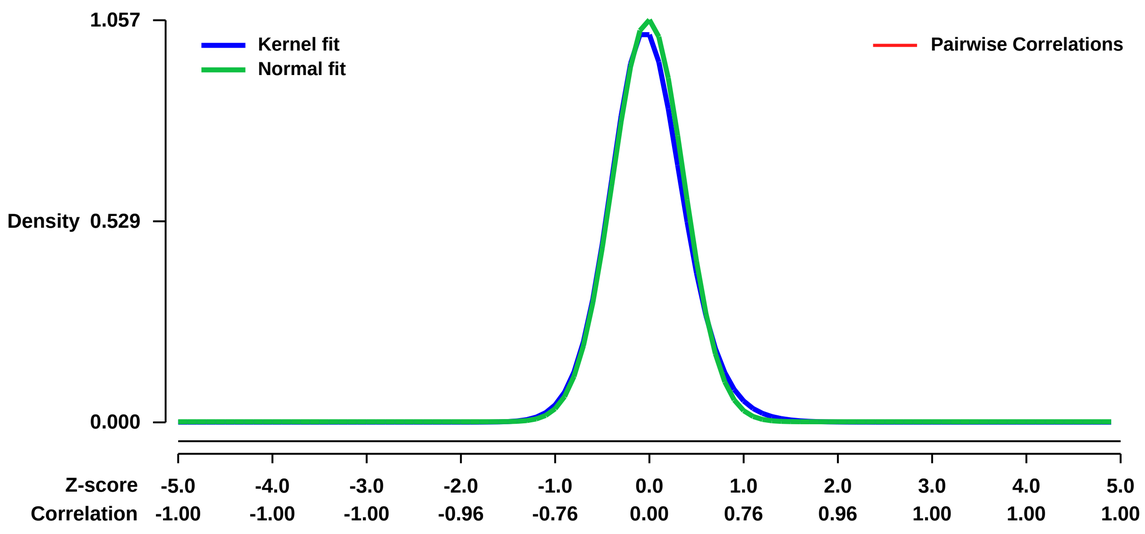

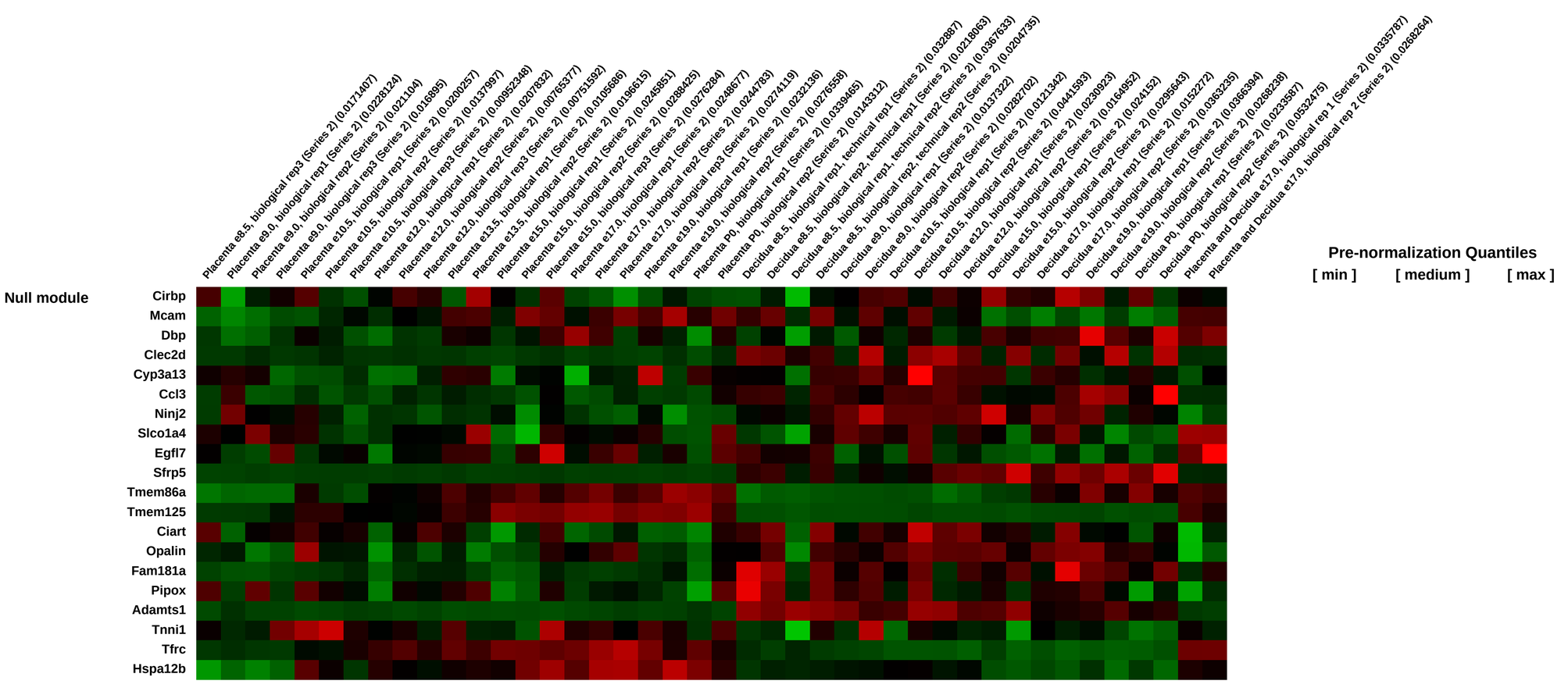

GEO Series "GSE19796" Expression Profiles

Num of samples in this series: 7

Scale of expression profile Z-scores

-3.0 -2.0 -1.0 0.0 1.0 2.0 3.0

GEO Link:	http://www.ncbi.nlm.nih.gov/geo/query/acc.cgi?acc=GSE19796
Status:	Public on Feb 21 2011
Title:	Expression data from Bmi1-null c-Kit+Sca-1+Lineage marker- (KSL) hematopoietic stem/progenitor cells
Organism:	Mus musculus
Experiment type:	Expression profiling by array
Platform:	GPL1261
Pubmed ID:	22351929
Summary & Design:	**Summary:** Bmi1 is a component of polycomb repressive complex 1 and its role in the inheritance of the stemness of adult somatic stem cells has been well characterized. Bmi1 maintains the self-renewal capacity of adult stem cells, at least partially, by repressing the Ink4a/Arf locus that encodes a cyclin-dependent kinase inhibitor, p16Ink4a, and a tumor suppressor, p19Arf 14. Deletion of both Ink4a and Arf in Bmi1-deficient mice substantially restored the defective self-renewal capacity of HSCs and neural stem cells. **Overall design:** Purified KSL cells from BM of wild-type, Bmi1-/-, Ink4a-/-Arf-/-, and Bmi1-/- Ink4a-/-Arf-/- mice were subjected to RNA extraction and hybridization on Affymetrix microarrays.

Background corr dist: KL-Divergence = 0.0650, L1-Distance = 0.0222, L2-Distance = 0.0007, Normal std = 0.5242

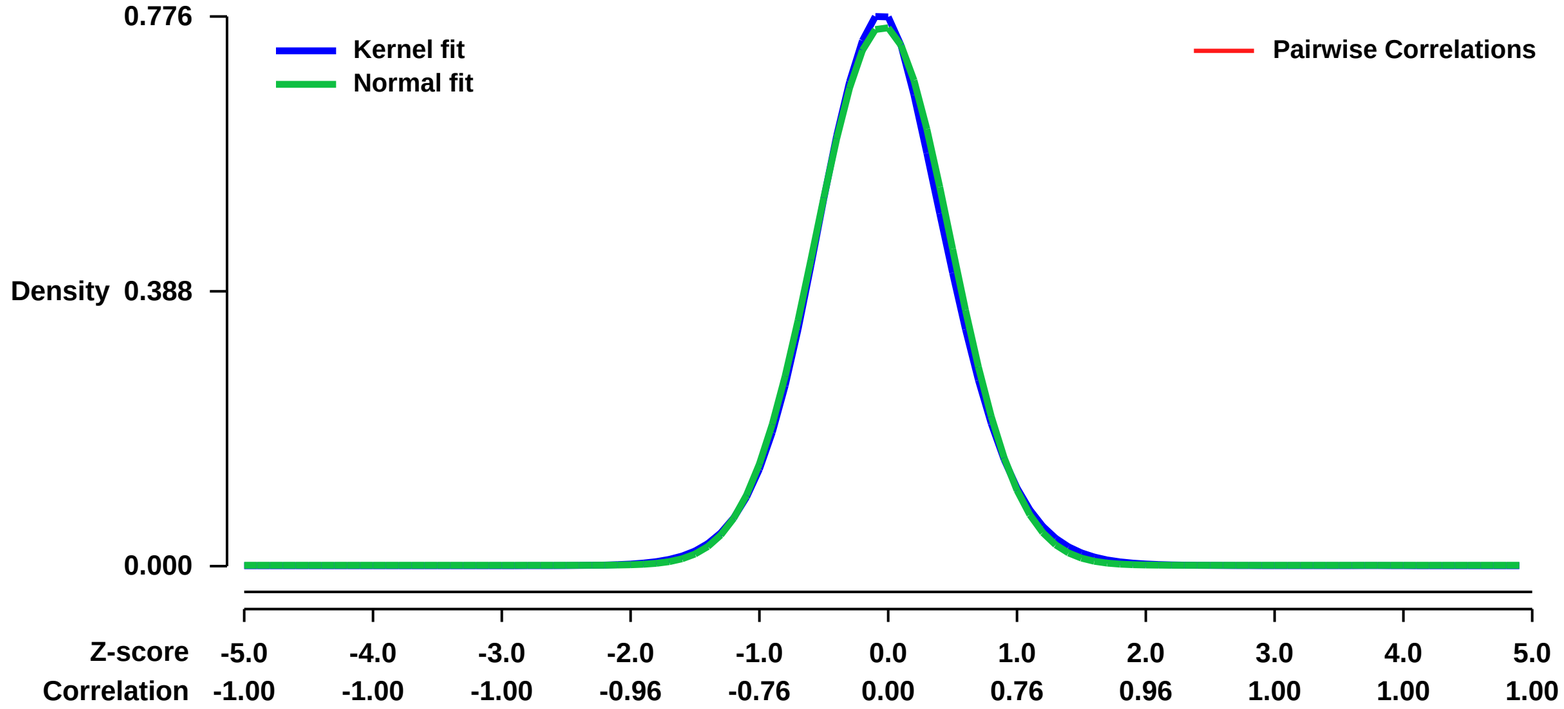

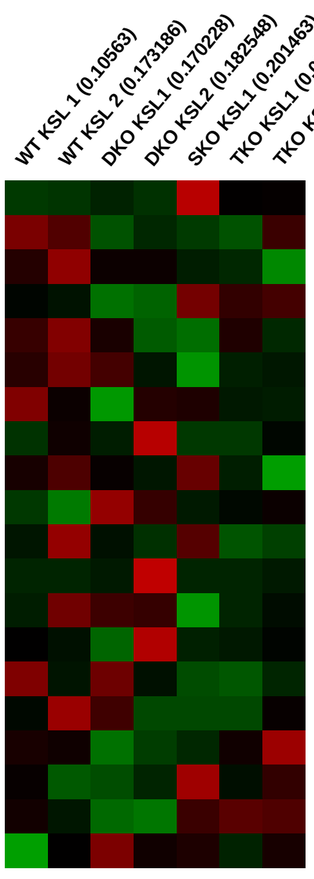

GEO Series "GSE20352" Expression Profiles

Num of samples in this series: 6

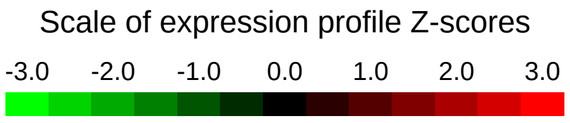

GEO Link:	http://www.ncbi.nlm.nih.gov/geo/query/acc.cgi?acc=GSE20352
Status:	Public on Feb 16 2010
Title:	The Apcmin mouse has altered hematopoietic stem cell function and provides a model for MPD/MDS
Organism:	Mus musculus
Experiment type:	Expression profiling by array
Platform:	GPL1261
Pubmed ID:	20197553
Summary & Design:	**Summary:** Apc, a negative regulator of the canonical Wnt signaling pathway, is a bona-fide tumor suppressor whose loss of function results in intestinal polyposis. APC is located in a commonly deleted region on human chromosome 5q, associated with myelodysplastic syndrome (MDS) suggesting that haploinsufficiency of APC contributes to the MDS phenotype. Analysis of the hematopoietic system of mice with the Apcmin allele that results in a premature stop codon and loss of function, showed no abnormality in steady state hematopoiesis. Bone marrow derived from Apcmin mice showed enhanced repopulation potential, indicating of a cell intrinsic gain of function in the long-term hematopoietic stem cell (HSC) population. However, Apcmin bone marrow was unable to repopulate secondary recipients due to loss of the quiescent HSC population. Apcmin mice developed a myelodysplastic/ myeloproliferative phenotype. Our data indicate that Wnt activation through haploinsufficiency of Apc causes insidious loss of HSC function that is only evident in serial transplantation strategies. These data provide a cautionary note for HSC expansion strategies through Wnt pathway activation, provide evidence that cell extrinsic factors can contribute to the development of myeloid disease and indicate that loss of function of APC may contribute to the phenotype observed in patients with MDS and del(5q). **Overall design:** LKS+ cells were isolated from Apcmin or WT mice using high-speed multiparameter flow cytometry. At least 2x104 cells per mouse were isolated with confirmed purity in excess of 90%. The cells were treated with RLT lysis buffer (Qiagen) containing beta-mercaptoethanol to stabilize RNA. RNA was extracted using Qiagen RNeasy Micro Kit according to manufacturers instruction. The RNA was amplified using a linear amplification protocol (Nugen Ovation V2 amplification system). cDNA was fragmented and biotinylated before hybridization onto Affymetrix mouse genome 430 2.0 Array chips

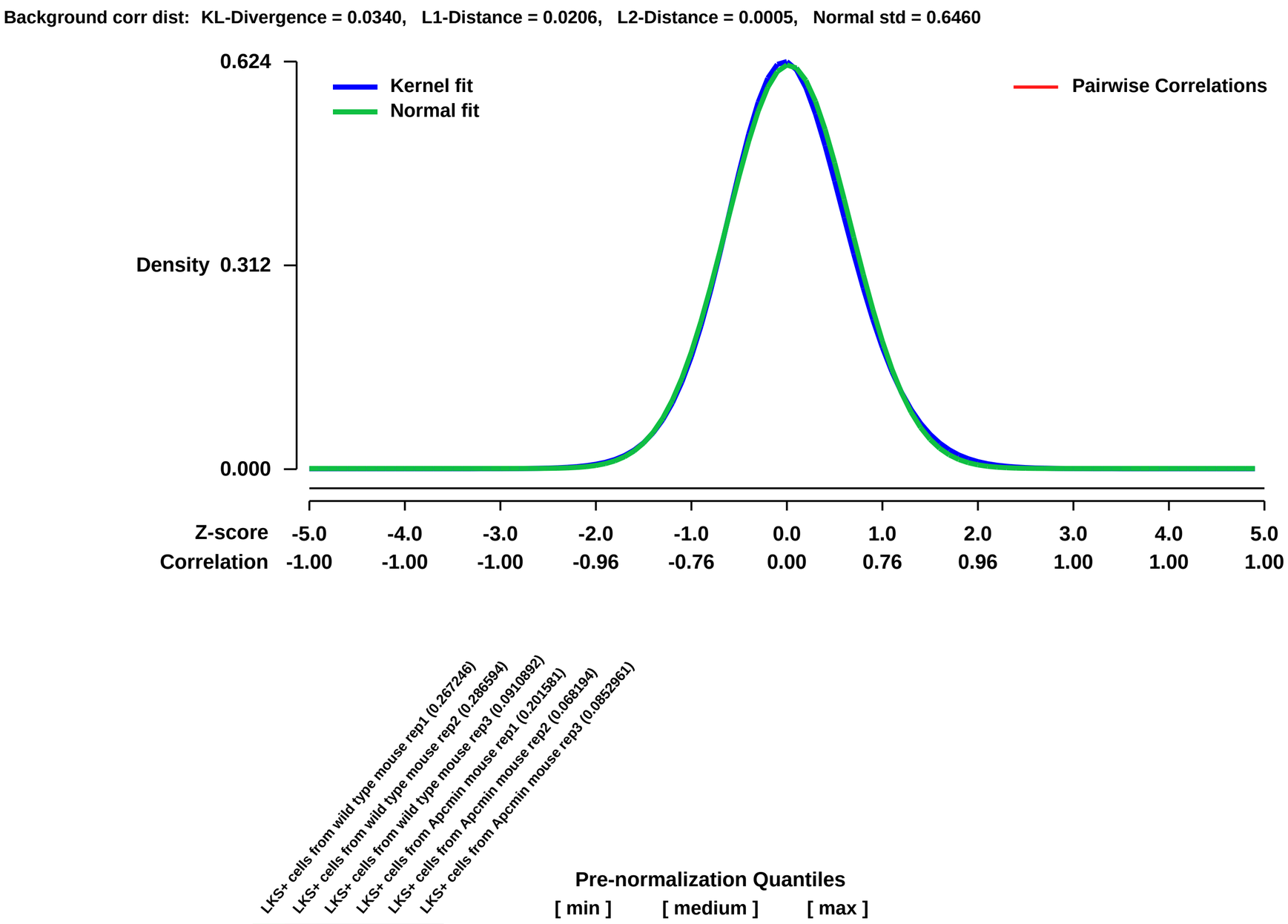

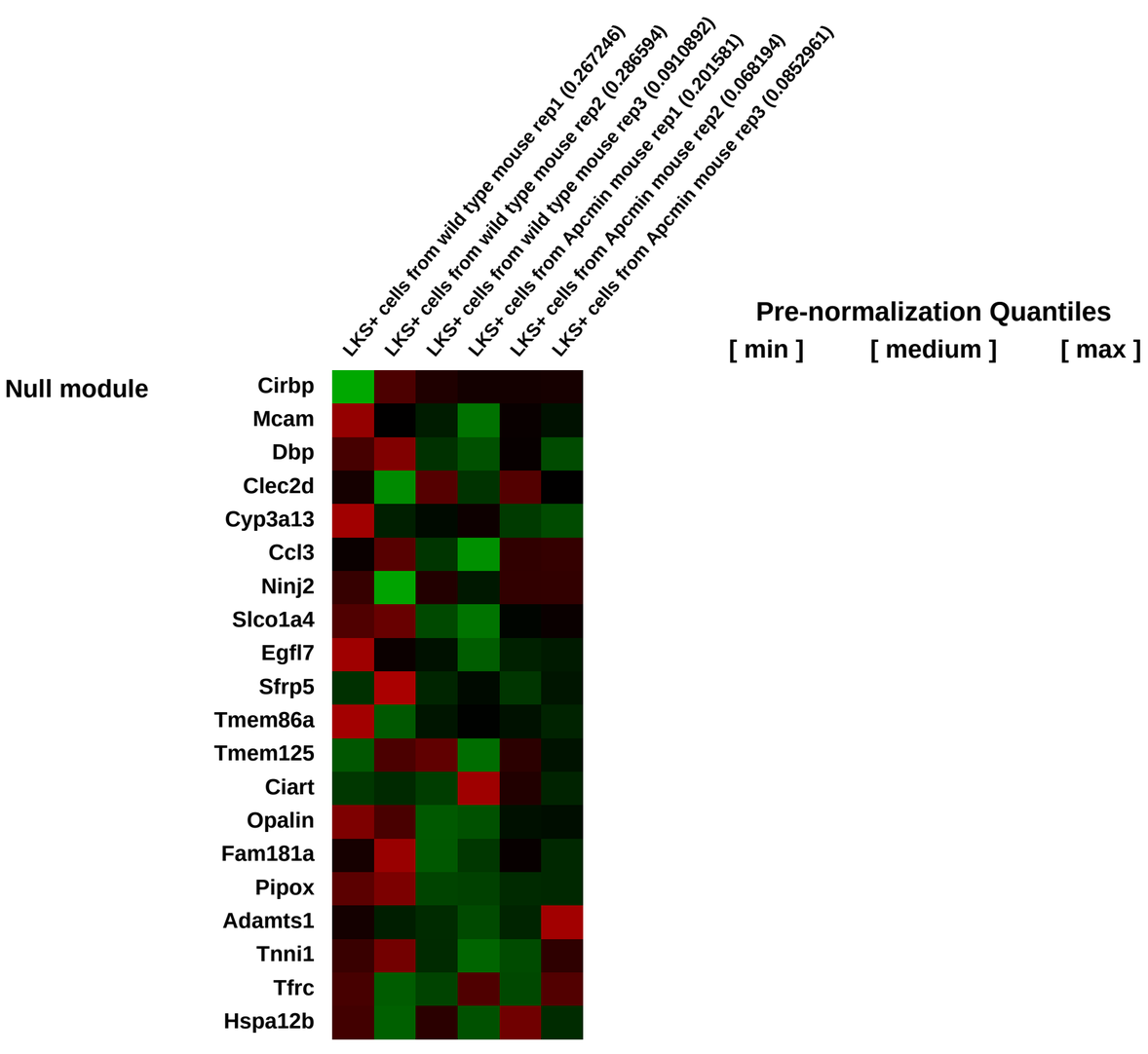

GEO Series "GSE16676" Expression Profiles

Num of samples in this series: 11

Scale of expression profile Z-scores

-3.0 -2.0 -1.0 0.0 1.0 2.0 3.0

GEO Link:	http://www.ncbi.nlm.nih.gov/geo/query/acc.cgi?acc=GSE16676
Status:	Public on Aug 01 2010
Title:	Rescue of murine Gata1s mutant M7 leukemic cells by full-length Gata1
Organism:	Mus musculus
Experiment type:	Expression profiling by array
Platform:	GPL1261
Pubmed ID:	20679399
Summary & Design:	**Summary:** In this project, we studied a mouse model of human Down Syndrome (DS) megakaryocytic leukemia involving mutations in the GATA1 transcription factor (called GATA1s mutation). The model was generated through retroviral insertional mutagenesis in Gata1s mutant fetal liver progenitors. In this study, we analyzed the dependency of these leukemic cells on the Gata1s mutant protein. Here we report Gata1s mutant leukemic cells were dependent on this mutant protein. Introduction of the full-length Gata1 protein to these cells led to their reduced proliferation and increased differentiation along the megakaryocytic lineage. **Overall design:** We transduced leukemic cells with Gata1/estrogen receptor fusion cDNA (Gata1-ER) and generated stable cell lines. Addition of beta-estradiol to culture medium led to activation of the full-length Gata1 protein in synchronized leukemic cells. Gene expression profiles were collected at multiple time points.

Background corr dist: KL-Divergence = 0.1370, L1-Distance = 0.0323, L2-Distance = 0.0018, Normal std = 0.3869

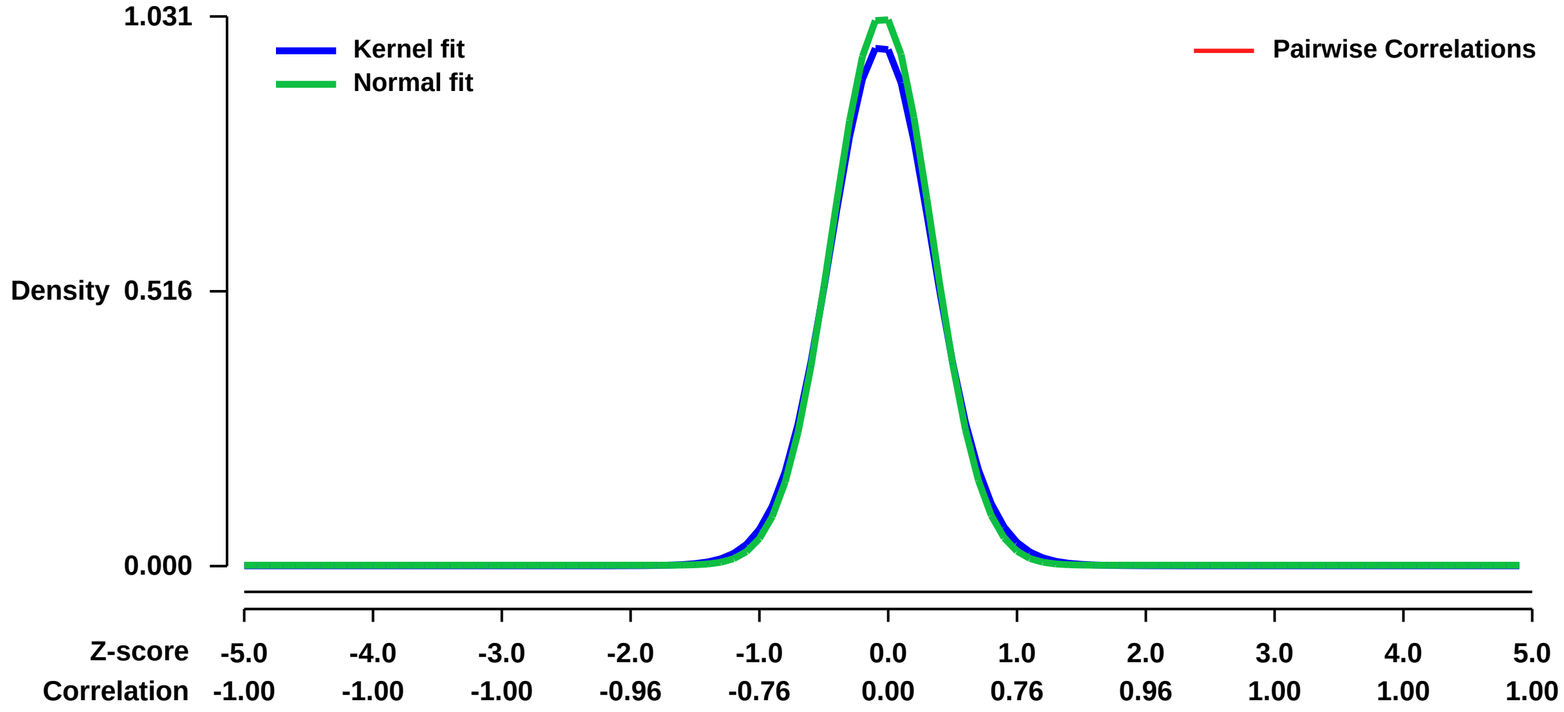

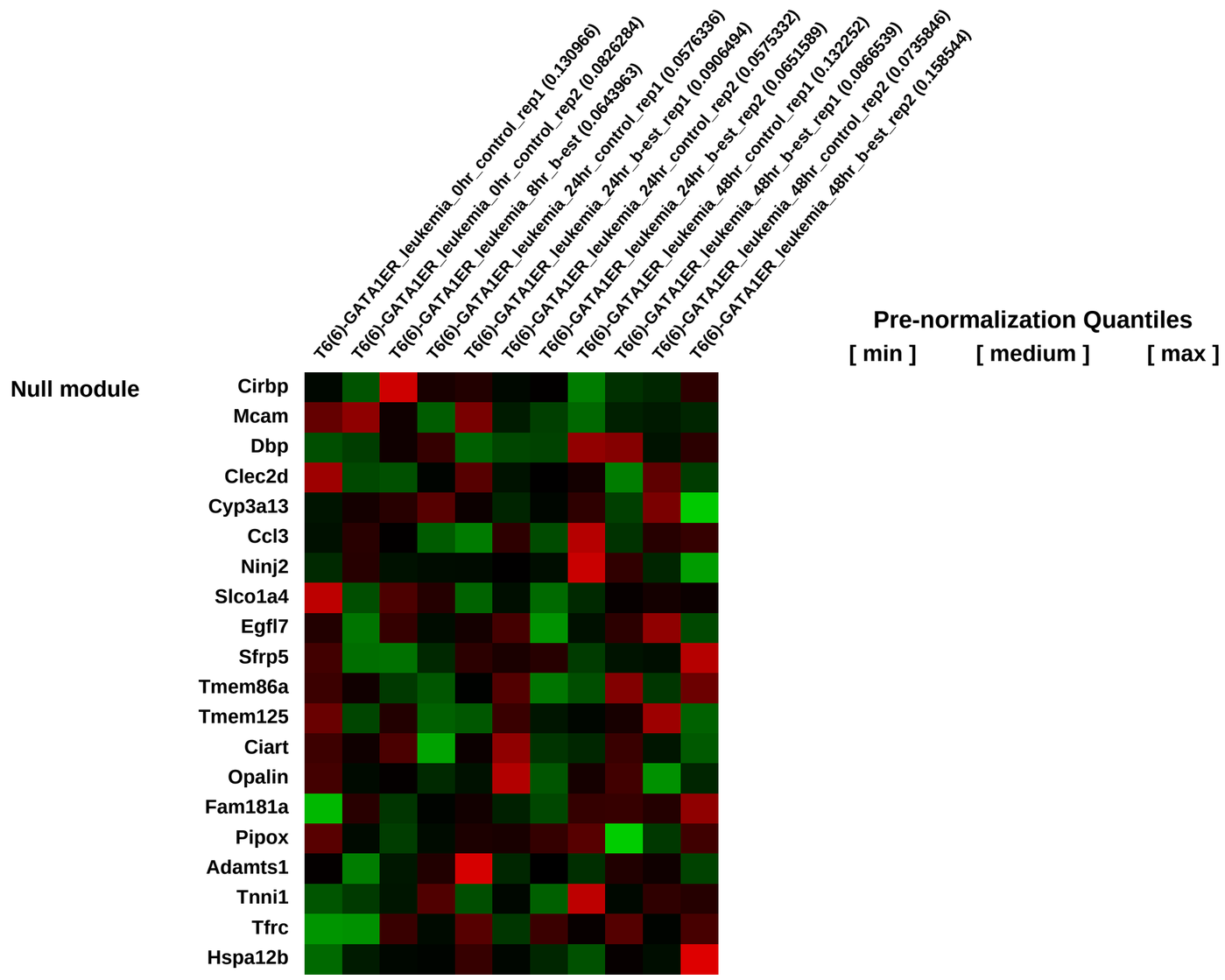

GEO Series "GSE4307" Expression Profiles

Num of samples in this series: 20

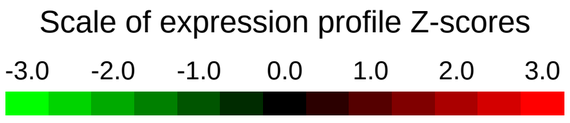

GEO Link:	http://www.ncbi.nlm.nih.gov/geo/query/acc.cgi?acc=GSE4307
Status:	Public on Apr 26 2006
Title:	Expression data from single cells from ICMs of mouse blastocysts at E3.5
Organism:	Mus musculus
Experiment type:	Expression profiling by array
Platform:	GPL1261
Pubmed ID:	16547197
Summary & Design:	**Summary:** The inner cell mass (ICM) of the early blastocyst at E3.5, a source of ES cell derivation, is a morphologically homogeneous population of undifferentiated pluripotent cells that give rise to all embryonic lineages. The immediate application of the newly developed V1V3 method to single cells in this stage of mouse embryos revealed the presence of two populations of cells, one with primitive endoderm expression and the other with pluripotent epiblast-like gene expression. The genes expressed differentially between these two populations were well preserved in morphologically differentiated primitive endoderm and epiblast in the embryos one day later (E4.5), demonstrating that the method successfully detects subtle but essential differences in gene expression at the single-cell level among seemingly homogeneous cell populations. This study provides a strategy to analyze biophysical events in medicine as well as in neural, stem cell, and developmental biology, where small numbers of distinctive or diseased cells play critical roles. **Keywords:** Single cell analysis **Overall design:** We isolated blastocysts at E3.5 and dissociated the ICM into single cells by trypsin-EDTA treatment. To prepare cDNA samples, we then randomly picked a total of 55 single cells. cDNAs were synthesized and amplified by the V1V3 method, and screened by gene-specific PCR using Oct4 and Cdx2 to remove trophectoderm cells, and 50 cells were identified as Oct4-positive and Cdx2-negative, ICM cells.

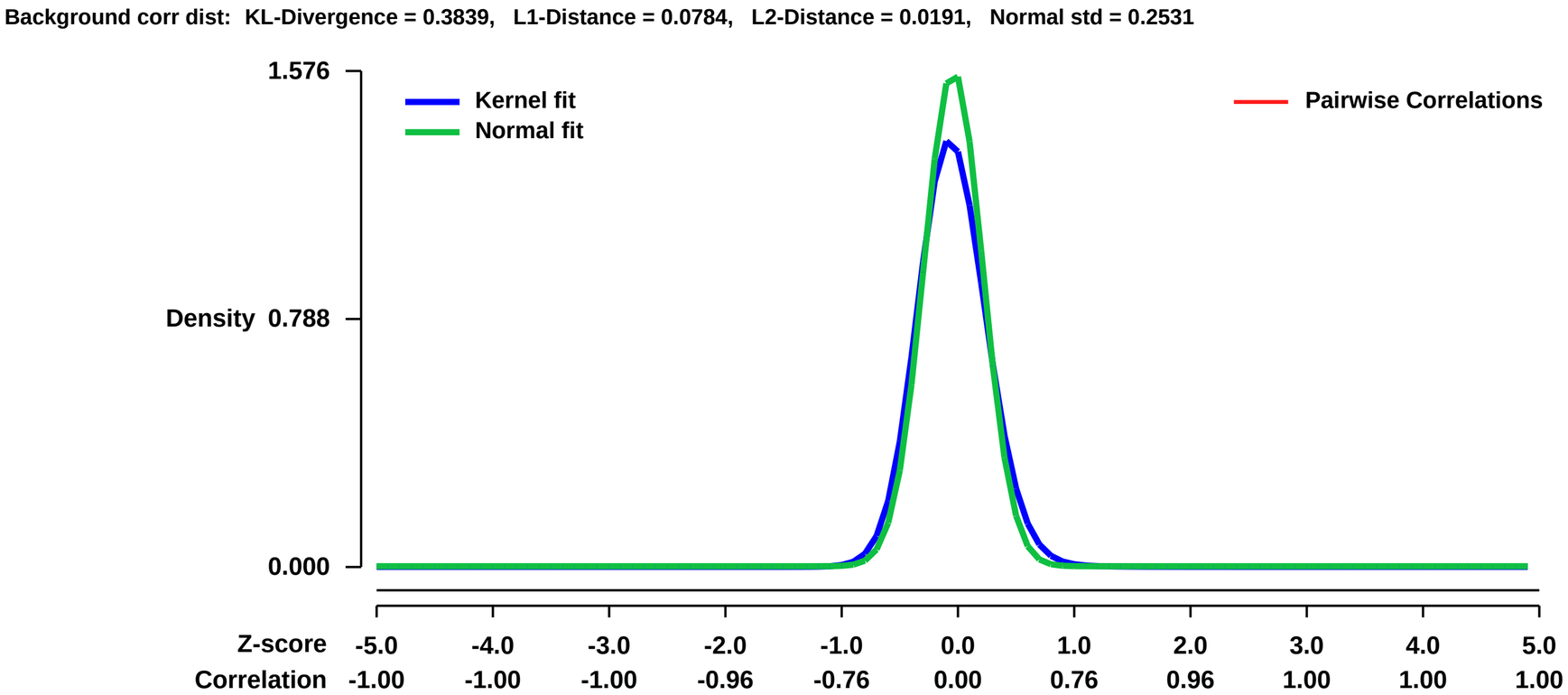

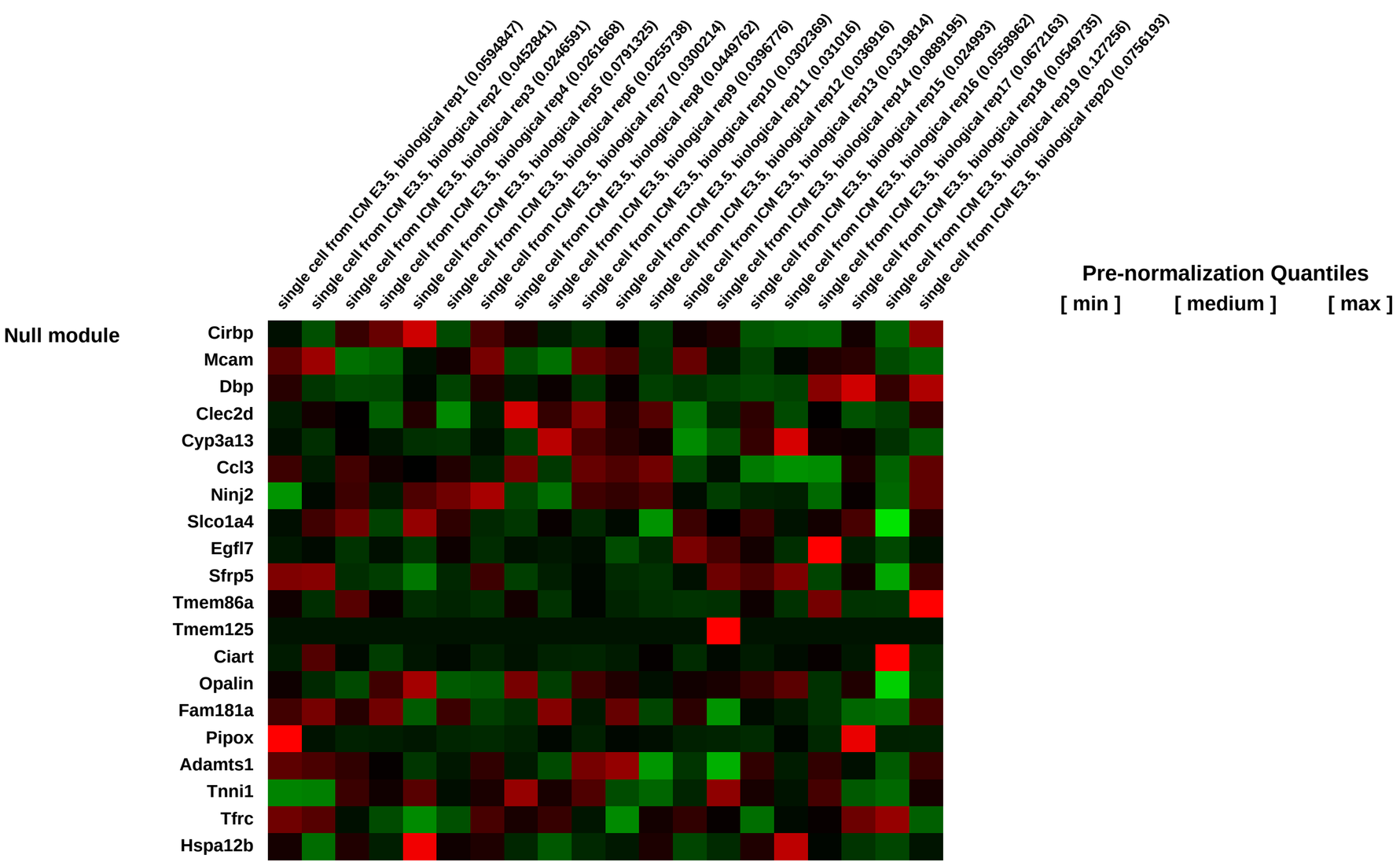

GEO Series "GSE29485" Expression Profiles

Num of samples in this series: 12

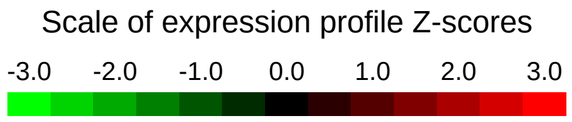

GEO Link:	**http://www.ncbi.nlm.nih.gov/geo/query/acc.cgi?acc=GSE29485**
Status:	**Public on Jul 01 2011**
Title:	**Expression data from Mouse embryo**
Organism:	**Mus musculus**
Experiment type:	**Expression profiling by array**
Platform:	**GPL1261**
Pubmed ID:	**22186409**
Summary & Design:	**Summary:** **Mice lacking the function of the PcG protein CBX2 (also known as M33) show defects in gonadal, adrenal, and splenic development. In particular, XY knockout mice develop ovaries but not testes, and the gonads are hypoplastic in both sexes.** **To clarify the molecular basis of the defects, RNA prepared from both wild type and KO gonads were subjected to microarray analyses.** **Overall design:** **Mouse embryonic gonads of Cbx2 knockout (KO) were sectioned and recovered at E11.5 for RNA extraction and hybridization on Affymetrix microarrays. Four different genotypes of embryos at E11.5 (XY WT, XX WT, XY Cbx2 KO, and XX Cbx2 KO) were frozen in OCT compound without fixation. They were sectioned to 30 ¿…m slices and stained with hematoxylin. The developing gonadal cells localized by GATA4 immunostaining and morphology were prepared using a Laser Microdissection System. The specimens prepared from two or three individuals were combined into one group, and three groups were prepared for each genotype.**

Background corr dist: KL-Divergence = 0.0809, L1-Distance = 0.0245, L2-Distance = 0.0009, Normal std = 0.4711

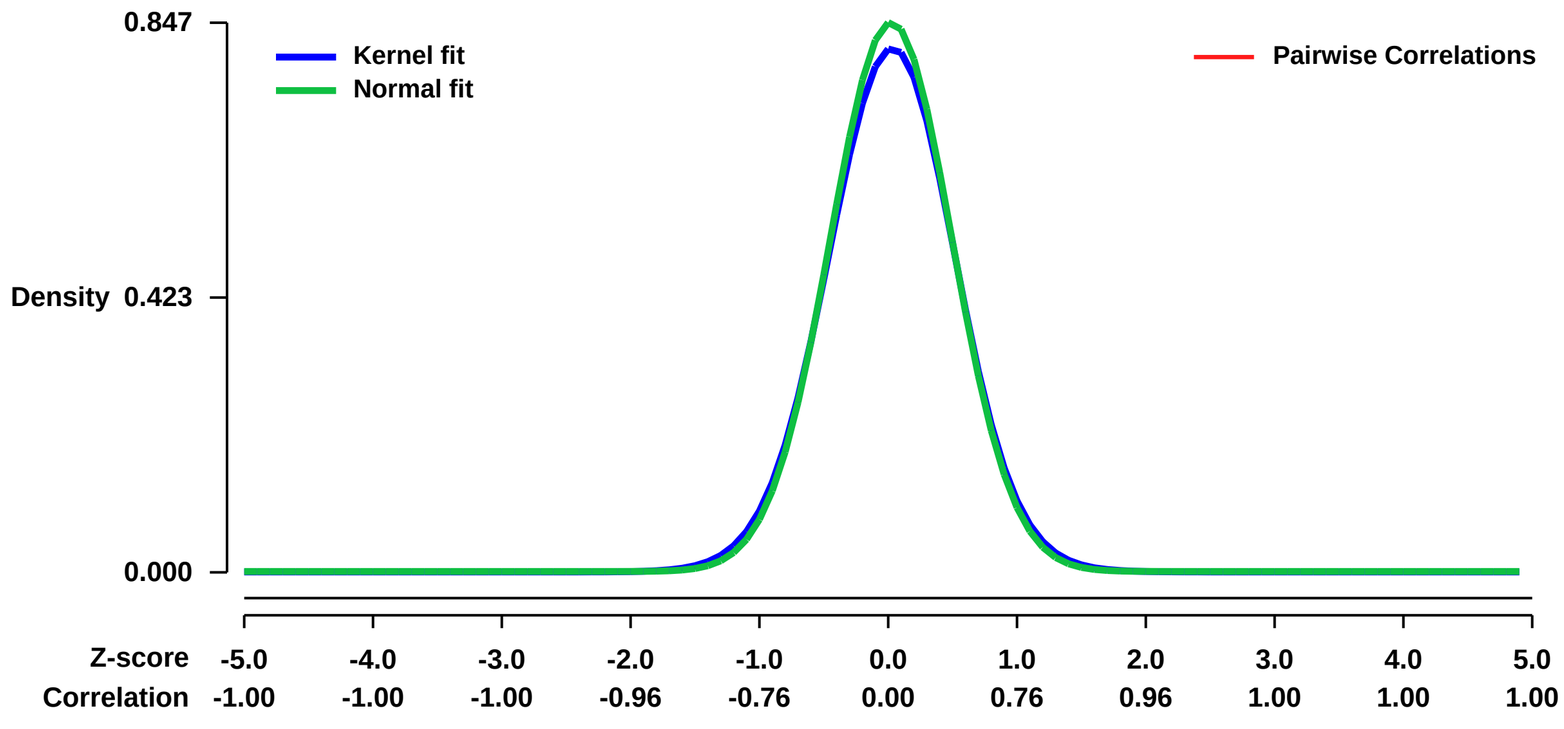

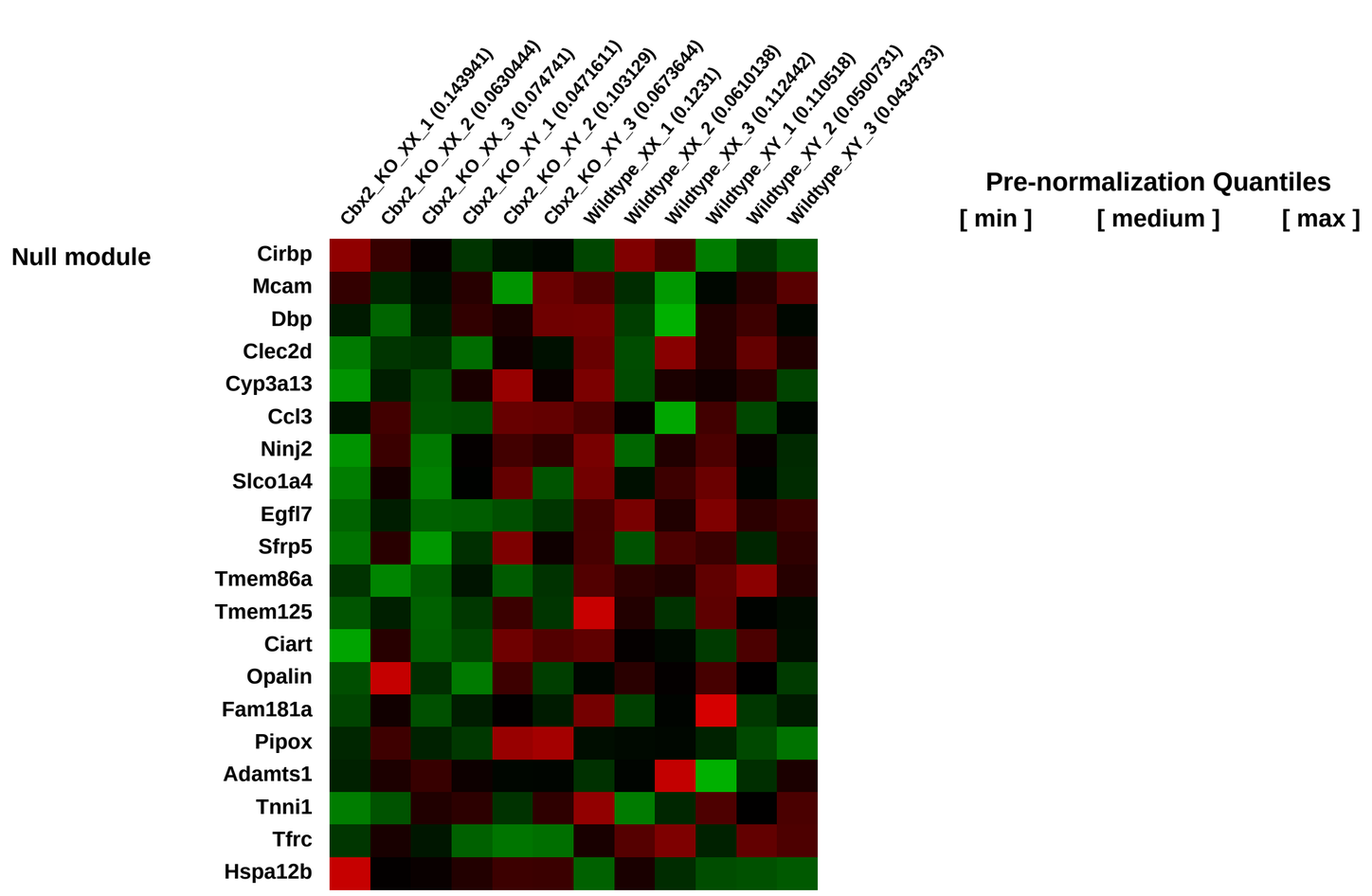

GEO Series "GSE44091" Expression Profiles

Num of samples in this series: 32

Scale of expression profile Z-scores

-3.0 -2.0 -1.0 0.0 1.0 2.0 3.0

GEO Link:	http://www.ncbi.nlm.nih.gov/geo/query/acc.cgi?acc=GSE44091
Status:	Public on Jul 30 2013
Title:	Genome-wide expression of the epithelial layer cells of mice injected with Clostridium difficile Toxin A and B
Organism:	Mus musculus
Experiment type:	Expression profiling by array
Platform:	GPL1261
Pubmed ID:	23897615
Summary & Design:	**Summary:** Toxin A (TcdA) and Toxin B (TcdB), of the pathogen Clostridium difficile, are virulence factors that cause gross pathologic changes (e.g. inflammation, secretion, and diarrhea) in the infected host, yet the molecular and cellular pathways leading to observed host responses are poorly understood. To address this gap, TcdA and/or TcdB were injected into the ceca of mice and the genome-wide transcriptional response of epithelial layer cells was examined. Bioinformatic analysis of gene expression identified sets of cooperatively expressed genes. Further analysis of inflammation associated genes revealed dynamic chemokine responses. **Overall design:** In total, 32 samples were analyzed (one microarray per mouse). The sample groups are separated by two factors: Toxin (TcdA, TcdB, TcdA+TcdB, or Sham injection) and endpoint (2, 6, or 16h). TcdA+B at 16h was not included, leaving 11 sample groups. Each sample group included biological triplicates, except TcdA+TcdB at 6h (one array) and Sham injection at 16h (four arrays).

Background corr dist: KL-Divergence = 0.2592, L1-Distance = 0.0407, L2-Distance = 0.0031, Normal std = 0.3015

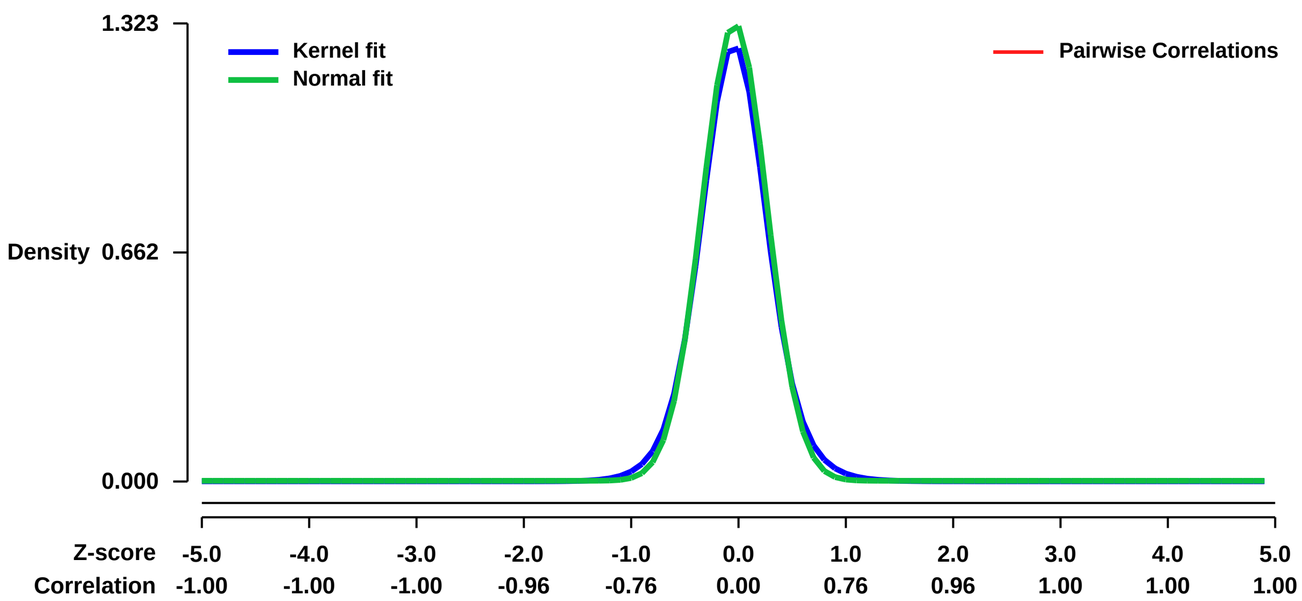

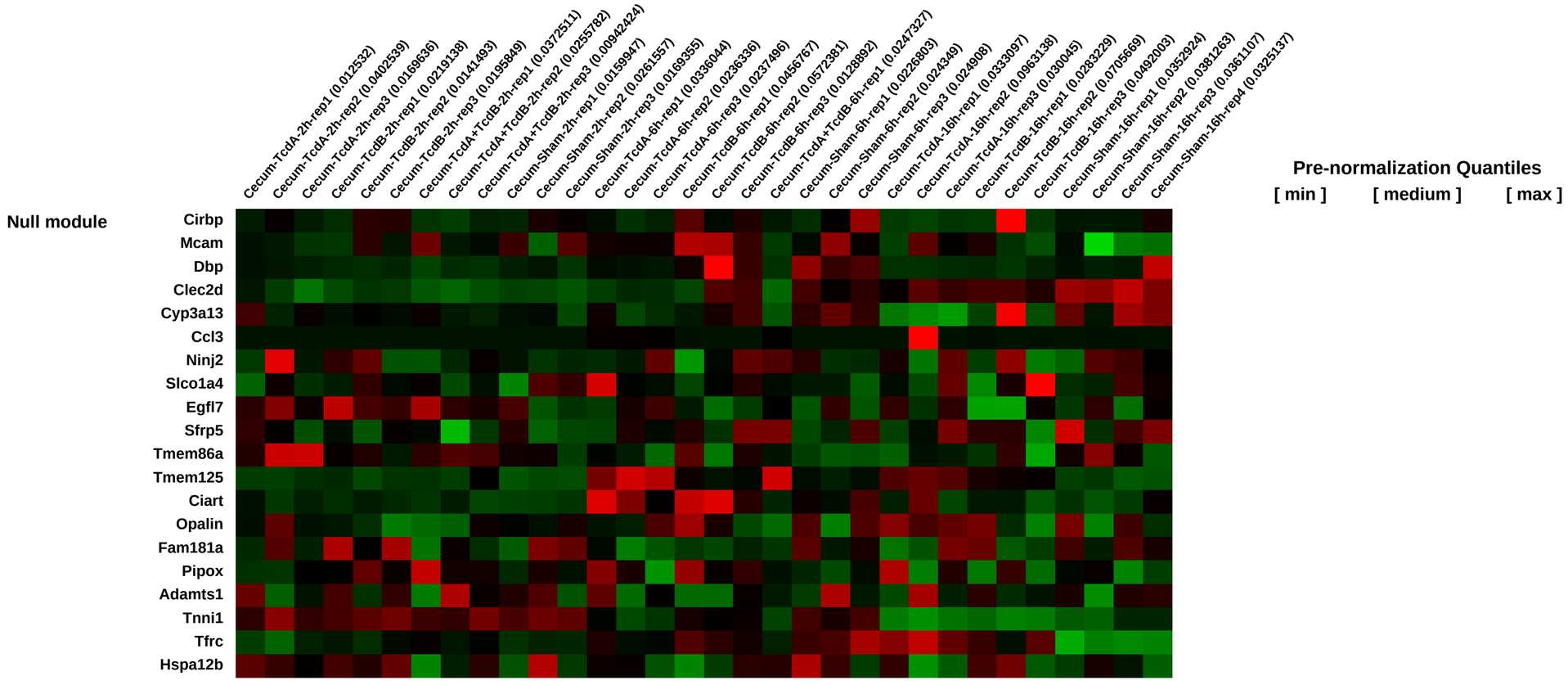

GEO Series "GSE4481" Expression Profiles

Num of samples in this series: 18

Scale of expression profile Z-scores

-3.0 -2.0 -1.0 0.0 1.0 2.0 3.0

GEO Link:	**http://www.ncbi.nlm.nih.gov/geo/query/acc.cgi?acc=GSE4481**
Status:	**Public on Dec 15 2006**
Title:	**C-type natriuretic peptide regulates endochondral ossification through p38 MAP kinase-dependent pathways_2**
Organism:	**Mus musculus**
Experiment type:	**Expression profiling by array**
Platform:	**GPL1261**
Pubmed ID:	
Summary & Design:	**Summary:** **C-type natriuretic peptide (CNP) has been recently identified as an important anabolic regulator of endochondral bone growth, but the molecular mechanism mediating these effects are not completely understood. Here we demonstrate that CNP activates the p38 MAP kinase pathway in chondrocytes and that pharmacological inhibition of p38 blocks the anabolic effects of CNP in a tibia organ culture system. We further show that CNP stimulates endochondral bone growth largely through expansion of the hypertrophic zone of the growth plate, while delaying mineralization. Both effects are reversed by p38 inhibition. We performed Affymetrix microarray analyses to identify CNP target genes in the organ culture system. These studies confirmed that hypertrophic chondrocytes are the main targets of CNP signaling in the growth plate, potentially because cGMP-dependent kinases I and II, important transducers of CNP signaling and are expressed at much higher levels in these cells than in other areas of the tibia. One of the genes most strongly induced by CNP was the Ptgs2 gene, encoding Cox2. Real-time PCR confirmed that Cox2 expression was induced by CNP in hypertrophic chondrocytes, but surprisingly in a p38-independent manner. Moreover, Cox2 inhibition â in contrast to p38 inhibition - did not block the anabolic effects of CNP. In summary, our data identify novel target genes of CNP and demonstrate that the p38 pathway is a novel, essential mediator of CNP effects on endochondral ossification, with potential implications for numerous skeletal diseases.** **Keywords: Growth plate zone comparison and treatment response analysis** **Overall design:** **Tibiae from E15.5 day old embryonic mice were isolated and cultured in minimal media in the presence of vehicle, BSA/HCl (1mM), or C-type natriuretic peptide, CNP (10-6M). On the sixth day of treatment cultured tibias were micro-dissected into the resting/proliferating, hypertrophic, and mineralized areas. Distinct zones from approximately 24 bones were pooled together, from which RNA was isolated using the Qiagen RNeasy Lipid Extraction Kit. Once the quality of total RNA from three independent trials was determined using the Agilent 2100 bioanalyzer, microarray analyses were performed at the London Regional Genomics Centre using MOE430_2.0 Affymetrix arrays. Results were analyzed using GeneSpring 7.2 software.**

Background corr dist: KL-Divergence = 0.1409, L1-Distance = 0.0266, L2-Distance = 0.0011, Normal std = 0.3892

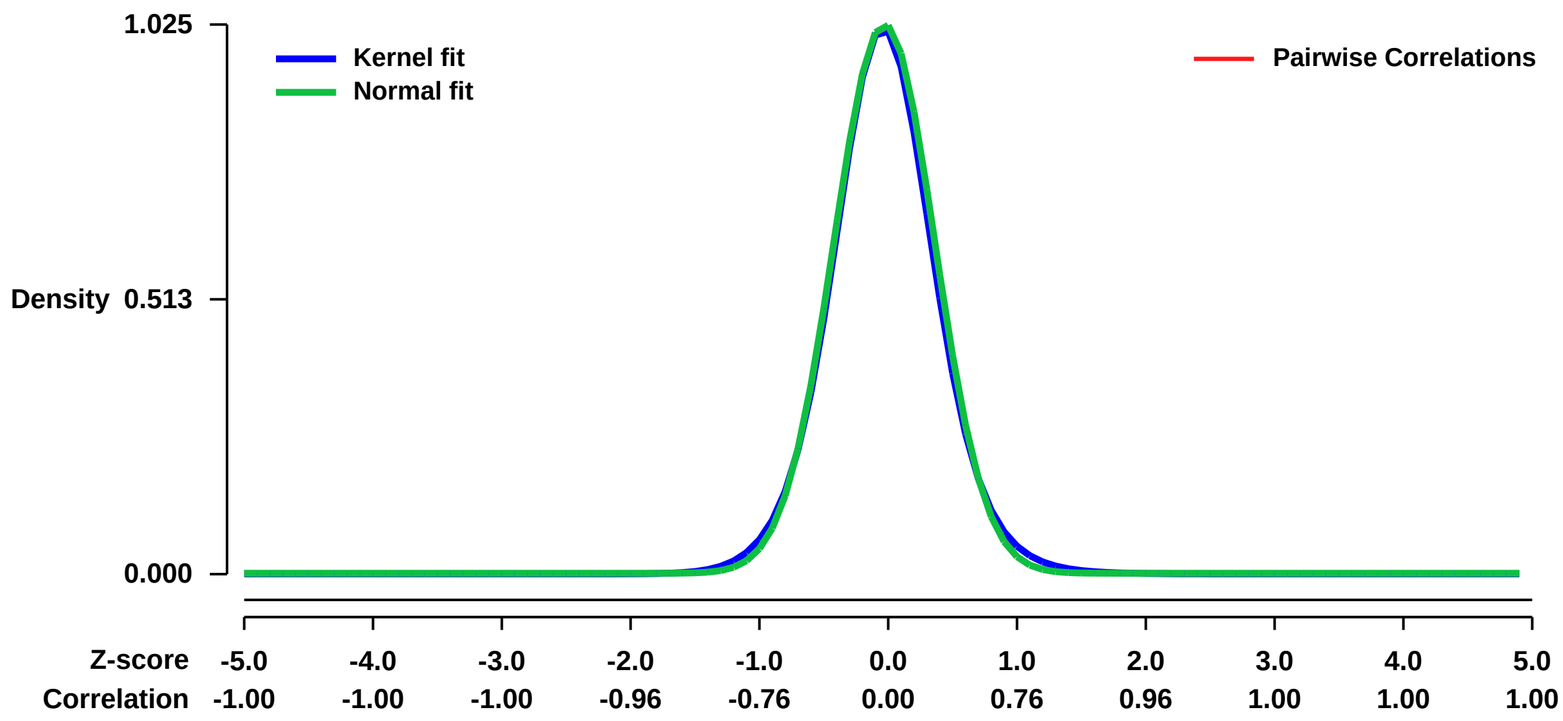

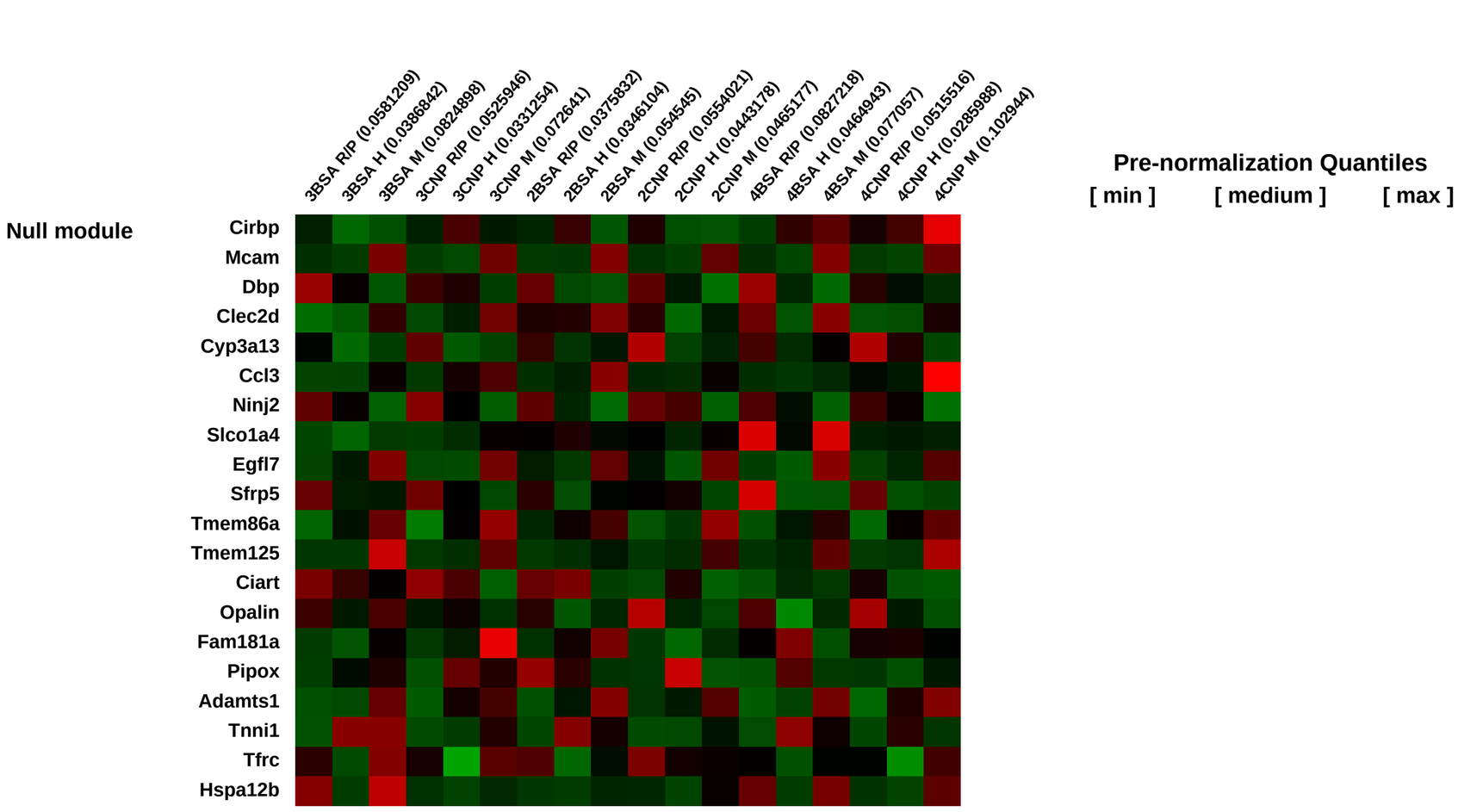

GEO Series "GSE13582" Expression Profiles

Num of samples in this series: 6

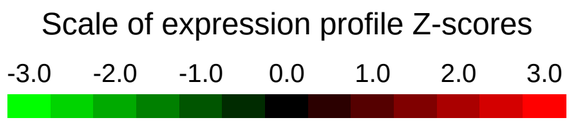

GEO Link:	http://www.ncbi.nlm.nih.gov/geo/query/acc.cgi?acc=GSE13582
Status:	Public on Jan 22 2009
Title:	Expression data from BAT of the KRAP deficient mice
Organism:	Mus musculus
Experiment type:	Expression profiling by array
Platform:	GPL1261
Pubmed ID:	19156225
Summary & Design:	**Summary:** KRAP (Ki-ras-induced actin-interacting protein) is a cytoskeleton-associated protein and a ubiquitous protein among tissues, originally identified as a cancer-related molecule. KRAP-deficient (KRAP-/-) mice show enhanced metabolic rate, decreased adiposity, improved glucose tolerance, hypoinsulinemia and hypoleptinemia. KRAP-/- mice are also protected against high-fat diet-induced obesity and insulin resistance despite of hyperphagia. **Overall design:** Total RNA was extracted from BAT of three pairs of littermates (KO1 vs. WT1, KO2 vs. WT2 and KO3 vs. WT3) fed normal chow.

Background corr dist: KL-Divergence = 0.0475, L1-Distance = 0.0257, L2-Distance = 0.0008, Normal std = 0.5908

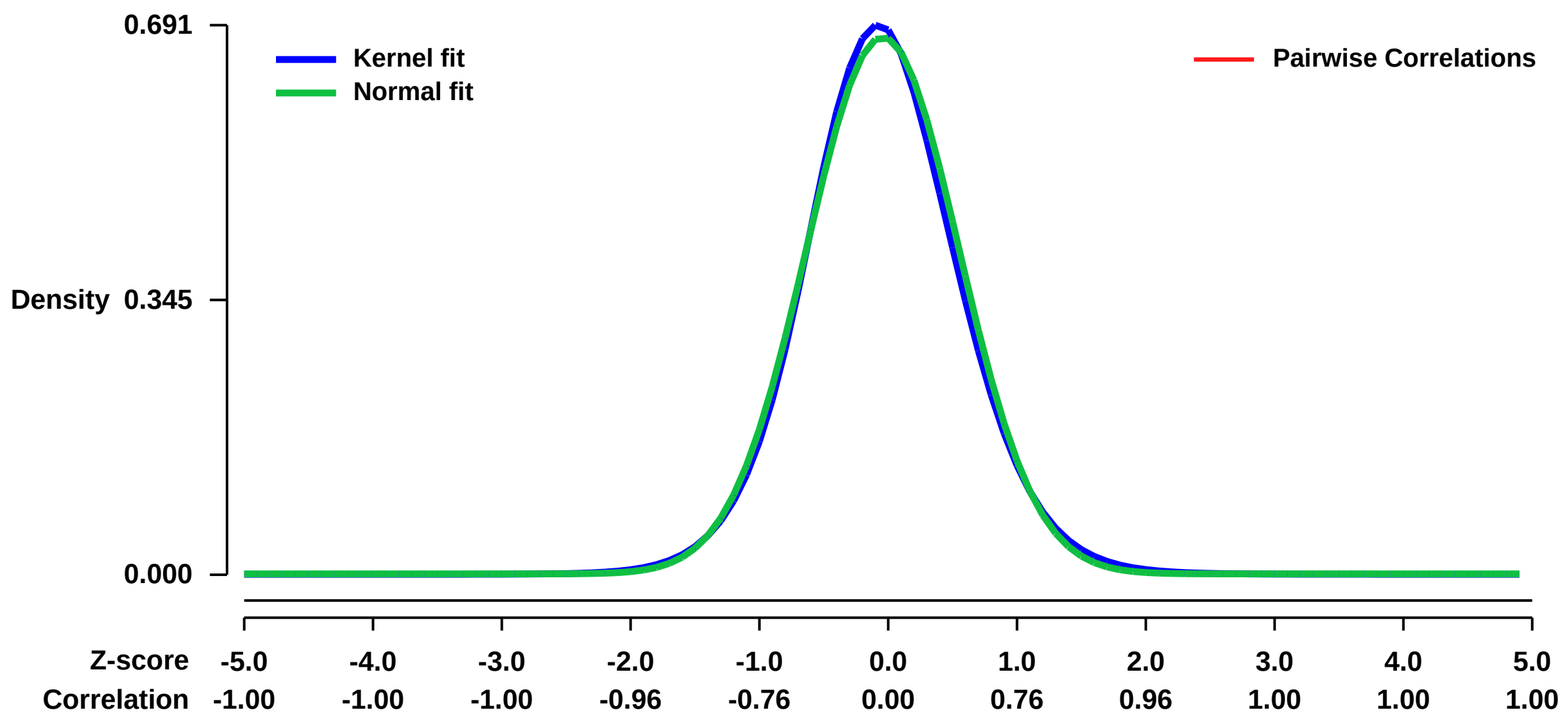

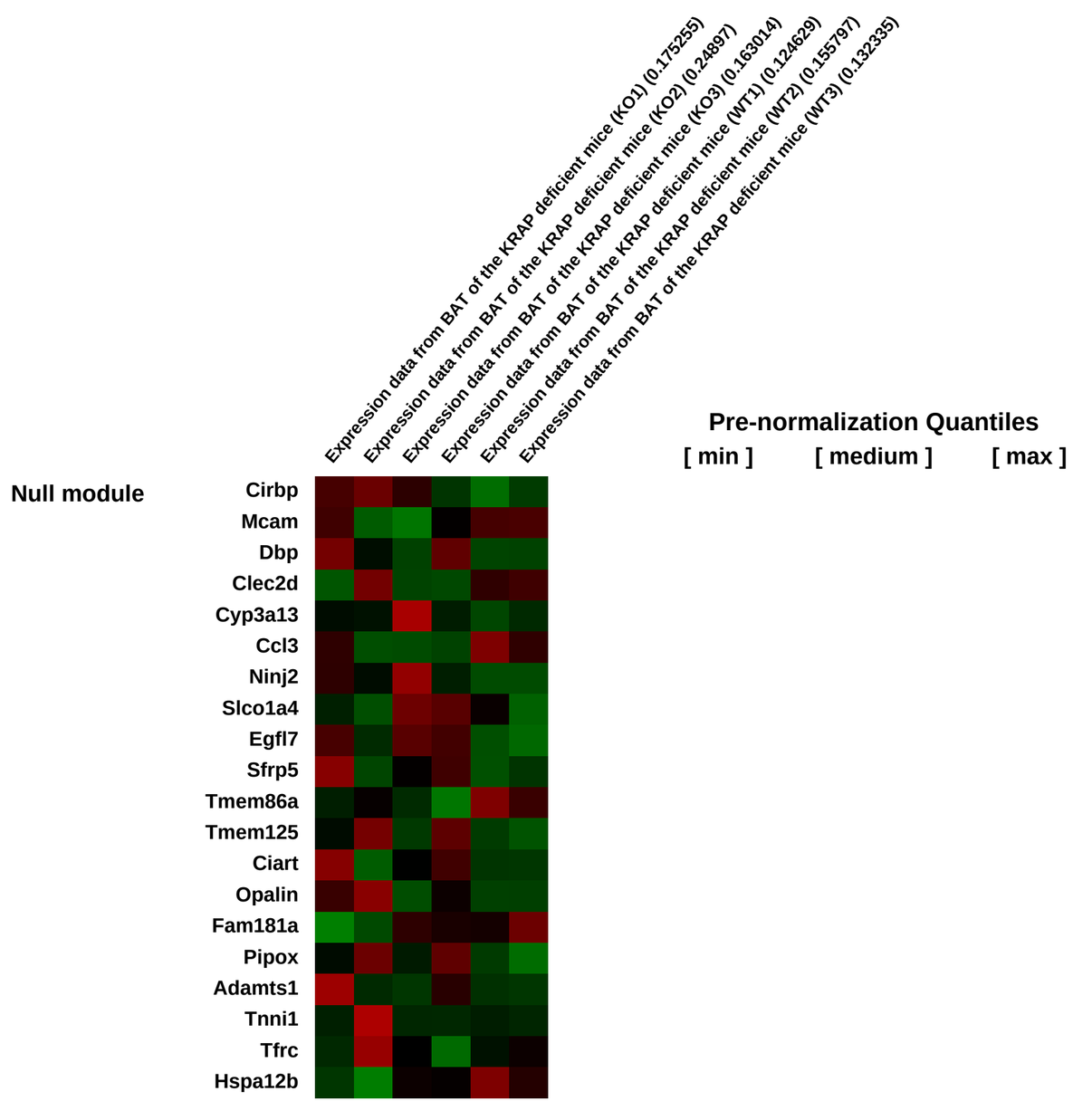

GEO Series "GSE26771" Expression Profiles

Num of samples in this series: 12

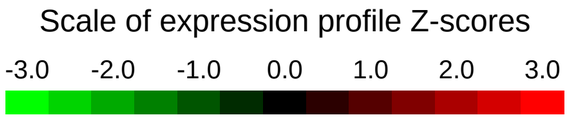

GEO Link:	**http://www.ncbi.nlm.nih.gov/geo/query/acc.cgi?acc=GSE26771**
Status:	**Public on Jan 22 2011**
Title:	**Expression data from primary mammary epithelial cells expressing ectopic p190B RhoGAP**
Organism:	**Mus musculus**
Experiment type:	**Expression profiling by array**
Platform:	**GPL1261**
Pubmed ID:	
Summary & Design:	**Summary:** **P190B RhoGAP is required for mammary gland development, and its overexpression disrupts mammary gland branching morphogenesis. To better understand the mechanisms by which p190B regulates mammary gland development we performed gene expression microarray analysis on mammary epithelial cells isolated from p190B overexpressing transgenic mice compared to control mice.** **Overall design:** **The mice used in this study were previously developed to inducibly overexpress p190B selectively in the mammary gland (Vargo-Gogola 2006). FVB/N mice carrying the MMTV-rtTA and TetO-p190B-IRES-luciferase transgenes or the MMTV-rtTA transgene only (Gunther EJ, FASEB) were fed doxycycline (Dox) chow (2 g/kg) for 7 d prior to removal of mammary glands and isolation of primary mammary epithelial cells at 6 weeks of age.**

Background corr dist: **KL-Divergence = 0.1492, L1-Distance = 0.0372, L2-Distance = 0.0027, Normal std = 0.3734**

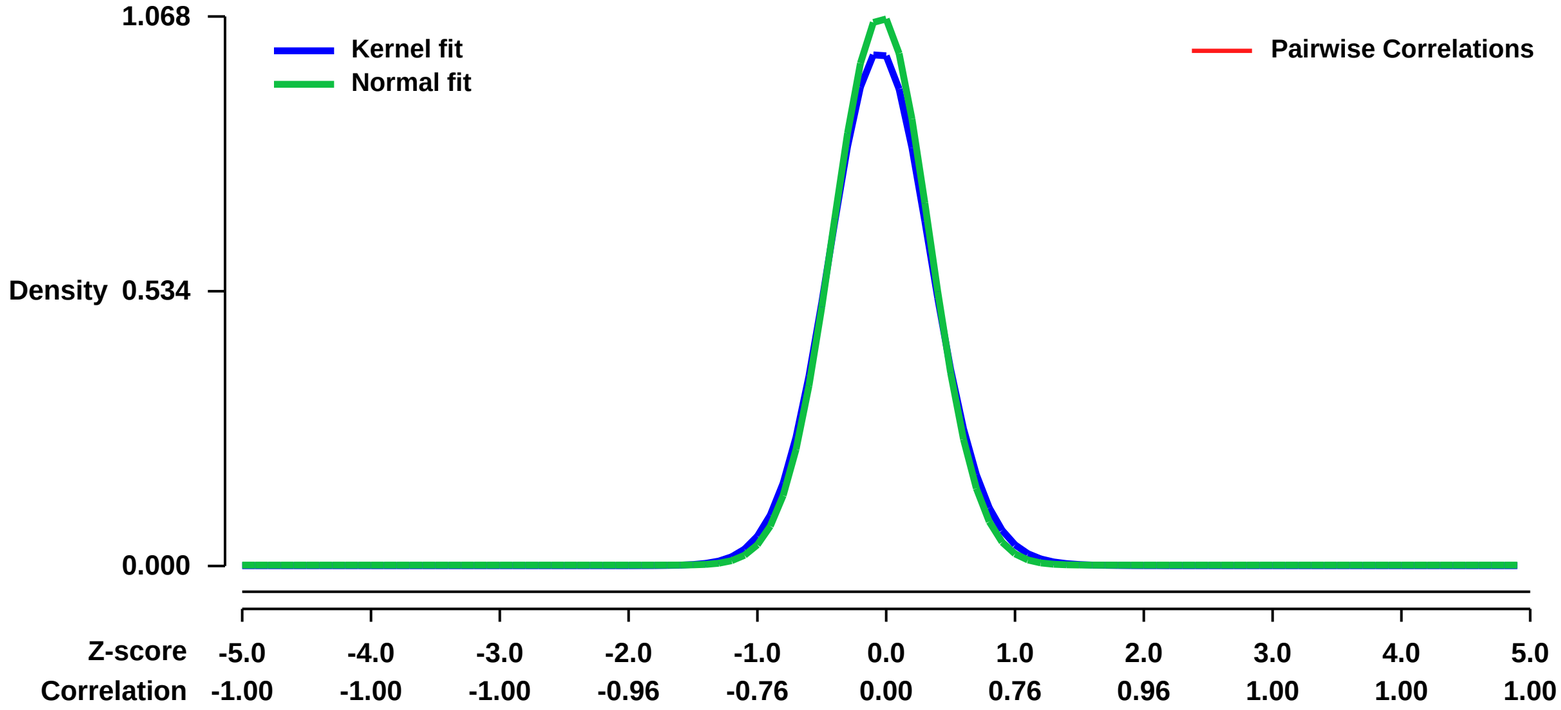

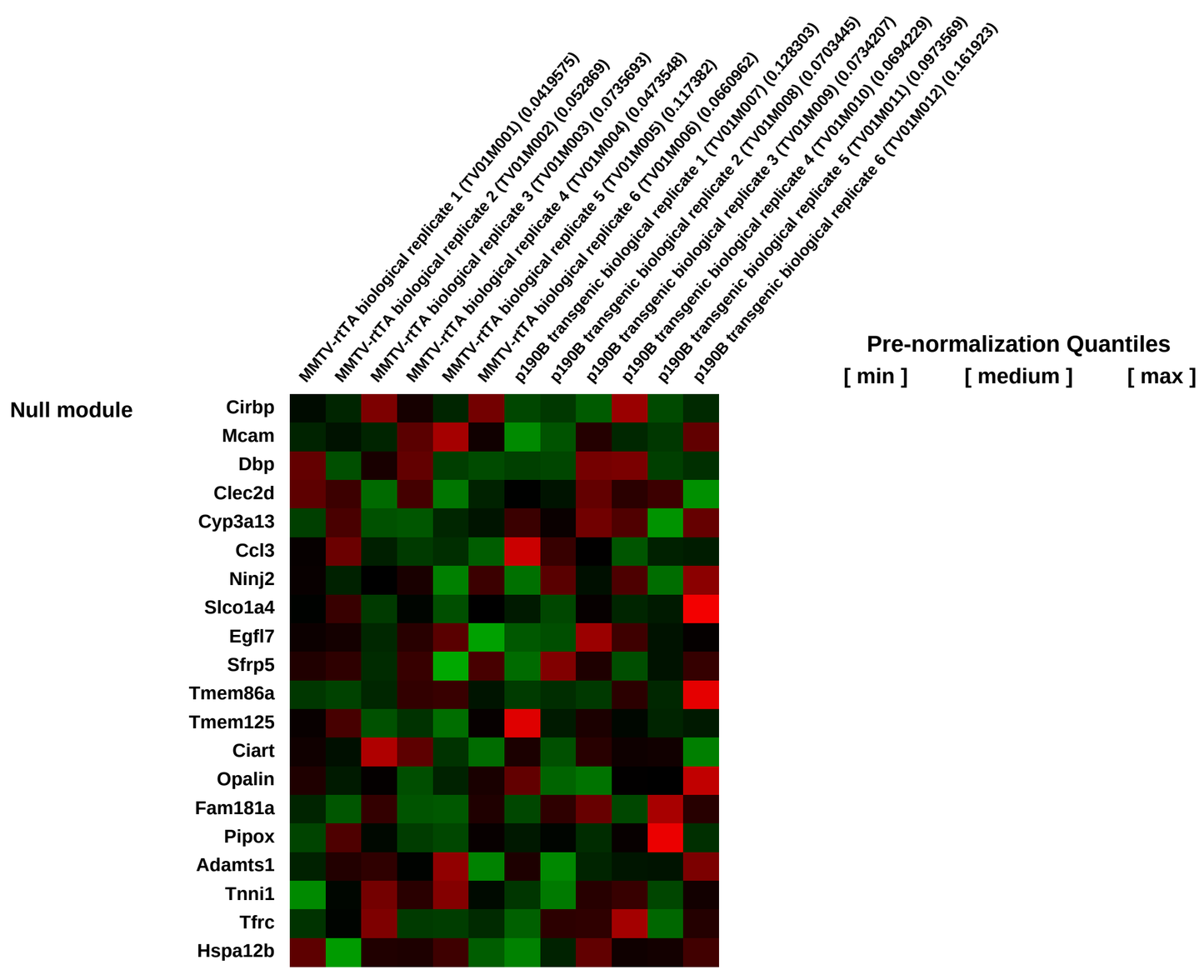

GEO Series "GSE13408" Expression Profiles

Num of samples in this series: 14

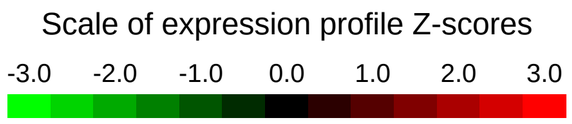

GEO Link:	http://www.ncbi.nlm.nih.gov/geo/query/acc.cgi?acc=GSE13408
Status:	Public on Sep 01 2009
Title:	Cell cycle exit and terminal differentiation independent of the Rb gene family during embryonic development
Organism:	Mus musculus
Experiment type:	Expression profiling by array
Platform:	GPL1261
Pubmed ID:	21059851
Summary & Design:	**Summary:** The retinoblastoma cell cycle regulator pRb and the two related proteins p107 and p130 are thought to suppress cancer development both by inhibiting the G1/S transition of the cell cycle in response to growth-arrest signals and by promoting cellular differentiation. Here, we investigated the phenotype of Rb family triple knock-out (TKO) embryonic stem cells as they differentiate in vivo and in culture. Confirming the central role of the Rb gene family in cell cycle progression, TKO mouse embryos did not survive past mid-gestation and differentiating TKO cells displayed increased proliferation and cell death. However, patterning and cell fate determination were largely unaffected in these TKO embryos. Furthermore, a number of TKO cells, including in the neural lineage, were able to exit the cell cycle in G1 and terminally differentiate. This ability of Rb family TKO cells to undergo cell cycle arrest was associated with the repression of target genes for the E2F6 transcription factor, uncovering a pRb-independent control of the G1/S transition of the cell cycle. These results show that the Rb gene family is required for proper embryonic development but is not absolutely essential to induce G1 arrest and differentiation in certain lineages. **Overall design:** Genome-wide gene expression was analyzed for wild-type and TKO ESC and EB cells. Three biological replicates were isolated for wild-type ESCs, TKO ESCs, and wild-type EBs, while five biological replicates were isolated for TKO EBs.

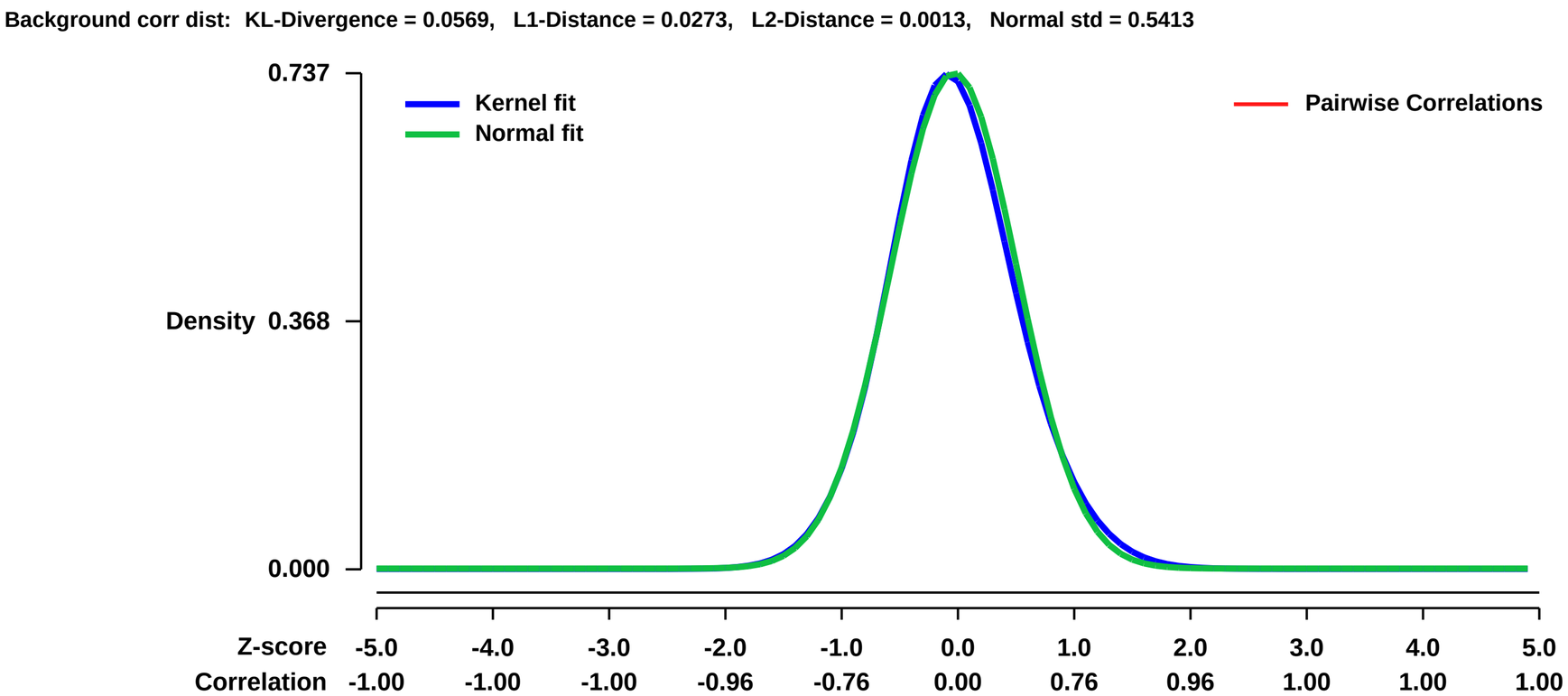

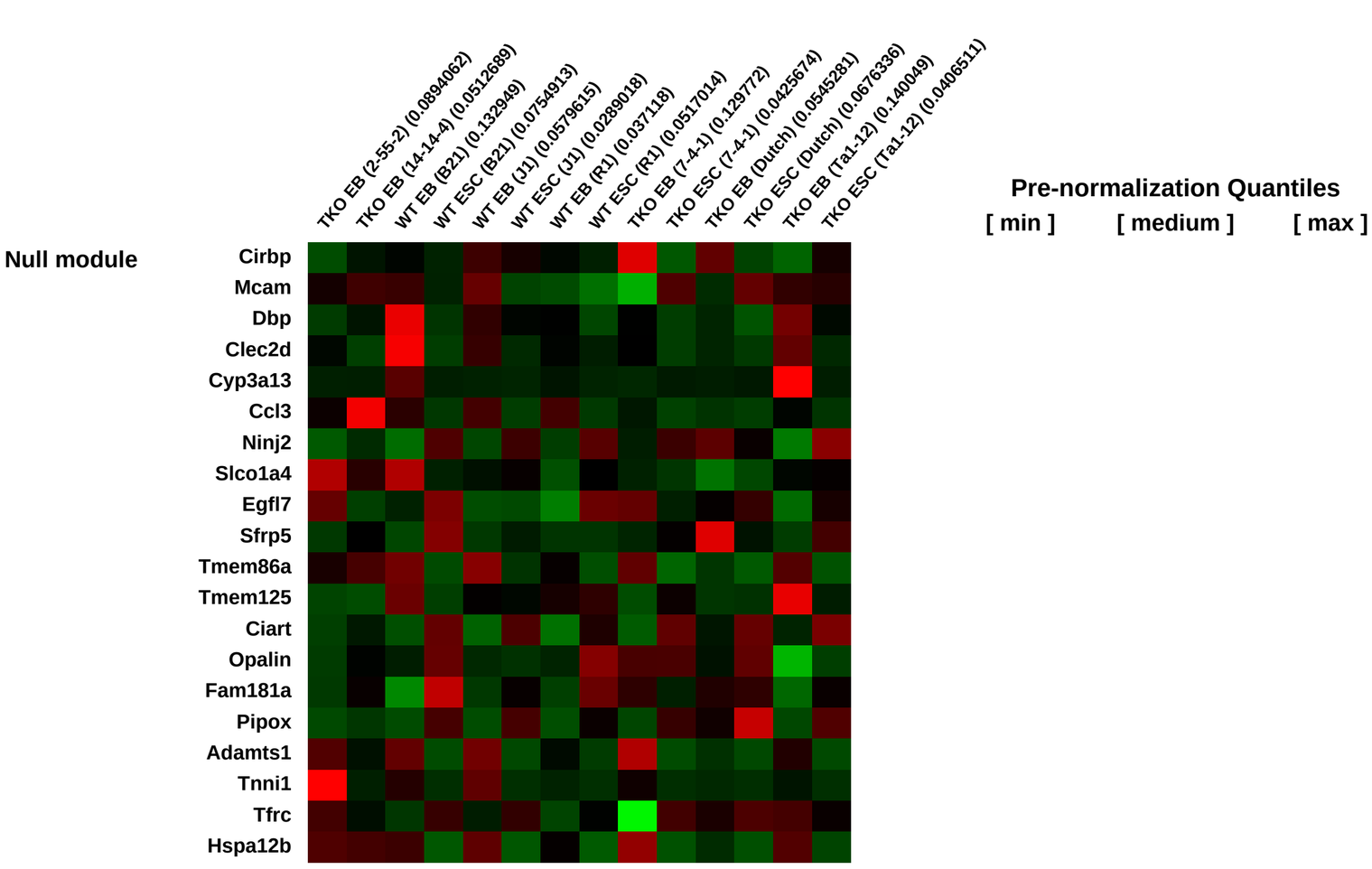

GEO Series "GSE34279" Expression Profiles

Num of samples in this series: 30

Scale of expression profile Z-scores

-3.0 -2.0 -1.0 0.0 1.0 2.0 3.0

GEO Link:	http://www.ncbi.nlm.nih.gov/geo/query/acc.cgi?acc=GSE34279
Status:	Public on Dec 20 2012
Title:	Retinoic acid (RA) induction time-course to profile gene expression during mES cell differentiation
Organism:	Mus musculus
Experiment type:	Expression profiling by array
Platform:	GPL1261
Pubmed ID:	23260668
Summary & Design:	**Summary:** Murine ES cell gene expression before RA induction are used to compare gene expression for time-points of 8, 12, 16, 24, 36, 48, 60 and 72 hours post-induction. **Overall design:** KH2 ES Cell RA Differentiation Time-course

Background corr dist: KL-Divergence = 0.0761, L1-Distance = 0.0220, L2-Distance = 0.0006, Normal std = 0.4833

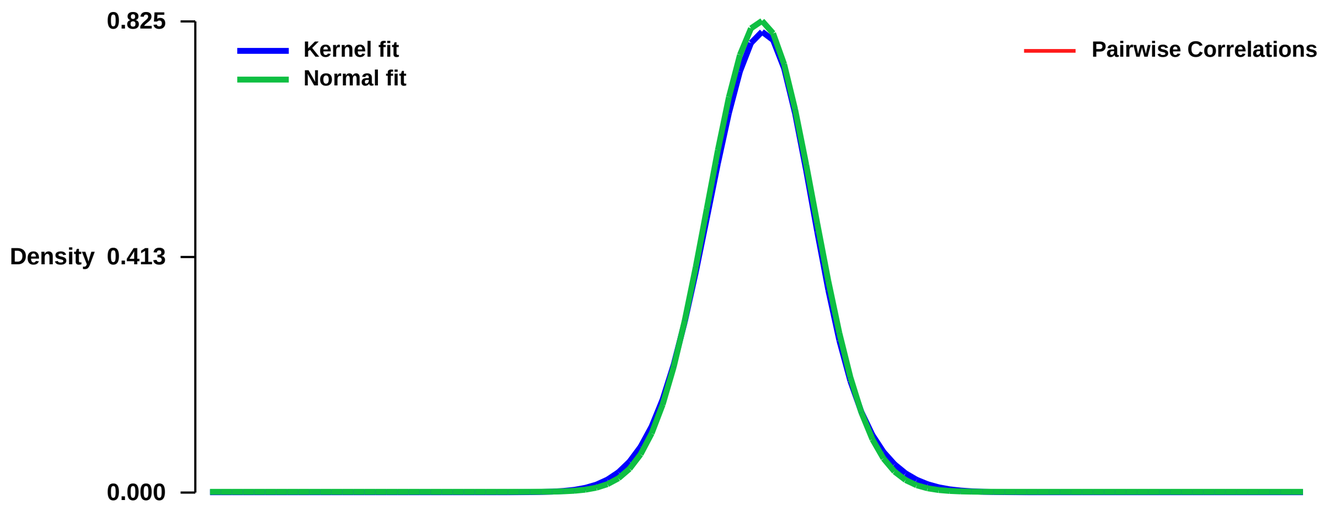

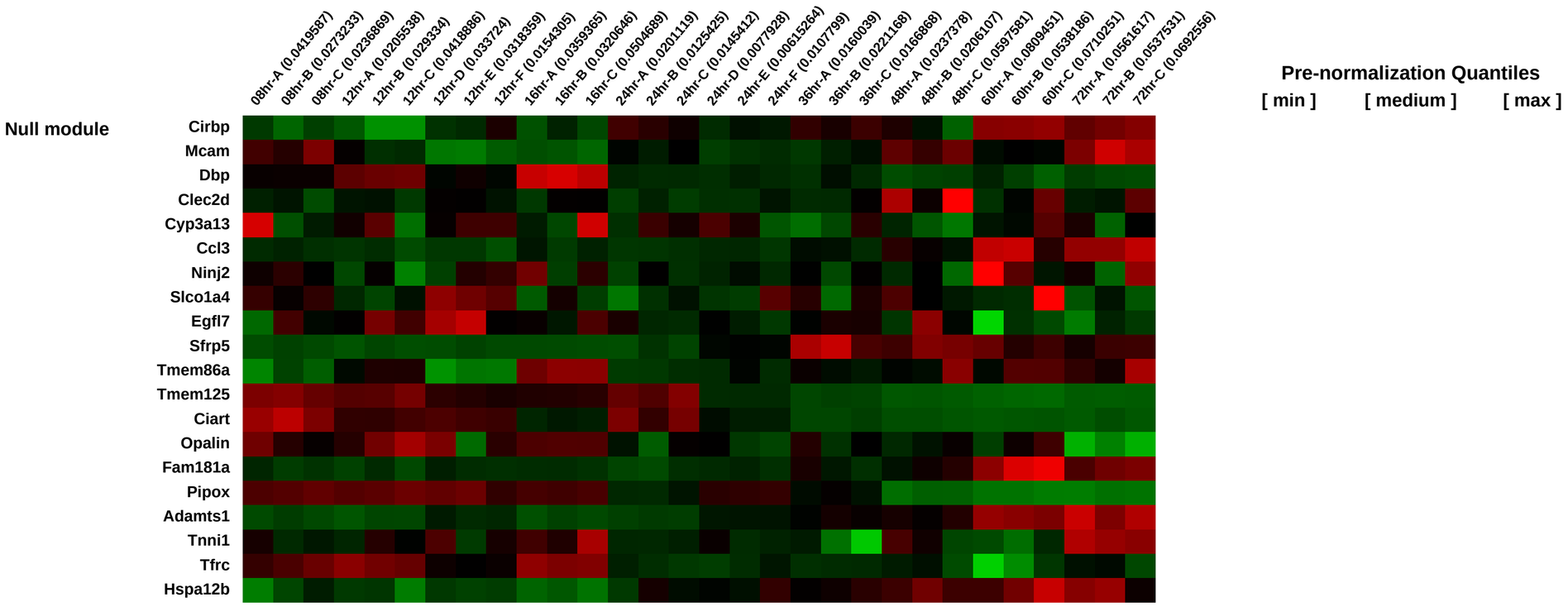

GEO Series "GSE36237" Expression Profiles

Num of samples in this series: 64

Scale of expression profile Z-scores

-3.0 -2.0 -1.0 0.0 1.0 2.0 3.0

GEO Link:	http://www.ncbi.nlm.nih.gov/geo/query/acc.cgi?acc=GSE36237
Status:	Public on Mar 09 2012
Title:	Tg2576 and wild-type mice treated with PDE9A-inhibitor
Organism:	Mus musculus
Experiment type:	Expression profiling by array
Platform:	GPL1261
Pubmed ID:	
Summary & Design:	**Summary:** Many forms of synaptic plasticity are critically dependent upon production of cGMP to trigger activity-dependent increases in synaptic size and strength. Phosphodiesterase 9A (PDE9A) is a high affinity, cGMP-specific phosphodiesterase with widespread distribution in the central nervous system. Inhibition of PDE9A results in significant accumulation of cGMP in brain tissue and cerebrospinal fluid (CSF) of rodents, and increases CSF cGMP in human volunteers. We hypothesized that chronic exposure to a PDE9A inhibitor, and the associated elevations in brain cGMP could provide a therapeutic benefit to vulnerable synapses chronically exposed to A,† in transgenic mice over-expressing human mutant amyloid precursor protein (Tg2576 mice). A total of N=20 animals per group of 4 month old Tg2576 mice and non-transgenic littermates (WT) were implanted with Alzet osmotic minipumps to deliver vehicle or the PDE9A inhibitor PF-04447943. Neurobehavioral outcomes were measured as conditioned fear response after 28 days of treatment and subsequently brains were harvested for measurement of A,†, gene expression profiling or synaptic density as assessed by Golgi staining of dendrites. Dendritic spine density on apical dendrites of CA1 neurons exhibited a small but significant deficit in the density of dendritic spines in vehicle treated Tg2576 mice as compared to WT mice. This deficit was ameliorated by 30 days of exposure to PF-04447943. No significant drug effect was observed in WT mice. No significant effects of drug treatment were observed on A,† levels in Tg2576 mice. Behavioral analysis of Tg2576 mice showed deficits in fear conditioning as early as 2 months old, and therefore were considered unlikely to be due to the accumulation of oligomeric A,†. These deficits were not affected by drug treatment. Transcriptional profiles of Tg2576 mice treated with drug compared to vehicle showed evidence of regulation of pathways related to synaptic plasticity and remodeling of the dendritic cytoskeleton, consistent with stabilization of vulnerable spine structure. These data supports the hypothesis that PDE9A inhibition can stabilize vulnerable synapses early in the Alzheimerâ s disease process. **Overall design:** 4-month old Tg2576 mice and non-transgenic (WT) littermates were implanted with minipumps to deliver vehicle or the PDE9A-inhibitor, PF-04447943, for 28 days. At the end of the study, hippocampus and frontal cortex were dissected from n=8 mice per group, RNA was isolated, and hybridized to Affymetrix 430 2.0 mouse whole genome microarray.

Background corr dist: KL-Divergence = 0.1705, L1-Distance = 0.0379, L2-Distance = 0.0029, Normal std = 0.3549

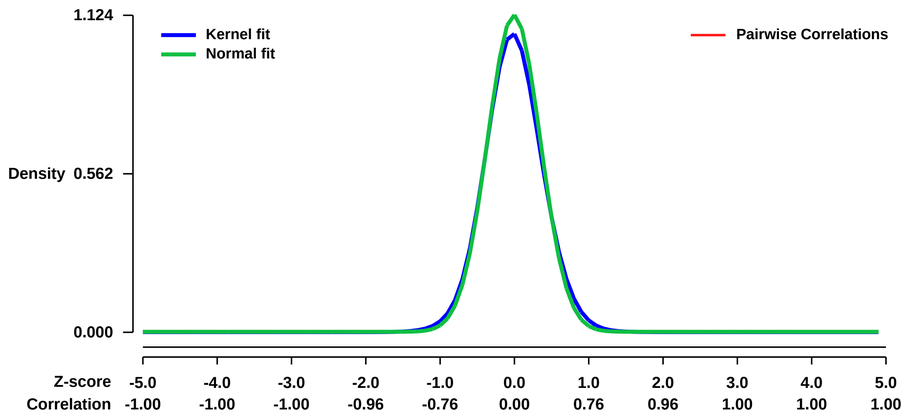

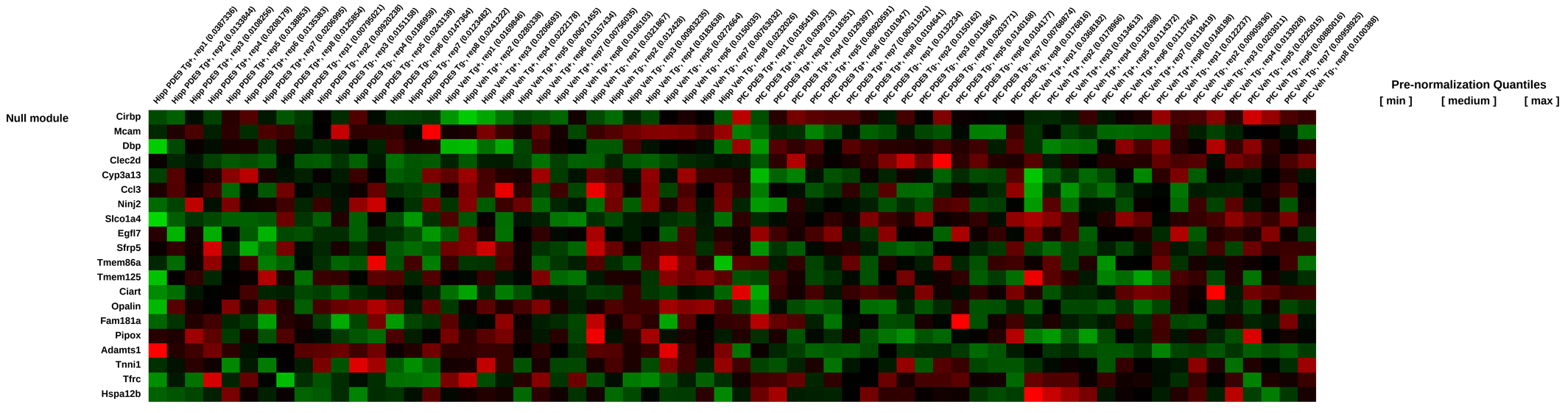

GEO Series "GSE8199" Expression Profiles

Num of samples in this series: 9

Scale of expression profile Z-scores

-3.0 -2.0 -1.0 0.0 1.0 2.0 3.0

GEO Link:	http://www.ncbi.nlm.nih.gov/geo/query/acc.cgi?acc=GSE8199
Status:	Public on Jul 10 2007
Title:	E18.5 Estrogen-related Receptor gamma Knockout Mouse Heart
Organism:	Mus musculus
Experiment type:	Expression profiling by array
Platform:	GPL1261
Pubmed ID:	17618853
Summary & Design:	**Summary:** **3 ventricles from E18.5 male mice were pooled for each array. Three arrays per genotype.** **Title: ERR‚Ä° Directs and Maintains the Transition to Oxidative Metabolism in the Post-Natal Heart** **Abstract: At birth the heart undergoes a critical metabolic switch to transition from a predominant dependence on carbohydrates during fetal life to a greater dependence on postnatal oxidative metabolism. This remains the principle metabolic state throughout life; although pathologic conditions such as heart failure and cardiac hypertrophy reactivate components of the fetal genetic program to increase carbohydrate utilization. Disruption of the ERR‚Ä° gene, which is expressed at high levels in the fetal and postnatal mouse heart, blocks this switch resulting in lactatemia, electrocardiographic (ECG) abnormalities and death during the first week of life. Genomic ChIP-on-chip and expression analysis at E18.5 clearly identifies ERR‚Ä° as both a direct and indirect regulator of a nuclear-encoded mitochondrial genetic network that coordinates the postnatal metabolic transition. These findings reveal an unexpected and essential molecular genetic component of the oxidative metabolic gene program in the heart and highlight ERR‚Ä° in the study of cardiac hypertrophy and failure.** **Keywords: ChIP-on-chip, electrocardiography, fetal gene program, OXPHOS, PGC-1a, sodium current, Single time point (E18.5) to compare genotype differences** **Overall design:** **Fetal mice were collected by caesarean secation. Hearts were stored in RNALater (Qiagen)**

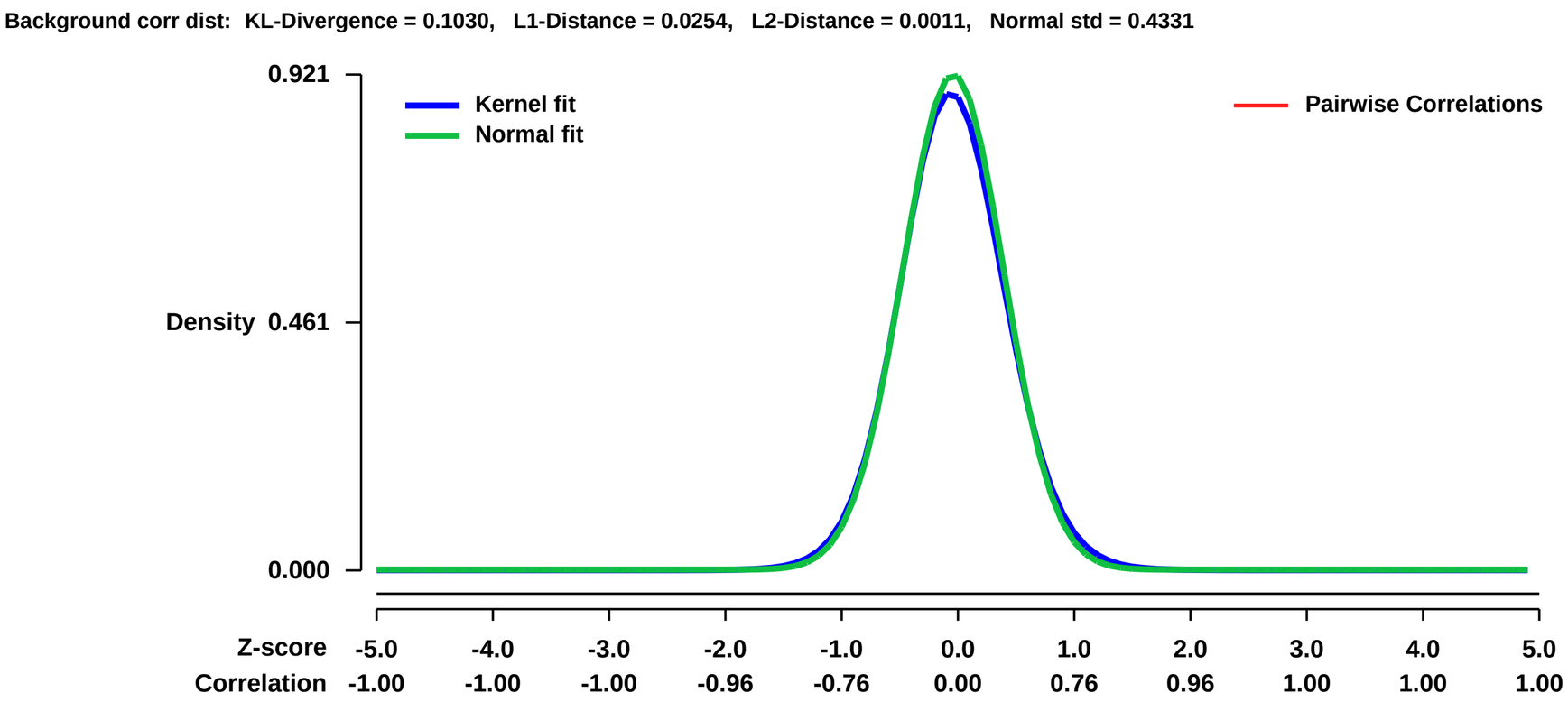

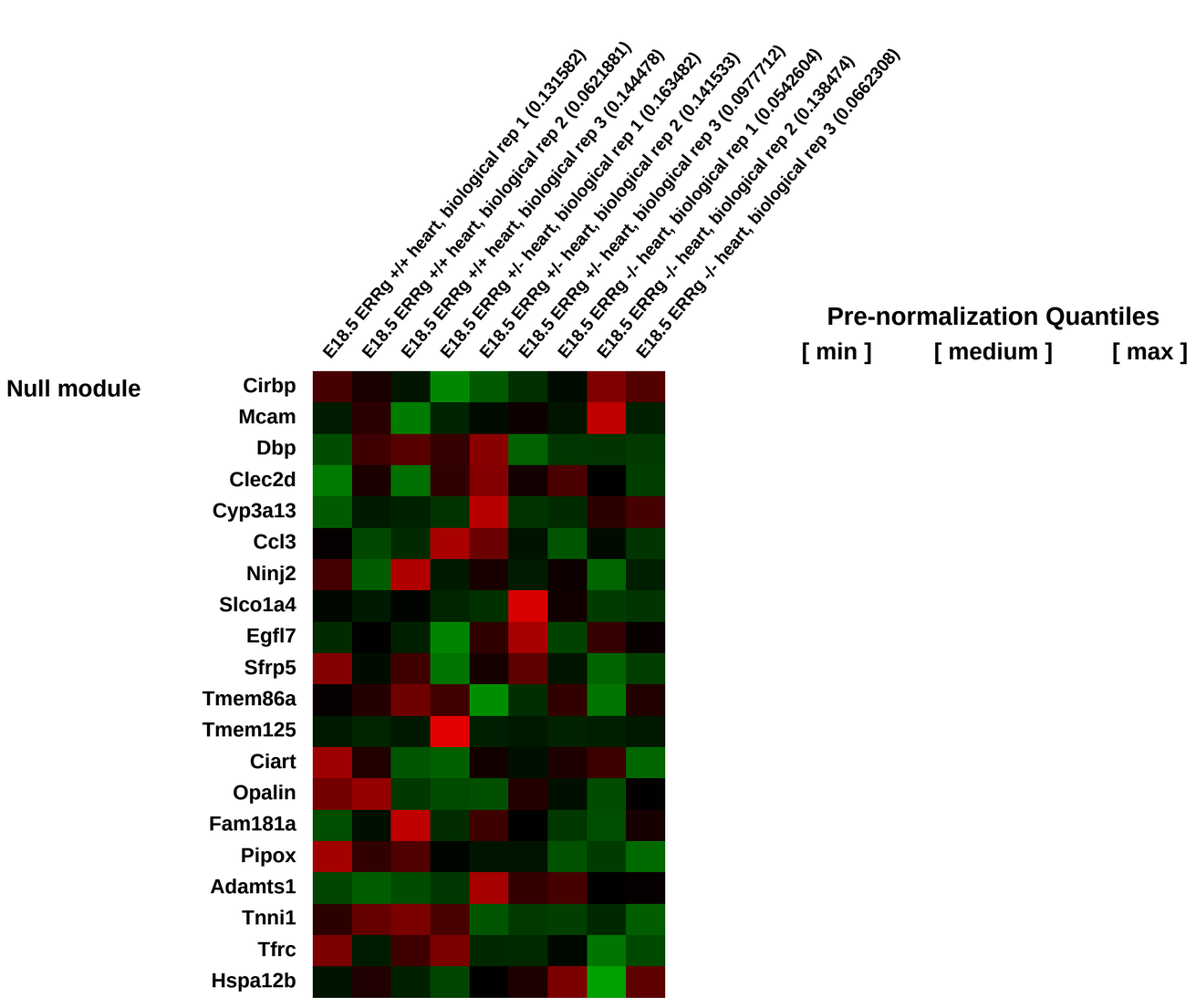

GEO Series "GSE29262" Expression Profiles

Num of samples in this series: 12

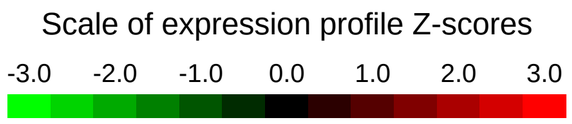

GEO Link:	http://www.ncbi.nlm.nih.gov/geo/query/acc.cgi?acc=GSE29262
Status:	Public on Dec 08 2011
Title:	Functional Plasticity of Regulatory T Cell Function
Organism:	Mus musculus
Experiment type:	Expression profiling by array
Platform:	GPL1261
Pubmed ID:	22013112
Summary & Design:	**Summary:** **Regulatory T cells (Tregs) can suppress a wide variety of cell types, in diverse organ sites and inflammatory conditions. While Tregs possess multiple suppressive mechanisms, the number required for maximal function is unclear. Furthermore, whether any inter-relationship orcross-regulatory mechanisms exist that areused to orchestrate and control their utilization is unknown. Here we assessed the functional capacity of Tregs lacking the ability to secrete both interleukin-10 (IL-10) and IL-35, which individually are required for maximal Treg activity. Surprisingly, IL-10/IL-35-double deficient Tregswere fully functionalin vitro and in vivo. Loss of IL-10 and IL-35 was compensated for by a concurrent increase in cathepsin E (CTSE) expression, enhanced TRAIL (Tnfsf10)expression and soluble TRAIL release, rendering IL-10/IL-35-double deficient Tregsfunctionally dependent on TRAIL in vitro and in vivo. Lastly, while C57BL/6 Tregs are IL-10/IL-35-dependent, Balb/c Tregs, which express high levels of CTSE and enhanced TRAIL expression, are TRAIL-dependent.These data reveal that cross-regulatory pathways exist, which control the utilization of suppressive mechanisms,thereby providing Tregfunctional plasticity.** **Overall design:** **Isolate natural Tregs from the different knockout mouse**

Background corr dist: KL-Divergence = 0.1244, L1-Distance = 0.0267, L2-Distance = 0.0012, Normal std = 0.4039

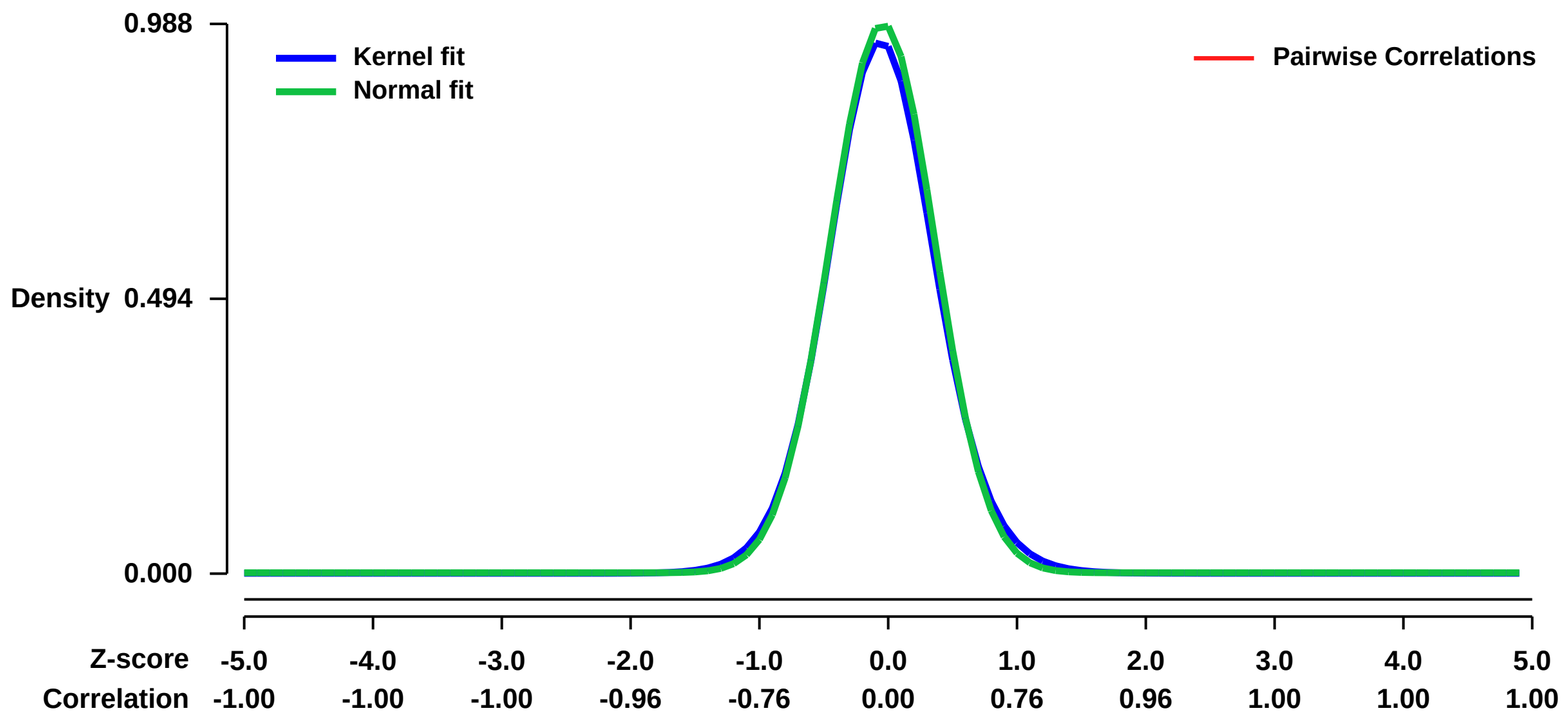

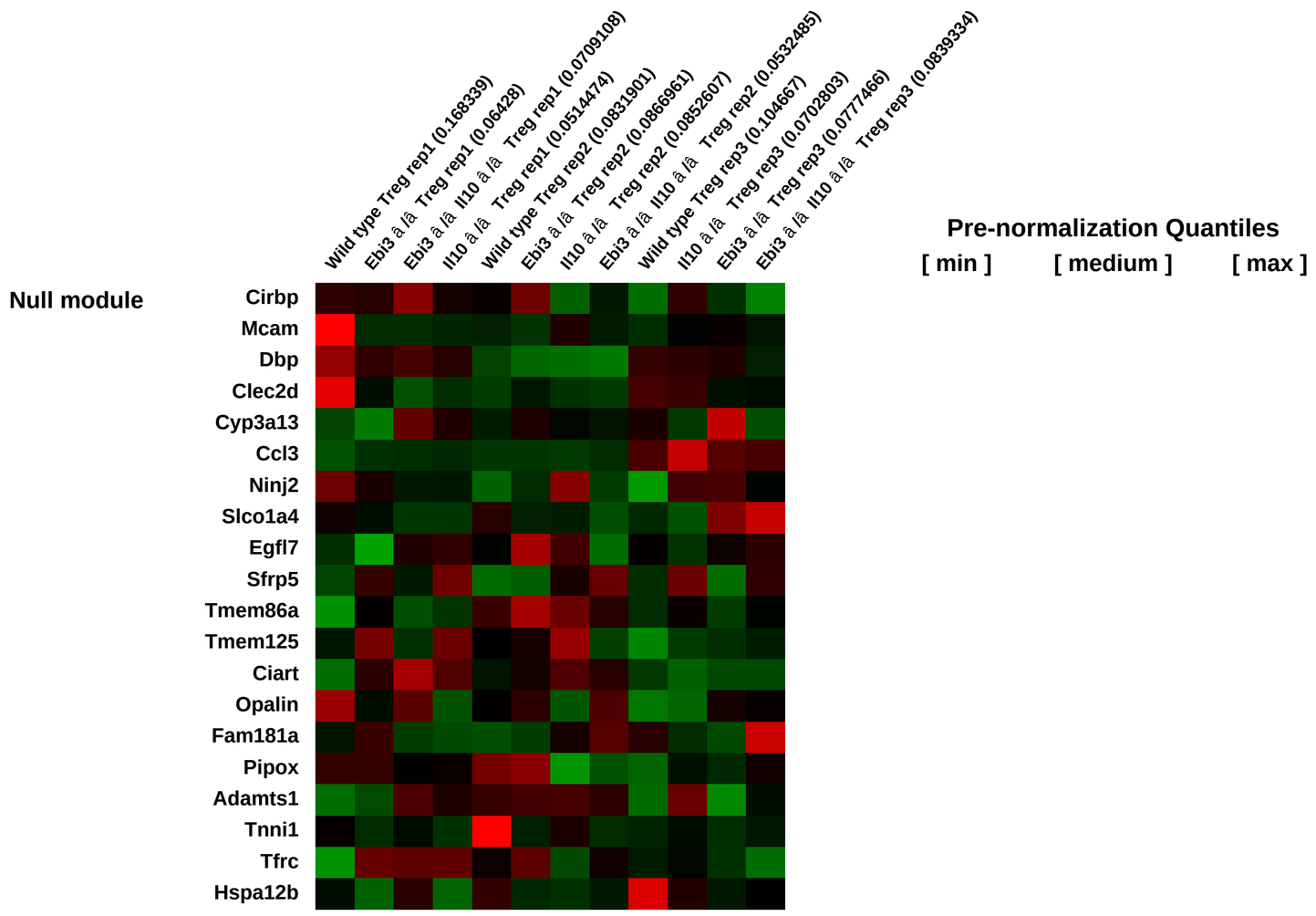

GEO Series "GSE21549" Expression Profiles

Num of samples in this series: 6

Scale of expression profile Z-scores

-3.0 -2.0 -1.0 0.0 1.0 2.0 3.0

GEO Link:	http://www.ncbi.nlm.nih.gov/geo/query/acc.cgi?acc=GSE21549
Status:	Public on Sep 01 2010
Title:	Expression profiles of EDTA-dissociated colon epithelial cells of wild-type mice and vil-Cre-Bcl9-/-/Bcl9l-/- mice.
Organism:	Mus musculus
Experiment type:	Expression profiling by array
Platform:	GPL1261
Pubmed ID:	20682801
Summary & Design:	**Summary:** To assess potential changes in Wnt signaling more comprehensively, EDTA-dissociated colon epithelial cells from three pools of wild-type and Bcl9/Bcl9l-mutant mice were subjected to an exploratory comparative gene expression profiling. **Overall design:** Total RNA of three samples of EDTA-dissociated colon epithelial cells of wild-type mice and three samples of vil-Cre-Bcl9-/-/Bcl9l-/- mice, each sample consisting of material of two or three different mice, was collected and resulting amplified cDNA hybridized to Affymetrix Mouse Genome 430 2.0 arrays. Samples are labeled as follows: Genotype_PoolID _UniqueID_NumberOfMice.

Background corr dist: KL-Divergence = 0.0455, L1-Distance = 0.0200, L2-Distance = 0.0005, Normal std = 0.5924

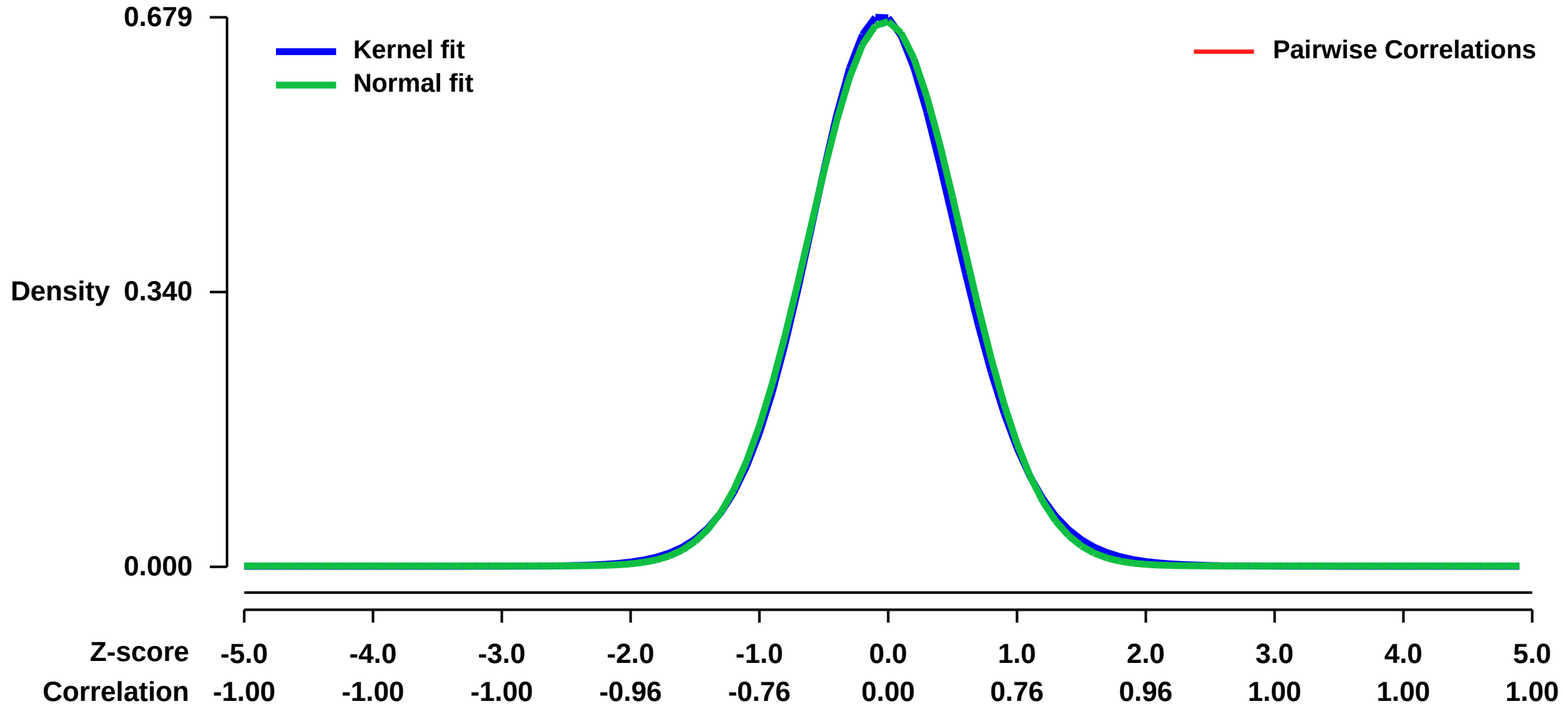

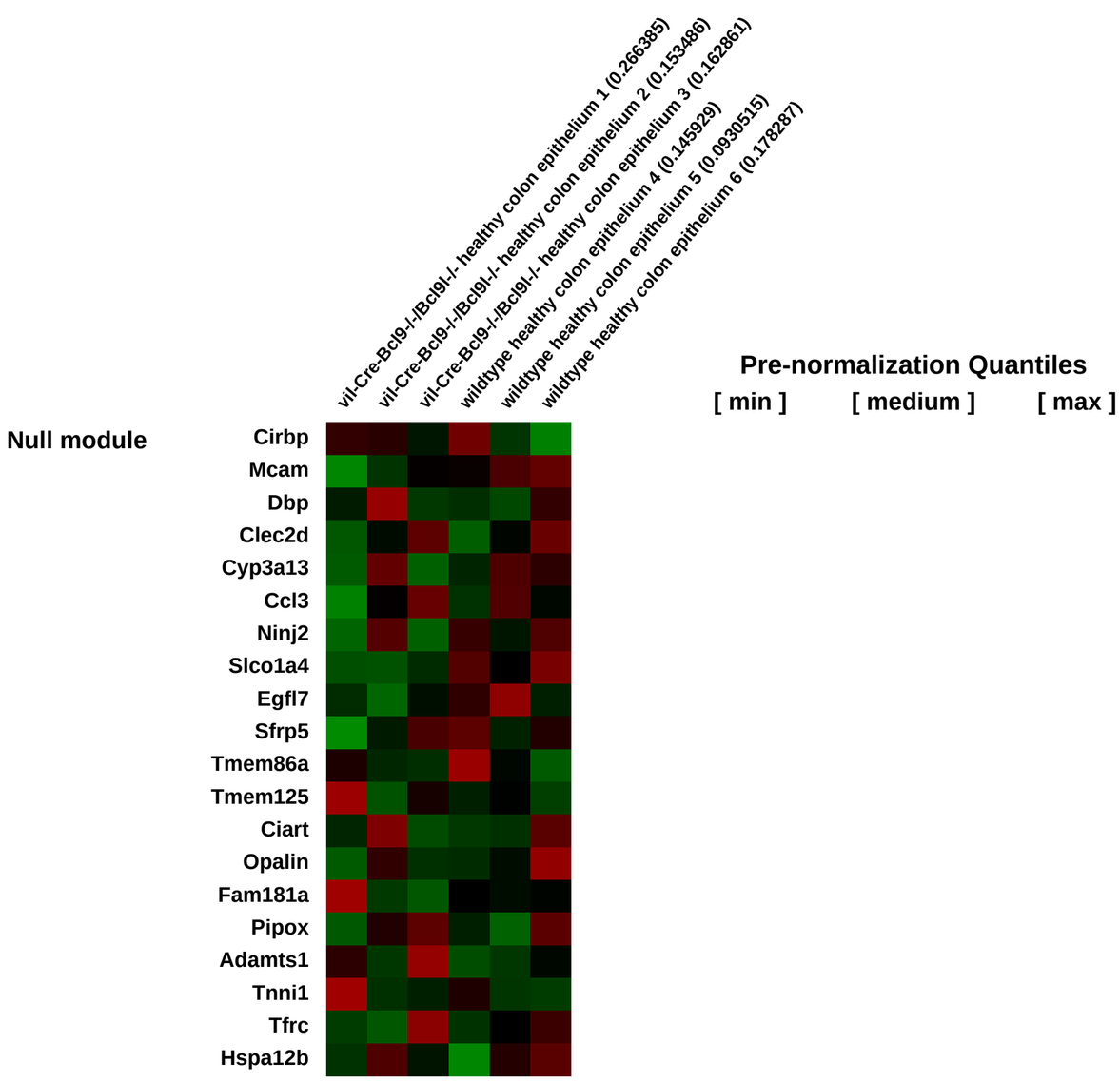

GEO Series "GSE4238" Expression Profiles

Num of samples in this series: 24

Scale of expression profile Z-scores

-3.0 -2.0 -1.0 0.0 1.0 2.0 3.0

GEO Link:	http://www.ncbi.nlm.nih.gov/geo/query/acc.cgi?acc=GSE4238
Status:	Public on Aug 08 2006
Title:	rhythmic transcriptome in the murine wt adrenal
Organism:	Mus musculus
Experiment type:	Expression profiling by array
Platform:	GPL1261
Pubmed ID:	16998155
Summary & Design:	**Summary:** This study was performed to characterize the rhythmic transcirptome of the murine adrenal gland with a focus on the corticosterone synthesis pathway. **Keywords: time course** **Overall design:** LD entrained male animals were released into DD and from the second day on whole adrenals were prepared from 12 time points at 4 hrs intervals.

Background corr dist: KL-Divergence = 0.1034, L1-Distance = 0.0281, L2-Distance = 0.0012, Normal std = 0.4307

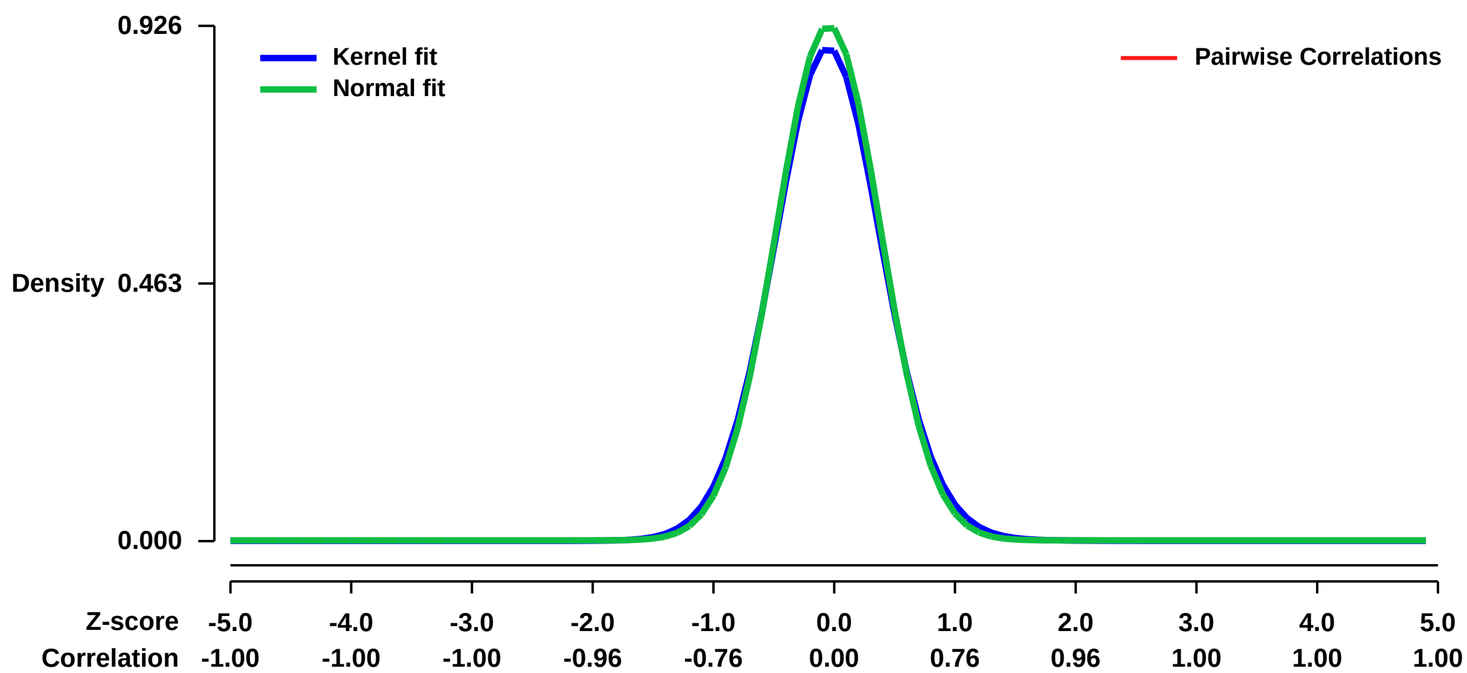

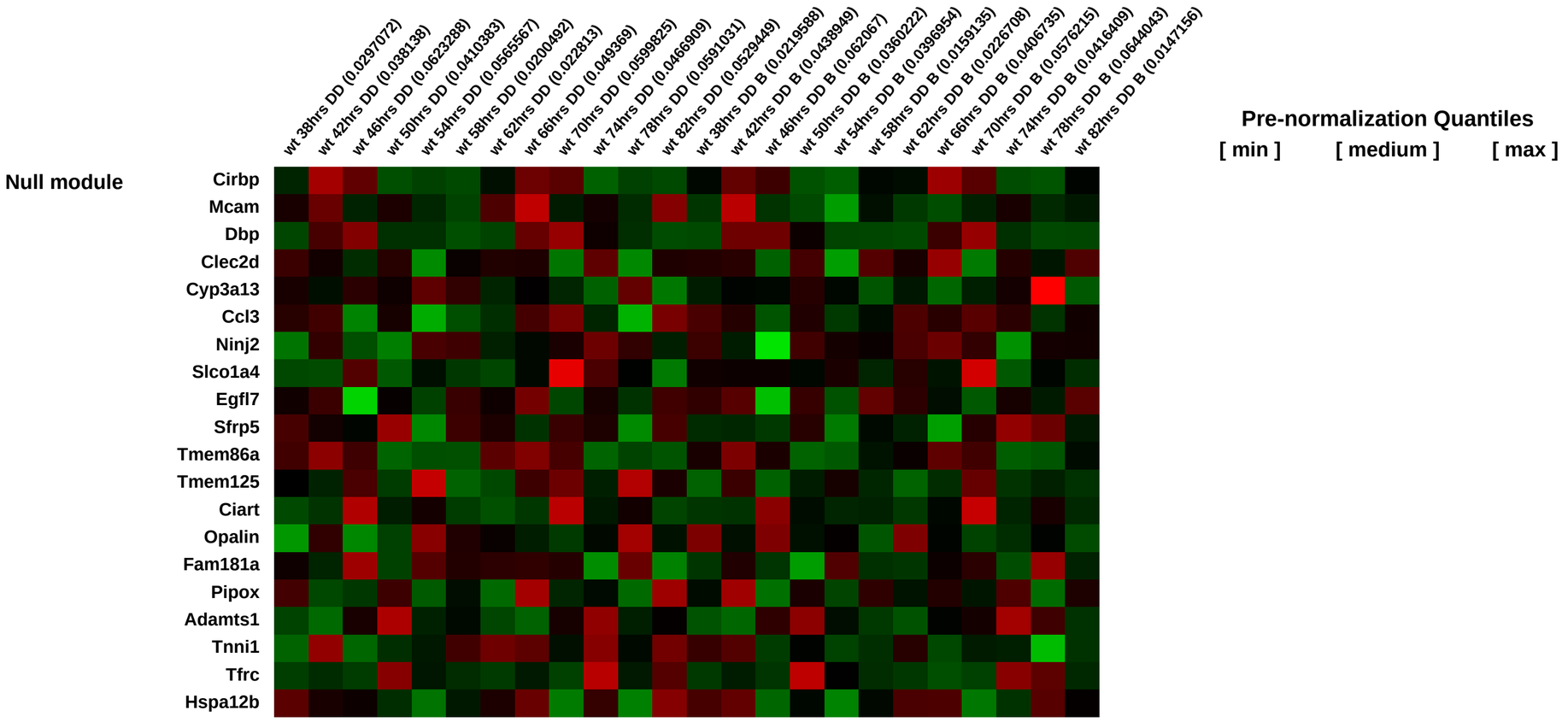

GEO Series "GSE47607" Expression Profiles

Num of samples in this series: 12

Scale of expression profile Z-scores

-3.0 -2.0 -1.0 0.0 1.0 2.0 3.0

GEO Link:	http://www.ncbi.nlm.nih.gov/geo/query/acc.cgi?acc=GSE47607
Status:	Public on Jun 11 2014
Title:	Environmental factors transmitted by aryl hydrocarbon receptor influence severity of psoriatic skin inflammation [Affymetrix]
Organism:	Mus musculus
Experiment type:	Expression profiling by array
Platform:	GPL1261
Pubmed ID:	24909886
Summary & Design:	**Summary:** Environmental stimuli are known to contribute to psoriasis pathogenesis and that of other autoimmune diseases, but the mechanism is unknown. Here we show that the aryl hydrocarbon receptor (AhR), a transcription factor that senses environmental stimuli, modulates pathology in psoriasis. AhR-activating ligands reduced inflammation in the lesional skin of psoriasis patients, whereas AhR antagonists upregulated inflammation. Similarly, AhR signaling via the endogenous FICZ ligand reduced the inflammatory response in the imiquimod-induced model of psoriasis and AhR deficient mice exhibited a substantial exacerbation of the disease, compared to AhR sufficient controls. Non-haematopoietic cells, in particular keratinocytes, were responsible for this hyper-inflammatory response, which involved increased reactivity to IL-1beta and upregulation of AP-1 family members of transcription factors. Thus, our data suggest a critical role for AhR in the regulation of inflammatory responses and open the possibility for novel therapeutic strategies in chronic inflammatory disorders. **Overall design:** Total RNA obtained from skin explants taken from AhR heterozygous or knock-out mice treated pericutaneously with imiquimod for 0 and 2d.

Background corr dist: KL-Divergence = 0.0682, L1-Distance = 0.0241, L2-Distance = 0.0009, Normal std = 0.4997

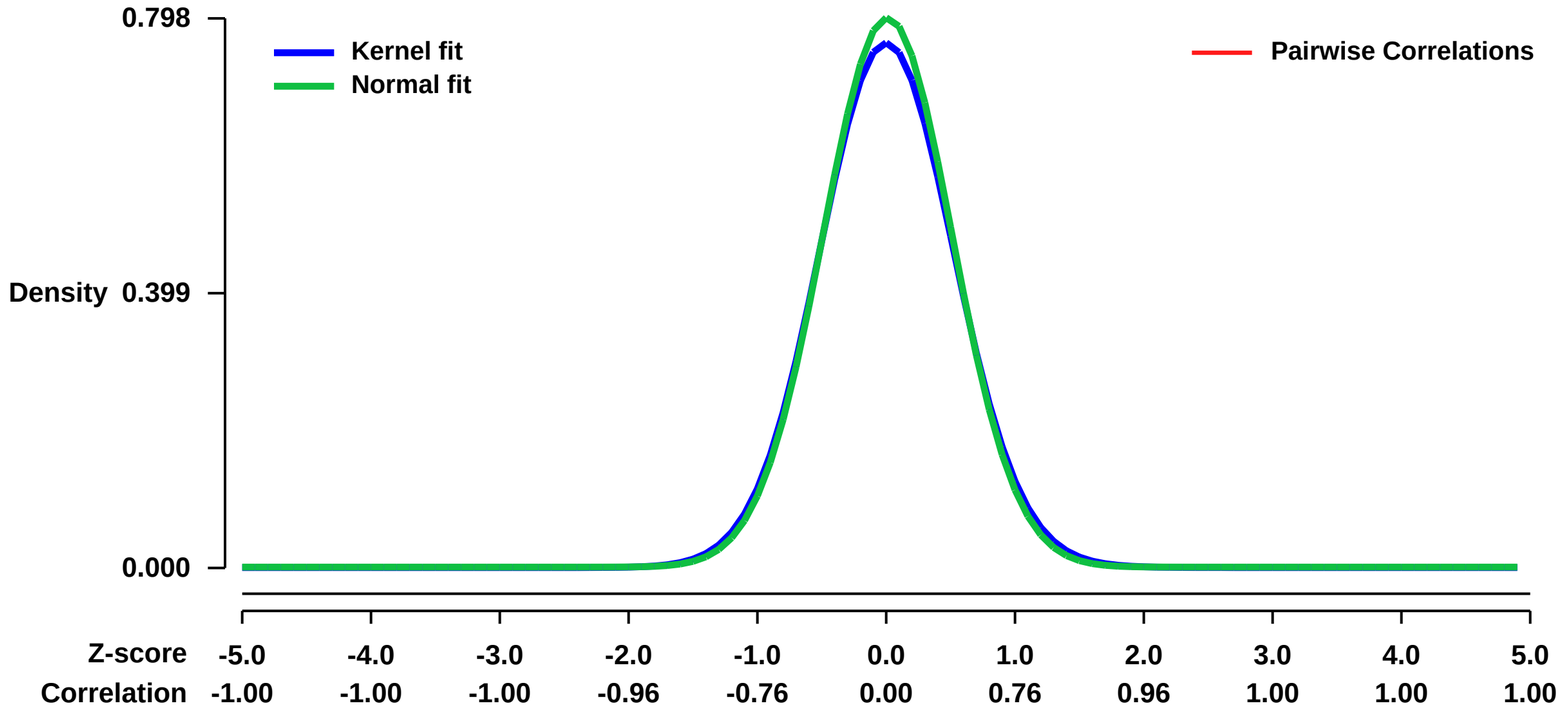

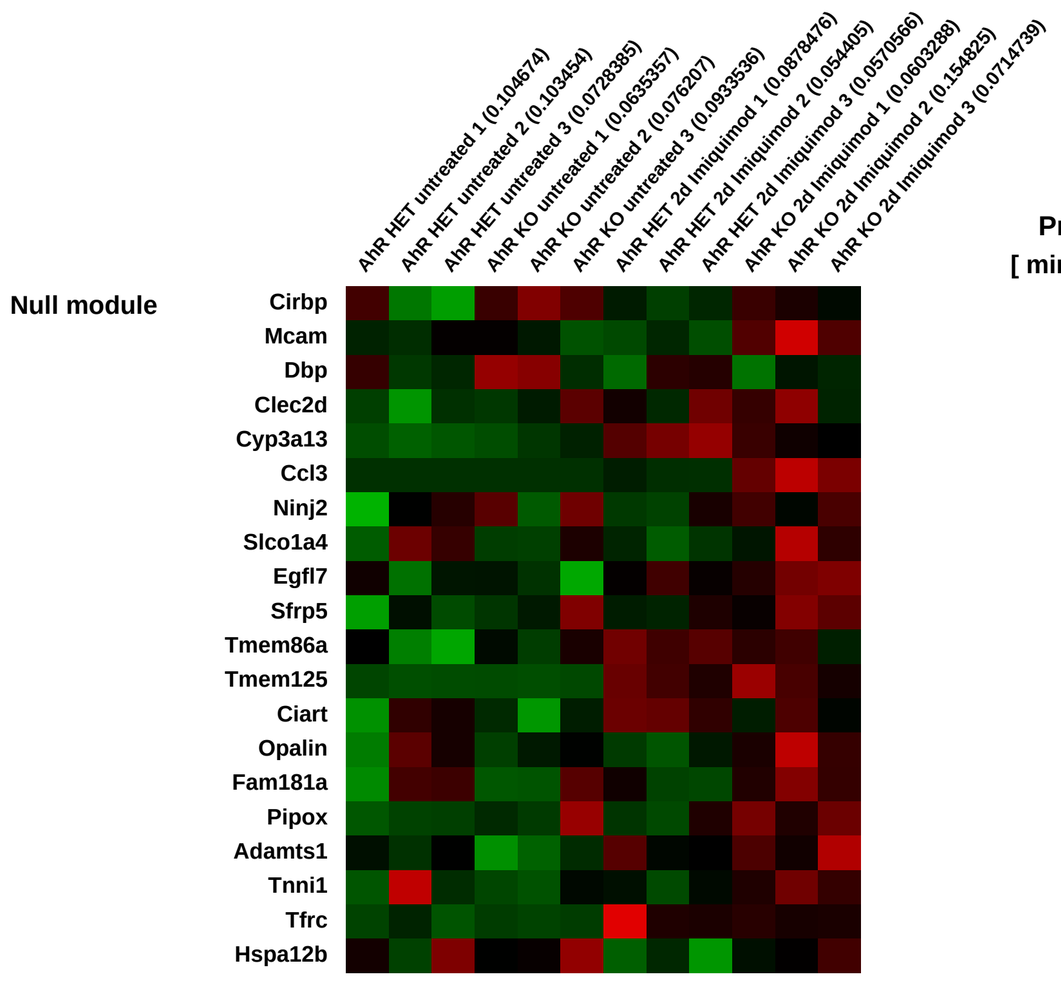

GEO Series "GSE28203" Expression Profiles

Num of samples in this series: 9

Scale of expression profile Z-scores

-3.0 -2.0 -1.0 0.0 1.0 2.0 3.0

GEO Link:	**http://www.ncbi.nlm.nih.gov/geo/query/acc.cgi?acc=GSE28203**
Status:	**Public on Mar 31 2012**
Title:	**Mouse oral tumors induced by activation of Ras and p53 mutations**
Organism:	**Mus musculus**
Experiment type:	**Expression profiling by array**
Platform:	**GPL1261**
Pubmed ID:	
Summary & Design:	**Summary:** **The p53 gain of function p53R172H promotes accelerated tumor growth and progression to carcinoma. To identify gene expression changes associated with the oncogenic function of mutant p53 we compared the expression profiles of oral tumors induced by activation of oncogenic K-ras and p53 gain- or loss-of-function mutations** **Oral tumors were induced by activation of endogenous oncogenic K-rasG12D and p53 loss- or gain-of-function mutations (p53R172H)** **Overall design:** **Oral tumors from mice carrying the p53R172H mutation or deletion of p53 were collected for gene expression analysis**

Background corr dist: **KL-Divergence = 0.0700, L1-Distance = 0.0257, L2-Distance = 0.0011, Normal std = 0.5020**

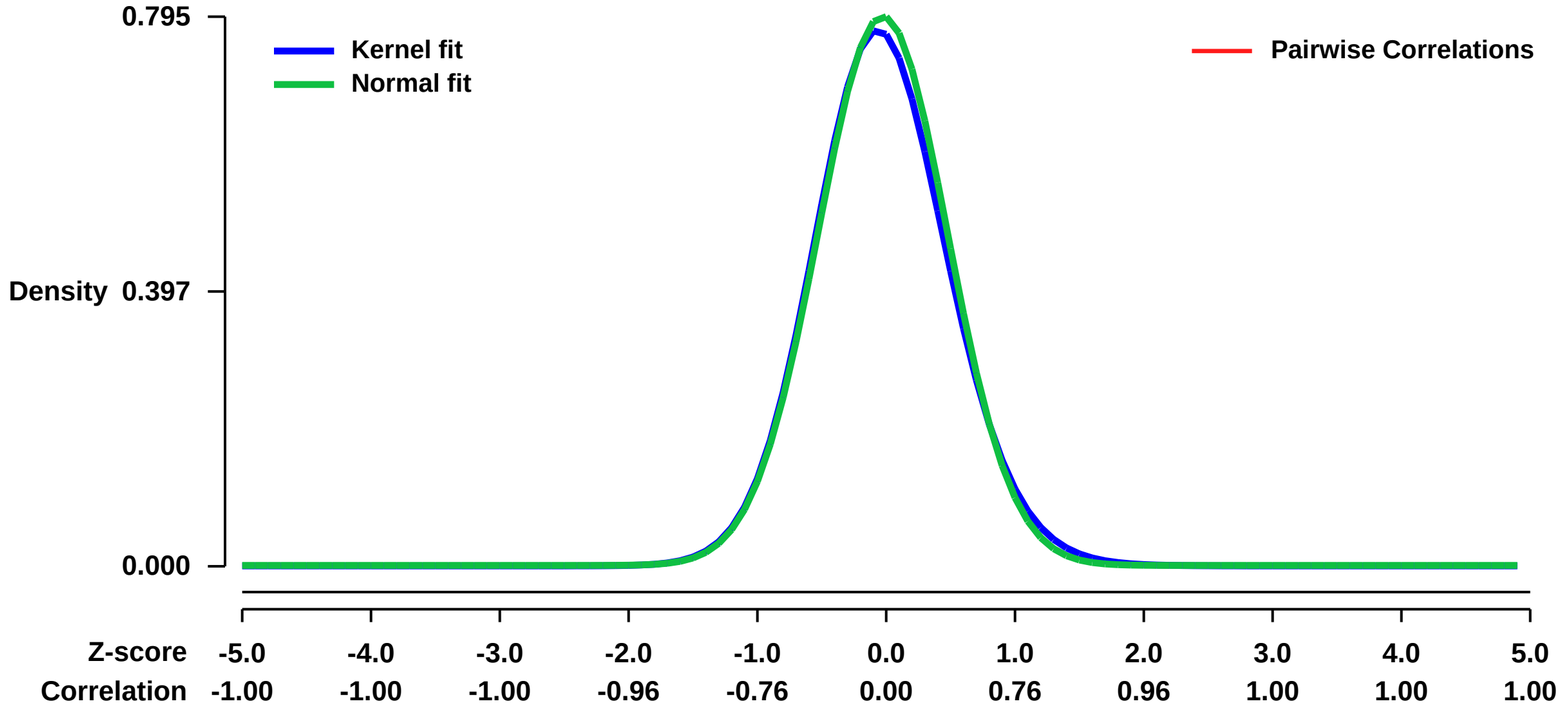

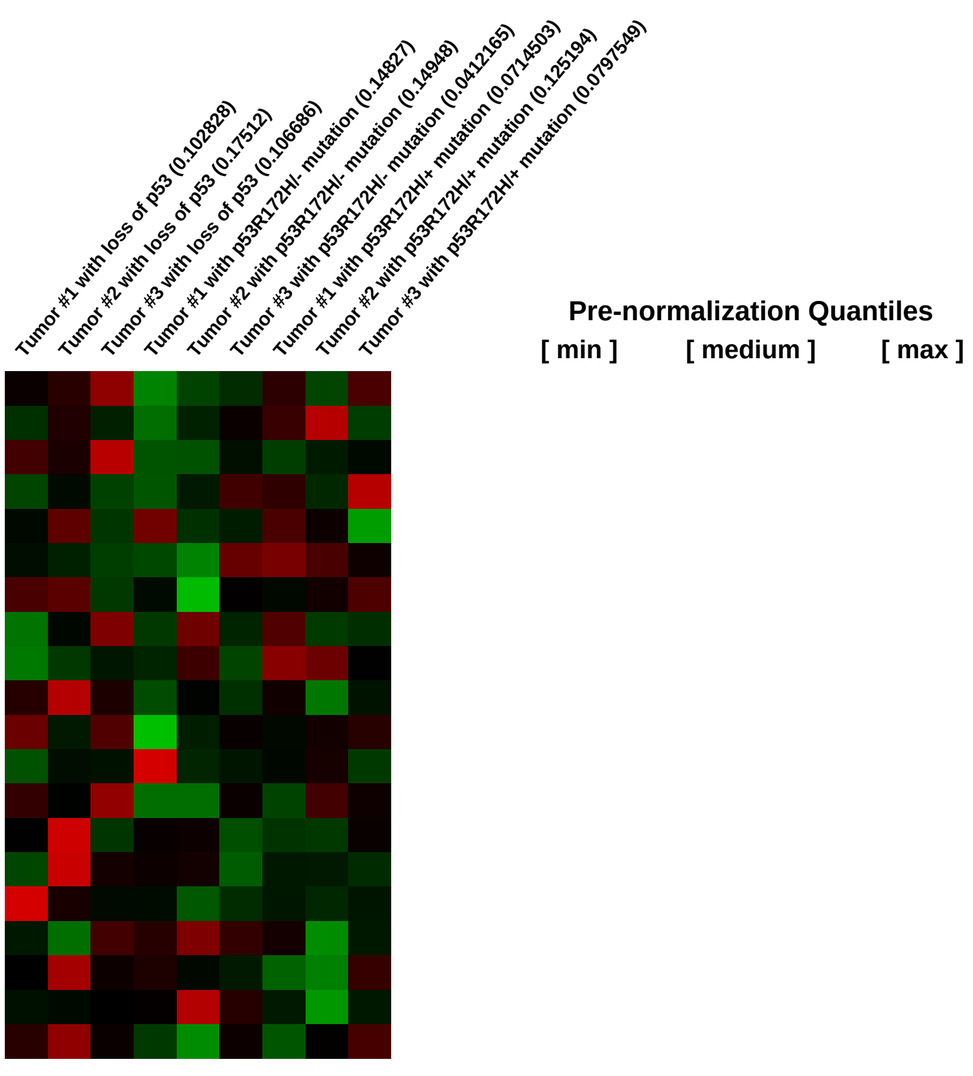

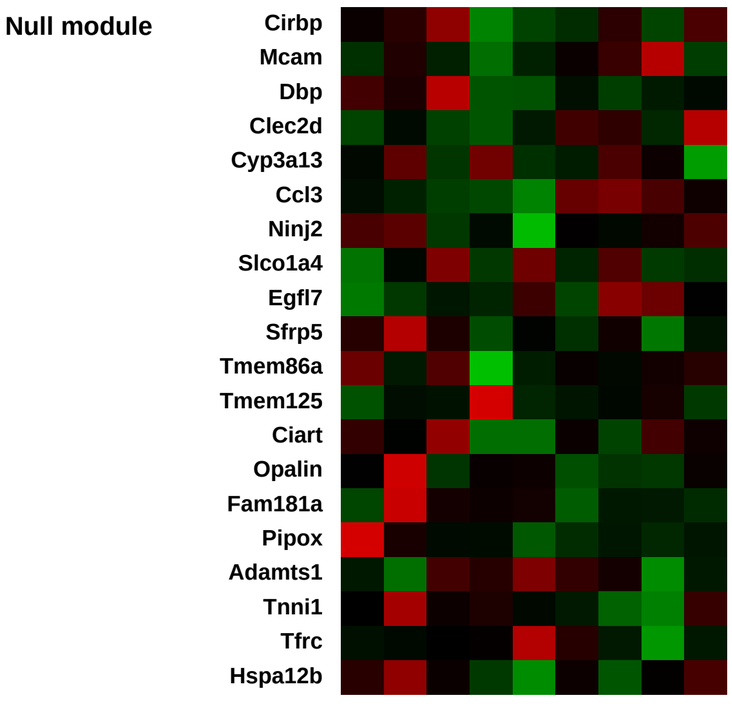

GEO Series "GSE4535" Expression Profiles

Num of samples in this series: 6

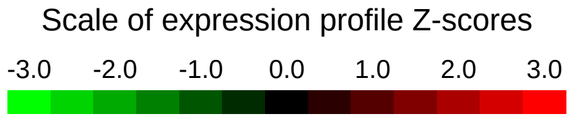

GEO Link:	http://www.ncbi.nlm.nih.gov/geo/query/acc.cgi?acc=GSE4535
Status:	Public on Oct 04 2006
Title:	primary FDC
Organism:	Mus musculus
Experiment type:	Expression profiling by array
Platform:	GPL1261
Pubmed ID:	17015706
Summary & Design:	**Summary:** expression profiles of FDC and BMDC are compared **Keywords: cell type comparison** **Overall design:** expression profiles of FDC and BMDC are compared

Background corr dist: KL-Divergence = 0.0390, L1-Distance = 0.0480, L2-Distance = 0.0034, Normal std = 0.6676

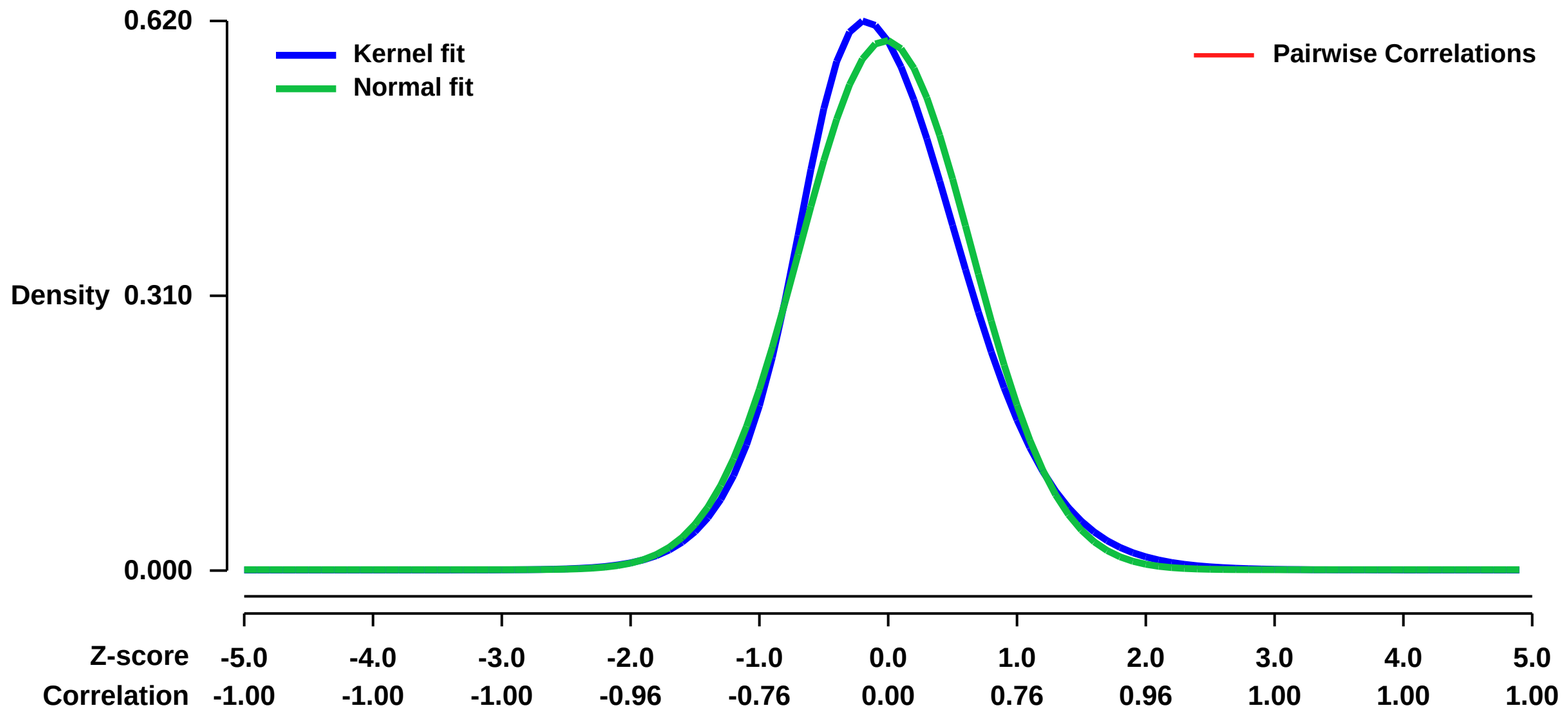

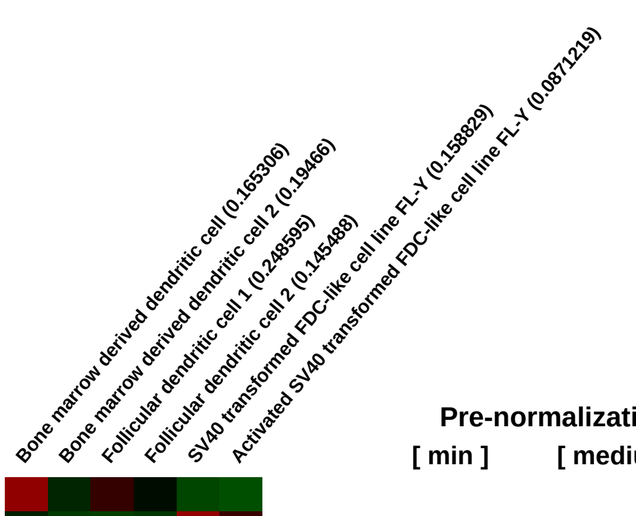

Pre-normalization Quantiles

[min] [medium] [max]

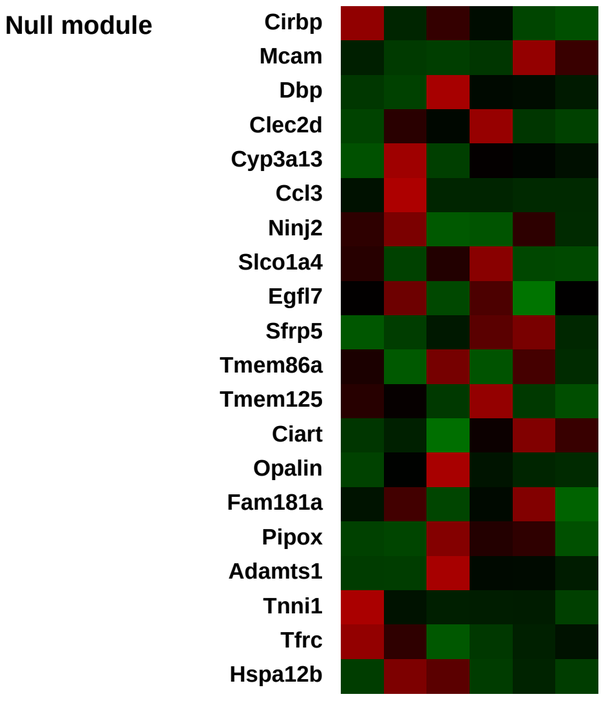

GEO Series "GSE30160" Expression Profiles

Num of samples in this series: 6

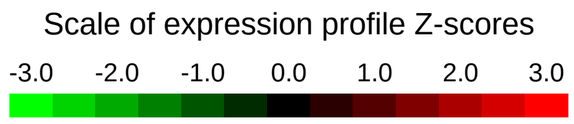

GEO Link:	**http://www.ncbi.nlm.nih.gov/geo/query/acc.cgi?acc=GSE30160**
Status:	**Public on Jul 05 2011**
Title:	**The RANK IVVY Motif-regulated Genes in Osteoclastogenesis**
Organism:	**Mus musculus**
Experiment type:	**Expression profiling by array**
Platform:	**GPL1261**
Pubmed ID:	
Summary & Design:	**Summary:** **By carrying out a systematic structure/function study of the RANK cytoplasmic domain, we previously identified a specific 4-a.a. RANK motif (IVVY535-538) which plays a critical role in osteoclastogenesis by mediating commitment of macrophages to the osteoclast lineage. We have recently validated the role of this IVVY motif in osteoclastogenesis in vivo by generating knockin (KI) mice bearing inactivating mutations in the RANK IVVY motif. This microarray experiment was performed to determine whether the IVVY motif is involved in regulating gene expression in osteoclastogenesis.** **We used microarrays to detail the global programme of gene expression underlying cellularisation and identified distinct classes of up-regulated genes during this process.** **Overall design:** **Bone marrow macrophages isolated from wild-type (WT) or knockin (KI) mice were plated in 60-mm tissue culture dishes and treated with M-CSF (44ng/ml) and RANKL (100ng/ml) for 24 hours. Each genotype has three triplicates. Total RNA was isolated for microarray analysis using mouse chips (type 430.2.0) at the Microarray Shared Facility at the University of Alabama at Birmingham.**

Background corr dist: KL-Divergence = 0.0193, L1-Distance = 0.0421, L2-Distance = 0.0019, Normal std = 0.8277

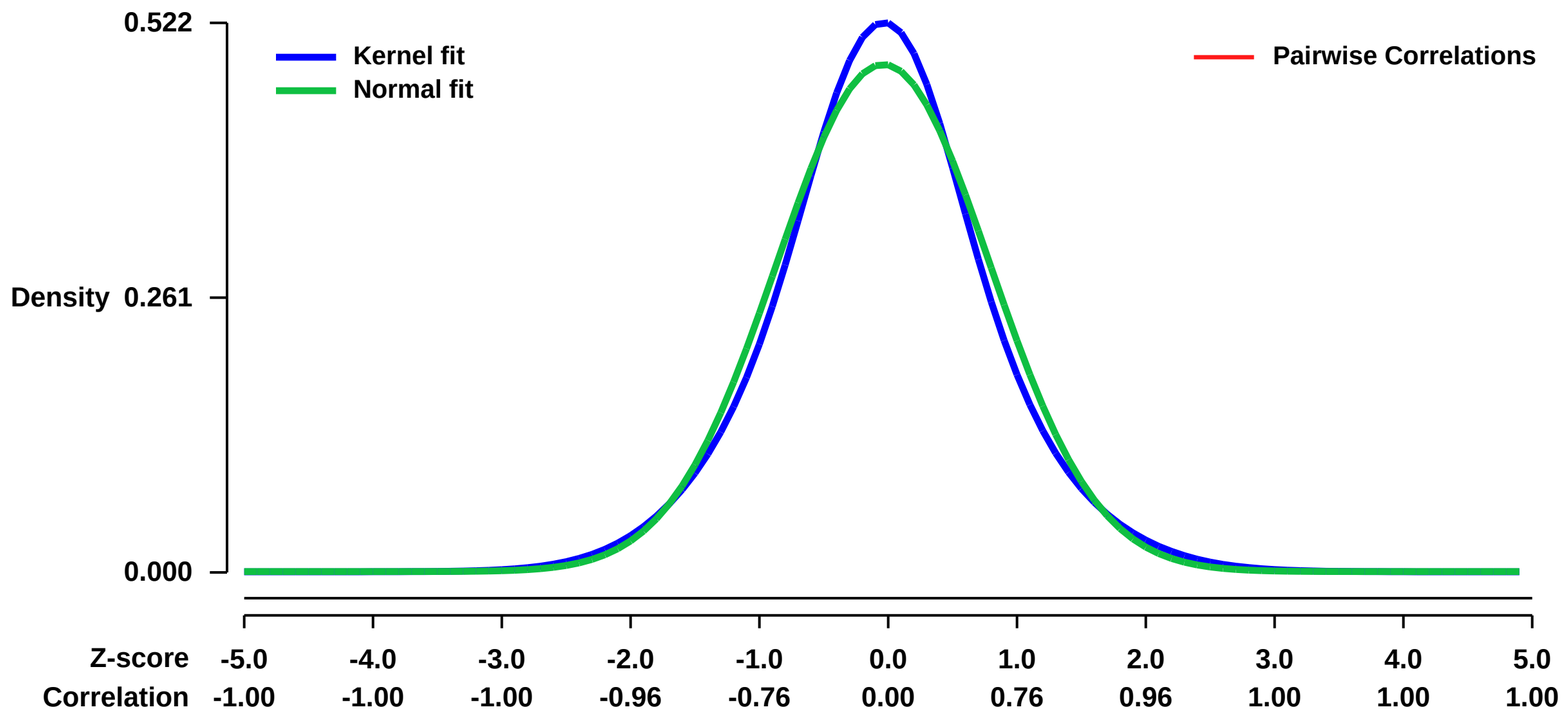

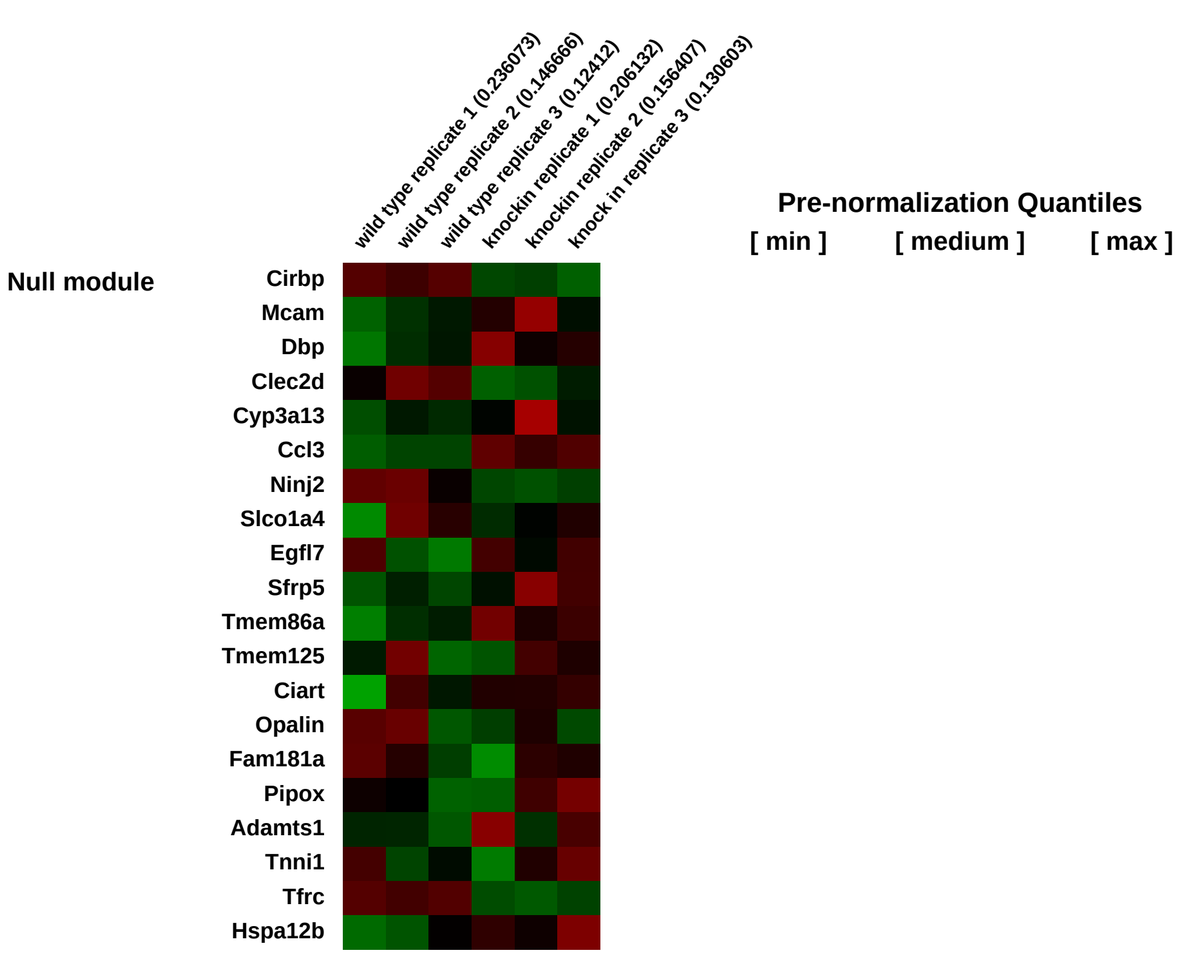

GEO Series "GSE58483" Expression Profiles

Num of samples in this series: 14

Scale of expression profile Z-scores

-3.0 -2.0 -1.0 0.0 1.0 2.0 3.0

GEO Link:	http://www.ncbi.nlm.nih.gov/geo/query/acc.cgi?acc=GSE58483
Status:	Public on Jun 14 2014
Title:	Expression data from chemokine-deficient mus musculus subjected to traumatic brain injury (TBI)
Organism:	Mus musculus
Experiment type:	Expression profiling by array
Platform:	GPL1261
Pubmed ID:	
Summary & Design:	**Summary:** We inflicted TBI to chemokine-deficient mouse lines in order to establish involvement of various signalling pathways that may be addressed therapeutically. Interacting chemokine pathways in brain regulate distinct inflammatory cells. Activated microglia are separate from invading phagocytes and dendritic cells. Findings show potential targets to interfere with specific inflammatory responses after brain injury. **Overall design:** TBI was carried out in Ccl3-/- and Ccr2-/- mice, total RNA prepared from injured cerebral neocortex after three days. RNA samples were from uninjured Ccl3-/- and Ccr2-/- mice as reference for hybridization on Affymetrix microarrays.

Background corr dist: KL-Divergence = 0.1640, L1-Distance = 0.0337, L2-Distance = 0.0020, Normal std = 0.3613

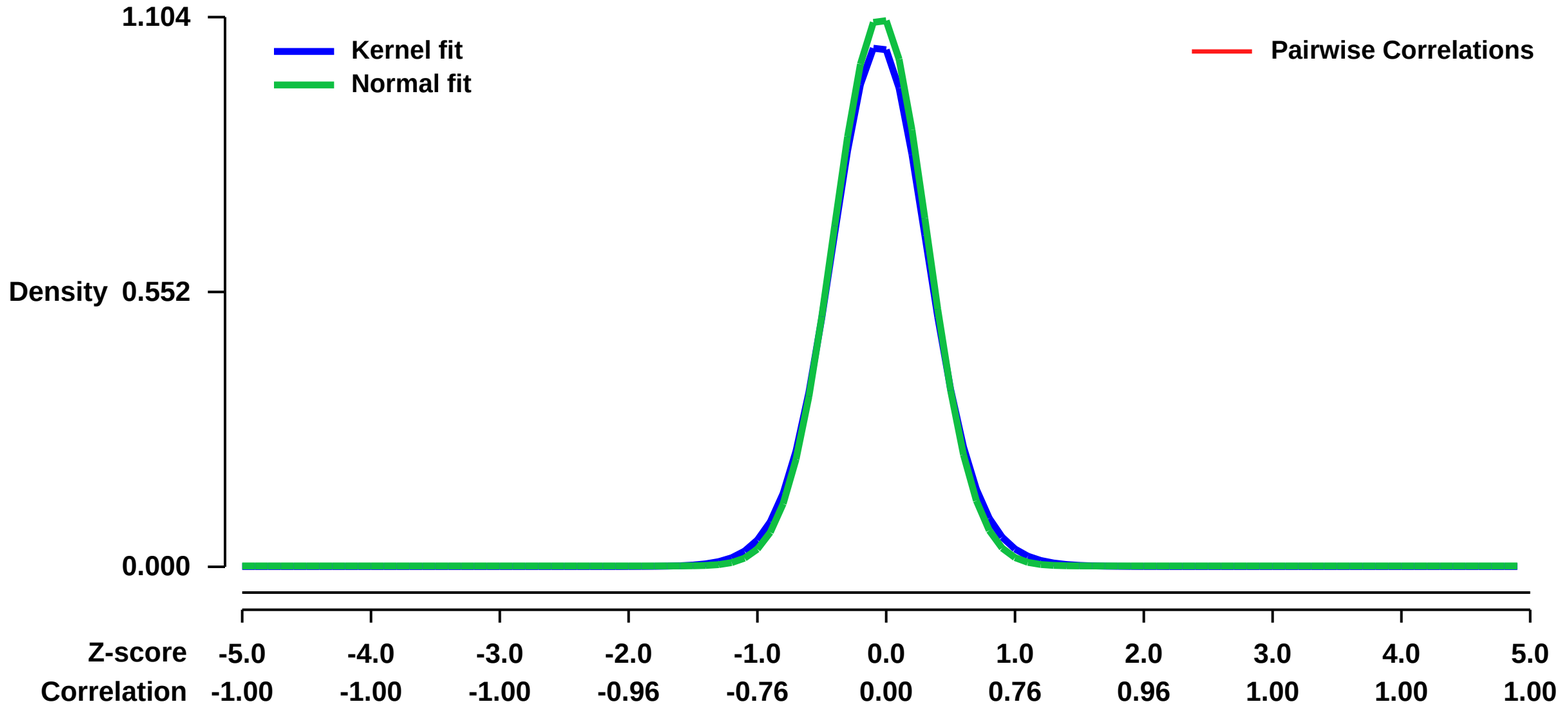

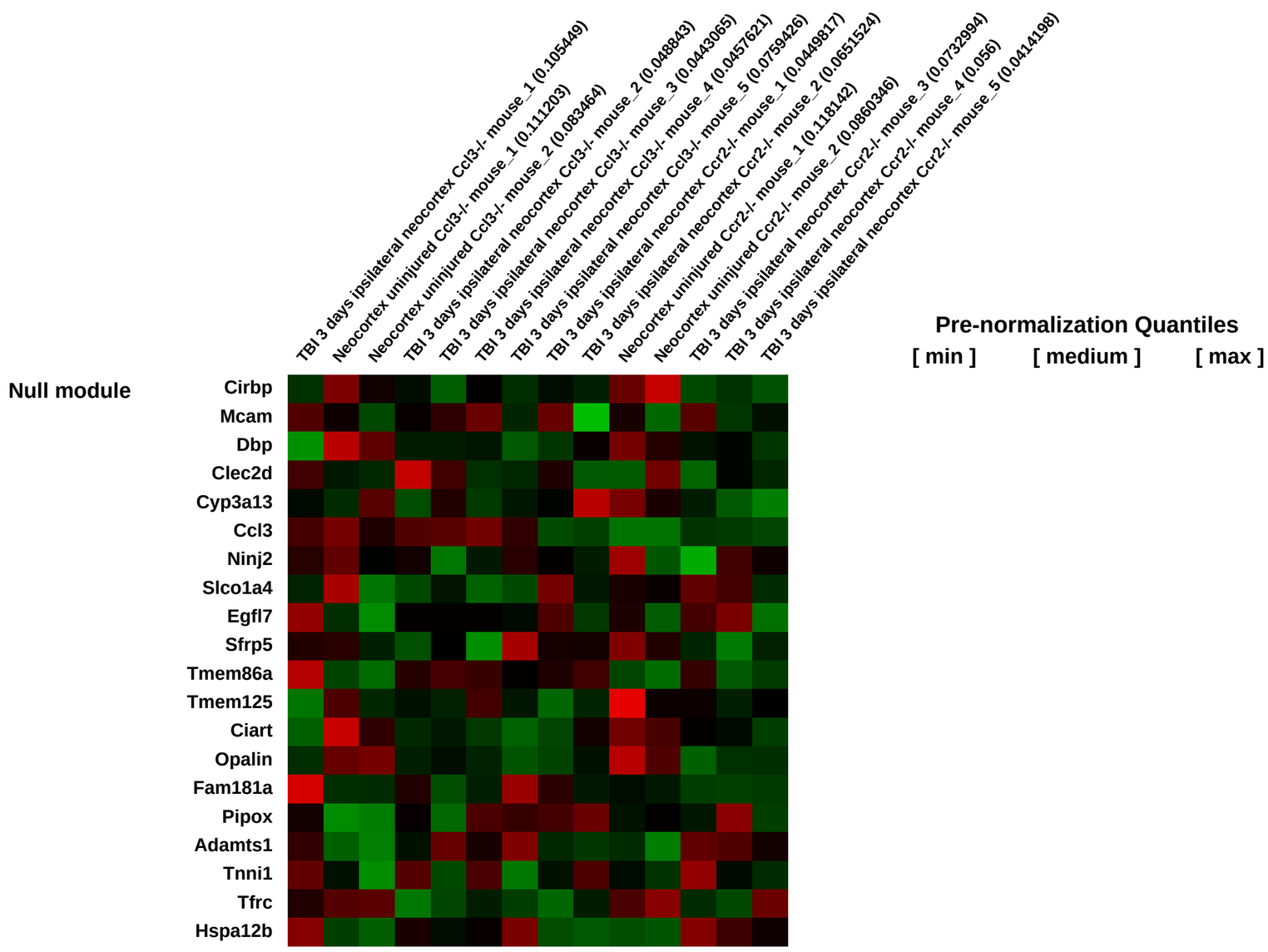

GEO Series "GSE14361" Expression Profiles

Num of samples in this series: 6

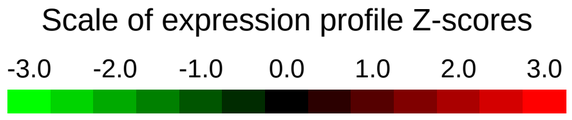

GEO Link:	http://www.ncbi.nlm.nih.gov/geo/query/acc.cgi?acc=GSE14361
Status:	Public on Jan 15 2009
Title:	IFNa activates dormant HSCs in vivo
Organism:	Mus musculus
Experiment type:	Expression profiling by array
Platform:	GPL1261
Pubmed ID:	19212321
Summary & Design:	**Summary:** Maintenance of the blood system is dependent on dormant haematopoietic stem cells (HSCs) with long-term self-renewal capacity. Upon injury these cells are induced to proliferate in order to quickly re-establish homeostasis. The signalling molecules promoting the exit of HSCs out of the dormant stage remain largely unknown. Here we show that in response to treatment of mice with interferon-alpha (IFN¸–), HSCs efficiently exit G0 and enter an active cell cycle. HSCs respond to IFN¸– treatment by increased phosphorylation of STAT1 and PKB/Akt, expression of IFN¸– target genes and up-regulation of stem cell antigen-1 (Sca-1). HSCs lacking either the interferon-¸–/¸† receptor (IFNAR), STAT1 or Sca-1 are insensitive to IFN¸– stimulation, demonstrating that STAT1 and Sca-1 mediate IFN¸– induced HSC proliferation. Although dormant HSCs are resistant to the anti-proliferative chemotherapeutic agent 5-FU1, HSCs pre-treated (primed) with IFN¸– and thus induced to proliferate are efficiently eliminated by 5-FU exposure in vivo. Conversely, HSCs chronically activated by IFN¸– are functionally compromised and are rapidly out competed by non-activatable IFNAR-/- cells in competitive repopulation assays. In summary, while chronic activation of the IFN¸– pathway in HSCs impairs their function, acute IFN¸– treatment promotes the proliferation of dormant HSCs in vivo. These data may help to clarify the so far unexplained clinical effects of IFN¸– on leukemic cells and raise the possibility for novel applications of type I interferons to target cancer stem cells. **Overall design:** cDNA microarray analysis was performed on sorted Lin neg, cKit+, CD150+, CD48neg HSCs from IFN¸– treated (16h after treatment) and untreated (littermate) mice. Per condition 3 independent biological replicates were analysed.

Background corr dist: KL-Divergence = 0.0491, L1-Distance = 0.0400, L2-Distance = 0.0025, Normal std = 0.5949

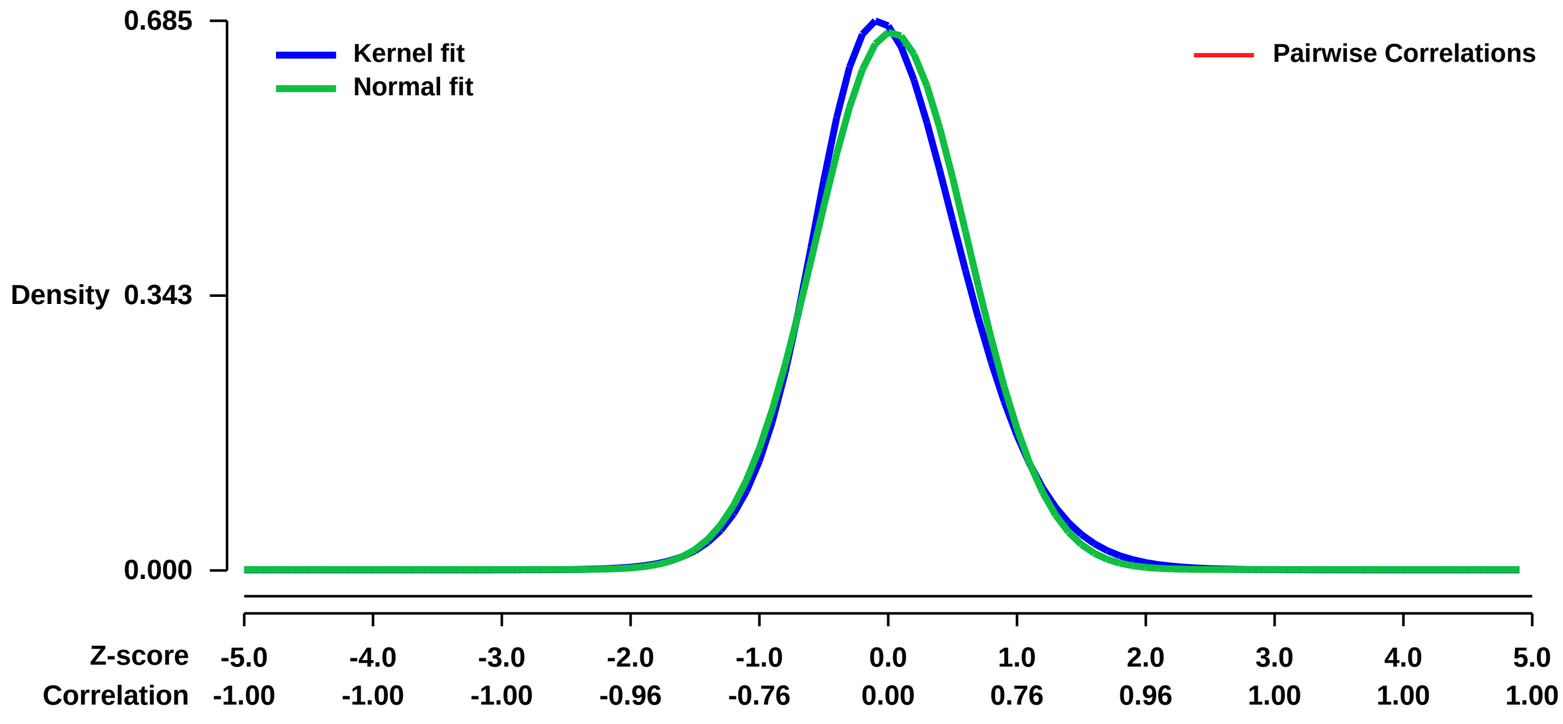

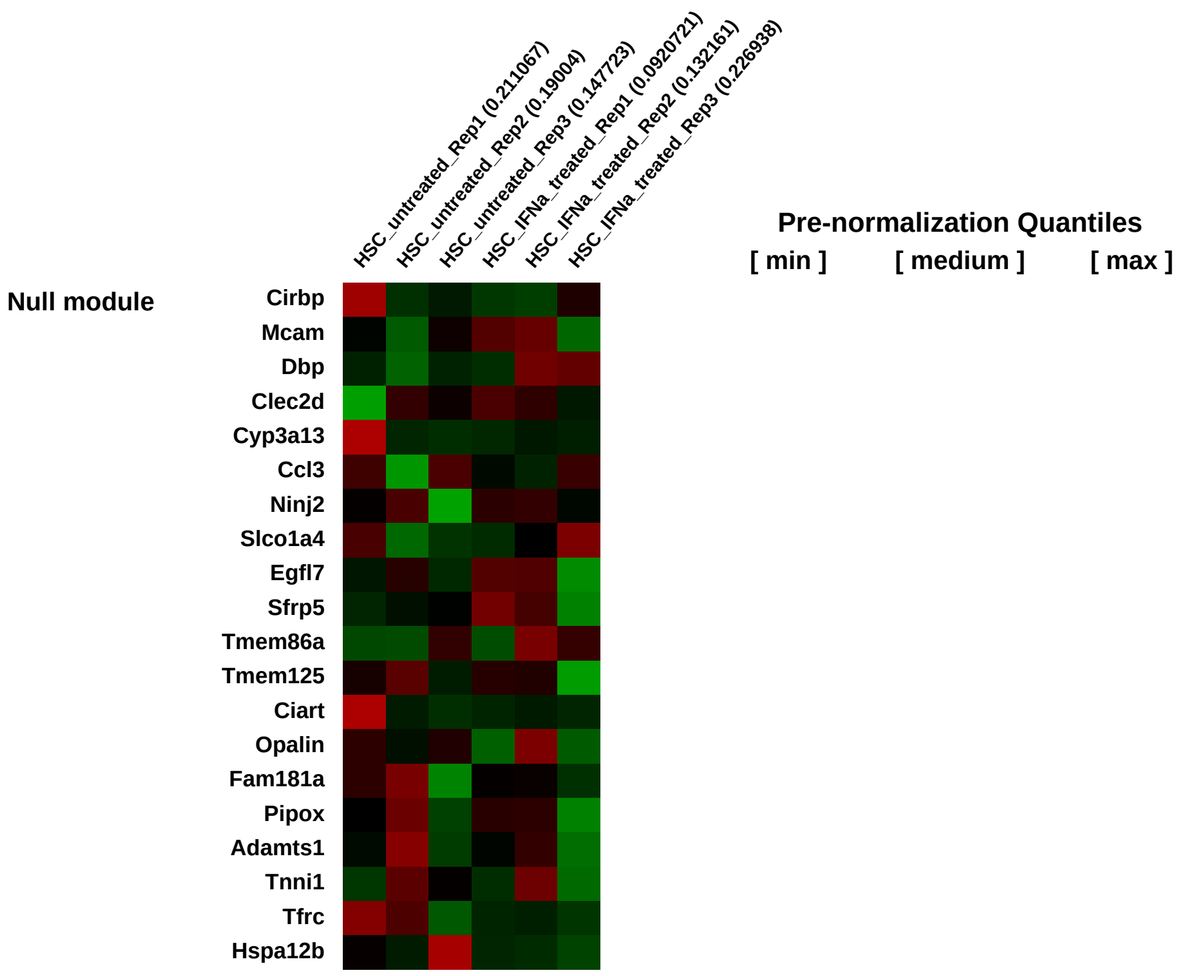

GEO Series "GSE40282" Expression Profiles

Num of samples in this series: 6

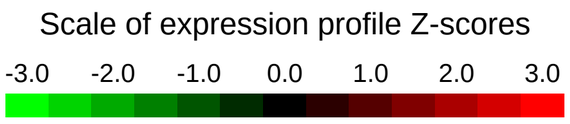

GEO Link:	http://www.ncbi.nlm.nih.gov/geo/query/acc.cgi?acc=GSE40282
Status:	Public on Jun 25 2013
Title:	Gene expression data of Lsd1fl/fl and Lsd1fl/fl Mx1Cre Gr1dim Mac1 granulocytic progenitor cells.
Organism:	Mus musculus
Experiment type:	Expression profiling by array
Platform:	GPL1261
Pubmed ID:	23795291
Summary & Design:	**Summary:** We discovered that mice with hematopoietic-specific deletion of Lsd1 lacked Gr-1+ Mac1+ neutrophilic granulocytes whereas the numbers of Gr-1dim Mac1+ granulocytic progenitor cells was increased. To determine the genes altered by Lsd1-loss, Gr-1dim Mac1+ granulocytic progenitor cells from Lsd1fl/fl and Lsd1fl/fl Mx1Cre mice were FACS-purified to be analyzed by gene expression profiling. **Overall design:** Primary Gr-1dim Mac1+ granulocytic progenitor cells were isolated from the bone marrow of Lsd1fl/fl and Lsd1fl/fl Mx1Cre animals by FACS-sorting, one week after the final p(I:C) dose. Total RNA from three biological replicates per genotype was extracted and used to hybridize to Affymetrix expression arrays using the Mouse Genome 430 2.0 array platform.

Background corr dist: KL-Divergence = 0.0230, L1-Distance = 0.0230, L2-Distance = 0.0005, Normal std = 0.7340

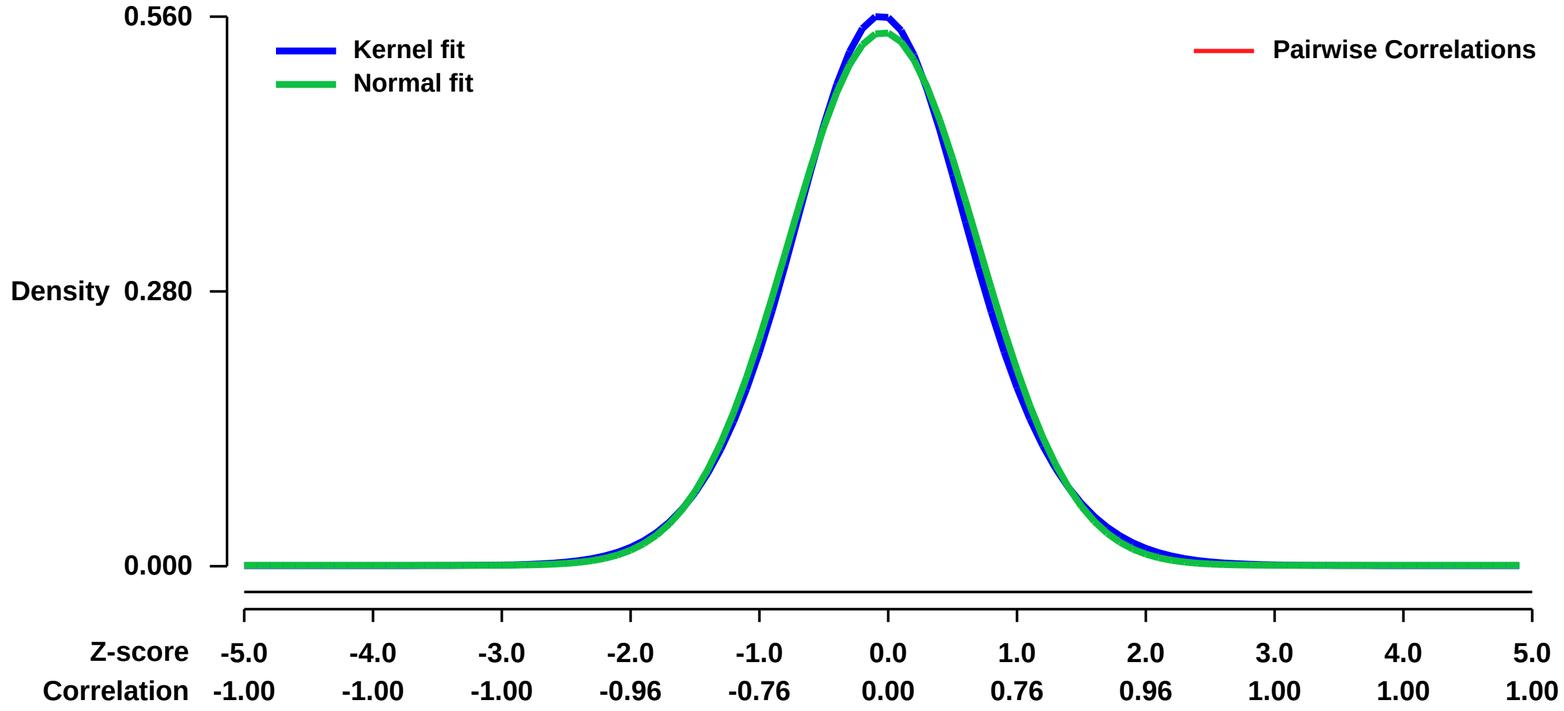

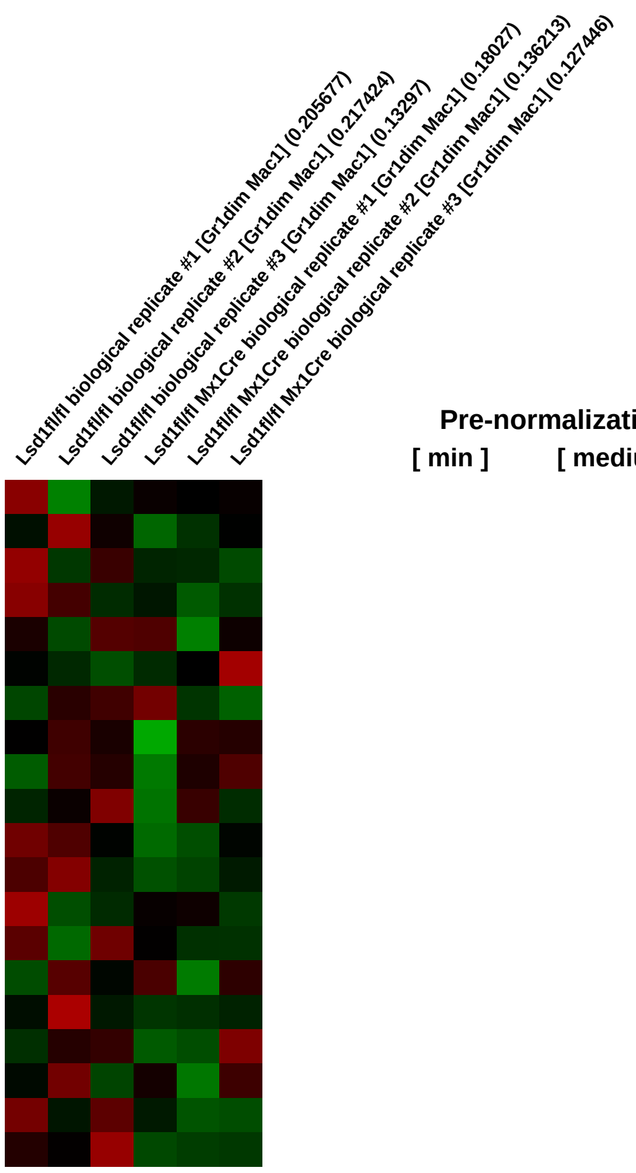

GEO Series "GSE4288" Expression Profiles

Num of samples in this series: 36

Scale of expression profile Z-scores

-3.0 -2.0 -1.0 0.0 1.0 2.0 3.0

GEO Link: http://www.ncbi.nlm.nih.gov/geo/query/acc.cgi?acc=GSE4288
Status: Public on Feb 05 2008
Title: Polysomal, free mRNP, and total cellular mRNA of J774.1 before and after LPS stimulation
Organism: Mus musculus
Experiment type: Expression profiling by array
Platform: GPL1261
Pubmed ID: 18230670

Summary & Design:

Summary:
Bacterial lipopolysaccharide(LPS) dramatically activates macrophages. So far, dozen of papers indicated that many proinflammatory molecules are transcriptionaly regulated during response. Despite of this,translational regulation is not fully elucidated especially in a comprehensive fashion. In this series, we investigated expression profiles of translation active (polysome) inactive (free mRNP) mRNAs of a typical mouse macrophage cell line, J774.1. Moreover, we also measured total cellular RNA level as a reference.

Keywords: time-course

Overall design:
Triplicates for each time points are included.

Background corr dist: KL-Divergence = 0.1306, L1-Distance = 0.0311, L2-Distance = 0.0019, Normal std = 0.3960

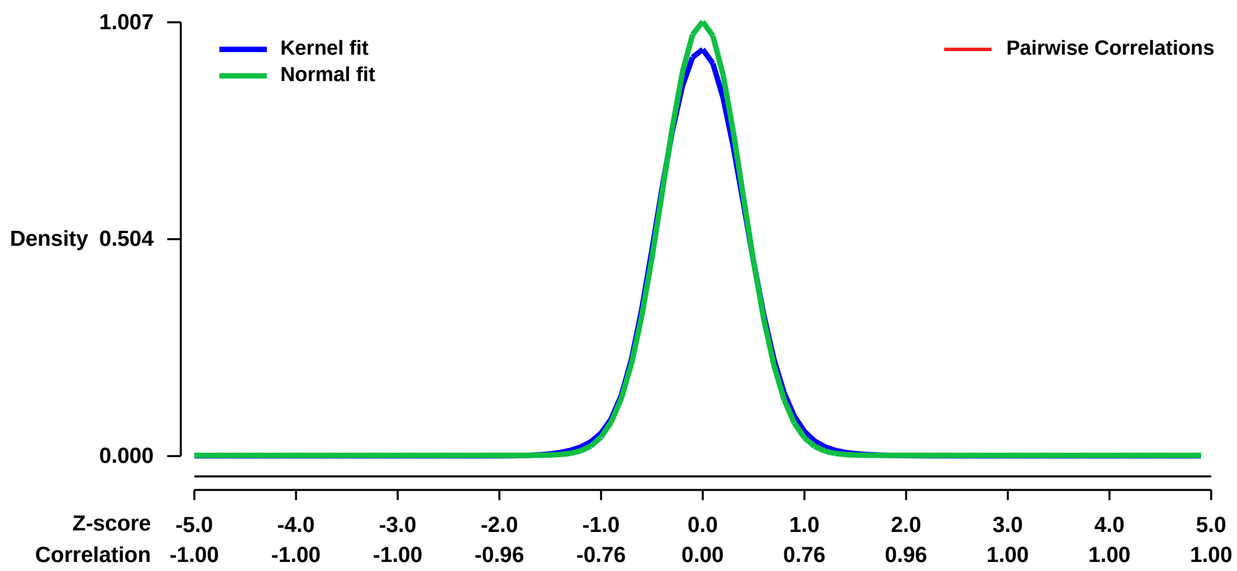

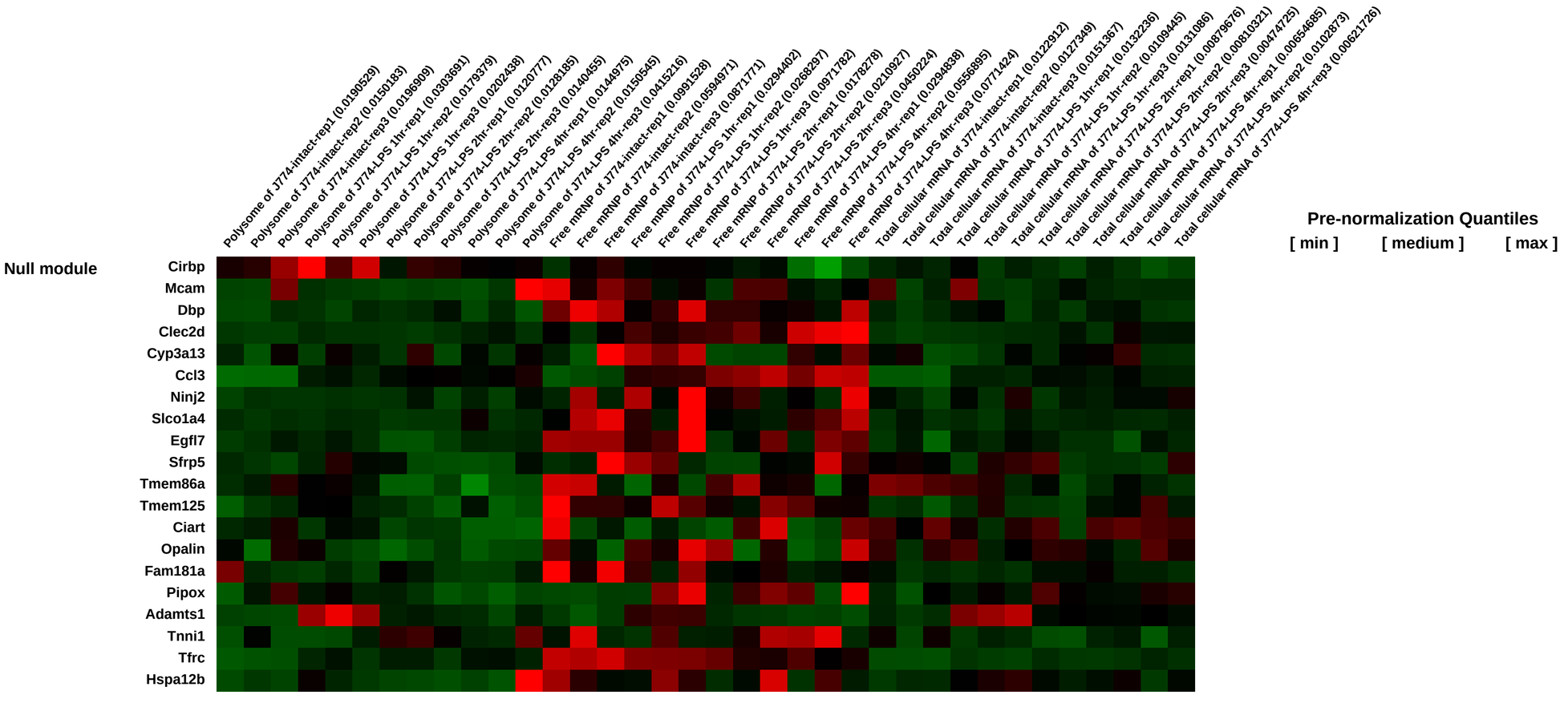

GEO Series "GSE17509" Expression Profiles

Num of samples in this series: 57

Scale of expression profile Z-scores

-3.0 -2.0 -1.0 0.0 1.0 2.0 3.0

GEO Link: http://www.ncbi.nlm.nih.gov/geo/query/acc.cgi?acc=GSE17509

Status: Public on Aug 20 2009

Title: Reduced levels of protein tyrosine phosphatase CD45 protect mice from the lethal effects of Ebola virus infection

Organism: Mus musculus

Experiment type: Expression profiling by array

Platform: GPL1261

Pubmed ID: 19683682

Summary & Design:

Summary:
To gain insight into the changes in gene expression pattern upon Ebola infection, CD45+/+ (100% protein level) and CD45+/- (62% protein level) mice were challenged with mouse adapted Ebola virus. At time-points day 0, 1, 3, 5, 7, 9, 11 and 13, spleen tissue was harvested and splenocytes isolated. Total RNA was isolated for mRNA expression analysis. The mouse genome 430 2.0 array (Affymetrix, Inc.), which consists of over 39,000 genes in a single array, was used. Based on gene expression patterns, the variable genes were grouped into sixteen clusters. Each cluster contained genes associated with cellular immune processes, signaling, cell-cycle, complement coagulation cascade, biosynthesis/metabolism, ubiquitous genes involved in several cascades, and genes of unknown function. Interestingly, gene expression in clusters 2 and 3 were significantly downregulated by day 1 following EBOV challenge in CD45100% mice. In contrast, at day 1 following EBOV infection, the CD45 62% mice maintained gene expression patterns similar to day 0. The differences in gene expression patterns between the CD45 100% and CD45 62% splenocytes were less apparent at day 3 following infection and by days 5 and 7 they became very similar. At day 9, when wild-type mice had succumbed to the disease, the pattern in CD45 62% mice remained similar to the day 7 patterns of CD45 100% and CD45 62% mice. The pattern at days 11 and 13 in the CD45 62% mice had returned to that of day 0 CD45 100% or CD45 62% mice. These results suggested that in CD45 100% mice, subversion of the cell transcriptional machinery during the early stages of EBOV infection (day 1) might represent a major factor leading to death of the mice. In CD45 62% mice, early control of gene regulation likely provided the appropriate antiviral responses leading to regulated inflammation, immune co-stimulation, and survival.

Overall design:
RNA expression in CD45 100% and 62% mice were compared at each time point: days 0, 1, 3, 5, and 7, using an empirical Bayes procedure. From 3 to 8 biological replicates were in each group. Samples for days 9, 11, and 13 (4 biological replicates each) were also available for only CD45 62%. Median expression values for highly variable genes within each group were clustered using agglomerative nesting over all available time points.

Background corr dist: KL-Divergence = 0.2878, L1-Distance = 0.0465, L2-Distance = 0.0049, Normal std = 0.2883

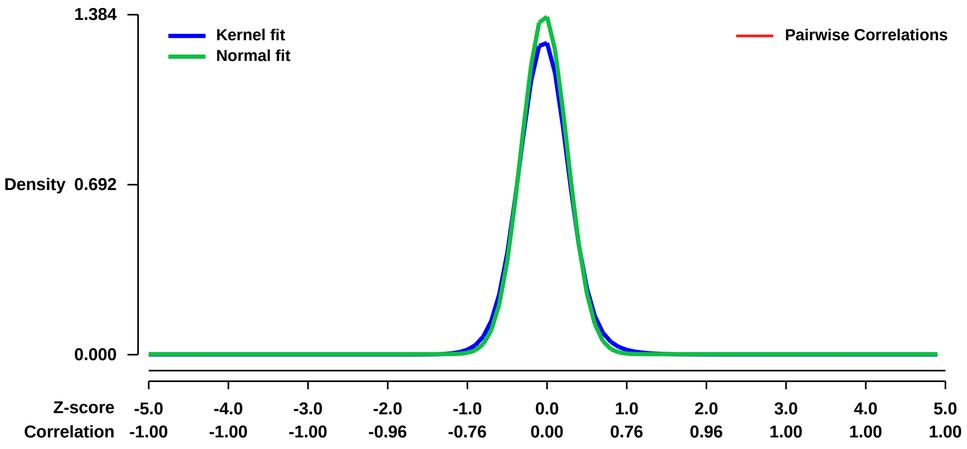

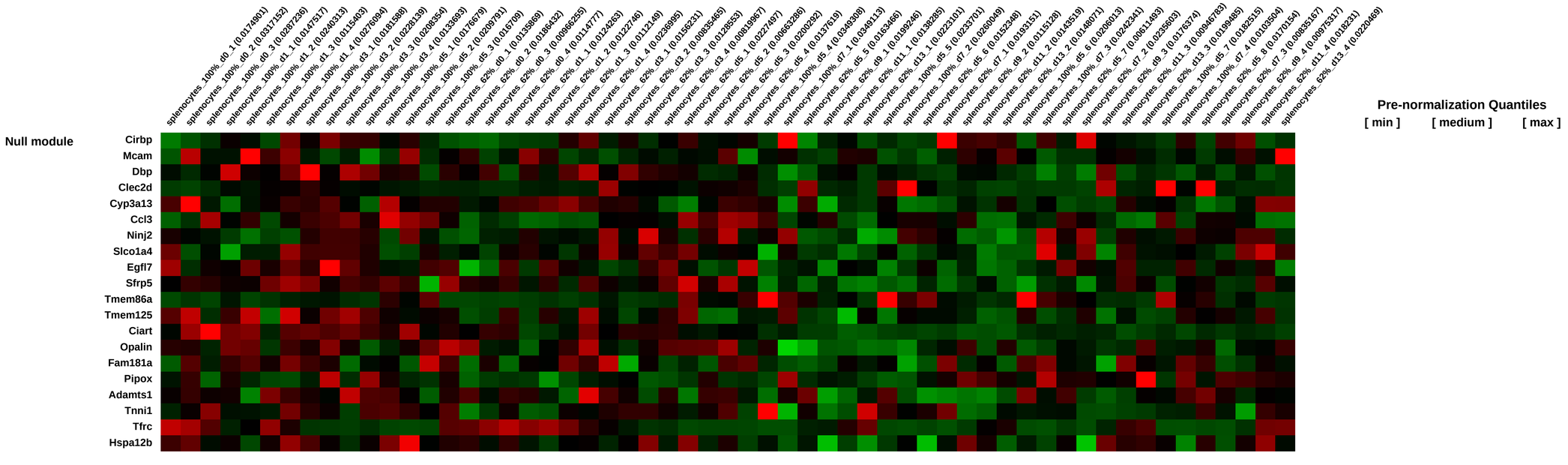

GEO Series "GSE15069" Expression Profiles

Num of samples in this series: 15

Scale of expression profile Z-scores

-3.0 -2.0 -1.0 0.0 1.0 2.0 3.0

GEO Link:	**http://www.ncbi.nlm.nih.gov/geo/query/acc.cgi?acc=GSE15069**
Status:	**Public on Apr 30 2009**
Title:	**Inhibitor trials in chondrocytes - MAS 5.0 normalization**
Organism:	**Mus musculus**
Experiment type:	**Expression profiling by array**
Platform:	**GPL1261**
Pubmed ID:	**20111593**
Summary & Design:	**Summary:** **Objectives: To identify similarities and differences in gene expression data in the MEK/ERK and PI3K pathways and to determine how histone modification affects these same pathways. Goal: To identify and functionally characterize novel targets of these signaling pathways in the context of chondrocyte differentiation.** **Keywords: Treatment, signaling, one-colour array, signaling pathway comparison** **Overall design:**

Background corr dist: **KL-Divergence = 0.0933, L1-Distance = 0.0484, L2-Distance = 0.0037, Normal std = 0.4765**

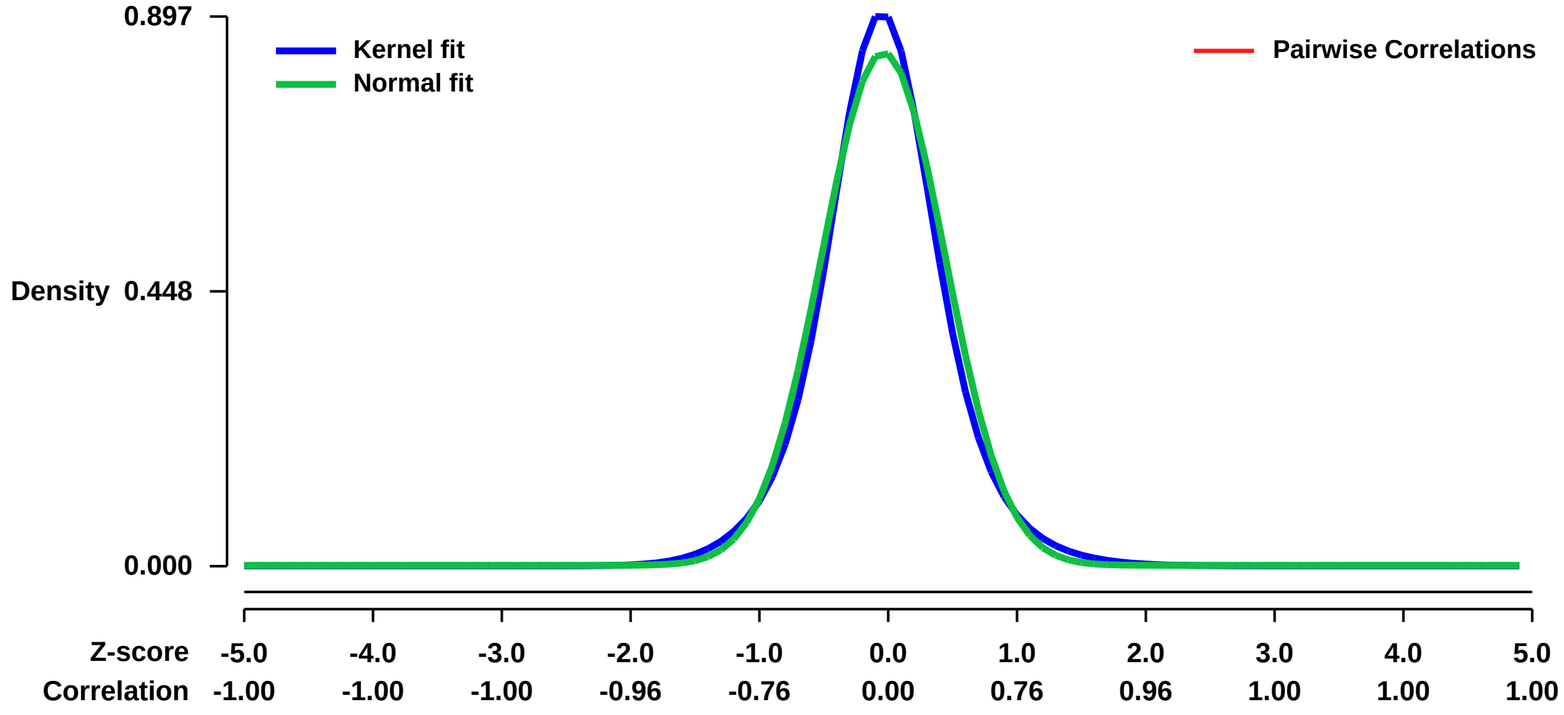

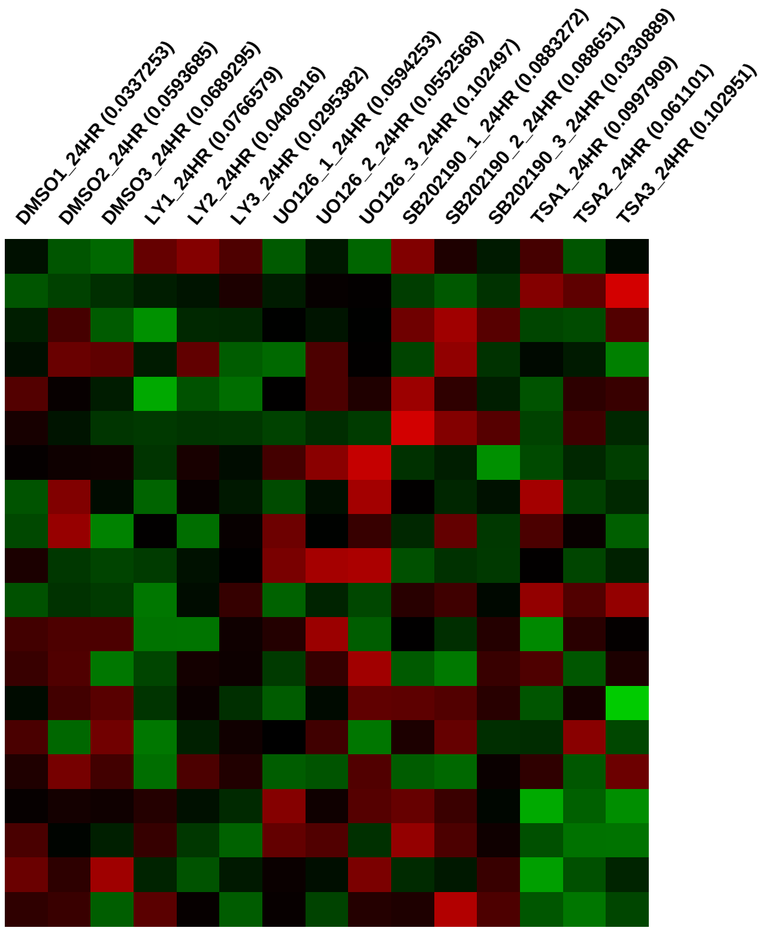

GEO Series "GSE9131" Expression Profiles

Num of samples in this series: 6

Scale of expression profile Z-scores

-3.0 -2.0 -1.0 0.0 1.0 2.0 3.0

GEO Link:	**http://www.ncbi.nlm.nih.gov/geo/query/acc.cgi?acc=GSE9131**
Status:	**Public on Sep 22 2007**
Title:	**Pparg<ldi/+> white Adipose Tissue expression differentials**
Organism:	**Mus musculus**
Experiment type:	**Expression profiling by array**
Platform:	**GPL1261**
Pubmed ID:	**17921248**
Summary & Design:	**Summary:** **Identifying gene expression changes in adipose tissue of lipodystrophic Pparg<ldi/+> targeted mice** **Keywords: Genetic modification** **Overall design:** **RNA from epididymal white adipose pads of three 10-week-old Pparg<ldi/+> males and three litter-matched WT controls was analyzed by MOE430v2.0 GeneChipâ¢ arrays, one mouse per array.**

Background corr dist: **KL-Divergence = 0.0333, L1-Distance = 0.0274, L2-Distance = 0.0008, Normal std = 0.6683**

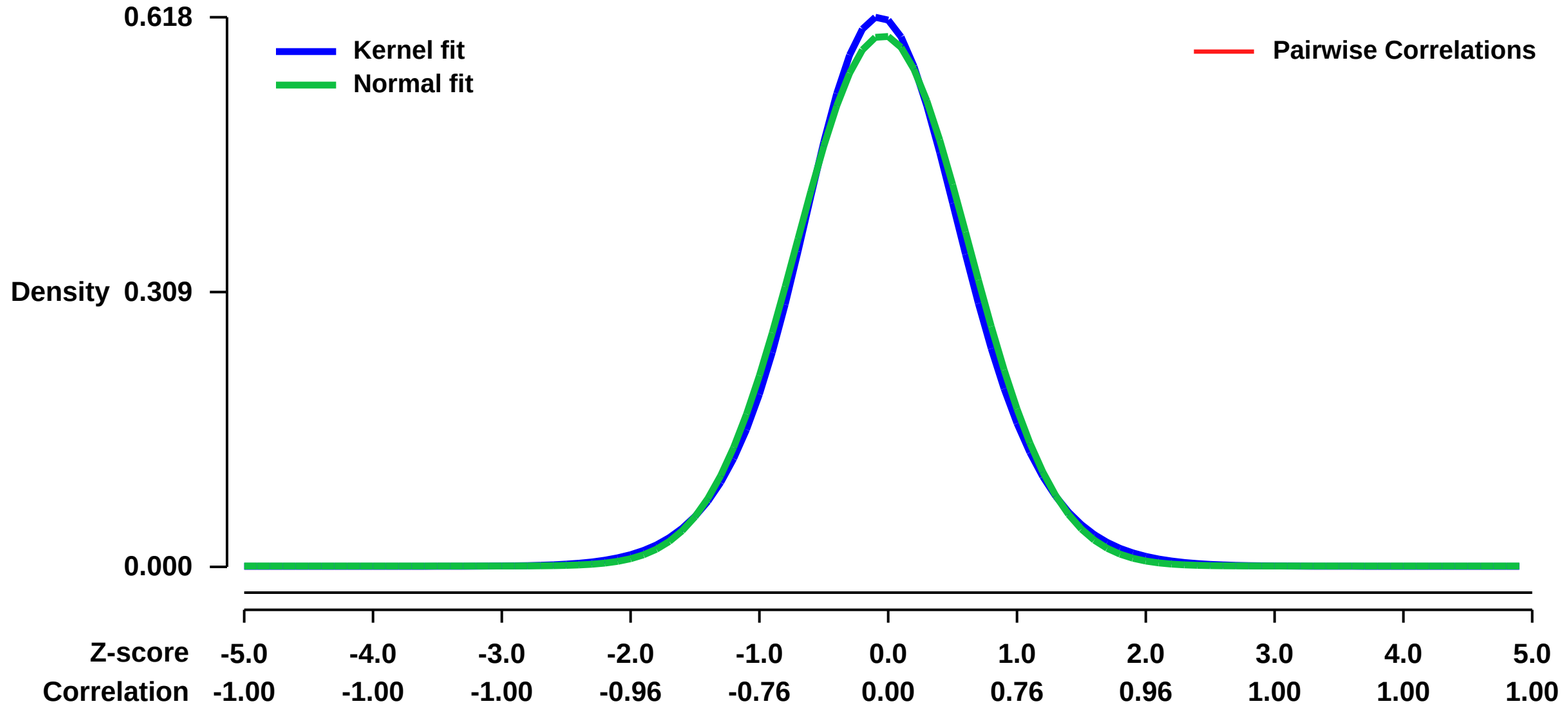

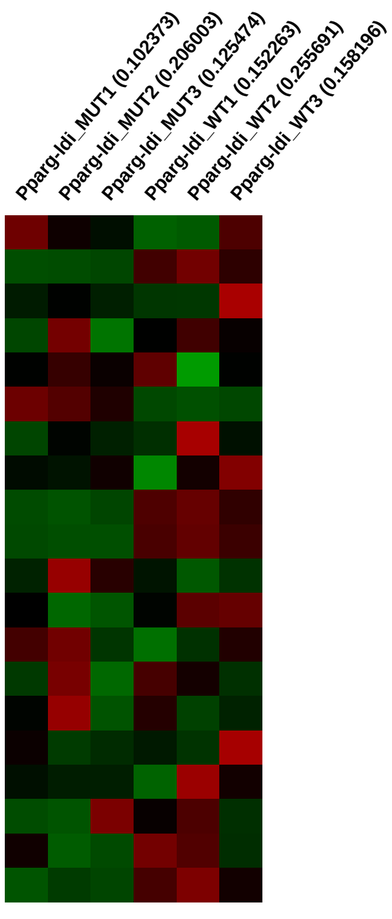

GEO Series "GSE13522" Expression Profiles

Num of samples in this series: 33

Scale of expression profile Z-scores

-3.0 -2.0 -1.0 0.0 1.0 2.0 3.0

GEO Link:	http://www.ncbi.nlm.nih.gov/geo/query/acc.cgi?acc=GSE13522
Status:	Public on Jan 02 2009
Title:	Transcriptional response in skin of mouse 24 hours after intradermal infection with Trypanosoma cruzi
Organism:	Mus musculus
Experiment type:	Expression profiling by array
Platform:	GPL1261
Pubmed ID:	19201883
Summary & Design:	**Summary:** To investigate the early host response triggered by three different strains of Trypanosoma cruzi at a local infection site, changes in host gene expression were monitored in a murine intradermal infection model using Affymetrix oligonucleotide arrays. Robust induction of IFN-stimulated genes (ISGs) was observed in excised skin 24 hours post-infection where the level of ISG induction was parasite strain-dependent with the least virulent strain triggering a muted IFN response. Infection of mice immunodepleted of IFN‚‡-producing cells or infection of IFN‚‡-deficient mice had minimal impact on the IFN response generated in T. cruzi infected mice. In contrast, infection of mice lacking the type I IFN receptor demonstrated that type I IFNs are largely responsible for the IFN response generated at the site of infection. These data highlight type I IFNs as important components of the innate immune response to T. cruzi the site of inoculation and their role in shaping the early transcriptional response to this pathogen. We used microarrays to detail the local host transcriptional response to intradermal T. cruzi infection in WT mice and mice depleted of NK cells, or deficient in IFN-gamma or type I IFN responses. Additionally we compared the local host-transcriptional response generated to infection with 3 different strains of Trypanosoma cruzi (Y, Brazil, and G). **Keywords: disease state analysis** **Overall design:** Mice were infected by intradermal injection of 10^6 T. cruzi trypomastigotes in 100uL of saline split between 2 adjacent sites on the shaved side flank. Control mice were injected with an equal volume of saline. 24 hours post-injection approximately 75mm^2 of skin immediately surrounding the injection site was excised and RNA was isolated from the tissue. Balb/c mice were used for most experiments and IFN-gamma KO mice were on the Balb/c background. WT 129 mice were also used as IFNAR-/- mice were on the 129 background. In total 33 arrays were performed. 7 WT (Balb/c) control, 3 Y strain infected, 3 Brazil strain infected, 3 G strain infected, 2 IFN-gamma KO control, 2 IFN-gamma KO infected, 1 NK cell depleted control, 1 NK cell depleted infected, 3 WT (129) control, 3 WT (129) infected, 3 IFNAR KO control, 3 IFNAR KO infected

Background corr dist: KL-Divergence = 0.1154, L1-Distance = 0.0494, L2-Distance = 0.0056, Normal std = 0.4145

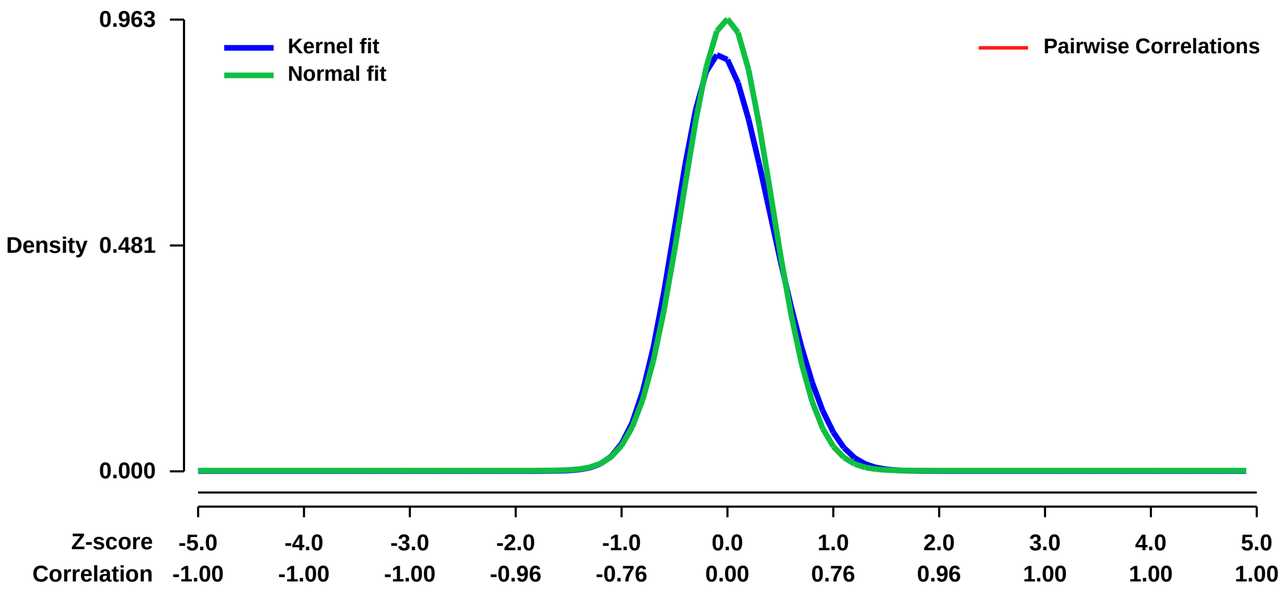

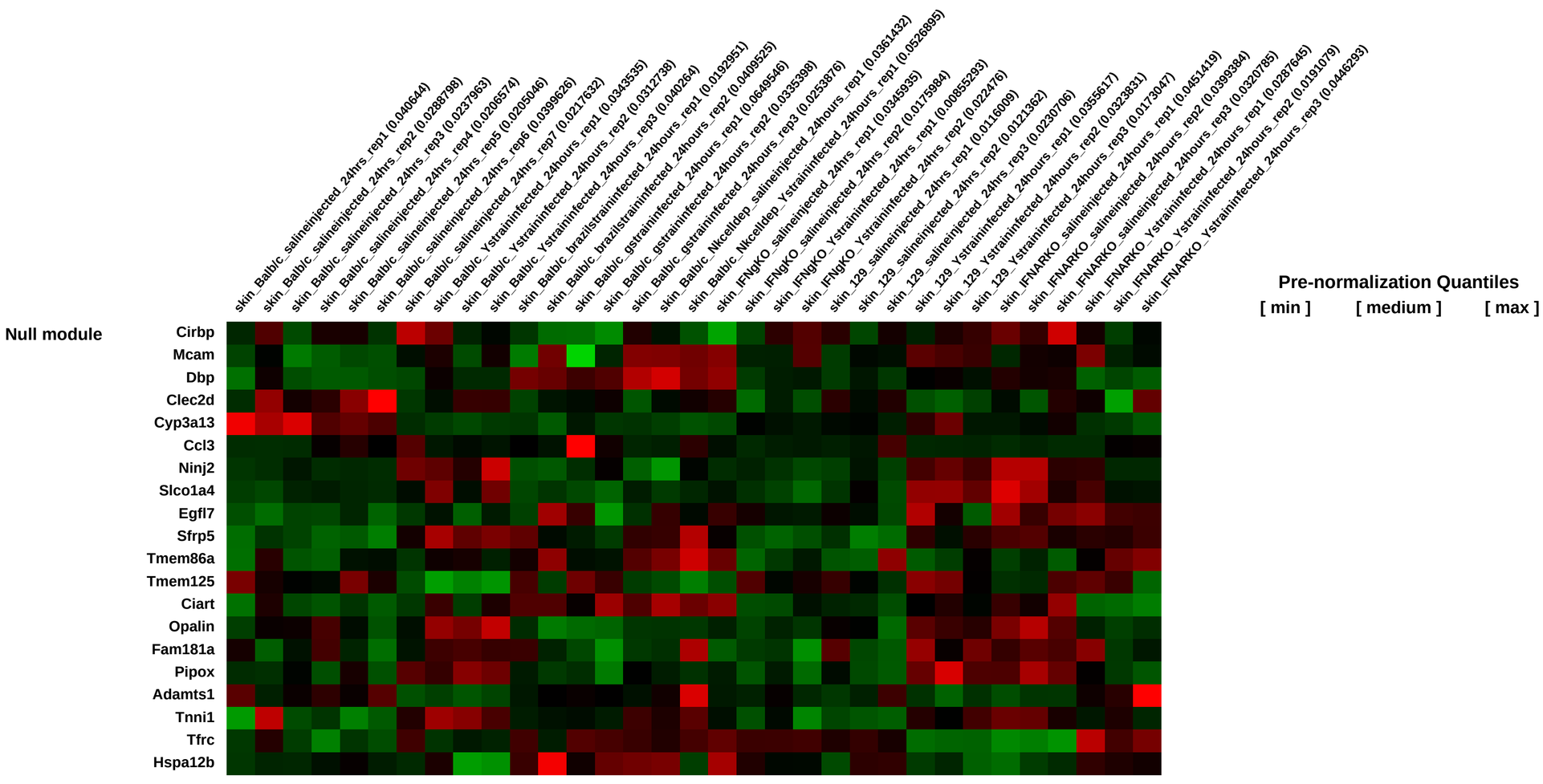

GEO Series "GSE8434" Expression Profiles

Num of samples in this series: 6

Scale of expression profile Z-scores

-3.0 -2.0 -1.0 0.0 1.0 2.0 3.0

GEO Link:	http://www.ncbi.nlm.nih.gov/geo/query/acc.cgi?acc=GSE8434
Status:	Public on Aug 01 2007
Title:	Transcriptional regulation by Errb (Nr3b2) in stria vascularis
Organism:	Mus musculus
Experiment type:	Expression profiling by array
Platform:	GPL1261
Pubmed ID:	17765677
Summary & Design:	**Summary:** Transcriptional profiles were compared in microdissected lateral walls of the inner ears from Errb mutant mice and wild type littermate controls. The goal is to identify transcriptional targets of Errb and candidate genes for inner ear diseases. **Keywords: genetic mutant analysis** **Overall design:** Errb mutant mice were generated by conditional knock-out strategy. Inner ears from 10 mice were pooled for each sample and 3 replicates of wild type and mutant samples were analyzed.

Background corr dist: **KL-Divergence = 0.0097, L1-Distance = 0.0148, L2-Distance = 0.0002, Normal std = 0.8623**

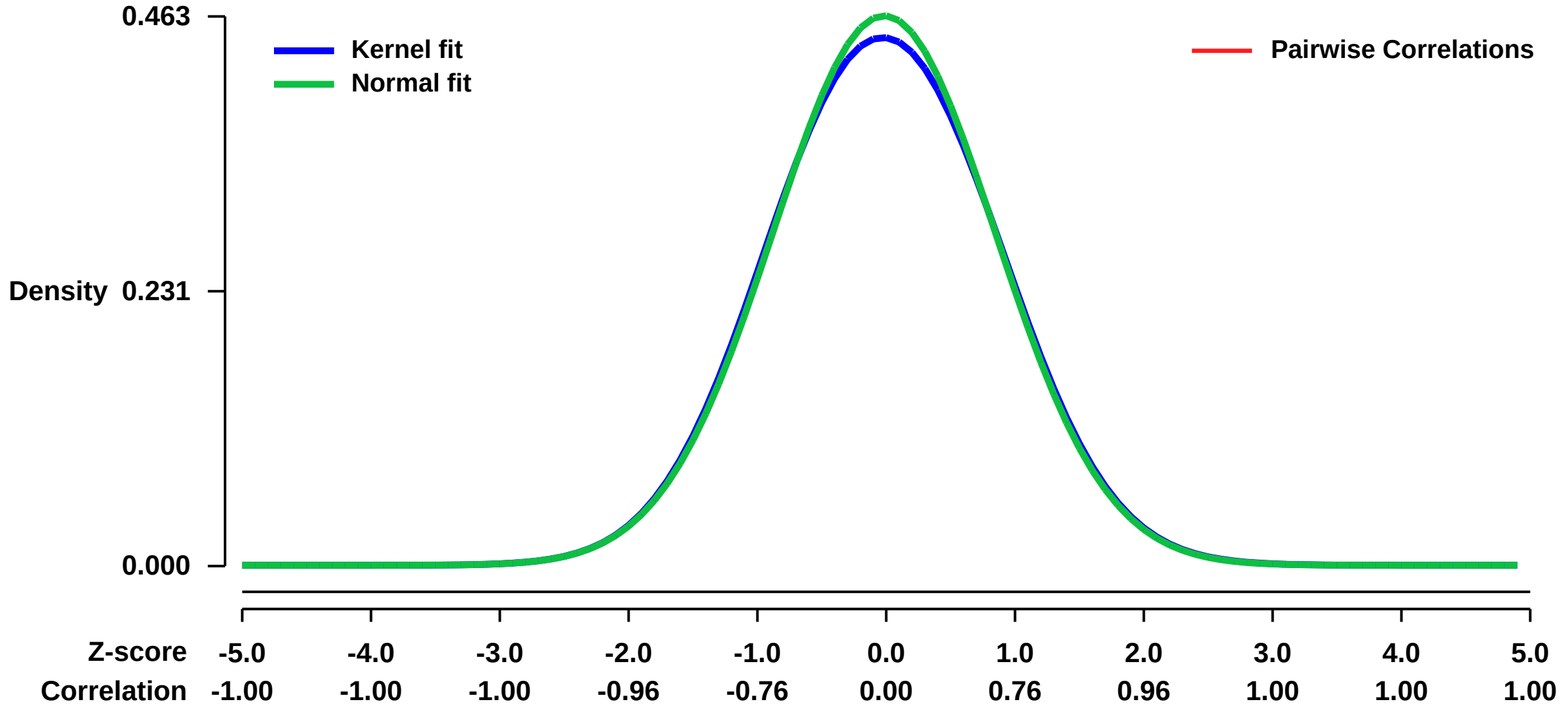

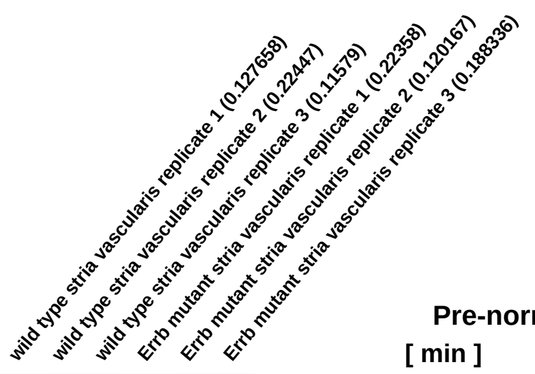

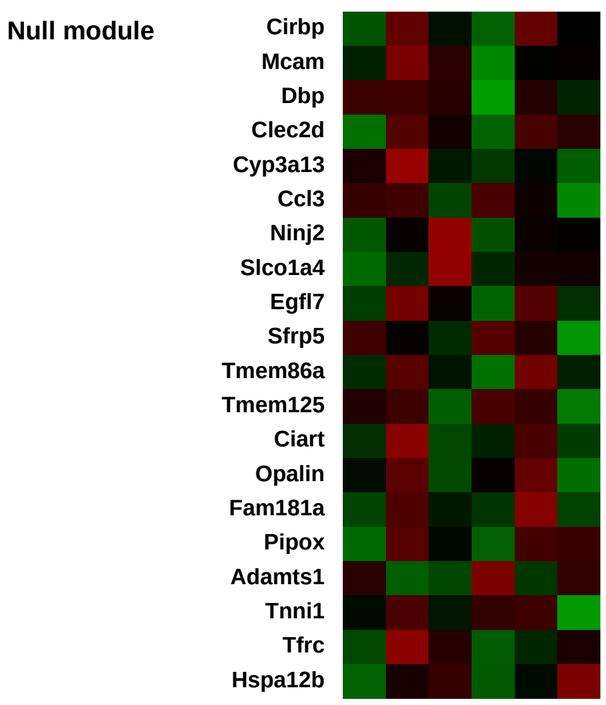

GEO Series "GSE6676" Expression Profiles

Num of samples in this series: 8

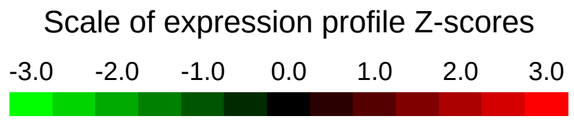

GEO Link:	**http://www.ncbi.nlm.nih.gov/geo/query/acc.cgi?acc=GSE6676**
Status:	**Public on Jan 09 2007**
Title:	**Comparison of corneas from wildtype mice to those from mice under the influence of high doses of TGF-beta russe-affy-mouse-372894**
Organism:	**Mus musculus**
Experiment type:	**Expression profiling by array**
Platform:	**GPL1261**
Pubmed ID:	
Summary & Design:	**Summary:** **Characteristic structural details of the cornea are transparency, the absence of blood vessels, and the presence of numerous sensory nerve endings. The corneal epithelium is one of the most densely innervated tissues of the body. The characteristics of the cornea are established during fetal development, and are lost in adult life when the cornea regenerates after injury. The common reaction of the cornea to injury is the formation of opaque scars, the ingrowth of blood vessels, and distinct changes in the innervation pattern. Scar formation of the cornea is critically modulated by the expression of transforming growth factor-beta (TGF-beta).** **To identify genes that are important for corneal transparency, dense innervation and absence of blood vessels by comparing corneas from wildtype mice with those that are under the influence of high doses of TGF-beta.** **Transparency, dense innervation, and absence of blood vessels in the cornea all depend on the expression of a critical set of genes that are not expressed when TGF-beta is present.** **Mice were generated that overexpress TGF-beta under control of a strong lens-specific promoter. These mice developed opaque corneas that are vascularized and lack sensory nerves. In addition, these corneas were densely populated with cells expressing neural cell adhesion protein.** **RNA was isolated from corneas of transgenic animals and wildtype littermates in order to analyze differentially expressed genes and to identify those that are only expressed in transparent, avascular, and densely innervated wildtype corneas.** **Keywords: TGF-beta overexpression** **Overall design:**

Background corr dist: **KL-Divergence = 0.0715, L1-Distance = 0.0250, L2-Distance = 0.0011, Normal std = 0.5009**

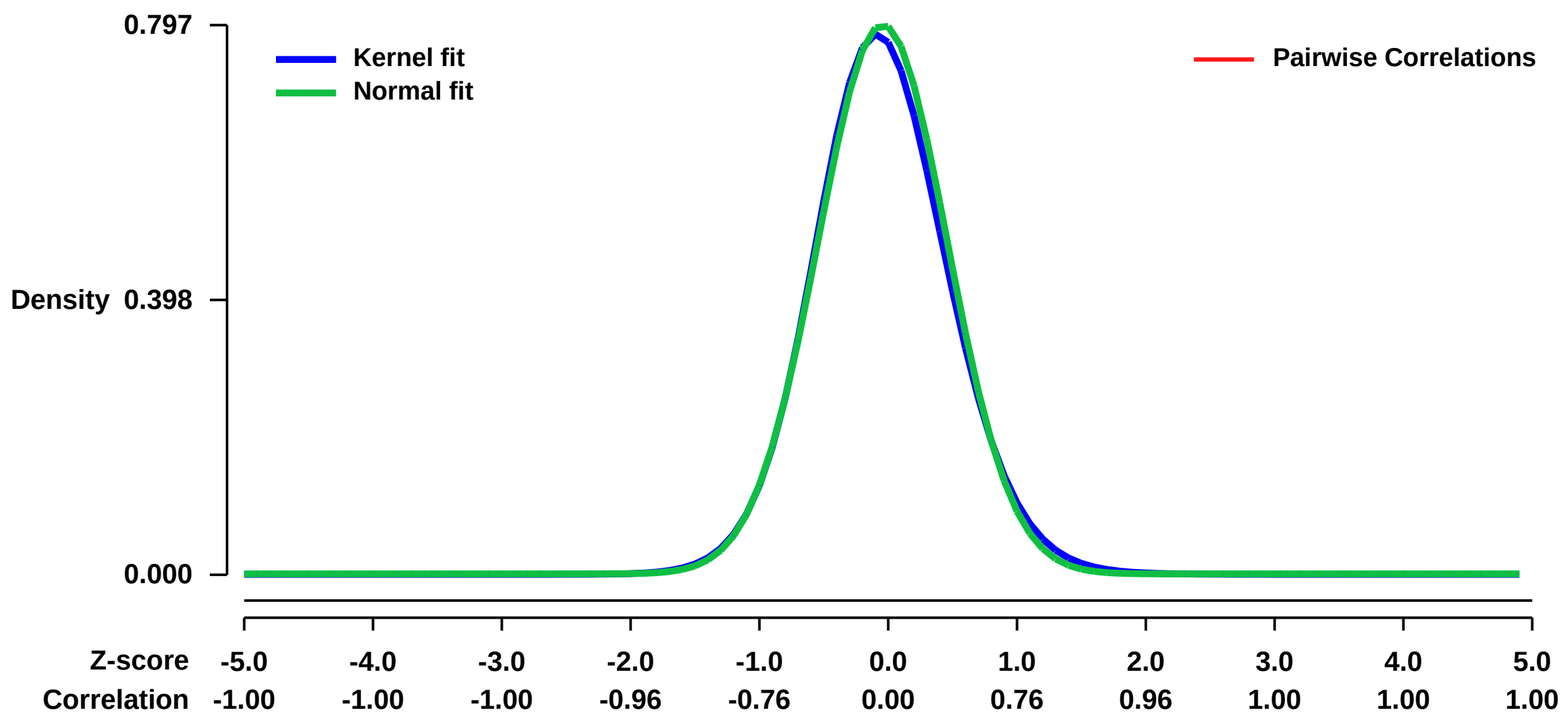

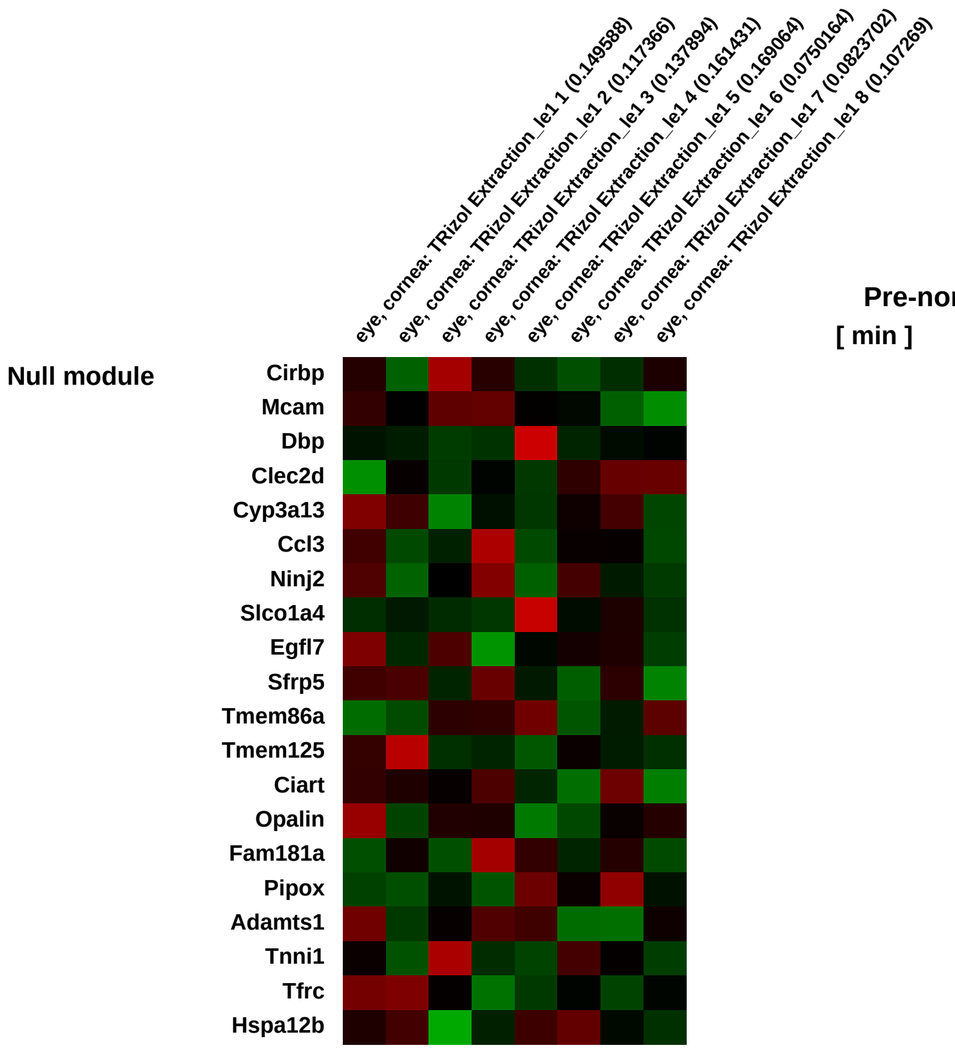

GEO Series "GSE15541" Expression Profiles

Num of samples in this series: 12

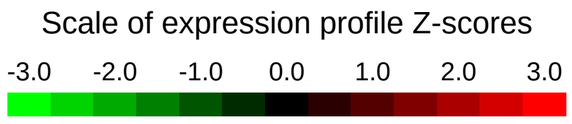

GEO Link:	http://www.ncbi.nlm.nih.gov/geo/query/acc.cgi?acc=GSE15541
Status:	Public on Apr 09 2009
Title:	Linkage of Meis1 leukemogenic activity to multiple downstream effectors including Trib2 and Ccl3
Organism:	Mus musculus
Experiment type:	Expression profiling by array
Platform:	GPL1261
Pubmed ID:	18375036
Summary & Design:	**Summary:** **OBJECTIVE: MEIS1, a HOX cofactor, collaborates with multiple HOX and NUP98-HOX fusion proteins to accelerate the onset of acute myeloid leukemia (AML) through largely unknown molecular mechanisms. MATERIALS AND METHODS: To further resolve these mechanisms, we conducted a structure-function analysis of MEIS1 and gene-expression profiling, in the context of NUP98-HOXD13 (ND13) leukemogenesis. RESULTS: We show, in a murine bone marrow transplantation model, that the PBX-interaction domain, the homeodomain, and the C-terminal domain of MEIS1, are all required for leukemogenic collaboration with ND13. In contrast, the N-terminal domain of MEIS1 is dispensable for collaboration with ND13, but is required for Flt3 upregulation, indicating additional roles for MEIS1 in induction of leukemia independent of alterations in Flt3 expression. Gene-expression profiling of a cloned ND13 preleukemic cell line transduced with wild-type or Meis1 mutant forms revealed deregulation of multiple genes, including a set not previously implicated as MEIS1 targets. Chromatin immunoprecipitation revealed the in vivo occupancy of MEIS1 on regulatory sequences of Trib2, Flt3, Dlk1, Ccl3, Ccl4, Pf4, and Rgs1. Furthermore, engineered overexpression of Trib2 complements ND13 to induce AML while Ccl3 potentiates the repopulating ability of ND13. CONCLUSION: This study shows that Meis1-induced leukemogenesis with ND13 can occur in the absence of Flt3 upregulation and reveals the existence of other pathways activated by MEIS1 to promote leukemia.** **Overall design:** **Establishment of pre-leukemic bone marrow cell lines following transduction with ND13 have been previously described (Pineault, Abramovich et al. 2005). In brief, lines were established from BM cells previously treated with 5-fluorouracil (5-FU) from (C57Bl/6Ly-Pep3b x C3H/HeJ) F1 (PepC3) (Ly5.1+/Ly5.2+) mice freshly transduced with the ND13-GFP or ND13pac virus and maintained in liquid culture. To generate ND13+Meis1 or ND13+Meis1 mutant BM cell lines, the ND13 BM cells were transduced by co-cultivation on irradiated (4,000 cGy) E86 producers for Meis1-YFP (or Meis1 mutant forms), respectively, for a period of 2 days in the presence of 5 ´µg/ml of protamine sulfate. Three independent experiments were performed for each of the four different conditions included in the study.**

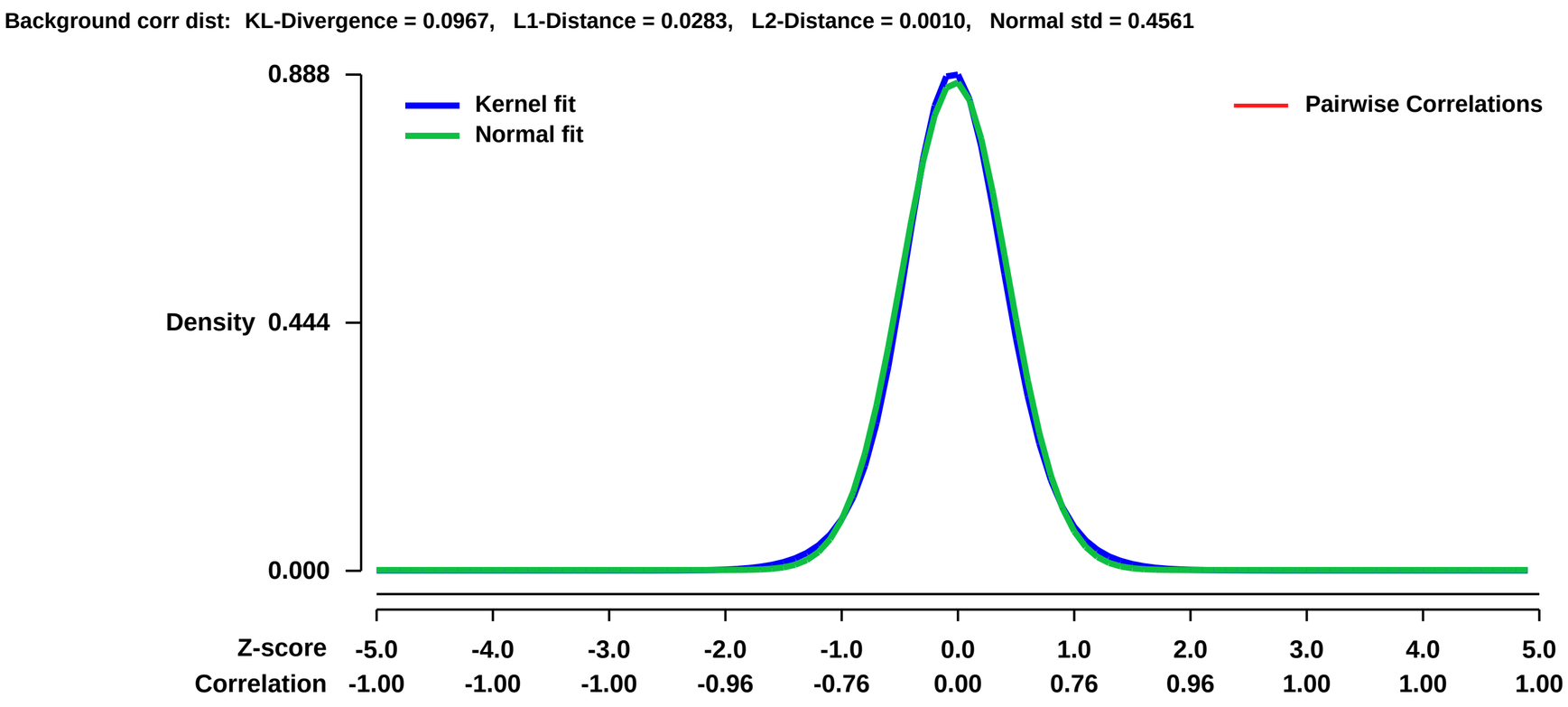

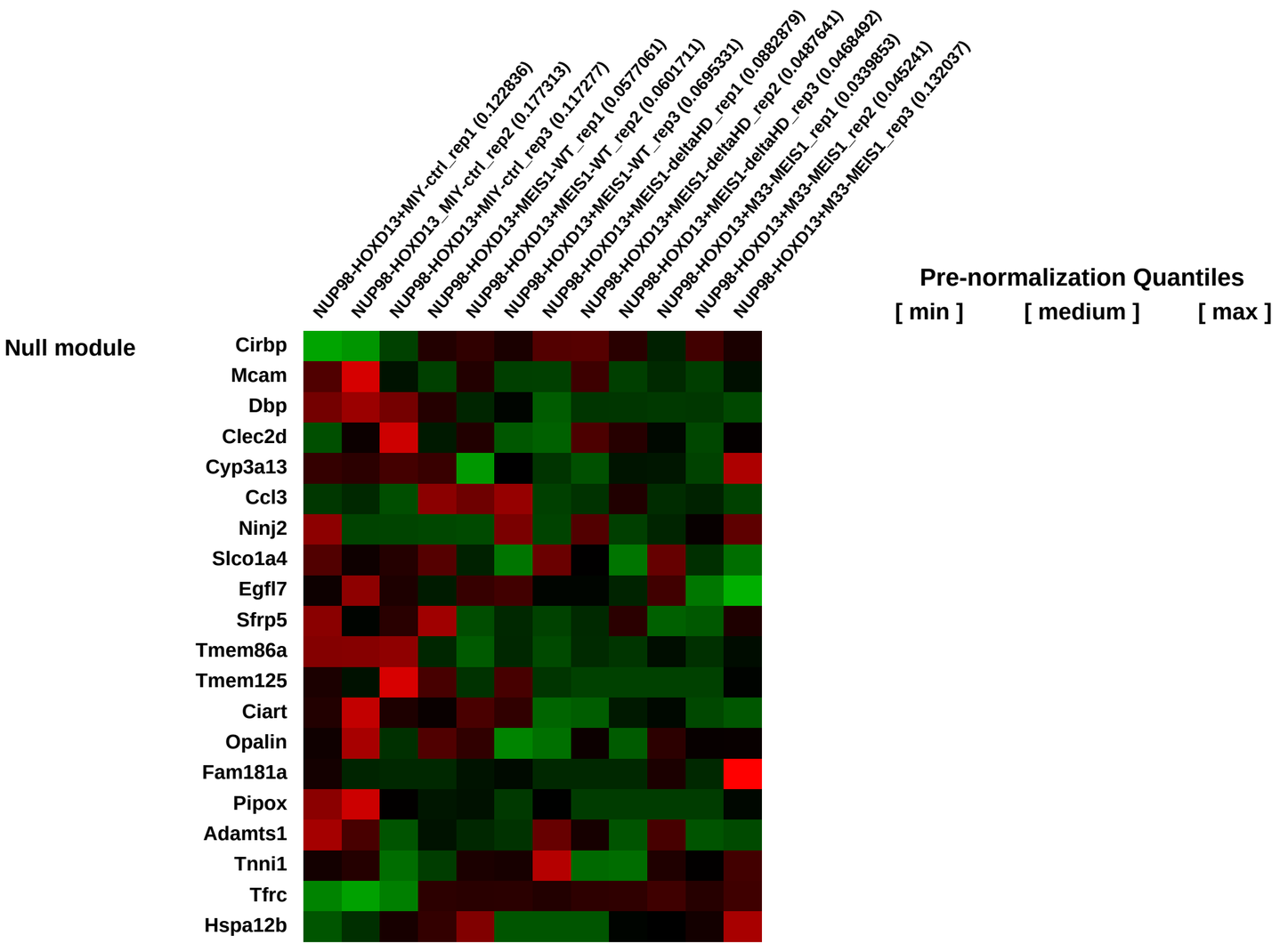

GEO Series "GSE15580" Expression Profiles

Num of samples in this series: 14

Scale of expression profile Z-scores

-3.0 -2.0 -1.0 0.0 1.0 2.0 3.0

GEO Link:	http://www.ncbi.nlm.nih.gov/geo/query/acc.cgi?acc=GSE15580
Status:	Public on Apr 29 2009
Title:	Molecular Signatures of Fetal and Adult Prostate Stem Cells
Organism:	Mus musculus
Experiment type:	Expression profiling by array
Platform:	GPL1261
Pubmed ID:	19478945
Summary & Design:	**Summary:** The global gene expression profiles of adult and fetal murine prostate stem cells were determined to define common and unique regulators whose misexpression might play a role in the development of prostate cancer. A distinctive core of transcriptional regulators common to both fetal and adult primitive prostate cells was identified as well as molecules that are exclusive to each population. Elements common to fetal and adult prostate stem cells include expression profiles of Wnt, Shh and other pathways identified in stem cells of other organs, signatures of the aryl-hydrocarbon receptor, and up-regulation of components of the aldehyde dehydrogenase/retinoic acid receptor axis. There is also a significant lipid metabolism signature, marked by overexpression of lipid metabolizing enzymes and the presence of the binding motif for Srebp1. The fetal stem cell population, characterized by more rapid proliferation and self-renewal, expresses regulators of the cell cycle, such as E2f, Nfy, Tead2 and Ap2, at elevated levels, while adult stem cells show a signature in which TGF-¿† has a prominent role. Finally, comparison of the signatures of primitive prostate cells with previously described profiles of human prostate tumors identified stem cell molecules and pathways with deregulated expression in prostate tumors including chromatin modifiers and the oncogene, Erg. Our data indicate that adult prostate stem or progenitor cells may acquire characteristics of self-renewing primitive fetal prostate cells during oncogenesis and suggest that aberrant activation of components of prostate stem cell pathways may contribute to the development of prostate tumors. **Overall design:** In order to identify molecules and pathways that are active in primitive prostate populations we determined the transcriptional profiles of four populations of cells: (i) fetal urogenital sinus epithelial cells, enriched in fetal prostate stem cells, (ii) Sca-1Hi, cells that express high levels of Sca-1, enriched in adult prostate stem cells, (iii) Sca-1Lo, cells that express medium to low levels of Sca-1 and are enriched in transit-amplifying cells, and (iv) Sca-1Neg, cells with no Sca expression, that represent the most mature population and have almost no in vivo regenerative potential.

Background corr dist: KL-Divergence = 0.0772, L1-Distance = 0.0539, L2-Distance = 0.0056, Normal std = 0.5032

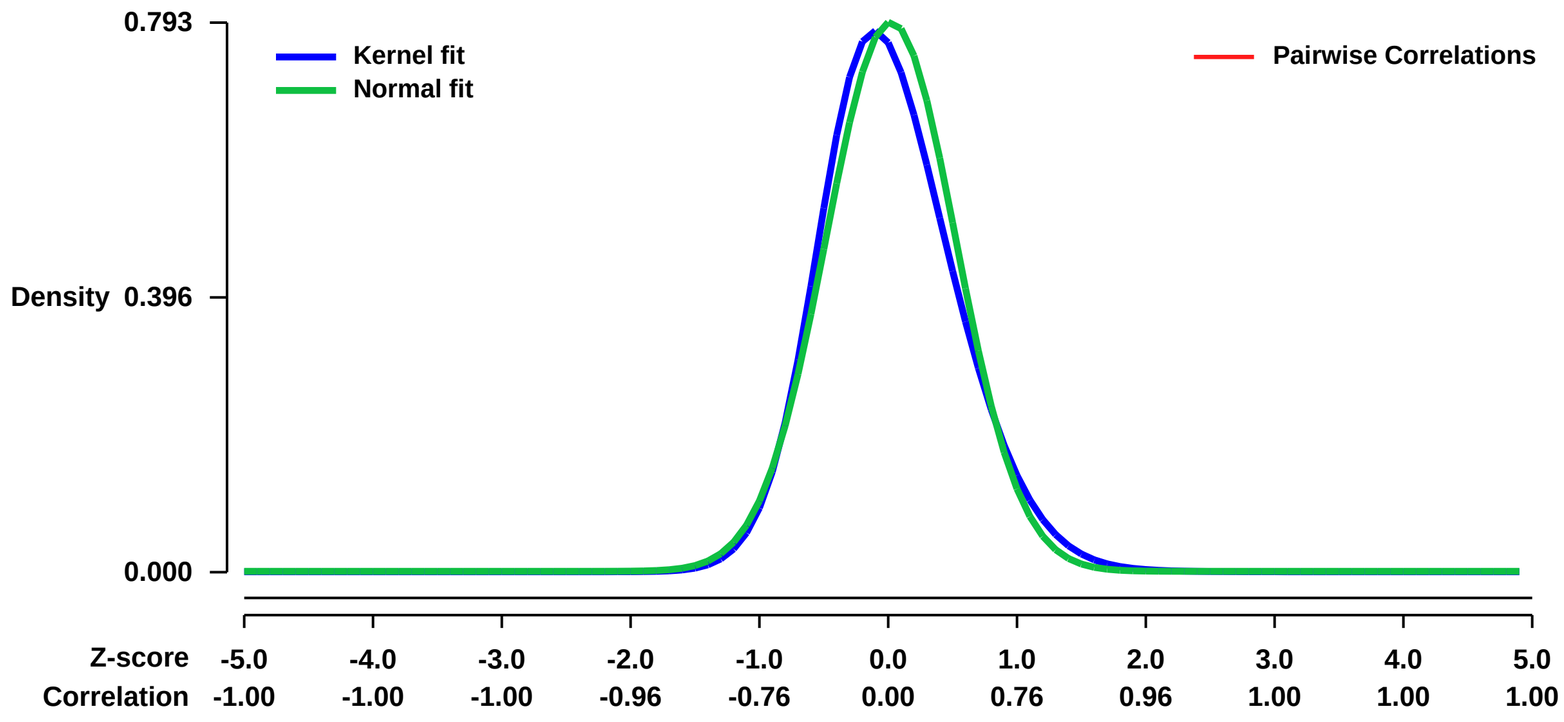

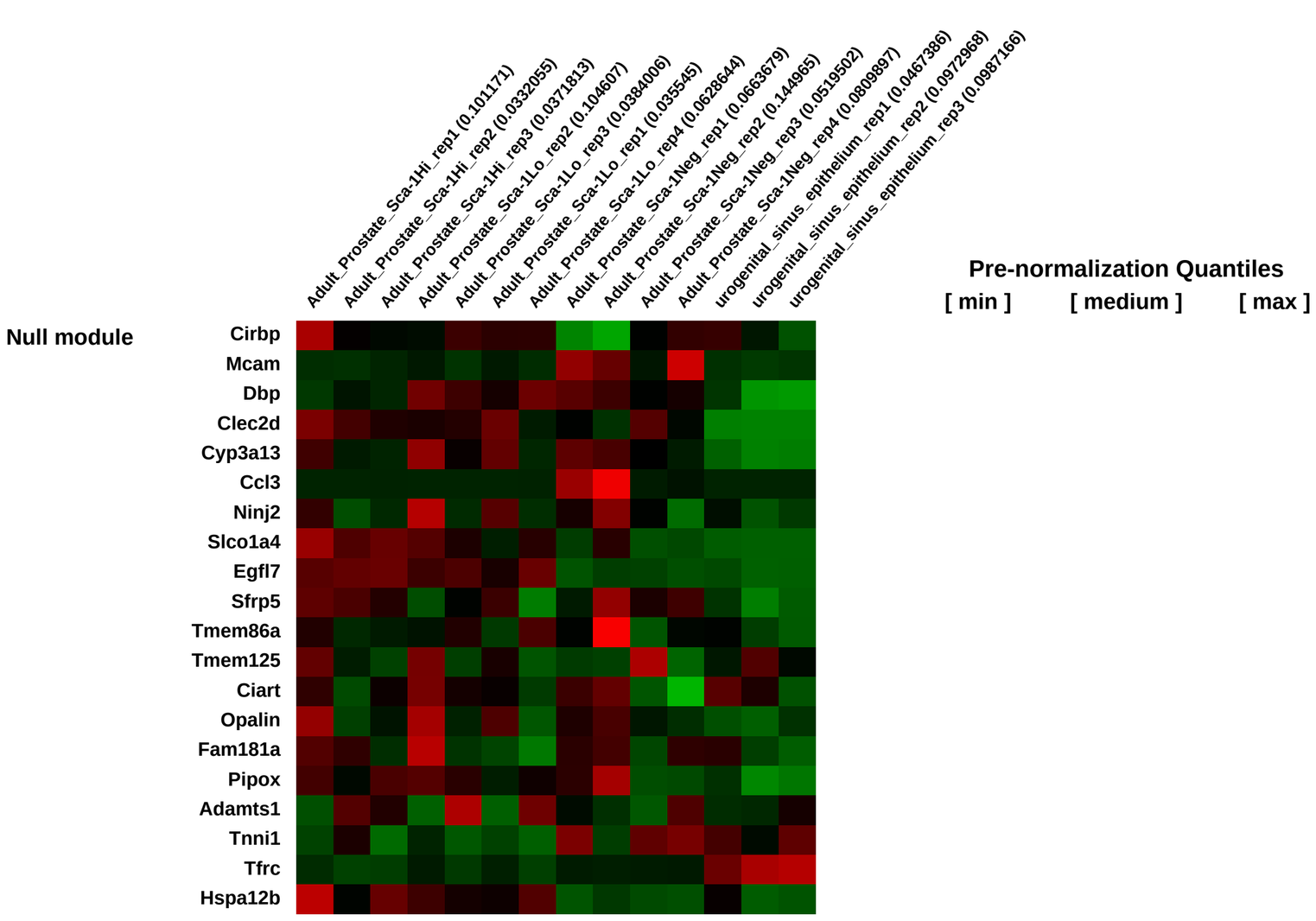

GEO Series "GSE34729" Expression Profiles

Num of samples in this series: 6

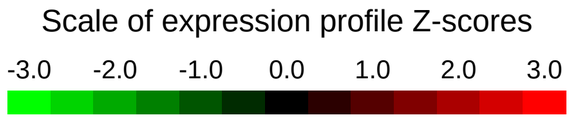

GEO Link:	http://www.ncbi.nlm.nih.gov/geo/query/acc.cgi?acc=GSE34729
Status:	Public on Jan 09 2013
Title:	Gene expression changes induced by overexpression of EVI1 in Lin- hematopoietic cells [Lin]
Organism:	Mus musculus
Experiment type:	Expression profiling by array
Platform:	GPL1261
Pubmed ID:	23212151
Summary & Design:	**Summary:** The transcription factor Evi1 is essential for the formation and maintenance of hematopoietic stem cells, and induces clonal dominance with malignant progression upon constitutive activation by chromosomal rearrangements or transgene integration events. To understand the immediate and adaptive response of primary murine hematopoietic cells to the transcriptional upregulation of Evi1, we developed an inducible lentiviral vector system with a robust expression switch. We found that Evi1 delays differentiation and promotes survival in myeloid culture conditions, orchestrating a battery of genes involved in stemness (Aldh1a1, Ly6a [Sca1], Abca1, Epcam, among others). Importantly, Evi1 suppresses Cyclins and Cyclin-dependent kinases (Cdk), while it upregulates Cdk inhibitors, inducing quiescence in various proliferation-inducing cytokine conditions and operating in a strictly dose-dependent manner. Hematopoietic cells with persisting Evi1-induction tend to adopt a relatively low expression level. We thus classify Evi1 as a dormancy-inducing oncogene, likely requiring epigenetic and genetic compensation for cell expansion and malignant progression. **Overall design:** Lin- Rosa26rtTA cells were isolated, transduced in S3F11 cytokines, induced the next day with DOX [1 ¸…g/ml] and 20 hours later sorted for negative/low or highly EGFP expressing cells, from which total RNA was extraced and subjected to Microarray Analysis

GEO Series "GSE31570" Expression Profiles

Num of samples in this series: 6

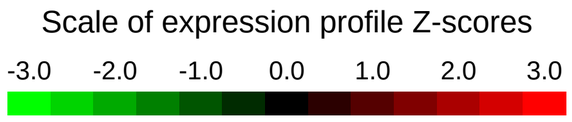

GEO Link:	http://www.ncbi.nlm.nih.gov/geo/query/acc.cgi?acc=GSE31570
Status:	Public on Oct 13 2011
Title:	The Dynamic Architecture of Hox Gene Clusters
Organism:	Mus musculus
Experiment type:	Genome binding/occupancy profiling by high throughput sequencing
Platform:	GPL1261
Pubmed ID:	24843030
Summary & Design:	**Summary:** The spatial and temporal control of Hox gene transcription is essential for patterning the vertebrate body axis. Although this process involves changes in histone posttranslational modifications, the existence of particular three-dimensional (3D) architectures remained to be assessed in vivo. Using high-resolution chromatin conformation capture methodology, we examined the spatial configuration of Hox clusters in embryonic mouse tissues where different Hox genes are active. When the cluster is transcriptionally inactive, Hox genes associate into a single 3D structure delimited from flanking regions. Once transcription starts, Hox clusters switch to a bimodal 3D organization where newly activated genes progressively cluster into a transcriptionally active compartment. This transition in spatial configurations coincides with the dynamics of chromatin marks, which label the progression of the gene clusters from a negative to a positive transcription status. This spatial compartmentalization may be key to process the collinear activation of these compact gene clusters. **Overall design:** Examination of gene expression in 3 cell types. Examination of 2 different histone modifications in 2 cell types.

Background corr dist: KL-Divergence = 0.0292, L1-Distance = 0.0210, L2-Distance = 0.0004, Normal std = 0.6864

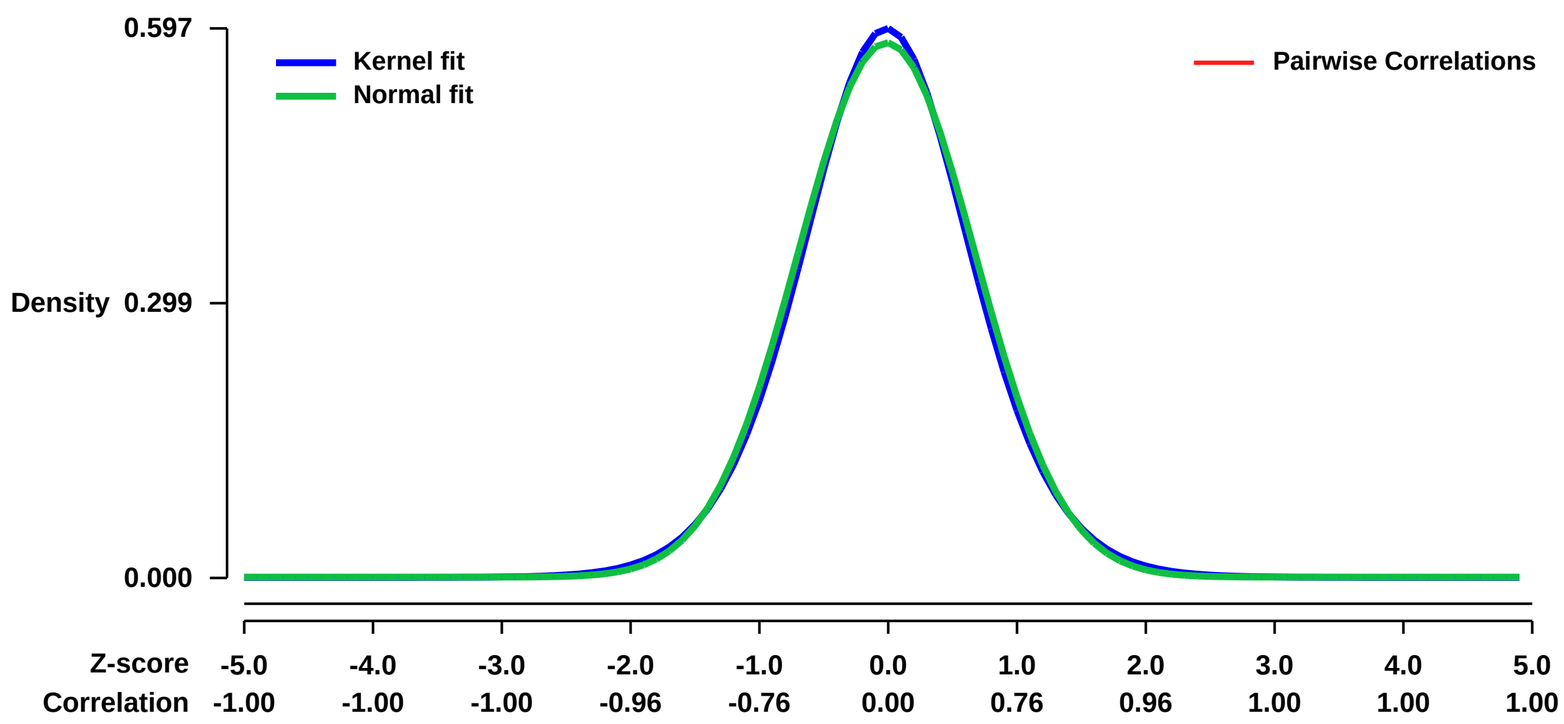

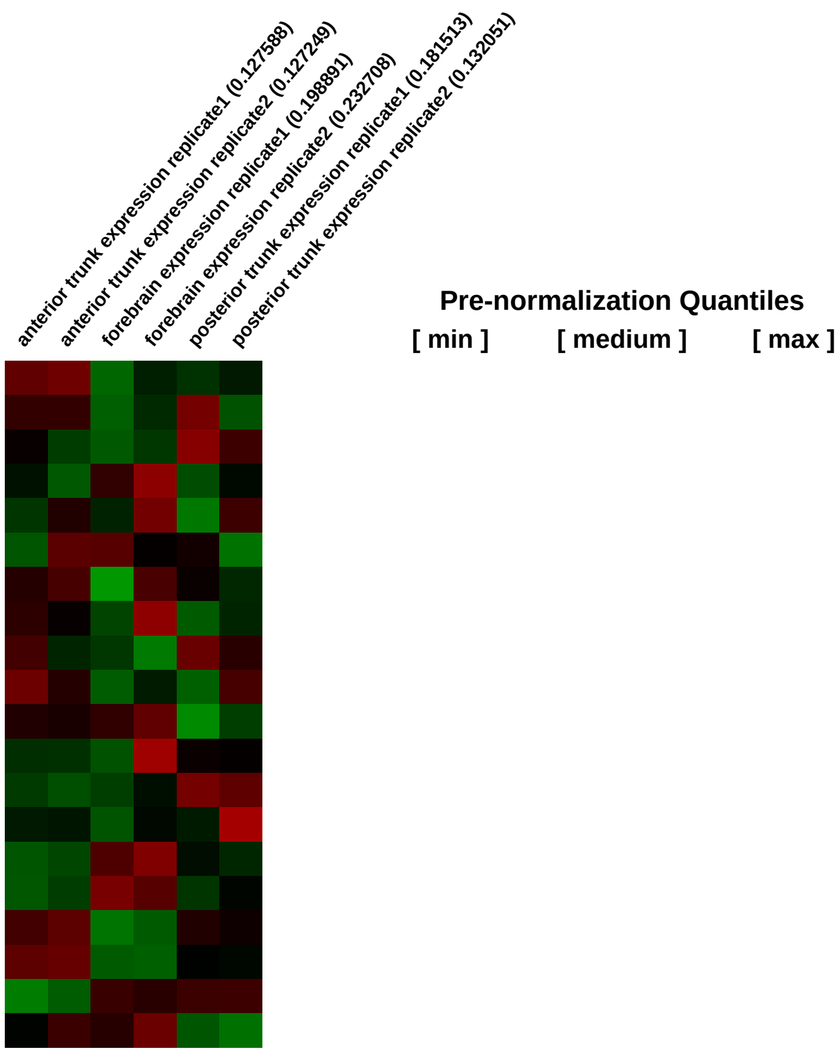

GEO Series "GSE12982" Expression Profiles

Num of samples in this series: 53

Scale of expression profile Z-scores

-3.0 -2.0 -1.0 0.0 1.0 2.0 3.0

GEO Link:	http://www.ncbi.nlm.nih.gov/geo/query/acc.cgi?acc=GSE12982
Status:	Public on Dec 12 2008
Title:	Expression data from mouse ES cells and various differentiated cell types
Organism:	Mus musculus
Experiment type:	Expression profiling by array
Platform:	GPL1261
Pubmed ID:	19026780
Summary & Design:	**Summary:** We used microarrays to detail the role of Polycomb proteins including Ezh2 and Eed in maintaining ES cell identity and executing pluripotency. Keywords: cell type and time course **Overall design:** To assay the global effects of the loss of polycomb proteins (Ezh2 or Eed) in embryonic stem (ES) cells , we compared the expression profiles of homologuous Ezh2 or Eed knockout ES cells to wild-type ES cells in undifferentiated or differentiated condition.

Background corr dist: KL-Divergence = 0.2375, L1-Distance = 0.0390, L2-Distance = 0.0037, Normal std = 0.3143

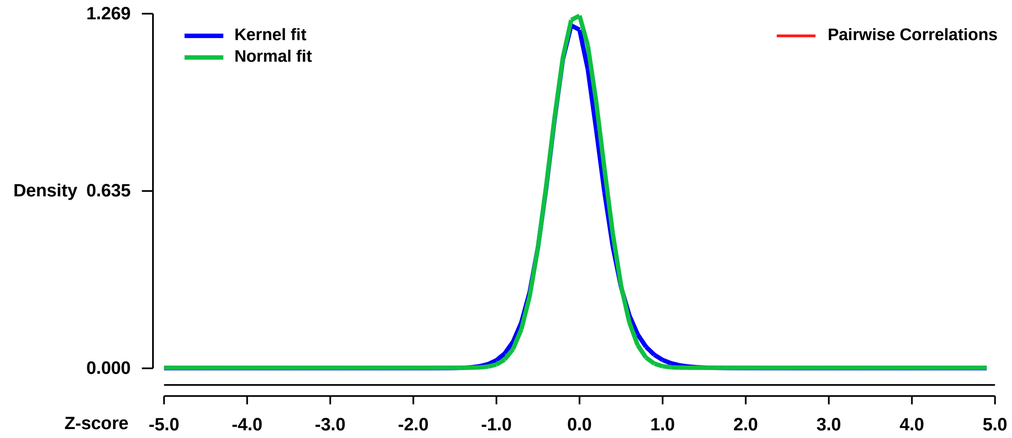

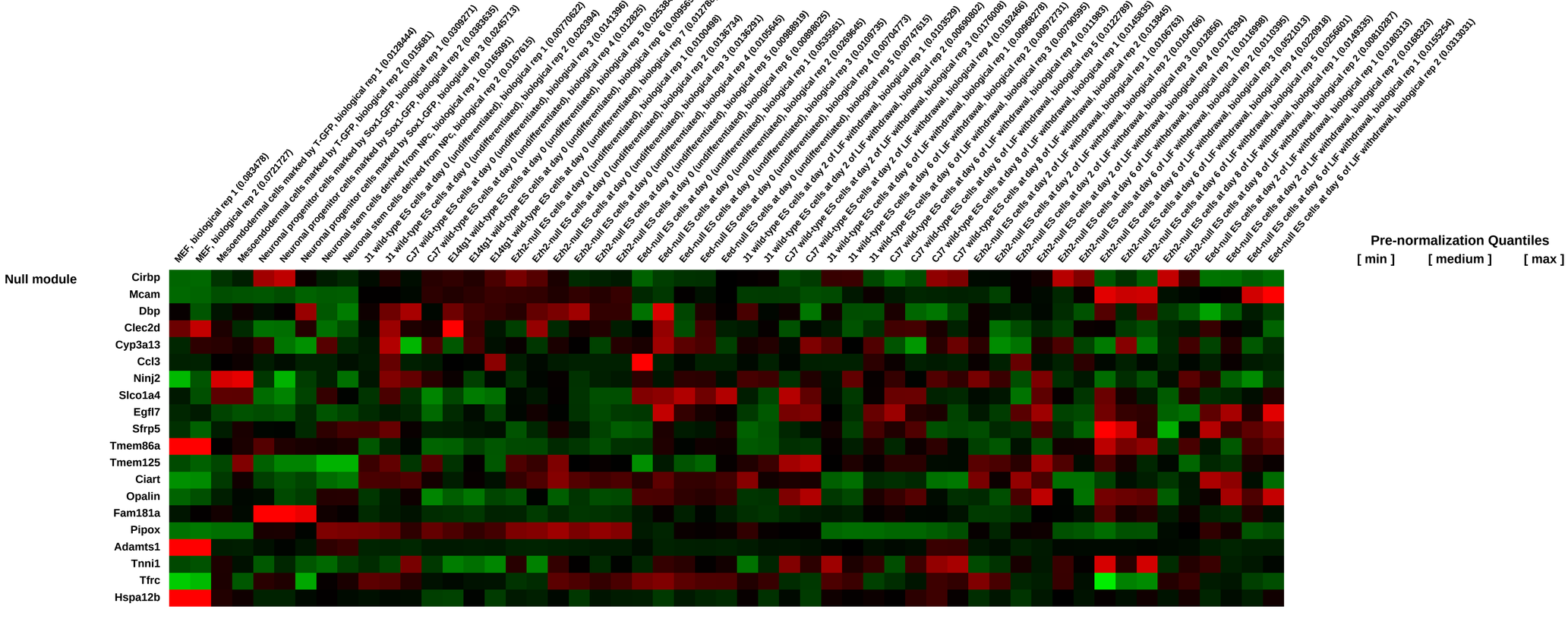

GEO Series "GSE10210" Expression Profiles

Num of samples in this series: 16

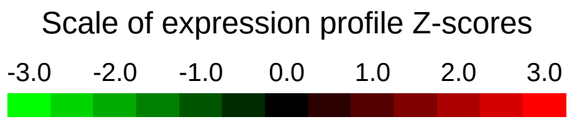

GEO Link:	http://www.ncbi.nlm.nih.gov/geo/query/acc.cgi?acc=GSE10210
Status:	Public on Jul 14 2008
Title:	Gene expression analysis of embryonic stem cells expressing VE-cadherin (CD144) during endothelial differentiation
Organism:	Mus musculus
Experiment type:	Expression profiling by array
Platform:	GPL1261
Pubmed ID:	18498633
Summary & Design:	**Summary:** Endothelial differentiation occurs during normal vascular development in the developing embryo. Mouse embryonic stem (ES) cells were used to further define the molecular mechanisms of endothelial differentiation. By flow cytometry a population of VEGF-R2 positive cells was identified as early as 2.5 days after differentiation of ES cells, and a subset of VEGF-R2 + cells, that were CD41+ positive at 3.5 days. A separate population of VEGF-R2+ stem cells expressing the endothelial-specific marker CD144 (VE-cadherin) was also identified at this same time point. Microarray analysis of >45,000 transcripts was performed on RNA obtained from cells expressing VEGF-R2, CD41, and CD144. **Keywords:** expression analysis **Overall design:** We identified four populations of cells; cells expressing VEGF-R2 (day 2.5), CD41 expressing cells (day 3.5), cells expressing CD144 (VE-Cadherin, day 3.5), and cells expressing CD144 (day 6.5). In addition to this, we have also obtained the negative control cells at each time such as VEGF-R2 (day 2.5) negative, CD41 negative (day 3.5), CD144 negative (VE-Cadherin, day 3.5), and negative CD144 (day 6.5). RNA for the microarray experiments were obtained in duplicate from two separately conducted experiments using the murine embryonic stem cells..

Background corr dist: KL-Divergence = 0.0996, L1-Distance = 0.0266, L2-Distance = 0.0013, Normal std = 0.4386

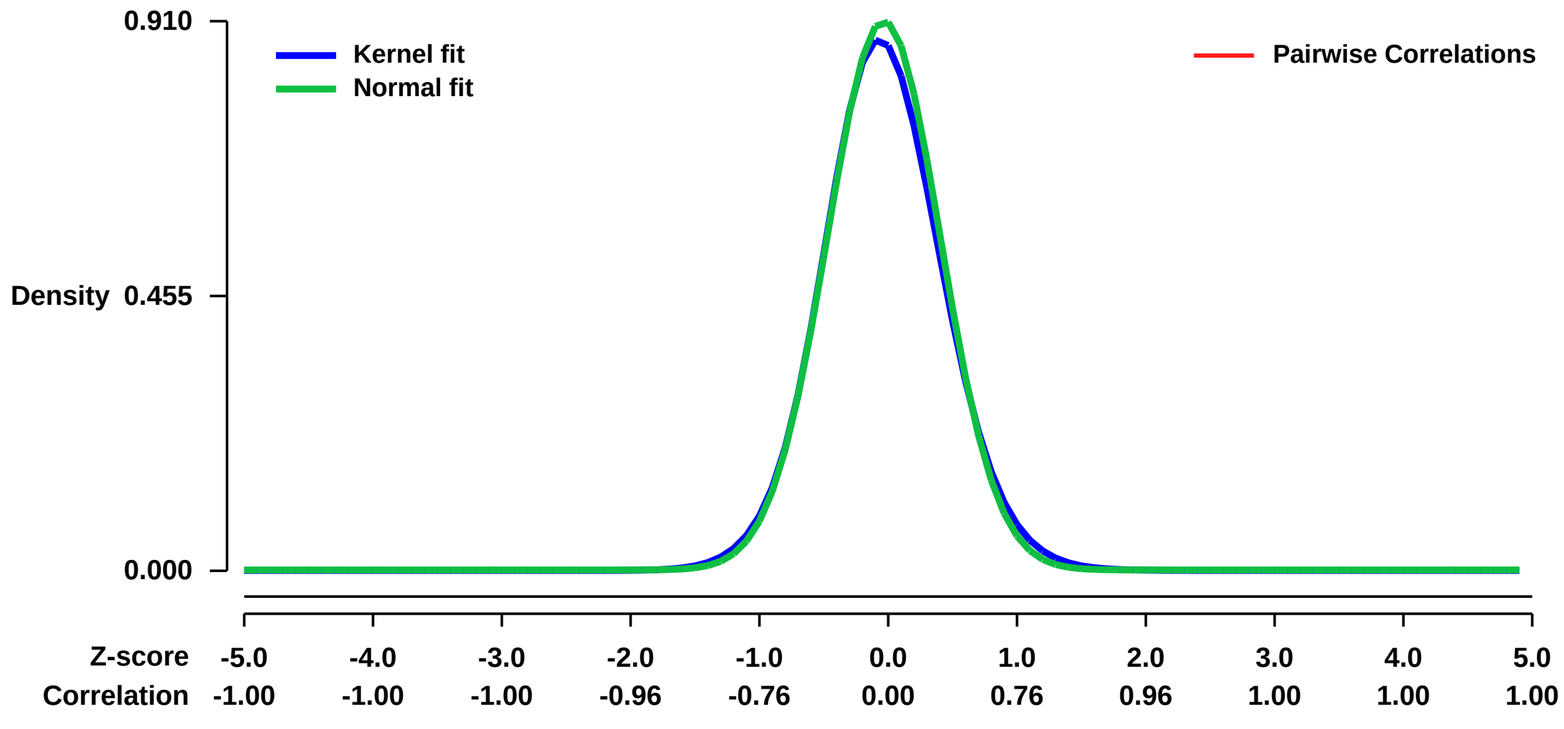

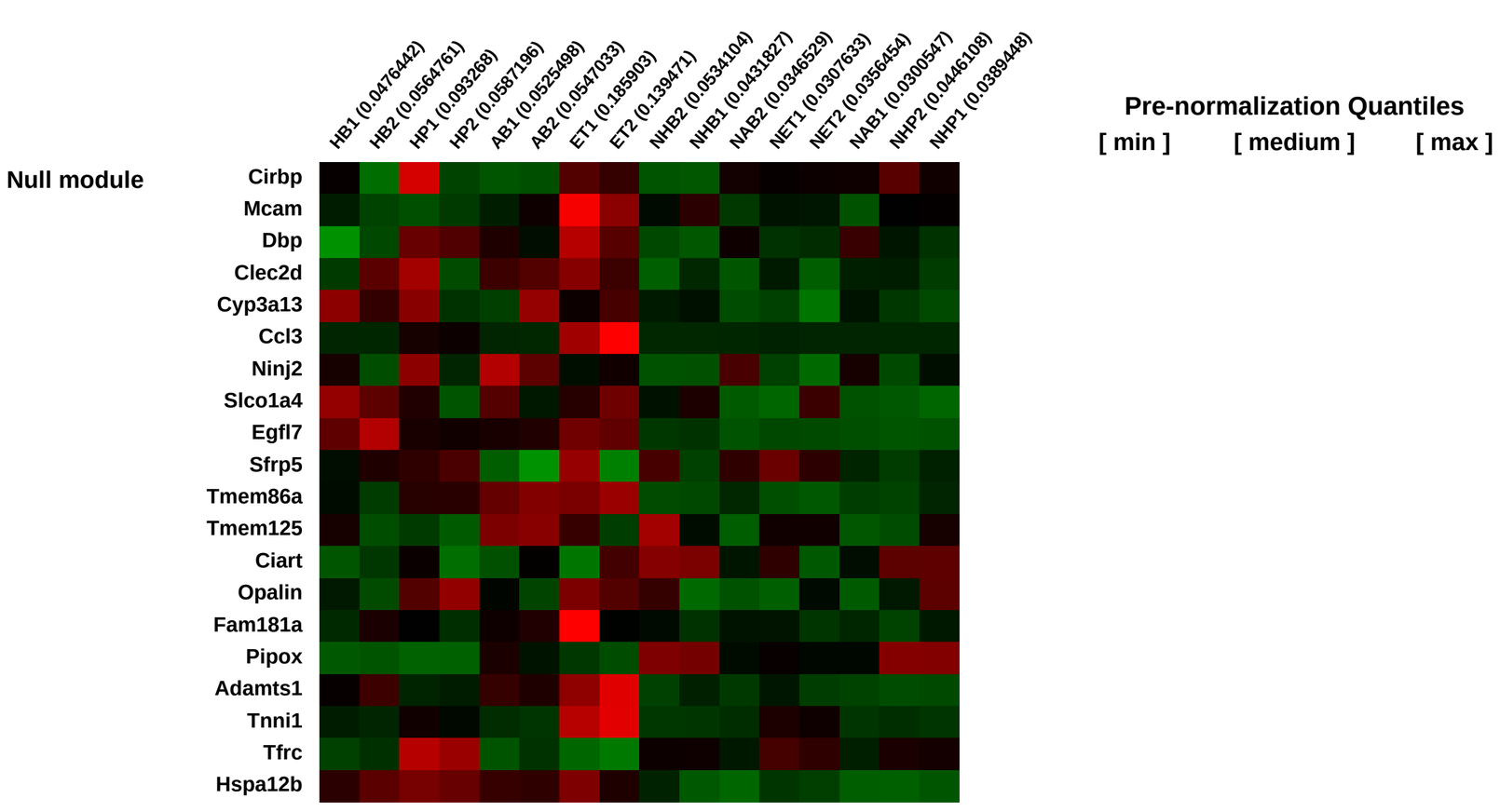

GEO Series "GSE12430" Expression Profiles

Num of samples in this series: 21

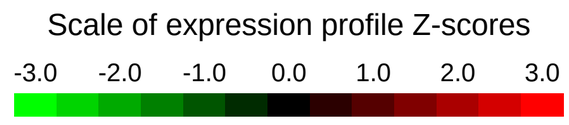

GEO Link:	**http://www.ncbi.nlm.nih.gov/geo/query/acc.cgi?acc=GSE12430**
Status:	**Public on Feb 09 2009**
Title:	**Loss of PATCHED (wechs-affy-mouse-512645)**
Organism:	**Mus musculus**
Experiment type:	**Expression profiling by array**
Platform:	**GPL1261**
Pubmed ID:	**19185848**
Summary & Design:	**Summary:** **We are examining the genes that control initiation and progression of murine medulloblastomas that result from loss of patched. Approximately 25% of human medulloblastomas have mutations in patched or in other elements of the sonic hedgehog pathway. However, the cells from which these tumors originate (neural progenitors or stem cells), the cells that are responsible for tumor propagation (cancer stem cells), and the genes that are required for tumor progression are poorly understood. To address these questions, we have developed conditional patched knockout mice in which the gene is deleted in neural stem cells or progenitors. In addition, we have isolated a population of tumor-propagating cells from these tumors. By studying these models we will gain insight into the mechanisms of tumorigenesis and identify new targets for therapy.** **To identify the molecular mechanisms that underlie tumor initiation and propagation, we will compare gene expression in tumors resulting from loss of patched in neural stem cells vs. progentors, and in cancer stem cells vs. non-cancer stem cells.** **We hypothesize that medulloblastomas initiated in neural stem cells (using GFAP-Cre) are more aggressive than those initiated in neural progenitors (using Math1-Cre), and will express more genes associated with self-renewal. In addition, we hypothesize that cancer stem cells (CD15+ cells) from a given tumor will express higher levels of self-renewal genes than non-stem cells (CD15- cells) from the same tumor.** **Cells from 5 GFAP-Cre tumors, 5 Math1-Cre tumors, and 5 conventional patched-knockout tumors will be isolated using enzymatic digestion and Percoll gradient centrifugation. These procedures have been found to result in 85-95% pure tumor cell populations. In addition, 5 tumors will be FACS-sorted to isolate CD15+ and CD15- populations. RNA will be prepared from each of these samples using an RNeasy kit from Qiagen. Samples of 2 micrograms will be resuspended in 10 microliters of RNase-free water, and sent to the Consortium for labeling, hybridization and analysis. Cells from the three types of tumors, and CD15+ and CD15- cells, will be compared to one another.** **Overall design:**

Background corr dist: KL-Divergence = 0.2096, L1-Distance = 0.0409, L2-Distance = 0.0036, Normal std = 0.3273

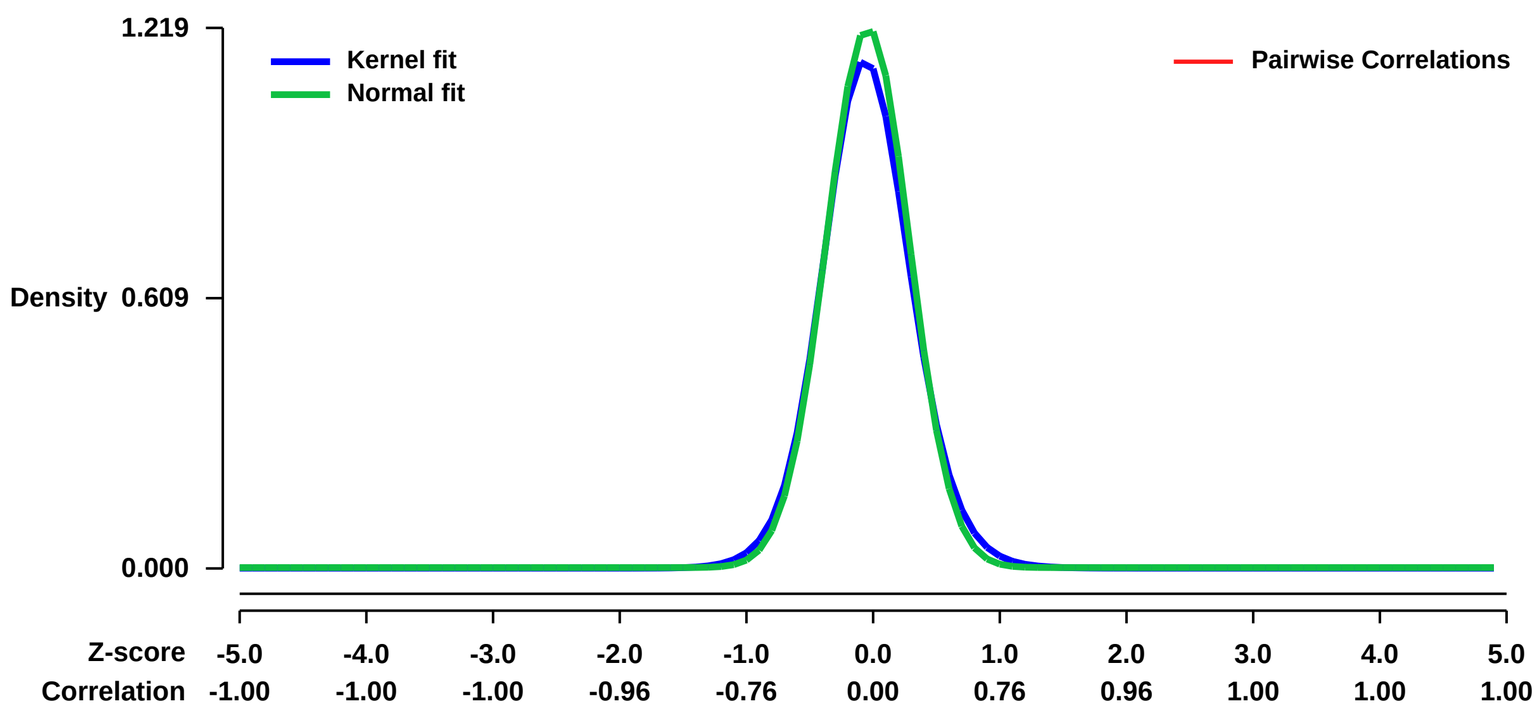

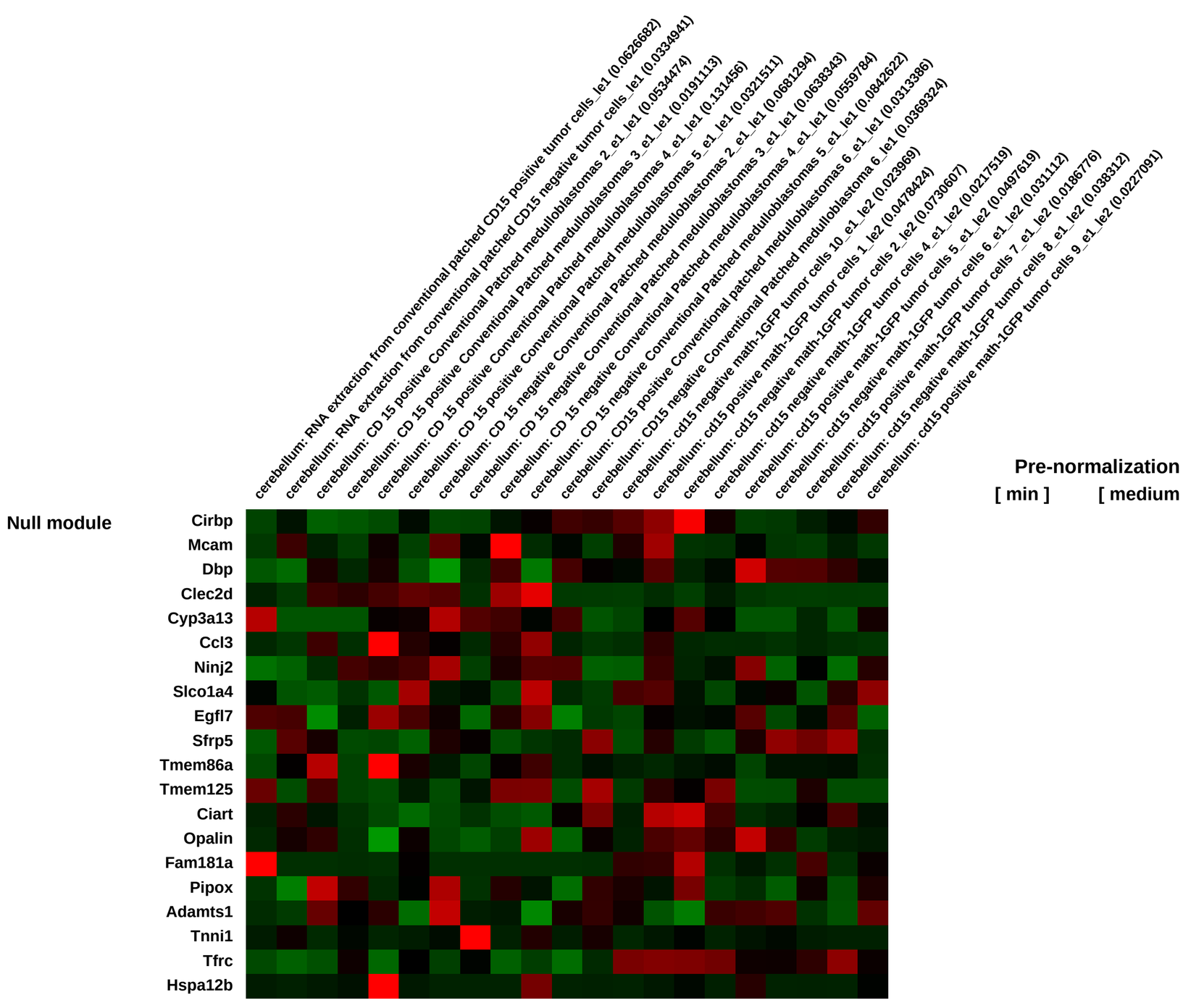

GEO Series "GSE15772" Expression Profiles

Num of samples in this series: 8

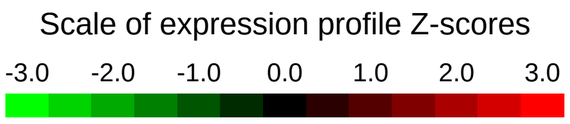

GEO Link:	http://www.ncbi.nlm.nih.gov/geo/query/acc.cgi?acc=GSE15772
Status:	Public on May 20 2009
Title:	WT Dorsal Skin Time Course
Organism:	Mus musculus
Experiment type:	Expression profiling by array
Platform:	GPL1261
Pubmed ID:	19494835
Summary & Design:	**Summary:** Skin and bladder epithelia form effective permeability barriers through the activation of distinct differentiation gene programs. Employing a genome-wide gene expression study, we identified transcription regulators whose expression correlates highly with that of differentiation markers both in bladder and skin, including the Grainyhead factor Get1/Grhl3, already known to be important for epidermal barrier formation. In the bladder, Get1 is most highly expressed in the differentiated umbrella cells and its mutation in mice leads to a defective bladder epithelial barrier formation due to failure of apical membrane specialization. Genes encoding components of the specialized urothelial membrane, the uroplakins, were downregulated in Get1-/- mice. At least one of these genes, Uroplakin II, is a direct target of Get1. The urothelial-specific activation of the Uroplakin II gene is due to selective binding of Get1 to the Uroplakin II promoter in urothelial cells, most likely regulated by histone modifications. These results demonstrate a key role for Get1 in urothelial differentiation and barrier formation. **Overall design:** To gain insights into common and unique transcriptional regulatory programs during epidermal differentiation, we profiled global gene expression in mouse dorsal skin at E14.5, E16.5, and E18.5.

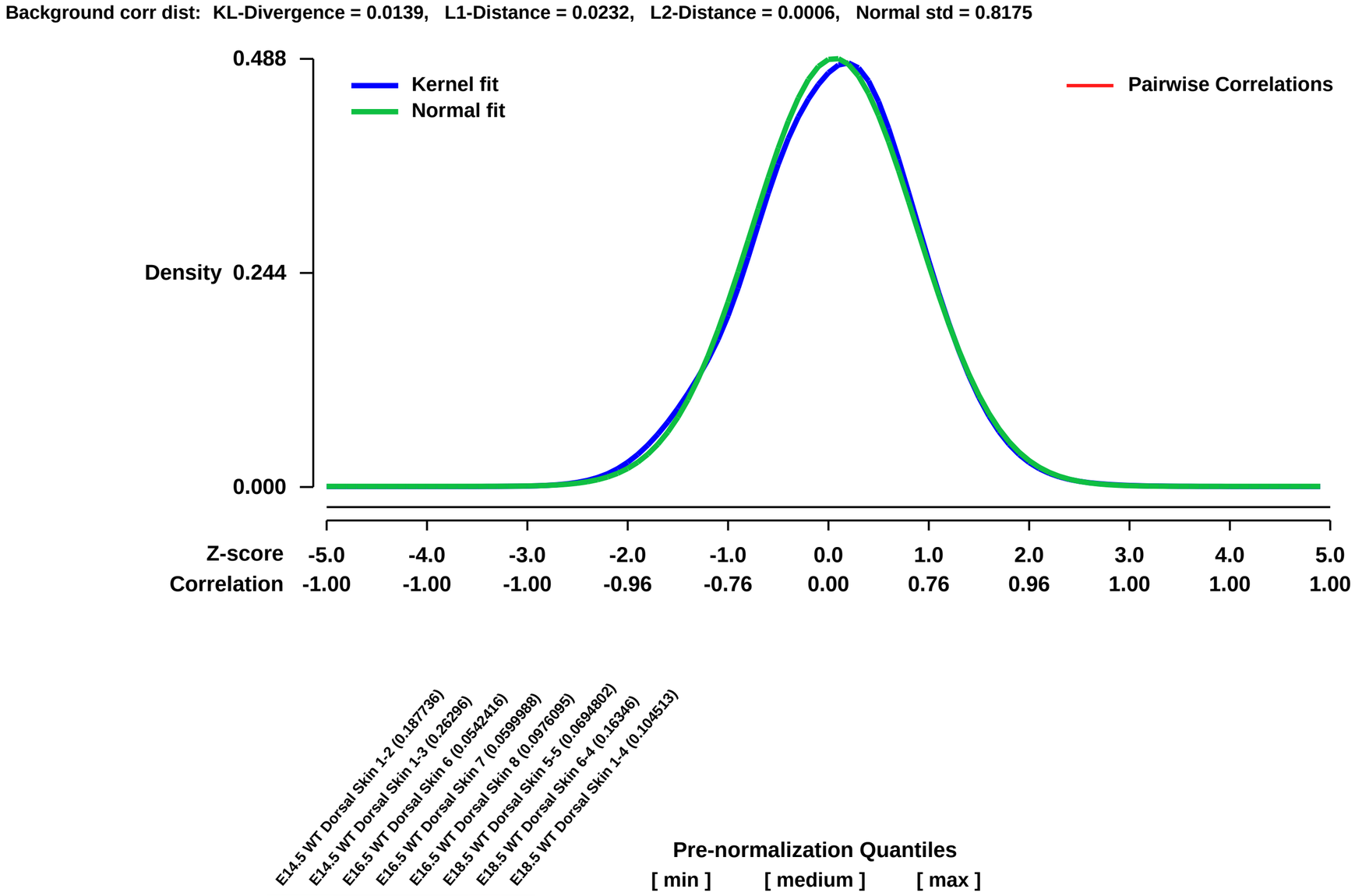

GEO Series "GSE12389" Expression Profiles

Num of samples in this series: 8

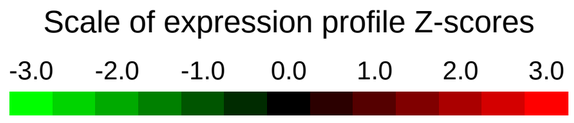

GEO Link:	http://www.ncbi.nlm.nih.gov/geo/query/acc.cgi?acc=GSE12389
Status:	Public on Oct 31 2008
Title:	Interferon-¸‡-dependent regulatory circuits in immune inflammation highlighted in diabetes
Organism:	Mus musculus
Experiment type:	Expression profiling by array
Platform:	GPL1261
Pubmed ID:	18981116
Summary & Design:	**Summary:** We demonstrate diverse roles of interferonâ gamma (IFN-¸‡) in the induction and regulation of immune-mediated inflammation using a transfer model of autoimmune diabetes. The diabetogenic CD4+BDC2.5 (BDC) T cell clone upon transfer into NOD.scid mice induced destruction of islets of Langerhans leading to diabetes. Administration of a neutralizing antibody to IFN-¸‡ (H22) resulted in long term protection (LTP) from diabetes, with inflammation but persistence of a significant, albeit decreased numbers of ¸†-cells. BDC T cells were a mixture of cells expressing high, intermediate and low levels of the T cell receptor. Clonotype-low BDC T cells were required for LTP. Furthermore, islet infiltrating leukocytes in the LTP mice contained Foxp3+CD4 T cells. Islet inflammation in both diabetic and LTP mice was characterized by heavy infiltration of macrophages. Gene expression profiles indicated that macrophages in diabetic mice were M1-type, while LTP mice contained M2-differentiated. The LTP was abolished if mice were treated with either an antibody depleting CD4 T cells, or a neutralizing antibody to CTLA-4, in this case, only at a late stage. Neutralization of IL-10, TGF-¸†, GITR or CD25 had no effect. Transfer of only clonotype-high expressing BDC T cells induced diabetes but in contrast, H22 antibodies did not inhibit diabetes. While clonotype high T cells induced diabetes even when IFN-¸‡ was neutralized, paradoxically, there was reduced inflammation and no diabetes if host myeloid cells lacked IFN-¸‡ receptor. Hence, using monoclonal CD4 T cells, IFN-¸‡ can have a wide diversity of roles, depending on the setting of the immune process. **Overall design:** Pancreatic islets were laser-capture microdissected from mice injected with diabetogenic T cells. One cohort of mice also received injections with anti-interfereon gamma monoclonal antibody, which protected those mice from developing diabetes. RNA prepared from islets was amplified and analyzed by Affymetrix GeneChips. Each GeneChip was prepared from RNA pooled from 5 mice at each timepoint. GeneChips were prepared from RNA extracted at different days following injection of T cells. The following days were assayed day 0 (i.e., untreated), day 3 (for diabetic and protected islets), day 4 (diabetic and protected), day 5 (only for protected, as diabetic islets were too edematous to dissect), day 8 (diabetic and protected).

Background corr dist: KL-Divergence = 0.0589, L1-Distance = 0.0528, L2-Distance = 0.0047, Normal std = 0.5629

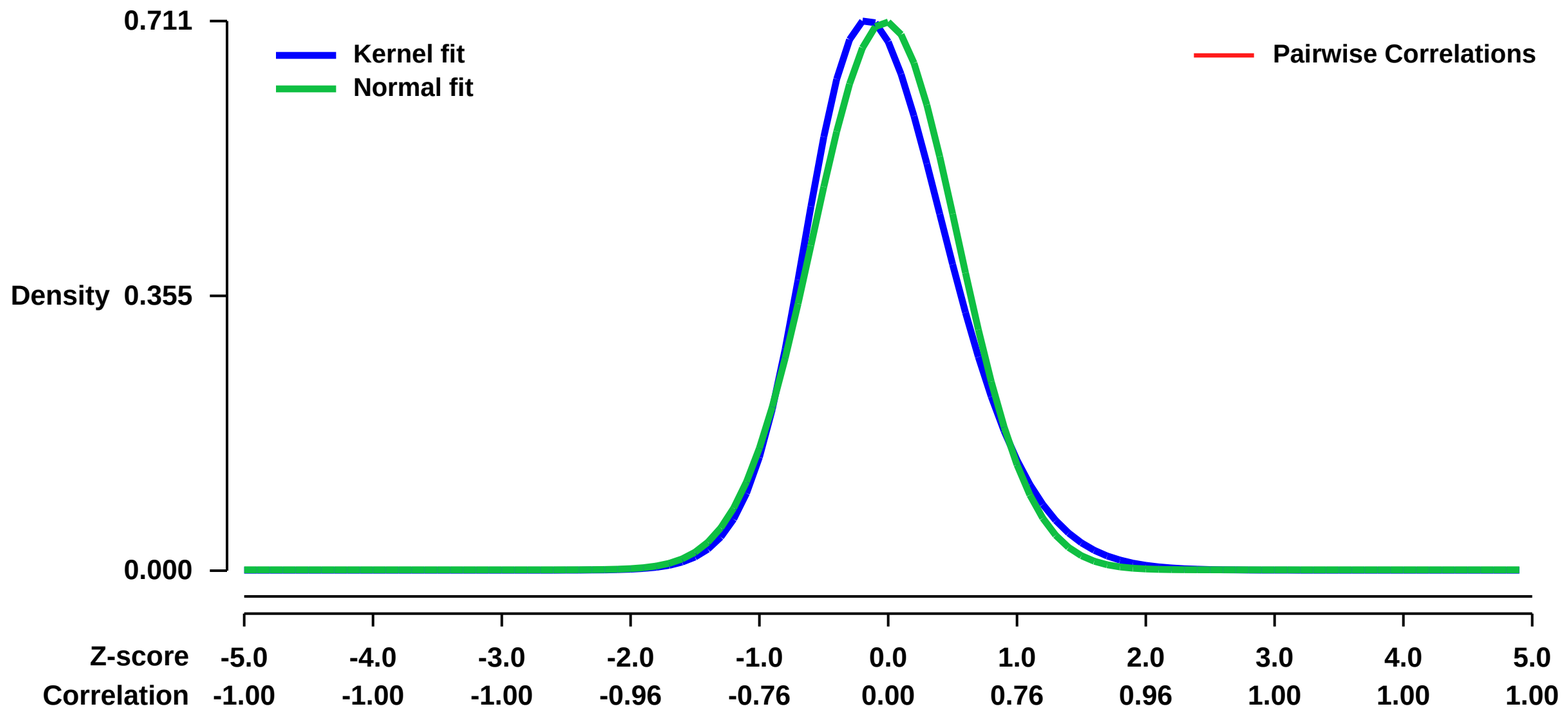

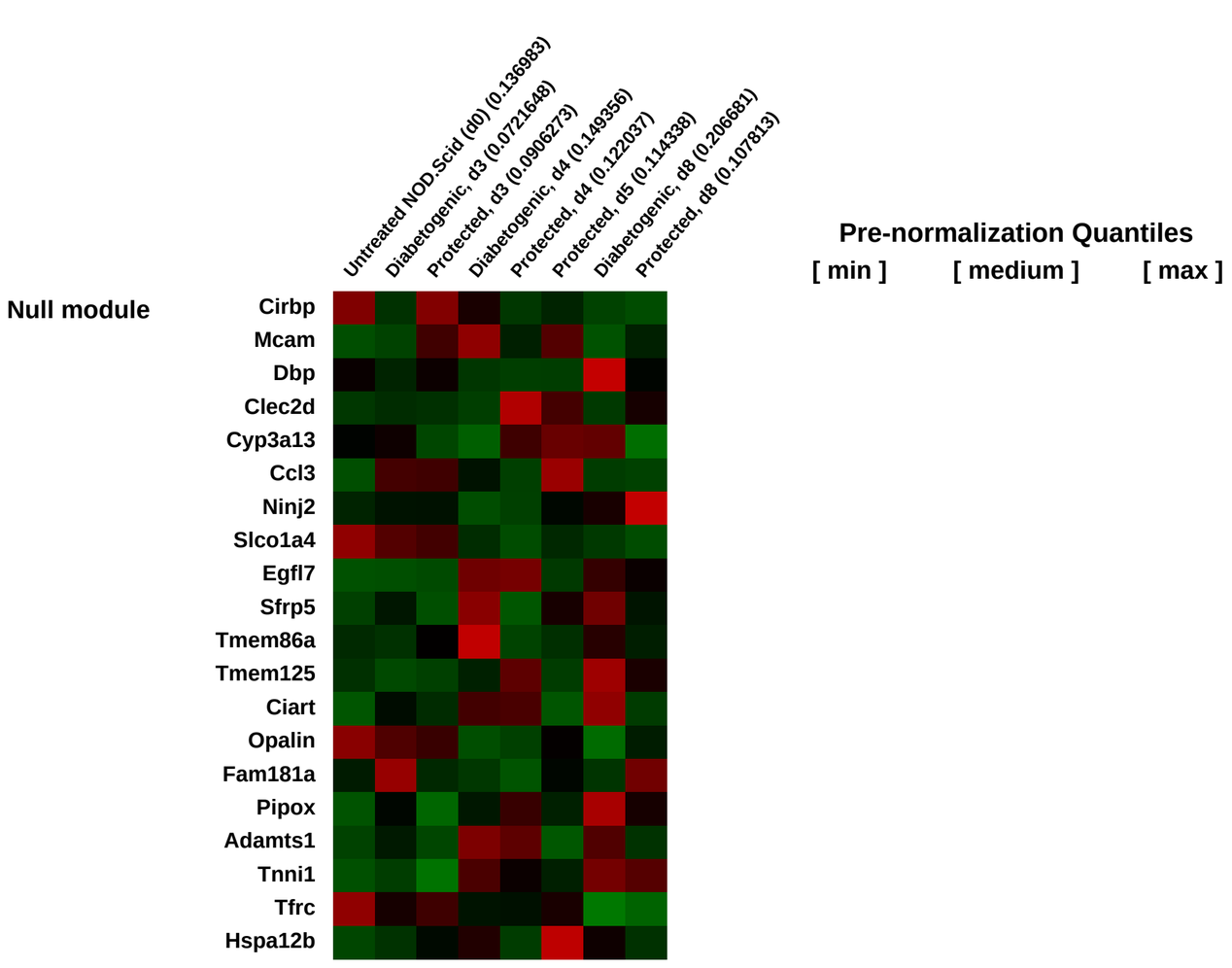

GEO Series "GSE8682" Expression Profiles

Num of samples in this series: 8

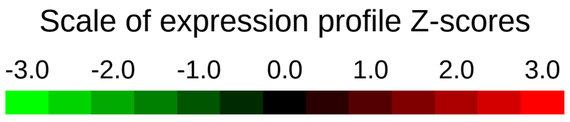

GEO Link:	http://www.ncbi.nlm.nih.gov/geo/query/acc.cgi?acc=GSE8682
Status:	Public on Jan 11 2008
Title:	Gene expression in mouse 3T3-L1 adipocyte tissue culture treated with tunicamycin
Organism:	Mus musculus
Experiment type:	Expression profiling by array
Platform:	GPL1261
Pubmed ID:	17878318
Summary & Design:	**Summary:** Tunycamcin induces UPR/ISR and Inflammation in mouse 3T3-L1 adipocyte tissue culture. The early transcriptome changes were analyzed using high-density microarrays to better characterize the signaling pathways responding to tunicamycin, to be compared with similar experiments with CLA as the treatment. Their gene expression responses between 4 to 12 hr after treatment showed a common set of early gene expression changes indicative of a UPR/Inflammation stress response. **Keywords: control/treatment time course** **Overall design:** Mouse 3T3-L1 RNA for each time point was isolated from control and treatment samples for analysis on microarrays with two biological reps.

Background corr dist: KL-Divergence = 0.0724, L1-Distance = 0.0702, L2-Distance = 0.0125, Normal std = 0.5281

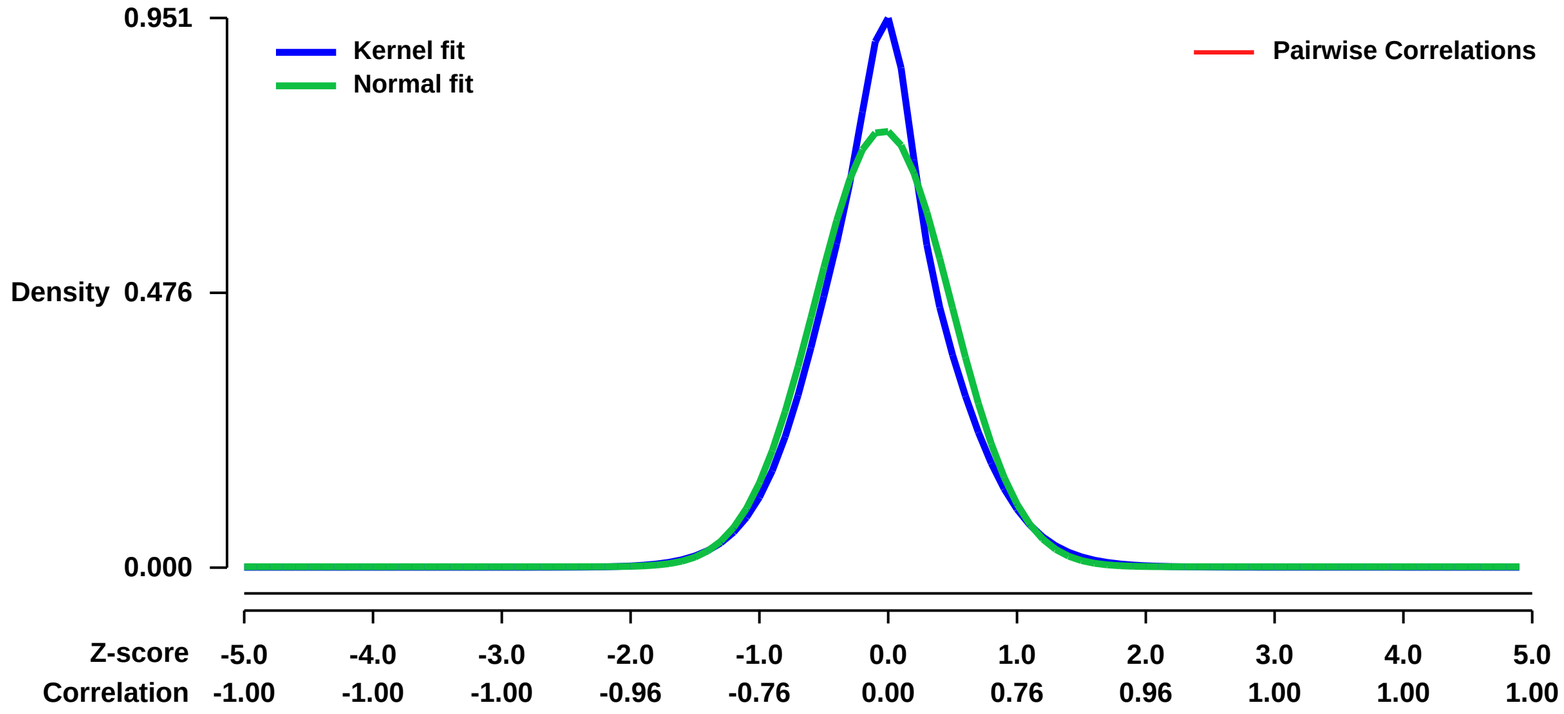

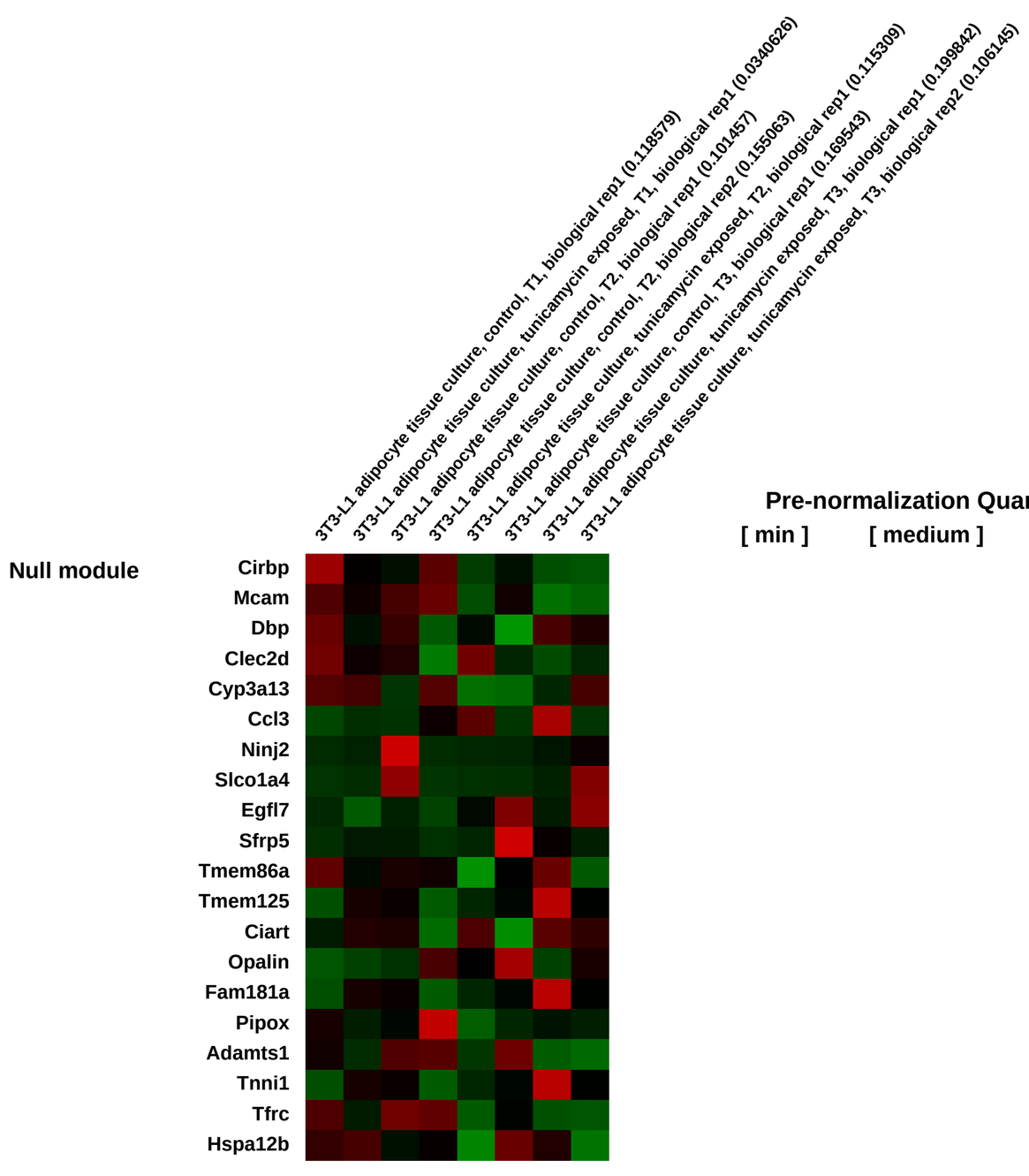

GEO Series "GSE58307" Expression Profiles

Num of samples in this series: 20

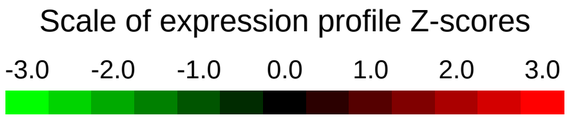

GEO Link:	**http://www.ncbi.nlm.nih.gov/geo/query/acc.cgi?acc=GSE58307**
Status:	**Public on Jun 09 2014**
Title:	**Expression profiling of KRas ablation surviving cells and matched Kras expressing spheres in pancreatic tumors**
Organism:	**Mus musculus**
Experiment type:	**Expression profiling by array**
Platform:	**GPL1261**
Pubmed ID:	
Summary & Design:	**Summary:** **In this dataset, we include the expression data obtained from KRas expressing tumors, matched Kras expressing tumor spheres, surviving cells and surviving cells after KRas re-expression for 24hs** **Overall design:** **Data reported here are obtained from 5 independent tumors (from 1 to 5). For each tumor, expression data for the original Tumor (in vivo bulk tumor lesion), the KRas Expressing Spheres derived from the bulk tumor, the matched surviving cells after 8 days of KRas ablation (SCs) and Surviving Cells after 24 hours of KRas re-expression are reported.**

Background corr dist: **KL-Divergence = 0.1687, L1-Distance = 0.0397, L2-Distance = 0.0034, Normal std = 0.3583**

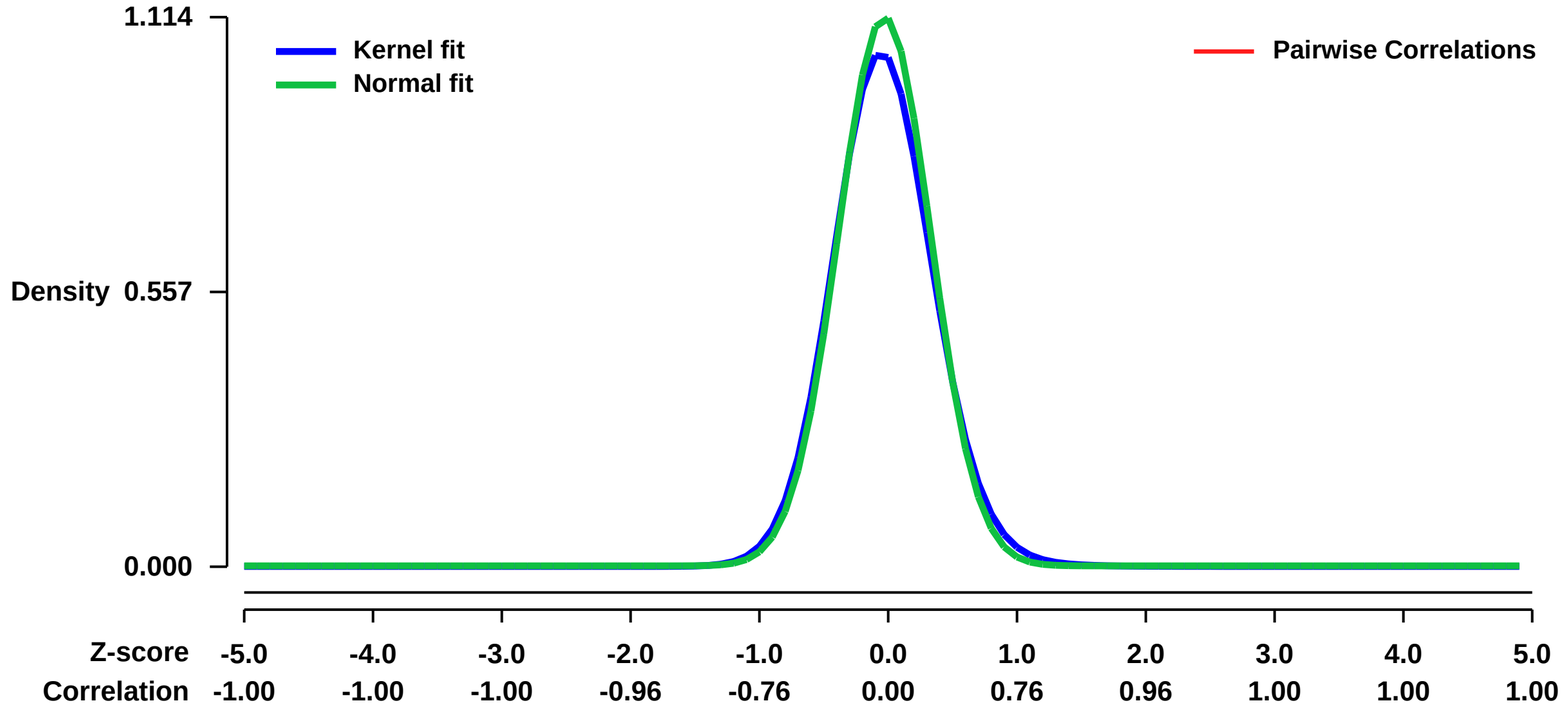

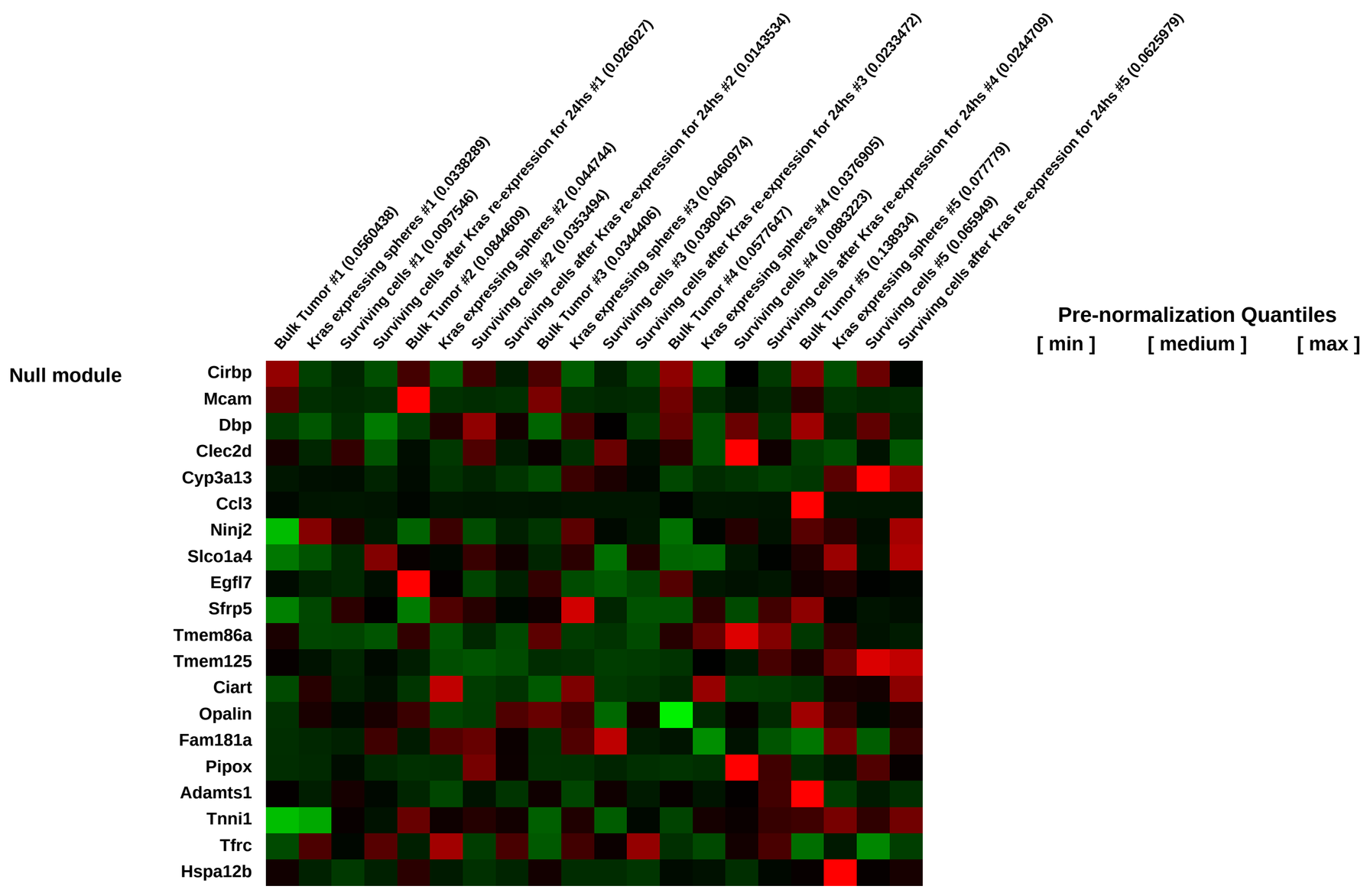

GEO Series "GSE42877" Expression Profiles

Num of samples in this series: 14

Scale of expression profile Z-scores

-3.0 -2.0 -1.0 0.0 1.0 2.0 3.0

GEO Link:	**http://www.ncbi.nlm.nih.gov/geo/query/acc.cgi?acc=GSE42877**
Status:	**Public on Dec 13 2012**
Title:	**Expression data from mice peritoneal cells**
Organism:	**Mus musculus**
Experiment type:	**Expression profiling by array**
Platform:	**GPL1261**
Pubmed ID:	
Summary & Design:	**Summary:** **Sodium methyldithiocarbamate (SMD) is one of the most abundantly used conventional pesticides in the U.S. At dosages relevant to occupational exposure, it causes major effects on the immune system in mice, including a decreased resistance to sepsis. This lab has identified some of the mechanisms of action of this compound and some of the immunological parameters affected, but the global effects have not previously been assessed.** **We used microarrays to analyze the effect of SMD on lipopolysaccharide-induced mediators important in innate immunity and inflammation and reveal a broad effect on expression of transcription factors involved in Toll-like Receptors 4 (TLR4) signaling.** **Overall design:** **Female (C57Bl/6 x C3H F1) mice at 12-16 weeks old were housed in filter top shoebox cages with 5 mice per cage in a temperature (70-78´ºF) and humidity (40-60%) controlled environment. Then the mice were anesthetized with halothane and 50 ´µl of SMD solution was placed on the nares. SMD was administered by inhalation at (1) 100 mg/kg, (2) 200 mg/kg or (3) 300 mg/kg. 30 minutes after administering SMD the mice were challenged with ultra pure LPS from Salmonella minnesota at 60 ´µg/mouse (in PBS) intravenously in a tail vein.**

Background corr dist: KL-Divergence = 0.1419, L1-Distance = 0.0366, L2-Distance = 0.0025, Normal std = 0.3931

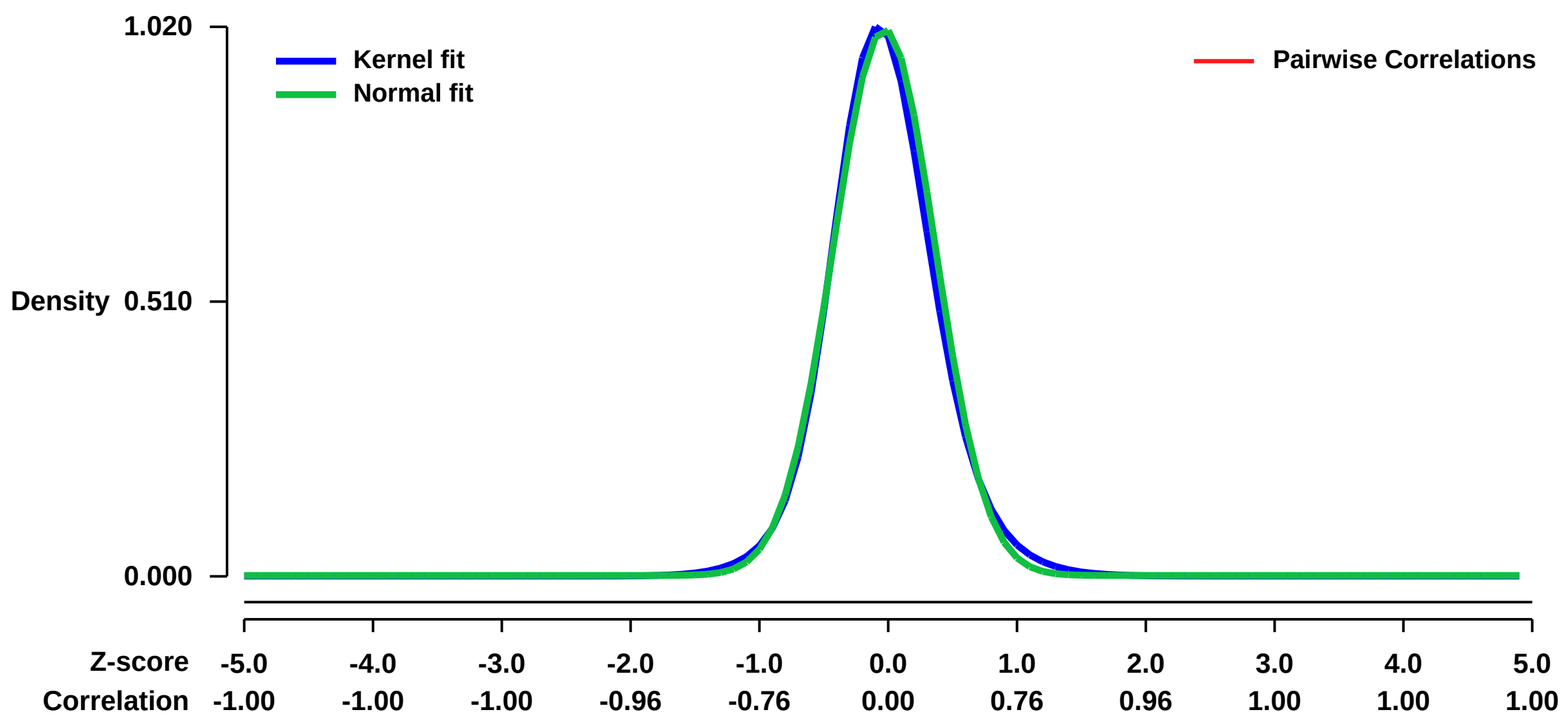

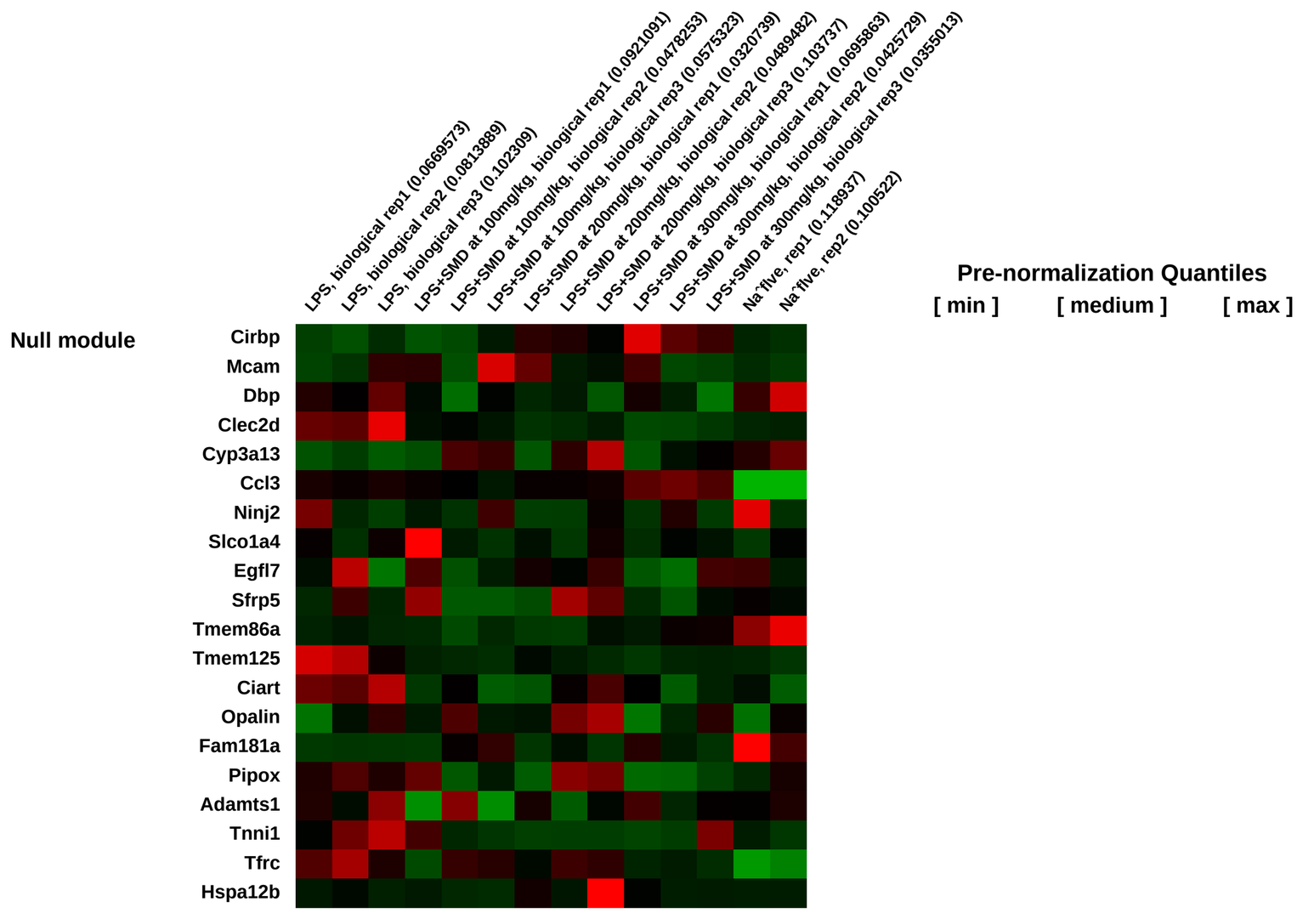

GEO Series "GSE35961" Expression Profiles

Num of samples in this series: 12

Scale of expression profile Z-scores

-3.0 -2.0 -1.0 0.0 1.0 2.0 3.0

GEO Link:	http://www.ncbi.nlm.nih.gov/geo/query/acc.cgi?acc=GSE35961
Status:	Public on Feb 21 2012
Title:	Expression data from mouse liver treated with metformin
Organism:	Mus musculus
Experiment type:	Expression profiling by array
Platform:	GPL1261
Pubmed ID:	23028442
Summary & Design:	**Summary:** **Optimal treatment for nonalcoholic steatohepatitis (NASH) has not yet been established, particularly for individuals without diabetes.** **We examined the effects of metformin, commonly used to treat patients with type 2 diabetes, on liver pathology in a non-diabetic NASH mouse model.** **Overall design:** **Eight-week-old C57BL/6 mice were fed a methionine- and choline-deficient (MCD) + high fat (HF) diet with or without 0.1% metformin for 8 weeks.**

Background corr dist: **KL-Divergence = 0.0889, L1-Distance = 0.0223, L2-Distance = 0.0007, Normal std = 0.4619**

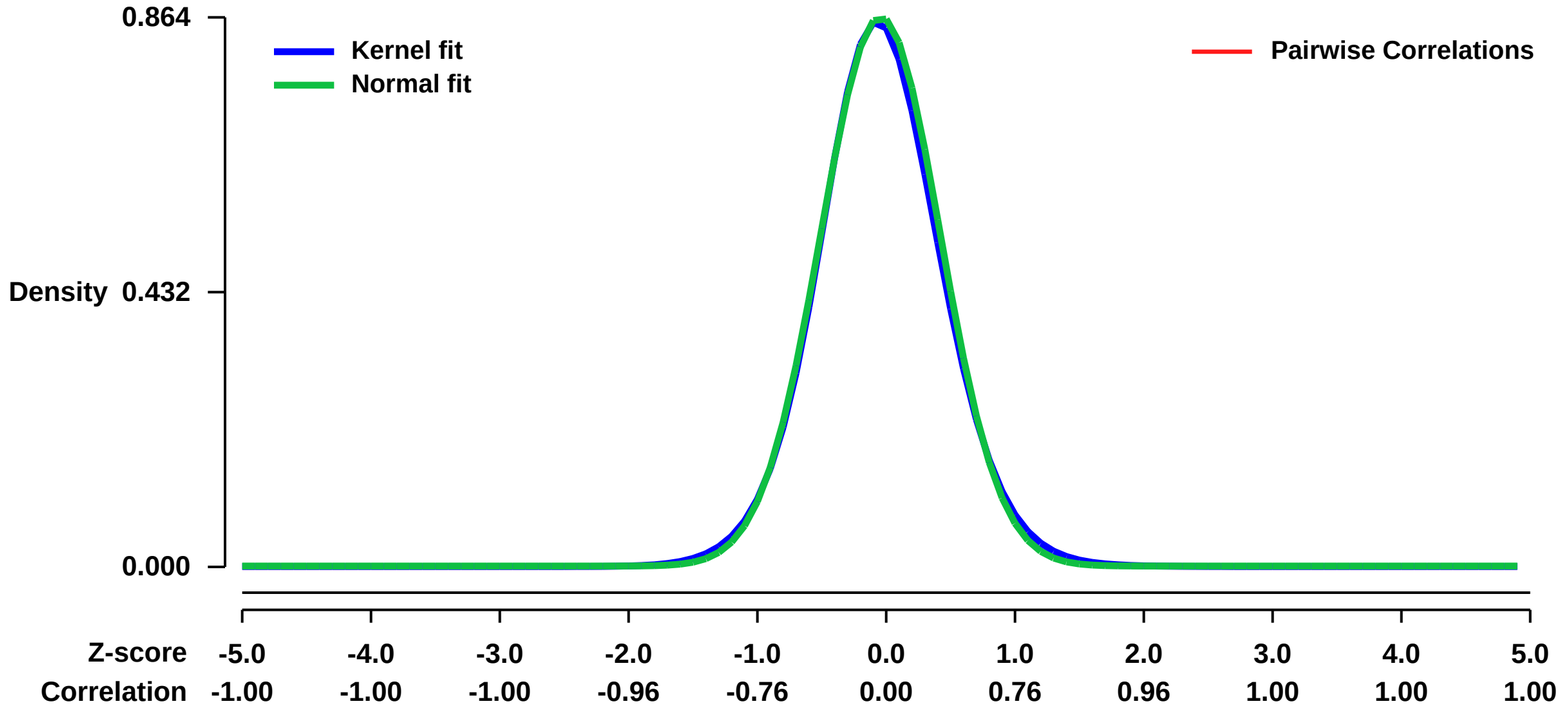

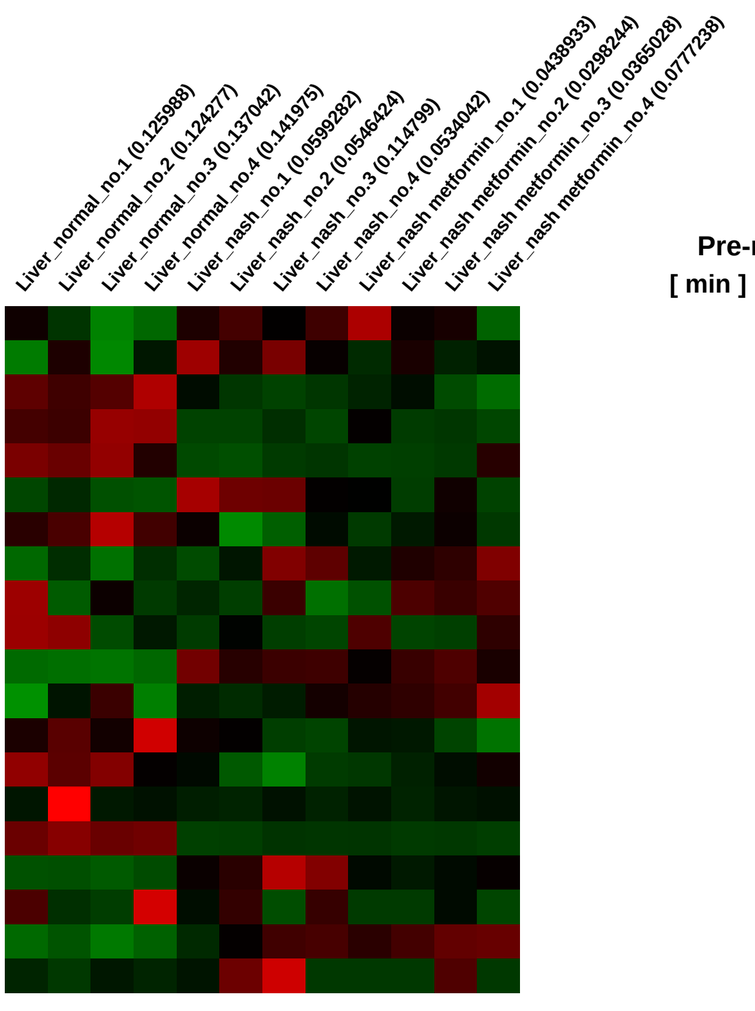

GEO Series "GSE27302" Expression Profiles

Num of samples in this series: 16

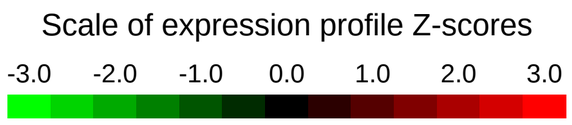

GEO Link:	**http://www.ncbi.nlm.nih.gov/geo/query/acc.cgi?acc=GSE27302**
Status:	**Public on Jan 11 2013**
Title:	**Expression data from mouse colon tissue response to T cell transfer at week 0, 2, 4 and 6**
Organism:	**Mus musculus**
Experiment type:	**Expression profiling by array**
Platform:	**GPL1261**
Pubmed ID:	**22179924**
Summary & Design:	**Summary:** **Temporal geneome profiling of T cell transfer colitis model** **T cells critically regulate clinical inflammatory bowel diseases and T cell dependent experimental colitis models have gained prominent favor as useful models to identify potential pathogenic mechanisms. The naˆflve CD4+CD45Rbhigh cell transfer model into recombinase activating gene-1 deficient (RAG-/-) mice induces both colitis and small bowel inflammation reflecting Crohn's disease with unclear pathogenic mechanisms. Given the pathological similarities between the T cell transfer model of colitis and clinical disease, we sought to identify changes in whole genome expression profiles over time during the delelopment of colitis.** **Overall design:** **Male RAG-1-/- C57BL/6 mice were injected with a half million CD4+CD45RBhigh T cells from healthy wild type C57BL/6 male mice. The colon tissue from individual cohorts were collected at weeks 0, 2, 4 and 6. Total RNA were extracted from the colon tissue and detected by Affymetrix GeneChip Mouse Genome 430 2.0 Array.**

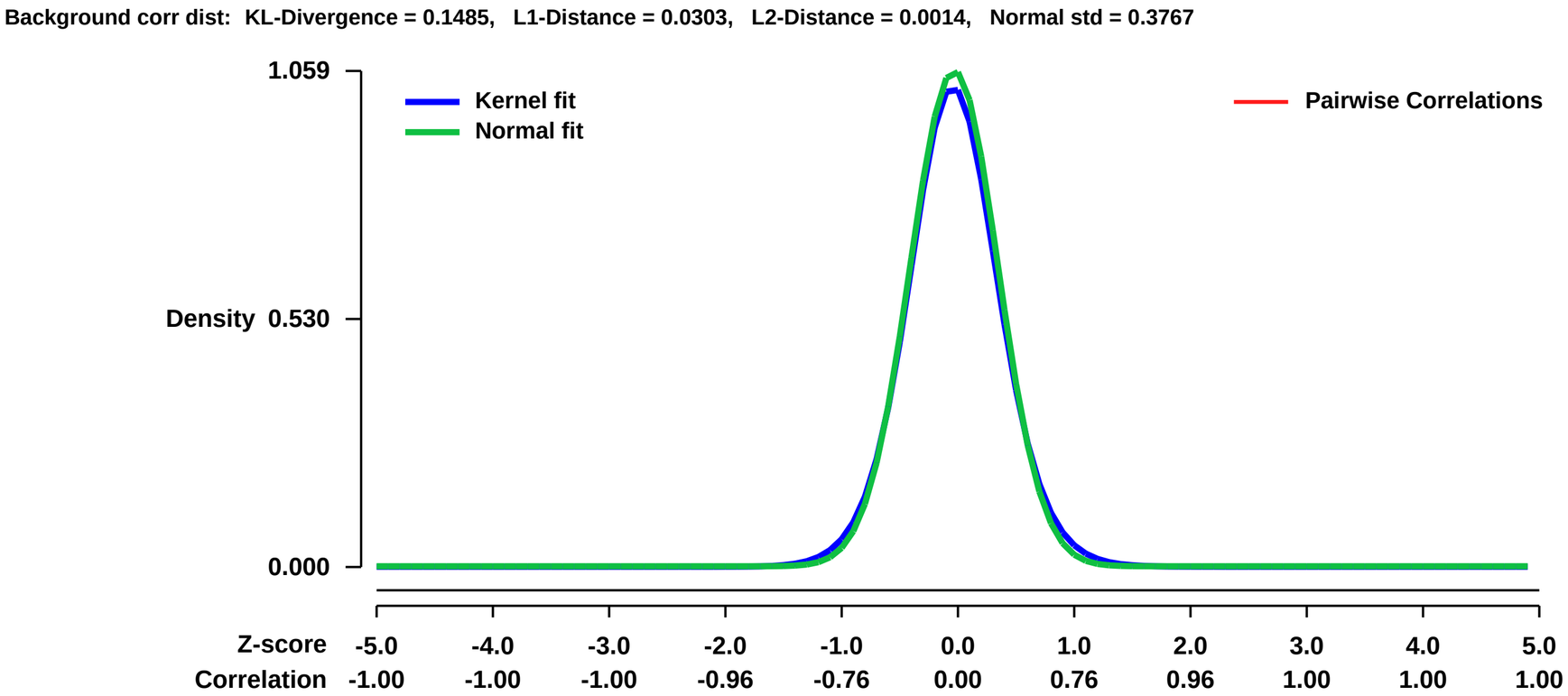

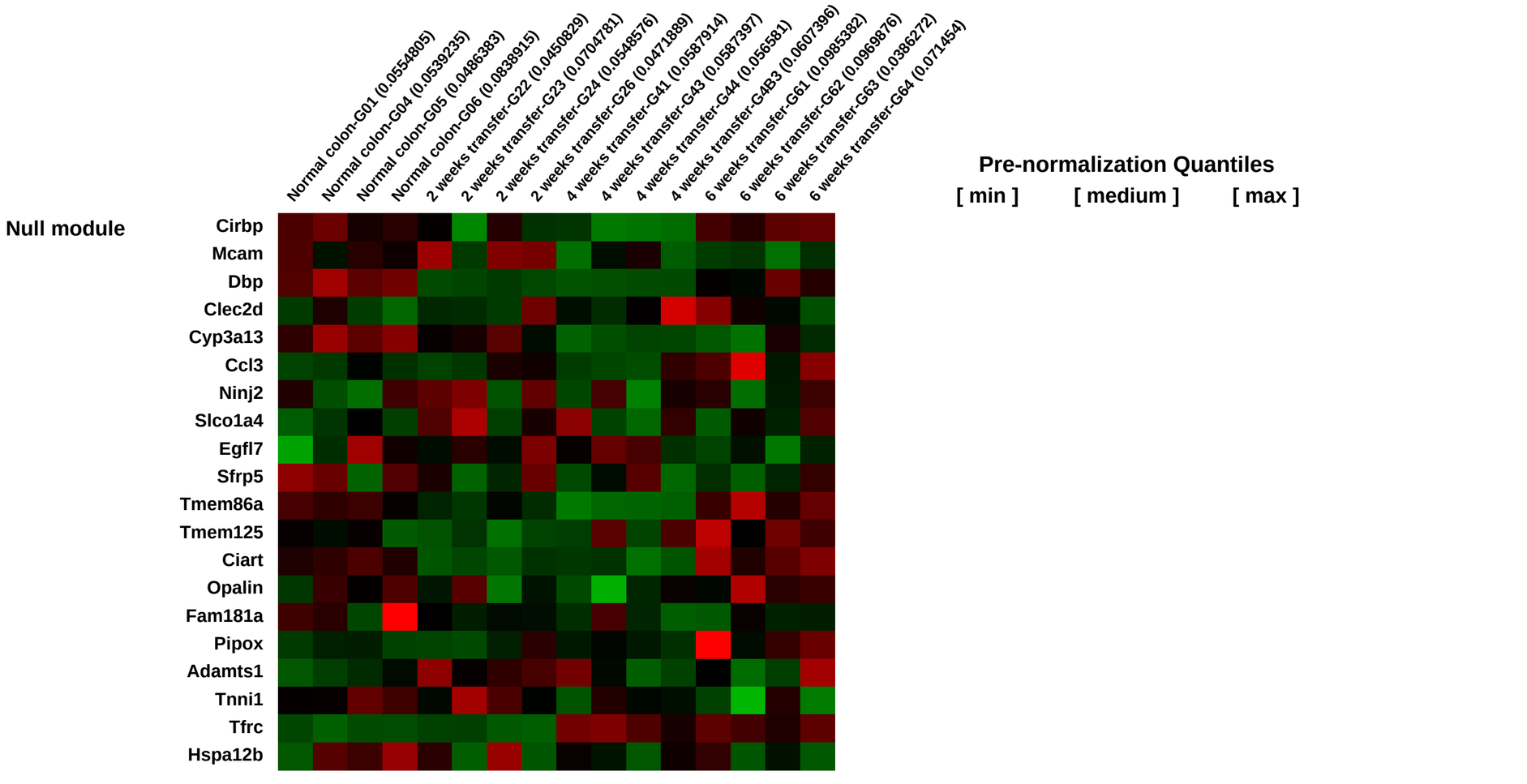

GEO Series "GSE46116" Expression Profiles

Num of samples in this series: 8

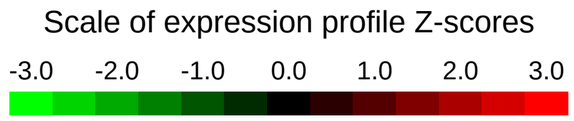

GEO Link:	**http://www.ncbi.nlm.nih.gov/geo/query/acc.cgi?acc=GSE46116**
Status:	**Public on Jul 01 2013**
Title:	**Changes in gene expression upon co-treatment of cells with Dex and E2**
Organism:	**Mus musculus**
Experiment type:	**Expression profiling by array**
Platform:	**GPL1261**
Pubmed ID:	**23803465**
Summary & Design:	**Summary:** **We report changes in gene expression upon co-treatment with Dex and E2 when compared to Dex or E2 treatments alone.** **Overall design:** **We examine expression under four different treatments (unt, Dex, E2, and Dex + E2).**

Background corr dist: **KL-Divergence = 0.0581, L1-Distance = 0.0199, L2-Distance = 0.0005, Normal std = 0.5293**

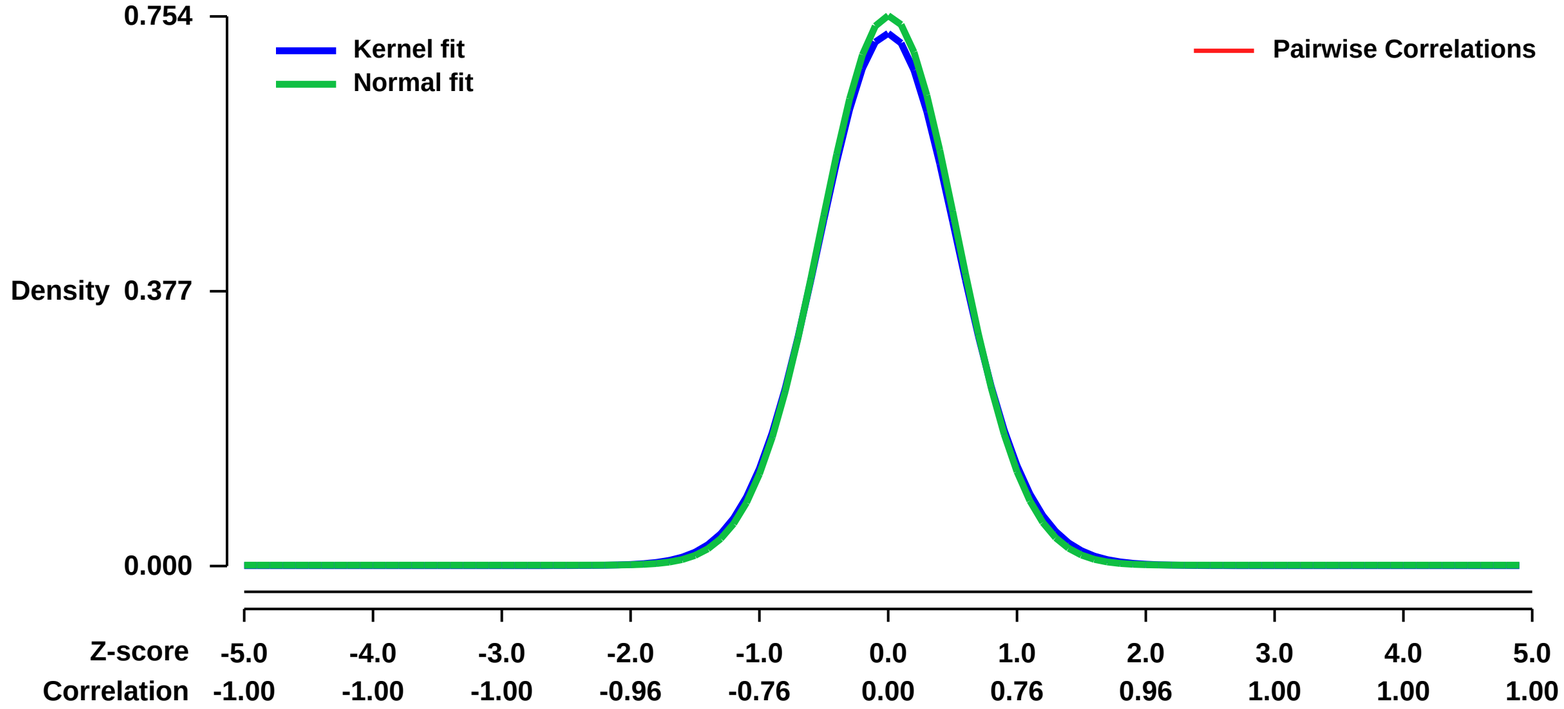

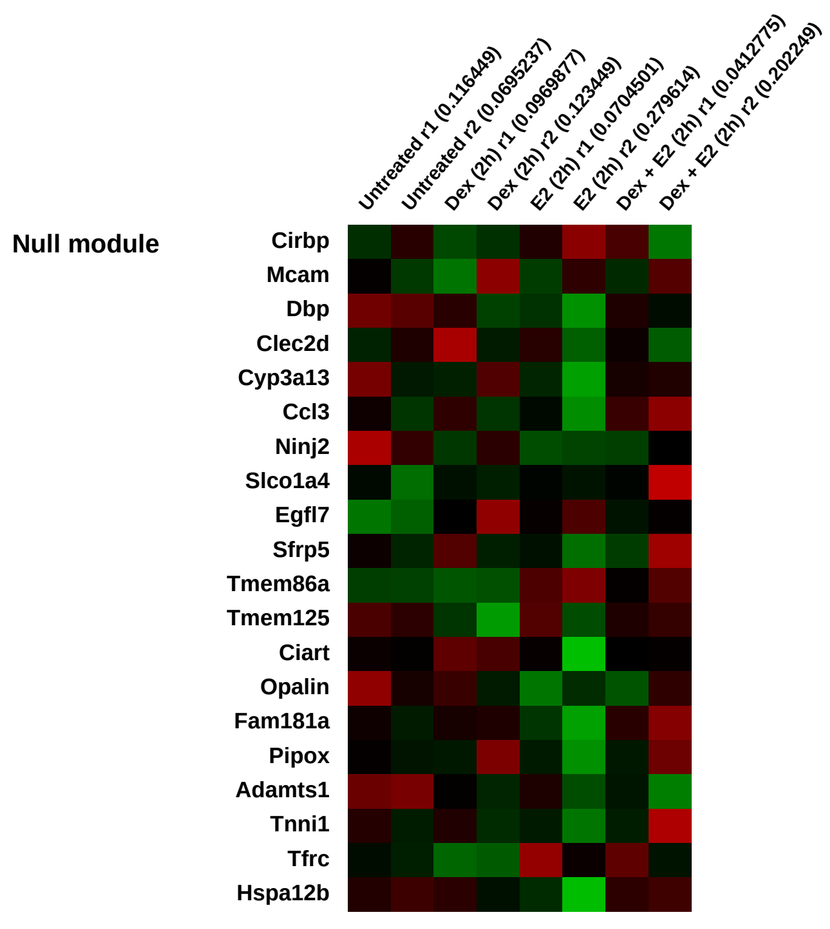

GEO Series "GSE1999" Expression Profiles

Num of samples in this series: 15

Scale of expression profile Z-scores

-3.0 -2.0 -1.0 0.0 1.0 2.0 3.0

GEO Link:	**http://www.ncbi.nlm.nih.gov/geo/query/acc.cgi?acc=GSE1999**
Status:	**Public on Nov 24 2004**
Title:	**Neuroprotective effects of erythropoietin. Wilson-5R01NS028208-15**
Organism:	**Mus musculus**
Experiment type:	**Expression profiling by array**
Platform:	**GPL1261**
Pubmed ID:	
Summary & Design:	**Summary:** **Hypoxic-ischemic (HI) injury in the developing brain is a common cause of disability in children, and there are no effective treatments at this time. Erythropoietin (EPO) has recently gained interest as a neuroprotective drug, and EPO and its receptor are expressed within the central nervous system. We have recently shown that pretreatment with EPO markedly reduced brain injury caused by unilateral hypoxic-ischemic insult in 7 day old mice. EPO did not reduce early signs of neuronal injury at 6 hours, but significantly protected the neonatal brain when assessed 24 hours and 7 days after HI. The mechanism of this delayed protection is unclear, but is thought to involve transcription of neuroprotective genes, possibly subsequent to activation of NFkB. By comparing gene expression in EPO- and vehicle-(VEH) treated mice after HI, we should gain insight into the mechanisms underlying the neuroprotective effects of EPO and may identify additional targets for therapeutic interventions.** **We will compare gene expression patterns in 7-day old mouse forebrain after 1) VEH pretreatment plus sham surgery, 2) VEH pretreatment plus HI, and 3) EPO pretreatment plus HI. We will thus identify genes induced by HI in the developing brain and characterize changes in gene expression caused by EPO pretreatment. We will use the model of neonatal hypoxic-ischemic injury and EPO treatment parameters that were used in our prior studies demonstrating neuroprotection. Based on the time-course of neuroprotection defined in our prior study and the pharmacokinetic profile of EPO, we will examine gene expression 18 hours after HI.** **We hypothesize that changes in gene expression after EPO pretreatment underlie the neuroprotective effects of this cytokine after neonatal hypoxic ischemic injury.** **We will examine gene expression in 3 groups: 1) 1) VEH pretreatment + sham surgery, 2) VEH pretreatment + HI, and 3) EPO pretreatment + HI. EPO (5U/g, i.p.) or VEH was injected in 7 day old mice, drawn from 4 litters, with 3 to 4 pups per treatment group in each litter. One hour later, the right common carotid artery was ligated under isoflurane anesthesia, animals were allowed to recover for 90 min and were then placed in hypoxic chambers (10% oxygen, balance nitrogen) for 50 min. The animals subjected to sham surgery received isoflurane anesthesia for a comparable period, incision and dissection to visualize the common carotid artery, but no ligation and no hypoxia. Eighteen hrs later, animals were anesthetized with isoflurane and the right hemisphere was rapidly dissected and placed in RNA Later (Qiagen) at 4C. Total RNA was isolated using an RNeasy lipid tissue mini kit (QIAzol lysis and RNeasy purification, Qiagen). RNA concentrations were determined spectrophotometrically and an aliquot of each sample was examined by gel electrophoresis to screen for degradation. Samples were stored at -80C. After quality control screening, we selected 5 male and 5 female samples per treatment group (extra samples were reserved). We plan to pool 1 male and 1 female for each microarray sample and we plan to run 5 microarrays from each treatment group, for a total of 15 microarrays. We would like to have Agilent Bioanalyzer quality control assays on the individual samples carried out by the consortium before pooling. We will send 10 micrograms of each sample for Agilent QC and subsequent pooling of equimolar amounts. We would like to use Affymetrix mouse gene chips (please advise which specific chips are available; are you using the GeneChip Mouse Expression array 430A or the GeneChip Mouse Genome 430 2.0 Array?).** **Keywords: dose response** **Overall design:**

Background corr dist: KL-Divergence = 0.1184, L1-Distance = 0.0326, L2-Distance = 0.0019, Normal std = 0.4083

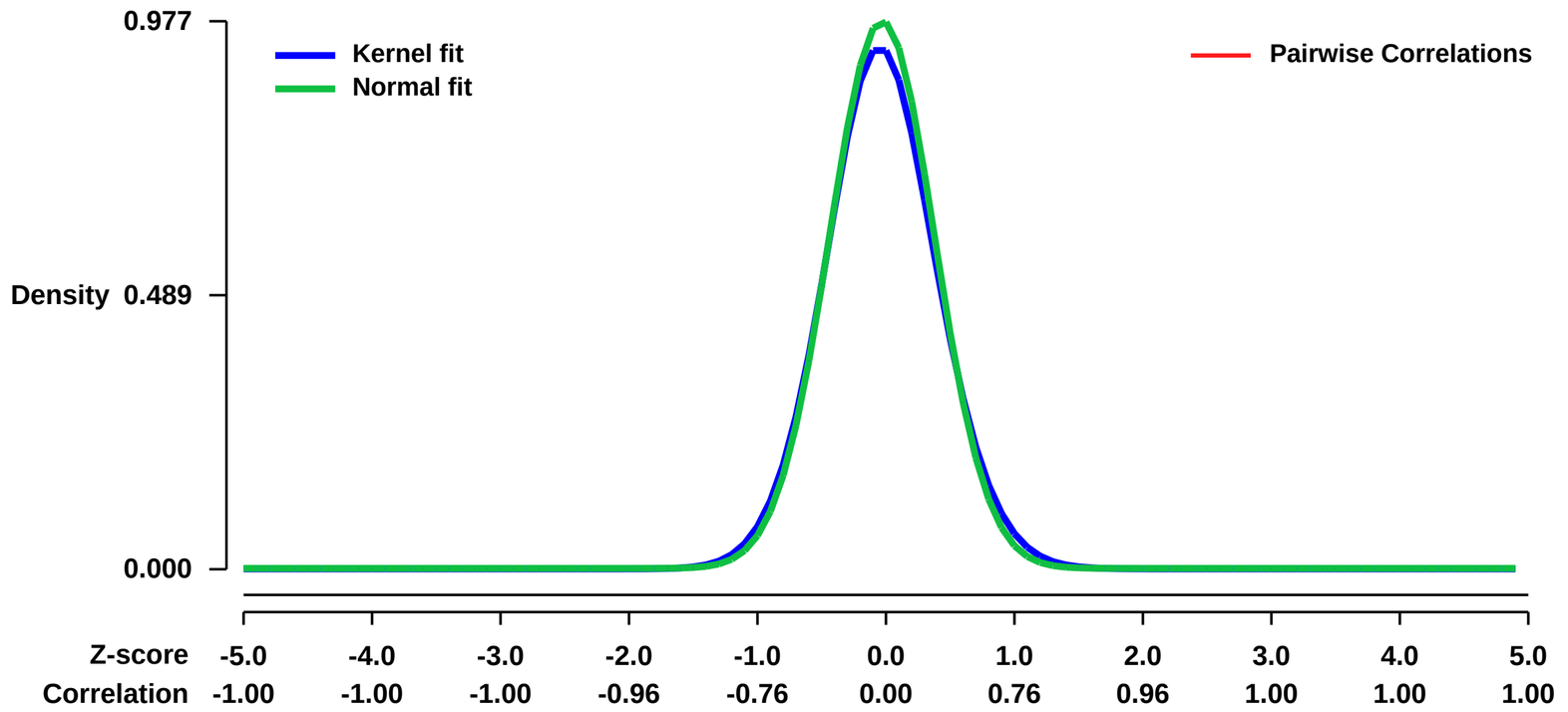

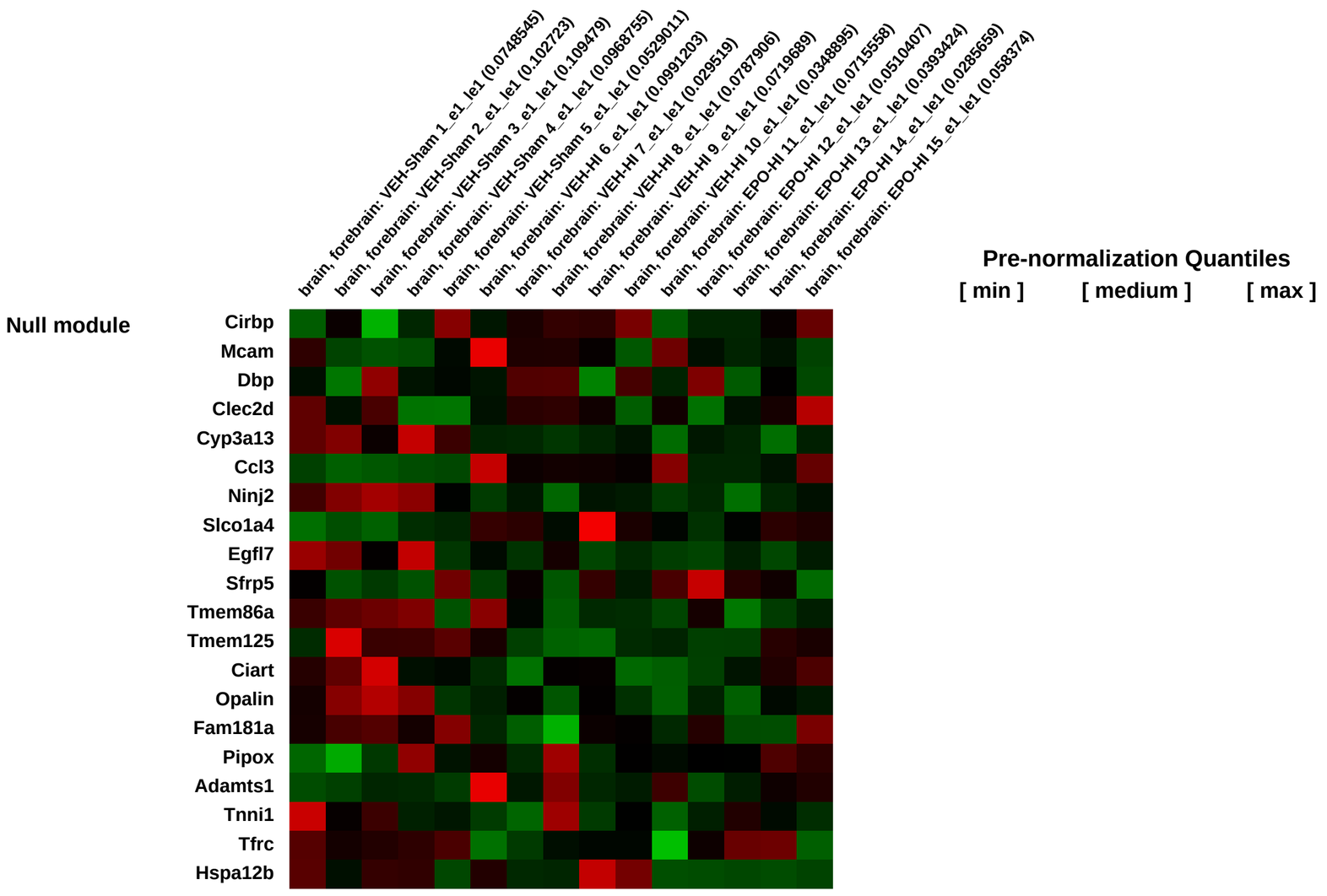

GEO Series "GSE46600" Expression Profiles

Num of samples in this series: 44

Scale of expression profile Z-scores

-3.0 -2.0 -1.0 0.0 1.0 2.0 3.0

GEO Link:	http://www.ncbi.nlm.nih.gov/geo/query/acc.cgi?acc=GSE46600
Status:	Public on Jun 20 2014
Title:	Transcriptome and Molecular Pathways Analysis of CD4 T-Cells from Young NOD Mice
Organism:	Mus musculus
Experiment type:	Expression profiling by array
Platform:	GPL1261
Pubmed ID:	24918037
Summary & Design:	**Summary:** Type 1 diabetes is a multigenic disease caused by T-cell mediated destruction of the insulin producing ˛†-cells. Although conventional (targeted) approaches of identifying causative genes have advanced our knowledge of this disease, many questions remain unanswered. Using a whole molecular systems study, we unraveled the genes/molecular pathways that are altered in CD4 T-cells from young NOD mice prior to insulitis (lymphocytic infiltration into the pancreas). Many of the CD4 T-cell altered genes lie within known diabetes susceptibility regions (Idd), including several genes in the diabetes resistance region Idd13 and two genes (Khdrbs1 and Ptp4a2) in the CD4 T-cell diabetogenic activity region Idd9/11. Alterations involved apoptosis/cell proliferation and metabolic pathways (predominant at 2 weeks), inflammation and cell signaling/activation (predominant at 3 weeks), and innate and adaptive immune responses (predominant at 4 weeks). We identified several factors that may regulate these abnormalities: IRF-1, HNF4A, TP53, BCL2L1 (lies within Idd13), IFNG, IL4, IL15, and prostaglandin E2, which were common to all 3 ages; AR and IL6 to 2 and 4 weeks; and Interferon (IFN-I) and IRF-7 to 3 and 4 weeks. Others were unique to the various ages (e. g. MYC, JUN, and APP to 2 weeks; TNF, TGFB1, NFKB, ERK, and p38MAPK to 3 weeks; and IL12 and STAT4 to 4 weeks). Our data suggest that diabetes resistance genes in Idd13 and Idd9/11, and BCL2L1, IL6-AR and IFNG-IRF-1-IFN-I/IRF-7-IL12 pathways play an important role in CD4 T-cells in the early pathogenesis of autoimmune diabetes. Thus, the alternative approach of investigation at the molecular systems level has captured new information, which combined with validation studies, offers the opportunity to test hypotheses on the role played by the genes/molecular pathways identified in this study, to understand better the mechanisms of autoimmune diabetes in CD4 T-cells, and to develop new therapeutic strategies for the disease. **Overall design:** CD4 T-cells were purified from spleen leukocytes collected from 2-, 3- and 4-week old NOD mice and two age-matched control strains, NOR, and C57BL/6, (n=5 for each strain and each age group; except NOD2wk). NOR is an insulitis- and diabetes-free control strain that shares shares ~88% of its genome with NOD mice, including the diabetogenic H2g7 MHC haplotype and several important non-MHC T1D susceptibility loci. C57BL/6 is also a diabetes-resitant strain, but it is more genetically distantly related to NOD.

Background corr dist: KL-Divergence = 0.4129, L1-Distance = 0.0601, L2-Distance = 0.0093, Normal std = 0.2468

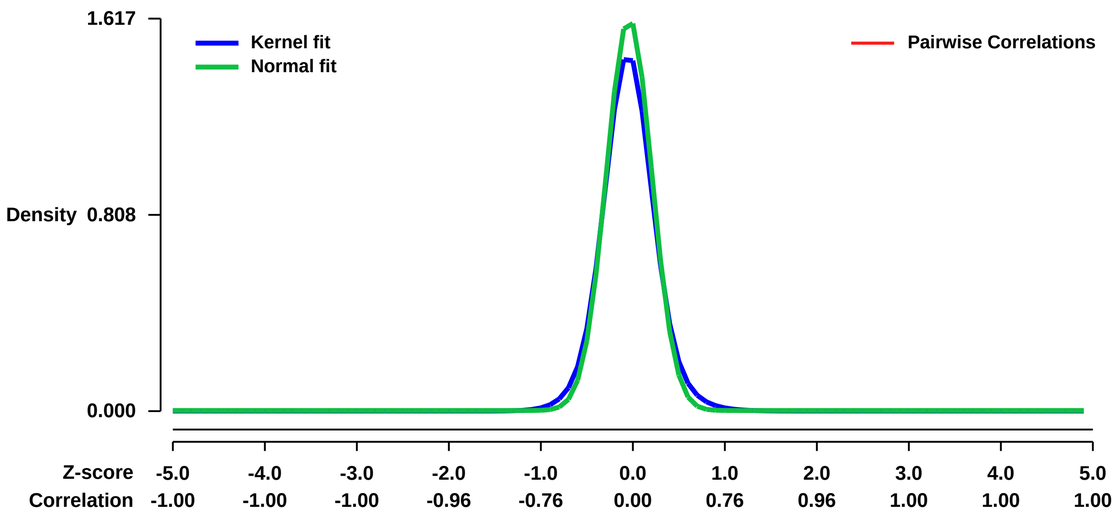

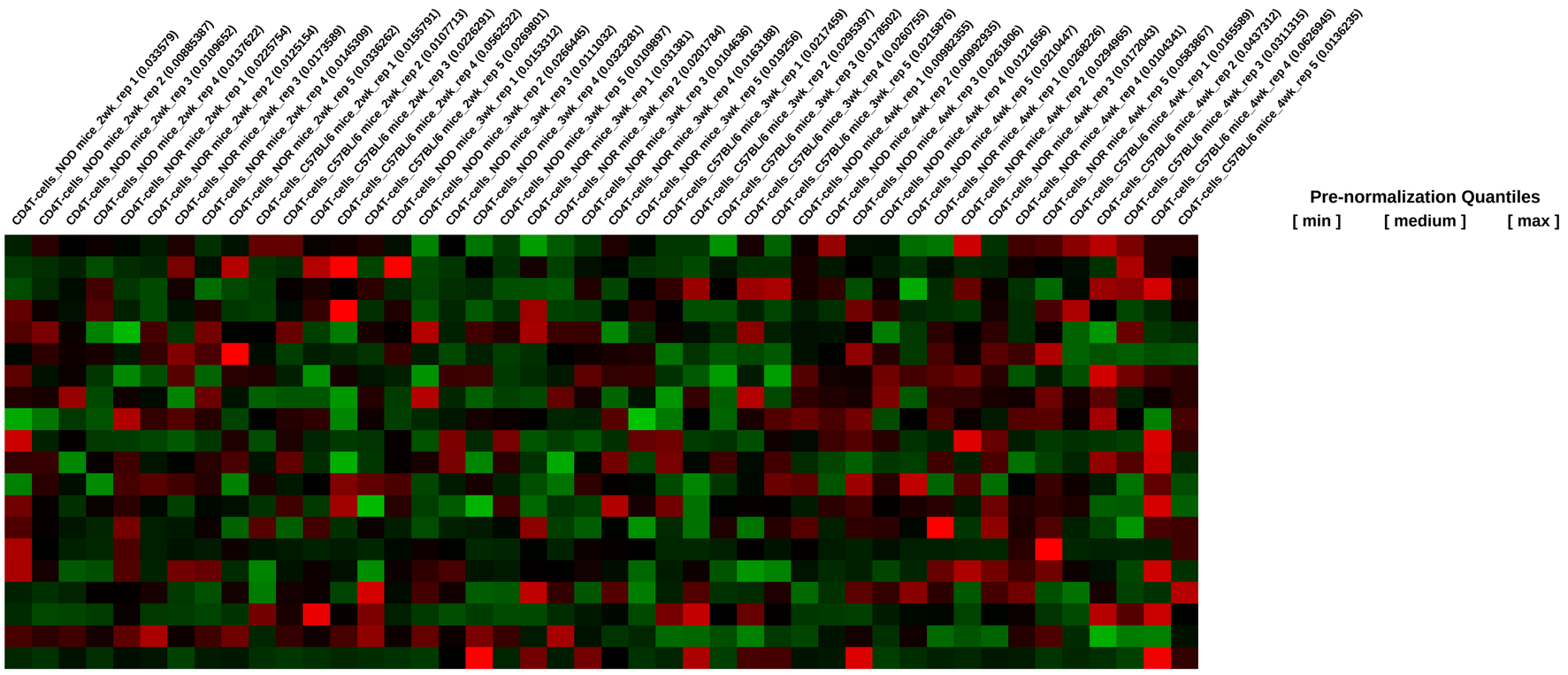

GEO Series "GSE28091" Expression Profiles

Num of samples in this series: 12

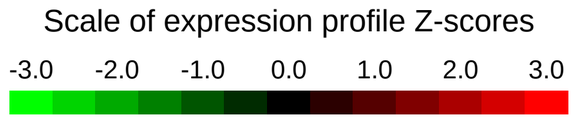

GEO Link:	**http://www.ncbi.nlm.nih.gov/geo/query/acc.cgi?acc=GSE28091**
Status:	**Public on Jun 01 2011**
Title:	**Expression profiles of mouse glioma-initiating cells.**
Organism:	**Mus musculus**
Experiment type:	**Expression profiling by array**
Platform:	**GPL1261**
Pubmed ID:	**21360625**
Summary & Design:	**Summary:** **To identify factors involved in glioma-initiating cells (GICs), we compared gene expressions between GIC-like cells and non-GICs.** **Overall design:** **p53-deficient Neural stem cells (NSCs), oligodendrocyte precursor cells (OPCs), and astrocytes (ASTs) were transfected with pCMS-EGFP-HRasL61 and pBabe-neo by electroporation and cultured in 0.5 mg/ml neomycin. The GFP-positive stable NSCs (NSCL61s), OPCs (OPCL61s) and ASTs (ASTL61s) were purified by flow cytometry. Total RNA was prepared using a RNeasy Mini Kit (QIAGEN) and used for the expression analysis.[a]**

Background corr dist: **KL-Divergence = 0.0893, L1-Distance = 0.0277, L2-Distance = 0.0014, Normal std = 0.4734**

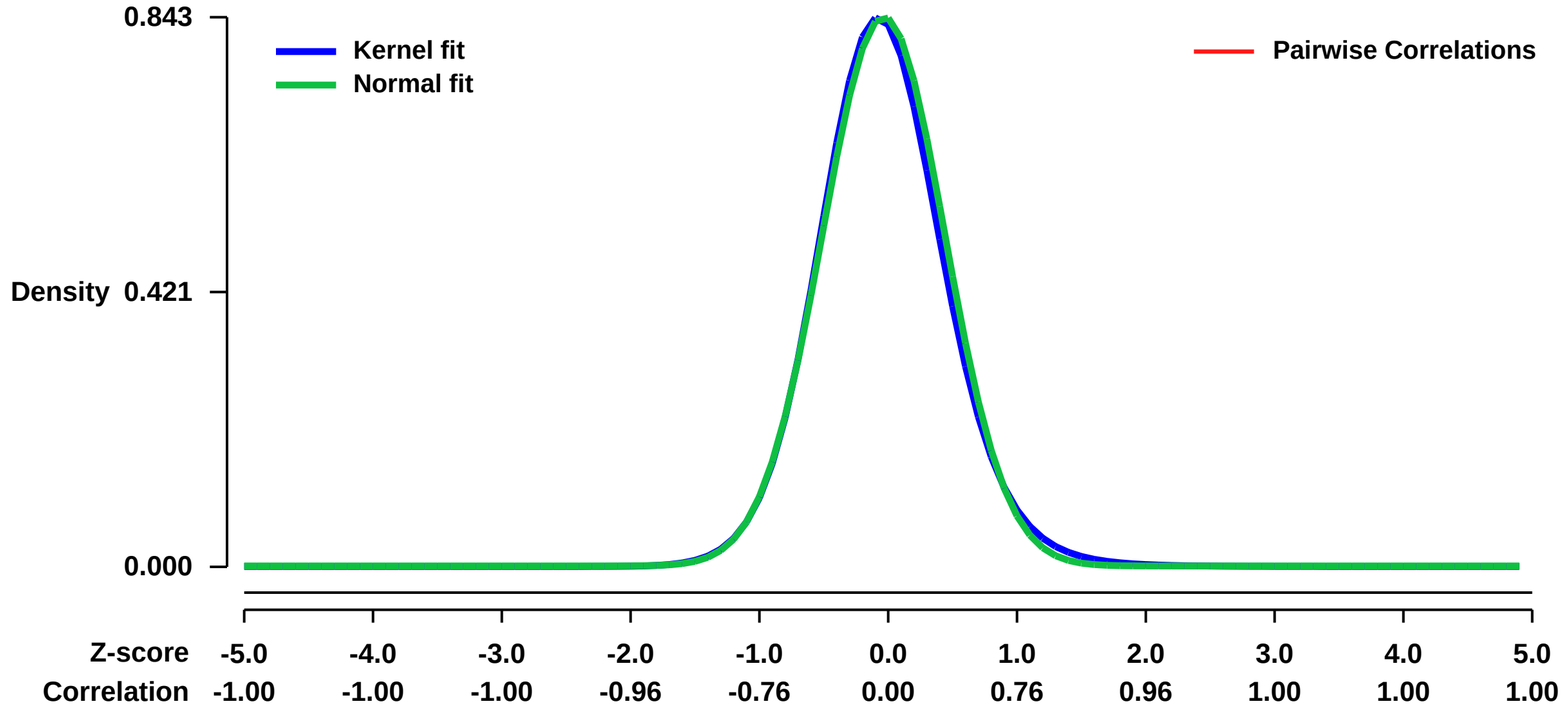

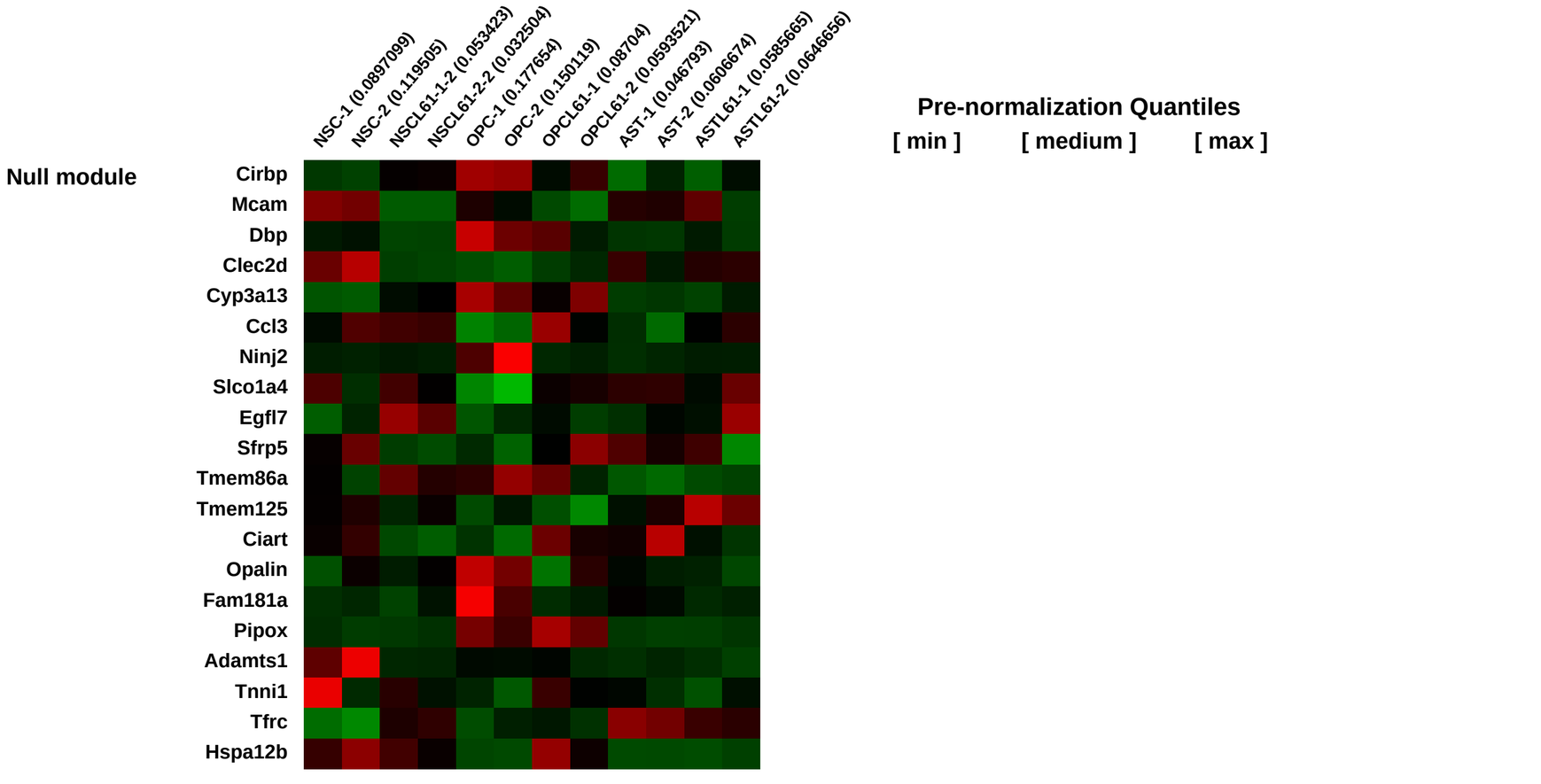

GEO Series "GSE26822" Expression Profiles

Num of samples in this series: 8

Scale of expression profile Z-scores

-3.0 -2.0 -1.0 0.0 1.0 2.0 3.0

GEO Link:	http://www.ncbi.nlm.nih.gov/geo/query/acc.cgi?acc=GSE26822
Status:	Public on Jan 01 2012
Title:	Expression data from postnatal mouse apical and basal organ of Corti from Dicer1 conditional knockout and littermate control cochleae.
Organism:	Mus musculus
Experiment type:	Expression profiling by array
Platform:	GPL1261
Pubmed ID:	21360794
Summary & Design:	**Summary:** Cre recombinase-mediated conditional knockout of floxed Dicer1 alleles causes depletion of small RNAs including microRNAs, which function to repress target mRNA expression by inhibiting translation and/or stimulating mRNA degradation. We used microarrays to examine gene expression in apical versus basal organ of Corti from the cochleae of control and mutant mice in which Dicer1 was deleted and microRNAs were depleted specifically in sensory hair cells by Atoh1 promoter-driven Cre recombinase expression. **Overall design:** Each biological replicate represents the combined apical or combined basal segments of organ of Corti from both cochleae of a single mouse. Two biological replicates for apical and basal organ of Corti from Dicer1 conditonal knockout and littermate controls were collected for RNA extraction and microarray analysis.

Background corr dist: KL-Divergence = 0.0736, L1-Distance = 0.0220, L2-Distance = 0.0008, Normal std = 0.4919

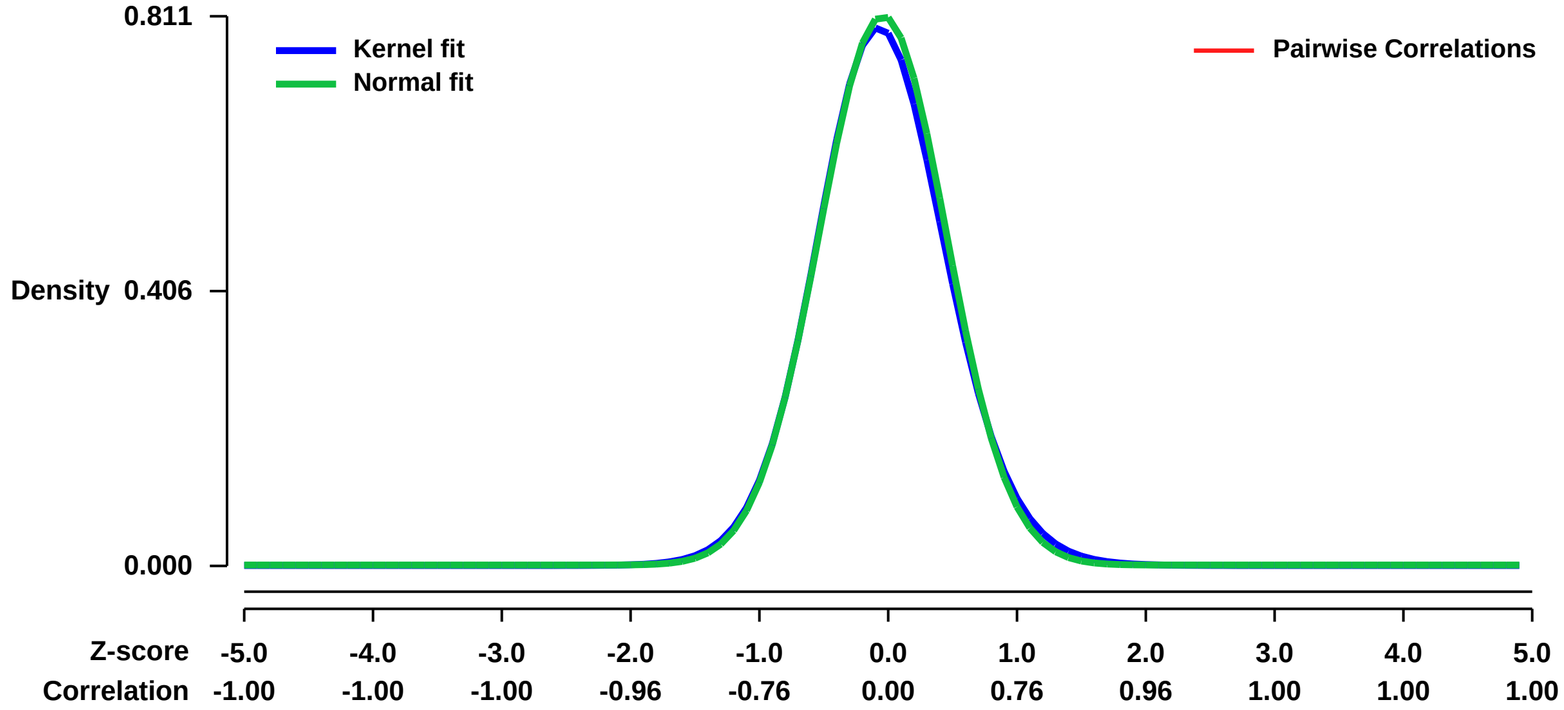

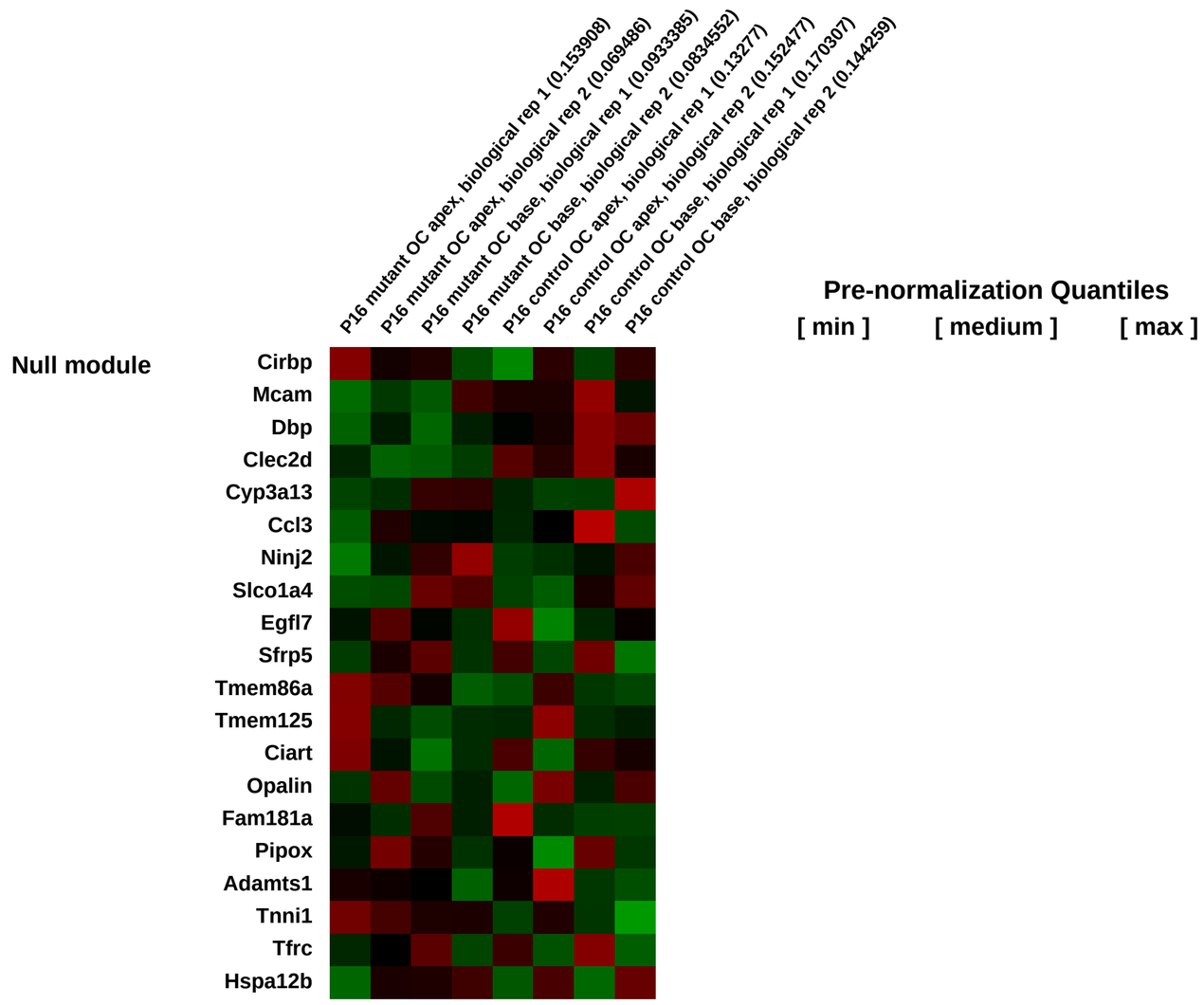

GEO Series "GSE9044" Expression Profiles

Num of samples in this series: 6

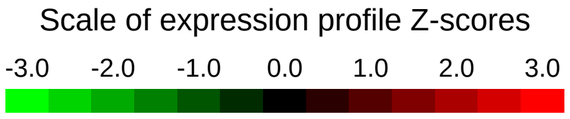

GEO Link:	http://www.ncbi.nlm.nih.gov/geo/query/acc.cgi?acc=GSE9044
Status:	Public on Sep 19 2007
Title:	HOXB4 target genes in ES cell-derived embryoid bodies (EBs)
Organism:	Mus musculus
Experiment type:	Expression profiling by array
Platform:	GPL1261
Pubmed ID:	17940039
Summary & Design:	**Summary:** To unravel the molecular mechanism by which HOXB4 promotes the expansion of early hematopoietic progenitors within differentiating ES cells, we analzed the gene expression profiles of embryoid bodies (EBs) in which transcription of HOXB4 had been induced or not induced. A substantial number of the identified HOXB4 target genes are involved in signaling pathways important for controlling self-renewal, maintenance and differentiation of stem cells. Furthermore, we demonstrate that HOXB4 activity and FGF-signaling are intertwined. HOXB4-mediated expansion of ES cell-derived early progenitors was enhanced by specific and complete inhibition of FGF-receptors. In contrast, the expanding activity of HOXB4 on hematopoietic progenitors in day4-6 embryoid bodies was blunted in the presence of basic FGF (FGF2) indicating a dominant negative effect of FGF-signaling on the earliest hematopoietic cells. Taken together, we show that modulation of FGF signaling is an essential feature of HOXB4 activity in the context of embryonic hematopoiesis. **Keywords:** plus/minus induction of HOXB4 gene expression by treatment with doxycycline (Dox) **Overall design:** Biological replicates: 3

Background corr dist: KL-Divergence = 0.0351, L1-Distance = 0.0254, L2-Distance = 0.0008, Normal std = 0.6458

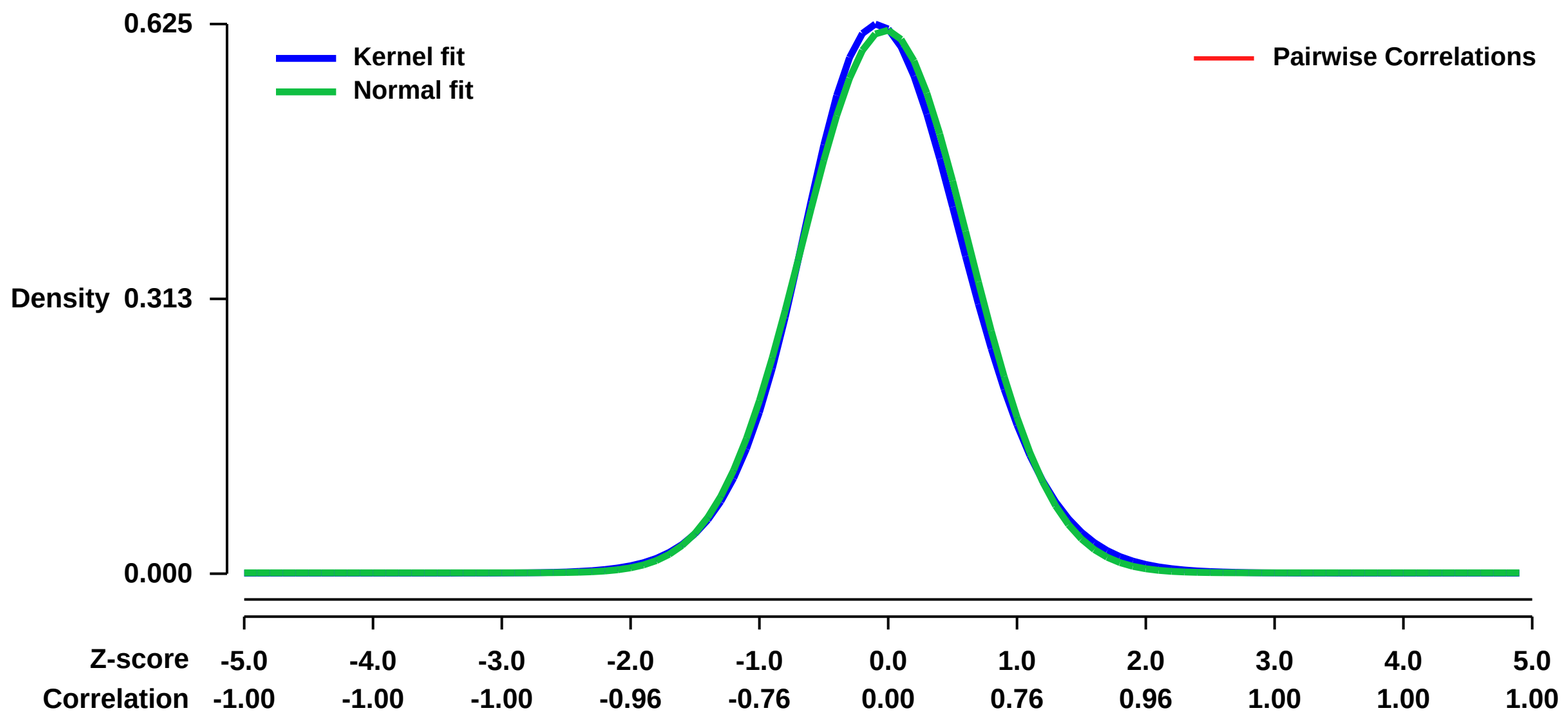

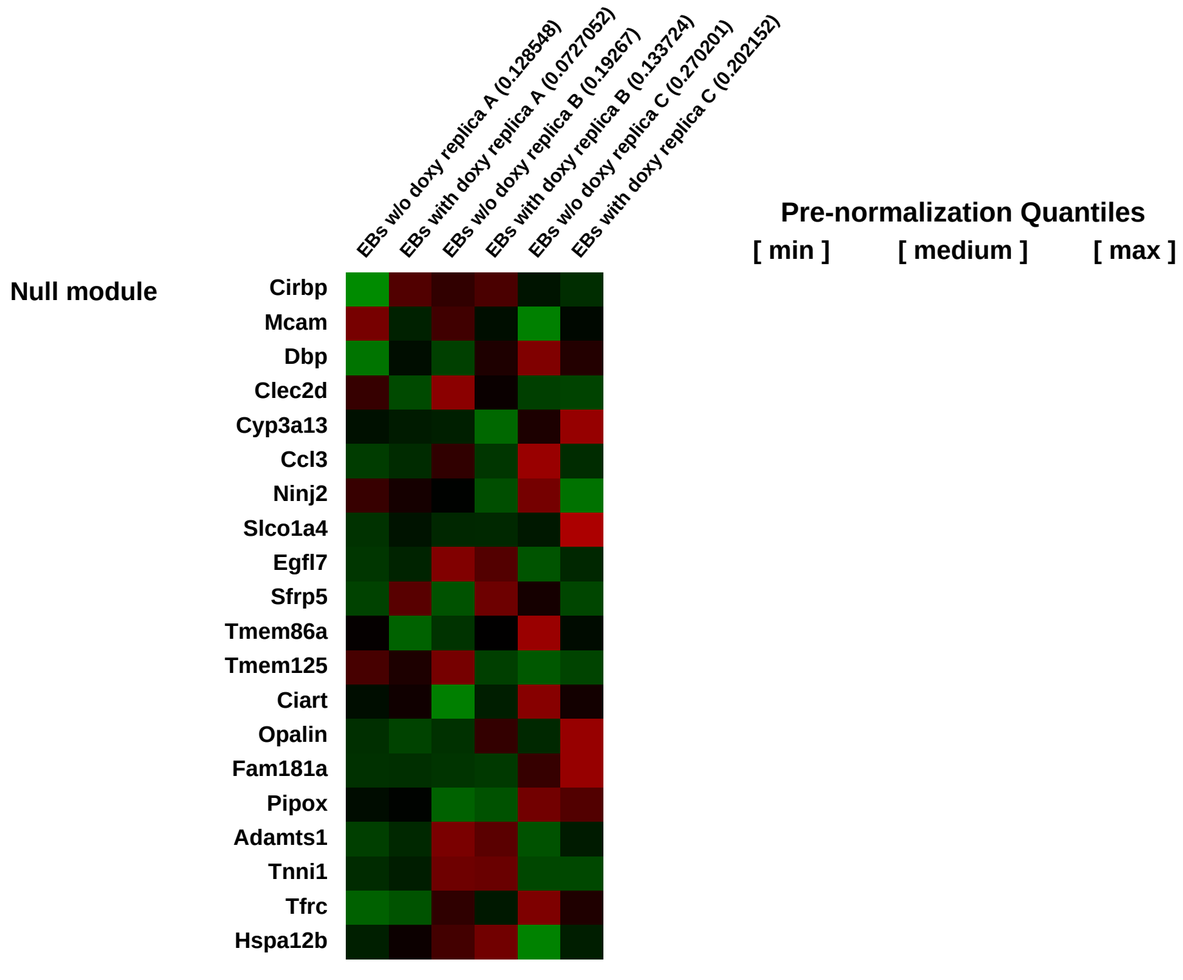

GEO Series "GSE55356" Expression Profiles

Num of samples in this series: 6

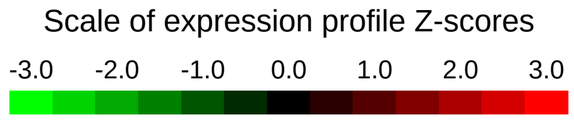

GEO Link:	**http://www.ncbi.nlm.nih.gov/geo/query/acc.cgi?acc=GSE55356**
Status:	**Public on Jul 01 2014**
Title:	**p38a-dependent gene expression in the colonic mucosa**
Organism:	**Mus musculus**
Experiment type:	**Expression profiling by array**
Platform:	**GPL1261**
Pubmed ID:	
Summary & Design:	**Summary:** **Gene expression in the colonic mucosa of wild-type and p38a-knockout intestinal epithelial cells (IECs) were compared.** **C57BL/6 wild-type mice, and intestinal epithelial cell-specific p38a-knockout mice on a C57BL/6 background were used for isolation of colonic mucosa** **Overall design:** **Gene expression in each genotype was analyzed in triplicate.**

Background corr dist: **KL-Divergence = 0.0251, L1-Distance = 0.0199, L2-Distance = 0.0005, Normal std = 0.7025**

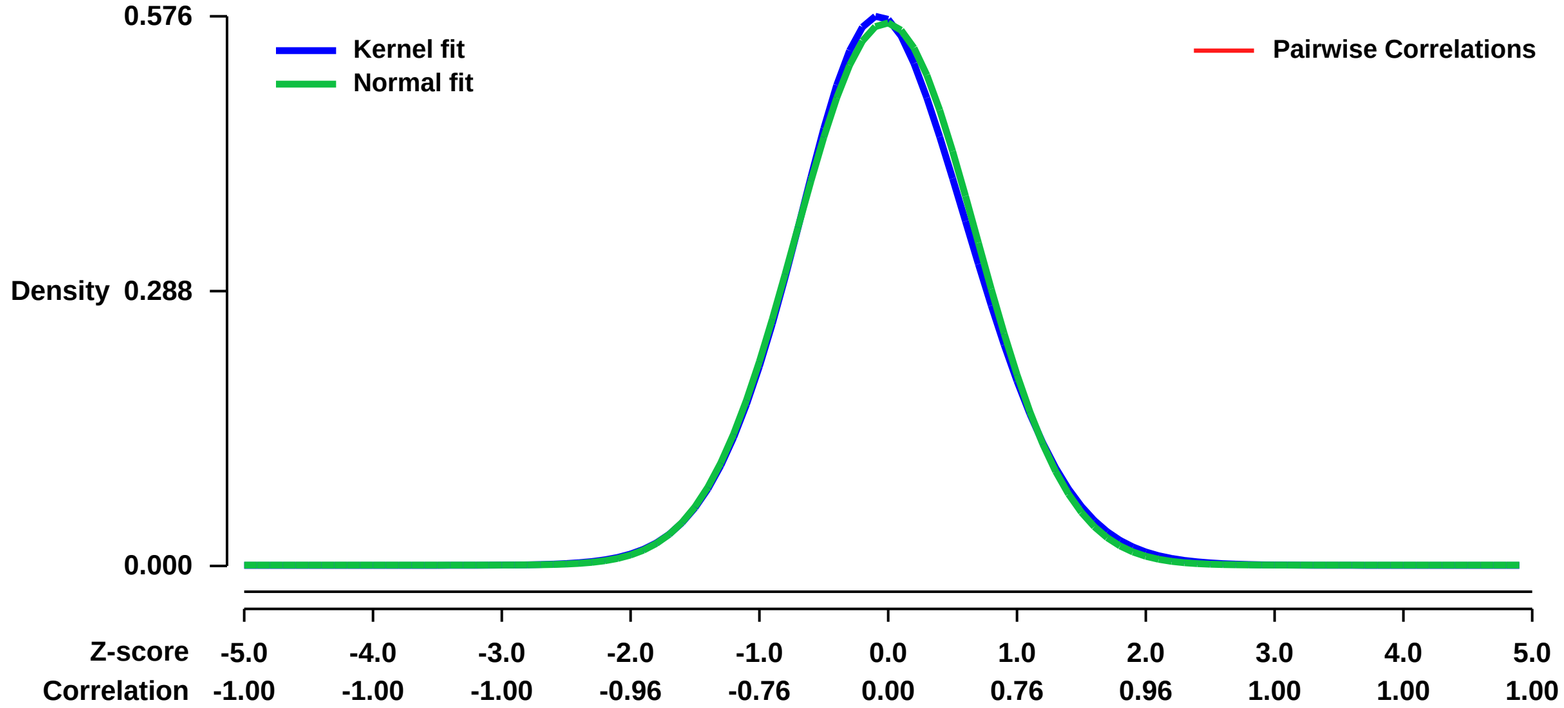

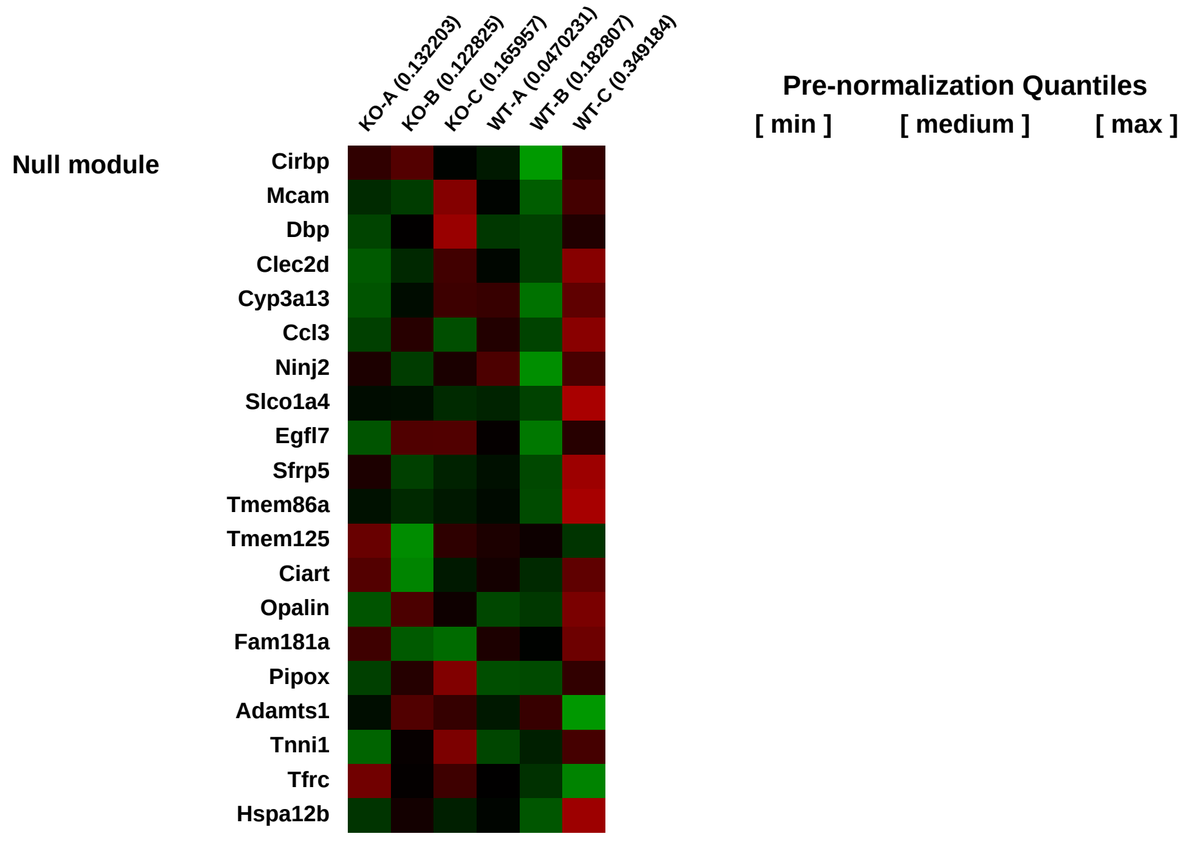

GEO Series "GSE45744" Expression Profiles

Num of samples in this series: 12

Scale of expression profile Z-scores

-3.0 -2.0 -1.0 0.0 1.0 2.0 3.0

GEO Link:	http://www.ncbi.nlm.nih.gov/geo/query/acc.cgi?acc=GSE45744
Status:	Public on Apr 04 2013
Title:	Whole-genome expression data from normal FVB mouse lung tissue, transgenic cyclin E overexpressing (CEO) normal mouse lung tissue, and transgenic CEO lung adeno
Organism:	Mus musculus
Experiment type:	Expression profiling by array
Platform:	GPL1261
Pubmed ID:	23621985
Summary & Design:	**Summary:** FVB mice were engineered to express wild-type human cyclin E under control of the human surfactant C promoter (CEO mice; Ma et al, PNAS 2007). These mice develop spontaneous lung tumors, which were shown to be adenocarcinoma by histological analysis. Here we compare whole-genome RNA expression levels between the tumors and normal lung of 4 CEO mice as well as 4 nontransgenic animals. **Overall design:** RNA was isolated from the lungs of 4 FVB mice and adjacent normal and tumor tissue from 4 FVB transgenes harboring human surfactant protein C- driven wild-type human cyclin E, all 7-11 months in age. These samples were divided into 3 groups of four, and 12 independent hybridizations were performed for analysis with Affymetrix GeneChip Mouse 430 2.0 arrays.

Background corr dist: KL-Divergence = 0.0712, L1-Distance = 0.0260, L2-Distance = 0.0008, Normal std = 0.5016

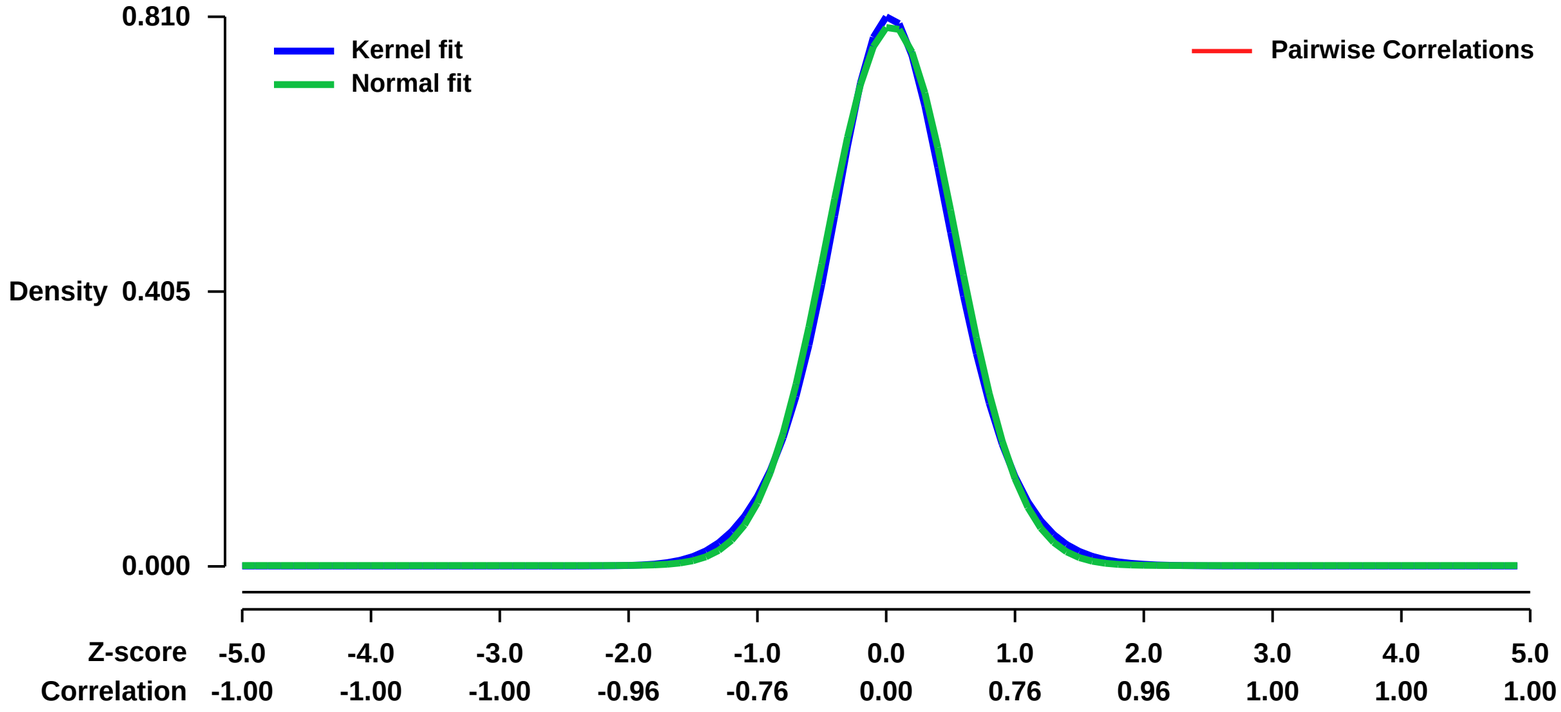

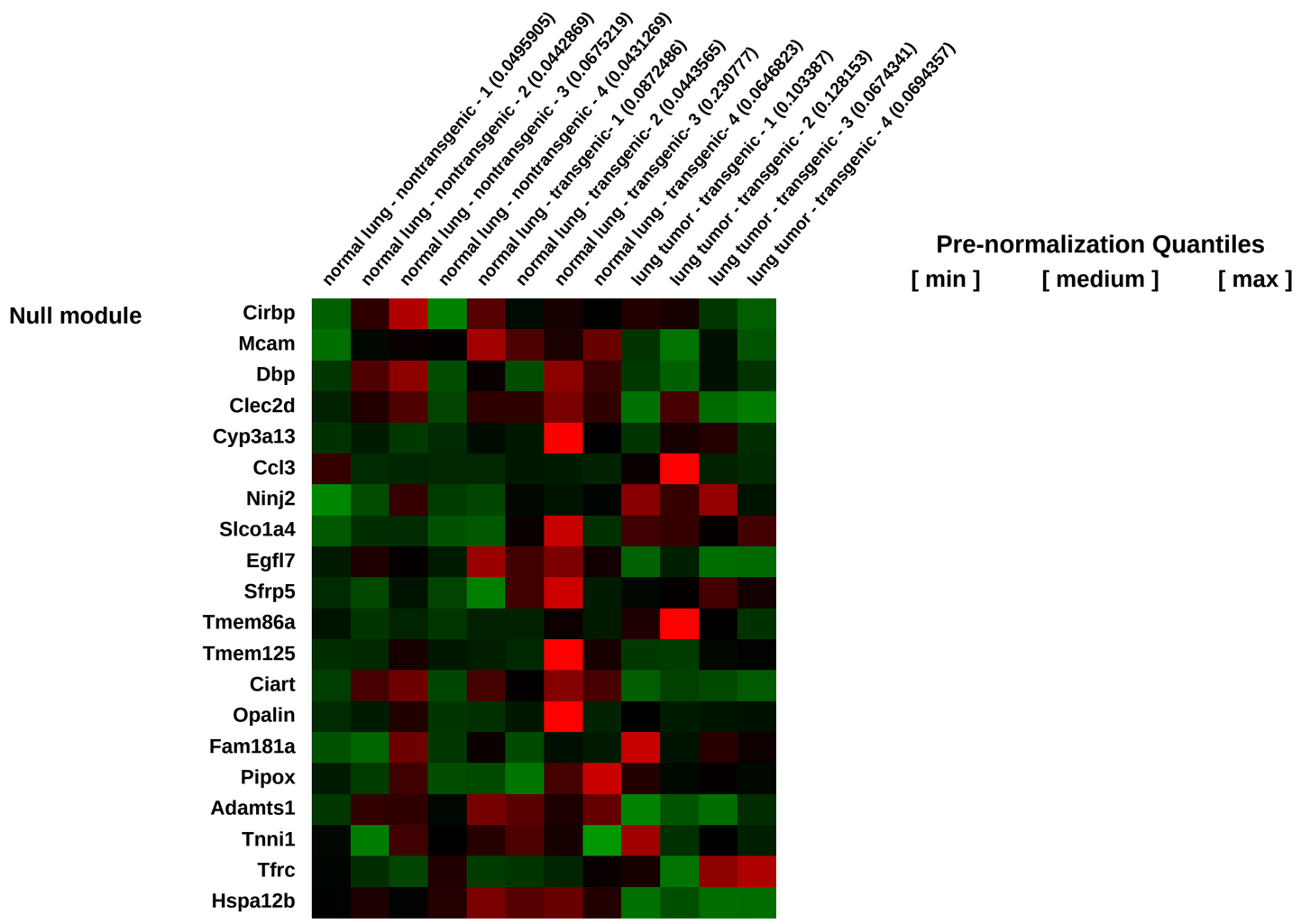

GEO Series "GSE11194" Expression Profiles

Num of samples in this series: 9

Scale of expression profile Z-scores

-3.0 -2.0 -1.0 0.0 1.0 2.0 3.0

GEO Link:	http://www.ncbi.nlm.nih.gov/geo/query/acc.cgi?acc=GSE11194
Status:	Public on Sep 01 2008
Title:	GATA4 conditional knockout in the small intestine
Organism:	Mus musculus
Experiment type:	Expression profiling by array
Platform:	GPL1261
Pubmed ID:	18812176
Summary & Design:	**Summary:** Background and Aims: Although the zinc finger transcription factor GATA4 has been implicated in regulating jejunal gene expression, the contribution of GATA4 in controlling jejunal physiology has not been addressed. Methods: We generated mice in which the Gata4 gene was specifically deleted in the small intestinal epithelium. Measurements of plasma cholesterol and phospholipids, intestinal absorption of dietary fat and cholesterol, and gene expression were performed on these animals. Results: Mice lacking GATA4 in the intestine displayed a dramatic block in their ability to absorb cholesterol and dietary fat. Comparison of the global gene expression profiles of control jejunum, control ileum, and GATA4 null jejunum by gene array analysis demonstrated that GATA4 null jejunum lost expression of 53% of the jejunal-specific gene set and gained expression of 47% of the set of genes unique to the ileum. These alterations in gene expression included a decrease in mRNAs encoding lipid and cholesterol transporters as well as an increase in mRNAs encoding proteins involved in bile acid absorption. Conclusion: Our data demonstrate that GATA4 is essential for jejunal function including fat and cholesterol absorption and confirm that GATA4 plays a pivotal role in determining jejunal versus ileal identity. **Keywords:** genetic modification **Overall design:** Jejunum was defined as 10 cm from the pyloric sphincter, and ileum was defined as 1 cm from the cecum. The animals used to harvest control jejunum and ileum were independent of each other.

Background corr dist: KL-Divergence = 0.0854, L1-Distance = 0.0221, L2-Distance = 0.0008, Normal std = 0.4649

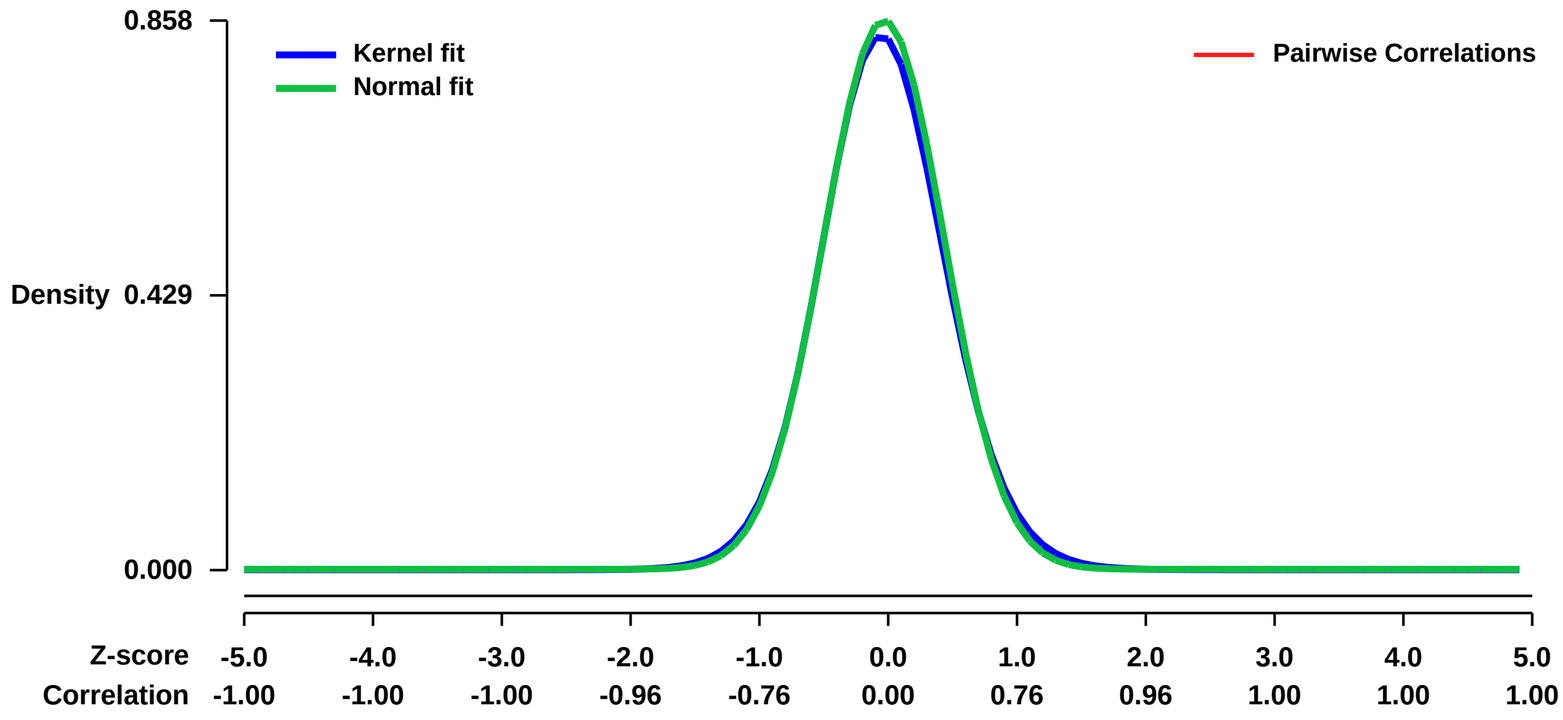

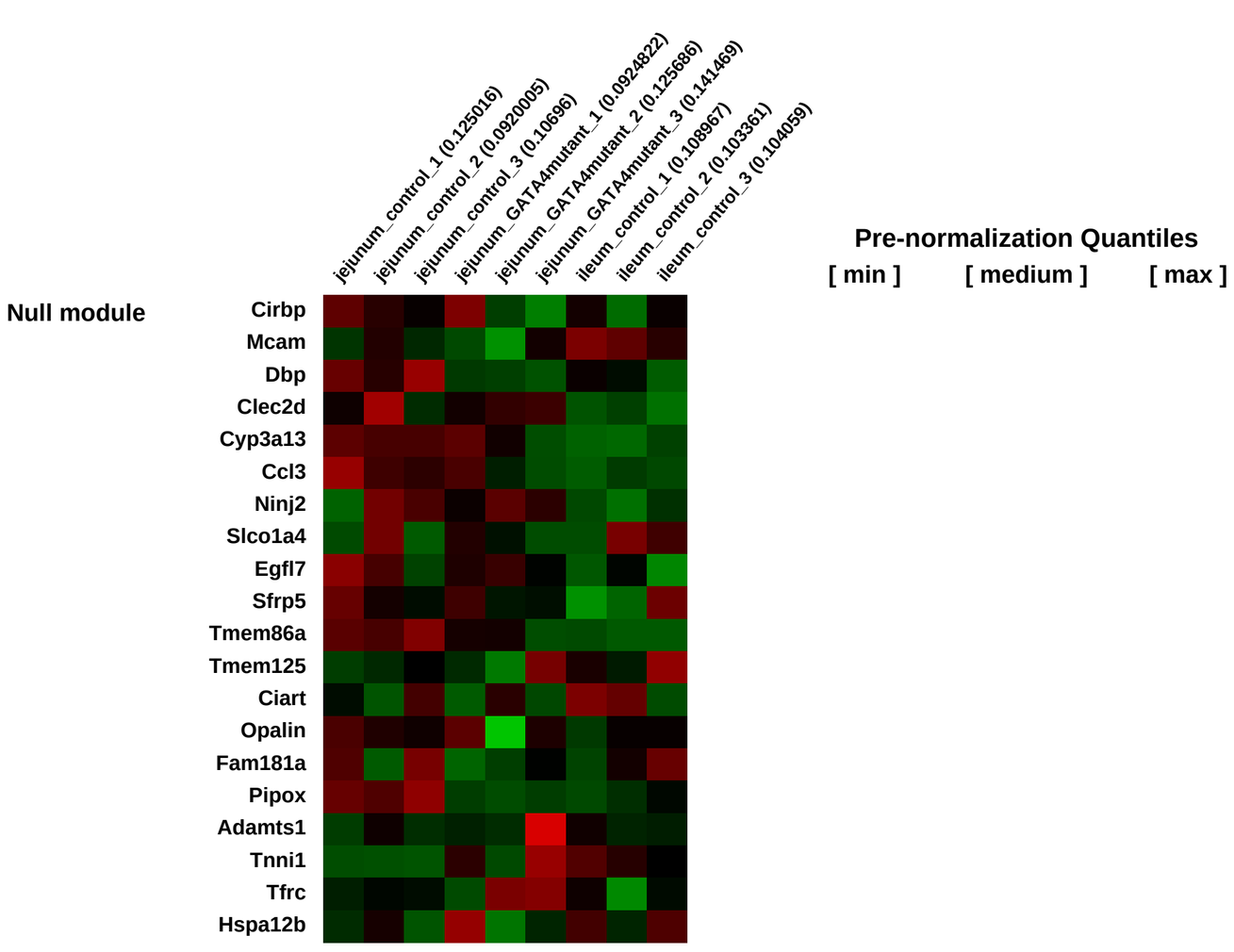

GEO Series "GSE15891" Expression Profiles

Num of samples in this series: 8

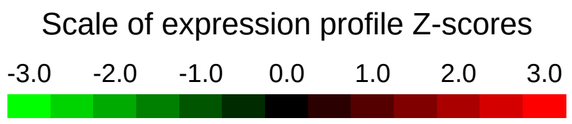

GEO Link:	**http://www.ncbi.nlm.nih.gov/geo/query/acc.cgi?acc=GSE15891**
Status:	**Public on Apr 30 2009**
Title:	**Gene expression of Mus exposed to chronic hypoxia**
Organism:	**Mus musculus domesticus**
Experiment type:	**Expression profiling by array**
Platform:	**GPL1261**
Pubmed ID:	**20103700**
Summary & Design:	**Summary:** **High altitude environments are characterized by the unique and unavoidable stress of chronic hypoxia. While much is known about gene expression responses to acute or in vitro hypoxia, less is known about the gene expression profiles of animals exposed to systemic chronic hypoxia, such as that experienced at high elevations. Here we simulated the hypoxic environment of two high altitude elevations,and a third chamber recieved ambient Reno air. Mice were housed in the hypoxic chambers for 32 days.** **We used microarrays to characterize the differential gene expression in the livers of mice housed in hypoxic environment of 4500 m versus 3000 and 1400 m. We used this data to draw hypotheses related to novel physiological responses to chronic systemic hypoxia** **Overall design:** **Mice were housed one of three chambers; the first received ambient Reno air (1400 m) and the other two received air mixed with nitrogen such that one chamber simulated the hypoxic environment of 3000 m and the third chamber simulated hypoxic environment of 4500 m. Twelve mice were housed in each chamber for 32 days. Liver were extracted, and RNA from livers of 4 mice were pooled such that each treatment was represented by 3 pooled samples.**

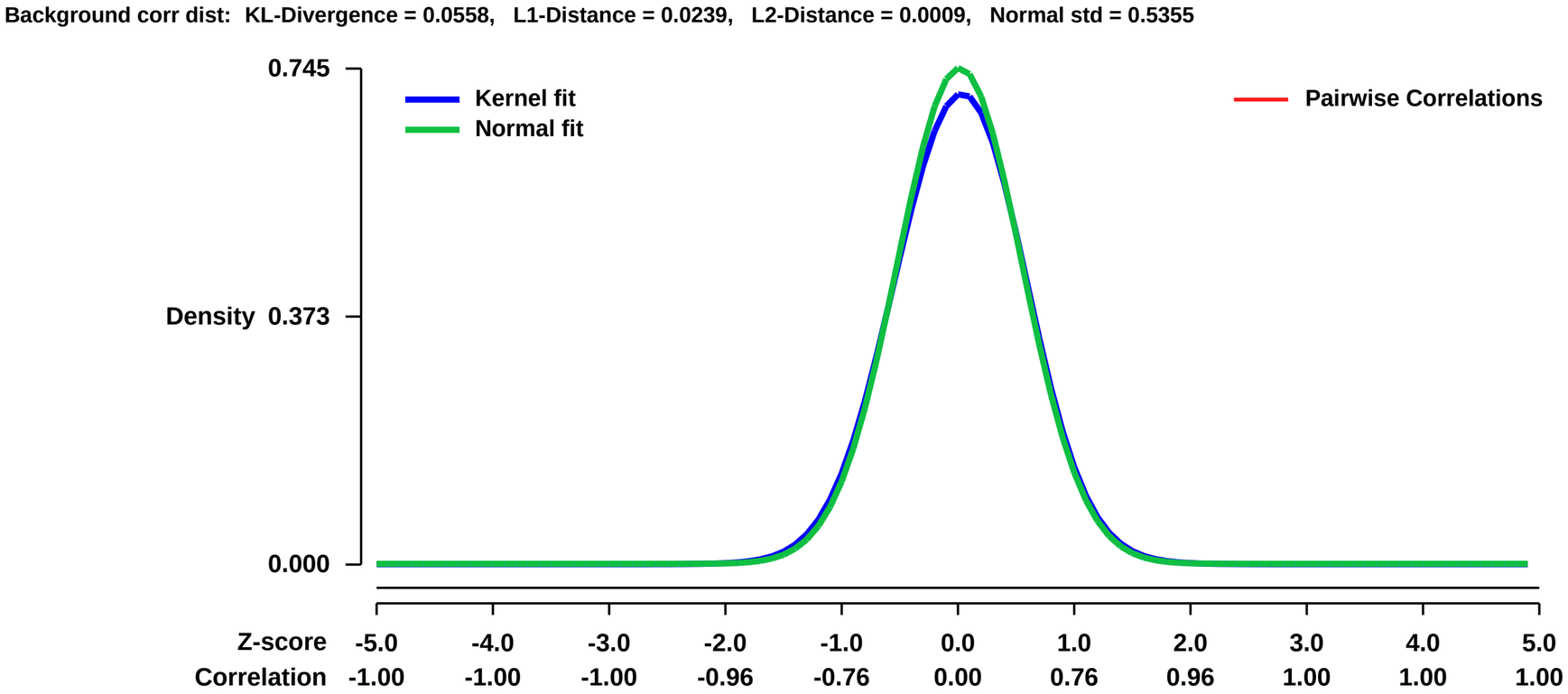

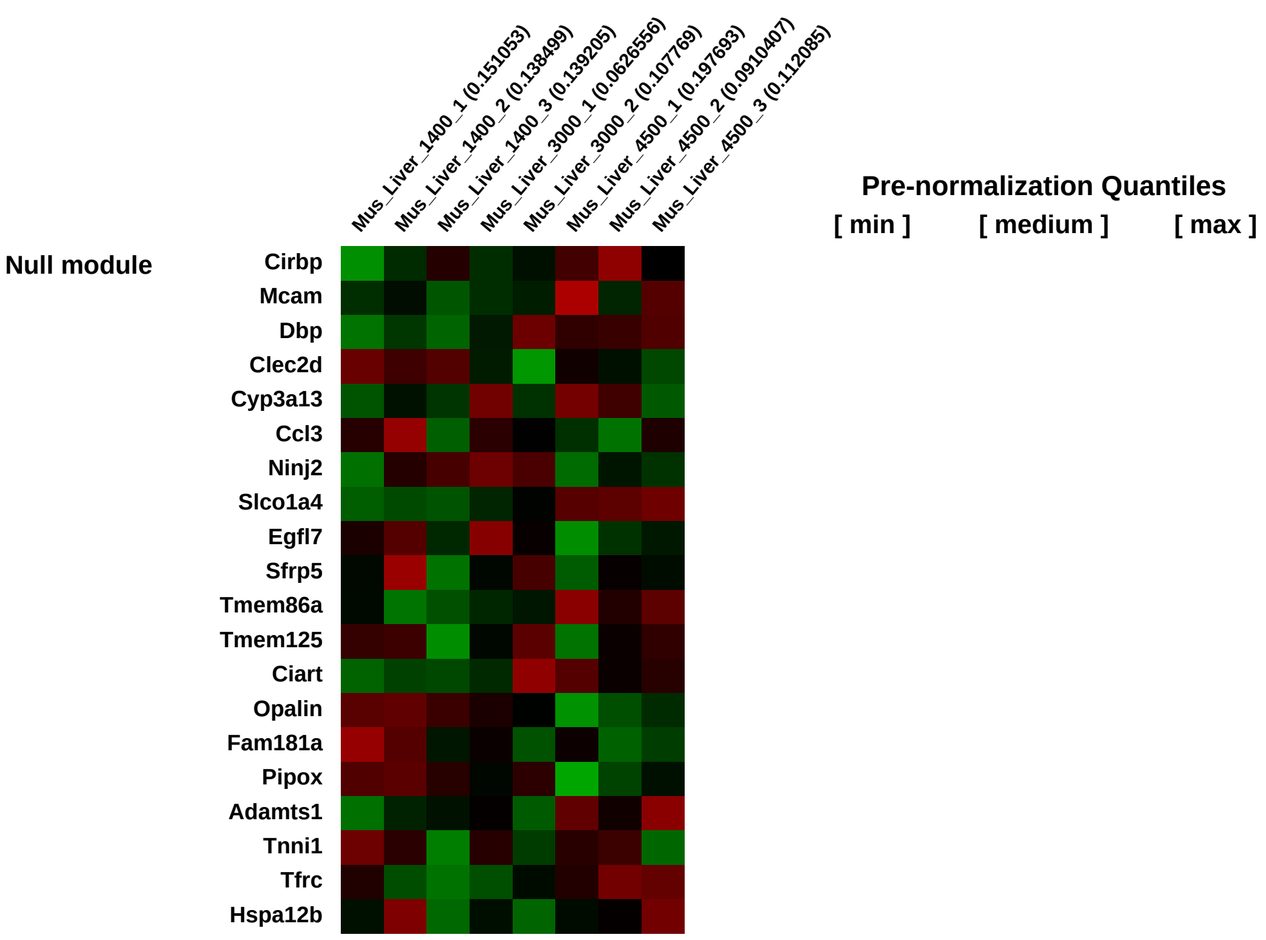

GEO Series "GSE18771" Expression Profiles

Num of samples in this series: 6

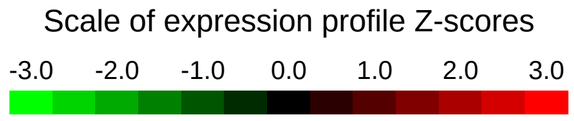

GEO Link:	**http://www.ncbi.nlm.nih.gov/geo/query/acc.cgi?acc=GSE18771**
Status:	**Public on Nov 04 2009**
Title:	**Mouse KIAA1718 knockdown ES cells**
Organism:	**Mus musculus**
Experiment type:	**Expression profiling by array**
Platform:	**GPL1261**
Pubmed ID:	
Summary & Design:	**Summary:** **Compare the gene expression profiles of ESCs stably expressing control and KIAA1718 short hairpin RNA, using Affymetrix microarray.** **Overall design:** **Mouse ES cells R1 were transformed with the respective lenti-virus expressing Luc shRNA or KIAA1718 shRNA1. The transformed ES cells were sorted for GFP. Total RNAs were extracted from cells using Trizol reagent (Invitrogen, Carlsbad, CA). For microarray experiments, RNA was processed and hybridized to Mouse Genome 430 2.0 arrays (Affymetrix) according to the manifactureâ s instruction.**

Background corr dist: **KL-Divergence = 0.0460, L1-Distance = 0.0328, L2-Distance = 0.0017, Normal std = 0.5977**

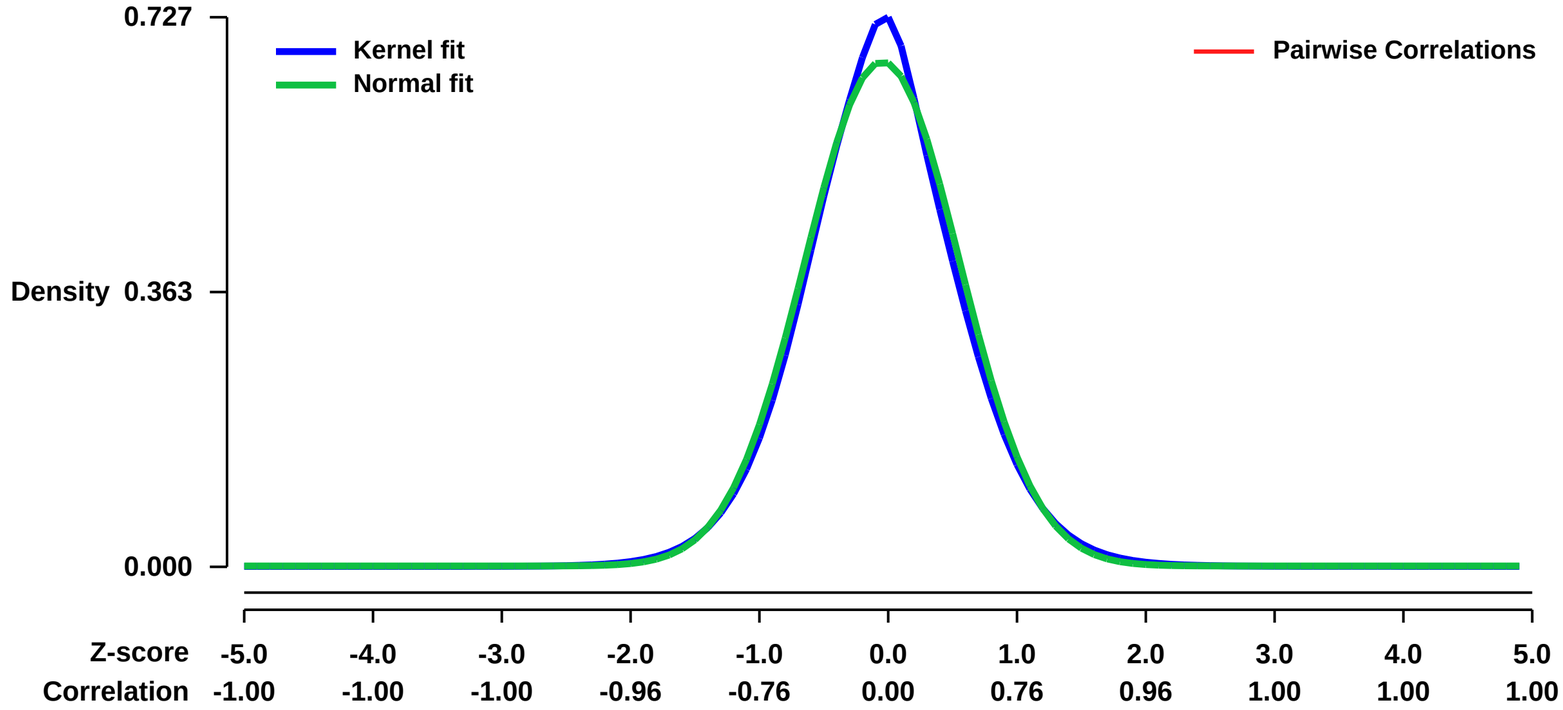

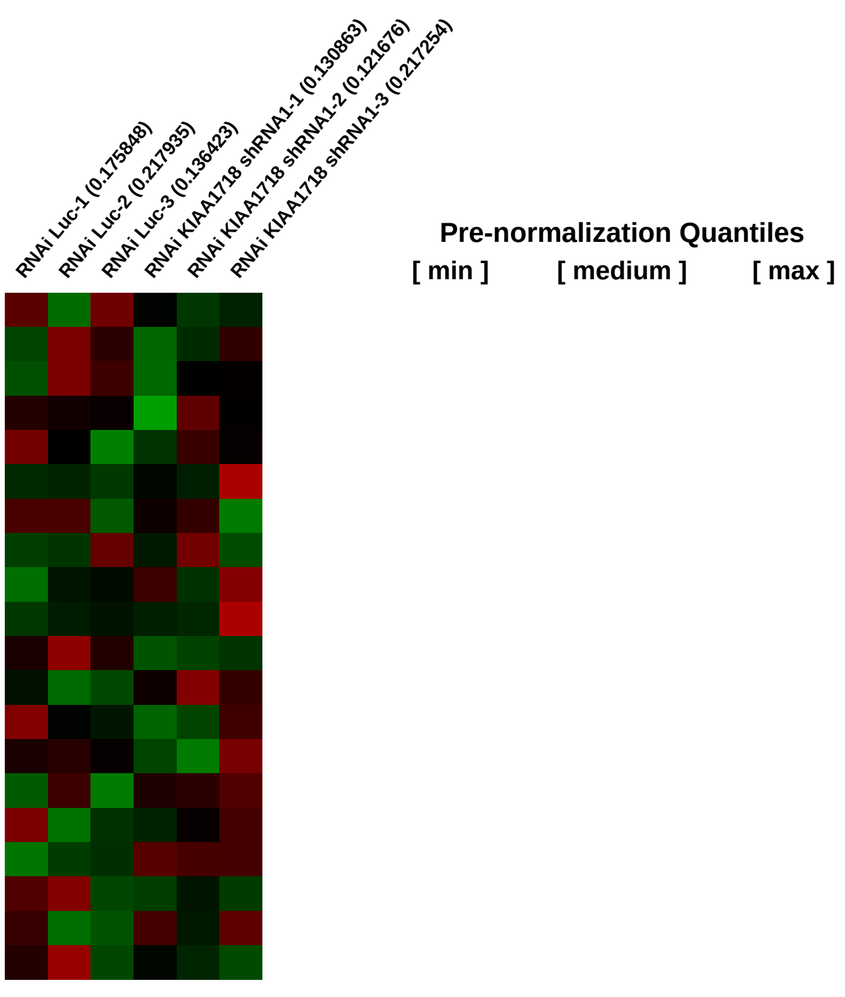

GEO Series "GSE8681" Expression Profiles

Num of samples in this series: 25

Scale of expression profile Z-scores

-3.0 -2.0 -1.0 0.0 1.0 2.0 3.0

GEO Link:	http://www.ncbi.nlm.nih.gov/geo/query/acc.cgi?acc=GSE8681
Status:	Public on Jan 11 2008
Title:	Gene expression in mouse 3T3-L1 adipocyte tissue culture treated with CLA
Organism:	Mus musculus
Experiment type:	Expression profiling by array
Platform:	GPL1261
Pubmed ID:	17878318
Summary & Design:	**Summary:** Trans-10, Cis-12 conjugated linoleic acid (t10c12 CLA) causes fat loss in mouse 3T3-L1 adipocyte tissue culture. The early transcriptome changes were analyzed using high-density microarrays to better characterize the signaling pathways responding to t10c12 CLA. Their gene expression responses between 4 to 24 hr after treatment showed a common set of early gene expression changes indicative of an integrated stress response (ISR). **Keywords: control/treatment time course** **Overall design:** Mouse 3T3-L1 RNA for each time point was isolated from control and treatment samples for analysis on microarrays with two to four biological reps.

Background corr dist: KL-Divergence = 0.1410, L1-Distance = 0.0407, L2-Distance = 0.0032, Normal std = 0.3886

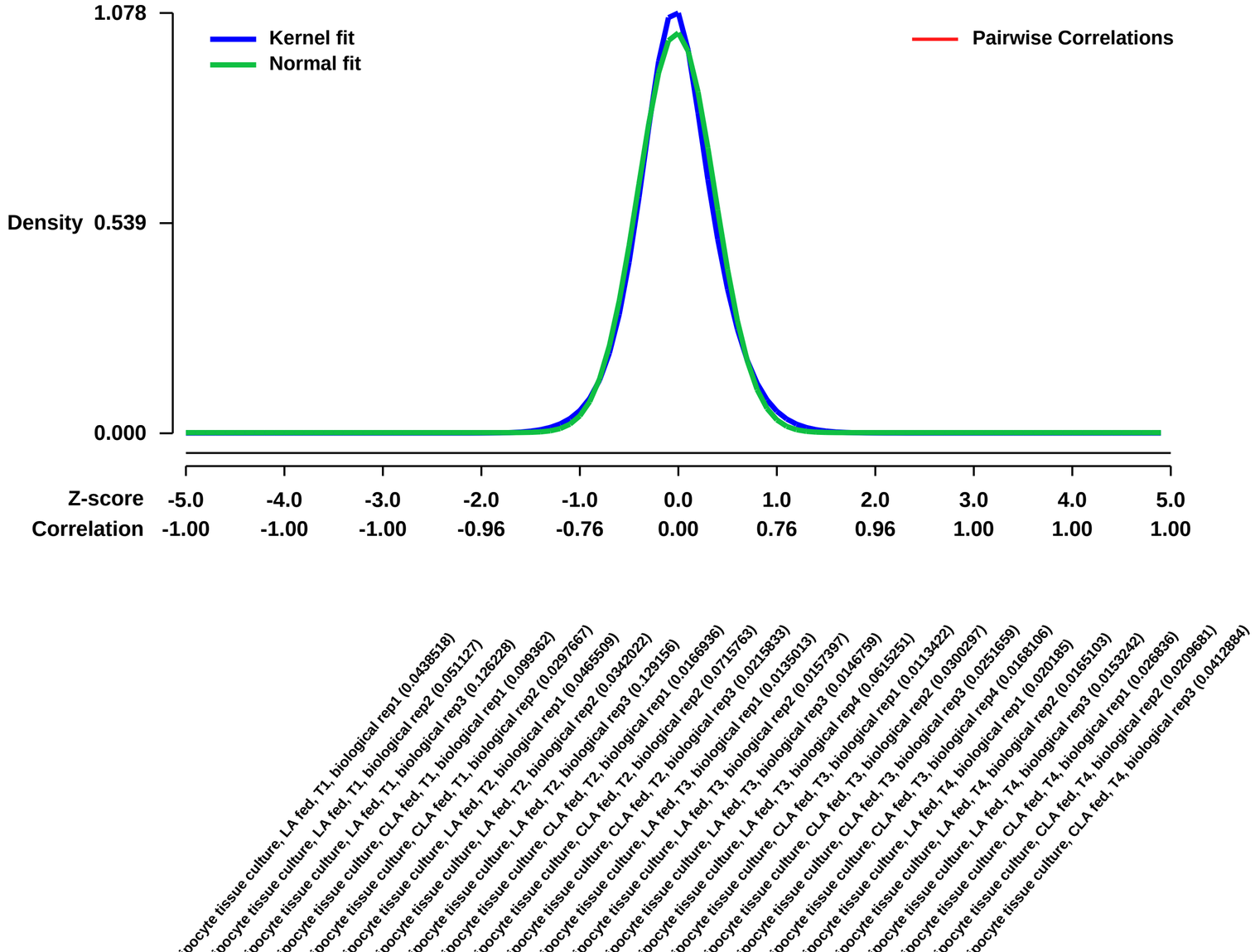

GEO Series "GSE13807" Expression Profiles

Num of samples in this series: 10

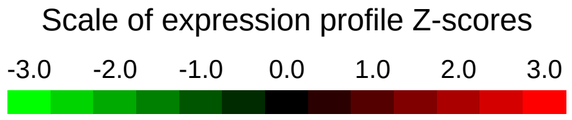

GEO Link:	**http://www.ncbi.nlm.nih.gov/geo/query/acc.cgi?acc=GSE13807**
Status:	**Public on Jan 31 2011**
Title:	**Identification and validation of gene expression changes upon removal of Dicer in the murine limb mesenchyme**
Organism:	**Mus musculus**
Experiment type:	**Expression profiling by array**
Platform:	**GPL1261**
Pubmed ID:	
Summary & Design:	**Summary:** **Wild type and Dicer null embryonic mouse limbs were analaysed using Affymetrix arrays to identify gene expression changes. Genes that were up-regulated in Dicer-null limbs were canidates for being miRNA targets.** **Potential miRNA target genes were validated using qRTPCR.** **Overall design:** **Mice carrying a heterozygous Dicer floxed allele and the prxcre driver allele were crossed to homozygous Dicer Floxed mice. Embryos were harvested from pregent moms and genotyped to determine heterozygous, Wild type and mutant limb buds. These limb buds were used to prepare RNA for array analysis.**

Background corr dist: **KL-Divergence = 0.0730, L1-Distance = 0.0212, L2-Distance = 0.0005, Normal std = 0.4901**

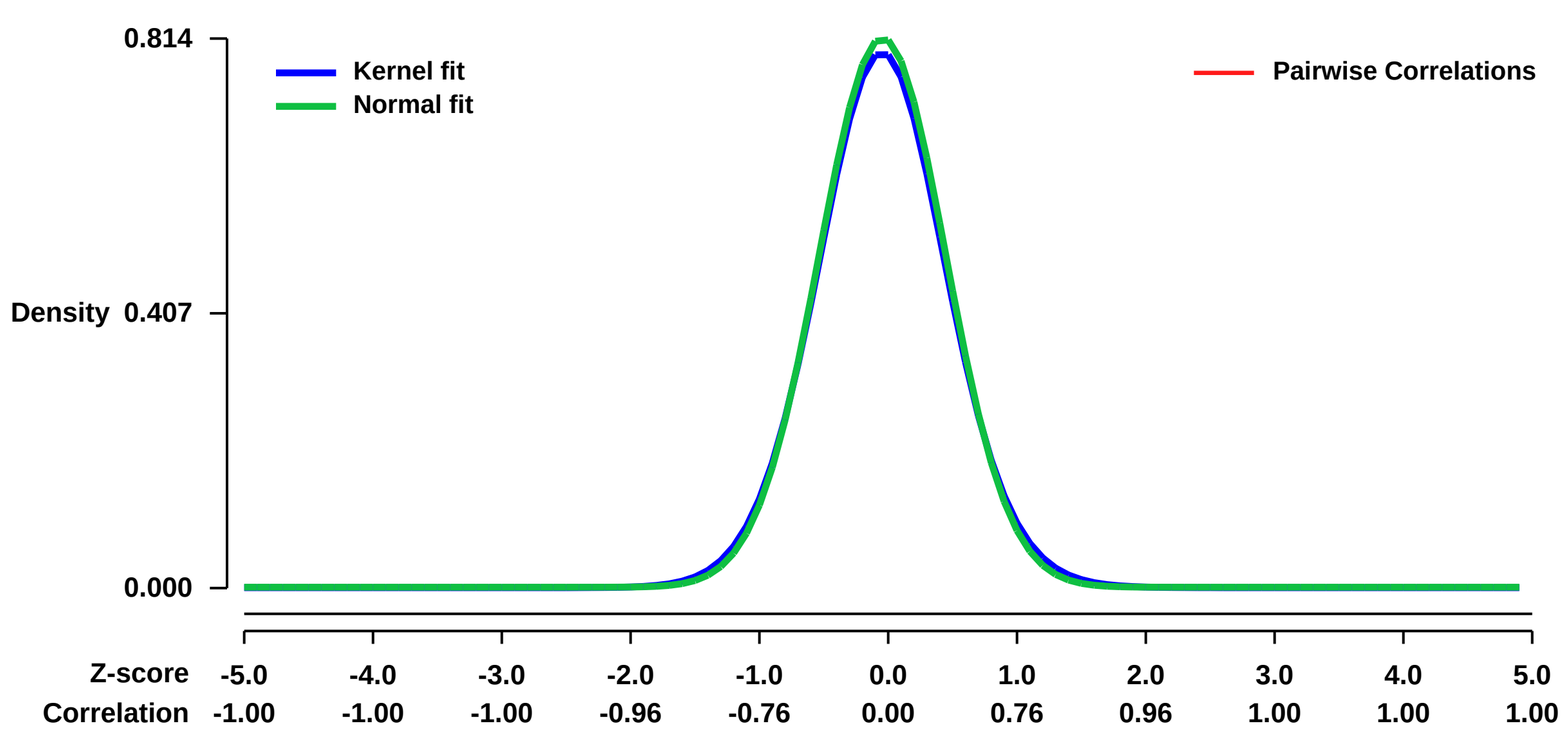

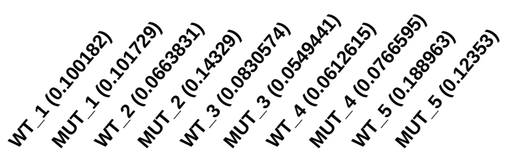

Pre-normalization Quantiles

[min] [medium] [max]

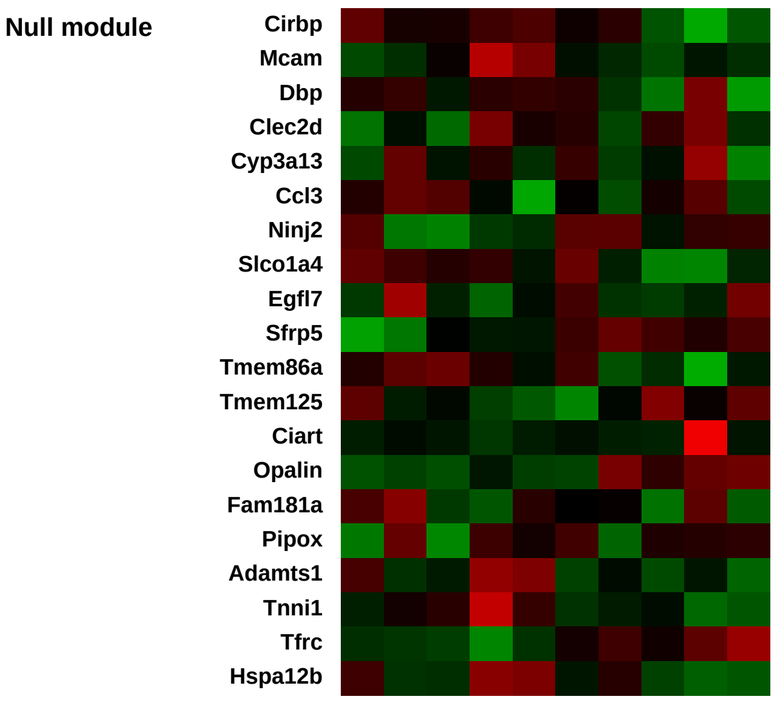

GEO Series "GSE13010" Expression Profiles

Num of samples in this series: 20

Scale of expression profile Z-scores

-3.0 -2.0 -1.0 0.0 1.0 2.0 3.0

GEO Link: http://www.ncbi.nlm.nih.gov/geo/query/acc.cgi?acc=GSE13010

Status: Public on Nov 01 2008

Title: Heat shock effects on testes from C57BL/6 and AKR/N mouse strains

Organism: Mus musculus

Experiment type: Expression profiling by array

Platform: GPL1261

Pubmed ID:

Summary & Design:

Summary:
Cryptorchidism and scrotal heating result in abnormal spermatogenesis but the mechanism(s) proscribing this temperature sensitivity are unknown. It was previously reported that the AKR/N or MRL/MpJ-+/+ mouse testis is more heat resistant than the testis from the C57BL/6 strain. We have attempted to probe into the mechanism(s) involved in heat sensitivity by examining global gene expression profiles of normal and heat-treated testes from C57BL/6, AKR/N and MRL/MpJ-+/+ mice by microarray analysis. In the normal C57BL/6 testis, 415 and 416 transcripts were differentially expressed (at least two-fold higher or lower) when compared to the normal AKR/N and MRL/MpJ-+/+ testis, respectively. The AKR/N and MRL/MpJ-+/+ strains revealed 268 differentially expressed transcripts between them. There were 231 transcripts differentially expressed between C57BL/6 and two purported heat-resistant strains, AKR/N and MRL/MpJ-+/+. Next, the testes of C57BL/6 and AKR/N mice were exposed to 43´"C for 15 min and harvested at different time points for TUNEL studies and microarrays. An increase of TUNEL-positive germ cell numbers was significant 8 hr after heat exposure in the C57BL/6 mouse. However, this increase was not observed in the AKR/N mouse until 10 hr after heat exposure. All tubules showed germ cell loss and disruption in C57BL/6 testis 24 hr after heat shock. In contrast, although a number of seminiferous tubules showed an abnormal morphology 24 hr post-heat shock in the AKR/N mouse, many tubules still retained a normal structure. Numerous transcripts exhibited differential regulation between the two strains within 24 hours after heat exposure. The differentially expressed transcripts in the testes 8 hr after heat exposure were targeted to identify the genes involved in the initial response rather than those due to germ cell loss. Twenty transcripts were significantly down-regulated and 19 genes were up-regulated by hyperthermia in C57BL/6 and did not show a parallel change in the AKR/N testis. Conversely, heat shock resulted in 30 up-regulated transcripts and 31 down-regulated transcripts in AKR/N that were not similarly regulated in C57BL/6. A number of genes shared similar differential expression patterns and differential regulation by hyperthermia in both strains of mice. Taken together, the present study indicates the diverse genetic backgrounds in the three strains lead to major differences in normal testis gene expression profiles while the differences in heat shock responses involves a significantly smaller number of genes. The data generated may provide insights regarding gene networks and pathways involved in heat stress and their relationship to spermatogenesis.

Overall design:
Total RNA of testes from two different strains of mice, C57BL/6 and AKR/N were analyzed using microarray 430.20 chip. Duplicates were used in controls and treated samples at 8hr, 10hr, 12hr, 24hr after heat shock at 43C for 15 min. All mice were 8 weeks old.

Background corr dist: KL-Divergence = 0.1793, L1-Distance = 0.0324, L2-Distance = 0.0017, Normal std = 0.3508

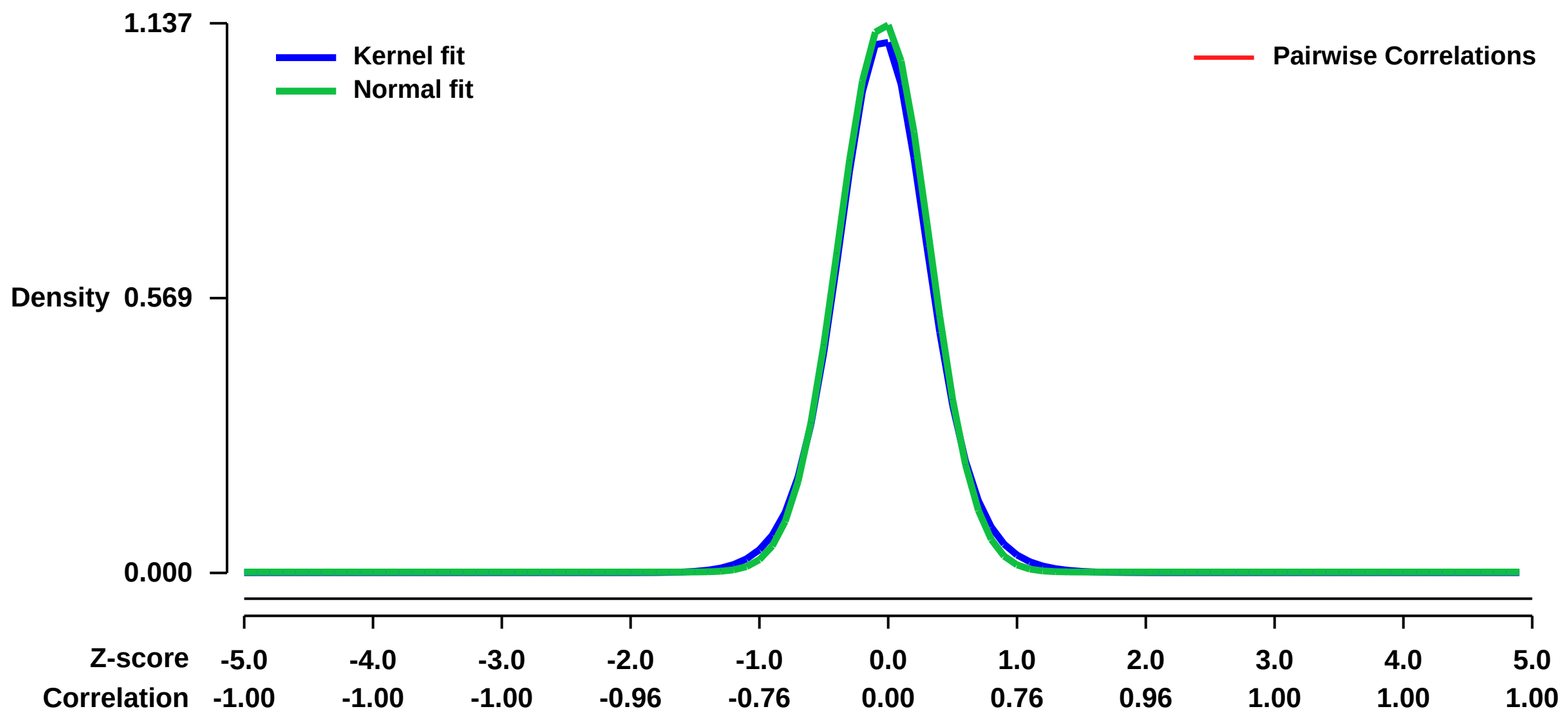

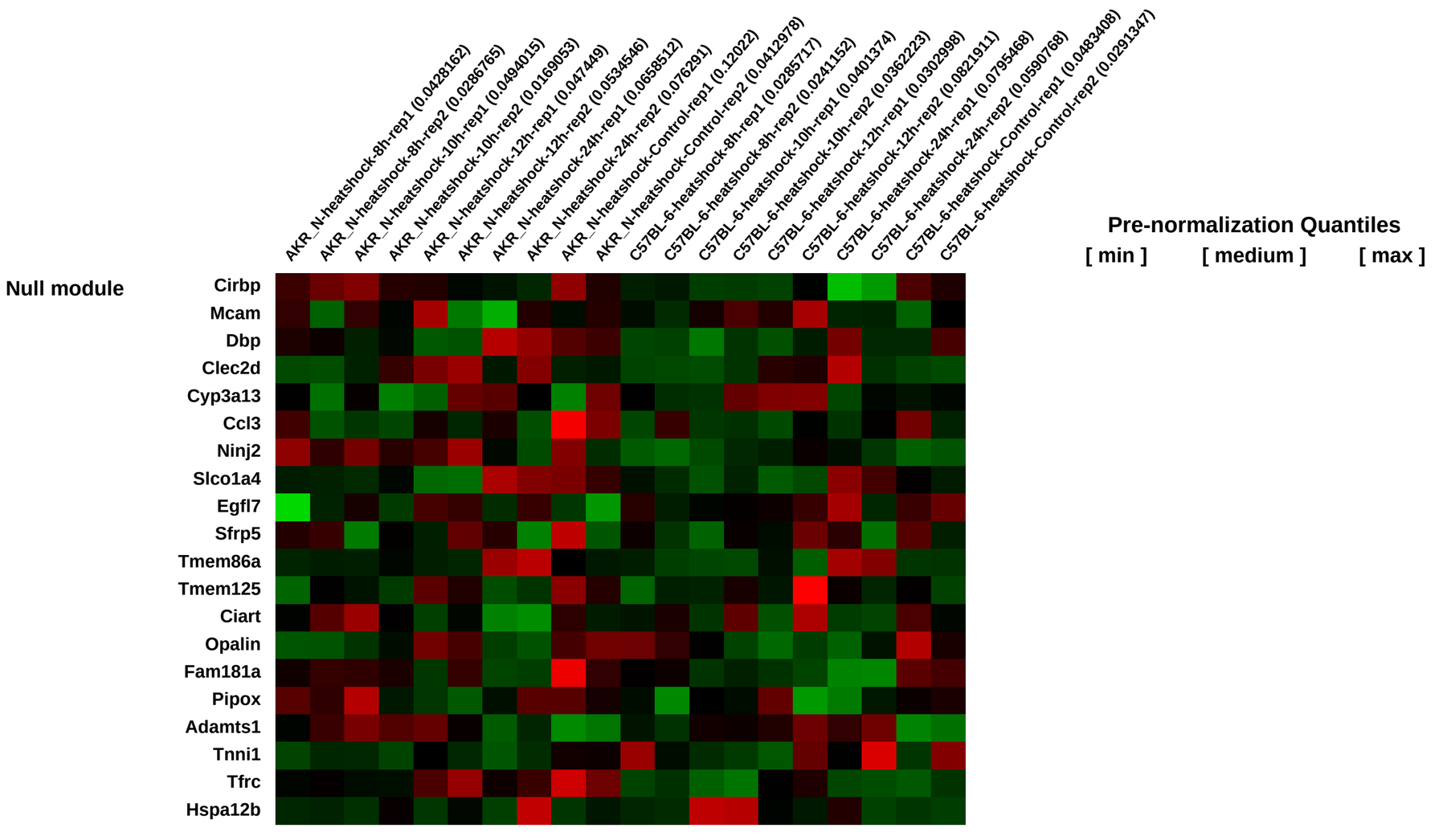

GEO Series "GSE56492" Expression Profiles

Num of samples in this series: 12

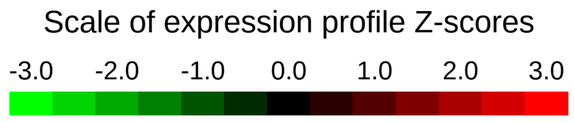

GEO Link:	**http://www.ncbi.nlm.nih.gov/geo/query/acc.cgi?acc=GSE56492**
Status:	**Public on Apr 15 2014**
Title:	**Identification of targets regulated by MLL1 in response to HSP90 inhibitors**
Organism:	**Homo sapiens**
Experiment type:	**Expression profiling by array**
Platform:	**GPL1261**
Pubmed ID:	
Summary & Design:	**Summary:** **MLL1 WT or KO MEF with and without HSP90 inhibitor treatment** **Overall design:** **MEF cells were seeded in 6-well plates for 3d with 100ng/ml doxycycline prior to treatment with 0.1% DMSO or 100nM AUY922 for 3h**

Background corr dist: **KL-Divergence = 0.0311, L1-Distance = 0.0822, L2-Distance = 0.0115, Normal std = 0.7736**

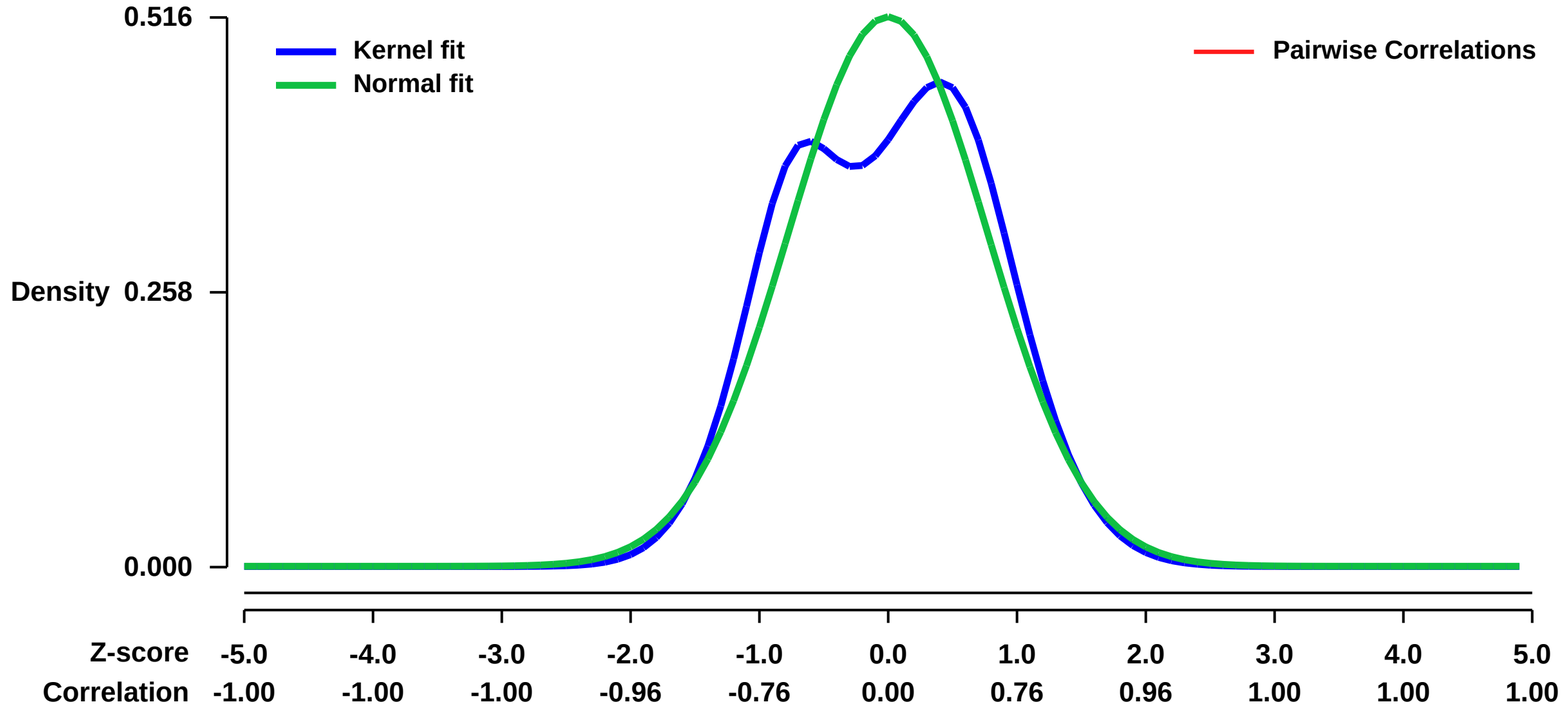

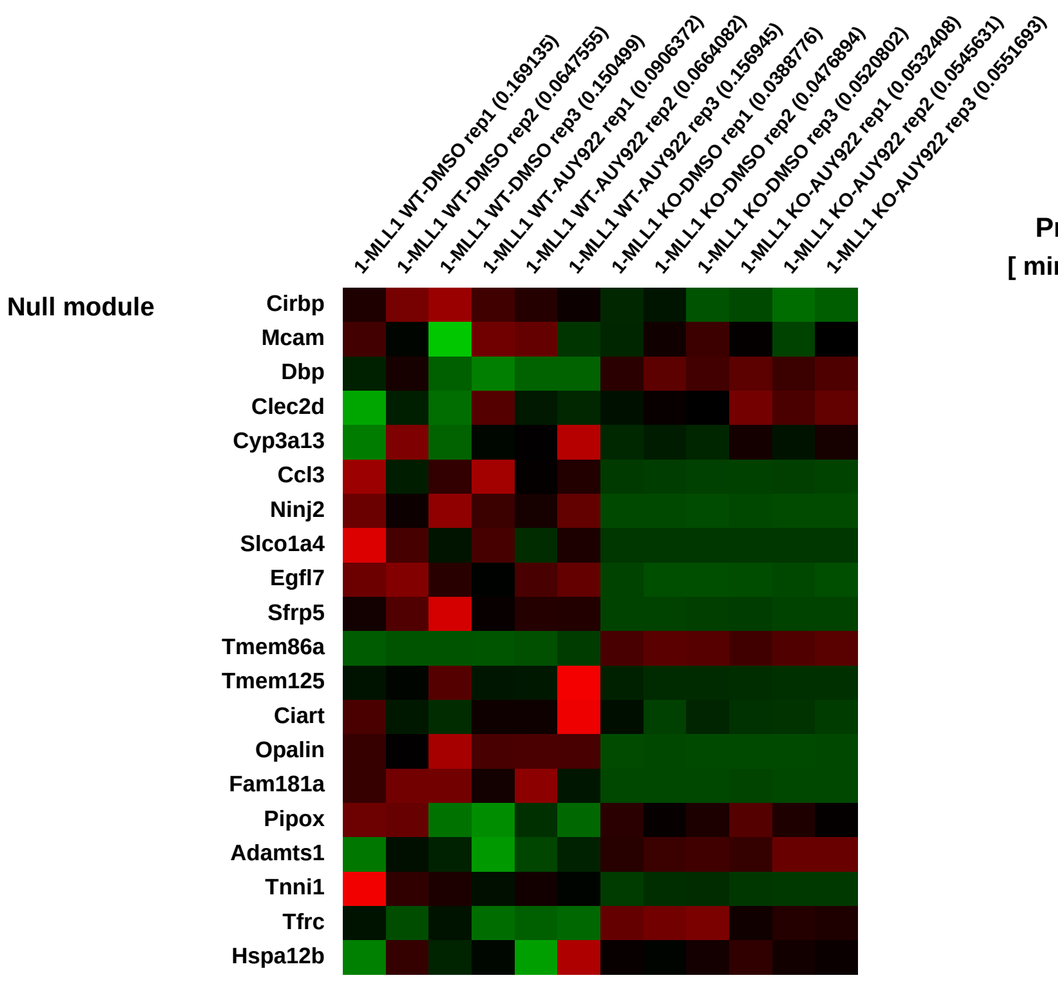

GEO Series "GSE14101" Expression Profiles

Num of samples in this series: 10

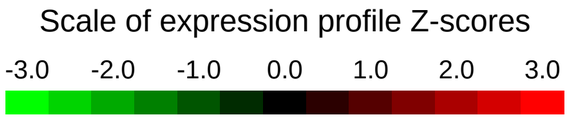

GEO Link:	**http://www.ncbi.nlm.nih.gov/geo/query/acc.cgi?acc=GSE14101**
Status:	**Public on Dec 23 2008**
Title:	**Genes regulated by Meis1 in murine Mll-AF9 leukemia cells**
Organism:	**Mus musculus**
Experiment type:	**Expression profiling by array**
Platform:	**GPL1261**
Pubmed ID:	**19109563**
Summary & Design:	**Summary:** **Leukemias with MLL-rearrangements are characterized by high expression of the homeo box gene MEIS1. In these studies, we knocked down Meis1 expression by shRNA lentivirus transduction in murine Mll-AF9 leukemia cells. Meis1 knockdown resulted in decreased proliferation and survival of murine Mll-AF9 leukemia cells. We also observed reduced clonogenic capacity and increased monocytic differentiation. The establishment of leukemia in transplant recipients was significantly delayed by Meis1 knockdown. Gene expression profiling of cells transduced with Meis1 shRNA showed reduced expression of genes associated with cell cycle entry and progression. shRNA mediated knockdown of MEIS1 in human MLL-fusion gene leukemia cell lines resulted in reduced cell growth. These results show that MEIS1 expression is important for MLL-rearranged leukemias and suggest that MEIS1 promotes cell cycle entry. Targeting MEIS1 may have therapeutic potential for treating leukemias expressing this transcription factor.** **Keywords: Gene expression** **Overall design:** **Murine Mll-AF9 leukemia (4166) cells were transduced with lentivirus expressing shRNA against Meis1 or control lentivirus (empty vector). Gene expression profiles were compared at 48 hours post transduction, using Puromycin as selection agent for transduced cells.**

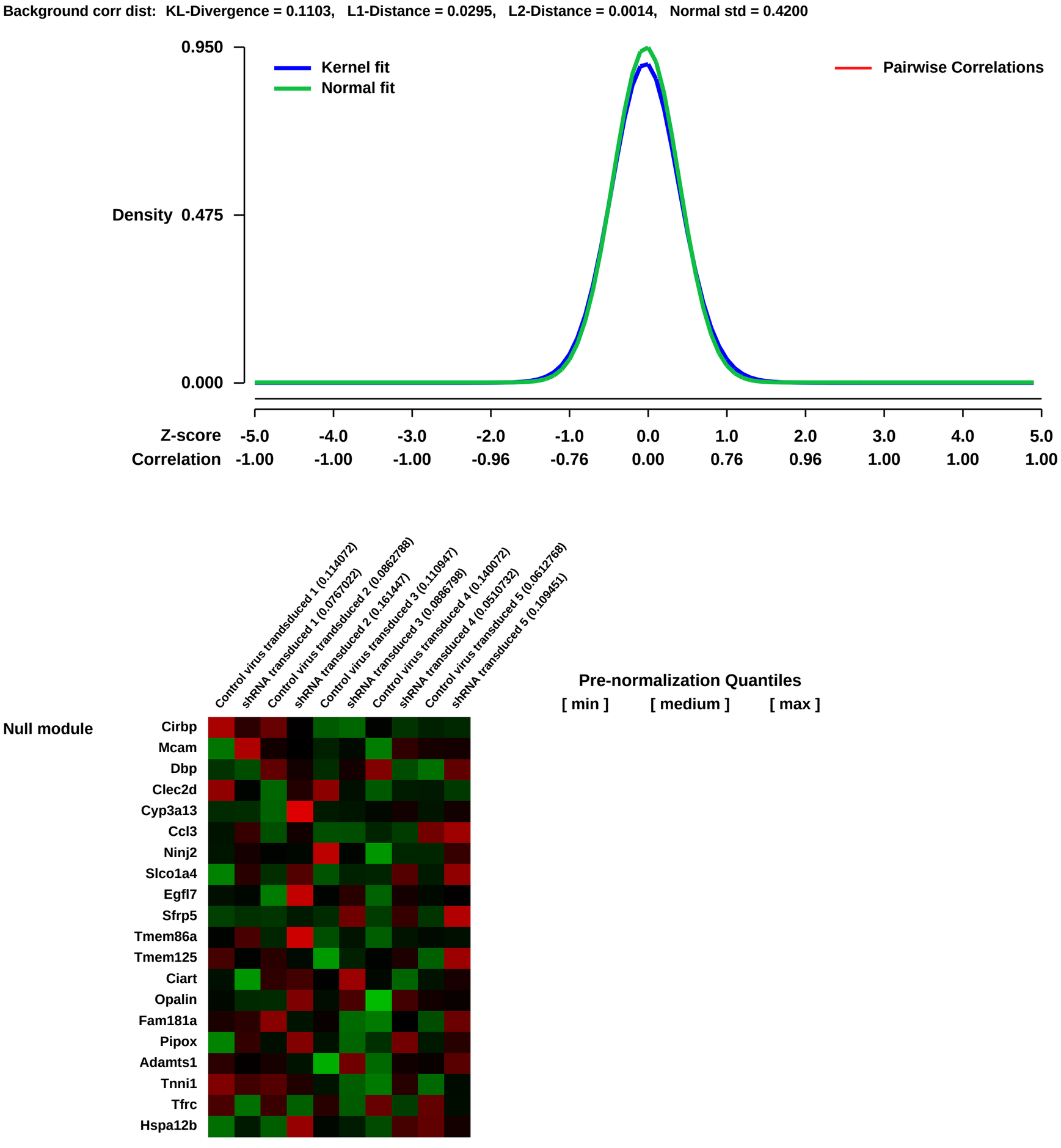

GEO Series "GSE35206" Expression Profiles

Num of samples in this series: 14

Scale of expression profile Z-scores

-3.0 -2.0 -1.0 0.0 1.0 2.0 3.0

GEO Link:	http://www.ncbi.nlm.nih.gov/geo/query/acc.cgi?acc=GSE35206
Status:	Public on Dec 05 2012
Title:	Specific transcriptional response of four blockers of estrogen receptors on estradiol-modulated genes in the mouse mammary gland
Organism:	Mus musculus
Experiment type:	Expression profiling by array
Platform:	GPL1261
Pubmed ID:	22678160
Summary & Design:	**Summary:** The efficacy and exceptionally good tolerance of estrogen blockade in the treatment of breast cancer is well recognized but novel agents are required, especially to take advantage of the multiple consecutive responses obtained in breast cancer progressing following previous hormone therapy, thus delaying the use of cytotoxic chemotherapy with its usually serious side effects. Acolbifene (ACOL) is a novel and unique antiestrogen completely free of estrogen-like activity in both the mammary gland and uterus while preventing bone loss. From the preclinical and clinical data so-far available, this new antiestrogen represents a unique opportunity for a highly potent and specific blockade of estrogen action in the mammary gland and uterus while exerting estrogen-like beneficial effects in other tissues (selective estrogen receptor modulator or SERM activity). In order to better understand the specificity of action of acolbifene, we have used Affymetrix GeneChips containing 45,000 probe sets to analyze 34,000 genes to determine the specificity of this compound compared to the pure antiestrogen fulvestrant, as well as the mixed antagonists/agonists tamoxifen and raloxifene to block the effect of estradiol (E2) and to induce effects of their own on gene expression in the mouse mammary gland. The genes modulated by E2 were those identified in two separate experiments and validated by quantitative real-time PCR (Q_RT-PCR). Three hours after the single subcutaneous injection of E2 (0.05 ug), the simultaneous administration of acolbifene, fulvestrant, tamoxifen and raloxifene blocked by 98%, 62%, 43% and 92% the number of E2-upregulated genes, respectively. On the other hand, 70%, 10%, 25% and 55% of the genes down-regulated by E2 were blocked by the same compounds. Acolbifene was also the compound which, when used alone, modulated the smallest number of genes also influenced by E2, namely 4%, thus possibly explaining the potent tumoricidal action of this compound in human breast cancer xenografts where 61% of tumors disappeared, thus bringing a new paradigm in the hormonal therapy of breast cancer. **Overall design:** Female C57BL6 mice were ovariectomized (OVX). One week after OVX, mice were treated with EM-652.HCl (acolbifene), tamoxifen citrate, raloxifene or ICI 182780 (fulvestrant). Compounds were administered to OVX mice or to OVX mice simultaneously treated with 17b-estradiol (E2). Control groups received an injection of the vehicle alone. All animals were sacrificed after 3h of treatment.Mammary glands from all mice of the same group were collected and pooled. Total mRNA was isolated and converted to biotinylated cRNA.A microarray analysis was performed using Murine U74Av2 Affymetrix microarrays.

Background corr dist: KL-Divergence = 0.1067, L1-Distance = 0.0402, L2-Distance = 0.0033, Normal std = 0.4237

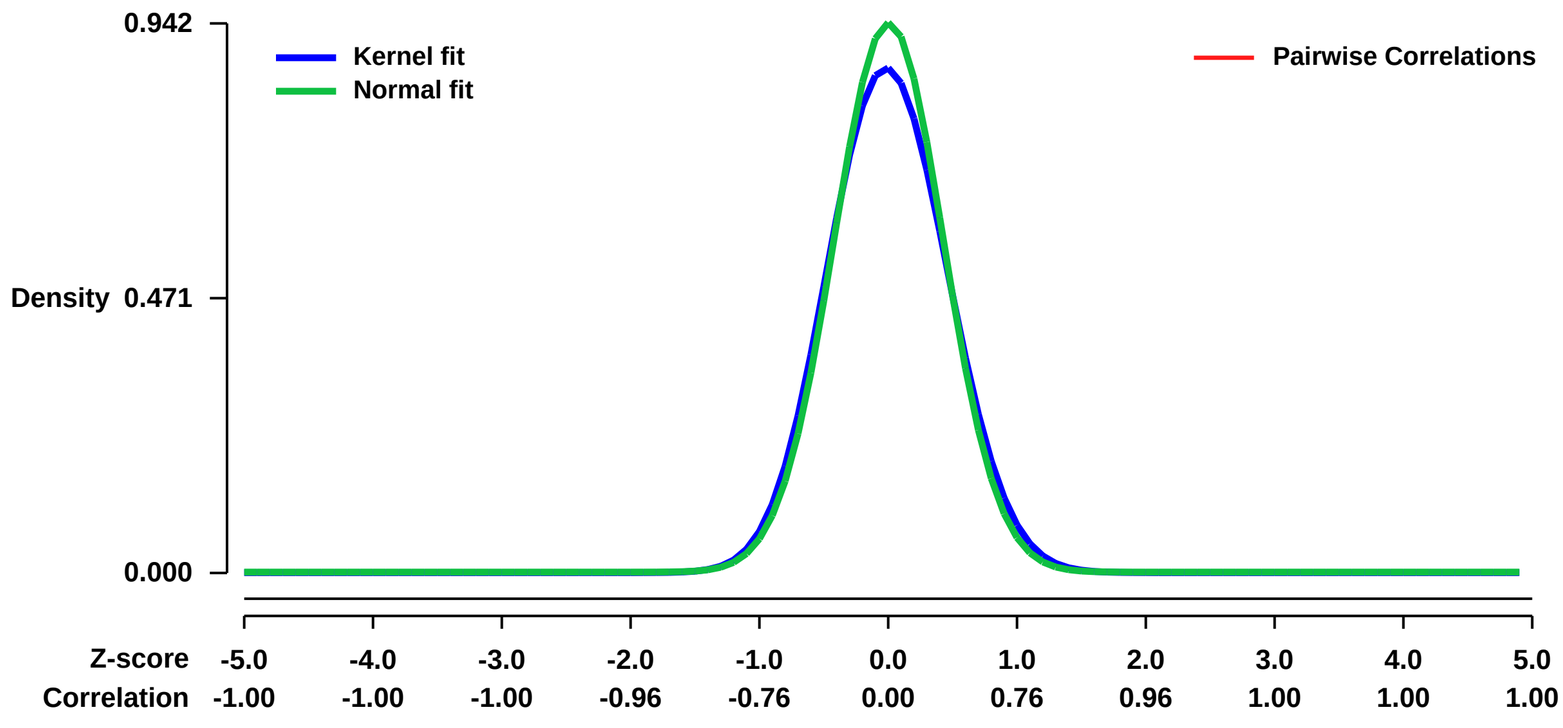

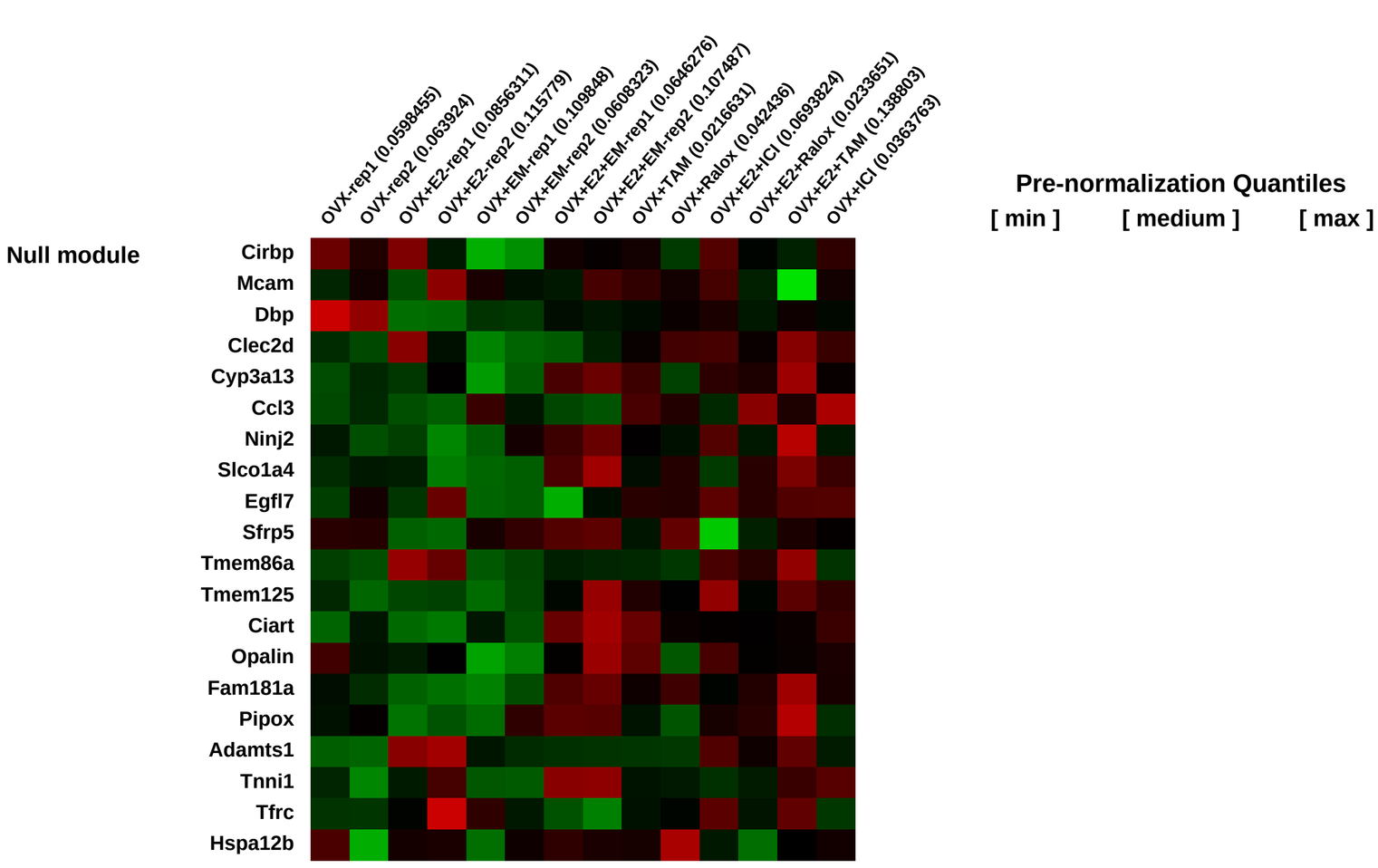

GEO Series "GSE26616" Expression Profiles

Num of samples in this series: 6

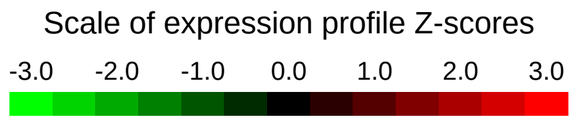

GEO Link:	http://www.ncbi.nlm.nih.gov/geo/query/acc.cgi?acc=GSE26616
Status:	Public on Jun 09 2011
Title:	EZH1 and EZH2 Co-Govern Histone H3-K27 Trimethylation and Are Essential for Hair Follicle Homeostasis and Wound Repair
Organism:	Mus musculus
Experiment type:	Expression profiling by array
Platform:	GPL1261
Pubmed ID:	21317239
Summary & Design:	**Summary:** Polycomb protein group (PcG)-dependent trimethylation on H3-K27(H3K27me3) regulates identity of embryonic stem cells (SCs). How H3K27me3 governs adult SCs and tissue development is unclear. Here, we conditionally target H3-K27-methyltransferases Ezh2 and Ezh1 to address their roles in mouse skin homeostasis. Postnatal phenotypes appear only in doubly-targeted skin, where H3K27me3 is abolished, revealing functional redundancy in EZH1/2 proteins. Surprisingly, while Ezh1/2-null hair follicles (HFs) arrest morphogenesis and degenerate due to defective proliferation and increased apoptosis, epidermis hyperproliferates and survives engraftment. mRNA-microarray studies reveal that despite these striking phenotypic differences, similar genes are upregulated in HF and epidermal Ezh1/2-null progenitors. Featured prominently are a) PcG-controlled non-skin lineage genes, whose expression is still significantly lower than in native tissues, and b) the PcG-regulated Ink4a/Inkb/Arf locus. Interestingly, even though Ink4a/Arf/Ink4b genes are fully activated in HF cells, they only partially so in epidermal-progenitors. Importantly, transduction of Ink4b/Ink4a/Arf shRNAs restores proliferation/survival of Ezh1/2-null HF progenitors in vitro, pointing towards the relevance of this locus to the observed HF phenotypes. Our findings reveal new insights into Polycomb-dependent tissue control and provide a new twist to how different progenitors within one tissue respond to loss of H3K27me3. **Overall design:** RNAs from FACS-purified WT and Ezh1/2 2KO ORS, matrix and epidermal cells (Rendl et al., 2005) were provided to the Genomics Core Facility, MSKCC for quality control, quantification, reverse transcription, labeling and hybridization to MOE430A 2.0 microarray chips (Affymetrix). Arrays were scanned per the manufacturerâ s specifications for the Affymetrix MOE430v2 chip. Images were background-subtracted. Probesets were identified as differentially expressed when the absolute fold change was â¥2. Probesets selected for visualization were log2 transformed and were analyzed with hierarchical clustering (Pearson correlation, average linkage), and visualized with heatmaps to assist in interpretation.

Background corr dist: KL-Divergence = 0.0410, L1-Distance = 0.0331, L2-Distance = 0.0015, Normal std = 0.6238

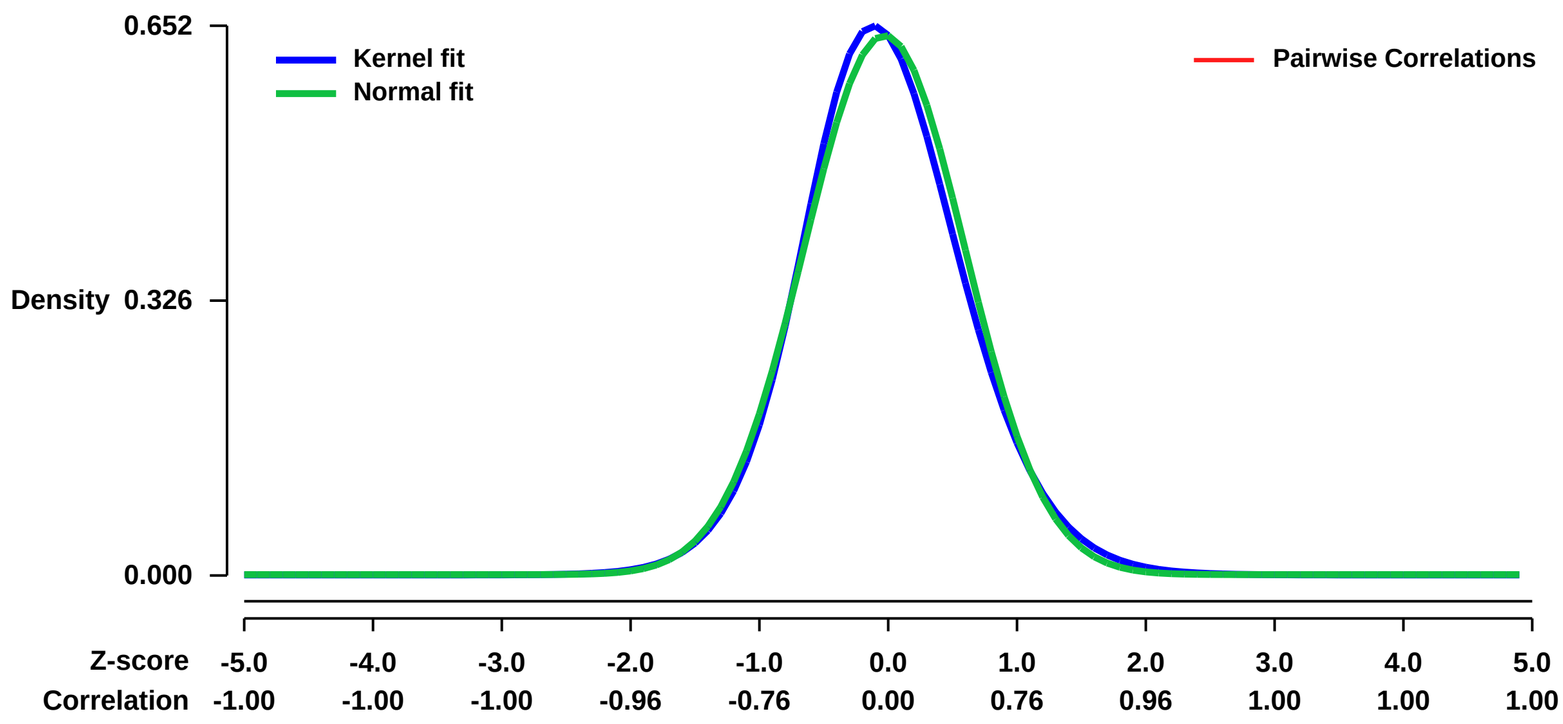

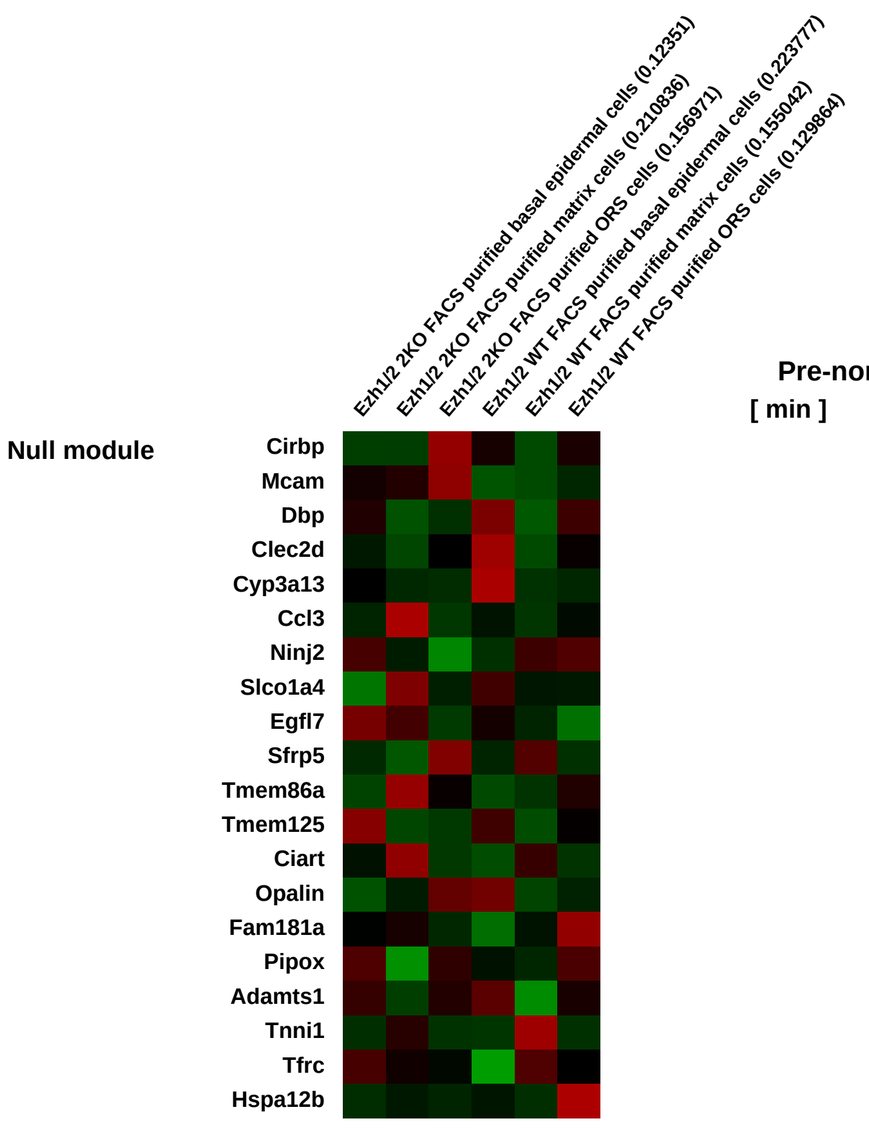

GEO Series "GSE30684" Expression Profiles

Num of samples in this series: 6

Scale of expression profile Z-scores

-3.0 -2.0 -1.0 0.0 1.0 2.0 3.0

GEO Link:	http://www.ncbi.nlm.nih.gov/geo/query/acc.cgi?acc=GSE30684
Status:	Public on Feb 16 2012
Title:	Stem Cell Antigen-1 (Sca-1) Regulates Mammary Tumor Development and Cell Migration
Organism:	Mus musculus
Experiment type:	Expression profiling by array
Platform:	GPL1261
Pubmed ID:	22140470
Summary & Design:	**Summary:** Stem cell antigen-1 (Sca-1 or Ly6A) is a member of the Ly6 family of glycosyl phostidylinositol (GPI)-anchored cell surface proteins. To determine the potential mechanisms by which Sca-1 regulates cell migration, adhesion, and tumor development; we performed an Affymetrix mouse genome 430A 2.0 array on cDNA comparing shLuc and shSca-1 from cells grown in vitro. **Overall design:** We performed an Affymetrix mouse genome 430A 2.0 array on cDNA comparing shLuc and shSca-1 from cells grown in vitro. Experimental groups were profiled in biological triplicate.

Background corr dist: KL-Divergence = 0.0380, L1-Distance = 0.0371, L2-Distance = 0.0017, Normal std = 0.6765

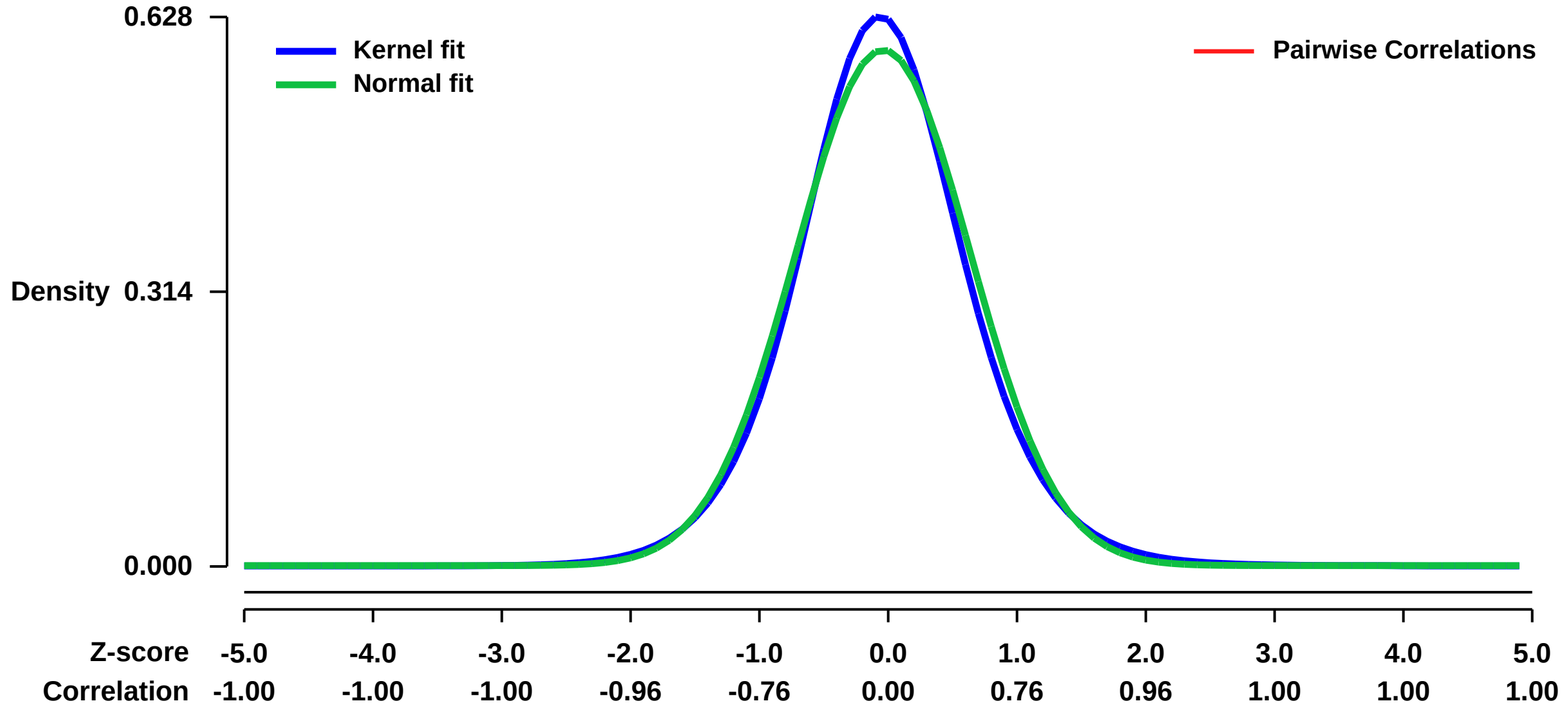

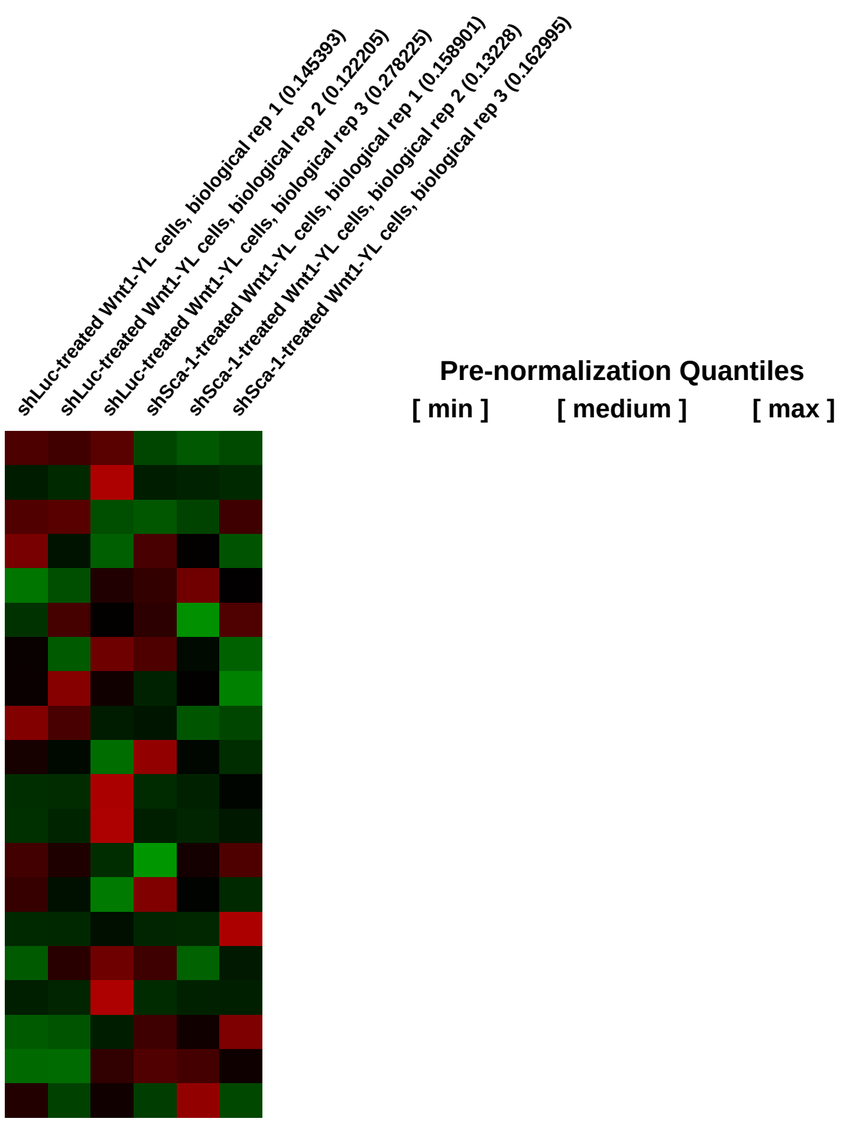

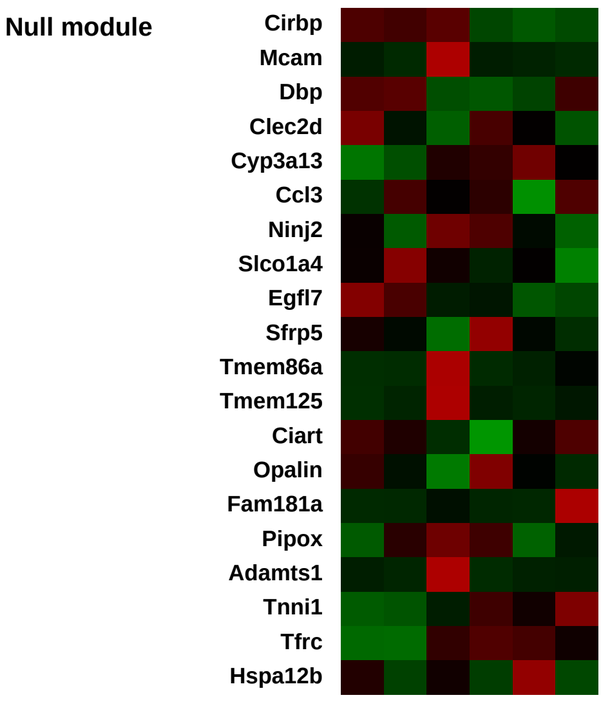

GEO Series "GSE11862" Expression Profiles

Num of samples in this series: 6

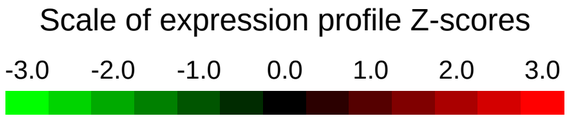

GEO Link:	http://www.ncbi.nlm.nih.gov/geo/query/acc.cgi?acc=GSE11862
Status:	Public on Sep 01 2008
Title:	Early Gene expression changes after axonal injury
Organism:	Mus musculus
Experiment type:	Expression profiling by array
Platform:	GPL1261
Pubmed ID:	19284657
Summary & Design:	**Summary:** We used optic nerve injury as a model to study early signaling events in the neuronal soma following axonal injury. Optic nerve injury results in the selective death of retinal ganglion cells (RGCs). The time course of cell death takes place over a period of days with the earliest detection of RGC death at about 48 hr post injury. We hypothesized that in the period immediately following axonal injury, there are changes in the soma that signal surrounding glia and neurons and that start programmed cell death. In the current study, we investigated early changes in cellular signaling and gene expression that occur within the first 6 hrs post optic nerve injury. We detected differences in phosphoproteins and gene expression within this time period that we used to interpret temporal events. Our studies revealed that the entire retina has been signaled by the RGC soma within 30 min after optic nerve injury and that pathways that modulate cell death are likely to be active in RGCs within 6 hrs following axonal injury **Keywords: Stress Response** **Overall design:** In the treated animals, axons of the optic nerve were crushed with fine forceps for 10 sec, 1 mm posterior to the globe, under direct visualization, within an intact meningeal sheath. Controls were contralateral eyes from the same animals in each group that had not been injured. After 6 hr eyes were enucleated and processed for tissue sectionin

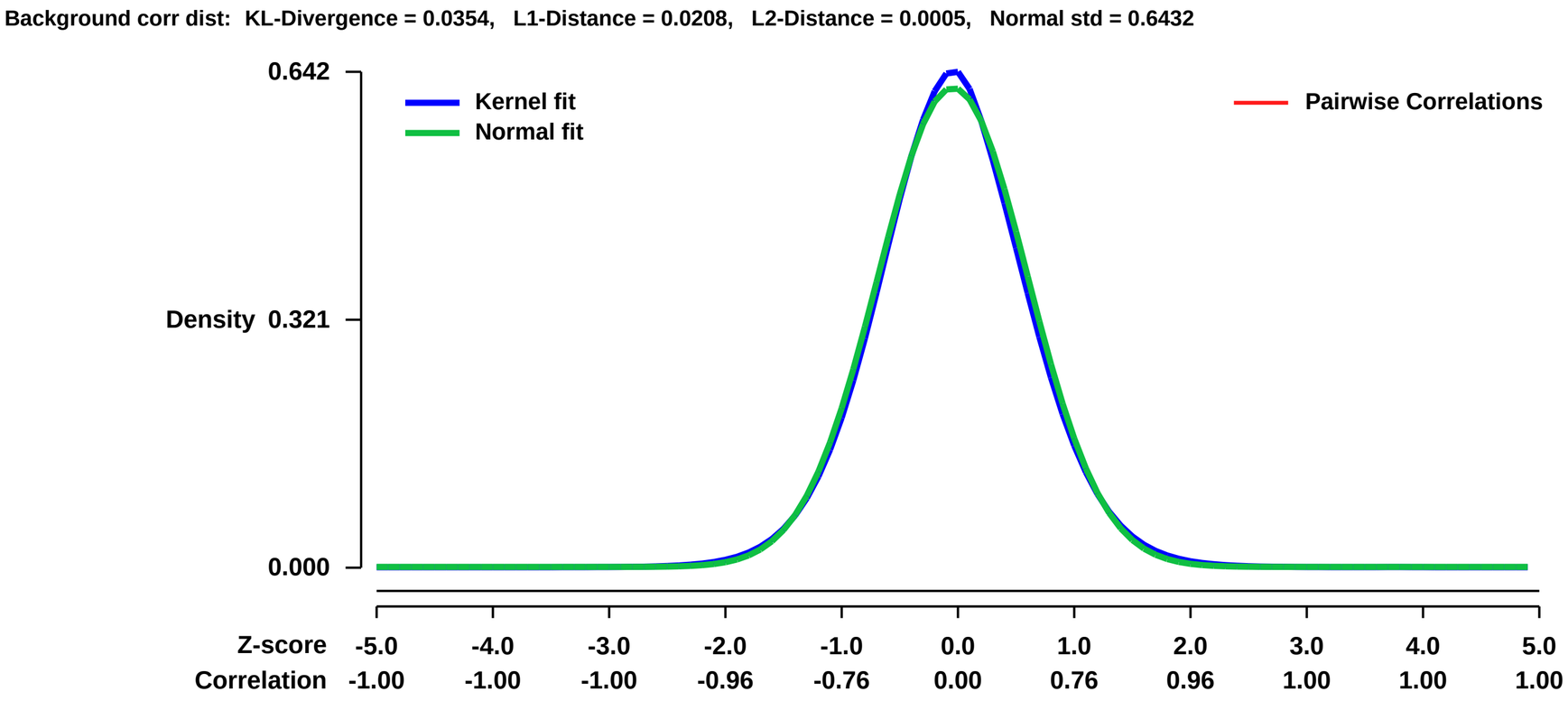

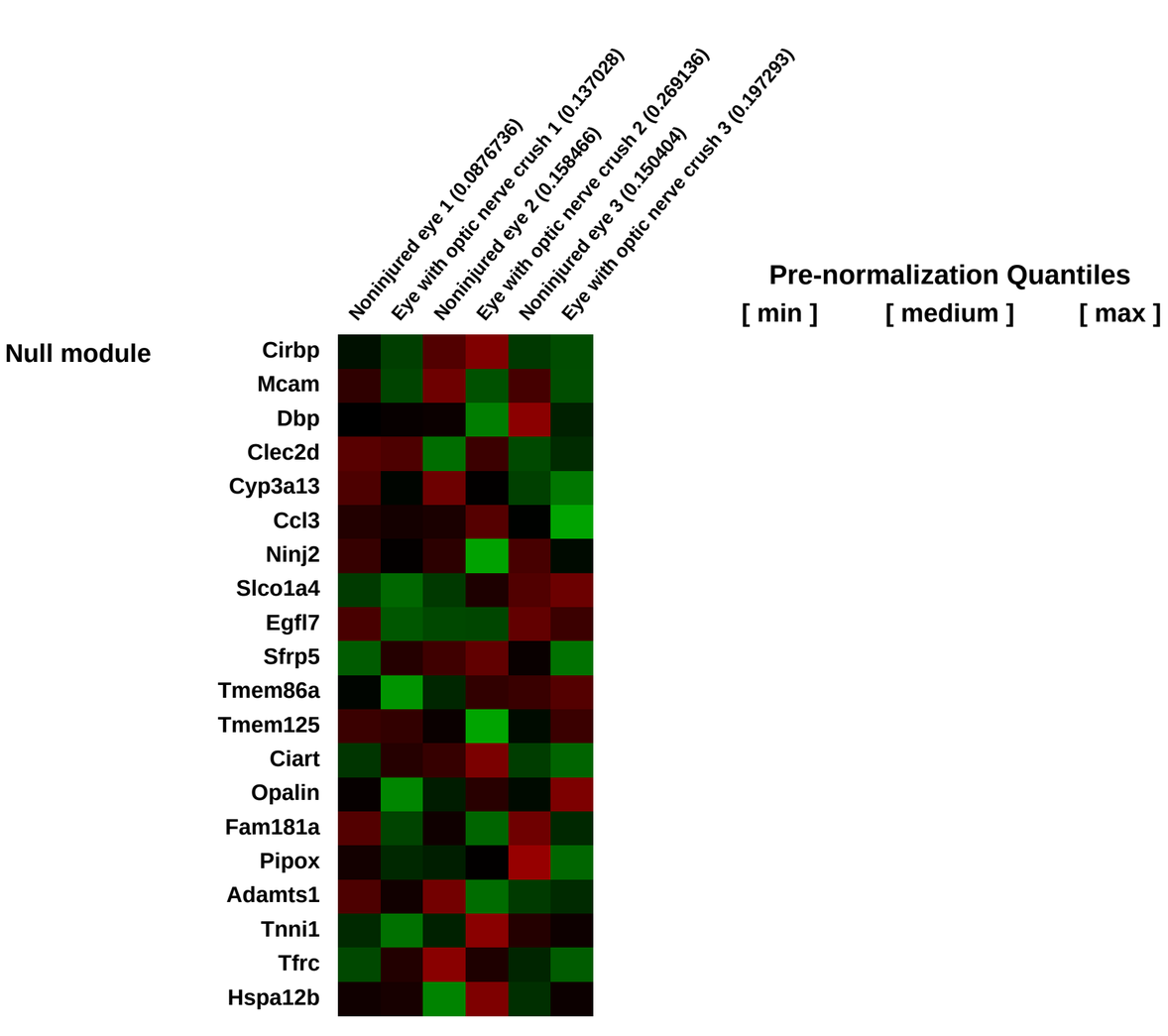

GEO Series "GSE20372" Expression Profiles

Num of samples in this series: 6

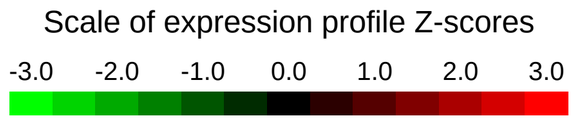

GEO Link:	**http://www.ncbi.nlm.nih.gov/geo/query/acc.cgi?acc=GSE20372**
Status:	**Public on Feb 15 2011**
Title:	**Gene expression in E14 TG2a cells grown with or without LIF and sorted for 5T4 expression**
Organism:	**Mus musculus**
Experiment type:	**Expression profiling by array**
Platform:	**GPL1261**
Pubmed ID:	**20376365**
Summary & Design:	**Summary:** **E14 TG2a cells grown with LIF were disaggregated and FACS sorted for cell surface 5T4 negativity versus E14 TG2a cells grown without LIF for 3 days and sorted for 5T4 positivity.** **Overall design:** **Two samples in triplicate. 5T4- vs. 5T4+**
Background corr dist:	**KL-Divergence = 0.0286, L1-Distance = 0.0298, L2-Distance = 0.0012, Normal std = 0.6906**

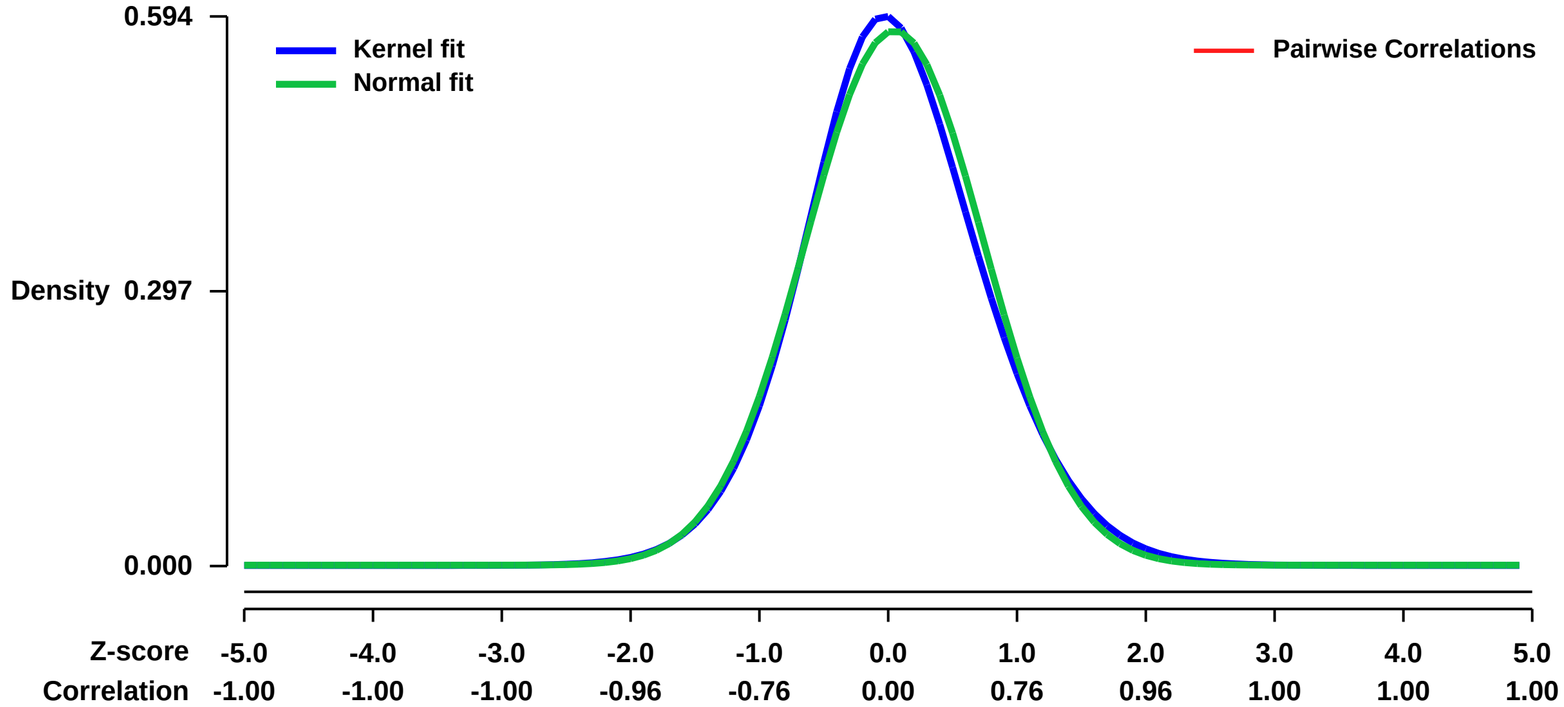

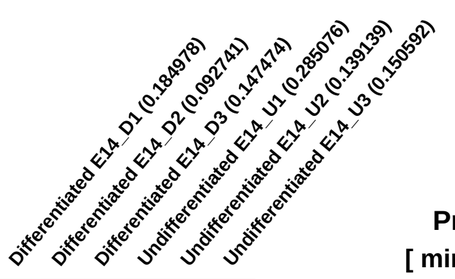

Pre-normalization Quantiles

[min] [medium] [max]

Null module

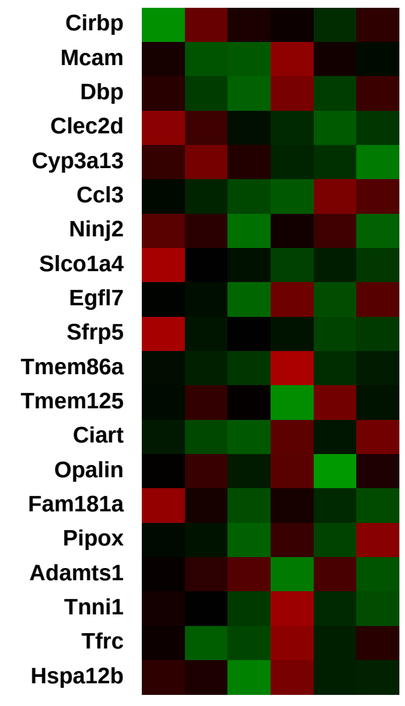

GEO Series "GSE28895" Expression Profiles

Num of samples in this series: 6

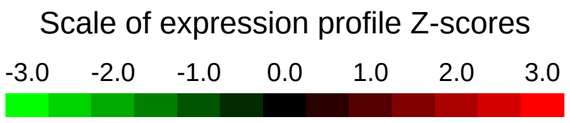

GEO Link:	http://www.ncbi.nlm.nih.gov/geo/query/acc.cgi?acc=GSE28895
Status:	Public on Apr 28 2011
Title:	Expression data from stomach of germ-free and gnotobiotic mice
Organism:	Mus musculus
Experiment type:	Expression profiling by array
Platform:	GPL1261
Pubmed ID:	21803885
Summary & Design:	**Summary:** The aim of this study was to examine the role of indigenous lactobacilli in the physiological development of the stomach in mice using microarray analysis. In lactobacilli-associated gnotobiotic mice, an increased expression of the genes related to the muscle system development, such as nebulin and troponin, was observed. On the other hand, the expression of the gastrin gene dramatically decreased. A microarray analysis of the stomachs infected with H. pylori also showed both the up-regulation of muscle cell genes and the down-regulation of gastrin genes. **Overall design:** Male germfree BALB/c mice were orally inoculated with 109 CFU lactobacilli and their stomachs were excised after 10 days for analyses. In the other experiment, 8-week-old mice were orally inoculated using a stomach tube on three consecutive days with 109 CFU of H. pylori. The stomachs of the germfree mice were used as controls. For the DNA microarray analysis, RNA was prepared from the stomach and then applied to a genome array.

Background corr dist: KL-Divergence = 0.0381, L1-Distance = 0.0198, L2-Distance = 0.0004, Normal std = 0.6266

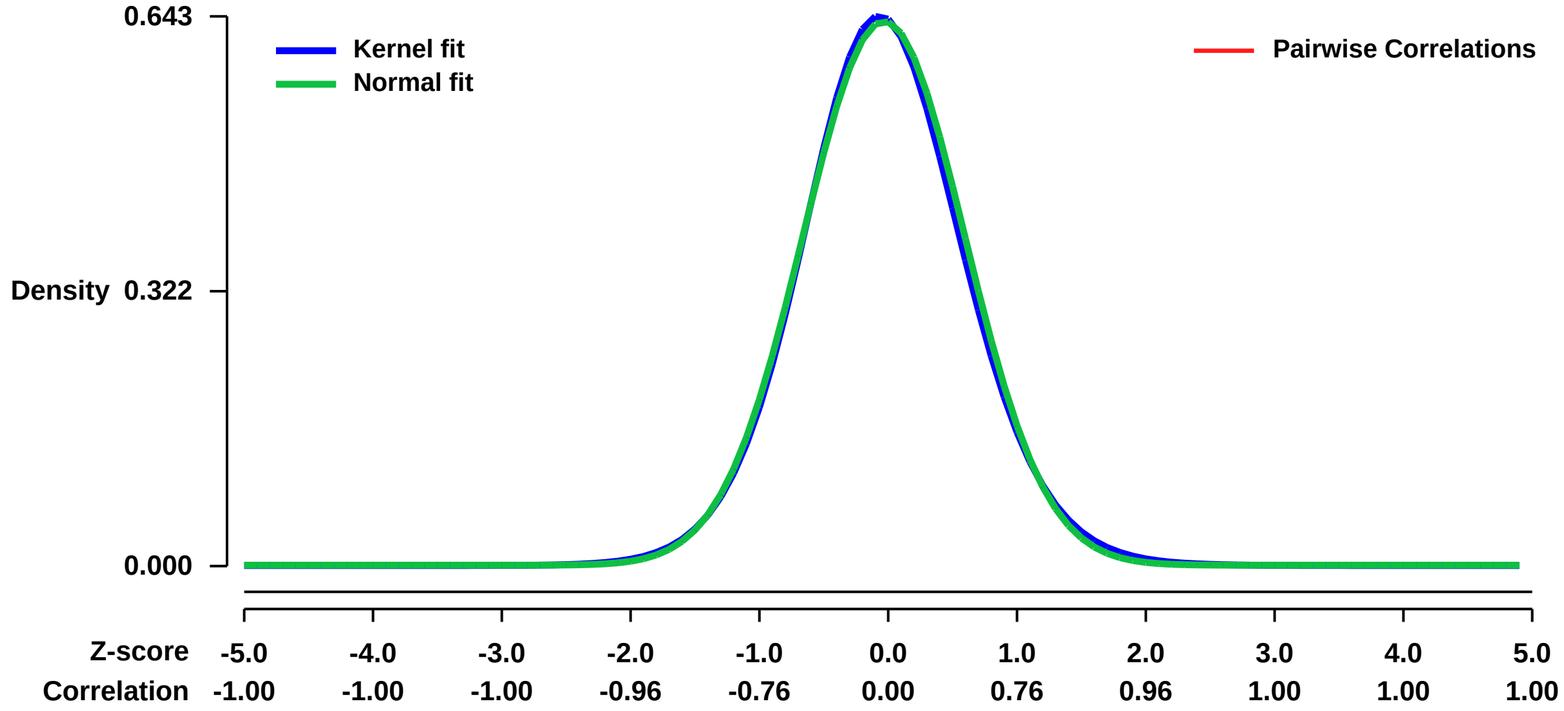

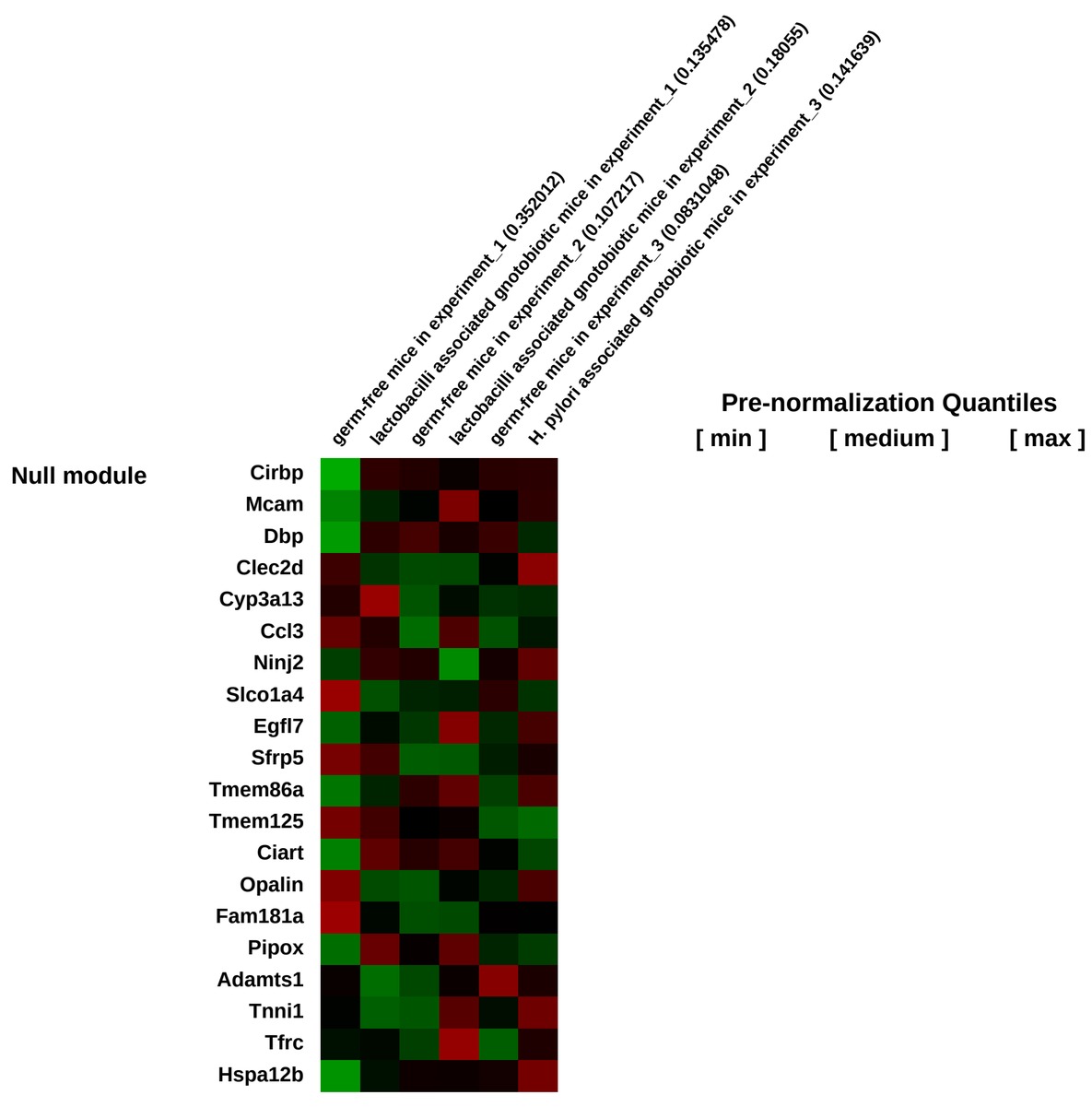

GEO Series "GSE10740" Expression Profiles

Num of samples in this series: 6

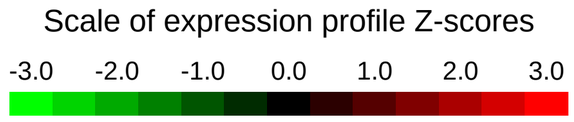

GEO Link:	**http://www.ncbi.nlm.nih.gov/geo/query/acc.cgi?acc=GSE10740**
Status:	**Public on Mar 06 2008**
Title:	**Expression data from the colon of wild-type and Slc9a3 (NHE3)-deficient mice**
Organism:	**Mus musculus**
Experiment type:	**Expression profiling by array**
Platform:	**GPL1261**
Pubmed ID:	**18467500**
Summary & Design:	**Summary:** **Na+/H+ exchanger 3 (NHE3) provides a major route for intestinal Na+ absorption. It has been considered as a target of proinflammatory cytokines and enteropathogenic bacteria and impaired NHE3 expression and/or activity may be responsible for inflammation-associated diarrhea.** **We used microarray analysis to detail the global programme of colonic gene expression in the absence of functional NHE3.** **Keywords: knockout effect** **Overall design:** **Whole colon was dissected from 6-8 week old NHE3-deficient mice and their wild-type littermates and total RNA isolated for microarray analysis using Affymetrix murine MOE430 2.0 arrays**

Background corr dist: KL-Divergence = 0.0390, L1-Distance = 0.0210, L2-Distance = 0.0005, Normal std = 0.6231

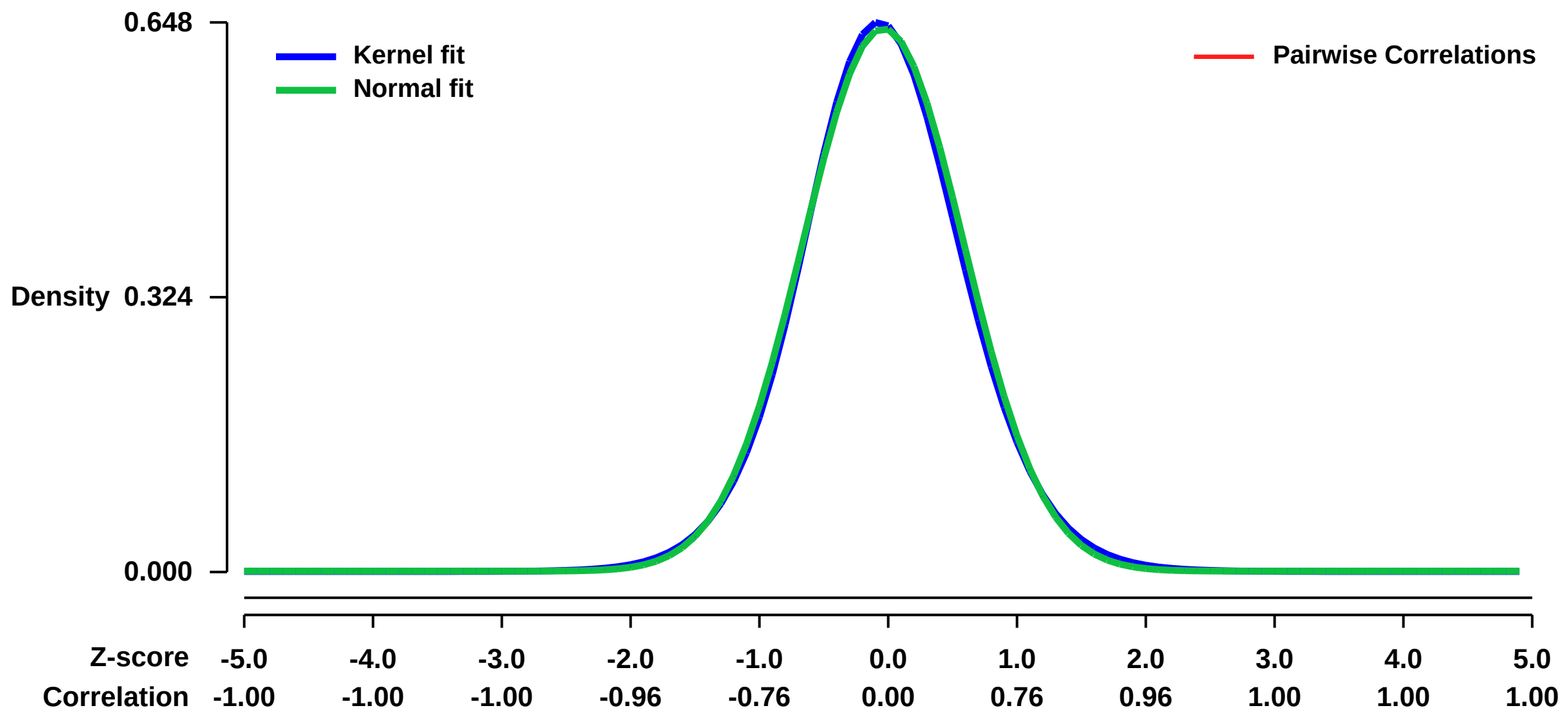

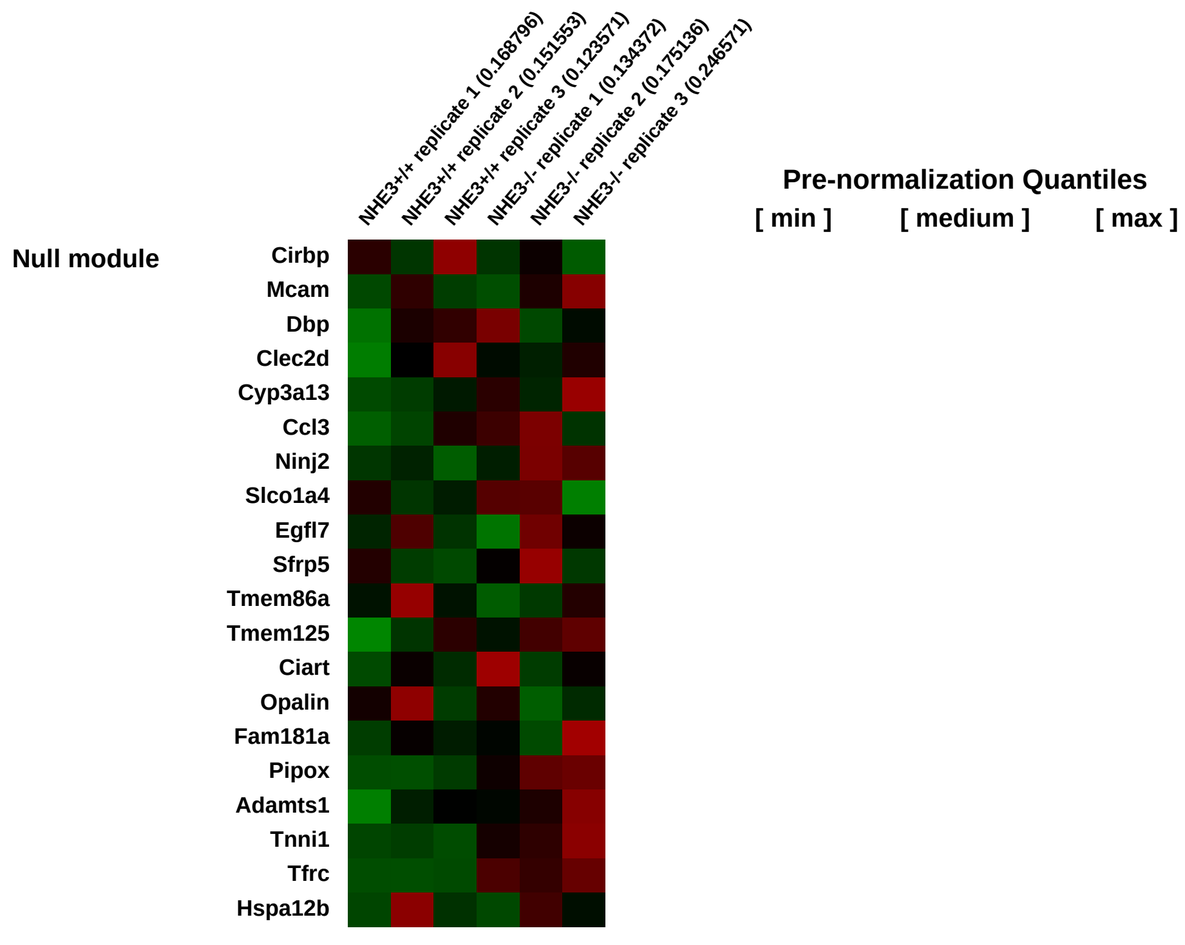

GEO Series "GSE15268" Expression Profiles

Num of samples in this series: 16

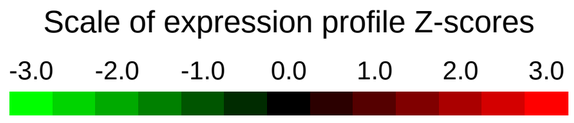

GEO Link:	http://www.ncbi.nlm.nih.gov/geo/query/acc.cgi?acc=GSE15268
Status:	Public on Jul 13 2010
Title:	Cell-context dependent Notch target genes
Organism:	Mus musculus
Experiment type:	Expression profiling by array
Platform:	GPL1261
Pubmed ID:	20628604
Summary & Design:	**Summary:** Notch signaling regulates a variety of developmental cell fates decisions in a cell-context dependent manner. Although Notch signaling directly regulates transcription via the RBP-J/CSL DNA binding protein, little is known about the genes in the respective tissues that are directly activated by Notch. To analyze how Notch signaling mediates its context dependent functions, we utilized a Tamoxifen(OHT)-inducible system (NERT) to activate Notch1 in embryonic stem cells (ESC) at different stages of mesodermal differentiation combined with global transcriptional analyses. **Overall design:** Notch1 signaling pathway was analysed in mouse embryonic stem cells (mESCs) that were kept under self-renewal conditions enabling ectodermal, or mesodermal gene expression (ESCe or ESCm respectively), or were differentiated into mesodermal progenitors. NotchIC were induced or not induced by hydroxytamoxifen (OHT) and addititionally in some experiments the cells were treated with protein synthesis inhibitor cycloheximide (CHX) for 4 h.

Background corr dist: KL-Divergence = 0.0742, L1-Distance = 0.0383, L2-Distance = 0.0021, Normal std = 0.5061

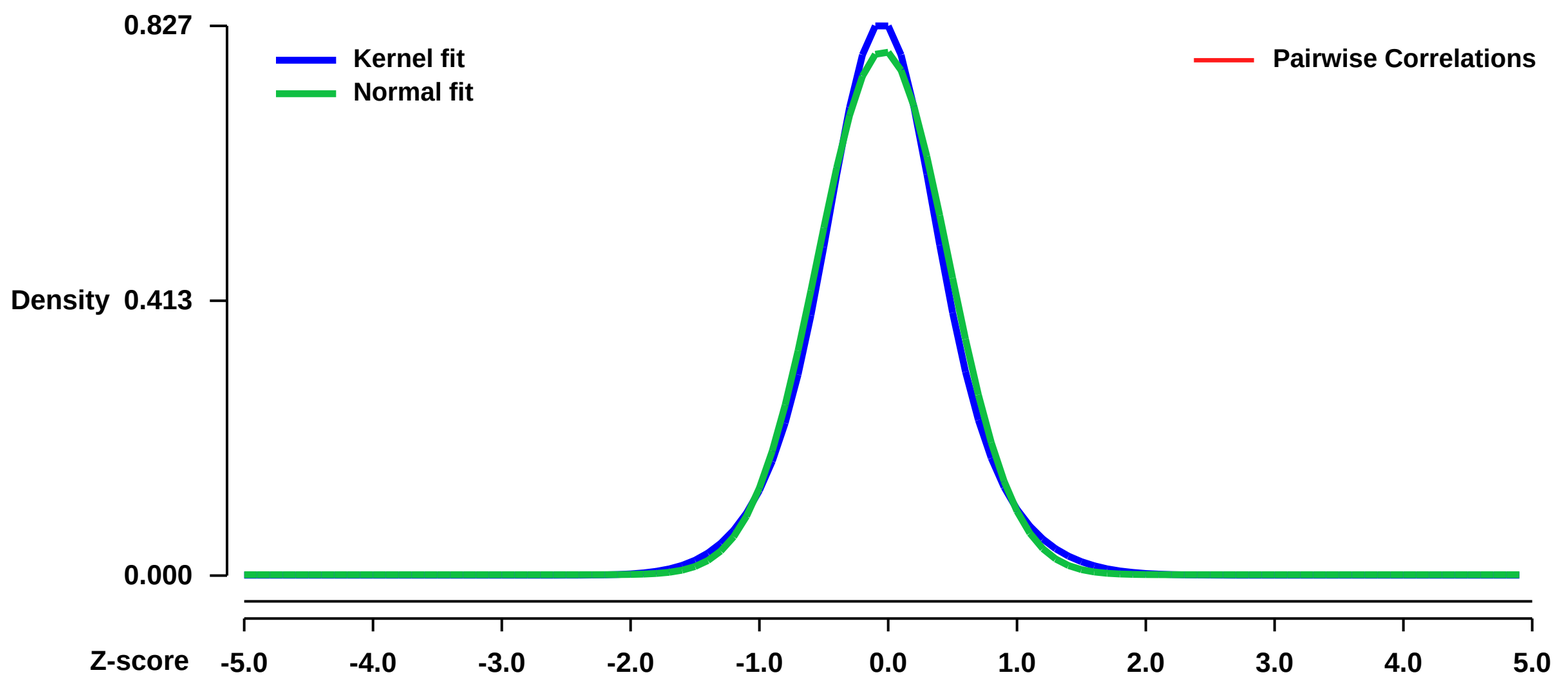

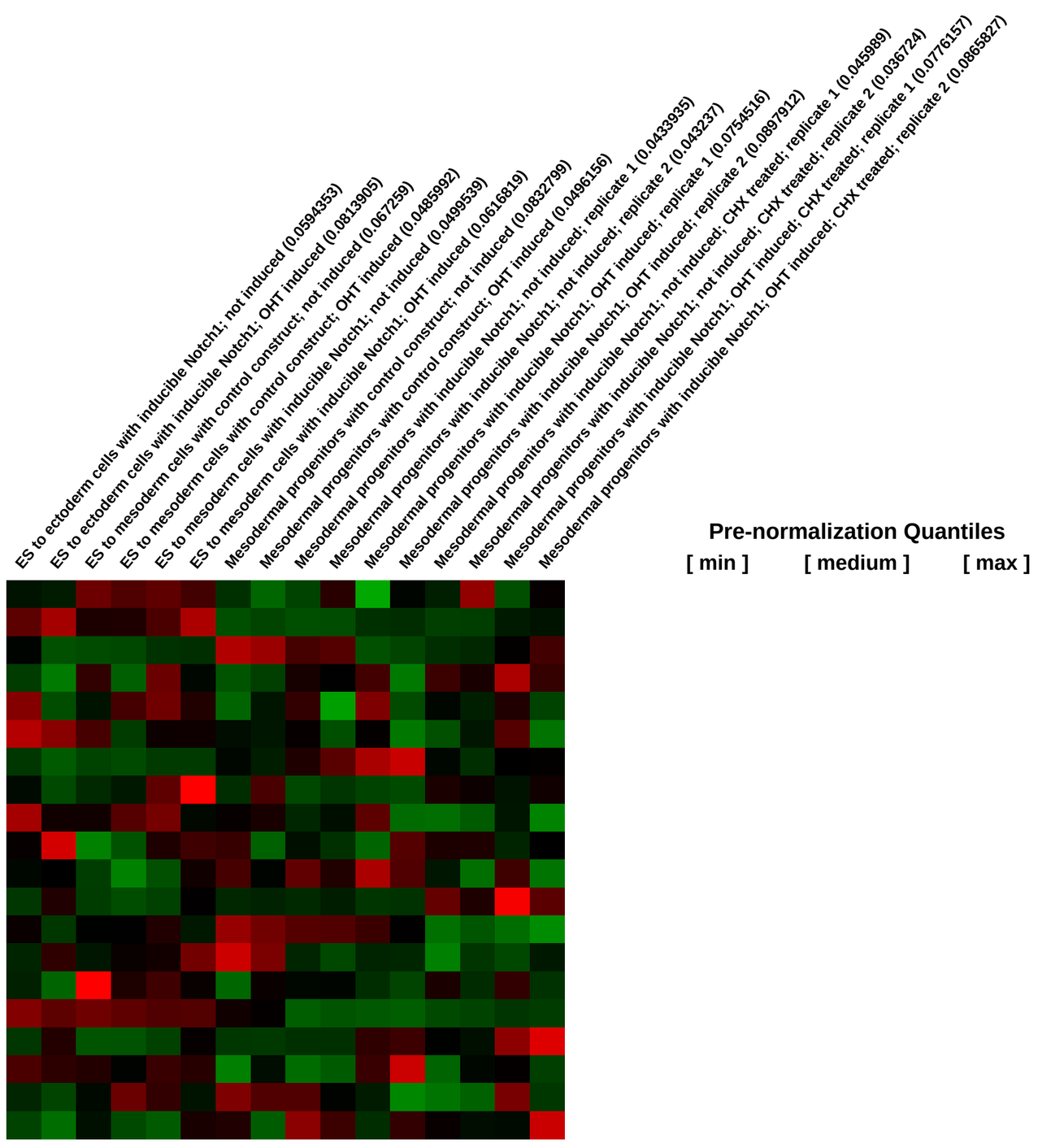

GEO Series "GSE22989" Expression Profiles

Num of samples in this series: 10

Scale of expression profile Z-scores

-3.0 -2.0 -1.0 0.0 1.0 2.0 3.0

GEO Link:	http://www.ncbi.nlm.nih.gov/geo/query/acc.cgi?acc=GSE22989
Status:	Public on Nov 29 2011
Title:	Gene expression profiling of Tgfbr2 mutant mouse models of cleft palate
Organism:	Mus musculus
Experiment type:	Expression profiling by array
Platform:	GPL1261
Pubmed ID:	22123828
Summary & Design:	**Summary:** The overall goal of this project is to investigate the role of TGF-beta signaling in palate development in order to discover candidate therapeutics for preventing and treating congenital birth defects. Here, we conducted gene expression profiling of embryonic palatal tissue from wild type mice as well as those with a neural crest specific conditional inactivation of the Tgfbr2 gene. The latter mice provide a model of cleft palate formation. **Overall design:** To investigate the mechanism of cleft palate resulting from mutations in TGFBR2, we analyzed neural crest specific conditional inactivation of Tgfbr2 in mice (Tgfbr2fl/fl;Wnt1-Cre). We performed microarray analyses using the palatal tissue of Tgfbr2fl/fl;Wnt1-Cre mice at embryonic day E13.5 (prior to palatal fusion, n=6 per genotype) and E14.5 (during palatal fusion, n=5 per genotype) to examine the genes regulated by Tgf-beta during palate formation.

Background corr dist: KL-Divergence = 0.0820, L1-Distance = 0.0225, L2-Distance = 0.0007, Normal std = 0.4701

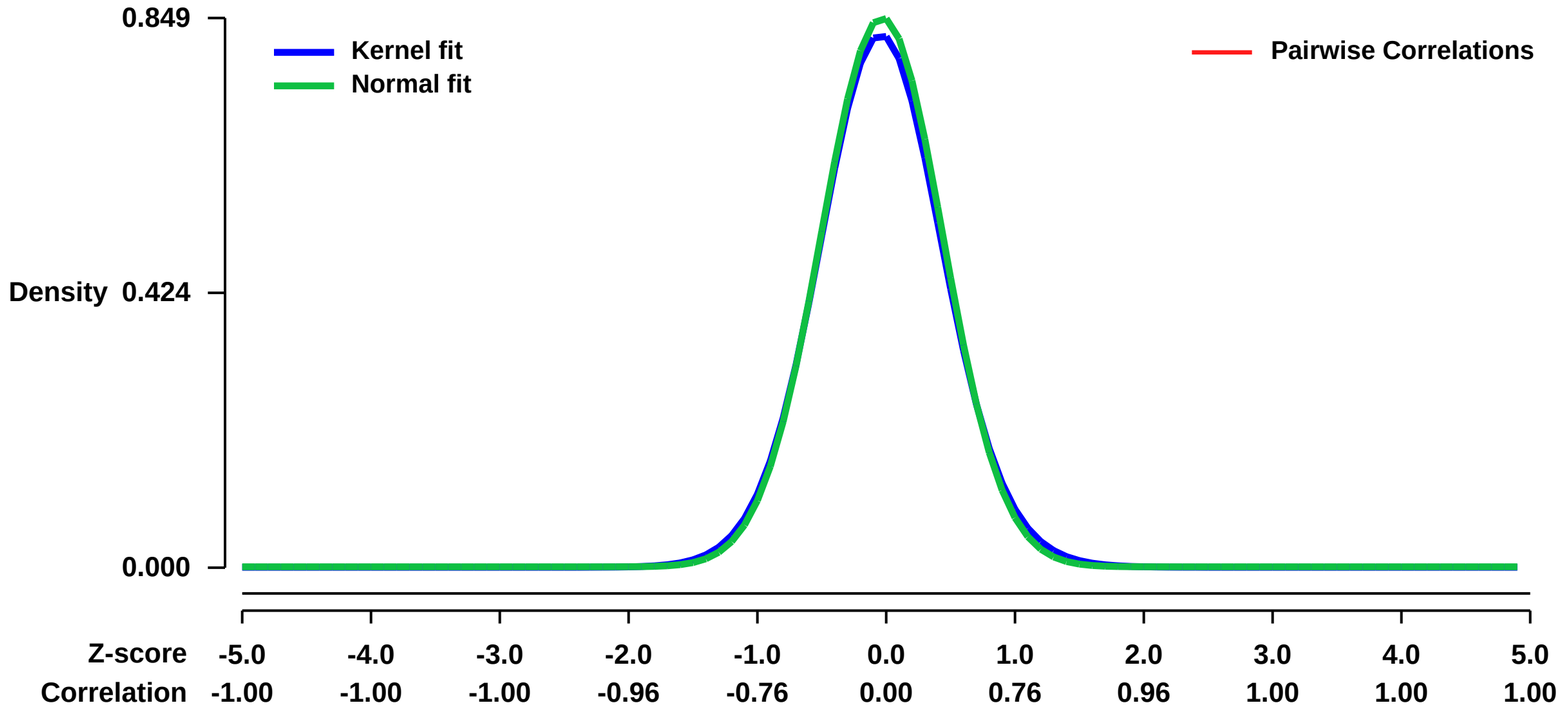

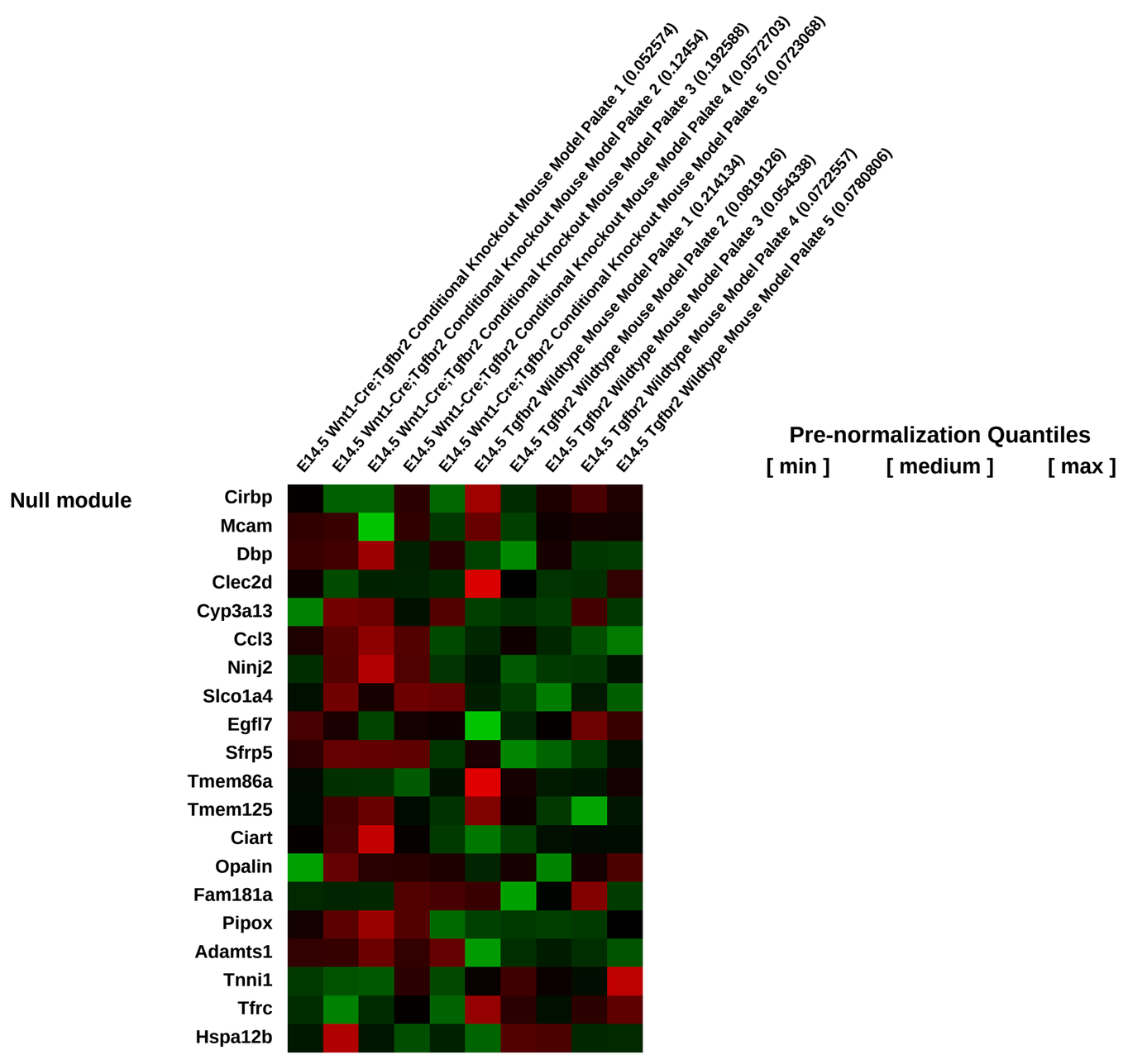

GEO Series "GSE11990" Expression Profiles

Num of samples in this series: 20

Scale of expression profile Z-scores

-3.0 -2.0 -1.0 0.0 1.0 2.0 3.0

GEO Link:	http://www.ncbi.nlm.nih.gov/geo/query/acc.cgi?acc=GSE11990
Status:	Public on Jul 20 2010
Title:	Gene expression profiling of mouse p53-deficient epidermal carcinoma defines molecular determinants of human cancer malignancy (training dataset)
Organism:	Mus musculus
Experiment type:	Expression profiling by array
Platform:	GPL1261
Pubmed ID:	20630075
Summary & Design:	**Summary:** The epidermal specific ablation of Trp53 gene leads to the spontaneous development of aggressive tumors in mice through a process that is accelerated by the simultaneous ablation of Rb gene. Since alterations of p53-dependent pathway are common hallmarks of aggressive, poor prognostic human cancers, these mouse models can recapitulate the molecular features of some of these human malignancies. To evaluate this possibility, gene expression microarray analysis was performed in mouse samples. The mouse tumors display increased expression of cell cycle and chromosomal instability associated genes. Remarkably, they are also enriched in human embryonic stem cell gene signatures, a characteristic feature of human aggressive tumors. Using cross-species comparison and meta-analytical approaches, we also observed that spontaneous mouse tumors display robust similarities with gene expression profiles of human tumors bearing mutated TP53, or displaying poor prognostic outcome, from multiple body tissues. We have obtained a 20-gene signature whose genes are overexpressed in mouse tumors and can identify human tumors with poor outcome from breast cancer, astrocytoma and multiple myeloma. This signature was consistently overexpressed in additional mouse tumors using microarray analysis. Two of the genes of this signature, AURKA and UBE2C, were validated in human breast and cervical cancer as potential biomarkers of malignancy. Our analyses demonstrate that these mouse models are promising preclinical tools aimed to search for malignancy biomarkers and to test targeted therapies of prospective use in human aggressive tumors and/or with p53 mutation or inactivation. **Overall design:** Control skin was compared with skin tumors arising in k14Cre;p53loxP/loxP and k14Cre;p53loxP/loxP;pRbloxP/loxP animals, giving a mouse p53-tumor signature

Background corr dist: KL-Divergence = 0.1609, L1-Distance = 0.0435, L2-Distance = 0.0043, Normal std = 0.3697

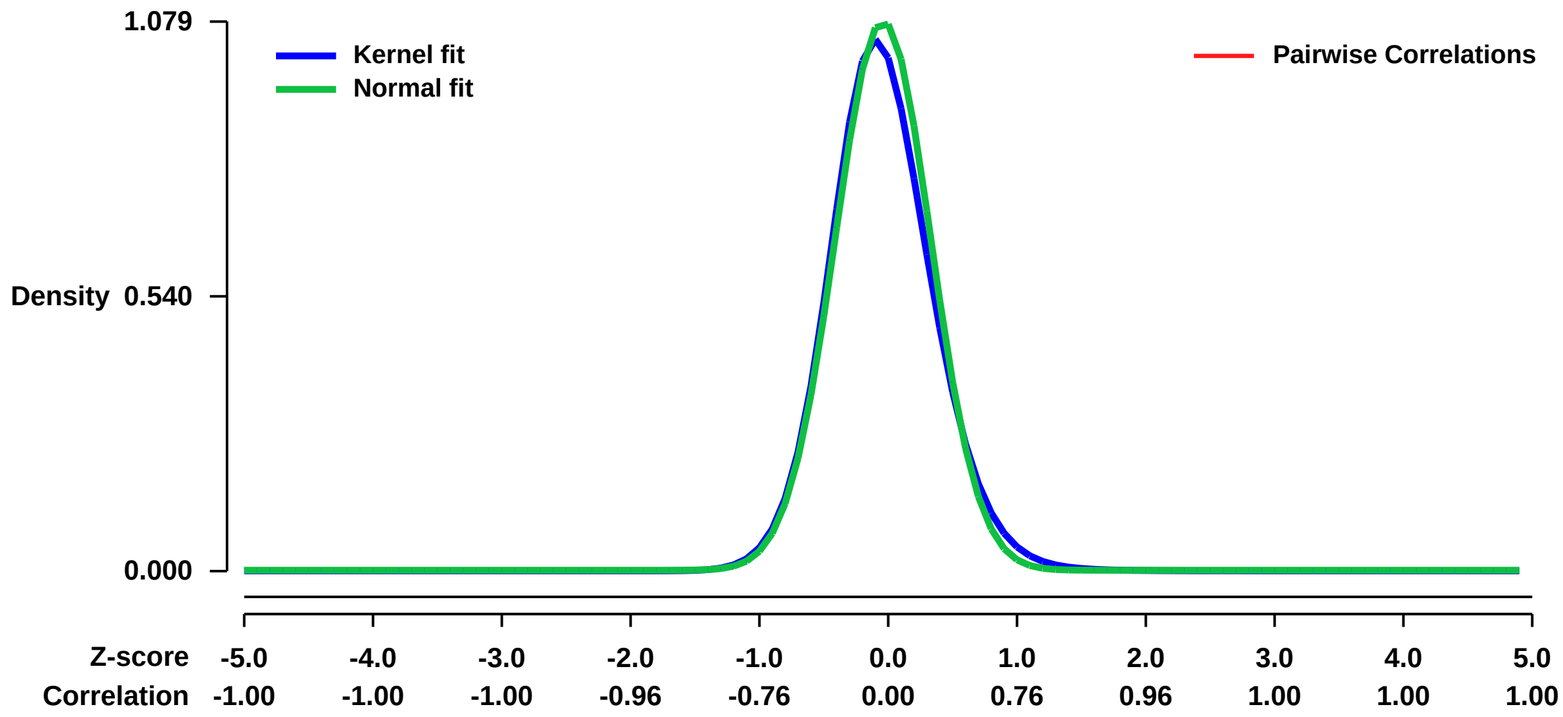

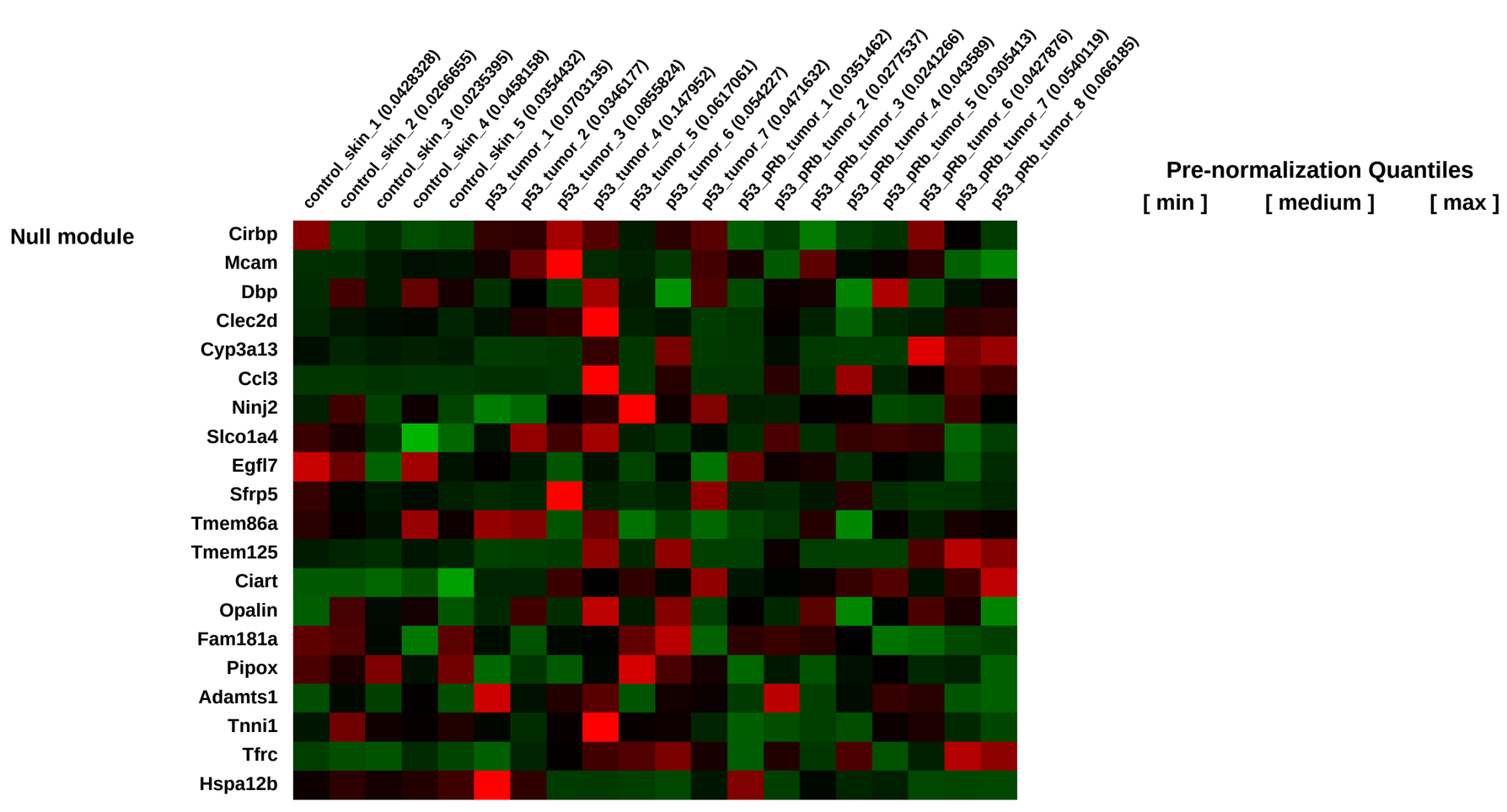

GEO Series "GSE7141" Expression Profiles

Num of samples in this series: 6

Scale of expression profile Z-scores

-3.0 -2.0 -1.0 0.0 1.0 2.0 3.0

GEO Link:	http://www.ncbi.nlm.nih.gov/geo/query/acc.cgi?acc=GSE7141
Status:	Public on Jan 01 2008
Title:	mRNA expression analysis of undifferentiated Dicer +/- (D4) and Dicer -/- (27H10) embryonic cell lines
Organism:	Mus musculus
Experiment type:	Expression profiling by array
Platform:	GPL1261
Pubmed ID:	18311153
Summary & Design:	**Summary:** We have analyzed the transcript expression levels in Dicer heterozygous and Dicer knock-out embryonic stem (ES) cells in order to identify which transcripts are regulated by RNAi pathway in mouse ES cells. **Keywords: Cell type comparison of cell line with or without knock-out** **Overall design:** Two cell lines were analysed in an undifferentiated state. Triplicates of both cell lines were analyzed.

Background corr dist: KL-Divergence = 0.0260, L1-Distance = 0.0446, L2-Distance = 0.0022, Normal std = 0.7653

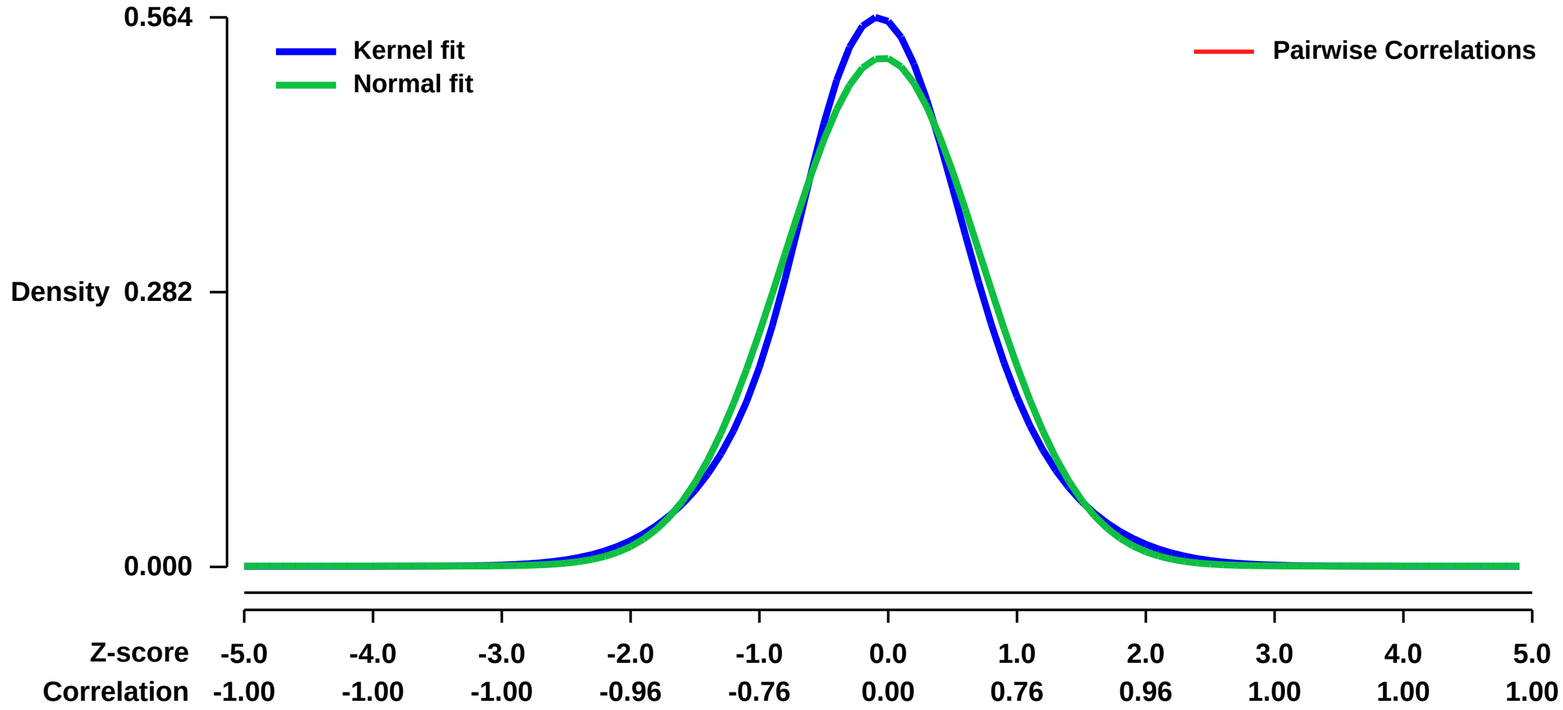

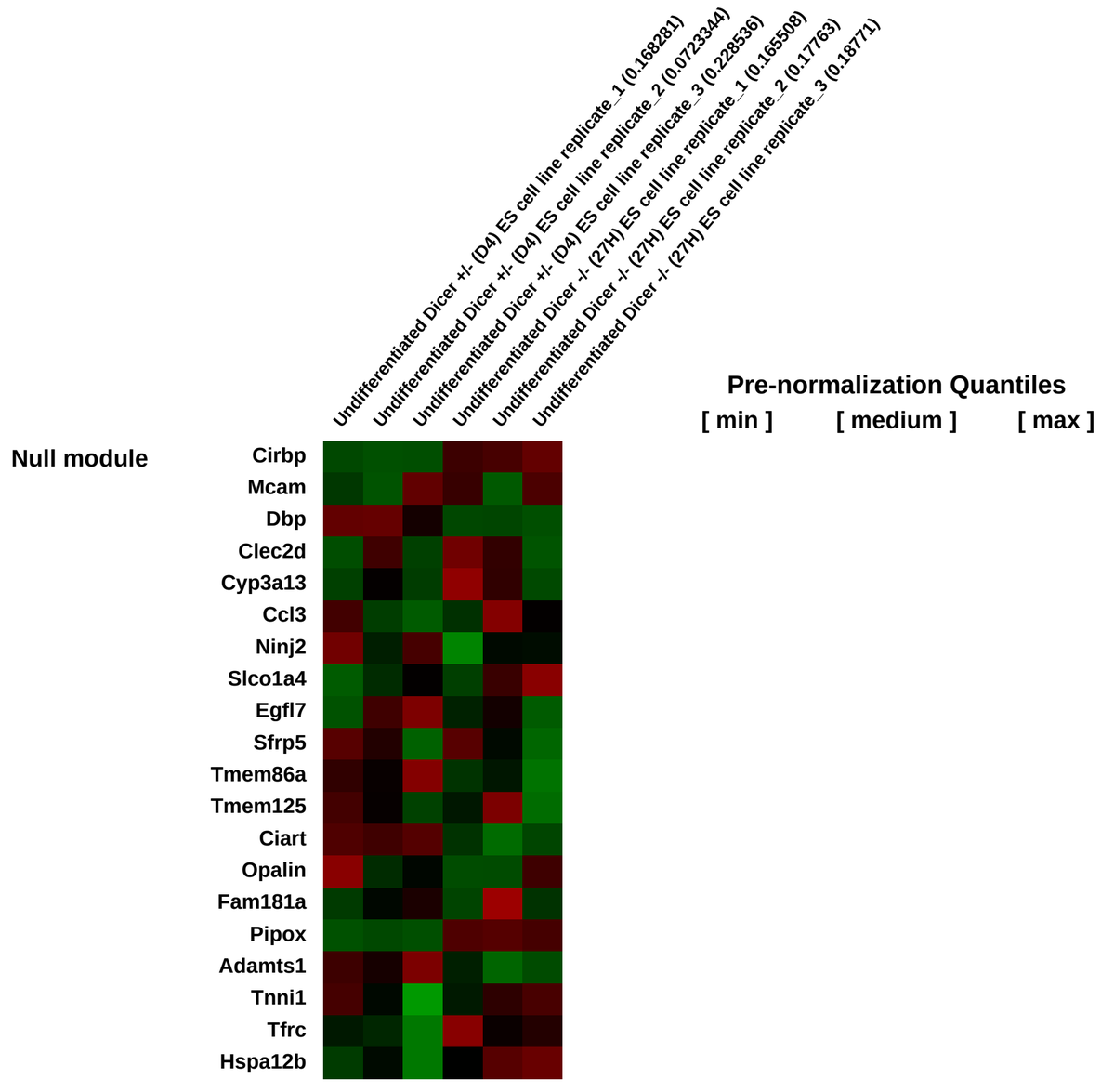

GEO Series "GSE58262" Expression Profiles

Num of samples in this series: 18

Scale of expression profile Z-scores

-3.0 -2.0 -1.0 0.0 1.0 2.0 3.0

GEO Link:	**http://www.ncbi.nlm.nih.gov/geo/query/acc.cgi?acc=GSE58262**
Status:	**Public on Jun 06 2014**
Title:	**Impact of gamma chain cytokines on the differentiation of recently antigen-activated CD8 T cells**
Organism:	**Mus musculus**
Experiment type:	**Expression profiling by array**
Platform:	**GPL1261**
Pubmed ID:	
Summary & Design:	**Summary:** **Analysis of how different gamma chain family cytokines influence CD8 T cell differentiation.** **Overall design:** **Naˆflve CD8 T cells were isolated from the spleens OT-I Thy1.1 TCR Tg mice. Whole splenocytes from wild-type C57BL/6 mice were used as stimulator cells. Purified naˆflve wild-type OT-I (1ˆ 106/well) were stimulated with OVA peptide (SIINFEKL) pulsed (5 ´µg/ml) and irradiated (2,000 rads) syngeneic splenocytes (6ˆ 106/well) in 24-well plates. Forty-eight hours later, activated OT-I T cells were harvested and viable cells were enriched over a Ficoll-paque gradient and washed with cRPMI prior to being reseeded in cRPMI (5ˆ 105 cells/ml) and treated with the media supplemented with various ¸‡c cytokines (IL-2, IL-4, IL-7, IL-15 and IL-21). Experimental samples were treated with 100 ng/ml of their respective gamma chain cytokine and incubated at 37´”C for 24 hours. RNA was isolated using either the RNeasy Mini kit, or a combination of TRIzol reagent and the Direct-zol RNA miniprep kit, all following manufacturer protocols. Two biological replicates for mRNA analysis were prepped using the RNeasy kit. The third replicate was prepped using the Trizol/Direct-zol approach. The quality and quantity of RNA samples was further analyzed on the Bioanalyzer. Labeled target cDNA was prepared from total RNA samples using the Ambion MessageAmp Premier protocol (3â IVT assay). Each sample target was hybridized to a Mouse 430 2.0 GeneChip array. Image processing and expression analysis were performed using Affymetrix GeneChip Command Console (AGCC) v. 3.1.1 and Affymetrix Expression Console v.1.1 software, respectively. Data from all biological replicates and conditions was imported into the Affymetrix Expression Console and normalized (RMA). RNA processing and microarray hybridization were performed by the Oregon Health & Science University Gene Microarray Shared Resource core facility in Portland, Oregon.**

Background corr dist: KL-Divergence = 0.0628, L1-Distance = 0.0441, L2-Distance = 0.0034, Normal std = 0.5375

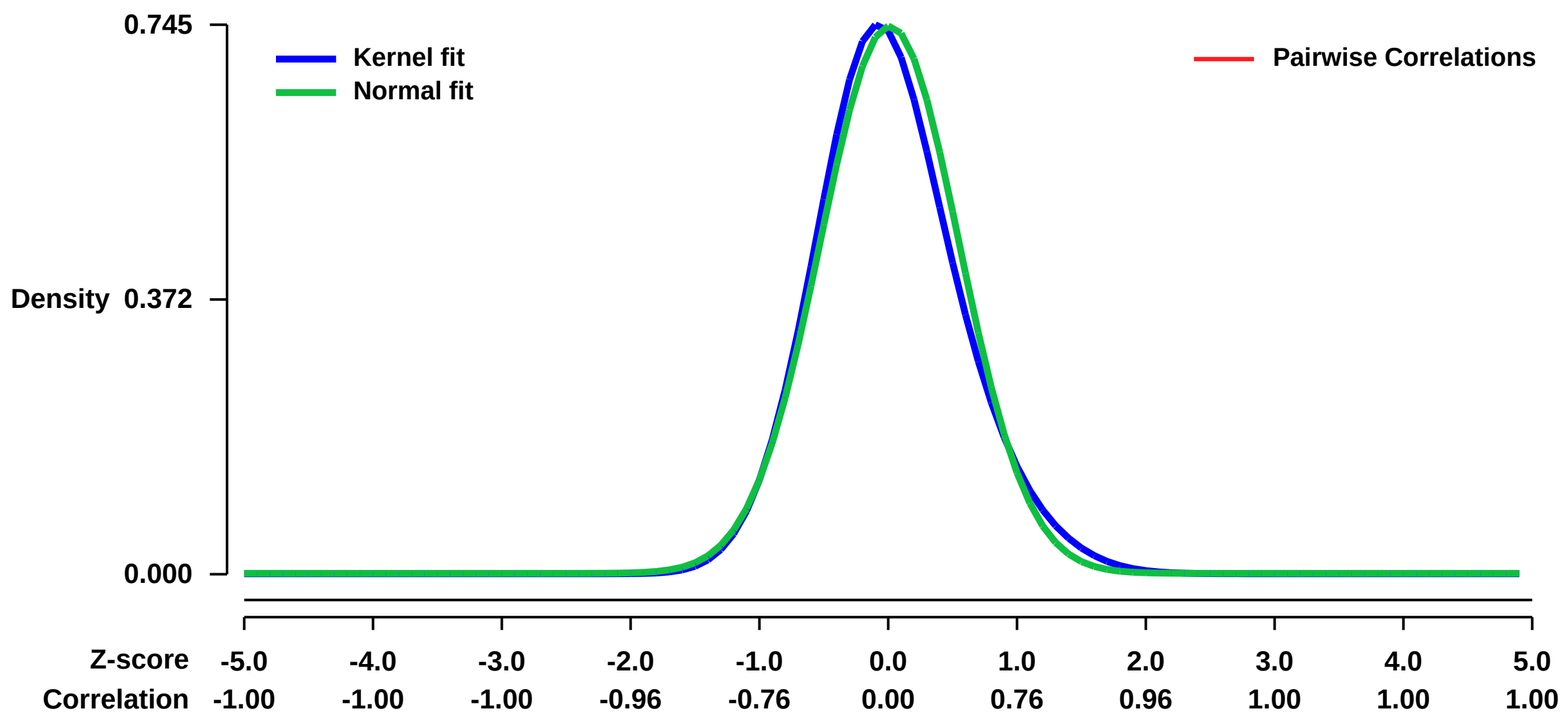

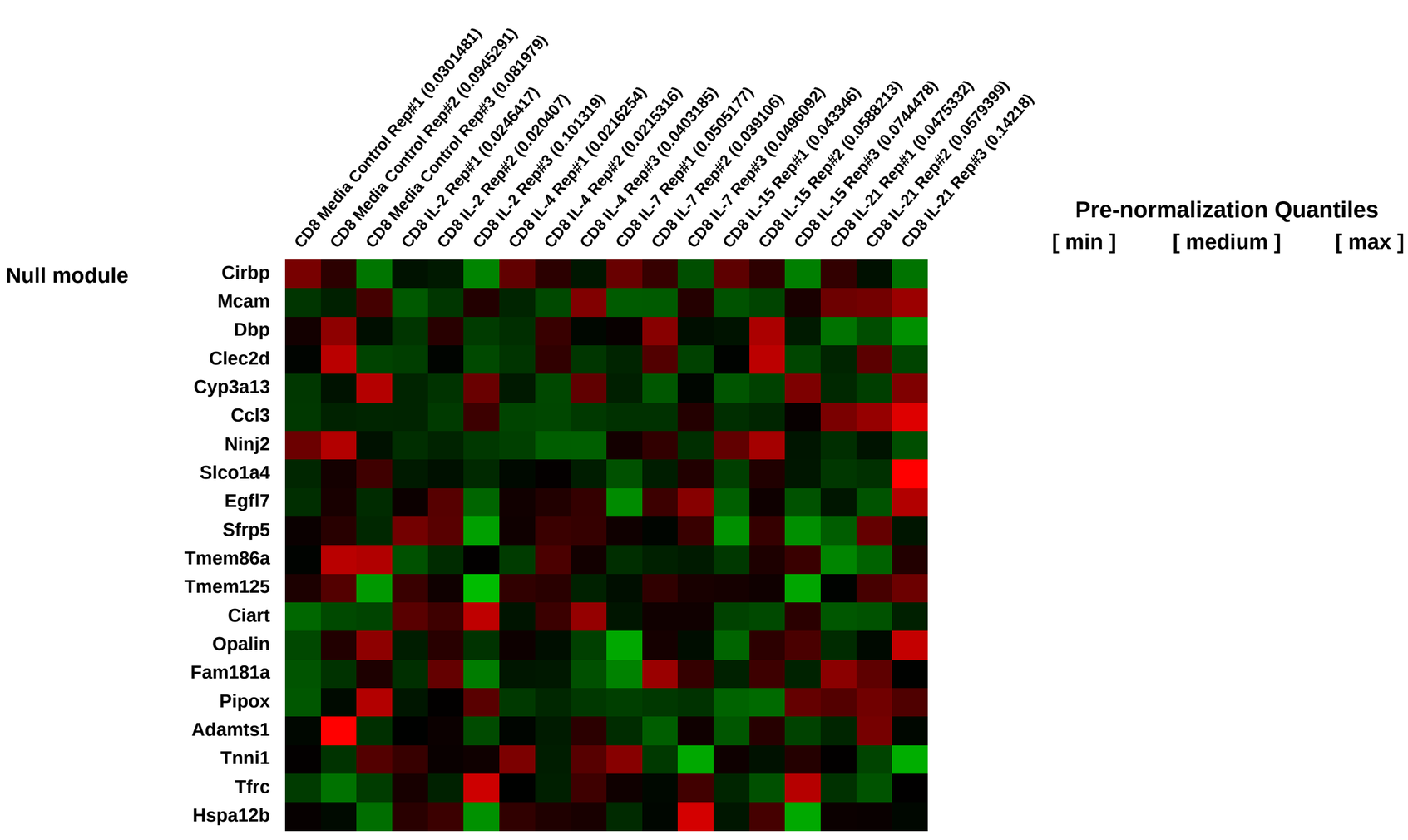

GEO Series "GSE12948" Expression Profiles

Num of samples in this series: 9

Scale of expression profile Z-scores

-3.0 -2.0 -1.0 0.0 1.0 2.0 3.0

GEO Link:	http://www.ncbi.nlm.nih.gov/geo/query/acc.cgi?acc=GSE12948
Status:	Public on Oct 27 2008
Title:	Oncogenesis of T-ALL and non-malignant consequences of overexpressing NOTCH1
Organism:	Mus musculus
Experiment type:	Expression profiling by array
Platform:	GPL1261
Pubmed ID:	20007543
Summary & Design:	**Summary:** We have determined the consequences of ICN1 overexpression from retroviral vectors introduced into bone marrow cells. Even though the tumors consist of phenotypically heterogeneous cells, no evidence for tumor stem cells was found. **Overall design:** Expression analysis, array-based comparative genomic hybridization and spectral karyotyping.

Background corr dist: KL-Divergence = 0.0309, L1-Distance = 0.0439, L2-Distance = 0.0027, Normal std = 0.6826

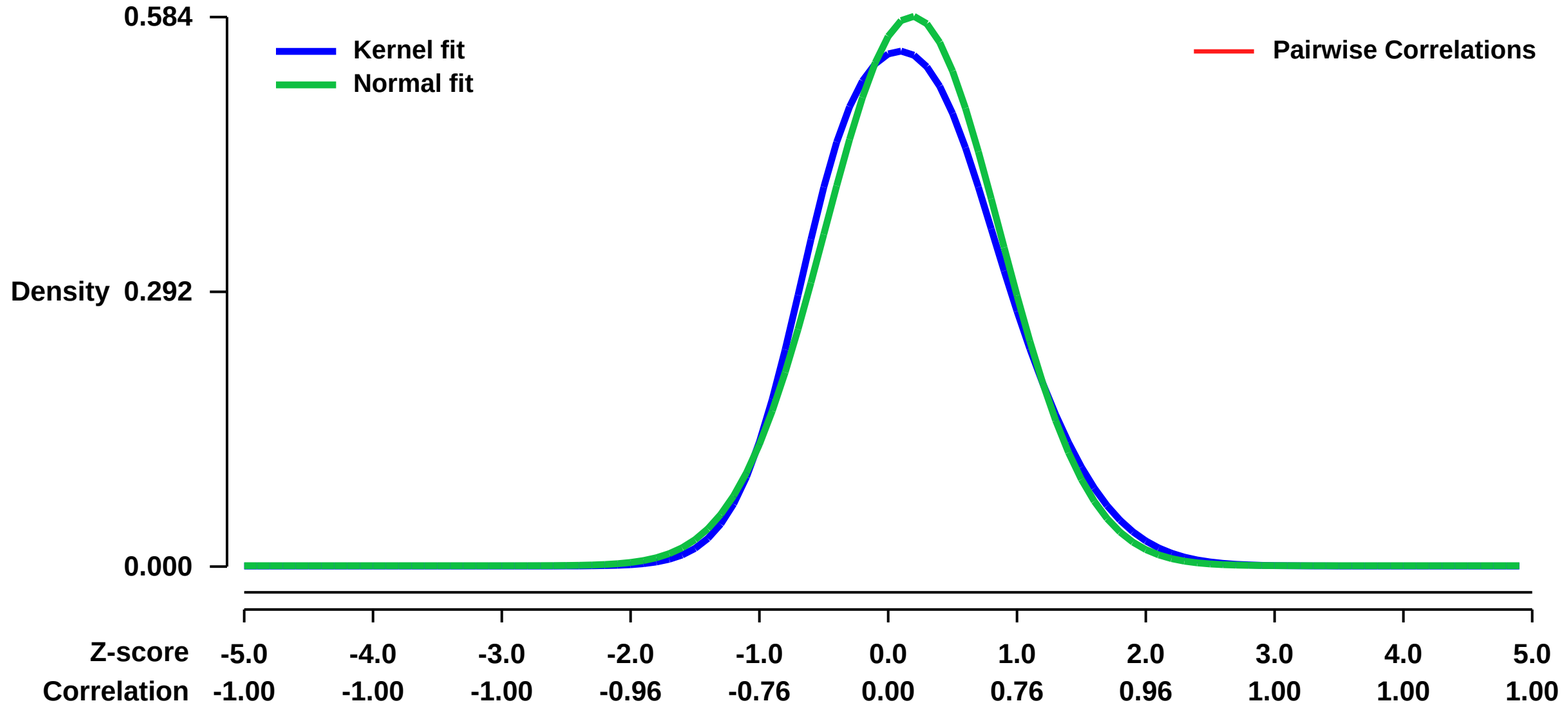

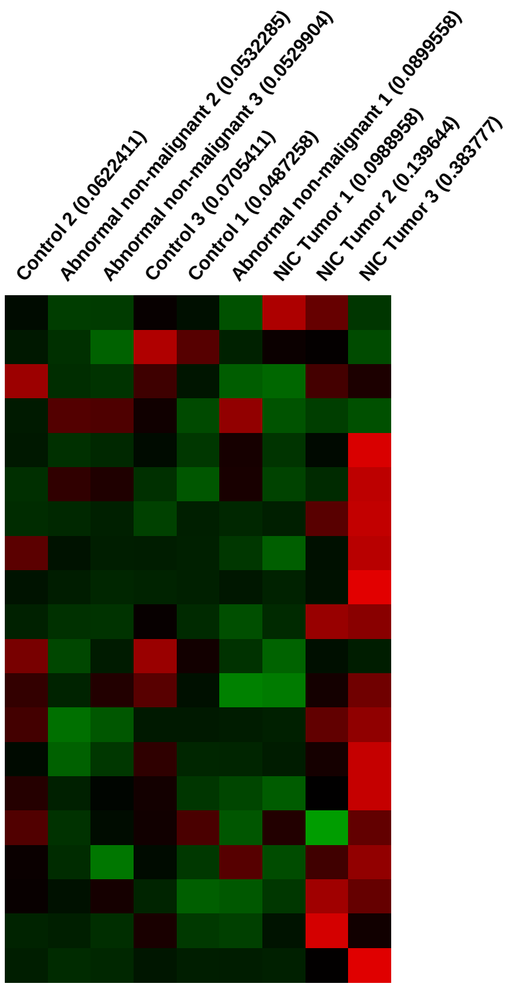

GEO Series "GSE8564" Expression Profiles

Num of samples in this series: 20

Scale of expression profile Z-scores

-3.0 -2.0 -1.0 0.0 1.0 2.0 3.0

GEO Link:	http://www.ncbi.nlm.nih.gov/geo/query/acc.cgi?acc=GSE8564
Status:	Public on Jul 22 2008
Title:	Analysis of Aire effects on individual mice of different genetic backgrounds
Organism:	Mus musculus
Experiment type:	Expression profiling by array
Platform:	GPL1261
Pubmed ID:	18838677
Summary & Design:	**Summary:** We compared gene expression profiles of aire-deficient and wild-type littermate thymic medullary epithelial cells. This was done in order to determine whether Aire's effects differed among strains, and also among individuals of the same strain. **Keywords: genetic modification** **Overall design:** Individual thymi were digested with collagenase, dispase and DNAse, and meduallary epithelial cells with the phenotype CD45-G8.8+Ly51intMHCclasssIIhi were isolated by FACS.

Background corr dist: KL-Divergence = 0.1413, L1-Distance = 0.0434, L2-Distance = 0.0041, Normal std = 0.3817

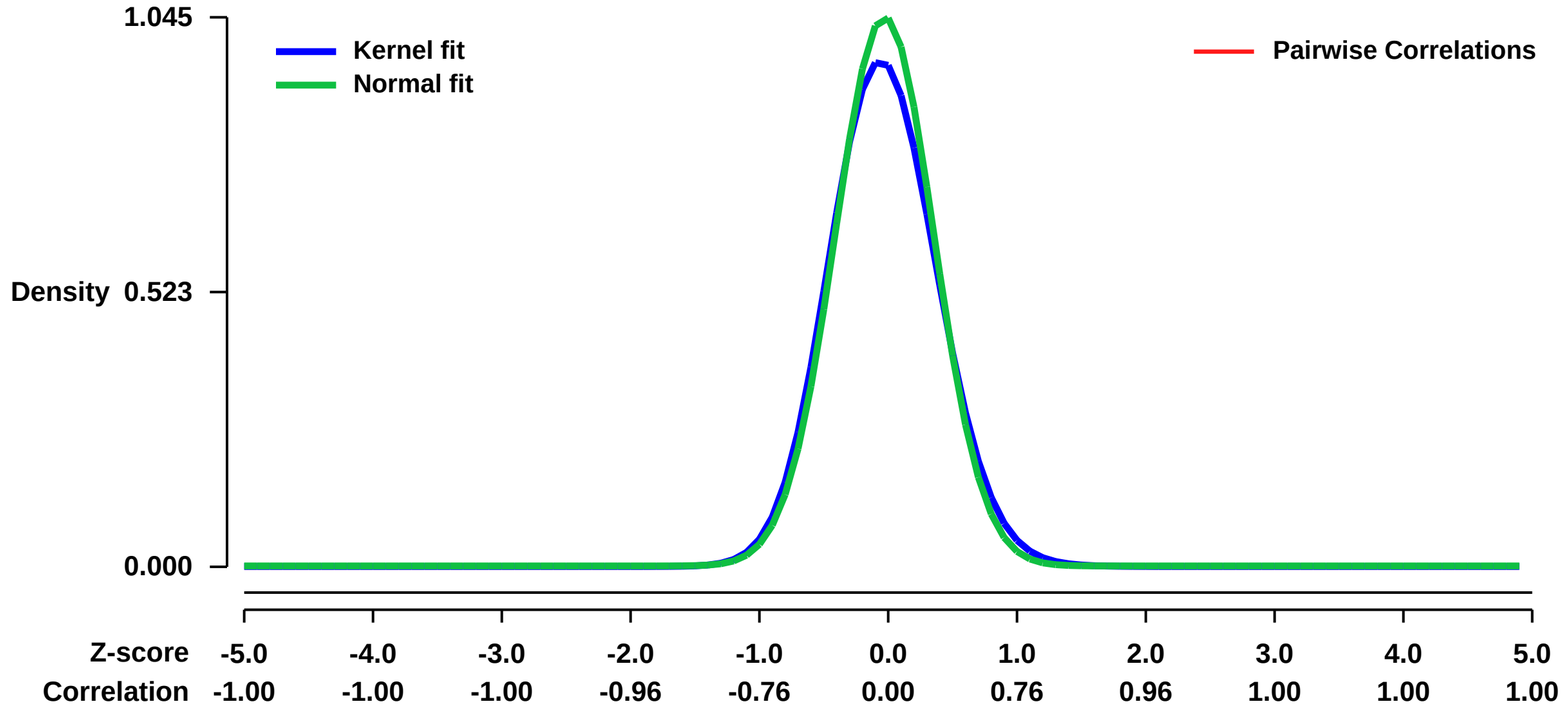

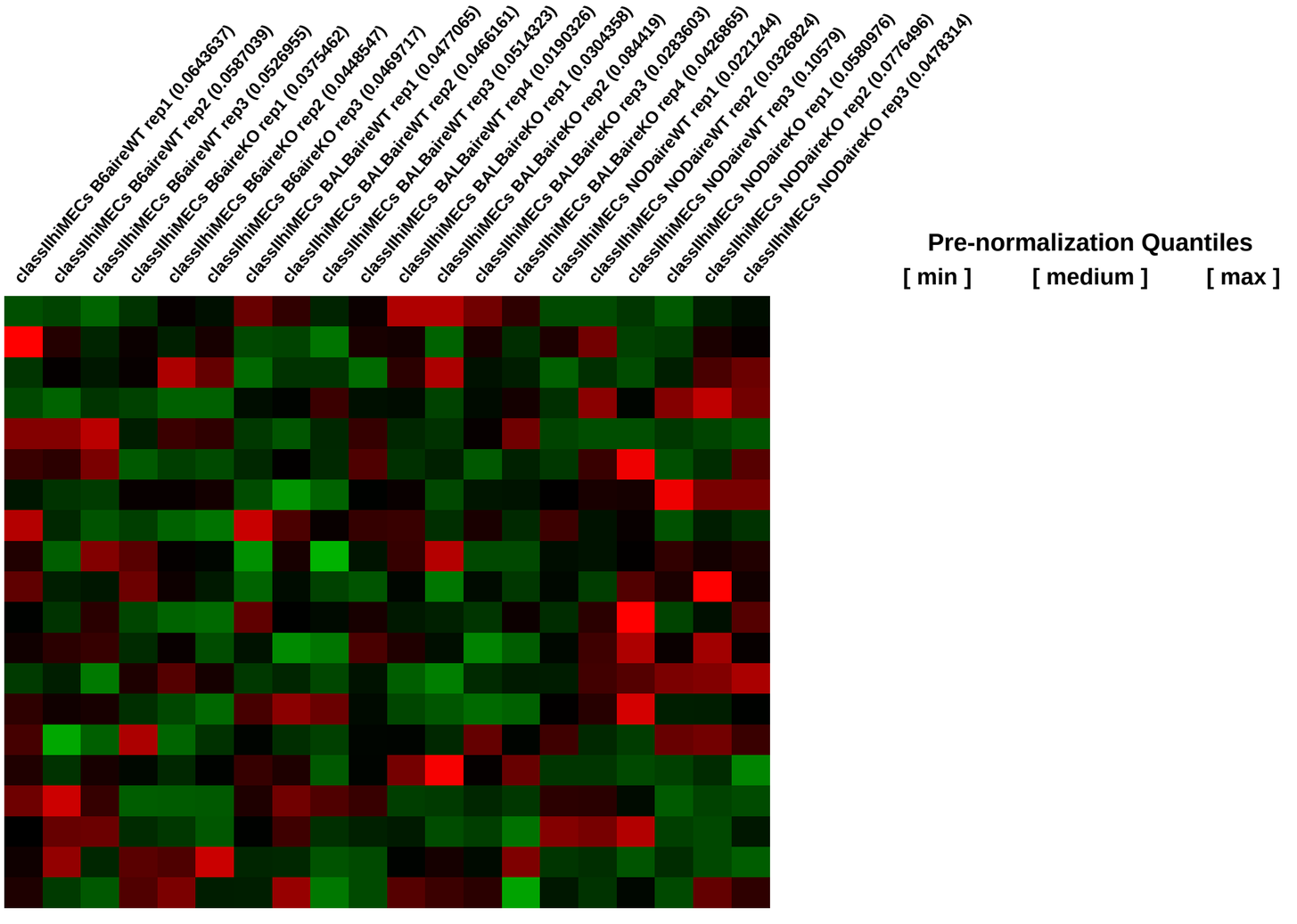

GEO Series "GSE39030" Expression Profiles

Num of samples in this series: 6

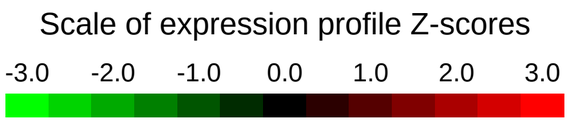

GEO Link:	http://www.ncbi.nlm.nih.gov/geo/query/acc.cgi?acc=GSE39030
Status:	Public on Oct 29 2013
Title:	Impact of ectopic expression of SNAIL2, ZEB2, ZEB1 or TWIST1 on BRAF-target genes in the murine melanocytic melan-a cell line
Organism:	Mus musculus
Experiment type:	Expression profiling by array
Platform:	GPL1261
Pubmed ID:	24075834
Summary & Design:	**Summary:** We have demonstrated that the oncogenic activation of B-RAF (using a truncated delta-BRAF-ER version inducible with tamoxifen) in the melan-a melanocyte cell line triggers the activation of Zeb1 and Twist1 at the expanse of Zeb2 and Snail2. Enforced maintenance of Zeb2 or Snail2 expression reduces the B-RAF oncogenic potential while ectopic expression of Zeb1 or Twist1 cooperates with B-RAF in melan-a cell transformation. To get an insight into the properties of these embryonic transcription factors, gene expression profiles of melan-a-derived cell lines either expressing a non-activated B-RAF (- tamoxifen) or an activated BRAF (+ tamoxifen) alone or in combination with Snail2, Zeb2, Twist1 or Zeb1 have been established. **Overall design:** Ectopic expression of SNAIL2, ZEB2, ZEB1 or TWIST1 on BRAF-target genes in the murine melanocytic melan-a cell line.

Background corr dist: KL-Divergence = 0.0343, L1-Distance = 0.0304, L2-Distance = 0.0011, Normal std = 0.6606

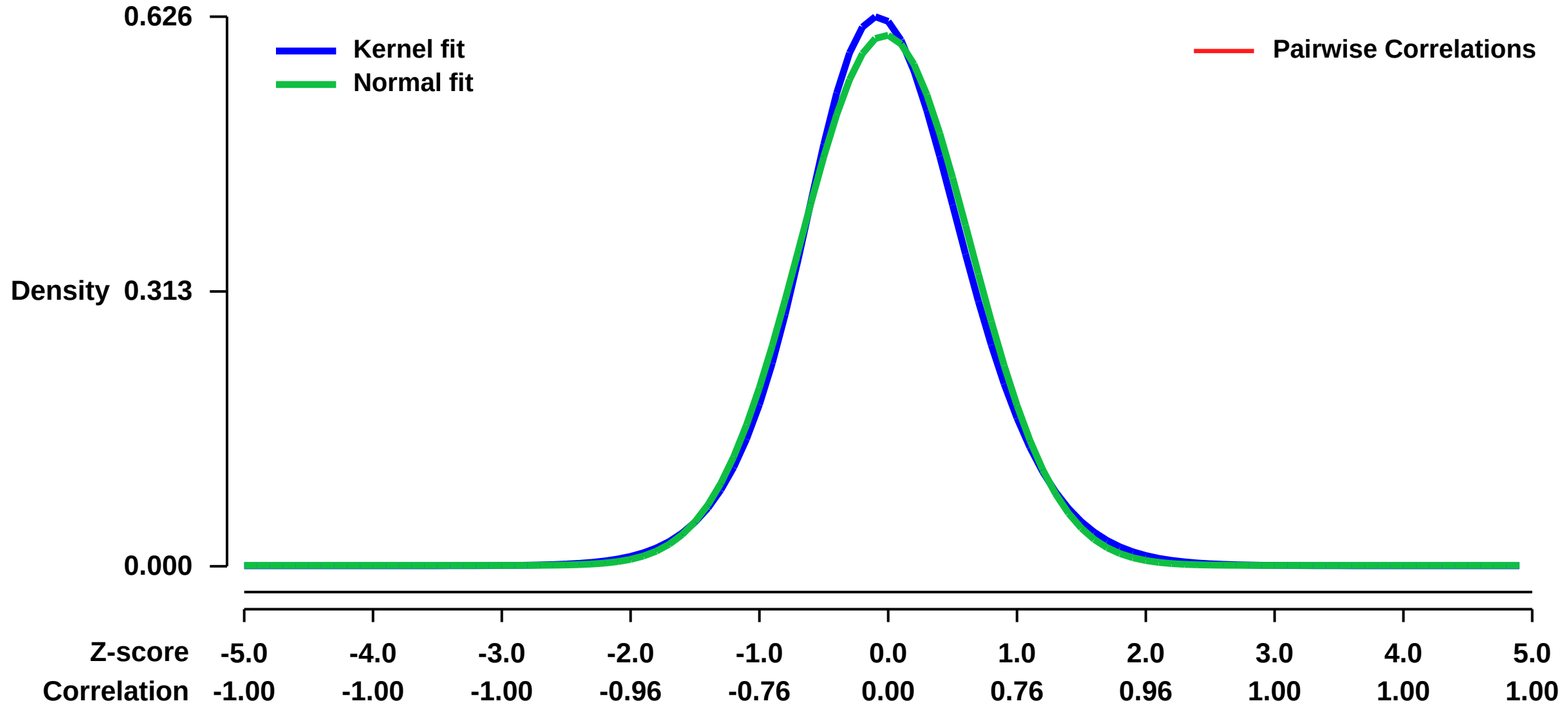

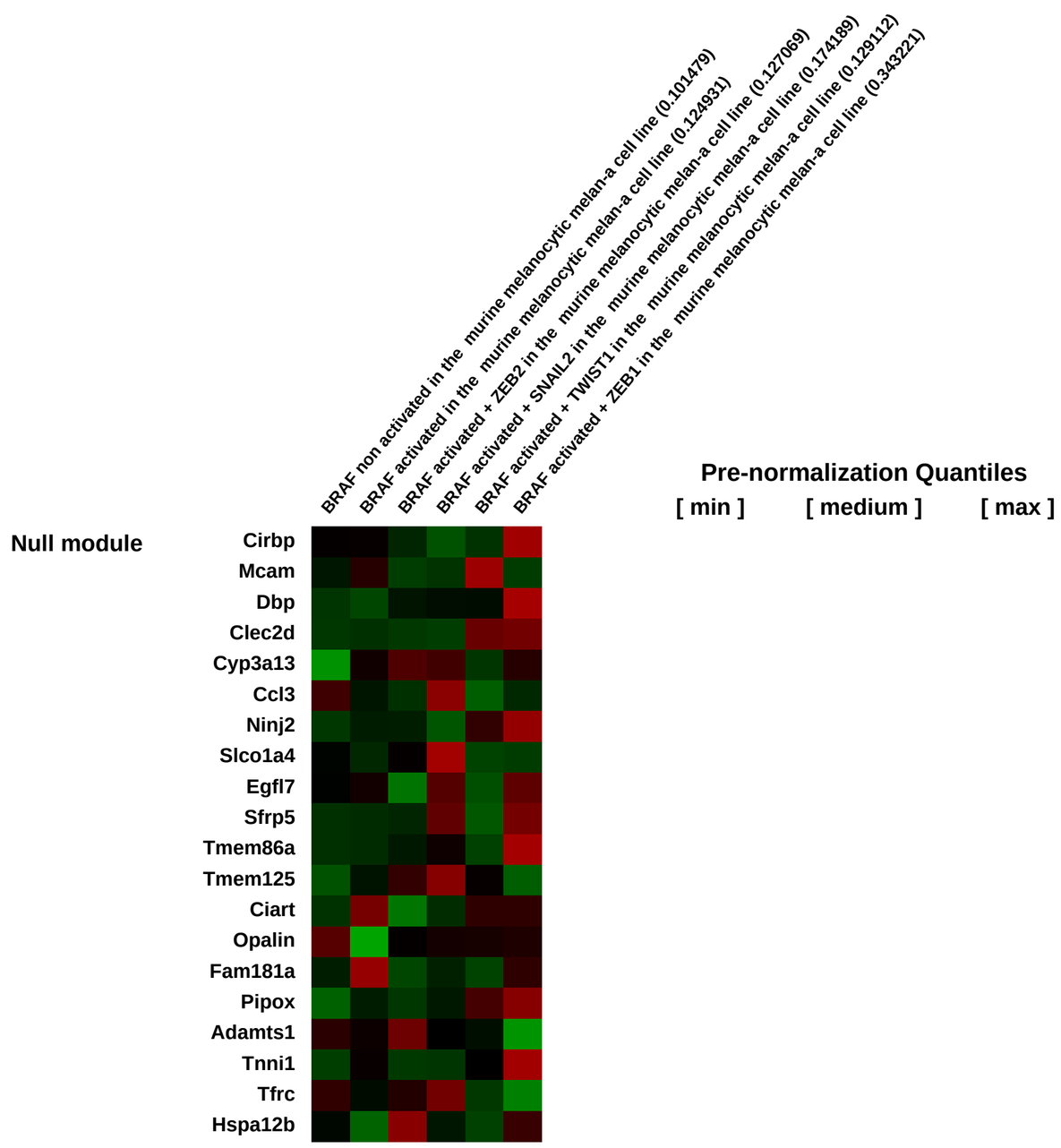

GEO Series "GSE27429" Expression Profiles

Num of samples in this series: 8

Scale of expression profile Z-scores

-3.0 -2.0 -1.0 0.0 1.0 2.0 3.0

GEO Link:	http://www.ncbi.nlm.nih.gov/geo/query/acc.cgi?acc=GSE27429
Status:	Public on Feb 22 2011
Title:	Expression data at 24 hours after the blocking of Shh signaling in tooth germs at embryonic day 14
Organism:	Mus musculus
Experiment type:	Expression profiling by array
Platform:	GPL1261
Pubmed ID:	21447550
Summary & Design:	**Summary:** The genetic mechanism governing the spatial patterning of teeth still remains to be elucidated. Sonic hedgehog (Shh) is one of key signaling molecules involved in the spatial patterning of teeth. By utilizing maternal transfer of 5E1 (an IgG1 monoclonal antibody against Shh protein) through the placenta to block Shh signaling, we investigated the changes in tooth patterning and in gene expression. We used microarrays to detect specific genes related with Shh signaling in tooth germs and identified some specific genes up- or down-regulated after blocking of Shh signaling activity. **Overall design:** Gene-chip expression analysis was performed with RNA from mandibular tooth germs from embryos of pregnant mice at one´ day after injection of 5E1 (an IgG1 monoclonal antibody against Shh protein; number of replicates =2), 40-1a (an IgG1 monoclonal antibody against ¸†-galactosidase; number of replicates=2), cyclopamine (a specific Smo antagonist; number of replicates=2) or PBS (Phosphate buffered saline; number of replicates=2), using a Affymetrix mouse gene microarray.

Background corr dist: KL-Divergence = 0.0607, L1-Distance = 0.0181, L2-Distance = 0.0004, Normal std = 0.5258

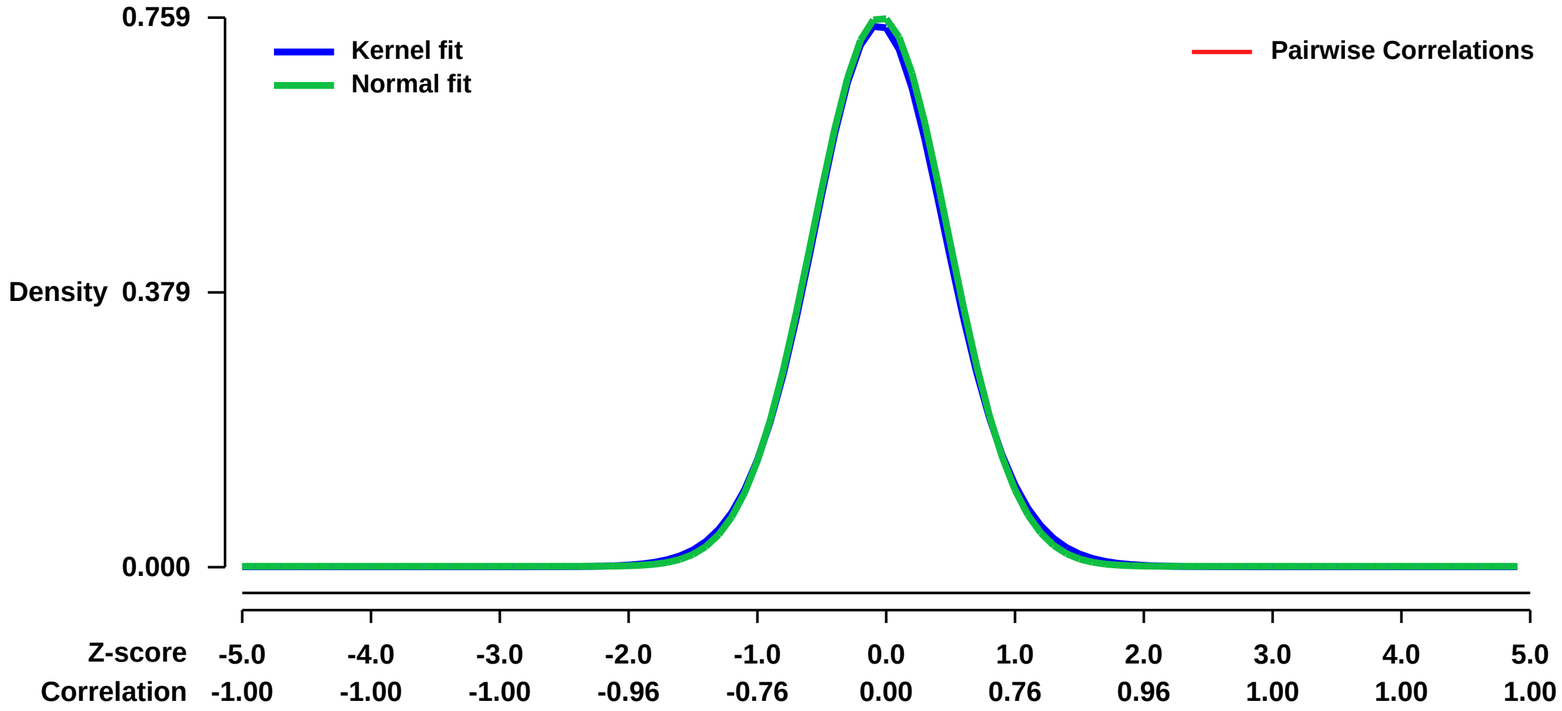

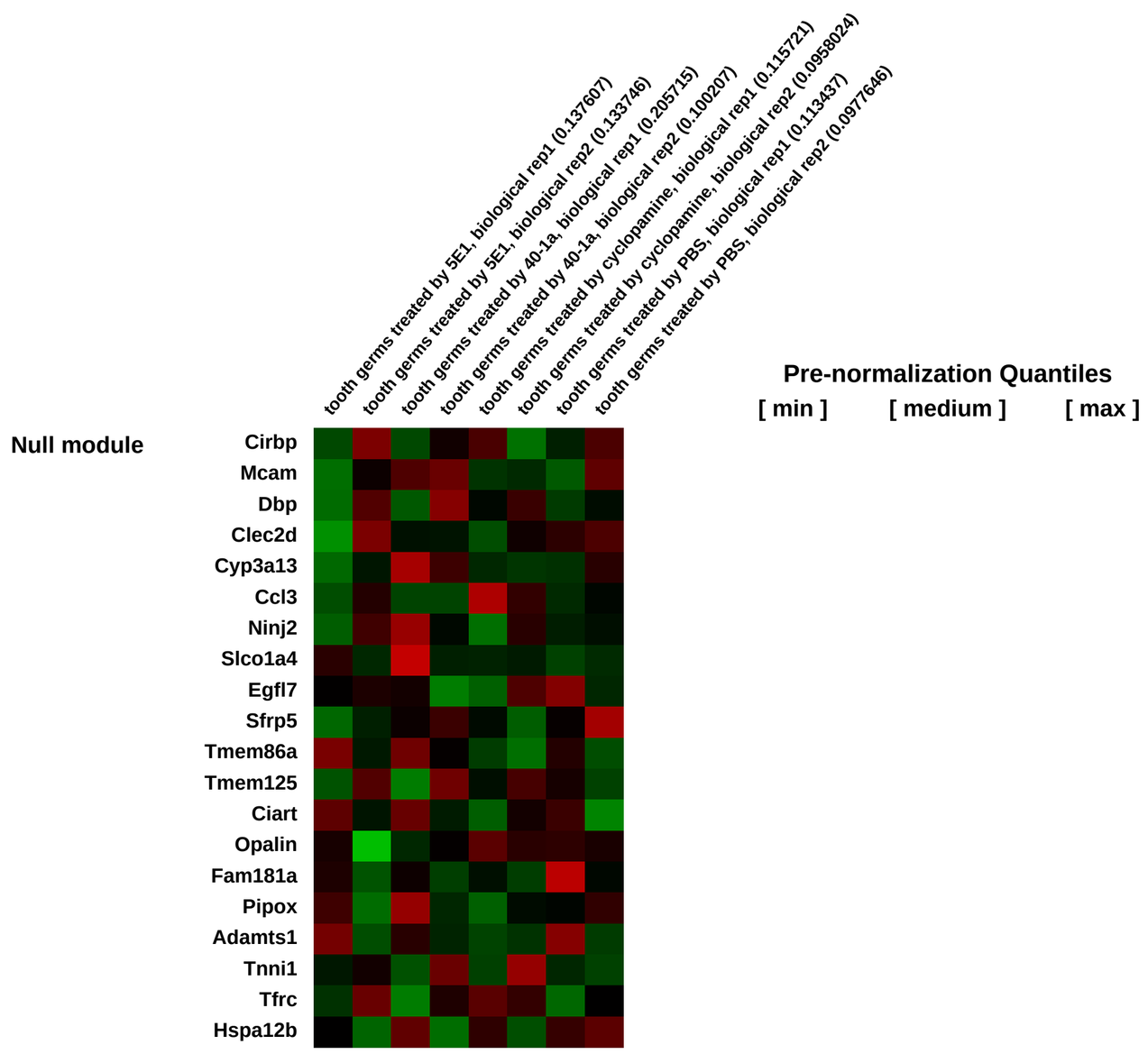

GEO Series "GSE21155" Expression Profiles

Num of samples in this series: 8

Scale of expression profile Z-scores

-3.0 -2.0 -1.0 0.0 1.0 2.0 3.0

GEO Link:	http://www.ncbi.nlm.nih.gov/geo/query/acc.cgi?acc=GSE21155
Status:	Public on Mar 29 2011
Title:	Accelerated leukemogenesis by truncated CBFb-SMMHC defective in high-affinity binding with RUNX1
Organism:	Mus musculus
Experiment type:	Expression profiling by array
Platform:	GPL1261
Pubmed ID:	20478528
Summary & Design:	**Summary:** Dominant RUNX1 inhibition has been proposed as a common pathway for CBF-leukemia. CBFb-SMMHC, a fusion protein in human acute myeloid leukemia (AML), dominantly inhibits RUNX1 largely through its RUNX1 high-affinity binding domain (HABD). We generated knock-in mice expressing CBFb-SMMHC with a HABD deletion, CBFb-SMMHCd179-221. These mice developed leukemia highly efficiently, even though hematopoietic defects associated with Runx1-inhibition were partially rescued. To identify changes in gene expression with the deletion of the HABD, we compared the gene expression profile in leukemia samples from mice expressing CBFb-SMMHCd179-221 with those from mice expressing full length CBFb-SMMHC. **Overall design:** Spleen cells were isolated from leukemic knock-in mice with full length CBFb-SMMHC at 2 months after ENU treatment and 2 leukemic CBFb-SMMHCd179-221 expressing chimeric mice at 3 weeks after birth. For each genotype, we performed two independent experiments with 4 Affymetrix GeneChip 430 chips.

Background corr dist: KL-Divergence = 0.0542, L1-Distance = 0.0201, L2-Distance = 0.0005, Normal std = 0.5550

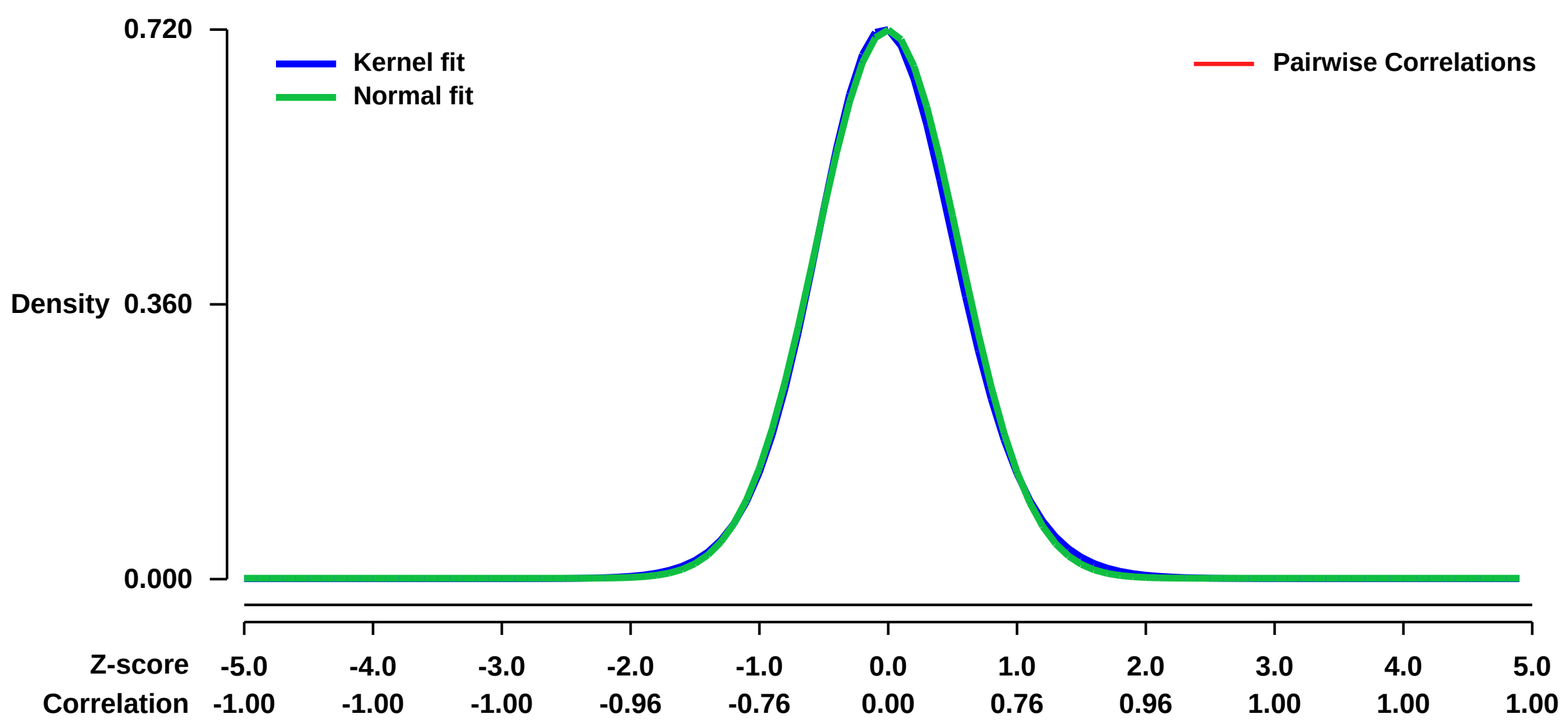

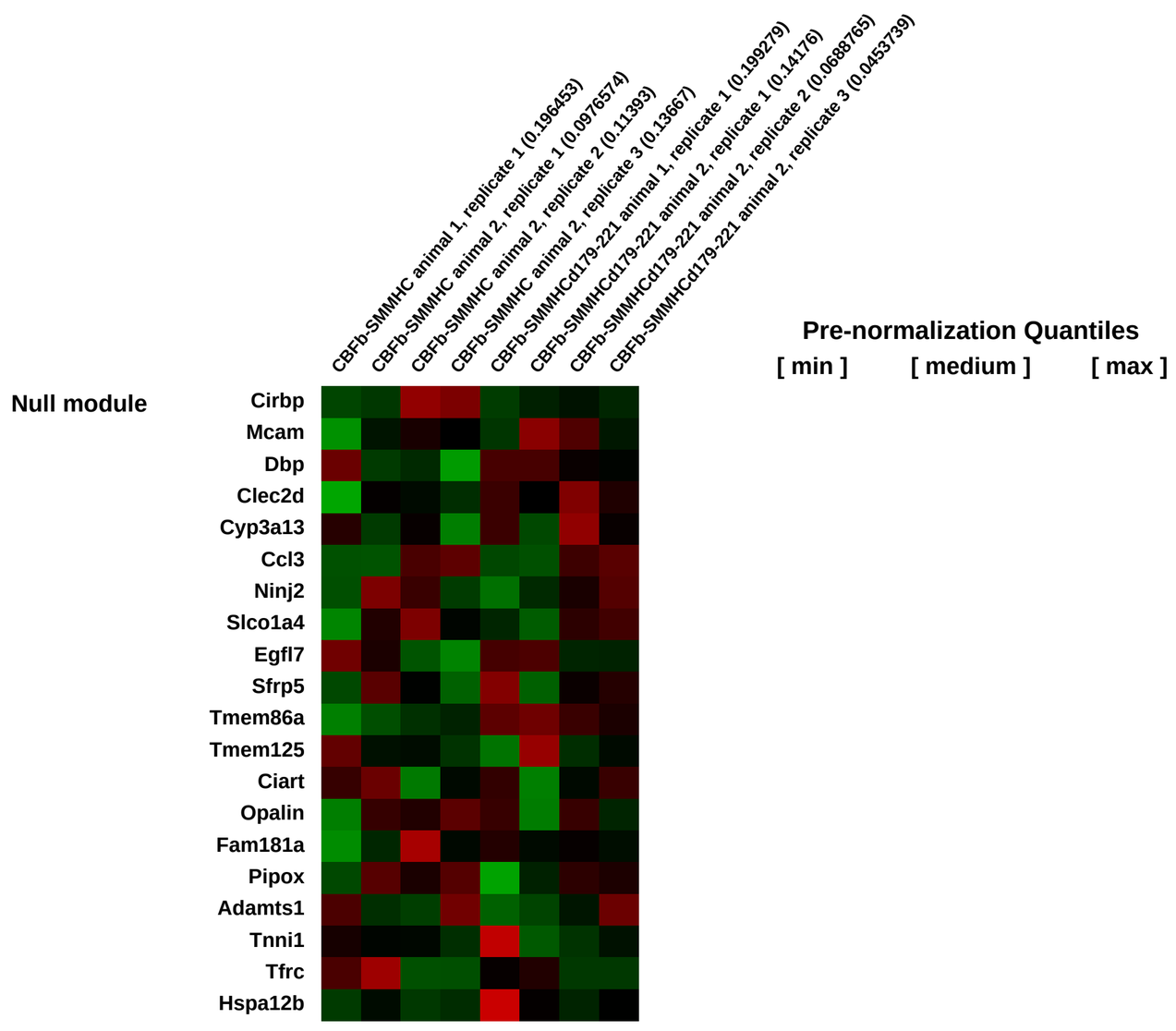

GEO Series "GSE10634" Expression Profiles

Num of samples in this series: 16

Scale of expression profile Z-scores

-3.0 -2.0 -1.0 0.0 1.0 2.0 3.0

GEO Link:	http://www.ncbi.nlm.nih.gov/geo/query/acc.cgi?acc=GSE10634
Status:	Public on Oct 01 2008
Title:	Aquaporin-11 knockout effect on kidney
Organism:	Mus musculus
Experiment type:	Expression profiling by array
Platform:	GPL1261
Pubmed ID:	18606867
Summary & Design:	**Summary:** Aquaporin-11 (AQP11), a new member of the aquaporin family, is localized in the endoplasmic reticulum (ER). Aqp11â /â mice neonatally suffer from polycystic kidneys derived from the proximal tubule. Its onset is proceeded by the vacuolization of ER. However, the mechanism for the formation of vacuoles and the development of cysts remain to be clarified. Here, we show that Aqp11â /â mice and polycystic kidney disease animals share a common pathogenic mechanism of cyst formation. Keywords: Geneexpression profile of Aqp11 knokout mouse kidney Overall design: Aqp11+/â mice, originally generated in a 129/SvEvBrd background (4), were back-crossed 10â 11 times to a C57/BL6 background. Heterozygous mice were interbred to obtain knockout (Aqp11â /â) and wild-type littermates (Aqp11+/+). The genotypes of offsprings were analyzed by PCR using tail DNA as a template. All animal experiments were approved by the Animal Care Committee of the University of Tokyo. One-week-old mice were sacrificed by cervical dislocation. Kidneys were rapidly excised on ice, washed in ice-cold phosphate-buffered saline, immersed in RNAlater (Ambion) and stored at â 20´℃. Total RNA was isolated using TRIzol Reagent (Invitrogen) and cleaned up using an RNeasy minikit with DNase treatment (Qiagen). The RNA quality and quantity were examined by agarose-gel electrophoresis and a spectrophotometer (GE Healthcare). Five pairs of Aqp11+/â mice were interbred, and we obtained 7 Aqp11+/+ and 9 Aqp11â /â offsprings. Three micrograms of total RNA obtained from each kidney was individually reverse-transcribed, amplified, and labeled using GeneChip One-Cycle Target Labeling and Control Reagent package (Affymetrix) according to the manufacturerâ s protocol. Labeled cRNA was hybridized to GeneChip Mouse Genome 430 2.0 Array (Affymetrix) (a total of 16 samples on 16 different arrays). The arrays were washed, stained using Fluidics Station (Affymetrix), and then scanned with the GeneChip Scanner (Affymetrix). Data collection was performed using GeneChip Operating Software (Affymetrix). The quality of collected data was checked by scatter plot analysis.

Background corr dist: KL-Divergence = 0.1852, L1-Distance = 0.0379, L2-Distance = 0.0028, Normal std = 0.3436

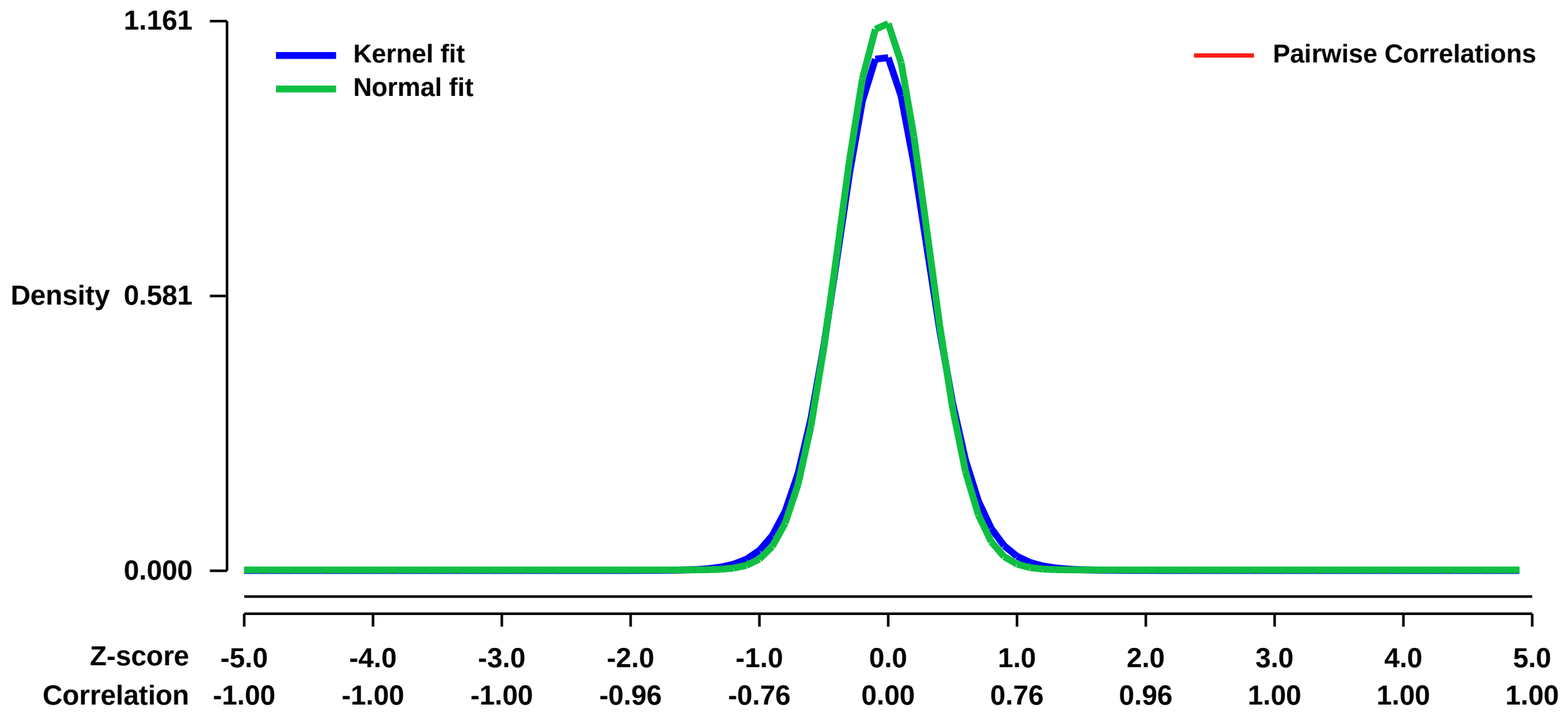

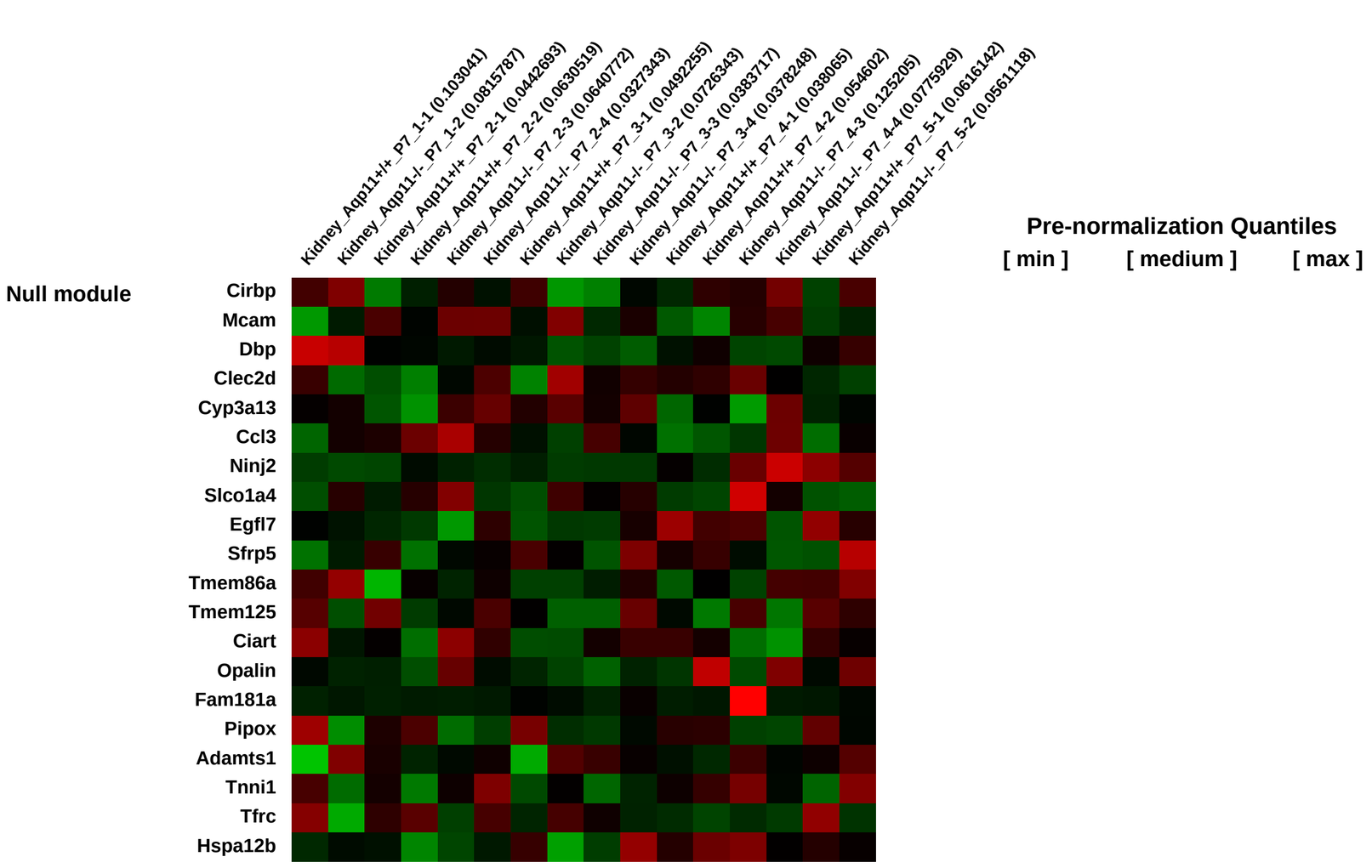

GEO Series "GSE21841" Expression Profiles

Num of samples in this series: 18

Scale of expression profile Z-scores

-3.0 -2.0 -1.0 0.0 1.0 2.0 3.0

GEO Link:	http://www.ncbi.nlm.nih.gov/geo/query/acc.cgi?acc=GSE21841
Status:	Public on May 15 2010
Title:	Expression data from LPS-stimulated RAW 264.7 mouse macrophages treated with Hypericum perforatum fraction and bioactive constituents
Organism:	Mus musculus
Experiment type:	Expression profiling by array
Platform:	GPL1261
Pubmed ID:	20303133
Summary & Design:	**Summary:** Hypericum perforatum extracts have been used as dietary supplements to treat conditions including mild-moderate depression and inflammation. A group of four bioactive constituents were identified from an active fraction of the extract. In order to identify the mechanism for the potential anti-inflammatory activity of the identified compounds, we used Affymatrix microarray to study the gene expression profile impacteded by these compounds, as well as the active fraction in LPS-stimulated mouse macrophages. **Overall design:** We treated RAW264.7 mouse macrophages with DMSO control, active fraction from Hypericum perforaum extract, and a combination of the 4 putative bioactive compounds, called the 4-component system, all with and without LPS induction. A total of six treatment combinations were included in the final gene expression analysis using microarray.

Background corr dist: KL-Divergence = 0.1757, L1-Distance = 0.0331, L2-Distance = 0.0020, Normal std = 0.3605

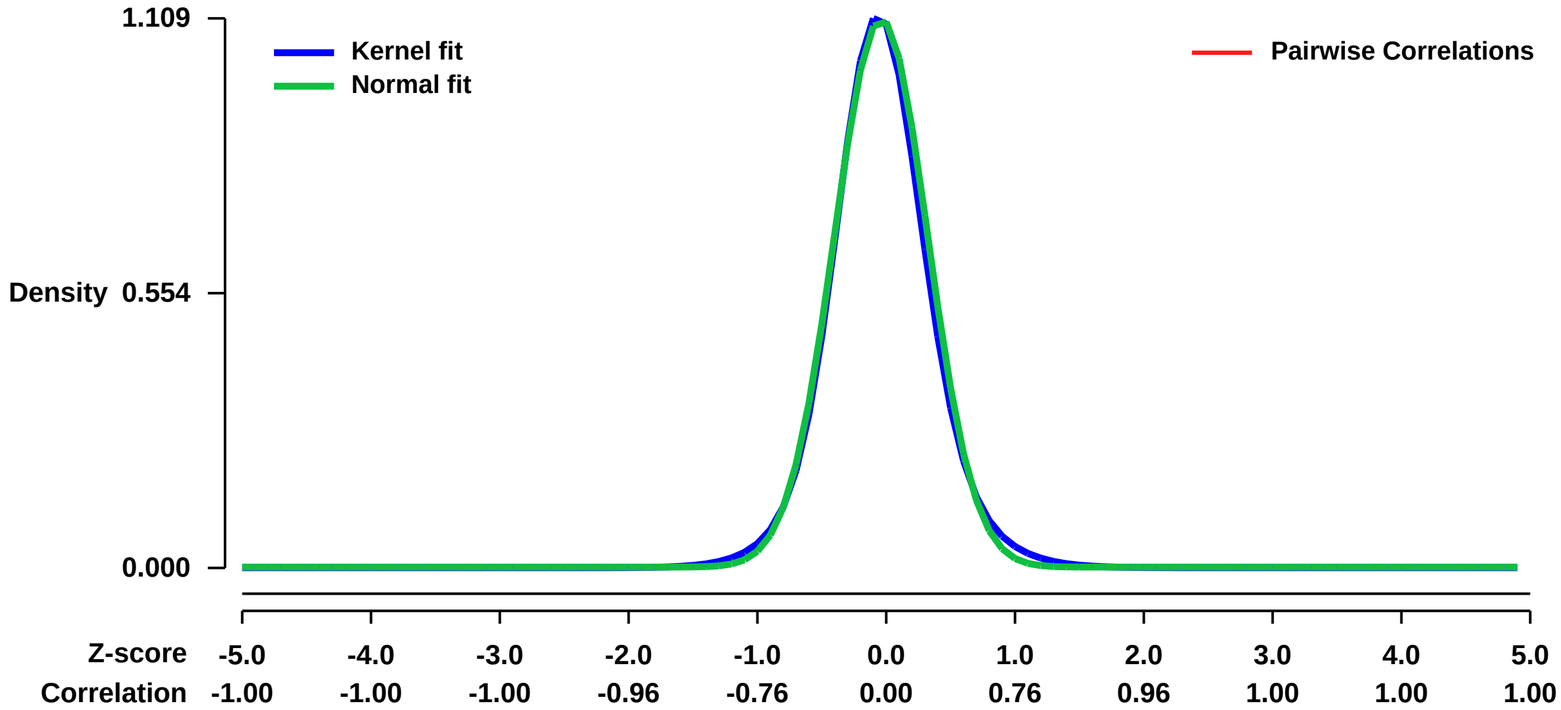

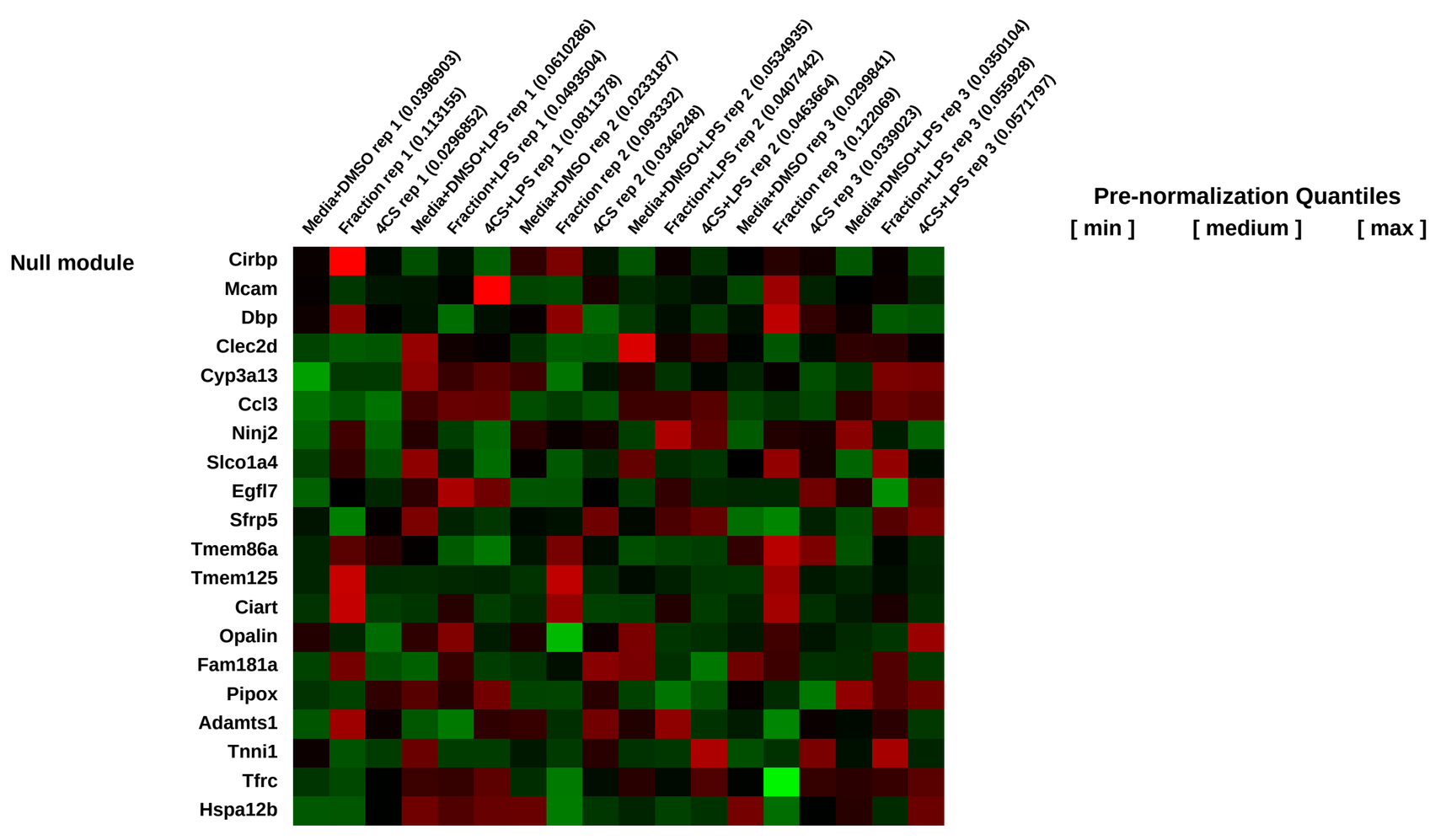

GEO Series "GSE20371" Expression Profiles

Num of samples in this series: 12

Scale of expression profile Z-scores

-3.0 -2.0 -1.0 0.0 1.0 2.0 3.0

GEO Link:	**http://www.ncbi.nlm.nih.gov/geo/query/acc.cgi?acc=GSE20371**
Status:	**Public on Dec 31 2013**
Title:	**PPARd target genes in MEFs**
Organism:	**Mus musculus**
Experiment type:	**Expression profiling by array**
Platform:	**GPL1261**
Pubmed ID:	
Summary & Design:	**Summary:** **The PPAR (Peroxisome proliferator-activated receptor) family of nuclear receptors has three members: PPARg, PPARa and PPARd. Although they share similar structures, their biological functions are distinct. PPARg controls lipid storage and adipogenesis, while PPARd is associated with fat burning. The highly specific synthetic ligand for PPARd, GW501516, is a promising drug candidate for obesity and diabetes. Here we use Affymetrix microarray to analyze gene expression profile in mouse embryo fibroblasts treated with 100 nM GW501516 for 0, 2, 8 and 24 hours. These data may provide new clues into the molecular mechanism by which GW501516 ameliorates obesity and diabetes.** **Overall design:** **Wild type mouse embryonic fibroblasts (MEFs) stably infected with retroviruses MSCVpuro expressing PPARd were plated at 0.5 million per 10 cm dish. After overnight incubation, cells were treated with 100nM GW501516 for 0h, 2h, 8h and 48h. Cells were collected at subconfluent condition. Total RNAs were sequentially purified with Trizol (Invitrogen) and RNeasy kit (Qiagen) and analyzed in triplicate on Mouse Genome 430 2.0 Array (Affymetrix) at NIDDK Microarray Core Facility following standard protocols.**

Background corr dist: **KL-Divergence = 0.1745, L1-Distance = 0.0430, L2-Distance = 0.0040, Normal std = 0.3502**

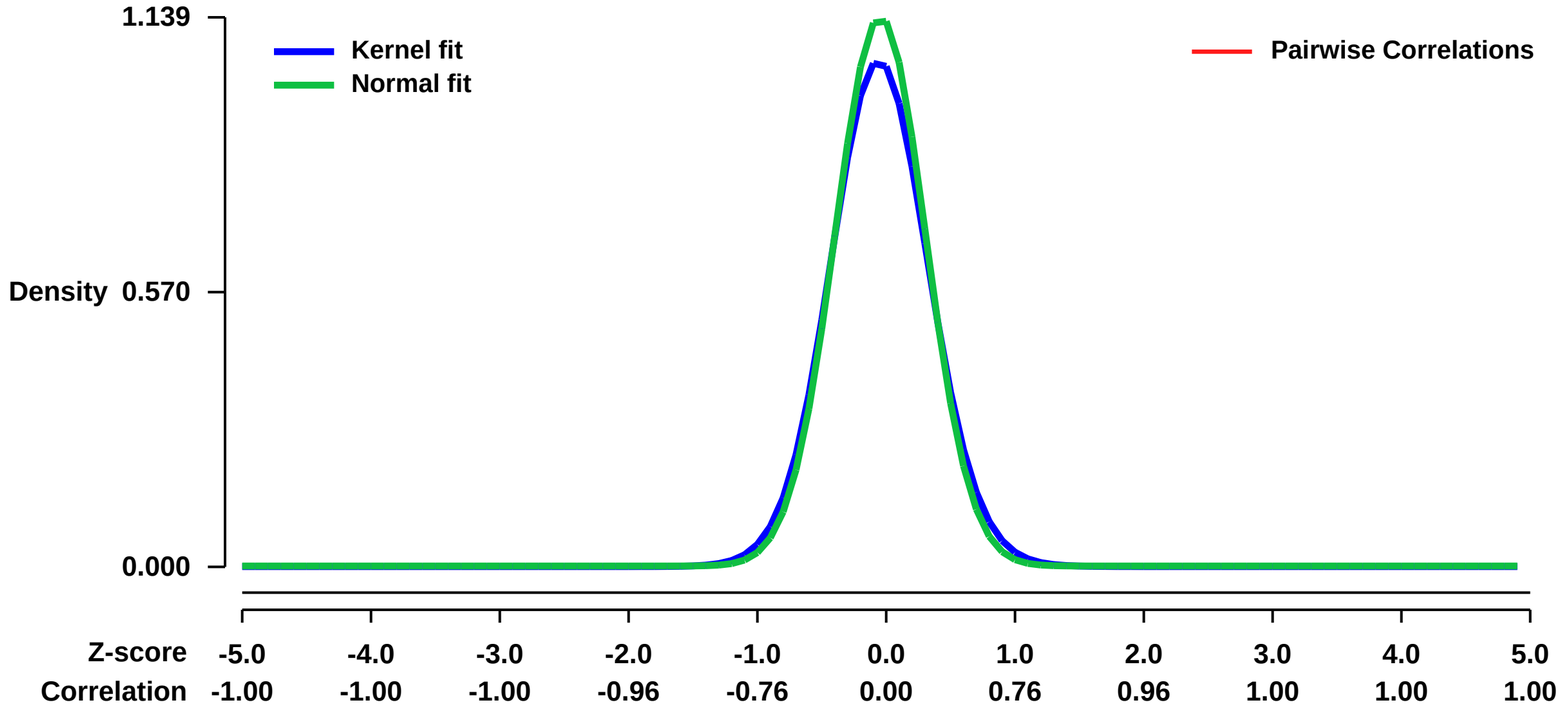

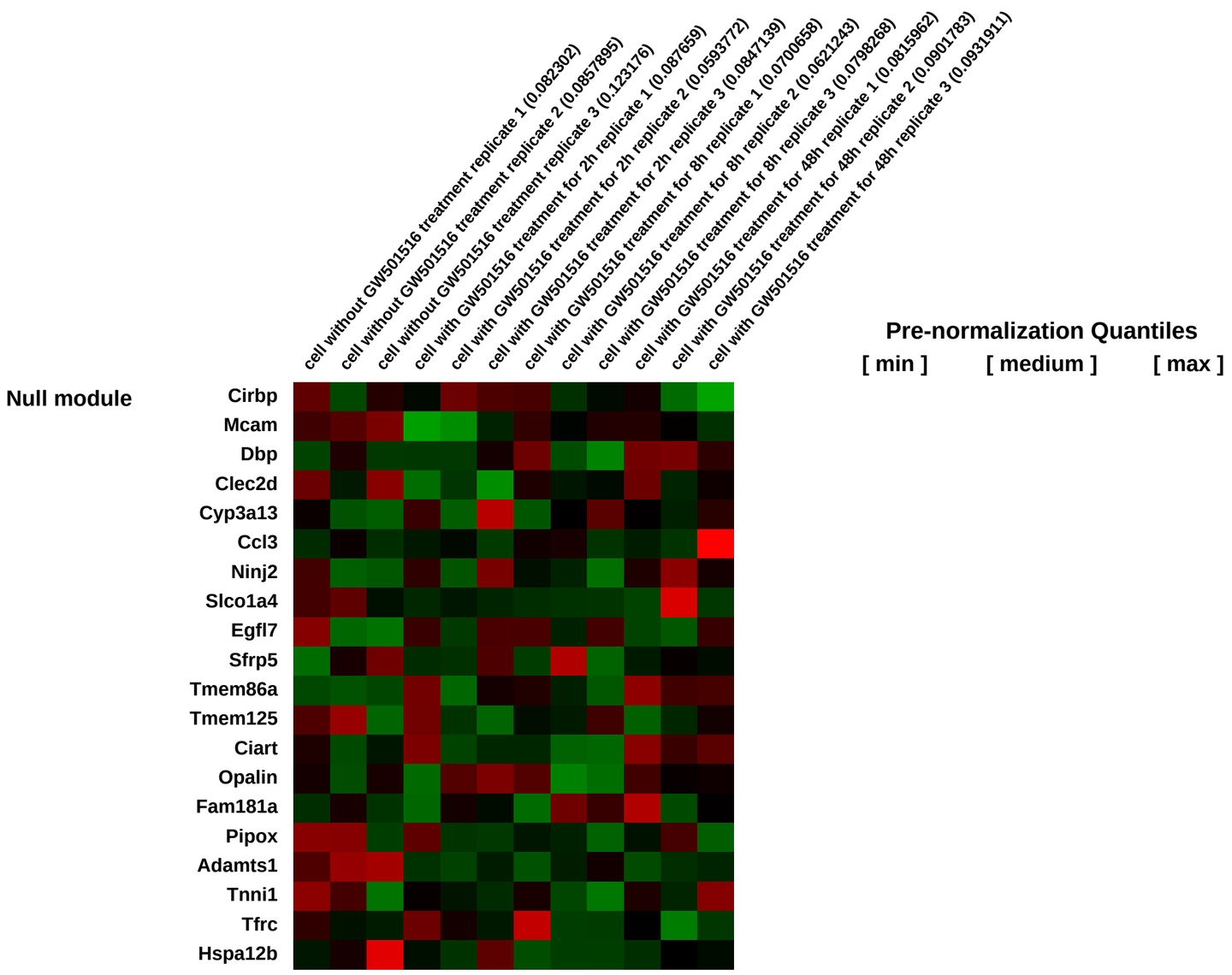

GEO Series "GSE8683" Expression Profiles

Num of samples in this series: 11

Scale of expression profile Z-scores

-3.0 -2.0 -1.0 0.0 1.0 2.0 3.0

GEO Link:	http://www.ncbi.nlm.nih.gov/geo/query/acc.cgi?acc=GSE8683
Status:	Public on Jan 11 2008
Title:	Gene expression in 3T3-L1 mouse tissue (preadipocytes) treated with Trans-10,Cis-12 conjugated linoleic acid(t10c12 CLA)
Organism:	Mus musculus
Experiment type:	Expression profiling by array
Platform:	GPL1261
Pubmed ID:	17878318
Summary & Design:	**Summary:** Trans-10, Cis-12 conjugated linoleic acid (t10c12 CLA) causes fat loss in mouse white adipose tissue (WAT) and 3T3-L1 adipocyte tissue culture; however in preadipocyte tissue (this series) the UPS/ISR and fat loss is not detected. The early transcriptome changes in 3T3-L1 preadipocyte tissue culture were analyzed using high-density microarrays to better characterize the signaling pathways responding to t10c12 CLA. Their gene expression responses between 4 to 12 hr after treatment do not show a set of genes indicative of an integrated stress response (ISR). **Keywords:** control/treatment time course **Overall design:** Mouse 3T3-L1 RNA for each time point was isolated from two control (LA) and two treatment (CLA) samples for analysis on four microarrays.

Background corr dist: KL-Divergence = 0.0965, L1-Distance = 0.0724, L2-Distance = 0.0128, Normal std = 0.4696

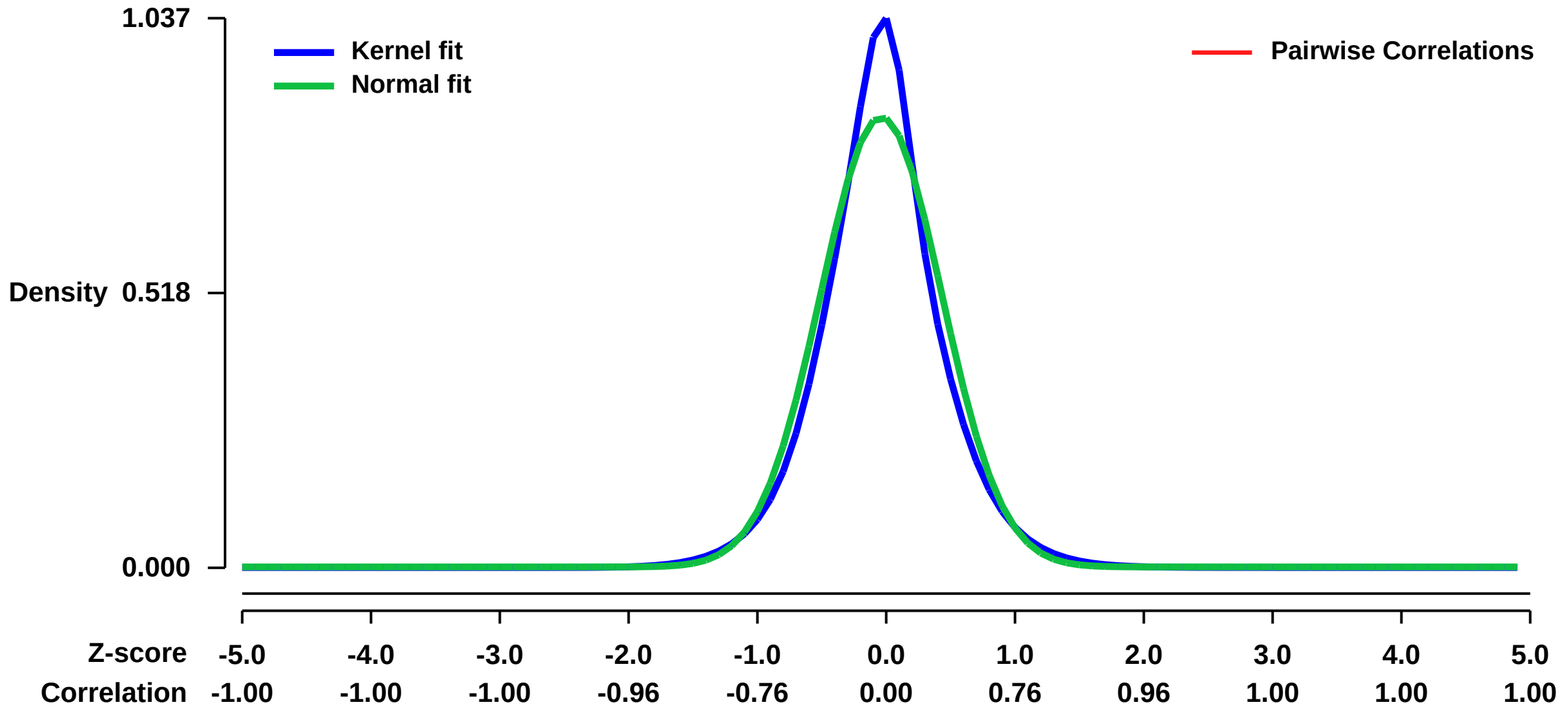

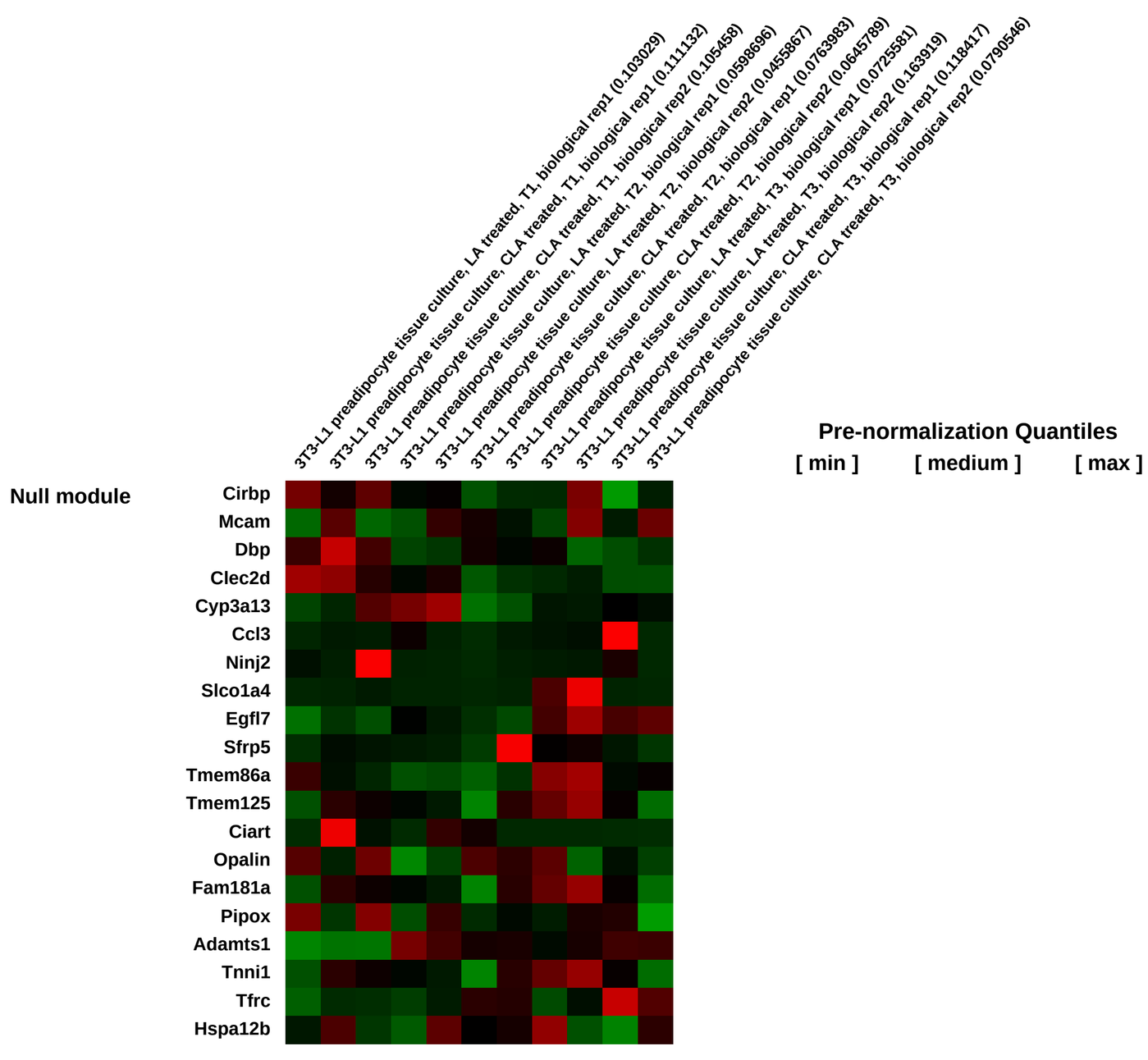

GEO Series "GSE10871" Expression Profiles

Num of samples in this series: 32

Scale of expression profile Z-scores

-3.0 -2.0 -1.0 0.0 1.0 2.0 3.0

GEO Link:	http://www.ncbi.nlm.nih.gov/geo/query/acc.cgi?acc=GSE10871
Status:	Public on May 28 2008
Title:	Differentiated, partially- and fully-reprogrammed MEFs/B-cells
Organism:	Mus musculus
Experiment type:	Expression profiling by array
Platform:	GPL1261
Pubmed ID:	18509334
Summary & Design:	**Summary:** Expression profiles generated during dissection of the molecular mechanisms underlying direct reprogramming of somatic cells to a pluripotent state (induced pluripotent stem cells, iPS). **Keywords: Cell type comparison/Timecourse** **Overall design:** 2 technical replicates of B lymphocytes, partially reprogrammed (MCV8, MCV6, BIV1), MEF-iPS(Oct4) and B-iPS(Nanog) cell lines.

Background corr dist: KL-Divergence = 0.2296, L1-Distance = 0.0483, L2-Distance = 0.0064, Normal std = 0.3326

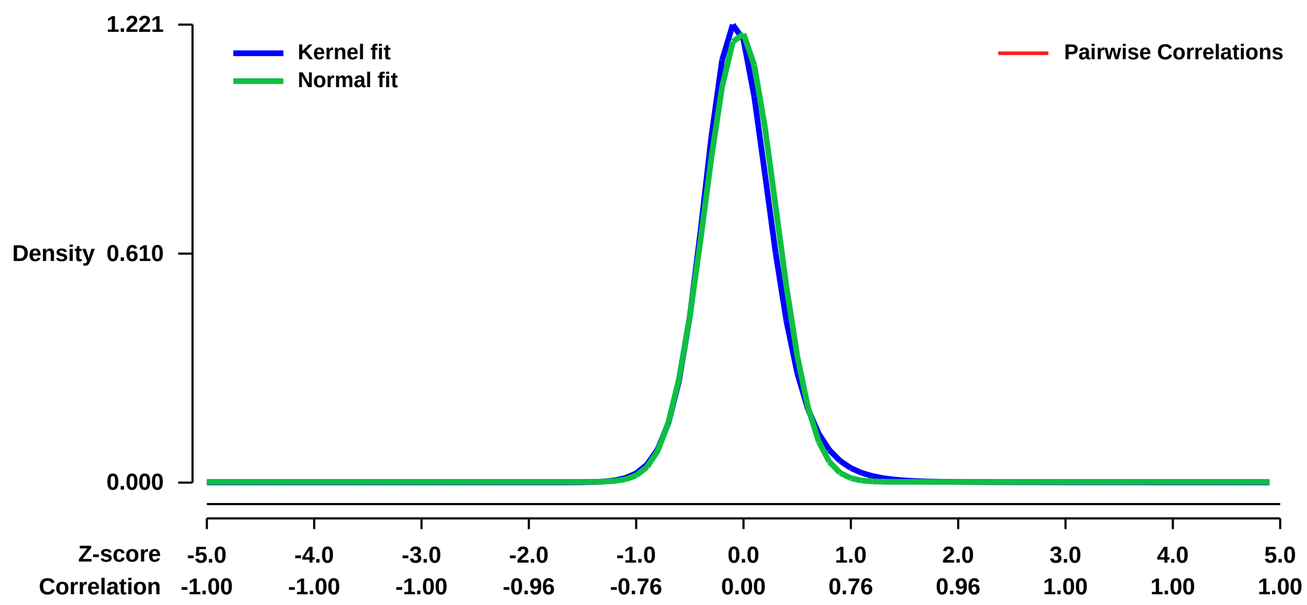

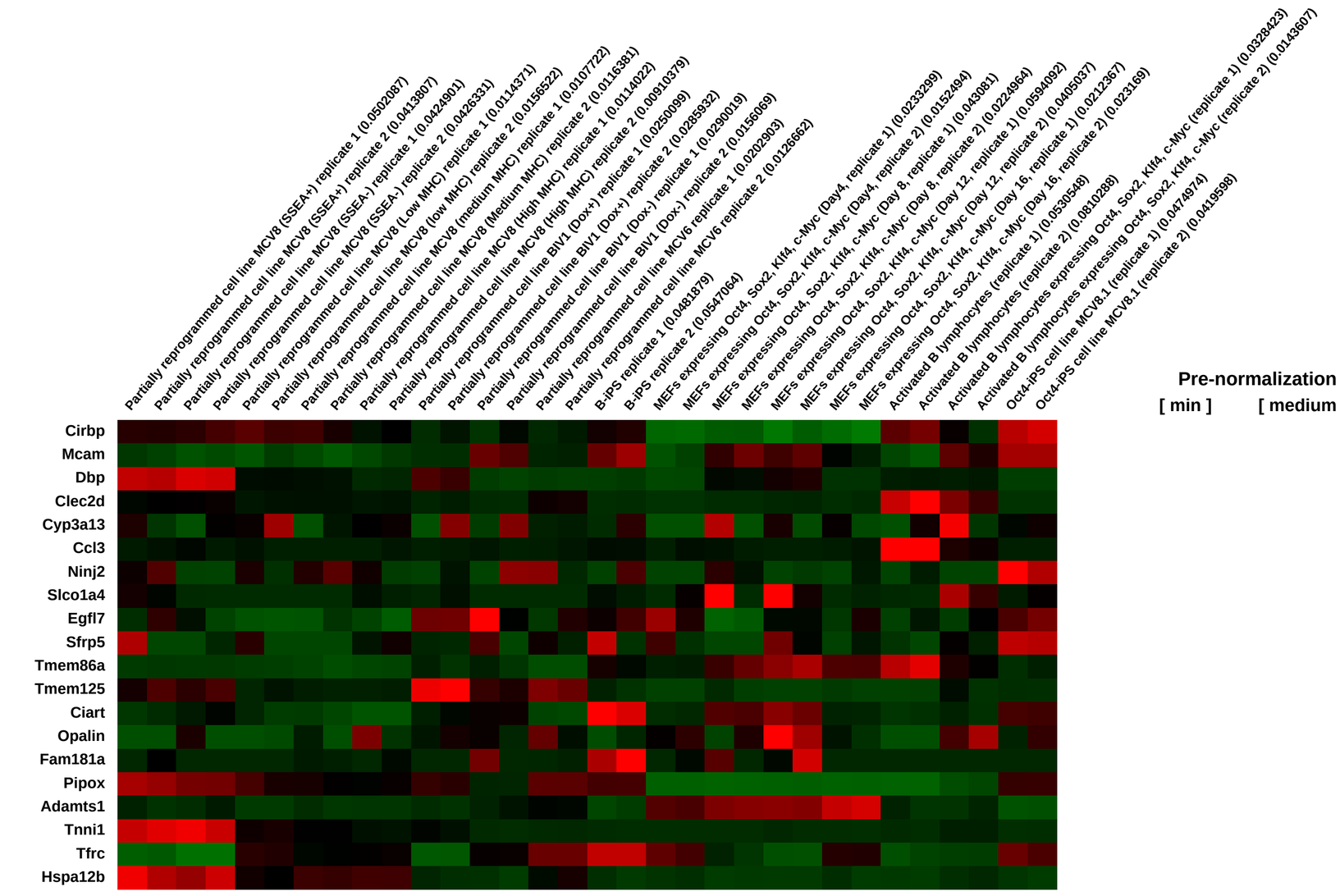

GEO Series "GSE34064" Expression Profiles

Num of samples in this series: 6

Scale of expression profile Z-scores

-3.0 -2.0 -1.0 0.0 1.0 2.0 3.0

GEO Link:	http://www.ncbi.nlm.nih.gov/geo/query/acc.cgi?acc=GSE34064
Status:	Public on Jan 01 2013
Title:	Expression data from mesodermal Tbx1-knockout otic vesicles at E11.5
Organism:	Mus musculus
Experiment type:	Expression profiling by array
Platform:	GPL1261
Pubmed ID:	
Summary & Design:	**Summary:** The T-box transcription factor Tbx1 is expressed in the otic vesicle and surrounding periotic mesenchyme during inner ear development. Mesenchymal Tbx1 is essential for inner ear development, with conditional mutants displaying defects in both auditory and vestibular systems. We have previously identified reduced expression of retinoic acid metabolic genes in the periotic mesenchyme of mesoderm conditional Tbx1 mutants, using the T-Cre mouse line, implicating retinoic acid in mesenchymal-epithelial signaling downstream of Tbx1 in the periotic mesenchyme. In order to identify downstream effectors of mesenchymal-epithelial signaling downstream of mesenchymal Tbx1, we have utilized a gene profiling approach comparing embryonic day 11.5 otic vesicle tissue from T-Cre-mediated conditional Tbx1 mutants (Mest-KO) and conditional heterozygous control litter mates (control). **Overall design:** E11.5 T-Cre-mediated conditional Tbx1 mutants (Mest-KO) and control (T-Cre conditional Tbx1 heterozygotes) embryos were microdissected to isolate the otic vesicle. Left and right ears from 3 embryos of the same genotype were pooled for each chip.

Background corr dist: KL-Divergence = 0.0459, L1-Distance = 0.0284, L2-Distance = 0.0011, Normal std = 0.5991

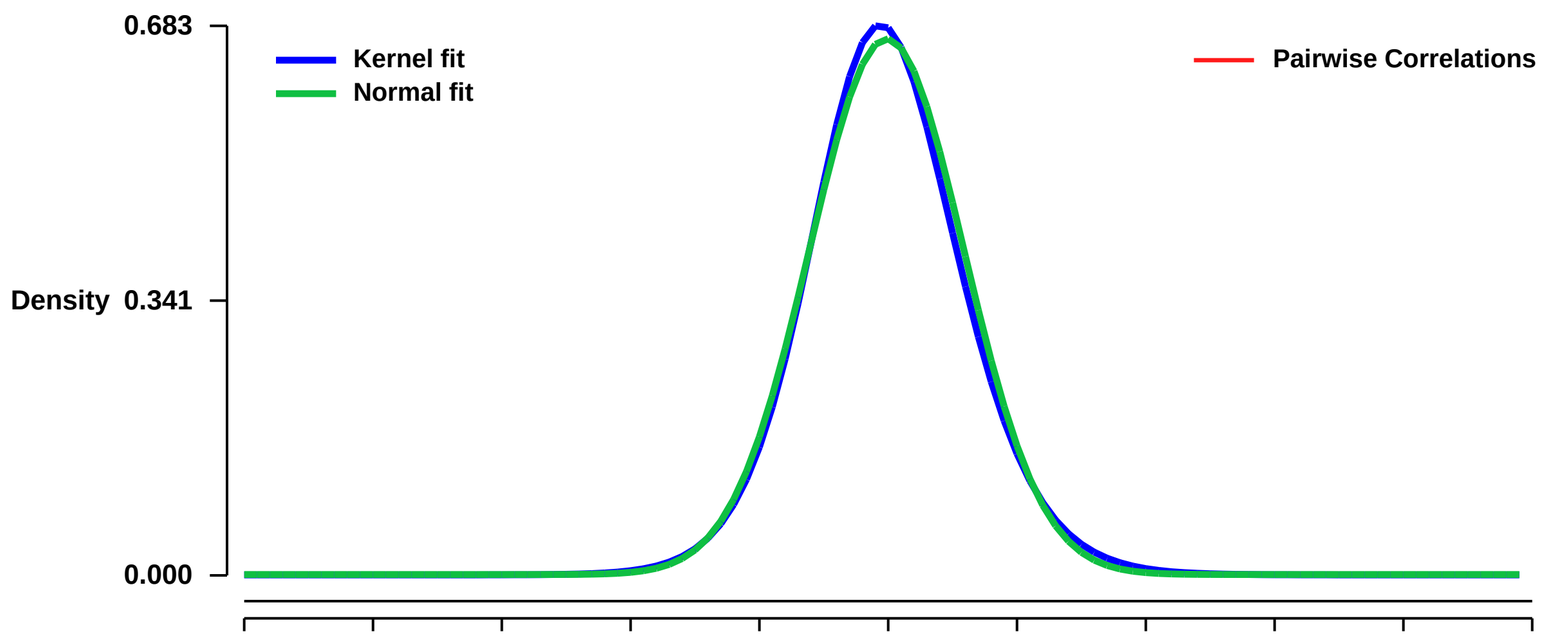

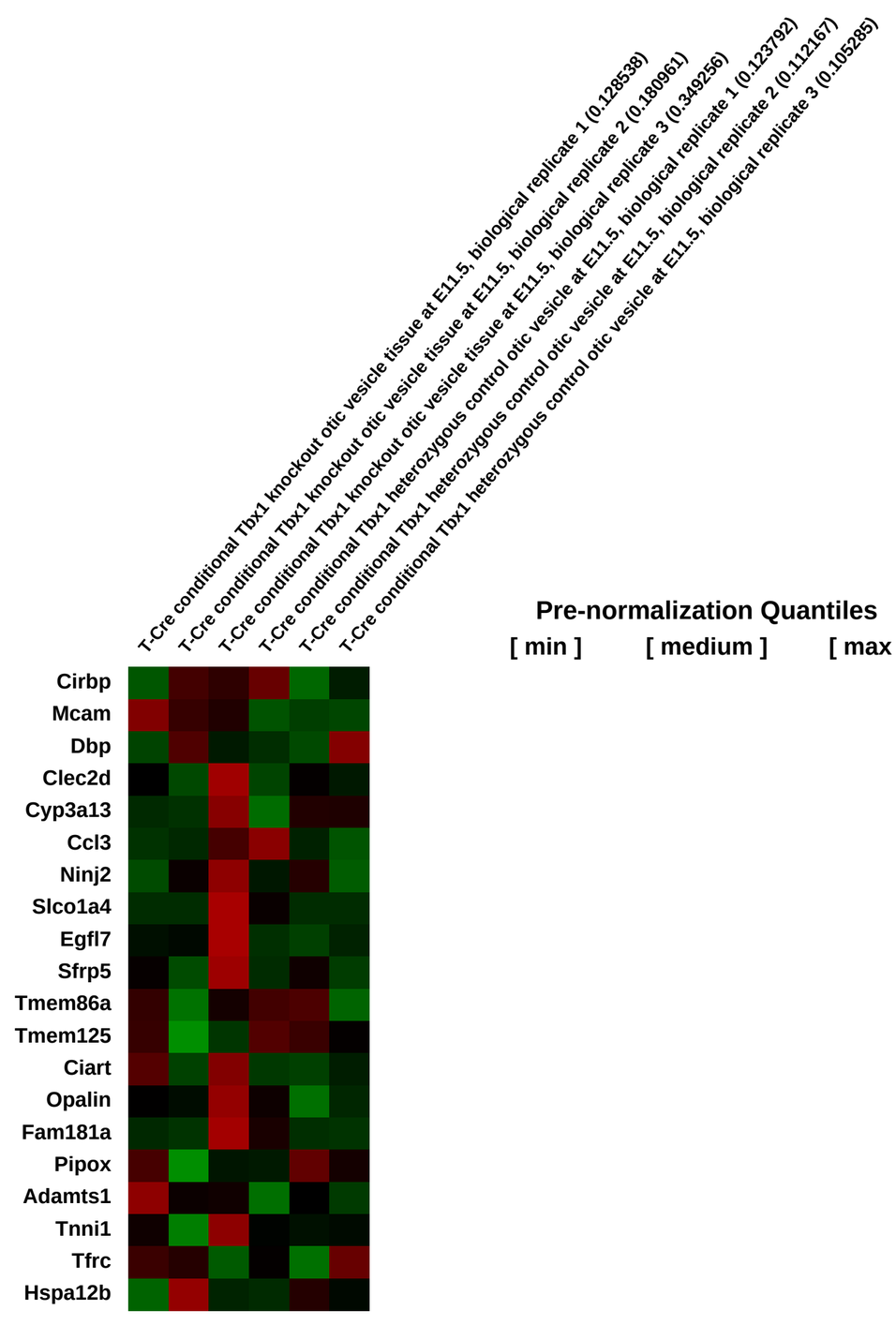

GEO Series "GSE52338" Expression Profiles

Num of samples in this series: 12

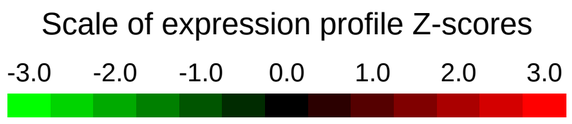

GEO Link:	**http://www.ncbi.nlm.nih.gov/geo/query/acc.cgi?acc=GSE52338**
Status:	**Public on Nov 14 2013**
Title:	**Expression data from peritoneal macrophages stimulated with trehalose-6,6'-dimycolate (TDM)**
Organism:	**Mus musculus**
Experiment type:	**Expression profiling by array**
Platform:	**GPL1261**
Pubmed ID:	
Summary & Design:	**Summary:** **Macrophage-inducible C-type lectin (Mincle, Clec4e) is a pathogen sensor that recognizes pathogenic fungi and Mycobactrium tuberculosis. We perfomed microarray analysis using peritoneal macrophages stimulated with TDM, a mycobacterial cell wall glycolipid that is known to be a Mincle ligand.** **Many chemokine and cytokine genes were upregulated in wildtype macrophages stimulated with TDM. Upregulation of these genes were completely abolishd in Mincle KO macrophages.** **Overall design:** **Peritoneal macrophages from WT and Mincle KO mice were stimulated with TDM or vehicle for 24 h (3 samples each). Microarray analysis was performed using Affymetrix Mouse 430 2.0.**

Background corr dist: **KL-Divergence = 0.1547, L1-Distance = 0.0266, L2-Distance = 0.0011, Normal std = 0.3748**

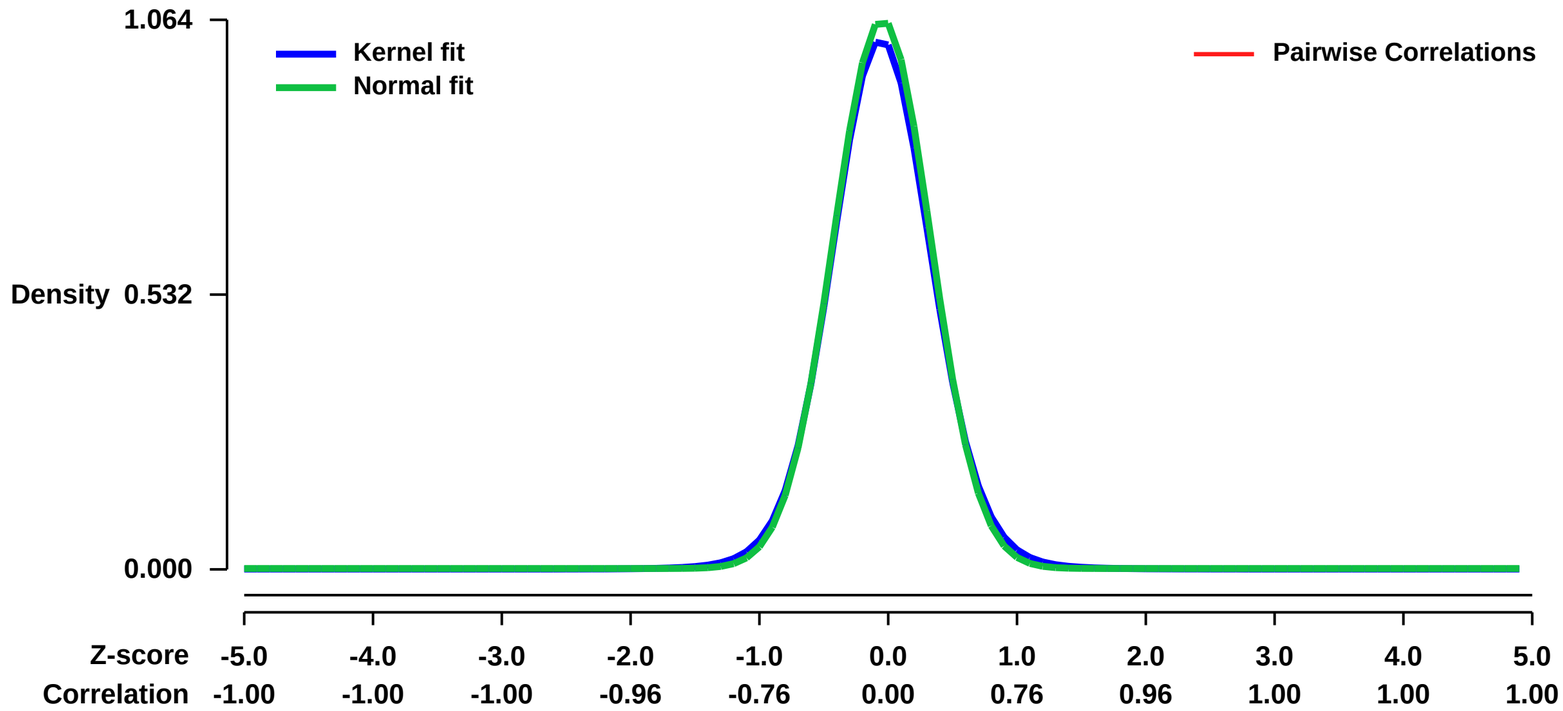

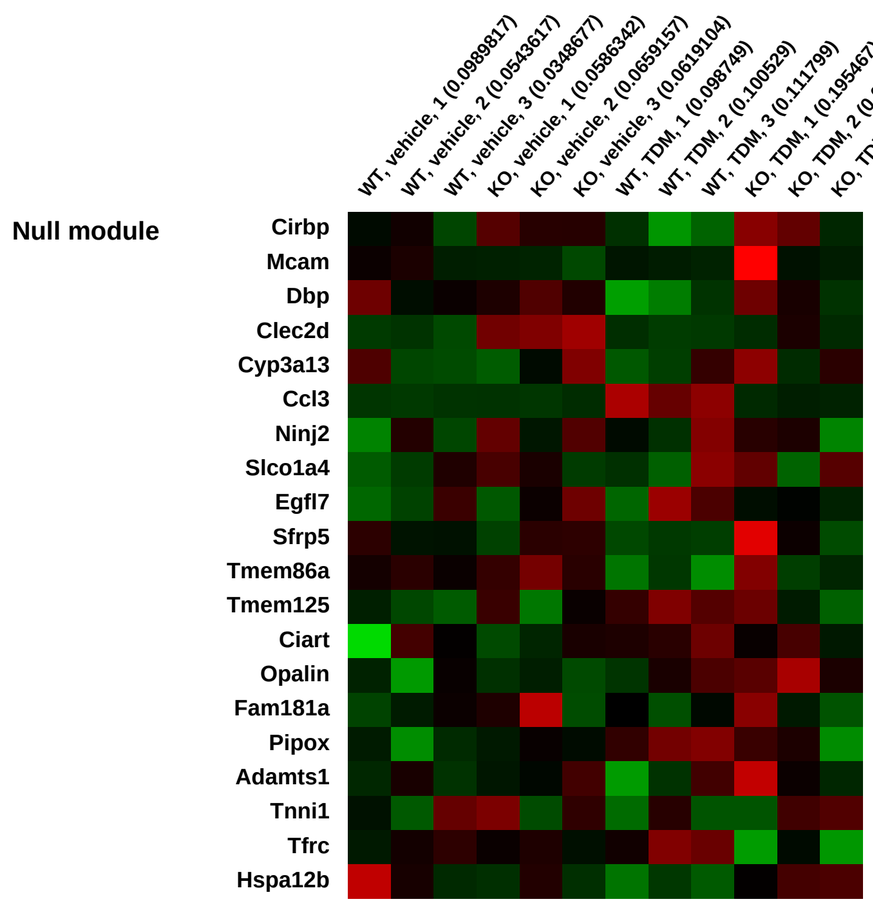

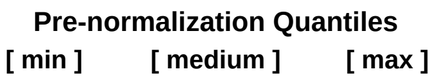

GEO Series "GSE50059" Expression Profiles

Num of samples in this series: 8

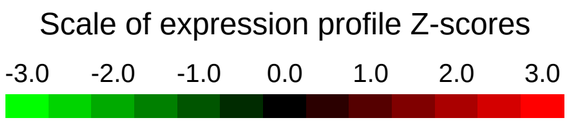

GEO Link:	http://www.ncbi.nlm.nih.gov/geo/query/acc.cgi?acc=GSE50059
Status:	Public on Jan 01 2014
Title:	Endothelin2 signaling in the neural retina promotes the endothelial tip cell state and inhibits angiogenesis
Organism:	Mus musculus
Experiment type:	Expression profiling by array
Platform:	GPL1261
Pubmed ID:	24043815
Summary & Design:	**Summary:** Endothelin signaling is required for neural crest migration and homeostatic regulation of blood pressure. Here we report that constitutive over-expression of Endothelin-2 (Edn2) in the mouse retina perturbs vascular development by inhibiting endothelial cell (EC) migration across the retinal surface and subsequent EC invasion into the retina. Developing endothelial cells exist in one of two states: tip cells at the growing front, and stalk cells in the vascular plexus behind the front. This division of endothelial cell states is one of the central organizing principle of angiogenesis. In the developing retina, Edn2 over-expression leads to over-production of endothelial tip cells by both morphologic and molecular criteria. Spatially localized over-expression of Edn2 produces a correspondingly localized endothelial response. Edn2 over-expression in the early embryo inhibits vascular development at mid-gestation, but Edn2 over-expression in developing skin and brain has no discernable effect on vascular structure. Inhibition of retinal angiogenesis by Edn2 requires expression of Endothelin receptor A (Ednra) but not Ednrb in the neural retina. Taken together, these observations imply that the neural retina responds to Edn2 by synthesizing one or more factors that promote the endothelial tip cell state and inhibit angiogenesis. The response to Edn2 is sufficiently potent that it over-rides the activities of other homeostatic regulators of angiogenesis, such as vascular endothelial growth factor. **Overall design:** Z/Edn2 females were crossed to Six3-Cre; Six3-Cre males. Postnatal P8 pups were genotyped for the Z/Edn2 allele by detection of Laz-Z activity in tail clips. Retinas from 2 - 3 pups were pooled for each data point.

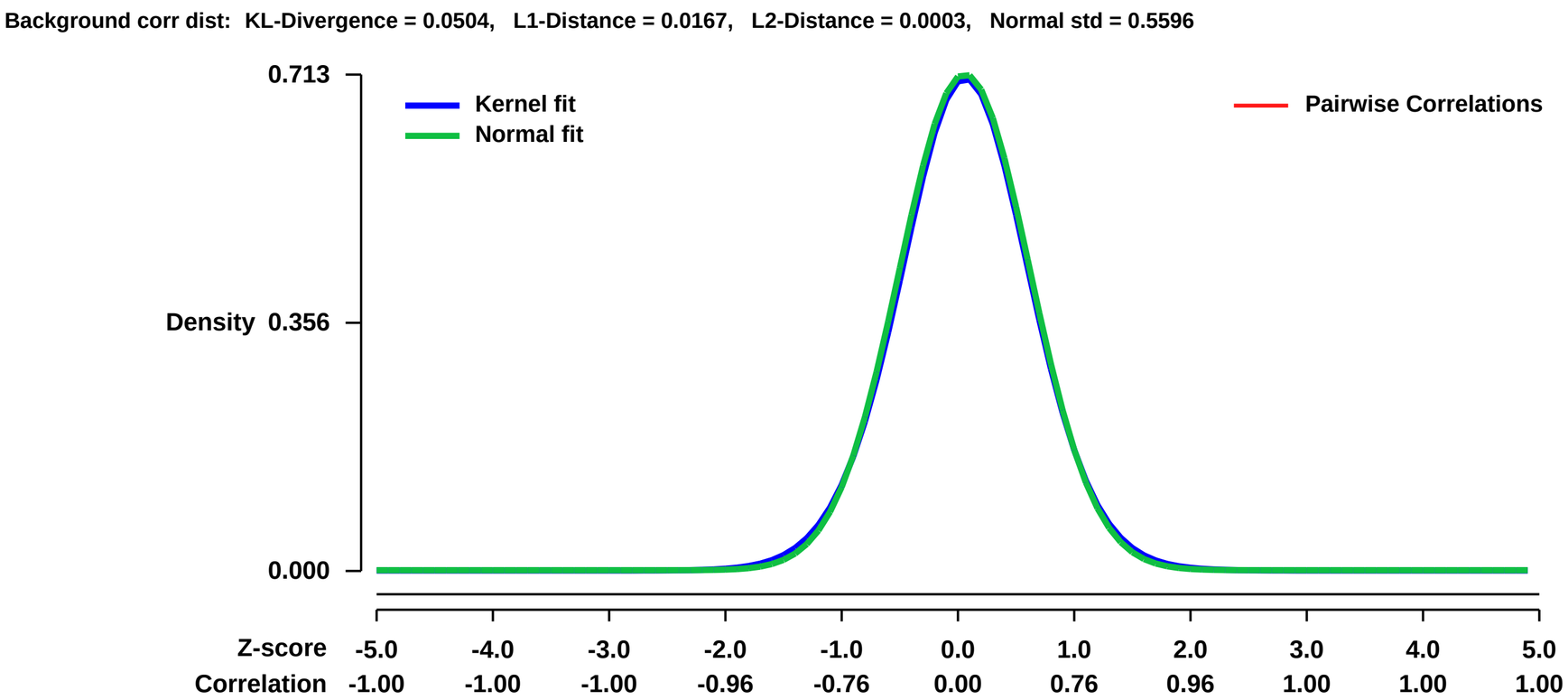

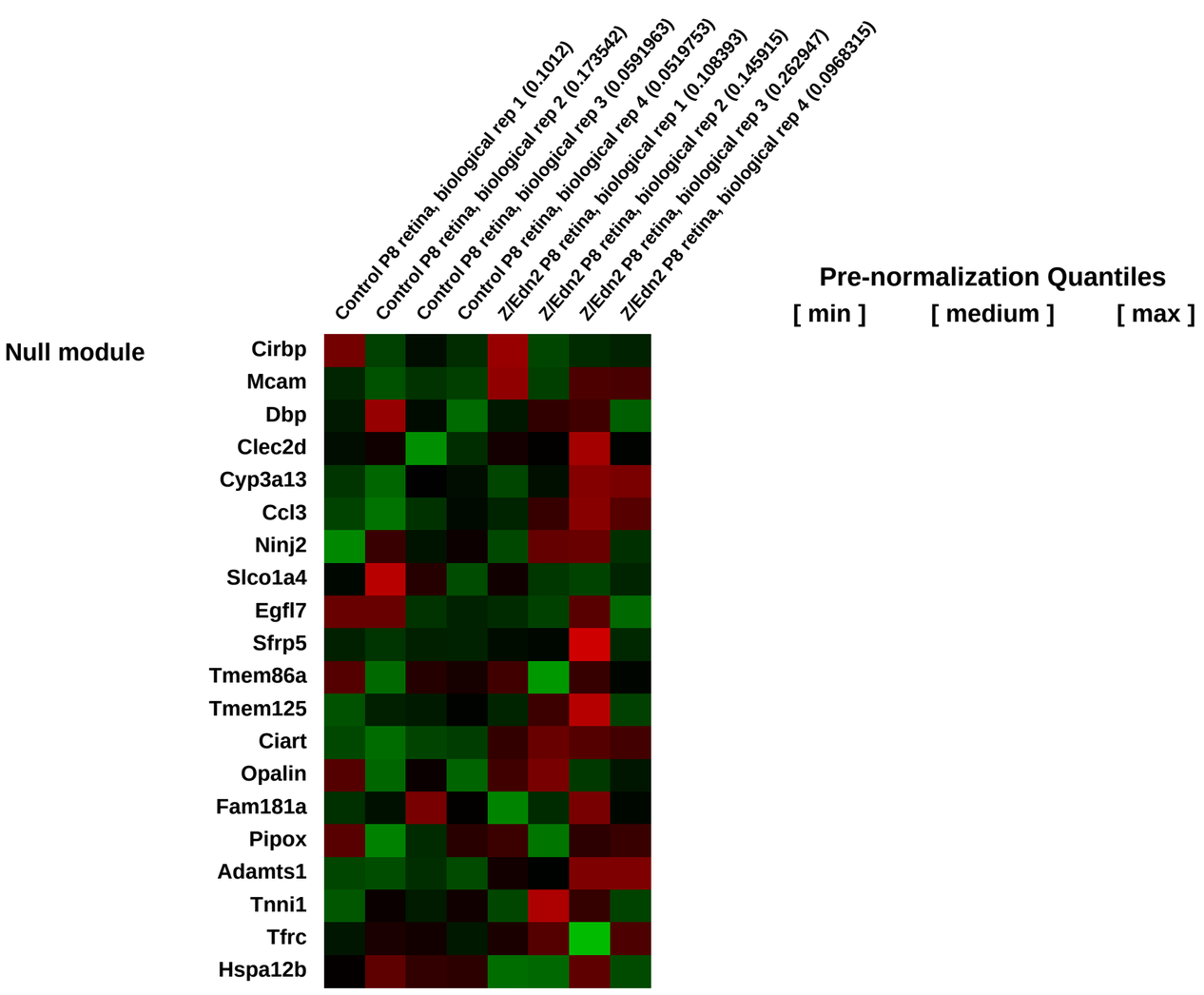

GEO Series "GSE27932" Expression Profiles

Num of samples in this series: 14

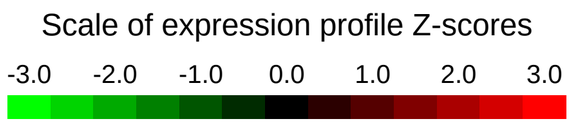

GEO Link:	**http://www.ncbi.nlm.nih.gov/geo/query/acc.cgi?acc=GSE27932**
Status:	**Public on Mar 16 2011**
Title:	**FoxOs are lineage-restricted redundant tumor suppressors and regulate endothelial cell homeostasis.**
Organism:	**Mus musculus**
Experiment type:	**Expression profiling by array**
Platform:	**GPL1261**
Pubmed ID:	**17254969**
Summary & Design:	**Summary:** **Activated phosphoinositide 3-kinase (PI3K)-AKT signaling appears to be an obligate event in the development of cancer. The highly related members of the mammalian FoxO transcription factor family, FoxO1, FoxO3, and FoxO4, represent one of several effector arms of PI3K-AKT signaling, prompting genetic analysis of the role of FoxOs in the neoplastic phenotypes linked to PI3K-AKT activation. While germline or somatic deletion of up to five FoxO alleles produced remarkably modest neoplastic phenotypes, broad somatic deletion of all FoxOs engendered a progressive cancer-prone condition characterized by thymic lymphomas and hemangiomas, demonstrating that the mammalian FoxOs are indeed bona fide tumor suppressors. Transcriptome and promoter analyses of differentially affected endothelium identified direct FoxO targets and revealed that FoxO regulation of these targets in vivo is highly context-specific, even in the same cell type. Functional studies validated Sprouty2 and PBX1, among others, as FoxO-regulated mediators of endothelial cell morphogenesis and vascular homeostasis.** **Overall design:** **Mice were engineered with negative control (MxCre- Fk1 L/L Fk2 L/L Afx L/L) and experimental (MxCre+ Fk1 L/L Fk2 L/L Afx L/L) genotypes. RNAs were isolated from Lung endothelial cells (2 negative controls, 2 experimental), liver sinusoidal endothelial cells (3 negative controls, 3 experimental) and thymus cells (2 negative controls, 2 experimental), and profiled on Affymetrix Mouse Genome 430 2.0 Array.**

Background corr dist: KL-Divergence = 0.0486, L1-Distance = 0.0400, L2-Distance = 0.0023, Normal std = 0.5970

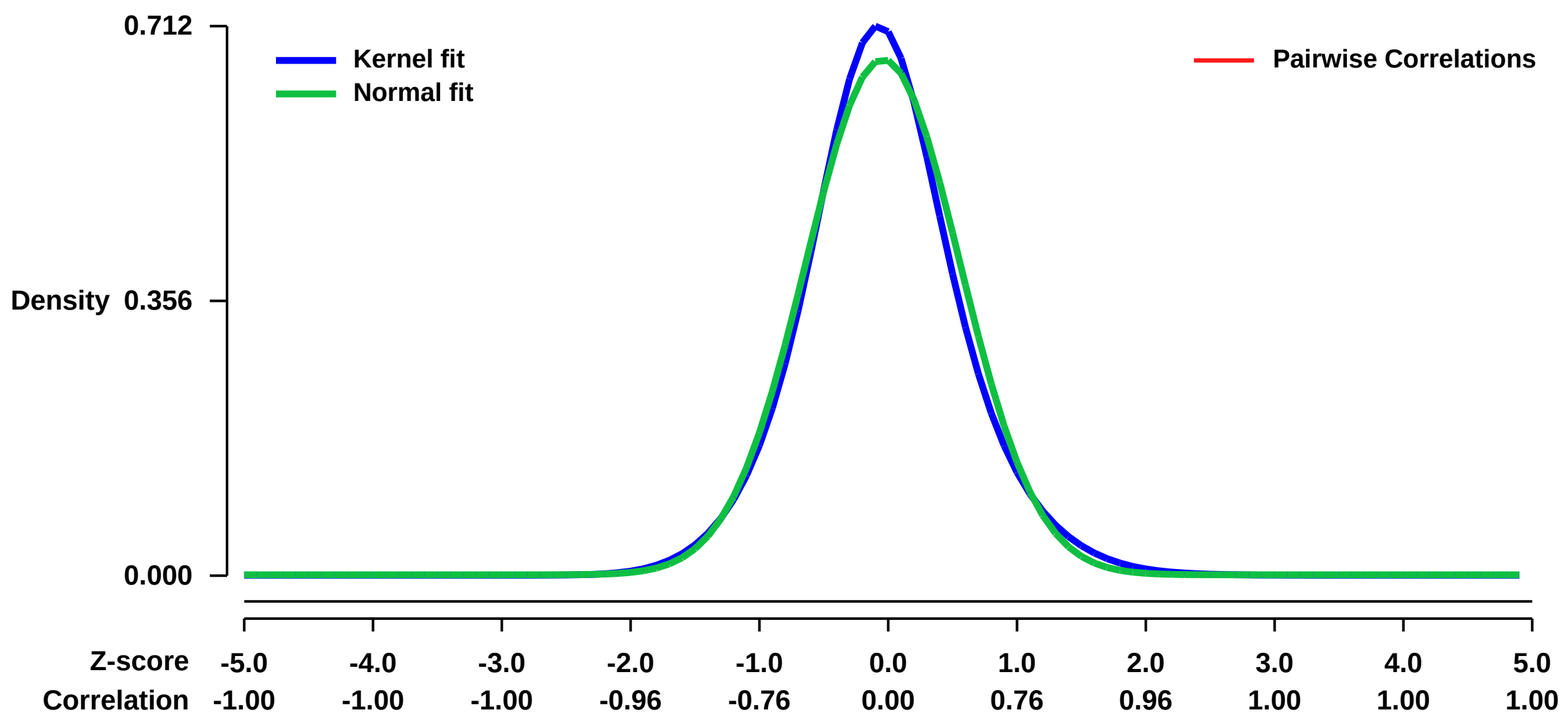

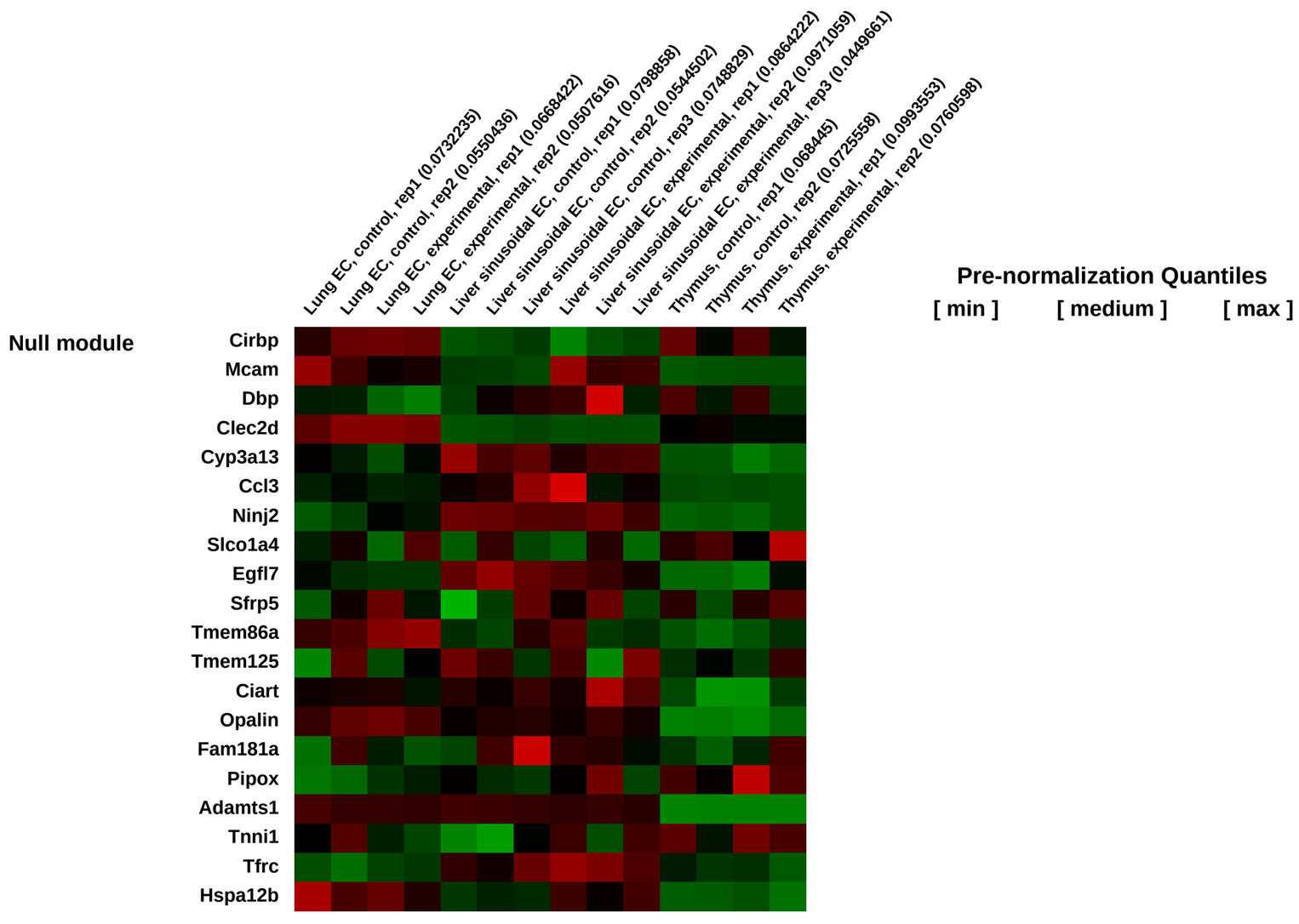

GEO Series "GSE37546" Expression Profiles

Num of samples in this series: 20

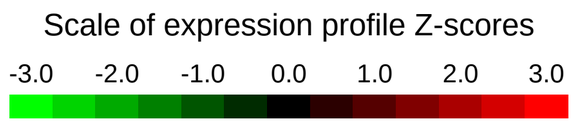

GEO Link:	http://www.ncbi.nlm.nih.gov/geo/query/acc.cgi?acc=GSE37546
Status:	Public on Apr 26 2012
Title:	Disturbed Hepatic Carbohydrate Management During High Metabolic Demand in Medium-Chain Acyl-CoA Dehydrogenase (MCAD)-deficient Mice
Organism:	Mus musculus
Experiment type:	Expression profiling by array
Platform:	GPL1261
Pubmed ID:	18459129
Summary & Design:	**Summary:** Medium-chain acyl-coenzyme A (CoA) dehydrogenase (MCAD) catalyzes crucial steps in mitochondrial fatty acid oxidation, a process that is of key relevance for maintenance of energy homeostasis, especially during high metabolic demand. To gain insight into the metabolic consequences of MCAD deficiency under these conditions, we compared hepatic carbohydrate metabolism in vivo in wild-type and MCAD-/- mice during fasting and during a lipopolysaccharide (LPS)-induced acute phase response (APR). MCAD-/- mice did not become more hypoglycemic on fasting or during the APR than wild-type mice did. Nevertheless, microarray analyses revealed increased hepatic peroxisome proliferator-activated receptor gamma coactivator-1a (Pgc-1a) and decreased peroxisome proliferator-activated receptor alpha (Ppar a) and pyruvate dehydrogenase kinase 4 (Pdk4) expression in MCAD-/- mice in both conditions,suggesting altered control of hepatic glucose metabolism. Quantitative flux measurements revealed that the de novo synthesis of glucose-6-phosphate (G6P) was not affected on fasting in MCAD-/- mice. During the APR, however, this flux was significantly decreased (-20%) in MCAD-/- mice compared with wild-type mice. Remarkably, newly formed G6P was preferentially directed toward glycogen in MCAD-/- mice under both conditions. Together with diminished de novo synthesis of G6P, this led to a decreased hepatic glucose output during the APR in MCAD-/- mice; de novo synthesis of G6P and hepatic glucose output were maintained in wild-type mice under both conditions. APR-associated hypoglycemia, which was observed in wild-type mice as well as MCAD-/- mice, was mainly due to enhanced peripheral glucose uptake. Conclusion: Our data demonstrate that MCAD deficiency in mice leads to specific changes in hepatic carbohydrate management on exposure to metabolic stress. This deficiency, however, does not lead to reduced de novo synthesis of G6P during fasting alone, which may be due to the existence of compensatory mechanisms or limited rate control of MCAD in murine mitochondrial fatty acid oxidation. **Overall design:** Total RNA obtained from Liver (20 samples) , where comparing 4 groups, consisting out of 5 biological replicates, all groups where fasted for 12 hrs, and half of them where injected with LPS (100ug/20gr BW) or vehicle

Background corr dist: KL-Divergence = 0.1254, L1-Distance = 0.0278, L2-Distance = 0.0011, Normal std = 0.4081

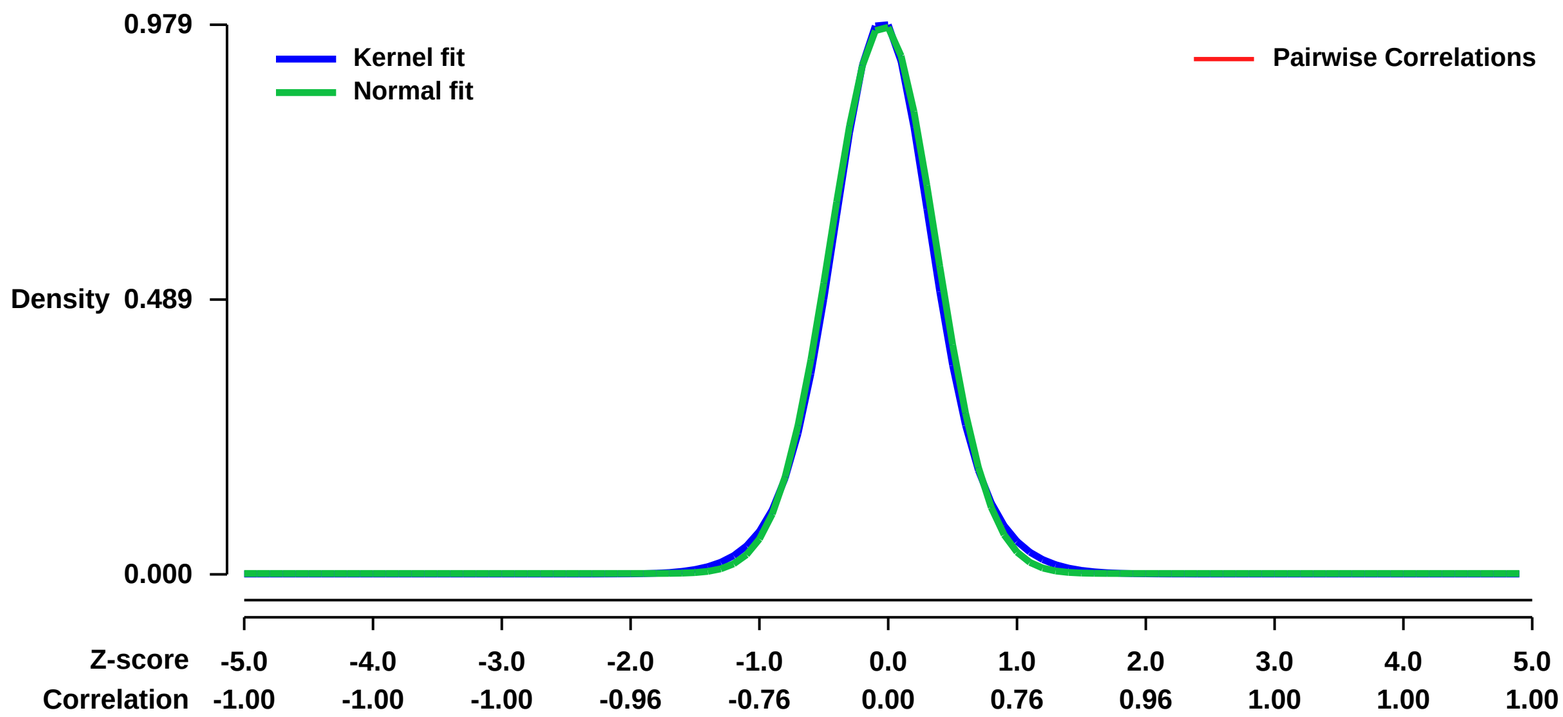

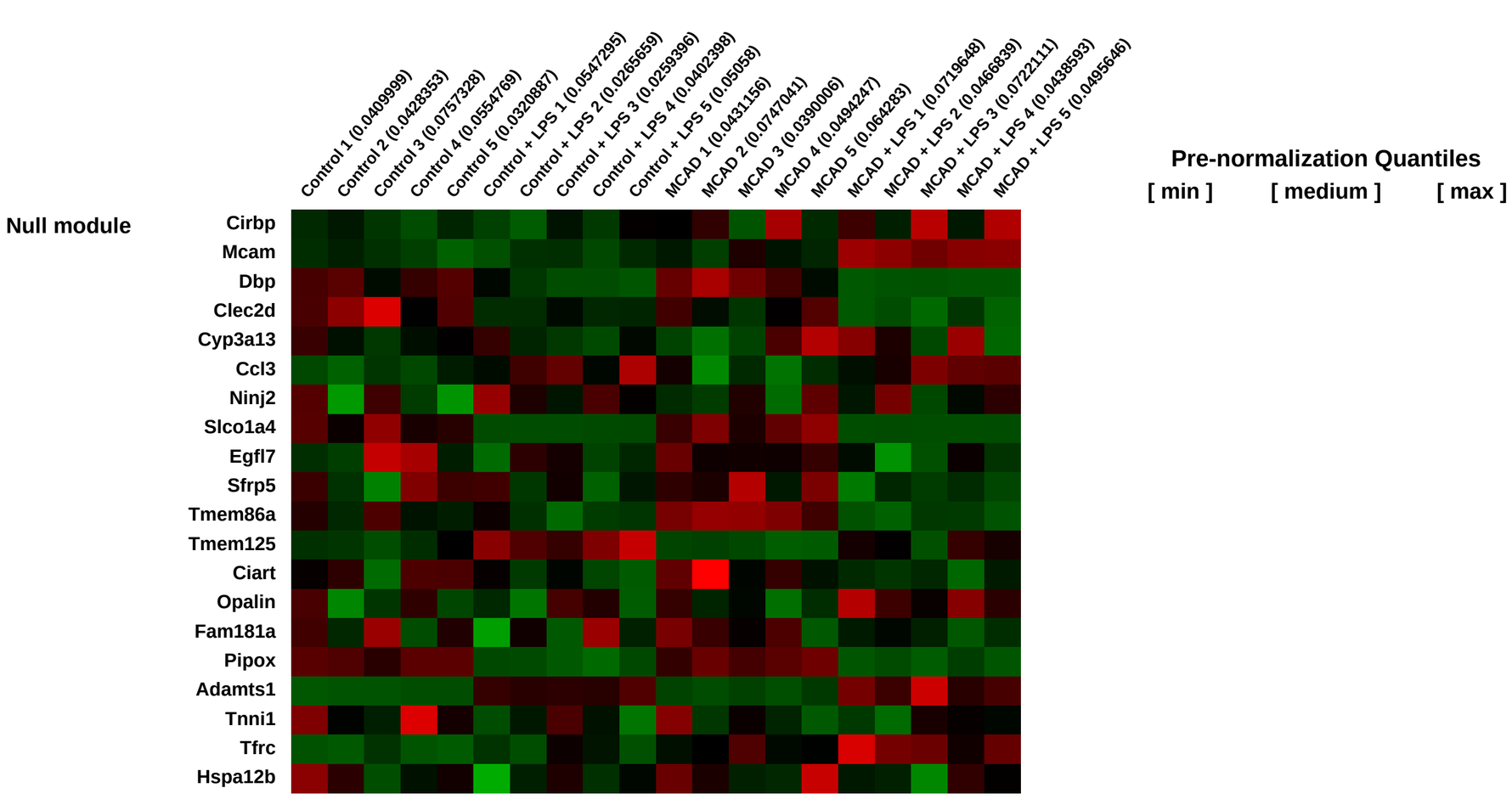

GEO Series "GSE42234" Expression Profiles

Num of samples in this series: 17

Scale of expression profile Z-scores

-3.0 -2.0 -1.0 0.0 1.0 2.0 3.0

GEO Link:	http://www.ncbi.nlm.nih.gov/geo/query/acc.cgi?acc=GSE42234
Status:	Public on Nov 14 2012
Title:	C/EBPa controls acquisition and maintenance of adult hematopoietic stem cell quiescence
Organism:	Mus musculus
Experiment type:	Expression profiling by array
Platform:	GPL1261
Pubmed ID:	23502316
Summary & Design:	**Summary:** In blood, the transcription factor C/EBPa is essential for myeloid differentiation and has been implicated in regulating self-renewal of fetal liver hematopoietic stem cells (HSCs). However, its function in adult HSCs is unknown. Here, using an inducible knockout model, we found that C/EBPa deficient adult HSCs underwent a pronounced expansion with enhanced proliferation, characteristics resembling fetal liver HSCs. Consistently, transcription profiling of C/EBPa deficient HSCs revealed a gene expression program similar to fetal liver HSCs. Moreover we observed that age-specific C/EBPa expression correlated with its inhibitory effect on the HSC cell cycle. Mechanistically, we identified N-Myc as a C/EBPa downstream target. C/EBPa upregulation during HSC transition from an active fetal state to a quiescent adult state was accompanied by down-regulation of N-Myc, and loss of C/EBPa resulted in de-repression of NMyc. Our data establish that C/EBPa acts as a molecular switch between fetal and adult states of HSC in part via transcriptional repression of the proto-oncogene N-Myc. **Overall design:** HSCs of Pu.1 knock-in (PU.1ki/ki) mice were used for RNA extraction and hybridization on Affymetrix microarrays. We compared these microarray samples with the corresponding wild type.

Background corr dist: KL-Divergence = 0.2630, L1-Distance = 0.0440, L2-Distance = 0.0062, Normal std = 0.2994

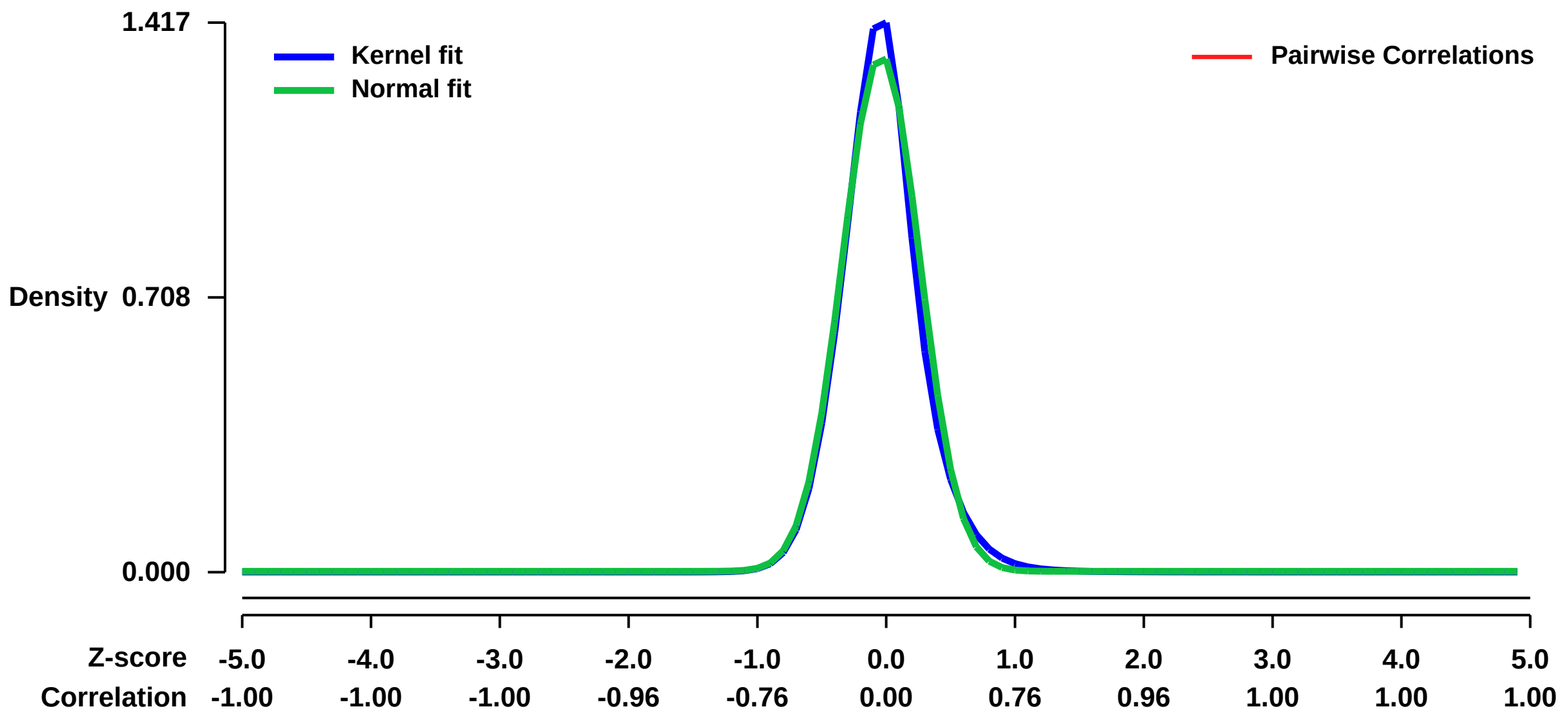

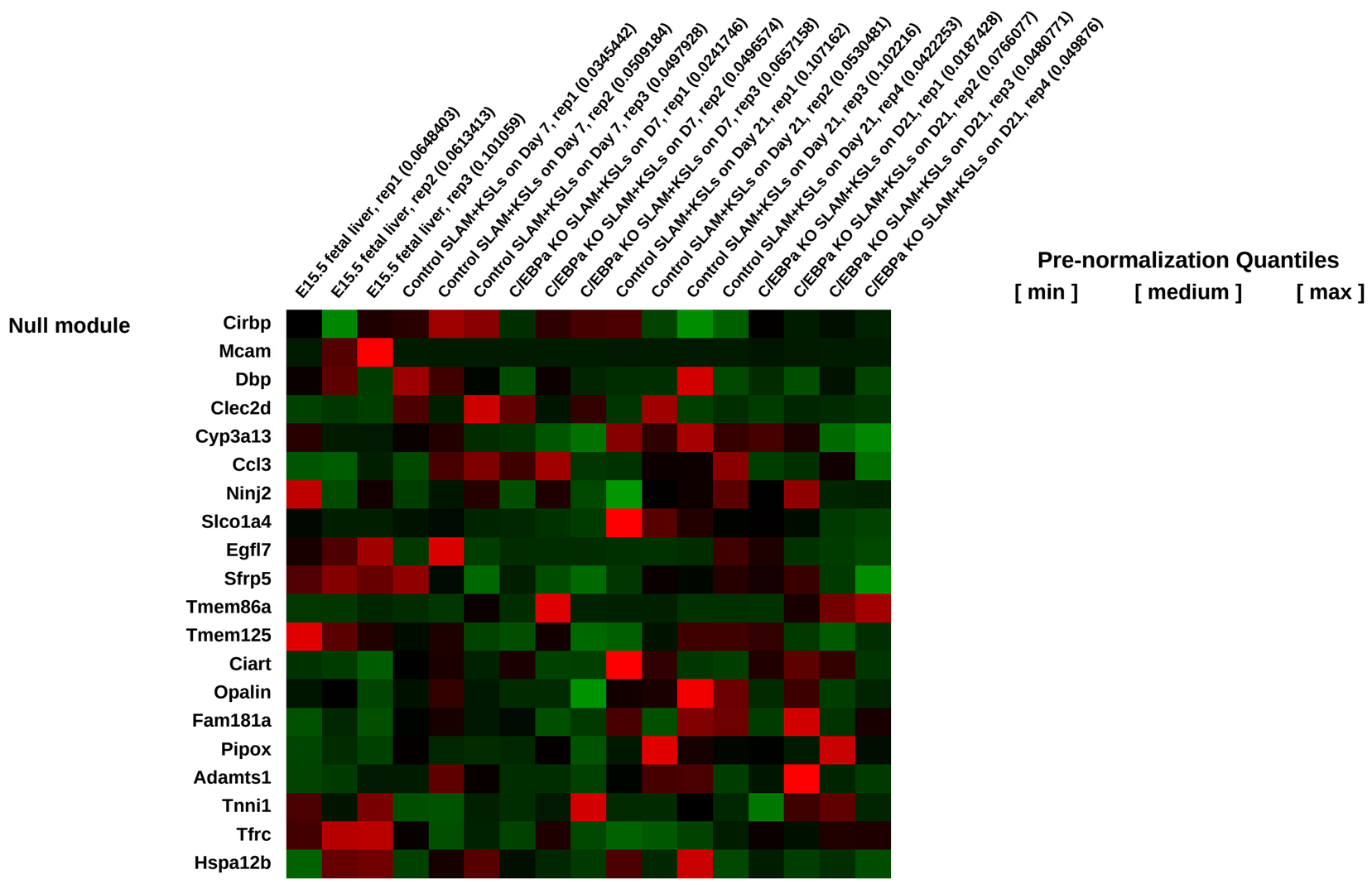

GEO Series "GSE15121" Expression Profiles

Num of samples in this series: 6

Scale of expression profile Z-scores

-3.0 -2.0 -1.0 0.0 1.0 2.0 3.0

GEO Link: http://www.ncbi.nlm.nih.gov/geo/query/acc.cgi?acc=GSE15121
Status: Public on Jan 01 2010
Title: Expression data from E10 cells with miR-129 over-expression
Organism: Mus musculus
Experiment type: Expression profiling by array
Platform: GPL1261
Pubmed ID:

Summary & Design:

Summary:
miRNAs are known to regulate gene expression by suppressing translation, but there is also a wealth of data showing that they can act as critical regulators of mRNA stability of their targets. In this experiment, we analyzed the mRNA expression profiles of E10 with high expression of miR-129 as compared to control cells to identify miR-129 targets.

E10 cells infected with miR-129 over-expressing lentivirus or the control lentivirus were cultured for 48 hours. More than 80% of cells were infected. Total RNA samples were isolated using Trizol (invitrogen), and subjected to labeling, fragmentation and hybridization, according to manufacturerâ s protocols. Mouse Genome 430 2.0 Array (Affymetrix) was used for mRNA expression profiling.

Overall design:
We compared the mRNA expression profiles between cells infected with miR-129 expressing lentivirus and the cells infected with control lentivirus

Background corr dist: KL-Divergence = 0.0330, L1-Distance = 0.0387, L2-Distance = 0.0017, Normal std = 0.6967

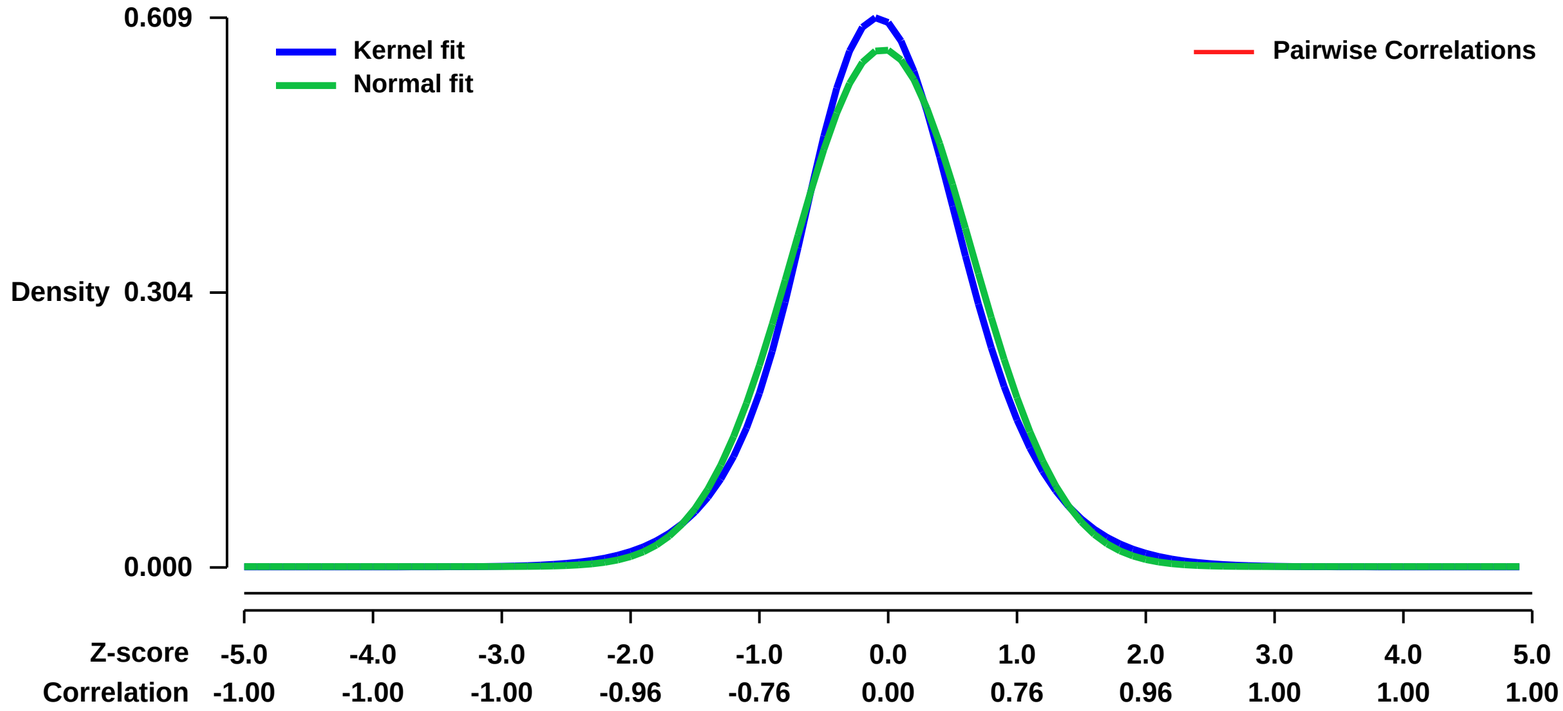

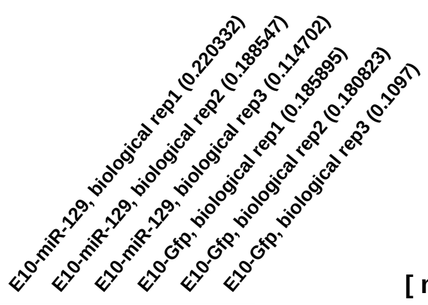

Pre-normalization Quantiles
[min] [medium] [max]

Null module

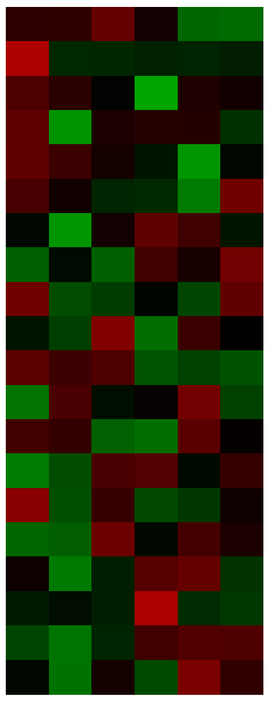

GEO Series "GSE28333" Expression Profiles

Num of samples in this series: 6

Scale of expression profile Z-scores

-3.0 -2.0 -1.0 0.0 1.0 2.0 3.0

GEO Link:	http://www.ncbi.nlm.nih.gov/geo/query/acc.cgi?acc=GSE28333
Status:	Public on Mar 22 2012
Title:	Expression data from BCL11A-null and wild-type bone marrow erythroid pregenitors
Organism:	Mus musculus
Experiment type:	Expression profiling by array
Platform:	GPL1261
Pubmed ID:	21998251
Summary & Design:	**Summary:** BCL11A is a critical mediator of hemoglobin switching and gamma-globin silencing. In this study, we showed the BCL11A is required in vivo for developmental silencing of gamma-globin genes in adult animals. We used microarray to determine the changes in gene expression profile after loss of BCL11A in adult erythroid cells **Overall design:** CD71+Ter119+ erythroid progenitor cells were FACS-sorted from bone marrows of 6-week old control (Bcl11a +/+) and BCL11A knockout (Bcl11a fl/fl EpoR-Cre+) mice.

Background corr dist: KL-Divergence = 0.0415, L1-Distance = 0.0210, L2-Distance = 0.0005, Normal std = 0.6102

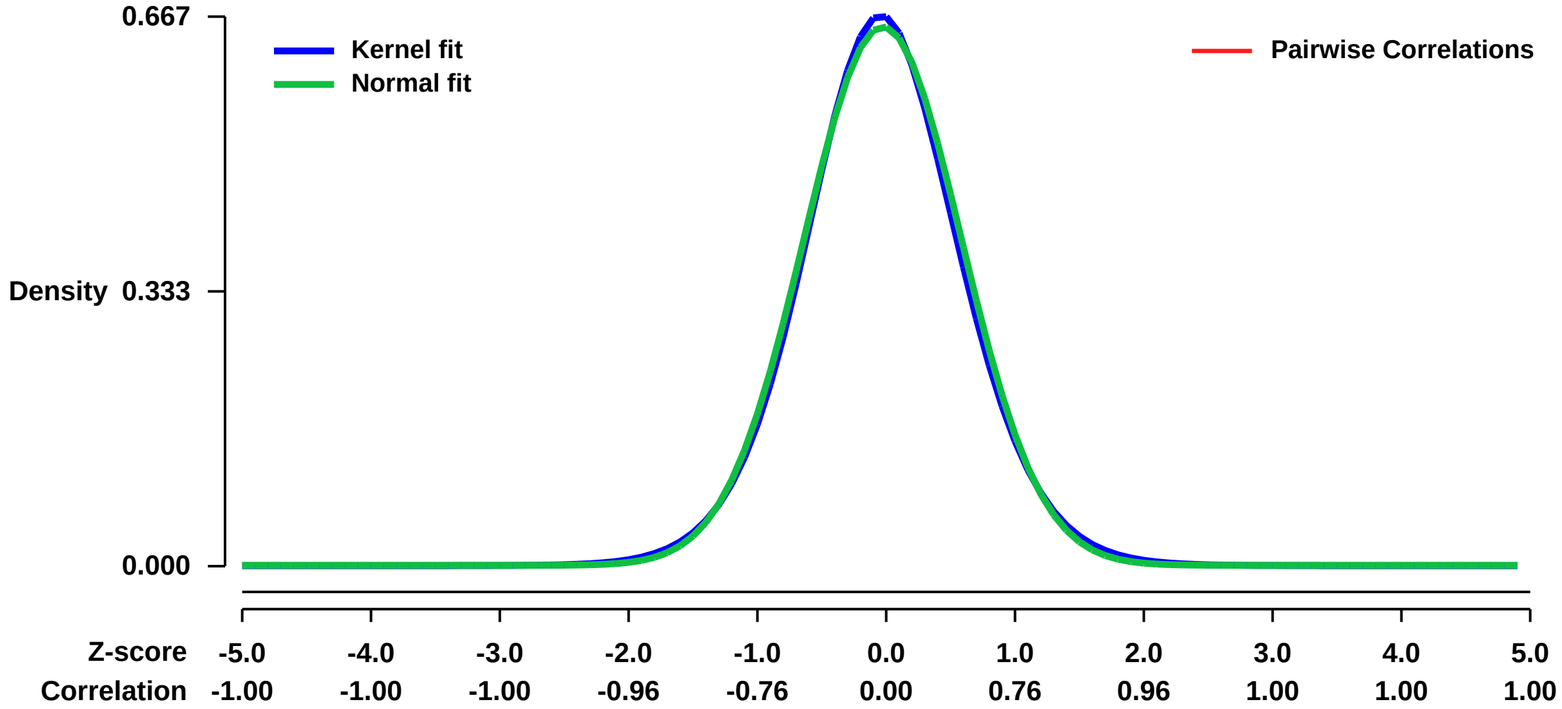

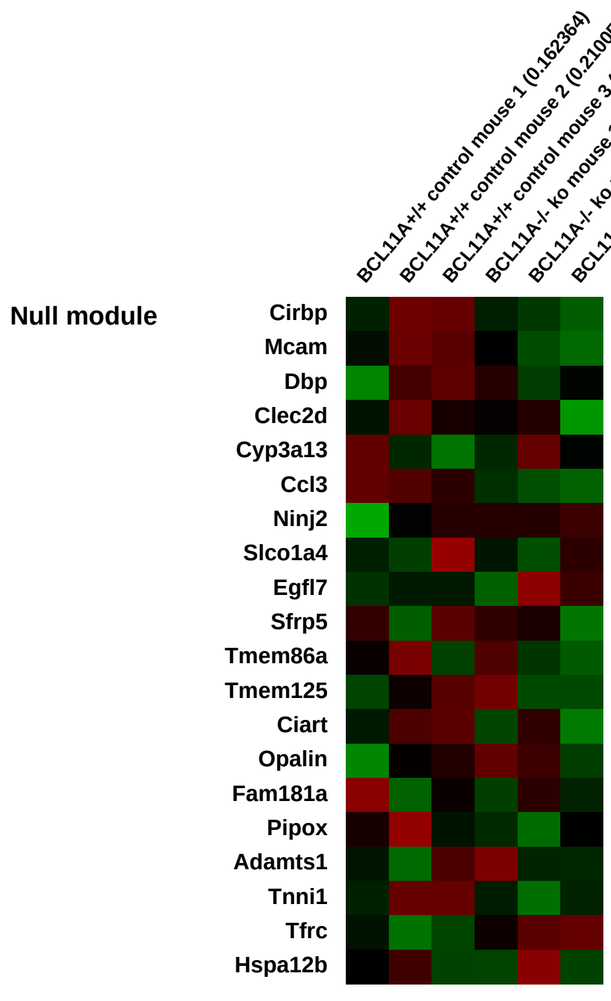

GEO Series "GSE10344" Expression Profiles

Num of samples in this series: 6

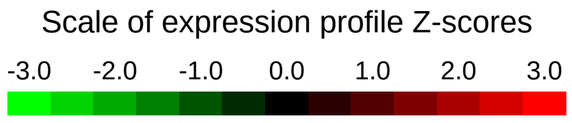

GEO Link:	**http://www.ncbi.nlm.nih.gov/geo/query/acc.cgi?acc=GSE10344**
Status:	**Public on Dec 31 2008**
Title:	**Expression data from garlic-fed mouse**
Organism:	**Mus musculus**
Experiment type:	**Expression profiling by array**
Platform:	**GPL1261**
Pubmed ID:	
Summary & Design:	**Summary:** **Garlic is a popular flavor enhancer in modern cuisines. Although anti-atherosclerotic, anti-proliferative, hypolipidemic and chemopreventative effects of garlic are known for a long time, the mechanisms of garlic as a dietary supplement ramain largely unknown.** **We used microarrays to analyze the global programme of gene expression in control (cellulose) and garlic-fed mice and identified erythropoietic and heme biosynthetic genes that could, in part, be responsible for the pleiotropic effects of garlic on health** **Keywords: diet, garlic** **Overall design:** **8-week old male C57BL/6J mice were divided into two diet groups and maintained at an SPF facility. Mice were fed (ad libitum) a special diet (Yeh and Yeh, 1994) with 4% cellulose (Control group, 3 mice) or 4% lyophilized raw garlic powder (Treatment group, 3 mice). At the end of the 15-week treatment, spleen organs were used for RNA isolation and arraying.**

Background corr dist: **KL-Divergence = 0.0471, L1-Distance = 0.0191, L2-Distance = 0.0004, Normal std = 0.5847**

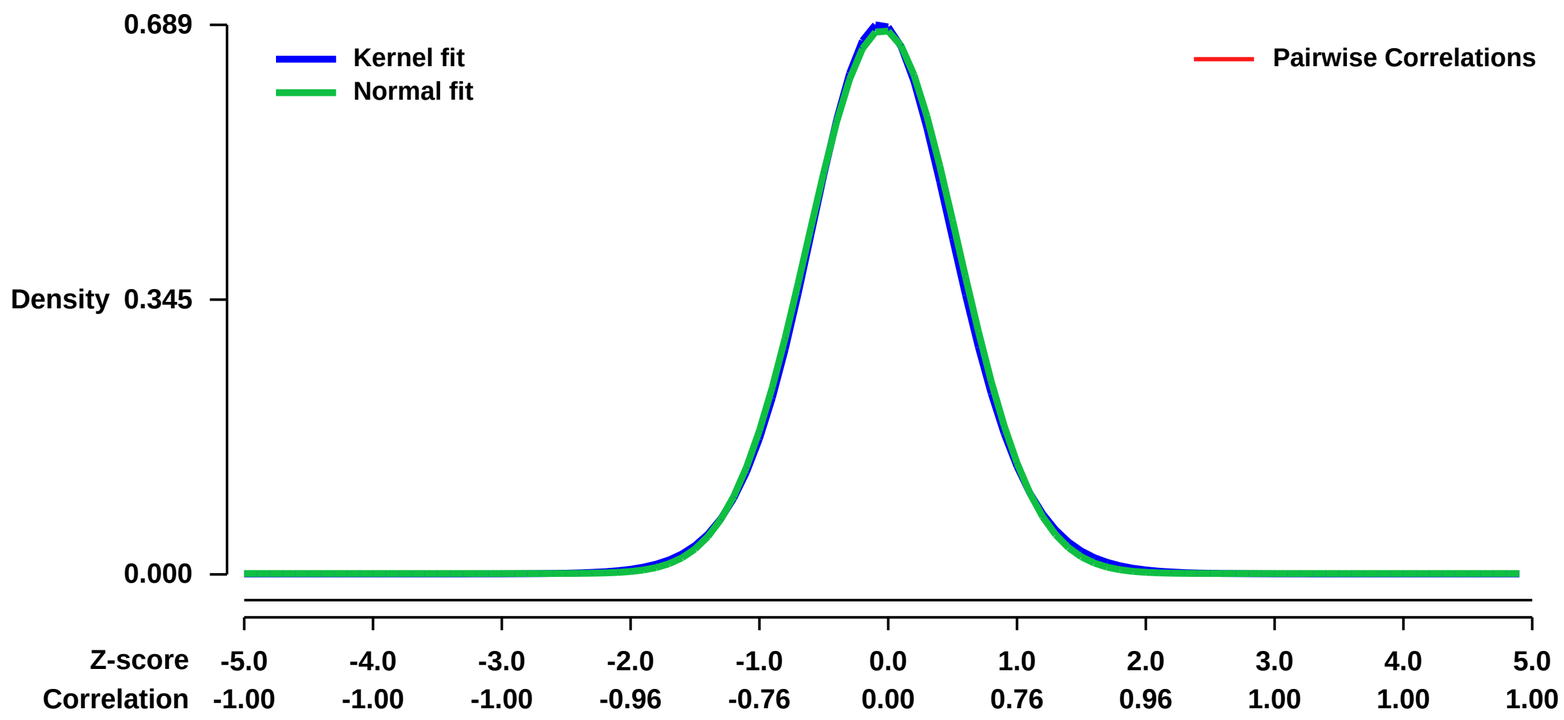

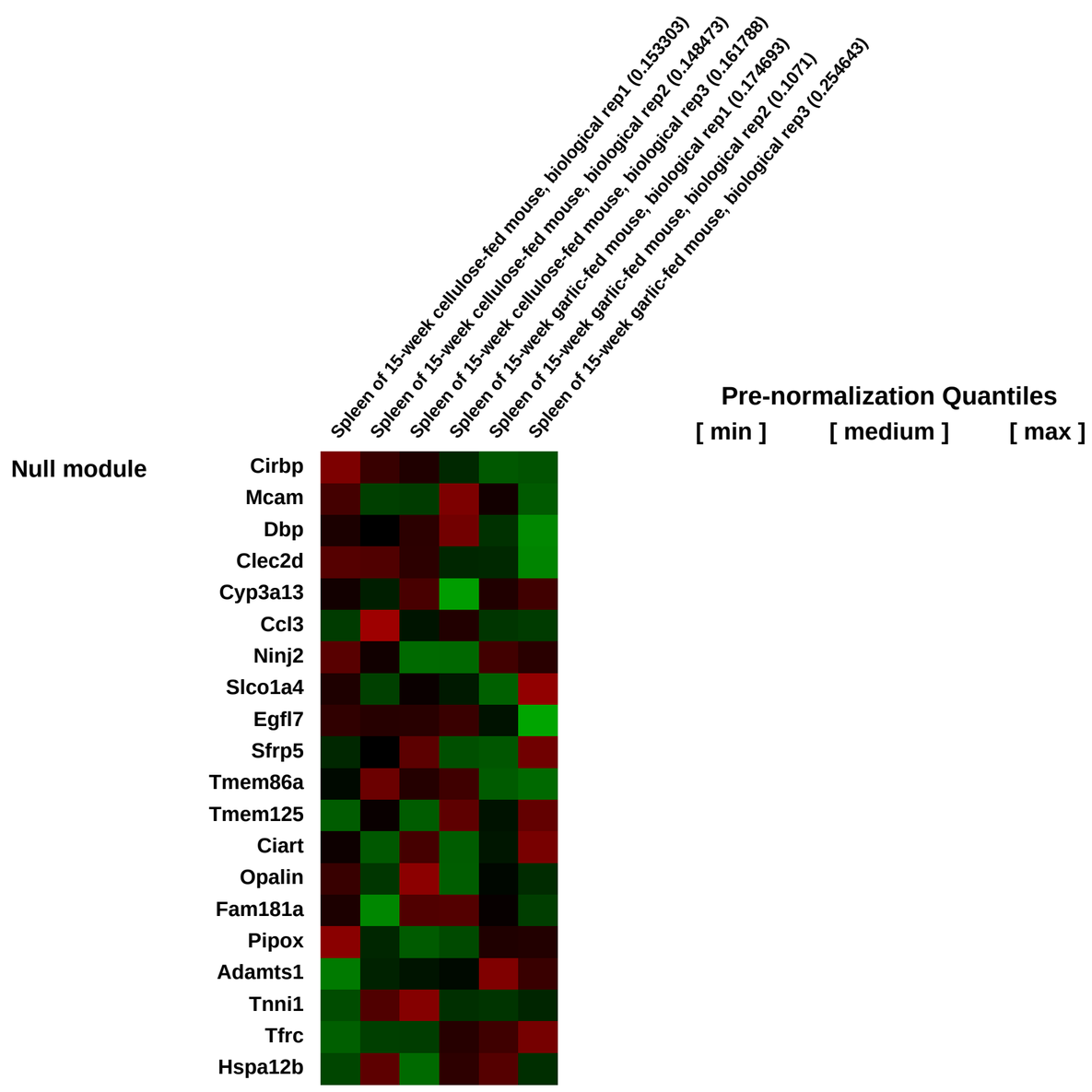

GEO Series "GSE8367" Expression Profiles

Num of samples in this series: 12

Scale of expression profile Z-scores

-3.0 -2.0 -1.0 0.0 1.0 2.0 3.0

GEO Link:	http://www.ncbi.nlm.nih.gov/geo/query/acc.cgi?acc=GSE8367
Status:	Public on Dec 31 2009
Title:	Sustained L-type Calcium Channel Blockade Alters Gene Regulation in the Adult Mouse Ventricle
Organism:	Mus musculus
Experiment type:	Expression profiling by array
Platform:	GPL1261
Pubmed ID:	
Summary & Design:	**Summary:** **Objective: L-type calcium channels (LTCC) homeostatically regulate calcium on a beat by beat basis, but also provide Ca that over long time scales may contribute to transcriptional regulation. We previously showed that sustained LTCC blockade (CCB) elicits LTCC remodeling in ventricular cardiac myocytes (CM). Here we hypothesize that sustained CCB has broad effects on the expression of genes involved in calcium handling. Methods and Results: Therefore, we subjected adult mice to sustained CCB for 24 hours and performed gene expression profiling. In comparison to vehicle-only control animals, 231 genes were up-regulated, and 111 genes were down-regulated by sustained LTCC blockade (p <0.01). Gene ontology analysis suggested that the CaMKIIdelta signaling pathway was up-regulated in these cells. Unexpectedly, phosphorylation of phospholamban (PLN) at threonine17 (Thr17), an index of CaMKIIdelta activity, was not changed by sustained CCB; however, the degree of phosphorylation of the neighboring PLN-Ser16 substrate site for PKA was significantly reduced by sustained CCB compared to control. Gene expression profiling suggested no change in PKA, but it showed that protein phosphatase 2A (PP2A) mRNA increased, and immunoblots demonstrated that PP2Ac-alpha protein was significantly increased by sustained CCB. Consistent with elevated PP2Ac-alpha protein expression LTCC exhibited decreased phosphorylation of the C-terminal Ser1928 PKA substrate site. Conclusions: We conclude that sustained CCB elicits a spectrum of transcriptional events, including compensatory up-regulation of LTCC and PP2Ac-alpha. Although this study is restricted to mouse, these results suggest the new hypothesis that clinically-relevant sustained LTCC blockade in humans results in changes in gene regulation in the heart.** **Keywords: L-type calcium channel, calcium channel blockade, verapamil** **Overall design:** **Left ventricular free wall from female mice was rapidly excised and either snap frozen at -80oC or used immediately for RNA isolation. Three VER treated mice and 3 vehicle treated mice were used to generate RNA for microarray. Total RNA was isolated using the RNAqueous -4PCR kit (Ambion) and quantitated spectrophotometrically at 260nm. Contaminating genomic DNA was eliminated by DNase treatment (Ambion). RNA quality was assessed using the Agilent 2100 Bioanalyzer. Microarray data was obtained using the Affymetrix 430 V2 GeneChip (representing 45,101 probe sets), in accordance with the manufacturerâ s specifications.**

Background corr dist: **KL-Divergence = 0.1573, L1-Distance = 0.0392, L2-Distance = 0.0031, Normal std = 0.3657**

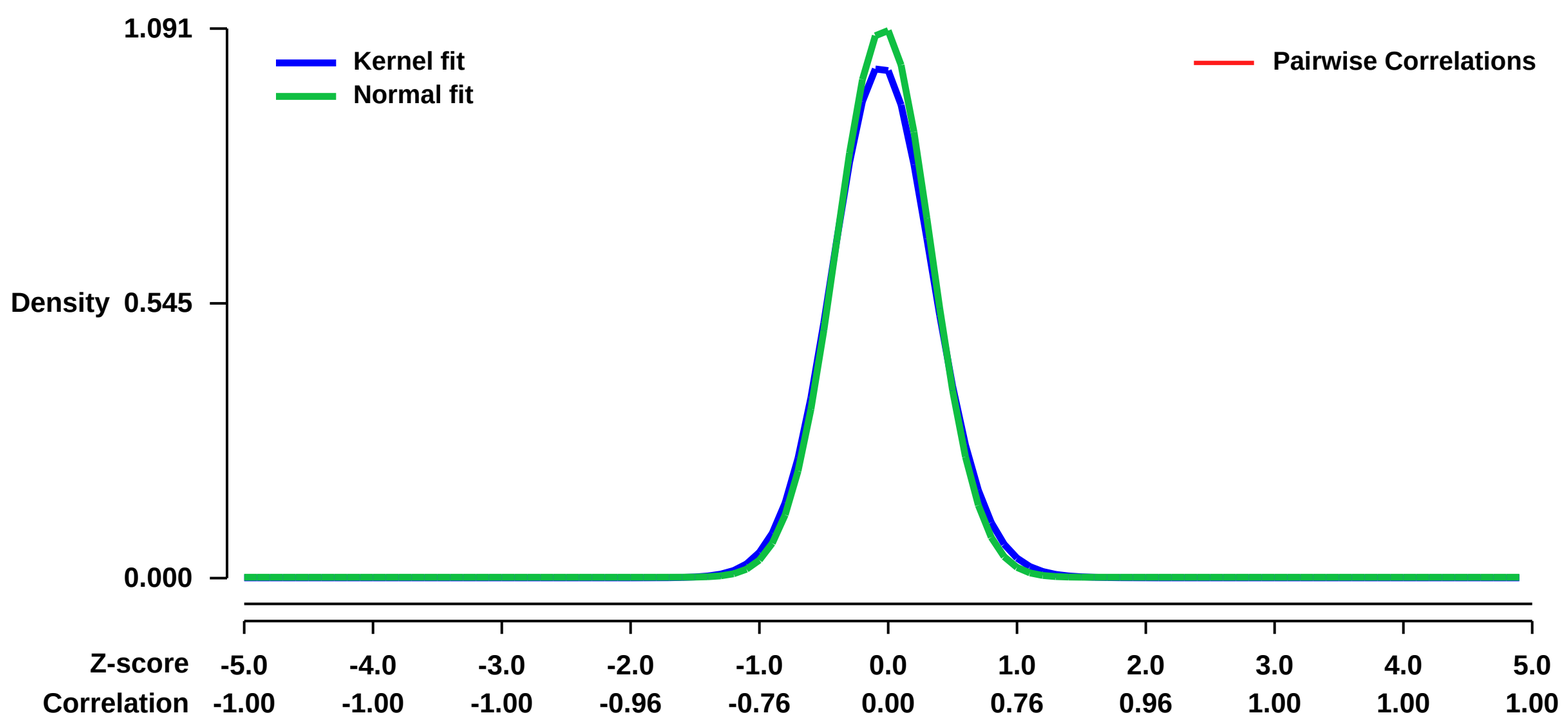

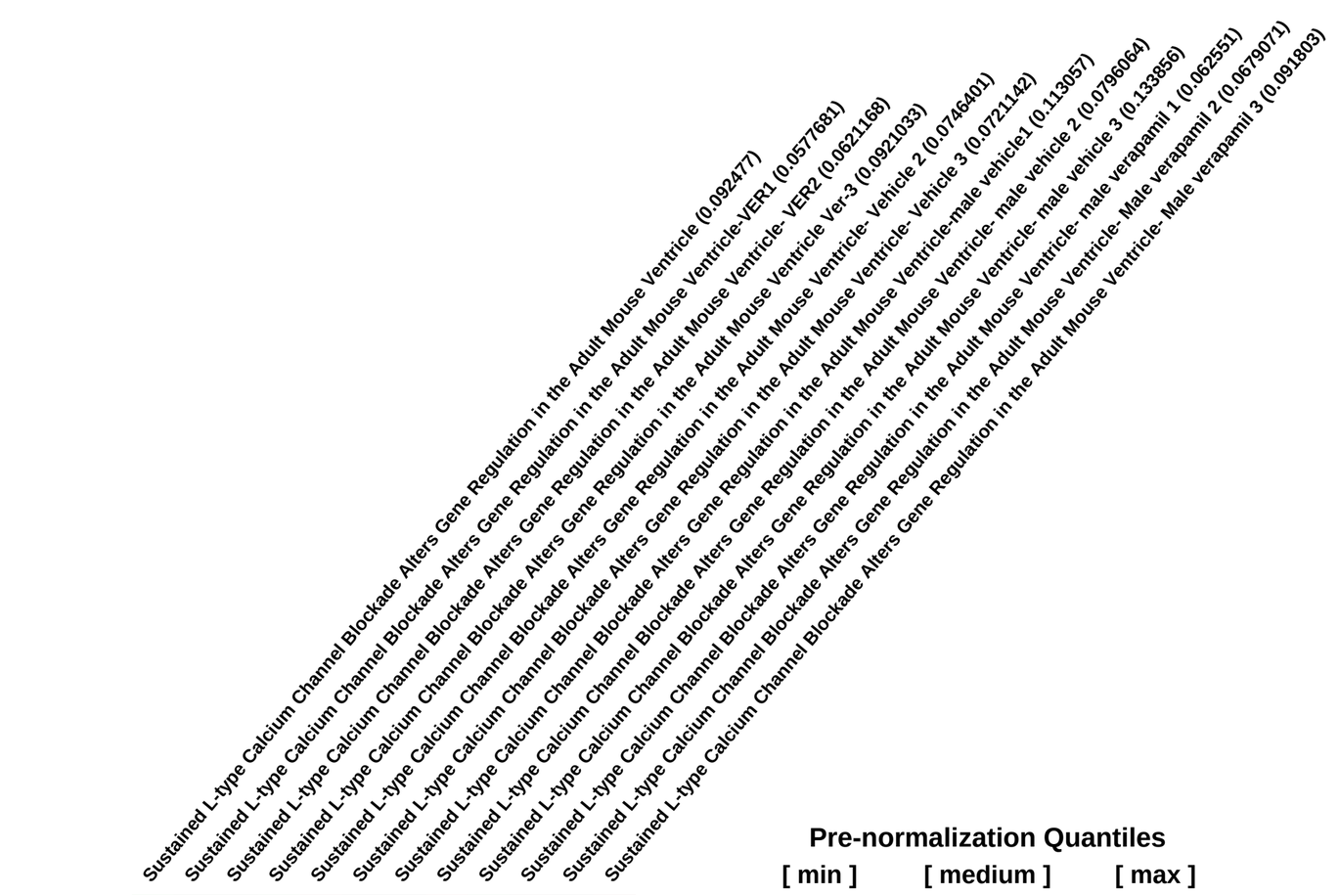

GEO Series "GSE45487" Expression Profiles

Num of samples in this series: 9

Scale of expression profile Z-scores

-3.0 -2.0 -1.0 0.0 1.0 2.0 3.0

GEO Link:	http://www.ncbi.nlm.nih.gov/geo/query/acc.cgi?acc=GSE45487
Status:	Public on Mar 26 2013
Title:	Identification of genes responsive to low-intensity pulsed ultrasound (LIPUS) in MC3T3-E1 preosteoblast cells
Organism:	Mus musculus
Experiment type:	Expression profiling by array
Platform:	GPL1261
Pubmed ID:	24252911
Summary & Design:	**Summary:** Although LIPUS has been shown to enhance fracture healing, the underlying mechanism of LIPUS remains to be fully elucidated. Here, to understand the molecular mechanism underlying cellular responses to LIPUS, we investigated gene expression profiles in mouse MC3T3-E1 preosteoblast cells using a GeneChip´fi system. **Overall design:** The mouse preosteoblast MC3T3-E1cells were treated with LIPUS (30 mW/cm2) for 20 min followed by culturing for 6 and 24 h at 37C. Mock-treated cells were served as control. Total RNA samples were prepared from the cells, and quality of the RNA was analyzed using a Bioanalyzer 2100. Gene expression was monitored by an Affymetrix GeneChip system with a Mouse Genome 430 2.0 array. Sample preparation for array hybridization was carried out as described in the manufacturer's instructions.

Background corr dist: KL-Divergence = 0.0154, L1-Distance = 0.0176, L2-Distance = 0.0004, Normal std = 0.7802

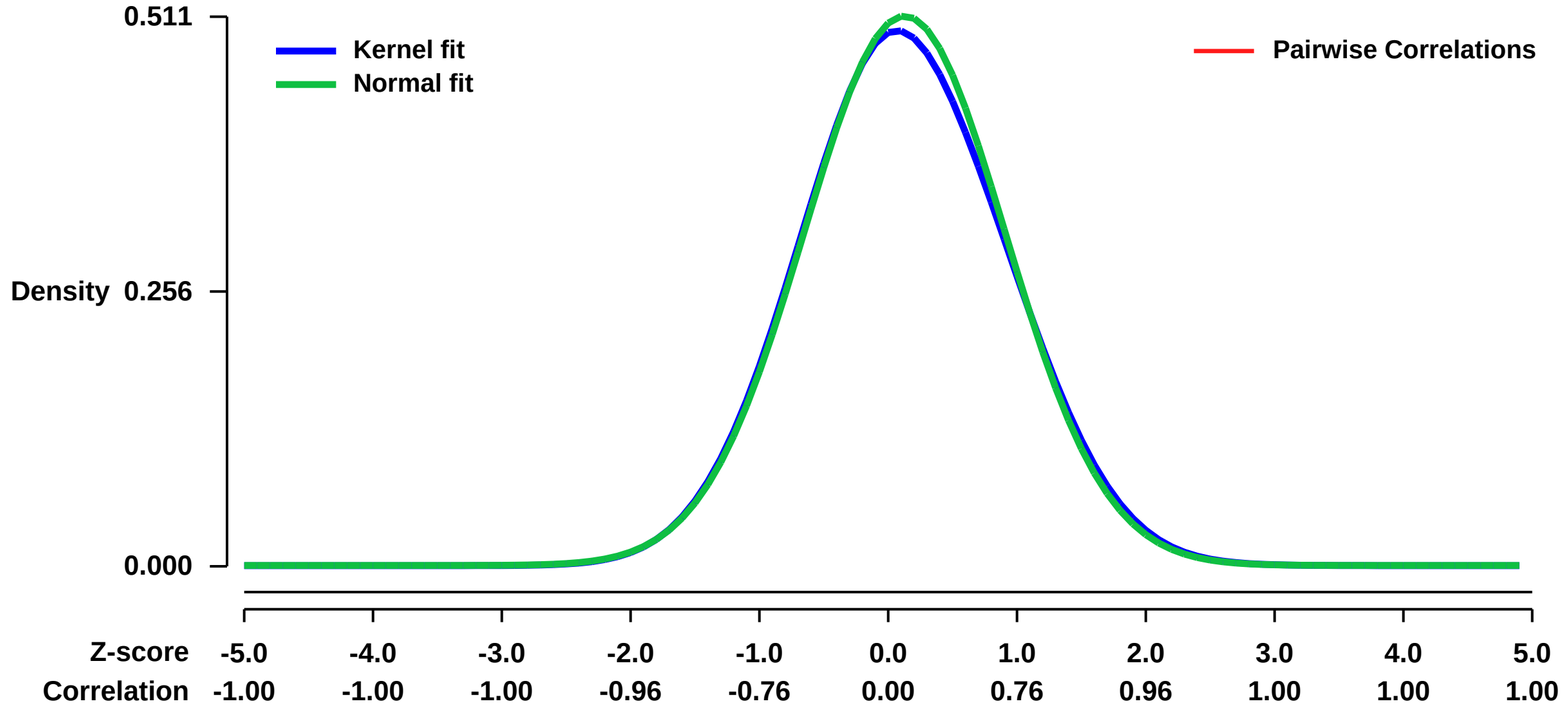

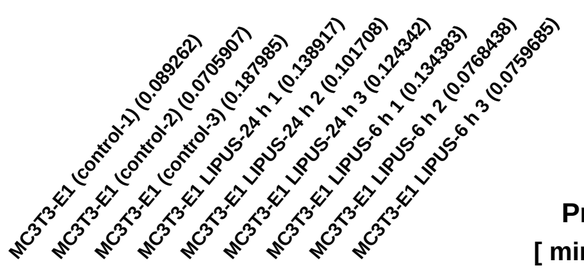

Pre-normalization Quantiles

[min] [medium] [max]

Null module

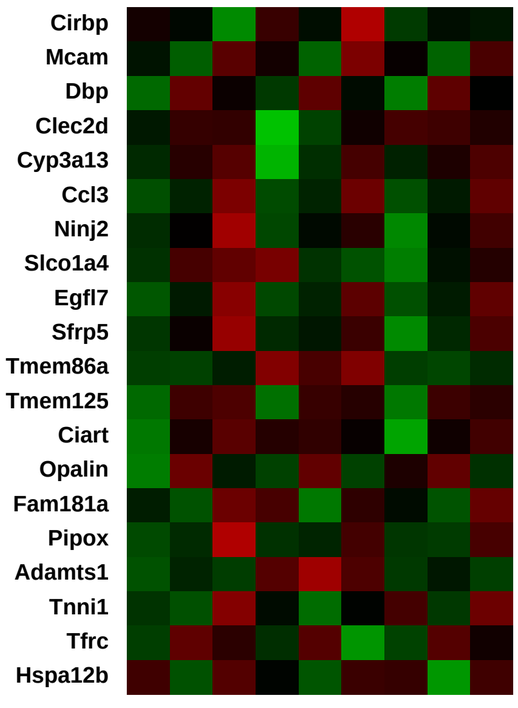

GEO Series "GSE13120" Expression Profiles

Num of samples in this series: 10

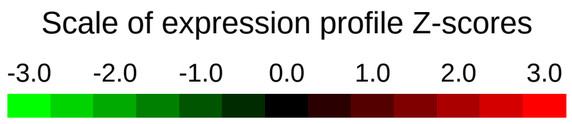

GEO Link:	http://www.ncbi.nlm.nih.gov/geo/query/acc.cgi?acc=GSE13120
Status:	Public on Nov 26 2008
Title:	Age-related gene expression changes in mouse neocortex
Organism:	Mus musculus
Experiment type:	Expression profiling by array
Platform:	GPL1261
Pubmed ID:	19041753
Summary & Design:	**Summary:** Aging is associated with major nuclear changes affecting genomic integrity and gene expression. Here we compare the gene expression profiles in the neocortex of young (5 months old) and old (30 months old) B6xC3 F1 mice. In a related study, we compare genes that change expression with age to SIRT1 associated genes identified by ChIP on chip (NimbleGen) and find a significant overlap, indicating that SIRT1 target genes are preferentially deregulated with age. Keywords: gene expression comparison, age-comparison **Overall design:** Total neocortex RNA was hybridized on Affymetrix M430 2.0 arrays. RNA was isolated from five young (5 months) and 5 old (30 months) B6xC3 F1 mice, samples were hybridized individually.

Background corr dist: KL-Divergence = 0.0674, L1-Distance = 0.0204, L2-Distance = 0.0005, Normal std = 0.5033

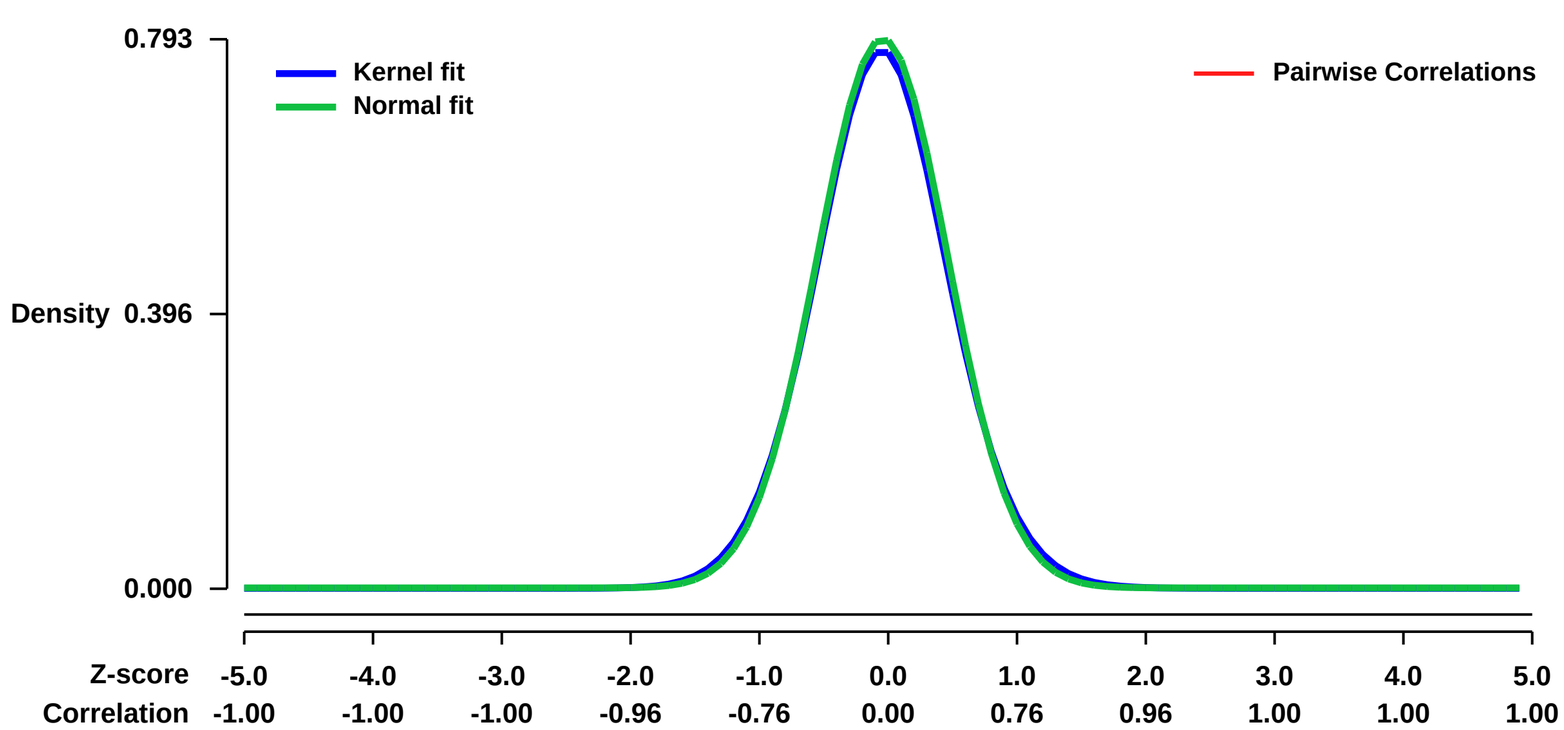

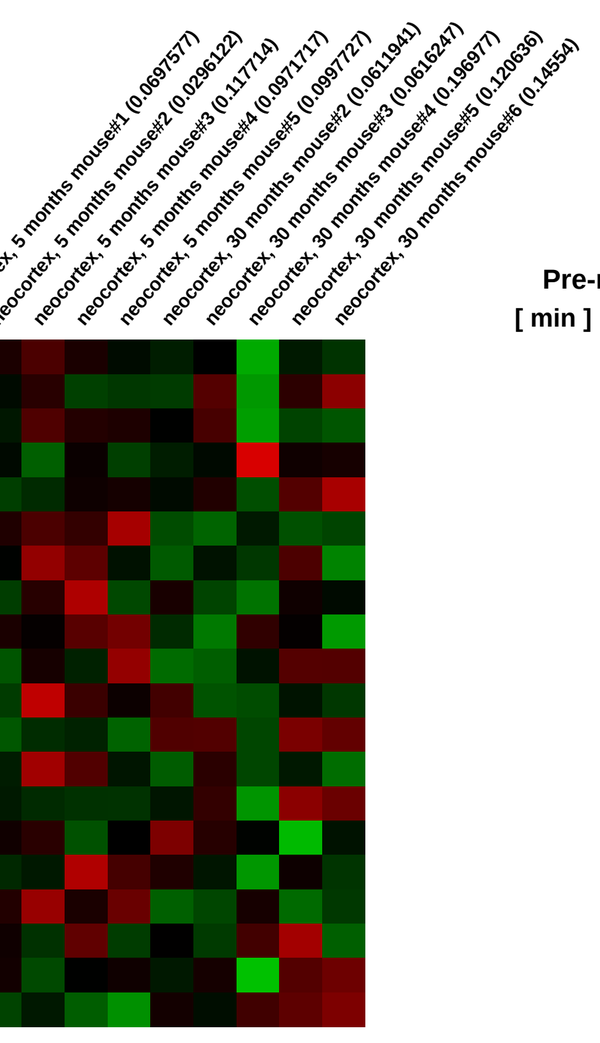

GEO Series "GSE3196" Expression Profiles

Num of samples in this series: 12

Scale of expression profile Z-scores

-3.0 -2.0 -1.0 0.0 1.0 2.0 3.0

GEO Link:	http://www.ncbi.nlm.nih.gov/geo/query/acc.cgi?acc=GSE3196
Status:	Public on Oct 24 2005
Title:	Gene expression in hypoxic MEFs having only p300 and CBP with deleted CH1 domains
Organism:	Mus musculus
Experiment type:	Expression profiling by array
Platform:	GPL1261
Pubmed ID:	16237459
Summary & Design:	**Summary:** The CH1 protein interaction domain of the transcriptional coactivators p300 and CBP is thought to interact with HIF-1alpha and this interaction is thought to be critical to the expression of HIF-1alpha target genes in response to hypoxia. To test the requirement of the CH1 domain for gene expression in response to hypoxia, rimary mouse embryonic fibroblasts (MEFs) were generated from C57Bl/6x129/Sv F2 e14.5 embryos that contain a deletion in the CH1 domain of three of four alleles of CBP and p300. The remaining allele of p300 or CBP was a conditional knock out allele. Control MEFs with only a single conditional knockout allele of p300 or CBP were also generated. At passage 3 MEFs were infected with Cre Adenovirus and grown until they had expanded at least 100 fold. Subconfluent MEFs were treated with 21% oxygen (normoxia) or 0.1% oxygen (hypoxia) with 5% carbon dioxide at 37 C in a humid chamber for 6hrs. At the start of treatment, medium was removed and replaced with medium (DMEM+10% FBS+pen-strep+ l-glu) that had been preequilibrated overnight in normoxia or hypoxia as appropriate. Immediately after treatment, cells were lysed in Trizol for RNA extraction. **Keywords: genetic modification, dose response** **Overall design:** 12 samples; 4 genotypes [CBP+/flox (flox1), p300 +/flox (flox2), CBP CH1/flox;p300 CH1/CH1 (triCH1flox1),CBP CH1/CH1;p300 CH1/flox (triCH1flox2)] , 2 treatments (normoxia and hypoxia).

Background corr dist: KL-Divergence = 0.1522, L1-Distance = 0.0360, L2-Distance = 0.0026, Normal std = 0.3713

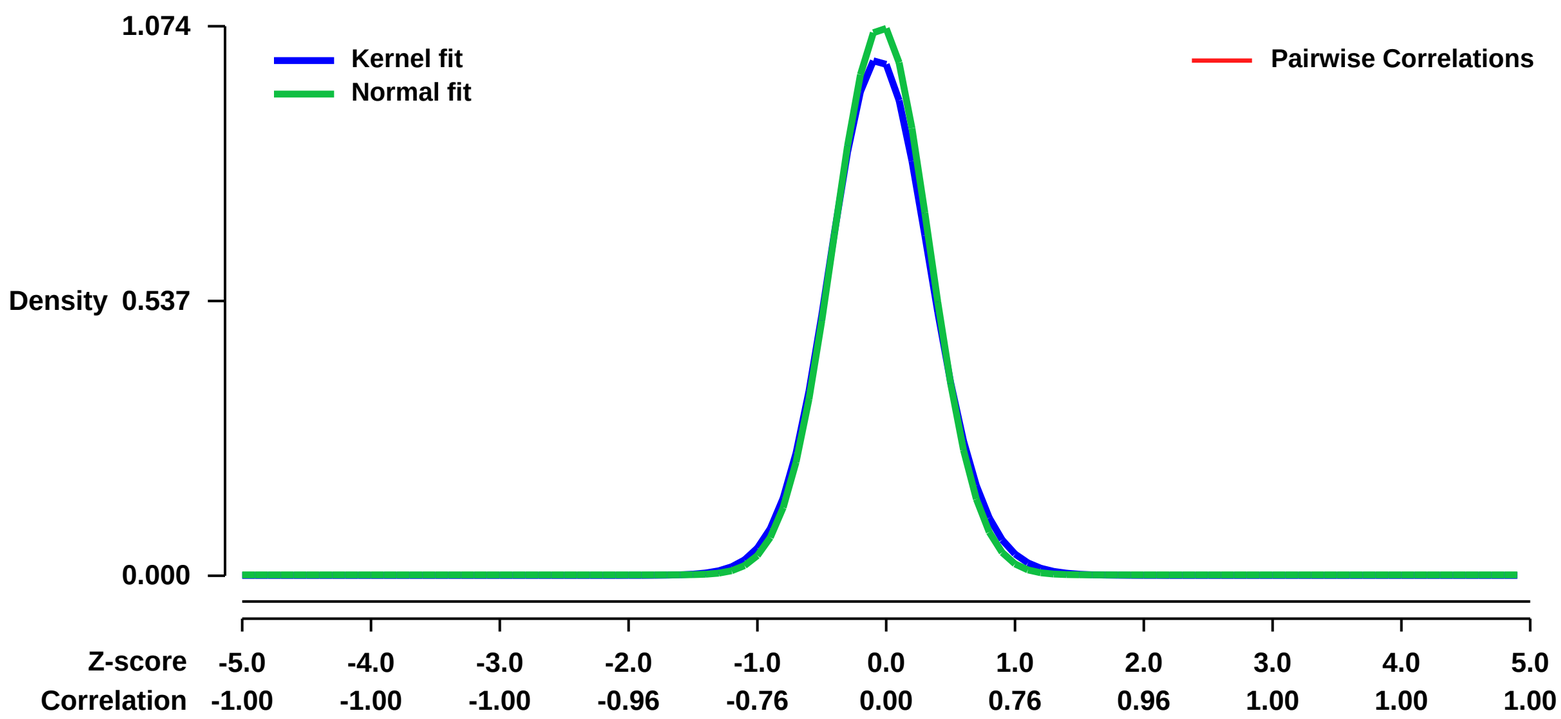

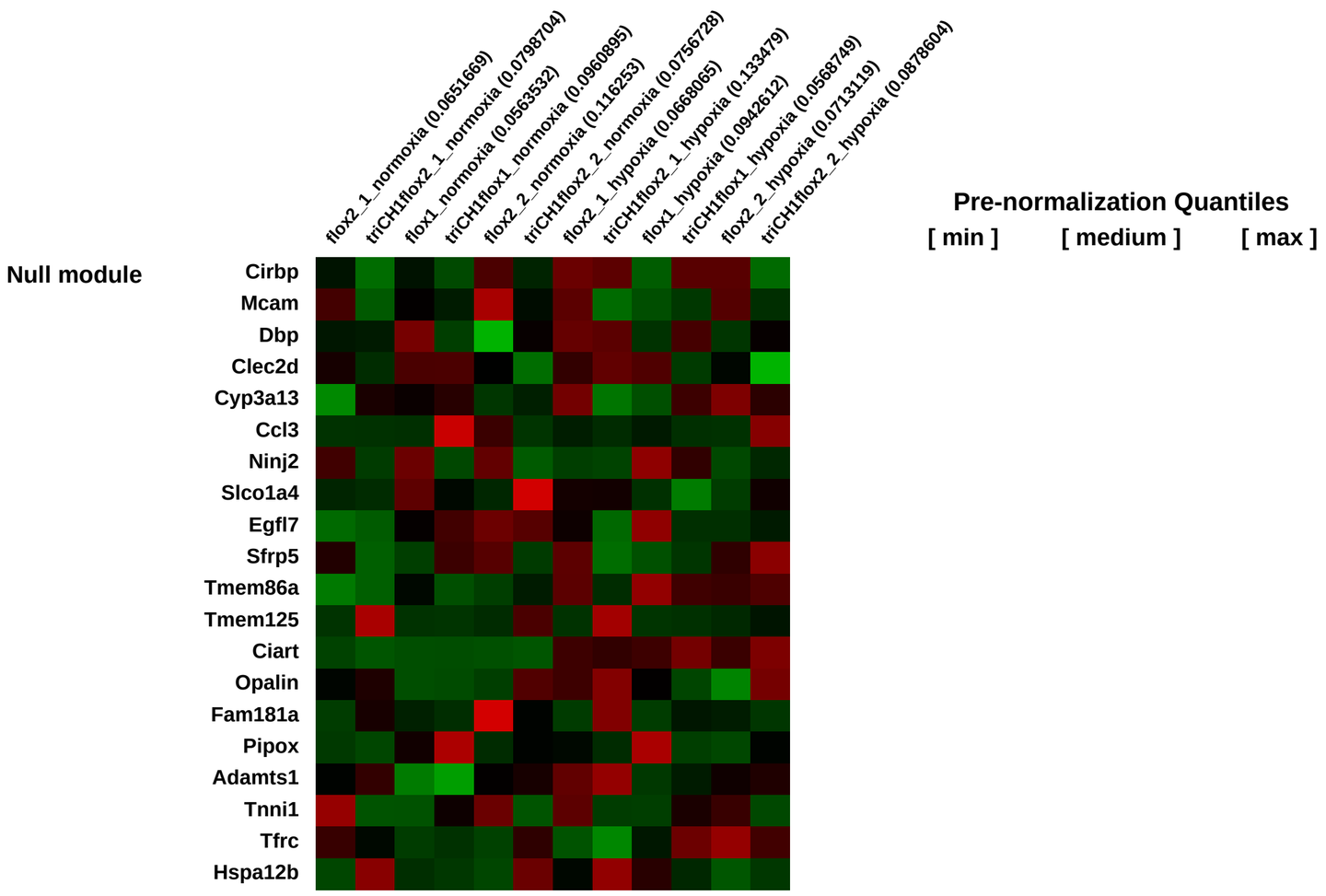

GEO Series "GSE19668" Expression Profiles

Num of samples in this series: 50

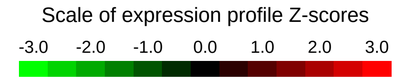

GEO Link:	http://www.ncbi.nlm.nih.gov/geo/query/acc.cgi?acc=GSE19668
Status:	Public on Aug 01 2010
Title:	Genetic Determinants for Susceptibility to Staphylococcus aureus Infection in A/J and C57BL/6J
Organism:	Mus musculus
Experiment type:	Expression profiling by array
Platform:	GPL1261
Pubmed ID:	20824097
Summary & Design:	**Summary:** Although it has recently been shown that A/J mice are highly susceptible to Staphylococcus aureus sepsis as compared to C57BL/6J, the specific genes responsible for this differential phenotype are unknown. Using chromosome substitution strains (CSS), we found that factors on chromosomes (chr) 8, 11, and 18 are responsible for susceptibility to S. aureus sepsis in A/J mice. F1 mice from C57BL/6J X CSS8 cross (C8A) and C57BL/6J X CSS18 (C18A) were also susceptible to S. aureus (median survival < 48 h), whereas F1 mice from C57BL/6J X CSS11 cross (C11A) were resistant (median survival > 120 h) to S. aureus. Bacterial loads in the kidney were consistent with F1 median survivals, with higher bacterial counts in susceptible mice. No sexlinked associations with susceptibility were noted in F1 intercrosses. Using whole genome transcription profiling, we identified a total of 192 genes on chromosomes 8, 11, and 18 which are differentially expressed between A/J and C57BL/6J in the setting of S. aureus infection. Of these, 28 genes had Gene Ontology annotations indicating a potential immune response function. These 28 genes are associated with susceptibility to S. aureus in A/J mice, and are potential determinants of susceptibility to S. aureus infection in humans. **Overall design:** To identify genes for which differential expression between A/J and C57BL/6J mice could contribute to host susceptibility to S. aureus infection, we compared the gene expression profiles between uninfected A/J and C57BL/6J mice and between infected A/J and C57BL/6J mice at 2, 4, 6, and 12 hours after infection.

Background corr dist: KL-Divergence = 0.1340, L1-Distance = 0.0649, L2-Distance = 0.0110, Normal std = 0.3963

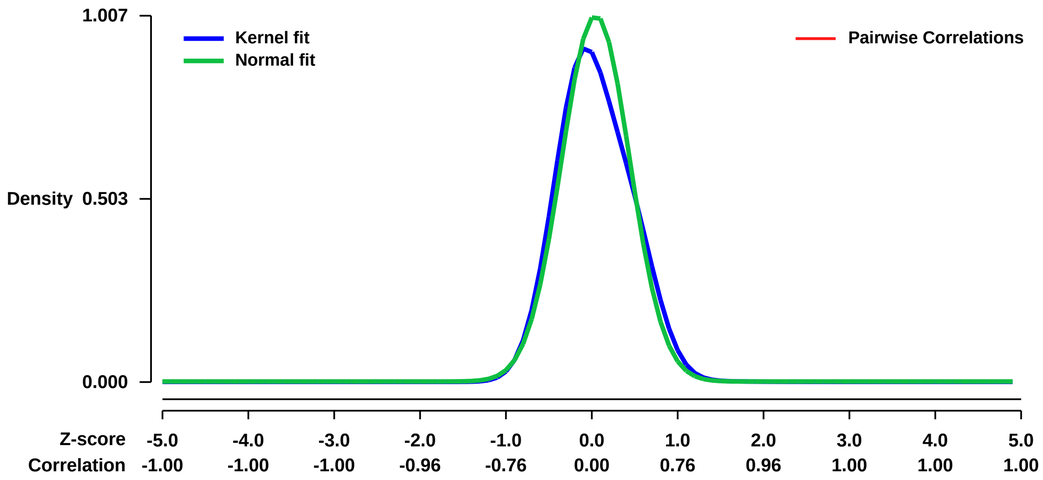

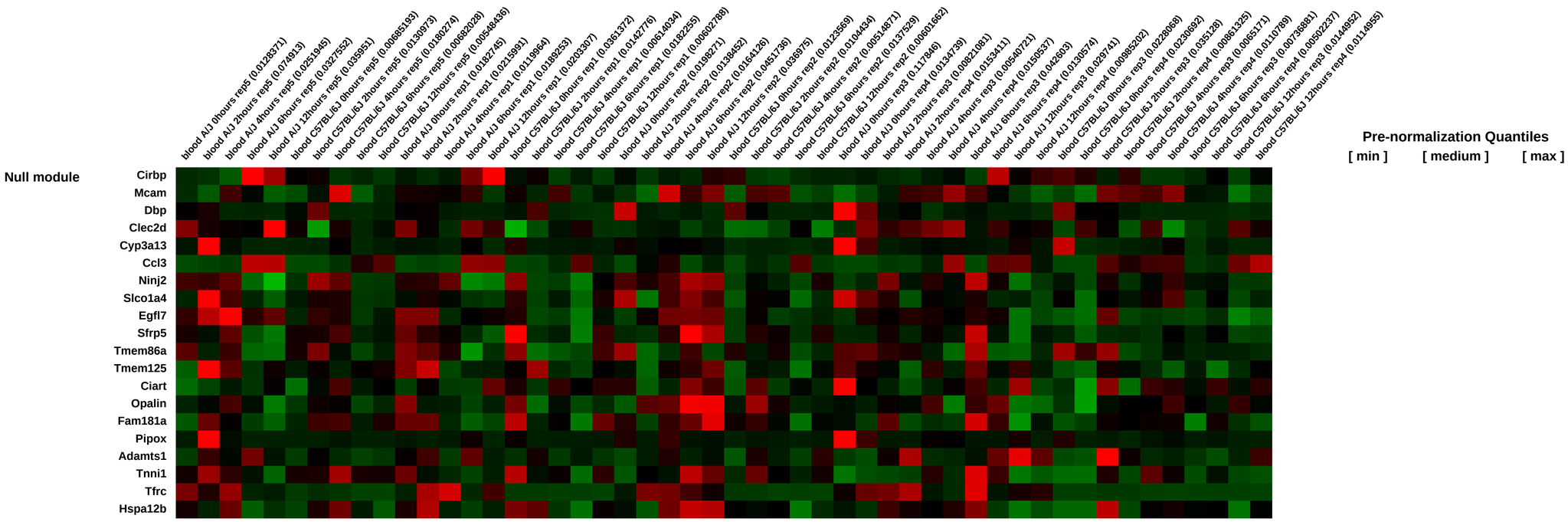

GEO Series "GSE34629" Expression Profiles

Num of samples in this series: 6

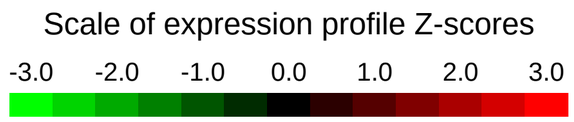

GEO Link:	**http://www.ncbi.nlm.nih.gov/geo/query/acc.cgi?acc=GSE34629**
Status:	**Public on Dec 22 2012**
Title:	**Comparing expression profiles of NIH3T3 cells with and without LPAR1 mutation**
Organism:	**Mus musculus**
Experiment type:	**Expression profiling by array**
Platform:	**GPL1261**
Pubmed ID:	
Summary & Design:	**Summary:** **To explore the signaling pathways of mutant LPAR1, we performed gene expression profiling for NIH3T3 cells expressing wild-type and mutant LPAR1 receptors using Affymetrix mouse 430 2.0 arrays** **Overall design:** **6 RNA samples from the same cell line. 3 samples contained LPAR1 mutant and 3 samples were wild-type. Cells were harvested at 0, 60, and 120 minutes.**
Background corr dist:	**KL-Divergence = 0.0350, L1-Distance = 0.0225, L2-Distance = 0.0005, Normal std = 0.6473**

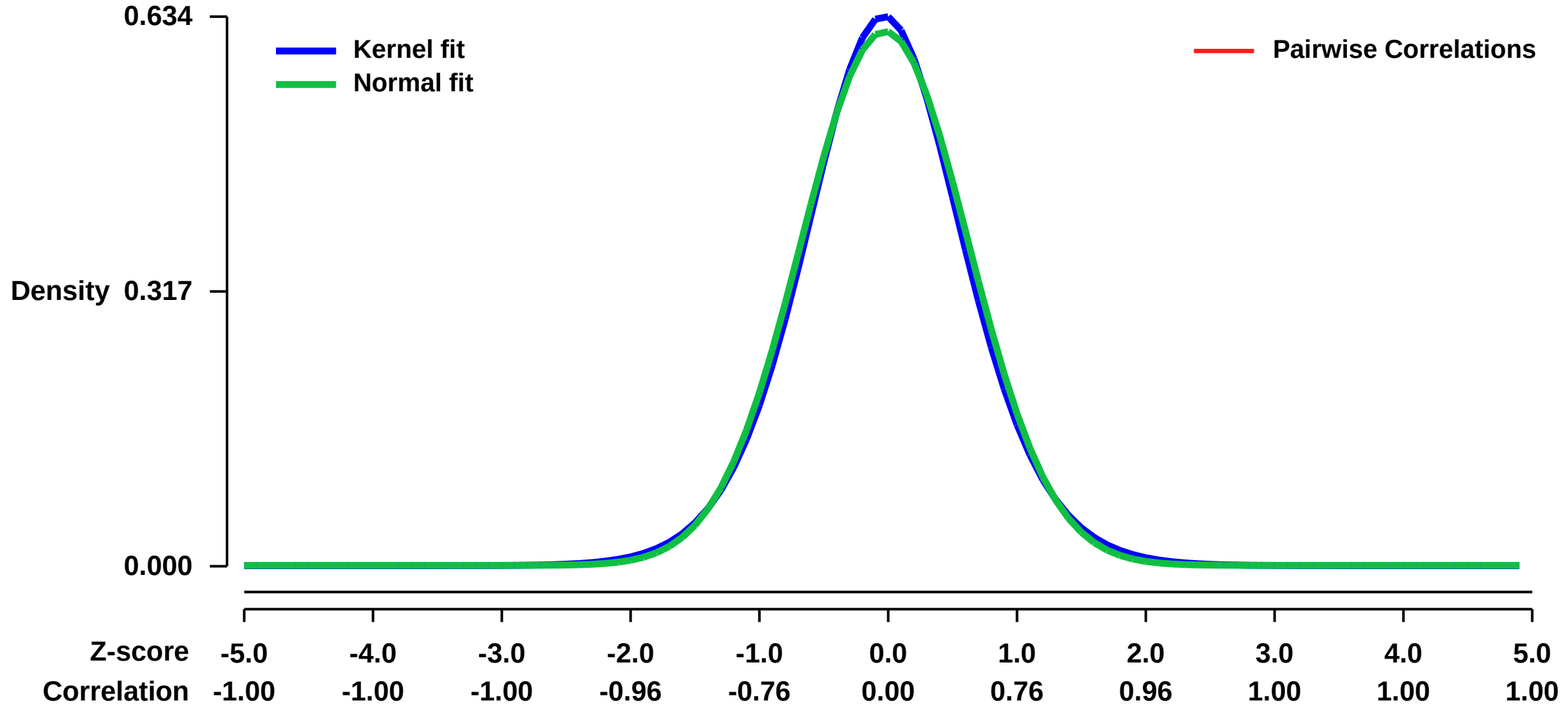

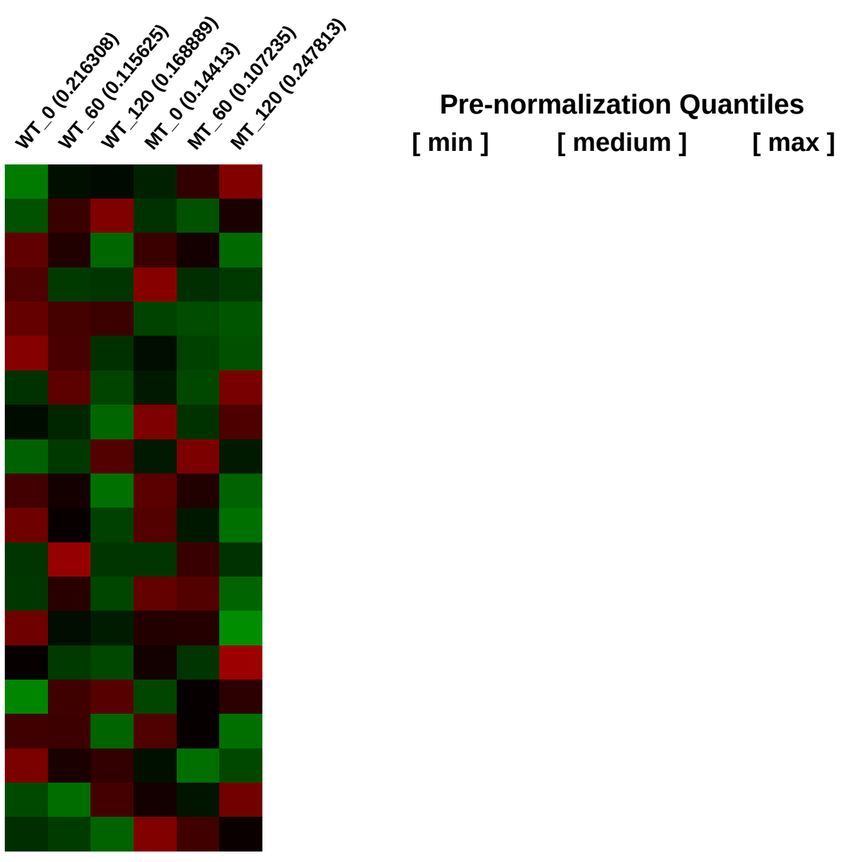

GEO Series "GSE2019" Expression Profiles

Num of samples in this series: 12

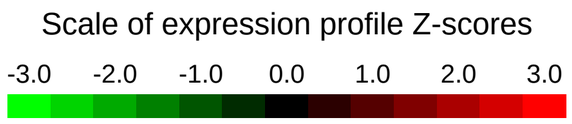

GEO Link:	http://www.ncbi.nlm.nih.gov/geo/query/acc.cgi?acc=GSE2019
Status:	Public on Dec 21 2004
Title:	Microarray Based Comparison of three Amplification Methods For Nanogram Amounts of Total RNA
Organism:	Mus musculus
Experiment type:	Expression profiling by array
Platform:	GPL1261
Pubmed ID:	15613496
Summary & Design:	**Summary:** **Two T7 based methods One round of Amplification (Affymetrix) and Two round of Amplification were compared to two Ribo-SPIA based systems, RiboSPIA and pico Ribo SPIA systems. Data for Pico-RiboSPIA are listed here.** **All Hybridisation were performed using Affymetrix Mouse 430-2 gene chips. Data were all scaled to 500.** **For 12 chips performed with pico Ribo SPIA the scaling factor average was 2.0 +/- 0.3, background intensities 74.4 +/- 12.7 , noise 3.9 +/- 0.6, rawQ 2.5 +/- 0.3** **Keywords: ordered** **Overall design:**

Background corr dist: KL-Divergence = 0.0933, L1-Distance = 0.0666, L2-Distance = 0.0072, Normal std = 0.5386

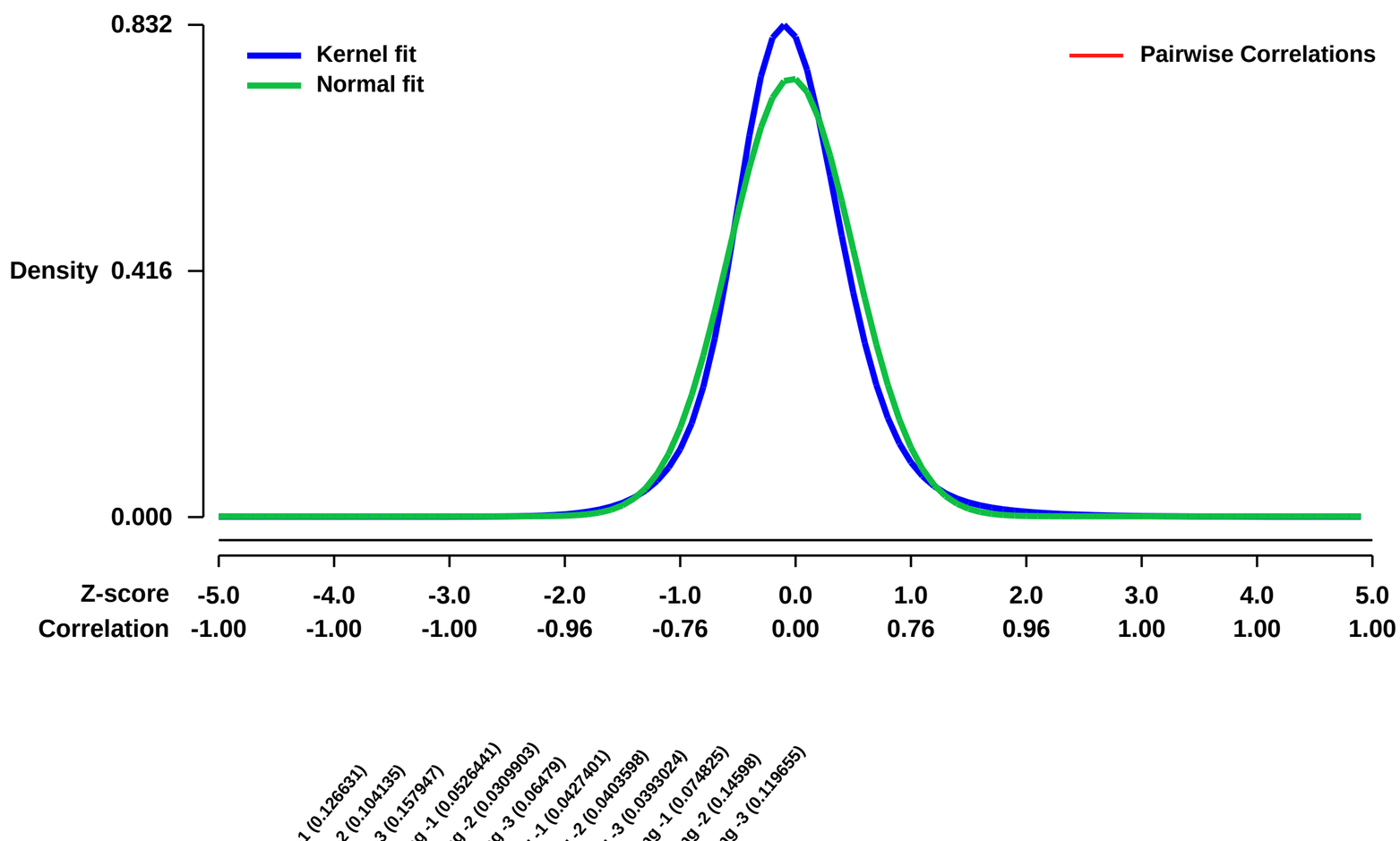

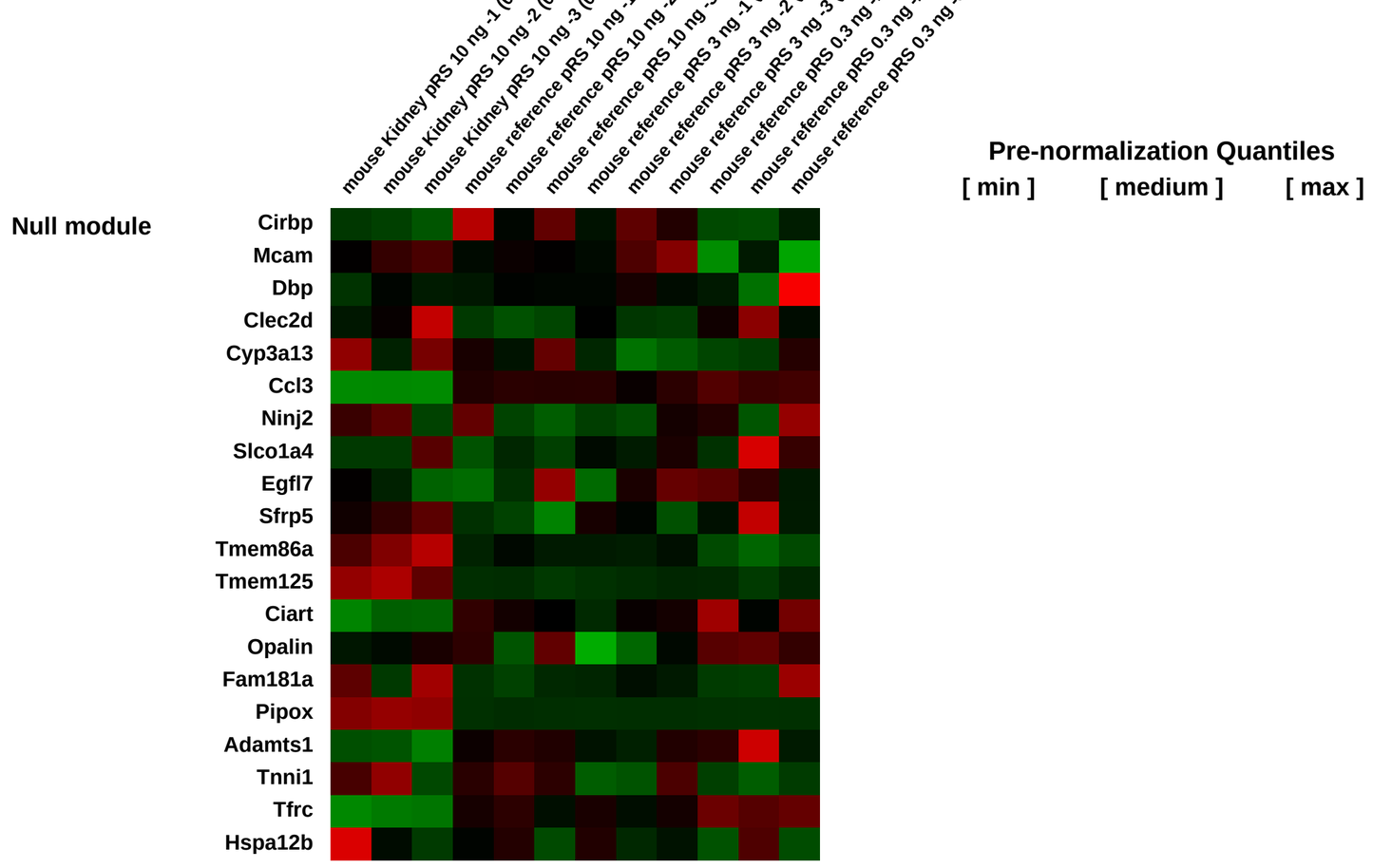

GEO Series "GSE15808" Expression Profiles

Num of samples in this series: 29

Scale of expression profile Z-scores

-3.0 -2.0 -1.0 0.0 1.0 2.0 3.0

GEO Link:	http://www.ncbi.nlm.nih.gov/geo/query/acc.cgi?acc=GSE15808
Status:	Public on Oct 08 2009
Title:	Global changes in processing of 3'-UTR characterize clinically distinct tumor types
Organism:	Mus musculus
Experiment type:	Expression profiling by array
Platform:	GPL1261
Pubmed ID:	19934316
Summary & Design:	**Summary:** We used a novel probe-level microarray analysis, revealing connections between mRNA processing and lymphoid neoplasia, in a mouse leukemia model. Characteristic differences in mRNA processing, primarily in the 3â -untranslated region, distinguished histologically similar tumor subtypes with different survival characteristics. Gene sets with specific processing in each tumor subtype defined signatures useful for tumor subclassification, as demonstrated by internal cross-validation with up to 80% discrimination accuracy. A combination of mRNA expression and sequence analysis suggested that differences in isoform abundance likely arose from both alternative polyadenylation and differential degradation. **Overall design:** 5 types of samples were analyzed with multiple biological replicates. Progenitor B-cells, mature B-cells were the control. LPC, APC, APN were the tumor cells. LPC (Lig4/P53 deficient cells developed pro-B lymphoma with c-myc amplification), APC (Artemis/P53 deficient cells developed pro-B lymphoma with c-myc amplification), APN (Artemis/P53 deficient cells developed pro-B lymphoma with N-myc amplification)

Background corr dist: KL-Divergence = 0.2247, L1-Distance = 0.0458, L2-Distance = 0.0045, Normal std = 0.3312

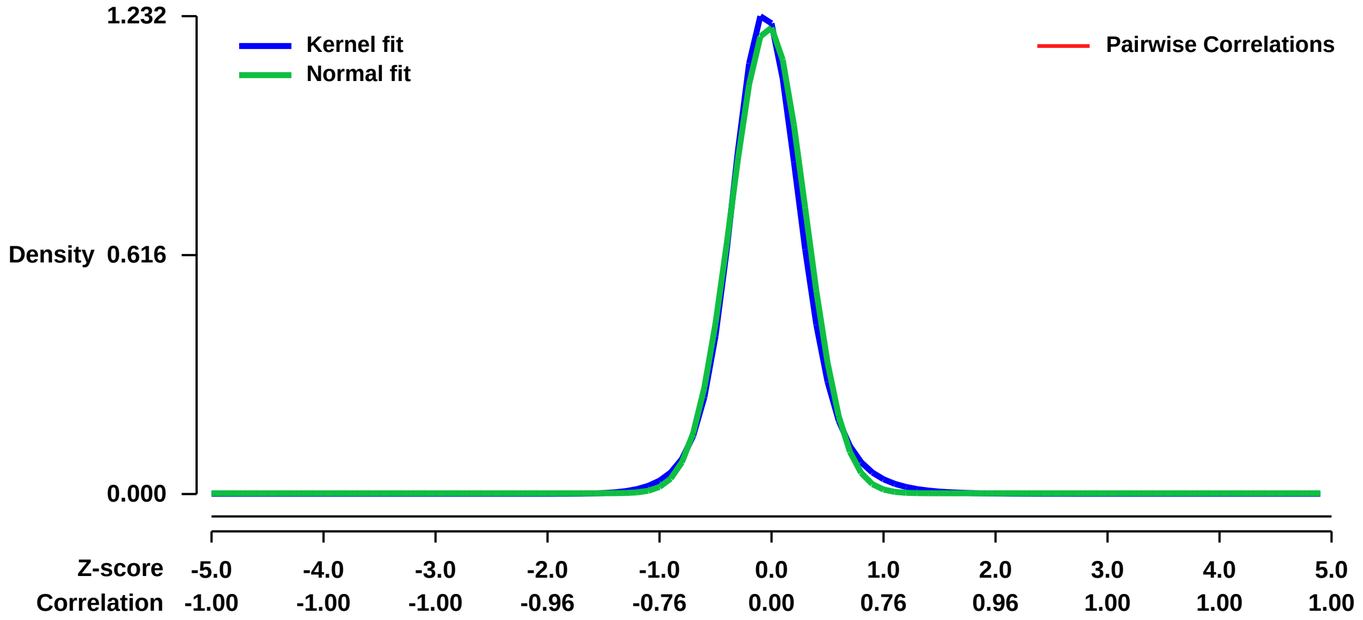

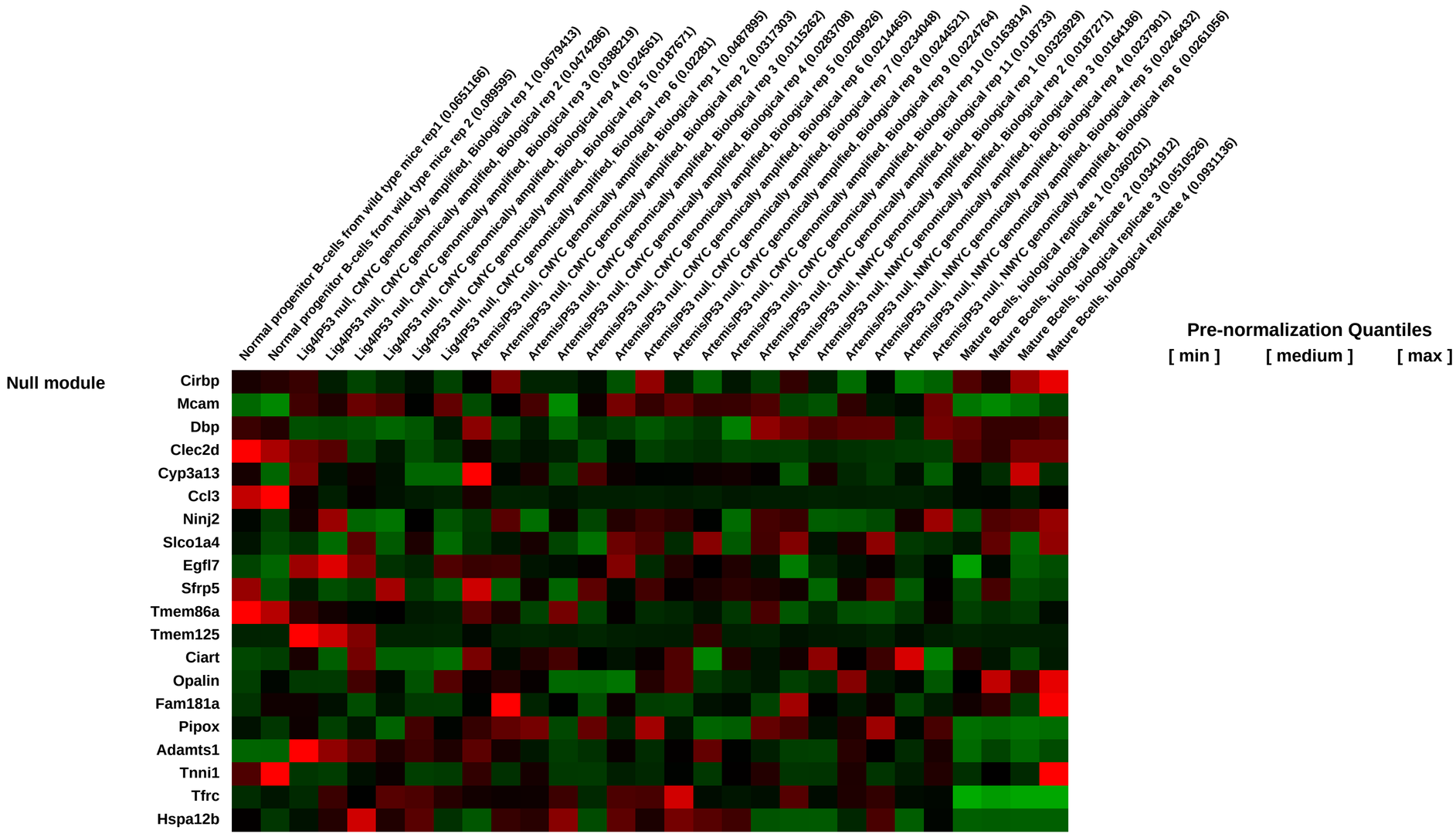

GEO Series "GSE37975" Expression Profiles

Num of samples in this series: 8

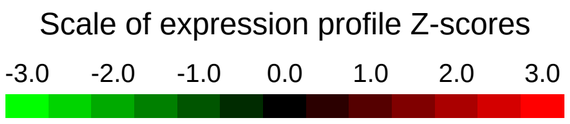

GEO Link:	http://www.ncbi.nlm.nih.gov/geo/query/acc.cgi?acc=GSE37975
Status:	Public on Jul 18 2012
Title:	Comparison of matched primary and metastasis 4T1.2 syngeneic mammary tumor model of spontaneous bone metastasis
Organism:	Mus musculus
Experiment type:	Expression profiling by array
Platform:	GPL1261
Pubmed ID:	22820642
Summary & Design:	**Summary:** Breast cancer metastasis to bone is a critical determinant of long-term survival after treatment of primary tumors. We used a mouse model of spontaneous bone metastasis to determine new molecular mechanisms. Differential transcriptome comparisons of primary and metastatic tumor cells revealed that a substantial set of genes suppressed in bone metastases were highly enriched for promoter elements for the type I interferon (IFN) regulatory factor, Irf7, itself suppressed in mouse and human metastases. The critical function of the Irf7 pathway was demonstrated by restoration of exogenous Irf7 or systemic interferon administration, which significantly reduced bone metastases and prolonged metastasis-free survival. Using mice deficient in the type I receptor (Ifnar1-/-) or mature B, T and NK cell responses (NOD Scid IL-2r‚‡-/- mice), we demonstrated that Irf7-driven suppression of metastasis was reliant on IFN signaling to host immune cells. Metastasis suppression correlated with decreased accumulation of myeloid-derived suppressor cells and increased CD4++, CD8 T cells and NK cells in the peripheral blood and was reversed by depletion of CD8+ cells and NK cells. Clinical importance of our findings was demonstrated as increased primary tumor Irf7 expression predicted prolonged bone and lung metastasis-free survival. Thus we report for the first time, a novel innate immune pathway, intrinsic to breast cancer cells, whose suppression in turn restricts systemic immunosurveillance to enable metastasis. This pathway may constitute a novel therapeutic target for restricting breast cancer metastases. **Overall design:** Microarrays were used to profile transcriptional alterations inherent in tumor cells growing in bone when compared to matched primary tumor cells in the 4T1.2 murine mammary tumor model. Primary and metastasized tumor were isolated from the same mouse with 4 independent biological replicates.

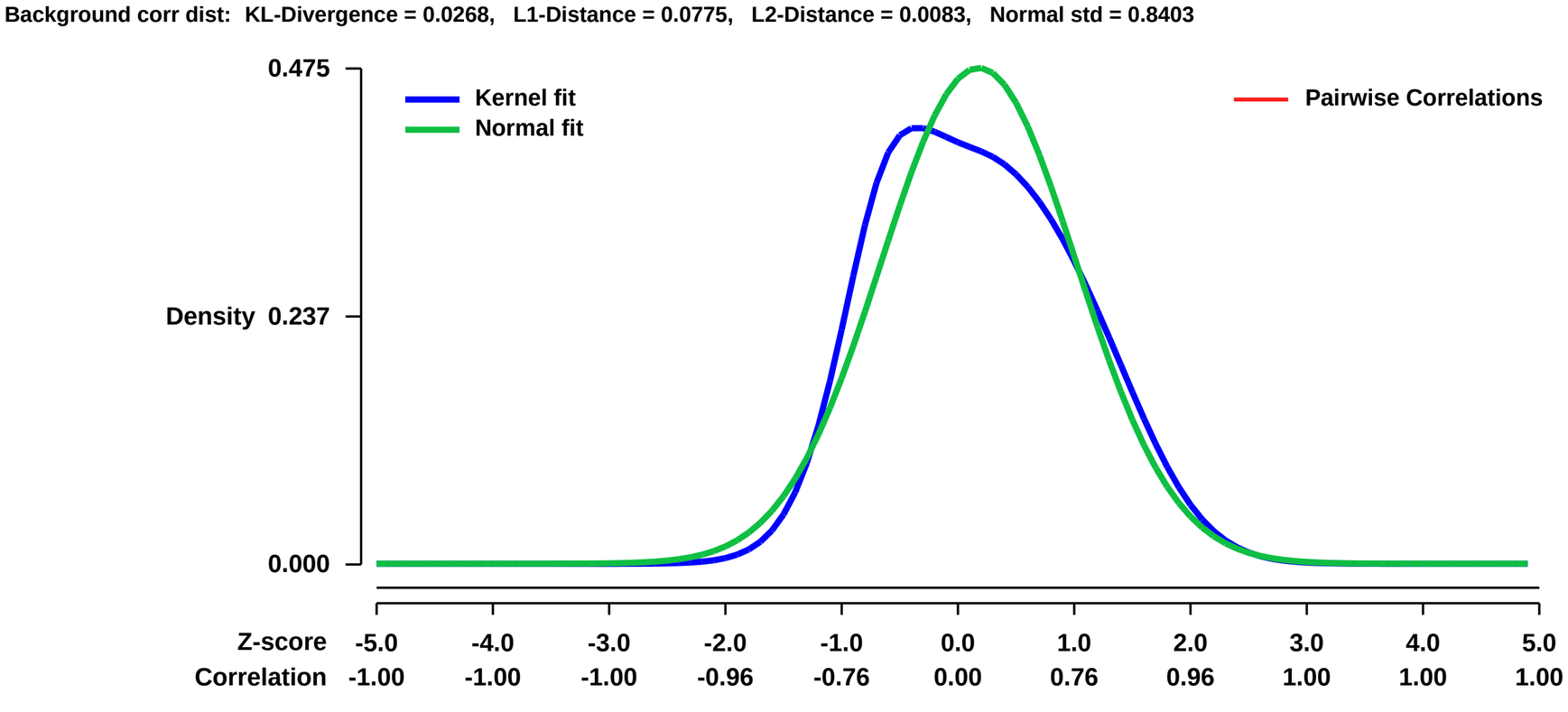

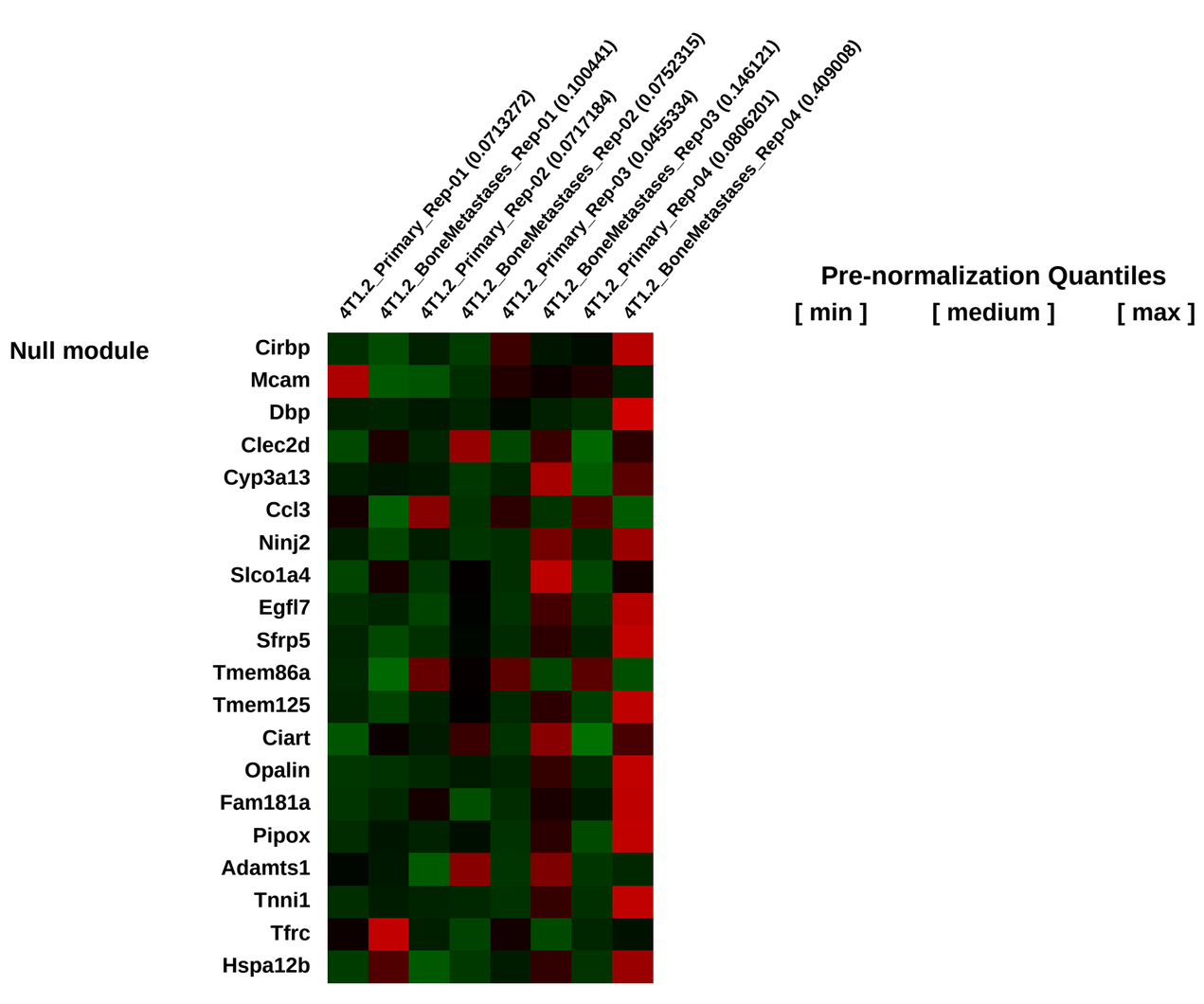

GEO Series "GSE41084" Expression Profiles

Num of samples in this series: 6

Scale of expression profile Z-scores

-3.0 -2.0 -1.0 0.0 1.0 2.0 3.0

GEO Link:	http://www.ncbi.nlm.nih.gov/geo/query/acc.cgi?acc=GSE41084
Status:	Public on Jul 01 2013
Title:	Expression data after irradiating mMSCs for 12 hours with broadband terahertz source
Organism:	Mus musculus
Experiment type:	Expression profiling by array
Platform:	GPL1261
Pubmed ID:	23378916
Summary & Design:	**Summary:** We report that terahertz (THz) irradiation of mouse mesenchymal stem cells with a pulsed broadband (centered at 10 THz) source, or a single-frequency, 2.52 THz, (SF) laser source, both with weak average power (<1mW/cm2), results in specific heterogenic changes in gene expression. The insignificant differential expression of heat shock and stress related genes as well as our temperature measurements imply a non-thermal response. The microarray survey and RT-PCR experiments demonstrate that at different irradiation conditions distinct groups of genes are activated. Stem cells irradiated for 12 hours with the broadband THz source exhibit an accelerated differentiation toward adipose phenotype, while the 2-hour (broadband or SF) irradiation affects genes transcriptionally active in pluripotent stem cells. Phenotypic and gene expression differences suggest that the THz effect depends on irradiation parameters such as duration and type of THz source, and on the level of stem cell differentiation. Computer simulations of the core promoters of two pluripotency markers reveal association between gene upregulation and propensity for DNA breathing. We propose that THz radiation has potential for non-contact control of cellular gene expression. **Overall design:** Growing in petri dish mouse mesenchymal stem cell cultures are irradiated for 12 hours with pulsed ultrafast (35 fs) broadband (centered at ~10 THz) source. Three independent biological experiments were conducted. In each experiment, a control mMSC culture was placed adjacent to the irradiated sample, and the temperature was kept at 26-27´”C for both the control and the irradiated sample. Immediately after completing the irradiation, total RNA was extracted from the irradiated sample and the control, and microarrays were used to identify differential changes in gene expression between the irradiated sample and its respective control. In each experiment, the mMSC cultures were synchronized to be at the same differentiation time point immediately before the irradiation.

Background corr dist: KL-Divergence = 0.0339, L1-Distance = 0.0126, L2-Distance = 0.0001, Normal std = 0.6395

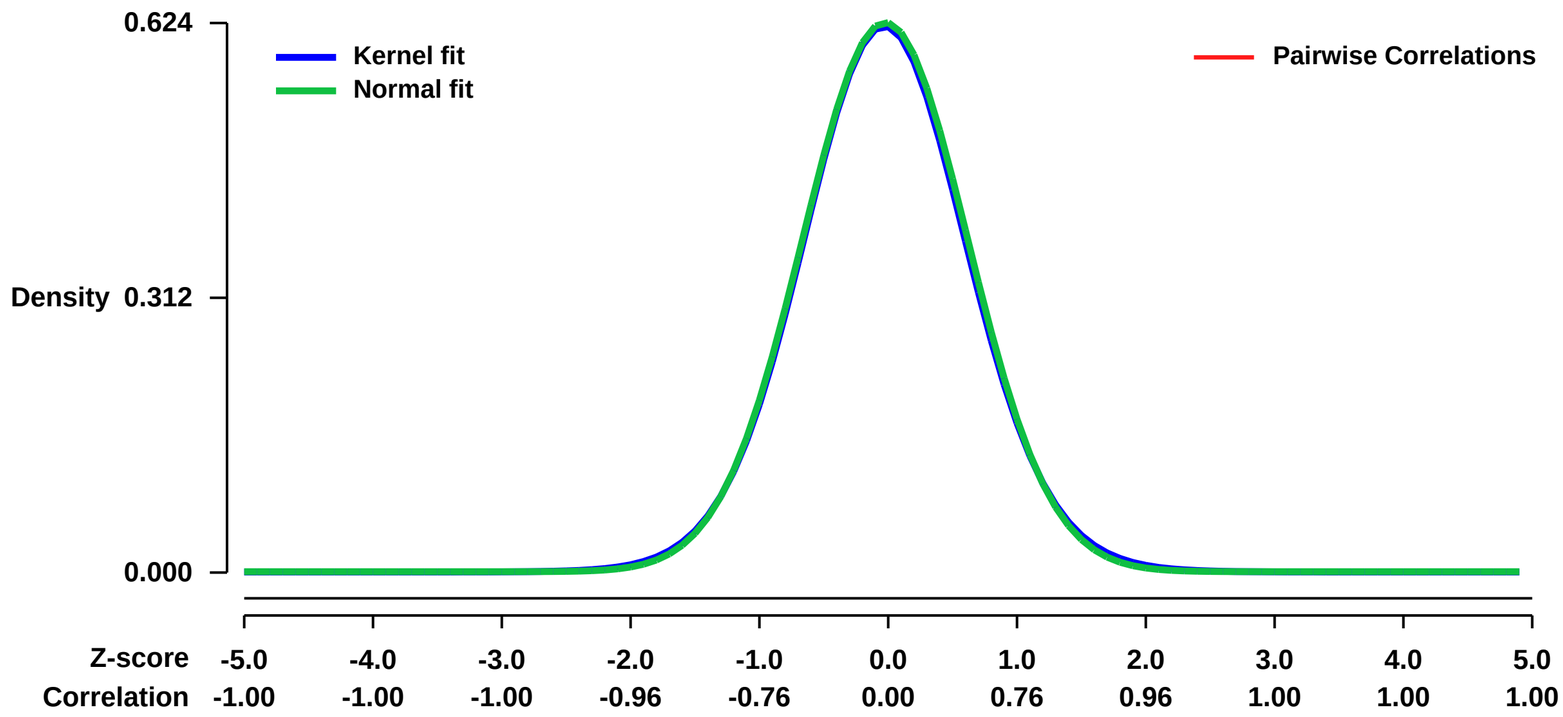

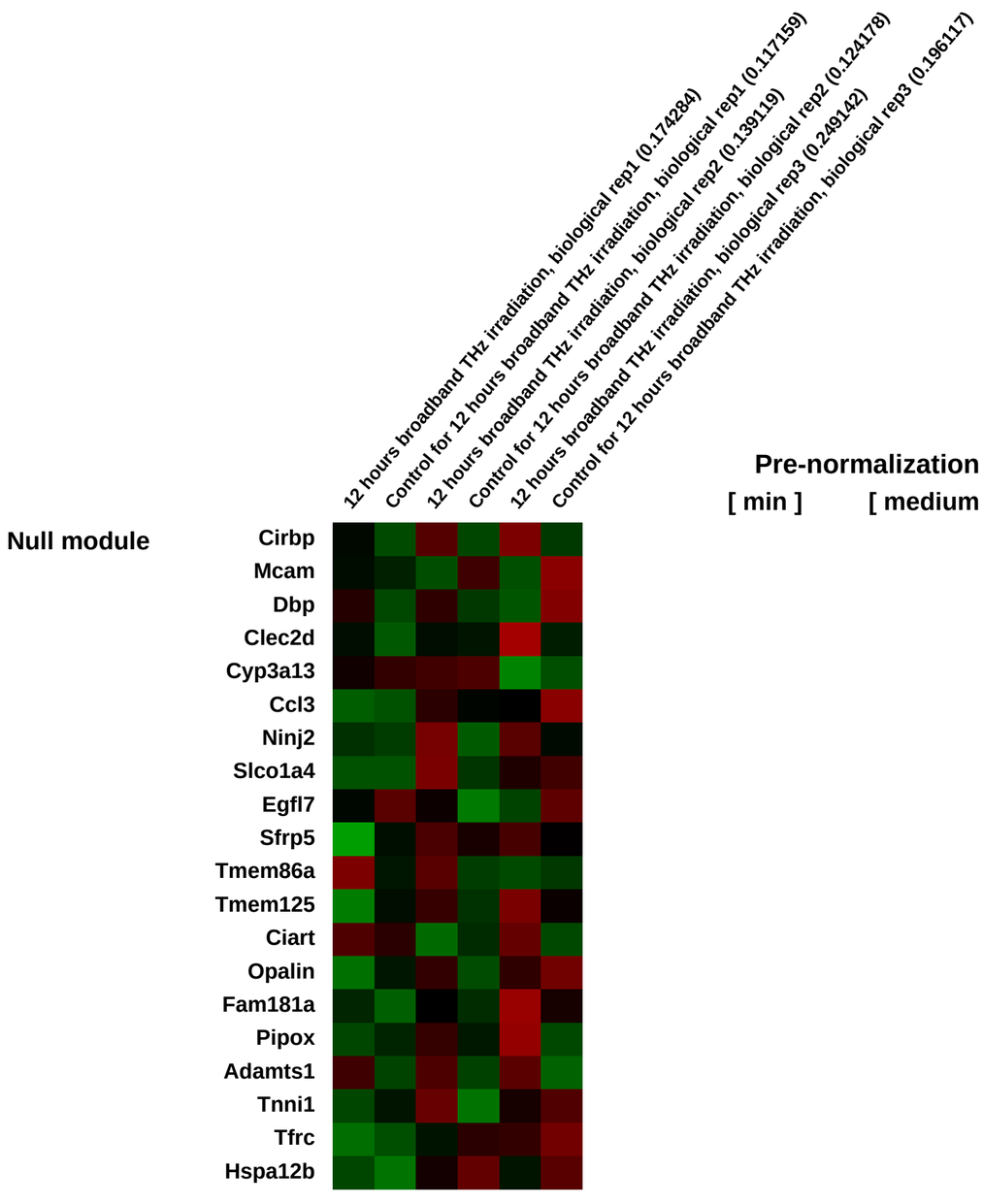

GEO Series "GSE46150" Expression Profiles

Num of samples in this series: 8

Scale of expression profile Z-scores

-3.0 -2.0 -1.0 0.0 1.0 2.0 3.0

GEO Link:	http://www.ncbi.nlm.nih.gov/geo/query/acc.cgi?acc=GSE46150
Status:	Public on Oct 01 2013
Title:	Gene expression profiling of primary mouse embryonic palatal mesenchymal cells in Tgfbr2 mutant mouse models
Organism:	Mus musculus
Experiment type:	Expression profiling by array
Platform:	GPL1261
Pubmed ID:	23975680
Summary & Design:	**Summary:** The overall goal of this project is to investigate the role of TGF-beta signaling in regulating the cellular metabolism of cranial neural crest (CNC) cells during palate development. Here, we conducted gene expression profiling of primary mouse embryonic palatal mesenchymal (MEPM) cells from wild type mice as well as those with a neural crest specific conditional inactivation of the Tgfbr2 gene. The latter mice provide a model of cleft palate, which is among the most common congenital birth defects and observed in many syndromic conditions. **Overall design:** To investigate the adverse effects of dysfunctional TGF-Beta signaling on the cellular metabolism of palatal mesenchyme during palatogenesis, we analyzed mice with a neural crest cell-specific conditional inactivation of Tgfbr2 (Tgfbr2fl/fl;Wnt1-Cre). We performed microarray analyses of primary mouse embryonic palatal mesenchymal cells of Tgfbr2fl/fl;Wnt1-Cre mutant mice and Tgfbr2fl/fl control mice, collected at embryonic day 13.5 (n=4 per genotype) and cultured with standard media (DMEM with supplements). Cells were collected after 2 passages.

Background corr dist: KL-Divergence = 0.0453, L1-Distance = 0.0160, L2-Distance = 0.0003, Normal std = 0.5769

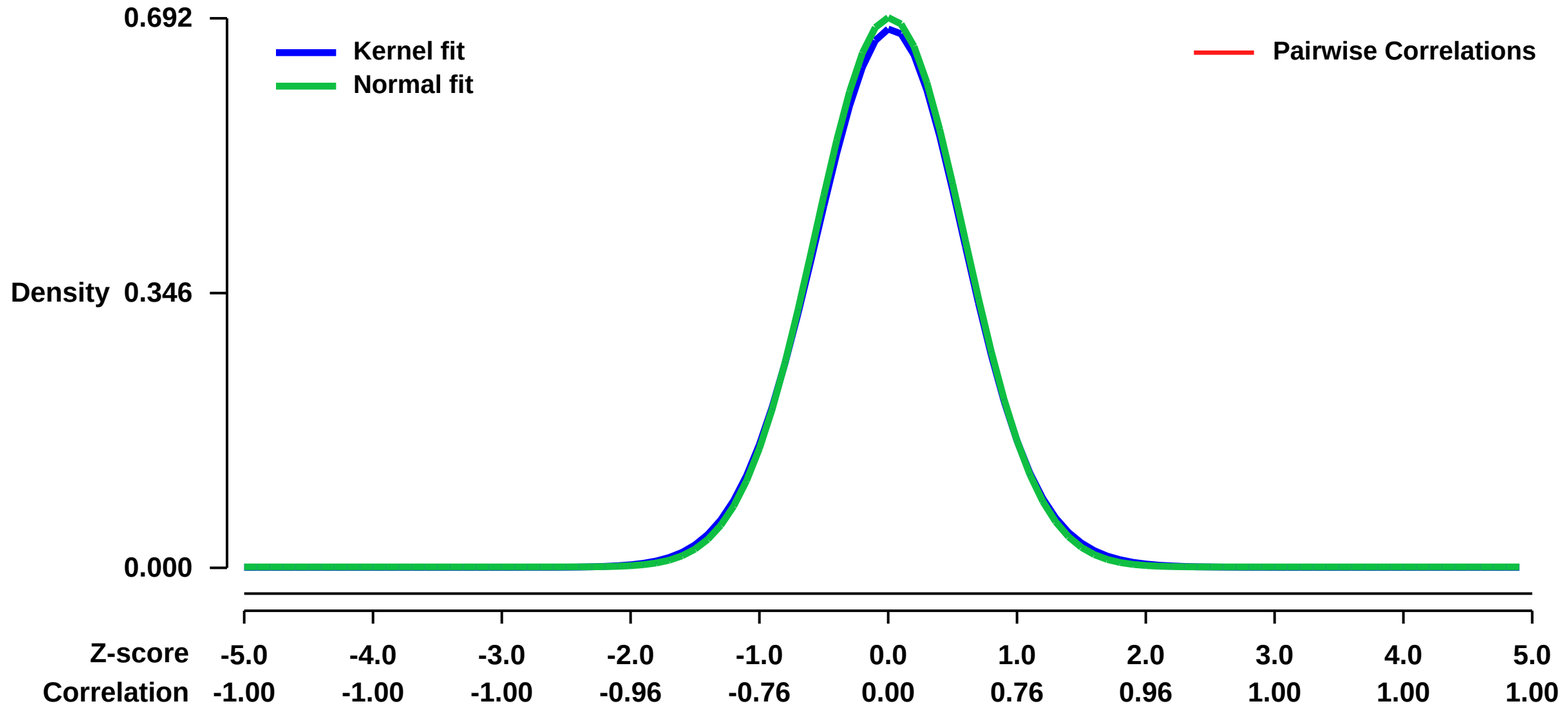

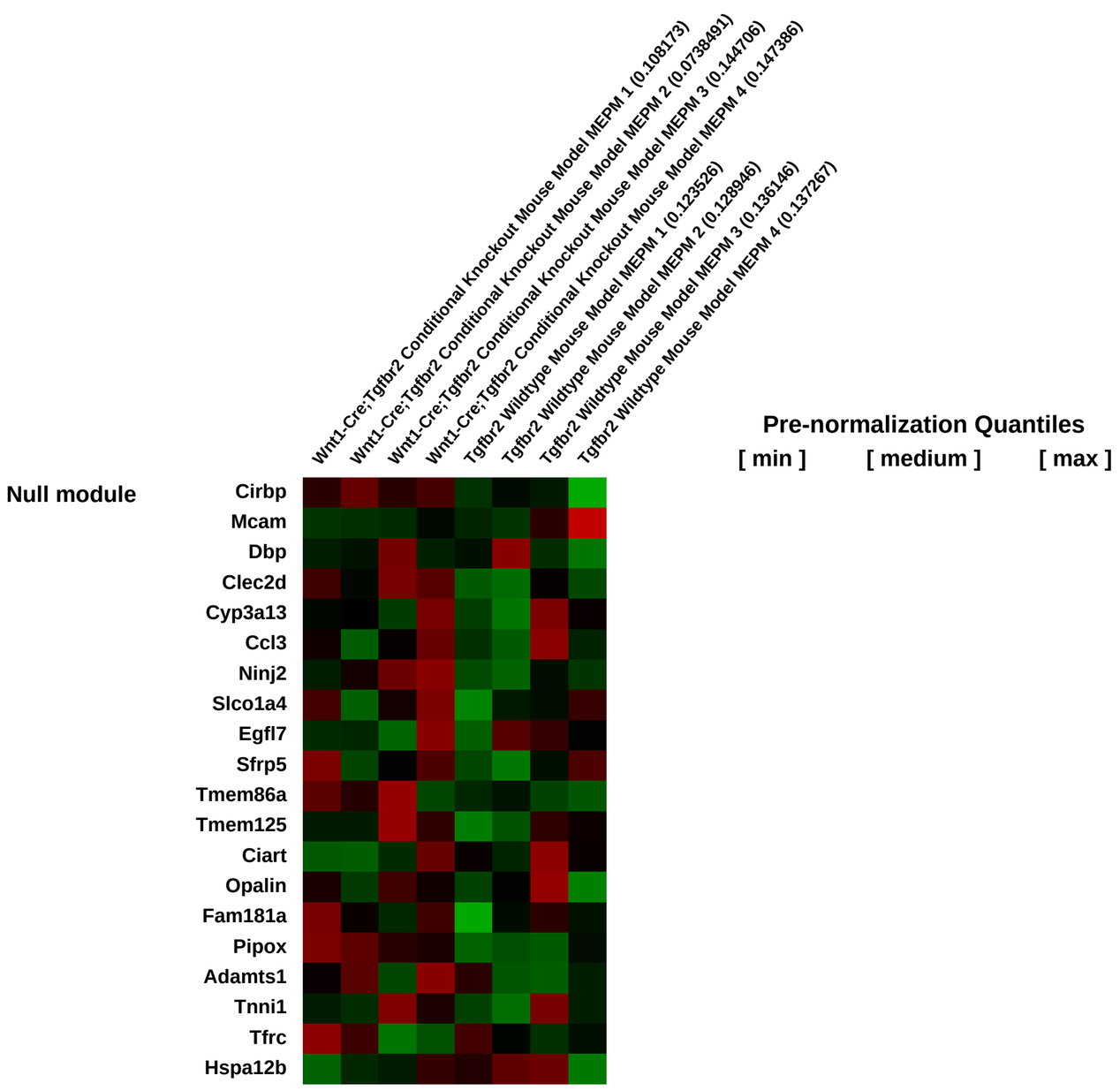

GEO Series "GSE19732" Expression Profiles

Num of samples in this series: 20

Scale of expression profile Z-scores

-3.0 -2.0 -1.0 0.0 1.0 2.0 3.0

GEO Link:	http://www.ncbi.nlm.nih.gov/geo/query/acc.cgi?acc=GSE19732
Status:	Public on Feb 01 2010
Title:	Identification of genes characteristic of committed preadipocyte fibroblasts
Organism:	Mus musculus
Experiment type:	Expression profiling by array
Platform:	GPL1261
Pubmed ID:	20200519
Summary & Design:	**Summary:** In order to identify the molecular mechanisms controlling preadipocyte commitment we derived new sublines of Swiss 3T3 fibroblasts with varying potential for adipogenesis. Swiss 2, Swiss 8, Swiss 9, and Swiss 19 differentiate into fat cells while Swiss 3, Swiss 5, and Swiss 22 have a lower propensity to differentiate into fat cells. The overall goal was to identify genes whose expression in the fibroblast state correlates with the ultimate potential of the cells to undergo adipogenesis **Overall design:** 4 preadipose fibroblast cell lines (Swiss 2, Swiss 8, Swiss 9, and Swiss 19 in triplicate or duplicate) were compared to 3 non-adipogenic fibroblast cell lines (Swiss 3, Swiss 5, Swiss 22 in triplicate)

Background corr dist: KL-Divergence = 0.2375, L1-Distance = 0.0460, L2-Distance = 0.0048, Normal std = 0.3101

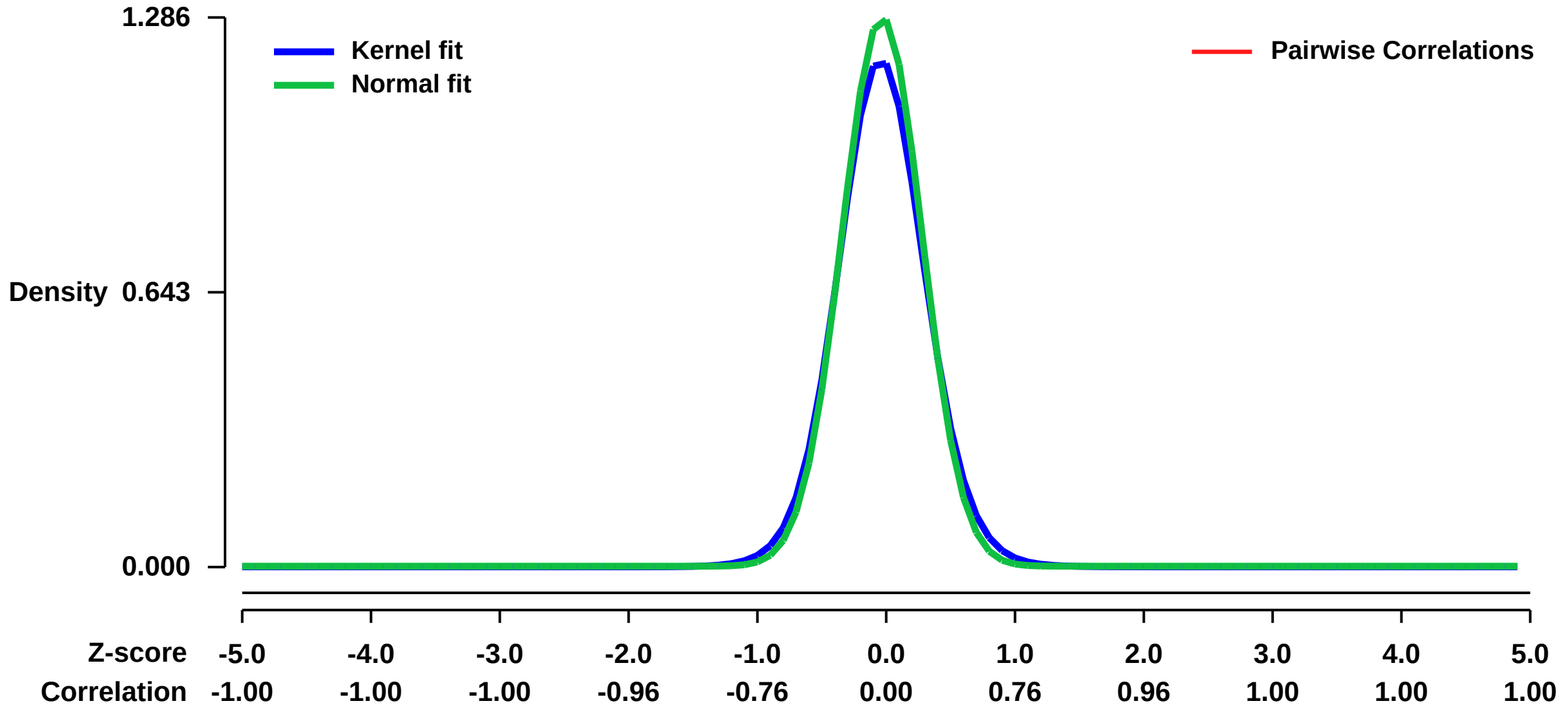

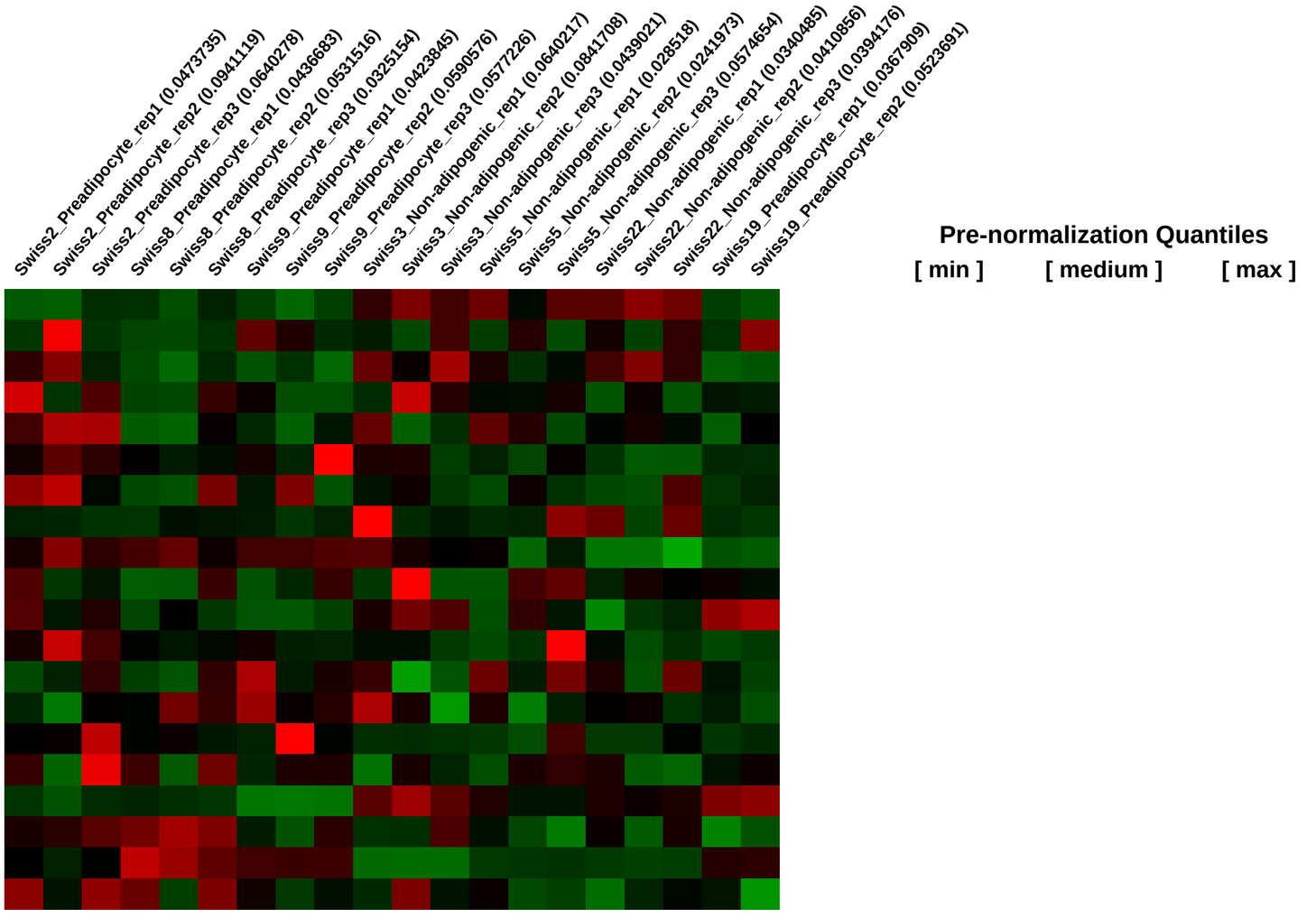

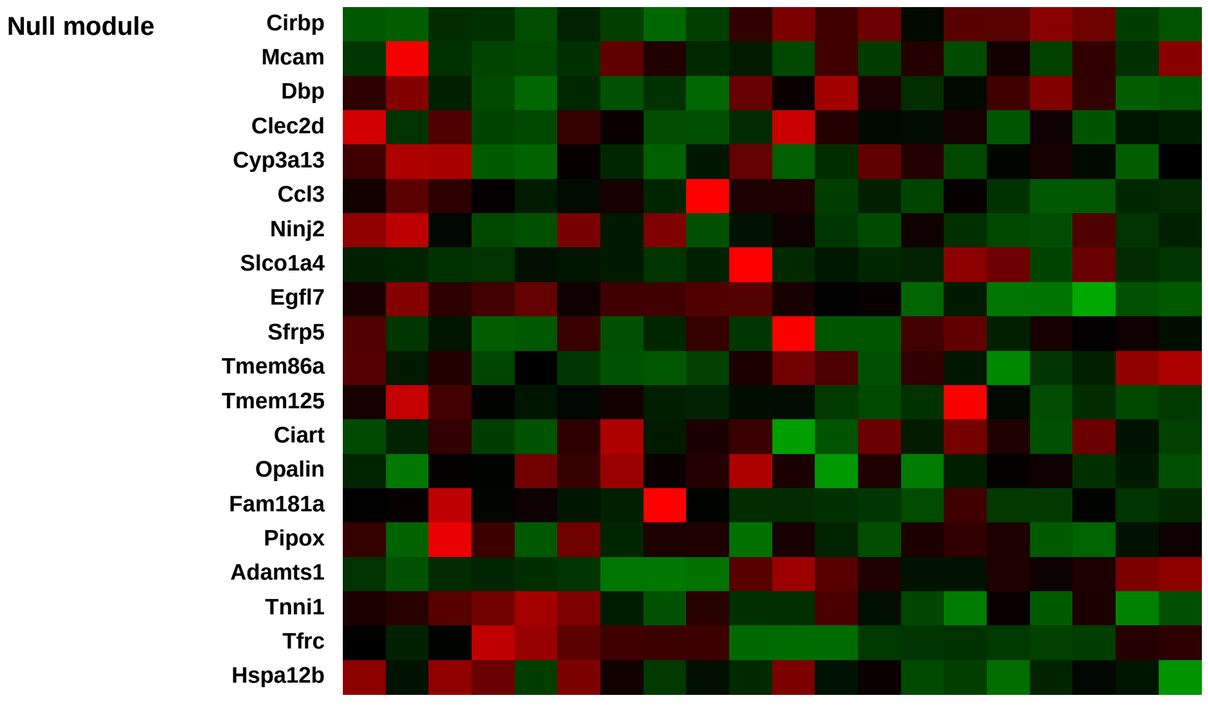

GEO Series "GSE43224" Expression Profiles

Num of samples in this series: 6

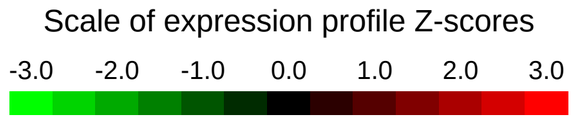

GEO Link:	http://www.ncbi.nlm.nih.gov/geo/query/acc.cgi?acc=GSE43224
Status:	Public on Feb 01 2013
Title:	Expression data from WT and E2A-deficient murine DN2 cells
Organism:	Mus musculus
Experiment type:	Expression profiling by array
Platform:	GPL1261
Pubmed ID:	23297135
Summary & Design:	**Summary:** The E2A transcription factors promote the development of thymus-seeding cells but it remains unknown whether these proteins play a role in T lymphocyte lineage specification or commitment. By examining E2A-dependent genes in developing T cells, we will address whether these proteins are involved in these processes. **Overall design:** DN2 cells from WT and E2A-deficient murine fetal thymi were FACS sorted. Subsequently RNA was extracted, labelled and hybridized to Affymetrix microarrays. The goal of this study is to investigate E2A-dependent genes in developing T cells

Background corr dist: KL-Divergence = 0.0381, L1-Distance = 0.0132, L2-Distance = 0.0001, Normal std = 0.6183

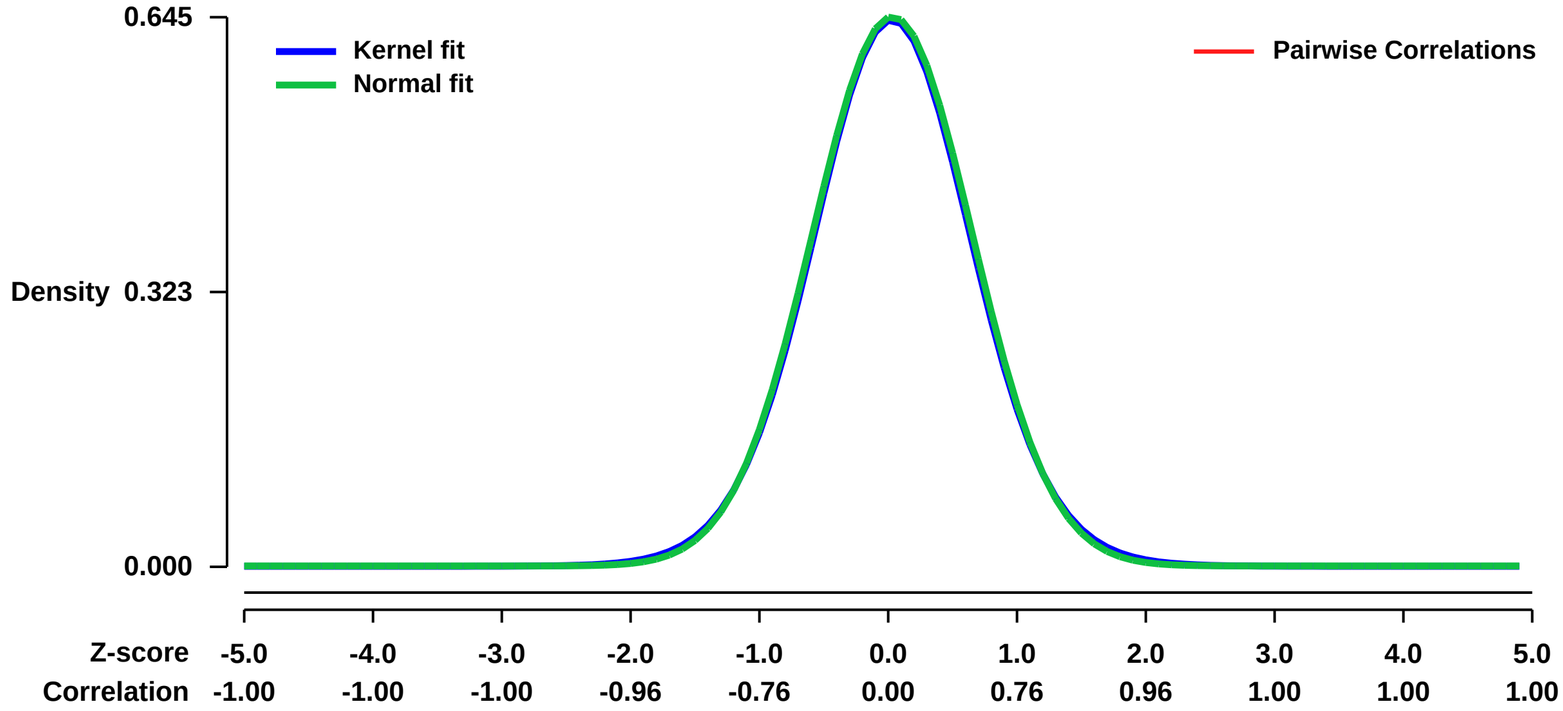

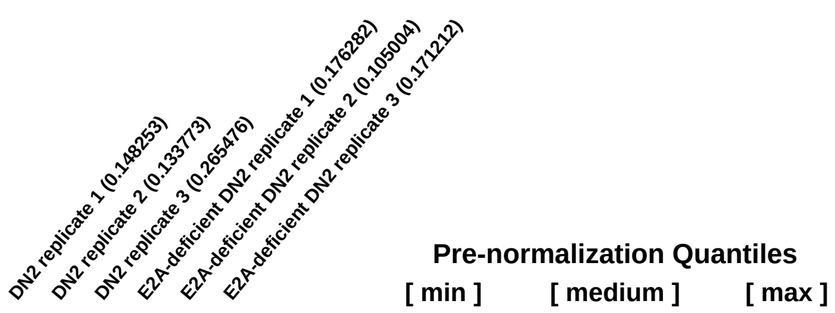

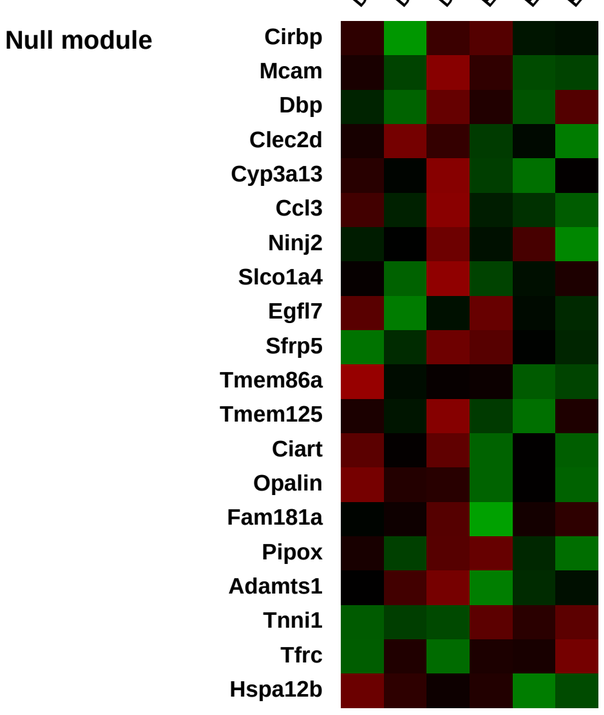

GEO Series "GSE11664" Expression Profiles

Num of samples in this series: 10

Scale of expression profile Z-scores

-3.0 -2.0 -1.0 0.0 1.0 2.0 3.0

GEO Link:	http://www.ncbi.nlm.nih.gov/geo/query/acc.cgi?acc=GSE11664
Status:	Public on Jun 05 2008
Title:	gene expression of CTCF-depleted mouse oocyte
Organism:	Mus musculus
Experiment type:	Expression profiling by array
Platform:	GPL1261
Pubmed ID:	18614575
Summary & Design:	**Summary:** CTCF is a multifunctional nuclear factor involved in epigenetic regulation. We have used transgenic RNA interference to deplete maternal stores of CTCF from growing mouse oocytes, and identified the potential target genes **Overall design:** We profiled the global gene expression in the wild type and CTCF-depleted GV oocytes, and identified a set of target genes.

Background corr dist: KL-Divergence = 0.1157, L1-Distance = 0.0232, L2-Distance = 0.0009, Normal std = 0.4149

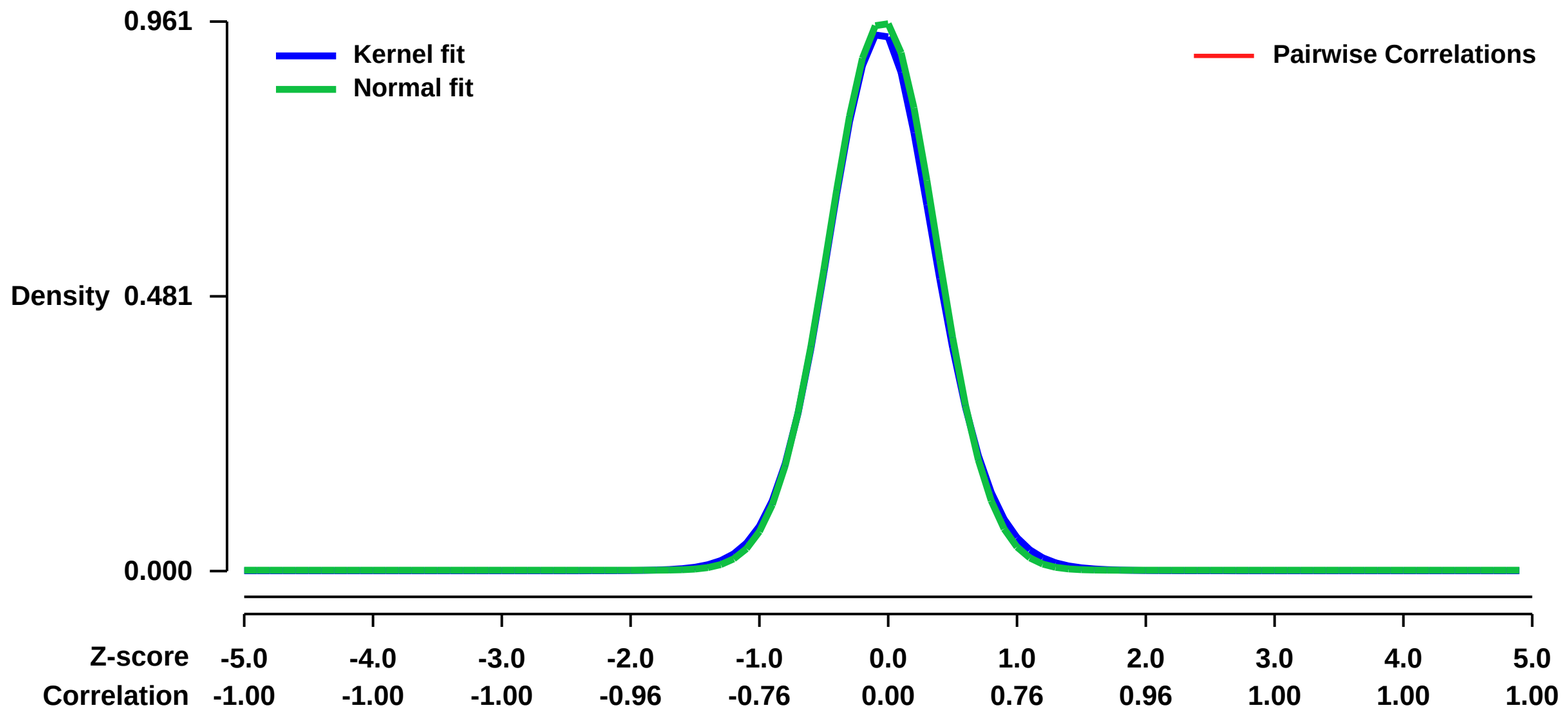

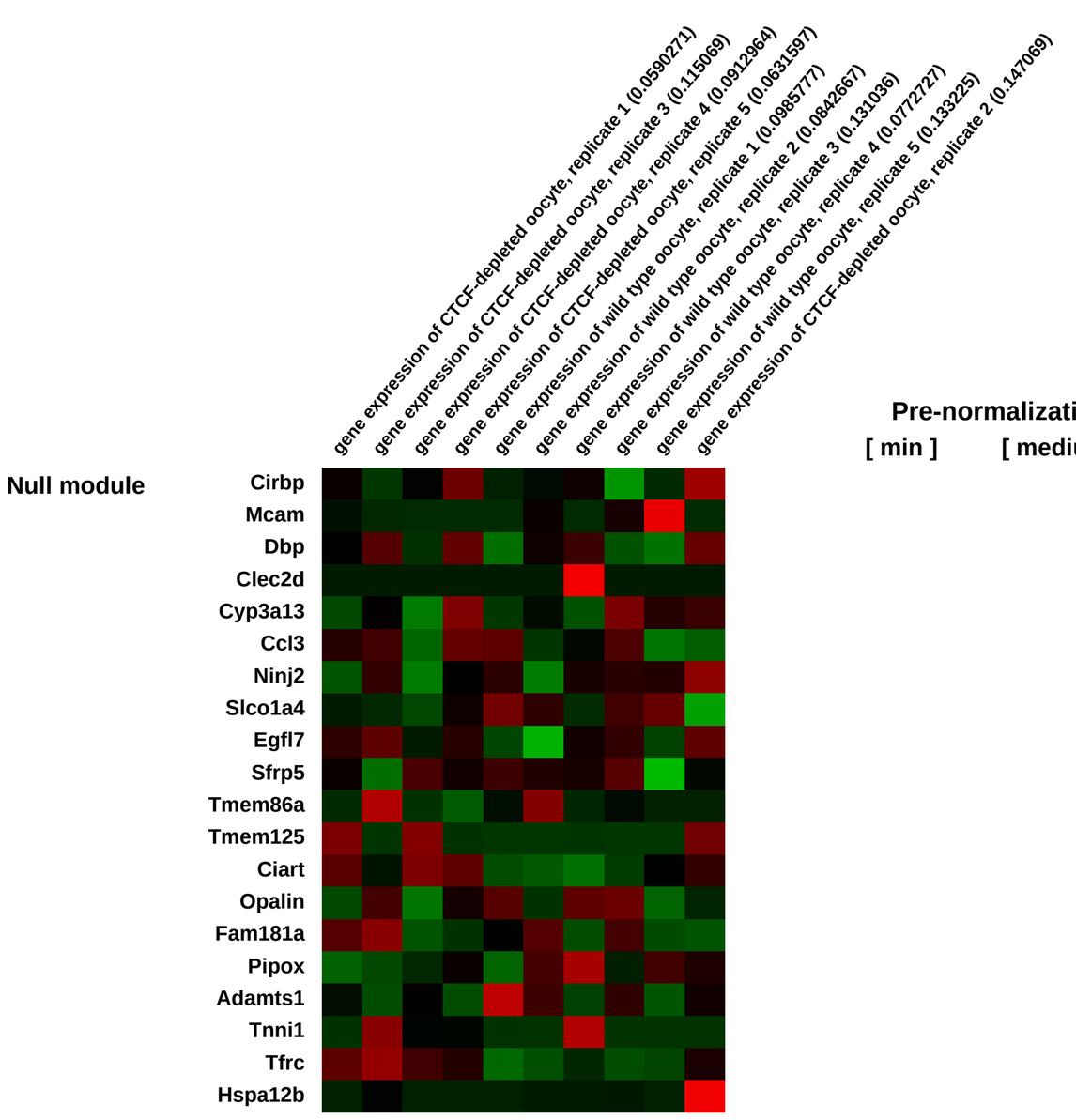

GEO Series "GSE43556" Expression Profiles

Num of samples in this series: 8

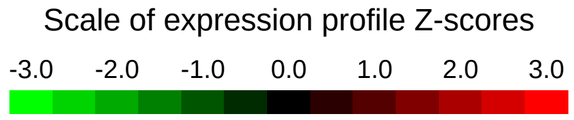

GEO Link:	http://www.ncbi.nlm.nih.gov/geo/query/acc.cgi?acc=GSE43556
Status:	Public on Feb 20 2013
Title:	MicroRNA-34a regulates cardiac ageing and function
Organism:	Mus musculus
Experiment type:	Non-coding RNA profiling by array
Platform:	GPL1261
Pubmed ID:	23426265
Summary & Design:	**Summary:** We compared the heart of 6-weeks-old mice (young) with 18-months-old mice (old) **Overall design:** hearts of 6 week old and 18 month old mice

Background corr dist: KL-Divergence = 0.0832, L1-Distance = 0.0207, L2-Distance = 0.0006, Normal std = 0.4697

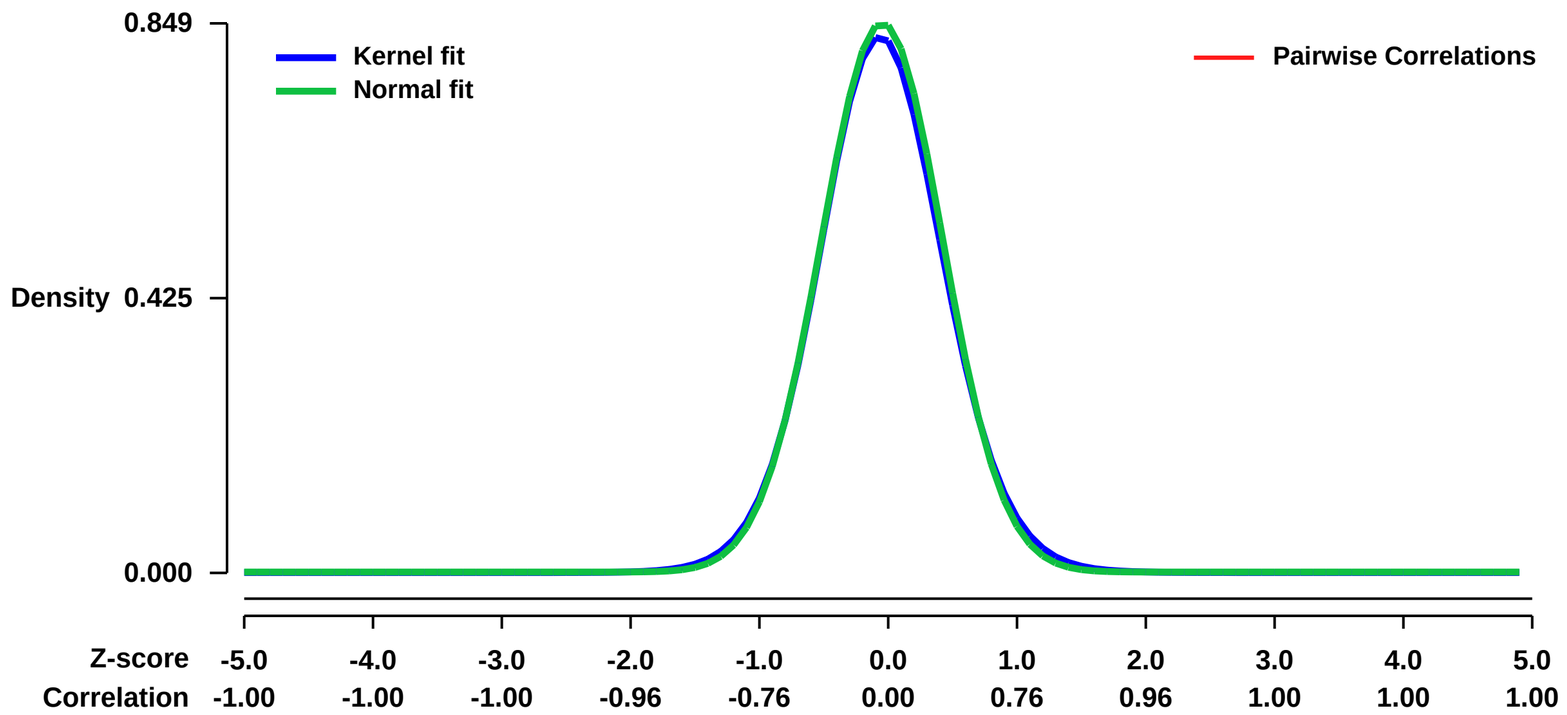

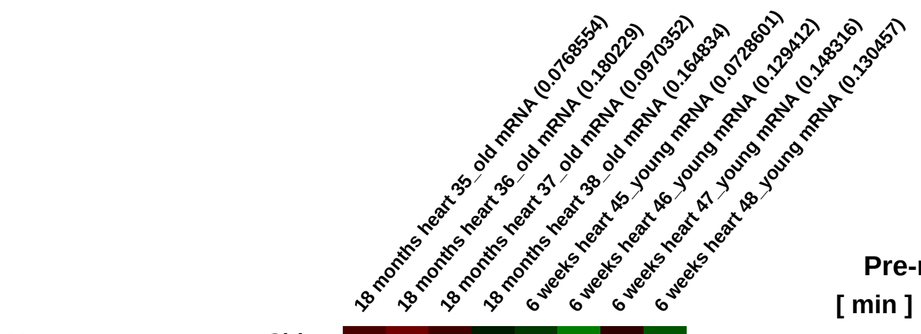

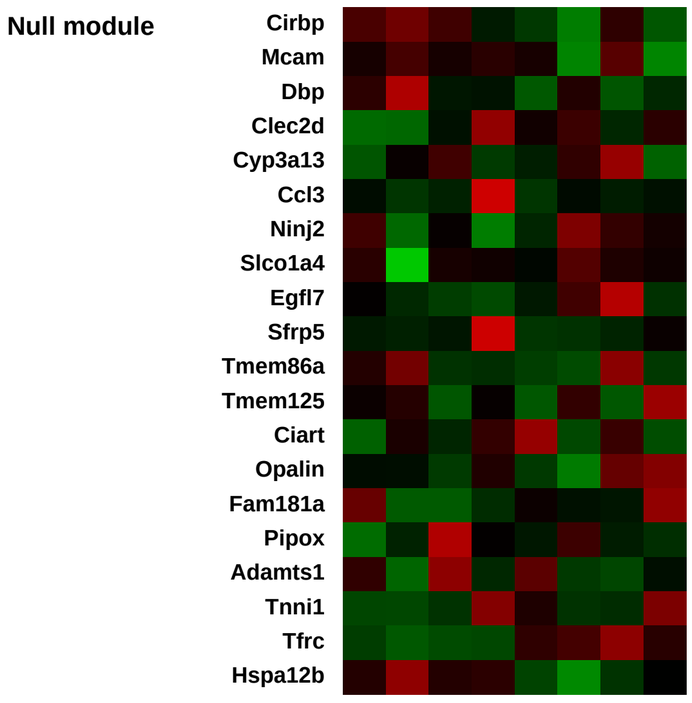

GEO Series "GSE27811" Expression Profiles

Num of samples in this series: 9

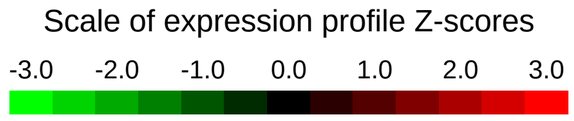

GEO Link:	**http://www.ncbi.nlm.nih.gov/geo/query/acc.cgi?acc=GSE27811**
Status:	**Public on May 12 2011**
Title:	**Expression data from LSK WT, GMP WT and GMP NcstnKO**
Organism:	**Mus musculus**
Experiment type:	**Expression profiling by array**
Platform:	**GPL1261**
Pubmed ID:	**21562564**
Summary & Design:	**Summary:** **Notch signaling is one of the central regulators of differentiation in a variety of organisms and tissue types. Within the hematopoietic system, Notch is essential for the emergence of definitive HSC during fetal life and controls adult HSC differentiation to the T-cell lineage. Notch activation is controlled by the gamma-secretase complex complex, composed of presenilin, nicastrin (Ncstn), anterior pharynx-1 (Aph1), and presenilin enhancer-2** **To determine other role of Notch signaling in HSC we designed a conditional mouse model of Nicastrin deletion. WT and KO HSC were analysed to determined genes controlled by Notch signaling.** **Overall design:** **Bone marrow lineage negative, cKit+, Sca1+ and lineage negative, cKit+, Sca1- CD34+ FcgammaRII/III+ cells were sorted from WT and Ncstn KO littermates for RNA extraction and hybridization on Affymetrix microarrays**

Background corr dist: **KL-Divergence = 0.0285, L1-Distance = 0.0206, L2-Distance = 0.0006, Normal std = 0.6601**

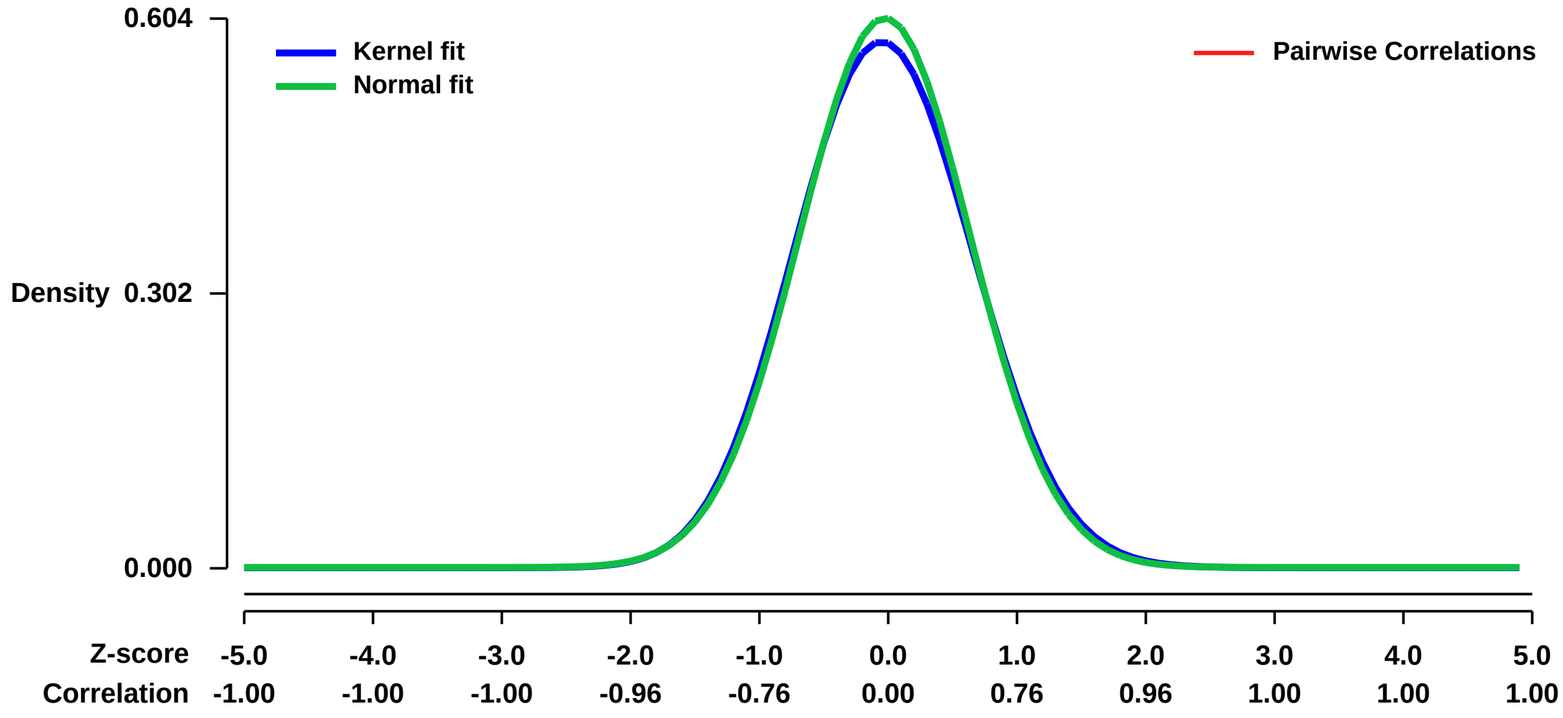

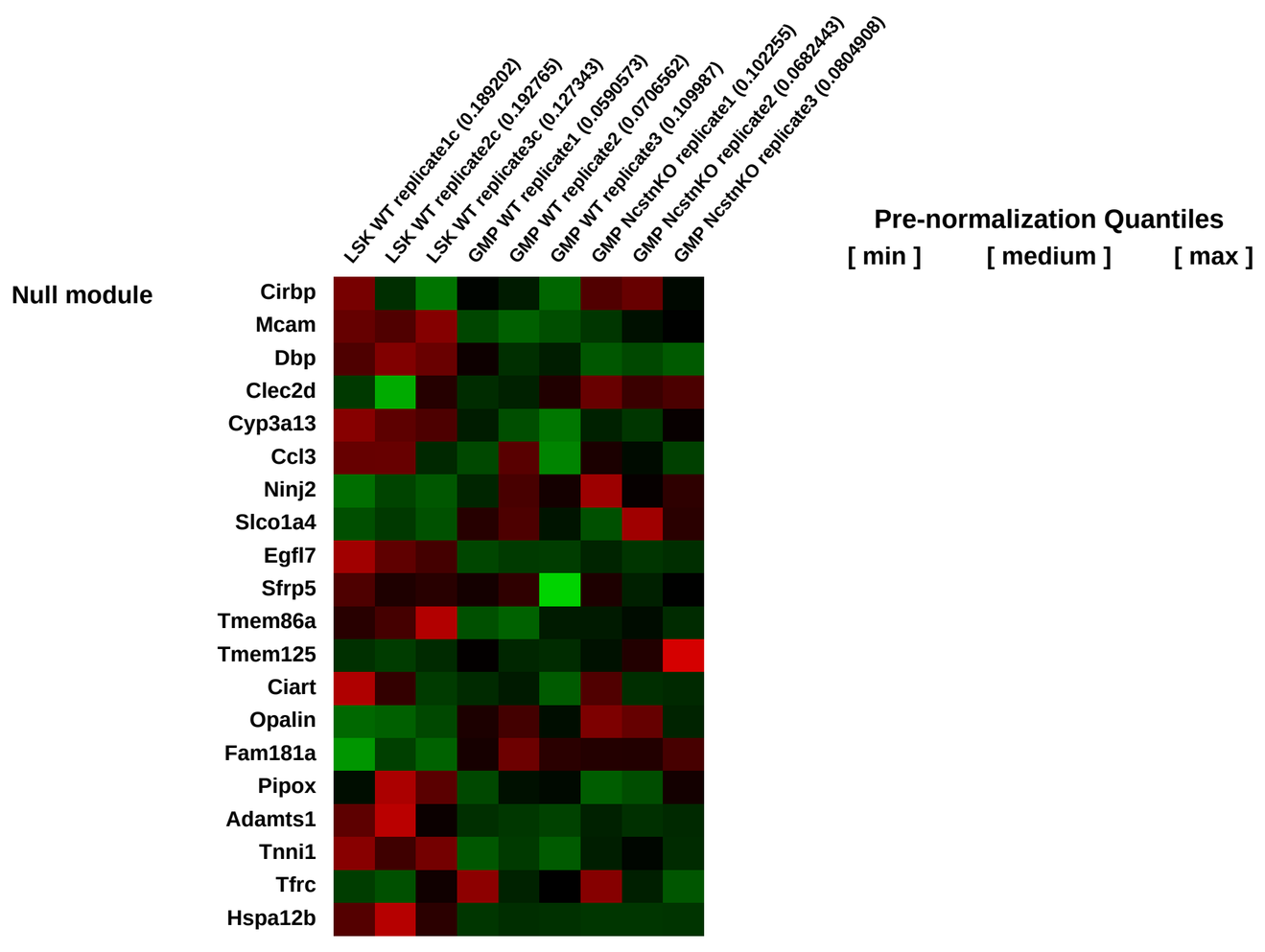

GEO Series "GSE29813" Expression Profiles

Num of samples in this series: 18

Scale of expression profile Z-scores

-3.0 -2.0 -1.0 0.0 1.0 2.0 3.0

GEO Link:	http://www.ncbi.nlm.nih.gov/geo/query/acc.cgi?acc=GSE29813
Status:	Public on Dec 07 2012
Title:	Global gene expression profiling of hepatocellular carcinomas in B6C3F1 mice induced by Ginkgo biloba extract by gavage for two years
Organism:	Mus musculus
Experiment type:	Expression profiling by array
Platform:	GPL1261
Pubmed ID:	23262642
Summary & Design:	**Summary:** Ginkgo biloba leaf extract (GBE) has been used for centuries in traditional Chinese medicine and today is used as an herbal supplement for various indications such as improving neural function, anti-oxidant and anti-cancer effects. As part of the herbal supplement industry, these compounds are largely unregulated, and may be consumed in large concentrations over extended periods of time. This is of particular concern, because the long-term effects in terms of toxicity and carcinogenicity data is lacking for many herbal products, including GBE. The 2-year B6C3F1 mouse carcinogenicity bioassay indicated a marked dose-related increase in hepatocellular carcinoma (HCC) development associated with exposure to GBE. We have shown that the mechanism of this increase in tumorigenesis is related to a marked increase in the incidence of ˛†-catenin mutation, and report a novel mechanism of constitutive ˛†-catenin activation through post-translational modification leading to constitutive Wnt signaling and unregulated growth signaling and oncogenesis. Furthermore, using global gene expression profiling, we show that GBE-induced HCC exhibit overrepresentation of gene categories associated with human cancer and HCC signaling including upregulation of relevant oncogenes and suppression of critical tumor suppressor genes, as well as chronic oxidative stress, a known inducer of calpain-mediated degradation and promoter of hepatocarcinogenesis in humans. These data provide a molecular mechanism to GBE-induced HCC in B6C3F1 mice that is relevant to human cancer, and provides relevant molecular data that will provide the groundwork for further risk assessment of unregulated compounds, including herbal supplements. **Overall design:** Six hepatocellular carcinomas induced by GBE, six spontaneous hepatocellular carcinomas, and six normal liver samples, three technical replicates each.

Background corr dist: KL-Divergence = 0.2189, L1-Distance = 0.0448, L2-Distance = 0.0045, Normal std = 0.3213

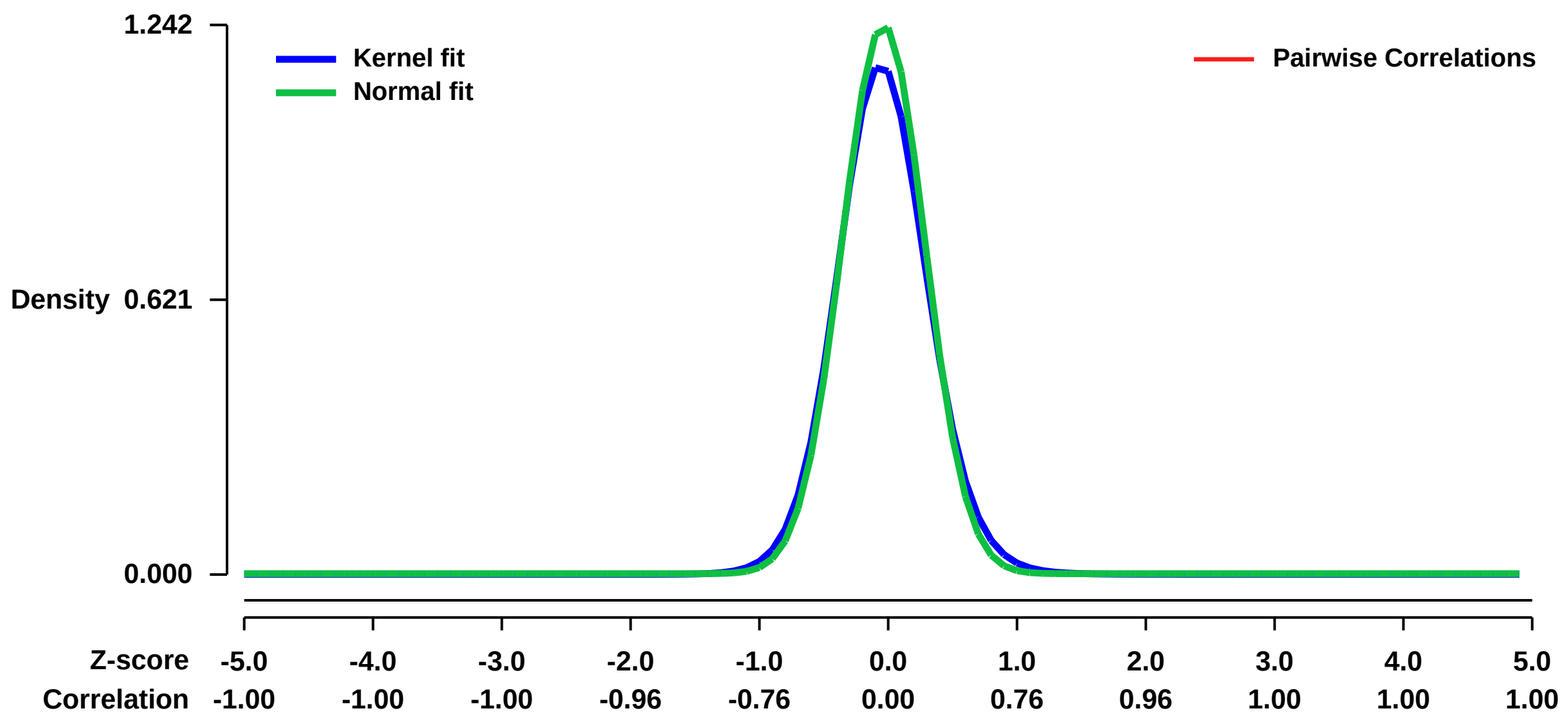

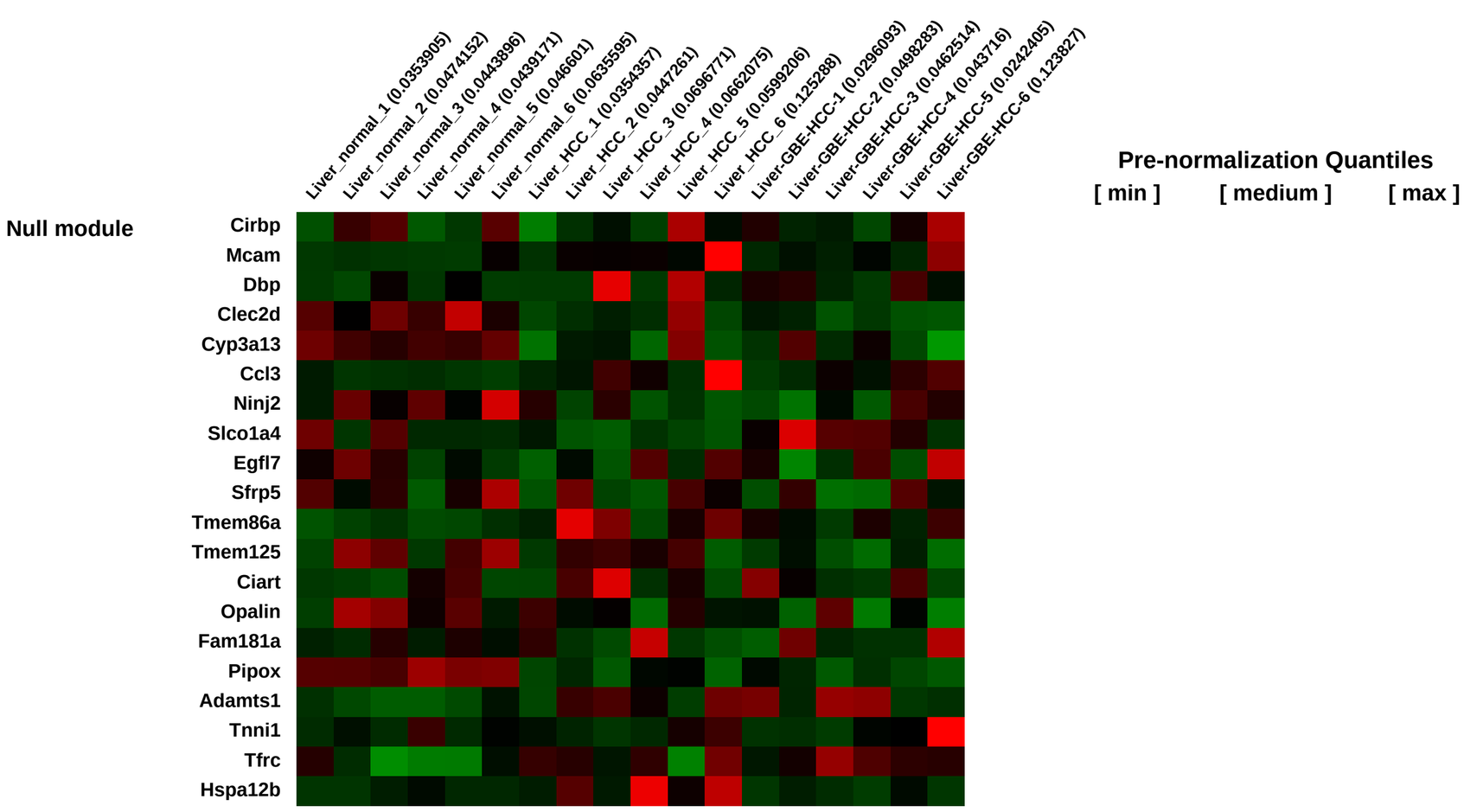

GEO Series "GSE5309" Expression Profiles

Num of samples in this series: 7

Scale of expression profile Z-scores

-3.0 -2.0 -1.0 0.0 1.0 2.0 3.0

GEO Link:	http://www.ncbi.nlm.nih.gov/geo/query/acc.cgi?acc=GSE5309
Status:	Public on Jul 15 2006
Title:	Transcriptional Profiling of Mammary Gland Side Population Cells
Organism:	Mus musculus
Experiment type:	Expression profiling by array
Platform:	GPL1261
Pubmed ID:	16282442

Summary & Design:

Summary:
Similar to the bone marrow, the mammary gland contains a distinct population of Hoechst-effluxing side population cells, MG-SPs. To better characterize MG-SPs, their microarray gene profiles were compared to the remaining cells, which retain Hoechst dye (MG-NSPs). For analysis, gene ontology (GO) that describes genes in terms of biological processes and ontology traverser (OT) that performs enrichment analysis were utilized. OT showed that MG-SP specific genes were enriched in the GO categories of cell cycle regulation and checkpoints, multi-drug resistant transporters, organogenesis, and vasculogenesis. The MG-NSP upregulated genes were enriched in the GO category of cellular organization and biogenesis which includes basal epithelial markers, p63, smooth muscle actin (SMA), myosin, alpha-6 integrin, cytokeratin (CK) 14, as well as luminal markers, CK8 and CD24. Additional studies showed that a higher percentage of MG-SPs exist in the G1 phase of the cell cycle compared to the MG-NSPs. G1 cell cycle block of MG-SPs may be explained by higher expression of cell cycle negative regulatory genes such as TGF-beta2 (transforming growth factor-beta2), IGFBP-5 (insulin like growth factor binding protein-5), P18 INK4C and Wnt-5a (wingless-5a). Accordingly, a smaller percentage of MG-SPs expressed nuclear b-catenin, possibly as a consequence of the higher expression of Wnt-5a. In conclusion, microarray gene profiling suggests that MG-SPs are a lineage deficient mammary gland sub-population expressing key genes involved in cell cycle regulation, development and angiogenesis.

Supplemental File Descriptions:

Table 1 is a list of 1632 Genes differentially expressed by MG-SP and MG-NSP; Criteria for comparison included 1.2-fold difference in expression levels, false discovery rate (FDR) 9.4%, P value less than 0.05.

Table 2 is a list of 771 Genes differentially expressed by MG-SP and MG-NSP; Criteria for comparison included 1.5-fold difference in expression levels, FDR 3.4%, P value less than 0.05.

Table 3 is a list of 335 Genes differentially expressed by MG-SP and MG-NSP; Criteria for comparison included 2-fold difference in expression levels, FDR 0%, P value less than 0.05.

Table 4 is a list of 90 Genes differentially expressed by MG-SP and MG-NSP; Criteria for comparison included 2-fold difference in expression levels, FDR 0%, P value less than 0.01.

Keywords: Normal C57BL/6 Mammary Gland Epithelial Cells

Overall design:
Gene expression profiles were obtained by hybridizing amplified RNA from four replicate MG-SP and MG-NSP samples to Affymetrix 430 2.0 microarray chips. To isolate MG-SP and MG-NSPs, mammary gland cells were stained using the Hoechst dye 33342 and fluorescence displayed at two wavelength emissions, blue and red. The MG-SP and MG-NSP regions were indicated by trapezoids on the left (R1) and right (R2), respectively. We and others have previously shown that the R1 region is composed of side population cells since verapamil blocks their appearance. The cells in each region (R1 and R2) were sorted, their RNA isolated and amplified by two rounds of in vitro amplification and applied to Affymetrix chips. Hybridization, scanning, and production of raw data files were performed according to the Affymetrix standard protocols. Normalization and model-based expression measurements were performed with dChip. Two of the chips were eliminated from further analysis due to the high percentage of probe sets called an array outlier after model based expression analysis by dChip (Not included). The genes were filtered to eliminate those with very low expression values in most samples. From 45,000 probe sets, 16,744 probe sets were retained and used for further analysis. For normalization purposes and to allow for data comparison with other centers, universal mouse reference RNA (Stratagene) was hybridized to two chips. All other arrays were normalized to one of the universal mouse reference RNA arrays expressing average intensity closest to the median intensity of all chips (Stratagene Ref 2).

Background corr dist: KL-Divergence = 0.0531, L1-Distance = 0.0342, L2-Distance = 0.0017, Normal std = 0.5752

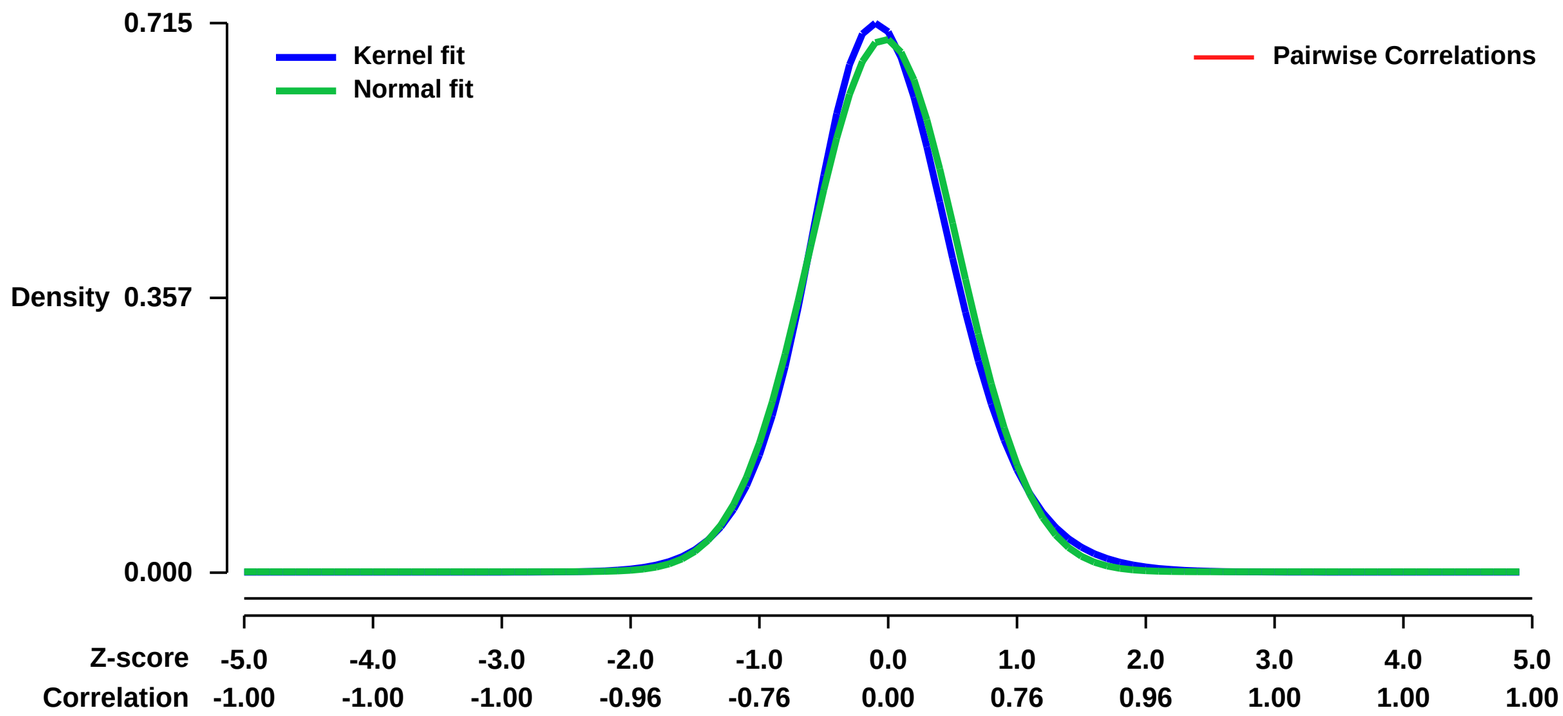

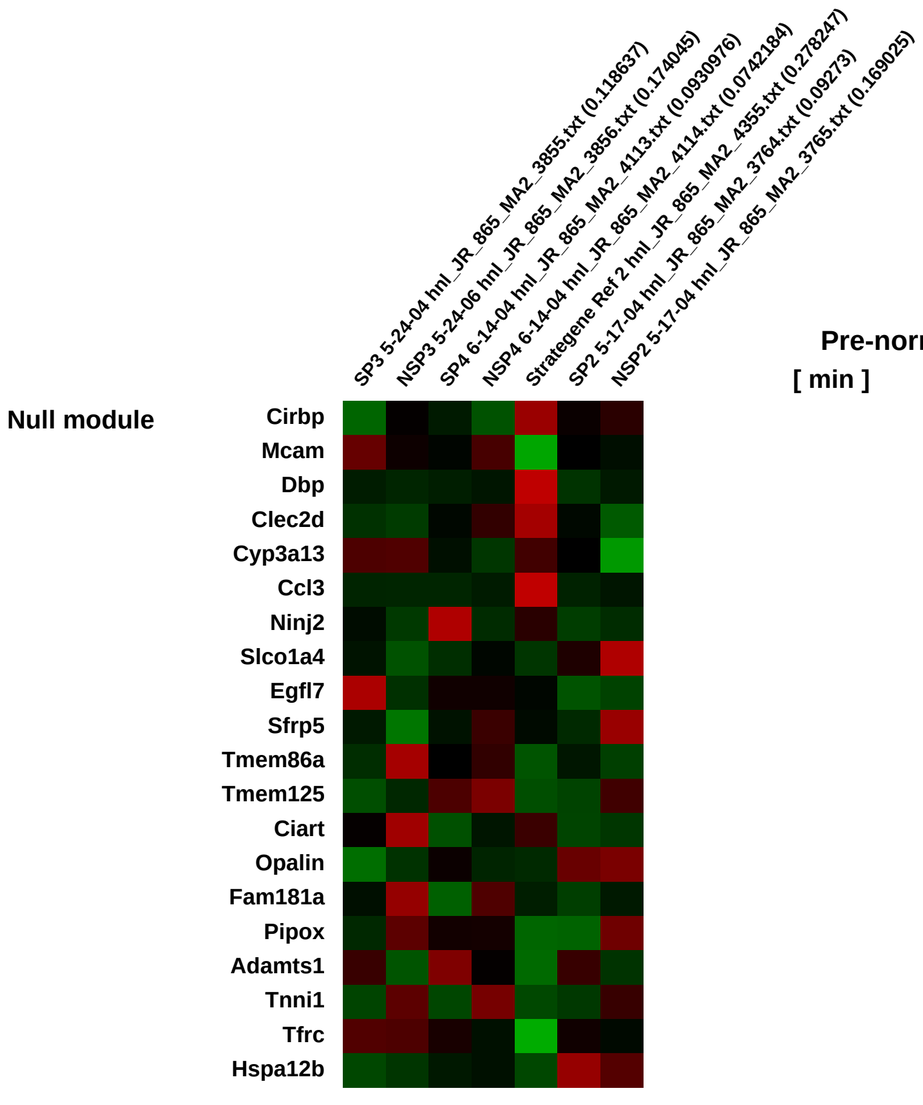

GEO Series "GSE5035" Expression Profiles

Num of samples in this series: 12

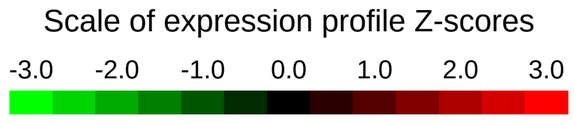

GEO Link:	**http://www.ncbi.nlm.nih.gov/geo/query/acc.cgi?acc=GSE5035**
Status:	**Public on Jun 09 2006**
Title:	**zhang-affy-arabi-50806**
Organism:	**Mus musculus**
Experiment type:	**Expression profiling by array**
Platform:	**GPL1261**
Pubmed ID:	

Summary & Design:

Summary:
In our original grant we proposed to use the NR3B-null mouse model to study the role of NR3B subunit in motor neuron function. We have now successfully generated NR3B null mice. Interestingly, NR3B-null mice invariably die at age P4-P8. Our preliminary examination indicates that the motor strength of these mice is severely impaired prior to death. As we continue to explore the cause of death in NR3B null mice, we propose to conduct gene profiling experiments to search for transcription changes in the brain related to ablation of the NR3B gene. We would like to use the facility provided by the NINDS/NIMH Microarray Consortium to identify true outlier genes that show abnormal expression patterns in these mice. Analysis of these outlier genes will help to identify changes in networks and pathways that may cause the death of NR3B-null mice. These studies will further help to elucidate the functional role of NR3B in motor neurons.

We will compare samples from the hindbrain and spinal cord of wild type and NR3B null mice to identify true outlier genes that show abnormal expression patterns, which may be implicated in the death of NR3B-null mice

We hypothesize that genes with their transcription level changing significantly by ablation of NR3B will be associated with the molecular mechanism underlying the death of motor neurons in NR3B null mice.

As NR3B is expressed primarily in the hindbrain and spinal cord, we will first collect and analyze the hindbrain and spinal cord samples from NR3B null mice and wild-type controls in triplicate at two time points (P0 and P5). Total RNA from total 12 samples will be purified. Extracted RNAs will be treated for with DNase I to remove contaminating genomic DNA. The purified RNA will be sent to the NINDS/NIMH Microarray Consortium to generate biotin-labeled probe according to the Affymetrix protocol. These probes will be used to hybridize the GeneChip Mouse Genome 430 2.0 Array. The hybridization, scanning, and initial data analysis of these GeneChips will be conducted by the Consortium staff. We will analyze the collected data further after data collection. We will use computer software, GeneSpring (Silicon Genetics, Redwood City, CA), to analyze data from microarray experiments. We will first identify genes that show significant changes between wild-type and NR3B null mice by applying ANOVA analysis to sample groups of different ages. The genes identified in this manner will then be subjected to hierarchical (Gene tree) and nonhierarchical (K-means) cluster analysis, in order to group them according to similar expression patterns. Another clustering method, the self-organizing map, will be used to determine whether one gene cluster is a variant of another. Finally, the Principal Components Analysis (PCA) will be employed to analyze large sample groups, which may include experimental variability with respect to age, anatomical location and genotype. We will determine from these analysis whether further experiments are needed using different array platforms, such as Agillent Oligo Array.

Keywords: time-course

Overall design:

Background corr dist: KL-Divergence = 0.1035, L1-Distance = 0.0235, L2-Distance = 0.0007, Normal std = 0.4373

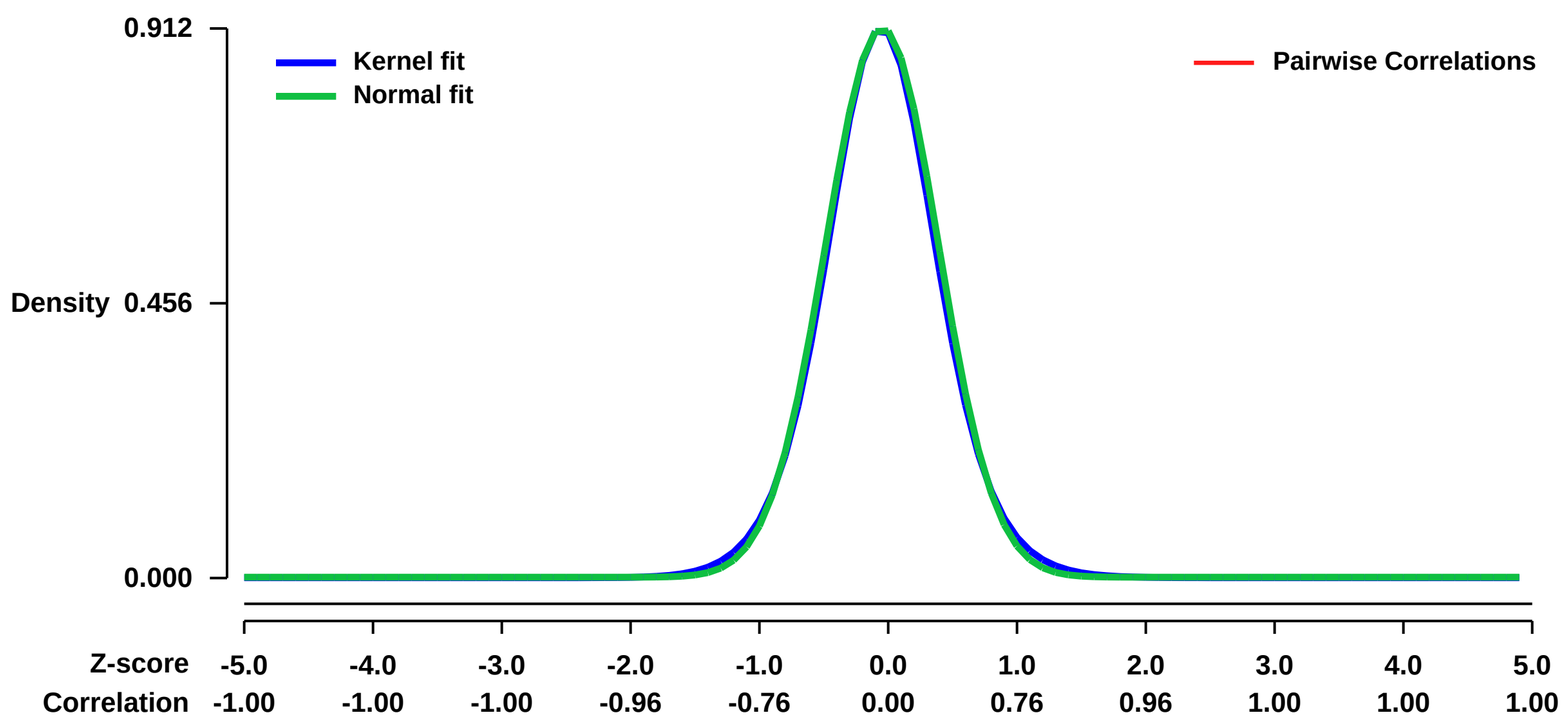

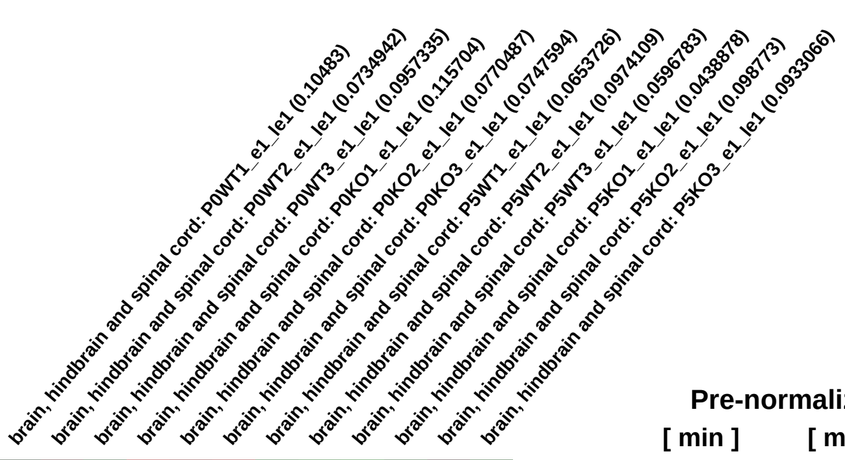

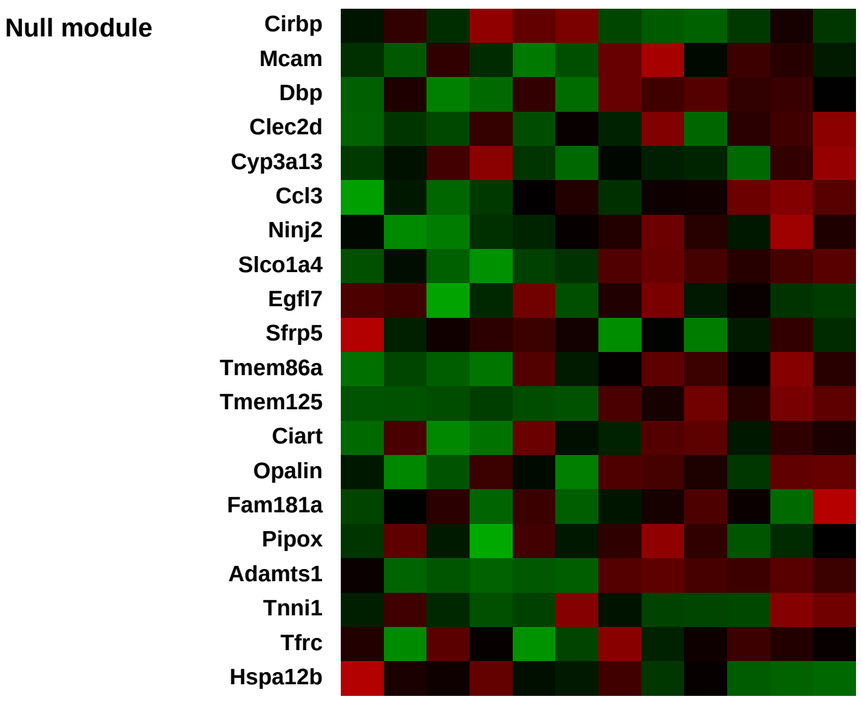

GEO Series "GSE6223" Expression Profiles

Num of samples in this series: 13

Scale of expression profile Z-scores

-3.0 -2.0 -1.0 0.0 1.0 2.0 3.0

GEO Link:	**http://www.ncbi.nlm.nih.gov/geo/query/acc.cgi?acc=GSE6223**
Status:	**Public on Nov 18 2006**
Title:	**Gene expression profiles of E14 bladder, urogenital sinus and urethra isolated from SMGA (Actg2) transgenic mice. (GUDMAP Series ID: 6)**
Organism:	**Mus musculus**
Experiment type:	**Expression profiling by array**
Platform:	**GPL1261**
Pubmed ID:	
Summary & Design:	**Summary:** **The long term objective is to create an encyclopedia of the expression levels of all genes in multiple components of the developing bladder. The central thesis is straightforward. The combination of microdissected and laser capture microdissection (LCM) plus microarray analysis offers a powerful, efficient and effective method for the creation of a global gene expression atlas of the developing urogenital system. Microarrays with essentially complete genome coverage can be used to quantitate expression levels of every gene. The ensuing rapid read-out provides an expression atlas that is more sensitive, more economical and more complete than would be possible by in situ hybridizations alone. The data submitted here represents the gene expression profiles of the embryonic day 14 bladder, urogenital sinus, and urethra.** **Keywords: Gene expression comparison from developing regions of the mouse embryonic day 14 urogenital system** **Overall design:** **Bladder, urogenital sinus, and urethra regions from embryonic day 14 SMGA/EGFP animals were microdissected and total RNA isolated for gene expression analysis using the Affymetrix MOE430 microarray chip.**

Background corr dist: KL-Divergence = 0.0992, L1-Distance = 0.0390, L2-Distance = 0.0030, Normal std = 0.4599

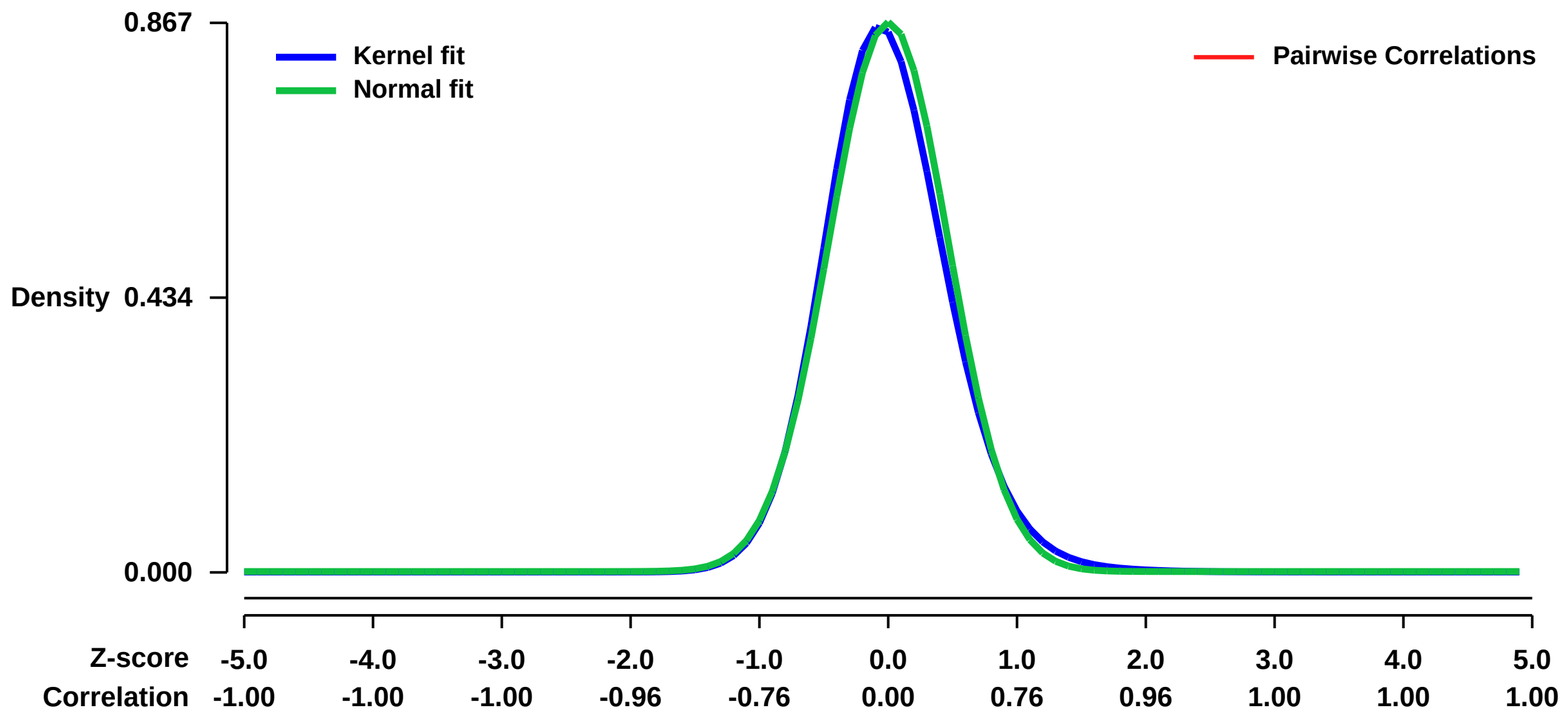

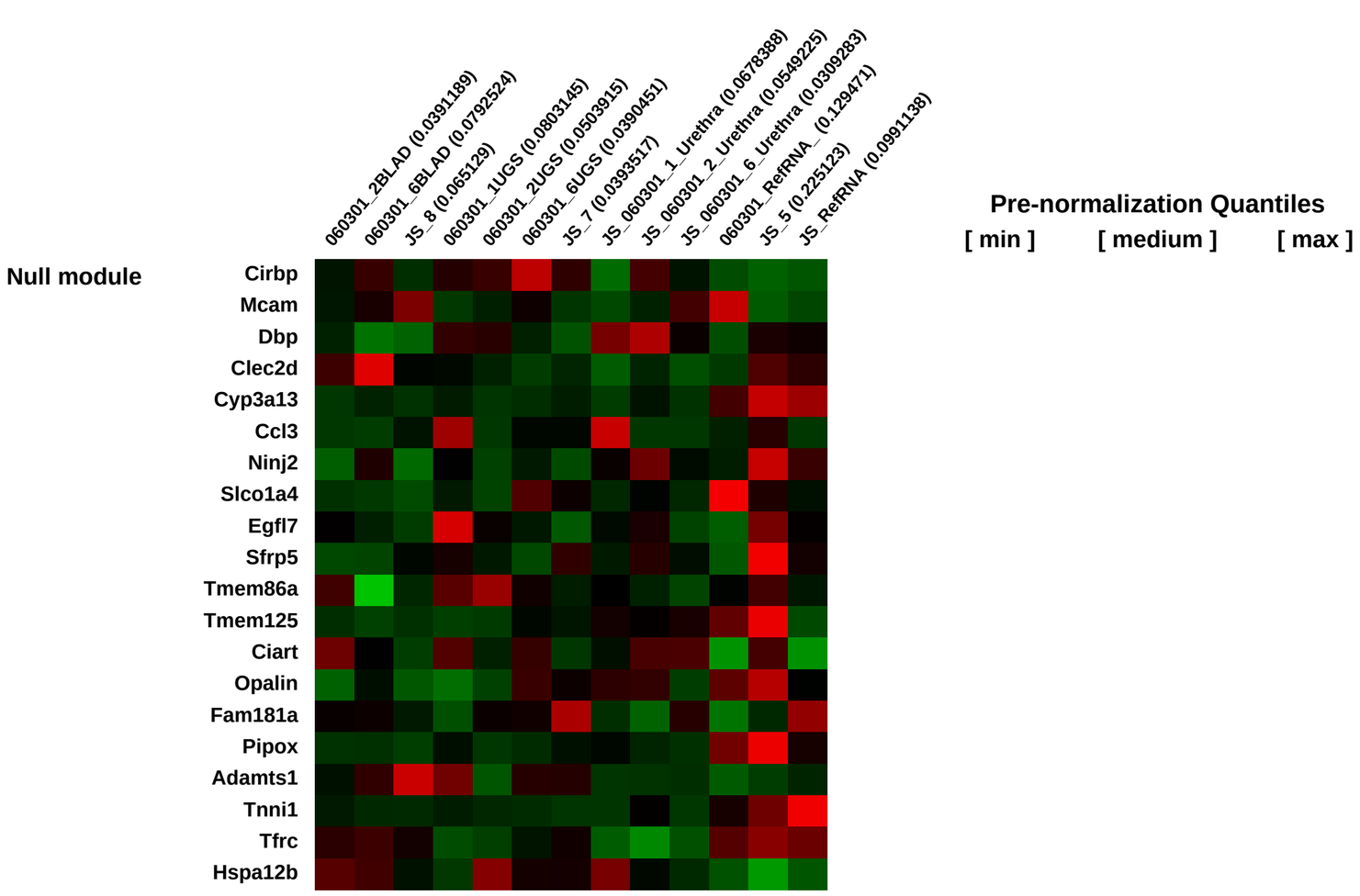

GEO Series "GSE42008" Expression Profiles

Num of samples in this series: 6

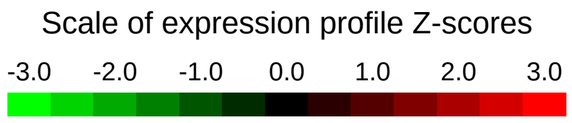

GEO Link:	http://www.ncbi.nlm.nih.gov/geo/query/acc.cgi?acc=GSE42008
Status:	Public on Jul 01 2013
Title:	Expression data from NcGFP ki/+, NcGFP ki/ki and wt (W4) ES cells
Organism:	Mus musculus
Experiment type:	Expression profiling by array
Platform:	GPL1261
Pubmed ID:	24036274
Summary & Design:	**Summary:** We generated a gene replacement allele of the E-cadherin locus that express an N-cadherin-GFP fusion in ES cells. Expression profiles of homozygous and heterozygous knock-in ES cells were analyzed in comparison to wt ES cells. The GEO Samples were compared to published data of E-cadherin knock-out ES cells (ArrayExpress, accession number E-MEXP-2836). The comparison data are linked below. **Overall design:** RNA was extracted from two independent experiments per genotype, data analysis was performed using the R/Bioconductor Limma software. Quality of the data set was controlled by the simpleaffy package and normalized by quantile normalization with the GCRMA alogrithm.

Background corr dist: KL-Divergence = 0.0266, L1-Distance = 0.0110, L2-Distance = 0.0001, Normal std = 0.6873

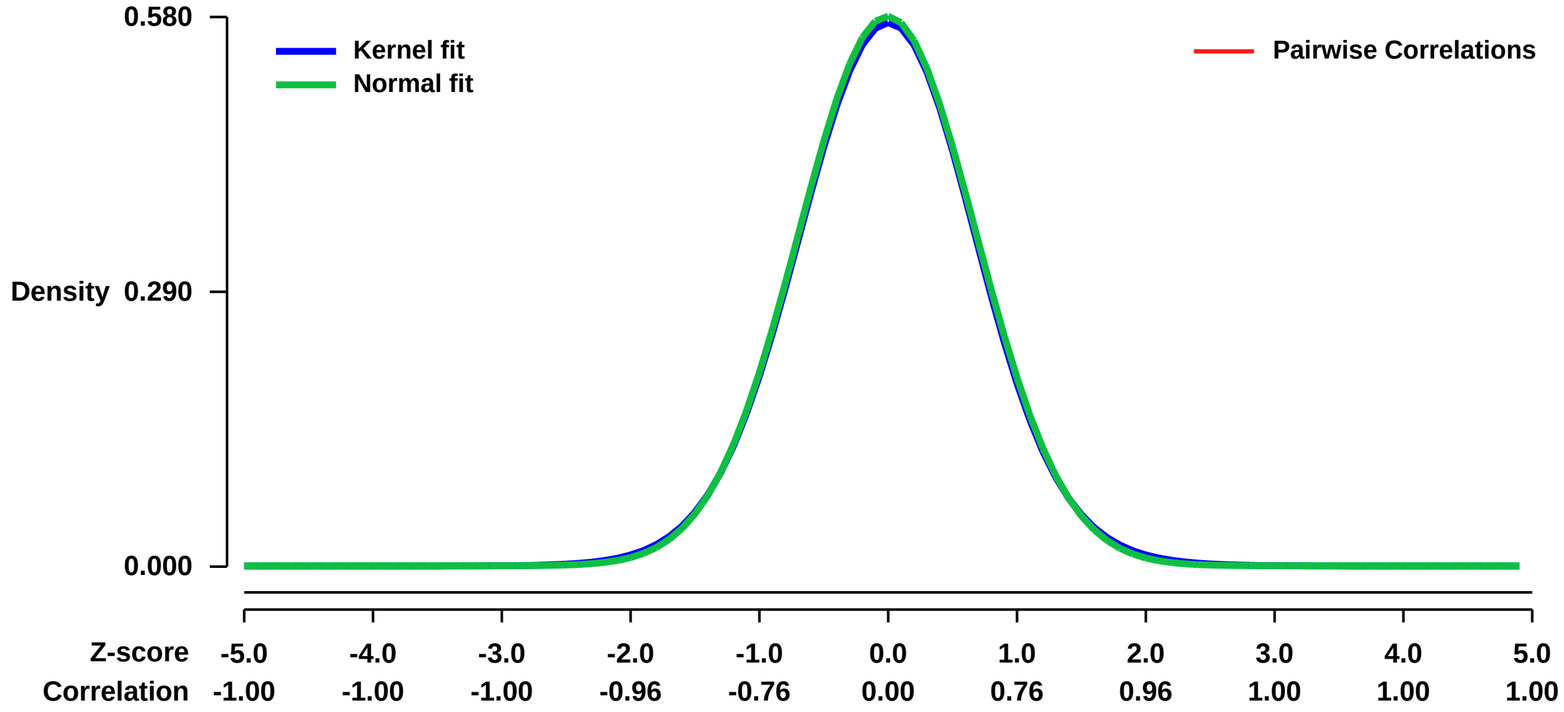

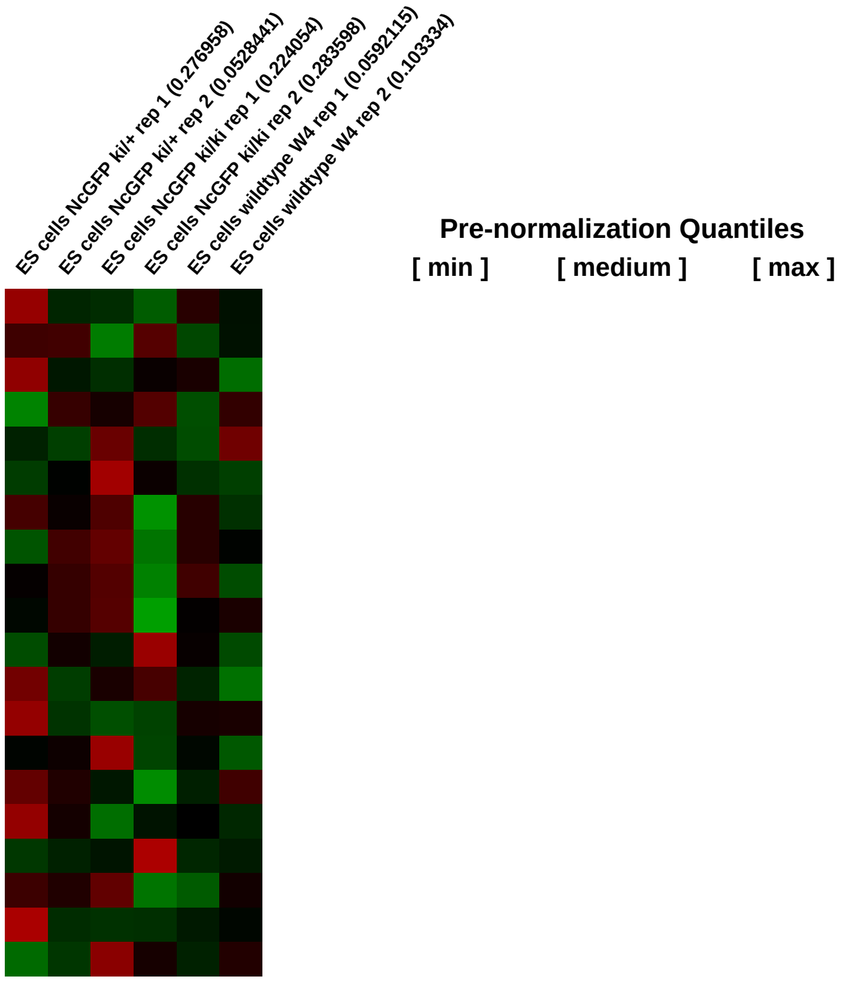

GEO Series "GSE41997" Expression Profiles

Num of samples in this series: 6

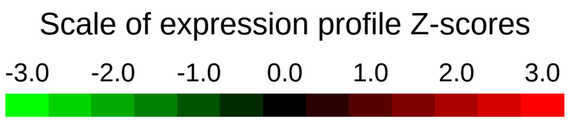

GEO Link:	http://www.ncbi.nlm.nih.gov/geo/query/acc.cgi?acc=GSE41997
Status:	Public on Dec 12 2013
Title:	Expression data from Dmp1-GFP sorted osteocytes
Organism:	Mus musculus
Experiment type:	Expression profiling by array
Platform:	GPL1261
Pubmed ID:	24333171
Summary & Design:	**Summary:** Estrogens are well known steroid hormones necessary to maintain bone health. In addition, mechanical loading, which estrogen signaling may intersect with the Wnt/¸†-catenin pathway, is also essential for bone health. As osteocytes are known as the major mechanosensory cells embedded in mineralized bone matrix, osteocyte ER¸– deletion mice (ER¸–¸ Ocy/¸ Ocy) were generated by mating ER¸– floxed mice with Dmp1-Cre mice to determine functions of ER¸– in osteocytes. Trabecular bone mineral density of female, but not male ER¸–¸ Ocy/¸ Ocy mice was significantly decreased. Bone formation parameters in ER¸–¸ Ocy/¸ Ocy were significantly decreased while osteoclast parameters were unchanged. This suggests that ER¸– in osteocytes exerts osteoprotective function by positively controlling bone formation. To identify potential targets of ER¸–, gene array analysis of Dmp1-GFP osteocytes FACS sorted from ER¸–¸ Ocy/¸ Ocy and control mice was performed. Expression of Mdk and Sostdc1, both known inhibitors of Wnt, were significantly increased without alteration of the mature osteocyte marker Sost or ¸†-catenin. Hindlimb unloading exacerbated the trabecular bone loss, but surprisingly cortical bone was resistant. These studies show that ER¸– in osteocytes has osteoprotective effects in trabecular bone through regulating expression of Wnt antagonists, but conversely plays a negative role in cortical bone loss due to unloading. **Overall design:** Wild type and osteocyte-specific Estrogen Receptor alpha knock-out mice were generated. The number of both genotypes of mice was three. Calvarial osteocytes of both genotypes harboring Dmp1-GFP were extracted by sequential enzymatic digestion, followed by FACS Aria sorting and total RNAs were purified for Affymetix GeneChip microarray analysis without pooling.

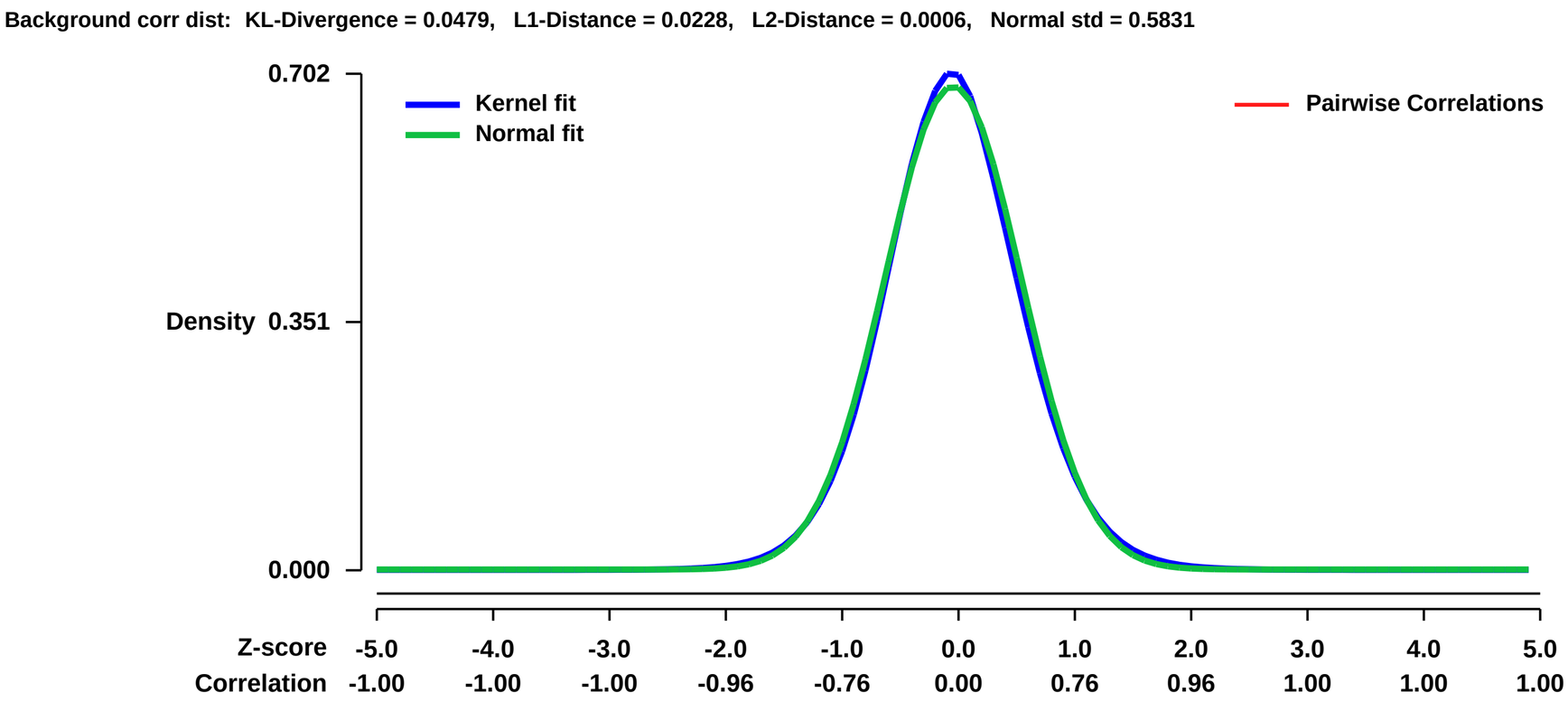

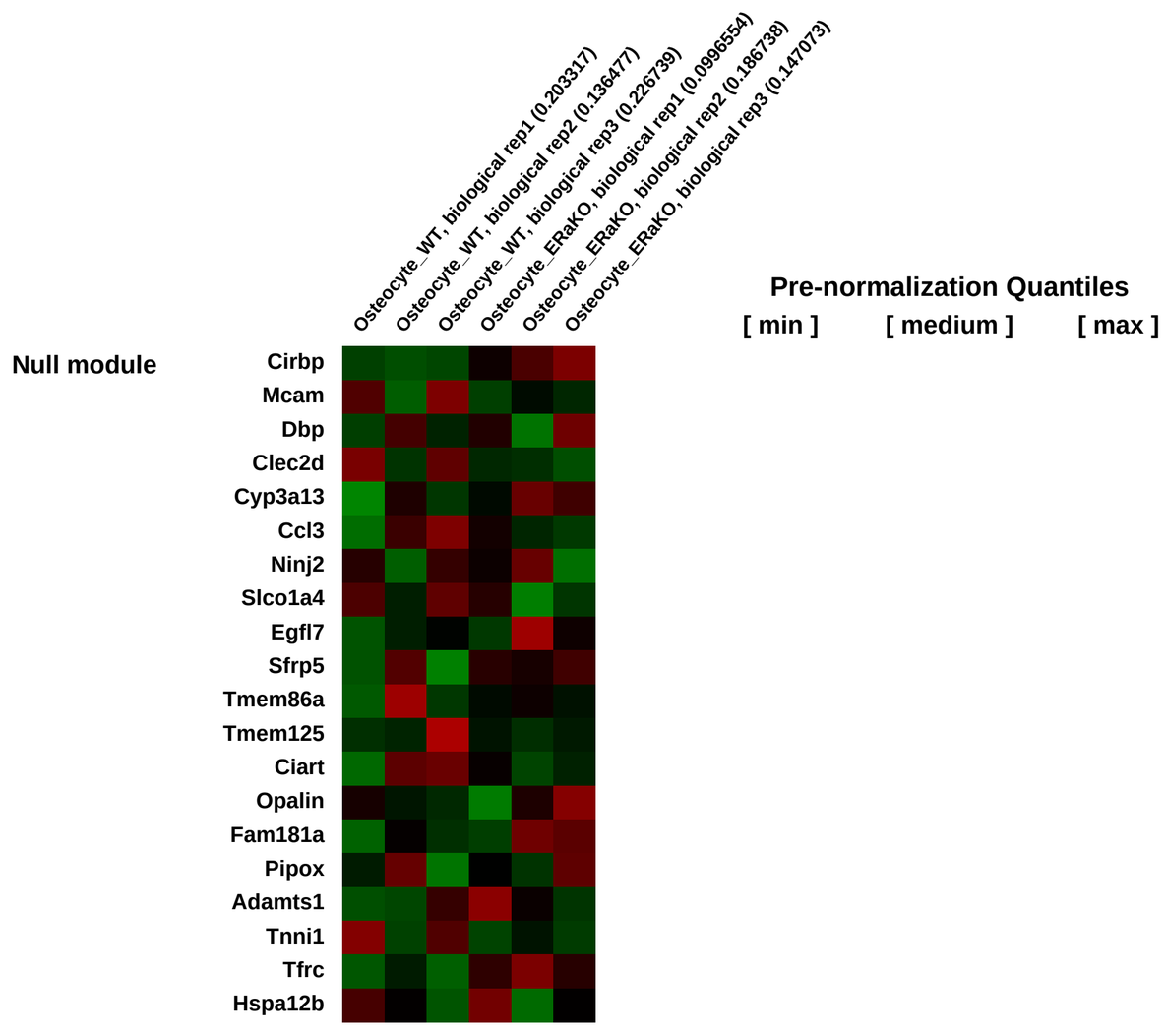

GEO Series "GSE14243" Expression Profiles

Num of samples in this series: 6

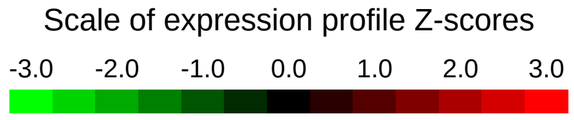

GEO Link:	http://www.ncbi.nlm.nih.gov/geo/query/acc.cgi?acc=GSE14243
Status:	Public on May 01 2009
Title:	Gene expression changes in As4.1 cells during treatment with interleukin (IL) or hydrogen peroxide (HP)
Organism:	Mus musculus
Experiment type:	Expression profiling by array
Platform:	GPL1261
Pubmed ID:	19433777
Summary & Design:	**Summary:** As4.1 cells are a renin-expressing cell line commonly used to study the molecular regulation of the mouse renin gene. In the present study, the global gene expression profile was assessed in these cells under control conditions (VEHICLE) and after treatment with interleukin (IL) or hydrogen peroxide (HP), both of which negatively regulate mouse renin gene expression. **Overall design:** For each experimental group, 2 separate cultures of As4.1 cells were used. Cells were treated with interleukin (IL), hydrogen peroxide (HP) or vehicle control (VEHICLE). Cellular RNA was prepared using conventional methods and quality was assessed using the Bioanalyzer 2100 (Agilent Technologies). All the microarray procedures were conducted at the University of Iowa DNA Core facility using standard Affymetrix protocols. In brief, approximately 5 ug of total RNA was used as input to a one-step amplification procedure to generate biotin-labeled RNA fragments for hybridization to the Affymetrix GeneChip Mouse Genome 430 2.0 array.

Background corr dist: KL-Divergence = 0.0412, L1-Distance = 0.0213, L2-Distance = 0.0005, Normal std = 0.6135

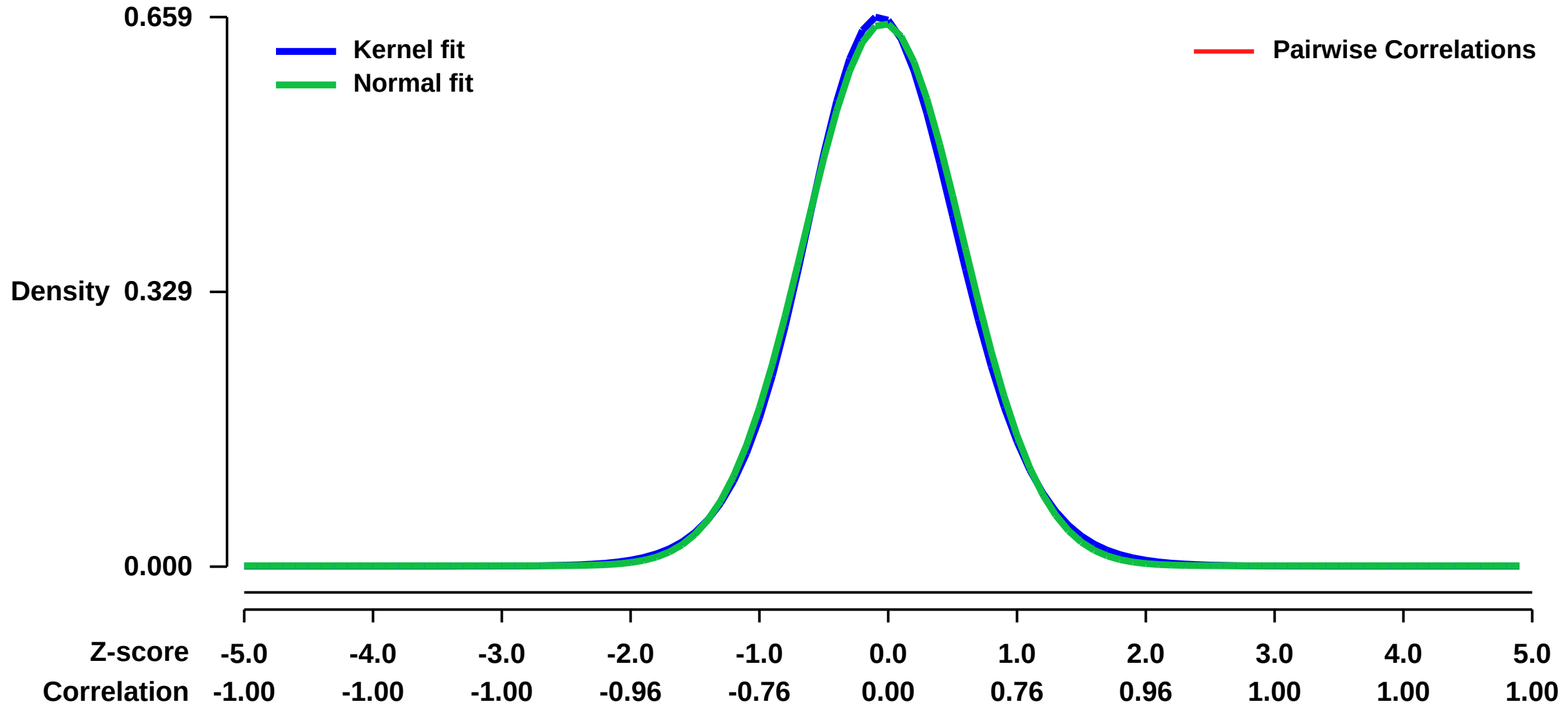

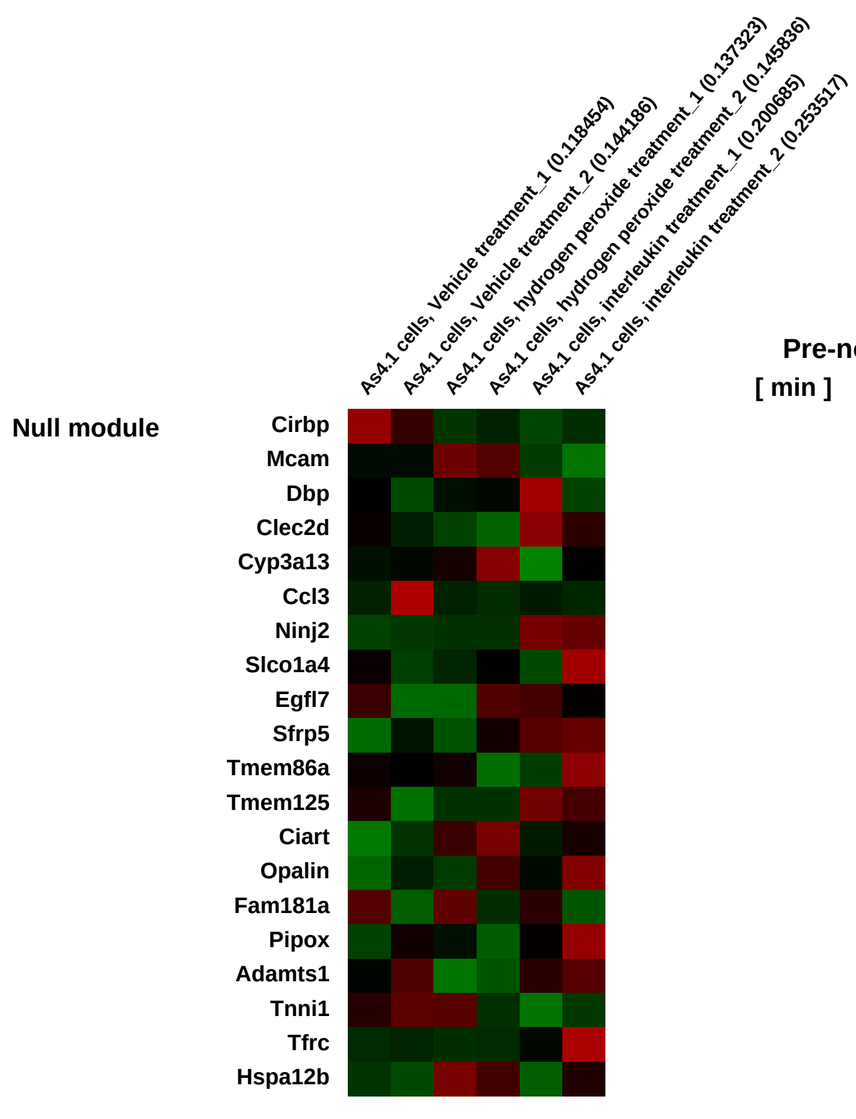

GEO Series "GSE30744" Expression Profiles

Num of samples in this series: 6

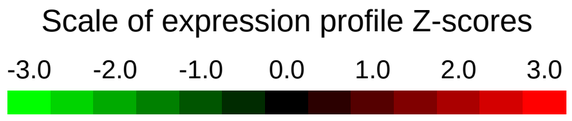

GEO Link:	**http://www.ncbi.nlm.nih.gov/geo/query/acc.cgi?acc=GSE30744**
Status:	**Public on Jul 23 2011**
Title:	**Expression analysis of haploid and diploid ES cells in 2i medium**
Organism:	**Mus musculus**
Experiment type:	**Expression profiling by array**
Platform:	**GPL1261**
Pubmed ID:	**21900896**
Summary & Design:	**Summary:** **gene expression differences were analysed between haploid and diploid ES cells** **Overall design:** **biological triplicates of haploid and diploid ES cell lines were analysed on an Affymetrix GeneChip 430 array**

Background corr dist: **KL-Divergence = 0.0237, L1-Distance = 0.0121, L2-Distance = 0.0002, Normal std = 0.7036**

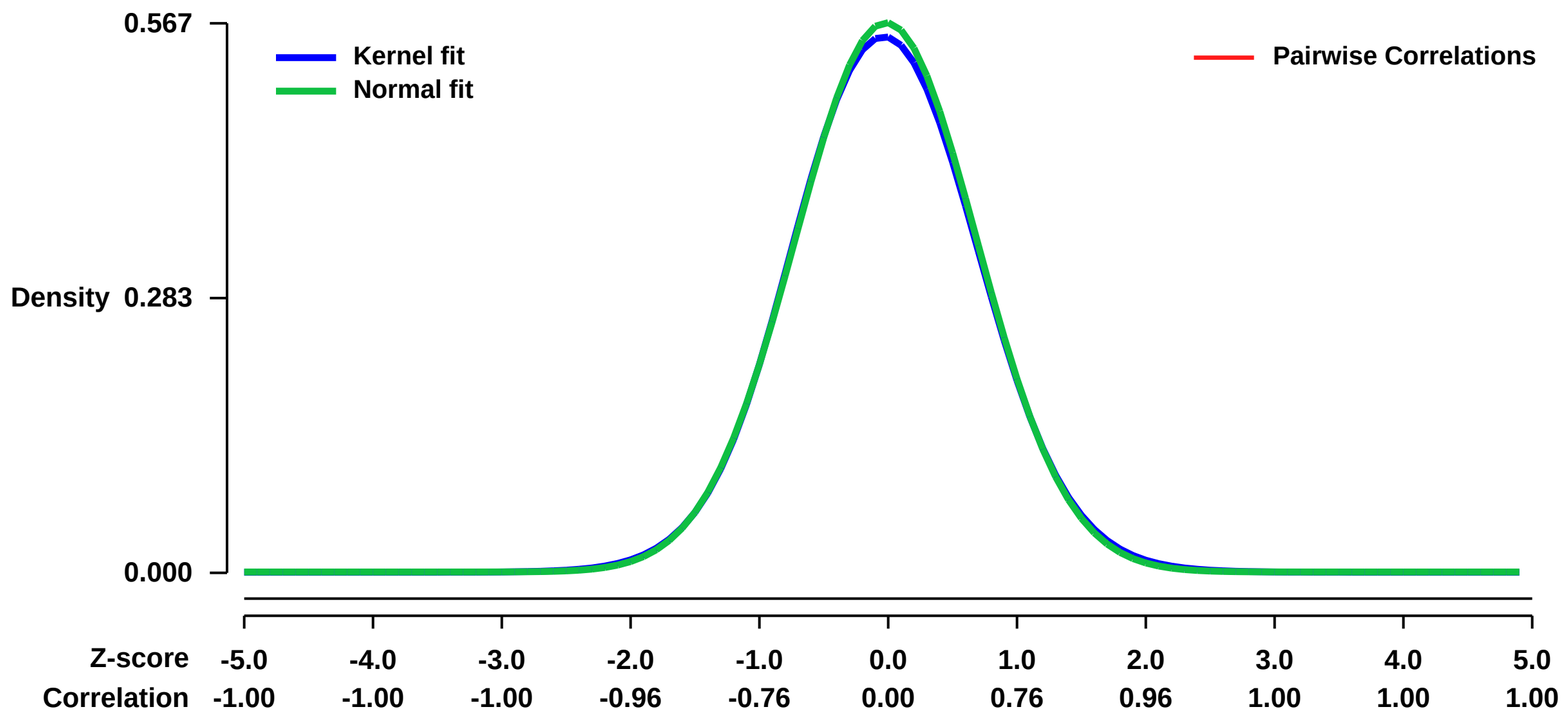

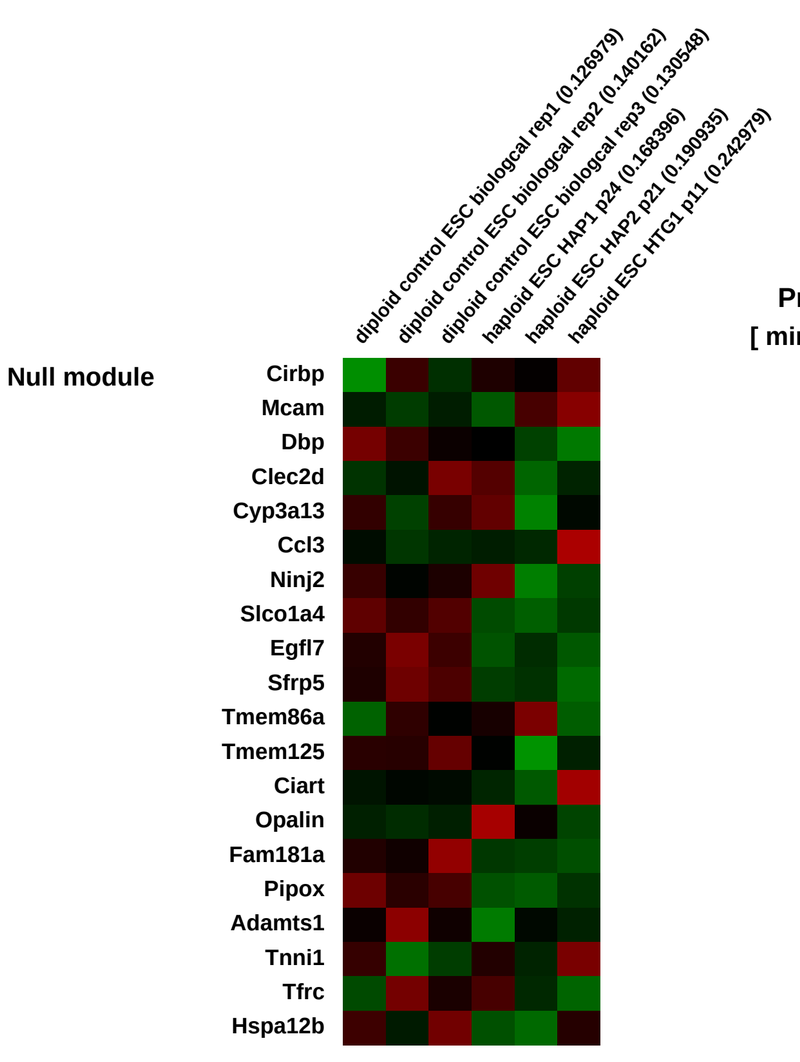

GEO Series "GSE53131" Expression Profiles

Num of samples in this series: 15

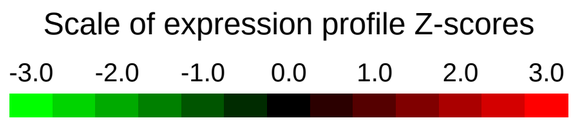

GEO Link:	http://www.ncbi.nlm.nih.gov/geo/query/acc.cgi?acc=GSE53131
Status:	Public on Dec 10 2013
Title:	Expression data from livers of C57BL/6J mice fed a high-fat diet and coffee
Organism:	Mus musculus
Experiment type:	Expression profiling by array
Platform:	GPL1261
Pubmed ID:	
Summary & Design:	**Summary:** The present study was conducted to evaluate the effects of the intake of three types of coffee (caffeinated, decaffeinated, and green unroasted coffee) on the livers of C57BL/6J mice fed a high-fat diet, and to extensively elucidate the physiological responses to coffee intake by analysing the findings obtained from a comprehensive transcriptomic analysis using DNA microarrays. The present study was conducted to evaluate the effects of the intake of three types of coffee (caffeinated, decaffeinated, and green unroasted coffee) on the livers of C57BL/6J mice fed a high-fat diet, and to extensively elucidate the physiological responses to coffee intake by analysing the findings obtained from a comprehensive transcriptomic analysis using DNA microarrays. **Overall design:** Briefly, 7-week-old male C57BL/6J mice purchased from Charles River Laboratories Japan (Yokohama) were divided into the following five groups. The normal diet group (ND group) was fed D12450B (10 kcal% fat, Research Diets, New Brunswick, NJ, USA). The high-fat diet group (HF group) was fed D12492 (60 kcal% fat, Research Diets, New Brunswick, NJ, USA). The caffeinated coffee group (HFCC group) was fed a high-fat diet containing 2% caffeinated freeze-dried coffee. The decaffeinated coffee group (HFDC group) was fed a high-fat diet containing 2% decaffeinated freeze-dried coffee. The green unroasted coffee group (HFGC group) was fed a high-fat diet containing 2% unroasted caffeinated freeze-dried coffee. The mice had ad libitum access to their diets and drinking water. After 9 weeks, mice were sacrificed and the livers were subjected to the Affymrtix DNA microarray experiment.

Background corr dist: KL-Divergence = 0.1748, L1-Distance = 0.0409, L2-Distance = 0.0034, Normal std = 0.3502

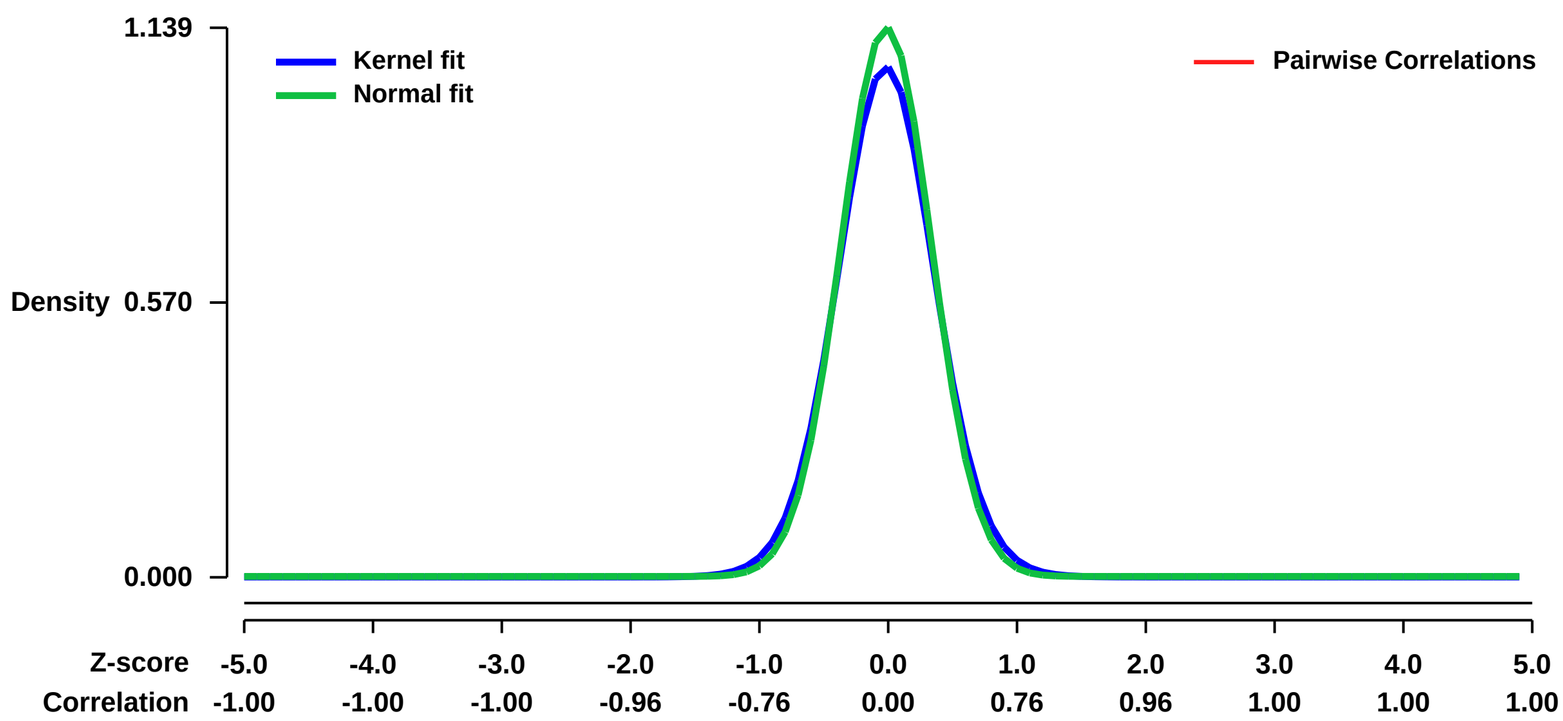

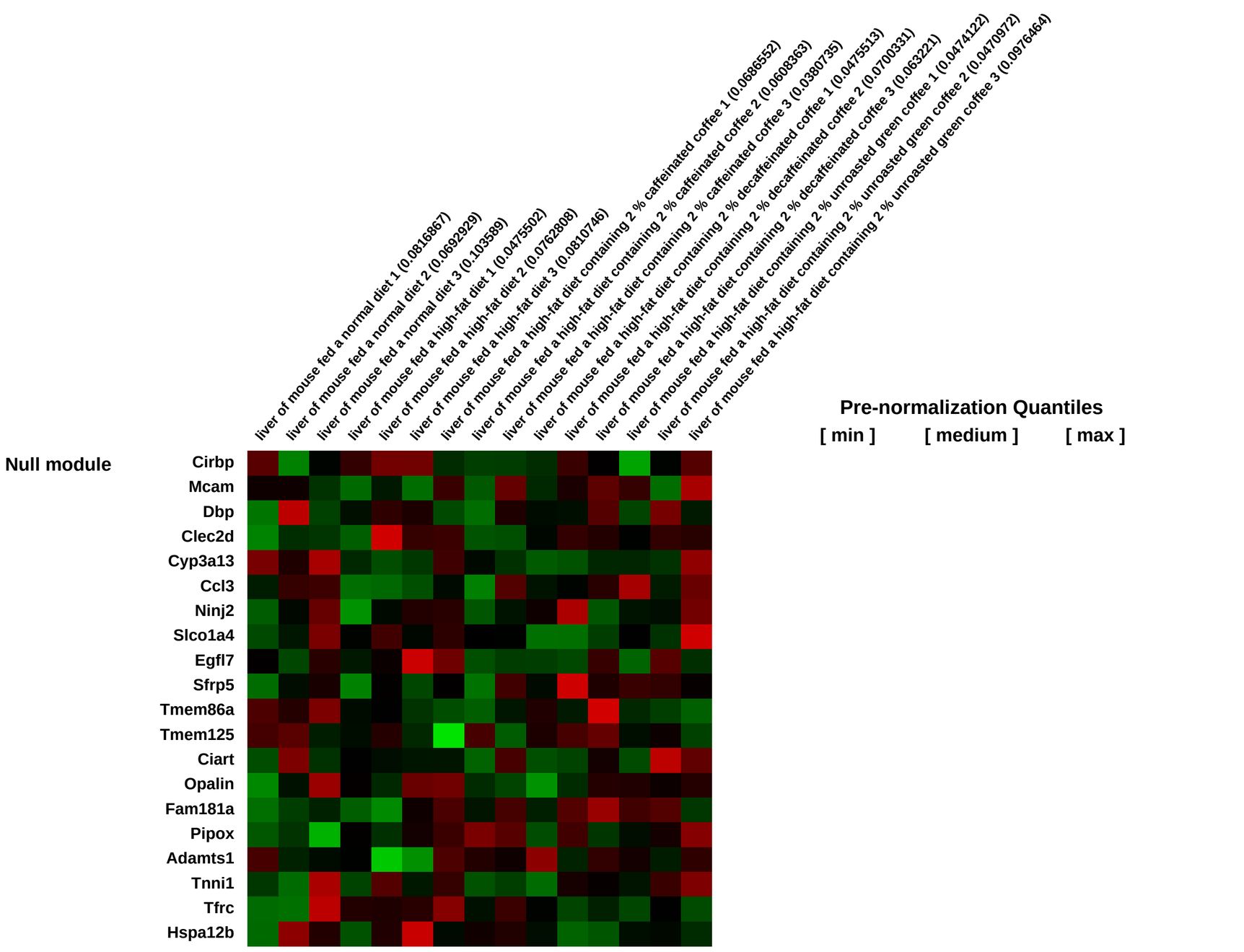

GEO Series "GSE54285" Expression Profiles

Num of samples in this series: 12

Scale of expression profile Z-scores

-3.0 -2.0 -1.0 0.0 1.0 2.0 3.0

GEO Link:	http://www.ncbi.nlm.nih.gov/geo/query/acc.cgi?acc=GSE54285
Status:	Public on Jan 23 2014
Title:	Analysis of impact of Toxoplasma effector MAF1 during Type II infection in WT MEFs and during Type I infection in WT and MAVS KO MEFs
Organism:	Mus musculus
Experiment type:	Expression profiling by array
Platform:	GPL1261
Pubmed ID:	24781109
Summary & Design:	**Summary:** The goals of the microarray experiment were to determine the role of MAF1, the Toxoplasma gondii mediator of host mitochondrial association, on host cell gene expression by comparing infection of WT cells with Type II and Type II:MAF1 parasites. We also explored the role of MAF1 on host cell gene expression by comparing profiles of WT and MAVS KO MEFs infected with Type I and Type Imaf1KO parasites. We used microarrays to detail the global programme of gene expression underlying cellularisation and identified distinct classes of up-regulated genes during this process. **Overall design:** WT MEFs were infected with Type II and Type II:MAF1 parasites at an MOI of 5. At 8 hpi RNA was harvested using TriZol. The Affymetrix IVT (16h) express kit was used for cDNA synthesis and labeling.

Background corr dist: KL-Divergence = 0.0168, L1-Distance = 0.0175, L2-Distance = 0.0003, Normal std = 0.7584

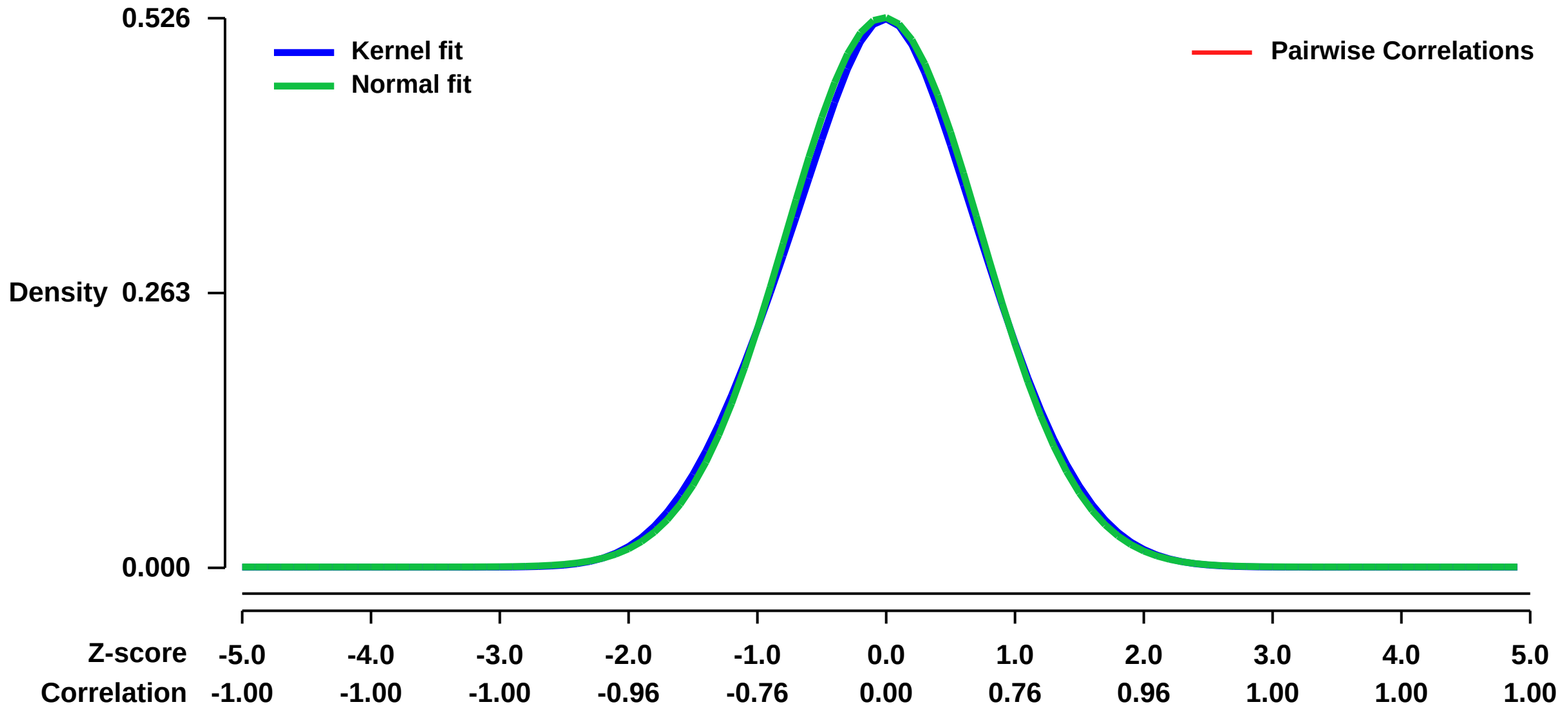

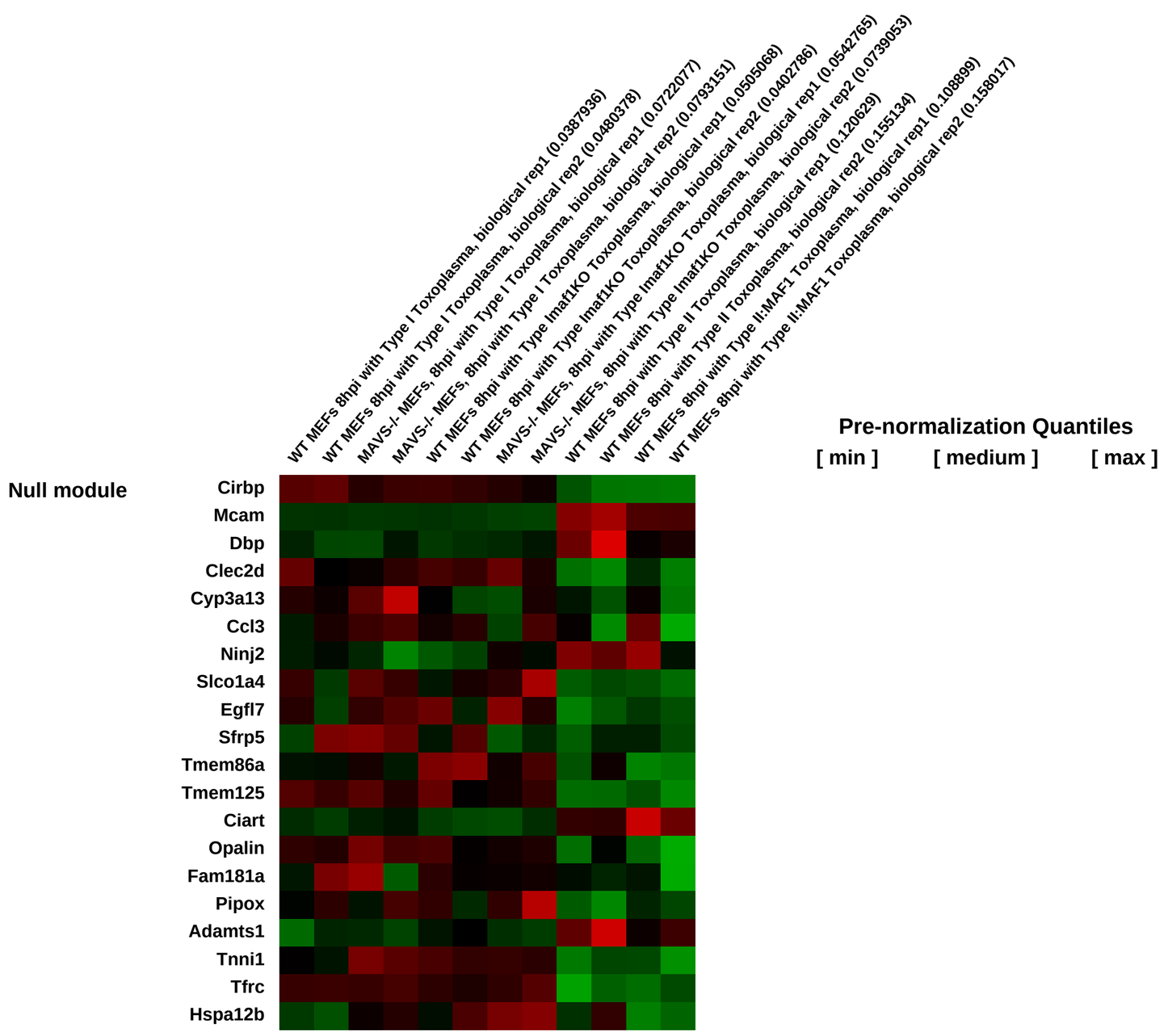

GEO Series "GSE38822" Expression Profiles

Num of samples in this series: 22

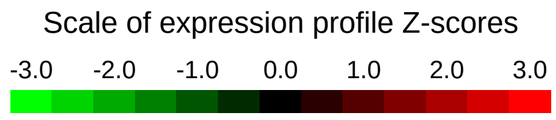

GEO Link:	http://www.ncbi.nlm.nih.gov/geo/query/acc.cgi?acc=GSE38822
Status:	Public on Aug 08 2012
Title:	Gene expression profiling of experimental granulation tissue in Mmp13-/- mice compared to wild type mice
Organism:	Mus musculus
Experiment type:	Expression profiling by array
Platform:	GPL1261
Pubmed ID:	22880047
Summary & Design:	**Summary:** Proteinases play a pivotal role in wound healing by degrading molecular barriers, regulating cell-matrix interactions and availability of bioactive molecules. Matrix metalloproteinase-13 (MMP-13, collagenase-3) is a wide spectrum proteinase. Its expression and function is linked to the growth and invasion of many epithelial cancers such as squamous cell carcinoma. Moreover, the physiologic expression of MMP-13 is associated e.g. to scarless healing of human fetal skin and adult gingival wounds. While MMP-13 is not found in the normally healing skin wounds in human adults, it is expressed in mouse skin during wound healing. Thus, mouse wound healing models can be utilized for studying the role of MMP-13 in the events of wound healing. As the processes such as the migration and proliferation of keratinocytes, angiogenesis, inflammation and activation of fibroblasts are components of wound repair as well as of cancer, many results received from wound healing studies are also adaptable to cancer research. Classically, the process of wound healing can be devided into three phases which are histologically and functionally separate but temporally overlapping: 1) hemostasis and inflammation, 2) re-epithelialization and granulation tissue formation, and 3) matrix remodeling. Granulation tissue is formed into the wound via fibroplasia, angiogenesis and extracellular matrix (ECM) deposition by fibroblasts. Granulation tissue is rich in inflammatory cells, fibroblasts, myofibroblasts and blood vessels. After epidermal recovery, the granulation tissue is resolved via matrix remodeling and cell apoptosis. A sterile viscose cellulose sponge (VCS) characterized by defined size and structure can be used to experimentally induce formation of subcutaneous granulation tissue. Compared to normal granulation tissue, this model allows easy examination of the granulation tissue in its entirety but leaving out epidermal keratinocytes in the sample preparation. In this study, we studied the role of MMP-13 in the formation of mouse VCS-induced granulation tissue. We performed gene expression profiling of the granulation tissue samples of Mmp13-/- (KO) and wild type (WT) mice harvested at day 7, day 14 and day 21 after VCS implantation. **Overall design:** Mmp13-/- (KO) mice were generated as described (Inada et al. 2004, PNAS, 101: 17192-17197) and used in these experiments after backcrossing at least seven generations into C57BL6 mice. The WT mice were generated from the backcrossed heterozygote Mmp13-/- (KO) mice. Granulation tissues were harvested at three time points (7d, 14d, 21d) from Mmp13-/- (KO) and WT mice. One sample of each mouse was analyzed (n=3, 7d; n=4, 14d; n=4, 21d; for each genotype). The samples were processed for RNA extraction and Affymetrix 3'IVT DNA microarray gene expression analysis.

Background corr dist: KL-Divergence = 0.1290, L1-Distance = 0.0326, L2-Distance = 0.0019, Normal std = 0.3952

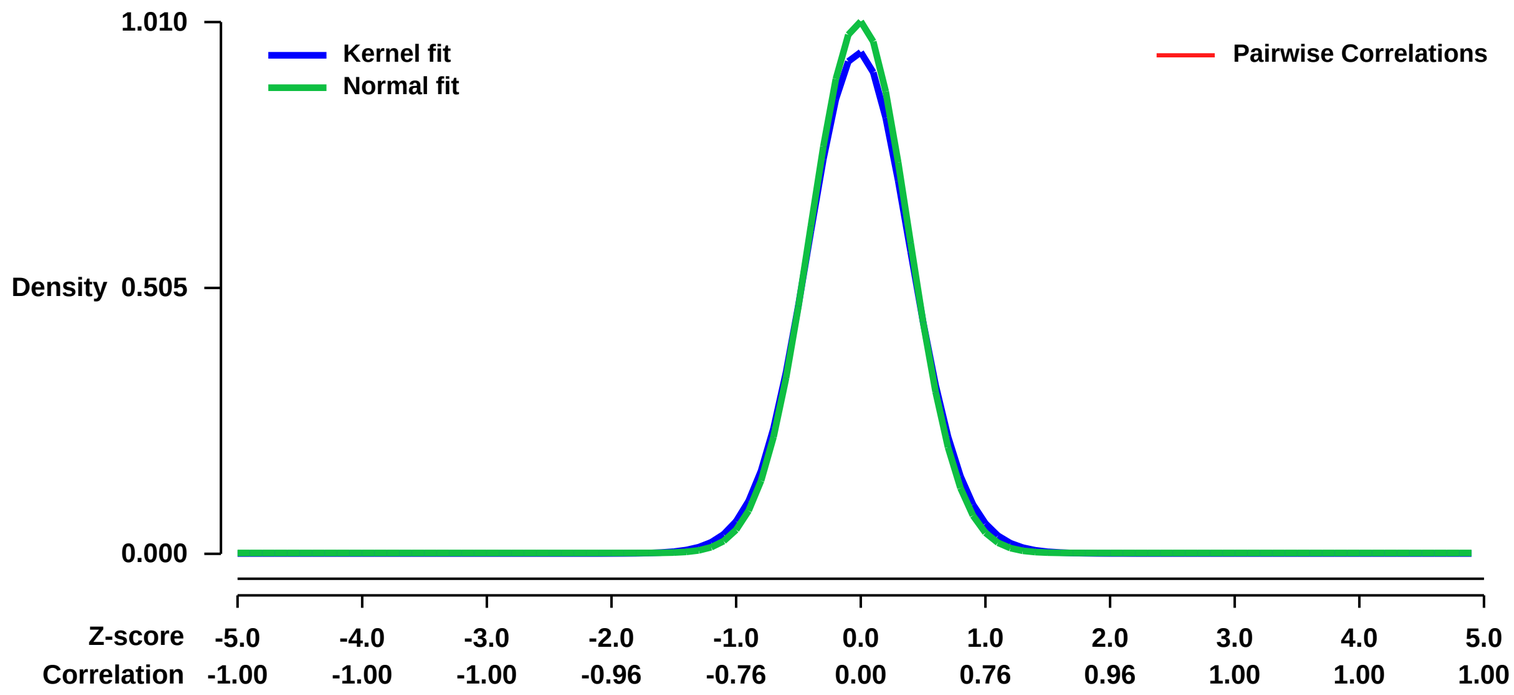

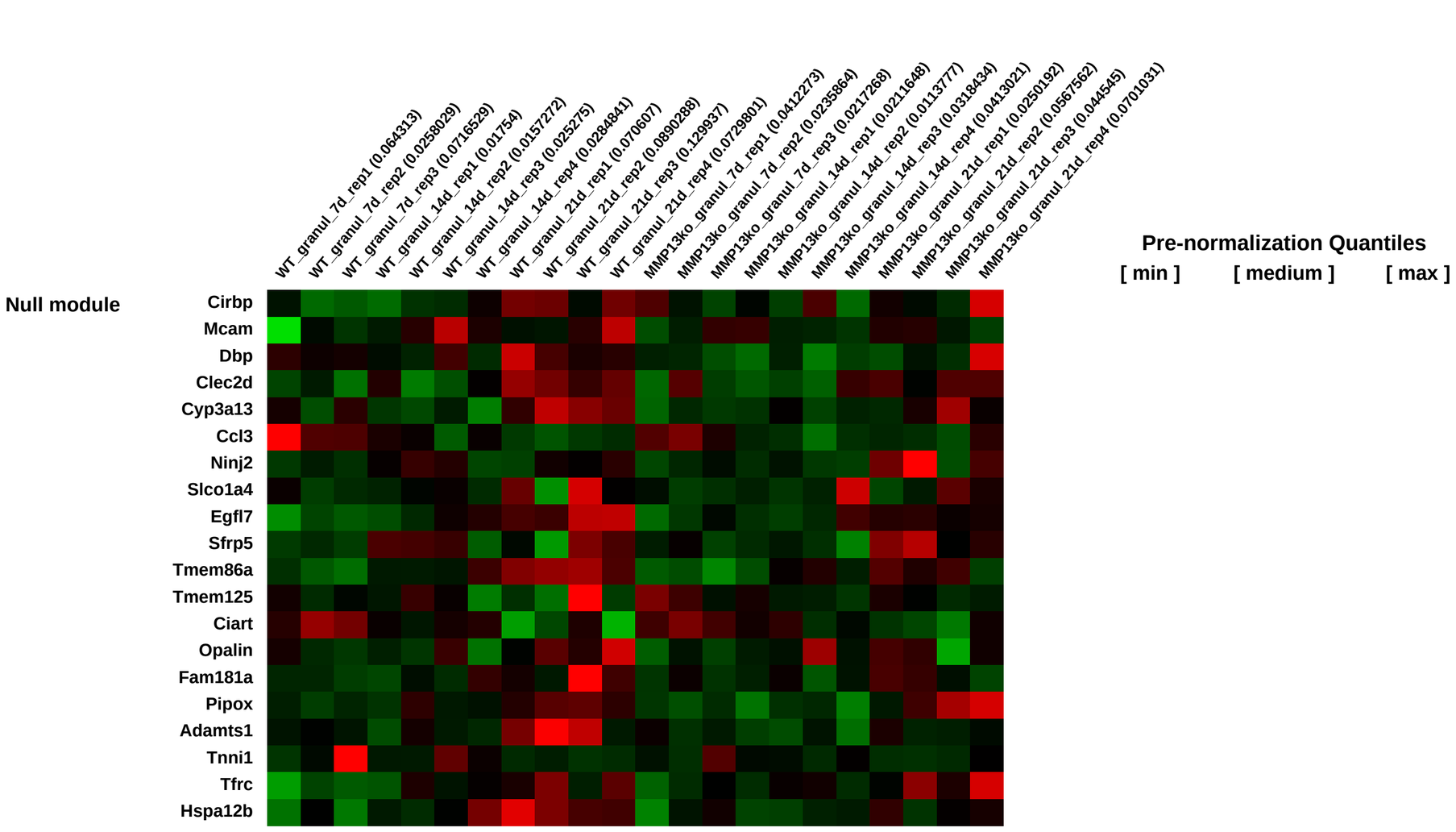

GEO Series "GSE21143" Expression Profiles

Num of samples in this series: 6

Scale of expression profile Z-scores

-3.0 -2.0 -1.0 0.0 1.0 2.0 3.0

GEO Link:	http://www.ncbi.nlm.nih.gov/geo/query/acc.cgi?acc=GSE21143
Status:	Public on Jun 14 2010
Title:	PLAGL2 regulates Wnt signaling to impede differentiation in neural stem cells and glioma
Organism:	Mus musculus
Experiment type:	Expression profiling by array
Platform:	GPL1261
Pubmed ID:	20478531
Summary & Design:	**Summary:** A hallmark feature of glioblastoma (GBM) cells is its strong self-renewal potential and immature differentiation state -- stem cell-like properties which may contribute to the plasticity and intense therapeutic resistance of GBM. The molecular basis of the immature differentiation profile remains an area of active investigation. Here, integrated genomic and biological analyses identified PLAGL2 as a potent proto-oncogene targeted for amplification/gain in malignant gliomas as well as in colorectal cancers. High level of PLAGL2 expression strongly suppresses neural stem cell (NSC) and glioma-initiating cell (GIC) differentiation while promoting their proliferation and self-renewal capacity under differentiation induction conditions. On the mechanistic level, the PLAGL2 transcriptome analysis revealed that these differentiation suppressive activities are attributable in part to PLAGL2 modulation of Wnt/beta-catenin signaling via up-regulation of Wnt6 ligand as well as Fzd9 and Fzd2 receptor expression. Correspondingly, inhibition of Wnt signaling in PLAGL2-expressing NSC partially restores their differentiation capacity. The identification of PLAGL2 as a glioma oncogene highlights the importance of a growing class of cancer genes functioning to impart stem cell-like characteristics on malignant cells. **Overall design:** p53-null mouse NSCs are infected with retrovirus expressing either control vector or PlagL2. Total RNA were collected upon differentiation in 1% FBS for 24 hr. 3 replicates each.

Background corr dist: KL-Divergence = 0.0436, L1-Distance = 0.0242, L2-Distance = 0.0007, Normal std = 0.6035

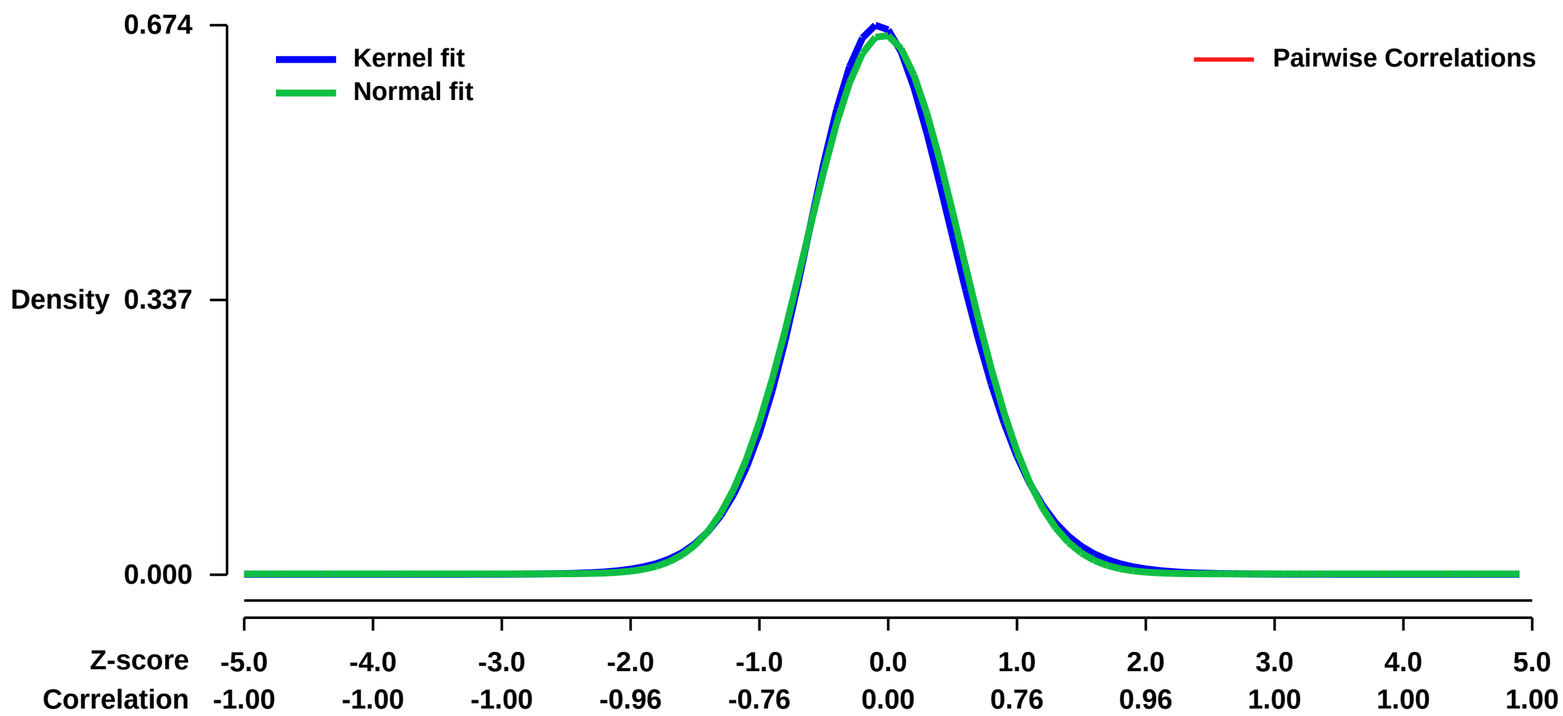

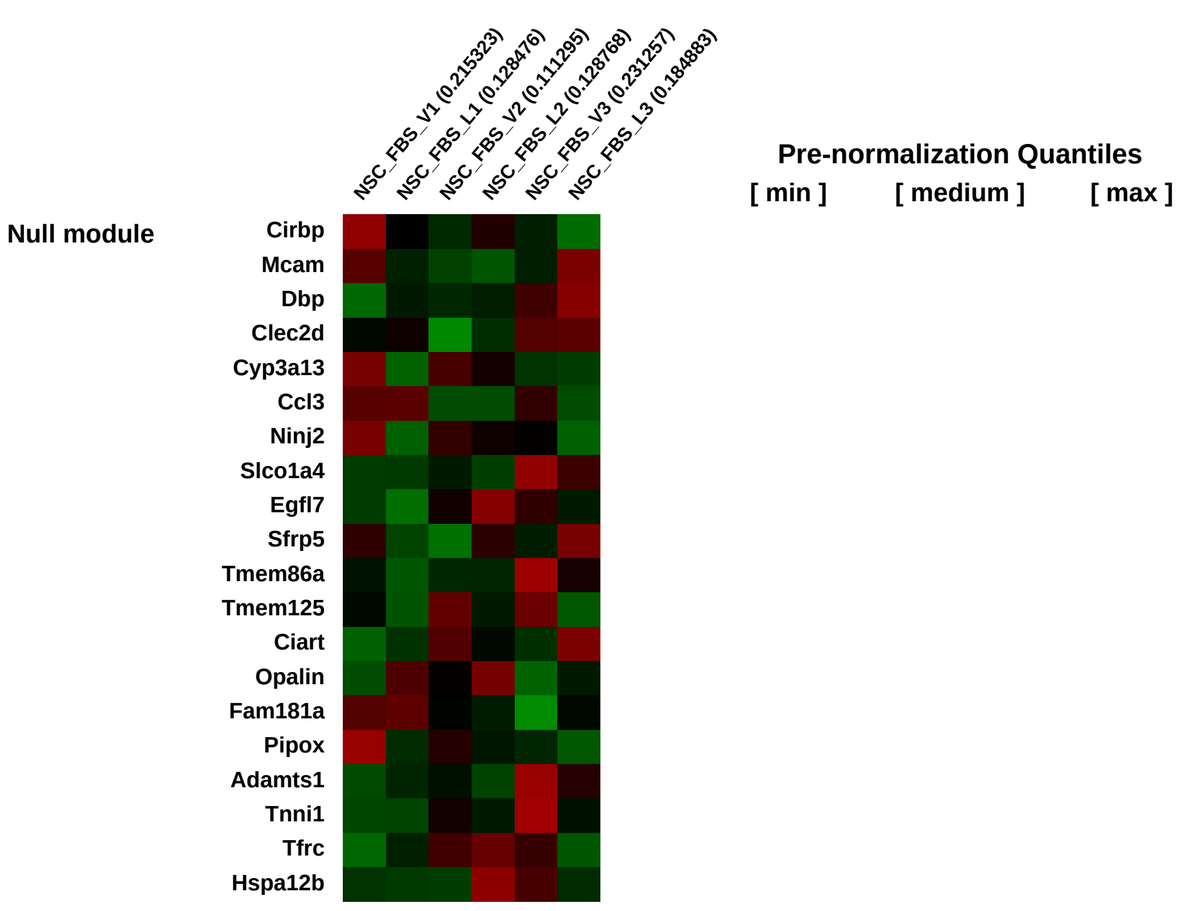

GEO Series "GSE40377" Expression Profiles

Num of samples in this series: 42

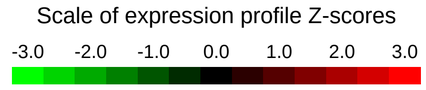

GEO Link:	http://www.ncbi.nlm.nih.gov/geo/query/acc.cgi?acc=GSE40377
Status:	Public on Aug 25 2012
Title:	Microarray profiling of WT or PDE10A KO mice treated with vehicle or a PDE10 inhibitor
Organism:	Mus musculus
Experiment type:	Expression profiling by array
Platform:	GPL1261
Pubmed ID:	20923867

Summary & Design:

Summary:
Inhibition of phosphodiesterase 10A (PDE10A) promotes cyclic nucleotide signaling, increases striatal activation, and decreases behavioral activity. Enhanced cyclic nucleotide signaling is a well established route to producing changes in gene expression. We hypothesized that chronic suppression of PDE10A activity would have significant effects on gene expression in the striatum. A comparison of the expression profile of PDE10A knockout (KO) mice and wild-type mice after chronic PDE10A inhibition revealed altered expression of 19 overlapping genes with few significant changes outside the striatum or after administration of a PDE10A inhibitor to KO animals. Chronic inhibition of PDE10A produced up-regulation of mRNAs encoding genes that included prodynorphin, synaptotagmin10, phosphodiesterase 1C, glutamate decarboxylase 1, and diacylglycerol O-acyltransferase and a down-regulation of mRNAs encoding choline acetyltransferase and Kv1.6, suggesting long-term suppression of the PDE10A enzyme is consistent with altered striatal excitability and potential utility as a antipsychotic therapy. In addition, up-regulation of mRNAs encoding histone 3 (H3) and down-regulation of histone deacetylase 4, follistatin, and claspin mRNAs suggests activation of molecular cascades capable of neuroprotection. We used lentiviral delivery of cAMP response element (CRE)-luciferase reporter constructs into the striatum and live animal imaging of 2-{4-[-pyridin-4-yl-1-(2,2,2-trifluoro-ethyl)-1H-pyrazol-3-yl]-phenoxymethyl}-quinoline succinic acid (TP-10)-induced luciferase activity to further demonstrate PDE10 inhibition results in CRE-mediated transcription. Consistent with potential neuroprotective cascades, we also demonstrate phosphorylation of mitogen- and stress-activated kinase 1 and H3 in vivo after TP-10 treatment. The observed changes in signaling and gene expression are predicted to provide neuroprotective effects in models of Huntington's disease.

Overall design:
n=4-6 per group. WT mice used as a control for PDE10A KO mice, vehicle control for PDE10A inhibitor treatment.

Background corr dist: KL-Divergence = 0.1400, L1-Distance = 0.0243, L2-Distance = 0.0008, Normal std = 0.3898

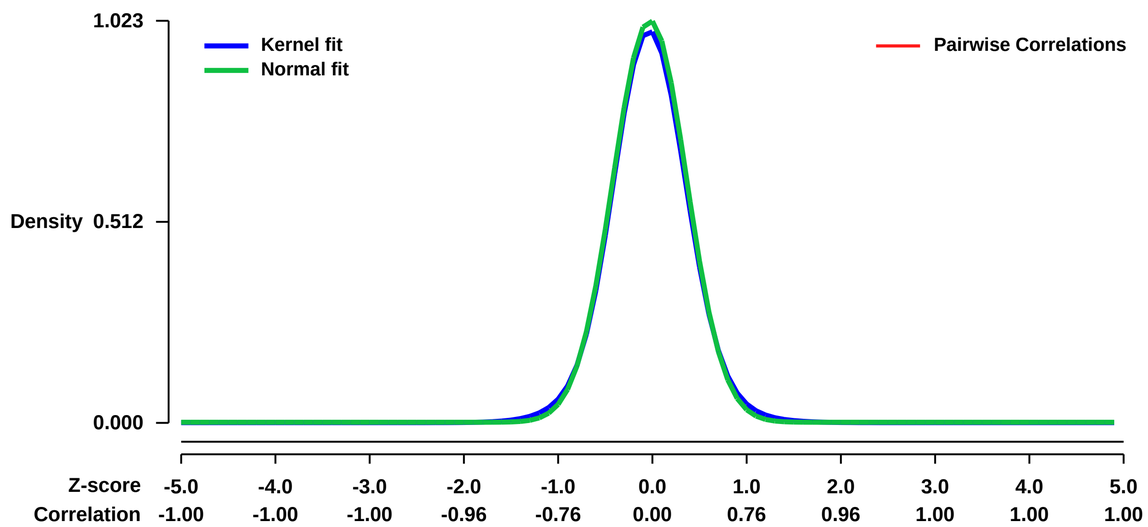

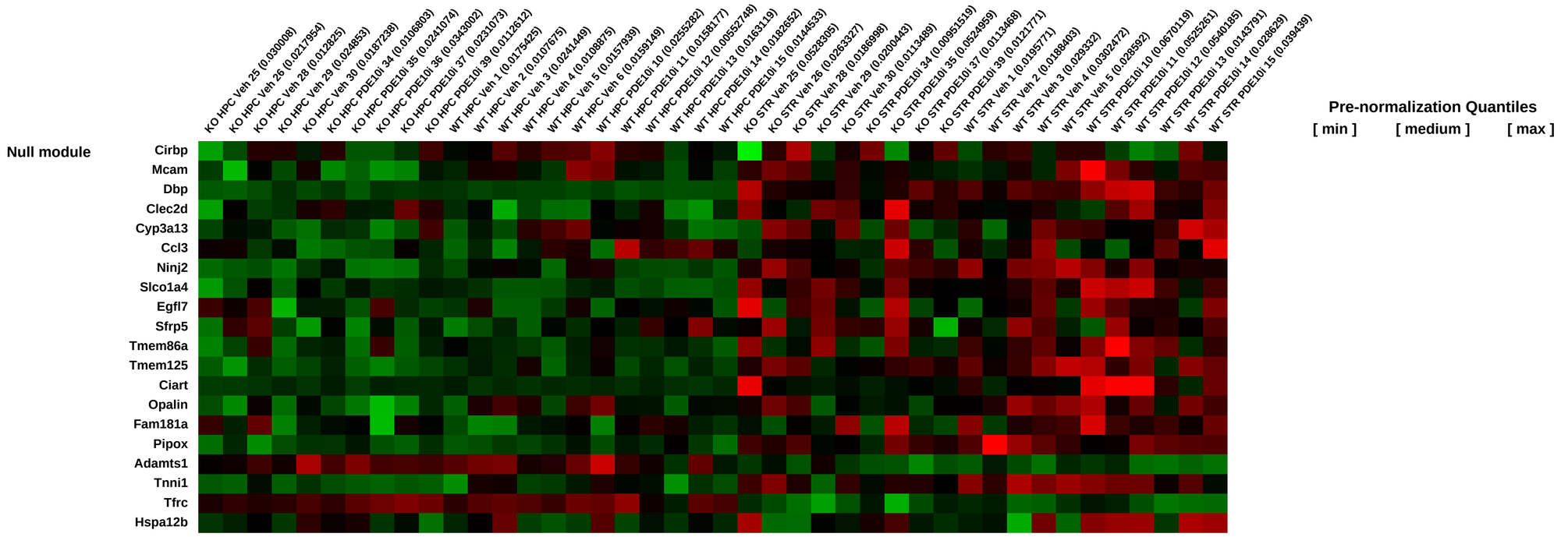

GEO Series "GSE48369" Expression Profiles

Num of samples in this series: 36

Scale of expression profile Z-scores

-3.0 -2.0 -1.0 0.0 1.0 2.0 3.0

GEO Link:	http://www.ncbi.nlm.nih.gov/geo/query/acc.cgi?acc=GSE48369
Status:	Public on Aug 20 2013
Title:	Expression data of sleeping, waking, and sleep deprived in adult heterozygous Cnp â eGFP-L10a mice
Organism:	Mus musculus
Experiment type:	Expression profiling by array
Platform:	GPL1261
Pubmed ID:	24005282
Summary & Design:	**Summary:** Transcriptomic studies revealed that hundreds of mRNAs show differential expression in the brains of sleeping versus awake rats, mice, flies, and sparrows. Although these results have offered clues regarding the molecular consequences of sleep and sleep loss, their functional significance thus far has been limited. This is because the previous studies pooled transcripts from all brain cells, including neurons and glia. In the following experiment, we studied the specific effects of sleep and wake conditions on glia cells of mouse cerebral cortex using the genetically targeted translating ribosome affinity purification (TRAP) methodology. We used bacterial artificial chromosome (BAC) transgenic mice expressing EGFP tagged ribosomal protein L10a in oligodendrocytes which constitute a defined cellular population of the mouse brain. Using this approach, we could extract only the oligodendrocitic mRNAs, and only those already committed to be translated into proteins (L10a is part of the translational machinery). **Overall design:** Six mice for each vigilant state group (sleep (S), waking (W), and sleep deprivation (SD)) were considered. For each animal, one forebrain sample was immediately processed. Samples were immunoprecipitated to isolate oligodendrocytes. The precipitated portion formed the bound sample (IP) containing olidodendrocytes and the remaining part formed the unbound sample (UB) containing all the remaining cell types (neurons and other glia cells). Then, both IP and UB samples were processed and RNA was extracted.

Background corr dist: KL-Divergence = 0.0780, L1-Distance = 0.0388, L2-Distance = 0.0022, Normal std = 0.4968

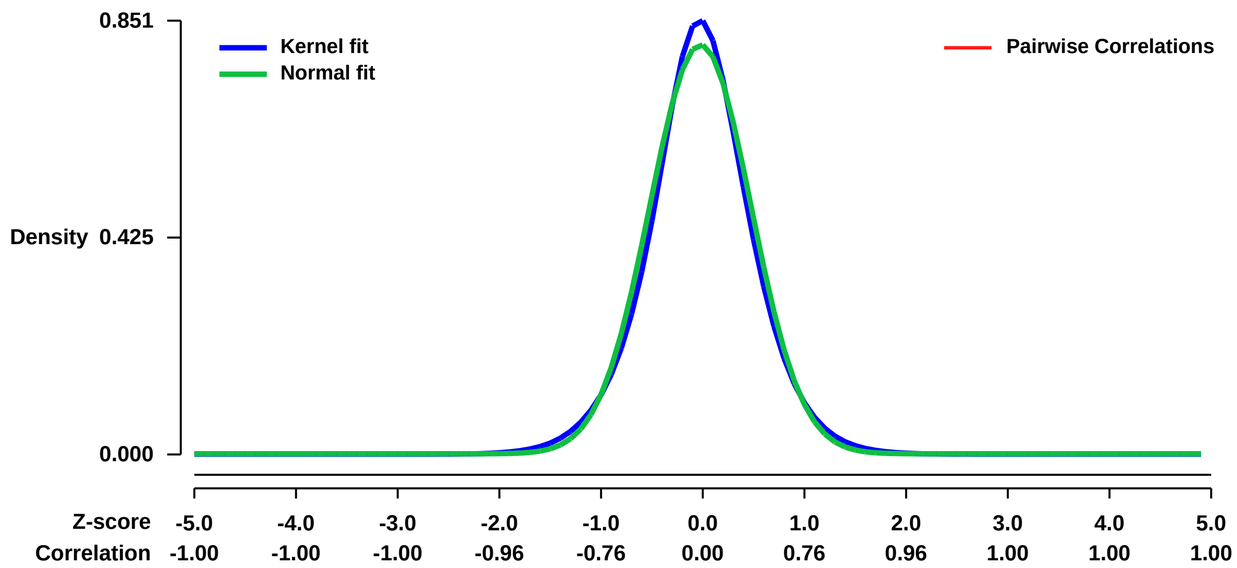

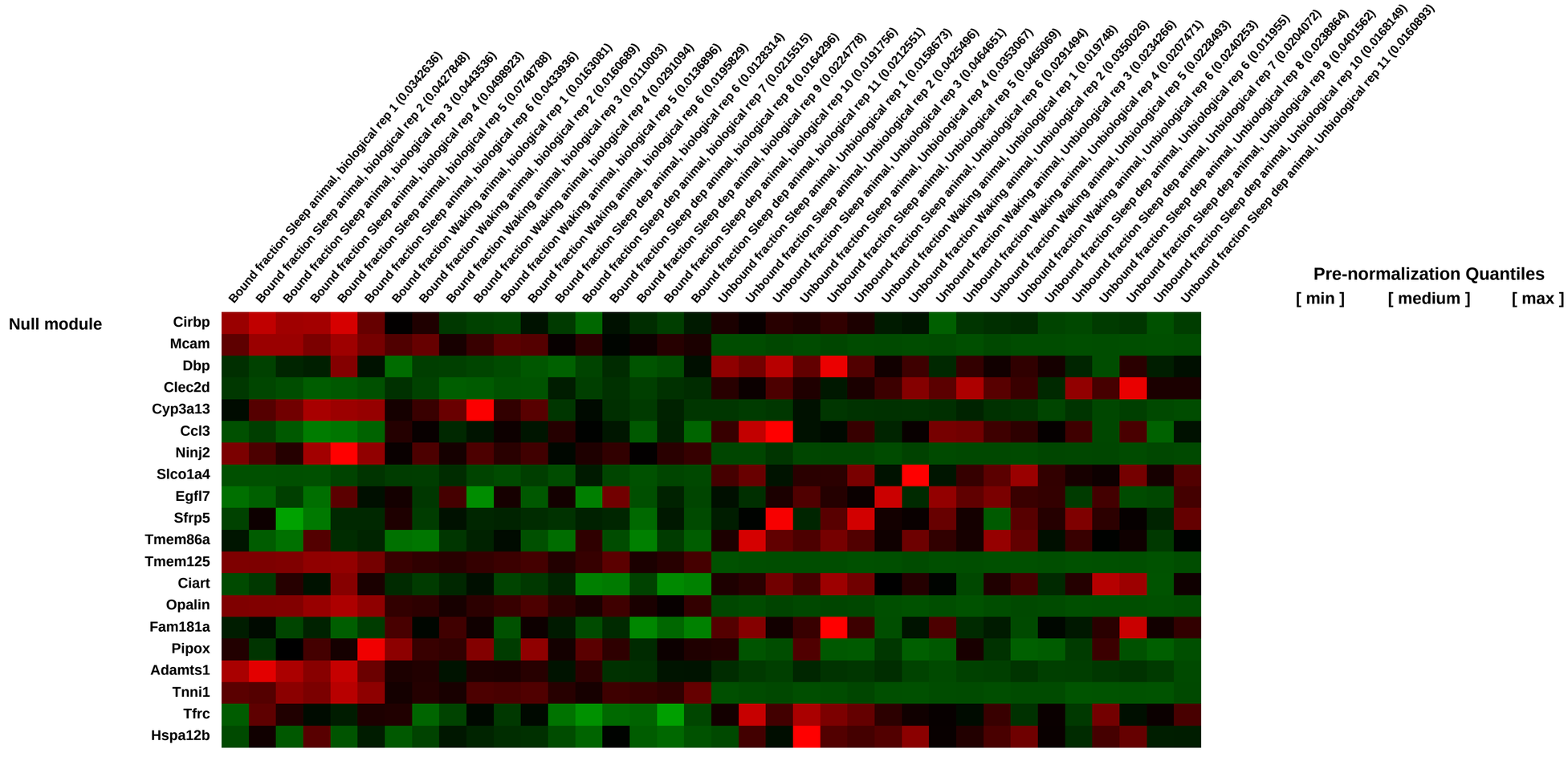

GEO Series "GSE18765" Expression Profiles

Num of samples in this series: 14

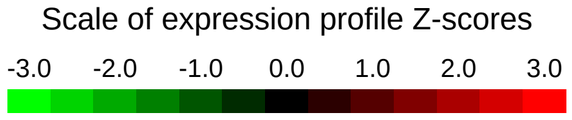

GEO Link:	http://www.ncbi.nlm.nih.gov/geo/query/acc.cgi?acc=GSE18765
Status:	Public on Nov 19 2010
Title:	The transcriptome of prospectively isolated adult neural stem cells
Organism:	Mus musculus
Experiment type:	Expression profiling by array
Platform:	GPL1261
Pubmed ID:	21112568
Summary & Design:	**Summary:** **Since the discovery of adult neural stem cells, their exact identity is still under discussion. Moreover, the lack of a reproducible procedure to purify neural stem cells prospectively rather than by growing them in vitro has so far precluded their study at the transcriptome level. Here we demonstrate a novel procedure to prospectively isolate neural stem cells from the adult mouse subependymal zone on the basis of their GFAP- and prominin1-expression by fluorescence-activated cell sorting. All self-renewing, multipotent stem cells are contained in this fraction at 70% purity. The stem cell identity of these double-positive cells is further demonstrated in vivo, by using a novel split-Cre-technology for fate mapping.** **Comparison of the transcriptome of these prospectively isolated neural stem cells to the transcriptomes of other astrocytes or ependymal cells revealed a distinct clustering of the stem cells, highlighting their unique features, as well as profound similarities to the astrocyte as well as ependyma transcriptome.** **Overall design:** **FACS-sorting was used to isolate prospective neural stem, astrocytes and ependymal cells from brain regions of hGFAP eGFP expressing mice. Total RNA from these cells was hybridised on Affymetrix MOE430 2.0 arrays and expression patterns were analysed.**

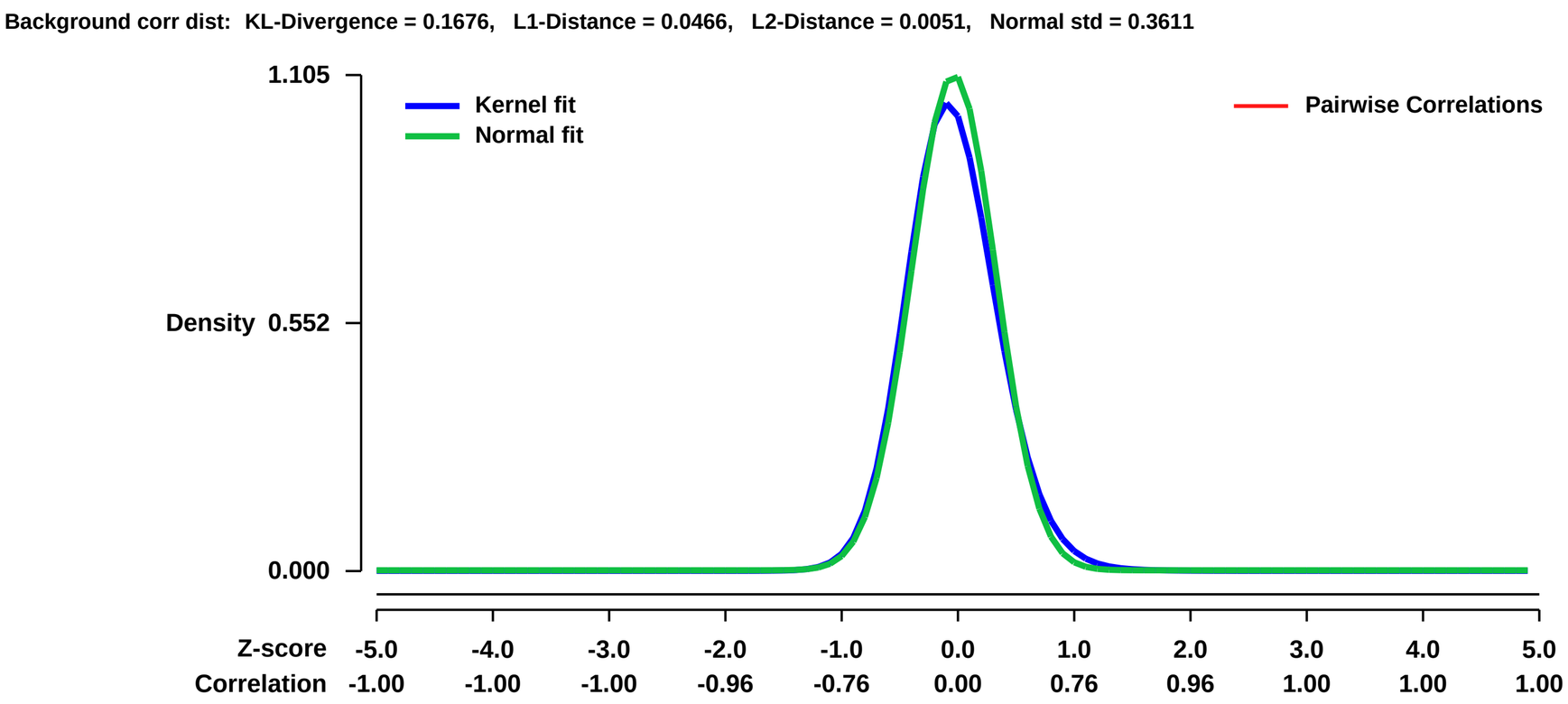

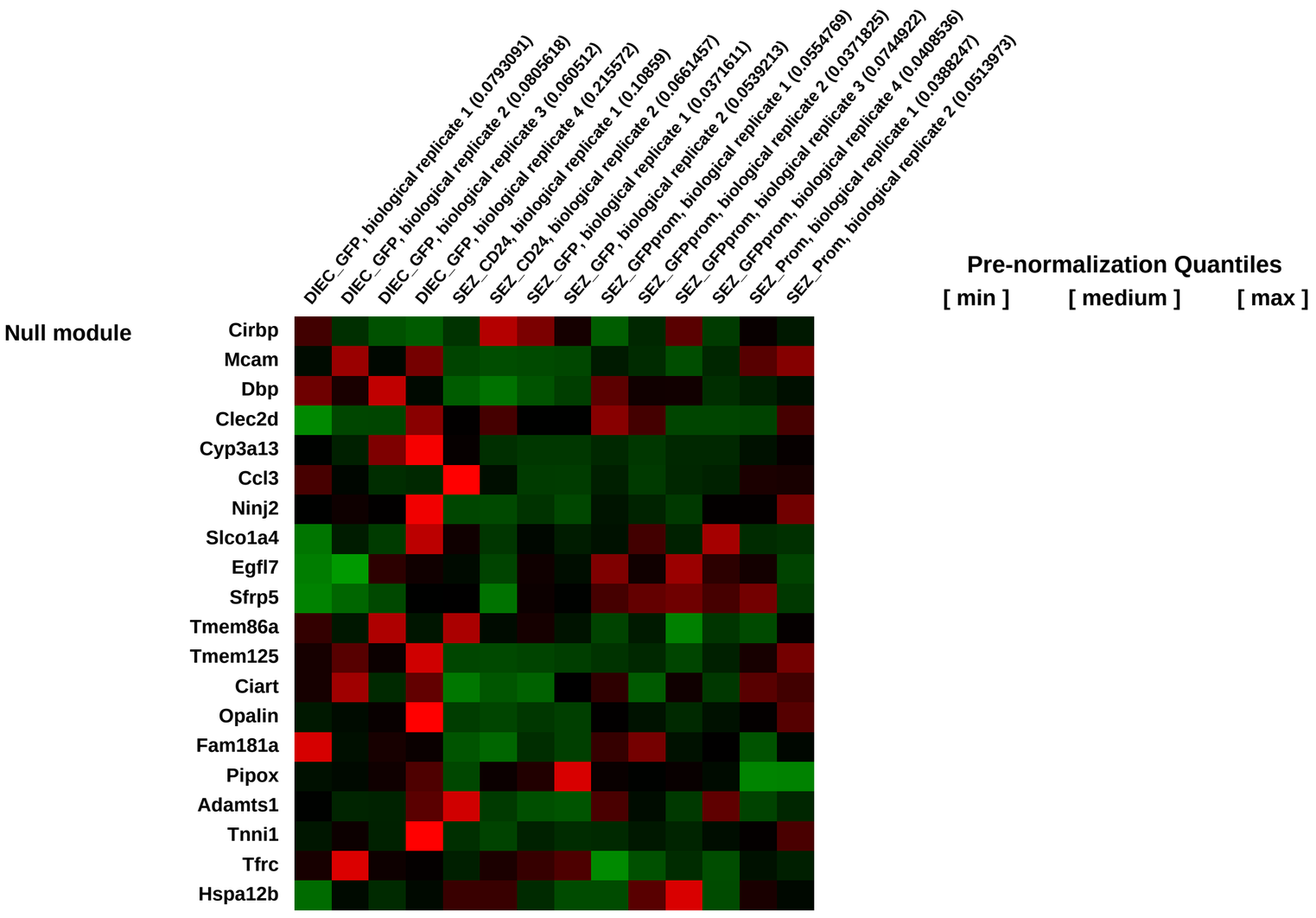

GEO Series "GSE21299" Expression Profiles

Num of samples in this series: 12

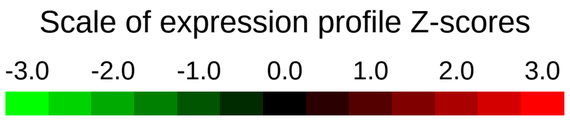

GEO Link:	http://www.ncbi.nlm.nih.gov/geo/query/acc.cgi?acc=GSE21299
Status:	Public on Feb 01 2011
Title:	Expression data from murine cell line transduced with epitope tagged forms of Hoxa9
Organism:	Mus musculus
Experiment type:	Expression profiling by array
Platform:	GPL1261
Pubmed ID:	20541477
Summary & Design:	**Summary:** **Importantly increasing evidence shows that Hox genes such as Hoxa9 are key regulators of stem cell self-renewal and hematopoiesis. Hoxa9 is expressed in early hematopoietic progenitor cells and promotes stem cell expansion. In contrast Hoxa9 down regulation is associated with hematopoietic differentiation. In addition to its role in development, HOXA9 has been intensively studied because of its central role in human acute leukemias. Despite their obvious biomedical importance, the mechanisms through which Hoxa9 and its partner proteins exert their downstream functions are poorly understood.** **Using whole-genome gene expression profiling, we identified direct targets of Hoxa9 in murine MHPs after 4-OHT withdraw, resulting in cell differentiation.** **Overall design:** **Bone marrow cells were harvested from 5-Fluorouracil treated female 6-8 week old C57BL/6 mice and transduced with an MSCV-based retrovirus expressing Hoxa9 fused to a modified estrogen receptor ligand binding domain (Hoxa9-ER). Hoxa9-ER cells were washed 3x and resuspended in IL-3+ media with/without 100 nM 4-OHT (Sigma). At selected intervals, cells were removed for flow cytometric analysis using anti-Gr1 and anti-Mac1 antibodies (BD biosciences), morphologic assessment by cytocentrifugation and staining with Diff-Quick reagents (Intl. Med. Equip.), and RNA collection. For RNA, Pellets were lysed in Trizol reagent (Invitrogen) and RNA was extracted following manufacturer's instructions until phase separation, after which RNeasy columns (Qiagen) were employed for further purification. cRNA probes were synthesized at the University of Michigan microarray core. Probes were hybridized to Affymetrix Mouse 430 2.0 array.**

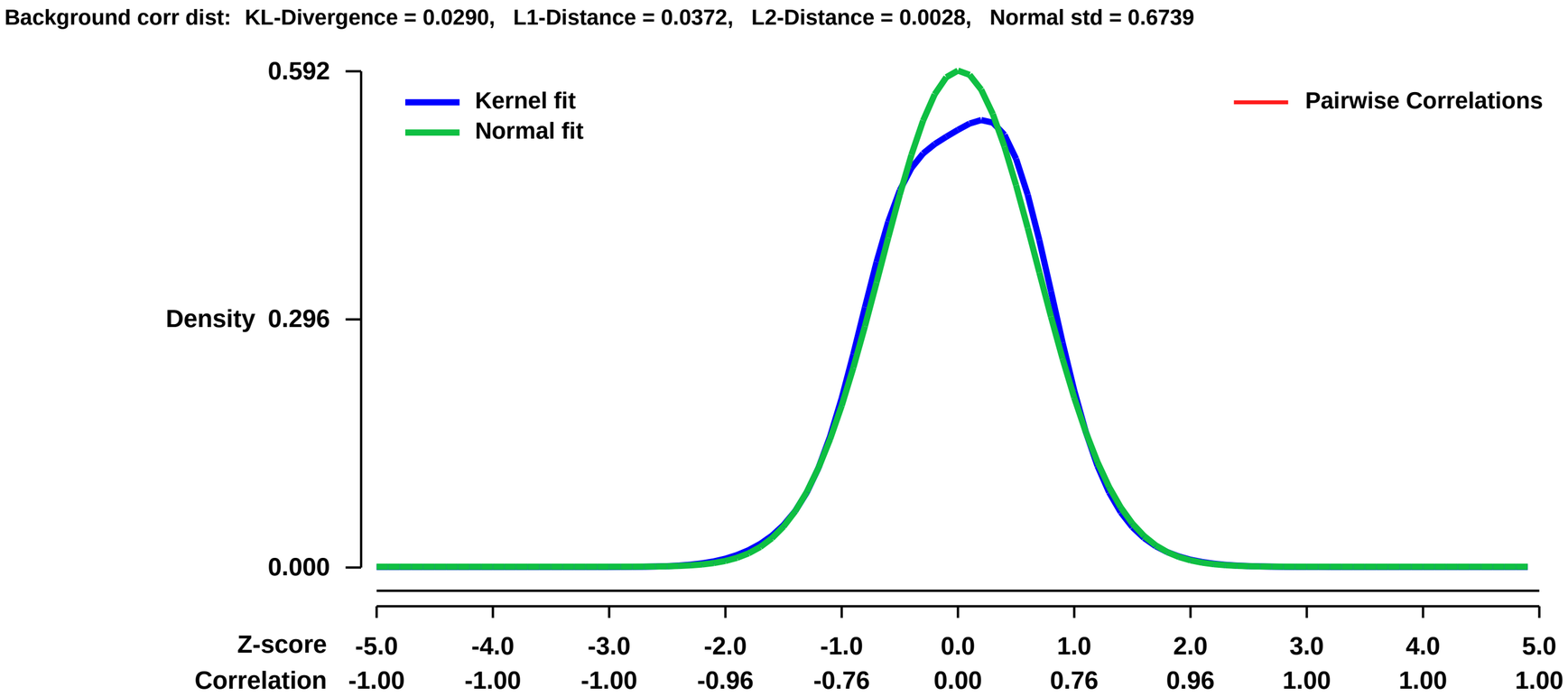

GEO Series "GSE34189" Expression Profiles

Num of samples in this series: 6

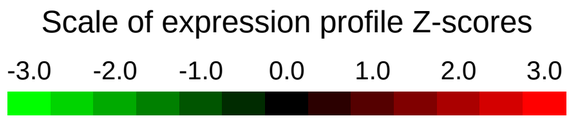

GEO Link:	**http://www.ncbi.nlm.nih.gov/geo/query/acc.cgi?acc=GSE34189**
Status:	**Public on Dec 07 2011**
Title:	**Neural invasion induces cachexia via astrocytic activation of neural route in pancreatic cancer**
Organism:	**Mus musculus**
Experiment type:	**Expression profiling by array**
Platform:	**GPL1261**
Pubmed ID:	
Summary & Design:	**Summary:** **Pancreatic cancer is characterized by a high frequency of cachexia, pain and neural invasion (N-inv). Neural damage is occurred by N-inv and modulates pain and muscle atrophy via the activation of astrocyte in the connected spine. The activated astrocyte by N-inv, thus, may affect cachexia in pancreatic cancer. Clinical studies in patients and autopsy cases with pancreatic cancer have revealed that N-inv is related to cachexia and astrocytic activation. We established a novel murine model of cancer cachexia using N-inv of human pancreatic cancer cells. Mice with N-inv showed a loss of body weight, skeletal muscle, and fat mass without appetite loss, which are compatible with an animal model of cancer cachexia. Activation of astrocytes in the spinal cord connected with N-inv was observed in our model. Experimental cachexia was suppressed by disrupting neural routes or inhibiting the activation of astrocytes. These data provide the first evidence that N-inv induces cachexia via astrocytic activation of neural route in pancreatic cancer.** **Overall design:** **We produced neural invasion (N-inv) model using intraneural injection of Capan-1 cells to left sciatic nerve of male SCID mouse. For controls, subcutaneous model (SC) and PBS model were produced. Microarray analysis was performed using the first lumbar cord (L1) from PBS, SC, and N-inv mice at 6 w (n = 2 each).**

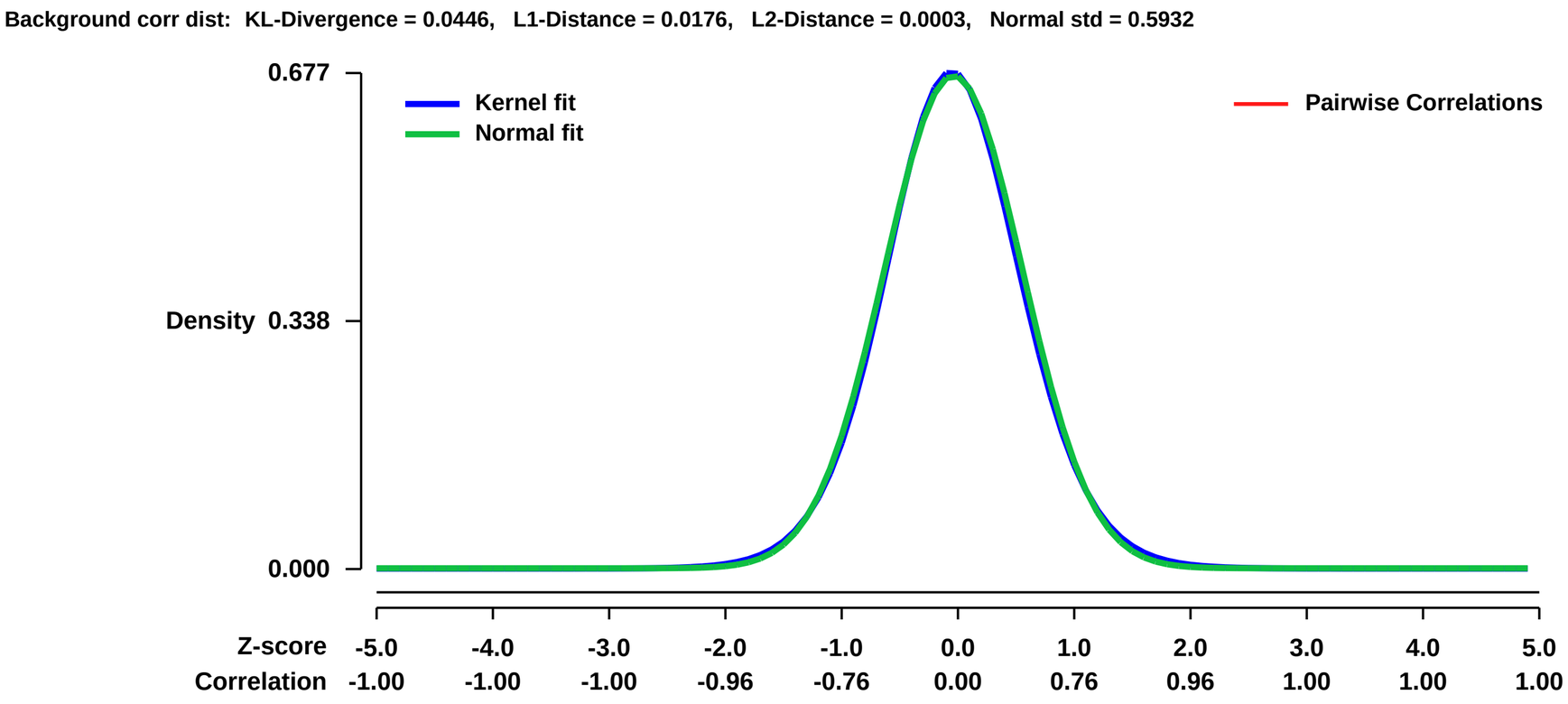

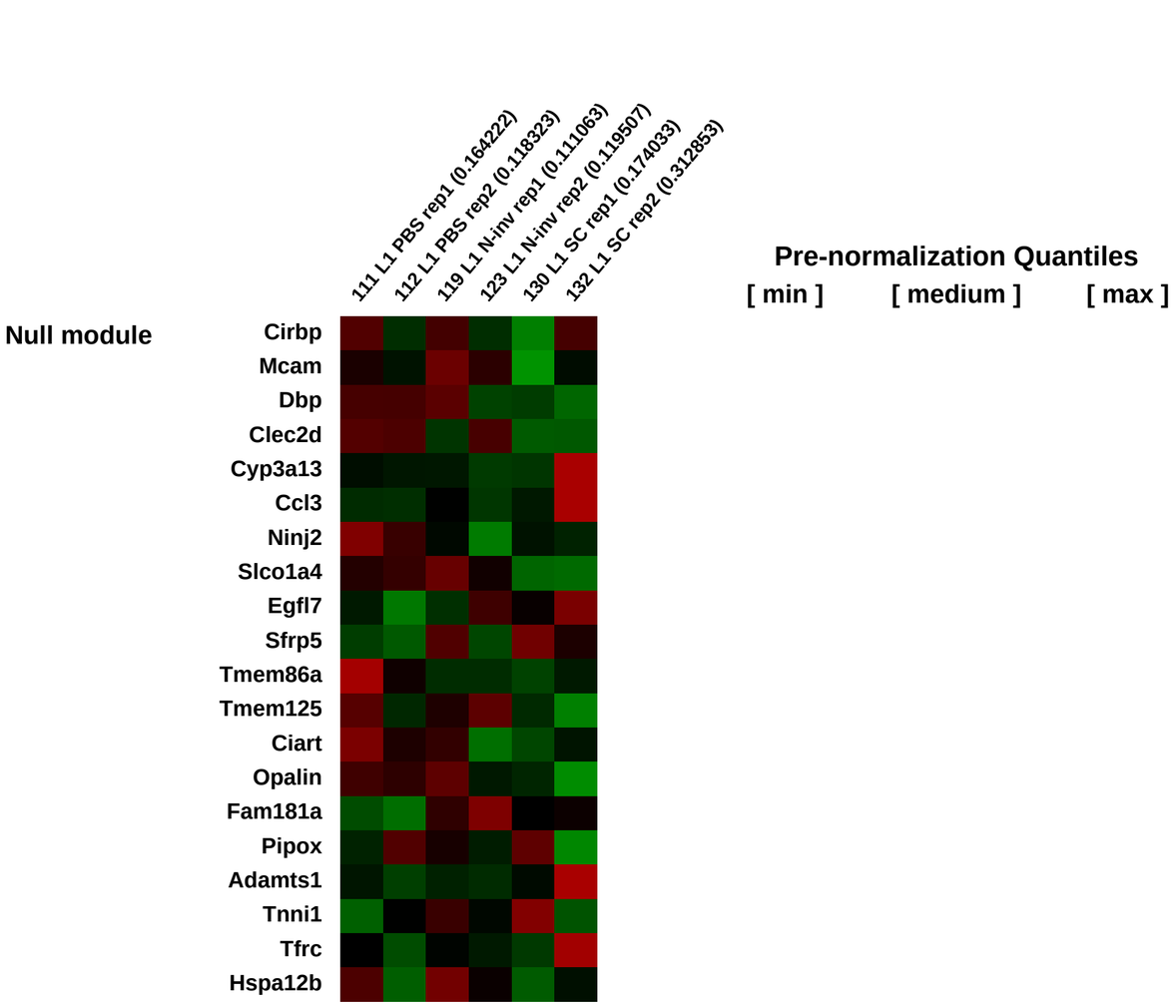

GEO Series "GSE15267" Expression Profiles

Num of samples in this series: 8

Scale of expression profile Z-scores

-3.0 -2.0 -1.0 0.0 1.0 2.0 3.0

GEO Link:	http://www.ncbi.nlm.nih.gov/geo/query/acc.cgi?acc=GSE15267
Status:	Public on Mar 18 2009
Title:	Expression data of induced pluripotent stem cell
Organism:	Mus musculus
Experiment type:	Expression profiling by array
Platform:	GPL1261
Pubmed ID:	20595395
Summary & Design:	**Summary:** We present a robust serum-free system for the rapid and efficient reprogramming of mouse somatic cells by Oct4, Sox2 and Klf4. The elimination of fetal bovine serum and oncogene c-Myc allowed reprogramming cells to be detected as early as Day 2 and reached greater than 10% of the population at Day 7 post retroviral transduction. The resulting iPS colonies were isolated with high efficiency to establish pluripotent cell lines. Based on this method, we further developed iPS-SF1 as a dedicated reprogramming medium for chemical screening and mechanistic investigations. Comparasion of iPS cell lines derived from serum-free culture condition, MEF cells cultured in serum and serum-free condition and ES cell lines was shown. **Overall design:** Selected induced pluripotent stem cell lines and its original mouse embroynic fibroblast were comparaed to defined mouse embroynic stem cell lines: R1 and CGR8.

Background corr dist: KL-Divergence = 0.0267, L1-Distance = 0.0218, L2-Distance = 0.0006, Normal std = 0.7121

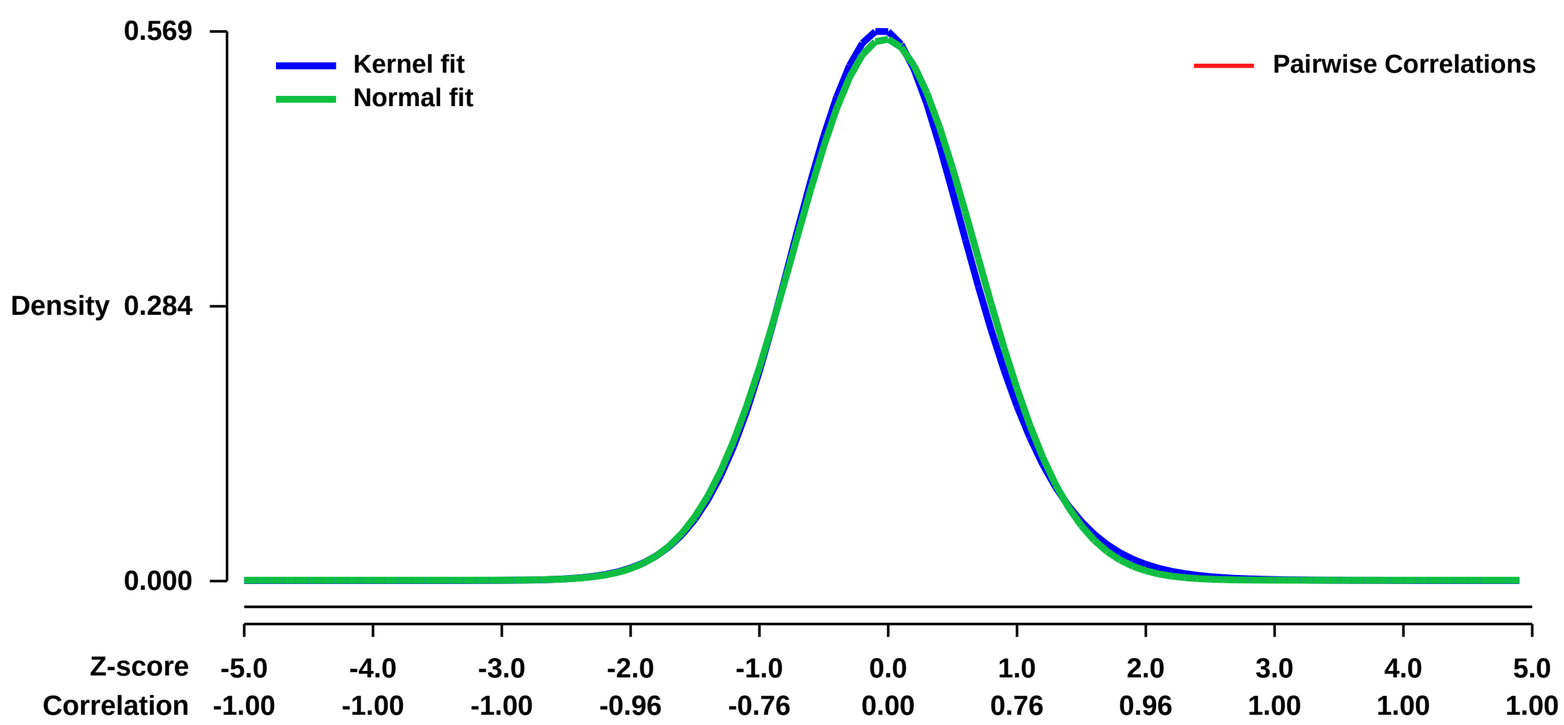

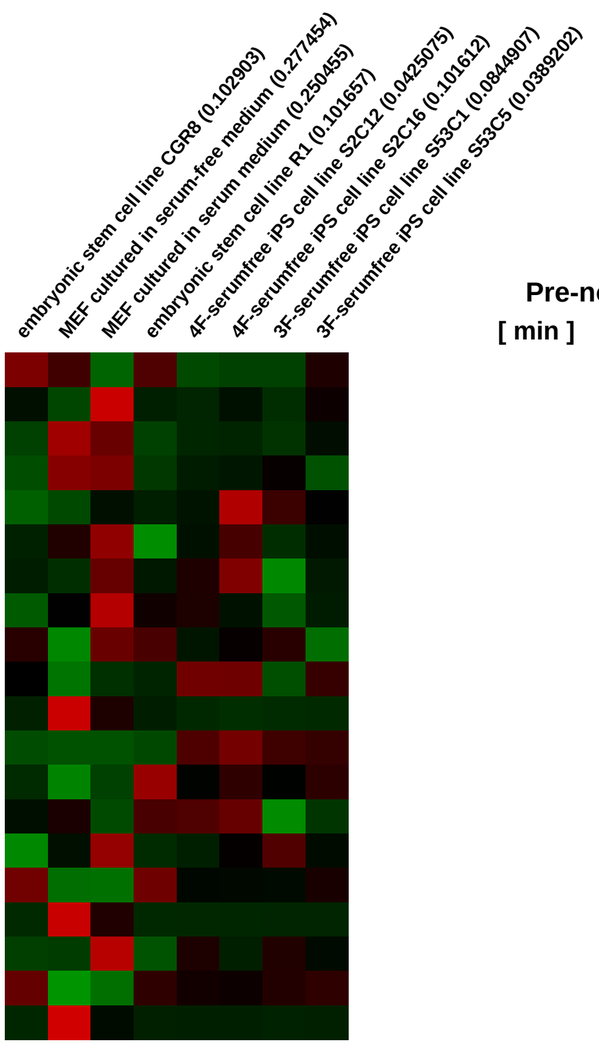

GEO Series "GSE28783" Expression Profiles

Num of samples in this series: 12

Scale of expression profile Z-scores

-3.0 -2.0 -1.0 0.0 1.0 2.0 3.0

GEO Link:	http://www.ncbi.nlm.nih.gov/geo/query/acc.cgi?acc=GSE28783
Status:	Public on May 20 2011
Title:	Effect of anti-miR-33 treatment on gene expression in mouse macrophages from atherosclerotic plaques.
Organism:	Mus musculus
Experiment type:	Expression profiling by array
Platform:	GPL1261
Pubmed ID:	21646721
Summary & Design:	**Summary:** Inhibition of miR-33 results in increased cholesterol efflux and HDL-cholesterol levels in mice. In this study we examined the effect of miR-33 inhibition in a mouse model of atherosclerosis and observed significant reduction in atherosclerotic plaque size. At the end of the study, gene expression in macrophages from the atherosclerotic plaques was assessed. The results demonstrated a reduction in inflammatory gene expression and increased levels of mRNAs containing miR-33 binding sites. **Overall design:** LDLR-/- mice on a Western diet with established atherosclerosis were switched to normal chow and treated with anti-miR-33, control anti-miR, or saline (n=4/group) for 4 weeks. Gene expression profiling was performed on macrophages in aortic plaques isolated at the end of the treatment period by laser capture microdissection.

Background corr dist: KL-Divergence = 0.1533, L1-Distance = 0.0402, L2-Distance = 0.0035, Normal std = 0.3721

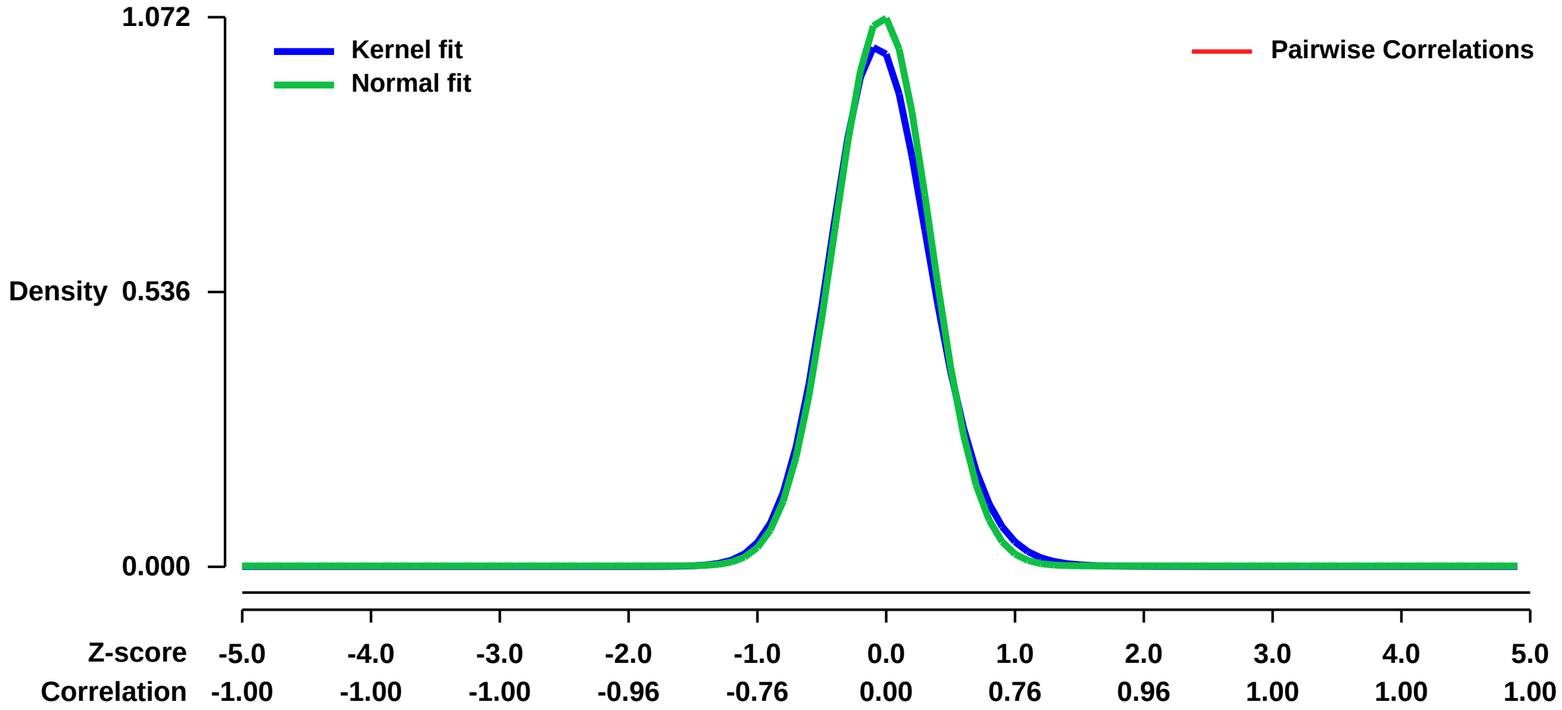

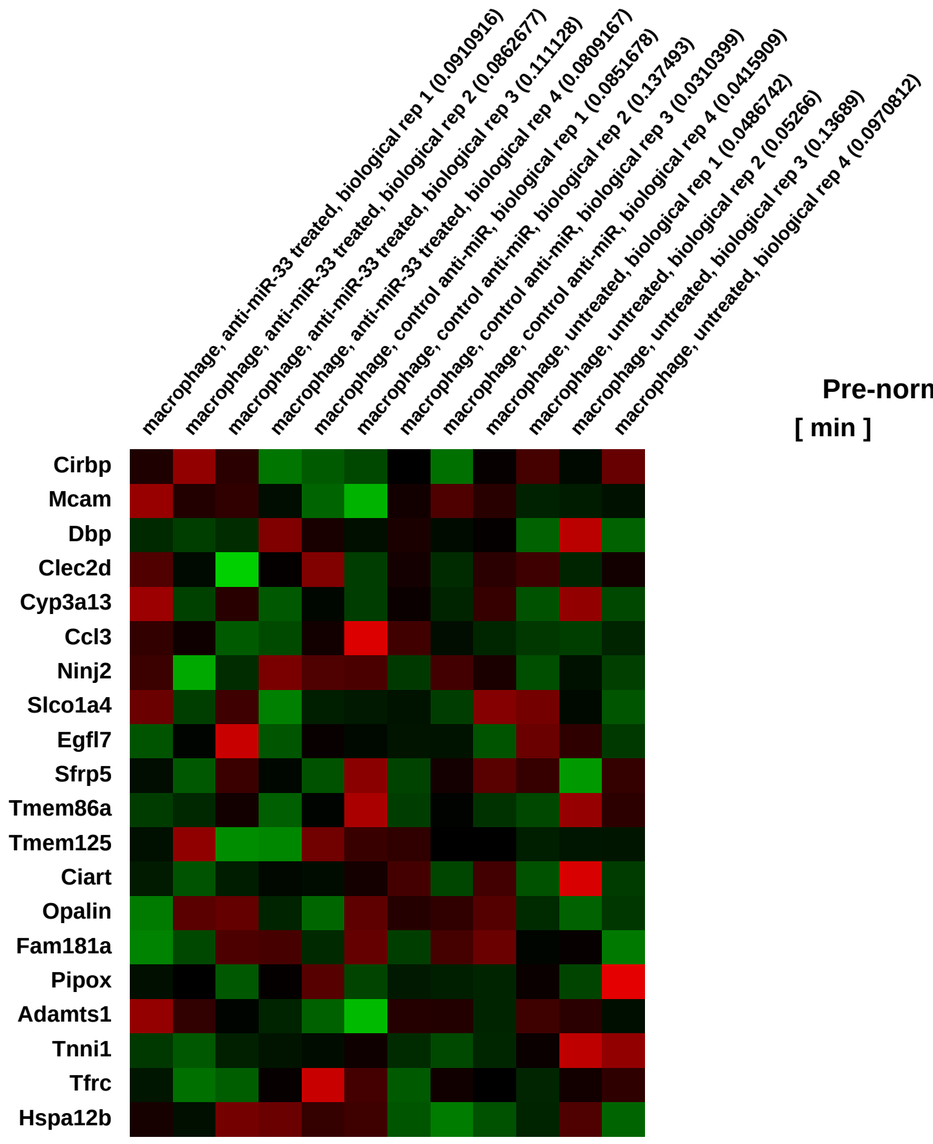

Pre-normalization Quantiles

[min] [medium] [max]

GEO Series "GSE11343" Expression Profiles

Num of samples in this series: 19

Scale of expression profile Z-scores

-3.0 -2.0 -1.0 0.0 1.0 2.0 3.0

GEO Link:	http://www.ncbi.nlm.nih.gov/geo/query/acc.cgi?acc=GSE11343
Status:	Public on May 10 2008
Title:	Rosiglitazone Treatment Reduces Diabetic Neuropathy in STZ treated DBA/2J mice
Organism:	Mus musculus
Experiment type:	Expression profiling by array
Platform:	GPL1261
Pubmed ID:	18583417
Summary & Design:	**Summary:** Diabetic Neuropathy (DN) is a common complication of diabetes. Currently, there is no drug treatment to prevent or slow the development of DN. Rosiglitazone (Rosi) is a potent insulin sensitizer and may also slow the development of DN by a mechanism independent of its effect on hyperglycemia. A two by two design was used to test the effect of Rosi treatment on the development of DN. Streptozotocin-induced diabetic DBA/2J mice were treated with Rosi. DN and oxidative stress were quantified, and gene expression was profiled using the Affymetrix Mouse Genome 430 2.0 microarray platform. An informatics approach identified key regulatory elements activated by Rosi. Diabetic DBA/2J mice developed severe hyperglycemia, DN and elevated oxidative stress. Rosi treatment did not affect hyperglycemia but did reduce oxidative stress and prevented development of thermal hypoalgesia. Two novel transcription factor binding modules were identified that may control genes correlated to changes in DN following Rosi treatment: SP1F_ZBPF and EGRF_EGRF. Rosi treatment reduced oxidative stress and DN independent of its insulin sensitizing effects. Gene expression profiling identified two novel targets activated by Rosi treatment. These targets may be useful in designing drugs with the same efficacy as Rosi in treating DN but with fewer undesirable effects. **Keywords: disease and treatment analysis** **Overall design:** Affymetrix chips were run on five mice from each group. One chip (in the Control group) failed quality control measures and was excluded.

Background corr dist: KL-Divergence = 0.0893, L1-Distance = 0.0337, L2-Distance = 0.0021, Normal std = 0.4560

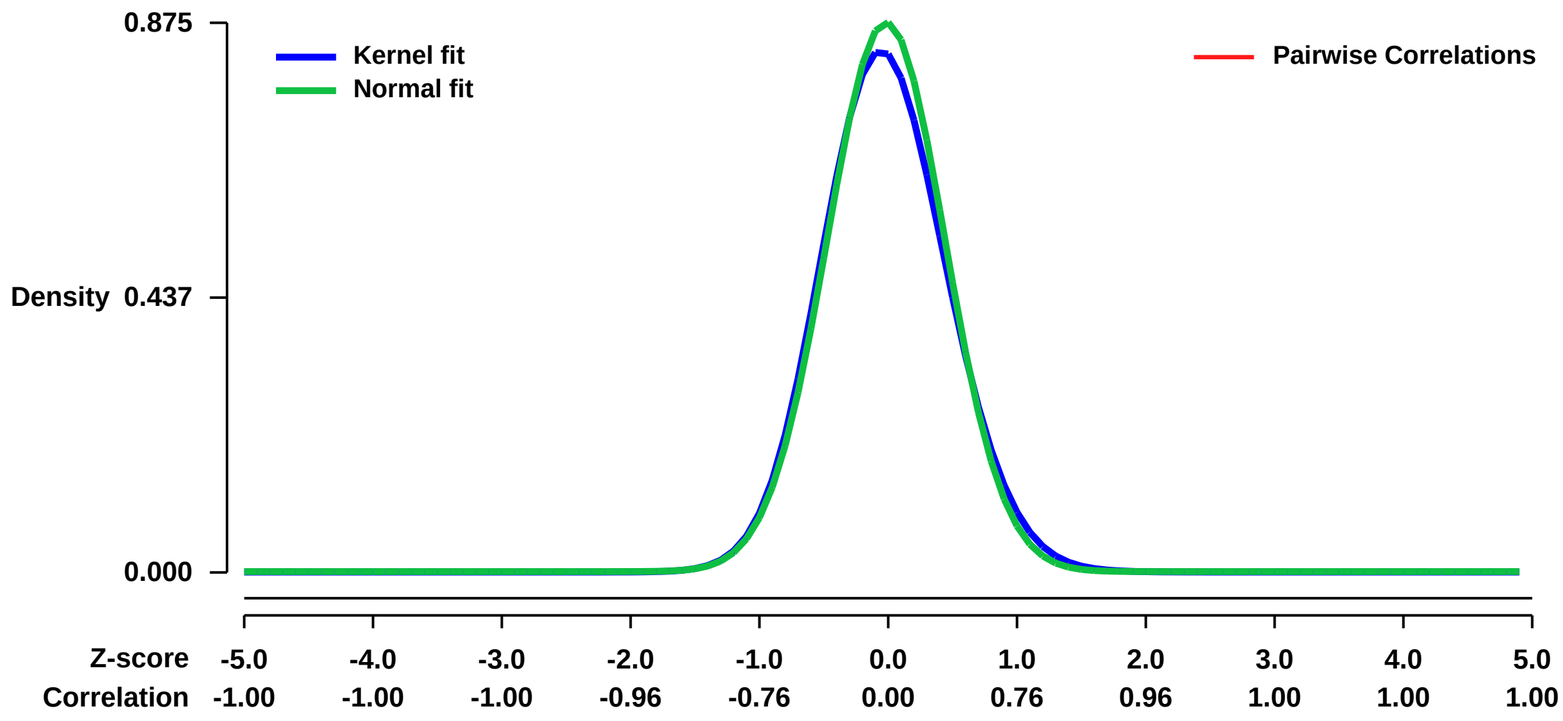

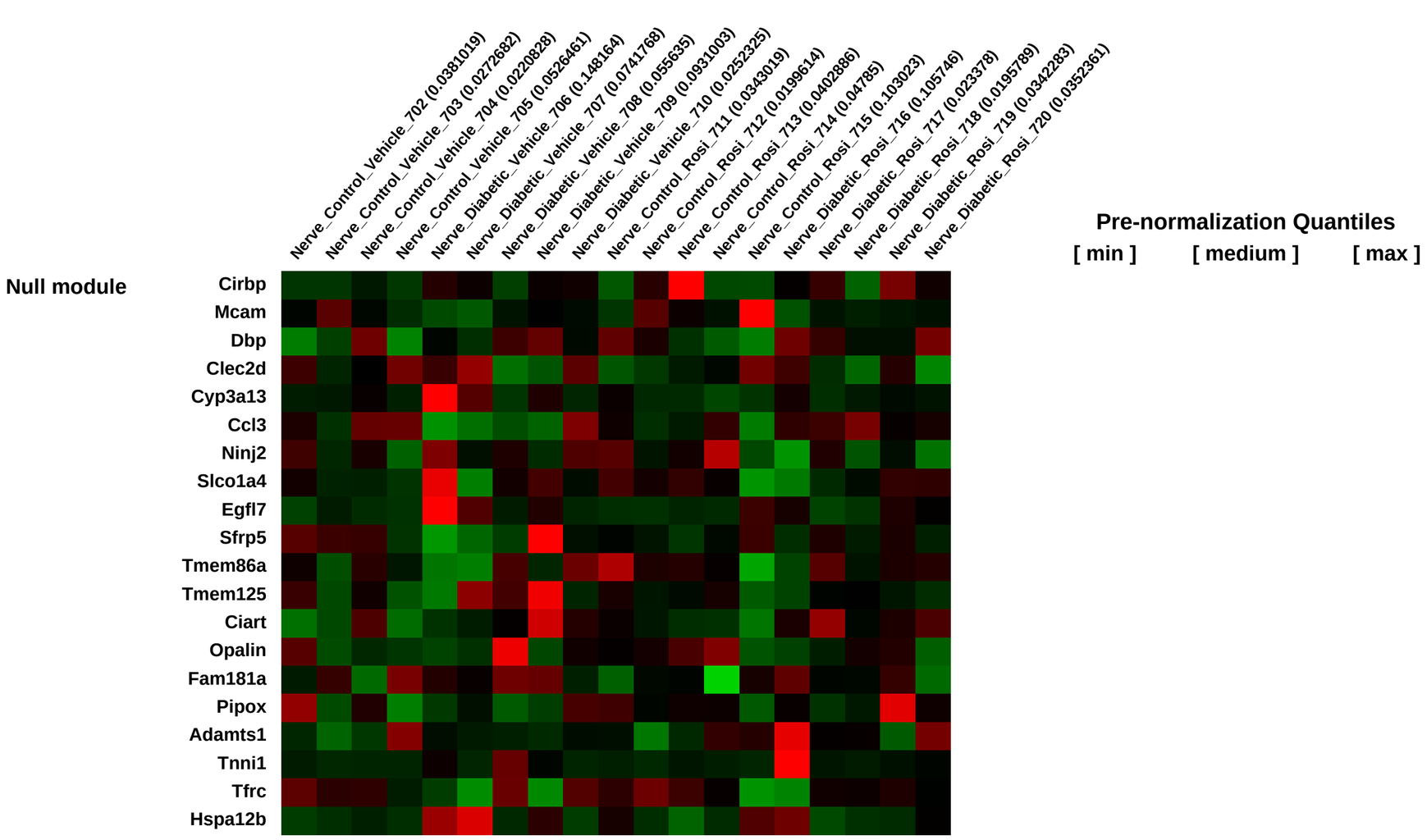

GEO Series "GSE17794" Expression Profiles

Num of samples in this series: 44

Scale of expression profile Z-scores

-3.0 -2.0 -1.0 0.0 1.0 2.0 3.0

GEO Link:	http://www.ncbi.nlm.nih.gov/geo/query/acc.cgi?acc=GSE17794
Status:	Public on Jan 11 2010
Title:	Expression data from B6C3F1 mice treated with 2-butoxyethanol
Organism:	Mus musculus
Experiment type:	Expression profiling by array
Platform:	GPL1261
Pubmed ID:	19812364
Summary & Design:	**Summary:** Mice were dosed with 2-BE (900mg/kg) or vehicle by oral gavage and sacrificied either after 4 hours of a single dose or after 7 days of daily dosing. **Overall design:** Mice were euthanased by cervical dislocation under ketamine / acepromazine (100 mg/kg / 5 mg/kg, I.P) anesthesia. The bone marrow from the right humerus, a portion of the left lateral liver lobe and half a cross-section of the spleen were harvested and the RNA was isolated from these tissues using standard Qiagen reagents. Standard Affymetrix protocols were used for GeneChip probe preparations. 44 arrays.

Background corr dist: KL-Divergence = 0.0249, L1-Distance = 0.0283, L2-Distance = 0.0013, Normal std = 0.6953

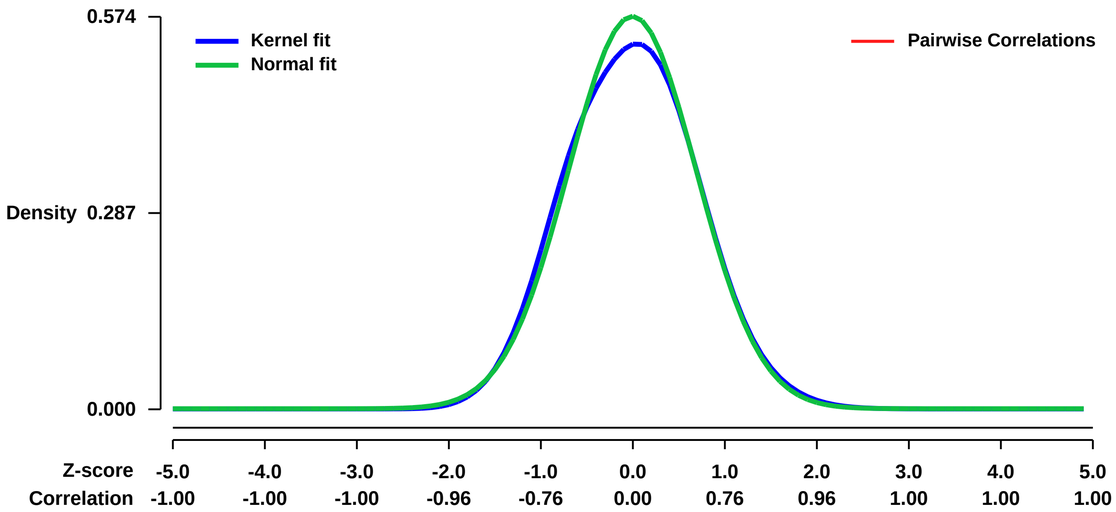

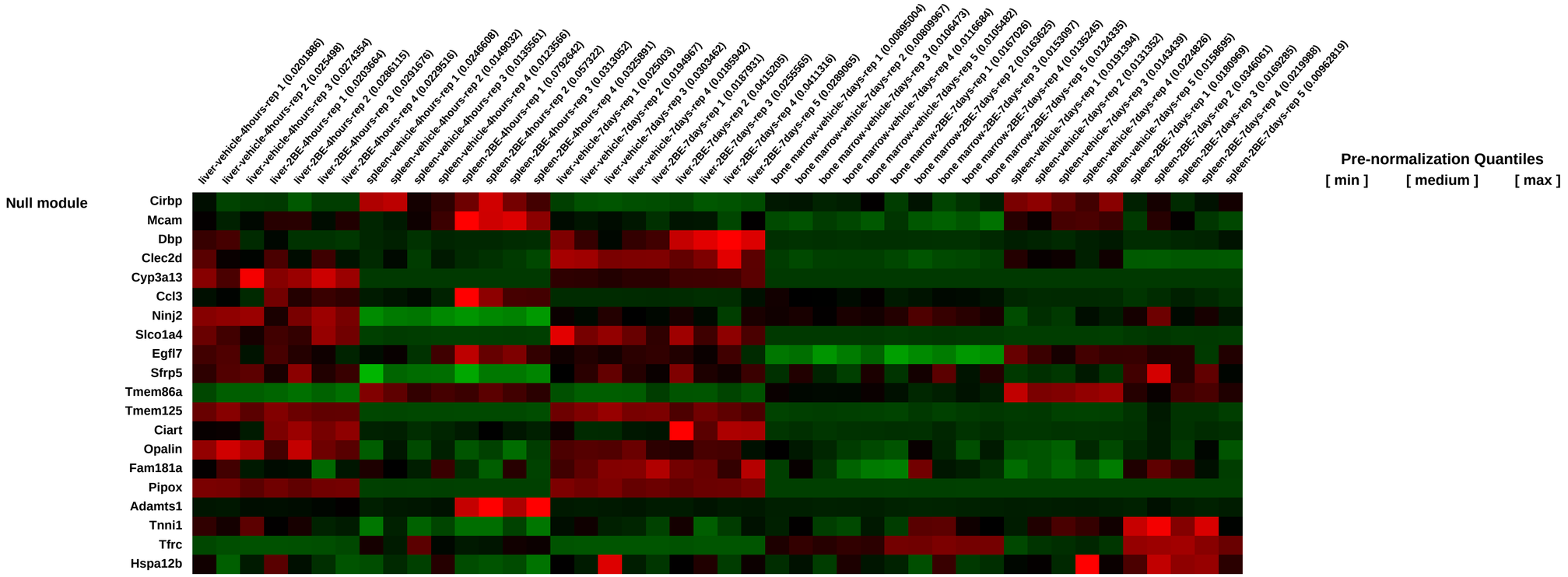

GEO Series "GSE7958" Expression Profiles

Num of samples in this series: 12

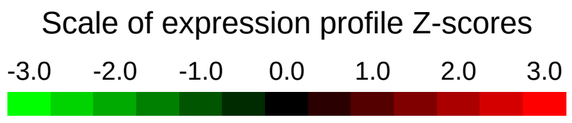

GEO Link:	http://www.ncbi.nlm.nih.gov/geo/query/acc.cgi?acc=GSE7958
Status:	Public on Jul 01 2007
Title:	Striatal gene expression data from 3- and 18-month-old Q92 mice and control mice.
Organism:	Mus musculus
Experiment type:	Expression profiling by array
Platform:	GPL1261
Pubmed ID:	17519223
Summary & Design:	**Summary:** Achieving a mechanistic understanding of disease and initiating preclinical therapeutic trials necessitate the study of huntingtin toxicity and its remedy in model systems. To allow the engagement of appropriate experimental paradigms, Huntingtonâ s disease (HD) models need to be validated in terms of how they recapitulate a particular aspect of human disease. In order to examine transcriptome-related effects of mutant huntingtin, we compared striatal mRNA profiles from seven genetic mouse models of disease to that of postmortem human HD caudate using microarray analysis. Transgenic models expressing short N-terminal fragments of mutant huntingtin (R6/1 and R6/2 mice) exhibited the most rapid effects on gene expression, consistent with previous studies. Although changes in the brains of knock-in models of HD took longer to appear, 15-month and 22-month CHL2Q150/Q150, 18-month HdhQ92/Q92 and 2-year-old YAC128 animals also exhibited significant HD-like mRNA signatures. When the affected genes were compared across models, a robust concordance was observed. Importantly, changes concordant across multiple lines mice were also in excellent agreement with the mRNA changes seen in human HD caudate. Although it was expected that the expression of full-length huntingtin transprotein might result in unique gene expression changes compared to those caused by expression of an N-terminal huntingtin fragment, no discernable differences between full-length and fragment models were detected. There was, however, an overall concordance between transcriptomic signature and disease stage. We thus conclude that the transcriptional changes of HD can be modelled in several available lines of transgenic mice, comprising lines expressing both N-terminal and full-length mutant huntingtin proteins. The combined analysis of mouse and human HD transcriptomes provides an important chronology of mutant huntingtin's gene expression effects. **Keywords:** genetic modification **Overall design:** Striatal samples from 6 Q92 mutant mice (3 3-month-old and 3 18-month-old) and 6 age-matched wild-type mice.

Background corr dist: KL-Divergence = 0.1336, L1-Distance = 0.0375, L2-Distance = 0.0027, Normal std = 0.3898

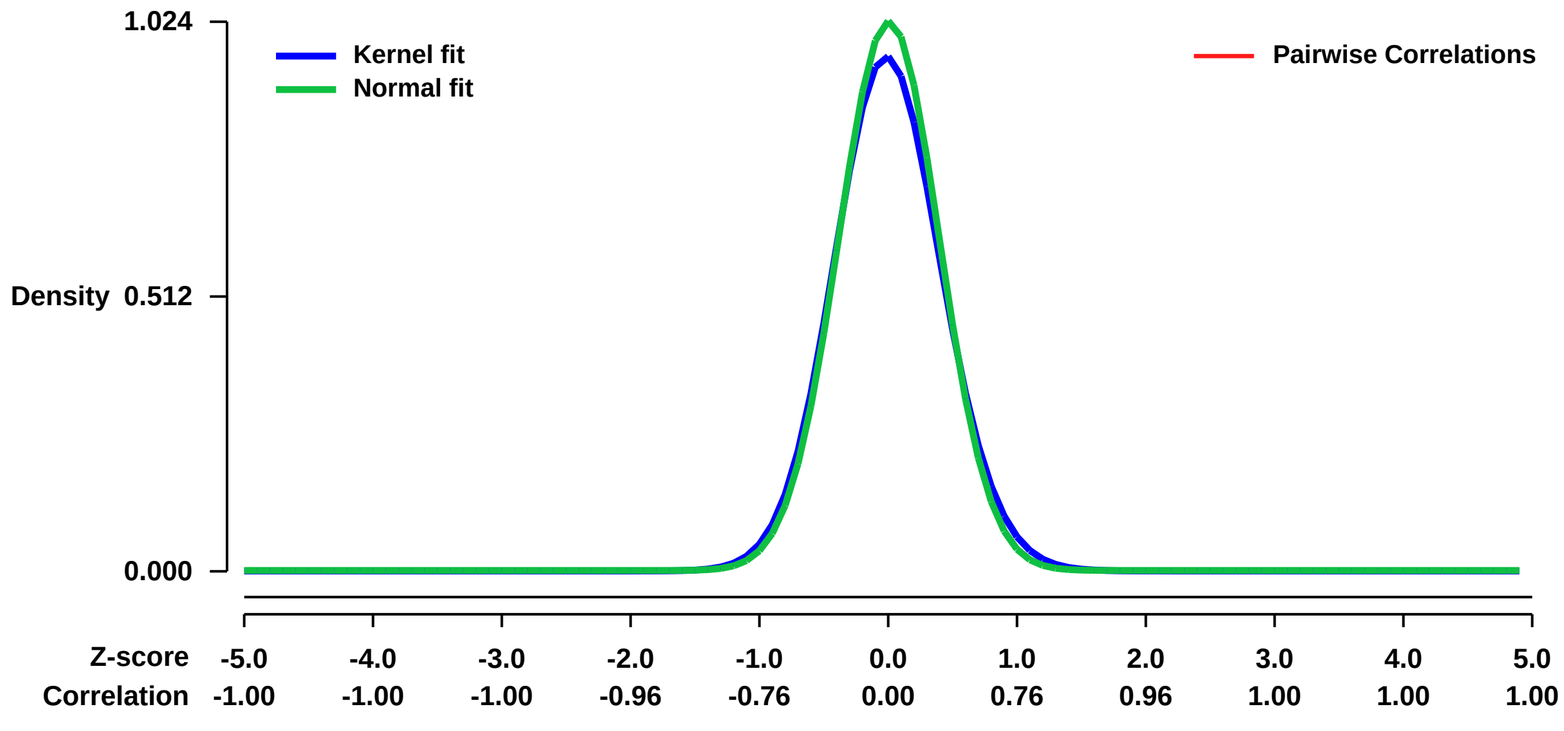

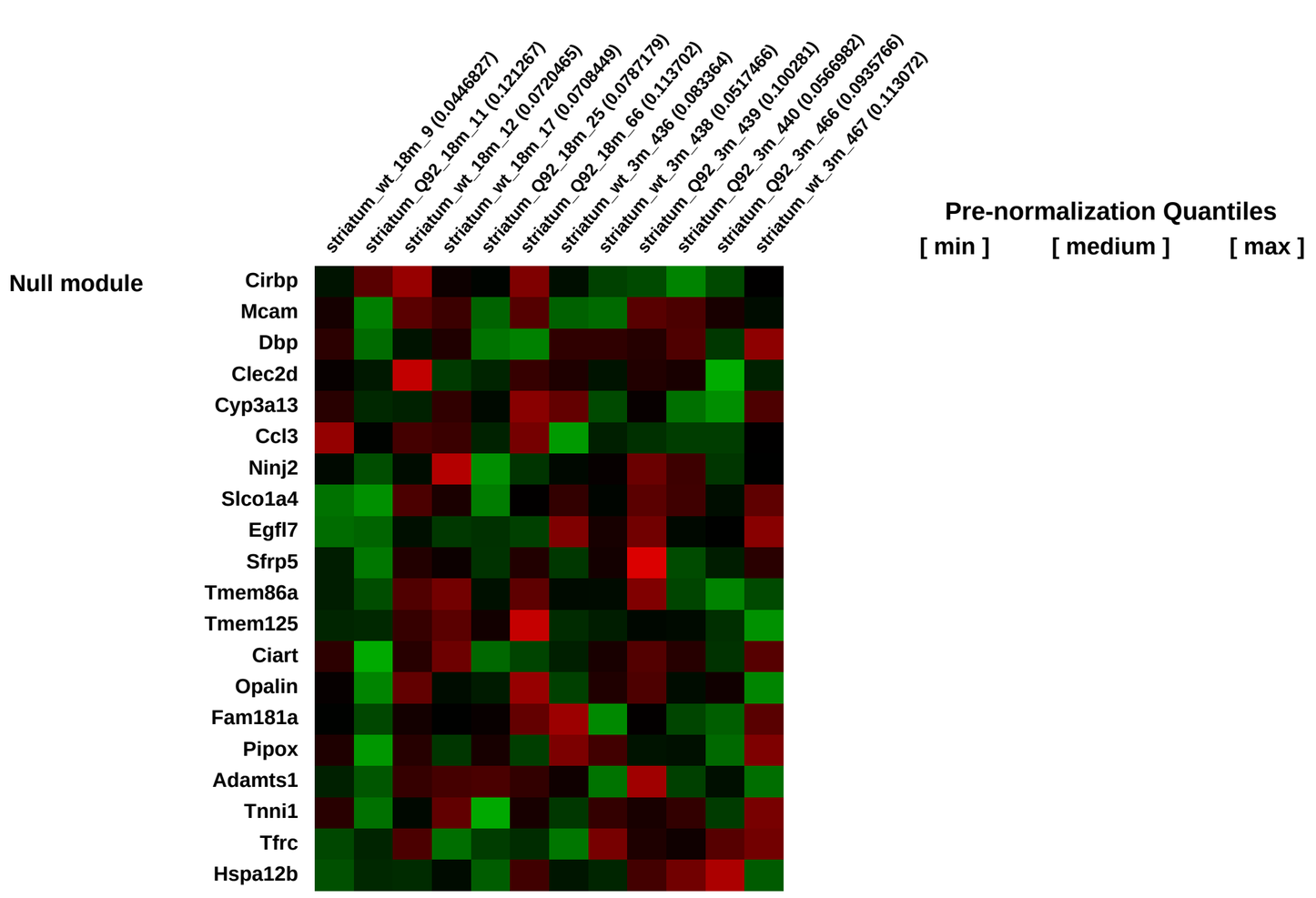

GEO Series "GSE8726" Expression Profiles

Num of samples in this series: 7

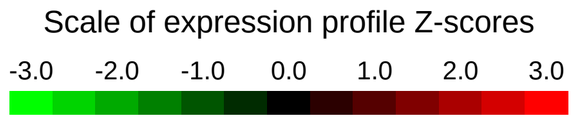

GEO Link:	**http://www.ncbi.nlm.nih.gov/geo/query/acc.cgi?acc=GSE8726**
Status:	**Public on Aug 06 2008**
Title:	**Expression Data from Sod2-/- and Sod2+/+ Mouse Erythroblasts.**
Organism:	**Mus musculus**
Experiment type:	**Expression profiling by array**
Platform:	**GPL1261**
Pubmed ID:	

Summary & Design:

Summary:
The mitochondrial superoxide dismutase (SOD2) is a major antioxidant protein which detoxifies superoxide anion radicals generated by mitochondrial respiration (Weisiger and Fridovich, J. Biol. Chem. 1973). We designed a model of oxidative stress-induced anemia caused by SOD2-deficiency (Friedman et al. J. Exp. Med. 2001). Our previous work showed that mice reconstituted with SOD2-deficient hematopoietic stem cells develop an anemia with striking similarity to human sideroblastic anemia (SA) (Friedman et al. Blood 2004; Martin et al. Exp Hematol 2005). Our overall goal was to define early events in the pathogenesis of SOD2-deficiency SA and, in particular, to identify genes involved in the response of erythroid progenitors to oxidative stress. We compared gene expression of sorted TER-119+ CD71+ erythroblasts from SOD2-/- (’KO’) versus Sod2+/+ (’WT’) hematopoietic stem cell recipients using cDNA microarrays.

Samples used in this study were re-hybridized with GLYCOv2 oligonucleotide arrays. GLYCOv2 oligonucleotide arrays are custom Affymetrix GeneChip arrays (Affymetrix, Santa Clara, CA) designed for the Functional Glycomics Gateway, collaboration between the Consortium for Functional Glycomics (CFG, http://www.functionalglycomics.org/) and Nature Publishing Group. A complete description of the array can be found at http://www.functionalglycomics.org/static/consortium/resources/resourcecoree.shtml . Hybridization results and quality control details can be found at https://www.functionalglycomics.org/glycomics/publicdata/microarray.jsp , by clicking on the â Raw Dataâ icon link for microarray experiment â Jeff Friedman 1: Sod2 KO anemic miceâ . Briefly but importantly, one Sod2-/- sample, which was prepared separately, and whose GAPDH 3’/5’ ratio was off range, was legitimately removed from the analysis of the GLYCOv2 and 430 2.0 arrays.

Keywords: Genotype comparison, genetic modification

Overall design:
We sorted Sod2-/- and Sod2+/+ size-matched mouse erythroblasts based on the expression of two developmental surface markers, CD71 and TER-119. Total RNA from 4 biological replicates per genotype were extracted and hybridized on 8 Affymetrix Mouse Genome 430 2.0 arrays (Affymetrix, Santa Clara, CA). After quality controls (see scan protocol), analysis was performed with GeneSifter (VizX Labs, Seattle, WA) using 4 Sod2+/+ (control samples, WT) and 3 Sod2-/- (KO) replicates.

Background corr dist: KL-Divergence = 0.0320, L1-Distance = 0.0795, L2-Distance = 0.0104, Normal std = 0.7538

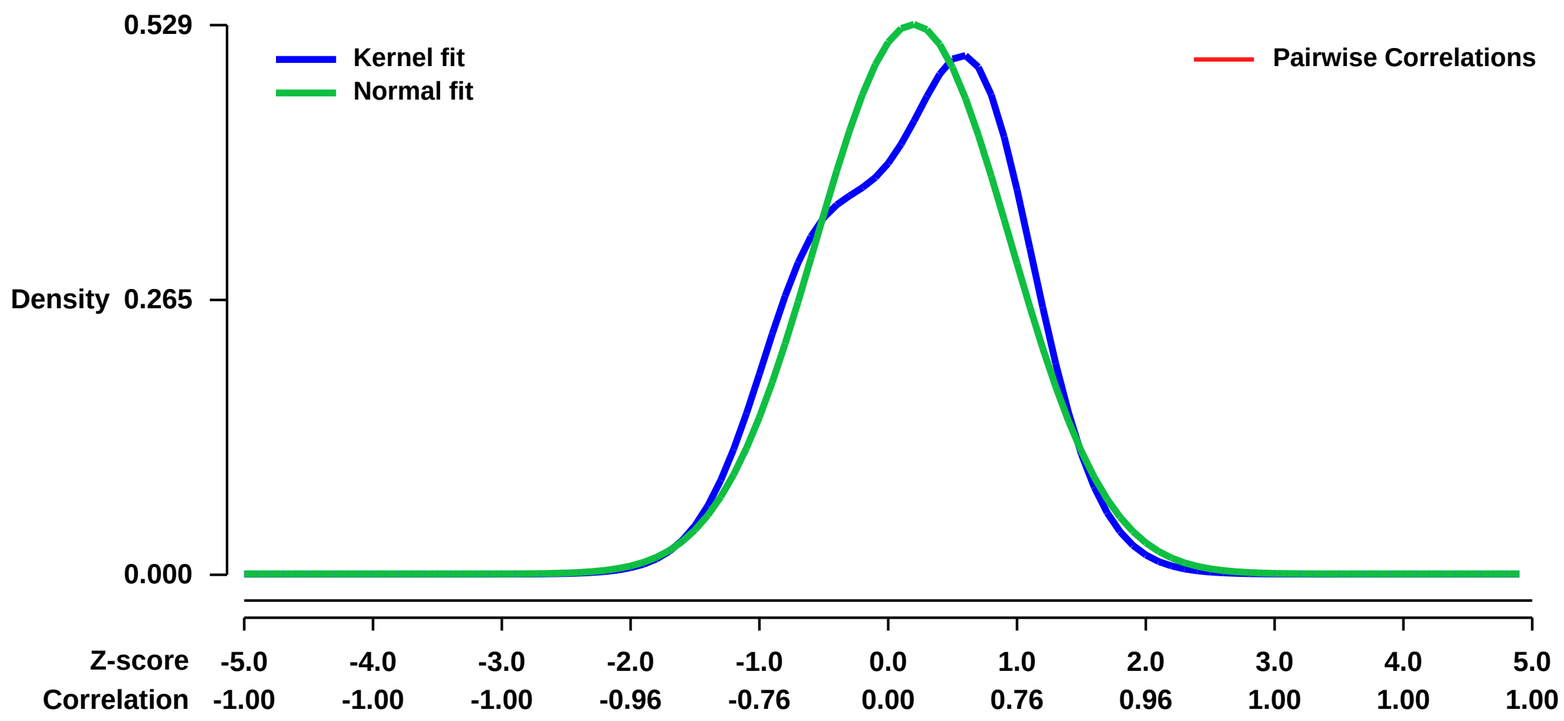

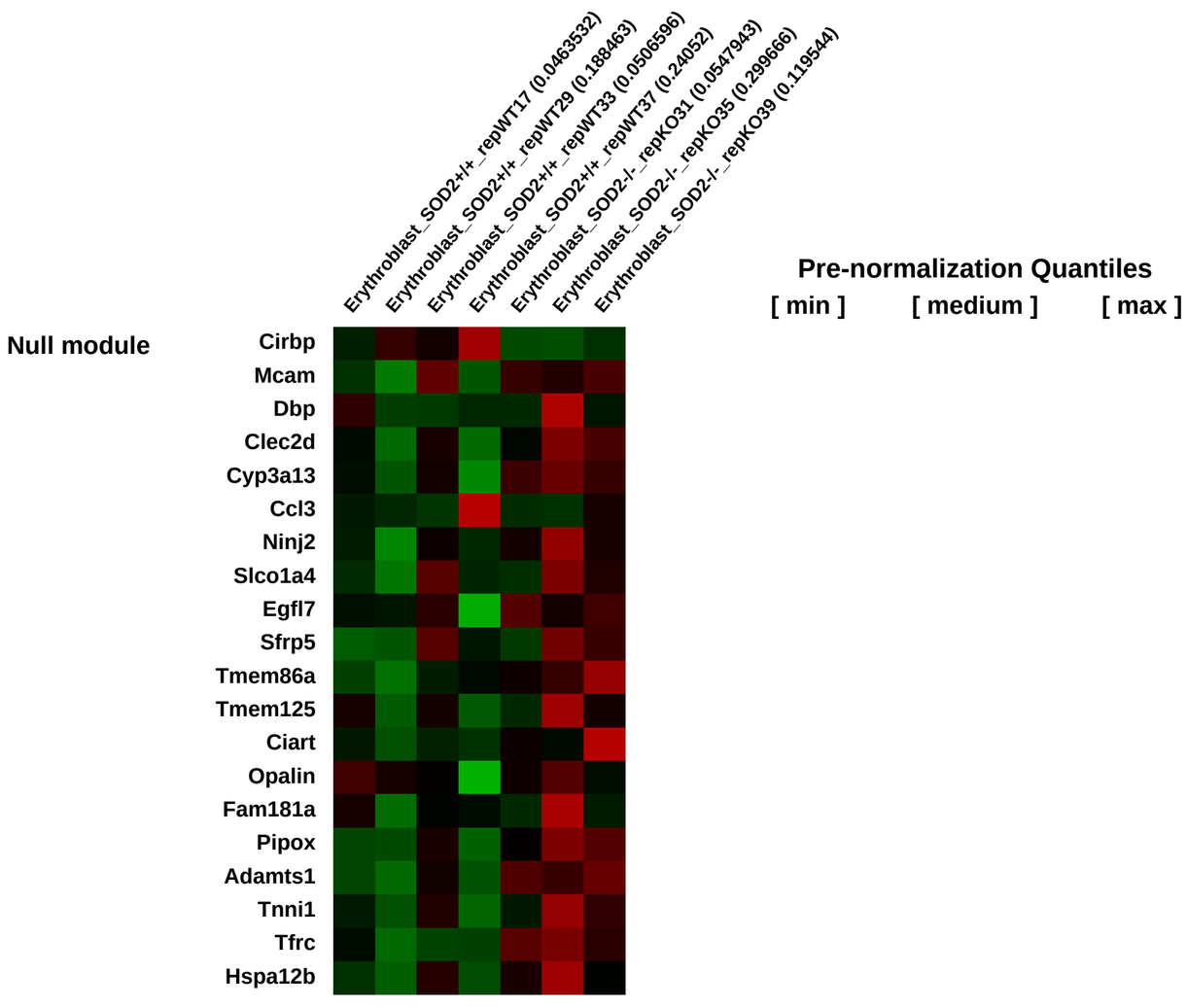

GEO Series "GSE5198" Expression Profiles

Num of samples in this series: 18

Scale of expression profile Z-scores

-3.0 -2.0 -1.0 0.0 1.0 2.0 3.0

GEO Link:	http://www.ncbi.nlm.nih.gov/geo/query/acc.cgi?acc=GSE5198
Status:	Public on Jul 07 2006
Title:	Transcriptional profiling of mouse ileum in response to colonization with a zebrafish or mouse gut microbiota
Organism:	Mus musculus
Experiment type:	Expression profiling by array
Platform:	GPL1261
Pubmed ID:	17055441
Summary & Design:	**Summary:** We compared gene expression in the small intestine (ileum) of mice that were either (i) germ-free, (ii) colonized with a conventional mouse cecal microbiota, (iii) colonized with a conventional zebrafish gut microbiota, or (iv) colonized with Pseudomonas aeruginosa PAO1. **Keywords:** response to microbial colonization **Overall design:** Adult germ-free NMRI mice were colonized with either (i) a conventional mouse cecal microbiota harvested from adult Swiss-Webster mice (5 biological replicates), (ii) a conventional zebrafish intestinal microbiota harvested from adult C32 zebrafish (3 biological replicates), or (iii) a culture of Pseudomonas aeruginosa PAO1 (5 biological replicates). 14 days after colonization, total RNA was prepared from the ileum of each animal, with total RNA prepared from adult germ-free NMRI mouse ileum serving as negative controls (5 biological replicates). RNA was used as template to generate cRNA for hybridization to Affymetrix 430 v2 Mouse GeneChips.

Background corr dist: KL-Divergence = 0.1427, L1-Distance = 0.0373, L2-Distance = 0.0028, Normal std = 0.3795

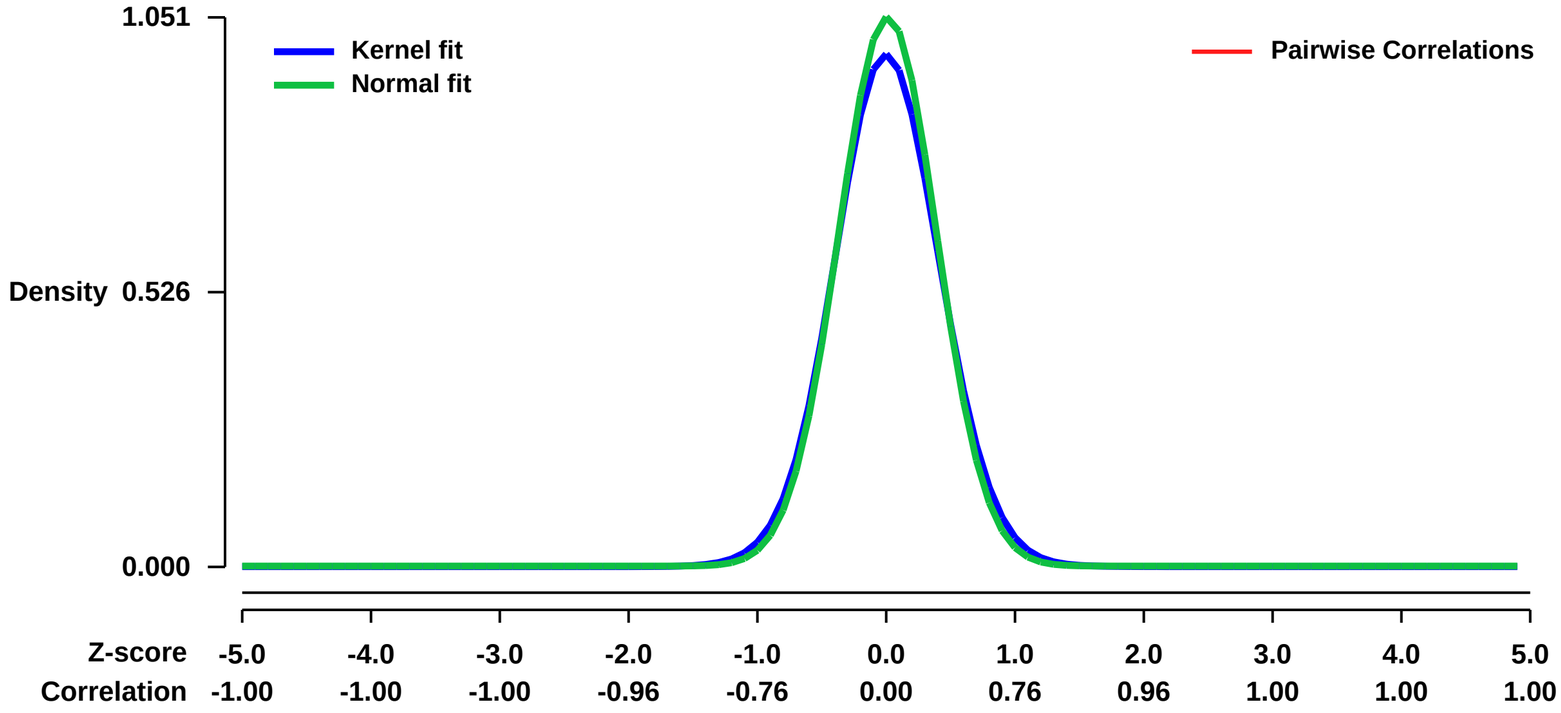

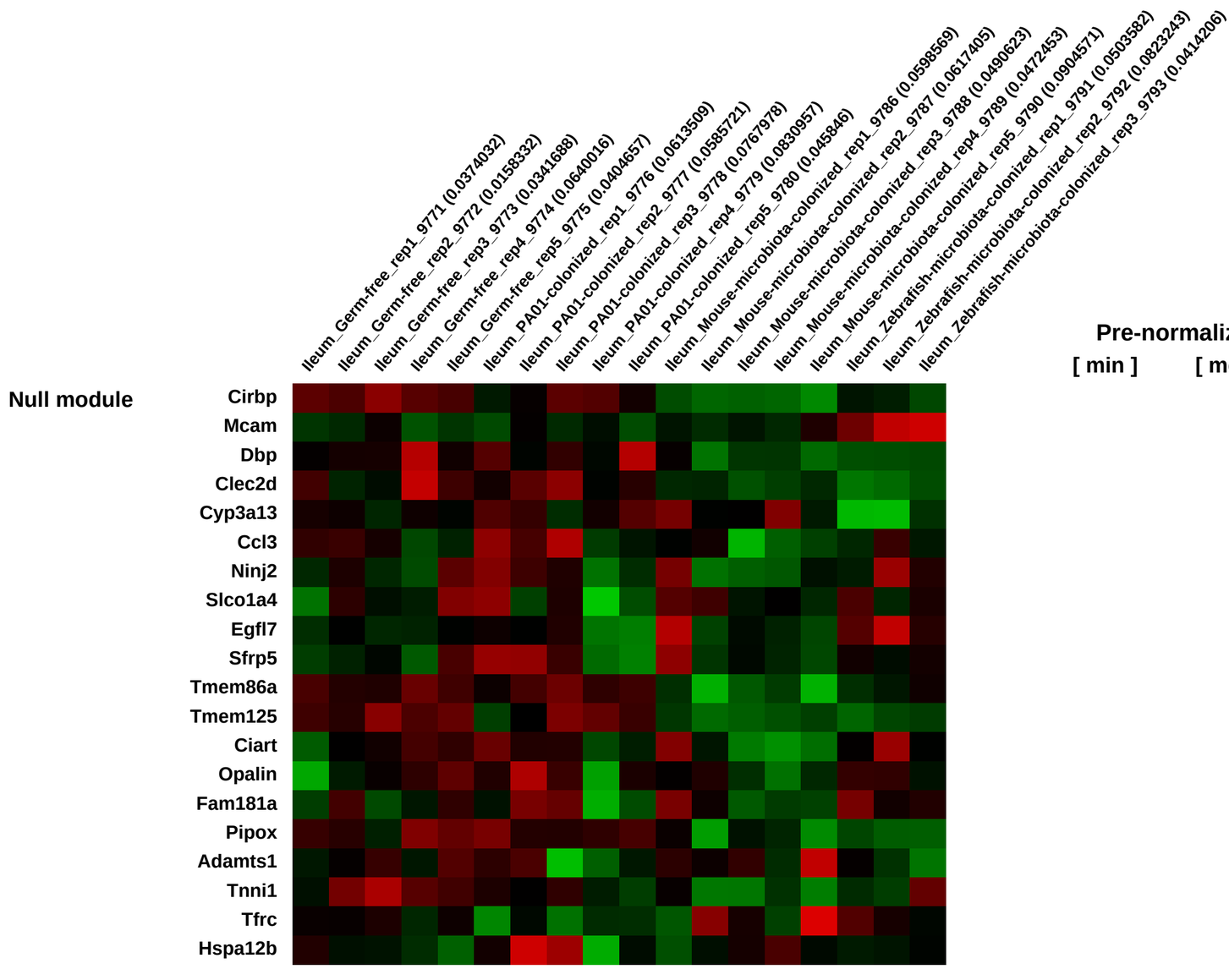

GEO Series "GSE43381" Expression Profiles

Num of samples in this series: 26

Scale of expression profile Z-scores

-3.0 -2.0 -1.0 0.0 1.0 2.0 3.0

GEO Link:	http://www.ncbi.nlm.nih.gov/geo/query/acc.cgi?acc=GSE43381
Status:	Public on Jan 15 2013
Title:	Expression profiling across mouse epithelial tissues
Organism:	Mus musculus
Experiment type:	Expression profiling by array
Platform:	GPL1261
Pubmed ID:	24142692
Summary & Design:	**Summary:** To characterize genes, pathways, and transcriptional regulators enriched in the mouse cornea, we compared the expression profiles of whole mouse cornea, bladder, esophagus, lung, proximal small intestine, skin, stomach, and trachea. **Overall design:** Total RNA was purified from esophagus, lung, proximal small intestine, skin, stomach, and trachea. Data from previous studies in the lab (cornea, GSE43155; bladder, GSE15770; and E18.5 skin, GSE15772) were utilized in the comparison.

Background corr dist: KL-Divergence = 0.0408, L1-Distance = 0.0400, L2-Distance = 0.0029, Normal std = 0.6123

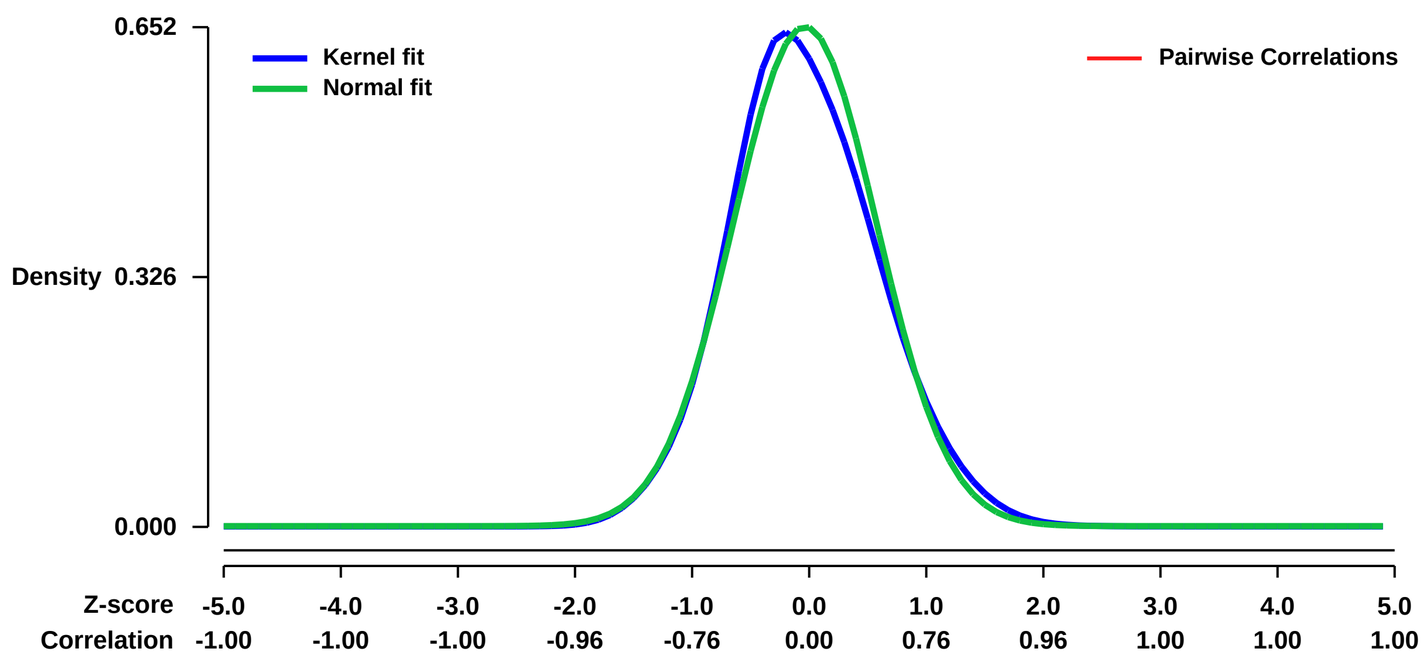

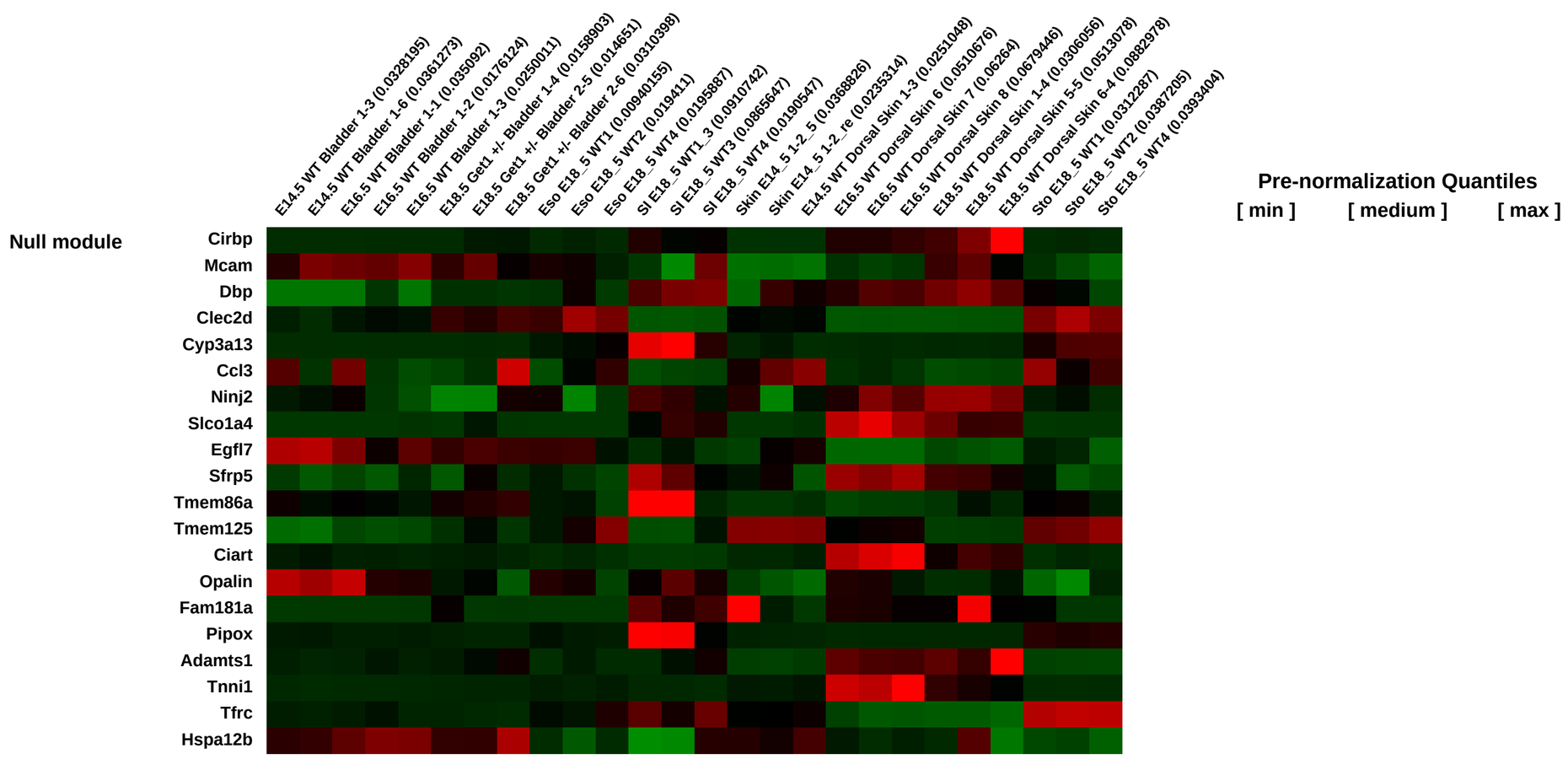

GEO Series "GSE54785" Expression Profiles

Num of samples in this series: 6

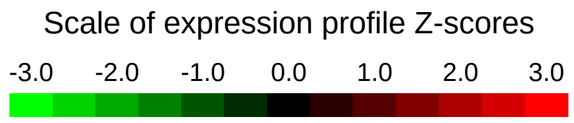

GEO Link:	http://www.ncbi.nlm.nih.gov/geo/query/acc.cgi?acc=GSE54785
Status:	Public on Feb 08 2014
Title:	The acetylome regulators Hdac1 and Hdac2 differently modulate intestinal epithelial cell dependent homeostatic responses in experimental colitis
Organism:	Mus musculus
Experiment type:	Expression profiling by array
Platform:	GPL1261
Pubmed ID:	24525021

Summary & Design:

Summary:
Histone deacetylases (Hdac) remove acetyl groups from proteins, influencing global and specific gene expression. Hdacs control inflammation, as shown by Hdac inhibitor-dependent protection from DSS-induced murine colitis. While tissue-specific Hdac knockouts show redundant and specific functions, little is known of their intestinal epithelial cell (IEC) role. We have shown previously that dual Hdac1/Hdac2 IEC-specific loss disrupts cell proliferation and determination, with decreased secretory cell numbers and altered barrier function. We thus investigated how compound Hdac1/Hdac2 or Hdac2 IEC-specific deficiency alters the inflammatory response. Floxed Hdac1 and Hdac2 and villin-Cre mice were interbred. Compound Hdac1/Hdac2 IEC-deficient mice showed chronic basal inflammation, with increased basal Disease Activity Index (DAI) and deregulated Reg gene colonic expression. DSS-treated dual Hdac1/Hdac2 IEC-deficient mice displayed increased DAI, histological score, intestinal permeability and inflammatory gene expression. In contrast to double knockouts, Hdac2 IEC-specific loss did not affect IEC determination and growth, nor result in chronic inflammation. However, Hdac2 disruption protected against DSS colitis, as shown by decreased DAI, intestinal permeability and caspase-3 cleavage. Hdac2 IEC-specific deficient mice displayed increased expression of IEC gene subsets, such as colonic antimicrobial Reg3b and Reg3g mRNAs, and decreased expression of immune cell function-related genes. Our data show that Hdac1 and Hdac2 are essential IEC homeostasis regulators. IEC-specific Hdac1 and Hdac2 may act as epigenetic sensors and transmitters of environmental cues and regulate IEC-mediated mucosal homeostatic and inflammatory responses. Different levels of IEC Hdac activity may lead to positive or negative outcomes on intestinal homeostasis during inflammation

Overall design:
Total RNAs from the colon of three control and three Hdac2 IEC-specific knockout mix background (CD-1/129/C57BL/6) mice were isolated with the Rneasy kit (Qiagen, Mississauga, ON, Canada).

Background corr dist: KL-Divergence = 0.0343, L1-Distance = 0.0202, L2-Distance = 0.0004, Normal std = 0.6501

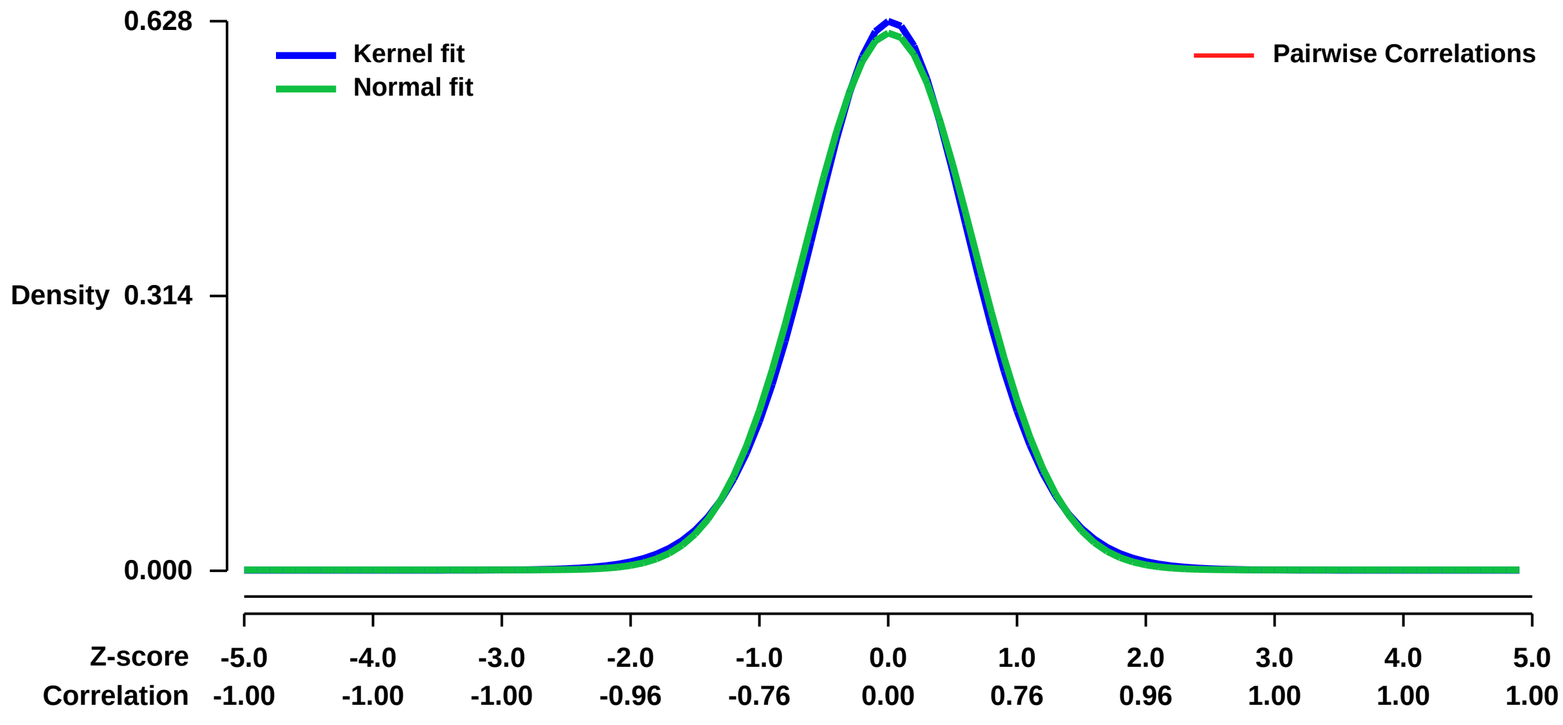

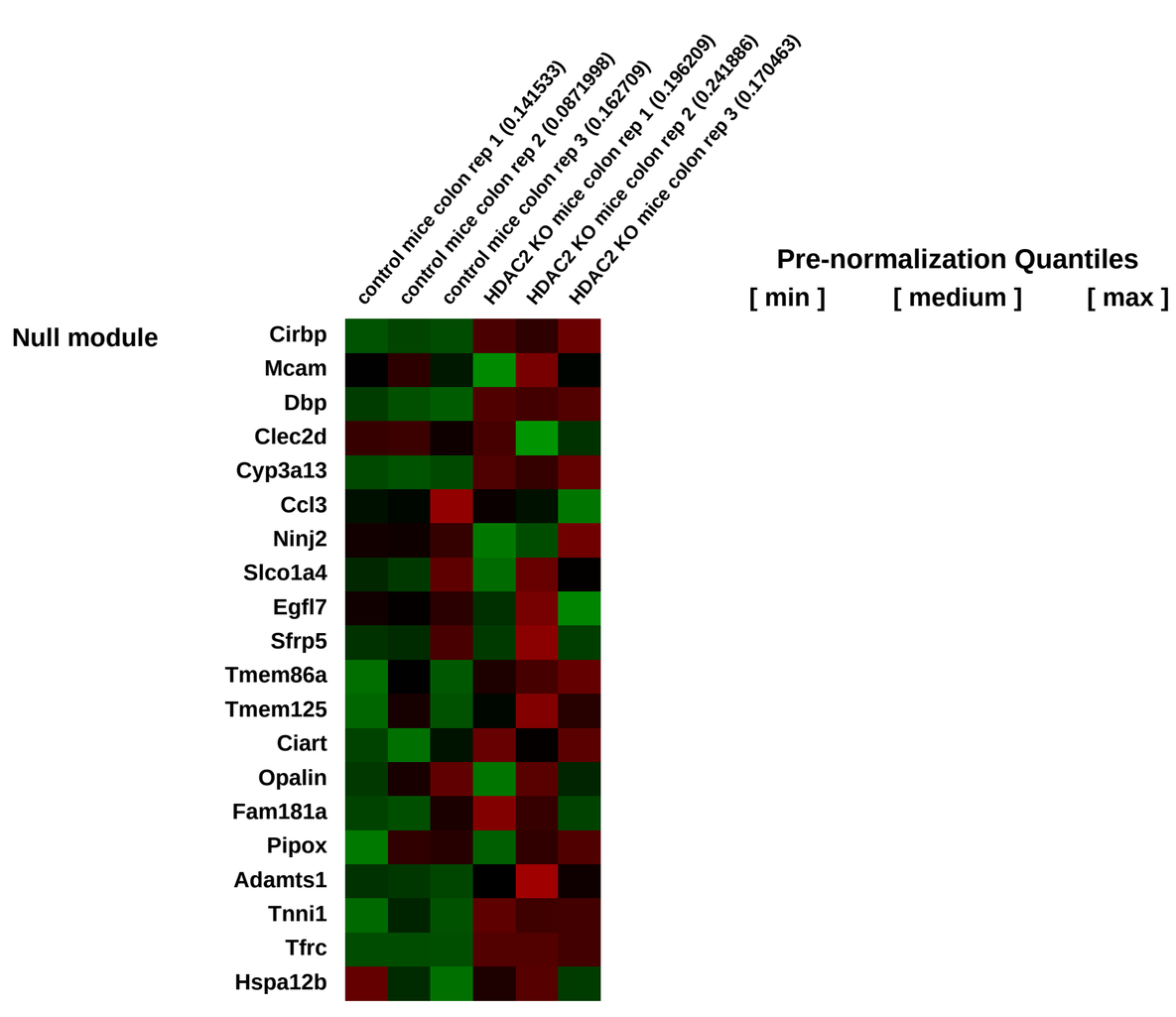

GEO Series "GSE10954" Expression Profiles

Num of samples in this series: 8

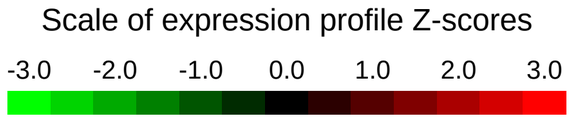

GEO Link:	http://www.ncbi.nlm.nih.gov/geo/query/acc.cgi?acc=GSE10954
Status:	Public on May 31 2008
Title:	Transcription Profiling of Lung Adenocarcinomas of c-Myc-Transgenic Mice
Organism:	Mus musculus
Experiment type:	Expression profiling by array
Platform:	GPL1261
Pubmed ID:	18498649
Summary & Design:	**Summary:** The transcriptional regulator c-Myc is the most frequently deregulated oncogene in human tumors. Targeted overexpression of this gene in mice results in distinct types of lung adenocarcinomas. By using microarray technology, alterations in the expression of genes were captured based on a female transgenic mouse model in which, indeed, c-Myc overexpression in alveolar epithelium results in the development of bronchiolo-alveolar carcinoma (BAC) and papillary adenocarcinoma (PLAC). In this study, we analyzed exclusively the promoters of induced genes by different in silico methods in order to elucidate the c-Myc transcriptional regulatory network. Keywords: c-myc transgenic versus non-transgenic **Overall design:** For gene expression analysis, RNA was isolated from lung tissue of either 16 c-Myc-transgenic or 16 non-transgenic control female mice. Identical amounts of RNA from 4 individuals of one group were pooled, such that 4 pools of 4 mice per group could be analyzed. Each pool was analysed in one microarray experiment.

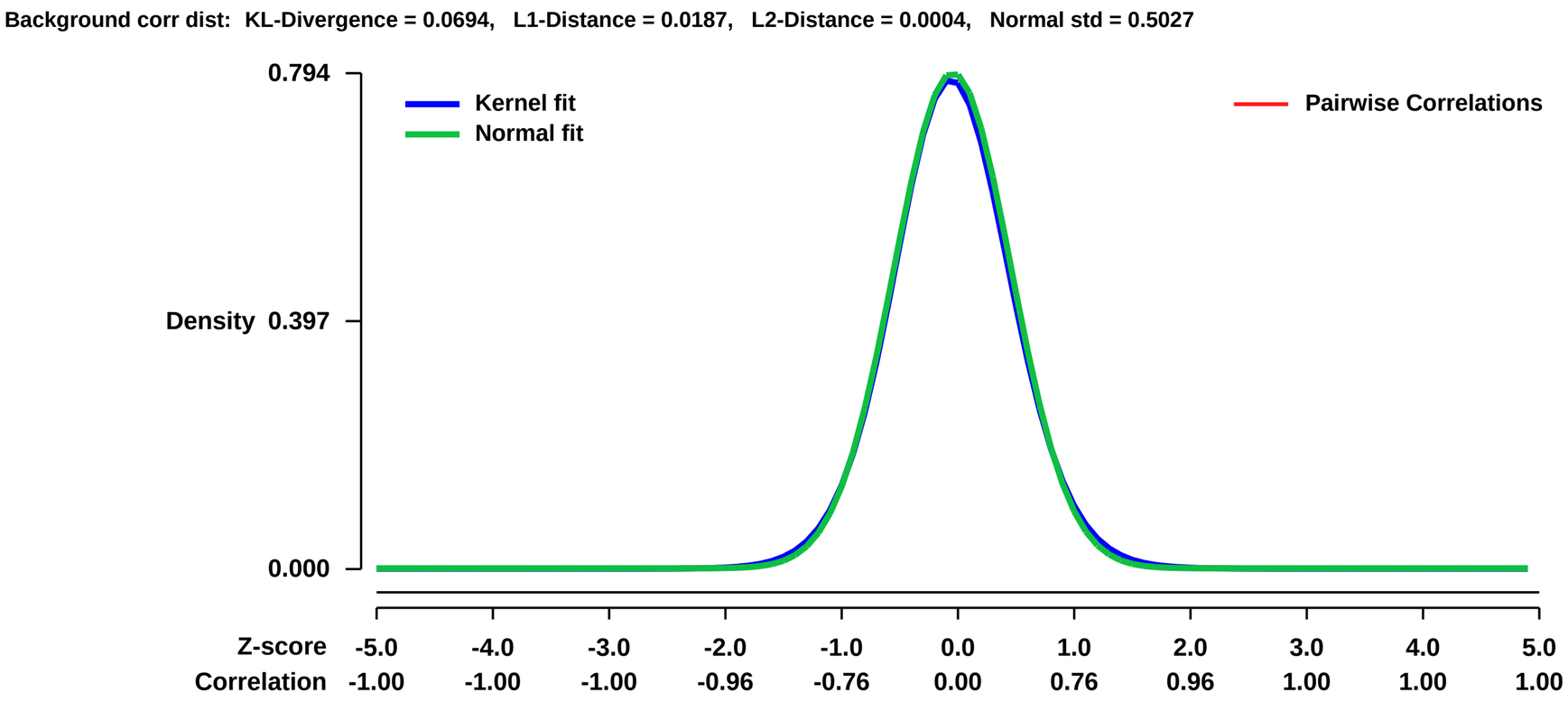

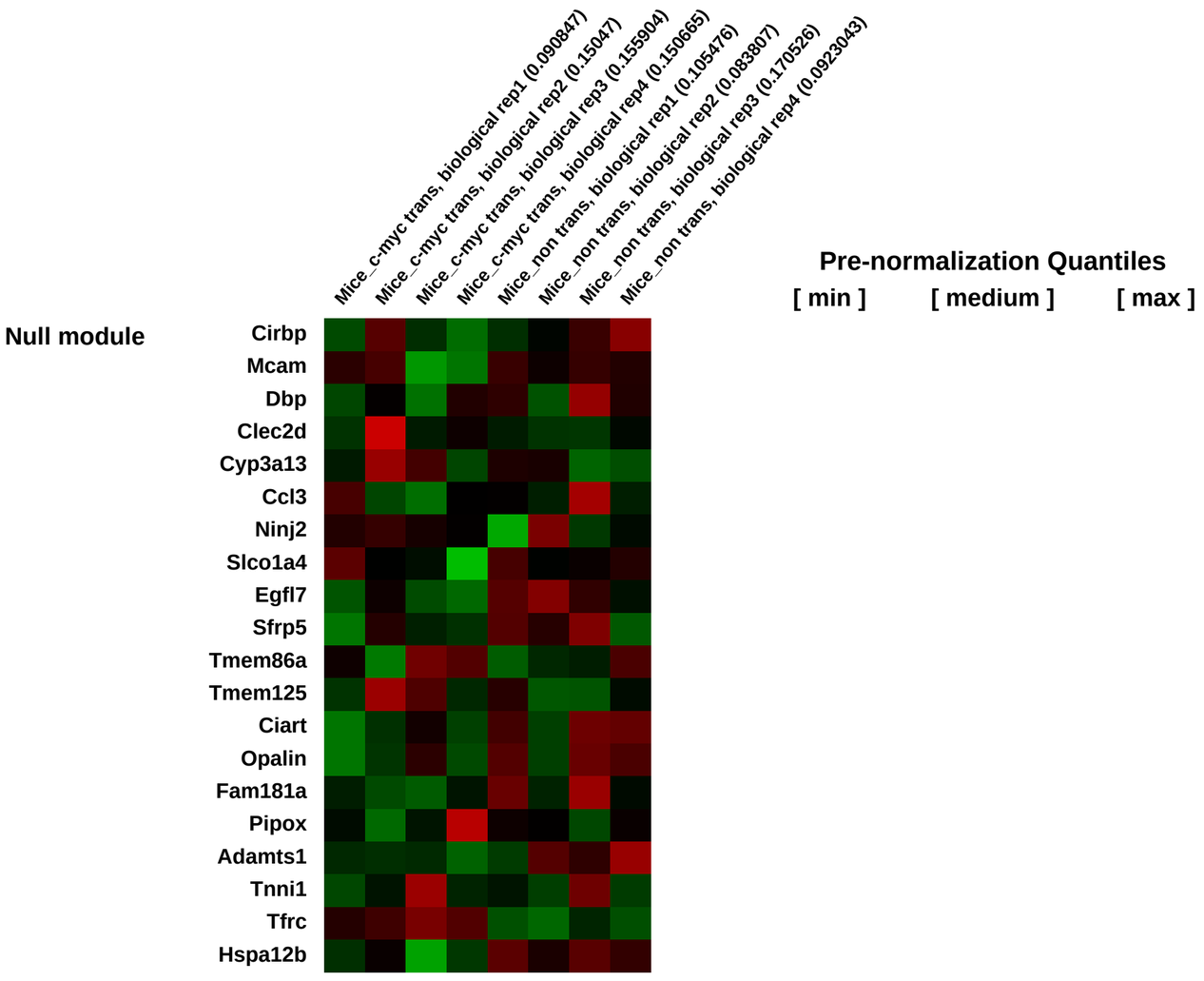

GEO Series "GSE23782" Expression Profiles

Num of samples in this series: 18

Scale of expression profile Z-scores

-3.0 -2.0 -1.0 0.0 1.0 2.0 3.0

GEO Link:	http://www.ncbi.nlm.nih.gov/geo/query/acc.cgi?acc=GSE23782
Status:	Public on Sep 15 2010
Title:	Adult epidermal Notch activity induces dermal accumulation of stromal cells
Organism:	Mus musculus
Experiment type:	Expression profiling by array
Platform:	GPL1261
Pubmed ID:	20940224
Summary & Design:	**Summary:** **K14NICDER transgenic and wildtype littermate mice were treated with 4OHT for 14 days to activate the transgene** **Epidermis and dermis preparations from Transgenic and Wild type mice plus whole skin** **Overall design:** **We sought to compare gene expression patterns in K14NICDER transgenic epidermis and dermis to wild type controls**

Background corr dist: **KL-Divergence = 0.0858, L1-Distance = 0.0370, L2-Distance = 0.0027, Normal std = 0.4638**

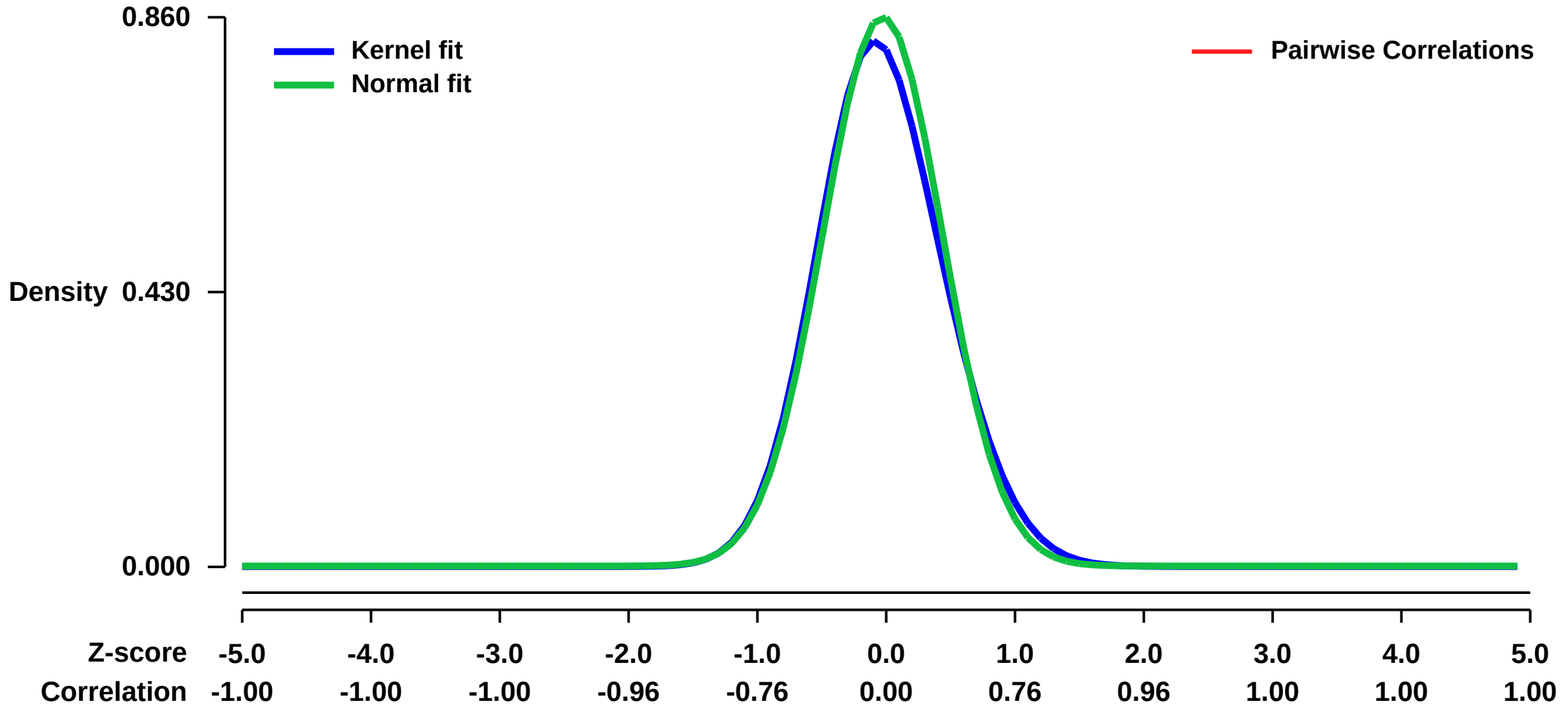

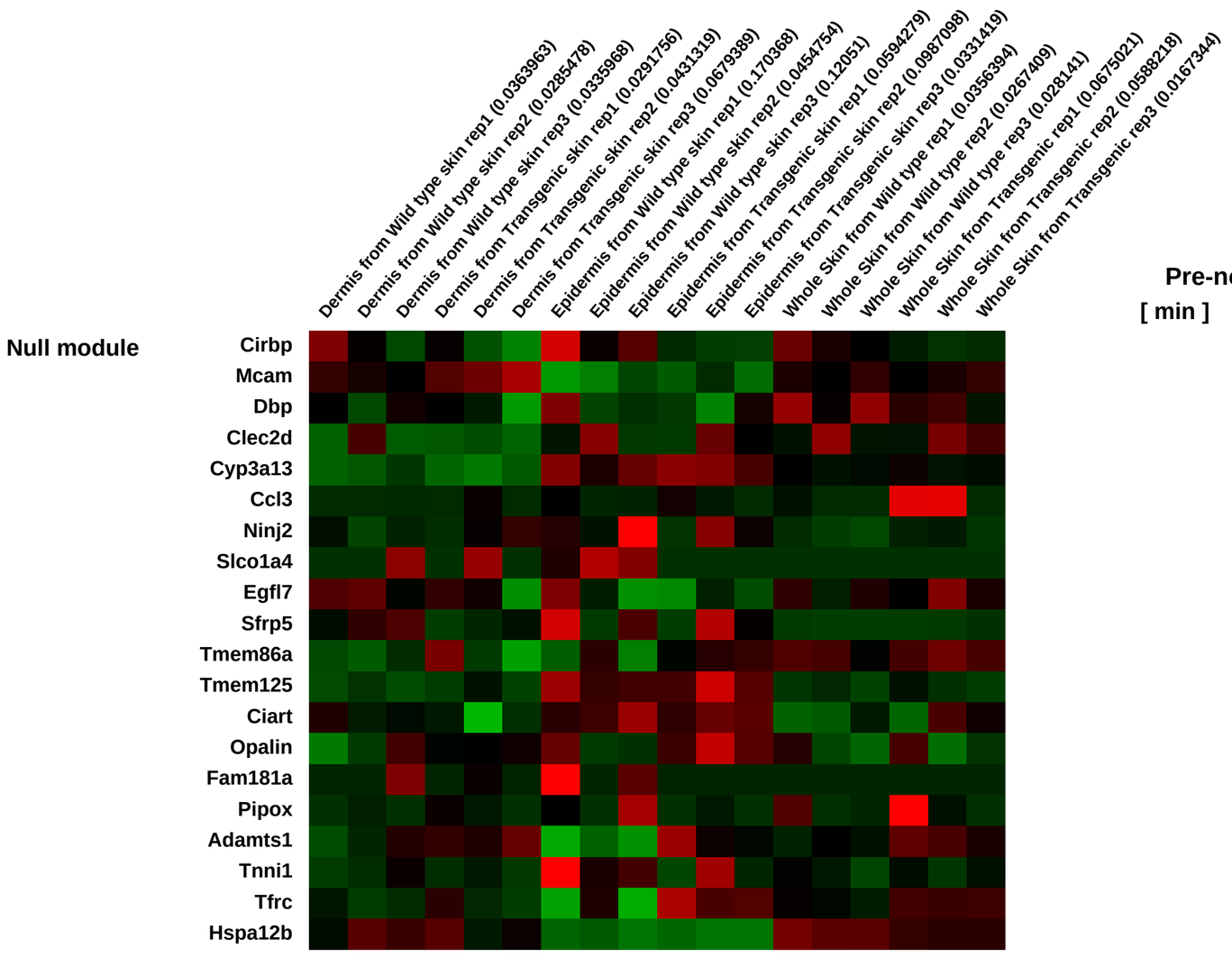

GEO Series "GSE23398" Expression Profiles

Num of samples in this series: 7

Scale of expression profile Z-scores

-3.0 -2.0 -1.0 0.0 1.0 2.0 3.0

GEO Link:	http://www.ncbi.nlm.nih.gov/geo/query/acc.cgi?acc=GSE23398
Status:	Public on Sep 18 2012
Title:	IL-2 regulated genes in scurfy CD4+ T-cells
Organism:	Mus musculus
Experiment type:	Expression profiling by array
Platform:	GPL1261
Pubmed ID:	21169543
Summary & Design:	**Summary:** The goal of the study was to identify the genes which are regulated by Interleukin-2 in the CD4+ T cells of the scurfy mice during regulatory T-cell deficiency. Scurfy (Sf) mice bear a mutation in the forkhead box P3 (Foxp3) transcription factor, lack regulatory T-cells (Treg), develop multi-organ inflammation, and die prematurely. The major target organs affected are skin, lungs, and liver. Sf mice lacking the Il2 gene (Sf.Il2-/-), despite devoid of Treg, did not develop skin and lung inflammation, but the inflammation in liver, pancreas, submandibular gland and colon remained. Genome-wide microarray analysis revealed hundreds of genes were differentially regulated among Sf, Sf.Il2-/-, and B6 CD4+ T-cells but the most changes were those encoding receptors for trafficking/chemotaxis/retention and lymphokines. Our study suggests that IL-2 controls the skin and lung inflammation in Sf mice in an apparent ""organ-specific"" manner through two novel mechanisms: by regulating the expression of genes encoding receptors for T-cell trafficking/chemotaxis/retention and by regulating Th2 cell expansion and lymphokine production. Thus, IL-2 is a master regulator for multi-organ inflammation and an underlying etiological factor for various diseases associated with skin and lung inflammation. Methods: CD4+ T cells were purified by Fluorescence Assisted Cell Sorting from the peripheral lymph nodes of (A) three individual Scurfy (Sf; B6.Cg-Foxp3sf/J) male mice, (B) three individual Sf.Il2-/- male mice (Scurfy mice carrying a null Interleukin (IL)-2 gene (B6.129P2-Il2tm1Hor/J)) and (C) a pooled sample of lymph nodes from two B6 (C57BL/6J) mice. All the mice were 3 weeks old. Total RNA was prepared using RNeasy mini kit (Qiagen). RNA samples were converted to cRNA, labeled and hybridized to Affymetrix Mouse 430_2 chips (Mouse Genome 430 2.0 Array, Affymetrix, Santa Clara, CA) at the University of Virginia DNA Sciences Core Facility. **Overall design:** 3. RNA from CD4+ T cells purified from peripheral lymph nodes of Sf.Il2-/- mice - 3 biological replicates.

Background corr dist: KL-Divergence = 0.0394, L1-Distance = 0.0267, L2-Distance = 0.0011, Normal std = 0.6124

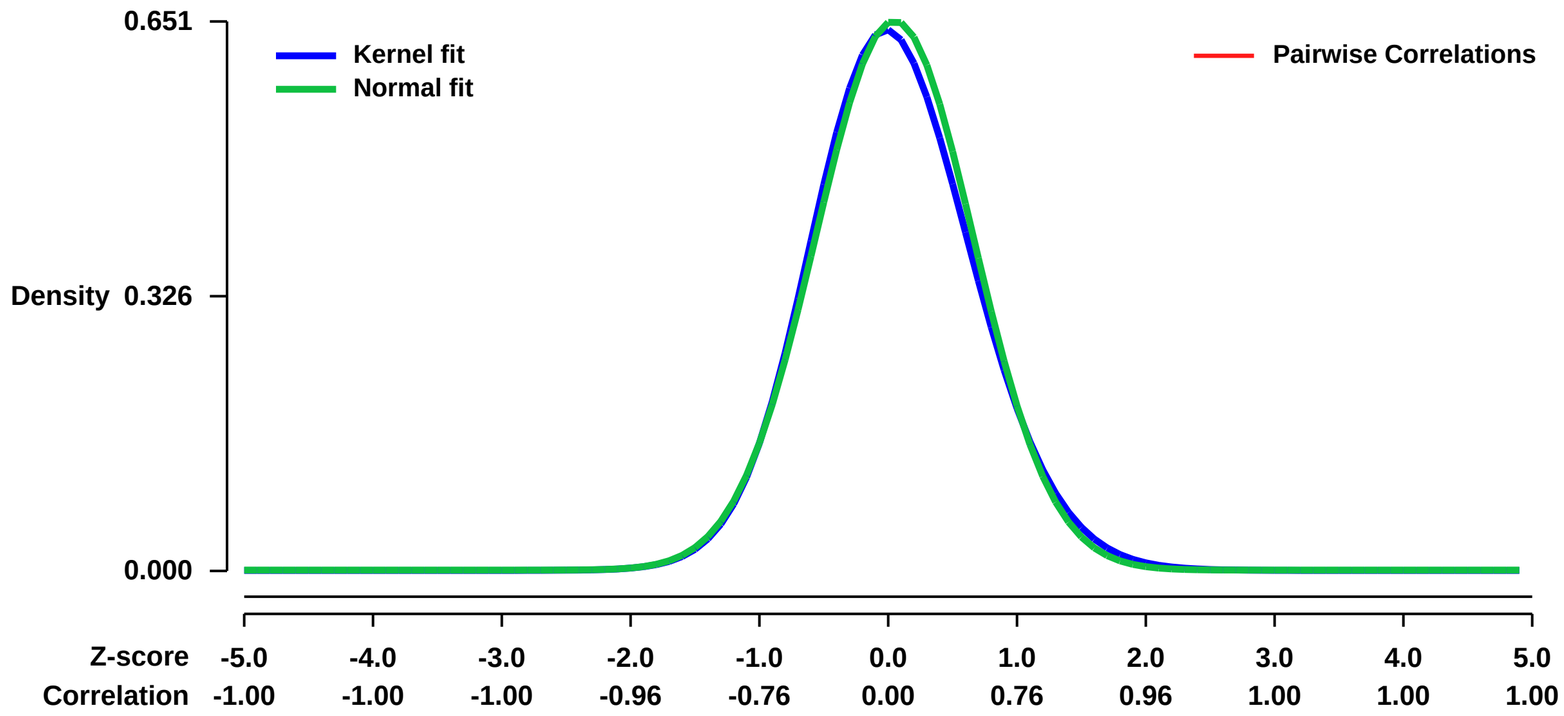

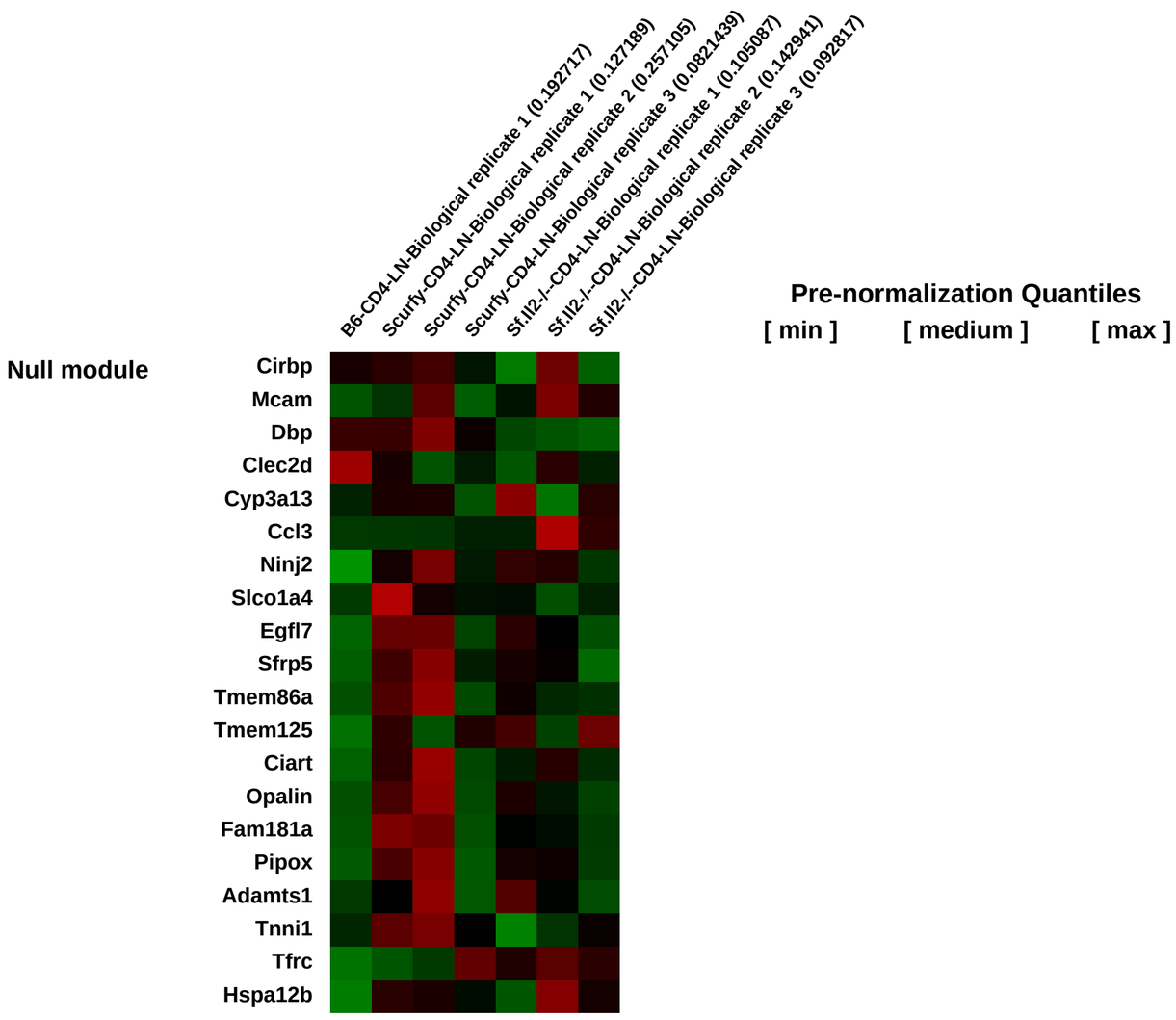

GEO Series "GSE5786" Expression Profiles

Num of samples in this series: 6

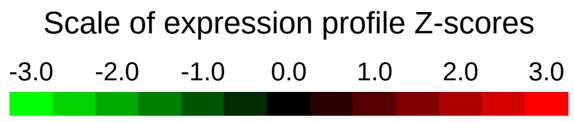

GEO Link:	http://www.ncbi.nlm.nih.gov/geo/query/acc.cgi?acc=GSE5786
Status:	Public on Oct 05 2006
Title:	Gene Expression Profiling of PGC-1a KO mouse striata
Organism:	Mus musculus
Experiment type:	Expression profiling by array
Platform:	GPL1261
Pubmed ID:	17018277
Summary & Design:	**Summary:** Huntingtonâ s Disease (HD) is an inherited neurodegenerative disease caused by a glutamine repeat expansion in huntingtin protein. Transcriptional deregulation and altered energy metabolism have been implicated in HD pathogenesis. We report here that mutant huntingtin causes disruption of mitochondrial function by inhibiting expression of PGC-1a, a transcriptional coactivator that regulates several metabolic processes including mitochondrial biogenesis and respiration. Mutant huntingtin represses PGC-1a gene transcription by associating with the promoter and interfering with the CREB/TAF4-dependent transcriptional pathway critical for the regulation of PGC-1a gene expression. Crossbreeding of PGC-1a knockout mice with HD knock-in mice leads to increased neurodegeneration of striatal neurons and motor abnormalities in the HD mice. Importantly, expression of PGC-1a partially reverses the toxic effects of mutant huntingtin in cultured striatal neurons. Moreover, lentiviral-mediated delivery of PGC-1a in the striatum provides neuroprotection in the transgenic HD mice. These studies suggest a key role for PGC-1a in the control of energy metabolism in the early stages of HD pathogenesis. **Keywords: PGC-1a, striatum** **Overall design:** Total RNA was extracted from striata of 3 pgc1¸– KO mice and 3 littermate controls using the RNeasy Mini Kit (Qiagen) according to manufacturerâ s protocol. Samples were analyzed using RNA 6000 Nano LabChip kit on a 2100 Bioanalyzer (Agilent Technologies) to ensure integrity of RNA.

Background corr dist: KL-Divergence = 0.0498, L1-Distance = 0.0184, L2-Distance = 0.0004, Normal std = 0.5732

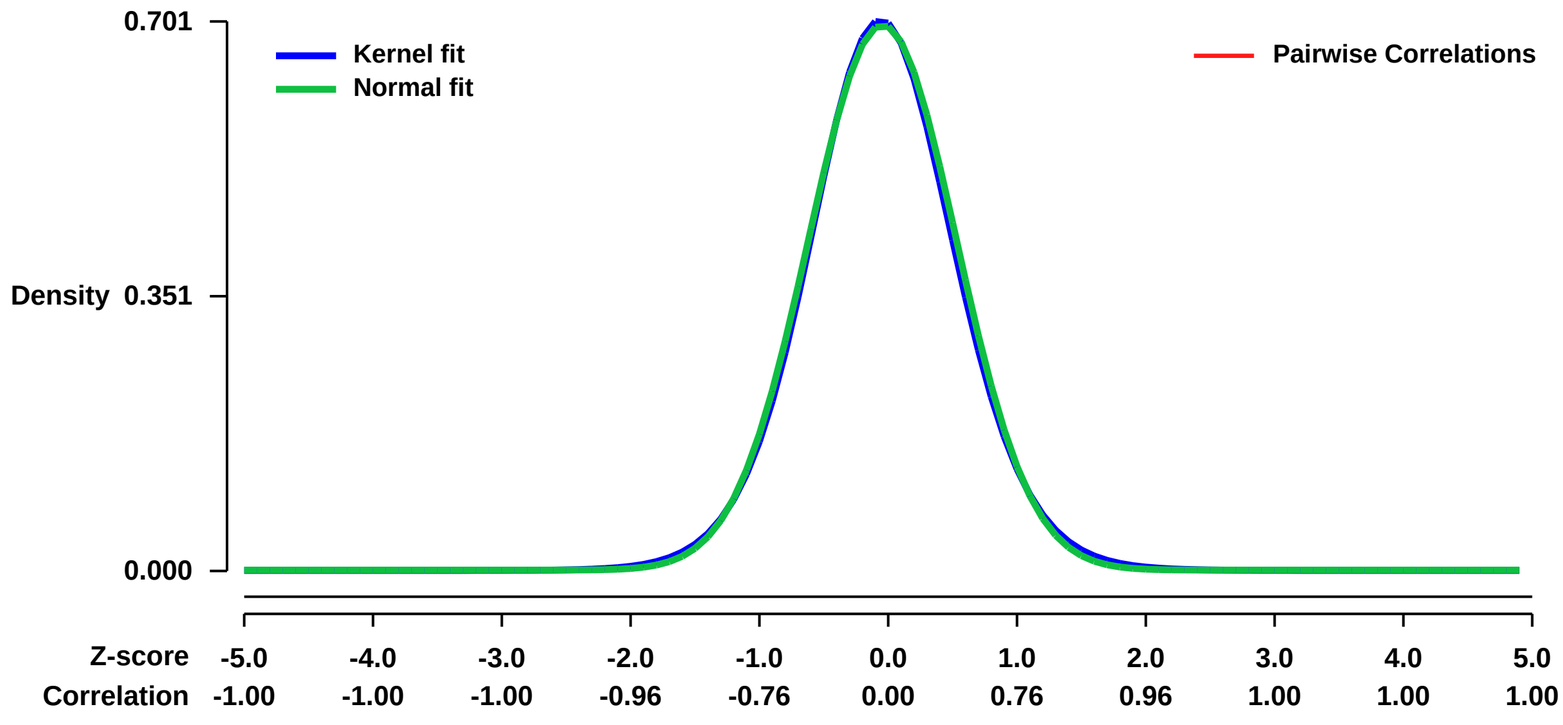

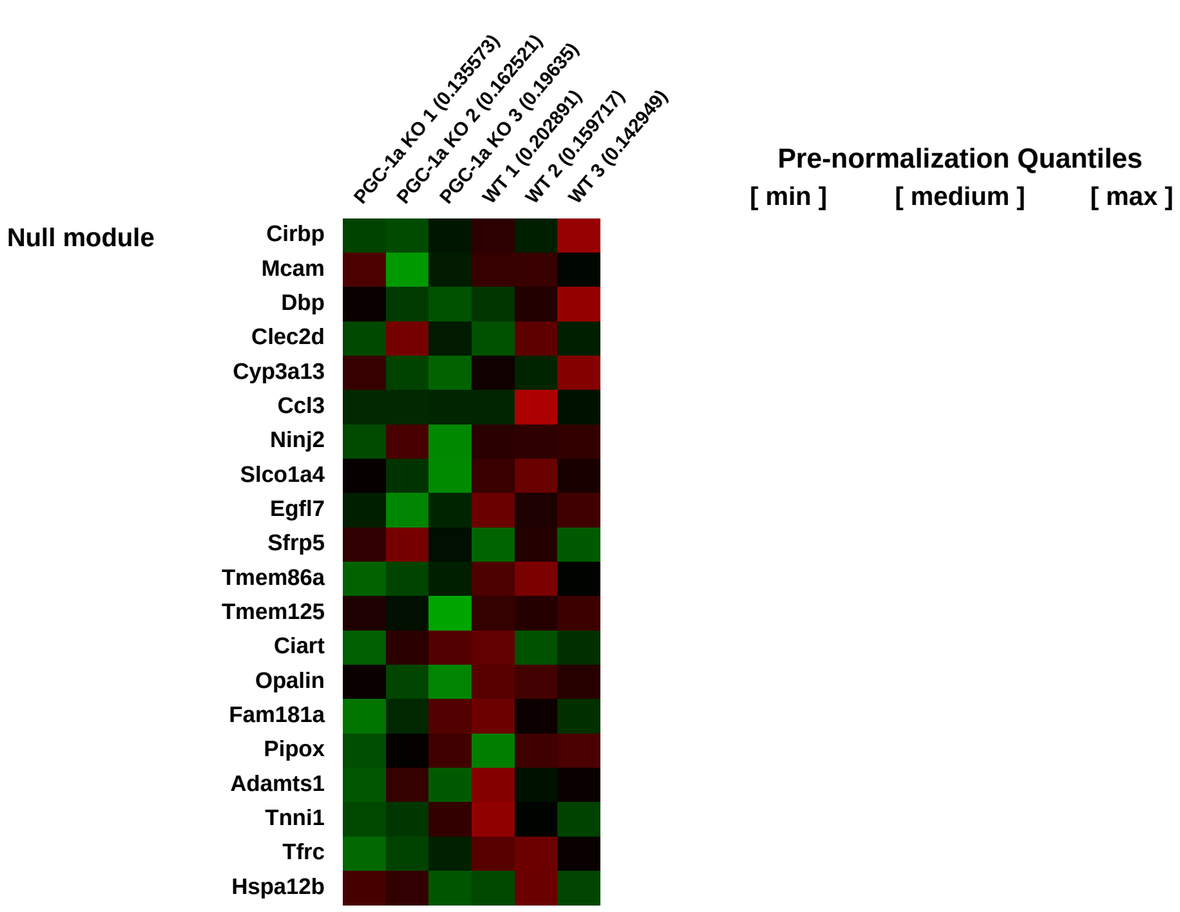

GEO Series "GSE28408" Expression Profiles

Num of samples in this series: 6

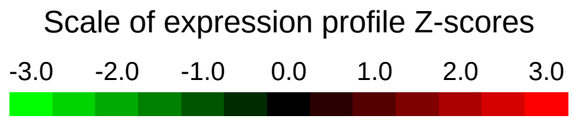

GEO Link:	**http://www.ncbi.nlm.nih.gov/geo/query/acc.cgi?acc=GSE28408**
Status:	**Public on Feb 01 2013**
Title:	**Expression data from Ly6G+ and Ly6G- dendritic cells (DC)**
Organism:	**Mus musculus**
Experiment type:	**Expression profiling by array**
Platform:	**GPL1261**
Pubmed ID:	**23305731**
Summary & Design:	**Summary:** **To investigate the functional properties of Ly6G+ DC, we employed GeneChip analysis to compare the gene expression profiles between Ly6G+ DC and Ly6C- DC.** **Overall design:** **Crude bone marrow (BM) cells prepared from C57BL/6 mice were cultured in the presence of GM-CSF. On day 6, CD11c+/MHC II+/Ly6G+ cells and CD11c+/MHC II+/Ly6G- cells were simultaneously sorted from the same cultures by FACSAria. Total RNA were extracted and hybridized on Affymetrix microarrays.**

Background corr dist: **KL-Divergence = 0.0392, L1-Distance = 0.0299, L2-Distance = 0.0012, Normal std = 0.6277**

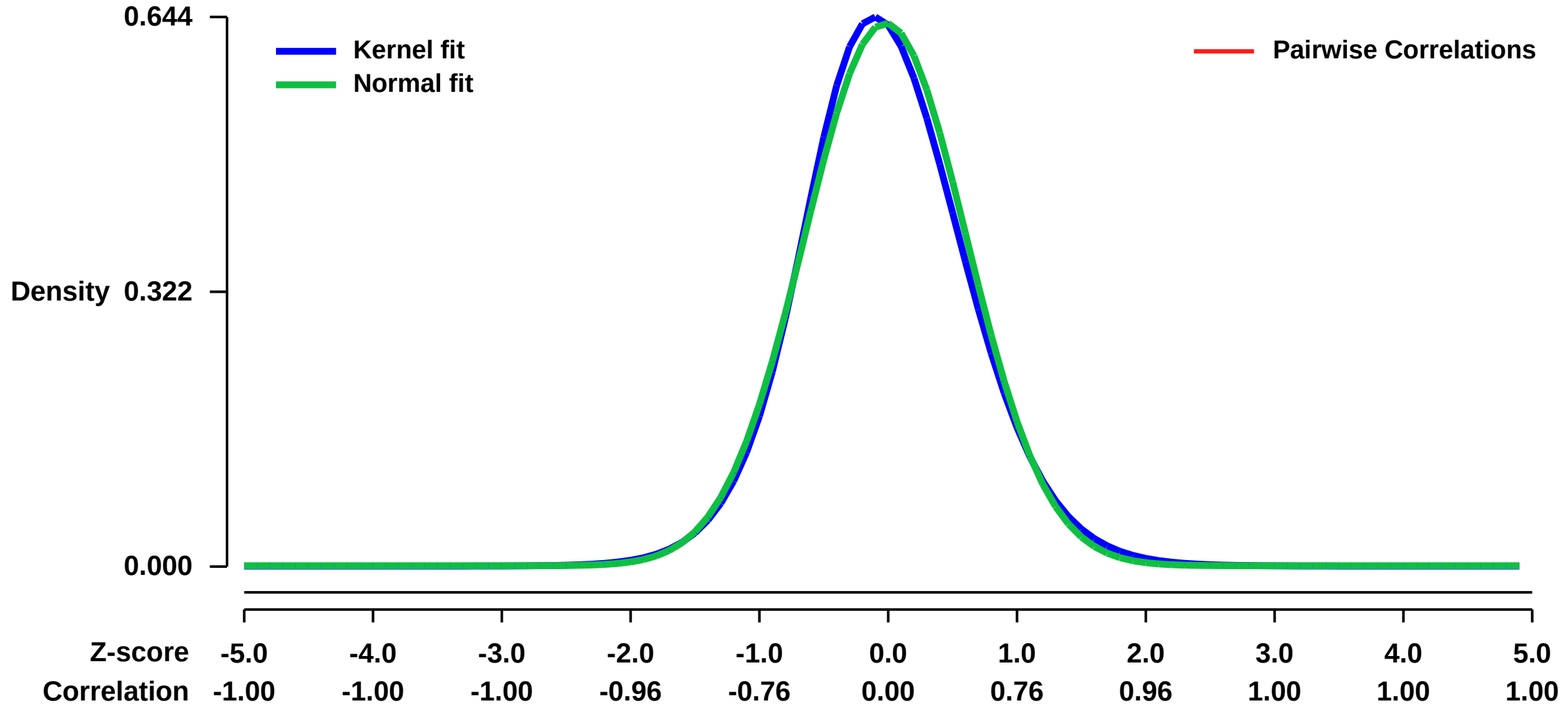

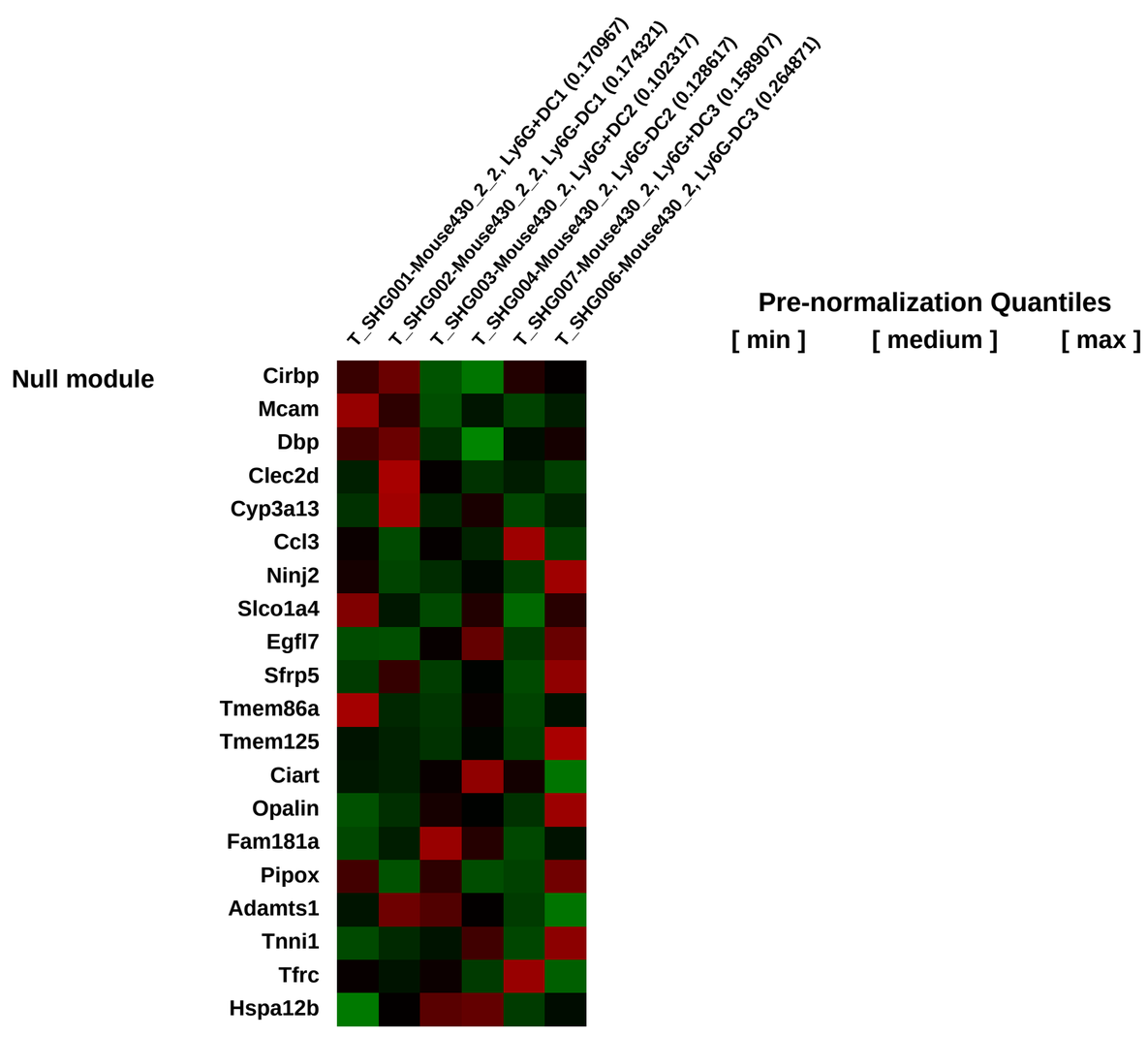

GEO Series "GSE35761" Expression Profiles

Num of samples in this series: 6

Scale of expression profile Z-scores

-3.0 -2.0 -1.0 0.0 1.0 2.0 3.0

GEO Link:	http://www.ncbi.nlm.nih.gov/geo/query/acc.cgi?acc=GSE35761
Status:	Public on Jun 01 2012
Title:	Effect of fluoxetine treatment on translational profiles of S100a10 cortical pyramidal cells
Organism:	Mus musculus
Experiment type:	Expression profiling by array
Platform:	GPL1261
Pubmed ID:	22632977
Summary & Design:	**Summary:** Molecular phenotyping of cell types and neural circuits underlying pathological neuropsychiatric conditions and their responses to therapy provides one avenue for the development of more specific and effective treatments. In this study, we identify a cell population in the cerebral cortex that shows robust and specific molecular adaptations following long-term SSRI treatment. We employed the bacTRAP strategy, which uses BAC transgenic mice expressing EGFP-tagged ribosomal protein L10a in specific cell populations, to affinity purify polysome-bound mRNAs from S100a10-expressing corticostriatal projection neurons. We show that the S100a10 cells are a unique population of cortical cells that are strongly and specifically responsive to chronic SSRI administration and that this response requires p11 (the protein product of S100a10). Our data demonstrate that the beneficial actions of antidepressant therapy can be mediated by a single cell type that is positioned to normalize activity between cortical and subcortical sites, and suggest that development of drugs that specifically target the activity of these cells may result in improved therapies to treat depression. **Overall design:** S100a10 bacTRAP mice were administered either fluoxetine (FLX) or vehicle (VEH) in their drinking water for 15-18 days. Three independent TRAP replicates from the cortex of each group were then collected. Total RNA from the immunoprecipitates was amplified and hybridized. Data were normalized with the GCRMA algorithm and replicates were averaged across conditions. We recommend filtering data to remove probe sets with normalized expression values less than 50 in at least one condition. Because the S100a10 BAC labels some non-neuronal cells, we recommend only probe sets listed in Table S1 of the accompanying paper be included in the analysis.

Background corr dist: KL-Divergence = 0.0516, L1-Distance = 0.0503, L2-Distance = 0.0038, Normal std = 0.6364

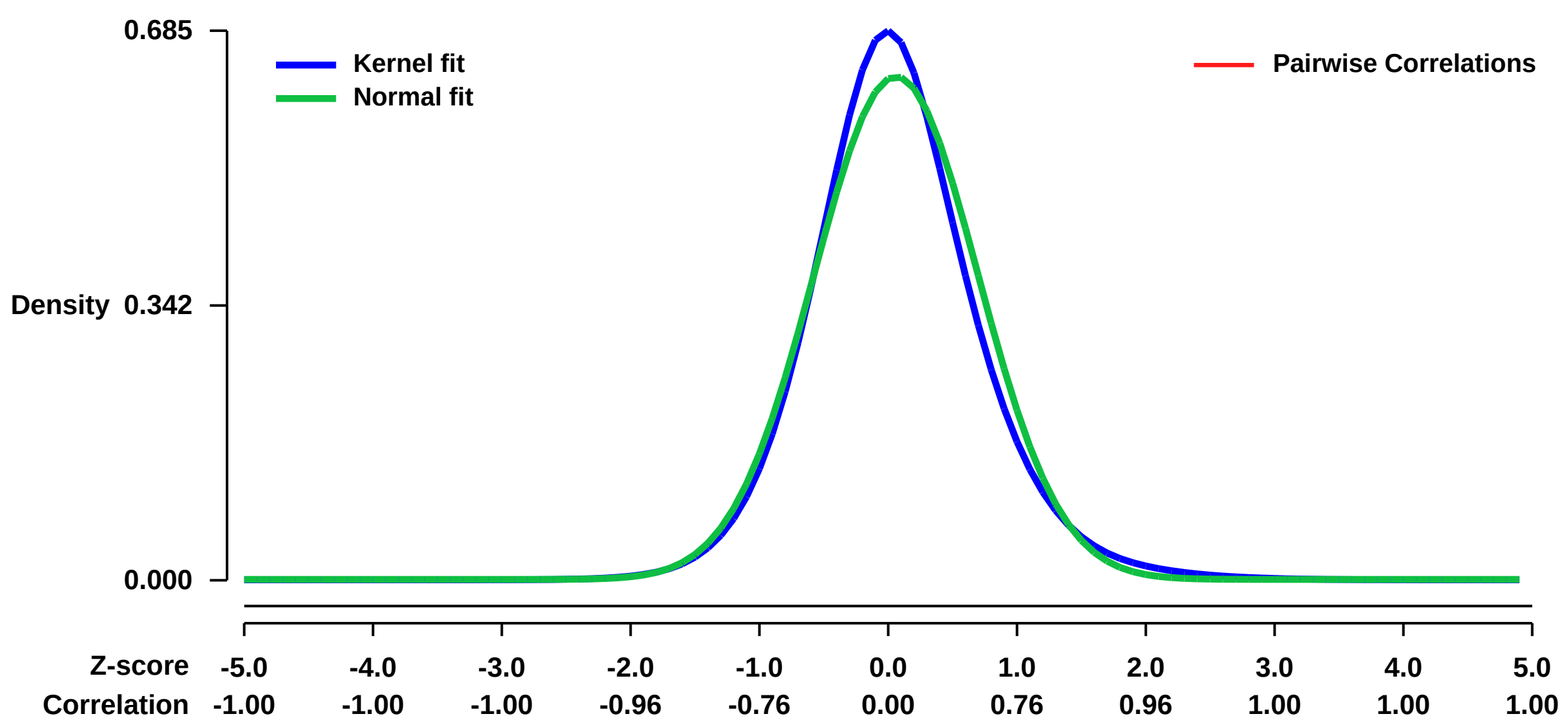

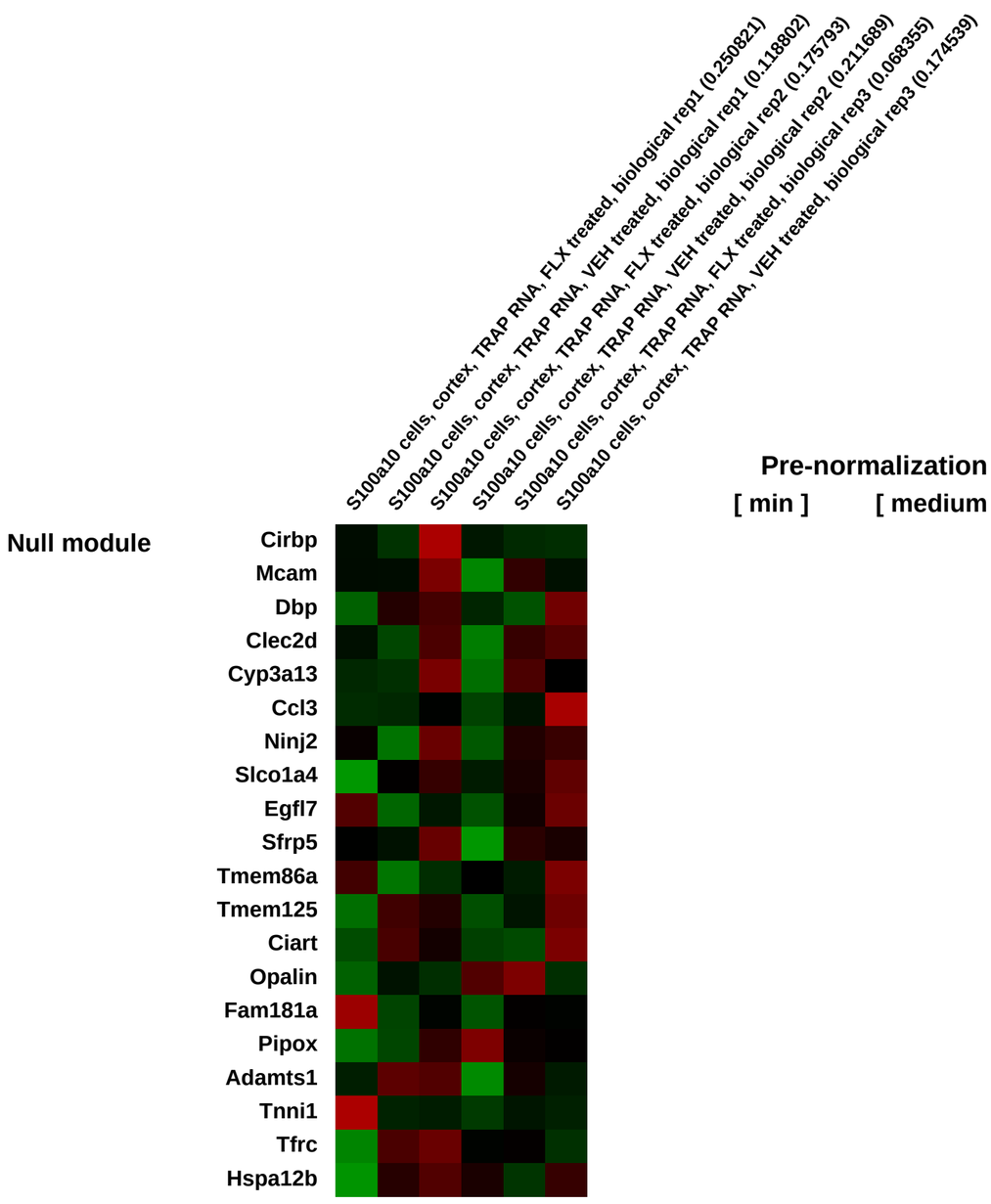

GEO Series "GSE59319" Expression Profiles

Num of samples in this series: 6

Scale of expression profile Z-scores

-3.0 -2.0 -1.0 0.0 1.0 2.0 3.0

GEO Link:	**http://www.ncbi.nlm.nih.gov/geo/query/acc.cgi?acc=GSE59319**
Status:	**Public on Jul 11 2014**
Title:	**Expression data of LPS-stimulated macrophages in wild-type and LysM-Cre+;Akirin2fl/fl mice**
Organism:	**Mus musculus**
Experiment type:	**Expression profiling by array**
Platform:	**GPL1261**
Pubmed ID:	
Summary & Design:	**Summary:** **Akirin2 is an evolutionally conserved nuclear protein involved in the regulation of a set of inflammatory gene expression in various cell types.** **We used microarrays to examine the effect of Akirin2 deficiency in LPS-inducible gene expression in macrophages** **Overall design:** **Peritoneal macrophages from wild-type and LysM-Cre+;Akirin2fl/fl mice were stimulated with LPS for 0, 2 and 4 hours, followed by RNA extraction and microarray analysis.**

Background corr dist: **KL-Divergence = 0.0412, L1-Distance = 0.0187, L2-Distance = 0.0004, Normal std = 0.6094**

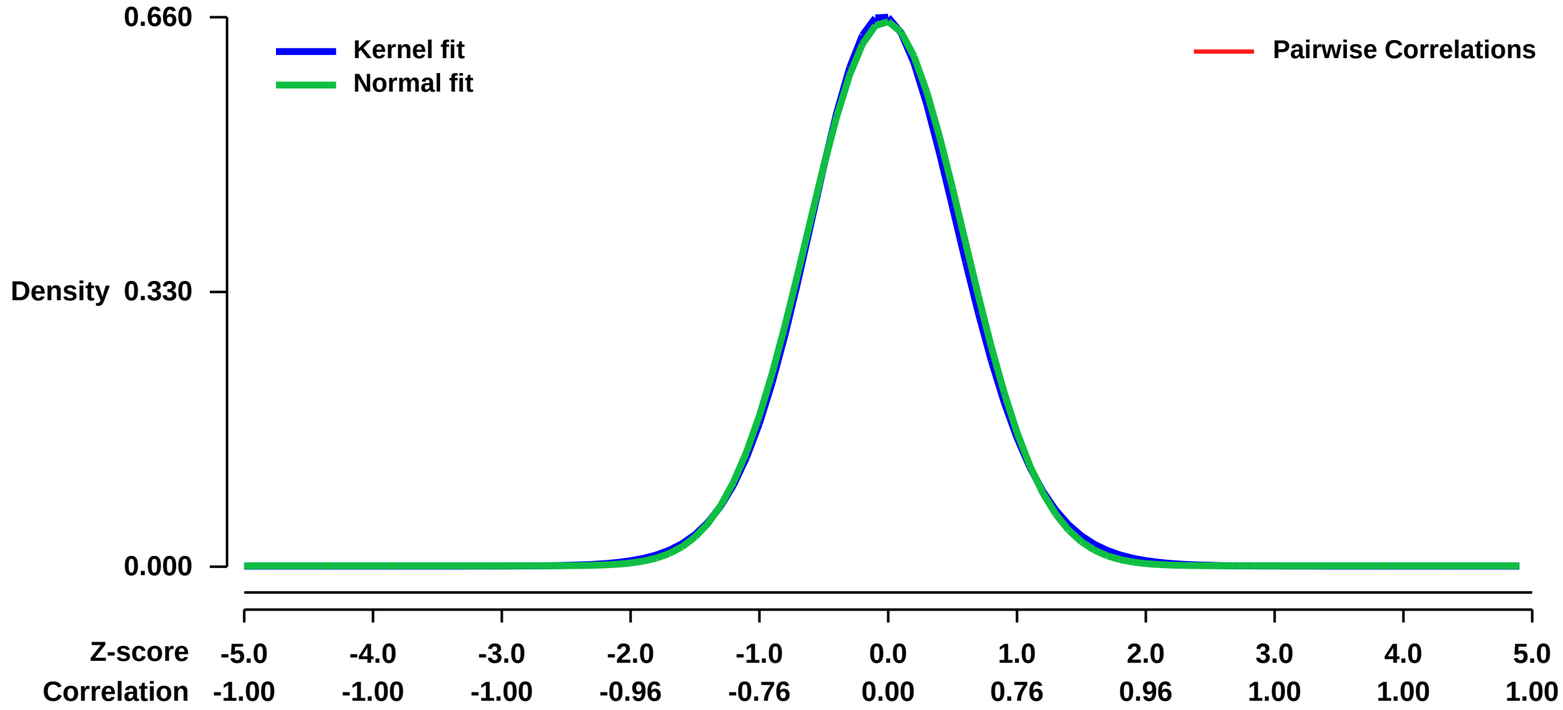

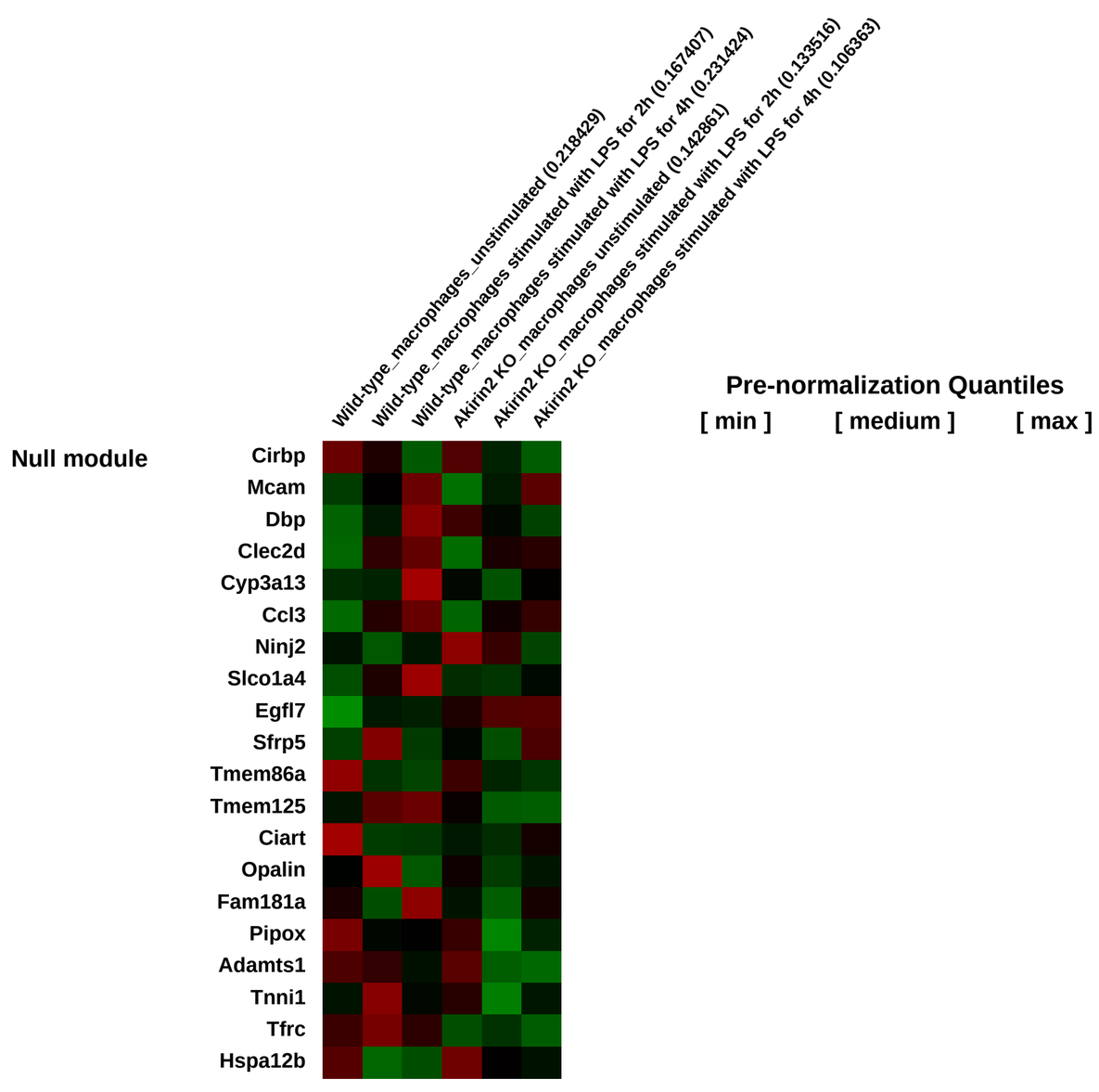

GEO Series "GSE41185" Expression Profiles

Num of samples in this series: 8

Scale of expression profile Z-scores

-3.0 -2.0 -1.0 0.0 1.0 2.0 3.0

GEO Link:	http://www.ncbi.nlm.nih.gov/geo/query/acc.cgi?acc=GSE41185
Status:	Public on Sep 06 2013
Title:	Potentiation of regulatory T cell stability and function via a neuropilin-1:semaphorin-4a axis
Organism:	Mus musculus
Experiment type:	Expression profiling by array
Platform:	GPL1261
Pubmed ID:	23913274
Summary & Design:	**Summary:** Regulatory T cells (Treg) represent a critical immunoregulatory component of the immune system. The signals that maintain Treg stability and potentiate their function remain obscure. Here we show that the immune cell surface ligand semaphorin-4a (Sema4a) **Overall design:** Sema treated and NRP1 knock outs were compared to untreated wild type T cell controls

Background corr dist: KL-Divergence = 0.0434, L1-Distance = 0.0294, L2-Distance = 0.0015, Normal std = 0.5876

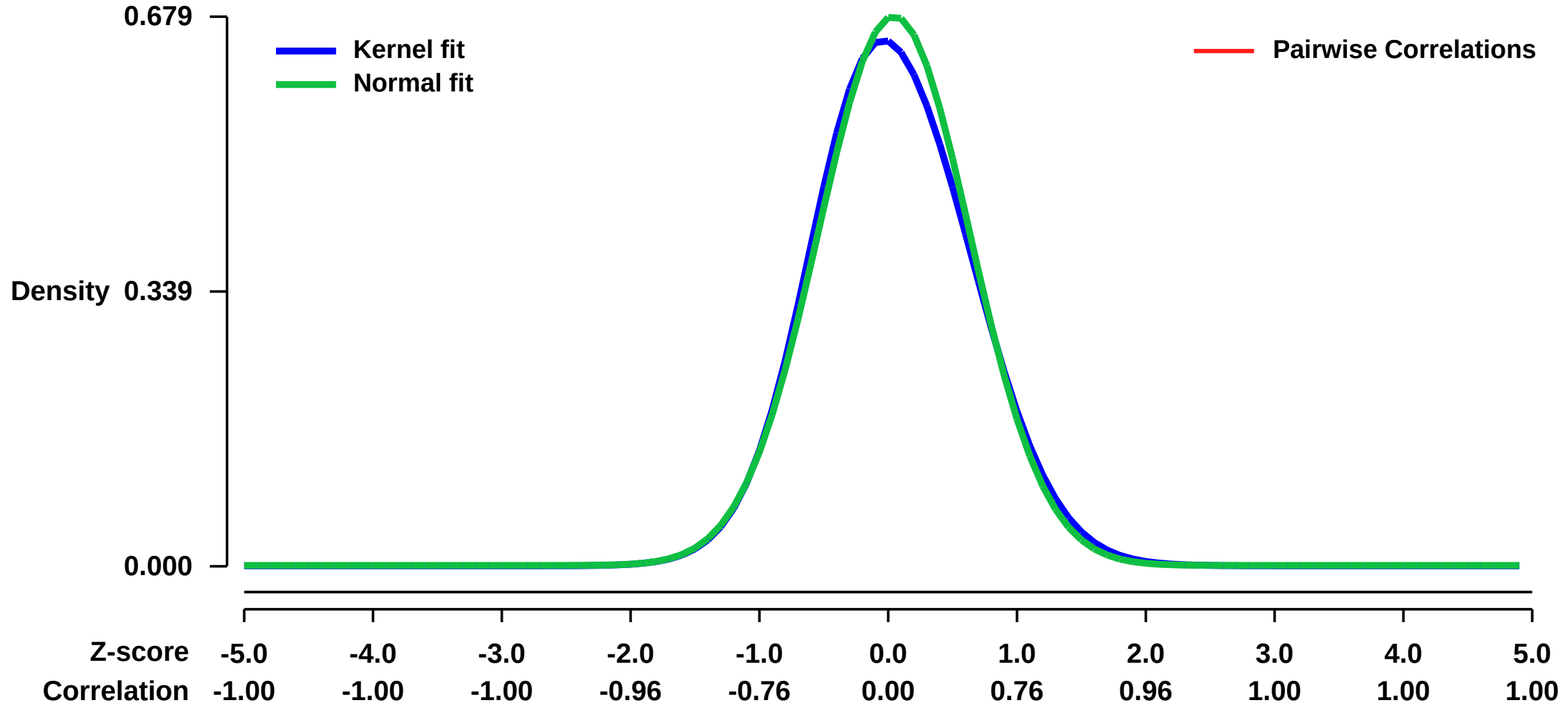

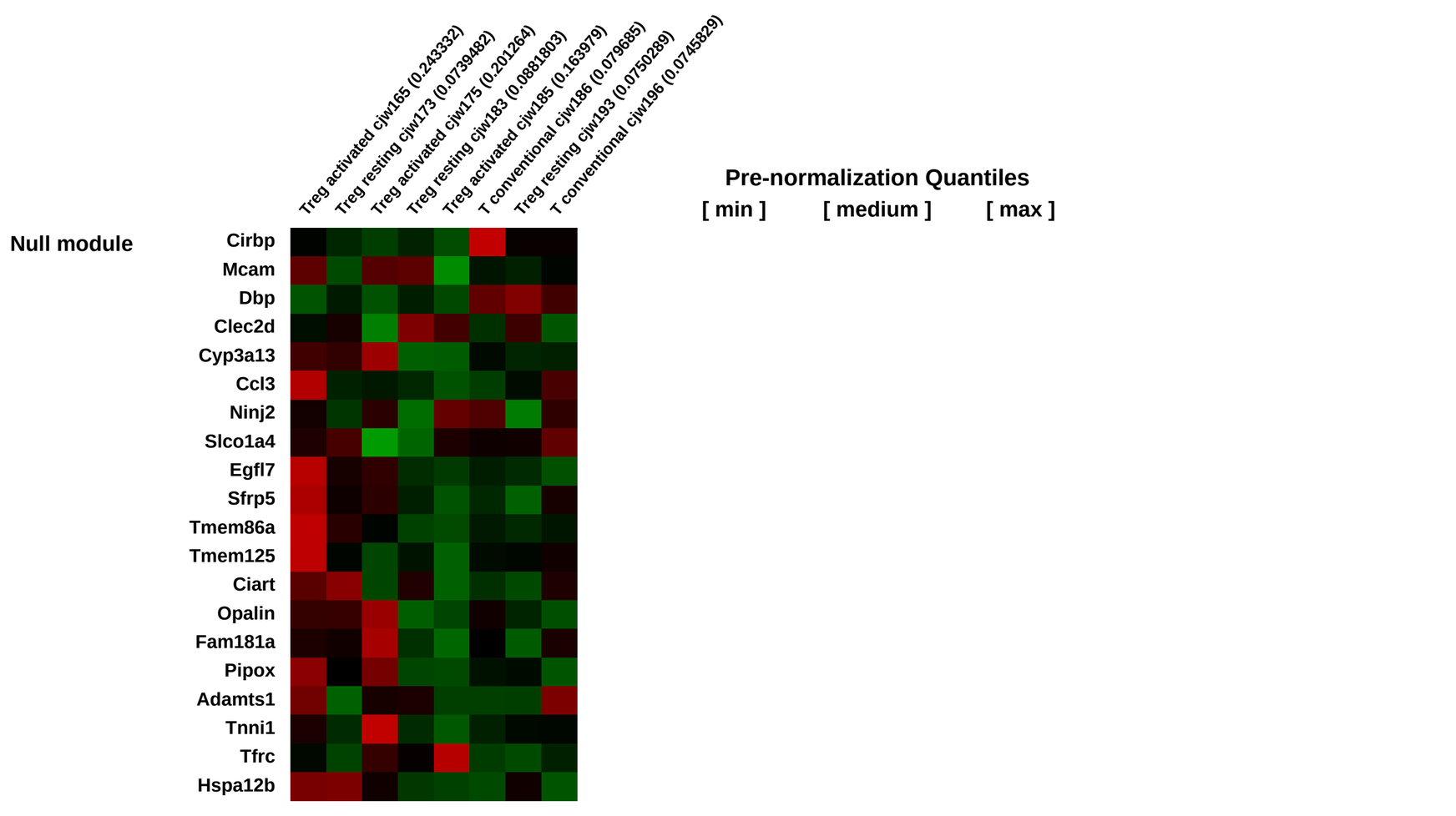

GEO Series "GSE10970" Expression Profiles

Num of samples in this series: 12

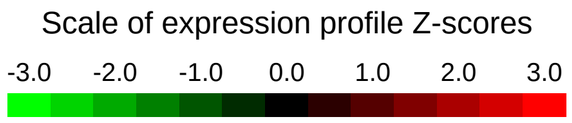

GEO Link:	http://www.ncbi.nlm.nih.gov/geo/query/acc.cgi?acc=GSE10970
Status:	Public on Mar 05 2009
Title:	Efficient Array-based Identification of Novel Cardiac Genes through Differentiation of Mouse ESCs
Organism:	Mus musculus
Experiment type:	Expression profiling by array
Platform:	GPL1261
Pubmed ID:	18478100
Summary & Design:	**Summary:** Cardiac disease accounts for the largest proportion of adult mortality and morbidity in the industrialized world. However, progress toward improved clinical treatments is hampered by an incomplete understanding of the genetic programs controlling early cardiogenesis. To better understand this process, we set out to identify genes whose expression is enriched within early cardiac fated populations, obtaining the transcriptional signatures of mouse embryonic stem cells (mESCs) differentiating along a cardiac path. We compared the RNA profiles of cardiac precursors cells (CPCs) with time-matched non-CPCs and undifferentiated mESCs, using a transgenic mESC line harboring an Nkx2-5 cardiac-specific regulatory sequence driving green fluorescent protein (GFP) to facilitate selection of CPCs. Approximately 24% (43/176) of the transcripts enriched in the CPC population have known roles in cardiac function or development. Importantly, we evaluated the biological relevance of a subset 31/133 (23%) of the remaining candidate genes by in situ hybridization and report that all were expressed in key cardiac structures during cardiogenesis (embryonic day, E7.5 - 9.5), many of which were previously uncharacterized. These data demonstrate the power of mESC differentiation to model specific developmental processes and provide a valuable resource that may be mined to further elucidate the genetic programs underlying cardiogenesis. **Keywords:** time course, differentiated cardiac cell fate **Overall design:** Cells from day 6 were then sorted using the BD Biosciences FACSAriaâ¢ Cell sorting system into GFP+ and GFP- fractions into RLT buffer (RNeasy, Qiagen). This sorting separates cells into two groups reflecting their differentiation into those fated to a non-cardiac lineage (GFP negative) and to a cardiac lineage (GFP positive).

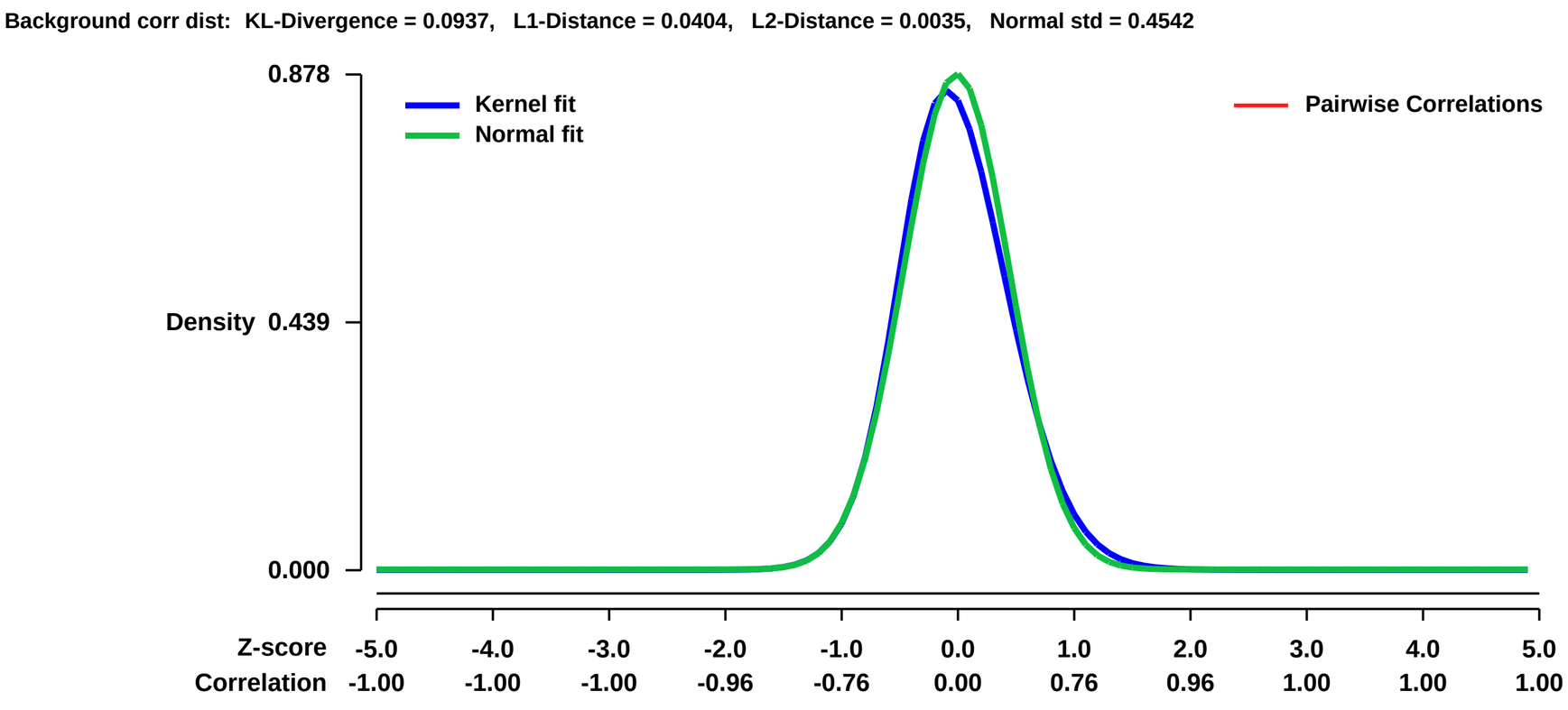

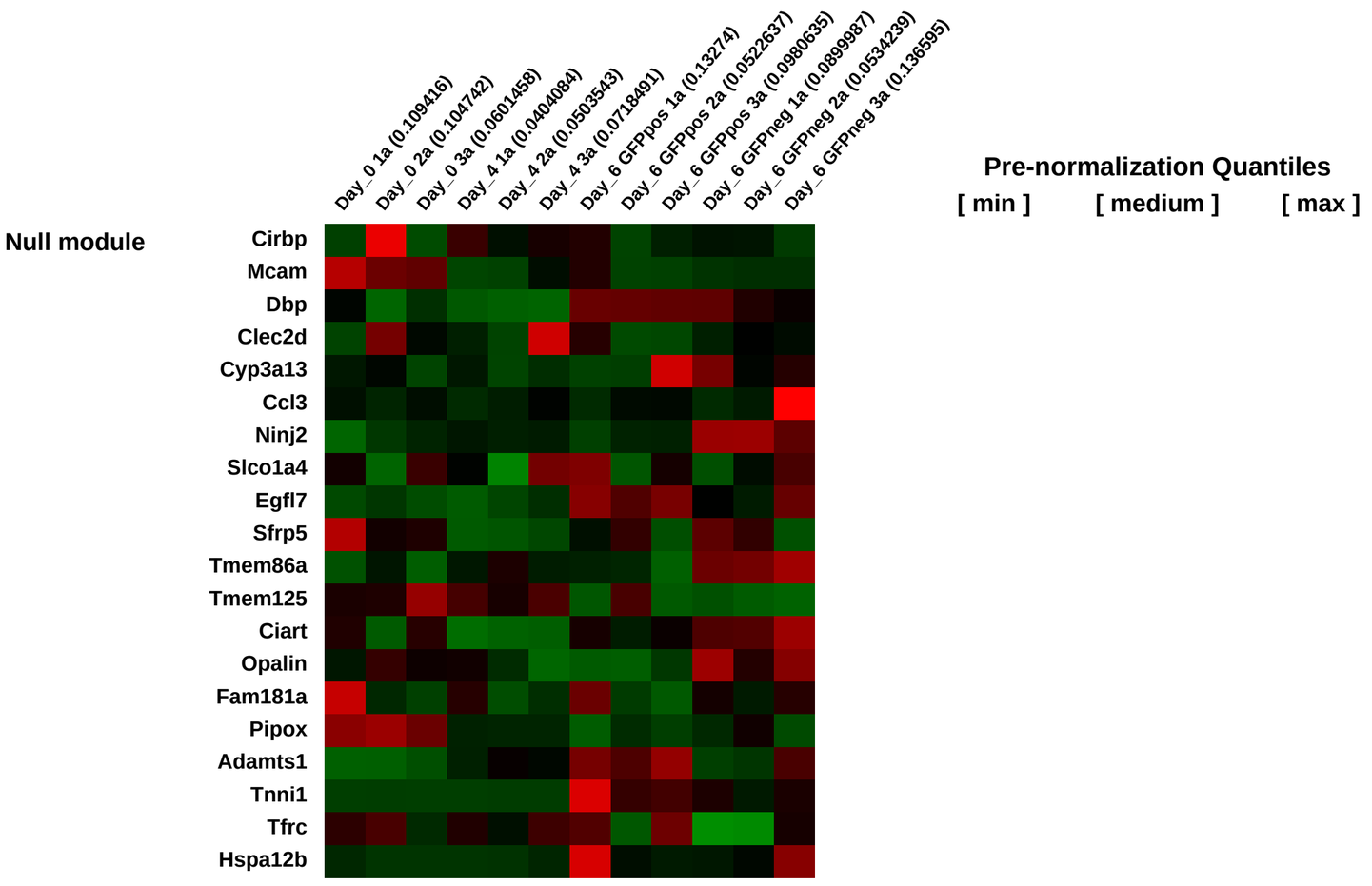

GEO Series "GSE44025" Expression Profiles

Num of samples in this series: 6

Scale of expression profile Z-scores

-3.0 -2.0 -1.0 0.0 1.0 2.0 3.0

GEO Link:	**http://www.ncbi.nlm.nih.gov/geo/query/acc.cgi?acc=GSE44025**
Status:	**Public on Nov 06 2013**
Title:	**Expression data from Sh2b3 Knock-out NOTCH1-induced leukemias**
Organism:	**Mus musculus**
Experiment type:	**Expression profiling by array**
Platform:	**GPL1261**
Pubmed ID:	**23908464**
Summary & Design:	**Summary:** **To formally address the tumor suppressor activity of Sh2b3 in vivo, we tested the interaction between oncogenic NOTCH1 and Sh2b3 loss in a retroviral- transduction bone marrow transplantation model of NOTCH-induced T-ALL** **Forced expression of activated NOTCH1 in this model typically results in full leukemia transformation 5-10 weeks later.** **Overall design:** **We performed microarray gene expression analysis of Sh2b3 wild type and Sh2b3â /â NOTCH1 induced leukemias**

Background corr dist: **KL-Divergence = 0.0428, L1-Distance = 0.0195, L2-Distance = 0.0004, Normal std = 0.6009**

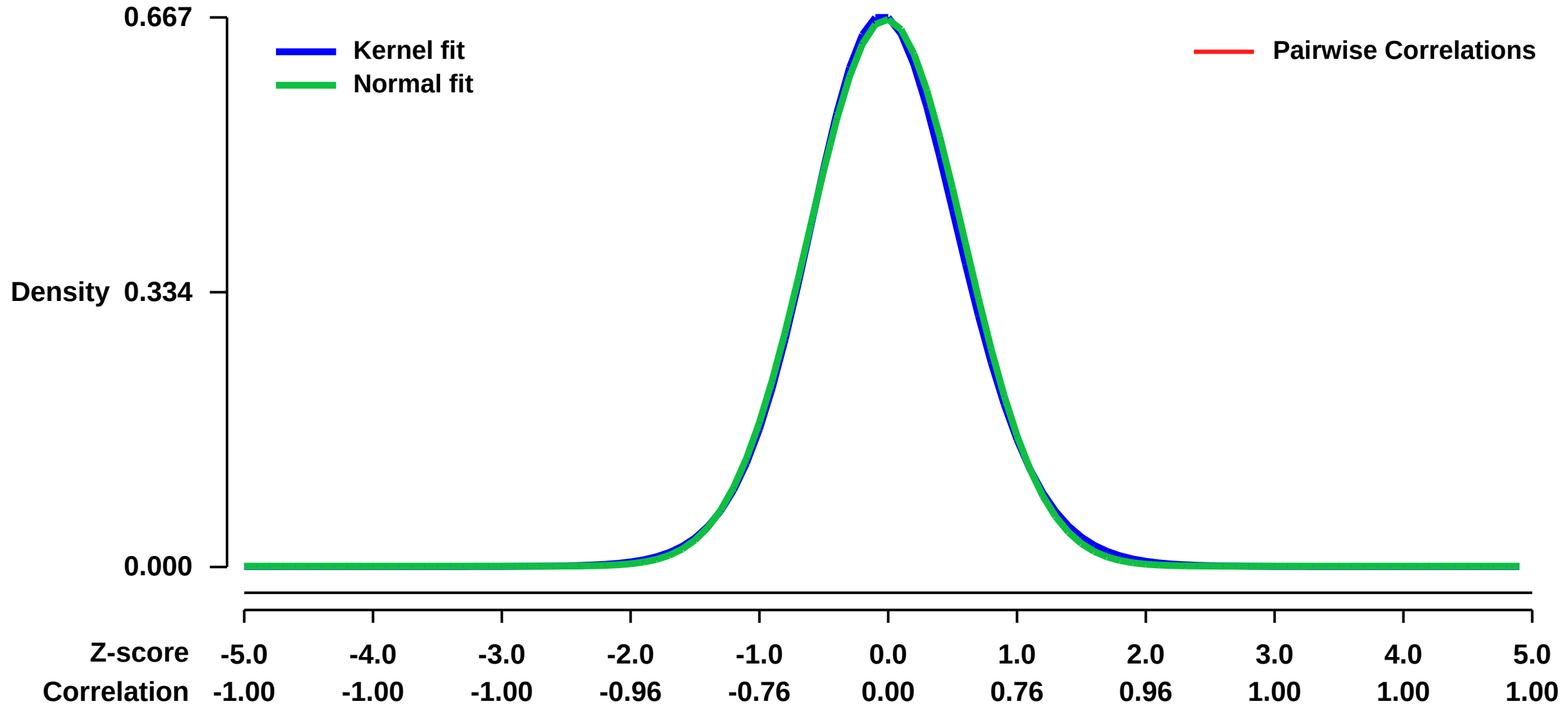

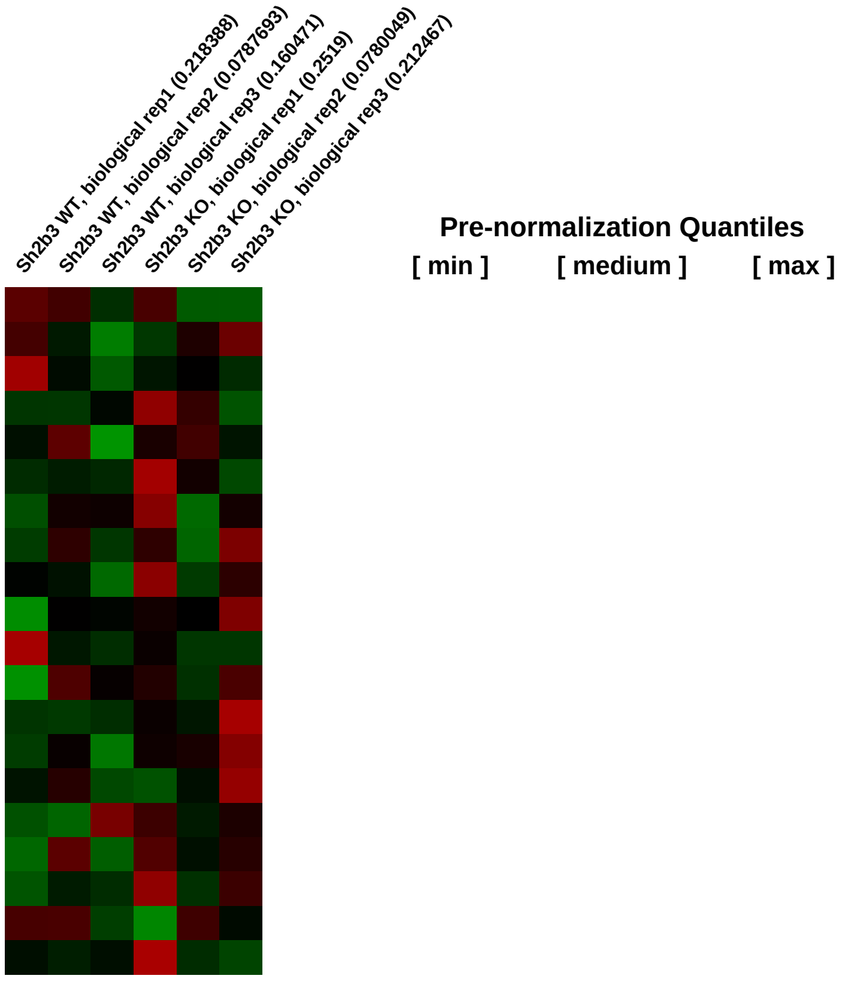

GEO Series "GSE17266" Expression Profiles

Num of samples in this series: 59

Scale of expression profile Z-scores

-3.0 -2.0 -1.0 0.0 1.0 2.0 3.0

GEO Link:	http://www.ncbi.nlm.nih.gov/geo/query/acc.cgi?acc=GSE17266
Status:	Public on Jan 12 2010
Title:	Expression data from B6C3F1 mice treated with baclofen
Organism:	Mus musculus
Experiment type:	Expression profiling by array
Platform:	GPL1261
Pubmed ID:	19812364
Summary & Design:	**Summary:** Mice were treated with either 100mg/kg baclofen or 0.5% methylcellulose alone by oral gavage for 1 or 5 days. **Overall design:** Mice were sacrificed by cervical dislocation after either a single dose (1day) or 5 daily doses (5 days) of either baclofen or 0.5% methylcellulose two hours after the last dose. The bone marrow from the right humerus, a portion of the left lateral liver lobe and half a cross-section of the spleen were harvested and the RNA was isolated from these tissues using standard Qiagen reagents. Standard Affymetrix protocols were used for GeneChip probe preparations. 59 arrays.

Background corr dist: KL-Divergence = 0.0198, L1-Distance = 0.0483, L2-Distance = 0.0033, Normal std = 0.7864

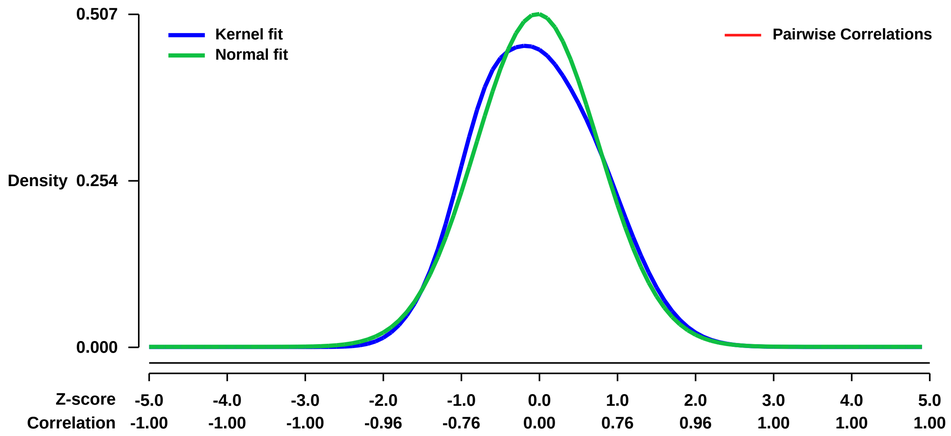

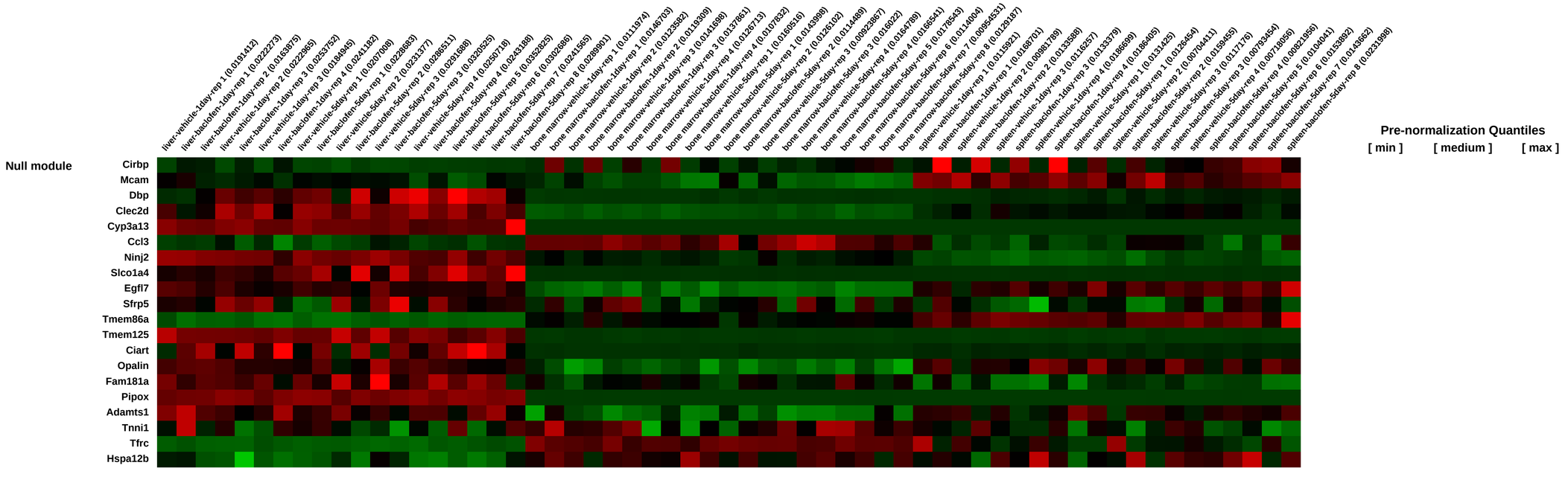

GEO Series "GSE9249" Expression Profiles

Num of samples in this series: 28

Scale of expression profile Z-scores

-3.0 -2.0 -1.0 0.0 1.0 2.0 3.0

GEO Link:	http://www.ncbi.nlm.nih.gov/geo/query/acc.cgi?acc=GSE9249
Status:	Public on Nov 01 2007
Title:	Gene expression analysis of B-NHL from ¸»MYC, ¸»MYC/I´µHABCL6, ¸»MYC/AIDKO and ¸»MYC/I´µHABCL6/AIDKO mouse models
Organism:	Mus musculus
Experiment type:	Expression profiling by array
Platform:	GPL1261
Pubmed ID:	18066064
Summary & Design:	**Summary:** Most human B cell lymphomas (B-NHL) are derived from germinal centers (GCs), the structure where B-cells undergo class switch recombination (CSR) and somatic hypermutation (SHM) and are selected for high-affinity antibody production. The pathogenesis of B-NHL is associated with distinct genetic lesions, including chromosomal translocations and aberrant somatic hypermutation, which appear to arise from mistakes occurring during CSR and SHM. To ascertain the role of CSR and SHM in lymphomagenesis, we crossed three oncogene-driven (MYC, BCL6, MYC/BCL6) mouse models of B cell lymphoma with mice lacking activation-induced cytidine deaminase (AID), the enzyme required for both processes. We show that AID deficiency prevents BCL6-dependent, GC-derived B-NHL, while it has no impact on the formation of MYC-driven, pre-GC lymphomas. Accordingly, abrogation of AID is associated with the disappearance of both CSR- and SHM-mediated structural alterations, including cMYC-IgH chromosomal translocations and aberrant SHM. These results demonstrate that AID is required for GC-derived lymphomagenesis, providing direct support to the notion that errors in AID-mediated antigen-receptor gene modification events represent major contributors to the pathogenesis of human B-NHL. **Keywords:** Phenotypic characterization of tumors developing in oncogene-driven mouse models of lymphomas **Overall design:** Nodal B-NHL from 5 MYC, 7 MYC/AIDKO, 12 MYC/HABCL6 and 6 MYC/HABCL6/AIDKO mice were analyzed in this study. Total RNA was extracted from frozen tumor biopsies and processed according to Affymetrix standard protocols

Background corr dist: KL-Divergence = 0.3116, L1-Distance = 0.0597, L2-Distance = 0.0098, Normal std = 0.2778

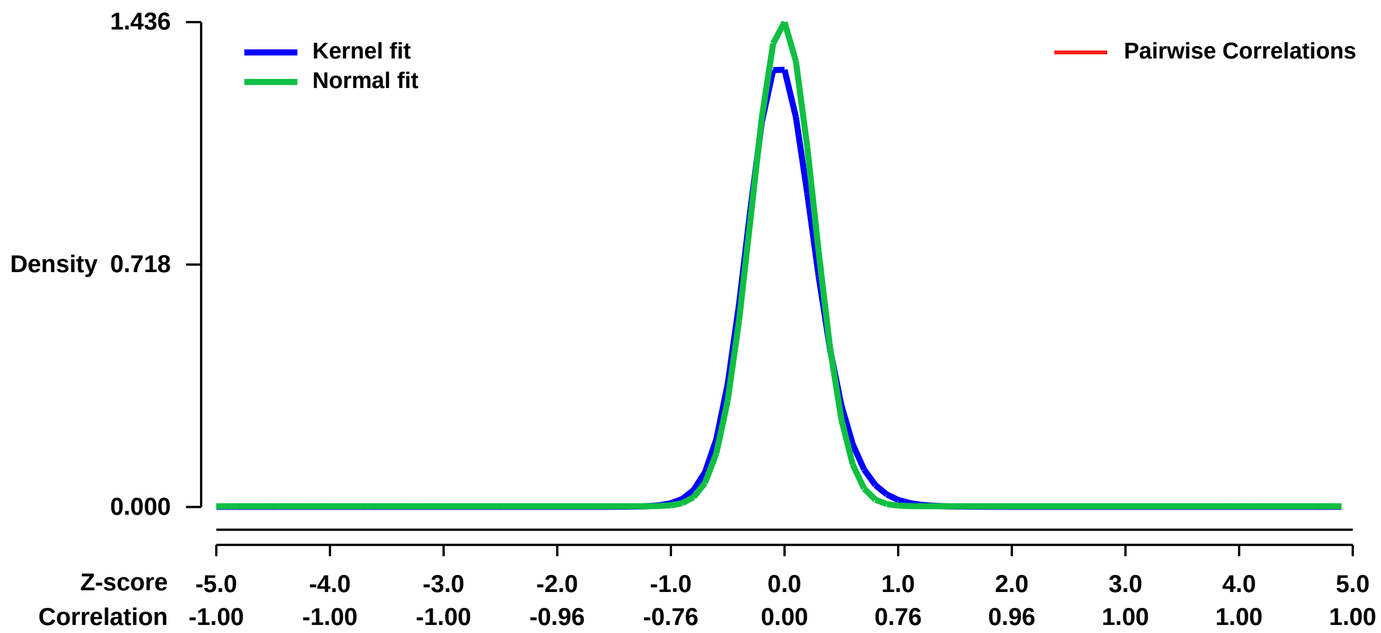

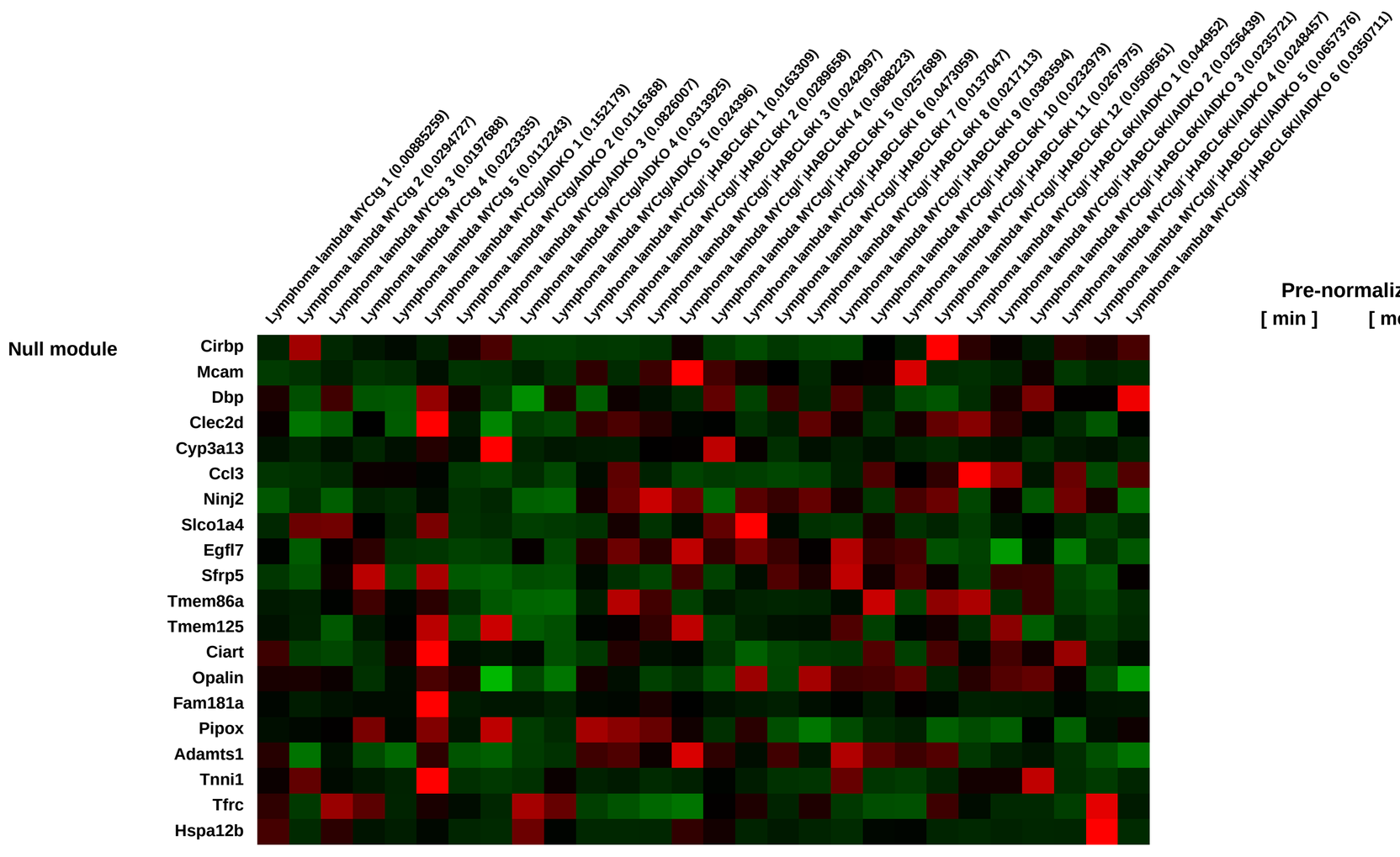

GEO Series "GSE36618" Expression Profiles

Num of samples in this series: 6

Scale of expression profile Z-scores

-3.0 -2.0 -1.0 0.0 1.0 2.0 3.0

GEO Link:	http://www.ncbi.nlm.nih.gov/geo/query/acc.cgi?acc=GSE36618
Status:	Public on Mar 20 2012
Title:	Mechanisms of terminal erythroid differentiation defect in EKLF-deficient mice
Organism:	Mus musculus
Experiment type:	Expression profiling by array
Platform:	GPL1261
Pubmed ID:	18852285
Summary & Design:	**Summary:** EKLF is a Krˆ…ppel-like transcription factor identified as a transcriptional activator and chromatin modifier in erythroid cells. EKLF-deficient (Eklf -/-) mice die at day 14.5 of gestation from severe anemia. In this study, we demonstrate that early progenitor cells fail to undergo terminal erythroid differention in Eklf -/- embryos. To discover potential EKLF target genes responsible for the failure of erythropoiesis, transcriptional profiling was performed with RNA from wild type and Eklf -/- early erythroid progenitor cells. These analyses identified significant perturbation of a network of genes involved in cell cycle regulation, with the critical regulator of the cell cycle, E2f2, at a hub. E2f2 mRNA and protein levels were markedly decreased in Eklf -/- early erythroid progenitor cells, which showed a delay in the G1-to-S-phase transition. Chromatin immunoprecipitation analysis demonstrated EKLF occupancy at the proximal E2f2 promoter in vivo. Consistent with the role of EKLF as a chromatin modifier, EKLF binding-sites in the E2f2 promoter were located in a region of EKLF-dependent DNase I sensitivity in early erythroid progenitor cells. We propose a model in which EKLF-dependent activation and modification of the E2f2 locus is required for cell cycle progression preceding terminal erythroid differentiation. **Overall design:** RNA was isolated from flow-sorted early erythroid progenitors in 13.5 day old fetal livers from EKLF knock out mice (n=3 fetal livers) and wild-type control mice (n=3 fetal livers) for gene expression analysis

Background corr dist: KL-Divergence = 0.0121, L1-Distance = 0.0188, L2-Distance = 0.0005, Normal std = 0.8297

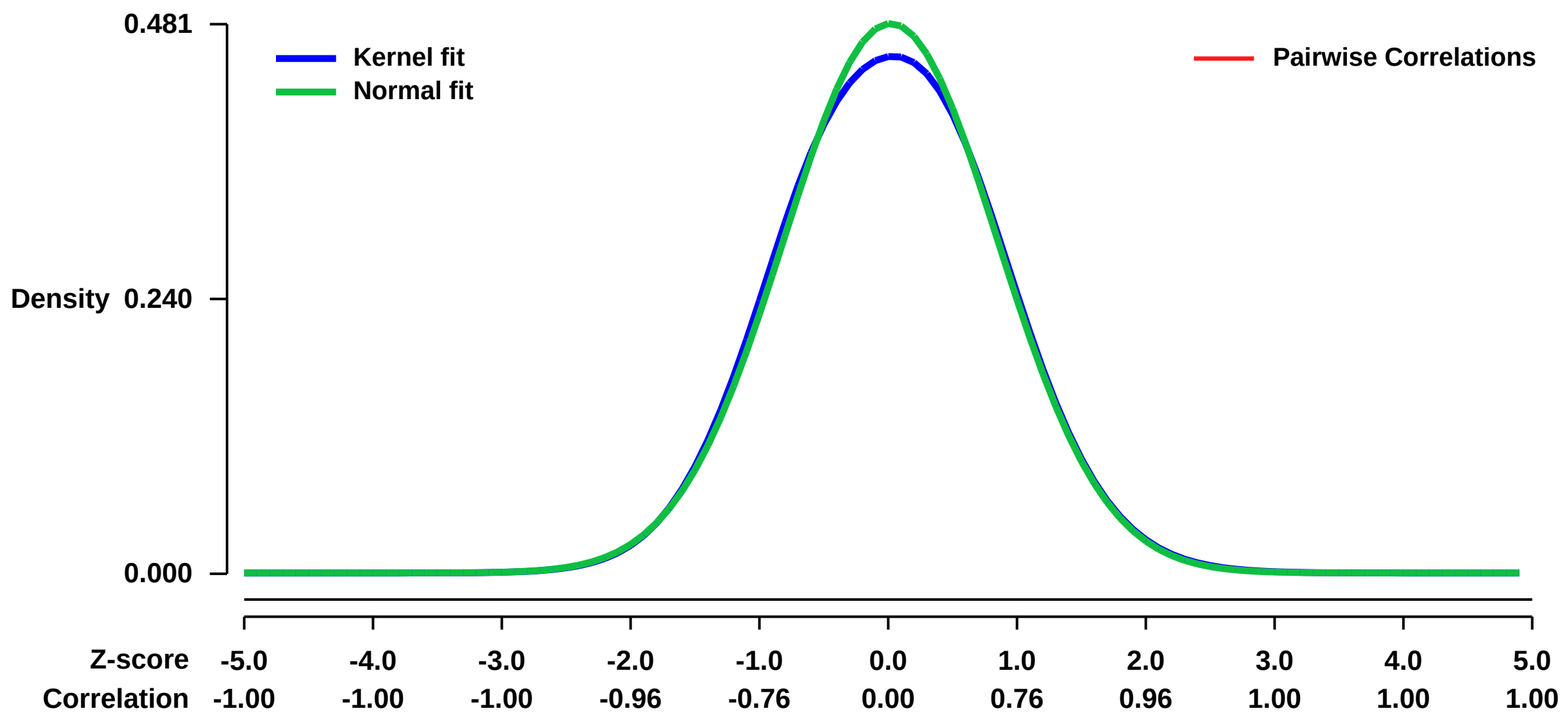

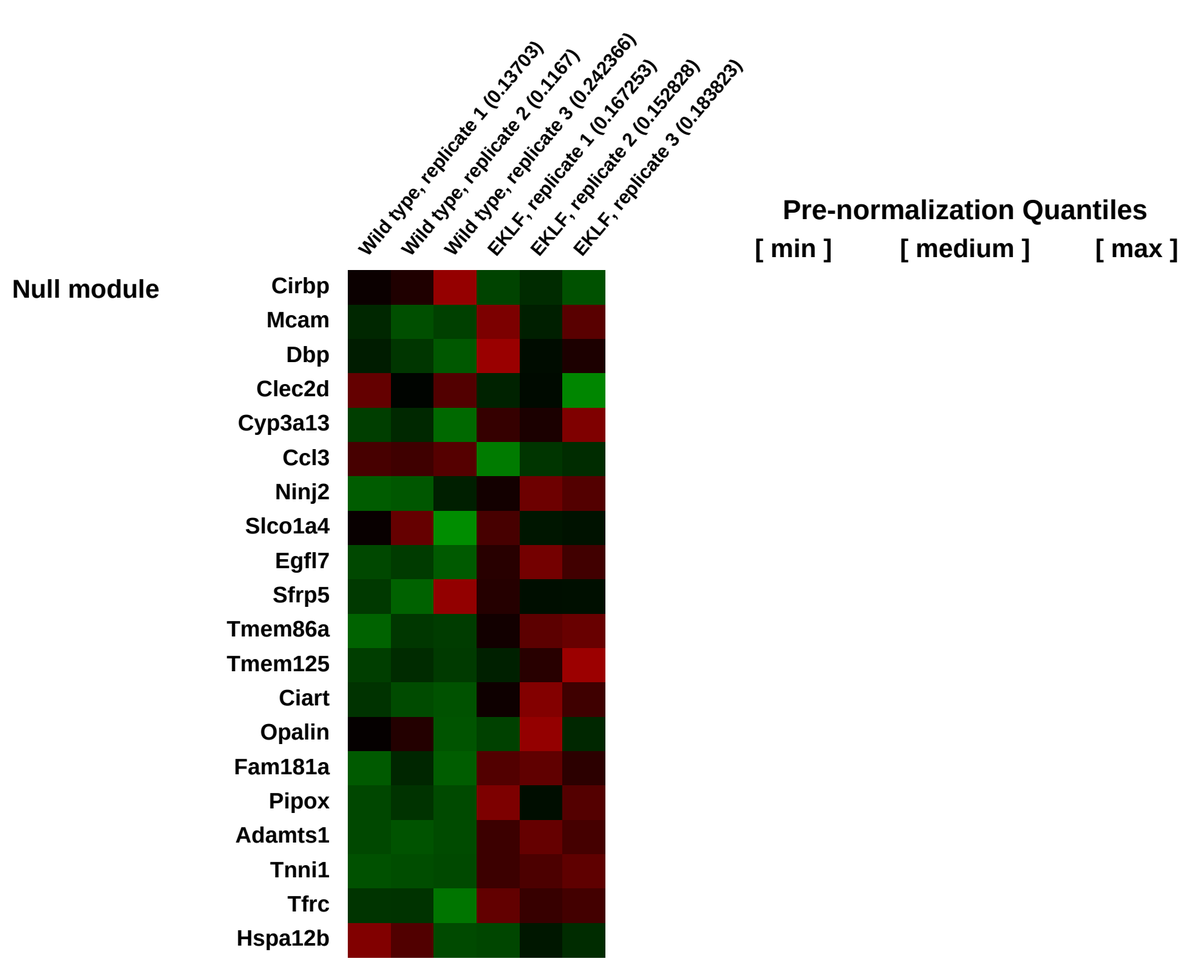

GEO Series "GSE9954" Expression Profiles

Num of samples in this series: 70

Scale of expression profile Z-scores

-3.0 -2.0 -1.0 0.0 1.0 2.0 3.0

GEO Link:	http://www.ncbi.nlm.nih.gov/geo/query/acc.cgi?acc=GSE9954
Status:	Public on Dec 20 2007
Title:	Large-scale analysis of the mouse transcriptome
Organism:	Mus musculus
Experiment type:	Expression profiling by array
Platform:	GPL1261
Pubmed ID:	18365009
Summary & Design:	**Summary:** We used microarrays to compare gene expression across different murine tissues. **Keywords: Other** **Overall design:** Different tissues were dissected from 10-12 week old C57Bl6 mice for RNA extraction and hybridization on Affymetrix microarrays.

Background corr dist: KL-Divergence = 0.3484, L1-Distance = 0.0923, L2-Distance = 0.0272, Normal std = 0.2989

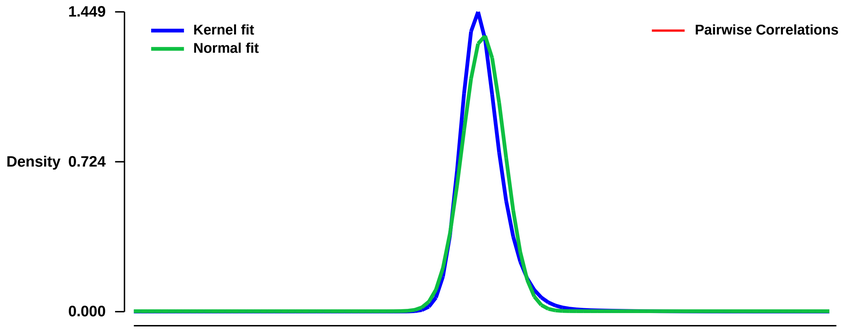

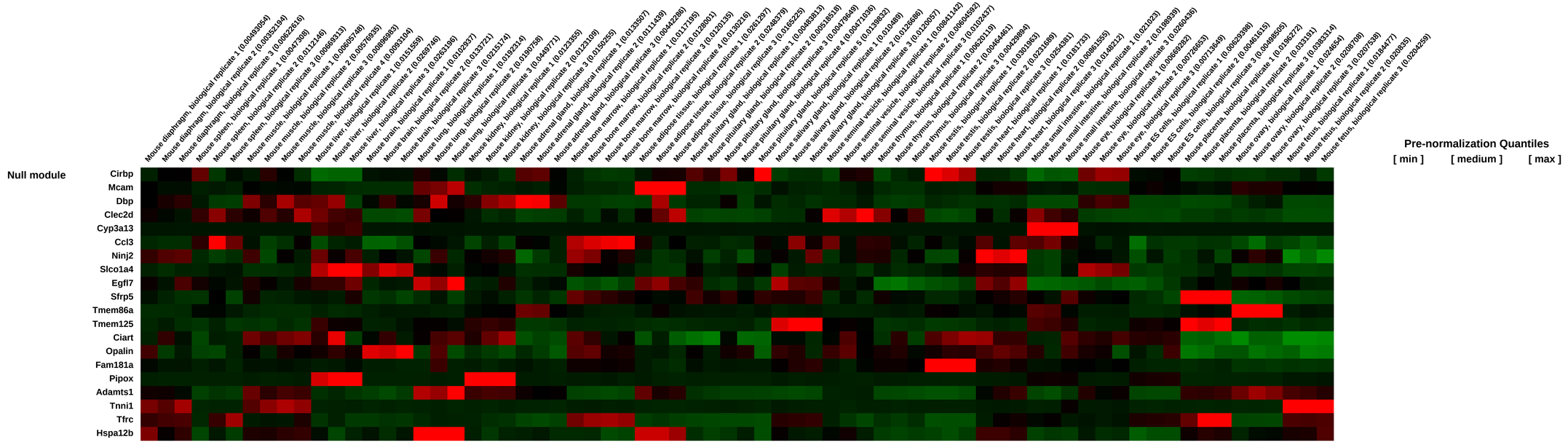

GEO Series "GSE7069" Expression Profiles

Num of samples in this series: 8

Scale of expression profile Z-scores

-3.0 -2.0 -1.0 0.0 1.0 2.0 3.0

GEO Link:	http://www.ncbi.nlm.nih.gov/geo/query/acc.cgi?acc=GSE7069
Status:	Public on Apr 20 2007
Title:	Zfx controls the self-renewal of embryonic and hematopoietic stem cells
Organism:	Mus musculus
Experiment type:	Expression profiling by array
Platform:	GPL1261
Pubmed ID:	17448993
Summary & Design:	**Summary:** Stem cells (SC) exhibit a unique capacity for self-renewal in an undifferentiated state. It is unclear whether the self-renewal of pluripotent embryonic SC (ESC) and of tissue-specific adult SC such as hematopoietic SC (HSC) is controlled by common mechanisms. The deletion of transcription factor Zfx impaired the self-renewal but not the differentiation capacity of murine ESC; conversely, Zfx overexpression facilitated ESC self-renewal by opposing differentiation. Furthermore, Zfx deletion abolished the maintenance of adult bone marrow HSC, but did not affect erythromyeloid progenitors or fetal HSC. In both ESC and HSC, Zfx activated a common set of direct target genes. In addition, the loss of Zfx resulted in the induction of immediate-early and/or stress-inducible genes in both SC types but not in their differentiated progeny. These studies identify the first shared transcriptional regulator of ESC and HSC, suggesting a common molecular basis of self-renewal in embryonic and adult SC. **Keywords:** Global gene expression data analysis in Zfx-deficient murine ESC and HSC **Overall design:** arrays (Affymetrix) at the Columbia University Microarray Project core facility according to the manufacturer's instructions. Samples were hybridized in duplicates, with the correlation between duplicate samples calculated at 0.995-0.997. Quality control and normalization were performed using positive and negative hybridization controls (Affymetrix) spiked into the RNA prior to labeling. Linear amplification of RNA was confirmed for every sample. Array scanning and raw data processing were done using GCOS 1.4 software (Affymetrix).

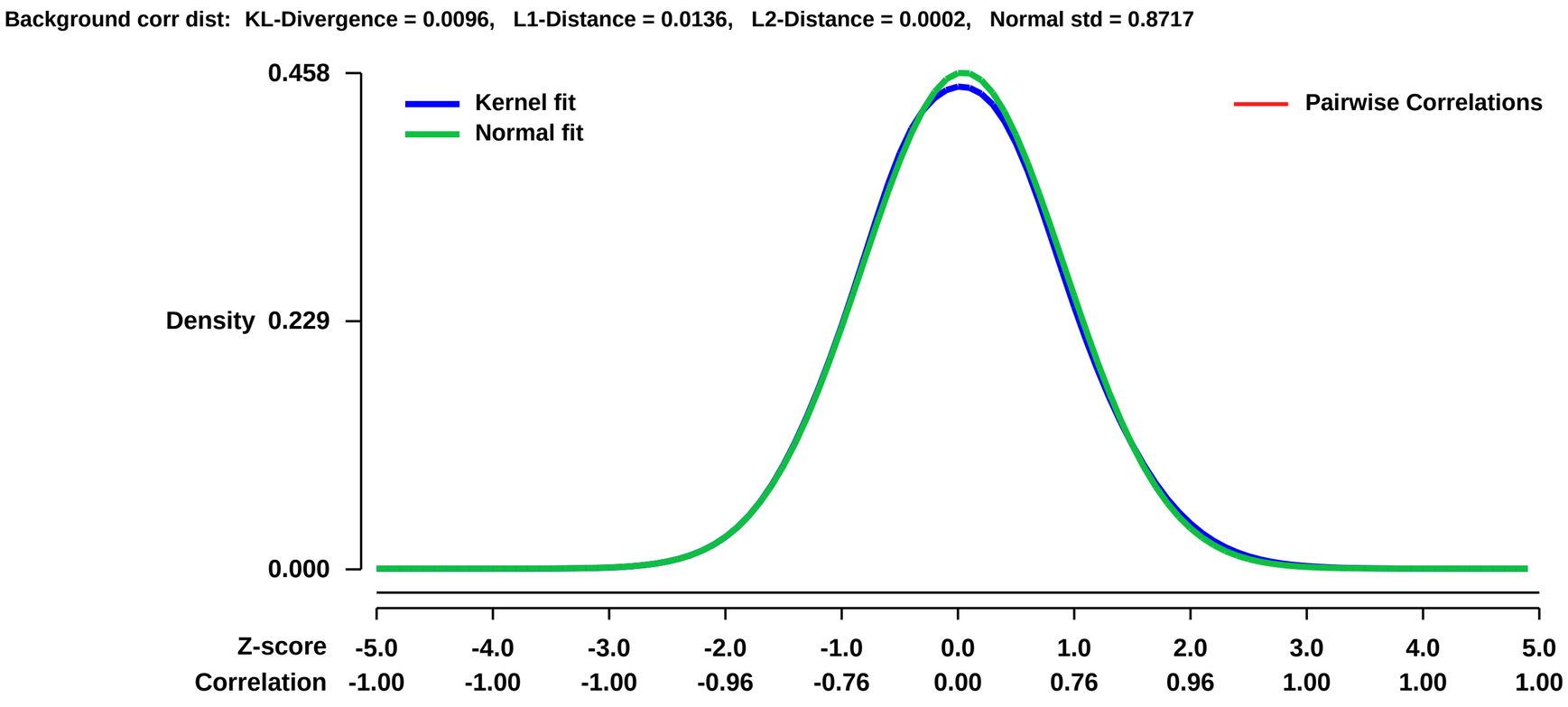

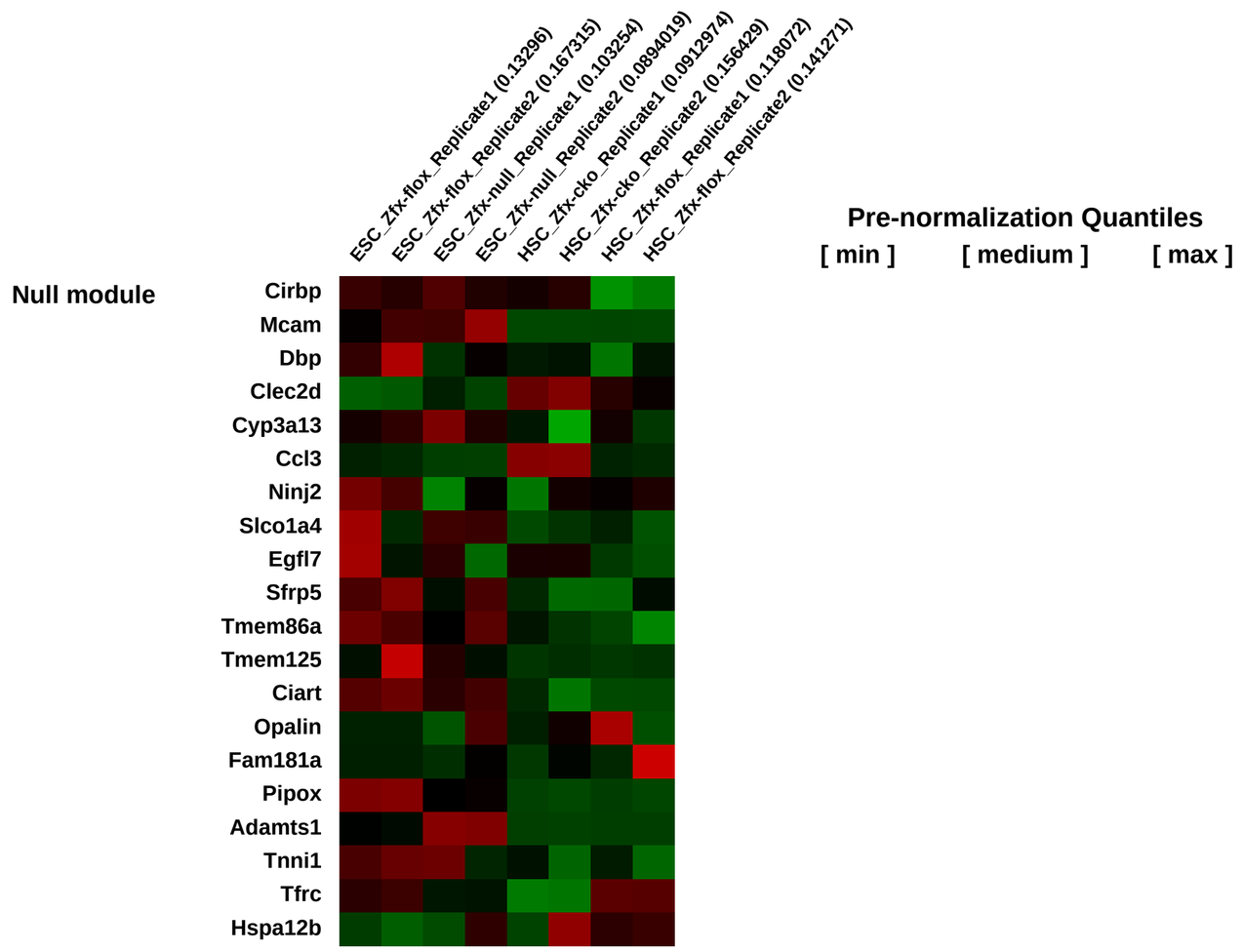

GEO Series "GSE3889" Expression Profiles

Num of samples in this series: 20

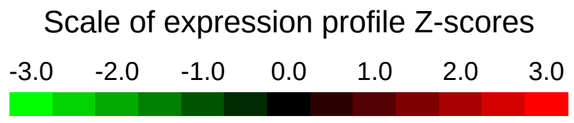

GEO Link:	http://www.ncbi.nlm.nih.gov/geo/query/acc.cgi?acc=GSE3889
Status:	Public on Dec 23 2005
Title:	Scd1 Knockout Mice on very low fat diet
Organism:	Mus musculus
Experiment type:	Expression profiling by array
Platform:	GPL1261
Pubmed ID:	17005996
Summary & Design:	**Summary:** Stearoyl-CoA desaturase 1-deficient (SCD1-/-) mice have impaired monounsaturated fatty acid (MUFA) synthesis. When maintained on a very low-fat, high-carbohydrate (VLF-HC) diet, SCD1-/- mice develop severe hypercholesterolemia characterized by an increase in apolipoprotein B-containing lipoproteins and the appearance of lipoprotein-X. Additionally, high-density lipoprotein cholesterol is dramatically reduced in VLF-HC SCD1-/- mice. The concomitant presence of elevated plasma bile acids, bilirubin and aminotransferases in the VLF-HC SCD1-/- mouse are indicative of hepatic dysfunction. Supplementation of the VLF-HC diet with unsaturated fat (canola oil), but not saturated fat (coconut oil), prevents these plasma phenotypes. However, dietary oleate was not as effective as canola oil in reducing low-density lipoprotein cholesterol, signifying an additional role for dietary polyunsaturated fatty acid deficiency in the development of this phenotype. These results indicate that lack of SCD1 results in an increased requirement for dietary unsaturated fat to compensate for impaired MUFA synthesis and to prevent hypercholesterolemia and hepatic dysfunction. **Keywords: repeat (genotype and diet)** **Overall design:** We used Affymetrix Mouse430v2.0 microarray chips to search for gene expression changes unique to the VLF-HC SCD1-/- group. These chips contain 45,101 probe sets representing over 39,000 transcripts and variants from over 34,000 mouse genes. We studied SCD1+/+ and SCD1-/- mice on chow or the VLF-HC diet, analyzing five individual livers from each subgroup for a total of twenty microarrays.

Background corr dist: KL-Divergence = 0.0559, L1-Distance = 0.0742, L2-Distance = 0.0112, Normal std = 0.5746

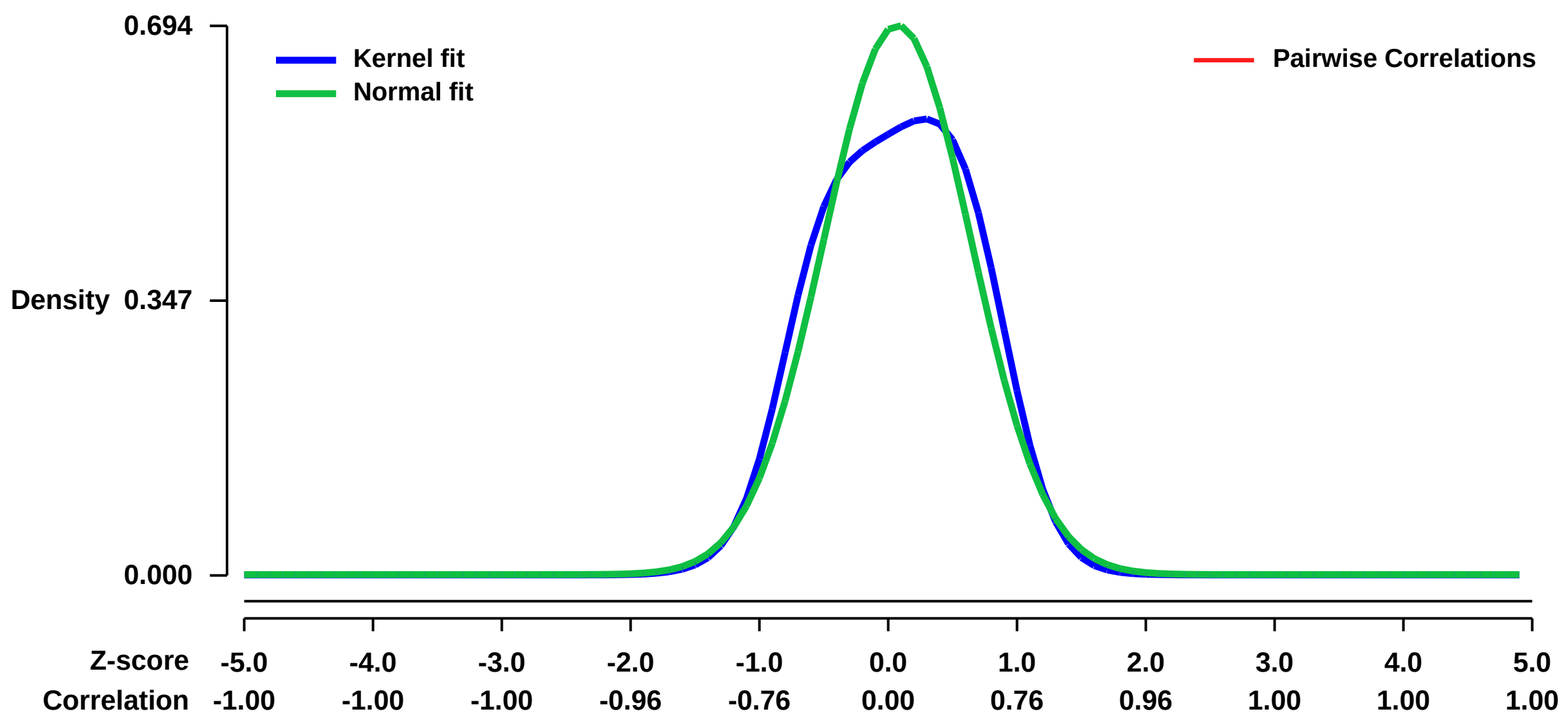

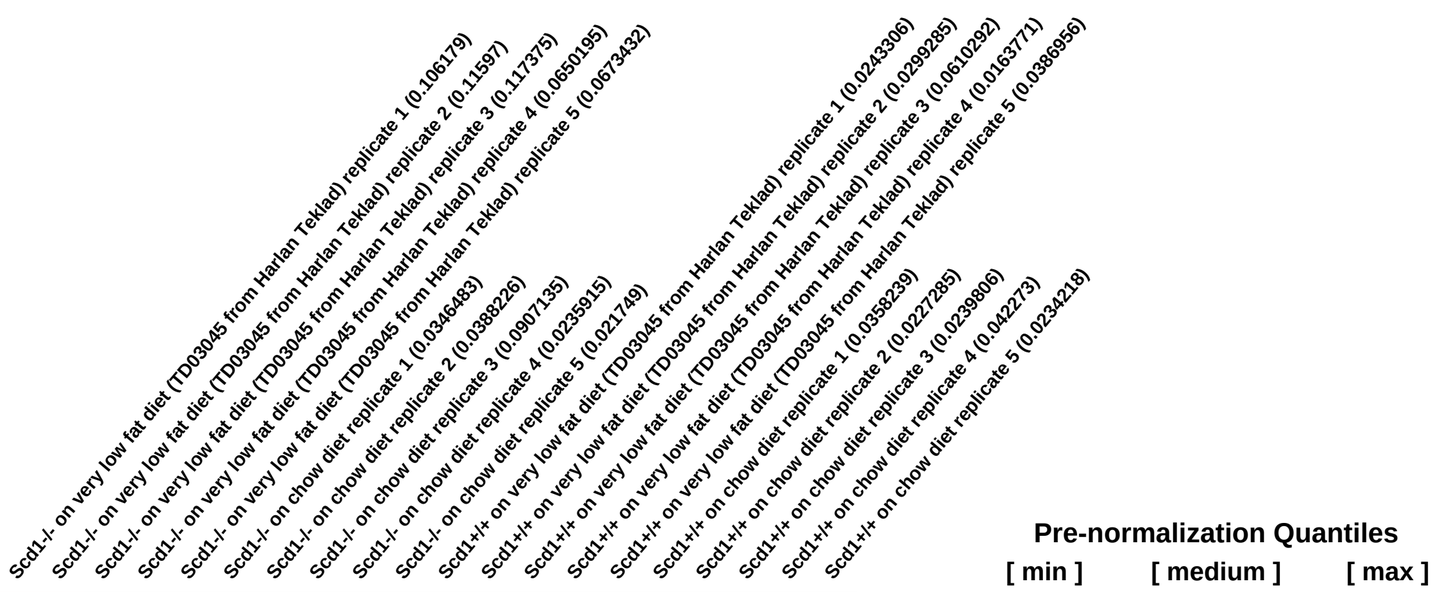

GEO Series "GSE10246" Expression Profiles

Num of samples in this series: 182

Details of this dataset are not shown due to large number of samples and the page size limit.

Find details in http://www.ncbi.nlm.nih.gov/geo/query/acc.cgi?acc=GSE10246
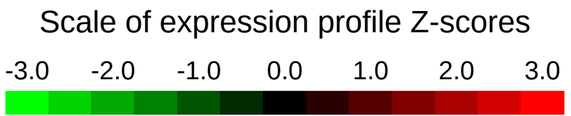
Background corr dist: KL-Divergence = 0.5414, L1-Distance = 0.1198, L2-Distance = 0.0520, Normal std = 0.2635